ARTIFICIAL NEURAL NETWORKS (A NEW STATISTICAL APPROACH) METHOD IN LENGTH-WEIGHT RELATIONSHIPS OF *ALBURNUS MOSSULENSIS* IN MURAT RIVER (PALU-ELAZIĞ) TURKEY

OZCAN, E. I.

Faculty of Fisheries, Munzur University, 62100 Tunceli, Turkey
e-mail: ebruozer@munzur.edu.tr; phone: +90-531-740-9095

(Received 24th Jan 2019; accepted 21st Mar 2019)

Abstract. Artificial Neural Networks (ANNs) is a reliable and alternative method used specially in the growth characteristics of some fish species. The purpose of this work was to compare with length-weight relationships and Artificial Neural Networks, the length-weight relation of 415 (232 female and 183 male) *Alburnus mossulensis* captured from Murat River between January 2018 and December 2018. The total length and the weight of the fish changed between 7.2-19.9 cm (12.81±0.095) and 3.24-40.6 g (13.51±0.30) respectively. The length-weight relationships were determined for females, males and all individuals as $W=0.0097L^{2.812}$ ($R^2=0.95$), $W=0.0168L^{2.599}$ ($R^2=0.95$) and $W=0.0130L^{2.701}$ ($R^2=0.95$), respectively. The growth type of *A. mossulensis* was negative allometric growth for female, male and all individuals. Regression analysis showed that length has high significantly correlation with weight (R = 0.97, R^2 = 0.95, $F_{1,413}$ = 79550.3, P <0.001) and 95% remain in weight was due to length remain. t-test results was used for the importance condition of the regression coefficients (t=89.193, P<0.01). Length-length relations were highly significant with R^2 values greater than 0.97. The condition factor values were ranged between 0.430 and 0.975 for all individuals. According to the comparison of the results obtained with MAPE (%), ANNs provided better results than the LWRs. With this study, it can be seen that ANNs can be used as an alternative useful method for population parameters prediction.
Keywords: *ANNs, MAPE (%), length-weight relation, negative allometric growth, Murat River*

Introduction

Alburnus mossulensis is a freshwater fish species from cyprinid, inhabiting the Euphrates, Tigris and Ceyhan rivers and in their near basins in Iran (Kuru, 2004; Geldiay and Balık, 2007; Coad, 2010). Ergene (1993) studied the reproduction and growth of this species in the Euphrates Basin of Turkey. Başusta (Girgin) (2000) investigation and growth and changes of in blod cells this species living in Keban Dam Lake. Turkmen and Akyurt (2000) and Yıldırım et al. (2003) studied the population structure and growth properties of the species in Karasu River. Başusta and Cicek (2006) studied the length-weight relationships for this fish in Ataturk Dam Lake in southeastern Anatolia, Turkey. Yıldırım et al. (2007) studied the reproduction and growth of this species in the Euphrates Basin of Turkey. Ghorbani (2011) studied the reproductive biology and population dynamics of the fish in Bibi-Sayyedan River of Tigris basin in Iran. Mousavi-Sabet et al. (2013, 2014) determined the length-weight relationships of the fish in Iran. Esmaeili et al. (2014) studied the LWR in this species in Iran. Abdul-Razak et al. (2015) studied some biological aspects of this species in the southern reaches of Euphrates River, Iraq. Alkan Uckun and Gokce (2015) assessed the age, growth, and reproduction of *A. mossulensis* in Karakaya Dam Lake (Turkey). Keivany et al. (2015, 2016); Radkhah (2016) and Keivany and Zamani-Faradonbeh (2017) studied the length-weight relationship and condition factor of *A. mossulensis* in Beheshtabad River, Bibi-Sayyedan River, Hamzeh-Ali Spring and Jarrahi River.

http://www.aloki.hu ● ISSN 1589 1623 (Print) ● ISSN 1785 0037 (Online)
DOI: http://dx.doi.org/10.15666/aeer/1705_1025310266

Keivany et al. (2017) studied the reproductive biology and morphological diversity of *Alburnus mossulensis* populations in Iran. Serdar et al. (2017) some population parameters of *Alburnus mossulensis* in the Karasu River.

ANNs have been used in differ branches of aquatic science and in biology more than in other sciences (Tureli Bilen et al., 2011). With ANNs models; Maravelias et al. (2003) estimated the distributions of demersal fish species, Mastrorillo et al. (1997) estimated the existences of small fish in a river, Park et al. (2003) estimated aquatic macro-invertebrate varieties, Obach et al. (2001) predicted population dynamics of aquatic insects, Joy and Death (2004) estimated and spatially mapping freshwater fish and assemblies of decapods and Benzer and Benzer (2016) fish population predicted. Benzer et al. (2015, 2017) and Benzer and Benzer (2018) predicted growth properties of crayfish (*Astacus leptodactylus*). Ozcan and Serdar (2018a) estimated some population parameters of tigris loach (*Oxynoemacheilus tigris*). Sangun et al. (2019) estimated body weight of *Sparus aurata* with artificial neural network. Many authors reported that ANNs gave better results than other methods (Tureli Bilen et al., 2011; Benzer et al., 2015, 2017; Benzer and Benzer, 2016, 2018; Ozcan and Serdar, 2018a). ANNs is an alternative method for other methods in non linear situations for predict modeling (Joy and Death, 2004).

This study is the first record ANNs as a new and alternative approach to predicting basic biological characteristics for *A. mossulensis* in Murat River. The results showed high proximity between the measured and predicted data. Predicted and observed values are compared by Mean Absolute Percent Error (%). The values obtained with Artificial Neural Networks are much closer to their real values. For this reason, in this study it can be concluded that ANNs model applied made a more effective and reliable analysis than other methods. The aim of this study is to show the reliability of ANNs, which is an alternative method for the calculation of length-weight relationships.

Materials and Methods

Murat River, which is born from Aladağ in the north of Lake Van, flows into the Palu and Keban Dam Lake. The coordinates of Murat River (Palu-Elazığ) sampling 1. stations (38°41'08.9"N, 39°52'51.9"E) and 2. stations (38°40'05.1"N, 39°50'59.5"E) are given in *Figure 1*.

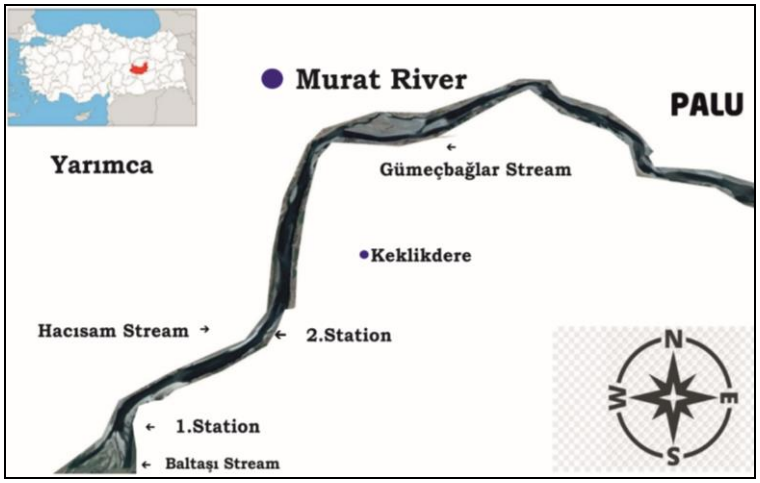

Figure 1. *Sampling stations of Murat River (Palu, Elazığ)*

http://www.aloki.hu ● ISSN 1589 1623 (Print) ● ISSN 1785 0037 (Online)
DOI: http://dx.doi.org/10.15666/aeer/1705_1025310266

Fishes were as monthly caught with gillnet by researcher and local fishermen during January 2018 and December 2018. Fishes were carried to the laboratory and fixed with 5% formaldehyde. Fish samples were measured for total length, fork length, standard length, weight and sexes identified by macroscopic observation of gonads; sex ratios were checked by a chi-square test (differed from 1:1).

The total length-weight relationship was determined with the below equation (*Eq. 1*) (Ricker, 1975). The degree of relation between the changeables was calculated with the determination coefficient, R^2 (King, 1995). (W is weight (W), L is total length (TL), a is the intercept, and b is the slope).

$$W = a*L^b \quad \text{(Eq.1)}$$

Length-length relationships were calculated with linear regression analysis (*Eq. 2*) (Zar, 1999).

$$TL=a+bFL,\ FL=a+bSL,\ SL=a+bTL \quad \text{(Eq.2)}$$

The condition factor values of fish are obtained by the below equation (*Eq. 3*) (W is weight; TL is total length and b is the coefficient of allometric of relationship) (Le Cren, 1951).

$$K=(W/TL^b)*100 \quad \text{(Eq.3)}$$

Artificial neural networks (ANNs) are biologically computer programs designed to adapt the human brain. ANNs identify the relationships in the data and learn through experiment and add their knowledge. An ANN is comprise of hundreds of single units, artificial neurons or processing elements. Neurons in a network are interconnected by the power of neural calculations. The behavior of these neural networks is determined by the transmission process and learning rule of their neurons. The activation signal is taked place transfer function to generate a single output of the neuron. Transmission process introduces non-linearity to the network. Throughout the course of the training, the connections are optimized until you reach the minimum and the best accuracy of the error. After the network is trained and tested, new data for output can be displayed (Agatonovic-Kustrin and Beresford, 2000). This model is an interrelatedness group of artificial neurons that process information in parallel. In general, an ANN is a system that varies according to internal and external information flowing through the network. Briefly summarized, neural networks are regression analysis, statistical, data-modelling tools used for modelling sophisticate relationships between inputs and outputs in data (Cabreira et al., 2009). Basically, there are 3 different layers in a neural network:

1. Input Layer (All the inputs are fed in the model through this layer (Length/weight, sex)).

2. Hidden Layers (There can be more than one hidden layers which are used for processing the inputs received from the input layers).

3. Output Layer (The data after processing is made available at the output layer (Weight/length)) (URL, 1); (*Fig. 2*).

The mathematical equation of the neuron model is as follows (*Eq.4*) (Krenkel et al., 2011). ($yi(k)$ is output value in discrete time k, F is a transfer function, $wi(k)$ is weight

http://www.aloki.hu ● ISSN 1589 1623 (Print) ● ISSN 1785 0037 (Online)
DOI: http://dx.doi.org/10.15666/aeer/1705_1025310266

value in discrete time *k* where i goes from *0* to *m*, *xi*(*k*) is input value in discrete time *k* where *i* goes from *0* to *m*, *b* is bias).

$$y(k) = F(\sum_{i=0}^{m} wi(k).xi(k) + b) \quad \text{(Eq.4)}$$

MAPE was used to compare ANNs and other methods. The smaller the MAPE values, the closer are the predicted values to the actual values (Benzer et al., 2017). MAPE is as follows equality (*Eq.5*). Yi is actual observation value, ei is difference between the actual value and the prediction value, n is number of total observations.

$$MAPE = \frac{1}{n}\sum_{i=1}^{n}\left|\frac{ei}{Yi}\right| x100 \ldots\ldots\ldots\ldots \quad \text{(Eq.5)}$$

Neural Network Toolbox of MATLAB (Ver R2016a) was used for ANNs. Created in MATLAB software are made up of three parts. These are "training", "testing", and "validation". In this study, for ANN model, 70% for training step, 15% for validation step and 15% for test step.

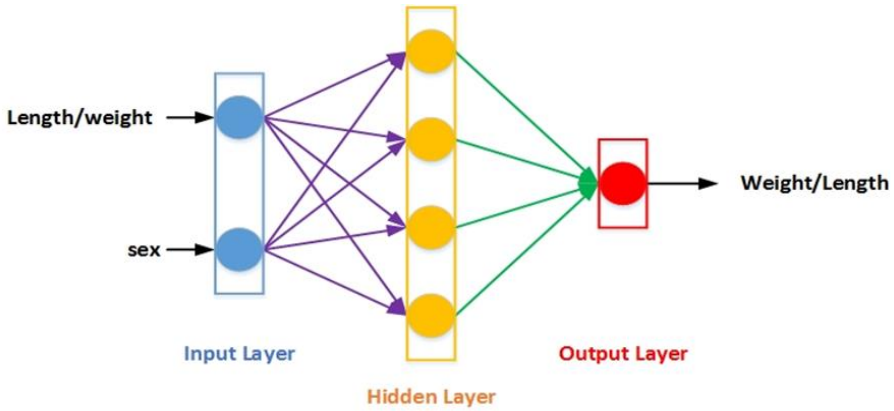

Figure 2. *Representation an ANN formed of 2 input layers, a hidden layer and an output layer to be estimated*

Results

A total of 415 (232 female and 183 male) specimens were caught in this study, the length and weight of females ranged from 8.7 to 19.9 cm (12.76 ± 0.12) and 5.0 to 40.60 g (13.32 ± 0.38) and those of males from 7.2 to 19.6 cm (12.82 ± 0.14) and 3.24 to 38.70 g (13.53 ± 0.45), respectively. The specimens were composed of 56% females and 44% males. The sex ratio of female to male was 1:0.79, chi-square test showed that significantly different from the expected 1:1 ratio ($P<0.05$). The difference in the lengths of females and males were not statistically important (*t*-test, $p>0.05$). The total length, weight-frequency is presented in *Figure 3*. The length group interval 11.0-12.9 cm (43.61%) and weight group 10.0-16.9 g (55.66%) were the most aboundant for all specimens. The females were larger in length and weight.

Length-weight relationships of *A. mossulensis* were found as $W=0.0097*L^{2.812}$, $R^2=0.95$, SE of $b=0.0025$ and 95% confidence intervals of $b=2.557$-2.836, *t*-test $P<0.05$ for females; $W=0.0168*L^{2.599}$, $R^2=0.95$ SE of $b=0.0028$ and 95% confidence intervals of $b=2.575$-2.865, *t*-test $P<0.05$ for males and $W=0.0130*L^{2.701}$, $R^2=0.95$ SE of $b=0.0019$

http://www.aloki.hu ● ISSN 1589 1623 (Print) ● ISSN 1785 0037 (Online)
DOI: http://dx.doi.org/10.15666/aeer/1705_1025310266

and 95% confidence intervals of *b*=2.557-2.865, *t*-test *P*<0.05 for all individuals (*Fig. 4*); (*Table 1*). The growth type of *A. mossulensis* was negative allometric growth for female, male and all individuals. Regression analysis showed that length has high significantly correlation with weight (R = 0.97, R^2 = 0.95, $F_{1,413}$ = 79550.3, P<0.001) and 95% remain in weight was due to length remain. *t*-test results was used for the importance condition of the regression coefficients (*t*=89.193, *P*<0.01).

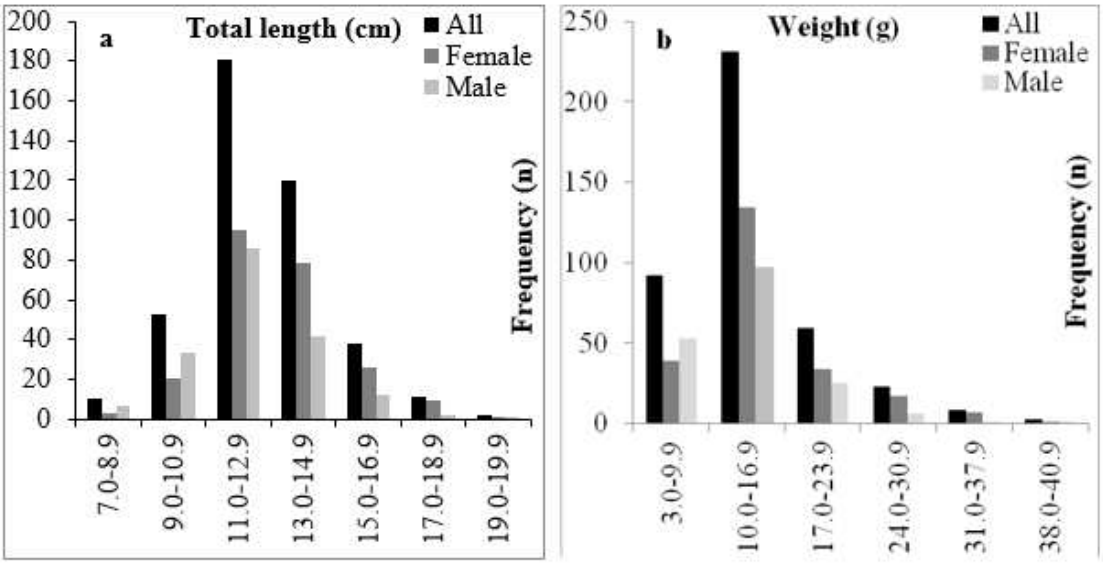

Figure 3. *Total-length (a) and weight (b) frequency of Alburnus mossulensis in Murat River*

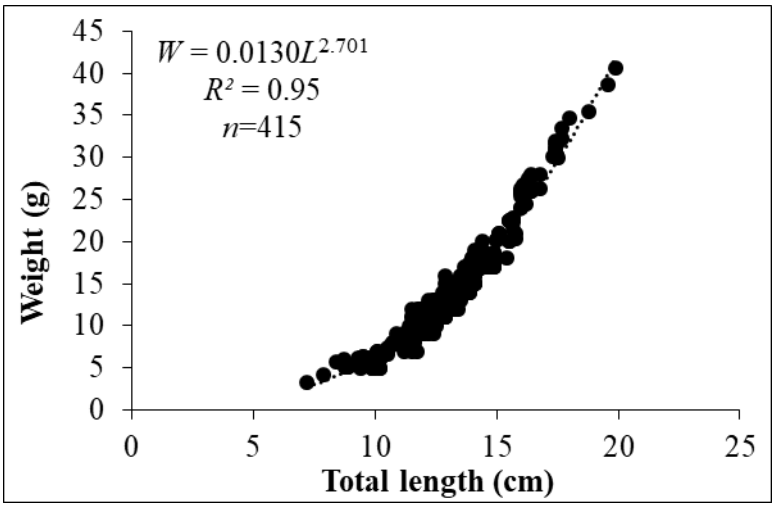

Figure 4. *Length-weight relationships of A. mossulensis for all individuals from Murat River*

The length and weight measurements, number of individuals (*n*), regression parameters *a* and *b* of the LWRs, 95% confidence intervals of *b,* coefficients of determination (R^2) and condition factor (*CF*) of the *A. mossulensis* were given in *Table 1*.

Regression analysis between the total, fork, standard length measurements for *A. mossulensis* sexes separately are shown in *Table 2*. Length- length relationships were highly significant with R^2 values greater than 0.97.

http://www.aloki.hu ● ISSN 1589 1623 (Print) ● ISSN 1785 0037 (Online)
DOI: http://dx.doi.org/10.15666/aeer/1705_1025310266

Table 1. *Length-weight relationships of A. mossulensis in Murat River*

Sex	*n*	Length range (cm)	Weight Range (g)	*a*	*b*	*95% CI of b*	R^2	*CF*
Female	232	8.7-19.9	5.0-40.6	0.0097	2.812	2.557-2.836	0.95	0.430-0.911
Male	183	7.2-19.6	3.24-38.7	0.0168	2.599	2.575-2.865	0.95	0.460-0.975
All	415	7.2-19.9	3.24-40.6	0.0130	2.701	2.557-2.865	0.95	0.430-0.975

n: number of individuals, *a*: intercept, *b*: slope, *CI*: confidence limits, R^2: coefficient of determination, CF: condition factor

Table 2. *Length–length relationships of A. mossulensis in Murat River*

Sex	Equation	*a*	*b*	R^2
Female	*TL= a + bFL*	1.0685	0.2454	0.98
	FL= a + bSL	1.0248	0.7082	0.98
	SL= a + bTL	0.8828	-0.5386	0.97
Male	*TL= a + bFL*	1.0958	-0.0541	0.98
	FL= a + bSL	1.0297	0.6071	0.99
	SL= a + bTL	0.8692	-0.3433	0.99
All	*TL= a + bFL*	1.0822	0.0916	0.98
	FL= a + bSL	1.0298	0.6258	0.99
	SL= a + bTL	0.8742	-0.4125	0.98

TL: Total length, *FL*: fork length, *SL*: Standard length

Figure 5 shows the coefficients of regression. The linear regression line, which is most appropriate between targets and outputs, is determined with a durable line.

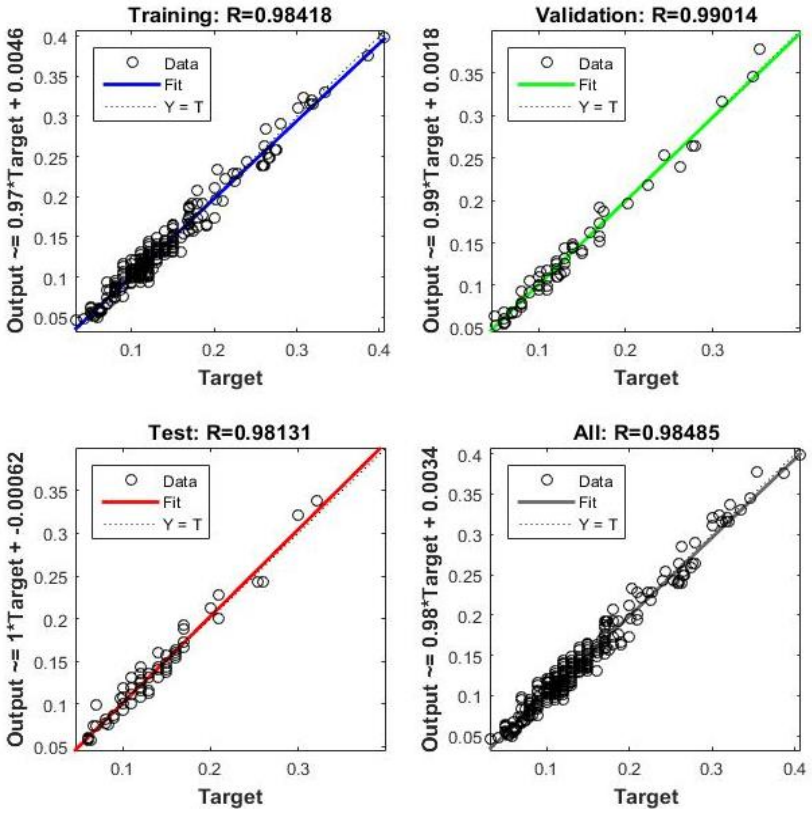

Figure 5. *Coefficients of regression in artificial neural networks model*

http://www.aloki.hu ● ISSN 1589 1623 (Print) ● ISSN 1785 0037 (Online)
DOI: http://dx.doi.org/10.15666/aeer/1705_1025310266

R value shows the relationship between outputs and targets. According to *Figure 5*, the targeted output *R* value was 0.98418 for training, 0.99014 for validation, 0.98131 for testing and 0.98485 for corresponding all response. *R*=0.98485 value confirmes that the ANN output precise linear relevance with the target (excellently match). All these results confirm that the training gives the best results. Because all of the coefficients are close to 1, the accuracy of the training is highly acceptable and gave better predictions than regression relationship (0.98485) (*Fig. 5*).

Figure 6 shows the best validation performance. The mean squared error of all data (performance chart) is occurred on a logarithmically. The training mean squared error must have a declining trend in order for the training plot to shows an excellent training.

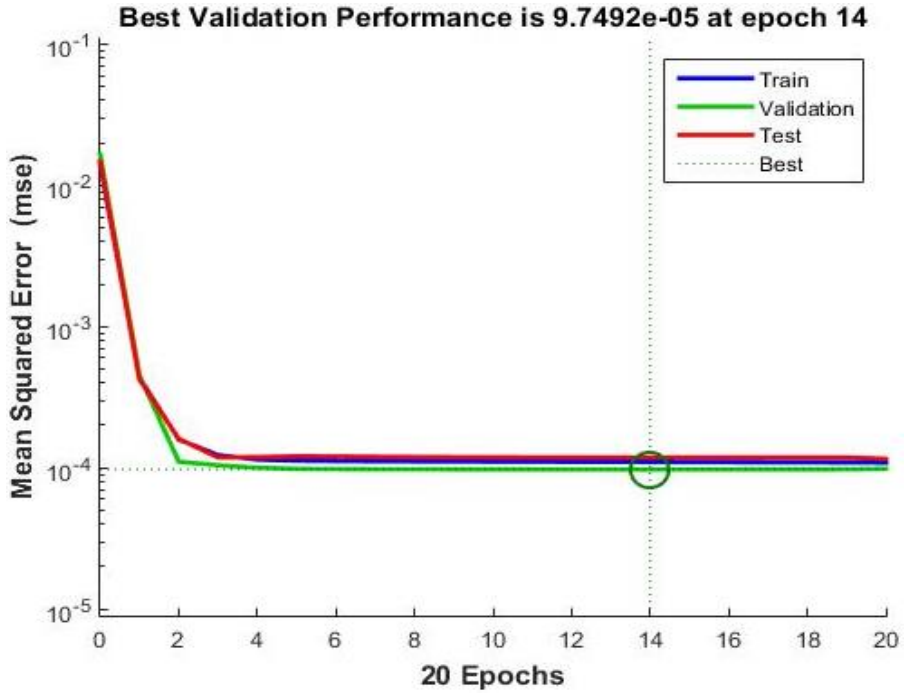

Figure 6. *Best validation performance of artificial neural networks*

In *Figure 6*, when the validation error increased to 20 epochs, the training was ended and the best validation performance was seen as 9.7492e-05 at 14th epoch. The optimum epoch is 20 for *A. mossulensis* there is no benefit to the system of increasing epoch after that.

Figure 7 shows the corresponding validation checks and the gradient of epochs. For the training state of artificial neural networks model, the validation checks was attained as 6, at epoch 20 and gradient=0.00032946, at epoch 20.

Actual values, ANNs and LWRs data of *A. mossulensis* are shown in *Table 3*. All values were classified by length groups and sexes. *Table 3* was obtained by comparison with ANNs and LWRs of *A. mossulensis*. The values we obtained with ANNs and LWRs were calculated one by one. It was determined that the ANNs MAPE (%) values were better than MAPE values calculated in length-weight relation.

http://www.aloki.hu ● ISSN 1589 1623 (Print) ● ISSN 1785 0037 (Online)
DOI: http://dx.doi.org/10.15666/aeer/1705_1025310266

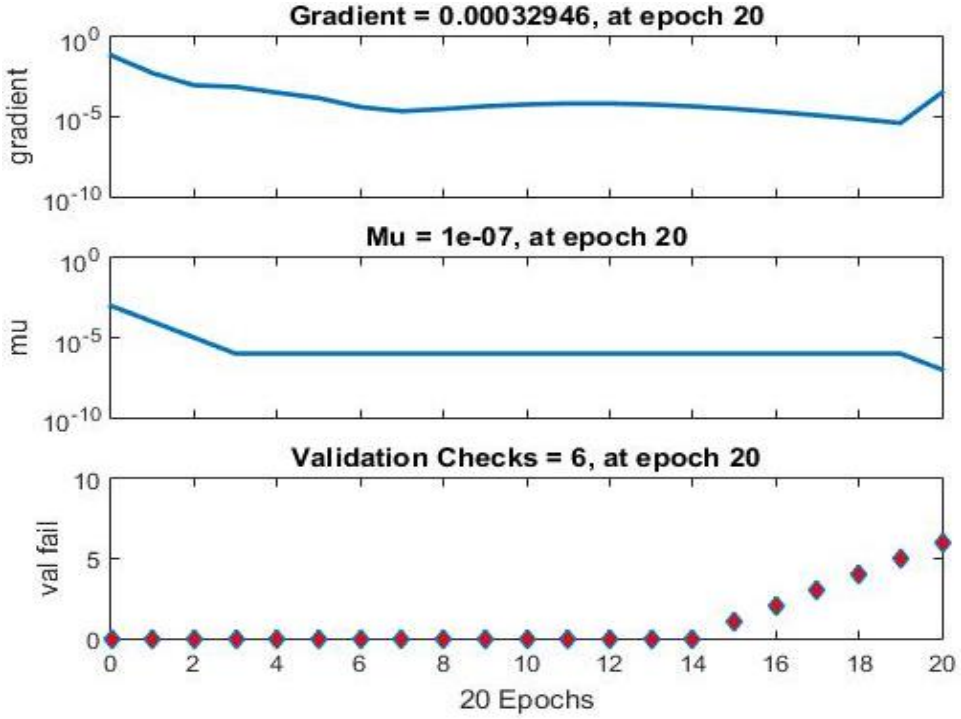

Figure 7. *Training state of artificial neural networks*

Table 3. *Comparison of real and calculated values by sex for A. mossulensis ANNs and LWRs*

Length groups (cm)	Sex	Real Data		ANNs		MAPE(%)		LWRs		MAPE (%)	
		TL	*W*	*TL*	*W*	*TL*	*W*	*TL*	*W*	*TL*	*W*
7.0-8.9	Female	8.77	5.373	9.005	5.353	2.680	0.372	9.294	4.577	5.975	14.815
	Male	8.40	4.917	8.875	4.893	5.655	0.488	8.968	4.123	6.762	16.148
	All	8.51	5.054	8.900	5.031	4.582	0.455	9.066	4.259	6.533	15.730
9.0-10.9	Female	10.305	6.870	10.424	6.716	1.555	2.242	10.153	7.124	1.475	3.697
	Male	10.110	6.682	10.068	6.754	0.415	10.078	10.060	6.769	0.495	1.302
	All	10.183	6.753	10.202	6.739	0.187	0.207	10.095	6.903	0.864	2.221
11.0-12.9	Female	12.216	11.142	12.246	11.256	0.246	1.023	12.151	11.252	0.532	0.987
	Male	12.121	11.009	12.151	10.994	0.248	0.136	12.104	11.025	0.140	0.145
	All	12.171	11.079	12.201	11.132	0.246	0.478	12.129	11.144	0.345	0.587
13.0-14.9	Female	13.742	15.296	13.696	15.427	0.335	0.856	13.677	15.478	0.473	1.189
	Male	13.386	14.800	13.478	15.763	0.687	6.507	13.848	15.765	3.451	6.520
	All	13.776	15.470	13.659	15.544	0.849	0.478	13.737	15.579	0.283	0.705
15.0-16.9	Female	15.888	24.208	15.909	23.823	0.132	1.590	16.218	22.855	2.077	5.589
	Male	15.742	22.867	15.655	22.710	0.553	0.687	15.865	22.284	0.781	2.550
	All	15.842	23.784	15.829	23.472	0.082	1.311	16.106	22.675	1.667	4.662
17.0-18.9	Female	17.670	32.233	17.627	32.773	0.243	1.675	18.046	30.420	2.128	5.625
	Male	17.550	31.500	18.015	32.697	2.650	3.800	17.900	29.840	1.994	5.270
	All	17.645	32.100	17.698	32.759	0.300	2.052	18.021	30.314	2.131	5.563
19.0-19.9	Female	19.900	40.600	19.802	39.793	0.492	1.988	19.665	41.893	1.181	3.184
	Male	19.600	38.700	19.458	38.247	0.724	1.170	19.319	40.209	1.434	3.899
	All	19.750	39.650	19.630	39.020	0.608	1.589	19.492	41.051	1.306	3.533
Average MAPE (%)						**1.118**	**1.866**			2.001	4.949

TL: Total length, *W*: Weight

http://www.aloki.hu ● ISSN 1589 1623 (Print) ● ISSN 1785 0037 (Online)
DOI: http://dx.doi.org/10.15666/aeer/1705_1025310266

Discussion

In this study, the maximum length for females was 19.90 cm and that for males was 19.60 cm; females are longer and heavier than males as seen in other fish species. The maximum total length reported for this fish from Ataturk reservoir was 38.20 cm (Başusta and Cicek, 2006), from Karakaya Dam Lake was 20.4 cm (Alkan Uckun and Gokce, 2015) and from Karasu River was 21.4 cm (Serdar et al., 2017).

Many researchers have found in different estimates for the length-weight relationship in fish. Le Cren (1951) because the oil and water content of the fish may vary depending on the temperature, stated that the length-weight relationship of the fish depends on the seasonal changes. It may also affect the *b* value in geographic location and environmental conditions such as and water temperature, which is the determining factor of feeding capacity, stomach fullness, disease and parasite loads (Bagenal and Tesch, 1978; Froese, 2006). Also, if the value of *b* is less than 3, the fish indicates negative allometric growth, and if the value of *b* is greater than 3, the fish indicates positive allometric growth (Weatherley and Gill, 1987). The *b* values reported for differ fish species ranged from 2.5 to 4.0 (Hile, 1936; Martin, 1949), 2 to 4 (Bagenal and Tesch, 1978) and 2.5 to 3.5 (Froese, 2006). In addition, high values of R^2 show that the length-weight relationships are linear observed range of values (*Table 4*). In the present study, length and weight relations of *A. mossulensis* were similar to those of Alkan Uckun and Gokce (2014) and Serdar et al. (2017).

Table 4. *Total length-weight relationship values for A. mossulensis from different regions*

Habitat	Sex	*a*	*b*	R^2	Author
Askale region of River Karasu	Female	0.0080	3.082	0.95	Turkmen and Akyurt, 2000
	Male	0.0100	2.828	0.94	
Karasu River	Female	0.0073	3.136	0.96	Yıldırım et al., 2003
	Male	0.0129	2.913	0.99	
Karakaya Dam Lake	Female	0.2060	2.065	0.95	Alkan Uckun and Gokce, 2015
	Male	0.1190	2.138	0.93	
	All	0.1350	2.120	0.94	
Karasu River (Erzincan-Erzurum)	Female	0.0131	2.800	0.93	Serdar et al., 2017
	Male	0.0125	2.820	0.92	
	All	0.0128	2.810	0.93	
Fırat River	All	0.0080	3.030	0.97	Keskin, 2016
Murat River	Female	0.0097	2.812	0.95	In this study
	Male	0.0168	2.599	0.95	
	All	0.0130	2.701	0.95	

Length-length relationships are generally used for population parameters of fish species (Başusta et al., 2013; Ozcan and Serdar, 2018a, 2018b). LLRs were significant (P<0.001) for all individuals with all R^2 values greater than 0.97. These results are in agreement with those of Serdar et al. (2017) work done in the Karasu River.

Ergene, (1993) reported the mean condition factor as 0.86. Turkmen and Akyurt, (2000) reported it as 1.023 in males and as 1.047 in females. In this study, the max-min condition factors were 0.430-0.911 for females and 0.460-0.975 for males. The condition factor allows us to be informed about the physiological status of fish in relation to health (Kumolu and Ndimele, 2010). The fact that the condition factor is high shows that the environmental conditions are quite suitable for population dynamics studies (Blackwell et al., 2000). In this study, it can be said that the environmental

http://www.aloki.hu ● ISSN 1589 1623 (Print) ● ISSN 1785 0037 (Online)
DOI: http://dx.doi.org/10.15666/aeer/1705_1025310266

conditions are not suitable for *A. mossulensis* in this region since the condition factor value is less than 1.

The values obtained with Artificial Neural Networks are much closer to their real values (*Table 3*). ANNs is required for future predictions along with other methods. However, in the majority of these studies it is seen that the ANNs results are better than the results of other conventional methods (Brosse et al., 1999). In this study, according to results of *Table 3*, ANNs provided very good results compared to LWRs. Thus, ANNs can be used as an alternative and reliable method in fisheries for length-weight relation. MAPE values of the predict of ANNs for length and weight were 1.118 and 1.866 and the value of LWRs were 2.001 and 4.949. Lewis (1982) categorized models with a MAPE value of less than 10% as "very good" in predicting, 10%-20% as "good", 20%-50% as "acceptable" and over 50% are classified as "wrong and faulty" models. In many studies are determined that MAPE of ANNs values are quite low (Benzer and Benzer, 2016, 2018; Benzer et al., 2017; Ozcan and Serdar, 2018a).

According to Ekici and Aksoy (1993), *R* is successful when the values are between 0.95-1. In addition, Saleem et al. (2017), for a very good fit, the distribution of data should be along a 45° line indicating that the network outputs are equal to the targets. The forecasting of length-weight relation using artificial neural network was found to be 0.98485 as the *R* values for all individuals. With ANNs seen that the output tracks are very good targets for training (*R*-value = 0.98418), validation (*R*-value = 0.99014), and testing (*R*-value = 0.98131). These results show the success of the relationship between length-weight. With this study obtained high correlation coefficient (*R*) between the measured and predicted output variables, reaching up to 0.99 (validation).

Conclusions

The results of this study showed high proximity between the measured and predicted data. The values obtained with Artificial Neural Networks are much closer to their real values. For this reason, the ANNs model used in this study has a highly acceptable accuracy and reliability.

Acknowledgements. Author thank Dr. Ibrahim MAKINIST and Mustafa AKDENIZ for helping collecting the fish samples; Prof. Dr. Ahmet Bedri OZER and Arş. Gör. Canan TASTIMUR for helping Artificial Neural Networks (ANNs); (MATLAB; Ver R2016a) calculations.

REFERENCES

[1] Abdul-Razak, M. M., Aufy, L. A., Jasim, B. M. (2015): Some biological aspects of the bleak, *Alburnus mossulensis* in the southern reaches of Euphrates River, Iraq. – Asian Journal of Applied Sciences 3(2): 277-285.

[2] Agatonovic-Kustrin, S., Beresford, R. (2000): Basic concepts of artificial neural net-work (ANN) modeling and its application in pharmaceutical research. – Journal of Pharmaceutical and Biomedical Analysis 22(5): 717-727. https://doi.org/10.1016/S0731-7085(99)00272-1.

[3] Alkan Uckun, A., Gokce, D. (2015): Assessing age, growth, and reproduction of *Alburnus mossulensis* and *Acanthobrama marmid* (Cyprinidae) populations in Karakaya Dam Lake (Turkey). – Turkish Journal of Zoology 39: 1-14. https://doi:10.3906/zoo-1211-13.

http://www.aloki.hu ● ISSN 1589 1623 (Print) ● ISSN 1785 0037 (Online)
DOI: http://dx.doi.org/10.15666/aeer/1705_1025310266

[4] Bagenal, T. B., Tesch, F. W. (1978): Age and Growth. – In: Bagenal, T. B. (ed.) Methods of assessment of fish production in fresh waters. Oxford Blackwell Scientific Publication, 101-136.
[5] Başusta (Girgin), A. (2000): Investigation and growth and changes of in blood cells *Acanthobrama marmid* (Heckel, 1843), *Chondrostoma regium* (Heckel, 1843) and *Chalcalburnus mossulensis* (Heckel, 1843) fishes living in Keban Dam Lake. – PhD. Thesis, Firat University.
[6] Başusta, N., Cicek, E. (2006): Length-weight relationships for some teleost fishes caught in Ataturk Dam Lake on southeastern Anatolia, Turkey. – Journal of Applied Ichthyology 22: 297-280. https://doi:10.1111/j.1439-0426.2006.00778.x.
[7] Başusta, A., Başusta, N., Ozer, E. I., Girgin, H., Aslan, E. (2013): Some population parameters of the lessepsian suez puffer (*Lagocephalus suezensis*) from Iskenderun Bay, Northeastern Mediterranean, Turkey. – Pakistan Journal of Zoology 45(6): 1779-1782.
[8] Benzer, S., Karasu Benli, C., Benzer, R. (2015): The comparison of growth with length–weight relation and artificial neural networks of crayfish, *Astacus leptodactylus*, in Mogan Lake. – Journal of Black Sea/Mediterranean Environment 21(2): 208-223.
[9] Benzer, S., Benzer, R. (2016): Evaluation of growth in pike (*Esox lucius* L., 1758) using traditional methods and artificial neural networks. – Applied Ecology and Environmental Research 14(2): 543-554. https://doi:10.15666/aeer/1402_543554.
[10] Benzer, S., Benzer, R., Gunal, A. C. (2017): Artificial neural networks approach in length-weight relation of crayfish (*Astacus leptodactylus* Eschscholtz, 1823) in Eğirdir Lake, Isparta, Turkey. – Journal of Coastal Life Medicine 5(8): 330-335. https://doi:10.12980/jclm.5.2017J7-19.
[11] Benzer, S., Benzer, R. (2018): New perspectives for predicting growth properties of crayfish (*Astacus leptodactylus* Eschscholtz, 1823) in Uluabat Lake. – Pakistan Journal of Zoology 50(1): 35-45. https://doi:10.17582/journal.pjz/2018.50.1.35.45.
[12] Blackwell, B. G., Brown, M. L., Willis, D. W. (2000): Relative weight (W*r*) status and current use in fisheries assessment and management. – Reviews in Fisheries Science 28: 1-44. https://doi.org/10.1080/10641260091129161.
[13] Brosse, S., Guegan, J., Tourenq, J., Lek, S. (1999): The use of artificial neural networks to assess fish abundance and spatial occupancy in the littoral zone of a mesotrophic lake. – Ecological Modelling 120(2-3): 299-311. https://doi.org/10.1016/S0304-3800(99)00110-6.
[14] Cabreira, A. G., Tripode, M., Madirolas, A. (2009): Artificial neural networks for fish-species identification. – ICES Journal of Marine Science 66: 1119-1129. https://doi.org/10.1093/icesjms/fsp009.
[15] Coad, B. W. (2010): Freshwater fishes of Iraq. – Sofia, Bulgaria: Pensoft Publishers, 274p.
[16] Ekici, B. B., Aksoy, U. T. (1993): Prediction of building energy consumption by using artificial neural networks. – Advances in Engineering Software 40: 356-362. https://doi.org/10.1016/j.advengsoft.2008.05.003.
[17] Ergene, S. (1993): The growth rates of *Chalcalburnus mossulensis* (Heckel, 1843), (Pisces, Cyprinidae) in Karasu. – Turkish Journal of Zoology 17(4): 367-377.
[18] Esmaeili, H. R., Gholamifard, A., Vatandoust, S., Sayyadzadeh, G., Zare, R., Babaei, S. (2014): Length–weight relationships for 37 freshwater fish species of Iran. – Journal of Applied Ichthyology 30(5): 1073-1076. https://doi.org/10.1111/jai.12433.
[19] Froese, R. (2006): Cube law, condition factor and weight–length relationships: history, meta-analysis and recommendations. – Journal of Applied Ichthyology 22: 241-253. https://doi.org/10.1111/j.1439-0426.2006.00805.x.
[20] Geldiay, R., Balık, S. (2007): Freshwater Fishes of Turkey. – V. Edition, Ege University Press, Bornova, Izmir, 638p.

http://www.aloki.hu ● ISSN 1589 1623 (Print) ● ISSN 1785 0037 (Online)
DOI: http://dx.doi.org/10.15666/aeer/1705_1025310266

[21] Ghorbani, M. (2011): Reproductive biology of Mossul bleak (*Alburnus mossulensis*) in Bibi-Sayyedan River of Semirom, in Isfahan Province. – MSc Thesis. Department of Natural Resources, Isfahan University of Technology, Isfahan, Iran.
[22] Hile, R. (1936): Age and Growth of the Cisco, *Leucichthys artedi* (Le Sueur), in the Lakes of the North-eastern High Lands, Wisconsin. – From Bulletin of the Bureau of Fisheries 48: 211317.
[23] Joy, K. M., Death, R. G. (2004): Predictive modelling and spatial mapping of freshwater fish and decapod assemblages using GIS and neural Networks. – Freshwater Biology 49: 1306-1052. https://doi. org/10.1111/j.1365-2427.2004.01248.x.
[24] Keivany, Y., Aalipour, M., Siami, M., Mortazavi, S. (2015): Length–weight and length–length relationships of three fish from the Beheshtabad River, western Iran. – Iranian Journal of Ichthyology 2(4): 296-298.
[25] Keivany, Y., Dopeikar, H., Ghorbani, M., Kiani, F., Paykan-Heyrati, F. (2016): Length–weight and length–length relationships of three cyprinid fish from the Bibi-Sayyedan River, western Iran. – Journal of Applied Ichthyology 32(3): 507-508. https://doi.org/ 10.1111/jai.13006.
[26] Keivany, Y., Zamani-Faradonbeh, M. (2017): Length–weight and length–length relationships for eight fish species from Jarrahi River, southwestern Iran. – Journal of Applied Ichthyology 33(4): 864-866. https://doi.org/10.1111/jai.13396.
[27] Keivany, Y., Ghorbani, M., Paykan-Heyrati, F. (2017): Reproductive biology of Mossul bleak (*Alburnus mossulensis*) in Bibi-Sayyedan River of Tigris basin in Iran. – Caspian Journal of Environmental Sciences 15(2): 135-145.
[28] Keskin, S. B. (2016): Determination of some population dynamical parameters of *Alburnus mossulensis* (Heckel, 1843) from lower Euprates basin. – M.Sc. Thesis, Nevşehir Hacı Bektaş Veli University, Graduate SchooL of Natural and Applied Sciences.
[29] King, M. (1995): Fisheries biology, assessment and management. – Fishing News Books, Blackwell Science, Oxford, UK.
[30] Krenker, A., Bešter, J., Kos, A. (2011): Introduction to the Artificial Neural Networks. – Artificial Neural Networks-Methodological Advances and Biomedical Applications. https://doi.org/10.5772/15751.
[31] Kumolu, C. A., Ndimele, P. E. (2010): Length Weight Relationships and Condition Factors of Twenty-One Fish Species in Ologe Lagoon, Lagos, Nigeria. – Asian Journal of Agricultural Sciences 2(4): 174-179.
[32] Kuru, M. (2004): Recent Systematic Status of Inland Water Fishes of Turkey. – Gazi Eğitim Fakültesi Dergisi 24: 1-21.
[33] Le Cren, C. D. (1951): The length-weight rela-tionship and seasonal cycle in gonad weight and condition in the Perch (*Perca fluviatilis*). – Journal of Animal Ecology 20: 201-219.
[34] Lewis, C. D. (1982): Industrial and business forecasting methods. – Butterworths, London.
[35] Maravelias, C. D., Haralabous, J., Papaconstantinou, C. (2003): Predicting demersal fish species distributions in the Mediterranean Sea using artificial neural networks. – Marine Ecology 255: 249-258. https://doi.org/10.3354/meps255249.
[36] Martin, W. R. (1949): The Mechanics of Enivironmental Control of Body Form in Fishes. – Univ. Toronto Stud. Biol. 58 (Publ. Ont. Fish. Res. Lab). 70: 1-19.
[37] Mastrorillo, S., Lek, S., Dauba, F., Belaud, A. (1997): The use of artificial neural networks to predict the presence of small-bodied fish in river. – Freshwater Biology 38: 237-246. https://doi.org/10.1046/j.1365-2427.1997.00209.x.
[38] Mousavi-Sabet, H., Abdollahpour, S., Salehi-Farsani, A., Vatandoust, S., Langroudi, H. F., Jamalzade, H. R., Nasrollahzadeh, A. (2013): Length-weight and length-length relationships and condition factor of Alburnus mossulensis (Heckel, 1843) from the

http://www.aloki.hu ● ISSN 1589 1623 (Print) ● ISSN 1785 0037 (Online)
DOI: http://dx.doi.org/10.15666/aeer/1705_1025310266

Persian Gulf basin. – Aquaculture, Aquarium, Conservation & Legislation International Journal of the Bioflux Society 6: 297-302. http://www.bioflux.com.ro/aacl.

[39] Mousavi-Sabet, H., Khataminejad, S., Vatandoust, S. (2014): Length-weight and length-length relations of the Seven Endemic Alburnus Species (Actinopterygii: Cypriniformes: Cyprinidae) In Iran. – Acta Ichthyologica et Piscatoria 44: 157-158. https://doi.org/10.3750/AIP2014.44.2.10.

[40] Obach, M., Wagner, R., Werner, H., Schmidt, H. H. (2001): Modelling population dynamics of aquatic insects ith artificial neural networks. – Ecology Modelling 146: 207-217. https://doi.org/10.1016/S0304-3800(01)00307-6.

[41] Ozcan, E. I., Serdar, O. (2018a): Artifical neural networks as new alternative method to estimating some population parameters of tigris loach (*Oxynoemacheilus tigris* (Heckel, 1843)) in the Karasu River, Turkey. – Fresenius Environmental Bulletin 27(12B/2018): 9840-9850.

[42] Ozcan, E. I., Serdar, O. (2018b): Length-weight and length-length relationships of red-spotted trout (*Salmo trutta macrostigma* (Dumeril, 1858)) in Karasu River (East Anatolia, Turkey). – Ecolojical Life Sciences 13(1): 27-31.

[43] Park, Y. S., Verdonschot, P. F. M., Chon, T. S., Lek, S**.** (2003): Patterning and predicting aquatic macro invertabrate diversities using artificial neural network. – Water Research 37: 1749-1758. https://doi.org/10.1016/S0043-1354(02)00557-2.

[44] Radkhah, A. (2016): A study on length-weight relationship and condition factor of *Alburnus mossulensis* in Hamzeh-Ali Region from Chaharmahal and Bakhtiari Province, Iran. – International Journal of Fisheries and Aquatic Studies 4(1): 124-125.

[45] Ricker, W.E. (1975): Computation and interpretation of biological statistics of fish populations. Bull. Fish. Res. Board Can. 191: 382-391.

[46] Saleem, W., Zain-ul-abdein, M., Ijaz, H., Mahfouz, A. S. B., Ahmed, A., Asad, M., Mabrouki, T. (2017): Computational Analysis and Artificial Neural Network Optimization of Dry Turning Parameters AA2024-T351. – Applied Sciences 7: 642. https://doi.org/10.3390/app7060642.

[47] Sangun, L., Guney, O. I., Ozalp, P., Başusta, N. (2019): Estimation of body weight of *Sparus aurata* with artificial neural network (MLP) and M5P (nonlinear regression) – LR algorithms. – Iranian Journal of Fisheries Sciences https://doi.org/10.22092/ijfs.2018.117010 (In press).

[48] Serdar, O., Ozcan, E. I., Aydın, R. (2017): Length-weight and length-length relationships of *Alburnus mossulensis* and *Acanthobrama marmid* (Heckel, 1843) in the Karasu River (Turkey). – Yunus araştırma Bülteni. https://doi.org/10.17693/yunusae.vi.278434.

[49] Tureli Bilen, C., Kokcu, P., Ibrikci, T. (2011): Application of artificial neural networks (ANNs) for weight predictions of blue crabs (*Callinectes sapidus* Rathbun, 1896) using predictor variables. – Mediterranean Marine Science 12(2): 439-446. https://doi.org/10.12681/mms.43.

[50] Turkmen, M., Akyurt, I. (2000): The population structure and growth properties of *Chalcalburnus mossulensis* (Heckel, 1843) caught crom Askale region of River Karasu. – Turkish Journal of Biology 24: 95-111.

[51] URL 1. (2018): Shubh Saxena, Artificial Neuron Networks (Basics). Introduction to Neural Networks. https://becominghuman.ai/artificial-neuron-networks-basics-introduction-to-neural-networks-3082f1dcca8c (21.12.2018).

[52] https://becoming human. ai/artificial-neuron-networks-basics-introduction-to neural-networks-3082f1dcca8c.

[53] Weatherly, A. H., Gill, H. S. (1987): The biology of fish growth. – London, academic Press: 433-443.

[54] Yıldırım, A., Haliloglu, H. I., Erdogan, O., Turkmen, M. (2003): Age and growth characteristics of *Chalcalburnus mossulensis* (Heckel, 1843) living in Karasu River (Erzurum-Turkey). – Turkish Journal of Zoology 27: 1091-1096.

http://www.aloki.hu ● ISSN 1589 1623 (Print) ● ISSN 1785 0037 (Online)
DOI: http://dx.doi.org/10.15666/aeer/1705_1025310266

[55] Yıldırım, A., Haliloglu, H. I., Erdogan, O., Turkmen, M. (2007): Some reproduction characteristics of *Chalcalburnus mossulensis* (Heckel, 1843) inhabiting the Karasu River (Erzurum, Turkey). – Turkish Journal of Zoology 31: 193-200.
[56] Zar, J. H. (1999): Biostatistical Analysis. – 4th ed. Prentice-Hall, New Jersey.

http://www.aloki.hu ● ISSN 1589 1623 (Print) ● ISSN 1785 0037 (Online)
DOI: http://dx.doi.org/10.15666/aeer/1705_1025310266

YIELD AND CHEMICAL COMPOSITION OF FIELD PEA/OAT (*PISUM SATIVUM* L./*AVENA SATIVA* L.) MIXTURES GROWN FOR GREEN MATTER

PŁAZA, A. – GĄSIOROWSKA, B. – RZĄŻEWSKA, E.*

Agrotechnology Department, Faculty of Natural Sciences, Siedlce University of Natural Sciences and Humanities, Siedlce, Poland
(e-mail: anna.plaza@uph.edu.pl; barbara.gasiorowska@uph.edu.pl)

**Corresponding author*
e-mail: emilia.rzazewska@uph.edu.pl

(Received 28th Jan 2019; accepted 6th Mar 2019)

Abstract. The paper presents results of a research conducted between 2010 and 2012 to determine the effect of the proportion of components in a mixture and harvest date on yield and chemical composition of field pea/oat (*Pisum sativum* L.*, Avena sativa* L.*)* mixtures. Two factors were examined in the study: factor I − proportion of components in a mixture: field pea 100%, oat 100%, field pea 75% + oat 25%, field pea 50% + oat 50%, field pea 25% + oat 75%; factor II − harvest date: the stage of field pea flowering and the stage of flat green pod of field pea. The following characteristics were examined: green matter yield of field pea/oat mixtures, nutrient content, NDF and ADF content. The results were statistically analysed. The highest fresh matter yield was produced by the 50% + 50% mixture of field pea and oat. Field pea/oat mixtures harvested at the stage of field pea flowering contained more total protein, crude ash and digestible nitrogen-free extracts. The mixtures harvested at the stage of flat green pod of field pea were higher in crude fibre, fibre fractions (NDF, ADF) and crude fat.
Keywords: *nutrient content, crude fibre, total protein, crude ash, fresh matter*

Introduction

Crop plants cultivated in mixtures usually produce higher yields compared to pure stands (Księżak and Staniak, 2013). It is the result of better utilisation of habitat conditions, including minerals and water from soil reserves. Spring cereals use roots to penetrate the surface soil layer whereas legumes reach the deeper layer. Also, plant species have different periods of critical demand for water and nutrients (Rutkowska and Pikuła, 2016).

Pisum sativum L. is a valuable component of legume/cereal mixtures. As the species includes various morphological forms (short or long stem, leafed and narrow-leafed), its potential to be mixed with spring cereals varies. Leafed cultivars seem to be the most suited to cultivation for green matter (Blagojevic et al., 2017). Oat may be a component mixed with field pea and sown on soils representing the rye good complex. One of its advantages is lower soil requirements compared with other cereal species (Shoaib et al., 2013).

A major issue which needs to be considered when cultivating legume/cereal mixtures is selection of an optimal harvest date which, paired with plant growth stage, makes it possible to rationally use the obtained yield. Also, when cultivating mixtures, one has to pay attention to nutrient content which determines the quality of harvested livestock feed. Feed digestibility is limited by plant cell wall components called fractions of neutral detergent fibre (NDF) and acid detergent fibre (ADF). Many authors (Rodrigues et al., 2008; Belanger et al., 2013; Stejskalova et al., 2013; Truba et al., 2017) believe

http://www.aloki.hu ● ISSN 1589 1623 (Print) ● ISSN 1785 0037 (Online)
DOI: http://dx.doi.org/10.15666/aeer/1705_1026710276

that modern livestock feeding systems (of cows in particular), take into account neutral detergent fibre (NDF) and acid detergent fibre (ADF) contents instead of or in addition to crude fibre. There are few works which assess the nutritive value of *Pisum sativum* L./*Avena sativa* L. mixtures in terms of the content of NDF and ADF fractions. The present paper is an attempt to at least partially fill this gap. The objective of the work is to determine the effect of the proportion of components in a mixture and harvest date on yielding and chemical composition of *Pisum sativum* L./*Avena sativa* L.

Materials and methods

Field research was conducted between 2010 and 2012 at the Zawady Experimental Farm (52°03' 39" N, 22° 33' 80" E) which belongs to Siedlce University of Natural Sciences and Humanities. The experimental soil was Albic Luvisol (Arenic), its reaction was neutral and it had average available phosphorus, potassium and magnesium contents. Humus content was 1.37%. The experimental design was a split-plot arrangement with three replicates. Two factors were examined in the study: factor I − proportion of components in a mixture: field pea 100%, oat 100%, field pea 75% + oat 25%, field pea 50% + oat 50%, field pea 25% + oat 75%; factor II − harvest date: the stage of field pea flowering, the stage of flat green pod of field pea. A detailed description of the mixtures and their sowing rates is as follows: field pea 170 kg∘ha^{-1}, oat 180 kg∘ha^{-1}, field pea 128 kg∘ha^{-1} + oat 45 kg∘ha^{-1}, field pea 85 kg∘ha^{-1} + oat 90 kg∘ha^{-1}, field pea 43 kg∘ha^{-1} + oat 135 kg∘ha^{-1}.

Each study years, the mixtures were preceded by winter triticale. In autumn, phosphorus and potassium fertilisers were applied at the rates of pure element dependent on the soil chemical composition, i.e.: 35.2 kg∘ha^{-1} P and 99.6 kg∘ha^{-1} K. In spring, nitrogen fertiliser, at the rate of 30 kg∘ha^{-1} N, was applied to all the units (excluding pure stand field pea) prior to seed sowing. An additional N rate, 50 and 30 kg∘ha^{-1}, was applied to oat and field pea/oat mixtures, respectively, at the stage of stem elongation. Seeds of field pea cv. Roch and oat cv. Zuch were sown in early April. Harvest was performed in late June (the stage of field pea flowering) and early July (the stage of flat green pod of field pea). During harvest, fresh matter yield was determined in each plot, and average fresh matter samples were collected to perform chemical analyses. The following characteristics were determined in the dry matter of the plant material sampled: total protein, crude ash, crude fibre and contents of fractions of neutral detergent fibre and acid detergent fibre (by near-infrared reflectance spectrometry NIRS using a NIRFlex N-500 spectrometer) as well as crude fat (by Soxlet method). Based on the determined nutrient contents, digestible nitrogen-free extracts were calculated as a difference between four components and the sum 1000.

Each characteristic studied was subjected to variance analysis appropriate for the split-block design. Tukey test was used to separate means when significant sources of variation had been found.

Results

The fresh matter yield content of field pea/oat mixtures

The fresh matter yield of field/oat was significantly affected by the experimental factors and their interaction (*Table 1*). The highest fresh matter yield was produced by

http://www.aloki.hu ● ISSN 1589 1623 (Print) ● ISSN 1785 0037 (Online)
DOI: http://dx.doi.org/10.15666/aeer/1705_1026710276

the 50% + 50% mixture of field pea and oat. Yields of the remaining mixtures were significantly lower. The yield of oat fresh matter was significantly higher compared with the 75% + 25% mixture. The highest fresh matter yield was produced by field pea grown in pure stand. Harvest date had a significant effect on fresh matter yield, it being higher for field pea/oat mixtures harvested at the stage of flat green pod of field pea compared with mixtures harvested at the stage of field pea flowering. An interaction was confirmed indicating that the highest fresh matter yield was produced by the 50% + 50% mixture of field pea and oat harvested at the stage of flat green pod of field pea, it being the lowest for pure stand field pea harvested at the flowering stage.

Table 1. *Fresh matter yield of field pea/oat mixtures (means across 2010-2012), t∘ha^{-1}*

Proportion of components in the mixture, % (I)		**Harvest date (II)**		**Means**
Pea	**Oat**	**Flowering stage of field pea**	**Flat green pod stage of field pea**	
100	0	58.2a	70.9a	64.6a
0	100	64.5c	76.8c	70.7c
75	25	62.1b	72.8b	67.5b
50	50	69.5e	80.9d	75.2d
25	75	66.7d	75.3c	71.0c
Means		64.2A	75.3B	-

Values in columns followed by the same small letter and values in rows followed by the same capital letter do not differ significantly at $P < 0.05$

The total protein content of field pea/oat mixtures

Statistical analysis revealed a significant influence of the experimental factors and their interaction on total protein content in field pea/oat mixtures (*Table 2*). The highest concentration of total protein was recorded in field pea cultivated in pure stand. Mixtures had a lower total protein content; of these the 75% + 25% mixture had the highest content of this component. An increase in the proportion of oat in the mixture was followed by a decline in total protein content, it being the lowest in pure stand oat. Harvest date had a significant effect on total protein content in mixtures. Field pea/oat mixtures harvested at the stage of field pea flowering had a higher concentration of total protein than mixtures harvested at the stage of flat green pod. An interaction was detected which indicated that pure stand field pea harvested at the flowering stage had the highest total protein content, it being the lowest in pure stand oat and field pea/oat mixtures with the component proportion of 50% + 50% and 25% + 75% harvested at the stage of flat green pod of field pea.

The crude fibre content of field pea/oat mixtures

Crude fibre content in field pea/oat mixtures was significantly affected by the experimental factors and their interaction (*Table 3*). The lowest crude fibre content was determined in pure stand field pea, it being the highest in oat. The presence of oat in mixtures with field pea contributed to an increase in crude fibre content. Of the test mixtures, the highest crude fibre content was recorded in the 75 + 25% and 50 + 50% mixtures. Also, harvest date had a significant effect on crude fibre content in mixtures

http://www.aloki.hu ● ISSN 1589 1623 (Print) ● ISSN 1785 0037 (Online)
DOI: http://dx.doi.org/10.15666/aeer/1705_1026710276

which was higher in mixtures harvested at the stage of flat green pod of field pea than the stage of field pea flowering. An interaction between the experimental factors was confirmed. It indicated that the lowest crude protein content was characteristic of pure stand field pea and the 75 + 25% mixture, both harvested at the stage of field pea flowering, it being the highest in oat cultivated in pure stand and harvested at the stage of flat green pod of field pea.

Table 2. *Total protein content in field pea/oat mixtures (means across 2010-2012), g⊙kg^{-1} d.m.*

Proportion of components in the mixture, % (I)		Harvest date (II)		Means
Pea	Oat	Flowering stage of field pea	Flat green pod stage field of pea	
100	0	146c	140c	143c
0	100	128a	118a	123a
75	25	134b	126b	130b
50	50	130a	122a	126a
25	75	128a	121a	125a
Means		133B	125A	-

Values in columns followed by the same small letter and values in rows followed by the same capital letter do not differ significantly at P < 0.05

Table 3. *Crude fibre content in field pea/oat mixtures (means across 2010-2012), g⊙kg^{-1} d.m.*

Proportion of components in the mixture, % (I)		Harvest date (II)		Means
Pea	Oat	Flowering stage of field pea	Flat green pod stage of field pea	
100	0	234a	259a	247a
0	100	276c	306d	291d
75	25	243a	263a	253a
50	50	252b	275b	264b
25	75	268c	287c	278c
Means		255A	278B	-

Values in columns followed by the same small letter and values in rows followed by the same capital letter do not differ significantly at P < 0.05

The neutral detergent fibre (NDF) content of field pea/oat mixtures

Statistical analysis revealed a significant influence of the experimental factors and their interaction on the content of neutral detergent fraction (NDF) in field pea/oat mixtures (*Table 4*). The lowest NDF content was recorded in field pea cultivated in pure stand, it being the highest in oat. As the proportion of field pea in mixture was reduced and oat proportion increased, an increase in the NDF content was observed. Of the test mixtures, the lowest NDF content was determined in the 75 + 25% mixture. Harvest date had a significant effect on NDF content in field pea/oat mixtures. The content was lower in mixtures harvested at the field pea flowering stage than at the stage of flat

http://www.aloki.hu ● ISSN 1589 1623 (Print) ● ISSN 1785 0037 (Online)
DOI: http://dx.doi.org/10.15666/aeer/1705_1026710276

green pod. There was observed an interaction between the experimental factors which indicated that the lowest NDF content was recorded in pure stand field pea and harvested at the flowering stage, it being the highest in oat harvested at the stage of flat green pod of field pea.

Table 4. *Neutral detergent fibre (NDF) content in field pea/oat mixtures (means across 2010-2012), g◎kg^{-1} d.m.*

Proportion of components in the mixture, % (I)		Harvest date (II)		Means
Pea	Oat	Flowering stage of field pea	Flat green pod stage of field pea	
100	0	400a	486a	443a
0	100	519e	629e	574e
75	25	431b	511b	471b
50	50	456c	548c	502c
25	75	479d	582d	531d
Means		457A	551B	-

Values in columns followed by the same small letter and values in rows followed by the same capital letter do not differ significantly at P < 0.05

The acid detergent fibre (ADF) content of field pea/oat mixtures

The content of acid detergent fibre (ADF) was significantly influenced by the experimental factors and their interaction (*Table 5*). The lowest ADF content was recorded in field pea cultivated in pure stand and the highest in oat. The more oat was added to the mixture, the higher the ADF content. Of the test mixtures, the lowest ADF content was recorded in the 75 + 25% mixture of field pea and oat. A interaction was detected indicating that the lowest ADF content was characteristic of pure stand field pea harvested at the flowering stage, it being the highest in oat harvested at the stage of flat green pod of field pea.

Table 5. *Acid detergent fibre (ADF) content in field pea/oat mixtures (means across 2010-2012), g◎kg^{-1} d.m.*

Proportion of components in the mixture, % (I)		Harvest date (II)		Means
Pea	Oat	Flowering stage of field pea	Flat green pod stage of field pea	
100	0	303a	334a	319a
0	100	359d	387d	373e
75	25	318b	340a	329b
50	50	326b	354b	340c
25	75	341c	369c	355d
Means		329A	357B	-

Values in columns followed by the same small letter and values in rows followed by the same capital letter do not differ significantly at P < 0.05

http://www.aloki.hu ● ISSN 1589 1623 (Print) ● ISSN 1785 0037 (Online)
DOI: http://dx.doi.org/10.15666/aeer/1705_1026710276

The crude fat content of field pea/oat mixtures

Statistical analysis demonstrated a significant effect of the experimental factors and their interaction on crude fat content in field pea/oat mixtures (*Table 6*). The highest crude fat content was determined in pure stand oat, it being the lowest in field pea. An addition of oat to mixtures with field pea contributed to an increase in crude fat content. Of the test mixtures, the highest crude fat content was recorded in the 25 + 75% mixture. Harvest date had a significant effect on crude fat content in mixtures. More crude fat was determined in mixtures harvested at the stage of flat green pod of field pea compared with the flowering stage. An interaction was found: the highest crude fat content was determined in oat cultivated in pure stand and harvested at the stage of flat green pod of field pea, it being the lowest in field pea harvested at the flowering stage.

Table 6. *Crude fat content in field pea/oat mixtures (means across 2010-2012), g◎kg^{-1} d.m.*

Proportion of components in the mixture, % (I)		**Harvest date (II)**		**Means**
Pea	**Oat**	**Flowering stage of field pea**	**Flat green pod stage of field pea**	
100	0	24.0a	25.5a	24.8a
0	100	29.6e	30.6e	30.1e
75	25	25.7b	27.0b	26.4b
50	50	27.1c	28.3c	27.7c
25	75	28.5d	29.4d	29.0d
Means		27.0A	28.2B	-

Values in columns followed by the same small letter and values in rows followed by the same capital letter do not differ significantly at $P < 0.05$

The crude ash content of field pea/oat mixtures

Crude ash content in field pea/oat mixtures was significantly affected by the proportion of components in a mixture, harvest date and their interaction (*Table 7*). Pure stand field pea and the 75 + 25% mixture had the highest crude ash content, it being the lowest in pure stand oat. In the remaining mixtures, crude ash content was lower than in field pea, and it differed insignificantly from oat content. Harvest date had a significant effect on crude ash content in mixtures. A higher concentration of crude ash was recorded in field pea/oat mixtures harvested at the stage of field pea flowering compared with the stage of flat green pod of field pea. There was found an interaction between the experimental factors which indicated that the highest crude ash content was determined in field pea cultivated in pure stand as well as mixed with oat at the following proportions: 75 + 25% and 50 + 50% and harvested at the flowering stage, it being the lowest in oat and the 50 + 50% and 25 + 75% mixtures of field pea and oat harvested at the stage of flat green pod of field pea.

The digestible nitrogen-free extracts of field pea/oat mixtures

Statistical analysis demonstrated a significant influence of the experimental factors and their interaction on digestible nitrogen-free extracts in field pea/oat mixtures (*Table 8*). The highest content of digestible nitrogen-free extracts was determined in the 75 + 25% and 50 + 50% mixtures of field pea and oat, it being the lowest in pure stand

http://www.aloki.hu ● ISSN 1589 1623 (Print) ● ISSN 1785 0037 (Online)
DOI: http://dx.doi.org/10.15666/aeer/1705_1026710276

oat and the 25 + 75% mixture. Harvest date had a significant effect on digestible nitrogen-free extracts in field pea/oat mixtures.

Table 7. *Crude ash content in field pea/oat mixtures (means across 2010-2012), g⊙kg^{-1} d.m.*

Proportion of components in the mixture, % (I)		Harvest date (II)		Means
Pea	Oat	Flowering stage of field pea	Flat green pod stage of field pea	
100	0	84.2b	73.8b	79.0b
0	100	79.2a	68.3a	73.8a
75	25	82.9b	72.1b	77.5b
50	50	81.0a	70.7a	75.9a
25	75	80.3a	69.0a	74.7a
Means		81.5B	70.8A	-

Values in columns followed by the same small letter and values in rows followed by the same capital letter do not differ significantly at $P < 0.05$

Table 8. *Digestible nitrogen-free extracts in field pea/oat mixtures (means across 2010-2012), g⊙kg^{-1} d.m.*

Proportion of components in the mixture, % (I)		Harvest date (II)		Means
Pea	Oat	Flowering stage of field pea	Flat green pod stage of field pea	
100	0	512b	502b	507b
0	100	529c	477a	503b
75	25	514b	512c	513c
50	50	510b	504c	507b
25	75	495a	494b	495a
Means		512B	498A	-

Values in columns followed by the same small letter and values in rows followed by the same capital letter do not differ significantly at $P < 0.05$

Their concentration was higher in mixtures harvested at the stage of field pea flowering compared with the stage of flat green pod of field pea. There was found an interaction between the experimental factors indicating that the highest content of digestible nitrogen-free extracts was determined in pure stand oat harvested at the stage of field pea flowering, and the lowest in pure stand oat harvested at the stage of flat green pod of field pea.

Discussion

Legume/cereal mixtures are predominantly grown for grain and fodder seed but they can be successfully cultivated for green matter to be used as fodder for cattle. On light soils, which predominate in Poland, field pea and oat may be valuable components used for cultivation in mixtures. In the present study, the highest fresh matter yield was

http://www.aloki.hu ● ISSN 1589 1623 (Print) ● ISSN 1785 0037 (Online)
DOI: http://dx.doi.org/10.15666/aeer/1705_1026710276

produced by the 50 + 50% mixture of field pea and oat. According to Huńady and Hochman (2014), mixtures of field pea (60%) with wheat or spring barley had the highest yields. Also Bedoussac and Justes (2009), Eskandari et al. (2009), Neuman et al. (2009), Kontturi et al. (2011), Księżak and Staniak (2013), Bojarczuk et al. (2014) and Neugschwandtner et al. (2014) demonstrated that mixed stands produce better yields than pure stands as mixtures are better at utilising changeable habitat conditions. In the experiment reported here, the fresh matter yield of the remaining mixtures was significantly lower although still higher than pure stand field pea. Harvest date had a significant effect on the fresh matter yield of field pea/oat mixtures. The yield was higher for mixtures harvested at the stage of flat green pod of field pea. Also studies by Staniak et al. (2012), Bojarczuk et al. (2014) and Rutkowska and Pikuła (2016) revealed that legume/cereal mixtures harvested at a later growth stage produced more biomass.

In the present study, the highest total protein content, crude ash content and digestible nitrogen-free extracts were found in pure stand field pea and in the 75 + 25% mixture of field pea and oat. Also Lithourgidis et al. (2006), Eskandari et al. (2009), Alizahed and Jat (2013), Huńady and Hochman (2014) Neugschwandtner and Kaul (2016) and Blagojevic et al. (2017) reported that leguminous plants grown in pure stand or constituting a high proportion in mixtures with cereals, oat in particular, produced the highest quality green fodder. In the study discussed here, pure stand field pea had the lowest crude fat content as well as the content of neutral detergent fibre (NDF) fraction and acid detergent fibre (ADF) fraction. Also Lithourgidis et al. (2006) found that common vetch cultivated in pure stand and in mixtures with spring triticale or oat had the lowest content of crude fibre and its fractions. In the study reported here, pure stand oat contained the most crude fibre, NDF, ADF and crude fat. According to many authors (Shoaib et al., 2013; Płaza et al., 2017), oat is the cereal that has the highest crude fat content. Also, cereals contain more crude fibre compared with legumes, which makes them less digestible. The factors which limit livestock feed uptake and digestibility include components of plant cell walls which are determined as fractions of neutral detergent fibre (NDA) and acid detergent fibre (ADF) (Belanger et al., 2013; Baert and Van Was, 2014; Truba et al., 2017).

Harvest date is a factor which affects nutrient content and, as a result, livestock feed quality. In the present study, field pea/oat mixtures harvested at the stage of field pea flowering contained more total protein, crude ash and digestible nitrogen-free extracts, which corresponds to findings reported by Lithourgidis et al. (2006), Shoaib et al. (2013), Płaza et al. (2017) and Uzun et al. (2017). In the experiment reported here, green fodder harvested at the earlier growth stage was of better quality, contained less crude fibre and fibre fractions, which made the green fodder more digestible. Research by Lithourgidis et al. (2006), Pires et al. (2006), Rondahl et al. (2006), Rutkowska et al. (2016) and Płaza et al. (2017) demonstrated that legume/cereal mixtures harvested at later development stages were of poorer quality. Primarily, they contained more crude fibre which reduces livestock feed digestibility. However, with fresh matter yield in mind, later harvest of legume/cereal mixtures, that is at the stage of flat green pod of field pea, should be encouraged. The highest fresh matter yield was produced by the 50 + 50% mixture of field pea and oat, and the most favourable chemical composition was determined for the 75 + 25% mixture.

http://www.aloki.hu ● ISSN 1589 1623 (Print) ● ISSN 1785 0037 (Online)
DOI: http://dx.doi.org/10.15666/aeer/1705_1026710276

Conclusions

1. The highest fresh matter yield was produced by the 50 + 50% mixture of field pea and oat.

2. Field pea grown in pure stand and mixed with oat at the proportion of 75 + 25% contained the most total protein, crude ash and digestible nitrogen-free extracts.

3. Pure stand oat had the highest crude fibre content, NDF, ADF and crude fat.

4. Field pea/oat mixtures harvested at the stage of field pea flowering contained more total protein, crude ash and digestible nitrogen-free extracts whereas mixtures harvested at the stage of flat green pod of field pea had more crude fibre, NDF, ADF and crude fat.

5. For further research, the selection of other species of legumes and cereals for cultivation in mixtures should be recommended. It will be very important to broaden the research with the features that define the feed value of the mixtures, i.e. the digestibility of the organic matter and the digestibility of the dry matter. The green matter from mixtures of legume and cereal plants can be used for silage used in cattle feeding.

REFERENCES

[1] Alizadeh, K., Jat, S. (2013): Mixed cropping of annual feed legumes with barley improves feed quantity and crude protein content under dry-land conditions. – Maejo Inter. J. Sci. Tech. 7(1): 42-47.

[2] Baert, J., Van Waes, C. (2014): Improvement of the digestibility of tall fescue (Festuca arundinacea Schreb.) inspired by perennial ryegrass (*Lolium perenne L.*). The future of European grasslands. – Grassl. Sci. Europe 19: 172-174.

[3] Bedoussac, L., Justes, E. (2010): Dynamic analysis of competition and complementarity for light and N use to understand the yield and the protein content of a durum wheat-winter pea intercrop. – Plant Soil 330: 37-54.

[4] Belanger, G., Virkajarvi, P., Tremblay, G. F., Saarijarvi, K. (2013): Herbage nutritive value in less-favoured areas of cool regions. The role of grasslands in a green future. – Grassl. Sci. Europe 18: 57-70.

[5] Blagojevic, M., Dordevic, N., Dinic, B., Vasic, T., Milenkovic, J., Petrovic, M., Markovic, J. (2017): Determination of green forage and silage protein degradability of some pea (*Pisum sativum* L.) plus oat (*Avena sativa* L.) mixtures grown in Serbia. Tarim Bilim. Der. – J. Agric. Sci. 23(4): 415-422.

[6] Bojarczuk, J., Księżak, J., Staniak, M. (2014): Evaluation of yielding of oat-pea mixtures cultivated in organic farming. – J. Res. Appl. in Agric. Eng. 59(3): 12-17 (in Polish).

[7] Eskandari, H., Ghanbari, A., Javanmard, A. (2009): Intercropping of cereals and legumes for forage production. – Not. Sci. Biol. 1(1): 7-13.

[8] Huńady, I., Hochman, M. (2014): Potential of legume-cereal intercropping for increasing yields and yield stability for self-sufficiency with animal fodder in organic farming. – Czech. J. Genet. Plant Breed. 50(2): 185-194.

[9] Kontturi, M., Laine, A., Niskanen, M., Hume, T., Hyovela, M., Peltonen-Sainio, P. (2011): Pea-oat intercrops to sustain lodging resistance and yield formation in northern European conditions. – Acta Agric. Scan., Sec. B-Soil and Plant Sci. 61(7): 612-621.

[10] Księżak, J., Staniak, M. (2013): Evaluation of mixtures of blue lupine (Lupinus angustifolius L.) with spring cereals grown for seeds in organic farming system. – J. Foof Agric. and Env. 11(4-4): 1670-1676.

[11] Lithourgidis, A. S., Vasilakoglou, I. B., Dhima, K. V., Dordas, C. A., Yiakoulaki, M. D. (2006): Forage yield and quality of common vetch mixtures with oat and triticale in two seeding ratios. – Field Crop Res. 99: 106-113.

http://www.aloki.hu ● ISSN 1589 1623 (Print) ● ISSN 1785 0037 (Online)
DOI: http://dx.doi.org/10.15666/aeer/1705_1026710276

[12] Neugschwandtner, R. W., Kaul, H. P. (2014): Sowing ratio and N fertilization affect yield and yield components of oat and pea in intercrops. – Field Crops Res. 155: 159-163.
[13] Neumann, A., Werner, J., Rauber, R. (2009): Evaluation of yield-density relationships and optimization of intercrop composition of field-grown pea-oat intercrops using the replacement series and the response surface design. – Field Crop Res. 114(2): 286-294.
[14] Płaza, A., Makarewicz, A., Gąsiorowska, B., Cybulska, A. (2017): Nutrient content in narrow-leaved lupine/oat mixture as affected by component proportion and harvest date. – Pol. J. Agron. 28: 35-42 (in Polish).
[15] Rodrigues, A. M., Andueza, D., Picard, F., Cecato, U., Farruggia, A., Baumont, R. (2008): Classification of mountain permanent grasslands based on their feed value. Biodiversity and animal feed. – Grass. Sci. Eur. 13: 501-503.
[16] Rondahl, T., Bertisson, J., Lindgren, E., Martinsson, K. (2006): Effects of stage of maturity and conservation strategy on fermentation, feed intake and digestibility of whole-crop pea oat silage used in dairy production. – Acta Agric. Scan., Sect. A-Anim. Sci. 56(3-4): 137-147.
[17] Rutkowska, A., Pikuła, D. (2016): Efficacy of N-15-nitrogen in fertilization of pea mixtures with wheat, barley, and oat. – Plant Soil Env. 62(8): 367-372.
[18] Shoaib, M., Ayub, M., Zamir, M. S. I., Akhtar, M. J. (2013): Dry matter yield of oat-Egyptian clover mixture under varying proportions and different growth stage of oat. – Inter. J. Agric. Biol. 15(4): 673-679.
[19] Staniak, M., Księżak, J., Bojarczuk, J. (2012): Estimation of productivity and nutritive value of pea-barley mixtures in organic farming. – J. Food Agric. Env. 10(2): 318-323.
[20] Stjskalova, M., Hejcman, M. (2013): Forage value of fodder main European broad-leaved woody species. The role of grassland in a green future. – Grass. Sci. Eur. 18: 85-87.
[21] Truba, M., Wiśniewska-Kadżajan, B., Jankowski, K. (2017): The influence of biology preparations and mineral fertilization NPK on fiber fraction in Dactylis glomerata and Lolium perenne. – Frag. Agron. 34(1): 107-116 (in Polish).
[22] Uzun, A., Asik, F. F., Acikgoz, E. (2017): Effects of different seeding rates on forage yield and quality components in pea. – Tur. J. Field Crops 22(1): 126-133.

http://www.aloki.hu ● ISSN 1589 1623 (Print) ● ISSN 1785 0037 (Online)
DOI: http://dx.doi.org/10.15666/aeer/1705_1026710276

PLANKTON DIVERSITY AND COMMUNITY STRUCTURE OF ASARAMA ESTUARY IN THE NIGER DELTA IN RELATION TO PHYSICO-CHEMISTRY

DIRISU, A. R.[1*] – UWAGBAE, M. A.[1,2] – EDWIN-WOSU, N. L.[3] – IMOOBE, T. O. T.[1]

[1]*Department of Animal and Environmental Biology, Faculty of Life Sciences, University of Benin, Benin City, Edo State, P.M.B. 1154, Nigeria*

[2]*Wetlands International, 3a Oromineke Street, D-Line, Port Harcourt, Nigeria*

[3]*Department of Plant Science and Biotechnology, University of Port Harcourt, Choba, Port Harcourt, Nigeria*

**Corresponding author*
e-mail: dedonrahman10@yahoo.com

(Received 21st Feb 2019; accepted 15th May 2019)

Abstract. Biodiversity of Asarama estuary at Andoni flat in the Niger Delta was surveyed in the wet and dry seasons of 2016/17; in order to ascertain the diversity, composition and community structure of plankton. Qualitative plankton samples, were collected from different sources including surface water and analysed in the laboratory. The results for the analyses for water chemistry showed optimal to near high values for the parameters, which were within the normal range of normality in tropical brackish waters. Biodiversity analyses revealed eight divisions of phytoplankton in the given order; (bacillariphyta constituting 84% > cyanophyta 8% > chlorophyta 6%, > euglenophyta 1%, ≥ dinophyta 1%, > ochrophyta < 1%, ≥ charophyta < 1%, ≥ oligohymenophorea < 1%) and three groups of zooplankton which were cyclopoida (composed of 98% of the species), harpaticoida and rotifera (which had 1% of the constituent species each). Species diversity and composition were low for zooplankton and very high for phytoplankton. Meanwhile, unregulated boat traffic and illegal pollution with crude oil products pose major challenges to the biotic communities. Nutrient enrichment may perhaps become an issue in the near future if no monitoring efforts backed with legislature are imposed on the maricultural practices of bivalves at the upstream.
Keywords: *Andoni, inter-tidal, phytoplankton, salinity, zooplankton*

Introduction

Estuaries are shallow open systems that are strongly influenced by river inflows, mixing with the coastal ocean and exchanging sediment including the cleaning of the atmosphere and the water interfaces. They usually have distinct salinity gradients in their lower part and a tidal influence in their upper freshwater part providing specific hydrological properties when compared to rivers. Importantly, estuaries form transition zones between freshwater and marine environments, and are thus characterised by a large variability in their biophysical and chemical properties under both the influence of climate change and intense anthropogenic activities (Pearle et al., 2010; Lancelot and Muylaert, 2011; Yang et al., 2014). Asarama estuary is one of the most important navigable waterways in the far reaches within Andoni land and it connects several communities therein. Besides, it is exposed to both the natural factors and human exploitation activities daily (Ansa and Francis, 2007).

The estuarine environment represents an ecotone between freshwater and marine ecosystems and is influenced by both, but is in many ways more complex than either of

http://www.aloki.hu ● ISSN 1589 1623 (Print) ● ISSN 1785 0037 (Online)
DOI: http://dx.doi.org/10.15666/aeer/1705_1027710292

them (Cearreta et al., 2000; Elliott and De Jonge, 2002; Elliott and McLusky, 2002; Yang et al., 2014). Both river flow and tidal motions drive the riverine and marine communities towards estuaries (Waniek et al., 2005) and hence shape the diversity and abundance of estuarine communities (Elliott and McLusky, 2002; Waniek, 2003; Froneman, 2004; Cloern et al., 2014). Despite the well-documented role of zooplankton in the transfer of carbon and energy, and in ichthyofaunal abundance, relatively few studies have dealt with the determinants of zooplankton assemblages in estuarine ecosystems (Carlsson et al., 1995; Dalal and Goswami, 2001; Tan et al., 2004; Thor et al., 2005; Hwang et al., 2010).

The productivity of any water body is determined by the amount of plankton therein as they are the major primary and secondary producers. Plankton communities serve as a base for the food chain that supports the commercial fisheries (Townsend et al., 2000; Godhantaraman et al., 2003; Conde et al., 2007; Davies et al., 2009; Ogbuagu et al., 2011). They are essential tools for biomonitoring programme (Davies et al., 2009) and as such their relative high abundance and diversity is crucial.

Some available studies in the Niger Delta brackish waters dealing with phytoplankton and zooplankton include Opute (1990) on the phytoplankton of Warri/Focados estuary in Delta State; Kadiri (2006) on the survey of phytoplankton on the western Niger Delta; Davies et al. (2009) on the phytoplankton of Elechi creek, and Ogbuagu et al. (2011) on the myco-plankton of Imo River in the Niger Delta).

There is a huge dearth of knowledge on the plankton communities of Asarama estuary regarding its checklist, diversity and community structure; as no such known study was documented prior to this work upon search. Hence, this study was timely and addresses the influence of environmental activities upon the composition, diversity and community structure of the plankton of Asarama estuary at Andoni flat in the Niger Delta. Therefore, the aim and objectives of this study were to document the diversity, community composition and the physicochemical environment associated with the plankton of Asarama estuary. We used Multivariate approach such as canonical correspondence (CC) analysis to test for the associations between plankton communities and the physicochemical environment in the study area.

Materials and methods

Study area

Asarama estuary at Adoni land in Rivers State is located within the coordinates (04°30’37”N, 007°27’05”E and 04°31’35”N, 007°28’44”E). It is a semi-diurnal tidal estuary system with a bridge across to other communities near shore (*Fig. 1*). The sampling stations (which are designated as points 1 to 5, in yellow ink along the water course on the map) were fixed by using a hand held Global Positioning System (GPS) and were maintained throughout the study period.

Sampling stations

The ecosystem is characterised by rich flora communities of white and red mangroves, Nipa palm forests and other halophytes. At station 1, is located a forest of mangroves named; Aso mangrove forest which is over 200 years old (personal communication, 2016). The forest is a host to several species of birds, monkeys, reptiles, bees and insects as observed during field studies. Stations 2 is rich in

http://www.aloki.hu ● ISSN 1589 1623 (Print) ● ISSN 1785 0037 (Online)
DOI: http://dx.doi.org/10.15666/aeer/1705_1027710292

mangroves as well. Decapods and bivalves were commonly seen on mangrove branches here. Stations 3 is characterised by an admixture of white mangrove and nipa palms. The sediment was mostly silty and contained a lot of dead decaying organic matter like dead woods, dead leaves and dead shells of molluscs. Station 4 is located far downstream after the bridge by the fishing wooden traps. The substratum was a mixture of sandy-muddy bed. A film of soot from an illegal petroleum local refinery was observed on the water surface throughout the study. Station 5 is equally located downstream of station 4. A lot of nipa palms were found here with so much decomposition activities of the palm fronds and their seeds. The substratum was mostly muddy at the upper most reaches.

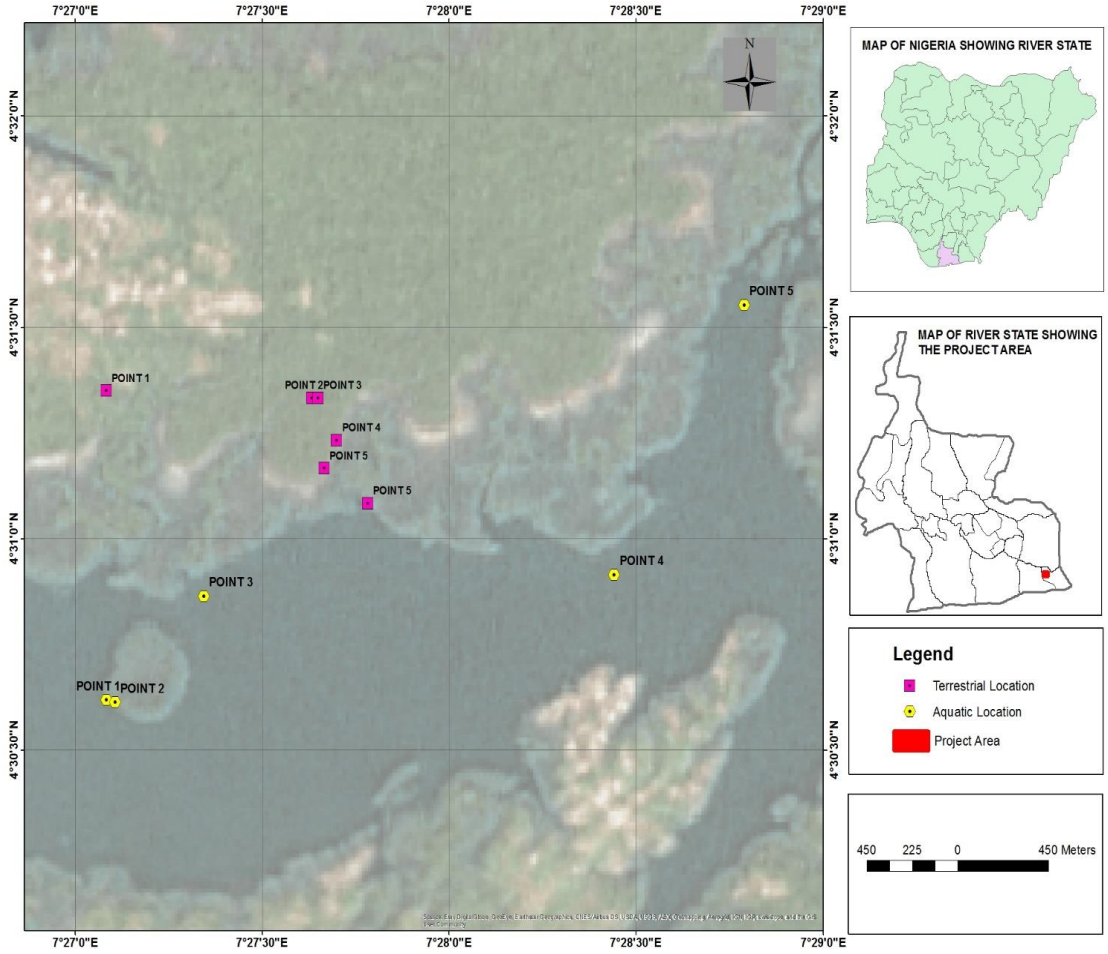

Figure 1. *Map of the study area*

Human activities and land used pattern

The major human activities in the locality include land and water transportations using cars, motor-bikes and boats, fishing with fish nets, gears and fish traps. Mariculture of Oysters (*Castrostrea* sp) and Periwinkles (*Tympanotonus fuscatus* Var. *Radular*) were predominant. At low tides particularly between 08:30 and 10:00 some of the locals were engaged in harvesting periwinkles indiscriminately without regulations.

http://www.aloki.hu ● ISSN 1589 1623 (Print) ● ISSN 1785 0037 (Online)
DOI: http://dx.doi.org/10.15666/aeer/1705_1027710292

Illegal local refinery of petroleum products was observed far upstream off the estuary at the north-western bank which was emitting soot into the atmosphere.

Surface water sampling and analyses

Surface water samples were collected, preserved where applicable and analysed either in the field or laboratory according the methods of Eaton et al. (2005). A HANNAH field pH meter was used for the determination of pH in-situ. Turbidity was determined in the laboratory by using a HACH DR - 2000 spectrophotometer (Hach instrument). Salinity was determined in the laboratory by using HACHCO150 Model for Total Dissolved Solid/Conductivity/Salinity. This was determined using a HACHCO150 TDS/Conductivity/Salinity meter. Azide modification of Winkler's method was used to determine dissolved oxygen content of the water samples. Also, the Azide modification of Winkler's method was used to determine BOD content of the water samples. Nitrate was determined using HACH ER 2000 spectrophotometer. Determination of sulphate was done using a HACH DR 2000 spectrophotometer.

Plankton sampling and laboratory analyses

We used qualitative method to collect both phyto and zooplankton communities from the subsurface water in August 2016, the peak of wet season in the Niger Delta and March 2017 (driest month in the dry season) across five sampling stations (designated as points 1 to 5 on the map) by towing a 55 micron plankton net tied to a 25 HP engine-powered boat cruising at a speed of about 5 km h^{-1} for not more than 3 minutes in all. Plankton samples were then preserved with few drops of 10% buffered formaldehyde solution in 250 ml plastic bottles (polypropylene bottles) (Davies et al., 2009; Imoobe and Adeyinka, 2009). Samples were observed in the postgraduate laboratory of the Department of Animal and Environmental biology, University of Benin, Benin, Nigeria; using the Olympus binoculars microscope (CH). Identification and classification to species level where possible, was carried out with the appropriate literatures (Newell and Newell, 1966; Prescott, 1975; Needham and Needham, 1978 and Van De Velde, 1984; Jeje and Fernando, 1986).

Data analyses

Physicochemical data were subjected to the Analysis of Variance (One-way ANOVA) using SPSS (version 16.0). Plankton results were tested for biological diversity indices such as species richness, Shannon diversity index and species evenness with the aid of Palaeontological Statistics software (PAST 1.99 version) and canonical correspondence analysis (CCA) was also performed to test for any existing association between environmental condition and the biota (Hammer et al., 2001; Uwagbae et al., 2017). Plankton data were equally analysed by using basic tools for the measurement of central tendency such as graphics and percentage distribution.

Results

Physico-chemical environment of Asarama estuary

The physical and chemical condition of Asarama estuary surface water is presented in *Tables 1* and *2,* respectively.

http://www.aloki.hu ● ISSN 1589 1623 (Print) ● ISSN 1785 0037 (Online)
DOI: http://dx.doi.org/10.15666/aeer/1705_1027710292

Table 1. *Summary of the seasonal mean and standard deviation of the physicochemical condition in surface water of Asarama estuary (between August, 2016 and March, 2017)*

Parameters	Station 1 Mean±SD	Station 2 Mean±SD	Station 3 Mean±SD	Station 4 Mean±SD	Station 5 Mean±SD	Significant values
Air temperature (°C)	30.00±2.83	30.00±4.24	30.00±4.24	30.50±3.54	31.00±4.24	0.998
Water temperature (°C)	28.00±2.83	27.75±1.77	28.00±2.83	29.00±4.24	28.50±3.54	0.996
pH	7.20±0.14	7.30±0.14	7.30±0.14	7.15±0.21	7.00±0.28	0.554
Turbidity (NTU)	9.00±1.41	19.00±8.49	10.00±4.24	11.00±1.41	14.00±1.41	0.259
EC ($mSCm^{-1}$)	8.35^{a}±0.28	9.37^{a}±0.08	7.82^{a}±0.71	7.05^{a}±0.15	5.22^{b}±1.27	0.022
TDS (mgL^{-1})	5.12^{a}±1.38	5.53^{a}±5.30	4.95^{a}±3.75	4.94^{a}±7.01	3.04^{b}±389	0.010
DO (mgL^{-1})	7.21±0.72	7.32±0.28	7.74±0.59	7.45±0.42	7.88±0.40	0.669
BOD (mgL^{-1})	0.98^{c}±0.01	0.99^{c}±0.01	1.89^{a}±0.16	1.18^{bc}±0.03	1.49^{ab}±0.38	0.014
Salinity (‰)	4.95±0.49	5.25±0.07	4.55±0.78	4.25±0.64	3.20±1.27	0.234
Total hardness ($CaCO_3$) (mgL^{-1})	1160.00±70.71	1430.00±14.14	1075.00±91.92	1075.00±162.63	1210.00±424.26	0.545
Nitrate (mgL^{-1})	0.13±0.03	0.10±0.01	0.14±0.03	0.12±0.04	0.09±0.01	0.378
Phosphate (mgL^{-1})	0.30^{c}±0.03	0.34^{bc}±0.04	0.42^{ab}±0.04	0.44^{ab}±0.04	0.46^{a}±0.04	0.033
Sulphate (mgL^{-1})	358.50±44.55	455.00±91.92	350.00±42.43	311.00±26.87	254.00±79.20	0.157

Significant < 0.05: significant difference. Superscript denotes the source of significant variation

Table 2. *Mean values of the investigated parameters in surface water across wet and dry seasonal during the study*

Parameters	Wet season Mean±SD	Dry season Mean±SD	Significant
Air temperature (°C)	27.60±0.55	33.00±0.71	0.000
Water temperature (°C)	26.10±0.22	30.40±1.14	0.000
pH	7.06±0.17	7.32±0.08	0.015
Turbidity (NTU)	15.00±5.87	10.20±2.77	0.107
EC ($mSCm^{-1}$)	7.21±1.85	7.91±1.29	0.480
TDS (mgL^{-1})	4.61±1.19	4.84±0.86	0.700
DO (mgL^{-1})	7.86±0.29	7.18±0.33	0.008
BOD (mgL^{-1})	1.38±0.47	1.23±0.33	0.599
Salinity (‰)	3.98±1.09	4.90±0.51	0.139
Total hardness ($CaCO_3$) (mgL^{-1})	1108.00±199.67	1272.00±202.53	0.223
Nitrate (mgL^{-1})	0.13±0.03	0.10±0.02	0.038
Phosphate (mgL^{-1})	0.42±0.07	0.36±0.07	0.252
Sulphate (mgL^{-1})	386.00±82.04	305.40±69.91	0.132

Significant < 0.05: significant difference

Air and water temperatures closely followed each other. The differences between air and water temperatures was not more than 4 °C. Mean air temperature ranged between 30 and 31 °C across the stations. Likewise water temperature varied from 27.75 °C at station 2 to 29 °C at station 4. There was however no significant differences between the two parameters ($P > 0.05$).

The mean spatial and temporal concentrations of hydrogen ion concentration (pH) values showed an alkaline condition ranging between 7.00 at station 5 and 7.30 at stations 2 and 3 respectively. The mean values across stations 1 to 5 in wet and dry seasons were between 7.06 and 7.32. Turbidity mean wet and dry season values ranged from 10.20 to 15.00 NTU. Turbidity mean concentration values were between 900 NTU at station 1 and 19.00 NTU at station 2. Electrical conductivity (EC) mean seasonal concentrations were between 5.22 $mScm^{-1}$ at station 5 and 9.37 $mScm^{-1}$ at station 2.

http://www.aloki.hu ● ISSN 1589 1623 (Print) ● ISSN 1785 0037 (Online)
DOI: http://dx.doi.org/10.15666/aeer/1705_1027710292

Total hardness and nutrients (phosphate, sulphate and nitrate) exhibited condition tenable in the marine environment. Mean values of total hardness varied from 1075.00 mgL^{-1} at station 3 and 4 respectively to 1430.00 mgL^{-1} at station 2. Its mean concentration value in the water was between 1108.00 mgL^{-1} in the wet season and 1272.00 mgL^{-1} in the dry season. Nitrate and phosphates both had low range of values. The mean temporal and spatial concentration values were less than 0.5 mgL^{-1}. However, sulphate recorded very high values of between 386.00 mgL^{-1} during the wet season and 305.40 mgL^{-1} during the dry season. Sulphate mean concentration were between 254.00 mgL^{-1} at station 5 and 455.00 mgL^{-1} at station 2. The seasonal values of dissolved oxygen (DO) ranged between 7.18 mgL^{-1} in the dry season and 7.86 mgL^{-1} in the wet season. Mean values across the stations ranged from 7.21 mgL^{-1} at station 1 to 788 mgL^{-1} at station 5. Biological oxygen demand (BOD_5) seasonal values ranged from 1.23 mgL^{-1} in the dry season to 1.38 mgL^{-1} in the wet season. And mean values showed variations from 0.98 mgL^{-1} at station 1 to 1.89 mgL^{-1} at station 3.

Salinity mean concentrations varied from 3.20 ppm at station 5 to 4.95 ppm at station 1. Seasonal concentrations varied between 3.98 ppm in wet season and 4.90 ppm in the dry season.

Plankton studies

Both phyto- and zooplankton were characterised and presented in this section.

Phytoplankton

Phytoplankton analysis revealed a total of eight divisions dominated by the Bacillariphyta constituting about 84%. Others were in the order Cyanophyta (8%) > Chlorophyta (6%), > Eglenophyta (1%), ≥ Dinophyta (1%), > Ochrophyta (< 1%), ≥ Charophyta (< 1%), ≥ Oligohymenophorea (< 1%) (*Figs. 2* and *3*). The total number of individuals is represented by 9,276 individuals per meter squared, amongst 57 taxa. Phytoplankton taxa had higher percentage composition and distribution across the study stations except at station 5 and were significantly higher during the dry season of the study in 2017 (*Table 3*).

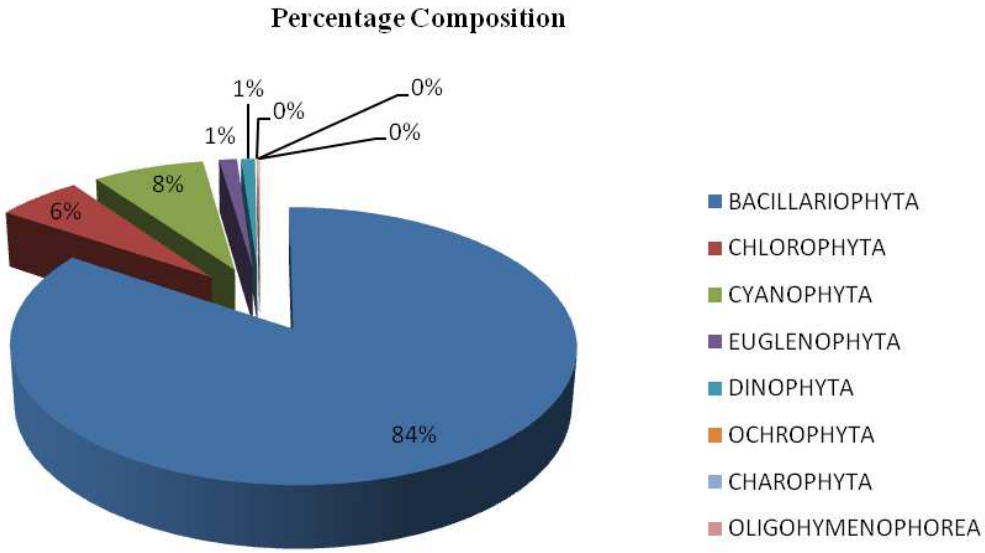

Figure 2. *Percentage composition of phytoplankton divisions*

http://www.aloki.hu ● ISSN 1589 1623 (Print) ● ISSN 1785 0037 (Online)
DOI: http://dx.doi.org/10.15666/aeer/1705_1027710292

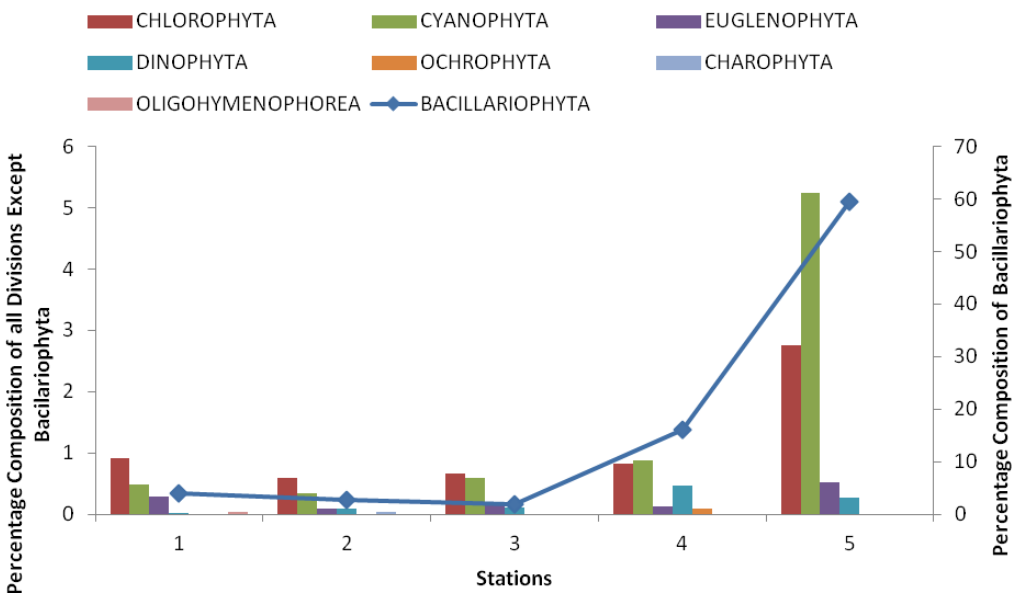

Figure 3. *Percentage composition and distribution of phytoplankton groups across the study stations*

Table 3. *Summary of the composition and distribution of phytoplankton species across the study stations*

Phytoplankton species	Stations					
	1	**2**	**3**	**4**	**5**	**Total**
DIVISION: BACILLARIOPHYTA						
Actinoptychus splendens	0	2	0	0	0	2
Amphiprora alata	0	3	0	0	0	3
Bacillaria paradoxa	10	18	32	244	1446	1750
Bacillaria sp.	0	0	0	0	48	48
Biidulphia regia	0	6	0	0	0	6
Chaetoreros sp.	4	0	0	0	0	4
Coscinodiscus cencinnus	1	0	0	0	0	1
Eunotia flexuosa	4	0	0	0	0	4
Flagillaria javanica	0	0	0	0	1200	1200
Flagillaria sp.	79	31	96	1216	2664	4086
Melosira granulata	4	0	0	0	0	4
Pinnularia cardinaliculus	4	0	0	0	0	4
Pinnularia sp.	0	0	6	12	24	42
Surirella robusta	1	0	0	0	0	1
Surirella sp.	3	0	0	0	60	63
Synedra acus	152	76	24	0	0	252
S. ulna	112	80	20	0	0	212
Tabellaria floculosa	0	40	0	0	0	40
TOTAL BACILLARIOPHYTA	374	256	178	1472	5442	7722
DIVISION: CHLOROPHYTA						
Clostrerium gracile	4	4	0	0	0	8
Cosmarium bretum	0	0	0	0	48	48
Cosmarium connatum	4	0	0	0	0	4

http://www.aloki.hu ● ISSN 1589 1623 (Print) ● ISSN 1785 0037 (Online)
DOI: http://dx.doi.org/10.15666/aeer/1705_1027710292

Cosmarium pseudoconnatum	4	0	0	0	0	4
Cosmarium resiforme	0	0	4	0	0	4
Eudorina elegans	0	11	0	0	0	11
Mougeotia sp.	4	0	0	0	0	4
Pandorina morum	18	0	0	0	0	18
Pandorina sp.	18	8	40	0	0	66
Pediastrum gracillinum	0	0	0	0	72	72
Pleodorina illinosensis	0	1	0	0	0	1
Scenedesemus dimorphus	0	0	0	8	0	8
Scenedesemus opollensis	0	0	0	8	0	8
Sirogonium melanosporum	26	8	8	8	48	98
Spirogyra karnalae	0	0	0	0	24	24
Spirogyra sp.	4	0	0	0	0	4
Volvox africana	2	10	0	32	36	80
Volvox aureus	0	12	8	20	24	64
TOTAL CHLOROPHYTA	84	54	60	76	252	526
DIVISION: CYANOPHYTA						
Aphanothecae sp.	0	0	16	0	0	16
Coelosphaerium sp.	24	8	32	32	168	264
Coelosphaerium pallidum	0	0	0	48	288	336
Microcystis aeruginosa	3	0	0	0	0	3
Microcystis flos-aquae	0	0	0	0	24	24
Oscillatoria bornettia	11	0	0	0	0	11
Oscillatoria sp.	0	24	0	0	0	24
Plectonema sp.	6	0	0	0	0	6
Lyngba aestuarri	0	0	6	0	0	6
TOTAL CYANOPHYTA	44	32	54	80	480	690
DIVISION: EUGLENOPHYTA						
Euglena sp.	18	0	0	8	48	74
Euglena spirogyra	0	8	16	0	0	24
Euglena viridia	5	0	0	0	0	5
Phacus tontus	1	0	0	0	0	1
Trachelomonas eurysloma	3	0	0	0	0	3
Trachelomonas oblonga	0	0	0	4	0	4
TOTAL EUGLENOPHYTA	27	8	16	12	48	111
DINOPHYTA						
Gymnodinium fuscum	1	9	10	42	24	86
TOTAL DINOPHYTA						
OCHROPHYTA						
Gonyostomum semen	0	0	0	8	0	8
TOTAL OCHROPHYTA	0	0	0	8	0	8
CHAROPHYTA						
Actinotaenium cucurbitinum	12	0	28	32	0	72
Euastrum elegans	0	0	0	24	24	48
Nitella gracilis	6	0	0	0	0	6
Straurodesmus leptodermus	0	3	0	0	0	3
TOTAL CHAROPHYTA	0	3	0	0	0	3
OLIGOHYMENOPHOREA						
Epistylis plicatilis	4	0	0	0	0	4
TOTAL OLIGOHYMENOPHOREA	4	0	0	0	0	4

http://www.aloki.hu ● ISSN 1589 1623 (Print) ● ISSN 1785 0037 (Online)
DOI: http://dx.doi.org/10.15666/aeer/1705_1027710292

Zooplankton

The zooplankton taxa were poorly represented and distributed in three groups; Cyclopoida, Harpaticoida and Rotifera of the phylum Arthropoda and sub-phylum Crustacea. A total of 1,299 individuals per unit area represented in 15 taxa were recorded in this aspect of the study. The group Cyclopoida constituted 98% of species while Harpaticoida and Rotifera had 1% each. Taxa composition and distribution varied irregularly across the sampled stations (*Figs. 4* and *5*). Meanwhile, Rotifera was highest at station 5. There was no zooplankton recorded at station 4 throughout the study (*Table 4*).

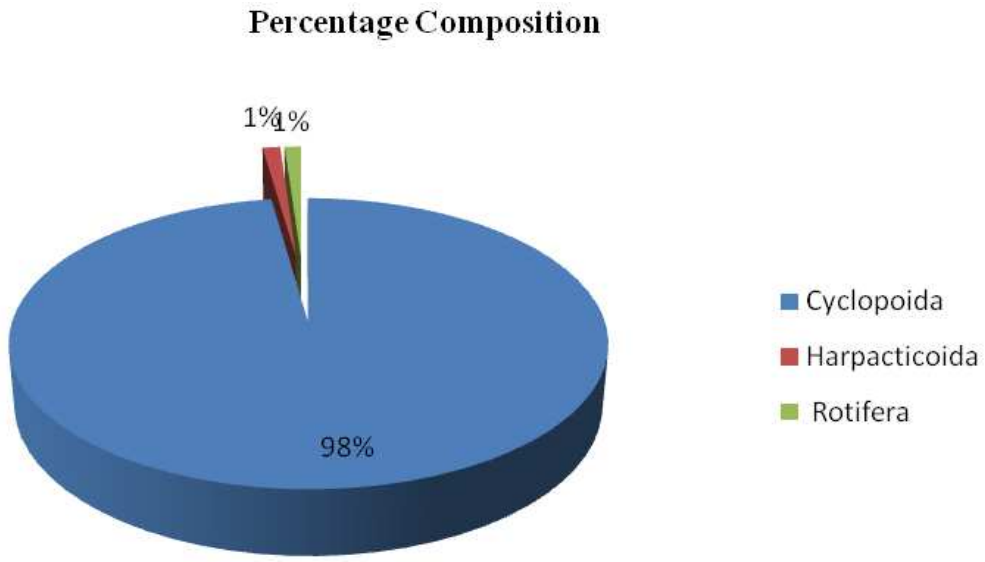

Figure 4. *Percentage composition of zooplankton taxa in study area*

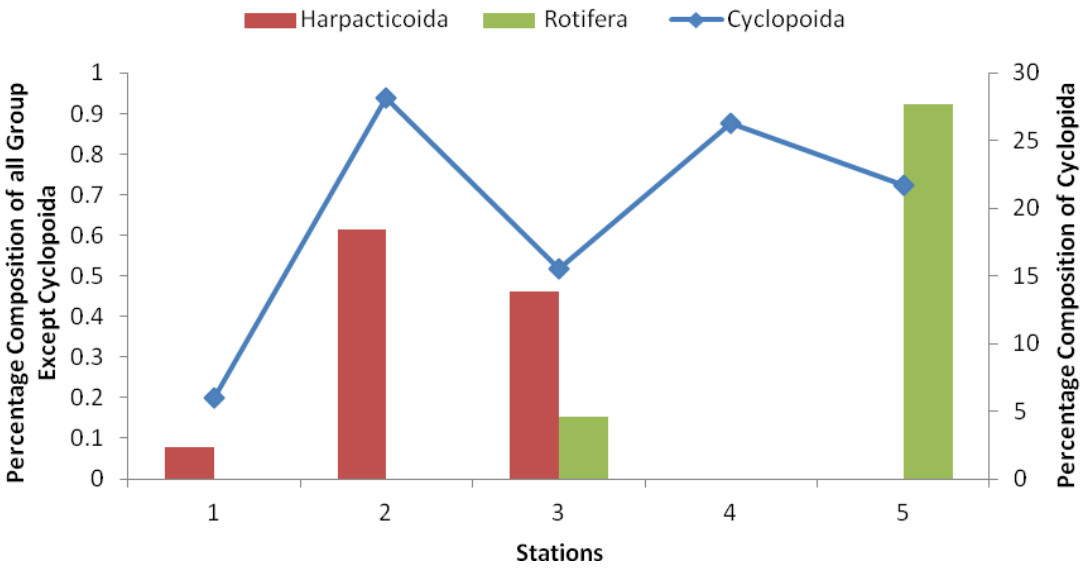

Figure 5. *Percentage composition and distribution of zooplankton species across the sampled stations*

http://www.aloki.hu ● ISSN 1589 1623 (Print) ● ISSN 1785 0037 (Online)
DOI: http://dx.doi.org/10.15666/aeer/1705_1027710292

Table 4. *Summary of the composition and distribution of zooplankton taxa across the study stations*

Zooplankton species	Stations					
	1	**2**	**3**	**4**	**5**	**Total**
Phylum: Arthropoda						
Subphylum: Crustacea						
Subclass: Copepoda						
Cyclopoida						
Thermocyclops neglectus	26	46	100	38	90	300
Mesocyclops bodanicola	32	256	84	272	120	764
Metacyclops minutus	4	0	0	0	0	4
Microcyclops javanus	0	0	2	0	24	26
Acanthocyclops sp.	6	48	8	0	48	110
Eucyclops macruroides	10	0	8	32	0	50
Achidius (Neotachidius) triangular	0	16	0	0	0	16
Harpacticoida						
Shizopera neglecta	1	8	6	0	0	15
TOTAL COPEPODA	79	374	208	342	282	1285
Rotifera						
Keratella hiemalis	0	0	0	0	12	12
Rotaria neptunia	0	0	2	0	0	2
TOTAL ROTIFERA	0	0	2	0	12	14

Diversity indices for plankton

Biological diversity index for phytoplankton with respect to species richness was highest at station 1 and least at station 2. Species were only evenly distributed at stations 2 and 3. Meanwhile species dominance was highest at station 4 and Shannon diversity was least at stations 4 and 5 respectively (*Table 5*).

Table 5. *Phytoplankton diversity index*

Description	STN 1	STN 2	STN 3	STN 4	STN 5	Total
Taxa_S	32	20	15	16	18	**101**
Individuals	552	362	346	1746	6270	**9276**
Dominance_D	0.1469	0.1253	0.1291	0.5074	0.2737	
Shannon_H	2.455	2.434	2.352	1.217	1.659	
Simpson_1-D	0.8531	0.8747	0.8709	0.4926	0.7263	
Evenness_e^H/S	0.364	0.57	0.7004	0.2111	0.292	
Menhinick	1.362	1.051	0.8064	0.3829	0.2273	
Margalef	4.91	3.225	2.395	2.009	1.944	
Equitability_J	0.7084	0.8123	0.8685	0.4389	0.5741	
Fisher_alpha	7.398	4.559	3.196	2.433	2.272	
Berger-Parker	0.2754	0.221	0.2775	0.6964	0.4249	

http://www.aloki.hu ● ISSN 1589 1623 (Print) ● ISSN 1785 0037 (Online)
DOI: http://dx.doi.org/10.15666/aeer/1705_1027710292

For the zooplankton, species richness was observed at stations 1 and 3 only, and evenness was least at stations 3. Dominance of species occurred at station 4 and fairly at station 4 (*Table 6*).

Table 6. *Zooplankton diversity index*

Description	STN 1	STN2	STN 3	STN 4	STN 5	Total
Taxa_S	6	5	7	3	5	**26**
Individuals	79	374	210	342	294	**1299**
Dominance_D	0.2969	0.5024	0.3907	0.6536	0.2953	
Shannon_H	1.396	0.9978	1.159	0.6479	1.359	
Simpson_1-D	0.7031	0.4976	0.6093	0.3464	0.7047	
Evenness_e^H/S	0.6729	0.5425	0.4553	0.6372	0.7786	
Margalef	1.144	0.6752	1.122	0.3428	0.7038	
Equitability_J	0.7789	0.62	0.5956	0.5898	0.8445	

Application of canonical correspondence analysis (CCA) on the biota

We used Canonical correspondence analyses to characterise the relationships between the abiotic and biotic components of Asarama estuary.

For phytoplankton several associations were found at axis 2 of the CCA (*Fig. 6*). There was a positive association between phosphorus, sulphur and Ochrophyta species at plot 4. At plot 1, there was a positive association between pH and Charophyta. Meanwhile, Cyanophyta and Euglenophyta showed some positive correlations with nitrate respectively.

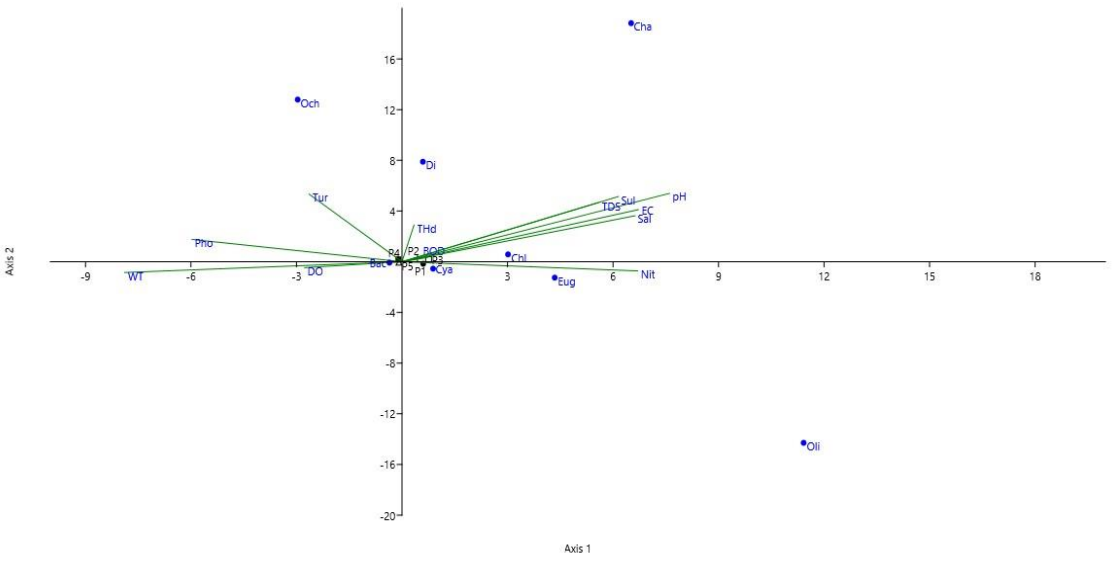

Figure 6. *Canonical corresponded analysis (CCA) for phytoplankton community*

However, for the zooplankton taxa (*Fig. 7*) there was a strong negative correlation between cyclopoida taxa and water temperature at axis 1. Also at axis 1, positive

http://www.aloki.hu ● ISSN 1589 1623 (Print) ● ISSN 1785 0037 (Online)
DOI: http://dx.doi.org/10.15666/aeer/1705_1027710292

association between biological oxygen demand (BOD), dissolve oxygen (DO) and rotifers was observed. Importantly, pH, EC, salinity, turbidity, sulphate and nitrate showed strong negative association with harpacticoida taxa during the study.

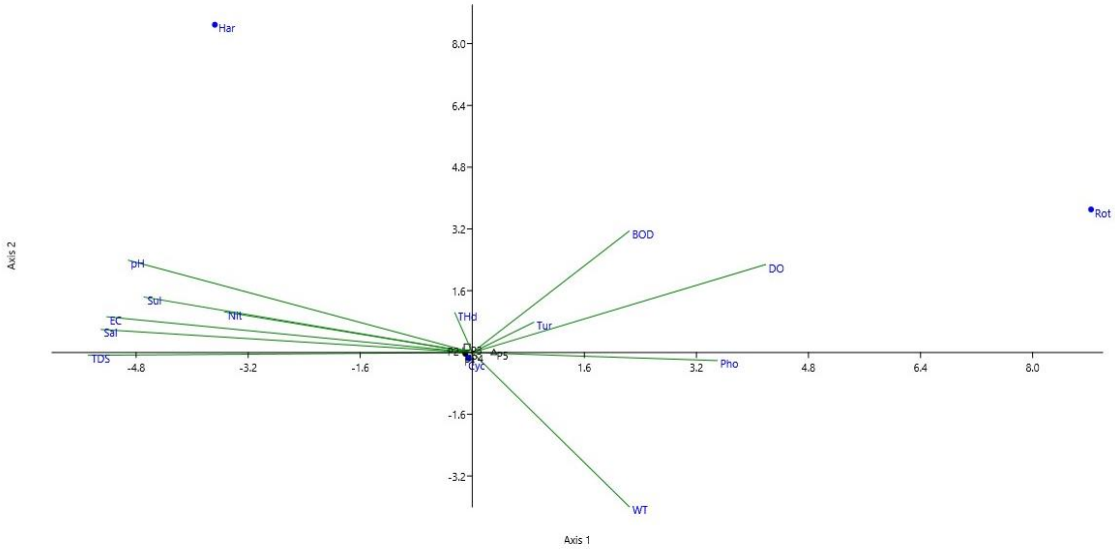

Figure 7. *Canonical corresponded analysis (CCA) for zooplankton community*

Discussion

The result of phytoplankton showed high species diversity, abundance and a robust community structure. In a given healthy aquatic environment, phytoplankton high population density is expected particularly in the shallow water depth rich in nutrient materials (Castro and Huber, 1997; Kadiri, 2006; Davies, 2009; Cloern et al., 2014; Dalu et al., 2016) except otherwise in contaminated or polluted waters. The dominance of Bacillariophyta division amongst the eight divisions recorded in this study corroborate the study by Kadiri (2006) and Egborge et al. (2001) in the western Niger Delta explaining that most inter-tidal waters in the zone are likely to be in this nature. Davies (2009) demonstrated that day light event (sun shine rays) play very important role in the production activities of both the primary and secondary producers as the latter is dependent on the former. The taxa among the division Bacillariophyta which were well represented across the study irrespective of the prevailing season were; *Bacillaria paradoxa, Flagillaria sp* and *Synedra acus* and were occasionally sampled at stations 1, 2, 3 and 5 respectively. The reason why the divisions Dinophyta, Ochrophyta and Oligohymenophorea recorded one species each throughout this study could not be well ascertained. However, the pattern of phytoplankton diversity is similar to what was reported (Kadiri, 2006) across waterways in the western Niger Delta of Nigeria. The pattern of diversity and species abundance observed in this study whereby some stations did not record any individual was affirmed by the output of the performance of diversity indices such as species richness and Shannon wiener diversity, and was earlier acclaimed (Kadiri, 2006 in the Niger Delta; and Lancelot and Muylaert, 2011). Environmental conditions such as temperature, pH, DO, BOD, salinity and EC in the surface water of Asarama estuary greatly influenced the production (particularly of phytoplankton), distribution and stability of the biotic community (typical for the zooplankton).

http://www.aloki.hu ● ISSN 1589 1623 (Print) ● ISSN 1785 0037 (Online)
DOI: http://dx.doi.org/10.15666/aeer/1705_1027710292

The zooplankton of Asarama estuary were in conformity to what have been documented for some coastal or brackish waters in the Niger Delta of Nigeria (Davies, 2009; Ogbuagu et al., 2011). Though, the zooplankton community structure had more taxa of the sub-class copepod which consist of the order cyclopoida and harpaticoida, and the class rotifer respectively. The dominance of copepods in this study as a finding is in consistency with some earlier studies (Kolo et al., 2001; Davies, 2009) in Nigerian coastal environments and Hwang et al. (2010) for a study in Taiwan. Zooplankton-cyclopoida was represented by seven species of which; *Thermocyclops neglectus and Mesocyclops bodanicola* were the most dominant and abundant species recorded across the five sampled stations. *Shizopera neglecta* (Harpacticoida) and the two species of Rotifers only (*Keratella hiemalis and Rotaria neptunia*) were recorded at station 4. We strongly attribute this phenomena to the presence of soot and oil film on the surface water which could perhaps inhibit the activities of primary producers. The restriction of the occurrence of Rotifers species to stations 3 and 5 only could not be fully ascertained in this study. Importantly, the dominance of copepods in a given aquatic environment as in this study, is an indication of a perturbed or stressed environment (Davies, 2009). Imoobe and Adeyinka (2009) reported a high species diversity for rotifers and copepods for an inland stream in Benin, Nigeria, which proved contrary to our findings for the same group of zooplankton. Environmental perturbation was found to be associated with Asarama estuary resulting from intense human activities such as transportation/navigation and over harvesting of periwinkle (*T. fuscatus)*. Despite the diversity of phytoplankton, the zooplankton diversity was low however, a situation that was least expected since Asarama estuary is typically a shallow inter-tidal ecosystem rich in nutrient resulting in high productivity in the littoral zone. However, we believe that the effect of vertical migration in zooplankton and the choice of sampling the subsurface water using qualitative method only could have accounted for the low zooplankton species abundance and species composition.

The application of canonical correspondence analysis in data analysis (*Fig. 7*) has been used as clarification method to establish any relationships or associations between biota and environmental variables in recent ecological studies (Lengendr and Lengendr, 1998; Yang et al., 2014 and Uwagbae et al., 2017). The positive association between BOD, DO and members of the rotifer group suggests that they have affinity for environment rich in dissolved oxygen as well as requiring low biological oxygen demand for decomposition activity. This finding was not farfetched from the observation in the Asarama estuary as there were a lot of decomposing woods and leaf litter, and dead mollusc shells in the river bed. The positive relationship that was observed between DO, BOD and rotifers was truly reflected at station 5 of *Tables 1* and *2* in which case, DO and BOD had higher mean concentrations. In addition, environmental perturbation was lesser at station 5 except for dead nipa palm trees remains. Meanwhile, the negative association or correlation between harpacticoida species with several environmental factors such as salinity, EC, nutrient and pH; foretell that they may be more tolerant to waters of very low salinity and electrical conductivity with moderate nutrient such as in inland waters. Conversely, it also suggested that total hydrocarbon content affected abundance of the already mentioned taxa. This is evident and further explains the phenomenon of the low species abundance at station 4 in particular. The same negative correlated relationship was observed for pH and rotifers, implying that they perhaps prefer habitats with non-acidic pH condition (i.e. between 6.8 and 8.2) which is contrary to our finding. Equally, at station 4, CCA proved that

http://www.aloki.hu ● ISSN 1589 1623 (Print) ● ISSN 1785 0037 (Online)
DOI: http://dx.doi.org/10.15666/aeer/1705_1027710292

cyclopoida-zooplankton were negatively influenced by water temperature, which is attributed to the total effect of direct sun heating of the littoral zone and the due to the absence of floral community that plays temperature regulation role by providing canopy effect as well as due to the presence of soot and petroleum slick on the water surface. The combination of these environmental factors can greatly influence the abundance, diversity and community structure of biota in any give aquatic ecosystem. The work by Lancelot and Muylaert (2011) satisfactorily explains the relationships between light, temperature and turbidity in shallow estuaries which supports our finding on the negative correlation between zooplankton and water temperature in the study area. However, it could also be attributed to the phenomena of tidal action still in shallow estuaries.

Conclusion

We conclude that the species diversity and composition for zooplankton was very low when compared with the result of the phytoplankton diversity in this study. The low zooplankton composition and diversity may be attributed to the phenomenon of vertical migration in shallow water coupled with the choice of sampling which was strictly restricted to the subsurface water considering the effect of sun rays on the shallow water in terms of increasing productivity.

However, the abundance of phytoplankton and diversity is attributed to the high effect of sun light and nutrient enrichment of the shallow estuary. Nevertheless, the indiscriminate human activities such as the unregulated transportation of goods and services, shipment of petroleum fractions from an illegal local refinery at upstream (though, they have relocated their activities as at early 2017) via wooden boats including bivalve mariculture, tend to pose danger to the biodiversity sustainability, and the environmental quality. Though this study is preliminary, we advocate that a major funded survey on the biodiversity of Asarama estuary should be carried out particularly on the influence of environmental factors on the fauna and flora organisms with a broadened scope. Besides, a comprehensive study on the physicochemical oceanography of Asarama estuary is of paramount importance amidst the rapid developments in the Niger Delta of Nigeria.

It is also very important to have a formal environmental legislature in place that seeks to protect the estuary and its kinds in the region, which allows its sustainable use of the resources amongst the locals. This way, the indiscriminate human impact on the environment would be greatly reduced sustainably.

Acknowledgements. We (particularly ARD and MAU) are very thankful to Duke University and Oak Foundation of the United States for the award of Duke University Marine Laboratory mini grant for marine conservation project, which greatly supported this work. We are grateful to the following persons: Obediah Owoh (Asarama community liaison officer and local curator), Godswill Amos (boat coxswain), Ikechuckwu Odoemenam (local diver) and Hakeem Okunola (taxi driver) for their various assistance during this project. We equally extend our thanks to Mr Isaac Adewole, a research fellow of the department of Animal and Environmental Biology, University of Benin, Benin for assisting in the laboratory work.

http://www.aloki.hu ● ISSN 1589 1623 (Print) ● ISSN 1785 0037 (Online)
DOI: http://dx.doi.org/10.15666/aeer/1705_1027710292

REFERENCES

[1] Ansa, E. J., Francis, A. (2007): Sediment characteristics of the Andoni Flats, Niger delta, Nigeria. – Journal of Applied Science and Environmental Management 11(3): 21-25.
[2] Castro, P., Huber, M. E. (1997): Marine Biology. 2nd Ed. – The WCB/McGraw-Hill Company, New York.
[3] Carlsson, P. E., Tester, G. P., Boni, L. (1995): Influences of riverine humic substances on bacteria, protozoa, phytoplankton, and copepods in a coastal plankton community. – Marine Ecology Progress Series 127: 213-221.
[4] Cearreta, A., Irabien, M. J., Leorri, E., Yusta, I., Croudace, I. W., Cundy, A. B. (2000). Recent anthropogenic impacts on the Bilbao Estuary, northern Spain: geochemical and microfaunal evidence. – Estuary Coastal and Shelf Science 50: 571-592.
[5] Cloern, J. E, Foster, S. Q., Kleckner, A. E. (2014): Phytoplankton primary production in the World's estuarine-coastal ecosystems. – Biogeosciences 11: 2477-2501.
[6] Conde, D., Bonilla, S., Aubriot, L., de León, R., Pintos, W. (2007): Relative contribution of planktonic and benthic microalgae production in a eutrophic coastal lagoon of South America. – J. Limnol. 78: 202-212.
[7] Dalal, S. G., Goswami, S. C. (2001): Temporal and ephemeral variations in copepod Community in the estuaries of Mandovi and Zuari - west coast of India. – Journal of Plankton Research 23: 19-26.
[8] Dalu, T., Bere, T., Froneman, P. W. (2016): Assessment of water quality based on diatom indices in a small temperate river system, Kowie River, South Africa. – Water SA 42(2): 183-193.
[9] Davies, O. A. (2009): Spatio-temporal distribution, abundance and species composition of zooplankton of Woji-Okpoka creek, Port Harcourt, Nigeria. – Research Journal of Applied Sciences, Engineering and Technology 1(2): 14-34.
[10] Davies, O. A., Abowei, J. F. N., Tawari, C. C. (2009): Phytoplankton community of Elechi creek, Niger delta, Nigeria. A nutrient-polluted tropical creek. – American Journal of Applied Sciences 6(6): 1143-1152.
[11] Eaton, A. D., Clesceri, L. S., Rice, E. W., Greenberg, A. E., Franson, M. A. H. (2005): Standard Methods for the Examination of Water and Wastewater. 21st Ed. – APHA, Washington, DC.
[12] Egborge, A. B. M., Idu, M. C., Kadiri, M. (2001): The Plants. – In Egborge, A.B.M. (Ed): Water Pollution in Nigeria. Vol. 2. Pollution of Warri River at Opete. Ben Miller Books Ltd, Nigeria, pp. 64-75.
[13] Elliott, M., De Jonge, V. N. (2002): The management of nutrients and potential Eutrophication in Estuaries and other restricted water bodies. – Hydrobiologia 475/476: 513-524.
[14] Elliott, M., McLusky, D. S. (2002): The need for definition in understanding estuaries. – Estuary Coastal and Shelf Science 55: 815-827.
[15] Froneman, P. W. (2004): Zooplankton community structure and biomass in a South African temporarily open/closed estuary. – Estuary Coastal and Shelf Science 60: 125-132.
[16] Godhantaraman, N., Uye, S. (2003): Geographical and seasonal variations in taxonomic composition, abundance and biomass of microzooplankton across a brackish-water lagoonal system of Japan. – Journal of Plankton Research 25(5): 465-482.
[17] Hammer, Ø., Harper, D. A. T., Ryan, D. A. T. (2001): PAST: Palaeontological Statistics Software Package for Education and data analysis. – Palaeontologia Electronica 4: 1-9. http://clade.ansp.org/entomology/mongolia/maishome.html.
[18] Hwang, J. S., Kumar, R., Hsieh, C. W., Kuo, A., Souissi, S., Hsu, M. H., Wu, J. T., Liu, W. C., Wang, C. F., Chen, Q. C. (2010): Patterns of zooplankton distribution along the marine, estuarine, and riverine portions of the Danshuei ecosystem in northern Taiwan. – Zoological Studies 49(3): 335-352.

http://www.aloki.hu ● ISSN 1589 1623 (Print) ● ISSN 1785 0037 (Online)
DOI: http://dx.doi.org/10.15666/aeer/1705_1027710292

[19] Imoobe, T. O. T., Adeyinka, M. L. (2009): Zooplankton-based assessment of the trophic state of a tropical forest river in Nigeria. – Archive for Biological Sciences 61(4): 733-740.
[20] Jeje, C. Y., Fernando, C. H. (1986): A Practical Guide to the Identification of Nigerian Zooplankton. – Kainji Lake Research Institute Nigeria.
[21] Kadiri, M. O. (2006): Phytoplankton survey in the Western Niger Delta, Nigeria. – African Journal of Environment and Pollution Health 5(1): 48-58.
[22] Kolo, R. J., Mani, I. A., Musa, H. A. (2001): Effects of different fertilizers on plankton productivity in earthen ponds. – Journal of Aquatic Science 16(2): 127-131.
[23] Lancelot, C., Muylaert, K. (2011): Trends in Estuarine Phytoplankton Ecology. – Elsevier Inc., Amsterdam.
[24] Legendre, P., Legendre, L. (1998): Developments in Environmental Modelling. – Numerical Ecology 24: 41-46.
[25] Needham, J. G., Needham, P. R. (1978): A Guide to the Study of Freshwater Biological Holden. – Devy Inc., San Francisco.
[26] Newell, G. E., Newell, R. C. (1966): – Marine Plankton: A Practical Guide. Revised Edition. – Hutchinson, London.
[27] Ogbuagu, D. H., Ayoade, A. A., AC-Chukwuocha, N. B. (2011): Spatial dynamics in physicochemistry and bacterio- and myco-plankton assemblages of Imo River in a Niger Delta community in Nigeria. – African Journal of Microbiology Research 5(8): 872-887. DOI: 10.5897/AJMR10.612.
[28] Opute, I. F. (1990): Phytoplankton flora in the Warri/Forcados Estuary of Southern Nigeria. – Hydrobiologia 208: 101-109.
[29] Pearl, H. W., Rossignol, K. L., Hall, N. S., Peierls, P. L., Wetz, M. S. (2010): Phytoplankton Community indicators of short and long term ecological changes in the anthropogenically and climatically impacted Neuse River estuary, North Carolina, USA. – Estuaries and Coast 33: 485-497.
[30] Prescott, G. W. (1975): How to Know the Freshwater Algae. – Brown Co. Publishers, Dubuque, Iowa.
[31] Townsend, C. R., Harper, J. L., Begon, M. (2000): Essentials of Ecology. 3rd Edn. – Blackwell Science Publishers, London.
[32] Tan, Y., Huang, L., Chen, Q. C., Huang, X. (2004): Seasonal variation in zooplankton composition and grazing impact on phytoplankton standing stock in the Pearl River Estuary, China. – Continental Shelf Research 24: 1949-1968.
[33] Thor, P., Nielson, T. G., Tiselius, P., Juul-Pederson, T., Michel, C., Møller, E. F. et al. (2005): Post-spring bloom community structure of pelagic copepods in the Disko Bay, Western Greenland. – Journal of Plankton Research 27: 341-356.
[34] Uwagbae, M. A., El Surtasi, E. I., Rotimi, J., Dirisu, A. R., Gbarakoro, T. N., Richard, G., Oratokhai, R. A., Agwu, J. E. (2017): Land Reclamation, Soil Quality and Agriculture. – In: Bharti, P. K., Chauhan, A. (eds.) Upshots of Age of Oil Spill and Influence of Physico-Chemical Properties on the Diversities of Soil Dwelling Insects. Discovery Publishing House, Pvt, Ltd, New Delhi, pp. 22-45.
[35] Van De Velde, I. (1984): Revision of the African species of the genus - Mesocyclops Sars, 1914 (Copepoda; Cyclopidae). – Hydrobiologia 109: 3-66.
[36] Waniek, J. J. (2003): The role of physical forcing in initiation of spring blooms in the northeast Atlantic. – Journal of Marine Systems 39: 57-82.
[37] Waniek, J. J., Holliday, N. P., Davidson, R., Brown, L., Henson, S. A. (2005): Freshwater control of onset and species composition of Greenland shelf spring bloom. – Marine Ecology Progress Series 288: 45-57.
[38] Yang, Z. F., Sun, T., Zhao, R. (2014): Environmental flow assessments in estuaries related to preference of phytoplankton. – Hydrology and Earth System Sciences 18: 1785-1791.

http://www.aloki.hu ● ISSN 1589 1623 (Print) ● ISSN 1785 0037 (Online)
DOI: http://dx.doi.org/10.15666/aeer/1705_1027710292

EFFECT OF HOT-WATER TREATMENT AND BULB STORAGE TEMPERATURE ON PROPAGATION OF *NARCISSUS TAZETTA* BY THE CHIPPING AND TWIN-SCALING TECHNIQUES

KHALAFALLA, M. M.[1] – ELTARAWY, M.[1] – SAAD, M. E. A.[2] – HEGAZY, A.[1*]

[1]*Hort. Dept., Fac. Agric., Kafrelsheikh Univ., Kafrelsheikh 33516, Egypt*

[2]*Hort. Res. Inst., Agric. Res. Center, Giza, Egypt*

**Corresponding author*
e-mail: ahmed.ebad@rocketmail.com

(Received 26th Feb 2019; accepted 24th May 2019)

Abstract. In the current study there were 6 treatment of all combinations of two propagation methods (chipping and twin-scaling), two propagating bulb storage temperatures (pre-cooling and no pre-cooling), two hot-water treatments (hwt and no hwt). Treatments were applied to measure the effects on the propagation of *Narcissus tazetta* cv. "Ziva" bulbs. The major effects were those of propagation methods and pre-propagating bulb storage temperatures. Chipping, pre-cooling and hwt consistently affected the bulblet formation in both seasons and bulblet weight per chip in the first season only but had no effect on number of bulblets. Chipping method increased all parameters (bulblet formation, weight and circumference of bulblet and number of bulblets per chip, number and length of leaves and roots per-chip). However, chipping resulted in lager, but fewer bulblets than twin-scaling. Pre-cooling increased bulblet formation and both weight and circumference of bulblet in the first season only but reduced number and length of leaves and roots in the second one only. Hot-water treatment increased bulblet formation in both seasons but reduced number and length of leaves and roots in the first season only.
Keywords: *Narcissus, chipping, twin-scaling, bulblet, hot-water treatments, bulb storage temperature*

Introduction

Narcissus, a genus of the Amaryllidaceae family, consisting of about 62 species, classified into 12 sections (Kington1989). These bulbs are well known garden perennial, cut flowers, and can also be used as flowering potted plant. In addition to its horticultural values, the genus *Narcissus* provides numerous alkaloids, some of which exhibit pharmaceutical importance (Bastida et al., 2011). The natural vegetative propagation rate of narcissus under field conditions is very slow, with the mother bulb produce few daughter bulbs, approximately 1.6 bulbs per year (Rees, 1972, 1992). In vitro propagation through tissue culture has been successfully used for narcissus (Malik and Bach, 2017). However, compared to chipping and twin-scaling, in vitro propagation is costly. Chipping and twin-scaling are two of conventional propagation techniques for rapidly propagating narcissus bulbs, enabling an increase from 1 to 1000 in 5–6.5 years instead of 15–25 years (Hanks, 1993). In chipping, bulbs are divided into 8 or 16 longitudinal segments depending on bulb size, but these are not subdivided further (Andrade-Rodringuez et al., 2015; Kharrazi et al., 2107), while in twin-scaling are further divided by removing scale pieces in pairs by cutting through the attached basal plate. In this technique bulb is cut into 50 to 100 twin-scales, depending on its size (Hanks, 1993; Zahng et al., 2013). Pretreatment of bulbs may profoundly affect the bulblets production from chipping and twin-scaling. Studies found in literature have reported the successful use of hot-water treatment before narcissus bulb cutting to increase bulblet yields, and control bulb mite

http://www.aloki.hu ● ISSN 1589 1623 (Print) ● ISSN 1785 0037 (Online)
DOI: http://dx.doi.org/10.15666/aeer/1705_1029310301

(Hanks, 1993). However, bulb storage temperature, has been reported to increase (0–10 weeks at 5–30 °C; Hanks et al., 1986) or decrease (5 days at 35 °C; Rees and Hanks, 1984) bulblets production, to be without effect (5 weeks 9 °C; Hanks and Rees, 1978). This study aimed to investigate chipping and twin-scaling techniques and to determine the effect of bulb storage temperature and hot-water treatment on propagation of *Narcissus tazetta* to achieve a high yield of bulblets.

Materials and methods

Bulbs of paperwhite *Narcissus tazetta* cv. "Ziva" were obtained from a commercial source Sperli- GmbH. In an experiment there were 8 treatments, consisting of all combinations of two hot water treatments (hwt and non-hwt) two pre-cutting storage temperatures (pre-cooled and non-pre-cooled bulbs) and two methods for propagation (chipping and twin-scaling). On July 1st, 2014/2015 and 2015/2016 bulb were graded, single-nosed, round bulbs 12–14 cm in circumference were selected, cleaned and divided into two groups of 48 bulbs each. In the first group the bulbs were given a hot water treatment (hwt) at 43.5 °C for 3h, with 1.5% (v/v) formalin, while in the second one they were soaked in a tap-water with 1.5% (v/v) formalin (non-hwt). After drying, the bulbs were stored at ambient temperature (27 ± 3 and 20 ± 3 °C day/night, RH 67–70%) until 6 weeks, prior to bulbs cutting time. Both groups were further divided into two subgroups of 24 bulbs each, the first subgroup was moved to a controlled chamber at a constant temperature of 9 °C, RH 65–70% (pre-cooled bulbs), while the second one was left in the same ambient temperature (non-cooled bulbs) as described above until the start of the bulbs cutting treatments. On October 3rd in both seasons, half of the bulbs of each group were propagated by chipping technique, while the other half was propagated by twin-scaling. Finally, each experiment included 12 bulbs (3 replication × 4 bulbs).

Methods of bulb cutting

After removing the outer brown tunicated scales, and outer crust of basel plate, the top of bulbs was cut off for about 2.5 cm. For chipping, bulbs were longitudinally cut into eight equal sized segments. For twin-scale cuttings, segments of each bulb were divided into pairs of scales (twin-scales) by cutting through the basal plate, however the outer papery scales and the very small ones were discarded (stored to reject any outside the range 0.8–1.0 g) hence each segment gave about 4 twin-scales (Hanks, 1985). Both chips and twin-scales were dipped in a fungicide solution with 1% captan plus 0.4% benomyl (benlate) for 30 min. After dipping and draining, either 12 chips or 16 twin-scales were placed in thin polyethylene bags (20 × 30 cm) filled with 500 ml sterile *vermiculite* previously mixed with 40 ml sterile distilled water and sealed by ensuring air space at top. The bags were incubated in single layer in the dark at 20–22 °C and relative humidity of 70–80%. After 15 weeks of incubation, the bulblet formation calculated as the percentage of chips and twin-scales with visible bulblet, number of bulblets per chip and twin-scale, number and length (the longest, cm) of leaves and roots and circumference (cm) and weight (g) of each bulblet were determined. The experimental design was factorial in a complete randomized with three replicates. The data were subjected to statistical analysis and means were compared according to Duncan's multiple range test (Snedecor and Cochran, 1980).

The following is an explanation of the shape of the cutting methods used:

http://www.aloki.hu ● ISSN 1589 1623 (Print) ● ISSN 1785 0037 (Online)
DOI: http://dx.doi.org/10.15666/aeer/1705_1029310301

Chipping

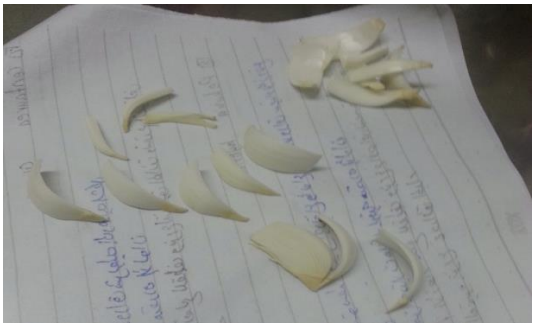

Twin-scaling

Chips and twin-scales were dipped in a fungicide solution with 1% captan +0.4% benomyl (benlate) for 30 min

Thin polyethylene bags (20 x 30 cm) filled with 500 ml sterile *vermiculite* previously mixed with 40 ml sterile distilled water and sealed by ensuring air space at top

Results

Bulblet formation

Data presented in *Table 1* reveal that there were significant effect of propagation methods (chipping or twin-scaling), pre-propagating storage temperature (pre-cooled or non-pre-cooled bulbs) and hot-water treatment (bulb given hot-water treatment (hwt) or non hwt) on the percentage of bulblet formation. In comparison with the alternative treatments, chipping, pre-cooling, hwt increased bulblet formation in both seasons. The interaction between cutting methods, bulb storage temperature and hwt also

http://www.aloki.hu ● ISSN 1589 1623 (Print) ● ISSN 1785 0037 (Online)
DOI: http://dx.doi.org/10.15666/aeer/1705_1029310301

significantly affected bulblet formation in the second season only (*Fig. 1*). In this interaction, the bulblet formation of the chips was in 100% irrespective of the pre-propagating storage temperature or whether not hot-water treatment was performed. In twin-scales, the highest bulblet formation (96.67%) was obtained in bulbs given pre-cooling, hwt.

Table 1. *The effects of cutting methods (C.M), hot-water treatments (hwt), bulb storage temperature (S), and their combination on bulblet formation (%), circumference (cm) and fresh weight (FW) of bulblet (g), number of bulblets per propagules (No.), number and length (L, cm) of leaves and roots in the first and second seasons*

Season	Bulblet form.		Bulblet fw		Bulblet circ.		No. bulblets		No. leaves		L. leaves		No. roots		L. roots	
	1st	2nd	1st	2nd	1st	2nd	1st	2nd	1st	2nd	1st	2nd	1st	2nd	1st	2nd
Cutting methods																
Chipping	86.68a	100.00a	0.34a	0.35a	2.58a	2.29a	1.50a	1.42a	2.09a	1.62a	2.31a	2.01a	2.34a	1.80a	2.65a	1.84a
Twin-scaling	76.86b	86.25b	0.17b	0.25b	2.04b	1.89b	1.34b	1.00b	1.63b	1.49b	1.59b	1.80b	1.58b	1.53b	1.84b	1.38b
Hot-water treatment																
Non-hwt	78.49b	92.01b	0.26	0.31	2.30	2.20	1.50	1.25	1.99a	1.50	2.07a	2.04	2.06a	1.63	2.47a	1.55
Hwt	85.05a	94.08a	0.25	0.29	2.31	1.98	1.34	1.17	1.73b	1.61	1.84b	1.78	1.85b	1.70	2.02b	1.67
Bulb storage temp.																
Non-pre-cooling	79.03b	89.50b	0.23b	0.31	2.22b	2.07	1.34	1.25	1.84	1.68a	1.95	2.16a	2.07	1.74a	2.35	1.78a
Pre-cooling	84.51a	96.59a	0.28a	0.26	2.39a	2.11	1.50	1.17	1.88	1.44b	1.96	1.65b	1.84	1.59b	2.14	1.44b
Significances																
C.M	*	*	*	*	*	*	*	*	*	*	*	*	*	*	*	*
Hwt	*	*	ns	ns	ns	ns	ns	ns	*	ns	*	ns	*	ns	*	ns
S	*	*	*	ns	*	ns	ns	ns	ns	*	ns	*	ns	*	ns	*
C.M × hwt	ns	*	ns	ns	*	ns	ns	ns	ns	ns	ns	ns	ns	ns	*	ns
C.M × S	ns	*	*	ns	*	ns	ns	ns	ns	ns	ns	*	ns	ns	ns	ns
Hwt × S	*	*	ns	ns	ns	ns	ns	ns	*	ns	ns	ns	ns	ns	*	ns
C.M × hwt × S	ns	*	*	ns	ns	ns	ns	ns	ns	ns	ns	ns	ns	ns	ns	ns

Main effect followed by different letters with in a column are significantly different at $P < 0.05$, Duncan's multiple range test
ns: not significant; *significant at $P < 0.05$, 1st first season; 2nd second season; Temp.: temperature; form.: formation; circ.: circumference

The fresh weight, circumference and number of bulblets:

Chipping method significantly increased fresh weight, circumference and number of bulblets in both seasons *Table 1*, while pre-cooling increased both fresh weight and circumference of bulblet in the first season only. However, hot-water treatment had no effect. In the first season the interaction revealed that, chipping method, pre-cooled bulbs produced a heavier maximum weight and circumference of bulblet than twin-scaling method, non-cooled bulbs (*Figs. 2* and *3*). However, chipping method, hwt produced a wider maximum circumference of bulblet than twin-scaling, hwt. There were also significant effects of cutting method, pre-propagating storage temperature and hwt on fresh weight of bulblet in the first season (*Fig. 2*). Chipping, pre-cooling and hwt produced bulblets that were heavier than those of twin-scaling, pre-cooling and hwt. There were non-significant effects of pre-cooling, hwt and all combinations on bulblet numbers per both chip and twin-scale in both seasons.

http://www.aloki.hu ● ISSN 1589 1623 (Print) ● ISSN 1785 0037 (Online)
DOI: http://dx.doi.org/10.15666/aeer/1705_1029310301

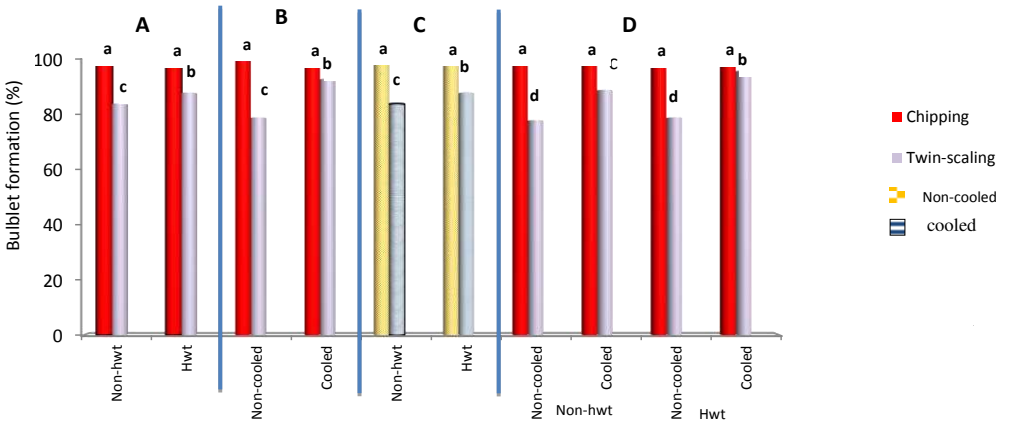

Figure 1. *Effect of cutting methods (chipping; twin-scaling) and hot water treatments (hwt; non-hwt) (A), cutting methods and bulb storage temperatures (cooled; non-cooled) (B), hot water treatments and bulb storage temperatures (C), and cutting methods and hot water treatments, bulb storage temperatures (D) on bulblet formation (%) in the second season. Columns with different letters are significantly different at 0.05 level based on Duncan's multiple range test*

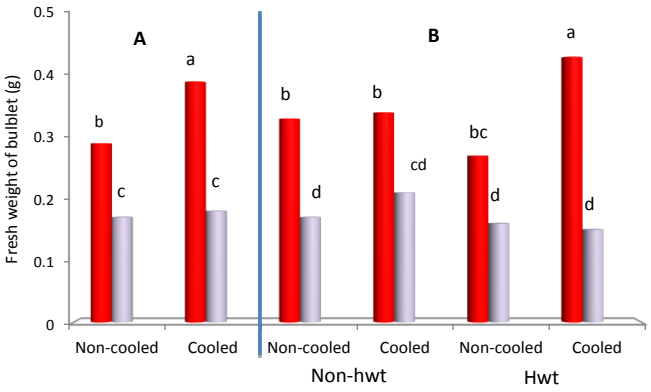

Figure 2. *Effect of cutting methods and bulb storage temperature (A), and cutting methods, hot water treatments and bulb storage temperatures (B) on fresh weight of bulblet (g) in the first season (other details are as in Fig. 1)*

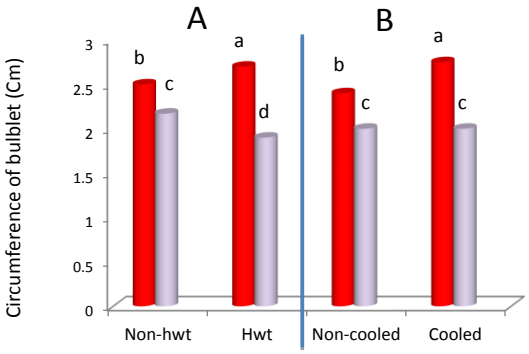

Figure 3. *Effect of cutting methods and hot water treatments (A) and cutting methods and bulb storage temperatures (B) on circumference of bulblet (cm) in the first season (other details are as in Fig. 1)*

http://www.aloki.hu ● ISSN 1589 1623 (Print) ● ISSN 1785 0037 (Online)
DOI: http://dx.doi.org/10.15666/aeer/1705_1029310301

Number and length of leaves and roots per bulblet:

Data presented in *Table 1* show that, chipping method significantly increased number and length of leaves and roots in both seasons, while pre-cooling treatment in the second season and hwt in the first one significantly decreased both number and length of leaves and roots. However, the interaction revealed that pre-cooling resulted the shortest leaves in both the chipping and twin-scaling methods in the second season only (*Fig. 4*). However, hot-water treatment resulted the shortest roots per bulblet on the chipping method in the first season only (*Fig. 5*). In cooling-stored bulbs, number of leaves and length of roots, were declined with hot-water treatment in first season (*Figs. 4* and *5*).

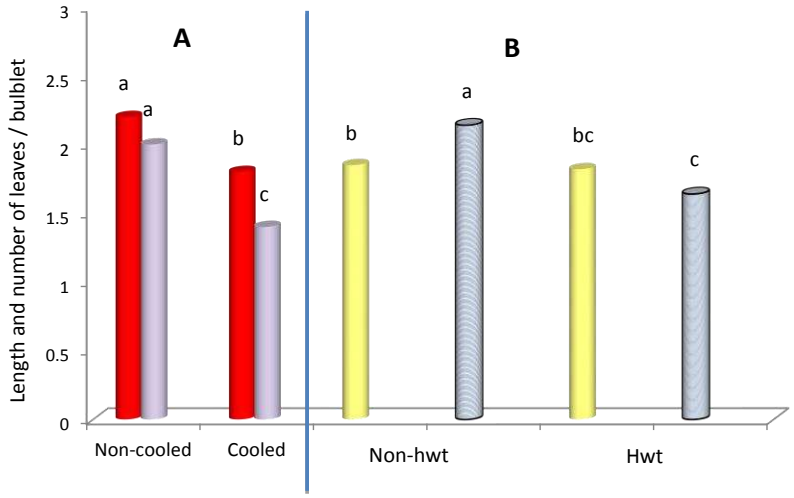

Figure 4. *Effect of cutting methods and bulb storage temperature on length of leaves (cm) in the second season (A), and hot-water treatments and bulb storage temperature on number of leaves in the first one (B) (other details are as in Fig. 1)*

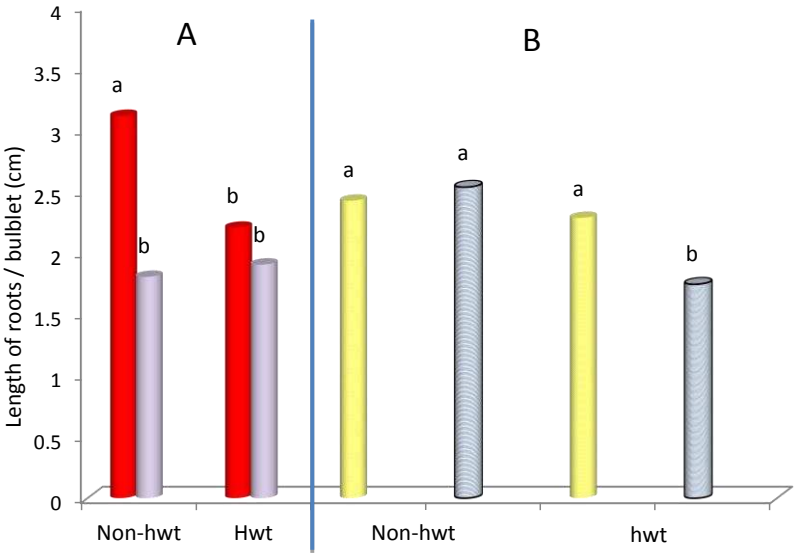

Figure 5. *Effect of cutting methods and hot water treatments (A), and hot water treatments and bulb storage temperatures on length of roots/bulblet (cm) in the first season (B) (other details are as in Fig. 1)*

http://www.aloki.hu ● ISSN 1589 1623 (Print) ● ISSN 1785 0037 (Online)
DOI: http://dx.doi.org/10.15666/aeer/1705_1029310301

Discussion

Chipping method consistently affected the bulblet formation and gave greater bulblet weight, circumference and number of bulblets per propagule. The advantage of propagation by the chipping method are simpler and rapid multiplication that produces large quantities of good quality bulb with a relatively short period, but it is less productive (Hanks, 1993). As known, chips had more scales and wider basal plate than twin-scales, suggesting that a higher content of nutrients was stored in the chips. However, the variation in bulblet formation, weight and circumference of bulblet and number and length of leaves and roots observed in *Table 1*, may be a result of variation in amount of food reserve (Hanks, 1985; Chen and Ziv, 2005; Zahng et al., 2013). The obtained results are similarly to the findings of Roxas et al. (2000) who reported that bulblet formation from cutting mother bulbs of *Lycoris* species into $^1/_4$ and $^1/_8$ sections (chips) was higher than that from $^1/_{16}$ sections. Thus, as pointed out by Seyidoglu and Zencirkiran (2008), Fenlon et al. (1990), Kharrazi et al. (2017) and Zhu et al. (2005) in several Amaryllidaceae species, a linear relationship between bulblet weight per chip and initial chip weight, based on parent bulb weight (which would reflect chip weight) and number of chips per bulb (cutting rate). Some species require a cold treatment for subsequent initiation and development of bulblet primordia and for rapid, synchronous growth (Khodorova and Boitel-Conti, 2013). The effect of previous bulb storage temperature on the performance of chips and twin-scales propagation was reported in earlier studies on *Narcissus*. Rees and Hanks (1984) found that pre-chipping storage temperature (5 days at 35 °C) reduced bulblet formation, whereas pre-cooling (5 weeks at 9 °C) alone or after a warm storage did not affected bulblets formation. Hanks et al. (1986) showed that pre-twin-scaling storage temperature (0–10 weeks at a range of 5–30 °C) produced bulblets in all cases, while the greatest bulblet formation was produced in bulbs stored at 15 and 30 °C for 6–7 weeks. Chen and Ziv (2005) reported that, in vitro, the twin-scales isolated from the *Narcissus tazetta* "Ziva" bulbs after 12 weeks in storage at 30 °C and a 6 weeks cold treatment at 15 °C produced high number of uniform adventitious buds and were able to regeneration on the semi-solid medium. They observed also that, higher starch levels were found to correlate to higher regeneration potentials in twin-scales. Our experiments show that, twin-scales required a cold treatment to induce bulblets formation more than those with chips. However, 86 and 100% (in both seasons, respectively) of chips produced bulblets, while bulblet formation for twin-scales did not reach 100% in any treatment, but 84.51 and 96.59% of twin-scales produced bulblets in pre-cooling treatment. Hot-water treatment is the established method for controlling nematodes and bulb scale mite in *Narcissus* planting stocks (Hanks, 1991, 1993). The effectiveness of hwt may vary depending on pre-hwt storage temperature and date of application. However, pre-hwt storage temperatures around 30 °C are used for preventing damage, lower temperatures are also effective if used for longer durations (Hanks, 1991). Vreeburg and van der Weijden (1987) stated that bulblet yields was greatest in bulbs given hwt (2 h at 43.5 °C) with formaldehyde before chipping with 5 days. In the study, bulblet formation was significantly greater due to either hwt or to pre-cooling and hwt interaction in both seasons, while there were insignificant differences in fresh weight and circumference of bulblet. Although, for Horticultural application or production purposes, twin-scaling method is used for propagation because of its potentially greater multiplication rates.

http://www.aloki.hu ● ISSN 1589 1623 (Print) ● ISSN 1785 0037 (Online)
DOI: http://dx.doi.org/10.15666/aeer/1705_1029310301

Conclusion

The current study showed that in chipping technique the segments produce larger but fewer bulblets per bulb than those produce by twin-scaling and may reach flowering size more quickly. However, hot-water treatment, pre-cooling of bulbs before twin-scaling improved bulblet formation and yields. Although relatively labor-intensive, twin-scaling dose have an important role to play in bulking-up schemes, because of its potentially greater multiplication rate. On the other hand, in chipping method, size of parent bulb and number of chips per bulb must be taken into consideration.

REFERENCES

[1] Bastida, J., Berkov, S., Torras, L., Pigni, N. B., De Andrade, J. P., Martinoz, V., Codina, C., Viladomat, F. (2011): Chemical and Biological Aspects of Amaryllidaceae Alkaloids. – In: Munoz-Torrero, D. (ed.) Recent Advances in Pharmaceutical Sciences. Transworld Research Network, Kerala, pp. 65-100.

[2] Chen, J., Ziv, M. (2005): The effects of storage condition on starch metabolism and regeneration potentials of twin-scales and inflorescence explants of *Narcissus tazetta*. – In-vitro Cell. Dev. Biol. Plant 41: 816-821.

[3] Fenlon, J. S., Jones, S. K., Hanks, G. R., Langton, F. A. (1990): Bulb yields from *Narcissus* chipping and twin-scaling. – J. Hortic. Sci. 65: 441-450.

[4] Hanks, G. R. (1985): Factors affecting yields of adventitious bulblets during propagation of *Narcissus* by the twin-scaling technique. – J. Hortic. Sci. 60: 531-543.

[5] Hanks, G. R. (1991): Pre-Warming of Narcissus, prior to Hot-Water Treatment, in Lincolnshire. – Hort. Development Council, Petersfield. HDC Project BOFIS. HRI Project 30284.

[6] Hanks, G. R. (1993): Narcissus. – In: De Hertogh, A. A., Le Nard, M. (eds.) The Physiology of Flowering Bulbs. – Elsevier Sci. Pub., Amsterdam, pp. 463-558.

[7] Hanks, G. R., Rees, A. R. (1978): Factors affecting twin-scale propagation of narcissus. – Sci. Hort. 9: 399-411.

[8] Hanks, G. R., Shaik, G., Jones, S. K. (1986): Bulblet production in *Narcissus*: the effect of temperature and duration of storage on bulb unit development and subsequent propagation by twin-scaling. – Ann. Appl. Biol. 109: 417-425.

[9] Kharrazi, M., Tehranifar, A. Nemati, H., Bagheri, A. (2017): Vegetative propagation of amaryllis (*Hippeastrum*×*johnsonii*) by different cutting methods. – Horticultural Science and Technology 35(3): 373-380.

[10] Khodorova, N. V., Boitel-Conti, M. (2013): The role of temperature in the growth and flowering of geophytes. – Plants 2: 699-711.

[11] Kington, S. (1989): The International Daffodil Checklist. – Royal Horticultural Society, London.

[12] Malik, M., Bach, A. (2017): High-yielding repetitive somatic embryogenesis in cultures of *Narcissus* L. 'Carlton'. – Acta Sci. Pol. Hortorum Cultus 16(2): 107-112.

[13] Andrade-Rodríguez, M., Guillén-Sanchez, D., Villegas-Torres, O. G., Ayala-Hernández, J. J., López-Martinez,V., Vargas-Araujo, J. (2015): Bulb cutting methods to propagate *Hippeastrum hybridum.* – Hort. Rev. Chapingo Ser. Hortic. 21(1): 57-69.

[14] Rees, A. R. (1972): The Growth of Bulbs. – Academic Press, London.

[15] Rees, A. R. (1992): Ornamental Bulbs, Corms, and Tubers. – CAB International, Wallingford, UK.

[16] Rees, A. R., Hanks, G. R. (1984): Storage treatments for very early forcing of narcissus. – J. Hortic. Sci. 59: 229-239.

[17] Roxas, U. A., Lapichino, G., Zizzo, G. V. (2000): Effect of different bulb sections on *Lycoris* bulblet multiplication by chipping. – Acta Hortic. 517: 99-106.

http://www.aloki.hu ● ISSN 1589 1623 (Print) ● ISSN 1785 0037 (Online)
DOI: http://dx.doi.org/10.15666/aeer/1705_1029310301

[18] Seyidoglu, N., Zencirkiran, M. (2008): Vegetative propagation of *Sternbergia lutea* (L) Ker Gawl. ex Sprengel (Winter Daffodil) By chipping techniques. – J. Biol. Sci. 8: 966-969.
[19] Snedecor, G. W., Cochran, W. G. (1980): Statistical Methods. 7th Ed. – Iowa State Univ. Press, Ames, Iowa.
[20] Vreeburg, P. J. M., Van der Weijden, G. J. M. (1987): Parteren van narcissen. – Waarom, wanneer en hoe Bloembollencultuur 98(25): 14-15.
[21] Zhang, W., Song, L., da Silva, J. A. T., Sun, H., (2013): Effects of temperature, plant growth regulators and substrates and changes in carbohydrate content during bulblet formation by twin-scale propagation in *Hippeastrum vittatum* 'Red lion'. – Scientia Horticulturae 160: 230-237.
[22] Zhu, Y., Liu, K. S., Yiu, J. C. (2005): Effects of cutting method on bulb production of *Hippeastrum hybridum* in Taiwan. – ISHS Acta Horticulture 673: 531-535.

http://www.aloki.hu ● ISSN 1589 1623 (Print) ● ISSN 1785 0037 (Online)
DOI: http://dx.doi.org/10.15666/aeer/1705_1029310301

ROLE OF URBANIZATION AND URBAN INCOME IN CARBON EMISSIONS: REGIONAL ANALYSIS OF CHINA

SARWAR, S.[1,2*] – ALSAGGAF, M. I.[1]

[1]*Finance and Insurance Department, University of Jeddah, Jeddah, Kingdom of Saudi Arabia (e-mail: msaggaf@uj.edu.sa)*

[2]*School of Economics, Shandong University, Shandong, China*

**Corresponding author*
e-mail: ch.sulemansarwar@gmail.com

(Received 12th Feb 2019; accepted 12th Jul 2019)

Abstract. The study aims to analyze the impact of urbanization and urban income on carbon emission, in the case of China. Panel data estimations use the data from 30 Chinese provinces from 1998 to 2016. Empirical result of urbanization confirms significant and positive coefficient, whereas, urban income has a negative coefficient. This illustrates that higher urbanization trend escalates the carbon emission, while this urban-based carbon emission can be controlled by increasing the per capita income of the urban population. Moreover, economic growth, industrialization, coal, and oil consumption are responsible for carbon emission, as reported by the significant and positive coefficients. The findings of the regional analysis are in line with the full sample results. Based on the results, the study provides practical implications for policy makers to curtail the environmental degradation process.
Keywords: *economic growth, industrialization, coal consumption, oil consumption, GMM*

Introduction

There are a number of challenges that are to be faced by the developing countries with the higher pace of economic growth such as, urbanization and greenhouse gas emission. The increase in urbanization leads to a higher demand for fossil fuels which ultimately results in higher carbon emission (Kumar and Madlener, 2016), but the contribution mechanism of urbanization in carbon emission varies due to underlying factors, such as economic condition, dependence on fossil fuels, industrialization, energy consumption etc. However, it is required to analyze the role of urbanization in carbon emissions for China, specifically. Furthermore, it is also important to study the factors that are helpful to control the urban based carbon emission.

A number of studies have been made in order to analyze relationship of urbanization and carbon emission (Parikh and Shukla, 1995; York, 2007; Kasman and Duman, 2015; Sun et al., 2016; Shahbaz et al., 2016; He et al., 2017; Ding and Li, 2017; Khoshnevis et al., 2018; Dai et al., 2018), the results have confirmed the role of urbanization in carbon emission. Several types of research have documented a positive relationship between urbanization and carbon emission (Parshall et al., 2010; Zhang and Lin, 2012; Fang et al., 2015; Hao et al., 2016; He et al., 2017; Ding and Li, 2017). On contrary, a number of researches have put forward the statement that the urbanization can be a reason for the decrease in carbon emission (Liddle, 2004; Mishra et al., 2009). Moreover, Martínez-Zarzoso and Maruotti (2011) confirmed a U-shaped association between urbanization and carbon emission.

Moreover, Xu and Lin (2015) have worked upon the effects of urbanization and industrialization on carbon emissions in China over the period of 1990-2011. The

http://www.aloki.hu ● ISSN 1589 1623 (Print) ● ISSN 1785 0037 (Online)
DOI: http://dx.doi.org/10.15666/aeer/1705_1030310311

regression estimations have reported U-shaped relationship. Likewise, a large number of studies has analyzed the relationship of urbanization and carbon emissions in accordance with Environmental Kuznets Curve (EKC). The study concluded that urbanization is in the favor of environmental development only if the economic development reached at a specific level (Martínez-Zarzoso and Maruotti, 2011; Hao and Peng, 2017; Yao et al., 2018). Recently, Chikaraishi et al. (2015) analyzed different factors that are responsible for urban-based carbon emission. For instance, the country's per capita gross domestic product and the ratio of service industries are one of the most important factors that influence the relationship between the urbanization and carbon emissions. Beside this, there are various factors that affect carbon emissions (such as, technological progress, energy consumption structure, economic development, and industrial structure (Jiang and Lin, 2012; Shahbaz et al., 2016; Waheed et al., 2018; Song and Wang, 2018).

Alkhathlan and Javid (2015) reported a non- linear trend between carbon emission and economic growth of Saudi Arabia, the reason for the positive relationship is the dependence on oil for energy, transportation and industrial activities. Kumar and Madlener (2016) confirmed that higher economic growth is among the major causes of carbon emission in India. Adewuyi and Awodumi (2017) reported that oil consumption and energy consumption have a significant impact on economic growth which further boosts the carbon emission. Previous studies have affirmed that industrialization is also a source of carbon emission (Sadorsky, 2013; Yuan et al., 2014; Lin et al., 2015; Zhu et al., 2017; Ding and Li, 2017; Liu and Bae, 2018).

In addition, the role of coal and oil consumption is considered as the main contributor to carbon emission in China (IPCC, 2014). As China is among the fastest growing economy as well as the biggest carbon emitter of the world (WDI, World Development Indicator, 2017); that is responsible for the around 30% of global carbon emission. According to the Information Energy Administration (2014), China is the second largest oil consumer in the world, the oil consumption of China 11.96 million bpd in 2015. Hence, on one side, the oil is important for economic growth, but, on the other side, the oil consumption has an adverse impact on the environment. The oil consumption, in form of industrial process, transportation, energy generation etc., is one of the main contributors of carbon emission. According to a recent statistics, the demand for oil will increase in the next few decades (Cook and Cherney, 2017). Coal is the main element of energy generation in China which contains around 65% of total energy mix (China Electric Council, 2016).

Previously, the studies have investigated the impact of economic growth, urbanization, industrialization, coal and oil consumption in carbon emission. However, after identifying the role of economic growth, urbanization, industrialization in carbon emission, current paper contributes to the existing literature through analyses the role of urban income to control the carbon emission, which is missed by the previous researches.

The current study has following objectives: the study analyzes the role of urbanization in carbon emission. Furthermore, the role of urban income to control the urban-based carbon emission is another objective. The main contribution of given study is to examine the role of annual average urban income to control the urban based carbon emission. It is known that the higher urbanization tends to boost the carbon emission by different channels: (i) forest need to cut down to extend the urban lands which causes to increase the carbon emission; (ii) higher urbanization triggers the industrialization,

http://www.aloki.hu ● ISSN 1589 1623 (Print) ● ISSN 1785 0037 (Online)
DOI: http://dx.doi.org/10.15666/aeer/1705_1030310311

transportation and energy consumption etc. which are the major carbon emitters (Shahbaz et al., 2016; Ding and Li, 2017)[1]. In concise, higher urbanization directly or indirectly boost the carbon emission. On the other side, the urbanization trend is increasing since few decades and it will be higher in upcoming decades, as mentioned in *Figure 1*. However, it is required to explore the counter measures that support to reduce carbon emission that is caused by urbanization. On this basis, this study assumes that higher urban income enables the urban population to invest in eco-friendly products that require less energy (e.g. advanced energy efficient home appliances, hybrid or electricity vehicles etc.) that assist to control the environmental degradation process. However, it is clear that urbanization increases the rate of carbon emission as well as it can also contribute to the green technology and its innovation (Martínez-Zarzoso and Maruotti, 2011). Finally, the regional based analysis is used to examine the carbon contributors and the role of higher urban income to mitigate the carbon emission. The findings can assist the policy maker to define the environmental policies to control the carbon emission.

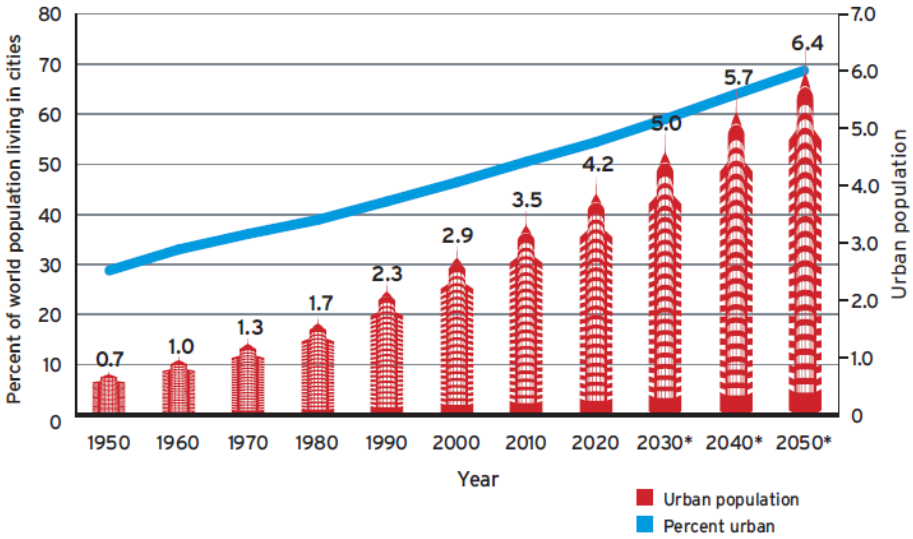

Figure 1. *Urbanization population and percentage of world population living in urban areas. (Source: UN, Department of Economic & Social Affairs, Population Division)*

Materials and methods

Current study investigates the urbanization, urban income, economic growth, industrialization, coal consumption and oil consumption on carbon emission. For empirical estimations, panel data of 30 Chinese provinces are collected over the period 1998 to 2016. Mainly, the paper concerns the role of urbanization on carbon emission and the corrective measures to reduce the urbanization based carbon emission in China. The bulk literature has confirmed the adverse effect of urbanization on carbon emission;

[1]Industrialization requires higher energy for operational activities that contribute in carbon emission, similarly, the waste of industries is also a source of carbon emission. The higher urbanization trend stimulates the buying of cars and the use of other transportation mean (Zhang, 2014), which use the fossil fuels and in turn increase the carbon level. Similarly, the urbanization increases the electricity consumption by city authorities for street lights, electricity sign boards and households (Shahbaz et al., 2016).

http://www.aloki.hu ● ISSN 1589 1623 (Print) ● ISSN 1785 0037 (Online)
DOI: http://dx.doi.org/10.15666/aeer/1705_1030310311

higher urbanization leads to increase the carbon emission (York, 2007; Wang et al., 2016; Kasman and Duman, 2015; Shahbaz et al., 2016; He et al., 2017; Zhu et al., 2017; Yao et al., 2018). This adverse relationship can be due to multiple reasons: firstly, there is a need to cut down the forests to increase the urban land which reduces the carbon balance. Secondly, higher urbanization requires the higher energy to meet the electricity demands, for transportation etc., however, this higher energy consumption causes to boost the carbon emission. It is necessary to find practicable solutions to control the urban based carbon emission. In light of this, we propose that the government should increase the per capita income of urban people and motivate them to buy energy efficient and environmental friendly products. In such domain, we use two assumptions: firstly, the industries are producing green and energy efficient equipment for industrial and household uses. Secondly, the urban population are motivated to purchase latest green technology household items; meaning that higher per capital income enables them to have environmental friendly items. The general form of studied model is given below:

$$CO_2 = f(U, UI, EG, I, C, O)$$

The log form of model is below:

$$\ln CO_{2\,it} = \beta_0 + \beta_1 CO_{2\,i,t-1} + \beta_2 U_{it} + \beta_3 UI_{it} + \beta_4 EG_{it} + \beta_5 I_{it} + \beta_6 C_{it} + \beta_7 O_{it} + \varepsilon_{it}$$

where $CO_{2\,it}$ and $CO_{2\,i,t-1}$ is current carbon emission and lagged carbon emission in million tons (Mt), respectively, which is calculated by using energy consumption based methodology. Energy consumption based carbon emission follows Intergovernmental Panel on Climate Change (IPCC, 2006). U_{it} is the urbanization (10,000 people) and UI_{it} is the proxy of urban income which measured as per capita income in Yuan. EG_{it} is the economic growth measured as gross regional product for each province (100 million Yuan). I_{it} represents the industrialization measured in 100 million Yuan. C_{it} and O_{it} presents the coal consumption and oil consumption (10,000 tons).

Difference-GMM, system-GMM and dynamic mean group (DMG) are employed for econometric estimations. We emphasize on panel data estimations due to following reasons: firstly, it assists to control the heterogeneity issues; secondly, is deals with the increase in degree of freedom. Thirdly, it is useful to control the multicollinearity issues.

Results and discussion

Table 1 reports the empirical estimations of difference-GMM, system-GMM and dynamic mean group (DMG). The findings of difference-GMM confirm the significant and positive coefficients of lagged carbon emission, urbanization, economic growth industrialization, coal, and oil consumption. These findings imply that higher urbanization trend, economic and industrialization activities, coal and oil consumption in different economic sectors are the main culprits of environmental degradation in China. On contrary, the coefficient of urban income has reported statistically significant and negative coefficient, which validates our hypothesis that higher urban income causes to reduce the carbon emission. The reason for this relationship is that the higher

http://www.aloki.hu ● ISSN 1589 1623 (Print) ● ISSN 1785 0037 (Online)
DOI: http://dx.doi.org/10.15666/aeer/1705_1030310311

urbanization leads to the advance and green technology innovation (Mishra et al., 2009; Martínez-Zarzoso and Maruotti, 2011). However, the increase in urban income raises the chances that urban population buys advanced green technologies that are useful to control the carbon emission from urbanization.

Table 1. *Econometric estimations*

	Difference-GMM		***System-GMM***		***DMG***	
	Coefficient	**p-value**	**Coefficient**	**p-value**	**Coefficient**	**p-value**
$CO_{2\,i,t-1}$	0.415	0.000	0.348	0.000	0.366	0.000
U_{it}	0.035	0.000	0.041	0.000	0.055	0.000
UI_{it}	-0.631	0.000	-0.230	0.001	-0.278	0.000
EG_{it}	0.051	0.015	0.024	0.000	0.132	0.022
I_{it}	0.136	0.001	0.097	0.038	0.110	0.061
C_{it}	0.302	0.000	0.311	0.000	0.229	0.000
O_{it}	0.106	0.010	0.086	0.041	0.081	0.039

CO_2 is lagged carbon emission, U represents the urbanization and UI is the urban income. EG mentions the economic growth, whereas, I is the industrialization. And C and U are the coal and oil consumption, respectively

System-GMM has reported similar results; the positive relationship of lagged carbon emission, urbanization, economic growth, industrialization, coal consumption and oil consumption (there is a slight difference; the coefficients of industrialization and oil consumption are statistically significant at 5% level). The coefficient of urban income is statistically significant and negative, at 1% level, which illustrates that higher carbon emission can be managed by increasing the urban income. The estimations of the dynamic mean group present the positive coefficient of urbanization, economic growth, coal consumption and oil consumption, whereas, industrialization turns out to be insignificant. The coefficient of urban income is still significant and negative.

Regional analysis

Empirical results of the regional analysis provide more insight that is useful for environmental policymakers, as the factors of carbon emission vary across different economic and geographical basis. The Chinese provinces are divided into six geographical regions to estimate the regional analysis. In *Table 2,* the coefficient of urbanization has reported significant and positive coefficients in five out of six regions, Southwest region reports insignificant coefficient. These significance and positive coefficients of urbanization exhibit that higher urbanization movement induces the carbon emission in most of the Chinese provinces. In case of urban income, the results are statistically significant and negative in five out of six provinces. The results confirm the role of urban income in carbon mitigation in most of the regions, however, it is suggested that urban-based carbon emission can be managed by increasing the per capita income of urban population. Moreover, motivate the urban population to have eco-friendly home appliances and vehicles.

Economic growth is a source of carbon emission in all six regions of China, as mentioned by the positive coefficients. The coefficients of industrialization are significant and positive in four out of six regions (North, Northeast, East and

http://www.aloki.hu ● ISSN 1589 1623 (Print) ● ISSN 1785 0037 (Online)
DOI: http://dx.doi.org/10.15666/aeer/1705_1030310311

Southcentral), whereas, insignificant in two regions (Southwest and Northwest). It is not hard to conclude that industry is also responsible for higher carbon emission in China. Estimated results of coal and oil consumption mentioned statistically significant and positive coefficients in all six regions, which indicate that fossil fuels are among the main sources of carbon emission. As China is a developing economy that requires fossil fuels (coal and oil) for industrial process, transportation, electricity generation etc., however, it is quite difficult for China to suddenly replace the fossil fuels with renewable energy.

Table 2. *Regional analysis*

	North	Northeast	East	South Central	Southwest	Northwest
$Lag\ CO_2$	0.162***	0.041***	0.167***	0.513**	0.527***	0.014***
U	0.061**	0.042***	0.031***	0.052***	0.033	0.142**
UI	-0.131***	-0.204***	-0.092***	-0.105	-0.117***	-0.032***
EG	0.010**	0.025***	0.031***	0.064***	0.462***	0.140***
I	0.016***	0.008**	0.067***	0.105**	0.019	0.062
C	0.257***	0.634***	0.138***	0.335***	0.614***	0.556***
O	0.082***	0.034**	0.415***	0.320***	0.014**	0.185***

CO_2 is lagged carbon emission, *U* represents the urbanization and *UI* is the urban income. *EG* mentions the economic growth, whereas, *I* is the industrialization. And *C* and *U* are the coal and oil consumption, respectively.
***, ** represents the significance level of 1% and 5%, respectively

Conclusion

There are two main objectives of given study: firstly, investigate the role of urbanization in carbon emission; secondly, examines the role of the urban income in carbon mitigation. The data from 30 Chinese provinces are used for empirical estimations that cover the time period of 1998-2016. Estimated findings have validated that higher urbanization causes the environmental degradation in China. In case of urban income, the coefficients present significant and negative results, which affirm our hypothesis that higher urban income likely to reduce the carbon emission by changing the buying behavior of urban population. The increase in income enables the urban population to have advance and green technology that uses less energy and have lesser emission than conventional technologies. The findings of economic growth, industrialization, coal and oil consumption are responsible for carbon emission in China. Similar findings are confirmed by regional based analysis; the higher per capita urban income assists to control the role of urbanization in carbon emission.

On the basis of above results, the study proposes significant policy implications that are useful to control the environmental degradation process. The study examines, the urban and central authorities should increase the urban income and motivate the urban population to acquire green technologies. The studies proposed that the government should impose the carbon tax on industries that force them to install carbon treatment plants. Lastly, the Chinese government needs to replace the non-renewable source of energy (coal and oil) to renewable energy (e.g. water, solar, wind, biomass etc.).

The authors have faced some limitations during the data collection and assigning the proxies; such as, the data before 1998 is missing in China statistical database which forces to limit the time series. For future studies, the authors can gather the previous

http://www.aloki.hu ● ISSN 1589 1623 (Print) ● ISSN 1785 0037 (Online)
DOI: http://dx.doi.org/10.15666/aeer/1705_1030310311

data by using some other available sources, to examine the robustness of results. Another limitation of current study is the base of two assumptions; firstly, the industries have to produce green and energy efficient equipment for industrial and household uses. Secondly, the urban population are motivated to purchase latest green technology household items; proposing that higher per capital income enables them to have environmental friendly items. However, for future direction, there is a strong need to find some alternate proxies to examine the role of urban income.

REFERENCES

[1] Achard, F., Eva, H., Mayaux, P., Stibig, H., Belward, A. (2004): Improved estimates of net carbon emissions from land cover change in the Tropics for the 1990's. – Global Biogeochemical Cycles 18(2).

[2] Arellano, M., Bover, O. (1995): Another look at the instrumental variable estimation of error-components models. – Journal of Econometrics 68(1): 29-51.

[3] Bekhet, H. A., Othman, N. S. (2017): Impact of urbanization growth on Malaysia CO2 emissions- Evidence from the dynamic relationship. – Journal of Cleaner Production 154: 374-388.

[4] Blundell, R., Bond, S. (1998): Initial conditions and moment restrictions in dynamic panel data models. – Journal of Econometrics 87(1): 115-143.

[5] Brown, S., Dushku, A., Pearson, T., Shoch, D., Winsten, J., Sweet, S., Kadyszewski, J. (2004): Carbon Supply from Changes in Management of Forest, Range, and Agricultural Lands of California. – Winrock International for California Energy Commission, Arlington, VA.

[6] Ding, Y., Li, F. (2017): Examining the effects of urbanization and industrialization on carbon dioxide emission: evidence from China's provincial regions. – Energy 125: 533-542.

[7] Dong, F., Bian, Z., Yu, B., Wang, Y., Zhang, S., Li, J., ... Long, R. (2018): Can land urbanization help to achieve CO2 intensity reduction target or hinder it? Evidence from China. – Resources, Conservation & Recycling 134: 206-215.

[8] EIA (Energy Information Administration) (2011, February 09): History of energy consumption in the United States 1775-2009. – https://www.eia.gov: https://www.eia.gov/todayinenergy/detail.php?id=10.

[9] Fang, C., Wang, S., Li, G. (2015): Changing urban forms and carbon dioxide emissions in China: A case study of 30 provincial capital cities. – Applied Energy 158: 519-531.

[10] He, Z., Xu, S., Shen, W., Long, R., Chen, H. (2016): Impact of urbanization on energy related CO2 emission at different development levels: regional difference in China based on panel estimation. – Journal of Cleaner Production. https://doi.org/10.1016/j.jclepro.2016.08.155.

[11] IPCC (2006): Greenhouse Gas Inventory: IPCC Guidelines for National Greenhouse Gas Inventories. – United Kingdom Meteorological Office, Bracknell, UK.

[12] Kasman, Adnan, and Yavuz Selman Duman. 2015. "CO2 Emissions, Economic Growth, Energy Consumption, Trade and Urbanization in New EU Member and Candidate Countries: A Panel Data Analysis." *Economic Modelling* 44 (January). North-Holland: 97–103. doi:10.1016/J.ECONMOD.2014.10.022.

[13] Lai, L., Huang, X., Yang, H., Chuai, X., Zhang, M., Zhong, T., ... Thompson, J. (2016): Carbon emissions from land-use change and management in China between 1990 and 2010. – Science Advances. DOI: 10.1126/sciadv.1601063.

[14] Li, K., Lin, B. (2015): Impacts of urbanization and industrialization on energy consumption/CO2 emissions: does the level of development matter? – Renewable and Sustainable Energy Reviews 52: 1107-1122.

http://www.aloki.hu ● ISSN 1589 1623 (Print) ● ISSN 1785 0037 (Online)
DOI: http://dx.doi.org/10.15666/aeer/1705_1030310311

[15] Liddle, Brant. 2004. "Demographic Dynamics and Per Capita Environmental Impact: Using Panel Regressions and Household Decompositions to Examine Population and Transport." *Population and Environment* 26 (1). Kluwer Academic Publishers-Plenum Publishers: 23–39. doi:10.1023/B:POEN.0000039951.37276.f3.
[16] Lin, B., Omoju, O., Okonkwo, J. (2015): Impact of industrialisation on CO2 emissions in Nigeria. – Renewable and Sustainable Energy Reviews 52: 1228-1239.
[17] Liu, X., Bae, J. (2018): Urbanization and industrialization impact of CO2 emissions in China. – Journal of Cleaner Production 172: 178-186.
[18] Liu, Y., Gao, C., Lu, Y. (2017): The impact of urbanization on GHG emissions in China: the role of population density. – Journal of Cleaner Production 157: 299-309.
[19] Lund, H., Kempton, W. (2008): Integration of renewable energy into the transport and electricity sectors through V2G. – Energy Policy 3578-3587.
[20] Madlener, R., Sunak, Y. (2011): Impacts of urbanization on urban structures and energy demand: what can we learn for urban energy planning and urbanization management? – Sustainable Cities and Society 1(1): 45-53.
[21] Martínez-Zarzoso, Inmaculada, and Antonello Maruotti. 2011. "The Impact of Urbanization on CO2 Emissions: Evidence from Developing Countries." *Ecological Economics* 70 (7). Elsevier: 1344–53. doi:10.1016/J.ECOLECON.2011.02.009.
[22] Parikh, Jyoti, and Vibhooti Shukla. 1995. "Urbanization, Energy Use and Greenhouse Effects in Economic Development: Results from a Cross-National Study of Developing Countries." *Global Environmental Change* 5 (2): 87–103. doi:https://doi.org/10.1016/0959-3780(95)00015-G.
[23] Pata, U. K. (2018): Renewable energy consumption, urbanization, financial development, income and CO2 emissions in Turkey- Testing EKC hypothesis with structural breaks. – Journal of Cleaner Production 187: 770-779.
[24] Pinghui, Z. (2017, March 03): Thousands tackling huge forest fire in northern China. – South China Morning Post: http://www.scmp.com/news/china/society/article/2092663/thousands-tackling-huge-forest-fire-northern-china.
[25] Routa, J., Kelomaki, S., Kilpelainen, A., Peltola, H., Strandman, H. (2011): Effects of forest management on the carbon dioxide emissions of wood energy in integrated production of timber and energy biomass. – Global Change Biology Bioenergy 3: 483-497.
[26] Shahbaz, M., Loganathan, N., Muzaffar, A. T., Ahmed, K., Jabran, M. A. (2016): How urbanization affects CO2 emissions in Malaysia? The application of STIRPAT model. – Renewable and Sustainable Energy Reviews 57: 83-93.
[27] Schlamadinger, B., Marland, G. (1999): Net effect of forest harvest on CO2 emissions to the atmosphere: a sensitivity analysis on the influence of time. – Tellus B: Chemical and Physical Meteorology 51(2): 314-325.
[28] Shen, A. (2017, November 17). Forest fire burns across mountainside in western China. – South China Morning Post. http://www.scmp.com/news/china/society/article/2120376/forest-fire-burns-across-mountainside-western-china.
[29] Shi, A. (2003): The impact of population pressure on global carbon dioxide emissions 1975-1996: Evidence from pooled cross-country data. – Ecological Economics 44: 29-42.
[30] Shi, X., Li, X. (2018): Research on three-stage dynamic relationship between carbon emission and urbanization rate in different city groups. – Ecological Indicators 91: 195-202.
[31] Stern, N. (2006): Stern Review: The Economics of Climate Change. HM Treasury. – Cambridge University Press, Cambridge, UK.
[32] Sarwar, Suleman. 2019. "Role of Urban Income, Industrial Carbon Treatment Plants and Forests to Control the Carbon Emission in China." *Environmental Science and Pollution Research* 26 (16): 16652–61. doi:10.1007/s11356-019-04854-3.

http://www.aloki.hu ● ISSN 1589 1623 (Print) ● ISSN 1785 0037 (Online)
DOI: http://dx.doi.org/10.15666/aeer/1705_1030310311

[33] Sun, Chuanwang, Xiang Yuan, and Xin Yao. 2016. "Social Acceptance towards the Air Pollution in China: Evidence from Public's Willingness to Pay for Smog Mitigation." *Energy Policy* 92 (May). Elsevier: 313–24. doi:10.1016/J.ENPOL.2016.02.025.

[34] Thuy, P. T., Moeliono, M., Locatelli, B., Brockhaus, M., Gregorio, M. D., Mardiah, S. (2014): Integration of adaptation and mitigation in climate change and forest policies in Indonesia and Vietnam. – Forests 2016-2036.

[35] Waheed, R., Chang, D., Sarwar, S., Chen, W. (2017): Forest, agriculture, renewable energy, and CO2 emission. – Journal of Cleaner Production. https://doi.org/10.1016/j.jclepro.2017.10.287.

[36] Wang, S., Fang, C., Wang, Y. (2016): Spatiotemporal variations of energy-related CO2 emissions in China and its influencing factors: an empirical analysis based on provincial panel data. – Renewable and Sustainable Energy Reviews 55: 505-515.

[37] Wang, S., Li, G., Fang, C. (2018): Urbanization, economic growth, energy consumption, and CO2 emissions: Empirical evidence from countries with different income levels. – Renewable and Sustainable Energy Reviews 81: 2144-2159.

[38] Wang, Y., Li, L., Kubota, J., Han, R., Zhu, X., Lu, G. (2016): Does urbanization lead to more carbon emission? Evidence from a panel of BRICS countries. – Applied Energy 168: 375-380.

[39] Wang, Z., Feng, C., Zhang, B. (2014): An empirical analysis of China's energy efficiency From both static and dynamic perspective. – Energy 74: 322-330.

[40] Xu, B., Lin, B. (2015): How industrialization and urbanization process impacts on CO2. Evidence from nonparametric additive. – Energy Economics 48: 188-202.

[41] Yao, X., Kou, D., Shao, S., Li, X., Wang, W., Zhang, C. (2018): Can urbanization process and carbon emission abatement be harmonious. New evidence from China. – Environmental Impact Assessment Review 71: 70-83.

[42] Yeh, J.-C., Liao, C.-H. (2017): Impact of population and economic growth on carbon emissions in Taiwan using an analytic tool STIRPAT. – Sustainable Environment Research 27: 41-48.

[43] York, R. (2007): Demographic Trends and Energy Consumption in European Union Nations, 1960–2025. – Social Science Research 36 (3). Academic Press: 855–72. doi:10.1016/J.SSRESEARCH.2006.06.007.

[44] Yuan, J., Xu, Y., Hu, Z., Zhao, C., Xiong, M., Guo, J. (2014): Peak energy consumption and CO2 emissions in China. – Energy Policy 68: 508-523.

[45] Zhang, C., Lin, Y. (2012): Panel estimation for urbanization, energy consumption and CO2 emissions: a regional analysis in China. – Energy Policy 49: 488-498.

[46] Zhang, N., Yu, K., Chen, Z. (2017): How does urbanization affect carbon dioxide emissions? A cross-country panel data analysis. – Energy Policy 107: 678-687.

[47] Zhu, Z., Liu, Y., Tian, X., Wang, Y., Zhang, Y. (2017): CO2 emissions from the industrialization and urbanization processes in the manufacturing center Tianjin in China. – Journal of Cleaner Production 168: 867-875.

[48] Zi, C., Jie, W., Hong-Bo, C. (2016): CO2 emissions and urbanization correlation in China based on threshold analysis. – Ecological Indicators 61(2): 193-201.

http://www.aloki.hu ● ISSN 1589 1623 (Print) ● ISSN 1785 0037 (Online)
DOI: http://dx.doi.org/10.15666/aeer/1705_1030310311

NUMERICAL SIMULATION OF BLASTING DUST POLLUTION IN OPEN-PIT MINES

HUANG, Z.[1,2*] – GE, S.[1,2,3] – JING, D.[1,2] – YANG, L.[1,2]

[1]*College of Safety Science and Engineering, Liaoning Technical University, Fuxin 123000, China*

[2]*Key Laboratory of Mine Thermodynamic Disasters and Control of Ministry of Education, Fuxin 123000, China*

[3]*Taiyuan University of Technology, Taiyuan 030024, China*

**Corresponding author*
e-mail: huangzhihui666@sina.com

(Received 27th Sep 2018; accepted 16th Jul 2019)

Abstract. To solve the problem of dust pollution caused by bench blasting in open-pit mines and to solve the current situation of blasting dust control efficiency in most open-pit mines, the blasting dust removal mechanism and migration law were studied in this paper. In this paper, taking the bench blasting in Fushun China open-pit mines as an example, a real-time simulation of blasting dust pollution in open-pit mines was conducted through the numerical simulation by Fluent software and field test using the theories of gas-solid two-phase flow and explosion mechanics. The results showed that in the stage of impact movement and mushroom cloud formation, the explosive gas produced by blasting expanded rapidly, and a large amount of dust rushed into the atmospheric space under the effect of blasting impact kinetic energy, and then diffused. The migration velocity of dust was very lowly without wind. The dust with a particle size of 60-100 μm settled slowly, and the dust with a particle size of below 40 μm settled with difficulty due to the strong disturbance by air flow. Based on the law of dust pollution, this paper provides a basis for the design of reasonable parameters of dustproof net and related parameters of remote mist emitter, and provides a theoretical and practical basis for the control of blasting dust in other open pit mines.
Keywords: *blasting dust, dust migration law, numerical simulation, gas-solid two-phase flow, strip mine*

Introduction

With the continuous expansion of production scale of open-pit mines, the problem of blasting dust pollution is becoming more and more serious. Blasting is mainly a process of rapid expansion of explosive gas with huge energy, in which a large amount of dust rushes into the atmospheric space under the effect of blasting impact kinetic energy, and then diffuses. The dust expands rapidly at the beginning of blasting, then gradually slows down, and finally tends to be stable. The dust of large particle size settles slowly, and most of the dust of small particle size diffuses slowly with the explosive gas (Jing et al., 2007; Ghose and Majee, 2001; Yang et al., 1996; Chen et al., 2013).

The local blasting dust concentration reached thousands of milligrams per cubic meter. Therefore, it not only endangers the health of workers, affects the normal operation of nearby production equipment, but also may endanger the health of surrounding residents (Baxter and Smith, 1993). A lot of studies have been done on explosive dust, for example, Jiang (2007) conducted real-time simulation of dust diffusion motion shape based on coal dust particle system, and developed BSMS simulation software. Their research has a lot of advantages, but due to the limitations of

http://www.aloki.hu ● ISSN 1589 1623 (Print) ● ISSN 1785 0037 (Online)
DOI: http://dx.doi.org/10.15666/aeer/1705_1031310333

computer performance at that time, they failed to simulate the law of blasting dust pollution more visually. On the basis of summarizing the predecessors, in this paper, taking the bench blasting in Fushun China open-pit mines as an example, a reasonable simplification was conducted according to the actual conditions of blasting site, and a corresponding mathematical model was established, and the movement track of dust particles was tracked by Fluent software (Fu and Liu, 2017; Shen et al., 2017; Lenart, 2017), and the simulation results were analyzed, and simple and effective dust control measures were taken, finally, the dust control measures were tested through the numerical simulation and field test of dust (Zhang et al., 2018; Nongqwenga and Modi, 2017; Peng et al., 2018; Wang et al., 2018; Wu, 2016). By analyzing the law of dust pollution, the reasonable proportion of water stemming and solid stemming and the reasonable height of dust screen are calculated.

General situation of blasting dust pollution and determination of basic characteristics of dust in east open pit mine in Fushun, China

Description of the diffusion process of dust

Fushun China East Open-pit Mine is located in the northern temperate zone. It is located in the east longitude 99° north latitude 47°. The pit is 5.7 km long from east to west, 1.9 km wide from north to south, and covers an area of 9.2 km^2. The deep-hole loosening blasting was adopted in 32# station working face, and the blasting parameters are shown in *Table 1*. The blasting pile did not form an obvious blasting funnel in the original place after blasting, and the degree of crushing of blasting body can meet the requirements of subsequent collision transportation, improve working efficiency and service life of equipment.

Through the observation and data analysis on the blasting site of East Open-pit Mine, it was found that in the process of open-pit blasting, the blasting dust rushed into the atmospheric space after leaving the blasting body under the effect of blasting impact kinetic energy (Yang et al., 2018; Zamora Figueroa et al., 2017; Jiang et al., 2017). Dust movement in the atmosphere can be roughly divided into three stages: (1) impact movement stage; (2) mushroom cloud formation stage; (3) diffusion stage. In this stage, the dust particles generated and excited by blasting vary greatly in the movement state. Although it lasted a short time, the dust concentration was high, as the local blasting dust concentration reached thousands of milligrams per cubic meter, as shown in *Figure 1*.

Figure 1. *Blowing dust after blasting*

http://www.aloki.hu ● ISSN 1589 1623 (Print) ● ISSN 1785 0037 (Online)
DOI: http://dx.doi.org/10.15666/aeer/1705_1031310333

Table 1. *Blasting mesh parameters (unit: m)*

Aperture	0.155 m	Bench blasting	7 m
Borehole row spacing	4 m	Super depth	1-2 m
Borehole column spacing	6 m	Packing length	3 m
Borehole depth	7-8 m	Burden	4.5 m

Materials and methods for testing the physical properties of dust

(1) Sampling requirements for testing the basic characteristics of dust

1) Sampling site for testing the basic characteristics of dust

a. Determination of dust concentration: the damage of dust to human body is determined by the concentration of free silica. Generally, the suspended dust 1.5 m above the ground (respiratory zone height) was determined;

b. Determination of dust dispersion: the dispersion of dust usually refers to a collection of percentages of particles with different particle sizes. Generally, the dust of different concentrations at different places were collected for many times.

2) The basic characteristics of dust in working face should be tested by taking into account the influence of air humidity, temperature, wind speed and so on. The following points should be considered in selecting the right time to test it:

a. The dust concentration was determined at the same place and the same wind speed.

b. The change value of dust concentration was determined at different times after blasting and the same wind speed.

In the course of testing the basic characteristics of dust, the following test instruments were used: AH-91A Dust Sampler produced in Wuxi (depending on the actual situation); glass fiber filters produced by Sephorlebo (Φ75 mm if the dust concentration was greater than 200 mg/m^3; Φ40 mm if the dust concentration was less than 200 mg/m^3); scales, tweezers, drying boxes, etc.

(2) Detection contents of dust dispersion

To deeply reveal the influence of dust on human body and equipment, and to design a more simple and effective dust removal scheme, we introduced the dispersion test.

1) Detection methods and specific contents

It was mainly detected by quantity and quality dispersion, and the observation method by microscope was most commonly used for the quantity dispersion. The dust sample was made into a standard sheet, tested by a microscope, and the content was calculated, and the dispersion was finally determined. *Equation 1* was used to calculate it:

$$P_{n_i} = (n_i / \sum n_i) \times 100\% \quad \text{(Eq.1)}$$

where: P_{ni}—Particle size dispersion; n_i—The sum of the number of dust particles of specified particle size, pcs; Σn_i—The sum of the number of dust particles of different particle sizes, pcs.

http://www.aloki.hu ● ISSN 1589 1623 (Print) ● ISSN 1785 0037 (Online)
DOI: http://dx.doi.org/10.15666/aeer/1705_1031310333

Weight dispersion: within a given range, the ratio of the sum of the mass of dust particles contained in each particle size interval to the sum of the mass of total dust particles was usually expressed as a percentage. *Equation 2* was used to calculate it:

$$P_{wi} = \frac{wi}{\sum wi \times 100\%} \quad \text{(Eq.2)}$$

Where: wi—The sum of the mass of dust particles in a certain particle size range; Pwi—The percentage of the mass of dust particles in a certain particle size range, %.

2) Main test instruments

Perchloroethylene fiber filter membrane; butyl acetate solvent; glass slide; microscope; computer microimage processing system; etc.

Determination results of dust

Because of the particularity and danger of determination of dust, it was necessary to use advanced testing instruments and means to test the concentration and dispersion and other important parameters of dust in a comprehensive and systematic way, which provided an important basis for selecting suitable dust control schemes. The test results are shown in *Tables 2* and *3*. Dust particles are irregular in shape and the equivalent diameter of the dust is usually used to describe the size of the dust particles. Dust particles vary and the particle size of dust is in accordance with Rosin-Rammler distribution after experimental analysis. *Figure 2* is drawn from the test dust sampling results, and the median particle size value is the particle diameter $\overline{d}$ = 170 when Y_d = 0.368.

Table 2. *Dust concentration of 32# station working face on the blasting site*

Test number	Test site	Dust concentration mg/m³	Test time	Test condition
1	Station working face on the blasting site	306.7	10	60S after blasting, no wind
2		273.5	10	60S after blasting, no wind
3		311.2	10	60S after blasting, no wind

Table 3. *Dust dispersion of 32# station working face on the blasting site*

Test number	Test site	Test time	Mass dispersion % (mean)				
			<30	30-90	90-150	150-270	>270
11	Station working face on the blasting site	10	6	10	34	43	7
22		10	5	10	35	45	5
33		10	4	10	36	47	3

http://www.aloki.hu ● ISSN 1589 1623 (Print) ● ISSN 1785 0037 (Online)
DOI: http://dx.doi.org/10.15666/aeer/1705_1031310333

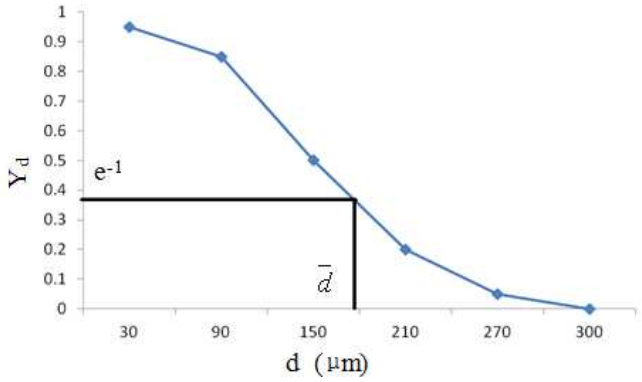

Figure 2. *Size distribution of accumulate particle quality of total dust*

Establishment of mathematical model and determination of parameters

According to the dust migration law, the discrete phase model of Euler-Lagrangian method was used to calculate the effect of turbulent velocity on particle motion by using random orbits.

Mathematical model of continuous phase flow field

(1) Turbulence model

It was generally recognized that the natural air flow was dominated by turbulent motion state, which thus directly affected the diffusion range of dust. It was necessary to briefly introduce the basic characteristics of turbulent motion.

Through a large number of tests, it can be concluded that: if the Reynolds number did not reach the critical value, we defined this flow as laminar flow (orderly flow between the flow layers); if the Reynolds number exceeded the critical value, we defined this flow as turbulence (chaotic and irregular flow of fluid). In the Cartesian coordinate system, the vector of velocity in the three coordinate axes (X-axis, Y-axis, Z-axis) was represented by u, v and w respectively, and the governing *Equations 3* and *4* can be expressed as:

$$div\vec{u} = 0 \tag{Eq.3}$$

$$\begin{cases} \dfrac{\partial u}{\partial t} + div\left(u\vec{u}\right) = -\dfrac{1}{\rho}\dfrac{\partial p}{\partial x} + v\,div\left(gradu\right) \\ \dfrac{\partial v}{\partial t} + div\left(v\vec{u}\right) = -\dfrac{1}{\rho}\dfrac{\partial p}{\partial y} + v\,div\left(gradv\right) \\ \dfrac{\partial w}{\partial t} + div\left(w\vec{u}\right) = -\dfrac{1}{\rho}\dfrac{\partial p}{\partial z} + v\,div\left(gradw\right) \end{cases} \tag{Eq.4}$$

where: grada=$\dfrac{\partial a}{\partial x}+\dfrac{\partial a}{\partial x}+\dfrac{\partial a}{\partial x}$; V—Kinematic viscosity coefficient, m^2/s; p—Pressure on a fluid microelement, pa.

http://www.aloki.hu ● ISSN 1589 1623 (Print) ● ISSN 1785 0037 (Online)
DOI: http://dx.doi.org/10.15666/aeer/1705_1031310333

The pulsation can be taken into account by using the Reynolds averaging method, that is, the time average of the variable ϕ can be expressed as *Equation 5:*

$$\bar{\phi}=\frac{1}{\Delta t}\int_{t}^{t+\Delta t}\phi(t)dt \tag{Eq.5}$$

where: "–"—Time average; ϕ —Instantaneous value; $\bar{\phi}$ —Time average; ϕ' — Pulsation value. ϕ, $\bar{\phi}$, ϕ' —The three were as *Equation 6:*

$$\phi=\bar{\phi}+\phi' \tag{Eq.6}$$

If the instantaneous value was replaced by the sum of the time average and pulsation value that is following as *Equation 7:*

$$u=\bar{u}+u' \quad v=\bar{v}+v' \quad w=\bar{w}+w' \quad p=\bar{p}+p' \tag{Eq.7}$$

By substituting the *Equation* 7 in the *Equation* 3, *Equation* 4, the following formulas can be obtained:

1) Continuity equation (Almstedt, 2003)

Continuity equation is as *Equation 8*.

$$\frac{\partial}{\partial x_i}(\rho u_i)=0 \tag{Eq.8}$$

where: ρ —Gas density, km/m^3; u_i—Gas velocity vector.

2) Momentum equation (N-S equation)

Momentum equation is as *Equation 9.*

$$\frac{\partial}{\partial x_j}(\rho u_i u_j)=-\frac{\partial}{\partial x_j}\left(\mu\frac{\partial u_i}{\partial x_j}-\rho\overline{u_i'u_j'}\right) \tag{Eq.9}$$

where: xi—Coordinates in the x, y, z direction, m; ui—The velocity of gas in the x, y, z direction, m/s; p—Effective turbulent pressure, Pa; μ—Dynamic viscosity coefficient Pa•s.

(2) Standard k-ε equation model

The standard k-ε equation model was first introduced by Launder and Spalding in the late last century. Up to now, it is also very popular in the field of turbulence simulation. The turbulent dissipation rate ε can be expressed by *Equation 10:*

$$\varepsilon=\frac{\mu}{\rho}\overline{\left(\frac{\partial u_i'}{\partial x_k}\right)\left(\frac{\partial u_i'}{\partial x_k}\right)} \tag{Eq.10}$$

http://www.aloki.hu ● ISSN 1589 1623 (Print) ● ISSN 1785 0037 (Online)
DOI: http://dx.doi.org/10.15666/aeer/1705_1031310333

The turbulent viscosity coefficient μ_t was a function of k and ε, that is, *Equation 11:*

$$\mu_t = \rho C_\mu \frac{k^2}{\varepsilon} \quad \text{(Eq.11)}$$

where: ρ— Gas density, kg/m^3; C_μ—Empirical constant; k—Turbulence kinetic energy, m^2/s^2; ε— Turbulent kinetic energy dissipation rate, m^2/s^3.

In the standard k-ε model, k and ε were two fundamental unknown quantities, and the corresponding transport equations were *Equations 12* and *13:*

$$\frac{\partial(\rho\varepsilon u_i)}{\partial x_j} = \frac{\partial}{\partial x_j}\left[\left(\mu + \frac{\mu_t}{\sigma_k}\right)\frac{\partial k}{\partial x_j}\right] + G_k + G_b - \rho\varepsilon - Y_M + S_k \quad \text{(Eq.12)}$$

$$\frac{\partial(\rho\varepsilon u_i)}{\partial x_j} = \frac{\partial}{\partial x_j}\left[\left(\mu + \frac{\mu_t}{\sigma_\varepsilon}\right)\frac{\partial \varepsilon}{\partial x_j}\right] + G_{1\varepsilon}\frac{\varepsilon}{k}\left(G_K + G_{3\varepsilon}G_b\right) - G_{2\varepsilon}\rho\frac{\varepsilon^2}{k} + S_\varepsilon \quad \text{(Eq.13)}$$

where: G_k— he generating term of turbulent kinetic energy caused by average velocity gradient; G_b—Turbulent kinetic energy caused by buoyancy; Y_M—Contribution of pulsation expansion in compressible turbulence; $G_{1\varepsilon}, G_{2\varepsilon}, G_{3\varepsilon}$—Empirical constants; $\sigma_k, \sigma_\varepsilon$—The Prandtl number corresponding to the turbulent kinetic energy k and dissipation rate ε; S_k, S_ε—User-defined source item.

When the fluid was steady-state incompressible, regardless of user-defined source item, G_b=0 , $G_{3\varepsilon}$=0 , Y_M=0 , S_k=0 , S_ε=0 , then the standard k-ε model were *Equations 14* and *15:*

$$\frac{\partial(\rho\varepsilon u_i)}{\partial x_j} = \frac{\partial}{\partial x_j}\left[\left(\mu + \frac{\mu_t}{\sigma_k}\right)\frac{\partial k}{\partial x_j}\right] + G_k - \rho\varepsilon \quad \text{(Eq.14)}$$

$$\frac{\partial(\rho\varepsilon u_i)}{\partial x_j} = \frac{\partial}{\partial x_j}\left[\left(\mu + \frac{\mu_t}{\sigma_\varepsilon}\right)\frac{\partial \varepsilon}{\partial x_j}\right] + G_{1\varepsilon}\frac{\varepsilon}{k}G_k - G_{2\varepsilon}\rho\frac{\varepsilon^2}{k} \quad \text{(Eq.15)}$$

where: $G_k = \mu_t \frac{\partial u_i}{\partial x_j}\left(\frac{\partial u_i}{\partial x_j} + \frac{\partial u_j}{\partial x_i}\right)$.

By deriving from experimental data and theoretical derivation, $G_{1\varepsilon}$ = 1.44, $G_{2\varepsilon}$ = 1.92, σ_k = 1.0, σ_ε = 1.3 were obtained.

The discrete phase model of Euler-Lagrangian method was adopted according to the dust migration law.

http://www.aloki.hu ● ISSN 1589 1623 (Print) ● ISSN 1785 0037 (Online)
DOI: http://dx.doi.org/10.15666/aeer/1705_1031310333

Mathematical model of discrete phase

According to the force balance on the droplet (particle), the equation of motion of the particle in Lagrangian coordinate system can be obtained (O'Rourke, 1981; Jin, 2010; Guo, 2006; Luo and Shen, 2006) as *Equations 16* and *17:*

$$\frac{du_p}{dt} = F_D(u-u_p) + g_x(\rho_p - \rho)/\rho_p + F_x \quad \text{(Eq.16)}$$

$$F_D = \frac{18\mu}{\rho_p D_p^2}\frac{C_D \mathrm{Re}}{24} \quad \text{(Eq.17)}$$

where: u— Continuous phase velocity, m/s; u_p— Particle velocity, m/s; μ— Molecular viscosity coefficient of the fluid, Pa•s; ρ, ρ_p— The density of the fluid and the particle respectively; kg/m^3; D_p— Particle diameter, m; Re was a relative Reynolds number, which was defined as *Equation 18:*

$$\mathrm{Re} = \frac{\rho D_p |u_p - u|}{\mu} \quad \text{(Eq.18)}$$

The resistance coefficient $C_D = \alpha_1 + \frac{\alpha_2}{\mathrm{Re}} + \frac{\alpha_3}{\mathrm{Re}^2}$, α_1, α_2, α_3 was a constant, which was given according to the experimental results of smooth spherical particles.

The other method for determining C_D was *Equation 19:*

$$C_D = \frac{24}{\mathrm{Re}}(1 + b_1 \mathrm{Re}^{b_2}) + \frac{b_3 \mathrm{Re}}{b_4 + \mathrm{Re}} \quad \text{(Eq.19)}$$

The form factor was defined as $\varphi = s/S$, s was the surface area of the sphere of the same volume as the particle; S was the actual surface area of the particle. Then the above constants were *Equations 20–23:*

$$b_1 = 2.3288 - 6.4581\phi + 2.4486\phi^2 \quad \text{(Eq.20)}$$

$$b_2 = 0.0964 + 0.5565\phi \quad \text{(Eq.21)}$$

$$b_3 = 4.905 - 13.8944\phi + 18.4222\phi^2 - 10.2599\phi^3 \quad \text{(Eq.22)}$$

$$b_4 = 1.4681 + 12.2584\phi - 20.7300\phi^2 + 15.8855\phi^3 \quad \text{(Eq.23)}$$

If the particle size was below micron, the Stokes resistance formula was used as *Equation 24:*

http://www.aloki.hu ● ISSN 1589 1623 (Print) ● ISSN 1785 0037 (Online)
DOI: http://dx.doi.org/10.15666/aeer/1705_1031310333

$$F_D = \frac{18\mu}{D_p^2 \rho_p C_c} \quad \text{(Eq.24)}$$

where C_c was the Cunningham correction coefficient, as *Equation 25:*

$$C_c = 1 + \frac{2\lambda}{D_p}[1.257 + 0.4e^{\frac{1.1D_p}{2\lambda}}] \quad \text{(Eq.25)}$$

where λ was the mean molecular free path.

Equation of motion of dust particle trajectory

The equation of motion of dust particle trajectory can be solved step by step in discrete time step. The particle velocity at every position on the particle orbit can be obtained by integrating *Equation 26.*

$$\frac{d_x}{dt} = u_p \quad \text{(Eq.26)}$$

By solving the governing equations on each coordinate axis, the discrete phase dust particle trajectory can be obtained.

Establishment of geometric model and generation of meshes

(1) Overview of the establishment of geometric model

To simulate and analyze the practical problems, it was necessary to establish a similar model to approximate the practical engineering problems, so we established a geometric model according to the actual situation of the receiving station.

(2) Division of meshes

The meshes adopted in this paper are shown in *Figure 3.*

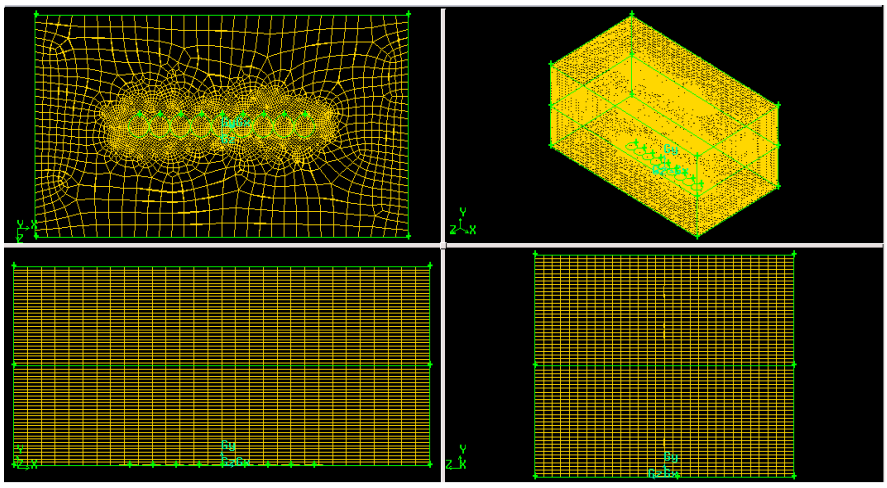

Figure 3. *3D mesh diagrams*

http://www.aloki.hu ● ISSN 1589 1623 (Print) ● ISSN 1785 0037 (Online)
DOI: http://dx.doi.org/10.15666/aeer/1705_1031310333

Establishment of boundary conditions

(1) Establishment of continuous phase boundary conditions

The boundary conditions, wall boundary conditions, and inlet and outlet boundary conditions involved in the simulation are shown in the *Tables 4* and *5*.

Table 4. *Setting list of model*

Model	Define
Solver	Segregated Implicit Transient
Viscous model	k-ε
Energy	On
Discrete phase model	On

Table 5. *Setting list of operating conditions*

Operating conditions	Setting
Operating pressure (pa)	101325
Gravitational acceleration	X 0 Y 0 Z -9.8
Air density kg/m^3	1.225
Air viscosity Pa•s	0.000018
Dust density kg/m^3	1830
Pressure-velocity	SIMPLEC
Pressure discretization	Standard
Discretization	Second order upwind
Convergence criterion	0.001

(2) Establishment of discrete phase boundary conditions

The assumption of mathematical model of dust movement was that when facing complex dust particles, we need to understand the main characteristics of dust, and we can ignore some subtle characteristics which have little influence on the calculation results, which can not only simplify the calculation, but also show the migration law of dust correctly. Therefore, we made the following assumptions, as shown in *Table 6:*

1) The dust particles were perceived as spheres
2) Initial velocity of dust ejection
3) The interaction between dust particles was neglected
4) The dust ejected steadily instantly

Iterative calculation

The unsteady numerical simulation by Fluent software according to the parameters and boundary conditions given above showed good convergence. The partial residual curve is shown in *Figure 4.*

http://www.aloki.hu ● ISSN 1589 1623 (Print) ● ISSN 1785 0037 (Online)
DOI: http://dx.doi.org/10.15666/aeer/1705_1031310333

Table 6. *Setting list of dust source parameters*

Injection	Define
Injection type	Surface
Material	Fenchen
Diameter distribution	Rosin-Rammler
Min. diameter (m)	1.0×10^{-6}
Max. diameter (m)	3.0×10^{-4}
Mean diameter (m)	1.7×10^{-4}
Spread parameter	2.42
Total flow rate (kg/s)	120
Turbulent dispersion	Stochastic tracking
Number of tries	500000
Time scale constant	0.16

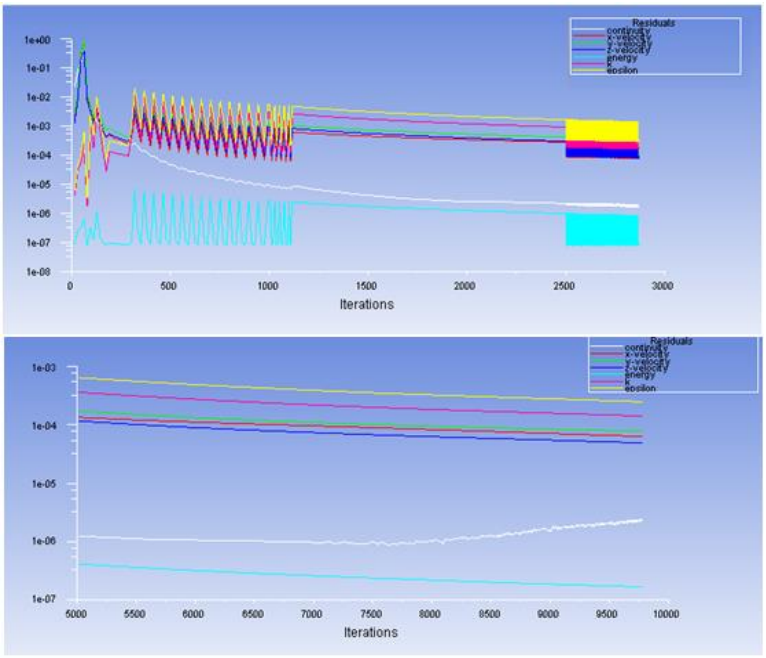

Figure 4. *Partial residual curve diagram*

The analysis and discussion of the numerical simulation results of blasting blowing dust law

To understand the movement state of dust more intuitively, a numerical simulation of the migration law of dust was conducted according to the field situation and relative conditions of blasthole arrangement (as shown in *Figs. 5* and *6*).

Dust particle trajectory diagrams at different times after blasting

The results showed that the change of the shape and migration velocity of dust was complex with the increase of time.

http://www.aloki.hu ● ISSN 1589 1623 (Print) ● ISSN 1785 0037 (Online)
DOI: http://dx.doi.org/10.15666/aeer/1705_1031310333

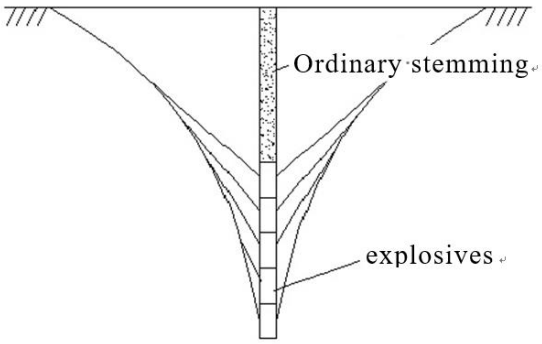

Figure 5. *Deep-hole blasting stress curve diagram*

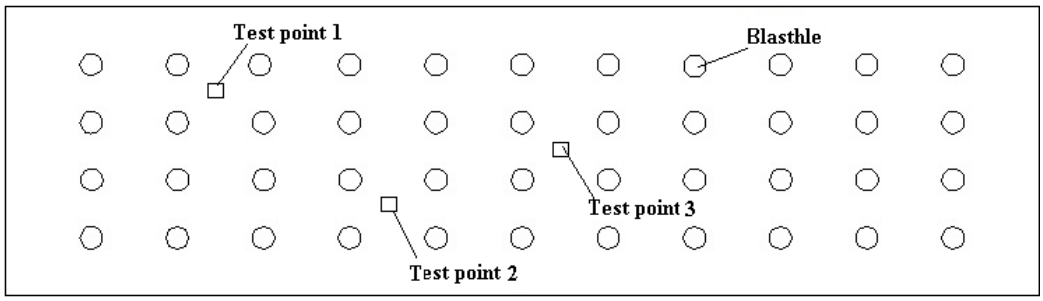

Figure 6. *Blasthole arrangement and test point diagram*

a. At the beginning of blasting, the initial velocity of dust was 50-65 m/s, and the average velocity of dust decreased to 30-40 m/s after the 0.1th second, and to 5-8 m/s after 0.5 s (*Fig. 7*), and to below 3.5 m/s after the 3rd second (*Fig. 8*). In the stage of impact movement of dust, the impact force was strong, the velocity of dust varied greatly. The inertia of dust particles was greater than that of gas phase, and the inertia of dust of large particle size was greater than that of dust of small particle size. Therefore, the front end of blasting dust cloud was dust particles, which moved by inertia.

b. With the increase of time, the velocity of dust decreased gradually under the effect of air resistance, and the average velocity of dust decreased to 1.04-2.78 m/s at the 6th second (*Fig. 9*), and was not obvious after the 6th second (*Fig. 10*), and became stable after this period of time. The heat carried by most of the explosive gases had basically been discharged into the atmosphere. Due to the release of huge blast energy, local pressure difference was produced, and a large amount of air came in because of the pressure difference, which slowly rose and diffused carrying dust.

c. The velocity of dust decreased to 0.6-1 m/s after the 25th second (*Figs. 11* and *12*) and varied slightly. Then, the diffusion stage began, and the range of dust pollution was also determined by this stage.

Dust concentration diagrams at different times after blasting

As can be seen from the dust concentration diagrams, the maximum dust concentration reached thousands of milligrams per cubic meter at the 0.1th second. At the 3rd second (*Fig. 13*), the maximum dust concentration reached 1,660 mg/m^3. The change of dust concentration in the inertial motion stage mainly depended on the change

http://www.aloki.hu ● ISSN 1589 1623 (Print) ● ISSN 1785 0037 (Online)
DOI: http://dx.doi.org/10.15666/aeer/1705_1031310333

of the velocity of dust inertial motion (*Fig. 14*). At the 25th second (*Fig. 15*), the maximum dust concentration was 459 mg/m^3, and the average dust concentration was 270 mg/m^3. After 35 s of settlement (*Fig. 16*), the maximum dust concentration was 339 mg/m^3, and the average dust concentration was 170 mg/m^3. At this point, some of the dust of large particle size began to settle, and the change of dust concentration was determined by both the diffusion and settlement velocity of the dust. The change of dust concentration was very slow at later time points (*Fig. 17*).

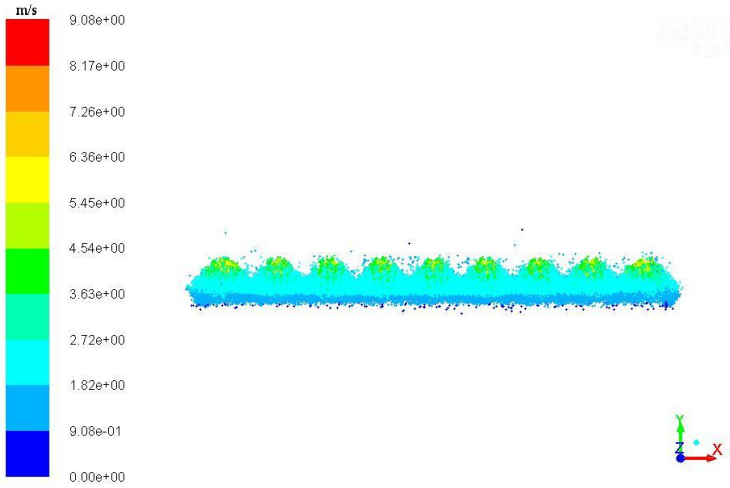

Figure 7. *Dust particle trajectory diagram (0.5 s)*

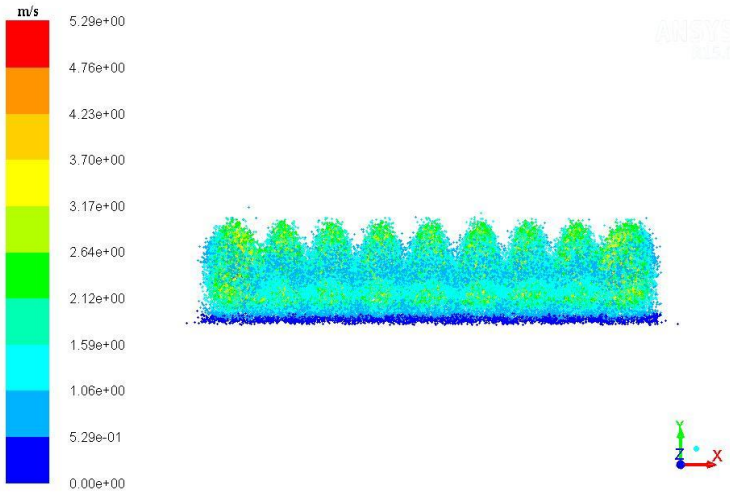

Figure 8. *Dust particle trajectory diagram (3 s)*

Dust particle size distribution diagrams at different heights at the same time after blasting

In the process of numerical simulation of dust, a disk area was established every 5 m in the vertical direction. By capturing the dust particles passing through every plane, the probability distribution diagrams of the discrete amount of average diameter of dust at different vertical heights were obtained. Through the interpolation fitting by tecplot

http://www.aloki.hu ● ISSN 1589 1623 (Print) ● ISSN 1785 0037 (Online)
DOI: http://dx.doi.org/10.15666/aeer/1705_1031310333

software, the probability distribution curve diagrams of dust particle size distribution at different heights were obtained. Through the analysis of each curve, it can be seen that at the 6th second (*Fig. 18*), the average diameter of the dust with a particle size of 200-300 μm was about 5-10 m. After the 25th second (*Figs. 19* and *20*), the settling velocity of the dust with a particle size of greater than 250 μm was very fast, and almost all of them had fallen to the ground. With the increase of vertical height of observation plane, the particle size of dust was becoming smaller and smaller, and the dust of large particle size can rapidly settle by its own gravity, but the dust of small particle size can suspend in the air for a long time under natural conditions. Due to the disturbance by air flow and the action of air resistance, the floating effect of the dust of large particle size decreased gradually. Some of the dust of large particle size settled by overcoming the buoyancy by its gravity, and the dust with a particle size of greater than 100 μm began to settle at a fast settling velocity with the increase of settling time. Almost all the dust with a particle size of about 250 μm fell to the ground after about 30 s, the dust with a particle size of 60-100 μm settled slowly, and the dust with a particle size of below 40 μm settled difficultly due to the strong disturbance by air flow.

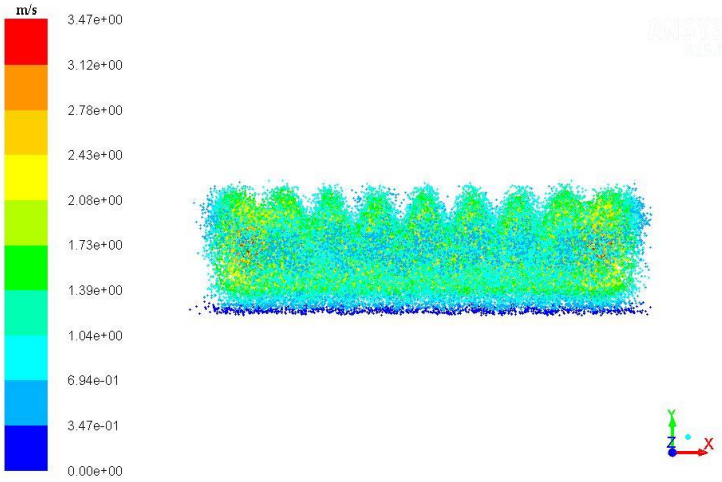

Figure 9. *Dust particle trajectory diagram (6 s)*

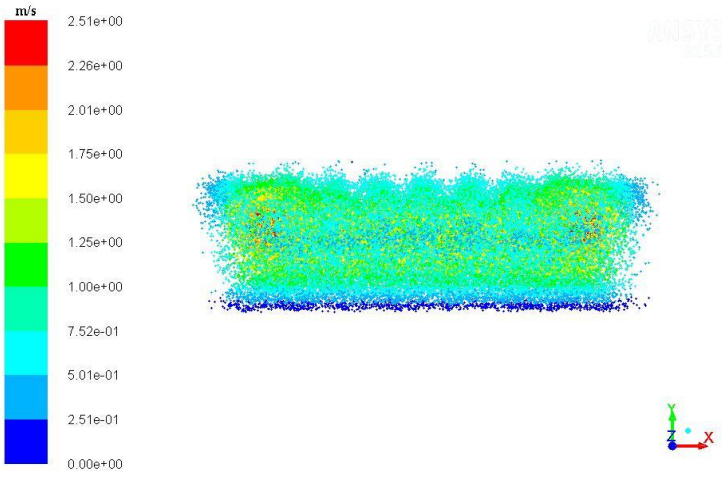

Figure 10. *Dust particle trajectory diagram (10 s)*

http://www.aloki.hu ● ISSN 1589 1623 (Print) ● ISSN 1785 0037 (Online)
DOI: http://dx.doi.org/10.15666/aeer/1705_1031310333

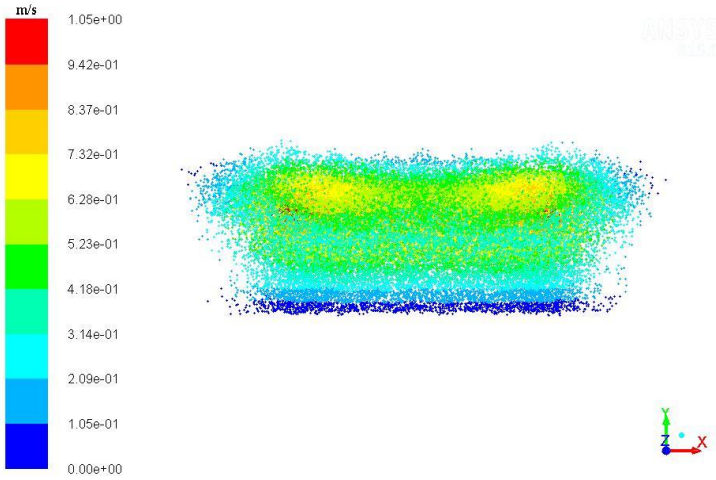

Figure 11. *Dust particle trajectory diagram (25 s)*

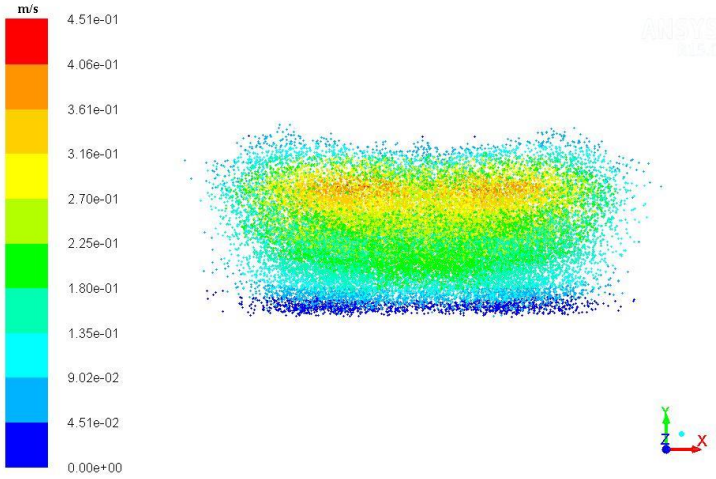

Figure 12. *Dust particle trajectory diagram (60 s)*

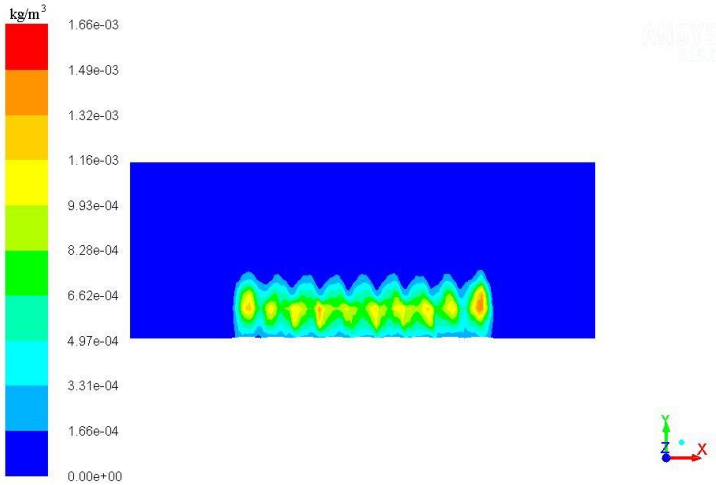

Figure 13. *Dust concentration diagram (3 s)*

http://www.aloki.hu ● ISSN 1589 1623 (Print) ● ISSN 1785 0037 (Online)
DOI: http://dx.doi.org/10.15666/aeer/1705_1031310333

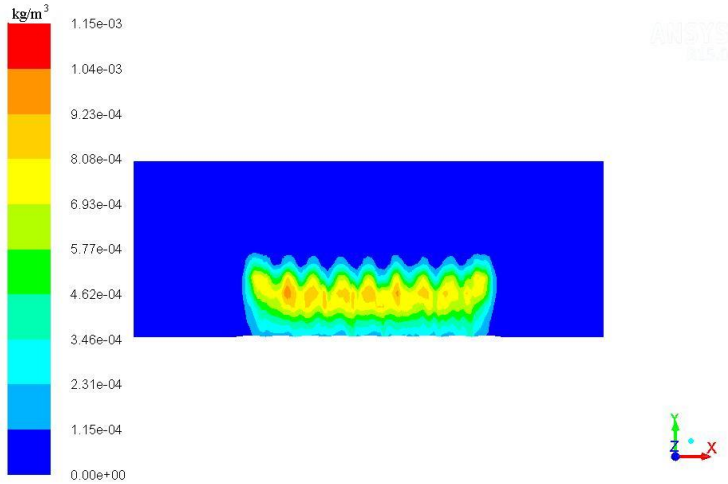

Figure 14. *Dust concentration diagram (6 s)*

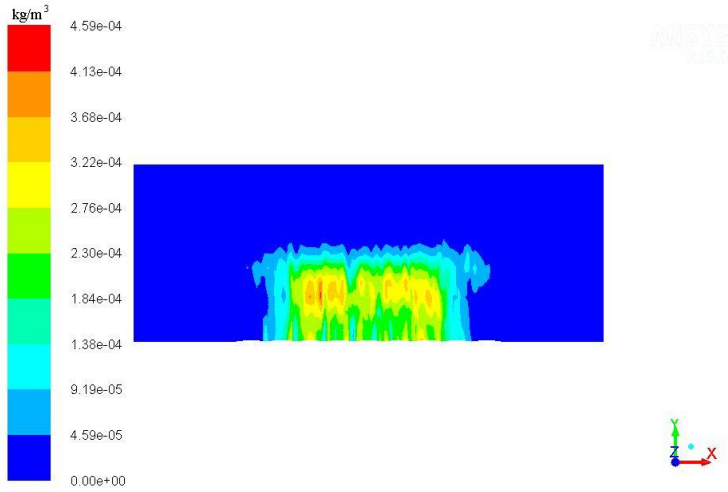

Figure 15. *Dust concentration diagram (25 s)*

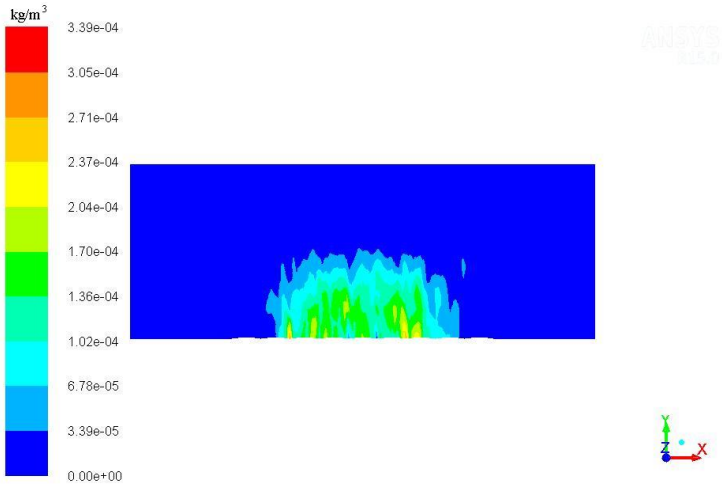

Figure 16. *Dust concentration diagram (60 s)*

http://www.aloki.hu ● ISSN 1589 1623 (Print) ● ISSN 1785 0037 (Online)
DOI: http://dx.doi.org/10.15666/aeer/1705_1031310333

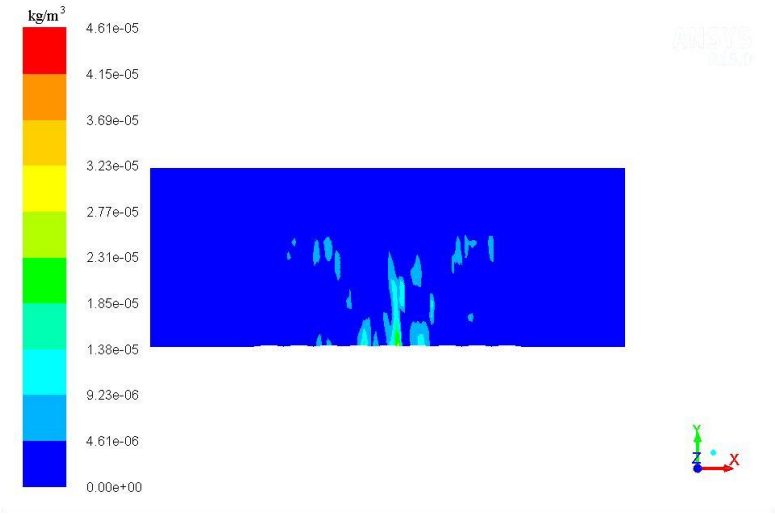

Figure 17. *Dust concentration diagram (360 s)*

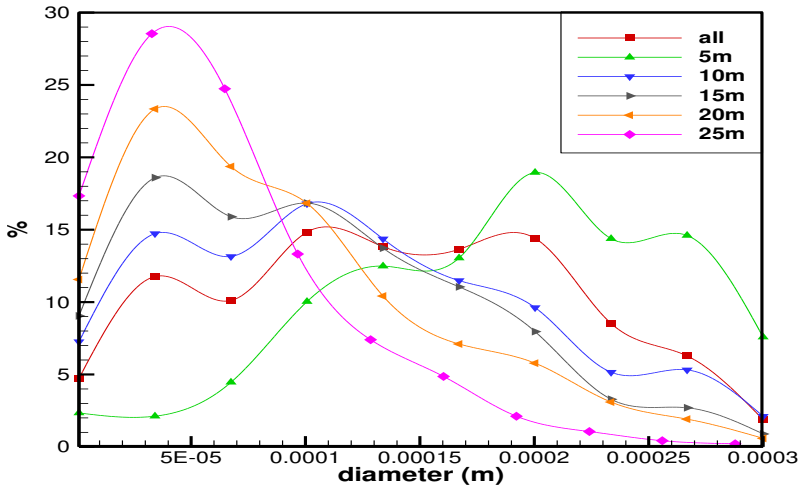

Figure 18. *Probability distribution diagram of the discrete amount of average diameter (6 s)*

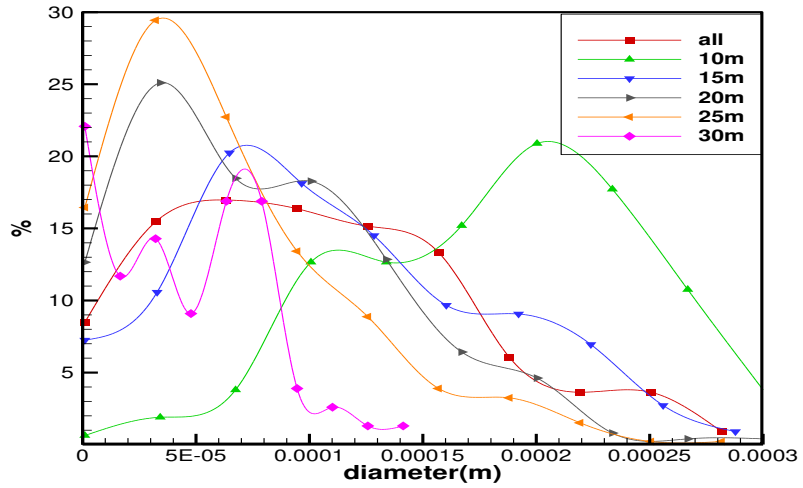

Figure 19. *Probability distribution diagram of the discrete amount of average diameter (25 s)*

http://www.aloki.hu ● ISSN 1589 1623 (Print) ● ISSN 1785 0037 (Online)
DOI: http://dx.doi.org/10.15666/aeer/1705_1031310333

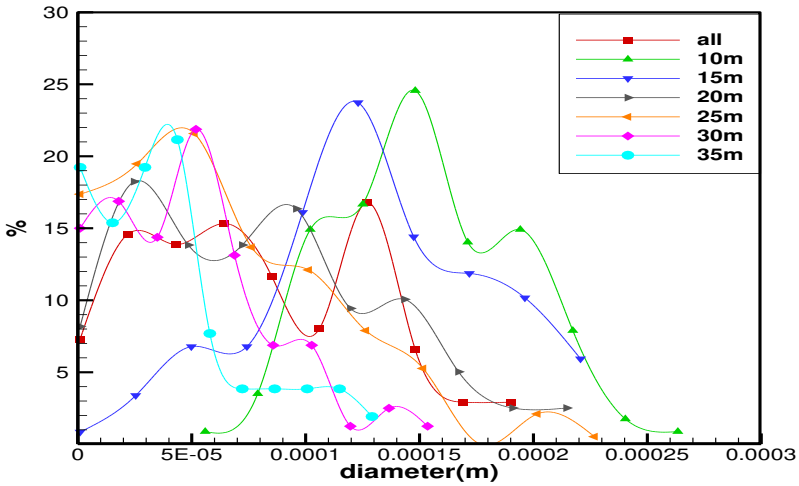

Figure 20. *Probability distribution diagram of the discrete amount of average diameter (60 s)*

Result verification

To verify the validity of the data, three test points were arranged at the blasting working face, and two direct reading dust testers were placed in each test point (the readings of the two testers were averaged). The dust concentration was measured at the 25th second (*Fig. 21*) and the 60th second (*Fig. 22*).

Figure 21. *Blowing dust after blasting (25 s)*

Figure 22. *Blowing dust after blasting (60 s)*

http://www.aloki.hu ● ISSN 1589 1623 (Print) ● ISSN 1785 0037 (Online)
DOI: http://dx.doi.org/10.15666/aeer/1705_1031310333

The test results are shown in *Tables 7* and *8*. In the 25 s after blasting, the average relative error of measured data and simulation data of three measuring points is 2.84%, 2.69% and 3.01%, both lower than 5%, in the 60 s after blasting, the average relative error of measured data and simulation data of three measuring points is 3.26%, 2.59% and 2.39% respectively, the relative error of measured data and simulation data of the test point 1, 2, 3 is under 5%, all show relatively reliable numerical simulation results and the reasonable model, The model can be used in subsequent studies to test the difficult law of blasting dust and its influencing factors.

Table 7. *Comparison of average dust concentration and simulated concentration in blasting working face (25 s)*

Height perpendicular to the ground	Measuring point 1			Measuring point 2			Measuring point 3		
	Measuring (mg/m^3)	Simulation (mg/m^3)	Error rate	Measuring (mg/m^3)	Simulation (mg/m^3)	Error rate	Measuring (mg/m^3)	Simulation (mg/m^3)	Error rate
5 m	225	231	2.67%	233	224	3.86%	221	228	3.17%
10 m	168	162	3.57%	171	165	3.51%	174	169	2.87%
15 m	371	378	2.16%	364	369	1.37%	359	353	1.67%
20 m	439	432	1.59%	428	433	1.17%	437	428	2.06%
25 m	231	241	4.32%	247	241	2.43%	242	251	3.72%
30 m	146	150	2.73%	158	152	3.80%	152	159	4.61%
Average relative error			2.84%			2.69%			3.01%

Table 8. *Comparison of average dust concentration and simulated concentration in blasting working face (60 s)*

Height perpendicular to the ground	Measuring point 1			Measuring point 2			Measuring point 3		
	Measuring (mg/m^3)	Simulation (mg/m^3)	Error rate	Measuring (mg/m^3)	Simulation (mg/m^3)	Error rate	Measuring (mg/m^3)	Simulation (mg/m^3)	Error rate
5 m	191	183	4.06%	188	190	1.06%	201	192	4.48%
10 m	181	187	3.31%	173	179	3.47%	185	176	4.86%
15 m	321	327	1.87%	325	317	2.46%	318	325	2.20%
20 m	174	167	4.02%	169	164	2.96%	177	172	2.82%
25 m	106	103	2.83%	105	107	1.90%	109	106	2.75%
30 m	85	82	3.52%	82	79	3.66%	78	80	2.56%
Average relative error			3.26%			2.59%			2.39%

Conclusions

(1) In this paper, a real time simulation of blasting dust pollution in open-pit mines was conducted through the numerical simulation and field test of dust. In the stage of impact movement of dust, a large amount of dust rushed into the atmospheric space instead of settling under the effect of inertia.

(2) Almost all the dust with a particle size of about 250 μm fell to the ground after about 30 s, and the dust with a particle size of 60-100 μm settled slowly, and the dust with a particle size of below 40 μm settled difficultly due to the strong disturbance by air flow.

Acknowledgements. Fund number 51704146, the project name Study on Dust Mesoscale Movement Characteristics and Dust Control Mechanism of Magnetized Spiral Pneumatic Mist Curtain in Fully Mechanized Heading Face Supported by National Natural Science Foundation of China.

http://www.aloki.hu ● ISSN 1589 1623 (Print) ● ISSN 1785 0037 (Online)
DOI: http://dx.doi.org/10.15666/aeer/1705_1031310333

REFERENCES

[1] Almstedt, A. E. (2003): Methods for multiphase computational fluid dynamics. – Chemical Engineering Journal 44(12): 39-152.
[2] Baxter, L. L., Smith, P. J. (1993): Turbulent dispersion of particles: the STP model. – Enemy and Fuels 7: 852-859
[3] Chen J., Wang, Y., Jiang, Z. (2013): Numerical simulation of blasting dust concentration distribution and diffusion regularities in stope. – Journal of China Coal Society 38(z1): 147-152.
[4] Fu, H., Liu, X. A (2017): Study on the impact of environmental education on individuals' behaviors concerning recycled water reuse. – Eurasia Journal of Mathematics Science and Technology Education 13(10): 6715-6724.
[5] Ghose, M. K., Majee, S. R. (2001): Air pollution caused by opencast mining and its abatement measures in India. – Environ Manag 63(3): 193-199.
[6] Guo, Y. (2006): Discussion on the application of the water-stem in the blasting operation. – SCI-Tech Information Development and Economy 16(11): 280-281.
[7] Jiang, L., Tao, T., Zhang, C., Jiang, H., Wang, J. (2017): Summary of the port shoreline resource evaluation based on triangular fuzzy analytic hierarchy process. – Polish Maritime Research 24(SI): 16-22.
[8] Jin, L. (2010): Mine Dust Prevention and Control Theory. – Science Publishing Company, Bejing.
[9] Jing, Z. (2007): Simulated study of the blasting smog-dust movement on account of particle system. – Journal of University of Science and Technology Beijing 2: 25-29.
[10] Jing, Z., Wan, S., Sun, J. (2007): Simulated study of the blasting smog-dust movement on account of particle system. – Journal of University of Science and Technology Beijing 29(2): 25-29.
[11] Lenart, A. S. (2017): Sphere-to-spheroid comparison - numerical analysis. – Polish Maritime Research 24(4): 4-9.
[12] Luo, Y., Shen, Z. (2006): Influence of borehole stemming on blasting effect. – Engineering Blasting 12(1): 16-18.
[13] Nongqwenga, N., Modi, A. T. (2017): Phosphorus and potassium quantity/intensity properties of selected South African soils (Kwazulu-Natal) and their correlation with selected soil parameters. – Applied Ecology and Environmental Research 15(3): 1-14.
[14] O'Rourke, P. J. (1981): Collective Droplets on Vaporizing Liquid Sprays. – University of Princeton, Princeton.
[15] Peng, W., Maleki, A., Rosen, M. A., Azarikhah, P. (2018): Optimization of a hybrid system for solar-wind-based water desalination by reverse osmosis: comparison of approaches. – Desalination 442: 16-31.
[16] Shen, Y., Zhao, N., Xia, M., Du, X. (2017): A deep q-learning network for ship stowage planning problem. – Polish Maritime Research 24(SI): 102-109.
[17] Wang, L., Wang, T., Liu, J., Wang, J. (2018): Correlation analysis of erectile dysfunction with lower urinary tract symptoms (LUTS) degree and clinical features in LUTS patients. – Iranian Journal of Public Health 47(5): 658-665.
[18] Yang, G., Li, H., Cheng, X. (1996): Mechanical analysis of blasting dust particles in movement. – Journal of Hebei Institute of Technology 18(4): 1-5.
[19] Yang, L., Yin, P., Li, K., Fan, H., Xue, Q., Li, X., Sun, L., Liu, Y. (2018): Seasonal dynamics of constitutive levels of phenolic components lead to alterations of antioxidant capacities in Acer truncatum leaves. – Arabian Journal of Chemistry 11(1): 14-25.
[20] Zamora Figueroa, A. C., Ramos Oropeza, J. R., Arias, M., Hernandez Valencia, I. (2017): Response of the microbial community to the biotreatment of a soil contaminated with a medium crude. – Revista Internacional De Contaminacion Ambiental 33(4): 629-639.
[21] Zhang, G., Li, L., Hao, C., Ren, J., Zhang, H., Jiao, J., Gao, L., Ding, S., Yao, S., Yao, W., Wu, W. (2016): Screening and preliminary verification of a phage display single-

http://www.aloki.hu ● ISSN 1589 1623 (Print) ● ISSN 1785 0037 (Online)
DOI: http://dx.doi.org/10.15666/aeer/1705_1031310333

chain antibody library against coal workers' pneumoconiosis. – Journal of Occupational and Environmental Medicine 58(12): 1264-1269.

[22] Zhang, N., Zhou, C., Xia, W., Nguyen, A. V. (2018): Volatilization of mercury in coal during conventional and microwave drying and its potential guidance for environmental protection. – Journal of Cleaner Production 176: 1-6.

http://www.aloki.hu ● ISSN 1589 1623 (Print) ● ISSN 1785 0037 (Online)
DOI: http://dx.doi.org/10.15666/aeer/1705_1031310333

SIMULATION STUDY ON THE INFLUENCE OF GREENING RATE OF URBAN RESIDENTIAL CLUSTERS ON THE DISTRIBUTION OF SUSPENDED PARTICULATE MATTERS

MA, X.* – ZHAO, J.

School of Architecture, Chang'an University, Xi'an 710064, China
(e-mail: 2232390994@qq.com)

**Corresponding author*
e-mail: maxina861005@126.com

(Received 27th Sep 2018; accepted 16th Jul 2019)

Abstract. Micro-climatic factors of landscape green space have provided dynamic conditions and thermal conditions for the distribution of suspended particulate matters. In this paper, the data of greening rate and micro-climatic factor of 88 residential areas were acquired, by means of field survey, spot test and CFD (Computation Fluid Dynamics) analog simulation. Through analysis of the previous relevant theoretical research and work, with the greening rate of residential clusters in Chinese Shanxi Province Xi'an as the research object, this study has reasonably set the value of the greening rate and built the physical models of the greening rate. In this study, the relationship among the various factors was obtained by analyzing the measured data. Meanwhile, CFD numerical models were verified, and the influence of the greening rate on wind speed, turbulence characteristics and concentration of suspended particulate matters were simulated. Finally, it concluded that the optimal cluster plan is 35% and 40% greening rate, while the cluster plan of 0% and 25% greening rate is inappropriate.
Keywords: *green area ratio, residential groups, CFD simulation, suspended particulate matter*

Introduction

Winston Churchill, British Prime Minister, once said that we shape our dwellings and afterward our dwellings shape. There is no doubt that modern urban construction will change the climate and living environment and directly affect the quality of life of residents (Periáñez, 2005). Urbanization has now become the main theme of the world's social and economic development. From a worldwide perspective, the world's urban population only accounted for 3% in 1800. After the industrial revolution, urbanization accelerated development and up to 2000, the world's urban population accounted for 55%, which is also the first time in human history that the urban population is larger than the rural population. In the face of the global urbanization development, the population changes of all countries show different pace. As shown in *Figure 1*, in the developed countries, due to the early start of urbanization and the high level of urbanization, the infrastructure of villages and towns is relatively perfect. With the increasing demand for urban environmental quality, the growth of urban population tends to be stable, and the phenomenon of population flowing back to villages and towns makes the cities of developed countries suburbanized; however, in the developing China, the urbanization starts late, the level is low and the development speed is very fast. Because of the abnormal development of the urban economy, the urban population grows rapidly. In order to meet the needs of the fast-growing population, the urban starts to expand construction blindly and unrestrictedly, which leads to the rapid decline of the environmental quality, serious traffic congestion and poor living conditions and other environmental and social problems. In China, the growth of urban population

http://www.aloki.hu ● ISSN 1589 1623 (Print) ● ISSN 1785 0037 (Online)
DOI: http://dx.doi.org/10.15666/aeer/1705_1033510356

shows a sharp trend. As shown in *Figure 2,* in 1950, China's population was 545 million, of which only 12% was 654 million. In 2000, there were 453 million people in urban areas. It is estimated that by 2025, 851 million people will live in cities (World population forecast by United Nations: Demographic Data of 2009, http://esa.un.org/upod/wup/dov_highights.htm).

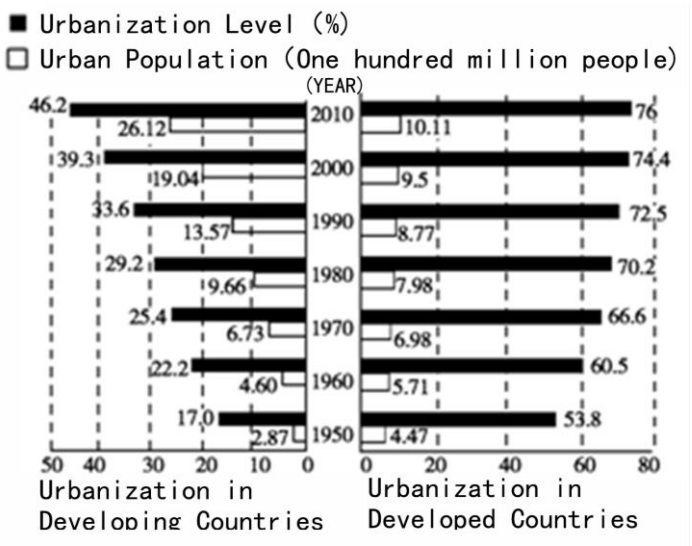

Figure 1. *World urbanization process*

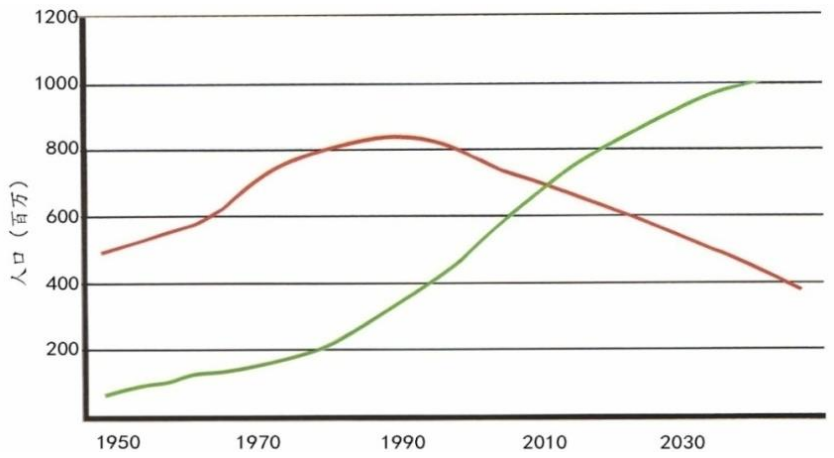

Figure 2. *The increase of rural population (red) and urban population (green) in China*

In the process of such rapid urbanization, not only the number of urban residents has increased, but also the urban land cover has been replaced by artificial paving materials from natural landforms. At the same time, the production and life of the city is maintained by the throughput of energy and raw materials (urban flow). In this process, it is inevitable to produce pollutant deposition in the form of energy and substance in the environment. These pollutants change the composition of urban atmospheric thermal structure and material form and affect urban climate and environment. Different forms and functions of urban areas form different local microclimates, which directly affect the quality of near-ground environment (*Fig. 3*). At present, the most concerned and

http://www.aloki.hu ● ISSN 1589 1623 (Print) ● ISSN 1785 0037 (Online)
DOI: http://dx.doi.org/10.15666/aeer/1705_1033510356

discussed phenomenon of urban environmental pollution is haze, which has the greatest impact on human life and production. The air quality is related to the concentration distribution of suspended particulate matter, which has been paid close attention by scholars, managers and builders in various fields and even ordinary residents. There have been many pollution incidents about air pollution all over the world, which are due to the serious impact and harm of gaseous pollutants on local people in foggy weather or solid pollutants in bad weather conditions. In recent years, a wide range of haze in China has seriously affected the health and normal life of residents, whose fundamental reason is the atmospheric environmental pollution caused by suspended particulate matter. A large number of studies have also shown that the concentration of atmospheric suspended particulate matter, especially small particle size, has a significant impact on the health of human and animal respiratory system and shows a significant positive correlation. Particularly, small granule matters are very easy to adsorb organic pollutants, acid oxides, heavy metals, viruses and bacteria in the air, which are suspended in the atmosphere for a long time. It is harmful to human body and other animals through large-scale wind transmission (Ding, 2011; Peng, 2002).

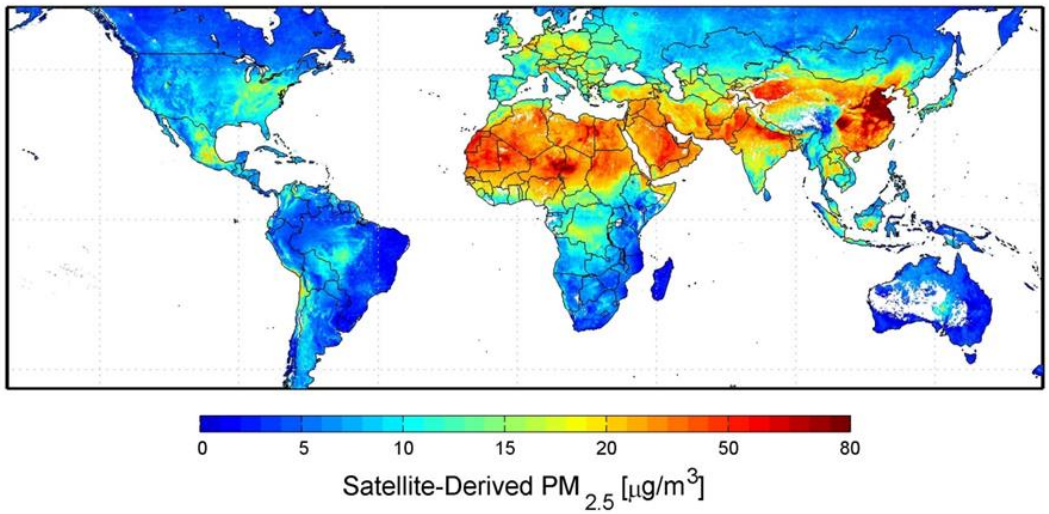

Figure 3. *Global air quality map released by NASA in September 2010*

Landscape garden is the most important place for urban activity and outdoor space in urban area, and the micro-climate changes in its spatial form affect the distribution of suspended particulate matters directly. *Figure 4* has shown the interactional relationship between climate and artificial environment. Climate acts on the environment where people live, people create an urban environment, which is better for living and production. However, with urban development and construction, urban spatial form conducts feedback to the atmospheric environment, where heat of the smooth and impervious underlying surface of the city conducts convection directly on the city surface due to lack of moisture and vegetation. The T thermal energy then rises and is transmitted to the atmosphere. Meanwhile, the nearby air temperature changes rapidly, enabling the city to be covered under the dry and warm lid. The difference between microclimate and the background climate occurs in certain areas of the city. In addition, under the influence of microclimate, a variety of special climatic phenomena, such as heat island and haze appearing in some areas and they differ from natural climate.

http://www.aloki.hu ● ISSN 1589 1623 (Print) ● ISSN 1785 0037 (Online)
DOI: http://dx.doi.org/10.15666/aeer/1705_1033510356

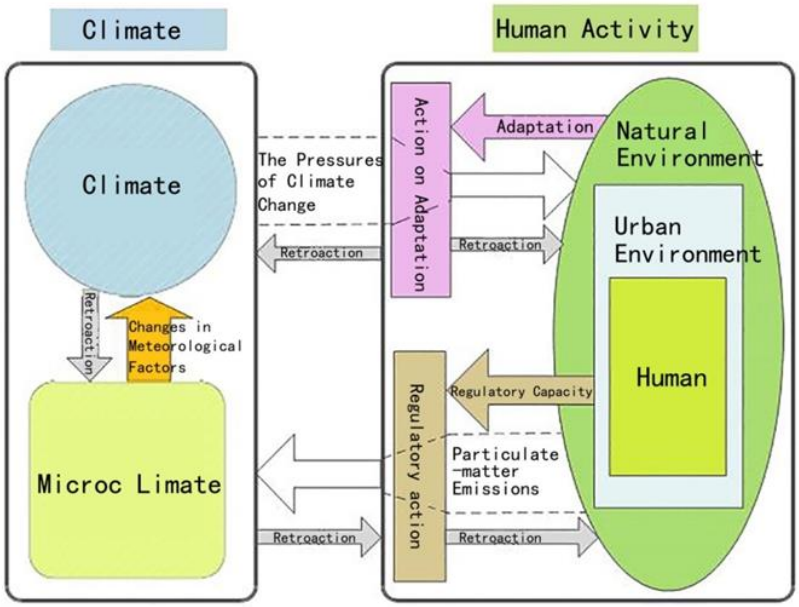

Figure 4. *Interaction among microclimate, climate and artificial environment (Dai Tianxing, 2006)*

According to aerodynamic equivalent diameter, air pollution particulate matters can be classified into TSP (≤ 100 μm), PM10 ≤ 10 μm) and PM2.5 (≤ 2.5 μm), etc., where the particulate matters with the grain size of less than 10μm are known as inhalable particulate matters. Since they closely relate to human health, they have raised extensive attention (Zhang, 2015). *Figure 5* shows data comparison of major air pollutants in Xi'an from 2007 to 2017, indicating that the concentration of inhalable particulate matters is far higher than SO_2 and CO_2, and the pollution is especially obvious in winter. Therefore, the inhalable particulate matters have become the major air pollutants, which cannot be ignored.

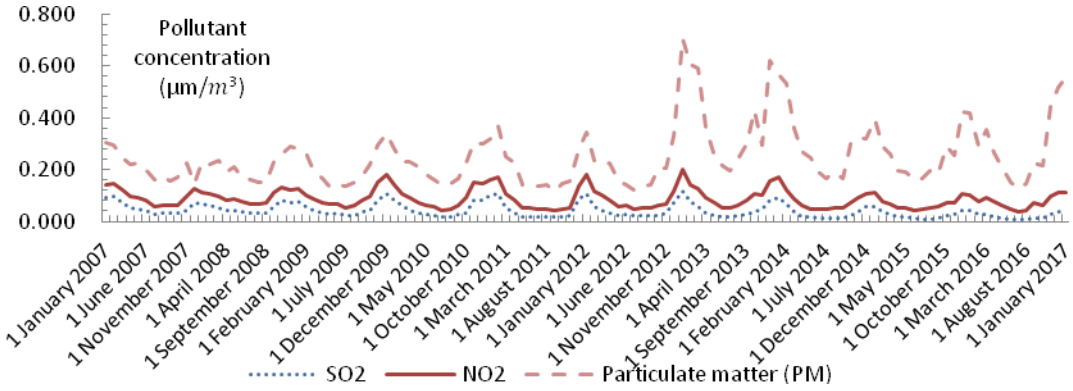

Figure 5. *Comparison of monthly mean concentration of air pollutants from 2007 to 2017 made by Xi'an Meteorological Bureau*

The concentration of ground pollutants is the major research object of this paper. This index mainly targets at the pollution of suspended particulate matters in people's

http://www.aloki.hu ● ISSN 1589 1623 (Print) ● ISSN 1785 0037 (Online)
DOI: http://dx.doi.org/10.15666/aeer/1705_1033510356

daily life. This is because human activities are mainly outdoor, while the outdoor ground pollutants directly harm human body. This index can be obtained via either air pollution level or field test. This paper conducted comparison of the PM2.5 concentration of the rigid pavement and green space in the Dependent's Area of Chang'an University, Xiaozhai Commercial District, Xi'an. This study collected data at 11:00 a.m. On each day from January 30, 2015 to March 23, 2015, which was obtained by the Meteorological Bureau. Moreover, what have been published by Xi'an Municipal Environmental Protection Bureau indicate that the law of the two are almost the same. However, the measured values are obviously greater than the published meteorological data. According to the *Technical Guidelines for Fugitive Emission Monitoring of Air Pollutants HJ/T55-2000* and *Ground Meteorological Planning* issued in 2004: the data of wind environment and pollutants are usually obtained through tests on the meteorological tower in suburb area, which is higher than 10 m. While the values in this paper were acquired at the human respiration altitude of 1.5 m away from the ground, as the near-surface concentration values, for which *Figure 6* shows the obvious difference between the two. Therefore, the practical research value of the measured values is greater (*Fig. 7*).

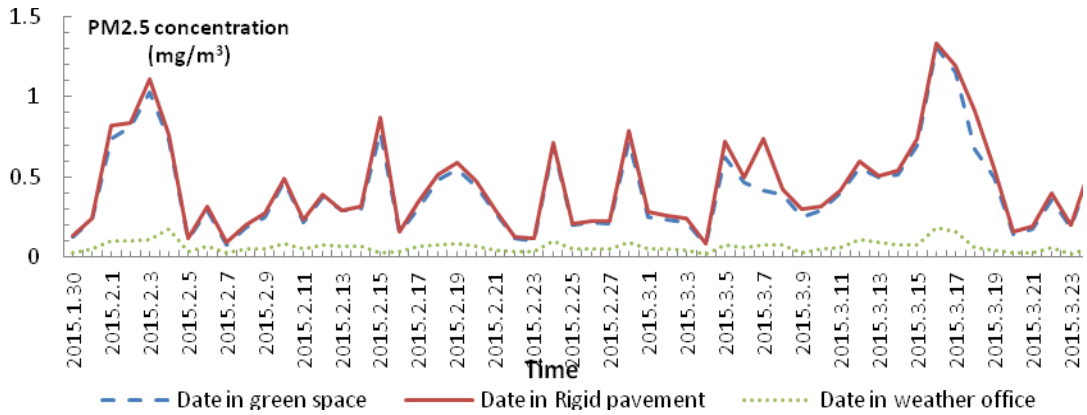

Figure 6. *Comparison of the measured data and published meteorological data of PM2.5 from January to March 2015*

Figure 7. *The near-surface test equipment 1.5 m away from the ground and meteorological observation iron tower*

http://www.aloki.hu ● ISSN 1589 1623 (Print) ● ISSN 1785 0037 (Online)
DOI: http://dx.doi.org/10.15666/aeer/1705_1033510356

In landscape garden, the dust settling effect of plants mainly results from the absorption and settling of particulate matters in the air by blocking the wind speed enabled by plant leaves. Buccolieri et al. (Nikolopoulou et al., 2001) found through wind tunnel test and CFD simulation that arbors on urban streets can improve wind environment and settle pollutants. However, due to different thickness of leaves and density of branches and leaves of various vegetation in greenbelts, dust retention differs per plant species It was found by Meir et al. (2000) through research that dust retention of trees and shrubs is far greater than that of lawns. In park green space and roadside green space, dust retention of shrubs per unit leaf area is higher than that of arbors. Many researches have proved that arbor leaves mainly retain large-grained flying dust, while shrubs set dust materially since they can better prevent pollution caused by the near-ground particulate matters (Zhou, 2001). In some researches, the relationship between the form of greenbelts and concentration of particulate matters is discussed from the perspective of the spatial arrangement of greenbelts. Feng et al. (2014) and Feng and Chu (2017) investigated and compared the urban green space, and concluded that pollutant dispersion presents positive relationship with green land area, and different green land area of residential areas, especially different trees and shrubs majorly contribute to dust retention of residential areas. There have been quite a few domestic and foreign scholars (Zhu et al., 2002; Che and Song, 2002; Su et al., 2002; Chai et al., 2002; Fanger and Toftum, 2002) with dedicated researches on the elimination rate of greenbelts of different structures towards particulate matters, with a consistent finding: under the same community structure, the effect of PM2.5 reduction by greenbelts is better than that of PM10 reduction.

The above research shows that suspended particulate matters are closely related to greening rate and characteristics of plant leaves due to the effect of microclimate. Moreover, dust retention of shrubs per unit leaf area is the best among other plant species. Therefore, by analyzing microclimate characteristics in this paper, shrubs were selected as the vegetation for research, and the design threshold of greening rate in residential clusters was preset reasonably, to study the distribution of PM2.5 of inhalable suspended particulate matters.

Materials and methods

Establishment of physical models

In this paper, residential quarters with 1,000-3,000 residents or 300-1,000 households in Xi'an were screened according to the study on the characteristics of urban residential clusters. Based on the scale characteristics of residential clusters, visit and investigation were carried out on 88 selected residential clusters in Xi'an, and the greening rate of the various community clusters were sorted out and analyzed. *Figure 8* indicates that the greening rate of the residential living clusters in Xi'an is mainly around the ranges of 30%, 35% and 40%.

It is expressly stipulated in the *Code of Urban Residential Areas Planning and Design GB50180-93 (2002)* that for the construction of new residential areas, the greening rate shall not be lower than 30%, and the greening rate shall not be lower than 25% for the reconstruction of old residential areas. It is stated by Article 14 in *Regulations of Xi'an Municipality on the Administration of Urban Greening* executed on June 1, 2014 that the greening rate of new residential areas shall not be lower than 35%, while the greening rate of residential areas under old city reconstruction shall be

http://www.aloki.hu ● ISSN 1589 1623 (Print) ● ISSN 1785 0037 (Online)
DOI: http://dx.doi.org/10.15666/aeer/1705_1033510356

5% lower in comparison, namely 30%. When building the models, the assumed greening rate of 25%, 30%, 35%, 40% and 0% shall be adopted combining the relevant standards and the practical cognitions of Xi'an to enhance the comparability of simulated results, as shown in *Figure 9*.

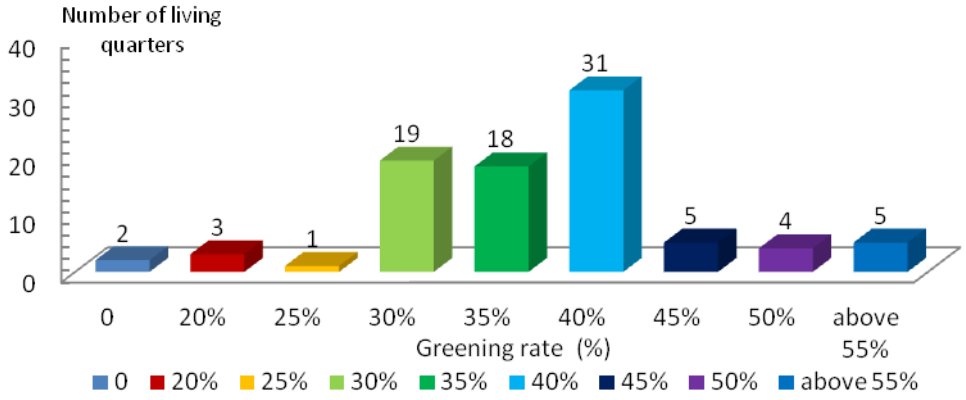

Figure 8. *Statistics of the greening rate in Xi'an through field survey*

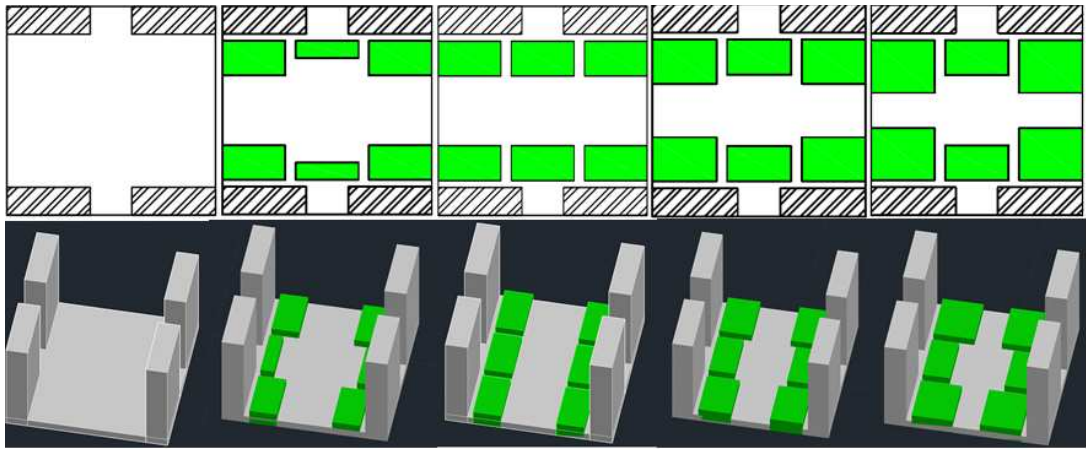

Figure 9. *Plane and aerial view of different greening rate models*

CFD numerical calculation model

According to the residential cluster space studied in this paper, Autodesk Simulation CFD was selected for the outdoor microclimate research thereof, given the fact that Autodesk Simulation CFD has high intelligence, strong automatic mesh generation technology, powerful analysis functions, high degree of humanization of post processing, and can conduct comparative analysis, etc. Its main functions are simulated analysis of fluid flow, heat transfer and movement (Hu, 2002). In this paper, the distribution of suspended particulate matters and flow field in the residential cluster space of different building height were simulated elaborately, with the powerful automatic mesh partitioning technology of the most common and mature turbulence model as well as Autodesk Simulation CFD, through the discretization and solution of differential equation.

http://www.aloki.hu ● ISSN 1589 1623 (Print) ● ISSN 1785 0037 (Online)
DOI: http://dx.doi.org/10.15666/aeer/1705_1033510356

Standard* $k-\varepsilon$ *turbulence model

In the study on urban outdoor environment, the most frequently used model is the standard $\mathbf{k}-\boldsymbol{\varepsilon}$ turbulence model. Such model focus on the turbulent dissipation rate and turbulence function. Suppose that both the inside and outside of the flow field are turbulence, the viscosity between molecules are ignored, and the standard model $\mathbf{k}-\boldsymbol{\varepsilon}$ is built and functioning effectively (Hu, 2002; MOHURD, 2010). In this paper, this model was taken as the research model. As a semi-rational formula, its equation is as follows:

$$\frac{\partial k}{\partial t}+\frac{\partial}{\partial t_j}(u_j k)=\frac{\partial}{\partial t_j}\left[\left(v_0+\frac{v_t}{\sigma_k}\right)\frac{\partial k}{\partial x_j}\right]+G-\varepsilon \quad \text{(Eq.1)}$$

$$\frac{\partial \varepsilon}{\partial t}+\frac{\partial}{\partial t_j}(u_j \varepsilon) \quad =\frac{\partial}{\partial t_j}\left[\left(v_0+\frac{v_t}{\sigma_\varepsilon}\right)\frac{\partial \varepsilon}{\partial x_j}\right]+\frac{C_1 \varepsilon}{k}G-C_2\frac{\varepsilon^2}{k} \quad \text{(Eq.2)}$$

where k—turbulence energy; ε—turbulent energy dissipation rate; σ_k、σ_ε、$C_1$and C_2 —empirical constant; G—generation of turbulent energy, expressed as:

$$G=v_t\left(\frac{\partial u_i}{\partial x_j}+\frac{\partial u_j}{\partial x_t}\right)\frac{\partial u_i}{\partial x_j} \quad \text{(Eq.3)}$$

Discretization and solution of differential equation

The study in this paper has adopted the Finite Volume Method (FVM), with which, the entire computation field was first divided into several control volumes for mesh processing. Then, the differential equation was set for discretization processing with related schemes. Finally, the boundary conditions and initial conditions were supplemented, unknown parameters of all points of the space were solved, and a satisfactory result was finally obtained through repeated iteration. FVM has high computational efficiency, as it can indicate accurately integral conservation when the meshes are not very precise (Ma et al., 2017).

Mesh size and division

In the process of numerical simulation, mesh division of the models played an important part affecting the calculation of simulation values. To reduce the impact of the mesh boundary on its central area, and reduce the calculation of excessive loss due to oversize mesh, fineness of the mesh partition unit for the models of the residential areas was adjusted to around 0.3. In large blocks, Uniform Mesh was adopted, while Non-uniform Mesh was brought in small blocks, providing possibilities for depicting more precise flow fields.

Initial value of PM2.5 concentration field

The annual mean PM2.5 concentration of Xi'an in 2014 was higher than the secondary national ambient air quality standard by 1.17 times (Ma et al., 2017). The 24-

http://www.aloki.hu ● ISSN 1589 1623 (Print) ● ISSN 1785 0037 (Online)
DOI: http://dx.doi.org/10.15666/aeer/1705_1033510356

h mean concentration of the 95th percentile was 194, higher than the secondary standard of the daily mean value of national ambient air quality standards by 1.59 times (Pape et al., 2014). The daily mean value of the monitoring points was 11-506 mg/m^3, and the maximum surpassing times was 5.75 times higher *(Code for planning and design of urban residential areas GB50180-2002, 2002)*. Since urban buildings have high density, the emission sources of single suspended particulate pollutants lead to low emissions. However, if they are in great quantity, emission sources can be considered as the spread mode of non-point source pollution (Feng and Wang, 2004). In this paper, only the background concentration of PM2.5 is considered, instead of the automobile exhaust or the influence of other complex surroundings. In the United States and Western Europe, the background concentration is about 3-5 μg/m^3, and 5 μg/m^3 (Sun et al., 2010; Peng Jiang, 2002; Salamanca et al., 2009) in Australia. There is still no public data available for China. According to the new *Ambient Air Quality Standard* published by Chinese government in March 2012, the value of 150 μg/m^3 executed previously is still reserved as the daily mean concentration limit of PM10, the daily mean concentration of PM2.5–75 μg/m^3 was set according to the proportion of PM2.5 to PM10–50% (Horemans, 2007; Zhao and Liu, 2001).

Experimental test

Summer experiment

The experiment was conducted from January 16 to 17, 2015. In this group of experiments, 88 residential areas of Xi'an were selected with two measurement points for each residential area. The central square, open place and the space between two buildings were respectively selected as measurement points. For each measurement point, there were 1056 data. The theoretical analysis has showed that the air humidity of the greenbelts increases through plant transpiration, and wind environment of some areas could be improved through photosynthesis. Therefore, concentration of PM2.5 would decrease along with the increase of greening rate. The data was separated for summarization. The single factor greening rate was taken as the major cause for comparison with the concentration of PM2.5, and a trend chart was drawn accordingly. The analysis of the design factors and the data of PM2.5 concentration of the 88 residential areas has showed that the greening rate is negatively related to PM2.5 concentration (*Figs. 10* and *11*).

Winter experiment

Selection of comparison group of green space rate

The comparison group compared the influence of green space rate on PM2.5 diffusion distribution under the same heat island and volume rate. As shown in *Table 1,* the locations are Jinduicheng Garden District and Shengshi Chang'an, which have similar volume ratios of 2.8 and 2.55 respectively and are located in Chang'an District in the northern suburbs of Xi'an. Chang'an District surrounds Xi'an City from the south and west and Qinling Mountains in the south. The intensity of heat island is weak and the concentration of PM2.5 is at a low level. The difference of green rate between the two districts is obvious of which the green space rate of Jinduicheng Garden District is only 18%, and that of Shengshi Chang'an is 65%. The location and detailed test points of the two districts are shown in *Figures 12* and *13* and *Table 2*.

http://www.aloki.hu ● ISSN 1589 1623 (Print) ● ISSN 1785 0037 (Online)
DOI: http://dx.doi.org/10.15666/aeer/1705_1033510356

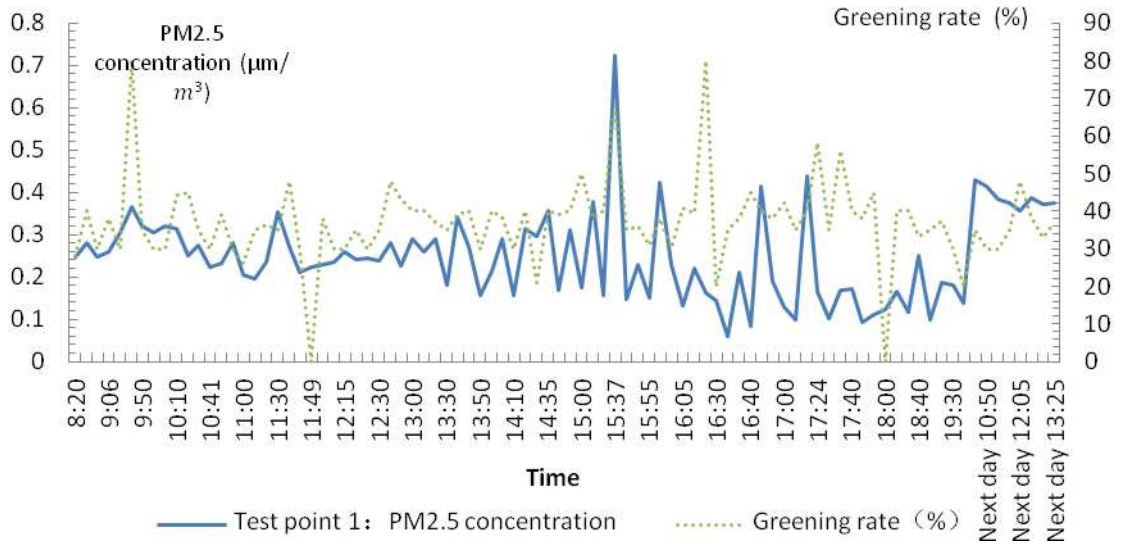

Figure 10. *Comparison of the changes between open place greening rate and PM2.5 concentration*

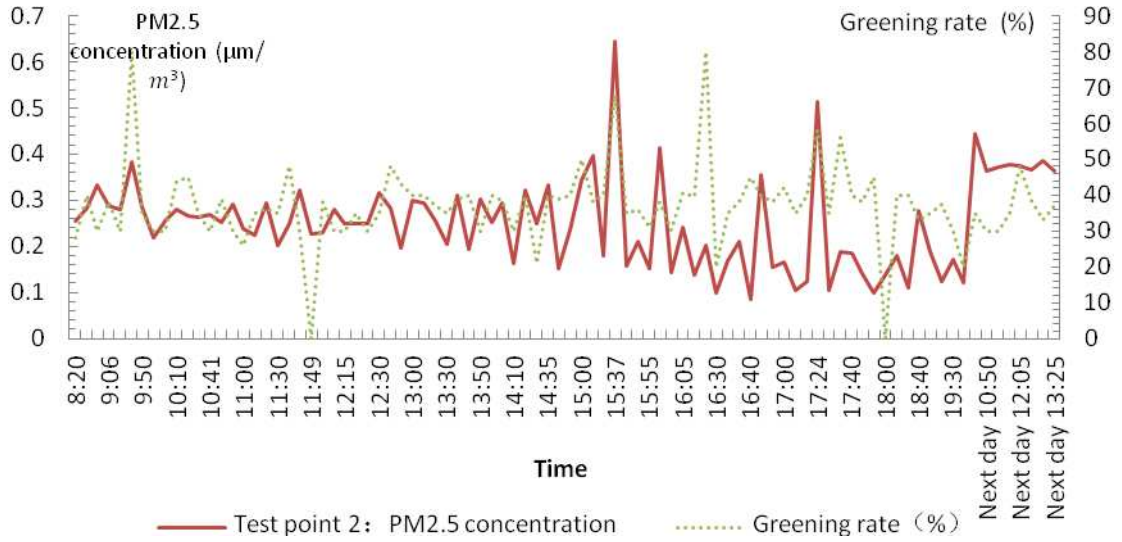

Figure 11. *Comparison of the changes between the greening rate of the space between two buildings and PM2.5 concentration*

Table 1. *Comparison survey of grouping factors*

Name	Location	Volume rate	Green space rate
Jinduicheng Garden District	Chang'an	2.8	18%
Shengshi Chang'an	Chang'an	2.55	65%

http://www.aloki.hu ● ISSN 1589 1623 (Print) ● ISSN 1785 0037 (Online)
DOI: http://dx.doi.org/10.15666/aeer/1705_1033510356

Table 2. *Maps of green space comparison groups*

Distrct name	Test point	Test point satellite map	Test point photo	Test point perspective
Jinduicheng District	Test point 1	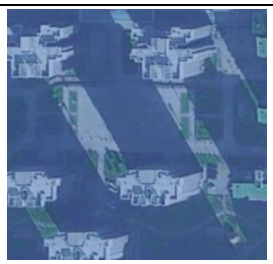		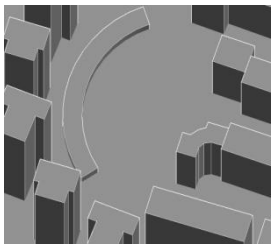
	Test point 2	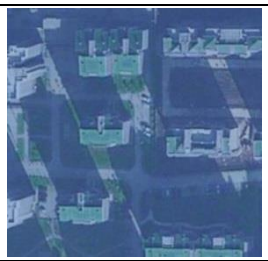		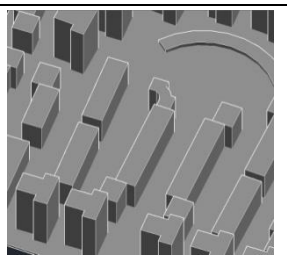
Shengshi Chang'an	Test point 1			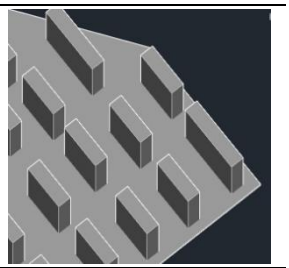
	Test point 2			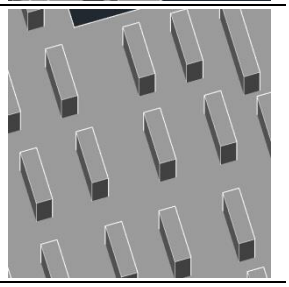

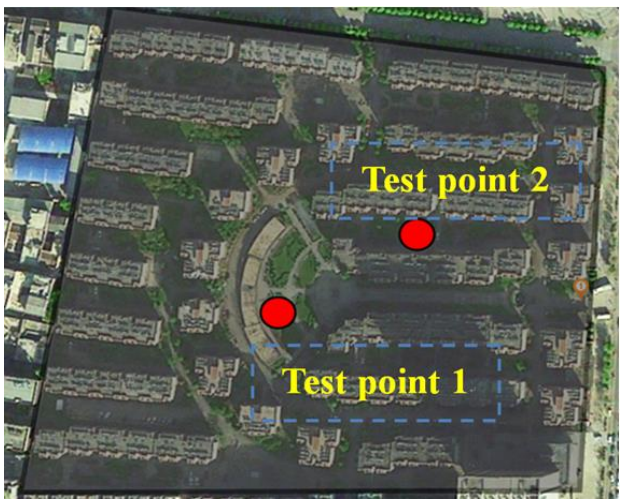

Figure 12. *Distribution of test points in Jinduicheng District*

http://www.aloki.hu ● ISSN 1589 1623 (Print) ● ISSN 1785 0037 (Online)
DOI: http://dx.doi.org/10.15666/aeer/1705_1033510356

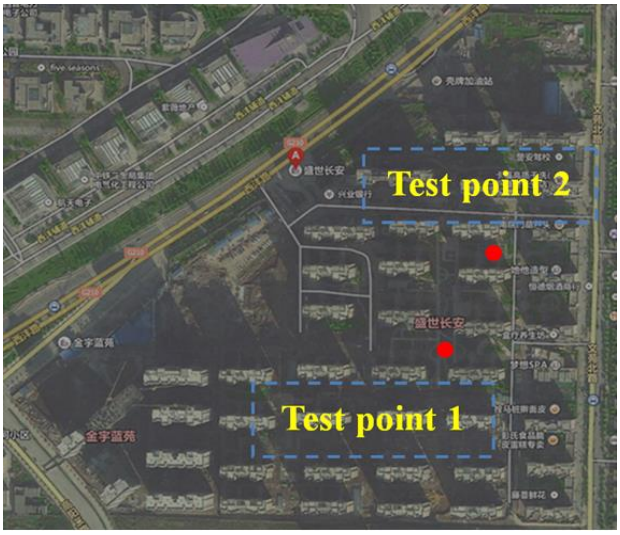

Figure 13. *Distribution of test points of Shengshi Chang'an*

Test of the influence of green space rate on PM2.5 concentration

During the experiment, every test point in each district is tested every hour. The test time is from 10:00 on January 15, 2015 to 10:00 on January 16, 2015. Detailed PM2.5 concentration analysis of the two districts is as follows:

It can be seen from *Figures 14* and 15 that the concentration of PM2.5 in Shengshi Chang'an is basically lower than that in Jinduicheng District, but during the period from 8:00 to 17:00 in the daytime, the construction site near Shengshi Chang'an has affected the high concentration of particulate matter in the district. The two residential areas are located in Chang'an District, where the intensity of heat island is weak and the volume ratio is basically the same. It can be seen that the difference of PM2.5 concentration between the two residential areas is caused by the difference of green space rate. Plants can alleviate PM2.5 pollution due to their retention on particulate matter. From the experimental data, it can be seen that green space can reduce PM2.5 concentration to a certain extent. As shown in *Figures 16* and *17*, as a whole, because the test point 1 is located in the open central square and the test point 2 is located in the hard ground between the two buildings where the ventilation is not smooth. Because the greening around the test point 1 is higher than that around the test point 2 which causes higher PM2.5 concentration of the test point 2. The data at 5:00 in Shengshi Chang'an are obviously higher, which may be caused by the passing cars.

To define the microclimate factors affecting PM2.5 concentration, this paper has introduced linear-regression analysis, to study the relationship among temperature, humidity, wind speed and PM2.5, by following 3 processes. Firstly, choose analyze → regression → linear, and activate the dialog boxes popping up in sequence. To follow that, there shall be further analysis. Finally, review the output; make the regression equation and inspection. The final analysis results are shown by *Table 3,* where, 3.126 is the constant term, while the coefficient of temperature, humidity, wind speed and PM2.5 concentration are respectively -2.198, 0.153, 0.045 and 0.190.

Since residuals are always assumed to obey normal distribution in the models, *Table 3* demonstrates whether the actual residuals after regression fit this assumption. Besides, it shows that the degree of influence imposed by various influencing factors on

http://www.aloki.hu ● ISSN 1589 1623 (Print) ● ISSN 1785 0037 (Online)
DOI: http://dx.doi.org/10.15666/aeer/1705_1033510356

PM2.5 concentration from high to low respectively: wind speed (m/s) > temperature (°C) > humidity (%RH), where wind speed exerts the greatest influence on PM2.5 concentration, while humidity exerts the lowest influence. Since it is difficult to subside PM2.5, gas pollution can be deemed as in the atmosphere, while wind speed is just a direct performance indicator of gas flow. Upon actual measurement, the most relevant micro-climatic factor of the distribution of PM2.5 concentration shall be wind environmental impact. Due to the difficult of PM2.5 reduction, increase of humidity has no significant effect on its settlement.

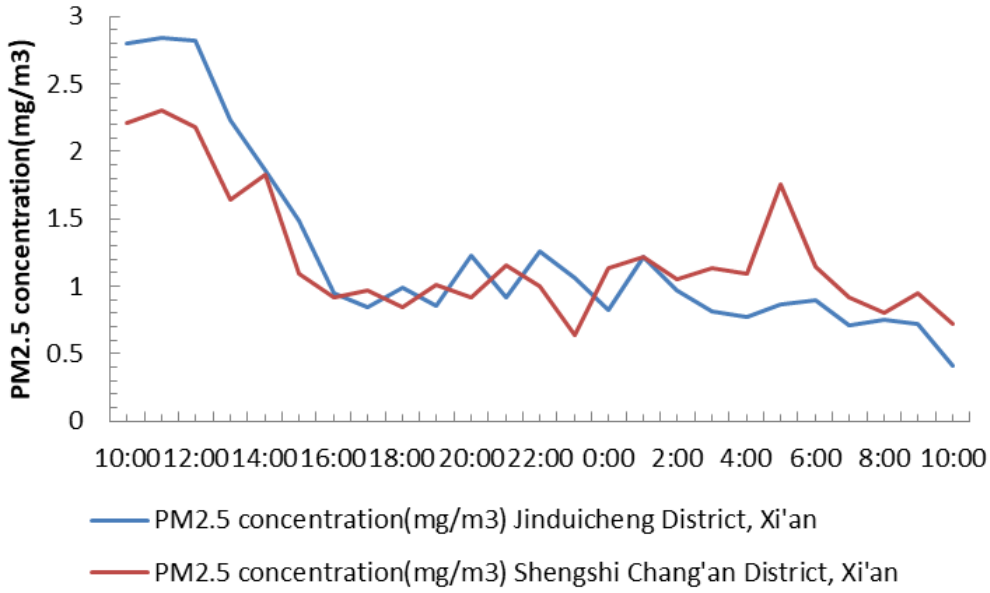

Figure 14. *Comparison of PM2.5 concentration data at test point 1*

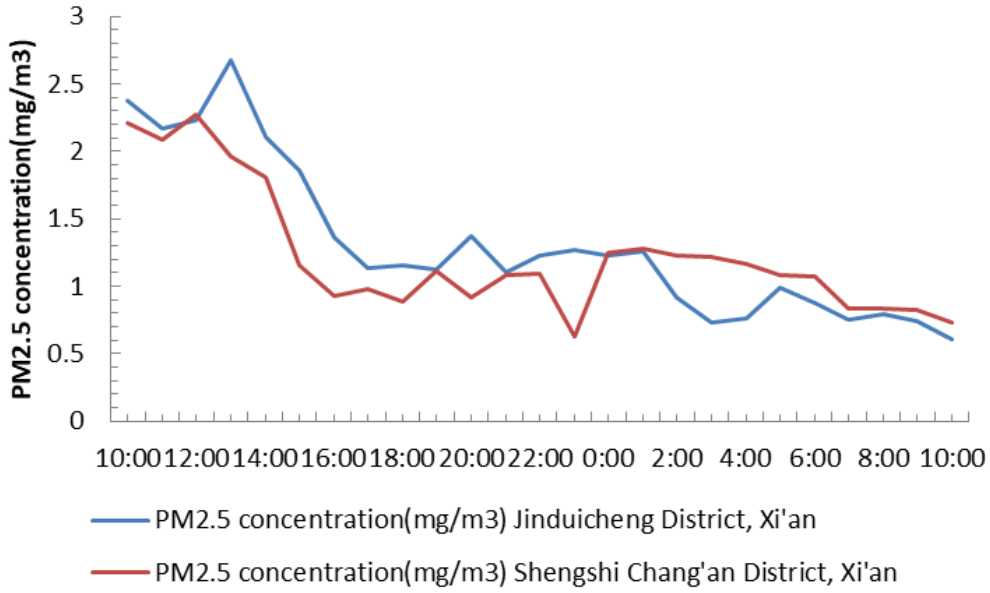

Figure 15. *Comparison of PM2.5 concentration data at test point 2*

http://www.aloki.hu ● ISSN 1589 1623 (Print) ● ISSN 1785 0037 (Online)
DOI: http://dx.doi.org/10.15666/aeer/1705_1033510356

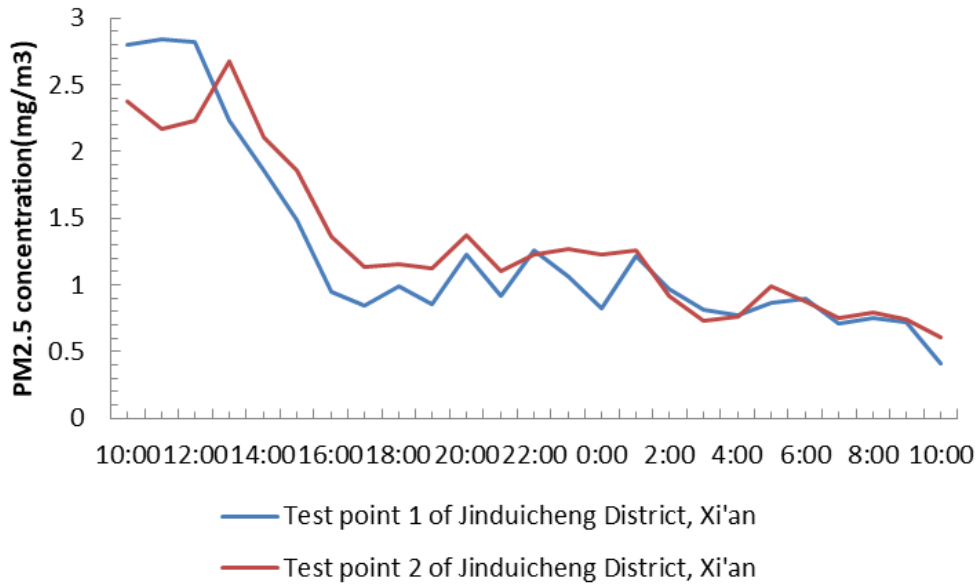

Figure 16. *Comparison of PM2.5 concentration between test point 1 and test point 2 in Jinduicheng District*

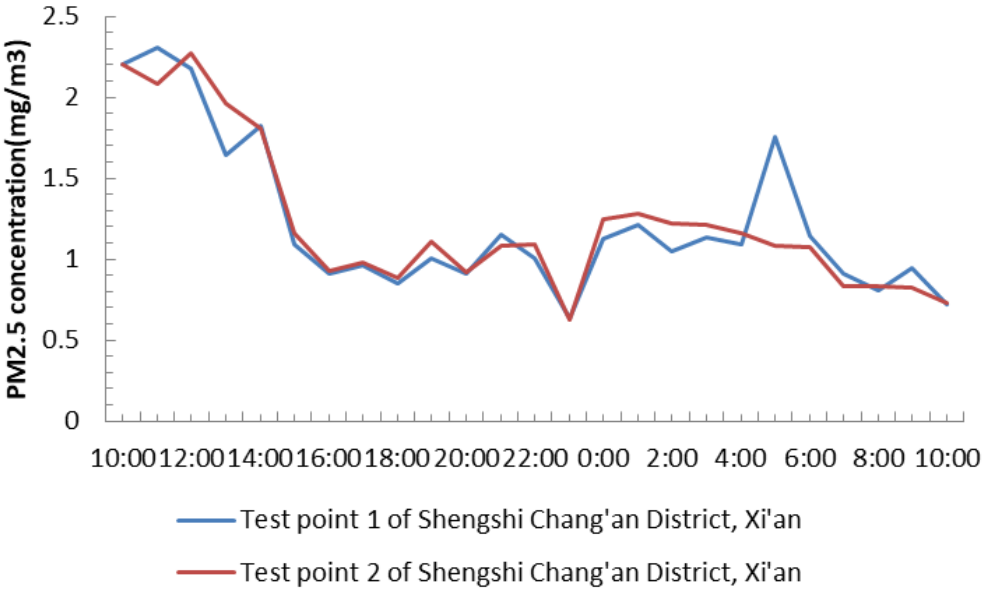

Figure 17. *Comparison of PM2.5 concentration between Shengshi Chang'an test point 1 and test point 2*

Results

Study in this paper conducted thermal pollution coupling calculation simulation of the greening rate of residential clusters in Xi'an, by building the physical model and CFD numerical calculation model. Furthermore, this paper has analyzed the effect of micro-climatic factors on improving the concentration distribution of suspended particulate matters through the influence of greening rate. After measurement

http://www.aloki.hu ● ISSN 1589 1623 (Print) ● ISSN 1785 0037 (Online)
DOI: http://dx.doi.org/10.15666/aeer/1705_1033510356

verification, micro-climatic factors of wind environment are found mostly related to PM2.5 concentration (Li et al., 2017; Tian et al., 2017; Liu et al., 2017). Therefore, during the simulation, comparative analysis was only made on wind speed, turbulence characteristics, PM2.5 concentration and the greening rate.

Table 3. *Coefficient of regression*

Coefficient[a]					
Model	**Unstandardized coefficient**		**Standardized coefficient**	**t**	**Sig.**
	B	**Standard error**	**Trial version**		
(Constant)	-2.198	.139		-15.809	.000
Temperature	.153	.010	.546	15.135	.000
Humidity	.045	.002	.804	22.275	.000
Wind speed	.190	.058	.112	3.288	.001

[a]Dependent variable: PM2.5 concentration

Wind speed

Figure 18 shows the planar wind speed distribution of different green land rates at an altitude of 1.5 m, under the condition of perpendicular to the northeast wind. *Figure 19* shows the comparison on the wind data of the gap between two green land parcels at an altitude of 1.5 m from north to south, at the fluid outlet on the west of the residential clusters. The comparison shows that wind speed in urban residential cluster space is negatively related to the greening rate. However, as the greening rate grows, its impact on wind speed weakens gradually. This is mainly because when the green land area is too large, airflow generated through transpiration of the plants can adjust the surrounding breeze or wind environment, and wind speed will not slow down linearly (Zamora Figueroa et al., 2017; Kmita et al., 2018). When the green land area is large enough, improvement made by the plants on the wind environment of the internal cluster space would be enhanced, and wind speed increases.

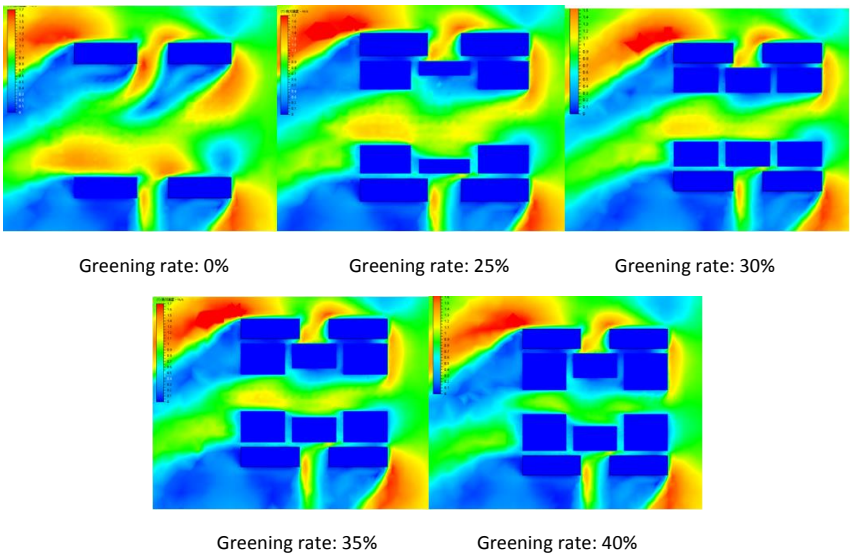

Figure 18. *Planar fluid spread of clusters with different greening rates at an altitude of 1.5 m*

http://www.aloki.hu ● ISSN 1589 1623 (Print) ● ISSN 1785 0037 (Online)
DOI: http://dx.doi.org/10.15666/aeer/1705_1033510356

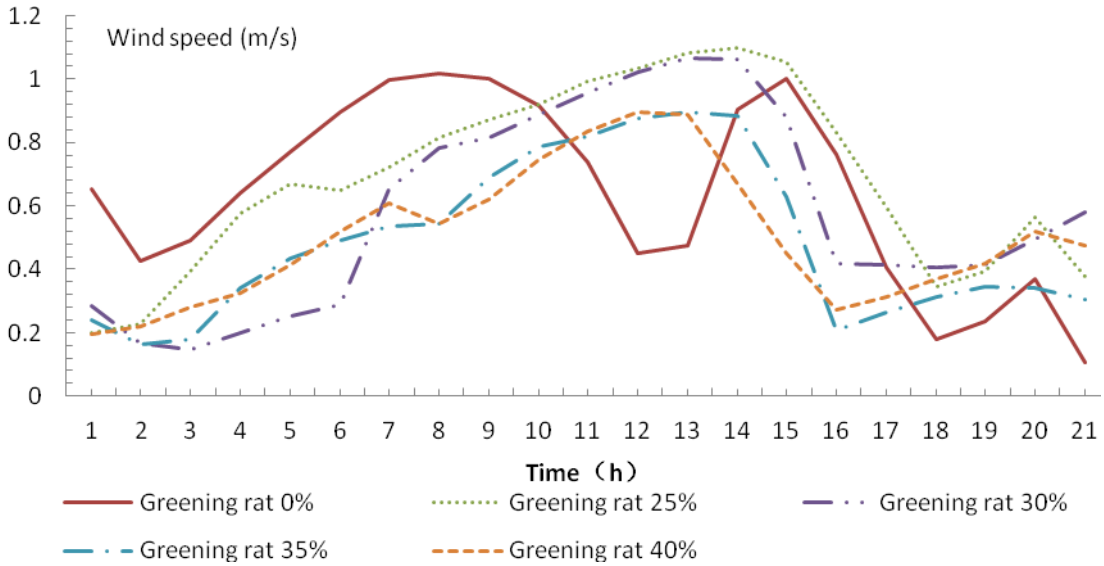

Figure 19. *Distribution of wind speed on the west-side air outlet in the cluster space with different greening rates at an altitude of 1.5 m*

Turbulence characteristics

Figure 20 shows a section view of each cluster on the west-side air outlet, indicating the influence of cluster space with different greening rate of fluid. When under the condition that the buildings are unchanged, it is clear that the degree of changes made by different green land area towards internal fluid of the space vary, and it is especially significant on the surface of the buildings.

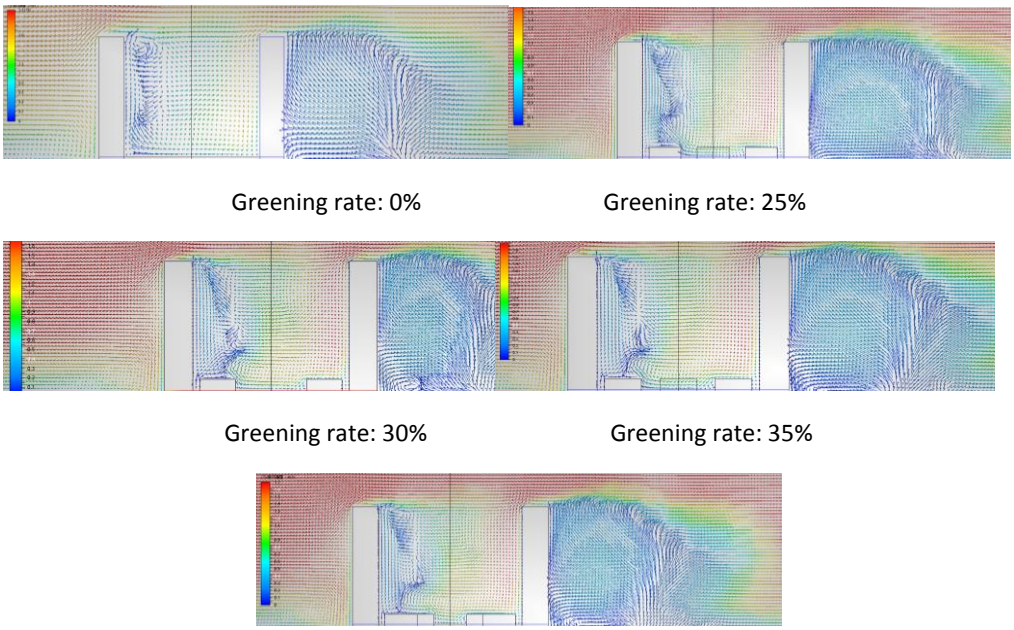

Figure 20. *Section view of wind velocity vector on the west-side outlet of fluid for clusters with different greening rates*

http://www.aloki.hu ● ISSN 1589 1623 (Print) ● ISSN 1785 0037 (Online)
DOI: http://dx.doi.org/10.15666/aeer/1705_1033510356

Spread of pollutants in cluster space

Figures 21 and *22* show the planar fluid spread distribution of different greening rates at an altitude of 1.5 m and the concentration distribution of fine particulate matters. As demonstrated, the concentration data of particulate matters from north to south in the gap between two west-side green land parcels of planar clusters at an altitude of 1.5 m was selected for comparison that is shown in *Figure 22*.

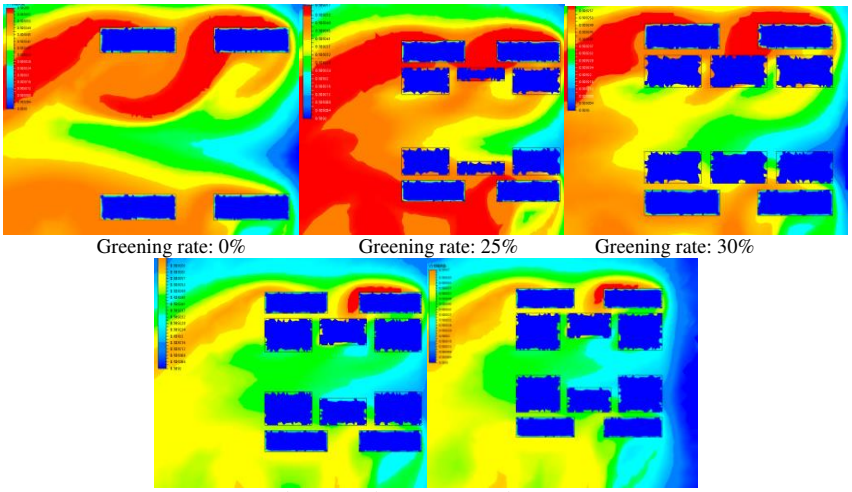

Figure 21. *Distribution of fine particulate matters of clusters with different greening rates*

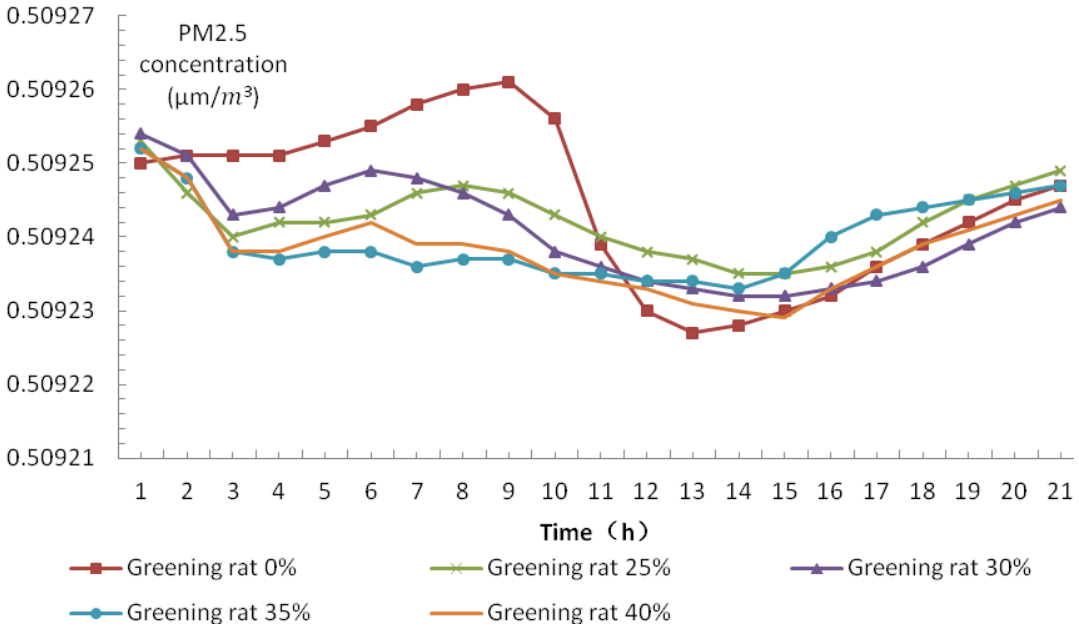

Figure 22. *Distribution of fine particulate matters on west-side air outlet in the cluster space with different greening rates at an altitude of 1.5 m*

The comparison discovers that the concentration of particulate matters in the space of urban residential clusters is negatively related to the greening rate, which is especially

http://www.aloki.hu ● ISSN 1589 1623 (Print) ● ISSN 1785 0037 (Online)
DOI: http://dx.doi.org/10.15666/aeer/1705_1033510356

significant in open space. However, a node appears. When a greening rate reaches a certain height, the concentration will decrease with the elevation of greenbelts, tending to be stable. This means that when the green land area reaches a certain height, excessively blocking and influencing field wind environment, wind speed will be largely reduced, dynamic factors for the spread of suspended particulate matters will wear off gradually, while the decrease of concentration of suspended particulate matters will also wear off gradually till reach the steady state.

Discussion

In the current residential group development process, in order to pursue the maximum unit area yield of commercial real estate, various types of residential areas are trying to approach or break through the volume ratio index and building density index defined by the regulatory plan to the maximum extent. Under the premise of determining the total building amount, the overall cluster layout cannot effectively combine local regional characteristics, climatic conditions and other factors, ignoring that the overall layout of residential areas will have a negative impact on the distribution of suspended particulate matter in the city.

The micro-climate environment has an important impact on the design of urban residential groups. Masatoshi M. Yoshino classifies the local climate dimensions in Japan, which can be concluded that the environmental factors of climate usually include temperature, solar radiation intensity, wind speed, humidity, etc. As shown in *Figure 23,* microclimate influences the surrounding environment and climate through the coupling of various climatic factors. Under the same solar radiation condition, influenced by the roughness of underlying surface, the greater the roughness of underlying surface, the more it can promote the flow and heat transfer of wind. By understanding the interaction principle between microclimate factors and urban underlying surface, we can find the characteristic factors of microclimate environment of residential groups (Chauhan et al., 2012).

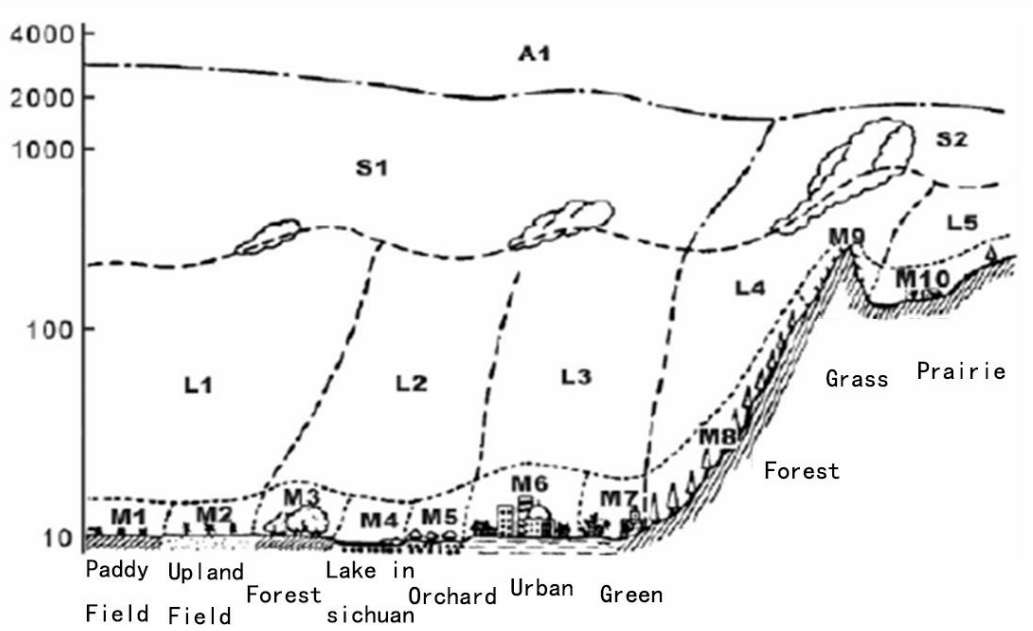

Figure 23. *Climate range map (Chauhan et al., 2012)*

http://www.aloki.hu ● ISSN 1589 1623 (Print) ● ISSN 1785 0037 (Online)
DOI: http://dx.doi.org/10.15666/aeer/1705_1033510356

Based on the research and analysis of the influence factors of microclimate, it is concluded that the microclimate factors which have great influence on the spatial form of urban residential groups are as follows: 1. Air circulation is reflected in the impact of the layout of buildings and buildings on microclimate. 2. Solar radiation and biological cooling are reflected in the change of microclimate caused by the absorption of heat radiation by greening vegetation communities. Vegetation can not only consume a lot of heat energy through transpiration in summer with intense sunshine radiation, but also increase the reflectivity of solar radiation by tree crowns. At the same time, plants can convert solar energy into biological energy, which reduces the fluctuation range of urban air layer. 3. Sun blocking effect refers to the use of buildings and trees, etc to shield the solar radiation, so as to reduce the absorption of solar radiation on the urban surface, so it will produce the climatic effect of reducing the environmental temperature in the shadows that appear in the shield (Sun et al., 2013); 4. Surface reflectance and temperature are reflected in the use of building surface materials and the impact of landscape paving materials on the temperature of microclimate 5. Evaporation and humidity; First of all, humidity is an important factor affecting natural ecological climate differences such as clouds, rain, fog and so on and is also an important factor affecting human comfort. In urban residential groups, this can increase and decrease air humidity through evaporation of underlying surfaces with different water seepage rates to achieve “passive” cooling (Sun et al., 2013). Many factors around residential group space influence the generation of microclimate, as shown in *Table 4*.

Table 4. *Signature characteristics of microclimate influencing factors and residential group composition factors*

Correlation factors	Signature characteristics	Effect on microclimate
Space shape	Plane form and elevation form	Air circulation
Green space	Greening Area, tree species	Wind speed reduction
Shaded condition	Buildings, trees	Direct radiation heating
Topographic roughness	Building distribution, average height, orientation and volume; extent of spatial openness	Scattering radiation warming
Surface reflectance	Building and ground material	Radiation warming
Evaporation of underlying surface	Green space and water body	Decalescence

The research in this paper was taken as a new method and new thought to conduct quantitative analysis and predict the microclimate with the greening rate of urban residential clusters, based on the spread of suspended particulate matters, further advancing the ecologicalization and scientification of the landscape architecture discipline. The findings of this paper have provided application value for the construction of similar areas. The following perceptions are summarized:

(1) Indication factors of this paper were set by combining the specific regional characteristics of Xi’an city. Therefore, in the future researches of other cities, such as Guanzhong, or even cities of lower temperature on average, the corresponding index parameters can be adjusted combining regional and cultural characteristics.

(2) Since spatial arrangement of urban greenbelts can be viewed from the plane and vertical plane perspectives, near ground microclimate is related to the greening

http://www.aloki.hu ● ISSN 1589 1623 (Print) ● ISSN 1785 0037 (Online)
DOI: http://dx.doi.org/10.15666/aeer/1705_1033510356

structure, quantity of greenbelts, spatial form of greenbelts and landscape pattern, etc., there are still factors in need of exploration in a further way.

(3) To certain extent, meteorological simulation software has relatively larger mesh calculation scale. Therefore, when studying micro-climatic factors, CFD is more suitable for the purpose of numerical simulation.

Conclusion

The increase of urban greenbelts and the improvement of urban underlying surfaces can realize the temperature reduction. On one hand, a great amount of greening volume can reduce the concentration of suspended particulate matters by alleviating heat island effect. On the other hand, greenbelts can greatly purify and retain particulate matters, and the wider range of greenbelts, the more effective.

In the space of residential clusters, different greening rates have been obtained through CFD simulation: concentration of particulate matters in the space of residential clusters is negatively related to the greening rate overall, and is especially significant in open space. However, a node appears. When the greening rate exceeds 40%, the degree of the concentration reduction with the elevation of greenbelts decreases, with the tendency to be stable. By making comprehensive analysis on the preferences of sectional turbulence characteristics and preferences of pollutant concentration of the cluster examples, this study has come to the conclusion that the optimal plan of greening rate is the cluster plan with the greening rate of 35% and 40%. The plan with the greening rate of 30% is optional, the plans with the greening rate of 0% and 25% are inappropriate, as shown in *Figure 24*.

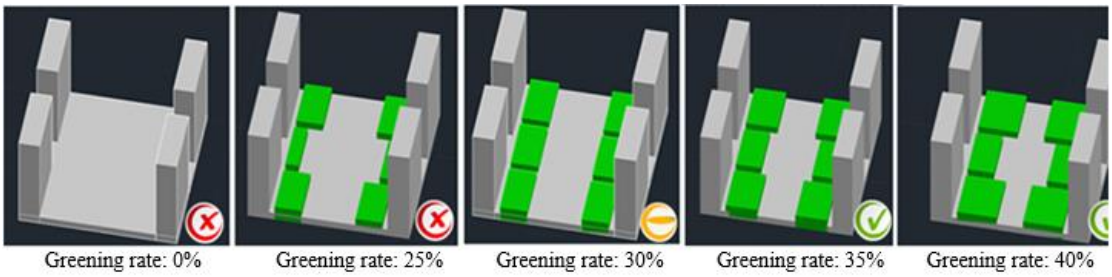

Figure 24. *Judgement on the sections of particulate matter concentration with different greening rates*

Acknowledgements. This paper is supported by The Project Supported by Natural Science Basic Research Plan in Shaanxi Province of China (Program No. 2019JQ-567) & Natural Science Foundation of China (NSFC): Influence Mechanism and Control of Urban Space Constitution on the Distribution of Suspended Particulate Matters (Program No. 51678058) & The Project Supported by Social Science Basic Research Plan in Shaanxi Province of China (Program No. 2018S18).

REFERENCES

[1] Chai, Y., Zhu, N., Han, H. (2002): Dust retention effect of urban greening species – take Harbin for example. – Chinese Journal of Applied Ecology 9: 1121-1126.

http://www.aloki.hu ● ISSN 1589 1623 (Print) ● ISSN 1785 0037 (Online)
DOI: http://dx.doi.org/10.15666/aeer/1705_1033510356

[2] Chauhan O S, Kader U S A, Vaidya P, et al. Dispersal and sink pathways of suspended particulate matter from the orographically enhanced SWM regime of the SE Arabian Sea[J]. International Journal of Remote Sensing, 2012, 33(14):4393-4407.
[3] Che, S., Song, Y. (2002): Analysis of the landscape pattern of Shanghai Municipal Park green space. – Journal of Shanghai Jiaotong University (Agricultural Sciences) 4: 322.
[4] Cheng, X., Hu, N., Cui, G., et al. (2004): Numerical study of pollutant dispersion in urban area. – Urban Environment and Urban Ecology 17(4): 1-4.
[5] Dai, T. (2006): Urban Environmental Ecology. – China Building Materials Press, Beijing.
[6] Ding T P, Gao J F, Tian S H, et al. Silicon isotopic composition of dissolved silicon and suspended particulate matter in the Yellow River, China, with implications for the global silicon cycle[J]. Geochimica Et Cosmochimica Acta, 2011, 75(21):6672-6689.
[7] Fanger, P. O., Toftum, J. (2002): Extension of the PMV model to non-air-conditioned buildings in warm climates. – Energy and Buildings 34(6): 533-536.
[8] Feng, X., Chu, Y. (2017): Study of the local microclimate effect of urban greenbelts based on aerodynamics simulation. – Chinese Landscape Architecture 2: 29-34.
[9] Feng, X., Gao, K., Zhong, S. (2014): Study of the influence of green layout of urban greenbelts on microclimate of some areas based on GRAPES numerical simulation. – South Architecture 3: 10-16.
[10] Feng, X., Wang, S. (2004): Model study of urban architectural ecological layout. – Proceedings of 2004 annual Meeting of Urban and Rural Planning: Urban Ecological Planning, pp. 525-529.
[11] Horemans B. Assessment of the water soluble ionic species of suspended particulate matter, collected at a coastal spot, De Haan, Belgium[J]. Journal of Neurophysiology, 2007, 76(3):1439-56.
[12] Hu, S. (2002): Three dimensional transient gas release of gas source diffusion of. – Science and Technology of Labour Protection 3(20): 28-30.
[13] Jasinski, R. (2017): Problems of the starting and operating of hydraulic components and systems in low ambient temperature (Part V). Methods ensuring correct start-up of hydraulic components of ship's onboard devices in low ambient temperatures. – Polish Maritime Research 24(4): 47-56.
[14] Kmita, A., Fischer, C., Hodor, K., Holtzer, M., Roczniak, A. (2017): Thermal decomposition of foundry resins: a determination of organic products by thermogravimetry-gas chromatography-mass spectrometry (Tg-Gc-Ms). – Arabian Journal of Chemistry 11(3): 380-387.
[15] Li, D., Wang, L., Peng, W., Ge, S., Li, N., Furuta, Y. (2017): Chemical structure of hemicellulosic polymers isolated from bamboo bio-composite during mold pressing. Polymer Composites 38(9): 2009-2015.
[16] Liu, Y., Li, T., Guo, L., Zhang, R., Feng, X., Liu, K. (2017): The mediating role of sleep quality on the relationship between perceived stress and depression among the elderly in urban communities: a cross-sectional study. – Public Health 149: 21-27.
[17] Ma, X., Zhao, J., Guo, P. (2017): Influence of the plane form of courtyard-type residential clusters on the spread of PM2.5. – Journal of Architecture and Civil Engineering 34(4): 120-126.
[18] Meir, P., Grace, J., Miranda, A. C. (2000): Photographic method to measure the vertical distribution of leaf area density in forests. – Agricultural and Forest Meteorology 102(2): 105-111.
[19] Ministry of Housing and Urban-Rural Development of the people's Republic of China (MOHURD) (2002): Code for Planning and Design of Urban Residential Areas. – GB50180-2002.
[20] Ministry of Housing and Urban-Rural Development of the people's Republic of China (MOHURD) (2010): Design Standard for Energy Efficiency of Residential Buildings in Severe Cold and Cold Zones. – JGJ 26-2010.

http://www.aloki.hu ● ISSN 1589 1623 (Print) ● ISSN 1785 0037 (Online)
DOI: http://dx.doi.org/10.15666/aeer/1705_1033510356

[21] Nikolopoulou, M., Baker, N., Steemers, K. (2001): Thermal comfort in outdoor urban spaces: understanding the human parameter. – Solar Energy 70(3): 227-235.
[22] Pape P L, Morin G, Jouvin D, et al. Zinc Speciation in the Suspended Particulate Matter of an Urban River (Orge, France): Influence of Seasonality and Urbanization Gradient[J]. Environmental Science & Technology, 2014, 48(20):11901-9.
[23] Peng, X., Jiang, J. (2002): Development of urban air pollutant diffusion simulation system. – High Altitude Meteorology 21(2): 139-144.
[24] Periáñez R. Modelling the transport of suspended particulate matter by the Rhone River plume (France). Implications for pollutant dispersion.[J]. Environmental Pollution, 2005, 133(2):351-364.
[25] Safaei-Ghomi, J., Enayat-Mehri, N., Eshteghal, F. (2018): 4-(4 -Diamino-Di-Phenyl)-Sulfone Supported On Hollow Magnetic Mesoporous Fe3O4@Sio2 Nps: As a Reusable and Efficient Catalyst for the Synthesis of Ethyl 2-Amino-5, 10-Dihydro-5, 10-Dioxo-4-Phenyl-4H Benzo Chromene-3-Carboxylates. – Journal of Saudi Chemical Society 22(4): 485-495.
[26] Salamanca, F., Martili, A., Tewari, M. et al. (2009): A study of the urban boundary layer using different urban parameterisation and high-resolution urban canopy parameters with WRF.– Journal of Applied Meteorology and Climatology 48: 484-501.
[27] Su, Z., Liu, Y., Peng, Q. (2002): Research of the dust retention effect of different greenbelt types in cities. – Arid Environmental Monitoring 3: 162-163.
[28] Sun J, Khelifa A, Zheng X, et al. A laboratory study on the kinetics of the formation of oil-suspended particulate matter aggregates using the NIST-1941b sediment.[J]. Marine Pollution Bulletin, 2010, 60(10):1701-1707.
[29] Sun J, Zhao D, Zhao C, et al. Investigation of the kinetics of oil ‐ suspended particulate matter aggregation[J]. Marine Pollution Bulletin, 2013, 76(1-2):250-257.
[30] Tian, A. L., Li, G. X., Elsheikha, H. M., Gardner, D. S., Zhang, X. Y., Dong, W., Yang, X. P., Luo, Y. Y., Li, H. L., Cong, W., Zhu, X. Q. (2017): Seroepidemiology of Toxoplasma gondii infection in patients with liver disease in eastern China. – Epidemiology and Infection 145(11): 2296-2302.
[31] Wahi, N., Bhatia, A. K., Bhadauria, S. (2018): Impact of Protozoan vahlkampfia sp on the growth of algae Chlorella vulgaris Glamtr. – Journal of Environmental Biology 39(1): 109-115.
[32] Zamora Figueroa, A. C., Ramos Oropeza, J. R., Arias, M., Hernandez Valencia, I. (2017): Response of the microbial community to the biotreatment of a soil contaminated with a medium crude. – Revista Internacional De Contaminacion Ambiental 33(4): 629-639.
[33] Zhang, W. (2015): Simulation study of the influence of green layout of residential areas on microclimate. – Master Thesis of Nanjing University.
[34] Zhao, J., Liu, J. (2001): Garden style summer thermal environment research. – Journal of Northwest Institute of Architectural Engineering (Natural Science Edition) 18(1): 8-11.
[35] Zhou, J. (2001): Urban green volume calculation mode and information system. – Acta Geographica Sinica 1: 14-23.
[36] Zhu, N., Li, M., Chai, Y. (2002): Analysis of the ecological functions of the green space system in Harbin greenbelts. – Chinese Journal of Applied Ecology 9: 1117-1120.

http://www.aloki.hu ● ISSN 1589 1623 (Print) ● ISSN 1785 0037 (Online)
DOI: http://dx.doi.org/10.15666/aeer/1705_1033510356

EFFECT OF ROOTING MEDIUM, CUTTING TYPE AND AUXIN ON ROOTING OF PEPINO (*SOLANUM MURICATUM* AITON) CUTTING

AGHDAEI, M.[1] – NEMATI, S. H.[1*] – SAMIEE, L.[2] – SHARIFI, A.[3]

[1]*Department of Horticultural Science, Faculty of Agriculture, Ferdowsi University of Mashhad, Iran*

[2]*Department of Ornamental Plants, Research Center for Plant Sciences, Ferdowsi University of Mashhad, Iran*

[3]*Department of Ornamental Plant Biotechnology, Academic Center for Education, Culture and Research, Branch of Khorasan Razavi, Iran*

[*]*Corresponding author*
e-mail: nemati@um.ac.ir

(Received 27th Nov 2018; accepted 2nd Jul 2019)

Abstract. To investigate the effect of rooting medium, cutting type and auxin (indole butyric acid (IBA)) on rooting of pepino cuttings (*Solanum muricatum* Aiton), two separate experiments were carried out in a factorial based on completely randomized design. In the first experiment, the effects of two types of cuttings (middle and distal) and eleven rooting media, and in the second experiment, the effects of three levels of IBA (0, 500 and 1000 mg L^{-1}) and seven rooting media (selected based on the results of the first experiment) on the rooting rate of cuttings and some growth characteristics including root length, the longest root length, stem length, fresh and dry weights of root and plant were evaluated. The results of the first experiment showed that the distal cuttings showed better rooting than the middle ones. The highest number of roots (40.5) was found in peat moss + perlite rooting medium. The highest averages of root length and length of the longest root were related to the distal cuttings planted in water and then in peat moss + perlite medium. The greatest root fresh weight was recorded in cuttings planted in peat moss + perlite medium, and the highest root dry weight and plant fresh and dry weights were obtained in distal cuttings planted in peat moss + sand medium. The results of the second experiment also showed that the highest (66) and lowest (26.76) numbers of roots were due to peat moss + perlite and water media, respectively. The greatest root length and length of the longest root was observed in the treatment of 0 mg L^{-1} IBA in water medium which was higher than in other treatments Moreover, the highest root fresh and dry weights were related to a treatment of 500 mg L^{-1} IBA in peat moss + sand medium. In general, the most suitable combination for pepino cultivation is the use of distal cuttings treated with a concentration of 500 mg L^{-1} IBA and planting in the rooting medium of peat moss + perlite, followed by peat moss + sand medium.
Keywords: *IBA, peat moss + perlite medium, root number and length, distal cutting, root fresh weight*

Introduction

Pepino (*Solanum muricatum* Aiton), a member of the Solanaceae family, is a tropical and semi-tropical crop and native to the Andean Mountains. It is grown commercially in countries such as Bolivia, Colombia, Ecuador, Peru, Australia and New Zealand for its edible fruits, which are juicy, fragrant, sweet and rich in color and shape. It contains 92% water, low calories, high minerals, thiamine, niacin, riboflavin and ascorbic acid (Prohens et al., 1996; Sudha at al., 2011). Pepino is a greenhouse crop with growing season longer than most greenhouse crops and has a yield of 70-80 tons per hectare (Prohens and Nuez, 1999).

http://www.aloki.hu ● ISSN 1589 1623 (Print) ● ISSN 1785 0037 (Online)
DOI: http://dx.doi.org/10.15666/aeer/1705_1035710369

Pepino propagation is possible through sexual and asexual methods, and most of the pepino cultivars are fertile and produce live seeds (5 to 30 seeds per fruit). Low percentage of seed germination, high levels of heterozygosity, and low quality of plants are the most important problems resulting from seed propagation (Pauli, 1988; Hernando and Leon, 1994; Pierik, 1997; Nemati and Tehranifar, 2007). There is not much information about the sexual reproduction of this plant, and generally reproductive propagation has been reported to be difficult and with low success. The germination rate of pepino seeds in soil has been reported to be only 4%, so cutting is the main propagation method of this plant (Bhardwaj et al., 1996; Hrbans et al., 1996; Prohens et al., 2005; Nemati and Tehranifar, 2007).

In various studies, it has been determined that type and position of cutting and rooting medium have a significant effect on the success of rooting. So that in some herbaceous species such as olive (Aboutalebi Jahromi and Hassanpoor, 2003) and *Azadirachta indica* (Palanisamy and Kumar, 1997), distal cuttings had better rooting than the middle or basal ones. Culture medium is composed of substances that can replace natural soil for plant growth, in which roots grow continuously by absorbing water and nutrients (Douglass et al., 2009). Use of culture media started in the 1960s by using organic substrates such as peat (Schie, 1997), and today the use of granulated substrates for planting greenhouse vegetables has become very common and becomes more important every year (Gül et al., 2005). An ideal growth environment for the plant should include features such as being affordable and accessible, appropriate efficiency for physical support of the plant, ability to store water and food, adequate oxygen exchange for root respiration, high water holding capacity and appropriate drainage. Moreover, culture medium should be free of pathogenic organisms (bacteria, nematodes, fungi and insects), weeds, toxic substances and chemical residues (pesticides) (Johnson et al., 1985; Cantliffe et al., 2003). Although different materials are used to prepare plants growth medium, the final selection of the material type depends on the inherent characteristics of the culture medium to maintain the desired growth of the plant (Verdonck et al., 1982). In a study, the effects of cutting type, different levels of naphthalene acetic acid and three substrates were investigated on sum of root length of 'Consuelo' pepino cuttings. Using middle cuttings treated with naphthalene acetic acid at concentration of 500 mg/l and planted in perlite medium was reported as the best combined treatment (Nemati and Tehranifar, 2007). Although use of cutting is considered as the main propagation method of pepino plant and many reports indicated that pepino cuttings stablish roots easily, none of them intensively compared rooting intensity of cutting type, effects of various rooting medium and growth regulators (IBA) on it. Moreover, there is a report on unsuccessful rooting and vegetation propagation of the cuttings of the plants grown from the seeds of the Ramses and Consuelo cultivars (Nemati and Tehranifar, 2007). Since low success of pepino propagation through seeds is a major problem in the development of this crop cultivation, this study was conducted to investigate the effects of rooting substrate, cutting type and different concentrations of indole butyric acid on the rooting of pippino cuttings of the 'Ramses' cultivar.

Materials and methods

In this research, in order to evaluate the effect of rooting medium, cutting type (cuttings position) and auxin (indole butyric acid) on rooting of pepino cuttings, two separate experiments were carried out based on a completely randomized design with

http://www.aloki.hu ● ISSN 1589 1623 (Print) ● ISSN 1785 0037 (Online)
DOI: http://dx.doi.org/10.15666/aeer/1705_1035710369

three replications in Ferdowsi University of Mashhad, Iran in 2016. In the first experiment, the effects of cutting type (distal and middle cuttings) and 11 rooting media including peat moss, perlite, cocopeat, sand, water, peat moss + perlite, peat moss + cocopeat, peat moss + sand, perlite + cocopeat, perlite + sand and cocopeat + sand were investigated on rooting of pepino cuttings (*Fig. 1*). Pepino seeds were purchased from Plant World Seed Company, UK, and planted in a greenhouse under temperature of 25°C and relative humidity of 50%.

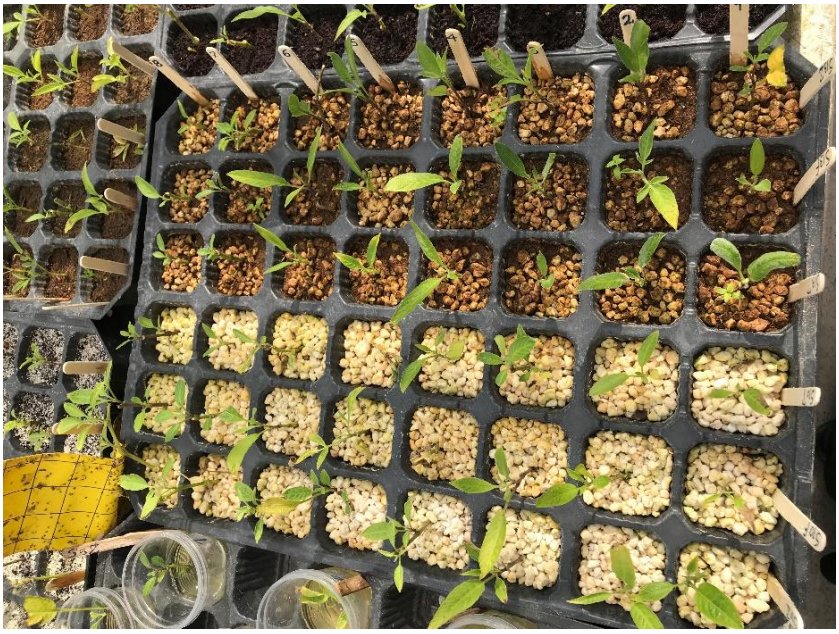

Figure 1. *Culture media and cuttings*

Two types of middle and distal cuttings with the length of 15 cm were prepared from the plants grown from seeds (seedlings) and planted in different media disinfected with benomyl fungicide. In the second experiment, the effects of different concentrations of indole butyric acid (IBA) (0, 500 and 1000 mg/l) and seven rooting media including peat moss, perlite, sand, water, peat moss + perlite, peat moss + sand and perlite + sand in six replications were evaluated on rooting of the cuttings and some growth parameters of pepino cuttings. Plants were grown in the greenhouse condition and temperature was set between 20ºC day/15ºC night and pots were tap watered each 3 days. It should be noted that the choice of cuttings type and rooting media in the second experiment was carried out based on the results of the first experiment. For this purpose, 5 cm of the basal portion of the cuttings was treated with different levels of indole butyric acid for 10 seconds, and after drying, they were planted in different rooting media disinfected with benomyl fungicide. After four weeks, characteristics including total number of roots, root length (cm), length of the longest roots (cm), root fresh and dry weight (g), stem length (cm) and plant fresh and dry weight (g) were evaluated. Data were analyzed using analysis of variance (ANOVA) procedure. The comparison of means were tested with the least significant difference test (LSD) at 5% probability level. The SAS software (version 9.3) was used for analysis.

http://www.aloki.hu ● ISSN 1589 1623 (Print) ● ISSN 1785 0037 (Online)
DOI: http://dx.doi.org/10.15666/aeer/1705_1035710369

Results and Discussion

Data showed that distal cuttings had better rooting. The highest number of roots and greatest root fresh weight were recorded in cuttings grown in peat moss + perlite medium. Moreover, the highest averages of root length and length of the longest root were observed in water and then in peat moss + perlite medium. However, the highest root dry weight and plant fresh and dry weights were obtained in distal cuttings planted in peat moss + sand medium. Investigating the effect of application of IBA on distal cuttings grown in seven media selected from the first experiment also showed that cuttings grown in peat moss + perlite and water media had the highest and lowest number of roots, respectively. Cuttings treated with 0 mg L^{-1} IBA and grown in water medium showed the greatest root length and length of the longest root. While, the highest root fresh and dry weights were observed under treatment of 500 mg L^{-1} IBA in peat moss + sand medium. Overall, distal cuttings treated with a concentration of 500 mg L^{-1} IBA and grown in the rooting medium of peat moss + perlite, followed by peat moss + sand medium were the best treatments for pepino vegetative propagation.

Effect of rooting medium and cutting type on rooting and growth characteristics of cuttings

Number of roots

Culture medium and cutting type had a significant effect on the total number of roots, while the interaction of medium × cutting type on this trait was not significant (*Table 1*). Based on the results of means comparison of simple effect of culture medium, the highest average number of roots (40.5) was observed in cuttings planted in peat moss + perlite rooting medium with no statistical significant difference from peat moss + sand. The lowest number of roots was obtained in peat moss + cocopeat medium. In other words, the number of roots in cuttings planted in peat moss + perlite and peat moss + sand was 1.7 and 2 times higher than the number of roots observed in peat moss + cocopeat medium, respectively (*Fig. 2*). The results of the simple effect of cuttings type showed that distal cuttings were more effective than middle ones so that the average number of roots in distal cuttings (31.4) was approximately 1.5 times that of middle ones (21.5).

Average root length, length of the longest root and stem length

Root length and length of the longest root were significantly affected by the culture medium, type of cutting and the interaction of culture medium × cutting type, while stem length was only affected by the interaction of culture medium × cutting type (*Table 1*). The results obtained from means comparison of the interaction of culture medium × cutting type showed that the highest averages of root length and length of the longest root were related to distal cuttings in water, while the lowest averages of root length and length of the longest root were observed, respectively, in middle and distal cuttings planted in peat moss + cocopeat medium. Besides, the greatest stem length was observed in cuttings planted in peat moss + sand medium and the shortest stem length was related to the cuttings planted in peat moss + perlite medium (*Table 1*).

The results of analysis of variance showed that fresh and dry weights of root were significantly affected by culture medium, cutting type and interaction of culture medium × cutting type, while fresh weight of the plant was affected only by culture medium and interaction of the culture medium × cutting type and plant dry weight index

http://www.aloki.hu ● ISSN 1589 1623 (Print) ● ISSN 1785 0037 (Online)
DOI: http://dx.doi.org/10.15666/aeer/1705_1035710369

was only affected by the culture medium × cutting type (*Table 2*). Based on the results of means comparison of the data, the greatest root and plant dry weights and plant fresh weight were related to distal cutting planted in peat moss + sand, while the lowest root dry weight was related to middle cuttings planted in cocopeat + perlite medium and the lowest fresh and dry weights of the plant were recorded in distal cuttings planted in cocopeat + perlite medium. Furthermore, the highest root fresh weight was related to distal cuttings planted in peat moss + perlite medium and the lowest root fresh weight was recorded in the middle cuttings planted in cocopeat + perlite and peat moss substrates (*Table 2*).

Table 1. *Effect of culture medium and cutting type on total number of root, root length of the cuttings, length of the longest root and length of the stem*

Culture medium	Cutting type	Total number of root	Root length (cm)	Length of the longest root (cm)	Length of the stem
Peat moss	Distal	25^{a}	5.86^{bcde}	8.50^{ab}	14.07^{bc}
	Middle	20.33^{a}	5.93^{bcd}	6.40^{fg}	$8.58^{efghijk}$
Perlite	Distal	34.33^{a}	5.44^{cdef}	$7.47^{abcdefg}$	8.98^{fefghi}
	Middle	21^{a}	4.37^{efghi}	8.00^{abcde}	6.75^{ghijkl}
Cocopeat	Distal	24.33^{a}	4.31^{fghij}	$7.47^{abcdefg}$	6.52^{hijk}
	Middle	19^{a}	4.99^{defgh}	8.40^{abc}	7.25^{ghijk}
Sand	Distal	38.33^{a}	6.83^{abc}	7.00^{bcdefg}	$7.83^{efghijk}$
	Middle	24.5^{a}	5.38^{cdefg}	7.60^{abcdef}	8.75^{efghij}
Water	Distal	27.33^{a}	7.78^{a}	7.67^{abcdef}	25.17^{a}
	Middle	17.50^{a}	4.59^{defghi}	8.15^{abcdd}	5.75^{jk}
Peat moss + Perlite	Distal	29.67^{a}	7.27^{ab}	6.00^{g}	16.00^{b}
	Middle	15.00^{a}	6.09^{bcd}	7.00^{bcdefg}	9.75^{defg}
Peat moss + Cocopeat	Distal	43.67^{a}	3.08^{ij}	7.67^{abcdef}	5.50^{k}
	Middle	37.33^{a}	2.79^{j}	6.50^{efg}	$7.75^{efghijk}$
Peat +Sand	Distal	24.67^{a}	5.67^{cdef}	8.97^{a}	14.33^{bc}
	Middle	16.00^{a}	5.83^{bcdef}	6.90^{cdefg}	$8.67^{efghijk}$
Perlite + Cocopeat	Distal	38.67^{a}	5.39^{cdefg}	7.83^{abcdef}	10.33^{def}
	Middle	30.00^{a}	3.16^{ij}	6.67^{defg}	5.90^{ijk}
Perlite + Sand	Distal	24.67^{a}	3.84^{jhij}	$7.50^{abcdefg}$	9.33^{efgh}
	Middle	18.50^{a}	3.53^{hij}	$7.50^{abcdefg}$	12.67^{cd}
Cocopeat + Sand	Distal	35.00^{a}	5.27^{defg}	7.17^{bcdefg}	10.17^{def}
	Middle	17.50^{a}	4.79^{defgh}	6.75^{defg}	10.50^{ef}
Significance					
Culture medium		**	**	**	NS
Cutting type		**	**	**	NS
Culture medium * Cutting type		NS	*	**	*

Means with the same letters in each column were not significantly different using least significant difference test (LSD) at $p < 0.05$. *, ** and NS are significant at $p \leq 0.05$, at $p \leq 0.01$ and not significant, respectively

Effect of rooting medium and indole butyric acid on rooting and growth characteristics of seedlings

Total number of roots

The results of analysis of variance showed that total root number was significantly affected by culture medium and indole butyric acid, while the interaction effect of culture medium × indole butyric acid on this index was not significant (*Table 3*). Based on the results of means comparison, the highest average number of roots (66) was found in peat + perlite culture medium, which showed a significant difference from other substrates, while the lowest mean number of roots (26.7) was seen in water medium

http://www.aloki.hu ● ISSN 1589 1623 (Print) ● ISSN 1785 0037 (Online)
DOI: http://dx.doi.org/10.15666/aeer/1705_1035710369

(*Fig. 3*). In other words, the number of roots observed in distal cuttings of pepino planted in peat + perlite culture medium was about 2.47 times higher than what was observed in the cuttings planted in water medium (*Fig. 3*). The simple effect of indole butyric acid hormone showed that the highest number of roots was related to the cuttings treated with indole butyric acid at concentration of 500 mg/l, which showed a statistically significant difference from two other concentrations (0 and 1000 mg/l) (*Fig 4*).

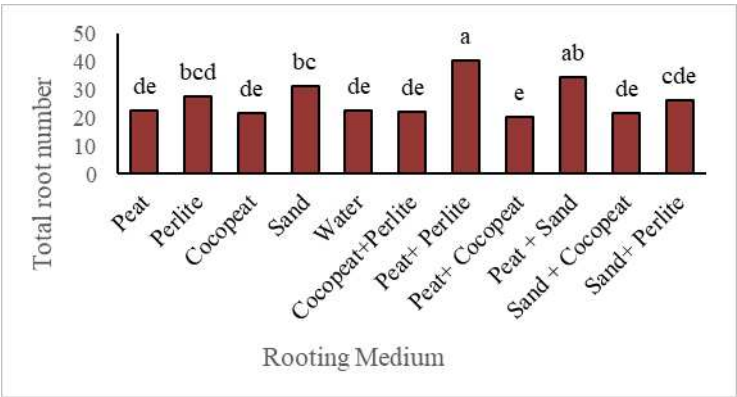

Figure 2. *Effect of culture media on root number*

Table 2. *Effect of culture medium and cutting type on root and plant fresh and dry weights*

Culture medium	Cutting type	Root fresh weight (g)	Root dry weight (g)	Plant fresh weight (g)	Plant dry weight (g)
Peat moss	Distal	0.233^{bc}	0.026^{bcd}	1.253^{ab}	0.145^{ab}
	Middle	0.030^{h}	0.013^{fghijk}	0.690^{fg}	0.138^{ab}
Perlite	Distal	0.120^{defg}	0.014^{fghijk}	0.833^{cdefg}	0.104^{bc}
	Middle	0.065^{efgh}	0.008^{jk}	0.915^{bcdef}	0.132^{ab}
Cocopeat	Distal	0.107^{defgh}	0.009^{ijk}	0.730^{efg}	0.098^{bc}
	Middle	0.185^{cd}	0.013^{fghijk}	1.085^{bcde}	0.168^{a}
Sand	Distal	0.140^{cde}	$0.016^{efghijk}$	0.770^{defg}	0.097^{bc}
	Middle	0.080^{efgh}	0.008^{jk}	0.990^{bcdef}	0.164^{a}
Water	Distal	0.107^{defgh}	0.024^{cde}	0.733^{efg}	0.167^{a}
	Middle	0.045^{fgh}	0.011^{jhijk}	0.650^{fg}	0.105^{bc}
	Middle	0.135^{cde}	0.021^{def}	0.870^{cdefg}	0.144^{ab}
Peat moss + Perlite	Distal	0.317^{a}	0.035^{ab}	1.193^{abc}	0.147^{ab}
	Middle	0.135^{cde}	0.021^{def}	0.870^{cdefg}	0.144^{ab}
Peat moss + Cocopeat	Distal	0.067^{efgh}	$0.016^{efghijk}$	1.247^{ab}	0.161^{a}
	Middle	0.040^{gh}	0.008^{jk}	1.125^{bcd}	0.125^{abc}
Peat+ Sand	Distal	0.293^{ab}	0.038^{a}	1.567^{a}	0.172^{a}
	Middle	0.142^{cde}	0.032^{ab}	0.870^{cdefg}	0.118^{abc}
Perlite + Cocopeat	Distal	0.063^{efgh}	0.010^{hijk}	0.530^{g}	0.070^{c}
	Middle	0.030^{h}	0.007^{k}	0.755^{defg}	0.140^{ab}
Perlite + Sand	Distal	0.130^{def}	0.018^{defghi}	0.867^{bcdef}	0.123^{abc}
	Middle	0.105^{defgh}	0.020^{defg}	0.920^{cdefg}	0.139^{ab}
Cocopeat + Sand	Distal	0.130^{def}	0.019^{defgh}	0.840^{cdefg}	0.120^{abc}
	Middle	0.085^{efgh}	$0.017^{defghij}$	0.935^{bcdef}	0.162^{a}
Significance					
Culture medium		**	**	**	NS
Cutting type		**	**	NS	NS
Culture medium *Cutting type		**	*	**	**

Means with the same letters in each column were not significantly different using least significant difference test (LSD) at $p < 0.05$. *, ** and NS are significant at $p \leq 0.05$, at $p \leq 0.01$ and not significant, respectively

http://www.aloki.hu ● ISSN 1589 1623 (Print) ● ISSN 1785 0037 (Online)
DOI: http://dx.doi.org/10.15666/aeer/1705_1035710369

Table 3. *Effect of culture medium and indole butyric acid on total number of root, root length, longest root, root quality and stem length*

Culture medium	IBA	Total number of root	Root length (cm)	Longest root (cm)	Root fresh weight (g)	Root dry weight (g)
Peat moss	0	30.50^{a}	5.86^{bcd}	13.07^{cde}	0.27^{abc}	0.025^{cd}
	500	39.33^{a}	6.01^{bcd}	11.25^{def}	0.30^{ab}	0.024^{cde}
	1000	36.66^{a}	4.49^{efgh}	11.83^{cdef}	0.25^{abc}	0.030^{bc}
Perlite	0	34.33^{a}	5.27^{bcdef}	8.98^{fgh}	0.12^{ef}	0.014^{0fg}
	500	42.16^{a}	4.68^{defgh}	10.96^{def}	0.11^{f}	0.014^{efg}
	1000	41.25^{a}	5.00^{cdefg}	11.75^{cdef}	0.13^{def}	0.013^{fg}
Sand	0	38.33^{a}	5.46^{bcdef}	7.33^{h}	0.14^{def}	0.013^{fg}
	500	46.66^{a}	3.85^{gh}	7.63^{gh}	0.12^{ef}	0.012^{g}
	1000	38.00^{a}	4.88^{defgh}	10.75^{defg}	0.16^{def}	0.018^{defg}
Water	0	27.16^{a}	7.78^{a}	24.83^{a}	0.11^{f}	0.024^{cd}
	500	29.66^{a}	5.47^{bcdef}	13.33^{cde}	0.08^{f}	0.015^{defg}
	1000	23.5^{a}	5.54^{bcde}	11.17^{def}	0.12^{ef}	0.019^{defg}
Peat moss + Perlite	0	51.83^{a}	6.44^{b}	14.00^{cd}	0.27^{abc}	0.035^{ab}
	500	66.66^{a}	5.73^{bcdef}	10.83^{defg}	0.20^{cde}	0.024^{cd}
	1000	49.58^{a}	5.27^{bcdef}	11.70^{cdef}	0.15^{def}	0.018^{defg}
Peat moss + Sand	0	38.66^{a}	5.01^{cdefg}	14.83^{bc}	0.33^{ab}	0.031^{ab}
	500	50.00^{a}	6.26^{bc}	17.50^{b}	0.34^{a}	0.041^{a}
	1000	31.66^{a}	5.85^{bcd}	10.67^{efg}	0.21^{cd}	0.020^{defg}
Perlite + Sand	0	36.66^{a}	3.84^{gh}	9.33^{fgh}	0.13^{def}	0.018^{defg}
	500	40.83^{a}	4.14^{fgh}	10.33^{efgh}	0.16^{def}	0.023^{cdef}
	1000	36.00^{a}	3.61^{h}	9.50^{fgh}	0.14^{def}	0.022^{cdef}
Significance						
Culture medium		**	**	**	**	**
IBA		**	*	**	NS	NS
Culture medium * IBA		NS	*	**	*	**

Means with the same letters in each column were not significantly different using least significant difference test (LSD) at $p < 0.05$. *, ** and NS are significant at $p \leq 0.05$, at $p \leq 0.01$ and not significant, respectively

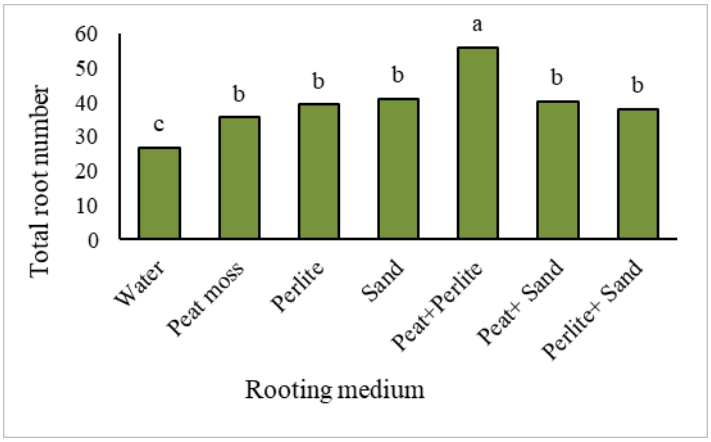

Figure 3. *Effect of rooting substrate on root number*

Average root length and length of the longest root

Mean root length and length of the longest root were significantly affected by the culture medium, indole butyric acid and culture medium × indole butyric acid interaction (*Table 3*). Among the different treatments, the greatest root length and the longest root length were related to 0 mg/l indole butyric acid in water, which resulted in

http://www.aloki.hu ● ISSN 1589 1623 (Print) ● ISSN 1785 0037 (Online)
DOI: http://dx.doi.org/10.15666/aeer/1705_1035710369

a statistically significant difference compared to other treatments. The lowest root length and the shortest root length were obtained in 1000 mg/l indole butyric acid in perlite + sand medium and 0 mg/l indole butyric acid in sand medium (*Table 3*).

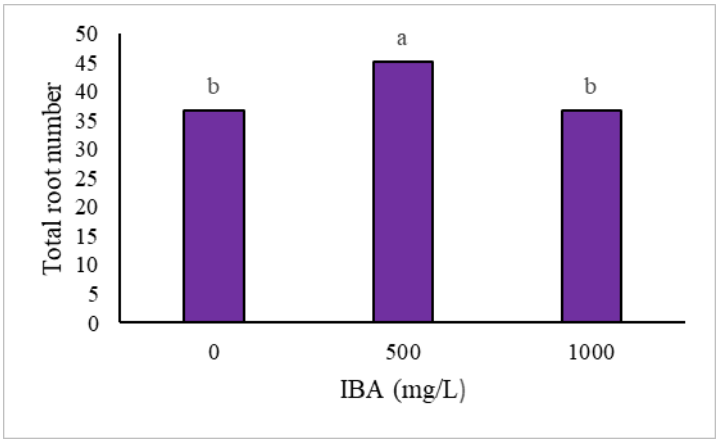

Figure 4. *Effect of indole butyric acid on root number*

Fresh and dry weights of root

Culture medium and culture medium × indole butyric acid interaction had a significant effect on root fresh and dry weights, while the simple effect of indole butyric acid on these two indices was not statistically significant (*Table 3*). The results of culture medium × indole butyric acid interaction showed that the highest root fresh and dry weights were due to the cuttings treated with 500 mg/l indole butyric acid in peat moss + sand medium. Moreover, the lowest root fresh and dry weights were recorded in the cuttings treated with indole butyric acid at concentration of 500 mg/l in water and sand substrates (*Table 3*).

Discussion

The results of the first experiment indicated better rooting of distal cuttings of pepino in comparison with the middle cuttings, and also greater suitability of peat moss + sand and peat moss + perlite substrates for rooting and vegetative growth of seedlings compared to other substrates. The significant effect of culture medium on different root characteristics such as number and length of root (Ercisli et al., 2005), weight, thickness, length and volume of root (Ahmad et al., 2000), and number of primary roots and amount of root dry matter (Kreen et al., 2002) has been reported in different studies. Culture medium is one of the most important indicators for successful rooting of cutting. Cuttings of azalea, privet and almond in a mixture with equal ratios of peat and sand had a remarkably good rooting, indicating that this combination (peat + sand) can be very useful for many cuttings which have poor rooting in either peat or sand (Hitchcock, 1928). Peat, perlite and sand substrates for rooting of tomato cuttings were more suitable than sand + soil + organic fertilizer mixture, so that the highest number of leaves and greatest fresh and dry weights of seedling were observed in peat medium and the longest root length and greatest seedling fresh weight were reported in peat and sand rooting media (Gül et al., 1993). Moreover, the increase found in rooting percentage and

http://www.aloki.hu ● ISSN 1589 1623 (Print) ● ISSN 1785 0037 (Online)
DOI: http://dx.doi.org/10.15666/aeer/1705_1035710369

number of primary root in kiwifruit cuttings planted in peat + perlite medium was associated to proper water holding of this medium (Ercişli et al., 2002). Due to having suitable physical and chemical characteristics such as density, porosity, air capacity, water holding capacity, pH, electrical conductivity, cation exchange capacity and carbon to nitrogen ratio, peat is a suitable medium for planting most horticultural species (Abad et al., 2001). The maintenance of adequate ventilation in the rooting environment, along with reduced water losses from cuttings, is one of the important tasks of propagation systems. On the one hand, the presence of proper ventilation around the roots in culture media containing peat moss is effective in the induction and growth of roots in cuttings (Hartman et al., 1990; Jinks, 1995), and, on the other hand, the positive and desirable effect of peat moss + sand on rooting can be due to better water holding by this mixture compared to sand, as well as due to other potential benefits affected by peat moss (Hitchcock, 1928). Superiority of peat moss can be due to high cation exchange capacity and appropriate moisture holding. Use of perlite in combination with traditional media containing peat can be effective in plant growth and development due to better aeration (Smith and Hall, 1994).

The results of this study showed that root length in water medium was longer than other rooting media. In line with the results obtained in this study, Nemati and Tehranifar (2007) also reported that the total root length of pepino cuttings planted in perlite and water media was greater than that in other substrates. However, rooted cuttings in water medium did not have good establishment in soil. The effect of rooting media on the extension of the appeared roots was more than induction of rooting (Long, 1932). Although pepino can withstand flood conditions for several days (Prohens et al., 1996), formation of long roots in water medium can be a sign of flood stress (Gibberd et al., 2001; Grzesiak et al., 2014). These long roots are likely to be aerotropic roots that plant expands under flood stress conditions to search for air and oxygen (Gibberd et al., 2001).

Cutting position affects the rate of rooting success, so that better rooting of distal cuttings compared to middle ones has been reported in different plants, such as olive (Aboutalebi Jahromi and Hassanpoor, 2003) and neem (Palanisamy and Kumar, 1997), which is consistent with the results obtained in this study. As the plant grows older, the production of rooting inhibitors increases and there is a direct correlation between the reduction of rooting and tissues of lower cuttings (Paton et al., 1970). Phenols act as auxin cofactor, and reduction in rooting potential, along with aging of plants, can be due to the reduction of phenolic compounds (Khandan-Mirkohi et al., 2015). The absence of terminal bud in cutting and consequently depriving of cutting from internal auxin can lead to a decrease in the number of cells in root primordia. On the other hand, the aging of the root primordia and increase in the number of its cells reduce the effect of internal auxin, indicating greater rooting in juvenile cuttings with terminal bud (Haissig, 1972; Khandan-Mirkohi et al., 2015). Generally, the increase in rooting in distal cuttings containing terminal buds relative to cuttings with no bud can be attributed to high concentrations of internal rooting stimulator produced in the terminal bud and hence the pre-formation of a number of root initials affected by these materials (Davies and Hartmann, 1988; Hartman et al., 1990). Better rooting of distal cuttings in comparison with the middle ones can be due to the presence of higher auxin content at distal end of the shoot, so it is possible that auxin concentration decreases with increased distance from shoot tip and, consequently, rooting decreases (Palanisamy and Kumar, 1997).

http://www.aloki.hu ● ISSN 1589 1623 (Print) ● ISSN 1785 0037 (Online)
DOI: http://dx.doi.org/10.15666/aeer/1705_1035710369

Based on the results of this study, rooting rate of pepino cuttings was influenced by the use of auxin hormone (IBA). The ability of cuttings for rooting is dependent upon phenolic compounds, enzymes and their auxin content (Loreti and Morini, 1985), so that success in rooting of some carnation species without application of plant growth regulators was related to their internal auxin (Guerrero et al., 1999). Auxin has a positive role in induction of rooting, formation of root initials, and increase of speed and percentage of cuttings rooting. Despite the synthesis of auxin in various plant organs (including young shoots and leaves), application of synthetic auxin for successful rooting and prevention of cutting death is useful (Štefančič et al., 2007; Kasim and Rayya, 2009). Through stimulating pericycle cells in the upper parts of root hairs, auxin hormone can stimulate the division of cell in this region and eventually lead to root formation (Hillman, 1984; Davies, 1995; Laskowski et al., 1995). Generally, the positive effect of auxin on rooting can be attributed to the increase of auxin-based food supply, increase of protein content and peroxidase enzyme activity (Husen and Pal, 2007) as well as its role in stimulating the division of the first cell of root initials (Hartman et al., 1990; Loach, 1996). In addition, the effect of rooting auxin hormone on the increase of root length can be due to the effect of this growth regulator on the stimulation of cell division.

Although it has been reported that pepino, due to the easy rooting of its cuttings, is mainly propagated vegetatively by using cutting and in most cases it is not necessary to use mist system or plant hormones (National Research Council, 1989; Spooner et al., 1993; Prohens et al., 1996), there is a report regarding unsuccessful rooting and vegetative propagation by using cuttings obtained from seedlings of Ramses and Consuelo varieties in Iran (Nemati and Tehranifar, 2007). Furthermore, the results of this study showed that application of rooting hormones can increase the success rate of pepino vegetative propagation. Use of IBA (especially at concentration of 500 mg/l) improved rooting and grwoth characteristics of seedlings in the present study. On the other hand, it has been shown that application of high concentration of IBA (1000 mg/l) in comparison with concentration of 500 mg/l decreased rooting and growth characteristics of seedlings, showing bell characteristic of hormones. Although IBA is one of the most effective compounds stimulating rooting in many species (Hartmann and Kester, 1990), its effect can vary based on the type of cuttings (Tworkoski and Takeda, 2007) and the concentration used. It has been reported that use of IBA at concentration of 1000 mg/l reduced the number of leaves and root fresh weight in lateral cuttings of tomato compared with the control (distilled water) (Gül et al., 1993). High concentrations of auxin can cause degradation of the basal tissues of cuttings, interference in hormonal balance in plant, damage to the cells, reduction of rooting, and inhibition of buds growth and even shoot development (Hartmann and Kester, 1990; Blythe et al., 2004; Ranjbar and Ahmadi, 2016).

Conclusion

Cutting position and type of culture medium influenced the success rate and percentage of rooting and different growth characteristics (number of roots, root length, length of the longest root, stem length, and fresh and dry weights of root and plant) in pepino cuttings. In conclusion, the results of the first experiment indicated the superiority of terminal cuttings over the middle ones and also more suitability of peat moss + perlite and peat moss + sand substrates compared to other substrates for the

http://www.aloki.hu ● ISSN 1589 1623 (Print) ● ISSN 1785 0037 (Online)
DOI: http://dx.doi.org/10.15666/aeer/1705_1035710369

propagation of pepino. Study of the effect of auxin hormone and rooting medium in the second experiment showed that treatment of the cuttings with 500 mg/l IBA was more effective than concentration of 1000 mg/l. Peat moss + perlite and peat moss + sand substrates were more suitable than other substrates. In general, it was found in this study that the best treatment combination to increase the rooting of cuttings and to improve the growth characteristics of pepino seedlings is the use of terminal cutting, rooting hormone of IBA at concentration of 500 mg/l, and planting of cuttings in peat moss + perlite and peat moss + sand media. Finally, it is highly recommended that future investigators compare rooting of different cultivars of pepino simultaneously under different light and carbon dioxide regimes.

Acknowledgements. The authors would like to thank the staff of the Department of Horticulture and Green Space Engineering and Research Center for Plant Sciences of Ferdowsi University of Mashhad for cooperation and provision of greenhouse and laboratory facilities for this project.

REFERENCES

[1] Abad, M., Noguera, P., Burés, S. (2001): National inventory of organic wastes for use as growing media for ornamental potted plant production: case study in Spain. – Bioresource Technology 77(2): 197-200.

[2] Aboutalebi Jahromi, A., Hassanpoor, A. (2003): Investigating the effects of time, location of cutting, rooting media and auxin on rooting of olive cuttings of Zard cultivar. – Iranian Journal of Horticultural Science and Technology 4(3-4): 105-114.

[3] Ahmad, N., Ishtiaq, M., Zeb, A. (2000): Response of bottle brush seedling to different soil media. – Sarhad Journal of Agriculture 16(5): 503-509.

[4] Bhardwaj, H. L., Hankins, A., Mebrahtu, T., Mullins, J., Rangappa, M., Abaye, O., Welbaum, G. E. (1996): Alternative crops research in Virginia. – In: Janick, J. (ed.) Progress in new crops. ASHS Press, Alexandria, VA. p. 87-96.

[5] Blythe, E. K., Sibley, J. L., Ruter, J. M., Tilt, K. M. (2004): Cutting propagation of foliage crops using a foliar application of auxin. – Scientia Horticulturae 103(1): 31-37.

[6] Cantliffe, D. J., Funes, J., Jovicich, E., Paranje, A., Rodriguez, J., Shaw, N. (2003): Media and containers for greenhouse soilless grown cucumber, melons, peppers and strawberries. – Acta Horticulturae 614: 199-203.

[7] Davies, F. T., Hartmann, H. T. (1988): The physiological basis of adventitious root formation. – Acta Horticulturae 227: 113-120.

[8] Davies, P. J. (1995): Introduction. The Plant Hormones. – Kluwer Academic Publishers pp. 1-38.

[9] Douglass, F. J., Thomas, D. L., Luna, T. (2009): Growing Media. – In: Dumroese, R. K., Luna, T., Landis, T. D. (eds.) Nursery manual for native plants: A guide for tribal nurseries. Volume 1: Nursery management. Agriculture Handbook 730. Washington, D.C.: U.S. Department of Agriculture, Forest Service. p. 77-93.

[10] Ercişli, S., Anapali, Ö., Eşitken, A., Şahin, Ü. (2002): The effects of IBA, rooting media and cutting collection time on rooting of kiwifruit. – Gartenbauwissenschaft 67(1): 34-38.

[11] Ercisli, S., Sahin, U., Esitken, A., Anapali, O. (2005): Effects of some growing media on the growth of strawberry cvs.'Camarosa'and'Fern'. – Acta Agrobotanica 58(1).

[12] Gibberd, M. R., Gray, J. D., Cocks, P. S., Colmer, T. D. (2001): Waterlogging tolerance among a diverse range of Trifolium accessions is related to root porosity, lateral root formation and 'aerotropic rooting'. – Annals of Botany 88(4): 579-589.

[13] Grzesiak, M. T., Ostrowska, A., Hura, K., Rut, G., Janowiak, F., Rzepka, A., Hura, T., Grzesiak, S. (2014): Interspecific differences in root architecture among maize and

http://www.aloki.hu ● ISSN 1589 1623 (Print) ● ISSN 1785 0037 (Online)
DOI: http://dx.doi.org/10.15666/aeer/1705_1035710369

triticale genotypes grown under drought, waterlogging and soil compaction. – Acta Physiologiae Plantarum 36(12): 3249-3261.
[14] Guerrero, J. R., Garrido, G., Acosta, M., Sanchez-Bravo, J. (1999): Influence of 2, 3, 5-triiodobenzoic acid and 1-N-naphthylphthalamic acid on indoleacetic acid transport in carnation cuttings: relationship with rooting. – Journal of Plant Growth Regulation 18(4): 183-190.
[15] Gül, A., Tüzel, Y., Yoltas, T. (1993): Possibilities of using side shoots as propagation material in greenhouse tomato production. – II Symposium on Protected Cultivation of Solanacea in Mild Winter Climates 366: 271-278.
[16] Gül, A., Eroğul, D., Ongun, A. R. (2005): Comparison of the use of zeolite and perlite as substrate for crisp-head lettuce. – Scientia Horticulturae 106(4): 464-471.
[17] Haissig, B. E. (1972): Meristematic activity during adventitious root primordium development: influences of endogenous auxin and applied gibberellic acid. – Plant physiology 49(6): 886-892.
[18] Hartman, H. T., Kester, D. E., Davies, F. T. (1990): Plant propagation: Principleand Practices. – Prentice-Hall. 647 pp.
[19] Hernando, J. E., Leon, J. (1994): Neglected crops from a different perspective. – Plant Production and Protection Series No. 26. FAO, Rome Italy. p. 181-191.
[20] Hillman, J. R. (1984): Apical dominance. – In: Wilkins, M. B. (ed.) Advanced Plant Physiology. London: Pitman Publishing, pp. 127-148.
[21] Hitchcock, A. E. (1928): Effect of peat moss and sand on rooting response of cuttings. – Botanical Gazette 86(2): 121-148.
[22] Hrbans, L., Hankins, A., Mebrahtu, T., Mullins, J., Rangappa, M. (1996): Alternative crops research in Virginia. – Progress in new crops. ASHS press p: 87-96.
[23] Husen, A., Pal, M. (2007): Metabolic changes during adventitious root primordium development in Tectona grandis Linn. f. (teak) cuttings as affected by age of donor plants and auxin (IBA and NAA) treatment. – New Forests 33(3): 309-323.
[24] Jinks, R. L. (1995): The effects of propagation environment on the rooting of leafy cuttings of ash (Fraxinus excelsior L.), sycamore (Acer pseudoplatanus L.) and sweet chestnut (Castanea sativa Mill.). – New Forests 10: 183-195.
[25] Johnson, H., Hochmuth, G. J., Maynard, D. N. (1985): Soilless culture of greenhouse vegetables. – Bulletin/Florida Cooperative Extension Service (USA).
[26] Kasim, N. E., Rayya, A. (2009): Effect of different collection times and sometreatments on rooting and chemical interminal constituents of bitter almond hardwood cutting. – Journal of Agriculture and Biological Sciences 5(2): 116-122.
[27] Khandan-Mirkohi, A., Moshrefi-Araghi, A., Haghdoost, L., Rashid- Rostami, F., Sahraii, S. (2015): The effect of rooting medium, cutting type and auxin (IBA) treatment on propagation of Arizona cypress (Cupressus arizonica var. glabra). – Journal of Science and Technology of Greenhouse Culture 5(4): 193-202. (In Persian).
[28] Kreen, S., Svensson, M., Rumpunen, K. (2002): Rooting of clematis micro shoots and stem cuttings in different substrates. – Scientia Horticulturae 96: 351-357.
[29] Laskowski, M. J., Williams, M. E., Nusbaum, H. C., Sussex, I. M. (1995): Formation of lateral root meristems is a two-stage process. – Development 121: 3303-3310.
[30] Loach, K. (1996): Environmental conditions for rooting cutting: importantce, measurment and control. – Acta Horticulturae 374: 632-636.
[31] Long, J. C. (1932): The influence of rooting media on the character of roots produced by cuttings. – American Society for Horticultural Science 29(3): 352-355.
[32] Loreti, F., Morini, S. (1985): Rooting responses to BS, B2 and GF677 rootstocks cuttings. – Acta Horticulturae 173: 261-269.
[33] National Research Council. (1989): Lost crops of the incas: little-known plants of the Andes with promise for worldwide cultivation. – Washington, DC: The National Academies Press.

http://www.aloki.hu ● ISSN 1589 1623 (Print) ● ISSN 1785 0037 (Online)
DOI: http://dx.doi.org/10.15666/aeer/1705_1035710369

[34] Nemati, H., Tehranifar, A. (2007): Investigation of sexual and asexual propagation of a new vegetable called pepino in Iran (Solanum muricatum, Atio, pepino). – Mashhad, Journal of Agricultural Science and Technology 21: 3-9. (In Persian).
[35] Palanisamy, K., Kumar, P. (1997): Effect of position, size of cuttings and environmental factors on adventitious rooting in neem (Azadirachta indica A. Juss). – Forest Ecology and Management 98(3): 277-280.
[36] Paton, D. M., Willing, R. R., Nicholls, W., Pryor, L. D. (1970): Rooting of stem cuttings of Eucalyptus: a rooting inhibitor in adult tissue. – Australian Journal of Botany 18(2): 175-183.
[37] Pauli, R. (1988): Micropropagation of pepinos (Solanum muricalum Ait.). – Acta Horticulturae 227: 387-389.
[38] Pierik, R. L. M. (1997): Micropropagation of Solanum muricatum Ait. (Pepino). – High-Tech and Micropropagation V: 160-172.
[39] Prohens, J., Ruiz, J. J., Nuez, F. (1996): The pepino (Solanum muricatum, Solanaceae): A "new" crop with a history. – Economic Botany 50: 355-368.
[40] Prohens, J., Nuez, F. (1999): Strategies for breeding a new greenhouse crop, the pepino (Solanum muricatum Aiton). – Canadian Journal of Plant Science 79: 269-275.
[41] Prohens, J., Rodríguez-Burruezo, A., Nuez, F. (2005): Utilization of genetic resources for the introduction and adaptation of exotic vegetable crops: The case of pepino (Solanum muricatum, Ait.). – Euphytica 146: 133-142.
[42] Ranjbar, A., Ahmadi, N. (2016): The effects of IBA and NAA, and rooting media on propagation of miniature rose cuttings (Rosa hybrida). – Journal of Horticultural Science 30(3): 250-528. (In Persian).
[43] Schie, W. V. (1997): Standardization of substrates. – International Symposium on Growing Media and Hydroponics 481: 71-78.
[44] Smith, C. A., Hall, D. A. (1994): The development of perlite as a potting substrate for ornamental plants. – Acta Horticulturae 361: 159-166.
[45] Spooner, D. M., Anderson, G. J., Jansen, R. K. (1993): Chloroplast DNA evidence for the interrelationships of tomtoes, potatoes, and pepinos (Solanaceae). – American Journal of Botany 676-688.
[46] Štefančič, M., Štampar, F., Veberič, R., Osterc, G. (2007): The levels of IAA, IAAsp and some phenolics in cherry rootstock 'GiSelA 5'leafy cuttings pretreated with IAA and IBA. – Scientia Horticulturae 112(4): 399-405.
[47] Sudha, G., Priya, M. S., Shree, R. I., Vadivukkarasi, S. (2011): In vitro free radical scavenging activity of raw pepino fruit (Solanum muricatum aiton). – International Journal of Current Pharmaceutical Research 3(2): 137-140.
[48] Tworkoski, T., Takeda, F. (2007): Rooting response of shoot cuttings from three peach growth habits. – Scientia Horticulturae 115(1): 98-100.
[49] Verdonck, O., De Vleeschauwer, D., De Boodt, M. (1982): The influence of the substrate to plant growth. – Acta Horticulturae 126: 251-258.

http://www.aloki.hu ● ISSN 1589 1623 (Print) ● ISSN 1785 0037 (Online)
DOI: http://dx.doi.org/10.15666/aeer/1705_1035710369

CORRELATION BETWEEN PLANT DIVERSITY AND THE PHYSICOCHEMICAL PROPERTIES OF SOIL MICROBES

SUN, Y.[1] – SHI, Y.[1,2] – TANG, Y.[1,2] – TIAN, J.[1,2] – WU, X.[2*]

[1]*College of Pharmacy and Biological Engineering, Chengdu University, Chengdu 610106, China*

[2]*Key Laboratory of Coarse Cereal Processing Ministry of Agriculture, Chengdu University, Chengdu 610106, China*

**Corresponding author*
e-mail: 2206681513@qq.com

(Received 27th Sep 2018; accepted 16th Jul 2019)

Abstract. OBJECTIVE: To study the correlation between plant diversity and the physicochemical properties of soil microbes. METHODS: The determination of the chemical properties of farmland soil in the research area can be achieved by potentiometer method, automatic analyzer method, molybdenum-antimony anti-colorimetric method and gas chamber method. Based on the determination results, the relationship between plant diversity and soil microbial physical and chemical properties in the national nature reserve in rocky desertification area can be analyzed. RESULTS: The physical and chemical properties of soil in different grades of rocky desertification were significantly different. With the increase of rocky desertification, soil physical and chemical properties showed a response process from degradation to improvement. Soil organic matter, nitrogen, capillary water holding capacity, bulk density and porosity were significantly correlated with plant diversity, which played an important role in improving soil physical and chemical properties and promoting the restoration of plant diversity. Factor analysis showed that plant diversity at different levels in national nature reserves had different correlation with soil physical and chemical factors at different levels. The ratio between the significant correlation factors and the number of plants showed that the diversity of trees was greater than that of shrubs, and the diversity of shrubs was greater than that of herbaceous plants. Tree plant diversity factor plays a leading role. CONCLUSION: With the proposed method the physicochemical properties of soil microbes can be effectively studied.
Keywords: *plant diversity, soil, microbes, physical and chemical properties, rocky desertification, the related factors*

Introduction

Rocky desertification refers to the unreasonable social and economic activities of human beings in a fragile ecological environment, resulting in contradictions between people and land, vegetation destruction, soil erosion, gradual exposure of rocks, declining or even loss of land productivity, and presenting an evolutionary process or result similar to a desertified landscape (Steinauer and Tilman, 2016). The poverty-stricken population in the southwestern part of China is relatively concentrated, and the contradiction between people and land is very prominent (Bazerman et al., 2017; Jiang et al., 2017; Sun et al., 2016). Once the vegetation on the slope is destroyed, the soil erosion of the farmland is intensified, resulting in the loss of all the thin soil layers and serious rocky desertification, and the water and nutrient storage capacity is rapidly reduced. Rocky desertification has become a major ecological problem that restricts regional economic and social development in southwest China (He and Tang, 2016). Rock desertification governance has become an important part of Chinese social and economic construction. However, the current research on rock desertification restoration

http://www.aloki.hu ● ISSN 1589 1623 (Print) ● ISSN 1785 0037 (Online)
DOI: http://dx.doi.org/10.15666/aeer/1705_1037110388

ecology lags far behind the practice of rock desertification control (Thakur and Milcu, 2015). The restoration and reconstruction of rocky desert ecosystems seriously lacks the scientific support of relevant theoretical research, resulting in insignificant results of rocky desertification control. There are a series of problems such as simple structure, poor stability and weak resistance, which are difficult to maintain the governance results after the treatment of rocky desertification (Nyemb et al., 2018; Sudhan et al., 2018).

Species diversity is a manifestation of biodiversity at the species level, which can characterize the structural complexity of a biome, reflecting the structure type, organization level, development stage, stability level and habitat level of the community. It is an important organic component of biodiversity and is a research hotspot in the field of ecology (Zhalnina and Dias, 2015). At the same time, the restoration of species diversity is one of the most important features in the process of vegetation restoration. The farmland soil is an important part of the terrestrial ecosystem, and it is the carrier of many ecological processes of the ecosystem. It is an indispensable research content in the process of plant community renewal and succession. Through the study of the changes of soil physicochemical properties in the process of ecosystem succession under specific environmental conditions (Li and Zhang, 2015a), it will help to understand the interaction and mechanism of above-ground and underground interactions in the evolution of ecosystems, and then provide a scientific basis for the process of artificially regulating forest regeneration succession (Lloret and Mattana, 2015). But so far, although the research on the single ecological process of ecosystem is deep, the research on the correlation between ecosystem plant diversity and soil physicochemical properties is lack of in-depth research, and there is no research on the response of its spatial and temporal differentiation and its succession to rocky desertification (Camara et al., 2018; Shen et al., 2017; Xiao et al., 2018). After artificial regeneration and succession of rocky desertification environment, there is still a lack of research on what are the characteristics and trends of plant diversity and soil physicochemical properties, how the succession of artificial vegetation affects the evolution of underground farmland soil, and what kind of forest vegetation can be constructed to improve the soil properties of farmland in this area (Weidner and Koller, 2015). Therefore, this study in 2017, and national nature reserve in rocky desertification area as the research object, research on plant diversity and soil physical and chemical properties and their relations, and explore the plant diversity and changes of soil physical and chemical properties and their reaction mechanism, in order to provide theoretical support for forest ecological protection and ecosystem restoration and reconstruction of rocky desertification in Guizhou, even in Southwest China.

Material and methods

Overview of the study area

In this study, three typical rocky desertification areas and one national nature reserve as research areas are selected, which represents the different climates, topography, vegetation zoning and farmland soil conditions in a rocky desertification area.

The research area 1 is mainly located in the plateau mountainous areas of the Guizhou Province. The terrain is undulating and the elevation is 1400-1742 m. The annual average rainfall of the basin is 863 mm, the annual maximum precipitation is 995 mm, and the annual minimum precipitation is 618 mm. Rainfall is mainly distributed from July to September, accounting for 52% of the total annual rainfall. The

http://www.aloki.hu ● ISSN 1589 1623 (Print) ● ISSN 1785 0037 (Online)
DOI: http://dx.doi.org/10.15666/aeer/1705_1037110388

rock is dominated by carbonate-like limestone, with some Jurassic purple sand shale and shale distribution (Mellado-Vázquez and Lange, 2016). The farmland soil is dominated by yellow loam and purple sand. The vegetation is a subtropical evergreen deciduous coniferous and broad-leaved mixed forest, and the native vegetation is basically destroyed. It is now dominated by secondary forests (Kolton and Graber, 2016). The wild vegetation is vines, thorns, shrubs, which are mainly Pyracantha angustifolia, Rosa roxbunghii, Pyracantha fortuneana, Clematis florida and sporadic distribution of Cyclobalanopsis glauca, Pinus massoniana, Betula luminifera.

Study Area 2 is located in the township of the Guizhou Province, 12 km away from the county seat. The landform type is a typical plateau basin. The slope of the central part of the dam is slow, and the elevation in the basin is 1271-1451 m. The annual average rainfall of the basin is 1215 mm, and the rainfall is mainly distributed from April to August, accounting for 75% of the total annual rainfall. The rocks are mostly Triassic dolomite, argillaceous dolomite and shale. The farmland soil is dominated by yellow soil and yellow lime soil. Natural vegetation accounts for a small proportion of the area. The common arbor is mainly cedar (Vej and Lamentowicz, 2015), and the shrub layer is mostly typical limestone thorn bush, with Viburnum chinshanense, Pyracantha fortuneana, Rubus corchorifolius, and Rhamnus hemsleyana, etc., common species of the herbaceous layer are Imperata cylindrica, Miscanthus floridulu, Miscanthus sinensis, Arthraxon hispidus, Clematis florida, etc.

The study area 3 is located on the banks of the canyon of the Guizhou Province. The landform types are divided into two parts: the plateau area and the canyon area. There are mainly five types of landforms in the basin, and four types are karst landforms with an altitude of 450-1450 m. The difference is 1000 m. The annual average rainfall of the basin is 1100 mm, and the rainfall is mainly distributed from May to October, accounting for 83% of the total annual rainfall. The rocks are mostly Triassic dolomite, argillaceous dolomite and shale (Zhang and Johnston, 2017). The farmland soil is dominated by yellow soil and yellow lime soil. The vegetation is a subtropical evergreen deciduous coniferous and broad-leaved mixed forest, and the primary vegetation is basically destroyed. It is now dominated by secondary forests. The wild vegetation is vines, thorns, shrubs, which are mainly Pyracantha angustifolia, Rosa roxbunghii, Pyracantha fortuneana, Clematis florida and sporadic distribution of Cyclobalanopsis glauca, Pinus massoniana, Betula luminifera

Study area 4 is carried out in a certain test area of the Guizhou Province. The test area is located in a national nature reserve in the Guizhou Province. Except for a small amount of sand shale leakage, it is mainly composed of pure dolomite and limestone with exposed peak clusters, peak forests and Canyon landforms, as well as limestone soil and evergreen deciduous broad-leaved mixed forest (Zhou and Zhang, 2016). The test area belongs to the mid-subtropical mountain monsoon humid climate, with an average annual temperature of 15.3 °C, an average temperature of 5.2 °C in January, an average temperature of 23.5 °C in July, a growth period of 237 d, annual rainfall of 1752.5 mm, and concentrated distribution from April to October. The annual average relative humidity is 83%, and there are 827 species of 408 families and 408 genera of vascular plants, such as calcicole (Manglietia calcarea, Rhammus calcicolus, Cinnamomum calcarea, Phoebe calcarea, Stachyurus lipoensis, Camellia rubimuricata, Indosasa lipoensis, Acer liponsis, Hoya lipoensis and Tengia scopulorum), and national key protected plants (Handeliodendron bodimieri, Amentotaxus argotaenia,

http://www.aloki.hu ● ISSN 1589 1623 (Print) ● ISSN 1785 0037 (Online)
DOI: http://dx.doi.org/10.15666/aeer/1705_1037110388

Euryocrymbus cavalerier, Emmenopterys henryi, Tetrathyrium subcordatum and Calocedrus macrolepis). *Figure 1* shows the map of zserve in zovince.

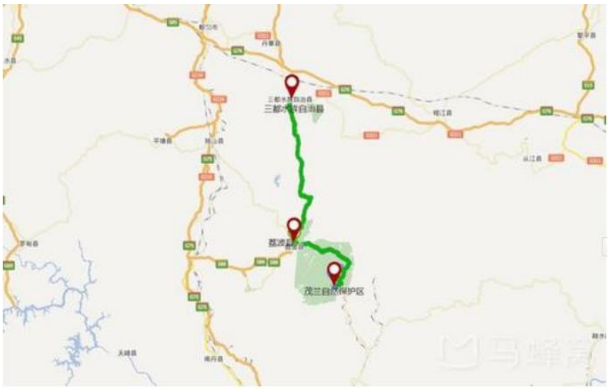

Figure 1. *Map of Maolan Nature Reserve, Guizhou Province*

Research methods

Sample setting

Based on the detailed investigation of the rocky desertification research area, five typical stages in the process of rock desertification succession are selected as the research objects, namely rockless desertification, potential rocky desertification, mild rocky desertification, moderate rocky desertification and intensity rocky desertification. The classification of rocky desertification is based on the results of expert research (Sun and Müllerschärer, 2015). For the five rocky desertification eco-environments, 45 research samples are set up in each of the four research areas, each of which has an area of 20 m × 20 m. The details of the sample are shown in *Table 1*. To analyze the physical and chemical properties of soil microorganisms, the basic information of the soil samples for the experiment should be clearly known. The basic information of the sample soil is given in *Table 1*.

In a national nature reserve, survey lines are set along the core area, buffer zone and test area, and the outer edge of the protected area. The number of forest survey plots established in different functional areas (interference levels) series are 12, 17, 9 and 3, respectively. One. The survey plot area is 20 m × 20 m, and the altitude, slope direction, slope position, slope, parent rock and farmland soil type are recorded (Baćmaga and Wyszkowska, 2016). Each plot is investigated for three layers of plants: arbor, shrub and grass. Diameter at breath height (abbreviated as DBH, the same below) ≥ 5 cm is classified as arbor and DBH < 5 cm is classified as shrub. The sample area is 10 m × 10 m in the arbor layer, 10 m × 10 m in the shrub layer, and 10 m × 10 m in the herb layer and the litter layer. The shrub layer, herb layer and litter layer are respectively set up three, representing that the development of each layer of plants or forest litter quantity is better, general, poor type. Among the vegetation survey indicators, the plants in arbor layer include the species name, DBH, tree height, number of plants, height under the branches, crown width and coverage, the plants in shrub layer include species name, ground diameter, height, number of plants and coverage, and plants in herbaceous layer include species, number of plants, height and coverage (Markowicz and Woźniak, 2015). The field sample is completed once in the first half of August of the survey year 2017.

http://www.aloki.hu ● ISSN 1589 1623 (Print) ● ISSN 1785 0037 (Online)
DOI: http://dx.doi.org/10.15666/aeer/1705_1037110388

Table 1. *Basic information of the study area and sample square setting*

Experiment sites	Location	Altitude (m)	Landform	Soil type	Degree of rocky desertification	Percentage of exposed rock (%)	Sum (serial number) of square
1	Saraci, Bijie City, Guizhou Province	1400-1742	Karst plateau mountains	Yellow soil, yellow lime soil	Intensive	30-35	1(1-3)
					Moderate	20-29	1(4-6)
					Mild	0-5	1(7-9)
					Potential	0-5	1(10-12)
					Nothing	0	1(13-15)
2	Hongfeng Lake in Qingzhen, Guizhou Province	1271-1451	Karst plateau basin	Yellow soil, yellow lime soil	Intensive	30-35	2(1-3)
					Moderate	20-29	2(4-6)
					Mild	0-5	2(7-9)
					Potential	0-5	2(10-12)
					Nothing	0	2(13-15)
3	Anshun, Guizhou	450-1450	Karst plateau canyon	Yellow soil, yellow lime soil	Intensive	30-35	3(1-3)
					Moderate	20-29	3(4-6)
					Mild	0-5	3(7-9)
					Potential	0-5	3(10-12)
					Nothing	0	3(13-15)
4	Maolan, Guizhou	430-1078	Karst plateau nature reserve	Yellow soil, yellow lime soil	Intensive	30-35	3(1-3)
					Moderate	20-29	3(4-6)
					Mild	0-5	3(7-9)
					Potential	0-5	3(10-12)
					Nothing	0	3(13-15)

Analysis of plant diversity

In October 2017, the density (strain/ m^2), average crown width (m^2 /strain) and coverage (%, That is, the proportion of the total area of the crown and the total area of all the trees), average DBH (cm/strain), average height (m/strain), and aboveground biomass are used to calculate community diversity (Yan and Zhang, 2016). The diversity measure indicators are:

Richness:

$$R = S \quad \text{(Eq.1)}$$

Shannon-Wiener index of diversity:

$$H = -\sum_{i=1}^{s} (Pi \ln Pi) \quad \text{(Eq.2)}$$

Uniformity index:

$$E = H / \ln S \quad \text{(Eq.3)}$$

http://www.aloki.hu ● ISSN 1589 1623 (Print) ● ISSN 1785 0037 (Online)
DOI: http://dx.doi.org/10.15666/aeer/1705_1037110388

Simpson dominance index, $D = \sum_{i=1}^{s} Pi^2$, S represents the total number of species in the community, Pi is the proportion of the number of individuals of species i to the total number of individuals in the community, i.e. $Pi = n_i / N$, n_i is the number of individuals of species i, N is the total number of individuals observed.

Collection of farmland soil samples and analysis of their physicochemical properties

(1) Collection of farmland soil samples in the rocky desertification research area

In the center of each plot, three sampling points are selected in a serpentine manner, and the spacing between the points is within 5 m. In October 2017, samples are taken 3 times at each point with a cutting ring (0-15 cm) and uniformly mixed to form a soil sample to be tested (Li and Zhang, 2015b). In a rocky desertification area, the farmland soil is very thin, and some of it is only about 15 cm. Therefore, it is used as a research object in the 0-15 cm farmland soil layer.

(2) Determination of soil physical properties in farmland

The volumetric weight, field water holding capacity, natural water content and capillary water holding capacity are determined by cutting ring method; total porosity is calculated by $p_t = 93.947 - 32.995 \times b$, b is bulk density, p_t is total porosity; capillary porosity is determined by cutting ring method; $p_o = p_t - p_c$ is used to calculate non-capillary porosity, p_o is non-capillary porosity, p_c is capillary porosity; permeability characteristics are determined by double-ring permeation.

(3) Determination of soil chemical properties in the study area

The pH value is determined by the potentiometer method using a water-to-earth ratio of 2.5:1. The organic matter is determined by oxidation of potassium dichromate with sulfuric acid to volumetric method; the whole nitrogen is potassium borate with copper sulfate as the selenium powder, and the automatic analyzer is determined by nitrogen analyzer. Hydrolyzed nitrogen is determined by alkali diffusion method; total phosphorus is determined by sulfuric acid for perchloric acid digestion and molybdenum anti-colorimetric method; effective phosphorus is determined by sodium bicarbonate extraction for molybdenum antimony colorimetric method; Hydrofluoric acid is determined by perchloric acid decoction flame photometer; available potassium is determined by flame photometric method using neutral ammonium acetate extraction (Ma and Baskin, 2017); farmland soil respiration is determined by gas chamber method.

(4) Collection and analysis of farmland soil samples in a national nature reserve

Combined with the plot survey, farmland soil sampling points are set up in each plot according to the three types of good, general and poor under-forest vegetation development. After removing the litchi cover layer of the sampling point, only the layer A of the farmland soil, or the layer A and the layer B, are sampled separately. The total weight of the soil sample of each layer is about 1 kg, and the soil sample is brought back to the laboratory under natural conditions. After air drying, the roots and gravel visible to the naked eye and the roots and coarse sand with a 1 mm mesh sieve are

http://www.aloki.hu ● ISSN 1589 1623 (Print) ● ISSN 1785 0037 (Online)
DOI: http://dx.doi.org/10.15666/aeer/1705_1037110388

removed, and the main chemical indicators of the farmland soil after grinding are determined (Baleshta and Simard, 2015). At the same time, according to the soil profile of farmland, the ring knife and sealant seal are extracted and brought back to the laboratory to analyze the main physical indexes of farmland soil, record the rock exposure rate of the sample plot, soil thickness, color, texture, root volume and amount of gravel.

Data processing and analysis

Drawing is performed using Excel software, and statistical analysis of variance analysis, t-test, multiple comparison (Duncan test), correlation analysis and principal component analysis are performed using SPSS 16.0 software (Økland and Nordbakken, 2016).

Calculation of plant diversity index:

Important value of arbor layer species:

$$IV = \frac{RD + RF + RT}{300} \quad \text{(Eq.4)}$$

In *Equation 4,* RD is the relative dominance, RF is the relative frequency, and RT is the relative density.

Species richness – Margalef index:

$$Mar = \frac{S - 1}{\ln N} \quad \text{(Eq.5)}$$

Ecological dominance – Simpson index:

$$Sim = 1 - \sum_{s=1}^{s} \frac{N_i(N_i - 1)}{N(N - 1)} \quad \text{(Eq.6)}$$

Information diversity – Shannon-Wiener index of:

$$Sha = -\sum_{s=1}^{s} P_i \ln P_i \quad \text{(Eq.7)}$$

Uniformity index – Pielon index:

$$Pie = \frac{H}{\ln S} \quad \text{(Eq.8)}$$

In the above equations, S represents the number of species, and N_i and N represent the number of species and all species, respectively

$$P_i = N_i / N \quad \text{(Eq.9)}$$

http://www.aloki.hu ● ISSN 1589 1623 (Print) ● ISSN 1785 0037 (Online)
DOI: http://dx.doi.org/10.15666/aeer/1705_1037110388

Results

Vegetation species composition and plant diversity of different grades of rocky desertification environment

Species composition

Vegetation species survey results show that the vegetation composition of rocky desertification environment is simple, and with the deepening of rocky desertification, the vegetation species composition shows a decreasing trend, and the Huajiang River with the highest degree of rocky desertification (Research Area 3) has the simplest vegetation community. There are only 8 families, 12 genera and 13 species in the layer, and there are only 10 families, 13 genera and 13 species in the wood layer. The richness of vegetation species in a rocky desertification area is also very low. Most species are 1 family, 1 genera and 1 species, and only 1 has Compositae, Rosaceae, and Gramineae. The families of Caprifoliaceae, Moraceae, Euphorbiaceae, and Rhamnaceae are mostly of many life types, indicating that these groups have better adaptation to the rocky desertification environment.

Among them, the Rosaceae species have more genus, species and life-type distribution in the potential and mild rocky desertification environment, but the distribution in the rocky desertification environment drops sharply, showing the adaptability of same species for different grades of rocky desertification environment has significant differences. The important value study of species also shows that there are significant differences between the established and dominant species of plant communities in different grades of rocky desertification. In the potential-light rocky desertification environment, species such as Saccharum arundinaceum, Robinia pseudoacacia, Ligustrum lucidum, and Artemisia dubia are dominant or established species of plant communities; In the light-moderate rocky desertification environment, the dominant or established species of plant communities are Miscanthus floridulus, Setaria viridis, Pteris multifida, Leptorhabdos parviflora, Viburnum propinquum, Itea yunnanensis and other species; in the moderate-intensity rocky desertification environment, the dominant species or plant species of the plant community are foxtail, Arthraxon hispidus, Broussonetia papyrifera, Lonicera japonica, Ampelocalamus calcareous, etc. *Table 2* shows the adaptability differences of rocky desertification environments at different levels.

Plant diversity

The plant diversity of four research areas was detected by Hashi Amtax NA8000 ammonia nitrogen automatic monitor. The following results were obtained. The results show that the four indices of plant diversity in rocky desertification environment are low (*Table 3*), indicating that the rocky desertification plant ecosystem has been destroyed, and the restoration succession is at a lower stage. The results also show that the four indexes of plant diversity in different grades of rocky desertification environment are significantly different: (1) The uniformity index of rockless desertification environment is significantly larger than the potential rocky desertification, and the potential rocky desertification is significantly larger than the mild, moderate and intensity rock desertification. (2) The environmental richness index of rockless desertification and mild rocky desertification is significantly larger than that of potential rocky desertification. (3) The environmental diversity index of rockless

http://www.aloki.hu ● ISSN 1589 1623 (Print) ● ISSN 1785 0037 (Online)
DOI: http://dx.doi.org/10.15666/aeer/1705_1037110388

desertification, potential rocky desertification and mild rocky desertification is significantly smaller than that of intensity rock desertification. There is no significant difference between rockless desertification, potential rocky desertification and mild rocky desertification. (4) The dominance index of potential rocky desertification environmental is significantly larger than other rocky desertification environments. It can be seen that among the four indices of plant diversity of rocky desertification environment, only the uniformity index change is significantly coupled with the succession of rocky desertification grade, showing a trend of decreasing with the increase of rocky desertification degree.

Table 2. *Adaptability differences of rocky desertification environment in different grades*

	Light-moderate rocky desertification environment	**Potential-light rocky desertification environment**	**Moderate-intensity rocky desertification environment**
Dominant species	Miscanthus floridulus, Setaria viridis, Pteris multifida, Leptorhabdos parviflora, Viburnum propinquum, Itea yunnanensis and other species	Saccharum arundinaceum, Robinia pseudoacacia, Ligustrum lucidum, and Artemisia dubia are dominant or established species of plant communities	foxtail, Arthraxon hispidus, Broussonetia papyrifera, Lonicera japonica, Ampelocalamus calcareous, etc

Table 3. *Plant diversity indices in different grades of rocky desertification environment*

Degrees of rocky desertification	**Evenness index**	**Richness index**	**Shannon-Wiener index**	**Dominance index**
Nil	12.65 ± 0.35a	12.65 ± 0.63a	2.26 ± 0.63ab	0.28 ± 0.09b
Potential	1.33 ± 0.26b	6.53 ± 0.35b	1.82 ± 0.52a	0.58 ± 0.09b
Low	0.38 ± 0.12c	12.17 ± 0.28a	2.48 ± 0.67ab	0.32 ± 0.08b
Middle	0.42 ± 0.11c	10.75 ± 1.02ab	2.91 ± 0.57bc	0.17 ± 0.05b
High	0.75 ± 0.13c	9.26 ± 0.67ab	3.28 ± 0.74c	0.13 ± 0.05b

The numerator value is the layer A of farmland soil and the denominator is the layer B of farmland soil

Correlation between plant diversity and soil physicochemical properties

The results of the correlation between plant diversity and soil physicochemical properties shows that (*Table 4*), there is a significant correlation between plant diversity in rocky desertification and soil physicochemical properties: (1) the richness index is negatively correlated with bulk density, total porosity, field water content, capillary water content, upper saturated permeability, organic matter, total nitrogen, total phosphorus and hydrolyzed nitrogen, and positively correlated with pH value, available potassium and soil respiration. (2) Diversity index is negatively correlated with bulk density, but positively correlated with total porosity, field water content, capillary water content, pH value, organic matter, total nitrogen and hydrolyzed nitrogen, and positively correlated with available phosphorus and available potassium. (3) The uniformity index had a significant negative correlation with pH and available phosphorus, a significant negative correlation with total phosphorus, a significant positive correlation with total potassium, and a significant positive correlation with soil respiration in farmland. (4)

http://www.aloki.hu ● ISSN 1589 1623 (Print) ● ISSN 1785 0037 (Online)
DOI: http://dx.doi.org/10.15666/aeer/1705_1037110388

The dominance index has a significant negative correlation with capillary porosity, and has a significant negative correlation with field water holding capacity, pH value, total nitrogen, total phosphorus and hydrolyzed nitrogen, and a significant positive correlation with the lower layer saturated permeability. There is a significant positive correlation with non-capillary porosity. It can be seen that changes in soil physicochemical properties of farmland in rocky desertification environment can easily affect the characteristics of plant diversity.

Table 4. *Correlation between physical and chemical factors of rocky desertification and plant diversity*

Soil physical-chemical factors	Richness index	Shannon-Wiener index	Evenness index	Dominance index
Bulk density/(g/cm^3)	-0.454**	-0.408**	-0.013	0.174
Capillary porosity/%	0.157	0.211	-0.114	-0.335**
Non-capillary porosity/%	0.136	0.043	0.134	0.251*
Total porosity/%	0.346**	0.311**	0.009	-0.104
Natural moisture content/%	0.179	-0.014	0.152	0.052
Field moisture content/%	0.518**	0.516**	0.17	-0.266**
Capillary moisture content/%	0.499**	0.532**	-0.001	-0.193
Upper strata saturated permeability/(mm/min)	0.365**	0.241	-0.063	0.17
Lower strata saturated permeability/(mm/min)	0.223	-0.008	-0.171	0.359**
pH value	0.248*	0.398**	-0.541**	-0.284*
Organic matter content/(mg/kg)	0.635**	0.349**	0.143	-0.092
Total nitrogen content/(g/kg)	0.719**	0.572**	-0.088	-0.262*
Total phosphorus content/(g/kg)	0.306**	0.213	-0.34*	-0.24*
Total potassium content/(g/kg)	-0.018	-0.199	0.396**	0.175
Hydrolysis nitrogen content/(mg/g)	0.759**	0.385**	-0.011	-0.226*
Available phosphorus content/(mg/kg)	0.092	0.247*	-0.309**	-0.085
Available potassium content/(mg/kg)	0.26*	0.253*	0.127	0.015
Soil respiration/	0.405*	-0.107	0.327*	-0.029

(In the table, * means general correlation, ** means significant correlation.)

The degree of dimensionality of plant diversity index and soil main physical index of a national nature reserve is obvious (factor extraction value > 1.0), and the cumulative variance contribution rate of trees, shrubs, herbaceous plant diversity factors and other factors in soil layer A and layer B is 90.00%, 91.49%. The cumulative variance contribution of the water holding capacity factor dominated by soil density, maximum water holding capacity and field water holding capacity, and the porosity factor dominated by non-capillary porosity, capillary porosity and total porosity in layer A and B is 95.75%, 94.63%. The main chemical index value of the soil has a large dimensionality difference (factor extraction value > 0.5). The common factor includes the fertility factor dominated by organic mass, total nitrogen and hydrolyzed nitrogen, and the amount of cation exchange, exchangeable salt base and the total phosphorus-dominated nutrient factor, the nitrogen factor dominated by total nitrogen, exchangeable salt base and pH, and the layer A also has a phosphorus factor dominated by total phosphorus, available phosphorus and cation exchange, potassium factor dominated by

http://www.aloki.hu ● ISSN 1589 1623 (Print) ● ISSN 1785 0037 (Online)
DOI: http://dx.doi.org/10.15666/aeer/1705_1037110388

potassium, organic matter and hydrolyzed nitrogen, and phosphorus factor in soil layer B dominated by effective phosphorus and exchangeable salt base, potassium factor dominated by total potassium, available potassium and cation exchange. The cumulative variance of soil fertility, nutrient, nitrogen, phosphorus and potassium factors in layer A and B is 83.06% and 87.60%.

Changes in main physicochemical indicators of farmland soil in a national nature reserve

There are no significant differences in the main physical indices of farmland soils between different forest types (*Table 5*). Farmland soil density, capillary porosity and total porosity, as well as maximum water holding capacity and field water holding capacity shows a trend of layer A > layer B. The non-capillary porosity values in the type I, III and V show the trend of layer A > layer B, in line with the general law; analysis of type II and IV showing the trend of layer B > layer A is due to the fact that there are many fractures in the parent rock at the sampling point part of the farmland soil in 50% of the plot, and the underground erosion of the layer Bin farmland causes the non-capillary porosity to be higher, and the other 50% of the sample is still in the trend of layer A > layer B. Type IV forest land has high rock exposure rate, low farmland soil density value, non-capillary porosity and total porosity, and maximum water holding capacity and field water holding capacity; Type III forest rock has low bare exposure rate, thin soil layer, small farmland soil density value, non-capillary porosity and total porosity, and maximum water holding capacity and field water holding capacity. The rock exposure rate and soil physicochemical indicators of type I and II forests are middle and the change is large.

Table 5. *Change of main physical indexes of soil of different karst forest types*

Types	Profile property				Porosity			Water holding capacity	
	Slope/(°)	Bare rock rate/%	PD/cm	Density/ (g/cm^3)	Capillary porosity/%	Non-capillary porosity/%	Total porosity/%	Field capacity/ ($\times 10^2 g/kg$)	Maximum water capacity/ ($\times 10^2 g/kg$)
Study area I	13.66	34.4	17.8	1.138/1.212	45.95/42.32	7.50/4.84	53.45/47.16	4.172/3.520	4.927/3.989
Study area II	11.22	25.96	11.48	1.281/1.331	41.80/36.70	6.0/7.85	47.80/44.55	3.138/2.639	3.740/3.347
Study area III	15.67	15.67	11.33	1.086/1.360	48.70/40.00	6.57/5.83	55.27/45.83	4.353/2.921	5.107/3.420
Study area IV	16.25	69.5	12.25	0.958/1.203	56.30/44.78	3.08/4.50	59.38/49.28	5.743/3.810	6.384/4.106

In the table, the numerator value is the layer A of farmland soil and the denominator is the layer B of farmland soil.

There are no significant differences in the main chemical indices of farmland soils between different forest types (*Tables 6* and *7*). The pH value and total potassium content of farmland soil shows the trend of layer A < layer B; the trend of soil organic matter quality, cation exchange amount, exchangeable salt base amount, total nitrogen amount, total phosphorus amount, hydrolyzed nitrogen amount, available phosphorus amount and available potassium is layer A > layer B. The change trend of total phosphorus and total potassium in layer A and B layer of farmland soil is different from other types, among which 50% of farmland soil total phosphorus and 75% of farmland soil total potassium change are contrary to the general law, which is related to the heterogeneity of farmland soil sample sites and farmland soil heterogeneity and the

http://www.aloki.hu ● ISSN 1589 1623 (Print) ● ISSN 1785 0037 (Online)
DOI: http://dx.doi.org/10.15666/aeer/1705_1037110388

underground erosion formed by the parent rock fissures. The soil fertility and nutrient index of type IV farmland are higher, the soil fertility and nutrient index of type III farmland are lower, and the soil fertility and nutrient index of type I, II and IV are middle, with larger variation.

Table 6. *Change of main soil fertility indexes of different karst forest types*

Types	pH	Organic mass/$(\times 10 g / kg)$	Cation exchange capacity/$(\times 10 cmol^{*} / kg)$	Exchangeable base amount/$(\times 10 cmol^{*} / kg)$
Study area I	6.55/6.62	6.32/3.34	3.89/2.44	1.08/1.07
Study area II	6.38/6.41	2.49/1.89	2.22/1.30	0.86/0.86
Study area III	6.05/6.22	6.14/2.16	4.24/2.82	1.50/1.18
Study area IV	6.46/6.63	5.95/3.40	6.30/4.63	3.34/3.08

The numerator value is the layer A of farmland soil and the denominator is the layer B of farmland soil.

Table 7*. Changes of main nutrient indexes of soil of different karst forest types*

Types	Total nitrogen content/(g/kg)	Total phosphorus content/(g/kg)	Total potassium content/ $(\times 10 g / kg)$	Hydrolysis nitrogen content/ $(\times 10^{2} mg / kg)$	Available phosphorus content/(mg/k)	Available potassium content/$(\times 10^{2} mg / kg)$
Study area I	2.63/2.52	0.30/0.29	3.99/4.02	2.65/1.64	2.76/1.85	1.68/0.91
Study area II	2.25/1.28	0.29/0.27	3.75/3.97	1.59/1.21	5.02/3.51	1.22/1.00
Study area III	4.87/0.98	0.22/0.13	4.15/4.38	2.97/0.90	1.65/1.46	2.54/1.32
Study area IV	4.92/2.02	0.35/0.40	4.53/4.38	3.10/1.51	2.13/1.56	2.49/1.51

The numerator value is the layer A of farmland soil and the denominator is the layer B of farmland soil

The correlation between different stratified plant diversity factors and soil physicochemical factors in different soil layers is different, which is consistent with the general characteristics of growth and development during the natural restoration process of trees, shrubs and herbaceous plants. According to the proportional relationship between relevant important factors and quantity in *Table 7*, the more nitrogen, phosphorus and potassium content in the study area, the richer plant diversity in the study area. The contents of nitrogen, phosphorus, potassium and other important factors in each class landform forest can fully explain the following results: The relevant significant factor-to-quantity ratios shows the trend of arbor layer (36.38%) > shrub layer (27.27%) > herb layer (18.9%), layer A in farmland soil (45.45%) < layer B (54.55%). The plant diversity factor of arbor layer plays a leading role.

Correlation between plant diversity index of arbor layer and soil physicochemical indicators in a national nature reserve

The correlation coefficient between the plant diversity index of forest arbor layer and the soil physicochemical index of farmland shows a trend of quadratic polynomial (QC) ≥ linear (SL). The significant indicators are 46.09% and 39.84%, respectively, showing the trend of the Layer A (QC = 21.88%, SL = 18.75%, the same below) < layer B (24.22%, 21.09%), Pielou index (14.06%, 13.28%) > Simpson index (12.50%, 10.94%) > Shannon-Wiener index (10.16%, 8.59%) > Margalef index (9.38%, 7.03%) as shown in *Table 8*. Among the related significant quantitative rate, the soil physical index of farmland is quadratic polynomial (66.67%) > linear (62.50%), layer A > layer

http://www.aloki.hu ● ISSN 1589 1623 (Print) ● ISSN 1785 0037 (Online)
DOI: http://dx.doi.org/10.15666/aeer/1705_1037110388

B, and the soil fertility index of farmland is quadratic polynomial (37.50%) > linear (31.25%), layer A > layer B, farmland soil nutrient index is quadratic polynomial (31.25%) > linear (22.92%), layer A < layer B in farmland soil. Significant correlations between plant diversity index in arbor layer and soil physical, fertility and nutrient indices are found. The logarithmic quantitative rate varies with species of diversity index, soil layers and types of physical and chemical indices, but the trend does not change with model types.

Table 8. *Correlation between plant diversity index and soil physical and chemical indexes in karst forest trees*

	Indicators			Simpson index		Shannon-Wiener index		Pielou index	
		A horizon	B horizon	A horizon	B horizon	A horizon	B horizon	A horizon	B horizon
Physical indicators	Density	-0.512**	-0.405*	-0.526**	-0.436*	-0.553**	-0.405**	-0.568**	-0.413*
		-0.514**	-0.534**	-0.569**	-0.512**	-0.553**	-0.506**	-0.574**	-0.484**
	Capillary porosity	-0.148	0.29	0.191	0.431*	-0.058	0.325	0.17	0.387*
		-0.243	0.292	0.246	0.439*	-0.264	0.326	0.229	0.387*
	Non-capillary porosity	0.433**	0.049	0.245	-0.075	0.402*	0.029	0.301	-0.003
		0.476**	0.352	0.379*	-0.328	0.433**	0.088	0.315	-0.046
	Total porosity	0.252	0.286	0.421**	0.328	0.314	0.303	0.452**	0.336
		0.252	0.351	0.436**	0.354	0.334	0.311	0.457**	0.337
	Field capacity	0.351*	0.4*	0.465**	0.453*	0.391*	0.389*	0.462**	0.426*
		0.359*	0.447*	0.478**	0.474*	0.396*	0.455*	0.47**	0.435*
	Maximum water capacity	0.439**	0.411*	0.419**	0.415*	0.449**	0.392*	0.445**	0.402*
		0.443**	0.49**	0.456**	0.474*	0.453**	0.465*	0.45**	0.439**
Fertility indicators	pH	0.186	0.08	0.186	0.07	0.231	0.127	0.228	0.159
		0.195	0.094	0.266	0.244	0.305	0.26	0.313	0.28
	Organic mass	0.348*	0.272	0.474**	0.424*	0.338*	0.302	0.452**	0.381*
		0.368*	0.277	0.476**	0.443*	0.381*	0.306	0.453**	0.382*
	Cation exchange capacity	0.182	0.362	0.313	0.365	0.277	0.416*	0.393	0.43
		0.273	0.382*	0.313	0.376	0.359*	0.419*	0.41*	0.435*
	Exchangeable base amount	0.105	0.122	0.272	0.178	0.182	0.174	0.361*	0.279
		0.12	0.13	0.283	0.181	0.215	0.183	0.387*	0.279
Nutrient indicators	Total nitrogen content	0.112	0.207	0.29	0.44*	0.184	0.29	0.351*	0.417*
		0.197	0.27	0.295	0.451*	0.307	0.302	0.378*	0.421*
	Total phosphorus content	-0.221	0.098	-0.095	0.232	-0.164	0.16	0.022	0.299
		-0.238	0.201	-0.101	0.313	-0.215	0.197	0.027	0.333
	Total potassium content	0.049	0.149	0.193	0.293	0.158	0.235	0.259	0.36
		0.249	0.453*	0.302	0.43*	0.192	0.321	0.305	0.399*
	Hydrolysis nitrogen content	0.23	0.369	0.337*	0.456*	0.23	0.384*	0.268	0.434*
		0.283	0.378	0.363*	0.538**	0.313	0.387*	0.287	0.436*
	Available phosphorus content	-0.094	-0.008	-0.202	-0.099	-0.142	-0.074	-0.156	-0.114
		-0.19	-0.203	-0.205	-0.112	-0.171	-0.103	-0.159	-0.176
	Available potassium content	0.145	0.381*	0.227	0.494**	0.16	0.49**	0.201	0.609**
		0.365*	0.569**	0.242	0.505**	0.3	0.536**	0.309	0.635**

(In the table, * means general correlation, ** means significant correlation.)

http://www.aloki.hu ● ISSN 1589 1623 (Print) ● ISSN 1785 0037 (Online)
DOI: http://dx.doi.org/10.15666/aeer/1705_1037110388

According to *Table 8*, based on the difference between the quadratic polynomial and the linear correlation between the plant diversity index and the farmland soil physicochemical indicators, it can be divided into three types. (1) The correlation is not significant, including farmland soil pH, total phosphorus and available phosphorus, the indicator rate is 53.91%, which is farmland soil layer A (28.13%) > B layer (25.75%)/Margale index (15.63%) > Shannon-Wiener Index (14.84%) > Simpson Index (12.50%) > Pielou Index (10.94%). (2) Only the significant type of curve correlation, including total potassium of layer B in farmland soil, etc., the indicator pair rate is 5.47%, showing the trend of layer A in farmland soil (2.34%) < layer B (3.13%), Pielou index (0.78%) < Simpson index (1.56%) = Shannon-Wiener index (1.56%) < Margalef index (2.34%).(3) Significant type of correlation. Both linear and quadratic polynomial correlations are significant, including farmland soil density, field water holding capacity and maximum water holding capacity, organic quality of layer A in farmland soil and available potassium of B layer. The indicator rate is 40.63%, which shows the trend of layer A (19.53%) < layer B (21.09%) and Margalef index (7.03%) < Shannon-Wiener index (8.59%) < Simpson index (10.94%) < Pielou index (13.28%).

Discussion

Discussion on the plant diversity of rocky desertification environment and the physicochemical properties of farmland soil

Compared with the experimental results of traditional methods, the results of this paper show that there is no obvious coupling relationship between the richness index, diversity index and dominance index of rocky desertification plant community at different levels and the succession of rocky desertification. This should be the result of human interference. After the natural state is superimposed by human activities, the natural law of vegetation restoration is disturbed. The change of evenness index has remarkable coupling relation with the succession of rocky desertification degree. With the increase of rocky desertification level, the evenness index showed a trend of gradual decrease, indicating that the evenness index of plant diversity should be an important basis for plant community evaluation in rocky desertification areas. The deterioration of rocky desertification environment leads to the decrease of plant diversity. The evolution of farmland soil properties under rocky desertification is not a process of degradation with the increase of rocky desertification level, but a gradual process of degradation and then improvement. The reason is the result of soil erosion of rocky desertification and soil nutrient accumulation of bare rocky desertification. With the increase of rocky desertification, the accumulation effect of bare rock increased gradually, and the input of soil nutrients in farmland increased. With the increase of rocky desertification, soil loss can be reduced, soil erosion is weakened, and soil nutrient loss of corresponding farmland is weakened. The combination of these processes leads to the gradual improvement of degraded farmland soils. The evolution process of the physical and chemical properties of farmland soil in rocky desertification is as follows: when forest vegetation is destroyed in rocky desertification environment, the loss of soil nutrients in farmland increases with the increase of soil and water loss, the input of organic matter in garbage decreases, the bulk density of farmland soil increases, nitrogen and water capacity decrease, and farmland soil degradation. The accumulation of nutrients and karst products in the atmosphere increased, and the input of organic matter and nitrogen in farmland soil increased. At the same time, with the increase of rocky desertification

http://www.aloki.hu ● ISSN 1589 1623 (Print) ● ISSN 1785 0037 (Online)
DOI: http://dx.doi.org/10.15666/aeer/1705_1037110388

degree, soil loss can be reduced, soil erosion weakened, soil nutrient loss in farmland reduced, soil nutrient and farmland physical properties gradually improved.

Discussion on plant diversity and soil physicochemical properties of a national nature reserve

In this paper, the distribution of the same type of cross-adjacent functional area exists in the forest type by the important value of the arbor layer species. Because the important value only reflects the dominant degree of the species in the community, does not reflect its growth and development stage, and there are different functional areas, the type of division can still be interpreted. The application of other indicators may better express the types of forests in different functional areas, but the main indicators and related trends of vegetation-farm soil systems will not change. In this paper, the significant differences in soil organic matter, total nitrogen, hydrolyzed nitrogen, available phosphorus and available potassium are different. The plant diversity index is similar to that of farmland soil. The correlation coefficient of the index value decreases or increases with the increase of the soil layer thickness. The correlation significant index shows the trend of the layer A < layer B, which is different from the non-natural secondary forest and similar to other natural secondary forests. It indicates that the correlation between forest plant diversity index and soil physicochemical index values is specific between soil layers.

Restoration and reconstruction of degraded ecosystems in rocky desertification area

The rocky desertification ecosystem has a simple vegetation community and a very low abundance. The rocky desertification environment has significant stress on its plant distribution. The plants in rocky desertification environment must have the characteristics of stone nature, calcium tolerance and drought tolerance, but also have a well-developed and strong root system, which has important guiding significance in the restoration and reconstruction of degraded ecosystems in rocky desertification area. The plants of Compositae, Rosaceae, Gramineae, Lonicerae, Euphorbiaceae and other plants are mostly distributed in rocky desertification environment, indicating that these groups have strong adaptability to rocky desertification environment, which provides an important reference for the application of vegetation restoration technology and the selection of pioneer species. Among them, the Rosaceae plants have more genus distribution in the potential and mild rocky desertification environment, while the number of species distributed in the intensity rocky desertification environment decreases significantly, indicating that the adaptability of adaptable species in different grades of rocky desertification environment are is significantly different. Therefore, in the process of controlling desertification and selecting species by rocky desertification, it is necessary to screen not only the species that adapt to the rocky desertification environment, but also the adaptive pioneer species for different grades of rocky desertification environment, so that it can achieve the expected goal of vegetation restoration in rocky desertification control. The degradation of fragile ecosystems is driven by strong human disturbances, with vegetation reduction as the cause, degradation of land productivity as the essence, and a composite process marked by similar desertification landscapes. The diversity and structural index of vegetation community in rocky desertification environment are low, and the stability is poor. Therefore, the vegetation with strong primitiveness and without disturbance should keep

http://www.aloki.hu ● ISSN 1589 1623 (Print) ● ISSN 1785 0037 (Online)
DOI: http://dx.doi.org/10.15666/aeer/1705_1037110388

the status quo and develop naturally. The disturbed rocky desertification ecosystem should supplement the post-successive propagules, paying special attention to the introduction of some top or sub-top species; secondary forest areas should be properly trimmed to maintain reasonable density, which is conducive to sexual reproduction and renewal chain as soon as possible. Recovery and rapid growth of forests promote the uniform distribution of species composition, rationalize the diversity, and achieve rapid restoration and formation of plant communities.

Conclusions

In this paper, a rocky desertification area and a national nature reserve are used as research objects to analyze the correlation effects of plant species diversity on the physicochemical properties of soil microbes. Three typical rock desertification areas and one national level nature protection are selected as the sample area. Through the collection and analysis of the physicochemical properties of the farmland soil samples in the rock desertification area, the results of the physical properties of the soils, such as the bulk density, field water capacity, natural water content, capillary water capacity, total porosity, capillary porosity, and non-capillary porosity, and the determination results of the chemical properties of the farmland soils such as pH, organic matter, total nitrogen, total phosphorus, total potassium, available phosphorus and available potassium are obtained. Based on this, the correlation between plant diversity and the physicochemical properties of farmland soil in the rocky desertification environment and the correlation between plant diversity and soil microbes in a national nature reserve are studied. After measuring the physicochemical indicators of farmland soil, the plant diversity index is calculated to study the physicochemical properties of farmland soils of different forest types. The change of index value is used to study the correlation between plant diversity of national nature reserve and soil microbes in farmland.

REFERENCES

[1] Baćmaga, M., Wyszkowska, J., Kucharski, J. (2016): The effect of the Falcon 460 EC fungicide on soil microbial communities, enzyme activities and plant growth. – Ecotoxicology 25(8): 1-13.

[2] Baleshta, K. E., Simard, S. W., Roach, W. J. (2015): Effects of thinning paper birch on conifer productivity and understory plant diversity. – Scandinavian Journal of Forest Research 30(8): 699-709.

[3] Bazerman, C., Applebee, A. N., Berninger, V. W., Brandt, D., Graham, S., Matsuda, P. K., Murphy, S., Rowe, D. W., Schleppegrell, M. (2017): Taking the long view on writing development. – Research in the Teaching of English 51(3): 351-360.

[4] Camara, E. M., Caramaschi, E. P., Di Dario, F., Petry, A. C. (2018): Short-term changes in two tropical coastal lagoons: effects of sandbar openings on fish assemblages. – Journal of Coastal Research 34(1): 90-105.

[5] He, Q. H., Tang, X. J., Tang, X. J. (2016): Research on soil parameter identification of excavator digging. – Computer Simulation 33(2): 361-366.

[6] Jiang, S. C., Ge, S. B., Wu, X., Yang, Y. M., Chen, J. T., Peng, W. X. (2017): Treating n-butane by activated carbon and metal oxides. – Toxicological and Environmental Chemistry 99(5-6): 753-759.

http://www.aloki.hu ● ISSN 1589 1623 (Print) ● ISSN 1785 0037 (Online)
DOI: http://dx.doi.org/10.15666/aeer/1705_1037110388

[7] Kolton, M., Graber, E. R., Tsehansky, L. (2016): Biochar-stimulated plant performance is strongly linked to microbial diversity and metabolic potential in the rhizosphere. – New Phytologist 213(3): 1393-1404.
[8] Li, J. H., Zhang, H., Li, W. J. (2015): Plant–soil feedbacks in a sub-alpine meadow ecosystem with high plant diversity on the Qinghai-Tibetan Plateau. – Plant Ecology 216(12): 1659-1674.
[9] Li, P., Zhang, J., Xie, H. (2015): Effects of Misgurnus anguillicaudatus and Cipangopaludina cathayensis on pollutant removal and microbial community in constructed wetlands. – Water 7(5): 2422-2434.
[10] Lloret, F., Mattana, S., Curiel, Y. J. (2015): Climate-induced die-off affects plant-soil-microbe ecological relationship and functioning. – FEMS Microbiology Ecology 91(2): 1-12.
[11] Ma, M., Baskin, C. C., Yu, K. (2017): Wetland drying indirectly influences plant community and seed bank diversity through soil pH. – Ecological Indicators 80(80): 186-195.
[12] Markowicz, A., Woźniak, G., Borymski, S. (2015): Links in the functional diversity between soil microbes and plant communities during natural succession in coal mine spoil heaps. – Ecological Research 30(6): 1005-1014.
[13] Mellado-Vázquez, P. G., Lange, M., Bachmann, D. (2016): Plant diversity generates enhanced soil microbial access to recently photosynthesized carbon in the rhizosphere. – Soil Biology and Biochemistry 94: 122-132.
[14] Nyemb, J. N., Magnibou, L. M., Talla, E., Tchinda, A. T., Tchuenguem, R. T., Henoumont, C., Laurent, S., Mbafor, J. T. (2017): Lipids constituents from Gardenia aqualla Stapf and Hutch. – Open Chemistry. 16(1): 371-376.
[15] Økland, T., Nordbakken, J. F., Lange, H. (2016): Short-term effects of whole-tree harvesting on understory plant species diversity and cover in two Norway spruce sites in southern Norway. – Scandinavian Journal of Forest Research 31(8): 766-776.
[16] Shen, Y., Zhao, N., Xia, M., Du, X. (2017): A deep Q-learning network for ship stowage planning problem. – Polish Maritime Research 24(SI): 102-109.
[17] Steinauer, K., Tilman, D., Wragg, P. D. (2016): Plant diversity effects on soil microbial functions and enzymes are stronger than warming in a grassland experiment. – Ecology 96(1): 99-112.
[18] Sudhan, S. P. N., Ahmed, R. N., Kiyani, H., Mansoor, S. S. (2018): Ionic liquid 1-butyl-3-methylimidazolium bromide: a green reaction media for the efficient synthesis of 3-methyl-1,4-diphenyl-1,4,5,7-tetrahydro-pyrazolo [3,4-d]pyrimidine-6-ones/thiones using phthalimide-n-sulfonic acid as catalyst. – Journal of Saudi Chemical Society 22(3): 269-278.
[19] Sun, J., Lu, J., Wang, W., Mu, Y., Zhao, J., Liu, C., Chen, L., Shi, L., Li, Q., Yang, T., Yan, L., Wan, Q., Wu, S., Liu, Y., Wang, G., Luo, Z., Tang, X., Chen, G., Huo, Y., Gao, Z., Su, Q., Ye, Z., Wang, Y., Qin, G., Deng, H., Yu, X., Shen, F., Chen, L., Zhao, L., Bi, Y., Xu, M., Xu, Y., Dai, M., Wang, T., Zhang, D., Lai, S., Ning, G. (2016): Prevalence of diabetes and cardiometabolic disorders in spouses of diabetic individuals. – American Journal of Epidemiology 184(5): 400-409.
[20] Sun, Y., Müllerschärer, H., Maron, J. L. (2015): Origin matters: diversity affects the performance of alien invasive species but not of native species. – American Naturalist 185(6): 725-736.
[21] Thakur, M. P., Milcu, A., Manning, P. (2015): Plant diversity drives soil microbial biomass carbon in grasslands irrespective of global environmental change factors. – Global Change Biology 21(11): 4076-4085.
[22] Vej, J., Lamentowicz, Ł., Bjm, R. (2015): Plant functional diversity drives niche-size-structure of dominant microbial consumers along a poor to extremely rich fen gradient. – Journal of Ecology 102(5): 1150-1162.

http://www.aloki.hu ● ISSN 1589 1623 (Print) ● ISSN 1785 0037 (Online)
DOI: http://dx.doi.org/10.15666/aeer/1705_1037110388

[23] Weidner, S., Koller, R., Latz, E. (2015): Bacterial diversity amplifies nutrient-based plant–soil feedbacks. – Functional Ecology 29(10): 1341-1349.
[24] Xiao, Q., Li, D., Guo, R., Zheng, L., An, X., Zeng, Z. (2018): In vivo and in vitro toxicities of diethyl phthalate to flounder fish Paralichthys olivaceus and its gill cell line (fg cells). – Journal of Environmental Biology 39(1): 73-81.
[25] Yan, X., Zhang, Y., Luo, X. (2016): Effects of uranium on soil microbial biomass carbon, enzymes, plant biomass and microbial diversity in yellow soils. – Radioprotection 51(3): 207-212.
[26] Zhalnina, K., Dias, R., Quadros, P. D. D. (2015): Soil pH determines microbial diversity and composition in the park grass experiment. – Microbial Ecology 69(2): 395-406.
[27] Zhang, X., Johnston, E. R., Barberán, A. (2017): Decreased plant productivity resulting from plant group removal experiment constrains soil microbial functional diversity. – Global Change Biology 23(10): 4318-4332.
[28] Zhou, D., Zhang, H., Bai, Z. (2016): Exposure to soil, house dust and decaying plants increases gut microbial diversity and decreases serum immunoglobulin E levels in BALB/c mice. – Environmental Microbiology 18(5): 1326-1337.

http://www.aloki.hu ● ISSN 1589 1623 (Print) ● ISSN 1785 0037 (Online)
DOI: http://dx.doi.org/10.15666/aeer/1705_1037110388

COMPARATIVE EFFICACY OF DOMESTIC GARLIC (*ALLIUM SATIVUM*) AND NEEM (*AZADIRACHTA INDICA*) AGAINST *HAEMONCHUS CONTORTUS* IN SMALL RUMINANTS

AZRA, A.[1] – KALEEMULLAH, M.[1] – KHATTAK, B.[2*] – ASMA, N.[1] – SAFI, A. U. R.[2] – QAISER, J.[2] – AFZAL, M.[3] – TAHIR, U.[4] – SINDHU, Z. U. D.[5] – FARHAN, Y.[6]

[1]*Depatrment of Zoology, Kohat University of Science and Technology, Kohat, Pakistan*

[2]*Department of Microbiology, Kohat University of Science and Technology, Kohat, Pakistan*

[3]*Zhejiang Provincial Key Laboratory of Agricultural Resources and Environment, Hangzhou, China*

[4]*College of Veterinary Sciences and Animal Husbandry, Abdul Wali Khan University, Mardan, Pakistan*

[5]*Department of Parasitology, University of Agriculture, Faisalabad, Pakistan*

[6]*Sulaiman Bin Abdullah Aba Al-Khail Centre for Interdisciplinary Research in Basic Sciences, International Islamic University, Islamabad, Pakistan*

**Corresponding author*
e-mail: baharkk75@gmail.com; phone: +92-334-9073-552

(Received 5th Dec 2018; accepted 1st May 2019)

Abstract. Livestock plays an important role in the economy of Pakistan. Small ruminants like sheep and goats, are highly susceptible to internal parasites, particularly gastrointestinal nematodes (GINs) including *Haemonchus contortus*. The present study was conducted in Pakistan to test the larvicidal and ovicidal activities with different concentrations of extracts of bulbs of domestic garlic (*Allium sativum*) and leaves of neem tree (*Azadirachta indica*) against *H. contortus*. In case of larval mortality, the highest mortality was recorded as 87% at 100% extract of neem leaves, while 100% extract of garlic bulb showed 67% mortality. The highest egg hatching inhibition (94%) was noted when neem leaves extract was used at 100% concentration, while in case of garlic extract, 100% concentration showed 80% inhibition of the eggs hatching. It was concluded that all the extracts of *A. indica* showed higher mortality and eggs hatching inhibition of *H. contortus* than *A. sativum*.
Keywords: *parasites, medicinal plants, eggs hatch assay, larval mortality assay*

Introduction

Agriculture always played a major role in the economy of Pakistan. In National Gross Domestic Product (GDP), agriculture contributes 24% in which share of livestock is 12%. According to the Ministry of National Food Security & Research the estimated population of domestic sheep (*Ovis aries*) was 30.5 million while domestic goats (*Capra aegagrus hircus*) were 74.1 million during 2017-18. It is also estimated that about 40000 tons of meat from sheep and 915000 tons from goats were obtained during the year 2017-18 (Economic Survey of Pakistan 2017-2018). But this important sector of agriculture is highly susceptible to gastrointestinal nematodes (GINs). Among GINs, *Haemonchus contortus*, a blood-sucking nematode that belongs to the family *Trichostrongylidae* and class *Secernentea,* causing a serious disease in small ruminants called Haemonchosis (Khattak et al., 2018).

http://www.aloki.hu ● ISSN 1589 1623 (Print) ● ISSN 1785 0037 (Online)
DOI: http://dx.doi.org/10.15666/aeer/1705_1038910397

The clinical symptoms of this disease include hemorrhagic anemia, hypo-protein anemia, and parasitic gastroenteritis in animals especially in small ruminants like sheep and goats (Mola, 2018). *Haemonchus contortus* infestation causes major health problems including reduction in animal productivity in terms of meat, milk and wool. The major impacts of *H. contortus* in small ruminants are associated with the blood sucking activity that results in extensive blood loss (Bowman et al., 2009). Each parasite sucks 0.05 ml of blood per day. As a result, there is a decrease in total erythrocytes count, hemoglobin, packed cell volume, body weight, milk production and wool growth (Hepworth, 2006; Urquhart et al., 1996; Rasool et al., 1995). It is estimated that a sheep can lose 250 ml blood/day if infected with 5000 *H. contortus* worms. Life cycle of this parasite takes around 21 days to complete. Its life cycle is direct i.e. no secondary host is involved in cycle completion. Every adult female parasite lays 5000-10,000 eggs per day which are then passed out in the feces (Emery et al., 2016) as shown in *Figure 1*.

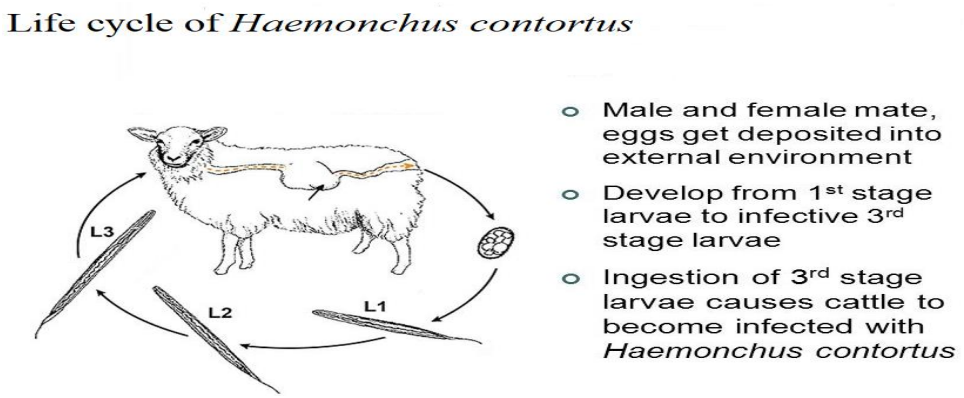

Figure 1. *Life cycle of Haemonchus contortus. (Reproduced from SlidePlayer.com)*

The frequent and un-judicial use of anthelmintic drugs has led to a growing problem of parasitic resistance against the conventional therapies. *Haemonchus contortus* is showing resistance to the most commonly used broad spectrum anthelmintics belonging to the classes; Benzimidazoles, imidazothiazoles and Macro cyclic lactones (Kaplan, 2004; Jackson and Coop, 2000; Sangster, 1999; Miller et al., 1987).

Garlic (*Allium sativum*) has been reported to be a parasiticide, amoebicide, larvicide and immune-stimulant (Duke, 2002). Essential oil of these plants can also be used as alternative or supplement to the current anthelmintics therapies (Anthony et al., 2004). Neem plant, (*Azadirachta indica)* is known for its medicinal properties and has been used against gastrointestinal nematodes and related problems in many parts of the world (Biswas et al., 2002). Therefore, the present study was designed with the objective to evaluate the anthelmintic properties of the crude extracts of Garlic and Neem plants against *H. contortus* in small ruminants.

Materials and methods

Sampling area

Adult *H. contortus* were collected from the infected abomasums of small ruminants from slaughter houses in district Kohat of Khyber Pakhtunkhwa, Pakistan as shown in

http://www.aloki.hu ● ISSN 1589 1623 (Print) ● ISSN 1785 0037 (Online)
DOI: http://dx.doi.org/10.15666/aeer/1705_1038910397

Figure 2. The climate in Kohat is referred to as a local steppe climate. There is little rainfall throughout the year. This location is 33°34'47.1"N/71°26'29.3"E, elevation is 395 m/1296 feet and barometric pressure is 97KPa. The temperature here averages 22.8 °C. The average annual rainfall is 529 mm.

Figure 2. *Sampling area of district Kohat. (Reproduced from Google Maps)*

Collection and isolation of H. contortus

After collection of the adult parasites, female *H. contortus* worms were separated and placed in the Petri dish containing Phosphate Buffer Saline (PBS). Petri dish containing worms were kept in incubator at 37 °C. The identification of *H. contortus* was carried out on the basis of morphological features using standard keys (Urquhart et al., 1996) as shown in *Figure 3*.

Cultivation of infective larvae

After separation of female parasites from male parasites, eggs were recovered by grinding the female with pistol and mortar by adding 5 ml PBS. Eggs were incubated at room temperature for 72 h for the development of the infective larvae (L3). After cultivation, the infective larvae (L3) were maintained in the laboratory at 25-30 °C in sterile conditions.

Collection of plant materials

Fresh and healthy plant parts of Garlic (bulbs) and Neem (leaves) (disease free) were collected from various parts of the Khyber Pakhtunkhwa, Pakistan. After collection, the plants were washed with distilled water and dried with clean clothes and then kept in the laboratory for further processing.

Preparation of plant extracts

After drying, the plant materials were cut into small pieces followed by grinding into fine powder. The powdered material was mixed with methanol in conical flask and filtered through Whattman filter paper No. 1. The filtrate was then allowed to evaporate and make them concentrated.

http://www.aloki.hu ● ISSN 1589 1623 (Print) ● ISSN 1785 0037 (Online)
DOI: http://dx.doi.org/10.15666/aeer/1705_1038910397

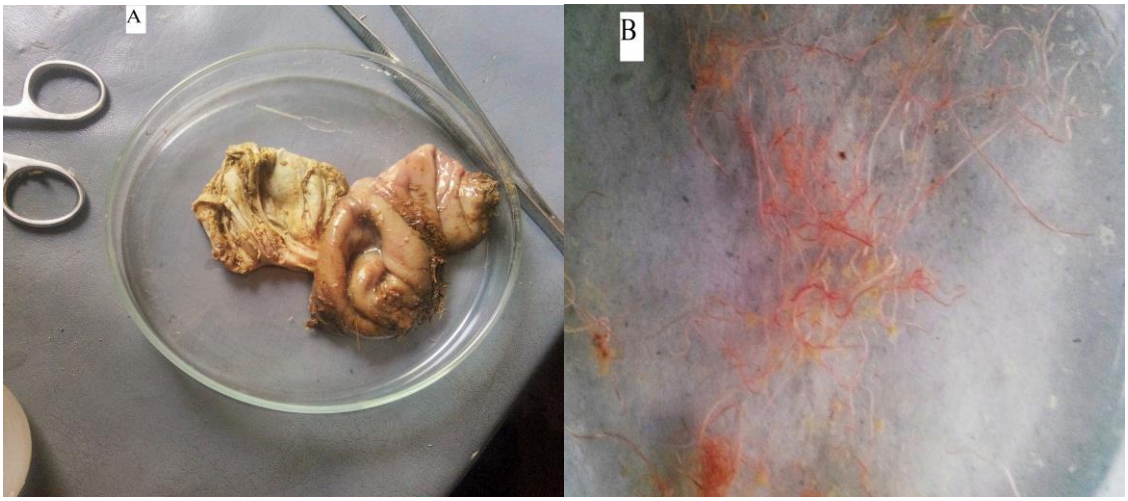

***Figure 3. A** Abomasum of infected sheep. **B** Adult worms harvested from infected abomasum*

Preparation of methanol extracts

10 gm of the Neem and Garlic powdered materials first weighted and then dissolved in 100 ml methanol solution in separate beakers in order to make 10% solution and mixed properly by magnetic stirrer for 15 min. The solutions were kept on rotary shaker for 24 h and the mixtures were then passed through Whattman filter paper No.1 to prepare filtrate. The filtrate was taken into cork labeled bottle in sterilized condition. Different concentrations of filtrate were made i.e. 50%, 25%, 12.5% and 6.25% by adding 2.5 ml PBS and 2.5 ml filtrate in separate petri dishes by serial dilution method. A 100% (5 ml) pure extract solution was taken as a mother solution having no PBS, where PBS (5 ml) was used as a control group.

Effects of plant extract on Haemonchus contortus

Mortality of *H. contortus* was checked after 6 h treatment to the various concentrations of Garlic (*Allium sativum*) and Neem (*Azadirachta indica*) extracts.

Statistical analysis

Student *t* test was used to statistically analyze the data and the significance level was kept as $P < 0.05$.

Results

Mean percentage mortality of L3 stage Larvae after 6 h post-exposure of various percentages of methanol neem extracts

The selected plants of different concentration of methanol extract, Neem (100%) was significantly effective against L3 stage larvae of *Haemonchus contortus.* The efficacy of methanol extracts of plants at different concentration presented in *Figure 4*. At 100% concentration, 87% mortality was observed. 53%, 43%, 37% and 23% mortality have showed by 50%, 25%, 12.5%, 6.25% concentrations, respectively. In case of L3, Neem showed highest mortality as compared to Garlic extract. In positive control there was 100% mortality as shown in *Figure 4*.

http://www.aloki.hu ● ISSN 1589 1623 (Print) ● ISSN 1785 0037 (Online)
DOI: http://dx.doi.org/10.15666/aeer/1705_1038910397

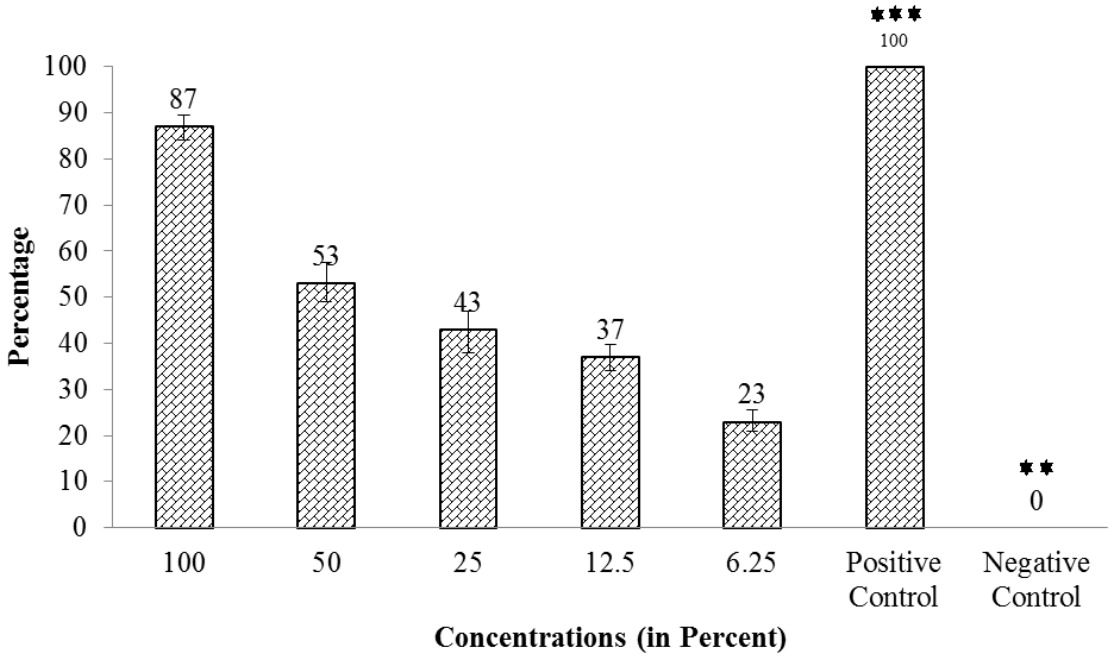

Figure 4. *Mean percent mortality of L3 stage larvae after 6 h post-exposure of various concentrations of methanol neem extracts*

Mean percentage mortality of L3 larvae after 6 h post-exposure against various percentages of garlic methanol extracts

It is evident from the data that Garlic diluted filtrate showed anthelmintics activity against L3 larvae but highest mortality has showed by 100% concentration which was noted as 67%. Moreover, 50%, 33%, 23% and 3% mortalities were shown by 50%, 25%, 12.5% and 6.25% solution, respectively. Whereas, in control group no mortality was noted as shown in *Figure 5.*

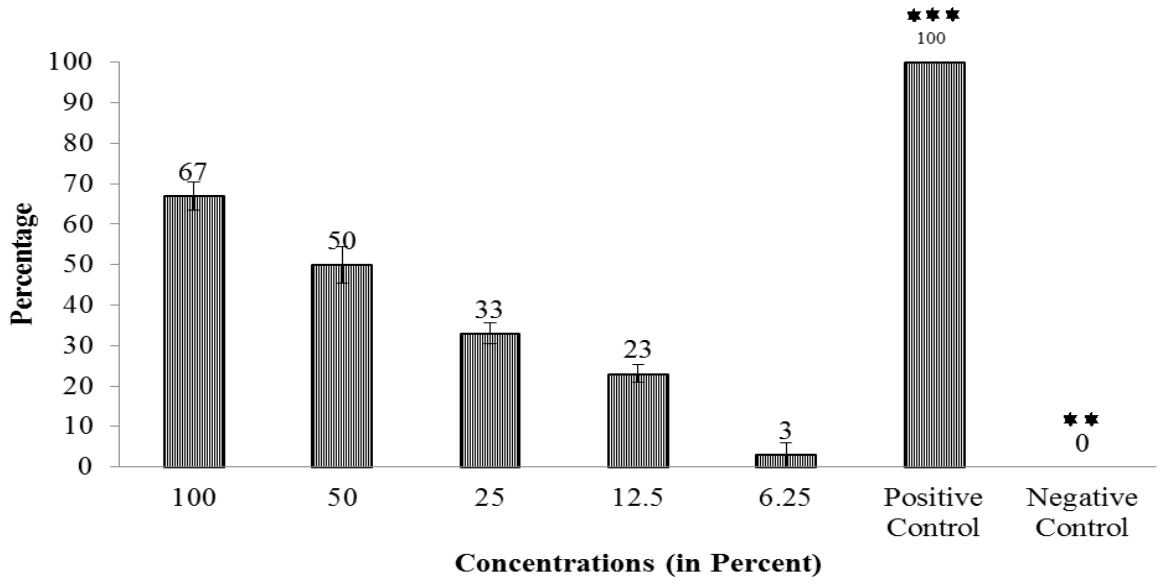

Figure 5. *Mean % mortality of larvae after treating 6 h with various concentration of methanol-based garlic extracts*

http://www.aloki.hu ● ISSN 1589 1623 (Print) ● ISSN 1785 0037 (Online)
DOI: http://dx.doi.org/10.15666/aeer/1705_1038910397

Percent inhibition of eggs hatching of H. contortus against Neem extract

At 100% Neem extract showed highest egg hatch inhibition which was 94% (*Table 1*). Second highest egg hatch inhibition was recorded for 50% methanol extract of Neem (72%), followed by 25% (54%) and 12.5% extract (33%). The lowest inhibitions were observed for 6.25% and 3.125% that were 20% and 8%, respectively.

Table 1. *Percent inhibition of eggs hatching of H. contortus against neem extract*

Concentration (%)	No. of egg inhibition in 1st trial	No. of egg inhibition in 2nd trial	No. of egg inhibition in 3rd trial	Mean of egg inhibition
100	94	96	92	94
50	75	70	72	72
25	58	53	50	54
12.5	35	32	33	33
6.25	20	18	21	20
3.125	8	9	7	8
Control	0	0	0	0

P = 0.9992 > 0.05, non-significant

Percent inhibition of eggs hatching of H. contortus against garlic extract

The 100% Garlic extract showed highest egg hatching inhibition i.e. 80% as shown in *Table 2*. At 50%, 25%, 12.5%, 6.25% and 3.125% egg hatching inhibition was recorded as 65%, 49%, 31%, 15% and 5%. The results infer that concentration is directly proportional to egg hatching inhibition**.**

Table 2. *Percent inhibition of eggs hatching of H. contortus against garlic extract*

Concentration (%)	No. of eggs after 3 days in 1st trial	No. of egg inhibition in 2nd trial	No. of egg inhibition in 3rd trial	Mean of egg inhibition
100	80	82	78	80
50	65	68	62	65
25	50	47	51	49
12.5	30	31	32	31
6.25	15	13	17	15
3.125	5	5	6	5
Control	0	0	0	0

P = 01.0000 > 0.05, Non-significant

Discussion

To control *Haemonchus contortus*, common anthelmintics are applied but not enough to erase this parasite completely as it is reported to be resistant to all three broad spectrum families of anthelmintics viz. benzimidazole, lmidazothiazole and ivermectin and against drugs with narrow spectrum of activity such as salicylanilides anthelmintics (Kaplan and Vidyashankar, 2012; Eckert, 2008). *H. contortus* is one of the most prevalent nematode parasites of small ruminants i.e. sheep and goats (Coles et al., 2005). Keeping in view the importance of this blood sucker, there is need of alternative

http://www.aloki.hu ● ISSN 1589 1623 (Print) ● ISSN 1785 0037 (Online)
DOI: http://dx.doi.org/10.15666/aeer/1705_1038910397

methods other than common anthelmintics to prevent sheep and goats from this highly dangerous nematode parasite.

The present study was undertaken to check the mean percentage of egg hatching inhibition. Extract filtrate obtained from *Allium sativum* at different concentration showed mean of inhibited eggs of *H. contortus* in the range from 5% to 80% which is much similar when compared with work of (Hammad et al., 2012) who reported that there was a dose and time dependent antinematicidal activity of crude aqueous methanol extract (CAME) of *N. tabacum* leaves with estimated LC_{50} values of 0.566 in EHA. Another study conducted in Pakistan by (Sindhu et al., 2009) showed a similar result that in egg hatching test, based on the LC_{50} values, most effective plants (LC50 in ppm) in their order of activity were; *N. tabacum* (0.10), *S. lappa* (0.73), *A. indica* (1.73), *C. arvensis* (2.51), *T. chebula* (5.55) and *A. vasica* (15.74). The allicin may have an important role in penetration of nematode egg surface, resulting in death of juveniles inside hard and protective barriers. The Azadirachtin of *Azadirachta indica* may have an important role in penetration of nematode egg surface, resulting in death of juveniles inside hard and protective barriers.

The third stage larvae (L3) of *H. contortus* in the present study were treated with different concentrations of the selected plants. In case of larvae, the mortality was found to be 87% at 100% methanol *Azadirachta indica*. Whereas, in case of *Allium sativum* the highest mean percent mortality was 67% at 100% extract. The methanolic diluted filtrate extract of *Azadirachta indica* showed approximately same result to the published paper of Rahman (2002). Rahman (2002) recorded the highest efficacy of neem leaves in alcoholic extract whereas aqueous extract has the lower efficacy (92%) than alcoholic extract against gastrointestinal nematodiasis in goat. Sujon et al. (2008) also recorded that the efficacy of methanol extract of neem was 80% and 100% at 5% and 10% concentration, respectively. Niddhi et al. (2007), Rahman et al. (2011) and Radhakrishnan et al. (2007) also showed the efficacy of neem against Haemonchus contortus adult and L3 stage larvae.

Conclusion and recommendations

Medicinal plants traditionally used against *Haemonchus contortus* control showed therapeutic activity. The selected medicinal plants contain active agents especially Allicin in garlic and Azadirachtin in Neem. These plant extracts at absolute (100%) form have the ability to lower the *H. contortus* infestation in small ruminants i.e. sheep and goats. *Azadirachta indica* contain potent anthelmintics compounds and therefore this plant is strongly recommended for further research studies. Mode and mechanism of action of anthelmintics plants also need to be studied in detail.

Acknowledgements. We sincerely acknowledge Pakistan Science Foundation Islamabad for providing us financial support with grant number (PSF/NSLP/KP-KUST-298).

http://www.aloki.hu ● ISSN 1589 1623 (Print) ● ISSN 1785 0037 (Online)
DOI: http://dx.doi.org/10.15666/aeer/1705_1038910397

REFERENCES

[1] Ahmed, M., Ansari, J. A. (1989): Effect of Haemonchosis on hematology and non-specific phosphomono esterase activities in sheep and goats. – Helminthologia 26: 295-302.
[2] Anthony, J. P., Fyfe, L., Smith, H. (2005): Plant active component-a resource for antiparasitic agents. – Trends in Parasitology 21: 462-468.
[3] Biswas, K., Chattopadhyay, I., Banerjee, R. K., Bandyopadhyay, U. (2002): Biological activities and medicinal properties of Neem (*Azadirachta indica*). – Current Science 82: 1336-1345.
[4] Bowman, D. D. (2009): Georgis Parasitology for Veterinarians. 9th Ed. – Saunders Elsevier, Philadelphia, PA, pp. 161-162.
[5] Coles, G. C., Rhodes, A. C., Wolstenholme, A. J. (2005): Rapid selection for ivermectin resistance in *Haemonchus contortus*. – Veterinary Parasitology 129: 345-347.
[6] Duke, J. A. (2002): Handbook of Medicinal Herbs. 2nd ed. – Boca Raton, FL, CRC Press.
[7] Eckert, J., Friedhoff, K. T., Zahner, H., Deplazes, P. (2008): Lehrbuch der Parasitologie für die Tiermedizin. – Enke Verlag, Stuttgart.
[8] Economic Survey of Pakistan (2017-2018): http://www.finance.gov.pk/survey_1718.html.
[9] Emery, D. L., Hunt, P. W., Le Jambre, L. F. (2016): Haemonchus contortus: the then and now, and where to from here? – International Journal for Parasitology 46(12): 755-769.
[10] Hamad, K. K., Iqbal, Z., Ud, Z., D., Sindhu, Z., Muhammad, G. (2013): Antinematicidal activity of Nicotiana tabacum L. leaf extracts to control benzimidazole-resistant Haemonchus contortus in sheep. – Pakistan Veterinary Journal 33(1): 85-90.
[11] Hepworth, K., Neary, M., Hutchens, T. (2006): Managing Internal Parasitism in Sheep and Goats. – Purdue University Cooperative Extension Service, West Lafayette, pp. 1-10.
[12] Iqbal, Z., Nadeem, Q. K., Khan, M. N., Akhtar, Waraich, F. N. (2001): In vitro anthelmintic activity of *Haemonchus contortus* of sheep. *Allium sativum, Zingiber officinale, Curcurbi mexicana* and *Ficus religiosa*. – International Journal of Agricultural Biology 3(4): 454-457.
[13] Jackson, F., Coop, R. L. (2000): The development of anthelmintic resistance in sheep nematodes. – Parasitology 120: 95-107.
[14] Kaplan, R. M. (2004): Drug resistance in nematodes of veterinary importance: a status report. – Trends in Parasitology 20: 477-481.
[15] Khattak, B., Safi, A. U. R., Sindhu, Z. U. D., Attaullah, M., Jamal, Q. (2018): Biological control of *Haemonchus contortus* by fungal antagonists in small ruminants. – Applied Ecology and Environmental Research 16(5): 5825-5835.
[16] Miller, J. E., Hembry, F. G., Kearney, M. T., Williams, J. C., Stag, L. C., Sims, D. (1987): Efficacy of levamisole and netobimin against Haemonchus contortus in lambs in Louisiana. – American Journal of Veterinary Research 48(9): 1403-1406.
[17] Mola, S. (2018): Review on control of haemonchus contortus in sheep and goat. – Journal of Veterinary Medicine and Research 5(5): 1139.
[18] Niddhi, A., Vihan, V. S., Sharma, S. D., Ashok, K. (2007): Evaluation of anthelmintic activity of Azadirachta indica (Neem) against Haemonchus contortus infection in goats. – Indian Journal of Veterinary Medicine 27(2): 95-98.
[19] Radhakrishnan, L., Gomathinayagam, S., Balakrishnan, V. (2007): Evaluation of anthelmintic effect of Neem (Azadirachta indica) leaves on Haemonchus contortus in goats. – Journal of Parasitology Research 2(1): 57-62.
[20] Radostits, O. M., Gay, C. C., Hinchcliff, K. W., Constable, P. D. (2006): Veterinary Medicine: A Textbook of the Diseases of Cattle, Horses, Sheep, Pigs and Goats. – Elsevier Health Sciences, Amsterdam.

http://www.aloki.hu ● ISSN 1589 1623 (Print) ● ISSN 1785 0037 (Online)
DOI: http://dx.doi.org/10.15666/aeer/1705_1038910397

[21] Rahman, M. (2002): In vitro and in vivo anthelmintic activity of some plants against gastrointestinal nematodes of goats. – MS Thesis, Department of Parasitology, Bangladesh Agricultural University, Mymensingh.
[22] Rahman, W. A., Lee, R., Sulaiman, S. F. (2011): In vitro anthelmintic activity of Neem plant (Azadirachta indica) extract against third-stage Haemonchus contortus larvae from goats. – Global Veterinary 7(1): 22-26.
[23] Rasool, G., Iqbal, Z., Misarkhan, M., Hayat, B. (1995): Hematological disturbance associated with Haemonchosis in sheep. – Pakistan Veterinary Journal 15: 159-162.
[24] Sangster, N. C. (1999): Anthelmintic resistance: past, present, and future. – International Journal for Parasitology 29(1): 115-124.
[25] Sindhu, Z. U. D., Iqbal, Z., Asim, M., Ahmad, A., Abbas, R. Z., Aslam, B. (2014): In vitro ovicidal and wormicidal activity of six medicinal plants against Haemonchus contortus. – International Journal of Agricultural Biology 16: 1199–1203.
[26] Sujon, M. A., Mostofa M, Jahan, M. S., Das, A. R., Rob, S. (2008): Studies on medicinal plants against gastrointestinal nematodes of goats. – Bangladesh Journal of Veterinary Medicine 166(12): 373-374.
[27] Urquhart, G. M., Armout, J. Duncan, J. L., Jennings, F. W. (1996): Veterinary Parasitology. 2nd Ed. – The University of Glasgow, Scotland, pp. 228-276.

http://www.aloki.hu ● ISSN 1589 1623 (Print) ● ISSN 1785 0037 (Online)
DOI: http://dx.doi.org/10.15666/aeer/1705_1038910397

A NEW QUANTITATIVE ETHNOECOLOGICAL APPROACH TO ASSESSING THE CONSERVATION STATUS OF PLANTS: A CASE STUDY OF DISTRICT TOR GHAR, PAKISTAN

SHAH, A. H.[1*] – MEHMOOD, A.[2] – FAROOQ, M.[1] – KHAN, K. R.[1] – NAWAB, B.[5] – SHAH, A. H.[4] – HUSSAIN, M.[4] – ZOHRA, L.[5] – KHAN, S. M.[3] – AHMAD, H.[6]

[1]*Department of Botany, Govt. Post Graduate College, Mansehra, Pakistan*

[2]*Department of Botany, Govt. Post Graduate College, Mandian, Pakistan*

[3]*Department of Plant Sciences, Quaid-i-Azam University, Islamabad, Pakistan*

[4]*Department of Botany, Hazara University, Mansehra, Pakistan*

[5]*Department of Botany, GPGJC Saidu Sharif, Swat, Pakistan*

[6]*Islamia College University, Peshawar, Pakistan*

**Corresponding author*
e-mail: abshah2086@gmail.com

(Received 28th Jan 2019; accepted 24th May 2019)

Abstract. Ethnoecological knowledge refers to the local wisdom, innovations, traditional life style and practices of aboriginal communities. This knowledge also contributes a lot to understanding of conservation stata of culturally significant flora of a region. The present research work is the first one to focus on this particular aspect of cultural knowledge to assessing preliminary conservation status of 295 culturally significant plant species of district Tor Ghar. In such remote and less privileged areas interaction between plants and people is much stronger. Multistage random selection of 700 informants was made. The data was obtained through EPA, group discussion and semi structured interviews. The conservation status of all culturally significant plant species were assessed quantitatively by developing a new special mathematical relation that is CS = K (OC + AV + CE)/TF × RP. A scale was devised on the basis of CS value index and all 295 species were assigned to different IUCN categories. According to this classification 20 species were found critically endangered, 35 endangered, 56 vulnerable, 58 near threatened (rare) and 126 least concerned (secure). This categorization depicts a miniature of ethno-conservation of plants at local level. The current study leads to an enhanced understanding of cultural knowledge on mountain vegetation within the context of anthropogenic impacts and the role of indigenous communities in regional plant conservation strategies and future outlooks.
Keywords: *local wisdom, aboriginal, endangered, threatened, ethno-conservation*

Introduction

Biodiversity and culture of a region affect each other reciprocally. Local wisdom of communities popularly known as traditional knowledge, cultural knowledge, indigenous knowledge or local ecological knowledge. The body of knowledge usually includes understandings, beliefs, and practices that human societies develop longitudinally in relationship with their natural environment, and which are dynamic and co-evolving with social and ecological changes (Berkes, 2000; Zent, 2001; Von, 2011). This knowledge incorporates spiritual connections with the natural environment and the sustainable use of natural resources, and association between people, which are reflected in their language, narratives, social organisation, values, beliefs, and cultural

http://www.aloki.hu ● ISSN 1589 1623 (Print) ● ISSN 1785 0037 (Online)
DOI: http://dx.doi.org/10.15666/aeer/1705_1039910419

laws and customs (Andrews, 2006). Every aspect of life is touched and covered by the culture of a particular region. According to Larid (1999) culture facilitates the association between humans and their environment. The perception of culture provides the basis of scientific disciplines such as ecological anthropology and scientific concepts such as bio-cultural diversity (Berkes et al., 2000).

According to Declaration of Belem (1988) there is an "inextricable link" between biological and cultural diversity. The term bio-cultural diversity was coined to describe the concept indicating the link (Posey, 1999). Human beings and their societies are an essential part of biodiversity, and according to their way of utilizing natural resources, they can be promoters of its sustainable use or drivers of its loss (Calvo, 2003). Wild biological resources are especially important for populations in rural areas, because these people depend directly on the extraction of local species to fulfill part of their daily requirements, such as wood, food, medicine, and timber (Boom, 1987; Prance et al., 1987; Phillips et al., 1994).

Participation of indigenous communities in decision making related to natural resource management has been regarded as a potential effort that can boost local well-being without harming biodiversity and ecosystem functions (United Nations, 1992; Schwartzman et al., 2000; Adams and Hutton, 2007; Berkes, 2007).

Local communities have more close association with biodiversity and their cultural practices and life styles influence biodiversity greatly. According to Convention on Biological Diversity, local communities showing a socially and geographically defined group of people may not homogeneous, living close to biodiversity and protected areas. They may have customary rights of use, distinctive knowledge and skills and direct impact on biodiversity as individuals or groups of individuals. These people are also described as having a close and unique relationship to their natural resources as a community. Locals communities may be dynamic in response to changing rural conditions, and therefore, may change their cultural practices and their perspectives on the importance of natural resources and biodiversity (Wiersum and Shackleton, 2005).

In order to protect and manage a particular ecological system, its cultural context is considered to be the most important one. Human relation to the natural environment has so for been studied mostly in biophysical terms; but there is now a growing acknowledgment that societies themselves have created detailed procedures to conserve and manage their resources. These methods are entrenched in their cultural values that have to be taken in to consideration if sustainable and reasonable human development is to become a truth (Bridgewater, 2002). These new trends have resulted in a change from a top down to a more community- based approach which aims to work closely with local people, depend on their cultural knowledge, and contribute to their livelihoods (Grimble and Laidlaw, 2002).

The convention on Biological Diversity (CBD) from 1992 stressed on parties to respect, preserve, and maintain knowledge, innovations and practices of indigenous and local communities having traditional lifestyles relevant for the conservation and sustainable use of biological diversity, and facilitate their wider involvement with the approval of bearers of such knowledge, innovations and practices, and encourage the reasonable sharing of the gains obtaining from the use of such knowledge, innovations and practices (McNeely, 2000).

Global environmental conservation policies and discourses have been increasingly influenced since 1980s, either verbally or practically, by the idea that conservation demands the coexistence of humans and nature (Adams et al., 2004; Wells and

http://www.aloki.hu ● ISSN 1589 1623 (Print) ● ISSN 1785 0037 (Online)
DOI: http://dx.doi.org/10.15666/aeer/1705_1039910419

McShane, 2004). According to Cotton (1996) over long time, indigenous people have developed their own locality specific knowledge on plant use management and conservation. The United Nations Convention Environment and Development (UNCED, 1992) mentioned the important roles that indigenous populations play in both the conservation and sustainable use of natural resources while in turn maintaining biodiversity. Current use of cultural knowledge in conservation led to the novel idea of "ethnoconservation" in the late 1990s which is now well known conservation approach around the world (Rajeswar, 2001; Jules et al., 2008; Negi, 2010).

In a context where numerous conservation goals must be attained, local ecological knowledge can be a donor to a multidisciplinary conservation approach as well as foster transdisciplinary approaches when locals become partners and co-workers (Aswani, 2018). Assessment of conservation status cannot be absolute and needs periodic revision but taking various criteria at a time validates the conclusion for a considerable period of time or for a specific geographic locality (Domínguez Lozano et al., 2003; Broennimann et al., 2005).

In the present investigation local ecological knowledge has been incorporated in IUCN red list and used as a tool for assessing conservation status of culturally significant flora of district Tor Ghar with special reference to the following objectives.

1. To assess the existing threats to culturally significant plants in the study area
2. To evaluate how the cultural values of plant biodiversity contribute towards conservation.
3. To quantify the local wisdom regarding conservation status of the flora

Materials and methods

Study area

District Tor Ghar, a rigorous mountainous area of northern Pakistan located between 34° 32' and 34° 50' N, and 72° 48' and 72° 58' E in Lesser Himalayas having strong cultural and traditional background besides rich plant biodiversity. The study area is inhabited by five well known tribes namely Basikhel, Akazai, Nusratkhel, Hassanzai and Medakhel (*Fig. 1*). Plants and peoples of the study area have close association and plants provide a number of societal benefits. Human culture is the main driver of plant biodiversity. Hence cultural knowledge was used as a tool for assessing conservation status of ethnospecies of the district.

Data collection

Villages of each tribal society as well as informants were selected randomly.700 informants shared their cultural knowledge related to conservation status through semi structured interviews, questionnaires, Ethnobotanical Participatory Appraisal (EPA) and group discussion.

Field trips

Extensive field trips of the study area were carried out during 2014 and 2015. Threatened and secure plant species were studied in their local habitats. Threatening factors and conservation efforts of indigenous tribes were recorded. Pressed, dried and poisoned specimens in triplicate deposited in herbarium of Hazara University, Mansehra, Pakistan.

http://www.aloki.hu ● ISSN 1589 1623 (Print) ● ISSN 1785 0037 (Online)
DOI: http://dx.doi.org/10.15666/aeer/1705_1039910419

Figure 1. *Map of district Tor Ghar showing different tribal belts*

Data analysis

Recorded data from the questionnaires was shifted on Microsoft Excel sheet for further processing and evaluation. Whole conservation related data was analyzed successfully by developing a new simple mathematical relation named as CS equation.

Development of a new equation

A new mathematical equation was developed for assessment of conservation status, which is a novel approach in the field of ethnobiology for quantification of local wisdom. The idea was born during data collection and field visits that local wisdom if quantified properly to assessing conservation status of a plant species in a particular

http://www.aloki.hu ● ISSN 1589 1623 (Print) ● ISSN 1785 0037 (Online)
DOI: http://dx.doi.org/10.15666/aeer/1705_1039910419

area, it would depict its conservation in a better way. During the study it has also been observed that locals adopted conservatory measures for protecting plant biodiversity. They protect the plants of their interest from fire and grazing and also cultivate useful plants. In this regard, a questionnaire was designed to get maximum information from the locals about conservation status of culturally significant flora of the area. Availability for the last ten years was recorded (increased, decreased or persistent). Occurrence of a plant species (abundance, moderate or rare) was noted. The most cited three important threatening factors of the study area (over exploitation, fire and grazing) were enlisted. Similarly, information regarding regeneration potential (high, moderate and low) was gathered. Data obtained from informants was cross checked by direct field observations during extensive field trips and analyzed by the following mathematical relation developed first time by the authors (*Eq. 5*).

As Conservation Status (CS) of a species is directly proportional to Occurrence (OC), Availability (AV) and Conservation Efforts (CE). This may be expressed mathematically as:

$$CS \alpha OC + AV + CE \quad \text{(Eq.1)}$$

Similarly Conservation Status (CS) is also directly proportional to Reproductive Potential (RP) of a species and can be represented as follows:

$$CS \alpha RP \quad \text{(Eq.2)}$$

where CS is inversely proportional to Threatening Factors (TF) shown mathematically as:

$$CS \alpha 1 / TF \quad \text{(Eq.3)}$$

By combining *Equations 1, 2* and *3,* the following equation obtained:

$$CS \alpha (OC + AV + CE) / TF \text{ X } RP \quad \text{(Eq.4)}$$

By substituting the sign of proportionality with constant K, the final equation was thus obtained.

$$CS = K (OC + AV + CE) / TF \text{ X } RP \quad \text{(Eq.5)}$$

where CS is the conservation status of a plant species, OC is occurrence, AV is availability for the last ten years, CE is conservation efforts by locals, TF is threatening factors and RP is regeneration potential of a plant species in a particular habitat.

The constant K was assigned a value 1. Degree of occurrence was evaluated by giving values 3 for abundance, 2 for moderate and 1 for rare. Values for availability for the last ten years are 3 for increasing, 2 for persistent and 1 for decreasing. The most cited four conservation efforts by locals were considered in this equation and assigned a sum of value 4 to these (1 for each conservation effort). Conservation efforts are protection from grazing, cutting and fire. Cultivation of a plant species is also a conservation effort. Threatening factors considered in this formula on the basis of local perception were Over-exploitation, fire and overgrazing/overbrowsing. Each threatening

http://www.aloki.hu ● ISSN 1589 1623 (Print) ● ISSN 1785 0037 (Online)
DOI: http://dx.doi.org/10.15666/aeer/1705_1039910419

factor was assigned a value 3 for extensive, 2 for moderate, 1 for low and 0 for absence of a threatening factor. Similarly, the values assigned to regeneration potential were 3 for high, 2 for moderate and 1 for low.

All 295 culturally significant plant species of the study area were assessed by the equation of CS in order to quantify the local wisdom. Keeping in view the CS index values, a scale was devised for assigning IUCN categories to the flora under investigation.

2-scale for IUCN categories

On the basis of C S values index plant species were described according to IUCN classification as critically endangered, endangered, vulnerable, near threatened (rare) and least concerned (secure) (*Table 1*).

Table 1. *Scale for IUCN categories*

Name of category	C S values
Critically endangered	0.1 to 1
Endangered	1.1 to 1.5
Vulnerable	1.6 to 2.0
Rare	2.1 to 2.5
Least concerned (secure)	2.6 and above

Results

Conservation status of 295 plant species was assessed tribewise and mean value was calculated for each recorded species (*Table 2*).

Table 2. *Tribewise CS values and IUCN categorization*

Name of species	Habit	Tribe wise CS values						
		Basikhel	Nusratkhel	Akazai	Hassanzai	Medakhel	Mean	Categories
Podophyllum emodi Wall. ex Royle.	Herb	0.5	0.5	0.5	0.5	NR	0.5	CE
Gentiana kurroo Royle.	Herb	0.85	0.85	NR	NR		0.85	CE
Dioscorea deltoidea Wall.exKunth.	Herb	0.66	1.33	0.66	0.132	2	0.95	CE
Incarvellia emodi	Herb			0.6		1.32	0.96	CE
Arisaema utile Hook.f.ex. Schott.	Herb	1					1	CE
Picris hieraciodes L.	Herb			1			1	CE
Citrullus colocynthis (Linn.) Schrad.	Herb	1			1.32	1	1.1	E
Asparagus officinalis L.	Herb			1.3	1.5	1	1.2	E
Caralluma tuberculata N.E. Brown.	Herb	1	1.5	1.3	1.32	1.5	1.32	E
Asparagus adscandens Roixb.	Herb	0.5			1.5	2	1.33	E
Astragalus graveolens Buch.-Ham.exBenth.	Herb	2	0	2			1.33	E
Colchicum luteum Baker.	Herb	1	2	1			1.33	E
Allium griffithianum Boiss.	Herb				1.5	1.2	1.35	E
Arisaema flavum (Forssk.)Schott.	Herb	1	2	1.33			1.44	E
Aerva sanguinolenta(Linn.) Blume.	Herb				1	2	1.5	E
Agave sisalana Perrine ex Engelm.	Herb				2	1	1.5	E
Crotolaria mediginea Lamk.	Herb					1.5	1.5	E
Geranium lucidum L.	Herb					1.5	1.5	E
*Rumex vesicarius*L.	Herb	1.5			1	2	1.5	E

http://www.aloki.hu ● ISSN 1589 1623 (Print) ● ISSN 1785 0037 (Online)
DOI: http://dx.doi.org/10.15666/aeer/1705_1039910419

Name of species	Habit	Tribe wise CS values						
		Basikhel	Nusratkhel	Akazai	Hassanzai	Medakhel	Mean	Categories
Geranium wallichianum D.Don ex Sweet.	Herb	1.6	1.6		1.5		1.56	V
Salvia lanata Roxburgh.	Herb	1	1	1.5		3	1.62	V
Impatiens bicolor Royle.	Herb	2	1.5				1.75	V
Bergenia ciliate Sternb.	Herb	1.3	2	2			1.76	V
Asparagus capitatus Baker.	Herb	1	1.2		2	3	1.8	V
Polygonatum verticillatum	Herb	2.6		1			1.8	V
Hypericum perforatum L.	Herb	1.6	2	2			1.86	V
Salvia moorcroftiana Wall.ex Benth.	Herb	2	2	2	1.5		1.87	V
Valeriana jatamansi Jones.	Herb	1.5	1.2	2.4	2.6		1.92	V
Arthraxon prionodes (Steud.) Dandy.	Herb					1.98	1.98	V
Alliaria petiolata (M.Bieb)Cavara& Grande.	Herb	2	2				2	V
Arisaema jacquemontii Blume.	Herb	2					2	V
*Cichorium intybu s*L.	Herb	2	2				2	V
Codonopsis clematidea(Schrenk) C.B.Clarke.	Herb					2	2	V
Convolvulus arvensis L.	Herb	2	2				2	V
Corchorus trilocularis L.	Herb				2	2	2	V
Erophila verna L.	Herb	2					2	V
Euphorbia hispida Boiss.	Herb					2	2	V
Evolvulus alsinoides (L.)	Herb				2		2	V
Fumaria officinalis L.	Herb					2	2	V
Mirabilis jalapa L.	Herb					2	2	V
Poa bulbosa L.	Herb	2	2	2			2	V
Polygonatum multiforum (L.) All.	Herb	2	2				2	V
Swertia ciliata(G. Don) B.L. Burtt.	Herb	2	2				2	V
Thymus linearis Benth.	Herb	2					2	V
Vicia hirsute (Linn.) S.F.Gray.	Herb					2	2	V
Viola odorata L.	Herb	2.4	1.6				2	V
Bistorta amplexicaulis (D.Don) Greene.	Herb	3	0	2.6	2.6		2	V
Cissampelo spareira L.	Herb				2.6	1.5	2	V
Artemisia scoparia Waldst. & Kit.	Herb	2	2		2	2.25	2	V
Ajuga bracteosa Wall., Benth.	Herb	2	1.6	2.6			2	V
Tulipa clusiana(Hook.) Regel.	Herb	2	2	2.4	2		2.1	R
Taraxicum officinale Webb.	Herb	2	2	2	2.25	2.4	2.13	R
Aristida depressa Retz.	Herb	2.14	2.14	2.14			2.14	R
Narcissus tazetta L.	Herb	3	1.5			2	2.16	R
Astragalus amherstianus Royle ex Benth.	Herb	2	2	2.6			2.2	R
Calendula arvensis L.	Herb	2	2	2.6			2.2	R
Cardamine hirsute L.	Herb	2	2			2.6	2.2	R
Clematis Montana Buch.	Herb	2	2.6	2			2.2	R
Dicliptera bupleuroides Nees.	Herb	2.6	2	2			2.2	R
Lepidium aucheri Boiss.	Herb	2	2		2.6		2.2	R
Silene vulgaris (Moench) Garcke.	Herb	2.4			2		2.2	R
Vernonia Sinerea (L.)Lees.	Herb	2.4		2			2.2	R
Brachiaria ramosa(Linn.) Stap.	Herb				1.98	2.49	2.23	R
Bothriochloa ischaemum (L.) Keng.	Herb					2.25	2.25	R
Commelina benghalensis L.	Herb	2.5	2.5	2	2		2.25	R
Apluda aristata L.	Herb	2.14	2.14	2.14	2.5	2.49	2.28	R
Commelina poludosa Blume.	Herb	1.6			3		2.3	R

http://www.aloki.hu ● ISSN 1589 1623 (Print) ● ISSN 1785 0037 (Online)
DOI: http://dx.doi.org/10.15666/aeer/1705_1039910419

Name of species	Habit	Tribe wise CS values						
		Basikhel	Nusratkhel	Akazai	Hassanzai	Medakhel	Mean	Categories
Cynoglossum lanceolatum Forssk.	Herb	2.6	2				2.3	R
Senesio chrysanthemoides DC.	Herb	2	2.6				2.3	R
Verbena officinalis L.	Herb				2	2.6	2.3	R
Sisymbrium irrio L.	Herb	1.6	1.6	2.6	2.8	3	2.32	R
Artemisia absinthium L.	Herb	2	2	3			2.33	R
Achillea millifolium L.	Herb	2.6	2.6	2			2.4	R
Achyranthus aspera L.	Herb	3	2	2	2.6		2.4	R
Acorus calamus L.	Herb	2	2.6		2.6		2.4	R
Tragus roxburghii Panigrahi.	Herb					2.4	2.4	R
Stellaria media (L.) Vill.	Herb	2.4			2.25	2.6	2.41	R
Calamagrostis decora Hook. f., Fl. Bri.	Herb	2.4	2.4	2.4	2.5	2.4	2.42	R
Deschampsiacae spitosa L.	Herb	2.4	2.4	2.4	2.5	2.4	2.42	R
Trifolium pratense L.	Herb	2.5			2.4	2.4	2.43	R
Datura stramonium L.	Herb	2.6	2	2	2.6	3	2.44	R
Imperata cylindrical (L)P. Beauv.	Herb	2.66		2.4	2.4		2.48	R
Dactylotenium aegyptium(L) P.Beauv.	Herb	2.4	2.4	2.4	3	2.25	2.49	R
*Chrysopogon serrulatus*Trin.	Herb					2.49	2.49	R
Eragrostis ciliaris(L.) R.Br.	Herb					2.49	2.49	R
Agrostis stolonifera L.	Herb	2.5	2.5	2.5		2.49	2.49	R
Euphorbia wallichii Hk.	Herb	2.5	2.5				2.5	R
Impatiens edgeworthii Hk. F.	Herb	3	2				2.5	R
Phragmites australis(Cay.) Trin.	Herb				2.4	2.6	2.5	R
Colocasia esculenta (Linn.) Schott.	Herb	2.6	3		1.5	3	2.5	R
Ricinus communis L.	Herb	3	2		2.6	2.6	2.5	R
*Carthmusoxycantha*M.Bieb.	Herb	2	2	2.6	3.32	3	2.58	S
Avena fetua L.	Herb	3		2.4	1.98	3	2.59	S
Achyranthes bidentata Blume.	Herb	2.6	2.6				2.6	S
Amaranthus spinesus L.	Herb	3	2		2.4	3	2.6	S
Borreria articularis (L.F.) FN . Will.	Herb					2.6	2.6	S
Caltha alba Camb.	Herb	2.6					2.6	S
Campanula benthamii Wall.	Herb					2.6	2.6	S
Cardiospermum halicacabum L.	Herb	2.6			2.6	2.6	2.6	S
Centaurea iberica Trevir&Spreng.	Herb	2.6					2.6	S
Gagea lutea (L) Ker-Gawl.	Herb	2.6					2.6	S
Galium aparine L.	Herb	2.6					2.6	S
Lactuca serriola L.	Herb	2.6					2.6	S
Oenthera rosea L.	Herb					2.6	2.6	S
*Onosma hispida*Wall. Ex G. Don.	Herb	2.6	2.6				2.6	S
Persicaria hydropiper (L.) Spach.	Herb					2.6	2.6	S
Polygonum aviculare L.	Herb	2.6	2.6	2.6			2.6	S
Polygonum plebejum R. Br.	Herb					2.6	2.6	S
Stachys parviflora Benth.	Herb	2.6	2.6		2.6	2.6	2.6	S
Torilislepto phyla (L.) Reichb.	Herb					2.6	2.6	S
Sorghum haleeparse (L) Pers.	Herb	2.66		2.4	3	2.4	2.61	S
Phalaris minor Retz.	Herb	3		2.5	2.5	2.49	2.62	S
Fumaria indica(Hausskn) Pusley.	Herb	2.5	2.5		2.6	3	2.65	S
Aethusa cynapium L.	Herb	2.66					2.66	S
Bupleurum falcatum L.	Herb	2.66					2.66	S
Nepeta cataria L.	Herb	2.66					2.66	S
Dichanthium annulatum(Forssk) Stapf.	Herb	3		3	2.15	2.5	2.66	S
Artemisia vulgaris L.	Herb	2.5	2.5			3	2.66	S

http://www.aloki.hu ● ISSN 1589 1623 (Print) ● ISSN 1785 0037 (Online)
DOI: http://dx.doi.org/10.15666/aeer/1705_1039910419

Name of species	Habit	Tribe wise CS values						
		Basikhel	Nusratkhel	Akazai	Hassanzai	Medakhel	Mean	Categories
Cuscuta gigantea Griff.	Herb	3			3	2	2.66	S
Mentha spicata L.	Herb	3	3			2	2.66	S
Pulicaria crispa(Forssk.) Oliv.	Herb	2			3	3	2.66	S
Silene conidia L.	Herb	3	3		2		2.66	S
Digitaria nodosa Perl.	Herb	2.5	3	3	2.5	2.49	2.69	S
Cynodon dactylon(L) Pers.	Herb	2.5	2.5	3	2.5	3	2.7	S
*Viola canescens*Wall. ex Roxb.	Herb	3		2.4			2.7	S
*Rumex hastatus*D. Don. Prodr.	Herb	2.4	3	3	2.4	3	2.76	S
Medicago polymorpha L.	Herb	3	3	3	2.5	2.4	2.78	S
Clematis grata Wall.	Herb	2.6				3	2.8	S
Fragaria nubicola(Hook.f.) Lindl. ex Lacaita.	Herb	3		3	2.4		2.8	S
Chenopodium murale L.	Herb	3			3	2.6	2.86	S
Rumex acetosa L.	Herb	2.6	3	3			2.86	S
Solanum incanum L.	Herb	3			2.6	3	2.86	S
Chenopodium album L.	Herb	2.4	2.4	3		3.75	2.88	S
Desmostachya bipinnata(L) Stapf.	Herb	3	3	3	3	2.49	2.89	S
Rumex dentatus L.	Herb	3	3	3		2.6	2.9	S
Ajuga reptan L.	Herb	3					3	S
Alloteropsis cimicina (L.) Stapf.	Herb					3	3	S
Asplenium septentrionale(Linnaeus) Hoffmann.	Herb	4	2				3	S
Canna indica L.	Herb					3	3	S
Chenopodium botrys L.	Herb	3				3	3	S
Cleome scaposa DC. Prodr.	Herb					3	3	S
Coronopus didymus (L.) Sm.	Herb	2	2	5		3	3	S
Euphorbia hirta L.	Herb	4			2	3	3	S
Euphorbia prostrate Aiton.	Herb					3	3	S
Lathyrus aphaca L.	Herb	3	3	3	3		3	S
Leptochloa panicea(Retz.) Ohwi	Herb					3	3	S
Malva neglecta Wall.	Herb	3	3	3	3	3	3	S
Malva sylvestris L.	Herb	3			3	3	3	S
Marrubium vulgare L.	Herb	4		2			3	S
Melilotus officinalis (L.)Desr.	Herb	3	3	3			3	S
*Oxalis carniculatus*L.	Herb	3	3	3	3	3	3	S
Plantago major L.	Herb	3	3				3	S
Trifolium repens L.	Herb	3	3	3	3	3	3	S
Verbascum thapsus L.	Herb	3			4	2	3	S
Trichodesma indicum (L.) R. Br. Prodr.	Herb	2.6			3.9	2.6	3	S
Sonchus asper (L) Hill.	Herb	3	2	3.6	3	3.75	3	S
Aerva javanica (Burm.f) Juss.	Herb	2	4	4	2	3.75	3.15	S
Amaranthus caudatus L.	Herb	3	3.75	3	3	3	3.15	S
Duchesnea indica(Andr.)Focke.	Herb	3.75	2.5	3	3	3.75	3.2	S
Plantago lanceolata L.	Herb	3		3	3.9	3	3.2	S
Amaranthus viridis L.	Herb	3.5	3				3.25	S
Chamaemelum nobile(L.) All.	Herb	3.3					3.3	S
Cuscuta reflexa Roxb.	Herb	2.6	2.6		4	4	3.3	S
Equisetum ramosissimum Desf.	Herb	3			3	4	3.33	S
Solanum nigrum L.	Herb	2.5	3	3.75	3.75	3.75	3.35	S
Nasturtium officinale R. Br.	Herb	3.75	3	5	3	2.25	3.4	S
Conyza canadensis (L.) Corgn.	Herb	3.75	3.75		3.75	2.5	3.43	S
Arundo donax L.	Herb	3	3.75	3.75	3.75	3	3.45	S

http://www.aloki.hu ● ISSN 1589 1623 (Print) ● ISSN 1785 0037 (Online)
DOI: http://dx.doi.org/10.15666/aeer/1705_1039910419

Name of species	Habit	Tribe wise CS values						
		Basikhel	Nusratkhel	Akazai	Hassanzai	Medakhel	Mean	Categories
Neslia apiculata Fisch.	Herb				3.9	3	3.45	S
Capsella bursa-pestoris L.	Herb	2.6	2.5		3.75	4.98	3.45	S
Cyperus cyperoides L.	Herb	2.5	2.5		4.98	4	3.49	S
Anisomeles indica(L.) O. Kuntze.	Herb	4		3			3.5	S
Urtica dioica L.	Herb	3		4			3.5	S
Chenopodium ambrosioides L.	Herb	3			3.9	4	3.63	S
Aloe vera(L.) Burm.	Herb	3	4		4	4	3.75	S
Cannabis sativa L.	Herb	4		4	3.75	4	3.93	S
Silybum marianum(L) Gaertn.	Herb	5	2.6	3.9	4.98	3.32	3.96	S
Adiantum incisum Forssk.	Herb	4					4	S
Galinsoga parviflora Cavanilles.	Herb				4		4	S
Portulaca oleracea L.	Herb	4					4	S
Pteris cretica L.	Herb				4		4	S
Ranunculus arvensis L.	Herb	4		4			4	S
Ranunculus scleratus L.	Herb	4				4	4	S
Solena amplexicaulis(Lam.)Gandhi.	Herb	4					4	S
Boenninghausenia albiflora(Hook.) Reichb.	Herb	4					4	S
Foeniculum vulgare Mill.	Herb	4.5	4		3.75		4	S
Adiantum capillus- veneris L.	Herb	5	4		4		4.33	S
Xanthium strumarium L.	Herb	5	5	3.3			4.43	S
Mentha longifolia(L.) Huds.	Herb	5	4	4		4.98	4.49	S
Mentha arvensis L.	Herb	5	5	5	4		4.75	S
*Adiantum venustum*D. Don.	Herb				5		5	S
Eryngium Sp. L.	Herb	5					5	S
Polystichum lonchitis L.	Herb	5					5	S
Ranunculus muricatus L.	Herb	5	5				5	S
Euphorbia helioscopia L.	Herb	7.5			4.98	4.98	5.82	S
Skimmia laureola(DC.) Sieb. &Zucc. ex Walp.	Shrub	0.5	0.4	0.5	0.5	0.5	0.48	CE
Woodfordia fruticosa(L.)S.Kurz.	Shrub	1	0.33	0.4	1	1.2	0.78	CE
Periploca aphylla Dcne.	Shrub	1	0.66	1			0.88	CE
Opuntia dillenii Haw.	Shrub	1	0.75	1	1	1.32	1	CE
Hedra nepalensis K.Koch.	Shrub	0.5	1	1.5			1	CE
Nannorrhops ritchieana (Griff.) Aitchison.	Shrub				1	1	1	CE
Vitis jacquemontii Parker.	Shrub		1				1	CE
*Viburnum grandiflorum*Wall. ex DC.	Shrub	0.6		1.5			1	CE
Viburnum cotinifolium D. Don.	Shrub	1.2	1.2		1		1.13	E
Buxus wallichiana Bill.	Shrub	1		1.3			1.15	E
Buddleja crispa Bth.	Shrub	1	1	2	1.5	1.5	1.4	E
Vitis parvifolia Roxb.	Shrub			1.5			1.5	E
Carissa opaca Stapf. en Haines.	Shrub	1.5	2	1	1.2	2	1.54	V
Hypericum oblongifolium L.	Shrub	2		1	1.2	2	1.55	V
Colebrookia oppositifolia Smith.	Shrub	0.75	0.75	1	2.6	3.32	1.68	V
*Cotoneaster bacillaris*Wall. ex Lindl.	Shrub	1.5		2			1.75	V
Justicia adhatoda L.	Shrub	2	1.5	2	2	1.5	1.8	V
Caesalpinia decapitala(Roth) Alston.	Shrub	1.5		2	1.5	2.4	1.85	V
Cotoneaster nummularia Fish &Mey.	Shrub	1.2		2	2.4		1.86	V
Bambusa glaucescens(Willd.) Sieb.	Shrub	1			3		2	V
Daphne mucronata Royle.	Shrub	2			2	2	2	V
Jasminum nudiflorum Lindl.	Shrub	2	2				2	V

http://www.aloki.hu ● ISSN 1589 1623 (Print) ● ISSN 1785 0037 (Online)
DOI: http://dx.doi.org/10.15666/aeer/1705_1039910419

Name of species	Habit	Tribe wise CS values						
		Basikhel	Nusratkhel	Akazai	Hassanzai	Medakhel	Mean	Categories
Otostegia limbata(Bth) Boiss.	Shrub	2		2	2	2	2	V
Yucca aloifolia L.	Shrub				2	2	2	V
Ziziphus oxyphylla Edgew.	Shrub	2					2	V
Maytenus royleanus(Wall. ex Lawson) Cufodontis.	Shrub	2	2	1.6	2.6	2	2	V
*Berberis lycium*Royle.	Shrub	2.5	2.1	2.4	1	2.49	2	V
Debregeasia salicifolia(D.Don) Rendle.	Shrub	2.4	1.6	2.4			2.1	R
Isodon rugosus(Wall. ex Benth.) Codd.	Shrub	2	2	2.6		2	2.15	R
Sarcococca saligna (D.Don) Muell.	Shrub	2	3	1.5			2.16	R
Nerium oleander L.	Shrub	2.6	2			2	2.2	R
*Rubus fructicosus*Hook .f.	Shrub	2	2.5	2.4		2	2.25	R
Andrachne cordifolia(Wall. ex Decne.) Muell.	Shrub	2.4	2.4	2	2.6	2	2.28	R
Jasminum humile L.	Shrub	2		2	3		2.33	R
Vitex negundo L.	Shrub	2	2.6	2.5	2	2.6	2.34	R
Zanthoxylum armatum DC.	Shrub	2	2.6	3	2	2.4	2.4	R
Cotinus coggyria Scop.	Shrub	2.4	2.4	2.6	2.4		2.45	R
Vitis vinifera L.	Shrub	2.6					2.6	S
Myrsine Africana L.	Shrub	3	3	3	2.4	2.4	2.76	S
*Indigofera heterantha*Wall.ex rand.	Shrub	2.5	2.5	3	2.5	3.6	2.82	S
Calotropis procera(Ait.) Ait. F.	Shrub	2.6	2.6	4	2	3	2.84	S
Rubus ellipticus Smith.	Shrub	2.5		3	3	3	2.87	S
Ziziphus nummularia(Burm. f.) Wight &Arn.	Shrub	2.6			2.4	3.75	2.91	S
Withania somnifera(L.) Dunal.	Shrub					3	3	S
Dodonaea vescosa(L.) Jacq.	Shrub	3.75	2.6	3	3	3	3	S
Mallotus philippensis(Lam.)Muess.	Shrub	4	3.75	2	3.75	3	3.3	S
*Nerium indicum*Mill.	Shrub	4				2.6	3.3	S
Cedrus deodara(Roxb. ex D. Don), G. Don.	Tree	0.5	0.4	0.5	0.66	0.66	0.54	CE
*Pistacia integerrima*J.L.Stewart. Brandis.	Tree	0.66	0.5	0.66	0.66	0.66	0.62	CE
Taxus wallichiana(Zucc.)Pilger.	Tree	0.66		1			0.83	CE
*Ficus carica*Forsk.	Tree	0.66		1	0.66	1.32	0.91	CE
Cornus macrophylla Wall. ex Roxb.	Tree	1	1	1			1	CE
Bauhinia variegate L.	Tree	1.2	1.2	1	1	1	1	CE
Quercus dilatata Lindle. ex Royle.	Tree	1.2		1			1.1	E
Quercus leucotrichophora A. Camus.	Tree	0.75		1.5			1.12	E
*Quercus floribundla*Lindl.	Tree	1		1.3			1.15	E
*Quercus incana*Roxb.	Tree	1	0.6	1.3		2	1.22	E
Populus alba L.	Tree	1.3	1.3		1.3	1.3	1.3	E
Abies pindrow Royle.	Tree	0.66		2			1.33	E
Picea smithiana(Wall.) Boiss.	Tree	0.66		2			1.33	E
*Butea monosperma (*Lam.) O. Kuntz.	Tree	1		1.5	1.5	1.5	1.37	E
Grewia optiva Drummond .exBurret.	Tree	1.6	0.75	1.42	1.6	1.66	1.4	E
Bombax ceiba L.	Tree	1	0.75	2	2.6	1	1.47	E
Celtis australis L.	Tree	1.2	1.2	1.5	2	1.5	1.48	E
Alnus nitida(Spach.) Endl.	Tree	0.66	1	3	1.32		1.49	E
Cydonia oblonga Miller.	Tree	1.5				1.5	1.5	E
Morus alba L.	Tree	1.5		1.5	2	1	1.5	E
Phoenix dactylifera L.	Tree			1.5			1.5	E
Phoenix sylvestris(L.) Roxb.	Tree				1	2	1.5	E

http://www.aloki.hu ● ISSN 1589 1623 (Print) ● ISSN 1785 0037 (Online)
DOI: http://dx.doi.org/10.15666/aeer/1705_1039910419

Name of species	Habit	Tribe wise CS values						
		Basikhel	Nusratkhel	Akazai	Hassanzai	Medakhel	Mean	Categories
Pinus wallichiana A. B. Jackson.	Tree	1.5	1.5	1.5	1.5	1.5	1.5	E
*Sapindus mukorossi*Gaertn.	Tree	1.5					1.5	E
Acacia nilotica L.	Tree	1	1	2	2	2	1.6	V
Ficus benghalensis L.	Tree	1.5	1.5	2	1.5	1.5	1.6	V
Aesculus indica(Wall.exCamb.)Hk.	Tree	1.33		1.5		2	1.61	V
Albezzia procera(Roxb) Benth.	Tree	1.5	1.5	3	1.5	1	1.7	V
Pyrus communis L.	Tree	1.5		2			1.75	V
Ziziphus jujube Mill.	Tree	1.6	1.6	2	1.2	2.6	1.8	V
Albezzia lebbek(L) Benth.	Tree	1.5		2	2		1.83	V
Pyrus pashia Ham ex D. Don.	Tree	2	1.33	2	2	2	1.86	V
Ficus racemosa L.	Tree	2	2	2	2		2	V
*Ilex dipyrena*Wall.	Tree	2					2	V
Cedrella serrata Royle.	Tree	2		1.5	3	2	2.12	R
Azadiracha indica L.	Tree	2.66	3.3	2	1	2	2.19	R
Delbergia sisso Roxb.	Tree	2	2	2.6	2.6	2.5	2.34	R
Punica granatum L.	Tree	2.5	2.6	2	2	2.6	2.34	R
Diospyrus lotus L.	Tree	2.5	2.3	2.5			2.43	R
Salix tetrasperma Roxb.	Tree	1.5			2	4	2.5	R
Olea ferruginea Royle.	Tree	3	2.4	2.5	3	3	2.78	S
Pinus roxburghii Sargent.	Tree	2	2	3.32	3.32	3.32	2.7	S
Ficus palmate Forsk.	Tree	3	3.5	2.5	3	2.5	2.9	S
Ailanthus altissima(Mill.) Swingle.	Tree	3	3	2	4		3	S
Robinia pseudoacacia L.	Tree	3	2.25	3	2.5	4.5	3	S
Moras nigra L.	Tree	3	3	3.5	3	2.8	3	S
Melia azedarach L.	Tree	3	3.5	3	3	3	3.1	S
Acacia modesta Wall.	Tree	3	3	3.75	3	3	3.15	S
Juglans regia L.	Tree	3	4.2	3	3	3	3.24	S
Prunus armeniaca L.	Tree	3	3.6				3.3	S
Euclaptus sp.	Tree	2			6	4	4	S
Broussonetia papyrifera(L.)L' Herit ex Vent.	Tree	4.5	4.5	5	4.98	4.98	4.79	S
Platanus orientalis L.	Tree	5					5	S

NR: not reported, CS: conservation status, CE: critically endangered, E: endangered, V: vulnerable, R: rare, S: secure

Conservation status of herbs

Six species of herbs were found critically endangered (CE) showing CS values up to 1.0 These species are *Podophyllum emodi* (0.5), *Gentiana kurroo* (0.85), *Dioscoreadeltoidea* (0.88), *Incarvellia emodi* (0.96), *Arisaema utile* (1.0) and *Picris hieraciodes (1.0)* (*Fig. 2*). Thirteen species of herbs were mentioned as endangered ranging CS values from 1.1 to 1.5. Vulnerable species were found 31, rare 41 and secure 104 (*Table 2*).

Conservation status of shrubs

Among shrubs 9 species were found critically endangered. These were Skimmia laureola (0.48), Woodfordiafruticosa (0.78), Periploca aphylla (0.88), Hedra nepalensis (01), Nannorrhops ritchieana(01), Vitis jacquemontii (01), Viburnum grandiflorum (01) and Opuntia dillenii(01) (*Fig. 3*). Endangered species were recorded 4, vulnerable 15, rare 11 and secure 9 (*Table 2*).

http://www.aloki.hu ● ISSN 1589 1623 (Print) ● ISSN 1785 0037 (Online)
DOI: http://dx.doi.org/10.15666/aeer/1705_1039910419

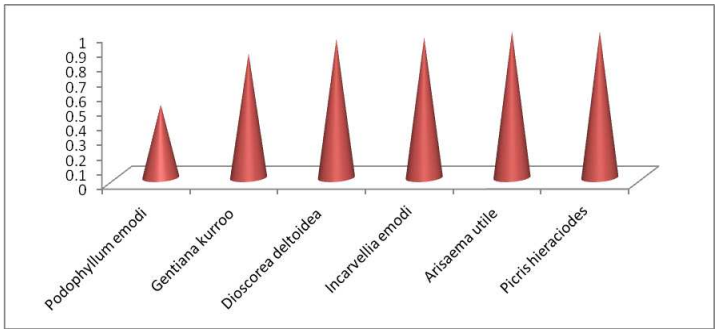

Figure 2. *Critically endangered herbs of district Tor Ghar*

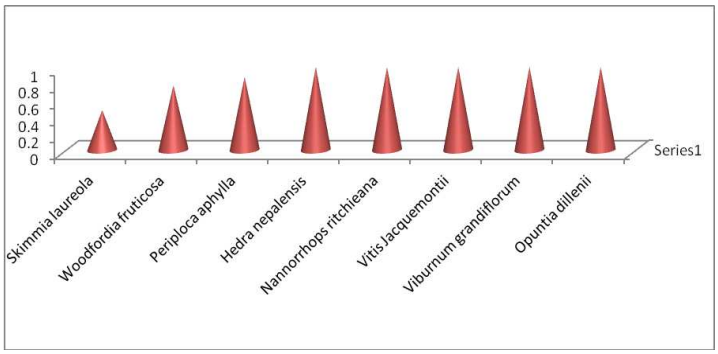

Figure 3. *Critically endangered shrubs of district Tor Ghar*

Conservation status of trees

Six trees species were declared critically endangered. These were *Cedrus deodara* (0.54), *Pistacia integerrima* (0.62), *Taxus wallichiana* (0.83), *Ficus carica* (0.91), *Cornus macrophylla* (1) and *Bauhinia variegata* (1) (*Fig. 4*). Eighteen species of trees were mentioned as endangered, 10 vulnerable, 6 rare and 13 secure (*Table 2*).

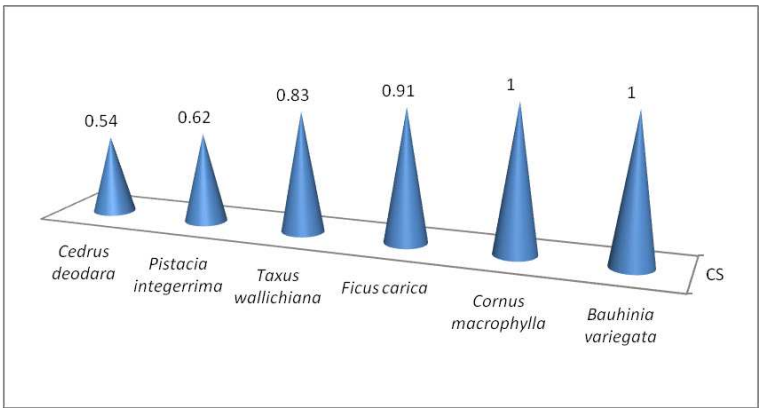

Figure 4. *Critically endangered trees of district Tor Ghar*

Herbs are found secure mostly in the region and least critically endangered whereas trees are more endangered and least critically endangered and rare. Shrubs are more vulnerable and least endangered (*Fig. 5*).

http://www.aloki.hu ● ISSN 1589 1623 (Print) ● ISSN 1785 0037 (Online)
DOI: http://dx.doi.org/10.15666/aeer/1705_1039910419

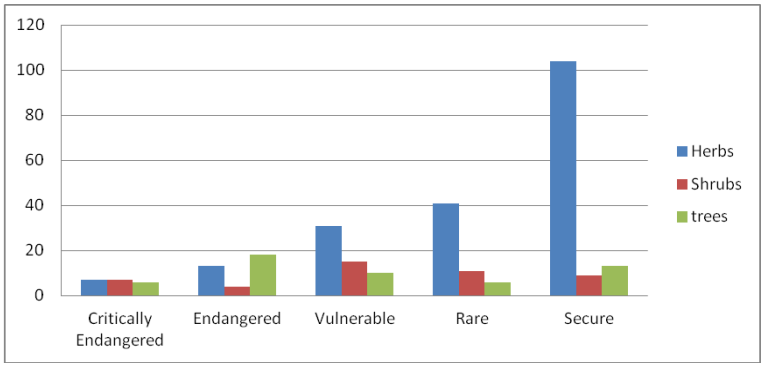

Figure 5. *Number of species of all life forms and IUCN categories*

Overall 20 species of all life forms were declared critically endangered, 35 endangered, 56 vulnerable, 58 rare and 126 secure (*Fig. 6*).

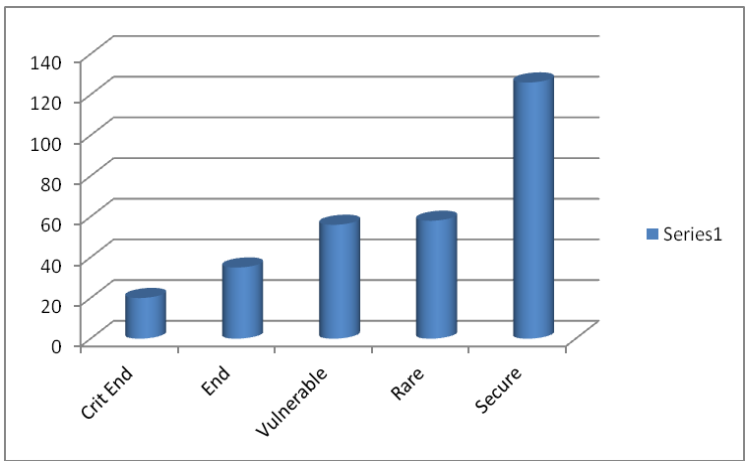

Figure 6. *Total number of species assigned to IUCN categories*

The percentage of threatened flora 38% (7% critically endangered, 12% endangered, 19% vulnerable) 19% near threatened (rare) was higher as compare to secure (least concerned) flora 43% (*Fig. 7*).

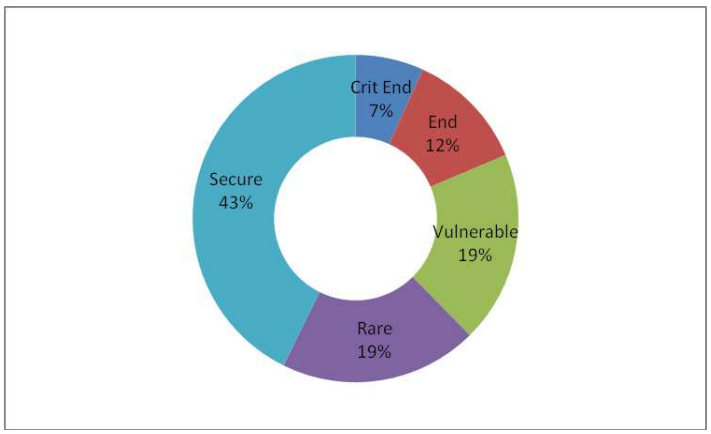

Figure 7. *Percentage of threatened and secure species of Tor Ghar*

http://www.aloki.hu ● ISSN 1589 1623 (Print) ● ISSN 1785 0037 (Online)
DOI: http://dx.doi.org/10.15666/aeer/1705_1039910419

Discussion

The current investigation finds out the role of ethnoecological knowledge in evaluating the conservation status of culturally significant flora of district Tor Ghar. The United Nations Convention Environment and Development (UNCED, 1992) also highlighted the important roles that indigenous peoples play in both the conservation and sustainable use of natural resources while in turn maintaining biodiversity. In the present study local wisdom was explored and conservation status of 295 plants species in terms of IUCN categories was calculated on the basis of newly developed equation. The results depict 7% critically endangered flora, 12% endangered, 19% vulnerable and 19% near threatened (rare). The rest of the flora that is 43% found secure (least concerned). Such categorization was also found in a number of other ethnobotanical studies (Gilani et al., 2006; Afzal et al., 2009; Haq, 2012; Akhter et al., 2013; Bibi et al., 2014; Shah et al., 2015). Hamayun et al., 2006) also evaluated conservation status of 49 medicinal plant species and found 24 species threatened. Out of which 9 were found endangered, 7 vulnerable and 8 rare. The study also revealed that locals particularly plants collectors had useful information about plants occurrence, distribution and sites of their maximum availability. This information was cross checked through field surveys and visits. The field observations include, range extent and area of occupancy, exploitation level, availability, habitat alteration, conservation efforts, plant collection methods, part collected, invasive species and threats to plant biodiversity. On the basis of these observations, the species were then categorized according to IUCN categories as critically endangered, endangered, vulnerable, rare (near threatened) and secure (least concerned).

The results obtained by applying this equation show accuracy and found in accordance with the majority of results of other studies conducted in adjacent areas as well as different parts of Pakistan. According to this equation six species of herbs were found critically endangered (CE) showing CS values up to 1. These species are *Podophyllum emodi* (0.5), *Gentiana kurroo* (0.85), *Dioscorea deltoidea* (0.88), *Incarvellia emodi* (0.96), *Arisaema utile* (1) and *Picris hieraciodes* (01). Thirteen species of herbs were mentioned as endangered ranging CS values from 1.1 to 1.5. Vulnerable species are 31 (1.6-2), rare 41 (2.1-2.5) and secure 104 (CS value above 2.5). Gilani et al. (2006) documented 21 ethnomedicinal herbs from AyubiaNational Park, district Abbottabad and found *Podophyllum emodi* and *Viola canescens*as vulnerable species due to overexploitation. While according to the findings of the present study *Podophyllum emodi* (0.5) is critically endangered but *Viola canescens* (2.7) is secure. *Podophyllum emodi* is under great harvesting pressure, showing minimum occurrence, availability for the last 10 years decreases and its regeneration potential could not keep pace with its overexploitation. Whereas *Viola canescens* shows the criteria of secure in this study. Afzal et al. (2009) studied that some plant species *Colchicum luetum, Bergenia ciliata, Pimpinella stewartii, Valleriana jatamonsii, Viola serpens* and *Dioscorea deltoids* etc. are rapidly depleting and may become locally extinct in near future. Some of these have also been reported and assessed in present investigation. *Colchicum luetum* (1.33), *Bergenia ciliate* (1.76) and *Valleriana jatamonsii* (1.92) were found vulnerable. While *Dioscorea deltoids* (.95) found critically endangered at local level.

Among shrubs 8 species were found critically endangered. These are *Skimmia laureola* (0.48), *Woodfordia fruticosa* (0.78), *Hedra nepalensis* (1.0), *Nannorrhops ritchieana* (1.0), *Vitis jacquemontii* (1.0), *Periploca aphylla* (01), *Opuntia dillenii* (01)

http://www.aloki.hu ● ISSN 1589 1623 (Print) ● ISSN 1785 0037 (Online)
DOI: http://dx.doi.org/10.15666/aeer/1705_1039910419

and *Viburnum grandiflorum* (1). Endangered species are 4, vulnerable 15, rare 11 and secure 9 (*Table 2*).

Six trees species were declared critically endangered. These are *Cedrus deodara* (0.54), *Pistacia integerrima* (0.62), *Taxus wallichiana* (0.83), *Ficus carica* (0.91), *Cornus macrophylla* (1) and *Bauhinia variegate* (1.0). Eighteen species of trees were declared as endangered, 10 vulnerable, 6 rare and 13 secure (*Table 2*).

Similarly Haq (2012) also conducted ethnoconservation survey of 12 threatened species from district Battagram (adjacent district to Tor Ghar). These species were *Acer caesium, Betula utilis, Cedrus deodara, Opuntia dilleni, Paeonia emodi, Pistacia integerrima, Populus alba, Quercus glauca, Skimmia laureola, Taxus wallichiana, Ulmus wallichiana* and *Viscum album*. Their conservation status was assessed through direct field observation and the information gathered by locals. The present research work also declared 6 plants *Cedrus deodara, Opuntia dilleni, Pistacia integerrima, Populus alba, Skimmia laureola* and *Taxus wallichiana* as critically endangered species of district Tor Ghar.

Shah et al. (2012) explored *Olea ferruginea* along with mixed tree species of *Monotheca buxifolia* and *Acacia modesta* as dominant ethnoflora of sacred jungles of Kurd sharif and Sho of district Karak showing a traditional way of conserving plant biodiversity. Similar findings of this research show *Olea ferruginea* (2.78) and *Acacia modesta* (3.15) as secure species of the study area. *Olea ferruginea* is protected in graveyards and considered one of the most important sacred plant species of Graveyards and is not cut for any purpose. *Olea ferruginea*is also protected by locals from fire by making small circular stony walls around trees (Shah et al., 2015)

Ahmad et al. (2012) found 5 plants species critically endangered, 6 endangered, 10 vulnerable, 11 secure and 6 rarely distributed in Sharda, Neelam valley Azad Jammu and Kashmir. This study further revealed the over exploited species are *Aconitum heterophyllum, Geranium wallichianum, Ajuga bracteosa, Traxicum officinale, Quercus incana, Berberis lycium, viola canescens* and *Dyosporus lotus.* Majority of them are at the verge of local extinction due to extensive harvesting pressure. The CS values index also shows *Geranium wallichianum* (1.56), *Ajuga bracteosa* (02) and *Berberis lyceum* (02) as vulnerable species, whereas *Traxicum officinale* (2.13) and *Dyosporus lotus* (2.4) as rare species. Whereas *Quercus incana* (1.22) as endangered species *and viola canescens* (2.7) as secure species. The result of *viola canescens* (2.7) as secure species is only different. It may be due to its habitat adjustment or reduced overexploitation. Therefore, *viola canescens* (2.7) is not considered the threatened species of the district. The field observations also show its moderate occurrence.

In Chakesar valley district Shangala, a plant resource assessment project was carried out ethnobotanically to explore conservation status of some important medicinal plants. Conservation of 127 plant species was evaluated through IUCN criteria. Among these species 47 were endangered (E), 32 vulnerable (VU), 36 rare (R) and 12 species were infrequent (IF). Some of the important endangered species of the region are *Abies pindrow*, *Acer oblongum, Aesculus indica, Alnus nitida, Berberis kunawarensis, Celtis australis, Desmodium elegans, Hedrane palensis, Juglan regia, Olea ferruginea, Paeonia emodi, Picea smithiana, Pinus gerardiana, Pisticia integrima, Quercus semicarfifolia, Vibernum grandiflorum* and *Woodfordia fruticosa* (Shah and Hussain, 2012). When the results of this study were compared with the results of present research, majority of the species showed similarity in results and however, a few species showed different conservation stata e.g. *Abies pindrow, Alnus nitida, Celtis australis*

http://www.aloki.hu ● ISSN 1589 1623 (Print) ● ISSN 1785 0037 (Online)
DOI: http://dx.doi.org/10.15666/aeer/1705_1039910419

and *Picea smithiana* were declared as endangered species while *Hedrane palensis, Vibernum grandiflorum* and *Woodfordia fruticosa* as critically endangered species of the research area. *Aesculus indica* was mentioned as vulnerable species of the district. In these results category of threatening is different. However, *Juglan regia* and *Olea ferruginea* showed different results being culturally significant species. These are well protected by local culture and therefore, attained the secure status. *Juglan regia* is the most popular wild edible plant of the study area. This tree species provides a number of services to the locals in the form of furniture wood, cosmetics and tasteful dry fruit having prolonged storage life. This important species is facing overexploitation pressure but due to cultivation and protection by locals showing secure status in the district Tor Ghar (Shah et al., 2015).

Akhtar et al. (2013) assessed ethnobotanically that *Aconitum violaceum, Colchicum luteum* and *Jasminum humile* as vulnerable due to over exploitation. According to the present study *Colchicum luteum* (1.33) is endangered and *Jasminum humile* (2.33) is rare. However, *Aconitum violaceum* was not reported by any tribe in the current study.

Bibi et al. (2014) pointed out the highest under pressure species *Caralluma tuberculata, Citrullus colocynthis, Malva neglecta* and *Mentha longifolia* in district Mastung of Baluchistan. *Caralluma tuberculata* (1.32) and *Citrullus colocynthis* (1.1) were also declared as endangered species, whereas *Malva neglecta* (3) and *Mentha longifolia* (4.49) as the most secured species of the area showing highest values of CS. *Malva neglecta* is an agricultural land associated plant species and is found abundantly in the study area. Similarly, *Mentha longifolia* was found secure and grows excessively near aquatic habitats of Tor Ghar.

Mussarat et al. (2014) indicated *Morus alba* and *Dalbergia sissoo* under great overexploitation pressure and threatened species in the area. While in the present exploration *Morus alba* (1.5) is endangered and *Dalbergia sissoo* (2.3) is rare. *Dalbergia sissoo* is under great overexploitation pressure especially for furniture wood. *Morus alba* is also depleting alarmingly in the region. No conservatory measures are taken to secure *Morus alba* in Tor Ghar.

Amjad et al. (2015) indicated *Ajuga bracteosa, Mallotus philippensis, Micromeriabiflora, Butea monosperma*and *Zanthoxylum armatum* as critically endangered in Kotli, Azad Jammu and Kashmir. The present research work show *Ajuga bracteosa* (2) as vulnerable, *Mallotus philippensis* (3.3) as secure, *Butea monosperma* (1.37) as endangered species and *Zanthoxylum armatum* (2.4) as rare species.

In the current study *Taxus wallichiana* (0.83) was found critically endangered while *Pinus wallichiana* (1.5) and *Abies pindrow* (1.33) were found endangered. The study of Adnan et al. (2006) also mentioned these species as rapidly decreasing species in Miandam vally of district Swat.

Cedrus deodara in this study showing (0.54) CS value and declared critically endangered. Sheikh et al. (2002) also pointed out that *Cedrus deodara* had completely eradicated from Naltar valley, northern western Karakorum range.

When the results of present study were matched with IUCN red list criteria at regional level two species were found critically endangered (CE) in the study area. These species were *Cedrus deodara* (0.54) and *Gentiana kurroo* (0.85). Two species were found Endangered/Threatened (EN) in the region i.e., *Picea smithiana* (1.33) and *Viburnum cotinifolium* (1.13). While *Geranium wallichianum* (1.56) and *Salvia moorcroftiana* (1.87) were mentioned endangered in IUCN criteria but vulnerable species at district Tor Ghar level. *Bergenia ciliata* (1.76) is vulnerable in IUCN list as

http://www.aloki.hu ● ISSN 1589 1623 (Print) ● ISSN 1785 0037 (Online)
DOI: http://dx.doi.org/10.15666/aeer/1705_1039910419

well as in the present research. *Pinus wallichiana* (1.5) was found endangered in this study but vulnerable in IUCN red list. *Viola canescens* (2.7) is considered as secure locally but vulnerable regionally. This species showed quite different conservation status from the published literature and IUCN red list indicating its conservation status secured locally.

Conclusion

Local ecological knowledge has been proved a successful tool for evaluating conservation stata of flora of the study site. This empirical study revealed that a higher proportion (57%) of flora is undergoing various degrees of threatening at local level that is 7% critically endangered, 12% endangered, 19% vulnerable and 19% rare in terms of IUCN categories. However, forty three percent flora of the district is secure. The findings of the present study indicating that flora of Tor Ghar is under high anthropogenic pressure. This is first ever attempt of quantifying the local wisdom regarding conservation status of the plants. Local perception of the flora also reflects its conservation status which may be considered in futures researches as base line study. The above discussion revealed that the mathematical relation designed during the study has been proved useful tool for evaluating ethno-conservation of local flora. The equation can be generalized and applied to any floristic area of the world. Conservation researchers should quantify the local wisdom while applying IUCN criteria to any floristic territory especially where anthropogenic disturbances are at alarming rate. This will reinforce the results and more clarify the picture of conservation status of plant biodiversity of a region.

Acknowledgements. Indigenous tribes of district Tor Ghar are highly acknowledged for their permission of gathering data and cooperation and guidance during field trips.

Conflict of interests. The authors declare that they have no competing interests.

REFERENCES

[1] Adams, W. M., Hutton. J. (2007): People, parks and poverty: political ecology and biodiversity conservation. – Conservation and Society 5: 147-183.

[2] Adams, W. M., Aveling, R., Brockington, D., Dickson, B., Elliott, J., Hutton, Roe, D., Vira, B., Wolmer, W. (2004): Biodiversity conservation and the eradication of poverty. – Science 306(5699): 1146-1149. http://dx.doi.org/10.1126/science.1097920.

[3] Adnan, S. M., Khan, A. A., Latif, A., Shinwari. Z. K. (2006): Threats to the sustainability of ethno-medicinal uses in northern Pakistan. A case study of Miandam valley, district Swat, NWFP province, Pakistan. – Lyonia 11(2): 19-100.

[4] Afzal, S., Afzal, N., Awan, M. R., Khan, T. S., Gilani, A., Khanum, R., Tariq, S. (2009): Ethno-botanical studies from Northern Pakistan. – Journal of Ayub Medical College Abbottabad 21(1): 52-56.

[5] Ahmad, K. S., Qureshi, R., Hameed, M., Ahmad, M. F., Nawaz, T. (2012): Conservation assessment and medicinal importance of some plants resources from Sharda, Neelumvalley, Azad Jammu and Kashmir, Pakistan. – International Journal of Agriculture and Biological Sciences 14: 997–1000.

http://www.aloki.hu ● ISSN 1589 1623 (Print) ● ISSN 1785 0037 (Online)
DOI: http://dx.doi.org/10.15666/aeer/1705_1039910419

[6] Akhtar, N., Rashid, A., Murad, W. E., Bergmeier, E. (2013): Diversity and use of ethno-medicinal plants in the region of Swat, North Pakistan. – J. Ethnobio. & Ethnmed. DOI: 10.1186/1746-4269-9-25.
[7] Amjad, M. S., Arshad, M. R., Quershi, M. (2015): Ethnomedicinal inventory and folk uses of indigenous plants from Pir Nasoora National Park, Azad Jammu and Kashmir. Asian Pacific J. Trop. Biomed. 5(3): 234-241. 9: 25.
[8] Andrews, G., Daylight, C., Hunt, J. (2006): Aboriginal cultural heritage landscape mapping of coastal NSW. – Prepared for the Comprehensive Coastal Assessment by the NSW Department of Natural Resources, Sydney, NSW.
[9] Anonymous (1992): CBD (Convention on Biological Diversity). – The Convention on Biological Diversity, Rio de Janeiro.
[10] Aswani, S., Lemahieu, A., Sauer, W. H. H. (2018): Global trends of local ecological knowledge and future implications. – PLoS One 13(4): e0195440. https://doi.org/10.1371/journal.pone.0195440.
[11] Berkes, F. (2007): Community-based conservation in a globalized world. – Proceedings of the National Academy of Sciences of the United States of America 104(39): 15188-15193.
[12] Berkes, F., Colding, J., Folke, C. (2000): Rediscovery of traditional ecological knowledge as adaptive management. – Ecol Appl. Ecological Society of America 10: 1251-1262.
[13] Bibi, T., Ahmad, M., Tareen, R. B., Tareen, N. M., Jabeen, R., Rehman, S. U., Sultana, S., Zafar, M., Yasee, G. (2014): Ethnobotany of medicinal plants in district Mastung of Balochistan Province-Pakistan. – J. Ethnopharmacol. 157: 79-89.
[14] Boom, B. M. (1987): Ethnobotany of the Chacobo Indians, Beni, Bolivia. – Adv. in Econ. Bot. 1-68.
[15] Bridgewater, P. B. (2002): Biosphere reserves: special places for people and nature. – Environ. Sci. & Policy 5: 9-12.
[16] Broennimann, O., Vittoz, P., Moser, D., Guisan, A. (2005): Rarity types among plant species with high conservation priority in Switzerland. – Bot. Helv. 115: 95-108.
[17] Calvo, L.M. (2003): EI humano y la gestion de la biodiversidad biologica: Problemas, potencialidades y tendencies. – In: Ibish, P. L., Merida, G. (eds.) Biodiversidad: Lariqueza de Bolivia. Estado de conocimiento y Conservacion. Ministerio de Desarrollo Sostenible. Editorial FAN, Santa Cruz de la Sierra, Bolivia.
[18] Cotton, C. M. (1996): Ethnobotany. Principles and Applications. – John Wiley and Sons, New York.
[19] Domínguez Lozano, F., Moreno Saiz, J. C., SainzOllero, H. (2003): Rarity and threat relationships in the conservation planning of Iberian flora. – Biodivers. & Conserv. 12: 1861-1882.
[20] Gilani, S. A., Quershi, R. A., Gilani, S. J. (2006): Indigenous uses of some important ethnomedicinal herbs of Ayubia National Park, Abbottabad, Pakistan. – Ethnobotany Leaflets 10: 285-293.
[21] Grimble, R., Laidlaw, M. (2002): Biodiversity management and local livelihoods: Rio plus 10. – ODI Natural Resource Perspectives Papers 73: 1-4.
[22] Hamayun, M., Khan, S. A., Sohn, E. Y., Lee, I. J. (2006): Folk medicinal knowledge and conservation status of some economically valued medicinal plants of district Swat, Pakistan. – Lyonia 11(2): 101-113.
[23] Haq, F. (2012): The critically endangered flora and fauna of district Battagram, Pakistan. – Advances in life Sciences 2(4): 118-123.
[24] Jules, P. (2008): How Do Biodiversity and Culture Intersect? Sustaining Cultural and Biological Diversity in a Rapidly Changing World: Lessons for Global Policy, 2-5 April 2008. – American Museum of Natural History's Center for Biodiversity and Conservation, IUCN-The World Conservation Union/Theme on Culture and Conservation, and Terralingua, pp. 1-17.

http://www.aloki.hu ● ISSN 1589 1623 (Print) ● ISSN 1785 0037 (Online)
DOI: http://dx.doi.org/10.15666/aeer/1705_1039910419

[25] Larid, S. A. (1999): Forests, Culture and Conservation. – In Posey, D. A. (ed.) Cultural and Spiritual Values of Biodiversity. – UNEP and Intermediate Technology Publications: London, pp. 345-396.
[26] McNeely, J. A. (2000): Cultural Factors in Conserving Biodiversity. – In Wilkes, A., Tillman, H., Salas, M., Grinter, T., Shaoting, Y. (eds.) Links between Cultures and Biodiversity. Proceedings of the Cultures and Biodiversity Congress. Yunnan Science and Technology Press, Yunnan, P. R. China, pp. 128-142.
[27] Meijaard, E., Mengersen, K., Buchori, D., Nurcahyo, A., Ancrenaz, M., Wich, S. (2011): Why don't we ask? A complementary method for assessing the status of great apes. – PLoS One 6(3): e18008. https://doi.org/10.1371/journal.pone.0018008.
[28] Mussarat, S., Salam, N. M. A., Tariq, A., Wazir, S. M., Ullah, R., Adnan, M. (2014): Use of ethnomedicinal plants by the people living around Indus River. Evid. based complement. – Alternat. Med. 2014: 2.
[29] Negi, C. S. (2010): Traditional culture and biodiversity conservation: examples from Uttarakhand, Central Himalaya. – Mounain Research & Development30: 259-265.
[30] Phillips, O., Gentry, A. H. (1993b): The useful plants of Tambopata, Peru: 11. Additional hypothesis testing in quantitative ethnobotany. – Economic Botany 47: 33-43.
[31] Posey, D. A. (1999): Cultural and Spiritual Values of Biodiversity. A Complementary Contribution to the Global Biodiversity Assessment. – In Posey, D. A. (ed.) Cultural and Spiritual Values of Biodiversity. UNEP and Intermediate Technology Publications, London, pp. 1-19.
[32] Posey, D. A., Overal, W. L., Goeldi, M. P. E. (1990): Ethnobiology: implications and applications. Proceedings of the First International Congress of Ethnobiology, Belém, 1988.
[33] Prance, G. T., Balee, W., Boom, B. M., Carneiro, R. L. (1987): Quantitative ethnobotany and the case for conservation in Amazonia. – Conservation Biology 1: 296-310.
[34] Rajeswar, J. (2001): Conservation ethics versus development: How to obviate the dichotomy. – Sustainable Development 9: 16-23.
[35] Schwartzman, S., Nepstad, D., Moreira, A. (2000): Arguing tropical forest conservation: people versus Parks. – Conservation Biology 14: 1370-1374.
[36] Shah, A. H., Khan, S. M., Shah, A. H., Mehmood, A., Rehman, I. U., Ahmad, H. (2015): Cultural uses of plants among Basikhel tribe of district Tor Ghar, Khyberpakhtunkhwa, Pakistan. – Pakistan Journal of Botany 47(SI): 17-31.
[37] Shah, A. S., Hussain, S., Din, N. U., Bhatti, K. H., Khan, A., Marwat, S. K., Zafar, M., Ahmad, M. (2012): Sacred jungles. A traditional way of conserving endangered ecosystems and biodiversity in semi- tribal area Kurd Sharif & Sho (District Karak, Khyber Pakhtunkhawa) Pakistan. – Science Technology and Development 31(4): 312-326.
[38] Shah, M., Hussain, F. (2012): Conservation assessment of plant resources of Chakaser valley, District Shangla, KPK, Pakistan. – Pakistan Journal of Botany 44(SI): 179-186.
[39] Sheikh, K., Ahmad, T., Khan, M. A. (2002): Use, exploitation and prospects for conservation: people and plant biodiversity of Naltar Valley, northern western Karakorum, Pakistan. – Biodiversity and Conservation 11(4): 715-742.
[40] United Nations (1992): United Nations Framework Convention on Climate Change. – United Nations, New York.
[41] Von Glasenapp, M., Thornton, T. F. (2011): Traditional ecological knowledge of Swiss alpine farmers and their resilience to socioecological change. – Human Ecology 39: 769-781.
[42] Wells, M. P., McShane, T. O. (2004): Integrating protected area management with local needs and aspirations. – AMBIO: A Journal of the Human Environment 33: 513-519.
[43] Wiersum, K. F., Shackleton, C. M. (2005): Rural Dynamics and Biodiversity Conservation in Southern Africa. – In Ros-Tonen, M. A. F., Dietz, T. (eds.) African

http://www.aloki.hu ● ISSN 1589 1623 (Print) ● ISSN 1785 0037 (Online)
DOI: http://dx.doi.org/10.15666/aeer/1705_1039910419

Forests between Nature and Livelihood Resources: Interdisciplinary Studies in Conservation and Forest Management. Edwin Mellen Press, UK.

[44] Zent, S. (2001): Acculturation and Ethnobotanical Knowledge Loss among the Piaroa of Venezuela: Demonstration of a Quantitative Method for the Empirical Study of Traditional Environmental Knowledge Change. – In: Maffi, L. (ed.) On Biocultural Diversity: Linking Language, Knowledge, and the Environment. Smithsonian Institution Press, Washington, DC, pp. 190-211.

http://www.aloki.hu ● ISSN 1589 1623 (Print) ● ISSN 1785 0037 (Online)
DOI: http://dx.doi.org/10.15666/aeer/1705_1039910419

MONITORING AND EVALUATION OF COASTAL WATER QUALITY PARAMETERS IN FETHIYE BAY, TURKEY

YILDIRIM, P. – BALAS, L.*

Sea and Aquatic Sciences Application and Research Center, Gazi University, Ankara, Turkey

**Corresponding author*
e-mail: lalebal@gazi.edu.tr

(Received 5th Mar 2019; accepted 20th Aug 2019)

Abstract. The physical, microbiological quality parameters and plankton abundance have been monitored and evaluated in coastal waters of Fethiye Inner Bay, Turkey. The temporal and areal variations of quality parameters have been investigated through the monthly measurements at 14 locations between March 2016 and February 2017. The physical parameters measured throughout the water column were water temperature, salinity, pH, and turbidity. Besides, water samples were taken from the surface waters, and total coliform, fecal coliform, fecal streptococci, *Escherichia coli*, *Pseudomonas aeruginosa*, *Salmonella* detection, phytoplankton and zooplankton abundance analyses were performed in the laboratory. By using the related Turkish Standards Institution (TSE) standards, biochemical oxygen demand and dissolved oxygen levels were also determined. Results were evaluated to understand the microbiological water quality of Fethiye Inner Bay, by the Turkish Regulations for the Surface Water Quality (2016) and the Quality of Bathing Water (2006), and Directive 2006/7/EC on bathing water. For the evaluation of the results, geographic information systems (GIS) based HYDROTAM-3D that is the first coastal waters hydrodynamic, transport and water quality model developed in Turkey, was used (http://www.hydrotam3d.com/fethiye). A microbiological parameters database was established for Fethiye Inner bay coastal waters by using HYDROTAM-3D model water quality management system, accessible over the internet.
Keywords: *marine environment, pollution, HYDROTAM-3D, microbiological parameters, phytoplankton, zooplankton, biochemical oxygen demand, dissolved oxygen, Fethiye Bay*

Introduction

People take the water from the hydrological cycle for their vital and economic needs, and the water used returns back to the cycle. In this cycle, substances that enter the water cause the pollution by changing the physical, chemical and biological properties of the water. The main factors that accelerate water pollution are population growth and rapid industrialization (Liyanage and Yamada, 2017). Water is a vital source of infections that can be transmitted through the digestive system. Pathogenic bacteria and other microorganisms mix with water in feces and similar ways depending on many factors such as the geographical location of the region, infrastructure facilities, sewage processes, the socio-economic structure of the community. Viruses, pathogenic bacteria, and parasites can be found in the water as harmful biological agents for human health (Griffin et al., 2003).

The increasing use of water due to population increase and developing industrialization is a crucial factor accelerating water pollution. Pollutants discharged from the point sources such as domestic and industrial sea outfalls or discharged from the distributed sources also pollute the water resources and prevent other uses of receiving waters. Protection of water resources, development, prevention of deterioration in quality and sustainable use of water for long-term conservation of water resources is necessary.

http://www.aloki.hu ● ISSN 1589 1623 (Print) ● ISSN 1785 0037 (Online)
DOI: http://dx.doi.org/10.15666/aeer/1705_1042110444

Fecal coliforms and fecal streptococci are dangerous indicators of health associated with fecal contamination (Barcina et al., 1991). The main entranceway of enteric bacteria and viruses such as *Escherichia coli* to coastal areas is by urban and agricultural wastes (Rees et al., 2010). Enteric bacteria exposed to the marine environment simultaneously, different to their natural habitat, encounter a variety of abiotic and biotic challenges that is marked (Rozen and Belkin, 2001). Biotic stress arises from natural seawater microbiota, which are better scavengers for limited nutrients available and may also prey and graze on the enteric newcomers. Abiotic stress faced by enteric bacteria in seawater include sunlight temperature, pH, lack of nutrients, salinity, current and turbulence and (possibly) hydrostatic pressure (Troussellier et al., 1998; Barcina et al., 1991; Rozen and Belkin, 2001). Lack of water quality management of coastal waters can lead to both health and income losses at shellfish trade centers and fishing places (Rees et al., 2010). Continuous water quality management at coastal waters are vital for human health. In this study, measurements and evaluations of physical, microbiological quality parameters and plankton abundance were performed for Fethiye Inner Bay. The monthly variations of microbiological quality parameters were investigated through the site measurements conducted in between March 2016 and February 2017.

The Fethiye Bay is located in the Eastern Mediterranean coast of Turkey. It is a sheltered area against currents and waves approaching from north, west and southeast directions. Fethiye Inner Bay is an enclosed water body having limited water exchange from the openings on both sides of the Şövalye (Zeytin) Island located in the Fethiye Bay (Cebe, 2016) and it is surrounded by the town of Fethiye. The primary economic activity in the town is tourism. Besides the tourism, its economy is mainly based on agriculture and animal husbandry (Cebe, 2016). Due to the compatibility of climate and physical conditions, irrigated agriculture is mostly performed in the town. The drainage waters of agricultural lands flow to the waters of Fethiye Bay via Murt (Mersinli) and other channels. Low flushing rate of the enclosed Inner Bay waters increases the sensitivity to pollutants.

The wastewater of the Fethiye Town is transferred to the treatment plant and then discharged to the Inner Bay from the eastern part of the Şövalye (Zeytin) Island (*Fig. 1*). The treated wastewater is rich in nitrogen and phosphorus, and it has been discharged into Fethiye Inner Bay together with the agricultural drainage waters that are also rich in nitrogen and phosphorus salts carried by the Murt River. The pollution in Murt River alone has a potential to affect the inner bay of Fethiye. Also, seven channels discharge the agricultural drainage waters directly into Fethiye Inner Bay without any treatment or sedimentation (*Fig. 2*). Likewise, settlements located in the Şövalye (Zeytin) Island and in the west of the bay constitute one of the primary sources of pollution because they are not connected to the wastewater system, and are not subject to the treatment. Other sources of pollution are Fethiye Marina and wastewaters emptied from the boats (Yılmaz et al., 2017). In this study, it is aimed to determine the coastal pollution level in Fethiye Inner Bay, to analyze the temporal and areal changes of water quality parameters and establish a database for evaluations.

Measurements and analysis

The field study has been conducted monthly between March 2016 and February 2017, in the Fethiye Inner Bay coastal waters in Turkey shown in *Figure 2*. Fourteen

http://www.aloki.hu ● ISSN 1589 1623 (Print) ● ISSN 1785 0037 (Online)
DOI: http://dx.doi.org/10.15666/aeer/1705_1042110444

(14) measurement points were located at the site, and their names, water depths, and coordinates are listed in *Table 1*. Measurements of physical parameters were performed at every 2 meters throughout the water column. The total number of measurements at the site is 1164 for the water temperature, salinity, pH, and 168 for the turbidity, each repeated at least three times. Measurement devices used are listed in *Table 2*.

Figure 1. *Location of Fethiye Inner Bay and Fethiye Town in Turkey (Google Earth, 2018)*

Table 1. *Coordinates of the measurement points at the site*

Point name	Coordinate (degree-minute)	Water depth (m)	Point name	Coordinate (degree-minute)	Water depth (m)
F1	36°38.657'K- 29°5.787'D	25.3	F8	36°38.581'K- 29°6.997'D	4.5
F2	36°38.384'K- 29°5.820'D	17.1	F9	36°38.707'K- 29°6.499'D	15.4
F3	36°38.176'K- 29°6.120'D	15.4	F10	36°38.944'K -29°6.266'D	16.2
F4	36°37.448'K- 29°5.690'D	14.7	F11	36°38.905'K- 29°6.843'D	4.6
F5	36°37.680'K- 29°6.153'D	15.3	F12	36°39.184'K- 29°6.528'D	16.3
F6	36°38.057'K- 29°7.076'D	5.3	F13	36°39.666'K- 29°6.367'D	15.2
F7	36°38.270'K- 29°6.621'D	15.2	F14	36°39.098'K- 29°5.060'D	46

Table 2. *Measurement devices*

Measurement device	Measurement	Sensitivity range
YSI Pro Plus Model Quatro (20 m cable)	pH (mV, pH)	± 0.2
	Temperature (°C, °F, K)	± 0.2 °C
	Salinity (ppt, psu)	± 1.0%; ± 0.1 ppt
	DO (mg/L, ppm) (-5 to 50 °C)	0 to 20 mg/L ± 2% 20 – 50 mg/L; ± 6%
HF MicroTPI field portable turbidimeter	Turbidity (0.01–1100 ntu/ftu)	± 2% of reading or 0.01 ntu (0-500 ntu) ± 3% of reading (500-1100 ntu)

http://www.aloki.hu ● ISSN 1589 1623 (Print) ● ISSN 1785 0037 (Online)
DOI: http://dx.doi.org/10.15666/aeer/1705_1042110444

Figure 2. *Fethiye Inner Bay measurement points (Google Earth, 2018)*

Total coliform, fecal coliform, fecal streptococci, *Escherichia coli, Pseudomonas aeruginosa*, and *Salmonella* analysis have been performed in 168 water samples taken for the temporal and spatial analysis of the changes of the bacteriological water quality parameters in the coastal waters. Phytoplankton and zooplankton abundance analyzes have been carried out in the laboratory for water samples taken from the surface and the bottom layer at depths exceeding 8 m using plankton nets. Biochemical Oxygen Demand (BOD) and Dissolved Oxygen (DO) requirements were determined by the relevant Turkish Standards Institution (TSE) standards for comparison with the changes in bacteriological parameters.

Microbiological laboratory test-methods are given in *Table 3* (TS EN ISO 9308-1, 2014; TS EN ISO 16266, 2009; TS EN ISO 7899-2, 2000), BOD and DO test-methods are listed in *Table 4* (TS EN ISO 5814, 2012; TS EN ISO 10707, 2005). BOD and DO were detected in 168 and 1164 samples, respectively.

55-micron Hydro-Bios plankton nets were used through the water column vertically to collect phytoplankton and zooplankton samples during the study. Then, both phytoplankton and zooplankton samples were fixed with 4% formaldehyde buffer solution until counting and identification activities.

http://www.aloki.hu ● ISSN 1589 1623 (Print) ● ISSN 1785 0037 (Online)
DOI: http://dx.doi.org/10.15666/aeer/1705_1042110444

Table 3. *Microbiological test-methods*

Microbiological analysis	Used standards
Enumeration of coliform bacteria	TS EN ISO 9308-1 Water quality- Detection and enumeration of *Escherichia coli* and coliform bacteria Part-1 Membrane filtration method
Enumeration of *Escherichia coli*	TS EN ISO 9308-1 Water quality- Detection and enumeration of *Escherichia coli* and coliform bacteria Part-1 Membrane filtration method
Enumeration of *Pseudomonas aeruginosa*	TS EN ISO 16266 Water quality - Detection and enumeration of *Pseudomonas aeruginosa* -- Method by membrane filtration
Enumeration of intestinal enterococci	TS EN ISO 7899-2 Water quality - Detection and enumeration of intestinal enterococci - Part 2: Membrane filtration method

Table 4. *Chemical test-methods*

Chemical analysis	Used standards
DO	TS EN ISO 5814 Water quality-determination of dissolved oxygen electrochemical probe method
BOD	TS EN ISO 10707 Water quality - Evaluation in an aqueous medium of the "ultimate" aerobic biodegradability of organic compounds - Method by analysis of biochemical oxygen demand (closed bottle test)

APHA Standard Methods (1995) were used during the counting of phytoplankton and zooplankton samples with Leica DM500 binocular microscope, and Sedgewick-Rafter Counting Chamber was employed as the counting chamber unit. The Sedgewick Rafter Counting Cells are designed primarily for the quantitative measurement of the exact number of particles in a precise volume of a fluid. This chamber itself is 50 mm in length, 20 mm in width and 1 mm in depth. The base part of the chamber is also grid marked with 100 x1 mm squares. Before transferring to the counting chamber, each sample was shaken at least 1 min, and 1 ml of sample were placed in the chamber. During the counting and identification, the number phytoplankton and zooplankton on each counting cell were recorded under the light microscope. Countings were repeated on 8 subsamples (Harris et al., 2000).

Physical parameters

Physical parameters were measured every 2 m from the surface to the bottom at each of the 14 stations. Salinity and temperature recorded at all measurement points are given in *Figure 3*. As a result of 12-month measurements carried out between March 2016 and February 2017, it was observed that the seawater salinity in Fethiye Inner Bay changed between 30.37 ppt (at F06) and 39.43 ppt (at F14) at the surface and the lowest salinity value was recorded in September, and the highest value was recorded in August. The salinity of surface waters is lower in all seasons than in the bottom layers. Towards the sea bottom from the surface, the average salinity increase is 4.35 ppt in the spring, 1.49 ppt in summer, 2.89 ppt in autumn, and 2.85 ppt in winter. Similarly, seawater temperatures were ranging in between 12.7 and 30.8 °C. The seasonal temperature averages decreased from the surface to the bottom of the water column from 20.7 to 18.6 °C in the spring, from 29.2 to 25.1 °C in summer, and they remained almost unchanged along the water column with a slight increase from 22.5 to 22.8 °C in the autumn and 16.8 to 16.8 °C in winter. Measured pH values ranged from 7.55 to 8.38.

http://www.aloki.hu ● ISSN 1589 1623 (Print) ● ISSN 1785 0037 (Online)
DOI: http://dx.doi.org/10.15666/aeer/1705_1042110444

The surface layer pH and turbidities measured at all points are given in *Figure 4*. Turbidity recorded at point F14 (water depth is 46 m.) changed in between 0.54 and 3.2 ntu, whereas at all other points ranged in between 1.02 and 4.81 ntu. The lowest values were recorded in autumn. All turbidity values were less than 5 ntu that is the acceptable limit for recreational purposes in coastal waters.

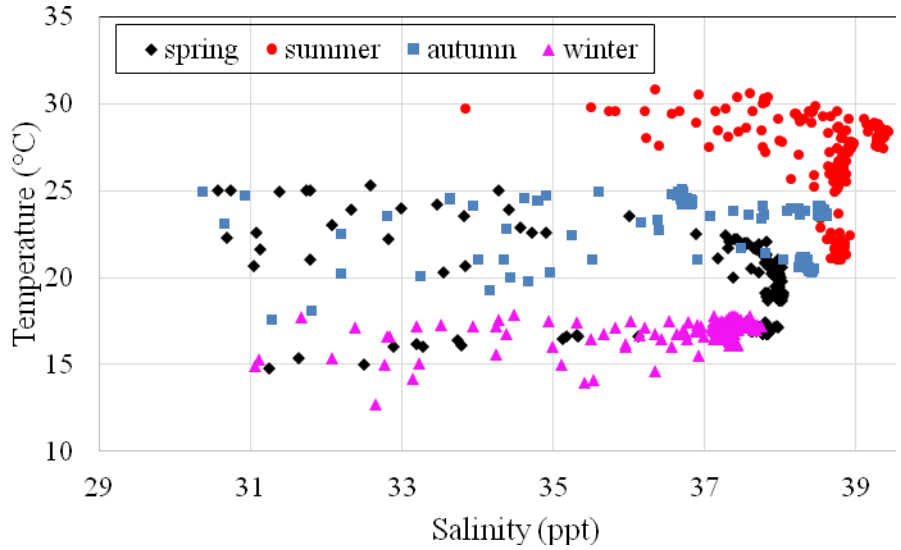

Figure 3. *Salinity and temperature recorded at all measurement points*

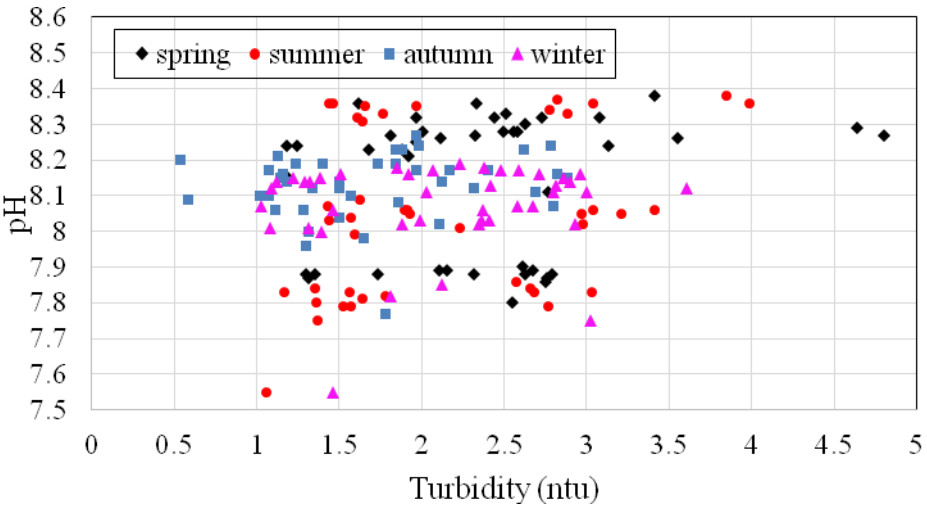

Figure 4. *Surface turbidity (ntu) and pH recorded at all measurement points*

Microbiological parameters

Coliform bacteria are bacteria that show the contamination of coastal waters. These bacteria are found in soil and plants as well as in the feces of warm-blooded animals. Such bacteria are fast-breeding species, and their presence indicates that disease-causing organisms (pathogens) from the feces of humans or animals could be existent in the coastal waters. Coliform bacteria are grouped as total coliform or fecal coliform

http://www.aloki.hu ● ISSN 1589 1623 (Print) ● ISSN 1785 0037 (Online)
DOI: http://dx.doi.org/10.15666/aeer/1705_1042110444

according to general characteristics. Total coliforms (TC) are common in soil or vegetation and do not show that water is contaminated by feces (Gao et al., 2015).

According to the 12-month measurements made between March 2016 and February 2017, the temporal changes in total coliform values at all measurement points are given in *Table 5*.

Table 5. *Temporal variations in TC (cfu/100 ml) at all measurement points*

		F01	**F02**	**F03**	**F04**	**F05**	**F06**	**F07**	**F08**	**F09**	**F10**	**F11**	**F12**	**F13**	**F14**
2016	Mar	57	300	30	55	200	300	230	102	30	45	650	120	48	46
	Apr	414	704	40	160	100	60	240	60	60	40	840	180	160	240
	May	1050	600	130	170	430	360	100	40	40	60	900	850	648	260
	Jun	300	100	100	120	40	60	20	120	180	40	50	12	13	10
	Jul	50	50	30	30	20	22	12	30	60	120	1040	180	20	0
	Aug	410	525	40	100	60	43	70	1040	70	30	140	120	15	6090
	Sep	779	413	50	20	20	320	70	40	220	170	450	254	140	0
	Oct	650	0	0	420	20	0	10	0	0	0	0	1440	0	1680
	Nov	1160	2	10	26	130	100	520	50	130	120	26	3650	460	100
	Dec	650	4	43	52	128	58	378	60	192	417	30	2850	682	192
2017	Jan	90	7	70	80	150	50	240	280	250	750	400	2150	900	390
	Feb	140	170	0	0	420	600	260	130	0	50	0	200	50	140

Measured coliform bacteria values provide guidance value (500 cfu/100 ml) of the Quality Criteria Table to be provided by Bathing Water Quality for Swimming and Recreation purposes, Annex-1 of Regulation for the Quality of Bathing Water (2006). The 15.5% of samples were above the guide standard however they were all less than the mandatory standard (10000 cfu/100 ml). In 91.7% of the samples TC was recorded. According to measured values, it is seen that the total coliform bacteria density is low in Fethiye Inner Bay coastal waters. However, coliform contamination was found at the mouth of Murt River (F11), along with the Çalış Beach (F12, F13), and in holiday village swimming bay (F01, F02) during the rainy spring and winter months. While this pollution is lower than the mandatory standard, its presence suggests that there may also be pathogens from the feces of humans or animals in the water.

Coliform bacteria originate as organisms in soil or vegetation and the intestinal tract of warm-blooded animals (fecal coliform). Fecal coliform (FC) bacteria are indicators of fecal contamination and the potential presence of pathogens associated with wastewater or sewage sludge. The total group includes FC bacteria such as *Escherichia coli*, as well as other types of coliform bacteria that are naturally found in the soil. The presence of fecal coliform in water may indicate recent contamination of the water by sewage or feces which could contain other bacteria, viruses, or disease-causing organisms. This is why coliform bacteria are considered "indicator organisms"; their presence warns of the potential presence of disease-causing organisms and should alert the person responsible for the water to take precautionary action (Gao et al., 2015).

The temporal variations in fecal coliform values at all measurement points according to the 12-month measurements made between March 2016 and February 2017 are shown in *Table 6*.

http://www.aloki.hu ● ISSN 1589 1623 (Print) ● ISSN 1785 0037 (Online)
DOI: http://dx.doi.org/10.15666/aeer/1705_1042110444

Table 6. *Temporal variations in FC (cfu/100 ml) at all measurement points*

		F01	F02	F03	F04	F05	F06	F07	F08	F09	F10	F11	F12	F13	F14
2016	Mar	15	100	5	32	15	200	18	55	18	12	211	60	34	33
	Apr	252	448	20	160	20	60	60	60	40	20	380	100	60	20
	May	150	130	20	50	50	60	20	30	40	20	900	850	136	170
	Jun	200	80	20	110	20	20	50	40	160	20	12	12	13	0
	Jul	50	58	43	30	24	18	12	10	15	20	220	50	100	0
	Aug	130	147	110	40	32	10	70	1040	30	5	20	100	10	6090
	Sep	201	82	54	32	20	120	10	10	220	100	50	166	40	0
	Oct	130	0	0	150	10	0	10	0	0	0	0	360	0	1680
	Nov	60	1	0	0	50	40	28	1	5	12	22	1120	30	4
	Dec	22	0	23	28	28	23	22	0	23	13	2	760	82	11
2017	Jan	20	30	500	150	5	9	20	50	40	14	8	460	150	19
	Feb	0	0	0	0	128	10	40	0	0	0	0	40	0	20

Measured FC bacteria values satisfy the guide standard (100 cfu/100 ml) of the Regulation for the Quality of Bathing Water (2006), Annex-1: Quality Criteria Required for Swimming and Recreation Waters, only at F07 in all of the measurements. In 85.7% of the samples FC was recorded. The 21.4% of samples were above the guide standard. At F14, the FC count was almost three times higher than the mandatory level (2000 cfu/100 ml) in August. Measurements indicate that there is substantial fecal pollution in Fethiye Inner Bay coastal waters. The source might be wastewater, sludge, septage, or animal excreta, resulted from the intensive anthropogenic facilities.

Escherichia coli is a member of the fecal coliform group and a more specific indicator of fecal pollution and commonly used to identify the presence of pathogenic microorganisms (Feng et al., 2012). It can be found in the digestive system of humans and warm-blooded animals. They cause digestive system infection. It is most commonly transmitted to humans by swimming in or swallowing the polluted water. Its presence in seawater indicates the entrance of sewage (Craig et al., 2004). There is a strong correlation between the increased *E. coli* levels in recreational waters, and the gastrointestinal disease even though the vast majority of them are not pathogenic (Blaustein et al., 2013). The temporal variations in *E. coli* values at all measurement points according to the 12-month measurements made between March 2016 and February 2017 are given in *Table 7*.

No limit value is defined for *E. coli* in the Regulation for the Quality of Bathing Water (2006). According to the bathing water quality standards for coastal and transitional waters in Directive 2006/7/EC of The European Parliament and the Council, Annex I, excellent quality and sufficient values of *E. coli* are stated as 250 and 500 cfu/100 ml, respectively. Similarly, in "Standard Values Required for Coastal and Transitional Waters Used for Recreational Use" (Regulation for the Surface Water Quality, 2016, Annex-5, *Table 6*) provides a guide standard of 250 cfu/100 ml and the mandatory standard of 500 cfu/100 ml. Measurements indicate that in rainy spring and autumn, *E. coli* significantly increases. Along the beach (Çalış Beach, F12 and F13 Points), *E. coli* values have doubled to the mandatory standard. In 38.1% of the samples *E. coli* was recorded. The 3.6% and 1.8% of samples were above the guide standard and the mandatory standard, respectively.

http://www.aloki.hu ● ISSN 1589 1623 (Print) ● ISSN 1785 0037 (Online)
DOI: http://dx.doi.org/10.15666/aeer/1705_1042110444

Table 7. *Temporal variations in E. coli (cfu/100 ml) at all measurement points*

		F01	F02	F03	F04	F05	F06	F07	F08	F09	F10	F11	F12	F13	F14
2016	Mar	0	0	0	0	0	0	8	0	0	0	42	22	0	0
	Apr	224	392	0	0	20	40	40	40	20	20	63	40	60	0
	May	0	0	0	0	0	40	0	0	0	0	51	94	850	119
	Jun	0	0	0	0	0	0	0	0	0	0	0	0	0	0
	Jul	0	0	0	0	0	0	0	0	0	0	0	0	2	0
	Aug	87	147	0	0	0	0	10	0	0	0	0	0	0	0
	Sep	201	0	0	0	0	0	0	0	110	0	0	71	20	0
	Oct	43	0	0	0	0	0	0	0	0	0	0	0	0	0
	Nov	36	1	0	0	38	40	28	1	2	0	20	933	25	2
	Dec	5	0	13	12	22	6	18	0	20	7	16	678	43	9
2017	Jan	0	0	500	150	5	9	10	0	40	14	8	460	75	19
	Feb	0	0	0	0	0	0	13	0	0	0	0	0	0	10

Fecal streptococci (FS) are also known as enterococci and of intestinal origin. They are a more resistant group of bacteria to be used as fecal pollutant indicators (Sinton et al., 1993). Especially they live in sea waters longer. The temporal variations in FS at all measurement points according to the 12-month measurements made between March 2016 and February 2017 are presented in *Table 8*.

Table 8. *Temporal variations in FS (cfu/100 ml) at all measurement points*

		F01	F02	F03	F04	F05	F06	F07	F08	F09	F10	F11	F12	F13	F14
2016	Mar	12	39	0	0	0	0	0	1	0	2	12	2	10	3
	Apr	69	137	0	1	0	1	15	2	1	5	235	3	11	39
	May	16	6	0	5	59	4	3	2	0	0	800	147	40	3
	Jun	0	0	0	0	1	0	0	0	1	0	2	1	1	0
	Jul	0	0	0	0	1	0	0	0	1	0	2	1	1	0
	Aug	27	86	0	1	0	0	0	0	1	0	4	1	3	1
	Sep	82	23	0	0	0	0	0	1	5	17	105	56	28	2
	Oct	25	9	0	0	0	1	9	2	4	34	11	17	4	0
	Nov	11	21	5	0	2	2	11	9	5	13	15	18	16	0
	Dec	8	11	35	60	16	47	17	83	102	14	52	65	228	18
2017	Jan	10	0	63	125	25	95	24	155	205	14	100	115	469	38
	Feb	0	12	0	0	10	0	0	0	0	0	0	20	10	0

Measured FS values at F01, F03, F05, F06, F07, F10, and F14, all satisfy the guide standard (100 cfu/100 ml) of the Regulation for the Quality of Bathing Water (2006), Annex-1: Table of Quality Criteria Required for Swimming and Recreation Waters. However, they exceed the guide standard at F02 in April, at F04 and F08 in January, at F09 and F13 in December and January, at F11 in April, May, September, and January, at F12 in May and January. All the measured values are less than the mandatory standard (1000 cfu/100 ml). In 66.1% of the samples FS was recorded. The 7.7% samples were above the guide standard.

http://www.aloki.hu ● ISSN 1589 1623 (Print) ● ISSN 1785 0037 (Online)
DOI: http://dx.doi.org/10.15666/aeer/1705_1042110444

Microbial degradation of waters used for drinking, irrigation or recreational purposes is monitored using concentration levels of fecal indicator bacteria (the United States Environmental Protection Agency, 2002). However, other bacteria, including gram-negative opportunistic pathogens of humans, *Pseudomonas aeruginosa*, and HPC bacteria, may also be useful in characterizing the quality of seawater (Carter et al., 2000). *P. aeruginosa* especially exists in coastal and transitional waters that interact with land (Kimata et al., 2004; Mena and Gerba, 2009). The increase in indicator bacteria in seawater and sediment has been associated with the risk of pathogenic microorganism-induced disease in humans (Donovan et al., 2008). Gastrointestinal diseases, skin infections, and risk of acute respiratory tract infections are increasing in people exposed through the recreational use of coastal waters intensified by indicator bacteria (Karbasdehi et al., 2017). Although not yet in Turkey, many regulations define measures to control *P. aeruginosa* pollution in recreational waters foreseeing such risks (Centers for Diseases Control and Prevention, 2014). The temporal variations in *P. aeruginosa* values at all measurement points according to the 12-month measurements made between March 2016 and February 2017 are summarized in *Table 9*.

Table 9. *Temporal variations in P. aeruginosa (cfu/100 ml) at all measurement points*

		F01	**F02**	**F03**	**F04**	**F05**	**F06**	**F07**	**F08**	**F09**	**F10**	**F11**	**F12**	**F13**	**F14**
2016	Mar	163	4	2	2	4	89	120	56	52	11	78	825	93	163
	Apr	223	242	8	4	9	13	10	5	2	1	18	77	23	172
	May	9	13	3	19	84	20	10	0	0	0	0	9	106	9
	Jun	0	0	16	1	1	0	0	0	0	0	0	2	7	0
	Jul	0	0	30	0	12	0	5	0	0	89	0	240	200	123
	Aug	336	1500	0	0	0	0	0	21	40	60	71	250	200	150
	Sep	920	800	0	0	0	0	0	16	25	40	500	230	35	0
	Oct	60	0	0	0	1	4	10	6	10	122	29	40	3	2
	Nov	320	60	50	0	0	16	0	10	70	0	30	1520	184	2
	Dec	210	20	221	115	123	348	45	33	56	145	138	2400	520	45
2017	Jan	0	0	410	250	270	720	90	60	40	320	285	3350	870	80
	Feb	270	920	240	80	820	1150	740	300	100	20	120	1750	100	240

The highest values of *P. aeruginosa* as a pathogenic bacteria was measured at F12 in winter time. No limit value is defined in the regulations for this bacteria in coastal waters. In Italian regulations, it is defined as 1 cfu/100 ml (Guida et al., 2016) in swimming pool waters. *P. aeruginosa* was detected as well in the absence of the TC, FC and FS. In 76.2% of the samples *P. aeruginosa* was recorded.

Salmonella is a pathogenic bacterial species, and it is dangerous for human health. They may enter to coastal waters by land-based anthropological sources, wastewaters, surface flows and ballast waters of marine vessels (Altuğ, 2012). The temporal variations in *Salmonella* values at all measurement points according to the 12-month measurements made between March 2016 and February 2017 are given in *Table 10*.

Measured *Salmonella* values are generally at high levels. They exceed the limit value (0 cfu/100 ml) of the Regulation for the Quality of Bathing Water (2006), Annex-1: Table of Quality Criteria Required for Swimming and Recreation Waters. The highest values have been reached at F11, F14 and F02 in August. *Salmonella* was detected as

http://www.aloki.hu ● ISSN 1589 1623 (Print) ● ISSN 1785 0037 (Online)
DOI: http://dx.doi.org/10.15666/aeer/1705_1042110444

well in the absence of the TC, FC and FS. In 93% of the samples *Salmonella* was recorded.

Table 10. *Temporal variations in Salmonella (cfu/100 ml) values at all measurement points*

		F01	F02	F03	F04	F05	F06	F07	F08	F09	F10	F11	F12	F13	F14
2016	Mar	18	22	42	0	12	82	8	15	6	0	3	52	14	9
	Apr	12	180	26	12	3	98	320	280	850	25	5	28	26	125
	May	150	340	0	0	0	240	700	700	800	0	0	460	100	530
	Jun	410	1230	1780	820	700	2560	450	660	640	9580	2650	1750	2310	200
	Jul	128	37	58	146	437	56	22	48	23	33	35	487	126	95
	Aug	4050	10800	250	1450	650	5150	580	2400	1240	3260	18550	600	5250	17500
	Sep	6350	3450	350	100	150	300	40	850	900	650	2650	550	300	100
	Oct	0	5500	2600	400	150	550	600	350	150	500	350	0	500	0
	Nov	1560	900	100	300	980	2200	2260	740	860	200	540	2210	500	720
	Dec	654	330	95	178	501	1100	1120	323	540	95	252	1120	260	347
2017	Jan	11	30	100	100	50	50	50	21	200	50	18	250	50	23
	Feb	30	30	60	0	20	150	20	40	10	0	10	60	20	20

Plankton abundance

The temporal changes in the phytoplankton and zooplankton abundance values as number per ml (#/ml) at the surface layer of the water and at the depth of -8 m from the surface in Fethiye Inner bay are shown in *Tables 11–14* according to the monthly measurements between March 2016 and February 2017.

Table 11. *Temporal change of surface layer phytoplankton abundance (number per ml) at all measurement points*

	2016										2017	
	Mar	Apr	May	Jun	Jul	Aug	Sep	Oct	Nov	Dec	Jan	Feb
F01	55833	11641	221839	38089	8299	6963	2820	5368	16287	45965	81752	27166
F02	46527	9086	219607	76055	10443	8091	13261	31080	61605	46987	31857	45398
F03	32843	7179	101325	89226	5729	6921	11706	7582	18469	34742	55280	70518
F04	112444	20161	69361	315769	8741	4047	11088	17608	54267	70721	93718	63724
F05	8031	14671	76132	39142	16929	10448	13725	11834	84207	54321	19369	81138
F06	8934	16641	114803	88872	7882	6966	9317	21008	29176	62391	99364	91007
F07	86218	18043	293864	51258	18763	5168	7362	7881	24748	25098	25754	35920
F08	70297	17760	67343	268413	9602	4993	8827	27911	23648	61238	109721	28246
F09	55096	7815	81279	34553	8247	7168	7769	38407	18604	57432	94822	43181
F10	115702	16923	109821	87645	6378	6882	5862	12567	28379	51867	79752	38131
F11	123704	10123	387105	99421	7122	10963	8487	28095	18737	19746	20281	48803
F12	117518	10964	123619	156963	11967	4569	3768	27960	34183	30545	26635	25279
F13	93821	15567	125742	77363	8043	5802	6668	33986	21864	25143	29183	21149
F14	97404	7439	121095	153750	4861	4089	3347	4158	31268	33613	37006	20869

http://www.aloki.hu ● ISSN 1589 1623 (Print) ● ISSN 1785 0037 (Online)
DOI: http://dx.doi.org/10.15666/aeer/1705_1042110444

Table 12. *Temporal change of phytoplankton abundance (number per ml) at -8 m from the surface at all measurement points*

	2016										2017	
	Mar	**Apr**	**May**	**Jun**	**Jul**	**Aug**	**Sep**	**Oct**	**Nov**	**Dec**	**Jan**	**Feb**
F01	71508	4729	80751	81796	5567	6043	3101	6287	40233	30245	20917	20133
F02	135865	9361	89611	52609	10439	8922	5327	16933	30173	27158	25363	23704
F03	142303	13684	246129	59803	8954	5963	7669	9611	8386	27149	46375	57352
F04	153108	31528	258198	172448	8086	3247	15179	9843	91279	86954	83106	87611
F05	165708	32642	117305	181249	11097	6019	9043	18052	38719	35732	34118	58792
F06	131038	11569	204311	112679	7083	8687	4783	28155	49811	44498	40247	76619
F07	34917	14048	121374	100826	15929	9281	7463	11743	23823	50139	82415	82193
F08	64923	13926	205103	81339	8051	7246	3569	7027	19403	45436	77369	47351
F09	92309	13466	71233	61287	16122	12844	3241	38406	44611	41213	38261	23769
F10	104627	14079	37581	270811	23901	12847	7746	5827	15332	24157	32669	18351
F11	119062	14602	73427	80643	8125	5521	6781	4427	14482	25941	40137	61837
F12	71508	4729	80751	81796	5567	6043	3101	6287	40233	30245	20917	20133
F13	135865	9361	89611	52609	10439	8922	5327	16933	30173	27158	25363	23704
F14	142303	13684	246129	59803	8954	5963	7669	9611	8386	27149	46375	57352

Table 13. *Temporal change of surface layer zooplankton abundance (number per ml) at all measurement points*

	2016										2017	
	Mar	**Apr**	**May**	**Jun**	**Jul**	**Aug**	**Sep**	**Oct**	**Nov**	**Dec**	**Jan**	**Feb**
F01	113	327	194	194	457	1308	301	171	73	84	93	201
F02	98	244	143	146	568	749	458	396	44	75	117	184
F03	85	138	179	337	640	725	745	179	88	98	109	189
F04	76	290	143	284	498	378	201	85	83	89	93	218
F05	101	402	163	225	884	540	626	208	62	98	143	139
F06	99	347	129	211	766	1211	436	288	93	120	149	129
F07	103	325	165	218	726	2684	377	201	58	89	123	152
F08	108	284	346	127	523	1812	781	379	137	142	158	121
F09	197	315	303	78	735	1359	801	601	147	125	102	117
F10	176	344	276	126	342	832	409	248	81	89	95	217
F11	133	322	101	66	504	761	609	463	99	118	138	189
F12	210	205	165	261	542	747	222	284	105	123	147	163
F13	218	228	663	461	478	1244	377	492	150	120	86	153
F14	298	456	104	237	264	564	323	163	115	98	81	161

Samples from F01 and F02 were dominated by Copepod and copepod nauplii individuals during March 2016. A few numbers of Cladocerans were also observed from the same sample. The dominance of Copepod and copepod nauplii groups were also observed between April and August 2016. Diatoms were the abundant phytoplankton group for the same period. While filamentous and green algae were dominated the April sample for F01 and F02, the system was shifted to filamentous

http://www.aloki.hu ● ISSN 1589 1623 (Print) ● ISSN 1785 0037 (Online)
DOI: http://dx.doi.org/10.15666/aeer/1705_1042110444

algae dominance during May 2016. However, diatoms were the most abundant group in the August sample.

Table 14. *Temporal change of zooplankton abundance (number per ml) at -8 m from the surface at all measurement points*

	2016										2017	
	Mar	**Apr**	**May**	**Jun**	**Jul**	**Aug**	**Sep**	**Oct**	**Nov**	**Dec**	**Jan**	**Feb**
F01	178	347	92	213	544	642	299	198	127	132	120	114
F02	162	298	179	145	551	901	468	164	114	105	128	145
F03	106	209	126	266	566	477	369	189	97	61	136	109
F04	89	372	118	249	431	359	371	156	104	71	148	150
F05	76	375	376	115	610	699	384	79	137	124	152	158
F06	68	417	106	185	969	2548	627	315	147	129	172	163
F07	43	283	141	37	1059	1904	1104	503	114	101	129	194
F08	46	399	90	259	472	745	209	237	152	165	144	195
F09	57	361	225	258	583	1026	265	415	221	279	161	134
F10	149	403	153	159	549	1014	463	317	92	77	109	109
F11	339	395	136	342	439	638	456	207	98	81	113	187
F12	178	347	92	213	544	642	299	198	127	132	120	114
F13	162	298	179	145	551	901	468	164	114	105	128	145
F14	106	209	126	266	566	477	369	189	97	61	136	109

Samples from stations F03 and F04 were Copepod and copepod nauplii dominated during March 2016. Moreover, few Cladoceran individuals were spotted at samples from 4 m depth. Copepod and copepod nauplii were both the abundant groups at the same stations between April and August. Phytoplankton samples for the same stations were dominated with diatoms between March and August. Therefore, filamentous and green algae domination was observed during April and May 2016. While Copepod nauplii and Rotifera groups were dominant at F05 during March, Copepod, Copepod nauplii, and Cladocera groups were observed in April from the same spot. Moreover, Copepod and copepod nauplii abundance was observed between May and September. Diatoms were the dominant phytoplankton group in March for F05. Both filamentous algae and diatom were the observed during April as well. However, the system was shifted to filamentous algae dominance during May. Diatoms were the dominant group at August sampling.

Rotifer and Copepod nauplii were dominant at F06 during March sampling. However, Cladocera, Copepod and Copepod nauplii were found to be the dominant groups in April (2016). Afterward, the abundance of Copepod and Copepod nauplii groups were reached to their highest number from May to the end of August. Diatoms were the dominant phytoplankton group in March among all phytoplankton. Both filamentous and green algae were the most dominant groups together with diatoms in April 2016 samples. While the system was shifted to filamentous algae dominance at May, diatom abundance was observed in August samples.

Copepod and Copepod nauplii group were dominant at F07, F08 and F09 from April to the end of August. Cladocera individuals were also observed at F07 and F09 during the investigation of 8 m samples in April. Filamentous algae dominance was observed

http://www.aloki.hu ● ISSN 1589 1623 (Print) ● ISSN 1785 0037 (Online)
DOI: http://dx.doi.org/10.15666/aeer/1705_1042110444

between April and May for both stations, and a few individuals of green algae and diatoms were also observed in the same samples. Followingly, diatoms dominated the system during August. The abundant groups were Copepod and Copepod nauplii for F10, F11, F12 and F13 from April until the end of August. Additionally, Cladocera individuals were observed at F11 during April.

Diatoms, filamentous and green algae were found to be the dominant groups for the same stations in April. After that the system was first shifted to filamentous algae dominance during May, then diatom dominance was observed during August. Copepod and Copepod nauplii groups were dominant at F14 between March and August. Additionally, Cladocera individuals were observed in March and April samples. While the diatoms were dominant in March, the system was shifted to diatom, filamentous and green algae dominance in April. Filamentous algae abundance was observed in May, and diatom dominance was found during August.

Copepod and Copepod nauplii were the dominant zooplankton group at F02, F05, F06, F07, F08, F09, F10, F12, F13 and F14 during June. Moreover, some Cladoceran individuals were observed at F01 and F03. Copepod nauplii were the only zooplankton group that was observed at F11. If we summarize phytoplankton distribution, filamentous algae dominance was observed for all stations.

Copepod and Copepod nauplii were dominant zooplankton groups at F01 and F02 during September 2016 sampling. Additionally, Appendicularia individuals were observed in October at both stations for the same period. Copepod and Copepod nauplii were dominant zooplankton groups together with Cladoceran individuals for November 2016 and January 2017 samples. Copepod and Copepod nauplii were the abundant zooplankton groups as well as in March 2017 sampling. Henceforth, members of Rotifera, Cladocera and Appendicularia were observed in the sample. During the investigation of phytoplankton distribution of the stations, diatom dominance was observed for September and October 2016. Small amounts of diatoms and filamentous algae were dominated the November 2016 sample while January 2017 samples were full of green algae and a few diatom species. Diatom dominance was observed at all samples in March 2017.

Copepod and Copepod nauplii dominance was observed between September and November 2016 for F03 and F04. Additionally, a few Appendicularia class individuals were found in 4 m samples. The abundant groups were Copepod and Copepod nauplii for F03 and F04, and a small number of Cladocera individuals were found in January 2017 samples. Copepod, Copepod nauplii, Cladocera and Appendicularia individuals were observed in March for both stations as well. The phytoplankton samples of F03 and F04 were dominated by diatoms and a few dinoflagellates during September and November 2016. However, filamentous algae dominance were observed in November 2016 for the same spots. January 2017 samples were abundant with green algae and a few diatoms. Diatom dominance was observed at all samples in March 2017.

Copepod and Copepod nauplii were dominant between September and November 2016 for F05, F06, F07, and F08 together with a few Appendicularia class individuals. On the other hand, Copepod, Copepod nauplii, and Rotifera groups were mostly found in January 2017 samples with a small amount of Cladoceran and Appendicularia individuals. The same phytoplankton distribution pattern was observed for F05, F06, F07, and F08. While Diatoms and dinoflagellates were dominated the system during September and October 2016, filamentous algae abundance was found in November 2016 samples. Green algae were dominant in November 2016, and a few diatom species

http://www.aloki.hu ● ISSN 1589 1623 (Print) ● ISSN 1785 0037 (Online)
DOI: http://dx.doi.org/10.15666/aeer/1705_1042110444

were observed in January 2017. The system was shifted to diatom dominance during March 2017.

Copepod and Copepod nauplii were the dominant zooplankton groups for F09, F10, and F11 between September and November 2016. Also, Cladoceran and Appendicularia individuals were found in samples. Sampling points were dominated by Copepod and Copepod nauplii zooplankton groups during January 2017. However, Rotifera abundance was observed together with a few Cladoceran and Appendicularia individuals for March 2017. Phytoplankton distributions of the points showed the same pattern as F05, F06, F07, and F08.

Copepod and Copepod nauplii were the abundant zooplankton groups for F12, F13, F14, and F15 between September and November 2016. Additionally, Cladoceran and Rotifera individuals were observed in October 2016. Copepod and Copepod nauplii were found to be the dominant zooplankton groups in January 2017. Moreover, few Rotifera and Cladoceran individuals were observed in January 2017. Copepod and Copepod nauplii were the dominant zooplankton group in March 2017 together with a small number of Rotifera, Cladocera, and Appendicularia individuals. Phytoplankton distribution of the same stations showed diatom dominance with a few individuals of dinoflagellate for September and October 2016. Filamentous algae were dominant in November 2016. Green algae have dominated the samples during January 2017, and a few diatom species were found in the sample. Diatom abundance was observed in the system in March 2017 samples.

Dissolved oxygen and biochemical oxygen demand

Dissolved Oxygen (DO) level is one of the most critical parameters in monitoring water quality and is an essential indicator of water mass's ability to support healthy ecosystems (Manivanan et al., 2013). DO is the amount of oxygen present in molecular form to provide life in seawater. The DO can enter the marine environment, directly through mixing and diffusion, or as a by-product of photosynthesis. Therefore, the level of DO in the water may increase due to strong wind and wave motions and the presence of plants and algae. On the other hand, it decreases by respiration and decay. When the plant population is very intense, oxygen consumption increases. Organisms such as bacteria, phytoplankton, and zooplankton need oxygen and consume dissolved oxygen in large quantities. Degradation of organic matter is the most significant oxygen consumer in the system. In general, a dissolved oxygen level of at least 4 mg/L is required to support live life. In marine environments, chronic oxygen deficiency occurs when the DO amount is between 2.0 and 6.0 mg/l, and hypoxic conditions (acute oxygen deficiency) threaten livelihood occur when DO is lowered than 2.0 mg/l. When the DO level drops below 0.2 mg/l, anoxic or oxygen-free conditions occur (O'Boyle et al., 2009). As temperature and salinity increase, the oxygen concentration in the seawater decreases.

The 12-month measurements between March 2016 and February 2017 were made at every 2 m from the surface to the sea bottom. The temporal changes of DO measurements at the water surface and at -14 m below the surface are presented in *Tables 15* and *16,* respectively. The seasonal and annual averages of DO (mg/l) at all measurement points are summarized in *Table 17*. The measured dissolved oxygen values are in between 3.83 and 9.12 mg/l, and the values are decreasing in the summer when the temperature is the warmest. In summer, mean DO values are below 6 mg/l,

http://www.aloki.hu ● ISSN 1589 1623 (Print) ● ISSN 1785 0037 (Online)
DOI: http://dx.doi.org/10.15666/aeer/1705_1042110444

and chronic oxygen deficiency condition is seen. All of the measurements were higher than 2 mg/l higher and hypoxic or anoxic condition was not observed.

Table 15. *Temporal change of surface dissolved oxygen (mg/l) at all measurement points*

	2016										2017	
	Mar	**Apr**	**May**	**Jun**	**Jul**	**Aug**	**Sep**	**Oct**	**Nov**	**Dec**	**Jan**	**Feb**
F01	9.12	6.47	7.95	6.2	5.58	5.6	6.08	5.91	6.78	6.78	6.78	7.52
F02	8.96	6.76	7.46	6.47	5.52	5.29	5.77	5.97	6.94	6.51	6.23	7.26
F03	8.97	6.93	8.01	6.14	5.01	5.34	6.79	6.13	6.79	6.32	7.51	7.56
F04	7.77	7.57	7.26	5.97	5.56	5.27	6.35	6.01	7.96	6.81	7.28	7.35
F05	7.96	7.66	8.18	6.42	5.32	5.96	6	6.16	8.48	6.73	6.87	6.73
F06	8.21	7.2	8.57	6.41	5.41	5.37	6.26	6.62	5.68	6.8	7.55	6.95
F07	8.18	8.16	8.32	6.95	5.07	5.91	6.7	6.09	6.72	6.3	6.02	7.69
F08	7.89	8.66	6.79	7.26	5.23	5.99	6.01	6.81	6.43	7.1	7.55	7.32
F09	8.8	7.6	7.57	6.9	5.53	5.3	6.23	6.52	7.25	6.74	7.64	7.1
F10	8.55	6.55	8.34	6.05	5.33	5.38	5.9	6.17	6.53	6.95	7.23	7.8
F11	8.25	7.69	8.48	6.98	5.15	5.38	5.46	6.48	6.35	7.12	7.64	7.64
F12	8.55	7.25	7.37	6.32	5.15	5.89	5.79	6.41	5.31	6.28	6.94	6.48
F13	9.03	7.33	7.33	6.41	5.37	5.64	6.53	5.99	5.43	6.27	6.84	6.76
F14	9.03	6.64	7.07	6.34	5.56	5.43	6.44	5.92	6.26	6.49	6.62	7.98

Table 16. *Temporal change of dissolved oxygen (mg/l) at -14 m below the surface at all measurement points*

	2016										2017	
	Mar	**Apr**	**May**	**Jun**	**Jul**	**Aug**	**Sep**	**Oct**	**Nov**	**Dec**	**Jan**	**Feb**
F01	7.57	7.46	7.09	6.72	6.06	5.39	5.99	5.85	6.24	6.08	5.98	6.31
F02	7.15	7.29	6.89	6.89	6.06	5.28	5.71	5.66	6.23	6.08	5.98	6.25
F03	7.07	6.95	6.95	6.75	5.3	4.65	6.08	5.8	6.33	5.97	5.74	6.33
F04	7.04	7.26	6.86	6.41	3.83	4.89	5.93	5.81	6.36	6.24	6.17	6.32
F05	7.11	7.19	6.95	6.65	5.35	4.88	5.86	5.77	6.25	6.16	6.1	6.1
F07	7.01	7.26	6.91	6.75	5.55	5.63	5.99	5.82	6.22	6.02	5.9	6.37
F09	7.51	7.22	6.79	6.42	5.73	5	5.93	5.71	6.11	6.11	5.97	6.28
F10	7.18	6.73	6.99	6.84	5.9	5.36	5.48	5.36	6.06	5.63	6	6.41
F12	7.28	7.38	7.01	6.78	6.09	4.17	5.94	5.87	6.11	5.66	5.36	5.64
F13	7.36	7.22	7.06	6.09	4.21	5.58	5.33	5.08	5.56	5.47	5.42	5.43
F14	8.1	7.85	7.29	7.02	6.2	5.68	5.88	5.8	6.38	6.33	6.3	6.56

Table 17. *Dissolved oxygen (mg/l) seasonal and annual averages*

	Spring	**Summer**	**Autumn**	**Winter**	**Annual**
Surface	7.87	5.79	6.34	7.00	6.75
-4 m	7.56	5.78	5.99	6.44	6.44
-8 m	7.55	5.87	5.99	6.22	6.41
-12 m	7.28	5.85	5.98	6.07	6.29
-14 m	7.18	5.76	5.89	6.02	6.21

http://www.aloki.hu ● ISSN 1589 1623 (Print) ● ISSN 1785 0037 (Online)
DOI: http://dx.doi.org/10.15666/aeer/1705_1042110444

Biochemical Oxygen Demand (BOD) is a measure of the amount of oxygen that is consumed by microorganisms to break down organic substances. As the water temperature values increase, the BOD values also increase. When the water temperature rises, photosynthesis rate of plants increases, plants grow faster and die. Decay the dead plants by the bacteria requires oxygen, and as a result, the BOD values rise. For this reason, the BOD values in the summer months are higher than the winter months values. The increase in nitrate and phosphate increases the rate of plant growth and death, and thus the organic pollutant load that will be broken down by bacteria in the marine environment. For this reason, the increase in nitrate and phosphate values is also effective in increasing BOD levels. As the BOD level rises, the dissolved oxygen (DO) values used by bacteria are reduced. In the months of intense rainfall, there is an increase in the mixing of the organic materials found in the soil with the sea water. Generally, in the uncontaminated waters, the BOD level is less than 4 mg/l, while it can reach 8-150 mg/l in the wastewater (Regulation of Surface Water Quality, 2016).

According to the 12-month measurements between March 2016 and February 2017, the temporal changes of the BOD values at the surface of Fethiye Inner Bay are presented in *Table 18*. All measured BOD values range from 2.3-6.8 mg/l.

Table 18. *Temporal change of biological oxygen demand (mg/l) at the surface layer for all measurement points*

	2016										2017	
	Mar	**Apr**	**May**	**Jun**	**Jul**	**Aug**	**Sep**	**Oct**	**Nov**	**Dec**	**Jan**	**Feb**
F01	2.41	5.03	3.66	4.92	3.98	5.26	5.51	5.45	3.89	3.64	3.42	3.58
F02	3.21	5.48	4.52	4.74	4.16	5.40	5.20	3.76	3.55	3.66	3.93	3.53
F03	2.32	3.09	3.43	4.82	5.34	4.97	4.54	3.86	3.69	3.76	4.13	3.43
F04	2.70	4.90	3.21	5.04	5.37	5.43	4.79	5.87	4.37	3.43	3.82	3.75
F05	3.03	3.15	4.06	4.82	5.24	5.03	4.59	4.08	4.52	4.36	3.99	4.24
F06	3.20	3.53	3.71	4.96	5.35	4.98	5.13	3.92	4.57	4.00	3.89	4.36
F07	3.11	3.26	3.18	4.54	4.97	4.71	4.46	4.10	4.63	4.13	4.32	3.64
F08	2.65	2.50	2.85	4.60	4.55	6.22	5.16	4.36	4.65	3.40	3.25	3.43
F09	2.40	2.82	2.72	4.36	4.54	4.85	4.16	4.16	3.94	3.81	3.77	3.20
F10	2.43	3.21	3.43	4.55	5.31	5.09	4.77	3.64	3.40	3.71	3.42	3.10
F11	4.39	5.98	6.85	5.46	5.60	4.96	5.52	5.13	4.85	4.80	4.75	4.57
F12	2.92	3.43	4.91	4.00	5.52	4.60	4.63	4.80	6.72	5.97	5.18	4.53
F13	2.94	3.10	4.37	4.13	4.82	4.64	3.47	4.08	4.53	4.25	3.87	3.42
F14	2.37	3.28	3.47	3.36	3.53	5.12	3.37	4.10	3.40	3.01	3.31	2.81

In this study, a three-dimensional coastal waters hydrodynamic (Balas and Özhan, 2003), wave propagation, transport and water quality (Cebe and Balas, 2016) numerical model HYDROTAM-3D, was used and a water quality monitoring and evaluation database system based on geographical information system (GIS) was established. The database system is available at www.hydrotam3d.com/fethiye by username: fb and user password: fb. Coordinated and temporal access is provided to all data.

http://www.aloki.hu ● ISSN 1589 1623 (Print) ● ISSN 1785 0037 (Online)
DOI: http://dx.doi.org/10.15666/aeer/1705_1042110444

Results and discussion

The monthly variations of water quality parameters were investigated through the site measurements conducted in between March 2016 and February 2017. Once at every month, at selected 14 locations, water samples were collected, and total coliform, fecal coliform, fecal streptococci, *Escherichia coli, Pseudomonas aeruginosa, Salmonella* detection, phytoplankton and zooplankton abundance analyses were performed in the laboratory. By using the related TSE standards, biochemical oxygen demand (BOD) and dissolved oxygen (DO) levels were determined, and water samples were collected from surface and -8 meters below if possible. The physical parameters measured throughout the water column were water temperature, salinity, pH, and turbidity. Changes in parameters measured between March 2016 and February 2017 were summarized in *Table 19*.

Table 19. *The measured ranges of physical and chemical parameters suitable to water samples in Fethiye Inner Bay*

Number of samples	Parameters	Mean	Minimum	Maximum
14	Water Depth (m)	16.2	4.5	46
1164	Salinity (S, ppt),	37.5	30.4	39.4
1164	Temperature (T,°C)	21.4	12.7	30.8
1164	pH	8.09	7.55	8.38
168	Turbidity (Turb.,ntu)	2.08	0.54	4.81
168	Total coliform (TC, cfu/100 ml)	298	0	6090
168	Fecal coliform (FC, cfu/100 ml)	131	0	6090
168	Fecal streptococci (FS, cfu/100 ml)	28	0	800
168	*E. coli* (cfu/100 ml)	37	0	933
168	*P. aeruginosa* (cfu/100 ml)	174	0	3350
168	*Salmonella* (cfu/100 ml)	930	0	18550
1164	DO (mg/l)	6.4	3.83	9.12
168	BOD (mg/l)	4.2	2.3	6.8

Pearson correlation matrix and related p-values were carried out on all the data set of water samples to describe the relations between measured parameters. In *Table 20,* coefficient of correlations (r) were listed, and significant correlations at $p < 0.05$ were indicated. After examination of several scatter plots, it is decided to refer the correlation as a weak correlation if $0.1 < r < 0.3$, a moderate correlation if $0.3 < r < 0.5$ and a strong correlation if $0.5 < r < 1.0$.

According to the correlation analysis, it is seen that temperature shows a weak positive significant correlation with the salinity ($r = 0.28$), pH ($r = 0.15$) and turbidity ($r = 0.25$). In line with a moderate positive correlation ($r = 0.3$), as water temperature increases, zooplankton counts increases as well. pH values show a weak negative correlation with DO ($r = -0.17$) and phytoplankton counts ($r = -0.15$) and a weak and moderate positive correlations with turbidity ($r = 0.19$) and zooplankton counts ($r = 0.32$) respectively. Zooplankton shows a reduction in numbers at the lower pH levels.

http://www.aloki.hu ● ISSN 1589 1623 (Print) ● ISSN 1785 0037 (Online)
DOI: http://dx.doi.org/10.15666/aeer/1705_1042110444

Table 20. *Correlation (r) matrix between all parameters analyzed in Fethiye Inner Bay coastal waters*

	T	S	pH	DO	BOD	Turb.	TC	FC	FS	Phyto	Zoo
T	1.00										
S	**0.28***	1.00									
pH	**0.15***	-0.08	1.00								
DO	0.04	**-0.15***	**-0.17***	1.00							
BOD	0.06	**0.33***	0.14	**-0.61***	1.00						
Turb.	**0.25***	**-0.29***	**0.19***	0.12	0.09	1.00					
TC	0.03	0.02	0.03	-0.12	**0.34***	-0.03	1.00				
FC	0.10	0.01	0.02	-0.12	**0.24***	-0.06	**0.85***	1.00			
FS	0.13	-0.08	0.12	0.15	**0.24***	**0.20***	**0.17***	0.12	1.00		
Phyto	-0.02	**-0.27***	**-0.15***	**0.43***	-0.10	0.14	-0.01	-0.01	**0.33***	1.00	
Zoo	**0.30***	0.10	**0.32***	**-0.45***	**0.35***	0.08	-0.02	0.07	**-0.13***	**-0.30***	1.00

*significant at $p < 0.05$

As the salinity of coastal waters decreases in rainy seasons, DO (r = -0.15) and phytoplankton counts (r = -0.27) increase and BOD decreases (r = 0.33). The measured DO decreases in the summer, as the water temperature increases. In 32% of the measurements, DO values are below 6 mg/l, and chronic oxygen deficiency condition is seen. DO and BOD values show a strong inverse relation (r = -0.61) as shown in *Figure 5*. DO values reach the highest values in the spring, while BOD values are the lowest. It is seen that, as phytoplankton counts (r = 0.43) increase and zooplankton counts (r = -0.45) decrease, DO increases in coastal waters of Fethiye Inner Bay. Whereas zooplankton counts show a positive moderate correlation with BOD (r = 0.35).

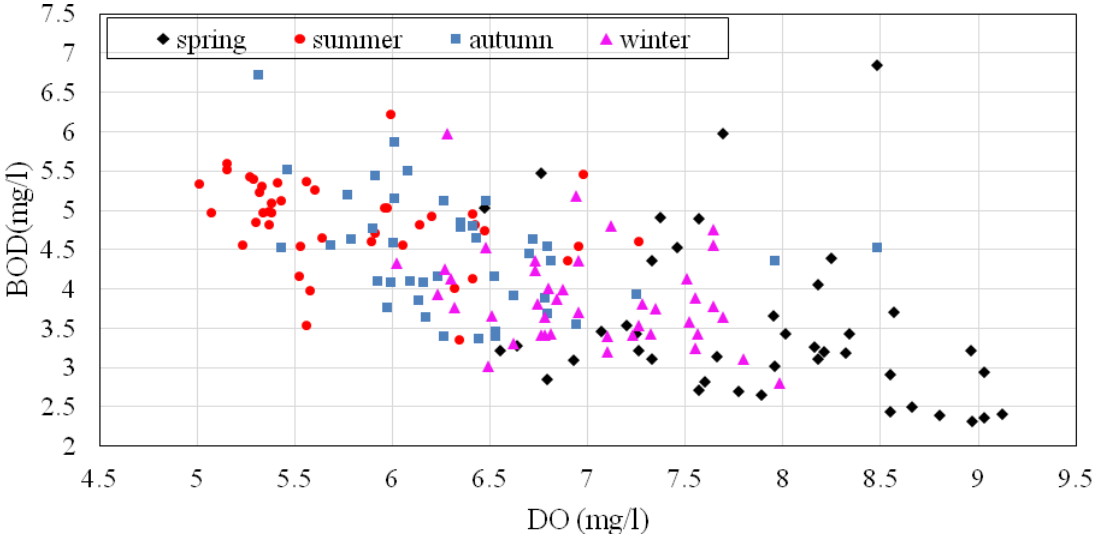

Figure 5. *Seasonal change of dissolved oxygen and biological oxygen demand*

BOD tends to increase in summer and autumn. This is due to the increase in microorganisms that requires dissolved oxygen to oxidize organic matter. BOD values

http://www.aloki.hu ● ISSN 1589 1623 (Print) ● ISSN 1785 0037 (Online)
DOI: http://dx.doi.org/10.15666/aeer/1705_1042110444

are higher than 4 mg/L in 55% of measured samples. It is seen that BOD values have a positive relation with TC (r = 0.34), FC (r = 0.24) and FS (r = 0.24). BOD increases as the concentration values of organic pollutants increase. As an example of this positive relation, timewise changes in BOD, total coliform, fecal coliform and fecal streptococci values at selected measuring points F06 and F12 are presented in *Figure 6*.

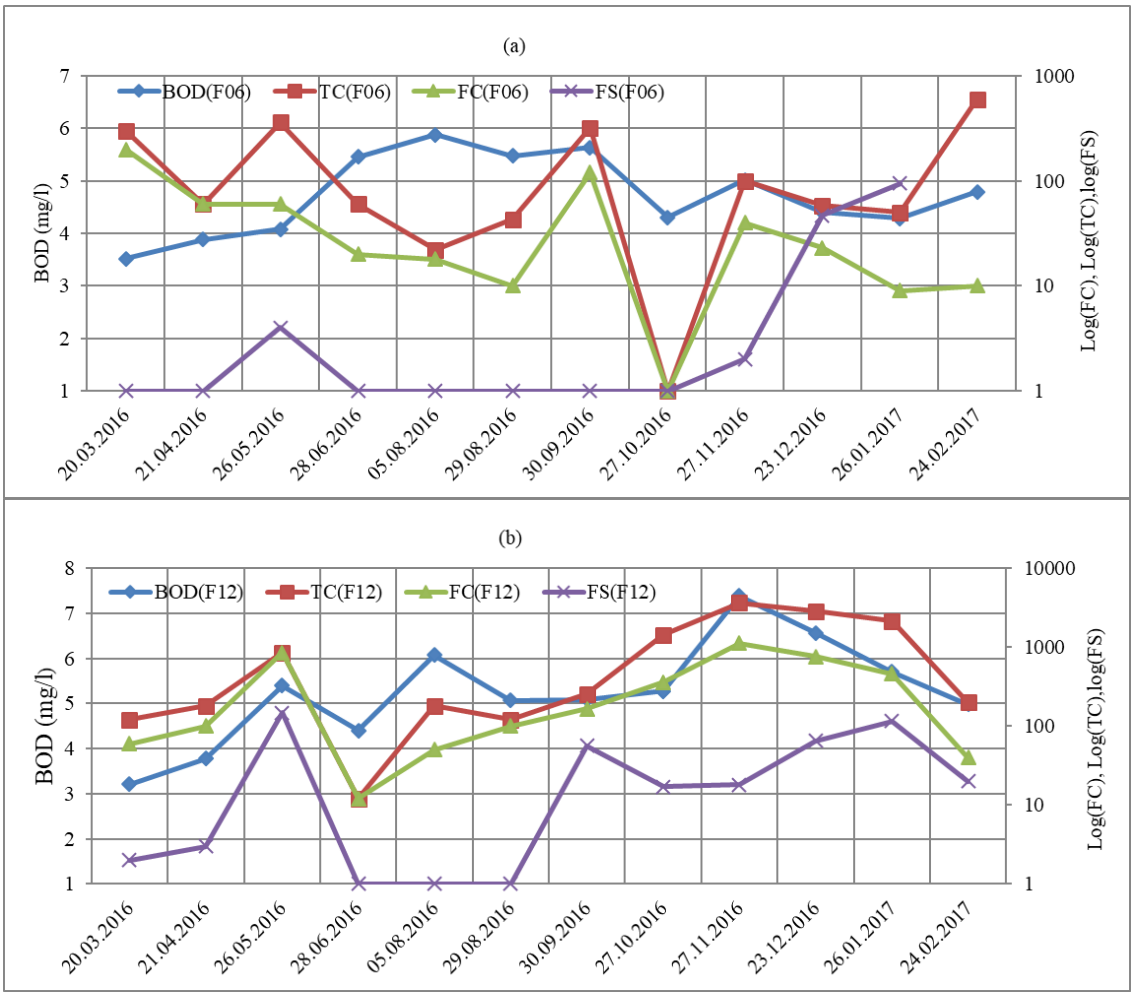

Figure 6. *Temporal changes in BOD, total coliform, fecal coliform and fecal streptococci values a) at point F06 b) at point F12*

It is seen that as TC amount increases, FC (r = 0.85) strongly increases and also FS (r = 0.17) shows an increase. In 91.7%, 85.7% and 66.1% of the samples TC, FC and FS were recorded respectively. In 15.5%, 21.4% and 7.7% of them were above the TC, FC and FS guide standards respectively. In 38.1% of the samples *E. coli* was recorded, and 3.6% and 1.8% were above the guide standard and the mandatory standard, respectively. It is seen that, FS amount has positive moderate correlation with phytoplankton count (r = 0.33).

In this study, "Spring Bloom" were observed between May and July which corresponds with the highest level phytoplankton abundance in the sampling points and the results are in line with Sverdrup's (1953) study (Colebrook, 1982; Martinez et al., 2011). During the "Spring Bloom", the amount of phytoplankton in aquatic

http://www.aloki.hu ● ISSN 1589 1623 (Print) ● ISSN 1785 0037 (Online)
DOI: http://dx.doi.org/10.15666/aeer/1705_1042110444

environments increase significantly due to less stratification, more stable dispersion of temperature and higher availability of surface nutrients.

After the spring bloom season, there was a decrease in phytoplankton and increase in zooplankton in all samples. Measurements show that there is an inverse correlation between zooplankton and phytoplankton counts (r = -0.3). Zooplankton numbers were reached to their maximum between August and September, then started to decrease in October. Moreover, a few phytoplankton peaks were also observed in the end of the fall bloom. This pattern corresponded with an event called "Fall Bloom". According to literature, the stratified water column started to mix due to an increase in the atmospheric events that cause an increase in nutrient levels as well in the aquatic ecosystem which results with a bloom in phytoplankton levels for a short period (Sverdrup, 1953). In this study, fall bloom was spotted starting from October, and it lasted for three months.

According to the results of the study performed, the number of total coliform bacteria had a significant increase during May and September. All measured microbiological parameters frequently increase in spring and winter, often exceeding guide standards. In a study by Kim et al. (2000), it was shown that increase in bacterial populations tended to be seasonal, which was in line with results of this study. The observations in the current study showed that zooplankton samples were mostly dominated by copepods which had a low grazing control of bacteria. Correspondingly, it is thought that the bacterial growth is not controlled by zooplankton in this study.

In conclusion, land-based pollutants transported with increasing surface runoff are thought to cause an increase in microorganism concentrations. Swimming in Çalış Beach coastal waters (F12 and F13) might be dangerous for human health. Seasonal averages and high BOD values indicate that the Fethiye Inner Bay is under considerable threat of continuous pollutant loadings. Measurements all indicate that immediate measures should be taken to reduce the land-based pollution causing degradation of coastal water quality in Fethiye Inner Bay.

Acknowledgements. This study was carried out with the support given by the Scientific and Technological Research Council of Turkey (TUBITAK) under the scope of the Project (No: 115Y468) entitled as 'Monitoring and evaluations of water quality parameters in coastal waters'. Authors would like to thank employees of DLTM Software Technologies Limited Company due to their support for field measurements.

REFERENCES

[1] Altuğ, G. (2012): The Occurrence of Salmonella in Various Marine Environments in Turkey. – In: Barakat, S. M. M. (ed.) Salmonella - A Dangerous Foodborne Pathogen. InTech, Rijeka, pp. 73-90.

[2] APHA (1995): Standard Methods for the Examination of Water and Wastewater. 19th Ed. – American Public Health Association, Washington, DC.

[3] Balas, L., Özhan, E. (2003): A baroclinic three dimensional numerical model applied to coastal lagoons. – Lecture Notes in Computer Science 2658: 205-212. DOI: 10.1007/3-540-44862-4_23.

[4] Barcina, I., Gonzalez, J. M., Iriberri, J., Egea, L. (1991): Role of protozoa in the regulation of enteric bacteria populations in seawater. – Marine Microbial Food Webs 5(2). 179-187.

http://www.aloki.hu ● ISSN 1589 1623 (Print) ● ISSN 1785 0037 (Online)
DOI: http://dx.doi.org/10.15666/aeer/1705_1042110444

[5] Blaustein, R. A., Pachepsky, Y., Hill, R. L., Shelton, D. R., Whelan, G. (2013): Escherichia coli survival in waters: Temperature dependence. – Water Research 47(2): 569-578. DOI: https://doi. org/10.1016/j.watres.2012.10.027.

[6] Carter, J. T., Rice, E. W., Buchberger, S. G., Lee, Y. (2000): Relationships between levels of heterotrophic bacteria and water quality parameters in a drinking water distribution system. – Water Research 34(5): 1495-1502. DOI: 10.1016/S0043-1354(99)00310-3.

[7] Cebe, K. (2016): Water Quality Modelling in Coastal Waters. – PhD Thesis. Gazi University, Graduate School of Natural and Applied Sciences, Civil Engineering Program, Ankara.

[8] Cebe, K., Balas, L. (2016): Water quality modelling in Kaş Bay. – Applied Mathematical Modelling 40(3). 1887-1913. DOI: 10.1016/j.apm.2015.09.037.

[9] Centers for Diseases Control and Prevention (CDC) (2014): The Model Aquatic Health Code. Atlanta, GA. – https://www.cdc.gov/mahc/.

[10] Colebrook, J. M. (1982): Continuous plankton records: seasonal variations in the distribution and abundance of plankton in the North Atlantic Ocean and the North Sea. – Journal of Plankton Research 4: 435-462. DOI: 10.1093/plankt/4.3.435.

[11] Craig, D. L., Fallowfield, H. F., Cromar, N. J. (2004): Use of microcosms to determine persistence of Escherichia coli in recreational coastal water and sediment and validation with in situ measurements. – Journal of Applied Microbiology 96(5): 922-930. DOI: 10.1111/j.1365-2672.2004.02243.x.

[12] Directive 2000/60/EC of the European Parliament and of the Council Establishing a Framework for Community Action in the Field of Water Policy. – OJ L327.

[13] Directive 2006/7/EC of the European Parliament and of the Council of 15 February 2006 Concerning the Management of Bathing Water Quality and Repealing. – Directive 76/160/EEC.

[14] Donovan, E., Unice, K., Roberts, J. D., Harris, M., Finley, B. (2008): Risk of gastrointestinal disease associated with exposure to pathogens in the water of the lower Passaic River. – Applied and Environmental Microbiology 74(4): 994-1003. DOI: 10.1128/AEM.00601-07.

[15] Feng, P., Weagant, S., Grant, M., Burkhardt, W., Shellfish, M., Water, B. B. (2012): Enumeration of Escherichia Coli and the Coliform Bacteria. – In: Food and Drug Administration (FDA) (ed.) Bacteriological Analytical Manual Online. 8th Ed., Silver Spring, Berlin. https://www.fda.gov/Food/FoodScienceResearch/LaboratoryMethods/ucm2006949.htm.

[16] Gao, G., Falconer, R. A., Lin, B. (2015): Modelling the fate and transport of faecal bacteria in estuarine and coastal waters. – Marine Pollution Bulletin 100(1): 162-168. DOI: https://doi.org/10.1016/j.marpolbul.2015.09.011.

[17] Griffin, D. W., Donaldson, K. A., Paul, J. H., Rose., J. B. (2003): Pathogenic human viruses in coastal waters. – Clinical Microbiology Reviews 16(1): 129-143. DOI: 10.1128/CMR.16.1.129-143.2003.

[18] Guida, M., Di Onofrio, V., Gallè, F., Gesuele, R., Valeriani, F., Liguori, R., … Liguori, G. (2016): Pseudomonas aeruginosa in swimming pool water: evidences and perspectives for a new control strategy. – International Journal of Environmental Research and Public Health 13(9): 919. DOI: 10.3390/ijerph13090919.

[19] Harris, R. P., Wiebe, P. H., Lenz, J., Skjoldal, H. R., Huntley, M. (2000): ICES Zooplankton Methodology Manual. – Academic Press, London.

[20] Karbasdehi, V. N., Dobaradaran, S., Nabipour, I., Ostovar, A., Arfaeinia, H., Vazirizadeh, A., … Khalifei, F. (2017): Indicator bacteria community in seawater and coastal sediment: the Persian Gulf as a case. – Journal of Environmental Health Science and Engineering 15(1): 6. DOI: 10.1186/s40201-017-0266-2.

http://www.aloki.hu ● ISSN 1589 1623 (Print) ● ISSN 1785 0037 (Online)
DOI: http://dx.doi.org/10.15666/aeer/1705_1042110444

[21] Kim, H.-W., Hwang, S.-J., Joo, G.-J. (2000): Zooplankton grazing on bacteria and phytoplankton in a regulated large river (Nakdong River. Korea). – Journal of Plankton Research 22(8): 1559-1577. DOI: 10.1093/plankt/22.8.1559.
[22] Kimata, N., Nishino, T. F., Fau, S. S., Kogure, K. (2004): Pseudomonas aeruginosa isolated from marine environments in Tokyo Bay. – Microbial Ecology 47(1): 41-47. DOI: 10.1007/s00248-003-1032-9.
[23] Liyanage, C. P., Yamada, K. (2017): Impact of population growth on the water quality of natural water bodies. – Sustainability 9: 1405. DOI: 10.3390/su9081405.
[24] Manivanan, R. P., Sinha, J. S., Kanetkar, C. N. (2013): Development and application of dissolved oxygen (DO) and biological oxygen demand (BOD) model for Panshet and Ujjani Reservoirs, Maharashtra, India. – Lakes and Reservoirs: Research and Management 18(3): 217-226. DOI: 10.1111/lre.12033.
[25] Martinez, E., Antoine, D., D'Ortenzio, F., de Boyer Montégut, C. (2011): Phytoplankton spring and fall blooms in the North Atlantic in the 1980s and 2000s. – Journal of Geophysical Research: Oceans 116(C11). DOI: 10.1029/2010JC006836.
[26] Mena, K. D., Gerba, C. P. (2009): Risk assessment of Pseudomonas aeruginosa in water. – Reviews of Environmental Contamination and Toxicology 201: 71-115. DOI: 10.1007/978-1-4419-0032-6_3.
[27] O'Boyle, S., McDermott, G. F., Wilkes, R. (2009): Dissolved oxygen levels in estuarine and coastal waters around Ireland. – Marine Pollution Bulletin 58(11). DOI: 1657-1663. 10.1016/j.marpolbul.2009.07.002.
[28] Regulation for the Quality of Bathing Water (2006): Rebulic of Turkey Ministry of Environment and Forestry. – Official Gazette date: January 9, 2006. No: 26048. http://www.resmigazete.gov.tr/eskiler/2006/01/20060109-2.htm.
[29] Regulation for the Surface Water Quality (2016): Republic of Turkey Ministry of Forest and Water Management. – Official Gazette date: August 10, 2016. No: 2979. http://www.resmigazete.gov.tr/eskiler/2016/08/20160810-9.htm.
[30] Regulation for the Water Pollution Control (2004): Republic of Turkey Ministry of Environment and Forestry. – Official Gazette date: December 31, 2004. No: 25687. http://www.mevzuat.gov.tr/Metin.Aspx?MevzuatKod=7.5.7221&sourceXmlSearch=&MevzuatIliski=0.
[31] Rozen, Y., Belkin, S. (2001): Survival of enteric bacteria in seawater. – FEMS Microbiology Reviews 25(5): 513-529. DOI: 10.1111/j.1574-6976.2001.tb00589.x.
[32] Sinton, L. W., Donnison, A. M., Hastie, C. M. (1993): Faecal streptococci as faecal pollution indicators: A review. Part II: Sanitary significance, survival and use. – New Zealand Journal of Marine and Freshwater Research 27(1): 117-137. DOI: 10.1080/00288330.1993.9516550.
[33] Sverdrup, H. U. (1953): On conditions for the vernal blooming of phytoplankton. – ICES Journal of Marine Science 18(3): 287-295. DOI: 10.1093/icesjms/18.3.287.
[34] Troussellier, M., Bonnefont, J.-L., Courties, C., Derrien, A., Dupray, E., Gauthier, M., … Pommepuy, M. (1998): Responses of enteric bacteria to environmental stresses in seawater. – Oceanologica Acta 21(6): 965-981. DOI: https://doi.org/10.1016/S0399-1784(99)80019-X.
[35] TS EN ISO 7899-2 (2000): Water quality - Detection and enumeration of intestinal enterococci - Part 2: Membrane filtration method. – Turkish Standards Institution, Ankara, Turkey.
[36] TS EN ISO 10707 (2005): Water quality - Evaluation in an Aqueous Medium of the "Ultimate" Aerobic Biodegradability of Organic Compounds - Method by Analysis of Biochemical Oxygen Demand (Closed Bottle Test). – Turkish Standards Institution, Ankara, Turkey.
[37] TS EN ISO 16266 (2009): Water Quality - Detection and Enumeration of Pseudomonas Aeruginosa - Method by Membrane Filtration. – Turkish Standards Institution, Ankara, Turkey.

http://www.aloki.hu ● ISSN 1589 1623 (Print) ● ISSN 1785 0037 (Online)
DOI: http://dx.doi.org/10.15666/aeer/1705_1042110444

[38] TS EN ISO 5814 (2012): Water Quality-Determination of Dissolved Oxygen Electrochemical Probe Method. – Turkish Standards Institution, Ankara, Turkey.
[39] TS EN ISO 9308-1 (2014): Water Quality - Enumeration of Escherichia Coli and Coliform Bacteria - Part 1: Membrane Filtration Method for Waters with Low Bacterial Background Flora. – Turkish Standards Institution, Ankara, Turkey.
[40] United States Environmental Protection Agency (EPA) (2002): National Water Quality Inventory: Report to Congress. – 2002 Reporting Cycle, Washington DC. https://www.epa.gov/sites/production/files/2015-09/documents/2007_10_15_305b_2002report_report2002305b.pdf.
[41] Rees, G., Pond, K., Kay, D., Bartram J., Santo Domingo, J. (2010): Safe Management of Shellfish and Harvest Waters: Minimizing Health Risks from Sewage-Contaminated Shellfish. – World Health Organization, Geneva and IWA, London.
[42] Yılmaz, N., Cebe, K., Yıldırım, F. P., İnan, A., Balas, L. (2017): The need for the integration of land use planning and water quality modeling in the case of Fethiye Bay. – Journal of Polytechnic 20(2): 427-435. DOI: 10.2339/2017.20.2 427-435.

http://www.aloki.hu ● ISSN 1589 1623 (Print) ● ISSN 1785 0037 (Online)
DOI: http://dx.doi.org/10.15666/aeer/1705_1042110444

SCREENING OF WHEAT-*THINOPYRUM BESSARABICUM* ADDITION AND TRANSLOCATION LINES FOR DROUGHT TOLERANCE

SHAFQAT, N.[1*] – AHMED, H.[2] – SHEHZAD, A.[3] – CHAUDHRY, S. K.[4] – SHAH, S. H.[5] – ISLAM, M.[6] – KHAN, W.[7] – MASOOD, R.[8] – KHAN, U.[8]

[1]*Department of Agriculture, Hazara University, Mansehra, Pakistan*

[2]*Islamia College, Peshawar, Pakistan*

[3]*National Institute for Genomics and Advanced Biotechnology (NIGAB), National Agricultural Research Centre (NARC), Islamabad, Pakistan*

[4]*Department of Botany, The University of Lahore, Sargodha Campus, Sargodha, Pakistan*

[5]*Department of Agricultural Sciences, Allama Iqbal Open University, Islamabad, Pakistan*

[6]*Department of Genetics, Hazara University, Mansehra, Pakistan*

[7]*Department of Environmental Sciences, Comsats Institute of Information Technology, Abbottabad Campus, Abbottabad, Pakistan*

[8]*Department of Botany, Hazara University, Mansehra, Pakistan*

**Corresponding author*
e-mail: noshinshafqat@gmail.com

(Received 2nd Mar 2019; accepted 2nd Jul 2019)

Abstract. Domestication of the crop plants has narrowed the genetic base of the crops and thereby mounting their exposure towards global climate change, disease and insect epidemics. Genetic variability of modern days crops must be broadened to make crop production more sustainable against various biotic and abiotic stresses which are posturing major threats to the world. It is therefore, crucial to identify novel additional sources of durable resistance. Wheat wild relatives have provided valuable sources of genetic diversity for various biotic, abiotic and quality components. In this respect wide hybridization has become a promising breeding method for introducing new variability in crop plants by using the crop wild relatives. In the present research work wheat-*Th. Bessarabicum* amphiploid, addition and translocation lines have been screened. These genetic stocks were exposed to 15% polyethylene glycerol (PEG) stress, to find out the drought tolerant addition and translocation lines by studying different physiological parameters. The screening of drought stress revealed that addition lines 2JJ, 4JJ, 5JJ, 7JJ and translocation line Tr-7 exhibited tolerance attitude towards water deficient conditions.
Keywords: *chlorophyll contents, proline, superoxide dismutase, drought tolerance, wheat (Thinopyrum bessarabicum) addition and translocation lines*

Introduction

The negative effect of non-living factors on the growth and development of living organism is termed as abiotic factors. Abiotic stress factors occurred naturally that may cause harm to the plants and animals in the effected area. Abiotic stress is the most destructive one concerning the growth and productivity of crops worldwide. It has also been found that abiotic factors are very harmful when they occur together in

http://www.aloki.hu ● ISSN 1589 1623 (Print) ● ISSN 1785 0037 (Online)
DOI: http://dx.doi.org/10.15666/aeer/1705_1044510461

combinations (Milter, 2006). The most important abiotic stress factors include salinity, drought and water logging which cause harm to the plants.

Water deficit condition imposes severe influences on growth and development of plants by causing changes at the physiological, metabolic and molecular levels (Zu et al., 2017). Drought is the prolonged period without precipitation that is injurious to crops plants. It is the most important environmental factor that limits the plant growth and productivity than any other environmental stresses (Jones and Corlett, 1992). Approximately 32% of wheat growing culture faces different types of drought stress throughout the growing season in developing countries (Morris et al., 1991). About 15 million ha of cultivated land in Pakistan is affected by this environmental factor (Mujtaba and Alam, 2002). About one-third of the total annual cereal production is obtained from wheat alone. The response of plants for drought stress depends upon the severity, frequency, duration of exposure and the plant growth stage (Bray, 1993).

Germination, tillering and the reproductive stages are considered to be the most sensitive to drought in wheat (Passioura, 2007). The best way to encounter this problem is to develop high yielding drought tolerant crop varieties. Genetic diversity of cultivated plants has become drastically narrowed due to selection pressure in breeding programs thereby minimizing tolerance to environmental stresses (Nevo, 2004). Global warming followed by rising drought and salinity has threatened the world's food security. One of the economical and sustainable solutions for increasing crop stability and productivity is by making improvement in crops genetic structure for higher tolerance against abiotic stresses (Blum, 1998; Ashraf et al., 2009). This can be achieved by the utilization of several methods; one of the method is by identifying agronomically important novel genes and QTLs from the wild genotypes to improve the cultivars (Xie and Nevo, 2008).

The crop wild relatives that adapt to drought stress environment are expected to have genes or alleles for drought and salt tolerance. These drought tolerant genes and/or QTLs could be introgressed or cloned to increase crop tolerance (Araus et al., 2003). Addition of barley chromosome segment into wheat has shown tolerance to drought (Hoffmann et al., 2011). *Th. bessarabicum,* a wheat wild relative grows on the sea shore of the Crimea (Gorham et al., 1985) are highly salt tolerant. Wild relatives that show salt tolerance also exhibit drought tolerance (Farooq and Azam, 2001). Soil water potential is decreased in drought stress which ultimately reduces plants osmotic potential for water absorption by congestion of soluble carbohydrates and proline and in other words osmotic regulation is performed (Martin et al., 1993). Consequently osmotic regulation will help to improve plant growth and development in water stress (Pessarkli, 1999).

Drought tolerance can be enhanced if selection is made on the basis of physiological mechanisms or characters conferring tolerance. Drought stress tolerance in crop plants is associated with various physiological traits such as proline accumulation for osmoregulation (Nayyar and Walia, 2003; Larkunthod et al., 2018) increased activity of antioxidant enzymes like superoxide dismutase (SOD), peroxidases (POX) to protect membrane integrity (Sairam and Saxena, 2000) and various yield components (Majid et al., 2007; Lonbani and Arzani, 2011). One of the ways to develop drought tolerant crop, these parameters can be used to screen the genetic stock to identify the new sources of tolerance for developing drought tolerant crop species/varieties. Drought tolerant selection at seedling stage is mostly carried out through Polyethylene glycol (PEG)-treated hydroponic conditions which induce negative osmotic potential comparable with

http://www.aloki.hu ● ISSN 1589 1623 (Print) ● ISSN 1785 0037 (Online)
DOI: http://dx.doi.org/10.15666/aeer/1705_1044510461

moisture deficit stress (Robin et al., 2015). The aim of present experiment was to find out the suitable drought tolerant wheat-*Th. bessarabicum* genetic stocks. The evaluation was made on the basis of physiological responses like accumulation of proline, superoxide dismutase enzymes activity and chlorophyll contents.

Materials and methods

Plant material

The germplasm consisted of wheat-*Th. bessarabicum* addition and translocation lines along with some other drought tolerant and susceptible cultivated wheat varieties (Bano et al., 2012) as a check. The material was obtained from Wheat Wide Crosses Program at NARC Islamabad. Pedigree of these genetic stocks is given in *Table 1*.

Table 1. *Pedigree of wheat-Th. bessarabicum genetic stocks*

Genetic stock	Pedigree
Tr-1	6BS.6BL-6J (CS/Th.bess//CSph/3/4*Prinia
Tr-2	1DS.1JS
Tr-3	3JS.3BL, (CS/Th.bess//CSph/3/3*Prinia
Tr-4	1AS.1AL-1JL
Tr-5	7DS.7DL-4J, (CS/Th.bess//CSph/3/4*Prinia
Tr-6	6JS.7DL, (CS/Th.bess//CSph/3/4*Prinia
Tr-7	5JS.5DS.5DL
Amphiploid	CS/*Thinopyrum bessarabicum*
1JJ	CS + 1JJ (2n = 6x = 42 + 2 = AABBDD + 1JJ)
2JJ	CS + 2 JJ (2n = 6x = 42 + 2 = AABBDD + 2JJ)
3JJ	CS + 3 JJ (2n = 6x = 42 + 2 = AABBDD + 3JJ)
4JJ	CS + 4 JJ (2n = 6x = 42 + 2 = AABBDD + 4JJ)
5JJ	CS + 5JJ (2n = 6x = 42 + 2 = AABBDD + 5JJ)
6JJ	CS + 6JJ (2n = 6x = 42 + 2 = AABBDD + 6JJ)
7JJ	CS + 7JJ (2n = 6x = 42 + 2 = AABBDD + 7JJ)
3JJ42	CS + Tr 3J(2n = 6x = 42 = AABBDD + Tr3J)
3JJ44	CS + Tr 3JJ(2n = 6x = 42 + 2 = AABBDD + Tr3JJ)
Chakwal-97, Punjab-96	Drought tolerant and susceptible wheat cultivars (Bano et al., 2012)

Laboratory procedure

The genetic stock was evaluated for several physiological and biochemical traits analysis in hydroponics with Polyethylene glycerol (PEG) induced drought under controlled environmental conditions of laboratory (*Fig. 1*). In the first phase, all the genetic stocks with two check cultivars were evaluated for drought analysis under two treatments namely control (Hoagland solution) and 15% PEG. Fifteen seeds/genetic stock were germinated in petri plates. After confirming the chromosomes number, the germinated seedlings of 3-4 days were shifted in small pot trays containing 2:3 of compost and sand. After 10 days, seedlings were transferred to holes on the 5 L hydroponics boxes containing half strength Hoagland's nutrient solution (Hoagland and Arnon, 1950). The pH of nutrient solution was maintained between 5.5-6.0 with 1N HCl

http://www.aloki.hu ● ISSN 1589 1623 (Print) ● ISSN 1785 0037 (Online)
DOI: http://dx.doi.org/10.15666/aeer/1705_1044510461

or KOH. Air pumps were fitted for providing oxygen to the roots throughout the growing period. For inducing drought, polyethylene glycol (PEG 6000) was used. Young leaf samples of three plants from each genetic stock were collected for different biochemical analyses after seven days of 15% PEG for drought stress.

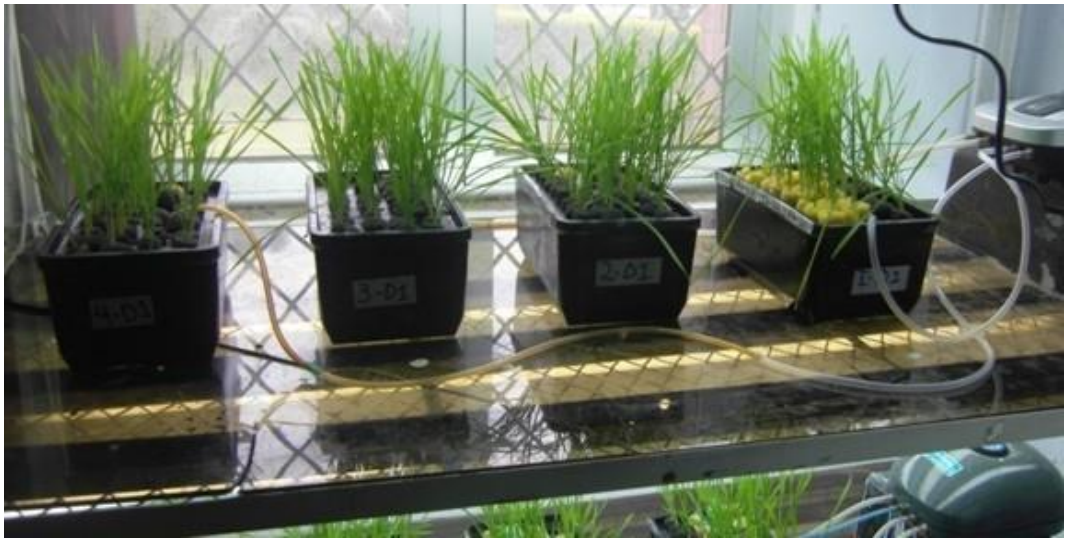

Figure 1. *Hydroponic experiments for screening tolerance against drought in Thinopyrum bessarabicum genetic stock at 15% PEG treatment*

Proline contents determination

Analysis of proline contents was done by the method of Bates et al. (1973). Fresh leaves of each sample weighing 0.25 g were homogenized in 10 mL of 3% aqueous sulfosalicylic acid and solution was filtered through Whatman 42 filter paper. 2 mL acid-ninhydrin and 2 mL of glacial acetic acid was added in filtrate and placed in a water bath for 1 h at 100 °C. After that the mixture was extracted with 4 mL toluene and readings were taken at 520 nm wavelength using a spectrophotometer.

Superoxide dismutase (SOD) determination

The SOD activity was calculated by measuring the ability of the enzyme to inhibit phytochemical reduction of nitrobluetetrazolium (NBT) according to the method of Giannopolitis and Ries (1977). Fresh leaf sample (0.25 g) was homogenized with 1 mL of 100 mML^{-1} sodium phosphate buffer containing 1% polyvinyl pyrollidone (PVP) in an ice bath. Then centrifugation was done at 10,000 rpm for 15 min at 4 °C. For SOD activity, the reaction mixture (3 mL) contained: K-Na-phosphate buffer (60 mM, pH 7.8), methionine (13 mM L^{-1}), riboflavin (12 mM L^{-1}), P-tetrazoleum blue (80 µM), EDTA (0.1 mM) and 100 µL of enzyme extract. The reaction mixture was left for 10 min under 15 W fluorescent light. After 10 min, light was switched off to stop the reaction. The absorbance of the mixture was measured by using spectrophotometer at A560 nm wavelength. For control the reaction mixture without the enzyme extract was utilized and a dark control mixture acted as a blank. One unit of SOD activity was taken as the quantity of enzyme that is able to inhibit tetrazoleum blue reduction by 50% as determined at 650 nm wavelength. SOD activity was expressed in arbitrary units per mg of fresh weight.

http://www.aloki.hu ● ISSN 1589 1623 (Print) ● ISSN 1785 0037 (Online)
DOI: http://dx.doi.org/10.15666/aeer/1705_1044510461

Chlorophyll contents determination

Crude extract from each sample was taken and readings were measured at spectrophotometer (RS-110) at wavelength 645 nm and 663 nm immediately with care to minimize exposure to light. Chlorophyll contents were calculated according to Arnon (1949).

Statistical analysis

Completely Randomized Design (CRD) was followed with three replications. The data were analyzed by analysis of variance technique and comparison among treatment means was made by Least Significant Difference (LSD) test by using Statistix 8.1 computer software at $p \leq 0.05$.

Results

Proline contents

Statistical analysis showed significant differences among wheat-*Th. bessarabicum* genetic stocks at 15% PEG stress at $p \leq 0.05$ for proline contents (*Table 2*). In this experiment, free proline contents were increased in almost all the drought stressed-seedlings of wheat genetic stock (*Fig. 2*). Maximum increase was observed in 3JJ (99%) followed by 7JJ (96%) and 5JJ (93%) disomic addition lines and in amphiploid (90%) as compared to the non-stressed plants. These addition lines represented the increased proline contents as compared to CS parent and drought tolerant check cultivar Chakwal-97, while addition lines 1JJ and 2JJ represented minimum increase in proline contents. All the translocation lines showed increase in proline contents than that of CS parent and tolerant check cultivar Chakwal-97. Translocation line Tr-6, Tr-7 and Tr-5 showed maximum increase of 97%, 95% and 94%, respectively which is greater than that of the drought tolerant genotype Chakwal-97, CS parent and CS/*Th. bessarabicum* amphiploid.

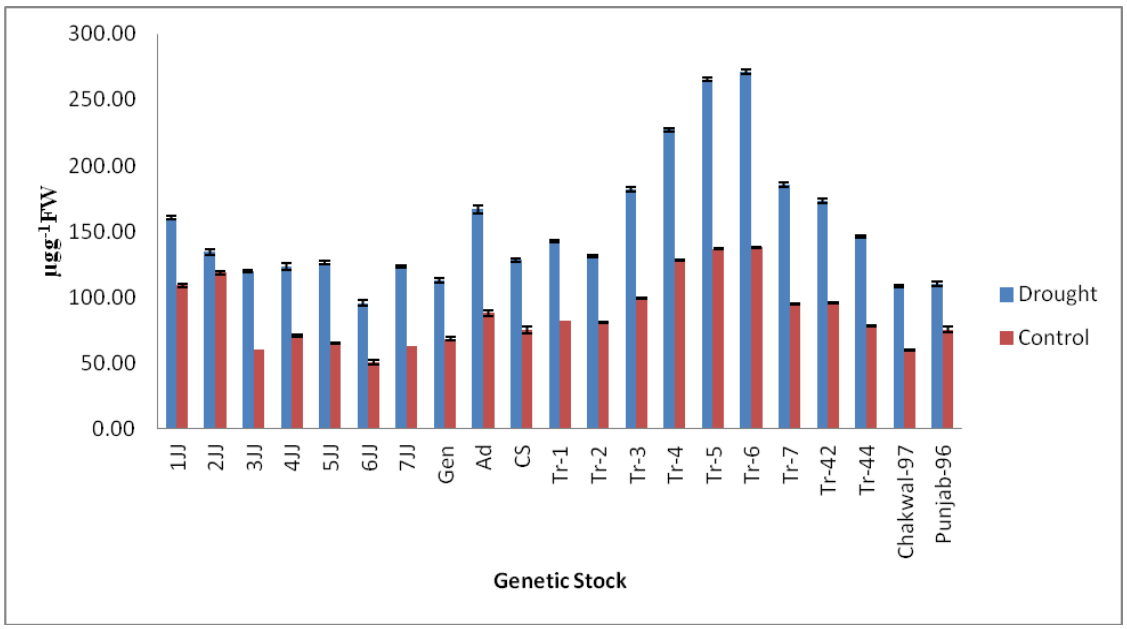

Figure 2. *Proline contents in leaves at control and 15% PEG treatments*

http://www.aloki.hu ● ISSN 1589 1623 (Print) ● ISSN 1785 0037 (Online)
DOI: http://dx.doi.org/10.15666/aeer/1705_1044510461

Table 2. *Means for proline contents at 15% PEG stress*

Genotypes	Control	Treatment	Mean
1JJ	109.31 pq	160.34 g	134.83 e
2JJ	118.72 o	134.42 ij	126.57 f
3JJ	60.38 yz	120.05 no	90.21 m
4JJ	70.73 uv	123.35 mn	97.04 k
5JJ	65.23 wx	126.20 lm	95.72 kl
6JJ	53.80 a	95.68 r	74.74 o
7JJ	62.90 xy	123.10 mn	93.00 lm
Gen	68.24 vw	112.91 p	90.58 m
Ad	74.62 tu	166.71 f	120.66 g
CS	75.12 t	128.36 kl	101.74 j
Tr-1	82.11 s	142.49 h	112.30 h
Tr-2	80.74 s	131.39 jk	106.07 i
Tr-3	127.68 kl	227.44 c	177.56 c
Tr-4	98.98 r	181.89 d	140.44 d
Tr-5	136.85 i	265.36 b	201.11 b
Tr-6	137.26 i	271.39 a	204.32 a
Tr-7	95.48 r	185.34 d	140.41 d
Tr-42	78.38 st	173.10 e	125.74 f
Tr-44	58.99 yz	146.12 h	102.55 j
Chakwal-97	57.72 za	108.74 q	83.23 n
Punjab-96	75.63 t	110.25 pq	92.94 lm

Inter critical value for comparison was 2.8, while general critical value for comparison was 3.96

Superoxide dismutase (SOD)

Statistical analysis showed significant differences among wheat-*Th. bessarabicum* genetic stocks at 15% PEG stress at $p \leq 0.05$ for superoxide dismutase activity (*Table 3*). The result showed SOD activity enhanced significantly in all the genotypes. The magnitude of the increment was different in various addition and translocation lines (*Fig. 3*). Under drought stress, maximum SOD activity was recorded in amphiploid (96%), translocation line Tr-2 (71%), Tr-7 (75%) and addition lines 1JJ (87%), 2JJ (90%), 5JJ (85%), 7JJ (83%) showed maximum SOD activity which was higher than that of the drought tolerant genotype Chakwal-97 (56%). Other translocation and addition lines along with amphiploid showed high to medium increase in SOD activity.

Chlorophyll A contents

Statistical analysis showed significant differences among wheat-*Th. bessarabicum* genetic stocks at 15% PEG stress at $p \leq 0.05$ for chlorophyll A contents (*Table 4*). Drought stress reduced significantly on leaf chlorophyll A contents of wheat genetic stock (*Fig. 4*). Comparison of wheat genetic stock revealed that addition lines 1JJ (9.6%), 2JJ (17%) and 4JJ (12%) represented reduction in chlorophyll A contents as compared to control and drought tolerant check. Similarly translocation line Tr-7 (11%),

http://www.aloki.hu ● ISSN 1589 1623 (Print) ● ISSN 1785 0037 (Online)
DOI: http://dx.doi.org/10.15666/aeer/1705_1044510461

Tr-6(19%) closely followed by Tr-3 (21%) and Tr-4 (21%) depicted minimum reduction in chlorophyll A contents. On the other hand, addition line 5JJ represented an increase in chlorophyll A contents.

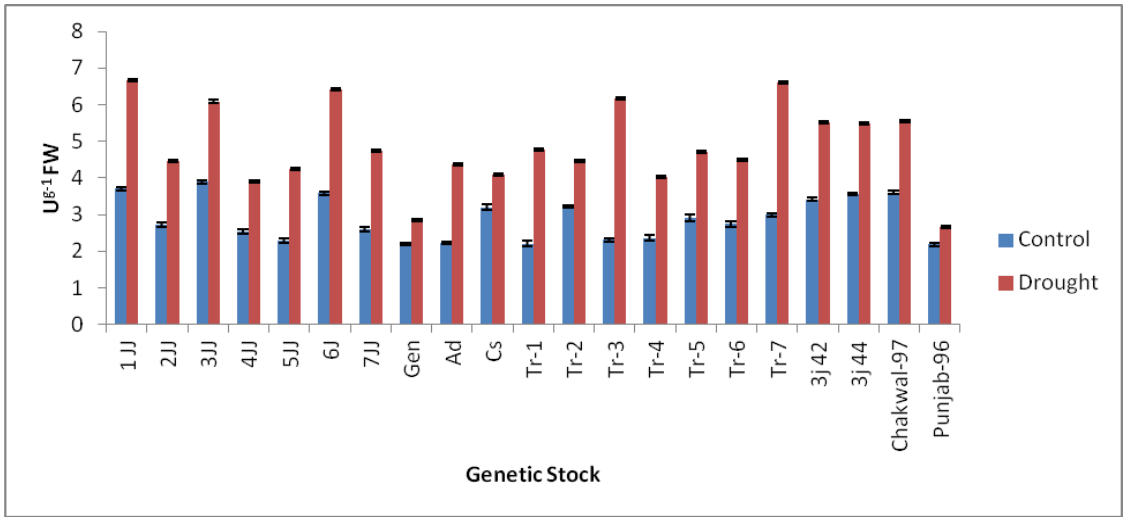

Figure 3. *Superoxide dismutase (SOD) activity in leaves at control and 15% PEG treatments*

Table 3. *Means for SOD contents at 15% PEG stress*

Genotypes	Control	Treatment	Mean
1JJ	3.70 o	9.17 b	6.43 a
2JJ	2.71 t	7.96 e	5.34 g
3JJ	3.89 n	6.07 j	4.98 i
4JJ	2.53 u	5.17 l	3.85 m
5JJ	2.28 vwx	9.61 a	5.95 d
6JJ	3.57p	8.90 c	6.23 c
7JJ	2.58 u	7.24 g	4.91 j
Gen	2.19 xy	5.34 k	3.77 n
Ad	2.22 wxy	7.61 f	4.91 ij
CS	3.19 r	5.32 k	4.26 l
Tr-1	2.20 wxy	9.25 b	5.73 e
Tr-2	3.20 r	2.93 s	3.07 p
Tr-3	2.30 vw	6.19 i	4.25 l
Tr-4	2.35 v	6.52 h	4.44 k
Tr-5	2.92 s	7.20 g	5.06 h
Tr-6	2.74 t	4.49 m	3.61 o
Tr-7	2.99 s	8.12 d	5.55 f
Tr-42	3.40 q	9.26 b	6.33 b
Tr-44	3.55 p	7.99 e	5.77 e
Chakwal-97	3.60 p	7.55 f	5.57 f
Punjab-96	2.18 y	3.91 n	3.05 p

Inter critical value for comparison was 0.09, while general critical value for comparison was 0.06

http://www.aloki.hu ● ISSN 1589 1623 (Print) ● ISSN 1785 0037 (Online)
DOI: http://dx.doi.org/10.15666/aeer/1705_1044510461

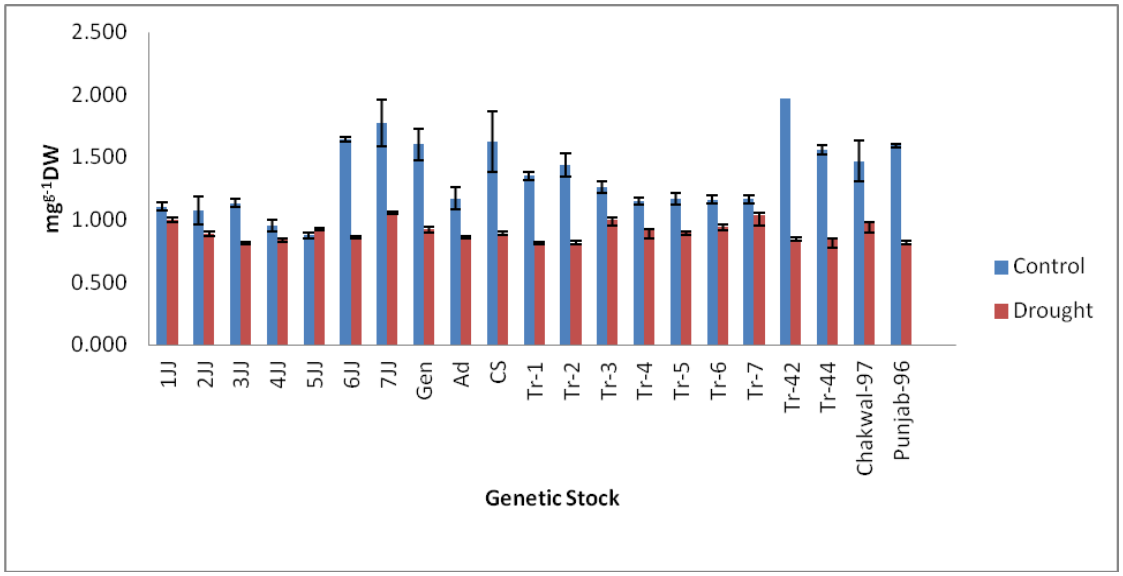

Figure 4. *Chlorophyll A contents in leaves at control and 15% PEG treatments*

Table 4. *Means for chlorophyll A contents at 15% PEG stress*

Genotypes	Control	Treatment	Mean
1JJ	1.10 h-l	0.99 i-o	1.05 ef
2JJ	0.85 m-p	0.88 m-p	0.87 h
3JJ	1.13 h-k	0.80 p	0.96 fgh
4JJ	0.95 k-p	0.83 op	0.89 gh
5JJ	0.8743 m-p	0.91 l-p	0.89 gh
6JJ	1.6440 bc	0.85 m-p	1.24 bc
7JJ	1.77 b	1.04 i-m	1.41 a
Gen	1.60 bcd	0.92 l-p	1.26 b
Ad	1.36 ef	0.85 m-p	1.11 cde
CS	1.62 bcd	0.88 m-p	1.25 b
Tr-1	1.35 fg	0.80 op	1.07 def
Tr-2	1.43 def	0.81 op	1.12 b-e
Tr-3	1.25 fgh	0.99 i-p	1.12 b-e
Tr-4	1.14 hij	0.91 l-p	1.03 efg
Tr-5	1.16 ghi	0.89 m-p	1.02 efg
Tr-6	1.16 g-j	0.94 k-p	1.05 ef
Tr-7	1.16 ghi	1.03 i-n	1.10 def
Tr-42	1.97 a	0.84 nop	1.40 a
Tr-44	1.55 cde	0.83 op	1.19 bcd
Chakwal-97	2.00 a	0.96 j-p	1.48 a
Punjab-96	1.59 bcd	0.81 op	1.20 bcd

Inter critical value for comparison was 0.19: while general critical value for comparison was 0.13

http://www.aloki.hu ● ISSN 1589 1623 (Print) ● ISSN 1785 0037 (Online)
DOI: http://dx.doi.org/10.15666/aeer/1705_1044510461

Chlorophyll B contents

Statistical analysis showed significant differences among wheat-*Th. bessarabicum* genetic stocks at 15% PEG stress at $p \leq 0.05$ for chlorophyll B contents (*Table 5*). Water deficit significantly reduced leaf chlorophyll B contents of all the wheat genetic stock (*Fig. 5*). Results revealed that all the wheat genetic stock addition lines 1JJ (24%), 4JJ (38%) 7JJ (39%) and translocation line Tr-1 (18%), Tr-9 (22%) represented the lowest reduction in chlorophyll B contents as compared to control and drought tolerant genotype. While addition line 5JJ (61%) and translocation line Tr-8 (61%) depicted maximum decrease in chlorophyll B contents.

Total chlorophyll contents

Statistical analysis showed significant differences among wheat-*Th. bessarabicum* genetic stocks at 15% PEG stress at $p \leq 0.05$ for total chlorophyll contents (*Table 6*). Results revealed that addition line 1JJ (14%), 2JJ (10%) and 4JJ (18%) showed minimum reduction in total chlorophyll contents, while addition lines 5JJ (24%), 6JJ (24%) and 7JJ (25%) depicted moderate decrease in total chlorophyll contents (*Fig. 6*). Similarly translocation lines Tr-5 and Tr-7 represented lower reduction in total chlorophyll contents.

Table 5. *Means for chlorophyll B contents at 15% PEG stress*

Genotypes	Control	Treatment	Mean
1JJ	0.43 e-l	0.32 i-p	0.37 c-f
2JJ	0.45 d-k	0.29 k-p	0.37 def
3JJ	0.49 d-h	0.23 op	0.36 def
4JJ	0.41 f-n	0.25 m-p	0.33 f
5JJ	0.68 ab	0.26 l-p	0.47 a-d
6JJ	0.49 d-i	0.25 m-p	0.37 def
7JJ	0.60 a-d	0.37 g-o	0.48 abc
Gen	0.53 b-g	0.24 op	0.38 b-f
Ad	0.48 d-j	0.24 nop	0.36 def
CS	0.41 f-m	0.28 k-p	0.35 ef
Tr-1	0.50 c-g	0.41 f-m	0.45 a-e
Tr-2	0.48 d-i	0.20 p	0.34 ef
Tr-3	0.54 b-f	0.27 l-p	0.41 a-f
Tr-4	0.69 ab	0.29 k-p	0.49 abc
Tr-5	0.54 b-f	0.28 l-p	0.41 a-f
Tr-6	0.72a	0.32 j-p	0.52 a
Tr-7	0.66 abc	0.33 h-p	0.49 ab
Tr-42	0.67 ab	0.26 m-p	0.46 a-d
Tr-44	0.41 f-n	0.31 k-p	0.36 def
Chakwal-97	0.59 a-e	0.25 m-p	0.42 a-f
Punjab-96	0.51 c-g	0.26 l-p	0.38 b-f

Inter critical value for comparison was 0.16, while general critical value for comparison was 0.11

http://www.aloki.hu ● ISSN 1589 1623 (Print) ● ISSN 1785 0037 (Online)
DOI: http://dx.doi.org/10.15666/aeer/1705_1044510461

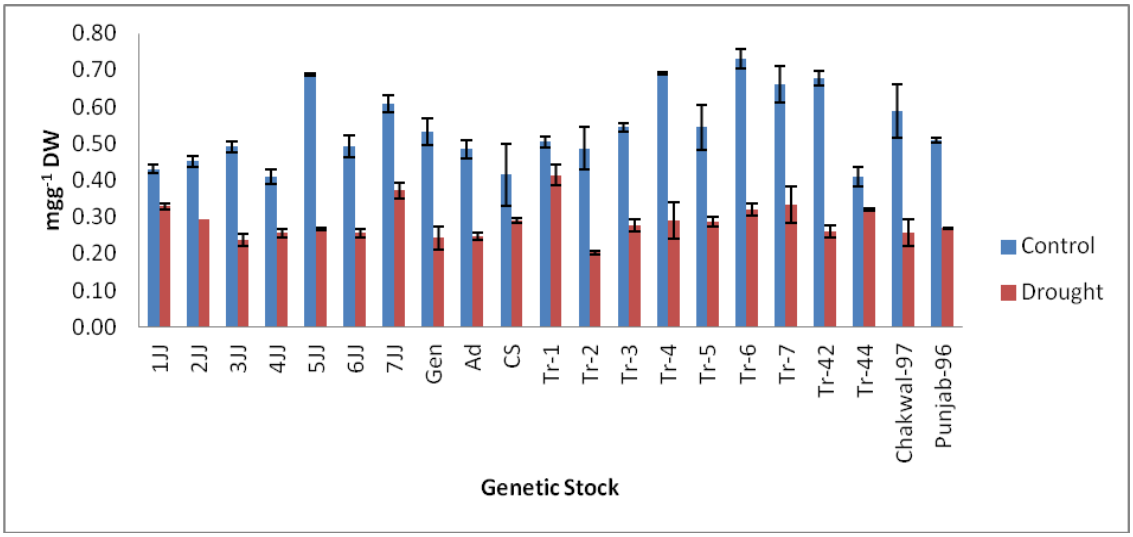

Figure 5. *Chlorophyll B contents in leaves at control and 15% PEG treatments*

Table 6. *Means for total chlorophyll contents at 15% PEG stress*

Genotypes	Control	Treatment	Mean
1JJ	1.53 jk	0.62 mn	1.08 def
2JJ	1.31 k	0.47 l-o	0.89 g
3JJ	1.62 hij	0.33 o	0.98 fg
4JJ	1.36 k	0.39 no	0.87 g
5JJ	1.56 ijk	0.48 l-o	1.02 efg
6JJ	2.13 cd	0.40 mno	1.27 bc
7JJ	2.38 bc	0.72 l	1.55 a
Gen	2.13 cd	0.46 l-o	1.29 b
Ad	1.85 e-h	0.40 no	1.12 b-f
CS	2.04 def	0.47 l-o	1.26 bcd
Tr-1	1.76 g-j	0.31 o	1.04 efg
Tr-2	1.92 d-g	0.31 o	1.11 b-f
Tr-3	1.80 f-i	0.57 l-o	1.18 b-e
Tr-4	1.84 e-h	0.50 l-o	1.17 b-e
Tr-5	1.71 g-j	0.47 l-o	1.09 c-f
Tr-6	1.89 d-g	0.56 l-o	1.22 bcd
Tr-7	1.82 f-i	0.67 lm	1.24 bcd
Tr-42	2.65 a	0.40 no	1.52 a
Tr-44	1.96 d-g	0.45 mno	1.20 b-e
Chakwal-97	2.59 ab	0.52 l-o	1.55 a
Punjab-96	2.10 de	0.38 no	1.24 bcd

Inter critical value for comparison was 0.26, while general critical value for comparison was 0.05

http://www.aloki.hu ● ISSN 1589 1623 (Print) ● ISSN 1785 0037 (Online)
DOI: http://dx.doi.org/10.15666/aeer/1705_1044510461

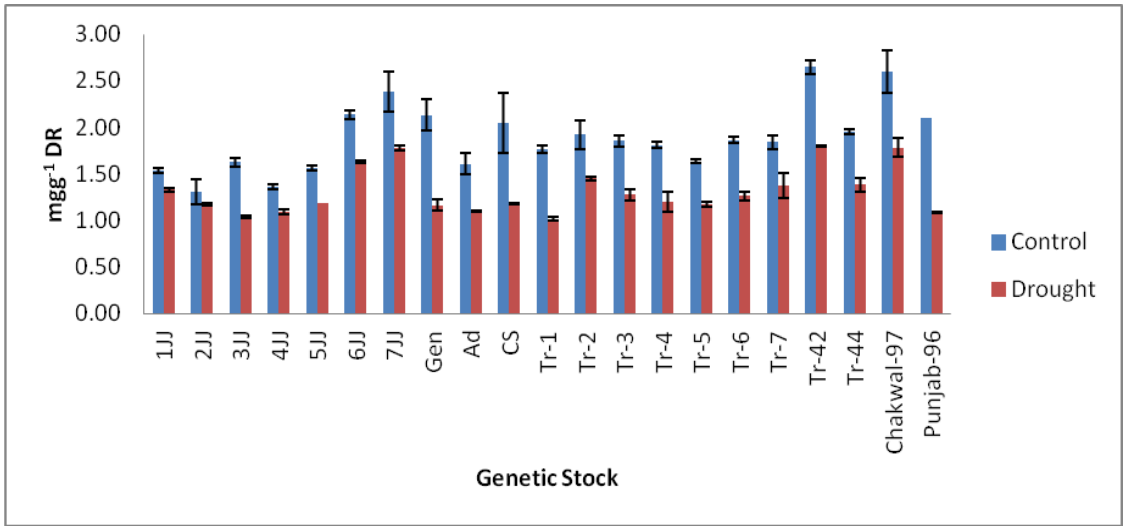

Figure 6. *Total chlorophyll contents in leaves at control and 15% PEG treatments*

Discussion

CS-*Th. bessarabicum* addition and translocation lines might possess tolerant genes for drought. Salt tolerant species might prove drought tolerant in the areas where water deficit prevails was inferred from the study of Farooq and Azam (2001). Whereas *Th. bessarabicum* (2n = 2x = 14, JJ or EbEb) is a perennial maritime wheatgrass that possesses salinity tolerances and can be an important gene source for wheat improvement (Gorham et al., 1985; William and Mujeeb-Kazi, 1993; King et al., 1997a). Majority of the traits associated with improved performance under drought stress have complex nature and controlled by several genes each having a small effect (Rebetzke et al., 2007; Yang et al., 2007).

Drought causes oxidative damages by producing reactive oxygen species (ROS) such as hydroxyls (OH), superoxide (O^{-}_{2}), peroxide hydrogen (H_2O_2). These ROS may initiate disturbance in lipid peroxidation, chlorophyll, protein oxidation, and nucleic acid (Scandalios, 1993). To combat the effects of drought–induced oxidative stress, plants develop complex mechanisms of antioxidant system via induction of drought tolerant genes (Bowler et al., 1992). Increase in ROS causes the enhanced SOD activity which is a major scavenger of O_2^- and it can catalytic the disproportionate reaction of superoxide radical anions into oxygen and hydrogen peroxide (Scandalios, 1993). As a consequence, H_2O_2 accumulation was possibly due to the activation of SOD. Thus, the balance between ROS and the antioxidative system is crucial for survival and adaptation to stress (Weng et al., 2015). Amphiploid, addition lines 1JJ 2JJ, 5JJ, 7JJ and translocation lines Tr-2, Tr-7 might have tried to maintain oxidative stress by exhibiting maximum SOD production. These addition lines possess 1J, 2J, 5J and 7J chromosomes pairs, while translocation lines have translocated segments of 1J and 5J from *Thinopyrum bessarabicum* chromosomes, respectively probably possess genes conferring resistance to drought via overproduction of SOD to scavenge ROS to protect against drought stress. SOD genes were mapped to the long arms of the homologous group-2 and group-7 chromosomes of wheat, respectively (Guohai et al., 1999). Zhao Xinhua et al. (2005) also found QTLs for SOD on chromosomes 1D, 2B and 5A of wheat. Higher SOD activity has also been reported in drought tolerant genotypes of

http://www.aloki.hu ● ISSN 1589 1623 (Print) ● ISSN 1785 0037 (Online)
DOI: http://dx.doi.org/10.15666/aeer/1705_1044510461

wheat (Sariam and Saxena, 2000). Din et al. (2009) also reported enhanced SOD activity in drought tolerant germplasm of wheat.

Drought stress influences the transcription of some of the genes to synthesize different types of drought stress related proteins, and proline is one of them. Proline is a crucial protein that has a vital function in water stress tolerance. Free proline might be involved in membrane stabilization during water stress (Kocheva and Georgiev, 2003), or it might be a reserve of readily mobilizable N available upon relief of stress (Hare et al., 1998). It has been reported that proline accumulation in the cytosol might be enough for osmotic adjustment by activating other mechanisms, such as the formations of strong H-bonded water around protein for protecting protein structures and scavenger of free radicals (Rascio et al., 1994; Alia et al., 2001; Ghoulam et al., 2002).

Results showed that addition lines 3JJ, 7JJ, 5JJ and translocation lines Tr-5, Tr-6 Tr-7 exhibited the highest proline accumulation at 15% PEG treatment indicating that these addition and translocation lines might possess genes on *Th. bessarabicum* chromosomes/chromosomal arms, which were induced during water deficit condition to maintain their turgor through osmotic adjustment. Research studies have shown that drought stresses increased leaf proline contents as compared to the control in drought tolerant lines (Dehnavi et al., 2017; Larkunthod et al., 2018). It was indicated by Gariba et al. (1992) that chromosome 4B, 5A and 5D of wheat may carry genes associated with the control of proline accumulation induced by osmotic stress. Ma et al. (2008) indicated an enzyme P5CR is the last enzyme in the cascade for proline synthesis. The TaP5CR gene was located on chromosome 3D of wheat genome. Its expression was upregulated by salt, PEG, ABA and heat stress. On the basis of above mentioned observation it can be suggested that enhanced level of proline accumulation in 5JJ and 3JJ addition line might be due to extra dosage of genes associated with the control of proline accumulation present on 5J and 3J chromosomes of *Th. bessarabicum*. The 7JJ addition lines might possess some other genes on *Th. bessarabicum* chromosomes which might be involved directly or indirectly in enhancing proline accumulation under drought stress. While translocation line Tr-5 contains chromosomal segment of 4J, Tr-6, while Tr-7 contains 6JS and 5JS chromosomal arm of *Th. Bessarabicum*, respectively that might possess some more genes responsible for inducing stress tolerant genes and accumulation of the highest level of proline under drought condition. Accumulation of osmolyte like proline has also been noticed in variety of crop species. Transgenic tobacco plants over expressing proline synthesis genes have been claimed to induce osmotic adjustment and have increased drought tolerance (Kishore et al., 1995). Under stress condition, proline concentration has been shown to be generally higher in stress-tolerant than that of stress-sensitive plants in many plant species such as rice (Shereen et al., 2007), alfalfa (Petrusa and Winicov, 1997), maize (Sharp et al., 1994), pigeon pea (Waheed et al., 2006) and potato (Rahnama and Ebrahimzadeh, 2004).

Concentration of chlorophyll contents in chloroplast affects photosynthetic capacity of crops and thereby considered a significant adaptation trait under water deficit condition (Chernyad'ev and Monakhova, 2003). Tolerance to drought comprises of maintaining high chlorophyll contents under water deficit to support photosynthetic capacity of plants (Yasmin et al., 2013). Drought stress causes decrease in the contents of chlorophyll by producing ROS such as O_2 and H_2O_2, thereby causing lipid peroxidation which consequently results in chlorophyll destruction (Mirnoff, 1993; Foyer et al., 1994). It has been expressed that tolerant genotypes of wheat and corn possessed higher chlorophyll contents than that of

http://www.aloki.hu ● ISSN 1589 1623 (Print) ● ISSN 1785 0037 (Online)
DOI: http://dx.doi.org/10.15666/aeer/1705_1044510461

sensitive genotypes during oxidative stress (Pastori and Trippi, 1992; Dehnavi et al., 2017). Disomic addition lines 1JJ, 2JJ, 4JJ possess a pair of 1J, 2J, 4J chromosomes and translocation lines Tr-7, Tr-6, Tr-3, Tr-4 possess chromosomal arms 5JS, 6JS, 3JS and 1JL, respectively from *Th. bessarabicum*, emphasizing the importance of these chromosomes/chromosomal arms in determining the tolerance of these genetic stock as these genetic stocks showed minimum reduction in chlorophyll A contents. While 5JJ addition line exhibited an increase in chlorophyll A contents under drought stress might possess gene(s) which were directly or indirectly involved in over expression of the chlorophyll A synthesis genes. It has also been found that the chlorophyll contents of leaves are increased in resistant cultivars under drought stress (Shahriari, 1999).

Reduction in chlorophyll contents of various crops has been previously reported by many researchers under drought stress. Results of chlorophyll B showed that addition lines 1JJ, 4JJ, 7JJ and translocation lines Tr-1 and Tr-9 exhibited minimum reduction in chlorophyll B, while addition lines 1JJ, 2JJ, 4JJ, 5JJ, 6JJ, 7JJ, amphiploid and translocation lines Tr-5 and Tr-7 depicted minimum decrease in total chlorophyll contents under water stress environment. Minimum reduction of chlorophyll B and total chlorophyll contents in these addition and translocation lines under drought stress might be linked to the presence of chromosomes/chromosomal arms from *Th. bessarabicum*.

It has been demonstrated that chlorophyll concentration in plants is a quantitative trait. Seven QTLs for chlorophyll contents on chromosomes 2B, 4A, 5B, 6A, 7A, and 7D under Nitrogen sufficient environment, while nine QTLs for chlorophyll contents on chromosomes 2D, 3A, 4B, 5B, and 6A when wheat seedlings are grown under nitrogen deficient environment were identified (Cao et al., 2004). Yang et al. (2007) mapped four additive QTLs controlling chlorophyll contents under water deficient and well watered on chromosomes 1A, 5A, and 7A in wheat. All these observations specify that controlling of chlorophyll contents in various environments is governed by multiple gene loci distributed on different chromosomes authenticating it as quantitative trait. Similar kinds of increased stress tolerance through presence of alien chromosomes of *Th. Elongatum* have also been reported by Taeb et al. (1993). Several alien substitution and translocation lines of wheat (*Triticum aestivum* L.) have shown genetic diversity for desirable traits of the alien donors (Rabinovich, 1998; Ko et al., 2002).

Conclusion

Wheat-*Th. bessarabicum* genetic stocks were given 15% PEG stress to evaluate their drought tolerance. The results indicated that amphiploid and the addition lines 1JJ, 5JJ, and translocation line Tr-7 have performed best in most of the physiological parameters studied in drought stress, and are considered to be tolerant under water stress condition. Other addition lines including 2JJ, 4JJ and 7JJ can be categorized as moderately tolerant to water deficit condition on the basis of their performance in traits studied under drought stress. These addition and translocation lines are recommended as sources of introducing drought tolerance into drought susceptible wheat cultivars.

Acknowledgements. This work is a part of Ph.D. Dissertation and supported by the Hazara University and National Agriculture Research Centre (NARC), Pakistan.

http://www.aloki.hu ● ISSN 1589 1623 (Print) ● ISSN 1785 0037 (Online)
DOI: http://dx.doi.org/10.15666/aeer/1705_1044510461

REFERENCES

[1] Alia, P. M., Matysik, J. (2001): Effect of proline on the production of singlet oxygen. – Amino Acids 21: 195-200.
[2] Araus, J. L., Bort, J., Steduto, P., Villegas, D., Royo, C. (2003): Breeding cereals for Mediterranean conditions: ecophysiological clues for biotechnology application. – Annals of Applied Biology 142: 129-141.
[3] Arnon, D. I. (1949): Copper enzymes in isolated chloroplast polyphenol oxidase in *Beta vulgaris*. – Plant Physiology 24: 1-15.
[4] Ashraf, M., Ozturk, M., Athar, H. R. (2009): Salinity and Water Stress. Improving Crop Efficiency. – Springer-Verlag, Berlin.
[5] Bano, A., Ullah, F., Nousheen, A. (2012): Role of abscisic acid and drought stress on the activities of antioxidant enzymes in wheat. – Plant Soil Environment 58: 181-185.
[6] Bates, L. S., Waldren, R. P., Teare, L. D. (1973): Rapid determination of free proline for water stress studies. – Plant Soil 39: 205-207.
[7] Blum, A. (1998): Improving wheat grain filling under stress by stem reserve mobilization. – Wheat: Prospects for Global Improvement 100: 77-83.
[8] Bowler, C., Montagu, V., Inze, M. D. (1992): Superoxide dismutase and stress tolerance. – Annual Review of Plant Physiology and Plant Molecular Biology 43: 83-116.
[9] Bray, E. A. (1993): Molecular responses to water deficit. – Plant Physiology 103: 1035-1040.
[10] Cao, W. D., Jia, J. Z., Jin, J. Y. (2004): Identification and interaction analysis of QTL for chlorophyll content in wheat seedlings. – Plant Nutrition and Fertilizer Science 10: 473-478.
[11] Chernyadev, I. I., Monakhova, O. F. (2003): Effects of cytokinin preparations on the pools of pigments and proteins of wheat cultivars differing in their tolerance to water stress. – Applied Biochemistry and Microbiology 39: 524–531.
[12] Din, J., Khan, S. U., Ali, I. (2009): Physiological assessment of drought tolerance in wheat (*Triticum aestivum* L.) varieties under moisture stress conditions. – Biologia Pakistan 55: 1-9.
[13] Dehnavi, M. M., Zare, T., Khajeeyan, R., Merajipoor, M. (2017): Drought and salinity impacts on bread wheat in a hydroponic culture: a physiological comparison. – Journal of Plant Physiology and Breeding 7: 61-74.
[14] Farooq, S., Azam, F. (2001): Co-existence of salt and drought tolerance in *Triticeae*. – Hereditas 135: 205-210.
[15] Foyer, C. H., Descourvieres, P., Kunert, K. J. (1994): Photo oxidative stress in plants. – Plant Physiology 92: 696-717.
[16] Galiba, G., Simon-Sarkadi, L., Kocsy, G., Salgo, A., Sutka, J. (1992): Possible chromosomal location of genes determining the osmoregulation of wheat. – Theoretical Applied Genetics 85: 415-418.
[17] Ghoulam, C. H., Foursy, A., Fares, K. (2002): Effects of salt stress on growth, inorganic ions and proline accumulation in relation to osmotic adjustment in five sugar beet cultivars. – Environmental and Experimental Botany 47: 39-50.
[18] Giannopolitis, C. N., Ries, S. K. (1977): Superoxide dismutases: I. Occurance in higher plants. – Plant Physiology 59: 309-314.
[19] Gorham, J., McDonnell, E., Budrewicz, E., Wynn Jones, R. G. (1985): Salt tolerance in the *Triticeae:* growth and solute accumulation in leaves of *Thinopyrum bessarabicum*. – Journal of Experimental Botany 36: 1021-1031.
[20] Guohai, W., Ronald Wilen, W., Robertson, J. A., Gusta, L. V. (1999): Isolation, chromosomal localization, and differential expression of mitochondrial manganese superoxide dismutase and chloroplastic copper/zinc superoxide dismutase genes in heat. – Plant Physiology 120: 513-520.

http://www.aloki.hu ● ISSN 1589 1623 (Print) ● ISSN 1785 0037 (Online)
DOI: http://dx.doi.org/10.15666/aeer/1705_1044510461

[21] Hare, P. D., Cress, W. A., Staden, J. (1998): Dissecting the role of osmolyte accumulation during stress. – Plant Cell and Environment 21: 535-553.
[22] Hoffmann, W. A., Marchin, R. M., Abit, P., Lau, O. L. (2011): Hydraulic failure and tree dieback are associated with high wood density in a temperate forest under extreme drought. – Global Change and Biology 17: 2731-2742.
[23] Jones, H. G., Corlett, J. E. (1992): Current topics in drought physiology. – Journal of Agricultural Science 119: 291-296.
[24] King, I. P., Forster, B. P., Law, C. C., Cant, K. A., Orford, S. E., Gorham, J., Reader, S., Miller, T. E. (1997a): Introgression of salt-tolerance genes from *Thinopyrum bessarabicum* into wheat. – New Phytology 137: 75-81.
[25] Kishore, K. P. B., Hong, Z., Miao, G. H., Hu, C. A. A., Verma, D. P. S. (1995): Over expression of Delta (1)-pyrroline-5-carboxylate synthetase increases proline production and confers osmotolerance in transgenic plants. – Plant Physiology 108: 1387-1394.
[26] Ko, J. M., Seo, B. B., Suh, D. Y., Do, G. S., Park, D. S., Kwack, Y. H. (2002): Production of a new wheat line possessing the 1BL.1RS wheat-rye translocation derived from Korean rye cultivar Paldanghomil. – Theoretical Applied Genetics 104: 171-176.
[27] Kocheva, K., Georgiev, G. (2003): Evaluation of the reaction of two contrasting barley (*Hordeum vulgare* L.) cultivars in response to osmotic stress with PEG 6000. – Belgium Journal of Plant Physiology 2003(Special Issue): 290-294.
[28] Larkunthod, P., Nounjan, N., Siangliw, J. L., Toojinda, T., Sanitchon, J., Jongdee, B., Theerakulpisut, P. (2018): Physiological responses under drought stress of improved drought-tolerant rice lines and their parents. – Notulae Botanicae Horti Agrobotanici Cluj-Napoca 46: 679-687.
[29] Lonbani, M., Arzani, A. (2011): Morpho-physiological traits associated with terminal drought stress tolerance in triticale and wheat. – Agronomy Research 9: 315-329.
[30] Ma, L., Zhou, E., Gao, L., Mao, X., Zhou, R., Jia, J. (2008): Isolation, expression analysis and chromosomal location of P5CR gene in common wheat (*Triticum aestivum* L.) S. – African Journal of Botany 74: 705-712.
[31] Majid, S. A., Asghar, R., Murtaza, G. (2007): Yield stability analysis conferring adaptation of wheat to pre-and post-anthesis drought conditions. – Pakistan Journal of Botany 39: 1623-1637.
[32] Martin, M., Micell, F., Morgan, J. A., Scalet, M., Zerbi, G. (1993): Synthesis of osmotically active substances in winter wheat leaves as related to drought resistance of different genotypes. – Journal of Agronomy and Crop Science 171: 176-184.
[33] Mirnoff, N. (1993): The role of active oxygen in the response of plants to water deficit and desiccation. – New Phytology 125: 27-58.
[34] Mittler, R. (2006): Abiotic stress, the field environment and stress combination. – Trends in Plant Science 11: 15-19.
[35] Morris, M. L., Blaid, A., Byerlee (1991): Wheat and Barley Production in Rain Fed Marginal Environments of the Developing World. Part I of 1990-91. – CIMMYT, Mexico.
[36] Mujtaba, S. M., Alam, S. M. (2002, April): Drought phenomenon and crop growth. – Industry & Economy. Retrieved from http://www.pakistaneconomist.com/issue2002/issue13/i&e4.htm
[37] Nayyar, H., Walia, D. P. (2003): Water stress induced proline accumulation in contrasting wheat genotypes as affected by calcium and abscisic acid. – Biology of Plant 46: 275-279.
[38] Nevo, E. (2004): Genomic Diversity in Nature and Domestication. – In: Henry, R. (ed.) Diversity and Evolution of Plants. Genotypic and Phenotypic Variation in Higher Plants. CAB International, Wallingford, UK, pp. 287-316.
[39] Passioura, J. B. (2007): The drought environment: physical, biological and agricultural perspectives. – Journal of Experimental Botany 58: 113-117.

http://www.aloki.hu ● ISSN 1589 1623 (Print) ● ISSN 1785 0037 (Online)
DOI: http://dx.doi.org/10.15666/aeer/1705_1044510461

[40] Pastori, G. M., Trippi, V. S. (1992): Oxidative stress induces high rate of glutathione reductase synthesis in a drought-resistant maize strain. – Plant Cell Physiology 33: 957-961.
[41] Pessarkli, M. (1999): Handbook of Plant and Crop Stress. – Marcel Dekker Inc., New York.
[42] Petrusa, L. M., Winicov, I. (1997): Proline status in salt tolerant and salt sensitive alfalfa cell lines and plants in response to NaCl. – Plant Physiology and Biochemistry 35: 303-310.
[43] Rabinovich, S. V. (1998): Importance of wheat-rye translocations for breeding modern cultivars of *Triticum aestivum* L. – Euphytica 100: 323-340.
[44] Rahnama, H., Ebrahimzadeh, H. (2004): The effect of NaCl on proline accumulation in potato seedlings and calli. – Acta Physiology of Plant 26: 263-270.
[45] Rascio, A., Plantani, C., Sealfati, G., Tonti, A., Di Fonzo, N. (1994): The accumulation of solutes and water binding strength in durum wheat. – Physiology of Plant 90: 554-558.
[46] Rebetzke. G. J., Ellis, M. H., Bonnett, D. G., Richards, R. A. (2007): Molecular mapping of genes for coleoptile growth in bread wheat (*Triticum aestivum* L.). – Theoretical Applied Genetics 114: 1173-1183.
[47] Robin, A. H. K., Uddin, M. J., Bayazid, K. N. (2015): Polyethylene glycol (PEG)-treated hydroponic culture reduces length and diameter of root hairs of wheat varieties. – Agronomy 5: 506-518.
[48] Sairam, R. K., Saxena, D. C. (2000): Oxidative stress and antioxidants in wheat genotypes: possible mechanism of water stress tolerance. – Journal of Agronomy and Crop Science 184: 55-61.
[49] Scandalios, J. G. (1993): Oxygen stress and superoxide dismutases. – Plant Physiology 101: 7-12.
[50] Sharp, R. E., Wu, Y., Voetberg, G. S., Saab, I. N., LeNoble, M. E. (1994): Confirmation that abscisic acid accumulation is required for maize primary root elongation at low water potentials. – Journal of Experimental Botany 45: 1717-1743.
[51] Shereen, A., Ansari, R. U., Yasmin, S., Raza, S., Mumtaz, S., Khan, M. A., Mujtaba, S. M. (2007): Physiological response of rice (*Oryza sativa* L.) to saline stress. – Pakistan Journal of Botany 39: 2527-2534.
[52] Taeb, M., Koebner, R. M. D., Forster, B. P. (1993): Genetic variation for water logging tolerance in the Triticeae and the chromosomal location of genes conferring water logging tolerance in *Thinopyrum elongatum*. – Genome 36: 825-830.
[53] Waheed, A., Hafiz, I. A., Qadir, G., Murtaza, G., Mahmood, T., Ashraf, M. (2006): Effect of salinity on germination, growth, yield, ionic balance and solute composition of pigeon pea (*Cajanus cajan* (L.) Mill sp). – Pakistan Journal of Botany 38: 1103-1117.
[54] Weng, M., Cui, I., Liu, F., Min, Z., Shan, I., Yang, S., Deng, X. (2015): Effects of drought stress on antioxidant enzymes in seedlings of different wheat genotypes. – Pakistan Journal of Botany 47: 49-56.
[55] William, M. D. H., Mujeeb-Kazi, A. (1993): *Thinopyrum bessarabicum*: Biochemical and cytological markers for the detection of genetic introgression in its hybrid derivatives with *Triticum aestivum* L. – Theoretical Applied Genetics 86: 365-370.
[56] Xie, W., Nevo, E. (2008): Wild emmer: Genetic resources, gene mapping and transfer for wheat improvement. – Euphytica 164: 603-614.
[57] Yang, D. L., Jing, R. L., Chang, X. P., W, Li. (2007): Identification of quantitative trait loci and environmental interactions for accumulation and remobilization of water-soluble carbohydrates in wheat (*Triticum aestivum* L.) stems. – Genetics 176: 571-584.
[58] Yasmeen, A., Basra, S. M. A., Wahid, A., Farooq, M., Nouman, W., Rehman, H. U., Hussain, N. (2013): Improving drought resistance in wheat (*Triticum aestivum*) by exogenous application of growth enhancers. – International Journal of Agriculture and Biology 15: 1307-1312.

http://www.aloki.hu ● ISSN 1589 1623 (Print) ● ISSN 1785 0037 (Online)
DOI: http://dx.doi.org/10.15666/aeer/1705_1044510461

[59] Zhao, L. Y., Deng, X. P., Shan, L. (2005): Effects of osmotic stress on chlorophyll fluorescence parameters of wheat seedling. – Chinese Journal of Applied Ecology16: 1261-1264.
[60] Zu, X., Lu, Y., Wang, Q., Chu, P., Miao, W., Wang, H., La, H. (2017): A new method for evaluating the drought tolerance of upland rice cultivars. – The Crop Journal 5: 488-498.

http://www.aloki.hu ● ISSN 1589 1623 (Print) ● ISSN 1785 0037 (Online)
DOI: http://dx.doi.org/10.15666/aeer/1705_1044510461

ASSESSING COMPLIANCE OF CONSERVATION SUSTAINABLE PRODUCTION STANDARDS AND PROFIT EFFICIENCY IN SMALL-SIZED FARMS IN KENYA

GICHUKI, C. N.[1] – HAN, J.[1*] – QIANG, L.[1] – NJAGI, T.[2] – NJINJU, S. M.[3]

[1]*College of Economics and Management Nanjing Agricultural University, Nanjing, China (e-mail: ngumbucg@gmail.com (Gichuki, C. N.); nideliuqiang@163.com (Qiang, L.))*

[2]*Tegemeo Institute of Agricultural Policy and Development, Egerton University, Nairobi, Kenya (e-mail: tnjagi@tegemeo.org)*

[3]*Kenya Agricultural and Livestock Research Organization, Nairobi, Kenya (e-mail: mugosimon7@yahoo.co.uk)*

[*]*Corresponding author*
e-mail: jhan@njau.edu.cn; phone: +1-3815-875-653

(Received 20th Dec 2018; accepted 10th Apr 2019)

Abstract. Sustainable Conservation Standards (SCS) promote the need for preserving soil life system and minimal use of farm chemicals including fertilizer to replenish the soil. The standards also guide farmers to meet international food safety and production standards such as Global Good Agricultural Practices (GLOBALGAP). The study was conducted in Kenya examined and compared levels of compliance to Sustainable Conservation Standards between GLOBALGAP certified and Non-GLOBALGAP Certified farms. Also, the study examined profit efficiency between GLOBALGAP certified and Non-GLOBALGAP Certified farms. The sample size comprised of 429 randomly selected smallholder farmers from three major snap bean producing regions in Kenya. The result revealed that the majority of GLOBALGAP certified farmers were likely to comply to Sustainable Conservation Standards techniques such as low usage of pesticides, herbicides, and fertilizer than None GLOBALGAP certified farmers. The showed that compliance to SCS and food safety and production standards enables snap bean smallholder farmers to directly access advanced value chains and ultimately receive higher prices for produce. We conclude by noting that the cost of implementing international food safety and production standards is still expensive to smallholder farmers especially in Sub-Saharan Africa.
Keywords: *GLOBALG.A.P., food safety, production standards, conservation agriculture*

Introduction

Globally food production system has been experiencing the transformation that greatly impacts on the global food supply value chains (Muller et al., 2017). One of the primary concern for changes in the production system is climate change and its impending threats to food and nutrition security. The effects will probably impact more in the developing countries that heavily depend on agriculture for livelihoods. For instance in Sub-Saharan Africa, agricultural production is the major employer in rural areas and also cushions against perennial food shortages (Stevenson et al., 2014). In the region, majority of the farmers are considered to own small parcels of land and are poor with low financial resources to cushion them against the adverse effects of climate change. The second concern to global food production is intensive agricultural production that advocates for excessive use of external inputs. This has been noted to increase the degradation of soil, water, and genetic resources over time. The increase in degradation of national resources not only pose a threat to global food security but

http://www.aloki.hu ● ISSN 1589 1623 (Print) ● ISSN 1785 0037 (Online)
DOI: http://dx.doi.org/10.15666/aeer/1705_1046310474

destabilizes livelihoods of larger populations. A study by Tilman et al. (2011) noted that annually more than 10 million hectares of quality productive land is lost due to soil degradation process, this will affect more than 1.5 billion people who depend directly on the land.

Generally, the trends in the degradation of national resources are seen to be on the increase despite policies put in place to reduce the growing threats. In developing countries, the agricultural production system is facing an even greater magnitude of soil and water degradation in prime agrarian lands (Whitfield et al., 2015). In particular, smallholder farms are experiencing falling groundwater table, declining organic carbon and soil matter, intensive soil tillage, imbalance of soil nutrients, increase in the use of pesticides and herbicides. The factors are believed to have contributed to declining crop yields and the rising cost of production and high wages. While on the supply marketing chain, smallholder farmers are not only limited to access to advanced markets but are also experiencing low prices for agricultural commodities. Besides, farmers are facing pressure from consumer's increasing demand for higher food quality and safety standards (Annor et al., 2016).

To sustain food production, overcome modern agrarian challenges and ensure that producers have stable livelihoods, policies on the adoption of sustainable conservation standards have been promoted. Mainly sustainable conservational agricultural practices ensure that farmers observe i) surface-incorporation of crop residues ii) reduced tillage or soil disturbance iii) increase production of cover crops for both annual and perennial crops. The concept is aimed at enriching and promoting soil health by enhancing natural biological processes above and below the soil surface. Also, SCS emphasizes the need for preserving soil life system and allows for minimal use of farm chemicals, including fertilizer to replenish the soil. However, the chemicals inputs quantities used in Sustainable Conservation farming are lower in comparison to conventional farming (Milder et al., 2015).

Over the years' sustainable production standards have merged to be a promising response to challenges of the degradation of national resources. Most of the agricultural sustainable production standards mainly address issues related to environmental quality and biodiversity conservation (Bain et al., 2013). Globally agricultural sustainability conservation standards are applied in production of major crops such as cocoa (22%), palm oil (15%), and tea (12%), coffee (38%) sugar (3%), soybeans (2%), and other crops (Potts et al., 2014). Good Agricultural Practices (GLOBALGAP) production is one of the standards put in place to minimize the negative impact of agriculture on the environment while meeting consumer concerns of food safety. Specifically, GLOBALGAP aims to reduce the use of fertilizer, management of waste, minimize the use of pesticides and efficiently use of non-renewable resources. Also, the standards ensure farmers invest in worker's safety and traceability systems (Chan, 2016).

In Sub-Saharan Africa (SSA), land productivity and per capita food availability have been on the declining in comparison to other regions in the world. Declining soil fertility and high-cost inputs are mainly linked to low agricultural productivity in the region. The problem is more profound among poorly endowed smallholder farmers. Majority of the farmers lack knowledge, resources, and techniques to adopt sustainable agricultural production standards (Whitfield et al., 2014). Nevertheless, a considerable number of smallholder farmers have been supported and trained in sustainable conservation farming practices. Farmers targeting the export market have been forced by marketing agents to comply with agricultural conservation practices (Blaikie and

http://www.aloki.hu ● ISSN 1589 1623 (Print) ● ISSN 1785 0037 (Online)
DOI: http://dx.doi.org/10.15666/aeer/1705_1046310474

Brookfield, 2015). On the contrary, large-scale farmers have resources to comply with the required food production standards easily. The concept of sustainable conservation standards is not only confined to improve environmental ecology and food safety but also archive acceptable profits sustained production level, and marketability of crops.

Studies in developing countries provide varied analysis of the increased competitiveness, in marketing and productivity in horticulture crops. While providing market linkage that has a positive impact on farmers' incomes, in most of the cases only farmers directly linked to advanced value chains tend to receive higher prices for their produce (Aasprong, 2013). Despite the associated benefits of being guaranteed market access, smallholder farmers are constantly under pressure to maintain sustainable production standards and sometime observe the set consumers food safety standards (Lockie et al., 2015). Prior studies have examined the returns on investments and social, economic benefits of horticultural crop production in developing economies (Henson et al., 2011). Conventionally, in Sub-Saharan Africa, farmers' profits are measured using financial gains in the form of gross margins. However, the techniques used don't show how exogenous factors such as farm characteristics, investments in sustainable conservation standards affected farms profit efficiencies levels.

In Asia, profit frontier function was used to estimate the profit efficiency of rice producers (Rahman, 2003; Chang et al., 2017). In computing profit efficiency, farmers can easily identify output level production, establish firms revenues and evaluate the benefits of investing in conservation agriculture (Abdulai and Huffman, 1998; Rahman, 2003). With this understanding, the objective of this study will examine variances in profit efficiency between certified GLOBALGAP farms and Non certified GLOBALGAP farms. Further, the study will examine utilization levels of sustainable conservation agriculture between certified GLOBALGAP farms and Non certified GLOBALGAP farms. The present study contributes to the debate on smallholder farmers producing efficiently in a perfectly competitive market while observing sustainable conservation agricultural production standards.

Materials and Methods

In Kenya, most of the snap beans are produced in the Central and Eastern regions. Snap beans are produced in well-drained silty loam to heavy clay soil that has pH range of between 6.5 to 7.5. Also, the beans grow well in optimum temperatures ranging between 20^{o}C and 25^{o}C. Snap beans do well in the altitude range of 1000 to 2100 meters. While the preferred rainfall for cultivation range is 900 to 1200 mm that is distributed throughout the year. Over the years there has been a decline in snap bean production that is mainly linked to i) erratic weather patterns, ii) declining soil fertility iii) use of banned pesticides such as dimethoate.

Study area and sampling procedures

The study employed multi-stage sampling technique to select 429 respondents who participated in the study. The first stage was purposively selecting major snap beans producing counties (Kirinyaga, Murang'a and Embu) in Kenya (*Figure 1*). A sampling frame of 3200 snap beans smallholder farmers from the three regions was obtained from ministry of Agriculture office. Using households sampling methodology formula 429 farmers were selected using simple random sampling procedure to participate in the

http://www.aloki.hu ● ISSN 1589 1623 (Print) ● ISSN 1785 0037 (Online)
DOI: http://dx.doi.org/10.15666/aeer/1705_1046310474

study. The data used in the study was collected between June 2016 and September 2016 in three major snap beans producing Counties in Kenya.

Data was collected through household surveys involving a face-to-face interview; this allowed interviewers to make a clarification on questions and to probe the respondents for accurate answers. The questionnaire was administered in local languages, to farmers who were farming snap beans in the last six years. The enumerators only interviewed respondents who were above 18 years and made most farming decision in the household (household head or spouse, farm employee). The identified farmers answered a detailed questionnaire on snap bean farming management, production, harvesting, and marketing of the beans. Also, farmers were presented with probing questions on perceptions and knowledge awareness of sustainable conservation agriculture and Global Good Agricultural Practices Good Agricultural Practices (GLOBALGAP) (The respondents provided information on household characteristics, land size, social capital, as well as non-income indicators.

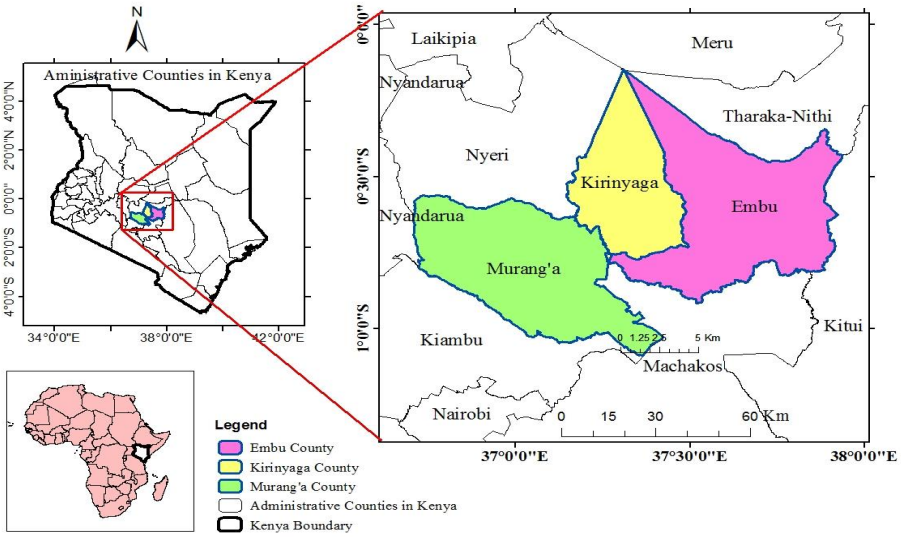

Figure 1. *Map of the study area*

Empirical analysis of profit efficiency

Traditionally, the farm production process has been measured using production function while efficiency has been estimated using deterministic or parametric approaches (Aigner et al., 1977; Van den Broeck et al., 1994). However, the profit frontier theory assumes that producers are always willing to maximize their profits, but not all are fully technically efficient. In a perfect competitive market, profits are assumed to be zero in the long run, producers operating at a negative profit are bound to exit the industry (Kumbhakar et al., 2015). Equally, if the profits are positive more will be attracted to in the industry. In the long run this increases market competition and drive profits to zero. Theoretically, firms are also seen to have short and long runs sequence of operating within profits as well as negatives. Thus profit efficiency is used in the present study to compare snap bean profit frontier function for certified GLOBALGAP farms and Non-GLOBALGAP farms in a perfectly competitive market.

Past studies in Africa and Asia have applied stochastic profit frontier models by considering estimation of the cost function (Ali and Flinn, 1989; Abdulai and Huffman,

http://www.aloki.hu ● ISSN 1589 1623 (Print) ● ISSN 1785 0037 (Online)
DOI: http://dx.doi.org/10.15666/aeer/1705_1046310474

1998; Chang et al., 2017). However, there is the assumption that cost function ignores the variances of profits and cost. In addition, the profit function takes into account that commodity prices are not homogeneous for all producers. The efficiency estimated by profit function can be used to evaluate management efficiency of producing high-quality products. In this study, we use one-step estimation and a Translog profit function. The efficiency determinant factors are included as the inefficiency term and estimated with the selected estimation function. Rahman (2003) argues that one-step estimation solves the statistical problem of consistency. The profit frontier function can simply be expressed as;

$$1n\Pi_i 1n\pi_i = \alpha_0 + \sum_{j=1}^{j} \alpha_j lnx_{ij} + v_i - u_i \quad \text{(Eq.1)}$$

where Π_i is the profit of the ith farm, xi's are the cost of different production inputs such, seed, water, labor (hired and own) and fertilizers (manure and chemical fertilizers). The error component v_i is assumed to be random variables identical independently distributed (iii) $N(0, \sigma_v^2)$ that contains statistical noise. $u_i$denotes the Non-negative random accounting for profit inefficiency expected to be truncated at zero $N(0, \sigma_v^2)$ distribution. Technical efficiency enables us to know variables that affect farm inefficiency. The equation is written as;

$$u_i = \delta_0 + \sum_{k=1}^{k} \delta_d z_{ik} + \omega_i \quad \text{(Eq.2)}$$

Input costs and farm characteristics are assumed to influence the profit efficiency of both GLOBALGAP certified, and None GLOBALGAP certified farms, in the equation Zi are the explanatory variables that explain inefficiency. The list of inefficiency variables used in different models includes farmer's characteristics, distance to market, number of extension contacts, subsidy support, and farmer's group membership. Inefficiency is denoted by E [exp(-u)|υ], and is a truncated normal distribution as outlined by (Battese and Coelli, 1995; Kumbhakar et al., 2015).

Results and discussion

Socioeconomic characteristics of respondents

Table 1 presented descriptive statistics for the survey; in general farmers in the study allocated an average of 1.2 hectares of land to snap bean production. Also we noted that only 58% of the farmers produced snap beans with GLOBALGAP certification. Despite the fact that snap bean production venture require smallholder farmers to have skills to comply with the Good Agricultural Practices standards, only 40 percent received regular extension visit. Further results showed that only 47 percent of the farmers received subsidy support from marketers, saving and credit co-operatives groups, Governmental and Nongovernmental organizations. However, 24 percent of the farmers accessed credit from formal banks to invest in the snap bean production venture in the year of the survey.

Table 2 presented the difference in characteristics of GLOBALGAP certified and Non-certified farmers. The analysis revealed that farmers who had GLOBALGAP certification were older and had more years in education than the None certified

http://www.aloki.hu ● ISSN 1589 1623 (Print) ● ISSN 1785 0037 (Online)
DOI: http://dx.doi.org/10.15666/aeer/1705_1046310474

farmers. Farmers with fully GLOBALGAP certification owned 1.087 hectors of snap beans farm size while None GLOBALGAP farmers owned 1.433. Generally, farmers with GLOBALGAP certification incurred 176.29$ on the cost of inputs such as seedlings, fertilizers, and pesticides. Also, they had additional input cost on soil/water testing and preservation, hygiene and sanitation units, packaging crates and traceability systems. While the None certified GLOBALGAP farmers only incurred input cost of $132.68 mainly related to seedlings, fertilizers, and pesticides. Despite farmers with GLOBALGAP certification incurring high cost if inputs, they also received higher returns of $1008.27 compared to $307.32 received by None GLOBALGAP certified farmers. Further, we noted that none GLOBALGAP farmers incurred more cost in land preparation than GLOBALGAP certified farmers.

Table 1. *Definition of variables (Source: Research findings)*

Variables	Description	Mean	St.Dev
GAP certification	1 if a farmer has GLOBALGAP certificate otherwise 0	0.580	0.494
Age	Age of the Household Head in years	44.64	12.83
Education	Number of years of schooling	9.669	2.578
Farm size	Total farm size under snap beans in hectares	1.232	1.089
Co-operative membership	1 of farmers belong to farmers groups otherwise 0	0.765	0.424
Extension contact	1 if farmer visited extension services on Snap bean production other wise 0	0.408	0.492
Access to credit	1 if farmer received a loan to finance snap bean venture otherwise 0	0.242	0.429
Under contract farming	1 if farmer is under contract farming other wise 0	0.540	0.497
Years of GLOBALGAP certification	Years of GLOBALGAP has certification	2.840	1.802
Farmers subsidy support	1 farmer received support from NGO otherwise 0	0.471	0.499
Distance to market	Distance to collection center market in kilometers	4.379	3.345

Table 2. *Differences in characteristics between GLOBALGAP compliance and Non-compliance farmers (Source: Research findings)*

	GLOBALGAP certified ***n=249***		**None-GLOBALGAP** ***n=180***		**T-test**	
	Mean	**(Sd)**	**Mean**	**(Std)**	***T***	**P**
Age Years	46.48	(12.96)	42.106	(12.24)	-3.534***	0.002
Education Years	9.751	(2.397)	9.556	(2.813)	0.774	0.439
Land size (ha)	1.087	(1.002)	1.433	(1.172)	3.288	0.999
Quantity snap bean produced Kgs	1486	(2934.9)	848.0	(1681.4)	-2.620***	0.004
Ave. returns in $	1008.27	(1.534)	307.32	(30151)	-4.546***	0.008
Ave. Input cost in $	176.29	(2721)	132.68	(23529)	1.613	-1.910
Land preparation Cost in $	24.87	(4169)	21.85	(2827)	-0.841	0.200

The last two column gives the t test statistics for equal means in the GLOBALGAP Certified and None-GLOBALGAP group. *** p<0.01, ** p<0.05, * p<0.1

Compliance to sustainable conservation standards

Figure 2, presented comparative analysis on the levels of compliance to sustainable conservation standards between GLOBALGAP certified and None certified farmers. Generally, the results indicated that more than 73 percent of the farmers applied water conservation techniques in their farms.

http://www.aloki.hu ● ISSN 1589 1623 (Print) ● ISSN 1785 0037 (Online)
DOI: http://dx.doi.org/10.15666/aeer/1705_1046310474

Further results revealed that 45 percent of the GLOBALGAP certified farmers used organic fertilizer in comparison, only 17 percent of the None certified farmers. We noted that GLOBALGAP certified farmers were less likely to apply pesticides, herbicides, and fertilizer than None GLOBALGAP certified farmers. The results indicated that only 20 percent of None GLOBALGAP certified farmers applied soil conservation technique minimum tillage while 65.9 percent of the GLOBALGAP certified applied the technique.

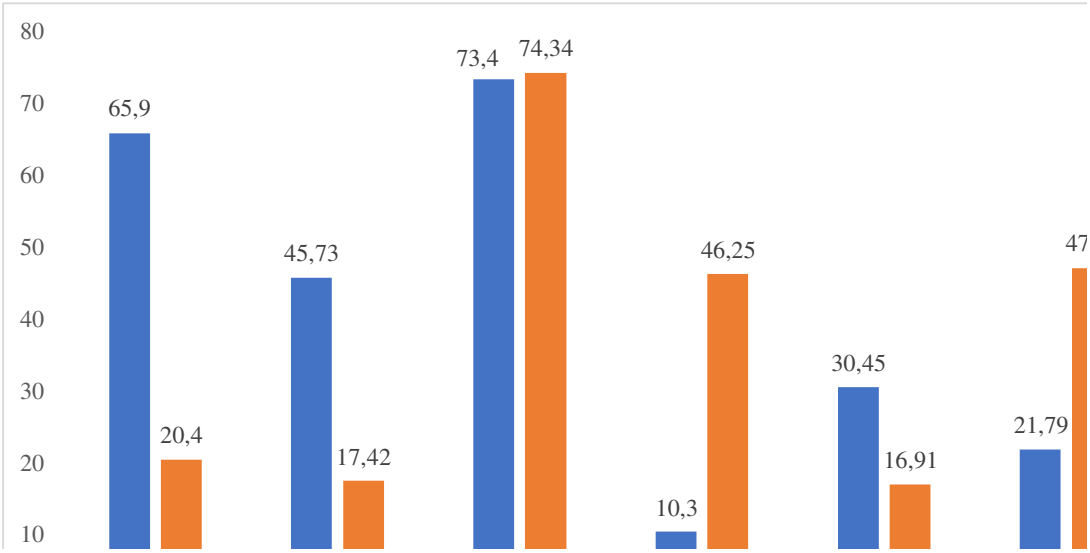

Figure 2. *Compliance to Sustainable Conservation Standards by Snap bean farmers*

Profit efficiency estimation

The maximum likelihood estimates of profit frontier function are presented in *Table 3*. The dependent variable is snap bean profits from the output of the whole year. The coefficient estimates parameter follows the normal profit function based on the assumption of a competitive market. The study results revealed that investing and complying to GLOBALGAP Ln(GAPC) farming standards negatively and significantly impacted profits of non- certified farmers. Also, General Input Cost (Ln GIC) negatively impact on none GLOBALGAP certified farms profits by 2.2%. Further results showed that land size would positively and significantly influence on profit efficiency of GLOBALGAP certified farms. While General Input Cost (Ln GIC) negatively impact on profits GLOBALGAP certified farms. Regarding characteristics that determine profit inefficiency, the results showed that farmers age, education years, years of GAP farming, distance to Market, GLOBAL GAP application in the farm, and contract farming would significantly influence on inefficiency for GLOBALGAP certified farms. While farmers age experience and distance to market determined on profit efficiency of Non- GLOBALG.A.P Certified farms

Table 4 shows the decile frequency distribution between GLOBALGAP certified, and non- GLOBALGAP certified farms. In general, the results revealed that the average measure of profit efficiency for GLOBALGAP certified farmers was 0.625 percent. This, implied that GLOBALGAP certified farmers got an average of about 62.5 percent of maximum profit potential.

http://www.aloki.hu ● ISSN 1589 1623 (Print) ● ISSN 1785 0037 (Online)
DOI: http://dx.doi.org/10.15666/aeer/1705_1046310474

Table 3. *Frontier Profit Function (Source: Research findings)*

	Parameters	GLOBALG.A.P Certified		Non- GLOBALG.A.P Certified	
		Coef	Std-err	Coef	Std-err
Ln(GIC)	β_1	0.005	0.021	-0.022	0.060
Ln(GAP)	β_2	-0.001	0.006	-0.099**	0.043
Ln (Landsize)	β_3	1.002***	0.017	0.008	0.002
Ln(GIC)× Ln(GAP)	β_4	0.001	0.008	-0.001	0.001
Ln(GIC)× Ln (Landsize)	β_5	-0.002	0.003	0.035	0.004
Ln(GAP)× Ln (Landsize)	β_6	0.001	0.014	0.027***	0.003
Ln(GIC) × Ln(GIC)	β_7	0.0015	0.011	0.568***	0.201
Ln(GAP) × Ln(GAP)	β_8	-2.800	4.400	0.006***	0.342
Ln (LS) × Ln (LS)	β_7	0.033***	0.012	0.640***	0.052
cons		-.4104	0.113	-14.14	20.09
Determinants of efficiencies					
Ln(farmer's age)	δ_1	0.029***	0.005	-0.005	0.012
Ln(HH Edu years)	δ_2	0.051***	0.008	0.007	0.011
Ln (Years of GAP farming)	δ_3	0.010***	0.002	-0.001	0.004
Ln(Distance to Market)	δ_4	0.005**	0.002	-0.007	0.002
ln (extent of GLOBAL GAP application in farm)	δ_5	0.025***	0.004	-0.004	0.003
Dummy for GAP extension	D_1	0.004	0.003	-0.003	0.004
Dummy if buyer is GAP certified	D_2	0.005	0.003	0.070	0.007
Dummy for membership to GLOBAL GAP farmers group	D_3	0.022	0.004	0.002	0.005
Dummy for GLOBAL GAP subsidy support	D_4	0.006	0.035	0.073	0.050
Dummy for contract farming	D_5	0.007***	0.038	-0.053	0.005
Usigma_cons		-14.38*	8.267	-14.14	20.09
Vsigma_cons		0.026	-7.291	-7.092	0.112
λ		0.028		0.029	

Note: ***,**,* Significant at 1, 5, 10, percent levels respectively Abbreviations: Log (Ln), General Input Cost (GIC), Good Agricultural Cost(GAPC), Land Size (LS)

Table 4. *Deciles Frequency Distribution of Profit Efficiencies of Snap bean Farmers (Source: Research findings)*

Efficiency level	GLOBALGAP certified farms		Non- GLOBALGAP farms	
	Frequency	Relative Efficiency %	Frequency	Relative Efficiency %
<0.010	4	1.61	59	32.78
0.21-0.40	37	14.86	50	27.78
0.41-60	48	19.28	21	11.67
0.61-0.80	73	29.32	22	12.22
0.81-1.00	87	34.94	28	15.56
Total	**249**	**100**	**180**	**100**
Minimum	0.030		0.017	
Maximum	0.999		0.876	
Mean	0.625		0.409	
Std Deviation	0.237		0.313	

This was gained due to production efficiency while the remaining shortfall of the discrepancy between observed profit and the frontier profit can be attributed to both technical and allocative inefficiencies as had earlier been confirmed by the likelihood ratio test. Further results showed non-GLOBALGAP farmers got an average of about 40.9 percent of maximum potential profit from snap bean venture.

http://www.aloki.hu ● ISSN 1589 1623 (Print) ● ISSN 1785 0037 (Online)
DOI: http://dx.doi.org/10.15666/aeer/1705_1046310474

Discussion

The main objective of this study was to examine the levels of compliance with sustainable conservation standards and estimate the profit efficiency of snap bean production between GLOBALGAP and Non-GLOBALGAP. The data was based on 429 smallholder farmers in Kenya. The comparative analysis on levels of utilization of sustainable conservation standards revealed that GLOBALGAP certified farmers were likely to apply soil conservation technique minimum tillage than Non-GLOBALGAP farms. Presently, extension messages in developing countries emphasize the use of reduced tillage. However, there, are indications that farmers are slow in adopting such practices (Luangduangsitthideth et al., 2018). Soil fertility experts recommend integration of organic matter from livestock and post-harvest crop waste to raise soil carbon levels. The study showed that the application of organic manure was less than 50 percent for both GLOBALGAP certified and Non- certified farmers. Previous studies reported that organic utilization of manure enhanced soil structure, improved soil carbon components while availing nutrients and mineral fertilizers to plants (Boström et al., 2015). We noted that low levels of inorganic fertilizer use by GLOBALGAP certified farms than for Non-certified farmers. Whitfield et al. (2015) reported that organic manure use improved the efficiency of fertilizer use by farmers.

The results of the study also indicated that the profit efficiency of GLOBALGAP certified farms was significantly higher than that Non-GLOBALGAP certified farms. The international food safety compliance literature showed that smallholder farmers in developing countries were locked out of the export market for non-compliance with sustainable conservation standards. In most of the cases, farmers were unable to meet requirements on environmental management, traceability standards, product safety, and the health safety of the workers (Kleemann et al., 2014). Thus, compliance with sustainable conservation standards such as GLOBALGAP would be prohibitive to farmers with low capital investment, a factor that affected the snap bean profit margins. Similarly, Lockie et al. (2013) reported that the use of safer pesticides required farmers to incur a higher cost of pest and disease management. Also, the cost of implementing GLOBALG.A.P certification could cost smallholder farmers up to 65 percent of the production cost (Muriithi et al., 2011). According to (Bain et al., 2013) compliance with sustainable production standards necessitated an increase in the cost of operation hence affecting the revenues.

The present study pointed out that farmer's group created inefficiencies for non-GLOBALGAP and GLOBALG.A.P Certified farms. However, Fernandez-Stark et al. (2011) study that farmers co-operatives are likely to get better returns when dealing directly with marketing companies or supermarket chains than middlemen. Also, collective action by farmer's organizations increased credit acquisition chances, the ability to negotiate prices, and market assurance. Supporting farmers with inputs, credit, and extension services resulted in reduced profit inefficiency, especially for GLOBALG.A.P certified farmers. The support services would help farmers to observe sustainable conservation standards required by buyers. Also, Aasprong (2013) notes that agricultural extension support system facilitated dissemination of suitable technologies to farmers reduced the inefficiency in Madagascar.

http://www.aloki.hu ● ISSN 1589 1623 (Print) ● ISSN 1785 0037 (Online)
DOI: http://dx.doi.org/10.15666/aeer/1705_1046310474

Conclusion

In conclusion, we noted that food production and certification standards such as GLOBALG.A.P significantly facilitate smallholder farmers to observe sustainable conservation practices. In particular, the standards help reduction in pesticide use, inorganic fertilizer use, minimum soil disturbance. However, the governments and other stakeholders in Sub-Saharan Africa have to mobilize and create awareness on the benefits of sustainable conservation standards. Also, there is a need to have a policy shift and address the perception that inorganic fertilizer is the panacea for smallholder productivity.

We also noted that smallholder snap bean farmers need to increase profit efficiency marginally. Much of the policy emphasis must be directed towards increasing compliance to sustainable conservation standards not only for the export target market but also local Kenyan market. However, high rejection rate resulting from Non-compliance sustainable conservation standards will likely lead farmers to produce for local market where they invest less and still get marginal profits from the snap beans. While compliance to sustainable conservation standards such as GLOBALG.A.P standards guarantees a ready market for the snap bean, there is need to scale up subsidies relating to sustainable conservation standards certification and compliance for snap bean venture to be more profit efficient. This will enhance smallholder's snap bean farmers in Kenya to efficiently produce and maintain competitiveness in the global market that is becoming more dynamic, especially with regards to environmental and food safety standards.

Acknowledgements. This paper was made possible through financial support of East Africa's Agricultural Policy and its impact on Sino-East Africa Agricultural Cooperation project and Priority Academic Program Development of Jiangsu Higher Education (PAPD). Grant no KYGB201802.

REFERENCES

[1] Aasprong, H. (2013): Entangled standardizing networks: the case of GLOBALGAP and Fairtrade in St Vincent's banana industry. – Int. J. Sociol. Agric. Food 20:91-108.
[2] Abdulai, A., Huffman, W. E. (1998): An examination of profit inefficiency of rice farmers in Northern Ghana. – Iowa State University, Department of Economics, Staff General Research Paper.
[3] Aigner, D., Lovell, C. K., Schmidt, P. (1977): Formulation and estimation of stochastic frontier production function models. – Journal of econometrics 6: 21-37.
[4] Ali, M., Flinn, J. C. (1989): Profit efficiency among Basmati rice producers in Pakistan Punjab. – American Journal of Agricultural Economics 71: 303-310.
[5] Aloui, O., Kenny, L. (2005): The cost of compliance with SPS standards for Moroccan exports: a case study. – World Bank Agriculture and Rural Development Discussion Paper. World Bank, Washington DC.
[6] Annor, B. P., Mensah-Bonsu, A., Jatoe, J. B. D. (2016): Compliance with GLOBALGAP standards among smallholder pineapple farmers in Akuapem-South, Ghana. – Journal of Agribusiness in Developing and Emerging Economies 6: 21-38.
[7] Asfaw, S., Mithöfer, D., Waibel, H. (2010): Agrifood supply chain, private-sector standards, and farmers' health: evidence from Kenya. – Agricultural Economics 41: 251-263.

http://www.aloki.hu ● ISSN 1589 1623 (Print) ● ISSN 1785 0037 (Online)
DOI: http://dx.doi.org/10.15666/aeer/1705_1046310474

[8] Bain, C., Ransom, E., Higgins, V. (2013): Private agri-food standards: Contestation, hybridity and the politics of standards. – International Journal of Sociology of Agriculture and Food 20: 1.
[9] Battese, G. E., Coelli, T. J. (1995): A model for technical inefficiency effects in a stochastic frontier production function for panel data. – Empirical economics 20: 325-332.
[10] Blaikie, P., Brookfield, H. (2015): Land degradation and society. – Routledge.
[11] Boström, M., Jönsson, A. M., Lockie, S., Mol, A. P., Oosterveer, P. (2015): Sustainable and responsible supply chain governance: challenges and opportunities. – Journal of Cleaner Production 107: 1-7.
[12] Chan, K. (2016): Manual on good agricultural practices (GAP). – Asian Productivity Organization (APO).
[13] Chandra, A., Idrisova, A. (2011): Convention on Biological Diversity: a review of national challenges and opportunities for implementation. – Biodiversity and Conservation 20: 3295-3316.
[14] Chang, T., Takahashi, D., Yang, C.-K. (2017): Profit efficiency analysis of rice production in Taiwan. – China Agricultural Economic Review 9: 32-47.
[15] Delgado, J. A., Groffman, P. M., Nearing, M. A., Goddard, T., Reicosky, D., Lal, R., Kitchen, N. R., Rice, C. W., Towery, D., Salon, P. (2011): Conservation practices to mitigate and adapt to climate change. – Journal of soil and water conservation 66: 118A-129A.
[16] Fernandez-Stark, K., Bamber, P., Gereffi, G. (2011): The Fruit and Vegetable Global Value Chain: Workforce Development and Economic Upgrading. – Durham: Center for Globalization. Governance and Competitiveness.
[17] Giller, K. E., Corbeels, M., Nyamangara, J., Triomphe, B., Affholder, F., Scopel, E., Tittonell, P. (2011): A research agenda to explore the role of conservation agriculture in African smallholder farming systems. – Field crops research 124: 468-472.
[18] Henson, S., Masakure, O., Cranfield, J. (2011): Do fresh produce exporters in sub-Saharan Africa benefit from GlobalGAP certification? – World Development 39: 375-386.
[19] Humphrey, J. (2008): Private standards, small farmers and donor policy: EUREPGAP in Kenya. – Working paper series, 308. Brighton: IDS.
[20] Joshi, P. (2011): Conservation agriculture: an overview. – Indian Journal of Agricultural Economics 66: 53.
[21] Kleemann, L., Abdulai, A., Buss, M. (2014): Certification and access to export markets: Adoption and return on investment of organic-certified pineapple farming in Ghana. – World Development 64: 79-92.
[22] Kumbhakar, S. C., Wang, H., Horncastle, A. P. (2015): A practitioner's guide to stochastic frontier analysis using Stata. – Cambridge University Press.
[23] Lockie, S., McNaughton, A., Thompson, L.-J., Tennent, R. (2013): Private food standards as responsive regulation: the role of national legislation in the implementation and evolution of GLOBALG. AP. – International Journal of Sociology of Agriculture & Food 20.
[24] Lockie, S., Travero, J., Tennent, R. (2015): Private food standards, regulatory gaps and plantation agriculture: social and environmental (ir) responsibility in the Philippine export banana industry. – Journal of Cleaner Production 107: 122-129.
[25] Luangduangsitthideth, O., Limnirankul, B., Kramol, P. (2018). Farmers' knowledge and perceptions of sustainable soil conservation practices in Paklay district, Sayabouly province, Lao PDR. – Kasetsart Journal of Social Sciences, available at: https://doi.org/10.1016/j.kjss.2018.07.006.
[26] Milder, J. C., Arbuthnot, M., Blackman, A., Brooks, S. E., Giovannucci, D., Gross, L., Kennedy, E. T., Komives, K., Lambin, E. F., Lee, A. (2015): An agenda for assessing and

http://www.aloki.hu ● ISSN 1589 1623 (Print) ● ISSN 1785 0037 (Online)
DOI: http://dx.doi.org/10.15666/aeer/1705_1046310474

improving conservation impacts of sustainability standards in tropical agriculture. – Conservation biology 29: 309-320.
[27] Minten, B., Randrianarison, L., Swinnen, J. (2007): Spillovers from high-value agriculture for exports on land use in developing countries: evidence from Madagascar. – Agricultural Economics 37: 265-275.
[28] Mugunzwe, H., Tshirley, D. (2006): Understanding Zambia's Domestic Value Chains for Fresh Fruits and Vegetables. Food Security Research Project, Zambia. – http://ageconsearch. umn. edu/bitstream/54621/2/ps17. pdf.
[29] Muller, A., Ferré, M., Engel, S., Gattinger, A., Holzkamper, A., Huber, R., Müller, M., Six, J. (2017): Can soil-less crop production be a sustainable option for soil conservation and future agriculture? – Land Use Policy 69: 102-105.
[30] Muriithi, B. W., Mburu, J., Ngigi, M. (2011): Constraints and determinants of compliance with EurepGap standards: a case of smallholder french bean exporters in Kirinyaga district, Kenya. – Agribusiness 27: 193-204.
[31] Okello, J. J., Swinton, S. M. (2010): From circle of poison to circle of virtue: pesticides, export standards and Kenya's green bean farmers. – Journal of agricultural economics 61: 209-224.
[32] Potts, J., Lynch, M., Wilkings, A., Huppé, G. A., Cunningham, M., Voora, V. A. (2014): The state of sustainability initiatives review 2014: Standards and the green economy. – International Institute for Sustainable Development Winnipeg, MB.
[33] Rahman, S. (2003): Profit efficiency among Bangladeshi rice farmers. – Food policy 28: 487-503.
[34] Saei, M., Mohammadi, H., Ziaee, S., Barkhordari, S. (2018): Economic effect of climate alteration on grain production in Iran. – Applied Ecology and Environmental Research 16: 6691-6707.
[35] Stevenson, J. R., Serraj, R., Cassman, K. G. (2014): Evaluating conservation agriculture for small-scale farmers in Sub-Saharan Africa and South Asia. – Elsevier.
[36] Tilman, D., Balzer, C., Hill, J., Befort, B. L. (2011): Global food demand and the sustainable intensification of agriculture. – Proceedings of the National Academy of Sciences 108: 20260-20264.
[37] Van den Broeck, J., Koop, G., Osiewalski, J., Steel, M. F. (1994): Stochastic frontier models: A Bayesian perspective. – Journal of Econometrics 61: 273-303.
[38] Van der Meer, C. (2006): Exclusion of small-scale farmers from coordinated supply chains. – Agro-food Chains and Networks for Development, Amsterdam 209-218.
[39] Whitfield, S., Dougill, A., Wood, B., Chinseu, E., Mkwambisi, D. (2014): Conservation Agriculture in Malawi: Networks, Knowledge Gaps and Research Planning. – Report on the National Conservation Agriculture Research Planning Workshop, Lilongwe, 6th May, 2014.
[40] Whitfield, S., Dougill, A. J., Dyer, J. C., Kalaba, F. K., Leventon, J., Stringer, L. C. (2015): Critical reflection on knowledge and narratives of conservation agriculture. – Geoforum 60: 133-142.
[41] Wysokinski, M., Golasa, P., Bienkowska, W. (2012): The importance of GLOBAL GAP for food safety in the supply chain. – Logistyka 6.

http://www.aloki.hu ● ISSN 1589 1623 (Print) ● ISSN 1785 0037 (Online)
DOI: http://dx.doi.org/10.15666/aeer/1705_1046310474

CDYNAMIC CHANGE CHARACTERISTICS OF ECOSYSTEM FLUXES IN COLD ZONE WETLANDS IN NORTHEAST CHINA

WEI, H.[1,2] – ZHANG, J.[1,2] – WANG, F.[1,2*]

[1]*North China University of Water Resources and Electric Power, Zhengzhou 450045, China*
[2]*Collaborative Innovation Center of Water Resources Efficient Utilization and Support Engineering, Zhengzhou 450045, China*

**Corresponding author*
e-mail: wangfuqiang@ncwu.edu.cn; phone/fax: +86-0371-6912-7399

(Received 27th Sep 2018; accepted 16th Jul 2019)

Abstract. In order to promote the understanding of the dynamic change characteristics of ecosystem flux in cold zone wetlands and to provide scientific basis for the accurate simulation of wetland flux, this study applied the eddy covariance (EC) flux measurement system for long-term continuous flux of Harbin Jinhewan Wetland Botanical Garden. A preliminary analysis of one-and-a-half-year measurements of water, heat, and CO_2 fluxes showed that: (1) The diurnal variation of CO_2 flux shows a single-valley character, and the annual variation is consistent with the vegetation growth trend; the diurnal variation of CO_2 concentration shows a single-peak and single-valley character, the annual change process is opposite to the vegetation growth trend. (2) The average daily CO_2 absorption rate of Jinhewan Wetland is only 0.13 mg/(m^2·s), with weak carbon sink function and great carbon sequestration potential. (3) The diurnal variations of sensible heat flux (SHF), latent heat flux (LHF) and Bowen ratio (except for winter) of Jinhewan Wetland are basically single-peaked; SHF is highest in spring and LHF is highest in summer; LHF is only smaller than SHF in winter, while in summer LHF is much larger than SHF and minimum is two times that of SHF.
Keywords: *Eddy covariance, sensible heat flux, latent heat flux, carbon dioxide flux, Bowen ratio*

Introduction

The exchange of mass and energy in the Soil-Plant-Atmosphere Continuum (SAPC system) plays an important role in global climate, environmental change, and hydrological and ecological processes (Chen et al., 2016; Wang, 1999). The mass exchange of water and CO_2 is the carrier for the biosphere to acquire and store energy, which is mainly achieved through the photosynthesis and transpiration of crops. CO_2 concentration also significantly affects the earth temperature. Heat exchange plays an important role in atmospheric movement, which affects the formation of weather and climate on a larger spatial scale (Wang et al., 2013). Observing and studying the relationship among ground-air water, heat and CO_2 exchange is of great significance to water cycle analysis, water resources management, and weather and climate forecast (Zheng, 2013). Since the 1980s, long-term observations of the fluxes have attracted extensive attention (Baldocchi et al., 2001).

The measurement methods for water, heat and CO_2 fluxes include Eddy Covariance (EC for short), BREB method (Bowen Ratio-Energy Balance, BREB for short), aerodynamic method, and profile gradient iterative method (Liu and Yu, 1997; Shen et al., 2005; Wang et al., 2009). Among them, the EC technique uses the sensor's measurement result of the wind speed fluctuation and a certain physical quantity pulsation in the atmosphere, and the fluxes of various substances and energy are obtained by calculating the covariance between them (Roland, 1991). This technique is simple, easy, and can be directly observed (Xu et al., 2008). With the rapid development

http://www.aloki.hu ● ISSN 1589 1623 (Print) ● ISSN 1785 0037 (Online)
DOI: http://dx.doi.org/10.15666/aeer/1705_1047510490

of measuring instruments and computing technology, the EC technique has been widely used in field observations (Liu et al., 2006), and it has achieved continuous, long-term, automatic observation of surface fluxes, while exerting minimal interference on the environment and ecosystems (Baldocchi, 2003). At present, the EC technique has become a standard method for measuring water, heat, and CO_2 fluxes, and is widely used for measurement of water, heat, and carbon fluxes between the earth's surface and atmosphere (Hutley et al., 2005; Kang et al., 2001). Many factors such as undulating terrain, unfavorable weather conditions will affect the accuracy of flux measurement results by using EC technique (Massman and Lee, 2002), and to some extent hinder the application of the technique. However, the study area is flat and the elevation difference is only 5 m. During the monitoring period, the temperature in the study area was between -30 and 30 °C, and the daily precipitation was within 21 mm (moderate rain), except for the two maximum days of 54 mm (storm) and 28 mm (heavy rain), with no adverse weather such as extreme temperatures and precipitation. Therefore, the effects of topography and climate can be ignored in this study.

Among the currently known terrestrial ecosystems, wetland, as one of the three largest ecosystems (land, sea, and wetland), is the second most important carbon stock next to the forest. Although accounting for only 6% of the land area (Gao et al., 2008), wetland stores 10%-30% of the carbon of the global terrestrial ecosystem (Nahlik and Fennessy, 2016; Smith et al., 2004; Edwards, 2001). At present, there is no conclusion on the carbon source/carbon sink function of wetlands (Shoemaker et al., 2015; Duman and Schäfer, 2018). The estuarine wetland of the Niuesi River in southern Texas has carbon sink characteristics under sufficient water conditions, but it appears carbon source characteristics when there is insufficient moisture (Heinsch et al., 2004). Affected by the wetland age, geographical location, climate and other environmental conditions, the wetland ecosystem will present a carbon source or carbon sink function accordingly (Kayranli et al., 2010). In addition, when the rate of methane released by sediments exceeds the rate of carbon sequestration in the plant photosynthesis, even reed wetlands with vigorous growth of vegetation will become carbon sources (Brix et al., 2001). The absorption of CO_2 in the Zoige wetland in southwestern China in 2008 and 2009 was 173 g/m^2/a and 292 g/m^2/a (Hao et al., 2001), respectively, and played a significant carbon sink function. Affected by tides, the Yangtze River estuary wetland alternates with the function of carbon sources and carbon sinks (Guo et al., 2009). In the alpine wetland ecosystem of the Tibetan Plateau, carbon absorption mainly occurred during the growing and withering stages of vegetation, while carbon release by respiration occurred during non-growing stage of vegetation (Cao et al., 2017). However, in the cold regions of northeastern China, long-term observations of wetland ecosystem fluxes are few (Chen, 1996; Yang and Lyu, 1999) and their research is not deep (He et al., 2006).

Jinhewan Wetland Botanical Garden is a demonstration area for the protection and restoration of aquatic ecosystems in Harbin, and is an important part of the ecological project of the "Hectares of Songjiang Wetland and Long-stretching Ecological Corridor". The water-heat cycle and the carbon source/carbon sink function of the wetland have an important effect on the protection and restoration of the ecosystem. This study used the EC flux measurement system to conduct long-term continuous observations of water, heat, and CO_2 fluxes at Jinhewan Wetland, and characteristics of changes in water, heat and CO_2 fluxes in the wetland was analyzed by using the monitoring results for one and a half year from August 1, 2015 to December 31, 2016.

http://www.aloki.hu ● ISSN 1589 1623 (Print) ● ISSN 1785 0037 (Online)
DOI: http://dx.doi.org/10.15666/aeer/1705_1047510490

And then the characteristics of the water-heat cycle and the carbon source/carbon sink function are further analyzed, thus providing technical support for the protection and restoration of the ecosystem in the demonstration area.

Test area and instrument

Test area

The test area is located in Jinhewan Wetland Botanical Garden, Harbin, Heilongjiang Province, China (N 45°46'35.2"-45°46'58.9", E 126°29'07.7"-126°29'45.1"; see *Fig. 1*). Located on the left bank of the main urban area of Harbin, Songhua River, on the beach between the West Fourth Ring Bridge and the East Third Ring Bridge, it is 3,800 m in length, 1500 m in width, 3.5 km^2 in area, and 115 m-120 m in altitude. The extremely gentle terrain effectively avoids the influence of topographic relief on the accuracy of flux observations by using EC technique.

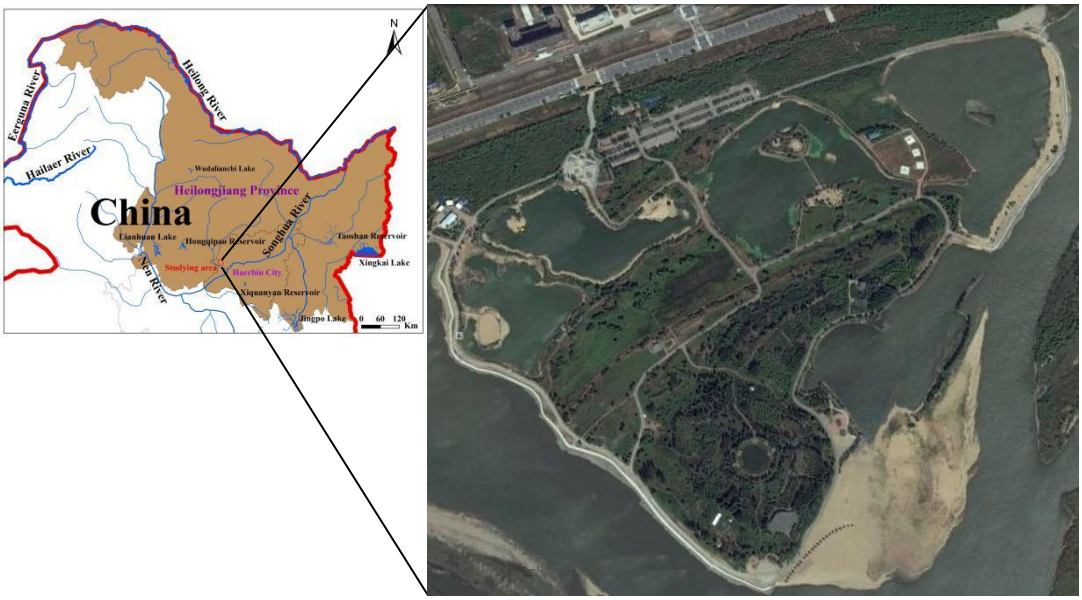

Figure 1. *Harbin Jinhewan Wetland Botanical Garden*

The test area is located in the middle temperate zone, which features a semi-humid continental monsoon climate with four distinct seasons, short winters and long summers. According to the meteorological data from 1951 to 2013, the average annual sunlight duration is 2636.3 h, and the annual sunlight rate is 55-66%. The average annual temperature is 3.2 °C, January is the coldest month, the average monthly temperature is -19.7 °C, and the extremely low temperature is -41.1 °C; in the hottest month in July, the average monthly temperature is 23.1 °C, and the extremely high temperature is 39.1 °C. The frost-free period averages 135 days. The average annual precipitation in Harbin City where the test area is located is 570 mm, and the maximum annual precipitation is 1015 mm. Affected by the alternating of southeast ocean air mass and the northwest continental air mass, the distribution of rainfall season is uneven. The average annual precipitation in June-September is 341.5 mm, accounting for about 60% of the whole year. Rainstorms are mostly concentrated in July and August, accounting

http://www.aloki.hu ● ISSN 1589 1623 (Print) ● ISSN 1785 0037 (Online)
DOI: http://dx.doi.org/10.15666/aeer/1705_1047510490

for about 84% of the year's heavy rain. The largest rainfall in history is 146.5 mm (July 28, 1914). The experimental area is surrounded by grasslands and pagoda wetland plants.

Data acquisition and processing

The EC technique can directly measure the water, heat, and CO_2 fluxes (Baldocchi et al., 2000) between the atmosphere and the earth's surface in the atmospheric boundary layer, of which the basic principle is to use atmospheric turbulence theory to collect CO_2 concentration, water vapor content, temperature, horizontal wind speed and vertical wind speed, and then to determine the CO_2 and water and heat fluxes between the surface and the atmosphere via statistical analysis of the data. The specific analysis process (Wang, 2012) is: within a certain average period, the turbulent transport flux of a scalar x is described by *Equation 1:*

$$Q_x = \overline{w\,(\rho x)} = \rho\,\overline{wx} \quad \text{(Eq.1)}$$

where the over-line indicates the time average; w is the vertical wind speed (m/s); ρ is the air density (kg/m^3), which is generally set to be constant within the average time period taken. Through Reynolds decomposition, each quantity is divided into two parts: average volume and pulse volume, as described in *Equations 2* and *3:*

$$w = \bar{w} + w' \quad \text{(Eq.2)}$$

$$x = \bar{x} + x' \quad \text{(Eq.3)}$$

Supposing that the time average of vertical wind speed is 0, that is, $\bar{w} = 0$

$$Q_x = \rho\,\bar{w}\bar{x} + \rho\,\overline{w'x'} = \rho\,\overline{w'x'} \quad \text{(Eq.4)}$$

Then CO_2 flux (F_C, mg•m^{-2}•s^{-1}), SHF (H, W/m^2) and LHF (LE, W/m^2) can be expressed as in *Equations 5, 6* and *7:*

$$F_C = \rho\,\overline{w'C'} \quad \text{(Eq.5)}$$

$$H = C_P\rho\,\overline{w'T'} \quad \text{(Eq.6)}$$

$$LE = \lambda\,\rho\,\overline{w'q'} \quad \text{(Eq.7)}$$

where is the CO_2 concentration fluctuating value (kg/kg); C_P is the air constant-pressure specific heat (J•kg^{-1}•K^{-1}), the general value is 1004.7 J•kg^{-1}•K^{-1}; T' is the ultrasonic virtual temperature fluctuation value (°C); λ is the latent heat of evaporation (J/kg); q' is the water vapor concentration (specific humidity) fluctuating value (kg/kg). ρ and λ are respectively calculated by the following formulas:

$$\rho = 100 \times \frac{P}{287.1 \times (T_a + 273.15) \times (1 + 0.61 \times q)} \quad \text{(Eq.8)}$$

$$\lambda = (2.501 - 0.00237 \times T_0) \times 10^6 \quad \text{(Eq.9)}$$

http://www.aloki.hu ● ISSN 1589 1623 (Print) ● ISSN 1785 0037 (Online)
DOI: http://dx.doi.org/10.15666/aeer/1705_1047510490

In *Equations 8* and *9,* P indicates the atmospheric pressure (hPa); T_a indicates the temperature (°C); T_0 indicates the surface temperature (°C).

In the actual calculation, the data first needs to be corrected (Webb et al., 1980; Wilczak et al., 2001; Finnigan et al., 2003) by removing the outliers caused by environmental factors such as rain, snow, dust and unstable power supply; then by performing slope correction and frequency loss correction, ultrasonic virtual temperature (humidity effect) correction for SHF, WPL correction for LHF and CO_2 fluxes (air density pulsation correction). Meanwhile, quality control and evaluation (Foken and Wichura, 1996) must also be carried out, such as whether the working status of the sensor is normal, whether the instantaneous value or the mean value is within a reasonable threshold, etc., and the similarity and stability of the final products (mainly the individual fluxes) need to be checked.

The eddy covariance (EC) flux measurement system was employed in this research, including the 3D ultrasonic anemometer–thermometer (CSAT3, Campbell Scientific Inc., USA), the fast-response infrared gas analyzer (Li-7500, LI- COR Inc., USA), and the data collector (CR5000, Campbell Scientific Inc., USA) and preprocessor (Eddy Reprocessing, or EdiRe, University of Edinburgh, UK, http://www.geos.ed.ac.uk/research/micromet/EdiRe). The measurement system was installed at the end of June in 2015, at the southwest corner in the Wetland Botanical Garden, with a location of N 45°46'40.3", E 126°29'23.9". This measurement has an installation height of 10 m from the ground, with a data acquisition frequency of 10 Hz and a set average period of 30 min. The main vegetation species at the measurement site are *Labiatae* and *reed*. The final data used to conduct analysis was recorded from August 1, 2015 to December 31, 2016, with a duration of one and a half years.

Results

In order to promote the understanding of the dynamic change characteristics of wetland ecosystems, we analyzed the daily changes and seasonal changes of CO_2 flux, CO_2 concentration, SHF, LHF and Bowen ratio (ratio of SHF to LHF) of Jinhewan Wetland based on one-and-a-half EC flux measurements.

Characteristics of changes in water and heat fluxes

Characteristics of daily changes in water and heat fluxes

January, April, July and October were selected as the representative months of the year (in which the data took the average of the data for October 2015 and October 2016) to analyze the average monthly diurnal variation of water and heat fluxes near the underlying surface ecosystem of Jinhewan Wetland in spring, summer, autumn and winter, and SHF and LHF were put in a contrastive analysis by using the Bowen ratio (the absolute value of which reflects the strong and week relationship between the sensible and latent heat exchange), as shown in *Figure 2*.

Sensible heat refers to the heat exchange in the form of turbulence that occurs between the atmosphere and the underlying surface due to temperature changes. Heat is positive when it is transported from the underlying surface to the atmosphere, and vice versa. The daily changes of SHF of Jinhewan Wetland throughout the year show single-peaked features. Before 8:30 in the morning of January, SHF was always negative, which is because the surface temperature is lower than the atmosphere at night, and heat

http://www.aloki.hu ● ISSN 1589 1623 (Print) ● ISSN 1785 0037 (Online)
DOI: http://dx.doi.org/10.15666/aeer/1705_1047510490

is transported from the atmosphere to the ground. The heat supplied to the ground is offset by the amount of radiation on the ground, making the temperature difference between surface and atmosphere stable. Therefore, the SHF floats up and down at -10 W/m^2. As the sun rises, solar radiation appears and gradually increases, and the ground continues to heat up, the temperature difference between the surface and the atmosphere begins to decrease and the SHF gradually becomes larger; SHF becomes positive at around 9:00, indicating that the surface temperature begins to rise above the atmosphere, and sensible heat is transferred to the atmosphere from the ground; then SHF increases rapidly and peaks at 12:00, indicating that the temperature difference between the surface and atmosphere reaches a maximum, as a result, the transport of sensible heat from the ground to the atmosphere achieves the highest rate of about 50 W/m^2; then the SHF decreases sharply, because the surface radiation of high-temperature surface is strong, and the solar radiation weakens again, as a result, the surface temperature drops rapidly and approaches atmospheric temperature as soon as 16:00, and the SHF is about 0 W/m^2; as ground radiation continues to cool down the earth's surface, the surface temperature begins to fall below the atmosphere, and sensible heat is transported from the atmosphere to the ground. The flux is negative, and it stabilizes after 17:00, indicating that the monthly SHF is positive for about 7 h. Due to the difference in sun rise and fall times in different seasons, the time course of monthly SHF change in April and July was different from that in January, where SHF starts to increase slowly from a negative value at about 5:00, and becomes positive at about 6:00 when the sensible heat starts to be transported from the ground to the atmosphere; it also reaches its maximum at around 12:00, which is close to 150 W/m^2 and 80 W/m^2 respectively; SHF is reduced to 0 W/m^2 at 18:00, and maintains a stable state of small-scale fluctuations by approaching 19:00; these two representative monthly SHF takes 12 h to be transported from the ground to the atmosphere. The rise of SHF in October was similar to that in April and July, and the decline was in sync with January; the peak was around 90 W/m^2, indicating that the monthly SHF is positive for 9 h. It can be seen that Jinhewan Wetland has the shortest SHF time in winter and the lowest peak value, while in the spring and summer, the SHF diurnal variation is more synchronous, the positive and negative flux values have the equal time. The peak value of spring flux is the highest, and the positive duration of SHF in autumn is slightly longer than in winter, and the peak value is close to summer, which is in the middle of the peak of the four seasons' flux.

Latent heat mainly refers to the heat energy absorbed or released from one phase to another by water under isothermal pressure conditions. When LHF is greater than 0 W/m^2, it mainly absorbs heat through soil evaporation and vegetation transpiration. When LHF is less than 0 W/m^2, heat is released mainly through dew, frost, and icing. The daily changes of LHF of Jinhewan Wetland in the four seasons also have a single-peaked feature, except that the feature is not significant in January. In January, in addition to the increase in LHF from about 0 W/m^2 to 10 W/m^2 in peak value between 10:00 and 16:00, it is reduced to 0 W/m^2, and LHF fluctuates up and down around 0 W/m^2 in 3/4 time of the entire day/night. In the other three representative months, LHF is greater than 0 W/m^2. Among them, LHF increases rapidly from 6:00 in April and October, reaching the peak 160 W/m^2 and 110 W/m^2 at 13:00, and then continues to decrease, and basically maintains between 20 W/m^2-40 W/m^2 from 20:30. July increases from 3:30 and peaks at around 220 W/m^2 before 13:00, and it also begin to fluctuate around 30 W/m^2 at 20:30. The results show that Jinhewan Wetland not only

http://www.aloki.hu ● ISSN 1589 1623 (Print) ● ISSN 1785 0037 (Online)
DOI: http://dx.doi.org/10.15666/aeer/1705_1047510490

transports water from the atmosphere to the ground during the night in winter, but also transports it from the ground to the atmosphere through evapotranspiration, indicating the strong water cycle characteristics of wetlands. In addition, the evapotranspiration is relatively weak in winter and is strong in spring and autumn, and during the summer daytime, due to the higher temperature, the evaporation of soil moisture can be promoted, and the vegetation also reduces its own temperature by enhancing transpiration, so the underlying surface evapotranspiration plays the most important role.

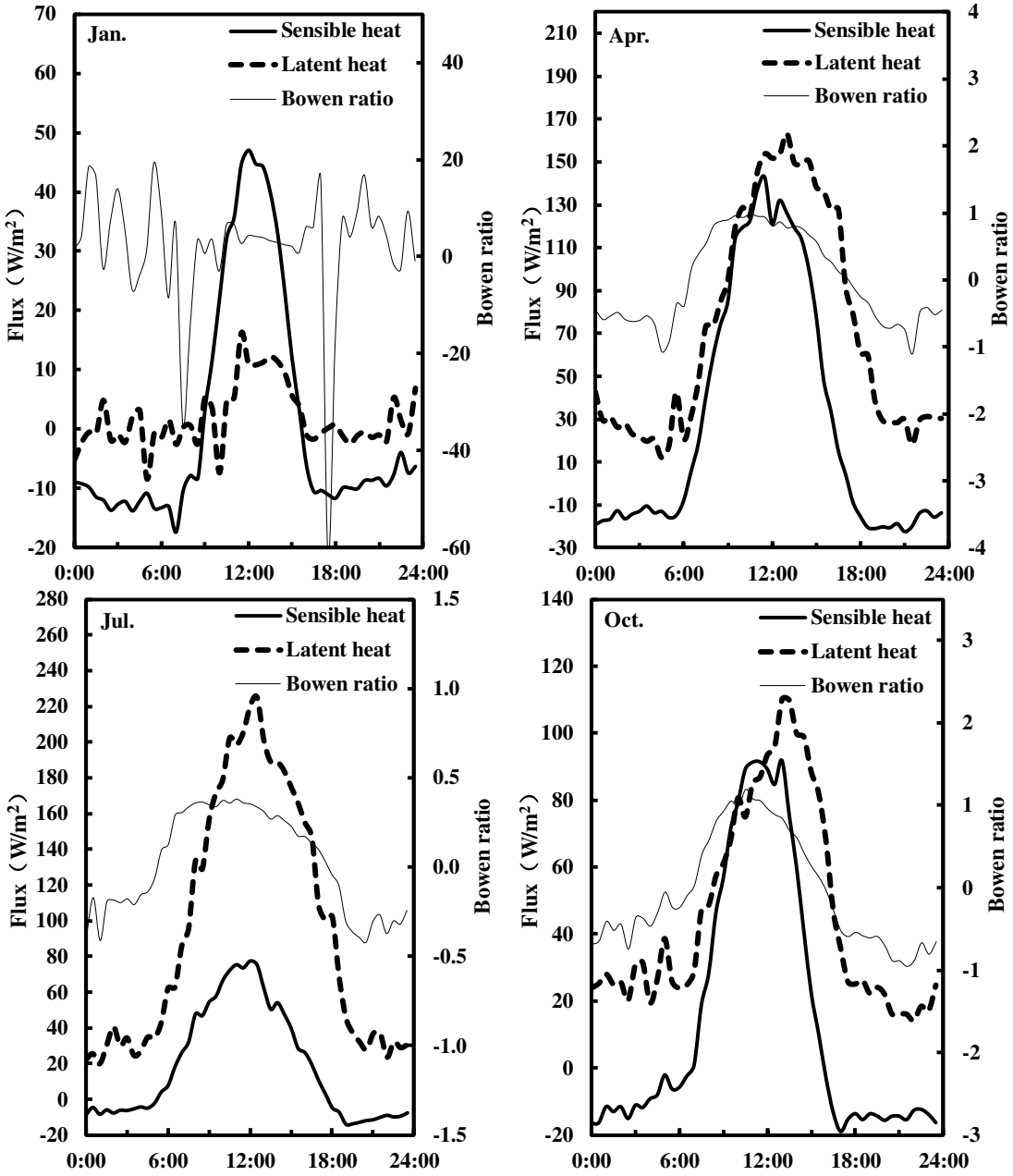

Figure 2. *Diurnal variation of monthly averaged water and heat fluxes in representative months from different seasons in Jinhewan Wetland*

http://www.aloki.hu ● ISSN 1589 1623 (Print) ● ISSN 1785 0037 (Online)
DOI: http://dx.doi.org/10.15666/aeer/1705_1047510490

By analyzing the size of the Bowen ratio, the SHF and LHF at any time during the average monthly diurnal variation (without considering the energy transfer direction of the sensible heat and the latent heat, only considering the size of the flux) are compared. LHF is less than SHF only in January, and because LHF is very small and even less than 1 W/m^2, the fluctuation of the Bowen ratio (absolute value) in January is relatively large. Without considering extreme cases, the range of variation is 1-20. LHF is almost always greater than SHF during the monthly diurnal variation in spring, summer and autumn. Among them, in April and October, the Bowen ratio (absolute value) fluctuates in the range of 0-1 (except that LHF is slightly smaller than SHF at some time in October, and the Bowen ratio is within 1-1.1). The overall difference between LHF and SHF is relatively small. Bowen ratio (absolute value) is greater than 0.5 about 65% of the time, the two are almost equal especially between 9:00-12:00, and the Bowen ratio is above 0.92. In July, the fluctuation range of Bowen ratio (absolute value) is only 0-0.5, and LHF is much larger than SHF.

Seasonal changes in water and heat fluxes

According to the observations of Jinhewan Wetland from August 2015 to December 2016, the daily average water and heat fluxes were calculated, and seasonal variations of water and heat fluxes were analyzed according to the annual change process. *Figure 3a, b,* and *c* show the change of annual mean value of the sensible heat, latent heat, and Bowen ratio, respectively.

Over the nearly one-and-a-half-year observation period, the average daily SHF ranged from -49.97 to 90.63 W/m^2, and the annual average daily change was smaller (see *Fig. 3a*). Daily SHF averaged 13.78 W/m^2; in the winter (December-February), the average was the lowest, only 3.57 W/m^2; in the spring (March-May), the average was the highest, reaching 19.13 W/m^2; in the summer and autumn (June-August and September-November, respectively), the average daily SHF average was mediate, with summer slightly higher than autumn, at 18.65 W/m^2, and the autumn average was close to the average during the observation period, which was 14.71 W/m^2.

Average daily LHF fluctuated more intensively, ranging from -12.28 W/m^2 to 213.40 W/m^2 (see *Fig. 3b*). The average value over a one-year observation period was 50.27 W/m^2; Characteristics of daily average LHF was the same as SHF in winter, only 3.87 W/m^2, which is far lower than the average of the other three seasons; the summer average was as high as 91.40 W/m^2; average daily LHF during the spring and autumn determines the average value of the observation period, and it was always fluctuating around 50 W/m^2; seasonal averages were 70.88 W/m^2 and 42.77 W/m^2, respectively.

Dividing the daily average SHF by the daily average LHF, we can get the annual variation of the daily scale Bowen ratio during the observation period (see *Fig. 3c*). Except for the late autumn period (from November 13 to November 30 for 2015 and 2016) and winter, and due to the continuous fluctuation of the daily average LHF around 0 W/m^2, the Bowen ratio varied greatly and changed narrowly within -3.08-3.33 for most of the spring, summer and autumn. Bowen ratio not only varied greatly in winter, but also fluctuated drastically, with only 30% of the time ranging from -1 to 1, indicating that the daily average SHF in winter is generally greater than the daily average LHF; while in the summer Bowen ratio ranged from -0.40 to 0.68, the daily average LHF was not only larger than the daily average SHF, but also at least 1.47 times that of the latter; in the spring and autumn, the daily average LHF was usually greater than the daily average SHF, with 70% of the time Bowen ratio ranging from -1 to 1.

http://www.aloki.hu ● ISSN 1589 1623 (Print) ● ISSN 1785 0037 (Online)
DOI: http://dx.doi.org/10.15666/aeer/1705_1047510490

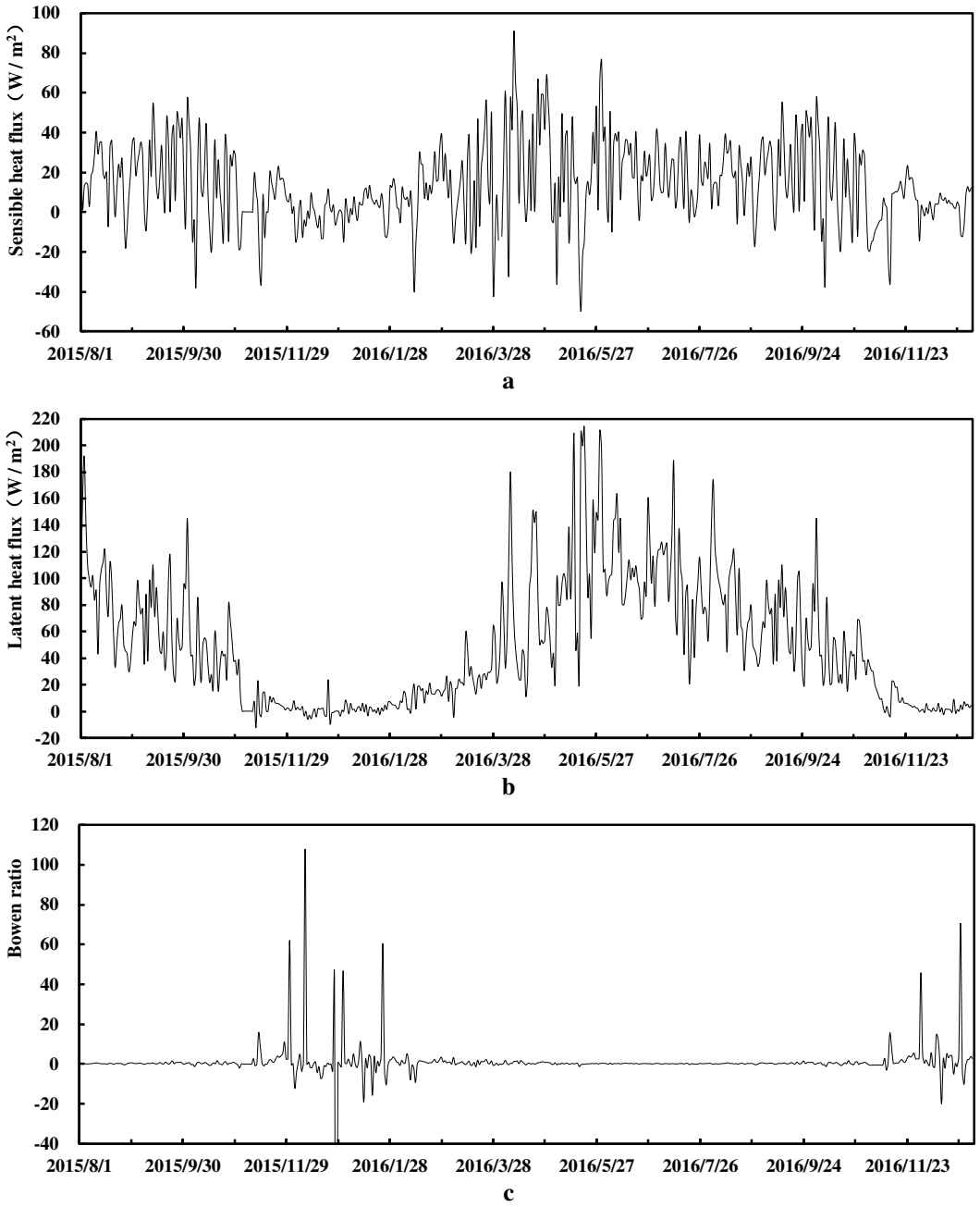

Figure 3. *Annual daily average change of Jinhewan Wetland sensible heat flux (a), latent heat flux (b) and Bowen ratio (c) during August 2015–December 2016*

Characteristics of CO_2 flux change

Figure 4 shows the average monthly diurnal variation and the average daily diurnal variation of the Jinhewan Wetland CO_2 flux in January and July. When the CO_2 flux is negative, it indicates that the surface absorbs CO_2 from the atmosphere due to photosynthesis and other reasons; when it is positive, it indicates that the surface releases CO_2 into the atmosphere under the effects of vegetation and soil microbial respiration. As can be seen from the figure, the CO_2 flux has the diurnal variation characteristics of the single-valley character. Due to the lack of sunlight at night, the

http://www.aloki.hu ● ISSN 1589 1623 (Print) ● ISSN 1785 0037 (Online)
DOI: http://dx.doi.org/10.15666/aeer/1705_1047510490

vegetation cannot absorb CO_2 via photosynthesis, instead they release CO_2 through stable respiration of vegetation and soil microorganisms, therefore the nighttime CO_2 flux is greater than 0 mg/(m^2•s) with little change. Jinhewan Wetland shows weak carbon source attribute, which fluctuates around 0.02 mg/(m^2•s) in January, and shows strong respiration with vigorous vitality of vegetation, and CO_2 flux fluctuates around 0.10 mg/(m^2•s); average annual CO_2 flux at night is about 0.05 mg/(m^2•s) and the maximum is 0.08 mg/(m^2•s). After sunrise, the vegetation begins to undergo photosynthesis, and as the sunlight increases, the photosynthesis intensity also slowly increases. The CO_2 absorption rate increases from 0 mg/(m^2•s) and gradually equals the release rate, and its flux begins to decrease and approach 0 mg/(m^2•s) step by step, which drops to 0 mg/(m^2•s) before 10:00 and 5:30 in January and July, and drops to 0 mg/(m^2•s) before 6:30 on an annual average. As sunlight becomes stronger, the rate of CO_2 absorption by vegetation through photosynthesis is greater than the release rate, and the CO_2 flux becomes negative and decreases. Jinhewan Wetland begins to play a carbon sink role; at noon time, the sunlight reaches the strongest and CO_2 flux reaches the least value, which reduce to -0.05 mg/(m^2•s) and -0.41 mg/(m^2•s) in January and July, respectively, and the average annual minimum flux is -0.13 mg/(m^2•s). As the sunlight weakens in the afternoon, photosynthesis is weakened and the CO_2 absorption rate begins to decrease. When it is again equal to the rate of CO_2 release, the flux turns to 0 mg/(m^2•s) again, reaching 0 mg/(m^2•s) after 15:00 and 18:00 in January and July, and averaging 0 mg/(m^2•s) after 17:30 on a yearly basis. Photosynthesis continues to weaken until it stops, and the respiration of vegetation and soil microorganisms begins to dominate. CO_2 flux increases again and becomes positive after being stable. In general, Jinhewan Wetland has a carbon sink function only 5 h a day in winter, and the CO_2 absorption rate is within 0.05 mg/(m^2•s). In summer, the carbon sink function is slightly stronger and it plays a carbon sink role for about 13 h per day. Absorption rate is relatively high, up to 0.41 mg/(m^2•s); the annual average carbon sink function is 11 h a day, and CO_2 absorption rate is up to 0.13 mg/(m^2•s), less than half of the highest absorption rate of Panjin wetland (0.3 mg/(m^2•s) (Wang and Zhou, 2006) that has the reputation of "the capital of wetlands".

To analyze the seasonal variation characteristics of CO_2 flux, CO_2 flux data with a time step of 30 min was taken for a 6 h sliding average treatment (as shown in *Fig. 5*). In the non-growing season of vegetation (from late autumn to early spring, approximately from November to March of the following year), CO_2 flux (absolute value) was small and it was greater than 0 in most of the time, indicating that vegetation photosynthesis was weak or even absent from photosynthesis during this period, atmospheric carbon exchange process is achieved mainly through vegetation and soil respiration. In the growing season of vegetation, the amplitude of CO_2 flux increased. In particular, during vigorous growth periods (July and August), vegetation has the most intense life activities: intense photosynthesis during the day brings rapid absorption of CO_2 and a large negative value of CO_2 flux; at night, vegetation respiration was also strong, and the release rate of CO_2 was also large. Regardless of whether CO_2 is transported from the atmosphere to the surface during the day or when CO_2 is transported from the surface to the atmosphere at night, the CO_2 flux during the vigorous growth of vegetation is higher than at the initial stage of growth (April to June) or at the end of growth (September and October), while the CO_2 flux in the growing season was higher than that in the non-growing season, and the change pattern of the year coincided with the vegetation growth trend.

http://www.aloki.hu ● ISSN 1589 1623 (Print) ● ISSN 1785 0037 (Online)
DOI: http://dx.doi.org/10.15666/aeer/1705_1047510490

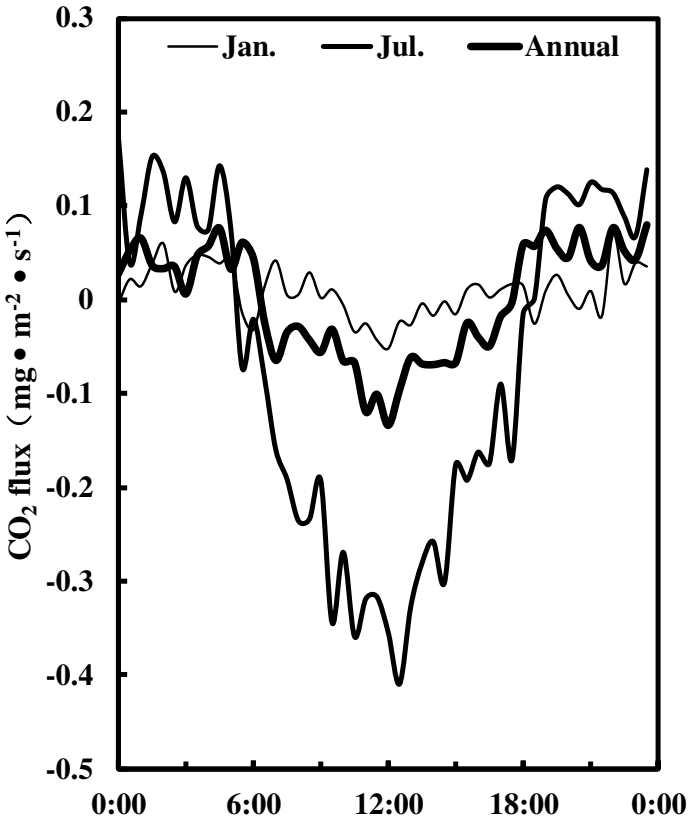

Figure 4. *Diurnal variation of monthly and yearly averaged CO_2 flux in Jinhewan Wetland*

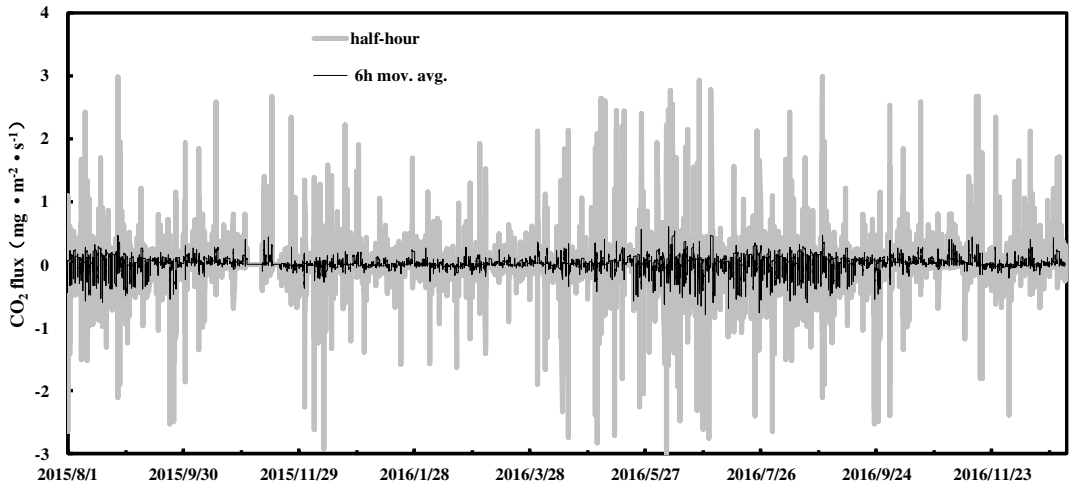

Figure 5. *Annual change process of Jinhewan Wetland CO_2 flux during August 2015–December 2016*

Characteristics of CO_2 concentration changes

The average monthly diurnal variation of the Jinhewan Wetland CO_2 concentration in January and July showed a single-peak and single-valley character (see *Fig. 6*). As a carbon source, the CO_2 flux of Jinhewan Wetland at night was always greater than 0 mg/(m^2•s), and near-surface CO_2 concentrations continued to accumulate, showing an

http://www.aloki.hu ● ISSN 1589 1623 (Print) ● ISSN 1785 0037 (Online)
DOI: http://dx.doi.org/10.15666/aeer/1705_1047510490

upward trend. After sunrise, with the CO_2 absorption from the photosynthesis of vegetation, when the CO_2 flux approaches 0 mg/(m^2•s), the concentration peaks: reaching 720 mg/m^3 at 8:00 in January, and 670 mg/m^3 at 4:30 in July, with an annual average peak value of 700 mg/m^3. As the CO_2 flux became negative, the wetland began to function as a carbon sink and the CO_2 concentration began to decrease. When the CO_2 flux increased to 0 mg/(m^2•s) due to the weakening of sunlight, the CO_2 concentration dropped to the bottom: reaching 670 mg/m^3 and 590 mg/m^3 around 16:00 in January and July, with an annual average of 650 mg/m^3. Then the CO_2 flux became positive and remained stable, so the concentration began to rise again. The difference between the peak value and bottom value of CO_2 concentration in July was greater than that in January, indicating that the photosynthesis and respiration of vegetation in summer had greater impact on CO_2 concentration than in winter. In summer, not only photosynthesis was strong from the strong sunlight, but vegetation was also in the growing season, with strong vitality and respiration.

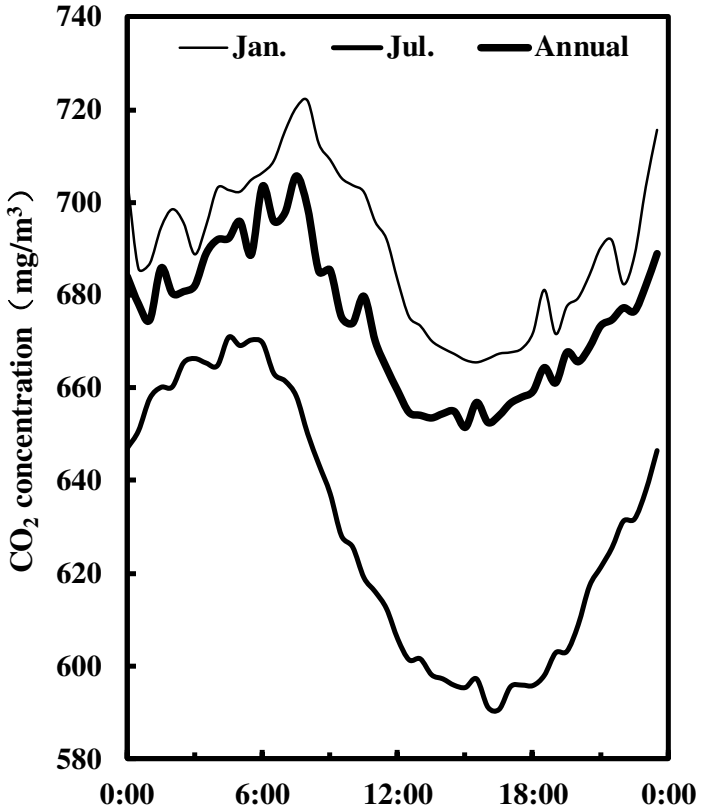

Figure 6. *Annual diurnal variation process of Jinhewan Wetland CO_2 concentration*

The seasonal variation characteristics of the CO_2 concentration is analyzed based on its 6 h rolling average data (see *Fig. 7*). The average CO_2 concentration during the observation period was 679.45 mg/m^3. Among them, the average CO_2 concentration during the vigorous growth period of vegetation was only 655.97 mg/m^3, and the CO_2 concentration was relatively stable, basically fluctuating within the range of 500-800 mg/m^3; while the average value of CO_2 concentration in other periods was 684.86 mg/m^3, with intense fluctuation and a maximum of 2000 mg/m^3.

http://www.aloki.hu ● ISSN 1589 1623 (Print) ● ISSN 1785 0037 (Online)
DOI: http://dx.doi.org/10.15666/aeer/1705_1047510490

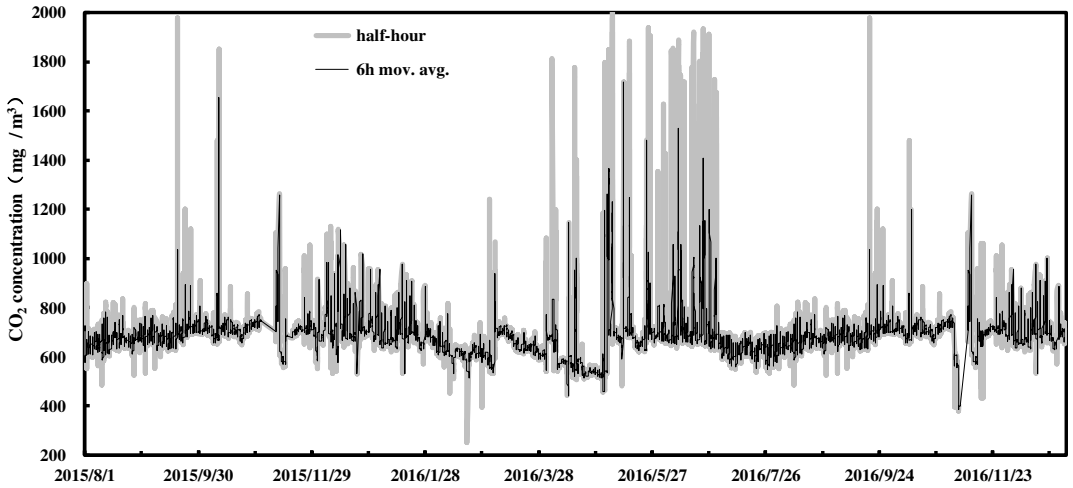

Figure 7. *Annual change process of Jinhewan Wetland CO2 concentration during August 2015–December 2016*

Discussion and conclusion

The material and energy exchange process on the ground-air interface of the cold zone wetland ecosystem in northeast China plays an important role in its climate change research and eco-protection. Jinhewan Wetland, as an example of Harbin's key ecological wetland for the protection and restoration of aquatic ecosystems, uses the EC flux measurement system to conduct long-term continuous flux observations. Based on the one-and-a-half year flux observations, this study initially analyzed the dynamic change characteristics of Jinhewan Wetland's water, heat, and CO_2 fluxes.

The SHF, LHF and Bowen ratio of Jinhewan Wetland basically has the characteristics of single-peaked diurnal variation; in summer, LHF is generally higher than in the other three seasons due to the highest temperature and strongest evapotranspiration; in spring, SHF is usually the largest because summer vegetation is in the vigorous growing period when most of the net radiation is consumed by strong evapotranspiration of vegetation, so SHF is smaller in summer than in spring; in case of the same season, LHF is smaller than SHF in winter, and LHF is almost always greater than SHF in the other three seasons; the two has the biggest difference in summer.

The diurnal variations of CO_2 flux and concentration show a single-valley character and a single-peak and single-valley character respectively. The annual average diurnal variation of flux shows that the daily maximum absorption rate of CO_2 is only 0.13 mg/(m^2•s), which is far less than the Panjin wetland and carbon sequestration has not been fully exerted. There may be two reasons. On the one hand, the Panjin Wetland has a warm temperate monsoon climate, where the temperate of Jinhewan Wetland in the mid-temperate zone is relatively cold. On the other hand, the Panjin Wetland meets the needs of the public for citizen activities by making small areas of land hardening based on natural plow fields and artificial paddy fields. While Jinhewan Wetland, with a higher degree of artificiality, takes into account the needs of the citizens for leisure and entertainment and their landscape functions, thus the green land area is relatively small and the vegetation coverage is low. In view of Jinhewan Wetland's weak carbon sink function, investment in vegetation construction can be increased and the potential for carbon sequestration in wetland ecosystems can be fully tapped. The annual change process of the flux is consistent with the vegetation growth trend, the more vigorous the

http://www.aloki.hu ● ISSN 1589 1623 (Print) ● ISSN 1785 0037 (Online)
DOI: http://dx.doi.org/10.15666/aeer/1705_1047510490

vegetation growth, the greater the flux (absolute value), and the annual change process of the concentration is just the opposite. The dynamic change characteristics of Jinhewan Wetland's flux are similar to flux changes in forest, grassland, and farmland ecosystems (Song et al., 2004; Liu et al., 2006; Wang et al., 2009).

The preliminary analysis results show that Jinhewan Wetland has a large room for the improvement of water-heat cycle and carbon sink function, and can further promote its role in the water-heat cycle and carbon sink function by strengthening vegetation construction and expanding the green area. Many factors such as undulating terrain, unfavorable weather conditions will affect the accuracy of flux measurement results by using EC technique (Massman and Lee, 2002), and to some extent hinder the application of the EC technique. However, the study area is flat and the elevation difference is only 5 m. During the monitoring period, the temperature in the area was between -30 and 30 °C, and the highest monthly precipitation was 154 mm, with no adverse weather such as extreme temperatures and precipitation. Therefore, the effects of topography and climate in this study can be ignored (Eda et al., 2016; Evadzi et al., 2017; Kuang et al., 2017; Liu, 2018; Meng et al., 2018).

The material and energy exchange process on the ground-air interface plays an important role in its climate change research and eco-protection. Jinhewan Wetland, as an example of Harbin's key ecological wetland for the protection and restoration of aquatic ecosystems, by conducting long-term continuous monitoring on it, using ground-based fixed-point observation data and combining large-scale remote-sensing data, it is possible to achieve scale conversion of flux data from ground-based observations to surface mean values, thereby providing technical support for regulating regional microclimates, preventing soil erosion and protecting ecological environment (Wani et al., 2018).

Acknowledgements. This work was supported by the Natural Science Foundation of China under Project No. 51409103, No. 51379079 and No. 51809093 and PhD Research Initiation Project of North China University of Water Resources and Electric Power No. 201904001.

REFERENCES

[1] Baldocchi, D. (2003): Assessing the eddy covariance technique for evaluating carbon dioxide exchange rates of ecosystems: past, present and future. – Global Change Biology 9: 479-492.

[2] Baldocchi, D., Finnigan, J., Wilson, K., et al. (2000): On measuring net ecosystem carbon exchange over tall vegetation on complex terrain. – Boundary-Layer Meteorology 96: 257-291.

[3] Baldocchi, D., Falge, E., Gu, L., et al. (2001): FLUXNET: a new tool to study the temporal and spatial variability of ecosystem scale carbon dioxide, water vapor and energy flux densities. – Bulletin of the American Meteorological Society 82: 2415-2434.

[4] Brix, H., Sorrell, B. K., Lorenzen, B. (2001): Are Phragmites-dominated wetlands a net source or net sink of greenhouse gases? – Aquatic Botany 69: 313-324.

[5] Cao, S., Cao, G., Feng, Q., et al. (2017): Alpine wetland ecosystem carbon sink and its controls at the Qinghai Lake. – Environmental Earth Sciences 76(5): 210.

[6] Chen, C., Cleverly, J., Zhang, L., et al. (2016): Modelling seasonal and inter-annual variations in carbon and water fluxes in an arid-zone acacia savanna woodland, 1981–2012. – Ecosystems 19(4): 625-644.

[7] Chen, G. Q. (1996): Marsh in Sanjiang Plain. – Science Press, Beijing, pp. 165-168.

http://www.aloki.hu ● ISSN 1589 1623 (Print) ● ISSN 1785 0037 (Online)
DOI: http://dx.doi.org/10.15666/aeer/1705_1047510490

[8] Duman, T., Schäfer, K. V. R. (2018): Partitioning net ecosystem carbon exchange of native and invasive plant communities by vegetation cover in an urban tidal wetland in the New Jersey Meadowlands (USA). – Ecological Engineering 114: 16-24.
[9] Eda, M., Lu, P., Kikuchi, H., et al. (2016): Reevaluation of early holocene chicken domestication in northern China. – J Archaeol Sci 67: 25-31.
[10] Edwards, G. C., Dias, G. M., Thurtell, G. W., et al. (2001): Methane fluxes from a wetland using the flux-gradient technique. The measurement of methane flux from a natural wetland pond and adjacent vegetated wetlands using a TDL-based flux-gradient technique. – Water Air and Soil Pollution 1: 447-454.
[11] Evadzi, P. I. K., Zorita, E., Huenicke, B. (2017): Quantifying and predicting the contribution of sea-level rise to shoreline change in Ghana: information for coastal adaptation strategies. – J Coastal Res 33(6): 1283-1291.
[12] Finnigan, J. J., Clement R., Malhi Y., et al. (2003): A re-evaluation of long-term flux measurement techniques, Part I: averaging and coordinate rotation. – Boundary Layer Meteorology 107(1): 1-48
[13] Foken, T., Wichura, B. (1996): Tools for quality assessment of surface based flux measurements. – Agricultural and Forest Meteorology 78: 83-105.
[14] Gao, J. Q., Xu, X. L., Zhang, F. (2008): Distribution characteristics of soil labile carbon along water table gradient of alpine wetland soils. – Journal of Soil and Water Conservation 22(3): 126-131.
[15] Guo, H. Q., Noormets, A., Zhao, B., et al. (2009): Tidal effects on net ecosystem exchange of carbon in an estuarine wetland. – Agricultural and Forest Meteorology 149: 1820-1828.
[16] Hao, Y. B., Cui, X. Y., Wang, Y. F., et al. (2011): Predominance of precipitation and temperature controls on ecosystem CO2 exchange in zoige alpine wetlands of Southwest China. – Wetlands 31(2): 413-422.
[17] He, Q. J., Zhou, G. S., Zhou, L. (2006): A comparative study of calculation methods for water and heat fluxes in Phragmites wetland in Panjin. – Journal of Meteorology and Environment 22(4): 35-41.
[18] Heinsch, F. A., Heilman, J. L., Mcinnes K. J., et al. (2004): Carbon dioxide exchange in a high marsh on the Texas Gulf Coast: effects of freshwater availability. – Agricultural and Forest Meteorology 125(1): 159-172.
[19] Hutley, L. B., Leuning, R., Beringer, J., et al. (2005): The utility of the eddy covariance techniques as a tool in carbon accounting: tropical savanna as a case study. – Australian Journal of Botany 53(7): 663-675.
[20] Kang, X., Hao, Y., Li, C., et al. (2011): Modeling impacts of climate change on carbon dynamics in a steppe ecosystem in Inner Mongolia, China. – Journal of Soils and Sediments 11(4): 562-576.
[21] Kayranli, B., Scholz, M., Mustafa, A., et al. (2010): Carbon storage and fluxes within freshwater wetlands: a critical review. – Wetlands 30: 111-124. https://doi.org/10.1007/s13157-009-0003-4.
[22] Kuang, Y., Qu, X., Yan, Y. (2017): Will higher traffic flow lead to more traffic conflicts? A crash surrogate metric based analysis. – Plos One 12(e01824588).
[23] Liu, C. M., Yu, H. N. (1997): Experimental Study on Moisture Movement in Soil-Crop-Atmosphere System. – Meteorological Press, Beijing, pp. 1-17.
[24] Liu, H. Z., Tu, G., Dong, W. J., et al. (2006): Diurnal variation and seasonal variation of water vapor and carbon dioxide fluxes at the ground-atmosphere interface in the semi-arid region. – Chinese Journal of Atmospheric Sciences 30(1): 108-118.
[25] Liu, Z. (2018): Economic analysis of methanol production from coal/biomass upgrading. – Energ Source Part B 13(1): 66-71.
[26] Massman, W. J., Lee, X. (2002): Eddy covariance flux corrections and uncertainties in long term studies of carbon and energy exchanges. – Agricultural and Forest Meteorology 113: 121-144.

http://www.aloki.hu ● ISSN 1589 1623 (Print) ● ISSN 1785 0037 (Online)
DOI: http://dx.doi.org/10.15666/aeer/1705_1047510490

[27] Meng, L., Zhong, Y., Wang, Z., et al. (2018): Supergravity separation for Cu recovery and precious metal concentration from waste printed circuit boards. – ACS Sustain Chem Eng 6(1): 186-192.
[28] Nahlik, A. M., Fennessy, M. S. (2016): Carbon storage in US wetlands. – Nature Communications 7: 13835.
[29] Roland, B. S. (1991): An Introduction to Boundary Layer Meteorology. – China Meteorological Press, Beijing.
[30] Shen, Y., Liu, Y. F., Wang, Y. (2005): Application progress of eddy correlation method for calculating hydrothermal and CO2 fluxes at home and abroad. – Journal of Nanjing Institute of Meteorology 28(4): 560-566.
[31] Shoemaker, W. B., Anderson, F., Barr, J. G., et al. (2015): Carbon exchange between the atmosphere and subtropical forested cypress and pine wetlands. – Biogeosciences 12(8): 2285-2300.
[32] Smith, L. C., MacDonald, G. M., Velichko, A. A., et al. (2004): Siberian peatlands a net carbon sink and global methane source since the early Holocene. – Science 303(5656): 353-356.
[33] Song X., Liu, Y. F., Xu, X. F., et al. (2004): Observation and analysis of carbon, water, and heat fluxes in planted forests in the hilly region of the red earth during winter and spring. – Resource Science 26(3): 98-104
[34] Wang, C., Yuan, R. M., Luo, T., et al. (2013): Comparison of near-surface flux observations in urban and suburban areas of Nanjing. – Journal of China University of Science and Technology 43(2): 87-96.
[35] Wang, H. Y., Zhou, G. S. (2006): Long-term flux observation of reed ecosystem in Panjin wetland. – Journal of Meteorology and Environment 22(4): 18-24
[36] Wang, J. M. (1999): Land surface process experiments and ground-air interaction studies: from HEIFE to IMGRASS and GAME-Tibet/TIPEX. – Plateau Meteorology 18(3): 280-294.
[37] Wang, J. M. (2012): Eddy-Related Flux Observation Instruction Manual. https://wenku.baidu.com/view/890bdd52f01dc281e53af0d3.html
[38] Wang, W. Z., Xu, Z. W., Liu, S. M., et al. (2009): Analysis of characteristics of water and heat flux in different underlying surfaces in the Heihe River Basin. – Advances in Earth Science 24(7): 714-723.
[39] Wani, S. A., Najar, G. R., Akhter, F. (2018): Characterization of available nutrients that influence pear productivity and quality in Jammu and Kashmir, India. – J Environ Biol 39(1): 37-41.
[40] Webb, E. K., Pearman, G. I., Lenning, R. (1980): Correction of flux measurements for density effects due to heat and water vapour transfer. – Quarterly Journal of the Royal Meteorological Society 106: 85-100. DOI: 10.1002/qj.49710644707.
[41] Wilczak, J. M., Oncley, S. P., Stage, S. A. (2001): Sonic anemometer tilt correction algorithms. – Boundary-Layer Meteorology 99(1): 127-150.
[42] Xu, Z. W., Liu, S. M., Gong, L. J., et al. (2008): Processing and quality evaluation of observational data of eddy covariance instrument. – Advances in Earth Science 23(4): 357-370.
[43] Yang, Q., Lyu, X. G. (1999): A preliminary study on the dynamic changes of soil respiration in the wetland ecosystem of the Sanjiang Plain. – Journal of Soil 30(6): 254-256.
[44] Zheng, N. (2013): The Turbulence Theory Analysis of the sensible Heat Flux in Forest Ecosystems Accurately Measured by the Scintillation Method. – Chinese Academy of Forestry, Beijing.

http://www.aloki.hu ● ISSN 1589 1623 (Print) ● ISSN 1785 0037 (Online)
DOI: http://dx.doi.org/10.15666/aeer/1705_1047510490

EFFECTS OF DIFFERENT FERTILISATION TECHNOLOGIES AND CULTIVATION TECHNOLOGY ON SOIL ORGANIC CARBON CONTENT

LIU, T.

College of Economics and Management, Nanjing Agricultural University, Nanjing 210095, China (e-mail: ysghge@163.com)

(Received 27th Sep 2018; accepted 16th Jul 2019)

Abstract. Due to the different stability of organic carbon with different protection mechanisms, the response and evolution of organic carbon components of yellow loam paddy soil to long-term fertilization was studied. Our aim was to study the effects of organic carbon on soil fertility from two aspects: fertilization treatment protection mechanism and tillage treatment protection mechanism. The long-term test site is located in an agricultural science research institute in a certain province of China. The fitting analysis found that the content of soil organic carbon and its components increased with time between 2006 and 2014 under the four fertilization protection mechanisms. Except for biochemical protection of organic carbon, the linear increase of the remaining components of organic carbon is more obvious than that of single fertilizer (NPK) treatment. Compared with traditional tillage treatment, the organic carbon contents have increased by 22.9% and 21.8% respectively, and the organic carbon reserves have increased by 21.8% and 16.7%, respectively. The carbon sequestration rates are 0.09 and 0.06 T $C \cdot hm^{-2} \cdot a^{-1}$. Unprotected free organic carbon is the largest part of organic carbon in soil, and is most sensitive to fertilization.

Keywords: *protection mechanism; organic matter, soil fertility, yellow soil, physical protection, chemical protection, biochemical protection*

Introduction

Soil organic carbon is one of the most active carbon pools in the Earth's surface system, and it plays the important role in regulating the physical, chemical and biochemical processes of soil. It is not only the indicator for assessing soil fertility, but also the important part of the global carbon cycle. Organic carbon with different protection mechanisms has different bioavailability and fertility effects (Herencia and Maqueda, 2016). The scientific basis for the assessment of soil carbon sequestration potential in farmland soils in Southwest China is provided by studying the changes in organic carbon composition of different protective mechanisms of yellow paddy soil with long-term fertilization (Ouyang et al., 2017; Wang et al., 2016; Zhang et al., 2015).

Kang Rifeng's analysis of long-term monitoring data of 17 national arable land in the black soil region of Northeast China shows that after 10-26 years of evolution, the organic matter content has increased overall, which is 33.9% higher than that before monitoring (Kintché et al., 2015). Hu Mingfang studied the evolution of soil organic carbon in double-crop paddy fields in Poyang Lake area under long-term fertilization (Kunlanit et al., 2014). The results show that the carbon content increases with the fertilization period under organic fertilizer treatment, which is consistent with Xu Minggang's research on the law of change of soil organic matter. The organic carbon reserves of 0-20 cm ploughed layer estimated by GATTINGER show that the cumulative rate of SOC (Soil organic carbon) is 0.24-0.46 $t \bullet hm^{-2} \bullet a^{-1}$. The evolution characteristics of organic carbon components in grey desert soils under different fertilization models analyzed by Li Sheng (Li et al., 2016) shows that the organic

http://www.aloki.hu ● ISSN 1589 1623 (Print) ● ISSN 1785 0037 (Online)
DOI: http://dx.doi.org/10.15666/aeer/1705_1049110507

carbon components show the significant increase trend under the long-term application of organic and inorganic fertilizers. In view of this, in accordance with the different solid-state mechanisms of organic carbon, the physical-chemical joint grouping method is proposed by the STEWART team to separate organic carbon into components of various protection mechanisms such as physical, chemical and biochemical protection. The role of soil micro-aggregates and minerals in the sequestration and transformation of organic carbon is emphasized, which provides the advanced method for the research on the changing characteristics of organic carbon and the transformation process.

At present, the research on the evolution characteristics of SOC under long-term fertilization mainly focuses on surface soil and particulate organic carbon, and has insufficient connection with SOC stability mechanism (Cruz Campas et al., 2017; Manjunatha et al., 2018). The differences and evolution characteristics of SOC components of different protection mechanisms are rarely noticed. Based on the previous work, the evolution characteristics of different stable organic carbons in time series are further revealed in this paper to explore their future trends.

As a sustainable agricultural technology, conservation tillage has far-reaching implications for improving soil fertility and carbon sequestration. SOC is the core material of soil nutrient cycling and fertility supply. The evolution law of the soil can reflect the difference of management measures. However, due to the obvious difference in carbon sequestration ability of different micro-aggregates in soil, the study on the evolution law of organic carbon is very important. At present, the research on farmland organic carbon at home and abroad mainly focuses on the protection mechanism of different tillage treatments (Amelian et al., 2018; Hu et al., 2017). The research on the law of soil organic carbon under the long-term tillage treatment protection mechanism needs to be strengthened.

Combined with long-term localization experiments and laboratory analysis, the physical-chemical of SOC combined grouping method is used to determine the content and distribution of unprotected organic carbon of free active, chemical protection and biochemically protection between micro-aggregates, and to analyze the role of soil micro-aggregates and mineral combinations in SOC sequestration and transformation. The change rate of organic carbon in yellow paddy soil with fertilization time and the effective of fertilization on improving SOC pool under different protection mechanisms are elucidated. At the same time, the carbon input and soil carbon sequestration of farmland under different tillage treatment mechanisms are analyzed, and the effects of long-term farming on the carbon reserves of 0-10 cm soil layer in farmland soil are discussed, these provide the reference for the improvement of soil fertility and the choice of carbon sequestration technology on the Loess Plateau.

Materials and methods

The general situation of the research area

The long-term test site is located in an agricultural science research institute in a certain province of China (106°39’52”E, 26°29’49”N). It is located in the hilly area of central Guizhou and has the subtropical monsoon climate with the average elevation of 1071 m and the average annual temperature of 15.3 °C, the annual average sunshine hours is about 1354 h, the relative humidity is 75.5%, the annual frost-free period is about 270 d, and the annual precipitation is 1100-1200 mm. The test site is yellow loess paddy soil, and the parent material is triassic limestone and sand shale weathering. It

http://www.aloki.hu ● ISSN 1589 1623 (Print) ● ISSN 1785 0037 (Online)
DOI: http://dx.doi.org/10.15666/aeer/1705_1049110507

began in 1995. In 1994, the basic soil samples were collected. The soil properties of the cultivated layer (0-20 cm) are: organic matter 31.15 g•kg^{-1}, total nitrogen 1.76 g•kg^{-1}, total potassium 13.84 g•kg^{-1}, alkali nitrogen 134.4 mg•kg^{-1}, available phosphorus 21.1 mg•kg^{-1}, available potassium 157.9 mg•kg^{-1}, and pH 6.6.

Methods

Experimental design

(1) Fertilization treatment

A ploughing field is selected as the experimental field. Before the experiment, the ploughing layer soil (0-20 cm) had a pH value of 8.70-9.10, and the conductivity is 0.362-0.702 dS/m, the mass fraction of organic carbon is 3.10-4.70 g/kg, the mass fraction of total nitrogen is 250-400 mg/kg, the mass fraction of organic phosphorus is 3.0-7.0 mg/kg, and the mass fraction of available potassium is 110.23 mg/kg. According to the needs, 5 fertilization treatments are selected from 11 treatment methods (Roy et al., 2018): control (CK), single application of chemical fertilizer (NPK), single application of organic fertilizer (M), low-level organic and inorganic fertilizer application (0.5MNPK) and the high amount of organic and inorganic fertilizers (MNPK) (Naab et al., 2015). The test uses the large-area comparison test with a plot area of 201 m^2 (35.7 m * 5.6 m) without repetition. The type of the applied organic fertiliser is: The chemical fertilizer is urea (including N 46%), superphosphate (including P_2O_5 16%), potassium chloride (including K_2O 60%); organic fertilizer contains C 413.8 g•kg^{-1}, N 2.7 g•kg^{-1}, P_2O_5 1.3 g•kg^{-1}, K_2O 6.0 g•kg^{-1}. The NPK treatment method is applied annually with N 165 kg•hm^{-2}, P_2O_5 82.5 kg•hm^{-2}, K_2O 82.5 kg•hm^{-2}, the annual application of organic fertilizer in the M treatment is 61.1 t•hm^{-2}; the amount of fertilizer applied by MNPK is the amount of fertilizer applied by M treatment plus NPK treatment. The amount of nitrogen applied by NPK treatment, M treatment, and 0.5MNPK treatment was the same (Qiu et al., 2014). The application amount of chemical nitrogen fertilizer is adjusted according to the nutrient content of organic fertilizer every year, as shown in *Table 1*. From 2002 to 2006, due to the destruction of the irrigation facilities at the test base, rice cultivation could not be satisfied and corn is replanted. The rice varieties planted are as follows: Jinma Stick (1995-1998), Nonghuhe (1999-2001), Xiangliangyou 875 (2007-2008), Yanyou United No. 2 (2009) and Maoyou 601 (2010-2014).

(2) Tillage treatment

The trial began in 1999 and the crop planted in the plot is rice. There are 4 treatments and 3 repetitions (Zhang et al., 2016). RT: When the rice is harvested, leave 10 cm, the straw and rice ears are taken away, and the soil is ploughed 20 cm after harvesting, and then simmered; NT: When the rice is harvested, leave 30 cm, and the remaining straw is threshed and left in the ground; SM: When the rice is harvested, leave 30 cm, and the remaining straw will be left in the ground after threshing. The soil will be separated by 60 cm and ploughed 30-35 cm after harvesting. CT: When rice is harvested, it leaves 10 cm, and the straw and rice ears are taken away. After harvesting, the soil is ploughed by 20 cm. Carry out the second ploughing, fertilize, simmer, and sow before planting. The fertilization amount of each treatment is N 150 kg•hm^{-2}, P_2O_5 105 kg•hm^{-2}, and K_2O 45 kg•hm^{-2}.

http://www.aloki.hu ● ISSN 1589 1623 (Print) ● ISSN 1785 0037 (Online)
DOI: http://dx.doi.org/10.15666/aeer/1705_1049110507

Table 1. *Annual amount of pure nutrient treatment in each treatment*

Handle	Stable manure ($t•hm^{-2}$)	N ($kg•hm^{-2}$)	P_2O_5 ($kg•hm^{-2}$)	K_2O ($kg•hm^{-2}$)
CK	0	0	0	0
NPK	0	165	82.5	82.5
0.5MNPK	30.6	165	81	224.6
M	61.1	165	79.4	366.6
MNPK	61.1	330	161.9	449.1

Collection of samples

Soil samples of 0-20 cm of ploughed soil in each district are collected in October 2014. The zones are equally divided into 3 plots (67 m^2), and each plot is uniformly distributed to collect 5 points to form the mixed sample, and 3 soil samples are collected from each plot. After removing the animal and plant residues, mix them. After the soil sample is air-dried, pass through the sieve with the pore size of 2 mm and set aside. The same method is used to collect soil samples for 2006, 2008, 2010 and 2012. They are air dried and sealed in the ziplock bag.

SOC grouping and measuring method

By referring to STEWART and other methods, SOC is divided into four carbon pools, which are free active organic carbon, physically protected organic carbon, chemically protected organic carbon and biochemically protected organic carbon (Wang et al., 2014). The specific operation steps are as follows.

The first step is to group the micro-aggregates: air dried soil samples over the 2 mm sieve are placed in the microaggregate separator and 30 glass beads having the diameter of 4 mm are added. After the separator is operated for 20 min, the component remaining on the 250 μm sieve is coarse particulate organic matter, and the free colloidal particles could pass through the 53 μm sieve. They are then centrifuged at 900 r/min and 3200 r/min for 7 min and 15 min, respectively, and d-Silt and d-C lay are obtained, respectively.

The second step is density grouping: the microaggregate fraction obtained in the first step is floated by 1.70 $g•cm^{-3}$ of sodium iodide, and the float is fine particulate organic matter. The recombinant part is dispersed in 5 $g•L^{-1}$ six sodium polyphosphate solution for 18 h, passed through the 53 μm sieve, and left on the sieve as physical protective organic matter. The particles smaller than 53 μm are then separated by centrifugation to obtain μ-Silt and μ-Clay.

The third step is the acid hydrolysis process: all the particles and cosmid fractions are refluxed for 16 h in 6 $mol•L^{-1}$ HCl at 95 °C less than 25 mL. The acid hydrolysis solution is filtered off, and the residue is the biochemical protective organic component (NH-Silt and NH-C lay). The acidolysis moiety is the difference between the full component and the non-acidolytic component, namely the chemically protected organic component (H-Silt and H-Clay).

The elemental analyzer (Lehman, EA3000) is used to determine the carbon content.

http://www.aloki.hu ● ISSN 1589 1623 (Print) ● ISSN 1785 0037 (Online)
DOI: http://dx.doi.org/10.15666/aeer/1705_1049110507

Calculation method

(1) Organic carbon reserve and micro-aggregate organic carbon reserve:

$$M_{soi1}=SOC\times BD\times H\times 10^{-1} \quad \text{(Eq.1)}$$

where M_{soi1} is the SOC reserve of 0-10 cm layer (t C•hm^{-2}); BD is the soil bulk density of 0-10 cm (g•cm^{-3}); H is the thickness of the soil layer, 10 cm;

$$M_i'=C_i\times SOC_i\times BD\times H\times 10^{-1} \quad \text{(Eq.2)}$$

where M_i' is organic carbon reserves of i-level micro-aggregates (t C•hm^{-2}); C_i is the relative mass fraction of the i-th micro-aggregates; SOC_i is the organic carbon content of the i-level micro-aggregates (g•kg^{-1}).

(2) The amount of straw carbon returned to the field and the amount of roots carbon returned to the field:

$$Y_{straw}=Y_{grain}\times\rho \quad \text{(Eq.3)}$$

where Y_{straw} is straw yield (t•hm-2); Y_{grain} is measured grain yield (t•hm-2); ρ is is straw grain ratio, taken 1.1.

$$Input-C_{straw}=Input-Y_{straw}\times C_{straw} \quad \text{(Eq.4)}$$

where $Input-C_{straw}$ is the amount of straw carbon returned to the field $Input-Y_{straw}$ is The amount of straw returned to the field. No-tillage and deep pine treatment are 100% of the yield, less tillage tradition and two sorghums is only 15% of the yield, and C_{straw} is the carbon content of the straw, which is 40%.

$$Y_{root}=\left(Y_{straw}+Y_{grain}\right)\times\alpha\times\beta \quad \text{(Eq.5)}$$

where α is the ratio of root to shoot, which is the ratio obtained after root exudates, and which is 0.6; β is the rate of returning to the roots, and the rate of returning the roots of 0-10 cm soil layer is 70%.

$$Input-C_{root}=Input-Y_{root}\times C_{root} \quad \text{(Eq.6)}$$

where C_{root} is the carbon content of the roots, which is 40%.

Data analyses

Data collation and mapping are performed using Excel 2016, and statistical analysis is performed using SPSS 24.0. All soil measurements are expressed as the average of 3 measurements. The least significant difference method (LSD) is used to test for differences between different fertilization treatments ($P < 0.05$) (Wentzel et al., 2015).

http://www.aloki.hu ● ISSN 1589 1623 (Print) ● ISSN 1785 0037 (Online)
DOI: http://dx.doi.org/10.15666/aeer/1705_1049110507

The average annual rate of change is expressed by the slope of the equation. The linear function is used to fit the relationship between the total organic matter and its components in the soil and the times of fertilization, and to test the significance of the equation.

Experiment analyses

From 2006 to 2014, the changes of soil organic carbon in the original yellow soil paddy soil are shown in *Figure 1*. Under the condition of long-term fertilizer, the changes of soil organic carbon components in yellow soil paddy soil are shown in *Figure 2*. According to the statistical results of *Figure 2,* the ratio of soil organic carbon to total organic carbon under long-term fertilizer conditions (5-year average) is given, as shown in *Figure 3*. *Figure 4* shows the increasing trend of total soil organic carbon content under long-term fertilizer conditions.

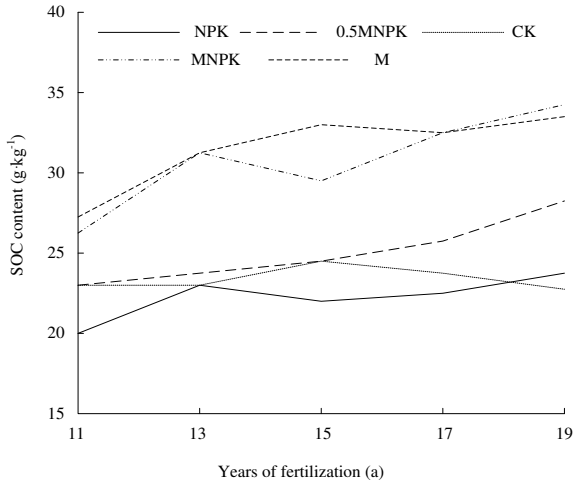

Figure 1. *Changes of soil organic carbon in yellow soil paddy soil from 2006 to 2014*

It can be seen from *Figure1* that the total organic matter content of the soil with 19 organic fertilizer is significantly higher than that of single fertilizer treatment and no fertilizer treatment, and the total organic matter is increased by 15-39%, and the increase of constant organic-inorganic application is the highest. Fitting analysis find that between 2006 and 2014, the SOC content of the four fertilization treatments increased with time, and the increasing trend of organic fertilizer treatment is more obvious than that of single fertilizer application. The annual average rate of increase of total organic matter content treated with organic fertilizer is 1.5-1.6 times and 3.5-3.7 times that of non-fertilizer and single-fertilizer treatment, respectively. This indicates that long-term application of organic fertilizer can significantly increase soil organic carbon content. In order to further verify this result, the annual growth rate of the total amount of organic carbon and its components in the paddy soil of yellow soil was calculated, as shown in *Table 2*.

It can be known from the results in *Table 2* that long-term application of organic fertilizer does increase the soil organic carbon content and can effectively increase rice yield.

http://www.aloki.hu ● ISSN 1589 1623 (Print) ● ISSN 1785 0037 (Online)
DOI: http://dx.doi.org/10.15666/aeer/1705_1049110507

Table 2. *Annual growth rate of total organic carbon and its components in yellow soil paddy soil from 2006 to 2014 under long-term fertilization*

Treatment	CK	NPK	M	0.5MNPK	MNPK
SOC	0.17	0.39	0.62	0.59**	0.61*
Unprotected C	-0.02	0.25	0.38	0.33**	0.47
Physically protected C	0.02	0.02	0.08**	0.07**	0.09*
Chemically protected C	0.01	0.00	0.10*	0.07	0.17*
Biochemically protected C	0.12	0.13*	0.15	0.12*	0.09

*, **, respectively, indicated that the fitted linear equation reached a significant level ($P < 0.05$) and a very significant level ($P < 0.01$)

It can be seen from *Figure 2* that compared with no fertilizer application and single application of chemical fertilizer, the application of organic fertilizer significantly increased the soil free activity, physical protection and chemical protection organic carbon content ($P < 0.05$), and the increase amount is 18-61%, 30-44% and 27-56%. Among them, the increase of the organic-inorganic fertilization with the constant is the highest. In general, it can be seen that long-term non-fertilization and single-fertilizer treatment cannot maintain the turnover of the organic carbon pool, which is more detrimental to the accumulation of SOC components.

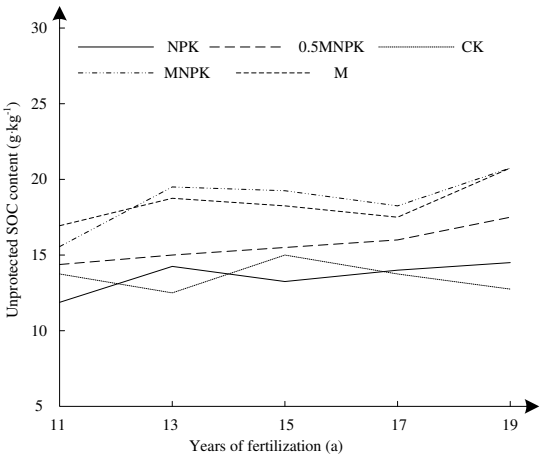

(a) Unprotected SOC content

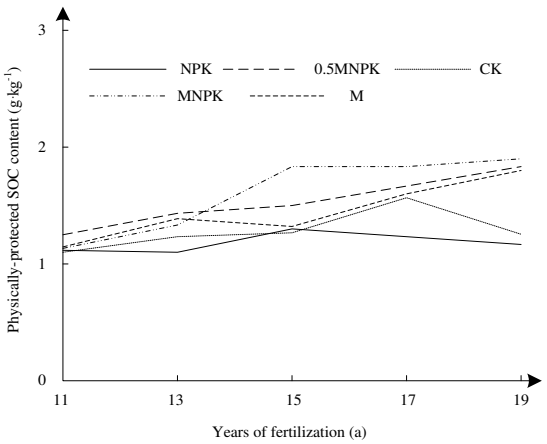

(b) Physically-protected SOC content

http://www.aloki.hu ● ISSN 1589 1623 (Print) ● ISSN 1785 0037 (Online)
DOI: http://dx.doi.org/10.15666/aeer/1705_1049110507

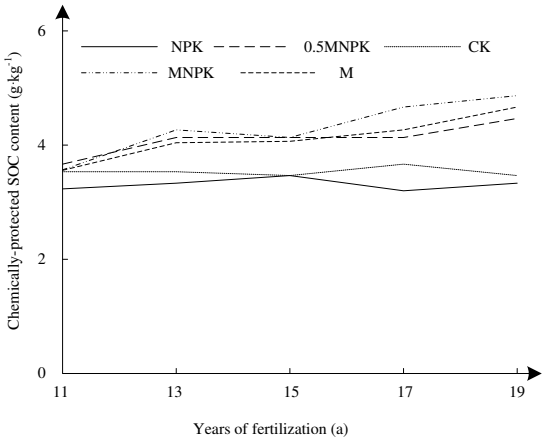

(c) Chemically-protected SOC content

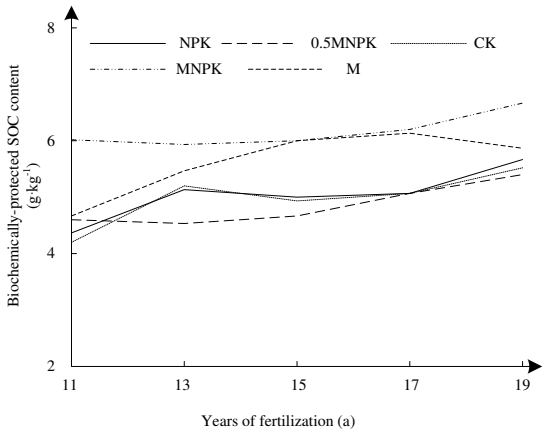

(d) Biochemically-protected SOC content

Figure 2. *Changes of soil organic carbon fractions in yellow soil paddy soil during 2006 to 2014 under long-term fertilization*

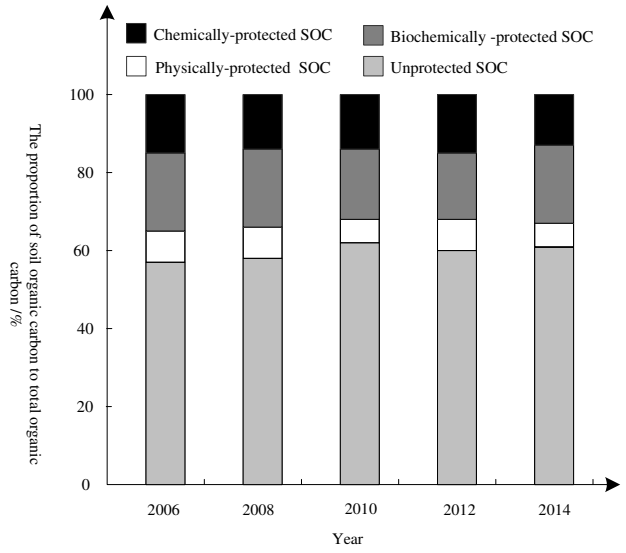

Figure 3. *The proportion of soil organic carbon to total organic carbon (average value of 5 years) under long-term fertilization*

http://www.aloki.hu ● ISSN 1589 1623 (Print) ● ISSN 1785 0037 (Online)
DOI: http://dx.doi.org/10.15666/aeer/1705_1049110507

It can be seen that the difference in the ratio of organic carbon between the NPK treatment and the CK treatment is not obvious. In contrast, the ratio of organic fertilizer treatment is higher, and the ratio of the other two organic carbons is lower.

It can be seen from *Figure 4* that except for CK treatment, the SOC content and the fertilization time in other cases show the very significant linear positive correlation ($P < 0.01$). The SOC content under CK treatment increased by 3.7% compared with that in 2006; the annual growth rate of SOC content under chemical fertilizer treatment is 23.9% and 20.6%.

The annual growth rate of SOC content under organic fertilizer treatment is higher, ranging from 20.6 to 21.3%. This indicates that long-term application of organic fertilizer can significantly increase the SOC content.

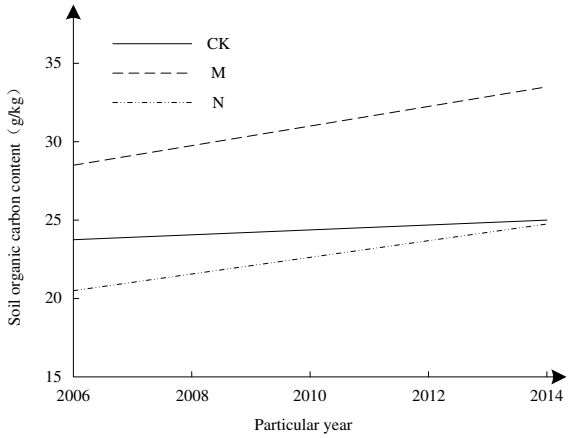

(a)

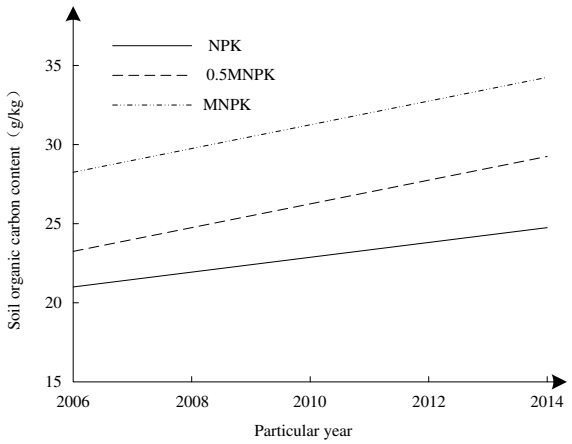

(b)

Figure 4. *Growth trend of soil organic carbon content in yellow soil paddy field from 2006 to 2014 under long-term fertilization (n=15)*

It can be seen from *Table 3* that the effects of different fertilization treatments on soil carbon-N ratio are not significant. This indicates that the conversion relationship of soil carbon-N under various management measures tends to be stable with the change of fertilization years. It can be seen from the experiment that the soil carbon-N ratio of each fertilization treatment in 2006 is significantly higher than that of other years,

http://www.aloki.hu ● ISSN 1589 1623 (Print) ● ISSN 1785 0037 (Online)
DOI: http://dx.doi.org/10.15666/aeer/1705_1049110507

indicating that land use patterns and farmland management changes can quickly affect the soil carbon-N ratio and quickly reach a new equilibrium. The general study suggests that the carbon-N ratio of dry-land is lower than that of paddy fields, but this study is different, and the reasons for further research are needed.

Table 3. *Soil carbon and nitrogen ratio in paddy fields under long-term fertilization (g/kg^{-1})*

Soil carbon and nitrogen ratio	CK	M	N	NPK	0.5MNPK	MNPK	Average value	Standard deviation
1995 year	11.7a	11.7a	11.8a	11.9a	11.1b	9.6c	11.3	0.9
1996 year	14.7a	10.5d	11.4c	10.8cd	11.4c	12.2b	11.8	1.5
2006 year	12.0d	18.2a	12.0d	15.2b	13.3c	15.4b	14.3	2.4
2008 year	11.8b	11.7b	10.1c	13.3a	10.5c	12.6ab	11.7	1.2
2010 year	10.5b	12.5a	9.3c	12.5a	11.0b	12.0a	11.3	1.3
2012 year	13.0a	12.6b	11.8cd	12.0c	11.5d	11.8cd	12.1	0.6
2014 year	12.3a	12.1a	12.6a	12.6a	11.9a	12.1a	12.3	0.3
Average value	12.3	12.8	11.3	12.6	11.5	12.2		
Standard deviation	1.3	2.5	1.2	1.4	0.9	1.7		

According to the analysis of *Figure 5,* there is no significant difference in soil bulk density of 0-10 cm layer in different long-term cultivation.

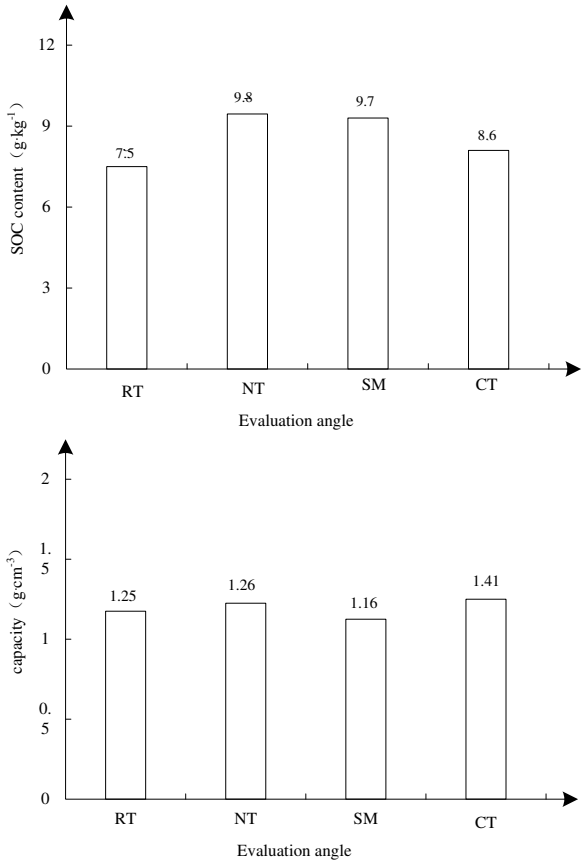

http://www.aloki.hu ● ISSN 1589 1623 (Print) ● ISSN 1785 0037 (Online)
DOI: http://dx.doi.org/10.15666/aeer/1705_1049110507

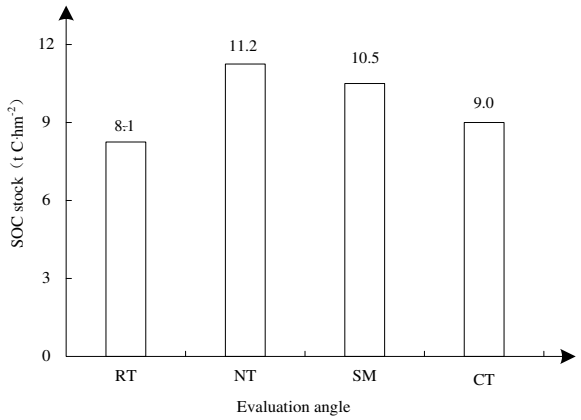

Figure 5. *Effects of long-term tillage on soil organic carbon content, capacity and organic carbon storage*

It can be seen from *Figures 6* and *7* that the carbon sequestration and carbon sequestration rate can be used as characteristic parameters for the evolution of organic carbon.

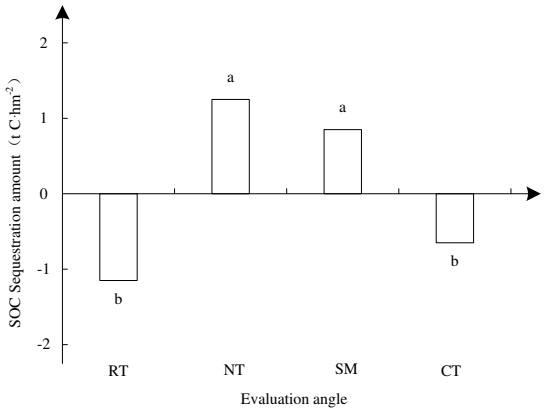

Figure 6. *Carbon fixation in long term different tillage treatment*

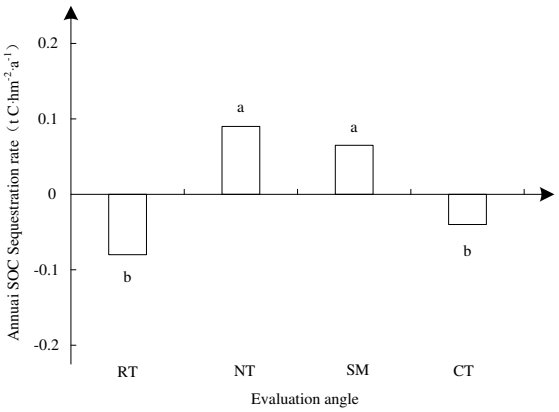

Figure 7. *Carbon fixation rate of long term different tillage treatment*

http://www.aloki.hu ● ISSN 1589 1623 (Print) ● ISSN 1785 0037 (Online)
DOI: http://dx.doi.org/10.15666/aeer/1705_1049110507

This study showed that under 15 years of conservation tillage, the soil organic carbon content of no-tillage and deep pine treatment with straw mulching as the main feature showed the upward trend.

Taking the year of 2006-2014 as the influencing factor, the changes of soil organic carbon content in yellow soil paddy field were analyzed under the condition of no fertilizer and long-term fertilizer, respectively. In order to fully verify the effectiveness of the proposed method, the variance of the change of organic carbon content is calculated and counted, and the results are shown in *Figure 8.*

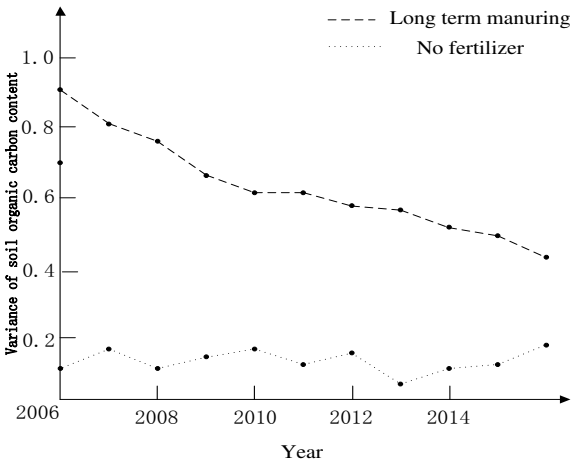

Figure 8. *Variance of soil organic carbon content*

Figure 8 shows that the variance of the change of organic carbon content is small under the condition of no fertilizer, and the influence of different years on the change of organic carbon content is small. Under the condition of long-term fertilizer, the variance of organic carbon content is larger, and the influence of different years on the change of organic carbon content is greater.

In order to further verify the effectiveness of the proposed method, the research accuracy of this method is compared with that of the traditional method, and the results are shown in *Table 4*.

Table 4. *Comparison of research accuracy*

Number of experiments/times	Paper method (%)	Traditional method (%)
5	89	76
10	88	75
15	90	74
20	92	72
15	93	80

The analysis *Table 4* shows that the research accuracy of this method is obviously higher than that of the traditional method, which shows that the research method has some advantages.

http://www.aloki.hu ● ISSN 1589 1623 (Print) ● ISSN 1785 0037 (Online)
DOI: http://dx.doi.org/10.15666/aeer/1705_1049110507

Discussion

Effect of NPK on soil organic matter composition

This study shows that in all treatments, the free active organic carbon belonging to high-activity organic carbon accounts for the relatively high proportion. It consists of unprotected coarse-grained organic carbon and fine-grained organic carbon, and is often used as one of the indicators of organic carbon change. Biochemically protected organic carbon and chemically protected organic carbon belong to the category of inert mineral-bound organic carbon (Song et al., 2015), which has strong stability. No change in chemically protected organic carbon indicates that long-term application of chemical fertilizer is not conducive to the accumulation of chemically protected organic carbon. The reason is that chemically protected organic carbon is mainly composed of humus, and the input of organic matter by NPK fertilizer is not enough to make up for its mineralization loss. During the period of 2006-2014, there was no significant change in physical protection of organic carbon under NPK treatment, indicating that it is less affected by chemical fertilizers.

Effect of single application of organic fertilizer on soil organic matter components

In this study, compared with single application of chemical fertilizer, the SOC and organic carbon content of each component were significantly increased with the fertilization period, which fully indicated its positive effect on increasing SOC reserves. The reason is that the application of organic fertilizer can not only increase crop yield, but also increase the direct input of carbon. This PANDEY et al study also shows that long-term application of organic fertilizer can increase the content of high-activity organic carbon and mineral-bound organic carbon in soil (Madejón et al., 2016). This PANDEY et al study also showed that long-term application of organic fertilizer can increase the content of high-activity organic carbon and mineral-bound organic carbon in soil. In this study, the proportion of mineral-bound organic carbon in the treatment with single application of organic fertilizer decreased slightly. The reason may be that the amount of soil fungi is increased in this case, so that the clay particles are converted into micro-aggregate particles. It increases the amount of animal and plant residues and secretions in the free active organic carbon. Yan Xiaogang et al. shows that the proportion of physical protection organic carbon in fluvo-aquic soil is 5.0-8.9%, which is mainly due to the physical protection of micro-aggregates, it reduces the decomposition of SOC by microorganisms and thus the effect of sequestering organic carbon.

Effect of NPK combined with organic fertilizer on organic matter components

The SOC content and annual variation of the MNPK treatment in this study are higher than 0.5MNPK treatment, which is consistent with most studies (Madejón et al., 2016). The SOC content mainly depends on the balance between the input and degradation of organic carbon, that is, the combination of constant organic fertilizer and chemical fertilizer. On the one hand, chemical fertilizer can increase microbial activity and increase crop root exudates.

On the other hand, organic fertilizer directly provides organic substances and promotes the increase of SOC. The study also shows that MNPK treatment improves the content of organic carbon in each component better than 0.5MNPK treatment, which

http://www.aloki.hu ● ISSN 1589 1623 (Print) ● ISSN 1785 0037 (Online)
DOI: http://dx.doi.org/10.15666/aeer/1705_1049110507

is consistent with the results of Zhang Jingye and Liang Shuming (Bahr et al., 2015). Yan Xiaogang's research shows that the content of free-particle organic carbon increased significantly under MNPK treatment, and there are differences in the proportion of organic carbon in each component under the same management measures and different fertilizer application rates. 0.5MNPK and MNPK still show the largest proportion of free active organic carbon. Compared with M treatment, their proportion of free active organic carbon is low. Because the long-term cooperation between NPK and organic fertilizers makes the non-protected active organic carbon form the stable Humin, it provides biochemical protection for organic carbon; it may also be that microbial metabolism promotes the accumulation of clay organic carbon.

Evolution characteristics of SOC in yellow soil paddy field under long-term fertilization

In this study, the SOC content shows the downward trend from 1995 to 2006. From 2006 to 2014, the SOC content under various conditions shows the very significant linear increase trend. This is due to changes in the farming system. Due to lack of water, the test site is changed to dry land during 2002-2006 and rice is replanted in 2007. The high permeability of dry land is conducive to the activity of soil microbes, resulting in the consumption of soil organic matter. The flooding and anoxic conditions of paddy fields inhibit their activities, which in turn is conducive to the accumulation of organic matter; on the other hand, paddy field conditions can effectively protect SOC. Other studies have also shown that the SOC content of paddy fields under the same conditions is significantly higher than that of dry land (Liu and Zhou, 2017).

Effect of long-term fertilization on carbon-N ratio in paddy yellow soil

Soil carbon-N ratio can reflect the coupling relationship between soil carbon and nitrogen, and is the important indicator for evaluating soil quality. The difference in soil carbon-N ratio between the fertilization treatments is not significant at around 12.3. This is consistent with the results of Luo Kun's research that the effect of fertilization measures on carbon-N ratio is not significant (Wander and Aref 2015). The soil carbon-nitrogen ratio is mainly related to the degree of soil organic matter. The carbon-nitrogen ratio of fresh organic matter tends to be higher, and the carbon-nitrogen ratio decreases with the increase of humification degree. Therefore, while increasing nitrogen input, the return level of carbon and nitrogen should be also paid attention. Vigorously promote the application of organic fertilizer and straw returning to maintain the stable increase in soil carbon-N ratio.

Carbon sequestration effect of conservation tillage

On the contrary, the less tillage treatment without straw returning decreased by 10.7%, which indicates that the conservation tillage of straw returning could increase soil organic carbon, while the no-tillage with reduced tillage frequency and intensity did not significantly improve organic carbon. Wang Chengji's research also shows that the organic carbon of conservation tillage with no increase in straw returning to the field is very small, and the no-tillage based on tillage management has great uncertainty on the accumulation of SOC in farmland.

http://www.aloki.hu ● ISSN 1589 1623 (Print) ● ISSN 1785 0037 (Online)
DOI: http://dx.doi.org/10.15666/aeer/1705_1049110507

Conclusions

The results of this study indicate that the soil organic matter content of yellow loam paddy soil is still at low level, which has the large carbon sequestration potential and capacity. Free active organic carbon is the largest part of SOC. The combination of organic and inorganic fertilizers also significantly increased the unprotected free activity, physical protection and chemically protected organic carbon content of the soil, and the highest increase is achieved under the condition of constant organic-inorganic application. The effect of single application of chemical fertilizer on the increase of SOC content and total nitrogen content is relatively small. The alone application of organic fertilizer or organic and inorganic fertilizer could significantly increase the SOC content and total nitrogen content. When applying organic fertilizer, the application of nitrogen fertilizer is more conducive to soil carbon sequestration. When applying nitrogen fertilizer, it is more beneficial to soil nitrogen conservation and maintain proper carbon-N ratio and carbon-N coupling relationship. Therefore, the constant combination of organic and inorganic fertilizers is the most effective mode to increase soil organic carbon storage.

The organic carbon reserves of no-tillage and deep pine cover treatment is significantly higher than that of less tillage and traditional tillage, and the soil carbon sequestration increased significantly with the increase of cumulative carbon input. To maintain the stability of SOC reserves, the minimum of 2.4 t C•hm^{-2} carbon is required each year. Through long-term conservation tillage, the organic carbon storage of the soil and micro-aggregate in the high loess slope area is improved, which is the farmland management measure that is conducive to the increase of carbon in the soil.

REFERENCES

[1] Amelian, S., Manian, M., Abtahi, S. M., Goli, A. (2018): Moisture sensitivity and mechanical performance assessment of warm mix asphalt containing by-product steel slag. – Journal of Cleaner Production 176: 329-337.

[2] Bahr, E., Chamba-Zaragocin, D., Fierro-Jaramillo, N. (2015): Modeling of soil nutrient balances, flows and stocks revealed effects of management on soil fertility in south Ecuadorian smallholder farming systems. – Nutrient Cycling in Agroecosystems 101(1): 55-82.

[3] Cruz Campas, M., Villalba Villalba, A. G., Ramirez Leal, R. (2017): Editorial. – Revista Internacional De Contaminacion Ambiental 33(SI): I-I.

[4] Dietrich, A. L., Lind, L., Nilsson, C. (2014): The use of phytometers for evaluating restoration effects on riparian soil fertility. – Journal of Environmental Quality 43(6): 1916.

[5] Herencia, J. F., Maqueda, C. (2016): Effects of time and dose of organic fertilizers on soil fertility, nutrient content and yield of vegetables. – Journal of Agricultural Science 154(8): 1343-1361.

[6] Hu, H., Chen, X., Sun, Z. (2017): Effect of water flows on ship traffic in narrow water channels based on cellular automata. – Polish Maritime Research 24(SI): 130-135.

[7] Jiang, G., Xu, M., He, X. (2014): Soil organic carbon sequestration in upland soils of northern China under variable fertilizer management and climate change scenarios. – Global Biogeochemical Cycles 28(3): 319-333.

[8] Kagawa, M., Matsubara, K., Kimura, K. (2014): Impacts of organic matter amendments on carbon and nitrogen dynamics in grassland soils. – Soil Biology and Biochemistry 68(1): 52-61.

http://www.aloki.hu ● ISSN 1589 1623 (Print) ● ISSN 1785 0037 (Online)
DOI: http://dx.doi.org/10.15666/aeer/1705_1049110507

[9] Kintché, K., Guibert, H., Bonfoh, B. (2015): Long-term decline in soil fertility and responsiveness to fertiliser as mitigated by short fallow periods in sub-Sahelian area of Togo. – Nutrient Cycling in Agroecosystems 101(3): 333-350.
[10] Kunlanit, B., Vityakon, P., Puttaso, A. (2014): Mechanisms controlling soil organic carbon composition pertaining to microbial decomposition of biochemically contrasting organic residues: evidence from midDRIFTS peak area analysis. – Soil Biology and Biochemistry 76(1): 100-108.
[11] Li, S., Gu, X., Zhuang, J. (2016): Distribution and storage of crop residue carbon in aggregates and its contribution to organic carbon of soil with low fertility. – Soil and Tillage Research 155(2): 199-206.
[12] Li, Y., Yu, H., Chappell, A. (2014): How much soil organic carbon sequestration is due to conservation agriculture reducing soil erosion? – Soil Research 52(7): 717-726.
[13] Liu, C. A., Zhou, L. M. (2017): Soil organic carbon sequestration and fertility response to newly-built terraces with organic manure and mineral fertilizer in a semi-arid environment. – Soil and Tillage Research 172(X): 39-70.
[14] Madejón, P., Alaejos, J., García-Álbala, J. (2016): Three-year study of fast-growing trees in degraded soils amended with composts: Effects on soil fertility and productivity. – Journal of Environmental Management 169(8): 18-26.
[15] Manjunatha, J. G., Deraman, M., Basri, N. H., Talib, I. A. (2018): Fabrication of poly (solid red a) modified carbon nano tube paste electrode and its application for simultaneous determination of epinephrine, uric acid and ascorbic acid. – Arabian Journal of Chemistry 11(2): 149-158.
[16] Naab, J. B., Mahama, G. Y., Koo, J. (2015): Nitrogen and phosphorus fertilization with crop residue retention enhances crop productivity, soil organic carbon, and total soil nitrogen concentrations in sandy-loam soils in Ghana. – Nutrient Cycling in Agroecosystems 102(1): 33-43.
[17] Ouyang, H., Hou, K., Wang, L., Peng, W. (2017): Optimization protocol for the microwave-assisted extraction of antioxidant components from *Pinus elliottii* needles using response surface methodology. – Bioresources 12(1): 478-494.
[18] Qiu, S., Xie, J., Zhao, S. (2014): Long-term effects of potassium fertilization on yield, efficiency, and soil fertility status in a rain-fed maize system in northeast China. – Field Crops Research 163(1): 1-9.
[19] Roy, S., Handique, G., Bora, F. R., Rahman, A. (2018): Evaluation of certain non-conventional plant based oils against red spider mite of tea. – Journal of Environmental Biology 39(1): 1-4.
[20] Sang, S. L., Shah, H. S., Awad, Y. M. (2015): Synergy effects of biochar and polyacrylamide on plants growth and soil erosion control. – Environmental Earth Sciences 74(3): 2463-2473.
[21] Song, Z. W., Zhu, P., Gao, H. J. (2015): Effects of long-term fertilization on soil organic carbon content and aggregate composition under continuous maize cropping in Northeast China. – Journal of Agricultural Science 153(2): 236-244.
[22] Wander, M. M., Aref, S. (2015): Long-term trends of corn yield and soil organic matter in different crop sequences and soil fertility treatments on the Morrow Plots. – Advances in Agronomy 62(08): 153-197.
[23] Wang, Y., Tang, J., et al. (2014): Aggregate-associated organic carbon and nitrogen impacted by the long-term application of fertilizers, rice straw, and pig manure. – Soil Science 179(10-11): 522-528.
[24] Wang, Y., Yang, Y., Shi, X., Mao, S., Shi, N., Hui, X. (2016): The spatial distribution pattern of human immunodeficiency virus/acquired immune deficiency syndrome in China. – Geospatial Health 11(2): 104-109.
[25] Wentzel, S., Schmidt, R., Piepho, H. P. (2015): Response of soil fertility indices to long-term application of biogas and raw slurry under organic farming. – Applied Soil Ecology 96(4): 99-107.

http://www.aloki.hu ● ISSN 1589 1623 (Print) ● ISSN 1785 0037 (Online)
DOI: http://dx.doi.org/10.15666/aeer/1705_1049110507

[26] Zhang, F., Li, C., Wang, Z. (2016): Long-term effects of management history on carbon dynamics in agricultural soils in Northwest China. – Environmental Earth Sciences 75(1): 1-9.
[27] Zhang, J. H., Wang, Y., Li, F. C. (2015): Soil organic carbon and nitrogen losses due to soil erosion and cropping in a sloping terrace landscape. – Soil Research 53(1): 87-96.
[28] Zhang, S., Pan, X., Wang, S., Yang, C., Gao, X., Wang, Z., Li, M., Ren, Z., Zheng, Q., Ma, W., Zhao, F., Qiao, Y. (2015): Knowledge of human papillomavirus vaccination and related factors among parents of young adolescents: a nationwide survey in China. – Annals of Epidemiology 25(4): 231-235.

http://www.aloki.hu ● ISSN 1589 1623 (Print) ● ISSN 1785 0037 (Online)
DOI: http://dx.doi.org/10.15666/aeer/1705_1049110507

A NOVEL REGIONAL ECOLOGICAL ASSESSMENT TECHNOLOGY BASED ON IMPROVED ELECTRE METHOD

YU, J.-P.* – YU, W.-Y.

School of Economics and Management, Yanshan University, Qinhuangdao 066004, PR China

Research Center of Regional Economic Development of Yanshan University, Qinhuangdao 066004, PR China

**Corresponding author*
e-mail: 3398849494@qq.com

(Received 27th Sep 2018; accepted 16th Jul 2019)

Abstract. A lot of efforts have been made in ecological assessment and applications. At present, Chinese government attaches great importance to regional economic development, so this research takes China as the research object. For this reason, a novel regional ecological assessment technology is proposed based on improved ELECTRE method. In the improved ELECTRE method, concordance index, non-concordance index, credibility index, consistent credibility, non-consistent credibility and net credibility are defined firstly, and the preference matrix, the relation of group individuals is also defined. Based on these definitions, it can be sorted for the quality of all alternatives according to the net credibility. Experimental results suggest that the proposed improved ELECTRE method is feasible and valid to the regional ecological assessment.
Keywords: *concordance index, non-concordance index, credibility index, consistent credibility, non-consistent credibility, net credibility, relation of group individuals, sort of group decision*

Introduction

In the eastern coastal areas and western areas to be developed in China, massive forest lands and wetlands have been damaged, leading to a situation of combined environmental pollution and massive ecological degradation (Anbari, 2003; Bi et al., 2015; Zuo et al., 2015). By ecological assessment, the key area for ecological environmental protection and restoration can be determined, ecological function zoning can be carried out, and proper protective measures and development plans can be made for different areas, to provide a scientific reference for determining urban development scale, land use arrangement and urban system configuration (Heilmann, 2013).

So far, a lot of efforts have been made in ecological assessment and application domestically and overseas (Nichols and Wahlen, 2004; Yang, 2015). The research contents include selection and analysis of sensitivity indexes of ecological environment, assessment of ecosystem service function and value, ecological risk analysis and pre-warning. The research range covers ecological sensitivity analysis under the context of global climate change, analysis of regional or watershed ecosystem dynamic change and difference, and provincial and municipal ecosystem assessment and ecological functional zoning (Zou et al., 2015; Zhao, 2003; Changdar et al., 2015; Lin and Lin, 2014). Diversified research methods have been adopted, such as ecological environment dynamic change monitoring and analysis with GIS and remote sensing monitoring technique, ecological environment sensitivity research based on fuzzy mathematical method, ecological environment vulnerability assessment with neural network method (Zhang et al., 2014; Belaqziz et al., 2013; Aloisio et al., 1997, 1999, 2005).

http://www.aloki.hu ● ISSN 1589 1623 (Print) ● ISSN 1785 0037 (Online)
DOI: http://dx.doi.org/10.15666/aeer/1705_1050910523

Investigation and survey indicate that most researches on ecological assessment at home and abroad focus on areas at national, provincial or county (municipal) levels, and few on areas at lower levels (Karamchand, 2006; Tehraniana et al., 2006; Wen et al., 2015). This paper is intended to analyze the ecological sensitivity and ecological risk of Manas County in Xinjiang from the aspects of land cover type, vegetation coverage index, geographic and geomorphic data, meteorological data, and soil type, and plan the areas of county development suitability and put forward ecological planning suggestions for different areas on this basis (Xiang et al., 2008; He and Xing, 2012; Zhang et al., 2016).

In this paper, a novel regional ecological assessment technology is proposed using improved ELECTRE method. In the proposed method, concordance index, non-concordance index, credibility index, consistent credibility, non-consistent credibility and net credibility are defined firstly, and the preference matrix, the relation of group individuals is also defined. Based on these definitions, it can be sorted for the quality of all alternatives according to the net credibility. Experimental results suggest that the proposed improved ELECTRE method is feasible and valid to the regional ecological assessment.

Improved ELECTRE method

In order to be specific and not lose the generality, $C_j\,(j=1,2,\cdots,m)$ are all supposed to be benefit attributes. p_j, q_j and v_j signify strictly superior to the threshold value, indifference threshold value and veto threshold value respectively between projects on C_j, For the first kind of threshold value, suppose that p_j is less than the difference between values of project a_j and project a_k on C_j, then we consider that the relation between a_j and a_k is that the former strictly superior to the latter; for the second kind of threshold value, suppose that q_j is more than the difference between values of project a_j and project a_k on C_j, then it can be considered that there is indifference relation between these two projects; for the last threshold value, suppose that v_j is less than or equal to the difference between values of project a_j and project a_k on C_j (the value of a_k is more than a_j), then we can vote down that the overall level of a_j is superior to a_k, This shows that $0 \le q_j \le p_j \le v_j$,

The improvements of the proposed ELECTRE method can be summarized as follows. Three novel indexes, Concordance Index, Non-concordance Index and Credibility Index are defined. Based on these indexes, a new Preference Matrix is constructed. Also, the Consistent Credibility, Non-consistent Credibility and Net Credibility are established. At the final, one novel approach is proposed to the Relation of Group Individuals and Sort of Group Decision.

Definition of three indexes

(1) Concordance Index, which can be expressed as $c(a_i, a_k)$, This index refers to the supporting degree to thesis that 'the level of a_i is higher than a_k', which can be defined as

http://www.aloki.hu ● ISSN 1589 1623 (Print) ● ISSN 1785 0037 (Online)
DOI: http://dx.doi.org/10.15666/aeer/1705_1050910523

$$c(a_i, a_k) = \frac{1}{w}\sum_{j=1}^{m} w_j c_j(a_i, a_k) \quad \text{(Eq.1)}$$

where

$$w = \sum_{j=1}^{m} w_j \quad \text{(Eq.2)}$$

$$c_j(a_i, a_k) = \begin{cases} 0 & if \quad y_j(a_i)+p_j \le y_j(a_k) \\ 1 & if \quad y_j(a_i)+q_j \ge y_j(a_k) \\ \dfrac{y_j(a_i)+p_j-y_j(a_k)}{p_j-q_j} & other \end{cases} \quad \text{(Eq.3)}$$

This index refers to the degree that project a_i is superior to project a_k on C_j,

(2) Non-concordance Index, which refers to the denying degree to thesis that 'the level of a_i is higher than a_k', which can be defined as

$$d_j(a_i, a_k) = \begin{cases} 0 & if \quad y_j(a_i)+p_j \ge y_j(a_k) \\ 1 & if \quad y_j(a_i)+v_j \le y_j(a_k) \\ \dfrac{y_j(a_k)-y_j(a_i)-p_j}{v_j-p_j} & other \end{cases} \quad \text{(Eq.4)}$$

(3) Credibility Index, which refers to the credibility of that 'the level of a_i is higher than a_k', the value of which can be defined as

$$s(a_i, a_k) = \begin{cases} c(a_i, a_k) & if \quad \forall C_j, d_j(a_i, a_k) \le c(a_i, a_k) \\ c(a_i, a_k) \times \prod_{c_j} \dfrac{1-d_j(a_i, a_k)}{1-c(a_i, a_k)} & if \quad \forall C_j, d_j(a_i, a_k) > c(a_i, a_k) \end{cases} \quad \text{(Eq.5)}$$

Build the preference matrix

Every decision maker has his own point of view to judge and different preferences, so that they often use different dimensions and standards to make decisions (Duan et al., 2018; You et al., 2018; Liu et al., 2017; McKane et al., 2017). After finishing the ranking of alternatives by using ELECTRE-III method, we cannot simply use the

http://www.aloki.hu ● ISSN 1589 1623 (Print) ● ISSN 1785 0037 (Online)
DOI: http://dx.doi.org/10.15666/aeer/1705_1050910523

average method or Borda method to integrate single decision result as the overall result, which does not conform to actual situations. Therefore, we need to put forward a new method to make the group reflect different dimensions and standards during the sorting process. Here, credibility index and the rating placement of project have greater relation with these dimensions and standards. We need to consider the following two questions at the same time: the relative interval of project while assigning the credibility index as $s(a_k, a_i)$ and $s(a_i, a_k)$, the relative rating placement of project on $s(a_i, a_k)$.

(1) Supposing that $\Delta Q_l(a_i, a_k)$ refers to the relative placement of project on (a_i, a_k) in the sort. $Q_l(a_i)$ refers to the order made by person l for project a_i. If there are m projects to be ordered, person l thinks that project a_i is the best among all the projects, then the $Q_l(a_i)$ is defined as 1. If person l thinks that project a_i is the worst one among all projects, then the $Q_l(a_i)$ is defined as m. There are five situations between the relative placement $\Delta Q^l(a_i, a_k)$ in ranking all projects and the project

$$\Delta Q_l(a_i, a_k) = \begin{cases} Q_l(a_i) >> Q_l(a_k) & if \quad Q_l(a_k) - Q_l(a_i) > \dfrac{n}{2} \\ Q_l(a_i) > Q_l(a_k) & if \quad 0 < Q_l(a_k) - Q_l(a_i) \le \dfrac{n}{2} \\ Q_l(a_i) = Q_l(a_k) & if \quad Q_l(a_k) - Q_l(a_i) = 0 \\ Q_l(a_i) < Q_l(a_k) & if \quad 0 < Q_l(a_i) - Q_l(a_k) \le \dfrac{n}{2} \\ Q_l(a_i) << Q_l(a_k) & if \quad Q_l(a_i) - Q_l(a_k) > \dfrac{n}{2} \end{cases} \qquad \text{(Eq.6)}$$

where $Q_l(a_i) >> Q_l(a_k)$ refers that person l thinks project a_i is much better than project a_k, $Q_l(a_i) > Q_l(a_k)$ refers that person l thinks project a_i is a little better than project a_k, $Q_l(a_i) < Q_l(a_k)$ refers that person l thinks project a_i is a little worse than project a_k, $Q_l(a_i) << Q_l(a_k)$ refers that person l thinks project a_i is much worse than project a_k,

When it is necessary to determine the quality sequence of projects, traditional ELECTRE method usually consider that there exists outranking relation while $s(a_i, a_k) \ge \lambda_{\max} - \beta$ is found, $\lambda_{\max} = \max_{a_i, a_k \in A} s(a_i, a_k)$, β is the intercepting threshold, the value of which is setting by decision makers themselves according to their own experience. Among all these outranking relations, the quality sequence of project a_i can be determined according to the difference between the number of outflowing directed arc of project a_i and the number of inflowing directed arc of project a_i. Therefore, there are four situations existed while defining the relative interval of credibility index $s_l(a_i, a_k)$ and $s_l(a_k, a_i)$ among each pair-projects

Zone I: $s_l(a_i, a_k) \ge \lambda_{\max} - \beta,\ s_l(a_k, a_i) \ge \lambda_{\max} - \beta$

http://www.aloki.hu ● ISSN 1589 1623 (Print) ● ISSN 1785 0037 (Online)
DOI: http://dx.doi.org/10.15666/aeer/1705_1050910523

$$Zone\ II:\ s_l(a_i,a_k) \geq \lambda_{\max} - \beta,\ s_l(a_k,a_i) < \lambda_{\max} - \beta$$

$$Zone\ III:\ s_l(a_i,a_k) < \lambda_{\max} - \beta,\ s_l(a_k,a_i) \geq \lambda_{\max} - \beta$$

$$Zone\ IV:\ s_l(a_i,a_k) < \lambda_{\max} - \beta,\ s_l(a_k,a_i) < \lambda_{\max} - \beta$$

(2) Build the Preference Evaluation Matrix (*Table 1*). Preference Evaluation Matrix is used to measure the quality between project a_i and project a_k.

Table 1. *Preference evaluation matrix*

	Zone I	**Zone II**	**Zone III**	**Zone IV**
$Q_l(a_i) >> Q_l(a_k)$	$a_i O_s a_k$	$a_i O_s a_k$	$a_i O_w a_k$	$a_i O_s a_k$
$Q_l(a_i) > Q_l(a_k)$	$a_i O_w a_k$	$a_i O_s a_k$	$a_i I a_k$	$a_i O_w a_k$
$Q_l(a_i) = Q_l(a_k)$	$a_i I a_k$	$a_i O_w a_k$	$a_i B_w a_k$	$a_i I a_k$
$Q_l(a_i) < Q_l(a_k)$	$a_i B_w a_k$	$a_i I a_k$	$a_i B_s a_k$	$a_i B_w a_k$
$Q_l(a_i) << Q_l(a_k)$	$a_i B_s a_k$	$a_i B_w a_k$	$a_i B_s a_k$	$a_i B_s a_k$

$a_i O_s a_k$ refers that project a_i is much better (O_s) than project a_k; $a_i O_w a_k$ refers that project a_i is little better (O_w) than project a_k; $a_i I a_k$ refers that there is no difference (I) between project a_i and project a_k; $a_i B_w a_k$ refers that project a_i is little worse (B_w) than project a_k; $a_i B_s a_k$ refers that project a_i is much worse (B_s) than project a_k

Consistent credibility, non-consistent credibility and net credibility

(1) Consistent credibility $\Phi^+(a_i)$ indicates the degree that project a_i superior to other projects, which can be defined as

$$\Phi^+(a_i) = \sum_{a_k \in A} s(a_i,a_k), \forall a_k \in A \qquad \text{(Eq.7)}$$

(2) Non-consistent credibility $\Phi^-(a_i)$ is used to show the degree that other projects superior to project a_i, which can be defined as

$$\Phi^-(a_i) = \sum_{a_k \in A} s(a_k,a_i), \forall a_k \in A \qquad \text{(Eq.8)}$$

(3) Net credibility $\Phi(a_i)$ can express the difference between consistent credibility and non-consistent credibility, which can be defined as

$$\Phi(a_i) = \Phi^+(a_i) - \Phi^-(a_i)$$

http://www.aloki.hu ● ISSN 1589 1623 (Print) ● ISSN 1785 0037 (Online)
DOI: http://dx.doi.org/10.15666/aeer/1705_1050910523

It can be sorted of the quality for all alternatives according to the value of net credibility $\Phi(a_i)$. The greater the value of the net credibility $\Phi(a_i)$ of a project, the better the project is.

Relation of group individuals

(1) Group concordance index $C_G(a_i, a_k)$ refers to the credibility of supporting thesis that 'project a_i is better than project a_k' from the perspective of group, which can be defined as

$$C_G(a_i, a_k) = \sum_{l=1}^{m} v_l f_l(a_i, a_k) \quad \text{(Eq.9)}$$

where

$$f_l(a_i, a_k) = \begin{cases} 1 & if \quad a_i O_s a_k \\ 0.75 & if \quad a_i O_w a_k \\ 0.5 & if \quad a_i I a_k \\ 0.25 & if \quad a_i B_w a_k \\ 0 & if \quad a_i B_s a_k \end{cases} \quad \text{(Eq.10)}$$

(2) Group non-concordance index $D_G(a_i, a_k)$ refers to the credibility of denying thesis 'project a_i is better than project a_k' from the perspective of group, which can be defined as

$$D_G(a_i, a_k) = \sum_{l=1}^{m} v_l g_l(a_i, a_k) \quad \text{(Eq.11)}$$

where

$$g_l(a_i, a_k) = \begin{cases} 1 & if \quad \left(a_i B_w a_k \ or \ a_i B_s a_k\right) \& \left(Q_l(a_i) << Q_l(a_k)\right) \\ 0 & other \end{cases} \quad \text{(Eq.12)}$$

(3) Group credibility index $S_G(a_i, a_k)$ refers to the credibility of thesis that 'project a_i is better than project a_k', which can be defined as

$$S_G(a_i, a_k) = C_G(a_i, a_k) \cdot (1 - D_G(a_i, a_k)) \quad \text{(Eq.13)}$$

Sort of group decision

(1) Group consistency credibility $\Phi_G^+(a_i)$ refers to estimate the credibility that project a_i is better than other projects from the perspective of group, which can be defined as

http://www.aloki.hu ● ISSN 1589 1623 (Print) ● ISSN 1785 0037 (Online)
DOI: http://dx.doi.org/10.15666/aeer/1705_1050910523

$$\Phi_G^+(a_i) = \sum_{k=1}^{n} S_G(a_i, a_k) \quad \text{(Eq.14)}$$

(2) Group non-consistency credibility $\Phi_G^-(a_i)$ refers to estimate the credibility that other projects are better than project a_i from the perspective of group, which can be defined as

$$\Phi_G^-(a_i) = \sum_{k=1}^{n} S_G(a_k, a_i) \quad \text{(Eq.15)}$$

(3) Group net credibility $\Phi_G(a_i)$ refers to the difference between $\Phi_G^+(a_i)$ and $\Phi_G^-(a_i)$, which can be defined as

$$\Phi_G(a_i) = \Phi_G^+(a_i) - \Phi_G^-(a_i) \quad \text{(Eq.16)}$$

It can be sorted for the quality of all alternatives according to the value of $\Phi_G(a_i)$. In general, the greater the value of the group net credibility of a project, the better the project is.

Experimental results

In the experimental section, we take the Manas County (see *Fig. 1*) as the research object, which located at Xinjiang autonomous region, P. R. China. Manas County is located in the middle section of North Slope of the Tian-Shan Mountains, bordered by Hu-Tu-Bi County in the east, Shi-He-Zi and Sha-Wan city in the west, He-Jing County in the south, and Hoboksar Mongol Autonomous County in the north. In respect of geographical coordinates, it stretches from 43°28′29″ to 45°38′52″north latitude and from 85°41′16″ to 86°43′10″ east longitude. Manas County takes the shape of strip long from north to south and narrow from west to east. It is 235 km long to the most and 118 km wide to the most. The whole county covers an area of 10.196.4 km^2, and has seven towns, four villages, two farms and one station, as well as Xin-Hu Farm of the Sixth Agricultural Division of Xin-Jiang Production and Construction Corps, and four regimental farms of the Eighth Agricultural Division, namely 147 regiment, 148 regiment, 149 regiment and 150 regiment. Geomorphically, Manas County can be divided into three units from south to north, namely southern mountain area, central plan, and northern desert, of which the altitude ranges from 5,222 m to 650 m, from 650 m to 320 m and from 320 m to 280 m respectively. Manas County falls into the dry and semi-dry temperate continental climate region, of which the climate features are severe cold winter, hot summer, abundant sunshine, aridness, and little rainfall, with annual average temperature of 6.9 °C and average annual precipitation of 173.3 mm.

Basic data

The main data used in this research covers land cover type, Normalized Differential Vegetation Index (NDVI), geographic and geomorphic data, meteorological data, soil

http://www.aloki.hu ● ISSN 1589 1623 (Print) ● ISSN 1785 0037 (Online)
DOI: http://dx.doi.org/10.15666/aeer/1705_1050910523

type, distribution data of geological disaster, and administrative map. *Table 2* shows the data sources and details.

Table 2. *Data contents and sources*

Data name	Data source	Description
Land cover type	Institute of Geographic Sciences and Natural Resources Research, CAS	Vector data of year 2017
NDVI	Environmental and Ecological Science Data Center for West China, National Natural Science Foundation of China	SPOT VGT NDVI 1 km resolution data of year 2009-2017
Digital elevation data	NASA SRTM3 data	90 m resolution grid data of year 2017
Geomorphic data	Land and Resource Department of Manas County	Geomorphic unit zoning of year 2017
Meteorological data	Manas County Meteorological Service	Data of rainfall, snow and meteorological disaster of year 2017
Soil type data	Manas County Bureau of Agriculture	Soil distribution and type of year 2017
Distribution of geological disaster	Land and Resource Department of Manas County	Distribution of places prone to and classifications of geological disasters of year 2017
Administrative division	Land and Resource Department of Manas County	Vector boundary diagram of Manas County and villages and towns of year 2017

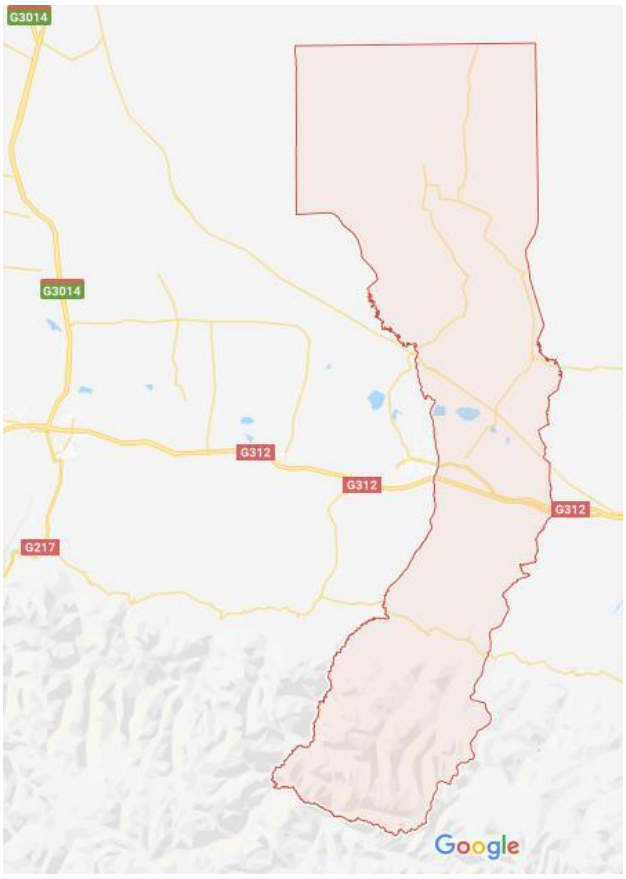

Figure 1. *The location of Manas County*

http://www.aloki.hu ● ISSN 1589 1623 (Print) ● ISSN 1785 0037 (Online)
DOI: http://dx.doi.org/10.15666/aeer/1705_1050910523

Considering that the data is from different sources, it is necessary to preprocess the data before ecological analysis, including correction of remote sensing image data, scanning vectorization and registration of grid data, mergence and clipping of grid data based on administrative boundary map of county region. Essential data on the survey region has been generated with Xi-An trimetric projection zone coordinate system based on the preprocessed data.

Ecological sensitivity analysis

The term of ecological sensitivity analysis in this research refers to the level of sensitivity of inhabiting area of major species in an ecosystem to interference of human activity, or the adaptive capacity of inhabiting area of major species in an ecosystem to external disturbance, which, with respect to selection of ecological factor, complies with the principles of representativeness, reliability, combination of qualitative analysis and quantitative analysis, and data availability (Sheikhhosseini, 2018; Fang et al., 2018; Dong et al., 2018). For constructing the indicator system, comprehensive consideration of natural factors and anthropogenic influence has been taken, and the selected sensitivity assessment indicators including land cover factor, vegetation factor, slope, geomorphic type, and groundwater protection zone factor. For land cover factor, land-use type is taken as the assessment indicator, and national forest parks and major wetlands are taken into full consideration; for vegetation factor, NDVI is taken as the assessment indicator; for geomorphic factor, geomorphic division type is taken as the assessment indicator (Zhang et al., 2017; Obraczka et al., 2017).

In this research, the attributes of the assessment indicators are assessed, and a value ranging from 1 to 9 is assigned to each indicator. High value indicates high level of ecological sensitivity (as shown in *Table 3*, '/' indicates that it would contain non-relevant information). A weight is assigned to land cover factor, NDVI, slope, geomorphology, and underground water factor respectively, which is 0.4, 0.1, 0.2, 0.2 and 0.1 respectively. A 30 m × 30 m grid cell is taken as analytical unit, and the weighted sum of the factors is calculated with grid calculator in ArcGIS 9.3. Based on the calculations, the ecologically sensitive region is divided into five levels with 5-level division method, namely high sensitive area, relatively highly sensitive area, medium sensitive area, low sensitive area and non-sensitive area.

Table 3. *Manas County ecosystem sensitivity assessment indicator*

Item	1	2	3	4	5	6	7	8	9
Land cover	Urban	/	/	Farmland	/	Deseed	Grassland	Other	Forest, wetland
NDVI	≤ 0	/	(0, 0.25]	/	(0.25-0.5]	/	(0.50-0.75]	/	(0.75-1]
Slope	≤ 5°	/	(5°-15°]	/	(15°-25°]	/	> 25°	/	/
Geomorphology	/	Fine soil plain	Inclined plain	Desert	/	Hill	Middle mountain	/	High mountain
Underground water	Non-protective zone	/	/	/	/	/	/	/	Protection zone

http://www.aloki.hu ● ISSN 1589 1623 (Print) ● ISSN 1785 0037 (Online)
DOI: http://dx.doi.org/10.15666/aeer/1705_1050910523

Ecological risk analysis

For purpose of this research, comprehensive ecological risk assessment method is adopted. According to field research and materials and documents, the three major ecological risks in Manas County include flood, desert, and geological disaster. An ecological risk assessment model has been built based on the results of risk exposure in combination with the intensity and frequency of risk. For the analysis, the collected research data is digitized first, and then further collated, verified and edited. On this basis, a database is built on the ArcGIS platform, and calculation and analysis are made according to the needs of assessment.

The flood types in Manas County mainly include snow (ice)-melted flood, rainstorm-type flood and blended-type flood. In the research, analysis is made on runoff of snow, rainstorm and small watershed, the probability of occurrence of flood is determined according to different catchment areas, and a certain area on both sides of river reach prone to flood is taken as the risky place. In the research on desertization risk, vegetation index, soil type, and average annual precipitation are taken as the assessment factors of desertization risk grade, and desertization risk classification is made. In the research on risk of landslide and debris flow, a geological disaster ecological risk formula of Manas County is established with slope, rainstorm and vegetation coverage as the assessment factors. At last, on the basis of main ecological risk analysis, the three risks set out above are normalized and graded respectively (as shown in *Table 4*), a weight of 0.40, 0.35 and 0.25 is assigned to flood risk, desertization risk and geologic risk respectively, and weighting calculation is conducted. Limited to human recognition, 1, 3, 5, 7, 9 are often used to distinguish the difference between two objects. Based on the results, the ecological risk area is divided into high risk area, relatively high risk area, moderate risk area, relatively low risk area and low area with the 5-level division method.

Table 4. *Manas County ecological risk assessment indicators*

Degree of risk	1	3	5	7	9
Flood risk	(0.04,0.08]	(0.08,0.17]	(0.17,0.33]	(0.33,0.58]	(0.58-1]
Desertization risk	(0.44,0.53]	(0534,0.60]	(0.60,0.65]	(0.65,0.70]	(0.70,0.85]
Geological risk	(0.11,0.25]	(0.25,0.34]	(0.34,0.45]	(0.45,0.56]	(0.56,0.80]

Suitability analysis of county development

According to the normalization with equal weight of the results of ecological sensitivity analysis and ecological risk analysis of Manas County and suitability analysis of county development, the highly ecologically sensitive area and highly ecological risk area are unsuitable for county development, relatively high ecologically sensitive area and relatively high risk area are barely suitable for county development, medium ecologically sensitive area and medium ecological risk area are moderately suitable for county development, and low ecologically sensitive area and low ecological risk area are highly suitable for county development. The ecology, safety, resources, environment and urban functions of areas unsuitable and barely suitable for county development are vulnerable, which are difficult to restore or will lead to heavy losses once being damaged. Proper control measures should be taken in areas moderately

http://www.aloki.hu ● ISSN 1589 1623 (Print) ● ISSN 1785 0037 (Online)
DOI: http://dx.doi.org/10.15666/aeer/1705_1050910523

suitable for county development according to the requirements of ecology, safety, resources and environment. Concentrated construction is feasible in areas highly or relatively highly suitable for county development.

Results of comprehensive ecological sensitivity analysis

According to the ecosystem sensitivity assessment indicators of Manas County, the highly sensitive area in the whole Manas County mainly covers the water conservation area in the south, wetlands in the central part, and desert in the north, and other areas most are moderately sensitive areas. The proportions of highly sensitive area, relatively highly sensitive area, moderately sensitive area, low sensitive area, and non-sensitive area to the total area of the survey region are 41.31%, 16.17%, 16.44%, 7.07% and 19.01% respectively.

Results of comprehensive ecological risk analysis

According to the ecological risk assessment system, the high-ecological-risk area of Manas County is mainly distributed in the south of Taxihe Village, the middle part and south of Qing-Shui-He Village, and the north of Guang-Dong-Di Village. The ecological risk level of the area along the downstream of Taxihe and the area along the downstream of Manas River is also relatively high, and that of other areas is low.

Results of suitability analysis of Manas County development

The suitability analysis results of county development are classified into five grades. The area highly suitable for county development mainly covers most areas of Manas town, Lan-Hou-Wan town, the west area of 147 regimental farm, Bei-Wu-Cha, the southeast of Liu-Hu-Di, as well as the east of 148 regimental farm, 149 regimental farm and 150 regimental farm; the area relatively highly suitable for county development mainly covers the middle part of the four regimental farms, the south of Lan-Zhou-Wan, Le-Tu-Yi and the south of Bao-Jia-Dian; the area moderately suitable for county development mainly covers Xin-Hu Farm and most area of Guang-Dong-Di village; the rest area is barely suitable or unsuitable for county development, mainly covering the northern desert, southern mountain, the area along Manas River and Taxihe, and reservoirs and swags in plain area.

Manas County construction regionalization

Manas County is regionalized according to the suitability analysis of Manas County development, by which the areas barely suitable or unsuitable for county development are classified into prohibited-construction areas, and the areas relatively highly or highly suitable for county development into construction-suitable areas. The prohibited-construction areas mainly cover the southern mountains, wetlands in the plain area, and the northern desert. The north slope of the Tian-Shan Mountains is highly sensitive water conservation area; most primeval forest and vegetation have been damaged in the process of bringing wasteland into cultivation; the area of the north desert has been put under proper control with the expansion of cultivated land and the construction of wind break, but it is still an ecologically sensitive area needing intensive protection. These areas set out above should be prohibited for development in urban construction (*Fig. 2*).

http://www.aloki.hu ● ISSN 1589 1623 (Print) ● ISSN 1785 0037 (Online)
DOI: http://dx.doi.org/10.15666/aeer/1705_1050910523

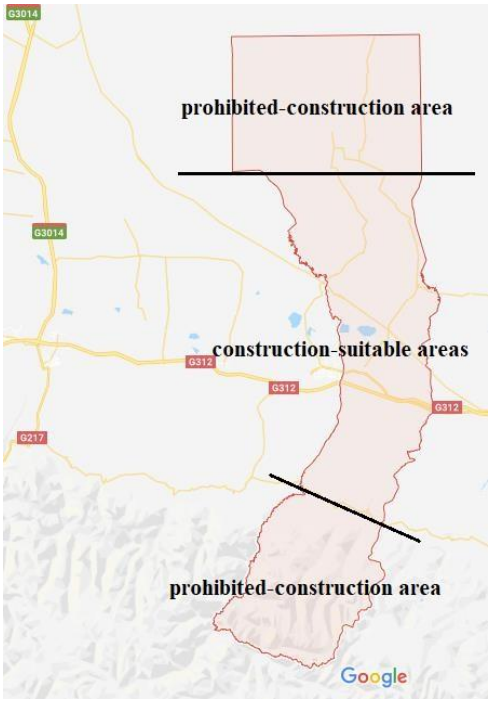

Figure 2. *The prohibited-construction area and construction-suitable area of Manas County*

Conclusions

In this paper, relatively comprehensive ecological assessment of Manas County has been made through ecological sensitivity analysis and ecological risk analysis by combining expert knowledge with the analytic hierarchy process and bringing the spatial analysis capability of GIS into full play, providing new ideas for ecological quality assessment and urban development planning. In the scope of Manas County, the highly sensitive area is mainly distributed in the water conservation area in the south mountains, wetlands in the central part, and desert in the north; the proportions of highly sensitive area, relatively highly sensitive area, moderately sensitive area, low sensitive area, and non-sensitive area to the total area of the survey region are 41.31%, 16.17%, 16.44%, 7.07% and 19.01% respectively; the highly ecological risk area is mainly distributed in the south of Taxihe Village, the middle part and south of Qing-Shui-He Village, and the north of Guang-Dong-Di Village, as well as the middle and lower reaches of Taxihe and the lower reaches of Manas River. According to ecological sensitivity analysis and ecological risk analysis, county development suitability analysis has been made in this research, and the survey region is classified into prohibited-construction area, construction expansion restricted zone, and construction-suitable area on this basis. The construction of any unrelated building should be prohibited in the prohibited-construction area, measures should be taken to avoid occupying urban construction land in the constructive expansion restricted zone as far as possible, and rational development on the premise of ecological environmental protection is allowed in the construction-suitable area.

According to the ecological sensitivity analysis and ecological risk analysis, the middle and lower reaches of Manas River and the upper and middle reaches of Taxihe are flood-prone area, of which the comprehensive ecological safety assessment index takes on a down trend. A special fund allocated by the Ministry of Water Resources was

http://www.aloki.hu ● ISSN 1589 1623 (Print) ● ISSN 1785 0037 (Online)
DOI: http://dx.doi.org/10.15666/aeer/1705_1050910523

used for flood control of Manas River in 2011. The feasible measures for flood control include consolidating the construction of small and medium size reservoirs and infrastructure of flood control and drainage of cities, and mitigating damage to Manas River and Taxihe. For severe desertification region, it needs to strengthen the construction of vegetation, river, road, and other ecological corridors in the junction zone between desert and city, to prevent desertification erosion. For the highly sensitive and risk areas such as the high mountains and gorge areas in Manas County, ecological emigration from the steep slope area along Manas River and Taxihe can be considered to resettle the scattered residents in an area of low ecological risk centrally. For county development, the construction of unrelated buildings should be prohibited in the prohibited-construction area; measures should be taken to avoid occupying urban construction land in the constructive expansion restricted zone as far as possible, or proper ecological assessment, compensation measures and the procedure for examination and approval should be subject to if it needs to occupy any urban construction land in special circumstance; the principles of construction following planning, optimal land utilization, intensive development, and rational exploitation on the premise of ecological environmental protection should be adhered to for the construction-suitable area.

Acknowledgements. This study was supported by Key project of important topic of humanities and social sciences research of Hebei province (project number: ZD201719), and Fund of key research base of humanities and social sciences of institutions of higher learning of Hebei province (project number: JJJD1710).

REFERENCES

[1] Aloisio, G., Cafaro, M., Williams, R., et al. (1997): A distributed web-based meta-computing environment. – Proceedings of High-Performance Computing and Networking (Lecture Notes in Computer Science) 1225: 480-486.

[2] Aloisio, G., Cafaro, M., Fiore, S., et al. (2005): A grid-based architecture for earth observation data access. – ACM Symposium on Applied Computing, Santa Fe, New Mexico, USA, pp. 701-705.

[3] Aloisio, G., Cafaro, M., Williams, R. (1999): The digital Puglia project: an active digital library of remote sensing data. – Proceedings of the 7th International Conference on High Performance Computing and Networking Europe 1593: 563-572.

[4] Anbari, F. T. (2003): Earned value project management method and extensions. – Project Management Journal 12: 12-23.

[5] Belaqziz, S., Khabba, S., Er-Raki, S., et al. (2013): A new irrigation priority index based on remote sensing data for assessing the networks irrigation scheduling. – Agricultural Water Management 119: 1-9.

[6] Bi, W., Dandy, G. C., Maier, H. R. (2015): Improved genetic algorithm optimization of water distribution system design by incorporating domain knowledge. – Environmental Modelling and Software 69: 370-381.

[7] Changdar, C., Mahapatra, G. S., Pal, R. K. (2015): An improved genetic algorithm based approach to solve constrained knapsack problem in fuzzy environment. – Expert Systems with Applications 42(4): 2276-2286.

[8] Dong, Q., Yuan, J., Chen, X., Ma, X. (2018): Reduction of moisture susceptibility of cold asphalt mixture with Portland cement and bentonite nanoclay additives. – Journal of Cleaner Production 176: 320-328.

http://www.aloki.hu ● ISSN 1589 1623 (Print) ● ISSN 1785 0037 (Online)
DOI: http://dx.doi.org/10.15666/aeer/1705_1050910523

[9] Duan, M., Liu, Z., Yan, D., Peng, W., Baghban, A. (2018): Application of LSSVM algorithm for estimating higher heating value of biomass based on ultimate analysis. – Energy Sources Part A - Recovery Utilization and Environmental Effects 40(6): 709-715.
[10] Fang, L., Wang, X., Guo, L., Liu, Q. (2018): Antioxidant, anti-microbial properties and chemical composition of cumin essential oils extracted by three methods. – Open Chemistry 16(1): 291-297.
[11] He, R. J., Xing, L. N. (2012): A learnable ant colony optimization to the disasters monitoring task allocation problem. – Research Journal of Chemistry and Environment 16(S2): 18-26.
[12] Heilmann, R. (2003): Discrete optimization a branch-and-bound procedure for the multi-mode resource-constrained project scheduling problem with minimum and maximum time lags. – European Journal of Operational Research 144: 348-365.
[13] Karamchand, S. S. (2006): Operator Scheduling in a Distributed Stream Management System for Remotely Sensed Imagery. – University of California, Davis, USA.
[14] Lin, C. H., Lin, P. L. (2014): Improving the non-dominated sorting genetic algorithm using a gene-therapy method for multi-objective optimization. – Journal of Computational Science 5(2): 170-183.
[15] Liu, Y., Li, T., Guo, L., Zhang, R., Feng, X., Liu, K. (2017): The mediating role of sleep quality on the relationship between perceived stress and depression among the elderly in urban communities: a cross-sectional study. – Public Health 149: 21-27.
[16] McKane, A., Therkelsen, P., Scodel, A., Rao, P., Aghajanzadeh, A., Hirzel, S., Zhang, R., Prem, R., Fossa, A., Lazarevska, A. M., Matteini, M., Schreck, B., Allard, F., Alcantar, N. V., Steyn, K., Hurdogan, E., Bjorkman, T., O'Sullivan, J. (2017): Predicting the quantifiable impacts of iso 50001 on climate change mitigation. – Energy Policy 107: 278-288.
[17] Nichols, D. C., Wahlen, J. M. (2004): How do earnings numbers relate to stock returns, a review of classic accounting research with updated evidence. – Accounting Horizons 18(4): 263-286.
[18] Obraczka, M., Beyeler, M., Magrini, A., Legey, L. F. (2017): Analysis of coastal environmental management practices in subregions of California and Brazil. – Journal of Coastal Research 33(6): 1315-1332.
[19] Sheikhhosseini, E. (2018): Design and effective synthesis of novel furo[2,3-d]pyrimidine derivatives containing ethylene ether spacers. – Journal of Saudi Chemical Society 22(3): 337-342.
[20] Tehraniana, S., Zhao, Y. S., Harveya, T., et al. (2006): A robust framework for real-time distributed processing of satellite data. – Journal of Parallel Distributed Computing 66: 403-418.
[21] Wen, X. Z., Shao, L., Xue, Y., et al. (2015): A rapid learning algorithm for vehicle classification. – Information Sciences 295(1): 395-406.
[22] Xiang, B., Li, G. Q., Liu, D. S., et al. (2008): Research on task management and scheduling of high performance remote sensing satellite ground pre-processing system. – Journal of Astronautics 29(4): 1443-1446.
[23] Yang, Y. S., Xu, B. W., Li, J. J. (2015): An improved genetic algorithm for fast configuration design of large-scale container cranes. – Journal of Information and Computational Science 12(11): 4319-4330.
[24] You, J., Sun, Y., Bo, Y., Zhu, Y., Duan, D., Cui, H., Lu, Q. (2018): The association between dietary isoflavones intake and gastric cancer risk: a meta-analysis of epidemiological studies. – BMC Public Health 18(510).
[25] Zhang, L., Sun, J., Guo, C. (2017): A novel multi-objective discrete particle swarm optimization with elitist perturbation for reconfiguration of ship power system. – Polish Maritime Research 24(SI): 79-85.

http://www.aloki.hu ● ISSN 1589 1623 (Print) ● ISSN 1785 0037 (Online)
DOI: http://dx.doi.org/10.15666/aeer/1705_1050910523

[26] Zhang, W. F., Wang, L. Z., Ma, Y., et al. (2014): Design and implementation of task scheduling strategies for massive remote sensing data processing across multiple data centers. – Software-Practice and Experience 44(7): 873-886.
[27] Zhang, Y. H., Sun, X. M., Wang, B. W. (2016): Efficient algorithm for K-barrier coverage based on integer linear programming. – China Communications 13(7): 16-23.
[28] Zhao, Z. J. (2003): An analysis of the deviation of stock market price from its intrinsic value. – Economic Research Journal 10: 66-74.
[29] Zou, Y. Y., Zhang, Y. D., Li, Q. H., et al. (2015): Improved multi-objective genetic algorithm based on parallel hybrid evolutionary theory. – International Journal of Hybrid Information Technology 8(1): 133-140.
[30] Zuo, X. Q., Chen, C., Tan, W., et al. (2015): Vehicle scheduling of an urban bus line via an improved multi-objective genetic algorithm. – IEEE Transactions on Intelligent Transportation Systems 16(2): 1030-1041.

http://www.aloki.hu ● ISSN 1589 1623 (Print) ● ISSN 1785 0037 (Online)
DOI: http://dx.doi.org/10.15666/aeer/1705_1050910523

EFFECT OF INORGANIC NUTRIENT POLLUTANTS ON OVIPOSITION PREFERENCE, EGG HATCHING RATE AND LARVAL DEVELOPMENT OF *CULEX QUINQUEFASCIATUS*

ILAHI, I.[1*] – YOUSAFZAI, A. M.[2] – HAQ, T. U.[3] – ATTAULLAH, M.[1] – RAHIM, A.[1] – ALI, H.[1] – MUHAMMAD, H.[1] – HALIMULLAH[1] – FAROOQ, M.[1] – ALI, Y.[1] – ROGHANI, K.[1] – BIBI, J.[1] – KHAN, S.[1] – MEHMOOD, A.[1]

[1]*Department of Zoology, University of Malakand*
Chakdara, Dir Lower, Khyber Pakhtunkhwa, Pakistan

[2]*Department of Zoology, Islamia College Peshawar*
Peshawar, Khyber Pakhtunkhwa, Pakistan

[3]*Department of Biotechnology, University of Malakand*
Chakdara, Dir Lower, Khyber Pakhtunkhwa, Pakistan

[*]*Corresponding author*
e-mail: ikramilahi@uom.edu.pk

(Received 30th Jan 2019; accepted 21st Mar 2019)

Abstract. The present research aims to evaluate the effects of ammonium (NH_4^+), nitrate (NO_3^-) and phosphate (PO_4^{-3}) on oviposition preference, hatching rate, time to pupation, pupation rate, time to adult emergence, adult emergence rate and female to male ratio of *Culex quinquefasciatus* mosquito, under laboratory conditions. The mosquito preferred to oviposit in containers containing 5 ppm NH_4^+, 45 ppm NO_3^- or 30 ppm PO_4^{-3} solution. No significant effect of these polutants on egg hatching rate was observed. The larvae that existed in containers containing 5 ppm NH_4^+, 45 ppm NO_3^- or 30 ppm PO_4^{-3} solution reached earlier to pupal and adult stages. The presence of NH_4^+ (5 ppm), NO_3^- (45 ppm) or PO_4^{-3} (30 ppm) in aqueous medium, resulted in decreased time to pupation or adult emergence and increased pupation and adult emergence rates. The adults emerged from these larvae showed significantly higher female to male ratio as compared to control adults ($P<0.05$). From the findings of the present research, it is concluded that the levels of NH_4^+, NO_3^- or PO_4^{-3} set in effluents for wastewater reuse in agricultural irrigation by WHO (2006) are favorable for the survival and development of *Cx. quinquefasciatus* mosquito, however higher levels of NH_4^+, NO_3^- or PO_4^{-3} are not favorable for the survival and development of this mosquito. These results help in identification of concentration ranges of the ammonium, nitrate and phosphate that make the larval habitat favorable for survival and reproduction of *Culex* mosquitoes. This could be helpful in effective control of mosquito borne diseases.
Keywords: *oviposition preference, hatching rate, pupation rate, time to pupation, emergence rate, time to adult emergence, female to male ratio*

Introduction

Mosquito larval habitats are influenced by many physical, chemical and biological factors. The results of several studies have shown the relationship between habitat characteristics and mosquito larval abundance and distribution (Kenea et al., 2011). Ammonium (NH_4^+), nitrate (NO_3^-) and phosphate (PO_4^{-3}) are the well-known inorganic nutrient pollutants of water bodies. The NH_4^+, NO_3^- and other ionic forms of inorganic nitrogen enter the surface water bodies both from natural and anthropogenic sources (Wetzel, 2001; Rabalais, 2002). Phosphate is also an important inorganic nutrient in aquatic ecosystem and surface water receives it from various

http://www.aloki.hu ● ISSN 1589 1623 (Print) ● ISSN 1785 0037 (Online)
DOI: http://dx.doi.org/10.15666/aeer/1705_1052510541

sources such as agricultural use of fertilizers, domestic and industrial wastewater, and atmospheric deposition (Tchobanoglous and Burton, 1991; Grubb et al., 2000).

The inorganic nutrient pollutants such as NH_4^+, NO_3^- and PO_4^{-3} in mosquito breeding sites influences the development of mosquito larvae (Noori et al., 2015). Breeding sites with higher NH_4^+, NO_3^- and PO_4^{-3} concentration provide better microbial food source for mosquito larvae (Dowling et al., 2013). Knowledge of mosquito breeding habitats is useful for identifying the most productive water bodies in a given area and developing efficient control approaches (Noori et al., 2015). Noori et al. (2015) designed a mesocosm experiment for investigating the relationships between inorganic nutrient pollutants (i.e., NH_4^+, NO_3^- and PO_4^{-3}) concentrations and larval development of *Cx. quinquefasciatus*. High concentrations of nitrate and phosphate favored the larval development and survival rates. High NO_3^- concentration suppressed the development of female mosquito but favored the development of male mosquitoes. The adult mosquitoes which emerged in high NO_3^- concentration solution were found to be faster in development. It was further observed that in the absence of NO_3^-, the addition of PO_4^{-3} slow the larval development. Schletzbaum (2013), evaluated the influence of water nutrient pollutant on the sequence of larval hatching of two mosquito species, *Culex pipiens* and *Anopheles albopictus* in container habitats. Higher NO_3^- concentration in the larval environment resulted in larger *Anopheles albopictus* females and higher emergence rate and shorter time to emergence for *Culex pipiens*.

Increased level of different forms of inorganic nitrogen in water is toxic to fresh water invertebrates, fishes and amphibian (Hickey and Vickers, 1994; Camargo et al., 2005). Phosphate (PO_4^{-3}) toxicity with aquatic invertebrates has also been reported (Kim et al., 2013). According to Williams et al. (1986), the elevated levels of nitrates, ammonia and phosphorus in the surface waters (in both marine and fresh water), can affect invertebrate diversity in feeding grounds. According to the compendium of standards for wastewater reuse in the Eastern Mediterranean region, the maximum permissible concentrations of NH_4^+, NO_3^- and PO_4^{-3} in effluents for reuse in agricultural irrigation are 5, 45 and 30 ppm, respectively (WHO, 2006). Irrigation water for agriculture has the potential to create mosquito breeding habitats within the storage system for water along the water supplying channels or in the field that receive water.

Monitoring of pollutants in aquatic environment is necessary for investigating the status of pollution in such environment for protection of human life and wildlife. From environmental, ecological and economic point of view, regular assessment of the pollutant levels and their destiny in different media of environment is essential. Regulation and re-evaluation of the threshold levels of different pollutants set by different international and national organizations is very important. The present research aims to evaluate the effects of threshold levels of three inorganic nutrient pollutants (NH_4^+, NO_3^- and PO_4^{-3}) set by WHO (2006) compendium of standards for wastewater reuse in agricultural irrigation in the Eastern Mediterranean region on the life-history of a common and economically important insect (*Culex quinquefasciatus* Say, 182) in water under laboratory conditions. The study contributes to the science of the effects of increasing level of inorganic nutrient pollutants on insect populations.

http://www.aloki.hu ● ISSN 1589 1623 (Print) ● ISSN 1785 0037 (Online)
DOI: http://dx.doi.org/10.15666/aeer/1705_1052510541

Materials and methods

During the present research, the effects of NH_4^+, NO_3^- and PO_4^{-3} on oviposition preference, hatching rate and larval development of *Culex quinquefasciatus* (Say, 182) were studied in laboratory condition. During larval development, the effects of above inorganic nutrient pollutants on time to pupation, pupation rate, time till first appearance of adult, adult emergence rate, and female to male ratio were studied.

Required chemicals

The chemicals used included ammonium chloride (NH_4Cl) of Merck Co. (Darmstadt, Germany) for NH_4^+, sodium nitrate ($NaNO_3$) of Sigma-Aldrich (USA) for NO_3^- and sodium phosphate dibasic (Na_2HPO_4) of Sigma-Aldrich (USA) for PO_4^{-3}. The following are the detail of molar mass of the compounds and the related ions used during the present research:

- Ammonium chloride (NH_4Cl) molar mass is 53.5 g and contains 18 g of NH_4^+.
- Sodium nitrate ($NaNO_3$) molar mass is 85.5 g and contains 62 g of NO_3^{-1}.
- Sodium phosphate dibasic (Na_2HPO_4) molar mass is 144 g and contains 97 g of PO_4^{-3}.

Preparation of solutions

Initially 1000 ppm stock solution of each pollutant was prepared. For preparation of stock solution of 1000 ppm (1000 mg/L) of NH_4^+, 2.9 gram of NH_4Cl was required. For preparation of stock solution of 1000 ppm (1000 mg/L) of NO_3^-, 1.4 gram of $NaNO_3$ was required. For preparation of stock solution of 1000 ppm (1000 mg/L) of PO_4^{-3}, 1.5 gram of Na_2HPO_4 was required.

Laboratory rearing of Cx. quinquefasciatus

Experiments were conducted on the effects of NH_4^+, NO_3^{-1} and PO_4^{-3} on larval mortality, egg laying preference, egg hatching rate and larval development of *Cx. quinquefasciatus*. Laboratory colonies of *Cx. quinquefasciatus* were maintained during April and May 2016.

Laboratory conditions

The experiments were conducted during April and May 2016. Inside the laboratory, minimum temperature was $\geq$ 20°C and maximum temperature was $\leq$ 33°C. The laboratory was wide, well ventilated and receiving sun light at the day time through glass windows.

Bioassay for effect of inorganic nutrient pollutants on oviposition preference

According to the standards for wastewater reuse in the Eastern Mediterranean Region, the maximum permissible concentrations of NH_4^+, NO_3^{-1} and PO_4^{-3} in effluents for reuse in agricultural irrigation are 5, 45 and 30 ppm, respectively (WHO, 2006). Irrigation water for agriculture has the potential to create mosquito breeding habitats within the storage system for water along the water supplying channels or in the field that receive water. The present study aimed to investigate the effect of NH_4^+, NO_3^{-1} and PO_4^{-3} on oviposition preference of *Cx. quinquefasciatus* at the concentrations which are permissible in effluents for reuse in agricultural irrigation (WHO, 2006). The effect of

http://www.aloki.hu ● ISSN 1589 1623 (Print) ● ISSN 1785 0037 (Online)
DOI: http://dx.doi.org/10.15666/aeer/1705_1052510541

NH_4^+, NO_3^{-1} and PO_4^{-3} on oviposition preference of *Cx. quinquefasciatus* was also studied at concentrations higher than WHO recommended concentrations of these nutrient pollutants in effluents for reuse in agricultural irrigation (WHO, 2006). Thus, two concentrations of NH_4^+ (5 and 10 ppm), NO_3^{-1} (45 and 90 ppm) and PO_4^{-3} (30 and 60 ppm) were tested for their effect on oviposition preference of *Cx. quinquefasciatus* gravid female adult. The main purpose was to investigate the effect of NH_4^+, NO_3^{-1} and PO_4^{-3} on oviposition preference of *Cx. quinquefasciatus* at concentrations which are permissible in effluents for reuse in agricultural irrigation (WHO, 2006). Three mosquito cages (cage 1-3) were used during this experiment (*Figure 1*).

Figure 1. *Picture showing mosquito cages used during the present research*

During the study of effect of NH_4^+ on oviposition preference of *Cx. quinquefasciatus* gravid female adult, two NH_4^+ solutions of 5 and 10 ppm (300 ml each) in two 400 ml polyethylene containers were placed in mosquito cage (45 cm × 45 cm × 45 cm). In addition, a control polyethylene container containing 300 ml non-chlorinated tap water was also placed inside the mosquito cage along with NH_4^+ solution. For studying the effect of NO_3^{-1} on oviposition preference, two NO_3^{-1} solutions of 45 and 90 ppm (300 ml each) in two 400 ml polyethylene containers were placed in mosquito cage. In addition, a control polyethylene container containing 300 ml non-chlorinated tap water was also placed inside the mosquito cage along with NO_3^{-1} solution. For studying the effect of PO_4^{-3} on oviposition preference, two PO_4^{-3} solutions of 30 and 60 ppm (300 ml each) in two 400 ml polyethylene containers were placed in a mosquito cage. In addition, a control polyethylene container containing 300 ml non-chlorinated tap water was also placed inside the mosquito cage along with PO_4^{-3} solution. The experiment was run in triplicate.

For each mosquito cage, 100 blood fed and gravid female adult mosquitoes (5 days of age after emergence from pupae) were caught from the existing laboratory colony of *Cx. quinquefasciatus* through mouth aspirator and then introduced into the cage. The gravid female mosquitoes laid egg into the containers after 2 or 3 days of introduction. The number of egg rafts laid by female mosquitoes in each jar was counted under stereo binocular microscope with digital camera (Labomed Inc, USA) so that to determine the effect of inorganic nutrient pollutants on the egg laying preference of *Cx. quinquefasciatus* female adult mosquitoes. Schematic of experiment on the effect of inorganic nutrient pollutants on oviposition preference and egg hatching rate is shown in *Figure 2*. Egg rafts and eggs within rafts have been shown in *Figures 3-4*.

http://www.aloki.hu ● ISSN 1589 1623 (Print) ● ISSN 1785 0037 (Online)
DOI: http://dx.doi.org/10.15666/aeer/1705_1052510541

Bioassay for effect of inorganic nutrient pollutants on egg hatching rate

The egg rafts laid by the gravid female mosquitoes during oviposition assays for NH_4^+, NO_3^- and PO_4^{-3}, hatched into first instar larvae. After two days of hatching, all the containers were brought out of the mosquito cages and the total number of eggs and the number of hatched out larvae were counted.

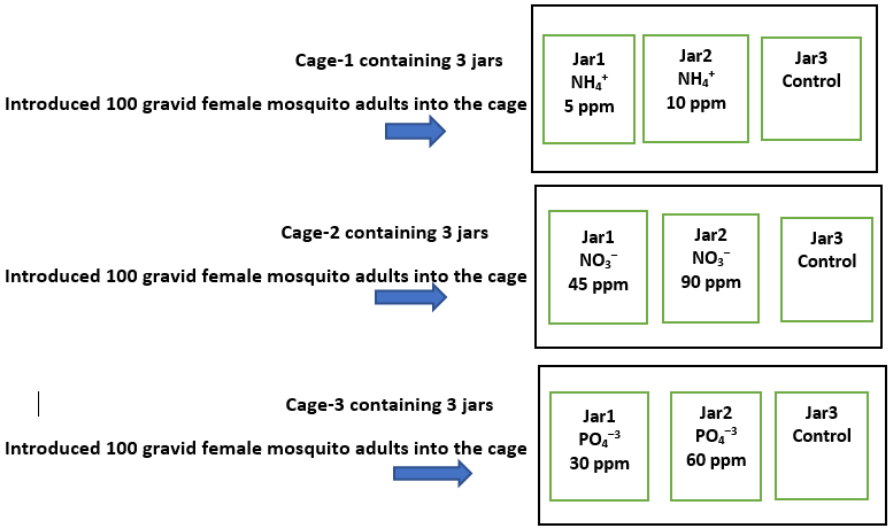

Figure 2. *Schematic of experiment on the effect of inorganic nutrient pollutants on oviposition preference and egg hatching rate*

Figure 3. *Egg rafts deposited by Culex quinquefasciatus during the present experiments*

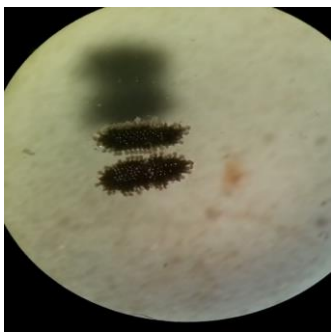

Figure 4. *Microscopic picture of Culex quinquefasciatus eggs in rafts taken during the present experiments*

http://www.aloki.hu ● ISSN 1589 1623 (Print) ● ISSN 1785 0037 (Online)
DOI: http://dx.doi.org/10.15666/aeer/1705_1052510541

Bioassay for effect of inorganic nutrient pollutant on larval development

The effect of high concentration of NH_4^+ (5 ppm), NO_3^- (45 ppm) and of PO_4^{-3} (30 ppm) in water on larval development of *Cx. quinquefasciatus* were also studied as these concentrations are allowable according to a compendium of standards for wastewater reuse in the Eastern Mediterranean Region (WHO, 2006). The schematic of experiment on the effect of inorganic nutrient pollutants on larval development of *Cx. quinquefasciatus* is shown in *Figure 5*. Thus 5 ppm concentration of NH_4^+, 45 ppm concentration of NO_3^- and 30 ppm concentration of PO_4^{-3} were prepared in three 1000 ml polyethylene jars. The solutions were prepared from stock solutions in sieved pond water for ensuring the presence of natural communities of microflora (Noori et al., 2015). The volume of each testing solution was 500 ml. In addition, a control 1000 ml polyethylene jar containing only 500 ml sieved river water was also arranged. Dried leaf litter of *Chenopodium album* was collected along the boundary wall of University of Malakand as there was no history of pesticides application. The leaf litter was ground into powder. During this experiment, 100 mg of leaf litter powder was added to each jar including control jar for providing source of carbon (Schletzbaum, 2013; Noori et al., 2015).

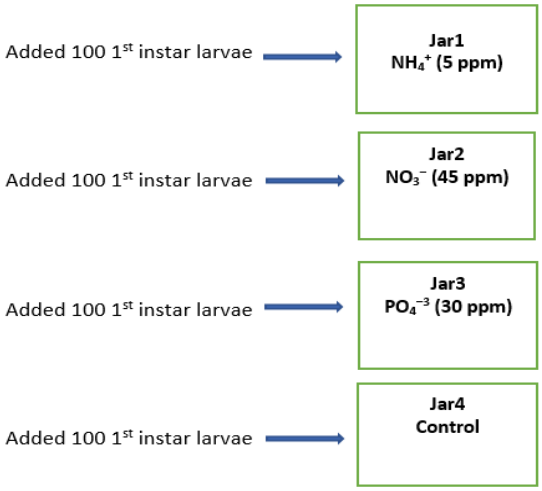

Figure 5. *Schematic of experiment on the effect of inorganic nutrient pollutants on larval development of Cx. quinquefasciatus*

One hundred newly hatched 1st instar larvae (a day after hatching) larvae of *Cx. quinquefasciatus* from laboratory colony were transferred to each polyethylene jar. This experiment was run in four replicates. The jars were capped with gauze to prevent the escape of emerging adult mosquitoes. The jars were daily checked for the appearance of pupae and adults. The observations were continued till all the larvae or pupae in all the jars have died or emerged as adults. The effect of NH_4^+, NO_3^- and PO_4^{-3} on time to pupation, pupation rate, time to adult emergence, adult emergence rate and female to male ratios were studied. All the mosquito adults were counted and the female to male ratio was determined by dividing the total number of female adults by the total number of male adults (Neira et al., 2014). Time to pupation or adult emergence was calculated by the following method (Kosalwat and Knight, 1987) (*Eq.1*):

http://www.aloki.hu ● ISSN 1589 1623 (Print) ● ISSN 1785 0037 (Online)
DOI: http://dx.doi.org/10.15666/aeer/1705_1052510541

$$T = \sum (D \times N) / \sum N \quad \text{(Eq.1)}$$

where T represents the average time to pupation or adult emergence (in days), D represents the number of days from day zero of exposure of first instar larvae to pupation or adult emergence and N represents the number of pupae or adults produced. *Figure 6* shows the pictures of egg, larval, pupal and adult stages of life history of *Culex quinquefasciatus* mosquito. The pictures have been taken in the laboratory during the present experiments.

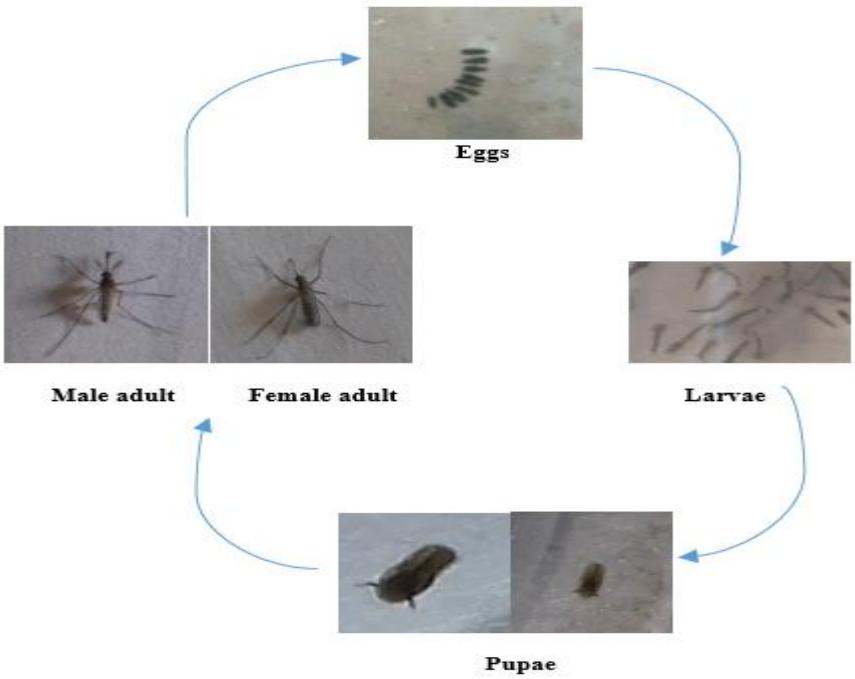

Figure 6. *Picture showing the egg, larval, pupal and adult stages of life history of Culex quinquefasciatus mosquito. The figure has been produced from the pictures taken in the laboratory during the present experiments*

Statistical analysis

The data was initially analyzed by normality test of Shapiro-Wilk. If the P value was less than 0.05 then the data was analyzed by Kruskal-Wallis test for comparison (Schlotzhauer and Little, 1987). When the P value in Kruskal-Wallis test was less than 0.05 then the Kruskal-Wallis test was followed by Bonferroni's post hoc test for pairwise comparison. The data was presented as the mean rank. If the value of P in normality test was greater than 0.05 then the data was analyzed by Dunnett's Test at P>0.05 significance level for assessing significant difference between control and each of the treatment solution. In this case the data was presented as mean with standard error. The LC_{50} values were compared by 95 % confidence limits overlap method (Wheeler et al., 2006).

http://www.aloki.hu ● ISSN 1589 1623 (Print) ● ISSN 1785 0037 (Online)
DOI: http://dx.doi.org/10.15666/aeer/1705_1052510541

Results

Oviposition preference of Cx. quinquefasciatus

The effect of NH_4^+ (5 ppm and 10 ppm), NO_3^- (45 ppm and 90 ppm) and PO_4^{-3} (30 ppm and 60 ppm) on oviposition preference of *Cx. quinquefasciatus* is shown in *Table 1*. Data is presented as means (with standard error of means) and mean ranks of egg rafts. Based on normality test of Shapiro-Wilk, the data was not normally distributed, therefore the data was analyzed by Kruskal-Wallis test at $P<0.05$ significance level for determining significant difference.

During the study of effect of NH_4^+ on oviposition preference, the Kruskal Wallis χ^2 value was 6.0 and the P value was 0.05. The overall test showed significant difference in the mean ranks of egg rafts across the control and treatment containers (5 ppm and 10 ppm NH_4^+ solutions). The mean rank of egg rafts in 5 ppm NH_4^+ solution container (mean rank = 8.0) was significantly higher when compared to control container ($P<0.05$). The control container and 10 ppm NH_4^+ solution container showed similar mean rank of egg rafts (mean rank = 3.5 each).

Table 1. *Effect of inorganic nutrient pollutants in water on oviposition preference of Cx. quinquefasciatus (n=3)*

Pollutants	Concentration	N. of egg rafts Mean± SE	Mean rank of egg rafts
Ammonium (NH_4^+)	Control	1.6±0.3	3.5
	5 ppm	7.3±0.7*	8
	10 ppm	1.6±0.6	3
			KW, χ^2=6.0
			P=0.05
Nitrate (NO_3^-)	Control	1.3±0.3	2
	45 ppm	8.0±1.2*	8
	90 ppm	3.6±0.3	5
			KW, χ^2=7.3
			P=0.03
Phosphate (PO_4^{-3})	Control	2.6±0.3	4
	30 ppm	12.7±1.8*	8
	90 ppm	2.3±0.3	3
			KW, χ^2=6
			P=0.049

KW - Kruskal-Wallis, *-.significantly different from the control at $P<0.05$ significance level in Kruskal-Wallis test

During the study of effect of NO_3^- on oviposition preference, the Kruskal Wallis χ^2 value was 7.3 and P value was 0.03. The overall test showed significant difference in mean ranks of egg rafts across the control and treatment containers (45 ppm and 90 ppm NO_3^- solutions). The mean rank of egg rafts in 45 ppm NO_3^- solution container (mean rank = 8.0) was significantly higher when compared to control container (mean rank = 2) ($P<0.05$). There was no significant difference ($P>0.05$) in the mean rank of 90 ppm NO_3^- solution container (mean rank = 5) and control container (mean rank = 2).

During the study of effect of PO_4^{-3} on oviposition preference, the Kruskal Wallis χ^2 value was 6.0 and P value was 0.050. The overall test showed significant difference in mean ranks of egg rafts across the control and treatment containers (30 ppm and 60 ppm PO_4^{-3} solutions). The mean rank of egg rafts in 30 ppm PO_4^{-3} solution container

http://www.aloki.hu ● ISSN 1589 1623 (Print) ● ISSN 1785 0037 (Online)
DOI: http://dx.doi.org/10.15666/aeer/1705_1052510541

(mean rank = 8.0) was significantly higher when compared to control container (mean rank = 4) ($P<0.05$). The mean rank of egg rafts of 60 ppm PO_4^{-3} solution container (mean rank = 3) was insignificantly lower ($P>0.05$) when compared to control container (mean rank = 4).

Hatching rate of Cx. quinquefasciatus

The effect of NH_4^+, NO_3^- and PO_4^{-3} on hatching rate of *Cx. quinquefasciatus* is shown in *Table 2*. Based on normality test of Shapiro-Wilk, the data was normally distributed, therefore the data was analyzed by Dunnett's Test at $P<0.05$ significance level for determining significant difference between control container and each of the inorganic nutrient pollutant solution containers. Data is presented as means with standard error of means. During this study, no significant difference in egg hatching rate of *Cx. quinquefasciatus* eggs was observed between the control container and any of the treatment containers ($P>0.05$).

Table 2. *Effect of inorganic nutrient pollutants in water on egg hatching rate of Cx. quinquefasciatus (n=3)*

Pollutants	Concentration (ppm)	Number of Eggs (Mean ± SE)	Number of hatched larvae (Mean ±SE)	Hatching rate (Mean % ± SE)
Ammonium (NH_4^+)	Control	153.3 ± 31.8	134.6 ± 32.8	86.9±4.6
	5	724.7 ± 68.7	703.3 ± 69.9	97± 0.6
	10	160.0 ± 35.1	140.0 ± 27.5	88.8±3.2
				P>0.05
Nitrate (NO_3^-)	Control	136.3 ± 35.4	123.7 ± 31.9	96.7±1.9
	45	780.0 ± 118.4	758.3 ± 118.7	97.03±1.3
	90	353.3 ± 34.4	337.7 ± 31.2	96.6.6±1.6
				P>0.05
Phosphate (PO_4^{-3})	Control	262.3 ± 41.2	239.3 ± 40.01	90.7±1.7
	30	1417.3 ± 123.2	1320.7 ± 115.8	93.2±0.6
	60	223.3 ± 26.2	212.0 ± 29.1	93.8±2.8
				P>0.05

There was no significant difference ($P>0.05$) in egg hatching rate between control and treatments

Larval development of Cx. quinquefasciatus

During the present research, the effect of 5 ppm NH_4^+, 45 ppm NO_3^- and 30 ppm PO_4^{-3} on larval development of *Cx. quinquefasciatus* were studied in the laboratory conditions. In addition, each container (including control) was also containing 100 grams leaf litter powder. The larval development study included the effect of above inorganic nutrient pollutants on time to pupation, pupation rate, time to adult emergence, adult emergence rate and female to male ratios. Following are the details:

Time to pupation of Cx. quinquefasciatus

The effect of 5 ppm NH_4^+, 45 ppm NO_3^- and 30 ppm PO_4^{-3} on time to pupation in *Cx. quinquefasciatus* is shown in *Table 3*. During this study, a total of one hundred first instar larvae were exposed to each nutrient pollutant. The value of significance in normality test of Shapiro-Wilk showed that the data is normally distributed, therefore the data was analyzed by Dunnett's Test (significance level=0.05) for determining significant difference between control and each of the inorganic nutrient pollutants. Data is presented as the mean and standard error of mean of four replicates. Each

http://www.aloki.hu ● ISSN 1589 1623 (Print) ● ISSN 1785 0037 (Online)
DOI: http://dx.doi.org/10.15666/aeer/1705_1052510541

pollutant caused a decrease in time to pupation. The minimum number of days to pupation was observed for PO_4^{-3} solution (8.5±0.6 days) followed by NO_3^- (12.5±0.6 days), NH_4^+ (13.5±0.6) and control (14.5±0.6). The difference in time to pupation between the control and PO_4^{-3} solution container was significant ($P<0.05$). However, the difference between the control and the rest of the pollutants i.e., NH_4^+ or NO_3^- was insignificant ($P>0.05$).

Table 3. *Effect of inorganic nutrient pollutants in water on time to pupation in Cx. quinquefasciatus (n=4)*

Treatment	Days (Means ± SE)	95% Confidence Intervals		Minimum	Maximum
		Lower limit	Upper limit		
Control	14.5 ± 0.6	12.4	16.6	13.0	16.0
Ammonium (NH_4^+)	13.5 ± 0.6	11.4	15.6	12.0	15.0
Nitrate (NO_3^-)	12.5 ± 0.6	10.4	14.6	11.0	14.0
Phosphate (PO_4^{-3})	8.5 ± 0.6*	6.4	10.6	7.0	10.0
Statistics	F= 16.6, DF within groups= 12, P=0.000				

*- Significantly different from the control at P<0.05 significance level

Pupation rate of Cx. quinquefasciatus

The effect of NH_4^+ (5 ppm), NO_3^- (45 ppm) and PO_4^{-3} (30 ppm) on pupation rate in *Cx. quinquefasciatus* is shown in *Table 4*. The value of significance in normality test of Shapiro-Wilk showed that the data is normally distributed, therefore the data was analyzed by Dunnett's Test (significance level≤0.05) for determining significant difference between control and each of the pollutants. Data is presented as the mean and standard error of mean of four replicates. Pupation rates in NH_4^+ solution container (52.0±9.9%) and PO_4^{-3} solution container (51.8±9.6%) were significantly higher ($P<0.05$) when compared to control containers (27.0±4.9%). Pupation rate in NO_3^- solution container (33.0±3.4%) was insignificantly higher than pupation rate in control container ($P>0.05$).

Table 4. *Effect of inorganic nutrient pollutants in water on pupation rate in Cx. quinquefasciatus (n=4)*

Treatment	Pupation rate (% Means ± SE)	95% Confidence Intervals		Minimum	Maximum
		Lower limit	Upper limit		
Control	27.0 ± 4.9	11.4	42.6	18.0	39.0
Ammonium (NH_4^+)	52.0 ± 9.9*	9.6	94.4	36.0	70.0
Nitrate (NO_3^-)	33.0 ± 3.4	22.2	43.8	25.0	40.0
Phosphate (PO_4^{-3})	51.8 ± 9.6*	21.04	82.5	30.0	77.0
Statistics	F= 3.2, DF within groups= 12, P<0.066				

*- Significantly different from the control at P<0.05 significance level

Time to adult emergence of Cx. quinquefasciatus

The effect of 5 ppm NH_4^+, 45 ppm NO_3^- and 30 ppm PO_4^{-3} in water on time to adult emergence in *Cx. quinquefasciatus* is shown in *Table 5*. The value of significance in normality test of Shapiro-Wilk showed that the data is normally distributed, therefore

http://www.aloki.hu ● ISSN 1589 1623 (Print) ● ISSN 1785 0037 (Online)
DOI: http://dx.doi.org/10.15666/aeer/1705_1052510541

the data was analyzed by Dunnett's Test (significance level=0.05) for determining significant difference between control and each of the inorganic nutrient pollutants. Data is presented as the mean and standard error of mean of four replicates. The minimum number of days to adult emergence was observed for PO_4^{-3} solution (11.5±1.7 days) followed by NO_3^- (15.0±1.4 days), NH_4^+ (17.0±1.4 days) and control (18.5±2.08 days). The difference in time to adult emergence between the control and PO_4^{-3} or NO_3^- solution container was significant ($P<0.05$). However, the difference between the control and NH_4^+ was insignificant ($P>0.05$).

Table 5. *Effect of inorganic nutrient pollutants in water on time to adult emergence in Cx. quinquefasciatus (n=4)*

Treatment	Days (Means ± SE)	95% Confidence Intervals		Minimum	Maximum
		Lower limit	Upper limit		
Control	18.5 ± 2.08	15.2	21.8	16.0	21.0
Ammonium (NH_4^+)	17.0 ± 1.4	14.7	19.3	16.0	19.0
Nitrate (NO_3^-)	15.0 ± 1.4*	12.7	17.3	13.0	16.0
Phosphate (PO_4^{-3})	11.5 ± 1.7*	8.74	14.3	10.0	14.0
Statistics	F= 12.9, DF within groups= 12, P<0.01				

*- Significantly different from the control at P<0.05 significance level

Adult emergence rate of Cx. quinquefasciatus

The effect of NH_4^+ (5 ppm), NO_3^- (45 ppm) and PO_4^{-3} (30 ppm) in water on adult emergence rate in *Cx. quinquefasciatus* is shown in *Table 6*. Data was presented as the mean and standard error of mean of emergence rates (n=4). The value of significance in normality test of Shapiro-Wilk showed that the data is normally distributed, therefore the data was analyzed by Dunnett's Test (significance level≤0.05) for determining significant difference between control and each of the pollutant solution.

Table 6. *Effect of inorganic nutrient pollutants in water on adult emergence rate of Cx. quinquefasciatus (n=4)*

Treatment	Emergence rate (%) (Mean ± SE)	95% Confidence Intervals		Minimum	Maximum
		Lower limit	Upper limit		
Ammonium (NH_4^+)	31.5 ± 4.4	17.5	45.6	22.3	40.01
Nitrate (NO_3^-)	61.9 ± 8.7*	34.3	89.5	44.3	83.3
Phosphate (PO_4^{-3})	61.5 ± 1.9*	55.4	67.4	56.8	65.0
Ammonium (NH_4^+)	57.1 ± 11.5*	20.5	93.8	32.5	86.6
Statistics	DF=12, F=3.6, P<0.05				

*- Significantly different from the control at P<0.05 significance level

Significantly higher number of adults emerged in the NH_4^+, NO_3^- or PO_4^{-3} solution container when compared to control container ($P<0.05$). Maximum adult emergence rates were observed in NH_4^+ (61.9±8.7%) and NO_3^- solution container (61.5±1.9%).

http://www.aloki.hu ● ISSN 1589 1623 (Print) ● ISSN 1785 0037 (Online)
DOI: http://dx.doi.org/10.15666/aeer/1705_1052510541

Female to male ratio of Cx. quinquefasciatus

All the adults were counted and the percentage of female and male mosquitoes to the total number of adults produced were determined for each jar. Female to male ratio was obtained through dividing the number of female adult mosquitoes by the number of male adult mosquitoes. Data was presented as the mean of percentage of female and male *Cx. quinquefasciatus* mosquito and mean female to male ratio (*Table 7*). The value of significance in normality test of Shapiro-Wilk showed that the data is distributed normally, therefore the data was analyzed by Dunnett's Test (significance level≤0.05) for determining significant difference between control and each of the pollutant solutions.

Table 7. *Effect of inorganic nutrient pollutants in water on female to male ratio of Cx. quinquefasciatus (n=4)*

Treatment	% Female (Mean ± SE)	% Male (Mean ± SE)	Female to male ratio (Mean ± SE)
Control	42.9 ± 2.3	57.1 ± 2.3	0.7 ± 0.07
Ammonium (NH_4^+)	52.4 ± 0.9*	47.7 ± 0.9*	1.1. ± 0.94*
Nitrate (NO_3^-)	62.7 ± 2.2*	37.3 ± 2.1*	1.7 ± 0.13*
Phosphate (PO_4^{-3})	60.8 ± 1.2*	39.2 ± 1.2*	1.6 ± 0.08*

*- Significantly different from the control at P<0.05 significance level

The female to male adult ratio for NH_4^+, NO_3^- and or PO_4^{-3} solution container was significantly higher than control container (P<0.05). Maximum female to male ratio was observed for NO_3^- solution container that was 1.7±0.13 (62.7±2.2% females, 37.3±2.1% males). After NO_3^-, maximum female to male ratio was noted for PO_4^{-3} that was 1.6±0.08 (60.8±1.2% females, 39.2±1.2% males). The lowest female to male ratio was observed for control container that was 0.7±0.07 (42.9±2.3% females, 57±2.3% males).

Discussion

During the present study, the effects of NH_4^+, NO_3^- and PO_4^{-3} on oviposition preference, hatching rate and larval development parameters of *Cx. quinquefasciatus* were studied under laboratory conditions. During the study of effect of these pollutants on oviposition preference, the effect of two environmentally realistic concentrations of NH_4^+ (5 ppm and 10 ppm) on oviposition preference of gravid female adult *Cx. quinquefasciatus* was studied. Gravid female *Cx. quinquefasciatus* adults preferred the container containing 5 ppm NH_4^+ solution but did not prefer the container containing 10 ppm NH_4^+ solution or control container (containing only non-chlorinated tap water) (*Table 1*). For example, the number of egg rafts in the container containing 5 ppm NH_4^+ was significantly higher than control container where as the number of egg rafts in the container containing 10 ppm NH_4^+ was insignificantly lower than control container (P>0.05). Nguyen et al. (2012) observed higher number of mosquito egg rafts in water containing NH_4^+ above 2 ppm when temperature was high (> 32°C). They observed lower number of egg rafts at the same concentration of NH_4^+ when temperature was lower. During the present research, minimum temperature was ≥ 20°C and maximum temperature was ≤ 33°C in which NH_4^+ at 5 ppm concentration acted as oviposition attractant for *Cx. quinquefasciatus*. During the study of effect of NO_3^- (at 45 ppm and 90 ppm) on oviposition preference of *Cx. quinquefasciatus,* the results

http://www.aloki.hu ● ISSN 1589 1623 (Print) ● ISSN 1785 0037 (Online)
DOI: http://dx.doi.org/10.15666/aeer/1705_1052510541

show that gravid female *Cx. quinquefasciatus* mosquito preferred water bodies with lower NO_3^- concentration (45 ppm) for oviposition. Water without NO_3^- and water with higher NO_3^- concentration (90 ppm) were less preferred for oviposition. These results suggest that NO_3^- in water attract the gravid female *Cx. quinquefasciatus* mosquito for oviposition, however water with higher NO_3^- concentration is not highly preferred for oviposition by *Cx. quinquefasciatus* mosquito (*Table 1*). To the author knowledge, limited studies have been conducted on the effect of NO_3^- on the oviposition preference of mosquitoes. For example, Nguyen et al. (2012) studied seasonal, weather, nutrients, and conspecific presence impacts on *Cx. quinquefasciatus* mosquito in combined sewage overflows. It was observed that high NO_3^- concentration i.e. >1 ppm is associated with decrease in the number of oviposited egg rafts. During the present research, the same trend of association of decreased number of egg rafts with high NO_3^- concentration was observed. During the experiment of Grech and Juliano (2017), the female *Cx. restuans* mosquito laid more eggs in containers having low amount of plant detritus but high concentration of total dissolved nitrogen, however after some days the gravid female *Cx. restuans* preferred those containers for oviposition which were containing high amount of plant detritus but low concentration of total dissolved nitrogen and high phosphate concentration. They concluded that the concentrations of total dissolved nitrogen and phosphorus have differential effect on the oviposition preference of the gravid female *Cx. restuans*, and the mosquitoes favor different nutrients in different circumstances and do not always oviposit preferentially in containers rich in plant detritus. During the study of effect of PO_4^{-3} (at 30 ppm and 60 ppm) on oviposition preference of *Cx. quinquefasciatus*, the gravid female *Cx. quinquefasciatus* preferred the container for oviposition having lower PO_4^{-3} concentration (30 ppm), however they oviposited less number of egg rafts in containers containing no PO_4^{-3} (control) or containing higher concentration of PO_4^{-3} (60 ppm). A breeding site rich in PO_4^{-3} and NH_4^+ is an excellent larval habitat for *Cx. quinquefasciatus* (Nguyen et al., 2012). The NH_4^+ and PO_4^{-3} promote the growth of bacteria in breeding site; the bacteria serve as food source for mosquito larvae (Beehler and Mulla, 1995; Sunish and Reuben, 2001) and attract adult gravid female mosquito for oviposition (Beehler et al., 1994). Nguyen et al. (2012) studied the effect of seasons, weather, nutrients, and conspecific presence impacts on *Cx. quinquefasciatus* mosquito in combined sewage overflows. At lower PO_4^{-3} concentration, *Cx. quinquefasciatus* oviposited more eggs rafts, however at higher PO_4^{-3} concentration (>10 ppm), a decrease in the number of oviposited egg rafts was observed. Similar trend was observed during the present research. Agricultural fertilizers also influence the oviposition preference of adult gravid female mosquitoes. For example, Kibuthu et al. (2016) studied the effect of sub lethal concentrations of cypermethrin, glyphosate, ammonium sulfate and diammonium phosphate on oviposition preference of *Anopheles arabiensis* and *Culex quinquefasciatus* mosquitoes. Highest number of egg rafts were observed in diammonium phosphate and ammonium sulfate treatments.

During the study of effect of inorganic nutrient pollutants on egg hatching rate, no significant difference in egg hatching rate of *Cx. quinquefasciatus* in NH_4^+, NO_3^- or PO_4^{-3} solution container and control container was observed ($P>0.05$) (*Table 2*). To the author knowledge, there is no reported study about the effect of inorganic nutrient pollutants i.e., ammonium, nitrate and phosphate on the egg hatching rate in mosquitoes. The effect of temperature on hatching rate of mosquito eggs has been reported. For example, Oda et al. (1999) studied the effect of temperature on hatching

http://www.aloki.hu ● ISSN 1589 1623 (Print) ● ISSN 1785 0037 (Online)
DOI: http://dx.doi.org/10.15666/aeer/1705_1052510541

rate and adult survival of *Cx. pipiens molestus* and *Cx. quinquefasciatus*. The egg hatching rate of *Cx. pipiens molestus* became very low with rise in temperature, however no effect of temperature rises on egg hatching rate of *Cx. quinquefasciatus* was observed. Yang (2008) studied the effect of site deprivation on oviposition performance and egg hatching rate of naturally blood–fed gravid *Culex quinquefasciatus* in the laboratory. Gravid female adults failed to form egg rafts, and egg hatching rate decreased significantly. Vitek and Livdahl (2006) compared the hatching rates of *Ae. Albopictus* eggs in both field and laboratory settings. The hatching rates were compared for mosquitoes exposed to regular, periodic hatch stimulation and random hatch stimulation. The hatching rate in laboratory treatments was not significantly different from the field treatments. Ezeakacha (2015) reported increase in egg hatch rate of *Aedes albopictus*, *Aedes aegypti*, *Aedes triseriatus* and *Culex quinquefasciatus* with increase in relative humidity and egg storage period.

The present study also aimed to investigate the effect of NH_4^+, NO_3^-, and of PO_4^{-3} in water at concentration of 5 ppm, 45 ppm and 30 ppm, respectively, on larval development parameters (such as time to pupation, pupation rate, time to adult emergence, adult emergence rate and female to male ratios) of *Cx. quinquefasciatus*. During this experiment, 100 mg of leaf litter powder was added to each jar including control jar for providing source of carbon (Schletzbaum, 2013; Noori et al., 2015). During the study of the effect of NH_4^+ (5 ppm), NO_3^- (45 ppm) and PO_4^{-3} (30 ppm) on time to pupation, larvae of control container larvae took more days to reach pupation, however the larvae in the containers that were containing NH_4^+, NO_3^- or PO_4^{-3} reached earlier to pupation (*Table 3*). Among the inorganic nutrient pollutants, PO_4^{-3} caused a significant decrease in time to pupation when compared to control ($P<0.05$). To the author knowledge, very limited studies have been conducted on the effect of pollutants on time to pupation in mosquitoes. For example, Noori et al. (2015) studied the effect of NH_4^+, NO_3^- and PO_4^{-3} in water on larval development of *Cx. quinquefasciatus*. During their study, larvae that were exposed to phosphate at concentration range of 1 ppm to 12 ppm without leaf litter, took more time in reaching to pupation. During the present study, the phosphate solution which was also containing 100 gram of leaf litter powder, caused a decrease in time to pupation. This indicated that larvae exposed to higher phosphate concentration (30 ppm) in presence of leaf litter reach early to pupation.

During the study of effect of NH_4^+ (5 ppm), NO_3^- (45 ppm), and PO_4^{-3} (30 ppm) on pupation rate of *Cx. quinquefasciatus*, significantly higher number ($P<0.05$) of larvae reached to pupation in NH_4^+ and PO_4^{-3} solution containers when compared to control container (*Table 4*). These results agree with the findings of Sunish and Reuben (2001) as they reported a positive influence of ammonia nitrogen and PO_4^{-3} on aquatic stages of mosquitoes. Similarly, in another study, increase in the concentration of NH_4^+ or PO_4^{-3} was associated with increase in the number of *Cx. quinquefasciatus* larvae that reached to pupation (Noori et al., 2015). There was observed no significant effect of NO_3^- (at 45 ppm) on pupation rate when compared to control ($P>0.05$). Noori et al. (2015) also found no significant correlation between increase in NO_3^- concentration and pupation rate. The presence of NH_4^+, NO_3^- and PO_4^{-3} accelerate the multiplication of microorganisms (Sunish and Reuben, 2001) that in turn favors the survival of *Culex* larvae. Paul et al. (2006) suggested that higher concentration of phosphorus in agricultural stream is associated with faster breakdown rate of leaf litter. The faster breakdown rate of leaf litter in water bodies results in multiplication of microorganisms.

http://www.aloki.hu ● ISSN 1589 1623 (Print) ● ISSN 1785 0037 (Online)
DOI: http://dx.doi.org/10.15666/aeer/1705_1052510541

Microorganisms in mosquito breeding sites constitute the major food source of mosquito larvae.

During the study of effect of NH_4^+ (5 ppm), NO_3^- (45 ppm) and PO_4^{-3} (30 ppm) in water on time to adult emergence of *Cx. quinquefasciatus*, in each of the NH_4^+, NO_3^- and PO_4^{-3} solution containers, the larvae took less number of days to reach to adulthood than in the control container (*Table 5*). The first instar larvae exposed to 45 ppm NO_3^- or 30 ppm PO_4^{-3} solution took significantly lower ($P<0.05$) number of days in reaching to adulthood when compared to the control. The larvae exposed to PO_4^{-3} took longer in reaching to adulthood. The larvae exposed to 5 ppm NH_4^+ solution took insignificantly higher number of days in reaching to adulthood when compared to control ($P>0.05$). The early emergence of adults in NH_4^+, NO_3^- or PO_4^{-3} solution containers (each containing 100 g leaf litter powder) can be attributed to increasing microbial activities (major food source of *Culex* larvae) (Sunish and Reuben, 2001; Paul et al., 2006).

During the study of effect of NH_4^+ (5 ppm), NO_3^- (45 ppm) and PO_4^{-3} (30 ppm) in water on adult emergence rate of *Cx. quinquefasciatus*, significantly higher number of adults emerged in NH_4^+, NO_3^- and PO_4^{-3} solution containers when compared to control container ($P<0.05$) (*Table 6*). Noori et al. (2015) reported the boosting effect of NH_4^+, NO_3^- and PO_4^{-3}on adult emergence rate of *quinquefasciatus*. Schletzbaum (2013) also reported the positive effect of NO_3^- concentration on adult emergence rate of *Cx. pipiens*. Agricultural fertilizers have also been reported for their effect on adult emergence rate of mosquitoes. For example, Kibuthu et al. (2016) observed significantly higher emergence rate of *Cx. quinquefasciatus* in diammonium phosphate treatment. The high emergence rate in NH_4^+, NO_3^- or PO_4^{-3} solution container can be attributed to increasing microbial activities (Sunish and Reuben, 2001; Paul et al., 2006).

During the study of effect of NH_4^+ (5 ppm), NO_3^- (45 ppm) and PO_4^{-3} (30 ppm) in water on female to male ratio of *Cx. quinquefasciatus*, the female to male adult ratio for each nutrient solution container was significantly higher than control container ($P<0.05$) (*Table 7*). Maximum female to male ratio was observed for NO_3^- and PO_4^{-3} solution container. To the author knowledge, very limited studies have been conducted on the effect of inorganic nutrient pollutants on female to male ratio in mosquitoes. For example, Noori et al. (2015) reported that high NO_3^- levels in water without leaf litter favored the development of male mosquitoes and suppresses the development of female mosquitoes. They suggested that the development of females might need more PO_4^{-3} than male development. But the findings of the present study suggest that high concentration of NH_4^+, NO_3^- or PO_4^{-3} favors the development of females. For the control container (containing only 100 grams leaf litter), the percentage of males was higher than the percentage of females (42.9±2.3% females, 57±2.3% males).

Conclusion

It is concluded that the levels of NH_4^+, NO_3^- and PO_4^{-3} recommended in effluents for wastewater reuse in agricultural irrigation by WHO (2006) are favorable for the survival and development of *Cx. quinquefasciatus* mosquito, however higher levels of NH_4^+, NO_3^- and PO_4^{-3} are not favorable for the survival and development of this mosquito. These results help in identification of concentration ranges of the NH_4^+, NO_3^- and PO_4^{-3} that make the larval habitat favorable for survival and reproduction of *Culex* mosquitoes. This could be helpful in effective control of mosquito borne diseases.

http://www.aloki.hu ● ISSN 1589 1623 (Print) ● ISSN 1785 0037 (Online)
DOI: http://dx.doi.org/10.15666/aeer/1705_1052510541

REFERENCES

[1] Beehler, J. W., Millar, J. G., Mulla, M. S. (1994): Protein hydrolysates and associated bacterial contaminants as oviposition attractants for the mosquito *Culex quinquefasciatus*. – Med. Vet. Entomol. 8: 381-385.

[2] Beehler, J. W., Mulla, M. S. (1995): Effects of organic enrichment on temporal distribution and abundance of culicine egg rafts. – J. Am. Mosq. Control Assoc. 11: 167-171.

[3] Camargo, J. A., Alonso, A., Salamanca, A. (2005): Nitrate toxicity to aquatic animals: a review with new data for freshwater invertebrates. – Chemosphere 58: 1255-1267.

[4] Dowling, Z., Ladeau, Sh. L., Armbruster, P., Biehler, D., Leisnham, P. T. (2013): Socioeconomic status affects mosquito (Diptera: Culicidae) larval habitat type availability and infestation level. – J. Med. Entomol. 50: 764-772.

[5] Ezeakacha, N. F. (2015): Environmental Impacts and Carry-over Effects in Complex Life Cycles: The Role of Different Life History Stages. – Ph.D. Dissertations, Graduate School of the University of Southern Mississippi.

[6] Grech, M. G., Juliano, S. A. (2017): Complex Effects of Superior Competitors and Resources on Culex restuans (Diptera: Culicidae) Oviposition. – J. Med. Entomol. XX(X): 1-10.

[7] Grubb, D. G., Guimarates, M. S., Valenica, R. (2000): Phosphate immobilizationusing an acidic typeF fly ash. – J. Hazards. Mater. 76: 217-236.

[8] Hickey, C. W., Vickers, M. L. (1994): Toxicity of Ammonia to Nine Native New Zealand freshwater Invertebrate Species. – Arch. Environ. Contain. Toxicol. 26: 292-298.

[9] Kenea, O., Balkew, M., Gebre-MichaeL, T. (2011): Environmental factors associated with larval habitats of anopheline mosquitoes (Diptera: Culicidae) in irrigation and major drainage areas in the middle course of the rift valley, central Ethiopia. – J. Vector Borne Dis. 48: 85-92.

[10] Kibuthul, T. W., Njenga, S. M., Mbugua, A. K., Muturi, E. J. (2016): Agricultural chemicals: life changer for mosquito vectors in agricultural landscapes? – Parasit Vectors 9: 500.

[11] Kim, E., Yoo, S., Ro, H. Y., Han, H. J., Baek, Y. W., Eom, I. C., Kim, H. M., Kim, P., Choi, K. (2013): Aquatic Toxicity Assessment of Phosphate Compounds. – Environ. Health. Toxicol. 28: e2013002.

[12] Kosalwat, P., Knight, A. W. (1987): Chronic toxicity of copper to a partial life cycle of the midge, Chironomus decorus. – Arch. Environ. Contam. Toxicol. 16: 283-290.

[13] Neira, M., Lacroix, R., Cáceres, L., Kaiser, P. E., Young, J., Pineda, L., Black, L., Sosa, N., Nimmo, D., Alphey, L., McKemey, A. (2014): Estimation of Aedes aegypti (Diptera: Culicidae) population size and adult male survival in an urban area in Panama. Mem. Inst. – Oswaldo Cruz, Rio de Janeiro 109(7): 879-886.

[14] Nguyen, A. T., Williams–Newkirk, A., Kitron, U., Chaves, L. F. (2012): Seasonal Weather, Nutrients, and Conspecific Presence Impacts on the Southern House Mosquito Oviposition Dynamics in Combined Sewage Overflows. – J. Med. Entomol. 49(6): 1328-1338.

[15] Noori, N., Lockaby, B. G., Kalin, L. (2015): Larval development of *Culex quinquefasciatus* in water with low to moderatepollution levels. – Journal of Vector Ecology 40(2): 208-220.

[16] Oda, T., Uchida, K., Mori, A., Mine, M., Eshita, Y., Kurokawa, K., Kato, K., Tahara, H. (1999): Effects of high temperature on the emergence and survival of adult *Culex pipiens* molestus and *Culex quinquefasciatus* in Japan. – J. Am. Mosq. Control Assoc. 15(2): 153-156.

[17] Paul, M. J., Meyer, J. L., Couch, C. A. (2006): Leaf breakdown in streams differing in catchment land use. – Fresh w. Biol. 51: 1684-1695.

[18] Rabalais, N. N. (2002): Nitrogen in aquatic ecosystems. – Ambio. 31: 102-112.

http://www.aloki.hu ● ISSN 1589 1623 (Print) ● ISSN 1785 0037 (Online)
DOI: http://dx.doi.org/10.15666/aeer/1705_1052510541

[19] Schletzbaum, M. A. (2013): Aqueous nitrates and larval competition alter disease risk from two urban mosquito species. – Cary Institute of Ecosystem Studies, Millbrook, NY 12545 USA.
[20] Schlotzhauer, S. D., Littel, R. C. (1987): SAS System for Elementary Statistical Analysis. – SAS Intitute Inc., Cary, NC. 416 pp.
[21] Sunish, I. P., Reuben, R. R. (2001): Factors influencing the abundance of Japanese encephalitis vectors in rice fields in India. – Med. Vet. Entomol. 15: 381-392.
[22] Tchobanoglous, G., Burton, F. L. (1991): WastewaterEngineering. – McGrow-Hill.
[23] Vitek, C. J., Livdahl, T. P. (2006): Field and Laboratory Comparison Of Hatch Rates In Aedes Albopictus (Skuse). – J. Am. Mosq. Control Assoc. 22(4): 609-614.
[24] Wetzel, R. G. (2001): Limnology. – 3rd ed. Academic Press, New York.
[25] Wheeler, M. W., Park, R. M., Bailer, A. J. (2006): Comparing median lethal concentrationvalues using confidence interval overlap or ratio tests. – Environ. Toxicol. Chem. 25: 1441-1444.
[26] WHO. (2006): A compendium of standards for wastewater reuse in the Eastern Mediterranean Region.
[27] Williams, K. A., Green, D. W. J., Pascoe, D. (1986): Studies on the acute toxicity of pollutants to fresh water macroinvertebrates. – Archives fur Hydrobiolgie 106: 61-70.
[28] Yang, P. (2008): Effect of Oviposition Site Deprivation on Oviposition Performance and Egg Hatch Rate of Naturally Blood–fed Gravid Culex quinquefasciatus (Diptera: Culicidae). – Proc. Hawaiian Entomol. Soc. 40: 51-54.

http://www.aloki.hu ● ISSN 1589 1623 (Print) ● ISSN 1785 0037 (Online)
DOI: http://dx.doi.org/10.15666/aeer/1705_1052510541

EVALUATION OF REGION AND SUBREGION-BASED TOTAL VOLUME EQUATIONS FOR DAHURIAN LARCH IN NORTHEAST CHINA

MBANGILWA, M. M.[1*] – JIANG, L. C.[1*]

[1]*Key Laboratory of Sustainable Forest Ecosystem Management-Ministry of Education, School of Forestry, Northeast Forestry University, Harbin 150040, China*

**Corresponding authors*
e-mail: jlichun@nefu.edu.cn

(Received 30th Jan 2019; accepted 22nd May 2019)

Abstract. A total of 10 sub-regions were identified and tree total volume equations were developed for economically important Dahurian larch species in northeast China (Daxing'an Mountain region/Heilongjiang province). These equations were based on a simple power function and adjusted to the forest inventory data volumes of three mountainous regions, including the northwest of northern slope of Yilehuli Mountains (NWYLHLM), the southeast of northern slope of Yilehuli Mountains (SAYLHLM) and the eastern slope of northern part of Daxin'an Mountains (NDXAM). The volume equations were tested to determine if differences by ecoregion were statistically significant. Results varied by species, volume and ecoregion suggesting that the relationship between tree volume and tree diameter of Dahurian larch (*Larix gmelinii* Rupr) tree species is significantly different between the three geographic regions, depending on local climatic, soil and ecological conditions. This implies that the provincial and regional models of volume-diameter relationships are not appropriate for predicting tree volume at ecoregional level. In addition, the use of an ecoregional specific model will lead to significant bias in predicting the total volume of trees. The ecoregion-based volume models developed in this study could provide more accurate information on tree growth and development to forest resource managers and planners.
Keywords: *Larix gmelinii, Heilongjiang, forest inventory, mountainous regions, ecoregions*

Introduction

Boreal forests, the second largest biome in the world, cover about one-third of the Earth's forest area (Jia and Zhou, 2018). Dahurian larch (*Larix gmelinii* Rupr) is a dominant tree species in Chinese boreal forest. It's one of the main timber species in China and forms large forests in northeast China, including the northeastern part of the Inner Mongolia autonomous region and the Daxing'an Mountain range (Jin et al., 2015). It's the most commercially cultivated timber species in northeastern China due to its ecological prevalence and its superior wood attribute. However, its timber quality is largely driven by the crown architecture, i.e., the number, size and distribution of branches. The majority of branch-level models in the literature are focused on planted forests, which have substantially different crown architecture than that grown in natural mixed forests (Dong et al., 2016). Therefore, the purpose of this study is to develop the total volume model for Dahurian larch in three forest regions of northeastern China.

Accurate estimation and determination of stem standing volume is very useful for both research and practical purposes in forestry and contributes to the efficient and sustainable management of timber resources (Barrio et al., 2007). When preparing a cut for sale, the estimate of the volume of trees to be felled is necessary. The cubage can be done on a tree, as in the case of the volume of large trees and can also be done on a stand with an estimate of the overall volume of wood made by type of wood. The cubing of standing timber is governed by the standard Afnor NF B 53-017 "Estimated

http://www.aloki.hu ● ISSN 1589 1623 (Print) ● ISSN 1785 0037 (Online)
DOI: http://dx.doi.org/10.15666/aeer/1705_1054310564

volume of standing timber" for estimating the "solid volume" of a standing tree (Limousin, 2011). Previous studies have shown that, total volume equation has been widely used throughout eastern North America (Honer, 1967). In a study conducted in 1998 (Shailer et al., 1998) in New Brunswick, Honer's volume equations were shown to best predict total volume from a set of almost 20 different published volume equations for nine important commercial species.

Recently Lee et al. (2017) reported that, Stem volume models using diameter at breast height (DBH) and height were developed for *Pinus densiflora*, *Pinus koraiensis*, and *Larix kaempferi*. The data were obtained from Gangwon, Gyeonggi, and North Gyeongsang provinces in South Korea, and the sample trees felled were used to provide the parameter estimates of volume equations. The combined-variable function, $V = a + bD^2H$, was shown to be the best model through the validation of the equation. Also, the model using only DBH, $V = aD + bD^2$ was also evaluated to be applicable in the field. Similarly, Tsega et al. (2018) reported as well that, Stem volume equations were fitted for *Cupressus lusitanica* in Gergeda Forest, Ethiopia using six different established equation forms. A total of 260 trees were measured for their diameter at breast height (*D*), total height (*H*) and stem volume using destructive sampling methods. The data set was randomly divided into equal size for equation development and equation validation. Five fit statistics comprising of the fit index, root mean square error, bias (%), absolute mean deviation and coefficient of variation were used to evaluate the performance of each equation. Among the different equations, the Schumacher and Hall function of the form $V = b_1 D^{b_2} H^{b_3}$, which estimates volume (*V*) using diameter at breast height and total height as predicting variables, performed best and was then fitted to the combined data set for prediction of volume over-bark of *C. lusitanica* in Gergeda Forest.

These models revealed higher accuracy when compared with previous studies. Both equations are considered to be easily used in the field. In the recent past, the principles of multifunction, multipurpose and ecologically based forest management were approved in China. Therefore, in order to help forest managers and practitioners realize the differences in these relationships among different sub-regions then subregion-based height-diameter models are very important.

Previous studies have also revealed that, there is ecoregion differences exist in the height-diameter relationships in Ontario (Zhang et al., 2002; Peng et al., 2004) and in West Virginia (Brooks and Wiant, 2008; Jiang et al., 2005) and local merchantable board foot, cubic foot and weight equations have been developed for six economically important hardwood species in central Appalachia. Equations were based on a simple power function and fit to volumes from the USDA Forest Service Forest Inventory Analysis data for West Virginia and parts of Ohio, Pennsylvania, Maryland, Virginia, and Kentucky. Five ecoregions were identified and the volume equations were tested to determine if differences by ecoregion were statistically significant with results varying by species, volume type and ecoregion (Brooks and Wiant, Jr., 2004). Akinsanmi and Akindélé (1995) noted that, sustainable management of forest resources requires adequate data collection. These actions make it possible for the manager to have indicators on wood potential in order to develop a consequent management plan. Palm (1982), Pauwels and Rondeux (1999) and Thibaut et al. (1998), revealed that the low values of the statistical parameters of validation are obtained with the formula of the truncated cone. The graphical analysis of the residues of the truncated cone model shows a good distribution of the residues. Consequently, Fonton et al. (2009) confirmed

http://www.aloki.hu ● ISSN 1589 1623 (Print) ● ISSN 1785 0037 (Online)
DOI: http://dx.doi.org/10.15666/aeer/1705_1054310564

the hypothesis of the succession of cone trunks along the stem of *Isoberlinia spp, Anogeissus leiocarpa* and *Danielli aoliveri* stems from the study by on the modeling of drum volume tree for sustainable management of forest ecosystems. Rondeux (1999), Laumans (1991), Thibaut et al. (1998) and Fonton et al. (2002) agreed with the findings of the models obtained in the Fonton study, expressing the volume as a function of diameter squared (D^2), are the most relevant for estimating individual tree volume. Finally, Bontemps et al. (2012) found that the estimation of forest-impaired biomass and forest productivity explained that environmental changes involve redefining and expanding the ecosystem services provided by forests, while aiming for the sustainability of their management. The quantification of timber and wood energy resources and the carbon storage function requires new methods of assessing forest volume and biomass.

In this current study, the test is based on the ecoregional statistical analysis from forest management data in Dahurian larch region, in the Daxing'an mountainous region located in northeastern China (Heilongjiang Province). For the purpose of this study again, there are many situations in forest mensuration when the use of local volume tables is useful (Brooks and Wiant, 2008). These may include but are not limited to cursory forest inventory applications as well as timber trespass evaluations when stem diameter is estimated from an existing stump diameter. This study uses forest inventory data from the Daxing'an Mountains region in Heilongjiang Province in northeastern China.

The objectives of this study are to evaluate whether ecoregion based volume cubic meter, total volume equations are statistically justified to test for differences between ecoregions for the one species selected and to evaluate the bias associated when a region wide model is compared to individual ecoregion models. Consequences of inappropriately applying provincial, regional or other regulations were also evaluated among the ten subregions.

Materials and Methods

Study area and data

The study was conducted in the cold temperate forest regions in Heilongjiang Province (Daxing'an Mountains; from 121° 12′E to 127° 00′E and from 50° 10′N to 53° 33′N) and eastern part of Inner Mongolia, in Northeastern China) (*Figure 1*). The elevation of the area ranges from 300 to 700 m above the sea level. The soil in this region is mostly Haplum-brepts or Eutroboralfs (or dark brown forest soil in Chinese Taxonomic System). The area experinces continental monsoon climate with mean annual rainfall ranges from 500 to 750 mm and mean annual temperature is from -1 to -2.8°C.

These temperate forests are dominated by White birch (*Betula platyphylla*), Amur linden (*Tilia amurensis*), Maple (*Acer mono*), Dahurian birch (*Betula davuria*), Mongolianoak (*Quercus mongolica*), Dahurian poplar (*Populus davidiana*), and mixed hardwood forest dominated by Amurlinden (*Tilia amurensis*), Maple (*Acer mono*), Manchurian ash (*Fraxinus manshurica*), Manchurian walnut (*Juglans mandshurica*), Mongolian oak (*Quercus mongolica*) and Manchurian elm (*Ulmus laciniata*) (Dong et al., 2014).

Data and methods

Ten subregions for conifer trees were identify for this study based on the work conducted by Brooks and Wiant (2008) in USA (*Table 1*).

http://www.aloki.hu ● ISSN 1589 1623 (Print) ● ISSN 1785 0037 (Online)
DOI: http://dx.doi.org/10.15666/aeer/1705_1054310564

Table 1. *F-test for testing the difference between subregions*

Subregions	n	Full Model			Reduced Model			Extra sum of squares		
		SSE_F	PF	df_F	SSE_R	PR	df_R	$df_R - df_F$	F-value	P-value
Overal	**2411**	**26.2484**	**30**	**2384**	**32.3012**	**3**	**2408**	**24**	**22.9060**	**0.0000**
SL - JGDQ	738	8.0276	6	732	8.2117	3	735	3	5.5972	0.0008
SL - XL	404	5.6357	6	398	7.0271	3	401	3	32.753	0.0000
SL - TH	417	3.0916	6	413	3.3481	3	414	3	11.370	0.0000
SL - HZ	429	4.0404	6	423	5.5989	3	426	3	54.389	0.0000
SL - SBZ	451	3.4801	6	445	3.4992	3	448	3	0.8120	0.4876
SL - HJY	342	2.9661	6	336	3.1289	3	339	3	6.1497	0.0004
SL - XLJ	438	2.4011	6	432	2.5310	3	435	3	7.7918	0.0000
SL - TQ	405	5.2095	6	399	5.9319	3	402	3	18.442	0.0000
SL - AME	499	8.2247	6	493	8.3661	3	496	3	2.8245	0.0382
JGDQ - XL	714	9.4562	6	708	11.218	3	711	3	43.966	0.0000
JGDQ - TH	727	6.9120	6	721	7.1381	3	724	3	7.8624	0.0000
JGDQ - HZ	739	7.8608	6	733	9.5449	3	736	3	52.343	0.0000
JGDQ - SBZ	761	7.3006	6	755	7.4159	3	758	3	3.9758	0.0079
JGDQ - HJY	652	6.7865	6	646	6.8625	3	649	3	2.4089	0.0660
JGDQ - XLJ	748	6.2216	6	742	6.5218	3	745	3	11.933	0.0000
JGDQ - TQ	715	9.0299	6	709	9.9681	3	712	3	24.553	0.0000
JGDQ - AME	809	12.045	6	803	12.426	3	806	3	8.4645	0.0000
XL - TH	393	4.5201	6	387	4.7256	3	390	3	5.8629	0.0006
XL - HZ	405	5.4689	6	399	5.8731	3	402	3	9.8294	0.0000
XL - SBZ	427	4.9087	6	421	6.5642	3	424	3	47.329	0.0000
XL - HJY	318	4.3947	6	312	4.7316	3	315	3	7.9746	0.0000
XL - XLJ	414	3.8297	6	408	4.9515	3	411	3	39.839	0.0000
XL - TQ	381	6.6381	6	375	6.8315	3	378	3	3.6418	0.0129
XL - AME	475	9.6533	6	469	11.221	3	472	3	25.394	0.0000
TH - HZ	418	2.9248	6	412	3.6358	3	415	3	33.384	0.0000
TH - SBZ	440	2.3646	6	434	2.6741	3	437	3	18.936	0.0000
TH - HJY	331	1.8505	6	325	1.8929	3	328	3	2.4795	0.0611
TH - XLJ	427	1.2855	6	421	1.7295	3	424	3	48.458	0.0000
TH - TQ	394	4.0939	6	388	4.1496	3	391	3	1.7599	0.1543
TH - AME	488	7.1099	6	482	7.3279	3	485	3	4.9428	0.0021
HZ - SBZ	452	3.3131	6	446	5.3358	3	449	3	90.744	0.0000
HZ - HJY	343	2.7993	6	337	3.5644	3	340	3	30.703	0.0000
HZ - XLJ	439	2.2343	6	433	3.6992	3	436	3	94.628	0.0000
HZ - TQ	406	5.0427	6	400	5.8446	3	403	3	21.202	0.0000
HZ - AME	500	8.0579	6	494	9.6820	3	497	3	33.187	0.0000
SBZ - HJY	365	2.2391	6	359	2.4153	3	362	3	9.4182	0.0000
SBZ - XLJ	461	1.6741	6	455	1.8099	3	458	3	12.303	0.0000
SBZ - TQ	428	4.4825	6	422	5.1044	3	425	3	19.517	0.0000
SBZ - AME	522	7.4977	6	516	7.6256	3	519	3	2.9323	0.0330
HJY - XLJ	352	1.1600	6	346	1.5273	3	349	3	36.511	0.0000
HJY - TQ	319	3.9684	6	313	4.1198	3	316	3	3.9795	0.0083
HJY - AME	413	6.9837	6	407	7.1959	3	410	3	4.1227	0.0067
XLJ - TQ	415	3.4035	6	409	4.0321	3	412	3	25.182	0.0000
XLJ - AME	509	6.4187	6	503	6.6461	3	506	3	5.9405	0.0005
TQ - AME	476	9.2271	6	470	10.009	3	473	3	13.277	0.0000

Note: N – sample size, SSE_F – error sum of squares of the full model, df_F – degrees of freedom of SSE_F, SSE_R – error sum of squares of reduced model, df_R – degrees of freedom of SSE_R, P is the number of parameters.

http://www.aloki.hu ● ISSN 1589 1623 (Print) ● ISSN 1785 0037 (Online)
DOI: http://dx.doi.org/10.15666/aeer/1705_1054310564

A total of 5474 individual height-diameter measurements for four Conifer Forest tree species were collected in systematically/randomly selected square/circular (25.8 m x 25.8 m plots) using field Inventory from Daxing'an Mountains in the northeast of China (*Figure 1*). A county was assigned as part of a specific ecoregion if a majority of the land base fell within ecoregion boundaries. The selected ecoregions are a combination of the different subregions between them and the land base regions identified by the China Soil Conservation Service. In this study, only one species of tree, the Dahurian larch (*Larix gmelinii* Rupr*)* was selected, given the absence of some data for other tree species.

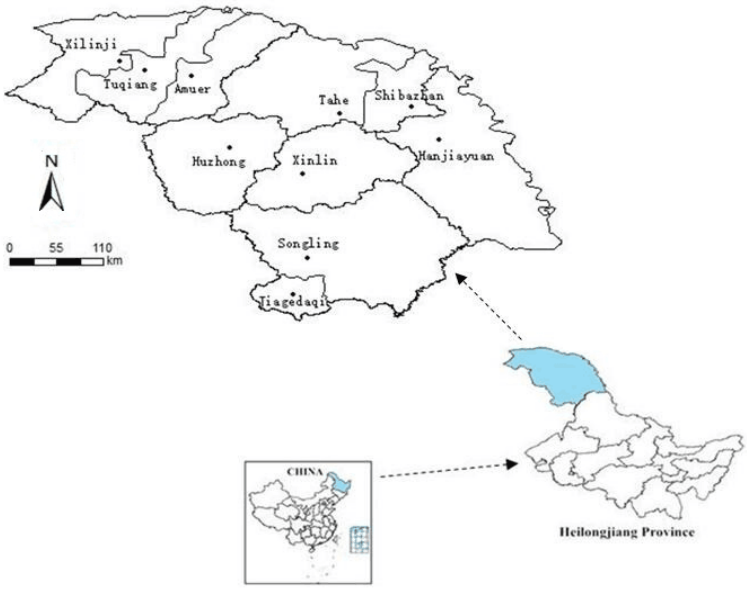

Figure 1. *The geographical location of study area and plot distribution in the Northeast China*

A total of 2411 destructively sampled Dahurian larch trees were used in this investigation. These trees were felled throughout the forest inventory areas of northeast China and all sampled trees were selected to ensure a representative distribution across a range of height and diameter classes within stands varying in density, height, site condition, age and stand structure. The data was then randomly divided into an adaptation dataset and a validation dataset (*Table 2*). For developing taper and individual tree volume equations the data set was initially used. Diameters at breast height were measured for all sampled trees (D, defined as 1.3 m above the ground) outside bark and total volume (V). Trees possessing broken tops, obvious cankers or crooked boles were excluded from the analysis. Summary statistics for tree diameter and total volume are provided for each subregion, the NDXAM, YLHLM-NW, and YLHLM-SA regions, and all data combined (Overall) in *Table 3*.

The three major regions employed are depicted in *Figure 1* above and include:

- Region1: The northwest of the northern slope of Yilehuli Mountains (NWYLHLM) which includes four subregions: Xilinji (XLJ), Tuqiang (TQ), Amuer (AME), Huzhong (HZ).
- Region2: The southeast of the northern slope of Yilehuli Mountains (SAYLHLM) which includes four subregions: Xinlin (XL), Tahe (TH), Shibazhan (SBZ), Hanjiayuan (HJY).

http://www.aloki.hu ● ISSN 1589 1623 (Print) ● ISSN 1785 0037 (Online)
DOI: http://dx.doi.org/10.15666/aeer/1705_1054310564

- Region3: The eastern slope of northern part of Daxing'an Mountains (NDXAM), which includes two subregions: Songling (SL), Jiagedaqi (JGDQ).

Table 2. *Summary of fitting and validation data sets for Dahurian larch (Larix gmelinii Rupr.) for the ten subregions in Northeastern China*

Subregions	Statistic	Fitting data			Validation data		
		D (cm)	Height (m)	Volume (m^3)	D (cm)	Height (m)	Volume (m^3)
	N°of observations	**214**	**214**	**214**	**214**	**214**	**214**
	Mean	29.15	19.59	0.81	25.87	40.21	0.70
SL	Minimum	5.50	7.10	0.01	4.10	7.50	0.01
	Maximum	55.10	29.20	2.55	50.20	87.50	2.28
	SD	14.07	5.41	0.70	12.88	19.56	0.62
	N°of observations	**524**	**524**	**524**	**524**	**524**	**524**
	Mean	27.27	18.30	0.66	23.99	37.55	0.54
JGDQ	Minimum	5.40	6.40	0.01	4.50	7.00	0.01
	Maximum	61.00	30.80	2.90	59.40	83.20	2.71
	SD	13.24	4.83	0.60	12.01	17.66	0.52
	N°of observations	**190**	**190**	**190**	**190**	**190**	**190**
	Mean	30.94	19.34	0.87	27.95	42.22	0.76
XL	Minimum	6.00	8.40	0.01	4.90	9.00	0.01
	Maximum	63.40	29.50	3.48	58.60	89.00	3.20
	SD	12.57	3.99	0.69	11.69	17.10	0.62
	N°of observations	**203**	**203**	**203**	**203**	**203**	**203**
	Mean	21.98	15.34	0.45	20.34	28.80	0.40
TH	Minimum	5.20	5.10	0.01	4.20	7.20	0.00
	Maximum	50.60	26.50	2.22	48.00	64.00	2.13
	SD	12.32	5.37	0.52	11.83	15.12	0.47
	N°of observations	**215**	**215**	**215**	**215**	**215**	**215**
	Mean	23.53	16.13	0.50	20.37	31.11	0.41
HZ	Minimum	5.10	4.50	0.01	4.10	6.00	0.01
	Maximum	48.80	25.90	2.34	45.80	64.50	2.04
	SD	11.61	4.69	0.51	10.07	14.73	0.67
	N°of observations	**237**	**237**	**237**	**237**	**237**	**237**
	Mean	27.46	17.93	0.64	24.49	39.13	0.54
SBZ	Minimum	5.40	6.10	0.01	4.40	6.40	0.01
	Maximum	56.60	26.10	2.11	50.60	91.00	1.84
	SD	13.33	4.72	0.54	12.30	19.50	0.47
	N°of observations	**128**	**128**	**128**	**128**	**128**	**128**
	Mean	26.79	17.72	0.62	23.78	37.11	0.52
HJY	Minimum	5.20	6.60	0.01	3.90	7.50	0.01
	Maximum	50.80	26.50	2.37	46.80	78.20	2.08
	SD	12.38	4.60	0.55	11.40	17.94	0.47
	N°of observations	**224**	**224**	**224**	**224**	**224**	**224**
	Mean	16.00	15.76	0.24	14.24	22.66	0.20
XLJ	Minimum	5.10	7.20	0.01	3.80	6.50	0.01
	Maximum	62.00	24.60	2.15	46.00	82.00	1.60
	SD	9.00	4.21	0.29	8.03	13.81	0.25
	N°of observations	**191**	**191**	**191**	**191**	**191**	**191**
	Mean	23.98	17.45	0.62	21.86	33.34	0.54
TQ	Minimum	5.20	6.50	0.01	4.60	6.40	0.01
	Maximum	56.00	28.50	2.70	53.00	96.00	2.42
	SD	14.59	5.25	0.68	13.74	20.63	0.60
	N°of observations	**285**	**285**	**285**	**285**	**285**	**285**
	Mean	33.68	22.37	1.08	30.36	47.93	0.95
AME	Minimum	5.10	7.33	0.01	4.60	6.30	0.01
	Maximum	72.20	33.98	3.99	62.60	89.10	3.39
	SD	13.00	4.87	0.75	11.70	18.70	0.67

D = diameter at breast height, SD=Standard of deviation

http://www.aloki.hu ● ISSN 1589 1623 (Print) ● ISSN 1785 0037 (Online)
DOI: http://dx.doi.org/10.15666/aeer/1705_1054310564

The individual tree database for each region was queried to select only those trees from the appropriate counties as well as selecting only those merchantable tree records having measured diameters and heights and non-zero volumes. The tree data selected was from the northwest of the northern slope of Yilehuli Mountains, the southeast of the northen slope of Yilehuli Mountains, the eastern slope of northern part of Daxin'an Mountains, located in Heilongjiang Province. The volume parameters examined included only total volume in cubic meter, as reported in the tree database. The number of trees species and ecoregions sampled after the combination of different ecoregions is shown in *Table 1*, and the state distribution parameter and the summary Tree diameter (DBH) statistics within volume (V) for regional and ecoregional datasets for Dahurian larch species are presented in *Table 3*. An initial evaluation was conducted using several families of nonlinear models to establish an appropriate volume model form (*Table 4*).

Table 3. *Summary statistics of tree diameter at breast (DBH), total height (H) and total volume (V) for regional and subregional data sets*

Ecoregions	DBH (cm)					H (m)				V (m^3)			
	N	Mean	STD	Min	Max	Mean	STD	Min	Max	Mean	STD	Min	Max
SL	214	29.15	14.07	5.50	55.10	19.59	5.41	7.10	29.20	0.81	0.70	0.01	2.55
JGDQ	524	27.27	13.24	5.40	61.00	18.30	4.83	6.40	30.80	0.66	0.60	0.01	2.90
XL	190	30.94	12.57	6.00	63.40	19.34	3.99	8.40	29.50	0.87	0.69	0.01	3.48
TH	203	21.98	12.32	5.20	50.60	15.34	5.37	5.10	26.50	0.45	0.52	0.01	2.22
HZ	215	23.53	11.61	5.10	48.80	16.13	4.69	4.50	25.90	0.50	0.51	0.01	2.34
SBZ	237	27.46	13.33	5.40	56.60	17.93	4.72	6.10	26.10	0.64	0.54	0.01	2.11
HJY	128	26.79	12.38	5.20	50.80	17.72	4.60	6.60	26.50	0.62	0.55	0.01	2.37
XLJ	224	16.00	9.00	5.10	62.00	15.76	4.21	7.20	24.60	0.24	0.29	0.01	2.15
TQ	191	23.98	14.59	5.20	56.00	17.45	5.25	6.50	28.50	0.62	0.68	0.01	2.70
AME	285	33.68	13.00	5.10	72.20	22.37	4.87	7.33	33.98	1.08	0.75	0.01	3.99
NWYLHLM	**915**	**24.94**	**13.86**	**5.10**	**72.20**	**18.26**	**5.53**	**4.50**	**33.98**	**0.64**	**0.68**	**0.01**	**3.99**
SAYLHLM	**758**	**26.75**	**13.10**	**5.20**	**63.40**	**17.56**	**4.93**	**5.10**	**29.50**	**0.65**	**0.60**	**0.01**	**3.48**
NDXAM	**738**	**27.82**	**13.50**	**5.40**	**61.00**	**18.67**	**5.03**	**6.40**	**30.80**	**0.70**	**0.64**	**0.01**	**2.90**
Overall	**2411**	**26.39**	**13.57**	**5.10**	**72.20**	**18.16**	**4.50**	**4.50**	**33.98**	**0.66**	**0.64**	**0.01**	**3.99**

Note: N-sample size (number of trees), STD-standard deviation, Min.-minimum, Max.-maximum

Table 4. *Volume equations used for model fitting and model validation*

Model code	Model of Volume Equations	Number of parameters
1	$V = aD^b$	2
2	$V = aD^bH^c$	3
3	$V = a(D^2H)^b$	2
4	$V = a+bD^2H$	2
5	$V = aD^2H$	1
6	$V = a1+aD^bH^c$	3

V = over-bark stem volume (in m^3), D = diameter at breast height (in cm), H = total tree height (in m), and a, b, c, and are parameters to be estimated from the data

Across all species and volume parameters, a simple power function proved to provide both consistent and accurate results (model code 2) and was thus selected as the basic model form for development (*Equation 1*):

$$V = aD^b H^c \quad \text{(Eq.1)}$$

http://www.aloki.hu ● ISSN 1589 1623 (Print) ● ISSN 1785 0037 (Online)
DOI: http://dx.doi.org/10.15666/aeer/1705_1054310564

Where V is volume in cubic meter (m^3), D is the tree diameter at breast height (DBH) (cm), H is the total height, a is the asymptotic parameter, b is the rate parameter, and c is the shape parameter. *Equation 1* was fit to (1) the Overall data (2411 Dahurian larch (*Larix gmelinii* Rupr) species of tree), (2) the region 1: The northwest of the northern slope of Yilehuli Mountains (NWYLHLM), (3) the region 2: The southeast of the northern slope of Yilehuli Mountains (SAYLHLM), (4) the region 3: The eastern slope of northern part of Daxing'an Mountains (NDXAM) and (5) each of the ten subregion separately. The PROC NLIN procedure in the Statistical Analysis System (SAS Institute, Inc. 1999) was utilized to estimate the model parameters and model statistics.

To test for differences between the overall model (region wide) and each ecoregion, a nonlinear extra sum of squares procedure was employed (Neter et al., 1996). This procedure involves the use of two indicator variables (k=2) who are needed in *Equation 2* for three regions in the full model form, while the reduced model form is represented by a three parameters model representing the volume relationship across all ecoregions (region wide). The full model form uses an indicator variable (k=2) approach to represent the tree regions.

- If region = NWYLHLM, $z_1 = 1$, $z_2 = 0$.
- If region = SAYLHLM, $z_1 = 0$, $z_2 = 1$.
- If region = NDXAM, $z_1 = 0$, $z_2 = 0$.

And to compare the difference of the volume relationships among different ecoregions, the non-linear extra sum of squares method was used (Bates and Watts, 1988; Huang et al., 2000). The method requires the fitting of full and reduced models.

The full model corresponds to different sets of parameters for each of the ecoregions involved, while the reduced model corresponds to the same set of parameters for all ecoregions.

Indicator (dummy) variables were used to facilitate the hypothesis tests as follows:

Test on the Overall model

In order to examine the sufficiency of the Overall model for the ten subregions, the full model for Darurian larch species and volume parameter was tested independently and is of the form:

$$V = \left(\alpha + \sum_{i=1}^{k} \alpha_i r_i\right) D^{\left(\beta + \sum_{i=1}^{k} \beta_i r_i\right)} H^{\left(\sigma + \sum_{i=1}^{k} \sigma_i r_i\right)} \quad \text{(Eq.2)}$$

Where:
V = volume parameter tested,
ri = indicator variable for ecoregion ri, i = 1,...,4,
D = tree dbh (in),
α,β, σ = parameters to be estimated from the data.
k= the number of indicator variables
The full model form has 10 parameters and an error sum of squares (SSEF) with N-10 degrees of freedom (dfF) where N is the total number of sample trees for each volume parameter and species tested. The form of the reduced model is that of *Equation 1* having three parameters and an error sum of squares (SSER) with N-3 degrees of freedom (dfR). The full model test has the following null and alternative hypotheses for each of the one species tests:
H_0: $\alpha_1=\alpha_2=\alpha_3=\alpha_4=\beta_1=\beta_2=\beta_3=\beta_4=\sigma_1=\sigma_2=\sigma_3=\sigma_4=0$ and
Ha: at least one parameter is not equal to 0.

http://www.aloki.hu ● ISSN 1589 1623 (Print) ● ISSN 1785 0037 (Online)
DOI: http://dx.doi.org/10.15666/aeer/1705_1054310564

Rejecting the null hypothesis would indicate that the volume-diameter relationship is not the same for all ecoregions. Failure to reject the null hypothesis would indicate that the reduced model form *Equation 2* would be adequate for all ecoregions. These tests were conducted independently for each of the major species investigated.

In addition to the overall ecoregion tests, similar tests were conducted for each of the ten pairwise ecoregions comparisons for each of one species and three volume units examined. The same indicator variable approach was applied to the specific ecoregion comparison tests having a full model.

Test on the region against regions

To compare the volume relationship between the region and regions, the following full model was used

$$V = (\alpha + \alpha_1 r_1) D^{(\beta+\beta_1 r_1)} H^{(\sigma+\sigma_1 r_1)} \quad \text{(Eq.3)}$$

Where all variables and parameters were as previously defined. The full model form has three parameters and an error sum of squares (SSE_F) with N-4 degrees of freedom (df_F). The reduced model form is that of *Equation 1*. For each species and volume type tested, the full model test has the following null and alternative hypotheses:

H_0: $\alpha_1=\beta_1=\sigma_1=0$

and

Ha: at least one parameter is not equal to 0.

Rejection of the null hypothesis would indicate that the volume-diameter relationship is not the same between the three ecoregions being tested. Failure to reject the null hypothesis would indicate that a single model (*Equation 1*) could be used for both ecoregions for that species and volume type. These tests were conducted independently for each species and volume type combination.

To evaluate the differences between the three regions

A total of three regions pairs were formulated to test the pairwise differences between the three regions. The three testing pairs require three full models that take the form of *Equation 2*, and three reduced models that take the form of *Equation 1*. For example, to test the difference between region NWYLHLM vs SAYLHLM, one indicator variable (k=1) can be defined: if subregion = NWYLHLM, Z1 =1; and if subregion = SAYLHLM, Z1 = 0. Similarly, the full model (*Equation 2*) has 6 estimable parameters. To evaluate the overall differences among subregions nine indicator variables (k=9) are needed in *Equation 3* for ten subregions. They are defined as follows:

- If subregion = SL, z1 = 1, all other zi = 0.
- If subregion = JGDQ, z2 = 1, all other zi = 0.
- If subregion = XL, z3 = 1, all other zi = 0.
- If subregion = TH, z4 = 1, all other zi = 0.
- If subregion = HZ, z5 = 1, all other zi = 0.
- If subregion = SBZ, z6 = 1, all other zi = 0.
- If subregion = HJY, z7 = 1, all other zi = 0.
- If subregion = XLJ, z8 = 1, all other zi = 0.
- If subregion = TQ, z9 = 1, all other zi = 0.
- If subregion = AME, all other zi = 0.

http://www.aloki.hu ● ISSN 1589 1623 (Print) ● ISSN 1785 0037 (Online)
DOI: http://dx.doi.org/10.15666/aeer/1705_1054310564

Test on the differences between the ten subregions

To test the pairwise differences between the ten subregions, a total of 45 subregions pairs for Dahurian larch species were formulated. The 45 testing pairs require 45 full models that take the form of *Equation 3*, and 45 reduced models that take the form of *Equation 1*. For example, to test the difference between subregions SL vs. XL, one indicator variable (k=1) can be defined: if subregions = SL, Z1 =1; and if subregion = XL, Z1 = 0. Similarly, the full model (*Equation 3*) has 6 estimable parameters. The reduced model takes the form of *Equation 1* with 3 parameters. The null and alternative hypotheses are:

H_0 (1): $a_1=b_1=C_1=0$

H_a (2): at the least one parameter is not equal to 0.

Rejecting the null hypothesis H_a (2) would indicate that there is a difference between the two subregions tested (subregion 1 (SL) and 2 (JGDQ) in this example).

Test statistic

The significance of the full and reduced model comparisons were based on an F-test of the form:

$$F = \frac{\frac{SSE_R - SSE_F}{df_R - df_F}}{\frac{SSE_F}{df_F}} \quad \text{(Eq.4)}$$

Where SSE_F is the error sum of squares of a full model with the degrees of freedom df_F, and SSE_R is the error sum of squares of a reduced model with the degrees of freedom df_R.

This test statistic is F-distributed for a non-linear model if the data used represent a large sample generally, the F-test is significant if the p-value for the test is less than 0.05.

In order to understand the consequences of inappropriate application of a volume model in different ecoregions, each of the ten models (global model, regional model 1 (NWYLHLM 1), regional model 2 (SAYLHLM 2), regional model 3 (NDXAM 3) (and 10 suregions models) was used to predict total volume of trees for each ecoregion.

And to quantify the magnitude of the prediction error when a specific region model is used, the average volume prediction error $(\bar{\varepsilon})$, the standard error of the prediction error (S_e), and the prediction bias as a percentage of average "real" volume (% bias) were calculated and defined as:

$$\bar{\varepsilon} = \frac{\sum_{i=1}^{m}(\hat{V}_i - V_i)}{m} \quad \text{(Eq.5)}$$

$$S_e = \sqrt{\frac{\sum_{i=1}^{m}(\epsilon - \bar{\varepsilon})^2}{m-1}} \quad \text{(Eq.6)}$$

$$Bias(\%) = {}^{\bar{\varepsilon}}/_{\bar{V}} \times 100 \quad \text{(Eq.7)}$$

Where:

m= number of tree volumes for each species and volume type,

V_i= data reported volume for tree i,

http://www.aloki.hu ● ISSN 1589 1623 (Print) ● ISSN 1785 0037 (Online)
DOI: http://dx.doi.org/10.15666/aeer/1705_1054310564

$\hat{V}_i$= predicted volume for tree i,

$\bar{V}$= mean data reported volume for each species and volume type. In this case $\bar{V}$ is the mean of observed tree volume. The t-test is used to test the null hypothesis and demonstrate that the mean prediction error is zero by

$$t = \frac{\bar{e}}{S_e/\sqrt{m}} \quad \text{(Eq.8)}$$

Large values for these measures of prediction error would indicate situations where selection of an ecoregion specific model may be justified. Parameter estimates for *Equation 1* were obtained using SAS Proc NLIN (SAS 2002) for each species, ecoregion and volume type combination.

Results and Discussion

Estimation and validation of volume equations

The initial volume model development was completed with six candidate model forms. For all of the models, the significance of each parameter was tested and proved before and after weighting. The estimated parameters and their MSE-model mean squared error of the weighted models are presented in *Table 5* who is the parth of the data who help us to form the model.

Table 5. *Parameter estimations and model MSE of volume function for the regional and ecoregional models*

Ecoregions	N	a	b	c	MSE
SL	214	0.0000565	1.6187	1.2814	0.00997
JGDQ	524	0.00009	1.8015	0.9107	0.0114
XL	190	0.000049	1.8909	1.0325	0.0189
TH	203	0.000070	1.7627	1.0569	0.00494
HZ	215	0.000052	2.2630	0.5791	0.00914
SBZ	237	0.000076	1.6698	1.1221	0.00588
HJY	128	0.000059	1.8506	0.9993	0.00690
XLJ	224	0.000077	1.4784	1.3240	0.00135
TQ	191	0.000041	1.6976	1.3134	0.0165
AME	285	0.000131	1.5815	1.0603	0.0217
NWYLHLM	**915**	**0.000157**	**1.7457**	**0.8174**	**0.0156**
SAYLHLM	**758**	**0.000051**	**1.8080**	**1.1025**	**0.0112**
NDXAM	**738**	**0.000080**	**1.7574**	**1.0044**	**0.0112**
Overal	**2411**	**0.000103**	**1.7658**	**0.9220**	**0.0134**

Note: N-sample size (number of tree), a, b, c-three parameters of volume model, MSE-model mean squared error

The volume equations were classified as two types of functions: volume = f(DBH) with an independent variable and volume = f(DBH, height) with two independent variables (*Table 4*) and the parameter estimates and fit statistics were computed by species and all equations (*Table 5*). For the volume equations with DBH, the parameter estimates were valid ($P < 0.05$), but the P-value of parameter b was not valid in Equation (model 1) for Dahurian larch. For this reason, Equation (model 1) failed to fit the model. Equation (model 3) had lower MSE than Equation (model 1).

http://www.aloki.hu ● ISSN 1589 1623 (Print) ● ISSN 1785 0037 (Online)
DOI: http://dx.doi.org/10.15666/aeer/1705_1054310564

For the volume equations with DBH and height, parameter estimates of Equations (model 4) to (model 6) were firstly evaluated, and all parameters were valid ($P < 0.05$). Compared to other equations, however, Equations (model 3) and (model 5), especially for Dahurian larch, had fit statistics with high MSE. Meanwhile, Equation (model 6) estimated using nonlinear regression analysis predicted the volume with negative number when DBH was smaller than 10 cm, which indicated the instability of parameter estimates. For these reasons, Equations (model 5) and (model 6) failed to be the best fit equations in this study.

Equation (model 2) has valid coefficients and good fit statistics for Dahurian larch species and is considered as the best model to predict the total volume. This result corresponded to previous studies, which concluded that Equation (model 2), the so-called combined-variable function, is the best fit model (Burkhart, 1977; Amateis and Burkhart, 1987; Sherrill et al., 2011; Lee et al., 2017).

Fitting the total volume equations to regional and subregional data

The sample sizes, parameter estimates and mean square errors (MSE) for all models are provided in *Table 5*.

The four regional models (Overall, Region 1: NWYLHLM, Region 2: SAYLHLM and Region 3: NDXAM) have similar model MSEs. The parameters of the Overall model were similar to those of the regional model 1, due to the fact that regional1 data were 37.9% of the Overall data set with similar DBH and volume ranges for Dahurian larch species (*Table 3*). Among the ten ecoregional models, the lowest MSE value was found in the subregion 8 (XLJ) with a value of 0.00135. The parameter estimates also varied among the ten subregions, indicating that each ecoregion may have a different volume relationship from others.

Comparison of the total volume equations among subregions and between regions

Tables 1 and 6 show the testing results for the differences in Volume relationships between the Overall regions and among the ten subregions. *Equation 2* was used to test if the Overall model using all data combined was sufficient for the ten subregions.

Table 6. *F-test for testing difference between regions*

Regions	n	Full Model			Reduced Model			Extra sum of squares		
		SSE_F	PF	df_F	SSE_R	PR	df_R	$df_R - df_F$	PF	P_VALUE
Overal	**2411**	**30.9453**	**9**	**2402**	**32.3012**	**3**	**2408**	**6**	**17.5411**	**0.0000**
NWYLHLM - SAYLHLM	1673	22.7335	6	1667	23.3796	3	1670	3	15.7934	<. 0.0001
NWYLHLM - NDXAM	1653	22.4578	6	1647	23.1683	3	1650	3	17.3701	<. 0.0001
SAYLHLM - NDXAM	1496	16.6992	6	1490	17.4872	3	1493	3	23.4346	<. 0.0001

Note: N – sample size, SSE_F – error sum of squares of the full model, df_F – degrees of freedom of SSE_F, SSE_R – error sum of squares of reduced model, df_R – degrees of freedom of SSE_R, P is the number of parameters

The null hypothesis H_0 (1) was rejected (p-value < 0.0001), indicating that the Overall model was not sufficient to describe the volume-diameter relationships for the ten suregions. The difference between the different regions was also tested using *Equation 3* and the null hypothesis H_0 (2) was rejected (p-value < 0.0001). This means

http://www.aloki.hu ● ISSN 1589 1623 (Print) ● ISSN 1785 0037 (Online)
DOI: http://dx.doi.org/10.15666/aeer/1705_1054310564

that the difference in Volume relationships between the three geographic regions was statistically significant. A pairwise test revealed that there were differences in Volume relationships among ten subregions, i.e., the F-values ranged from 0.81 to 94.63 and all p-values were not less than 0.0001 (*Table 1*). Each ecoregion appeared to have a unique tree Volume relationship.

Prediction errors of applying subregional equation to each subregion

According to the tests above, there were significant differences among the ten subregions in the volume relationships. Inappropriately "applying" a volume model in these ecoregions may result in prediction biases. To understand the consequences, all fourteen models (Overall model, regional 1 model, regional 2 model, regional 3 model and ten subregional models) were used to predict total tree volume for each given ecoregion individually. The mean prediction error ($\bar{\varepsilon}$), the prediction bias (%), and the t-test for testing the null hypothesis that the mean prediction error equals zero are shown in *Tables 7 to 8*.

Table 7. *Prediction error of applying the overall model for each subregions*

Subregions	N	$\bar{V}$(m)	$\hat{\bar{V}}$(m)	$\bar{\varepsilon}$	S_e	Bias (%)
SL	214	0.8126	0.8312	-0.0186	0.1039	-2.2859
JGDQ	524	0.6584	0.6852	-0.0267	0.1069	-4.0588
XL	190	0.8727	0.8241	0.0487	0.1572	5.5797
TH	203	0.4517	0.4489	0.0278	0.0721	0.6154
HZ	215	0.4977	0.4776	0.0201	0.1262	4.0371
SBZ	237	0.6442	0.6776	-0.0334	0.0833	-5.1780
HJY	128	0.6170	0.6295	-0.0124	0.0839	-2.0033
XLJ	224	0.2401	0.2513	-0.0112	0.0559	-4.6555
TQ	191	0.6234	0.5973	0.0262	0.1377	4.1955
AME	285	1.0806	1.0891	-0.0843	0.1526	-0.7798

Note: N – sample size, $\bar{V}$ – average of observed tree volume, $\hat{\bar{V}}$ – average of predicted tree volume from the model, S_e – standard deviation of prediction error

If the overall model was used to predict the volume of trees in each region, excessive or underestimated predictions were made for different ecoregions (The p values of the t tests would be less than 0.05 for each of the ten subregions). On average, the overall model under-estimated (i.e., positive Bias %) tree volume from 0.6% to 5.6% for subregions XL, TH and HZ, and over-estimated (i.e., negative Bias %) tree volume about -2% to -5.2% in subregions HJY and SBZ. In the three forest regions, the Overall model under-estimated tree volume in both subregion TQ (4,2%) to subregion XL (5,6%) (*Table 7*).

Prediction errors of applying regional and overall volume equations to each subregion

Applying the regional model to each subregion would result in similar patterns and magnitudes of the prediction errors as the Overall model. This model under-estimated tree volume in the NWYLHLM - TQ (1.6%). And over-estimated tree volumes in the NWYLHLM - XLJ (-9.8%), NWYLHLM - SBZ (-8.5%), NWYLHLM - JGDQ (-7.1%), NWYLHLM - HJY (-5.5%), NWYLHLM - SL (-4.2%), NWYLHLM - TH (-3.4%) and NWYLHLM - NWYLHLM (-1.8%).

http://www.aloki.hu ● ISSN 1589 1623 (Print) ● ISSN 1785 0037 (Online)
DOI: http://dx.doi.org/10.15666/aeer/1705_1054310564

Table 8. *Prediction errors of applying a specific subregion model to each subregion*

Subregions	N	$\bar{V}$(m)	$\hat{\bar{V}}$(m)	$\bar{\varepsilon}$	S_e	Bias (%)
SL 1						
SL - SL	214	0.8127	0.8185	-0.0588	0.0993	-0.7233
SL - JGDQ	524	0.6585	0.6612	-0.0277	0.1132	-0.4206
SL - XL	190	0.8728	0.7898	0.0829	0.1766	9.5095
SL - TH	203	0.4517	0.4277	0.0241	0.0813	5.3276
SL - HZ	215	0.4977	0.4516	0.0461	0.1474	9.2601
SL - SBZ	237	0.6442	0.6474	-0.0314	0.0772	-0.4877
SL - HJY	128	0.6171	0.6015	0.0156	0.0937	2.5228
SL - XLJ	224	0.2401	0.2480	- 0.0791	0.0456	-3.2931
SL - TQ	191	0.6234	0.5799	0.0435	0.1418	6.9854
SL - AME	285	1.0807	1.0908	-0.0101	0.1535	-0.9366
JGDQ 2						
JGDQ - SL	214	0.8127	0.7989	0.0138	0.1056	1.6923
JGDQ - JGDQ	524	0.6585	0.6577	0.0073	0.1065	0.1106
JGDQ - XL	190	0.8728	0.7922	0.0805	0.1652	9.2266
JGDQ - TH	203	0.4517	0.4297	0.0221	0.0774	4.8805
JGDQ - HZ	215	0.4977	0.4568	0.0408	0.1329	8.2106
JGDQ - SBZ	237	0.6442	0.6505	-0.0632	0.0799	-0.9811
JGDQ - HJY	128	0.6171	0.6036	0.0135	0.0866	2.1839
JGDQ - XLJ	224	0.2401	0.2380	0.0213	0.0532	0.8886
JGDQ - TQ	191	0.6234	0.5732	0.0501	0.1449	8.0476
JGDQ - AME	285	1.0807	1.0477	0.0329	0.1535	3.0486
XL 3						
XL - SL	214	0.8127	0.8871	-0.0745	0.1389	-9.1656
XL - JGDQ	524	0.6585	0.7193	-0.0609	0.1349	-9.2456
XL - XL	190	0.8728	0.8692	0.0356	0.1367	0.4075
XL - TH	203	0.4517	0.4611	-0.0937	0.0775	-2.0747
XL - HZ	215	0.4977	0.4869	0.0107	0.1085	2.1590
XL - SBZ	237	0.6442	0.7085	-0.0643	0.1179	-9.9776
XL - HJY	128	0.6171	0.6540	-0.0369	0.0937	-5.9855
XL - XLJ	224	0.2401	0.2479	-0.0777	0.0836	-3.2342
XL - TQ	191	0.6234	0.6285	-0.0509	0.1328	-0.8180
XL - AME	285	1.0807	1.1776	-0.0969	0.2066	-8.9667
TH 4						
TH - SL	214	0.8127	0.8546	-0.0419	0.1088	-5.1609
TH - JGDQ	524	0.6585	0.6968	-0.0384	0.1128	-5.8291
TH - XL	190	0.8728	0.8378	0.0350	0.1483	4.0124
TH - TH	203	0.4517	0.4518	-0.0009	0.0699	-0.0221
TH - HZ	215	0.4977	0.4786	0.0191	0.1228	3.8285
TH - SBZ	237	0.6442	0.6864	-0.0421	0.0889	-6.5414
TH - HJY	128	0.6171	0.6364	-0.0193	0.0834	-3.1301
TH - XLJ	224	0.2401	0.2523	-0.0121	0.0625	-5.0579
TH - TQ	191	0.6234	0.6089	0.0145	0.1310	2.3321
TH - AME	285	1.0807	1.1296	-0.0489	0.1651	-4.5282
HZ 5						
HZ - SL	214	0.8127	0.8855	-0.0729	0.1795	-8.9669
HZ - JGDQ	524	0.6585	0.7303	-0.0718	0.1778	-10.908
HZ - XL	190	0.8728	0.8963	-0.0235	0.1678	-2.6975
HZ - TH	203	0.4517	0.4666	-0.0149	0.1154	-3.3011
HZ - HZ	215	0.4977	0.4948	0.0291	0.0952	0.5849
HZ - SBZ	237	0.6442	0.7277	-0.0834	0.1827	-12.949
HZ - HJY	128	0.6171	0.6667	-0.0496	0.1354	-8.0448
HZ - XLJ	224	0.2401	0.2279	0.0122	0.1201	5.0896
HZ - TQ	191	0.6234	0.6339	-0.0105	0.1628	-1.6775
HZ - AME	285	1.0807	1.1606	-0.0799	0.2524	-7.3936
SBZ 6						
SBZ - SL	214	0.8127	0.8107	.0.0200	0.1007	0.2466
SBZ - JGDQ	524	0.6585	0.6613	-0.0281	0.1092	-0.4263
SBZ - XL	190	0.8728	0.7918	0.0809	0.1745	9.2726
SBZ - TH	203	0.4517	0.4308	0.0209	0.0797	4.6327
SBZ - HZ	215	0.4977	0.4566	0.0411	0.1427	8.2544
SBZ - SBZ	237	0.6442	0.6504	-0.0614	0.0763	-0.9533

http://www.aloki.hu ● ISSN 1589 1623 (Print) ● ISSN 1785 0037 (Online)
DOI: http://dx.doi.org/10.15666/aeer/1705_1054310564

Subregions	N	$\bar{V}$(m)	$\hat{\bar{V}}$(m)	$\bar{\varepsilon}$	S_e	Bias (%)
SBZ - HJY	128	0.6171	0.6046	0.0125	0.0909	2.0298
SBZ - XLJ	224	0.2401	0.2471	-0.0693	0.0463	-2.8855
SBZ - TQ	191	0.6234	0.5784	0.0450	0.1439	7.2243
SBZ - AME	285	1.0807	1.07152	0.0917	0.1501	0.8484
HJY 7						
HJY - SL	214	0.8127	0.82939	-0.0167	0.1082	-2.0599
HJY - JGDQ	524	0.6585	0.67592	-0.0175	0.1111	-2.6531
HJY - XL	190	0.8728	0.81559	0.0572	0.1478	6.5513
HJY - TH	203	0.4517	0.43620	0.0155	0.0713	3.4374
HJY - HZ	215	0.4977	0.46176	0.0359	0.1223	7.2192
HJY - SBZ	237	0.6442	0.66660	-0.0224	0.0891	-3.4731
HJY - HJY	128	0.6171	0.61655	0.0053	0.0824	0.0862
HJY - XLJ	224	0.2401	0.23754	0.0259	0.0646	1.0803
HJY - TQ	191	0.6234	0.59013	0.0333	0.1338	5.3383
HJY - AME	285	1.0807	1.09658	-0.0159	0.1671	-1.4709
XLJ 8						
XLJ - SL	214	0.8127	0.77025	0.0424	0.1178	5.2179
XLJ - JGDQ	524	0.6585	0.62573	0.0327	0.1309	4.9692
XLJ - XL	190	0.8728	0.74293	0.1298	0.2206	14.876
XLJ - TH	203	0.4517	0.40948	0.0423	0.1082	9.3531
XLJ - HZ	215	0.4977	0.43355	0.0641	0.1745	12.888
XLJ - SBZ	237	0.6442	0.61228	0.0319	0.0938	4.9585
XLJ - HJY	128	0.6171	0.57157	0.0455	0.1215	7.3756
XLJ - XLJ	224	0.2401	0.24797	-0.0784	0.0357	-3.2643
XLJ - TQ	191	0.6234	0.54921	0.0742	0.1725	11.9033
XLJ - AME	285	1.0807	1.02260	0.0581	0.1587	5.3743
TQ 9						
TQ - SL	214	0.8127	0.8856	-0.0729	0.1268	-8.9781
TQ - JGDQ	524	0.6585	0.7101	-0.0516	0.1280	-7.8375
TQ - XL	190	0.8728	0.8506	0.0221	0.1462	2.5369
TQ - TH	203	0.4517	0.4543	-.0.0261	0.0729	-0.5779
TQ - HZ	215	0.4977	0.4781	0.0196	0.1258	3.9439
TQ - SBZ	237	0.6442	0.6941	-0.0499	0.0954	-7.7461
TQ - HJY	128	0.6171	0.6428	-0.0257	0.0891	-4.1653
TQ - XLJ	224	0.2401	0.2569	-0.0167	0.0675	-6.9841
TQ - TQ	191	0.6234	0.6231	0.0033	0.1279	0.0525
TQ - AME	285	1.0807	1.1869	-0.1062	0.1951	-9.8283
AME 10						
AME - SL	214	0.8127	0.8327	-0.0199	0.1023	-2.4606
AME - JGDQ	524	0.6585	0.6865	-0.0280	0.1096	-4.2542
AME - XL	190	0.8728	0.8189	0.0538	0.1801	6.1619
AME - TH	203	0.4517	0.4539	-0.0216	0.0794	-0.4791
AME - HZ	215	0.4977	0.4831	0.0146	0.1425	2.9319
AME - SBZ	237	0.6442	0.6766	-0.0324	0.0767	-5.0306
AME - HJY	128	0.6171	0.6317	-0.0146	0.0928	-2.3688
AME - XLJ	224	0.2401	0.2681	-0.0279	0.0432	-11.634
AME - TQ	191	0.6234	0.5999	0.0236	0.1449	3.7786
AME - AME	285	1.0807	1.0914	-0.0107	0.1464	-0.9879

Note: N – sample size, $\bar{V}$ – average of observed tree volume, $\hat{\bar{V}}$ – average of predicted tree volume from the model, S_e – standard deviation of prediction error

Again, larger under-estimations occurred in the NWYLHLM - XL (2.9%) (*Table 9*). This was expected because the estimated parameters of the Overall model were close to those of the three regional models (*Table 5*).

On the other hand, the regional model has not been able to overestimate the volume of trees in the ten ecoregions of the different regions (*Table 9*).

When the ten ecoregional models were applied to each ecoregion, they generally performed well in the ecoregions in which the models were developed (p-values for the t-

http://www.aloki.hu ● ISSN 1589 1623 (Print) ● ISSN 1785 0037 (Online)
DOI: http://dx.doi.org/10.15666/aeer/1705_1054310564

tests > 0.05 for testing that the mean prediction error equals zero) and the models produced significant prediction errors. The prediction biases ranged from -3.3% to 9.5% in Model 1 (SL1), -0.9% to 9.2% in Model 2 (JGDQ2), -9.9% to 2.1% in Model 3 (XL3), -6.5% to 4% in Model 4 (TH4), -12.9% to 5.1% in Model 5 (HZ5), -2.8% to 9.3% in Model 6 (SBZ6), -3.5% to 7.2% in Model 7 (HJY7), -3.3% to 14.9% in Model 8 (XLJ8), -9.8% to 3.9% in Model 9 (TQ9) and -11.6 to 6.2% in Model 10 (AME10) (*Table 8*).

Table 9. *Prediction errors of applying regional models to each subregion*

Reg – Sub	N	$\bar{V}$(m)	$\hat{\bar{V}}$(m)	$\bar{\varepsilon}$	S_e	Bias (%)
NWYLHLM - SL	214	0.8126	0.8467	-0.0341	0.1062	-4.1954
NWYLHLM - JGDQ	524	0.6584	0.7048	-0.0464	0.1076	-7.0473
NWYLHLM - XL	190	0.8727	0.8470	0.0257	0.1569	2.9456
NWYLHLM - TH	203	0.4517	0.4668	-0.0151	0.0722	-3.3517
NWYLHLM - HZ	215	0.4977	0.4984	-0.0077	0.1227	-0.1553
NWYLHLM - SBZ	237	0.6442	0.6992	-0.0549	0.0871	-8.5312
NWYLHLM - HJY	128	0.6171	0.6510	-0.0339	0.0850	-5.5072
NWYLHLM - XLJ	224	0.2401	0.2636	-0.0235	0.0565	-9.7865
NWYLHLM - TQ	191	0.6234	0.6132	0.0101	0.1384	1.6296
NWYLHLM - AME	285	1.0807	1.1005	-0.0199	0.1503	-1.8412
SAYLHLM - SL	214	0.8126	0.8491	-0.0365	0.1128	-4.4898
SAYLHLM - JGDQ	524	0.6584	0.6879	-0.0295	0.1158	-4.4792
SAYLHLM - XL	190	0.8727	0.8284	0.0443	0.1453	5.0817
SAYLHLM - TH	203	0.4517	0.4423	0.0936	0.0704	2.0724
SAYLHLM - HZ	215	0.4977	0.4672	0.0304	0.1220	6.1162
SAYLHLM - SBZ	237	0.6442	0.6765	-0.0322	0.0913	-5.0072
SAYLHLM - HJY	128	0.6171	0.6257	-0.0868	0.0833	-1.4062
SAYLHLM - XLJ	224	0.2401	0.2433	-0.0320	0.0661	-1.3335
SAYLHLM - TQ	191	0.6234	0.6016	0.0217	0.1302	3.4885
SAYLHLM - AME	285	1.0807	1.1281	-0.0474	0.1757	-4.3865
NDXAM - SL	214	0.8126	0.8117	0.0094	0.1023	0.1158
NDXAM - JGDQ	524	0.6584	0.6649	-0.0647	0.1067	-0.9832
NDXAM - XL	190	0.8727	0.7993	0.0734	0.1639	8.4153
NDXAM - TH	203	0.4517	0.4332	0.0185	0.0755	4.1036
NDXAM - HZ	215	0.4977	0.4597	0.0379	0.1337	7.6241
NDXAM - SBZ	237	0.6442	0.6559	-0.0117	0.0787	-1.8260
NDXAM - HJY	128	0.6171	0.6088	0.0826	0.0858	1.3380
NDXAM - XLJ	224	0.2401	0.2426	-0.0247	0.0524	-1.0274
NDXAM - TQ	191	0.6234	0.5804	0.0429	0.1411	6.8916
NDXAM - AME	285	1.0807	1.0689	0.0117	0.1526	1.0849

Note: N – sample size, $\bar{V}$ – average of observed tree volume, $\hat{\bar{V}}$ – average of predicted tree volume from the model, S_e – standard deviation of prediction error

These results are expected because different ecoregions have large differences in climatic, soil and ecological conditions. As Peng et al. (2004) and Rivas et al. (2007) indicated, part of the differences in dbh and volume models among tree species may be caused by differences in genetics, growth conditions and site quality. Recent studies with different species also indicated differences in ecoregion-based height diameter models (Huang et al., 1999; Peng et al., 2004; Brooks and Wiant, 2005). For our case, the updated Ecoregion classification of Dahurian larch region (*Figure 1*) provides comprehensive information on changes in ecoregion-species relationships along the ecological and macroclimatic gradients of different regions. These ecoregions are characterized by large climatic patterns (temperature and precipitation, for example), soil moisture and nutrient

http://www.aloki.hu ● ISSN 1589 1623 (Print) ● ISSN 1785 0037 (Online)
DOI: http://dx.doi.org/10.15666/aeer/1705_1054310564

regimes, and succession and vegetation types (Hills, 1959, 1960; CEC, 1997; ELC Working Group, 2000).

In general, Dahurian larch species are larger in forest subregions (JGDQ and AME), mainly due to climate, abundant rainfall and the longer growing season. For example, the average annual temperatures of the different ecoregions are between -1°C to -2.8°C and -28°C to 20°C, respectively in Daxing'an Mountains region. Moreover the average air temperatures in January and July are about -28°C and 20°C, respectively while the mean annual precipitation is relatively higher in Daxing'an Mountains region (500 to 750 mm). More detailed analysis of climatic characteristics for each ecoregion can be found in Dong et al. (2014). In addition, local ecological conditions (vegetation type) also affect species growth and productivity in these ecoregions. For example, in the ten subregions studied, it has been shown that the stand of the Dahurian larch species is the most dominant in relation to others species. The latter which is our study species comprises a total of 2411 individuals for all ten subregions compared to a total of 1324 trees in all ten subregions for *Betula platyphylla* species (BH), 445 trees for Siberian larch (SY) species, 1294 trees for Korean pine (ZZS). Subregion 2 (JGDQ) has the largest number of trees (524 trees for Dahurian larch species only).

Therefore, the combination of all climatic, environmental and vegetation factors plays an important role in determining the different volume relationships among ten subregions.

These results are consistent with the recent findings reported by Huang (1999) quoted by Liunjun et al. (2002) and Huang et al. (2000) for Lodgepole pine and white spruce in the boreal forests of Alberta.

Illustration of different graphics in Figure 2

The different figures below illustrate average prediction errors on diameter classes of 5 cm for the ten subregions. Clearly, the overall model's negative biases in some subregions were due to overestimation for large trees. The larger positive model biases in the two subregions (XL (second line on the left) and TQ (fifth line on the left)) are due to the underestimation of all trees by the global model.

This limitation was initial pointed by Thalmann (1965), where advanced evaluation methods based on confirmed technical bases are necessary. These graphs show the mean prediction errors (m^3) in diameter classes of 5 cm when the global model is applied to predict the volume of trees in each of the ten subregions.

Solid lines with solid symbols: diamond, square, triangle, asterisk and circle are used to represent subregions:

- First line (SL and JGDQ: 3E (circles), 3W (squares), 2S (triangles), 3S (asterisks) and 3W (circles)).
- Second line (XL and TH: 3E (circles), 3W (asterisk), 3W (squares), 3S (triangles).
- Third line (HZ and SBZ: 3E (triangles), 3W (triangles), 3W (circles), 3W (squares), 4W (asterisks), 2W (circles).
- Fourth line (HJY and XLJ: 3E (circles), 2W (circles), 4W (asterisks), 1W (squares), 1S (rod).
- Fifth line (TQ and AME: 2E (rods), 2E (circles), 2W (diamond), 5w (asterisks), 3W (squares).

Therefore, trends in prediction errors in the 5 cm of diameter classes were very similar for some regional model and the overall model.

http://www.aloki.hu ● ISSN 1589 1623 (Print) ● ISSN 1785 0037 (Online)
DOI: http://dx.doi.org/10.15666/aeer/1705_1054310564

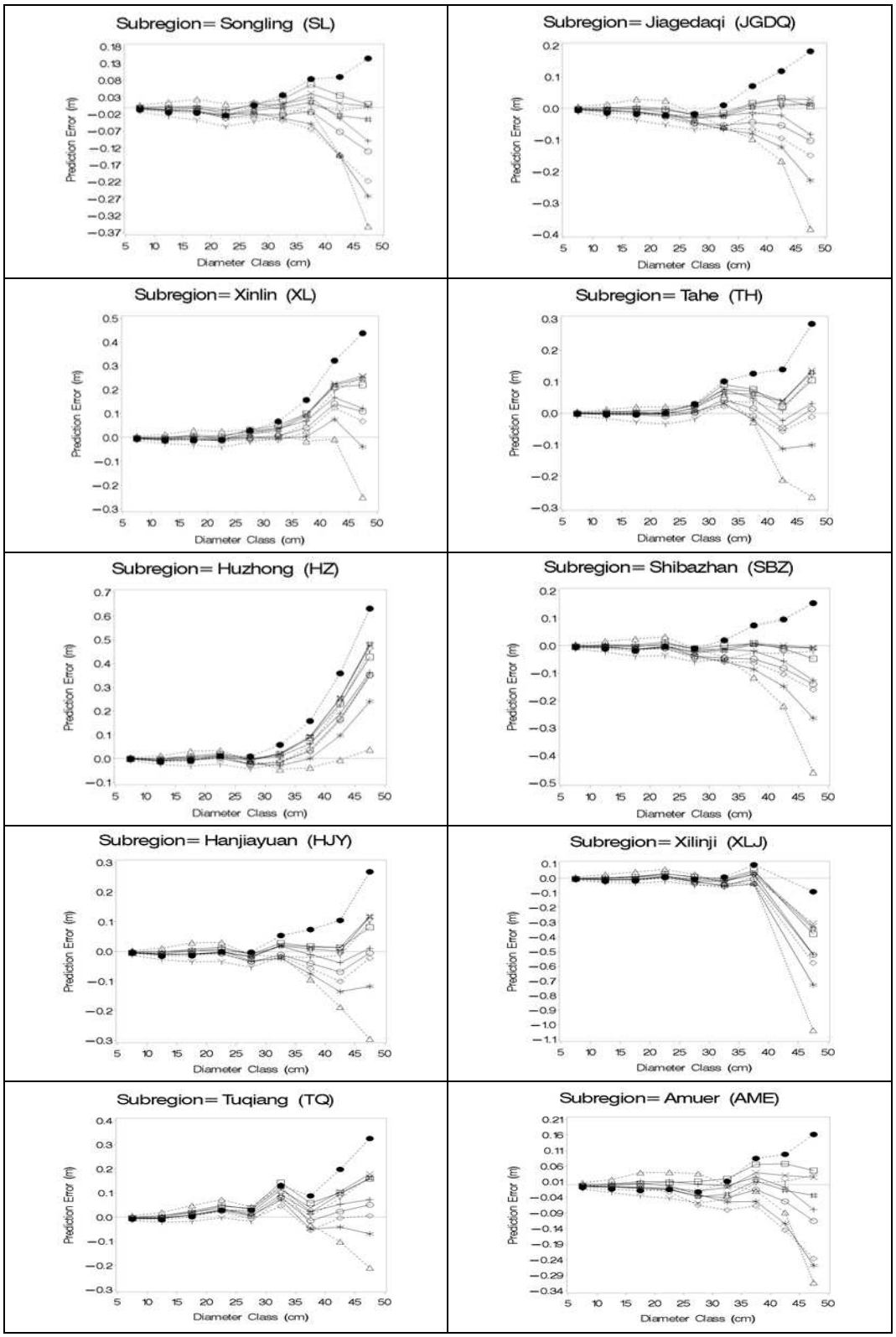

Figure 2. *Average prediction errors (m) across 5-cm diameter classes when each subregional model is applied to predict total volume in each of the ten subregions with symbols: SL (hash), JGDQ (square), XL (star),TH (circle), SBZ (X), HJY (plus), HZ (triangle), XLJ (dot), TQ (diamond) and AME (Y)*

http://www.aloki.hu ● ISSN 1589 1623 (Print) ● ISSN 1785 0037 (Online)
DOI: http://dx.doi.org/10.15666/aeer/1705_1054310564

On the other hand, other regional models overestimated tree volume (e.g. % bias) in some subregions of different regions including: HJY and SBZ and in others, underestimated, for example: XL, TH, HZ and finally TQ and XL. Some figures indicate that negative model biases result from overestimation of all trees in diameter classes of different subregions. The relatively high value for some subregions can be explained by the morphology of the Dahurian larch stem in the temperate mixed forests of the study regions.

Conclusion

With total tree volume equations being developed in the study for economically important hardwood species from northeastern China (Daxing'an Mountain region /Heilongjiang province), these equations were based on a simple function and adjusted to the forest inventory data volumes of three mountainous regions, including the north-west of the North Slope of the Yilehuli Mountains, the southeast of the North Slope of the Yilehuli Mountains, and the northeastern slope of the Daxin'an Mountains. Using dummy variables and an additional sum of squares procedure, the volume - diameter relationship was not the same for all ecoregions when tested by species and volume type. For ecoregion-specific comparisons, statistical differences in total volume were found across many ecoregions, which can be explained in part by the longitudinal, latitudinal, and elevation properties of differences between soils, the length of the season of growth and annual rainfall rate in the regions, which leads us to prove the significance of the relationship between the volume and diameter of the trees of the Dahurian larch tree species studied.

The main underlying factor is probably the differences in height-diameter relationships reported for the same ecoregions in northeastern China. Mean bias varied from -3.3% to 9.5% for (SL1), -0.9% to 9.2% for (JGDQ2), -9.9% to 2.1% for (XL3), -6.5% to 4% for (TH4), -12.9% to 5.1% for (HZ5), -2.8% to 9.3% for (SBZ6), -3.5% to 7.2% for (HJY7), -3.3% to 14.9% for (XLJ8), -9.8% to 3.9% for (TQ9) and -11.6% to 6.2% for (AME10) for the marketable value of timber in the three regions. Local tree volume equations specific to species and ecoregions are presented and can be easily used in wood intrusion situations. However, there are clear variations in volume relationships for Dahurian larch species in the ten subregions of the three regions studied in northeastern China (Heilongjiang Province). Inappropriate application of provincial or regional volume models to these different subregions can lead to significant errors in estimating tree height and total volumes. Ecoregion-based volume models can actually provide more accurate predictions of tree volume and height than models developed at the provincial or regional level.

Acknowledgements. This research was financially supported by National Key R &D Program of China (grant No. 2017YFB0502700), National Natural Science Foundation of China (grant No. 31570624), Applied Technology Research and Development Program of Heilongjiang Province (GA19C006-1) and the Fundamental Research Funds for the Central Universities.

http://www.aloki.hu ● ISSN 1589 1623 (Print) ● ISSN 1785 0037 (Online)
DOI: http://dx.doi.org/10.15666/aeer/1705_1054310564

REFERENCES

[1] Akinsanmi, F. A., Akindélé, S. O. (1995): Teak productivity in relation to soil conditions: A re-assessment of teak plantations in the dry high forest area of south-western Nigeria. – Nigerian Journal of Forestry 24: 7-10.
[2] Amateis, R. L., Burkhart, H. E. (1987): Tree volume and taper of loblolly pine varies by stand origin. – South J Appl For. 11: 185-189.
[3] Barrio, M., Diéguez-Aranda, U., Castedo-Dorado, F., Álvarez, J. G., Kv, G. (2007): Merchantable volume system for pediculate oak in northwestern Spain. – Ann for Sci 64: 511-520. [CrossRefGoogleScholar].
[4] Bates, D. M., Watts, D. G. (1988): Nonlinear regression analysis and its applications. – Wiley, New York.
[5] Bontemps, J. D., Longuetaud, F., Franceschini, T., Charru, M., Constant, T. (2012): Estimation of forest biomass and productivity in the face of environmental change. – AgroParisTech, ENGREF, UMR 1092 INRA / AgroParisTech Forest-Wood Resources Study Laboratory (LERFoB), Street 14 Girardet, F-54000 Nancy 14p.
[6] Brooks, J. R., Wiant, H. V. Jr. (2004): A simple technique for estimating cubic volume yields. – Forest Ecology and Management 203: 373-380.
[7] Brooks, J. R., Wiant, H. V. Jr. (2005): Evaluating ecoregion based height_diameter relationship of five economically important Appalachian hardwood species in West Virginia. – In: McRoberts, R. E., Reams, G. A., Van Deusen, P. C., McWilliams, W. H. (eds.) Proceedings of the seventh annual forest inventory and analysis symposium; October 3-6, 2005; Portland, ME. Gen. Tech. Rep. WO-77. Washington, DC: U.S. Department of Agriculture, Forest Service: 237-242.
[8] Brooks, J. R., Jiang, L., Ozçelik, R. (2008): Compatible stem volume and taper equations for Brutian pine, Cedar of Lebanon, and Cilicica fir in Turkey. – Forest Ecology and Management 256(1): 147-151.
[9] Burkhart, H. E. (1977): Cubic-foot volume of loblolly pine to any merchantable top limit. – South J Appl For. 1: 7-9.
[10] CEC (Commission for Environmental Cooperation). (1997): Ecological Regions of North America: Toward a common perspective. – CEC, Montreal. 71 p and maps.
[11] Corral-Rivas, J. J., Barrio-Anta, M., Aguirre-Calderon, O. A., Dieguez-Aranda, U. (2007): Use of stump diameter to estimate diameter at breast height and tree volume for major pine species in El Salto, Durango (Mexico). – Forestry 80: 29-40.
[12] CRPF FOGEFOR d, Limousin. (2011): The cubing of standing trees. 17 p.
[13] Dong, L.-H., Zhang, L., Li, F. (2014): Developing additive system of biomas equations for nine hardwood species in Norteast China. – Forest Ecology and Management 329: 306-317.
[14] Dong, L., Liu, Z., Bettinger, P. (2016): Nonlinear mixed-effects branch diameter and length models for natural Dahurian larch (Larix gmelini) forest in northeast China. – Trees 30(4): 1191-1206.
[15] ELC Working Group. (2000): The Ecoregions and Ecodistricts of Ontario. – Ecological Land Classification Program, Ont. Min. Nat. Resour., Sault Ste Marie, ON.
[16] Fonton, N. H., Glele Kakai, R., Rondeux, J. (2002): Étude dendrométrique d'Acacia auriculiformis A. Cunn. ex Benth. en mélange sur vertisol au Bénin. [Dendrometric study of Acacia auriculiformis A. Cunn. Ex Benth. in mixture on vertisol in Benin]. – Biotechnologie, Agronomie, Société et Environnement 6(1): 29-37.
[17] Fonton, N. H., Yabi, C. C., Dovonon, J. Z. D., Adoko, F. K., Titilayo. D. (2009): Tree Shaft Volume Modeling for Sustainable Management of Sudanese Forest Ecosystems. 100 p.
[18] Fonton, H. N., Dah-Dovonon, J. Z., Adoko, F. K., Dotchamou, T. (2009): Modélisation du volume du fût d'arbre pour une gestion durable des écosystèmes forestiers soudaniens.

http://www.aloki.hu ● ISSN 1589 1623 (Print) ● ISSN 1785 0037 (Online)
DOI: http://dx.doi.org/10.15666/aeer/1705_1054310564

[Modelling of tree stem volume for sustainable management of sudanian forest ecosystems]. – Bois et Forêt des Tropiques 300(2): 95-100.

[19] Hills, G. A. (1959): A Ready Reference to the Description of the Land of Ontario and its Productivity. – Preliminary Report. Ontario Department of Lands and Forests, Division of Research, Maple. 142p.

[20] Hills, G. A. (1960): Comparison of forest ecosystems (vegetation and soil) in different climatic zones. – Silva Fennica 105: 33-39.

[21] Honer, T. G. (1967): Standard volume tables and merchantable conversion factors for the commercial tree species of central and eastern Canada. – Can. Dept. Forestry Rural Devel., For. Mgmt. Res. And Serv. Inst. Info. Rep. FMR-X-5.

[22] Huang, S., Titus, S. J., Wiens, D. P. (1999): Comparison of nonlinear height_diameter functions for major Alberta tree species. – Canadian Journal of Forest Research 22: 1297-1304.

[23] Huang, S., Price, D., Morgan, D., Peck, K. (2000): Kozak's variable-exponent taper equation regionalized for white spruce in Alberta. – West J Appl For 15(2): 75-85. [CrossRefGoogle Scholar].

[24] Huang, S., Price, D., Titus, S. J. (2000): Development of ecologicalbased height–diameter models for white spruce in boreal forests. – For. Ecol. Manage. 129: 125-141. [CrossRefGoogleScholar].

[25] Jia, B., Zhou, G. (2018): Growth characteristics of natural and planted Dahurian larch in northeast China. – Earth System Science Data Discussions 6p.

[26] Jiang, L., Brooks, J. R., Wang, J. (2004): Compatible taper and volume equations for yellow-poplar in West Virginia. – For. Ecol. And Mgmt. 213: 399-409. [CrossRefGoogle Scholar].

[27] Jin, Q., Valsta, L., Heliövaara, K., Li, J., Luo, Y., Shi, J. (2015): Effects of Catastrophic Insect Outbreaks on the Harvesting Solutions of Dahurian Larch Plantations. – International Journal of Forestry Research, 12p.

[28] Laumans, P. (1991): Tables de cubage à deux entrées pour le volume bois sciable du Teck (Tectona grandis L. f.) au Sud Bénin. – Wittelsbacherstr 11, D-8016 Feldkirchen, 18p.

[29] Lee, D., Seo, Y., Choi, J. (2017): Estimation and validation of stem volume equations for Pinus *densiflora*, *Pinus koraiensis*, and *Larix kaempferi* in South Korea. – Forest Science and Technology 13(2): 77-82.

[30] Neter, J., Kutner, M. H., Nachtsheim, C. J., Wasserman, W. (1996): Applied linear statistical models. – McGraw-Hill, New York. 1048p.

[31] Newnham, R. (1992): Variable-form taper functions for four Alberta tree species. – Can J For Res 22: 210-223. [CrossRefGoogleScholar].

[32] Özcelik, R., Karatepe, Y., Gürlevik, N., Canellas, I., Crecente-Campo, F. (2016): Development of ecoregion-based merchantable volume systems for *Pinus brutia* Ten and *Pinus nigra* Arnold in southern Turkey. – Journal of Forestry Research 27(1): 101-117.

[33] Palm, R. (1982): Influence of the volume formula and the length of the ridges on the determination of the volume of felled trees. – Annals of Forest Science 39: 231-238.

[34] Palm, R., Iemma, A. F. (2002): Application conditions and variable transformations in linear regression. – Gembloux Belgium, University Faculty of Agricultural Sciences, Statistics and Computer Science Notes, 34p.

[35] Pauwels, D., Rondeux, J. (1999): Tarifs de cubage pour les petits bois de melèze (Larix sp.) en Ardenne. – Les Cahiers Forestiers de Gembloux, 11p.

[36] Peng, C., Zhang, L., Zhou, X., Dang, Q., Huang, S. (2004): Developing and evaluating tree height_diameter models at three geographic scales for black spruce in Ontario. – Northern Journal of Applied Forestry 21: 83-92.

[37] Rondeux, J. (1999): The measurement of trees and forest stands. – Gembloux, Belgium, The Agronomic Press of Gembloux, 2nd edition, 521p.

[38] SAS Institute Inc. (2002): SAS/STAT Online User's Guide, Version 9.0. – SAS Institute Inc., Cary, NC.

http://www.aloki.hu ● ISSN 1589 1623 (Print) ● ISSN 1785 0037 (Online)
DOI: http://dx.doi.org/10.15666/aeer/1705_1054310564

[39] Shailer, S., Kershaw, J. A., Zundel, P. (1998): Comparison of total volume equations for use in southwestern New Brunswick. – Research Report perpared for Georgia Pacific (The Timber Company), St. Croix district.
[40] Sherrill, J. R., Bullock, B. P., Mullin, T. J., McKeand, S. E., Purnell, R. C. (2011): Total and merchantable stem volume equations for midrotation loblolly pine (Pinus taeda L.). – South J Appl For. 35: 105-108.
[41] Thibaut, A., Rondeux, J., Claessens, H. (1998): Tarifs de cubage pour l'Aulne glutineux [Alnus glutineux (L.) Gaertn.] en Belgique méridionale. – Revue Forestière Française, L-3: 244-250.
[42] Tsega, M., Guadie, A., Teffera, Z. L., Belayneh, Y., Niu, D. (2018): Development and validation of a stem volume equation for Cupressus lusitanica in Gergeda Forest, Ethiopia. – Southern Forests: a Journal of Forest Science 81(1).
[43] Zhang, L., Peng, C., Huang, S., Zhou, X. (2002): Development and evaluation of ecoregion-based jack pine height-diameter models for Ontario. – Forestry Chronicle 78(4): 530-538.

http://www.aloki.hu ● ISSN 1589 1623 (Print) ● ISSN 1785 0037 (Online)
DOI: http://dx.doi.org/10.15666/aeer/1705_1054310564

ROLES OF HOMOARGININE IN THE CARDIOVASCULAR SYSTEM

EKUA, N. E. – CHE, D.* – ADAMS, S. – QIN, G. – ZHAO, B. – JIANG, H.

College of Animal Science and Technology, Jilin Agricultural University Changchun 130118, China

Jilin Provincial Key Lab of Animal Nutrition and Feed Science, Jilin Agricultural University Changchun 130118, China

Key Lab of Animal Production, Product Quality and Security, Ministry of Education, Jilin Agricultural University, Changchun 130118, China

**Corresponding author*
e-mail: chedongsheng@163.com; phone: +86-136-4431-9554

(Received 5th Mar 2019; accepted 13th Jun 2019)

Abstract. Homoarginine is a non-protein amino acid which is structurally similar to arginine. Research shows that homoarginine is produced in a small quantity in the body of humans and animals and it is suggested to be found in some organs such as the kidney, liver, brain and body fluids; blood and urine. Homoarginine is synthesized from arginine and lysine by the catalytic action of arginine: glycine amidinotransferase (AGAT) which is also responsible for the synthesis of guanidinoacetate, the precursor of creatine. High concentration of homoarginine has been reported to inhibit arginase which is a substrate in the synthesis of nitric oxide. Recent reports have also indicated that low homoarginine concentrations are a risk marker for cardiovascular diseases and death. More research needs to be done to improve knowledge on the physiological role of homoarginine and its application in clinical studies and pharmacy with the aim of coming up with possible medication and ways to combat cardiovascular diseases. This review seeks to summarize the role of homoarginine in the cardiovascular system.
Keywords: *arginine: glycine amidinotransferase, disease, nitric oxide, smooth muscle cells, synthesis*

Introduction

As a cationic amino acid, homoarginine has structural similarities to arginine (*Fig. 1*) and formed from lysine (Papageorgiou et al., 2015). Its synthesis occurs in the kidney and the liver (Ryan and Wells, 1964). The enzyme that is responsible for homoarginine synthesis remains unknown (Tsikas and Kayacelebi, 2014) however, it is assumed to be arginine: glycine amidinotransferase (AGAT) which may help in the synthesis of homoarginine from lysine and arginine in animals (Hou et al., 2015; Tsikas and Wu, 2015). According to research, homoarginine inhibits arginase and arginine transportation by cells (Hou et al., 2015). The level of homoarginine concentration in the body has been reported to be higher in children as compared to adults - children have a high level of protein synthesis to support growth (Atzler et al., 2014). Some researchers found that its concentration in the plasma declines with age, which results in cardiovascular, cerebrovascular diseases and death in animals and humans (Atzler et al., 2015; Hou et al., 2015). Studies have shown that homoarginine may impact nitric oxide metabolism, endothelial function, insulin secretion, and inhibit platelet aggregation; these are important for the maintenance of cardiovascular health (Bretscher et al., 2003; Stockebrand et al., 2015). Based on these functions, some scientists have showed that homoarginine is an independent risk biomarker of cardiovascular diseases (Tomaschitz

http://www.aloki.hu ● ISSN 1589 1623 (Print) ● ISSN 1785 0037 (Online)
DOI: http://dx.doi.org/10.15666/aeer/1705_1056510574

et al., 2014; Kayacelebi et al., 2015; Chafai et al., 2017; Seppälä et al., 2017). Current investigations on the usage of homoarginine in both human and animals in relations to different conditions such as disease states, growth promotion, nutrient transport and metabolism, foetal and neonatal growth and survival is increasingly gaining scientific attention. Homoarginine has been associated with different disease states in both human and animals however there are limited investigations involving homoarginine. Therefore, this current review seeks to summarize the role of homoarginine in the cardiovascular systems, including Atherosclerosis, Type 2 diabetes mellitus, and Stroke.

Synthesis of homoarginine

Arginine and asymmetric dimethylarginine (ADMA) are usually measured at the same time with homoarginine, which is a homolog of arginine (*Fig. 1*) (Teerlink et al., 2002; Davids et al., 2012b). Homoarginine is solid and it has a melting point of 213-215°C with a molecular weight of 188.231 g/mol. Its formation is endogenous (Seppälä et al., 2017). Some legumes are rich in nonprotein amino acids, including homoarginine; the grass pea (Lathyrus sativus L.), which is rich in homoarginine serves as food for humans and feed for domestic animals (Bell, 2003; Rao, 2011). Research shows that plasma concentration of homoarginine in healthy adults is about 2 μM (Hou et al., 2015; May et al., 2015; Hanff et al., 2016). A study on rats recorded 20 min as the half-life of homoarginine (Günes et al., 2017; Adams et al., 2019). It is known to play a role in the arginine/nitric oxide pathway by acting as a substrate (Haghikia et al., 2017). According to research, homoarginine's ability to inhibit either arginase or protein arginine methyltransferase (PRMTs) makes it increase the production of nitric oxide (Michel, 2013; Vogl et al., 2015) and this might have a positive impact on endothelial function (Valtonen et al., 2008). Recent reports have indicated that low homoarginine concentrations is a risk factor for cardiovascular conditions and death in people as well as kidney disease patients (Atzler et al., 2014; Pilz et al., 2014; Tomaschitz et al., 2014; Vogl et al., 2015).The physiological role of homoarginine is still being studied by some researchers.

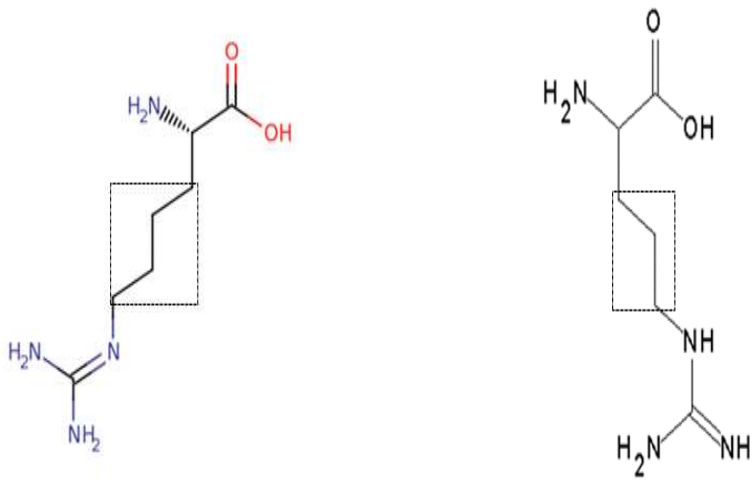

Homoarginine Arginine

Figure 1. *The structural formula of arginine and its homolog homoarginine which differs by a methylene group (-CH2-)*

http://www.aloki.hu ● ISSN 1589 1623 (Print) ● ISSN 1785 0037 (Online)
DOI: http://dx.doi.org/10.15666/aeer/1705_1056510574

Homoarginine metabolism in vascular system

Metabolism of Homoarginine

Studies over the past fifty years have led to an understanding of some of the physiological and biochemical roles of homoarginine in humans and animals (Hou et al., 2015). Homoarginine is produced in a small quantity in the body of humans and animals (Hou et al., 2015). It is suggested to be found in some organs such as the kidney, liver, brain and body fluids; blood and urine (Valtonen et al., 2008). A research on the possible pathways for homoarginine showed that a mitochondrial enzyme found in the kidney, which is arginine: glycine amidinotransferase (AGAT), catalyses the transformation of glycine and arginine to guanidinoacetate (GAA) and ornithine, and GAA is methylated to creatine with the help of guanidinoacetate N-methyltransferase (GAMT) for energy metabolism. Homoarginine is produced when AGAT uses lysine instead of glycine (Davids et al., 2012a) (*Fig. 2*). In the urea cycle, homoarginine is formed when ornithine is replaced by lysine. The ornithine transcarbamoylase (OTC) enzyme is important in this metabolic pathway. This enzyme catalyses the transamidination of lysine which facilitates the production of homoarginine (Davids et al., 2012a). Homoarginine also inhibits arginase and acts as a substrate for NO synthase to form NO, which performs a critical function in vasodilation and is important in the regulation of blood pressure (März et al., 2010).

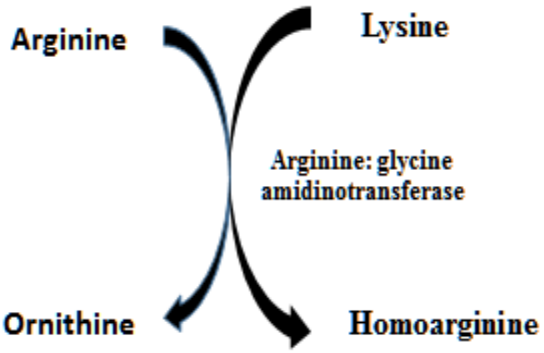

Figure 2. *A schematic diagram showing the synthesis of Homoarginine and Ornithine from Arginine and lysine using Arginine: glycine amidinotransferase*

Nitric Oxide and Nitric Oxide Synthases

Nitric oxide (NO) is formed during the complex oxidation reaction from arginine and oxygen (O2). NO is produced with the help of enzyme nitric oxide synthase (NOS), with the endothelial cells of blood vessels being its first location. The enzyme is called synthase, not synthetase, because there is no need of adenosine triphosphate (ATP) for its action (Arzumanian et al., 2003). The nitric oxide synthase plays active role in the production of NO. They are neuronal (nNOS), endothelial (eNOS) and inducible (iNOS). Oxygen, nicotinamide-adenine-dinucleotide phosphate (NADPH), tetrahydrobiopterin and flavin adenine nucleotides are known as the co-factors for NOS (Kassim et al., 2010; Tousoulis et al., 2012).

Expression of Neuronal NOS occurs in specific neurons in the brain with Ca^{2+} and calmodulin regulating the activities of enzymes (Zhou and Zhu, 2009). According to

http://www.aloki.hu ● ISSN 1589 1623 (Print) ● ISSN 1785 0037 (Online)
DOI: http://dx.doi.org/10.15666/aeer/1705_1056510574

immunohistochemistry, nNOS could be located in the spinal cord, the sympathetic ganglia and adrenal glands, in kidney macula densa cells, and in the vascular smooth muscle (Förstermann et al., 1994). nNOS is known to play a role in physiological functions such as memory, learning, and neurogenesis (Zhou and Zhu, 2009). Research has shown that the central regulation of blood pressure in the central nervous system (CNS) is assisted by NO formed by nNOS (Sakuma et al., 1992; El karib et al., 1993). A data on human studies indicated that nNOS perform a significant function in vascular tone regulation (Melikian et al., 2009). When eNOS becomes dysfunctional, low level of nNOS expressed in the vascular smooth muscle cells maintains vasodilation (Schwarz et al., 1999). The endothelial cells are known as the site for endothelial NOS production. Research has also shown that the isozyme is found in cardiac myocytes, platelets, LLC-PK1 kidney tubular epithelial cells and certain neurons of the brain, and in (Förstermann et al., 1994). Numerous essential cardiovascular functions appear to be regulated by eNOS which serves as a homeostatic regulator. Endothelial NOS-derived NO stimulates soluble guanylyl cyclase and increases cyclic guanosine monophosphate (cGMP) in smooth muscle cells thereby dilates all types of blood vessels (Förstermann and Sessa, 2011). Blood pressure rises as a result of deletion of the eNOS gene (Huang et al., 1995; Shesely et al., 1996). The inhibition of platelet aggregation and adhesion to the vascular wall occurs when nitric oxide is released towards the vascular lumen (Alheid et al., 1987). Evidence has also indicated that endothelial NO inhibits leucocyte adhesion and vascular inflammation. An early event in the development of atherosclerosis is leucocyte adherence and therefore, NO may act against the onset of atherogenesis (Förstermann and Sessa, 2011). Expression of inducible NOS can be instigated by bacterial lipopolysaccharide, cytokines, and other agents (Förstermann, 2000). The production of high quantity of NO by inducible NOS occurs when induced in macrophages which indicates a major cytotoxic principle of those cells (Nathan and Hibbs Jr, 1991). Arginine is utilized by all isoforms of NOS as the substrate, with molecular oxygen and decreased NADPH being utilized as co-substrates (Förstermann and Sessa, 2011).

Functions of homoarginine in vascular system

Nitric oxide synthesis

Nitric oxide which has been studied extensively due to its health effects in the body is an inorganic molecule that exists in mammalian biology (Ziolo et al., 2001). The formation of nitrogen oxides occurs when NO; an unstable free-radical gas reacts rapidly with oxygen. It is soluble and has a molecular weight of 30.006 g/mol. Nitric oxide has a half-life of ~6–30 s (Tousoulis et al., 2012). The nitric oxide synthases catalyse the oxidation of arginine to produce nitric oxide in mammals. eNOS and nNOS are constitutively expressed and are referred to as Ca^{2+}-dependent enzymes (Förstermann and Sessa, 2011). It serves as a main paracrine and autocrine mediator of immune regulation and vascular relaxation in the body (Moncada, 1991). In the endothelium, nitric oxide serves as a central signal transduction pathway (Ignarro et al., 1999). Homoarginine is a weak substrate for nitric oxide synthase (NOS) and can produce NO. When homoarginine hinders the activity of arginase, it may increase arginine and NO production (Hrabak et al., 1994). Nitric oxide aids in blood pressure regulation, inhibition of platelet aggregation, platelet adhesion inhibition, and neurotransmission (Loscalzo and Vita, 2000; Atzler et al., 2015). Arginine performs

http://www.aloki.hu ● ISSN 1589 1623 (Print) ● ISSN 1785 0037 (Online)
DOI: http://dx.doi.org/10.15666/aeer/1705_1056510574

various functions in living organisms (März et al., 2010; Haghikia et al., 2017), but the roles of homoarginine need more research (Seppälä et al., 2017). A study suggested that homoarginine competes with arginine, which causes a decrease in NO synthesis (Alesutan et al., 2016). An intravenous homoarginine infusion research done on rats showed an increase in serum concentration of homoarginine and ornithine (Dellera et al., 2016). According to the results obtained, it was suggested that anti-proliferative effects may be exerted by homoarginine; increasing the release of NO from vascular cells (Durante, 2013; Dellera et al., 2016), and by ornithine; acting as an arginase inhibitor to increase NO availability (Durante, 2013; Dellera et al., 2016). Homoarginine plays an important role in NO synthesis even though its concentration is little in the serum and plasma of humans and animals.

Cardiovascular diseases

Vascular smooth muscle cells perform a major function in vascular diseases (Qiu et al., 2014). Studies have shown that the abnormal proliferation and migration of vascular smooth cells are the main constituents of hypertension, atherosclerosis and vascular sterosis after vessel transplant (Kockx and Knaapen, 2000; González-Navarro et al., 2010). Homoarginine is a less efficient NOS substrate than arginine, but competes with arginine for NO synthesis by hindering the regular production of NO (März et al., 2010). Research has reported that critical cardiovascular conditions are as a result of both high and low hArg levels whereas increased vascular resistance is as a result of high homoarginine levels. Prospective research indicated that cardiovascular death and stroke were caused by low homoarginine levels (Tomaschitz et al., 2014; Chafai et al., 2017; Seppälä et al., 2017). Endothelium plays a main role in the vasculature by ensuring the promotion and maintenance of a protective environment via endothelial cell-derived vasoactive factors (Guzik et al., 2004; Papageorgiou et al., 2015). Some scientists investigated on how low level of homoarginine is related to dilation and a reduced function of the left ventricle and their findings indicated that high homoarginine is linked to lower left ventricle thickening, higher ejection fraction and lower N-terminal pro B-type natriuretic peptide (NTproBNP) (Bahls et al., 2018).

Atherosclerosis

Atherosclerosis, a disease of the arterial wall occurs at sensitive areas in the main arteries (Insull Jr, 2009). It starts off by lipid retention, oxidation, and modification, which leads to incurable swelling and causes thrombosis or stenosis (Insull Jr, 2009). Many factors may cause atherosclerosis by their effects on low-density lipoprotein (LDL) particles and inflammation (De Groot et al., 2000; Tomkin and Owens, 2012). These factors often include tobacco smoking, hypertension, obesity, diabetes, and genetic susceptibility (Insull Jr, 2009). Aortic stiffness, the inverse measure of aortic distensibility (AD), is also known as a cardiovascular risk marker aside the common factors for atherosclerosis (Kronzon and Tunick, 2006; Haghikia et al., 2017). Atherosclerosis has been reported as a main cause of death and morbidity across the globe. Studies have shown that homoarginine promotes vascular calcification (Alesutan et al., 2016; Haghikia et al., 2017) and it may be involved in the pathogenesis of atherosclerosis (Seppälä et al., 2017). However, there are inadequate information on the association between low homoarginine concentrations and the occurrence of atherosclerosis.

http://www.aloki.hu ● ISSN 1589 1623 (Print) ● ISSN 1785 0037 (Online)
DOI: http://dx.doi.org/10.15666/aeer/1705_1056510574

Type 2 diabetes mellitus

Type 2 diabetes mellitus (T2DM) is a metabolic disorder which is distinguished by insulin deficiency, hyperglycemia, and insulin resistance (Olokoba et al., 2012). An interaction between genetic, environmental and behavioural risk factors can also cause this disorder (Chen et al., 2012). Recent evidence has reported that homoarginine concentrations were lower at higher age, lower body mass index (BMI), lower albumin, lower haemoglobin, and were lower in females as compared to males (Drechsler et al., 2011). Low homoarginine concentrations were also associated with a longer history of diabetes mellitus and higher levels of C-reactive protein (Drechsler et al., 2011). Low serum concentration of homoarginine is independently associated with T2DM patients that can lead to death.

Stroke

Stroke is as a result of the cessation of blood flow to the brain which can cause disability and death. Ischemic stroke is caused by thrombosis due to atherosclerosis. Some common risk factors associated with stroke are hypertension, stress and age. In the LURIC study, low serum homoarginine concentrations were found to be a novel risk factor for fatal strokes (Pilz et al., 2011). A recent report on a homoarginine supplementation in stroke-infected mice indicated a noticeable decrease in homoarginine in the plasma from AGAT null mice, which is related to an increase in the size of stroke (Choe et al., 2013). According to Choe et al. (2013), there was a decrease in the death rate of patients with ischemic stroke which was independently associated with high homoarginine levels recorded. In the Harburg Stroke Study, which involved 137 patients affected with ischemic stroke, it was reported that plasma homoarginine concentrations were significantly decreased in patients who were near death, nonfatal recurrent stroke and nonfatal myocardial infarction compared with those without the condition (Choe et al., 2012).

Conclusion

It has become evident that homoarginine is a new biomarker for cardiovascular diseases by its involvement in NO production. Low serum concentration of homoarginine has been reported in subjects suffering from cardiovascular, cerebrovascular and renal diseases as compared to healthy subjects. More research needs to be done to understand the physiological role of homoarginine and its application in clinical studies and pharmacy as a possible medication for the cure of associated diseases.

Acknowledgements. The authors would like to appreciate the national key research and development program of China (2017YFD0502104), and the scientific project of Jilin province (20170309003NY) for providing the financial support to publish this review.

Declaration of interests. The authors declare that there is no conflict of interests.

http://www.aloki.hu ● ISSN 1589 1623 (Print) ● ISSN 1785 0037 (Online)
DOI: http://dx.doi.org/10.15666/aeer/1705_1056510574

REFERENCES

[1] Adams, S., Che, D., Qin, G., Farouk, M. H., Hailong, J., Rui, H. (2019): Novel Biosynthesis, Metabolism and Physiological Functions of L-Homoarginine. – Current Protein and Peptide Science 20(2): 184-193.

[2] Alesutan, I., Feger, M., Tuffaha, R., Castor, T., Musculus, K., Buehling, S. S., Heine, C. L., Kuro-o, M., Pieske, B., Schmidt, K. (2016): Augmentation of phosphate-induced osteo-/chondrogenic transformation of vascular smooth muscle cells by homoarginine. – Cardiovascular research 110(3): 408-418.

[3] Alheid, U., Frölich, J. C., Förstermann, U. (1987): Endothelium-derived relaxing factor from cultured human endothelial cells inhibits aggregation of human platelets. – Thrombosis research 47(5): 561-571.

[4] Arzumanian, V., Stankevicius, E., Laukeviciene, A., Kevelaitis, E. (2003): Mechanisms of nitric oxide synthesis and action in cells. – Medicina (Kaunas) 39(6): 535-541.

[5] Atzler, D., Gore, M. O., Ayers, C. R., Choe, C.-u., Böger, R. H., de Lemos, J. A., McGuire, D. K., Schwedhelm, E. (2014): Homoarginine and cardiovascular outcome in the population-based Dallas Heart Study. – Arteriosclerosis, thrombosis, and vascular biology:ATVBAHA. 114.304398.

[6] Atzler, D., Schwedhelm, E., Choe, C.-u. (2015): L-homoarginine and cardiovascular disease. – Current Opinion in Clinical Nutrition & Metabolic Care 18(1): 83-88.

[7] Bahls, M., Atzler, D., Markus, M., Friedrich, N., Böger, R., Völzke, H., Felix, S., Schwedhelm, E., Dörr, M. (2018): Low-Circulating Homoarginine is Associated with Dilatation and Decreased Function of the Left Ventricle in the General Population. – Biomolecules 8(3):63.

[8] Bell, E. A. (2003): Nonprotein amino acids of plants: significance in medicine, nutrition, and agriculture. – Journal of agricultural and food chemistry 51(10): 2854-2865.

[9] Bretscher, L. E., Li, H., Poulos, T. L., Griffith, O. W. (2003): Structural characterization and kinetics of nitric-oxide synthase inhibition by novel N5-(iminoalkyl)-and N5-(iminoalkenyl)-ornithines. – Journal of Biological Chemistry 278(47): 46789-46797.

[10] Chafai, A., Fromm, M. F., König, J., Maas, R. (2017): The prognostic biomarker L-homoarginine is a substrate of the cationic amino acid transporters CAT1, CAT2A and CAT2B. – Scientific Reports 7(1): 4767.

[11] Chen, L., Magliano, D. J., Zimmet, P. Z. (2012): The worldwide epidemiology of type 2 diabetes mellitus—present and future perspectives. – Nature reviews endocrinology 8(4): 228.

[12] Choe, C.-u., Nabuurs, C., Stockebrand, M. C., Neu, A., Nunes, P., Morellini, F., Sauter, K., Schillemeit, S., Hermans-Borgmeyer, I., Marescau, B. (2012): L-arginine: glycine amidinotransferase deficiency protects from metabolic syndrome. – Human molecular genetics 22(1): 110-123.

[13] Choe, C.-u., Atzler, D., Wild, P. S., Carter, A. M., Böger, R. H., Ojeda, F., Simova, O., Stockebrand, M., Lackner, K., Nabuurs, C. (2013): Homoarginine levels are regulated by L-arginine: glycine amidinotransferase and affect stroke outcome: results from human and murine studies. – Circulation: CIRCULATIONAHA. 112.000580.

[14] Davids, M., Ndika, J. D., Salomons, G. S., Blom, H. J., Teerlink, T. (2012a): Promiscuous activity of arginine: glycine amidinotransferase is responsible for the synthesis of the novel cardiovascular risk factor homoarginine. – FEBS letters 586(20): 3653-3657.

[15] Davids, M., Swieringa, E., Palm, F., Smith, D. E., Smulders, Y. M., Scheffer, P. G., Blom, H. J., Teerlink, T. (2012b): Simultaneous determination of asymmetric and symmetric dimethylarginine, L-monomethylarginine, L-arginine, and L-homoarginine in biological samples using stable isotope dilution liquid chromatography tandem mass spectrometry. – Journal of Chromatography B 900: 38-47.

http://www.aloki.hu ● ISSN 1589 1623 (Print) ● ISSN 1785 0037 (Online)
DOI: http://dx.doi.org/10.15666/aeer/1705_1056510574

[16] De Groot, L., Chrousos, G., Dungan, K., Feingold, K., Grossman, A., Hershman, J., Koch, C., Korbonits, M., McLachlan, R., New, M. (2000): The Role of Lipids and Lipoproteins in Atherosclerosis--Endotext.
[17] Dellera, F., Ganzetti, G., Froio, A., Manzini, S., Busnelli, M., Meinitzer, A., Sirtori, C., Chiesa, G., Parolini, C. (2016): L-homoarginine administration reduces neointimal hyperplasia in balloon-injured rat carotids. – Thrombosis and haemostasis 116(2): 400-402.
[18] Drechsler, C., Meinitzer, A., Pilz, S., Krane, V., Tomaschitz, A., Ritz, E., März, W., Wanner, C. (2011): Homoarginine, heart failure, and sudden cardiac death in haemodialysis patients. – European journal of heart failure 13(8): 852-859.
[19] Durante, W. (2013): Role of arginase in vessel wall remodeling. – Frontiers in immunology 4: 111.
[20] El karib, A. O., Sheng, J., Betz, A. L., Malvin, R. L. (1993): The central effects of a nitric oxide synthase inhibitor (Nω-nitro-L-arginine) on blood pressure and plasma renin. – Clinical and experimental hypertension 15(5): 819-832.
[21] Förstermann, U., Closs, E. I., Pollock, J. S., Nakane, M., Schwarz, P., Gath, I., Kleinert, H. (1994): Nitric oxide synthase isozymes. Characterization, purification, molecular cloning, and functions. – Hypertension 23(6 Pt 2): 1121-1131.
[22] Förstermann, U. (2000): Regulation of nitric oxide synthase expression and activity, Nitric Oxide. – Springer. p. 71-91.
[23] Förstermann, U., Sessa, W. C. (2011): Nitric oxide synthases: regulation and function. – European heart journal 33(7): 829-837.
[24] González-Navarro, H., Nabah, Y. N. A., Vinué, Á., Andrés-Manzano, M. J., Collado, M., Serrano, M., Andrés, V. (2010): p19ARFDeficiency Reduces Macrophage and Vascular Smooth Muscle Cell Apoptosis and Aggravates Atherosclerosis. – Journal of the American College of Cardiology 55(20): 2258-2268.
[25] Guzik, T. J., Sadowski, J., Kapelak, B., Jopek, A., Rudzinski, P., Pillai, R., Korbut, R., Channon, K. M. (2004): Systemic regulation of vascular NAD (P) H oxidase activity and nox isoform expression in human arteries and veins. – Arteriosclerosis, thrombosis, and vascular biology 24(9): 1614-1620.
[26] Günes, D. N., Kayacelebi, A. A., Hanff, E., Lundgren, J., Redfors, B., Tsikas, D. (2017): Metabolism and distribution of pharmacological homoarginine in plasma and main organs of the anesthetized rat. – Amino acids 49(12): 2033-2044.
[27] Haghikia, A., Yanchev, G. R., Kayacelebi, A. A., Hanff, E., Bledau, N., Widera, C., Sonnenschein, K., Haghikia, A., Weissenborn, K., Bauersachs, J. (2017): The role of L-arginine/L-homoarginine/nitric oxide pathway for aortic distensibility and intima-media thickness in stroke patients. – Amino acids 49(6): 1111-1121.
[28] Hanff, E., Kayacelebi, A. A., Yanchev, G. R., Maassen, N., Haghikia, A., Tsikas, D. (2016): Simultaneous stable-isotope dilution GC-MS measurement of homoarginine, guanidinoacetate and their common precursor arginine in plasma and their interrelationships in healthy and diseased humans. – Amino acids 48(3): 721-732. doi: 10.1007/s00726-015-2120-0.
[29] Hou, Y., Jia, S., Nawaratna, G., Hu, S., Dahanayaka, S., Bazer, F. W., Wu, G. (2015): Analysis of l-homoarginine in biological samples by HPLC involving precolumn derivatization with o-phthalaldehyde and N-acetyl-l-cysteine. – Amino acids 47(9): 2005-2014.
[30] Hrabak, A., Bajor, T., Temesi, A. (1994): Comparison of Substrate and Inhibitor Specificity of Arginase and Nitric Oxide (NO) Synthase for Arginine Analogs and Related Compounds in Murine and Rat Macrophages. – Biochemical and biophysical research communications 198(1): 206-212.
[31] Huang, P. L., Huang, Z., Mashimo, H., Bloch, K. D., Moskowitz, M. A., Bevan, J. A., Fishman, M. C. (1995): Hypertension in mice lacking the gene for endothelial nitric oxide synthase. – Nature 377(6546): 239.

http://www.aloki.hu ● ISSN 1589 1623 (Print) ● ISSN 1785 0037 (Online)
DOI: http://dx.doi.org/10.15666/aeer/1705_1056510574

[32] Ignarro, L. J., Cirino, G., Casini, A., Napoli, C. (1999): Nitric oxide as a signaling molecule in the vascular system: an overview. – Journal of cardiovascular pharmacology 34(6): 879-886.
[33] Insull Jr, W. (2009): The pathology of atherosclerosis: plaque development and plaque responses to medical treatment. – The American journal of medicine 122(1): S3-S14.
[34] Kassim, M., Achoui, M., Mansor, M., Yusoff, K. M. (2010): The inhibitory effects of Gelam honey and its extracts on nitric oxide and prostaglandin E2 in inflammatory tissues. – Fitoterapia 81(8): 1196-1201.
[35] Kayacelebi, A. A., Willers, J., Pham, V. V., Hahn, A., Schneider, J. Y., Rothmann, S., Frölich, J. C., Tsikas, D. (2015): Plasma homoarginine, arginine, asymmetric dimethylarginine and total homocysteine interrelationships in rheumatoid arthritis, coronary artery disease and peripheral artery occlusion disease. – Amino acids 47(9): 1885-1891.
[36] Kockx, M. M., Knaapen, M. W. (2000): The role of apoptosis in vascular disease. – The Journal of pathology 190(3): 267-280.
[37] Kronzon, I., Tunick, P. A. (2006): Aortic atherosclerotic disease and stroke. – Circulation 114(1): 63-75.
[38] Loscalzo, J., Vita, J. A. (2000): Nitric oxide and the cardiovascular system. – Springer Science & Business Media.
[39] März, W., Meinitzer, A., Drechsler, C., Pilz, S., Krane, V., Kleber, M. E., Fischer, J., Winkelmann, B. R., Böhm, B. O., Ritz, E. (2010): Homoarginine, cardiovascular risk, and mortality. – Circulation 122(10): 967-975.
[40] May, M., Kayacelebi, A. A., Batkai, S., Jordan, J., Tsikas, D., Engeli, S. (2015): Plasma and tissue homoarginine concentrations in healthy and obese humans. – Amino acids 47(9): 1847-1852. doi: 10.1007/s00726-015-1922-4.
[41] Melikian, N., Seddon, M. D., Casadei, B., Chowienczyk, P. J., Shah, A. M. (2009): Neuronal nitric oxide synthase and human vascular regulation. – Trends in cardiovascular medicine 19(8): 256-262.
[42] Michel, T. (2013): R is for arginine: metabolism of arginine takes off again, in new directions. – Circulation:CIRCULATIONAHA. 113.005924.
[43] Moncada, S. (1991): Nitric oxide: physiology, pathophysiology, and pharmacology. – Pharmacol rev 43: 109-142.
[44] Nathan, C. F., Hibbs Jr, J. B. (1991): Role of nitric oxide synthesis in macrophage antimicrobial activity. – Current opinion in immunology 3(1): 65-70.
[45] Olokoba, A. B., Obateru, O. A., Olokoba, L. B. (2012): Type 2 diabetes mellitus: a review of current trends. – Oman medical journal 27(4): 269.
[46] Papageorgiou, N., Androulakis, E., Papaioannou, S., Antoniades, C., Tousoulis, D. (2015): Homoarginine in the shadow of asymmetric dimethylarginine: from nitric oxide to cardiovascular disease. – Amino acids 47(9): 1741-1750. doi: 10.1007/s00726-015-2017-y.
[47] Pilz, S., Tomaschitz, A., Meinitzer, A., Drechsler, C., Ritz, E., Krane, V., Wanner, C., Böhm, B. O., März, W. (2011): Low serum homoarginine is a novel risk factor for fatal strokes in patients undergoing coronary angiography. – Stroke 42(4): 1132-1134.
[48] Pilz, S., Teerlink, T., Scheffer, P. G., Meinitzer, A., Rutters, F., Tomaschitz, A., Drechsler, C., Kienreich, K., Nijpels, G., Stehouwer, C. D. (2014): Homoarginine and mortality in an older population: the Hoorn study. – European journal of clinical investigation 44(2): 200-208.
[49] Qiu, J., Zheng, Y., Hu, J., Liao, D., Gregersen, H., Deng, X., Fan, Y., Wang, G. (2014): Biomechanical regulation of vascular smooth muscle cell functions: from in vitro to in vivo understanding. – Journal of The Royal Society Interface 11(90): 20130852.
[50] Rao, S. L. (2011): A look at the brighter facets of beta-N-oxalyl-l-alpha,beta-diaminopropionic acid, homoarginine and the grass pea. Food and chemical toxicology. – British Industrial Biological Research Association 49(3): 620-622. doi: 10.1016/j.fct.2010.06.054.

http://www.aloki.hu ● ISSN 1589 1623 (Print) ● ISSN 1785 0037 (Online)
DOI: http://dx.doi.org/10.15666/aeer/1705_1056510574

[51] Ryan, W. L., Wells, I. C. (1964): Homocitrulline and Homoarginine synthesis from lysine. – Science (New York, N.Y.) 144(3622): 1122-1127.
[52] Sakuma, I., Togashi, H., Yoshioka, M., Saito, H., Yanagida, M., Tamura, M., Kobayashi, T., Yasuda, H., Gross, S., Levi, R. (1992): NG-methyl-L-arginine, an inhibitor of L-arginine-derived nitric oxide synthesis, stimulates renal sympathetic nerve activity in vivo. A role for nitric oxide in the central regulation of sympathetic tone? – Circulation Research 70(3): 607-611.
[53] Schwarz, P. M., Kleinert, H., Förstermann, U. (1999): Potential functional significance of brain-type and muscle-type nitric oxide synthase I expressed in adventitia and media of rat aorta. – Arteriosclerosis, thrombosis, and vascular biology 19(11): 2584-2590.
[54] Seppälä, I., Oksala, N., Jula, A., Kangas, A. J., Soininen, P., Hutri-Kähönen, N., März, W., Meinitzer, A., Juonala, M., Kähönen, M. (2017): The biomarker and causal roles of homoarginine in the development of cardiometabolic diseases: an observational and Mendelian randomization analysis. – Scientific reports 7(1): 1130.
[55] Shesely, E. G., Maeda, N., Kim, H.-S., Desai, K. M., Krege, J. H., Laubach, V. E., Sherman, P. A., Sessa, W. C., Smithies, O. (1996): Elevated blood pressures in mice lacking endothelial nitric oxide synthase. – Proceedings of the National Academy of Sciences 93(23): 13176-13181.
[56] Stockebrand, M., Hornig, S., Neu, A., Atzler, D., Cordts, K., Böger, R. H., Isbrandt, D., Schwedhelm, E., Choe, C.-u. (2015): Homoarginine supplementation improves blood glucose in diet-induced obese mice. – Amino acids 47(9): 1921-1929.
[57] Teerlink, T., Nijveldt, R. J., De Jong, S., Van Leeuwen, P. A. (2002): Determination of arginine, asymmetric dimethylarginine, and symmetric dimethylarginine in human plasma and other biological samples by high-performance liquid chromatography. – Analytical biochemistry 303(2): 131-137.
[58] Tomaschitz, A., Meinitzer, A., Pilz, S., Rus-Machan, J., Genser, B., Drechsler, C., Grammer, T., Krane, V., Ritz, E., Kleber, M. E. (2014): Homoarginine, kidney function and cardiovascular mortality risk. – Nephrology Dialysis Transplantation 29(3): 663-671.
[59] Tomkin, G. H., Owens, D. (2012): LDL as a cause of atherosclerosis. – The Open Atherosclerosis & Thrombosis Journal 5(1): 13-21.
[60] Tousoulis, D., Kampoli, A.-M., Tentolouris Nikolaos Papageorgiou, C., Stefanadis, C. (2012): The role of nitric oxide on endothelial function. – Current vascular pharmacology 10(1): 4-18.
[61] Tsikas, D., Kayacelebi, A. A. (2014): Do homoarginine and asymmetric dimethylarginine act antagonistically in the cardiovascular system? – Circulation Journal 78(8): 2094-2095.
[62] Tsikas, D., Wu, G. (2015): Homoarginine, arginine, and relatives: analysis, metabolism, transport, physiology, and pathology. – Springer.
[63] Valtonen, P., Laitinen, T., Lyyra-Laitinen, T., Raitakari, O. T., Juonala, M., Viikari, J. S., Heiskanen, N., Vanninen, E., Punnonen, K., Heinonen, S. (2008): Serum L-homoarginine concentration is elevated during normal pregnancy and is related to flow-mediated vasodilatation. – Circulation Journal 72(11): 1879-1884.
[64] Vogl, L., Pohlhammer, J., Meinitzer, A., Rantner, B., Stadler, M., Peric, S. A., Hammerer-Lercher, A., Klein-Weigel, P., Fraedrich, G., Kronenberg, F., Kollerits, B. (2015): Serum concentrations of L-arginine and L-homoarginine in male patients with intermittent claudication: a cross-sectional and prospective investigation in the CAVASIC Study. – Atherosclerosis 239(2): 607-614.
[65] Zhou, L., Zhu, D.-Y. (2009): Neuronal nitric oxide synthase: structure, subcellular localization, regulation, and clinical implications. – Nitric oxide 20(4): 223-230.
[66] Ziolo, M. T., Katoh, H., Bers, D. M. (2001): Positive and negative effects of nitric oxide on Ca(2+) sparks: influence of beta-adrenergic stimulation. – American journal of physiology, Heart and circulatory physiology 281(6): H2295-2303. doi: 10.1152/ajpheart.2001.281.6.H2295.

http://www.aloki.hu ● ISSN 1589 1623 (Print) ● ISSN 1785 0037 (Online)
DOI: http://dx.doi.org/10.15666/aeer/1705_1056510574

DETERMINATION OF SOME QUALITY CRITERIA AND NUTRIENT CONTENTS OF LOCAL BLACK CHICKPEA GENOTYPES GROWTH IN DIFFERENT LOCATIONS

TOĞAY, Y.[1] – TOĞAY, N.[1] – ÇIĞ, F.[2*] – AKKOÇ, G.[2]

[1]*Fethiye ASMK Vocational School, Muğla Sıtkı Koçman University, Fethiye, Muğla, Turkey*

[2]*Department of Field Crops, Faculty of Agriculture, Siirt University, Siirt, Turkey*

[*]*Corresponding author*
e-mail: fatihcig@hotmail.com; phone: +90-533-777-1140

(Received 17th Jan 2019; accepted 2nd Jul 2019)

Abstract. This experiment was conducted in 7 different locations of Turkey (Diyarbakır/Dicle, Malatya, Mardin, Elazığ, Elazığ/Gezin, Iğdır and Hatay) and it was conducted on the black chickpea genotypes. The aim of this experiment is to determine the hydration capacity of black chickpea genotypes, seed ratio with hard seed coat, the weight of one hundred seed, the protein content in the grain, the fat content in the grain and the P, K, Ca, Mo, Fe, Zn, Cu and Mn (mg / kg) contents. In line with this aim, in 2015, it was carried out with three repetitions according to the Trial Plan of Random Parcels. At the end of the experiment, the obtained values were subjected to variance analysis and the differences among the means were tested according to the Duncan multiple comparison method. The difference among the genotypes in terms of hydration capacity was found to be statistically significant at 1%. The hydration capacities of genotypes varied between 0.9826-1.0856. While the genotype of Hatay has the highest hydration capacity, Gezin genotype was determined to have the lowest hydration capacity. In the study, no genotype was found to have seeds with hard seed coat (seed without water). All seeds are swollen as a result of taking water. The highest values were determined as follows: Iğdır genotype with a weight of 12.40 g for the hundred seed, Gezin genotype for the fat ratio in the grain and the ratio of protein in the grain is Elazığ genotype. The Elazığ genotype is prominent in terms of phosphorus, potassium, molybdenum, zinc and copper content in grain.
Keywords: *Cicer arietinum L., cooking time, hydration capacity, macroelements, microelemets*

Introduction

Chickpea (*Cicer arietinum* L.), which belongs to the genus *Cicer* of the family of legumes (Fabaceae), is a legume plant. Almost 10,000 years ago, wheat, barley, rye, peas, vetch and lentil plants together with chickpea, have been reported to be cultivated for the first time in the area called Fertile Crescent (in Turkish: Bereketli Hilal) (Redden and Berger, 2007). The chickpea genus is composed of some perennial species, such as *C. arietinum* L., as well as single-year species. The first chickpea plant cultivated in the area known as the old world is *Cicer arietinum* L. (Tanno and Willcox, 2006). Cultured chickpea *C. arietinum* L. diploid (2n = 16) is an edible legume plant (Sethy et al., 2006). According to a classification, plants in the genus *Cicer* are known to be single or multi-year. According to the morphological characterization, there are 39 species in the genus *Cicer* and after the revision studies, it was reported that *Cicer* genus consists of 44 species, 9 of which are single-year and 35 of which are multi-year (Van der Maesen et al., 2007). Total of 10 species belonging to the genus *Cicer* is located in Turkey and five of them are of endemic character (Öztürk, 2011).

As a result of research with genetic markers, it was detected that the Fertile Crescent Region, which is the homeland of chickpea, is the richest region in terms of chickpea

http://www.aloki.hu ● ISSN 1589 1623 (Print) ● ISSN 1785 0037 (Online)
DOI: http://dx.doi.org/10.15666/aeer/1705_1057510585

gene sources (Roorkiwal et al., 2014). Chickpea taxa shows to be most spread in Turkey in the following regions: Southeast Anatolia, Mediterranean, Eastern Anatolia and Aegean regions. The species spread in Turkey are: *C. arietinum, C. reticulatum, C. echinospermum, C. pinnatifidum, C. bijugum, C. incisum, C. montbretii, C. floribundum, C. isauricum, C. heterophyllum, C. uluderensis* and *C. anatolicum* türleridir (Van der Maesen, 1972; Öztürk, 2011; Akın, 2018) (*Fig. 1*).

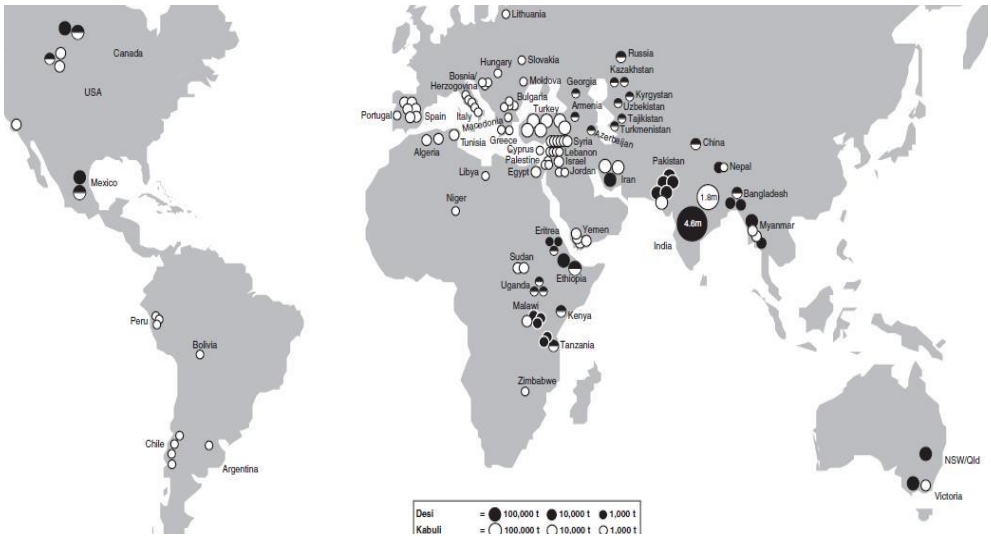

Figure 1. *Kabuli and Desi type chickpea production pattern of the world (Knights et al., 2007)*

Legumes contain high protein, low fat content, vitamins and minerals as nutritional values in their seeds (Pekşen and Artık, 2005). In addition, edible legumes contain 11% of insoluble dietary fibers that are beneficial for intestinal health due to their laxative effects (Anderson and Bryant, 1986; Marlett et al., 2002). Chickpea seed coat was found to be rich in dietary fiber and minerals. However, the contribution of the seed coat on nutritional benefits of the whole seed were determined to be limited (Savar and Karataş, 2017). If the benefits of chickpea in human nutrition are listed; Polyphenols are common constituents of foods of plant origin and major antioxidants in the human diet. These compounds possess diverse biological activities such as antioxidation, apoptosis, antiaging, anticancer, antiinflammation, antiatherosclerosis, cardiovascular protection, improvement of the endothelial function, as well as inhibition of angiogenesis and cell proliferation activity (Ozdemir, 2006; Han et al., 2007). Colored seeds contained up to 13-, 11-, and 31-fold more TPC (Total polyphenol content), TFC (Total flavonoid content), and antioxidant activity, respectively, than cream- and beige-color seeds. Thus, colored chickpea could be a potentially functional food in addition to its traditional role of providing dietary proteins and dietary fibers. colored chickpea might be considered a functional food in addition to its traditional role of providing dietary proteins. Colored chickpea might also contribute significantly to the management and/or prevention of degenerative diseases associated with free radical damage due to their high antioxidant activity. Due to their high antioxidant activity, future research should be conducted to verify that colored chickpeas can be used for management and/or prevention of degenerative disease (Segev et al., 2010).

http://www.aloki.hu ● ISSN 1589 1623 (Print) ● ISSN 1785 0037 (Online)
DOI: http://dx.doi.org/10.15666/aeer/1705_1057510585

While chickpea is the second most sown and farmed legume in the world among the edible legumes, it is ranked first in our country (Anonymous, 2016). While India ranks first in terms of cultivation area and production, 2/3 part of the world chickpea production takes place in this country. In terms of cultivation area Turkey is fourth after Pakistan and Iran and third in terms of production.

According to the studies conducted, *Cicer* species in the flora of Turkey (Davis et al., 1988) was represented by 9 species. With the work done in the following years *C. uluderensis* (Dönmez, 2011), *C. reticulatum* (Ladizinsky, 1975) and *C. heterophyllum* (Constandriopoulos et al., 1972) species were identified in Turkey and had been added to the world scientific literature as new species. On the other hand; *C. floribundum* var. *Amanicola* in Osmaniye, *C. heterophyllum* var. *Kasanii* in Antalya and *C. incisum* subsp. *Serpentinica* in Erzincan are introduced to the scientific world with relevant study (Öztürk, 2011) and the total number of taxa spreading in Turkey increased to 15. This study conducted on chickpea plant which has been spreading widely in Turkey, showed that it is crucial to reserve the black chickpea as a genetic resource due to its resistance to diseases and adverse environmental conditions, quality parameters and active substances.

In this study, it is aimed to emphasize the importance of black chickpea, which is rarely grown and scarcely found in our country and to restore it to agriculture and human life by looking at some quality criteria and nutrient element contents.

Literature review

It is known that black chickpea which belongs to the Desi variety, also known as Bengal Gram in India, has high fiber content and low glycemic. In India, black chickpeas are highly involved in human nutrition. Black chickpea is not given the necessary importance in our country. Black chickpea, which is important in the eating habits of our ancestors, has lost its importance today and has even been used as animal feed by producers. Today, the cultivation of black chickpea covers a very small area and cannot be evaluated statistically. Black chickpea, which had been produced in the past years, is now being produced by some farmers in regions such as Malatya, Elazığ, Elazığ/Gezin, Diyarbakır/Dicle, Mardin, Iğdır and Hatay. This production is done to meet the farmer's own needs and is usually given as supplementary food in animal feed.

Yarmaca and mekaşer are local food names of Eastern Anatolia. As well as being directly used in food, black chickpea is also used as ‘yarmaca’ and ‘mekaşer’ after being put through certain processes. Black chickpeas are more delicious than other chickpeas. Black chickpea is a versatile legume and is widely used in India and the Middle East. It is consumed as a fast snack in meals, humus and curries, soups and salads in Turkey.

It is produced by some farmers in regions such as Malatya, Elazığ, Elazığ/Gezin, Mardin, Diyarbakır/Dicle, Iğdır, Hatay and is consumed by a certain part of the population and finds buyers at very high prices. They are either put into food after being boiled or are added into food as yarmaca (Malatya region) or mekaşer (Diyarbakır-Dicle region) after certain processes and consumed that way. In contrast to the positive aspects of food legumes such as high protein content, the length of cooking times is seen as a negation for their consumption. It was observed that the cooking time was closely related to the hydration capacity of the seed and that there was a positive relationship between the hydration capacity and the cooking time and that the varieties with high hydration capacity were more rapidly cooked (Williams et al., 1983; Manan et

http://www.aloki.hu ● ISSN 1589 1623 (Print) ● ISSN 1785 0037 (Online)
DOI: http://dx.doi.org/10.15666/aeer/1705_1057510585

al., 1987; Singh et al., 1991). For this reason, it has been tried to increase the hydration capacity of seed with various breeding and growing techniques in edible legumes (Rao and Vakil, 1985).

Materials and methods

Material

Black chickpeas obtained from Diyarbakır / Dicle, Malatya, Mardin, Elazığ, Elazığ / Gezin, Iğdır and Hatay were used in the experiment.

All genotypes have taken their names from the provinces and districts where situated in South East, Meditereinan and Eastern Anatolia regions of Turkey. All collected genotypes were grown with the same methods without fertilization in dry conditions. The aim of the study is to determine the nutrient content of genotypes grown under farmer conditions. 1 kg of samples were collected from each genotype. Materials were obtained from seeds grown by farmers in traditional methods.

Methods

The study was carried out with three repetitions according to the Trial Plan of Random Parcels.

Determination of hydration capacity, hard seed coat and hydration index (%)

In the study, seed weight was detected by weighing 50 seeds from each genotype and these seeds were placed in a 250 ml erlenmayer with a wide mouth then 100 ml demineralized water was added to the seeds and the mouth of the erlenmayer was covered with aluminum foil for 16 hours at room temperature (22-25˚C). Seeds that were kept at room temperature for 16 hours were taken from the containers at the end of this period and were kept for a short time between drying papers in order to remove the water on them. Then, if there had been non-swelling seeds, they were separated as hard-coated seeds and the hydration capacities and hydration indices of the varieties were determined after various calculations were made by weighing the wet weights of the remaining seeds. The following equation was used to determine the hydration capacity. Hydration index was also determined by calculating the hydration capacity against the original seed weight (Williams et al., 1986) (*Eq. 1*).

$$Hydration\ Capacity = \frac{Y-\left(X-\left(\frac{X}{100}\right)N2\right)}{N1-N2} \quad \text{(Eq.1)}$$

where

- Y = Wet Seed Weight.
- X = Dry Seed Weight.
- N_1 = Original Seed Count.
- N_2 = Hard-Coated Seed Count (Non-Water Drawing Seed Count).

Weight of one hundred seed, (g)

The grains were randomly weighed in four groups of 100 pieces, on a 0.01 g sensitive scale, and averages of one hundred seed, were calculated.

http://www.aloki.hu ● ISSN 1589 1623 (Print) ● ISSN 1785 0037 (Online)
DOI: http://dx.doi.org/10.15666/aeer/1705_1057510585

Grain protein ratio (%)

After grinding the seeds, Kjeldahl method was applied and the amount of nitrogen was determined, and the resulting values were multiplied by 6.25 and the crude protein ratios in the grains of genotypes were detected.

Fat content in grain (%)

Spectra Star laboratory type NIR (Near Infrared) analyzer was used to determine the crude fat content in the grains of genotypes.

Determination of macro and micro nutrients in seeds

Phosphorus content in grain (%) was calculated according to Kacar (1984), with vanado molybdo phosphoric acid yellow color method. Mo, Fe, K, Ca, Zn, Cu and Mn (mg / kg) analyses were performed according to Kacar (1994).

At the end of the study, the obtained values were subjected to variance analysis and the differences among the means were tested according to Duncan's multiple comparison method ($P < 0.05$). In statistical analysis, information from Yurtsever (1984) and Düzgüneş et al. (1987) were used.

Results and discussions

The Duncan groups are shown in *Table 1*, which gives us the mean values of the weight of one hundred seed, protein content in the grain, fat content in the grain, hydration capacity, hydration index and the differences among the means belonging to the black chickpea genotypes grown in different locations in Turkey.

The weight of one hundred seed, is a genre specification and it shows significant changes compared to genotypes. As shown in *Table 1*, the average weight of one hundred seed, of genotypes used in the study ranged from 7.97-12.40 g. The lowest hundred seed weight was obtained from the Dicle genotype and the highest value was obtained from the Iğdır genotype. Karaköy (2008) reported that the weight of one hundred seed, of chickpeas varied between 37.6-51.5 g. The findings of this study were different with the findings of the researchers. The reason for this is that the black chickpeas used in this study have smaller grain size than the other chickpeas and they are not developed by any reclamation method.

The mean hydration capacity of the genotypes used in the study ranged between 0.9826-1.0856 g/seed and the lowest hydration capacity was detected in the Gezin genotype, but its difference from the Malatya genotype was not statistically significant. The highest hydration capacity was obtained from Hatay genotype and its difference compared to Mardin and Elazığ genotypes was statistically insignificant. In previous studies, it had been reported that the water absorption properties of legume seeds are related to seed size and seed coat thickness (Kaur et al., 2005). Toğay et al. (2001) stated in their study conducted within the chickpea varieties that have been registered in Turkey that the hydration capacity varies between 0.979-1.223 g/seed. In terms of this feature, the findings of the researchers seem to be supporting each other. In a study, unlike these research findings, the hydration capacity in Desi genus chickpea grown in Tunisia was found to be 0.64 g/seed (Ghribi et al., 2015).

As can be seen from *Table 1* the mean hydration index of the genotypes used in the study ranged from 16.23 to 23.66% and the lowest hydration index was obtained from

http://www.aloki.hu ● ISSN 1589 1623 (Print) ● ISSN 1785 0037 (Online)
DOI: http://dx.doi.org/10.15666/aeer/1705_1057510585

the Iğdır genotype but the difference between it and the Gezin genotype was statistically insignificant. The highest hydration index was obtained from the Dicle genotype. In this study, no statistical analysis was performed since there were no genotypes with hard seed coat among black chickpea genotypes. Considering the positive relationship between hydration capacity and cooking time reported in the previous studies regarding this topic (Williams et al., 1983; Manan et al., 1987; Singh et al., 1991), the Hatay genotype has been found to be more suitable for rapid cooking than the other varieties. The Gezin black chickpea genotype can be evaluated as the longest cooking type.

Table 1. *Duncan groups showing the average values and the differences among means of the weight of one hundred seed, hydration capacity, hydration index, protein content in the grain and fat content in the grain of the black chickpea genotypes grown in different locations in Turkey*

Genotypes	Weight of one hundred seed (g)*	Hydration capacity (g/seed)**	Hydration index (%)*	Protein content in the grain (%)*	Fat content in the grain (%)*
Dicle	7.97 d	1.0493 ab	23.66 a	19.60 c	3.25 c
Malatya	9.58 c	0.9986 c	21.30 b	19.58 c	3.17 c
Mardin	11.27 b	1.0583 a	18.56 c	19.75 c	3.20 c
Elazığ	10.98 b	1.0650 a	18.66 c	22.54 a	3.21 c
Gezin	11.55 ab	0.9826 c	16.50 d	19.91 c	3.55 a
Iğdır	12.40 a	1.0121 bc	16.23 d	19.33 c	3.37 b
Hatay	10.81 b	1.0856 a	19.53 c	20.83 b	2.93 d

**: $p<0.01$; *: $p<0.05$

The average protein content of the genotypes was varying between 19.33-22.54% and the lowest protein ratio was obtained from the Iğdır genotype, but the difference among it and the Dicle, Malatya, Mardin and Gezin genotypes was not statistically significant. The highest protein ratio in the grain was obtained from Elazığ genotype. Dry seed protein rate was stated to be between 12.4% and 31.5% (average 23%) (Özdemir, 2006). Dinç (2014) carried out an adaptation work with the chickpea varieties were registered in Turkey and the protein content in grain values were reported to vary between 20.32-24.5%. As a result of this study, the protein ratio values in the grain were found to be close to the values reached by different researchers like (Khan et al., 1995; Önder and Üçer, 1999; Erdin and Kulaz, 2014).

As it was seen on *Table 1*, the average fat content of genotypes in the study was 2.93-3.55% and the lowest fat content was obtained from Hatay genotype while the highest ratio was obtained from Gezin genotype. Özdemir (2006) stated the rate of the oil in chickpea seeds range between 3.8-12.2% and among the edible legumes, most oil was to be found in chickpeas. Şehirali (1988a) had reported that the fat content of chickpeas ranged from 1.5-6.8% while the adaptation study conducted by Dinç (2014) with the chickpea varieties which have been registered in Turkey, stated that the fat content in the grain varied between 4.01-4.93%. The low-fat content of black chickpea compared to other chickpeas is very important for low calorie nutrition and especially for cardiovascular diseases and cholesterol.

Duncan groups showing the mean values and the difference among mean values of black chickpea genotypes grown in different locations of Turkey in terms of iron,

http://www.aloki.hu ● ISSN 1589 1623 (Print) ● ISSN 1785 0037 (Online)
DOI: http://dx.doi.org/10.15666/aeer/1705_1057510585

molybdenum, manganese, copper and zinc content are shown in *Table 2*. Duncan groups showing the mean values and the differences among the mean values obtained in terms of calcium, phosphorus and potassium content are shown in *Table 3*.

Table 2. *Duncan groups showing the mean values and the difference among mean values of black chickpea genotypes grown in different locations of Turkey in terms of iron, molybdenum, manganese, manganese, copper and zinc content*

Genotypes	Iron Content (ppm)*	Molybdenum content (ppm)**	Manganese content (ppm)*	Copper content (ppm)*	Zinc content (ppm)*
Dicle	50.15 c	2.36 bc	23.62 d	15.06 ab	58.58 b
Malatya	73.20 a	2.30 cd	30.27 c	15.81 a	46.59 bc
Mardin	43.20 cd	2.16 d	25.27 d	12.76 c	40.10 c
Elazığ	47.09 cd	2.50 ab	41.33 b	15.58 a	96.33 a
Gezin	61.69 b	2.43 abc	27.86 cd	13.52 bc	35.36 c
Iğdır	40.67 d	2.43 abc	28.13 cd	12.76 c	36.49 c
Hatay	49.45 cd	2.60 a	46.00 a	12.58 c	32.40 c

**: $p<0.01$; *: $p<0.05$

As shown in *Table 2*, the iron content of the genotypes used in the study ranged from 40.67-73.20 ppm and the lowest iron content was obtained from Iğdır genotype, while the highest iron content was obtained from Malatya genotype. Özdemir (2006) reported that an average of 6.6 mg (66 ppm) iron mineral exists in 100 gr seed. The iron content of black chickpea was also found to be within the average of iron content of other chickpeas. Due to the high iron and calcium content of chickpea, it is especially recommended for preschool children, pregnant and lactating women.

The effect of black chickpea genotypes on molybdenum content in grain was statistically significant at 1% level. Average molybdenum content of the genotypes used in the study ranged from 2.16 to 2.60 ppm and the lowest molybdenum content was obtained from the Mardin genotype, while the highest molybdenum content in the grain was obtained from the Hatay genotype.

The manganese content of the genotypes used in the experiment varied between 23.62-46.00 ppm and the lowest manganese content was obtained from the Dicle genotype. Its difference from Mardin genotype was statistically insignificant. Mut and Gülümser (2005) stated that manganese content varies between 19-20.42 ppm in zinc and molybdenum applications with bacterial inoculation in chickpea. The manganese content of black chickpea which had not been subjected to any fertilizer application, was even higher than the normal average rate of chickpea.

As shown in *Table 2*, the average copper content in the grain of genotypes used in the study ranged from 12.58 to 15.81 ppm, while the lowest copper content was obtained from the Hatay genotype, its difference compared to the Iğdır and Mardin genotypes were found to be statistically insignificant. The highest copper content in grain was obtained from Malatya genotype but its difference from Elazığ genotype was found to be statistically insignificant. Mut and Gülümser (2005) stated that the copper content of zinc and molybdenum applied together with bacterial vaccination in chickpea ranged between 10-11.67 ppm on average in studies. In the study conducted by the

http://www.aloki.hu ● ISSN 1589 1623 (Print) ● ISSN 1785 0037 (Online)
DOI: http://dx.doi.org/10.15666/aeer/1705_1057510585

researchers, it is believed that the low content of manganese and copper is due to the applied zinc fertilizer.

The mean zinc content of the genotypes used in the study changed between 32.40-96.33 ppm and the lowest zinc content was obtained from Hatay genotype. Its difference from Iğdır, Gezin and Mardin genotypes was found to be statistically insignificant. The highest zinc content in grain was obtained from Elazığ genotype. Legumes are rich in zinc content and chickpea is reported to contain an average of 3.4 mg of zinc (Anonymous, 2015). It was observed in this study that zinc content of black chickpea is also quite high.

As can be seen in *Table 3*, the calcium content of the genotypes used in the study varies between 0.28-0.58%. Even though the lowest calcium content was obtained from Dicle genotype, the difference between it and Elazığ genotype was statistically insignificant. The highest calcium content in grain was obtained from Mardin genotype. Özdemir (2006) reported that the average calcium content in 100 gr seed is 185.6 mg (0.185%) while Şehirali (1988b) stated that there were 33-1980 mg of calcium in 100 grams of chickpea.

Table 3. *Duncan groups showing the mean values and the difference among mean values of black chickpea genotypes grown in different locations of Turkey in terms of calcium, phosphorus and potassium content*

Genotypes	Calcium content (%)*	Phosphorus Content (%)*	Potassium Content (%)*
Dicle	0.28 c	0.33 c	1.13 bc
Malatya	0.32 bc	0.28 d	1.02 cd
Mardin	0.58 a	0.29 d	1.00 d
Elazığ	0.31 c	0.42 a	1.20 ab
Gezin	0.45 b	0.43 a	1.30 a
Iğdır	0.35 bc	0.34 bc	0.97 d
Hatay	0.40 bc	0.36 b	1.25 a

*: $p<0.05$

The phosphorus content of the genotypes used in the experiment changed between 0.28-0.43% and the lowest phosphorus content was obtained from Malatya genotype but the difference between it and Mardin genotype was found statistically insignificant. The highest phosphorus content in grain was obtained from Gezin genotype and its difference from Elazığ genotype was not statistically significant. Özdemir (2006) reported that the phosphorus content in chickpea was 342.9 mg (0.34%) in 100 gr seed. The phosphorus content of black chickpea also appears to be around average values.

As shown in *Table 3*, the potassium content of the genotypes used in the study ranged from 0.97% to 1.30% and the lowest potassium content was obtained from the Iğdır genotype and the difference between it and the Mardin genotype was found to be statistically insignificant. The highest potassium content in grain was obtained from the Gezin genotype and the Hatay genotype was also in the same group.

http://www.aloki.hu ● ISSN 1589 1623 (Print) ● ISSN 1785 0037 (Online)
DOI: http://dx.doi.org/10.15666/aeer/1705_1057510585

Conclusion

The hydration capacity, which is an important criterion in chickpea consumption, was measured in studied chickpea genotypes. In genotypes with low hydration capacity, water is absorbed in a long time and the duration of cooking of seeds is increased. Hard seed crusted seeds cannot absorb water as fast as normal seeds, cannot germinate or cook quickly. As a result of this study, it was detected that the best black chickpea genotypes are the Hatay and Elazığ genotypes in terms of hydration capacity and cooking characteristics. These genotypes are good sources of genes with respect to their hydration capacity during breeding work. In addition, the resistance to anthracnose, which is known to be the most important factor limiting yield in chickpeas, especially in early planting and in areas with high humidity, should be considered. Elazığ genotype is prominent in terms of fat content in the grain, protein content in the grain, phosphorus, potassium, molybdenum, zinc and copper content. In terms of healthy eating; black chickpea has a high protein content, low fat content and rich in especially calcium, iron and zinc. In this way, it is very important that it regains its rightful place by taking part in nutrition programs.

REFERENCES

[1] Akın, F. (2018): Effects of Salt Stress on Germination and Growth in Black and White Chickpea (*Cicer arietinum* L.) Genotypes in vitro Conditions. – Necmettin Erbakan University Graduate School of Natural and Applied Sciences Department of Molecular Biology and Genetics (Master Thesis) (in Turkish).

[2] Anderson, W. J., Bryant, C. A. (1986): Dietary fiber: Diabetes and obesity. – Am. J. Gastroenterol. 81: 898-906.

[3] Anonymous (2015): http:// bodytr.com/2015/02.

[4] Anonymous (2016): World and Turkey Chickpea Data. – http// www.fao.org. (in Turkish).

[5] Constandriopoulos, J., Pamukçuoğlu, A., Quezel, P. (1972): A propos des *Cicer vivaces* du pourtour Mediterranéen Oriental. – Biologia Gallo-Hellenica 4(1): 3-18.

[6] Davis, P. H., Mill, Rr., Tan, K. (1988): Flora of Turkey and the East Aegean Islands. – Vol. 10. Edinburgh: Edinburgh University Press.

[7] Dinç, A. (2014): Türkiye'de Tescil Edilmiş Bazı Nohut (*Cicer arietinum* L.) Çeşitlerinin Van Koşullarında Verim ve Verim Öğelerinin Belirlenmesi. – (basılmamış) YYÜ. Feb Bilimleri Enstitüsü, Van. (Ms thesis) (in Turkish).

[8] Dönmez, A. A. (2011): *Cicer uludereensis* Dönmez: A new species of *Cicer* (Chickpea) (Fabaceae) from around the Fertile Crescent, SE Turkey. – Turkish Journal of Botany 35: 71-76.

[9] Düzgüneş, O., Kesici, T., Gürbüz, F. (1987): Research and Experimental Methods. – Ankara University Faculty of Agriculture Publications: 1021, Text Book: 295. - A.Ü. Printing House, Ankara. (in Turkish).

[10] Erdin, F., Kulaz, H. (2014): Cultivation of some chickpea (*Cicer arietinum* L.) varieties as a second product in Van-Gevaş ecological conditions. – Turkish Journal of Agricultural and Natural Sciences 1: 910-914. (in Turkish).

[11] Ghribi, A. M., Maklouf, I., Blecker, C., Attia, H., Besbes, S. (2015): Nutritional and compositional study of desi and kabuli chickpea (*Cicer arietinum* L.) flours from Tunisian cultivars. – Advances in Food Technology and Nutrition Sciences Open Journal 1(2): 38-47.

[12] Han, X., Shen, T., Lou, H. (2007): Dietary polyphenols and their biological significance. – Int J Mol Sci. 8: 950-88.

http://www.aloki.hu ● ISSN 1589 1623 (Print) ● ISSN 1785 0037 (Online)
DOI: http://dx.doi.org/10.15666/aeer/1705_1057510585

[13] Kacar, B. (1984): Plant Nutrition Practice Guide. – Ankara Univ. Agricultural Fac. Pub.: 899, Practice Guide: 250.
[14] Kacar, B. (1994): Chemical Analysis of Plant and Soil: III. Soil Analysis. – A.Ü.Z.F. Eğt. Araşt. ve Gel. Vakfı Yayın No: 3, Ankara. (in Turkish).
[15] Karaköy, T. (2008): A Research on Determination of Yield and Yield Characteristics of Some Local Chickpea (*Cicer arietinum* L.) Genotypes Grown from Çukurova and Central Anatolia Regions. – Çukurova University Institute of Science and Technology, Adana (Doctorate thesis) (in Turkish).
[16] Kaur, P., Gupta, A. K., Kaur, N. (2005): Embryo is not required for initiation of a-amylase activity in germinating cowpea seeds. – Ind. J. Biochem. Biophy. 42: 161-165.
[17] Khan, M. A., Akhtar, N., Ullah, I., Jaffery S. (1995): Nutritional evaluation of Desi and Kabuli chickpeas and their products commonly consumed in Pakistan. – International Journal of Food Sciences and Nutrition 46(3): 215-223.
[18] Knights, E. J., Açıkgöz, N., Warkentin, T., Bejiga, G., Yadav, S. S., Sandhu, J. S. (2007): Area, Production, and Distribution. – In: Yadav, S. S., Redden, R. J., Chen, W., Sharma, B. (eds.) Chickpea breeding and management. Wallingford: CABI, p. 169.
[19] Ladizinsky, G. (1975): A new *Cicer* L. from Turkey. – Notes Royal Botanic Garden Edinburgh 34(2): 201-202.
[20] Manan, F., Hussain, T., Alli, I., Iqbal, P. (1987): Effectes of cooking on phytic acid contend and nutritive value of pakistani peas and lentils. – J. Food Composition and Analysis 1(1): 65-70.
[21] Marlett, J. A., McBurney, M. I., Slavin, J. L. (2002): Health implicationsof dietary fiber. – Journal American. Diet Association 102: 993-1000.
[22] Mut, Z., Gülümser, A. (2005): Effects of zinc and molybdenum application on some quality characteristics of Damla-89 chickpea cultivation with bacterial inoculation. – Journal of Faculty of Agriculture, Ondokuz Mayıs University 20(2): 1-10. (in Turkish).
[23] Önder, M., Üçer, F. B. (1999): Cultivation of some chickpea varieties as second crop in Konya ecological conditions. – Selcuk University Journal of the Faculty of Agriculture 13(18): 1-8. (in Turkish).
[24] Özdemir, S. (2002): Legumes, 142. – Hasad Publishing, İstanbul. (in Turkish).
[25] Özdemir, S. (2006): Edible Legumes. – Hasad Publication. Publication No:239. p: 59-62.
[26] Öztürk, M. (2011): Revision of The Genus *Cicer* L. in Turkey via Morphological, Palynological, Cytotaxonomical, Molecular Phylogenetic Methods and Analyses of Seed Protein and Element Contents. – Selcuk University, Institute of Science and Technology (Doctorate thesis) (in Turkish).
[27] Pekşen, E., Artık, C. (2005): Antinutritional factors and nutritive values of food grain legumes. – Journal of Faculty of Agriculture, Ondokuz Mayıs University 20(2): 110-120. (in Turkish).
[28] Rao, V. S., Vakil, U. K. (1985): Effects of Gamma Radiation on Cooking Quality and Sensory Attributes of Four Legumes. – Faba Bean Abstract 1986 006-00092.
[29] Redden, R. J., Berger, J. D. (2007): History and Origin of Chickpea. – In: Yadav, S. S., Redden, R. J., Chen, W., Sharma, B. (eds.) Chickpea breeding and management. Wallingford: CABI, p. 1-13.
[30] Roorkiwal, M., von Wettberg, E. J., Upadhyaya, H. D., Warschefsky, E., Rathore, A., Varshney, R. K. (2014): Exploring germplasm diversity to understand the domestication process in *Cicer* spp. using SNP and DArT markers. – Plos One 9(7): e102016.
[31] Sayar, S., Karatas, S. C. (2017): Effect of seed coat on the physical, chemical and nutritional properties of whole chickpea. – The Journal of Food 42(4): 468-476.
[32] Segev, A., Badani, H., Kapulnik, Y., Shomer, I., Oren-Shamir, M., Galili, S. (2010): Determination of polyphenols, flavonoids, and antioxidant capacity in colored chickpea (*Cicer arietinum* L.). – Journal of Food Science 75: S115-S119.

http://www.aloki.hu ● ISSN 1589 1623 (Print) ● ISSN 1785 0037 (Online)
DOI: http://dx.doi.org/10.15666/aeer/1705_1057510585

[33] Sethy, N. K., Shokeen, B., Edwards, K. J., Bhatia, S. (2006): Development of microsatellite markers and analysis of intraspecific genetic variability in chickpea (*Cicer arietinum* L.). – Theoretical and Applied Genetics 112(8): 1416-1428.
[34] Singh, U., Subrahmanyam, N., Kumar, J. (1991): Cooking quality and nutritional attributes of some newly developed cultivars of chickpea (*Cicer arietinum* L.). – J. Sci. Food Agr. 55: 37-46.
[35] Şehirali, S. (1988a): Food Legumes. – Ankara University Faculty of Agriculture Publications, No: 314. Ankara University Press, Ankara. (in Turkish).
[36] Şehirali, S. (1988b): Edible Legumes. – A.Ü.Z.F. Publications: 1089. Ankara, 435p. (in Turkish).
[37] Tanno, K., Willcox, G. (2006): The origins of cultivation of *Cicer arietinum* L. and *Vicia faba* L.: Early finds from Tell El-Kerkh, North-West Syria, Late 10th Millennium B.P. – Vegetation History and Archaeobotany 15(3): 197-204.
[38] Toğay, N., Toğay, Y., Çiftçi, V. (2001): A Research on Determination of Hydration Capacity and Hard Seed Coat Rate of Pea Varieties That Are Registered in Turkey. – 5. Field Crops Congress of Turkey, 17-21 September 2001: 377-379. Tekirdağ. (in Turkish).
[39] Van der Maesen, L. J. G. (1972): *Cicer* L., a monograph of the genus, with special reference to the chickpea (*Cicer arietinum* L.), its ecology and cultivation. – H. Veenman & Zonen, Wageningen.
[40] Van der Maesen, L. J. G., Maxted, N., Javadi, F., Coles, S., Davies, A. M. R. (2007): Taxonomy of the genus *Cicer* Revisited. – In: Yadav, S. S., Redden, R. J., Chen, W., Sharma, B. (eds.) Chickpea breeding and management. Wallingford: CABI, p. 41-72.
[41] Williams, P. C., Singh, K. B., Nakkoul, H. (1983): Relation of some physical aspetcs of Kapuli type chickpeas to cooking time. – Journal of the Science of Food and Agriculture 34: 492-496.
[42] Williams, P. C., Jaby El Haramein, F., Sayegh, A. (1986): Crop Qualiyt Evaulation Methods and Guidelines. – ICARDA, Technical Manual No. 14, 142 p.
[43] Yurtsever, N. (1984): Experimental Statistical Methods. – T. C. Ministry of Forestry and Rural Affairs General Directorate of Rural Services Publications No: 121, Teknik Publication No: 56, Ankara, 624 p. (in Turkish).

http://www.aloki.hu ● ISSN 1589 1623 (Print) ● ISSN 1785 0037 (Online)
DOI: http://dx.doi.org/10.15666/aeer/1705_1057510585

INVESTIGATION OF LEAD AND CADMIUM CONTAMINATION IN MINE SOIL AND METAL ACCUMULATION IN SELECTED PLANTS GROWING IN A GOLD MINING AREA

LU, N.[1,2,3,4,5] – LI, G.[1,2,3,4,5] – HAN, J. C.[1,2,3,4,5*] – WANG, H. Y.[1,2,3,4,5] – YANG, W.[1,2,3,4,5] – SUN, Y. Y.[1,2,3,4,5]

[1]*Shaanxi Provincial Land Engineering Construction Group Co., Ltd. Xi'an 710075, China*

[2]*Shaanxi Key Laboratory of Land Consolidation, Xi'an 710075, China*

[3]*Institute of Land Engineering and Technology, Shaanxi Provincial Land Engineering Construction Group Co., Ltd., Xi'an 710075, China*

[4]*Key Laboratory of Degraded and Unused Land Consolidation Engineering, the Ministry of Natural Resources, Xi'an 710075, China*

[5]*Shaanxi Provincial Land Consolidation Engineering Technology Research Center Xi'an 710075, China*

[*]*Corresponding author*
e-mail: hanjc_sxdj@126.com; phone: (029)86625019

(Received 1st Mar 2019; accepted 21st May 2019)

Abstract. To fully understand and evaluate the impact of lead and cadmium on the surrounding soil pollution in tailings from gold ore dressings, 36 soil samples were collected at different depths near an abandoned concentrating mill in a gold mining area. By examining the lead and cadmium contents in the soil samples, the degree of lead and cadmium pollution over the soil profile was analyzed at different sampling points. Meanwhile, 12 typical plant samples, including *Bulrush (Phragmites communis (Cav.) Trin. ex Steud.), Capillary Wormwood (Artemisia capillaris), Heteropappusaltaicus (Artemisia gmelinii)* and *Stipa (Stipa capillata Linn.)* were collected at the soil sampling point. The lead and cadmium contents were determined in the aboveground and belowground organs, and the enrichment and transfer coefficients of each plant sample were calculated. The results showed that both lead and cadmium were moderately polluted within 0-10 m of the tailing dump. The lead and cadmium contents over the depth profile of 0-30 cm were higher at depths of 0-10 cm and 20-30 cm than at 10-20 cm. *Heteropappusaltaicus* showed more significant enrichment and transfer effects and large coverage and can thus be used as the phytoremediation material for the remediation of Cd- and Pb-polluted soil around tailing slag.
Keywords: *tailing slag, lead and cadmium pollution, phytoremediation, enrichment, migration*

Introduction

Mine tailings are by-products of mineral processing, usually, they are rich in significant quantities of heavy metals (Wang et al., 2017a). In modern society, heavy metal pollution in agricultural soil from mining has been becoming serious and widespread (Marrugo-Negrete et al., 2017; Yang et al., 2018). The National Communique on Soil Pollution Survey Bulletin issued in April 2014 showed that the soil environment in China was negative, and the environmental problems of industrial and mining wasteland were in evidence. Inorganics were the main type of pollution. Inorganic cadmium (Cd) and lead (Pb) pollutants were found in excesses of 7.0% and 1.5%, respectively in China (Luo and Tu, 2018). In 16.1% farmland soils, heavy metals

http://www.aloki.hu ● ISSN 1589 1623 (Print) ● ISSN 1785 0037 (Online)
DOI: http://dx.doi.org/10.15666/aeer/1705_1058710597

have exceeded the environmental quality standard (Mahar et al., 2016). The processes of industrial production, mining development, sewage irrigation and rock weathering are the main ways heavy metals enter the soil ecosystem (Pascaud et al., 2015; Sankhla et al., 2016; Ashraf et al., 2017; Jing et al., 2018). Pb and Cd also cause damage to human health. Heavy metals are difficult to decompose through biological cycling and energy exchange and are difficult to remove, resulting in heavy-metal-contaminated soils (Arora et al., 2015; Mahar et al., 2016; Wang et al., 2017b). Shaanxi province is rich in mineral resources. The development of mineral resources has brought great economic benefits as well as serious environmental problems. As the deposits are mostly related to or associated with metals, one can assume the metal smelting process leaches heavy metals. In addition, a single mining mode is mostly used in China at present, which coupled with the low recovery rate and the comprehensive utilization rate, is not only a great waste of resources but has also led to serious ecological destruction and environmental pollution.

Phytoremediation technology can be used for in situ remediation (Filippis, 2015) and is a clean, green and environmentally friendly technology for the treatment of heavy-metal-polluted soil. Compared with other technologies, phytoremediation does not cause secondary environmental problems but instead increases the soil organic matter content (Sarwar et al., 2017; Fiorentino et al., 2017; Ashraf et al., 2017), and the repair period is short and adaptable, making phytoremediation suitable for repairing large areas (Taj and Rajkumar, 2016; Kim et al., 2019).

Although some results in the scientific literature have shown that some plants have cumulative effects on Pb and Cd, there are large differences in growth status and enrichment characteristics under different geographical climates. Through the determination of heavy metals in Pb- and Cd-contaminated soils and surrounding plants in gold mining areas, several plants with tolerance to heavy metal pollution or the ability to enrich heavy metals were screened to provide a scientific reference for applying phytoremediation technology to heavy metal pollution in mining areas.

Materials and methods

Description of the research area

The research area is located in Yao Shang Village, Taiyao Town, Tongguan County. The geographic coordinates are E34°30′56″~34°31′21″, N110°19′23″~110°19′56″ (*Fig. 1)*. The small gold mining area in the Qinling Mountains is the second largest gold-producing area in China. It mainly exploits quartz-veined gold deposits and has a warm, temperate continental monsoon climate with four seasons, with an annual average temperature of 13ºC, sunshine duration of 2269 hours and frost-free period of 190 days. The ore dressing tailings were stacked at random along the river and bank slope, causing soil and water pollution.

Sample collection

Collection of plant samples

Sampling was carried out on August 23th and 24th, 2016. A total of 4 sampling sites of 10 m, 30 m and 50 m to the north of the tailing pile and slag pile were set up, and square sample boxes were used to investigate plants near the sampling points and collect a number of typical plants along with the roots, such as *Bulrush, Capillary*

http://www.aloki.hu ● ISSN 1589 1623 (Print) ● ISSN 1785 0037 (Online)
DOI: http://dx.doi.org/10.15666/aeer/1705_1058710597

Wormwood, *Heteropappusaltaicus* and *Stipa*. For each plant sample, 3 to 5 plants with similar growth periods that were well developed were selected from the area and packed in kraft paper bags for analysis.

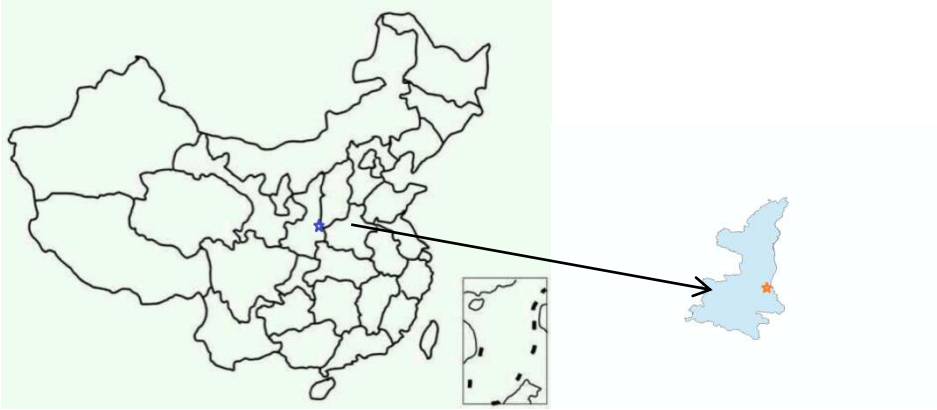

Figure 1. *Description of the research area*

Collection of soil samples

The tailings slag stacked in low-lying areas not far from the road in the open air. The top of the tailings slag was basically equal to the the height of the roadbed. The tailings slag thickness is about 30-40 cm, and it seems to be landfilling construction waste down there. Soil samples were collected by the plum sampling method along the main wind direction. The plum sampling method picks five samples based on the shape of a plum along with the center point at the diagonal intersection. At each sampling point, soil samples of 0-10 cm, 10-20 cm, 20-30 cm were collected (three times) and the remaining sample was approximately 1 kg using the quartile method. Soil samples were sealed in a plastic bag to avoid sample contamination. The sampling location and the surrounding environment were recorded accurately, and a total of 36 tailings (N34°30′58″ E110°19′45″) and 36 soil samples were collected.

Sample processing and determination

Treatment and determination of plant samples

The plant samples were separated into aboveground and underground organs, which were then treated separately. The samples were cleaned and washed with deionized water and placed in an oven at 105ºC for approximately 30 min. Then, the temperature was adjusted to 75°C until reaching a constant plant weight, which was taken as the dry weight (g) (Environment Pollution Analysis Method, 1987). The samples were milled by agate mortar and then sieved with a 0.25 mm nylon sieve. Weighed samples of approximately 0.5 g were placed in a polytetrafluoroethylene digestion tank along with 65-68% nitric acid and 30% hydrogen peroxide for digestion of the heavy metals to make them easy to measure. An AAS Zeenit 700P atomic absorption spectrometer was used to determine the Pb and Cd contents in the aboveground and underground organs. The reagents used in the test were excellent grade, with strict quality control.

http://www.aloki.hu ● ISSN 1589 1623 (Print) ● ISSN 1785 0037 (Online)
DOI: http://dx.doi.org/10.15666/aeer/1705_1058710597

Treatment and determination of soil samples

The soil samples were air-dried, crushed and ground with wood rods, sieved (<0.149 mm), and stored until measurement (Hu et al., 2014; Zhu et al., 2015; Vogelmann et al., 2015) of the Pb and Cd contents by the method outlined in GB/T 17141-1997. The pH was measured on the basis of NY/T 1377-2007.

Method for evaluation of heavy metal pollution

The grade II soil environmental quality standard was used as the evaluation criterion of soil Pb and Cd geoccumulation indices. The geoccumulative index (I_{Geo}) was used to evaluate the degree of Pb and Cd pollution. The I_{Geo} (*Eq.1*) was obtained in accordance with Muller (1969).

$$I_{Geo} = log_2\left(\frac{c_i}{kB_i}\right) \quad \text{(Eq.1)}$$

In the formula, I_{Geo} is the geoccumulation index, c_i is the measured mass concentration of heavy metal I (mg kg^{-1}), B_i is the environmental background level of the measured element (soil environmental quality standard grade II, in *Table 1*), and k is a correction factor because the diagenesis may cause a change in the background value (generally k =1.5) (Wang et al., 2015). According to the I_{Geo}, the pollution levels of heavy metals can be classified (*Table 2*), the higher I_{Geo} is, the more serious of the pollution.

Table 1. *Descriptive statistics of the Pb and Cd concentrations (mg kg^{-1}) in the tailings of the study area*

Distance from tailing slag	Elements	pH	Range (mg kg^{-1})	Mean (mg kg^{-1})	Standard deviation	Grade II of GB 15618-1995(mg kg^{-1})
0 m	Cd	7.48-7.60	0.47-5.34	2.64	2.51	0.6
	Pb		2506.90-3369.92	2471.70	1117.38	350
10 m	Cd	7.53-7.90	3.42-9.00	5.91	2.84	0.6
	Pb		1779.29-2612.68	2231.01	421.09	350
30 m	Cd	8.00-8.11	0.17-0.39	0.26	0.12	0.6
	Pb		32.12-75.61	71.40	37.36	350
50 m	Cd	7.54-7.84	0.16-0.47	0.33	0.16	0.6
	Pb		28.02-175.19	100.13	73.63	350

Table 2. *Heavy metals geoaccumulation index graduation standard*

I_{Geo}	Grade	Pollution level
≥5	6	Serious
4~5	5	Heavy
3~4	4	Biased
2~3	3	Moderate
1~2	2	Mild
0~1	1	Light
＜0	0	No pollution

http://www.aloki.hu ● ISSN 1589 1623 (Print) ● ISSN 1785 0037 (Online)
DOI: http://dx.doi.org/10.15666/aeer/1705_1058710597

Data processing

Plant bioaccumulation factor (BCF) was calculated by *Eq.2*:

$$BCF = \frac{C_p}{C_s} \quad \text{(Eq.2)}$$

In the formula, BCF is the bioaccumulation factor, C_p is the concentration of Pb or Cd in the ground or underground part of the plant (mg kg^{-1}), C_s is the content of Pb or Cd in the soil (mg kg^{-1}), BCF is an important index to measure the heavy metals enrichment capacity. The larger BCF is, the higher the enrichment efficiency of the plant. The larger BCF indicates the stronger mobility of the heavy metal.

The plant transfer coefficient (TF) was calculated as *Eq.3*:

$$TF = \frac{F_i}{R_i} \quad \text{(Eq.3)}$$

where TF is the transfer coefficient, F_i is the concentration of Pb or Cd in the ground part of the plant (mg kg^{-1}), R_i is the content of a certain element in the underground part of the plant (mg kg^{-1}).

Results and Discussion

Evaluation of soil pH and Pb and Cd accumulation indices

The pH values of the tailing samples and soil samples were all greater than 7.5 (*Table 1*). The Pb and Cd concentrations in the 0-30 cm soil samples are given in *Table 1*, along with the Pb and Cd geoccumulative pollution indices of the soil samples. The average and range of Cd and Pb concentrations in the samples taken from different distances from the tailing dumps were compared with the grade II limits (GB 15618-1995). The ratios of the average concentrations of Pb and Cd in the tailing samples to the standard limits were 7.06 and 4.40, respectively. At a distance of 10 m from the tailings, the samples had values of 9.85 and 6.37. The Cd and Pb concentrations in these samples significantly exceeded the soil environmental quality standard grade II.

The average geoccumulative indices of Cd and Pb were calculated by *Eq.1*. The average geoccumulative indices of Cd and Pb in the tailing slag were 0.82 and 1.72 (*Fig. 2*), respectively, which corresponded to mild and moderate pollution levels, respectively. The average Cd and Pb geoccumulative indices of the soil samples taken 10 m from the tailing slag indicated partial to moderate pollution. The average Cd and Pb cumulative indices of the soil samples taken 30 m and 50 m from the tailing slag were negative, indicating no pollution. The results showed that there were different degrees of Cd and Pb pollution in the tailing dumps itself and within 10 m of the tailing pile.

Pb and Cd concentrations in soil

The mean concentrations of Pb and Cd at different soil depths are presented in *Figures 3 and 4*. In this section, we analyzed the Pb and Cd concentrations at depths of 0-10 cm, 10-20 cm and 20-30 cm at each sampling point. Soil taken 30-50 m from the tailing slag showed much lower Pb and Cd concentrations than soil 0-10 m from the tailing slag (*Figures 3 and 4*). The contents of Pb and Cd in the tailings changed greatly

http://www.aloki.hu ● ISSN 1589 1623 (Print) ● ISSN 1785 0037 (Online)
DOI: http://dx.doi.org/10.15666/aeer/1705_1058710597

from surface to the lower layer. The average contents and the maximum values of Pb and Cd in the soil profiles of all layers were lower than the grade II soil environmental quality standards. However, the concentrations of Pb in the tailings in each section were higher than soil environmental quality standard (dotted lines). The content of Cd at 0-20 cm soil depth taken 0 m and 30-50 m from the tailing slag was no pollution. The concentration of Cd at a depth of 20-30 cm was 8.9 times that of 0.6 mg kg^{-1} obtained in soil taken 10 m from the tailing slag. At a distance of 0 m, the average concentrations of Pb and Cd in the 20-30 cm section reached 3369.9 and 5.34 mg kg^{-1}, respectively. After comparison with the literature, the cause of the above phenomenon may be that Pb and Cd were present in a migratable state and a bound state in the tailings, and the precipitation and oxidation of the surface layer promoted migration from the surface layer to the lower layer, resulting in the accumulation of Pb and Cd in the lower layer (20-30 cm) (Adeyi and Torto, 2014).

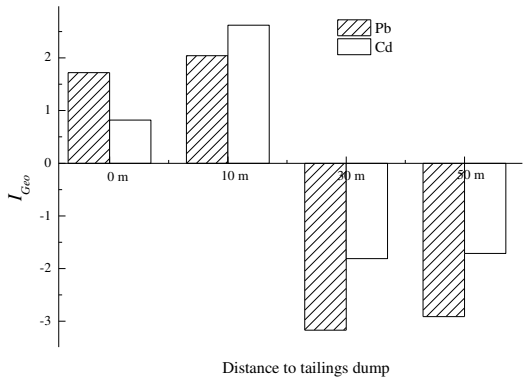

Figure 2. *The average I_{Geo} of Pb and Cd at different distances from the tailings dump*

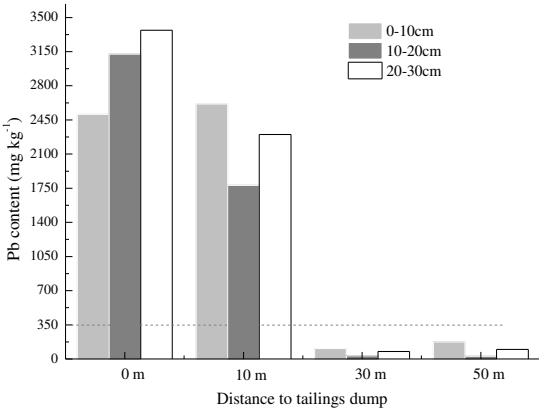

Figure 3. *The average contents of Pb in soil profile at each sampling point*

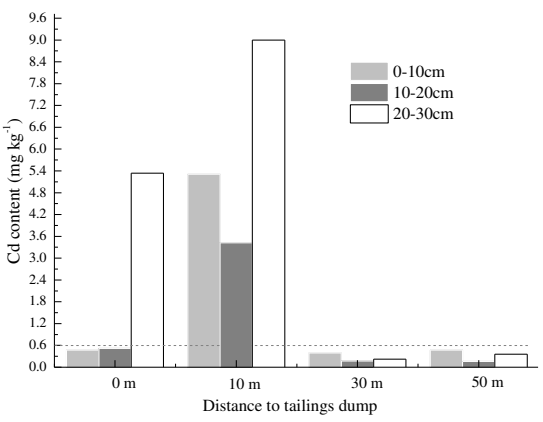

Figure 4. *The average contents of Cd in soil profile at each sampling point*

The average concentrations of Pb and Cd in the 0-10 cm soil were higher than those in the tailings. It is possible that the tailings accumulated for a long time, which led to the larger Pb and Cd accumulation at a depth of 20-30 cm at the sampling point. The main reason for the high concentrations of Cd and Pb in the 0-10 cm layer was that the location of the sampling point was affected by gusts of dust and particle sedimentation.

http://www.aloki.hu ● ISSN 1589 1623 (Print) ● ISSN 1785 0037 (Online)
DOI: http://dx.doi.org/10.15666/aeer/1705_1058710597

This might also be because the tailing pile pressure accounts for a large area of land, and the accumulation time of tailings was different.

Based on the above analysis, the Pb and Cd concentrations in the study area were highest 0-10 m from the tailing dump, and the maximum Pb and Cd concentrations were 9.6 and 15 times higher, respectively, than those given by GB15618-1995 (pH>7.5). The over-standard rates of Pb and Cd at the sampling points within an area of 0-10 m from the tailing dump were 100% and 83.3%, respectively. In the range of 30-50 m from the tailing dump, the Pb and Cd contents in the soil were lower than the environmental quality standard for soils, though the background soil in Shaanxi has a Pb content higher than 11.5 mg kg^{-1} (Xue et al., 1986).

The results showed that there were significant differences in Cd content in different depths (p=0.043<0.05). The Cd content of heavy metals did not change with the distance from the tailings slag (p=0.161>0.05). There were very significant differences in Pb content in different depths (p=0.000<0.01). The Pb content of heavy metals did not change with the distance from the tailings slag (p=0.31>0.05).

Distribution of Pb and Cd in various plant organs

In this section, the effects of Pb and Cd enrichment and transfer to plants at a distance of 10 m from the tailings dump were analyzed and compared with the corresponding soil environment (*Fig. 5*).

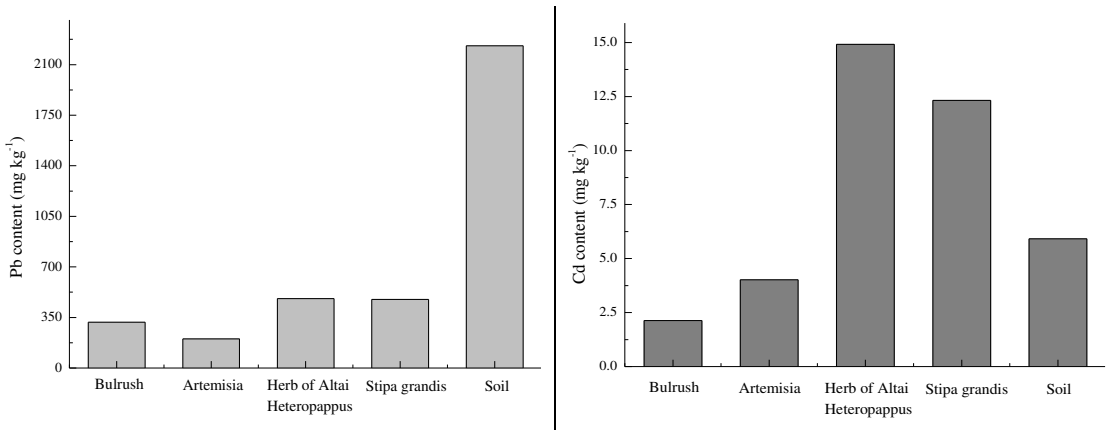

Figure 5. *Comparison of Pb and Cd concentrations and soil concentrations 10 m from tailings slag*

The bioaccumulation factor (BCF) and transfer coefficient (TF) of *Bulrush (Phragmites communis (Cav.) Trin. ex Steud.) (Poales family), Capillary Wormwood (Artemisia capillaries) (Compositae family), Heteropappusaltaicus (Artemisia gmelinii) (Compositae family), Stipa (Stipa capillata Linn.) (Gramineae family)* 10 m from tailing slag are shown in *Table 3*. The BCF and TF were calculated by *Eq.2* and *Eq.3*, respectively.

From *Table 3*, we can see that the values of the BCF of Cd for *Heteropappusaltaicus* and *Stipa* were more than 1 and the BCF of Pb was less than 0.3. Among the four plants, the BCF of Pb was similar for *Heteropappusaltaicus* and *Stipa*, and the two plants had similar Pb enrichment abilities. The TFs of *Capillary Wormwood, Heteropappus-altaicus* and *Stipa* for Pb and Cd were higher than 1.

http://www.aloki.hu ● ISSN 1589 1623 (Print) ● ISSN 1785 0037 (Online)
DOI: http://dx.doi.org/10.15666/aeer/1705_1058710597

The Cd and Pb distributions in various plant organs taken at a distance of 10 m from the tailing slag are shown in *Table 4*. At the sampling point 10 m from the tailing slag, the Cd and Pb concentrations in different organs of *Bulrush, Heteropappusaltaicus* and *Stipa* were compared. The results showed that the stem and leaves had higher Pb and Cd accumulation than the roots. *Heteropappusaltaicus* leaves had the highest Pb accumulation. Taking the results of *Table 3* and *Table 4* into consideration, *Heteropappusaltaicus* had better Pb and Cd accumulation ability. There might be two reasons for this. *Heteropappusaltaicus*, *Capillary Wormwood* and *Stipa* were the dominant crops around the tailing slag and thus had adapted to their growth environment and formed a specific tolerance mechanism. In addition, the stems and leaves of the *Heteropappusaltaicus* plants were covered with villus. These special physiological characteristics play a certain role in the accumulation of Cd and Pb, therefore, the Cd and Pb contents in the stem and leaf were generally higher than those in the underground organs. *Heteropappusaltaicus* had a large coverage in the local area. Theoretically, extraction this plant could reduce the degree of Cd and Pb pollution in soil around the tailing slag.

Table 3. *Plant bioaccumulation factor (BCF) and transfer factor (TF)*

Distance from tailings slag	Element	BCF				TF			
		Bulrush	*Capillary Wormwood*	*Heteropa-ppusaltaicus*	*Stipa*	*Bulrush*	*Capillary Wormwood*	*Heteropa-ppusaltaicus*	*Stipa*
10 m	Cd	0.279	0.785	2.97	2.26	0.557	2.55	2.11	1.42
	Pb	0.094	0.097	0.224	0.230	0.406	1.50	1.17	1.41

Table 4. *The distribution of Cd and Pb concentrations (mg kg^{-1}) in different plant organs*

Distance from tailings slag	Element	Plant					
		Bulrush root	*Bulrush* stem	*Bulrush* leaves	*Capillary Wormwood* root	*Capillary Wormwood* stem	*Capillary Wormwood* leaves
10 m	Cd	1.28	1.92	2.96	1.82	3.00	6.82
	Pb	163.27	244.94	517.18	144.85	140.12	320.04
Distance from tailings slag	**Element**	**Plant**				
		Heteropap-pusaltaicus root	*Heteropap-pusaltaicus* stem	*Heteropap-pusaltaicus* leaves	*Stipa* root	*Stipa* shoot
10 m	Cd	7.07	15.84	18.92	8.67	13.36
	Pb	410.5	453.7	562.4	337.39	513.57

One group of plants for phytoremediation lied in their excellent heavy metal accumulation capacity. Research had showed that Asteraceae species had the ability to remove heavy metal concentrations (Bolan et al., 2014). Some of them can absorb heavy metal ion in their tissues but usually have less biomass and slow growth rate. Because of the cosmopolitan distribution and local ecological adaptability (Rahman et al., 2008), Asteraceae could be used for removal the heavy metal pollutants. Nikolić and Stevović (2015) reported that family Asteraceae includes multiple species with phytoremediation potential including *T. vulgare (L)*, *T. parthenium (L.)* and *T.*

http://www.aloki.hu ● ISSN 1589 1623 (Print) ● ISSN 1785 0037 (Online)
DOI: http://dx.doi.org/10.15666/aeer/1705_1058710597

balsamita (L.) and *S. transcaspicus Nevski.* owes the ability to remove heavy metals. Xiao et al. (2018) observed that the coverage of Asteraceae family and herbs were most in the heavy metal pollution aera and *Symphytum officinale Linn.* has the ability to accumulate Cd and Pb. In the research of Hesami et al. (2018), the heavy metal uptake ability of 16 plants shoot from family Asteraceae was investigated by calculating (BCF), (TF) and the phytoremediation potential were evaluated. The maximum shoot concentrations of Pb (162 mg kg^{-1}) were found in *Taraxacum officinale F.H.Wigg* and Cd (13 mg kg^{-1}) in *Crepis sp*. The maximum BCF of Pb and Cd were 0.326 and 1.787, respectively. Comparing the results with the BCF of *Heteropappusaltaicus*, the BCF of Pb and Cd were 0.224 and 2.97, respectively.

Conclusion

The soil 30 m and 50 m from the tailing dump was not polluted by heavy metals. Soil 0-10 m from the tailing slag showed different degrees of Cd and Pb contamination, whereas soil 10 m from the tailings slaghad moderately high Cd and Pb concentrations.

The Cd and Pb concentrations at depths of 0 to 30 cm were analyzed. The Pb and Cd contents in the tailings gradually increased from the surface to the lower layer. It is possible that the tailings accumulated fora long time, which led to the larger accumulation of Pb and Cd at a depth of 20-30 cm at the sampling point. The high Pb and Cd contents in the surface layer (0-10 cm) may be due to the location of the sampling point, which was affected by gusts of dust and particle sedimentation, and large area of the tailing pile. There were significant differences in Cd (p=0.043<0.05) and Pb (p=0.000<0.05) content in different depths, respectively.

Among the four tested plants, *Heteropappusaltaicus* showed a strong comprehensive Cd and Pb transfer ability and can be used as a phytoremediation plant for Cd and Pb soil pollution around tailings slag. Based on the existing research results, taking soil Cd and Pb 10 m away from tailings slag as an example, the soil contaminated by heavy metals is restored to a safe planting level, which will require equal dry weight plants and take at least 5 years under ideal conditions of equal enrichment efficiency. But it is worth noting that each part of the plant has a certain enrichment effect on heavy metals. If the plants are not properly treated, it may lead to the re-entry of heavy metals enriched by plants into the soil system. These heavy metals are mostly soluble and will cause severer harm. Selecting more dominant plants of family Asteraceae for phytoremediation of environmental pollutants is the final target.

Acknowledgements. Financial support were provided by the Fund Project of Shaanxi Key Laboratory of Land Consolidation (2018-JC16) and the Research Project of Shaanxi Provincial Land Engineering Construction Group in China (DJNY2019-18).

REFERENCES

[1] Adeyi, A. A., Torto, N. (2014): Profiling heavy metal distribution and contamination in soil of old power generation station in Lagos, Nigeria. – J American Journal of Science and Technology 1(1): 1-10.

[2] Arora, B., Şengör, S. S., Spycher, N. F., Steefel, C. I. (2015): A reactive transport benchmark on heavy metal cycling in lake sediments. – Computational Geosciences 19(3): 613-633.

http://www.aloki.hu ● ISSN 1589 1623 (Print) ● ISSN 1785 0037 (Online)
DOI: http://dx.doi.org/10.15666/aeer/1705_1058710597

[3] Ashraf, M. A., Hussain, I., Rasheed, R., Iqbal, M., Riaz, M., Riaz, M., Arif, M. S. (2017): Advances in microbe-assisted reclamation of heavy metal contaminated soils over the last decade: A review. – Journal of Environmental Management 198(Part 1): 132-143.
[4] Bolan, N., Kunhikrishnan, A., Thangarajan, R., Kumpiene, J., Park, J., Makino, T., Kirkham, M. B., Scheckel, K. (2014): Remediation of heavy metal (loid) s contaminated soils–to mobilize or to immobilize? – Journal of Hazardous Materials 266: 141-166.
[5] Filippis, D. L. F. (2015): Chapter 8–Role of phytoremediation in radioactive waste treatment. – Soil Remediation and Plants: Prospects and Challenges 92(6): 207-254.
[6] Fiorentino, N., Ventorino, V., Rocco, C., Cenvinzo, V., Agrelli, D., Gioia, L., Mola, D., Adamo, P., Pepe, O., Fagnano, M. (2017): Giant reed growth and effects on soil biological fertility in assisted phytoremediation of an industrial polluted soil. – Science of the Total Environment 575: 1375-1383.
[7] Hesami, R., Salimi, A., Ghaderian, S. M. (2018): Lead, zinc, and cadmium uptake, accumulation, and phytoremediation by plants growing around Tang-e Douzan lead–zinc mine, Iran. – Environmental Science and Pollution Research 25(9): 8701-8714.
[8] Hu, M., Wu, J. Q., Peng, P. Q., Gan, G., Zhou, H., Liao, B. (2014): Assessment model of heavy metal pollution for arable soils and a case study in a mining area. – Acta Scientiae Circumstantiae 34(2): 423-430.
[9] Jing, F., Chen, X., Yang, Z., Guo, B. (2018): Heavy metals status, transport mechanisms, sources, and factors affecting their mobility in Chinese agricultural soils. – Environmental earth sciences 77(3): 104.
[10] Kim, J. H., Ryu, T. H., Lee, S. S., Lee, S., Chung, B. Y. (2019): Ionizing radiation manifesting DNA damage response in plants: An overview of DNA damage signaling and repair mechanisms in plants. – Plant Science 278: 44-53.
[11] Luo, Y., Tu, C. (eds.) (2018): Twenty years of research and development on soil pollution and remediation in China. – The research and development of technology for contaminated site remediation. 10.1007/978-981-10-6029-8 (Chapter 48): 785-798.
[12] Mahar, A., Wang, P., Ali, A., Awasthi, M. K., Lahori, A. H., Wang, Q., Li, R. H., Zhang, Z. (2016): Challenges and opportunities in the phytoremediation of heavy metals contaminated soils: A review. – Ecotoxicology and environmental safety 126: 111-121.
[13] Marrugo-Negrete, J., Pinedo-Hernández, J., Díez, S. (2017): Assessment of heavy metal pollution, spatial distribution and origin in agricultural soils along the Sinú River Basin, Colombia. – Environmental research 154: 380-388.
[14] Ministry of environmental protection, Ministry of land and resources. (2014): National survey of soil pollution status of China. – China Envir. Protect. Indus. 5: 10-14.
[15] Muller, G. (1969): Index of geoaccumulation in sediments of the Rhine River. – Geojournal 2(108): 108-118.
[16] Nikolić, M., Stevović, S. (2015): Family Asteraceae as a sustainable planning tool in phytoremediation and its relevance in urban areas. – Urban Forestry and Urban Greening 14(4): 782-789.
[17] Pascaud, G., Boussen, S., Soubrand, M., Joussein, E., Fondaneche, P., Abdeljaouad, S., Bril, H. (2015): Particulate transport and risk assessment of Cd, Pb and Zn in a Wadi contaminated by runoff from mining wastes in a carbonated semi-arid context. – Journal of Geochemical Exploration 152: 27-36.
[18] Rahman, A. H. M. M., Alam, M. S., Khan, S. K., Ahmed, F., Islam, A. K. M. R., Rahman, M. M. (2008): Taxonomic studies on the family Asteraceae (Compositae) of the rajshahi division. – Research Journal of Agriculture and Biological Sciences 4(2): 134-140.
[19] Research cooperation group of analysis method of environmental pollution. (1987): Environmental Pollution Analysis Method. – 2 edition. Beijing: Science Press.
[20] Sankhla, M. S., Kumari, M., Nandan, M., Kumar, R., Agrawal, P. (2016): Heavy metals contamination in water and their hazardous effect on human health—a review. – International Journal of Current Microbiology and Applied Sciences 5(10): 759-766.

http://www.aloki.hu ● ISSN 1589 1623 (Print) ● ISSN 1785 0037 (Online)
DOI: http://dx.doi.org/10.15666/aeer/1705_1058710597

[21] Sarwar, N., Imran, M., Shaheen, M. R., Ishaque, W., Kamran, M. A., Matloob, A., Rehim, A., Hussain, S. (2017): Phytoremediation strategies for soils contaminated with heavy metals: Modifications and future perspectives. – Chemosphere 171: 710-721.
[22] Taj, Z. Z., Rajkumar, M. (2016): Perspectives of plant growth-promoting actinomycetes in heavy metal phytoremediation. – In: Subramaniam, G., Arumugam, S., Rajendran, V. (eds.) Plant Growth Promoting Actinobacteria. Springer, Singapore: 213-231
[23] Vogelmann, E. S., Reichert, J. M., Prevedello, J., Awe, G. O., Reinert, D. J. (2015): Soil hydrophobicity: comparative study of usual determination methods. – Ciencia Rura 45(2): 260-266.
[24] Wang, F., Huang, Y. Z., Wang, X. L., Gao, Z., Yu, F. X., Xu, F., Bao, Q. L., Hu, Y., Qiao, M., Jin, S. L. (2015): Ecological risk assessment of heavy metals in the surrounding soil of tungsten ores: Comparison of different evaluation methods. – Environmental Chemistry 34(2): 225-233.
[25] Wang, L., Ji, B., Hu, Y., Liu, R., Sun, W. (2017a): A review on in situ phytoremediation of mine tailings. – Chemosphere 184: 594-600.
[26] Wang, G., Zhang, S., Xiao, L., Zhong, Q., Li, L., Xu, G., Deng, O. P., Pu, Y. (2017b): Heavy metals in soils from a typical industrial area in Sichuan, China: spatial distribution, source identification, and ecological risk assessment. – Environmental Science and Pollution Research 24(1): 1-13.
[27] Xiao, R., Shen, F., Du, J., Li, R., Lahori, A. H., Zhang, Z. (2018): Screening of native plants from wasteland surrounding a Zn smelter in Feng County China, for phytoremediation. – Ecotoxicology and environmental safety 162: 178-183.
[28] Xue, C. Z., Xiao, L., Wu, Q. F., Li, D. Y., Wang, K. X., Li, H. E., Wang, R. (1986): Studies of background values of ten chemical elements in major agricultural soils in Shaanxi Province. – Acta Universities Agriculturalis Boreali-Occidentalis (Natural Science Edition) 3: 30-53.
[29] Yang, Q., Li, Z., Lu, X., Duan, Q., Huang, L., Bi, J. (2018): A review of soil heavy metal pollution from industrial and agricultural regions in China: Pollution and risk assessment. – Science of the Total Environment 642: 690-700.
[30] Zhu, D. W., Zhong, H., Zeng, Q. L., Yin, Y. (2015): Prediction of methylmercury accumulation in rice grains by chemical extraction methods. – Environmental Pollution 199: 1-9.

http://www.aloki.hu ● ISSN 1589 1623 (Print) ● ISSN 1785 0037 (Online)
DOI: http://dx.doi.org/10.15666/aeer/1705_1058710597

EFFECT OF MIXING RATIO AND PLANTING YEARS ON THE MICRO STRUCTURE OF SOFT ROCK AND SAND COMPOUND SOIL: A SCANNING ELECTRON MICROSCOPE STUDY

LI, J.[1,2,3,4] – HAN, J. C.[1,2,3,4] – WANG, Y. K.[1,2,3,4] – GE, L.[1,2,3,4] – TIAN, C.[1,2,3,4] – SHI, C. D.[1,2,3,4] – WANG, H. Y.[1,2,3,4*] – GUO, H. [1,2,3,4]

[1]*Shaanxi Provincial Land Engineering Construction Group Co. Ltd. /Shaanxi key Laboratory of Land Consolidation, 710075 Xi'an, China*

[2]*Institute of Land Engineering Technology in Shaanxi Province Co. Ltd., 710075 Xi'an, China*

[3]*Key Laboratory of Degraded and Unused Land Consolidation Engineering Ministry of Nature and Resources PRC, 710075 Xi'an, China*

[4]*Shaanxi Provincial Land Consolidation Engineering Technology Research Center710075 Xi'an, China*

[*]*Corresponding author*
e-mail: 2644816206@qq.com; phone: +86-029-8662-5017; fax: +86-029-8662-5017

(Received 1st Mar 2019; accepted 21st May 2019)

Abstract. To illustrate the internal micro-mechanism of macro-properties for soft rock and sand compound soil. The compound soil with the mixing ratios of soft rock to sand 1:1, 1:2 and 1:5 which planted in six years, and the ratio of 1:2 planted in one, five and six years were characterized by scanning electron microscope (SEM) to observe the micro structures. The results showed that (1) in the 1:1 compound soil, the silt particles and sandy particles accounted for about 62.5% and 37.5%. Compared with sand, the content of silt particles in 1:1 compound soil increased by about 26%, while the sandy particles decreased by about 26%. (2) The coarse sandy particles (0.25~1 mm) decreased from 9.2% for 1:2 compound soil planted in one year to 2.0% that planted in six years. In contrast, the fine silt particles (0~0.01 mm) increased from 20.7% to 32.6%. With increasing wheat planting years, soil particles of compound soil became finer, which was consistent with the situation that adding soft rock into sand. (3) After six-year wheat planting, the number of soil aggregate for 1:5 and 1:1 compound soil were 1.0 and 2.5. While the number of soil aggregate was 2.0 for 1:2 compound soil after one-year wheat planting, which increased to 8.0 after six-year wheat planting. With the increase of soft rock into sand or wheat planting years, the number of soil aggregate increased also, thus the soil quality was greatly improved.
Keywords: *micro-mechanism, SEM, soil particles, soil aggregate, long-term planting*

Introduction

Soft rock refers to the interbed rock which is composed of thick sandstone, sand shale and argillaceous sandstone of Paleozoic Permian, Mesozoic Triassic, Jurassic and Cretaceous (Bazhenov et al., 1993; Martin et al., 1999; Zhang et al., 2009a). Soft rock is as hard as stone without water, while as soft as mud when it meets water. Water and wind erosion is poorly tolerable for soft rock, which can lead to a large amount of soil loss and

http://www.aloki.hu ● ISSN 1589 1623 (Print) ● ISSN 1785 0037 (Online)
DOI: http://dx.doi.org/10.15666/aeer/1705_1059910610

thus a disaster for local people (Yang et al., 2014). Soft rock is mainly distributed at the junction of Shanxi, Shaanxi and Inner Mongolia where partly overlaps with Mu Us Sandy Land. Soft rock and sand presents interphase distribution there (Zhang et al., 2009b). Sandy soil there is loose and has no structure which results in serious leakage of water and fertilizer and soil erosion problem. It has been proposed that soft rock can be blended with sand to form compound soil, which compensates the shortcomings in the structure of sandy soil that can be further used for planting (Wang et al., 2013). Compared to sand, the texture of compound soil has been improved (Zhu et al., 2017) and the water and fertilizer holding capacity has been significantly increased (Han et al., 2012; Wang et al., 2014, 2016).

The study of soil microstructure is helpful to the further understanding of soil properties and its intrinsic mechanism. Currently, scanning electron microscopy (SEM) is usually applied for studying the microstructure of soil (Montes et al., 2005; Sayen et al., 2009; Romero, 2013; Lin and Cerato, 2014; Jiang et al., 2014;). Chang et al. (2015) directly observed the morphology of sand, clay, and Red Yellow soil treated by Xanthan gum with SEM, showing the connection mechanism of Xanthan gum with soils of different particle sizes. SEM and energy dispersive spectrometer (EDS) can be jointly used for semi-quantitative analysis of matter elements. Ramamurthy and Kannan (2009) studied the effects of atmospheric pollution by analyzing heavy metals in soil and plants collected from an industrial area with SEM-EDS method. Through this, a perceptible variation in the trace element concentration of samples in different seasons can be found. For the study of soft rock, Li et al. (2016) used SEM to observe the microstructure of soft rock geopolymer materials and discussed the influences of fly ash content and curing age on the mechanical properties and microstructure of soft rock geopolymer material. However, the microstructure of soft rock and sand compound soil is still unclear. The study of the microstructure of compound soil is also helpful for improving the macro properties of compound soil by laying the theoretical and technical foundation in the micro level, which provides efficient support for the resource utilization of soft rock.

In this work, soft rock, sand and compound soil were observed by SEM to study the effect of mixing ratio and wheat planting year on the soil microstructure. Compound soil with the mixing ratios of soft rock to sand 1:1, 1:2, and 1:5 which planted in six years, and the ratio was 1:2 planted in one year, five years, and six years were characterized by scanning electron microscope (SEM) to observe the micro structures. Microstructures of soil with different treatments were qualitatively compared. Statistical analysis of the micro images showed the variation trends of particle size and aggregate number, etc., as a function of mixing ratio and wheat planting ages. The application of SEM can not only determine the microstructural changes observed in the soil, but also simultaneously determine the main components of the cement material in the process of sand becoming soil, and compare the particle size distribution information measured by laser particle size analyzer to reveal relationship between the microscopic and Macroscopic composite soil.

http://www.aloki.hu ● ISSN 1589 1623 (Print) ● ISSN 1785 0037 (Online)
DOI: http://dx.doi.org/10.15666/aeer/1705_1059910610

Materials and methods

Materials

Soft rock and sand were collected from Yuyang District, Yulin City (108.58°E to 110.24°E, 37.49 °N to 38.58°N). The altitude ranges from 1000 to 1600 m. The area is in medium-temperate arid climate zone. All the experimental fields were artificially sown. The tested wheat variety was Xiaoyan 22, with an average 1000-grain weight of 38 g and a wheat germination rate of 90.1%. The wheat yield is 150 kg / hm^2 and the line spacing is 20 cm. Before wheat planting, apply the base fertilizer (diammonium phosphate 300 kg / hm^2, urea 150 kg / hm^2). Winter irrigation treatment of urea 150 ~ 225 Kg / hm^2, spring application of urea 150 ~ 225 kg / hm^2, irrigation 3 times, winter irrigation 1 time, spring irrigation 1 time, filling period 1 time, chemical weeding 1 time in spring, a spray three defense after heading.In addition, soft rock and sand compound soil after six-year wheat planting with three proportions (1:1, 1:2, 1:5, respectively) and compound soil with ratio of 1:2 after one-year, five-year and six-year crop cultivation were collected respectively. Sample information was given in *Table 1*.

Table 1. *Details of soil samples*

Sample	Mixing Ratio of Soft Rock to Sand	Wheat Planting Year
Soft Rock		
Compound Soil	1:1	6
Compound Soil	1:2	1
Compound Soil	1:2	5
Compound Soil	1:2	6
Compound Soil	1:5	6
Sand		

Methods

The microscopic structure of collected soil samples was characterized by FEI Q45 SEM. Soil samples with a good flat surface were prepared on the sample stage, which were observed at the voltage of 25 kV. The magnification times gradually increased and photographs were taken at magnification times of 100, 500, 1000 and 2000, respectively. The obtained surface microstructure images of soil samples were analyzed and processed. The particle size was measured by the Nano Measure software. Specifically, the scale on the picture was used as a reference, and then lines were crossed on the maximum diameter of all the soil particles, including the attached clay and silty particles, to obtain the particle size. The measurement results were output and the number of particles classified by size into several levels was counted. Through the picture, the number of aggregates and other sample information were also obtained. The soil particle size composition, the number of aggregates, etc., were plotted as a function of mixing ratio of compound soil or wheat planting year.

http://www.aloki.hu ● ISSN 1589 1623 (Print) ● ISSN 1785 0037 (Online)
DOI: http://dx.doi.org/10.15666/aeer/1705_1059910610

According to the X-ray diffraction method, clay mineral samples with particle size less than 10 μm and less than 2 μm in 1:2 compound soil with wheat planting years of 1 year, 5 years and 6 years were extracted according to the Stokes settlement theorem. A clay mineral sample having a particle diameter of less than 10 μm is used for determining the total relative content of clay minerals; a clay mineral sample having a particle diameter of less than 2 μm is used to determine the relative content of each clay mineral.

Results and Discussion

Micro-morphology of compound soil

Microstructure of compound soil with different mixing ratios

The texture of soft rock and sand compound soil with different proportions has been studied by laser particle size analyzer (Zhu et al., 2017). The volume of soil particles with different grain sizes was measured by laser, so as to obtain the percentage of each grain size. Compared with this indirect measurement method, it was more intuitive to measure the particle size through micro-image obtained by SEM. In addition, the morphology of the soil particle surface and the interface between particles can be seen.

Fig. 1 showed the SEM images of compound soil with different proportions after wheat planting for six years. *Fig. 1(a-d)*, *Fig. 1(e-h)*, and *Fig. 1(i-l)* respectively illustrated the composite soils with ratios of 1:1, 1:2, and 1:5. The magnification times for images from top to bottom were 100, 500, 1000, and 2000, respectively. From the images of lower magnification times (100 and 500 times), it can be seen that there was more cementing matter between soil particles under the ratio of 1:1. As the content of sand increased, the particles became dispersed and the cementation material became less. In the images with higher magnification times of 1000 and 2000 times, it showed that there were more matter attached on the surface of soil particles under the ratio of 1:1 and 1:2 than that with the ratio of 1:5. With the increasing content of soft rock, the particles mostly presented face contact to each other and more cementing materials bonded them together, maintaining certain content of pores and good agglomeration property.

Microstructure of compound soil with different wheat planting ages

Fig. 2 showed the images of compound soil with the ratio of 1:2 which planted in different ages under SEM. *Fig. 2(a-d)*, *Fig. 2(e-h)* and *Fig. 2(i-l)* were the images of compound soil with one-year, five -year and six-year wheat planting ages, respectively. The magnification times from top to bottom were 100, 500, 1000 and 2000 times, respectively. In lower magnification images of 500 and 1000 times, it can be seen that the surface of soil particles after one-year planting was relatively smooth, while with the increasing wheat planting years, more attachments appeared on the surface of soil particles. Higher magnification images (1000 and 2000 times) indicated that the soils were relatively dispersive after one year wheat planting. The inter-particle boundaries

http://www.aloki.hu ● ISSN 1589 1623 (Print) ● ISSN 1785 0037 (Online)
DOI: http://dx.doi.org/10.15666/aeer/1705_1059910610

were clear and cementing matter was less. In contrast, the compound soil planted in five and six years presented closer connection, smaller pores and richer intergranular cementation. This was due to the increase of soil organic matter content during several years of crop cultivation, such as irrigation and fertilization. In addition, root exudates, soil biological activities and their products, and humus etc. can make the soil agglomeration better, so that the soil structure improved remarkably.

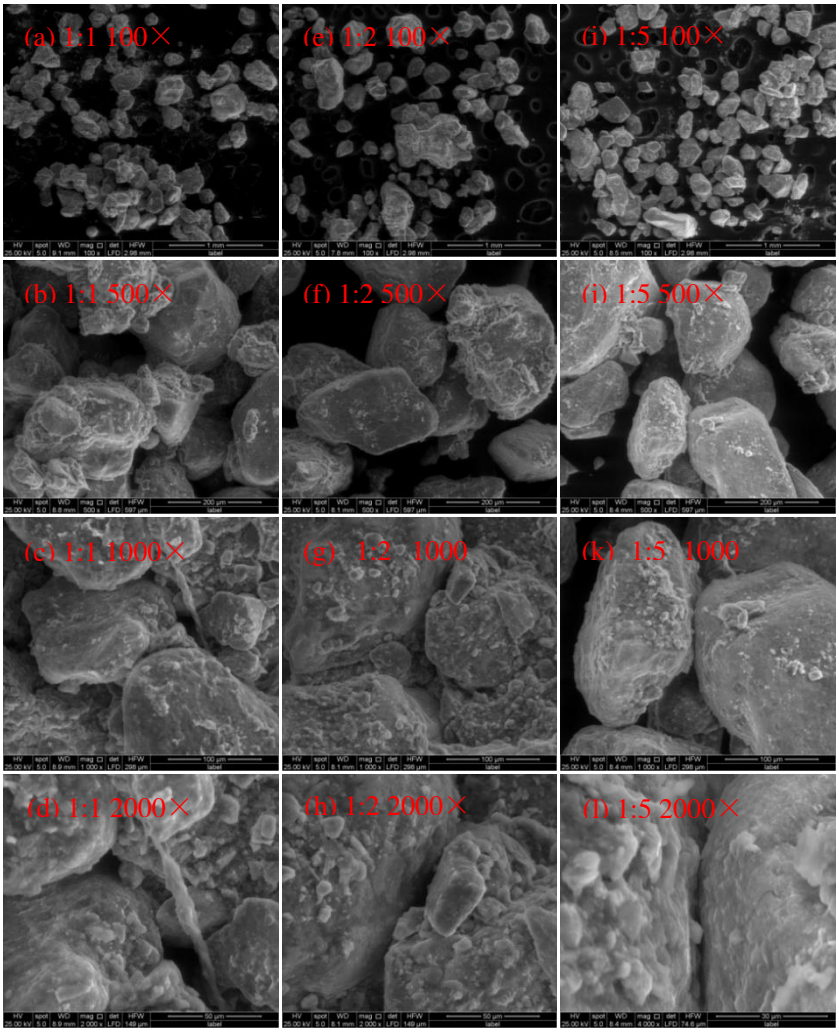

Figure 1. *SEM images of soft rock and sand compound soil with different ratios after six-year wheat planting. The ratios of soft rock to sand were 1:1, 1:2, and 1:5 for (a-d), (e-h), and (i-l), respectively. The magnification times were 100, 500, 1000, and 2000 respectively for (a, e, and i), (b, f, and j), (c, g, and k), and (d, h, and l)*

By section analysis of compound soil aggregates, backscattered electron imaging and X-ray energy spectrometer analysis showed that the elemental composition of cemented materials in compound soil was mostly O, Mg, Al, Si, K, Ca, Fe. In combination with Oades' research on soils with low organic matter content and high clay mineral and iron-aluminum oxide content, it is found that the formation of agglomerates mainly

http://www.aloki.hu ● ISSN 1589 1623 (Print) ● ISSN 1785 0037 (Online)
DOI: http://dx.doi.org/10.15666/aeer/1705_1059910610

depends on the cohesive force of cosmids and the cementation of iron-aluminum oxides. It is believed that the cemented material in the compound soil is mainly clay mineral and is closely packed between the bone particles.

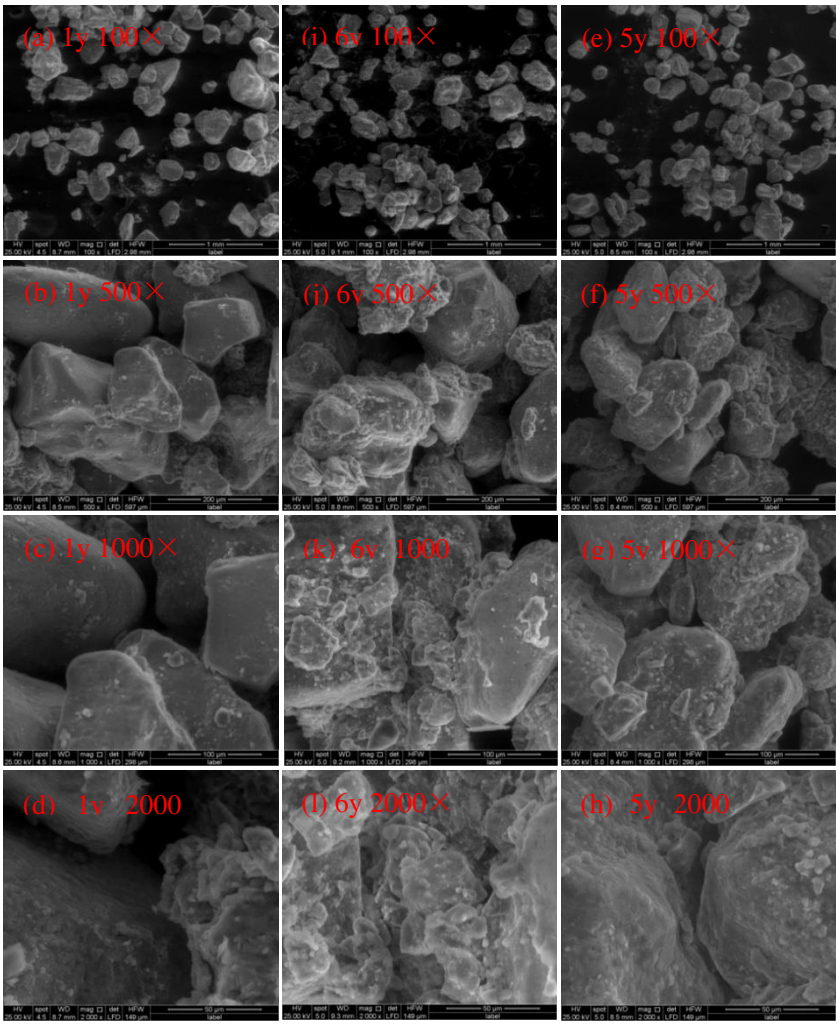

Figure 2. *SEM images of soft rock and sand compound soil with different wheat planting years. The ratio of soft rock to sand was 1:2, and the wheat planting years were one year, five years, and six years for (a-d), (e-h), and (i-l), respectively. The magnification times were 100, 500, 1000, and 2000 respectively for (a, e, and i), (b, f, and j), (c, g, and k), and (d, h, and l)*

According to the XRD analysis, the content of clay minerals in the compound soil increased with the increasing wheat planting years, shown as *Table 2* and increased from 18.2% after wheat planting in 1 year to 22.4% after 6 years wheat planting, which greatly improved the cementing property of the compound soil. There is a significant difference between the compound soil of 5 years and 6 years and the initial stage of compounding. The clay minerals in the compound soil were mainly water-sensitive illite-montmorillonite mixed layer, which accounts for 49~51% of clay minerals, and the proportion of different kinds of clay minerals was similar.

http://www.aloki.hu ● ISSN 1589 1623 (Print) ● ISSN 1785 0037 (Online)
DOI: http://dx.doi.org/10.15666/aeer/1705_1059910610

Table 2. *Content analysis of cementing materials in compound soil and aeolian sand soil*

Years of planting	Clay mineral content (%)	Relative content of clay minerals (%)			
		I/S	It	Kao	C
1	18.2	49	26	12	13
5	21.9	51	25	13	11
6	22.4	51	25	11	13

I/S: Illite-montmorillonite mixed layer; It: Illite

Particle gradation of compound soil

According to the soil texture classification of United States Department of Agriculture (USDA) (Drzymala, 2000), the range of sandy particle size 0.05 to 1 mm, while in this paper, the sandy particle was divided into fine sandy particles (0.05~0.25 mm) and coarse sandy particles (0.25~1 mm). The particles whose size ranged from 0.002 to 0.05 mm were called silty particles and that smaller than 0.002 mm were called clay particles. Since the resolution capacity is not enough for the Nano Measure software to distinguish the clay particles, the 0 to 0.05 mm particles were all denoted as silty particles in this work, in which 0 ~ 0.01 mm and 0.01 ~ 0.05 mm particles were denoted as fine and coarse silty particles, respectively.

Particle gradation of compound soil with different mixing ratios

As shown in *Fig. 3*, the content of sandy particles in sand was more than 63.5%, and the content of fine silty particles (0~0.01 mm) was only 2.3%. The content of sandy particles in soft rock was about 19.6%, and the content of fine silty particles was up to 32.3%. In addition, the content of coarse silty particles was also very high, about 48.1%.

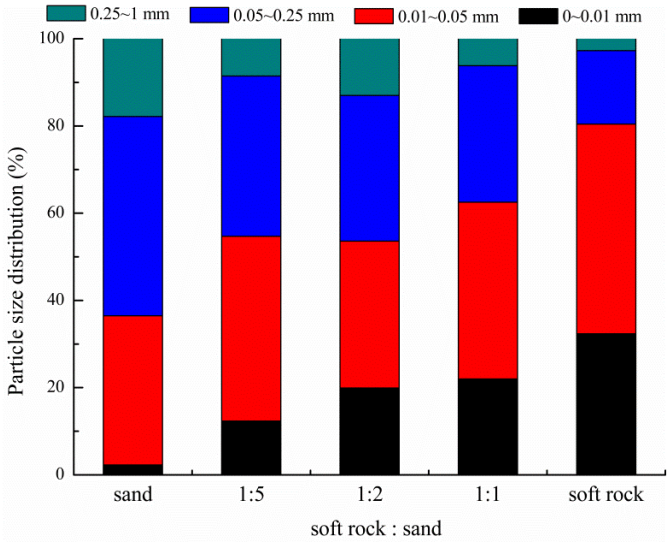

Figure 3. *The particle size distribution of soft rock and sand compound soil with different mixing ratios after six-year wheat planting*

http://www.aloki.hu ● ISSN 1589 1623 (Print) ● ISSN 1785 0037 (Online)
DOI: http://dx.doi.org/10.15666/aeer/1705_1059910610

By comparison, the measurement results of particle size by SEM and laser particle size analyzer (Zhang et al., 2015) were basically the same. It indicated that the riched fine particles in soft rock made up for the lack of fine particles in sand. The content of sandy particles in compound soil with the ratio of 1:1 was about 37.5%, in which about 6.2% was coarse sandy particles, and the content of silty particles was about 62.5%, in which the fine silty particles was about 40.5%. Compared with sand, the content of silty particles increased by about 26%, and the content of sandy particles decreased by about 26%. The particle size distribution of compound soil can be altered by adjusting the proportion of soft rock and sand. With the adding soft rock into sand, the percentage of coarse particles decreased while the fine particles increased. Furthermore, the trend was more obvious with the increasing proportion of soft rock in sand. The mixing of soft rock and sand not only significantly improved the soil texture but also increased the content of fine particles, which was beneficial to the formation of soil agglomeration and capillary pores, so as to enhance the water retention capacity of soil.

Particle gradation of compound soil with different wheat planting ages

Fig. 4 displayed the particle size distribution of compound soil with the ratio of 1:2 as a function of wheat planting year. It can be seen that the content of coarse sandy particles decreased with the increase of wheat planting period, from 9.2% for one-year tillage to 2.0% for six-year tillage.

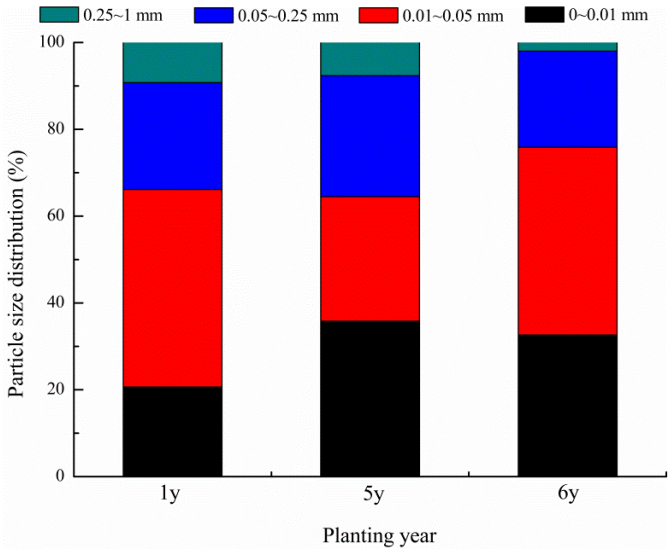

Figure 4. *The particle size distribution of soft rock and sand compound soil (the ratio is 1:2) with different wheat planting years*

Besides, the content of fine silty particles increased from 20.7% for one-year wheat planting to 32.6% for six-year wheat planting. With the increase of tillage time, the content of sandy particles decreased while silty particles increased, which was attributed to the comprehensive actions of tillage, irrigation, and activities of crop root, animal and

http://www.aloki.hu ● ISSN 1589 1623 (Print) ● ISSN 1785 0037 (Online)
DOI: http://dx.doi.org/10.15666/aeer/1705_1059910610

microorganism. By comparing the particle size distribution of compound soil after five-year and one-year wheat planting, it can be found that with the increasing wheat planting years, the coarse sandy particles crushed into fine sandy or silty particles and coarse silty particles crushed into fine silty particles under the action of root and microorganisms. Thus, the content of coarse sandy and coarse silty grains decreased, while the content of fine sandy and fine silty grains increased. After six-year wheat planting, soil particles continued to become finer gradually, therefore, the content of coarse and fine sandy granules declined, and the content of coarse and fine silty particles increased, which was conducive to the rational distribution of soil particles, the formation of pore structure with good performance of ventilation, water permeability, fertilizer holding, etc. Thus, the land quality was improved.

Aggregation characteristics of compound soil

Fig. 5 was the mean number of coacervates in multiple images (the magnification times was 100) of compound soil after six-year wheat planting as a function of the mixing ratio. With the increase of soft rock in sand, the number of coacervates also increased, raging from 1 for the ratio of 1:5 to 2.5 for the ratio of 1:1. From the ratio of 1:5 to 1:1, the number of coacervates increased by 75.0% and 42.9%, respectively.

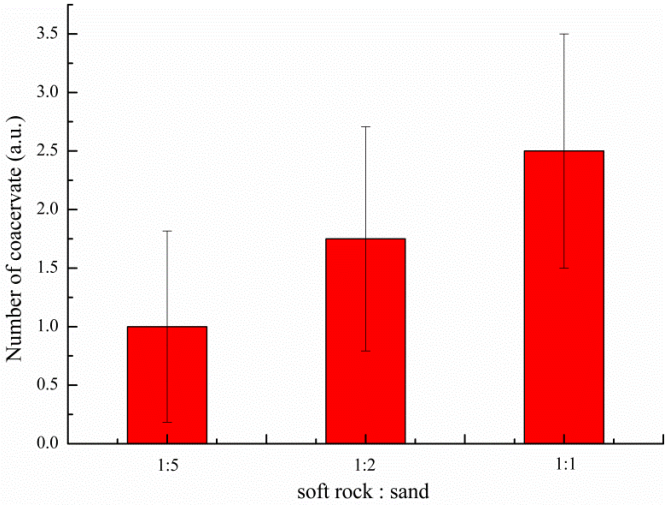

Figure 5. *The number of coacervate of soft rock and sand compound soil with different ratios after six-year wheat planting*

Fig. 6 was the mean number of coacervates in 100 times magnification of compound soil with ratio of 1:2, which plotted as a function of wheat planting year. With the increase of the wheat planting period, the number of coacervates increased too, varying from 2 for one-year wheat planting to 8 for the six-year wheat planting. Among three wheat planting, the increase in the number of coacervates was 100.0%. In terms of the relationship between particle size and formation of aggregates, it was considered that the more the fine particles, the stronger the soil aggregation ability. Aggregation refers

http://www.aloki.hu ● ISSN 1589 1623 (Print) ● ISSN 1785 0037 (Online)
DOI: http://dx.doi.org/10.15666/aeer/1705_1059910610

to the process of agglomeration of soil particles resulted from various forces. The main external forces included the effects of plant roots, fossorial animals, soil tillage, alternation of dry and wet, and alternation of freeze and thaw, etc. Section 3.2.1 indicated that after six years wheat planting, with the increasing proportion of soft rock in the compound soil, the content of sandy grains decreased while the silty grains increased. The finer particles would accelerate the formation of aggregates, which was consistent with the result shown in *Fig. 5*. It can be seen in section 3.2.2 that with the increasing wheat planting years, for the compound soil with the ratio of 1:2, the soil particles became finer, which was beneficial to the formation of aggregates.

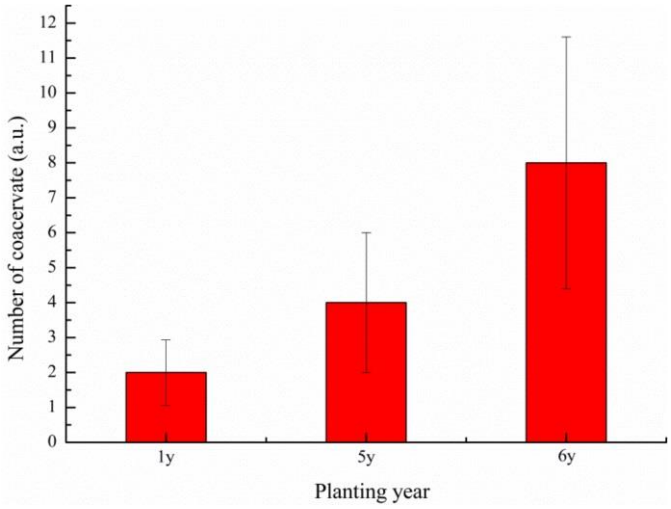

Figure 6. *The number of coacervate of soft rock and sand compound soil (the ratio was 1:2) with different wheat planting years*

In *Fig. 6*, the number of aggregates increased with the increasing wheat planting ages, resulting from the inserting, cutting, squeezing effect of plant roots and fossorial animal during the wheat planting period. In addition, the enwinding of mycelium to the soil particles played a role as forming power (Aspiras et al., 1971; Tisdall and Oades, 1980), and mycelial secretion played an important role of cementing soil particles (Martin et al., 1955). Timely and reasonable cultivation, intertillage, raking, repression and other measures with chopping, squeezing and other effects would also be conducive to the formation of aggregates.

Conclusion

The improvement effect of sandy soil properties by mixing soft rock and sand into compound soil was studied with the mono-factor analysis method under SEM. The samples were compound soil planted in six years with mixing ratio of 1:1, 1:2, 1:5, respectively, and compound soil planted in one, five and six years with the ratio of 1:2. The effect of mixing ratio and wheat planting ages on microstructure and properties of

http://www.aloki.hu ● ISSN 1589 1623 (Print) ● ISSN 1785 0037 (Online)
DOI: http://dx.doi.org/10.15666/aeer/1705_1059910610

compound soil was analyzed. It was found that with the increasing amount of soft rock in compound soil, the soil particles became much more fine. The grain composition of sandy soil was significantly improved by adding of soft rock. The content of silty particles for compound soil planted in six years with the ratio of 1:1 increased by 26% compared to the sandy soil, and the sandy particles decreased by about 26%. With the increase of wheat planting period, due to farming activities and activities of plant roots and soil microorganisms, etc., soil particles of compound soil continuously got finer, and the distribution of particle size became more reasonable. The content of coarse sandy particles decreased from 9.2% for one-year wheat planting to 2.0% for six-year wheat planting, while the content of fine silty particles increased from 20.7% to 32.6%. With the increasing content of soft rock in compound soil or the wheat planting period, the number of soil aggregates increased, raging from 1 for 1:5 ratio to 2.5 for 1:1 ratio planted in six years, and from 2 for one-year wheat planting to 8 for six-year wheat planting whose ratio was 1:2. In conclusion, soil quality has been improved with the addition of soft rock or the increase of planting years. Finally, the analysis of microstructure for compound soil laid a good foundation for the study of the inherent mechanism of macroscopic performance.

Acknowledgements. Supported by the Fundamental Research Funds for the Central Universities, CHD (300102279503); The Fund Project of Shaanxi Key Laboratory of Land Consolidation (2018-JC18, 2019-JC08); Shaanxi Provincial Land Engineering Construction Group Ltd., internal research project (DJNY2019-12, DJNY2018-12).

REFERENCES

[1] Aspiras, R. B., Allen, O. N., Chesters, G., Harris, R. F. (1971): Chemical and Physical Stability of Microbially Stabilized Aggregates. – Soil Science Society of America Journal 35: 283.

[2] Bazhenov, M. L., Chauvin, A., Audibert, M., Levashova, N. M. (1993): Permian and Triassic paleomagnetism of the southwestern Tien Shan: timing and mode of tectonic rotations. – Earth & Planetary Science Letters 118: 195-212.

[3] Chang, I., Im, J., Prasidhi, A. K., Cho, G. C. (2015): Effects of Xanthan gum biopolymer on soil strengthening. – Construction & Building Materials 74: 65-72.

[4] Drzymala, S. (2000): Comparison of soil texture classification according to the new Polish Standard, PTG and international classifications [FAO and USDA]. – Acta Agrophysica 35: 49-53.

[5] Han, J., Xie, J., Zhang, Y. (2012): Potential role of feldspathic sandstone as a natural water retaining agent in Mu Us Sandy Land, Northwest China. – Chinese Geographical Science 22: 550-555.

[6] Jiang, M., Zhang, F., Hu, H., Cui, Y., Peng, J. (2014): Structural characterization of natural loess and remolded loess under triaxial tests. – Engineering Geology 181: 249-260.

[7] Li, C., Wang, L., Zhang, T., Yang, D., Song, L. (2016): Preparation of geopolymer materials by Pisha sandstone. – Journal of Building Materials 19: 373-378.

http://www.aloki.hu ● ISSN 1589 1623 (Print) ● ISSN 1785 0037 (Online)
DOI: http://dx.doi.org/10.15666/aeer/1705_1059910610

[8] Lin, B., Cerato, A. B. (2014): Applications of SEM and ESEM in Microstructural Investigation of Shale-Weathered Expansive Soils along Swelling-Shrinkage Cycles. – Engineering Geology 177: 66-74.
[9] Martin, J. P., Martin, W. P., Page, J. B., Raney, W. A., Ment, J. D. D. (1955): Soil Aggregation. – Advances in Agronomy 7: 1-37.
[10] Martin, M. W., Jorge, C. R., Constantino, M. M. (1999): Late Paleozoic to Early Jurassic tectonic development of the high Andean Principal Cordillera, El Indio Region, Chile (29–30°S). – Journal of South American Earth Sciences 12: 33-49.
[11] Montes-H, G., Geraud, Y., Duplay, J., Reuschlé, T. (2005): ESEM observations of compacted bentonite submitted to hydration/dehydration conditions. – Colloids & Surfaces A Physicochemical & Engineering Aspects 262: 14-22.
[12] Ramamurthy, N., Kannan, S. (2009): SEM-EDS analysis of soil and plant (Calotropis gigantea Linn) collected from an industrial village, Cuddalore DT, Tamil Nadu, India. – Romanian Journal of Biophysics 19: 219-226.
[13] Romero, E. (2013): A microstructural insight into compacted clayey soils and their hydraulic properties. – Engineering Geology 165: 3-19.
[14] Sayen, S., Mallet, J., Guillon, E. (2009): Aging effect on the copper sorption on a vineyard soil: column studies and SEM-EDS analysis. – Journal of Colloid & Interface Science 331: 47.
[15] Tisdall, J. M., Oades, J. M. (1980): The effect of crop rotation on aggregation in a red-brown earth. – Australian Journal of Soil Research 18: 423-433.
[16] Wang, N., Xie, J., Han, J. (2013): A Sand Control and Development Model in Sandy Land Based on Mixed Experiments of Arsenic Sandstone and Sand: A Case Study in Mu Us Sandy Land in China. – Chinese Geographical Science 23: 700-707.
[17] Wang, N., Xie, J., Han, J., Luo, L. (2014): A comprehensive framework on land-water resources development in Mu Us Sandy Land. – Land Use Policy 40: 69-73.
[18] Wang, H., Han, J., Tong, W., Cheng, J., Zhang, H. (2016): Analysis of water and nitrogen use efficiency for maize (Zea mays L.) grown on soft rock and sand compound soil. – Journal of the Science of Food & Agriculture. doi: 10.1002/jsfa.8075.
[19] Yang, F. S., Cao, M. M., Li, H. E., Wang, X. H., Bi, C. F. (2014): Ecological restoration and soil improvement performance of the seabuckthorn flexible dam in the Pisha Sandstone area of Northwestern China. – Solid Earth Discussions 6: 2803-2842.
[20] Zhang, K., Xu, M., Wang, Z. (2009a): Study on reforestation with seabuckthorn in the Pisha Sandstone area. – Journal of Hydro-environment Research 3: 77-84.
[21] Zhang, K., Xu, M., Wang, Z., Duan, X., Bi, C. (2009b): Ecological impacts of seabuckthorn in the Pisha Sandstone area. Advances in Water Resources and Hydraulic Engineering. – Springer Berlin Heidelberg. doi: 10.1007/978-3-540-89465-0_193.
[22] Zhang, L., Han, J., Wang, H., Ma, Z. (2015): Grain size composition change after feldspathic sandstone and aeolian sandy soil compounding. – Science of Soil and Water Conservation 13: 44-49.
[23] Zhu, D., Han, J., Wang, H. (2017): The remediation method of sandy land in the feldspathic sandstone area-a review. – Carpathian Journal of Earth and Environmental Sciences 12: 49-60.

http://www.aloki.hu ● ISSN 1589 1623 (Print) ● ISSN 1785 0037 (Online)
DOI: http://dx.doi.org/10.15666/aeer/1705_1059910610

RESEARCH PROGRESS OF SOURCE AND MECHANISM OF AGRICULTURAL NON-POINT SOURCE POLLUTION IN CHINA

SHOU, C. G. – DU, H. S.* – LIU, X. P.

College of Tourism and Geographical Science, Jilin Normal University
NO.1301, Haifeng Street, Siping 136000, China
(phone: +86-185-4349-9109; fax: +86-434-329-2077)

**Corresponding author*
e-mail: duhs@163.com; phone: +86-151-4466-1359; fax: +86-434-329-2077

(Received 1st Mar 2019; accepted 21st May 2019)

Abstract. Agricultural non-point source pollution of aquifer, lake, riverbank and other ecosystems is caused by chemical fertilizer, pesticide, animal manure and other organic or inorganic pollutants through surface runoff and farmland leaching in agricultural production. The non-point source pollution has the characteristics of wide distribution, concealment, randomness, hysteresis and complex formation mechanism, and thus it is difficult to study and control this type of pollution. Understanding the mechanism of agricultural non-point source pollution and comprehensively being aware of the pollution sources are of great theoretical and practical significance for future research. In this paper, the mechanism of agricultural non-point source pollution was analysed in terms of rainfall and runoff process, soil erosion process, pollutant migration and transformation, and so on. In addition, the sources and sinks of nitrogen, livestock and poultry pollutants, pesticides, plastic film and other pollution sources were discussed, and the results could be informative for the formulation of agricultural sustainable development policies.
Keywords: *non-point source pollutants, agricultural runoff, livestock and poultry raising, pesticide pollution, contaminant transport, geographic information system*

Introduction

With the continuous strengthening of human economic activities, water environmental pollution has become a global problem. According to the types of pollution, it is divided into point source and non - point source. Point source pollution has been effectively treated by controlling industrial wastewater and urban sewage, but the problem of non-point source pollution has not been effectively solved. Agricultural non-point source pollution is caused by the non-point-source pollutants including chemical fertilizers, pesticides, livestock and poultry manure, and farmland leachate, produced in agricultural production processes (Wang et al., 2007). In recent years, agricultural non-point source pollution has been worsened and drawn more attention. Agricultural non-point source pollution can lead to surface water eutrophication and groundwater pollution, threatening aquatic habitats. Hence, it has been regarded as one of the main pollution sources of surface water and groundwater (Ma et al., 2003). Compared to point source pollution, non-point source pollution has a wider space-time range, greater uncertainty and affected by many factors such as geographical conditions, climate conditions, soil structures and vegetation coverage, thus increasing the difficulty of research, decontamination and management (Pei et al., 2010; Babin et al., 2016). At present, many scholars have studied on the agricultural non-point source pollution, and governments have also been involved in the management and abatement of agricultural non-point source pollution.

http://www.aloki.hu ● ISSN 1589 1623 (Print) ● ISSN 1785 0037 (Online)
DOI: http://dx.doi.org/10.15666/aeer/1705_1061110621

At present, the pollution composition is rapidly transformed in China (Chen et al., 2004). Especially, the excessive application of nitrogen and phosphorus fertilizers in China rural area has caused serious environmental problems. Because Livestock-poultry farming and domestic sewage was not centralized and treated, a large amount of manure was directly disposed of into the water body through surface runoff generated by rainstorm. Consequently, the problem of agricultural non-point source pollution in a watershed was aggravated. In this paper, pollutant sources and process and mechanism on non-point source pollution were reviewed and the information obtained could be beneficial for the formulation of agricultural sustainable development policies in China.

Sources of pollutants

Sources and sinks of nitrogen

In order to comprehensively understand the current situation of total nitrogen pollution in the water source area of the Middle Route Project of the South to North Water Diversion and effectively grasp the sources of pollution and formulate systematic countermeasures, Xin and Xu (2018) carried out the field monitoring and data collections of 7 reservoir sections, 16 reservoir tributaries and 62 typical reservoir bays in Danjiangkou Reservoir area. The environmental issues resulting from nitrogen have been extensively studied (Jacobsen et al., 2016; Walters et al., 2017), but most of the studies only focused on a specific problem, and rarely conducted comprehensive studies on the various links of nitrogen cycles in watersheds (Rowe et al., 2016). Therefore, the understanding of the nitrogen cycles in watersheds is usually one-sided and not qualified to provide scientific information for the decision-making of environmental management in the watersheds (*Table 1*).

Table 1. *China's pesticide application and main grain production from 2010 to 2016 (10^4t)*

Item	2010	2011	2012	2013	2014	2015	2016
Pesticide	175	179	181	180	181	179	175
Staple food	54648	57121	58958	60194	60703	62144	61625

Sha et al. (2018) carried out model analysis on the characteristics of the load flux and source composition of the total nitrogen pollutants in the water body, employed The regional nutrient management model (ReNuMa) to model the total nitrogen source apportionments of Lianjiang River and estimate the future pollution fluxes and contribution proportion under changed climate conditions, which were further compared to current status to estimate the response of watershed non-point source pollution to climate change. To date, the research on the deposition of atmospheric nitrogen has not been sufficiently done in China. Thus, the basic data are insufficient, and the research methods and technologies are still developing. At present, merely scattered data of rainwater nitrogen contents in China have been reported, and the quantitative studies on the dry and wet deposition intensities, space-time distribution and the sources of atmospheric nitrogen at watershed scales have not been documented (Singh and Pandey, 2018). Collected surface water samples from Guanzhong area, Shanxi, in the Weihe River Basin so as to prevent and control the nitrate nitrogen (NO_3^- - N) pollution of the surface water in the watershed. For this purpose, Zhang et al. (2018) have done the

http://www.aloki.hu ● ISSN 1589 1623 (Print) ● ISSN 1785 0037 (Online)
DOI: http://dx.doi.org/10.15666/aeer/1705_1061110621

hydrochemical assessment and nitrogen isotopic measurement to determine the pollution levels of nitrate by identifying its main pollution sources on the water surface. Limited by experimental conditions, the applications of stable nitrogen isotopes in the identification of atmospheric nitrogen deposition and nitrogen sources of surface water were rarely attempted in China (Xiao and Liu, 2002).

Livestock and poultry breeding pollutants

After the reform and opening in China, the livestock and poultry breeding industry in China has been developed rapidly (Qian et al., 2018), but some of the farms possessed poor equipment and bad management, resulting in pollution problems because of livestock and poultry waste (Huang et al., 2006). China began to recognize the harm of livestock and poultry waste to environment in 1990s (Wang et al., 2017a). However, the research on this kind of pollution was still developing in China. Ji et al. (2017) took the total nitrogen emission from livestock and poultry breeding in the Zhexi Reservoir Basin as the research object, calculated the water environment capacity and the total nitrogen pollutant emission load of livestock and poultry breeding on the small watershed scale, and determined the response relationship between the environment capacity of the river basin and the total nitrogen emission of the livestock and poultry according to the pollutant discharge contribution rates of different industries. Wang et al. (2017b) conducted hotspot analyses for total and respective livestock numbers in China for the years 1992, 2002, and 2012. Based on these analyses, the main livestock pollutants of the hot spot provinces were estimated using the discharge coefficient method. In order to characterize the spatial distribution of non-point source pollution in the Yanghe Reservoir watershed, based on land use, agricultural management, and other data, Chen et al. (2018) calculated the load of four pollutants (TN, TP, NH_3-N and COD). Pollutant sources included domestic wastewater, solid waste, livestock and poultry breeding, chemical fertilizer loss, soil erosion and urban runoff. The spatial distribution of sources was analyzed using ArcGIS. In practice, the rapid development of livestock and poultry breeding in China has significantly affected the regional environmental quality (Xu et al., 2018), and the surface water and groundwater in certain regions have been largely polluted. Due to the lack of understanding of the various loss routes of livestock and poultry breeding waste and the quantitative migration rules of nutritional elements, the environmental pollution issues ascribed to livestock and poultry breeding have not been quantitatively studied, which affects the development of livestock and poultry pollution management regulations.

Pesticides pollution

Excessive unreasonable application of pesticides causes pollution (Vryzas, 2018; Yang et al., 2018). According to the literatures, more than 84% of peasants applied pesticides in excess of the standards (Li and Yin, 2001). As a result, highly toxic and highly persistent pesticides would be discharged into the environment, polluting crops, soil, atmosphere and water (Yang et al., 2009). The excessive application leads to the majority of pesticides were discharged into the soil and atmosphere (Lai, 2017). Hu et al. (2016) collected rice and soil samples from 11 counties and cities around Poyang Lake according to the pollution status of organic chlorine pesticides (OCPS) pollution in rice and soil in the area around Poyang Lake, and used Gas chromatograph - electron capture detector (GC-ECD) technology to determine organo chlorine residue. The OCPs from the rice samples were evaluated with the health risk assessment model. With the

http://www.aloki.hu ● ISSN 1589 1623 (Print) ● ISSN 1785 0037 (Online)
DOI: http://dx.doi.org/10.15666/aeer/1705_1061110621

aim of ecological restoration for surface water that suffered from pesticides and domestic waste water pollution in a agricultural village, Jin et al. (2017) established a Vallisneria natans and Hydrilla verticillata demonstration area in August 2015, and evaluated the effect of submerged vegetation restoration on the control of seven pesticides, the recovery of macrozoobenthos and the reduction of conventional water quality indicators. At present, the relative research in China mainly focused on the highly persistent organ chlorine pesticides (Yuan et al., 2003; Kang et al., 2003). Because of their persistence, the pollution effect of organochlorine pesticides residues on the soil in China will last for a long time. In addition, at present, the research on widespread and highly toxic organophosphorus pesticides (Wu et al., 2018; Chahkandi et al., 2019) focused on the development of detection methodology and analysis of the residues over vegetables, fruits and crops (Wan et al., 2004; Yang et al., 2004).

White pollution

Since the 1980s, agricultural film mulching technology has been widely applied. This technology has brought economic benefits but caused serious environmental problems (Yang et al., 2009). The agricultural film has remarkable effects in resisting natural disasters, expanding planting area of crops and increasing yields. Meanwhile, the plastic residues harm the environment and soil (Yan et al., 2006). A large amount of residual agricultural film was dispersed in soil and could not be degraded, which not only reduced the permeability, water content, and drought resistance of farmlands, but also seriously affected the growth of plant roots and water-fertilizer transport, resulting in the reduction of crops yields (Hu and Zhang, 2003). To date, the number and distribution of agricultural film residues in local regions and the harm to soil and crops growth have been extensively studied, but long-term, systematic and large-scale follow-up studies and observation experiments are still insufficient.

Mechanism study

Surface runoff

The runoff formed by rainfall is a carrier for non-point source pollutants migration and transformation (Ma, 2019). Thus, the characteristics of runoff generation and confluence as a response to rainstorm events were usually investigated from the points of view of hydrology and hydrodynamics. At the beginning, a typical SCS-CN model (Soil Conservation Service-Curve Number, USDA-SCS, 1972) was usually adopted in the research on non-point source pollution. Afterwards, Lutz revised the SCS method by taking the soil moisture conditions (such as basic flow factor) in the early stage into account, which renders the Lutz method more accurate in the simulation of hydrological parameters. During the same period, a number of watershed hydrological models were also developed (Villamizar and Brown, 2016), such as the Stanford Watershed Model (SWM) (Crawford, 1996). In the early 1960s, the excess storage, excess infiltration and integrated runoff generation theories were proposed in China (Hu and Lu, 2019). These theories have been gradually applied in the studies on the non-point source pollution. In addition, in view of the small number of non-point source pollution monitoring data in China, Li (2000) proposed a simple and practical average-concentration algorithm for estimating the non-point source pollution load in watersheds based on the formation process of pollution. Liang et al. (2005) used a small-scale artificial rainfall simulator to

http://www.aloki.hu ● ISSN 1589 1623 (Print) ● ISSN 1785 0037 (Online)
DOI: http://dx.doi.org/10.15666/aeer/1705_1061110621

launch natural heavy rain experiments in four typical land-use types around the Guanting Reservoir. On the basis of the experiments, the migration process of nitrogen and phosphorus along with rainstorm runoff and runoff sediments was studied, and the loss rates of total nitrogen and total phosphorus in different land-use types were also estimated. In order to investigate effects of under different vegetation coverage (0%, 15%, 30%, 45%, 60%, 75%, 90%), slope lengths (3 m, 4 m, 5 m) and fertilizer treatments (control (CK) and compound N-P-K fertilizer (CF)) on runoff producing processes and nitrogen loss, Wu et al. (2019) conducted an artificial simulated rainfall experiment.

Soil erosion

Soil erosion issue is common in the world, and it affects the production and livings of people (Yuan et al., 2019). Soil erosion is one of the primary forms of agricultural non-point source pollution (Zhang et al., 2019). In the late 1960s, the Universal Soil Loss Equation (USLE) was prevalent in the simulation and estimation of long-term average soil loss in the erosion processes of slope lands (Wischmeier and Smith, 1978). Huang et al. (2003) predicted the non-point source pollution load discharged into the Yahekou reservoir using the USLE equation, which taking six factors of rainfall, soil erodibility, slope length, slope, and crop and management measures into account. This model was continuously revised and extended until a Revised Universal Soil Loss Equation (RUSLE) model (Daniel et al., 1994) was developed. Wang (2006) adopted the RUSLE equation and SCS hydrological model to estimate the nitrogen and phosphorus pollution loads in the Chaohu Lake Watershed. Zhou et al. (2015) systematically evaluated and analyzed the risks of agricultural non-point source pollution in the Ashi River Watershed based on a modified universal soil loss equation (MUSLE) model. In the early 1980s, a WEPP (Water Erosion Prediction Project) model was proposed to study the mechanism of soil erosion. On the basis of the meteorological data and soil erosion moduli of field runoff plots in Huajiang demonstration area in 2006 and 2010, Long et al. (2014) estimated the annual average soil erosion moduli at different rocky desertification levels, and evaluated the applicability of the WEEP model in Karst rocky desertification area. Likewise, on the basis of the meteorological data and monitoring data of field runoff plots in an experimental station in Binxian County, Heilongjiang Province in 2008, Liu et al. (2010) estimated the secondary rainfall runoff and soil loss in the black soil area of Northeast China using the WEPP model, and evaluated the applicability of WEPP model by comparing with the measured data. Wang et al. (2019) selected seven sub-basins of the Chaohu Basin as the target area, established a sediment delivery distribution model to quantitatively estimate the particulate phosphorus loading modules (PPLM) of the Chaohu Basin in 2015 and determined the differences in the loss of particulate phosphorus and their causes under different land use patterns.

Migration and transformation of pollutants

The migration of non-point source pollutants refers to the process of non-point source pollutants diffusing from the soil circle to other circles (Lu and Xie, 2018), especially the hydrosphere, under the action of external forces (rainfall, irrigation, etc.). Some of the agricultural non-point source pollutants were discharged into ditch wetland systems along with field drainage. After the interception and reduction by the ditch wetland systems, the residual pollutants were eventually discharged into rivers, lakes

http://www.aloki.hu ● ISSN 1589 1623 (Print) ● ISSN 1785 0037 (Online)
DOI: http://dx.doi.org/10.15666/aeer/1705_1061110621

and other water bodies (Wei et al., 2016), causing pollution to the surface water environment (Chen, 2000). A series of studies have been launched on the relationships between nitrogen and phosphorus loss due to farmland rainfall runoff and farmland tillage patterns, crops growth seasons, rainfall characteristics, land utilization, topographic conditions and vegetation cover (Hong et al., 2007). Liu et al. (1988) investigated the non-point source pollution in the Yuqiao Reservoir Watershed of Tianjin City and the results showed that vegetation was a key factor restricting the spatial variability of non-point source pollution (*Figure 1*).

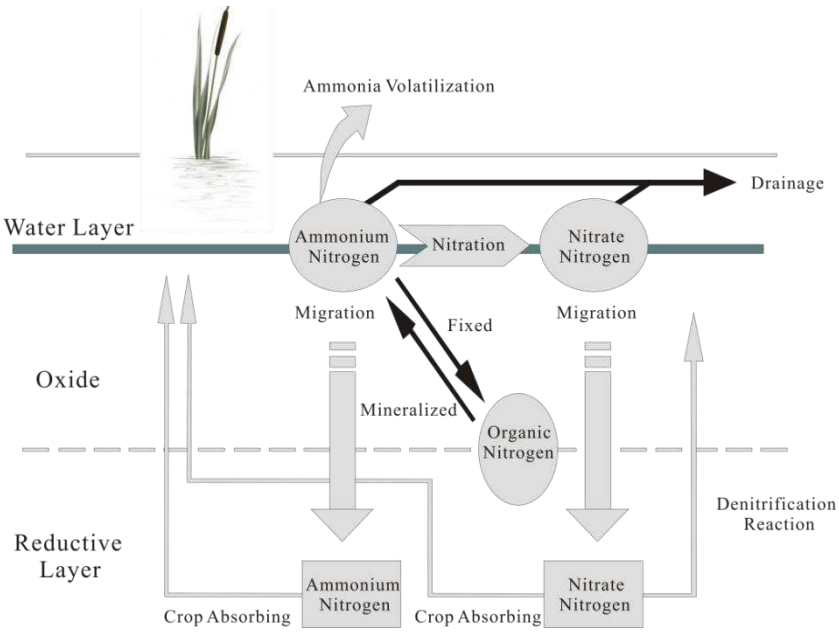

Figure 1. *Conversion of ammonium and nitrate nitrogen*

Shen et al. (2014) conducted a simulated experiment to determine the interception effectiveness of runoff, sediment, nitrogen, and phosphorus by artificial grass-like Vegetative filter strips (VFS) with different widths. The results indicate that grass VFS are very effective in reducing runoff, sediment, nitrogen, and phosphorus and controlling agricultural non-point source pollution. Kang et al. (2018) investigated and analysed the characteristics of application and surface runoff loss of nitrogen and phosphorus fertilizers in nine cities of Fujian Province during the years of 1985 to 2016. Additionally, they analysed the risk grades of farmlands pollution due to nitrogen and phosphorus fertilizers considering nitrogen and phosphorus fertilizers runoff loss, rainfall and river network density. At the same time, the spatial distribution characteristics of nitrogen and phosphorus contaminated regions were presented through the geographic information system (GIS) analysis. Li et al. (2017) divided paddy field water into surface and subsurface waters. The leaching of surface water and the dissolved solute NH_4^+, NO_3^- and PO_4^{3-} within it were calculated using water-balance method. Water in the soil was simulated numerically from transient flow equation, from which Li et al. (2017) calculated the discharge rate to drainage ditch. Water flow in the drainage network was simulated using the wave equation and the biochemical reaction of the solutes was described by first-order kinetics.

http://www.aloki.hu ● ISSN 1589 1623 (Print) ● ISSN 1785 0037 (Online)
DOI: http://dx.doi.org/10.15666/aeer/1705_1061110621

Conclusions and prospects

The mechanism of non-point source pollution was discussed in terms of rainfall and runoff processes, soil erosion process and pollutants migration and transformation processes in this paper. In addition, the non-point-source pollutant sources were analysed in terms of nitrogen sources and sinks, livestock and poultry breeding pollution, chemical fertilizer and pesticide pollution, and white pollution.

The future research should embark on the following: First, the basic monitoring should be enhanced because the agricultural non-point source pollution research should not be separated from field tests and monitoring data. Therefore, the field test, monitoring and management are required to be reinforced, and the correlations between the database of different regions and different watersheds should be increased. Secondly, the pollution research models suitable for China's situations should be established; the agricultural non-point source pollution research models suitable for China's different regions should be established; the agricultural non-point source pollution research in regions without data or with data difficult to derive should be done. Thirdly, the cross-research between related subjects and related fields should be conducted; the agricultural non-point source pollution research should be closely related with geography, ecology, economics, management and other disciplines.

Agricultural non-point source pollution control and management will be a long-term and gradual process, and we can make efforts in the following aspects. First, the simple and cheap alternative technology is the key to the control of agricultural non-point source pollution. Finding alternative economic, simple and feasible technical system to control agricultural non-point source pollution, establishing causality between economic behavior and pollution hazard is the basis of formulating control policy. Second, the promotion and demonstration project operation management mechanism.These include the construction of agricultural non-point source pollution control demonstration area, the formulation of agricultural non-point source pollution control project long-term management mechanism, the establishment of long-term supervision institutions and strengthening the construction of farmers' professional organizations. Third, there should be different management policies for different pollution sources. For example, the use of chemical fertilizers and pesticides can be controlled by levying taxes, subsidizing agricultural environmental policies and insuring against risks. Fourth, we should promote modern agricultural technologies, raise the level of agricultural production, implement multi-dimensional innovation, and comprehensively promote the prevention and control of agricultural non-point source pollution.

The mechanisms of agricultural non-point source pollution have been greatly developed. The relationships between the pollution and sustainable development of agriculture as well as the negative influences of the pollution on ecological environment and human health have been well agreed. The relative results have effectively promoted people's understanding of the serious environmental consequences of agricultural non-point source pollution.

Acknowledgements. The study was supported by the National Key Research and Development Program of China (2018YFD0300204).

http://www.aloki.hu ● ISSN 1589 1623 (Print) ● ISSN 1785 0037 (Online)
DOI: http://dx.doi.org/10.15666/aeer/1705_1061110621

REFERENCES

[1] Babin, N., Mullendore, N., Prokopy, L. (2016): Using social criteria to select watersheds for non-point source agricultural pollution abatement projects. – Land Use Policy 55: 327-333.
[2] Chahkandi, M., Amiri, A., Arami, S. R. S. (2019): Extraction and preconcentration of organophosphorus pesticides from water samples and fruit juices utilizing hydroxyapatite/Fe_3O_4 nanocomposite. – Microchemical Journal 144: 261-269.
[3] Chen, J. N., Li, G. H., Wang, H. T. (2004): Research on area source pollution controlling technology for the Dianchi Lake. – China Water Resources 9: 47-50.
[4] Chen, P., Fu, C. F., Ji, X. G. (2018): Spatial distribution characteristics of non-point source pollution load in yanghe reservoir basin. – Journal of Hydroecology 39(06): 58-64.
[5] Cheng, Q. G. (2000): Influence of non–point source pollutants on environment and trend analysis. – Environmental Protection and Re-Cycling Economy 5: 4-6.
[6] Crawford, N. H. (1966): Digital Simulation in Hydrology: Stanford Watershed Model IV. – Evapotranspiration 39.
[7] Daniel, T. C., Sharpley, A. N., Edwards, D. R., Wedepohl, R., Lemunyon, J. L. (1994): Minimizing surface water eutrophication from agriculture by phosphorus management. – Journal of Soil and Water Conservation 49(2): 30-38.
[8] Hong, H. S., Zhang, Y. Z., Cao, Z. W. (2007): Study on non-point source pollution in the Wuchun catchment of Jiulong River. – Beijing: Science Press 2007.
[9] Hu, Y., Zhang, H. J. (2003): Research progress of calculation and control of non- point source pollution. – Journal of Anhui Agricultural Sciences 31(5): 788-790.
[10] Hu, C. H., Chen, L. L., Li, Y. H. (2016): Pollution of paddy rice and soil organochlorine pesticides and health risk assessment in poyang lake area. – Environmental Chemistry 35(02): 355-363.
[11] Hu, J. H., Lu, J. (2019): Landscape patterns regulate non-point source nutrient pollution in an agricultural watershed. – Science of the Total Environment 669.
[12] Huang, J. H., Li, Q., Tian, K. (2003): Prediction of non-point pollution load for Yahekou Reservoir. – Water Resources Protection 19(2): 28-30.
[13] Huang, J. J., Lin, C. W., Chen, Y. B., Zhang, Q. Y. (2006): Actualities and counter measures of non-point pollution of agriculture in China. – Anhui Agricultural Science Bulletin (12): 47-48.
[14] Jacobsen, B. H., Hansen, A. L. (2016): Economic gains from targeted measures related to non-point pollution in agriculture based on detailed nitrate reduction maps. – Science of the Total Environment 556: 264-75.
[15] Ji, Z. B., Wang, W. J., Liu, X. F., Xu, C., Wang, Y., Bai, Y., Qiu, W. T., Luo, L. (2017): Design of discharge permit system of livestock and poultry breeding: a case study in Zhexi Reservoir Basin. – Journal of Environmental Engineering Technology 7(05): 621-628.
[16] Jin, C. C., Yang, Y., Liu, S. L. (2017): Ecological restoration of pesticides pollution in rural waste water. – Ecology and Environment 26(01): 142-148.
[17] Kang, Y. H., Liu, P. B., Wang, Z. J., Lv, Y. B., Li, Q. J. (2003): Persistent organochlorinated pesticides in water from Guanting Reservoir and Yongdinghe River, Beijing. – Journal of Lake Sciences 15(2): 125-132.
[18] Kang, Z. M., Zhang, R. X., Ye, Y. Z. (2018): Pollution risk assessment of nitrogen and phosphorus loss in surface runoff from farmland fertilizer in Fujian Province based on GIS. – Chinese Journal of Eco-Agriculture.
[19] Lai, W. Y. (2017): Pesticide Use and Health Outcomes: Evidence from Agricultural Water Pollution in China. – Journal of Environmental Economics and Management S0095069617303169.
[20] Li, H. E. (2000): Mean concentration method for estimation non-point source pollution load and its application. – Acta Scientiae Circumstantiae 20(4): 397-400.

http://www.aloki.hu ● ISSN 1589 1623 (Print) ● ISSN 1785 0037 (Online)
DOI: http://dx.doi.org/10.15666/aeer/1705_1061110621

[21] Li, B. G., Yin, C. Q. (2001): Water environment problems and control measures of 3-lakes in China. – Water Issues Forum (3): 36-39.
[22] Li, Y. Q., Zhang, C., Zhang, W. X. (2017): Simulating the transport and transformation of non-point contaminants in paddy field within an irrigated district 36(11): 29-35.
[23] Liang, T., Wang, H. P., Zhang, X. M. (2005): Simulation study of non-point source pollution under different land use in Guanting Reservoir watershed. – Acta Scientiae Circumstantiae 25(4): 483-490.
[24] Liu, F., Wang, H. D., Liu, P. T. (1988): The quantitative identification of non-point source pollution and its application in Yuqiao reservoir watershed. – Acta Geographica Sinica (4): 329-340.
[25] Liu, Y. L., Zheng, F. L., Wang, B., Wang, Y. X., Xie, Y. J., Fan, H. (2010): Assessment of WEPP model applicability in black soil zone of Northeast China-- A case study of slope gradient and soil and water conservation measures. – Bulletin of Soil and Water Conservation 30(1): 139-145.
[26] Long, M. Z., Wu, K. H., Xiong, K. N. (2014): Assessment of the applicability of the WEPP model (Hillslope Version) for soil erosion in karst rock desertification area, Guizhou Province. – Carsologica Sinica 33(2): 201-207.
[27] Lu, H., Xie, H. L. (2018): Impact of changes in labor resources and transfers of land use rights on agricultural non-point source pollution in Jiangsu Province, China. – Journal of Environmental Management 207.
[28] Ma, W. C., Chen, L. M., Li, J. Z. (2003): Progress in the research of non-point source pollution models of aquatic environment. – Advances in Earth Science 18(3): 358-366.
[29] Ma, H. (2019): Runoff simulation of agricultural non-point source pollution model in liaohe river basin. – Heilongjiang Science and Technology of Water Conservancy 2: 22-26.
[30] Pei, L., Wang, L. M., Yu, G. Q. (2010): Status of study on agricultural non-point source pollution and new progress of its application. – Water Resources and Hydropower Engineering 41(12): 58-61.
[31] Qian, Y., Song, K., Hu, T., Ying, T. (2018): Environmental status of livestock and poultry sectors in China under current transformation stage. – Science of The Total Environment 622-623: 702-709.
[32] Rowe, E. C., Jones, L., Dise, N. B., Evans, C. D., Mills, G., Hall, J., Stevens, C. J., Mitchell, R. J., Field, C., Caporn, S. J. M., Helliwell, R. C., Britton, A. J., Sutton, M. A., Payne, R. J., Vieno, M., Dore, A. J., Emmett, B. A. (2016): Metrics for evaluating the ecological benefits of decreased nitrogen deposition. – Biological Conservation S0006320716308552.
[33] Sha, J., Lu, R., Xu, Y. X. (2018): Estimation of watershed non-point source pollution response toward climate change: a coupled modeling approach. – Environmental Science and Technology 41(06): 181-187.
[34] Shen, X. B., Chen, C. S., Zhang, Z., Sun, X. T., Xiao, B. (2014): Interception of runoff, sediment, nitrogen and phosphorus by vegetative filter strips with different width in a simulated experiment. – Journal of Agro-environmental Science 33(04): 721-729.
[35] Singh, R., Pandey, J. (2018): Non-point source-driven carbon and nutrient loading to Ganga River (India). – Chemistry and Ecology 1-17.
[36] Villamizar, M. L., Brown, C. D. (2016): Modelling triazines in the valley of the River Cauca, Colombia, using the annualized agricultural non-point source pollution model. – Agricultural Water Management 177.
[37] Vryzas, Z. (2018): Pesticide fate in soil-sediment-water environment in relation to contamination preventing actions. – Current Opinion in Environmental Science and Health 5-9.
[38] Walters, C. G., Shumway, C. R., Huggins, D. R. (2017): Impacts of terrain attributes on economics and the environment: costs of reducing potential nitrogen pollution in wheat production. – Agricultural Economics 48(2): 143-152.

http://www.aloki.hu ● ISSN 1589 1623 (Print) ● ISSN 1785 0037 (Online)
DOI: http://dx.doi.org/10.15666/aeer/1705_1061110621

[39] Wan, Y. Q., Chen, Y. Q., Zhan, C. R. (2004): Determination of multi-organophosphorous pesticide residuals in sesame seeds by capillary gas chromatography. – Chinese Journal of Analysis Laboratory 23(7): 10-12.
[40] Wang, X. H. (2006): Study on non-point source pollution of Nitrogen and Phosphorus drainage evaluating and it's controlling on in ChaoHu watershed. – Hefei: Hefei University of Technology. (in Chinese).
[41] Wang, Z. M., Zhang, B., Song, K. S., Liu, D. W., Yan, B. X., Hu, L. J., Yang, H. J., Xu, J. P., Yang, F., Duan, H. T. (2007): Domestic and overseas advances of nonpoint source pollution studies. – Chinese Agricultural Science Bulletin 23(9): 68-68.
[42] Wang, H., Xu, J., Liu, X., Sheng, L., Zhang, D., Li, L., Wang, A. (2017a): Study on the pollution status and control measures for the livestock and poultry breeding industry in northeastern China. – Environmental Science and Pollution Research 4435-4445.
[43] Wang, J. X., Xu, F., Liu, R. M. (2017b): Analysis of spatial hot spots of total livestock and poultry production in China and calculation of major pollutants. – Journal of Agro-Environment Science 36(07): 1316-1322.
[44] Wang, Z. F., Lin, C., Xu, J. D., Jin, P. H., Xiong, J. F., Min, M., Ma, R. H. (2019): Spatial differences in non-point source particle phosphorus loads and critical influence factors in the Chaohu Basin. – Journal of agro-environmental sciences 38(03): 659-670.
[45] Wei, O. Y., Wei, J., Li, X. M., Giubilato, E., Critto, A. (2016): Long-term agricultural non-point source pollution loading dynamics and correlation with outlet sediment geochemistry. – Journal of Hydrology 540: 379-385.
[46] Wischmeier, W. H., Smith, D. D. (1978): Predicting rainfall erosion losses - a guide to conservation planning. – Agric Handbook 537.
[47] Wu, P., Zhang, Y., Chen, Z., Wang, Y. L., Zhu, F. F., Cao, B., Wu, Y., Li, N. (2018): The organophosphorus pesticides in soil was degradated by Rhodobacter sphaeroides after wastewater treatment. – Biochemical Engineering Journal 141.
[48] Wu, Y. H., Zhang, L. P., Qian, J. (2019): Research on multi-factor effect of nitrogen loss in slope runoff. – Journal of Natural Disasters 28(01): 44-53.
[49] Xiao, H. Y., Liu, C. Q. (2002): Sources of nitrogen and sulfur in wet deposition at Guiyang, southwest China. – Atmospheric Environment 36(33): 5121-5130.
[50] Xin, X. K., Xu, J. F. (2008): Countermeasures for total nitrogen pollution control in water source area of middle route project of south to north water diversion. – Yangtze river 49(15): 7-12.
[51] Xu, P. C., Zhou, X., Xu, D. F., Xiang, Y. B., Ling, W. T., Chen, M. D. (2018): Contamination and Risk Assessment of Estrogens in Livestock Manure: A Case Study in Jiangsu Province, China. – International Journal of Environmental Research and Public Health 15(1): 125-127.
[52] Yan, C. R., Mei, X. R., He, W., Zheng, S. (2006): Present situation of residue pollution of mulching plastic film and controlling measures. – Transactions of the Chinese Society of Agricultural Engineering 22(11): 269-272.
[53] Yang, J. L., Liu, L. P., Li, L. (2004): Simultaneous determination of organophosphorus pesticide in vegetables with chromatography. – Journal of Environment and Health 21(4): 251-252.
[54] Yang, S. J., Zhang, A. P., Yang, S. Q., Yang, Z. L. (2009): Status analysis of agricultural non-point source pollution and advances in domestic and overseas. – Chinese Journal of Agrometeorology 30(s1): 82-85.
[55] Yang, F. Y., He, Q., Chen, Y. Q. (2018): Evaluation of pesticide contamination and edible risk in enteromorpha entire body in subei shoal of southern yellow sea. – Journal of agricultural and environmental sciences 37(06): 1108-1116.
[56] Yuan, X., Wang, Y., Chen, J., Sun, C., Xu, N. (2003): Organochlorine residues of sediments in Taihu Lake and its risk evaluation. – Environmental Science 24(1): 121-125.

http://www.aloki.hu ● ISSN 1589 1623 (Print) ● ISSN 1785 0037 (Online)
DOI: http://dx.doi.org/10.15666/aeer/1705_1061110621

[57] Yuan, X. F., Han, J. C., Shao, Y. J., Li, Y. H., Wang, Y. S. (2019): Geodetection analysis of the driving forces and mechanisms of erosion in the hilly-gully region of northern Shaanxi Province. – Journal of Geographical Sciences 29(05): 779-790.
[58] Zhang, Y., Zhang, X., Bi, Z. L. (2018): Nitrate nitrogen pollution and source trace in the surface water of Guanzhong area, Shaanxi, in the Weihe River Basin. – Journal of Safety and Environment 18(06): 2395-2400.
[59] Zhang, T., Yang, Y. H., Ni, J. P., Xie, D. (2019): Adoption behavior of cleaner production techniques to control agricultural non-point source pollution: A case study in the Three Gorges Reservoir Area. – Journal of Cleaner Production 223: 897-906.
[60] Zhou, H., Lei, G. P., Feng, X. J. (2015): MUSLE -based risk evaluation of agricultural non -point source pollution in the Ash River watershed. – Research of Agricultural Modernization 36(3): 469-476.

http://www.aloki.hu ● ISSN 1589 1623 (Print) ● ISSN 1785 0037 (Online)
DOI: http://dx.doi.org/10.15666/aeer/1705_1061110621

MICROCYSTIN CHANGES AND PROTEOMIC RESPONSES OF *MICROCYSTIS AERUGINOSA* EXPOSED TO CADMIUM DURING COLONY FORMATION

BI, X. D.[1*] – DAI, W.[1*] – SUN, J. S.[2] – JIA, N.[3]

[1]*Key Laboratory of Aquatic-Ecology and Aquaculture of Tianjin, Department of Fisheries Sciences, Tianjin Agricultural University*
No. 22 Jinjing Road, Xiqing District, Tianjin 300384, China

[2]*Tianjin Key Laboratory of Animal and Plant Resistance, Tianjin Normal University*
No. 393 Binshui West Road, Xiqing District, Tianjin 300387, China
(phone: +86-022-2376-6539; fax: +86-022-2376-6000)

[3]*Key Laboratory of Systems Bioengineering (Ministry of Education), School of Chemical Engineering and Technology, Tianjin University*
No. 92 Weijin Road, Nankai District, Tianjin 300372, China
(phone: +86-022-2740-3902; fax: +86-022-2740-3902)

**Corresponding authors*
e-mail: yl80123@aliyun.com (X. D. Bi), daiweitj@126.com (W. Dai); phone: +86-022-2378-1299; fax: +86-022-2378-8970

(Received 1st Mar 2019; accepted 21st May 2019)

Abstract. *Microcystis* occurs as colonies in natural waters and always disaggregates into unicellular cells in the laboratory. Cadmium (Cd) could stimulate *Microcystis* colony formation in the laboratory. To elucidate the mechanism involved in cadmium-induced colony formation of *Microcystis*, microcystin (MC) changes and proteomic responses in *M. aeruginosa* treated with seven concentrations of Cd (0, 0.0125, 0.0250, 0.0500, 0.1000, 0.2000 and 0.4000 mg/L) for 40 h were studied. The results showed that seven concentrations of Cd except 0.4000 mg/L Cd could significantly induce colony formation ($P < 0.05$), and the Cd-induced colony-stimulating effects were accompanied with the increased intracellular MC-RR production. A total of 1170 proteins, including seven MC biosynthesis-related enzymes and seven polysaccharide biosynthesis-related enzymes, were identified using 2D-LC-MS/MS combined with isobaric tags for relative and absolute quantitation (iTRAQ). 0.4000 mg/L Cd could downregulate all the identified enzymes involved in MC and polysaccharide biosynthesis while most of these enzymes were upregulated during Cd-induced colony formation. Cd might stimulate *Microcystis* colony formation via increasing the biosynthesis of MC and polysaccharide.
Keywords: *cyanotoxin, polysaccharide, heavy metal ions, iTRAQ, Cyanobacteria colony*

Introduction

Cyanobacteria blooms have been paid more and more attention all over the world for their toxic impacts on freshwater environments and human health (O'Neil et al., 2012). *Microcystis* is a common cyanobacterial genus forming blooms (Shen and Song, 2007). In natural freshwaters, *Microcystis* cells always aggregate into colonies (Zhu et al., 2016). Colony formation provides *Microcystis* with a competitive advantage in preventing zooplankton grazing, viral and bacterial attack (Yang and Kong, 2012). However, the mechanism involved in *Microcystis* colony formation remains poorly understood.

In laboratory cultures, *Microcystis* is hard to keep colonial phenotype and colonial *Microcystis* usually disaggregates into single cells or a few paired cells (Huisman et al.,

http://www.aloki.hu ● ISSN 1589 1623 (Print) ● ISSN 1785 0037 (Online)
DOI: http://dx.doi.org/10.15666/aeer/1705_1062310636

2018). Previous studies have identified that zooplankton grazing pressure (Yang et al., 2012), ultraviolet radiation (Sommaruga et al., 2008), heterotrophic bacteria cocultivation (Shen et al., 2011), low light intensities and temperatures (Li et al., 2013) could stimulate colony formation of *Microcystis* cultured in the laboratory. Moreover, we found that the contents of lead (Pb), cadmium (Cd), chromium (Cr), aluminium (Al), ferrum (Fe), and manganese (Mn) in *Microcystis* cell were significantly positive with the colony size in natural freshwaters (Bi et al., 2015). Cd(II) could promote *Microcystis* colony formation in an appropriate concentration range (Bi et al., 2016). Moreover, Gan et al. (2012) found that microcystin (MC, a typical cyanotoxin), supplementation in medium could enhance the size of *Microcystis* colony and depletion of MC could dramatically decrease colony size. Different from above external biotic and abiotic environmental factors, MC released by toxic *Microcystis* might act as an internal signal factor influencing the aggregation of *Microcystis* cells.

Proteomics, the large-scale analysis of proteins, can link the upstream genome and the downstream metabolome (Wilmes and Bond, 2009). Proteomic analysis has been widely applied in reflecting functional protein dynamic responses of cyanobacteria under stress (Alexova et al., 2016). According to the proteomic responses of *M. aeruginosa* to N or P starvation, Yue et al. (2015) found that N limitation enhanced the expression of several proteins relating to cellular C metabolism and fixation while P limitation downregulated the proteins involved in protein synthesis and the assimilation of C and N. Proteomic response of *M. aeruginosa* revealed that long-term exposure of amoxicillin could affect the cellular biosynthesis process and the metabolism of nucleoside phosphate and carbohydrate (Liu et al., 2016).

To make clear how heavy metals affect colony formation of *Microcystis*, *M. aeruginosa* were treated with seven concentrations of Cd for 40 h, and their changes in the colony formation, intracellular MC contents and proteomic responses were investigated. The results will help us reveal the impact of heavy metals on the breakout of *Microcystis* blooms in natural waters.

Materials and methods

Algal culture conditions

M. aeruginosa FACHB-905 was purchased from the Institute of Hydrobiology, Chinese Academy of Sciences. Algae were cultured in BG11 medium (without EDTA) under a L:D (12 h: 12 h) cycle at a light intensity of 40 μmol/m^2/s at 25 °C. Stock solution of $CdCl_2$ (Merck, Germany) was added to algae cultured to the exponential phase, and the final concentrations of Cd were prepared as follows: 0.0125 (Cd_A), 0.0250 (Cd_B), 0.0500 (Cd_C), 0.1000 (Cd_D), 0.2000 (Cd_E) and 0.4000 mg/L (Cd_F). The culture without Cd was used as control group (CK). All groups were done in triplicate, and the initial density of *M. aeruginosa* was 5.2 $\times 10^6$ ind/L. After 40 h, samples were taken from algal cultures to study changes in cell densities, colony numbers, MC content and proteomic analysis.

Counting algal cell density and colony

Algal cell density and colony were counted using a hemocytometer under microscope. Samples were collected 1 cm below the medium surface, and the flasks

http://www.aloki.hu ● ISSN 1589 1623 (Print) ● ISSN 1785 0037 (Online)
DOI: http://dx.doi.org/10.15666/aeer/1705_1062310636

were shaken up slightly before sampling. Algal phenotype was classified as unicellular, two-cell aggregation and colony (aggregation of ≥ 3 cells).

Intracellular MC extraction and analysis

Intracellular MC was extracted and measured according to the method of Bi et al. (2017) using high-performance liquid chromatography (SPD-M20A, Shimadzu, Japan) equipped with a Shim-Pack VP-ODS column (250 mm × 4.6 mm). MC-RR was identified by its characteristic UV spectra and retention time, and spiked with purified standards of MC-RR (Sigma, USA).

Proteomic analysis

Sampling, proteins extraction and iTRAQ labeling

Samples were extracted with Lysis buffer (8 M Urea, 40 mM Tris-HCl or TEAB, pH 8.5) containing 2 mM EDTA and 1mM PMSF, and then added with 10 mM DTT after being kept on ice for 5 min, then were sonicated at 200 W for 1 min. After centrifugation (25000 g, 4 °C) for 20 min, the supernatants obtained were incubated at 56 °C for 1 h and cooled to room temperature, then incubated with 55 mM IAM (for alkylation) in darkness for 45 min, and then centrifuged (25000 g, 4 °C) for 20 min. Protein concentrations were quantified using Bradford method. The protein solution (100 μg) with 8 M urea was diluted 4 times with 100 mM TEAB. For iTRAQ analysis, proteins were digested with Trypsin Gold (Promega, Madison, WI, USA) with a protein-to-trypsin ratio of 40:1 at 37 °C overnight, and peptides were desalted with a Strata X C18 column and vacuum-dried. The peptides were dissolved in 30 ul 0.5 M TEAB via vortexing. ITRAQ labeling reagents recovered to ambient were transferred and combined with proper samples. Peptide labeling was performed using ITRAQ Reagent 8-plex Kit. The labeled peptides with different reagents were combined and desalted with a Strata X C18 column and vacuum-dried, the above experimental method refers to Wiese et al. (2007).

Peptide fractionation, HPLC, mass spectrometer detection

After being reconstituted with buffer A (5% ACN, 95% H_2O, adjusting pH to 9.8 with ammonia) to 2 mL, labeled peptides were fractioned using a Shimadzu LC-20AB HPLC pump system equipped with a high pH RP column at a flow rate of 1 mL/min with a gradient of buffer B (5% H_2O, 95% ACN, adjusting pH to 9.8 with ammonia): 5% for 10 min, 5-35% for 40 min, 35-95% for 1 min, 95% for 3 min, 95-5% within 1 min followed by 5% buffer for 10 min. Chromatograms were recorded at 214 nm, and fractions were collected at 1-min intervals. In total, 20 fractions were collected and vacuum-dried, dissolved in buffer (2% ACN, 0.1% FA in water) and centrifuged at 20,000 g for 10 min. Supernatants were loaded onto a C18 trap column using a LC-20AD nano-HPLC instrument (Shimadzu, Kyoto, Japan) and eluted, then separated with an analytical C18 column packed in-house at a flow rate of 300 nL/min with the following gradient of buffer (2% H_2O and 0.1% FA in ACN): 8-35% in 35 min; 35-60% in 5 min, 80% for 5 min, 80-5% in 0.1 min and equilibrating for 10 min. Data was acquired with a Triple TOF 5600 System equipped with a Nanospray III source (SCIEX, Framingham, MA, USA) and a pulled quartz tip emitter (New Objectives, Woburn, MA). This procedure was carried out by Beijing Genomics Institute

http://www.aloki.hu ● ISSN 1589 1623 (Print) ● ISSN 1785 0037 (Online)
DOI: http://dx.doi.org/10.15666/aeer/1705_1062310636

(Shenzhen, China), the above experimental method refers to Olson et al. (2013) and Lyu et al. (2016).

Protein identification, quantification and data analysis

For an MS/MS Ions Search, each query represented a complete MS/MS spectrum. The common protein databases: NCBInr, SwissProt (Magrane and UniProt Consortium, 2011), and UniProt were used for protein identification. ITRAQ quantification was applied by BGI's IQuant (Wen et al., 2014). Proteins with 1.2-fold change and Q-value less than 0.05 were determined as differentially expressed protein. Genes were annotated by using BLAST* (Altschul and Gish, 1996) against Clusters of Orthologous Groups of proteins database (COG) (Tatusov et al., 2003) and Kyoto Encyclopedia of Genes and Genomes database (KEGG) (Kanehisa et al., 2006). We set Cd_A/CK, Cd_B/CK, Cd_C/CK, Cd_D/CK, Cd_E/CK, Cd_F/CK, as comparison group.

Statistical analysis

Data expressed as means ± SD were subjected to one-way analysis of variance (SPSS ver. 10.0) to determine differences among groups, and least significant difference multiple-range test was used to determine significance differences ($P < 0.05$).

Results and discussion

Effects of Cd on the growth, colony formation and intracellular MC-RR content of M. aeruginosa

As shown in *Figure 1A,* with the increasing Cd concentrations, cell densities of *M. aeruginosa* increased first and then decreased, and the maximum cell density appeared in *M. aeruginosa* exposed to 0.0250 mg/L Cd. As compared to CK, all tested concentrations of Cd except 0.4000 mg/L Cd could significantly induce colony formation ($P < 0.05$), and 0.1000 mg/L Cd showed the best inductive effects (*Fig. 1B*). Intracellular MC-RR contents of *M. aeruginosa* exposed to 0.0250, 0.0500, 0.1000 and 0.2000 mg/L of Cd increased significantly as compared to CK (*Fig. 1C*). Cd could contribute to *M. aeruginosa* cells aggregation, and the Cd-induced colony-stimulating effects accompanied with the increased intracellular MC-RR contents. In our previous research, it was observed that the *Microcystis* colonies with smallest size in natural waters had the highest MC cellular production which decreased with the increasing colony size (Bi et al., 2017), suggesting toxic *Microcystis* might play a vital role in *Microcystis* colony formation via MCs production. Based on our above results, we speculated that Cd could increase the production of MC which acted as an internal signal stimulating the colony formation.

Proteomic analysis of M. aeruginosa exposed to Cd

A total of 405114 spectrums were generated, 7766 peptides and 1170 protein were identified (*Table A1*). According to the distribution of COG classification, it was found that in *M. aeruginosa* FACHB-905 genome, the number of genes relating to energy production and conversion (C), amino acid transport and metabolism (E), carbohydrate transport and metabolism (G) and cell wall/membrane/envelope biogenesis (M) was more than that of other function related genes (*Table A2*). Among all the KEGG

http://www.aloki.hu ● ISSN 1589 1623 (Print) ● ISSN 1785 0037 (Online)
DOI: http://dx.doi.org/10.15666/aeer/1705_1062310636

pathways, biosynthesis of secondary metabolites, antibiotics and amino acids accounted for 22.46%, 14.08% and 9.42%, respectively (*Table A3*).

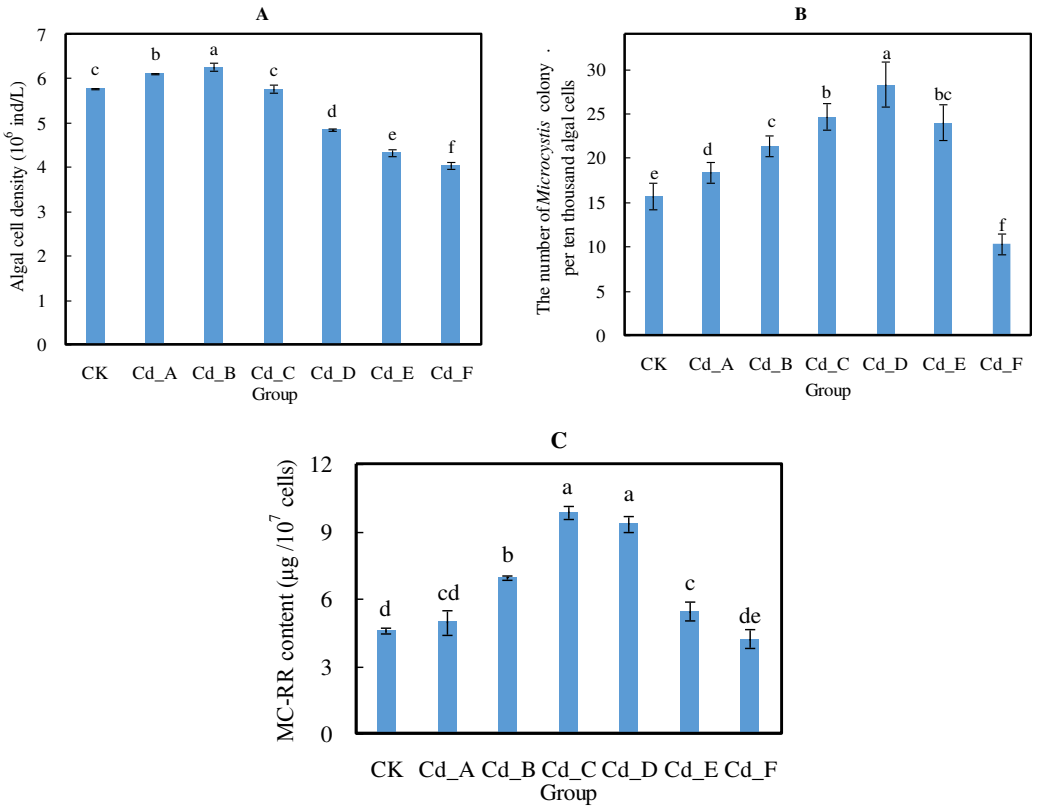

Figure 1. *Effects of Cd on the growth (A), colony formation (B) and intracellular MC-RR content (C) of M. aeruginosa*

MCs are synthesized by a large, modular enzyme complex, including peptide synthetases McyA, McyB, and McyC, a polyketide synthase McyD, two hybrid enzymes (McyE and McyG) consisting of peptide synthetase and polyketide synthase modules, and enzymes putatively involved in the tailoring (McyJ, McyF, and McyI) and transport (McyH) of MCs (Tillett et al., 2000). As shown in *Figure 2,* a total of seven MC biosynthesis-related enzymes, including McyB, McyC, McyD, McyE, McyG, McyI, and McyJ were identified using proteomic analysis. Consistent with the changes in MC-RR, 0.4000 mg/L Cd downregulated all these seven identified MC biosynthesis-related enzymes. 0.050 mg/L Cd upregulated all indentified MC biosynthesis-related enzymes except McyG, and 0.0125 mg/L Cd upregulated all indentified MC biosynthesis-related enzymes except McyJ. Other concentrations of Cd regulated MC biosynthesis-related enzymes to different degree. All tested concentrations of Cd except 0.4000 mg/L Cd could upregulated the expression level of McyC while McyD expression of *M. aeruginosa* exposed to 0.0125-0.0500 mg/L Cd was upregulated (*Table A4*).

Both soluble and total carbohydrates in colonial *Microcystis* cells and sheaths were significantly higher than those in disaggregated cells (Zhang et al., 2007). In colonial *Microcystis,* extracellular polysaccharides (EPS) were the main constituents of the

http://www.aloki.hu ● ISSN 1589 1623 (Print) ● ISSN 1785 0037 (Online)
DOI: http://dx.doi.org/10.15666/aeer/1705_1062310636

sheaths relating to cell aggregation (Plude et al., 1991). Previous researches have proved that biotic and abiotic factors could stimulate polysaccharide production (Xu et al., 2016; Yang et al., 2007). We also found that the contents of intracellular polysaccharide and bound extracellular polysaccharide in Cd-induced *M. aeruginosa* colony increased significantly, which could stimulate aggregation of algal cell and eventually promote colony formation (Bi et al., 2016). Many genes were involved in polysaccharides synthesis pathway, such as *capD*, *csaB*, *tagH*, *rfbB*, and *epsL* (Thurlow et al., 2009). Proteomic analysis showed that all identified polysaccharide biosynthesis-relate enzymes were downregulated in *M. aeruginosa* exposed to 0.4000 mg/L Cd which led to decreased colonies (*Fig. 3*). All concentrations of Cd except 0.4000 mg/L triggered upregulation of capsule biosynthesis protein CapD and sugar ABC transporter substrate-binding protein while rfbB NAD-dependent dehydratase and lipid-A-disaccharide synthase of *M. aeruginosa* exposed to 0.0125-0.0500 mg/L Cd were upregulated. These upregulated polysaccharide biosynthesis-relate enzymes might be responsible for Cd-induced increase in polysaccharides.

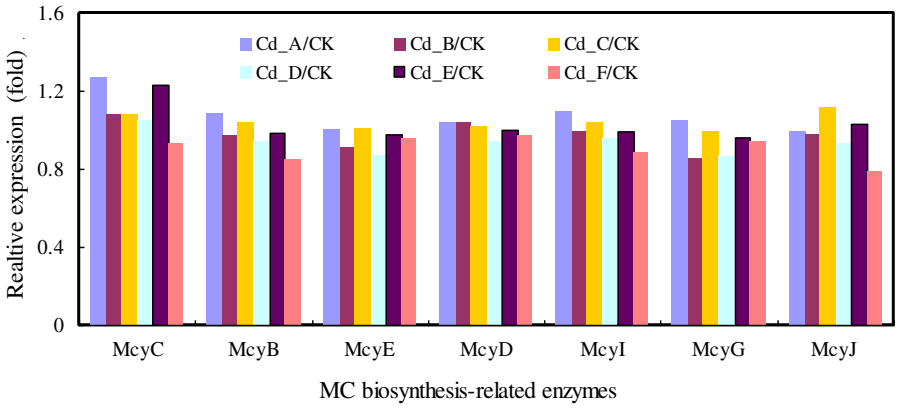

Figure 2. *Cd-induced changes in the expressions of MC biosynthesis-relate enzymes of M. aeruginosa*

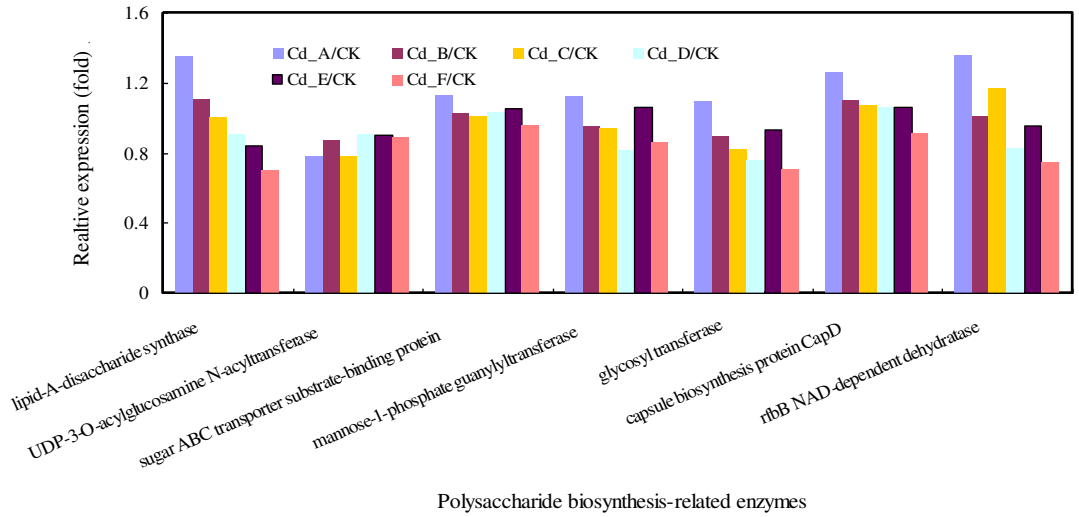

Figure 3. *Cd-induced changes in the expressions of polysaccharide biosynthesis-relate enzymes of M. aeruginosa*

http://www.aloki.hu ● ISSN 1589 1623 (Print) ● ISSN 1785 0037 (Online)
DOI: http://dx.doi.org/10.15666/aeer/1705_1062310636

The strong competition advantages of *M. aeruginosa* in plankton system are based on its high photosynthetic activity (Amorim et al., 2017). Cd remarkably influenced the porphyrin and chlorophyll metabolism (*Fig. 4*), and photosynthesis (*Fig. 5*) in *M. aeruginosa*. 16 related proteins were upregulated or downregulated significantly in *M. aeruginosa* exposed to 0.4000 mg/L Cd. The expression level of heme oxygenase and ferredoxin: protochlorophyllide reductase increased in all groups, thus preventing or minimizing ROS-induced damages (Zhou et al., 2006). Furthermore, the expression level of magnesium-protoporphyrin IX monomethyl ester cyclase, radical SAM protein, glutamate-tRNA ligase, photosystem II extrinsic protein and ATP synthase increased by more than 27% in *M. aeruginosa* exposed to 0.0125 and 0.0500 mg/L Cd. The increased global effects on photosynthesis could help *M. aeruginosa* enhancing the carbon fixation and energy transfer, and thus promoting the synthesis of polysaccharides and colony formation. When the Cd contention was up to 0.0500 mg/L, the expression level of allophycocyanin subunit beta/alpha and universal stress protein UspA increased by 1.5 fold as compared to the control group, thus protecting DNA against oxidative damage (Bhat and Madyastha, 2001).

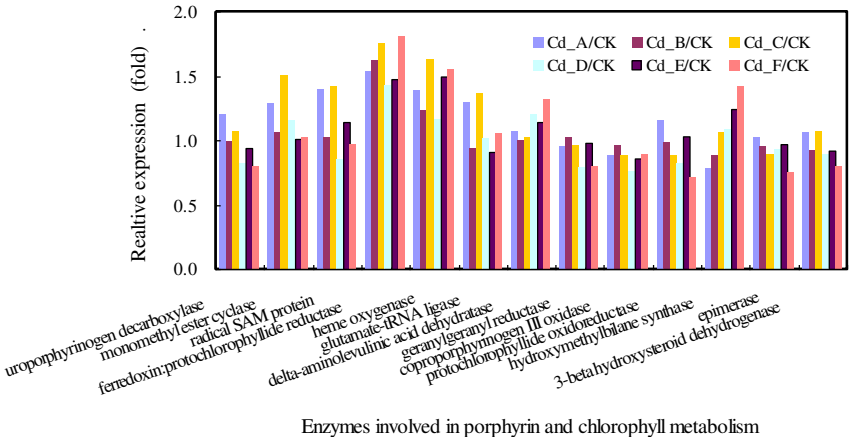

Figure 4. *Cd-induced changes in the expressions of enzymes involved in porphyrin and chlorophyll metabolism of M. aeruginosa*

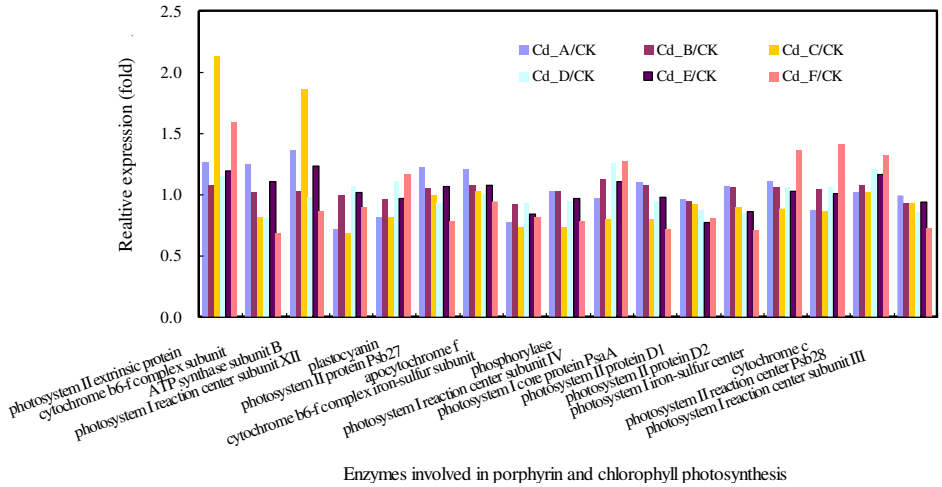

Figure 5. *Cd-induced changes in the expressions of enzymes involved in porphyrin and chlorophyll photosynthesis of M. aeruginosa*

http://www.aloki.hu ● ISSN 1589 1623 (Print) ● ISSN 1785 0037 (Online)
DOI: http://dx.doi.org/10.15666/aeer/1705_1062310636

Consolidate all our findings about the effects of heavy metal ions on the *Microcystis* colony formation, we believe that *Microcystis* could bioaccumulate heavy metal ions, such as Cd, in natural waters, and appropriate heavy metal ions enriched in *Microcystis* cell could promote the synthesis and secretion of polysaccharide and MC in *M. aeruginosa* by upregulated polysaccharide and MC biosynthesis-related enzymes. Heavy metal ions could increase *Microcystis* colony formation in natural waters with the assistance of low concentration of MC, which may act as an important internal signal stimulator.

Conclusions

Proper concentration of heavy metal ions could induce *Microcystis* colony formation. Heavy metal ions could increase *Microcystis* colony formation in natural waters with the assistance of low concentration of MC, which may act as an important internal signal stimulator. Further intensive study should be carried out to reveal the mechanism of synergistic reaction of MC and heavy metal ions.

Acknowledgements. This work is financially supported by National Natural Science Foundation of China (31772857) and Natural Science Foundation Grant of Tianjin (17JCYBJC29500, 18JCYBJC95900 and 16JCYBJC29900).

REFERENCES

[1] Alexova, R., Dang, T. C., Fujii, M., Raftery, M. J., Waite, T. D., Ferrari, B. C., Neilan, B. A. (2015): Specific global responses to N and Fe nutrition in toxic and non-toxic *Microcystis aeruginosa*. – Environmental Microbiology 18(2): 401-13.

[2] Altschul, S. F., Gish, W. (1996): Local alignment statistics. – Method in Enzymology 266: 460-480.

[3] Bhat, V. B., Madyastha, K. M. (2001): Scavenging of peroxynitrite by phycocyanin and phycocyanobilin from *Spirulina platensis*: protection against oxidative damage to DNA. – Biochemical and Biophysical Research Communications 285: 262-266.

[4] Bi, X. D., Dai, W., Zhang, S. L., Xing, K. Z., Zhang, X. F. (2015): Accumulation and distribution characteristics of heavy metals in different size *Microcystis* colonies from natural waters. – Fresenius Environmental Bulletin 24: 773-779.

[5] Bi, X. D., Yan, R., Li, F. X., Dai, W., Jiao, K. W., Zhou, Q. X., Liu, Q. (2016): Sequestration and distribution characteristics of Cd(II) by *Microcystis aeruginosa* and its role in colony formation. – BioMed Research International Article 9837598.

[6] Bi, X. D., Dai, W., Zhang, S. L., Dong, S. J., Zhang, D. J. (2017): Effects of toxic *Microcystis* genotypes on natural colony formation and mechanism involved. – Water Science and Technology 76(3-4): 885-894.

[7] Amorim, C. A., Ulisses, C., Moura, A. N. (2017): Biometric and physiological responses of *Egeria densa Planch.* cultivated with toxic and non-toxic strains of *Microcystis*. – Aquatic Toxicology 191: 201-208.

[8] Gan, N. Q., Xiao, Y., Zhu, L., Wu, Z. X., Liu, J., Hu, C. L., Song, L. R. (2012): The role of microcystins in maintaining colonies of bloom-forming *Microcystis* spp.. – Environmental Microbiology 14(3): 730-742.

[9] Huisman, J, Codd, G. A, Paerl, H. W, Ibelings, B. W, Verspagen, J. M. H, Visser, P. M. (2018): Cyanobacterial blooms. – Nature Reviews Microbiology 16(8): 471-483.

http://www.aloki.hu ● ISSN 1589 1623 (Print) ● ISSN 1785 0037 (Online)
DOI: http://dx.doi.org/10.15666/aeer/1705_1062310636

[10] Kanehisa, M., Goto, S., Hattori, M., Aoki-Kinoshita, K. F., Itoh, M., Kawashima, S., Katayama, T. (2006): From genomics to chemical genomics: new developments in KEGG. – Nucleic Acids Research 34(suppl 1): D354-D357.
[11] Li, M., Zhu, W., Gao, L., Lu, L. (2013): Changes in extracellular polysaccharide content and morphology of *Microcystis aeruginosa* at different specific growth rates. – Journal of Applied Phycology 25(4): 1023-1030.
[12] Liu, Y., Chen, S., Zhang, J., Gao, B. Y. (2016): Growth, microcystin-production and proteomic responses of *Microcystis aeruginosa* under long-term exposure to amoxicillin. – Water Research 93: 141-152.
[13] Lyu, K., Meng, Q., Zhu, X., Dai, D., Zhang, L., Huang, Y., Yang, Z. (2016): Changes in iTRAQ-based proteomic profiling of the cladoceran *Daphnia magna* exposed to microcystin-producing and microcystin-free *Microcystis aeruginosa*. – Environment Science Technology 50(9): 4798-4807.
[14] Magrane, M., UniProt Consortium (2011): UniProt Knowledgebase: a hub of integrated protein data. – Database bar009. DOI: 10.1093/database/bar009.
[15] Olson, K. C., Chen, G., Lynch, C. J. (2013): Quantification of branched-chain keto acids in tissue by ultra fast liquid chromatography-mass spectrometry. – Analytical Biochemistry 439(2): 116-22.
[16] O'Neil, J. M., Davis, T. W. Burford, M. A., Gobler, C. J. (2012): The rise of harmful cyanobacteria blooms: The potential roles of eutrophication and climate change. – Harmful Algae 14: 313-334.
[17] Omori, K., Datta, T., Amano, Y., Machida, M. (2019): Effects of different types of extracellular polysaccharides isolated from cyanobacterial blooms on the colony formation of unicellular Microcystis aeruginosa. – Environmental Science and Pollution Research 26(4): 3741-3750.
[18] Sommaruga, R., Chen, Y. W., Liu, Z. W. (2008): Multiple strategies of bloom-forming *Microcystis* to minimize damage by solar ultraviolet radiation in surface waters. – Microbial Ecology, DOI: 10.1007/s00248-008-9425-4.
[19] Shen, H., Song, L. R. (2007): Comparative studies on physiological responses to phosphorus in two phenotypes of bloom-forming *Microcystis*. – Hydrobiologia 592: 475-486.
[20] Shen, H., Niu, Y., Xie, P., Tao, M., Yang, X. (2011): Morphological and physiological changes in *Microcystis aeruginosa* as a result of interactions with heterotrophic bacteria. – Freshwater Biology 56: 1065-1080.
[21] Tatusov, R. L., Fedorova, N. D., Jackson, J. D., Jacobs, A. R., Kiryutin, B., Koonin, E. V., Krylov, D. M. (2003): The COG database: an updated version includes eukaryotes. – BMC bioinformatics 4: 41.
[22] Thurlow, L. R., Thomas, V. C., Hancock, L. E. (2009): Capsular polysaccharide production in *Enterococcus faecalis* and contribution of CpsF to capsule serospecificity. – Journal of Bacteriology 191(20): 6203-6210.
[23] Tillett, D., Dittmann, E., Erhard, M., von Döhren, H., Börner, T., Neilan, B. A. (2000): Structural organization of microcystin biosynthesis in *Microcystis aeruginosa* PCC7806: an integrated peptide-polyketide synthetase system. – Chemistry and Biology 7(10): 753-764.
[24] Wen, B., Zhou, R., Feng, Q., Wang, Q., Wang, J., Liu, S. (2014): IQuant: An automated pipeline for quantitative proteomics based upon isobaric tags. – Proteomics 14(20): 2280-2285.
[25] Wiese, S., Reidegeld, K. A., Meyer, H. E., Warscheid, B. (2007): Protein labeling by iTRAQ: a new tool for quantitative mass spectrometry in proteome research. – Proteomics 7(6): 1004.
[26] Wilmes, P., Bond, P. L. (2009): Microbial community proteomics: elucidating the catalysts and metabolic mechanisms that drive the Earth's biogeochemical cycles. – Current Opinion in Microbiology 12(3): 310-317.

http://www.aloki.hu ● ISSN 1589 1623 (Print) ● ISSN 1785 0037 (Online)
DOI: http://dx.doi.org/10.15666/aeer/1705_1062310636

[27] Xiao, M., Li, M., Reynolds, C. S. (2018): Colony formation in the cyanobacterium *Microcystis*. – Biological reviews 93(3): 1399-1420.
[28] Xu, F., Zhu, W., Xiao, M., Li, M. (2016): Interspecific variation in extracellular polysaccharide content and colony formation of *Microcystis* spp. cultured under different light intensities and temperatures. – Journal of Applied Phycology 28: 1533-1541.
[29] Yang, Z., Kong, F. X. (2012): Formation of large colonies: a defense mechanism of *Microcystis aeruginosa* under continuous grazing pressure by flagellate *Ochromonas* sp. – Journal of Limnology l71: 61-66.
[30] Yang, Z., Kong, F. X., Shi, X. L., Xing, P., Zhang, M. (2007): Effects of Daphnia-associated infochemicals on the morphology, polysaccharides content and PSII-efficiency in *Scenedesmus obliquus*. – International Review of Hydrobiology 92: 618-625.
[31] Yue, D., Peng, Y., Yin, Q., Xiao, L. (2015): Proteomic analysis of *Microcystis aeruginosa* in response to nitrogen and phosphorus starvation. – Journal of Applied Phycology 27: 1195-1204.
[32] Zhang, M., Kong, F., Tan, X., Yang, Z., Cao, H., Xing, P. (2007): Biochemical, morphological, and genetic variations in *Microcystis aeruginosa* due to colony disaggregation. – World Journal of Microbiology and Biotechnology 23: 663-670.
[33] Zhou, W., Juneau, P., Qiu, B. (2006): Growth and photosynthetic responses of the bloom-forming cyanobacterium *Microcystis aeruginosa* to elevated levels of cadmium. – Chemosphere 65(10): 1738-1746.
[34] Zhu, W., Zhou, X. H., Chen, H. M., Gao, L., Xiao, M., Li, M. (2016): High nutrient concentration and temperature alleviated formation of large colonies of Microcystis: Evidence from field investigations and laboratory experiments. – Water Research 101(2016): 167-175.

APPENDIX

Tables A1 and *A4* are electronic appendices.

Table A2. *The COG distribution of all identified proteins in M. aeruginosa FACHB-905*

Abbreviation	Functional categories	Number
B	Chromatin structure and dynamics	1
C	Energy production and conversion	111
D	Cell cycle control, cell division, chromosome partitioning	21
E	Amino acid transport and metabolism	125
F	Nucleotide transport and metabolism	35
G	Carbohydrate transport and metabolism	83
H	Coenzyme transport and metabolism	70
I	Lipid transport and metabolism	34
J	Translation, ribosomal structure and biogenesis	104
K	Transcription	41
L	Replication, recombination and repair	38
M	Cell wall/membrane/envelope biogenesis	88
N	Cell motility	7
O	Posttranslational modification, protein turnover, chaperones	84
P	Inorganic ion transport and metabolism	61
Q	Secondary metabolites biosynthesis, transport and catabolism	46
R	General function prediction only	166
S	Function unknown	69
T	Signal transduction mechanisms	57
U	Intracellular trafficking, secretion, and vesicular transport	19
V	Defense mechanisms	15

http://www.aloki.hu ● ISSN 1589 1623 (Print) ● ISSN 1785 0037 (Online)
DOI: http://dx.doi.org/10.15666/aeer/1705_1062310636

Table A3. *The KEGG distribution of all identified proteins in M. aeruginosa FACHB-905*

No	Different proteins in annotated pathways	Number (percentage)
1	Metabolic pathways	411 (42.55%)
2	Biosynthesis of secondary metabolites	217 (22.46%)
3	Biosynthesis of antibiotics	136 (14.08%)
4	Microbial metabolism in diverse environments	118 (12.22%)
5	Biosynthesis of amino acids	91 (9.42%)
6	Carbon metabolism	73 (7.56%)
7	Ribosome	43 (4.45%)
8	Purine metabolism	41 (4.24%)
9	Amino sugar and nucleotide sugar metabolism	31 (3.21%)
10	Photosynthesis	31 (3.21%)
11	ABC transporters	30 (3.11%)
12	Oxidative phosphorylation	29 (3%)
13	Glycolysis/Gluconeogenesis	29 (3%)
14	Porphyrin and chlorophyll metabolism	27 (2.8%)
15	Pyruvate metabolism	26 (2.69%)
16	2-Oxocarboxylic acid metabolism	25 (2.59%)
17	Two-component system	24 (2.48%)
18	Starch and sucrose metabolism	24 (2.48%)
19	Aminoacyl-tRNA biosynthesis	24 (2.48%)
20	Carbon fixation pathways in prokaryotes	23 (2.38%)
21	Methane metabolism	22 (2.28%)
22	Glyoxylate and dicarboxylate metabolism	22 (2.28%)
23	Alanine, aspartate and glutamate metabolism	22 (2.28%)
24	Pyrimidine metabolism	22 (2.28%)
25	Glycine, serine and threonine metabolism	21 (2.17%)
26	Fructose and mannose metabolism	21 (2.17%)
27	RNA degradation	21 (2.17%)
28	Cysteine and methionine metabolism	20 (2.07%)
29	Pentose phosphate pathway	19 (1.97%)
30	Carbon fixation in photosynthetic organisms	19 (1.97%)
31	Photosynthesis - antenna proteins	18 (1.86%)
32	Citrate cycle (TCA cycle)	17 (1.76%)
33	Fatty acid metabolism	17 (1.76%)
34	Fatty acid biosynthesis	16 (1.66%)
35	Nitrogen metabolism	16 (1.66%)
36	Glutathione metabolism	14 (1.45%)
37	Valine, leucine and isoleucine biosynthesis	14 (1.45%)
38	Arginine biosynthesis	13 (1.35%)
39	Propanoate metabolism	13 (1.35%)
40	Lysine biosynthesis	12 (1.24%)
41	Phenylalanine, tyrosine and tryptophan biosynthesis	12 (1.24%)
42	Butanoate metabolism	12 (1.24%)
43	Arginine and proline metabolism	12 (1.24%)
44	Histidine metabolism	11 (1.14%)
45	Nonribosomal peptide structures	11 (1.14%)
46	Sulfur metabolism	10 (1.04%)
47	Streptomycin biosynthesis	10 (1.04%)
48	C5-Branched dibasic acid metabolism	10 (1.04%)
49	Terpenoid backbone biosynthesis	10 (1.04%)
50	Ubiquinone and other terpenoid-quinone biosynthesis	10 (1.04%)
51	Nicotinate and nicotinamide metabolism	10 (1.04%)
52	Biotin metabolism	10 (1.04%)
53	Galactose metabolism	9 (0.93%)

http://www.aloki.hu ● ISSN 1589 1623 (Print) ● ISSN 1785 0037 (Online)
DOI: http://dx.doi.org/10.15666/aeer/1705_1062310636

54	Peptidoglycan biosynthesis	9 (0.93%)
55	Mismatch repair	9 (0.93%)
56	Pantothenate and CoA biosynthesis	9 (0.93%)
57	One carbon pool by folate	9 (0.93%)
58	Peroxisome	8 (0.83%)
59	Central carbon metabolism in cancer	8 (0.83%)
60	Cell cycle - Caulobacter	8 (0.83%)
61	Bacterial secretion system	8 (0.83%)
62	Tyrosine metabolism	8 (0.83%)
63	Homologous recombination	8 (0.83%)
64	Tuberculosis	8 (0.83%)
65	DNA replication	8 (0.83%)
66	Protein export	7 (0.72%)
67	Glucagon signaling pathway	7 (0.72%)
68	Nucleotide excision repair	7 (0.72%)
69	Cationic antimicrobial peptide (CAMP) resistance	7 (0.72%)
70	Carotenoid biosynthesis	7 (0.72%)
71	Biosynthesis of unsaturated fatty acids	6 (0.62%)
72	Legionellosis	6 (0.62%)
73	Fatty acid degradation	6 (0.62%)
74	Folate biosynthesis	6 (0.62%)
75	Thiamine metabolism	6 (0.62%)
76	Degradation of aromatic compounds	5 (0.52%)
77	Drug metabolism - other enzymes	5 (0.52%)
78	Selenocompound metabolism	5 (0.52%)
79	Monobactam biosynthesis	5 (0.52%)
80	Valine, leucine and isoleucine degradation	5 (0.52%)
81	Base excision repair	5 (0.52%)
82	Drug metabolism - cytochrome P450	5 (0.52%)
83	Inositol phosphate metabolism	5 (0.52%)
84	Phenylalanine metabolism	5 (0.52%)
85	Cyanoamino acid metabolism	5 (0.52%)
86	Vitamin B6 metabolism	5 (0.52%)
87	Salmonella infection	5 (0.52%)
88	Type I polyketide structures	4 (0.41%)
89	Protein processing in endoplasmic reticulum	4 (0.41%)
90	Chemical carcinogenesis	4 (0.41%)
91	Metabolism of xenobiotics by cytochrome P450	4 (0.41%)
92	Aminobenzoate degradation	4 (0.41%)
93	Tryptophan metabolism	4 (0.41%)
94	Polyketide sugar unit biosynthesis	4 (0.41%)
95	Glycerophospholipid metabolism	4 (0.41%)
96	Sulfur relay system	4 (0.41%)
97	Riboflavin metabolism	4 (0.41%)
98	Pentose and glucuronate interconversions	4 (0.41%)
99	Insulin signaling pathway	4 (0.41%)
100	Chloroalkane and chloroalkene degradation	4 (0.41%)
101	HIF-1 signaling pathway	4 (0.41%)
102	GABAergic synapse	4 (0.41%)
103	Biosynthesis of ansamycins	4 (0.41%)
104	Glycerolipid metabolism	4 (0.41%)
105	RNA polymerase	4 (0.41%)
106	Tetracycline biosynthesis	4 (0.41%)
107	Lipopolysaccharide biosynthesis	3 (0.31%)
108	AMPK signaling pathway	3 (0.31%)

http://www.aloki.hu ● ISSN 1589 1623 (Print) ● ISSN 1785 0037 (Online)
DOI: http://dx.doi.org/10.15666/aeer/1705_1062310636

109	Pathways in cancer	3 (0.31%)
110	Huntington's disease	3 (0.31%)
111	Viral carcinogenesis	3 (0.31%)
112	Toluene degradation	3 (0.31%)
113	Type II diabetes mellitus	3 (0.31%)
114	Biosynthesis of siderophore group nonribosomal peptides	3 (0.31%)
115	Chlorocyclohexane and chlorobenzene degradation	3 (0.31%)
116	Fluorobenzoate degradation	2 (0.21%)
117	PPAR signaling pathway	2 (0.21%)
118	Mineral absorption	2 (0.21%)
119	Limonene and pinene degradation	2 (0.21%)
120	N-Glycan biosynthesis	2 (0.21%)
121	Taurine and hypotaurine metabolism	2 (0.21%)
122	Synaptic vesicle cycle	2 (0.21%)
123	Sphingolipid metabolism	2 (0.21%)
124	Isoquinoline alkaloid biosynthesis	2 (0.21%)
125	Stilbenoid, diarylheptanoid and gingerol biosynthesis	2 (0.21%)
126	Phosphatidylinositol signaling system	2 (0.21%)
127	Insulin resistance	2 (0.21%)
128	Naphthalene degradation	2 (0.21%)
129	Benzoate degradation	2 (0.21%)
130	Atrazine degradation	2 (0.21%)
131	FoxO signaling pathway	2 (0.21%)
132	Lysine degradation	2 (0.21%)
133	Tropane, piperidine and pyridine alkaloid biosynthesis	2 (0.21%)
134	RNA transport	2 (0.21%)
135	Bisphenol degradation	2 (0.21%)
136	Adipocytokine signaling pathway	2 (0.21%)
137	Alzheimer's disease	2 (0.21%)
138	Phenylpropanoid biosynthesis	2 (0.21%)
139	Vasopressin-regulated water reabsorption	2 (0.21%)
140	Meiosis - yeast	2 (0.21%)
141	Type I diabetes mellitus	2 (0.21%)
142	Glutamatergic synapse	2 (0.21%)
143	Novobiocin biosynthesis	2 (0.21%)
144	Vancomycin resistance	2 (0.21%)
145	Endocytosis	1 (0.1%)
146	Flavonoid biosynthesis	1 (0.1%)
147	Isoflavonoid biosynthesis	1 (0.1%)
148	Renal cell carcinoma	1 (0.1%)
149	beta-Lactam resistance	1 (0.1%)
150	Polycyclic aromatic hydrocarbon degradation	1 (0.1%)
151	Linoleic acid metabolism	1 (0.1%)
152	Nitrotoluene degradation	1 (0.1%)
153	Influenza A	1 (0.1%)
154	Hepatitis B	1 (0.1%)
155	NOD-like receptor signaling pathway	1 (0.1%)
156	mRNA surveillance pathway	1 (0.1%)
157	PI3K-Akt signaling pathway	1 (0.1%)
158	Cocaine addiction	1 (0.1%)
159	Thyroid hormone synthesis	1 (0.1%)
160	Biosynthesis of type II polyketide products	1 (0.1%)
161	Toxoplasmosis	1 (0.1%)
162	Styrene degradation	1 (0.1%)
163	D-Glutamine and D-glutamate metabolism	1 (0.1%)

http://www.aloki.hu ● ISSN 1589 1623 (Print) ● ISSN 1785 0037 (Online)
DOI: http://dx.doi.org/10.15666/aeer/1705_1062310636

164	p53 signaling pathway	1 (0.1%)
165	Plant-pathogen interaction	1 (0.1%)
166	beta-Alanine metabolism	1 (0.1%)
167	Retinol metabolism	1 (0.1%)
168	Ethylbenzene degradation	1 (0.1%)
169	D-Alanine metabolism	1 (0.1%)
170	Parkinson's disease	1 (0.1%)
171	Non-alcoholic fatty liver disease (NAFLD)	1 (0.1%)
172	Prostate cancer	1 (0.1%)
173	Viral myocarditis	1 (0.1%)
174	Biosynthesis of 12-, 14- and 16-membered macrolides	1 (0.1%)
175	Colorectal cancer	1 (0.1%)
176	Alcoholism	1 (0.1%)
177	Amphetamine addiction	1 (0.1%)
178	Serotonergic synapse	1 (0.1%)
179	Steroid hormone biosynthesis	1 (0.1%)
180	Phosphonate and phosphinate metabolism	1 (0.1%)
181	Other glycan degradation	1 (0.1%)
182	Glycosaminoglycan biosynthesis - chondroitin sulfate/dermatan sulfate	1 (0.1%)
183	Ascorbate and aldarate metabolism	1 (0.1%)
184	Epithelial cell signaling in Helicobacter pylori infection	1 (0.1%)
185	Small cell lung cancer	1 (0.1%)
186	Progesterone-mediated oocyte maturation	1 (0.1%)
187	Synthesis and degradation of ketone bodies	1 (0.1%)
188	Apoptosis	1 (0.1%)
189	Amyotrophic lateral sclerosis (ALS)	1 (0.1%)
190	Renin-angiotensin system	1 (0.1%)
191	Carbapenem biosynthesis	1 (0.1%)
192	Herpes simplex infection	1 (0.1%)
193	Antigen processing and presentation	1 (0.1%)
194	Dopaminergic synapse	1 (0.1%)
195	Estrogen signaling pathway	1 (0.1%)
196	Butirosin and neomycin biosynthesis	1 (0.1%)
197	Biosynthesis of vancomycin group antibiotics	1 (0.1%)

http://www.aloki.hu ● ISSN 1589 1623 (Print) ● ISSN 1785 0037 (Online)
DOI: http://dx.doi.org/10.15666/aeer/1705_1062310636

EFFECT, IMMOBILIZATION AND COOPERATIVITY OF AMENDMENTS ON REMEDIATION OF PB-CONTAMINATED SOIL

CHANG, J. H.[1,2#] – LIU, Q. F.[1,2#] – YU, J.[1,2,*] – WANG, Y. T.[3] – PENG, W. D.[1,2] – CHEN, J. Y.[1,2] – LIU, W.[4]

[1]*Department of Environmental Science and Engineering, College of Architecture and Environment, Sichuan University, Chengdu 610065, China*

[2]*Institute of New Energy and Low Carbon Technology, Sichuan University, Chengdu 610065, China*

[3]*Chengdu Academy of Environmental Sciences, Chengdu 610072, China*

[4]*Chengdu Hydrogeological Engineering Geological Center, Chengdu 610081, China*

[#]*These authors contributed equally to this work and should be regard as co-first authors*

**Corresponding author*
e-mail: yuj@scu.edu.cn; phone: +86-189-8093-9168

(Received 1st Mar 2019; accepted 21st May 2019)

Abstract. In our study, zeolite, sepiolite, vermiculite and biochar were added to high-concentration lead-contaminated soils, respectively, and the metal fractions, toxicity leaching amount and leaching characteristics of lead (Pb) in soils were studied after 30 d. Besides, the feasibility of chemical immobilization to reduce Pb was investigated. In the soil immobilization experiments, compared with the control, the toxicity leaching amount of soils added zeolite, sepiolite, vermiculite and biochar decreased. The decreasing ratios were 40.12%, 41.28%, 25.50%, and 16.04%, respectively. It is clear that the treatment of zeolite showed the best effect. And the group matching curing agents (GMCAs) with a mass ratio of 2:1 for zeolite and sepiolite was the best, of which the Pb content in soil leaching solutions decreased by 41.4%. Meanwhile, through soil column leaching experiment, compared with the control, the pH of leachates generally increased, and the electrical conductivity (EC) of leachates presented a falling trend. The Pb content of accumulated leachates from treatments decreased, and the best effect treatment was at a mass ratio of 1:2 for zeolite andsepiolite with the highest decrease rate at 93.35%. And the immobilization effect was further verified. Therefore, the addition of curing agents could decrease the bioavailability and migration of Pb.
Keywords: *lead contamination, curing agents, stabilization, soil leaching column, environmental assessment*

Introduction

With the advancement of industrial and agricultural modernization, soil heavy metal contamination has become an extremely important and serious global environmental problem in recent decades (Liu et al., 2014). Pb is a common heavy mental pollutant owning to the fact that excessive intake of Pb can damage nerve and human organs such as kidney and liver, increasing the risk of cancer (Taylor et al., 2014; Cao et al., 2015; Schwab et al., 2005). Pb can easily be complexed with soil colloids and adsorbed on oxides and clays because of its hard degradation, limited soluble and chronicity in soils (Suman et al., 2005; Putra et al., 2013). In

http://www.aloki.hu ● ISSN 1589 1623 (Print) ● ISSN 1785 0037 (Online)
DOI: http://dx.doi.org/10.15666/aeer/1705_1063710654

recent decades, due to the industrial pollution caused by human activities such as electroplating, atmospheric deposition from combustion of leaded gasoline, metal smelting and coal mining, Pb concentration in soil has increased dramatically (Tai et al., 2013). Consequently, it is urgent to develop a method for the remediation of Pb-contaminated soils.

At present, the remediation methods of Pb-contaminated soils mainly focus on soil washing, electrodialysis and phytoremediation due to their outstanding effects (Amrate et al., 2005; Gupta et al., 2013; Xu et al., 2014; Suzuki et al., 2014). Although these methods may be effective to remediate Pb-contaminated soils, they usually tend to be expensive and time-consuming (Suman et al., 2005). On the contrary, immobilization as a main potential soil remediation technique has received considerable attention (Hwang et al., 2008; Kumpiene et al., 2008).

The immobilization of heavy mental is a remediation technique applied to decrease the mobility of elements by adding curing agents in soils, so that reducing the bioavailability and solubility of heavy metals (Mcgowen et al., 2001; Mignardi et al., 2012). Soil immobilization technique has been successfully applied to radioactive waste, sediment, and industrial sludge. Compared with other technologies, this technology can be applied widely and the processing time is short. Curing agents have different curing mechanism for heavy metals, such as soil pH, ions exchange, adsorption, coordinating action, co-precipitation, etc. (Suman et al., 2005). However, most studies on heavy metal immobilization treatments aimed at single curing agent remediation, rarely considering GMCAs remediation or verifying further immobilization effect by soil column leaching experiment.

Therefore, this study on batch immobilization experiments and soil column leaching experiment were conducted by selecting four kinds of curing agents, including zeolite, sepiolite, vermiculite and biochar. The purposes of the study were:(1) to compare immobilization effects of different curing agents on Pb-contaminated soils so that screening out the feasible curing agents; (2) to study the leaching characteristics and the rules of migration and transformation of Pb-contaminated soils under different treatments, and to assess the influence of the soils on the surrounding environment after immobilization.

Materials and methods

Soil sample and curing agents

The topsoil layer (0–20 cm) of the tested soil was collected from one battery plant in Chongzhou, Sichuan, China (30°34'N, 103°34'E). The collected soil was dried at room temperature, and then the uniform soils were obtained through a 2 mm nylon mesh. Zeolite, sepiolite, vermiculite and biochar were used in the immobilization experiment. Zeolite is an artificial zeolite. Sepiolite particle diameter is ≤ 74 um. Vermiculite particle size is 0.5~1.5 mm, 12 h after soaking by 7.5% potassium nitrate solution at 600~800 °C heating 5 to 7 min, and then through 100 mesh. Biochar particle size is less than 150 microns to corn starch and coconut shell as raw material, under the environment of low oxygen content at 600 °C high temperature pyrolysis, and then through 100 mesh. All reagents obtained as chemical pure were used in the study. All the solutions were prepared by deionized water. The physical and chemical properties of soil are shown in *Table 1*.

http://www.aloki.hu ● ISSN 1589 1623 (Print) ● ISSN 1785 0037 (Online)
DOI: http://dx.doi.org/10.15666/aeer/1705_1063710654

Table 1. *Physical and chemical properties of the tested soil*

pH	Organic matter g/kg	Total phosphorus mg/kg	Cation exchange capacity cmol/kg	Total nitrogen mg/kg	Pb concentration mg/kg	Silt %	Clay %	Sand %
6.71	18.2	465.6	7.23	910.8	2231.75	31.30	20.31	48.39

Design of experiment

Design of single curing agent immobilization experiment

Soils samples (50 g) were placed in the beakers (100 mL) and then curing agents (zeolite, sepiolite, vermiculite, and biochar) were added to them, respectively. Batch leaching experiments were conducted at different curing agent concentrations from 0 to 16 $g \cdot kg^{-1}$. Then each beaker was added 20 mL water. The soils dried at room temperature for 2 weeks were sampled by quartering, and then the uniform soils were obtained through a 2 mm nylon mesh. The soil were screened by 100 meshes, dried and frozen, then placed on the conductive adhesive. The morphological characteristics of the materials were observed by scanning electron microscopy (SEM) (JSM-6510LV). Afterwards, effect of curing agents on Pb immobilization in soil was tested by Toxicity Characteristic Leaching Procedure (TCLP). And the concentration of lead ion in filtrate was measured by Atomic Absorption Spectrophotometer (AAS) (AA800, America). In this experiment, three parallel samples were used for each data.

Design of GMCAs immobilization experiment

Soil samples (50 g) were placed in the beakers (100 mL) and then added different curing agents according to *Table 2*. Batch leaching experiments were carried out at curing agent concentration 8 $g \cdot kg^{-1}$. Two kinds of curing agent in each group matching were set at three ratios of 1:1, 1:2 and 2:1. Then each beaker was added 20 mL water. The soils dried at room temperature for 2 weeks were sampled by quartering, and then the uniform soils were obtained through a 2 mm nylon mesh. Afterwards, effect of GMCAs on Pb immobilization in soil was tested by TCLP. And the concentration of lead ion in filtrate was directly determined by AAS.

Table 2. *Twenty-two treatments in the experiment*

Number	Single curing agent	Number	Group matching curing agents	Number	Group matching curing agents
CK	Control	A5	$Zeolite_{(1)}$ + $Sepiolite_{(1)}$[a]	A14	$Vermiculite_{(1)}$ + $Biochar_{(1)}$
A1	Zeolite	A6	$Zeolite_{(1)}$ + $Sepiolite_{(2)}$ [b]	A15	$Vermiculite_{(1)}$ + $Biochar_{(2)}$
A2	Sepiolite	A7	$Zeolite_{(2)}$ + $Sepiolite_{(1)}$[c]	A16	$Vermiculite_{(2)}$ + $Biochar_{(1)}$
A3	Vermiculite	A8	$Zeolite_{(1)}$ + $Vermiculite_{(1)}$	A17	$Sepiolite_{(1)}$ + $Biochar_{(1)}$
A4	Biochar	A9	$Zeolite_{(1)}$ + $Vermiculite_{(2)}$	A18	$Sepiolite_{(1)}$ + $Biochar_{(2)}$
		A10	$Zeolite_{(2)}$ + $Vermiculite_{(1)}$	A19	$Sepiolite_{(2)}$ + $Biochar_{(1)}$
		A11	$Zeolite_{(1)}$ + $Biochar_{(1)}$	A20	$Sepiolite_{(1)}$ + $Vermiculite_{(1)}$
		A12	$Zeolite_{(1)}$ + $Biochar_{(2)}$	A21	$Sepiolite_{(1)}$ + $Vermiculite_{(2)}$
		A13	$Zeolite_{(2)}$ + $Biochar_{(1)}$	A22	$Sepiolite_{(2)}$ + $Vermiculite_{(1)}$

[a]$Zeolite_{(1)}$ + $Sepiolite_{(1)}$, zeolite mixing with sepiolite at a mass ratio of 1:1
[b]$Zeolite_{(1)}$ + $Sepiolite_{(2)}$, zeolite mixing with sepiolite at a mass ratio of 1:2
[c]$Zeolite_{(2)}$ + $Sepiolite_{(1)}$, zeolite mixing with sepiolite at a mass ratio of 2:1

http://www.aloki.hu ● ISSN 1589 1623 (Print) ● ISSN 1785 0037 (Online)
DOI: http://dx.doi.org/10.15666/aeer/1705_1063710654

Design of soil column leaching experiment

Preparation of acid rain

According to the pH of average rainfall and acid rain monitoring data in Southwest China during the period from 1995 to 2003 (Mei, 2006), the simulated acid rain was prepared. The chemical composition of rainfall was presented in *Table 3*. Simulated acid rain leaching experiment was carried out by adjusting pH and compounding the main anion and cation concentrations according to the rainfall characteristics of Southwest China. The acid rain solution (*Table 4*) was prepared by selecting corresponding salts and calculating its mass on the basis of ion composition and equivalence relation. The solution mixing sulfuric acid and nitric acid was compounded by the rainfall of Southwest China, in which the molar ratio of SO_4^{2-} to NO_3^- was 3:1 (Tang, 2006). And the pH of rainfall solution was set at 4.7 and was adjusted by adding diluted NaOH or/and HNO_3 solution.

Table 3. *The chemical composition and ion content of rain in Southwest China (umol/L)*

Ions	NH_4^+	Na^+	K^+	Ca^{2+}	SO_4^{2-}	Mg^{2+}	NO_3^-	Cl^-	F^-
Content	165.42	24.14	24.29	111.16	145.09	13.44	51.63	38.07	22.26

Table 4. *A variety of salt content in acid rain (mg/L)*

Salts	$MgCl_2 \cdot 6H_2O$	$CaSO_4 \cdot 2H_2O$	KNO_3	NaF	$(NH_4)_2SO_4$	NH_4NO_3
Content	2.731	19.120	2.519	0.974	10.130	0.951

Soil column leaching experiment

Soil samples (200 g) were placed in the beakers (500 mL) and then added single curing agents and GMCAs pre-screening. Batch leaching experiments were carried out at curing agent concentration 8 $g \cdot kg^{-1}$. The soils after immobilization dried at room temperature for 2 weeks were sampled by quartering, and then the uniform soils were obtained through a 2 mm nylon mesh. Then soil column leaching experiment was carried out. Soil column leaching apparatus was shown in *Figure 1*. The soils reacted for a certain time by using intermittent leaching to approach the natural rainfall state. The leachates kept leaching at 8 h every other day, which was collected for 10 times (a total of 1000 mL). Batch soil column leaching experiments were conducted to explore the effects of leaching variables including pH value, EC and the concentration of Pb in soils. Afterwards, the soils after leaching dried naturally at room temperature were sampled by quartering, and then the uniform soils were obtained through a 2 mm nylon mesh so that determining the fractions of Pb in soils. The concentration of lead ion in the solution was directly measured by AAS. Moreover, de-ionized water should be used to make the soil column saturated and moist before leaching.

Experimental analytical methods

Soil pH value was determined with H_2O at a 1:2.5 soil solution ratio. Soil organic carbon, total phosphorus and total nitrogen were measured by the Walkley–Black titrations, Digestion-Mo-Sb Anti spectrophotometric method and Kjeldahl method,

http://www.aloki.hu ● ISSN 1589 1623 (Print) ● ISSN 1785 0037 (Online)
DOI: http://dx.doi.org/10.15666/aeer/1705_1063710654

respectively (Bremmer and Mulvaney, 1982; Nelson and Sommers, 1996). The ammonium acetate method was applied to measure cation exchange capacity (CEC) in soils (Rhoades, 1982). The soil digestion method was applied to determine total heavy mental concentration at a volume ratio of 1:2:2 for HNO_3–HCl–$HClO_4$ mixture (Zhang et al., 2013). The exchangeable, reducible, oxidizable, and residual fractions ofPb in soils were determined to use the optimized Bureau of Reference (BCR) three-step sequential extraction procedure before and after leaching (Nemati et al., 2011; Pueyo et al., 2008). To determine the amount of Pb leaching in soil, America Environmental Protection Agency's TCLP was used (U.S. EPA, 1986). The concentration of Pb in the solution was measured by AAS. And soils after immobilization experiments were photographed by SEM operating at 15 kV.

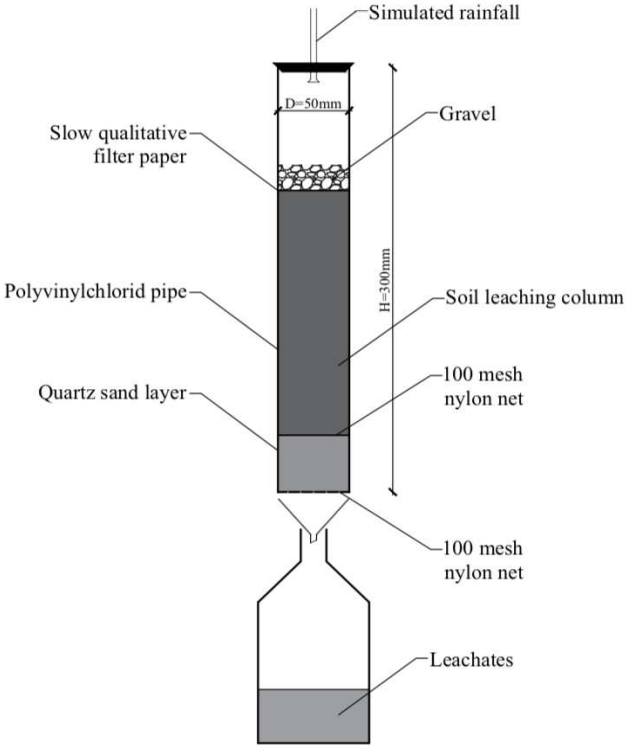

Figure 1. *Apparatus of soil column leaching experiment*

Statistical analysis

Statistical data analysis was done with software SPSS Version 19.0. The data were analyzed by Pearson's correlation analysis using a two-tailed test with significance levels of 0.05 and 0.01.

Results and discussion

Effect of single curing agent on Pb immobilization in soil

SEM analysis of soil after adding single curing agent

As shown in *Figure 2*, the soil samples were photographed by SEM before and after immobilization. It showed that new metal-containing phase was not found after adding

http://www.aloki.hu ● ISSN 1589 1623 (Print) ● ISSN 1785 0037 (Online)
DOI: http://dx.doi.org/10.15666/aeer/1705_1063710654

curing agents in soil by SEM analysis. And the surface particles presented a smoother morphology than the control soil. Therefore, results suggested the dissolution may not be the main immobilization mechanism for heavy metals. Moreover, the reduction of water solubility for heavy metal in soil was mainly attributed to surface ion exchange and co-precipitation, corresponding mineral crystals were formed to make the surface smoother. Similar results also found in the studies of He et al. (2013). It might be due to the addition of curing agents reacting with Pb in soils to form corresponding lead minerals, which were crystals, so the surface appears smoother. Similar results were also found in Mignardi et al.'s (2012) study. However, there is little difference between different curing agents, of which the mechanism needs to be further explored.

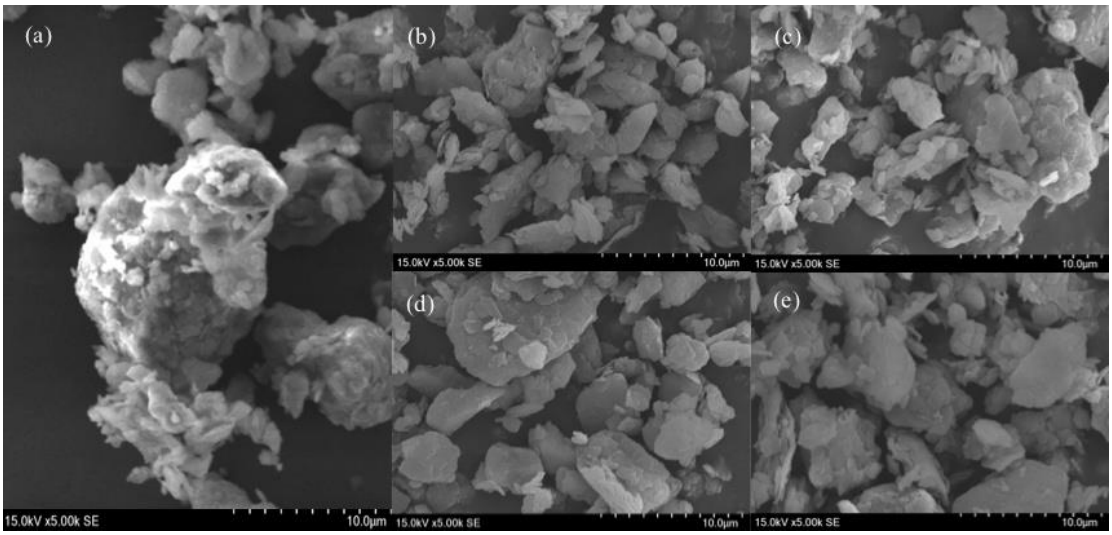

Figure 2. *SEM images of the control and the tested soil (a, the control soil; b, the soil added zeolite; c, the soil added sepiolite, d, the soil added vermiculite; e, the soil added biochar)*

Effect of single curing agent on soil pH value

As shown in *Figure 3,* the addition of zeolite, sepiolite, vermiculite, and biochar influenced the soil pH differently. With the concentration of curing agents increasing, soil pH increased gradually. Soil pH increases from 6.71 to 7.67, 6.95, 7.20, 6.92 for four curing agents, respectively, when the concentration of curing agents is 16 g/kg. It showed that zeolite influenced the soil pH most in four curing agents, of which the pH increase was 0.96. The increase of pH value was mainly due to the fact that the zeolite was a shelf-shaped silicate mineral of alkali and alkali earth metals, containing a large amount of Na^+, K^+, Ca^{2+}, Mg^{2+} ions, which could exchange with H^+ and Al^{3+} ions in the soil solution (Chi et al., 2017).

The pH of soil plays an important role on the remediation of heavy metal contamination. Generally speaking, with the increase of pH, the absorption capacity of heavy metals in soils will enhance. Because heavy metals will form hydroxide precipitates in soil solution as the OH^- increases (Begum et al., 2013; Elliott and Brown, 1989). Organic matter and Fe-Mn oxide are considered as the main carrier for heavy metal adsorption in soils, which can bind more strongly with heavy metals, so that reducing the bioavailability and biological activity of heavy metal in soils (Zhou et al., 2010).

http://www.aloki.hu ● ISSN 1589 1623 (Print) ● ISSN 1785 0037 (Online)
DOI: http://dx.doi.org/10.15666/aeer/1705_1063710654

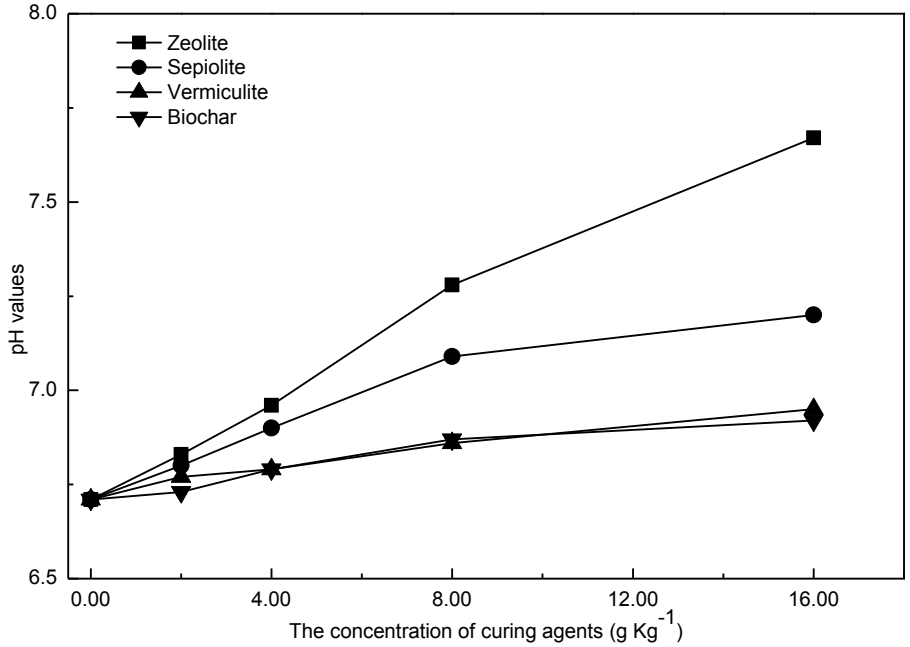

Figure 3. *Effect of curing agents on soil pH value*

Effect of single curing agent on Pb immobilization in soil

As shown in *Figures 4* and *5,* four kinds of curing agents could reduce the exchangeable Pb contents and Pb leaching amounts efficiently. Zeolite, sepiolite, vermiculite and biochar could reduce the exchangeable Pb contents. When the concentration of curing agents was 16.0 g/kg, the exchangeable Pb contents reduced by 93.59%, 100%, 59.35%, 46.91%, respectively. The activity of soil heavy metals depended on the exchangeable fraction (Zhou et al., 2010). Moreover, zeolite, vermiculite and sepiolite could decrease the Pb leaching amount (*Fig. 5*). The Pb leaching amount gradually reduced with further increasing of the curing agent concentration from 0 to 16.0 g/kg. When the concentration of zeolite, vermiculite and sepiolite all reached 16.0 g/kg, Pb leaching amount reduced by 40.12%, 25.50%, 41.28%, respectively.

Compared four kinds of curing agents, zeolite and vermiculite could reduce the exchangeable Pb contents, which inhibited the activity of Pb in soils. Moreover, zeolite and sepiolite could reduce Pb leaching amount effectively. The less leaching amount indicated that only less Pb took away with the surface runoff, which was less harmful to the environment. Above all, sepiolite was the best for Pb immobilization in soil, followed by zeolite and vermiculite. Sepiolite could absorb heavy metal ions or complexes with opposite charges in soil to reduce the activity and migration of heavy metals because of its large specific surface area and unique pore structure (Shirvani et al., 2006). Meanwhile, due to the layered chain structure of the crystal, some heavy metal ions would be absorbed into the interlayer crystal structure to become solidified ions so as to achieve solidification (Sun et al., 2012).

Through single factor correlation analysis, it can be found that the amount of four curing agent, soil pH value and curing effect indicators have a certain correlation. *Table 5* shows that soil pH value is significantly or extremely significantly positively

http://www.aloki.hu ● ISSN 1589 1623 (Print) ● ISSN 1785 0037 (Online)
DOI: http://dx.doi.org/10.15666/aeer/1705_1063710654

correlated with the amount of four curing agents applied. The reduction of exchangeable Pb contents in soil and the immobilization efficiency are positively correlated with the amount of four curing agents applied. *Table 6* shows that soil pH value is significantly or positively correlated with the reduction of exchangeable Pb contents in soil and the immobilization efficiency after applying curing agent. To some extent, the increase of soil pH reduced the bioavailability and migration of Pb in soil, inhibited the activity of heavy metals, and stabilized Pb in soil.

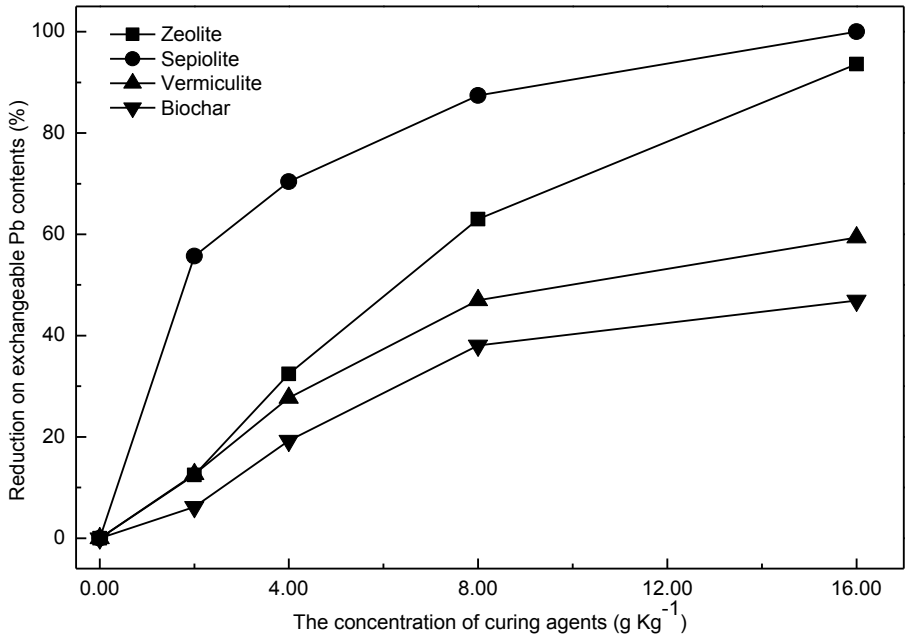

Figure 4. *Effect of different curing agents on exchangeable Pb contents in the soil*

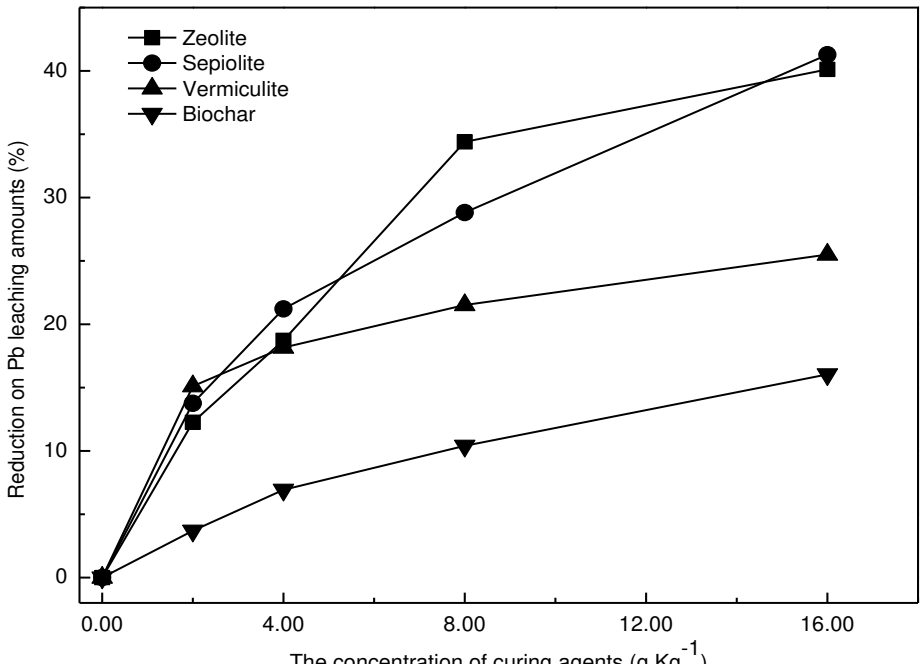

Figure 5. *Effect of different curing agents on Pb leaching contents in the soil*

http://www.aloki.hu ● ISSN 1589 1623 (Print) ● ISSN 1785 0037 (Online)
DOI: http://dx.doi.org/10.15666/aeer/1705_1063710654

Table 5. *Correlation coefficient analysis of dosage of four curing agents and test indexes*

Number	Concentration			
	Zeolite	**Sepiolite**	**Vermiculite**	**Biochar**
pH	0.995**	0.980*	0.987**	0.959*
The reduction of exchangeable Pb contents	0.982**	0.825	0.947*	0.947*
Immobilization efficiency	0.928*	0.949*	0.814	0.977**

**Extremely significant correlation ($p \leq 0.01$)
*Significant correlation ($p \leq 0.05$)

Table 6. *Correlation coefficient analysis of pH value and curing effect index*

Number	pH value			
	Zeolite	**Sepiolite**	**Vermiculite**	**Biochar**
The reduction of exchangeable Pb contents	0.994**	0.902*	0.976**	0.999**
Immobilization efficiency	0.954*	0.984**	0.888*	0.981**

**Extremely significant correlation ($p \leq 0.01$)
*Significant correlation ($p \leq 0.05$)

Effect of GMCAs on Pb immobilization in soil

Effect of GMCAs on soil pH value

It can be seen from *Figure 6* that, compared with the control (pH 6.71), single curing agents could increase soil pH, among which the zeolite increased soil pH most by 0.57. GMCAs could also increase the soil pH, but the increasing effect was not as good as single curing agents. Among all GMCAs, A5, A13 and A22 possessed a better capacity to increase the soil pH. The pH was increased by 0.36, 0.33, and 0.30, respectively. Therefore, GMCAs showed a general effect in adjusting soil pH.

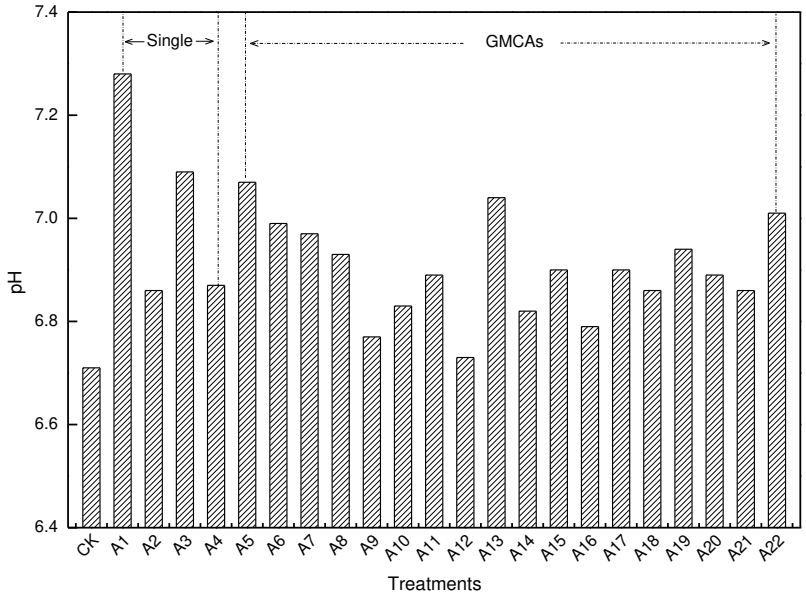

Figure 6. *Effect of different treatments on soil pH value*

http://www.aloki.hu ● ISSN 1589 1623 (Print) ● ISSN 1785 0037 (Online)
DOI: http://dx.doi.org/10.15666/aeer/1705_1063710654

Effect of GMCAs on Pb immobilization in the soil

As shown in *Figures 7* and *8*, when the concentration of GMCAs was 16.0 g/kg, the various treatments showed different curing efficiency. Besides, different mass ratios of curing agents also performed differently in the same GMCAs. Among all treatments, the GMCAs with a mass ratio of 1:2 or 2:1 for zeolite and sepiolite were the best, and the treatments of these GMCAs decreased the exchangeable Pb contents in soils by 90.2%, 86.4%, respectively. Moreover, A7 and A10 decreased Pb contents effectively in soil leaching solution by 41.4%, 42.1%, respectively. Obviously, zeolite mixing with sepiolite at a mass ratio of 2:1 could immobilize the soil Pb effectively. The combination of zeolite and sepiolite had synergistic effect. Similar results were also found in the studies of Liu (2014).

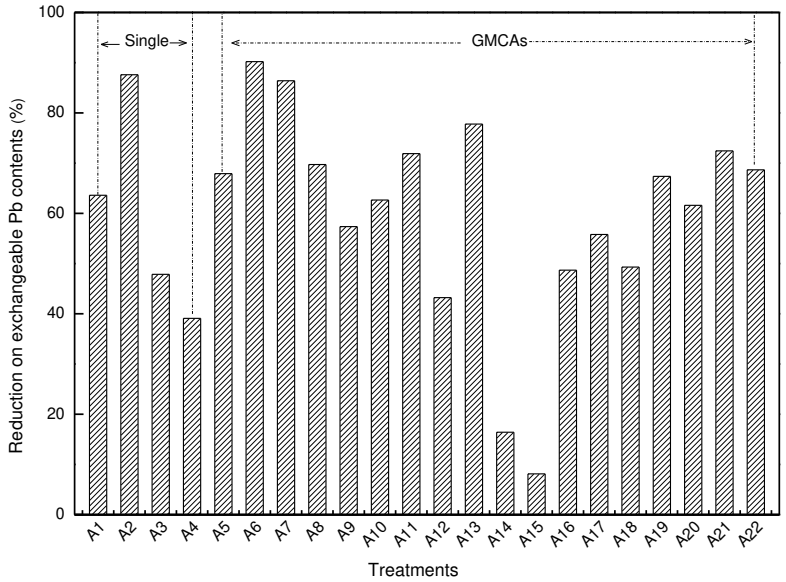

Figure 7. *Effect of GMCAs on exchangeable Pb contents in the soil*

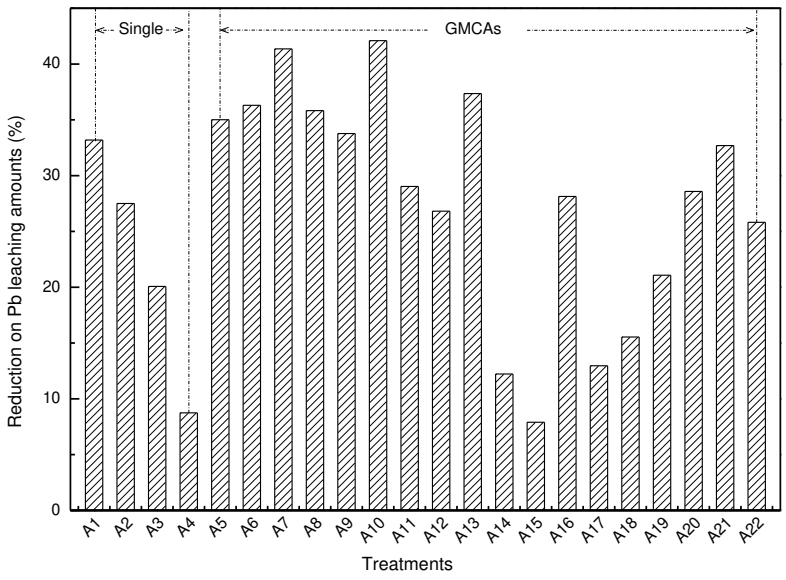

Figure 8. *Effect of GMCAs on Pb leaching contents in the soil*

http://www.aloki.hu ● ISSN 1589 1623 (Print) ● ISSN 1785 0037 (Online)
DOI: http://dx.doi.org/10.15666/aeer/1705_1063710654

However, compared with the single curing agent, two curing agents at different ratios have different effects on Pb in soil. Some of them have synergistic effects, while others have antagonistic effects.

The result and analysis of soil column leaching experiment

Variation of pH in leachates with leaching times

Considering the effects of curing agent immobilization preliminarily, soil column leaching experiment was conducted by choosing four single curing agents and four different kinds of GMCAs according to *Table 7*.

The results of soil leachates pH from different treatments were shown in *Figure 9,* which gave the change of the pH during the soil column leaching experiment. Compared with the pH of the control, the pH of other treatments was higher than the original leaching solution. Moreover, the pH of the leachates first increased and then decreased with the increase of leaching times. The maximum pH of the leachates was inconsistent in different times, but basically appeared after the fourth leaching. This is mainly determined by the rate of neutralization and exchange reaction between exchangeable base ions and H^+ input through acid rain. With the continuous reaction of exchangeable base ions and H^+ input, the pH of exchangeable base ions begins to decrease slowly after the complete exchange of exchangeable base ions in the mid-leaching stage. However, because the soil contains a large number of buffer ions, the decrease of pH is relatively small (Zhang et al., 2007; Yu et al., 2001; Fang, 2016; Ma, 2007). In addition, the anions contain in acid rain also coordinate with the hydroxyl groups on the surface of soil particles. Hence, under leaching of leachates, the hydroxyl group enters the solution and consumes H^+, which leads to the increase of pH of soil leachates (Xu et al., 2004). It indicated that the addition of curing agents was beneficial to alleviate the effect of acid rain and improved the soil buffering properties (Yu et al., 2001).

Among the different treatments, the most obviously increasing of pH was B1, followed by B6, and the third was B5. The maximum change of pH could reach 0.69, which occurring at the 5^{th} time of leaching. For B2, B3, B4, B7 and B8, the increase of pH was lower than B1, B6 and B5. It showed that the addition of zeolite has the greatest influence on soil pH, which indicated that zeolite increases the cation exchange capacity in soil and adsorbs the hydrogen ions in original solution, thereby increasing pH of leachates.

Table 7. *Nine treatments in the experiment*

Number	Curing agents
CK	Control
B_1	Zeolite
B_2	Sepiolite
B_3	Vermiculite
B_4	Biochar
B_5	$Zeolite_{(1)}$ + $Sepiolite_{(2)}$
B_6	$Zeolite_{(2)}$ + $Biochar_{(1)}$
B_7	$Sepiolite_{(1)}$ + $Vermiculite_{(2)}$
B_8	$Vermiculite_{(2)}$ + $Biochar_{(1)}$

http://www.aloki.hu ● ISSN 1589 1623 (Print) ● ISSN 1785 0037 (Online)
DOI: http://dx.doi.org/10.15666/aeer/1705_1063710654

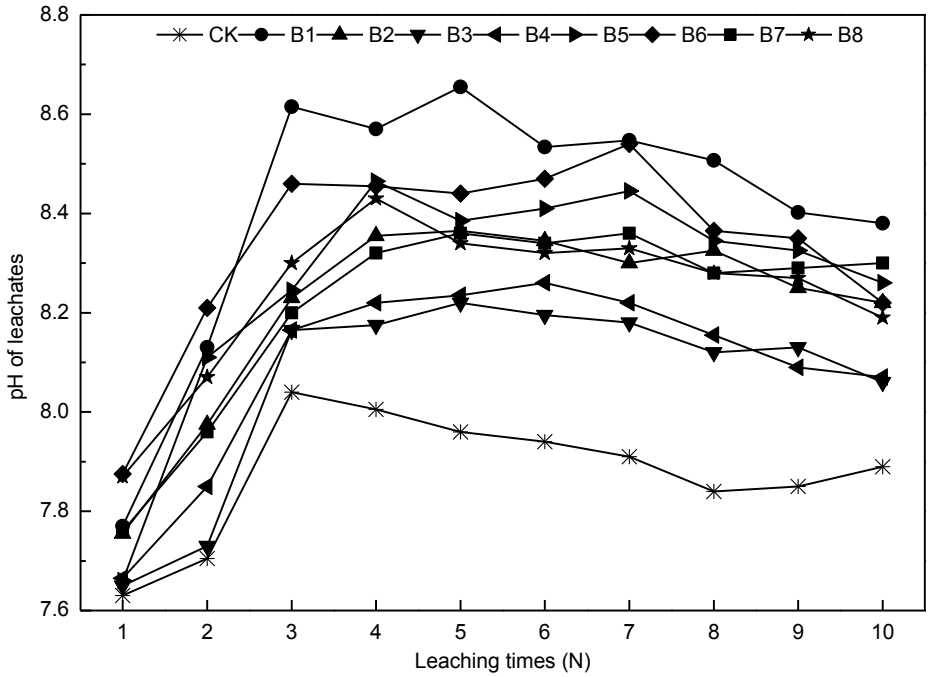

Figure 9. *Changes of pH with leaching times in leachates*

Variation of EC in leachates with leaching times

The EC of soil can be used to characterize soluble salt content in soil, and the content of soluble salt in soil shows a great effect on the EC of soil (Sun, 2000). The EC of each treatment was shown in *Figure 10* with the leaching of simulated acid rain (pH 4.7). It could be seen that the change of EC in each treatment was approximately the same, and leachates for the first time showed the highest EC. With the increase of the leaching times, the EC rapidly reduced. There was the highest rate at the beginning, and then their concentration was close to equilibrium and remained almost constant with further leaching. It showed that the release of base cation in soil gradually reduced with the increasing of the leaching times, and the initial release quantity was the largest, and then it flattened out. The EC changes can be divided into two stages: rapid decline and slow decline to a steady state. The early stage may be related to the rapid release of various base ions on the soil surface, some soluble oxide particles adsorbed on the soil surface and soluble salts into aqueous solutions. In the later stage, the exchangeable ions in soil become less and less, and the process of slowly releasing and tending to equilibrium is achieved (Zhang et al., 2007; Fang, 2016). At the same time, most of the curing agents are mineral materials. After acid rain leaching, a certain degree of weathering occurs to release the corresponding base ions. Some of them are lost with the leachates, and the other part is adsorbed in the soil, so the conductivity trend tends to balance finally. In addition, acid rain causes a large number of salt-based ions to dissolve, and H^+ in acid rain replaces salt-based ions in soil colloids. This may also explain that the leachates pH will decrease with the increase of leaching times (Zhang et al., 2007).

From *Figure 10* it could also be seen that the initial EC of each treatment was higher than CK under the leaching of simulated acid rain, indicating that the EC could increase the content of soluble salts and also could reduce the release of base cation after adding curing agents in soils (Rhoades et al., 1990).

http://www.aloki.hu ● ISSN 1589 1623 (Print) ● ISSN 1785 0037 (Online)
DOI: http://dx.doi.org/10.15666/aeer/1705_1063710654

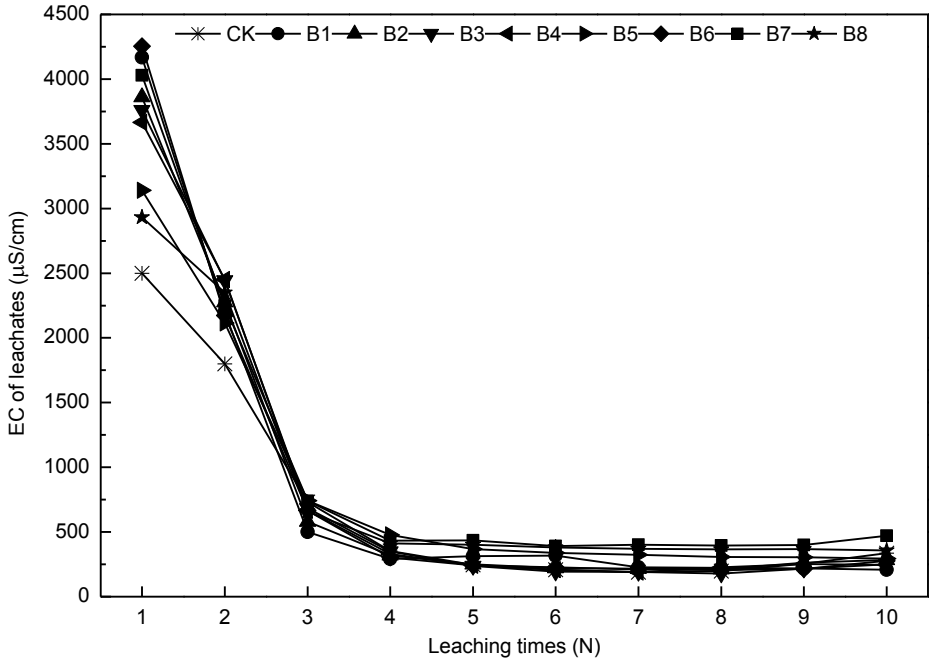

Figure 10. *Changes of EC with leaching times in leachates*

Correlation analysis was conducted between Pb content, pH, conductivity and leaching times in leachates under simulated acid rain leaching conditions, and the results were shown in *Table 8*.

Table 8. *The correlation coefficient of leaching times, pH, EC and Pb content*

The Pb concentration of leachates	Leaching times	pH	EC
CK	-0.804**	-0.725*	0.979**
B1	-0.838**	-0.794**	0.940**
B2	-0.853**	-0.872**	0.943**
B3	-0.902**	-0.805**	0.933**
B4	-0.881**	-0.845**	0.963**
B5	-0.717*	-0.918**	0.926**
B6	-0.758*	-0.848**	0.995**
B7	-0.813**	-0.901**	0.943**
B8	-0.650*	-0.879**	0.907**

**Extremely significant correlation ($p \leq 0.01$). *Significant correlation ($p \leq 0.05$)

On the whole, Pb content in the leachates is significantly negatively correlated with pH. It may be due to the loss of soluble Pb carbonate in the process of acid rain leaching. With the increase of leaching times, at the beginning, Pb in the water-soluble and exchangeable states was released quickly due to acid rain leaching, and then Pb carbonate was also dissolved by H^+ reaction, leading to loss, so there was a significant correlation (Shi et al., 2013). At the same time, the Pb content of leachates is significantly negatively correlated with the number of leaching times, and extremely significantly positively correlated with EC.

http://www.aloki.hu ● ISSN 1589 1623 (Print) ● ISSN 1785 0037 (Online)
DOI: http://dx.doi.org/10.15666/aeer/1705_1063710654

Influence of leaching on curing agent immobilization

The change trend of Pb concentration in leachates with leaching times was shown in *Figure 11* under the leaching of simulated acid rain. It indicated the Pb concentration significantly reduced with the increasing of leaching time when the leaching time was ≤ 2. With further leaching, the rate of reduction decreased. The Pb concentration of B5 decreased most slowly, which decreased from 5.86 μg/L to 0.61 μg/L.

Compared with the control (CK), the Pb concentration of leachates significantly reduced after adding curing agents in soils under the leaching of simulated acid rain. The Pb concentration of the control was 190.23 μg/L. And the maximum concentration of Pb after adding curing agents was 106.89 μg/L. The Pb content of accumulated leachates from B1 to B8 significantly decreased, and the decreasing rate was 76.03%, 73.01%, 44.02%, 44.74%, 83.97%, 79.64%, 61.82% and 55.21%, respectively. The highest decrease rate was 83.97% resulted from the treatment of zeolite mixed with sepiolite at a mass ratio of 1:2. Curing agent treatment can significantly reduce the leaching of lead in soil under acid rain conditions (Linet al., 2009). Similar results also found in the studies of Tao et al. (2015) and Rao et al. (2013).

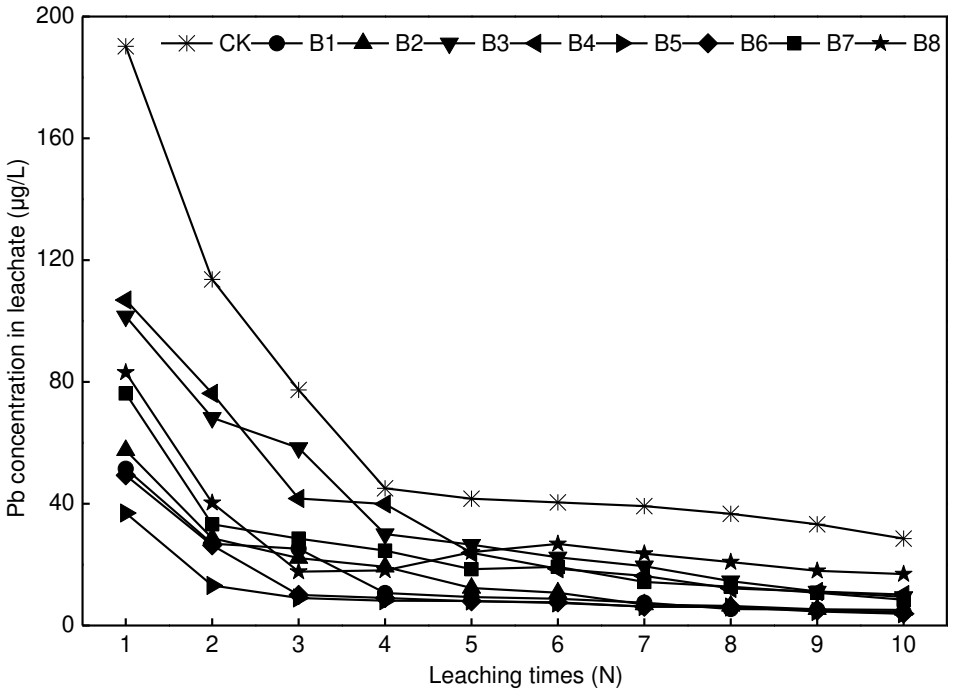

Figure 11. *Changes of Pb concentration with leaching times in leachate*

Influence of leaching on Pb fractions

The fractions of Pb in soil were determined by the BCR procedure before and after leaching. The changes of Pb fractions before and after leaching were presented in *Figure 12*. It indicated that the exchangeable Pb amount increased and the residual Pb amount decreased after leaching.

With the addition of different curing agents, the change of reducible and oxidizable Pb amount was not obvious, of which some increased and some decreased. Our results suggested that the residual Pb contents gradually transformed into exchangeable Pb,

http://www.aloki.hu ● ISSN 1589 1623 (Print) ● ISSN 1785 0037 (Online)
DOI: http://dx.doi.org/10.15666/aeer/1705_1063710654

reducible Pb and oxidizable Pb contents with the increasing of leaching times. In other words, simulated acid rain could activate the fractions of Pb, which increased its bioavailability and migration. However, the addition of curing agents could decrease the leaching Pb amounts, thus reducing the harm to the ecological environment around the soil (Brown et al., 2004; Geebelen et al., 2003).

The exchangeable Pb amount of nine treatments (CK and B1-B8) in soil leaching solutions increased by 9.95%, 6.69%, 6.98%, 7.44%, 7.81%, 4.56%, 6.54%, 9.19% and 7.84%, respectively. Among all treatments, the minimum increasing rate was the treatment of B5. That is to say, the activating ability of simulated acid rain was relatively small, namely this treatment posed the minimum potential side-effects to the ecological environment around the soil.

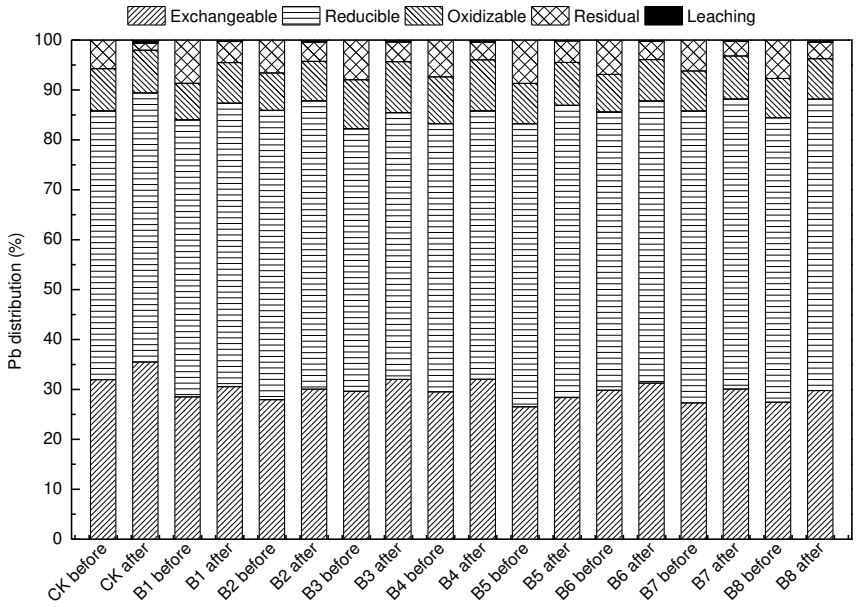

Figure 12. *Comparative distribution of Pb in soil for different treatments before and after leaching*

Conclusion

Four kinds of curing agents showed a better immobilization effect when further increasing of the concentration of curing agents. Compared with the control, the toxicity leaching amount of soils added zeolite, sepiolite, vermiculite and biochar decreased. The decreasing ratios were 40.12%, 41.28%, 25.50% and 16.04%, respectively. Moreover, the soil pH value was significantly or extremely significantly positively correlated with the amount of four curing agents applied. The soil pH value was significantly or positively correlated with the reduction of exchangeable Pb contents in soil and the immobilization efficiency after applying curing agent. The treatment of zeolite showed a best effect on reducing toxicity leaching amount of Pb in soil. Among various GMCAs, zeolite mixing with sepiolite at a mass ratio of 2:1 was the best agent which could immobilize Pb effectively. Under the leaching condition of pH 4.7, the pH of leachates generally increased compared with the control, and the EC of leachates presented a falling trend. The Pb content of accumulated leachates from treatments was decreased, and the highest decrease rate was 83.97%. The residual Pb contents

http://www.aloki.hu ● ISSN 1589 1623 (Print) ● ISSN 1785 0037 (Online)
DOI: http://dx.doi.org/10.15666/aeer/1705_1063710654

gradually transformed into exchangeable Pb, reducible Pb and oxidizable Pb contents with the increasing of leaching times. Moreover, Pb content in the leachates was significantly negatively correlated with pH, significantly negatively correlated with the number of leaching times, and extremely significantly positively correlated with EC. For all treatments, the treatment of zeolite mixing with sepiolite at a mass ratio of 1:2 showed a best effect on reducing leaching amount of Pb in soil. Meanwhile, the activating ability of simulated acid rain was relatively small, namely this treatment posed the minimum potential harm to the ecological environment around the soil. That is to say, the addition of curing agents could decrease the bioavailability and migration of Pb, thus reducing the harm to the ecological environment around the soil. In addition, the mechanism of Pb immobilization and the modification of curing agents need to be future explored.

Acknowledgements. The work was supported by National Key Research and Development Program (2018YFC1802605), Nature Science Foundation of Sichuan Province (2017GZ0383, 2017SZ0181).

REFERENCES

[1] Amrate, S., Akretche, D. E., Innocent, C., Seta, P. (2005): Removal of Pb from a calcareous soil during EDTA- enhanced electrokinetic extraction. – Science of the Total Environment 349(1): 56-66.

[2] Begum, Z. A., Rahman, I. M. M., Sawai. H. Mizutani, S., Maki, T., Hasegawa, H. (2013): Effect of extraction variables on the viodegradable Chelant-assisted removal of toxic metals from artificially contaminated European reference soils. – Water Air & Soil Pollution 224(3): 1381.

[3] Bremmer, J. M., Mulvaney, C. S. (1982): Nitrogen: Total. – In: Page, A. L., Miller, R. H., Keeney, D. R. (eds.) Methods of Soil Analysis. Part 2: Chemical and Microbiological Properties. ASA/SSSA, Madison, WI, pp. 595-641.

[4] Brown, S., Chaney, R., Hallfrisch, J., Ryan, J. A., Berti, W. R. (2004): In situ soil treatments to reduce the phyto- and bioavailability of lead, zinc, and cadmium. – Journal of Environmental Quality 33(2): 522.

[5] Cao, S., Duan, X., Zhao, X., Wang, B. B., Ma, J., Fan, D. L., Sun, C. Y., He, B., Wei, F. S., Jiang, G. B. (2015): Health risk assessment of various metal(loid)s via multiple exposure pathways on children living near a typical lead-acid battery plant, China. – Environmental Pollution 200: 16-23.

[6] Chi, S., Xu, W., Xiong, S. Wang, W. Z., Qin, Y. L., Zhao, W. Y., Zhang, C. L., Li, Y. H., Li, T., Zhang, J. Z., Xiong, Z. T., Wang, Z. Y., Xie, D. T. (2017): Effect of Nano Zeolites on pH, CEC in Soil and Cd fractions in plant and soil at different cadmium levels. – Environmental Science 38(4): 1654-1666.

[7] Elliott, H. A., Brown, G. A. (1989): Comparative evaluation of NTA and EDTA for extractive decontamination of Pb-polluted soils. – Water Air & Soil Pollution 45(3-4): 361-369.

[8] Fang, Z. (2016): Study on Stabilization Characteristics and Stabilization of Soil Heavy Metal Pollution in Lead and Zinc Mining Areas. – China University of Mining & Technology, Beijing.

[9] Geebelen, W., Adriano, D. C., Lelie, D. V. D., Mench, M., Carleer, R., Clijsters, H., Vangronsveld, J. (2003): Selected bioavailability assays to test the efficacy of amendment-induced immobilization of lead in soils. – Plant & Soil 249(1): 217-228.

[10] Gupta, D. K., Corpas, F. J., Huang. (2013): Lead tolerance in plants: strategies for phytoremediation. – Environmental Science and Pollution Research 20(4): 2150-2161.

http://www.aloki.hu ● ISSN 1589 1623 (Print) ● ISSN 1785 0037 (Online)
DOI: http://dx.doi.org/10.15666/aeer/1705_1063710654

[11] He, M., Shi, H., Zhao, X. Y., Yu, Y., Qu, B. (2013): Immobilization of Pb and Cd in contaminated soil using nano-crystallite hydroxyapatite. – International Symposium on Environmental Science and Technology. https://doi.org/10.1016/j.proenv.2013.04.090
[12] Lin, H., Shi, W. Shao, H. B., Shao, M. A. (2009): The remediation of the lead-polluted garden soil by natural zeolite. – Journal of Hazardous Materials 169: 1106-1111.
[13] Hwang, A., Ji, W., Kweon, B., Khim, J. (2008): Thephysico-chemical properties and leaching behaviors of phosphatic clay for immobilizing heavy metals. – Chemosphere 70(6): 1141-1145.
[14] Kumpiene, J., Lagerkvist, A., Maurice, C. (2008): Stabilization of As, Cr, Cu, Pb and Zn in soil using amendments—a review. – Waste Management 28(1): 215-225.
[15] Liu, G., Yu, Y., Hou, J., Xue, W., Liu, X. H., Liu, Y. Z., Wang, W. H., Alsaedi, A., Hayat, T., Liu, Z. T. (2014): An ecological risk assessment of heavy metal pollution of the agricultural ecosystem near a lead-acid battery factory. – Ecological Indicators 47: 210-218.
[16] Liu, H. (2014): Effects of Modifier on Heavy Metal Morphology and Remediation Efficiency of Polygonum. – Guangxi Normal University, Guilin, pp. 1-137.
[17] Ma, H. (2007): Morphological Distribution and Leaching Characteristics of Heavy Metals in Municipal Sludge. – Hohai University, Jiangsu, pp. 1-73.
[18] Mcgowen, S. L., Basta, N. T., Brown, G. O. (2001): Use of diammonium phosphate to reduce heavy metal solubility and transport in smelter-contaminated soil. – Journal of Environmental Quality 30(2): 493.
[19] Mei, Z. (2006): The Comprehensive analysis on the chemical consistent of precipitation and the formation of acid rain at Chengdu urban area. – Dissertation, Sichuan University, Chengdu, China.
[20] Mignardi, S., Corami, A., Ferrini, V. (2012): Evaluation of the effectiveness of phosphate treatment for the remediation of mine waste soils contaminated with Cd, Cu, Pb, and Zn. – Chemosphere 86(4): 354-360.
[21] Nelson, D. W., Sommers, L. E. (1996): Total Carbon, Organic Carbon, and Organic Matter: Laboratory Methods. – In: Sparks, D. L. (ed.) Methods of Soil Analysis. Part 3. SSSA Book Ser. No. 5. SSSA/ASA, Madison, WI, pp 961-1010.
[22] Nemati, K., Abu, Bakar. N. K., Abas, M. R., Sobhanzadeh, E. (2011): Speciation of heavy metals by modified BCR sequential extraction procedure in different depths of sediments from Sungai Buloh, Selangor, Malaysia. – Journal of Hazardous Materials 192(1): 402-410.
[23] Pueyo, M., Mateu, J., Rigol, A., Vidal, M., López-Sánchez, J. F., Rauret, G. (2008): Use of the modified BCR three-step sequential extraction procedure for the study of trace element dynamics in contaminated soils. – Environmental Pollution 152(2): 330-341.
[24] Putra, R. S., Ohkawa, Y., Tanaka, S. (2013): Application of EAPR system on the removal of lead from sandy soil and uptake by Kentucky bluegrass (Poapratensis, L.). – Separation & Purification Technology 102(1): 34-42.
[25] Rao, Z., Zhu, Q. Huang, D. Y., Liu, S. L., Cao, X. L., Ren, X. F., Wang, S., Wang, J. Y. (2013): Effects of sepiolite on cadmium and lead leaching in contaminated red soil under simulated acid rain conditions. – Journal of Soil and Water conservation 27(3): 24-27.
[26] Rhoades, J. D. (1982): Cation Exchange Capacity. – In: Page, A. L., Miller, R. H., Keeney, D. R. (eds.) Methods of Soils Analysis. Part 2: Chemical and Microbiological Properties. Series Agronomy No. 9. ASA/SSSA, Madison, WI, pp 149-157.
[27] Rhoades, J. D., Shouse, P. J., Alves, W. J., Manteghi, N. A., Lesch, S. M. (1990): Determining soil salinity from soil electrical conductivity using different models and estimates. – Soil Science Society of America Journal 54(1): 46-54.
[28] Schwab, A. P., He, Y., Banks, M. K. (2005): The influence of organic ligands on the retention of lead in soil. – Chemosphere 61(6): 856-866.

http://www.aloki.hu ● ISSN 1589 1623 (Print) ● ISSN 1785 0037 (Online)
DOI: http://dx.doi.org/10.15666/aeer/1705_1063710654

[29] Shi, W., Li, H., Du, S., Wang, K. B., Shao, H. B. (2013): Immobilization of lead by application of zeolite: Leaching column and rhizobox incubation studies. – Applied Clay Science 85: 103-108.
[30] Shirvani, M., Kalbasi, M., Shariatmadari, H. (2006): Sorption–desorption of cadmium in aqueous palygorskite, sepiolite, and calcite suspensions: isotherm hysteresis. – Chemosphere 65(11): 0-2184.
[31] Suman, Raj. D. S, Aparna, C., Rekha, P., Bindhu, V. M. (2005): Stabilization and solidification technologies for the remediation of contaminated soils and sediments. An overview. – Land Contamination & Reclamation 13(1): 23-48.
[32] Sun, Y. R. (2000): Experimental survey for the effects of soil water content and soil salinity on soil electrical conductivity. – Journal of China Agricultural University 5(4): 39-41.
[33] Sun, Y. B., Xu, Y. M., Shi, X., Wang, L., Liang, X. F. (2012): The effect of sepiolite on passivation and remediation of cadmium-contaminated red soil. – Journal of Environmental Science 32(06): 1465-1472.
[34] Suzuki, T., Niinae, M., Koga, T., Akita, T., Ohta, M., Choso, T. (2014): EDDS-enhanced electrokinetic remediation of heavy metal-contaminated clay soils under neutral pH conditions. – Colloids & Surfaces A Physicochemical & Engineering Aspects 440(2): 145-150.
[35] Tai, Y., Mcbride, M. B., Li, Z. (2013): Evaluating specificity of sequential extraction for chemical forms of lead in artificially-contaminated and field-contaminated soils. – Talanta 107(2): 183-188.
[36] Tang, S. (2006): The studies on the water environmental risk and chemical remediation of heavy mental in urban soils in Guangzhou. – Dissertation. South China Agricultural University, Guandong, China.
[37] Tao, Q., Yao, J., He, S. F., Yang, Y., Li, Y., Liang, Y. (2015): The leaching effect of modified zeolite on Pb and Zn in contaminated soil under acid rain was simulated. – Journal of Soil and Water Conservation 29(5): 305-308.
[38] Taylor, M. P., Mould, S. A., Kristensen, L. J., Rouillon, M. (2014): Environmental arsenic, cadmium and lead dust emissions from metal mine operations: Implications for environmental management, monitoring and human health. – Environmental Research 135(1): 296-303.
[39] U.S. EPA, Federal Register (1986): Toxicity Characteristic Leaching Procedure (TCLP). – 40CFR, Vol.50, No.286, Appendix 2, Part 268, pp 406-943.
[40] Xu, J., Kleja, D. B., Biester, H., Lagerkvist, A., Kumpiene, J. (2014): Influence of particle size distribution, organic carbon, pH and chlorides on washing of mercury contaminated soil. – Chemosphere 109: 99-105.
[41] Xu, Z., Xu, D., Liu, G. S., Liu, W. P. (2004): Release characteristics of aluminum, manganese and iron in red soil under acid rain. – Journal of Soil and Water Conservation 18(3): 21-27.
[42] Yu, Y., Ding, A. F., H, Jia., Meng, L. (2001): Effects of simulated acid rain on soil acidification and base ions transplant. – Journal of Nanjing Forestry University 25(2): 39-42.
[43] Zhang, J., Zhang, X., Wang, C. W., Liu, S. P., Liu, Y. H. (2007): Simulated acid rain on soil exchangeable cation migration and its effect on soil acidification in orchards. – Journal of Soil and Water Conservation 21(1): 15-17.
[44] Zhang, S., Lin, H., Deng, L., Gong, G. S., Jia, Y. X., Xu, X. X., Li, T., Li, Y., Chen, H. (2013): Cadmium tolerance and accumulation characteristics of Siegesbeckia orientalis, L. – Ecological Engineering 51(2): 133-139.
[45] Zhou, H., Zeng, M., Liu, J., Liao, B. H., Shi, H. (2010): Influence of application $CaCO_3$ on content of Pb, Cd, Zn exchangeable in soil and the cumulative distribution of soybean plants. – Journal of Soil & Water Conservation 24(4): 123-126.

http://www.aloki.hu ● ISSN 1589 1623 (Print) ● ISSN 1785 0037 (Online)
DOI: http://dx.doi.org/10.15666/aeer/1705_1063710654

EVALUATION OF SPATIOTEMPORAL CHARACTERISTICS OF PRECIPITATION EXTREMES VARIATIONS IN AMUR RIVER BASIN

YAN, B.[1] – XU, J.[1] – WANG, Y.[1*] – HUANG, F.[2] – HAN, X.[1] – ZHANG, L.[3] – GUO, L.[4]

[1]*Changjiang River Scientific Research Institute, Changjiang Water Resources Commission of the Ministry of Water Resources of China, Wuhan 430015, China*

[2]*College of Hydrology and Water Resources, Hohai University, Nanjing 210098, China*

[3]*School of Natural Resources, University of Nebraska-Lincoln, Lincoln, NE 68588, USA*

[4]*Business School of Hohai University, Nanjing 210098, China*

**Corresponding author*
e-mail: wangyq@mail.crsiri.cn; phone: +86-158-5066-0117

(Received 1st Mar 2019; accepted 21st May 2019)

Abstract. Between 25th July and 19th August 2013, Amur River basin received some of its most extreme precipitation on record. The floods caused by the heavy rain brought affected Amur River and its 4 major tributaries. Hailun and Hailar stations break daily maximum precipitation record with 153.6 mm in 30th July, and 85.8 mm in 27th July, respectively. Based on daily precipitation observations at 25 stations from 1954 to 2014, the trends, periodicities and abrupt changes of five extreme precipitation indices in Amur River basin were investigated to the Spatiotemporal Characteristics of the extreme precipitation. Area-averaged annual total wet-day precipitation (PRCPTOT), maximum 1-day precipitation amount (Rx1day), maximum 5-day precipitation amount (Rx5day), very wet days (R95) and extremely wet days (R99) had non-significant trends. By wavelet analysis for annual PRCPTOT, Rx1day, Rx5day, R95 and R99 series, the real part wavelet phase of main periods were mostly located at positive peaks in 2013, which were corroborated by abrupt change analysis. Multi-cycle superimposition of main periods is possibly the main cause for extreme precipitation in 2013. The record-breaking daily precipitation data improve 100-year recurrence interval (111.47 mm) to 130.61 mm in Hailun and raise 100-year recurrence interval from 78.95 mm to 87.91 mm in Hailar.
Keywords: *precipitation extremes trend analysis wavelet analysis abrupt change Amur River basin*

Introduction

Climate change is a severe issue all around the world, which received a lot of attention. The studies in the mean value for temperature and precipitation have made very rich and detailed achievements in different regions, such as China (Qian and Zhu, 2001; Shi et al., 2007), Italy (Moonen et al., 2002), Iran (Tabari and Talaee, 2011), Chile (Kumar et al., 1992), and South Africa (Minetti et al., 2003). The extreme climate events always accompanied by the disasters and the life and property losses directly (Easterling et al., 2000a; Changnon et al., 2000; Griggs and Noguer, 2002), attracts more and more interests of international organizations and scientific research personnel in recent years (Allen et al., 2015; Bordi et al., 2007; Furió and Meneu, 2011). Extreme events, generally defined as the extreme low or high values in the range of observation data (Field et al., 2012), are considered more important and necessary than the study of the mean values referred to human and natural system (Aguilar et al., 2009; Katz and Brown, 1992). As climate changes present poor-rich effects on different regions, the

http://www.aloki.hu ● ISSN 1589 1623 (Print) ● ISSN 1785 0037 (Online)
DOI: http://dx.doi.org/10.15666/aeer/1705_1065510669

intensity and frequency of the extreme events also show different variation characteristics on geographically. In particular, the extreme precipitation indices present both negative and positive trends in India (Revadekar and Preethi, 2012; Preethi et al., 2011) and China (Wang and Zhou, 2005; Fu et al., 2013). It is generally that the changes in precipitation is the result of global atmospheric circulation in large spatial and temporal scales (Trenberth, 1999), and easily affected by monsoon (Li and Liu, 2006; Turner and Slingo, 2009), the Arctic Oscillation (Scaife et al., 2008), El Niño (Easterling et al., 2000b; DeFlorio et al., 2013) and other factors in the small term, but the relations between extreme indices and these factors are not the focus in our analyses and detailed research will be considered in future.

As one of the most important international rivers in East Asia with plenty of water, vast area and diversity of ecological features, Amur River has been concerned universally. The main factor caused the 2013 flood is the big amount of moisture poured on the Amur River basin, influenced by the East Asian monsoon, the Siberia High, high-pressure of the Pacific Ocean, the Arctic oscillation (AO) and so on (Danilov-Danil'yan and Gel'fan, 2014). Therefore, it is necessary to explore the spatiotemporal characteristics of the extreme precipitation events and take measures to cut back the damage from the events.

The five extreme precipitation indices were chosen to identify the changes of extreme precipitation events firstly: PRCPTOT, Rx1day, Rx5day, R95 and R99, which were recommended by World Meteorological Organization (WMO), United Nations Environment Programme (UNEP), et al. (Tao et al., 2018; Li et al., 2018). Secondly, the Mann-Kendall test was used to calculate the magnitude of the trends for five extreme indices, and evaluate whether the trend is significant or not. Then the periodicities of the extreme indices were analyzed by wavelet transform, and the abrupt changes were detected by Mann-Kendall method. Compared with the results of the trends and periodicities, the changes of the five extreme indices time series were analyzed, and the changes could partly reveal the causes of the 2013 extreme precipitation. Finally, the extent of the 2013 extreme precipitation was measured by analyzing the typical station, and some conclusions were given. This paper aims to provide a reference for international river-related countries to deal with extreme weather events through the study of extreme precipitation in the Amur River Basin.

Study area and data

Study area

The Amur River (*Fig. 1*), with the other name as Heilong River in Chinese, has the tenth largest basin area on earth (Nicholson et al., 2014). The Amur River basin has an area of 1.86 million km^2 which covers the territories of Mongolia, Russia, China and North Korea. In addition to its transboundary location, the Amur River basin can be characterized by contrasts between other geographic aspects: Russia and Asia; continental and monsoon climates; and southern dense and northern sparse populations. The climate of eastern Amur basin is humid monsoon temperature climate, which impact can reach the northernmost latitude on earth (Semenov et al., 2014; Yu et al., 2013). The climate of areas in the west of this basin (upper reach of the Amur River) is sheltered from monsoon influence and arid. The arid western portion of this basin is smaller compared with the more humid eastern portion.

http://www.aloki.hu ● ISSN 1589 1623 (Print) ● ISSN 1785 0037 (Online)
DOI: http://dx.doi.org/10.15666/aeer/1705_1065510669

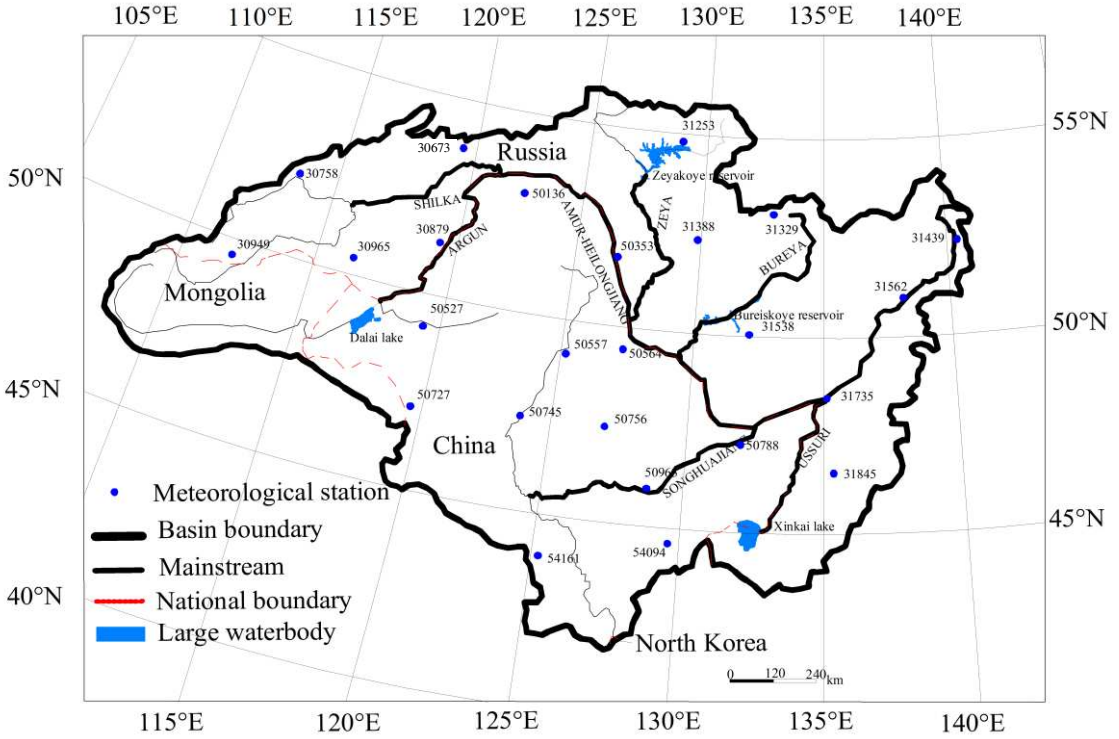

Figure 1. *Locations of the 25 meteorological stations in the Amur River basin*

Long-term observed precipitation data

The daily precipitation data from 1954 to 2014 were collected in 25 stations of which the 12 stations in China and 13 stations in Russia. *Figure 1* presented the geographical location of the stations and more information were shown in *Table 1*. The Chinese station data was provided from the National Climate Center, China Meteorological Administration, and the station data of Russia came from Russian Federal Service for Hydrometeorology and Environmental Monitoring. The data collected from authoritative departments in China and Russia are measured daily data of meteorological sites. Data quality control is necessary in the calculation and detecting the trends and periodicities of the extreme precipitation indices (Huang et al., 2013; You et al., 2014), although these data has been detected by primary quality control. The RHtestV.4 software package (http://etccdi.pacificclimate.org/software.shtml) was employed for homogeneity assessment (Wang, 2008a, b; Wang and Feng, 2013).

Methodology

In this study, five indices were chosen for variations evaluation of the extreme precipitation in Amur River basin, the definitions of these indices were presented in *Table 2,* and all these indices are from the core indices which were recommended by the Joint CCI-CLIVAR Expert Team for Climate Change Detection Monitoring and Indices (ETCCDMI) and applied in different countries (Liu et al., 2015; Altinsoy et al., 2013). These indices were used widely to study the variations of extreme climate events in many regions of the world.

http://www.aloki.hu ● ISSN 1589 1623 (Print) ● ISSN 1785 0037 (Online)
DOI: http://dx.doi.org/10.15666/aeer/1705_1065510669

Table 1. *List of 25 stations used in the study*

WMO number	Station	Latitude (°N)	Longitude (°E)	Altitude (m)
30673	Mogoca	53.75	119.73	624
30758	Chita	52.08	113.48	671
30879	Nerchinskij Zavod	51.32	119.62	621
30949	Kyra	49.57	111.97	907
30965	Borzja	50.40	116.52	675
31253	Bomnak	54.72	128.87	365
31329	Ekimchan	53.08	132.98	540
31388	Norsk	52.35	129.92	207
31439	Bogorodskoe	52.38	140.47	33
31538	Sutur	50.07	132.13	343
31562	Nizhnetambovskoe	50.93	138.18	20
31735	Habarovsk	48.57	135.17	75
31845	Krasnyj Jar	46.53	135.32	128
50136	Mohe	52.97	122.52	433
50353	Huma	51.72	126.65	177
50527	Hailar	49.27	119.75	610
50557	Nenjiang	49.17	125.23	242
50564	Sunwu	49.43	127.35	235
50727	Aershan	47.17	119.93	997
50745	Qiqihar	47.38	123.92	147
50756	Hailun	47.43	126.97	239
50788	Fujin	47.23	131.98	66
50963	Tonghe	45.97	128.73	109
54094	Mudanjiang	44.57	129.60	241
54161	Changchun	43.90	125.27	237

Table 2. *Definitions of five precipitation indices*

Index	Indicator name	Definitions	Units
PRCPTOT	Annual total wet-day precipitation	Annual total PRCP in wet days (RR ≥ 1 mm)	mm
Rx1day	Max 1-day precipitation amount	Monthly maximum 1-day precipitation	mm
Rx5day	Max 5-day precipitation amount	Monthly maximum consecutive 5-day precipitation	mm
R95	Very wet days	Annual total PRCP when RR > 95th percentile	mm
R99	Extremely wet days	Annual total PRCP when RR > 99th percentile	mm

The RClimDex software was employed to carry out the calculation of extreme precipitation indices. The non-parametric Mann-Kendall test (Ahmad et al., 2015; Yin et al., 2016; Yue et al., 2002) was used to estimate the magnitude of indices trend and verify whether the trend is significant. The Kendall slope is computed as *Equation 1:*

$$\beta = \mathrm{Median}\left(\frac{x_i - x_j}{i - j}\right) \quad \text{(Eq.1)}$$

Where $1 < j < i < n$ and β indicates the trend rate, and the unit is mm/year in this study. The threshold of significance test was set to 0.05 when assessing the trends of extreme indices.

http://www.aloki.hu ● ISSN 1589 1623 (Print) ● ISSN 1785 0037 (Online)
DOI: http://dx.doi.org/10.15666/aeer/1705_1065510669

Wavelet analysis (Lau and Weng, 1995), as an effective method to detect the periodicity in time series, was used to explore the extreme precipitation indices time series. In this study, Morlet wavelet was as the mother wavelet, to participate in the wavelet transform (Liu et al., 2015; Dai et al., 2003). The original data should be z-score standardized to eliminate the randomness before wavelet transform. The continuous transform is computed as *Equations 2–4:*

$$W_f(a,b) = |a|^{-\frac{1}{2}} \int_{-\infty}^{+\infty} f(t)\overline{\psi}\left(\frac{t-b}{a}\right)dt \quad \text{(Eq.2)}$$

$$\psi(t) = e^{ict}e^{-t^2/2} \quad \text{(Eq.3)}$$

$$\mathrm{Var}(a) = \int_{-\infty}^{+\infty} \left|W_f(a-b)\right|^2 db \quad \text{(Eq.4)}$$

Where *f(t)* is the extreme precipitation indices times series, $W_f(a,b)$ is the coefficient of wavelet transform, a and b are scale and time parameters, respectively. $\psi(t)$ is the morlet wavelet function, and Var(a) reveals the fluctuations of a in the annual indices series. When $c = 6.2$, the periodicity $T \approx a$, so c was set to 6.2 in this study. By the graph of Var(a) varying with a, the main periodicities can be marked by the peaks corresponding to a.

The generalized extreme value distribution (GEV) (Furió and Meneu, 2011; Burke et al., 2010), derived from the characterization of extreme event, was employed to fit the annual Rx1day series. The distribution formula is computed as *Equation 5:*

$$G(z;\mu,\theta,\sigma,\xi) = \exp\left\{-\left[1+\xi\left(\frac{z-\mu}{\sigma}\right)\right]^{-1/\xi}\right\} \quad \text{(Eq.5)}$$

Defined on $\{z:1+\xi(z-\mu)/\sigma>0\}$, $-\infty<\mu<\infty$ (location parameter), $\sigma>0$ (scale parameter) and $-\infty<\xi<\infty$ (shape parameter). The profile likelihood method is more reasonable to be used to estimate the multi-year return levels and 0.95 confidence intervals, compared with the maximum likelihood method (Huang et al., 2013).

Results and discussion

General characteristics of precipitation extreme indices

The changes of Percentage of precipitation anomalies in the area-averaged time series for five extreme precipitation indices were shown in *Figure 2,* and the basic statistical data was performed in *Table 3*. The changes of 5 indices are almost consistent, while the R99 fluctuate severely. The anomaly percentage of R99 varies from 73.50 to -80.76, while other indices fluctuate between -30 and 30. In particular, the variation coefficient (0.30) of R99 is largest, while PRCPTOT, Rx1day, Rx5day, and R95 are 0.10, 0.08, 0.09 and 0.18, respectively.

Figure 3 shows the distribution for the multi-year mean of extreme precipitation indices from 1954 to 2014 in the Amur River basin. Most of the extreme precipitation events generally occurred in the southeast of the Amur River basin, while the south area

http://www.aloki.hu ● ISSN 1589 1623 (Print) ● ISSN 1785 0037 (Online)
DOI: http://dx.doi.org/10.15666/aeer/1705_1065510669

are higher than other area for Rx1day. Spatially, the maximum value of the multi-year mean of extreme precipitation indices generally occurs in the south, while the minimum value generally occurs in the north. Specifically, the maxima of PRCPTOT, R95 and R99 occur in Krasnyj Jar Station (southeast of the basin), and the maxima of Rx1day and Rx5day occur in Changchun Station (southwest of the basin). The minima of PRCPTOT, Rx5day, R95 and R99 occur in Kyra Station (northwest of the basin), and the minimum value of Rx1day occurs in Mogoca Station (northwest of the basin). Particularly, the distributions are similar to the distribution pattern of the annual precipitation in Liu's view, although his study area is just one part of the Amur River basin (Liu et al., 2015).

Figure 2. *Percentage of precipitation anomalies changes in the time series for five extreme precipitation indices during 1954 to 2014 (comparison with the averages of 1954~2014). (PRCPTOT-annual total wet-day precipitation, Rx1day-maximum 1-day precipitation amount, Rx5day-maximum 5-day precipitation amount, R95-very wet days, R99-extremely wet days)*

Table 3. *Statistical information for five extreme precipitation indices time series*

Indices	Mean (mm)	Standard deviation	Coefficient of kurtosis	Coefficient of variation	Maxima (mm)	Minima (mm)	Range (mm)	Range/ mean (%)
PRCPTOT	500.69	49.16	-0.19	0.10	619.28	399.27	220.01	43.94
Rx1day	46.84	3.86	0.03	0.08	56.26	38.7	17.56	37.49
Rx5day	78.86	7.19	-0.26	0.09	98.79	66.56	32.23	40.87
R95	124.75	22.24	-0.05	0.18	180.88	82.38	98.50	78.96
R99	39.66	11.91	0.54	0.30	68.81	7.63	61.18	154.26

http://www.aloki.hu ● ISSN 1589 1623 (Print) ● ISSN 1785 0037 (Online)
DOI: http://dx.doi.org/10.15666/aeer/1705_1065510669

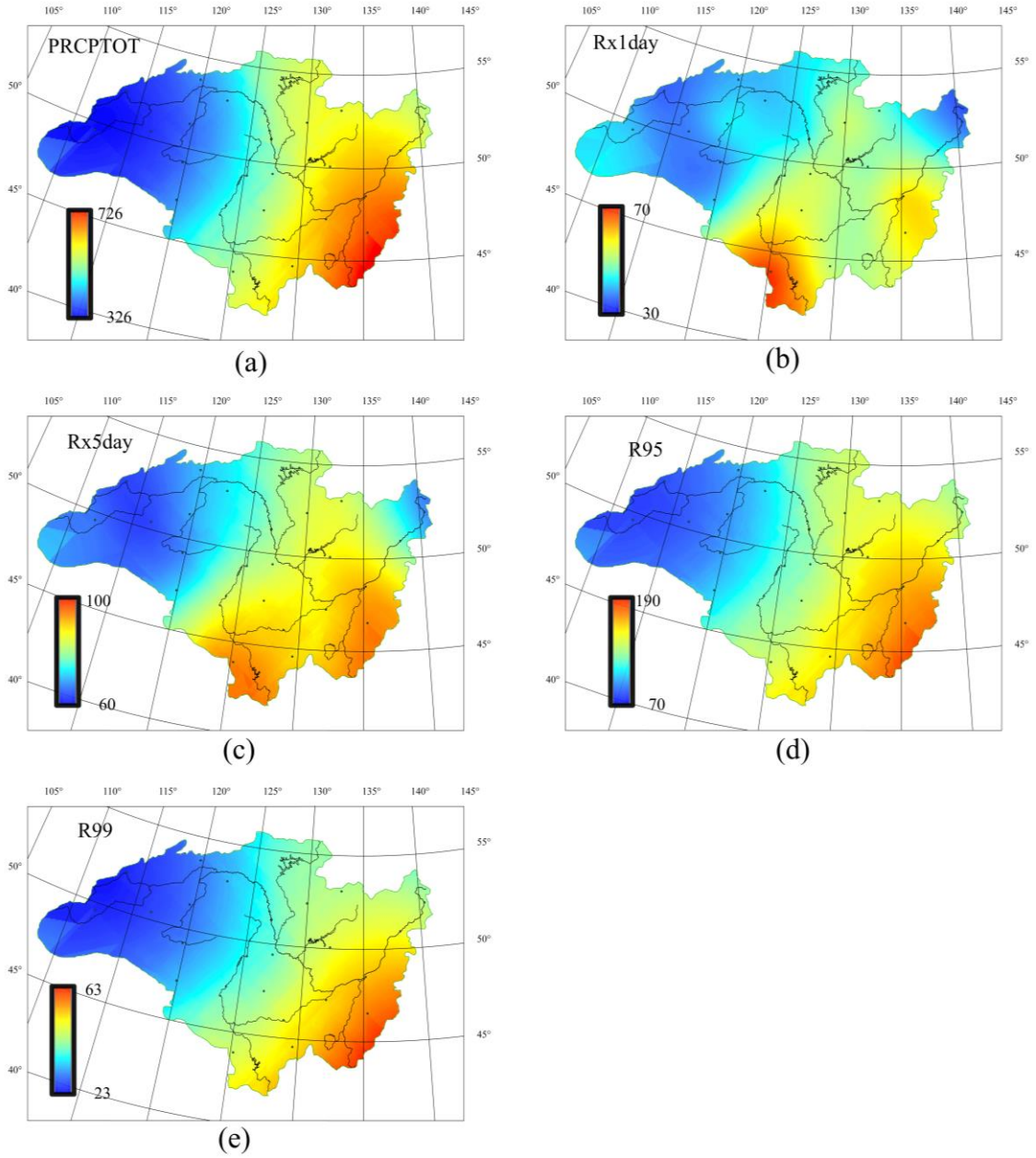

Figure 3. *Spatial distribution for the multi-year mean of extreme precipitation indices from 1954 to 2014 in the Amur River basin (unit mm). (PRCPTOT-annual total wet-day precipitation, Rx1day-maximum 1-day precipitation amount, Rx5day-maximum 5-day precipitation amount, R95-very wet days, R99-extremely wet days)*

Trends of extreme precipitation indices

For the five indices, the area-averaged trends are weak and statistical non-significant, the Kendall slopes for PRCPTOT, Rx1day, Rx5day, R95 and R99 are -0.28, 0.02, -0.04, 0.01 and 0.09 mm/year, respectively. For the spatial trends results (*Fig. 4*), only Nizhnetambovskoe station, the trends of Rx1day, Rx5day, R95 and R99 are notable and positive significantly, while the other stations fluctuate weakly in all indices during the study period.

http://www.aloki.hu ● ISSN 1589 1623 (Print) ● ISSN 1785 0037 (Online)
DOI: http://dx.doi.org/10.15666/aeer/1705_1065510669

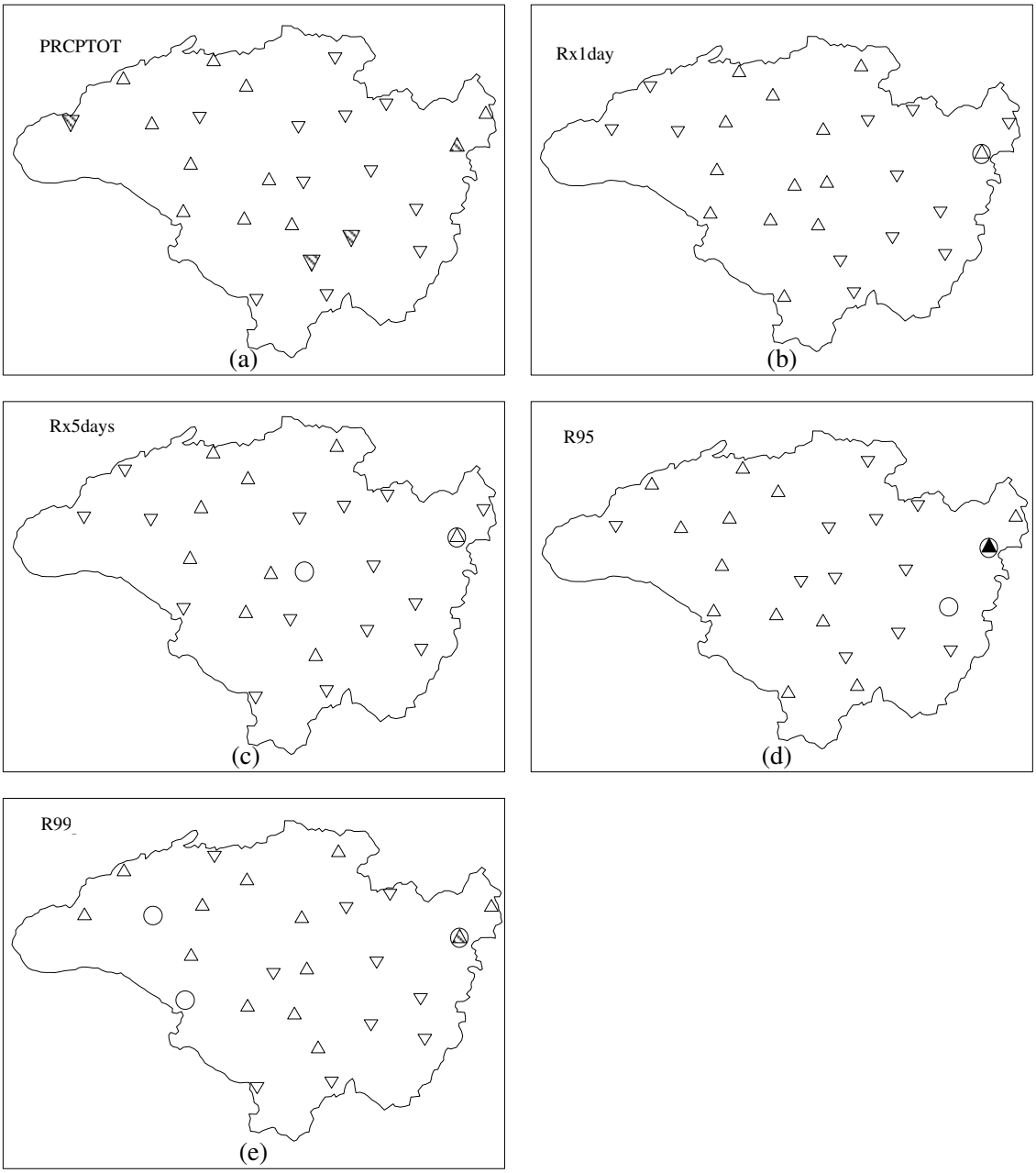

Figure 4. *Spatial pattern of trends for the extreme precipitation indices for 25 stations from 1954 to 2014 in the Amur River basin (▲,◬, ◭, ○, ▽, ▼, ▼ indicate $\beta > 2$ mm/year, $1 < \beta \leq 2$ mm/year, $0 < \beta \leq 1$ mm/year, $\beta = 0$, $-1 < \beta < 0$ mm/year, $-2 < \beta \leq -1$ mm/year, $\beta \leq -2$ mm/year, respectively; the triangles that are rounded indicate significant trend at 0.05 level). (PRCPTOT-annual total wet-day precipitation, Rx1day-maximum 1-day precipitation amount, Rx5day-maximum 5-day precipitation amount, R95-very wet days, R99-extremely wet days)*

Periodicities of extreme precipitation indices

Wavelet analysis is employed to judge the periodicities of the extreme precipitation indices. For PRCPTOT, three peaks can be found in the Periodicities diagnosis graphs of annual area-averaged indices series and they are located at time scale of 4, 13 and 29a. As the peak value means the oscillation strength, the first main period is 29a, and

http://www.aloki.hu ● ISSN 1589 1623 (Print) ● ISSN 1785 0037 (Online)
DOI: http://dx.doi.org/10.15666/aeer/1705_1065510669

the second and third are 13 and 4a respectively. The main periods are 30, 19 and 5a for Rx1day, 30, 14 and 6a for Rx5day, 30, 13 and 4a for R95, and 28, 11, 18 and 6a for R99, respectively.

Figure 5 shows the wavelet transform real part variation course of annual area-averaged indices series. The size of amplitude responses the periodic obviousness, and the amplitude of the first main period of 29a are larger than those of 13 and 4a in *Figure 5a*. For PRCPTOT, the amplitude of 13a time scale becomes gradually smaller in the entire study period, and even weaker than 4a after 1990. It reveals that the periodicity of 4a timescale was more obvious than 13a after 1990. Besides, the positive real part phase means abundant PRCPTOT, while the negative real part phase indicates scarce PRCPTOT. Taking 13a time scale as example, abundant PRCPTOT occurred in 1957-1962, 1969-1974, 1992-1998 and 2010-2014.

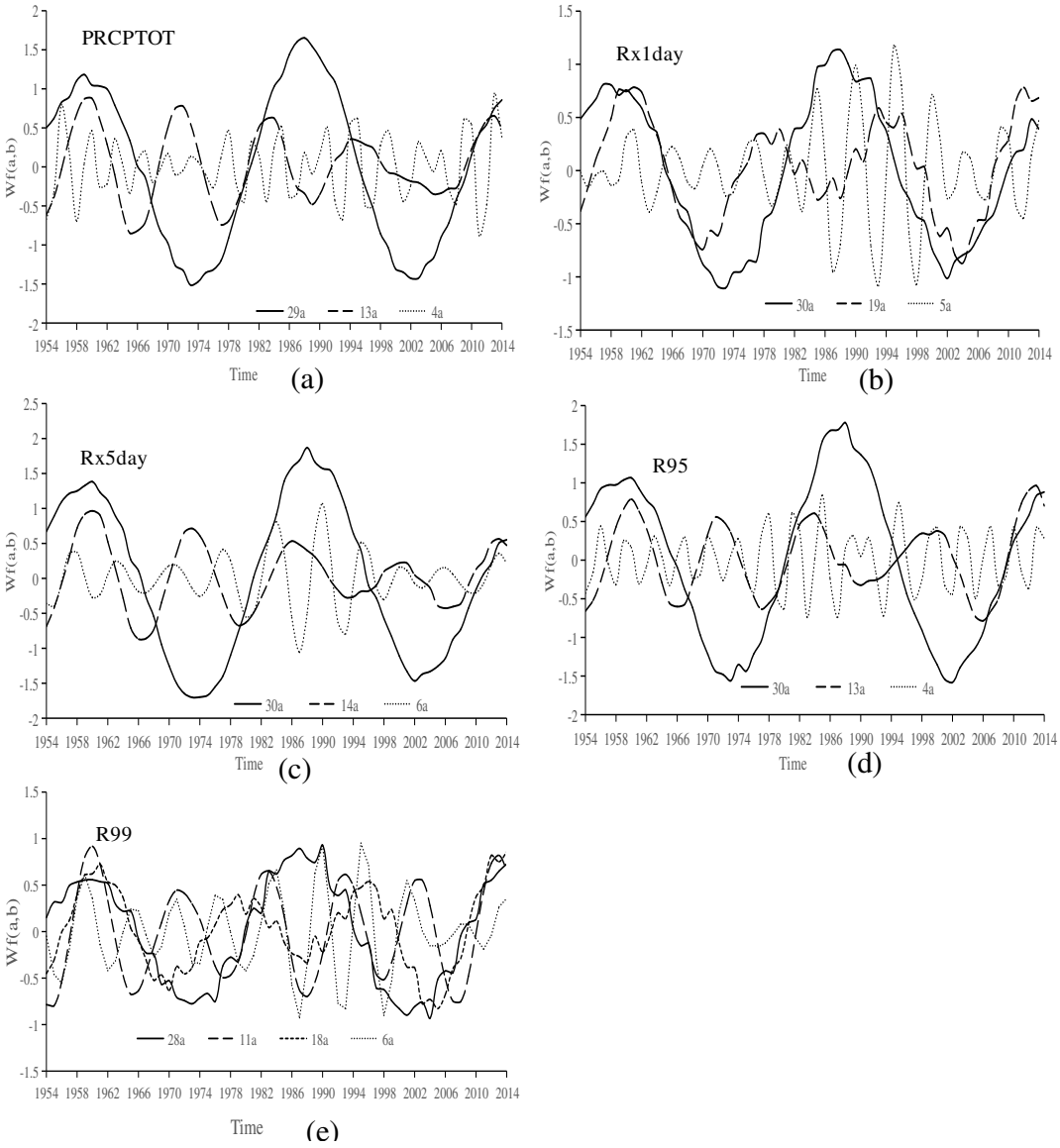

Figure 5. *The wavelet transform real part variation course of annual area-averaged indices series (PRCPTOT-annual total wet-day precipitation, Rx1day-maximum 1-day precipitation amount, Rx5day-maximum 5-day precipitation amount, R95-very wet days, R99-extremely wet days)*

http://www.aloki.hu ● ISSN 1589 1623 (Print) ● ISSN 1785 0037 (Online)
DOI: http://dx.doi.org/10.15666/aeer/1705_1065510669

Overall, the periodicities analysis of the annual extreme precipitation indices explains the cause of the extreme precipitation in Amur River basin in 2013. For PRCPTOT, Rx1day, Rx5day, R95 and R99, the real part wavelet phase of main periods were mostly located at positive peaks in 2013.

Abrupt changes of extreme precipitation indices

The Mann-Kendall method is used to perform abrupt change testing on extreme precipitation indices, which is widely used in hydrometeorology. *Figure 6* shows the Mann-Kendall abrupt change test of the five extreme precipitation indices from 1954 to 2014. It can be seen from the figure that there are similar abrupt change characteristics in the five extreme indices, with two change points around 1963 and around 1989. Both of these change points correspond to the peak of the first main period in *Figure 5,* which indicates that there is a certain relationship between the abrupt change and the periodic variation of the sequence. In addition, the lines of Rx1day, R95 and R99 have intersections in 2013, 2014 and 2012, respectively, while the other two indicators will intersect at the end of the evaluation period, which is almost the same as the peak of the first main period in *Figure 5*.

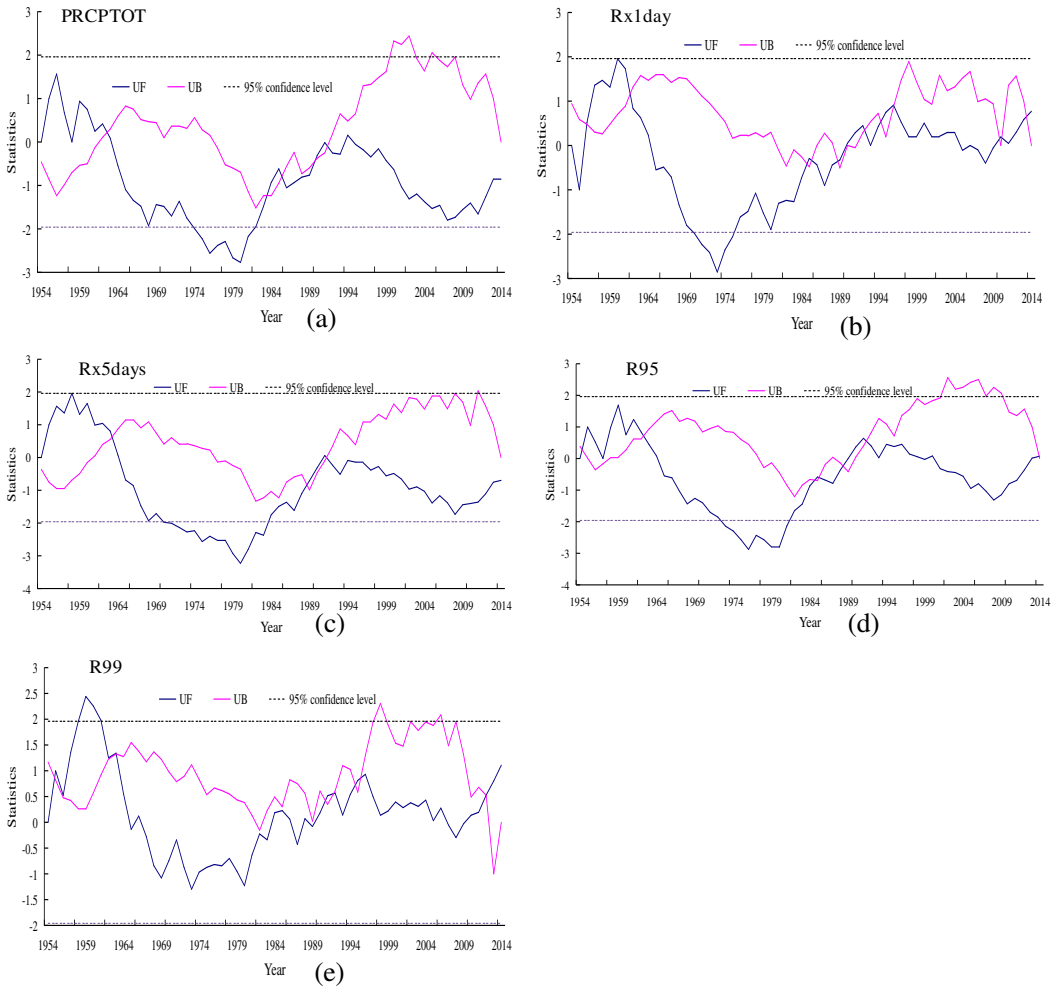

Figure 6. *The Mann-Kendall abrupt change test of annual area-averaged indices series. (PRCPTOT-annual total wet-day precipitation, Rx1day-maximum 1-day precipitation amount, Rx5day-maximum 5-day precipitation amount, R95-very wet days, R99-extremely wet days)*

http://www.aloki.hu ● ISSN 1589 1623 (Print) ● ISSN 1785 0037 (Online)
DOI: http://dx.doi.org/10.15666/aeer/1705_1065510669

Extreme precipitation analyses at typical stations in 2013 floods

The Hailun and Hailar Stations received record-breaking observations of daily maximum precipitation in 2013. The GEV distribution was fitted to the annual Rx1day series of Hailun and Hailar, and the profile likelihood method was employed to estimate the 10/50/100-year return levels (*Table 4*). For Hailun station, the record-breaking data (153.6 mm) was around 100-year return level in the evaluation period of 1954-2012, and improve the 10/50/100-year return levels (76.37, 100.90 and 111.47 mm) to 89.14, 114.62 and 130.61 mm. For Hailar station, the record-breaking observation (85.80 mm) was also around 100-year return level in the period of 1954-2012, and the 10/50/100-year return levels (51.99, 70.45 and 78.95 mm) were raised to 54.21, 76.80 and 87.91 mm.

Table 4. *The 10/50/100-year return levels and 0.95 confidence intervals (mm) estimated by the profile likelihood method for annual Rx1day series*

Region	Time series	10 years	50 years	100 years
Hailun	1954-2012	76.37(68.63,89.33)	100.90(87.37,136.47)	111.47(94.21,162.38)
	1954-2013	89.14(79.71,97.33)	114.62(94.96,161.45)	130.61(104.34,199.60)
Hailar	1954-2012	51.99(46.51,61.84)	70.45(59.46,101.75)	78.95(64.35,126.00)
	1954-2013	54.21(47.91,65.77)	76.80(63.16,115.72)	87.91(68.94,138.21)

This study analyzes the temporal and spatial variation characteristics of extreme precipitation indices for the trend, periodicity and abrupt change analysis of five extreme precipitation indices. The results of the trend, periodicity and abrupt change analysis are also mutually corroborated, indicating to some extent the correctness of the results of the analysis. This study has certain similarities with the results of other scholars studying Northeast Asia, but other scholars are limited by the availability of data, and the scope of research is limited to China (Deng et al., 2018; Liu et al., 2015) or Russia (Vyshkvarkova and Voskresenskaya, 2018). In addition, some scholars use large-scale meteorological products to analyze extreme precipitation (Zhu et al., 2018; Tao et al., 2018). Based on the analysis of spatio-temporal distribution characteristics of extreme precipitation, this paper uses GEV distribution to analyze the impact of the extremes on the return levels of typical stations by comparison two periods with or without the value of 2013, which is helpful to further understand the numerical value of the single extreme value for the entire evaluation period. Furthermore, the causes of extreme precipitation are not studied in this paper, and it is expected to be demonstrated in future research..

Conclusions

1. Generally, the changes of annual PRCPTOT, Rx1day, Rx5day, R95 and R99 series are almost consistent, while the R99 with the largest variation coefficient (0.30) fluctuate severely.
2. For PRCPTOT, Rx1day, Rx5day, R95 and R99 indices, not only area-averaged but also individual stations have weak and non-significant trends except for the Nizhnetambovskoe Station.

http://www.aloki.hu ● ISSN 1589 1623 (Print) ● ISSN 1785 0037 (Online)
DOI: http://dx.doi.org/10.15666/aeer/1705_1065510669

3. It was reasonable to use wavelet analysis to explore the periodicities for annual PRCPTOT, Rx1day, Rx5day, R95 and R99 series, and the real part wavelet phase of main periods were mostly located at positive peaks in 2013. It means that the periodicities of the extreme precipitation indices are the main cause for 2013 extreme precipitation event than the trends.
4. The correlation coefficients among PRCPTOT, Rx1day, Rx5day, R95 and R99 varied from 0.50 to 0.84, and all have passed 0.01 significant level.
5. The Hailun and Hailar stations suffered from record-breaking daily maximum precipitation in 2013, and their 10/50/100-year return levels were raised from 76.37/100.90/111.47 mm and 51.99/70.45/78.95 mm to 89.14/114.62/130.61 mm and 54.21/76.80/87.91 mm, respectively.

Acknowledgements. This work is funded by the National Key R&D Program of China (2017YFC0403600, 2017YFC0403606, 2017YFC1502404), National Public Research Institutes for Basic R&D Operating Expenses Special Project (CKSF2017061/SZ, CKSF2017057/SZ, CKSF2017008), the National Natural Science Foundation of China (No. 51779013, 51509009), Water Conservancy Science and Technology Innovation project of GuangDong Province (2017-03). Special thanks are given to the anonymous reviewers and editors for their constructive comments.

REFERENCES

[1] Aguilar, E., Barry, A. A., Brunet, M., Ekang, L., Fernandes, A., Massoukina, M., Mbah, J., Mhanda, A. D., Nascimento, D., Peterson, T. (2009): Changes in temperature and precipitation extremes in western central Africa, Guinea Conakry, and Zimbabwe, 1955–2006. – Journal of Geophysical Research: Atmospheres (1984–2012) 114(D2).

[2] Ahmad, I., Tang, D., Wang, T., Wang, M., Wagan, B. (2015): Precipitation trends over time using Mann-Kendall and spearman's RHO tests in swat river basin, Pakistan. – Advances in Meteorology. http://dx.doi.org/10.1155/2015/431860.

[3] Altinsoy, H., Ozturk, T., Turkes, M., Kurnaz, M. (2013): Simulating the Climatology of Extreme Events for the Central Asia Domain Using the RegCM 4.0 Regional Climate Model. – In: Helmis, C., Nastos, P. T. (eds.) Advances in Meteorology, Climatology and Atmospheric Physics. Springer, Berlin, Heidelberg, pp. 365-370.

[4] Bordi, I., Fraedrich, K., Petitta, M., Sutera, A. (2007): Extreme value analysis of wet and dry periods in Sicily. – Theoretical and Applied Climatology 87(1-4): 61-71.

[5] Burke, E. J., Perry, R. H. J., Brown, S. J. (2010): An extreme value analysis of UK drought and projections of change in the future. – Journal of Hydrology 388(1): 131-143.

[6] Changnon, S. A., Pielke, R. A., Changnon, D., Sylves, R. T., Pulwarty, R. (2000): Human factors explain the increased losses from weather and climate extremes. – Bulletin of the American Meteorological Society 81(3): 437-442.

[7] Dai, X., Wang, P., Chou, J. (2003): Multiscale characteristics of the rainy season rainfall and interdecadal decaying of summer monsoon in North China. – Chinese Science Bulletin 48(24): 2730-2734.

[8] Danilov-Danil'yan, V. I., Gel'fan, A. N. (2014): The extraordinary flood in the Amur River Basin. – Herald of the Russian Academy of Sciences 84(5): 335-343.

[9] Deflorio, M. J., Pierce, D. W., Cayan, D. R., Miller, A. J. (2013): Western US extreme precipitation events and their relation to ENSO and PDO in CCSM4. – Journal of Climate 26(12): 4231-4243.

[10] Deng, Y., Jiang, W., He, B., Chen, Z., Jia, K. (2018): Change in intensity and frequency of extreme precipitation and its possible teleconnection with large-scale climate index

http://www.aloki.hu ● ISSN 1589 1623 (Print) ● ISSN 1785 0037 (Online)
DOI: http://dx.doi.org/10.15666/aeer/1705_1065510669

over the china from 1960 to 2015. – Journal of Geophysical Research Atmospheres 123(4).

[11] Easterling, D. R., Evans, J. L., Groisman, P. Y., Karl, T. R., Ambenje, P. (2000a): Observed variability and trends in extreme climate events: a brief review. – Bulletin of the American Meteorological Society 81(3): 417-425.

[12] Easterling, D. R., Meehl, G. A., Parmesan, C., Changnon, S. A., Karl, T. R., Mearns, L. O. (2000b): Climate extremes: observations, modeling, and impacts. – Science 289(5487): 2068-2074.

[13] Field, C., Barros, V., Stocker, T. et al. (2012): Managing the Risks of Extreme Events and Disasters to Advance Climate Change Adaptation. A Special Report of Working Groups I and II of the Intergovernmental Panel on Climate Change. – Cambridge University Press, New York.

[14] Fu, G., Yu, J., Yu, X., Ouyang, R., Zhang, Y., Wang, P., Liu, W., Min, L. (2013): Temporal variation of extreme rainfall events in China, 1961–2009. – Journal of Hydrology 487: 48-59.

[15] Furió, D., Meneu, V. (2011): Analysis of extreme temperatures for four sites across Peninsular Spain. – Theoretical and Applied Climatology 104(1-2): 83-99.

[16] Griggs, D. J., Noguer, M. (2002): the scientific basis. Contribution of working group I to the third assessment report of the intergovernmental panel on climate change. – Weather 57(8): 267-269.

[17] Huang, F., Xia, Z., Guo, L., Yang, F. (2013): Climate change detection and annual extreme temperature analysis of the Irtysh Basin. – Theoretical and Applied Climatology 111(3-4): 465-470.

[18] Katz, R. W.; Brown, B. G. (1992): Extreme events in a changing climate: variability is more important than averages – Climatic Change 21(3): 289-302.

[19] Kumar, K. R., Pant, G. B., Parthasarathy, B., Sontakke, N. A. (1992): Spatial and subseasonal patterns of the long-term trends of Indian summer monsoon rainfall. – International Journal of Climatology 12(3): 257-268.

[20] Lau, K. M., Weng, H. (1995): Climate signal detection using wavelet transform: How to make a time series sing. – Bulletin of the American Meteorological Society 76(12): 2391-2402.

[21] Li, C., Walter, L. F., Wang, J., Hubert, F., Mariia, F., Hu, R., Yin, S., Bao, Y., Yu, S., Julian, H. (2018): An analysis of precipitation extremes in the inner mongolian plateau: spatial-temporal patterns, causes, and implications. – Atmosphere 9(8): 322.

[22] Li, J., Liu, B. (2006): The change character of monsoon rainband over Heilongjiang Province for the past 40 years. – Journal of Forestry Research 17(1): 71-74.

[23] Liu, B., Xiao, C., Liang, X. (2015): Evaluation of spatial and temporal characteristics of precipitation variations in Jilin Province, Northeast China. – Theoretical and Applied Climatology 122(1-2): 129-142.

[24] Liu, R., Liu, S., Cicerone, R., Shiu, C., Li, J., Wang, J., Zhang, Y. (2015): Trends of extreme precipitation in eastern China and their possible causes. – Advances in Atmospheric Sciences 32(8): 1027-1037.

[25] Minetti, J. L., Vargas, W. M., Poblete, A., Acuña, L., Casagrande, G. (2003): Non-linear trends and low frequency oscillations in annual precipitation over Argentina and Chile, 1931-1999. – Atmósfera 16(2): 119-135.

[26] Moonen, A. C., Ercoli, L., Mariotti, M., Masoni, A. (2002): Climate change in Italy indicated by agrometeorological indices over 122 years. – Agricultural and Forest Meteorology 111(1): 13-27.

[27] Nicholson, U., Poynter, S., Clift, P. D., Macdonald, D. I. M. (2014): Tying catchment to basin in a giant sediment routing system: a source-to-sink study of the Neogene–Recent Amur River and its delta in the North Sakhalin Basin. – Geological Society, London, Special Publications 386(1): 163-193.

http://www.aloki.hu ● ISSN 1589 1623 (Print) ● ISSN 1785 0037 (Online)
DOI: http://dx.doi.org/10.15666/aeer/1705_1065510669

[28] Preethi, B., Revadekar, J. V., Munot, A. A. (2011): Extremes in summer monsoon precipitation over India during 2001–2009 using CPC high-resolution data – International Journal of Remote Sensing 32(3): 717-735.
[29] Qian, W., Zhu, Y. (2001): Climate change in China from 1880 to 1998 and its impact on the environmental condition. – Climatic Change 50(4): 419-444.
[30] Revadekar, J., Preethi, B. (2012): Statistical analysis of the relationship between summer monsoon precipitation extremes and foodgrain yield over India. – International Journal of Climatology 32(3): 419-429.
[31] S. M. Allen, Gough, W. A., Mohsin, T. (2015): Changes in the frequency of extreme temperature records for Toronto, Ontario, Canada. – Theoretical and Applied Climatology 119(3-4): 481-491.
[32] Scaife, A. A., Folland, C. K., Alexander, L. V., Moberg, A., Knight, J. R. (2008): European climate extremes and the North Atlantic Oscillation. – Journal of Climate 21(1): 72-83.
[33] Semenov, E. K., Sokolikhina, N. N., Tatarinovich, E. V., Tudrii, K. O. (2014): Synoptic conditions of the formation of a catastrophic flood on the Amur River in 2013. – Russian Meteorology and Hydrology 39(8): 521-527.
[34] Shi, Y., Shen, Y., Kang, E., Li, D., Ding, Y., Zhang, G., Hu, R. (2007): Recent and future climate change in Northwest China. – Climatic Change 80(3-4): 379-393.
[35] Tabari, H. Talaee, P. H. (2011): Temporal variability of precipitation over Iran: 1966–2005. – Journal of Hydrology 396(3): 313-320.
[36] Tao, Y., Wang, W., Song, S., Ma, J. (2018): Spatial and temporal variations of precipitation extremes and seasonality over China from 1961~2013. – Water 10(6): 719.
[37] Trenberth, K. E. (1999): Conceptual Framework for Changes of Extremes of the Hydrological Cycle with Climate Change. – In: Karl, T. R. et al. (eds.) Weather and Climate Extremes. Springer, Dordrecht, pp. 327-339.
[38] Turner, A. G., Slingo, J. M. (2009): Uncertainties in future projections of extreme precipitation in the Indian monsoon region. – Atmospheric Science Letters 10(3): 152-158.
[39] Vyshkvarkova, E. V., Voskresenskaya, E. N. (2018): Changes of extreme precipitation in Southern Russia. – IOP Conference Series: Earth & Environmental Science 107(1): 012044.
[40] Wang, X., Wang, T., Yang, M., Zhang, N., Lu, D., Xu, T. (2018): Temporal and spatial distribution characteristics of surface vapor pressure and their influencing factors in Weifang. – Journal of Meteorology & Environment 34(3): 78-85.
[41] Wang, X. L. (2008a): Accounting for autocorrelation in detecting mean shifts in climate data series using the penalized maximal t or F test. – Journal of Applied Meteorology and Climatology 47(9): 2423-2444.
[42] Wang, X. L. (2008b): Penalized maximal F test for detecting undocumented mean shift without trend change. – Journal of Atmospheric and Oceanic Technology 25(3): 368-384.
[43] Wang, X. L., Feng, Y. (2013): RHtestsV4 User Manual. – Climate Research Division, ASTD, STB, Environment Canada.
[44] Wang, Y., Zhou, L. (2005): Observed trends in extreme precipitation events in China during 1961–2001 and the associated changes in large-scale circulation. – Geophysical Research Letters 32(9).
[45] Yin, J., Yan, D., Yang, Z., Yuan, Z., Yuan, Y., Wang, H., Shi, X. (2016): Research on historical and future spatial-temporal variability of precipitation in China. – Advances in Meteorology. http://dx.doi.org/10.1155/2016/9137201.
[46] You, C. H., Lee, D. I., Kang, M. Y. (2014): Rainfall estimation using specific differential phase for the first operational polarimetric radar in Korea. – Advances in Meteorology. http://dx.doi.org/10.1155/2014/413717.
[47] Yu, L., Xia, Z., Li, J., Cai., T. (2013): Climate change characteristics of Amur River. – Water Science and Engineering 6(2): 131-144.

http://www.aloki.hu ● ISSN 1589 1623 (Print) ● ISSN 1785 0037 (Online)
DOI: http://dx.doi.org/10.15666/aeer/1705_1065510669

[48] Yue, S., Pilon, P., Cavadias, G. (2002): Power of the Mann–Kendall and Spearman's RHO tests for detecting monotonic trends in hydrological series. – Journal of Hydrology 259(1): 254-271.
[49] Zhu, J., Huang, G., Wang, X., Cheng, G., Wu, Y. (2018): High-resolution projections of mean and extreme precipitations over china through PRECIS under RCPs. – Climate Dynamics 50(11-12): 4037-4060.

http://www.aloki.hu ● ISSN 1589 1623 (Print) ● ISSN 1785 0037 (Online)
DOI: http://dx.doi.org/10.15666/aeer/1705_1065510669

KINETIC MODELLING OF GAS GENERATED FROM ANAEROBIC FERMENTATION OF KITCHEN WASTE WITH MICROAEROBIC PRETREATMENT

FENG, L.[1] – LI, X.[1] – GU, S. Y.[2*] – LI, Y.[2] – ZHANG, M.[2] – YAN, Y. S.[2] – ZHANG, W. Y.[2]

[1]*Liaoning Province Clean Energy Key Laboratory, Shenyang Aerospace University, Shenyang Daoyi Street 37, Shenyang 110136, China*

[2]*Shenyang Agricultural University, Shenyang Dongling Street 120, Shenyang 110866, China*

**Corresponding author*
e-mail: syndgsy@126.com; phone: +86-137-0985-0916

(Received 1st Mar 2019; accepted 21st May 2019)

Abstract. Anaerobic fermentation is one of the effective ways to achieve the harmless, resource-reducing and reducing of kitchen waste. In this paper, the oxygen content under initial conditions in the anaerobic fermentation process of kitchen waste was changed by experiment (for micro-oxygen pretreatment). It was verified that trace oxygen can optimize the anaerobic fermentation system and increase the rate of anaerobic fermentation. Through the study of the gas production characteristics of the micro-oxygen experiment group, by using the Logistic model and the modified Gompertz model, the R^2 is above 0.99, and the fitting effect is better. The first-order hydrolysis model was combined with different particle reaction kinetic models to obtain a modified first-order gas production model. The results show that the air intake is suitable for the cylindrical particle model. The corresponding R^2 and k values for the air intake from 0 ml to 20 ml are: $\ln(y_m) + \ln(k) = 0.98298$, $k = 0.04339$; $\ln(y_m) + \ln(k) = 0.96149$, $k = 0.04706$; $\ln(y_m) + \ln(k) = 0.98219$, $k = 0.04611$; $\ln(y_m) + \ln(k) = 0.94356$, $k = 0.05039$; $R^2 = 0.9327$, $k = 0.05149$; the fitting effect is better. The population growth model and the modified primary gas production model can better describe the effect of oxygen content change on anaerobic fermentation gas production, and have important significance for the application of anaerobic fermentation in actual production and life processes.
Keywords: *kitchen waste, microaerobic pretreatment, kinetic analysis, population model, modified first-order gas-generation model*

Introduction

Waste and pollution of kitchen waste is a worldwide economic and environmental problem. Per capita production of 95-115 kg of kitchen waste per year in Europe and North America exceeds one third of the total food produced in the region. China is due to population base. Larger, with the rapid increase in the amount of organic waste and municipal sludge produced in recent years, the amount of kitchen waste produced in China reached 95 million tons in 2015, and the average daily waster output was as high as 260,000 tons per day The per capita annual output is 73 kg (Zeng, 2017). One of the effective ways to treat kitchen waste by anaerobic digestion has many advantages: Anaerobic digestion of food waste has many advantages: the generated biogas is an alternative to fossil fuels and thus can ease the energy shortage problem; processed biogas can be used as organic fertilizer, enabling a resource utilization of food waste; the process only produces a little amount of secondary pollution. Therefore, anaerobic digestion of food waste is in line with the "reduction, resource recovery, non-toxic" principle for waste treatment. Overall, this waste treatment process is not only environment-friendly, but also can promote a sustainable economic development (Melikoglu and Webb, 2013).

http://www.aloki.hu ● ISSN 1589 1623 (Print) ● ISSN 1785 0037 (Online)
DOI: http://dx.doi.org/10.15666/aeer/1705_1067110683

In the current research background, the three models commonly used in the study of organic matter hydrolysis kinetics model are the first-order hydrolysis model, the Monod model and the Contois model. Huang et al. (2017) used kitchen waste and activated sludge as substrates for anaerobic fermentation, and used the first-order kinetic model to fit the methane production and predict the late methane production, The predicted value and the actual measured value have less error; Sun et al. (2016) carried out anaerobic digestion experiments using cow dung and corn stover as raw materials, and simulated the Gompertz model. The R^2 of the fitting equation of cow dung and corn stover were 0.983 and 0.991, and the predicted and experimental measured values were 12.3% and 1.7%. Miao et al. (2014) and Syai-churrozi et al. (2013) also fitted anaerobic digestion methane production of cyanobacteria, pig manure and distiller's grains based on the revised Gompertz model, providing a scientific assessment method for predicting the methanogenic potential of various raw materials in the future, but the revised Gompertz model can only characterize the gas production potential of the fermentation substrate, and it is difficult to reflect the influence of influencing factors such as organic load and hydraulic retention time on the gas production rate. Liu et al. (2017) established the PSO-SVM anaerobic digestion gas production prediction model by controlling the temperature, pH, oxidation-reduction potential, and influent organic load as the input, and the gas production as the output, which improved the accuracy of the model. Jurado et al. (2016) first pretreated the pig manure by aqueous ammonia soaking method, and based on the ADM1 kinetic model, the anaerobic fermentation of the pretreated pig manure was fitted. The results show that the ADM1 model has poor prediction ability for anaerobic fermentation process after aqueous ammonia soaking treatment. The reason may be that the hydrolysis rate of the treated pig manure is increased, and the hydrolysis constant needs to be revised to meet the requirements. Lauwers et al. (2013) and other studies have shown that the ADM1 model is suitable for a single matrix substrate, the practical application process is more complicated, and the ADM1 model is more difficult to apply.

As a key factor in the anaerobic fermentation process, oxygen concentration has a significant impact on the generation of biogas. By changing the concentration of oxygen, the activity of the microflora in the system can be manipulated. Thus, increasing the biological activity of aerobic microorganisms and facultative anaerobic microorganisms in the anaerobic fermentation process represents a means for regulating the gas-generation in the system. However, there is currently no systematic kinetic model established for the anaerobic fermentation process of kitchen waste with microaerobic pretreatment, and both the kinetic and mechanistic analyses are lacking (Mata-Alvarez et al., 2000; Forster-Carneiro et al., 2008; Pavan et al., 2000). To this end, in this study, we established three models, namely, a population growth model, a modified Gompertz model and a modified first-order gas-generation model. With them, we explored the impact of oxygen concentration on the microaerobic pretreatment process and system gas-generation. Based on our data, we also provided suggestions for the subsequent industrialization of the process.

Materials and methods

Experimental materials

The raw materials used in this experiment mainly include kitchen waste and inoculated sludge, which were collected from the Southern District Canteen of

http://www.aloki.hu ● ISSN 1589 1623 (Print) ● ISSN 1785 0037 (Online)
DOI: http://dx.doi.org/10.15666/aeer/1705_1067110683

Shenyang Aerospace University and the sewage treatment plant in north Shenyang City (Liaoning province), respectively. First, mix the different kitchen wastes (including taro, vegetables, meat, eggs and other proteins). Remove other materials such as bones and paper scraps from the kitchen waste, stir them with a blender, and store them in cold storage; The inoculated mud was taken from the anaerobic digestion sludge of the sewage treatment plant in the northern part of Shenyang City, Liaoning Province.

Experimental methods

A wide-mouth reagent bottle (1 L) was used as the anaerobic fermentation tank (*Fig. 1*). The raw material for anaerobic fermentation was kitchen waste (simulation), and a certain amount of inoculated sludge was added to the anaerobic digestion tank. Anaerobic digestion was carried out in a water bath at 37 °C. Five parallel groups were set up. Group 1 was used as a control and it was carried out as a standard anaerobic fermentation. Groups 2–5 were experimental groups, and 5 ml, 10 ml, 15 ml, and 20 ml of air were respectively inflated to create different microaerobic conditions. The biogas generation in each group was measured once a day, and the total amount of biogas generation in each group was also calculated. The experimental period is 50 days, of which 1-10 days is the adaptation period. At this time, the microorganisms are in the adaptation stage, also called the start-up stage, mainly by hydrolyzing the fermenting bacteria group to act on starch and cellulose. Hydrogen-producing bacterial bacteria convert monosaccharides into volatile fatty acids (VFAs), H_2 and CO_2. 31-50 days is the deceleration period and the decay period. Since a large amount of organic matter in chicken manure and straw is consumed, the microorganisms enter the endogenous respiration stage and begin to sleep or die.

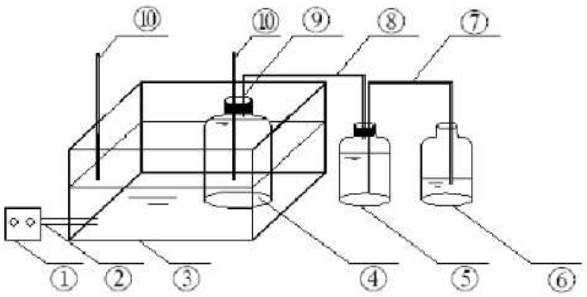

Figure 1. *Experimental set-up. 1 - Controller, 2 - Heater, 3 - Water bath, 4 - Sample reactor, 5 - Gas cylinders, 6 - Water collection bottle, 7 - Outlet pipe, 8 - Airway, 9 - Detection tube, 10 - thermometer*

Model establishment

A kinetics model for anaerobic fermentation

The hydrolysis kinetics model is mainly classified according to the type of organic matter and the hydrolysis process. There are three major categories: the ones based on organic matter concentration, the ones based on organic matter composition and the ones based on organic surface area. The most commonly used organic-concentrations-based hydrolysis kinetic models are the Monod model, the Contois model, and the first-order hydrolysis model.

http://www.aloki.hu ● ISSN 1589 1623 (Print) ● ISSN 1785 0037 (Online)
DOI: http://dx.doi.org/10.15666/aeer/1705_1067110683

The Monod model was proposed by the founder of modern cell growth kinetics, Monod, in 1942. This model describes the relationship between the limiting substrate concentration of cells and their growth rate during the equilibrium and log phase of the microbial growth.

The Contois model was proposed about 20 years later than the Monod model. It describes the growth of microorganisms over time. The Contois model was first applied to the hydrolysis process of the soluble organic matters in aerobic activated sludge, and later developed also for the anaerobic fermentation process of organic particulates. The Contois model is a modified Monod model, which assumes that saturation constant is proportional to the initial concentration of the substrate. However, this model also has disadvantages: for example, it does not consider the influence of temperature on the rate of hydrolysis (Rao and Singh, 2004; Fang and Yu, 2002; Song et al., 2004).

First-order hydrolysis model is the simplest model for the hydrolysis of organic matters. It assumes that the concentration of unhydrolyzed organic matter is proportional to the hydrolysis rate; thus, this model is not suitable for the lag phase. By comparing the actual anaerobic fermentation process with the simulation, First-order hydrolysis model is considered as the model of choice for simulating the hydrolysis of organic particulates (Rao and Singh, 2004). It can be improved by introducing the concept of specific surface area of hydrolyzed particles into the model (Song et al., 2004). Although the hydrolysis characteristics of the specific components in the hydrolysis model are not particularly clear because of the different compositions of organic particulates, the kinetic model regarding the mixture as a hydrolyzed whole, compared to the conventional one, undoubtedly provides some clues for future studies.

Anaerobic fermentation kinetics models for the SBR system

Population growth model

The Logistic equation is:

$$P = \frac{P_{max}}{1 + exp\left[\frac{4R_{max}(\lambda - t)}{p_{max}} + 2\right]} \quad \text{(Eq.1)}$$

where P is the cumulative amount of methane generation (ml/gVS) at time point t; Pmax is the potential maximum methane generation (ml/gVS); Rmax is the maximum methanogenic rate (ml/gVS/d); t is the reaction time; and λ is the delay time (d).

The modified Gompertz equation is:

$$M = P \times \exp\left\{-\exp\left[\frac{R_m \times e}{P}(\lambda - t) + 1\right]\right\} \quad \text{(Eq.2)}$$

where M is the accumulative amount of methane generation at time point t (ml/gVS); P is the potential maximum methane generation (ml/gVS); Rm is the maximum methanogenic rate (ml/g/VS/d); t is the reaction time; and λ is the delay time (d).

It can be seen from these two equations that the P, Pmax, and Rmax in the Logistic equation represent the same as the kinetic parameters, M, P and Rm in the modified Gompertz equation. In this study, we performed nonlinear regression analysis (a

http://www.aloki.hu ● ISSN 1589 1623 (Print) ● ISSN 1785 0037 (Online)
DOI: http://dx.doi.org/10.15666/aeer/1705_1067110683

function incorporated in the origin 8.0 software) of the kinetic parameters in the Logistic equation and the modified Gompertz equation.

First-order gas-generation model

Because of the proportional relationship between degradable organic matter and methane generation derived the first-order gas-generation model based on previous studies (Vavilin et al., 2008):

$$\frac{1}{t}\ln\left(\frac{dy_t}{d_t}\right)=\frac{1}{t}\left(\ln\left(y_m\right)+\ln k\right)-k \qquad \text{(Eq.3)}$$

where y_m is the theoretical methane generation per unit degradable organic matter (ml/gVS); y_t is the methane generation per unit degradable organic matter at time point t (ml/gVS); t is the reaction time (d); k is the hydrolysis constant (d^{-1}).

By combining *Equations 2* and *3,* we obtained the $Ln(y_m) + ln(k)$ and the k value of the corresponding organic matter, which were used for the following analysis.

Modified first-order gas-generation model

The modified first-order gas-generation model is based on the modified first-order hydrolysis model. Modified first-order hydrolysis models include pellet particle model, cylindrical particle model, and spherical particle model. The conclusions are shown in *Table 1*.

Table 1. *The conclusions of three hydrolysis models*

Pellet particle model	Cylindrical particle model	Spherical particle model
$c = c_0 e^{-kt}$	$c = c_0\left(\frac{1}{2}kt+1\right)^{-2}$	$c = c_0\left(\frac{2}{3}kt+1\right)^{\frac{3}{2}}$
$\frac{dc}{dt} = -kc$	$\frac{dc}{dt} = -k\frac{c^{\frac{3}{2}}}{c_0^{\frac{1}{2}}}$	$\frac{dc}{dt} = -k\frac{c^{\frac{5}{3}}}{c_0^{\frac{2}{3}}}$

For our modified first-order gas-generation model, we referred to the first-order hydrolysis model, and used cumulative methane generation to indicate the degree of hydrolysis of the substrate. Considering the proportional relationship between the gas generation rate of anaerobic fermentation and the degradation rate of organic matter, and the initial generation rate in the SBR system is 0, we have:

$$G=\frac{\alpha}{c_0}\left(c_0-c\right) \qquad \text{(Eq.4)}$$

Putting the conclusions shown in *Table 1* into *Equation 4,* we have:

http://www.aloki.hu ● ISSN 1589 1623 (Print) ● ISSN 1785 0037 (Online)
DOI: http://dx.doi.org/10.15666/aeer/1705_1067110683

$$G = \alpha\left(1 - e^{-kt}\right) \quad \text{(Eq.5)}$$

$$G = \alpha\left[1\text{-}\left(\frac{1}{2}kt + 1\right)\right] \quad \text{(Eq.6)}$$

$$G = \alpha\left[1\text{-}\left(\frac{2}{3}kt + 1\right)^{\frac{3}{2}}\right] \quad \text{(Eq.7)}$$

where t is the reaction time (d); k is the Hydrolysis constant (d^{-1}); c is the concentration of volatile solid matters (gVS); c_0 is the initial concentration of the volatile solid matters (gVS); G is the cumulative biogas generation (mL/gVS); α is the conversion rate of the volatile solid matters (mL/gVS). *Equations 5, 6* and *7* correspond to pellet particle, cylindrical particle, and spherical particle models, respectively. Using origin 8.0, we did a linear regression analysis to compare the hydrolysis constants of these models.

Experimental result analysis and model verification

Statistical analysis of experimental results

Through the statistics of the cumulative gas production of each group of experiments, it can be seen that the gas production of the system is lower under different micro-oxygen concentration conditions in the initial stage of the experiment. This is because the anaerobic digestion of kitchen waste is in the adaptation stage at the beginning of the experiment, and the activity of methanogens and other strains in the system is low; as the experiment progresses, the daily gas production begins to rise gradually. Each system of different oxygen concentrations reached the first peak around day 10, 511 ml (5 ml), 490 (10 ml), 607 (15 ml), 586 ml (20 ml), 498.5 (0 ml). Since a large amount of substrate is decomposed into small molecular organic substances and cannot be consumed in time, a large amount of organic acid accumulation changes the neutral environment suitable for the growth of methanogens, thereby inhibiting the activity of methanogens, resulting in a decrease in daily gas production. As the experiment progressed, the methanogens passed the inhibition phase and the gas production gradually recovered. The system of different oxygen concentrations reached the second peak of gas production around the 20th day, and then the gas production between different systems will also fluctuate slightly until the end of the experiment.

In the meantime, the gas production conditions of different oxygen concentration systems show different rules. Each system reached the first peak of gas production around the tenth day. At the beginning of the experiment, the daily gas production of the 20 ml experimental group was up to 586 ml, and the daily gas production of the 0 ml blank experimental group was only 314 ml. Therefore, the gas production rate of the 20 ml micro-oxygen test group at the initial stage of the experiment was higher than that of the 0 ml blank test group. This is because the presence of trace oxygen makes the system a small amount of organic matter consumed by aerobic bacteria in the initial stage of fermentation, so that the accumulation of organic acids is less, and the inhibitory effect on methanogens in the system is reduced. According to the statistical analysis of the data, it can be seen that since the initial materials are the same, the

http://www.aloki.hu ● ISSN 1589 1623 (Print) ● ISSN 1785 0037 (Online)
DOI: http://dx.doi.org/10.15666/aeer/1705_1067110683

cumulative gas production of each group is about 11.5 L. However, the experimental period of the micro-oxygen test group was shorter than that of the control group, and the reaction rate was faster as the oxygen content increased. The 0 ml control group entered the late stage of the experiment at about 40 days, and the 20 ml group entered the later stage of the experiment when it was about 25 days old, and the reaction rate increased by 37.5%. The experimental results show that micro-oxygen pretreatment can accelerate the reaction rate of anaerobic fermentation, which is of great significance to the actual production and life.

Discussion of the Logistic equation and the modified Gompertz equation

During the experiment, the other influencing factors (Temperature, pH, Organic matter concentration, Mass transfer efficiency) were constant, and the change in the gas-generation was achieved by manipulating the concentration of the air that was inflated. The data were input into the original 8.0 software for nonlinear fitting. The results were shown in *Figure 2*. It can be seen from *Table 2* that the fitting based on the Logistic equation gave high R^2 values (all > 0.99), indicating a well-fitting effect of the equation; thus, the anaerobic fermentation process can be accurately simulated. On the other hand, the Gompertz equation also performed very well, with only one R^2 value below 0.99 (R^2 of the 5 ml data), and it therefore also can be employed for the fermentation with microaerobic pretreatment (*Table 3*). Nevertheless, a detailed comparison between these two equations suggests that the Logistic equation performs slightly better (Duan et al., 2016).

Table 2. *The fitting parameters of the Logistic equation*

Microaerobic level	P_{max} (ml/gVS)	R_{max} (ml/gVS)	λ(b)	R^2	RMSE
0 ml	163.0659	4.9061	6.6926	0.9987	2.7806
5 ml	155.7169	5.5464	7.0825	0.9966	5.3478
10 ml	149.8337	4.8603	6.0728	0.9961	2.9435
15 ml	172.0383	6.1555	4.2376	0.9982	2.2739
20 ml	177.7048	7.3598	5.9396	0.9981	5.7349

Table 3. *The fitting parameters of the Gompertz equation*

Microaerobic level	P_{max} (ml/gVS)	R_{max} (ml/gVS)	λ(b)	R^2	RMSE
0 ml	192.9103	4.4659	4.8080	0.9966	1.7100
5 ml	173.8075	5.0624	5.3332	0.9881	2.8803
10 ml	167.6019	4.5520	4.6021	0.9974	2.3736
15 ml	186.169	5.7861	2.8244	0.9917	4.7257
20 ml	188.7640	6.9479	4.6672	0.9902	2.5224

As indicated by the R^2 values, the Gompertz equation had a better fitting effect for the 5 ml group and 10 ml group, whereas the Logistic equation had a better performance for 0 ml, 15 ml and 20 ml groups. Meanwhile, we can also conclude that under good fitting conditions, 20 ml of air intake had the highest gas-generation potential. This shows that the addition of a proper amount of oxygen can increase the activity of

http://www.aloki.hu ● ISSN 1589 1623 (Print) ● ISSN 1785 0037 (Online)
DOI: http://dx.doi.org/10.15666/aeer/1705_1067110683

facultative anaerobic bacteria in the system. These "active" bacteria subsequently promote the anaerobic digestion process, increasing the degradation efficiency of the substrate and improving the gas production potential of the whole system (Pontes and Pinto, 2006; Garcia-Ochoa et al., 1999).

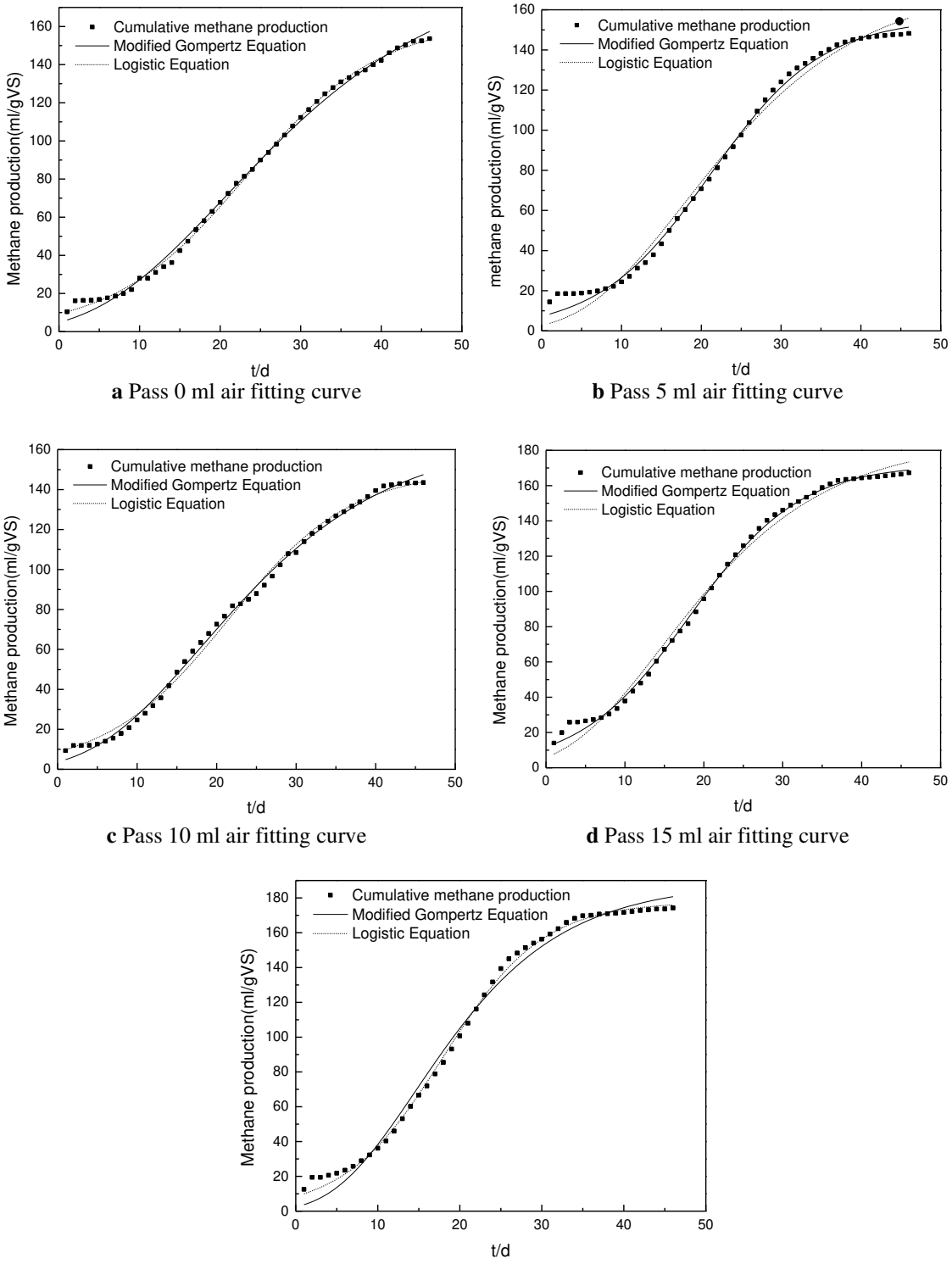

a Pass 0 ml air fitting curve

b Pass 5 ml air fitting curve

c Pass 10 ml air fitting curve

d Pass 15 ml air fitting curve

e Pass 20 ml air fitting curve

Figure 2. *Comparison of fitted function graphs of Logistic and Gompertz equations under different air concentrations*

http://www.aloki.hu ● ISSN 1589 1623 (Print) ● ISSN 1785 0037 (Online)
DOI: http://dx.doi.org/10.15666/aeer/1705_1067110683

Analysis of the first-order gas-generation kinetics model

Using the equation of the first-order gas-generation model, the fitting diagrams were shown in *Figure 3*. Except for 0 ml and 10 ml groups, the R^2 values were all greater than 0.97 (i.e., other R^2 values were below 0.97), indicating it was not able to simulate the experimental data.

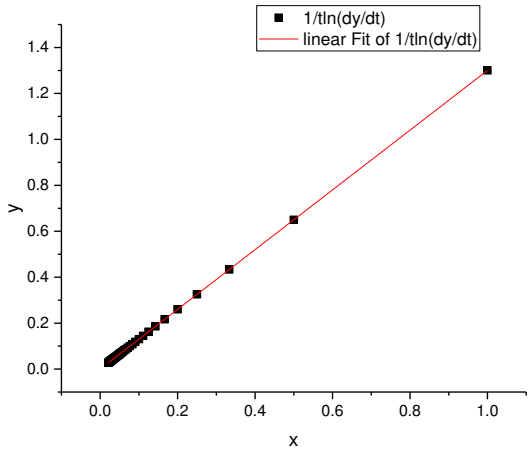

a Pass 0 ml air fitting curve

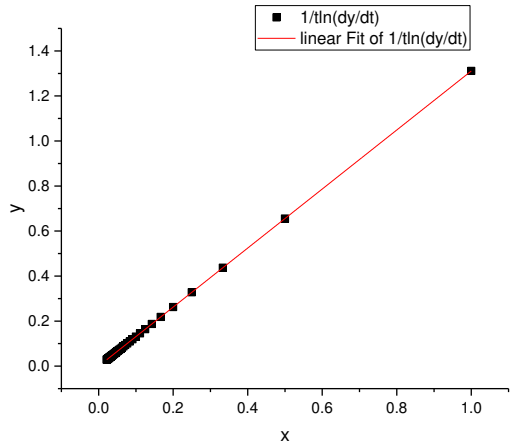

b Pass 5 ml air fitting curve

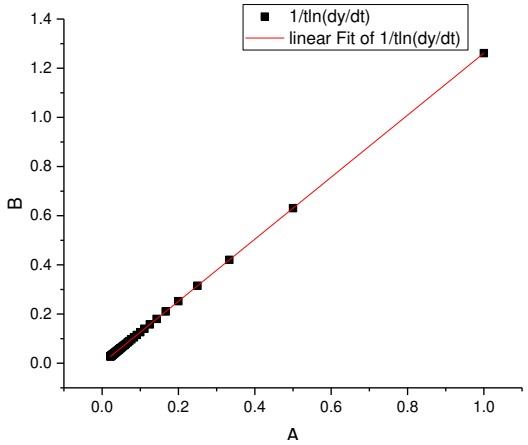

c Pass 10 ml air fitting curve

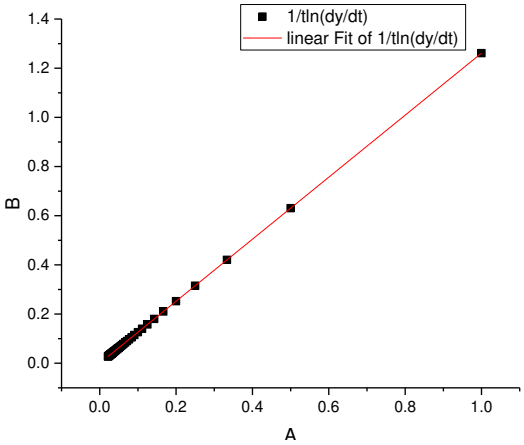

d Pass 15 ml air fitting curve

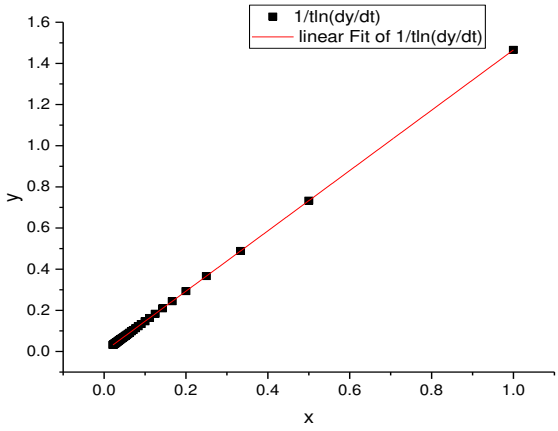

e Pass 20 ml air fitting curve

Figure 3. *First-order gas-generation fitting diagrams of each experimental group*

http://www.aloki.hu ● ISSN 1589 1623 (Print) ● ISSN 1785 0037 (Online)
DOI: http://dx.doi.org/10.15666/aeer/1705_1067110683

The k represents the degradation rate of the degradable portion of the substrate: the lower the value of k, the slower the reaction rate; otherwise, the faster the reaction. It can be concluded from *Table 4* that the k value of the 0 ml group is the highest (k = 0.00012), indicating that the reaction of this group was the fastest. The second highest k value (0.000051), which is only slightly lower, was found in the 5 ml group. The 20 ml group had the lowest reaction rate (k = 0.000010). These data also showed that in the 0 ml group, gas-generation peaked at the early stage of the experiment.

Table 4. *Parameters of the first-order gas-generation model for each group*

Microaerobic level	Parameters		
	$\ln(y_m) + \ln(k)$	k	R^2
0 ml	1.30019	0.00012	0.9843
5 ml	1.31103	0.000052	0.9608
10 ml	1.2613	0.000026	0.9824
15 ml	1.38128	0.000051	0.95225
20 ml	1.46557	0.000010	0.93532

y_m represents the amount of biogas generated by the reaction, and k represents the speed of the reaction. Neither y_m nor k along can fully characterize the gas -generation from the kitchen waste. However, $\ln(y_m) + \ln(k)$, a parameter combining y_m and k, can indicate the availability of the degradable part of the substrate. Therefore, it can be considered as an indicator of the methanogenesis characteristics, which include the speed of gas-generation and the amount of gas-generation. Thus, the larger this value, the better the gas-generation characteristics of the corresponding experimental group (Linke, 2006).

While the value of k obtained in our study can directly indicate the speed of reaction in each experimental group, to have a more comprehensive comparison, we also checked the value of $\ln y_m + \ln k$ for each group, which can directly indicate the methanogenesis characteristics. In our data, 20 ml group had the highest $\ln y_m + \ln k$ value (1.46557), suggesting it is of relatively optimal methanogenic characteristics in comparison with the other four groups. This is consistent with the conclusions drawn by using the Logistic equation. For other groups, from high to low, their $\ln y_m + \ln k$ values were 1.38128 (15 ml), 1.31103 (5 ml), 1.30019 (0 ml), and 1.2613 (10 ml). These data clearly demonstrate that the addition of micro-oxygen, if not destroying the microaerobic environment, can promote the degradation of the substrate and increase the methane yield.

Analysis of the modified first-order gas-generation model

Using the models described above, we revealed that the 5 ml experimental group had the longest delay time (8 d), followed by the 0 ml group (7 days) and the 20 ml group (6 days). The groups with the shortest delay time were the 10 ml and 15 ml groups (both 5 days). As mentioned previously, the modified first-order gas-generation model was derived from the modified first-order hydrolysis model, and the first-order hydrolysis model does not include the lag phase when estimating the hydrolysis constant k. Consequentially, for the anaerobic fermentation process with a significant lag phase, the estimation of the hydrolysis constant must exclude the lag period. The k values are

http://www.aloki.hu ● ISSN 1589 1623 (Print) ● ISSN 1785 0037 (Online)
DOI: http://dx.doi.org/10.15666/aeer/1705_1067110683

listed in *Table 5*. Our data suggest that cylindrical particle model is suitable for every oxygen concentration, followed by the pellet particle model, and the last is the spherical particle model. The hydrolysis constants of the cylindrical particle model for each concentration (from 0 ml to 20 ml) were 0.04339, 0.04706, 0.04611, 0.05039 and 0.05149, respectively.

Table 5. *Parameters of the modified first-order gas-generation model for each group*

Microaerobic level	Model	Pellet particle model	Cylindrical particle model	Spherical particle model
0 ml	R^2 K(1/d)	0.8841 0.0350	0.9830 0.0434	0.7987 0.0462
5 ml	R^2 K(1/d)	0.8641 0.0403	0.9615 0.0471	0.7692 0.0548
10 ml	R^2 K(1/d)	0.8911 0.0391	0.9822 0.0461	0.8008 0.0528
15 ml	R^2 K(1/d)	0.9035 0.0478	0.9436 0.0504	0.8046 0.0680
20 ml	R^2 K(1/d)	0.8810 0.0493	0.9327 0.0515	0.7778 0.0701

Based on the above analysis, including the ones for the lag phase and the modified first-order gas-generation model, the complete periodic equations can be obtained by inputting the value (from Population growth model) and the k value (from first-order gas-generation model) into the equation. For each group, they are:

$$G_1 = \begin{cases} -0.0351t^4 + 0.7142t^3 - 5.0891t^2 + 15.3286t, 1 \le t \le 7 \\ 163.0659\left[1 - \left(\frac{1}{2} \times 0.0434t + 1\right)\right], 8 \le t \le 46 \end{cases}$$

$$G_2 = \begin{cases} 0.0094t^5 - 0.2385t^4 + 2.3185t^3 - 10.6587t^2 + 23.0191t, 1 \le t \le 8 \\ 155.7169\left[1 - \left(\frac{1}{2} \times 0.0471t + 1\right)\right], 9 \le t \le 46 \end{cases}$$

$$G_3 = \begin{cases} -0.0761t^4 + 1.1732t^3 - 6.3810t^2 + 14.6148t, 1 \le t \le 5 \\ 149.8337\left[1 - \left(\frac{1}{2} \times 0.0461t + 1\right)\right], 6 \le t \le 46 \end{cases}$$

$$G_4 = \begin{cases} 0.2469t^3 - 3.4825t^2 + 16.5419t, 1 \le t \le 5 \\ 172.0383\left[1 - \left(\frac{1}{2} \times 0.0504t + 1\right)\right], 6 \le t \le 46 \end{cases}$$

$$G_5 = \begin{cases} 0.4875t^3 - 5.072t^2 + 17.5546t, 1 \le t \le 6 \\ 177.7048\left[1 - \left(\frac{1}{2} \times 0.0515t + 1\right)\right], 7 \le t \le 46 \end{cases}$$

http://www.aloki.hu ● ISSN 1589 1623 (Print) ● ISSN 1785 0037 (Online)
DOI: http://dx.doi.org/10.15666/aeer/1705_1067110683

Notably, this model is a modified model, which takes the lag phrase into consideration, thus better describing the individual stages of the anaerobic fermentation process. We anticipate that our analysis may guide the development of microaerobic pretreatment process and provides a theoretical basis for the kinetics analysis of sequencing anaerobic fermentation.

Conclusion

- Three Kinetic models of anaerobic fermentation of kitchen waste with microaerobic pretreatment were established. Among them, the Logistic model and the modified Gompertz model could better simulate the process since most of the R^2 values were higher than 0.99. Judging from the simulation results, the experimental group in which 20 ml of air were inflated had the largest gas generation capacity.
- For the modified first-order gas-generation model, the cylindrical particle model was suitable for every air concentration. The corresponding $\ln(y_m) + \ln(k)$ values and k values for each group are: 0 ml group, $\ln(y_m) + \ln(k) = 0.98298$, $k = 0.04339$; 5 ml group, $\ln(y_m) + \ln(k) = 0.96149$, $k = 0.04706$; 15 ml group, $\ln(y_m) + \ln(k) = 0.98219$, $k = 0.04611$; 20 ml group, $\ln(y_m) + \ln(k) = 0.94356$, $k = 0.05039$; 20 ml group, $\ln(y_m) + \ln(k) = 0.9327$, $k = 0.05149$. It is worth noting these results were obtained from three simulations for each group. Every experimental group had a significant lag phrase. The longest lag phrase was 8 d for the 5 ml experimental group, followed by the 0 ml group (7 days) and the 20 ml group (6 days). The groups with the shortest delay time were the 10 ml and 15 ml groups (both 5 days). Based on the modified first-order gas-generation model, the entire periodic equation taking the lag phrase into consideration was also generated.

Acknowledgements. This work was funded by Shenyang Science and Technology Plan Project: Study on biogas kinetics and process optimization of anaerobic fermentation of mixed raw materials (18-013-0-86).

REFERENCES

[1] Duan, X., Wang, X., Xie, J. et al. (2016): Effect of nonylphenol on volatile fatty acids accumulation during anaerobic fermentation of waste activated sludge. – Water Research 105: 209-217.
[2] Fang, H., Yu, H. Q. (2002): Mesophilic acidification of gelatinaceous wastewater. – Journal of Biotechnology 93(2): 99-108.
[3] Forster-Carneiro, T., Perez, M., Romero, L. I. (2008): Influence of total solid and inoculum contents on performance of anaerobic reactors treating food waste. – Bioresource Technology 99(15): 6994-7002.
[4] Garcia-Ochoa, F., Santos, V. E, Naval, L. et al. (1999): Kinetic model for anaerobic digestion of livestock manure. – Enzyme & Microbial Technology 25(1): 55-60.
[5] Huang, Y., Zhao, M., Yang, L. et al. (2017): Study on methane production performance and kinetics of mixed kitchen digestion and excess sludge. – Journal of Food Science and Biotechnology 36(05): 486-93.

http://www.aloki.hu ● ISSN 1589 1623 (Print) ● ISSN 1785 0037 (Online)
DOI: http://dx.doi.org/10.15666/aeer/1705_1067110683

[6] Jurado, E., Antonopoulou, G., Lyberatos, G. et al. (2016): Continuous anaerobic digestion of swine manure: ADM1-based modelling and effect of addition of swine manure fibers pretreated with aqueous ammonia soaking. – Applied Energy 172(190-8.
[7] Lauwers, J., Appels, L., Thompson, I. P. et al. (2013): Mathematical modelling of anaerobic digestion of biomass and waste: power and limitations. – Progress in Energy & Combustion Science 39(4): 383-402.
[8] Linke, B. (2006): Kinetic study of thermophilic anaerobic digestion of solid wastes from potato processing. – Biomass and Bioenergy 30(10): 892-6.
[9] Liu, L., Xie, B., Ma, W. et al. (2017): Mixed soft measurement model of gas production by anaerobic treatment of wastewater based on kinetics and PSO-SVM. – China Papers 36(3): 31-6.
[10] Mata-Alvarez, J., Mac, S., Llabr, S. P. (2000): Anaerobic digestion of organic solid wastes. An overview of research achievements and perspectives. – Bioresource Technology 74(1): 3-16.
[11] Melikoglu, M., Webb, C. (2013): Analysing global food waste problem: pinpointing the facts and estimating the energy content. – Central European Journal of Engineering 3(2): 157-64.
[12] Miao, H., Wang, S., Zhao, M. et al. (2014): Codigestion of Taihu blue algae with swine manure for biogas production. – Energy Conversion & Management 77(1): 643-9.
[13] Pavan, P., Battistoni, P., Mata-Alvarez, J., Cecchi, F. (2000): Performance of thermophilic semi-dry anaerobic digestion process changing the feed biodegradability. – Water Science & Technology 41(3): 75-81.
[14] Pontes, R. F. F., Pinto, J. M. (2006): Analysis of integrated kinetic and flow models for anaerobic digesters. – Chemical Engineering Journal 122(1): 65-80.
[15] Rao, M. S., Singh, S. P. (2004): Bioenergy conversion studies of organic fraction of MSW: kinetic studies and gas yield–organic loading relationships for process optimisation. – Bioresource Technology 95(2): 173-85.
[16] Song, Y. C., Kwon, S. J., Woo, J. H. (2004): Mesophilic and thermophilic temperature co-phase anaerobic digestion compared with single-stage mesophilic- and thermophilic digestion of sewage sludge. – Water Research 38(7): 1653-62.
[17] Sun, Z., Zhang, J., Liu, Y. et al. (2016): Potential and kinetics of methane production by anaerobic digestion of cattle manure and corn stover. – Journal of Environmental Engineering 10(03): 1468-74.
[18] Syaichurrozi, I., Budiyono, Sumardiono, S. (2013): Predicting kinetic model of biogas production and biodegradability organic materials: Biogas production from vinasse at variation of COD/N ratio. – Bioresource Technology 149(2): 390.
[19] Vavilin, V. A., Fernandez, B., Palatsi, J. et al. (2008): Hydrolysis kinetics in anaerobic degradation of particulate organic material: an overview. – Waste Management 28(6): 939-51.
[20] Zeng, Y. (2017): Overview of the status quo of urban kitchen waste treatment. – Science and Technology Economics Guide (14): 9-10.

http://www.aloki.hu ● ISSN 1589 1623 (Print) ● ISSN 1785 0037 (Online)
DOI: http://dx.doi.org/10.15666/aeer/1705_1067110683

SPATIAL AND TEMPORAL EVOLUTION AND COORDINATION ANALYSIS OF POPULATION, SPACE AND ECONOMY IN CENTRAL PLAIN CITY CLUSTER OF CHINA

ZHOU, P. C.[1] – YANG, Y. F.[2*]

[1]*School of Surveying and Urban Spatial Information, Henan University of Urban Construction, Pingdingshan 467036, China*
(phone: +86-158-9098-3715)

[2]*College of Environment and Planning, Henan University, Kaifeng 475004, China*

**Corresponding author*
e-mail: yyfnp@henu.edu.cn; phone: +86-182-3787-8989

(Received 1st Mar 2019; accepted 21st May 2019)

Abstract. Taking the Central Plain City Cluster of China as the research object, and using the center-of-gravity coupling model, unbalance index, and coordination measure model, this paper analyzed spatial and temporal evolution characteristics of coordination between urban population, built-up area, and economy in 2008-2016, and predicted their overall development trend in combination with the Logistic model. It obtained following results: (i) The growth rate of urban economy is faster than that of urban population and built-up area, and the stage characteristics and spatial differences of their evolution are significant. (ii) On the whole, the shift direction of population is opposite to that of built-up area and economic gravity, the coordination between population and built-up area and economy gradually declines, while the shift direction of built-up area is the same as that of the economic center-of-gravity, and the coordination between built-up area and economy is gradually strengthened. The unbalance index of population, built-up area and economy is on the rise, while unbalance index of population and built-up area remains stable. (iii) The spatial difference characteristics of the coordination between them are significant. Specifically, the coordination is poor between population and built-up area and economy, while the coordination is good between built-up area and economy. (iv) According to the prediction, the overall size of urban population, built-up area and economy of the Central Plain City Cluster will be 29.4 million, 4,355 km^2, and 4.549 billion yuan in 2026, and such prediction is very believable.
Keywords: *urbanization, center of gravity coordination model, unbalanced index, coupling,* coordination degree, logistic prediction

Introduction

As the world's fastest-growing economy, since the reform and opening up, China has been accelerating in the urbanization process, and both the speed and scale of its urbanization are unprecedented (Chan and Yao, 1999; Niu et al., 2014; Feng et al., 2014). According to the estimation by the Development Research Center of the State Council of China, the peak rate of urbanization in China is 70%-75%, and it will get close to 67% by 2030. In other words, in a long period of time in the future, China's urbanization process will still maintain a high development speed, and the city scale will be further expanded. Therefore, how to maintain coordinated and orderly development will become particularly important in the process of high-speed urbanization.

As an important characterization of the urbanization process, population, built-up area and economy have close connection and interaction in the scale, speed, structure, quality and benefits of urbanization (Shi, 2015; Wang et al., 2014). Urbanization should

http://www.aloki.hu ● ISSN 1589 1623 (Print) ● ISSN 1785 0037 (Online)
DOI: http://dx.doi.org/10.15666/aeer/1705_1068510702

be a complex process of interaction and coordinated development of the three-dimensional integrated system of "population – built-up area – economy". However, in the process of rapid urbanization development of small and medium-sized cities in China, there appear various problems such as excessive accumulation of population, low intensive use of urban land, lopsided industrial structure, and extensive economic development, leading to the imbalance between population, built-up area, and economic system (Di et al., 2016; Lin, 2007, 2006; Friedmann, 2010). Such imbalance has greatly restricted further development of China's urbanization (Fan et al., 2014; Tang, 2013). In this situation, the study on coordinated development of population, built-up area, and economy has great realistic significance for healthy and sustainable development of urbanization.

Some studies have shown that urbanization is the spatial and temporal evolution of regional socio-economic processes, mainly reflected in population, economy, space and society (Ameen et al., 2015; Liu et al., 2014). In the process of urbanization, any subsystem in the population, the built-up area, and economy gets ahead or lags behind the development of other subsystems will lead to an imbalance in the overall development of urban society (Chen, 2008; Liu and Yamauchi, 2013; Holden and Otsuka, 2014). With reference to the above studies, we believe that the healthy and sustainable development of the economy, population, and built-up area is the coordinated development of "population – built-up area – economy". Some scholars such as Henderson and Cohen demonstrated the importance of the coordination of urban population and economy to the healthy development of urbanization; they pointed out that population urbanization is the core and economic urbanization is the driving force, and the quantitative relationship between population urbanization and economic urbanization determines the basic trend and economic benefits of urbanization, while the lag of the development of built-up areas will lead to various problems of resources and environment (Henderson, 2002; Cohen, 2008; Ravallion et al., 2007; Murakami et al., 2005; Ameen et al., 2015). Based on the relatively independent and non-inclusive variables of urban built-up area and urban population, Yang Yanzhao et al. built the relationship model between urban built-up area expansion and population growth, and evaluated the coordination between urban built-up area expansion and population growth (Yang et al., 2013; Zhou et al., 2016). They found that the rapid expansion of built-up areas, as the main type of urban development, has weakened the coordination between built-up area expansion and population growth. From the perspectives of regional structure, construction land structure, and urban scale structure, Wang Chengxin et al. analyzed the relationship between urban population growth and built-up area expansion in China, and found that there is a significant regional and structural difference between urban population growth and built-up area expansion (Wang et al., 2016).

Some existing studies also explored methods of urban measurement. Using Logistic regression, Zhang Leqin et al. measured the relationship between urban built-up area expansion and economic development (Zhang et al., 2014). Using exploratory spatial data analysis and coupling coordination model, He Sanwei et al. analyzed the coupling coordination type and spatial distribution of population, land and economic urbanization in Beijing-Tianjin-Hebei region, and found that most cities have difficulties in achieving a good level of coordinated development (He and Shao, 2018). Different scholars have different judgment criteria for coordination, but the research results have indicated that there are obvious spatial differences in the coordination relationship

http://www.aloki.hu ● ISSN 1589 1623 (Print) ● ISSN 1785 0037 (Online)
DOI: http://dx.doi.org/10.15666/aeer/1705_1068510702

between population, built-up area and economic urbanization subsystems, and the uncoordinated phenomenon is very prominent. Through the above findings, we have a deeper understanding of the changes in the relationship between the development of urbanization subsystems and the spatial distribution of the coupling coordination state. However, there are still some shortcomings in the existing studies. (1) There are few studies on urban scale measurement, and most studies focus on the expansion model, model and dynamic mechanism (Xu et al., 2007; Liu and Yang, 2011). Some scholars discussed from the perspective of the population and built-up area (Li et al., 2011; Liu and Wang, 2011). There is no prediction about the urban population, the built-up area, and the future trend of the economy, so it is impossible to formulate preventive policies for relevant issues. (2) In terms of the research area, many studies focus on China's coastal areas (Li et al., 2018; You et al., 2017; Wang et al., 2018), but few studies care about the inland urban city cluster in the process of rapid urbanization, and such areas are exactly the areas with prominent problem in the coordination between the urban population, built-up area, and economy. This is mainly because there is still no clear definition of the theoretical connotation of urbanization coordination in the academic circle (*The concept of coordination comes from the "coordinated development of urban and rural areas" proposed by the central government. As a part of the harmonious society theory, it describes the state of balanced development between urban and rural areas.*). Besides, there is no criterion for measurement indicator system. In addition, the coordinated development is a description of dynamic interactions, and the specific evaluation conclusions need to be combined with local situations, so it is difficult to unify the weight of indicators. With reference to the existing studies, we believe that the population - built-up area - economic urbanization subsystems have the same effect on the overall coordinated development. Therefore, we used the proportion of the population, build-up area, and economic growth rate of each city to that of the Central Plain City Cluster to characterize the contribution share of each subsystem. If the contribution share of each subsystem is consistent, it will be deemed to be the theoretical optimal state. The Central Plain City Cluster is a central inland region of China with rapid urbanization. Problems exposed in the process of its urbanization development are representative. Thus, study on the coordination of "population - built-up area - economy" of this region is helpful for deeply understanding the quality and rules of its urbanization development, and has great realistic significance for healthy and sustainable development of the regional urbanization. On the basis of studies both at home and abroad, considering the relationship between population size, GDP and built-up area of the Central Plain City Cluster, we established a mathematical model to measure the coordination between urban population, built-up area and GDP of the Central Plain City Cluster. Besides, we introduced the center of gravity model and the imbalance index to study the spatial and temporal evolution characteristics and coordination relationship of the population, built-up areas and economy of 30 provincial cities in the Central Plain City Cluster in 2008-2016. Finally, using the Logistic model, we predicted the future development trend of urban population and built-up area in the Central Plain City Cluster of China, in the hope of providing certain references for properly adjusting the relationship between urban population, land use, and economic development, and promoting the coordinated development of urbanization.

http://www.aloki.hu ● ISSN 1589 1623 (Print) ● ISSN 1785 0037 (Online)
DOI: http://dx.doi.org/10.15666/aeer/1705_1068510702

Overview of the study area

The Central Plain City Cluster is located in the central eastern of China (*Fig. 1*). As an intersection of "two horizontal lines and three vertical lines" urbanization strategy, it is a core growth pole for undertaking the industrial transfer of foreign countries and China's eastern regions, resource output of western regions, and driving the development of central and western regions of China. This region has excellent natural endowments, the terrain is mainly plain, with hills and mountains; human resources are abundant, the industrial system is complete, and the advantages of industrial clusters are obvious and the innovation ability is continuously enhanced; the transportation location is superior, the three-dimensional transportation network is gradually improved, and all-direction accessible comprehensive transportation hub based on the railway transportation is gradually forming; urban system is complete, and it is gradually forming the coordinated development pattern of large, medium and small cities and small towns. The *Development Plan for Central Plain City Cluster*, issued by the State Council of China on December 28, 2016, clearly defined the scope of this region, and divided this region into 6 zones according to the city type and regional industrial structure: Zhengzhou Metropolitan Zone, Core Development Zone, Northern Trans-regional Coordinated Development Demonstration Zone, Eastern Industrial Transfer Demonstration Zone, Western Transformation and Innovation Development Demonstration Zone, and Southern High Efficiency Ecological Economic Demonstration Zone. By the end of 2016, the area of Central Plain City Cluster was 287,000 km^2, the total population was 162.1082 million, the GDP was 6,034.372 billion yuan with the per capita GDP of 37,200 yuan, making this region become the fourth growth pole of Chinese economy, following the Yangtze River Delta, the Pearl River Delta, and Beijing-Tianjin-Hebei economic circle. Therefore, how to realize the spatial optimization and coordinated development of population, built-up area and economy is an important issue confronted by the Central Plain City Cluster.

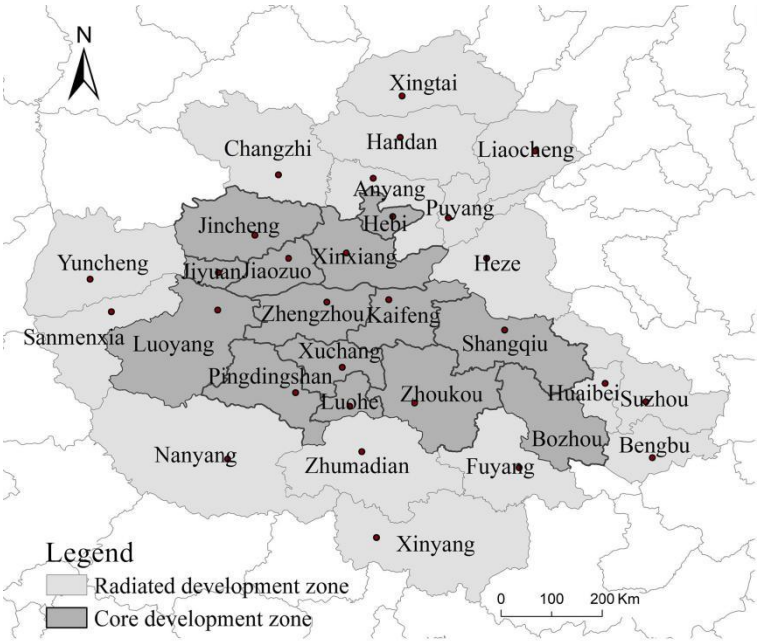

Figure 1. *Map for Central Plain City Cluster*

http://www.aloki.hu ● ISSN 1589 1623 (Print) ● ISSN 1785 0037 (Online)
DOI: http://dx.doi.org/10.15666/aeer/1705_1068510702

Study method and data source

Study method

Center of gravity coordination model

In this study, we adopted the center-of-gravity model and center-of-gravity spatial coupling trend to reflect the overall coupling trend of the growth of population, built-up area, and economy of 30 cities in Central Plain City Cluster. The center-of-gravity model is as follows (Zhou et al., 2016):

$$G_I(x, y) = \frac{\sum_j^n (Q(x_j, y_j))}{\sum_j^n I_j} \quad \text{(Eq.1)}$$

where G_I denotes the center of gravity of urban population, built-up area or economy; I = 1, 2, and 3 denotes population, built-up area, and economy, respectively; n denotes the number of study areas; I_j denotes the population, built-up area or economy of the j-th city; x_j and y_j denote the longitude and latitude of the j-th city.

Using the overlapping of spatial distribution and the consistency in track of center-of-gravity changes, we observed the spatial coupling trend in center of gravity of 30 cities in Central Plain City Cluster. The overlapping of spatial distribution can be calculated with the following formula (Zhou et al., 2016):

$$S = \sqrt{(\Delta x_G)^2 + (\Delta y_G)^2} \quad \text{(Eq.2)}$$

where S denotes the distance of center of gravity between urban population and built-up area, between population and economy, and between built-up area and economy; x_G and y_G denote the longitude and latitude of the center of gravity; closer distance means higher overlapping.

The consistency in track of center-of-gravity changes can be calculated with the following formula (Zhou et al., 2016):

$$C = \cos\theta = \frac{(\Delta x_A \Delta x_B) + (\Delta y_A \Delta y_B)}{\sqrt{(\Delta x_A^2 + \Delta y_A^2) + (\Delta x_B^2 + \Delta y_B^2)}} \quad \text{(Eq.3)}$$

where $\cos\theta$ denotes the cosine value of the vector angle θ of displacement of the center of gravity of urban population and built-up area, population and economy, and built-up area and economy in this time point relative to that in last time point, and it is in the range of [-1,1], and higher value means greater consistency of variation; Δx and Δy denote variation of the longitude and latitude of the center of gravity of this time point relative to the last time point. In this paper, Excel 2007 software is used to process data and charts.

Unbalance index

In order to study the distribution of urban population, built-up area and economy, with reference to previous studies, we constructed an unbalance index characterizing the

http://www.aloki.hu ● ISSN 1589 1623 (Print) ● ISSN 1785 0037 (Online)
DOI: http://dx.doi.org/10.15666/aeer/1705_1068510702

overall balance of urban population, built-up area, and economy. The unbalance index can be calculated with the following formula:

$$U = \sqrt{\frac{\sum_{i=1}^{n}\left[\frac{\sqrt{2}}{2}(X_i - Y_i)\right]^2}{n}} \quad \text{(Eq.4)}$$

where U denotes the unbalance index, n denotes the number of study unit, X_i and Y_i denote the proportion of population and built-up area, population and economy, and built-up area and economy to the total amount. The unbalance index reflects the coupling relationship between population and built-up area, population and economy, and built-up area and economy. The smaller the U value, the more balanced the distribution. In this paper, Excel 2007 software is used to process data and charts.

Spatial coordination measure model

The coordination degree is an indicator reflecting the degree of internal dependence of different factors. It can be used to judge the degree of interdependence and close relationship between urban population, built-up area and economy. Its function is:

$$C = \frac{X + Y}{\sqrt{X^2 + Y^2}} \quad \text{(Eq.5)}$$

where C is the coordination degree, representing the coordination degree between population and built-up area, between population and economy, and between built-up area and economy, with the value in the range of [-1.4142, 1.4142], the higher the C value, the better the coordination; X and Y denote the proportion of urban population, built-up area, and growth rate of economic scale to the total population, total built-up area, and growth rate of total economic scale, respectively. According to the proportional relationship between population, built-up area and economy, we divided the coordination degree into four types: $C \geq 1.3868$ means coordinated (difference below 0.5 times), $1.3868 > C \geq 1.3416$ means relatively coordinated (difference 0.5-1 times), $1.3416 > C \geq 1.2649$ means relatively uncoordinated (difference 1-2 times), and $C < 1.2649$ means uncoordinated (difference above 2 times). In this paper, Excel 2007 software is used to process data and ArcGIS 10 software is used to visualize the calculation results.

Logistic prediction model

Predicting the trend of changes in the urban population, built-up area, and economic scale is favorable for the control of urban size and making the development plan. In view of this, using Logistic model, we predicted the development trend of urban population, built-up area and economy, to provide theoretical recommendations for the promotion of urbanization construction in a scientific and proper manner. The Logistic growth model is as follows:

http://www.aloki.hu ● ISSN 1589 1623 (Print) ● ISSN 1785 0037 (Online)
DOI: http://dx.doi.org/10.15666/aeer/1705_1068510702

$$S_t = \frac{S_{max}}{1+(S_{max}/S_0-1)e^{-k_s t}} \quad \text{(Eq.6)}$$

where S_{max} denotes the maximum of simulated object, and k_s denotes the initial growth rate of simulated object. In this paper, Excel 2007 software is used to process data and charts.

Data source

The basic data involved in this study included population, built-up area and economy. For the population indicator, we took the resident population of the urban area; for the built-up area indicator, we used the area of the built-up area; for the economic indicator, we used the urban GDP. All data were selected from *China Urban Construction Statistical Yearbook (2008-2016).*

Result analysis

Characteristics of spatial and temporal evolution

Characteristics of temporal evolution

In 2008-2016, the urban population, built-up area, and economic scale of Central Plain City Cluster showed a linear growth trend. Specifically, the population increased from 20.68 million to 24.65 million, with an average annual growth rate of 2.22%; the built-up area scale increased from 2,073 km^2 to 3,031 km^2, with an average annual growth rate of 4.87%; the economic scale increased from 660.5 billion yuan to 1,775.4 billion yuan, with an average annual growth rate of 13.16%. From *Figure 2* it can be seen that the growth rate of urban population, built-up area and economy of Central Plain City Cluster showed a fluctuating trend.

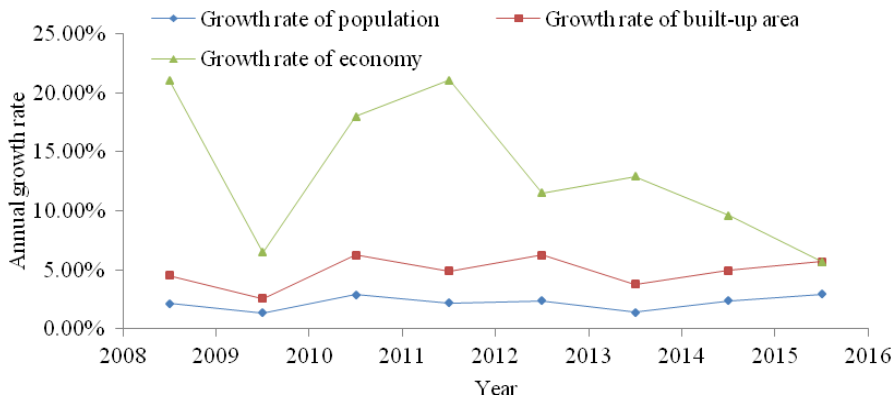

Figure 2. *Growth rate of urban population, built-up area, and economy of Central Plain City Cluster in 2008-2016*

Specifically, the variation trend of growth rate of built-up area expansion and population was basically consistent, while the growth rate of economy showed a significant decline. In 2008-2010, due to the impact of the international financial crisis, urban economic growth rate declined rapidly, the urban construction rate slowed down,

http://www.aloki.hu ● ISSN 1589 1623 (Print) ● ISSN 1785 0037 (Online)
DOI: http://dx.doi.org/10.15666/aeer/1705_1068510702

the employment opportunities decreased, leading to a decline in the growth rate of population and built-up area. In 2010-2014, with the support of the state policy of vigorously promoting urban infrastructure construction, a new round of urban development and industrial park construction drove the rapid economic development, which consequently led to the expansion of urban built-up area and the population agglomeration. Although external capital stimulus has promoted economic development in a short term, urban development lacks internal motivation, so that the growth rate of urban population, built-up area and economy fluctuated. In 2014-2016, the national economic stimulus policy came to an end, and the economic growth rate declined. With the gradual improvement of urban functions, urban population and built-up area entered a steady growth stage. On the whole, the variation in growth rate of urban population, built-up area and economy was not in the same proportion, the economic growth rate was the highest and the population growth rate was the lowest.

Characteristics of spatial evolution

Figure 3 depicted the spatial distribution of growth rate of urban population, built-up area, and economy of Central Plain City Cluster.

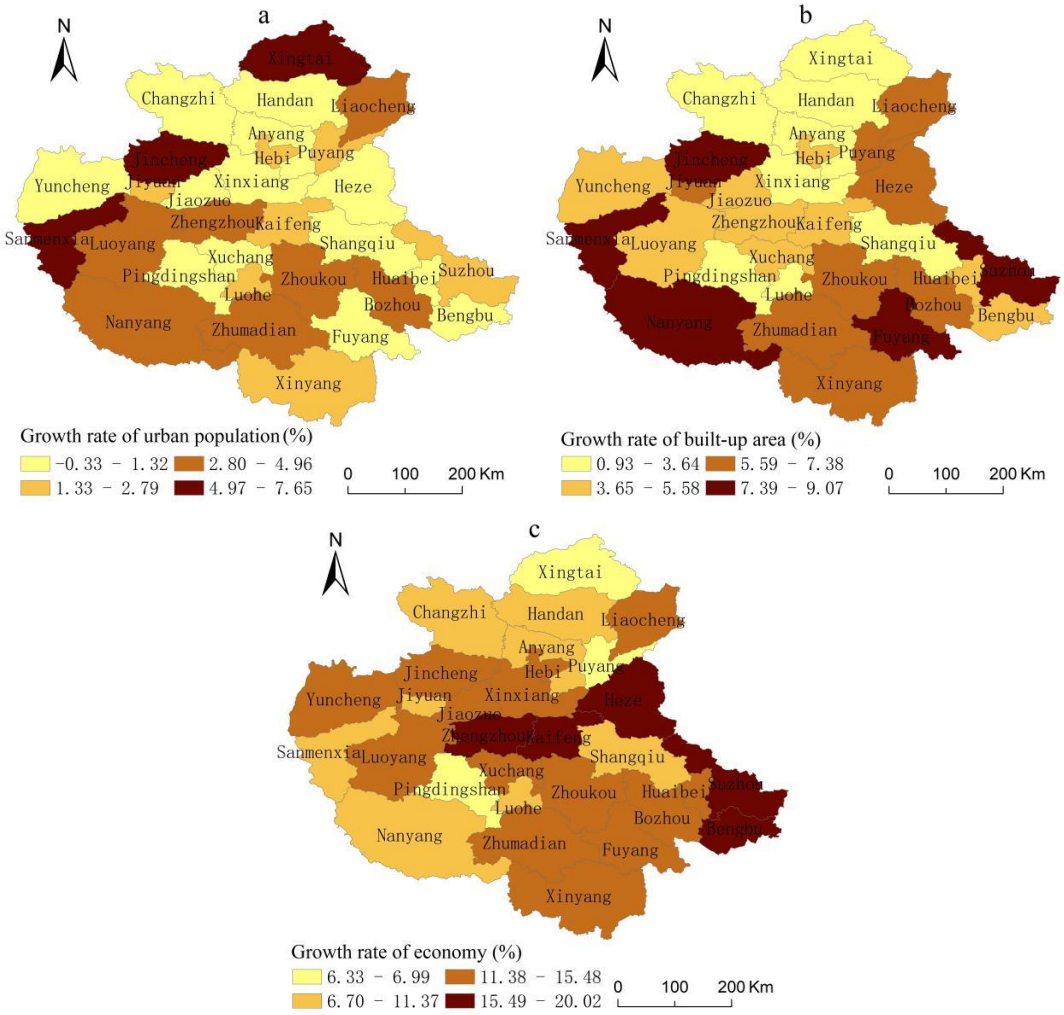

Figure 3. *Spatial distribution of growth rate of urban population (a), built-up area (b), and economy (c) of Central Plain City Cluster in 2008-2016*

http://www.aloki.hu ● ISSN 1589 1623 (Print) ● ISSN 1785 0037 (Online)
DOI: http://dx.doi.org/10.15666/aeer/1705_1068510702

It showed significant spatial difference in growth rate of population, built-up area, and economy. In the study period, the growth rate of urban population was mainly concentrated in the range of 1.33-2.79% and 2.80%-4.96%, accounting for 43.33% and 23.33% of the total number of cities respectively; the growth rate of population of different cities was relatively close to each other. In terms of built-up area rate, the number of cities in different grades is basically the same. The growth rate of built-up area was mainly concentrated in the range of 3.65%-5.58%, and both were in the Midwest of the city cluster, accounting for 30% of the total number of cities. In general, the growth rate of built-up area is faster than that of urban population. Driven by the tide of urbanization, land finance has become an essential means or urban development. The growth rate of urban economy was mainly concentrated in the range of 12.27%-16.22%, accounting for 50% of the total number of cities. The cities with faster economic growth were concentrated in the central and western parts of the Central Plain City Cluster, mainly because, except Zhengzhou Metropolitan Zone, the Eastern Industrial Transfer Demonstration Zone, Western Transformation and Innovation Development Demonstration Zone, and Southern High Efficiency Ecological Economic Demonstration Zone realized collaborative development, forming a multi-regional development pattern.

Analysis of coordination evolution

Overall coordination trend

(1) Coordination trend of the center of gravity

According to *Equation 1,* the track of changes in urban population, built-up area, and economic center of gravity is calculated (*Fig. 4*). From *Figure 4,* it can be seen that the center of gravity of urban population, built-up area, and economy of Central Plain City Cluster was located in the northwest of the geometric center of gravity.

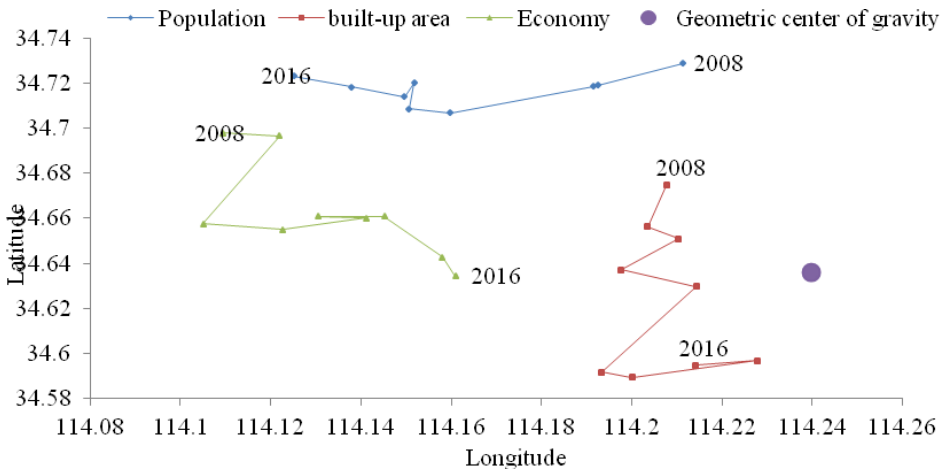

Figure 4. *Moving tracks of center of gravity of urban population, built-up area, and economy of Central Plain City Cluster in 2008-2016*

In 2008-2016, the center of gravity of urban population moved about 6.7 km to the west, with annual average moving distance of 1.33 km; the center of gravity of urban population moved about 8.37 km to the south, with annual average moving distance of

http://www.aloki.hu ● ISSN 1589 1623 (Print) ● ISSN 1785 0037 (Online)
DOI: http://dx.doi.org/10.15666/aeer/1705_1068510702

1.98 km; the center of gravity of urban economy moved about 9.16 km to the southeast, with annual average moving distance of 1.85 km. On the whole, the moving distance of three centers of gravity was small, indicating that the distribution of population, built-up area, and economy of cities of Central Plain City Cluster was basically reasonable. Combined with *Figure 3,* the movement direction and growth rate distribution of the center of gravity were basically consistent in the urban population, built-up area, and economy; the growth of built-up area was mainly concentrated in the regions of south of Yellow River, and the center of gravity moved to the south, close to the geometric center of gravity; the center of gravity of population generally moved to the west due to influence of southwestern cities with faster population growth including Nanyang, Luoyang, Sanmenxia, and Zhengzhou; the center of gravity generally moved to the southeast due to the influence of cities with faster economic growth rate of central and southeastern cities.

According to *Equations 2* and *3,* the spatial overlapping and variation consistency in the center of gravity of urban population, built-up area and economy is calculated (*Fig. 5*).

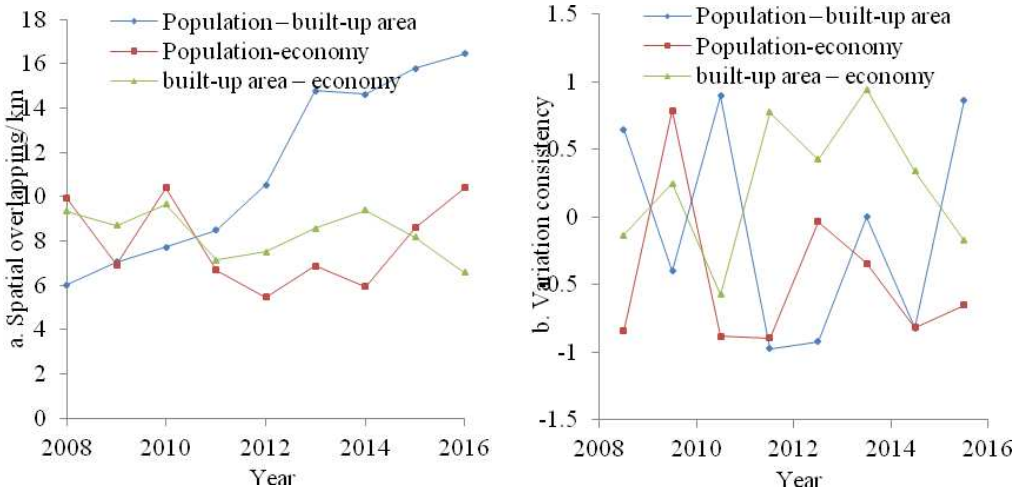

Figure 5. *Spatial overlapping (a) and variation consistency (b) of center of gravity of urban population and built-up area in Henan Province*

From *Figure 5,* it can be seen that: (i) The center-of-gravity distance between population and built-up area was generally on the rise, increasing from 6 km in 2008 to 16.5 km in 2016, with the average value of 10.9 km; the center-of-gravity overlapping was getting worse, and the coordination was declining; the variation consistency of the center of gravity between population and built-up area showed alternate changes of "the same direction – opposite direction", the variation consistency index was generally -0.12, indicating that the center of gravity of population and built-up area moved in the opposite direction and the distance between the centers of gravity was constantly increasing. (ii) The center-of-gravity distance between population and economy showed a general trend of "decline – rise", increasing from 9.9 km in 2008 to 10.4 km in 2016, with the average value of 8.1 km; the center-of-gravity overlapping showed a small fluctuation; the variation consistency index of the center of gravity between population and economy was negative (-2.69), indicating that the centers of gravity moved in the

http://www.aloki.hu ● ISSN 1589 1623 (Print) ● ISSN 1785 0037 (Online)
DOI: http://dx.doi.org/10.15666/aeer/1705_1068510702

opposite direction, and the distance between the centers of gravity first increased then decreased, the coordination was poor. (iii) The center-of-gravity distance between built-up area and economy showed a declining trend, from 9.3 km in 2008 to 6.6 km in 2016, with the average value of 8.4 km; the center-of-gravity overlapping declined; the variation consistency of the center of gravity between built-up area and economy showed alternate changes of "the same direction – opposite direction", the variation consistency index was generally 2.32, indicating that the centers of gravity generally moved in the same direction, and the coordination gradually became greater.

(2) Evolution of unbalance situation

According to *Equation 4,* we calculated the unbalance index of population and built-up area, population and economy, and built-up area and economy of Central Plain City Cluster. The calculation results were shown in *Figure 6.*

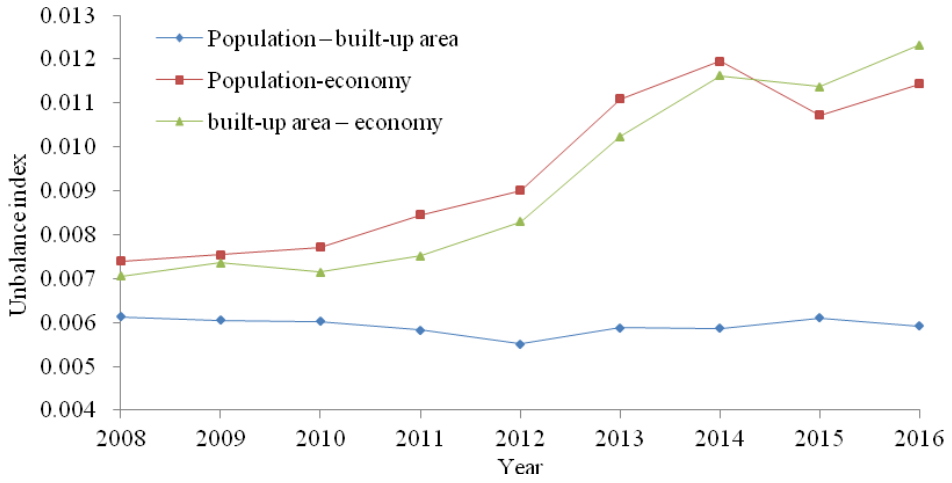

Figure 6. *Unbalance index of population, built-up area, and economy of Central Plain City Cluster*

Generally, the urban population–economy, and built-up area – economy unbalance index showed a fluctuation trend of "rise – decline – rise", and the variation trend of both was basically consistent, while the population - built-up area unbalance index was basically stable, showing a trend of "slow decline – slow rise". (i) In the study period, the population – built-up area unbalance index remained basically the same, with an average of 0.0059, indicating that the population and built-up area elements realized a balanced development in space. (ii) On the whole, the population–economy unbalance index rose from 0.0074 to 0.0114, and the built-up area – economy unbalance index rose from 0.0071 to 0.0123. Main reason was as follows: when carrying out the transfer of eastern industries, central core cities did not realize the corresponding agglomeration of population, so that the unbalance appeared between population, built-up area, and economy in space, till the urban population agglomeration effect became gradually stronger in the late period, then the spatial distribution balance of population and economic elements got gradually strengthened. For small and medium-sized cities, because built-up area expansion rate was much higher than the economic growth rate, the spatial distribution of built-up area and economic elements became out of balance.

http://www.aloki.hu ● ISSN 1589 1623 (Print) ● ISSN 1785 0037 (Online)
DOI: http://dx.doi.org/10.15666/aeer/1705_1068510702

Trend of spatial coordination

According to *Equation 5,* we calculated the coordination (*C*) between population and built-up area, between population and economy, and between built-up area and economy of 30 cities in Central Plain City Cluster, and divided the coordination into coordinated, relatively coordinated, relatively uncoordinated, and uncoordinated types (*Fig. 7*).

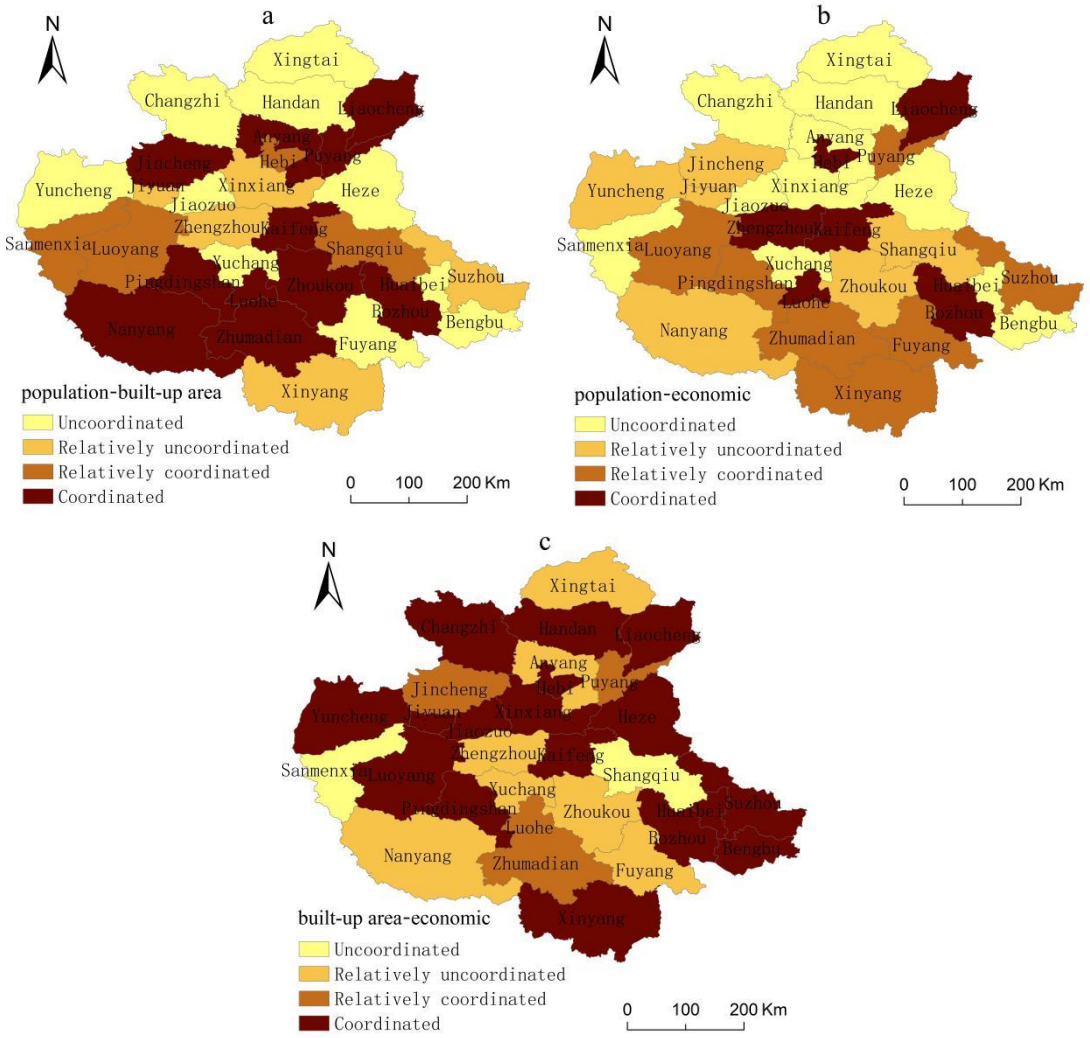

Figure 7. *Spatial distribution of population (a), built-up area (b) and economic (c) scale of 30 cities in 2008-2016*

(i) In the study period, the coordination relationship between population and built-up area of 30 cities in the Central Plain City Cluster was mainly coordinated and uncoordinated types, accounting for 36.67% and 33.33% of the total number of cities, respectively. The coordinated cities were mainly concentrated in the southern and northern parts of the City Cluster, and basically located in the transition area from the core city circle to edge city circle. They not only avoided the flow of urban population to Zhengzhou and outside Henan Province, but also avoided the problem of weak economic development due to geographical location, so the relationship between

http://www.aloki.hu ● ISSN 1589 1623 (Print) ● ISSN 1785 0037 (Online)
DOI: http://dx.doi.org/10.15666/aeer/1705_1068510702

population and built-up area was relatively balanced. Uncoordinated cities were mainly concentrated in the northern part, basically the fringe areas of the City Cluster. These cities received weak radiation of core city circle. Driven by the tide of urbanization, the built-up area expansion in these cities was faster than the population growth. Relatively coordinated and relatively uncoordinated cities were few and mainly distributed along the Longhai (Lianyungang-Lanzhou) Railway, accounting for 13.33% and 16.67% of the total number of cities, respectively.

(ii) The coordination relationship between population and economy was mainly uncoordinated type, accounting for 36.67% of the total number of cities. The number of coordinated, relatively coordinated and relatively uncoordinated cities is roughly equal, 20%, 23.33%, and 20%, respectively. Uncoordinated cities were mainly distributed in the northern part of the City Cluster, namely, north of the Yellow River. The expansion of Zhengzhou Metropolitan Zone and construction of all-direction accessible township industrial axis and belt promoted economic development of northern area and also made it absorbed numerous people from other places, so that urban economic growth of northern area was rapid but the population agglomeration was slow. Coordinated cities were scarcely distributed, mainly because these cities had high economic level, were located far from Zhengzhou, and situated in status of local core cities. The relatively coordinated and relatively uncoordinated cities were mainly distributed in the south of the Yellow River. These cities had stable economic development and population growth, and the relationship between economy and population was basically coordinated.

(iii) The coordination relationship between built-up area and economy was mainly coordinated type, accounting for 56.67% of the total number of cities. Relatively coordinated, relatively uncoordinated, and uncoordinated cities accounted for 13.33%, 23.33%, and 6.67% of the total number of cities, respectively. Roughly opposite to the coordination relationship between population and economy, the built-up area – economy coordinated cities were basically distributed along the Longhai Railway and the north of the Longhai Railway, while the relatively uncoordinated cities were basically distributed in the south of the Longhai Railway.

Logistic growth model

Urban development has its inherent laws. Predicting the development trend of population, built-up area and economy in the future urban development process has important realistic significance for rationally determining the scale of a city and coordinating the development of urban population, built-up area and economy. On the basis of the data of population, built-up area, and economy during 2008 (t = 1) and 2016 (t = 8), According to *Equation 6,* using the Brute Force search method, we established the Logistic prediction model for urban population, built-up area, and economy of the Central Plain City Cluster:

$$P_t = \frac{19648.15}{1 + 8.5822\, e^{-0.0217t}} \quad \text{(Eq.7)}$$

$$A_t = \frac{7936.97}{1 + 3.0806\, e^{-0.0695t}} \quad \text{(Eq.8)}$$

http://www.aloki.hu ● ISSN 1589 1623 (Print) ● ISSN 1785 0037 (Online)
DOI: http://dx.doi.org/10.15666/aeer/1705_1068510702

$$E_t = \frac{74577.44}{1+11.7325e^{-0.1531t}} \quad \text{(Eq.9)}$$

where P_t denotes the population size, A_t denotes the built-up area scale, and E_t denotes the economic scale. The goodness of fit of the model R^2 is higher than 0.97, so the fitting results are very credible. This model can reconstruct the population, built-up area and economic scale of the Central Plain City Cluster in 2008-2016 and predict the value of the following ten years (Chen and Zhang, 2014). As shown in *Figure 8,* the growth of each variable strictly followed the Logistic growth law, and the reconstruction results were very close to the actual scale of each variable. According to the prediction results, by 2026, the population, built-up area and economic scale of the Central Plain City Cluster were 29.4 million, 4,355 km^2, and 4.549 billion yuan, respectively, increasing by 4.75 million, 1,324 km, and 2.777 billion yuan, respectively compared with 2016. In 2016, the actual per capita built-up area was 123 m^2, the per capita GDP was 720,000 yuan, and the average built-up area GDP was 586 million yuan; in 2026, the per capita built-up area was 148 m^2, the per capita GDP was 154,700 yuan, and the average built-up area GDP was 1.045 billion yuan. On the whole, in the next decade, the urban population, built-up area and economic scale of the Central Plain City Cluster would show a steady growth trend, among which the economic growth rate will be the fastest, followed by the built-up area growth rate, and the slowest was the population growth rate.

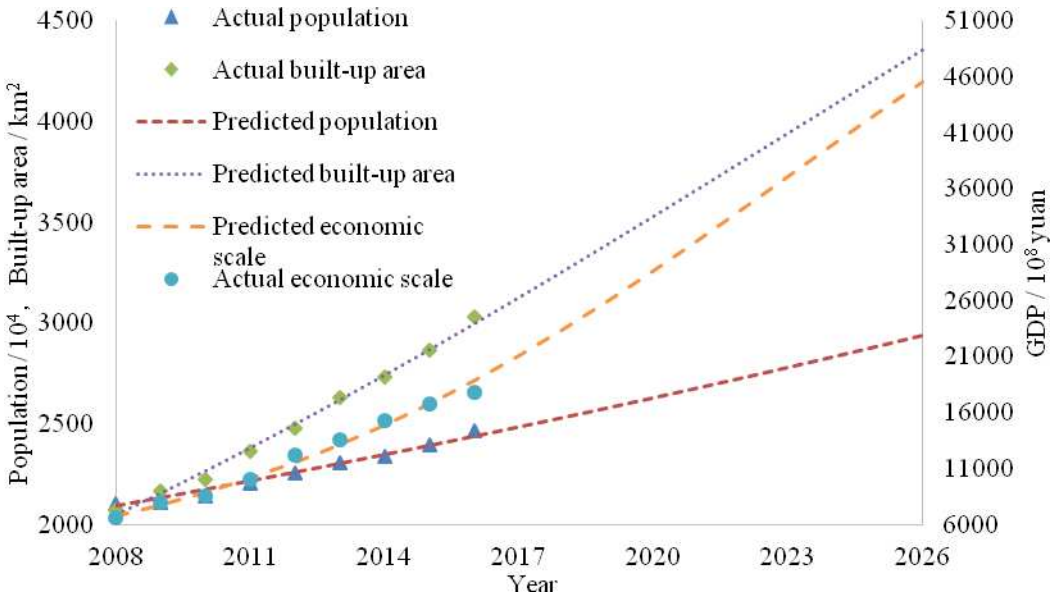

Figure 8. *Prediction of urban population, built-up area, and GDP of Central Plain City Cluster (2008-2026)*

Discussion

On the basis of previous studies, we analyzed the spatial and temporal evolution characteristics of the coordination of population - built-up area - economy of the Central Plain City Cluster and came up with some implications and conclusions. The

http://www.aloki.hu ● ISSN 1589 1623 (Print) ● ISSN 1785 0037 (Online)
DOI: http://dx.doi.org/10.15666/aeer/1705_1068510702

urbanization problem of the Central Plain City Cluster is mainly reflected in two aspects. First, the expansion of the urban built-up area leads to occupation of large area of farmland around the city, no guarantee for the life of landless farmers, and imbalance between the population growth, economic growth, and built-up area expansion. These are similar to the situation in other regions of China. Second, compared with the Yangtze River Delta, the Pearl River Delta, and the Beijing-Tianjin-Hebei region, the core cities of the Central Plain City Cluster are less efficient in promoting the surrounding areas. Once there the relationship between the population, built-up area, and economic development of surrounding areas is not coordinated, there will be adverse spatial effect between cities, which will be more unfavorable for the integrated development of the region. Therefore, it is necessary to improve the efficiency of economic growth, reduce the input of such productive resources as land, adjust the industrial structure, increase urban employment, and promote the coordinated and sustainable development of urbanization.

At present, there is still no unified standard for the evaluation system of urbanization coordination measurement. Combining the existing studies, we supplemented the existing theoretical connotation of "urbanization coordination" and stressed that the population - built-up area - economic urbanization subsystems have the same effect on the overall coordinated development. Besides, we built a preliminary framework for analysis of the urbanization coordination, namely, using the proportion of the population, build-up area, and economic growth rate of each city to that of the city cluster to characterize the contribution share of each subsystem; if the contribution share of each subsystem is consistent, it will be deemed to be the theoretical optimal state. The measurement of urban scale is very complicated. In this study, we calculated the future trend of urban population, built-up area and economy from the city cluster level and obtained reasonable results, indicating that our technical ideas are feasible and can be promoted. The calculation results can be used as an important reference for understanding the evolution process and future trend of the relationship between urban population, built-up area, and economy. Considering the complexity of urban scale prediction, especially the imbalance of urbanization development will reduce the accuracy of Logistic prediction, it is necessary to further explore a more comprehensive and effective technical method.

For example, the ecological factor should become an important indicator in the evaluation system of urbanization coordination. Both domestic and foreign theories of sustainable development of cities emphasized three important evaluation indicators "ecology, society, and economy". However, there is still no definite conclusion about how to quantify the weight of each indicator, and this is a difficult but important point of study. Therefore, we attempted to analyze the coordination between population and built-up area, and the conclusion can be used as a reference indicator for the evaluation of human settlement environment. However, we did not explore the coordinated relationship between ecological environment and urbanization. This is a weak point of our study. In the future study, we should analyze the urbanization and the connotation of the ecological environment from the perspective of complexity, and accordingly propose a reasonable analytical framework to explain the coordination mechanism between urbanization and ecological environment from multiple dimensions, so as to make clear the coordinated development relationship between urbanization and ecological environment, and ultimately promote the sustainable urban development.

http://www.aloki.hu ● ISSN 1589 1623 (Print) ● ISSN 1785 0037 (Online)
DOI: http://dx.doi.org/10.15666/aeer/1705_1068510702

Conclusions

Taking the Central Plain City Cluster as the research object, and using the center-of-gravity coupling model, unbalance index, and coordination measure model, this paper analyzed spatial and temporal evolution characteristics of coordination between urban population, built-up area, and economy in 2008-2016, and predicted their overall development trend according to the Logistic model. The results shown are as follows:

(i) The growth rate of urban population, built-up area and economy of Central Plain City Cluster shows a fluctuating trend. The economic growth is faster than that of population and built-up area. The variation trend of growth rate of built-up area expansion and population is basically consistent, while the growth rate of economy shows a significant decline, and the stage characteristics and spatial differences of their evolution are significant.

(ii) From the macro perspective, the shift direction of population is opposite to that of built-up area and economic gravity, the coordination between population and built-up area and economy gradually declines, while the shift direction of built-up area is the same as that of the economic center-of-gravity, and the coordination between built-up area and economy is gradually strengthened. The unbalance index of population, built-up area and economy is on the rise, while unbalance index of population and built-up area remains stable.

(iii) The coordination between population and built-up area and between population and economy is poor, with the population – built-up area and population –economy coordinated cities accounting for 36.67% and 20% of the total number of cities. The coordination between built-up area and economy is good, with built-up area – economy coordinated cities accounting for 56.67% of the total number of cities. The coordination between these three items presents significant spatial difference characteristics.

(iv) According to the prediction, the growth of each variable strictly follows the Logistic growth law, and the reconstruction results are very close to the actual scale of each variable. According the prediction, the overall size of urban population, built-up area and economy will be 29.4 million, 4,355 km2, and 4.549 billion yuan in 2026, and such prediction is very credible.

Acknowledgements. Great gratitude to the fund support of the National Natural Science Foundation of China (41771565), Henan provincial government decision research tendering project (2017B189).

REFERENCES

[1] Ameen, R. F. M., Mourshed, M., Li, H. (2015): A critical review of environmental assessment tools for sustainable urban design. – Environmental Impact Assessment Review 55: 110-125.

[2] Chan, R. C. K., Yao, S. M. (1999): Urbanization and sustainable metropolitan development in China: Patterns, problems and prospects. – GeoJournal 3: 269-277.

[3] Chen, C. (2008): Research on healthy development of urbanization. – Territory & Natural Resources Study 30(4): 7－9.

[4] Chen, Y. G., Zhang, L. (2014): An allometric analysis of the scaling relations between population and urban area of Xinyang. – Progress in geography 33(8): 1058-1067.

[5] Cohen, B. (2008): Urbanization in developing countries: current trends, future projections, and key challenges for sustainability. – Technology in Society 28(1): 63-80.

http://www.aloki.hu ● ISSN 1589 1623 (Print) ● ISSN 1785 0037 (Online)
DOI: http://dx.doi.org/10.15666/aeer/1705_1068510702

[6] Di, Q. B., Han, S. S., Han, Z. L. (2016): Spatial pattern of economic carrying capacity of cities at prefecture level and above in China. – Geographical Research 35(2): 337-352.
[7] Fan, H., Liu, W. D., Wu, Z. B., Zhang, H. Y. (2014): The coupling coordination evaluation between population urbanization and land urbanization in Zhejiang Province. – Economic Geography 34(12): 21-28.
[8] Feng, Z. M., Yang, Y. Z., You, Z., Zhang, J. H. (2014): Research on the suitability of population distribution at the county level in China. – Acta Geographica Sinica 69(6): 723-737.
[9] Friedmann, J. (2010): Four theses in the study of China's urbanization. – International Journal of Urban & Regional Research 30(2): 440-451.
[10] He, S. W., Shao, X. (2018): Spatial clustering and coupling coordination of population-land-economic urbanization in Beijing-Tianjin-Hebei region. – Economic Geography 38(1): 95-102.
[11] Henderson, V. (2002): Urbanization in developing countries. – New Zealand Geographer 17(1): 89-112.
[12] Holden, S. T., Otsuka, K. (2014): The roles of land tenure reforms and land markets in the context of population growth and land use intensification in Africa. – Food Policy 48: 88-97.
[13] Li, J. F., Yu, H. F., Fu, Y. C., Zhao, Y. L. (2018): Spatial-temporal changes of population-economy-land-society-ecology coordination level of urbanization and clustering: A case of Guangdong Province, China. – Progress in Geography 37(2): 287-298.
[14] Li, X. S., Zhang, S. L., Wang, Y. H. (2011): Quantitative study of construction land increase limit year in the economic transition stage in China. – Journal of Natural Resources 726(7): 1058-1059.
[15] Lin, G. C. S. (2006): Peri-urbanism in globalizing China: a study of new urbanism in Dongguan. – Eurasian Geography & Economics 47(1): 28-53.
[16] Lin, G. C. S. (2007): Chinese Urbanism in Question: State, Society, and the Reproduction of Urban Spaces. – Urban Geography 28(1): 7-29.
[17] Liu, A. M., Yang, D. C. (2011): City scale, resource allocation and economic growth. – Modern Economic Science 33(1): 106-113, 128.
[18] Liu, F. W., Xu, H. Z., Wang, S. (2014): Analysis on spatial-temporal coupling coordinate degree among population, land and economy urbanization: based on China provincial panel data. – Urban Development Studies 21(8): 7-11.
[19] Liu, Y., Yamauchi, F. (2013): Population density, migration, and the returns to human capital and land: Insights from Indonesia. – IFPRI Discussion Papers 48(1): 182-193.
[20] Liu, Y. G., Wang, F. L. (2011): Holistic forecast method of land use in leap-forward of urbanization. – Geographical Research 30(7): 1187-1197.
[21] Murakami, A., Zain, A. M., Takeuchi, K., Tsunekawa, A., Yokota, S. (2005): Trends in urbanization and patterns of land use in the Asian mega cities Jakarta, Bangkok, and Metro Manila. – Landscape & Urban Planning 70(3): 251-259.
[22] Niu, S. W., Lan, Z. C., Hu, Y. Y. (2014): Urbanization: population growth constraint and policy implication. – China Population, Resources and Environment 24(8): 49-56.
[23] Ravallion, M., Chen, S., Sangraula, P. (2007): New evidence on the urbanization of global poverty. – Population and Development Review 33: 667-701.
[24] Shi, Y. S. (2015): Dialectical examination of the relationship between land urbanization and population urbanization. – Shanghai Land & Resources 36(2): 9-13.
[25] Tang, Y. H. (2013): Research on the concept of urbanization and new definition. – Academic Forum 5: 113-116.
[26] Wang, C. X., Wang, B. T., Wang, X. Y. (2016): Study on population urbanization and land urbanization allometric growth in China based on the structure. – China Population, Resources and Environment 8(26): 135-141.

http://www.aloki.hu ● ISSN 1589 1623 (Print) ● ISSN 1785 0037 (Online)
DOI: http://dx.doi.org/10.15666/aeer/1705_1068510702

[27] Wang, F., Zhang, F., Lin, X. Y., Shi, T. W., Chen, H. T. (2018): Study on coupling coordination degree among "population, land, economy and society" urbanization in the Yangtze River Delta Region. – Journal of Industrial Technological Economics 4: 45-52.
[28] Wang, J., Fang, C. L., Li, Y. R. (2014): Spatio-temporal analysis of population and construction land change in urban and rural China. – Journal of Natural Resources 29(8): 1271-1281.
[29] Xu, Y. X., Chen, F., Pu, L. J. (2007): A retrospect and prospect on research of urban spatial and land use expansion. – Economic Geography 27(2): 296-301.
[30] Yang, Y. Z., Feng, Z. M., Zhao, Y. D., You, Z. (2013): Coordination between urban land expansion and population growth in China. – Geographical Research 32(9): 1168-1678.
[31] You, Z., Lei, Y. L., Feng, Z. M., Yang, Y. Z. (2017): Comparative study on the social and economic coordination of the population distribution and regional differences of Beijing-Tianjin-Hebei, Yangtze River Delta and Pearl River Delta city clusters. – Modern Urban Research 3: 78-84.
[32] Zhang, L. Q., Chen, S. P., Chen, B. P. (2014): The contribution of land to the economic growth and inflection point of its logistic curve in Anhui Province in recent 15 years. – Scientia Geographica Sinica 34(1): 40-46.
[33] Zhou, Y., Huang, X. J., Xu, G. L., Li, J. B. (2016): The coupling and driving forces between urban land expansion and population growth in Yangtze River Delta. – Geographical Research 35(2): 313-324.

http://www.aloki.hu ● ISSN 1589 1623 (Print) ● ISSN 1785 0037 (Online)
DOI: http://dx.doi.org/10.15666/aeer/1705_1068510702

HYDROLOGIC IMPACT OF CLIMATE CHANGE ON POYANG LAKE WETLAND, CHINA

ZHAN, M. J. – WANG, H. Q. – LI, B. Z. – YIN, J. M.*

Jiangxi Provincial Eco-meteorological Centre
No. 323 Aixihu 2nd Road, NanChang City, Jiangxi Province, China

**Corresponding author*
e-mail: yjm163@sina.com; phone: +86-791-8271-3183; fax: +86-791-8271-3189

(Received 1st Mar 2019; accepted 21st May 2019)

Abstract. This study developed hydrologic models based on satellite remote sensing data from 2002 to 2010. Daily meteorological and hydrological data (1959-2010) were used as model inputs to analyse the relationships between meteorological factors and water area, and to calculate the daily water area and mean reduced water area on an annual basis to analyse the trend of changes. By analysing BCC-CSM1-1 model data, the study derived a qualitative assessment of the future water area of the Poyang Lake Basin, China. The following results were found. (1) The water area had shrunk substantially since the 1990s, especially during the 2000s. Because of aridification, the water area had decreased by 22.5% from 1845 km^2 in the 1980s to 1430 km^2 in the 2000s. (2) Since 1990, the first day of its wet season had become delayed and the final day had advanced. Generally, the number of wet season days had reduced while that of the dry season has increased. (3) In all future scenarios, extreme events were projected to occur more frequently, suggesting dramatic volatility in water resources and great frequency of droughts, which would exacerbate the shrinking of Poyang Lake and represent a severe threat to its water security.
Keywords: *Poyang Lake, water area, wet season, dry season, RCPs scenario*

Introduction

Although wetlands cover only about 6% of the earth's surface, they provide many services for humans, such as food, water, recreation and space for living. Climate change is recognized as a threat to the health of wetland systems. Major changes in global climate can be summarized as follows: (1) changes in total precipitation and precipitation pattern; (2) increase temperature and evapotranspiration, especially in high latitude; and (3) an increase in extreme climate events (IPCC, 2013; Junk et al., 2013). These changes will certainly induce variations in the structure, pattern, and function of wetlands by modifying temperature, precipitation, hydrology, and evapotranspiration (Erwin and Gardner, 2009). In North America, climate change will change rainfall patterns, thus affecting runoff and groundwater inflows to wetlands. In general, a decrease in precipitation or an increase in evapotranspiration will result in less-frequent flooding of existing wetlands. The magnitude and rate of climate change could alter the hydrology of the Great Lakes and affect wetland ecosystems. Because of an increased frequency and duration of low water levels, key wetlands are at risk, particularly those that are impeded from adapting to the new water level conditions by man-made structures or geomorphic conditions (Sierszen, 2012).

In China, especially in north China, it is difficult to predict the loss of the wetlands because of the climate change. As the global mean temperature continues to increase, the glacier in Qinghai-Tibet Plateau accelerates dissolution. The area of some wetlands has shrunk, while some wetland areas have increased, such as Ulan Ula Lake (Yan et al., 2014). But in south China, due to the combined effect of human activities and

http://www.aloki.hu ● ISSN 1589 1623 (Print) ● ISSN 1785 0037 (Online)
DOI: http://dx.doi.org/10.15666/aeer/1705_1070310716

climate change, the wetland area is shrinking, such as Dongting Lake, Poyang Lake and so on (Liu et al., 2013; Cheng et al., 2016).

Located on the southern bank of the middle and lower reaches of the Yangtze River, Poyang Lake is the largest freshwater lake in China. It covers an area of 162,200 km^2 and it accounts for 9% of the Yangtze River Basin. The lake is one of the 10 largest ecological reserves in China and it is a major global ecoregion, as designated by the World Wide Fund for Nature. It plays an essential role in the protection of worldwide biodiversity, management of ecological security, safeguarding of people's livelihoods and property, and implementation of national water resource strategies (Hu et al., 2007). However, because of the impacts of climate change and anthropogenic activity, the wetland of Poyang Lake has "aged" rapidly in recent years, as evidenced in the lake sediments and by the shrinking of the lake and wetland areas (Jie et al., 2007; Qian and Dan, 2010; Jian et al., 2014).

The development of remote sensing technology has enabled extensive analysis of the water area of Poyang Lake to be conducted. For example, Zhang et al. (2012) adopted satellite remote sensing data acquired during 1991-2000 to analyze the water area dynamics of Poyang Lake. Using statistical analysis to couple the water area data with water levels measured by hydrologic stations during the same period, they established a relationship between water area and water level that modeled water area changes well, despite inherent errors between the wetland and water areas based on the remote sensing analysis. Dai et al. (2013) compared Landsat images of Poyang Lake from around 1990 and 2000 and they reported a substantial reduction in water area.

This study used remote sensing data to analyze the change of area of Poyang Lake's main body and its adjacent waters during 2000-2010. The objectives were to determine the relationship between meteorological conditions and water level, simulate the daily water area of Poyang Lake's wetland from 1959 to 2008, and discuss its annual trend of change over the past 50 years. Furthermore, the study adopted future Representative Concentration Pathways (RCPs) scenario data provided by the BCC-CSM1-1 model, developed by the National Climate Center of the China Meteorological Administration. These projections were used to discuss potential changes in climatic and basin factors, surface runoff and hydrologic extremum, and the potential impact of temperature change on the water area of Poyang Lake. The findings constitute a reference for the provision of management solutions by decision-making departments and science-based suggestions for sustainable socioeconomic development.

Data

Meteorological data

Daily meteorological data from Jan. 1, 1959 to Dec. 31, 2010 were provided by the Meteorological Bureau of Jiangxi Province. The dataset comprised almost complete and regular data records (20:00 to 20:00 Beijing time) from a reasonably dense and well-distributed network of 79 meteorological stations located within the lake basin (*Fig. 1*). Missing temperature and precipitation data in some stations records accounted for $\leq 0.5\%$ of the total dataset. The missing data were compensated based on inverse distance weighting using data from the nearest four stations (Appleton and Adlam, 2012); therefore, the missing data were considered not to compromise the mean value and the total value calculated on annual and monthly bases.

http://www.aloki.hu ● ISSN 1589 1623 (Print) ● ISSN 1785 0037 (Online)
DOI: http://dx.doi.org/10.15666/aeer/1705_1070310716

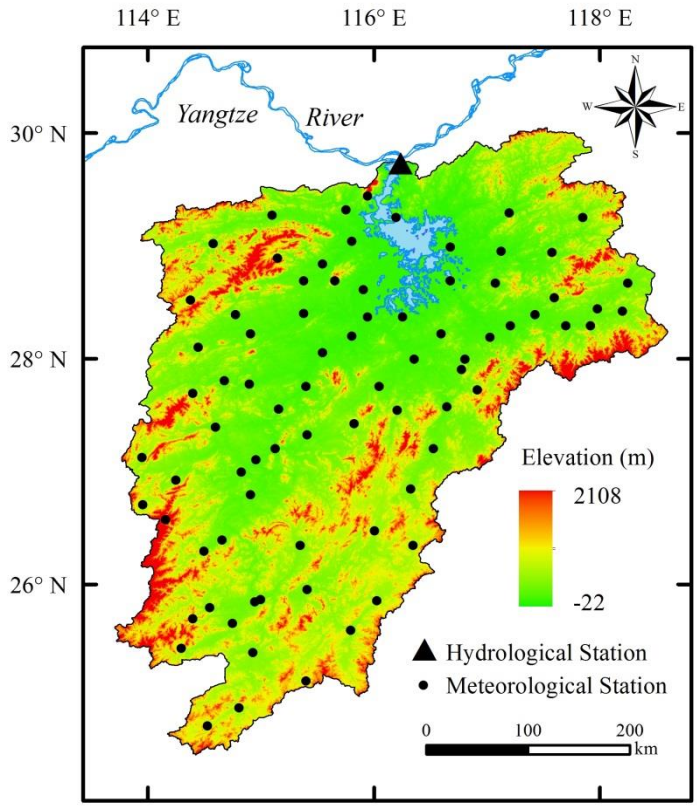

Figure 1. *Meteorological and hydrological (Hu Kou) stations in the Poyang Lake Basin*

Hydrological data

The Hukou Hydrologic Station is the control station located at the point where Poyang Lake discharges into the Yangtze River. The data recorded at Hukou reflect the level of Poyang Lake, which is governed by the levels of both the Yangtze River and the five major rivers that flow into the lake (*Fig. 1;* Hu et al., 2010). The hydrological data used in this study comprised daily water levels (Wusong Elevation) from 1961 to 2010 recorded at Hukou and Xingzi stations, provided by the Water Resources Department of Jiangxi Province.

Satellite remote sensing image data

The satellite remote sensing data of the water area of Poyang Lake (2002–2010) comprised 130 images acquired from the Poyang Lake Satellite Remote Sensing Data Bulletin released by the Meteorological Institute of Jiangxi Province. *Figure 2* shows the water area of Poyang Lake measured by remote sensing on June 4, 2010.

Climate model data

To predict future global and regional climate change, future emissions of greenhouse gases and sulfate aerosols need to be considered and these are included in the Special Report on Emissions Scenarios. In 2014, the IPCC suggested the use of radiation intensity per unit area to reflect Representative Concentration Pathway (RCP) scenarios

http://www.aloki.hu ● ISSN 1589 1623 (Print) ● ISSN 1785 0037 (Online)
DOI: http://dx.doi.org/10.15666/aeer/1705_1070310716

over the next 100 years. Different RCP scenarios (e.g., high, medium, and low) can be chosen based on projections of greenhouse gas emissions and equivalent CO_2 concentrations (IPCC, 2014; Metz et al., 2007).

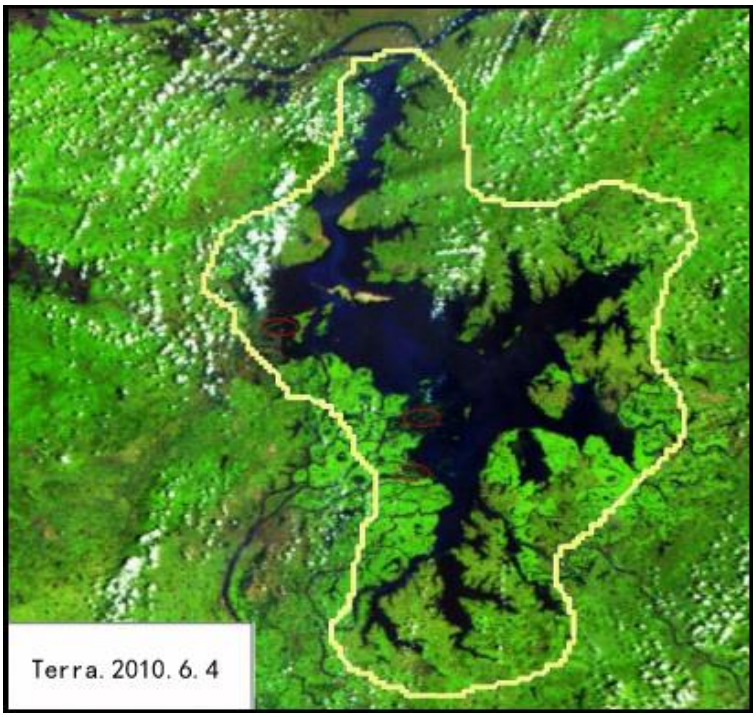

Figure 2. *Remote sensing image of Poyang Lake, acquired on June 4, 2010*

The study used data from the BCC-CSM1-1 model, developed by the National Climate Center. The model included three scenarios: RCP26, RCP45, and RCP85 with data resolution of 1° × 1°. The data comprised four parameters: mean temperature, highest and lowest temperatures, and precipitation spanning from Jan. 1, 1980 to Dec. 31, 2060. The model has been compared with other global climate models proposed for IPCC AR5, and it has been found to have better capacity in simulating climate (National Climate Center, 2012) in the monsoon belt of East Asia. Analysis of a control run of the BCC-CSM1-1 model by Zhang et al. (2011) and by Xin et al. (2013) indicated that it could satisfactorily reproduce the temperature and precipitation in China.

The simulation capability of the BCC-CSM1-1 model in terms of the daily temperature and precipitation in the area of Poyang Lake from 1986 to 2005 can be assessed using a Taylor diagram (Taylor, 2001; Xu et al., 2016). Comparisons of the correlation coefficients and the root mean square deviations of the observed data (1986–2005) with the BCC-CSM1-1 simulated data (1986–2005) show whether the model results are applicable to the Poyang Lake Basin. The Taylor diagram presented in *Figure 3* shows the correlation coefficients for the temporal and spatial distributions of temperature are 0.68 and 0.67, respectively, while those for precipitation are 0.58 and 0.45, respectively. All the root mean square deviations are < 0.5. Therefore, the BCC-CSM1-1 model is considered capable of simulating the daily temperature and precipitation at the station level for 1986–2005, indicating the suitability of the simulation data for the analysis of the spatiotemporal variations of temperature and precipitation.

http://www.aloki.hu ● ISSN 1589 1623 (Print) ● ISSN 1785 0037 (Online)
DOI: http://dx.doi.org/10.15666/aeer/1705_1070310716

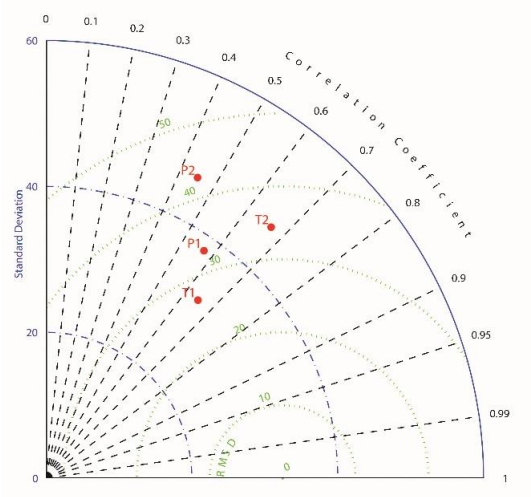

Figure 3. *Taylor diagram of temperature (Temporal distribution: T1; Spatial distribution: T2) and precipitation (Temporal distribution: P1; Spatial distribution: P2) for the BCC-CSM1-1 model*

Methodology

Classification of water area

This study classified the water area of Poyang Lake using the following scheme. The historically largest water boundary was taken as its outer boundary and its historically smallest water boundary was adopted as its inner boundary. We considered the area outside the outer boundary as land not submerged by water and the area inside the inner boundary as land covered by the lake. The water boundary of the lake moves within the outer and inner boundaries on a daily basis. The area between the water and inner boundaries was defined as the expanded water area and the area within the outer and water boundaries was defined as the reduced water area (see *Fig. 4*).

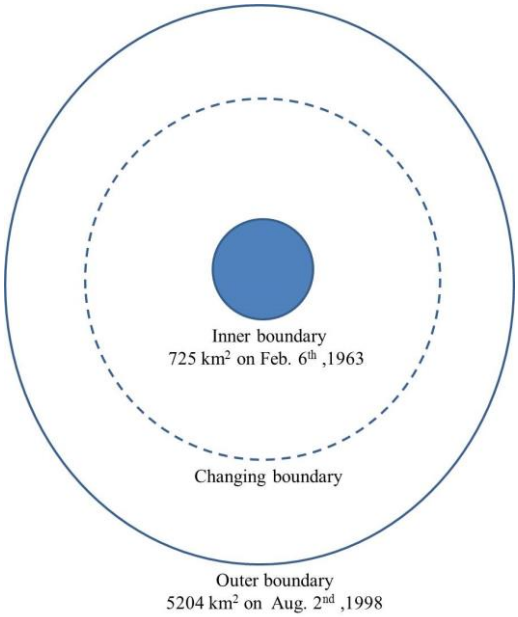

Figure 4. *Schematic of definition of water area of Poyang Lake*

http://www.aloki.hu ● ISSN 1589 1623 (Print) ● ISSN 1785 0037 (Online)
DOI: http://dx.doi.org/10.15666/aeer/1705_1070310716

Water area model of Poyang Lake

Land reclamation constitutes a major process via which the land resource of lake areas in the southern plains of China has been developed and exploited. The harnessing of reclaimed land to develop agriculture (Zhang et al., 2015) has long been practiced in the wetland area of Poyang Lake. Since the founding of the People's Republic of China, unchecked land reclamation has been undertaken. For example, the area of reclaimed land in the 1950s, 1960s, and 1970s was 394.9, 793.4, and 211.7 km^2, respectively. However, by the 1980s, the situation was more controlled with only 66.9 km^2 of land reclaimed. Since the flooding that occurred in 1998, a policy of returning farmland to lakes has been phased in (Zhu and Kang, 2017). By the end of 2001, 900,000 residents had been resettled and the water area increased by over 1000 km^2. To avoid the influence of anthropogenic activity on the water area of Poyang Lake, this study used data collected from 2002 to 2009, after the return of farmland to the lake had been completed. These data included 98 samples of water area measured by remote sensing, water level measured at Hukou Station, and mean temperature and precipitation measured by the meteorological stations surrounding the Poyang Lake wetland. Stepwise regression analysis (Arunajadai, 2009) revealed the strongest correlations between the water area determined by remote sensing and water level measured at Hukou Station, and between the 30-d accumulative mean temperature and accumulative precipitation. We established a functional relationship between water area, Hukou water level, and meteorological conditions as below:

$$Y = -1.029X1 + 0.202X2 + 312.476X3 - 991.585 \quad \text{(Eq.1)}$$

where Y is the simulated water area of Poyang Lake, X_1 is the 30-d accumulative mean temperature, X_2 is the 30-d accumulative mean precipitation, and X_3 is the water level at Hukou Station on that day. Based on 14 sets of remote sensing data of water area, water level measured at Hukou Station, and meteorological data, it was verified that this model could satisfactorily simulate the water area of Poyang Lake with a correlation coefficient of up to 0.986 and mean relative error of only 5.6% (*Table 1*). No significant difference between simulated and measured data by F-test. In general, the simulation achieves the desired effect.

Inputting the data on temperature, precipitation, and water level at Hukou Station during the study period into *Equation 1* produced the largest and smallest water areas of 5204 (August 2, 1998; Hukou water level: 22.53 m) and 725 km^2 (February 6, 1963; Hukou water level: 5.91 m), respectively. Therefore, this study adopted 5204 km^2 as the outer boundary and 725 km^2 as the inner boundary.

Results

Changing trends of drought and flood of the Poyang Lake Basin

To analyze the trend of change of the Poyang Lake wetland, we supposed the water area within the outer boundary and within the inner boundary was S_{MAX} and S_{MIN}, respectively, and the water area on a certain day was S. Therefore, we defined the following:

$$S_{\text{expanded lake area}} = S - S_{MIN}$$

http://www.aloki.hu ● ISSN 1589 1623 (Print) ● ISSN 1785 0037 (Online)
DOI: http://dx.doi.org/10.15666/aeer/1705_1070310716

and

$$S_{\text{reduced lake area}} = S_{\text{MAX}} - S.$$

We used *Equation 1* to calculate the daily water area from 1959 to 2008. Its difference from the outer and inner boundaries was determined as the daily expanded or reduced water areas, respectively. *Figure 5* shows the annual mean expanded or reduced water areas. According to the statistics in the Chronicle of Meteorological Disasters in China—Jiangxi Volume (CMA, 2010) and the Yearbook of Climate-Related Disasters in China (CMA, 2014), basin-wide severe flooding occurred in 1970, 1973, 1975, 1995, and 1998. Taking 1998 as an example, 1329 villages and towns from 79 counties (cities or districts) were badly affected with direct economic losses of RMB38.714 billion. Basin-wide severe drought has occurred in 1963, 1971, 1972, 1978, 1986, 1988, 2001, 2003, 2004, 2006, and 2007. Taking 2007 as an example, 352,000 ha of crops were affected by drought and 64,000 ha of winter crops could not be sown. Overall, 760,000 people and 310,000 large livestock lacked adequate supplies of drinking water.

Table 1. *Simulation tests of the water area of Poyang Lake in 2010*

Data	Water level of Hukou (m)	Remote sensing of water area (km^2)	Accumulated temperature of 30 days (°C)	Accumulated precipitation of 30 days (mm)	Simulated area (km^2)	Relative error
02.21	8.98	1582	236.1	145.9	1601	1.2
03.12	11.71	2298	285.2	196.8	2414	5.0
03.26	10.28	1757	410.4	224.0	1844	4.9
05.23	16.61	3300	642.2	329.1	3604	9.2
05.24	16.87	3390	646.8	330.9	3681	8.6
05.25	17.16	3429	652.1	330.9	3766	9.8
06.04	16.97	3367	673.0	364.9	3692	9.7
06.21	18.17	3855	711.1	369.0	4029	4.5
06.22	18.17	3855	714.4	338.4	4019	4.3
08.12	18.83	3688	897.4	100.8	3989	8.2
09.18	16.89	3293	834.8	136.3	3455	4.9
10.08	14.74	2922	734.1	74.2	2874	1.6
10.28	12.85	2342	590.0	70.7	2431	3.8
11.08	11.2	1932	519.3	62.5	1986	2.8
Average						5.6

The time series of changing wetland area presented in *Figure 5* reflects the occurrence of flood and drought disasters in the Poyang Lake Basin. *Figure 5* shows that since 1990 the wetland area of Poyang Lake has had a trend of reduction. Particularly since 2000, several severe droughts have exacerbated this trend (the trend passed the 0.01 reliability test). The water area of Poyang Lake has shrunk substantially from the 1990s, especially during the 2000s. Because of aridification, the water area has shrunk by 22.5% from 1845 km^2 in the 1980s to 1430 km^2 in the 2000s.

http://www.aloki.hu ● ISSN 1589 1623 (Print) ● ISSN 1785 0037 (Online)
DOI: http://dx.doi.org/10.15666/aeer/1705_1070310716

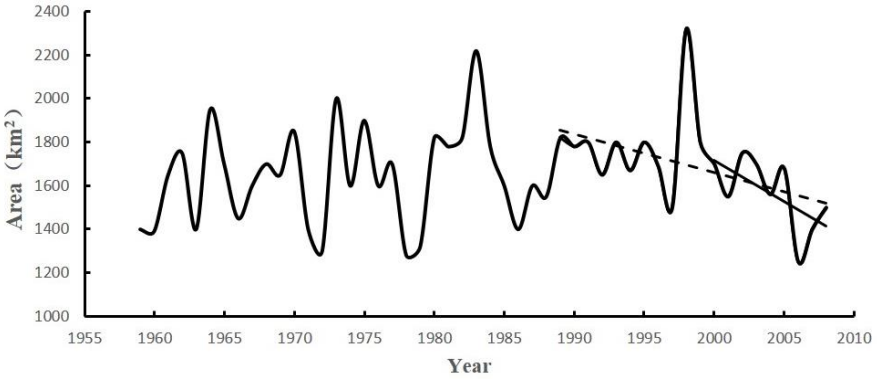

Figure 5. *Temporal variation of wetland area of the Poyang Lake Basin (1959–2008)*

Changing trend of wet season of Poyang Lake Basin

The wet and dry seasons of the Poyang Lake Basin were determined based on the water level at the Xingzi Hydrologic Station. When its water level was > 13.39 m, we considered the area to be in the wet season and the first day of such an occurrence was denoted the first day of the wet season (final day of the dry season). When its water level was < 10.22 m, we considered the area to be in the dry season and the first day of such an occurrence was denoted the first day of the dry season (final day of the wet season). The period between the first and final days of the wet season was called the wet season of Poyang Lake. Using daily hydrological data from Xingzi Station (1959–2009), we calculated the annual first and final days of the wet season and the number of wet season days.

According to *Figures 6–8*, the first day of the wet season of Poyang Lake has had a tendency to become delayed (the trend passed the 0.05 reliability test). Conversely, the final day of the wet season of Poyang Lake has had a tendency to become advanced (the trend did not pass the reliability test). Generally, the number of days of the wet season of Poyang Lake has decreased since 1990 (the trend passed the 0.05 reliability test). This reduction has led to large-scale wetland loss and degradation, stunting the growth and development of both plants and animals. Taking the dry season from August 2006 to April 2007 as an example, it is evident that the eco-environment of the lake area has been influenced by the effects of climate change. Droughts have given rise to serious ecological issues, including the drying up of lake branches, degradation of lakeside wetland, and desertification of the lakebed.

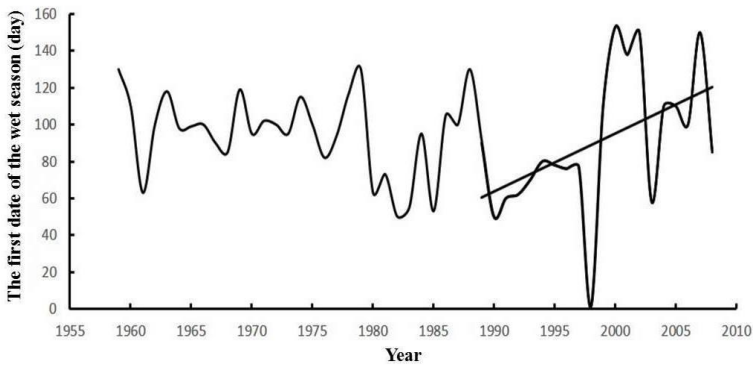

Figure 6. *Temporal variation of first day of the wet season (1959–2008)*

http://www.aloki.hu ● ISSN 1589 1623 (Print) ● ISSN 1785 0037 (Online)
DOI: http://dx.doi.org/10.15666/aeer/1705_1070310716

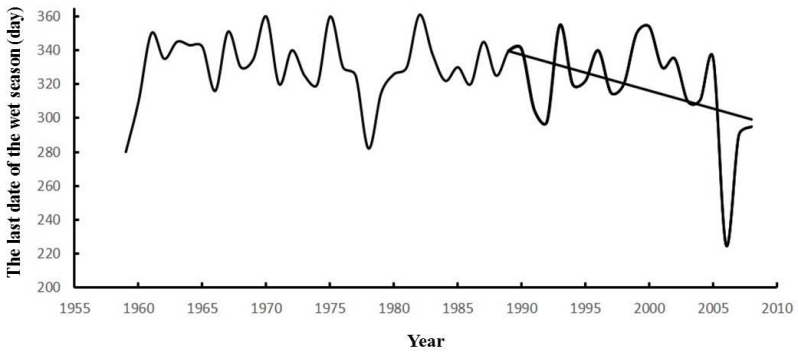

Figure 7. *Temporal variation of the final day of the wet season (1959–2008)*

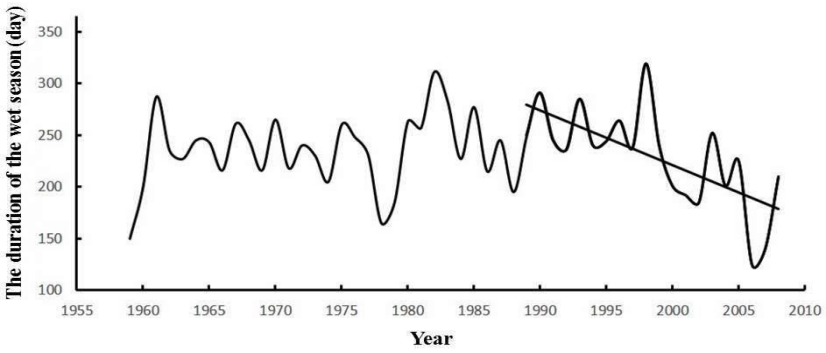

Figure 8. *Temporal variation of duration of wet season (1959–2008)*

Climate prediction

Data from the BCC-CSM1-1 model, developed by the National Climate Center, is capable of simulating the climatic conditions of the Poyang Lake Basin. Based on systematic analyses, Zhan et al. (2013) verified the capability of the BCC-CSM1-1 model in simulating the spatial and temporal trends of temperature.

Temperature prediction

As shown in *Figure 9,* under the three future climate change scenarios (RCP2.6, RCP4.5, and RCP8.5), the annual mean temperature of the Poyang Lake Basin would increase to different extents from 2011 to 2060. It would increase the least under the RCP2.6 scenario and it would increase the most under the RCP8.5 scenario. The rates of temperature rise under the RCP2.6, RCP4.5, and RCP8.5 scenarios would be 0.26, 0.37, and 0.44 °C/a, respectively. The mean temperature, however, would be highest (17.7 °C) under the RCP4.5 scenario and lowest (16.9 °C) under the RCP8.5 scenario.

Precipitation prediction

As shown in *Figure 10* and *Table 2*, under the three RCP climate change scenarios, precipitation in the Poyang Lake Basin from 2011 to 2060 would not change overall, although interannual fluctuation would be apparent. The annual mean precipitation would be lowest under the RCP8.5 scenario, while it would be similarly relatively

http://www.aloki.hu ● ISSN 1589 1623 (Print) ● ISSN 1785 0037 (Online)
DOI: http://dx.doi.org/10.15666/aeer/1705_1070310716

higher under the RCP2.6 and RCP4.5 scenarios. In terms of interdecadal precipitation distribution, the trends seen under the RCP2.6 and RCP4.5 scenarios would be consistent with a W–shaped pattern, i.e., reflecting a process of "fall–rise–fall." Under the RCP8.5 scenario, the Poyang Lake Basin could experience a prominent trend toward a hotter and wetter climate.

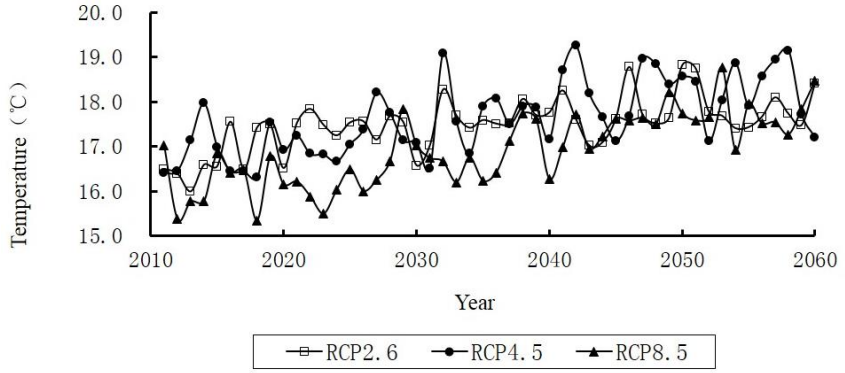

Figure 9. *Temporal variation of annual mean temperature under different RCP scenarios (2011–2060)*

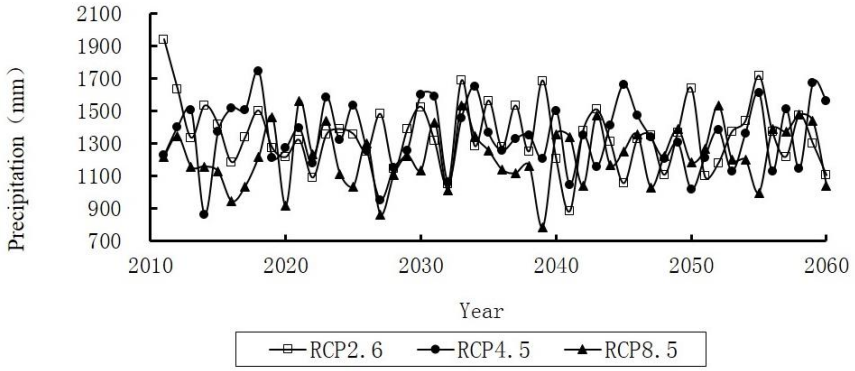

Figure 10. *Temporal variation of annual precipitation under different RCP scenarios (2011–2060)*

Table 2. *Decadal annual precipitation of the Poyang Lake Basin under different RCP scenarios (2011–2060)*

Precipitation (mm) / Scenarios	2010s	2020s	2030s	2010s	2010s	2011-2060
RCP2.6	1437	1329	1385	1292	1326	1354
RCP4.5	1362	1323	1376	1296	1371	1345
RCP8.5	1157	1200	1212	1245	1290	1221

Changing trend of precipitation extremum

Extreme precipitation events can be represented by two quantiles, e.g., the 10th and 90th percentiles of annual precipitation (Guan et al., 2015; Zhang et al., 2015). *Table 3*

http://www.aloki.hu ● ISSN 1589 1623 (Print) ● ISSN 1785 0037 (Online)
DOI: http://dx.doi.org/10.15666/aeer/1705_1070310716

lists the threshold values of extreme events in the Poyang Lake Basin. It is shown that from 2011 to 2060, dry years with 10% probability of occurrence would increase obviously under all three RCP scenarios but the increase would be greatest under the RCP4.5 and RCP8.5 scenarios. Over the past 50 years, wet years with 10% probability of occurrence remained largely constant under the RCP2.6 scenario but they decreased in number in both the RCP4.5 and the RCP8.5 scenarios. In general, under all three scenarios, extreme events would be expected to occur more frequently, suggesting dramatic volatility in water resources and greater frequency of droughts, which would exacerbate the shrinking of Poyang Lake and represent a severe threat to its water security.

Table 3. *Frequency of extreme events in the Poyang Lake Basin from 2011 to 2060 under the different RCP scenarios*

Extreme precipitation from 1981 to 2005 (mm)		**Extreme precipitation from 2011 to 2060 (mm)**		
The 10th percentile	**The 90th percentile**		**Times lower than the 10th percentile**	**Times higher than the 10th percentile**
1098	1607	RCP2.6	6	5
		RCP4.5	10	1
		RCP8.5	13	2

Conclusions and discussion

The Poyang Lake Basin is sensitive to the effects of climate change. Particularly since the 1990s, it has witnessed a rapid rise in temperature, fewer rainfall days, and increased precipitation intensity, which have increased the frequencies of floods in summer and of droughts in spring and autumn (Wang et al., 2009; Wei et al., 2015). Since the 2000s, with even greater temperature rises and slight falls in amounts of precipitation, the Poyang Lake Basin has faced severe challenges of aridification and shrinkage of the lake area. Based on hydrological data from the Wuhe and Xingzi stations (1956–2007), a study by Min and Dan (2010) yielded almost identical results to those derived from the present work.

1. A statistical model built using hydrological and meteorological data was verified capable of reflecting changes in the water area of Poyang Lake. Based on the difference between the water area and the outer and inner boundaries, this study redefined and reclassified the area of the Poyang Lake wetland. The results showed that the change of wetland area satisfactorily reflected the variation between flood and drought throughout the entire basin. Since 1990, and particularly since 2000, acute reduction of the wetland area has accelerated its aridification.

2. Using the water level of the Xingzi Station as a benchmark, the first and final days of the wet season (first and final days of the dry season) of Poyang Lake were analyzed. It was found that since 1990 the first day has become delayed and that the final day (first day of the dry season) has advanced. The number of wet season days has decreased significantly and the wetland area is in the process of dramatic shrinkage.

3. Under the RCP2.6, RCP4.5, and RCP8.5 scenarios, it was discovered that the temperature from 2011 to 2060 would continue to rise in the Poyang Lake Basin. Although the precipitation amounts would remain similar, extreme droughts would occur with greater frequency and the water area would fluctuate more substantially,

http://www.aloki.hu ● ISSN 1589 1623 (Print) ● ISSN 1785 0037 (Online)
DOI: http://dx.doi.org/10.15666/aeer/1705_1070310716

which would exacerbate the shrinkage and degradation of the water area, introducing greater instability to the ecological system.

Irrespective of whether based on observed or remotely sensed data, previous research has largely agreed that the area of Poyang Lake has shrunk from the 1960s to the 2000s (Min and Dan, 2010; Feng et al., 2011; Gan and Liu, 2011). However, considering the influence of the Three Gorges Dam (Wu et al., 2011; Mei et al., 2015; Liu et al., 2017), the future of the Poyang Lake Basin is more difficult to forecast. Based on future climate data, this study predicted exacerbation of the shrinkage of Poyang Lake. To overcome inadequacies identified in this research, our future work will use additional climate model data and a hydrological model to consider the effects of the Three Gorges Dam.

Acknowledgements. This study was supported by the CMA Climate Change Science Fund (CCSF (201607) and the CDM FUND "Jiangxi Climate Change Adaptation Program" (2014102).

REFERENCES

[1] Appleton, J. D., Adlam, K. A. M. (2012): Geogenic control on soil chemistry in urban areas: a novel method for urban geochemical mapping using parent material classified data. – Applied Geochemistry 27(1): 161-170.

[2] Arunajadai, S. G. (2009): Stepwise logistic regression. – Anesthesia and Analgesia 109(1): 285-285.

[3] Cheng, J. X., Xu, L. G., Jiang, J. H. et al. (2016): The research of runoff responses to climate change and human activities in the Dongting Lake catchment. – Journal of Ago-Environment Science 35(11): 2146-2153.

[4] China Meteorological Adminisitration (CMA) (2010): Chronicle of Meteorological Disasters in China—Jiangxi Volume. – China Meteorological Publishing, Beijing.

[5] China Meteorological Adminisitration (CMA) (2014): Yearbook of Climate Related Disasters China. – China Meteorological Publishing, Beijing.

[6] Dai, Z., Zhang, W., Chen, X. (2013): Monitoring TSM by HJ CCD imagery index in Poyang Lake. – Geomatics and Information Science of Wuhan University 38(11): 1303-1307.

[7] Erwin, K. L., Gardner, R. C. (2009): Wetlands and global climate change: the role of wetland restoration in a changing world. – Wetlands Ecology and Management 17(1): 71.

[8] Feng, L., Hu, C., Chen, X. et al. (2011): MODIS observations of the bottom topography and its inter-annual variability of Poyang Lake. – Remote Sensing of Environment 115(10): 2729-2741.

[9] Gan, X. Y., Liu, C. L. (2011): Analysis of drought in Poyang Lake. – Meteorological and Environmental Research 5: 38-40.

[10] Guan, Y., Zhang, X., Zheng, F. et al. (2015): Trends and variability of daily temperature extremes during 1960-2012 in the Yangtze River Basin, China. – International Journal of Climatology 124(3): 79-94.

[11] Hu, M. L., Wu, Z. Q., Liu, Y. L. (2010): Characteristics of water level and its effects on water environmental factors in Hukou area of Poyang Lake. – Journal of Hydrogeology 48: 542-553.

[12] Hu, Q., Feng, S., Guo, H. (2007): Interactions of the Yangtze River flow and hydrologic processes of the Poyang Lake, China. – Journal of Hydrology 347(1-2): 90-100.

[13] IPCC (2013): Climate Change 2013: The Physical Science Basis. Contribution of Working Group I to the Fifth Assessment Report of IPCC the Intergovernmental Panel on Climate Change. – Cambridge University Publishing, UK, and New York.

http://www.aloki.hu ● ISSN 1589 1623 (Print) ● ISSN 1785 0037 (Online)
DOI: http://dx.doi.org/10.15666/aeer/1705_1070310716

[14] IPCC (2014): Climate Change 2014: Impacts, adaptation and vulnerability. Contribution of Working Group II to the Fifth Assessment Report of IPCC the Intergovernmental Panel on Climate Change. – Cambridge University Publishing, UK and New York.
[15] Jian, H.G, Jia, J., Kettner, A. J. (2014): Changes in water and sediment exchange between the Changjiang River and Poyang Lake under natural and anthropogenic conditions, China. – Science of the Total Environment 481C(1): 542-553.
[16] Jie, E. L., Li, X. J., Liu, S. Y. (2007): Analysis of dynamic changes of the wetland of poyang lake and its causes. – Acta Agriculturae Universitatis Jiangxiensis 42: 36-45.
[17] Junk, W. J., An, S., Finlayson, C. M. et al. (2013): Current state of knowledge regarding the world's wetlands and their future under global climate change: a synthesis. – Aquatic Sciences 75(1): 151-167.
[18] Liu, Y., You, H., Cheng, X. et al. (2013): Estimation of variation of Poyang Lake area based on long-term MODIS observations. – Journal of Geo-Information Science 15(3): 469-475.
[19] Liu, Z., Guo, S., Guo, J. et al. (2017): The impact of Three Gorges Reservoir refill operation on water levels in Poyang Lake, China. – Stochastic Environmental Research and Risk Assessment 31(4): 879-891.
[20] Mei, X., Dai, Z., Du, J. et al. (2015): Linkage between Three Gorges Dam impacts and the dramatic recessions in China's largest freshwater lake, Poyang Lake. – Scientific Reports. DOI: 10.1038/srep18197.
[21] Metz, B., Davidson, O. R., Bosch, P. R. (2007): Climate Change 2007: Mitigation. Contribution of Working Group III to the Fourth Assessment Report of the Intergovernmental Panel on Climate Change. – Cambridge University Publishing, UK and New York.
[22] Min, Q., Dan, M. (2010): Drought change characteristics and drought protection countermeasures for Poyanghu Lake Basin. – Journal of China Hydrology 30(1): 84-88.
[23] National Climate Center (2012): Data set of Regional model prediction in China Version 2.0. – China Meteorological Publishing, Beijing.
[24] Qian, M., Dan, M. (2010): Drought change characteristics and drought protection countermeasures for Poyang Lake Basin. – Journal of China Hydrology 30(1): 84-88.
[25] Sierszen, M. E., Morrice, J. A., Trebitz, A. S. et al. (2012): A review of selected ecosystem services provided by coastal wetlands of the Laurentian Great Lakes. – Aquatic Ecosystem Health and Management 15(1): 92-106.
[26] Taylor, K. E. (2001): Summarizing multiple aspects of model performance in a single diagram. – Journal of Geophysical Research Atmospheres 106(D7): 7183-7192. DOI: 10.1029/2000JD900719.
[27] Wang, H. Q., Zhao, G. N., Peng, J. et al. (2009): Precipitation characteristics over five major river systems of Poyang drainage areas in recent 50 years. – Resources and Environment in the Yangtze Basin 18(7): 615-619.
[28] Wei, J., Knoche, H. R., Kunstmann, H. (2015): Contribution of transpiration and evaporation to precipitation: an ET-Tagging study for the Poyang Lake region in Southeast China. – Journal of Geophysical Research: Atmospheres 120(14): 6845-6864.
[29] Wu, L. H., Li, M., Guo, Y. Y. et al. (2011): Influence of Three Gorges Project on Water quality of Poyang Lake. – Procedia Environmental Sciences 10(1): 1496-1501.
[30] Xin, X. G., Wu, T. W., Li, J. L. et al. (2013): How well does BCC_CSM1.1 reproduce the 20th century climate change over China? – Atmospheric and Oceanic Science Letters 6(1): 21-26.
[31] Xu, Z., Hou, Z., Han, Y. et al. (2016): A diagram for evaluating multiple aspects of model performance in simulating vector fields. – Geoscientific Model Development 9(12): 1-25.
[32] Yan, Q., Liao, J. J., Shen, G. Z. (2014): Remote sensing analysis and simulation of change of Ulan-Ul Lake in the past 40 years. – Remote Sensing for Land and Resources 26(1): 152-157.

http://www.aloki.hu ● ISSN 1589 1623 (Print) ● ISSN 1785 0037 (Online)
DOI: http://dx.doi.org/10.15666/aeer/1705_1070310716

[33] Zhan, M. J., Yin, J. M., Kong, P. (2013): Prediction on possible climate change of Poyang Lake Basin in the future 50 years, under RCP scenario. – Science Technology and Engineering 13(34): 107-115.
[34] Zhang, J., Wei, H. U., Liu, Y. (2015): Response of soil microbial functional diversity to different land-use types in wetland of Poyang Lake, China. – Acta Ecologica Sinica 35(4): 234-245.
[35] Zhang, L., Dong, M., Wu, T. (2011): Changes in precipitation extremes over Eastern China simulated by the Beijing Climate Center - Climate System Model (BCC_CSM1.0). – Climate Research 50(2): 227-245.
[36] Zhang, L., Fraedrich, K. Zhu, X. et al. (2015): Interannual variability of winter precipitation in Southeast China. – Theoretical and Applied Climatology 119(1-2): 229-238.
[37] Zhang, N., Wen, W., Yin, W. (2012): Estimate the area of the Poyang Lake using satellite remote sensing data and analyze its relationship with water level. – Remote Sensing Technology and Application 36: 45-54.
[38] Zhu, H. G., Kang, L. Y. (2017): An analysis on farmers' alternative choice to substitute livelihood and its influencing factors in returning farmland to wetland. A case study of Poyang Lake area. – Journal of Jiangsu University 19(3): 7-14.

http://www.aloki.hu ● ISSN 1589 1623 (Print) ● ISSN 1785 0037 (Online)
DOI: http://dx.doi.org/10.15666/aeer/1705_1070310716

MAIZE YIELD AND LEAF PHOTOSYNTHETIC CHARACTERISTICS IN RESPONSE TO PLANTING DENSITIES AND APPLICATION OF YUHUANGJIN, AS A NEW PLANT GROWTH REGULATOR

TONG, T. – GU, W. R.* – LIU, X. M. – LI, C. F.

Department of Crop Cultivation and Farming System, College of Agriculture
Northeast Agricultural University, 150030 Harbin, PR China

**Corresponding author*
e-mail: wanronggu@163.com; phone: +86-451-5519-0472

(Received 1st Mar 2019; accepted 21st May 2019)

Abstract. This study aims to analyze the effects of plant growth regulator on the chlorophyll fluorescence characteristics and yield of spring maize under different planting densities in Northeast China. 'Dongnong 253' was used as the material in this experiment and was planted at the densities of 5, 6, 7 and 8 plants m^{-2}. The plants were sprayed at the jointing stage with the "Yuhuangjin" plant growth regulator. The results showed that increasing the planting density effectively increased the production of the maize populations, while it led to a decrease in the chlorophyll content, angle between the stem and leaf (ABSL) in the ear leaf, single plant dry weight and photosynthetic efficiency, as well as increases in the plant height, ear height and lodging risk. The application of "Yuhuangjin" decreased the plant height and ear height and increased the dry matter accumulation per plant and lodging resistance, increased the ABSL in the ear leaf, reduced the degree of overshadowing in the prophase, extended the duration of high leaf area index (*LAI*), delayed the senescence process of the leaf and improved the canopy aeration and transmittance capability. The application of "Yuhuangjin" improved the photosynthetic capacities and maintained higher stable photosynthesis by significantly improving the chlorophyll fluorescence parameters, such as *Fv/Fm*, *Y(II)*, and *qP* and decreasing *Y(NO)* and *qN*. This study showed that the highest yield was 11428.18 kg ha^{-1} after the "Yuhuangjin" treatment at the planting density of 7 plants m^{-2}. This experiment provided theoretical and experimental evidence for the effect of increased production from the use of plant growth regulator and high-density planting cultivation on spring maize in Northeast China.

Keywords: *maize, high-density planting, chlorophyll fluorescence characteristics, photosynthesis rate, Yuhuangjin, yield*

Introduction

Maize (*Zea mays* L.) plays an important role in ensuring world food security (Dong et al., 2013; Li et al., 2017). Increasing planting density is important to increase maize yields. The demand for maize is increasing with the rapidly increasing demands for food, livestock feed and bio-fuel at the global scale. Previous researchers have conducted extensive work in improving maize yield potentials and increasing yields per unit area (Diallo et al., 2015; Li et al., 2016; Biswas and Ma, 2017; Ren et al., 2017a). Previous studies have shown that increasing population density is an important method to achieve high yields (Rutger and Crowder, 1967; Roy et al., 2014). The analysis of 37 super-high-yield fields between 2006 and 2007 showed that the yields reached 15000 kg ha^{-1} in the high yield field, the densities were in the range of 79725~84630 ears ha^{-1} (Chen et al., 2008). However, the current density of maize in the United States is generally 8 plants m^{-2} or higher. Dense planting is the main measure used to improve maize yields (Zhao et al., 2006; Benari and Makowski, 2016). The

http://www.aloki.hu ● ISSN 1589 1623 (Print) ● ISSN 1785 0037 (Online)
DOI: http://dx.doi.org/10.15666/aeer/1705_1071710730

structure of the canopy group becomes poor with the increase in planting density, and increased density can cause the plants to shade each other. Increasing the planting density will also increase the competition for light, water and nutrients between plants (Kang et al., 2011; Farhad and Mehdi, 2015; Ren et al., 2017b). With the planting density increases, the individual plants in the group will shade each other, which will deteriorate the permeability of the canopy, decrease the photosynthetic performance, increase the plant height and increase the risk of lodging (Li et al., 2007; Sangakkara et al., 2012).

The maize in the area of Northeast China experiences low temperatures and rainy environments, which enable the root system to resist falling. Plant growth regulator is a synthetic substance that has the function of plant hormones (Yan et al., 2009). Plant growth regulator can effectively regulate the growth and development of plants and can effectively regulate the structural characteristics of the canopy. It is easy for the root system to fall in the later stages of growth and development, and this will cause many production cuts (Liao et al., 2014). Plant growth regulator technology can lower the height and ear height of maize plants (Meng et al., 2016). Plant growth regulators can enhance the anti-lodging ability, improve the chlorophyll content in leaves and prolong the duration of high leaf area index (*LAI*) values (Cheng and Liu, 2017). Plant growth regulator can truncate the elongation of internode cells, lower the center of the maize plant, increase the roughness of the stalks, improve the anti-lodging capacity (Fan et al., 2017), improve the leaf photosynthetic characteristics, photosynthetic efficiency and the rational distribution of assimilation products (Zhang et al., 2014). Moreover, plant growth regulator can also promote the absorption of the maize root system, promote the delivery of root secretions to the ground and promote the formation of grain yields (Cicchino et al., 2013).

Photosynthesis is the basis of plant growth and development (Inamoto et al., 2015). The photosynthetic rate is an important index that can reflect the photosynthetic capacity of a plant. The process of photosynthesis is composed of a series of complex photophysical and photochemical processes. During these processes, part of the light energy losses is released in the form of fluorescence. Chlorophyll fluorescence is closely related to photosynthesis (Hwang and Choo, 2016; Zhang et al., 2017).

"Yuhuangjin" plays an important role in the increase of maize planting in China. The plant growth regulator "Yuhuangjin" was provided by Fujian Haolun Biology Engineering Technology Co. Ltd, China. Its total effective component contents are the mixture of 3% diethyl aminoethyl hexanoate and 27% ethephon. Maize in Heilongjiang Province faces problems related to how both production and anti-lodging capacity can be synergistically increased. Previous researchers have conducted extensive work on the application of "Yuhuangjin", and it plays an important role in the mining potential of planting. In this experiment, we combined dense planting and plant growth regulator to study the photosynthetic characteristics of maize and the effects on yield. The results also provided an experimental basis for the reasonable application of "Yuhuangjin" in China.

Materials and methods

Experimental materials and treatments

The present experiment was carried out from 2013 to 2014 at the Xiang Fang experimental base, Northeast Agricultural University, Heilongjiang Province at 45°42′N

http://www.aloki.hu ● ISSN 1589 1623 (Print) ● ISSN 1785 0037 (Online)
DOI: http://dx.doi.org/10.15666/aeer/1705_1071710730

latitude and 126°36′E longitude. The soil is a typical black soil (typic hapludoll in USDA soil taxonomy). The soil contained organic matter (25.25 g kg^{-1}), total nitrogen (N) (1.70 g kg^{-1}), available potassium (K) (179.35 mg kg^{-1}), rapid available phosphorus (P) (65.34 mg kg^{-1}), and alkali hydrolysable nitrogen (N) (118.21 mg kg^{-1}). The climate in the region is temperate continental monsoon. The weather data from 2013 and 2014 are provided in *Table 1*.

Table 1. *Daily mean values of the weather variables at the experimental site during the six months of the maize growing season in 2013 and 2014*

Month	Average temperature (°C)		Precipitation (mm)		Sunshine hours (h)	
	2013	2014	2013	2014	2013	2014
April	4.4	10.3	10.8	6.1	202.3	267.0
May	17.9	14.3	73.5	91.4	240.7	127.5
June	21.4	22.9	86.4	56.8	151.7	216.8
July	23.9	23.1	198.0	115.5	195.1	159.9
August	22.5	21.9	125.7	83.8	163.7	208.1
September	15.8	15.5	31.5	32.2	230.1	184.4
Total [a]	17.7	18	525.9	385.8	1183.6	1163.7

[a] Precipitation and sunshine are monthly sums, while temperature is a monthly mean of daily means

Maize was hand-sown at 7 cm depth and 70 cm row distance on May 1 in 2013 and May 1 in 2014 in a plot size of 84 m^2. The supply trial variety was ‘Dongnong 253’. The tested planting densities were 5 plants m^{-2}, 6 plants m^{-2}, 7 plants m^{-2} and 8 plants m^{-2}. Using the same density of rope, 20 ml of "Yuhuangjin" was added to 30 kg of water. The solution was sprayed on six leaves and one bud, and water was used as a control. Diammonium phosphate (250 kg), urea (75 kg), and potassium sulfate (150 kg) were used as seed fertilizer, and nitrogen fertilizer was applied per hectare during the jointing stage.

Measurement of leaf area index (LAI)

The leaf area was measured using three randomly selected maize plants in each plot at the silking stage. The length and maximum width of each leaf were measured with a ruler. Leaf area index (*LAI*) = single plant leaf area × the number of plants per unit of land ÷ unit land area.

Measurement of chlorophyll content (SPAD)

The CCM-200+ (Beijing Aozuo Ecology Instrument Co, Ltd) chlorophyll meter was used to measure the relative chlorophyll content in leaves. In each treatment phase, three plants with uniform leaf ages were selected and marked. The determination time was between 8:30 and 10:00 am, and the ear-leaf content of each reproductive period was measured. The leaf tip, leaf center and leaf base of the leaves were determined, and the mean values were calculated as the determination value of the blade. The three measured values of each treatment were calculated, and the average value was taken as the *SPAD* value of the treatment. In the subsequent measurements, the marked plants were selected for measurement.

http://www.aloki.hu ● ISSN 1589 1623 (Print) ● ISSN 1785 0037 (Online)
DOI: http://dx.doi.org/10.15666/aeer/1705_1071710730

Measurement of net photosynthetic rate of leaves (Pn)

The net photosynthetic rate of the leaves was determined between 9:00 and 11:00 am, and a hand-held photosynthetic rate meter instrument CI-340 (Zealquest Scientific Technology Co., Ltd.) was used to measure the ear-leaf content. The mean value of the three measured values was used as the measured value for the treatment.

Measurement of chlorophyll fluorescence parameters

The middle of the selected plant was measured to determine the chlorophyll fluorescence parameters, and the measurement was collected between 8:30 and 10:00 am. First, a leaf clip was used to hold the middle of the ear leaf, and the ear leaf was kept in the dark treatment for 20 minutes; then, the leaf clip operation steps were followed. The mean value of the three measurements was taken as the measured value. The *PSII* maximum quantum yield (*Fv/Fm*), actual quantum yield (*Y(Ⅱ)*), non-regulating performance dissipation quantum yield (*Y(NO)*), non-photochemical quenching parameters (*qN*), and photochemical quenching parameters (*qP*) were calculated. The measurement instrument was a portable modulated chlorophyll fluorometer (PAM-2500) (KANGGAOTE Science and Technology Co., Ltd).

Measurement of biomass and yield

To determine the biomass and yield, two consecutive four-meter lengths were selected for each process. The rows per ear, number of ear, kernels row, number of row and hundred grain weight were calculated. After harvest, 20 ears were selected to calculate the kernels row, number of row, hundred grain weight, and the theoretical yield. The biomass was determined by the drying method, and the stalks and grains were dried separately. Each process was repeated three times, and the results were averaged.

Statistical analyses

According to the analysis of variance principles, data were statistically analyzed following standard statistical methods using Microsoft Excel 2010 and SPSS 12.0. Differences between treatments were determined by a posteriori Tukey's test at a significance level of 0.05.

Results

Effects of plant growth regulator on leaf area index of spring maize in different planting densities

During the reproductive process, the *LAI* first showed an increasing then a decreasing trend in both treatments (*Table 2*). The *LAI* peaks appeared around the time of silking, and the *LAI* also increased with the increase in planting density. In the "Yuhuangjin" treatment, the peak *LAI* values were 0.89% (5 plants m^{-2}), 3.95% (6 plants m^{-2}), 1.23% (7 plants m^{-2}) and 8.74% (8 plants m^{-2}) lower than the peak *LAI* values in the water treatment. From the silking stage to the dough stage, the *LAI* values were 3.75% (5 plants m^{-2}), 6.47% (6 plants m^{-2}), 7.14% (7 plants m^{-2}) and 14.60% (8 plants m^{-2}) lower than the peak values in the water treatment.

http://www.aloki.hu ● ISSN 1589 1623 (Print) ● ISSN 1785 0037 (Online)
DOI: http://dx.doi.org/10.15666/aeer/1705_1071710730

Effects of plant growth regulator on chlorophyll SPAD in the leaves of northeast spring maize under different planting densities

From the silking stage to the dough stage, the chlorophyll *SPAD* value decreased in the two treatments (*Table 3*). In the water treatment, the *SPAD* value decreased in every growth period with the increase in density. From the silking stage to the dough stage, the *SPAD* value declined by 16.72% (5 plants m^{-2}), 23.52% (6 plants m^{-2}), 25.01% (7 plants m^{-2}) and 25.73% (8 plants m^{-2}).

Table 2. *The effects of plant growth regulator on the LAI of spring maize under different planting densities in Northeast China*

Treatment	Density (plants m^{-2})	Jointing stage	Trumpet stage	Silking	Grain filling stage	Dough stage
Water	5	2.25±0.12^{ab}	3.55±0.06^{d}	4.05±0.09^{d}	3.79±0.07^{d}	3.28±0.07^{f}
	6	2.46±0.62^{ab}	4.13±0.12^{c}	4.39±0.13^{cd}	4.06±0.05^{c}	3.45±0.05^{ef}
	7	2.58±0.03^{ab}	4.73±0.16^{b}	4.89±0.07^{b}	4.49±0.12^{b}	3.72±0.08^{cd}
	8	2.88±0.09^{a}	5.22±0.06^{a}	5.59±0.08^{a}	4.71±0.05^{a}	3.84±0.06^{c}
Plant growth regulator	5	2.12±0.12^{b}	3.52±0.03^{d}	4.02±0.05^{d}	3.84±0.13^{d}	3.40±0.10^{ef}
	6	2.36±0.45^{ab}	4.11±0.22^{c}	4.22±0.23^{d}	4.16±0.07^{c}	3.58±0.12^{de}
	7	2.53±0.48^{ab}	4.71±0.29^{b}	4.83±0.48^{bc}	4.52±0.06^{b}	4.02±0.17^{b}
	8	2.67±0.12^{ab}	4.68±0.23^{b}	5.10±0.50^{b}	4.72±0.15^{a}	4.25±0.14^{a}

The values represent the mean ± SE (n=7). The values with the same letters in the columns are not significantly different at $P < 0.05$

Table 3. *The effects of plant growth regulator on the chlorophyll SPAD values of spring maize under different planting densities in Northeast China*

Treatment	Density (plants m^{-2})	Silking	Grain filling stage	Dough stage
Water	5	77.14±4.52^{ab}	74.50±4.03^{a}	64.24±9.82^{a}
	6	68.53±2.37^{bcd}	59.09±4.52^{b}	52.41±3.97^{bc}
	7	63.58±6.98^{cd}	59.18±3.49^{b}	47.68±3.66^{c}
	8	61.27±6.16^{d}	53.01±2.62^{c}	45.50±8.98^{c}
Plant growth regulator	5	82.66±9.52^{a}	71.17±1.78^{a}	65.34±2.09^{a}
	6	74.83±4.70^{abc}	63.60±1.95^{b}	62.46±1.19^{ab}
	7	68.57±6.24^{bcd}	65.24±4.62^{b}	60.13±3.95^{ab}
	8	66.64±4.06^{bcd}	62.50±2.86^{b}	55.51±2.71^{abc}

In the "Yuhuangjin" treatment, the *SPAD* value was higher than that in the water treatment in every growth period. The *SPAD* value in the "Yuhuangjin" treatment was higher than that in the water treatment by 7.14% (5 plants m^{-2}), 9.19% (6 plants m^{-2}), 7.85% (7 plants m^{-2}) and 8.77% (8 plants m^{-2}) at the silking stage. From the silking stage to the dough stage, *SPAD* value declined by 18.52% (5 plants m^{-2}), 16.54% (6 plants m^{-2}), 12.30% (7 plants m^{-2}) and 16.71% (8 plants m^{-2}) in the "Yuhuangjin" treatment. Except for the 5 plants m^{-2} density, the "Yuhuangjin" treatment decreased the chlorophyll degradation rate at varying degrees in the later stages of procreation.

http://www.aloki.hu ● ISSN 1589 1623 (Print) ● ISSN 1785 0037 (Online)
DOI: http://dx.doi.org/10.15666/aeer/1705_1071710730

Effects of plant growth regulator on the net photosynthetic rate (Pn) of leaves of northeast spring maize under different planting densities

From the silking stage to the dough stage, the net photosynthetic rate of the leaves decreased gradually in both treatments (*Table 4*). In the water treatment, the net photosynthetic rate was 43.29 μmol m^{-2} s^{-1} (5 plants m^{-2}), 40.42 μmol m^{-2} s^{-1} (6 plants m^{-2}), 38.79 μmol m^{-2} s^{-1} (7 plants m^{-2}) and 37.59 μmol m^{-2} s^{-1} (8 plants m^{-2}) at the silking stage. When the planting density increased, the net photosynthetic rate decreased. Compared to the 5 plants m^{-2} density, the net photosynthetic rate in the other densities reduced by 6.64% (6 plants m^{-2}), 10.40% (7 plants m^{-2}) and 13.17% (8 plants m^{-2}). At various densities, the net photosynthetic rate decreased by 46.23% (5 plants m^{-2}), 44.47% (6 plants m^{-2}), 44.72% (7 plants m^{-2}) and 49.70% (8 plants m^{-2}) from the silking stage to the dough stage.

Table 4. *The effects of plant growth regulator on the Pn of spring maize leaves under different planting densities in Northeast China*

Treatment	Density (plants m^{-2})	Jointing stage	Trumpet stage	Silking	Grain filling stage	Dough stage
Water	5	15.93 ± 0.09^{b}	29.40 ± 1.80^{b}	43.29 ± 1.31^{bc}	35.05 ± 0.88^{b}	23.28 ± 0.88^{cd}
	6	14.50 ± 0.16^{d}	26.53 ± 0.91^{de}	40.42 ± 0.32^{d}	32.22 ± 0.42^{e}	22.44 ± 0.43^{de}
	7	13.97 ± 0.07^{e}	25.23 ± 0.17^{ef}	38.79 ± 0.41^{ef}	31.02 ± 0.18^{f}	21.44 ± 0.17^{e}
	8	13.61 ± 0.22^{e}	24.58 ± 0.44^{f}	37.59 ± 1.21^{f}	29.90 ± 0.66^{f}	18.91 ± 0.66^{f}
Plant growth regulator	5	16.55 ± 0.41^{a}	32.52 ± 1.31^{a}	46.81 ± 0.88^{a}	37.23 ± 0.62^{a}	26.48 ± 0.88^{a}
	6	15.99 ± 0.09^{b}	29.28 ± 0.70^{b}	44.28 ± 0.32^{b}	34.80 ± 0.32^{bc}	25.28 ± 0.32^{b}
	7	15.84 ± 0.16^{bc}	28.41 ± 0.49^{bc}	42.65 ± 0.66^{c}	33.66 ± 0.74^{cd}	24.18 ± 0.38^{c}
	8	15.60 ± 0.22^{c}	27.16 ± 0.96^{cd}	39.99 ± 0.22^{de}	32.52 ± 1.05^{de}	19.87 ± 0.69^{f}

The net photosynthetic rate was higher in the "Yuhuangjin" treatment than in the water treatment in every growth period. The peak values were 46.81 μmol m^{-2} s^{-1} (5 plants m^{-2}), 44.28 μmol m^{-2} s^{-1} (6 plants m^{-2}), 42.65 μmol m^{-2} s^{-1} (7 plants m^{-2}) and 40.00 μmol m^{-2} s^{-1} (8 plants m^{-2}) at the silking stage. The net photosynthetic rates in the "Yuhuangjin" treatments were higher than those in the water treatment by 8.15% (5 plants m^{-2}), 9.55% (6 plants m^{-2}), 9.95% (7 plants m^{-2}) and 6.39% (8 plants m^{-2}).

From the silking stage to the dough stage, the net photosynthetic rate declined by 43.42% (5 plants m^{-2}), 42.90% (6 plants m^{-2}), 43.29% (7 plants m^{-2}) and 50.33% (8 plants m^{-2}). The net photosynthetic rate in the "Yuhuangjin" treatment was higher than that in the water treatment by 13.79% (5 plants m^{-2}), 12.64% (6 plants m^{-2}), 12.80% (7 plants m^{-2}) and 5.08% (8 plants m^{-2}) at the dough stage.

Effects of plant growth regulator on chlorophyll fluorescence parameters of the leaves of northeast spring maize under different planting densities

From the silking stage to the dough stage, the *PSII* maximum quantum yield showed a declining trend in the two treatments (*Table 5*). The *Fv/Fm* declined by 3.16% (5 plants m^{-2}), 3.40% (6 plants m^{-2}), 3.19% (7 plants m^{-2}) and 3.41% (8 plants m^{-2}) from the silking stage to the dough stage in the water treatment. The *Fv/Fm* declined by 3.07% (5 plants m^{-2}), 3.28% (6 plants m^{-2}), 2.65% (7 plants m^{-2}) and 2.17% (8 plants m^{-2}) from the silking stage to the dough stage in the "Yuhuangjin" treatment. Compared

http://www.aloki.hu ● ISSN 1589 1623 (Print) ● ISSN 1785 0037 (Online)
DOI: http://dx.doi.org/10.15666/aeer/1705_1071710730

with the water treatment, the *PSII* maximum quantum yield in the "Yuhuangjin" treatment decreased by a small amount. At the same time, the "Yuhuangjin" treatment increased the *PSII* maximum quantum yield.

With the increase in density, the *Y(II)* of the two treatments showed a decreasing trend (*Table 6*). From the silking stage to the dough stage, the *Y(II)* in the water treatment reduced by 7.04% (5 plants m^{-2}), 47.64% (6 plants m^{-2}), 47.40% (7 plants m^{-2}) and 57.49% (8 plants m^{-2}). The *Y(II)* in the "Yuhuangjin" treatment reduced by 42.44% (5 plants m^{-2}), 45.44% (6 plants m^{-2}), 46.38% (7 plants m^{-2}) and 53.42% (8 plants m^{-2}) from the silking stage to the dough stage. The "Yuhuangjin" treatment reduced the decrease in *Y(II)* in the later stages of procreation. Compared with the water treatment, the *Y(II)* in the "Yuhuangjin" treatment increased at varying degrees. In the silking stage, the *Y(II)* values in the "Yuhuangjin" treatment were 0.71% (5 plants m^{-2}), 1.32% (6 plants m^{-2}), 0.67% (7 plants m^{-2}) and 3.80% (8 plants m^{-2}) higher than those in the water treatment. In the dough stage, the *Y(II)* values in the "Yuhuangjin" treatment were 9.46% (5 plants m^{-2}), 5.58% (6 plants m^{-2}), 2.61% (7 plants m^{-2}) and 13.73% (8 plants m^{-2}) higher than those in the water treatment.

Table 5. *The effects of plant growth regulator on the Fv/Fm of spring maize leaves under different planting densities in Northeast China*

Treatment	Density (plants m^{-2})	Silking	Grain filling stage	Dough stage
Water	5	0.799 ± 0.002^{ab}	0.789 ± 0.006^{abc}	0.774 ± 0.009^{a}
	6	0.796 ± 0.002^{ab}	0.787 ± 0.005^{abc}	0.768 ± 0.002^{a}
	7	0.791 ± 0.010^{ab}	0.784 ± 0.003^{abc}	0.766 ± 0.011^{a}
	8	0.785 ± 0.004^{b}	0.780 ± 0.008^{c}	0.758 ± 0.009^{a}
Plant growth regulator	5	0.803 ± 0.004^{a}	0.797 ± 0.008^{a}	0.779 ± 0.001^{a}
	6	0.803 ± 0.013^{a}	0.794 ± 0.010^{ab}	0.779 ± 0.019^{a}
	7	0.793 ± 0.004^{ab}	0.784 ± 0.007^{abc}	0.772 ± 0.013^{a}
	8	0.786 ± 0.012^{b}	0.781 ± 0.006^{bc}	0.770 ± 0.013^{a}

Table 6. *The effects of plant growth regulator on the Y(Ⅱ) of spring maize leaves under different planting densities in Northeast China*

Treatment	Density (plants m^{-2})	Silking	Grain filling stage	Dough stage
Water	5	0.661 ± 0.002^{ab}	0.608 ± 0.024^{ab}	0.350 ± 0.093^{ab}
	6	0.654 ± 0.022^{ab}	0.593 ± 0.024^{abc}	0.343 ± 0.028^{ab}
	7	0.647 ± 0.048^{ab}	0.576 ± 0.030^{c}	0.340 ± 0.049^{ab}
	8	0.615 ± 0.039^{c}	0.532 ± 0.050^{d}	0.261 ± 0.047^{c}
Plant growth regulator	5	0.666 ± 0.005^{a}	0.614 ± 0.016^{a}	0.383 ± 0.048^{a}
	6	0.663 ± 0.007^{ab}	0.610 ± 0.006^{ab}	0.362 ± 0.040^{a}
	7	0.652 ± 0.024^{ab}	0.586 ± 0.014^{bc}	0.350 ± 0.054^{ab}
	8	0.638 ± 0.008^{bc}	0.548 ± 0.024^{d}	0.297 ± 0.032^{bc}

With the progress of procreation, the two *Y(NO)* treatments generally showed upward trends (*Table 7*). In the same growth period, the *Y(NO)* values of both treatments also increased with increasing density. Compared to the plant growth regulator treatment, the *Y(NO)* in the water treatment increased by 21.01% (5 plants

http://www.aloki.hu ● ISSN 1589 1623 (Print) ● ISSN 1785 0037 (Online)
DOI: http://dx.doi.org/10.15666/aeer/1705_1071710730

m^{-2}), 24.26% (6 plants m^{-2}), 34.38% (7 plants m^{-2}) and 41.60% (8 plants m^{-2}) from the silking stage to dough stage. The "Yuhuangjin" treatment increased the *Y(NO)* by 19.63% (5 plants m^{-2}), 18.78% (6 plants m^{-2}), 21.03% (7 plants m^{-2}) and 24.50% (8 plants m^{-2}) from the silking stage to the dough stage. The "Yuhuangjin" treatment reduced the *Y(NO)* at varying degrees. In the silking stage, the water treatment reduced the *Y(NO)* by 1.07% (5 plants m^{-2}), 4.16% (6 plants m^{-2}), 4.32% (7 plants m^{-2}) and 5.14% (8 plants m^{-2}) compared to the "Yuhuangjin" treatment. In the dough stage, the water treatment reduced the *Y(NO)* by 2.20% (5 plants m^{-2}), 8.39% (6 plants m^{-2}), 13.83% (7 plants m^{-2}) and 16.61% (8 plants m^{-2}) compared to the "Yuhuangjin" treatment.

Table 7. *The effects of plant growth regulator on the Y(NO) of spring maize leaves under different planting densities in Northeast China*

Treatment	Density (plants m^{-2})	Silking	Grain filling stage	Dough stage
Water	5	0.319 ± 0.004^{bc}	0.343 ± 0.001^{c}	0.386 ± 0.046^{c}
	6	0.334 ± 0.022^{abc}	0.356 ± 0.016^{c}	0.415 ± 0.024^{bc}
	7	0.357 ± 0.008^{ab}	0.406 ± 0.035^{ab}	0.479 ± 0.006^{ab}
	8	0.367 ± 0.037^{a}	0.414 ± 0.048^{a}	0.520 ± 0.018^{a}
Plant growth regulator	5	0.322 ± 0.010^{c}	0.339 ± 0.006^{c}	0.378 ± 0.002^{c}
	6	0.320 ± 0.030^{bc}	0.349 ± 0.009^{c}	0.381 ± 0.017^{c}
	7	0.341 ± 0.014^{abc}	0.366 ± 0.019^{bc}	0.413 ± 0.022^{bc}
	8	0.348 ± 0.004^{abc}	0.377 ± 0.029^{abc}	0.434 ± 0.019^{b}

With procreation, the *qN* values of the two treatments generally showed upward trends at the different densities (*Table 8*). From the silking stage to the dough stage, the *qN* value of the water treatment increased by 0.39% (5 plants m^{-2}), 0.43% (6 plants m^{-2}), 0.43% (7 plants m^{-2}) and 0.44% (8 plants m^{-2}). The *qN* value of the "Yuhuangjin" treatment increased by 0.37% (5 plants m^{-2}), 0.42% (6 plants m^{-2}), 0.41% (7 plants m^{-2}) and 0.44% (8 plants m^{-2}) from the silking stage to the dough stage.

Table 8. *The effects of plant growth regulator on qN of spring maize leaves under different planting densities in Northeast China*

Treatment	Density (plants m^{-2})	Silking	Grain filling stage	Dough stage
Water	5	0.038 ± 0.008^{d}	0.125 ± 0.015^{abc}	0.424 ± 0.008^{e}
	6	0.065 ± 0.011^{c}	0.145 ± 0.005^{ab}	0.490 ± 0.008^{cd}
	7	0.102 ± 0.011^{ab}	0.151 ± 0.002^{ab}	0.532 ± 0.025^{ab}
	8	0.113 ± 0.010^{a}	0.156 ± 0.005^{a}	0.554 ± 0.027^{a}
Plant growth regulator	5	0.023 ± 0.009^{d}	0.108 ± 0.008^{c}	0.395 ± 0.044^{e}
	6	0.059 ± 0.004^{c}	0.120 ± 0.020^{bc}	0.475 ± 0.007^{d}
	7	0.084 ± 0.011^{b}	0.124 ± 0.019^{bc}	0.496 ± 0.010^{bcd}
	8	0.086 ± 0.014^{a}	0.131 ± 0.031^{a}	0.523 ± 0.017^{a}

The "Yuhuangjin" treatment reduced the increase of the *qN* value and enhanced the photosynthetic performance of the leaves. With the increase in densities, the *qN* values of the two treatments showed increasing trends. In terms of the plant growth regulator,

http://www.aloki.hu ● ISSN 1589 1623 (Print) ● ISSN 1785 0037 (Online)
DOI: http://dx.doi.org/10.15666/aeer/1705_1071710730

the *qN* values of the blades declined under the "Yuhuangjin" treatment. In the dough stage, compared with the water treatment, the "Yuhuangjin" treatment resulted in low *qN* values of 6.83% (5 plants m^{-2}), 3.20% (6 plants m^{-2}), 6.75% (7 plants m^{-2}) and 5.63% (8 plants m^{-2}).

With the increase in densities, the *qP* values of the two treatments gradually decreased after the silking stage (*Table 9*). The water treatment reduced the *qP* values by 7.49% (5 plants m^{-2}), 37.15% (6 plants m^{-2}), 44.84% (7 plants m^{-2}) and 57.25% (8 plants m^{-2}) from the silking stage to the dough stage. The "Yuhuangjin" treatment reduced the *qP* values by 34.91% (5 plants m^{-2}), 36.31% (6 plants m^{-2}), 42.47% (7 plants m^{-2}) and 53.83% (8 plants m^{-2}) from the silking stage to the dough stage. Compared with the water treatment, the "Yuhuangjin" treatment exhibited varying degrees of improvement. In the silking stage, the maximum *qP* values were 2.05% (5 plants m^{-2}), 3.60% (6 plants m^{-2}), 4.56% (7 plants m^{-2}) and 4.94% (8 plants m^{-2}) higher than those in the water treatment.

Effects of plant growth regulator on yield of spring maize in different planting densities in northeast China

With the increase in densities, the water treatment first exhibited an increasing then decreasing trend in the yield (*Table 10*). The highest yield was measured in the 7 plants m^{-2} density (12346.40 kg ha^{-1}), which was 34.94%, 12.89% and 9.58% higher than the yields in the 5 plants m^{-2}, 6 plants m^{-2} and 8 plants m^{-2} densities, and these differences were significant.

Table 9. *The effects of plant growth regulator on qP of spring maize leaves under different planting densities in Northeast China*

Treatment	Density (plants m^{-2})	Silking	Grain filling stage	Dough stage
Water	5	0.839 ± 0.039^{abc}	0.754 ± 0.006^{a}	0.524 ± 0.076^{ab}
	6	0.814 ± 0.015^{abc}	0.734 ± 0.036^{a}	0.512 ± 0.042^{ab}
	7	0.798 ± 0.019^{bcd}	0.711 ± 0.045^{a}	0.440 ± 0.031^{bc}
	8	0.755 ± 0.049^{d}	0.647 ± 0.080^{b}	0.322 ± 0.025^{d}
Plant growth regulator	5	0.856 ± 0.002^{a}	0.763 ± 0.010^{a}	0.557 ± 0.099^{a}
	6	0.843 ± 0.024^{ab}	0.758 ± 0.005^{a}	0.537 ± 0.038^{ab}
	7	0.835 ± 0.010^{abc}	0.720 ± 0.029^{a}	0.480 ± 0.065^{ab}
	8	0.792 ± 0.012^{cd}	0.661 ± 0.046^{b}	0.366 ± 0.046^{cd}

Table 10. *The effects of plant growth regulator on yield factors of spring maize under different planting densities in Northeast China*

Treatment	Density (plants m^{-2})	Rows per ear	Kernels row	Hundred grain weight (g)	Yield (kg ha^{-1})
Water	5	16.05^{a}	33.95^{bc}	33.97^{a}	7868.41^{d}
	6	15.93^{a}	35.58^{abc}	32.31^{a}	9404.50^{c}
	7	16.39^{a}	33.89^{bc}	32.74^{a}	10618.44^{ab}
	8	16.00^{a}	31.50^{de}	29.47^{b}	9689.59^{bc}
Plant growth regulator	5	15.80^{a}	35.95^{ab}	34.49^{a}	7887.15^{d}
	6	15.95^{a}	33.50^{cd}	34.36^{a}	9450.90^{c}
	7	15.45^{a}	36.50^{a}	34.61^{a}	11428.18^{a}
	8	15.90^{a}	31.28^{e}	31.71^{ab}	10435.83^{abc}

http://www.aloki.hu ● ISSN 1589 1623 (Print) ● ISSN 1785 0037 (Online)
DOI: http://dx.doi.org/10.15666/aeer/1705_1071710730

Compared with the water treatment, the production in the "Yuhuangjin" treatment increased, and the highest yield was measured in the 7 plants m^{-2} density (13290.95 kg ha^{-1}), but this difference was not significant. Compared with the water treatment, the yields in the "Yuhuangjin" treatment increased by 6.14% (5 plants m^{-2}), 0.48% (6 plants m^{-2}), 7.65% (7 plants m^{-2}) and 3.81% (8 plants m^{-2}). With the increase in density, rows per ear, kernels row and hundred-grain weight did not obviously change, and the differences were not significant. For the "Yuhuangjin" treatment, the differences between row and kernel numbers of the different densities were not significant, while the hundred-grain weight increased, but not significantly.

Discussion

The main factors of maize yields include effective ear number, spike number and grain weight per unit area. The effective ear number of the group is easiest to control and is one of the main ways to increase maize yields. With the increase in density, the yield first increased and then decreased, the ear rows and the line grain number decreased, and kilo-grain weight decreased (Gilberto et al., 2013; Li et al., 2014; Niyogi, 2017). In this experiment, the changes in the yields at different densities in the two treatments are consistent with the results of previous studies. The maximum yields in both treatments occurred at the 7 plants m^{-2} density. The maximum yields were 10618.44 kg ha^{-1} (water treatment) and 11428.18 kg ha^{-1} ("Yuhuangjin" treatment). Compared with the water treatment, the "Yuhuangjin" treatment increased the yields by 0.24% (5 plants m^{-2}), 0.49% (6 plants m^{-2}), 7.63% (7 plants m^{-2}) and 7.70% (8 plants m^{-2}). The differences in the ear rows and the line grain number were not obvious. The experiment also showed that the "Yuhuangjin" treatment mainly increased the hundred-grain weight, which influenced the yield.

The formation of maize yield is a group production process and not simple individual accumulation. The production of a maize population is related to the *LAI*, canopy characteristics, photosynthetic productivity and assimilation products of the entire population (Khoshbakht et al., 2017). During the growth period, the *LAI* exhibited a curve with a single peak, and the peak *LAI* was reached in the silking stage. With the increase in density, the maize yield mainly depends on the photosynthetic characteristics of the leaf groups, especially the photosynthetic capacity of the upper part and the duration of high light. In this experiment, the change in the LAI with density was consistent with the results obtained by Bian (Bian et al., 2011) and the spraying of "Yuhuangjin" reduced the *LAI*. The *LAI* values in the "Yuhuangjin" treatment were 0.89% (5 plants m^{-2}), 3.95% (6 plants m^{-2}), 1.23% (7 plants m^{-2}) and 8.74% (8 plants m^{-2}) lower than those in the water treatment. Spraying "Yuhuangjin" can reduce the leaf area of the colony, and it can also reduce the mutual shading between individuals within a group and improve the permeability of the group. The positive effects of the "Yuhuangjin" treatment are greater than the losses caused by the decreases in the leaf area. From the silking stage to the dough stage, *LAI* decreased by 3.75% (5 plants m^{-2}), 6.47% (6 plants m^{-2}), 7.14% (7 plants m^{-2}) and 14.60% (8 plants m^{-2}) compared to the water treatment. The aging process slows in the later stages. With the increase in density, the *LAI* of the group also increased. Increased densities also increased the supply levels of the source. The pre-control effect of "Yuhuangjin" on the leaf area of the group increased the permeability of the group and delayed the aging process of the leaf blades.

http://www.aloki.hu ● ISSN 1589 1623 (Print) ● ISSN 1785 0037 (Online)
DOI: http://dx.doi.org/10.15666/aeer/1705_1071710730

Chlorophyll is an important material in the photosynthesis process. Chlorophyll is involved in the absorption of light energy by a plant and the conversion process. The change in chlorophyll content can be reflected in the blades during the aging process. The chlorophyll content can also reflect the photosynthetic performance and is closely linked to the yield formation (Ma and Dwyer, 1998). Increasing the planting density can decrease the chlorophyll contents of individual plant leaves in a group, and it can reduce the production capacity of single plants. The "Yuhuangjin" treatment increased the chlorophyll content of the leaves and increased the photosynthetic capacity of the leaves. The living environment of an individual plant worsens with the increase in the number of maize plants number per unit area. These density increases will result in the decrease of the net photosynthetic rate of the group. The results of the "Yuhuangjin" treatment in this experiment show that the net photosynthetic rate of the blades is improved by using "Yuhuangjin". The function time of the blade is extended, which created the conditions necessary for higher yields.

The light energy absorbed by the photosynthetic apparatus is mainly utilized in the following ways: to promote photochemical reactions, to dissipate in the form of heat energy and to emit in the form of fluorescence. These three paths are interrelated with each other. The fluorescence signals emitted by plant bodies contain rich photosynthetic information that can be used to predict crop yield potentials (Gong et al., 2006). With the increase of densities, the relative chlorophyll content (*SPAD*) will decrease, and plant growth regulators can improve the chlorophyll content of maize leaves (Li et al., 2011). This study shows that the *SPAD* value of the plants treated by "Yuhuangjin" increased at different degrees under different densities. The *SPAD* values in the "Yuhuangjin" treatment were 7.14% (5 plants m^{-2}), 9.19% (6 plants m^{-2}), 7.85% (7 plants m^{-2}) and 8.77% (8 plants m^{-2}) higher than those in the water treatment. By regulating the canopy structure of the group, "Yuhuangjin" reduced the shading of the plants and increased the light energy intercepted by the ear leaves. These conditions laid the foundation for the synthesis of chlorophyll. With the increase in density, the filling stage was reflected in the *PSII* center of the ear, while the *qP* and *qN* increased. A suitable planting density can help improve the apparent quantum efficiency of maize leaves, and it can increase the primary photochemical efficiency, *PSII* quantum yield, and photochemical quenching coefficient. A suitable planting density can also reduce the photochemical quenching coefficients of the blades (Yang et al., 2009). The chlorophyll fluorescence parameters of the "rod and three leaves" under the two strains showed a unique phenomenon. The "Yuhuangjin" treatment increased the photosynthetic capacity, and the actual quantum yield increased significantly (Xu et al., 2008). With the increase in densities, the *Fv/Fm*, *Y(II)* and *qP* decreased, while the *Y(NO)* and *qN* increased in the water treatment. This result suggested that increasing planting density can lead to worse population canopy conditions and can lower the fluorescence yield. Spraying "Yuhuangjin" increased the *Fv/Fm*, *Y(II)* and *qP*, while it decreased the *Y(NO)* and *qN*. The "Yuhuangjin" treatment improved the maximum quantum yield, improved the ability of the leaves to adapt to strong light, reduced the chemical quenching parameters, enhanced the leaf physiological functions and improved the utilization of energy and the actual quantum yield of the blade. Compared with the water treatment, the "Yuhuangjin" treatment resulted in smaller decreases in *Fv/Fm*, *Y(II)* and *qP*, higher reductions in *Y(NO)*, and reductions in the *qN*. Spraying "Yuhuangjin" delayed the senescence of the leaves and increased the duration of high photosynthetic efficiency, which laid the foundation for higher yields. The changes in

http://www.aloki.hu ● ISSN 1589 1623 (Print) ● ISSN 1785 0037 (Online)
DOI: http://dx.doi.org/10.15666/aeer/1705_1071710730

the net photosynthetic rate and chlorophyll fluorescence parameters of the leaf blades showed a unique phenomenon. Increasing the planting density can reduce the photosynthetic capacity of individual plants in the population. Spraying "Yuhuangjin" can improve the photosynthetic capacity of individual plants.

Conclusion

In the water treatment, the *LAI* increased, and the *SPAD* value of the group decreased with the increase in density. The group yield first increased and then decreased. The maximum yield was 10618.44 kg ha^{-1} (7 plants m^{-2}). The *Pn* decreased, and the chlorophyll fluorescence parameters *Fv/Fm*, *Y(II)* and *qP* decreased, while *Y(NO)* and *qN* increased. In the "Yuhuangjin" treatment, the *LAI* declined, the *SPAD* increased, the *Pn* increased, the chlorophyll fluorescence parameters *Fv/Fm*, *Y(II)* and *qP* increased, and the *Y(NO)* and *qN* decreased. The maximum yield was 11428.18 kg ha^{-1} (7 plants m^{-2}). The "Yuhuangjin" treatment slowed the aging process of the leaves, improved the photosynthetic capacity of the leaves and increased production. In maize production, it is important to pay more attention on obtain high yields by increasing the planting density in Heilongjiang Province. We still have a lot of work to do to reveal the effects of plant density and plant growth regulators on the physiological and molecular levels of maize.

Acknowledgements. This work was supported by Heilongjiang Provincial Funding for National Key R&D Programs of China (GX18B029), National Key R&D Program of China (2017YFD0300506, 2016YFD0300103) and "Academic Backbone" Project of Northeast Agricultural University (17XG23). We thank the anonymous reviewers and the editor for their valuable comments and suggestions, which distinctly contributed to the improvement of this paper.

Conflict of Interests. Authors state no conflict of interests.

REFERENCES

[1] Benari, T., Makowski, D. (2006): Analysis of the trade-off between high crop yield and low yield instability at the global scale. – Environmental Research Letters 11(10): 104005.

[2] Bian, D. H., Zhang, R. D., Duan, L. S., Li, J. M., Li, Z. H. (2011): Effects of partial spraying of plant growth regulator on canopy structure, chlorophyll fluorescence characteristic and yield of summer maize (Zea mays L.). – Acta Agriculture Boreali-Sinica 26(3): 139-145.

[3] Biswas, D. K., Ma, B. L. (2017): Effect of nitrogen rate and fertilizer nitroge source on physiology, yield, grain quality, and nitrogen use efficiency in corn. – Canadian Journal of Plant Science 96(3): 392-403.

[4] Chen, G. P., Yang, G. H., Zhao, M., Wang, L. C., Wang, Y. D., Xue, J. Q., Gao, J. L., Li, D. H., Dong, S. T., Li, C. H., Song, H. X., Zhao, J. R. (2008): Studies on maize small area super-high yield trails and cultivation technique. – Journal of Maize Sciences 16(4): 1-4.

[5] Cheng, S., Liu, N. (2017): Study on the effects of ethephon paclobutrazol and indoloacetic acid on the growth physiology and yield components of maize. – Agricultural Technology & Equipment 335(11): 17-18,21.

[6] Cicchino, M., Edreira, J., Otegui, M. (2013): Maize physiological responses to heat stress and hormonal plant growth regulators related to ethylene metabolism. – Crop Science 53(5): 2135-2146.

http://www.aloki.hu ● ISSN 1589 1623 (Print) ● ISSN 1785 0037 (Online)
DOI: http://dx.doi.org/10.15666/aeer/1705_1071710730

[7] Diallo, L., Cao, Q., Yang, F., Yang, Z., Cui, J., Gang, L., Dafaalla, T. I. M., Diarso, M., Ahmad, W. (2015): Seed priming effects of Yuhuangjin on spring maize. – Journal of Animal & Plant Sciences 25(3): 747-754.
[8] Dong, C. Y., Yang, X. G., Yang, J., Xie, W. J., Ye, Q., Zhao, J., Li, K. N. (2013): The temporal variation characteristics and spatial distribution laws of drought of spring maize in northern China. – Scientia Agricultura Sinica 46(20): 4234-4245.
[9] Fan, H. C., Gu, W. R., Wei, J. P., Wang, Y. L., Meng, Y., Zhang, L. G., Li, J., Wei, S. (2017): Mechanism of lodging resistance of maize improved by plant growth regulator. – Jiangsu Journal of Agricultural Sciences 33(2): 253-262.
[10] Farhad, S., Mehdi, R. (2015): Effect of different levels of drip irrigation, plant density and spacing on the yield of maize hybrid (KSC700). – Maydica 60(2): 19-26.
[11] Gilberto, O., Koteyeva, N. K., Voznesenskaya, E. V., Edwards, G. E., Sage, T. L., Rowan, S. F., Columbus, J. T. (2013): Evolution of leaf anatomy and photosynthetic pathways in portulacceae. – American Journal of Botany 100(12): 2388-2402.
[12] Gong, Q. Z., Lv, J. Y., Xu, B. C., Li, F. M., Zhang, H. B. (2006): Effect of water stress on chlorophyll fluorescence paramenters and WUE of wheat under different planting models. – Journal of Northwest Science-Technology University of Agriculture and Forestry (Natural Science Edition) 34(5): 83-92.
[13] Hwang, J. S., Choo, Y. S. (2016): Solute patterns and diurnal variation of photosynthesis and chlorophyll fluorescence in Korean coastal sand dune plants. – Photosynthetica 55(1): 1-14.
[14] Inamoto, K., Nagasuga, K., Yano, T., Yamazaki, H. (2015): Influence of light intensity on the rate of photosynthesis and dry matter accumulation in Oriental hybrid lily 'Siberia' at different developmental stages. – Journal of Pomology & Horticultural Science 90(3): 259-266.
[15] Kang, M. Z., Yang, L. L., Zhang, B. G., Reffye, P. D. (2011): Correlation between dynamic tomato fruit-set and source-sink ratio: a common relationship for different plant densities and seasons. – Annals of Botany 107(5): 805-815.
[16] Khoshbakht, D., Asghari, M. R., Haghighi, M. (2017): Influence of foliar application of polyamines on growth, gas exchange characteristics, and chlorophyll fluorescence in Bakraii citrus under saline conditions. – Photosynthetica 56(2): 731-742.
[17] Li, C. H., Zhao,Y. L., Yang, G. H., Luan, L. M., Wang, Q., Li, N. (2007): Effects of shading on photosynthetic characteristics of different genotype maize. – Chinese Journal of Applied Ecology 18(6): 1259-1264.
[18] Li, X. Y., Tang, Q. Y., Li, D. Q., Li, W. K., Li, H. L., Cai, Q. H. (2011): Effects of different plant densities on the photosynthetic-physiological characters and yield traits in spring maize grown on super-high yielding paddy field. – Acta Agriculturae Boreali-Sinica 26(5): 174-180.
[19] Li, J. H., Du, Y. Y., Yang, J., Huo, L. Y., Zhao, H. W. (2014): Effects of density and chemical control agent on agronomic traits and yield of compact corn Fengyu 4. – Seed 33(3): 89-93.
[20] Li, Y., Liu, H. J., Huang, G. H. (2016): The effect of nitrogen rates on yields and nitrogen use efficiencies during four years of wheat-maize rotation cropping seasons. – Agronomy Journal 108(5): 2076-2088.
[21] Li, S. K., Zhao, J. R., Dong, S. T., Zhao, M., Li, C. H., Cui, Y. H., Liu, Y. H., Gao, J. L., Xue, J. Q., Wang, L. C., Wang, P., Lu, W. P., Wang, J. H., Yang, Q. F., Wang, Z. M. (2017): Advances and prospects of maize cultivation in China. – Scientia Agricultura Sinica 50(11): 1941-1959.
[22] Liao, R. W., Liu, J. M., Bai, Y. M., An, S. Q., Liang, H., Lu, J. L., Le, Z. Y., Cao, Y. J. (2014): Spatial distribution and temporal variation of maize root in the soil under field conditions. – Chinese Journal of Eco-Agriculture 22(3): 284-291.
[23] Ma, B. L., Dwyer, L. M. (1998): Nitrogen uptake and use of two contrasting maize hybrids in leaf senescence. – Plant Soil 199(2): 283-291.

http://www.aloki.hu ● ISSN 1589 1623 (Print) ● ISSN 1785 0037 (Online)
DOI: http://dx.doi.org/10.15666/aeer/1705_1071710730

[24] Meng, X. M., Sun, N., Bian, S. F., Fang, X. Q., Zhao, H. X., Zhang, L. H., Tan, G. B., Yan, W. P. (2016): Effects of plant growth regulator on the stem agronomic characters and yield of spring maize. – Journal of Northeast Agricultural Sciences 41(6): 16-20.
[25] Niyogi, K. K. (2017): Editorial overview: Physiology and metabolism: Light responses from chemoreceptor to photosynthesis and photoprotection. – Current Opinion in Plant Biology 37: 4-5.
[26] Ren, B. Z., Fan, X., Dong, S. T., Liu, P., Zhao, B., Zhang, J. W. (2017a): Effect of plant density and nitrogen rate on yield, nitrogen uptake and use efficiency of summer maize hybrids with different plant height. – Journal of Plant Nutrition and Fertilizer 23(2): 269-277.
[27] Ren, B. Z., Liu, W., Zhang, J. W., Dong, S. T., Liu, P., Zhao, B. (2017b): Effects of plant density on the photosynthetic and chloroplast characteristics of maize under high-yielding conditions. – The Science of Nature 104(3-4): 12.
[28] Roy, A. K., Claudia, W. R., Deen, B., Lauzon, J., Bruulsema, T. (2014): Nitrogen application rate, timing and history effects on nitrous oxide emissions from corn (Zea mays L.). – Canadian Journal Soil Science 94(4): 563-573.
[29] Rutger, J. N., Crowder, L. V. (1967): Effect of population and row width on corn silage yields. – Agronomy Journal 59(5): 475-576.
[30] Sangakkara, R., Bandaranayake, S., Attanayake, U., Stamp, P. (2012): Impact of associated inter crops on growth and yield of maize (Zea mays L.) in major seasons of south Asia. – Maydica 57(1): 6-10.
[31] Xu, J. M., Gao, H. Q., Mao, S. G., Wang, X., Li, C. S., Ji, Y. Q., Lu, W. P. (2008): Effects of wide row space double plant cultivation on the characteristic of photosynthesis at later growth stage in maize (Zea Mays L). – Journal of Yangzhou University (Agricultural and Life Science Edition) 29(1): 66-70.
[32] Yan, Y. D., Jiang, Z. B., Xu, F. L., Wang, Y. K., Zou, C. (2009): Analysis of the soil texture and fertility status of hillside close-planting jujube field on the loess plateau. – Agricultural Research in the Arid Areas 27(3): 174-178.
[33] Yang, Y. W., Wu, X. D. (2009): Effect of the different planting densities on the photosynthetic characteristics chlorophyll fluorescence parameters and yield of waxy Maize. – Journal of Anhui Agricultural Sciences 37(18): 8403-8405.
[34] Zhang, Q., Zhang, L. Z., Jochem, E., Werf, W. V. D., Zhang, W. Q., Duan, L. S. (2014): Maize yield and quality in response to plant density and application of a novel plant growth regulator. – Field Crop Research 164(1): 82-89.
[35] Zhang, P., Wei, T., Cai, T., Ali, S., Han, Q. F., Ren, X. L., Jia, Z. K. (2017): Plastic-film mulching for enhanced water-use efficiency and economic returns from maize fields in semiarid China. – Frontiers in Plant Science 8. doi: 10.3389/fpls.2017.00512.
[36] Zhao, M., Li, J. G., Zhang, B., Dong, Z. Q., Wang, M. Y. (2006): Compensation mechanism of high yield and potential tapping of crops. – Acta Agronomica Sinica 32(10): 1566-1572.

http://www.aloki.hu ● ISSN 1589 1623 (Print) ● ISSN 1785 0037 (Online)
DOI: http://dx.doi.org/10.15666/aeer/1705_1071710730

QUALITY CONTROL OF CHINESE VELVET ANTLER BY PROFILING OF PESTICIDE RESIDUES AND HEAVY METALS

ZHANG, Z. Y.[1] – LIU, X. F.[2] – HOU, Y. T.[1] – WANG, R. R.[1] – LI, P. F.[1] – ZHAO, C. W.[3*]

[1]*School of Life Science and Medicine, Dalian University of Technology, DaGong Road, Panjin Liaoning 124221, China*

[2]*Department of Laboratory Medicine, Jilin Cancer Hospital, HuGuang Road, Changchun Jilin 130021, China*

[3]*Department of Orthopedics, Affiliated Hospital of Changchun University of Chinese Medicine, GongNong Road, Changchun Jilin 130021, China*

**Corresponding author*
e-mail: zcw_1980@126.com; phone: +86-135-9608-8558; fax: +86-431-8617-7151

(Received 1st Mar 2019; accepted 21st May 2019)

Abstract. Quality control is the most critical issue for Chinese medicines (CMs) as its increasing acceptance all around the world. This study measure and analyse the pollution of nine kinds of velvet antlers, which is one of the classical Chinese medicines, in different species and parts of Cervus Nippon and Cervus Elaphus in China. Following the relevant Chinese national standards to evaluate the pollution, we employed the Quick Easy Cheap Effective Rugged and Safe multiresidue method (QuEChERS), combinating with gas chromatography (GC), for the analysis of the organochlorine pesticides (OCPs) in velvet antler. The Inductively Coupled Plasma Mass Spectrometry (ICP-MS) method was used to detect lead, cadmium, copper and arsenic in nine kinds of velvet antlers. The content of mercury and the pollutants in the nine kinds of velvet antlers were all in line with the Chinese Pharmacopoeia. However, these results showed that velvet antler as the unique animal medicine also has a certain amount of pesticide residues, and the individual detection indicators in antler, such as heavy metal copper, are high, which suggests that, we still need to conduct reasonable testing and analysis of heavy metals and pesticide residues in velvet antler before giving it to patients to ensure the safety of clinical application.
Keywords: *organochlorine pesticides, heavy metal, Chinese medicines, medication safety*

Introduction

Traditional Chinese medicine (TCM) is one of the important components of the traditional medicine in the world. Chinese medicinal materials are rich and widely distributed in China. The Chinese medicinal materials have been accepted by the vast majority of patients because of the characteristics of mild pharmacology, specimens and treatment, persistent drug effects and small side effects (Huie, 2002). With a growing number of reports announcing that excessive heavy metals and pesticide residues in Chinese medicinal materials have came out, the quality of Chinese medicinal materials has becoming paid more and more attention. The contents of harmful elements, pesticide residues and microorganism have become an important cause of serious influence on the export of Chinese medicinal materials and the modernization of traditional Chinese medicine (Iavicoli et al., 2009). Therefore, accurately detecting and limiting the amount of harmful substances such as heavy metals and pesticide residues is the key to ensure the safety of medication and to promote the internationalization of Chinese medicine (Efferth and Kaina, 2011).

http://www.aloki.hu ● ISSN 1589 1623 (Print) ● ISSN 1785 0037 (Online)
DOI: http://dx.doi.org/10.15666/aeer/1705_1073110742

At present, the most toxic heavy metals are arsenic, cadmium, mercury and lead in environmental pollution, food safety and quality control of Chinese medicinal materials. However, heavy metals are parts of the natural environment. They are found in air, water and soil. In the process of Chinese herbal medicine, heavy metals can enter the medicinal materials through their growth environment, and then lead to heavy metal pollution through biological enrichment. The heavy metals in deer products are mainly derived from feeds which are fed, obviously this problem needs to be paid more attention during the processing and production, but it is often unavoidable. In addition, the production and processing of Chinese medicine preparation, the transportation and storage processing could also be polluted, these problems are accumulating and cause the heavy metal pollution of Chinese medicinal materials aggravating rapidly.

Pesticide residues, among the other potentially toxic compounds can be found in velvet antlers. According to the research status in recent years, pesticide residues in Chinese herbal medicines are universal (Kang et al., 2016; Yang et al., 2013), and organochlorine pesticide residues occupy a large proportion. The use of OCPs as insecticides and biocides has been widespread in agriculture and public health since the 1940s, and most of OCPs are resistant to photochemical, biological and chemical degradation for a long period of time (Yohannes et al., 2014). They persist in various media and some can be transported over long distances to regions where they have never been used. The use of most OCPs is now prohibited in China, but their low biodegradability means that they can still be detected in the environment (Barriada-Pereira et al., 2003). The nature drugs from animal body may also be polluted in the process of formation, such as exposing to pesticides and other routes.

Moreover, Chinese herbal medicines may also be exposed to pesticides and contaminated during transportation, storage and processing (Ting et al., 2013). In addition, the pesticide residues in Chinese medicinal materials are likely to be enriched in the traditional Chinese medicine preparation by processing. Which are easily accumulated in the body by patients already infirm, posing a threat to drug safety. Therefore, the determination of pesticide residues has been included in the Chinese medicine inspection methods and quality standards formulated by WHO.

Velvet antler as the animal medicine is a kind of immature horn of most male deer family, which is widely distributed all over the world. China is one of the largest amount of numbers and species of deers, including Sika deer, Wapiti, elk and so on. Velvet antler is the only regenerable mammalian organ (Li et al., 2014, 2016). It has special structural features, grows periodically and falls off each year, leaving no scars on the wound, the growth rate is very fast, reaching 1-2 cm per day. As a TCM, the pharmacological effects of velvet antler are enduring, which frequently performed to prevent and treat of osteoporosis (Tseng et al., 2014; Zhang et al., 2013), promoted cell proliferation (Xiao et al., 2017), repaired liver damage (Chunhua et al., 2017), anti-fatigue (Jang et al., 2014), anti-oxidation (Chunhui et al., 2017), anti-inflammatory (Ma et al., 2017; Lee et al., 2015) and showing other pharmacological activities. The composition of antler is extremely complex, the quality of different types of antler can be wildly different. In general, it can be divided into inorganic elements, organic components and bioactive ingredients.

The processing of velvet antler is according to the needs of Chinese medicine and pharmacy, putting dried velvet antler into Chinese Herbal Slices or other forms, for clinical use or variety of dosage forms. The Chinese Pharmacopoeia records two types of processing methods for velvet antler, “powder of velvet antler” and “tablets of velvet

http://www.aloki.hu ● ISSN 1589 1623 (Print) ● ISSN 1785 0037 (Online)
DOI: http://dx.doi.org/10.15666/aeer/1705_1073110742

antler". Take the velvet antler, lick the hair, scrape it, smash it into pieces, grind it into fine powder, then get the powder of velvet antler. The processing of tablets of velvet antler is more complicated: Take the velvet antler, lick the hair, scrape it, and wrap the body with a cloth belt, injecting hot white spirit from the small hole in the wound surface, continue to add spirit, until the run through or the liquor is slightly steamed, cross-cut, flattened and dried (China Pharmacopoeia Committee, 2015). The velvet antler is transected and the transverse section is divided into skin layer, interstitial layer and medulla layer from the outside to the inside. According to the industry standard NY/T1162-2006 promulgated by the Ministry of Agriculture, the velvet pieces made from the tip to the base can be divided into four parts: wax piece, powder piece, yarn piece and bone piece.

At present, the main extraction methods used in the analysis of pesticide residues are: ultrasonic extraction, microwave assisted extraction, supercritical fluid extraction, solid phase extraction, solid phase microextraction, accelerated solvent extraction, liquid phase microextraction, QuEChERS and so on. Among the above, QuEChERS is a novel sample preparation methodology for pesticide multiresidue analysis which was developed between 2000 and 2002 and firstly reported in 2003 (Anastassiades et al., 2003). Although it is a very new method, it has already been widely accepted by pesticide residue analysts in the international community, and a lot of publications already deal with this method in its original form or variations of it (Hu et al., 2012). QuEChERS has been validated for the extraction of OCPs in completely different matrices of TCM (Xu et al., 2011).

In order to solve the problem of quality and safety in the development of Chinese medicinal materials, the new technology of detection of pesticide residues, such as modern spectral analysis, chromatography analysis, spectrum and chromatography, is rapidly developing (Kong et al., 2015; Tadeo et al., 2012). The commonly used methods are GC, gas chromatography-mass spectrometry, high performance liquid chromatography, liquid chromatography mass spectrometry and so on. Among which, GC has become one of the most important analysis methods in agricultural residue detection because of its good stability, high sensitivity, good selectivity and ability to separate a variety of substances at the same time. GC can be used to meet the detection requirements of different kinds of pesticides by selecting different detectors. It is often used to detect the pesticide residues with small relative molecular weight, low boiling point and good thermal stability. Because of the content of heavy metals in Chinese herbal medicines is generally low, it is necessary to select suitable analytical instruments and methods for testing. The ICP-MS is characterized by high sensitivity, high accuracy, low detection line, rapid analysis, and simultaneous determination of various elements (Jiang et al., 2014). It is the most effective method of elemental analysis recognized currently. It has been included in the Chinese Pharmacopoeia as one of the methods for determining lead, cadmium, arsenic, mercury and copper in Chinese herbal medicines (China Pharmacopoeia Committee, 2015).

Materials

Sampling

In order to ensure the current pollution situation, samples were chosen: New Zealand plum velvet antler powder, red powder, wax tablets, Jilin sika deer antler red powder, yellow powder, wax tablets, Jilin red deer pilose antler powder tablets, sand tablets, wax

http://www.aloki.hu ● ISSN 1589 1623 (Print) ● ISSN 1785 0037 (Online)
DOI: http://dx.doi.org/10.15666/aeer/1705_1073110742

tablets both are purchased from a farm in Shuangyang District, Changchun City, Jilin Province, China. The feeding method is captive. (*Fig. 1*). The fodder are mainly corn, soybean and bean cake, and the roughage are silage corn stalk, grass and leaves. All the samples were ground and passed through 80-mesh sieve and stored at -20 °C prior analyses.

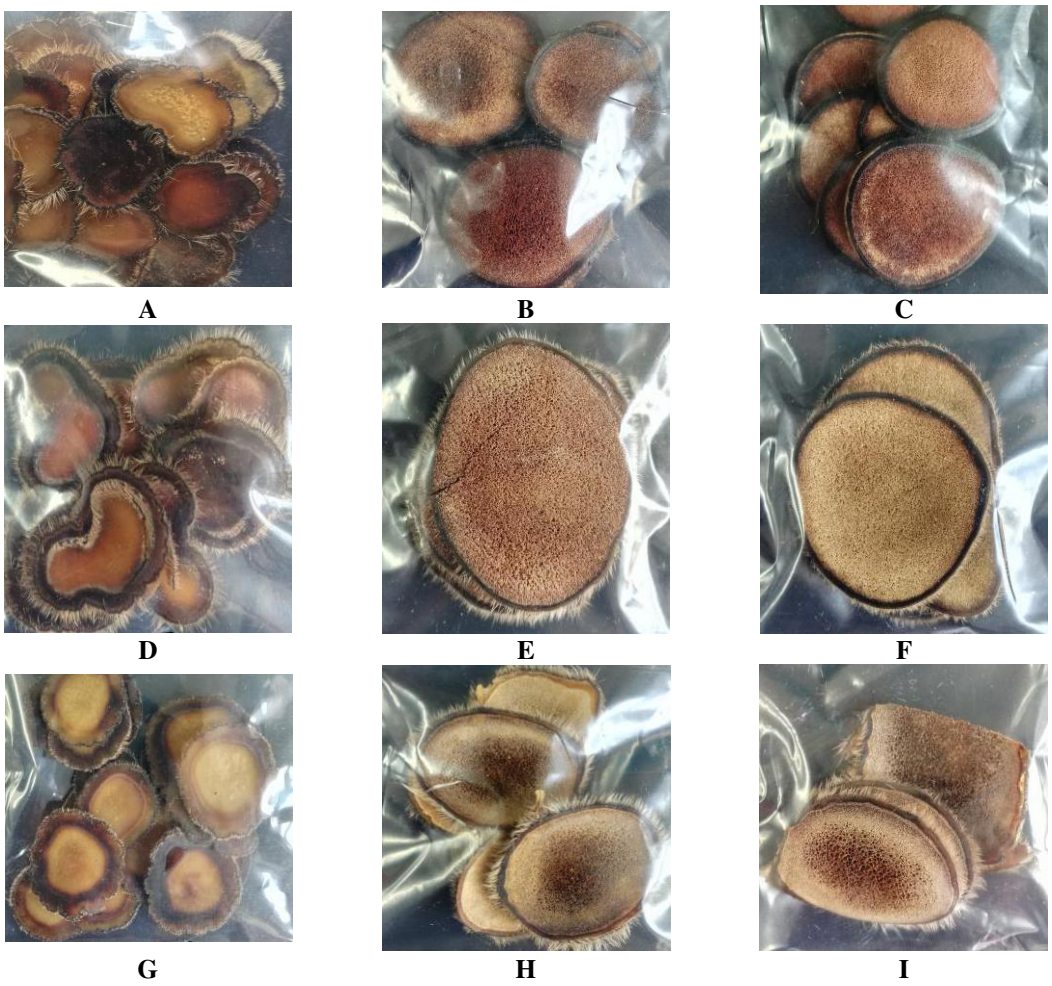

Figure 1. *Different varieties of velvet antlers. A: New Zealand sika deer antler wax tablets. B: New Zealand sika deer antler red powder. C: New Zealand sika deer antler powder. D: Jilin sika deer antler wax tablets. E: Jilin sika deer antler red powder. F: Jilin sika deer antler yellow powder. G: Jilin red deer pilose antler powder wax tablets. H: Jilin red deer pilose antler powder tablets. I: Jilin red deer pilose antler sand tablets*

Experimental method

Pesticide analysis by GC

Preparation of standard solution

All OCP standards (α-BHC, β-BHC, γ-BHC, δ-BHC, o, p'-DDD, p, p'-DDD, o, p'-DDT, p, p'-DDT, Pentachloronitrobenzene (PNCB) were purchased from the National Standards Research Center. A mixed stock solution was prepared by dissolving exact amounts of powdered samples in mixture of methanol and toluene (3:1, v/v) at a concentration of 100 ng/mL, and then diluted to a mixed standard solution with a

http://www.aloki.hu ● ISSN 1589 1623 (Print) ● ISSN 1785 0037 (Online)
DOI: http://dx.doi.org/10.15666/aeer/1705_1073110742

concentration of 10 ng/mL. A series of standard solutions with concentrations of 1, 5, 10, 50, and 100 ng/mL were prepared and the calibration curves were established after measurement.

Extraction and clean-up

Extraction and clean-up were carried out according to the QuEChERS method (Anastassiades et al., 2007). Nine samples were separately added to liquid nitrogen, ground and passed through a 80-mesh sieve. 0.5 g of sample was weighed into the 15 mL centrifuge tubes. The main extraction involved the addition of 1.5 g of sodium acetate, 10 mL of acidum aceticum-water-acetonitrile (1:4:95, v/v). The tube was closed and shaken vigorously by hand for 2 min. Then, 1.5 g of anhydrous $MgSO_4$ (burned in a high-temperature muffle furnace for 4 h) was added to the suspension. The tube was closed, shaken vigorously by hand for 2 min, and centrifuged for 5 min at 3000 r/min.

For clean-up, 1 mL of the upper organic phase was transferred into a 2-mL centrifugation tube already containing 25 mg PSA, 25 mg GCB and 150 mg anhydrous $MgSO_4$. The tube was closed, shaken vigorously by hand for 2 min, and centrifuged for 5 min at 12000 r/min. An upper organic phase was taken and concentrated by nitrogen to 200 μL for injection.

GC analyses

The measurement conditions were as follows: TG-5 quartz capillary column; The column temperature was maintained at 120 °C for 1 min, and then ramped at 6 °C min^{-1} up to 180 °C and kept for 2 min, then at 10 °C min^{-1} up to 280 °C and kept for 2 min; Detector temperature: 300 °C; Injector temperature: 230 °C; Carrier gas: N_2; Flow rate 40 mL/min; The sample injection volume was 1 μL, no splitting and external standard method for quantification.

Chemical analysis of the mineral composition

Preparation of standard solution

The elements standard solutions were prepared by 5% nitric acid solution diluting stock solution of 1000 μg/mL As, Cd, Pb, Hg and Cu (purchased from National Nonferrous Metals and Electronic Materials Analysis and Testing Center) to prepare a mixed standard stock solution with a concentration of 1000 μg/L. The mixture was further diluted to a mixed standard solution of 0.5, 1, 2, 10, 20, 50 μg/L and stored at 4 °C. Then the calibration curves were established after measurement.

Extraction

The heavy metals including As, Cd, Pb, Hg and Cu were analyzed by using ICP-MS. Before the analysis, samples were digested by using a microwave digestion system. Nine samples were separately added to liquid nitrogen, ground and passed through 80-mesh sieve. The sample was accurately weighed 0.5 g, placed in a microwave digestion tank and added 8 mL of nitric acid. The digestion procedures were carried out in a microwave oven according to the digestion setting (*Table 1*). After the temperature of the digestion solution dropped below 60 °C, the digestion tank is taken out. The samples were cooled to room temperature and ultrapure water was added to a total volume of 25 mL. The samples were stored at 4 °C before analysis.

http://www.aloki.hu ● ISSN 1589 1623 (Print) ● ISSN 1785 0037 (Online)
DOI: http://dx.doi.org/10.15666/aeer/1705_1073110742

ICP-MS analyses

The measurement conditions were: Plasma gas flow: 15.0 L/min; Spray chamber temperature: 2 °C; Auxiliary gas flow: 0.85 L/min; He gas flow: 5 mL/min; Carrier gas flow: 1 L/min; RF power: 1450 W; Data sampling mode: peak capture mode; Sampling depth: 8 mm; Number of sweeps: 100 times.

Table 1. *Microwave digestion procedure*

Step	Set temperature (°C)	Heating time (min)	Duration (min)
1	130	4	5
2	160	4	10
3	210		15

Statistical analysis

All data are expressed as average value of concentration and standard deviation. Descriptive statistics of the determined results were calculated by using MS Office Excel software, and the Excel add-in "Data Analysis suite" was applied for the linear regression analysis.

Results and discussion

Pesticide residue test results

Figure 2 shows typical gas chromatograms of standards for the nine pesticides. The calibration curves were obtained using the linear least squares regression procedure of the peak area versus the concentration. The results show that the concentration has a good linear relationship with the peak area, and the linearity is greater than 0.99. The calibration curves were enough for the detection OCPs in samples. The nine samples were extracted, clean-up and measured according to the method described in the section "Pesticide analysis by GC", while the OCPs were well separated (*Fig. 2*).

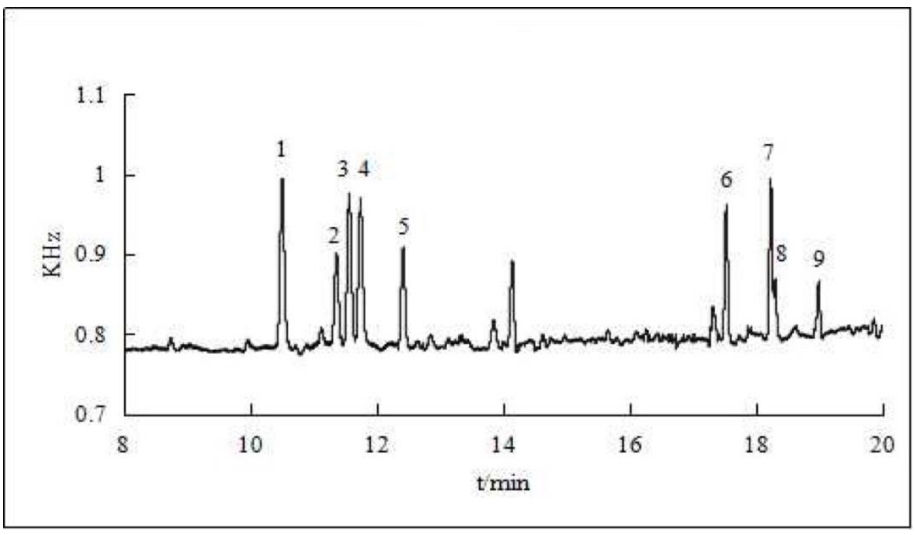

Figure 2. *Chromatogram of organochlorine pesticides standards. 1. α-BHC; 2. β-BHC; 3. γ-BHC; 4. PCNB; 5. δ-BHC; 6. o, p'-DDD; 7. p, p'-DDD; 8. o, p'-DDT; 9. p, p'-DDT*

http://www.aloki.hu ● ISSN 1589 1623 (Print) ● ISSN 1785 0037 (Online)
DOI: http://dx.doi.org/10.15666/aeer/1705_1073110742

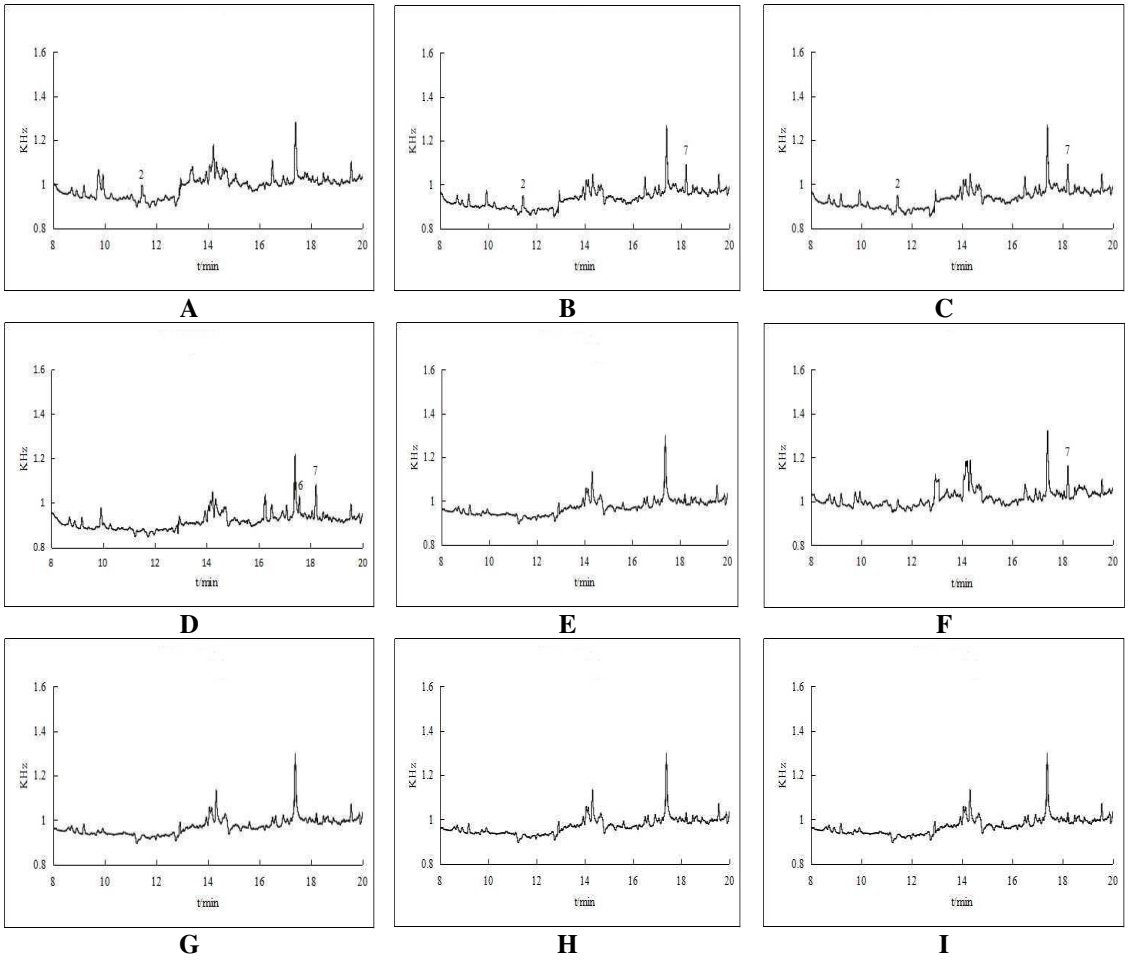

Figure 3. *Chromatogram of organochlorine pesticides of velvet antlers. A: New Zealand sika deer antler wax tablets. B: New Zealand sika deer antler red powder. C: New Zealand sika deer antler powder. D: Jilin sika deer antler wax tablets. E: Jilin sika deer antler red powder. F: Jilin sika deer antler yellow powder. G: Jilin red deer pilose antler powder wax tablets. H: Jilin red deer pilose antler powder tablets. I: Jilin red deer pilose antler sand tablets*

Nine velvet samples were quantified according to the peak area external standard method to calculate the residual amount of various organochlorine pesticides in the sample (*Fig. 3*). In this work, *Table 2* shows that the concentrations of contaminants detected in the nine samples did not exceed the maximum allowable residue limits (MRLs) which specified in the Chinese Pharmacopoeia (total BHC < 200 μg/kg and total DDT < 200 μg/kg) (Chinese Pharmacopoeia Commission, 2015).

The residual levels of some OCPs in environment seem to remaining approximately twenty years at least. In general, plant medicinal materials are in direct contact with the soil, so the pesticide content of botanicals is relatively high. During this study, the levels of OCPs in the nine samples were found to be in accordance with Chinese Pharmacopoeia standards. However, there is still a certain amount of pesticide residues in the antler, which indicates that the possibility of pesticide residues in animal drugs, and should be tested before giving to patients to ensure the medication safety. In addition, data support is provided to continually correct reasonable maximum residue limits (MRLs).

http://www.aloki.hu ● ISSN 1589 1623 (Print) ● ISSN 1785 0037 (Online)
DOI: http://dx.doi.org/10.15666/aeer/1705_1073110742

Table 2. *The content of organochlorine pesticides in different kinds of velvet antlers (n = 3)*

Antler species	Concentration (μg/kg)			
	β-BHC	δ-BHC	o, p'-DDD	p, p'-DDD
Jilin plum velvet wax tablets	—	—	3.87 ± 0.32	11.60 ± 1.22
Jilin plum antler yellow powder	—	—	—	10.08 ± 0.84
Jilin plum antler red powder	—	—	—	—
Jilin horse velvet wax tablets	—	—	—	11.40 ± 0.95
Jilin horse antler powder tablets	2.70 ± 0.15	3.60 ± 0.47	—	—
Jilin horse velvet sand	—	—	—	—
New Zealand sika antler wax tablets	2.90 ± 0.14	—	—	—
New Zealand sika antler powder	4.95 ± 0.29	—	—	10.56 ± 1.13
New Zealand plum antler red powder	—	—	4.00 ± 0.54	—

Heavy metal test results

^{63}Cu and ^{75}As with ^{72}Ge as the internal standard, ^{111}Cd with ^{115}In as the internal standard, ^{201}Hg and ^{208}Pb with ^{209}Bi as the internal standard. During the measurement, the internal standard samples tube were always inserted into the internal standard solution, and the samples tube of the instrument were inserted into the mixed standard solution with a concentration of 0.5, 1, 2, 10, 20, 50 μg/L and nine velvet samples for measurement. As *Table 3* showed that the calibration curves of the five heavy metal elements have a good linear relationship, and the correlation coefficients (r) were all above 0.99.

Table 3. *Standard curves and linear relations*

Measuring element	Regression equation	r
Cu	y = 3.2998x - 0.8663	0.9968
As	y = 0.0377x + 0.0113	0.9995
Cd	y = 0.0064x + 0.0167	0.9992
Hg	y = 0.0024x - 0.0013	0.9998
Pb	y = 0.0088x - 0.0034	0.9996

The results of determination of heavy metals were shown in *Table 4*, which can be seen that the nine velvet samples contain a certain amount of heavy metals and the content of Cu was relatively high. In addition, the heavy metal content of the wax sheet was higher than other parts of the velvet antler. In particular, Jilin plum velvet wax tablets have the highest content of heavy metals.

This study revealed that the contents of heavy metals from nine samples are in line with the permissible limits, but the level of Cu in the samples was generally higher, and the heavy metals remaining of the wax tablets were higher than the other parts of the antler. Food chain in the ecosystem is a process, which stored chemical energy in organic matter conducting layer by layer. The absorption and enrichment of heavy metal in CMs are the important factors causing the potential quality problems of clinical application. In the natural world, green plants are almost at the end of the bio-chain.

http://www.aloki.hu ● ISSN 1589 1623 (Print) ● ISSN 1785 0037 (Online)
DOI: http://dx.doi.org/10.15666/aeer/1705_1073110742

Heavy metal elements are absorbed by green plants and transported step by step along the chain, enforce accumulating and generating bio-magnification effects. Compared with green plants, animals are at the top of the bio-chain, which is more likely to be contaminated by heavy metals and harmful elements. The wax is the tip of the antler, thus the accumulation of heavy metals and harmful elements is higher. From this point of view, comprehensive and objective evaluation of the content of heavy metals in animal drugs can provide realistic data support for the safety of medication.

Table 4. *The content of 5 kinds of heavy metals in velvet antlers (n = 3)*

Antler species	Concentration (mg/kg)				
	Cu	**As**	**Cd**	**Hg**	**Pb**
Limit of detection	20	5	1	1	10
Jilin plum velvet wax tablets	4.577 ± 0.18	0.200 ± 0.014	0.011 ± 0.005	0.014 ± 0.007	0.688 ± 0.074
Jilin plum antler red powder	2.556 ± 0.13	0.103 ± 0.025	0.003 ± 0.0007	0.022 ± 0.014	0.372 ± 0.032
Jilin plum antler yellow powder	2.675 ± 0.16	0.093 ± 0.031	0.003 ± 0.0004	0.013 ± 0.003	0.512 ± 0.071
Jilin horse velvet wax tablets	5.065 ± 0.22	0.092 ± 0.01	0.001 ± 0.0003	0.008 ± 0.002	0.098 ± 0.002
Jilin horse velvet sand	1.033 ± 0.092	0.117 ± 0.011	0.001 ± 0.00	0.010 ± 0.001	0.588 ± 0.018
Jilin horse antler powder tablets	0.905 ± 0.06	0.062 ± 0.017	0.001 ± 0.00	0.010 ± 0.001	0.624 ± 0.049
New Zealand sika antler wax tablets	4.428 ± 0.11	0.109 ± 0.025	0.003 ± 0.0011	0.011 ± 0.005	0.104 ± 0.019
New Zealand sika antler powder	2.197 ± 0.15	0.041 ± 0.009	0.005 ± 0.002	0.113 ± 0.025	0.116 ± 0.16
New Zealand plum antler red powder	2.573 ± 0.17	0.172 ± 0.067	0.012 ± 0.003	0.275 ± 0.035	0.279 ± 0.008

Interestingly, studies have shown that there are excessive Cu and Cd contents in corn and soybean crops in Jilin Province (Liang et al., 2011). Therefore, we have reasons to suspect that the presence of heavy metals in velvet antlers may be enriched by food, and the food pathway only affects the content of heavy metals in antler. It could be related to the process of transportation and storage, so the reasons for the existence of heavy metals in antler must be further investigated to ensure the medication safety.

Conclusions

As a natural medicine, TCM has been favoured by patients because of its less side effects, good curative efficiency and medicine safety, which has been recognized and accepted by the international community gradually. TCM is a group of special products used by doctors to prevent and treat diseases, it would be rare for such plants or animal can use both as food and medicine to produce toxic effects on human body. It is the uniqueness of traditional Chinese medicine. However, due to the possibility that CMs may be contaminated by toxic and harmful substances during planting, processing, storage and so on, these pollution poses a certain threat to human health, which in turn affects the safety of its use. Animal medicine refers to the whole or parts of the body, the physiological or pathological product of the animal, the processed products, and the like, has taken a place for thousands of years. “Shen Nong’s Herbal Classic” contains 365 kinds of drugs, including 67 kinds of animal drugs, and the number of animal drugs in the “Compendium of Materia Medica” increased to 461 kinds. Animal medicine has the characteristics of strong activity and high curative effect, which is an indispensable component of TCM. Nowadays, there are many pharmacological studies on animal

http://www.aloki.hu ● ISSN 1589 1623 (Print) ● ISSN 1785 0037 (Online)
DOI: http://dx.doi.org/10.15666/aeer/1705_1073110742

drugs, but studies on safety issues such as residues of harmful substances are rare. Only a few analytical methods for determining pesticide residues in TCM have been reported.

Velvet antler is one of the representative animal drugs in TCM. Chinese deer industry has made great progress after continuous development. However, problems such as lack of talents, backward technology, extensive management, new technologies and methods have not been well promoted and applied in production practice are still exist. The world's leading exporters of velvet antler are New Zealand, Canada and Russia, of which New Zealand deer Antler has the greatest impact on Chinese antler industry.

The results show that although several OCPs detected in this subject have been banned for a while, some pesticide residues still can be found in velvet antlers. The content of heavy metal Cu in velvet antler is high, meanwhile the heavy metal pollution in the part of wax sheets is the worst, and provide a reference data for the further studies focused on the safety of herbal preparations. In addition, the source of heavy metal and pesticide pollution in antler is likely to be related to the management of farms, the processing of feed, medicine, transportation, storage and so on. Pharmacopoeia has only specified the source and type of deer antler, the method of identification, as well as the production methods of antler slices and powder. But the specification and quality description of the products of deer antler is too macroscopic; the identification method is too simple and not specific. Obviously, antler as traditional Chinese medicine needs to be further developed, clear breeding and regulatory standards should be established as soon as possible. Improving the more targeted analytical methods are useful for developing realistic MRLs and other regulatory guidelines for managing pesticide heavy metal residues in TCM products.

Acknowledgements. The English titles of books and the papers that are published in Chinese are translations made by the authors. This work was supported by the National Natural Science Foundation of China (grant no. 81503177 and 81573999), and the Fundamental Research Funds for the Central Universities (DUT19LK57).

REFERENCES

[1] Anastassiades, M., Lehotay, S. J., Stajnbaher, D., Schenck, F. J. (2003): Fast and easy multiresidue method employing acetonitrile extraction/partitioning and "dispersive solid-phase extraction" for the determination of pesticide residues in produce. – J AOAC Int 86(2): 412-31.

[2] Anastassiades, M., Tasdelen, B., Scherbaum, E., Stajnbaher, D. (2007): Recent Developments in QuEChERS Methodology for Pesticide Multiresidue Analysis. – In: Ohkawa, H., Miyagawa, H., Lee, P. W. (eds.) Pesticide Chemistry: Crop Protection, Public Health, Environmental Safety. Wiley-VCH, Weinheim.

[3] Barriada-Pereira, M., Concha-Grana, E., Gonzalez-Castro, M. J., Muniategui-Lorenzo, S., Lopez-Mahia, P., Prada-Rodriguez, D., Fernandez-Fernandez, E. (2003): Microwave-assisted extraction versus Soxhlet extraction in the analysis of 21 organochlorine pesticides in plants. – J Chromatogr A 1008(1): 115-22.

[4] China Pharmacopoeia Committee (2015): Chinese Pharmacopoeia. – China Medical Science and Technology Press, Beijing.

[5] Chunhua, M., Hongyan, L. (2017): Protective effect of pilose antler peptide on carbon tetrachloride-induced hepatotoxicity in mice. – International Journal of Biological Macromolecules 99(6): 648-654.

http://www.aloki.hu ● ISSN 1589 1623 (Print) ● ISSN 1785 0037 (Online)
DOI: http://dx.doi.org/10.15666/aeer/1705_1073110742

[6] Chunhui, Y., Wenjun, C., Hui, W., Liquan, S., Changwei, Z., Tianzhu, Z. (2017): Pilose antler peptide protects osteoblasts from inflammatory and oxidative injury through EGF/EGFR signaling. – Int J Biol Macromol 99: 15-20.
[7] Efferth, T., Kaina, B. (2011): Toxicities by herbal medicines with emphasis to traditional Chinese medicine. – Curr Drug Metab 12(10): 989-96.
[8] Hu, Y., Wan, L., Zhang, J., Yang, F., Cao, J. (2012): Rapid determination of pesticide residues in Chinese materia medica using QuEChERS sample preparation followed by gas chromatography–mass spectrometry. – Acta Pharmaceutica Sinica B 2(3): 286-293.
[9] Huie, C. W. (2002): A review of modern sample-preparation techniques for the extraction and analysis of medicinal plants. – Anal Bioanal Chem 373(1-2): 23-30.
[10] Iavicoli, I., Fontana, L., Bergamaschi, A. (2009): The effects of metals as endocrine disruptors. – Journal of Toxicology and Environmental Health, Part B 12(3): 206-223.
[11] Jang, S., Park, E. D., Suh, H. J., Lee, S. H., Kim, J. S., Park, Y. (2014): Enhancement of exercise endurance capacity by fermented deer antler in BALB/c mice. – Biosci Biotechnol Biochem 78(10): 1716-22.
[12] Jiang, J., Feng, L., Li, J., Sun, E., Ding, S. M., Jia, X. B. (2014): Multielemental composition of suet oil based on quantification by ultrawave/ICP-MS coupled with chemometric analysis. – Molecules 19(4): 4452-65.
[13] Kang, C. Z., Guo, L. P., Zhou, T., Zhao, D., Kang, L. P., He, Y. L., Wang, S., Zhou, L. Y. (2016): Discussion on present situation of study on pesticide residues in Chinese herbal medicines. – Zhongguo Zhong Yao Za Zhi 41(2): 155-159.
[14] Kong, L., Zhang, Y., Gu, L., He, B., Hu, J., Pang, H., Qin, G. (2015): Research Progress of Traditional Chinese Medicine Pesticide Residues. – Chinese Journal of Experimental Traditional Medical Formulae 21(21): 231-234.
[15] Lee, S. H., Yang, H. W., Ding, Y., Wang, Y., Jeon, Y. J., Moon, S. H., Jeon, B. T. (2015): Anti-inflammatory effects of enzymatic hydrolysates of velvet antler in RAW 264.7 cells in vitro and zebrafish model. – Excli J 14: 1122-32.
[16] Li, C., Chu, W. (2016): The regenerating antler blastema: the derivative of stem cells resident in a pedicle stump. – Front Biosci (Landmark Ed) 21(3): 455-467.
[17] Li, C., Zhao, H., Liu, Z., McMahon, C. (2014): Deer antler-a novel model for studying organ regeneration in mammals. – Int J Biochem Cell Biol.56: 111-122.
[18] Liang, X. H., Cao, T. H., Zhang, L., Yu, L., Liu, X. G. (2011): Content of heavy metals in farmland soil and accumulation in crops in Jilin province. – Journal of Jilin Agricultural Sciences 36(6): 59-62.
[19] Ma, C., Long, H., Yang, C., Cai, W., Zhang, T., Zhao, W. (2017): Anti-inflammatory role of pilose antler peptide in LPS-induced lung injury. – Inflammation 40(3): 904-912.
[20] Tadeo, J. L., Perez, R. A., Albero, B., Garcia-Valcarcel, A. I., Sanchez-Brunete, C. (2012): Review of sample preparation techniques for the analysis of pesticide residues in soil. – J AOAC Int 95(5): 1258-71.
[21] Ting, A., Chow, Y., Tan, W. (2013): Microbial and heavy metal contamination in commonly consumed traditional Chinese herbal medicines. – J Tradit Chin Med 33(1): 119-24.
[22] Tseng, S. H., Sung, C. H., Chen, L. G., Lai, Y. J., Chang, W. S., Sung, H. C., Wang, C. C. (2014): Comparison of chemical compositions and osteoprotective effects of different sections of velvet antler. – J Ethnopharmacol 51(1): 352-60.
[23] Xiao, X., Li, L., Xu, S., Mao, M., Pan, R., Li, Y., Wu, J., Huang, L., Zheng, X. (2017): Evaluation of velvet antler total protein effect on bone marrow-derived endothelial progenitor cells. – Mol Med Rep 16(3): 3161-3168.
[24] Xu, R., Wu, J., Liu, Y., Zhao, R., Chen, B., Yang, M., Chen, J. (2011): Analysis of pesticide residues using the Quick Easy Cheap Effective Rugged and Safe (QuEChERS) pesticide multiresidue method in traditional Chinese medicine by gas chromatography with electron capture detection. – Chemosphere 84(7): 908-912.

http://www.aloki.hu ● ISSN 1589 1623 (Print) ● ISSN 1785 0037 (Online)
DOI: http://dx.doi.org/10.15666/aeer/1705_1073110742

[25] Yang, Y. H., Dou, X. W., Kong, W. J., Yang, M. H., Chen, S. L., Xiao, Q. (2013): Status of pesticide registration and residue analysis for traditional Chinese medicine in China. – Zhongguo Zhong Yao Za Zhi 38(24): 4238-45.
[26] Yohannes, Y. B., Ikenaka, Y., Saengtienchai, A., Watanabe, K. P., Nakayama, S. M., Ishizuka, M. (2014): Concentrations and human health risk assessment of organochlorine pesticides in edible fish species from a Rift Valley lake - Lake Ziway, Ethiopia. – Ecotoxicol Environ Saf 95-101.
[27] Zhang, L. Z., Xin, J. L., Zhang, X. P., Fu, Q., Zhang, Y., Zhou, Q. L. (2013): The anti-osteoporotic effect of velvet antler polypeptides from Cervus elaphus Linnaeus in ovariectomized rats. – J Ethnopharmacol 150(1): 181-186.

http://www.aloki.hu ● ISSN 1589 1623 (Print) ● ISSN 1785 0037 (Online)
DOI: http://dx.doi.org/10.15666/aeer/1705_1073110742

SOIL ORGANIC MATTER VARIATION OF TOPSOIL UNDER INTENSIVE TILLAGE: THE CASE OF SANHU FARM, HUBEI PROVINCE, CHINA

WANG, L. Y.[1] – WANG, H. Z.[1,2*] – PAN, F. J.[1] – ZHOU, Y.[1,2*] – HA, J.[3] – LI, R. D.[4]

[1]*Key Lab for Geographical Process Analysis & Simulation of Hubei Province, Faculty of Urban & Environmental Science, Central China Normal University, Wuhan 430079, China*

[2]*Center of Land Science Research, Central China Normal University, Wuhan 430079, China*

[3]*School of Environmental and Sustainability Sciences, Kean University, New Jersey 07083, USA*

[4]*Institute of Geodesy and Geophysics, Chinese Academy of Sciences, Wuhan 430077, China*

[*]*Corresponding authors*
e-mail: wanghongzhi@mail.ccnu.edu.cn, yzhou@mail.ccnu.edu.cn

(Received 1st Mar 2019; accepted 21st May 2019)

Abstract. Soil organic matter (SOM) plays an important role both to condition soil properties and to mitigate climate change. SOM change pattern after intensive tillage is still not well revealed. Taking Sanhu Farm, Jiangling County, Hubei Province, China as a case area, based on topsoil survey samples of 1990, 1994 and 2000 respectively, the spatial distribution pattern and temporal change of SOM content was analyzed. The results show that (1) SOM content successively decreased with the increase of land exploitation history; (2) topsoil SOM value of the three survey years showed a similar spatial pattern whereby the highest SOM value was distributed in the center, and SOM value decreased incrementally as the distance from the center increased, which showed the SOM values were negatively correlated to the altitude of study area; (3) there was an overall tendency for the maximum or minimum value of SOM to approach to the average value over time; (4) SOM concentration changes were influenced by crop systems changes related to the price of crops and related policies. The study depicts SOM variability after the reclamation from virgin land to arable land at a landscape scale, which may contribute to research revealing spatial distribution patterns and controlling elements of SOM change.
Keywords: *land reclamation from lakes, SOM change pattern, land exploitation history, the kriging interpolation, spatial autocorrelation, crop systems*

Introduction

Soil organic matter (SOM) is the largest source of SOC, which is a key element to soil quality for its far reaching effect on soil physical, chemical and biological properties (Laik et al., 2009; Nadi et al., 2017). As an important feature of soil, even in small amounts, organic matter is very important to keep soil healthy (Osman, 2013). It has tremendous biological significance for providing food for microorganisms, storing nutrients, retaining water, and performing as a soil conditioner and aggregating agent (Manlay et al., 2007; Osman, 2013). The Soil surface comprises the largest carbon stock in terrestrial ecosystems, and soils to 1 m depth contain 74% of the total terrestrial C stocks (Lal, 2004; Batjes, 2016; Vitharana et al., 2019). The global soil organic carbon (SOC) pool is estimated to amount to 1200-1600 Pg carbon in the upper 1 m (Batjes, 1999), representing 2.5 times the carbon pool in vegetation, or 2 times the amount of carbon in the atmosphere. Change of soil organic matter (SOM) content under intensive

http://www.aloki.hu ● ISSN 1589 1623 (Print) ● ISSN 1785 0037 (Online)
DOI: http://dx.doi.org/10.15666/aeer/1705_1074310757

tillage has becomes a pivotal concern in soil research as an option for mitigation of climate change (Schulp et al., 2008b; Das et al., 2008).

Insight in variability of SOM quality and quantity is required to quantify the greenhouse gas mitigation potential of the landscape (Schulp et al., 2008a). Research shows that there is a direct link between SOM content and human impact, observed in land use patterns or land management systems, for example (Smith et al., 2000; Lettens et al., 2005; Abdollahi et al., 2014; Gmach et al., 2018; Wood et al., 2018). SOM contents are generally lower after intensive tillage (Degryze et al., 2004; Lettens et al., 2004a; Gerzabek et al., 2005; Papienik et al., 2007), especially the surface soil organic carbon and total nitrogen contents in cultivated areas (Schulp et al., 2008b; Barrett et al., 2015; Wood et al., 2018). Afforestation by different plantations increased soil C pools to different magnitudes (Laik et al., 2009; Kukuļs et al., 2019). Alternative management systems, like reduced tillage or organic farming, have been introduced that are considered to lead to more sustainable land use and increased sequestration of atmospheric C into agricultural soils (Pulleman et al., 2000). However Dutch research highlights some relationships between the SOM content variability and land condition before its exploitation. It is not a universal rule to lower SOM contents after intensive tillage (Webb, 1998; Schulp et al., 2008b; Abdullah, 2014).

At landscape scale, patterns of management, land use or land use history might better present the spatial variability of SOM pools (Veldkamp et al., 2001; Dendoncker et al., 2004; Schulp et al., 2008b) while soil and groundwater may dominate over other factors that influence SOM pools (quality and quantity) at a national scale. At temporal scales up to a few decades, SOM content changes are observed following land use conversions (Lettens et al., 2004b; Falloon et al., 2006; Gmach et al., 2018). Intensive cultivation is often exerted to land in China to support the large population. Soil pedons and characteristics including SOM contents are quite different to the natural ones under the Chinese special management patterns.

In this paper, we will try to reveal how the SOM contents have been changed under intensive tillage at landscape scale, using Sanhu Farm as a case study area, which belongs to Jiangling County, Hubei province, China. This site has been reclaimed farmland from a lake since 1960 and is currently dominated by anthrosols (Wang et al., 2010).

Materials and Methods

Case study area

Sanhu Farm (30°10'-30° 16' N, 112°29'-112° 35' E) is located in southeast of Jiangling County, Hubei province in central China, with an area of 63.5 km^2 (*Fig. 1*). There are 14,812 people in Sanhu Farm and 55.49% of them are peasants. The percentage of forest cover is only 1.92%. The max distance from north to south inside the farm is 11.2 km while from east to west is 7.75 km. The area is characterized by a subtropical humid monsoonal climate. The average monthly temperature reaches a maximum of 27.2°C in July and a minimum of 3.5°C in January. The average annual temperature is 16.1°C and the average annual precipitation is about 1100 mm. The altitude of Sanhu Farm ranges from 25.1 m to 29.3 m, with an average altitude of 25.8 m (Yellow Sea Height System). The relief of the farm is like a shallow dish, a little lower at the center and higher at the surrounding boundary. At the same time, it tilts

http://www.aloki.hu ● ISSN 1589 1623 (Print) ● ISSN 1785 0037 (Online)
DOI: http://dx.doi.org/10.15666/aeer/1705_1074310757

southwardly with a slope of about one five-thousandth. The parent soil material of Sanhu Farm is Quaternary sediments of fluvial or lacustrine deposits.

Sanhu Farm was once one of the Four Lakes in Jianghan Plain. Jianghan Plain is located in the middle reach of the Yangtze River basin where the Han River meets the Yangtze. This part of the basin was formed mainly by the alluviation and deposition of sediment from these two rivers. Jianghan Plain is one of the most important commodity grain and oil production bases of China and it is distinguished by its numerous shallow lakes. There were 1,141 lakes during the 1960s, but this number was reduced to 752 lakes in 1990s. There is a Four-Lake Area in Jianghan Plain, which named for the four biggest lakes of Jianghan Plain, one of which was Sanhu Lake which no longer exists (only two larger lakes remain of the original four). Sanhu Farm was named after Sanhu Lake.

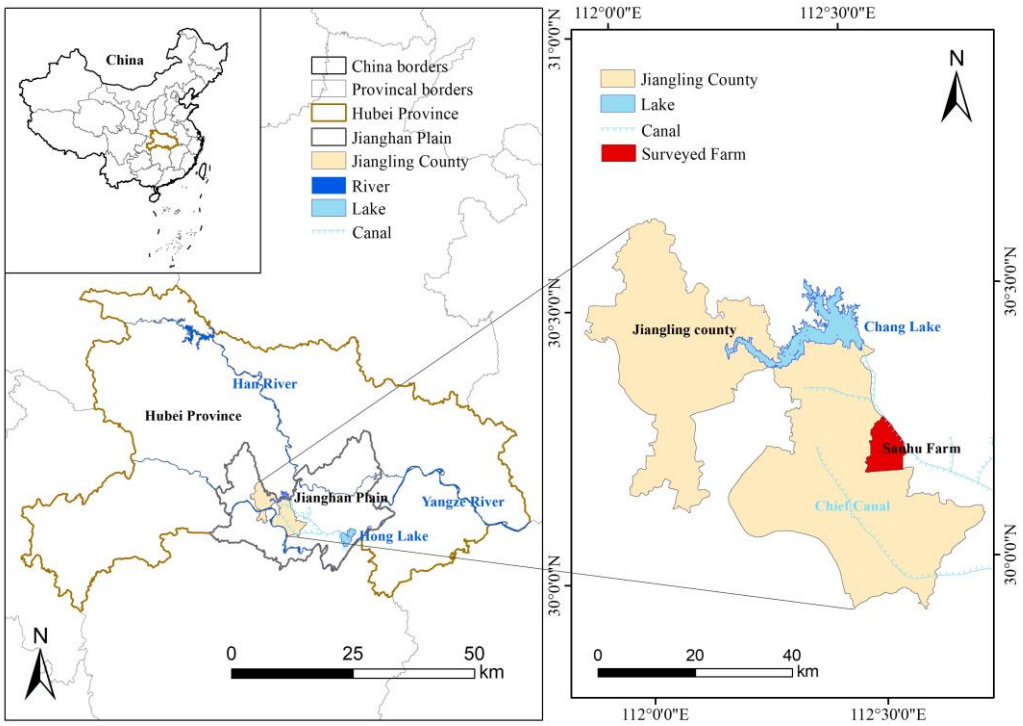

Figure 1. *Location of Sanhu Farm*

The plan of reclamation of Sanhu Lake began from 1960 just after the fulfillment of the construction of the Chief Canal of the Four Lake Area. There were two main objectives of the reclamation of Sanhu Farm. Firstly, there was a famine nationwide in China from 1958 to the early 1960s, and relieving the food problem was of utmost importance at that time. Secondly, many people were suffering from schistosome, a disease develops in the slack water environments. The reclamation of Sanhu Lake effectively addressed both of these concerns.

The Sanhu Lake area went through three land reclamation periods before reaching its present pattern. In the first stage, from 1962 to 1965, there were 33 km^2 of cultivated land reclaimed. In the second stage, from 1971 to 1973, 16.5 km^2 were reclaimed. In the third stage, from 1975 to 1979, 14 km^2 were reclaimed. By the end of 1979, the present pattern of Sanhu Farm had been formed.

http://www.aloki.hu ● ISSN 1589 1623 (Print) ● ISSN 1785 0037 (Online)
DOI: http://dx.doi.org/10.15666/aeer/1705_1074310757

Three sides of Sanhu Farm is bound by water bodies, that is, Chief Canal of Four-Lake Area (8.6 km) on the east, Cengda River on the south and Cenhe River on the west. There is a well-developed water drainage system in Sanhu Farm, consisting of 7 main canals, 28 sub-canals and hundreds of ditches, which is connected or controlled by culverts and Watergates Developed Artificial Water Systems: numerous canals and ditches (*Fig. 2*). The water drainage system has been efficient to drain logged water to the outside canals and to irrigate the farmland, as well. So the area maintains the outline of Sanhu Lake.

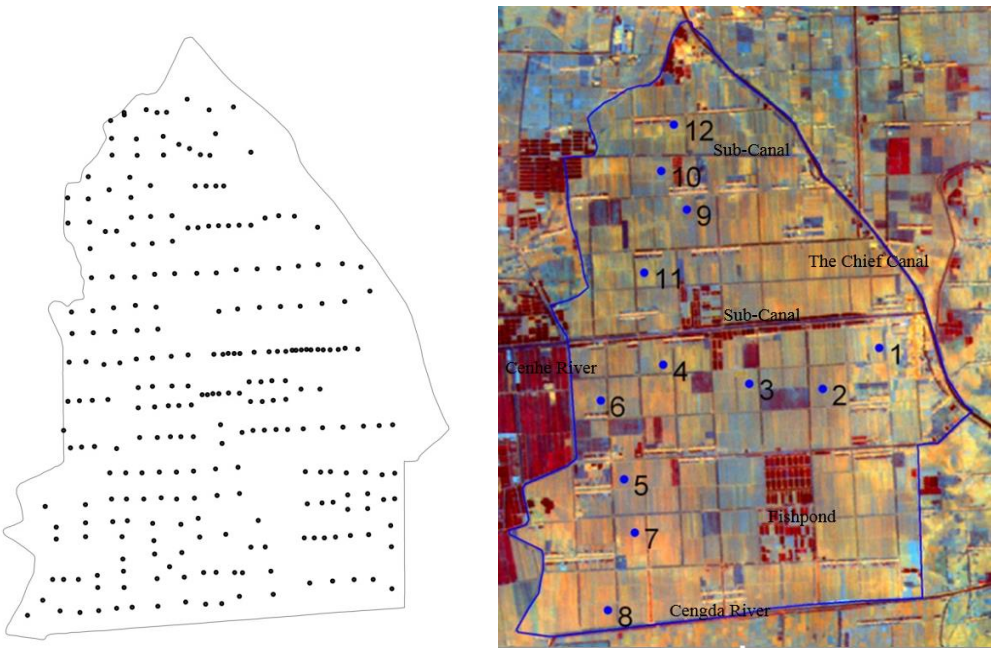

(a) Topsoil Samples *(b) Soil Profiles*

Figure 2. *Distribution Map of Topsoil Samples (a) or Soil Profiles (b)*

Before 1994, the main crop in Sanhu Farm was rice because of the enacting of the national policy "Food for the Program", due to the national famine from the late 1950s to the early 1960s. After 1994, most of the paddy land was changed to dry crops which were harvested twice per year (cotton and rapeseed, respectively). However, the area of paddy has been expanding again as a result of the National Commissariat Allowance Policy from 2004 and the rising price of rice (Wang et al., 2010), but the speed of expansion has been restricted due to the degradation of the local drainage system. As a result, it is necessary to study the variation of SOM caused by the fluctuation of land use and management and to evaluate the impact of land use change on soil properties and climate change at a landscape scale.

Data collection and processing

Soil samples processing and analyzing

Some temporal and typological data were sampled and collected, including soil survey data of topsoil random samples without spatial information from both 1980 (643 samples) and 1987 (516 samples), soil survey data of topsoil with spatial information of

http://www.aloki.hu ● ISSN 1589 1623 (Print) ● ISSN 1785 0037 (Online)
DOI: http://dx.doi.org/10.15666/aeer/1705_1074310757

262 random samples from 1990, 1994 and 2000, and soil horizontal sampling analysis data of 12 profiles from 2008 which have spatial points corresponding to former data.

Soil samples collection and pre-treatment were all carried out from October to November just after the harvest of rice in order to keep the seasonal consistency of the soil samples. Every topsoil sampling data was a mixture of arable horizon. 12 soil profiles (1.0 m wide×0.8 m thick×1.1 m deep) were dug at locations shown in *Fig. 2*. The geographic coordinates of every profile were recorded by GPS as well as photos of the landscape where the soil profiles were taken. Samples from every soil horizon in each profile were collected using a cutting ring. All soil samples were put in sterilized Kraft paper sacks with plastic bags outside to prevent water volatilization and were transported to a laboratory and kept at lower temperature. Samples were allowed to air dry and passed through a 1 mm bore diameter sieve first. One-fourth volume of every soil sample was collected for chemical analysis after passing through a 0.1 mm bore diameter sieve. The external heating method ($K_2Cr_2O_7$ at 0.4 mol/L-H_2SO_4) was used to determine the SOM content of all samples in the laboratory (Walkley and Black, 1934; Mirzaee et al., 2016; Singh et al., 2019).

Geographical data collection and data spatialization

A GIS based database of the study area was constructed containing a DEM of 1:10000 (1980), soil survey data of topsoil, and soil horizontal sampling data of several profiles and tables of soil survey data. The spatial system of the database is the Xi'an Geodetic Coordinate System 1980, Gauss-Krueger Projection. All the soil survey data with spatial information were digitalized in the format of DBF. According to the spatial information of the geographic coordinates of topsoil samples or soil profiles, the DBF data were converted to the point layer of the distribution of topsoil samples (*Fig. 2a*) or soil profiles (*Fig. 2b*) where the background is a TM image of May, 2005.

The kriging interpolation for the SOM spatial-temporal pattern prediction

There were 262 topsoil point observations from 1990, 1994 and 2000 which had exactly location information corresponding to the three different years. A DBF file of SOM content of 262 topsoil samples of the three years was connected to the point layer of the distribution of topsoil samples respectively under the ArcGIS10 platform environment. Then the Kriging interpolation technique was applied to depict the spatial pattern of SOM of the three years. The Kriging interpolation method is based on geostatistical models that include autocorrelation-that is the statistical relationships among the measured points. Kriging is a multistep process, includes exploratory statistical analysis of the data, variogram modeling, creating the surface, and (optionally) exploring a variance surface. The first step for the Kriging interpolation is to select the best fitted model which standardizes the mean near to zero, makes the Root-Mean-Square as small as possible, makes the average Standard Error near to the Root-Mean-Square, and standardizes the Root-Mean-Square Standardized near to one. Considering factors of error covariance analysis of every model type synthetically, the Exponential model best fits to identify the SOM for 1990 and the Spherical model best fits to identify the SOM for 1994 and 2000.

http://www.aloki.hu ● ISSN 1589 1623 (Print) ● ISSN 1785 0037 (Online)
DOI: http://dx.doi.org/10.15666/aeer/1705_1074310757

Results and analysis

The total trend of SOM concentration change

The average SOM concentration of every survey year was calculated by Excel according to all the topsoil random samples (*Table 1*). *Table 1* shows that the mean SOM concentration decreased from 1980 to 2008 with an average decrease rate of 1.01 g/kg per year. At the earliest stage, the SOM concentration decreased rapidly with a highest average yearly decrease rate of 2.57 g/kg. At the following stages, the mean yearly SOM decrease rate fluctuated under 0.78 g/kg. It tells us the SOM concentration successively decreased with the increase of the exploitation history.

Table 1. *The average concentration of SOM (Unit:g/kg)*

Year	1980	1987	1990	1994	2000	2008	Total
Types of Samples	topsoil	topsoil	topsoil	topsoil	topsoil	profile	
Spatial Located?	no	no	Yes	Yes	Yes	Yes	
Number of Samples	643	516	262	262	262	12	
SOM of topsoil	54.0	36.0	35.4	32.9	29.4	25.6	
Annual decrease rate	/	2.57	0.20	0.63	0.58	0.78	1.01

The samples of 1990, 1994 and 2000 were co-located in the three survey years, so the data may show more objective information. The annual decrease rate of SOM content was 0.63 g/kg from 1990 to 1994, and 0.58 g/kg from 1994 to 2000. The decrease of the former period was more rapid than that of the later period. The value of SOM greatly affects the soil productivity. Usually the SOM concentration value can be divided into three main grades as POOR, MEDIUM and ABUNDANT. When the SOM concentration value falls between 20-40 g/kg, it is MEDIUM; below 20 g/kg, POOR; above 40 g/kg, ABUNDANT. Sample numbers and percentages of every SOM concentration grade of the three survey years are shown in *Table 2*.

Table 2. *Sample numbers and percentage of every SOM concentration grade*

Year	Sample Numbers			Sample Number Percentage		
Grade	<20 g/kg Poor	[20-40g/kg] Medium	>40g/kg Abundant	<20 g/kg Poor	[20-40g/kg] Medium	>40g/kg Abundant
1990	32	155	75	12.2	59.2	28.6
1994	46	143	73	17.6	54.6	27.9
2000	19	193	51	7.3	73.7	19.5

Among the 262 samples, there are 75 samples graded as ABUNDANT in 1990, 73 samples in 1994, but only 51 samples in 2000; The percentage of samples graded as ABUNDANT decreased from 28.6% in 1990 to 19.5% in 2000. In the other end, there are 32 samples graded as POOR in 1990, 46 samples in 1994, but only 19 samples in 2000 (*Table 2*). In the long run, the SOM concentration differences of samples decreased after the land reclamation and intensive tillage.

The prediction of SOM spatial patterns and analysis

The distribution maps of the topsoil organic matter of the three survey years were depicted (*Fig. 3*) through the Kriging interpolation based on the topsoil sampling point

http://www.aloki.hu ● ISSN 1589 1623 (Print) ● ISSN 1785 0037 (Online)
DOI: http://dx.doi.org/10.15666/aeer/1705_1074310757

distribution layer under ArcGIS 10.1 platform with selected appropriate models (*Table 3*), and with 10 classes divided by Natural Breaks rule with a slight artificial interference. The maps (*Fig. 3*) show us that there was a high SOM center located in the south-middle part of the study area running through all the three survey years. In 1990, the SOM values decrease incrementally as the distance from the high SOM center increases. Compared with 1990, the highest SOM region of 1994 shrank considerably. By 2000, the highest SOM region divided into two centers, and the top two SOM classes (Legend) no longer existed, which were component classes of the SOM distribution maps of the former two survey years.

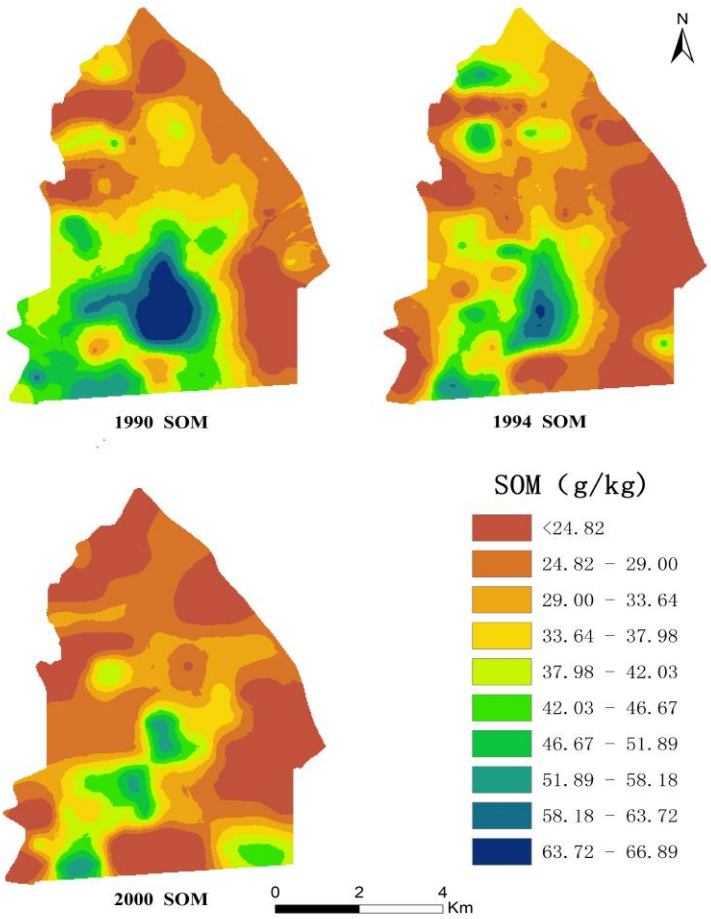

Figure 3. *The spatial pattern of SOM of topsoil of Sanhu Farm*

The selected model of 1990 is the Exponential and that of the other two years is the Spherical. The performance of Kriging models depends on spatial autocorrelation of the topsoil organic matter. The Range (*Table 3*) tells the scope that spatial autocorrelation works, which is one of the principles to set samples. Distances of neighboured samples are all less than the Range value, so the Kriging models can be used reliably.

The ratio of Nugget/Partial Sill (*Table 3*) reveals the factors that may affect the spatial autocorrelation of the SOM distribution. When the ratio is smaller than 0.25, the spatial autocorrelation of the SOM distribution is very strong and the SOM distribution is mainly controlled by structural factors such as climate, soil parent material, landform,

http://www.aloki.hu ● ISSN 1589 1623 (Print) ● ISSN 1785 0037 (Online)
DOI: http://dx.doi.org/10.15666/aeer/1705_1074310757

etc. When the ratio is bigger than 0.75, the random factors affect the SOM distribution more, such as fertilization, cropping pattern, etc. According to *Table 3*, the SOM spatial pattern of 1990 and 2000 were more decided by the structural factors, while that of 1994 was more decided by random factors.

Considering the area of Sanhu farm is only 64 km^2, the climate type does not change and its influence on the distribution of SOM can be omitted. So for the Suhan Farm area, we think that the landform and the soil parent material are key structural factors for SOM distribution. Meanwhile, Sanhu lake was a lake formed by low-lying land where the Yangtze river and its tributaries are found (He, 2002). The soil parent material changes with the distance from the center of the lake to the rivers. When the sample site is nearer to the center of the lake, the soil parent material has more clays; when it is nearer to the rivers, the soil parent material has more sands. In another words, the soil parent material is quite uniform with the height of the study area. On the other hand, the random factors in the Sanhu Farm area related to human activities, among which the cropping pattern was the key factor to influence the SOM spatial pattern.

Table 3. *Parameters of semivariogram fitted to SOM distribution patterns*

Year	Model	Nugget	Partial Sill	Range	Nugget/Partial Sill
1990	Exponential	0.312	1.651	3577.776	0.189
1994	Spherical	0.973	1.118	2161.201	0.870
2000	Spherical	0.082	0.628	2150.335	0.131

Driving factors of the SOM spatial pattern changes

Both structural and random factors affect the SOM spatial patterns. The SOM spatial pattern and its change are controlled by the mixture of the two types of factors. *Table 3* shows that the SOM spatial patterns of 1990 and 2000 are affected more by the structural factors while that of 1994 is affected more by random factors. We think the elevation is the key structural factor and the cropping system is the key random factor.

The SOM Spatial Patterns of the study area have been controlled by the micro-landform constantly. This area was reclaimed through a lake, the Sanhu Lake. It was formed by the extraction of lake water to the Main Canals, so the study area basically kept the landform of the Sanhu Lake. The elevation of study area is between from 25.1 m to 29.3 m (*Fig. 4*). Most of this area has a height of around 26-27 m. The center part of the former lake was lowest with the richest deposit of peats, a rich source of SOM. That's why there is always a high SOM value at the center (*Fig. 3*).

When the relation between the SOM values and the elevation was analyzed (*Fig. 5*), it was found that the SOM values in the three survey years all had a strong negative correlation with the height. In the other words, in different survey years, between the elevation and the SOM value, there showed a similar pattern in which the SOM values decreased as the height increased, though every survey year's decreasing gradient was slightly different. The decreasing gradient of 1990 was 0.2656; that of 1994, 0.2574; that of 2000, 0.3263. The SOM values of 2000 decreased with the decrease of height more rapidly than that of the other two survey years. Though the decreasing gradient of 1990 was quite similar to that of 1994, the value of 1994 was the smallest.

The SOM values of samples with their corresponding heights were used to make a scatter diagram (*Fig. 6*). The diagram clearly shows the pattern of the changes of the SOM values during different periods after the land reclamation and intensive tillage.

http://www.aloki.hu ● ISSN 1589 1623 (Print) ● ISSN 1785 0037 (Online)
DOI: http://dx.doi.org/10.15666/aeer/1705_1074310757

The red triangles in *Fig. 6* represent the SOM values of 1990, blue 1994 and green 2000. It is important to note that the highest SOM value is not just for the site with the lowest height. Rather, the mean value of SOM decreased constantly along the three survey years (*Table 4*). Compared to the SOM values of the three survey years, the data from 1994 had the highest standard deviation (*Table 4*) and the biggest ratio of Nugget/Partial Sill (*Table 3*), which was affected more by human activities.

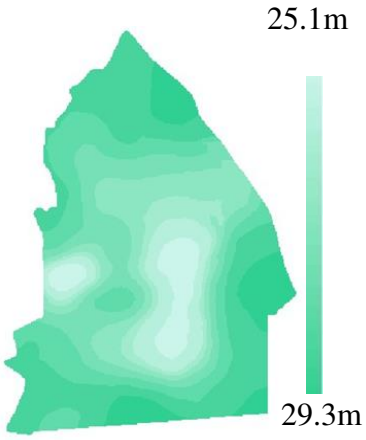

Figure 4. *The DEM of study area*

	Elevation	SOM_2000	SOM_1994	SOM_1990
Elevation	1.0000			
SOM_2000	-0.3263*	1.0000		
	0.0000			
SOM_1994	-0.2574*	0.3618*	1.0000	
	0.0000	0.0000		
SOM_1990	-0.2656*	0.4124*	0.5042*	1.0000
	0.0000	0.0000	0.0000	

Figure 5. *Relationship of SOM concentration and elevation*

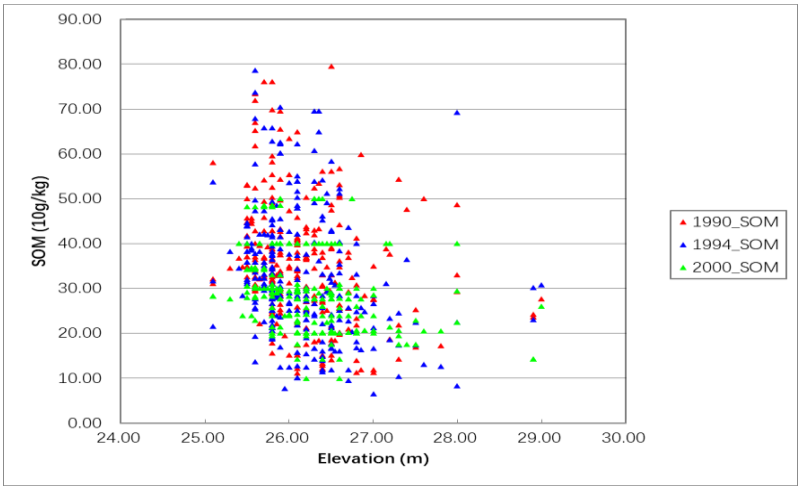

Figure 6. *Relationship between elevation & SOM concentration of every survey year*

When the cropping system and its changes were considered (*Fig. 7*), the cause of the speciality of the SOM spatial pattern from1994 can be identified. From 1980 to 1990, the paddy land accounted for 56.35% of the total arable land and the dry land accounted for 43.65% (*Fig. 7a*). By then early rice and late rice were planted in rotation in paddy land while the dry land was rotated by wheat, rapeseed and soybean. But from 1991 onward, China assigned cotton production responsibility nationally and the government supplied loans with low or free interest to encourage cotton planting. Additionally, the

http://www.aloki.hu ● ISSN 1589 1623 (Print) ● ISSN 1785 0037 (Online)
DOI: http://dx.doi.org/10.15666/aeer/1705_1074310757

price of cotton rose 10% in 1993 and continued to rise in 1994. This policy had strongly affected the cropping system of Sanhu Farm. The paddy land changed to dry land for cotton planting continuously in 1991. Until 1995, almost all paddy land was changed to dry land, where the paddy land accounted for 4.18% of the total arable land, and the dry land accounted for 95.82% (*Fig. 7b)*. The cropping system had been cotton and rapeseed in rotation from then. In 1998, however, the price of cotton depreciated significantly, and the government reformed the circulation system of cotton the following year. Cotton was no more the nationally critical materials, and the risk of cotton planting was no longer the joint responsibility of government and peasants (Sun, 2005). But the cropping system of Sanhu Farm had changed very little for the degeneration of irrigation system guaranteed the rice production till 2008 we did our last field investigation to the area.

Table 4. *The classical statistical features of SOM concentration data of Sanhu Farm*

Year	Sample Number	Mean (g/kg)	Standard deviation	Coefficient of variation (%)	Maximum (g/kg)	Minimum (g/kg)
1990	262	35.45	13.38	0.38	79.50	11.10
1994	262	32.92	14.36	0.44	78.70	6.50
2000	262	29.42	8.59	0.29	50.00	10.00

So 1994, a period of cropping system change emerged, which is why the ratio of Nugget/Partial Sill of SOM spatial pattern was very high (*Table 3*). We may suppose that, when the cropping system was steady and uniform, the micro-landform was the key controlling factor of the SOM spatial pattern of Sanhu farm. But as the cropping system changed, the influence of human activity can't be neglected for the SOM distribution. Regardless of whether the cropping system was steady, the amount of SOM decreased continuously after reclamation and intensive cultivation.

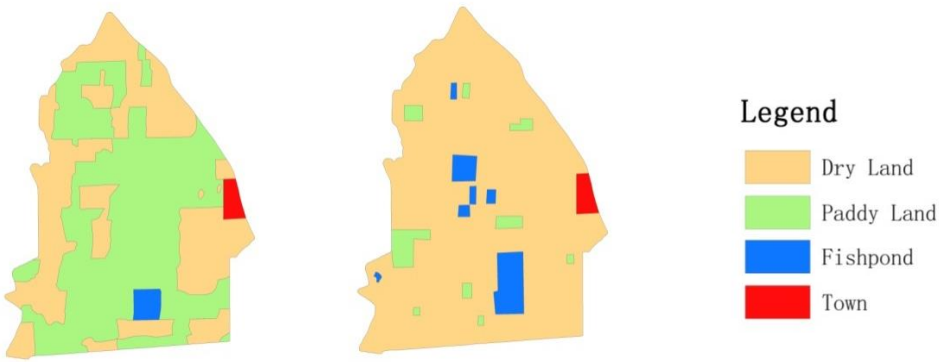

a. Land use of 1980 b. Land use of 2005

Figure 7. *Land use pattern of Sanhu Farm*

Discussion

Our research concerns two significant issues of the soil science domain.

The first issue is to ascertain the influencing factors and their influences on soil quality (Cambardella et al., 2004; Karlen et al., 2013a; Ontl et al., 2015) or carbon accounting (Ratayake et al., 2016).

http://www.aloki.hu ● ISSN 1589 1623 (Print) ● ISSN 1785 0037 (Online)
DOI: http://dx.doi.org/10.15666/aeer/1705_1074310757

Many researchers suggest that soil quality is influenced by inherent (such as parent material, climate, and topography) and anthropogenic (such as tillage and crop rotation) factors (Karlen et al., 1998; Schwanghart et al., 2011). Research teams from the USDA mainly focus on changes in soil quality indicators through long-term care or maintenance of the plots for elaborately designed tests of tillage operations over several decades (Cambardella et al., 2004; Karlen et al., 2013b). Karlen et al. (2013b) verified their hypothesis that long-term moldboard plowing would have the greatest negative effect on soil quality indicators, and they put forth that less aggressive tillage systems or cropping systems could significantly improve soil quality/health. Cambardella et al. (2004) found that soil quality degradation with tillage depends upon landscape position, suggesting that soil quality increases on the backslope, and that shoulder landform elements are responsible for higher watershed-scale soil quality in the ridge-tilled watershed. Ontl et al. (2015) analyzed the influence of different bioenergy cropping systems on soil aggregation and particulate organic matter. The result showed that root system properties of crops and soil texture influenced the shift of iPOM-C concurrently, and cropping system effects were not consistent among positions across landscape.

SOM is a very important indicator of soil quality (Cambardella et al., 2004). We emphasized spatial patterns and temporal change of SOM with sampling data from three different years, while the USDA observed changes in many indicator variables of soil quality among positions across landscape, or under different cropping systems and tillage types, by comparing soil layered sampling data from a single year. They elaborately designed different scenarios of cropping systems and tillage types on different plots which was helpful to get the oriented results, but we analyzed a real-world cropping system altered by the farmers' wills, and concomitantly affected by both the market and policy. Our study area Sanhu Farm was virgin land before the reclamations of the 1960s, so it supplied a nice perspective to observe the impact of anthropogenic factors. In a spatial visual style, our research supported the hypothesis that soil quality is influenced by inherent and anthropogenic factors.

In another aspect, previous researches on carbon counting achieved some creative results. Rice cropping under waterlogged conditions enhances the soil organic matter (SOM) accumulation (Lal, 2002; Ratnayake et al., 2016). Wu (2011) reported that SOC accumulation in paddy ecosystems was faster and more pronounced than in other arable ecosystems. Kölbl et al. (2014) found that lower lands with water logging get greater accumulation of SOC in soil. Ratnayake et al. (2016) went further to find that different upland crops make limited contribution to carbon accumulation, while rice fields in the lower land landscape exhibit greater potential to store SOC in terms of carbon sequestration compared with upland cropping systems. Our research results were in accord with theirs. Furthermore, we found that the upland cropping systems also generate a smaller standard deviation.

Another issue is on the spatial modelling of SOM (SOC) and model accuracy (Miller et al., 2016; Ratnayake et al., 2016), which mainly focus on sampling density, efficiency, and the simulating precision of models. Previous research designed the rules for model selection which were used in our research in the preceding introduction, and the average distance of sample sites was about 350 m, which satisfied the sampling distance need (>2150 m) of every model (*Table 3*). Kriging models we used for simulating the spatial-temporal change of SOM rely on spatial autocorrelation, which perform best when the distance between points is minimized and only appropriate to use for making predictions between points, and they are considered inappropriate for

http://www.aloki.hu ● ISSN 1589 1623 (Print) ● ISSN 1785 0037 (Online)
DOI: http://dx.doi.org/10.15666/aeer/1705_1074310757

extrapolating beyond the extent of sampling points (Miller et al., 2016). So, near the boundary of Sanhu Farm the simulating error of SOM is relatively higher than the remaining area for there is no sample outside of the boundary. The biggest advantage of the Kriging technique over many classical statistical procedures is that it incorporates the spatial correlation of the data. Considering the sampling rule of different years was the same, and we mainly cared about the change of SOM, and the boundary area was quite limited, so we did not discuss the possible error of the boundary area in our calculation.

Conclusion

SOM plays a very important role both to condition soil properties and to mitigate climate change. Sanhu Farm with an area of 64 km^2, which was a lake before the 1960s, was used as our study site to observe SOM variability after intensive tillage of the virgin land. Based on 262 topsoil survey samples of 1990, 1994 and 2000 respectively, the SOM spatial distribution pattern, as well as the temporal change of SOM content of the corresponding years, were analyzed.

The SOM content successively decreased with the increase of the land exploitation history. From 1990 to 2000, the sample numbers of SOM grade in Abundant had decreased from 28.6% to 19.5%; the SOM grade in Poor decreased from 12.2% to 7.3%; but the Medium grade increased from 59.2% to 73.7%. We depicted the topsoil SOM distribution maps of the three survey years with an appliance of a same legend of 10 classes divided by Natural Breaks rule under ArcGIS 10 (*Fig. 7*). Compared with the map of 1990, the distribution area of the top grade shrank greatly by 1994, and the top two grades were disappeared by 2000. there was an overall tendency for the maximum or minimum value of SOM to approach to the average value over time.

The altitude of Sanhu Farm thus played a controlling role throughout the three survey years.The SOM concentration of each survey year was negatively and significantly (at 5 percent level) correlated with the elevation. The topsoil SOM distribution of the three survey years showed a similar spatial pattern whereby the highest SOM concentration value grade was distributed in the center, and the SOM value decreased incrementally as the distance to the center increased ,which showed the SOM values were negratively correlated to the altitude of study area.

SOM concentration changes were influenced by crop systems changes which were affected crop prices and related policies. In particular, the crop system change from rice to cotton influenced the decrease of SOM significantly.

Acknowledgements. The work was funded by NSFC (NO. 41571487 & NO. 40771088). Many thanks to David W. Knight for the language editing to the manuscript, who is assistant Professor of Department of Human Dimensions of Natural Resources, Colorado State University.

REFERENCES

[1] Abdollahi, L., Schjønning, P., Elmholt, S., Munkholm, L. J. (2014): The effects of organic matter application and intensive tillage and traffic on soil structure formation and stability. – Soil and Tillage Research 136: 28-37.

http://www.aloki.hu ● ISSN 1589 1623 (Print) ● ISSN 1785 0037 (Online)
DOI: http://dx.doi.org/10.15666/aeer/1705_1074310757

[2] Abdullah, A. S. (2014): Minimum tillage and residue management increase soil water content, soil organic matter and canola seed yield and seed oil content in the semiarid areas of Northern Iraq. – Soil and Tillage Research 144: 150-155.
[3] Barrett, C. B., Bevis, L. E. M. (2015): The self-reinforcing feedback between low soil fertility and chronic poverty. – Nature Geoscience 8: 907-912.
[4] Batjes, N. H., Dijkshoorn, J. A. (1999): Carbon and nitrogen stocks in the soils of the Amazon Region. – Geoderma 89: 273-286.
[5] Batjes, N. H. (2016): Harmonized soil property values for broad-scale modelling (WISE30sec) with estimates of global soil carbon stocks. – Geoderma 269: 61-68.
[6] Cambardella, C. A., Moorman, T. B., Andrews, S. S., Karlen, D. L. (2004): Watershed-scale assessment of soil quality in the loess hills of southwest Iowa. – Soil and Tillage Research 78: 237-247.
[7] Das, B., Nordin, R., Mazumder, A. (2008): An alternative approach to reconstructing organic matter accumulation with contrasting watershed disturbance histories from lake sediments. – Environmental Pollution 155: 117-124.
[8] Degryze, S., Six, J., Paustian, K., Morris, S. J., Paul, E. A., Merckx, R. (2004): Soil organic carbon pool changes following land-use conversions. – Global Change Biology 10: 1120-1132.
[9] Dendoncker, N., Van Wesemael, B., Rounsevell, M. D. A., Roelandt, C., Lettens, S. (2004): Belgium's CO2 mitigation potential under improved cropland management. – Agriculture, Ecosystems & Environment 103: 101-116.
[10] Falloon, P., Smith, P., Bradley, R. I., Milne, R., Tomlinson, R. W., Viner, D., Livermore, M., Brown, T. (2006): RothCUK - a dynamic modelling system for estimating changes in soil C from mineral soils at 1-km resolution in the UK. – Soil Use and Management 22: 274-288.
[11] Gerzabek, M. H., Staunton, S. (2005): Editorial. – Journal of Environmental Radioactivity 81: 115-116.
[12] Gmach, M. R., Dias, B. O., Silva, C. A., Nóbrega, J. C. A., Lustosa-Filho, J. F., Siqueira-Neto, M. (2018): Soil organic matter dynamics and land-use change on Oxisols in the Cerrado, Brazil. – Geoderma Regional 14: e00178.
[13] He, B. (2002): The origin types and their characteristics of the lakes in Jianghan Plain. – Journal of central China normal university (natural science) 36: 241-244.
[14] Karlen, D. L., Kumar, A., Kanwar, R. S., Cambardella, C. A., Colvin, T. S. (1998): Tillage system effects on 15-year carbon-based and simulated N budgets in a tile-drained Iowa field. – Soil & Tillage Research 48: 155-165.
[15] Karlen, D. L., Cambardella, C. A., Kovar, J. L., Colvin, T. S. (2013a): Soil quality response to long-term tillage and crop rotation practices. – Soil and Tillage Research 133: 54-64.
[16] Karlen, D. L., Kovar, J. L., Cambardella, C. A., Colvin, T. S. (2013b): Thirty-year tillage effects on crop yield and soil fertility indicators. – Soil and Tillage Research 130: 24-41.
[17] Kölbl, A., Schad, P., Jahn, R., Amelung, W., Bannert, A., Cao, Z. H., Fiedler, S., Kalbitz, K., Lehndorff, E., Müller-Niggemann, C., Schloter, M., Schwark, L., Vogelsang, V., Wissing, L., Kögel-Knabner, I. (2014): Accelerated soil formation due to paddy management on marshlands (Zhejiang Province, China). – Geoderma 228-229: 67-89.
[18] Kukuļs, I., Kļaviņš, M., Nikodemus, O., Kasparinskis, R., Brūmelis, G. (2019): Changes in soil organic matter and soil humic substances following the afforestation of former agricultural lands in the boreal-nemoral ecotone (Latvia). – Geoderma Regional 15: e00213.
[19] Laik, R. (2004): Soil Carbon Sequestration Impacts on Global Climate Change and Food Security. – Science 304: 1623-1627.
[20] Laik, R., Kumar, K., Das, D. K., Chaturvedi, O. P. (2009): Labile soil organic matter pools in a calciorthent after 18 years of afforestation by different plantations. – Applied Soil Ecology 42: 71-78.

http://www.aloki.hu ● ISSN 1589 1623 (Print) ● ISSN 1785 0037 (Online)
DOI: http://dx.doi.org/10.15666/aeer/1705_1074310757

[21] Lal, R. (2002): Soil carbon dynamics in cropland and rangeland. – Environmrntal Pollution 116: 353-362.
[22] Lettens, S., Van Orshoven, J., Van Wesemael, B., Muys, B. (2004a): Soil organic and inorganic carbon contents of landscape units in Belgium derived using data from 1950 to 1970. – Soil Use and Management 20: 40-47.
[23] Lettens, S., Van Orshoven, J., Van Wesemael, B., Perrin, D., Roelandt, C. (2004b): The inventory-based approach for prediction of SOC change following land use change. – Biotechnologie, Agronomie, Societe et Environnement 8: 141-146.
[24] Manlay, R., Feller, C., Swift, M. J. (2007): Historical evolution of soil organic matter concepts and their relationships with the fertility and sustainability of cropping systems. – Agriculture, Ecosystems and Environment 119: 217-233.
[25] Miller, B. A., Koszinski, S., Hierold, W., Rogasik, H., Schröder, B., Van Oost, K., Wehrhan, M., Sommer, M. (2016): Towards mapping soil carbon landscapes: Issues of sampling scale and transferability. – Soil and Tillage Research 156: 194-208.
[26] Mirzaee, S., Ghorbani-Dashtaki, S., Mohammadi, J., Asadi, H., Asadzadeh, F. (2016): Spatial variability of soil organic matter using remote sensing dats. – Catena 145: 118-127.
[27] Nadi, M., Golchin, A., Sedaghati, E., Shafie, S., Hosseini fard, S. J., Füleky, G. (2017): Using Nuclear Magnetic Resonance 1H and 13C in soil organic matter covered by forest. – Journal of Water and Soil Science 21: 83-92.
[28] Ontl, T. A., Cambardella, C. A., Schulte, L. A., Kolka, R. K. (2015): Factors influencing soil aggregation and particulate organic matter responses to bioenergy crops across a topographic gradient. – Geoderma 255-256: 1-11.
[29] Osman, K. T. (2013): Soils: Principles, Properties and Management. – Springer Science + Business Media Dordrecht.
[30] Papienik, S. K., Lindstrom, M. J., Schumacher, T. E., Schumcher, J. A., Malo, D. D., Lobb, D. A. (2007): Charaterization of soil profiles in a landscape affected by long-term tillage. – Soil & Tillage Research 93: 335-345.
[31] Pulleman, M. M., Bouma, J., Van Essen, E. A., Meijles, E. W. (2000): Soil organic matter content as a function of different land use history. – Soil Science Society of America Journal 64: 689-693.
[32] Ratnayake, R. R., Karunaratne, S. B., Lessels, J. S., Yogenthiran, N., Rajapaksha, R. P. S. K., Gnanavelrajah, N. (2016): Digital soil mapping of organic carbon concentration in paddy growing soils of Northern Sri Lanka. – Geoderma Regional 7: 167-176.
[33] Schulp, C. J. E., Nabuurs, G., Verburg, P. H. (2008a): Future carbon sequestration in Europe—Effects of land use change. – Agriculture, Ecosystems & Environment 127: 251-264.
[34] Schulp, C. J. E., Veldkamp, A. (2008b): Long-term landscape – land use interactions as explaining factor for soil organic matter variability in Dutch agricultural landscapes. – Geoderma 146: 457-465.
[35] Schwanghart, W., Jarmer, T. (2011): Linking spatial patterns of soil organic carbon to topography — A case study from south-eastern Spain. – Geomorphology 126: 252-263.
[36] Singh, R. J., Deshwal, J. S., Sharma, N. K., Ghosh, B. N., Bhattacharyya, R. (2019): Effects of conservation tillage based agro-geo-textiles on resource conservation in sloping croplands of Indian Himalayan Region. – Soil and Tillage Research 191: 37-47.
[37] Smith, P., Powlson, D. S., Smith, J. U., Falloon, P., Coleman, K. (2000): Meeting the UK's climate change commitments: options for carbon mitigation on agricultural land. – Soil Use and Management 16: 1-11.
[38] Sun, Y., Wang, H., Huang, B. (2005): Analysis on the temporal and spatial change of cotton production of Hubei province. – Journal of Hubei University (Natural Science) 27: 385-388.

http://www.aloki.hu ● ISSN 1589 1623 (Print) ● ISSN 1785 0037 (Online)
DOI: http://dx.doi.org/10.15666/aeer/1705_1074310757

[39] Veldkamp, A., Kok, K., De Koning, G. H. J., Schoorl, J. M., Sonneveld, M. P. W., Verburg, P. H. (2001): Multi-scale system approaches in agronomic research at the landscape level. – Soil and Tillage Research 58: 129-140.
[40] Vitharana, U. W. A., Mishra, U., Mapa, R. B. (2019): National soil organic carbon estimates can improve global estimates. – Geoderma 337: 55-64.
[41] Walkley, A., Black, I. A. (1934): An examination of the degtjareff method for determining soil organic matter, and a proposed modification of the chromic acid titration method. – Soil Science 37: 29-38.
[42] Wang, H., Song, M., Xu, X., Tang, D., Ai, T. (2010): Land use pattern Diagnosis based on physical properties and vertical structures of anthrosols profiles. – The IASTED International Conference on Environmental management and Engineering. Banff, Canada.
[43] Webb, N. R. (1998): The Traditional Management of European Heathlands. – The Journal of Applied Ecology 35: 987-990.
[44] Wood, S., Tirfessa, D., Baudron, F. (2018): Soil organic matter underlies crop nutritional quality and productivity in smallholder agriculture. – Agriculture, Ecosystems and Envrinment 266: 100-108.
[45] Wu, J. (2011): Carbon accumulation in paddy ecosystems in subtropical China: evidence from landscape studies. – European Journal of Soil Science 62: 29-34.

http://www.aloki.hu ● ISSN 1589 1623 (Print) ● ISSN 1785 0037 (Online)
DOI: http://dx.doi.org/10.15666/aeer/1705_1074310757

DEVELOPMENT OF A MEASURING INSTRUMENT FOR RAPID DETECTION OF CADMIUM IONS IN WATER ENVIRONMENT

YANG, P.[1,2,3] – SHI, J. H.[1,2,3] – YU, Y. G.[1,2,3] – SUN, M.[1,2,3*]

[1]*College of Information and Electrical Engineering, China Agricultural University, Beijing 100083, China*

[2]*Key Laboratory of Agricultural Information Acquisition Technology, Ministry of Agriculture, Beijing 100083, China*

[3]*Beijing Engineering and Technology Research Center for Internet of Things in Agriculture, Beijing 100083, China*

**Corresponding author*
e-mail: sunming@cau.edu.cn; phone: +86-135-2055-7807

(Received 1st Mar 2019; accepted 21st May 2019)

Abstract. In this study, heavy metal cadmium ions (Cd^{2+}) in water environment were studied, and the existing Cd^{2+} colorimetric system was simplified. Based on colorimetry and spectroscopy, a portable analyzer for rapid detection of Cd^{2+} was developed. This study simplifies the tedious and complex pre-processing and completes the colorimetric experiment. The measuring instrument is mainly divided into an optical path module and a circuit module. The optical path module converts the concentration of cadmium ions into an optical signal, and the circuit module realizes functions of converting, amplifying, data processing, viewing management data, and uploading data of the optical signal. After the detector was completed, several system performance analyses were performed, and low power consumption, anti-interference, and repeatability tests were taken to verify the accuracy of the measurement. The experimental results show that the determination coefficient of the model and the chemical value of the colorimetric reaction is $R^2 = 0.934$, the detection limit is 0.1047 mg/L, the detection range is 0.1~1 mg/L, and the variation coefficient of cadmium content index is less than 1.0%. The test results show that the tester has good accuracy and repeatability. At the same time, compared with other related instruments, the meter also has the advantages of multiple functions, small size, portability, convenient use, and low power consumption.
Keywords: *cadmium ion, colorimetry, spectroscopy, analyzer, rapid detection*

Introduction

With the rapid development of modern industry, the danger of heavy metal pollution has become increasingly prominent. Cadmium is a highly toxic heavy metal and is a non-essential toxic element of the human body. It is called the "first of the five poisons" (Bairi et al., 2014; Chansuvarn, 2012). As early as 1974, the United Nations Environment Programme (UNEP) and the International Committee for Work Health and Heavy Metals identified it as a key pollutant . Numerous studies have shown that cadmium is carcinogenic, and the International Agency for Research on Cancer (IARC) classifies cadmium as the first class of human carcinogens (Chen et al., 2014; Chen et al., 2015). Wastewater containing cadmium is discharged into the environment. Cadmium has a strong enrichment effect in aquatic animals. Fish can be enriched 100,000 times. Once absorbed by the human body through the food chain, cadmium will selectively accumulate liver and kidney (Kim et al., 2012). Cadmium can also hinder the metabolism of bones, which is the main culprit for "pain sickness" (Fang,

http://www.aloki.hu ● ISSN 1589 1623 (Print) ● ISSN 1785 0037 (Online)
DOI: http://dx.doi.org/10.15666/aeer/1705_1075910766

2016). Therefore, it is especially important to study the efficient detection of cadmium ion concentration.

The current detection methods are: atomic emission spectroscopy, mass spectrometry, fluorescence analysis (Georgiev et al., 2014; Ghasemi, 2009), electrochemical analysis method (Han, 2013), spectrophotometry (Mohanty et al., 2018), atomic absorption spectrometry (Han et al., 2014; HJ-763, 2015). Atomic absorption spectroscopy (Huang et al., 2013; Huang et al., 2012) overcomes the shortcomings of the traditional method, which has the advantages of low detection line, easy operation, and fast analysis speed (Kai, 2015) However, the range of atomic absorption bands is narrow, and it is difficult to analyze complex samples. Spectrophotometry is simpler to choose from, simple and fast to operate, and has a wider range of applications, but it is relatively low in accuracy. Electrochemical analysis methods (Li, 2006), although the detection efficiency is high, the accuracy accuracy is limited. Mass spectrometry (Li, 2008;Mohan et al. ,2018) can quickly detect metal concentration on the basis of a small amount of reagents (Rajalakshmi, 2011;Banerjee et al. ,2008), but it has limitations in the field of organic mass spectrometry. The application of various methods provides different ideas for cadmium ion detection. (Wanget al. , 2003;Ying ,2013)

In recent years, there have been many research results for the measurement of cadmium ion colorimetry. Yuan Aiping used dry ashing to dissolve ash with warm 0.2 mol/L sulfuric acid, and added dithizone-carbon tetrachloride as a masking agent to eliminate copper interference in the matrix and used for cadmium in fish and meat foods. The detection limit of the method was 0.12 μg/L, and the recovery was 86%-112%. Fan Yueqin et al. studied the color reaction of the new reagent 4-methyl-2,5-disulfonylphenyldiazoaminoazobenzene with cadmium . In the presence of TritonX-100, the reagent forms a red complex with cadmium in a buffer solution of $Na_2B_4O_7$-NaOH at pH 10.5~11.5. The maximum absorption wavelength is 526 nm and the apparent molar absorptivity is 2.5×105 $L \cdot mol^{-1} \cdot cm^{-1}$. This study combines colorimetry and spectroscopy to simplify the complex and cumbersome pre-processing of colorimetric methods, transform Cd^{2+} into measurable compounds, construct detection models, and apply the model to portable spectrometers to develop low cost. Low detection limit, simple pre-treatment, suitable for a variety of heavy metal rapid detection instrument.

Materials and methods

Materials

The heavy metal cadmium ion (Cd^{2+}) was used as the research object. The test materials included dithizone, carbon tetrachloride, sodium tartrate, sodium hydroxide, hydroxylamine hydrochloride and distilled water. The instruments used are pH meters, beakers, electronic balances, centrifuge tubes, and the like. The test principle is that in a strong alkali sodium hydroxide solution, Cd^{2+} in the water sample can react with dithizone to form a red complex.

In the colorimetric experiment, dithizone was used as a color developer, and the solvent was carbon tetrachloride (CCl_4). In the experiment, sodium potassium tartrate solution was used as a masking agent to exclude magnesium, iron, calcium and aluminum ions to prevent these ions from forming hydroxide precipitates in an alkaline environment (Alfonso,2010; Zhang et al,2010). The colorimetric reaction can be carried

http://www.aloki.hu ● ISSN 1589 1623 (Print) ● ISSN 1785 0037 (Online)
DOI: http://dx.doi.org/10.15666/aeer/1705_1075910766

out under a strong alkaline environment and adjusted with a sodium hydroxide solution. As a color developing agent, dithizone has a molecular formula of $C_{13}H_{12}N_4S$, a blue-black crystalline powder, which is easily oxidized by air and can be protected by a hydroxylamine hydrochloride solution. (Zhang et al, 2015;Zhao et al,2011) Carbon tetrachloride is a colorless solution with large specific gravity, low viscosity, non-toxicity and good chemical stability. It is selected as a solvent for dithizone solution. After the dithizone is dissolved in carbon tetrachloride, the solution is blue-green, and the red complex formed by the colorimetric reaction with cadmium is obviously different, which meets the requirements of the colorimetric reaction.(Wu et al, 2015;Sponza et al,2011)

Methods

The specific test steps are as follows:

Solution preparation: test to simulate cadmium-containing water, prepare 66 gradients of cadmium solution from 0.001 to 1 mg/L with standard solution; configure 1 mg/L dithizone use solution, use carbon tetrachloride as solvent; configure 20% The hydroxylamine hydrochloride solution is used as a reducing medium; 10% sodium potassium tartrate solution is used as a masking agent; the colorimetric reaction can be carried out under a strong alkaline environment, and the sodium hydroxide solution is used for adjustment.

The maximum wavelength of the absorption of the magenta liquid after the reaction was measured by a visible spectrophotometer V-1300 was 530 nm, and did not change with the change of the concentration. Therefore, this study chose 530 nm as the incident light center wavelength.

The optical path portion is composed of an LED light source, a fiber optical path, and a silicon detector. The required light source band of the circuit is 530 nm. Select the LED plus filter to achieve the required narrow-band light source to ensure the monochromaticity of the light source. The filter has relatively stable performance, high transmittance, and can be well matched to the established model. After comparison, this study selected the LED light source of model E505-06 from Japan EPETEX and the filter of 530 nm center wavelength of INTOR Company of USA.

In order to enable the monochromatic light source to emit parallel light and vertically illuminate the detector, and simplify the structure of the instrument, this study uses a fixed fiber collimator as the optical path, and realizes the connection between the reaction black box and the circuit, as shown in *Figure 1*. One end of the fiber is the incident end, and the outside is a metal sleeve, which is used to fix the filter and the LED light source, to ensure the stability and reliability of the light source, and to reduce the experimental error. The structure is shown in *Figure 2*. In this study, a cuvette with a diameter of 1 cm was used as the absorption cell to carry the sample.

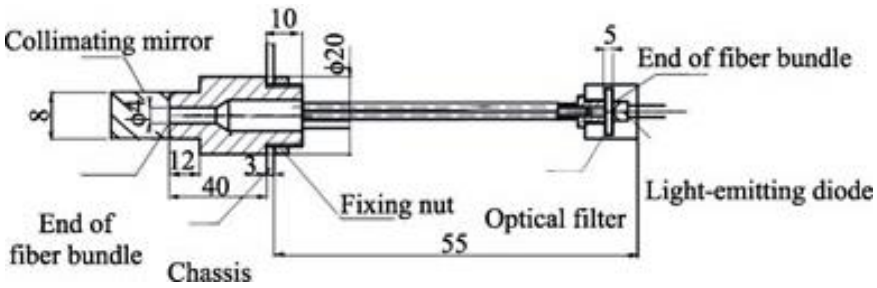

http://www.aloki.hu ● ISSN 1589 1623 (Print) ● ISSN 1785 0037 (Online)
DOI: http://dx.doi.org/10.15666/aeer/1705_1075910766

Figure 1. *Structure diagram of fiber channel*

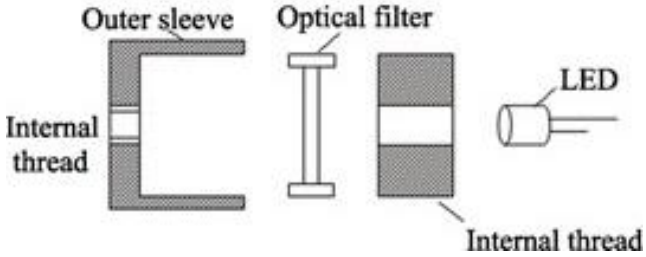

Figure 2. *Schematic diagram of metal sleeve*

The circuit module is mainly composed of a power supply circuit, a detection and amplification circuit, a keyboard circuit, a liquid crystal display circuit, etc., to realize conversion of an optical signal, amplification of an electric signal, attenuation of noise, and data processing and display functions. The instrument uses TI's low-power 16-bit microcontroller MSP430F149 as the controller of the system, with a 16-bit reduced instruction set to meet the rapid detection design of the analyzer.

The measuring instrument adopts a silicon material photodiode detector with a spectral response range of 300 to 1100 nm, and the model number is PS0308 (product of FIRST SENSOR, Germany), which effectively ensures the linearity of the instrument. Since the design circuit of this study works in a low frequency environment and requires good linearity, the photodiode is selected to work in zero bias mode without dark current error, and there is no need to design a reverse voltage bias circuit.

This design adopts full dot matrix graphic liquid crystal display CSME-12864, which has the advantages of low voltage, low consumption and good backlight mode. At the same time, this design uses membrane keyboard to realize functions of viewing, measuring, flipping, deleting, storing data, etc. powered by.

Results

The partial least squares method is combined with the above four different partitioning methods, combined with the MSC pretreatment method to establish a mathematical model of cadmium ion concentration and absorbance. The model has several evaluation indicators, and the model results are intuitive and specific through specific index values. Analysis, the results are shown in *Table 1*.

Table 1. *Comparison of different modeling set partitioning methods combined with PLS cadmium ion concentration prediction model*

Modeling set partitioning method	Main factor	Modeling set		Forecast set		RPD
		Rc	RMSECV	Rp	RMSEP	
RS	3	0.9427	0.1094	0.9131	0.1317	2.5074
KS	2	0.9619	0.0792	0.9201	0.1246	2.6101
SPXY	4	0.9662	0.0768	0.7068	0.1850	1.4455
Duplex	5	0.9550	0.0970	0.9549	0.0863	3.6142

http://www.aloki.hu ● ISSN 1589 1623 (Print) ● ISSN 1785 0037 (Online)
DOI: http://dx.doi.org/10.15666/aeer/1705_1075910766

From the analysis of *Table 1,* it can be known that the RS method divides the modeling set, the range does not cover all the samples, is not representative, and the established model is not stable enough. The model established by the Duplex method has the best detection and detection results. The RMSECV and RMSEP are 0.0970 mg/L and 0.0863 mg/L, respectively, which are small, and are smaller than other models. The RPD value is 3.3142 over 3, indicating that the model predicts better. Therefore, Duplex is selected as the model selection method of modeling set, and the PLS model of cadmium ion concentration is established by MSC pretreatment method. The model and prediction map of the obtained model are shown in *Figures 3* and *4,* and the sample is evenly distributed in the curve. Left and right, achieved a good prediction effect.

The test method is to prepare a set of lead standard solution 0.001~1 mg/L a total of 66 sets of gradient solution. The measurement was carried out by using a 530 nm light source with a bandwidth of 10 nm, and the linear regression analysis was obtained. The modeling results and test results are shown in *Figure 3.*

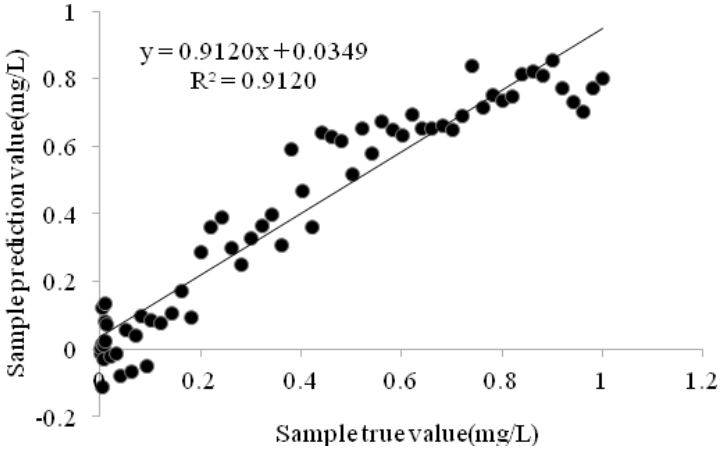

Figure 3. *Correlation between the actual value of Cd^{2+} concentration and the modeling set of predicted values*

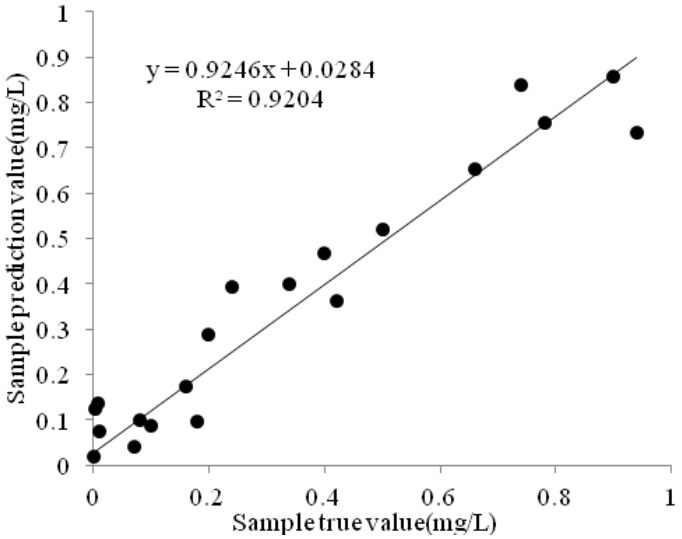

Figure 4. *Correlation between the true value of Cd^{2+} concentration and the validation set of predicted values*

http://www.aloki.hu ● ISSN 1589 1623 (Print) ● ISSN 1785 0037 (Online)
DOI: http://dx.doi.org/10.15666/aeer/1705_1075910766

The design is based on the colorimetric reaction of dithizone with cadmium ions, masking the interference of other heavy metal ions with masking agent, and optimizing the reaction environment, including pH, temperature and other influencing factors. The whole instrument is composed of optical path module and circuit module. The linear measurement range of the instrument is 0.1~1 mg/L, which can measure the low concentration of cadmium ions and achieve a certain precision. The national surface water environmental quality standard for cadmium ions is 0.01 mg/L, and the instrument meets the testing standards. The detection range of dithizone spectrophotometry in national standard is 0.01~0.3 mg/L. The detection range of this method meets the standard requirements, and the experimental operation is simple. Compared with the spectrophotometer, the optical path system of the instrument is simple in design, and the main structure is composed of LED, filter and optical fiber. The measurement room has good shading performance, can shield the influence of stray light, and has simple and reliable design. The instrument passed the repeatability test with a coefficient of variation of less than 1% and hardware and software anti-interference measures to make it have certain stability. The tester has certain innovations. The actual experimental verification results show that the prototype of this design has good repeatability and stability, and can be used for the measurement of cadmium ions in water.

Discussion

By comparing the detection range of the method to meet the standard requirements, the experimental operation is simple. Compared with the spectrophotometer, the optical path system of the instrument is simple in design, and the main structure is composed of LED, filter and optical fiber. The measurement room has good shading performance, can shield the influence of stray light, and the design is simple and reliable. The instrument passed the repeatability test with a coefficient of variation of less than 1% and hardware and software anti-interference measures to make it have certain stability. The tester has certain innovations. The actual experimental verification results show that the prototype of this design has good repeatability and stability, and can be used for the measurement of cadmium ions in water.

Conclusion and recommendation

In this study, heavy metal Cd^{2+} was used as the research object to simplify the existing Cd^{2+} colorimetric system, and a portable analyzer for Cd^{2+} rapid detection was developed.

(1) By analyzing the physicochemical properties of Cd^{2+} and the colorimetric reaction of cadmium with dithizone, the experimental scheme for the color reaction of dithizone with water-weight Cadmium metal in alkaline environment at normal temperature was determined, and a masking agent was used. Mask other ion interference.

(2) The detection range of the analyzer in this study is 0.1~1 mg/L, the coefficient of variation is less than 1%, and the repeatability test results are good. At the same time, the analyzer has simple and stable structure, low power consumption and portability. Further research on this analyzer can be carried out in future work to achieve rapid detection of various heavy metals in the actual water environment.

http://www.aloki.hu ● ISSN 1589 1623 (Print) ● ISSN 1785 0037 (Online)
DOI: http://dx.doi.org/10.15666/aeer/1705_1075910766

Acknowledgements. Fund for this research is provided by Development of the decision-making system in agricultural non-point source and heavy metal pollution management (No.2016YFD0800907).

REFERENCES

[1] Alfonso, M., Tarraga, A., Molina, P. (2010): Ferrocene-based multichannel molecular chemosensors with high selectivity and sensitivity for Pb(II) and Hg(II) metal cations. – Dalton Transactions 39(37): 8637-8645.

[2] Bairi, P., Chakraborty, P., Roy, B. (2014): Sensing of Hg^{2+}, and Ag^{+}, through a pH dependent FRET system: fabrication of molecular logic gates. – Sensors & Actuators B Chemical 193(3): 349-355 (in Chinese with English abstract).

[3] Banerjee, S., Kara, S., Santra, S. (2008): A simple strategy for quantum dot assisted selective detection of cadmium ions. – Chemical Communications 26: 3037-3039.

[4] Chansuvarn, W., Imyim, A. (2012): Visual and colorimetric detection of mercury(II) ion using gold nanoparticles stabilized with a dithia-diaza ligand. – Microchimica Acta 176(1): 57-64.

[5] Chen, G. H., Chen, W. Y., Yen, Y. C. (2014): Detection of mercury (II) ions using colorimetric gold nanoparticles on paper-based analytical devices. – Analytical Chemistry 86(14): 6843-6849.

[6] Chen, Z., Zhang, C., Tan, Y. (2015): Chitosan-functionalized gold nanoparticles for colorimetric detection of mercury ions based on chelation-induced aggregation. – Microchimica Acta 182(3): 611-616.

[7] Fang, Y. J., Xia, D. Z. (2016): Determination of cadmium ion binding ability of natural product extracts by spectrophotometry. – Chinese Journal of Traditional Chinese Medicine and Pharmacy 2: 295-298.

[8] Georgiev, N. I., Asiri, A. M., Qusti, A. H. (2014): Design and synthesis of pH-selective fluorescence sensing PAMAM light-harvesting dendrons based on 1,8-naphthalimides. – Sensors & Actuators B Chemical 190(1): 185-198.

[9] Ghasemi, J. B., Zohrabi, P. (2009): Spectrophotometric complexation study of 4-(2-Thiazolylazo) Resorcinol and Zn^{2+}, Cd^{2+}, Pb^{2+} and Cu^{2+} in 50% DMSO/water solution. – Chemia Analityczna 54(5): 1035-1049.

[10] Han, X. (2013): Detection of Heavy Metal Cadmium in Soil Based on Reagent Colorimetric and Spectral Analysis. – China Agricultural University, Beijing.

[11] Han, Z. X., Zhu, B. S., Wu, T. L., Yang, Q. Q., Xue, Y. L., Zhang, Z.,Wu, X. Y.(2014): A fluorescent probe for Hg^{2+}, sensing in solutions and living cells with a wide working pH range. – Chinese Chemical Letters 25(1): 73-76 (in Chinese with English abstract).

[12] HJ-763 (2015): Specifications and test procedures for automatic monitoring of cadmium in water.

[13] Huang, J., Li, M. X., Liang, X. F. (2013): Rapid determination of lead in tin alloy jewelry by dithizone colorimetric method. – Journal of Inspection and Quarantine 2: 5-8.

[14] Huang, X. W., Zhao, Z. X., Li, H. S., Wang, F. S. (2012): Determination of trace mercury by ultrasonic anodic stripping voltammetry. – Chemical Reagents 34(6): 532-534.

[15] Kai, Y. (2015): Determination of trace cadmium in soil by complex spectrophotometry. – Trace Elements and Health Research 32(1): 66-67.

[16] Kang, R. Q., Yang, S., Wang, Y. L. (2014): Determination of cadmium in cosmetics in a city by flame atomic absorption spectrophotometry. – Chemical Engineer 28(12): 21-23.

[17] Kim, H. N., Ren, W. X., Kim, J. S. (2012): Fluorescent and colorimetric sensors for detection of lead, cadmium, and mercury ions – Chemical society reviews 41(8):3210-3244.

[18] Kim, I. B., Bunz, U. H. (2011): Modulating the sensory response of a conjugated polymer by proteins: an agglutination assay for mercury ions in water. – Journal of the American Chemical Society 128(9): 2818-2819

http://www.aloki.hu ● ISSN 1589 1623 (Print) ● ISSN 1785 0037 (Online)
DOI: http://dx.doi.org/10.15666/aeer/1705_1075910766

[19] Li, M. Z. (2006): Spectral Analysis Technology and Its Application. – Science Press, Beijing.
[20] Li, Y. Q. (2008): Progress in the application of atomic absorption spectrometry in the analysis of heavy metal cadmium and cadmium. – Metallurgical Analysis 28(6): 33-41.
[21] Mohan, B. K., Padhy, R., Mohapatra, M., Sabat, G., Behera, S. K., Jena, S., Behera, J. K. (2018): Physio-Chemical analysisi of wastewater samples from drainage systems of Berhampur muncipality area of Odisha. – International Journal of Plant, Animal and Environmental Sciences 8(4): 1-5.
[22] Rajalakshmi, K., Haribabu, T. E., Sudha, P. N. (2011): Toxic kinetics of antioxidants from P. tricornutum and calendula exposed to heavy metal lead. – International Journal of Plant, Animal and Environmental Sciences 1(2): 105-109.
[23] Sponza, D., Karaogiu, N. (2002): Environmental geo chemistry and pollution studies of Aliage metal industry district.– Environment International 27:541-553.
[24] Wang, Z. K., Xu, J. W., Guo, M. (2003): Research progress in detection technology of heavy metal cadmium ions. – 68(486): 167-82.Xu, S. X., Wang, B. (2016): Determination of cadmium residues in vegetables by dithizone method. – Anhui Agricultural Sciences 44(14): 109-110.
[25] Wu, F., Mao, M., Cen,Y. (2017): Copolymerization of Eu(TTA) 3Phen doped styrene and methyl methacrylate nanoparticles and use in quantitative detection of pepsinogen – Rsc Advances 702(1): 102-108.
[26] Ying, H. J. (2013): Research and Development of Heavy Metal Ion Sensors. – Jiangnan University, Wuxi.
[27] Zhang, G., Zhao, G. Q., Jiang, J. J. (2010): Study on enzymatic detection of cadmium ions in foods. – Food Engineering: 51-53.
[28] Zhang, Z. H., Wang, Z. Q., Wang, H., Duan, Y. Y., Liu, G. (2015): Design and experiment of rapid detection system for soil cadmium element. – Journal of China Agricultural University 20(1): 157-163.
[29] Zhao, H., Nan. T., Tan, G. (2011): Development of two highly sensitive immunoassays for detection of copper ions and a suite of relevant immunochemicals – Analytica Chimica acta 702(1):102-108.

http://www.aloki.hu ● ISSN 1589 1623 (Print) ● ISSN 1785 0037 (Online)
DOI: http://dx.doi.org/10.15666/aeer/1705_1075910766

THE INFLUENCE OF EELGRASS (*ZOSTERA MARINA* L.) ON THE ENVIRONMENTAL FACTORS AND THE MICROBIAL COMMUNITIES IN SEDIMENT FROM SHUANGDAO BAY OF CHINA

LV, X. F. – YU, P. –WANG, X. L. – LI, Y. C.*

Marine College, Shandong University, Wenhua Xi Road 180, Weihai, Shandong, China

**Corresponding author*
e-mail: li_yuchun@sdu.edu.cn; phone: +86-135-6215-7118; fax: +86-631-568-8303

(Received 1st Mar 2019; accepted 21st May 2019)

Abstract. *Zostera marina* is a perennial seagrass that is widespread on temperate coasts around the world. Some studies have showed that the presence of *Z. marina* in marine environments influences the microbial communities in sediment collected from Shuangdao Bay of China. To investigate the impact of *Z. marina*, the environmental factors and microbial communities in sediments collected in the eelgrass beds and adjacent unvegetated area, were examined. Several environmental factors and microbial communities composition differed significantly between the two areas. The content of total-phosphate and NH_4^+-N in the sediments of eelgrass beds were lower than the sediments of the unvegetated area, while the bacterial abundance and diversity in eelgrass bed were greater than that of unvegetated area. The most abundant bacteria found in sediments were Proteobacteria, Bacteroidetes, Planctomycetes and Acidobacteria, while the bacterial community structures were significantly different between the two areas. The changes found in the environmental factors and microbial communities were mainly attributed to the presence of *Z. marina*. This study may provide further understanding of the effects of *Z. marina*, which may be vital to the regulation of the marine environment.
Keywords: *Zostera marina, environmental factors, microbial communities, marine sediments, marine environment*

Introduction

Seagrasses are a unique group of plants that comprise 60 monocotyledonous angiosperm species (Hemminga and Duarte, 2002) that grow in coastal sediments in shallow coastal zones (Fonseca, 1998; Lebreton et al., 2012). *Zostera marina* is one of the most common seagrasses and distributed mainly in temperate regions of the northern hemispheres (Short et al., 2007; Zhou et al., 2015). Eelgrass meadow can provide a valuable habitat and food source for many invertebrates and fishes (Gillanders, 2006).

In recent years, many studies on *Z. marina* have focused on its biological processes that are related to photosynthesis, nitrogen fixation and restoration (Goodman et al., 1995; McGlathery et al., 1998; Marion, 2010). Eelgrass link sediment and nutrient cycles providing several vital coastal ecosystem functions (Harlin et al., 1981), so their protection and restoration are important. Many bacterial species found in the sediments of eelgrass bed are absent in sediment habitats outside of eelgrass bed (Campbell et al., 1990; Shieh et al., 1997). Several studies showed that bacteria inhabit the roots of the eelgrasses (Kuo et al., 1981; Kurtz et al., 2003; Küsel et al., 1999; Nielsen et al., 1999) and may form synergistic relationships. Eelgrass can excrete amino acids and sugars from their roots, thereby create suitable niches for a wide variety of microorganisms in the rhizosphere (Lee et al., 2000; Holmer et al., 2001; Jensen et al., 2005). Double

http://www.aloki.hu ● ISSN 1589 1623 (Print) ● ISSN 1785 0037 (Online)
DOI: http://dx.doi.org/10.15666/aeer/1705_1076710779

gradient denaturing gradient gel electrophoresis (DG-DGGE) was used to investigate several factors' impact on bacterial community diversity, and the results suggests that vegetation and season exert stronger controls on microbial community structure (James et al., 2006). Jensen et al., found that eelgrass can affect microbial processes in the rhizoplane via the excretion of amino acids and sugars. Significant differences in the bacterial communities associated with the roots and the bulk sediment associated with *Z. marina* have been found (Jensen et al., 2007), and the presence of roots could favour the growth of particular bacteria. Few studies to date have examined the effects of the eelgrass meadow on the environmental factors and bacterial communities.

In this study, we used a variety of methods to measure the environmental factors in sediments collected from eelgrass meadow and unvegetated area. We then characterized the richness, diversity, similarity, and composition of the microbial communities. In addition, root-specific bacteria were also analysed.

Materials and methods

Study area and sampling

Shuangdao Bay is located in Weihai, which lies within the Shandong Peninsula in northern China (N37°28.5′-37°29.2′, E121°57.5′-122°58.5′). The sample S1 (N37°29.087′, E121°58.267′) was collected from the sediments in eelgrass meadow, while sample S2 (N37°29.045′, E121°58.286′) was collected from the sediments in adjacent unvegetated area (*Fig. 1*). S0, S40, and S80 were collected from the sediments of a single plant. The sediment taken from the root of *Z. marina* was designated S0 (N37°29.073′, E121°58.306′), and the sediments taken from 40 and 80 cm away from the root were designated as S40 and S80, respectively. The S40 and S80 samples are a mixture of four samples taken from the circumference of the sampling zone. Samples were collected in April 2015.

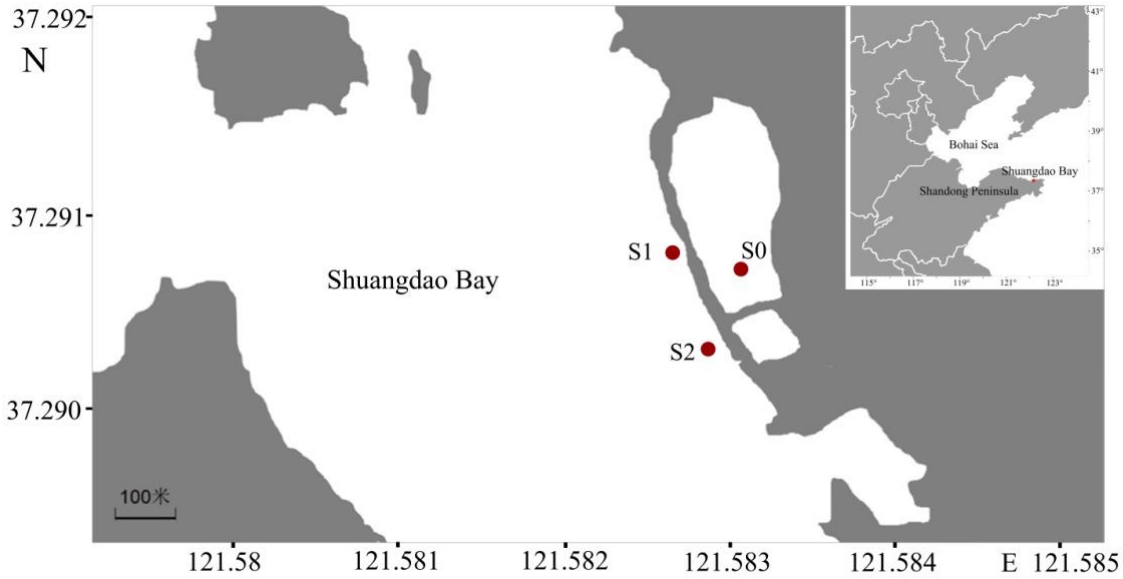

Figure 1. *Sampling area in Shuangdao Bay, Shandong Peninsula, China. Sediments were sampled in eelgrass beds (S1) and in adjacent unvegetated area (S2)*

http://www.aloki.hu ● ISSN 1589 1623 (Print) ● ISSN 1785 0037 (Online)
DOI: http://dx.doi.org/10.15666/aeer/1705_1076710779

In each sampling location, a composite sediment sample was collected at a depth of approximately 0–10 cm using a bottom sampler. Each fresh composite sample was subdivided into two subsamples, one of which was stored at -80 °C prior to bacterial 16S ribosomal ribonucleic acid (rRNA) gene sequencing, while the other was freeze-dried and tested to determine the levels of elemental factors that included salinity and nutrition factors such as sediment organic matter (SOM), total-nitrogen (TN), total-phosphate (TP), NO_3^-, NO_2^-, NH_4^+, PO_4^{3-} and water-soluble sulfide (WS).

Determination of environmental parameters in sediment

The contents of SOM and WS were determined by using the muffle furnace heating methodand $BaSO_4$ turbidimetry (Lv et al., 2018), respectively; three replicates were performed for each measurement. The TN/TP extract solution was obtained using a simultaneous preparation method (Li et al., 2007) and the contents of TN and TP were determined by using zinc cadmium reduction and the phosphomolybdenum blue method, which utilizes the reduction of ascorbic acid for specific ions according to the oceanographic survey GB17378.5-2007, respectively. NO_3^- was determined using zinc cadmium reduction, while NH_4^+ was detected using the indophenol blue method described in GB17378.5-2007. One-way ANOVA (Wolfram Mathematic 11.3) was used and the LSD-t tests were performed to compare TN, TP, WS, SOM, NH_4^+ and NO_3^- between different samples. Differences were deemed significant at $P < 0.05$ and extremely significant at $P < 0.01$. Values are means ± SD (n = 3).

DNA extraction, clone library construction, PCR amplification and high-throughput sequencing

The PowerSoil DNA Isolation Kit (TineGene Limited Company, Shanghai) was used to extract the genomic DNA. The DNA library was established using a two-step PCR amplification method, and the sequencing was conducted on an Illumina Miseq 16S rDNA system. The PCR primer sequences used to amplify the V4-V5 region within the bacterial DNA are shown in *Table 1*. The 16S rDNA sequences of S1 and S2 have been deposited in the NCBI Sequence Read Archive under accession number PRJNA506488. The 16S rDNA sequences of S0, S40 and S80 have been deposited in the NCBI Sequence Read Archive under accession number SRP158072.

Table 1. *The PCR primers sequences for amplifying bacterial DNA*

Primer name		Sequence (5'-3')
16SrDNA (1st amplification)	515F	AATGATACGGCGACCACCGAGATCTACACNNNNNNNNTCTTTCCCTAC ACGACGCTCTTCCGATCTGTGCCAGCMGCCGCGGTAA
	926R	CAAGCAGAAGACGGCATACGAGATNNNNNNNNGTGACTGGAGTTCCTT GGCACCCGAGAATTCCACCGTCAATTCMTTTGAGTTT
16SrDNA (2nd amplification)	515F (Inner)	TTCCCTACACGACGCTCTTCCGATCTGTGCCAGCMGCCGCGGTAA
	515F (Outer)	AATGATACGGCGACCACCGAGATCTACACNNNNNNNNTCTTTCCCTAC ACGACGCTC
	926R (Inner)	GAGTTCCTTGGCACCCGAGAATTCCACCGTCAATTCMTTTGAGTTT
	926R (Outer)	CAAGCAGAAGACGGCATACGAGATNNNNNNNNGTGACTGGAGTTCCTT GGCACCCGAGA

http://www.aloki.hu ● ISSN 1589 1623 (Print) ● ISSN 1785 0037 (Online)
DOI: http://dx.doi.org/10.15666/aeer/1705_1076710779

Data analyses

Paired-end reads were assigned to each sample based on their unique barcode and were truncated by cutting off the bar code and primer sequence. Split sequences for each sample were merged using FLASH V1.2.7 (Magoc and Salzberg, 2011), and the splicing sequences were called raw tags. Quality filtering on the rawtags was performed under specific filtering conditions to obtain the high-quality clean tags according to the QIIME quality-controlled process (Caporaso et al., 2011). The tags were compared with the reference database using UCHIME algorithm (Edgar et al., 2011; UCHIME, 2011) to detect chimera sequences, and then the chimera sequences were removed, finally obtaining the effective tags. Using the USEARCH and Perl scripts, the sequences retained were analyzed following the UPARSE pipeline to generate an operational taxonomic unit (OTU) table and pick representative sequences (Edgar, 2013). The sequences with a length shorter than 200 bp and singletons were removed. The retained sequences were were aligned with the 16S rDNA sequences using Silva 119 (http://www.arb-silva.de/) in order to annotate the species based on 97% sequence similarity using the average neighbour method. Taxonomical assignments of OTUs were executed using MOTHUR 1.33.3. OTU abundance information was normalized using a standard sequence number corresponding to the sample with the least sequences. Rarefaction analysis was performed to compare the relative levels of OTU richness across all sediment samples at an OTU cutoff of 0.03 (Xu et al., 2017). Principal components analysis (PCA) of the PCORD5 is used to examine the relationship between the microbial community (phyla) and environmental factors. All data are tested for normal distributions before ANOVA. Figures are prepared by PCORD5.

Results

Determination of environmental factors in sediment

Compared with S2, the contents of TP (LSD-t = 113.12, $p < 0.01$) and NH_4^+ (LSD-t = 7.41, $p < 0.01$) in S1 were significantly reduced, while the contents of other factors have no significant differences (*Fig. 2*). To explore whether these differences were caused by the presence of eelgrass, we examined these environmental factors in the sediment near its roots (S0), as well as 40 cm (S40) and 80 cm (S80) from the roots. The contents of NH_4^+ (LSD-t = 0.007825, $p < 0.05$) and TP (LSD-t = 0.02093, $p < 0.05$) in S0 were lower than that of S40 and S80 (*Fig. 3*). In conclusion, the sediment in eelgrass meadow contains lower levels of TP and NH_4^+ than that of unvegetaed area.

Microorganism richness and diversity

After processing, 33424 and 27009 high-quality sequences were obtained from S1 and S2, respectively. A total of 9640 OTUs were obtained for the samples at 3% dissimilarity (*Table 2*). The abundance indices (Chao and Ace indexes) of S1 were both higher than that of sample S2, while the diversity indices (Shannon and Simpson indexes) were lower than that of sample S2. These results suggested that the bacterial abundance and diversity in the sediment of eelgrass meadow were greater than that of unvegetated area. In the same way, we measured the microorganism richness and diversity in S0, S40 and S80. After processing, 72720, 53733 and 25842 high-quality sequences were obtained from these samples, and a total of 15232 OTUs were obtained

http://www.aloki.hu ● ISSN 1589 1623 (Print) ● ISSN 1785 0037 (Online)
DOI: http://dx.doi.org/10.15666/aeer/1705_1076710779

(*Table 2*). As shown in *Table 2*, the bacteria diversity and richness in the sediment near the roots (S0 and S40) were greater than that of sediment far from the roots (S80).

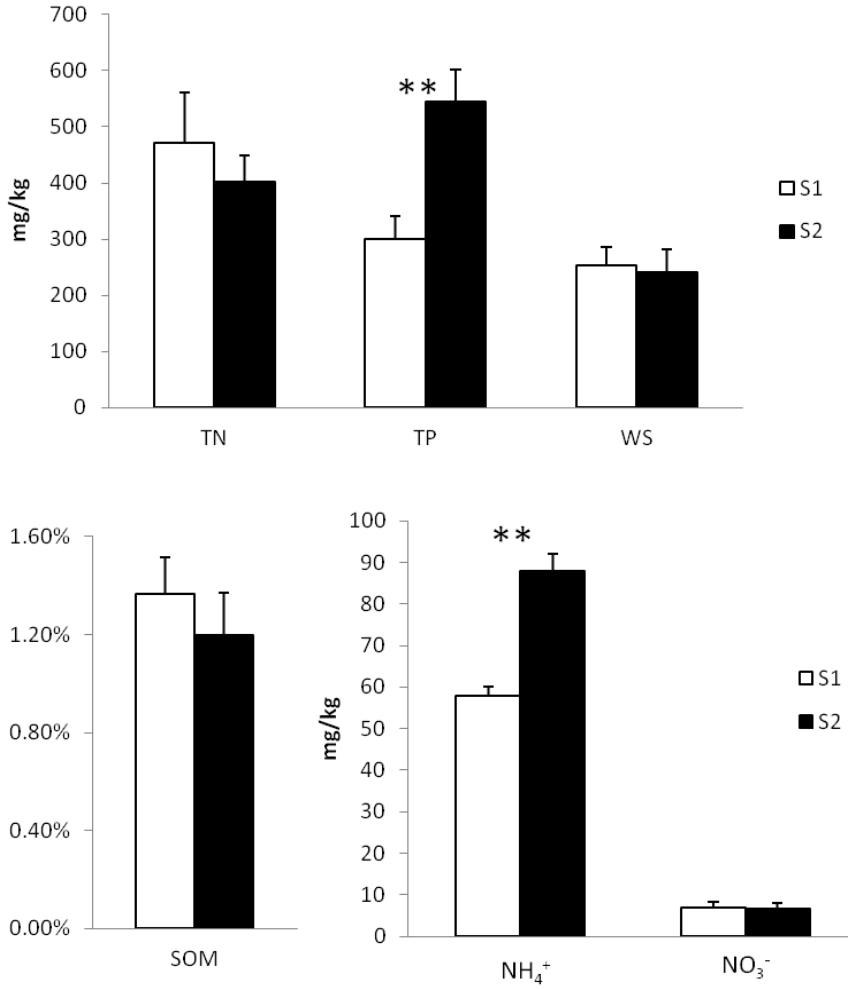

Figure 2. *The change of environmental factors in the sediments. Values are means ± SD (n = 3). *P < 0.01. TN: total-nitrogen; TP: total-phosphate; WS: water-soluble sulfide; SOM: sediment organic matter*

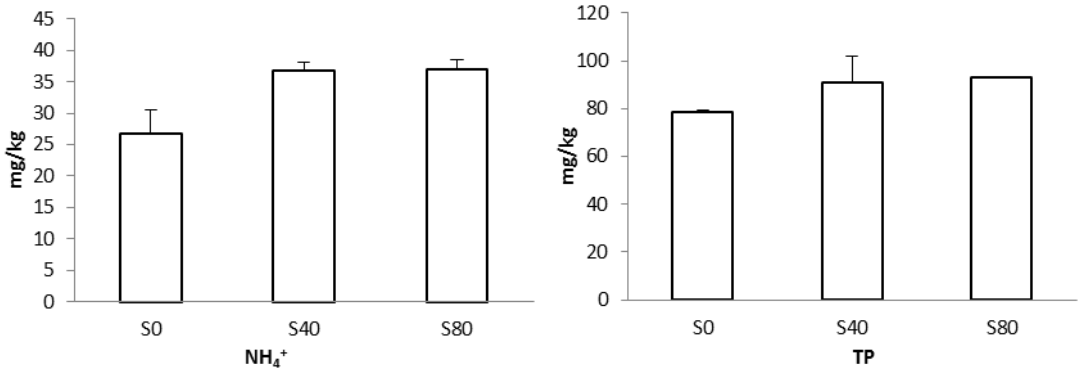

Figure 3. *The contents of NH_4^+ and TP in the S0, S40 and S80. Values are means ± SD (n = 3). * P < 0.05. TP: total-phosphate*

http://www.aloki.hu ● ISSN 1589 1623 (Print) ● ISSN 1785 0037 (Online)
DOI: http://dx.doi.org/10.15666/aeer/1705_1076710779

Table 2. *The community richness and diversity in different samples*

Sample	OTU numbers	Coverage	Chao index	Ace index	Shannon index	Simpson index
S1	5260	84.3	11668	24097	7.05	0.0042
S2	4380	85.8	10315	16090	7.03	0.0036
S0	5735	92.1	11957.1	16241.4	6.9	0.0049
S40	5455	88.3	12717.0	19374.8	7.0	0.0046
S80	4042	90.1	9225.0	14475.2	6.5	0.0067

Comparison of microbial communities among different samples

To assess the variation in the microbial communities, the compositions of taxa at the phyla and class levels are represented in a pie chart (*Figs. 4* and *5*). A significant difference in bacterial community was found between eelgrass beds and adjacent unvegetated area. At the level of phyla (*Fig. 4)*, the most abundant phylum represented within each sample was Proteobacteria, which comprised 48% and 53% of the reads from S1 and S2.

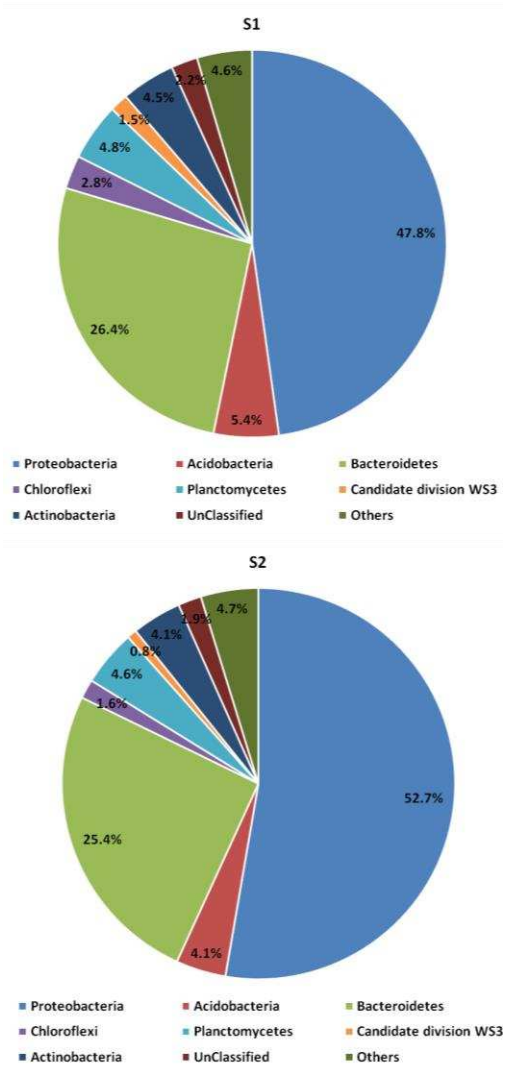

Figure 4. *The diagram for different samples's microbial communities at phylum level*

http://www.aloki.hu ● ISSN 1589 1623 (Print) ● ISSN 1785 0037 (Online)
DOI: http://dx.doi.org/10.15666/aeer/1705_1076710779

The relative abundances of Proteobacteria, Gemmatimonadetes, Cyanobacteria and Chlamydiae were higher in the sediment of eelgrass meadow, while the relative abundances of Bacteroidetes, Firmicutes, Deferribacteres, Planctomycetes and Chlorobi were higher ($P < 0.05$) in the sediment of adjacent unvegetated area. At the level of class (*Fig. 5)*, the relative abundance of Gemmaproteobacteria was higher in the presence of eelgrass, while the relative abundances of Alphaproteobacteria, Flavobacteriia, Sphingobacteriia and Planctomycetacia were higher ($P < 0.05$) in the absence of eelgrass.

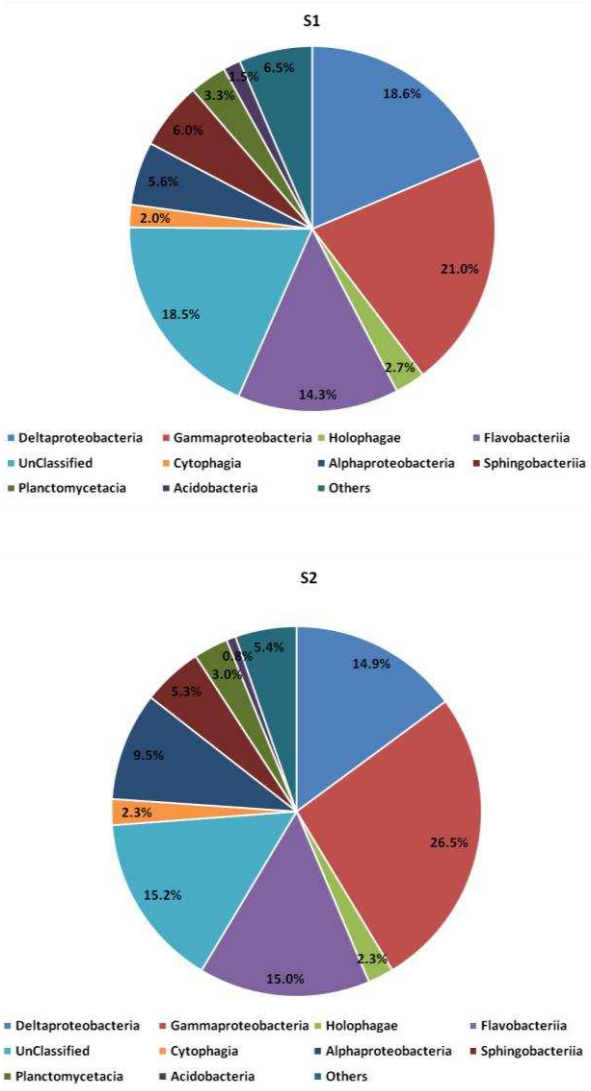

Figure 5. *The diagram for different samples's microbial communities at class level*

Microbial community and environmental conditions

Sediment properties are listed in *Figures 2* and *3*. The sediment in eelgrass meadow had much lower TP and NH_4^+ contents. The PCA analysis showed that PC1 and PC2 explained 56.246% and 18.277% of the bacterial phyla, respectively. The changes of microbial community composition in S1 and S2 were mainly attributed to NH_4^+, NO_3^- and TN (*Fig. 6*).

http://www.aloki.hu ● ISSN 1589 1623 (Print) ● ISSN 1785 0037 (Online)
DOI: http://dx.doi.org/10.15666/aeer/1705_1076710779

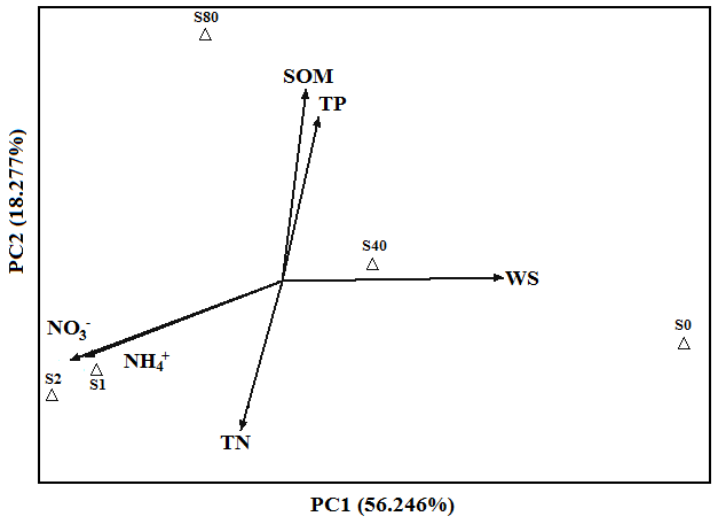

Figure 6. *Principal components analysis (PCA) of the microbial community composition and sediment properties on the basis of the relative abundance of bacterial phyla*

Root-specific bacteria

To obtain the root-specific bacteria of eelgrass, we analysed the OTUs specifically detected in S0. The results showed that there were 2654 unique OTUs detected within the roots of *Z. marina*, and the OTU size was 3464. Among these, 601 OTUs were identifiable at the family level, 302 at the genus level, and 11 at the species level. At the family level, the identified bacteria were Alicyclobacillaceae, Anaerolineaceae, Desulfobacteraceae, Desulfobulbaceae, Flavobacteriaceae, Planctomycetaceae and Spirochaetaceae. At the genus level, the identified bacteria were *Coxiella*, *Desulfococcus*, *Desulfobulbus*, *Acidiferrobacter*, *Geobacter*, *Sulfurovum*, *Rhodopirellula* and *Spirochete*. The eleven identified species were *Bacillus hwajinpoensis*, *Bacillus algicola*, *Brevundimonas bullata*, *Brevundimonas vesicularis*, *Paenibacillus provencensis*, *Roseiovarius aestuarii*, *Labrenzia marina*, *Lewinella nigricans*, *Sphingomonas paucimobilis*, *Ruditapes philippinarum*, and *Stenotrophomonas acidaminiphila*.

Discussion

Influence on environmental factors

The sediment in eelgrass meadow contains low levels of TP and NH_4^+ (*Figs. 2* and *3*). In this study, the content of NH_4^+ was significantly lower in eelgrass meadow which may be due to the vigorous ammonium absorption process in the roots (Hemminga et al., 1994). The contents of the other environmental factors such as organic matter have no significant difference in eelgrass meadow and unvegetated area which is consistent with previous research (Xu et al., 2016). From the above results, we speculate that nitrogen metabolism and phosphorus metabolism in the sediments inside eelgrass meadow are more vigorous than those outside eelgrass meadow, while there is no significant difference in carbon metabolism and sulfur metabolism. These environmental factors are considered to have been influenced by the presence of eelgrass, then influence the growth of particular bacteria.

http://www.aloki.hu ● ISSN 1589 1623 (Print) ● ISSN 1785 0037 (Online)
DOI: http://dx.doi.org/10.15666/aeer/1705_1076710779

Variation in the bacterial community and ecological functioning

The coverage index for all of the samples in this study was estimated to be between 84.3% and 92.1%, which indicated that the results of the high-throughput sequencing most likely encompass most of the microbial organisms in the sediment. The richness and diversity analysis indicated that the bacterial abundance and diversity in eelgrass meadow were greater than in the unvegetated areas (*Table 2*), which may be related to the metabolic cycle or root exudates of *Z. marina*.

Proteobacteria is the most abundant phylum of bacteria in many coastal areas (Hu et al., 2014; Li et al., 2016). In the present study, this phenomenon is laso observed, and the dominance of *Proteobacteria* does not change in different samples (*Fig. 4*). In this study, the microbial community structures were analyzed on the basis of two approaches: eelgrass meadow analysis (*Figs. 4* and *5*) and single eelgrass analysis (*Fig. 7*). The two different approaches did not return similar result. The results suggested that the bacteria communities in sediment were complex. The results indicate that the first approach is more representative of the effect of eelgrass on microbial communities in sediments, as the effects of individual plant is limited.

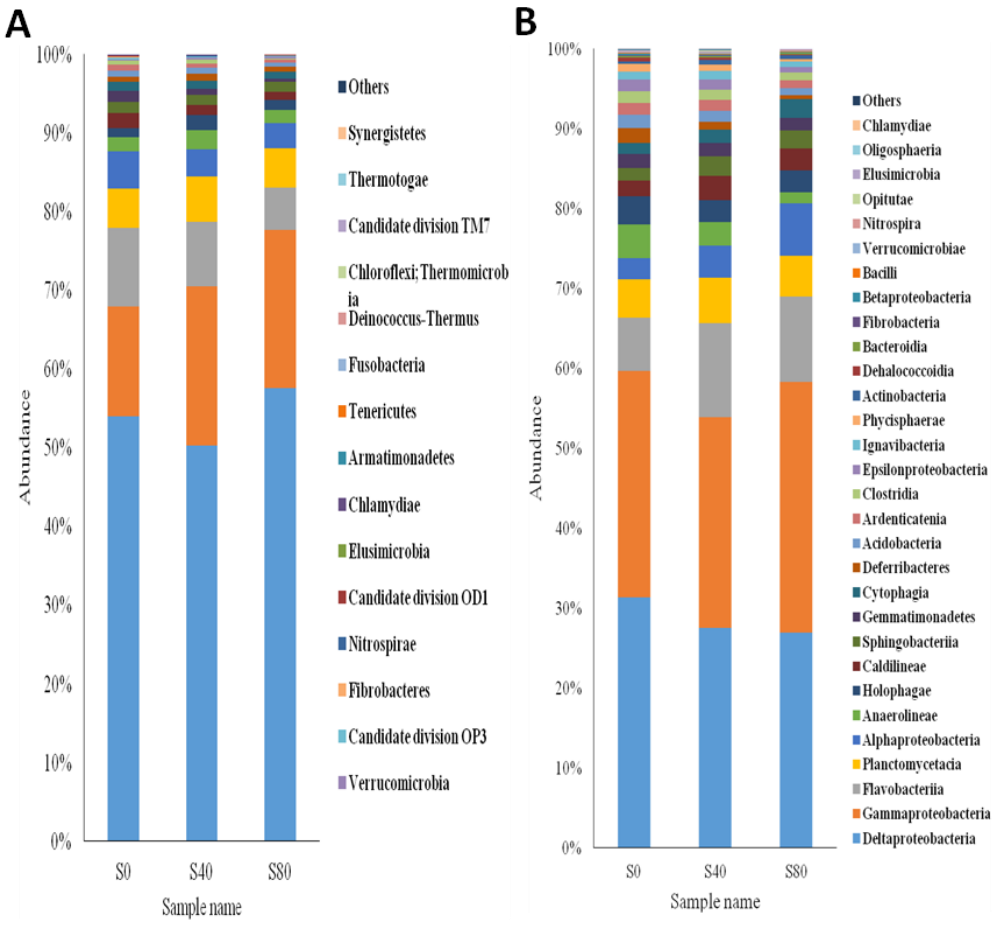

Figure 7. *The diagram for different samples' microbial communities at phylum level (A) and class level (B)*

Nutrient loading was reported to regulate the shifts in microbial structure and diversity in sediment along the river (Wang et al., 2018). Previous studies reported that

http://www.aloki.hu ● ISSN 1589 1623 (Print) ● ISSN 1785 0037 (Online)
DOI: http://dx.doi.org/10.15666/aeer/1705_1076710779

microbial biomass in saline environments was increased by an addition of easily decomposable substrate (Yan and Marschner, 2012), and TN is the main factor increasing the microbial biomass (Li et al., 2016). In this study, the S1 (in eelgrass meadow) and S2 (in unvegetated area) sites had apparently different bacterial phylum structure, which was found to be attributed to NH_4^+, NO_3^- and TN (*Fig. 6*). On the basis of the environmental properties results, we believe that NH_4^+ content in sediment influence the microbial community structure of eelgrass meadow.

Root-specific microorganisms

Root-specific microorganisms were analyzed through single eelgrass analysis. The results showed that there were 2654 unique OTUs detected within the roots of *Z. marina*, while there were 5735 OTUs detected. The result indicated that the microbial community structure and diversity in the area near the roots of eelgrass are significantly different from the surrounding environment. There abundance of *Rhodopirellula* in habitats with eelgrass was lower than that of unvegetated area. As a kind of Planctomycetes, *Rhodopirellula* has an anaerobic ammonium oxidation function (Wecker et al., 2010). It is speculated that the nitrogen cycle in sediments with eelgrass is more vigorous, and the conversion of ammonium is more rapid, which is also consistent with the ammonium content of the sample S1 below the sample S2 (*Fig. 2*). The microorganisms specifically detected in the roots of eelgrass may be closely related to their growth, which reflect the influence of eelgrass meadow on environmental factors and microbial community.

Based on the current and previous studies, we proposed that microbial community composition was closely related to environmental factors which may be influenced by the presence of eelgrass. However, more studies are needed on whether the sediments' microbial community compositions in different areas have the same trend.

Conclusions

Based on the measurements of the environmental factors, the sediments in eelgrass meadow have low levels of NH_4^+ and TP. The abundance and diversity of the microorganisms in the sediment with eelgrass were greater than in the sediment without eelgrass. In addition, significantly differences were observed in the microbial community composition between eelgrass meadow and unvegetated aera. Therefore, we speculate that the changes in the structure of the microbial community in the sediments with eelgrass are closely related to the vigorous N and P metabolism.

Acknowledgements. We thank Weiteng Mao and Zhaoyang Hua for sediment sampling, Haonan Wu for statistical analysis. This research was funded by the Shandong Province Natural Science Foundation (Grant No. ZR2014DP006) and Weihai Ocean Institute Project (Grant No. 1070413421424).

REFERENCES

[1] Campbell, R., Greaves, M. P. (1990): Anatomy and Community Structure of the Rhizosphere. – In: Lynch, J. M. (ed.) The Rhizosphere. John Wiley & Sons, Chichester, pp. 11-34.

http://www.aloki.hu ● ISSN 1589 1623 (Print) ● ISSN 1785 0037 (Online)
DOI: http://dx.doi.org/10.15666/aeer/1705_1076710779

[2] Caporaso, J. G., Lauber, C. L., Walters, W. A., Berg-Lyons, D., Lozupone, C. A. Turnbaugh, P. J., Fierer, N., Knight, R. (2011): Global patterns of 16S rRNA diversity at a depth of millions of sequences per sample. – Proceedings of the National Academy of Sciences of the United States of America 108(25): 4516-4522. DOI: 10.1073/pnas.1000080107.
[3] Edgar, R. C. (2013): UPARSE: Highly accurate OTU sequences from microbial amplicon reads. – Nature Methods 10(10): 996-998. DOI: 10.1038/NMETH.2604.
[4] Edgar, R. C., Haas, B. J., Clemente, J. C., Quince, C., Knight, R. (2011): UCHIME improves sensitivity and speed of chimera detection. – Bioinformatics 27(16): 2194-2200. DOI: 10.1093/bioinformatics/btr381.
[5] Fonseca, M., Julius, B. E., Kenworthy, W. J. (1998): Integrating biology and economics in seagrass restoration: how much is enough and why. – NOAA Conf. on Goal Setting and Success Criteria for Coastal Habitat Restoration, Charleston, SC, pp. 12-14. DOI: 10.1016/S0925-8574(00)00078-1.
[6] Gillanders, B. M. (2006): Seagrasses, Fish and Fisheries. – In: Larkum, A. D. W., Orth, R. J., Duarte, C. M. (eds.) Seagrasses: Biology, Ecology and Conservation. Springer, Dordrecht, pp. 503-536. DOI: 10.1007/978-1-4020-2983-7.
[7] Goodman, J. M., Dennison, W. C. (1995): Photosynthetic responses of eelgrass (*Zostera marina* L.) to light and sediment sulfide in a shallow barrier island lagoon. – Aquatic Botany 50(1): 37-47. DOI: 10.1016/0304-3770(94)00444-Q.
[8] Harlin, M. M., Thorne-Miller, B. (1981): Nutrient enrichment of seagrass beds in a Rhode Island coastal lagoon. – Mar Biol 65(3): 221-229. DOI: 10.1007/BF00397115.
[9] Hemminga, M. A., Duarte, C. M. (2002): Seagrass ecology. – Limnology and Oceanography 47(2): 611-611. DOI: 10.4319/lo.2002.47.2.0611.
[10] Hemminga, M. A., Koutstaal, B. P., Soelen, J. V., Merks, A. G. A. (1994): The nitrogen supply to intertidal eelgrass (*Zostera marina*). – Marine Biology 118(2): 223-227. DOI: 10.1007/ BF00349788.
[11] Holmer, M., Andersen, F. O., Nielsen, S. L., Boschker, H. T. S. (2001): The importance of mineralization based on sulfate reduction for nutrient regeneration in tropical seagrass sediments. – Aquat Bot 71(1): 1-17. DOI: 10.1016/s0304-3770(01)00170-x.
[12] Hu, Y., Wang, L., Tang, Y., Li, Y., Chen, J., Xi, X. et al. (2014): Variability in soil microbial community and activity between coastal and riparian wetlands in the Yangtze River estuary - potential impacts on carbon sequestration. – Soil Biology and Biochemistry 70: 221-228. DOI: 10.1016/j.soilbio.2013.12.025.
[13] James, J. B., Sherman, T. D., Devereux, R. (2006): Analysis of bacterial communities in seagrass bed sediments by double-gradient denaturing gradient gel electrophoresis of PCR-amplified 16S rRNA genes. – Microb Ecol 52(4): 655-661. DOI: 10.1007/s00248-006-9075-3.
[14] Jensen, S. I., Kuhl, M., Glud, R. N., Jorgensen, L. B., Prieme, A. (2005): Oxic microzones and radial oxygen loss from roots of *Zostera marina*. – Mar Ecol Prog Ser 293: 49-58.
[15] Jensen, S. I., Kuhl, M., Prieme, A. (2007): Different bacterial communities associated with the roots and bulk sediment of the seagrass *Zostera marina*. – FEMS MicrobiolEcol 62: 108-117. DOI: 10.1111/j.1574-6941.2007.00373.x.
[16] Kuo, J., McComb, A. J., Cambridge, M. L. (1981): Ultrastructure of the seagrass rhizosphere. – New Phytol 89(1): 139-143. DOI: 10.1111/j.1469-8137.1981.tb04756.x.
[17] Kurtz, J. C., Yates, D. F., Macauley, J. M., Quarles, R. L., Genthner, F. L., Chancy, C. A., Devereux, R. (2003): Effects of light reduction on growth of the submerged macrophyte Vallisneria Americana and the community of heterotrophic root-associated bacterial. – J Exp Mar Biol Ecol 291(2): 199-218. DOI: 10.1016/S0022-0981(03)00120-5.

http://www.aloki.hu ● ISSN 1589 1623 (Print) ● ISSN 1785 0037 (Online)
DOI: http://dx.doi.org/10.15666/aeer/1705_1076710779

[18] Küsel, K., Pinkart, H. C., Drake, H. L., Devereux, R. (1999): Acetogenic and sulfate-reducing bacteria inhabiting the rhizoplane and deep cortex cells of the sea grass Halodule wrightii. – Appl Environ Microbiol 65(11): 5117-5123.
[19] Lebreton, B., Richard, P., Galois, R., Radenac, G., Brahmia, A., Colli, G., Grouazel, M., André, C., Guillou, G., Blanchard, G. F. (2012): Food sources used bysediment meiofauna in an intertidal *Zostera noltii* seagrass bed: a seasonalstable isotope study. – Mar Biol 159(7): 1537-1550. DOI: 10.1007/s00227-012-1940-7.
[20] Lee, K. S., Dunton, K. H. (2000): Diurnal changes in pore water sulfide concentrations in the seagrass Thalassia testudinum beds: the effects of seagrasses on sulfide dynamics. – J Exp Mar Biol Ecol 255(2): 201-214. DOI: 10.1016/S0022-0981(00)00300-2.
[21] Li, X. G., Song, J. M., Li, N., Niu, L. F., Yuan, H. M., Dai. J. C. (2007): Simultaneous determination of nitrogen and phosphorus in sediments and its application in Jiaozhou Bay. – Rock and Mineral Analysis 26(2): 87-92 (in Chinese). DOI: 10.1631/jzus.2007.B0900.
[22] Li, Y. Q., Wang, Y. D., Xu, S. Q., Hu, B. B., Wang, Z. L. (2016): Effects of mariculture and solar-salt production on sediment microbial community structure in a coastal wetland. – Journal of Coastal Research 33(3): 573-582. DOI: 10.2112/JCOASTRES-D-16-00093.1.
[23] Lv, X., Yu, P., Mao, W., Li, Y. (2018): Vertical variations in bacterial community composition and environmental factors in the culture pond sediment of sea cucumber *Apostichopus japonicus*. – Journal of Coastal Research 84(sp1): 69-76. DOI: 10.2112/SI84-010.1.
[24] Magoc, T., Salzberg, S. L. (2011): FLASH: Fast length adjustment of short reads to improve genome assemblies. – Bioinformatics 27(21): 2957-2963. DOI: 10.1093/bioinformatics/btr507.
[25] Marion, S., Rao, R. J. (2010): Innovative techniques for large-scale seagrass restoration using *Zostera marina* (eelgrass) Seeds. – Restoration Ecology 18(4): 514-526. DOI: 10.1111/j.1526-100X.2010.00692.x.
[26] McGlathery, K. J., Risgaard-Petersen, N., Christensen, P. B. (1998): Temporal and spatial variation in nitrogen fixation activity in the eelgrass *Zostera marina* rhizosphere. – Marine Ecology Progress Series 168: 245-258. DOI: 10.3354/meps168245.
[27] Nielsen, J. T., Liesack, W., Finster, K. (1999): Desulfovibrio zosterae sp. nov., a new sulfate reducer isolated from surface-sterilized roots of the seagrass *Zostera marina*. – Int J Syst Bacteriol 2(2): 859-865. DOI: 10.1099/00207713-49-2-859.
[28] Shieh, W. Y., Yang, J. T. (1997): Denitrification in the rhizosphere of the two seagrasses *Thalassia hemprichii* (Ehrenb.) Aschers and *Halodule uninervis* (Forsk.) Aschers. – J Exp Mar Biol Ecol 218(2): 229-241. DOI: 10.1016/s0022-0981(97)00076-2.
[29] Short, F., Carruthers, T., Dennison, W., Waycott, M. (2007): Global seagrass distribution and diversity: a bioregional model. – J ExpMar Biol Ecol 350: 3-20. DOI: 10.1016/j.jembe.2007.06.012.
[30] UCHIME (2011): http://drive5.com/uchime/uchime_download.html.
[31] Wang, Y., Wang, Z. L. (2018): Shifts of sediment microbial community structure along a salinized and degraded river continuum. – Journal of Coastal Research 342: 443-450.
[32] Wecker, P., Klockow, C., Schüler, Margarete, Dabin, Jérôme, Michel, G., Glöckner, Frank, O. (2010): Life cycle analysis of the model organism *rhodopirellula baltica* sh 1t by transcriptome studies. – Microbial Biotechnology 3(5): 583-594. DOI: 10.1111/j.1751-7915.2010.00183.x.
[33] Xu, Q., Liu, B., Zhou, Y. (2016): Does the eelgrass meadow influence the macrobenthic community structure in swan lake, northern China? – Marine Biodiversity 1-8. DOI: 10.1007/s12526-016-0601-3.
[34] Xu, S., Wang, Y., Guo, C., Zhang, Z., Shang, Y., Chen, Q., Wang, Z.-L. (2017): Comparison of microbial community composition and diversity in native coastal wetlands

http://www.aloki.hu ● ISSN 1589 1623 (Print) ● ISSN 1785 0037 (Online)
DOI: http://dx.doi.org/10.15666/aeer/1705_1076710779

and wetlands that have undergone long-term agricultural reclamation. – Wetlands 37: 99-108. DOI: 10.1007/s13157-016-0843-7.

[35] Yan, N., Marschner, P. (2012): Response of microbial activity and biomass to increasing salinity depends on the final salinity, not the original salinity. – Soil Biology & Biochemistry 53: 50-55.

[36] Zhou, Y., Liu, X., Liu, B., Liu, P., Wang, F., Zhang, X., Yang, H. (2015): Unusual pattern in characteristics of the eelgrass *Zostera marina* L. in a shallow lagoon (Swan Lake), North China: implications on the importance of seagrass conservation. – Aquat Bot 120: 178-184. DOI: 10.1016/j.aquabot.2014.05.014.

http://www.aloki.hu ● ISSN 1589 1623 (Print) ● ISSN 1785 0037 (Online)
DOI: http://dx.doi.org/10.15666/aeer/1705_1076710779

SILICON AND THIOUREA MEDIATED STIMULATION OF SALT TOLERANCE VARYING BETWEEN THREE FODDER BEET (*BETA VULGARIS* L.) GENOTYPES

ALI, A.[1*] – KHAN, S. U.[1] – QAYYUM, A.[1] – BILLAH, M.[2] – AHMED, W.[3] – MALIK, S.[4]

[1]*Department of Agronomy, The University of Haripur, 22620 Haripur, Pakistan*

[2]*Department of Soil Science, The University of Haripur, 22620 Haripur, Pakistan*

[3]*Department of Horticulture, The University of Haripur, 22620 Haripur, Pakistan*

[4]*Soil and Water Testing Laboratory, 22620 Haripur, Pakistan*

**Corresponding author*
e-mail: aqayyum@uoh.edu.pk

(Received 6th Mar 2019; accepted 13th Jun 2019)

Abstract. Effect of exogenously applied Silicon (Si) and Thiourea (TU) were examined in fodder beet plants under saline conditions. Seedlings growth of three fodder beet genotypes (Jamon, Monro and Tarine) were maintained in pots containing soil salinized with 300 mM NaCl dissolved in irrigation water. Two levels of Si (100 mgL^{-1}, 200 mgL^{-1}) and TU (150 mgL^{-1}, 300 mgL^{-1}) respectively were applied exogenously through leaves of 40 to 50 days old pots transplanted fodder beet plants. Salinity stress significantly suppressed plant growth and fresh biomass and as well as altered some physiological parameters like total chlorophyll content, K^+, Na^+, and K^+/Na^+ ratio in all the investigated fodder beet genotypes. Yet, these reductions were higher in Tarine followed by Jamon than those of Monro. However, both treatments of Si and TU as foliar application were effective in mitigating the adverse effects of salinity stress on shoot growth and improvement in fresh weights of Monro. Salinity stress increased leaf Na^+ contents, whereas K^+ contents and K^+/Na^+ ratio decreased in fodder beet plants under saline regime. These reductions were improved by Si and TU application, increased the K^+ uptake and K^+/Na^+ ratio through ion selectivity and ultimately triggered activity of anti-oxidant enzymes: Superoxide dismutase (SOD), Peroxidase (POD), and Catalase (CAT) and proline accumulation needed to thrive best in saline stress conditions. The beneficial effects of applied Si and TU were reflected in the form of enhanced fodder beet growth as well as improvement in various physiological traits and antioxidant defensive mechanism.
Keywords: *fodder beet, winter fodder crop, salt stress, silicon, thiourea*

Introduction

Salinity intrusion is one of the major environmental issues throughout the world and a huge number of hectares of marginal lands also have limited the scope for crop production (Dasgupta et al., 2015). Salinity and drought are two of the most genuine abiotic stresses, which signify a threat on crop productivity worldwide (Guo et al., 2014). In many parts of the world, a significant region of watered arable land has been confronting a major issue of salinization. Even though it is very difficult to accurately determine the increasing salinized area and its phenomenon however, it was estimated that round about 20-21% of irrigated land (45 million ha) which contributes the on third of the world's coproduction is mainly salt affected (Shrivastava et al., 2015). The productivity of most crops was reduced by soil salinity, in spite of the fact that to a changing degree relying on species (Hussain et al., 2016). Pakistan has about 16.80 million ha irrigated agricultural area in which 6-7% is categorized as strongly Saline, 9-

http://www.aloki.hu ● ISSN 1589 1623 (Print) ● ISSN 1785 0037 (Online)
DOI: http://dx.doi.org/10.15666/aeer/1705_1078110791

10% slightly saline, 3-4% moderately and 6% miscellaneous, while 72% is listed as non-salt affected land (Khan etal., 2017). Salt stress has great impact on major and minor crop's yield and reduce up to 50% yield in many arid and semi-arid areas of the world (Dugasa et al., 2016). Production of practically every conventional crop around there is significant decreased under saline soil conditions. Henceforth the introduction of non-traditional salt tolerant fodder crops in these areas could be an appropriate alternative.

Fodder beet is salt tolerant crop when contrasted with other fodder and forages, similar to that it can be effectively grown on salt influenced lands and fed as fodder in numerous European countries and in Egypt. Farmers generally use all parts roots and leaves as animal feed, directly in fresh form or processed (Sakr et al., 2014). The cultivation of fodder beet crop on marginal lands gives a remarkable benefit to farmers in the form of high economic yield production on such type of barren lands (Abdallah et al., 2008). The beet crop is utilized by amalgamation with straw in European and in other different countries of the world. Both the underground part roots and above part leaves are used as animal feed, however the tuberous roots of fodder beet are mainly utilized as primary feed for animals (El-Sarag et al., 2013).

Some beneficial mineral supplements have been determined by different researchers which can balance the unfavorable impacts of salt stress. On earth crust after the oxygen, silicon is found the 2nd most abundant element and exist as 8th common element in nature (Sahebi et al., 2015). A number of ways like fertilizer or bio-stimulant silicon can be used which plays a vital role in plant growth development and yield productivity under various stress conditions (Sawas and Ntatsi, 2015). Silicon supplementation into the solution culture enhanced wheat development and K^+/Na^+ with reduction in Na^+ and upgraded K^+ take-up. It is useful for plants from numerous points of view as it enhances plant water status in setting of relative water content and transpiration rate, improves the hurtful impacts of salt stress on chlorophyll and plant biomass in both leaves and roots, it brings down fundamentally the Na^+ uptake by (Liu et al., 2015). The supplementation of Silicon under salt stress conditions has the ability to mitigate the adverse effects of Na^+ and uptake by plants by increasing the K^+ concentration and with the resultant increase in K^+/Na^+ ratio (Xu et al., 2015). Exogenous application of different concentrations of Silicon to salt stressed aloe sensitive plants and tolerant plants significantly improved the K^+ content in roots and translocation to leaves and other parts of plants consequently raising the K^+/Na^+ ratio, while decrease the Na^+ uptake and its translocation (Garg et al., 2016).

Thiourea is a nitrogen and sulfur containing compound and is being utilized for the improvement of crops yield. Addition of thiourea significantly improves plant's root and shoot weight, tallness and number of leaves and leaf area, which directly results in the enhancement of plant's growth and development under various stresses condition (Parveen et al., 2015). Thiourea has the ability to improve entire plant growth, by enhancing cellular development of plants under salt stress (Ikram and Javed, 2015). Saddiqui et al. (2006) also reported that exogenously applied Thiourea altogether enhanced the fresh and dry weights grown under salt stress condition.

The current research was undertaken to test the hypothesis that (1) Thiourea and Silicon exogenous application enhanced fodder beet salt tolerance both by improving the plant biomass and decreasing the ion toxicity; (2) Thiourea and silicon improved the plant water balance by enhancing the proline accumulation; (3) Both treatments alleviated the ion toxicity by triggering antioxidant enzymes which are involved in scavenging reactive oxygen species and ion homeostasis.

http://www.aloki.hu ● ISSN 1589 1623 (Print) ● ISSN 1785 0037 (Online)
DOI: http://dx.doi.org/10.15666/aeer/1705_1078110791

Materials and methods

Land preparation and nursery raising

A plot sized 2×2 m^2 was prepared for nursery raising of Fodder Beet genotypes. For seeds sowing, the seedbed was prepared by thoroughly mixing one part Farm Yard Manure (FYM) and two parts soil as collected from AP horizon of the Agriculture Research Farm, The University of Haripur. Phosphorus 120 mg kg^{-1} as single super phosphate and half dose of the nitrogen (60 mg kg^{-1} N) as urea were applied as starter dose for fodder beet genotypes at time of Nursery preparation. Remaining ½ of the N was applied in two equal splits, i.e. 30 mg kg^{-1} N was applied 15 days after sowing (DAS) and the remaining at 30 DAS. and the nursery plot was then irrigated immediately. The nursery was left for 45 days after sowing to develop their growth and irrigations were provided at 7 days intervals subsequently.

Pot filling and nursery transplantation

A surface soil (0-20 cm), clay loam soil, (Gee and Bauder, 1986) was collected from Agriculture research farm area Department of Agricultural Sciences, The University of Haripur, Pakistan. The soil contained 1.20 mg Kg^{-1} of total dissolved salts, 0.55% organic matter (Nelson and Sommers, 1996), 0.20% calcium chloride (Leoppert et al., 1996), 8.7 mgL^{-1} available Pphosphorous. Growth media was prepared by filling pots measuring (height 22 cm, base diameter 24 cm and top diameter 27.5 cm) with a mixture of field soil and Farm yard manure in 3:1 ratio. The base of each pot was covered with polyethylene bags in order to develop salinity stress condition.

Plant growth and treatments application

At field capacity, five plants were transplanted on 1st March, 2017 in each pot, replicated thrice using Completely randomized design (CRD) for each fodder beet variety. In order to develop salinity stress, 300 mM NaCl solution was applied to the growth medium of Twenty days old transplanted after transplantation in pots Twenty days after transplantation in pots, a dose of 300 mM NaCl solution was applied to each pot in order to develop salinity stress. All pots were placed in green house and Twenty days after salt application, Calcium silicate (Si) and Thiourea (TU) were applied exogenously on Fodder beet genotypes. Two levels of Si and TU at 100 mgL^{-1}, 200 mgL^{-1} and 150 mgL^{-1}, 300 mgL^{-1} respectively were applied at 40 days after transplantation in pots, nonetheless one treatment in each fodder beet variety was kept control in the absence of Si and TU application. At 60th day of transplantation in pots, the plants were harvested and roots were cleaned from soil for data recording of fresh shoot, root weight and length of shoot, root and total biomass. The third fresh leaf of each fodder beet plant was harvested at the end of experiment for K^+, Na^+ concentration, K^+/Na^+ ratio, proline content estimation and the activity of antioxidant enzymes (SOD, POD and CAT).

Statistical analysis

Data of the present study were subjected to analysis using Two-Way ANOVA according to Abdi and Williams (2010), using Statistix 8.1. The differences among means were tested using Tukey's Honest Significant Difference test at 0.01% probability level. Mean values were presented as mean value with standard errors calculated from three replications.

http://www.aloki.hu ● ISSN 1589 1623 (Print) ● ISSN 1785 0037 (Online)
DOI: http://dx.doi.org/10.15666/aeer/1705_1078110791

Results

Growth parameters

Shoot length and root length of all fodder beet genotypes reduced significantly ($P \leq 0.01$) under salinity stress (*Table 1*). However, the reduction in shoot length and root length was much lower in Jamon and Tarine respectively than all other fodder beet genotypes. Exogenously applied Silicon and Thiourea significantly improved the growth of fodder beet genotypes as compared to non-treated plants under salt stress conditions. Silicon and Thiourea increased the shoot length in Monro with Si @ 200 mg L^{-1} being statistically at par with Tarine under TU @ 300 mg L^{-1} application. Similarly, the root length of Jamon plants increased under Si @ 100 mg L^{-1} whereas TU @ 300 mg L^{-1} application increased root length of Monro plants as compared to other treatments.

Table 1. *Growth parameters of fodder beet genotypes grown in saline conditions as affected by exogenous application of silicon and thiourea*

Parameters	Genotypes	Treatments				
		Control (300 mM NaCl)	**Si (100 mg L^{-1})**	**Si (200 mg L^{-1})**	**TU (150 mg L^{-1})**	**TU (300 mg L^{-1})**
Shoot length (cm)	Jamon	32.43 ± 0.34	40.83 ± 0.56	35.30 ± 0.29	38.97 ± 0.38	37.23 ± 0.32
	Monro	36.10 ± 0.32	38.93 ± 0.28	44.50 ± 0.25	37.50 ± 0.41	38.70 ± 0.66
	Tarine	42.36 ± 0.32	41.90 ± 0.64	39.33 ± 0.71	39.80 ± 0.42	43.90 ± 0.48
Root length (cm)	Jamon	8.26 ± 0.08	10.86 ± 0.08	7.03 ± 0.12	8.73 ± 0.18	7.57 ± 0.09
	Monro	8.06 ± 0.14	9.13 ± 0.20	7.10 ± 0.26	8.33 ± 0.23	9.43 ± 0.15
	Tarine	8.33 ± 0.14	7.36 ± 0.17	8.90 ± 0.22	7.63 ± 0.20	8.47 ± 0.23
Shoot weight (g)	Jamon	73.53 ± 0.65	84.40 ± 0.82	62.83 ± 0.62	105.17 ± 0.42	61.60 ± 0.93
	Monro	56.83 ± 0.98	59.80 ± 1.08	111.97 ± 0.92	62.23 ± 0.64	102.00 ± 0.72
	Tarine	65.07 ± 0.12	62.10 ± 0.52	58.53 ± 0.60	54.67 ± 0.47	49.27 ± 0.62
Root weight (g)	Jamon	40.23 ± 0.26	40.26 ± 0.71	12.73 ± 0.55	48.93 ± 0.49	27.53 ± 0.52
	Monro	35.67 ± 0.75	39.73 ± 0.56	50.17 ± 1.27	39.83 ± 0.37	58.23 ± 0.52
	Tarine	34.66 ± 1.08	26.50 ± 0.70	32.13 ± 0.33	24.40 ± 0.32	25.73 ± 0.81
Total Biomass (g)	Jamon	103.77 ± 0.91	134.67 ± 1.52	117.53 ± 0.99	154.10 ± 0.66	89.13 ± 0.88
	Monro	92.50 ± 1.68	99.53 ± 1.38	162.13 ± 1.78	102.07 ± 0.96	160.23 ± 0.97
	Tarine	79.73 ± 1.07	98.60 ± 1.70	90.67 ± 1.36	79.07 ± 0.84	95.00 ± 1.28

Values in columns having the same letter are not significantly different at $p \leq 0.05$

Shoot weight and root weight was significantly different ($P \leq 0.01$) of all fodder beet plants grown with salinity in root environment (*Table 1*). However, the reduction in shoot weight and root weight due to root zone salinity was much lower in Tarine compared to other fodder beet genotypes. The exogenous application of silicon and Thiourea significantly affected the fodder beet shoot and root weight under saline conditions. The highest shoot weight and root weight was recorded with Silicon and Thiourea application in Monro which was statistically at par with Jamon. Imposed root zone salinity significantly affected ($P \leq 0.01$) the total biomass in fodder beet plants (*Table 1*). Salinity stress caused maximum reduction in biomass of Tarine plants as

http://www.aloki.hu ● ISSN 1589 1623 (Print) ● ISSN 1785 0037 (Online)
DOI: http://dx.doi.org/10.15666/aeer/1705_1078110791

compared to other fodder beet plants. Both Silicon and Thiourea were found to increase the total biomass under salt stress conditions. Monro produced maximum biomass under Silicon @ 200 mg L^{-1} and Thiourea @ 300 mg L^{-1} followed by Jamon under Silicon @ 100 mg L^{-1} and Thiourea @ 150 mg L^{-1} (*Fig. 1*).

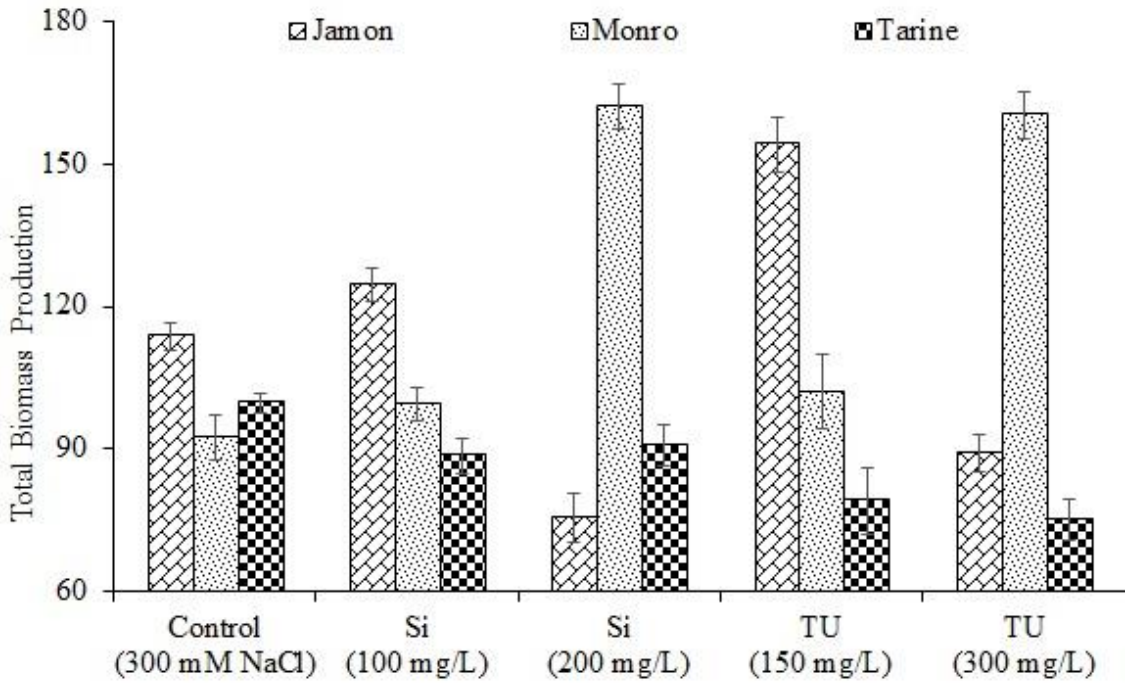

Figure 1. *Increase in total biomass production in fodder beet genotypes grown under salt stress conditions at different levels of silicon and thiourea. The bars indicates standard error (±SE) of mean (n = 3). All means are significantly different at p ≤ 0.05*

Physiological parameters

In all fodder beet plants, the potassium ion concentration was found significantly affected ($P \leq 0.01$) under salt stress conditions (*Table 2; Fig. 2*). The highest K^+ concentration was observed in Tarine under salt stress. Plants perform better in K^+ ions accumulation as Silicon and Thiourea were exogenously applied as compared to control treatment. The higher K^+ concentration in fodder beet shoots was recorded under exogenous application of Silicon @ 200 mg L^{-1} and Thiourea @ 150 mg L^{-1} in Tarine, statistically at par with Monro under control treatment. Root zone salinity significantly ($P \leq 0.01$) enhanced the sodium concentration in fodder beet shoots. The maximum Na^+ concentration was depicted in Monro under saline conditions. However, Silicon and Thiourea exogenous application were found to decrease the Na^+ ion accumulation in fodder plants under salt stress conditions as compared to control. Monro recorded with lowest Na^+ accumulation under Silicon @ 200 mg L^{-1} statistically at par with Tarine and Jamon under Silicon @ 100 mg L^{-1} and Thiourea @ 300 mg L^{-1} respectively. Monro recorded highest in K^+/Na^+ ration under Silicon @ 200 mg L^{-1} followed by Jamon under Thiourea @ 150 mg L^{-1} exogenous application respectively. Data revealed significant variation ($P \leq 0.01$) among fodder beet genotypes regarding proline accumulation under

http://www.aloki.hu ● ISSN 1589 1623 (Print) ● ISSN 1785 0037 (Online)
DOI: http://dx.doi.org/10.15666/aeer/1705_1078110791

saline conditions (*Table 2*). Salinity stress significantly reduced proline accumulation in Monro compared to other fodder beet genotypes. Both Silicon and Thiourea were found to positively influence proline accumulation in Fodder beet plants. Deceasing salinity stress also decreased proline accumulation in Tarine under Silicon @ 100 mg L^{-1} and Thiourea @ 300 mg L^{-1}, statistically at par with Janom and Monro under Thiourea application @ 300 mg L^{-1} respectively.

Table 2. *Concentration of K^+, Na^+, K^+/Na^+ ratio, proline content and antioxidant enzyme activities in fodder beet genotypes grown under saline conditions as affected by exogenous application of silicon and thiourea*

Parameters	Genotypes	Treatments				
		Control (300 mM NaCl)	Si (100 mg L^{-1})	Si (200 mg L^{-1})	TU (150 mg L^{-1})	TU (300 mg L^{-1})
K^+ concentration (mg g^{-1})	Jamon	76.67 ± 3.18	94.63 ± 3.76	86.87 ± 3.47	88.67 ± 2.88	102.87 ± 3.00
	Monro	129.17 ± 7.08	115.87 ± 5.44	80.50 ± 6.01	116.80 ± 5.42	101.90 ± 4.10
	Tarine	123.40 ± 8.24	96.37 ± 5.85	138.27 ± 4.10	141.97 ± 5.50	122.03 ± 7.89
Na^+ concentration (mg g^{-1})	Jamon	56.00 ± 5.29	48.00 ± 7.218	63.60 ± 4.86	56.33 ± 6.35	61.27 ± 5.91
	Monro	81.57 ± 10.46	76.57 ± 7.36	43.10 ± 8.92	64.37 ± 2.23	48.97 ± 6.80
	Tarine	105.27 ± 5.21	54.63 ± 6.22	94.47 ± 3.99	116.57 ± 4.13	77.63 ± 6.82
K^+/Na^+ ratio	Jamon	1.40 ± 0.18	1.65 ± 0.28	1.69 ± 0.10	2.05 ± 0.32	1.40 ± 0.17
	Monro	1.65 ± 0.26	1.85 ± 0.18	2.20 ± 0.32	1.52 ± 0.10	1.94 ± 0.24
	Tarine	1.17 ± 0.06	1.22 ± 0.08	1.58 ± 0.04	1.79 ± 0.16	1.47 ± 0.09
Proline content (mg g^{-1})	Jamon	146.67 ± 3.53	264.33 ± 2.85	245.67 ± 4.41	235.67 ± 4.26	248.33 ± 2.33
	Monro	122.0 ± 2.52	250.0 ± 6.08	234.0 ± 3.18	190.0 ± 5.03	243.33 ± 3.06
	Tarine	157.33 ± 5.24	304.67 ± 5.36	241.67 ± 2.65	240.67 ± 7.97	274.0 ± 7.26
SOD (unit.mg^{-1})	Jamon	154.0 ± 0.66	167.0 ± 0.83	196.0 ± 0.93	195.0 ± 0.68	178.0 ± 0.745
	Monro	172.0 ± 0.81	190.0 ± 0.90	209.0 ± 0.86	198.0 ± 0.69	186.0 ± 0.722
	Tarine	164.0 ± 0.70	197.0 ± 0.87	201.0 ± 0.79	191.0 ± 0.64	184.0 ± 0.766
POD (unit.mg^{-1})	Jamon	35.29 ± 0.40	51.42 ± 0.73	50.12 ± 0.61	50.23 ± 0.66	54.23 ± 0.810
	Monro	36.17 ± 0.49	51.58 ± 0.77	50.78 ± 0.69	51.12 ± 0.70	54.89 ± 0.848
	Tarine	36.82 ± 0.52	52.02 ± 0.79	50.33 ± 0.68	50.16 ± 0.60	55.07 ± 0.866
CAT (unit.mg^{-1})	Jamon	2.65 ± 0.66	3.01 ± 0.83	3.84 ± 0.93	2.69 ± 0.68	2.89 ± 0.745
	Monro	2.95 ± 0.81	3.22 ± 0.90	3.06 ± 0.86	2.75 ± 0.69	2.86 ± 0.722
	Tarine	2.81 ± 0.70	3.09 ± 0.87	2.98 ± 0.79	2.59 ± 0.64	2.93 ± 0.766

Values in columns having the same letter are not significantly different at $p \leq 0.05$

Anti-oxidant enzymatic activities

Anti-oxidant enzymes activity (SOD, POD and CAT) were significantly affected ($P \leq 0.01$) by induced salt stress in all fodder beet genotypes (*Table 2; Fig. 3*). Highest SOD and POD activity was found in Jamon while Tarine recorded higher CAT activity than rest of the genotypes under imposed salinity stress. Exogenous application of both Silicon and Thiourea enhanced the activity of antioxidant enzymes in fodder beet genotypes under salinity stress than that of untreated plants (control). Nonetheless, SOD, POD and CAT activity were increased significantly in fodder beet plants under Silicon @ 200 mg L^{-1} and Thiourea @ 150 mg L^{-1} when applied exogenously under salt stress conditions.

http://www.aloki.hu ● ISSN 1589 1623 (Print) ● ISSN 1785 0037 (Online)
DOI: http://dx.doi.org/10.15666/aeer/1705_1078110791

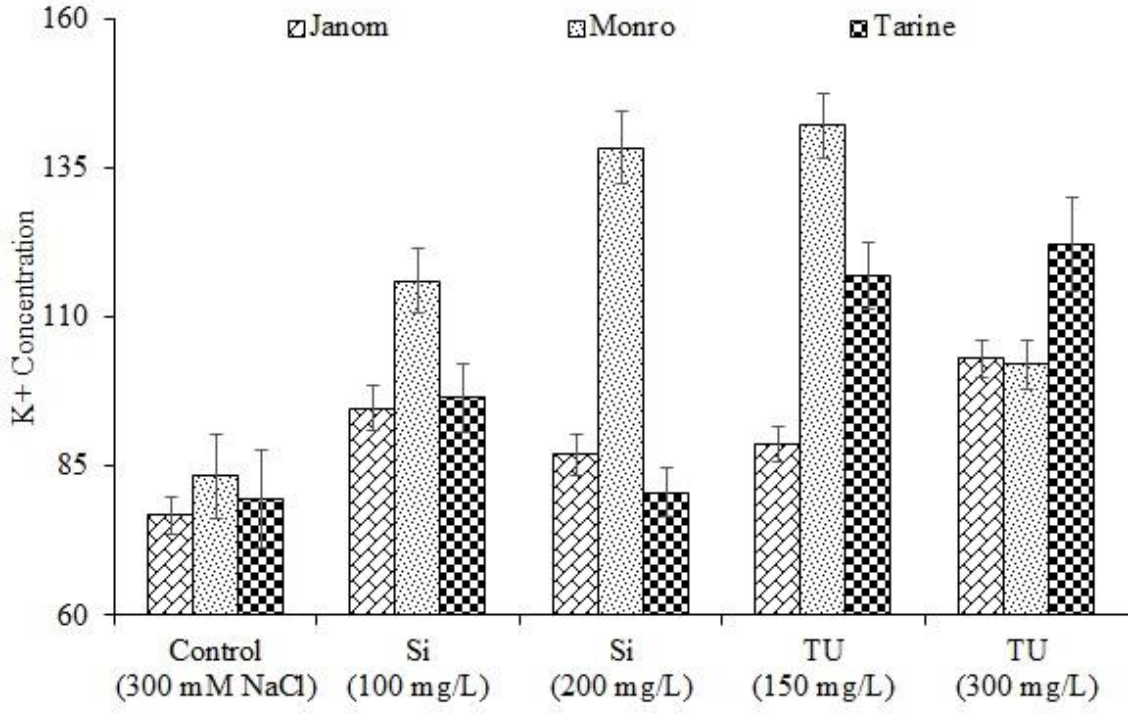

Figure 2. *Percent increase in shoot K^+ concentration in fodder beet genotypes grown under salt stress conditions at different levels of silicon and thiourea. The bars indicates standard error (±SE) of mean (n = 3). All means are significantly different at $p \leq 0.05$*

Discussion

The salinity stressed produced adverse effects on plants growth as mostly expressed as osmotic stress, explicit ion toxicity, damage to cellular membranes, vital nutrient deficiency and trigger in oxidants, etc. (Ashraf, 2009). To overcome salinity stress effects in plants, researchers are using various bio-stimulants which have been reported to influence various physiological processes (Perveen et al., 2014). In current study, the foliar application of silicon and Thiourea enhanced the growth of all Fodder beet plants as grown under salt stress condition. Various growth parameters including root and shoot length, root and shoot fresh weight, and total biomass were enhanced by Silicon and Thiourea under salt stress conditions (*Table 1*). Similar results to our research study have also been observed (Anjum et al., 2011) in two different wheat genotypes grown under 130 mM salt stress conditions. Likewise, some prior reports supported our results and revealed that Thiourea application mitigates the adverse effects of salinity and hence improved the final grain yield of many crops like, cereal crops (Sahu et al., 2006) and potato (Mani et al., 2012). Various research studies stated that exogenously applied Nitrogen containing compounds e.g. Thiourea has significant impact on the synthesis of green photosynthetic pigments which ultimately associated with high biomass production in salt stress conditions (Ashraf and Harris, 2013). Both Silicon and Thiourea exogenously applied are directly involved in the cellular osmotic adjustment of plants, which leads to enhance the biomass production of plants under salt stress condition (Burman et al., 2004; Seckin et al., 2009).

http://www.aloki.hu ● ISSN 1589 1623 (Print) ● ISSN 1785 0037 (Online)
DOI: http://dx.doi.org/10.15666/aeer/1705_1078110791

Figure 3. *Mechanism of silicon and thiourea mediated salinity tolerance in fodder beet*

Present study showed that salt stress caused the increased accumulation of Na^+ in shoots and roots of fodder beet genotypes. Due to presence of high concentration of Na^+ content, reduction was recorded in the concentration of K^+ which ultimately reduced the K^+/Na^+ ration in plant's tissues. The physiological window of ideal K^+ uptake by plants limits within the sight of expanding measure of Na^+. In the current research exogenous application of Silicon and Thiourea on fodder beet plants enhanced the K^+ and K^+/Na^+ by reducing Na^+ uptake (*Table 2; Fig. 2*). Silicon is also reported as to enhance the K^+/Na^+ ratio under salt stress (Al-aghabary et al., 2004). A critical decrease saw in Na^+ take-up demonstrates that TU-induced tolerance is because of salt stress mitigation strategy (Srivastava et al., 2011). To become salt stress tolerant, plants adopt various strategies and mechanisms like proline accumulation, formation of mannitol and glycine betaine etc which plays an important role in various plants processes just like, scavenging of Reactive Oxygen species in salt stress (Ali and Ashraf, 2011), stabilization of cell's membrane (Ashraf and Ali, 2008) and Osmotic adjustment of plants (Ashraf and Foolad, 2007). In this study, Tarine performed best in proline accumulation under salt stress conditions. Maximum proline content was found by Silicon exogenous application @ 100 mgL^{-1} (*Table 2; Fig. 3*). Silicon application improves proline and protein accumulation which ultimately trigger antioxidative defense mechanisms and decreases the lipid peroxidation under salt stress (Al-aghabary et al., 2004). Production of Reactive Oxygen Species such as SOD, POD, and hydroxyl radicals mainly damage the plants at cellular level which thrive in saline growth medium (Ashraf et al., 2009). In the current study we have detected that salt stress induces the SOD, POD and CAT activities as to alleviate salt stress in fodder beet plants. The exogenous application of Silicon and Thiourea showed to activate these activities more efficiently against salt stress conditions for ideal plant growth and development (*Table 2; Fig. 3*). Some prior studies concluded that Thiourea induced enhancement in the activities of antioxidant enzymes like, SOD, POD and CAT with remarkable decrease in Oxidative stress generated by the presence of Salinity stress

http://www.aloki.hu ● ISSN 1589 1623 (Print) ● ISSN 1785 0037 (Online)
DOI: http://dx.doi.org/10.15666/aeer/1705_1078110791

(Hammed et al., 2013). Likewise, another study also suggested that exogenous application of Thiourea in salt stress condition significantly lowered oxidative damage caused by ROS rather than unsprayed plants (Srivastava et al., 2011). It has been demonstrated recently that Silicon mitigates oxidative stress by stimulation of antioxidants, both enzymatic and non-enzymatic (Savvas and Ntatsi, 2015), such as superoxide dismutase (SOD), catalase (CAT), ascorbate peroxidase (APx), peroxidases (POD), and ascorbate (AA) etc. Li et al. (2016) showed that the provision of Si exogenously increased the SOD, POD and CAT activity of *Glycyrrhiza uralensis* seedlings grown under salt stress, after 20 days of treatment. Our research findings are analogous to earlier research studies which revealed that exogenously applied silicon can increase the anti-oxidant enzymatic activities such as; superoxide dismutase (SOD), peroxidase (POD) and catalase (CAT) under saline regimes.

Conclusions

Salt stress caused reduction in growth attributes, physiological and biochemical parameters of fodder beet plants. However, exogenously application of silicon and Thiourea improved to some extent stress tolerance in fodder beet plants by improving growth parameters as well as proline content, K^+ content, K^+/Na^+ ratio and decreasing Na^+ content in the shoots under saline conditions. Among all the three fodder beet genotypes evaluated under salt stress condition, Monro performed best having maximum SOD, POD and CAT activities. It was able to thrive best under saline conditions and hence produced prolific biomass, followed by Jamon and Tarine respectively. Furthermore; Silicon @ 200 mgL^{-1} and Thiourea @ 150 mgL^{-1} was found most effective in mitigating the salt stress conditions. To further investigate the salt ameliorating ability of silicon and Thiourea, a field experiment with more number of fodder beet genotypes is suggested.

Compliance with ethical standards. There is no potential conflict of interests and authors confirm that the field studies did not involve endangered or protected species.

REFERENCES

[1] Abdallah, E. F., Yassen, A. A. (2008): Fodder beet productivity under fertilization treatments and water augmentation. – Australian Journal of Basic and Applied Sciences 2: 282-287.

[2] Abdi, H., Williams, L. J. (2010): Newman-Keuls Test and Tukey Test. – In: Salkind, N. J. (ed.) Encyclopedia of Research Design. Sage, Thousand Oaks, CA, pp. 1-11.

[3] Al-aghabary, K., Zhu, Z., Shi, Q. (2004): Influence of silicon supply on chlorophyll content, chlorophyll fluorescence, and antioxidative enzyme activities in tomato plants under salt stress. – Journal of Plant Nutrition 27(12): 2101-2115.

[4] Ali, Q., Ashraf, M. (2011): Induction of drought tolerance in maize (*Zea mays* L.) due to exogenous application of trehalose; growth, photosynthesis, water relations and oxidative defence mechanism. – Journal of Agronomy and Crop Science 197(4): 258-271.

[5] Anjum, F., Wahid, A., Farooq, M., Javed, F. (2011): Potential of foliar applied thiourea in improving salt and high temperature tolerance of bread wheat (*Triticum aestivum*). – International Journal of Agriculture and Biology 13(2): 25-39.

http://www.aloki.hu ● ISSN 1589 1623 (Print) ● ISSN 1785 0037 (Online)
DOI: http://dx.doi.org/10.15666/aeer/1705_1078110791

[6] Ashraf, M. (2009): Biotechnological approach of improving plant salt tolerance using antioxidants as markers. – Biotechnology Advances 27(1): 84-93.
[7] Ashraf, M., Ali, Q. (2008): Relative membrane permeability and activities of some antioxidant enzymes as the key determinants of salt tolerance in canola (*Brassica napus* L.). – Environmental and Experimental Botany 63(3): 266-273.
[8] Ashraf, M., Foolad, M. (2007): Roles of glycine betaine and proline in improving plant abiotic stress resistance. – Environmental and Experimental Botany 59(2): 206-216.
[9] Ashraf, M., Harris, P. J. C. (2013): Photosynthesis under stressful environments. An overview. – Photosynthetica 51: 163 -190.
[10] Burman, U., Garg, B. K., Kathju, S. (2004): Interactive effects of thiourea and phosphorus on clusterbean under water stress. – Biologia Plantarum 48(1): 61-65.
[11] Dasgupta, S., Hossain, M. M., Huq, M., Wheeler, D. (2015): Climate change and soil salinity: the case of coastal Bangladesh. – Ambio 44(8): 815-826.
[12] Dugasa, T., B. Bebie, R. P., Tomer, S., Barnabas, J. (2016): Effect of seed priming on salt tolerance of bread wheat (*Triticumaestivum* L.) varieties tesfayedugasa. – Journal of Scientica 6(3): 139-153.
[13] El-Sarag, E. I. (2013): Response of fodder beet cultivars to water stress and nitrogen fertilization in semi arid regions. – American-Eurasian Journal of Agricultural & Environmental Sciences 13: 1168-1175.
[14] Garg, N., Bhandari, P. (2016): Interactive effects of silicon and arbuscular mycorrhiza in modulating ascorbate-glutathione cycle and antioxidant scavenging capacity in differentially salt-tolerant *Cicer arietinum* L. genotypes subjected to long-term salinity. – Protoplasma 253(5): 1325-1345.
[15] Gee, G. W., Bauder, J. W. (1986): Particle Size Analysis. – In: Klute, A. (ed.) Methods of Soil Analysis, Part 1: Physical and Mineralogical Methods. 2nd Ed. American Society of Agronomy Madison, Wisconsin pp. 383-412.
[16] Guo, J., Ling, H., Wu, Q., Xu, L., Que, Y. (2014): The choice of reference genes for assessing gene expression in sugarcane under salinity and drought stresses. – Scientific Reports 4: 70-42.
[17] Hameed. A., Jafri, L., Sheikh, M. A. (2013): Effect of thiourea on proteins, catalase, guaiacol peroxidase and protease activities in wheat leaves under H_2O_2 induced oxidative stress. – Iranian Journal of Plant Physiology 4: 857-864.
[18] Hussain, M. I., Lyra, D. A., Farooq, M., Nikoloudakis, N., Khalid, N. (2016): Salt and drought stresses in safflower: a review. – Agronomy for Sustainable Development 36(1): 4.
[19] Ikram, S., Javed, F. (2015): Cadmium stress alleviation by thiourea in barley. – International Journal of Innovation and Applied Studies 12(2): 384.
[20] Khan, M., Shafi, M., Bakht, J., Anwar, S. (2017): Effect of salinity and seed priming on growth characters of wheat varieties. – Sarhad Journal of Agriculture 33(3): 435-446.
[21] Liu, P., Yin, L., Wang, S., Zhang, M., Deng, X., Zhang, S., Tanaka, K. (2015): Enhanced root hydraulic conductance by aquaporin regulation accounts for silicon alleviated salt-induced osmotic stress in *Sorghum bicolor* L. – Environmental and Experimental Botany 111: 42-51.
[22] Li, Y. T., Zhang, W. J., Cui, J. J., Lang, D. Y., Li, M., Zhao, Q. P., Zhang, X. H. (2016): Silicon nutrition alleviates the lipid peroxidation and ion imbalance of Glycyrrhiza uralensis seedlings under salt stress. – Acta Physiologiae Plantarum 38(4): 96.
[23] Loeppert, R. H., Suarez, D. L. (1996): Carbonate and Gypsum. – In: Sparks, D. L., Page, A. L., Helmke, P. A. (eds.) Methods of Soil Analysis. Part 3: Chemical Methods. American Society of Agronomy Madison, WI, pp. 437-474.
[24] Mani, F., Bettaieb, T., Zheni, K., Doudech, N., Hannachi, C. (2012): Effect of hydrogen peroxide and thiourea on fluorescence and tuberization of potato (*Solanum tuberosum* L.). – Journal of Stress Physiology and Biochemistry 8(3): 14-19.

http://www.aloki.hu ● ISSN 1589 1623 (Print) ● ISSN 1785 0037 (Online)
DOI: http://dx.doi.org/10.15666/aeer/1705_1078110791

[25] Nelson, D. W., Sommers, L. E. (1996): Total Carbon, Organic Carbon, and Organic Matter. – In: Sparks, D. L., Page, A. L., Helmke, P. A. (eds.) Methods of Soil Analysis. Part 3: Chemical Methods. American Society of Agronomy Madison, WI, pp. 961-1010.
[26] Perveen, A., Wahid, A., Mahmood, S., Hussain, I., Rasheed, R. (2015): Possible mechanism of medium-supplemented thiourea in improving growth, gas exchange, and photosynthetic pigments in cadmium-stressed maize (*Zea mays*). – Brazilian Journal of Botany 38(1): 71-79.
[27] Perveen, S., Shahbaz, M., Ashraf, M. (2014): Triacontanol-induced changes in growth, yield, leaf water relations, oxidative defense system, minerals, and some key osmoprotectants in Triticum aestivum under saline conditions. – Turkish Journal of Botany 38(5): 896-913.
[28] Sahu, M. P., Kumawat, S. M., Ramaswamy, N. K., D'souza, S. F., Singh, G. (2006): Sulphydryl bioregulator technology for increasing wheat productivity. – Research Bulletin RAU-BARC 3: 1-56.
[29] Sakr, H. O., Awad, H. A., Seadh, S. E., Abido, W. A. E. (2014): Influence of irrigation withholding and potassium levels on forage yields and its quality of fodder beet. – Journal of Crop Science 5(1): 116-125.
[30] Savvas, D., Ntatsi, G. (2015): Biostimulant activity of silicon in horticulture. – Scientia Horticulturae 196: 66-81.
[31] Seckin, B., Sekmen, A. H., Türkan, I. (2009): An enhancing effect of exogenous mannitol on the antioxidant enzyme activities in roots of wheat under salt stress. – Journal of Plant Growth Regulation 28(1): 12.
[32] Shrivastava, P., Kumar, R. (2015): Soil salinity: a serious environmental issue and plant growth promoting bacteria as one of the tools for its alleviation. – Saudi Journal of Biological Sciences 22(2): 123-131.
[33] Siddiqui, Z. S., Shaukat, S. S., Zaman, A. U. (2006): Alleviation of salinity-induced dormancy by growth regulators in wheat seeds. – Turkish Journal of Botany 30(5): 321-330.
[34] Srivastava, A. K., Srivastava, S., Penna, S., D'Souza, S. F. (2011): Thiourea orchestrates regulation of redox state and antioxidant responses to reduce the NaCl-induced oxidative damage in Indian mustard (*Brassica juncea* (L.) Czern.). – Plant Physiology and Biochemistry 49(6): 676-686.
[35] Xu, C. X., Ma, Y. P., Liu, Y. L. (2015): Effects of silicon (Si) on growth, quality and ionic homeostasis of aloe under salt stress. – South African Journal of Botany 98: 26-36.

http://www.aloki.hu ● ISSN 1589 1623 (Print) ● ISSN 1785 0037 (Online)
DOI: http://dx.doi.org/10.15666/aeer/1705_1078110791

ASSESMENT OF GROWTH AND PRODUCTIVITY OF CUCUMBER (*CUCUMIS SATIVUS* L.) GENOTYPES UNDER SALT STRESS REGIME

SARWAR, M.[1*] – AHMAD, S.[1] – CHATTHA, M. B.[1] – CHATTHA, M. U.[2] – ALAM, M. W.[1] – ANJUM, S.[3] – SHAFEEQ, T.[1] – NASEEM, M. K.[1] – MANNAN, A.[1]

[1]*Institute of Agricultural Sciences, University of the Punjab (Quaid-e-azam campus) Lahore, Pakistan*

[2]*Depatment of Agronomy, Bahauddin Zakariya University, Multan, Pakistan*

[3]*Depatment of Botany, University of Agriculture, Faisalabad, Pakistan*

[*]*Corresponding author*
e-mail: mubeensarwar4@yahoo.com, mubeen.iags@pu.edu.pk

(Received 8th Mar 2019; accepted 3rd May 2019)

Abstract. The potential of cucumber (*Cucumis sativus* L.) genotypes for salt tolerance was investigated in a pot experiment under a lath house conditions. Salt stress substantially reduced plant growth and physiological traits in cucumber plants. On other hand, increase in accumulation of organic solutes i.e., proline as well as activity of anti-oxidant enzymes like SOD, POD and CAT were also observed. However, salinity also caused ionic imbalancement in studied genotypes and lead towards high leaf sodium and chloride (Na^+, Cl^-) content along with a significant reduction in leaf K^+ and Ca^+ levels. On the behalf of percent increment or reduction in observed, cucumber genotypes Marketmore & Green long were found to be salt resistant, while Summer green and 20252 catagerized as salt sensitive. Tolerant genotypes effectively maintained better dry biomass and high Ca^+ and K^+ content with least Na^+ and Cl^- in their leaves exposed to salt stress. Furthermore, maximum accumulation of proline contents and greater activity of antioxidants (SOD, POD and CAT) results in improved tolerance under salinity which indicate that salt tolerance induced in cucumber is greatly connected with level of organic osmolytes and antioxidant defense system.
Keywords: *photosynthesis, salinity tolerance, glycinbetaine, salinity stress, superoxide dismutase, peroxidase*

Introduction

Increasing salinity is threat for vegetable production, particularly in irrigated areas where 40% food of the world's is produce (Sarwar et al., 2016, 2017). Some vegetables i.e., onions, cucumbers, tomatoes, peppers and eggplants are sensitive to salinity (Yamaguchi and Blumwald, 2005; Sarwar et al., 2017). Stepien and Klobus (2006) and Sarwar et al. (2018) stated that cucumber considered is an important vegetable for human nutrition and diet and it is source of vitamins and dietary fiber; it has been used for 3,000 years in its native areas of Asia and Africa (Gopalan et al., 1982). But melicious impact of salt stress on cucumber crop caused a severe reduction in crop growth and yield (El-shraiy et al., 2011; Sarwar et al., 2016, 2017). Cucumber growth significantly affected by salinity higher than 25 mM, which caused a reduction in yield upto 13% (Chartzoulzkis, 1992; Dorota, 1997). Soil salinity is a very serious threat being faced by agriculture sector of the world as it restricts the plant growth and yield (Qin et al., 2010; Mahboob et al., 2017; Sarwar et al., 2017) modulates leaf gas

http://www.aloki.hu ● ISSN 1589 1623 (Print) ● ISSN 1785 0037 (Online)
DOI: http://dx.doi.org/10.15666/aeer/1705_1079310806

exchange traits (Maeda and Nakazawa, 2008) enhanced cell membranes leakage (Dogan et al., 2010) and caused nutrient deficiency (Yang et al., 2008).

Salt stress resistance in plants depends on types of salts which are present in soil, plant growth conditions, genotype, age and management practice (Sheekh-El et al., 2002; Ashraf et al., 2010) it prompts osmotic and ionic stress which affect the morpho-physio and biochemical modifications at cellular level (Murphy and Durako, 2003). Higher amount of salts in soil, reduced the water potential of plant cell and soil which restrict the plant roots to absorb necessary water (Lloyd et al., 1989) that lead dehydration and ultimately cause death of the cell. Soil salinity means Na^+ and Cl^- ions are dominant and higher level of such ions leads to ionic toxicity in salt sensitive crops (Garcia-Sanchez et al., 2002). Maximum amount of toxic ions in saline environment inhibits absorption of the essential nutrients i.e., K^+, Ca^+ and Mg^+ (Hasegawa et al., 2000) and moreover enhance the concentrations of toxic ions Na^+ or Cl^- in plant cells which results in enhanced permeability and/or destabilization of cellular membranes by subsituting Ca^+ and K^+ (Grattan and Grieve, 1992). Photosynthetic activity of plant decreased due to modulation in stomatal conductance under salinity (Sarwar et al., 2017). Loss of turgor by osmotic effect of salinity resulted in stomata will close, reduce the supply of carbon dioxide to leaves of plants. Though, in calvin cycle more reduction in photosynthetic rate was also reported due to degradation of green pigments; decreased leaf area by reducing photosynthetic enzyme activity (Misra et al., 1997; Ashraf et al., 2010). Salinity-induced oxidative stress has toxic reactions like, mutation, degradation of protein and lipid peroxidation that impaired photosynthesis (Mccord, 2000). Salinty and drought tolerance mechanism in plants comprises balance between osmotic adjustment, ions concentrations, osmotic adjustment is a water balance in cell due to accumulation of proline, sugars and their role as an osmolyte for osmotic adjustment. Sugars alcohols i.e. mannitol and sorbitol, and glycinebetaines are bring into mainly protect the protein of cytoplasm or keep away cell membranes desiccation (Ashraf et al., 2010; Balal et al., 2012).

Keeping in view the malicious impact of salt stress on plants, the objectives of our study were to figure out the physiological, biochemical and chemical responses of cucumber genotypes on scientific basis for elucidating the fundamental mechanisms involved in salt tolerance. Such information is also key for suggesting a suitable crop cultivar for salt-affected soils. Furthermore objective of this study was to determine the fluctuations in ionic homeostasis of cucumber genotypes in response to Nacl salinity.

Material and methods

Current investigation was planned to find out the potential of cucumber genotypes for their salt tolerance under lath house conditions (30–35°C and relative humidity 40-50%) in University of Agriculture, Faisalabad- Pakistan. Four contrasting cucumber genotypes (Marketmore, Green long, Summer green and 20252) have varying degree of salinity tolerance were used for this study. A sand culture experiment was comprised with seven treatments and replicated four times, every treatment contain 12 pots; so, total 84 pots were used for this study. Before start of experiment, seeds of uniform size and identical color were selected and sterilized by using 3% solution (v/v) of sodium hypo-chlorite for ten minutes. Distilled water was used to rinsed the seeds and air-dried the seeds at 25°C. Eight cucumber seeds were sown in each 9 L plastic pot, after one week of emergence, thinning was carried out to maintain four plants in each pot. Plants

http://www.aloki.hu ● ISSN 1589 1623 (Print) ● ISSN 1785 0037 (Online)
DOI: http://dx.doi.org/10.15666/aeer/1705_1079310806

were irrigated after two days interval, half strength Hogland solution was used as a nutrient source twice in a week. Salt stress was based on Nacl (MERCK, CAS #-7647-14-5), NaCl stress was imposed at 40 days old crop after sowing. Six levels of salinity were investigated i.e., (Control- no stress), 2, 3, 4, 5, 6 and 7 dS m^{-1} NaCl. To avoid the osmotic shock, salt stress was imposed by gradual increments untill final concentrations reached for each treatments. The levels of salinity were maintained through out the experiment by recording EC and pH of the growing media. After one weeks of NaCl induction data were recorded for evaluation.

Growth characteristics

Five plants selected from each treatment to calculate the morphological traits, e.g. shoot/root length of cucumber plants with meter rod. Fresh weight of both shoot/root was weighed by an electrical balance (g). For dry weight determination these shoot/root were placed in oven at 70ºC temperature for 72 hours and mean values were calculated.

Leaf gas exchange attributes

The gaseous characteristics were estimated with Infrared Gas Analyzer by the described method of Sarwar et al. (2017).

Chlorophyll contents (SPAD)

For each plant, quantification of chlorophyll were taken from fully expanded third to forth young leave (Khan et al., 2003).

Membrane leakage (%)

Membrane leakage was assessed by the procedure of Lutts et al. (1996). Ten leaf discs of approximately same size were selected from young fully expanded leaf. After washing to remove dirt from leaf, little leaf discs were dipped in test tube having 10 ml distilled water and these tubes leave for 24 hour under room temperature followed by the determination of (EC_1) of electrolyte rich solution with the help of EC meter. Later on, the samples were shifted to water bath at 72ºC for 20 minutes and subsequently cooled at room temperature. The EC of diffused tissues (EC_2) was recorded. Membrane leakage was deliberated as ratio between EC_1 and EC_2 and expressed into %age.

Antioxidant enzymes and proline contents

Superoxide dismutase activity was assessed via proposed procedure of (Giannopolitis and Ries, 1977). Catalase and peroxidase were determined by the method of Chance and Maehly (1955). Whereas proline and glycinebetaine were quantified by the techniques of Bates et al. (1973) and Grieve and Gratan (1983).

Determination of ionic content (Na^+, K^+ and Ca^+)

The concentrtion of sodium, potassium and calcium were quantify according to method of digested leave samples The content of Na^+ and K^+ in extracted solution was estimated by flame photometer (Model Jenway PFP-7; UK). A graded series of standards (ranging from 10- 100 mg L^{-1}) of Na^+ K^+ and Ca^+ were prepared to draw standard curves used to quantify final concentration.

http://www.aloki.hu ● ISSN 1589 1623 (Print) ● ISSN 1785 0037 (Online)
DOI: http://dx.doi.org/10.15666/aeer/1705_1079310806

Determination of Chloride

For determination of chloride ions, grounded plant material (1 gram) was taken in 50 ml test tube having 20 ml of distilled water and heated in an oven for overnight at 66°C. Then this solution filtered with "Whatmann-40 filter paper" and quantify of content with the help of Cl^- analyzer (Model: Corning-920, Germany).

Statistical analysis

The collected data was statistically analyzed under Completely Randomize Design (CRD) with factorial arrangement using (ANOVA) analysis of variance technique by Statistix 8.1 by implying HSD (Tukey's Test).

Results

Plant growth attributes

The present results revealed that increasing salt stress significantly and gradually reduced plant biomass in response of shoot/root length, fresh/dry weight and no. of leaves per plant. However, this decline was minimum in Marketmore, Green long genotypes who maintained better shootand root length, fresh and dry biomass by retaining maximum no. of leaves/plant as comparison to Summer green or 20252 genotypes (*Figs. 1, 2, 3a*).

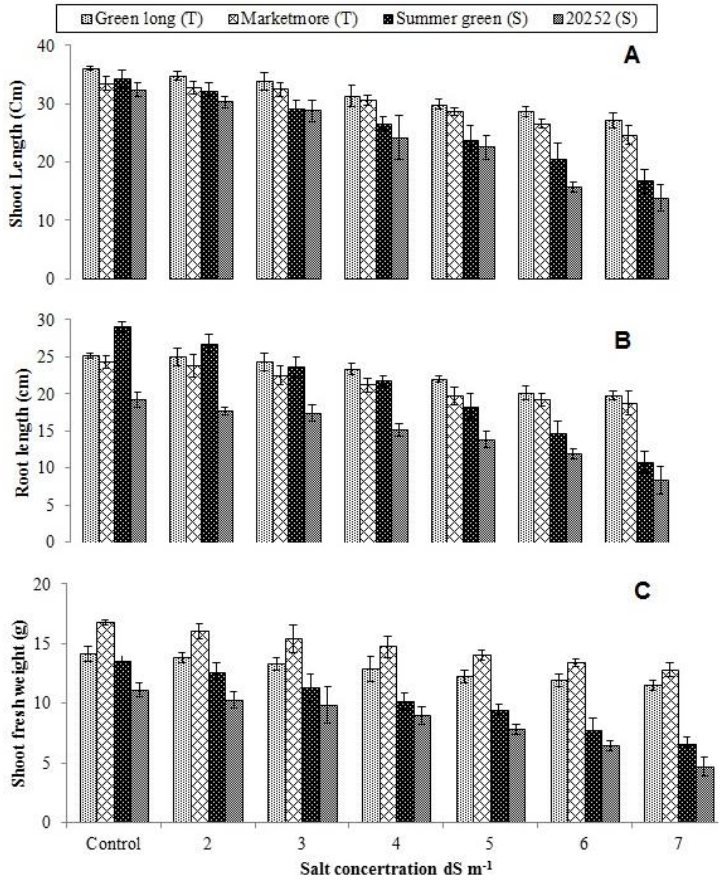

Figure 1. *Effect of salt stress on (a) shoot length (b) root length (c) Shoot fresh weight (g)*

http://www.aloki.hu ● ISSN 1589 1623 (Print) ● ISSN 1785 0037 (Online)
DOI: http://dx.doi.org/10.15666/aeer/1705_1079310806

Among the genotypes, Greenlong effectively neutralized the negative impects of salinity on plant growth and performed better than other genotypes under all salinity treatments. Hence, maximum shoot fresh weight was exhibited by market more under all experimental conditions. Cucumber 20252 showed maximum sensitivity towards salinity at all concentrations of salt stress and failed to manage considerable no. of leaves which produced lower shoot/root lengths with minimum fresh/dry weights.

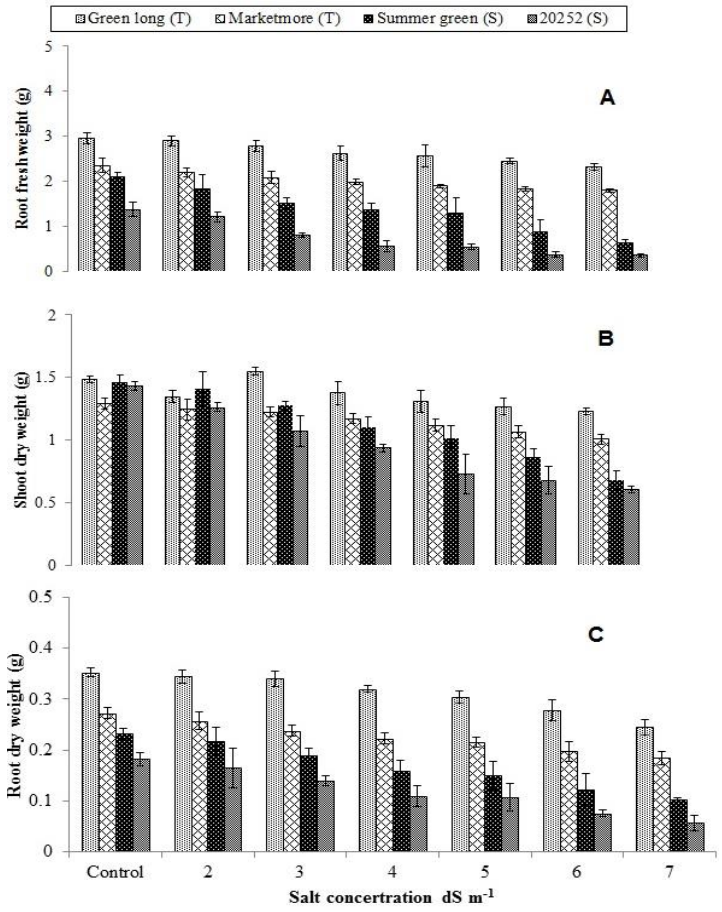

Figure 2. *Effect of salt stress on (a) Root fresh weight (b) Shoot dry weight (c) Root dry weight*

Leaf gas exchange attributes and chlorophyll content (SPAD)

Gas exchange attributes meaningfully decreased in tested cucumber genotypes (*Fig. 3*) at all salt levels however, significant decline in photosynthesis was induced by 6 dS m^{-1} salinity (*Fig. 3b,c*). Under highest salt level 7.0 dS m^{-1}, maximum reduction in gas exchange attributes were noted for Summer green or 20252 whereas, lowest for Marketmore or Green long in comparison to their controls. Increasing salt level caused decline in gas exchange attributes in tested genotypes, but higher decreased in these parameters was noted for genotype 20252 which is followed by Summer green. Maximum photosynthetic and respiration rate was exhibited by Marketmore under all salinity levels that is statistically at par with green long and behaved alike. Whereas, genotype 20252 showed highest stomatal conductance up to 3 dS m^{-1} salt stress but Green long maintained better stomatal conductance and improved water use efficiency even at higher level of salinity which is followed by Marketmore. Likewise, all the

http://www.aloki.hu ● ISSN 1589 1623 (Print) ● ISSN 1785 0037 (Online)
DOI: http://dx.doi.org/10.15666/aeer/1705_1079310806

evaluating genotypes illustrate significant degradation of leaf chlorophyll in answer to elevating salt stress (*Fig 4c*). Maximum decline was observed at 7 dSm^{-1}. Thus, Green long and marketmore produced maximum chlorophyll under all level of salinity which expressed their capacity to tolerate salinity stress. Contrarly, high levels of salinity significantly affected stay green ability of Summer green and 20252 by reducing chlorophyll pigment. Lowest chlorophyll content was recorded for same genotypes at highest stress of 7 dSm^{-1}.

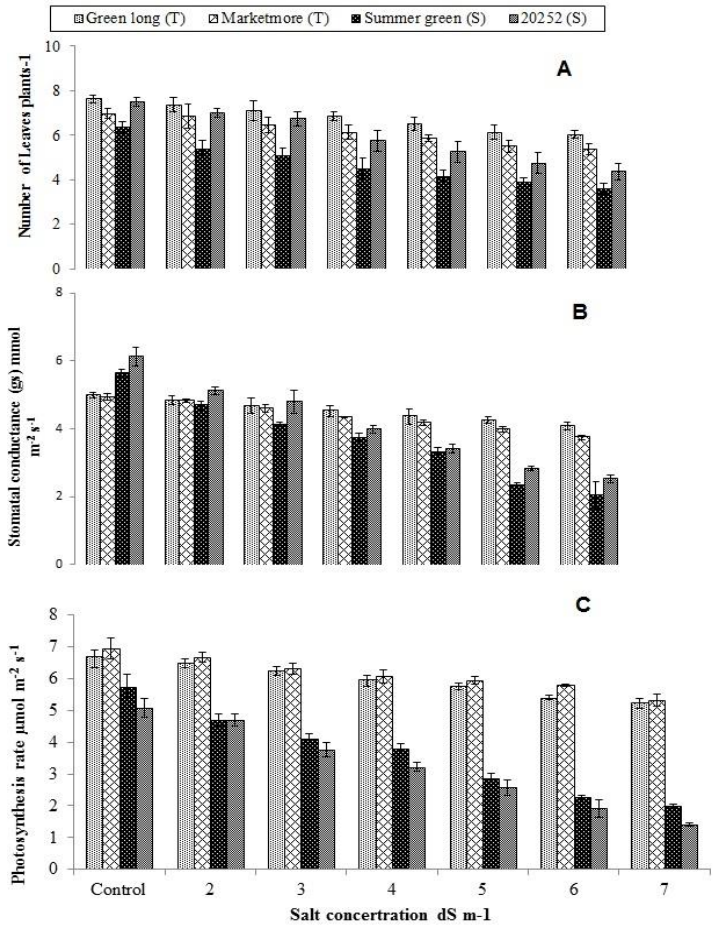

Figure 3. *Effect of salt stress on (a) number of leaves plant^{-1} (b) Stomatal conductance (c) Photosynthesis rate*

Electrolyte leakage(%)

It is obvious from data that all the cucumber genotypes showed a significant enhancement in electrolyte leakage when subjected to salt stress. Hence, the gradual increase in electrolyte leakage was observed with rising level of salinity and maximum increase was noted at 7 dSm^{-1} stress in genotype (20252) that was statistically at par with Summer green and behaved alike. Among the genotypes, Marketmore and Green long maintained better membrane stability and resulted in minimum electrolyte leakage under all salinity treatments over non-saline control. It indicates that electrolyte leakage % that can be used as potential approach for evaluating salt stress tolerance in cucumber plants.

http://www.aloki.hu ● ISSN 1589 1623 (Print) ● ISSN 1785 0037 (Online)
DOI: http://dx.doi.org/10.15666/aeer/1705_1079310806

Antioxidant enzymes and osmolytes

It is clear from presented data that imposition of different salts concentration had a significant impact on the production of proline content and enzymatic activities in tested cucumber genotypes (*Fig. 5b,c*). However, maximum accumulation of proline and antioxidant activity was observed at highest saline level (7 dSm^{-1}). In case of genotypes, highest activities of CAT, SOD, POD and proline was demonstrated by Marketmore that was proceeded by green long genotype on exposure to all salinity treatments. Whereas, summer green was unable to produce better proline content as presented in *Fig. 6* and releaved minimum values for proline at all stress levels. Likewise, lowest activities of SOD, CAT, POD antioxidant were also exhibited by summer green as compared to other genotypes uder control and salt stress as well (*Figs. 5 and 6*).

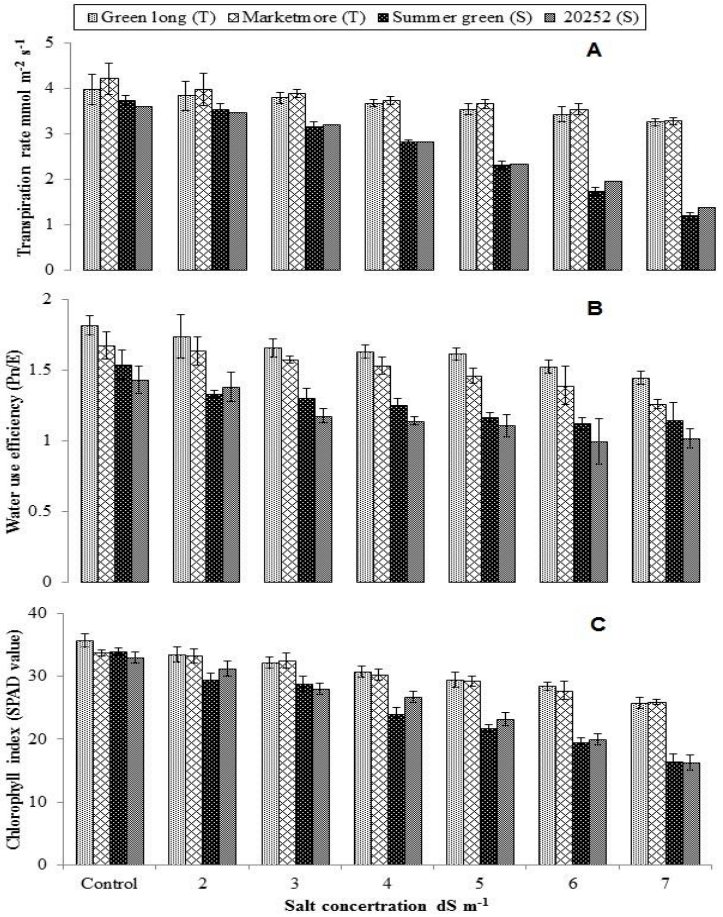

Figure 4. *Effect of salt stress on (a) Transpiration rate (b) Water use efficiency (WUE) (Pn/E) (c) Chlorophyll contents*

Leaf inorganic osmolytes

It is cleared from the results that rising levels of salinity modulated the concentration of in-organic osmolytes (Na^+, Cl^-, K^+, and Ca^+) in all cumcumber genotypes grown under salt stress (*Table 1*). Among the genotypes, 20252 and Summer green leaves had accumulated maximum contents of Na^+ and Cl^-, respectively, whereas Marketmore showed least build up of Na^+ and Cl^- contents in leaves in addition to improved

http://www.aloki.hu ● ISSN 1589 1623 (Print) ● ISSN 1785 0037 (Online)
DOI: http://dx.doi.org/10.15666/aeer/1705_1079310806

deposition of ionic content of K and Ca that was followed by green long under all saline regimes. These outcomes showed that at 70 mM level of salinity, cucumber genotypes Marketmore and Green long presented least increment in Na^+ and Cl^-, however, Summer green and 20252 exhibited maximum accumulation of these ions which indicated that resistant genotypes had lowest level of Na^+ and Cl^- in their leaves in comparison to sensitive cucumber genotypes. It can be concluded from the findings of this experiment is (Summer green or 20252) categorize as sensitive genotypes whereas, (Marketmore or Green long) are categorized as salt tolerant cucumber genotypes.

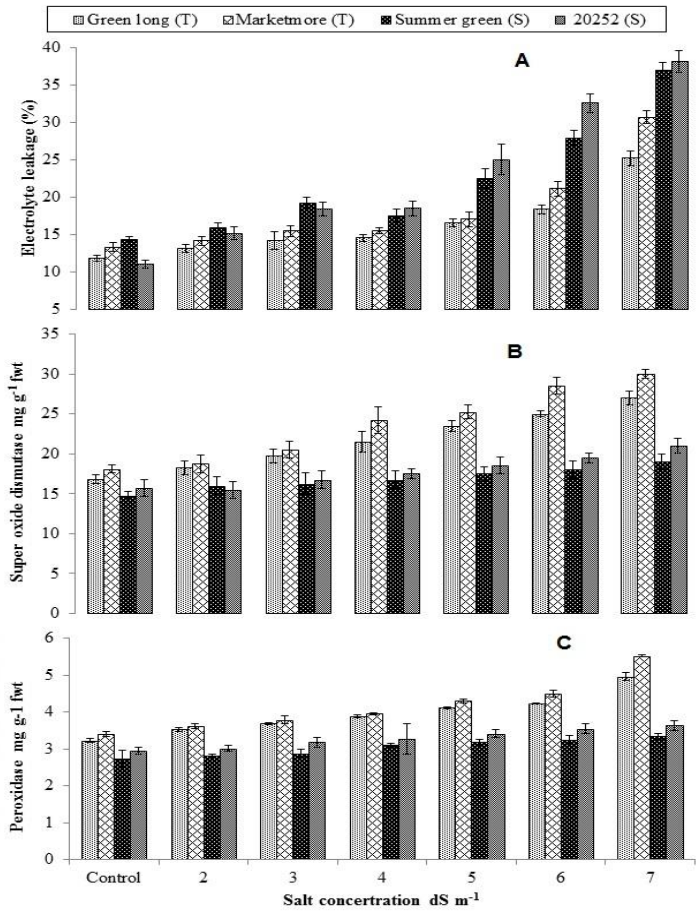

Figure 5. *Effect of salt stress on leaf (a) Electrolyte leakage (%) (b) Superoxide dismutase activity (c) Peroxidase activity*

Discussion

Inhibition in plant growth and development is very usual phenomena under salinity stress (Ashraf et al., 2009; Mahboob et al., 2017; Sarwar et al., 2017). Results illustrated that salts significantly decreased the root/shoot length, their fresh/dry biomasses and number of leaves per plants in all studied cucumber genotypes (*Figs. 1,2* and *3a*). Under stressed condition variation in total number of leaves $plant^{-1}$ is a important prevalence (Zhu et al., 2001). In present study, studied cucumber genotypes such as Marketmore and Green long was presented was little affected by salinity and presented maximum number of leaves while sumer green and 20252 failed to produce better number of

http://www.aloki.hu ● ISSN 1589 1623 (Print) ● ISSN 1785 0037 (Online)
DOI: http://dx.doi.org/10.15666/aeer/1705_1079310806

leaves under saline conditions. Likewise reduction in leaves per plants were also observed by (Hassine and Lutts, 2010) in potato crop and (Bakht et al., 2011) in maize plant. Such decline in number of leaves in term of salt stress might be because of negative effects of salts on cell elongation mechanisms (Ashraf and Harris, 2004; Iqbal and Ashraf, 2005; Sawar et al., 2017).

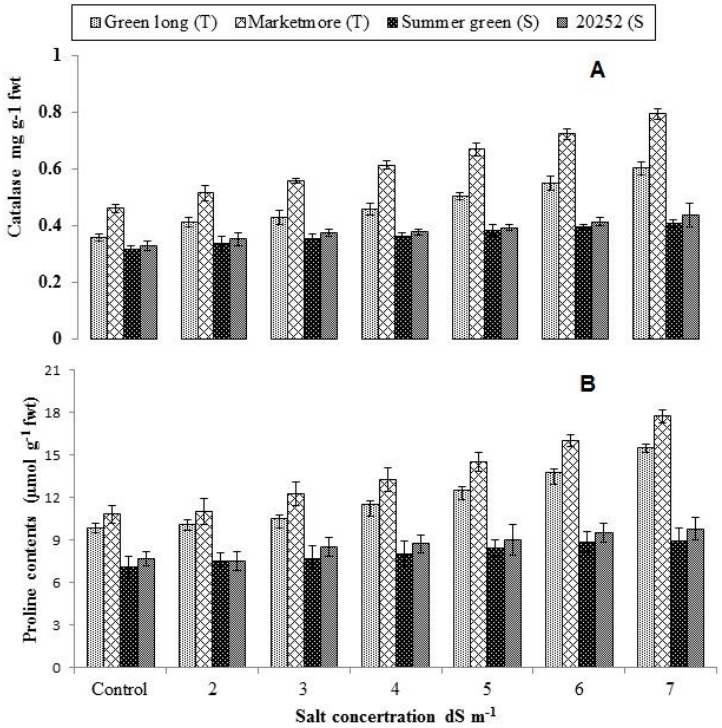

Figure 6. *Effect of salt stress on leaf (a) Catalase activity (b) Proline contents*

Table 1. *Effect of salt stress on leaf inorganic osmolytes of four cucumber genotypes*

	Na^+ *ions(mg* g^{-1} *D.W)*				K^+ *ions(mg* g^{-1} *D.W)*			
Salt Treatments	**Green long**	**Marketmore**	**Summer green**	**20252**	**Green long**	**Marketmore**	**Summer green**	**20252**
Control	8.79±0.28	8.46±0.45	8.95±0.30	10.00±0.43	28.5±0.64	30±0.91	28.75±0.85	28±0.91
2.0 dS m^{-1}	9.54±0.62	9.26±0.90	11.61±0.47	14.23±0.69	26.25±1.25	27.25±1.2	26.25±1.10	25±1.08
3.0 dS m^{-1}	11.19±0.42	10.66±1.0	15.76±0.82	17.77±0.96	24.25±1.10	25.75±1.2	24.25±1.10	23.5±1.19
4.0 dS m^{-1}	12.91±0.51	11.27±0.60	18.19±1.61	20.66±1.68	22.75±0.85	24.75±1.3	23±0.912	22±0.91
5.0 dS m^{-1}	15.89±0.57	12.27±0.98	23±1.164	23.27±0.87	20.75±0.85	22.75±0.85	19.75±0.75	21.5±1.75
6.0 dS m^{-1}	19.81±0.68	15.69±2.06	24.45±1.54	28.14±1.05	19.5±0.645	21.75±1.10	15.75±0.85	14.25±1.54
7.0 dS m^{-1}	22.71±0.72	20.99±0.84	32.35±1.38	37.09±1.97	18.75±0.85	21±0.91	13.5±0.64	11.5±1.70
Salt Treatments	Ca^+ *ions(mg* g^{-1} *D.W)*				Cl^- *ions(mg* g^{-1} *D.W)*			
Control	26.5±0.95	29.75±1.10	26.75±1.31	28.75±1.2	4.90±0.27	4.27±0.15	6.7±0.48	4.6±0.49
2.0 dS m^{-1}	24.75±0.85	29±0.40	25.25±1.3	25.75±0.85	5.32±0.30	4.45±0.41	8.11±0.48	5.85±0.60
3.0 dS m^{-1}	23.25±0.62	27.75±1.10	23.5±1.19	23.75±1.79	6.04±0.30	5.20±0.38	9.3±0.87	5.99±0.58
4.0 dS m^{-1}	22.75±0.85	26.5±0.64	20.75±0.85	20.5±1.93	6.62±0.75	6.092±0.56	11.60±1.03	8.30±0.70
5.0 dS m^{-1}	21.25±0.47	25.25±0.85	17.5±1.19	18.25±0.85	8.45±0.58	7.12±0.61	14.53±1.71	9.44±0.82
6.0 dS m^{-1}	20.5±1.32	23.75±1.4	15±1.47	16.5±1.70	9.4±0.47	7.975±0.54	16.31±1.66	11.07±1.55
7.0 dS m^{-1}	19.5±0.64	22.75±0.85	12.5±1.5	12±1.22	11.16±0.62	8.89±0.75	20.94±0.65	15.96±1.31

Data represent the means ± SE of four repeats. Means having different letters are significantly different at $P \leq 0.05$ according to HSD Tucky Test

http://www.aloki.hu ● ISSN 1589 1623 (Print) ● ISSN 1785 0037 (Online)
DOI: http://dx.doi.org/10.15666/aeer/1705_1079310806

The tested cucumber genotypes showed significant decreased in plant fresh and dry biomasses on exposure to various levels of salinity (*Fig. 2*), which established by the results of Mahboob et al. (2016) in *Triticum aestivum* (Noreen and Ashraf, 2008; Ashraf, 2009; Sarwar et al., 2016) in sunflower. However, under salt stress reduction in plant biomass might be due to lot of factors e.g, lack of turgor potential maintenance, sodium and chloride ions toxicity and variabilities in metabolic pathways. In the meantime, such factors disturb the gas exchange attributes that is ultimatelly cause decline in the activity of photosynthetic pigments (Sarwar et al., 2017). Subsequently, in this investigation reduction in plant biomass was due to decline in photosynthesis rate and a strong positive correlation was observed amongst dry weight of plants and gas exchange traits which revealed that those genotypes attained maximum dry biomass had higher rates of *gs* and *Pn.* The present results explained that photosynthesis was reduced due to maximum level of Na^+or Cl^- ions in plant cell which exhilarated the lethal impact on physiological mechanisms and functioning of leaf stomata. Bano (2010) also finds the same decreased in gas exchange traits in rice, when its exposed to saline stress. Results revealed that "Marketmore and Green long" presented lowest decreased in *Pn* and *gs* as compared to "Summer green and 20252", thus these attributes can be used as a screening tool for the salinity tolerance in cucumber plants. The previous researchers reported that the saline stress induced significant differences in *gs Pn* and *E* in sunflowers, rice and olive and these types of physiological traits can be measured as a potential signs of salinity tolerance (Nishimura et al., 2011). Since, salt stress have great impact on stomata function by losing the turgidity of guard cells ultimatelly it reduced transpiration rate in cucumber plants (Stepin and Klobus, 2006). Our findings are in agreement to Tezara et al. (2002), they described that sunflower showed a significant reduction in *E* on exposure to water stress. On the other hand, salts stress restrict the availability of various essentials nutrients to plants especially K^+ ions (Najafi et al., 2007; Mahboob et al., 2013) and K^+ is responsible for guard cell turgidity (Burman et al., 2003) so under salinity, variabilities in guard cell functioning may be reduced *gs* and *E* in cucumber plants. Those cucumber genotypes which keep the constant transpiration rate and stomatal conductance under stressed environments were successful to regulate them osmotically through production of glycinebetaine and proline. Thus, it is clear that Marketmore and Green long genotypes of cucumber have salt tolerance potential due to higher production of proline in plant cell. Increase in production of such osmoprotectant under salinity reported that for Seepweed and Glasswort by Moghaieb et al. (2004), in Maiz by Hajlaoui et al. (2010) and Mahboob et al. (2013). In this study, reduction in chlorophyll contentsdue to substitution of Mg^{2+} ions by toxic Na^+ ions,that caused the denaturation of chlorophyll. Under salinity in cotton crop same results were reported by Meloni et al. (2003) and in Maiz stated by Mahboob et al. (2013). In literature a positive relationship was observed amongst chlorophyll contents production and plant biomass growth. It is showed that salinity fragmented the cell membranes to a smaller extent in resistant genotypes in comparison to sensitives. In genotypes Marketmore and Green long were showed the sign of little electrolyte leakage; might be tolerant genotypes presented lower H_2O_2 and least (EL) than sensitives, this trait electrolyte leakage can be used to determine the saline stress damage's and potential of tolerance in plants. Likewise, Noreen and Ashraf (2009) complied different cucumber genotypes to many salt concentrations and observed a increment in LPO and H_2O_2 level with various salt concentrations. Higher activities of SOD, POD and CAT detoxify the (ROS) in plant cell (Sekmen et al., 2012). So, salt tolerance potential is connected with the production

http://www.aloki.hu ● ISSN 1589 1623 (Print) ● ISSN 1785 0037 (Online)
DOI: http://dx.doi.org/10.15666/aeer/1705_1079310806

of antioxidant enzymes activities (Balal et al., 2012). Same findings were comparised in this study a constant activities of antioxidant in tolerant cucumber genotypes with high potassium and calcium ions in their leaves, in results higher plant biomass, maximum photosynthesis activities as comparison to sensitive genotypes. As a result K^+ and Ca^+ ions concentrations can used as a screening parameter for the estimation of salt stress tolerance in cucumber cultivars. Conclusion of this findings is that saline stress had negative impact on the growth and yield of cucumber plant and potential of salinity tolerance is greatly connected with the quantity of proline contents and Ca^+, K^+ ions that play vital part in osmotic adjustment under salinity.

Conclusions

Salt stress harmfully affect the morpho-physiological and biochemical traits of cucumber genotypes by producing osmotic stress, ionic toxicity, altered stomatal functioning, impaired photosynthesis and restricted K^+ availability. Salt resistant cucumber genotypes were able to avoid most of the harmful implications of salt stress by Na^+ exclusion and maintenance of favorable levels of K^+ and Ca^{2+} that helped stabilize photosynthetic pigments and photosynthetic machinery under salinity stress resulting in comparatively better functioning and growth than salt sensitive genotypes. These cucumber genotypes can also serve for future studies dealing with salinity tolerance in cucumber, besides their worth in breeding programs and cultivation on soils where salinity seems inevitable

REFERENCES

[1] Ashraf, M., Haris, P. J. C. (2004): Potential biochemical indicators of salinity tolerance in plants. – Plant Science 166: 3-16.

[2] Ashraf, M., Rahmatullah, A. R., Bhatti, A. S., Afzal, M., Sarwar, A., Maqsood, M. A., Kanwal, S. (2010): Amelioration of Salt Stress in Sugarcane (Saccharum officinarum L.) by Supplying Potassium and Silicon in Hydroponics. – Pedosphere 20: 153-162.

[3] Bakht, J., Shafi, M., Jamal, Y., Sher, H. (2011): Response of maize (Zea mays L.) to seed priming with NaCl and salinity stress. – Spanish Journal of Agricultural Research 9: 252-261.

[4] Balal, R. M., Khan, M. M., Shahid, M. A., Mattson, N. S., Abbas, T., Ashfaq, M., Garcia-Sanchez, F., Ghazanfer, U., Gimeno, V., Iqbal, Z. (2012): Comparative studies on the physio-biochemical, enzymatic, and ionic modifications in salt tolerant and salt sensitive citrus rootstocks under NaCl stress. – Journal of the American Society for Horticultural Science 137: 1-10.

[5] Bano, A. (2010): Root-to-shoot signal transduction in rice under salt stress. – Pakistan Journal of Botany 42: 329-339.

[6] Bates, L. S., Waldron, R. P., Teaxe, W. I. (1973): Rapid determination of free proline for water stress studies. – Plant and Soil 39: 205-207.

[7] Burman, U., Garg, B. K., Kathju, S. (2003): Water relations, photosynthesis and nitrogen metabolism of Indian mustard (Brassica jucea) grown under salt and water stress. – Journal of Plant Biology 30: 55-60.

[8] Chance, M., Maehly, A. C. (1955): Assay of catalases and peroxidases. – Methods in Enzymology 2: 764-817.

[9] Chartzoulakis, K. S. (1992): Effects of NaCl salinity on germination, growth and yield of greenhouse cucumber. – Journal of Horticultural Science 67: 115-119.

http://www.aloki.hu ● ISSN 1589 1623 (Print) ● ISSN 1785 0037 (Online)
DOI: http://dx.doi.org/10.15666/aeer/1705_1079310806

[10] Dogan, M., Tipirdamaz, R., Demir, Y. (2010): Salt resistance of tomato species grown in sand culture. – Plant, Soil and Environment 56: 499-507.
[11] Dorota, Z. (1997): Irrigating with high salinity water. – Bulletin 322 Agricultural and Biological Engineering Dep; Florida Cooperative Extension service Institute of Food and Agriculture Sciences University of Florida.
[12] El-Shraiy, A. M., Mostafa, M. A., Zaghlool, S. A., Shehata, S. A. M. (2011): Alleviation of Salt Injury of Cucumber Plant by Grafting onto Salt Tolerance Rootstock. – Australian Journal of Basic and Applied Sciences 5(10): 1414-1423.
[13] FAO. (2012): The State of the World's Land and Water Resources for Food and Agriculture (SOLAW) managing systems at risk. – Food and Agriculture Organization of the United Nations, Rome and Earthscan, London.
[14] Garcia-Sanchez, F., Jifon, J. L., Carvaial, M., Syvertsen, M. (2002): Gas exchange, chlorophyll and nutrient contents in relation to Na^+ and Cl^- accumulation in 'Sunburst' mandarin grafted on different rootstocks. – Plant Science 162: 705-712.
[15] Giannopolitis, C. N., Ries, S. K. (1977): Superoxide dismutase I. Occurrence in higher plants. – Plant Physiology 59: 309-314.
[16] Gopalan, C., Rama, S. B. V., Balasubramanian, S. C. (1989): Nutritive value of Indian foods. – National Institute of Nutrition, Indian Council of Medical Research.
[17] Grattan, S. R., Grieve, C. M. (1992): Mineral element acquisition and growth response of plants grown in saline environment. – Agriculture Ecosystems & Environment 38: 275-300.
[18] Grieve, C. M., Gratan, S. R. (1983): Rapid assay for the determination of water soluble quaternary ammonium compounds. – Plant and Soil 70: 303-307.
[19] Hajlaoui, H., Ayeb, N. E., Garrec, J. P., Denden, V. (2010): Differential effects of salt stress on osmotic adjustment and solutes allocation on the basis of root and leaf tissue senescence of two silage maize (Zea mays L.) varieties. – Industrial Crops and Products 31: 122-130.
[20] Hasegawa, P. M., Bressnan, R. A., Zhu, J. K., Bohnert, H. J. (2000): Plant cellular and molecular responses to high salinity. – Annual Review of Plant Physiology and Plant Mololecular Biology 51: 463-499.
[21] Hassine, A. B., Lutts, S. (2010): Differential responses of saltbush Atriplex halimus L. exposed to salinity and water stress in relation to senescing hormones abscisic acid and ethylene. – Journal of Plant Physiology 167: 1448-1456.
[22] Heidari, M. (2010): Nucleic acid metabolism, proline concentration and antioxidants enzyme activity in canola (Brassica nupus L.) under salinity stress. – Agricultural Sciences in China 9: 504-511.
[23] Iqbal, M., Ashraf, M. (2005): Changes in growth photosynthetic activity and ionic relations in spring wheat. – Plant Growth Regulator 60: 41-52.
[24] Khan, W., Prithiviraj, B., Smith, P. (2003): Photosynthetic responses of corn and soybean to foliar application of salicylates. – Journal of Plant Physiology 20: 1-8.
[25] Lloyd, J., Kriedmann, P. E., Aspinall, D. (1989): Comperative sensitivity of prior lisbon lemon and valencia orange trees to foliar sodium and chloride concentrations. – Plant, Cell & Environment 12: 529-540.
[26] Lutts, S., Kinet, J. M., Bouharmont, J. (1996): NaCl-induced senescence in leaves of rice (Oryza sativa L.) cultivars differing in salinity resistance. – Annals Bot 78: 389-398.
[27] Maeda, Y., Nakazawa, R. (2008): Effects of the timing of calcium application on the alleviation of salt stress in the maize, tall fescue, and reed canary grass seedlings. – Biologia Plantarum 52: 153-156.
[28] Mahboob, W., Rehman, H., Basra, S. M. A., Afzal, I., Abbas, M. A., Naeem, M., Sarwar, M. (2015): Seed Priming Improves the Performance of Late Sown Spring Maiz (Zea mays) through better Crop Stand and Physiological Attributes. – Int. J. Agric. Biol 17(3): 491-498.

http://www.aloki.hu ● ISSN 1589 1623 (Print) ● ISSN 1785 0037 (Online)
DOI: http://dx.doi.org/10.15666/aeer/1705_1079310806

[29] Mahboob, W., Khan, M. A., Shirazi, M. U. (2016): Induction of salt tolerance in wheat (Triticum aestivum L.) seedlings through exogenous application of proline. – Pak. J. Bot 48(3): 861-867.
[30] Mahboob, W., Khan, M. A., Shirazi, M. U. (2017): Characterization of Salt Tolerant Wheat (Triticum aestivum) Genotypes on the Basis of Physiological Attributes. – Int. J. Agric. Biol 19: 726-734.
[31] McCord, J. M. (2000): The evolution of free redicals and oxidative stress. – The American Journal of Medicine 108: 652-659.
[32] Meloni, D. A., Oliva, M. A., Martinez, C. A., Cambraia, J. (2003): Photosynthesis and activity of superoxide dismutase, peroxidase and glutathione reductase in cotton under salt stress. – Environmental and Experimental Botany 49: 69-76.
[33] Misra, A. N., Sahu, S. M., Misra, M., Singh, P., Meera, I., Das, N., Kar, M., Shau, P. (1997): Sodium chloride induced changes in leaf growth, and pigment and protein contents in two rice cultivars. – Biologia Plantarum 39: 257-262.
[34] Moghaieb, R. E. A., Saneoka, H., Fujita, K. (2004): Effect of salinity on osmotic adjustment, glycinebetaine accumulation and the betaine aldehyde dehydrogenase gene expression in two halophytic plants, Salicornia europaea and Suaeda maritima. – Plant Science 166: 1345-1349.
[35] Murphy, K. S. T., Durako, M. J. (2003): Physiological effects of short term salinity changes on Ruppia maritima. – Aquatic Botany 75: 293-309.
[36] Najafi, F., Khavari-Nejad, R. A., Rastgar-Jazii, F., Sticklen, M. (2007): Growth and some physiological attributes of pea (Pisum sativum L.) as affected by salinity. – Pakistan Journal of Biology 10: 2752-2755.
[37] Nishimura, T., Cha-um, S., Takagaki, M., Ohyama, K., Kirdmanee, C. (2011): Survival percentage, photosynthetic abilities and growth characters of two indica rice (Oryza sativa L. spp. indica) cultivars in response to isosmotic stress. – Spanish Journal of Agricultural Research 9: 262-270.
[38] Noreen, S., Ashraf, M. (2008): Alleviation of adverse effects of salt stress on sunflower (Helianthus annuus L.) by exogenous application of salicylic acid: growth andphotosynthesis. – Pakistan Journal of Botany 40: 1657-1663.
[39] Noreen, Z., Ashraf, M. (2009): Assessment of variation in antioxidative defense system in salt- treated pea (Pisum sativum) cultivars and its putative use as salinity tolerance markers. – Journal of Plant Physiology 166: 1764-1774.
[40] Qin, J., Dong, W. Y., He, K. N., Yu, Y., Tan, G. D., Han, L., Dong, M., Zhang, Y. Y., Zhang, D., Li, Z. A., Wang, Z. L. (2010): NaCl salinity-induced changes in water status, ion contents and photosyn thetic properties of Shepherdia argentea (Pursh) Nutt. seedlings. – Plant, Soil and Environment 56: 325-332.
[41] Sarwar, M., Amjad, M., Ayyub, C. M., Ashraf, A., Tehseen, S., Manan, A., Butt, M., Hussain, T., Nawaz, M. A. (2016): Evaluation of cucumber germplasm for salinity tolerance based on early growth attributes and leaf inorganic osmolytes. – Transylvanian review 24: 1077-1086.
[42] Sarwar, M., Amjad, M., Ayyub, C. M. (2017): Alleviation of Salt stress in cucumber (Cucumis sativus L.) through seed priming with triacontanol. – International Journal of Agricultural Biology 19: 771-778.
[43] Sarwar, M., Anjum, S., Khan, M. A., Haider, M. S., Ali, S., Naseem, M. K. (2018): Assessment of sustainable and eco-friendly agricultural substrates for eminence production of chilies for kitchen gardening. – Int J Recycl Org Waste Agriculture 7: 365-374.
[44] Sekmen, A. H., Turkan, I., Tanyolac, Z. O., Ozfidan, C., Dinc, A. (2012): Different antioxidant defense responses to salt stress during germination and vegetative stages of endemic halophyte Gypsophila oblanceolata Bark. – Environmental and Experimental Botany 77: 63-76.

http://www.aloki.hu ● ISSN 1589 1623 (Print) ● ISSN 1785 0037 (Online)
DOI: http://dx.doi.org/10.15666/aeer/1705_1079310806

[45] Sheekh-EL, M. M., Omar, H. H. (2002): Effect of high salt stress on growth and fatty acids content of the unicellular green algae Chlorella vulgaris. – Journal of Microbiology 55: 181-191.
[46] Stepien, P., Klobus, G. (2006): Water relations and photosynthesis in Cucumis sativus L. leaves under salt stress. – Biologia Plantarum 50: 610-616.
[47] Tezara, W., Mitchell, V., Driscoll, S. P., Lawlor, D. W. (2002): Effects of water deficit and its interaction with CO_2 supply on the biochemistry and physiology of photosynthesis in sun flower. – Journal of Experimental Botany 53: 1781-1791.
[48] Yamaguchi, T., Blumwald, E. (2005): Developing salt-tolerant crop plants: challenges and opportunities. – Trends in Plant Science 10: 616-619.
[49] Yang, C. W., Wang, P., Li, C. Y., Shi, D. C., Wang, D. L. (2008): Comparison of effects of salt and alkali stresses on the growth and photosynthesis of wheat. – Photosynthetica 46: 107-114.
[50] Zhu, J. K. (2001): Plant salt tolerance. – Trends in Plant Science 6: 66-72.

http://www.aloki.hu ● ISSN 1589 1623 (Print) ● ISSN 1785 0037 (Online)
DOI: http://dx.doi.org/10.15666/aeer/1705_1079310806

ASSESSMENT OF INVASIVE PLANT SPECIES, *OPUNTIA* SPP. (PRICKLY PEAR) IN RAYDAH PROTECTED AREA, ASEER, SAUDI ARABIA

ALWADAI, H. M.

Department of Biology, College of Science, King Khalid University, Abha, Saudi Arabia (e-mail: hmalwadai@kku.edu.sa; hmwadei@gmail.com; phone: +966-17-241-7242; fax: +966-17-241-8412)

(Received 9th Mar 2019; accepted 13th Jun 2019)

Abstract. Raydah protected area in an important declared protected area in Aseer area, Kingdom of Saudi Arabia that is rich in biodiversity, and provides habitat for nine of the ten indigenous bird species in the kingdom. Invasive plant *Opuntia* spp. in Raydah could threaten the natural balance among the indigenous species and thereafter affect the biological components of the ecosystem. This study evaluates the prevalence of invasive species and vegetation cover trends in Raydah protected area to identify possible interventions to conserve and protect the protected area. The results provide important and necessary information for the conservation and management of the Raydah Area and the Aseer Area's south-western highlands. The study has demonstrated the potential of sentinel sensor for detection and mapping of invasive species such as *Opuntia* spp. with desirable accuracy. This encouraging result demonstrated the feasibility of developing a semi-automated process for mapping and analysing the distribution of *Opuntia* spp. and found better results compared to multispectral data with very high resolution. Assessment of the current situation of the *Opuntia* spp. in the protected area will provide scientific data base for future management plans to combat and control invasive plants and protect the protected area from their adverse effects.
Keywords: *ecosystem, biodiversity, Sarawat Mountains, Juniperus procera, Sentinel satellite data*

Introduction

Invasive plants pose significant threats to natural ecosystems (Gurevitch and Padilla, 2004), biodiversity (Gaertner et al., 2009), forests (Peerbhay et al., 2016), rangelands and agricultural productivity (Pimentel et al., 2005). In addition, invasive plants are known to reduce the abundance of native plant species (Gaertner et al., 2009), alter soil properties (Pejchar and Mooney, 2009), and homogenize the biodiversity of invaded landscapes (Joshi et al., 2004). Invasive species are the species, subspecies that occur outside their natural range and potential for dispersal, and include any part of those species that may survive and then reproduce (Turlings, 2000). The non-native species invasion process took place in three phases: arrival, establishment and spread.

The southwestern parts of the Kingdom of Saudi Arabia have witnessed negative impacts of invasive species on forest ecosystems over the past few decades. Among them, the *Opuntia* spp. is one of the most serious invasive plant species, colonizing large forest areas in the highlands of the Sarawat Mountains in the southwestern parts of the kingdom. It is rich in dense vegetation as part of the southwest mountain ecosystem of the Sarwat, and constitutes the highest density of vegetation and diversity in the kingdom. The Sarwat southwest mountains' main high altitude species include *Juniperus procera*, the main dominant species with a density of 95 percent at elevations of 2000-3000 m above sea level (Aref et al., 2013). It grows in lower elevations with other tree species, such as *Acacia* spp., *Oleaeuropaea* ssp. Africana (Mill.) P. Green. *Ziziphus spina christi* and *Tamarix aphylla* (El-Juhany and Aref, 2013). El-Juhany and

http://www.aloki.hu ● ISSN 1589 1623 (Print) ● ISSN 1785 0037 (Online)
DOI: http://dx.doi.org/10.15666/aeer/1705_1080710822

Aref (2013) noted that the following species of tree were reported only in the Aseer region: *Dobera glabra, Adenium obesum, Mimusop slaurifolia, Ficussy comorus* and *Tamarindus indica.*

In the southwestern highlands, Thomas et al. (2016) reported many invasive species such as *Opuntia* spp. To evaluate changes in vegetation and the spread of invasive species, it is therefore important to evaluate the status in the Raydah protected area. Invasive species are usually introduced from their native range to new plant species, either intentionally (Surendra et al., 2013) or accidentally, expanding into natural areas and disrupting native plant communities. They are equipped to adapt to new habitats, and with reproductive capacity they can grow aggressively. In the absence of natural enemies, their ability to compete and grow vigorously enables them to expand aggressively. These alien species are usually introduced into an ecosystem through seeds in imported soil, traveller fruits, deliberate introduction of certain species for their products, services or values, dispersal of seeds by natural means, and disposal of waste or soil containing alien plant seeds. Invasive species may have been introduced through human interference in the southwestern highlands of the kingdom and expanded due to clearing vegetation of large areas for road expansion, grazing and felling and removal of endemic forest trees.

Invasive plant expansion Raydah may have catastrophic effects on the habitat of the protected area in terms of overgrowth and displacement of native plants, resulting in disruption of the natural balance of native plant communities. Possible major consequences could include:

- Altering the plant species density and extinction of some species.
- Reducing the genetic base of the endemic species (resulting from biotic and abiotic stresses).
- Impact the balance and composition of endemic plant species - dependent wildlife components.
- Biodiversity reduction can adversely affect wildlife and alter natural processes such as fire or intensity and water flow.

Assessment of the current situation in the Raydah protected area will indicate and reveal the gravity of the situation and indicate possible interventions to control the invasive species Many methods have been developed to control or eradicate invasive species dependent on: available resources, plant species and habitat, and spread severity. These methods include: chemical control of invasive species by systematic herbicides, biological control by imported enemies, mechanical control by machines and hand tools, physical control (hand pulling, water drainage, flooding, burning and shading), or a combination of these methods (Integrated Management). Accordingly, this study address the situation of the invasive species in Raydah, with the general aim of conserving Raydah protected area, as part of an important ecosystem in the southwestern highlands of the kingdom, from their danger and threats. The unique plant association that provides habitat for nine of the ten indigenous bird species of Saudi Arabia should be managed and protected from the aggressiveness of the alien species.

Remote sensing data of high resolution have received considerable attention for invasive species inventory. The multi-date satellite imagery facilitates the monitoring and identification of phenological changes. It may be useful to integrate satellite information with other attributes in GIS to predict the spread of invasive species. Remote sensing of invasive plants has only been successful if the invasive is in a

http://www.aloki.hu ● ISSN 1589 1623 (Print) ● ISSN 1785 0037 (Online)
DOI: http://dx.doi.org/10.15666/aeer/1705_1080710822

riparian, grassland, desert environment, aquatic and wetland where the lack of a tree cover enables the sensors to see the invasive plant unhindered (Bradley and Mustard, 2006). Thus, hindered invasive poses a challenge. Many researchers used hyperspectral data to detect and map invasive species (Lawrence et al., 2004). A practical advantage of using hyperspectral imagery to map invasive species is its capability to determine relative or unmixed components, which can be particularly useful in determining the percentage of species coverage (Peerbhay et al., 2016; Peerbhay et al., 2015; Curatola Fernandez et al., 2013). As noted above, the success of alien invasion remote sensing depends on their unique spectral signatures being identified, facilitated by differences in biophysical and biochemical characteristics (Matongera et al., 2016). Numerous studies (e.g. Matongera et al., 2016; Peerbhay et al., 2016; Niphadkar and Nagendra, 2016; Rocchini et al., 2015; Bradley, 2014; Boyd and Foody, 2011; Joshi et al., 2004) have explored approaches to remote sensing to optimize AIP detection and mapping.

The study aims to evaluate the prevalence of invasive species and vegetation cover trends in Raydah protected area to identify possible interventions to conserve and protect the protected area. The results may provide important and necessary information for the conservation and management of the Raydah Area and the Aseer Area's southwestern highlands. The specific objectives of this study were: to evaluates the usefulness of Sentinel satellite dataset for *Opuntia* spp. detection and mapping with emphasis on automatic information extraction techniques, establishing a phenological trend for the extraction of understory invasive plant data from temporal Sentinel satellite data (i.e. *Opuntia* spp.), assessing the usefulness of Sentinel sensor for the detection and mapping of *Opuntia* spp.

Literature review

Invasive species are defined as those non-native species that threaten ecosystems, habitats and species (Convention on Biological Diversity, 2008). They have great impact and influence on of the global environmental change (Pysek and Richardson, 2010), seriously affecting ecosystem services that are important to human welfare (Branco et al., 2015; Hejda et al., 2009). Their threats to plant diversity was reported to increase in past decades (Pimentel et al., 2001), due to the increase in exchange of plant material, and consequently their genetic materials among countries (Van Wilgen et al., 2008). Their effect was ranked as second to human interferences in the cause of species endangerment and extinction (IUCN, 2011). The reported hazards include direct threats to human health, and loss or alteration of goods and services regarding fishery, farming, forestry, drinking water, hydrology, climate stabilization, pollination, culture and recreation (McNeely, 2005; Lovell et al., 2006). The invasive species affect and threaten biological diversity by reducing genetic variation and narrowing gene pools to the extinction of endemic species (Sax and Gaines, 2008). Consequently, costs associated with their impacts are very high worldwide.

The management of invasive alien species present a significant challenge for the conservation authorities. The main principles applied to managing invasive species may include: Prevention of invasive species from entering the ecosystem, regular monitoring and rapid response, eradication, and or containment if eradication is not realistic. Some control methods were suggested that range from chemical, biological, physical, manual and integrated management system. Berhanu and Tesfaye (2006) described the dilemma of *Prosopis* dilemma (an aggressive invasive species) and some controlling methods.

http://www.aloki.hu ● ISSN 1589 1623 (Print) ● ISSN 1785 0037 (Online)
DOI: http://dx.doi.org/10.15666/aeer/1705_1080710822

Similarly, invasive species can affect plant diversity in the Kingdom, and reach reaches its woodlands, forests, grasslands, agriculture lands, islands and inhabited areas (Thomas et al., 2016). They may have significant impacts on ecosystems and agriculture areas by eliminating or displacing many native species, particularly the highlands. The prevailing warm climate and the humid areas can enhance their spread in the kingdom by accelerating rapid seedling growth compared to native populations as indicated by Griffith et al. (2014).

Thomas et al. (2016) stated that "Approximately 37 alien plants have been reported from various habitats of southwestern region, majority of which are associated with specific plant associations". They indicated that on the higher elevations (800 to 2700 m) the common exotics according to severity are: "*Opuntia* spp., *N. glauca, Argemone ochroleuca, T. minuta, Verbesina encolioides, Tridax procumbens, Lantana camara, Amaranthus spinosus, Xanthium spinosum, Cenchrus setigerus* and *Bidens aurea"*. Further on, they indicated that six species have increased their distribution range both in the lowlands and highlands, and are therefore considered most troublesome ones in Saudi Arabia. The stated species in a descending order of were "*P. juliflora (Leguminosae), O. dellenii (Cactaceae), N. glauca (Solanaceae), T. portulacastrum (Aizoaceae), O. ficus-indica (Cactaceae) and Argemone ochroleuca (Papaveraceae)*".

The entry of invasive species to the highlands of Aseer Area could be attributed to human interferences like clearance of native plants for roads, as mentioned by Kingston and Waldren (2003). This is evident in the presence of some exotics along road sides in the southwestern high ranges (Thomas, 2016). Also, the highlands of Aseer Area was subjected to overgrazing (Abulfatih et al., 1989) and felling of forest trees that could have contributed to spread of opportunistic invasive species. Economic costs from invasive species include direct costs through reduction of ecosystem productivity and management costs. Indirect costs can occur through reduction in services and revenues. The key to reduce the threats and costs of invasive species damage and management is by early detection and rapid response. Warrag et al., 2019 reported the status of dieback of *Juniperus procera* (African pencil cedar) in natural stands and plantation in Alsouda highlands Saudi Arabia that is near to the studied location. They stated that with time, the NDVI showed a growing trend of greenness, especially in high rainfall seasons. The slope aspect effect was evident in the vegetation's dieback severity and greenness as detected by NDVI data.

Material and methods

Study area and field survey

Raydah watershed area, in an important declared protected area in Aseer area, Kingdom of Saudi Arabia (*Fig. 1*). Among the other protected areas in the kingdom, it has unique plant association and diversity in the highlands of the Sarawat Mountains in the southwestern parts of the kingdom (Mallick, 2016). The studied area is located between latitude of 18°10'50.859"N and 18°13'2.58"N and longitude of 42°21'58.042"E and 42°24'56.197"E and elevations 1330 to 2827 m.a.s.l.

The main features of Raydah protected area is described in Saudi Wildlife Authority as follows:

- It covers an area of 12.17 km^2.

http://www.aloki.hu ● ISSN 1589 1623 (Print) ● ISSN 1785 0037 (Online)
DOI: http://dx.doi.org/10.15666/aeer/1705_1080710822

- It protects dense stands of Juniper (*Juniperus procera)*.
- Its unique plant association provides habitat for nine of the ten indigenous bird species of Saudi Arabia.
- Also, the protected area attracts Caracal Lynx, and Arabian wolf.

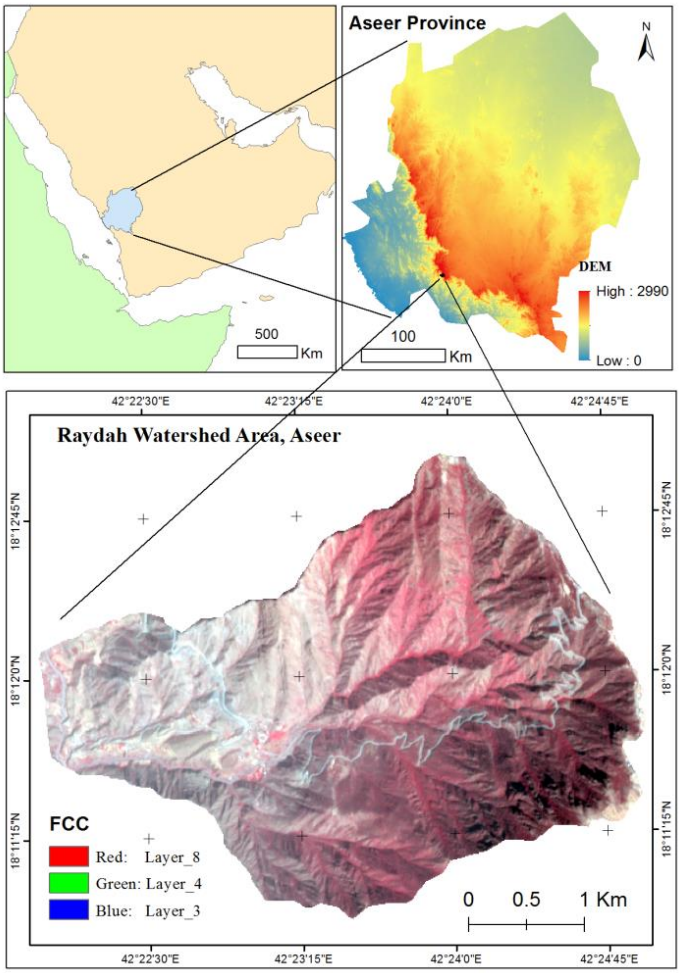

Figure 1. *Study area*

Sarawat Mountains in the south-western parts of the kingdom receives the highest southwestern monsoon annual rainfall in KSA, with variable annual patterns (Vincent, 2008). Precipitation is mainly from March to June during spring and summer growing seasons (Wheater et al., 1989; Mallick et al., 2014), and mean on the minimum of daily average temperature and mean on the maximum of daily average temperature are 19.3 °C and 29.70 °C, respectively. Rainfall data was obtained from the meteorological station situated 8 km northwest of the study area (Al-Sooda Station no. 00028, 18° 15' 08" N (latitude) and 42° 24' 15.7" E (longitude).

Ground surveys were conducted during 9th February 2019 to 23rd February 2019 for the understanding and distribution of vegetation classes and invasive plants. *Figure 2* shows the pictures of important location, in which Juniper procera were severely affected due to *Opuntia* spp. invasive species. The 50 × 50 m size of the sampling areas screened during the field survey.

http://www.aloki.hu ● ISSN 1589 1623 (Print) ● ISSN 1785 0037 (Online)
DOI: http://dx.doi.org/10.15666/aeer/1705_1080710822

Figure 2. *Natural stands status of the Raydah protected area. Opuntia spp. spread and effected Juniperus procera (1-4); Juniperus procera (5-6) and Sidr tree (Ziziphus spina-christi) (7)*

Data processing

The Sentinel-2 level-1C satellite datasets (Level 1C Radiometric and geometric corrections including ortho-rectification and global reference system spatial registration with accuracy of sub-pixels) over the Raydah protected area were used to prepare the Normalized Difference Vegetation Index (NDVI) and Land Use and Land Cover (LULC) maps. The Sentinel-2 L1C product DNs are unsigned integer values of reflectance that that can be multiplied by 10,000 to achieve TOA reflectance values. DEM acquired from ALOS PALSAR Radiometrically Terrain corrected (RTC) DEM. From DEM, elevation (1330-2827 m, with the mean of 2070 m), slope angle (0° to 89.54° with the mean of 29.08°) have been calculated using ArcGIS software. For the generation of texture features, the gray level co-occurrence matrix (GLCM) method (Haralick, 1986) with 3 × 3 pixel window size was used. The NIR band of Sentinel data generated six texture features, mean, variance, contrast, homogeneity, dissimilarity and entropy as input images. The mean, contrast, homogeneity and variance characteristics displayed maximum information and were therefore taken as classification input images. For maximum likelihood classification, the common training sites selected from the sentinel image were used. For classification accuracy assessment, the classified images were field-checked at 152 locations.

Results and discussion

Temporary analysis of September, February and April Sentinel satellite dataset (*Fig. 3*) was conducted to determine a trend in vegetation phenology and to detect changes in the composition and structure of the community. *Juniperus procera* forest maintained significant foliage during the month of June, resulting in high reflectance from the upper canopy and hindering under-story reflection. From June to October, therefore, it was not possible to separate *Opuntia* spp. from the story. Therefore, for

http://www.aloki.hu ● ISSN 1589 1623 (Print) ● ISSN 1785 0037 (Online)
DOI: http://dx.doi.org/10.15666/aeer/1705_1080710822

further analysis, Sentinel images were not used. The *Juniperus procera,* once established, individual trees can survive in hot and dry conditions, but in areas with low rainfall, trees are usually poor in shape and small in size. Where rainfall exceeds *Juniperus procera* dominated forests are gradually replaced by moister types of evergreen forests in which *Juniperus procera* becomes increasingly common. This region has the highest average rainfall in Saudi Arabia distributed over 4-6 months during the spring (Aug and Sept and summer growing seasons (March-June), while negligible rainfall during the rest of the year (Wheater et al., 1989; Mallick et al., 2018). Due to partial leaf shedding in the month of February, the under-story reflection also added to the overall reflection (appearing in light reddish tones on standard false color composite (FCC)).

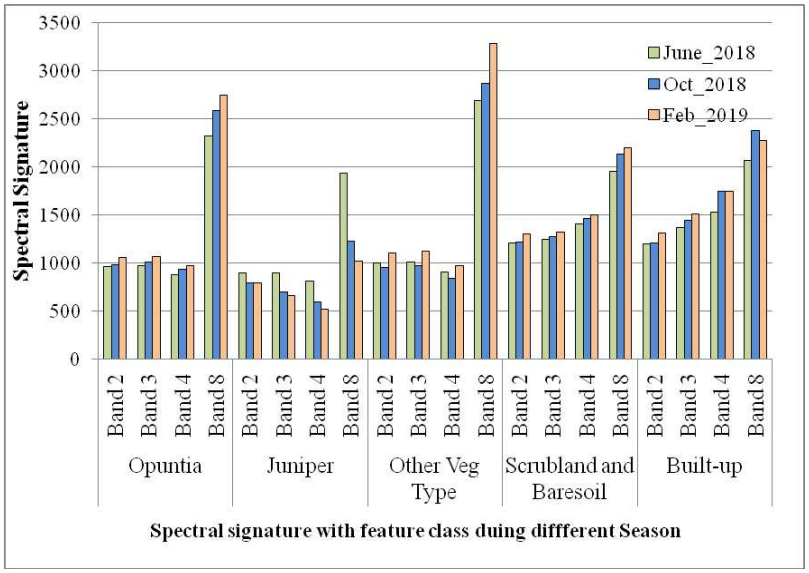

Figure 3. *Spectral reflectance of feature classes in June 2018, Oct. 2018 and Feb. 2019*

Although vegetation was visible in the February image under the story, it was not possible to delineate boundaries. Maximum reflection from vegetation occurred in the month of June - October due to full extent (moister types of evergreen forests) in evergreen tree (Sidr tree (*Ziziphus spina-christi*) and *Juniperus procera* forests (*Fig. 4*). This pattern in reflection showed that the data acquired between February were suitable for detecting *Opuntia* spp in the studied area. Every year, the best month varies due to annual temperature and precipitation differences. Statistically compared the Sentinel satellite data for various vegetation classes (*Table 1*). *Opuntia* spp's CV was slightly higher than *Juniperus procera*, indicating that discrimination against *Opentia* spp was possible to facilitate more accurate discrimination. *Table 2* shows the separability of different classes. In bands 3 and 8 of Sentinel data, the 2000 transformed divergence (TD) value showed very good separability of *Opuntia* spp from *Juniperus procera*. The 1997 and 1998 TD values between *Opuntia* spp and other tree (incl. Sidr tree) in bands 3 and 8 showed good separability, respectively. The texture classification was helpful in distinguishing the *Opuntia* spp from *Juniperus procera* successfully. In the vegetation classes, Band 8 of Sentinel data had the maximum variability compared to the other three bands (*Tables 1* and *2*). Band 8 of Sentinel data was therefore selected to analyze texture to extract *Opuntia* spp.

http://www.aloki.hu ● ISSN 1589 1623 (Print) ● ISSN 1785 0037 (Online)
DOI: http://dx.doi.org/10.15666/aeer/1705_1080710822

Table 1. *Transformed values of divergence (TD) showing separability (higher values mean greater separability)*

Satellite data	Bands	Average	Minimum	Class pairs				
				1:2	1:3	1:4	2:3	2:4
Sentinel data	Band2	1997	1987	2000	1987	1992	2000	2000
	Band3	2000	1997	2000	1997	2000	2000	2000
	Band4	1876	1257	2000	1257	2000	2000	2000
	Band8	2000	1998	2000	1998	2000	2000	2000

1 *Opuntia*, 2 Juniper, 3 Other tree, 4 Bare soil

Table 2. *Spectral reflectance (DN values) statistical analysis from different feature classes*

Feature class	Statistical parameters	Band1	Band2	Band3	Band4
Opuntia spp.	Min	1006	1022	914	2304
	Max	1112	1127	1037	2701
	Mean	1060.13	1067.53	975.33	2547.80
	Std. dev	26.402	28.658	35.479	112.579
	CV	2.490	2.684	3.638	4.419
	Skewness	0.129	0.615	0.041	-0.722
	Kurtosis	0.237	-0.301	-0.553	-0.081
Juniperus procera	Min	774	628	491	953
	Max	821	696	561	1168
	Mean	797.14	657.79	520.79	1016.93
	Std. dev	11.446	13.195	16.621	51.270
	CV	1.394	1.896	2.963	4.390
	Skewness	0.161	0.324	0.775	1.624
	Kurtosis	-0.524	1.802	0.834	2.912
Other types (incl. Sidr tree)	Min	1083	1096	943	3124
	Max	1150	1148	1050	3564
	Mean	1109.88	1128.38	974.75	3290.75
	Std. dev	21.457	16.928	34.640	170.984
	CV	1.933	1.500	3.554	5.196
	Skewness	0.011	-0.639	-0.221	0.183
	Kurtosis	0.144	0.411	-0.355	-1.451
Scrubland and bare soil	Min	1247	1248	1397	2108
	Max	1358	1378	1610	2296
	Mean	1305.33	1325.13	1505.40	2200.80
	Std. dev	29.978	35.341	58.261	66.520
	CV	2.297	2.667	3.870	3.023
	Skewness	0.805	-0.897	1.680	1.061
	Kurtosis	0.552	0.624	3.207	-0.467
Built-up	Min	1219	1429	1665	2148
	Max	1410	1572	1796	2342
	Mean	1311.33	1509.00	1750.33	2273.00
	Std. dev	95.657	73.000	73.962	108.448
	CV	7.295	4.838	4.226	4.771
	Skewness	0.297	-0.991	-1.719	-1.704
	Kurtosis	1.023	-1.866	-3.309	4.911

http://www.aloki.hu ● ISSN 1589 1623 (Print) ● ISSN 1785 0037 (Online)
DOI: http://dx.doi.org/10.15666/aeer/1705_1080710822

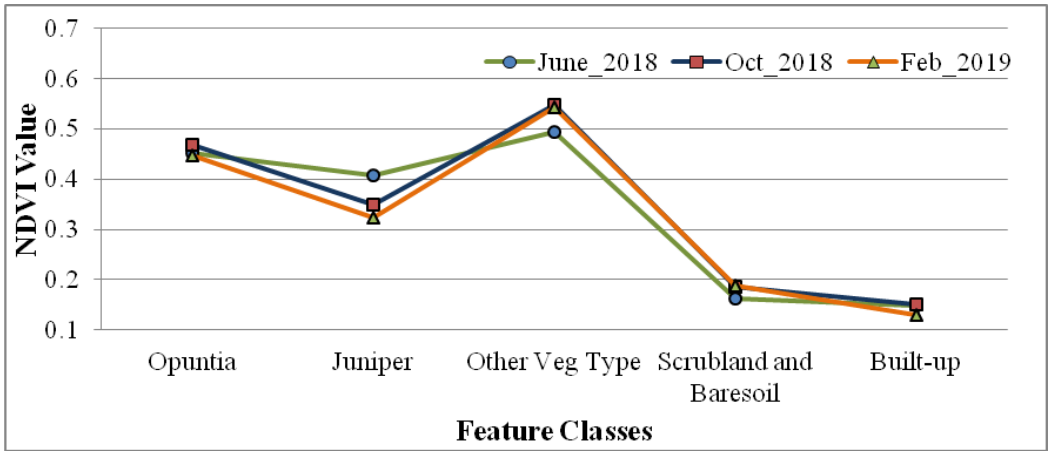

Figure 4. *NDVI value of different feature class over different period*

Taking into account the objectives, Sentinel satellite dataset were used to prepare the feature class map for the study area, i.e. built-up, exposed rocks, scrublands, *Juniperus procera, Opuntia* spp. and other tree (incl. Sidr tree). The total area of each category of feature class and percentage was calculated and presented in table. *Figure 5* shows the feature class type and the built - up area that also includes the road network lined from east to west direction and the building is mainly located in the western part of the study area towards the low land area. The *Juniperus procera* (45%) was the most dominant class in 2019, followed by scrublands (30.62%), exposed rocky area (12.66%) and *Opuntia* spp. (9.33%) shown in *Table 3*. Accuracy assessment was also evaluated to study the performance of the Sentinel sensor in feature class detection (specifically *Juniperus procera* and *Opuntia* spp.) for the classified output (*Table 4*).

Table 3. *Area (ha) of feature class estimated from the output of Sentinel sensors*

Sl. No	Feature class	Area in ha	Percent %
1	Built-up	17.70	1.45
2	Exposed rocks	154.93	12.66
3	Scrublands	374.61	30.62
4	*Juniperus procera*	550.54	45.00
5	*Opuntia* spp.	114.13	9.33
6	Other tree (Incl. Sidr)	11.53	0.94
Total area		1223.44	100.00

Table 4. *The producer's and user's accuracies*

Sl. No	Feature class	Producer's accuracy	User's accuracy
1	Built-up	76.52	92.85
2	Exposed rocks	93.15	94.61
3	Scrublands	88.90	92.47
4	*Juniperus procera*	96.14	94.82
5	*Opuntia* spp.	94.69	95.72
6	Other tree (incl. Sidr)	87.65	91.02

http://www.aloki.hu ● ISSN 1589 1623 (Print) ● ISSN 1785 0037 (Online)
DOI: http://dx.doi.org/10.15666/aeer/1705_1080710822

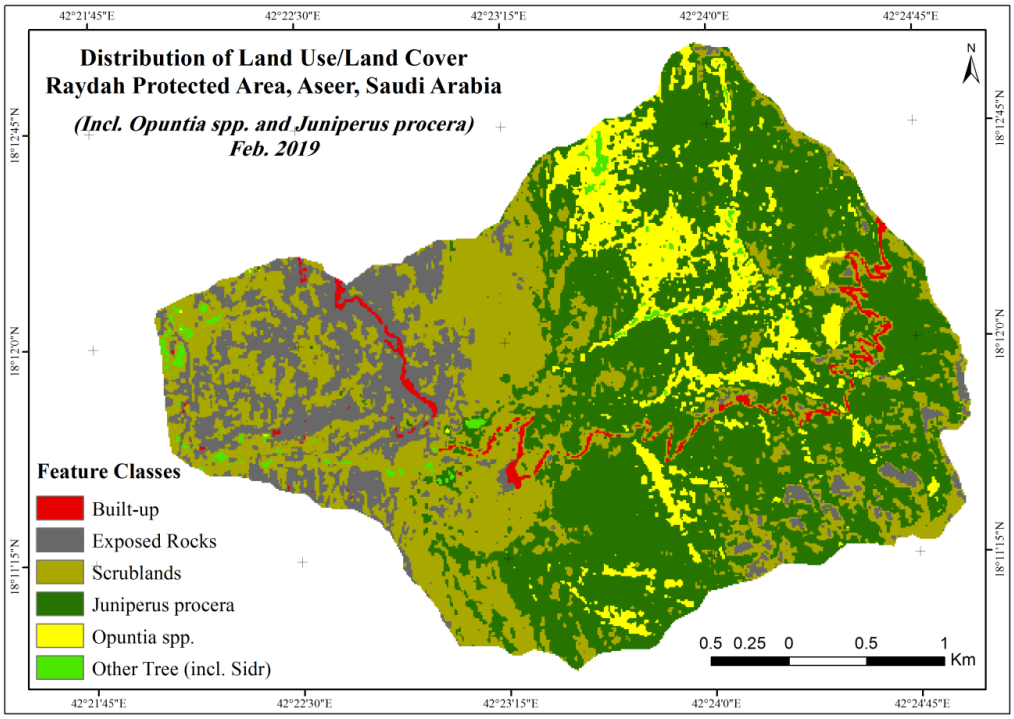

Figure 5. *Distribution of land use/land cover in Raydah protected area, Saudi Arabia*

The relationship between feature class and topography was analyzed using DEM. Figure shows the results of analysis of feature class in 2019 according to elevation (height). According to *Figure 6, Juniperus procera* are mostly located in regions with 1951-2827 m of height (Friis, 2009; Negash, 2010). It found as the dominant species in Raydah protected montane vegetation or mixed with other evergreen forests such as Sidr tree (*Ziziphus spina-christi*). The *Opuntia* spp. Mostly located in the regions with 1951-2550 m of height. Similarly, scrubland areas, mainly in regions with height of 1330-1950 m. This may be due to soil depth, week geology, and denuded high slope. With increasing altitude, the rock exposed class decreases.

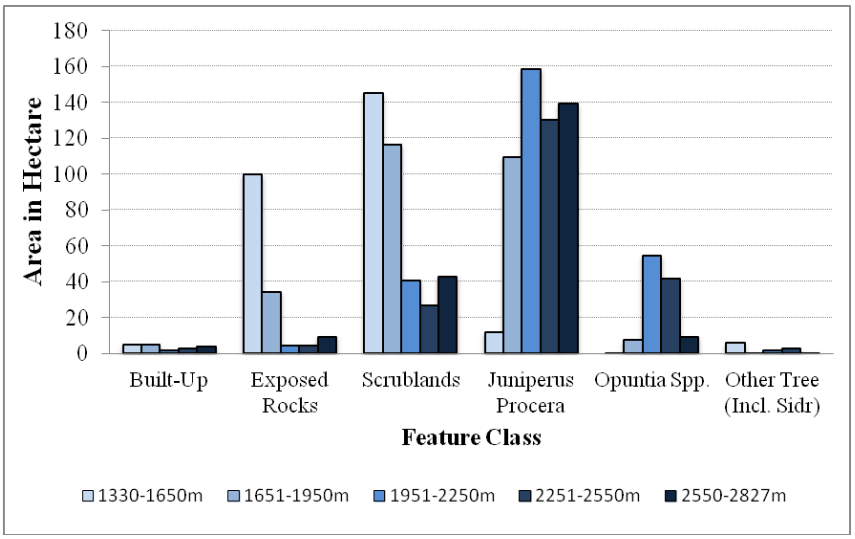

Figure 6. *Feature class according to elevation range*

http://www.aloki.hu ● ISSN 1589 1623 (Print) ● ISSN 1785 0037 (Online)
DOI: http://dx.doi.org/10.15666/aeer/1705_1080710822

The gradient of the slope influences the feature classes distribution in studied area. *Table 5* shows the statistical analysis of slope analysis with feature class at the particular elevation range. The Juniper procera having large variation of slope gradient (ranged approx. 80°) between 1951 and 2827 m of elevation range. Whereas in *Opuntia* spp. It is found that the variation of slope gradient is low (ranged approx. 48°) between 1951 and 2550 m of elevation range. This finding shows that the growth and expansion of *Opuntia* spp. maximum at the moderate slope gradient (*Fig. 7*). It will be noted that the amount of moisture (water) intake tends to slightly decrease with slope increase. On the more gentle slopes, especially the 1.15° slope or less, the largest intake of water was found. That the degree of slope affects the infiltration. Therefore, it can be concluded that the slope factor influences and accelerates the growth and expansion of *Opuntia* spp. in the studied area.

Table 5. *Statistics of feature class according to topography and slope*

	Statistical parameters	**BLT**	**EX**	**SCR**	**Jun. Pro**	**Op. Sp**	**OT**	**Total area**
Class-I Height 1330-1650 m	Area in Ha	4.80	99.88	145.28	11.77	0.23	5.86	267.81
	Min Slope	2.29	1.01	1.09	0.88	7.30	1.15	
	Max Slope	46.14	89.11	89.11	42.49	19.53	38.33	
	Mean Slope	22.13	21.28	21.84	21.1	14.28	14.03	
Class-II Height 1651-1950 m	Area in Ha	4.89	34.5	116.72	109.52	7.44	0.83	273.89
	Min Slope	1.15	2.56	1.81	2.29	9.69	16.39	
	Max Slope	41.54	88.35	67.67	69.25	39.65	35.25	
	Mean Slope	26.77	28.7	30.37	28.57	25.51	23.07	
Class-III Height 1951-2250 m	Area in Ha	1.56	4.39	40.91	158.61	54.64	1.81	261.92
	Min Slope	10.88	11.23	4.13	0.81	7.64	13.34	
	Max Slope	44.16	46.71	89.40	89.42	54.65	50.09	
	Mean Slope	28.64	30.4	33.8	31.89	32.17	30.02	
Class-IV Height 2251-2550m	Area in Ha	2.58	4.59	26.59	130.27	41.59	2.61	208.23
	Min Slope	18.08	17.30	10.89	3.34	9.66	20.24	
	Max Slope	48.24	89.49	89.49	89.48	58.33	46.13	
	Mean Slope	31.71	41.34	35.52	34.24	34.66	32.19	
Class-V Height 2551-2827 m	Area in Ha	3.84	9.39	42.86	139.34	9.42	0.28	205.14
	Min Slope	2.29	0.21	0.94	0.81	5.11	21.04	
	Max Slope	40.15	89.49	89.55	89.54	88.53	44.01	
	Mean Slope	28.05	30.04	25.57	30.84	26.42	30.77	
Total area in hectare								1217.00

BLT = Built-Up; EX = Exposed Rocks; SCR = Scrublands; Jun. Pro = *Juniperus Procera*; Op. Sp = *Opuntia* spp; OT = Other Tree (Incl. Sidr)

Over the past few decades, the southwest part of the Kingdom of Saudi Arabia has experienced negative impacts of invasive species on forest ecosystems, the *Opuntia* spp. among them. It is one of the most severe invasive plant species, colonizing large forest areas in the Sarawat Mountains highlands in the southwestern parts of the Kingdom. Assessing the current situation in the protected area of Raydah will indicate the gravity of the situation and indicate possible interventions to control the invasive species.

http://www.aloki.hu ● ISSN 1589 1623 (Print) ● ISSN 1785 0037 (Online)
DOI: http://dx.doi.org/10.15666/aeer/1705_1080710822

Remote sensing data of high resolution have received considerable attention for invasive species inventory. The image of the multi-date satellite, i.e. Sentinel dataset facilitates phenological change monitoring and identification. In order to predict invasive species spread, it may be useful to integrate satellite information with other attributes in GIS.

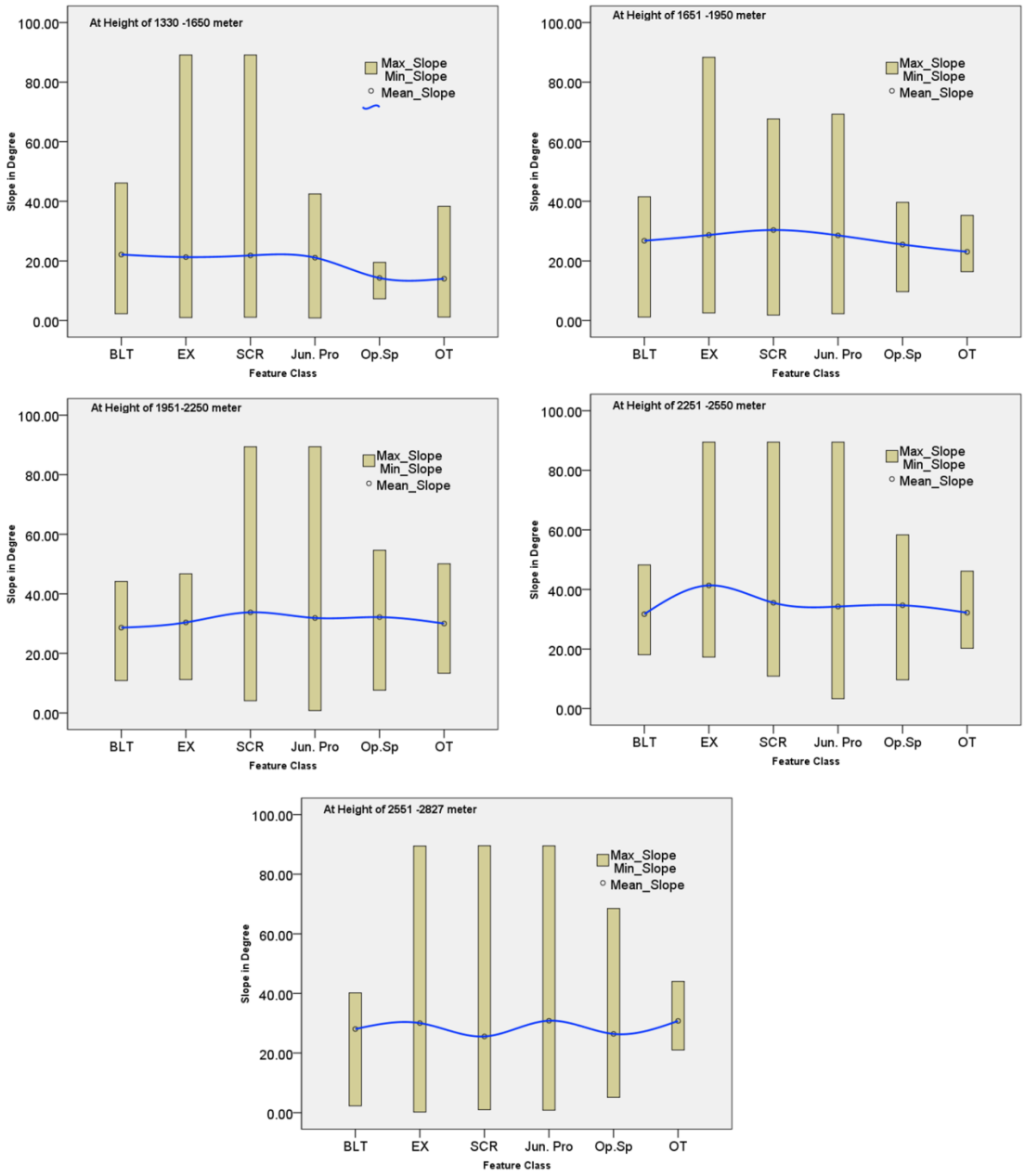

Figure 7. *Graphical representation of slope in degree (min, max and mean) at different feature classes*

The results of this study showed that *Juniperus procera* (45%) was the most dominant class in 2019, followed by scrublands (30.62%), exposed rocky area (12.66%) and *Opuntia* spp. (9.33%). The relationship between feature class and topography was

http://www.aloki.hu ● ISSN 1589 1623 (Print) ● ISSN 1785 0037 (Online)
DOI: http://dx.doi.org/10.15666/aeer/1705_1080710822

also analyzed using DEM. *Juniperus procera* are mostly located in regions with 1951-2827 m of height. It found as the dominant species in Raydah protected montane vegetation or mixed with other evergreen forests such as Sidr tree (*Ziziphus spina-christi*). The *Opuntia* spp. mostly located in the regions with 1951-2550 m of height. Similarly, scrubland areas, mainly in regions with height of 1330-1950 m. This may be due to soil depth, week geology, and denuded high slope. With increasing altitude, the rock exposed class decreases. The gradient of the slope influences the feature classes' distribution in studied area. *Juniper procera* has large variation of slope gradient (ranged approx. 80°) between 1951 and 2827 m of elevation range. Whereas in *Opuntia* spp. It is found that the variation of slope gradient is low (ranged approx. 48°) between 1951 and 2550 m of elevation range. It can be concluded that the slope factor influences and accelerates the growth and expansion of *Opuntia* spp. in the studied area.

Conclusions

Raydah protected area in an important declared protected area in Aseer area - Kingdom of Saudi Arabia that is rich in biodiversity, and provides habitat for nine of the ten indigenous bird species in the kingdom. Invasive plant species in Raydah could threaten the natural balance among the indigenous species and thereafter affect the biological components of the ecosystem. Assessment of the current situation of the invasive plants in the protected area will provide scientific data base for future management plans to combat and control invasive plants and protect the protected area from their adverse effects.

In this study, the temporal data (i.e. June, Oct and February months) were used to establish a trend in vegetation phenology and changes in species community composition and canopy structures. Comparison of the data from these three months revealed that February was adequate month to detect under story *Opuntia* spp. Maximum reflection from vegetation occurred in the month of June - October due to full extent (moister types of evergreen forests) in evergreen tree (Sidr tree (*Ziziphus spina-christi*) and *Juniperus procera* forests where as during February is shows less reflectance over Sidr tree (*Ziziphus spina-christi*) and *Juniperus procera* forests. This pattern in reflection showed that the data acquired between February were suitable for detecting *Opuntia* spp in the studied area. Every year, the best month varies due to annual temperature and precipitation differences. *Opuntia* spp's CV was slightly higher than Juniperus procera, indicating that discrimination against *Opuntia* spp was possible to facilitate more accurate discrimination. The study demonstrated the potential of sentinel sensor for invasive species such as *Opuntia* spp to be detected and mapped with desirable accuracy. This encouraging result demonstrated the feasibility of developing a semi - automated process for mapping and analysing the distribution of *Opuntia* spp in forest areas and found better results compared to multispectral data with very high resolution.

Acknowledgements. The author extends his appreciation to the Rector of King Khalid University for supporting this work. This research was conducted during a sabbatical leave.

http://www.aloki.hu ● ISSN 1589 1623 (Print) ● ISSN 1785 0037 (Online)
DOI: http://dx.doi.org/10.15666/aeer/1705_1080710822

REFERENCES

[1] Abulfatih, H. A., Emara, H. A., Hashish, A. E. (1989): The influence of grazing on vegetation and soil of Asir highlands in south western Saudi Arabia. – Arab Gulf J. Sci. Res. 7: 69-78.

[2] Aref, I. M., El Atta, H. A., Alshahrani, T., Alazba, A., Ahmad, A. I. (2013): Evaluation of the physiological and growth response of *Juniperus procera* Hochst. Endlicher to some types of microcatchments. – International Journal of Plant, Animal and Environmental Sciences 3(1): 234-241.

[3] Berhanu, A., Tesfaye, G. (2006): The *Prosopis* dilemma: impacts on dryland biodiversity and some controlling methods. – J. Dryl. 1(2): 158-164.

[4] Boyd, D. S., Foody, G. M. (2011): An overview of recent remote sensing and GIS based research in ecological informatics. – Ecol. Inf. 6(1): 25-36.

[5] Bradley, B. A. (2014): Remote detection of invasive plants: a review of spectral, textural and phenological approaches. – Biol. Invasions 16(7): 1411-1425.

[6] Bradley, B. A., Mustard, J. F. (2006): Characterizing the landscape dynamics of an invasive plant and the risk of invasion using remote sensing. – Ecological Applications 6: 1132-1147.

[7] Branco, S., Videira, N., Branco, M., Paiva, M. R. (2015): A review of invasive alien species impacts on eucalypt stands and citrus orchards ecosystem services: towards an integrated management approach. – J. Environ. Manage. 149: 17-26.

[8] Convention on Biological Diversity (2008): Alien Species that Threaten Ecosystems, Habitats or Species. – FAO, Rome.

[9] Curatola Fernández, G., Silva, B., Gawlik, J., Thies, B., Bendix, J. (2013): Bracken fern frond status classification in the Andes of southern Ecuador: combining multispectral satellite data and field spectroscopy. – Int. J. Rem. Sens. 34(20): 7020-7037.

[10] El-Juhany, L. I., Aref, I. M. (2013): The present status of the natural forests in the southwestern Saudi Arabia: Asir and East Jazan Forests. – World Applied Sciences Journal 21(5) 710-726.

[11] Friis, I. (2009): Cupressaceae. – In: Hedberg, I. et al. (eds.) Flora of Ethiopia and Eritrea. Vol. 1 Lycopodiaceae to Pinaceae. Addis Abeba University, Addis Ababa, Ethiopia & Uppsala, Sweden, pp. 193-195.

[12] Gaertner, M., Den Breeyen, A., Hui, C., Richardson, D. M. (2009): Impacts of alien plant invasions on species richness in Mediterranean-type ecosystems: a meta-analysis. – Prog. Phys. Geogr. 33(3): 319-338.

[13] Griffiths, B. S., Spilles, A., Bonkowski, M. (2012): C:N:P stoichiometry and nutrient limitation of the soil microbial biomass in a grazed grassland site under experimental P limitation or excess. – Ecol. Process. 1 1-11. 10.1186/2192-1709-1-6.

[14] Gurevitch, J., Padilla, D. K. (2004): Are invasive species a major cause of extinctions? – Trends Ecol. Evol. 19(9): 470-474.

[15] Hejda, M., Pysek, P., Jarosík, V. (2009): Impact of invasive plants on the species richness, diversity and composition of invaded communities. – J. Ecol. 97: 393-403.

[16] IUCN (2011): International Union for Conservation of Nature. – http://www.iucn.org/about/union/secretariat/offices/iucnmed/iucn_med_programme/species/invasive_species/.

[17] Joshi, C., De Leeuw, J., Van Duren, I. C. (2004): Remote sensing and GIS applications for mapping and spatial modelling of invasive species. – ISPRS 2004: Proceedings of the XXth ISPRS Congress: Geo-Imagery Bridging Continents, 12-23 July 2004, Istanbul, Turkey. Comm. VII., pp. 669-677.

[18] Kingston, N., Waldren, S. (2003): The plant communities and environmental gradients of Pitcairn island: the significance of invasive species and the need for conservation management. – Ann. Bot. 92: 31-40.

http://www.aloki.hu ● ISSN 1589 1623 (Print) ● ISSN 1785 0037 (Online)
DOI: http://dx.doi.org/10.15666/aeer/1705_1080710822

[19] Lawrence, R. L., Bunn, A., Powell, S., Zambon, M. (2004): Classification of remotely sensed imagery using stochastic gradient boosting as a refinement of classification of tree analysis. – Remote Sensing of Environment 90: 331-336.
[20] Lovell, S. J., Stone, S. F., Fernandez, L. (2006): The economic impacts of aquatic invasive species: a review of the literature. – Agric. Res. Econ. Rev. 35(2006): 195-208.
[21] Mallick, J., Singh, R. K., Khan, R. A., Singh, C. K., Kahla, N. B., Warrag, E. I., Islam, S., Rahman, A. (2018): Examining the rainfall - topography relationship using non-stationary modelling technique in semi-arid Aseer region, Saudi Arabia. – Arabian Journal of Geosciences. https://doi.org/10.1007/s12517-018-3580-9.
[22] Mallick, J. Geospatial-based soil variability and hydrological zones of Abha semi-arid mountainous watershed, Saudi Arabia. Arab J. Geosci. 9:281 (2016). DOI 10.1007/s12517-015-2302.
[23] Mallick, J., Y. Alashker, M. Shams, A. Mohd, and A.H. Mohd Risk assessment of soil erosion in semi-arid mountainous watershed in Saudi Arabia by RUSLE model coupled with remote sensing and GIS. Geocarto International. Taylor and Francis. UK.: 1–26 (2014).
[24] Matongera, T. N., Mutanga, O., Dube, T., Lottering, R. T. (2016): Detection and mapping of bracken fern weeds using multispectral remotely sensed data: a review of progress and challenges. – Geocarto Int. 1-16. https://doi.org/10.1080/10106049.2016.1240719.
[25] McNeely, J. A. (2005): Human Dimensions of Alien Invasive Species. – In: Mooney, H. A., Mack, R. N., McNeely, J. A., Neville, L. E., Schei, P. J., Waage, J. K. (eds.) Invasive Alien Species: A New Synthesis. Island Press, Washington, DC, pp. 285-309.
[26] Negash, L. (2010): A Selection of Ethiopia's Indigenous Trees: Biology, Uses and Propagation Techniques. – Addis Ababa University Press, Addis Ababa, Ethiopia.
[27] Niphadkar, M., Nagendra, H. (2016): Remote sensing of invasive plants: incorporating functional traits into the picture. – Int. J. Rem. Sens. 37(13): 3074-3085.
[28] Peerbhay, K., Mutanga, O., Lottering, R., Bangamwabo, V., Ismail, R. (2016): Detecting bugweed (Solanum mauritianum) abundance in plantation forestry using multisource remote sensing. – ISPRS J. Photogrammetry Remote Sens. 121: 167-176.
[29] Peerbhay, K. Y., Mutanga, O., Ismail, R. (2015): Random forests unsupervised classification: the detection and mapping of Solanum mauritianum infestations in plantation forestry using hyperspectral data. – IEEE J. Sel. Top. Appl. Earth Obs. Remote Sens. 8(6): 3107-3122.
[30] Pejchar, L., Mooney, H. A. (2009): Invasive species, ecosystem services and human wellbeing. – Trends Ecol. Evol. 24(9): 497-504.
[31] Pimentel, D., McNair, S., Janecka, J., Wightman, J., Simmonds, C., OConnell, C., Wong, E., Russell, L., Zern, J., Aquino, T., Tsomondo, T. (2001): Economic and environmental threats of alien plant, animal, and microbe invasions, Agric. – Ecosyst. Environ. 84: 1-20.
[32] Pysek, P., Richardson, D. M. (2010): Invasive species, environmental change and management: and health. – Annu. Rev. Environ. Res. 35 pp. 25-55.
[33] Rocchini, D., Andreo, V., Förster, M., Garzon-Lopez, C. X., Gutierrez, A. P., Gillespie, T. W., Hauffe, H. C., He, K. S., Kleinschmit, B., Mairota, P. (2015): Potential of remote sensing to predict species invasions: a modelling perspective. – Prog. Phys. Geogr. 39(3): 283-309.
[34] Sax, D. F., Gaines, S. D. (2008): Species invasions and extinction: the future of native biodiversity on islands. – Proc Nat Acad Sci USA 105: 11490-11497.
[35] Surendra, B., Ahmedin, A. M., Siraj, K. T., Raju, A. J., Solomon (2013): Invasive alien plant species assessment in urban ecosystem: a case study from Andhra University, Visakhapatnam, India. – Int. Res. J. Environment Sci. 2(5): 79-86.
[36] Thomas, J., Mohammed, A. E., Ahmed, H. A, Abdulrehman, Alatar, A., Sivadasan, M., Mohammed, B., Sami, A., Rajakrishnan, R. (2016): Impact of alien invasive species on habitats and species richness in Saudi Arabia. – Journal of Arid Environments. https://doi.org/10.1016/j.jaridenv.2015.10.009.

http://www.aloki.hu ● ISSN 1589 1623 (Print) ● ISSN 1785 0037 (Online)
DOI: http://dx.doi.org/10.15666/aeer/1705_1080710822

[37] Turlings, L. (2000): Invasive Plants and Animals: Is There Away Out? – Netherlands Committee for IUCN, Leiden.
[38] Van Wilgen, B. W., Reyers, B., Le Maitre, D. C., Richardson, D. M., Schonegevel, L. (2008): A biome-scale assessment of the impact of invasive alien plants on ecosystem services in South Africa. – J. Environ. Manage 89: 336-349.
[39] Vincent, P. (2008): Saudi Arabia: An Environmental Overview. – Taylor and Francis, London. https://doi.org/10.1201/9780203030882.
[40] Warrag, E. I., Mallick, J., Singh, R. K., Khan, R. A. (2019): Status of dieback of *Juniperus procera* (African pencil cedar) in natural stands and plantation in Alsouda Highlands, Saudi Arabia. – Applied Ecology and Environmental Research 17(2): 2325-2338.
[41] Wheater, H. S., Larentis, P., Hamilton, G. S. (1989): Design rainfall characteristics for south-west of Saudi Arabia. – Proc. Instn. Civ. Engrs. Part 2: 517-538.

http://www.aloki.hu ● ISSN 1589 1623 (Print) ● ISSN 1785 0037 (Online)
DOI: http://dx.doi.org/10.15666/aeer/1705_1080710822

THE EFFECT OF WHEAT BRAN ADDED TO CANOLA SILAGE ON FEED VALUE AND IN VITRO ORGANIC MATTER DIGESTIBILITY

GÜL, S.[1*] – COSKUNTUNA, L.[2] – KOÇ, F.[2] – ÖZDÜVEN, L.[2]

[1]*Vocational School of Technical Sciences Plant and Animal Production Department, Namık Kemal University, Tekirdağ, Turkey*

[2]*Department of Animal Science, Faculty of Agriculture, Namık Kemal University, Tekirdağ, Turkey*

[*]*Corresponding author*
e-mail: sgul@nku.edu.tr; phone: +90-282-250-4014; fax: +90-282-250-9934

(Received 13th Mar 2019; accepted 16th Jul 2019)

Abstract. This study was carried out to determine the effect of wheat bran as added to canola silage on the fermentation and in vitro organic matter digestibility. Canola was harvested and ensiled with 5% and 10% wheat bran in glass silos. With each treatment three parallel investigations were performed. Chemical, microbiological analyses and in vitro cellulase method were conducted on the silage which was opened on the 60th day of storage. According to the analysis of the control, 5% and 10% wheat bran treatments, crude protein reached 14.31%, 14.71% and 15.66%; ammonia-nitrogen reached 91.53, 85.43 and 85.34 g/kg TN; metabolisable energy reached 7.94, 8.27 and 8.51 MJ/kg KM; while organic matter digestibility was 61.45%, 63.93% and 62.92%, respectively. In conclusion, addition of wheat bran can increase dry matter content of canola silage.
Keywords: *canola, additive, silage quality, OM, digestibility*

Introduction

Canola seeds are mentioned frequently because of their contribution to the biodisel production. Canola is one of the oilseed plants that belong to brassica sp. Canola has tolerance to low temperatures and salinity (Sovero, 1993; Francois, 1994). Canola may be used as silage, straws, stubble and stover for roughage source in ruminant nutrition because of its palatability, and low levels of rejection (Sovero, 1993; Francois, 1994; Kincaid et al., 2012; Reta et al., 2015). Brassicas have metabolisable energy from 2.8 to 3.3 mcal/kg DM and dry matter digestibility of 81 to 89% before blooming (Hall and Jung, 2008; Barry, 2013). However, there are very restricted research studies about nutrient composition of canola forages. Sånchez-Duarte et al. (2011) reported a slight increase in feed consumption of eight month elder heifers fed with a 21% canola silage ratio, compared with heifers in the control group. Silage process is a method that contributes to diminish anti-nutritional effects concerning Brassicas and allows conservation without affecting nutritional value (Fales et al., 1987). But it requires an additive for proper conservation. Brassica forage contains 80-95% water (Lambert et al., 1987; Guillard and Alison, 1988). High moisture forages tend to lose their nutrients during ensiling. Canola forage must be wilted to 60-65% moisture before ensiling (Balakhial et al., 2008). A little scientific literature investigates the effect of wheat bran addition on the feed value and in vitro OM digestibility of canola silage. Addition of wheat bran can increase dry matter content of canola silage thanks to its relatively high dry matter content. The main objective of this study was to determine the effects of

http://www.aloki.hu ● ISSN 1589 1623 (Print) ● ISSN 1785 0037 (Online)
DOI: http://dx.doi.org/10.15666/aeer/1705_1082310829

different level of wheat bran addition on feed value and in vitro OM digestibility of canola silage.

Materials and methods

The study was conducted in 2016 in Tekirdağ (41.0 ºN, 27.5 ºE), western Turkey located at about 5 m altitude above sea level and with a total precipitation of 482 mm on average and an annual mean temperature of 10.5ºC. Caravel which is a kind of winter canola was sowed in October 2016. Canola forage was harvested when 2/3 of the were blooming. Forage was chopped 1.0-1.5 cm theoretical length of cut. Silage materials were divided into three trial groups for the control, 5% wheat bran and 10% wheat bran. The material mixed with additive was pressed in 36 (1.0-1 liter) glass jars (Weck, Wher-Oftlingen, Germany) equipped with lids that enabled gas release only. The jars were stored under constant room temperature (20±1ºC). Three jars per treatment from all groups were sampled on day 60 for pH, dry matter, water soluble carbohydrates, lactic acid (DM, WSC, LA) content measurement and LAB, mold and yeast enumeration.

Analytical procedure

Chemical analyses were performed on triplicate samples. The fresh and silage samples were dried at 60ºC for 72 h in a fan-assisted oven. After drying, samples were ground through a 1 mm mesh screen for chemical analysis. The dry matter (DM) was determined by drying the samples at 105ºC for 16 h. Crude protein and ash contents of samples were determined according to the methods of AOAC (2012). Hemicellulase, cellulase, dry matter digestibility and relative feed value was determined by calculation. Neutral detergent fibre (NDF), acid detergent fibre (ADF) and acid detergent lignin (ADL) content determined as described by Van Soest et al. (1991). Metabolisable energy (ME) content of fresh and silage samples were calculated from the chemical composition TSE (1991). In vitro organic matter digestibility of samples was determined according to the methods of Aufrère and Michalet-Doreau (1988). Ammonia nitrogen (NH_3-N) and pH values fresh and silage samples were determined according to MAFF (1986). Lactic acid (LA) was determined by the spectrophotometric method of Barker and Summerson (1941). Water soluble carbohydrate (WSC) contents of experiment were determined by spectrophotometer (Shimadzu UV-12ol, Kyoto Japan) after reaction with the Anthrone reagent (MAFF, 1986). Microbiological analyses were performed according to the methods reported by Seale et al. (1990). Accordingly as the incubation medium; MRS agar was used for LAB and malt extract was used for yeast and mold. LAB, mould and yeast counts of samples were obtained at 30 °C following 3 days incubation period. Lactic acid bacteria (LAB), yeast and mold counts of the samples were converted into logaritmic coloni forming unit (cfu/g).

Statistical analysis

Statistical analyses were performed with the general linear model (GLM) procedure of Duncan's multiple range test performed with the Statistical Analysis System (2005) Software (SAS, Cary, N.C.).

$$Y_{ij} = \mu + a_i + e_{ij} \quad \text{(Eq.1)}$$

http://www.aloki.hu ● ISSN 1589 1623 (Print) ● ISSN 1785 0037 (Online)
DOI: http://dx.doi.org/10.15666/aeer/1705_1082310829

where
Y_{ij} = studied traits; μ = overall mean; a_i = fixed effect of the treatment; e_{ij} = random effect.

For all statistical comparisons, a probability level of $P < 0.05$ was accepted as statistically significant. When significant associations were identified, the mean values for each effect were contrasted using Duncan test.

Results and discussion

The results of the chemical analysis of fresh and ensiled canola are given in *Table 1*. In the study, dry matter and crude protein contents of canola silages ranged between 21.79-28.82% and 14.31-15.66%, respectively, and the dry matter and crude protein contents of canola silages increased significantly with the increase of wheat bran usage rate ($P < 0.01$). The reason for this increase in silage dry matter and crude protein content is that the dry matter and crude protein content of wheat bran is higher than that of canola. DM content was higher compared with that reported by Balakhial et al. (2008), Kincaid et al. (2012) and Limón-Hernández et al. (2019). Limón-Hernández et al. (2019), reported a CP of 145 g/KM DM that is slightly lower than our mean content of 148 g/kg DM. The CP content of canola silages was higher than that provided by most of conserved cereals that have 60 to 100 g/kg DM. For that reason silage could meet the requirements of ruminants (Van Soest, 1994; NRC, 2000). Besides, the addition of wheat bran to the canola significantly decreased the crude ash and ammonia nitrogen of the silages ($P < 0.05$). The pH value of silages, water-soluble carbohydrates and lactic acid contents were not affected by the addition of additives ($P > 0.05$). The pH value (4.5) was higher than (3.9) reported by Limón-Hernández et al. (2019). Balakhial et al. (2008) reported pH value 4.8 that is higher than our mean value (4.5). In the study conducted by Balakhial et al. (2008), it was reported that the addition of urea to the canola silage increased pH and ammonia concentration of the silage and thus the silage quality was adversely affected. The research findings show that wheat bran supplement has a positive effect on silage quality.

Table 1. *Chemical analysis of canola silages*

Treatment	DM %	pH	CP %	Ash %	WSC g/kg KM	NH_3-N g/kg TN	LA %
0	23.66	5.87	14.65	11.39	49.42	98.95	-
Control	21.79±0.48^c	4.63±0.02	14.31±0.02^c	13.85±0.89^a	13.97±0.17	91.53±1.18^a	36.15±5.05
WB 5%	24.72±0.57^b	4.61±0.04	14.71±0.06^b	13.74±0.40^a	16.75 ±2.28	85.43±4.71^b	32.21±7.02
WB 10%	28.82±1.23^a	4.55±0.16	15.66±0.19^a	11.40±0.50^b	15.08±1.33	85.34±2.87^b	33.10±6.59
P	0.001	0.550	0.001	0,005	0.160	0.001	0.730

Values with different letters in the same column are statistically different (P<0.05 and 0.01). WB: wheat bran; DM: dry matter; CP: crude protein; WSC: water soluble carbohydrate; NH_3-N: ammonia nitrogen; LA: Lactic acid

The microbiological composition of the canola silage is given in *Table 2*. The number of lactic acid bacteria increased as the amount of wheat bran decreased, while the number of yeast and mold increased. Silage fermentation is a complex process

http://www.aloki.hu ● ISSN 1589 1623 (Print) ● ISSN 1785 0037 (Online)
DOI: http://dx.doi.org/10.15666/aeer/1705_1082310829

which depends on many factors. The silage characteristics that contribute to a good fermentation are: dry matter content, physiological properties of epiphytic bacteria and, most importantly, the quantity of soluble carbohydrates (Zanine et al. 2010). The decline in pH values inhibit the spoilage microorganism proliferation, which allows the silage nutritive values to be preserved. Thus, the best silage forages are the ones with high water soluble carbohydrate content, which should be sufficient to promote the fermentation and produce enough acid to preserve the silage. In the present experiment, content of WSC in all ensiled canola forages (4.2% DM, *Table 1*) was lower than the 6 to 7% content which is recommended for theoretical requirement to achieve well preserved fermentation (Wang et al. 2009). Thus the canola without additives was adequate for producing good quality silages.

Table 2. *Microbiological analysis of canola silages*

Treatment	LAB log_{10}cfu/g	YEAST log_{10}cfu/g	MOLD log_{10}cfu/g
0	4.77	4.76	3.57
Control	3.12±0.25^{a}	3.28±0.04^{b}	2.53±0.04^{b}
WB 5%	2.52±0.07^{b}	3.15±0.07^{b}	2.56±0.05^{b}
WB 10%	2.48±0.04^{b}	4.59±0.11^{a}	4.50±0.09^{a}
p	0.001	0.001	0.001

Values with different letters in the same column are statistically different (P<0.01). WB: wheat bran

NDF, ADF, ADL, hemicellulose, digestible dry matter (DDM), dry matter intake (DMI) and relative feed values (RFV) of canola silages are given in *Table 3*. In parallel with the increase in wheat bran ratio added to the canola, the NDF and ADF contents of the silages significantly reduced (P < 0.01).

Table 3. *The results of the analysis of the cell wall of canola silages*

Treatment	NDF %	ADF %	ADL %	HEM.CEL %	DDM	DMI	RFV
0	55.33	44.80	10.16	10.52	54.00	2.17	90.77
Control	54.32±0.22^{a}	41.20±1.43^{a}	19.37±1.70^{ab}	13.12±1.65	56.80±1.11^{b}	2.21±0.01^{b}	97.24±1.52^{b}
WB 5%	51.28±0.65^{b}	34.43±0.57^{b}	15.06±2.37^{b}	16.85±0.92	62.08±0.44^{a}	2.34±0.03^{a}	112.59±1.54^{a}
WB 10%	50.51±0.79^{b}	37.08±2.73^{b}	19.90±2.68^{a}	13.43±3.43	60.01±2.13^{a}	2.38±0.04^{a}	110.47±2.61^{a}
p	0.001	0.01	0.08	0.16	0.01	0.001	0.001

Values with different letters in the same column are statistically different (P<0.05 and 0.01). NDF: neutral detergent fiber; ADF: acid detergent fiber; ADL: acid detergent lignin; OMD: Organic matter digestion; DMI: dry matter intake; RFV: relative feed values

The degradation of the cell wall components in silages is thought to be resulted from the fact that the wheat bran has low NDF and ADF content and accelerates the activity of lactic acid bacteria in the environment, being a source of carbohydrates. The NDF and ADF findings were similar with Balakhial et al. (2008); and higher than Limón-Hernández et al. (2019) findings. Kincaid et al. (2012) reported a lower value of NDF

http://www.aloki.hu ● ISSN 1589 1623 (Print) ● ISSN 1785 0037 (Online)
DOI: http://dx.doi.org/10.15666/aeer/1705_1082310829

(29.82%) which can be attributed to an early harvest (60-70 days after sowing). Feeding behavior of animals, feed consumption, feed digestibility and feed conversion to animal products vary depending on the quality of feed (Van Soest, 1994).

Feed quality is determined by the relative feed value (RFV) index developed for clover in the USA and used in other roughages (Bozkurt, 2011; Canbolat, 2013). Neely et al. (2009) reported that RFV of canola silage was double that of corn, alfaalfa silage and more than three times higher than triticale silage. The lowest RFV was found as 97.24 in control group canola silage, whereas the RFV significantly increased with the addition of wheat ($P < 0.05$). The highest DDM ratio of silages was found as 62.08% and 5% in wheat bran group and the lowest DDM ratio was found as 56.80% in lean canola silage. DMI ratios of silages ranged between 2.21-2.38% and DMI ratio was found to be significantly higher in the groups with the addition of wheat bran than in the control group of canola silage. It is reported that increase in NDF, ADF and ADL levels, which are found in the structure of feeds and slow down the digestion, causes satiety and limits the feed consumption of animals (Canbolat and Karaman, 2009; Canbolat, 2013). The findings of this research also support this. The DDM and DMI values determined in the study were found to be similar with the findings of Canbolat and Karaman (2009) and Bozkurt (2011), who studied different legume feeds. In a study investigating the effects of urea and molasses on the quality of feed as an additive to canola silage, it was determined that the addition of molasses improved the quality of silage decreasing the content of ADF and NDF, but lowered the DDM value (Balakhail et al. 2008). DMI findings were slightly lower than Paula et al. (2017) findings. In the study, the addition of wheat bran to canola silage was found to increase the DMI value.

Organic matter digestion (OMD), metabolic energy (ME) contents of canola silages were determined and given in *Table 4*. Organic matter digestibility and metabolic energy values of canola silages increased with the addition of wheat bran. The highest organic matter digestibility was determined as 63.93% in canola silages with the addition of 5% wheat bran, while the highest metabolic energy value was found in the group with the addition of 10% wheat bran ($P < 0.05$). OMD findings were slightly lower than reported by Balakhial et al. (2008), Kincaid et al. (2012), Paula et al. (2017) and Limón-Hernández et al. (2019).

Table 4. *Organic matter digestion (OMD), metabolic energy (ME) content of canola silages*

Treatment	OMD %	ME MJ/kg KM
0	60.79	8.23
Control	61.45±0.67^{b}	7.94±0.20^{b}
WB 5%	63.93±0.02^{a}	8.27±0.06^{a}
WB 10%	62.92±0.72^{a}	8.51±0.07^{a}
p	0.01	0.00

Values with different letters in the same column are statistically different ($P<0.01$)

Conclusion

The results of this study show that canola forage has suitable nutrient composition. Therefore, it can be used for dairy cattle nutrition. It allows conservation without

http://www.aloki.hu ● ISSN 1589 1623 (Print) ● ISSN 1785 0037 (Online)
DOI: http://dx.doi.org/10.15666/aeer/1705_1082310829

affecting its nutritional value. High moisture content of canola forage is one of the dangerous factors concerning canola silage quality. It requires an additive for proper conservation. Addition of wheat bran improved DM and DDM content of canola silage.

REFERENCES

[1] Maff (1986): Preparation of Sample of Plant Material. In: The Analaysis of Agriculture Material. A Manual Methods used by the Agricultural Development and Advisory Servicei Reference Book. 472. Ministry of Agriculture, Fisheries and Food. Her Majesty's Satationery office. London

[2] TSE (1991): Animal feeds-Determination of metabolizable energy (chemical method). – Turkish Standards Institute (TSE), Publ. No. 9610, 1-3, Ankara, Turkey.

[3] AOAC (2012): Official Methods of Analysis. – 19th ed. Association of Official Analytical Chemists: International, USA.

[4] Aufrère, J., Michalet-Doreau, B. (1988): Comparison of methods for predicting digestibility of feeds. – Anim. Feed Sci. Technol. 20: 203-218.

[5] Balakhial, A., Naserian, A. A., Heravi Moussavi, A., Eftekbar Shadrodi, F., Vali, Z. R. (2008): Changes in chemical composition and In vitro DM digestibility of urea and molasses treated whole crop canola silage. – Journaal of Animal and Veterinary Advances 7(9): 1042-1044.

[6] Barker, S. B., Summerson, W. H. (1941): The colorimetric determination of lactic acid in biological material. – J. Biol. Chem. 138: 535-554.

[7] Bary, T. N. (2013): the feeding value of forage brassica plants for grazing ruminant livestock. – Animal Feed Science and Technology 181: 15-25.

[8] Bozkurt, K. A. (2011): Determination of relative feed value of some legume hays harvested at flowering stage. – Asian Journal of Animal and Veterinary Advances 6: 525-530.

[9] Canbolat, O., Karaman, Ş. (2009): Comparison of In vitro gas production, organic matter digestion, reative feed value and metabolic energy content of some legume forages. – Journal of Agricultural Science 15: 188-195.

[10] Canbolat, Ö. (2013): Effects of different ripening periods on potential nutrition value of rapeseed (Brassica napus L). – Journal of Ankara University Faculty of veterinary Medicine 60: 145-150.

[11] Fales, S. L., Gustine, S. C., Hoover, R. J. (1987): Concentrations of glucosinolates and S-methylcysteine sulfoxidein ensiled rape (Brassica napus L). – Journal of Dairy Science 70: 2402-2405.

[12] Francois, L. (1994): Growth, seed yield and oil content of canola grown under saline conditions. – Agronomy Journal 86: 233-237.

[13] Guillard, K., Allinson, D. L. (1988): Yield and nutrient content of summer and fall-grown forage Brassica crops. – Can. J. Plant Sci. 68: 721.

[14] Hall, M. H., Jung, J. (2008): Use of brassica crops to extend the grazing season. Pennsylvania State university Agricultural Cooperative Extension. – Agronomy Fact 33. Available at http://pubs.cas.psu.edu./FreePubs/pdfs/uc100 pdf (acces august, 2017).

[15] Kincaid, R. L., Johnson, K. A., Michal, J. J., Huisman, A. C., Hulbert, S. H., Pan, W. L. (2012): Case study: production of silage containing biennial canola and peas for use as forage in a dairy ration. – The Professional Animal Scientist 28: 120-124.

[16] Lambert, M. G., Abrams, S. M., Harpster, H. W., Jung, G. A. (1987): Effect of hay substitution on intake and digestibility of forage rape (Brassica napus) fed to lambs. – J. Anim. Sci. 65: 1639.

[17] Limón-Hernández, D., Rayas-Amor, A. A., Garcia-Martinez, A., Estrada-Flores, J. G., López, M. N., Cruz Monterrosa, R. G., Morales-Almaráz, E. (2019): Chemical composition, in vitro gas production, methane production and fatty acid profile of canola

http://www.aloki.hu ● ISSN 1589 1623 (Print) ● ISSN 1785 0037 (Online)
DOI: http://dx.doi.org/10.15666/aeer/1705_1082310829

silage (Brassica napus) with four levels of molasses. – Tropical Animal Health and Production. Available at. https//doi.org/10.1007/s11250-019-01849-7.

[18] Neely, C., Brown, J., Hunt, C., Davis, J. (2009): Increasing the value of winter canola crops by developing ensiling systems (canolage) to produce cattle feed. – Presented at the Idaho Alfalfa andvForage Conference 3-4 February, 27-31.

[19] NRC. National Research Council (2000). The nutrient requirements of dairy cattle. – 6th ed. Washington, DC, USA: National academy Press.

[20] Paula, E. M., Broderick, G. A., Danes, A. C., Lobos, N. E., Zanton, G. I., Faciolall, A. P. (2017): Effects of replacing soybean meal with canola meal or treated canola meal on ruminal digestion, omasal nutrient flow and performance in lactating dairy cows. – Journal of Dairy Science 101: 328-339.

[21] Reta, S. D. G., Serrato-Corona, J. S., Quiroga-Garza, H. M., Gaytán-Mascorro, A., Figueroa-Viramontes, U. (2015): Forage yield and chemical composition of canola (Brassica napus L.) as affected by sowing methods. – Grass and Forage Science 71(2): 281-290.

[22] Sánchez-Duarte, J. L., Reta-Sánchez, D. G., Ochoa-Martinez, E., Serrato-Corona, J. S. (2011): Ensilado de canola, una nueva alternative forrajera en la alimentaciòn del ganado lechero: primeras prucbas de ensilaje realizadas en la Comarca Lagunera. – Hoard's Dairyman en Español (Canola silage, a new alternative forage for feeding dairy cattle: first silage trials performed in the Comarca Lagunera) 201: 582-584.

[23] Seale, D. R., Pahlow, G., Spoelstra, S. F., Lindgren, S., Dellaglio, F., Lowe, J. F. (1990): Methods for the microbiological analysis of silage. – Proceeding of The Eurobac Conference, 147, Uppsala.digestibility of corn silage in sheep. Iranian J. Vet. Res. Shiraz Univ. 10: 110-118.

[24] Sovero, M. (1993): Rapeseed a new oilseed crop for the United States. – In: Janick, J., Simon, J. E. (eds.) New crops. New York, NY, USA Wiley, pp. 302-307. Available at: http//www.hort.purdue.edu./newcrop/proceedings 1993./V2-302 html#Cold Tolerance.

[25] Statical Analysis Sistem (2005): SAS User's Guide: Statistics. Version 6. – Cary, NC: SAS Institute.

[26] Van Soes, P. J., Robertson, J. B., Lewis, B. A. (1991): Methods for dietary fiber, neutral detergent fiber, and nonstarch polysaccharides in relation to animal nutrition. – Journal of Dairy Science 74: 3583-3597.

[27] Van Soest, P. J. (1994): Nutritional ecology of the ruminant. – 2nd ed. Ithaca: Cornell University Press.

[28] Wang, J., Wang, J. Q., Zhou, H., Feng, T. (2009): Effects of addition of previously fermented juice prepared from alfalfa on fermentation quality and protein degradation of alfalfa silage. – Anim. Feed Scince Technology. 151: 280-290.

[29] Williams, S. R. O., Moate, P. J., Deighton, M. H., Hannah, M. C., Wales, W. J., Jacobs, J. L. (2016): Milk production and composition, methane emissions from dairy cows fed Lucerne hay with forage brassica or chicory. – Animal Production Sience 56: 304-311.

[30] Zanine, A. M., Santos, E. M., Dorea, J. R. R., Dantas, P. A. S., Silva, T. C., Pereira, O. G. (2010): Evaluation of elephant grass with adition of cassava scrapings. – Revista Brasileira de Zootecnia 39(12): 2611-2616. ISSN 1806-9290.

http://www.aloki.hu ● ISSN 1589 1623 (Print) ● ISSN 1785 0037 (Online)
DOI: http://dx.doi.org/10.15666/aeer/1705_1082310829

DETERMINING THE TEMPORAL CHANGES IN AVIAN POPULATION INHABITING URBAN SEASONALLY WATERLOGGED AREAS IN HYDERABAD SINDH, PAKISTAN

RAJPAR, M. N.[1] – HASSAN-ABOUSHIBA, A. B.[2] – ULLAH, S.[1] – OZDEMIR, I.[3] – ULLAH, A.[4] – ZAKARIA, M.[5*]

[1]Department of Forestry, Faculty of Life Sciences, Shaheed Benazir Bhutto University Sheringal, Dir (Upper), Khyber Pakhtunkhwa 18051, Pakistan (e-mail: rajparnawaz@gmail.com, sami.ullah@sbbu.edu.pk)

[2]Department of Zoology, Faculty of Science, University of Sebha, Libya (e-mail: abushibaa@yahoo.com)

[3]Department of Wildlife Ecology and Management, Faculty of Forestry Isparta University of Applied Science, 32260 Cunur, Isparta, Turkey (e-mail: ibrahimozdemir@isparta.edu.tr)

[4]Department of Agricultural Extension Education and Communication, The University of Agriculture Peshawar, Pakistan (e-mail: ayat.ullah@zalf.de)

[5]Faculty of Forestry, Universiti Putra Malaysia, 43400 UPM Serdang, Selangor, Malaysia (e-mail: mzakaria@upm.edu.my)

[*]Corresponding author e-mail: mzakaria@upm.edu.my

(Received 14th Mar 2019; accepted 21st May 2019)

Abstract. Determining the temporal change in avian population is crucially important in order to understand whether their population is increasing or decreasing. The information about population parameters will help in conservation and protection efforts of avian species in future. Hence, the present study was carried out to determine the temporal changes in avian species in the 2014/15 and 2018/19 periods in urban waterlogged area of Hyderabad district Sindh, Pakistan. The highest relative abundance (28229 bird individuals representing 50 species and 14 families) was detected in 2018/19 rather than in 2014/15 (17454 individuals representing 38 bird species and 12 families). Out of the 50 bird species detected in 2018/2019, 30 were migrants (18965 individuals); 15 residents (5370 individuals), and 5 resident–migrants (3897 individuals) and while in the case of 2014/15 period, 22 species were migrants (11547 individuals), 15 residents (5247 individuals) and one resident–migrant (660 individuals). IUCN and BirdLife Status indicated that one migrant species was critically endangered; two species Rare/Accidental/Vulnerable and the rest of the 23 species were of the least concern. All resident bird species were totally protected (LC) while one resident–migrant species was data deficient. Foraging guild structure indicated that omnivore (32.489%) and Piscivore (12.808%) were the most dominant guilds of 2018/19 rather than 2014/15 while Carnivore was absent in detections of 2014/15. Alpha diversity analysis indicated that urban seasonal waterlogged was more diverse, rich and evenly distributed in 2018/19 than 2014/15. The findings of this study indicated that urban seasonal waterlogged area is suitable habitat (foraging sites and stopover) for a wide array of waterbird species especially migrant birds to refuel, rest, and forage.
Keywords: *waterbirds, population parameters, native, threatened, BirdLife*

Introduction

Waterbirds are directly or indirectly depend on the aquatic environment and foraged either near water body's edges or banks or on the surface. They are bioindicators of aquatic ecosystems due to cause–effect association with different microclimate and

http://www.aloki.hu ● ISSN 1589 1623 (Print) ● ISSN 1785 0037 (Online)
DOI: http://dx.doi.org/10.15666/aeer/1705_1083110843

vegetation composition. Waterbirds may exploit broad scale of habitat, responded quickly to any environmental change either microclimate or vegetation structure and composition. Waterbird can be easily detected and identified (i.e., they showed their presence through vocalization). They can be surveyed more efficiently over the large spatial scale, e.g., presence, abundance, and influenced by surrounded habitats as compared to other animals.

The urban seasonal waterlogged areas are the undeveloped residential low-lying landscape within the city that received the water from domestic sewage and rainfall drain. They are characterized with shallow water overlying the interspersed soil and dominated either by submerged and emergent aquatic vegetation (Zhang et al., 2010). Waterlogged areas have been considered highly productive habitats for diverse fauna species, such as birds, amphibians, reptiles and mammals (Ehrenfed, 2000; Gibbs et al., 2005; Van der Walk, 2006). Due to loss and degradation of natural wetland areas, urban sewage has become a hotspot habitat for a wide array of waterbird species, i.e., waterfowls, waders, grebes, gulls, cormorants, terns to refuel, rest, and forage. These areas provide an important stopover foraging habitat for migrant as well as resident waterbird species due to high productivity (Hoffmann and Dodson, 2005). The other reason could be that, these areas are rich in fishes, amphibians, aquatic invertebrates (i.e. snails, worms, larvae of dragonflies, and water beetles that mostly occurs in soft damp soils, ditches, ponds), and organic matter.

It has been stated that more than 50% of the world's population inhabit in cities (Mackintosh and Davis, 2013) that may cause huge domestic sewage. A rapid increased in urbanization i.e., draining and infilling of wetland for development may also have caused the disappearing of wetlands from landscape (Sutula and Stein, 2003). The loss and degradation of wetland areas have increased runoff from urban sewage and industrial plants, which has adversely affected the hydrology of waterways and the remaining rest of wetlands (Catford et al., 2007; Vermoden et al., 2009; Davis et al., 2010). It has also been reported that more 50% of natural wetlands had been lost and degraded (Fraser and Keddy, 2005) that caused almost 40% of migrant bird species (i.e., 200 bird species) to be declined worldwide (BirdLife, 2015).

Previously, no study has been conducted to examine the temporal changes in avian population parameters inhabiting urban seasonal waterlogged areas. Hence, this study was conducted to examine the temporal changes in the avian population (i.e., relative abundance, diversity, status, and foraging guild structure) that utilizing the urban seasonal waterlogged areas.

Materials and methods

Study Area

These urban seasonal waterlogged areas lie in within the heart of the city 25^0 22' 45" N and 68^0 22' 06" E along the east bank of the Indus River, Hyderabad Sindh, Pakistan (*Figure 1*). Hyderabad city is densely populated, i.e., 2.323 million urban inhabitants and covers a total area of 3,198 km^2. It received monsoon rainfall from mid–April to late June and mostly remains warm (i.e., 50^0F to 119^0F) year–round, but sometimes temperature may fall at 34^0F during winter. The urban seasonal waterlogged areas are undeveloped residential wastelands that are under control of the cantonment board. These areas encompass the ditches and low laying grounds that receive water from domestic sewage and rainfall.

http://www.aloki.hu ● ISSN 1589 1623 (Print) ● ISSN 1785 0037 (Online)
DOI: http://dx.doi.org/10.15666/aeer/1705_1083110843

Birds Survey

It has been known that avian populations fluctuate from time to time and habitat to habitats (Schieck, 1997; Blake and Loiselle, 2001). Determining the temporal changes is highly essential to understand the trends in avian population in the wetland areas (Thompson et al., 2002; DeSante et al., 2005). For this reason, the Distance Sampling Point Count Method is one of the most common quantitative survey technique that has been widely used to examine the temporal changes in avian populations (i.e. relative abundance, foraging guilds, and diversity) inhabiting different habitats (Verner and Purcell, 1999; Codesido and Bilenca, 2000). This method involves the visual and auditory detection of birds with fixed or variable radius plots, and it provides detailed information on avian population parameters (Verner and Ritter, 1985; Mills et al., 2000). The design of this study was encompassing of the following factors: (i) suitability for habitats, such as open water bodies and vegetated areas, i.e. submerged vegetation; (ii) suitability for surveying cryptic, shy, and skulking species; (iii) suitability for species–rich populations; (iv) suitability in situations where human access was restricted; and (v) areas best situated for bird–habitat studies.

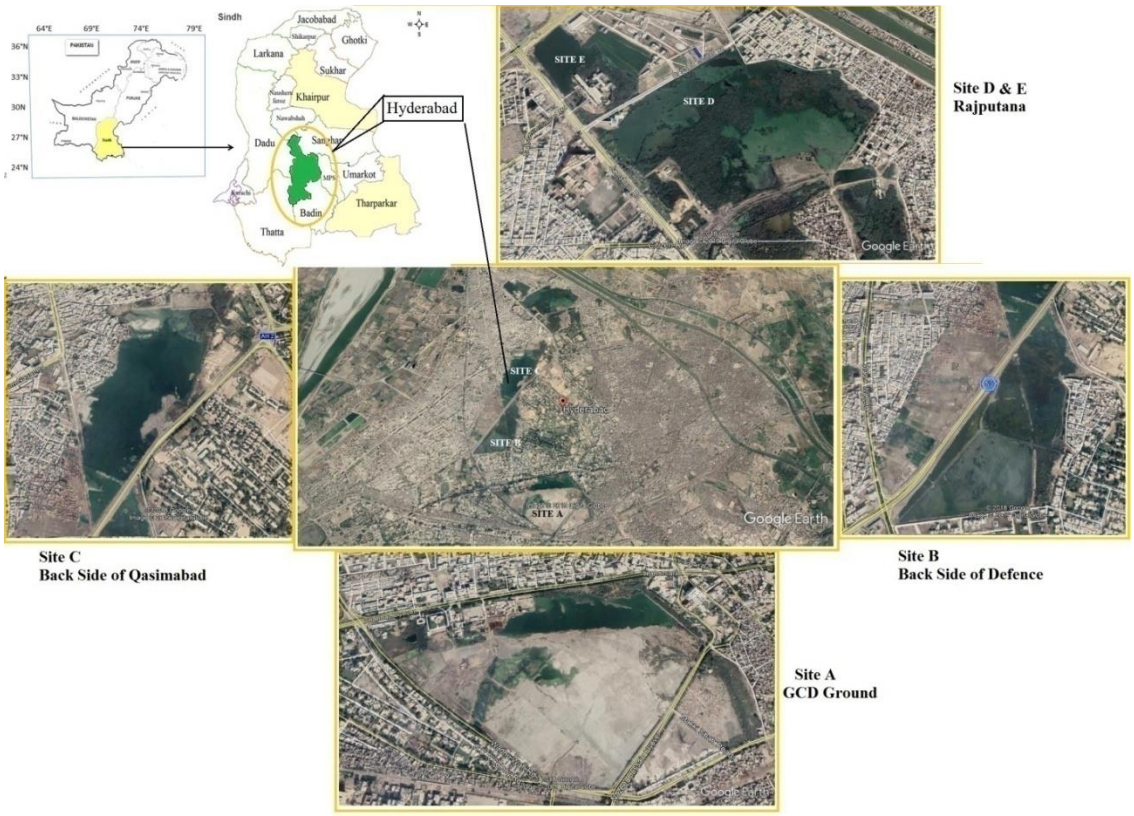

Figure 1. *Location map of the study area*

Avian species inventories at five selected sites were carried out from September 2014 to February 2015 and September 2018 to February 2019 employing Distance Sampling Point Count method. A total of 150 point count stations (i.e., in site 30 point count stations) were fixed at 300 m intervals along the edges of water bodies to avoid double counting the same bird individuals at more than one station (Meadows et al.,

http://www.aloki.hu ● ISSN 1589 1623 (Print) ● ISSN 1785 0037 (Online)
DOI: http://dx.doi.org/10.15666/aeer/1705_1083110843

2012; Wijesundara and Wijesundara, 2014; Adams et al., 2015). The birds were surveyed at each point count station for 15 minutes during each visit. The surveys were carried out during 0750–1100 hrs. This period of time is appropriate as most of the avian species remain active in search of food. The sampling methodology was followed as described by Richardson et al. (2001), Buckland et al. (2004), Aborn (2007), Nadeau et al. (2008), and Yu-Seong et al. (2008).

Data Analysis

Relative abundance revealed the common or rare species inhabiting in a particular area. It is the percentage composition of particular bird species among all detected bird species utilizing the waterlogged area (Simon and Okoth, 2016; Walag and Canencia, 2016; James and Bright, 2017). Relative abundance (%) of avian species was determined to employ the following formula;

$$\text{Relative Abundance} = \frac{ni}{N} \text{ X } 100 \qquad \text{(Eq.1)}$$

where, n*i* = is the number of individuals in the *i*th bird species, N = is total detected numbers of individuals of species detected in urban seasonal waterlogged areas (Bibby et al., 2000; Hubbell, 2001; McGill et al., 2007).

Avian diversity was analyzed using the Community Analysis Package (PCA) Version 4.0 by Henderson and Seaby (2007). The reliability of data of tested through Shapiro–Wilk normality test (Analytical Software version 8.1) by Razali (2011).

The status of avian species was identified and confirmed with the help of IUCN RedList and BirdLife International checklist.

Results

Relative Abundance

The results of 2018/19 stated that urban waterlogged areas had attracted highest relative abundance (i.e., 28229 bird individuals equal to 61.793%) representing 50 species and 14 families as compared to 2014/15 (i.e., 17454 bird individuals equal to 38.207%) represent 38 species and 12 families. This indicated that 23.586% higher numbers of bird individuals were detected in 2018/19. Furthermore, twelve new avian species namely; Common Teal – *Anas cerca*, Green–winged Teal – *Spatula discors*, Mallard – *Anas platyrhinchos*, Gadwall – *Meraca strepera*, Great Cormorant – *Phalacrocorax carbo,* Brown–headed Gull – *Larus brunnicephalus,* Black Kite – *Milvus migrans,* Bar–tailed Godwit – *Limosa lapponica,* Spoon–billed Ibis – *Platalea leucorodia,* Pied Avocet – *Recurvirostra avosetta,* Solitary Sandpiper – *Tringa solitaria,* Spotted Sandpiper – *Actitis macularius,* and White–tailed Lapwing – *Chettus ialeucura* were detected in 2018/19 as compared to 2014/15 (*Table 1*).

In addition, the results obtained using the One–Way ANOVA and Tukey's HSD test showed that the avian relative abundance of the urban seasonal waterlogged area was significantly different in the 2018/19 and 2014/15 periods (i.e., F_1, 86 = 4.46, $P < 0.05$; CV = 2/81).

http://www.aloki.hu ● ISSN 1589 1623 (Print) ● ISSN 1785 0037 (Online)
DOI: http://dx.doi.org/10.15666/aeer/1705_1083110843

Table 1. *Ranking of waterbird species recorded in urban seasonal waterlogged areas*

Family	Common Name	*Scientific name*	Detected Observation in 2014/15	%	Detected Observation in 2018/19	%
Anatidae	Northern Pintail	*Anas acuta*	1490	3.262	1958	4.286
Anatidae	Common Teal	*Anas cerca*	1870	4.093	1922	4.207
Anatidae	Green–winged Teal	*Spatula discors*	–	–	1870	4.093
Anatidae	Mallard	*Anas platyrhinchos*	–	–	1824	3.993
Anatidae	Gadwall	*Meraca strepera*	–	–	1760	3.853
Anatidae	Baikal Teal	*Sibirionetta formosa*	1260	2.758	1656	3.625
Anatidae	Northern Shoveler	*Spatula clypeata*	1630	3.568	1558	3.410
Anatidae	Falcated Duck	*Mareca falcate*	975	2.134	1234	2.701
Laridae	River Tern	*Sterna aurantia*	486	1.064	860	1.883
Anatidae	Garganey	*Spatula querquedula*	680	1.489	859	1.880
Scolopacidae	Black–winged Stilt	*Himantopus himantopus*	660	1.445	752	1.646
Phalacrocoracidae	Indian Cormorant	*Phalacrocorax fuscicollis*	610	1.335	752	1.646
Laridae	Common Tern	*Sterna hirundo*	640	1.401	742	1.624
Phalacrocoracidae	Great Cormorant	*Phalacrocorax carbo*	–	–	656	1.436
Laridae	Black-headed Gull	*Chroicocephalus ridibundus*	240	0.525	639	1.399
Phalacrocoracidae	Little Cormorant	*Micro carboniger*	780	1.707	576	1.261
Laridae	Brown–headed Gull	*Larus brunnicephalus*	–	–	545	1.193
Charadriidae	Red–wattled Lapwing	*Vanellus indicus*	130	0.284	537	1.175
Ardeidae	Little Egret	*Egretta garzetta*	870	1.904	460	1.007
Laridae	Short–billed Gull	*Larus brachyrhynchus*	235	0.514	458	1.003
Scolopiacidae	Little Stint	*Calidris minuta*	830	1.817	447	0.978
Ardeidae	Cattle Egret	*Bubulcus ibis*	567	1.241	439	0.961
Laridae	Short–tailed Gull	*Larus canus*	340	0.744	434	0.950
Accipitridae	Black Kite	*Milvus migrans*	–	–	430	0.941
Charadriidae	Yellow–wattled Lapwing	*Vanellus malarbaricus*	40	0.088	388	0.849
Scolopacidae	Bar–tailed Godwit	*Limosa lapponica*	–	–	376	0.823
Podicipedidae	Little Grebe	*Tachybaptus ruficollis*	589	1.289	348	0.762
Ardeidae	Intermediate Egret	*Egretta intermedia*	546	1.195	324	0.709
Ardeidae	Indian Pond Heron	*Ardeol grayii*	100	0.219	290	0.635
Scolopacidae	Marsh Sandpiper	*Tringa stagnatilis*	290	0.635	267	0.584
Motacillidae	Yellow Wagtail	*Motacilla flava*	181	0.396	220	0.482
Scolopacidae	Common Sandpiper	*Actis hypoleucos*	214	0.468	217	0.475
Motacillidae	White Wagtail	*Motacilla alba*	150	0.328	198	0.433
Ardeidae	Great Egret	*Casmerodius albus*	367	0.803	195	0.427
Scolopacidae	Terek Sandpiper	*Xenus cinereus*	209	0.458	194	0.425
Threskiornithidae	Spoon–billed Ibis	*Platalea leucorodia*	–	–	189	0.414
Phoenicopteridae	Greater Flamingo	*Phoenicopterus roseus*	34	0.074	180	0.394
Recurvirostridae	Pied Avocet	*Recurvirostra avosetta*	–	–	170	0.372
Scolopacidae	Wood Sandpiper	*Tringa glareola*	50	0.109	168	0.368
Alcedinidae	Pied Kingfisher	*Ceryle rudis*	20	0.044	160	0.350
Rallidae	Common Moorhen	*Gallinula chlorpus*	40	0.088	155	0.339
Scolopacidae	Green Sandpiper	*Tringa ochropus*	164	0.359	148	0.323
Scolopacidae	Solitary Sandpiper	*Tringa solitaria*	–	–	134	0.293
Scolopacidae	Spotted Sandpiper	*Actitis macularius*	–	–	130	0.285
Scolopacidae	Lesser Sand Plover	*Charadrius mongolus*	27	0.059	124	0.271
Charadriidae	White–tailed Lapwing	*Chettus ialeucura*	–	–	106	0.232
Scolopacidae	Grey Plover	*Pluvialis squatarola*	18	0.039	64	0.140
Rallidae	White–breasted Waterhen	*Amaurornis phoenicurus*	78	0.171	46	0.101
Alcedinidae	White–throated Kingfisher	*Halcysmyrnensis*	30	0.066	45	0.099
Scolopacidae	Sociable Lapwing	*Vanellus gregarius*	14	0.031	25	0.055
	Total 39 Species	**Total**	**17454**		**28229**	
				45683		

http://www.aloki.hu ● ISSN 1589 1623 (Print) ● ISSN 1785 0037 (Online)
DOI: http://dx.doi.org/10.15666/aeer/1705_1083110843

Relative Abundance of Migrant, Resident, Resident-Migrant Bird Species

Notably, 18965 bird individuals of 30 migrant species representing 6 families were detected in 2018/19 as compared to 11547 bird individuals of 22 species and 5 families detected in 2014/15. Likewise, 5370 individuals of 15 resident species were detected in 2018/19 and 5247 individuals of 15 resident species in 2014/15. However, 5 resident–migrant bird species (i.e. 3897 individuals) were detected in 2018/19 while 660 bird individuals of *Himantopus himantopus* resident–migrant species (i.e.) were detected in 2014/15. Out of 30 migrant bird species, one species was critically endangered; two species Ra/A/Vu (Rare/Accidental/Vulnerable) and the rest 23 species were least concern based on IUCN Status. All resident bird species were totally protected and one resident–migrant bird species as data deficient (*Table 2*).

Foraging Guilds Structure in the 2018/19 and 2014/15 Periods

Notably, the findings of foraging guild structure 2018/19 stated that currently, urban seasonal waterlogged areas had attracted a higher number of bird individuals than previous years (i.e., guild omnivore; 32.489% in 2018/19 and 17.562% in 2014/15). Likewise, the higher relative abundance of guild Piscivore was detected in 2019 (12.808%) rather than 2014/15 (7.292%). On the contrarily, lower number of bird individuals of guild Carnivore/Piscivore/Insectivore were detected in 2019 (4.188%) rather than 2014/15 (5.472%). Moreover, the member of guild Carnivore was detected in 2018/19 but no individuals of Carnivore was documented in 2014/15 period (*Table 3*).

Comparison of Diversity Indices

The results of the alpha diversity analysis indicated that urban seasonal waterlogged areas had attracted higher diversity of avian species in 2018/19 rather than 2014/15 (*Table 4*).

Discussions

The urban seasonal waterlogged areas investigated in this study encompasses of 30.0% rush and sedge aquatic plants while rest is shallow water open areas devoid of aquatic vegetation. Rush and sedge plants serve as hiding cover for avian species while open water areas as foraging grounds. The shallow water is rich in food resources, such as fishes, amphibians, insects, crustaceans and aquatic plants which is the major diet of avian species especially waterfowl, seagulls, cormorant, grebes, plovers, sandpipers, stilt, and egrets.

Urban seasonal waterlogged areas are a highly important habitat for a wide array of waterbirds and terrestrial birds. Their importance depends on many factors, namely; size, connectivity to surrounding areas, diversity of vegetation, water quality, occurrence of food resources and disturbance. Besides, determining the temporal changes in avian population parameters is highly important to obtain the population trend of different avian species utilizing these areas. Evidently, the results of the diversity analysis in the study indicated that the bird diversity during consequent time period might vary depending on the habitat suitability, richness of food resources, and feeding guilds in the wetland reserve.

http://www.aloki.hu ● ISSN 1589 1623 (Print) ● ISSN 1785 0037 (Online)
DOI: http://dx.doi.org/10.15666/aeer/1705_1083110843

Table 2. *List of migrant, resident, and resident–migrant bird species detected in urban seasonal waterlogged areas of Hyderabad, Sindh Pakistan in the 2014/15 and 2018/19 periods*

Family	Common Name	Scientific Name	Current Status	Detected Observation in 2014/15	%	Detected Observation in 2018/19	%
Migrant Bird Species							
Anatidae	Northern Pintail	*Anas acuta*	LC	1490	4.883	1958	6.417
Anatidae	Common Teal	*Anas cerca*	LC	1870	6.192	1922	6.299
Anatidae	Mallard	*Anas platyrhinchos*	LC	–	–	1824	5.978
Anatidae	Gadwall	*Meraca strepera*	LC	–	–	1760	5.768
Anatidae	Baikal Teal	*Sibirionetta formosa*	Ra/A/Vu	1260	4.130	1656	5.427
Anatidae	Northern Shoveler	*Spatula clypeata*	LC	1630	5.342	1558	5.106
Anatidae	Falcated Duck	*Mareca falcate*	Ra/A/Vu	975	3.195	1234	4.044
Anatidae	Garganey	*Spatula querquedula*	LC	680	2.229	859	2.815
Laridae	Common Tern	*Sterna hirundo*	LC	640	2.098	742	2.432
Laridae	Black-headed Gull	*Chroicocephalus ridibundus*	LC	240	0.787	639	2.094
Laridae	Brown–headed Gull	*Larus brunnicephalus*	LC	–	–	545	1.786
Laridae	Short–billed Gull	*Larus brachyrhynchus*	LC	235	0.770	458	1.501
Scolopiacidae	Little Stint	*Calidris minuta*	LC	830	2.720	447	1.465
Laridae	Short–tailed Gull	*Larus canus*	LC	340	1.114	434	1.422
Charadriidae	Yellow–wattled Lapwing	*Vanellus malarbaricus*	LC	40	0.132	388	1.272
Scolopacidae	Bar–tailed Godwit	*Limosa lapponica*	LC	–	–	376	1.232
Scolopacidae	Marsh Sandpiper	*Tringa stagnatilis*	LC	290	0.950	267	0.875
Motacillidae	Yellow Wagtail	*Motacilla flava*	LC	181	0.593	220	0.721
Scolopacidae	Common Sandpiper	*Actis hypoleucos*	LC	214	0.701	217	0.711
Motacillidae	White Wagtail	*Motacilla alba*	LC	150	0.492	198	0.649
Scolopacidae	Terek Sandpiper	*Xenus cinereus*	LC	209	0.685	194	0.636
Recurvirostridae	Pied Avocet	*Recurvirostra avosetta*	LC	–	–	170	0.557
Scolopacidae	Wood Sandpiper	*Tringa glareola*	LC	50	0.164	168	0.551
Scolopacidae	Green Sandpiper	*Tringa ochropus*	LC	164	0.537	148	0.485
Scolopacidae	Solitary Sandpiper	*Tringa solitaria*	LC	–	–	134	0.439
Scolopacidae	Spotted Sandpiper	*Actitis macularius*	LC	–	–	130	0.426
Scolopacidae	Lesser Sand Plover	*Charadrius mongolus*	LC	27	0.088	124	0.406
Charadriidae	White–tailed Lapwing	*Vanellus leucurus*	LC	–	–	106	0.347
Scolopacidae	Greater Sand Plover	*Charadrius leschenaultii*	LC	18	0.059	64	0.210
Scolopacidae	Sociable Lapwing	*Vanellus gregarious*	CE	14	0.046	25	0.082
		Sub-Total		**11547**		**18965**	
					30512		

http://www.aloki.hu ● ISSN 1589 1623 (Print) ● ISSN 1785 0037 (Online)
DOI: http://dx.doi.org/10.15666/aeer/1705_1083110843

Family	Common Name	Scientific Name	Current Status	Detected Observation in 2014/15	%	Detected Observation in 2018/19	%
Resident Bird Species							
Laridae	River Tern	*Sterna aurantia*	LC	486	4.579	860	8.103
Phalacrocoracidae	Indian Cormorant	*Phalacrocorax fuscicollis*	LC	610	5.747	752	7.085
Phalacrocoracidae	Little Cormorant	*Micro carboniger*	LC	780	7.349	576	5.427
Charadriidae	Red–wattled Lapwing	*Vanellus indicus*	LC	130	1.225	537	5.059
Ardeidae	Little Egret	*Egretta garzetta*	LC	870	8.197	460	4.334
Ardeidae	Cattle Egret	*Bubulcus ibis*	LC	567	5.342	439	4.136
Podicipedidae	Little Grebe	*Tachybaptus ruficollis*	LC	589	5.549	348	3.279
Ardeidae	Intermediate Egret	*Egretta intermedia*	LC	546	5.144	324	3.053
Ardeidae	Indian Pond Heron	*Ardeol grayii*	LC	100	0.942	290	2.732
Ardeidae	Great Egret	*Casmerodius albus*	LC	367	3.458	195	1.837
Phoenicopteridae	Greater Flamingo	*Phoenicopterus roseus*	LC	34	0.320	180	1.696
Alcedinidae	Pied Kingfisher	*Ceryle rudis*	LC	20	0.188	160	1.507
Rallidae	Common Moorhen	*Gallinula chlorpus*	LC	40	0.377	155	1.460
Rallidae	White–breasted Waterhen	*Amaurornis phoenicurus*	LC	78	0.735	46	0.433
Alcedinidae	White–throated Kingfisher	*Halcysmyrnensis*	LC	30	0.283	45	0.424
		Sub-Total		**5247**		**5367**	
					10614		
Resident–Migrant Bird Species							
Anatidae	Green–winged Teal	*Spatula discors*	LC	–	–	1870	41.036
Recurvirostridae	Black–winged Stilt	*Himantopus himantopus*	LC	660	14.483	752	16.502
Phalacrocoracidae	Great Cormorant	*Phalacrocorax carbo*	DD	–	–	656	14.395
Accipitridae	Black Kite	*Milvus migrans*	LC	–	–	430	9.436
Threskiornithidae	Eurasian Spoonbill Ibis	*Platalea leucorodia*	LC	–	–	189	4.147
		Sub-Total		**660**		**3897**	
					4557		
		Grand Total		**17454**	**-**	**28229**	
		Overall Total			**45683**		

(LC = Least Concern, Ra = Rare, A = Accidental, Vu = Vulnerable, CE = Critically Endangered, DD = Data Deficient, M = Migrant, Re = Resident, and R–M = Resident–Migrant)

http://www.aloki.hu ● ISSN 1589 1623 (Print) ● ISSN 1785 0037 (Online)
DOI: http://dx.doi.org/10.15666/aeer/1705_1083110843

Table 3. *List of foraging guild based on the number of species and the total number of detections*

Guild Name	Year 2014/15		Year 2018/19	
	Observations	Percentage	Observations	Percentage
Omnivore	8023	17.562	14842	32.489
Piscivore	3331	7.292	5851	12.808
Piscivore/Insectivore	3235	7.081	4595	10.058
Carnivore/Piscivore/Insectivore	2500	5.472	1913	4.188
Insectivore	331	0.725	418	0.915
Detritivore	34	0.074	180	0.394
Carnivore	–	–	430	0.941
Sub–Total	**17454**		**28229**	
Grand Total	**45683**			

Table 4. *Comparison of diversity indices of avian species inhabiting urban seasonally waterlogged areas in the 2018/19 and 2014/15 periods*

Indices	2018/19				2014/15			
	Overall	Migrant	Resident	Resident–Migrant	Overall	Migrant	Resident	Resident–Migrant
Shannon's Index								
H	17.48	11.38	7.399	2.232	8.04	4.866	3.036	0.502
Exp. H	82.6	48.47	27.43	4.762	55.54	31.21	20.96	4.527
Lower H @ 95%	12.2	7.737	4.757	0.558	8,04	4.866	3.038	0.562
Upper H @ 99%	14.84	10.01	6.342	2.232	8.04	4.866	3.036	0.502
Margalef's Index								
R_1	4.414	3.881	3.312	1.561	4.017	3.441	3.043	1.51
Lower H @ 95%	3.943	3.393	2.741	0.637	4.008	3.43	3.029	1.495
Upper H @ 99%	4.181	3.677	3.128	1.561	4.026	3.453	3.054	1.527
McIntosh's Index								
E	0.971	0.960	0.947	0.893	0.851	0.802	0.773	0.525
Lower H @ 95%	0.929	0.902	0.853	0.430	0.850	0.801	0.771	0.520
Upper H @ 99%	0.950	0.937	0.918	0.893	0.852	0.804	0.774	0.532

Evidently, the results of population parameters are noteworthy, in comparisons; the higher relative abundance, bird species, foraging guilds, and diversity indices were detected in the 2018/19 rather than 2014/15 period. This indicate that urban seasonal waterlogged areas has becomes more attractive habitat with the passage of time for avian species as compared to previous years. The recording of higher relative abundance, species composition, foraging guilds, and diversity indices could be that these areas are less disturbed even though they are located within the heart of the city. Because nobody hunting in these areas due to under administration of cantonment board. The other reason might be that these areas are rich in fish fingerlings, amphibians, insect larvae, and organic matter. These food resources are the major diet of waterbird as well as terrestrial bird species. The third reason could be that natural wetland areas of the Hyderabad have lost due to conversion into agriculture fields, water pollution, and aquaculture ponds, and urban settlements. Due to these reasons, urban seasonal waterlogged areas of the Hyderabad serve as an alternate habitat for a wide array of waterbird as well as terrestrial bird species, especially in winter.

Furthermore, it was observed that the relative abundance of waterbird was influenced by vegetation structure, food resources, and water level that affected the habitat selection. This could be that these factors indicated where and how the waterbirds used the urban waterlogged areas. For example; waterfowl, grebes and cormorant often

http://www.aloki.hu ● ISSN 1589 1623 (Print) ● ISSN 1785 0037 (Online)
DOI: http://dx.doi.org/10.15666/aeer/1705_1083110843

utilized open water areas devoid of aquatic vegetation for foraging (waterfowls, sandpipers, lapwings, stilts, cormorants, terns, and egrets) and dead fallen trees for perching (cormorants and egrets). Likewise, egrets, herons, sandpipers, plovers, and lapwings selected shallow waters for foraging and substrate for perching and avoided the deep waters. This could be that deep water may restrict their prey accessibility and reduced the prey–capturing success (Gawlik, 2002; Brönmark and Hansson, 2005).

Additionally, it was also observed that the richness and diversity of food resources may regulate the distribution and diversity of waterbird species in aquatic habitat (Johnson and Sherry, 2001; Sutula and Stein, 2003). Furthermore, this study highlighted that waterbird species are habitat specialist, they often selected habitat that offers ideal foraging and perching sites, shelter from predator and harsh weather. Relatively, water depth, vegetation structure and composition, richness and diversity of food resources, and dead fallen trees in urban waterlogged areas play a significant role in foraging guild structure (Kiviat and MacDonald, 2004; Benassi et al., 2007; Guadagnin et al., 2009; Tsai et al., 2012).

Conversely, seven foraging guilds were recorded in 2018/19 and six foraging guilds in 2014/15 period. Apparently, the recording of seven feeding guilds of the avian species in urban waterlogged areas in the 2018/19 showed that this seasonal fragile habitat provided suitable food and foraging sites for a wide array of avian species (i.e., waterbirds and terrestrial birds). Furthermore, the results of foraging guild structure revealed that urban seasonal waterlogged areas are rich in food diversity, vegetation structure, and water level that may play a crucial role to attract a higher diversity of avian species especially waterbirds. It was observed that piscivore, i.e., cormorant, egrets, heron, and kingfishers preyed on fishes especially in shallow waters, omnivore i.e., waterfowls foraged on animal (fishes, amphibians, invertebrates, etc.) and plant matter (aquatic plants) that floating at the surface of the water or occurs in shallow waters, insectivore, i.e., stilt, sandpipers, and lapwing, etc mostly preferred shallow water and soft mud to prey on aquatic invertebrates (Guadagnin et al., 2009).

Furthermore, the results foraging behavior also indicated that the waterbirds and terrestrial birds inhabiting in urban waterlogged areas were highly variable in their morphological structures, foraging behavior, and food capturing tactics, and habitat selections. The members of each foraging guild varied in their food selection due to morphological differences, bill and tarsus size, water depth and habitat preferences.

Conclusions

The findings of this study indicated that urban seasonal waterlogged area is suitable habitat (foraging sites and stopover) for a wide array of waterbird species especially migrant birds to refuel, rest, and forage. Unfortunately, these fragile areas have been shrinking at an alarm rate due to urban development. For conservationist, dealing with the human and maintaining the functional waterlogged ecosystem is the greatest challenge to conserve and protect these fragile aquatic habitats. The existence, sustainability, and future of avian species directly depend on protection and conservation of the urban waterlogged areas of Hyderabad and across the country. Hence, it is strongly recommended that the urban seasonal waterlogged areas should be declared as wetland reserve (wetland of global importance) due to harboring a variety of migrants as well as native waterbird species that belong to different taxonomic groups.

http://www.aloki.hu ● ISSN 1589 1623 (Print) ● ISSN 1785 0037 (Online)
DOI: http://dx.doi.org/10.15666/aeer/1705_1083110843

REFERENCES

[1] Aborn, D. A. (2007): Abundance, Density and Diversity of Neotropical Migrants at the Lula Lake Land Trust, GA. – Southeastern Naturalist 6(2): 293-304.
[2] Adams, H. L., Wes Burger, J. L., Riffel, S. (2015): Edge effects on avian diversity and density of native grass conservation buffers. – The Open Ornit. J. 8: 1-9.
[3] Benassi, G., Battisti, C., Luiselli, L. (2007): Area effect on bird species richness of an arcipelago of wetland fragments of Central Italy. – Comm. Ecol. 8: 229-237.
[4] Bibby, C. J., Burgess, N. D., Hill, D. A., Mustoe, S. (2000): Bird Census Techniques. – London; Academic Press, UK. Second Edition. Pp. 91-112.
[5] BirdLife International (2015): Migratory Birds and Flyways. – URL: http://www.birdlife.org/worldwide/ programme-additional-info/migratory-birds-and-flyways.
[6] Blake, J. G., Loiselle, B. A. (2000): Diversity of birds along an elevational gradient in the Cordillera Central, Costa Rica. – Auk 117: 663-686.
[7] Brönmark, C., Hansson, L.–A. (2005): The Biology of Lakes and Ponds. – Oxford University Press, Oxford, New York. Second Edition. Pp. 285.
[8] Buckland, S. T., Anderson, D. R., Burnhan, K. P., Lake, J. L., Borchers, D. L., Thomas, L. (2004): Advance Distance Sampling; Estimating Abundance of Biological Populations. – London; Campman and Hall. Pp. 141-172. ISBN: 0–19–850927–8.
[9] Catford, J. A., Walsh, C. J., Beadall, J. (2007): Catchment urbanization increases benthic micro algal biomass in streams under control light conditions. – Aquatic Science 69: 511-522.
[10] Codesido, M., Bilenca, D. N. (2000): Comparacion de los metodos de transecta de fajay de conteo de puntos de radio fijo en una comunidad de aves del bosque semiárido santiagueño. – El Hornero 15: 85-91.
[11] Davis, J., Sim, L., Chambers, J. (2010): Multiple stressors and regime shifts in shallow aquatic ecosystems in antipodean landscapes. – Freshwater Biology 55: 5-18.
[12] DeSante, D. F., Nott, M. P., Kaschube, D. R. (2005): Monitoring, modelling, and management: why base avian monitoring on vital rates and how should it be done. – In: Ralph, C. J., Rich, T. D. (eds.) Bird conservation implementation and integration in the Americas. U.S. Forest Service General Technical Report PSW-GTR-191. Albany, California, USA. Pp. 795-804.
[13] Ehrenfed, J. (2000): Evaluating wetlands within an urban context. – Ecological Engineering 15: 253-265.
[14] Fraser, L. H., Keddy, P. A. (2005): The World's Largest Wetlands: Ecology and Conservation. – Cambridge University Press, U.K.
[15] Gawlik, D. E. (2002): The effect of prey availability on the numerical response of wading birds. – Ecological Monographs 72: 329-346.
[16] Gibbs, J. P., Whiteleather, K. K., Schueler, F. W. (2005): Changes in frog and toad populations over 30 years in New york State. – Ecological Applications 15: 1148-1157.
[17] Guadagnin, D. L., Maltchik, L., Fonseca, C. R. (2009): Species–area relationship of Neotropical waterbird assemblages in remnant wetlands. – Diversity and Distributions 15: 319-327.
[18] Henderson, P. A., Seaby, R. M. H. (2007): Community Analysis Package 4.0. – Pisces Conservation Ltd, Lymington, UK.
[19] Hoffmann, M. D., Dodson, S. I. (2005): Land use, primary productivity and lake area as desciptors of zooplankton diversity. – Ecology 86: 255-261.
[20] Hubbell, S. P. (2001): The unified neutral theory of biodiversity and biogeography. – Princeton University Press, Princeton, N.J.
[21] James, A.–O., Emmanue, D., Bright, A. Y. (2017): Diversity and abundance of bird species in Mole National Park, Damongo, Ghana. – Journal of Natural Sciences Research 17(12): 20-33.

http://www.aloki.hu ● ISSN 1589 1623 (Print) ● ISSN 1785 0037 (Online)
DOI: http://dx.doi.org/10.15666/aeer/1705_1083110843

[22] Johnson, M. D., Sherry, T. W. (2001): Effects of food availability on the distribution of migratory warblers among habitats in Jamaica. – Journal of Animal Ecology 70: 546-560.
[23] Kiviat, E., MacDonald, K. (2004): Biodiversity pattern and conservation in the Hacensack Meadowlands, New Jersey. – Urban Habitats 2(1): 28-61.
[24] Mackintosh, T., Davis, J. (2013): The Importance of Urban Wetlands. – In: Paul, S. (ed.) Workbook for Managing Urban Wetlands in Australia. Sydney Olympic Park Authority. URL: https://www.sopa.nsw.gov.au/Resource–Centre/WET–eBook–Workbook–for–Managing–Urban–Wetlands–in–Australia#. First Edition, ISNB: 978–0–9874020–0–4.
[25] McGill, B. J., Etienne, R. S., Gray, J. S., Alonso, D., Anderson, M. J., Benecha, H. K., Dornelas, M., Enquist, B. J., Green, J. L., He, F., Hulbert, A. H., Magurran, A. E., Marquet, P. A., Maurer, B. A., Ostling, A., Soykan, C. U., Ugland, K. L., White, E. P. (2007): Species abundance of bird distributions: moving beyond single prediction theories to integration within an ecological framework. – Ecology Letters 10: 995-1015.
[26] Meadows, S., Moller, H., Weller, F. (2012): Reduction of bias when estimating bird abundance within small habitat fragments. – New Zeal. J. Ecol. 36(3): 1-8.
[27] Mills, T. R., Rumble, M. A., Flake, L. D. (2000): Habitats of birds in ponderosa pine and aspen/birch forest in the Black Hills, South Dakota. – Journal of Field Ornithology 71: 187-206.
[28] Nadeau, C. P., Conway, C. J., Smith, B. S., Lewis, T. E. (2008): Maximizing detection probability of wetland dependent bird during point count surveys in North-western Florida. – The Wilson Journal of Ornithology 120(3): 513-518.
[29] Razali, N. M. (2011): Power comparisons of Shapiro-Wilk, Kolmogorov–Smirnov, Lilliefors and Anderson–Darling test. – Journal of Statistical Modeling and Analytics 2(1): 21-33.
[30] Richardson, A. J., Taylor, I. R., Growns, J. E. (2001): The foraging ecology of egrets in rice fields in southern New South Whales, Australia. – Waterbirds 24(2): 255-264.
[31] Schieck, J. (1997): Biased detection of bird vocalizations affects comparisons of bird abundance among forested habitats. – Condor 99: 179-190.
[32] Simon, G. S., Okoth, E. O. (2016): Species richness and abundance of birds in and around Nimule National Park, South Sudan. – Sci. Lett. 4(1): 92-94.
[33] Sutula, M., Stein, E. (2003): Habitat value of natural and constructed wetlands used to treat urban runoff: a literature review. – Southern California Coastal Water Research Project. Technical Report No. 388.
[34] Thompson III, F. R., Burhans, D. E., Root, B. (2002): Effects of point count protocol on bird abundance and variability estimates and power to detect population trends. – Journal of Field Ornithology 73(2): 141-150.
[35] Tsai, J-S., Venne, L. S., Smith, L. M., McMurry, S. T., Haukos, D. A. (2012). Influence of local and landscape characteristics of avian richness and density in wet Playas of the southern great plains, USA. – Wetland 32: 605-618.
[36] van der Walk, A. G. (2006): The Biology of Freshwater Wetlands. – Oxford University Press, Oxford. ISBN-10: 9780198525400.
[37] Vermoden, K., Leuven, R., Van der Velde, G., Van Katwijk, M. M., Roelofs, J. G. M. (2007): Urban drainage systems: An undervalued habitat for aquatic macro invertebrates. – Biological Conservation 142: 1105-1115.
[38] Verner, J., Ritter, L. V. (1985): A comparison of transects and point counts in oak-pine woodlands of California. – Condor 87: 47-68.
[39] Verner, J., Purcell, K. L. (1999): Fluctuating populations of House Wrens and Bewick's Wrens in foothills of the western Sierra Nevada of California. – Condor 101: 219-229.
[40] Walag, A. M. P., Canencia, M. O. P. (2016): Physio–chemical parameters and macrobenthic invertebrates of intertidal zone of Gusa, Cagayan de Oro City, Philippine. – AES Bioflux 8(1): 71-82.

http://www.aloki.hu ● ISSN 1589 1623 (Print) ● ISSN 1785 0037 (Online)
DOI: http://dx.doi.org/10.15666/aeer/1705_1083110843

[41] Wijesundara, C., Wijesundara, M. (2014): Bird Diversity of Dekinda Forest Reserve, Balana, Sri Lanka: Implications for Conservation. – Ceylon J. of Sci. (Bio. Sci.) 43(1): 137-146.
[42] Yu-Seong, C., Kwon, I., Yoo, J. (2008): A study of feeding methods in five species of heron and egrets in Korea. – Journal of Field Biology 31(2): 147-151.
[43] Zhang, M., Lei, G., Lu, C. (2010): Wetland conservation in China: Status, Challenges and Strategies. – Wetland Science and Practice 27(2): 16-23.

http://www.aloki.hu ● ISSN 1589 1623 (Print) ● ISSN 1785 0037 (Online)
DOI: http://dx.doi.org/10.15666/aeer/1705_1083110843

BIO-FERTILIZING EFFICIENCY OF PHOSPHATE SOLUBILIZING BACTERIA IN NATURAL ENVIRONMENT: A TRIAL FIELD STUDY ON STRESS TOLERANT POTATO (*SOLANUM TUBEROSUM* L.)

JAHANGIR, G. Z.[1,3*] – ARSHAD, Q.-U.-A.[2] – SHAH, A.[1] – YOUNAS, A.[3] – NAZ, S.[3] – ALI, Q.[4*]

[1]*Centre for Applied Molecular Biology (CAMB), University of Punjab, Lahore, Pakistan*

[2]*Departments of Zoology, University of Punjab, Lahore, Pakistan*

[3]*Department of Biotechnology, LCWU, Lahore, Pakistan*

[4]*Institute of Molecular Biology and Biotechnology, University of Lahore, Lahore, Pakistan*

**Corresponding authors*
e-mail: zahra_jahangir@yahoo.com, saim1692@gmail.com

(Received 14th Mar 2019; accepted 24th May 2019)

Abstract. The present study aimed at the characterization of various strains of phosphate solubilizing bacteria (PSB) purified on Pikovskaya (PVK) agar medium, containing insoluble tricalcium phosphate (TCP). Maximum phosphate solubilization index (PSI) was calculated from 1.1 to 4.57 cm from clear halo zones around the microbial growth on the PVK. 26 highly efficient purified PSB isolates were also found effective for potassium solubilization on Aleksandrov medium. Maximum potassium solubilization index (KSI) was calculated as 1.1-4.66 cm. The phosphate and potassium solubilization is linked to the production of low molecular weight acids by bacterial cells. Therefore change/decline in the pH of liquid cultures was also observed and maximum decrease was recorded as 3.25 in 9AS strain. Most efficient strains were characterized by ribotyping and based on sequence studies were identified under genera *Klebsiella, Enterobacter, Bacillus,* Marine bacterium*, Staphylococcus,* and *Serratia*. Their sequences obtained MF465778, MF465779, MF465782, MF465781, MF465777, and MF465783, respectively (GenBank). Bio-fertilizing efficiency and possible plant growth promoting effect of selected PSB was evaluated by applying in potato (*Solanum tuberosum* L.) rhizosphere in trial field. An increase of, two-fold yield in plant height, number of lateral shoots, number of roots and root length was observed by *Bacillus licheniformis*, *Serratia marcescens*, and *Staphylococcus warneri*, as compared to un-inoculated controls. These results indicate that the isolated strains bear great potential to be used as source of bio fertilizer in crop fields.
Keywords: *PSB, KSB, biofertilizer, potato trial field, molecular characterization*

Introduction

Phosphorus (P) being an essential macro nutrient is indispensable for plant's growth (Leticia et al., 2015). Unlike nitrogen, there is no atmospheric reservoir available to augment its quantity in soil. Phosphorus in soil is present both in the form of organic and inorganic phosphates. Inorganic phosphates form large mineral complexes with other metals in the soil. While on the other hand, organic phosphates, which constitute 20-80% of total phosphorus contents in soil, are present as immobilized and insoluble phosphates (Diep et al., 2013). Phosphorus that is absorbable by plant roots exists in scarce amount in soil. The amount of P deviates between 200-2000 kg P/ha at upper 15 cm soil layer, having an average amount of about 1000 kg present in soil but its available quantity is a lower fraction of phosphorus available (Ali et al., 2013; Jahangir et al., 2016), that is roughly 10μM in different soils (Nobandegani et al., 2015). A recent

http://www.aloki.hu ● ISSN 1589 1623 (Print) ● ISSN 1785 0037 (Online)
DOI: http://dx.doi.org/10.15666/aeer/1705_1084510859

investigation suggested that although 95-99% of all phosphoric amount is in insoluble forms, however only 0.1% of it, is in plant's accessible form (Ali et al., 2014, 2016; Awais et al., 2017; Surapat et al., 2013). Thus, plants need assisting agents to convert immobilized and insoluble phosphorus into a form that can be absorbed readily through roots.

Nature has richly supplied the agricultural soils with phosphate solublizing bacteria (PSB). These bacteria are one of the many other types of Plant growth-promoting bacteria (PGPB) which aid plant growth and development through various mechanisms (Glick, 2001). PSB are found to convert insoluble phosphates, in a form accessible to plants, such as orthophosphate (Leticia et al., 2015), through solubilization and mineralization. Animal dung has long been used to increase the P contents of soil ignoring the microbial communities and their roles (Sharma et al., 2011). Thus, PSB application to increase the rhizospheric phosphorus levels by solubilization of re-precipitated P forms is favored (Shekhar et al., 2000; Sadiq et al., 2013). In addition, application of KSB biofertilizers is not only associated with the improvement of soil fertility but also increases the crop yield. It also assists in shielding the plants from hazardous diseases plus lowers the solicitation of various synthetic fertilizers being expensive. Application of the PSB also minimizes the cost of the synthetic fertilizers in a much eco-friendly manner (Sindhu et al., 2010; Sheng et al., 2003; Zameer et al., 2015).

The purpose of the present study aimed for the isolation and molecular characterization of efficient PSB strains through ribotyping. The potential of potent strains for the development of plant growth is also evaluated in natural open environment on potato trial field that showed significant results. The Present investigation reports *Bacillus licheniformis*, *Serratia marcescens*, and *Staphylococcus warneri* are potential candidates to develop economical source of phosphate fertilizers that enhance plant growth and also help to reuse the fixed soil phosphate.

Materials and methods

Soil sampling

To isolate growth promoting rhizobacteria, soil samples were collected from crop rhizosphere of different agricultural areas of Punjab in the months of August-October. Soil adhering to plant roots was taken from about 20-24 cm depth. The soil samples were collected in disinfected polythene bags and were carried to the research laboratory of the Centre for Applied Molecular Biology (CAMB) Lahore. Soil samples were kept at 4 ± 1 °C until further use.

Purification of PSB strains from rhizospheric soils

For the isolation of PSB strains, the tiny roots with adhering soil were removed weighing about 1 g (per sample) in a formerly sterilized mortar. 6 ml of normal saline was poured in individual sample and crushed moderately with sterilized pestles. The soil suspension from each sample was serially diluted by 10x factor in saline water to get better isolation. Serially diluted soil samples, 10 µl of diluent was spread on synthetic Pikovaskaya (PVK) agar medium (Merck, B.N. #JE2JF62127), and was sterilized at 121 °C and 105 kPa for 15 min, incubated at 28 °C (binder, MB64585923, 240 V and 50/60 Hz). After initial incubation of 48 h, single colonies that produced halo

http://www.aloki.hu ● ISSN 1589 1623 (Print) ● ISSN 1785 0037 (Online)
DOI: http://dx.doi.org/10.15666/aeer/1705_1084510859

zones were repeatedly streaked on PVK agar plates until purified cultures were obtained. Purified cultures were preserved in 20% glycerol at -80 °C.

Phosphate solubilization

Single colonies of purified PSB isolates were inoculated into 10 ml LB broth medium in 50 ml separate culture tubes. LB medium contained Tryptone (DIFCO#0349000), 10 g/L; NaCl, 10 g/L; Agar (bioworld#40100044-1), 15 g/L and Yeast Extract (Fluka#0001415579), 5 g/L, and was sterilized at 121 °C and 105 kPa for 15 min. For obtaining the optimal growth, these cultures were incubated overnight at 28 °C in constant shaking incubator (New Brunswick scientific classic C24KS). For pin point inoculation 10 µl of each of this fresh grown culture was dripped in the middle of respective labelled PVK agar plates and incubated for 7 days at 28 °C. The phosphate solubilization index (SI) of phosphate solubilizing bacteria was calculated on seventh day using the following formula:

$$\text{PSI} = \frac{\left(\text{Colony diameter} + \text{halo zone diameter}\right)}{\text{Colony diameter}}$$

Based on higher phosphate solubilization index, 11 superior isolates were selected for further characterization.

Potassium solubilization

The efficient PSB isolates with higher PSI were also analyzed for assessing their proficiency to dissolve bounded potassium. The solubilization of potassium was assessed by the same protocol and formula as the phosphate solubilization; however, Aleksandrove media was used to calculate the potassium solubilization index (KSI). This modified Aleksandrove medium/L contained $CaCO_3$: 0.10 g, Glucose: 5.0 g, $MgSO_47H_2O$: 0.50 g, $FeCl_3$: 0.006 g, $Ca_3(PO_4)_2$: 2.0 g, Insoluble Mica powder (insoluble potassium source): 3.0 g and Agar: 20.0 g, and was sterilized at 121 °C and 105 kPa for 15 min. Disinfected water was used for medium preparation with pH adjustment of 5.5-5.7.

pH change

Single purified colony of all PSB isolates was inoculated in 10 ml of PVK broth to assess the pH change of the medium. Cultures were incubated in the shaker incubator (New Brunswick scientific classic C24KS) at 120 rpm and 28 °C for ten days along with un-inoculated control. The pH of isolate was measured by a pH meter (Bante, 210) on 1st, 3rd, 7th and 10^{th} day of incubation.

Molecular characterization of PSB strains based on 16SrRNA conserved regions

11 superior isolates (based on their solubilizing efficiency) were selected for molecular characterization. Bacterial DNA was extracted using a buffer (50 ml) that contained 5 M NaCL, 5 ml; 0.5 M EDTA, 5 ml; Tris of pH 7.9, 5 ml and autoclaved distilled water, 35 ml. Other reagents of protocol include Phenol Chloroform Isoamylalcohol (25:24:1), 10% SDS, 70% Ethanol, Isopropanol and glass beads. 10 ml of sterilized LB broth medium was inoculated with single colony of each of the 11 PSB isolates in aseptic conditions. Cultures were incubated overnight, in shaker incubator at 28 °C to obtain

http://www.aloki.hu ● ISSN 1589 1623 (Print) ● ISSN 1785 0037 (Online)
DOI: http://dx.doi.org/10.15666/aeer/1705_1084510859

optimal growth. After incubation, the culture was dispensed into 1.5 ml microcentrifuge tubes and cells were harvested from each culture by tight centrifugation at 3000 rpm for about 10 min. Cell pellets were resuspended in DNA extraction buffer (500 µl/1.5 ml of each culture) and dispensed in correctly labeled 1.5 ml micro centrifuge tubes. Each tube was given a heat shock up to 65 °C for the duration of 30 min. After cooling for 5 min, 100 µl of 10% SDS was added and were again given the 65 °C heat shock for 10 min. After cooling for about 5 min, added the 200 µl of glass beads along with 200 µl of PCI. Each sample was subjected to vortex after 1 min incubation in freezer. After repeating this step three times, samples were centrifuged on 14000 rpm for 10 min and their supernatants were collected in a new 1.5 ml microcentrifuge tubes and added with equal volume of Isopropanol. Further, tubes were centrifuged at 14000 rpm for 10 min. Pellet was saved and washed with 500 µl of 70% Ethanol on 14000 rpm for 7 min. After washing, DNA pellets are dried for about 10 min at room temperature and then resuspended them in the 50 µl nuclese-free water and stored at -20 °C 4 µl of each sample was run on 11% agarose gel using 1 µl of 6X loading dye in 1XTAE buffer. Each sample of DNA was also quantified through nanodrop analysis. PCR was optimized to amplify 16S rRNA gene sequence using a universal primer (Laticia et al., 2015):

FORWARD PRIMER: 5'- GAGAGTTTGATCCTGGCTCAG-3'

REVERSE PRIMER: 5'- CTACGGCTACCTTGTTACGA-3'

Annealing temperature and other amplification conditions were optimized in Gradient thermal cycler (BIO-RAD T100^{TM}). PCR reaction mixture contained 100 ng/µl of template (4 µl of 14AS DNA), 1mM dNTPs, 1X PCR Buffer, 1.0 picomol, each of Forward and Reverse Primers, 2.5 mM $MgCl_2$, and 0.5 U of Taq Polymerase (Thermo Scientific). Final volume made up to 20 µl with nuclease free H_2O. The cycling conditions included initial denaturation at 95°C for 3 min followed by 35 incubation repeats of 45 s denaturation at 95 °C, 45 s annealing at gradient of 54 °C, 55 °C, 56 °C, 57°C, 58 °C, 59 °C and 1 min extension at 72 °C with the final extension of 7 min at 72 °C and infinity hold at 4 °C. After optimization, same cycling conditions were practiced for amplification of 16SrRNA gene sequences from all six best performing strains. PCR products were run on 1% agarose gel along with 100 bp DNA ladder (Thermo Scientific#SM0323) in 1XTAE buffer. Amplified bands were purified using Invitrogen, Purelink^{R} Quick Gel Extraction Kit # K2100-12).

Purified 16S rRNA PCR products were sequenced by DNA core facility of the CAMB. Sequence data was analyzed and used for molecular identification of the studied PSB strains. The obtained sequences were BLAST, aligned and compared with the standard sequences in NCBI of all bacterial lineage based on information related to 16SrRNA gene sequences available on the online portal of National Center for Biotechnology Information GenBank (http://www.ncbi.nlm.nih.gov/). Further analyses were made on MEGA 6, and the phylogenetic trees for PSB strains were constructed through neighbor-joining method.

Trial field experiments of PSB isolates on potato crop

Bacillus licheniformis, Staphylococcus warneri, and *Serratia marcescens* (14 AS, Rl, and 5Bl respectively) were applied in the rhizospheric region of 25 abiotic stress tolerant potato plants (Sante) in a trial field to test their biofertilizing efficiency in the

http://www.aloki.hu ● ISSN 1589 1623 (Print) ● ISSN 1785 0037 (Online)
DOI: http://dx.doi.org/10.15666/aeer/1705_1084510859

natural environment. Field trial study was conducted in the area of CAMB specified for potato trial field within trial field premises of CAMB during October-January 2017.

The trial field land was prepared by using different irrigational practices and was supplied with essential amount of fungicide and inorganic fertilizers for adequate crop growth. The soil of trial field was sandy loam and an adequate quantity of organic matter was mixed during softening of soil. The pH of trial field soil was 6.5 on the day of plantation. No extra fertilizer was applied during whole experiment. All other requirements of the field including watering and soil softening were provided as per need of the crop. The Lab grown complete plants of tissue cultured transgenic Sante variety (possessing Dehydrin-10 gene of Eucalyptus) was shifted to the trial field. Following the plantation pattern of Skogsmyr (1994), the plants were planted (shifted) to trial field soil at distance of 0.25 to 0.5 m. Overnight grown bacterial culture (10 ml per plant) was applied to the rhizosphere soil of plantlets in three repeated treatments on 7th, 21st, and 50th day of plantation. The potato field was harvested on 90^{th} day after shifting the plants into trial field from laboratory. The number of survived plants per experimental units, number of lateral shoots per plant, total number of roots and tubers (of all sizes) per plant, maximum root and shoot length per plant were measured and recorded for all three treatments and, negative control lanes.

Statistical analysis

The obtained experimental data were analyzed statistically by using Statistix software version 8.1 and the results were expressed as the mean. Means and standard errors (SE) separation was accomplished by LSD. Statistical analysis of the results was performed by using general linear model (GLM) and one-way analysis of variance (one-way ANOVA) up to 5 levels to access whether the different PSB isolates had a significant effect on plant growth parameters. Significance of the effect of treatment was determined by the magnitude of the value ($P < 0.05$).

Results and discussion

Purification and phosphate solubilization potential of PSB

Phosphate Solubilizing Microbial colonies that were purified on the Pikovskaya (PVK) agar medium containing insoluble tri-calcium phosphate (TCP), (*Fig. 1*). Insoluble P was consumed by all isolates to different extents but eleven samples namely 2CQlV, 2CQll, 2CQlll, 2CQV, 9AS, 2CQVl, 14AS, GRl, GRll, 5BI and 17AS exhibited greater halo zones on PVK agar plates, hence showed higher PSI (*Fig. 2*). 14AS showed highest halo zone measured as 3.2 cm with the PSI of 4.57cm. Whereas the lowest halo zone measurement was recorded as 1.1 cm in 3SQII. Similar methodology related to isolation and screening of PSB has been reported by scientists (Sadiq et al., 2013; Zameer et al., 2016; Jahangir et al., 2016). Values of Phosphate solubilizing index (PSI) based on their colony diameter and clear zones, differed for different PSB isolate. Similar results were stated by Yasmin et al. (2011).

K solubilization potential of the PSB isolates

PSB isolates with higher PSI were also evaluated for potassium solubilization efficiency. These potassium solubilizing microbes increase plants growth as a result of solubilization of insolvable K minerals like mica and feldspar (Sheng et al., 2003). All

http://www.aloki.hu ● ISSN 1589 1623 (Print) ● ISSN 1785 0037 (Online)
DOI: http://dx.doi.org/10.15666/aeer/1705_1084510859

of the tested PSB isolates consumed Aleksandrov medium yielding various sized colonial growth while 3SQIV isolate showed disperse pattern of growth. While, 14 PSB isolates namely 2CQII, 2CQV, 2CQIII, 63dII, 2CQIV, 5GQI, 2CQVI, 2CQVIII, 9AS, GRII, 14AS, GRl,17AS and 5B1 were found to be capable of solubilizing K from insoluble K-bearing minerals source and the zone of solubilization was measured from 4.66 to 1.1 cm (*Fig. 3*). The research by Zhang and Kong (2014), also demonstrated the ability of the potassium solubilization from insoluble potassium. Maximum measurement of the colony and halo zone diameter was recorded by 2CQVI (1.7 cm) and 2CQVIP (1.1 cm) respectively (*Fig. 3*). The overall highest recorded value of KSI was shown by 2CQVl as 4.66 cm (*Fig. 3*). The distinct patterns of P and K Solubilization on respective growth media for comparative efficiency of PSB isolates are presented in (*Figs. 4* and *5*).

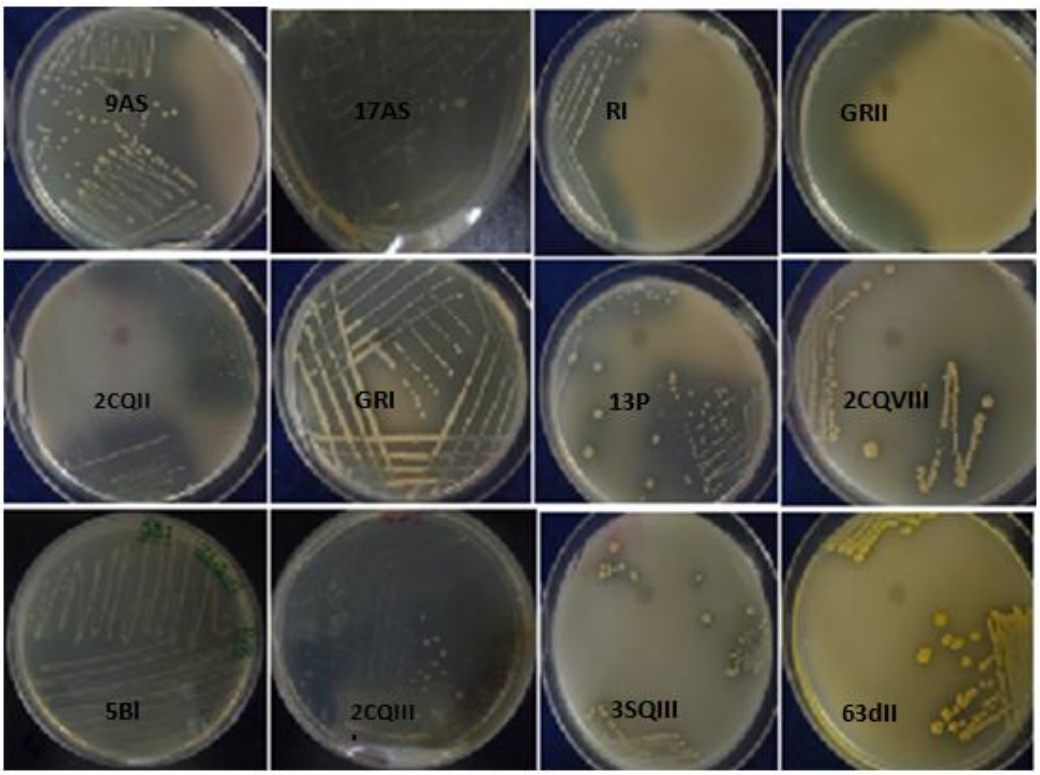

Figure 1. *Purified PSB isolates on PVK medium*

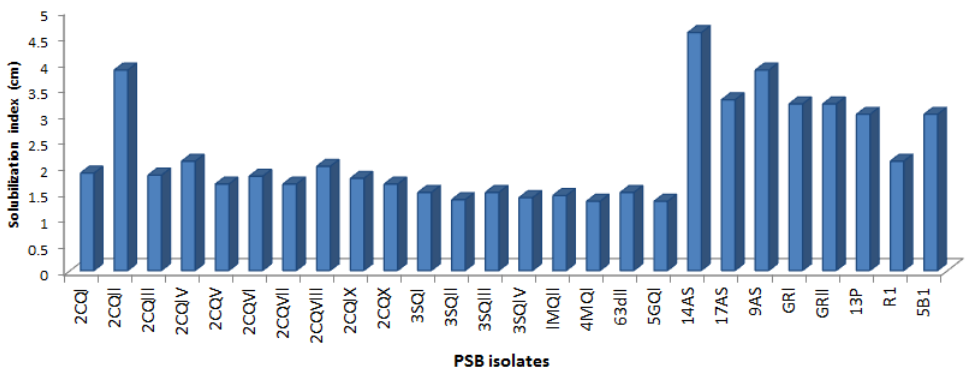

Figure 2. *PSI of purified PSB isolates on PVK*

http://www.aloki.hu ● ISSN 1589 1623 (Print) ● ISSN 1785 0037 (Online)
DOI: http://dx.doi.org/10.15666/aeer/1705_1084510859

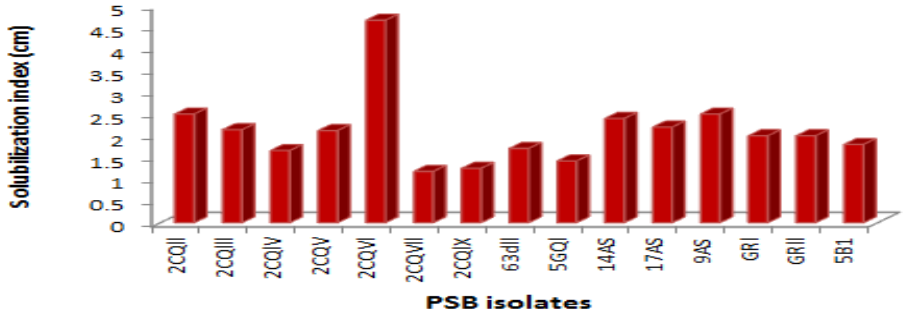

Figure 3. *KSI of selected PSB isolates on Aleksandrov medium*

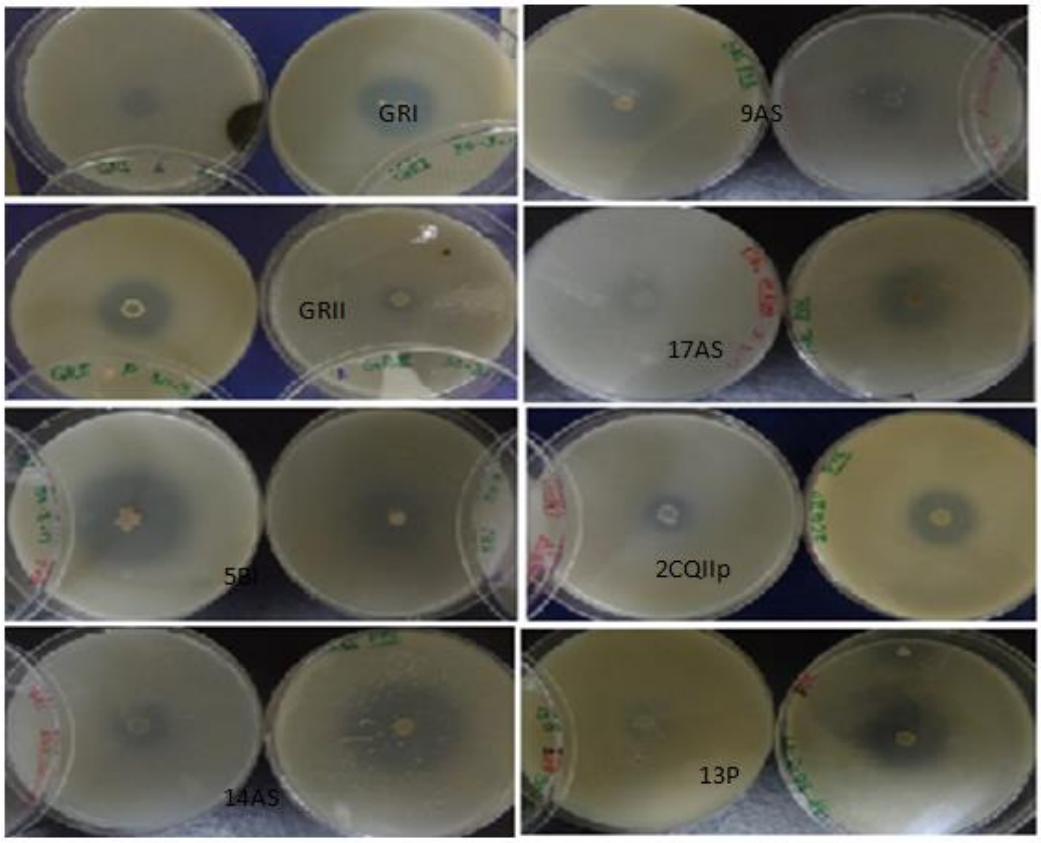

Figure 4. *Comparison of some PSB isolate's Solubilization index (SI) on Pikovskaya's and Aleksandrov media*

pH change

A successive decrease in all of the isolates was observed on 1st, 3rd, 7th and 10th days. Maximum recorded acidic value was of 9AS (3.25) depicting the highest medium discoloration because of breakdown of insoluble precipitates of tricalcium phosphate (*Fig. 6*). However, 5 cultures 2CQlll, 2CQlV, 2CQVl, 2CQX and 63dll, showed distinct patterns of PH change by giving much lower pH values at start then a bit increase in these values on successive day but showed overall trend towards acidic property (*Fig. 6*). The results of the presented study are in close accordance with the findings of

http://www.aloki.hu ● ISSN 1589 1623 (Print) ● ISSN 1785 0037 (Online)
DOI: http://dx.doi.org/10.15666/aeer/1705_1084510859

Perez et al. (2007), who reported 3.2-4.0 units decrease in the pH of medium due to phosphate solubilization.

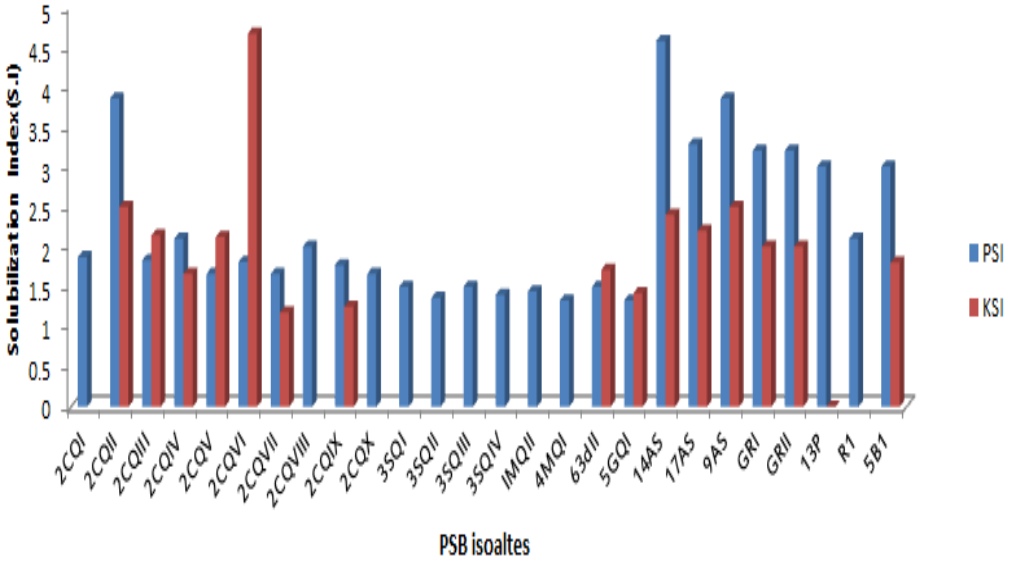

Figure 5. *Comparison of solubilization index of selected PSB isolates on PVK and Aleksandrov media*

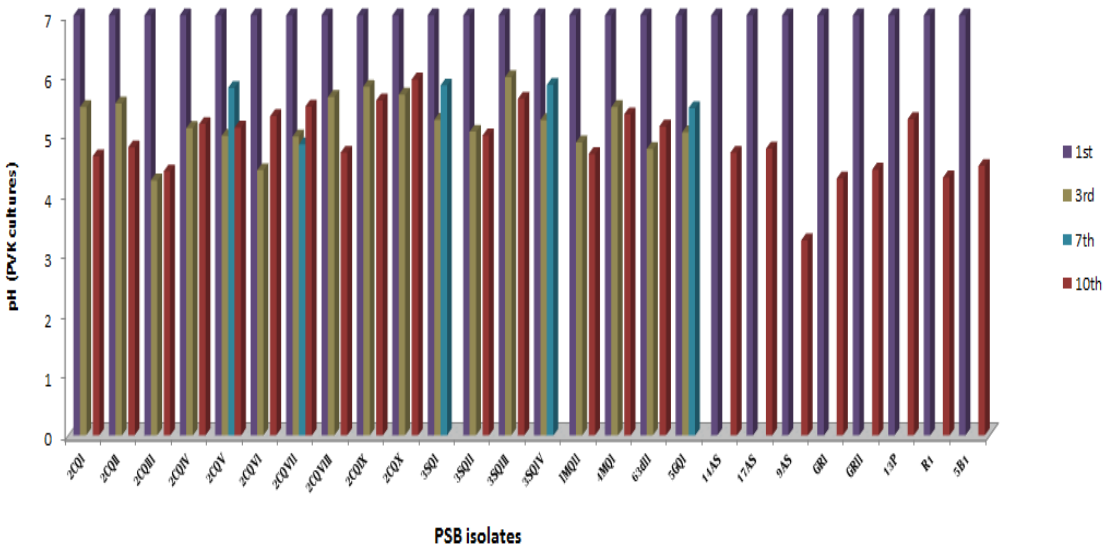

Figure 6. *pH change in PVK broth medium inoculated with different PSB isolates*

Molecular characterization/identification of bacterial isolates

For molecular characterization, genomic DNA of 9AS, 2CQll, 2CQlll, 14AS, 2CQlV, 2CQV, 17AS, 2CQVl, GR1, 5B1 and R1 PSB isolates was extracted and used as template for 16SrRNA amplification with universal primer set. DNA of 2CQlll isolate was used as a template for optimizing the primer set's annealing temperature and run its gradient PCR. It displayed the single prominent band at 54 °C, 55 °C and 56 °C

http://www.aloki.hu ● ISSN 1589 1623 (Print) ● ISSN 1785 0037 (Online)
DOI: http://dx.doi.org/10.15666/aeer/1705_1084510859

of approximately 1.2 kb size (*Fig. 7*). Following the optimized recycling conditions ribotyping PCR was carried with genomic DNA of 6 potent isolates 2CQll, 14AS, 2CQlll, 17AS, Rl and 5Bl as templates. In all strains PCR products of 1.2 kb was observed (*Fig. 8*). After ribotyping, the data for sequence analyses of PCR products were obtained from the DNA core facility of the CAMB and used it for molecular identification through in silico analysis. Thus by equating the 16SrRNA sequence database with all available data of gene bank through BLAST homology, inferred the isolates identification. On the base of close relations, experimental PSB isolates 2CQll, 14AS, 2CQlll, 17AS, Rl and 5B1 were identified as *Enterobacter* sp., Marine Bacterium, *Klebsiella* sp., *Bacillus licheniformis, Staphylococcus warneri* and *Serratia marcescens,* with the sequence similarity of 95%, 93%, 93%, 94%, 96% and 96% respectively. Accession no was obtained by submitting their sequence data to NCBI. The identified PSB isolates are mentioned in *Table 1*. Phylogenetic trees were constructed by MEGA 6 software, shown in the *Figure 9*. Similarly, different PSB from the plant rhizosphere have been purified, characterized and reported by other researcher (Tariq et al., 2014; Dar et al., 2014; Rodríguez et al., 2000).

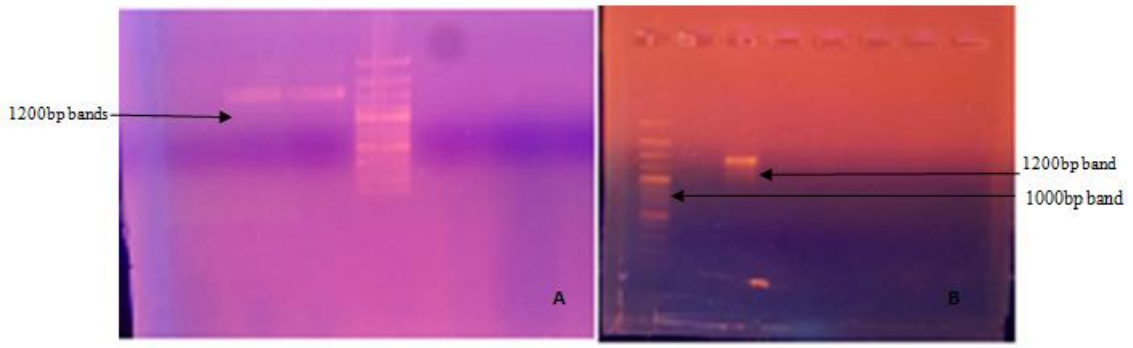

Figure7. *Gradient PCR displaying ribotyping PCR result (1% Agarose gel) of about 1200 bp band (A) at 54 °C and 55 °C (B) at 55 °C with DNA of 14AS (100 bp DNA ladder)*

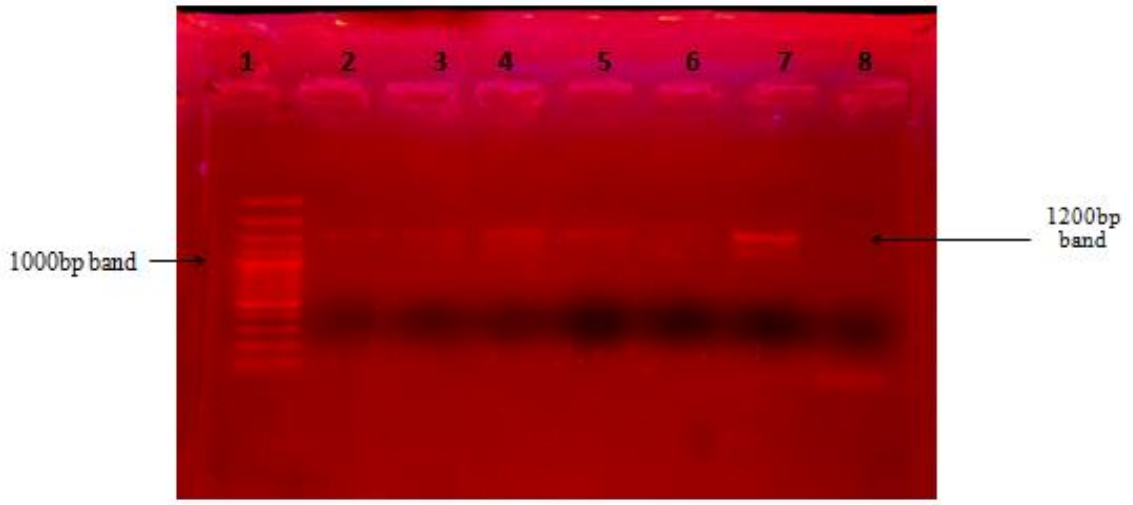

Figure 8. *Ribotyping PCR showing the results at 55 °C annealing T with 1.2 kb band of selected PSB isolates (from 2-8) in respective order of 2CQll, 17AS, 2CQlll, 14AS, 5Bl, R1 and control on 1% agarose gel with100 bp DNA ladder in first well*

http://www.aloki.hu ● ISSN 1589 1623 (Print) ● ISSN 1785 0037 (Online)
DOI: http://dx.doi.org/10.15666/aeer/1705_1084510859

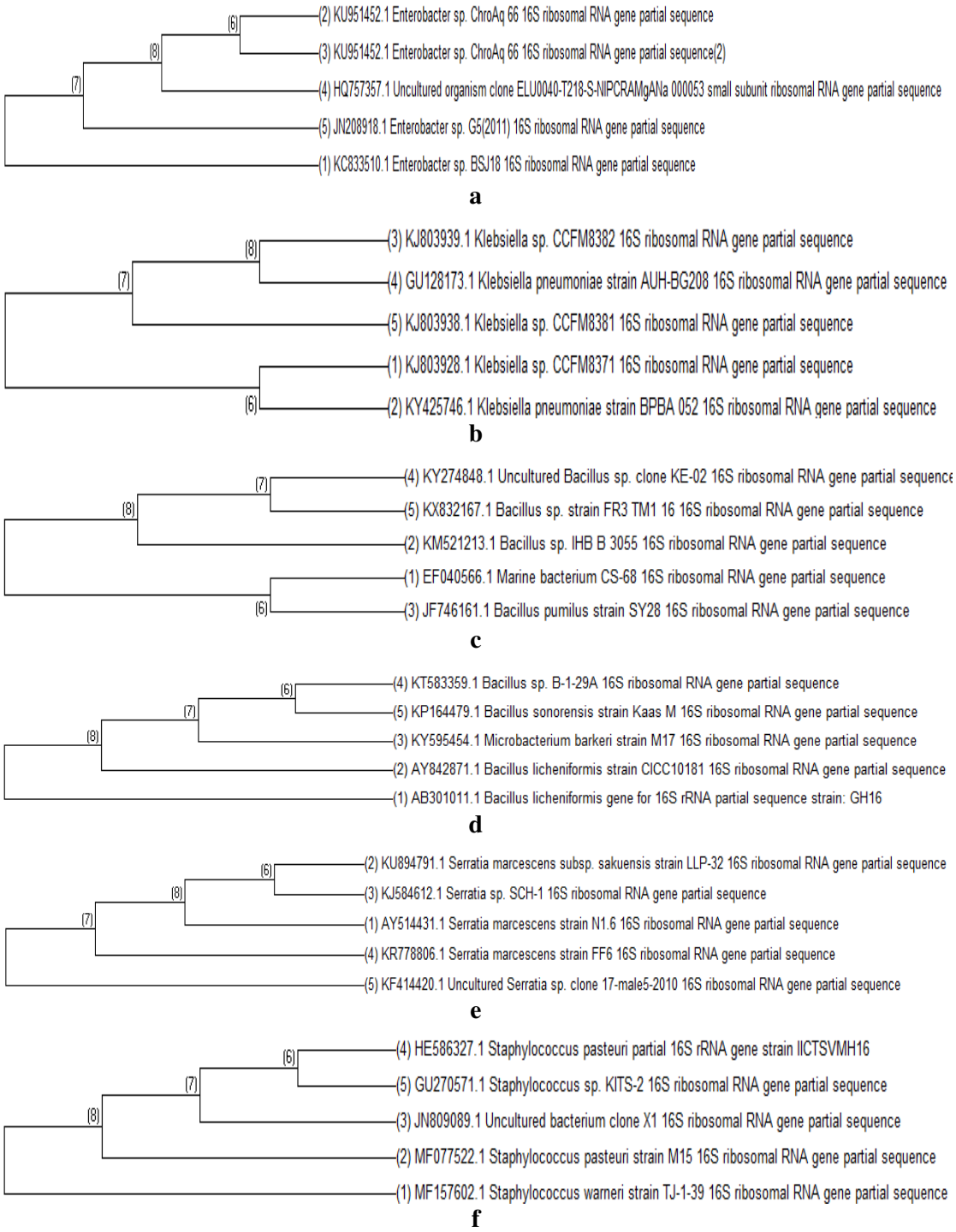

***Figure 9. a** Phylogenetic tree of 2CQll. **b** Phylogenetic tree of 2CQlll. **c** Phylogenetic tree of 14AS. **d** Phylogenetic tree of 17AS. **e** Phylogenetic tree of 5B1. **f** Phylogenetic tree of R1*

Field efficiency of CAMB biofertilizing agents in natural environment (on potato trial field)

To evaluate their efficiency as phosphate biofertilizers in natural environment, three bacterial strains, the *Bacillus licheniformis* (14AS), *Serratia marcescens* (5B1), and

http://www.aloki.hu ● ISSN 1589 1623 (Print) ● ISSN 1785 0037 (Online)
DOI: http://dx.doi.org/10.15666/aeer/1705_1084510859

Staphylococcus warneri (R1), were studied under natural environmental conditions. All three strains were found effective biofertilizers as more than double yield of potato tubers was obtained (*Figs. 10F*). Similar results were also reported by Malboobi et al. (2009) who evaluated efficiency of PSB on potato field trail and found significant yield in the growth of potato crops. Plants and tubers from control lanes and lanes treated with these three strains were compared. Very healthy and vigorous potato plants were observed in the experimental lanes that were treated with CAMB biofertilizer and showed significant results (*Table 2*). Harvesting of trial field with accumulated yield from all treatments and negative control are also shown in picture (*Fig. 10*). Significant differences ($P < 0.005$) were observed between the values obtained for plant growth, number of lateral shoots, number of roots and root length of potato plants as compared to un- inoculated control plants (*Table 2*). These findings are in close accordance of Sadiq et al. (2013) who have performed pot experiments of similar nature. They have applied PSB isolates in the rhizosphere of sugarcane plant and found positive impact of PSB isolates on the plant growth. Mayak et al. (2014) have performed experiments on stress tolerance effect of rhizobacteria on tomato. They isolated plant growth promoting rhizobacteria from soil and applied selected strain (*Achromobacter piechaudii*) in tomato rhizosphere in salty soil conditions. During their study they found that application of bacteria caused enhanced growth of tomato plants. Further they have linked enhanced salt stress tolerance of tomato plants with enhanced uptake of potassium and phosphorous. Findings of Mayak et al. (2014) and Hosni et al. (2016) support the outcome of presented study. Furthermore, our study explains that rhizospheric application of plant growth promoting bacteria (phosphate and potassium solubilizing bacteria) enhance absorbable phosphate and potassium in the root area of plants. Similar results have also been reported by many others who have concluded up with enhanced overall plant production in the influence of PSB application in rhizosphere of pot and trial field plants (Khalid et al., 2004; Çakmakçi et al., 2006; Wu et al., 2005). The results reported by Wu et al. (2005) have reported the highest biomass and seedling height in the plants of *Zea mays* trial field treated with PSB. Although several studies have been reported on the plant growth promoting effect of PSB in trial field, this is the first report on the rhizospheric application of PSB in the trial field of transgenic potato variety. The plants of treated lanes possessed dehydrin-10 gene of Eucalyptus globulus for tolerance against multiple abiotic stresses and produced about three folds enhanced potato yield and biomass over untreated lanes. The survival of tissue cultured plants in trial field lanes treated with PSB was also amazing and the higher survival rate may also be linked with antifungal activity of PSB strains as described by Jahangir et al. (2016).

Table 1. *Identified PSB isolates (based on sequencing and in silico studies) with assigned accession numbers*

Serial no.	Isolate code	Gene bank no.	Closely related in database	Maximum identity (%)	Accession no.
1	2CQll	KC833510.1	Enterobacter sp.	95	MF465779
2	14AS	AB301011.1	*Bacillus licheniformis*	94	MF465782
3	17AS	EF040566.1	Marine Bacterium	93	MF465781
4	2CQIII	KJ803928.1	*Klebsiella sp.*	93	MF465778
5	5B1	AY514431.1	*Serratia marcescens*	96	MF465783
6	R1	MF157602.1	*Staphylococcus warneri*	96	MF465777

http://www.aloki.hu ● ISSN 1589 1623 (Print) ● ISSN 1785 0037 (Online)
DOI: http://dx.doi.org/10.15666/aeer/1705_1084510859

Figure 10. *Different treatments upon potato plants in trial field and its harvesting.* ***A*** *Control line;* ***B–D*** *Experimental lines treated with Bacillus licheniformis, Serratia marcescens, and Staphylococcus warneri respectively.* ***E–F*** *Harvesting of trial field with accumulated yield from all treatments and negative control*

Table 2. *Effect of PSB on growth parameters in potato trial field*

Plant growth parameters (90 days)					
Sr. no	**Bacterial isolates**	**Plant height**	**No. of lateral shoots**	**No. of roots**	**Max root length**
1	5B1	21.7 ± 1.337^{a}	13.7 ± 0.969^{a}	35.3 ± 4.23^{a}	6.7 ± 0.471^{a}
2	R1	22.0 ± 0.785^{a}	13.7 ± 1.416^{a}	27.4 ± 2.008^{ab}	10.7 ± 3.504^{a}
3	14AS	20.9 ± 1.036^{ab}	11.5 ± 1.815^{a}	19.9 ± 1.086^{b}	7.6 ± 0.304^{a}
4	Control	18.6 ± 0.967^{b}	12.4 ± 1.286^{a}	32.6 ± 3.766^{a}	7.0 ± 0.365^{a}

Each value is an average of replicates; ± denotes standard error mean among these replicates and numbers followed by different letters differs significantly at $P < 0.005$

Conclusion

The effects of this study demonstrated that Phosphate Solubilizing Bacteria play a vital role in plant nutrition, convert the insoluble phosphorus into the available form to the florae and used as biofertilizers for agricultural crops. Phosphate solubilizing bacteria identified by molecular characterization performed efficiently in natural environment and more than double potato yield was obtained as compared to untreated control plants in potato trial field. On the basis of this investigation, further studies are necessary to investigate possible synergistic effects of rhizospheric bacteria since the use of these bio-fertilizers can be used in an ideal harvesting system with a control effects on the environment sustainable manner in agricultural soils. Furthermore, use of these beneficial microbes not only reduces need of phosphate fertilizer for crop plant

http://www.aloki.hu ● ISSN 1589 1623 (Print) ● ISSN 1785 0037 (Online)
DOI: http://dx.doi.org/10.15666/aeer/1705_1084510859

rather it plays some important role in plant growth parameter. Therefore, more research is needed to investigate the Phosphate Solubilizing Bacteria (PSB) as bio-inoculants to enhance the sustainable management of soil and agriculture that could help in economic stability and environment friendliness.

Acknowledgements. Very passionate thanks are paid to Mr. Islam Khan (CEMB) for his generous help. We are also very thankful to the CAMB DNA Core Facility (especially Mr. Muhammad Usman and Mr. Muhammad Akram) and Proteomics Lab CAMB for their kind cooperation during execution of this work.

REFERENCES

[1] Ali, Q., Ahsan, M., Ali, F., Aslam, M., Khan, N. H., Munzoor, M., Mustafa, H. S. B., Muhammad, S. (2013): Heritability, heterosis and heterobeltiosis studies for morphological traits of maize (Zea mays L.) seedlings. – Advancements in Life Sciences 1(1) 52-63.

[2] Ali, Q., Ali, A., Ahsan, M., Ali, S., Khan, N. H., Muhammad, S., Abbas, H. G., Nasir, I. A., Husnain, T. (2014): Line × Tester analysis for morpho-physiological traits of *Zea mays* L. seedlings. – Advancements in Life Sciences 1(4): 242-253.

[3] Ali, Q., Ahsan, M., Malook, S., Kanwal, N., Ali, F., Ali, A., Ahmed, W., Ishfaq, M., Saleem, M. (2016): Screening for drought tolerance: comparison of maize hybrids under water deficit condition. – Advancements in Life Sciences 3(2): 51-58.

[4] Awais, M., Tariq, M., Ali, A., Ali, Q., Khan, A., Tabassum, B., Nasir, I. A., Husnain, T. (2017): Isolation, characterization and inter-relationship of phosphate solubilizing bacteria from the rhizosphere of sugarcane and rice. – Biocatalysis and Agricultural Biotechnology 11: 312-321.

[5] Çakmakçi, R., Dönmez, F., Aydın, A., Şahin, F. (2006): Growth promotion of plants by plant growth-promoting rhizobacteria under greenhouse and two different field soil conditions. – Soil Biology & Biochemistry 38: 1482-1487.

[6] Dale, P. J., McPartlan, H. C. (1992): Field performance of transgenic potato plants compared with controls regenerated from tuber discs and shoot cuttings. – Theoretical and Applied Genetics 84(5-6): 585-591.

[7] Dar, A. I., Saleem, F., Ahmad, M., Tariq, M., Khan, A., Ali, A., Tabassum, B., Ali, Q., Khan, G. A., Rashid, B., Nasir, I. A. (2014): Characterization and efficiency assessment of PGPR for enhancement of rice (*Oryza sativa* L.) yield. – Advancements in Life Sciences 2(1): pp.38-45.

[8] Diep, C. N., Hieu, T. N. (2013): Phosphate and potassium solubilizing bacteria from weathered materials of denatured rock mountain, Ha Tien, Kien Giang Province, Vietnam. – American Journal of Science 1(3): 88-92.

[9] Glick, B. R. (2001): Phytoremediation, synergistic use of plant and bacteria to clean up the environment. – Biotechnology Advances 21(3): 83-393.

[10] Hosni, F., Asgharzadih, A., Ardakani, M., Hamidi, A. (2016): The impact of potato mini-tuber inoculation with plant growth promoting rhizobacteria on tuber yield and nutrients uptake. – Crops Improvement 17: 911-924.

[11] Jahangir, G. Z., Sadiq, M., Hassan, N., Nasir, I. A., Saleem, M. Z., Iqbal, M. (2016): The effectiveness of phosphate solubalizing bacteria as biocontrol agents. – Journal of Animal and Plant Science 26(5): 1313-1319.

[12] Khalid, A., Arshad, M. Zahir, Z. A. (2004): Screening plant growth promoting rhizobacteria for improving growth and yield of wheat. – Journal of Applied Microbiology 96: 473-480.

http://www.aloki.hu ● ISSN 1589 1623 (Print) ● ISSN 1785 0037 (Online)
DOI: http://dx.doi.org/10.15666/aeer/1705_1084510859

[13] Laticia, A., Fernandez, Agaras, B., Wall, L. G., Valverde, C. (2015): Abundance and ribotypes of phosphate-solubilizing bacteria in Argentinean agricultural soils under no-till management. – Annual Reviews of Microbiology 65(3): 1667-1678.
[14] Malboobi, M. A., Behbahani, M., Madani, H., Owlia, P., Deljou, A., Yakhchali, B., Moradi, M., Hassanabadi, H. (2009): Performance evaluation of potent phosphate solubilizing bacteria in potato rhizosphere. – World Journal of Microbiology and Biotechnology 25: 1479-1484. DOI: 10.1007/s11274-009-0038-y.
[15] Mayak, S., Tirosh, T., Glick, B. R. (2004): Plant growth-promoting bacteria confer resistance in tomato plants to salt stress. – Plant Physiology and Biochemistry 42(6): 565-572.
[16] Nobandegani, M. B. J., Saud, H. M., Yun, W. M. (2015): Phylogenetic relationship of phosphate solubilizing bacteria according to 16S rRNA genes. – BioMed Res. Intl. 2015: 1-5.
[17] Pérez, E., Sulbarán, M., Ball, M. M., Yarzábal, L. A. (2007): Isolation and characterization of mineral phosphate-solubilizing bacteria naturally colonizing a limonitic crust in the south-eastern Venezuelan region. – Soil Biology and Biochemistry 39: 2905-2914.
[18] Rodríguez, H., Gonzalez, T., Selman, G. 2000. Expression of a mineral phosphate solubilizing gene from *Erwinia herbicola* in two rhizobacterial strains. – J. Biotechnol. 84(2): 155-161.
[19] Sadiq, H. M., Jahangir, G. Z., Nasir, I. A., Iqtidar, M., Iqbal, M. (2013): Isolation and characterization of phosphate-solubilizing bacteria from rhizosphere soil. – Biotechnology Biotechnological Equipments 27(6): 4248-4255.
[20] Sharma, S., Kumar, V., Tripathi, R. B. (2011): Isolation of phosphate solubilizing microorganism (PSMs) from soil. – Journal of Microbiology and Biotechnology Research 1(2): 90-95.
[21] Shekhar, N. C., Bhaclauriay, S., Kumar, P., Lal, H., Mondal, R., Verma, D. (2000): Stress induced phosphate solubilization in bacteria isolated from alkaline soils. – FEMS Microbiology Letters 182(2): 291-296.
[22] Sheng, X. F., Xia, J. J., Chen, J. (2003): Mutagenesis of the Bacillus edaphicus strain NBT and its effect on growth of chilli and cotton. – Agricultural Sciences of China 2: 400-412.
[23] Sindhu, S. S., Dua, S., Verma, M. K., Khandelwal, A. (2010): Growth Promotion of Legumes by Inoculation of Rhizosphere Bacteria. – In: Khan, M. S. et al. (eds.) Microbes for Legume Improvement. – Springer, Vienna, pp. 195-235.
[24] Skogsmyr, I. (1994): Gene dispersal from transgenic potatoes to conspecifics: a field trial. – Theoretical and Applied Genetics 88(6-7): 770-774.
[25] Surapat, W., Pukahuta, C., Rattanachaikunsopon, P., Tadanori, A., Sophon, B. (2013): Characteristics of phosphate solubilization by phosphate-solubilizing bacteria isolated from agricultural chilli soil and their efficiency on the growth of chilli (Capsicum frutescens L. cv. Hua Rua). – Chiang Mai Journal of Science 40(1): 11-25.
[26] Tariq, M., Ali, Q., Khan, A., Khan, G. A., Rashid, B., Rahi, M. S., Ali, A., Nasir, I. A., Husnain, T. (2014): Yield potential study of Capsicum annuum L. under the application of PGPR. – Advancements in Life Sciences 1(4): 202-207.
[27] Wu, S. C., Cao, Z. H., Li, Z. G., Cheung, K. C., Wong, M. H. (2005): Effects of biofertilizer containing N-fixer, P and K solubilizers and AM fungi on maize growth: a greenhouse trial. – Geoderma 125(1-2): 155-166.
[28] Yasmin, H., Bano, A. (2011): Isolation and characterization of phosphate solubilizing bacteria from rhizosphere soil of weeds of khewra salt range and attock. – Pakistan Journal of Botany 43(3): 1663-1668.
[29] Zameer, M., Tabassum, B., Ali, Q., Tariq, M., Zahid, H., Nasir, I. A., Akram, W., Baqir, M. (2015): Role of PGPR to improve potential growth of tomato under saline condition: An overview. – Life Science Journal 12(3s): pp.54-62.

http://www.aloki.hu ● ISSN 1589 1623 (Print) ● ISSN 1785 0037 (Online)
DOI: http://dx.doi.org/10.15666/aeer/1705_1084510859

[30] Zameer, M., Zahid, H., Tabassum, B., Ali, Q., Nasir, I. A., Saleem, M., Butt, S. J. (2016): PGPR potentially improve growth of tomato plants in salt-stressed environment. – Turkish Journal of Agriculture - Food Science and Technology 4(6): pp.455-463.
[31] Zhang, C., Kong, F. (2014): Isolation and identification of potassium-solubilizing bacteria from tobacco rhizospheric soil and their effect on tobacco plants. – Applied Soil Ecology 82: 18-25.

http://www.aloki.hu ● ISSN 1589 1623 (Print) ● ISSN 1785 0037 (Online)
DOI: http://dx.doi.org/10.15666/aeer/1705_1084510859

METHODOLOGY FOR THE OPTIMIZATION OF GROUNDWATER QUALITY MONITORING NETWORKS ORIENTED TO SATISFY A SPECIFIC SPATIAL COVERAGE

ACEVES-DE-ALBA, J.[1,2] – JÚNEZ-FERREIRA, H. E.[1*] – GONZÁLEZ-TRINIDAD, J.[1] – CARDONA-BENAVIDES, A.[2] – BAUTISTA-CAPETILLO, C. F.[1]

[1]*Doctorado en Ciencias de la Ingeniería, Universidad Autónoma de Zacatecas, Av. Ramón López Velarde No. 801, Col. Centro, Zacatecas, Zacatecas, México, C.P. 98000 (phone: +52-492-924-2432; fax: +52-492-925-6690 ext. 1613)*

[2]*Facultad de Ingeniería, Universidad Autónoma de San Luis Potosí, Av. Dr. Manuel Nava No. 8, Zona Universitaria Poniente, San Luis Potosí, San Luis Potosí, México, C.P. 78290 (phone/fax: +52-444-826-2300)*

**Corresponding author*
e-mail: hejunez@uaz.edu.mx

(Received 19th Mar 2019; accepted 3rd May 2019)

Abstract. Through the optimal design of groundwater monitoring networks, it is possible to obtain the maximum level of information for certain variables (water level, some quality indicator parameters, and/or the presence of some contaminant) at minimum cost; the methodologies for this kind of designs follow a procedure to discard wells that provide redundant information. The information collected by monitoring networks is fundamental for supporting decision making that aims for a sustainable management of groundwater. In this paper, an existing methodology for the design of optimal groundwater quality monitoring networks is modified to include a new algorithm that allows to obtain alternative spatial distributions of the wells that provide the highest level of information, expressed in terms of the estimated uncertainty over an estimation grid. Additionally, different weights can be assigned to each monitoring site and to the analyzed variable(s) within the objective function in order to accomplish specific objectives without a significant loss of information. The final result represents a significant improvement to the original methodology by adjusting the spatial coverage of the optimal monitoring network to satisfy specific objectives.
Keywords: *geostatistics, Kalman filter, estimation grid, water management, sustainable*

Introduction

Groundwater is a vital resource for human beings; it provides 50% of the total water used worldwide (WWAP, 2016). This data shows the dependence of people on groundwater, mainly in regions with extensive cropping areas for food production and industrial activities (Li et al., 2015).

Considering the importance of groundwater, it is necessary to know, in detail, the spatial distribution of the groundwater flow systems and its physical-chemical characteristics to improve its management (Esquivel et al., 2015; Kim et al., 2007). It is relevant to assure sustainable levels of groundwater quality when it is used for water supply (Yang et al., 2018). The implementation of groundwater quality monitoring programs is of paramount importance; for instance, it was detected that in almost 15% of the monitoring stations in Europe, the standard for nitrates in drinking water established by the World Health Organization (WHO) was exceeded (WWAP, 2018). It is possible to characterize the groundwater quality in some areas of interest (AOI) by measuring some physical-chemical parameters of water extracted by wells and

http://www.aloki.hu ● ISSN 1589 1623 (Print) ● ISSN 1785 0037 (Online)
DOI: http://dx.doi.org/10.15666/aeer/1705_1086110882

estimating the spatial distribution of their concentrations; however, the costs and time involved in visiting and sampling all the existing wells are often not economically viable; specially in low income countries.

The optimal design of groundwater monitoring networks is an alternative to reduce time and costs associated to the acquisition of data to accomplish specific objectives (Júnez-Ferreira et al., 2016a); in addition the development of a sustainable strategy for groundwater extraction management is required.

The methodologies for the optimal design of groundwater monitoring networks can be subdivided in three main groups: 1) those based on elements of hydrogeological conceptual models, 2) those that execute data analysis with statistical techniques, and 3) those that use groundwater flow numerical models (Júnez-Ferreira et al., 2016a; Loaiciga et al., 1992; Herrera and Pinder, 2005; Zhang et al., 2005). The latter can be considered as the most robust framework, since it does not only consider hydrogeological aspects (as group one) but also takes into consideration groundwater levels evolution (in space and time). It is important to note that some methodologies combine aspects of two or the three groups.

The hydrogeological framework usually uses a Geographic Information System (GIS) in order to incorporate as much areal information as possible of the hydrogeological factors that control the groundwater functioning such as geology, recharge and discharge zones, rainfall data, groundwater levels, land use/land cover images derived from satellites, among others (Singh and Katpatal, 2017; Zhou et al., 2013). The statistical-based methodologies usually employ a variance-based objective function evaluated by an optimization method, they are commonly based on spatial and/or spatiotemporal geostatistical techniques, entropy theory, harmonic series models and principal component analysis (Mirzaie-Nodoushan et al., 2017; Júnez-Ferreira et al., 2016b; Andricevic, 1990; Kim et al., 2007; Júnez-Ferreira and Herrera, 2013), some of them are multicriteria (Hosseini and Kerachian, 2017a, b). The combination of hydrogeological criteria through the use of GIS and statistical techniques has been used in (Baalousha, 2010; Uddameri and Andruss, 2014; Sizirici and Tansel, 2015; Júnez-Ferreira et al., 2016a; Alizadeh and Mahjouri, 2017). The methodologies based on a numerical flow model include optimization methods and are always combined with a GIS (Kim, 2015) or with statistical estimation methods such as the Kalman Filter (KF), Monte Carlo simulations (Herrera and Pinder, 2005; Zhang et al., 2005; Kollat et al., 2011; Luo et al., 2016; Jiang et al., 2018), or can have characteristics of the three groups of methodologies for the optimal design of groundwater monitoring networks (Nobre et al., 2007).

Most of these methodologies require a large amount of information about the study site that includes a comprehensive database of sampling campaigns, geological data, and an advanced understanding of flow systems.

In those areas with scarce data, it is necessary to implement methodologies to start with the data generation. In the literature, the KF or different types of kriging have been widely used as estimation methods for the design of optimal monitoring networks oriented to the reduction of the estimate error variance in areas with few hydrogeological data (Júnez-Ferreira et al., 2016a; Júnez-Ferreira and Herrera, 2013); however, the spatial distribution of the wells with higher priority selected by these methodologies preferably covers the central area of a pre-defined estimation grid, frequently assigning a lower priority to those wells located at the periphery of the study area. This is considered as a deficiency because a poor spatial coverage of the

http://www.aloki.hu ● ISSN 1589 1623 (Print) ● ISSN 1785 0037 (Online)
DOI: http://dx.doi.org/10.15666/aeer/1705_1086110882

monitoring network may lead to the undesirable extrapolation of the monitored variable(s) at those areas. In addition, a resilient monitoring network in regard to sampling station distribution, in practice could be easier to implement and to explain to stakeholders. The design of an optimal monitoring network results in an academic exercise not feasible to real-world limitations (data availability, budget), hence the implementation of alternative methodologies is advisable (Bode et al., 2018).

In Mexico there are 653 administrative aquifers, 105 of them have been classified with intensive abstraction resulting in negative environmental effects such as the ongoing deterioration of water quality (Esteller et al., 2011), sea water intrusion problems, presence of brackish water (CONAGUA, 2017), and high fluoride and arsenic concentrations in groundwater (Banning et al., 2012; Cardona et al., 2018). However, the natural evolution of the groundwater quality has not received the required attention as a tool for management planning.

Mexico and a number of countries around the world are involved in the Sustainable Development Goals (SDG) to address global challenges such as environmental (water) degradation. Specifically, goal 6: Clean Water and Sanitation, indicator 6.3.2: Proportion of water bodies with good water quality requires the implementation of groundwater monitoring networks to compile data for some core parameters at existing sampling stations (UN WATER).

The lack of properly designed wells for groundwater quality monitoring purposes makes necessary employing the available long screened production wells. The spatial distribution of these production wells depends on factors such as the location of irrigation lands and populated areas. Therefore, it is relevant for water management institutions to consider methodologies that contribute to the design of optimal groundwater monitoring networks, with water quality data obtained from production wells. This is an important issue for making decisions regarding groundwater sustainable development, not only in Mexico, but in several other countries around the world.

This paper proposes a methodology for the design of multivariable groundwater monitoring networks. The approach includes 1) irregular shape estimation grid according with the spatial sampling station distribution 2) a ponderation grid map based on sampling station density per unit area 3) the definition of an objective function that considers simultaneously, the ponderation grid map, priority determination for any water quality parameters included in the monitoring network and/or for sampling stations and a KF for the reduction of the estimate uncertainty for each variable provided by the selected sampling stations. The methodology allows obtaining alternative spatial distributions of the wells that provide the highest level of information, expressed in terms of the estimated uncertainty over an estimation grid.

Materials and methods

The methodology presented in this paper is based on that proposed in Júnez-Ferreira et al. (2016a); the original methodology selects the optimal monitoring positions by using spatial correlations expressed as covariance matrices derived from semivariogram models obtained through geostatistical analyses to data of groundwater quality parameters. The optimization of the monitoring network is carried out by successive inclusions employing the KF as the estimation method, minimizing a function called the joint total (JT) normalized variance of the estimation error (Júnez-Ferreira et al., 2016a).

http://www.aloki.hu ● ISSN 1589 1623 (Print) ● ISSN 1785 0037 (Online)
DOI: http://dx.doi.org/10.15666/aeer/1705_1086110882

This methodology requires of a spatial estimation grid where the objective function is evaluated. During the optimization process, the addition of weights to the groundwater quality parameters, or different densities in the estimation grid have been useful to satisfy specific objectives, like assigning a higher priority to contaminated sites or to highly dangerous parameters (Júnez-Ferreira et al., 2016a; Esquivel et al., 2015).

For the proposed methodology, the objective function incorporates the spatial coverage of the available sampling stations (by means of a supplementary function, SF) besides a modified version of the joint total (JT) normalized variance of the estimation error. The modified JT, besides having a weight for each groundwater quality parameter includes a weight for each sampling station, this new algorithm is now called the weighted joint total normal variance of the estimation error (WJT). Both, the WJT and the SF are weighted in order to define different alternatives of the spatial coverage for the selected monitoring networks without a significant loss of information.

The objective function (OF) (*Eq. 1*) for the proposed methodology is:

$$OF = \mathrm{V} \times \mathrm{WJT} + W \times \mathrm{SF} \quad \text{(Eq.1)}$$

where V and W are the weigthing factors for the WJT and the SF, respectively; $V + W = 1$. Based in Júnez-Ferreira et al. (2016a) to obtain WJT, the KF is implemented through the use of $\hat{\mathrm{q}}^0$and P^0 that represent an initial state vector and the initial error covariance matrix, respectively. The KF process employs the following equations (*Eqs. 2, 3* and *4*):

$$\hat{\mathrm{q}}^{n+1} = \hat{\mathrm{q}}^n + \mathrm{K}_{n+1}(\mathrm{z}_{n+1} - \mathrm{H}_{n+1}\hat{\mathrm{q}}^n) \quad \text{(Eq.2)}$$

$$\mathrm{P}^{n+1} = \mathrm{P}^n - \mathrm{K}_{n+1}\mathrm{H}_{n+1}\mathrm{P}^n \quad \text{(Eq.3)}$$

$$\mathrm{K}_{n+1} = \mathrm{P}^n\mathrm{H}_{n+1}^{\mathrm{T}}(\mathrm{H}_{n+1}\mathrm{P}^n\mathrm{H}_{n+1}^{\mathrm{T}} + \mathrm{r}_{n+1}) \quad \text{(Eq.4)}$$

where K_{n+1} is the Kalman gain, H_{n+1} is the sampling matrix, z_{n+1} is the measurement vector, and r_{n+1} is the measurement error covariance. Superscripts refer to the number of measurements employed in the estimation; subscripts are used to indicate the transition when a new measurement is going to be used in the process.

The spatial covariance matrix for each parameter is calculated as follows (*Eq. 5*):

$$C(h) = C(0) - \gamma(h) \quad \text{(Eq.5)}$$

where $C(h)$ represent the covariance matrix, $C(0)$ is the variance for each analyzed parameter, and $\gamma(h)$ is the variogram model function.

The WJT value is calculated with (*Eq. 6*):

$$\mathrm{WJT} = \sum_{p=1}^{np} \sigma_{w,p}^2 \times \alpha_w \times \alpha_p \quad \text{(Eq.6)}$$

where $\sigma_{\mathrm{w,p}}^2$ represents the normalized estimate error variance (located at the principal diagonal of the corresponding updated covariance matrix) at each estimation position

http://www.aloki.hu ● ISSN 1589 1623 (Print) ● ISSN 1785 0037 (Online)
DOI: http://dx.doi.org/10.15666/aeer/1705_1086110882

for the p parameter, when the w well has been sampled, α_w represents the w well weight, α_p represents the p parameter weight, and np is the number of parameters.

The main advantages of this proposal are: a) it considers the possibility of obtaining alternative monitoring networks designs oriented to a desired spatial coverage b) it allows the assignation of different weights to a particular sampling point, which gives the opportunity to take into account specific hydrogeological conditions such as contaminated areas without affecting, within the optimization procedure, those wells located around this specific sampling point.

Custom estimation grid

As part of the proposed methodology, it has been developed an algorithm for the generation of a custom estimation grid (CEG). The KF estimates will be obtained and the OF evaluated at the CEG; it offers advantages when compared to a regular grid as implemented in commercial software such as XTools Pro 18 (XTools Pro), create fishnet (ArcGIS) and sampling design tool (Buja, 2012) because it avoids extrapolation areas since it is an adjusted envelope of the sampling points.

The definition of the CEG starts with the calculation of the distance between the extreme coordinates of the wells (maximum distance), followed by the calculation of the grid density with half the maximum distance divided by ten; this density (separation between the grid nodes) is selected to draw a rectangular grid that covers all the area where the wells with available data are located, an initial value of 0 is set to all these nodes. The CEG will be composed by values different than 0, the following procedure is carried out from the top (North) to the bottom (South) row of the original rectangular grid to the assignation of these values:

1. Values of 1 are assigned to the nodes that are next to the wells.
2. For each row it is given a value of 2 to the nodes that are between those with a value of 1.
3. A value of 3 is assigned to the nodes in empty rows to connect the nodes with values different to 0.
4. Values of 4 will be assigned to the nodes with an original value of 0 in such a manner that each row of the CEG cannot be longer one node to the West and one node to the East than the next row at the south.

The flowchart and pseudocode for this process are shown in *Figure 1*.

The colours in *Figure 2* are directly related to the value that indicates in which part of the algorithm the node for the CEG was selected.

Supplementary function

For the case study, the SF is proposed trying to establish a higher priority to those wells that have influence over the highest number of nodes of the estimation grid, and at the same time, with small influence of the other wells on their estimates (i.e., there is a poor spatial coverage of wells at that area). For that purpose, it is necessary to define a Custom Smooth Grid (CSG) based on the CEG and the maximum range used in the semivariogram models. For each node of the CEG, it is calculated the sum of wells located at a distance less than the model range, obtaining the values of the CSG (*Fig. 3*).

http://www.aloki.hu ● ISSN 1589 1623 (Print) ● ISSN 1785 0037 (Online)
DOI: http://dx.doi.org/10.15666/aeer/1705_1086110882

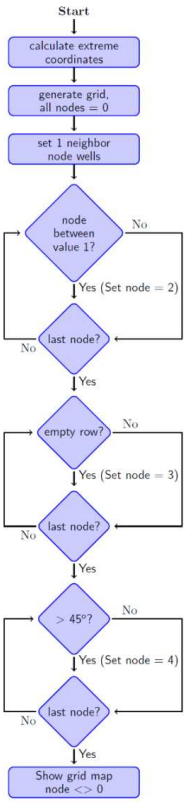

Calculate extreme coordinates based on the sampling stations

Initialize estimation grid (EG) to 0

While the EG node counter is less or equal to the total EG nodes

While the sampling station counter is less or equal to the total sampling stations

If the EG node is neighbor to the sampling station

Set EG node to 1

While the EG node counter is less or equal to the total EG nodes

If the EG node is between EG nodes equal to 1 in the same row

Set 2 to the EG node

While the EG node counter is less or equal to the total EG nodes

If all the row is 0 in the EG

Identify and sum the continuos rows with 0

Calculate the EG nodes per row based on the position and the rows with 0

While the row counter is less or equal to total rows with 0

While the number of node is less or equal to the number of nodes

Set the EG node to 3

While the grid node counter is less or equal to the total grid nodes

If previous and next position in the EG node is different to 0

If a below position is 0

Set 4 to the below EG node

While the EG node counter is less or equal to the total EG nodes

If the EG node is different to 0

Display EG node: pink (1), blue (2), brown (3) and green (4)

Figure 1. *CEG generation flowchart and pseudocode*

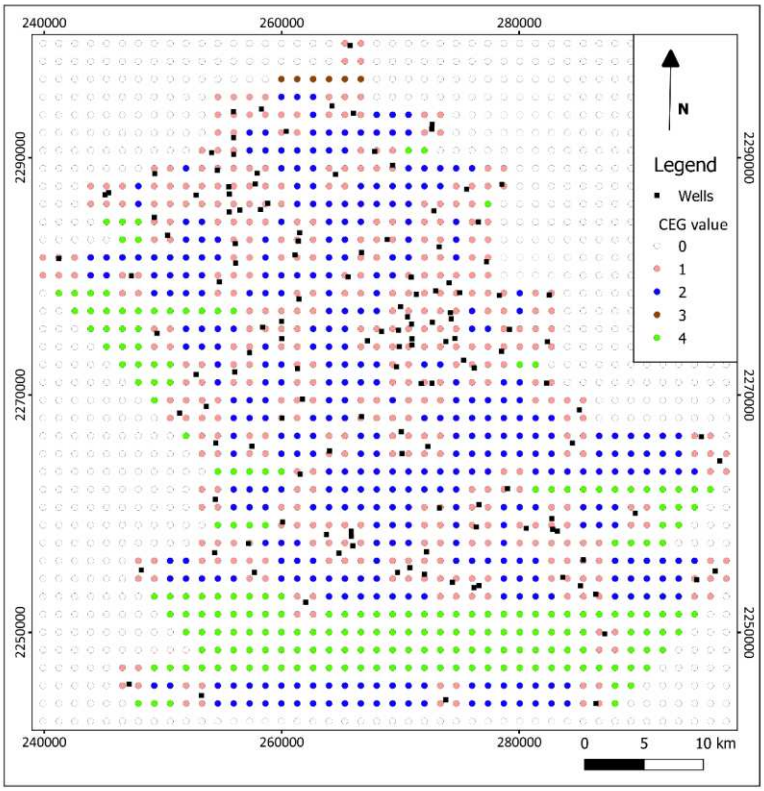

Figure 2. *Custom estimation Grid (CEG)*

http://www.aloki.hu ● ISSN 1589 1623 (Print) ● ISSN 1785 0037 (Online)
DOI: http://dx.doi.org/10.15666/aeer/1705_1086110882

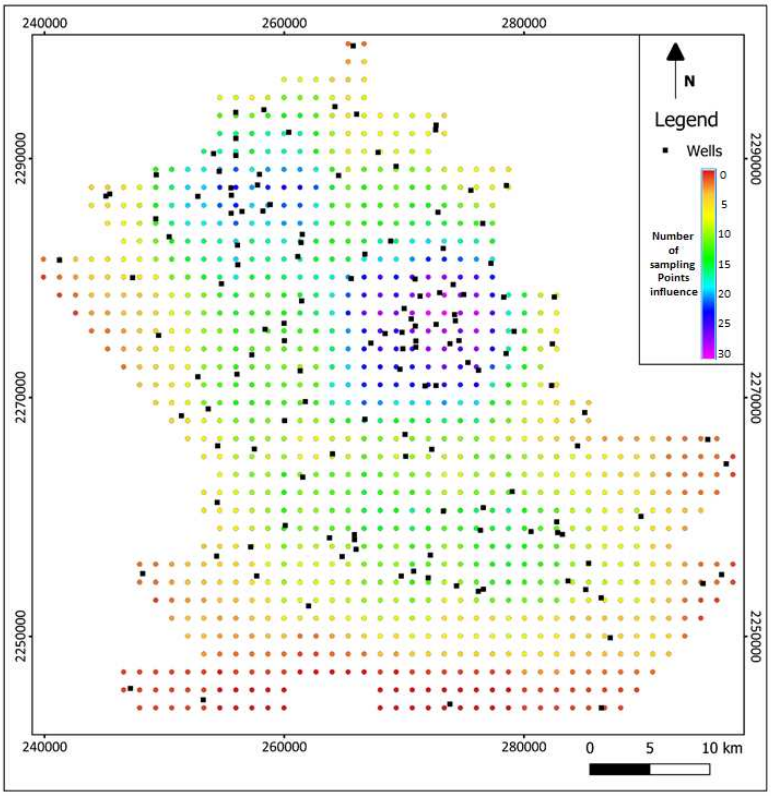

Figure 3. *Custom Smooth Grid (CSG)*

The SF is defined as follows:
The lower values in the CSG represent zones with a poor spatial coverage of wells.
The formulas for the values of the CSG are (*Eq. 7*):

$$ie_{w,p} = \sum_{n=1}^{nn} node_n \quad \text{(Eq.7)}$$

where $ie_{w,p}$ represents the influence of the well w over the nodes of the CEG, corresponding to the p parameter, $node_n$ is 1 when the node is inside a circumference with center on the w well and radius equal to the range of the semivariogram model in the p parameter; $node_n$ is 0 when the node is outside the circumference, nn is the total number of nodes in the CEG (*Eq. 8*);

$$iw_{n,p} = \sum_{w=1}^{nw} well_w \quad \text{(Eq.8)}$$

where $iw_{n,p}$ represents the influence of the sampling wells over the node n, corresponding to the p parameter, $well_w$ is 1 when the well is inside a circumference with center on the n node and radius equal to the range of the semivariogram model in

http://www.aloki.hu ● ISSN 1589 1623 (Print) ● ISSN 1785 0037 (Online)
DOI: http://dx.doi.org/10.15666/aeer/1705_1086110882

the p parameter, $well_w$ is 0 when the well is outside that circumference, nw is the total number of sampling wells (*Eq. 9*);

$$inw_{w,p} = \sum_{n=1}^{nn} (iw_{n,p} \times r_{n,p}) \quad \text{(Eq.9)}$$

where $inw_{w,p}$ represents the influence of the sampling wells over circular zones of the CEG, $r_{n,p}$ is 1 when the node is inside a circumference with center on the w well and radius equal to the range of the semivariogram model in the p parameter, $r_{n,p}$ is 0 when the node is outside the circumference (*Eq. 10*);

$$f_{w,p} = \frac{\alpha_w}{ie_{w,p} \times inw_{w,p}} \quad \text{(Eq.10)}$$

where $f_{w,p}$ represents the w well factor for the p parameter (*Eq. 11*);

$$ff_w = \sum_{p=1}^{np} f_{w,p}\alpha_p \quad \text{(Eq.11)}$$

where ff_w represents the w well final factor, np represents the total number of parameters considered in the network design.

In the case study, it is proposed that $SF = ff_w$.

Results

Case study: hydrogeological setting

In order to evaluate the performance of the proposed methodology, it was applied for the design of a monitoring network in the "El Bajío" Region of Central Mexico (*Fig. 4*). The Bajío Region, specifically the Irapuato-Valle aquifer has become recently a focus of attention due to the intensive water extraction regime for agricultural, population, and industrial use. Groundwater extraction (about 600 × 10^6 m^3/year) through more than 2900 production wells in the area supports the water supply for more than 900,000 inhabitants in urban and rural areas, the irrigation of approximately 60,000 hectares and the water consumption for a refinery, a power production plant and several industrial parks (Comisión Nacional del Agua, 2015; Esteller et al., 2011; Gómez and Sandoval, 2004). The rock units in the study area include a sequence of Mesozoic plutonic and vulcano-sedimentary rocks affected by several metamorphism stages and Tertiary intrusive rocks outcropping in the Sierra de Guanajuato located at the North of the study area that constitutes the hydrogeological basement. The Tertiary sequence include volcanic (ignimbrites, lava flow and tuffs) and continental sedimentary rocks (conglomerates and basin fill sediments). The Oligocene volcanic sequence is comprised of andesite and rhyolite; the overlying Miocene and Pliocene volcanic rocks are mainly andesite and basalt associated with the Mexican Neo-volcanic Belt (Nieto-samaniego et al., 2012). From the Oligocene, the Sierra de Guanajuato underwent a rapid uplift, the main geologic structures are NW-SE trending normal faults, displacing

http://www.aloki.hu ● ISSN 1589 1623 (Print) ● ISSN 1785 0037 (Online)
DOI: http://dx.doi.org/10.15666/aeer/1705_1086110882

more than 500 m the Oligocene volcanic sequence (Gómez et al., 1989; Nieto-samaniego, 1990). During this stage of deformation, several faults were reactivated, the N-S (Taxco-San Miguel de Allende fault) and NE-SW trending directions, together with the "El Bajío" Fault with NW-SE trend, formed half grabens, leading the formation of the "El Bajío" region (Botero-santa et al., 2015). At the same time, the erosion from the mountains led to transfer clastic material to the graben structure. The deposition of basin fill sediments in the graben structure produced a granular permeable regionally unconfined aquifer with a maximum thickness of 350 -400 m. Basin fill sediments are inter-bedded poorly consolidated fluvio-lacustrine sediments, including sands, inter-bedded sandy-clay and silts. From pumping test data, typical hydraulic conductivity values for that aquifer are 1 to 10 m/day (Júnez-Ferreira et al., 2016a). The Tertiary volcanic rocks are cut by a set of NW-SE and N-S normal faults, creating the possibility of a fractured heterogeneous aquifer (200-300 m thickness). The basaltic Pliocene rocks outcropping in the southern portion of the study area are in contact with the basin fill sediments, they confirm an unconfined aquifer with hydraulic conductivity values from 6 to 18 m/day (Júnez-Ferreira et al., 2016a). The Oligocene and Miocene volcanic rocks below the basin-fill sediments can also constitute a deep aquifer, fractured conditions along the NW-SE trending structures have been identified in deep wells (600-700 m deep) producing thermal groundwater (well-head temperature 35-45 °C).

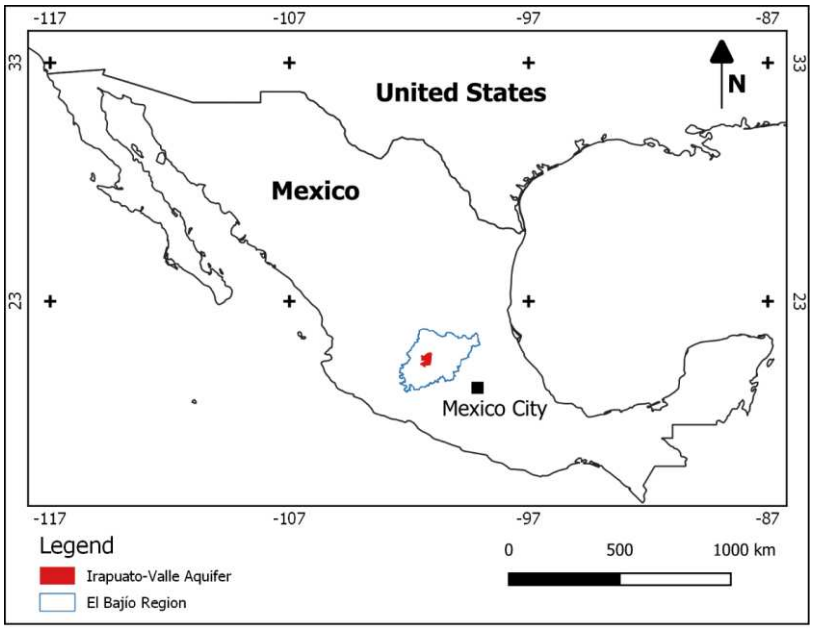

Figure 4. *Location map of the study area. (Sources: Simplified El Bajío Region map modified Suárez-mota and Villase, 2015; Irapuato-Valle Aquifer from National Water Information System, 2019; countries boundaries from Tapiquén, 2019)*

A sampling campaign for groundwater quality determination was carried out in December 2003 for laboratory measurement of 20 physicochemical parameters and in situ measurements of six field parameters (Júnez-Ferreira et al., 2016a), a total of 140 water samples were taken in production wells from the study area. A map displaying the sampled wells is presented in *Figure 2* (UTM coordinates datum WGS84, Zone 14N). Wells ranging from 46 to 700 m deep (mean 180 m, standard deviation 115 m), most of

http://www.aloki.hu ● ISSN 1589 1623 (Print) ● ISSN 1785 0037 (Online)
DOI: http://dx.doi.org/10.15666/aeer/1705_1086110882

them screened along the saturated length of the well, promoting intra-well artificial mixing. This implies that sampled water represents a mixture of several water-bearing layers. It was identified that water in recharge areas is HCO_3-Ca dominant type (650 mg/L of total dissolved solids in average). Along the groundwater flow, water chemistry evolves to dominant HCO_3-Mix and HCO_3-Na. Groundwater quality analysis indicates the contribution of geogenic and anthropogenic contamination sources. The volcanic rocks, especially those of rhyolitic composition and the basin fill sediments derived from them, are potential trace element sources specifically for Arsenic. The water samples were analyzed for arsenic composition (mean 0.011 mg/L, max. 0.083 mg/L), 35% of the samples exhibit concentrations in excess of the WHO guideline value (0.010 mg/L) (*Fig. 5a*). Dissolved arsenic is usually found as arsenic (III) in reducing environments, which usually develops at some depth within aquifers, while near the water table oxic condition prevails (Appelo and Postma, 2005). There is a lack of vertical water quality profiles information in wells, for this reason it is not possible to demonstrate the existence of any vertical transition between oxic and anoxic conditions in the tapped aquifer. However, aerobic and oxic conditions (dissolved oxygen above 1 mg/L, Eh values above 100 mV) were detected in all the groundwater samples, suggesting that oxic conditions should prevail in most of the water bearing geologic formations tapped by the production wells. Considering that the sample depth could be assigned to mid-well screen depth, no correlation between sample depth and arsenic values was identified ($R^2 = 0.07$), indicating that dissolved arsenic is not explained by desorption from Fe-(hydr)oxide minerals in reducing conditions (*Fig. 5b*). Most of the high arsenic water samples are associated with HCO_3-Na dominant type, indicating that leaching from volcanic rocks with rhyolitic composition is a major control. Evidence from north-central Mexico suggests that dissolution of volcanic glass of felsic composition seems to be the dominant process for arsenic release into groundwater (Banning et al., 2012); the concentration in the central and northwest region of the study area seem to be derived from this source. The basin fill sediment constitutes an additional source; arsenic values above the WHO drinking water standard in the southwest region of the study area are probably derived from the basin fill sediments. Decarbonatization of basin-fill sediments could constitute an additional process for arsenic mobilization (Banning et al., 2012). The identification of groundwater impacted from anthropogenic sources, considered water types such as Cl-Mg, Mixed-Ca, Mixed-Na, and SO_4-Mixed; they exemplify impacted groundwater by diffuse contamination. Impact of diffuse contamination produced by irrigation can be evaluated with a combination of indicators, such as chloride, sulphate, nitrate, phosphate among others (Cardona et al., 2008). Chloride is a conservative solute; it is useful to detect the infiltration of diffuse contamination from agricultural activities. In addition, electrical conductivity is a function of the total concentration and charge of the ions; the relationship between them is approximately linear in most of the cases. The relation between chloride and electrical conductivity for water samples from the study area is shown in *Figure 6*. The characteristics of the local surface water and wastewater are presented as an additional reference. Despite the scatter, there is an evident general trend for most of the samples, suggesting that infiltration of wastewater modify to some extent groundwater composition. A few samples are not following the general trend, especially high electrical conductivity values with low chloride values; for these samples high alkalinity values (> 500 mg/L $CaCO_3$) linked with low nitrate

http://www.aloki.hu ● ISSN 1589 1623 (Print) ● ISSN 1785 0037 (Online)
DOI: http://dx.doi.org/10.15666/aeer/1705_1086110882

concentration (about 4-5 mg/L N-NO_3), suggest a limited influence of irrigation return flow or wastewater infiltration.

From the above considerations, the methodology proposed in this paper was applied for the design of an optimal groundwater quality monitoring network oriented to characterize the spatial distribution within the study area of only three parameters of the database presented in Júnez-Ferreira et al. (2016a): arsenic, chloride and electrical conductivity. Six cases were analyzed: 1) $V = 1$ and $W = 0$ within the OF ("100 – 0"), 2) $V = 99.999$ and $W = 0.001$ ("99.999 – 0.001"), 3) $V = 99.995$ and $W = 0.005$ ("99.995 – 0.005"), 4) $V = 99.99$ and $W = 0.01$ ("99.99 – 0.01"), 5) $V = 0.5$ and $W = 0.5$ ("50 – 50") and 6) $V = 0$ and $W = 1$, but in this case the optimization procedure is applied in such a manner that the highest priority in wells is assigned to the highest estimate error variance ("Worst" case). For the six cases $\alpha_w = \alpha_p = 1$.

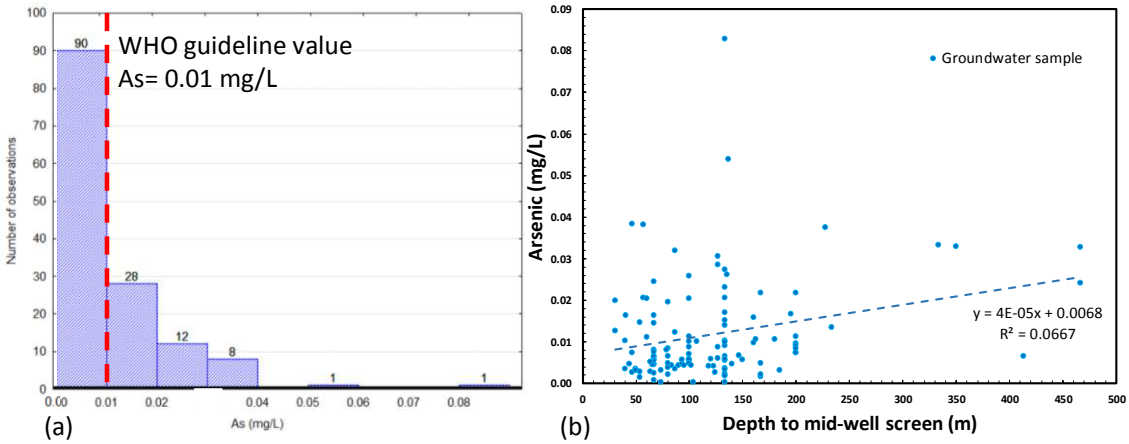

Figure 5. *Arsenic analysis in a) the number of samples for groups and the reference of the WHO, in b) the correlation between concentration and well depth*

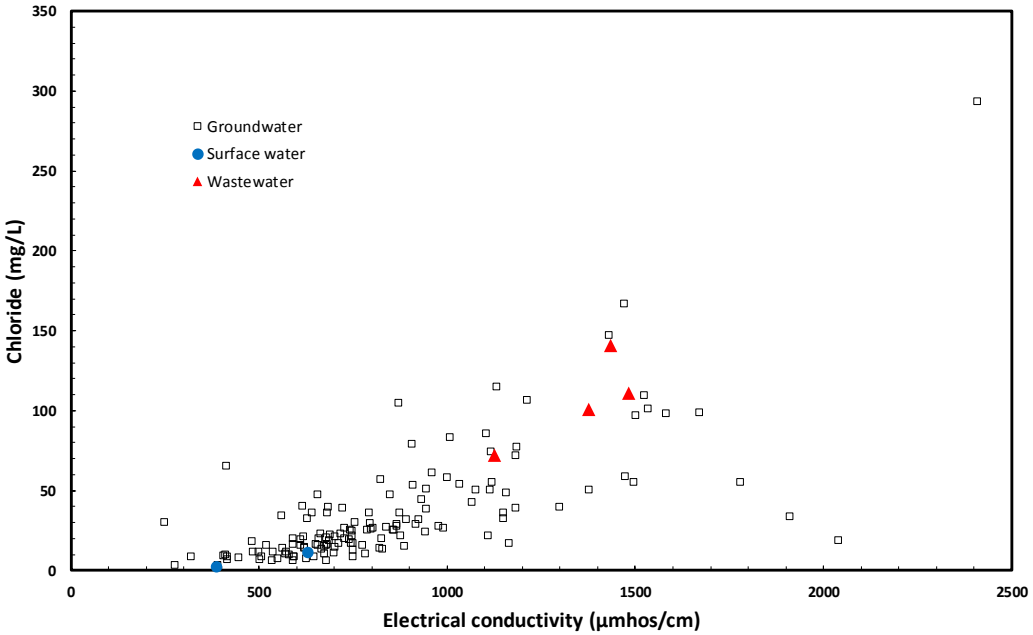

Figure 6. *Correlation between chloride and electrical conductivity*

http://www.aloki.hu ● ISSN 1589 1623 (Print) ● ISSN 1785 0037 (Online)
DOI: http://dx.doi.org/10.15666/aeer/1705_1086110882

Geostatistical analyses

As a result of the geostatistical analyses carried out to the selected groundwater quality parameters, semivariogram models for each parameter were obtained (*Table 1*). With these models, covariance matrices were derived and normalized for each parameter and used in the optimization process, using the CEG and the CSG values.

Table 1. *Semivariogram models used for the generation of the groundwater monitoring network*

Parameter	Model	Nugget (u^2)*	Sill (u^2)*	Range (m)
Electrical conductivity	Spherical	0	125097	6792
Arsenic	Spherical	$6.5x10^{-5}$	0.000142	4685
Chloride	Spherical	60.98	1490	6515

*u in (mg/L) for arsenic and chloride, in (μmhos/cm) for electrical conductivity

Discussion

The methodology proposed by Júnez-Ferreira et al. (2016a) considered the selection of sampling points by choosing the well positions that minimize the estimate error variance of the selected indicator parameters with the option to include priority zones according to the groundwater quality data. The optimization process is supported by a Kalman filter to calculate WJT. The comparison between Júnez-Ferreira et al. (2016a) and the methodology proposed in this paper was carried out for various weighted values of the Kalman filter and the ponderation map proposed also in this new methodology. For the first case (100 – 0), the 100 indicates the percentage used for the calculations of the WJT with the Kalman filter and 0 the percentage of the SF; meaning that this is the equivalent of the Júnez-Ferreira et al. (2016a) methodology.

Figure 7 shows the percentage of reduction of the initial WJT that is obtained on the CEG each time a new well is added to the monitoring network for the six analyzed cases. The fastest reduction in the WJT is, as expected, produced for case "100 – 0", on the other hand, the lowest reduction corresponds to what we called the "Worst" case. The introduction of non-zero values to the SF produces a slower reduction in the WJT compared to the "100 – 0", it can be shown that assigning the same weight to both functions of the OF ("50 – 50") results in a reduction of the WJT that is found approximately in the middle of the "100 – 0" and the "Worst" cases. Assigning a very small weight to the SF produces almost the same estimates than in the optimal case in terms of the estimate uncertainty value ("100 – 0"); however, a different set of wells is now selected.

Figure 8a shows that for the "100 – 0" case, the first 10 positions are selected mainly at the central part of the cloud of the sampling stations, when the optimal monitoring network includes 30 positions; it extends to cover a larger area of the cloud of available sampling stations. However, it does not include positions in the periphery. An optimal monitoring network with 50 positions reaches some of the peripheral sampling positions with a high density at the central zone of the cloud.

Even though a priority order was assigned to all the monitoring wells, only those with the highest priority will be monitored in an optimal scheme since they achieve the highest reduction in the estimation grid uncertainty. In order to compare the set of wells selected for cases "100 – 0", "99.999 – 0.001", "99.995 – 0.005", "99.99 – 0.01", and

http://www.aloki.hu ● ISSN 1589 1623 (Print) ● ISSN 1785 0037 (Online)
DOI: http://dx.doi.org/10.15666/aeer/1705_1086110882

"50 – 50", an analysis of *Figure 8* was done, where 10, 30 and 50 wells comprise the selected monitoring networks for each case. The resulting monitoring network for the "worst" case is not analyzed further; their WJT values were only used as a reference in *Figure 7,* to visualize how close the different cases are to the best and worst possible estimation scenarios.

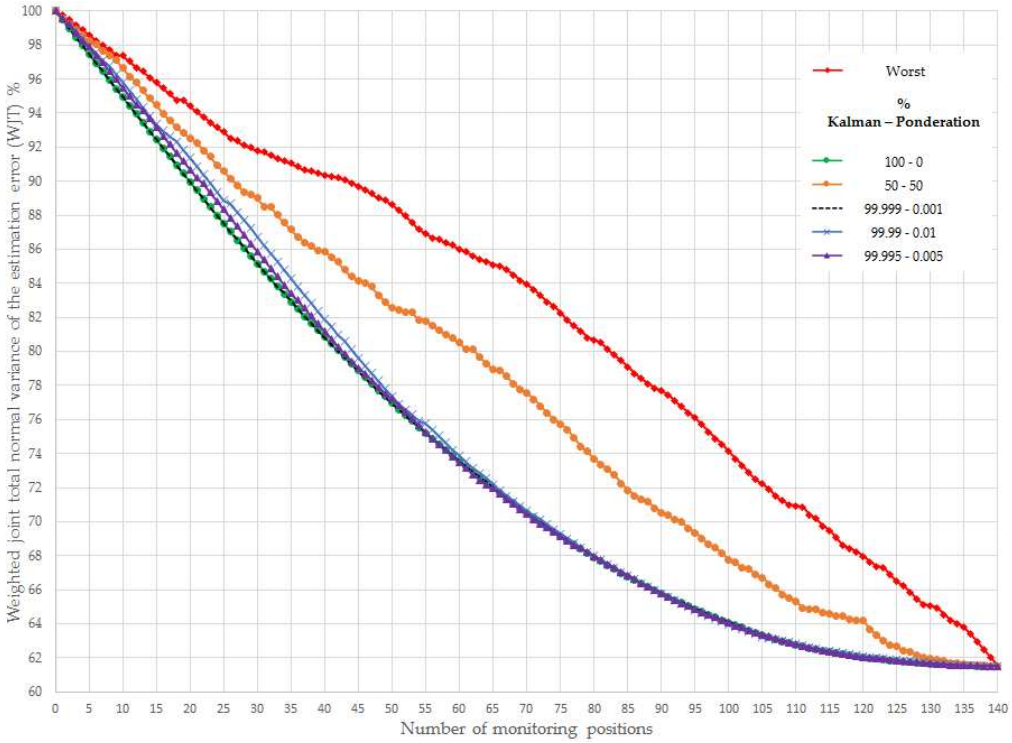

Figure 7. *Comparison of the WJT (%) vs number of monitoring positions*

When analyzing the "99.999 – 0.001" case (*Fig. 8b*), the first 10 positions are slightly biased to the south, including some of the peripheral wells. When 30 positions are selected, the wells are more homogeneously distributed within the cloud of points, but unlike the "100 – 0" case, the peripheral well with a priority value of 27 is included. With 50 positions, the same spatial coverage than the "100 – 0" case is virtually obtained.

For the "99.995 – 0.005" case shown in *Figure 8c,* the first 10 positions are notoriously biased to the extreme Southern part; only the position with a priority value of 9 is located at the Northwest. For 30 positions, the distribution is considerably better, with small areas uncovered at the central part. Finally, with 50 positions, the spatial coverage is better than in cases "100 – 0", "99.999 – 0.001", considering various wells at the Western periphery. The increase in the WJT value when selecting 50 wells for the "99.995 – 0.005" and the "100 – 0" cases is of 0.25%, this means that the loss of information is minimum for this alternative.

In *Figure 8d* it can be shown that for the "99.99 – 0.01" case, the first 10 and 30 selected positions are more biased to the south compared to the previously analyzed cases. When 50 positions are included in the monitoring network, the coverage is very similar to *Figure 8c;* however, the WJT value has increased in 0.40% with respect to the "100 – 0" case.

http://www.aloki.hu ● ISSN 1589 1623 (Print) ● ISSN 1785 0037 (Online)
DOI: http://dx.doi.org/10.15666/aeer/1705_1086110882

The "50 – 50" case (*Fig. 8e*), is clearly biased to the selection of wells along the Southern periphery when 10 positions are included in the monitoring network. The selection of 30 wells now includes the Western periphery and one well is selected at the North. When 50 positions are selected, the monitoring networks is denser at those peripheral zones, leaving the central part of the cloud uncovered.

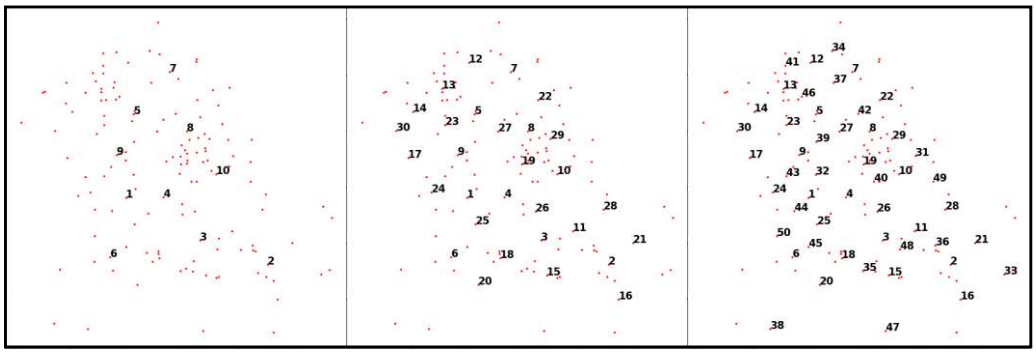

(a)

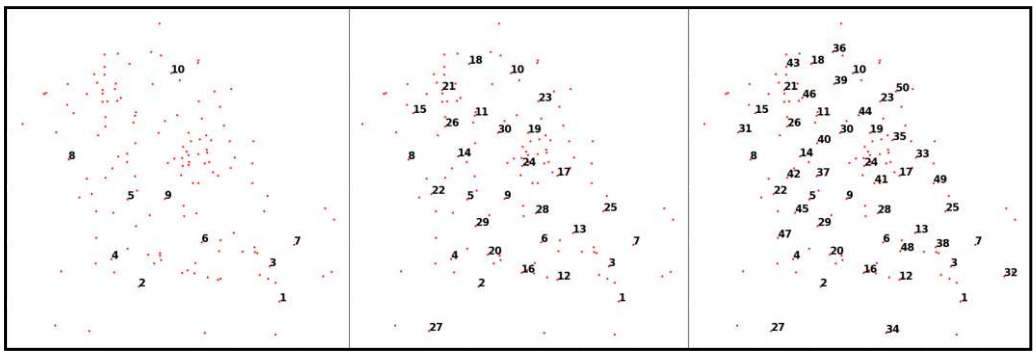

(b)

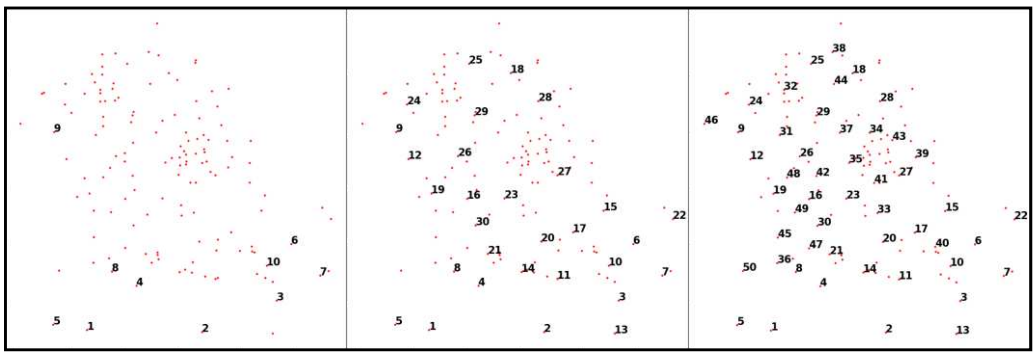

(c)

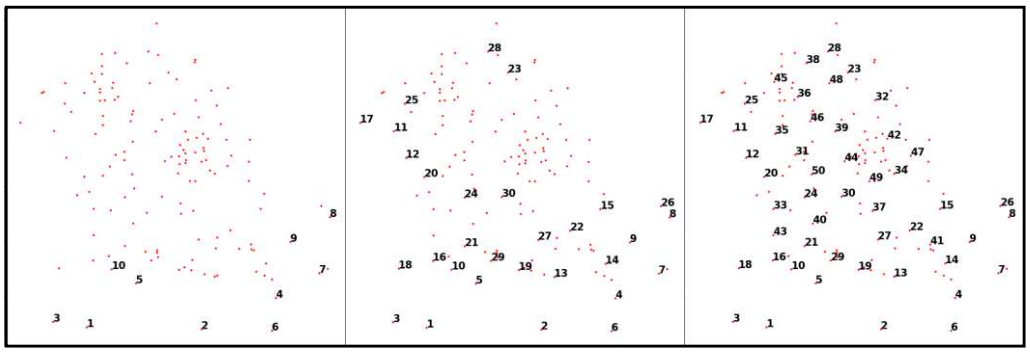

(d)

http://www.aloki.hu ● ISSN 1589 1623 (Print) ● ISSN 1785 0037 (Online)
DOI: http://dx.doi.org/10.15666/aeer/1705_1086110882

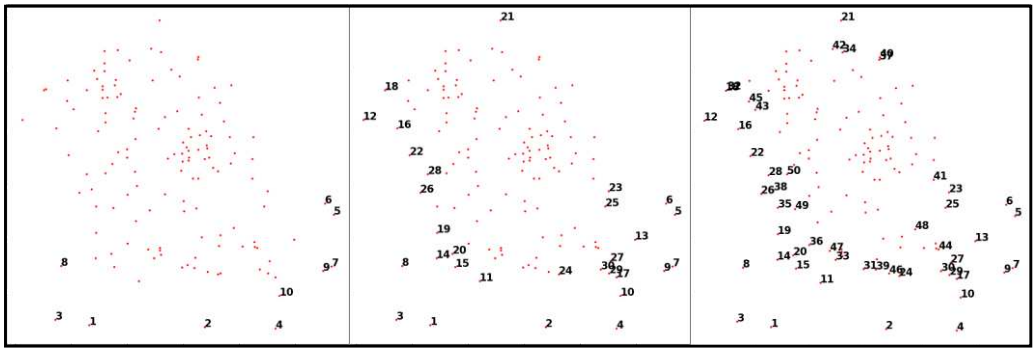

(e)

Figure 8. *Groundwater monitoring networks and priority order for cases: a) "0-100", b) "0.001-99.999", c) "0.005-99.995", d) "0.01-99.99" and e) "50-50"*

Conclusions

Various methodologies for the design of optimal groundwater monitoring networks are based on the reduction of the estimated error variance of the variable(s) involved in the design; these estimates are obtained over an estimation grid. In most cases, the shape of the estimation grid is square or rectangular; therefore, at poorly sampled peripheral areas, the estimates are extrapolations. On the other hand, these methodologies are biased to assign a higher priority to those wells that have more influence over a larger number of nodes of the estimation grid, thus assigning a low priority to those wells closer to the periphery of the estimation grid (Júnez-Ferreira et al., 2016a).

When the design is oriented to reduce the estimated error variance only, without assigning specific weights to the nodes of the estimation grid, the monitoring network could fail in covering some pre-defined priority zones or wells with valuable information. Therefore, it is necessary to evaluate alternative designs to consider those areas or sites of interest, minimizing the loss of information when estimating with the selected optimal monitoring network.

The proposed methodology includes a new algorithm for the definition of the estimation grid that takes into account the shape of the cloud of available sampling positions, trying to avoid extrapolation. The inclusion of a supplementary function in the optimization procedure allows the monitoring design to achieve a better spatial coverage, especially at the periphery of the estimation grid, without having a significant loss of information. The objective function considers also the assignment of weights to the wells; this aspect is important when some of them have been previously identified as relevant.

Through this methodology, it is possible to analyze alternative designs in which the spatial coverage of the monitoring networks changes, but its estimates are close to the optimal in terms of the estimate error variances.

Geochemistry evolution, along with groundwater flow in thick heterogeneous aquifers can be interpreted by specific methodologies; hydrogeochemistry is useful to solve questions of origin and attenuation of geogenic and anthropogenic contaminants. The proposed methodology considers statistical techniques to analyze the spatial distribution of specific water quality parameters as a result of sampling campaigns. In this regard, the understanding of groundwater chemical evolution and/or impacts of

http://www.aloki.hu ● ISSN 1589 1623 (Print) ● ISSN 1785 0037 (Online)
DOI: http://dx.doi.org/10.15666/aeer/1705_1086110882

diffuse contamination with the monitoring network is beyond of the scope of the proposed methodology. This methodology is useful for the selection of the most convenient set of sampling stations in selected areas from a number of alternatives, it was specifically oriented for the implementation of drinking water monitoring networks. Once the monitoring network is designed, the collected data will include information from the whole selected area, data redundancy will be avoided and WTJ customized accordingly for example with financial resources and/or available time. The implementation of this methodology should facilitate to decision makers the classification of water quality in aquifers.

Acknowledgements. Jorge Aceves De Alba greatly appreciates the support of the Consejo Nacional de Ciencia y Tecnología (CONACyT) for a scholarship grant from August 2014 to February 2016. Jorge Aceves De Alba would also like to acknowledge the support of the Programa para el Desempeño Profesional Docente (PRODEP) for a scholarship grant from August 2016 to July 2017, as well as the reviewers for their comments and suggestions which helped us to improve this paper. This work was partially financially supported by the National Council of Science and Technology (CONACyT) through grant 294537 (Consolidación del Laboratorio Nacional de Espectrometría de Masas con Aceleradores) and CONACyT-BMBF (Federal Ministry of Education and Research, Germany) through grant 0207586.

REFERENCES

[1] Alizadeh, Z., Mahjouri, N. (2017): A spatiotemporal Bayesian maximum entropy-based methodology for dealing with sparse data in revising groundwater quality monitoring networks: the Tehran region experience. – Environ. Earth Sci. 76(12): 1-15.

[2] Andricevic, R. (1990): Cost-effective network design for groundwater flow monitoring. – Stoch. Hydrol. Hydraul. 4(1): 27-41.

[3] Appelo, C. a. J., Postma, D. (2005): Geochemistry, Groundwater and Pollution. 2nd Ed. – A. A. Balkema Publishers, Leiden.

[4] ArcGIS, "Create Fishnet" – http://desktop.arcgis.com/en/arcmap/10.3/tools/data-management-toolbox/create-fishnet.htm (accessed: 21-Oct-2018).

[5] Baalousha, H. (2010): Assessment of a groundwater quality monitoring network using vulnerability mapping and geostatistics: A case study from Heretaunga Plains, New Zealand. – Agric. Water Manag. 97(2): 240-246.

[6] Banning, A., Cardona, A., Rüde, T. R. (2012): Applied geochemistry uranium and arsenic dynamics in volcano-sedimentary basins - an exemplary study in North-Central Mexico. – Appl. Geochemistry 27(11): 2160-2172.

[7] Bode, F., Ferré, T., Zigelli, N., Emmert, M., Nowak, W. (2018): Reconnecting stochastic methods with hydrogeological applications: a utilitarian uncertainty analysis and risk assessment approach for the design of optimal monitoring networks. – Water Resour. Res. 54(3): 2270-2287.

[8] Botero-Santa, P. A., Alaniz-Álvarez, S. A., Nieto-Samaniego, Á. F., López-Martínez, M., Levresse, G., Xu, S. (2015): Origin and development of the El Bajío basin in the central sector of the Transmexican Volcanic Belt [Origen y desarrollo de la cuenca El Bajío en el sector central de la Faja Volcánica Transmexicana]. – Rev. Mex. Ciencias Geológicas 23(1): 84-98.

[9] Buja, K. (2012): Sampling Design Tool (ArcGIS 10.0). – https://www.arcgis.com/home/item.html?id=ecbe1fc44f35465f9dea42ef9b63e785 (accessed: 10-Oct-2018).

[10] Cardona, A., Carrillo-Rivera, J. J., Castro Larragoitia, G. J., Graniel-Castro, E. H. (2008): Combined use of Indicators to Evaluate Waste-Water Contamination to Local Flow Systems in Semi-Arid Regions: San Luis Potosi. – In: Rivera, J. J. C., Guerrer, M. A. O.

http://www.aloki.hu ● ISSN 1589 1623 (Print) ● ISSN 1785 0037 (Online)
DOI: http://dx.doi.org/10.15666/aeer/1705_1086110882

(eds.) Mexico in Groundwater Flow Understanding from Local to Regional Scale. 1st Ed. CRC, London, pp. 85-104.

[11] Cardona, A., Banning, A., Carrillo-Rivera, J. J., Aguillón-Robles, A., Rüde, T. R., Aceves de Alba, J. (2018): Natural controls validation for handling elevated fluoride concentrations in extraction activated Tóthian groundwater flow systems: San Luis Potosí, Mexico. – Environ. Earth Sci. 77(4): 121.

[12] Comisión Nacional del Agua (2015): Update of the Average Annual Availability of Water in the Irapuato-Valle Aquifer (1119), State of Guanajuato [Actualización de la disponibilidad media anual de agua en el acuífero Irapuato-Valle (1119), Estado de Guanajuato]. – Comisión Nacional del Agua, Mexico.

[13] CONAGUA (2017): Water Statistics in Mexico [Estadísticas del agua en México]. – CONAGUA, Ciudad de México.

[14] Esteller, M. V., Rodríguez, R., Cardona, A. (2011): Evaluation of hydrochemical changes due to intensive aquifer exploitation : case studies from Mexico. – Environ Monit Assess 184(9): 5725-41.

[15] Esquivel, J. M., Morales, G. P., Esteller, M. V. (2015): Groundwater monitoring network design using GIS and multicriteria analysis. – Water Resour. Manag. 29(9): 3175-3194.

[16] Gómez, J. A. M., Sandoval, R. (2004): Use of groundwater in the Irapuato-Valle de Santiago aquifer region (Mexico) and its impact on the hydrogeological system [Uso del agua subterránea en la región acuífera Irapuato-Valle de Santiago (México) y su impacto sobre el sistema hidrogeológico]. – Boletín Geológico y Min. 115): 311-318.

[17] Gómez, J. J. A., Gómez, J. M. A., Samaniego, Á. F. N. (1989): Considerations about the tectonic evolution during the Cenozoic of the Sierra de Guanajuato and the southern part of the Mesa Central [Consideraciones acerca de la evolución tectónica durante el Cenozoico de la Sierra de Guanajuato y la parte meridional de la Mesa Central]. – Rev. del Inst. Geol. UNAM 8(1): 33-46.

[18] Herrera, G. S., Pinder, G. F. (2005): Space-time optimization of groundwater quality sampling networks. – Water Resour. Res. 41(12): 25-49.

[19] Hosseini, M., Kerachian, R. (2017a): A Bayesian maximum entropy-based methodology for optimal spatiotemporal design of groundwater monitoring networks. – Env. Monit Assess 189: 1-24.

[20] Hosseini, M., Kerachian, R. (2017b): A data fusion-based methodology for optimal redesign of groundwater monitoring networks. – J. Hydrol. 552: 267-282.

[21] Jiang, S., Fan, J., Xia, X., Li, X., Zhang, R. (2018): An effective Kalman filter-based method for groundwater pollution source identification and plume morphology characterization. – Water (Switzerland) 10(8). DOI: 10.3390/w10081063.

[22] Júnez-Ferreira, H. E., Herrera, G. S. (2013): A geostatistical methodology for the optimal design of space-time hydraulic head monitoring networks and its application to the Valle de Querétaro aquifer. – Environ. Monit. Assess. 185(4): 3527-3549.

[23] Júnez-Ferreira, H. E., Herrera, G. S., Gonzalez-Hita, L., Cardona, A., Mora-Rodriguez, J. (2016a): Optimal design of monitoring networks for multiple groundwater quality parameters using a Kalman filter: application to the Irapuato-Valle aquifer. – Environ. Monit. Assess. 188(1): 39.

[24] Júnez-Ferreira, H., González, J., Reyes, E., Herrera, G. S. (2016b): A geostatistical methodology to evaluate the performance of groundwater quality monitoring networks using a vulnerability index. – Math. Geosci. 48(1): 255-44.

[25] Kim, G.-B. (2015): Optimal distribution of groundwater monitoring wells near the river barrages of the 4MRRP using a numerical model and topographic analysis. – Environ. Earth Sci. 73(9): 5497-5511.

[26] Kim, G.-B., Lee, K.-K., Lee, J.-Y., Yi, M.-J. (2007): Case study for determination of a water level monitoring frequency for nationwide groundwater monitoring networks in Korea. – J. Hydrol. 342(3-4): 223-237.

http://www.aloki.hu ● ISSN 1589 1623 (Print) ● ISSN 1785 0037 (Online)
DOI: http://dx.doi.org/10.15666/aeer/1705_1086110882

[27] Kollat, J. B., Reed, P. M., Maxwell, R. M. (2011): Many-objective groundwater monitoring network design using bias-aware ensemble Kalman filtering, evolutionary optimization, and visual analytics. – Water Resour. Res. 47(2): 1-18.
[28] Li, Z., Deng, X., Wu, F., Hasan, S. S. (2015): Scenario analysis for water resources in response to land use change in the middle and upper reaches of the Heihe River Basin. – Sustain. 7(3): 3086-3108.
[29] Loaiciga, B. H. A., Member, A., Member, A., Rouhani, S. (1992): Review of ground-water quality monitoring network design. – J. Hydraul. Eng. 118(1): 11-37.
[30] Luo, Q., Wu, J., Yang, Y., Qian, J., Wu, J. (2016): Multi-objective optimization of long-term groundwater monitoring network design using a probabilistic Pareto genetic algorithm under uncertainty. – J. Hydrol. 534): 352-363.
[31] Mirzaie-Nodoushan, F., Bozorg-Haddad, O. Loáiciga, H. A. (2017): Optimal design of groundwater-level monitoring networks. – J. Hydroinformatics 19(6): 920-929.
[32] National Water Information System, "National Water Information System [Sistema Nacional de Información del Agua]" – http://sina.conagua.gob.mx/sina/ (accessed: 14-Apr-2019).
[33] Nieto-Samaniego, Á. F. (1990): Cenozoic faulting and stratigraphy in the southeastern part of the Sierra de Guanajuato [Fallamiento y estratigrafía cenozoicos en la parte sudoriental de la Sierra de Guanajuato]. – Rev. del Inst. Geol. UNAM 9(2): 146-155.
[34] Nieto-Samaniego, , Á. F., Ojeda-García, Á. C., Alaniz-Álvarez, S. A., Xu, S. (2012): Geology of the Salamanca region, Guanajuato, Mexico [Geología de la región de Salamanca, Guanajuato, México]. – Boletín la Soc. Geológica Mex. 64(3): 411-425.
[35] Nobre, R. C. M., Rotunno, O. C. Filho, Mansur, W. J., Nobre, M. M. M., Cosenza, C. a, N. (2007): Groundwater vulnerability and risk mapping using GIS, modeling and a fuzzy logic tool. – J. Contam. Hydrol. 94(3-4): 277-292.
[36] Singh, C. K., Katpatal, Y. B. (2017): Evaluating control of various hydrological factors on selection of groundwater-level monitoring networks in irrigated areas using a geospatial approach. – J. Irrig. Drain. Eng. 143(8): 05017003.
[37] Sizirici, B., Tansel, B. (2015): Parametric fate and transport profiling for selective groundwater monitoring at closed landfills : A case study. – Waste Manag. 38): 263-270.
[38] Suárez-Mota, M. E., Villase, J. L. (2015): The Bajio region, Mexico and the conservation of its floristic diversity. – Rev. Mex. Biodivers. 86: 799-808.
[39] Tapiquén, E. P. (2019): Efraín Porto Tapiquén Geography, GIS and Environmental Studies [Geografía, SIG y Estudios Ambientales]. – https://tapiquen-sig.jimdo.com/ (accessed: 14-Apr-2019).
[40] Uddameri, V., Andruss, T. (2014): A GIS-based multi-criteria decision-making approach for establishing a regional-scale groundwater monitoring. – Environ. Earth Sci. 71(6): 2617-2628.
[41] UN WATER, "Indicator 6.3.2 - Water quality" – http://www.sdg6monitoring.org/indicators/target-63/indicators632/ (accessed: 25-Oct-2018).
[42] WWAP (2016): Water and Jobs. – WWAP, Paris.
[43] WWAP (2018): Nature-Based Solutions for Water. – WWAP, Paris.
[44] XTools Pro, "XTools Pro 18." – https://help.xtools.pro/pro/18.0/en/XTools_Pro_Components/Analysis_Tools/Create_Fishnet.htm (accessed: 11-Oct-2018).
[45] Yang, Y., Xu, W., Chen, J., Chen, Q., Pan, Z. (2018): Hydrochemical characteristics and groundwater quality assessment in the diluvial fan of Gaoqiao, Emei Mountain, China. – Sustainability 10(12): 4507.
[46] Zhang, Y., Pinder, G. F., Herrera, G. S. (2005): Least cost design of groundwater quality monitoring networks. – Water Resour. Res. 41(8): 1-12.
[47] Zhou, Y., Dong, D., Liu, J., Li, W. (2013): Upgrading a regional groundwater level monitoring network for Beijing Plain, China. – Geosci. Front. 4(1): 127-138.

http://www.aloki.hu ● ISSN 1589 1623 (Print) ● ISSN 1785 0037 (Online)
DOI: http://dx.doi.org/10.15666/aeer/1705_1086110882

APPENDIX

Samples

UTM X	UTM Y	Electrical conductivity (µmhos/cm)	Arsenic (mg/l)	Chloride (mg/l)
255942	2293883	721	0.02835	38.85
258294	2294106	865	0.032	29.1
264225	2294358	563	0.0232	13.8
266037	2293737	698	0.0153	10.8
249273	2284968	248	0.0034	29.75
250397	2283463	739	0.0056	19.2
247341	2280044	581	0.0097	10
241239	2281506	674	0.0101	14.9
260375	2292217	1113	0.0107	50.22
264528	2288593	502	0.0069	6.84
269331	2289364	787	0.0066	25.43
254750	2279539	839	0.0057	26.9
256120	2281124	802	0.0059	26.7
256090	2282764	821	0.0051	13.7
258212	2285624	857	0.0053	25.43
266723	2282010	594	0.0061	8.56
268873	2283108	876	0.0068	21.77
274098	2279465	666	0.0085	13.45
270904	2279933	749	0.0101	12.96
261117	2281813	500	0.0038	11.25
265579	2279966	678	0.0047	20.3
261324	2272237	1471	0.0046	166.98
259981	2276218	748	0.0036	24.7
261502	2283669	482	0.0074	17.86
271738	2270976	1474	0.0102	58.96
272305	2265668	916	0.0146	29.1
272657	2271001	977	0.0165	27.64
264019	2265292	2410	0.0383	293.52
261750	2269664	1105	0.01285	85.48
278536	2287752	626	0.0042	7.09
275567	2287348	590	0.0068	6.06
276558	2284583	750	0.0047	8.31
272818	2285517	647	0.0171	8.56
273267	2282492	828	0.0232	13.45
261399	2282976	413	0.0041	65.43
257767	2287796	655	0.0263	15.9
256467	2285587	572	0.0136	11.49
255569	2285435	1378	0.00345	50.17
255547	2287556	1000	0.002	58.21
254566	2288936	663	0.0141	22.74
267229	2274569	1034	0.0085	53.81

http://www.aloki.hu ● ISSN 1589 1623 (Print) ● ISSN 1785 0037 (Online)
DOI: http://dx.doi.org/10.15666/aeer/1705_1086110882

270070	2266911	867	0.0206	27.39
265991	2257299	703	0.0056	14.75
264823	2256684	681	0.0082	16.38
277246	2281242	570	0.0102	10.27
278314	2278407	727	0.0205	26.58
282529	2278425	690	0.0176	22.01
258815	2286160	551	0.006	7.09
255955	2290276	485	0.008	11.69
254101	2290424	610	0.0114	19.56
252790	2286848	628	0.0042	32.28
249309	2288653	590	0.004	16.38
255582	2286945	933	0.0044	44.51
265851	2258103	673	0.0059	10.51
263772	2258257	746	0.0088	17.12
260077	2259299	703	0.0045	21.03
261545	2263341	1067	0.0297	42.395
257189	2257498	446	0.00365	8.055
285064	2268748	1299	0.0103	39.62
282307	2271012	1182	0.006	39.13
282371	2274499	686	0.01695	18.91
278506	2273692	925	0.0131	31.55
279172	2275540	943	0.0081	24.21
270591	2276591	748	0.0219	21.77
269822	2275460	1119	0.0046	55.28
269893	2274092	945	0.083	38.4
270976	2274737	823	0.054	56.75
270973	2274224	1076	0.0107	50.39
269655	2272381	1149	0.0096	32.29
262022	2252546	406	0.002	8.875
257694	2255060	782	0.004	10.27
254349	2256718	507	0.0034	8.8
254400	2261222	887	0.0035	14.84
257494	2265699	1779	0.01635	54.84
284469	2265951	1166	0.0047	16.63
283214	2258544	1117	0.0033	74.36
276376	2258892	520	0.0066	15.65
272009	2254911	1533	0.0029	100.77
276613	2253958	615	0.0057	40.11
271331	2278492	620	0.0218	14.43
272962	2278788	679	0.0206	15.41
274982	2278628	726	0.0114	19.81
268410	2275364	874	0.0057	35.96
270001	2277455	827	0.0205	19.57
272675	2276129	621	0.0168	13.94
270933	2275990	1430	0.0067	146.76
261448	2278096	775	0.0049	15.9

http://www.aloki.hu ● ISSN 1589 1623 (Print) ● ISSN 1785 0037 (Online)
DOI: http://dx.doi.org/10.15666/aeer/1705_1086110882

260003	2274766	792	0.0027	36.2
258394	2275726	680	0.0077	6.35
257289	2273581	1158	0.0147	48.76
279012	2262127	611	0.0103	15.41
280594	2258783	1523	0.0123	109.58
285398	2256122	1582	0.0044	97.84
274367	2254234	590	0.0032	19.57
273276	2260493	682	0.0071	36.2
269754	2255053	2040	0.0089	18.83
272189	2256803	945	0.0091	50.88
270786	2255466	1910	0.0027	33.37
251411	2268482	960	0.0178	61.15
254443	2265954	1495	0.0315	54.845
253651	2269050	859	0.0384	25.44
256054	2271954	1213	0.0092	106.65
266727	2268190	1670	0.0026	98.82
273817	2244339	756	0.0023	30.08
286457	2244021	991	0.0074	26.67
287199	2249886	796	0.0052	29.35
286441	2253231	892	0.0095	31.55
285147	2253929	848	0.0038	47.29
283668	2254647	559	0.0016	34
295339	2266495	1501	0.0024	96.86
296876	2264452	537	0.0007	11.5
252791	2271746	797	0.0112	25.93
282816	2258695	1009	0.0017	82.9
270132	2265073	1182	0.0112	71.9
276607	2260779	1131	0.0029	114.6
282733	2259587	907	0.0007	79.2
276186	2253776	642	0.0021	36.2
255951	2291694	716	0.0048	22.8
257925	2288696	658	0.0032	19.9
260031	2268069	1184	0.0197	77.2
265749	2299445	276	0.001	3.2
272667	2292812	632	0	11.1
272632	2292422	390	0	3.2
267827	2290531	535	0.0019	6.3
245432	2287054	593	0.0046	8.7
245118	2286870	712	0.0045	16.8
249504	2275210	751	0.005	17
265846	2258531	1109	0.0099	21.4
253236	2244695	410	0.00035	10
247158	2245650	417	0.0035	6.6
248184	2255261	619	0.0023	20.9
294946	2254438	320	0.00035	8.7
296494	2255175	417	0.0023	8.3

http://www.aloki.hu ● ISSN 1589 1623 (Print) ● ISSN 1785 0037 (Online)
DOI: http://dx.doi.org/10.15666/aeer/1705_1086110882

289764	2260054	1149	0.0023	35.9
273830	2274505	872	0.033	104.9
275319	2272939	684	0.0066	39.3
276204	2272290	909	0.0242	53.4
274578	2274772	657	0.0333	47.6
274275	2276426	743	0.0376	25
274206	2276950	650	0.0328	16.3

http://www.aloki.hu ● ISSN 1589 1623 (Print) ● ISSN 1785 0037 (Online)
DOI: http://dx.doi.org/10.15666/aeer/1705_1086110882

A RESEARCH ON THE DETERMINATION OF THE FACTORS AFFECTING THE IMPLEMENTATIONS OF AGRICULTURAL INNOVATIONS BY BEEKEEPERS IN MUĞLA PROVINCE, TURKEY

ÇUKUR, T.[1*] – ÇUKUR, F.[2]

[1]*Department of Marketing and Advertising, Milas Vocational School, Muğla Sıtkı Koçman University, 48200 Milas, Muğla, Turkey*

[2]*Department of Management and Organization, Milas Vocational School, Muğla Sıtkı Koçman University, 48200 Milas, Muğla, Turkey*

[*]*Corresponding author*
e-mail: tayfun.cukur@hotmail.com; phone: +90-252-211-3263; fax: +90-252-211-1879

(Received 22nd Mar 2019; accepted 13th Jun 2019)

Abstract. This study aims to detect the factors which are effective on the adoption and the implementation of the agricultural innovations by the farmers who are focused on the beekeeping in the Milas district Muğla province of Turkey. For this aim, a questionnaire is made with 62 farmers who are determined with the method of proportional sampling. The method of Logistic Regression Analysis is used with the aim of the determination of the factors which are effective on the implementation of the innovations related to the beekeeping by farmers. According to the results of the analysis, it is determined that young farmers, farmers who have problems related to production, who are members of cooperative and who do not store the honey implement the agricultural innovations which are related to beekeeping more.
Keywords: *beekeeping, agricultural extension, innovators, adoption, farmers*

Introduction

The growing population in the world increases the demand for foodstuffs. No doubt, this situation creates a pressure on ecosystem. As it is not easy to increase the areas of agricultural production, it will be possible to meet the demand for foodstuffs by increasing the fertilization of agricultural production. The most important way of increasing agricultural fertilization is to develop modern agriculture technologies and agricultural innovations. As it known, agriculture is the most important source of income and livelihood for people who live in rural areas. For this reason, to be able to increase the fertilization, it is quite important to reach the developed technologies and agricultural innovations to the rural areas.

Rogers (1976) defines innovation as an idea, implementation or an object which is approved as new by an individual or a respective department. So, everything which the individual perceives for the first time has the characteristics of being new for that individual (Özçatalbaş and Gürgen, 1998). Some characteristics of innovations affect their adoption. General characteristics of innovations can be classified in five groups. These groups are; usefulness, suitability, simplicity, trialability and observability (Cinemre and Demiryürek, 2005).

Innovations are accepted as critical for socio-economic development as they contribute to the growth in industry, trade and economy in every society. Innovation contributes to the fertilization, productivity, quality and competitiveness (Mutsvangwa-Sammiea et al., 2018). The adoption of agricultural innovations is an important factor to increase

http://www.aloki.hu ● ISSN 1589 1623 (Print) ● ISSN 1785 0037 (Online)
DOI: http://dx.doi.org/10.15666/aeer/1705_1088310897

agricultural fertilization, ensure food security, provide comprehensive growth and reduce poverty (Gebremariama and Tesfaye, 2018). The adoption of new technologies in terms of input and agricultural implementations has vital importance for the growth of agricultural sector. Together with the adoption of new technologies, the fertilization of land and labour force increases, natural sources are used effectively (Peter et al., 2018).

The time between the introduction of an innovation and the implementation of it is called "adoption process". Generally, the adoption of innovations takes time. It is detected that the adoption of innovations is not an instantaneous behaviour or act but a process which involves a series of acts and requires a specific time period. For example, the plantation of a new kind of a seed or the purchase and the use of a new drug when they are found out for the first time cannot be expected. Time is needed for this and this process sometimes lasts quite long (Cinemre and Demiryürek, 2005). All the individuals of rural population do not accept an innovation simultaneously. A part of the society becomes more eager in accepting and can adopt it years later when compared to the others (Özkaya, 1996).

One of the ways of minimizing the costs in businesses is to use new technologies which are effective on the cost. The implementation of technology in the businesses of husbandry hinges upon the degree of adoption of these innovations by the society in which these businesses take place (Türkyılmaz et al., 2003). The adoption and the propagation of innovations is a subject about which there are so many intensive debates and which does not lose its currency not only in agricultural area but also in branches such as health, marketing, business management, communication, sociology and geography (Aktaş, 2005).

Innovations in agricultural extension are new or improved inputs or methods which are handled in the process of agricultural production in an attempt to create behavioural change over farmers and obtain the desired result. The generalization of an innovation and making it be used by so many farmers can be possible by carrying out various agricultural extension activities effectively and within a long time period.

Agricultural innovation is not just a matter of adopting new technologies. It also necessitates a balance between the new techniques and alternative organization types (Klerks et al., 2012). It is accepted that the decision of adopting innovations is correlated with the social, economical and psychological characteristics of potential adopters. In adopting the innovations, not only the characteristics of the individuals but also the characteristics of the innovation are important (Longo, 1990). Adopting agricultural technologies is a complicated process because of the multidimensional nature of the technologies and mutual relations between the different explanatory factors (Jensen et al., 2014). The characteristics of the farmer and the agricultural enterprise, bio-physical characteristics of the agricultural enterprise, financial and administrative characteristics of the agricultural enterprise and the other factors occurring out of the farmers are effective on the decision of adopting new technology (Yigezu et al., 2018). When the litterateur is examined, it is seen that a great number of factors are effective on the adoption of the innovations by farmers.

Beekeeping is not seen as a source of side income for agricultural businesses any more rather it is seen as a main income source. Turkey occupies the first places in the world in terms of both the bee possession and the production of bee products. According to the 2018 data, the number of the beekeeping businesses in Turkey is 81.300 and the number of hives is 8.108.424. In 2018, the total amount of honey produced is 107.920 tons and the total amount of beeswax is 3.987 tons (TÜİK, 2018).

http://www.aloki.hu ● ISSN 1589 1623 (Print) ● ISSN 1785 0037 (Online)
DOI: http://dx.doi.org/10.15666/aeer/1705_1088310897

The aim of this study is to determine the implementation circumstances of innovations by farmers who are focused on beekeeping in the Milas district. In this context, the factors which are effective on the decisions of the farmers in terms of implementing innovations will be detected by examining the circumstances of following and implementing the innovations by farmers.

Materials and Methods

The primary material of the study composes of 62 questionnaires which are made with the farmers in 9 villages in the Milas district in Muğla province. Moreover, the previous research on the subject has been capitalized on to a great extent. The questionnaires were administered in April-May 2017.

In this study, purposive sampling method is used in choosing the villages with which the questionnaire is made. The study of questionnaire is made in 9 villages composing of Karahayıt, Sakarkaya, Akçalı, Çukurköy, Gölyaka, Kapıkırı, Fesleğen, Kalem and Karacahisar in which beekeeping is performed intensively in the Milas district Muğla province of Turkey (*Figure 1*).

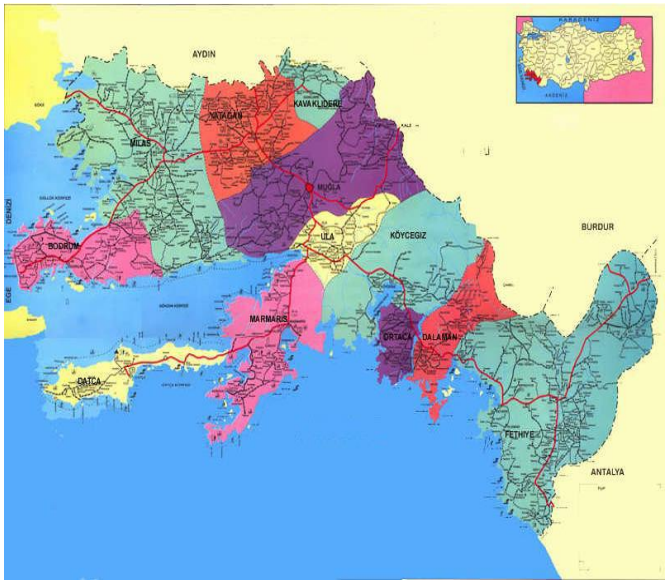

Figure 1. *Map of Muğla Province (Source: Anonymous, 2004)*

According to the information taken from Milas Agriculture and Forestry District Directorate, 721 farmers perform beekeeping activities in the district and these 721 farmers constitute the main population of the study (Anonymous, 2017). In the research, farmers who are determined with the proportional sample size are interviewed (Newbold, 1995). 90% confidence interval and 10% error margin are grounded on in the research. In *Equation 1*; n is the sample size, N is the population size, p is the ratio of the studied feature in the main population (the ratio of the beekeepers who implement innovations is accepted as 50% as it is desired to reach the maximum sample size and p=0.5 is taken).

$$n = \frac{Np(1-p)}{(N-1)\sigma_P^2 + p(1-p)} \qquad \text{(Eq.1)}$$

http://www.aloki.hu ● ISSN 1589 1623 (Print) ● ISSN 1785 0037 (Online)
DOI: http://dx.doi.org/10.15666/aeer/1705_1088310897

According to the calculation, the total number of the farmers who are to be interviewed is calculated as 62. The range of the applied questionnaires according to the districts is given on *Table 1*.

Table 1. *Villagers with whom the questionnaire is made in the scope of the research*

Villages	Beekeepers with whom the questionnaire is made (n)
Karahayıt	5
Sakarkaya	12
Akçalı	15
Çukurköy	13
Kapıkırı	3
Gölyaka	2
Fesleğen	6
Kalem	2
Karacahisar	4
TOTAL	62

Logistic regression analysis method is used in the research with the aim of determining the factors which are effective on the circumstances of adopting the innovations by farmers. The aim of the model is to create the most suitable model by also paying regard to the level of the relation between the dependent variable and the independent variable or variables when the dependent variable (Y) is bivalent or classified (Önder and Cebeci, 2002). Logistic regression is a method from which is benefited in detecting the cause and effect relation with explanatory variable when categorically; the response variable is observed in dual, trio and multiple categories. It is a regression method which helps perform the classification and appointment transactions in which the expected value of response variable is obtained as probability in accordance with the explanatory variables (Everest, 2015).

Logistic regression does not deal with estimating the value of dependent variable. Instead of this, the probability of taking the value of 1 of dependent variable is tried to be estimated. As the obtained result is a value of a probability, it can only take values between 0 and 1 (Alpar, 2011). The model of logistic regression estimates the result as any value between 0 and 1 and tries to detect the probability of being 1 of dependent variable (Hosmer and Lemeshow, 2000). The logistic regression model used in the study is given in the *Equation 2*.

$$\pi(x) = P(Y = 1 / X = x) = \frac{e^{\beta_0+\beta_1X_1+\beta_2X_2+...+\beta_pX_p}}{1+e^{\beta_0+\beta_1X_1+\beta_2X_2+...+\beta_pX_p}} = \frac{1}{1+e^{-(\beta_0+\beta_1X_1+\beta_2X_2+...+\beta_pX_p)}} \qquad \text{(Eq.2)}$$

where X: is the data matrix in relation to the independent variable and X = x is (when the value of X is known) the probability of the occurrence of the event (Y = 1) π. β = refers to constant, βi = refers to the to be estimated parameter for every explanatory (independent) variable, Xi = refers to the i^{th} independent variable. Logit conversion is applied to the logistic regression function which is given in the equilibrium and is not linear and it is linearized. When the model is fixed according to the datas of the study, *Equation 3* is formed. Accordingly, b1 shows how much alteration 1 unit alteration in independent variable x causes in dependent variable (Aldrich and Nelson, 1984).

http://www.aloki.hu ● ISSN 1589 1623 (Print) ● ISSN 1785 0037 (Online)
DOI: http://dx.doi.org/10.15666/aeer/1705_1088310897

$$g(x) = In\left[\frac{\pi(x)}{(1-\pi(x))}\right] = Ine^{\beta_0+\beta_1 X} = \beta_0 + \beta_1 X ... \quad \text{(Eq.3)}$$

In the research, a model which can identify the relation between the dependent and independent variables by using the least variables to have the best accord and which can be accepted as true statistically is established (Ertan and Gök, 2012). The farmers who implement the innovations related to beekeeping are coded as 1 and the farmers who do not implement the innovations are coded as 0. The functional form of the regression model estimating the factors which are effective on the adoption of the agricultural innovations by beekeepers is as in the following.

Y = f (X1, X2, X3, X4, X5, X6, X7, X8, X9, X10, X11, X12, X13)

Y; The circumstance of implementing the agricultural innovations yes; 1, no; 0 (Dummy).
X1; The age of the business manager.
X2; Educational level of the business manager.
X3; Beekeeping experience of the business manager.
X4; The amount of honey production.
X5; The circumstance of the business managers to get a loan yes; 1, no; 0 (Dummy).
X6; The circumstance of record keeping of the business yes; 1, no; 0 (Dummy).
X7; The circumstance of the business managers to have the information about the domestic market yes; 1, no; 0 (Dummy).
X8; The circumstance of the business managers to have the information about the foreign market yes; 1, no; 0 (Dummy).
X9; The circumstance of the business managers to have a problem about the production of bee products yes; 1, no; 0 (Dummy).
X10; The circumstance of the business managers to have a problem about the marketing of bee products yes; 1, no; 0 (Dummy).
X11; The circumstance of the business managers to be a member of the cooperative yes; 1, no; 0 (Dummy).
X12; The storage circumstance of the produced honey yes; 1, no; 0 (Dummy).
X13; The circumstance of participation in agriculture fairs yes; 1, no; 0 (Dummy).

Results

Socio-economical characteristics of beekeepers

The socio-economical characteristics of the farmers have important effects on their adoption of the innovations. Therefore, socio-economical characteristics of the beekeepers are examined. The ages, time periods of agricultural experience, time periods of beekeeping experience, education levels of the beekeepers, the number of hives and the sources of income take place among the socio-economical characteristics which are examined in the research.

It is detected that 41.94% of the producers are older than 51, 50% of the producers are at the age of 35-50 and 8.06% are younger than 35. As it is seen from these results, half of the beekeepers are at the age range of 35-50. The age average of the beekeepers is found as 48. It is seen that 61.29% of the beekeepers have the experience of agriculture for more than 21 years. It is detected that 12.90% of the beekeepers deal with the

http://www.aloki.hu ● ISSN 1589 1623 (Print) ● ISSN 1785 0037 (Online)
DOI: http://dx.doi.org/10.15666/aeer/1705_1088310897

agricultural production for less than 10 years, 25.81% of the beekeepers deal with the agricultural production for 10-20 years. It is seen that 45.16% of beekeepers have had the experience about beekeeping for more than 21 years. It is detected that 32.26% of beekeepers perform beekeeping for less than 10 years and 22.58% of beekeepers perform beekeeping for 10-20 years. It can be stated that the level of education can be effective on the information sources that the farmers who perform beekeeping use. According to the datas of the questionnaire, it can be said that the majority of the beekeepers are the graduates of primary school (80.65%). 14.52% of the beekeepers are the graduates of secondary/high school and one beekeeper is the graduate of college. It is detected that 33.87% of the beekeepers have less than 100 hives, 40.32% of beekeepers have 100-200 hives and 25.81% of beekeepers have more than 201 hives. It is seen that 74.19% of the beekeepers earn their lives only with agriculture and 25.81% of the beekeepers, together with agriculture, deal with some other job activities out of agriculture (*Table 2*).

Table 2. *Socio-economic characteristics of beekeepers*

Variables	Number	%
Age		
<35	5	8.06
35-50	31	50.00
51+	26	41.94
The duration of agricultural experience (year)		
<10	8	12.90
10-20	16	25.81
21+	38	61.29
The duration of beekeeping experience (year)		
<10	20	32.26
10-20	14	22.58
21+	28	45.16
Education		
Literate	2	3.22
Primary School	50	80.65
Secondary-High School	9	14.52
College	1	1.61
The number of hives		
<100	21	33.87
100-200	25	40.32
201+	16	25.81
Sources of income		
Agriculture	46	74.19
Agriculture+non-agricultural	16	25.81

The information needs and the information sources of farmers about beekeeping

Rogers states that innovations are adopted at five stages (Rogers, 1983). These stages are: awareness, interest, evaluation, trial and adoption. Farmers need information quite intensively especially at the stages of awareness and interest. Therefore, it is vital that the needs for the information should be detected for farmers to decide about innovation and these needs should be met, the information should be provided truly and on time for the farmers to adopt the agricultural innovations.

In the current study, it was found that the beekeepers are in need of information about various subjects related to beekeeping. It was determined that 79% of the farmers who took place in the research need information about beekeeping. The major need for information is about disease and pest control. 64.5% of the farmers need information

http://www.aloki.hu ● ISSN 1589 1623 (Print) ● ISSN 1785 0037 (Online)
DOI: http://dx.doi.org/10.15666/aeer/1705_1088310897

about disease and pest control. 32.3% of the farmers need information about marketing and 27.4% of the farmers need information about bee production (*Table 3*).

Table 3. *The subjects that the farmers need information about beekeeping*

	n*	**%**
Disease and pest control	40	64.5
Marketing	20	32.3
Queen bee production	17	27.4
The production of bee products	16	25.8
Management of colony	14	22.6
Agricultural supports	12	19.4
Subjects about farmer organization	7	11.3
The storage of bee products	1	1.6
Social and cultural subjects	1	1.6
Giving sugar and the time for it	1	1.6

*The total is over 100% as there are answers more than one

Information sources play an important role over getting into touch with new technologies, being aware of the information, creating an interest, making understanding easy and encouraging farmers to adopt (Pandey, 2014). In the study, it was determined that the beekeepers obtain information from different sources. In the research, Agriculture and Forestry District Directorate comes first as an information source of the farmers (38.7%). 37.1% of the farmers consult to the union of beekeepers and 24.2% of the farmers consult to their friends and relatives (*Table 4*).

Table 4. *Information sources of the farmers*

	n*	**%**
Agriculture and Forestry District Directorate	24	38.7
The Union of Beekeepers	23	37.1
Friends and relatives	15	24.2
Veterinary	8	12.9
I do not consult anybody	4	6.5
Internet	1	1.6
Municipality	1	1.6
The head of village or neighborhood	1	1.6

*The total is over 100% as there are answers more than one

The points of view of farmers towards agricultural extension

Innovativeness which is an adoption and implementation of an idea in a society for the first time is really important for the extension of the innovations. The aim in agricultural extension is to increase the number of innovators (Cinemre and Demiryürek, 2005). For this reason, the determination of the points of view of the farmers towards agricultural extension/extensionists is quite important as the agricultural extension/extensionists play an important role in the access and the implementation of innovations by farmers. Because the more powerful is the relation between the farmer and extensionist, the more high is the possibility of adopting the innovations by farmers. In the study, it was found that the beekeepers are not much in contact with extensionists. While 22.6% of farmers state that they do not get into touch with the extensionists, 53.2% of the farmers state that

http://www.aloki.hu ● ISSN 1589 1623 (Print) ● ISSN 1785 0037 (Online)
DOI: http://dx.doi.org/10.15666/aeer/1705_1088310897

they get into touch with the extensionists twice a year (*Table 5*). While 89.6% of the producers (48 producers) who state that they get into touch with the extensionists for the aim of getting information find the information that they get useful, 10.4% of the producers does not find the information useful.

Table 5. *The frequency of getting into touch with extensionists by farmers for the aim of getting information about beekeeping*

	n	**%**
Once a week	1	1.6
Once a month	6	9.7
Once in three months	5	8.1
Once a year	2	3.2
Twice a year	33	53.2
Thrice a year	1	1.6
I do not get into touch	14	22.6
Total	62	100.0

It can be argued that the beekeepers' contacts with extensionists generally occur in the village. The proportion of the farmers who say that "I get into touch with the extensionists when they come to the village" is found as 45.2% on the other hand, the proportion of the farmers who say that "I get into touch with the extensionists when I have a problem" is found as 32.3% (*Table 6*). 22.6% of the farmers states that they never get into touch with the extensionists.

Table 6. *The circumstance of getting into touch with the extensionists*

	n	**%**
I get into touch with the extensionists when I have a problem	20	32.3
I get into touch with the extensionists when they come to the village	28	45.1
I never get into touch	14	22.6

When the places where the beekeepers and extensionists get in contact were examined, it was found that nearly half of the contacts occurred in the tea house of the village. With a proportion of 45.2%, the village's tea house comes first for the farmers as a place for getting into touch with extensionists. The proportion of the farmers who state that they get into touch with the extensionists at Agriculture and Forestry District Directorate is detected as 45.2% (*Table 7*).

It can be stated that mass communication is effective on the adoption of innovations. The most important reason of this is that the attentions of the farmers can be drawn to the innovation and a specific level of knowledge about innovation can be created (Sezgin, 2010). It is detected in the research that 91.9% of the farmers watch agriculture programmes at the television while 37.1% of the farmers listen to the agricultural programmes at the radio. 59.7% of the farmers state that they read books, magazines and newspapers about agriculture. In the research, the proportion of the farmers who use internet for agricultural purposes is found as 24.2% (*Table 8*).

Demonstrations show a group that how a new work is done or how an old work is done better (Cinemre and Demiryürek, 2005). Demonstrations are some of the extension methods which enable farmers to learn by hearing, seeing and practicing. Demonstrations are accepted as the most effective method at the operations of agricultural extension and

http://www.aloki.hu ● ISSN 1589 1623 (Print) ● ISSN 1785 0037 (Online)
DOI: http://dx.doi.org/10.15666/aeer/1705_1088310897

they are used quite prevalently (Yurttaş and Atsan, 2007). In the research, the proportion of the farmers who attend the demonstrations about beekeeping is found as 16.1%. While the proportion the farmers who attend the course/seminar about beekeeping is detected as 24.2%, the proportion of the farmers who attend conference/panel activities is detected as 40.3% (*Table 8*).

Table 7. *The place of getting into touch with the extensionists by farmers*

	n*	**%**
Agriculture and Forestry District Directorate	28	45.2
Village chamber	4	6.5
Village's tea house	30	48.4
Terrain	2	3.2
Telephone	2	3.2
I get into touch at the meetings organized	8	12.9
I never get into touch	14	22.6

*The total is over 100% as there are answers more than one

Table 8. *The circumstances of the farmers to attend various activities*

	n	**%**
Watching agriculture programmes at television	57	91.9
Attending agriculture fairs and exhibitions	39	62.9
Reading materials like book, magazine, newspaper, leaflet etc. about agriculture	37	59.7
Being informed via telephone or sms about agriculture	34	54.8
Attending the farm or home visits	26	41.9
Attending the conference-panel activities	25	40.3
Listening to the programmes about agriculture at the radio	23	37.1
Using internet with the aim of agriculture	15	24.2
Attending course-seminar activities	15	24.2
Attending demonstration activities	10	16.1
Attending the trips with the aim of agriculture	6	9.7
Attending the competitions with the aim of agriculture	2	3.2

Agriculture fairs are important agricultural activities which provide information to the farmers about the new techniques and technologies in the agricultural sector. Farmers find the possibility to practice the new technology instantly thanks to the demonstration areas created at the fairs (Çukur and Çukur, 2017). It is detected in the research that 62.9% of the farmers attend the agriculture fairs and exhibitions (*Table 8*).

Results of Logistic Regression Analysis

The proportion of the farmers who state that they follow the innovations about beekeeping is found as 69.4%. 61.3% of the farmers state that they implement the innovations about beekeeping.

The ages of the farmers, the circumstances of the farmers to have a problem about production and the circumstances of them to be a member of a cooperative are found significant at 0.05 level of significance and the circumstance of storing the honey is found significant at 0.10 level of significance statistically, at the logistic regression analysis which is done for the aim of the determination of the factors which are effective on the implementations of agricultural innovations about beekeeping by farmers. That is, it is determined that young farmers, farmers who have problems related to production, who

http://www.aloki.hu ● ISSN 1589 1623 (Print) ● ISSN 1785 0037 (Online)
DOI: http://dx.doi.org/10.15666/aeer/1705_1088310897

are the members of the cooperative and who do not store the honey implement the agricultural innovations about beekeeping more (*Table 9*).

Table 9. *Logistic Regression Results*

INNOVATION	Coef.	Std. Err.	P>|z|
Age	-0.1149346	0.0535188	**0.032**
Education	-0.1166394	0.203393	0.566
Experience	0.0248924	0.0445552	0.576
Production	0.0000635	0.0001996	0.750
Credit	0.5355139	0.7737263	0.489
Record	-0.8402401	1.174613	0.474
Domestic	-0.8161603	0.8246815	0.322
Foreign	-0.2167684	0.9579789	0.821
Proprob	2.577754	1.233063	**0.037**
Marprob	0.6426032	1.028957	0.532
Coop	1.543304	0.7792494	**0.048**
Storage	-1.438156	0.7846837	**0.067**
Fair	0.7029553	0.7998101	0.379
Cons	3.160572	3.32936	0.342

Log likelihood = -28.575797
Number of obs = 61
LR $chi^2(13)$ = 23.69
Prob > chi^2 = 0.0341
Pseudo R^2 = 0.2930

Discussion

In this study which aims to determine the implementation of innovations by farmers who perform beekeeping at the district of Milas, it is determined that a great deal of the farmers adopt and implement the innovations about beekeeping (61.3%). In the research which is done by Kızılaslan and Ünal (2013), similar results are found and it is determined that 67.2% of the farmers implement the new agricultural informations and techniques. According to the research done by Kızılaslan (2009), the proportion of the farmers who state that they sometimes implement the innovations is detected as 71.67%. On the other hand, according to the research done by Özçatalbaş (2000), it is detected that the level of adopting the innovations at the majority of producers is under the level of intermediate and the proportion of the producers who have high adopting level is 8.7%. In the research done by Udofia and Edet (2016) at Ethiopia, the proportion of adopting the modern beekeeping techniques by beekeepers is found quite low and it is determined that only 16.80% of the beekeepers adopt modern beekeeping techniques. According to the research done by Chambo et al. (2018), more than half of the beekeepers adopt more than 74% of the suggestions about the harvest and after harvest. According to the research done by Kumar (2013), farmers adopt 45.71% of the innovations about bee feeding and 36.66% of the innovations about migratory beekeeping. These proportional differences occurring between the levels of adopting the innovations can arise from the differences at the personal characteristics of the beekeepers, social structure and the economical and financial situations of the beekeepers.

As there are differences between the levels of adopting the innovations by beekeepers, there are also differences in the factors which are effective on the adoption of the

http://www.aloki.hu ● ISSN 1589 1623 (Print) ● ISSN 1785 0037 (Online)
DOI: http://dx.doi.org/10.15666/aeer/1705_1088310897

innovations. In this study, it is detected that young farmers, farmers who have problems related to production, who are the members of the cooperative and who do not store the honey implement the agricultural innovations related to beekeeping more. According to the research done by Wodajo (2011), getting loan, the education level of the father of the family and attending the demonstrations have positive effects on the adoption of modern hives by farmers. In the research done by Adgaba et al. (2014), it is determined that farmers who have a crowded family, who have a high level of education and young farmers adopt the usage of modern hives more easily.

One of the most important factors in adopting the agricultural innovations by farmers is, no doubt, the practices of agricultural extension. In the research done by Fadare et al. (2008), it is detected that the proportion of adopting the innovations by beekeepers is low and the greatest reason of this is the low level of relation between the farmer and extensionist. According to the findings obtained from the research, it can be said that farmers do not get into touch with the extensionists very often. It is detected in the research that 53.2% of the beekeepers get into touch with the extensionists twice a year. In the research done by Ahmad et al. (2007), the majority of the farmers (82.5%) do not visit the local agricultural extension office. In the research done by Jan et al. (2008), the proportion of the farmers who says that "last year, extensionist came to the place that I live" is found as just 2.5%. In the research done by Kenea (2008) in Kenya, it is determined that 58.8% of the farmers did not get into touch with the extensionists last year, 38.8% of the farmers get into touch with the extensionists at least once a year and 8.5% of the farmers get into touch with the extensionists at least once a month.

The age of the owners of the business is an important factor in adopting the innovations. It is determined at the end of the research that the level of adopting the innovations by young farmers is higher and this result shows a parallelism with the data of litterateur. In the research done by Boz et al. (2011) and Sezgin et al. (2010), it is determined that there is an important relation between the age and the adoption of innovations.

In the research, it is determined that being a member of the cooperative has an important effect on the adoption of agricultural innovations by farmers. In the research done by Kolade and Harpham (2014) and Wossen et al. (2017), the same result is detected.

It is detected that an important part of the farmers (89.6%) finds the information that they get from the extensionist useful. In the research done by Apantaku et al. (2016), same results are found and it is detected that 53% of the farmers think that agricultural extension services develop the agricultural activities, 94% of the farmers think that agricultural extension services help farmers be educated about the better agricultural techniques. According to the research done by Muktar et al. (2016) in Nigeria, 10% of the farmers find the agricultural extension quite useful in terms of their production, 8.8% of the farmers find it useful and 45% of the farmers find it partially useful. In the research done by Yalçın and Boz (2007), it is emphasized that the importance of district and provincial directorates of agriculture, in terms of extension, decreases in the region.

First of all, farmers need to get true and confidential information about innovation to be able to adopt the innovations. It is detected in the research that an important part of the beekeepers needs information about illness and pest control and marketing. Similarly, in the research done by Sıralı and Doğaroğlu (2004), it is determined that 45.94% of beekeepers needs information about illness, pest and the control of them. According to the research done by Awino et al. (2018), farmers need information about the illnesses

http://www.aloki.hu ● ISSN 1589 1623 (Print) ● ISSN 1785 0037 (Online)
DOI: http://dx.doi.org/10.15666/aeer/1705_1088310897

and pests which affect the bees and producing and marketing the bee products. In the research done by Ibegbulem (2014), it is stated that farmers need information about the sources of the plants on which the bees gather pollens.

Today, farmers use mass communication (television, radio, internet, newspaper, book, magazine etc.) quite intensively to be informed about agricultural innovations and get information about new technologies. In the research, the proportion of watching agricultural programmes at television by farmers is found high and the proportion of listening to the programmes about agriculture is found relatively low. It is determined in the research done by Ahmad et al. (2007) that the proportion of farmers who regard radio as an information source is 83.75% and the proportion of farmers who regard television as an information source is 82.50%. In the research done by Akinbile and Alabi (2010), the proportion of the farmers who listen to the radio to update their knowledge is found as 75% and the proportion of the farmers who watch television to update their knowledge is found as 69.2%. In the research done by Anastasios et al. (2010) in Greece, it is detected that 80.41% of the farmers have television. According to the research done by Sezgin (2010), 41.4% of the farmers follow the programmes about agriculture at television/radio regularly.

59.7% of the farmers state that they read books, magazines and newspapers about agriculture. Similar results are found in the research done by and the proportion of the farmers who read newspaper is found as 61.7%. In the research done by Ijatuyi (2016) in Nigeria, it is detected that 18.75% of the farmers regard newspaper as a source of information. In the research done by Wangu (2014), it is detected that 30.6% of the farmers regard newspaper as a source of information and 9.2% of the farmers regard agricultural magazines as a source of information.

Approximately one fourth of the farmers who join in the research use internet for the aim of agriculture. Similar results are found in the research done by Okwu and Iorkaa (2011) and the proportion of the farmers who use internet for the aim of getting information is found as 23.9%. In the research done by Akinbile and Alabi (2010), the proportion of the farmers who use internet for the aim of getting information is found a bit low as 11.7%. In the research done by Anastasios et al. (2010) the proportion of the farmers who use the internet is found as 15.10%.

Conclusion

Consequently, the managers of the businesses should be young, the member of the cooperative and the farmers who do not store the honey to adopt and implement the innovations faster in the businesses of beekeeping in the district of Milas in Muğla province and accordingly, to perform a more fertile and profitable beekeeping by using modern agricultural techniques and technologies. Besides this, it should be remembered that the farmers who have a high level of information about agriculture, who are open to the innovations and the outer world and who trust the extensionists contribute to the development of beekeeping more. For this reason, performing the agricultural extension activities with the aim of increasing the levels of innovativeness of the beekeepers by considering their present situation is thought to be quite useful.

http://www.aloki.hu ● ISSN 1589 1623 (Print) ● ISSN 1785 0037 (Online)
DOI: http://dx.doi.org/10.15666/aeer/1705_1088310897

REFERENCES

[1] Adgaba, N., Al-Ghamdi, A., Shenkute, A. G., Ismaiel, S., Al-Kahtani, S., Tadess, Y., Ansari, M. J., Abebe, W., Abdulaziz, M. Q. A. (2014): Socio-economic analysis of beekeeping and determinants of box hive technology adoption in the Kingdom of Saudi Arabia. – The J. of Animal & Plant Sciences 24(6): 1876-1884.

[2] Ahmad, M., Ahmad, M., Akram, M., Rauf, R., Khan, I. A., Pervez, U. (2007): Interaction of extension worker with farmers and role of radio and television as sources of information in technology transfer: a case study of four villages of district Peshawar and Charsadda. – Sarhad J. Agric. 23(2): 515-518.

[3] Akinbile, L. A., Alabi, O. E. (2010): Use of ICTs among fish farmers in Oyo state. – Journal of Agricultural Extension 14(1): 22-30.

[4] Aktaş, Y. (2005): Entrance of Agricultural Extension and Communication. – Dilara Publishing House, Trabzon, 283p. (in Turkish).

[5] Aldrich, J. H., Nelson, F. D. (1984): Linear Probability, Logit, and Probit Models. – Thousand Oaks, CA: SAGE Publications, California, 95p.

[6] Alpar, R. (2011): Applied Multivariate Statistical Methods. – Detay Publishing, Ankara, 853p. (in Turkish).

[7] Anastasios, M., Koutsouris, A., Konstadinos, M. (2010): Information and communication technologies as agricultural extension tools: a survey among farmers in west Macedonia, Greece. – The Journal of Agricultural Education and Extension 16(3): 249-263.

[8] Anonymous (2004): Mugla Agriculture Master Plan. – Ministry of Agriculture and Rural Affairs, Muğla Province Directorate of Agriculture, Mugla.

[9] Anonymous (2017): Milas Agriculture and Forestry District Directorate Records. (in Turkish).

[10] Apantaku, S. O., Aromolaran, A. K., Shobowale, A. A., Sijuwola, K. O. (2016): Farmers and extension personnel view of constraints to effective agricultural extension services delivery in Oyo State, Nigeria. – Journal of Agricultural Extension 20(2). http://journal.aesonnigeria9.org/index.php/jae/article/view/869.

[11] Awino, O. I., Muya, S., Kabochi, S., Kutimaa, H., Kasina, M. (2018): Apiarists' awareness and responses to honey bee colony parasite and pathogen infections in Kenya. – International Journal of Natural Resource Ecology and Management 3(4): 46-52.

[12] Boz, I., Akbay, C., Bas, S., Budak, D. B. (2011): Adoption of innovaitions and best manegement practices among dairy farmers in the eastern mediterranean region of Turkey. – Journal of Animal and Veterinary Advances 10(2): 251-261.

[13] Chambo, E. D., Garcia, R. C., Cunha, F., Carvalho, C. A. L., Caldas, M. J. M., da Silva, N. L. S., Ronqui, L., Junior, C. S., Santos, P. R., Toledo, V. A. A. (2018): Development of Beekeeping: An Analysis Using the Technique of Principal Components. – Chapter 4. In Insect Science-Diversity, Conservation and Nutrition.

[14] Cinemre, H. A., Demiryürek, K. (2005): Agricultural Extension and Communication. – Ondokuz Mayıs University Agricultural Faculty Department of Agricultural Economics, Text Book No:17; Samsun, 150p. (in Turkish).

[15] Çukur, T., Çukur, F. (2017): Fair organizations from the participating firms in the agricultural fairs perspective and its contributions on the local economy: the case of Milas 2. south aegean agricultural fair. – Atatürk Univ. J. of the Agricultural Faculty 48(2): 93-98. (in Turkish).

[16] Ertan, A., Gök, M. (2012): Analysis of the effective factors of Egirdir agricultural producers' decision process on having an agricultural insurance. – ODU Journal of Social Sciences Research 3(5): 66-76. (in Turkish).

[17] Everest, B. (2015): A Research on the Perception of Cooperative Principles and Analysis of Factors Affecting Member Participation in the Cooperative Management of Agricultural Credit Cooperatives: Case of Regional Union of Agricultural Credit Cooperative in

http://www.aloki.hu ● ISSN 1589 1623 (Print) ● ISSN 1785 0037 (Online)
DOI: http://dx.doi.org/10.15666/aeer/1705_1088310897

Balıkesir. – Phd. thesis. Ege University Graduate School of Natural and Applied Science, Department of Agricultural Economics, İzmir. (in Turkish).
[18] Fadare, S. O., Ojo, S. O., Imoudu, P. B. (2008): Analysis of production performance of beekeeping in the niger delta area of Nigeria. – APIACTA 37-48.
[19] Gebremariam, G., Tesfaye, W. (2018): The heterogeneous effect of shocks on agricultural innovations adoption: Microeconometric evidence from rural Ethiopia. – Food Policy 74: 154-161.
[20] Hosmer, D. W., Lemeshow, S. (2000): Applied Logistic Regression. – Wiley-Interscience Publication, 392p.
[21] Ibegbulem, J. A. (2014): Evaluation of Honey from Some States in Nigeria by the Determination of Pollen Spectra, Physico-Chemical Parameters, Anti-Bacterial Activity and Consumers' Acceptance. – Phd thesis (unpublished). Department of Biological Sciences, Ahmadu Bello Unıversity, Zaria.
[22] Ijatuyi, E. (2016): Analysis of information sources used by fish farmers in Ife central local government area of Osun-State, Nigeria. – J. Hum. Ecol. 56(1-2): 91-98.
[23] Jan, I., Khan, H., Jalaluddin, M. (2008): Analysis of agricultural extension system: a discrepancy between providers and recipients of the extension services empirical evidence from north-west Pakistan. – Sarhad J. Agric. 24(2): 349-354.
[24] Jensen, L. P., Picozzi, K., de Almeida, O. C., da Costa, M. J., Spyckerelle, L., Erskine, W. (2014): Social relationships impact adoption of agricultural technologies: the case of food crop varieties in Timor-Leste. – Food Sec. 6: 397-409.
[25] Kenea, W. (2008): Rural Livelihood, Land Management and Biodiversity Community Participation for Biodiversity Conservation The case of Kakamega Forest in Western Kenya. – Phd thesis (unpublished). Fac. of Spatial Planning, Univ. of Dortmund.
[26] Kızılaslan, N. (2009): Attitudes and behaviors of the farmers towards agricultural extension (Tokat province research Yesilyurt county). – Tübav Science 2(4): 439-445. (in Turkish).
[27] Kızılaslan, N., Ünal, Y. (2013): Detection of farmers' awareness for agricultural extension (Tokat/Erbaa Case). – Gaziosmanpaşa Journal of Scientific Research 5: 1-19. (in Turkish).
[28] Klerks, L., van Mierlo, B., Leeuwis, C. (2012): Evolution of systems approaches to agricultural innovation: concepts, analysis and interventions. – In: Darnhofer, I., Gibbon, D., Dedieu, B. (eds.) Farming Systems Research into the 21st Century: The New Dynamic. Springer, Dordrecht, pp. 457-483.
[29] Kolade, O., Harpham, T. (2014): Impact of cooperative membership on farmers' uptake of technological innovations in Southwest Nigeria. – Development Studies Research 1(1): 340-353.
[30] Kumar, Y. (2013): A Multi-Dimensional Study on Production and Management System of Apiculture Farming in Jammu Region. – Phd thesis (unpublished). Division of Agricultural Extension Education, Sher-e-Kashmir University, Jammu.
[31] Longo, R. M. J. (1990): Information transfer and the adoption of agricultural innovations. – J. of The American Soc. for Information Sci. 41(1): 1-9.
[32] Muktar, B. G., Ahungwa, G. T., Nasiru, A. (2016): Farmers perception on the benefit of extension services in Jigawa State, Nigeria. – International Journal of Applied Research and Technology 5(8): 24-30.
[33] Mutsvangwa-Sammie, E. P., Manzungu, E., Siziba, S. (2018): Key attributes of agricultural innovations in semi-arid smallholder farming systems in south-west Zimbabwe. – Physics and Chemistry of the Earth 105: 125-135.
[34] Newbold, P. (1995): Statistics for Business and Economics. – Prentice-Hall International, New Jersey, 867p.
[35] Okwu, O. J., Iorkaa, T. I. (2011): An assessment of farmers' use of new information and communication technologies as sources of agricultural information in ushongo local government area, Benue state, Nigeria. – Journal of Sustainable Developmnet in Africa 13(2): 41-52.

http://www.aloki.hu ● ISSN 1589 1623 (Print) ● ISSN 1785 0037 (Online)
DOI: http://dx.doi.org/10.15666/aeer/1705_1088310897

[36] Önder, H., Cebeci, Z. (2002): Variable Selection in Logistic Regression. – Journal of Çukurova University Agricultural Faculty 17(2): 105-114. (in Turkish).
[37] Özçatalbaş, O., Gürgen, Y. (1998): Agricultural Extension and Communication. – Baki Bookstore, Adana, 385p. (in Turkish).
[38] Özçatalbaş, N. (2000): An analysis of attitude and behaviours of farmers on agricultural information and extension in Şanlıurfa province. – Journal of Mediterranean University Agricultural Faculty 13(2): 203-211. (in Turkish).
[39] Özkaya, T. (1996): Agricultural Extension and Communication. – Ege University Agricultural Faculty Publications No: 520, Ege University Agricultural Faculty Offset Printing, İzmir, 170p. (in Turkish).
[40] Pandey, D. K., De, H. K., Upadhaya, A. D. (2014): Information sourcing and utilisation by fish farmers of Tripura State in north-east India. – Indian J. Fish. 61(3): 99-103.
[41] Peter, B. G., Messina, J. P., Frake, A. N., Snapp, S. S. (2018): Scaling Agricultural Innovations: Pigeonpea in Malawi. – The Professional Geographer 70(2): 239-250.
[42] Rogers, E. M. (1976): New product adoption and diffusion. – J. of Consumer Res. 2(4): 290-301.
[43] Rogers, E. M. (1983): Diffusion of Innovations. – The Free Press, New York, 453p.
[44] Sezgin, A. (2010): Impact analysis of the mass media tools on the adoption of the innovations in animal production: the case of Erzurum province. – Journal of the Faculty of Veterinary Medicine, Kafkas University 16(1): 13-19. (in Turkish).
[45] Sezgin, A., Kaya, T., Külekçi, M., Kumbasaroğlu, H. (2010): Impact analysis on the adoption of the innovations generated for agricultural production: the case of Erzurum province. – IX Agricultural Economics Congress in Turkey, Şanlıurfa, 557-564p. (in Turkish).
[46] Sıralı, R., Doğaroğlu, M. (2004): Determination of some occupational and sociological characteristics of Thracian beekeepers. – Uludag Bee Journal February: 35-41.
[47] TÜİK (Turkish Statistical Institute) (2018): Livestock statistics. – https://biruni.tuik.gov.tr/hayvancilikapp/hayvancilik.zul.
[48] Türkyılmaz, M. K., Bardakçıoğlu, H. E., Nazlıgül, A. (2003): Socio-economic factors affecting the adoption of innovations in dairy enterprises in Aydın. – Turk J. Vet. Anim. Sci. 27: 1269-1275. (in Turkish).
[49] Udofia, S. I., Edet, I. B. (2016): Assessment of adoption level of beekeeping practices in Ikot Udo Abia community, Akwa Ibom State, Nigeria. – Nigerian J. of Agric., Food and Env. 12(4): 98-104.
[50] Wangu, K. C. (2014): Use of Social Media as a Source of Agricultural Information by Small Holder Farmers; A Case Study of Lower Kabete, Kiambu County. – Msc thesis (unpublished). School of Journalism and Mass Communication, University of Nairobi.
[51] Wodajo, W. A. (2011): Financial benefits of box hive and the determinants of its adoption in selected district of Ethiopia. – American J. of Economics 1(1): 21-29.
[52] Wossen, T., Abdoulaye, T., Alene, A., Haile, M. G., Feleke, S., Olanrewaju, A., Manyong, V. (2017): Impacts of extension access and cooperative membership on technology adoption and household welfare. – Journal of Rural Studies 54: 223-233.
[53] Yalçın, M., Boz, I. (2007): Information sources of greenhouse growers in Kumluca district. – Garden 36(1-2): 1-10. (in Turkish).
[54] Yigezu, Y. A., Mugera, A., El-Shater, T., Aw-Hassan, A., Piggin, C., Haddad, A., Khalil, Y., Loss, S. (2018): Enhancing adoption of agricultural technologies requiring high initial investment among smallholders. – Technological Forecasting & Social Change 134: 199-206.
[55] Yurttaş, Z., Atsan, T. (2007): Agricultural Extension and Communication Techniques. – Atatürk University Agricultural Faculty Publications No: 67, Erzurum, 100p. (in Turkish).

http://www.aloki.hu ● ISSN 1589 1623 (Print) ● ISSN 1785 0037 (Online)
DOI: http://dx.doi.org/10.15666/aeer/1705_1088310897

EFFICACY OF THE SPIDER WEB METABOLITES ACTIVITY AGAINST MULTI DRUG RESISTANCE (MDR) BACTERIA

HAQ, I. U.[1] – QASIM, M.[1] – RAHIM, K.[2,3*] – AMEEN, F.[4] – DAWOUD, T.[4] – BASIT, A.[5] – MUNIR, S.[6] – ALSHEHREI, F.[7]

[1]*Department of Microbiology, Kohat University of Science and Technology (KUST), Khyber Pakhtunkhwa Kohat 26000, Pakistan*

[2]*Department of Microbiology, Cholistan University of Veterinary and Animal Sciences (CUVAS), Punjab, Bahawalpur 63100, Pakistan*

[3]*Beijing Key Laboratory of Genetic Engineering Drug and Biotechnology, Institute of Biochemistry and Biotechnology, College of Life Sciences, Beijing Normal University, Beijing 100875, China*

[4]*Department of Botany & Microbiology, College of Science, King Saud University, Riyadh 11451, Saudi Arabia*

[5]*State Key Laboratory of Agro-Biotechnology, College of Biological Sciences, China Agricultural University, Beijing, China*

[6]*Faculty of Plant Protection, Yunnan Agricultural University, Kunming 650201, Yunnan, China*

[7]*Department of Biology, Jumom College Umm Al-Qura University Makkah 21955, Saudi Arabia*

**Corresponding author*
e-mail: kashifrahim@cuvas.edu.pk, kashifbangash073@gmail.com

(Received 24th Mar 2019; accepted 2nd Jul 2019)

Abstract. Antibiotic resistance, which is emerging among pathogenic bacteria, is a leading cause of treatment failure worldwide with particular reference to developing countries. Thus, there is a need to explore and discover novel antimicrobial agents. The objective of this study was to investigate antibacterial activity of spider web metabolites and characterize certain antibacterial compounds. Web solvent extract (methanol, ethanol and acetone) was biologically screened for antibacterial activity against seven multiple drug resistant bacteria including three Gram negative bacteria (*E. coli, A. baumannii,* and *S. typhi*) and four gram positive bacteria (*S. aureus, Bacillus, E. faecalis and S. pneumonae*) using well diffusion test. Solvent extracts with the concentrations of (3.3 mg/ml 4.95 mg/ml 6.6 mg/ml 8.25 mg/ml 9.9 mg/ml and 11.55 mg/ml) were used to check the efficiency against MDR bacteria. Solvent extract of web metabolites exhibited significant activity against all seven MDR bacteria, by producing clear growth inhibition zones ranging in diameter from 04 to 22 mm. Considerable activities was exhibited against *E. faecalis* (22 mm), *E. coli* (14 mm) *and S. typhi* (15 mm). Acetone solvent extracts showed high antibacterial activity against most MDR bacteria. Solvent extracts with concentrations less than 5 mg/ml did not exhibit sufficient activity. Higher activities were related to concentrations higher than 6 mg/ml. Findings of the current study indicated that spider web metabolites may show promising antimicrobial activity against MDR bacteria. Additionally, the results suggest that spider web may be a broad spectrum antimicrobial agent, wherein its individual constituents contribute to its antimicrobial activity.
Keywords: *antibiotics resistance, antibacterial metabolites, solvent extracts, MDR, Pakistan*

Introduction

A lack of proper antimicrobial agents capable of controlling the incidence of infectious diseases is a major issue facing the health sector worldwide. An increase in

http://www.aloki.hu ● ISSN 1589 1623 (Print) ● ISSN 1785 0037 (Online)
DOI: http://dx.doi.org/10.15666/aeer/1705_1089910908

microbial diseases resistant to antibiotics has reached worrisome proportions in the biosciences field (Cassini et al., 2018). Discovery of the first antibiotic, followed by technological advances in antimicrobial drug research, led to the protection of millions from microbial diseases. In the history of antibiotics, the first ever contribution was made by Sir Alexander Fleming who, in 1928, discovered that Penicillin derived from molds was capable of inhibiting bacteria. Following the discovery of this highly appreciated antibiotic, several other antibiotics were also discovered and used to treat infectious diseases (Davies et al., 2010)**.** However, towards the end of the 1900s, emergence of antimicrobial resistant species together with the capacity for resistant gene transfer between species became a cause for major concern in the life sciences community (Amare et al., 2011). The Emergence of MDR bacteria capable of resisting antibiotics directly and indirectly is the direct result of all these factors. Furthermore, extensive use of antibiotics during the past few decades, led to the application of selective pressure on vulnerable bacteria, favouring the survival of resistant strains, few of which are resilient to more than one antibiotic (Arason et al., 2002).

The emergence of MDR bacterial species increased gradually over the years. Currently numerous studies have described various pathogenic bacterial species including *Salmonella typhi, Acinetobacter baumannii, Staphylococcus aureus, Enterococcus faecalis, Streptococcus pneumonae* and *Escherichia coli* as highly antimicrobial resistant. These bacteria, which cause many different infectious diseases, are resistant to multiple antibiotics and cannot be treated with traditional antibiotics as reported in many studies (Singhal, 2014; Doi, 2015; Da Silva, 2016; Megan, 2016; Nilsson, 2012; Wattanathum, 2003; Noble, 1992). These strains may be untreatable in the near future unless substitute or novel antimicrobials are developed. Novel antibiotics may be derived from natural sources such as plants, animals or their secretions in the form of molecules and compounds. Spider web metabolites comprise different molecules which appear to be antimicrobial according to studies (Vollrath et al., 2000). Spider silk is also attracting attention due to its antimicrobial properties. There have been unsubstantiated reports regarding the antimicrobial potential of spider silk (Wright et al., 2012). This report indicated that microbes were unable to grow on spider silk due to its acidic properties, suggesting that spider silk either prevented. Biofilm formation by microorganisms or were bacteriostatic or bactericidal in nature (Saleem et al., 2010). Additionally, bacteriostatic activity of spider silk has also been attributed to the presence of potassium nitrate, which inhibits the growth of microbes such as *Bacillus subtilis* and *E. coli* (Chakraborty et al., 2009). Antibacterial and antifungal activity of spider webs is mentioned in literature. However, antimicrobial potential of spider webs against multi drug resistant bacteria (MDR) has not yet been examined in Pakistan. Multi-drug resistant (MDR) organisms are a global threat. Antibiotic resistance accounts for hundreds of thousands of deaths annually (Johan et al., 2018). Spider web been traditionally used as an antiseptic in rural areas of Pakistan, while Atypus spider webs were used by people in the Carpathian Mountains as a topical antiseptic (Wright et al., 2012). This was considered to be helpful as a disinfectant.

The aim of this study was to investigate antibacterial activity of spider web metabolites and characterize certain antibacterial compounds. Different concentrations of web extract were used against previously identified MDR bacteria. This study will be helpful to kill drug resistant bacteria and discovery of the novel antibiotics.

http://www.aloki.hu ● ISSN 1589 1623 (Print) ● ISSN 1785 0037 (Online)
DOI: http://dx.doi.org/10.15666/aeer/1705_1089910908

Materials and methods

Sampling

The current study and sampling of web were done in the district Kohat, Khyberpakhtunkhwa, Pakistan. Previously identified and characterized clinical bacterial isolates of *Salmonella typhi, Staphylococcus aureus, Enterococcus faecalis, Acinetobacter baumannii, bacillus, Streptococcus pneumonae,* and *Escherichia coli* were recruited for this study. These previously identified isolates were basically from chronic wounds origin. The samples were forwarded for re-culturing and re-identification. Biochemical test used for identification are given in details in *Table 1*.

Table 1. *Biochemical identification of test isolates*

Pathogens	Cell morphology		Biochemical tests				
	Shape	Gram	Cat	Oxi	Ind	DNase	Cit
Bacillus	Rod	+ ve	+ ve	variable	-ve	-ve	+ ve
A. baumannii	Rod	-ve	+ ve	-ve	-ve	-ve	+ ve
S. Aureus	Cocci	+ ve	+ ve	-ve	-ve	+ ve	+ ve
S. Typhi	Rod	-ve	+ ve	-ve	-ve	-ve	-ve
E. coli	Rod	-ve	+ ve	-ve	+ ve	-ve	-ve
S. pneumonae	Cocci	+ ve	-ve	-ve	-ve	-ve	-ve
E. faecalis	Cocci	+ ve	+ ve	-ve	-ve	-ve	+ ve

S. aureus = *staphylococcus aureus, S. Typhi* = *salmonella typhi, S. Pneumonae* = *streptococcus Pneumonae, E. faecalis* = *Enterococcus faecalis.* Cat = catalase, Cit = citrate, Ind = indole, Oxi = oxidase

Antibiotic resistance patterns

Antibiotic resistance patterns of the isolates were determined via the Kirby-Bauer disk diffusion method (Bauer et al., 1966) according to the recommendations of the Clinical and Laboratory Standard Institute (CLSI) (Shallu et al., 2015). The isolates were treated with a total of 11 antibiotics as follows; Clarithromycin, Doxycycline, Cefoperazone sulbactam, Cefoxitin, Kanamycin, Nitrofurantoin, Penicillin, Levofloxacin, Ciprofloxacin, Oxacillin and Clarithromycin. Briefly, Mullen-Hinton agar was prepared. A 0.5 McFarland turbidity standard equivalent to inoculation of a bacterial suspension was prepared and inoculated. Following 48 h of incubation, the diameters of inhibition zones around the disks were measured using a graduated ruler and results were interpreted according to CLSI guidelines.

Collection, processing and metabolites of spider web

Spider webs were collected from garages and ceilings of unused buildings in the district of Kohat, Pakistan. Webs were washed with distilled water in the laboratory and cleansed of other redundant ingredients and dust. Clean and wrapped web was air-dried at room temperature and preserved in ampoules. Organic solvents, such as methanol, ethanol and acetone, were screened for possible extraction of web metabolites which were to be tested against MDR species or specific pathogens considered sufficiently important or suitable for exploration (Tshipamba et al., 2018).

http://www.aloki.hu ● ISSN 1589 1623 (Print) ● ISSN 1785 0037 (Online)
DOI: http://dx.doi.org/10.15666/aeer/1705_1089910908

Pure web metabolites were extracted using standard methodology. Pure web portions weighing 6 g each were introduced into falcon tubes, each containing 60 mL of acetone, methanol, ethanol and distilled water, and set on an orbital shaker at different angles for 2 weeks. After shaking liberated excessive amounts of metabolites, solvents were filtered into a beaker. The filtrate of solvent extract was placed in a large beaker and allowed to evaporate for one week. Following evaporation, the solidified extract was dissolved in 6 mL DMSO and kept it in sterile falcon tubes.

Screening of webs

Biological screening of antimicrobial properties of the web metabolites was performed via the well diffusion method. Muller Hinton Agar (MHA) media was used to assess susceptibility patterns of isolated bacteria by applying solvent extracts using well diffusion (Jaja et al., 2018).

Results

All isolates of *S. typhi, S. aureus, E. faecalis, A. baumannii, bacillus, S. pneumonae* and *E. coli* were re-identified via culture characterization, gram staining and biochemical testing.

Antimicrobial sensitivity pattern of bacterial isolates

Antimicrobial patterns of isolated bacterial pathogens were determined using 11 different antibiotic groups. *E. coli*, *S. typhi* and *A. baumannii* showed resistance to 7 antibiotics widely used against these pathogens, whereas *S. aureus* was resistant to 8 antibiotics. *S. pneumonae* was resistant to 6 antibiotics. However, *Bacillus* and *E. faecalis* were resistant to 6 antibiotics (*Table 2*). After confirming MDR patterns of these pathogens, aqueous acetone, ethanol, and methanol extracts of spider web were evaluated in *vitro* against *Acinetobacter, bacillus, S. aureus, S. typhi, E. faecalis, S. pneumonae* and *E. coli.*

Table 2. *Assessment of test isolates*

Antibiotics	*E. coli*	*E. faecalis*	*S. aureus*	*Bacillus*	*Acinetobacter*	*S. typhi*	*S. pneumonae*
Chloramphenicol (30 µg)	NA	R	R	I	NA	R	R
Clarithromycin (2 µg)	S	I	I	R	R	I	I
Oxacillin (5 µg)	S	R	R	R	R	R	R
Doxycycline (30 µg)	R	R	R	R	I	R	R
SCF (105 µg)	I	S	S	S	R	S	S
Cefoxitin (30 µg)	R	I	I	R	R	R	R
Kanamycin (30 µg)	R	I	R	R	R	R	R
Nitroforantoin (300 µg)	I	R	R	I	I	I	I
Penicillin (6 µg)	R	R	R	R	R	R	R
Levofloxacin (5 µg)	R	S	S	S	I	S	S
Ciprofloxacin (5 µg)	S	S	R	S	R	S	I

R = Resistant, I = Intermediate, S = Sensitive, SCF = Cefoperazonesulbactum. NA = not applicable

http://www.aloki.hu ● ISSN 1589 1623 (Print) ● ISSN 1785 0037 (Online)
DOI: http://dx.doi.org/10.15666/aeer/1705_1089910908

Antimicrobial activity of solvent extract against MDR bacteria

A total of 6 trials were conducted to test the anti-MDR effects of web, using different solvent concentrations against each MDR bacterium. Following 24 h, a significant portion of 9.9 mg/ml and 11.55 mg/ml solvent extract concentrations showed prolific activity while those concentrations that were less than 9.9 mg/ml did not display sufficient activity. Activity was measured by zone of inhibition around the wells. The highest inhibition zone (22 mm) was recorded for *E. faecalis* while the lowest zone (04 mm) was formed against *E. coli* (*Fig. 1*).

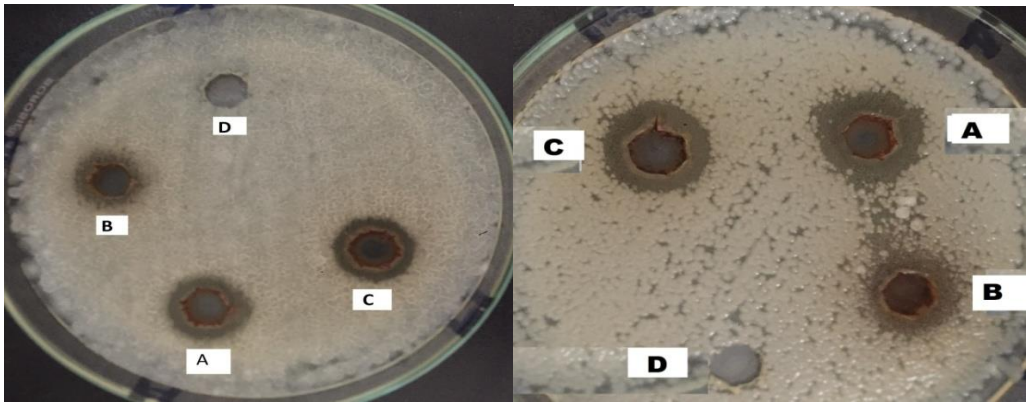

Figure 1. *Antimicrobial activity of the spider web was evaluated by means of well diffusion method by using different organic solvents acetone, ethanol and methanol as compared with control respectively (A, B, C and D). The web extract residues with different concentration (3.3 mg/ml 4.95 mg/ml 6.6 mg/ml 8.25 mg/ml 9.9 mg/ml and 11.55 mg/ml) showed promising activity. The presence of inhibition zones was measured, recorded and considered as indication for antibacterial activity. After 24 h a significant fragment of trials 9.9 mg/ml and 11.55 mg/ml solvent extract concentration showed proficient activity while the rest less than 9.9 mg/ml did not show enough activity. Activity was measured by zone of inhibition around the wells. The highest zone of inhibition (22 mm) was recorded for Enterococcus faecalis while lowest zone (04 mm) was formed against E. coli*

Anti-MDR bacterial potential of spider web metabolite extracts of the organic solvents acetone, ethanol, and methanol was analyzed. Solidified solvent extracts were dissolved in DMSO. An extract of distilled water was incorporated as the negative control**.** Results were described based on two parameters; organic solvents, and solvent extract concentrations.

Screening based on organic solvents

Spider silk was screened using different organic solvents to extract the web metabolites.

(i) Acetone

Acetone extract showed activity against all MDR bacteria, but higher activity was recorded against *E. coli, E. faecalis, and S. aureus*. The highest zone of inhibition (15 mm) was recorded for *E. coli,* whereas *E. faecalis, S. aureus, and S. typhi* each

http://www.aloki.hu ● ISSN 1589 1623 (Print) ● ISSN 1785 0037 (Online)
DOI: http://dx.doi.org/10.15666/aeer/1705_1089910908

exhibited 12 mm inhibitory zones on average. Inhibitory zones of 10, 09, and 07 mm were recorded for *Bacillus, S. pneumonae* and *A. baumannii,* respectively (*Table 3*).

Table 3. *Antimicrobial activity of web with the acetone extract*

Pathogens	Zone of inhibition (mm) of acetone extract					
	3.3 mg/ml	**4.95 mg/ml**	**6.6 mg/ml**	**8.25 mg/ml**	**9.9 mg/ml**	**11.55 mg/ml**
Bacillus	-	-	-	-	-	10
S. aureus	-	-	-	7	9	12
S. typhi	-	-	-	8	-	12
Acinetobacter	-	-	-	-	7	9
E. faecalis	-	-	-	13	13	13
E. coli	-	-	-	14	14	15
S. pneumonae	-	-	-	-	05	07

(ii) Ethanol

Ethanolic extract showed the highest inhibition zone (17 mm) against *bacillus.* The second highest zone of inhibition (15 mm) was recorded for *A. baumannii*. However, the inhibitory zones of *S. aureus, S. typhi* and *E. coli* were 12, 10 and 10 mm, while *S. pneumonae* showed resistance upto some extent, its zone of inhibition was 08 mm. *E. faecalis* appeared to be resistant to ethanol extract as shown (*Table 4*)

Table 4. *Antimicrobial activity of web with the ethanol extract*

Pathogens	Zone of inhibition (mm) of ethanolic extract					
	3.3 mg/ml	**4.95 mg/ml**	**6.6 mg/ml**	**8.25 mg/ml**	**9.9 mg/ml**	**11.55 mg/ml**
Bacillus	-	-	-	-	16	17
S. aureus	-	-	07	09	10	12
S. typhi	-	-	-	05	05	10
Acinetobacter	-	-	-	-	-	15
E. faecalis	-	-	-	-	-	-
E. coli	-	-	-	-	7	10
S. pneumonae	-	-	-	-	5	8

(iii) Methanol

The highest zone with methanol was recorded against *E. faecalis* (22 mm). Methanolic extracts showed average class inhibition zones against other MDR bacteria as follows; *S. aureus* (12 mm), *Bacillus* (13 mm), and *A. baumannii* and *S. typhi* 11 mm). The lowest inhibitory zones (06 mm) were recorded for *E. coli* and *S. pneumonae* (*Table 4*).

Screening based on solvent concentration

Web solvent extracts with the following solvent concentrations were tested; 3.3 mg/ml, 4.95 mg/ml, 6.6 mg/ml, 8.25 mg/ml, 9.9 mg/ml and 11.55 mg/ml. Sufficient activity was recorded only for concentrations ranging from 9.9 to 11.55 mg/ml.

http://www.aloki.hu ● ISSN 1589 1623 (Print) ● ISSN 1785 0037 (Online)
DOI: http://dx.doi.org/10.15666/aeer/1705_1089910908

(i) Inhibition zones with 11.55 mg/ml

The highest inhibition zone (22 mm) was recorded for the concentration of 11.55 mg/ml for *E. faecalis* with the methanolic extract, whereas the second highest zone of inhibition was recorded for *Bacillus* (17 mm) with the ethanolic extract. Both *A. baumannii* and *E. coli* showed 15 mm inhibitory zones while the pathogens *S. aureus* and *S. typhi* showed zones of 12 mm. Additionally, *S. pneumonae* showed a10 mm zone (*Table 4*).

(ii) Inhibition zones with 9.9 mg/ml

Solvent extracts with concentrations of 9.9–11.55 mg/ml showed high efficiency. The highest inhibition zone (16 mm) was recorded for *Bacillus* with ethanolic extract. *E coli* appeared to be more susceptible to acetone extract of 9.9 mg/ml as it produced a zone of 14 mm. Another high inhibition zone (13 mm) was recorded for *E. faecalis,* while11 mm inhibitory zones were observed against *S. typhi and S. aureus* and 06 and 07 mm inhibitory zones were recorded for *A. baumannii* and *S. pneumonae,* respectively (*Tables 3, 4* and *5*).

Table 5. *Antimicrobial activity of web with the methanol extract*

Pathogens	Zone of inhibition (mm) of methanol extract					
	3.3 mg/ml	4.95 mg/ml	6.6 mg/ml	8.25 mg/ml	9.9 mg/ml	11.55 mg/ml
Bacillus					10	12
S. aureus					11	13
S. typhi	-	-	-	07	11	11
Acinetobacter	-	-	-	-	-	11
E. faecalis	-	-	-	-	08	22
E. coli	-	-	-	-	04	06
S. pneumonae	-	-	-	-	06	06

Discussion

Accessibility to various antibiotics following the initial discovery of penicillin, initiated great enthusiasm in modern medicine (Sulaiman et al., 2014). The discovery of antimicrobials was one of the noteworthy discoveries in the history of microbial diseases. Following the discovery of antibiotics, humans became mostly free of harmful, deadly diseases. As a result of this medical miracle, people are able to live safe and healthy lives (Levy and Marshall, 2004). Currently, scientists are searching for natural sources of antibiotics that may help to develop antimicrobial agents against MDR bacteria. Novel antimicrobials have always been developed from natural sources. These sources may be microorganisms, plants and animals such as spiders and their metabolites. Spider silk is frequently cited as having antimicrobial properties in addition to several other scientifically verified biomedical properties (Chakraborty et al., 2009). Most studies on biomedical and mechanical properties of spider webs also mention their antimicrobial properties. Several studies describing antimicrobial properties of spider webs, may surface in literature reviews but these properties have not been tested against MDR bacteria. To our knowledge, this is the first study which addresses this crucial issue.

http://www.aloki.hu ● ISSN 1589 1623 (Print) ● ISSN 1785 0037 (Online)
DOI: http://dx.doi.org/10.15666/aeer/1705_1089910908

In this study, silk of common house spiders was investigated for its qualitative antimicrobial potential. Aqueous, acetone, ethanol and methanol web extracts were tested against MDR bacteria including *S. typhi, S. aureus, E. faecalis, A. baumannii, bacillus, S. pneumonae* and *E. coli.* We determined that silk from the common house spider may act as an antimicrobial agent under various *in vitro* conditions. The studies related to antimicrobial potential of spider silk has been previously reported (Saleem, 2010; Laxminarayan, 2003). Web solvent extracts appear to be effective against all the MDR bacteria. Maximum inhibitory effects of all bacteria corresponded to concentrations ranging from 9.9 mg/ml and 12.55 mg/ml following after 24 h incubation period.

The most significant inhibition zone (17 mm) corresponding to increased activity was recorded against *bacillus* following 24 h of incubation. However, after 24 h, activity was not significant and decreased. Web extracts showed significant activity against *E. coli*, *Bacillus, S. aureus* and *S. pneumonae* as indicated by the diameter of their inhibition zones, which confirmed the findings of other studies, in which inhibition zones were; *E. coli* (8 mm) *B. subtilis* (14 mm), *S. aureus* (16 mm) and for *Streptococcus* species (12 mm) (Wright et al., 2012).

Among all MDR bacteria tested, *S. aureus* appears to be susceptible to minimum concentrations as well as maximum concentrations of solvent extracts. *E. faecalis* appears to be resistant to all solvent extracts to some extent.

Spider silk comprises certain constituents having antimicrobial potential such as potassium hydrogen phosphate, compound potassium nitrate and amino acids. These amino acids display broad spectrum activity, especially against a diverse group of microorganisms, including gram positive and gram negative bacteria and fungi (Gomes et al., 2011). Antimicrobial peptides bind to the lipid bilayer membrane of bacteria. Through this interaction bactericidal peptides attain an amphiphilic three-D configuration whereby its positive side interacts directly with negatively charged lipid head-groups resulting in the formation of pores in the bacterial membrane (Havard, 2006).

Thereby**,** potassium hydrogen phosphate lowers pH to approximately 4 by releasing protons into the aqueous solution, causing it to turn acidic. Such low pH prevents microorganisms from digesting web constituents (Case et al., 1999). Consequently, microorganisms are unable to degrade the web easily. Potassium nitrate is a web constituent that prevents protein from denaturing in the acidic condition**.** Therefore, the above stated components make spider silk a good agent for preservation.

Spider silk constituents show potential as novel preservative agents which may be useful in food, pharmaceutical and diary industries, among others. These are efficient and moderately in expensive with increased shelf life and reduced side effects. Silk producing genes of spiders may be manipulated to obtain higher yields of better quality silk, which may be utilized for industrial purposes.

Conclusion

Spider web metabolites used in this study displayed promising antimicrobial activity against MDR bacteria. Results indicate that spider web may function as a broad spectrum antimicrobial agent. Individual components responsible for its antimicrobial activity should be evaluated via cell culture assays for toxicity, as well as via NMR and HPLC for their molecular structure.

http://www.aloki.hu ● ISSN 1589 1623 (Print) ● ISSN 1785 0037 (Online)
DOI: http://dx.doi.org/10.15666/aeer/1705_1089910908

Acknowledgements. This study was supported by King Saud University, Deanship of Scientific Research, College of Science Research Center.

Author contribution. All of the authors contributed equally in this project.

Conflict of interests. The authors confirm that this article content has no conflict of interests.

REFERENCES

[1] Amare, G. L., Abdurrahma, Z., Moges, B., Ali, J. S. (2011): Postoperative surgical site bacterial infections and drug susceptibility patterns at Gondar University Teaching Hospital, Northwest Ethiopia. – Journal of Bacteriology Parasitology 2: 126.

[2] Arason, V. A., Gunnlaugsson, A., Sigurdsson, J. A, Erlendsdottir, H., Gudmundsson, S., Kristinsson, S. (2002): Clonal spread of resistant pneumococci despite diminished antimicrobial use. – Microbiology Drug Resistance 8(3): 187-192.

[3] Bauer, A. W., Kirby. W. M., Sherris, J. C., Turck, M. (1966): Antibiotic susceptibility testing by a standardized single disk method. – American Journal of Clinical Pathology 45(4): 493-496.

[4] Case, S. T., Thornton, J. R. (1999): High molecular mass complexes of aquatic silk proteins. – International Journal of Biological Macromolecules 24(2-3): 89-101.

[5] Cassini, A., Colzani. E., Pini, A., Mangen, M. J., Plass, D., McDonald, S. A., Maringhini, G., Van, L. A., Haagsma, J. A., Havelaar, A. H., Kramarz, P. (2018): Impact of infectious diseases on population health using incidence-based disability-adjusted life years (DALYs): results from the Burden of Communicable Diseases in Europe study - European Union and European Economic Area countries 2009 to 2013. – Euro Surveillance 23(16).

[6] Chakraborty, D., Das, S. (2009): Antibacterial activities of cobweb protein. – Clinical Microbiology and Infection 4: S1-678.

[7] Da, Silva, G. J., Domingues, S. (2016): Insights on the horizontal gene transfer of carbapenemase determinants in the opportunistic pathogen *Acinetobacter baumannii*. – Microorganisms 4(3): 29.

[8] Davies, J., Davies, D. (2010): Origins and evolution of antibiotic resistance. – Microbiology Molecular Biology Reviews 74(3): 417.

[9] Doi, Y., Murray, G. L., Peleg, A. Y. (2015): *Acinetobacter baumannii:* evolution of antimicrobial resistance treatment options. – Seminars in Respiratory and Critical Care Medicenes 36: 85-98.

[10] Goms, S. C., Leonor, I. B., Mano, J. F., Reis, R. L., Kaplan, D. L. (2011): Antimicrobial functionalized genetically engineered spider silk. – Biomaterials 32(18): 4255-4266.

[11] Håvard, J., Pamela, H., Robert, E. W. (2006): Antimicrobial peptide agents. – Clinical Microbiology Reviews 19(3): 491-511.

[12] Jaja, I. F., Bhembe, N. L., Green, E., Oguttu, J., Muchenje, V. (2018): Molecular characterisation of antibiotic-resistant *Salmonella enterica* isolates recovered from meat in South Africa. – Acta Tropica 190: 129-136.

[13] Johan, B. P., Erik, K., Joakim, L. (2018): Environmental factors influencing the development and spread of antibiotic resistance. – FEMS Microbiology Reviews 42(1): fux053.

[14] Laxminarayan, R., Duse, A., Wattal, C., Zaidi, A. K., Wertheim, H. F., Sumpradit, N., Greko, C. (2013): Antibiotic resistance the need for global solutions. – Lancet Infectious Diseases 13(12): 1057.

[15] Levy, S. B., Marshall, B. (2004): Antibacterial resistance worldwide: causes, challenges and responses. – Nature Medicine 10(12s): S122.

[16] Megan, R. K., Alexander, E. P., Laynez, W., Annie, U. S., Sachinkumar, B. S., Timothy, D. S., Alexander, R. H. (2016): Development of an *in vitro* colonization model to

http://www.aloki.hu ● ISSN 1589 1623 (Print) ● ISSN 1785 0037 (Online)
DOI: http://dx.doi.org/10.15666/aeer/1705_1089910908

investigate *Staphylococcus aureus* interactions with airway epithelia. – Cell Microbiology 18(5): 720-731.

[17] Nilsson, O. (2012): Vancomycin resistant enterococci in farm animals - occurrence and importance. – Infection Ecology and Epidemiology 2. DOI: 10.3402/iee.v2i0.16959.

[18] Noble, W. C., Virani, Z., Cree, R. G. (1992): Co-transfer of vancomycin and other resistance genes from *Enterococcus faecalis* NCTC 12201 to *Staphylococcus aureus.* – FEMS Microbiology Letters 72(2): 195-198.

[19] Saleem, M., Nazir, M., Ali, M. S., Hussain, H., Lee, Y. S., Riaz, N., Jabbar, A. (2010): Antimicrobial natural products: an update on future antibiotic drug candidates. – Natural Product Reports 2 27: 238-254.

[20] Shallu, K., Pradeep, K. S., Cheshta, S., Anupam, P., Aradhana, M., Anil, K. J., Acques, F. M., Anuradha, C. (2015): Multidrug-Resistant *Candida auris* Misidentified as *Candida haemulonii*: Characterization by Matrix-Assisted Laser Desorption Ionization–Time of Flight Mass Spectrometry and DNA Sequencing and Its Antifungal Susceptibility Profile Variability by Vitek 2, CLSI Broth Microdilution, and Etest Method. – Journal of Clinical Microbiology 53(6): 1823-1830.

[21] Singhal, L., Gupta, P. K., Kale, P., Gautam, V., Ray, P. (2014): Trends in antimicrobial susceptibility of *Salmonella Typhi* from North India (2001-2012). – Indian Journal of Medical Microbiology 3(2): 149.

[22] Sulaiman, A. A., Milton, W., Tahani, A. A., Hashim, B. S., Asmaa, A. F., Arunachalam, C. (2014): What if Fleming had not discovered penicillin? – Saudi Journal of Biological Sciences 21(4): 289-293.

[23] Tshipamba, M. E., Lubanza, N., Adetunji, M. C., Mwanza, M. (2018): Molecular characterization and antibiotic resistance of foodborne pathogens in street-vended ready-to-eat meat sold in South Africa. – Journal of Food Protection 81(12): 1963-1972.

[24] Wattanathum, A., Chaoprasong, C., Nunthapisud, P., Chantaratchada, S., Limpairojn, N., Jatakanon, A., Chanthadisai, N. (2003): Community acquired pneumonia in Southeast Asia: the microbial differences between ambulatory and hospitalized patients. – Chest 123(5): 1512-1519.

[25] Wright, S., Goodacre, S. L. (2012): Evidence for antimicrobial activity associated with common house spider silk. – BMC Research Notes 5: 326.

[26] Vollrath, F. (2000): Strength and structure of spiders' silks. – Review Molecular Biotechnology 74(2): 67-83.

http://www.aloki.hu ● ISSN 1589 1623 (Print) ● ISSN 1785 0037 (Online)
DOI: http://dx.doi.org/10.15666/aeer/1705_1089910908

VALUATION OF WETLAND ECOSYSTEM SERVICES IN RAPIDLY URBANIZING REGION: A CASE STUDY OF THE NANJING JIANGBEI NEW AREA, CHINA

TANG, S.[1,2] – WANG, L. C.[1*] – WU, X. G.[1]

[1]*School of Geographic and Oceanographic Sciences, Nanjing University, Nanjing 210023, China*

[2]*Faculty of Humanities and Social Sciences, Jinling Institute of Technology, Nanjing 210038, China*

**Corresponding author*
e-mail: wang6312@263.net.cn; phone: +86-25-8359-3233

(Received 25th Mar 2019; accepted 2nd Jul 2019)

Abstract. Wetlands are considered as one of the most important ecosystems on the Earth. Rapidly urbanizing, being an intense way of human activities, has brought significant impact on the ecological functions of urban wetlands. This study focused on the urban wetland ecosystem in the Nanjing Jiangbei New Area, China, and presented a dynamic integrated approach to assess the monetized value of its services. A classification decision tree model was adopted to interpret the Landsat TM/ETM/OLI images to obtain the LUCC data of urban wetlands in different years. Then an integrated approach was employed to correct the equivalent values and their prices of various ecosystem services, dynamically evaluating the value of wetland ecosystem services. The results showed that the overall value of the wetland ecosystem services of the Jiangbei New Area was 893.99 million USD, 1365.63 million USD and 1016.46 million USD in 2002, 2009 and 2015, respectively. Among the service categories, the regulating service reaches the most and the provisioning service contributes the least to the total value. According to the analysis of annual valuation results, it was inevitable that the ecological conditions of wetlands in the rapidly urbanizing area would deteriorate and the capability to provide ecosystem services would degenerate. This research suggests that rapid urban development should adopt an ecosystem service oriented strategy to align sustainable utilization with conservation and to recognize the interaction between the wetland ecosystem services and the forces of urbanization.
Keywords: *LUCC, TCT, VTM, ecosystem services value, regulating services*

Introduction

As Millennium Ecosystem Assessment (MA) pointed, ecosystem services are the benefits people obtain from ecosystems. Every part of Earth produces a bundle of ecosystem services. These include provisioning services such as food and water; regulating services such as flood control; cultural services such as spiritual and recreational benefits; and supporting services, such as materials cycling (MA, 2003). All the services that the ecosystem provides maintain the conditions for life on Earth. Being known as the "kidney of the Earth", the wetland ecosystem is one of the most valuable ecosystems. As a significant land-water interacted ecosystem, the wetland provides us a multitude of benefits, including supply of materials, water storage, environmental protection, flood control, soil maintenance, climate regulation and maintenance of biodiversity, etc.(Keddy, 2010; Sharma et al., 2015; LePage, 2011). It also provides essential materials and ecological benefits to support life and economic growth in urbans and cities (Azous and Horner, 2000; Sullivan et al., 2014; Parker et al., 2018). As previous studies have shown, land-use and land-cover change (LUCC) caused

http://www.aloki.hu ● ISSN 1589 1623 (Print) ● ISSN 1785 0037 (Online)
DOI: http://dx.doi.org/10.15666/aeer/1705_1090910927

by human activities have significant impact on the urban wetland ecosystem (Zorrilla-Miras et al., 2014; Šabić et al., 2018). Around the globe, disorganized land use and development have led to a decrease in the total area covered by wetlands (Gardner et al., 2015), and to problems such as debilitated wetland structures and soil erosion, with urbanization exacerbating the decrease of wetland resources (Ehrenfeld, 2000; Kentula et al., 2014; MA, 2005; Davidson, 2014; Sica et al., 2016).

The impacts of human activities on ecosystems have increased rapidly in the last few decades. While a part of these activities can be considered beneficial to human well-being, there is increasing evidence of adverse effects, especially in areas with a concentrated population such as cities and urbans. Protection and recovery of urban wetland resources entails increased awareness of the ecological value of wetlands among the public, for which it is necessary the assessment of the value that wetland ecosystem services provide (Zhang et al., 2017a).

The concept of ecosystem services has been drawing more and more attention in the global community since the 1990s. On the basis of previous research (Costanza et al., 1997; Daily, 1997; Costanza and Mageau, 1999; De Groot et al., 2002; Costanza et al., 2014), MA put forward a guiding solution classifying ecosystem services into four categories: provisioning services, regulating services, cultural services and supporting services, and performed an assessment about them (MA, 2003, 2005a, b). Research on the value of ecosystem services provides an efficient tool to compare them and estimate the effect of environmental policies (McPherson, 1997; Tyrväinen and Miettinen, 2000; Jim and Chen, 2009). In this case, the assessments of urban wetland ecosystem services could specify the substantial contribution of this intricate system to human well-being. Meanwhile, the value-related studies also provide the conditions for the further research and practice of decision-making about urban wetland resources management.

According to existing publications, China has lost nearly 33% of its wetlands from 1978 to 2008 (Niu et al., 2012). The total area of wetlands in 2014 was 3.4 million hectares smaller than in 2003, an 8.82% decrease, and wetlands used for urban construction increased nearly tenfold (Geng, 2014). In recent years there have been efforts by Chinese researchers to probe into the field of valuation of wetland ecosystem services, with mainly focused on the comprehensive valuation of urban wetland ecosystem services, the value of ecosystem services of specific urban wetlands or the value of specific services, among others (Li and Wei, 2015; Xue et al., 2015; Cao et al., 2017; Zhang et al., 2017b, 2014, 2015a; Yang and Liu, 2018).

An assessment of the ecosystems services and their relation to human well-being requires an integrated approach. This enables a decision process to determine which service or set of services is valued most highly and how to develop approaches to maintain services by managing the system sustainably (MA, 2003). Nevertheless, due to limitations in data and research methodologies, research on dynamic monitoring of urban wetlands is still scarce, while in-depth quantitative and comparative studies on the value of ecosystem services are not available, making it difficult to provide a basis for urban planning and management (Zhang et al., 2017a). Based on previous methodologies published by Constanza et al (1997, 2014), Xie and other Chinese researchers optimized a unit area and equivalent value-based system, which is called Value Transfer Method (VTM), to assess the monetized value of ecosystem services (Xie et al., 2001, 2008, 2010, 2015a, b). This optimization was done to increase the reliability of the results and to provide a basis for building an efficient valuation system of ecosystem services of urban wetlands.

http://www.aloki.hu ● ISSN 1589 1623 (Print) ● ISSN 1785 0037 (Online)
DOI: http://dx.doi.org/10.15666/aeer/1705_1090910927

LUCC (land use/land cover change) analysis has already been recognized as an effective way to monitor changes in wetlands in a remote manner (Frohn et al., 2012). Through a discrimination method that combined the use of spectral information and supportive information, this study presents a comprehensive way that increases the precise level of land cover classification to improve accuracy of spatial information acquisition from the wetlands in research area. The study presented herein aims to develop an urban wetland ecosystem service valuation system based on the VTM combining modified equivalent values and LUCC data. It is an empirical study using the Nanjing Jiangbei New Area in the Jiangsu province in China as the study case.

Materials and methods

Research area

The Nanjing Jiangbei New Area in the Jiangsu province is located between 30°51′N and 32°27′N (latitude), 118°21′E and 119°03′E (longitude). It consists of three regions-Pukou District, Liuhe District and Baguazhou Sandbank, covering a total area of 2451 km^2, about 37% of the total of Nanjing (*Fig. 1*). With many rivers, polders and ponds, this area used to have abundant wetland resources which, however, were considerably reduced due to rapid urbanization and excessive reclamation. According to the "Overall Planning of Jiangbei New Area (2014-2030)", the urbanization rate of this new area is expected to reach 90% in 2030, while it was 66.3% in 2014, which means that urbanization initiatives will be accelerated and thus impose larger threats to the wetlands within the area.

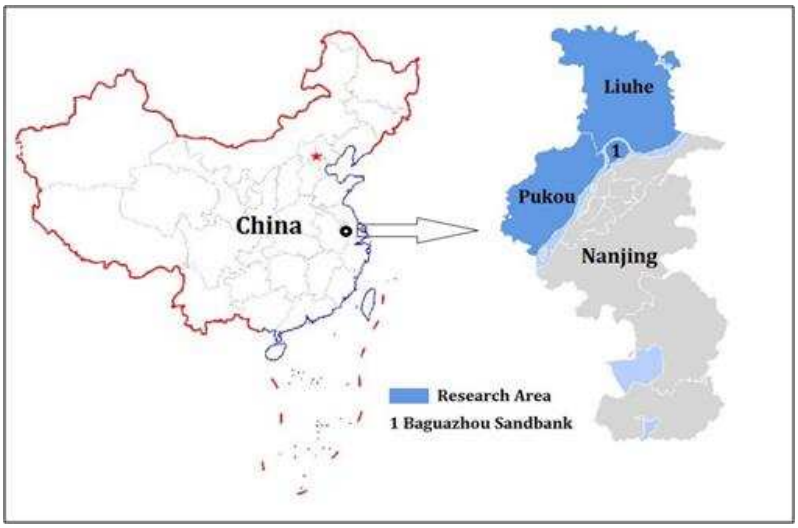

Figure 1. *The location of research area*

Remote sensing image processing

Data used in this study are remote sensing data collected in three periods during cloudless days in adjacent date (*Table 1*), including Landsat TM/ETM/OLI images captured in 2002, 2009 and 2015. The WGS-1984 coordinate system and the UTM projection are used to correct the images, and pre-processing steps including radiative correction, geometric correction and extraction of interested regions are taken before

http://www.aloki.hu ● ISSN 1589 1623 (Print) ● ISSN 1785 0037 (Online)
DOI: http://dx.doi.org/10.15666/aeer/1705_1090910927

utilization of the data. In light of the distribution of wetlands in the Jiangbei New Area and their main types, we took into consideration the features of valuation of remote images and put forward a system of classification of wetlands in the area (*Table 2*).

Table 1. *Remote sensing data source*

Satellite/sensor	Number of wavelengths	Resolution (m)	Date of obtain	Track number
Landsat7 ETM	7	30	2002-10-08	120/38
Landsat5 TM	8	30	2009-10-03	120/38
Landsat8 OLI	11	30	2015-09-02	120/38

Table 2. *Wetland classification system in research area*

Type of wetland	Main features
Lake wetland	A large area of planar water, including lakes, large reservoirs, etc.
River wetland	Regional permanent freshwater rivers
Pond wetland	Mainly refers to a small area of aquaculture water, irrigation reservoirs, etc.
Paddy fields	Mainly refers to paddy fields, also includes a small amount of cultivation of lotus root, artemisia and other aquatic plants arable land

Using spectral signatures, geometric features and environmental conditions of the main types of wetlands, our study followed the principle of "regional analysis followed by type recognition" and built a decision tree model of comprehensive indicators (*Fig. 2*).

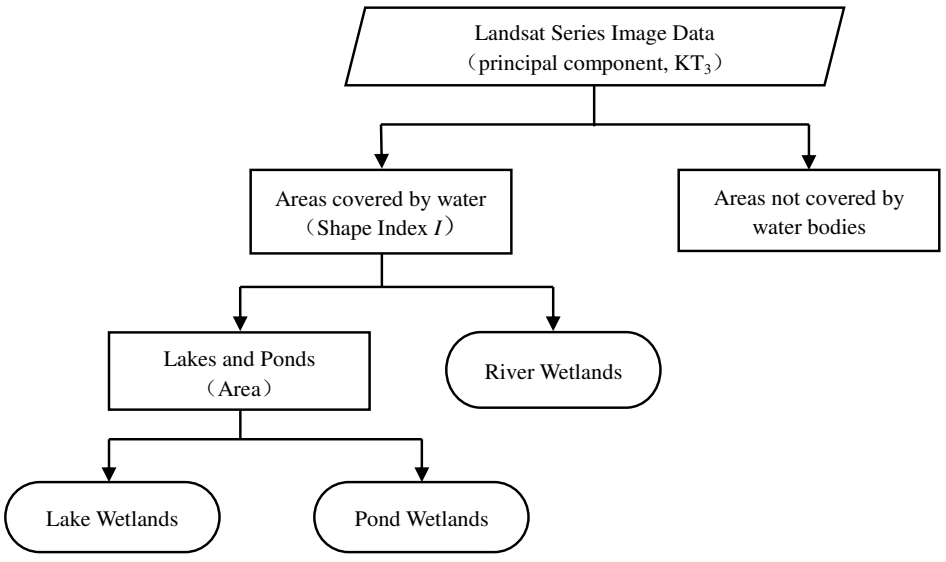

Figure 2. *Decision tree model for wetland information classification and extraction*

In the model, the Tasseled Cap transform (TCT), also known as Kauth–Thomas (K-T) transform, is performed to preprocess the images. The essence of TCT is similar to the principal component analysis by taking linear combinations of the original spectral

http://www.aloki.hu ● ISSN 1589 1623 (Print) ● ISSN 1785 0037 (Online)
DOI: http://dx.doi.org/10.15666/aeer/1705_1090910927

bands (Mostafiz and Chang, 2018). TCT is a widely used metric capable of capturing scene characteristics in related coordinate directions in a defined feature space and provides a mechanism for data volume reduction with minimal information loss and its spectral features can be directly associated with the important physical parameters of the land surface (Crist, 1985; Yarbrough et al., 2012). Consequently, the TCT conducting in TM imagery has been widely applied for ecological monitoring and other environmental studies, and its reliability and accuracy have been generally recognized (Zhang et al., 2002). In the studies of interpretation of land surface images, the TCT is usually employed to establish an automatic classification and recognition system (Thenkabail and Wu, 2012).

Valuation methods

Equivalent values

The MA definition follows Costanza and his colleagues in including both natural and human-modified ecosystems as sources of ecosystem services, and classify ecosystem services using categories of provisioning, regulating, cultural, and supporting services (MA, 2003). Among these services, 1) provisioning services refer to the products obtained from ecosystems, including food, fiber, wood, fresh water, etc.; 2) regulating services refer to the benefits obtained from the regulation of ecosystem processes, including gas regulation, climate regulation, soil erosion control, water purification and waste treatment, etc.; 3) cultural services are the nonmaterial benefits people obtain from ecosystems through spiritual enrichment, cognitive development, reflection, recreation, and aesthetic experiences, etc., 4) supporting services refer to those that are necessary for the production of all other ecosystem services, including primary production, production of oxygen, soil formation and retention, materials cycling and provisioning of habitat, etc.

Based on the previous studies, a basic equivalent system for ecosystem service value accounting is proposed by Xie and other Chinese researchers, within a basic idea of VTM (Xie et al., 2001, 2008, 2010, 2015a, b). Since 2008, the method has been optimized and improved many times, and its research adaptability has been fully proved. With the equivalent value per unit area of the ecosystem services set as the basis in the study (Xie et al., 2010, 2015), we could calculate the monetized value per unit area according to the price of the average national crop production. The equivalent values per unit area of different ecosystem services in 2015 are presented (*Table 3*).

Correction of equivalent values of water supply and flood control

Adapting to the specific situation of the study area, *Equation 1* is used to amend the equivalent values of two sub-category services, water supply and flood control. Considering both services are related to the hydrological processes of wetland ecosystems, the amount of precipitation is employed as a reliable modifying factor to amend the equivalent values.

$$R_i = W_i / \overline{W} \quad \text{(Eq.1)}$$

where R_i stands for the correction coefficient of equivalent values of water supply and flood control services in Region i, W_i refers to the annual precipitation in Region i, and $\overline{W}$ refers to the average annual precipitation in the whole nation.

http://www.aloki.hu ● ISSN 1589 1623 (Print) ● ISSN 1785 0037 (Online)
DOI: http://dx.doi.org/10.15666/aeer/1705_1090910927

Table 3. *Equivalent values of different ecosystems*

Ecosystem services		**Provisioning services**		**Regulating services**				**Supporting services**			**CS**
Category	Subcategory	MP	WS	GR	CR	WT	FC	SM	MC	BM	CS
Cropland	Dry field	1.25	0.02	0.67	0.36	0.10	0.27	1.03	0.12	0.13	0.06
	Paddy fields	1.45	-2.63	1.11	0.57	0.17	2.72	0.01	0.19	0.21	0.09
Forest	Coniferous	0.74	0.27	1.70	5.07	1.49	3.34	2.06	0.16	1.88	0.82
	Mixed	1.02	0.37	2.35	7.03	1.99	3.51	2.86	0.22	2.60	1.14
	Broad leaved	0.95	0.34	2.17	6.50	1.93	4.74	2.65	0.20	2.41	1.06
	Shrub	0.62	0.22	1.41	4.23	1.28	3.35	1.72	0.13	1.57	0.69
Grassland	Prairie	0.24	0.08	0.51	1.34	0.44	0.98	0.62	0.05	0.56	0.25
	Bush	0.94	0.31	1.97	5.21	1.72	3.82	2.40	0.18	2.18	0.96
	Meadow	0.55	0.18	1.14	3.02	1.00	2.21	1.39	0.11	1.27	0.56
Marshland	Marshland	1.01	2.59	1.90	3.60	3.60	24.23	2.31	0.18	7.87	4.73
Wilderness	Desert	0.04	0.02	0.11	0.10	0.31	0.21	0.13	0.01	0.12	0.05
	Bare land	0.00	0.00	0.02	0.00	0.10	0.03	0.02	0.00	0.02	0.01
Water area	River/lake	1.03	8.29	0.77	2.29	5.55	102.24	0.93	0.07	2.55	1.89
	Glacier snow	0.00	2.16	0.18	0.54	0.16	7.13	0.00	0.00	0.01	0.09

MP: Materials Production; WS: Water Supply; GR: Gas Regulation; CR: Climate Regulation; WT: Waste Treatment; FC: Flood Control; SC: Soil Maintenance; MC: Materials Cycling; BM: Biodiversity maintenance; CS: Cultural Services

Correction of equivalent value of soil maintenance

The ratio between the soil maintenance amount per unit area in the study regions and nationwide average level is taken as the correction coefficient of the equivalent value of the soil maintenance service. The equation is presented as *Equation 2:*

$$S_i = E_i / \bar{E} \quad \text{(Eq.2)}$$

where S_i stands for the correction coefficient of the equivalent value of soil maintenance in Region i, E_i refers to the soil maintenance amount per unit area in Region i, and $\bar{E}$ refers to the average amount of nationwide soil maintenance per unit area.

In most studies, the Universal Soil Loss Equation (USLE) is generally used to calculate the amount of soil erosion as it is a widely used mathematical model that describes soil erosion processes. The USLE was developed from erosion plot and rainfall simulator experiments. The USLE is composed of six factors to predict the long-term average annual soil loss in different situations. The equations take the simple product form as *Equations 3* and *4:*

$$SP_x = R_x \cdot K_x \cdot L \cdot S_x \cdot \quad \text{(Eq.3)}$$

$$SA_x = R_x \cdot K_x \cdot L \cdot S_x \cdot C_x \cdot P_x \quad \text{(Eq.4)}$$

where SP_x refers to the potential amount of average annual soil erosion, SA_x refers to the actual amount of average annual soil loss, while R_x, K_x, $L \cdot S_x$, C_x and P_x represent the rainfall erosivity factor, the soil erodibility factor, the land form factor, the land cover

http://www.aloki.hu ● ISSN 1589 1623 (Print) ● ISSN 1785 0037 (Online)
DOI: http://dx.doi.org/10.15666/aeer/1705_1090910927

and management factor and the land conservation measure factor, respectively. In addition, the potential amount of average annual soil erosion is a quantitative expression of the theoretical soil loss in the absence of vegetation and other management means.

According to *Equations 3* and *4,* we could obtain *Equation 5* to calculate average annual soil maintenance amount (SM_x):

$$SM_x = R_x \cdot K_x \cdot L \cdot S_x \cdot (1 - C_x \cdot P_x \quad \text{(Eq.5)}$$

Calculation of total values

The post-correction monetized value per unit area of each wetland ecosystem is calculated based on the equivalent values, the fundamental equivalent price and the correction coefficient. And the total value of ecosystem services is worked out based on the area of different types of wetlands in the research area. We first make calculations for different regions and then add them up to calculate the total value. The equation for this calculation is shown as *Equation 6:*

$$ESV = \sum A_{ki}\, m_{ki}\, n_{ki}\, C \quad \text{(Eq.6)}$$

where ESV refers to the amount of ecosystem services value (USD/a), A_{ki} refers to the area (hm^2) of Type *k* wetland in Region *i*; m_{ki} is the equivalent value of Type *k* wetland in Region *i*; n_{ki} is the correction coefficient of the equivalent value of Type *k* wetland in Region *i*, and C refers to the fundamental equivalent price of ecosystem services per unit area (USD/(hm^2·a)).

Results

LUCC data

Landsat images were often used to extract LUCC data, and land surface water is often identified by TCT (Mcfeeters, 1996; Chandrasekar et al., 2010; Adam et al., 2014; Fu and Burgher, 2015; Friedl et al., 2018). Meanwhile, the significant effectiveness of TCT in classification and extraction of wetland image has also been proved (Jiang et al., 2015; Luo and Tao, 2017; Mostafiz and Chang, 2018). The TCT method enhances the spectral information content of Landsat data for different implications of the earth's surface. Typically, there are three generally used dimensions in TCT, consisting by brightness (measure of soil), greenness (measure of vegetation), and wetness (measure of moisture) (Yarbrough et al., 2012; Adam et al., 2014; Fu and Burgher, 2015; Mostafiz and Chang, 2018). In this study, the water-covered areas were identified by the third principal component, KT_3 (wetness, mainly reflects the humidity information of ground objects), before extracting information of different types of wetlands according to the area and shape. Meanwhile, the area of paddy fields is taken as described from the yearbooks of Liuhe, Pukou and Baguazhou in different years. The results of the remote extraction and classification are shown below (*Figs. 3, 4* and *5*), and the areas of different types of wetlands are presented (*Table 4*).

Following the results from the extraction and classification of remote images from 2015, we identified the sampling sites through an stochastic method based on the proportion that each of the three types of wetlands (rivers, lakes and ponds) takes up in the total area of wetlands. On that basis, we verified the accuracy of extraction results

http://www.aloki.hu ● ISSN 1589 1623 (Print) ● ISSN 1785 0037 (Online)
DOI: http://dx.doi.org/10.15666/aeer/1705_1090910927

through comparison between the land use map and site surveying data. As the results of accuracy tests by the confusion matrix show, the classification accuracy rate of rivers and lakes are high, reaching 97.33% and 94.21%, respectively; while the extraction accuracy of ponds is lower, standing at 82.31%. The overall classification accuracy of the extraction results is 86.50% and the overall Kappa coefficient is 0.8433.

Table 4. *Area of wetlands in different years*

Wetland types	Regions	2002		2009		2015	
		Area (hm^2)	Proportion (%)	Area (hm^2)	Proportion (%)	Area (hm^2)	Proportion (%)
Lake wetland	Pukou	408.38	0.45	500.22	0.55	256.95	0.28
	Liuhe	2145.69	1.44	2658.78	1.79	2546.28	1.71
	Baguazhou	38.61	0.69	29.05	0.52	22.41	0.40
	Jiangbei	2592.68	1.06	3188.05	1.30	2825.64	1.15
River wetland	Pukou	274.54	0.30	598.05	0.66	222.66	0.24
	Liuhe	1222.34	0.82	1688.04	1.14	1038.33	0.70
	Baguazhou	69.70	1.24	107.64	1.92	69.54	1.24
	Jiangbei	1566.58	0.64	2393.73	0.98	1330.53	0.54
Pond wetland	Pukou	3114.59	3.42	3836.79	4.22	1493.73	1.64
	Liuhe	2061.59	1.39	3585.87	2.41	2076.12	1.40
	Baguazhou	46.85	0.84	46.77	0.84	32.22	0.58
	Jiangbei	5223.02	2.13	7469.43	3.05	3602.07	1.47
Paddy field	Pukou	9562.00	10.51	8566.33	9.41	8426.67	9.26
	Liuhe	26677.00	17.96	27300.00	18.38	26100.00	17.58
	Baguazhou	2333.00	41.66	2333.00	41.66	2333.00	41.66
	Jiangbei	38572.00	15.74	38199.33	15.59	36859.67	15.04
Total area	Pukou	13359.50	14.68	13501.39	14.84	10400.01	11.43
	Liuhe	32106.62	21.62	35232.69	23.73	31760.73	21.39
	Baguazhou	2488.16	44.43	2516.46	44.94	2457.17	43.88
	Jiangbei	47954.27	19.57	51250.54	20.91	44617.91	18.20

According to the interpretation results and relevant statistical data (*Figs. 3, 4,* and *5; Table 4*), during the three research periods, the total area of wetlands in Jiangbei New Area in 2002, 2009 and 2015 are 47954.27 hm^2, 51250.54 hm^2 and 44617.91 hm^2 respectively, accounting for 19.57%, 20.91% and 18.20% of the total land area respectively.

According to the dynamic change of the total wetland area in Jiangbei New Area, the total wetland area increased slowly during the period of 2002-2009 and decreased continuously during 2009-2015. On the basis of the long-term change from 2002 to 2015, the total wetland area decreased by 0.54% annually on average, showing a slowly decreasing trend on the whole. From 2002 to 2009, the area of other types of wetlands increased significantly except for paddy field wetlands, the most obvious increasing was shown as the average annual growth rate of river wetlands (7.54%) and pond wetlands (6.14%). From 2009 to 2015, by contrast, the area of all types of wetlands decreased relatively rapidly, and the average annual reduction rate of pond wetlands was the most significant (-8.63%).

http://www.aloki.hu ● ISSN 1589 1623 (Print) ● ISSN 1785 0037 (Online)
DOI: http://dx.doi.org/10.15666/aeer/1705_1090910927

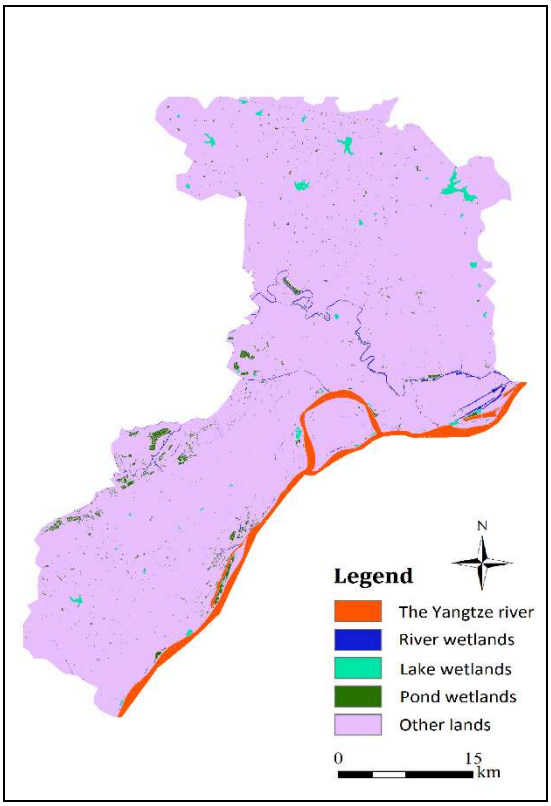

Figure 3. *Wetlands in the Jiangbei New Area (2002)*

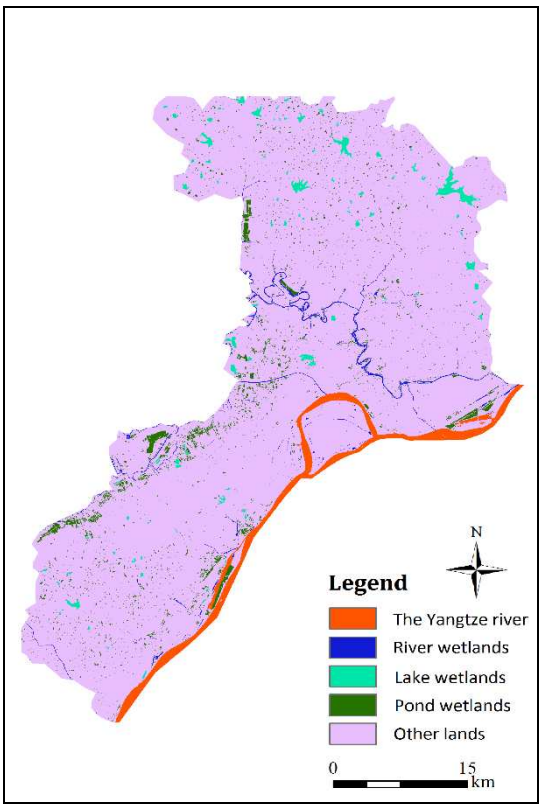

Figure 4. *Wetlands in the Jiangbei New Area (2009)*

http://www.aloki.hu ● ISSN 1589 1623 (Print) ● ISSN 1785 0037 (Online)
DOI: http://dx.doi.org/10.15666/aeer/1705_1090910927

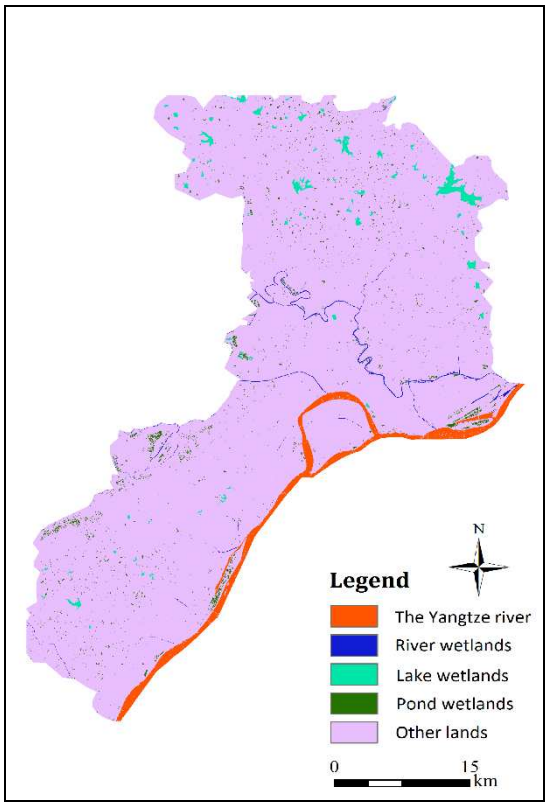

Figure 5. *Wetlands in the Jiangbei New Area (2015)*

Correction results

Fundamental equivalent price

Within the Value Transfer Method, the economic value of productivity per unit area of farmland is utilized as the basis of fundamental ecosystem service price calculating in unit area. Computation based on relevant data, the economic value of crops production per unit area in China in 2010 was 3406.5 RMB/hm^2 (Nie, 2011; Xie et al., 2015b; Zhang et al., 2016), converting to 503.21 USD/hm^2 according to the average exchange rate of RMB against US dollar in 2010 (6.7695). We obtained the corrected price of the standard equivalent by calculating the ratio between the value of crops production per unit area in Nanjing and the same value nationwide in 2010 (Nanjing Statistical Bureau, 2012), after which we then obtained a correction coefficient of 1.38. As a result, the economic value of the fundamental equivalent of ecosystem services per unit area in Nanjing was 4700.97 RMB/hm^2, converting to 694.43 USD/hm^2 according to the average exchange rate mentioned above.

Correction coefficients

Through the calculation of the ratio of annual precipitation in the Jiangbei New Area and the national average level, we obtained the correction coefficients for the equivalent values of the services of water supply and flood control (*Table 5*).

In 2010, the soil maintenance amount per unit area in China was 208.88 t hm^{-2} a^{-1} (Rao, 2015). The average soil erosion modulus (actual amount of average annual soil loss) in the Pukou District over several years was 2465 t km^{-2} a^{-1}, that in the Liuhe

http://www.aloki.hu ● ISSN 1589 1623 (Print) ● ISSN 1785 0037 (Online)
DOI: http://dx.doi.org/10.15666/aeer/1705_1090910927

District was 2357 t km^{-2} a^{-1} and 3546 t km^{-2} a^{-1} in the Baguazhou Sandbank, while the average *CP* value over those years in Nanjing was 0.0483 (Ma et al., 2011). Using *Equation 5* to calculate, we find that the average soil maintenance amount over those years in the Pukou is 485.70 t hm^{-2} a^{-1}, and that for the Liuhe and the Baguazhou Sandbank are 464.42 t hm^{-2} a^{-1} and 698.70 t hm^{-2} a^{-1}, respectively.

Table 5. *Correction coefficients of equivalent value of water supply and flood control services*

Year	Average annual precipitation in China	Annual precipitation & correction coefficients in Pukon		Annual precipitation & correction coefficients in Liuhe		Annual precipitation & correction coefficients in Baguazhou	
2002	660 mm	1083.6 mm	1.64	980.2 mm	1.49	1105.7 mm	1.68
2009	591.1 mm	1174.2 mm	1.99	1055.1 mm	1.78	1368.9 mm	2.32
2015	648.8 mm	1508.1 mm	2.32	1300.4 mm	2.00	1535.8 mm	2.37

Using the ratio between the average Soil maintenance amount in each region and the national average level, we calculated the correction coefficients of the equivalent value of the Soil maintenance service in the Pukou District, the Liuhe District and the Baguazhou Sandbank, which are 2.33, 2.22 and 3.34, respectively.

Valuation results

Using the previously stated *Equation 6* for the calculations, the results for the valuation of wetland ecosystem services in 2002, 2009 and 2015 in the Jiangbei New Area in Nanjing are presented (*Tables 6, 7* and *8*). The ecosystem services of wetlands in this area reached its highest value in 2009 at 1365.63 million USD, and reached its lowest in 2002 at 893.99 million USD, with the 2015 value of1016.46 million USD in the middle.

To sum up, the value of ecosystem services of wetlands in the Jiangbei New Area presents a variable trend: it moved up sharply from 2002 to 2009, with an annual increase rate of 7.50%, but underwent a tangible drop from 2009 to 2015, with an annual decrease rate of 4.26% (*Fig. 6*).

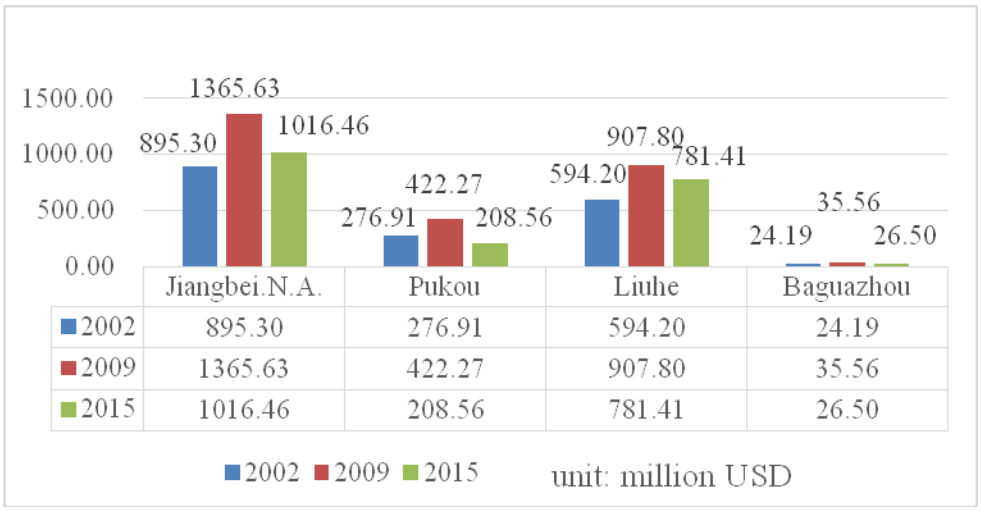

Figure 6. *Temporal change of wetland ecosystem services value in Jiangbei New Area*

http://www.aloki.hu ● ISSN 1589 1623 (Print) ● ISSN 1785 0037 (Online)
DOI: http://dx.doi.org/10.15666/aeer/1705_1090910927

Table 6. *Valuation results of wetland ecosystem services in Jiangbei New Area, 2002*

Category		Provisioning services		Regulating services				Supporting services			Cultural services
Subcategory		MP	WS	GR	CR	WT	FC	SM	MC	BM	CS
Lake	Pukou	1.98	26.10	1.48	321.89	4.40	10.65	4.36	0.13	4.90	3.63
	Liuhe	10.39	124.59	7.77	1536.60	23.10	55.98	21.92	0.71	25.72	19.06
	Baguazhou	0.19	2.53	0.14	31.18	0.42	1.01	0.59	0.01	0.46	0.34
	JNA	12.55	153.22	9.38	1889.67	27.91	67.64	26.87	0.85	31.08	23.04
River	Pukou	1.33	17.55	0.99	216.40	2.96	7.16	2.93	0.09	3.29	2.44
	Liuhe	5.92	70.98	4.42	875.36	13.16	31.89	12.48	0.40	14.65	10.86
	Baguazhou	0.34	4.56	0.25	56.28	0.75	1.82	1.07	0.02	0.84	0.62
	JNA	7.59	93.09	5.67	1148.04	16.86	40.87	16.49	0.52	18.78	13.92
Pond	Pukou	14.79	62.19	27.82	581.82	52.71	52.71	82.64	2.64	115.23	69.25
	Liuhe	9.79	37.40	18.41	349.89	34.89	34.89	52.30	1.74	76.27	45.84
	Baguazhou	0.22	0.96	0.42	8.96	0.79	0.79	1.79	0.04	1.73	1.04
	JNA	24.80	100.55	46.65	940.67	88.39	88.39	136.73	4.42	193.23	116.14
Paddy fields	Pukou	65.18	-193.88	49.90	200.52	25.62	7.64	1.10	8.54	9.44	4.05
	Liuhe	181.84	-491.44	139.20	508.25	71.48	21.32	2.93	23.83	26.34	11.29
	Baguazhou	15.90	-48.46	12.17	50.12	6.25	1.86	0.39	2.08	2.30	0.99
	JNA	262.92	-733.77	201.27	758.89	103.36	30.83	4.41	34.45	38.08	16.32
All	Pukou	83.27	-88.04	80.19	1320.62	85.68	78.17	91.03	11.40	132.86	79.37
	Liuhe	207.94	-258.46	169.81	3270.11	142.63	144.08	89.63	26.68	142.98	87.05
	Baguazhou	16.65	-40.41	12.98	146.54	8.21	5.48	3.84	2.16	5.33	2.99
	JNA	307.86	-386.92	262.98	4737.26	236.52	227.73	184.50	40.24	281.17	169.41
Total value		6060.77							(Unit: million RMB)		
		893.99 million USD, according to the average exchange rate of RMB against US dollar in 2010									

JNA: Jiangbei New Area; MP: Materials Production; WS: Water Supply; GR: Gas Regulation; CR: Climate Regulation; WT: Waste Treatment; FC: Flood Control; SC: Soil Maintenance; MC: Materials Cycling; BM: Biodiversity maintenance; CS: Cultural Services

Table 7. *Valuation results of wetland ecosystem services in Jiangbei New Area, 2009*

Category		Provisioning services		Regulating services				Supporting services			Cultural services
Subcategory		MP	WS	GR	CR	WT	FC	SM	MC	BM	CS
Lake	Pukou	2.42	38.79	1.81	478.43	5.38	13.05	5.34	0.16	6.00	4.44
	Liuhe	12.87	184.44	9.62	2274.63	28.62	69.37	27.16	0.87	31.87	23.62
	Baguazhou	0.14	2.63	0.11	32.39	0.31	0.76	0.45	0.01	0.35	0.26
	JNA	15.44	225.86	11.54	2785.46	34.32	83.18	32.95	1.05	38.22	28.33
River	Pukou	2.90	46.38	2.16	572.00	6.44	15.60	6.39	0.20	7.17	5.31
	Liuhe	8.17	117.10	6.11	1444.15	18.17	44.04	17.24	0.56	20.24	15.00
	Baguazhou	0.52	9.73	0.39	120.02	1.16	2.81	1.65	0.04	1.29	0.96
	JNA	11.59	173.21	8.66	2136.17	25.77	62.45	25.28	0.79	28.69	21.27
Pond	Pukou	18.22	92.96	34.27	869.69	64.93	64.93	101.80	3.25	141.95	85.31
	Liuhe	17.03	77.71	32.03	727.04	60.69	60.69	90.97	3.03	132.67	79.73
	Baguazhou	0.22	1.32	0.42	12.36	0.79	0.79	1.79	0.04	1.73	1.04
	JNA	35.46	172.00	66.72	1609.08	126.41	126.41	194.56	6.32	276.34	166.09

http://www.aloki.hu ● ISSN 1589 1623 (Print) ● ISSN 1785 0037 (Online)
DOI: http://dx.doi.org/10.15666/aeer/1705_1090910927

Paddy fields	Pukou	58.39	-210.76	44.70	217.97	22.95	6.85	0.98	7.65	8.46	3.62
	Liuhe	186.09	-600.79	142.45	621.35	73.15	21.82	3.00	24.38	26.95	11.55
	Baguazhou	15.90	-66.92	12.17	69.21	6.25	1.86	0.39	2.08	2.30	0.99
	JNA	260.38	-878.47	199.33	908.54	102.36	30.53	4.37	34.12	37.71	16.16
All	Pukou	81.93	-32.63	82.94	2138.10	99.71	100.43	114.52	11.26	163.57	98.70
	Liuhe	224.16	-221.55	190.22	5067.16	180.63	195.91	138.37	28.85	211.72	129.90
	Baguazhou	16.79	-53.24	13.09	233.98	8.51	6.22	4.27	2.17	5.67	3.24
	JNA	322.87	-307.41	286.25	7439.25	288.86	302.57	257.16	42.28	380.97	231.84
Total value		9244.62							(unit: million RMB)		
		1365.63 million USD, according to the average exchange rate of RMB against US dollar in 2010									

Table 8. *Valuation results of wetland ecosystem services in Jiangbei New Area, 2015*

Category		**Provisioning services**		**Regulating services**				**Supporting services**			**Cultural services**
Subcategory		MP	WS	GR	CR	WT	FC	SM	MC	BM	CS
Lake	Pukou	1.24	23.23	0.93	286.51	2.77	6.70	2.74	0.08	3.08	2.28
	Liuhe	12.33	198.46	9.22	2447.62	27.41	66.43	26.01	0.84	30.52	22.62
	Baguazhou	0.11	2.07	0.08	25.53	0.24	0.58	0.34	0.01	0.27	0.20
	JNA	13.68	223.76	10.23	2759.66	30.42	73.72	29.10	0.93	33.87	25.11
River	Pukou	1.08	20.13	0.81	248.28	2.40	5.81	2.38	0.07	2.67	1.98
	Liuhe	5.03	80.93	3.76	998.10	11.18	27.09	10.61	0.34	12.45	9.23
	Baguazhou	0.34	6.42	0.25	79.21	0.75	1.81	1.07	0.02	0.83	0.62
	JNA	6.44	107.48	4.82	1325.59	14.32	34.71	14.05	0.44	15.95	11.82
Pond	Pukou	7.09	42.19	13.34	394.73	25.28	25.28	39.63	1.26	55.26	33.21
	Liuhe	9.86	50.56	18.54	472.96	35.14	35.14	52.67	1.76	76.81	46.16
	Baguazhou	0.15	0.93	0.29	8.70	0.55	0.55	1.23	0.03	1.19	0.72
	JNA	17.10	93.68	32.17	876.39	60.96	60.96	93.53	3.05	133.26	80.09
Paddy fields	Pukou	57.44	-241.71	43.97	249.98	22.58	6.73	0.97	7.53	8.32	3.57
	Liuhe	177.91	-645.38	136.19	667.46	69.94	20.86	2.87	23.31	25.77	11.04
	Baguazhou	15.90	-68.36	12.17	70.70	6.25	1.86	0.39	2.08	2.30	0.99
	JNA	251.25	-955.44	192.34	988.14	98.77	29.46	4.22	32.92	36.39	15.59
All	Pukou	66.85	-156.15	59.05	1179.50	53.02	44.53	45.73	8.95	69.33	41.04
	Liuhe	205.12	-315.43	167.71	4586.14	143.66	149.52	92.15	26.25	145.55	89.05
	Baguazhou	16.50	-58.94	12.79	184.14	7.79	4.81	3.03	2.14	4.60	2.52
	JNA	288.48	-530.52	239.55	5949.78	204.47	198.85	140.90	37.34	219.47	132.62
Total value		9244.62							(unit: million RMB)		
		1016.46 million USD, according to the average exchange rate of RMB against US dollar in 2010									

The category-related components of ecosystem services of wetlands in the Jiangbei New Area are presented (*Table 9*). Among the presented components, the regulating service plays a vital role, taking up about 90% of the total value and even up to 95.81% in 2015, while the provisioning service contributes the least to the ecosystem services, with the proportion being negative in 2002 and 2015, accounting for the major losses in the ecosystem services of urban wetlands.

http://www.aloki.hu ● ISSN 1589 1623 (Print) ● ISSN 1785 0037 (Online)
DOI: http://dx.doi.org/10.15666/aeer/1705_1090910927

Table 9. *Category proportion of the wetland ecosystem services value*

Year	Provisioning services	Regulating services	Supporting services	Cultural services
2002	-1.30%	90.16%	8.35%	2.80%
2009	0.17%	89.96%	7.36%	2.51%
2015	-3.52%	95.81%	5.78%	1.93%

Discussion

The change and composition of value

The importance or "value" of ecosystems is viewed and expressed differently by different disciplines, cultural conceptions, philosophical views, and schools of thought (MA, 2003). The monetization of the value of ecosystem services is a more intuitively way to help people understanding the significance of ecosystem services to human well-being.

According to the valuation results, the value of ecosystem services of wetlands in the Jiangbei New Area reached 893.99 million USD, 1365.63 million USD and 1016.46 million USD in 2002, 2009 and 2015, respectively. In general, these results have the characteristics of temporal discretization, with notably changes in the values among different time periods, implicating a variable state of the wetland ecosystem. Among the three regions, Pukou shows the least stability with the sharpest and most obvious fluctuations over time. Consistent with findings of Zhang et al. (2015b), the change of wetland ecosystem service value is directly related to the change of land use pattern. Land use changes generally can be defined as a human-induced process that has great consequences for landscape and related ecosystems (Sawut et al., 2013).

Similar to the findings in Chaohu Lake Basin (Zhang et al., 2015b), the regulating service performances the core part of the ecosystem services of wetlands in study area. In this category, the flood control service has the highest value, which reflects the structural and functional stability of wetlands ecosystem is of vital importance for the ecological security in the Jiangbei New Area. Yet, the regulating services cannot be perceived or recognized directly by human observation. Located along the northern bank of the Yangtze River, the Jiangbei New Area is rich in precipitation and consists mainly of hilly lands; the landscapes and land covers have been largely damaged, leaving the area susceptible to inundation and waterlogging. Therefore, the regulating services, especially the flood control service, of the urban wetland ecosystem, deserves more attention as a key of the regional ecological security guarantee system.

The provisioning service contributes the least to the total value, with its contribution rate being negative in 2002 and 2015. This result is not consistent with the findings in Chaohu Lake Basin, Lakeside Wetland Park and other areas (Zhang et al., 2014, 2015b, 2017; Li and Gao, 2016). In previous research cases, the value calculation includes farmland, woodland and other types, so the provisioning service value is relatively high. Nevertheless, the land use type structure of our study area is different from that of lake basins, wetland parks or metropolis. Paddy fields and ponds wetland are the main components of production system in the study area. According to the calculation results, the value of the water supply service in 2015 was -78.37 million USD, mainly because the paddy fields take up the largest proportion in the total area of wetlands in the study area and these fields are largely water-consuming during the production process. Nonetheless, analysis of the hydrologic process of the paddy fields shows that these

http://www.aloki.hu ● ISSN 1589 1623 (Print) ● ISSN 1785 0037 (Online)
DOI: http://dx.doi.org/10.15666/aeer/1705_1090910927

fields are critical in water conservation (Xie et al., 2008) and, in particular, play an important role in underground water supply and water storage during floods; its function in water conservation has been included as a factor in the service type of flood control (Xie et al., 2015a, b). Therefore, respect to the direct benefits that humans receive from ecosystems, the water provisioning service of the paddy fields is obviously smaller compared to the water provisioning of other types of wetlands.

The impact of urbanization

Previous research has proved that regional massive urbanization had serious implications on the provision for ecosystem services, whether they be provisioning services or regulating services (Ai et al., 2015). Similarly, our research findings sufficiently proved that disorganized urbanization poses severe threats to the urban wetland ecosystem. A better understanding of the value of ecosystem services will facilitate protection and recovery of wetland resources in urban sprawl areas (Li et al., 2014). The rapidly urbanizing in Jiangbei New Are is acting as a violent form of human activity and causing obvious land use changes resulting in a great effect on the wetland ecosystem services.

According to this study, the area of wetlands in Pukou and the value of their ecological services witnessed a sharp drop between 2009 and 2015, because against the backdrop of fast urbanization driven by the planning of a new city center, wetlands were encroached and the original landscapes were destroyed, debilitating the ecosystem services. In the future, urban planners of Pukou should pay more attention to the ecological functions of urban wetlands, prevent the impertinently wetland occupying, protect and recover key wetlands and closely monitor wetland ecosystems in the city to build a stable ecosystem and support the development of the city center. Meanwhile, though there are no obvious losses in the value of ecosystem services of wetlands in Liuhe, protection and regional recovery of wetlands in this region should be given attention to maintain and improve the value of wetland ecosystem services. In particular, lake wetlands in the northern part of Liuhe and pond wetlands in the basin of the Chu River in the region's center should be protected and properly utilized to avoid severe value losses caused by future rapid urbanization, as Pukou has experienced.

Conclusion

This study has presented a dynamic model system to assess the value of ecosystem services of urban wetlands. Following the principle of "regional analysis followed by type recognition", our study developed a decision tree model for the automatic classification and extraction of remote images of urban wetlands. In addition, based on analysis of the spatial distribution and surrounding environment of urban wetlands, the model employed certain regulating factors to correct the fundamental price and the equivalent values, dynamically evaluating the value of wetland ecosystem services in different years in the research area. The study demonstrates that this approach is suitable for ecosystem services valuation in regional spatial scale and could accomplish a fast and convenient monitoring of the value of urban wetlands, supporting decision-making activities in urban management. Based on this study case, the application of VTM could be modified in other urban scale ecosystems.

The analysis empirically demonstrated that regional massive urbanization had serious implications on the provision for urban wetland ecosystem services. In the past period,

http://www.aloki.hu ● ISSN 1589 1623 (Print) ● ISSN 1785 0037 (Online)
DOI: http://dx.doi.org/10.15666/aeer/1705_1090910927

the local government of the Jiangbei New Area applied special stress on the construction of infrastructure in localized regions to pursue a high level of quality to the economy and urban development, yet ignored the effective protection of the wetlands ecosystem there. It was inevitable that the ecological conditions of wetlands in the rapidly urbanizing area would deteriorate and the capability to provide ecosystem services would degenerate.

The valuation results would also provide a more appropriate reference to decision makers, and draw more attention to the importance of wetland systems in the field of urban ecological security, seeking the synchronized development of human well-being and the nature. Specifically, the valuation can help the regional policy maker (i.e., government, community) to aware the value of ecological resources and formulate or adjust policies accordingly to protect and restore ecosystem services in one particular area. The results suggest that rapid urban development should adopt an ecosystem service oriented strategy to align sustainable utilization with conservation and to recognize the interaction between the wetland ecosystem services and the forces of urbanization. The local administrators and planners should pay enough attention to analysis the value change in and maintain the capability of wetland ecosystem services in urban area. There is an urgent need for conducting the conservation and rehabilitation of urban wetland as key policies in the regional planning, while scientific appraisal can serve as the basis for policy formulation and valuation. Therefore, to evaluate urban wetland ecosystems correctly and frequently is of great significance.

Acknowledgements. This research was financially supported by the Jiangsu University Philosophy and Social Science Fund Project (key subject) (Grant N0. 2018SJZDI092) and the Jiangsu University Philosophy and Social Science Fund Project (Grant No. 2017SJB0487).

REFERENCES

[1] Adam, E., Mutanga, O., Odindi, J., Abdel-Rahman, E. M. (2014): Land-use/cover classification in a heterogeneous coastal landscape using RapidEye imagery: evaluating the performance of random forest and support vector machines classifiers. – International Journal of Remote Sensing 35(10): 3440-3458.

[2] Ai, J. Y., Sun, X., Feng, L., Li, Y. F., Zhu, X. D. (2015): Analyzing the spatial patterns and drivers of ecosystem services in rapidly urbanizing Taihu Lake Basin of China. – Frontiers of Earth Science 9(3): 531-544.

[3] Azous, A., Horner, R. R. (2000): Wetlands and Urbanization: Implications for the Future. – CRC Press Inc., Boca Raton.

[4] Cao, Y., Tang, C. D., Ma, Q., Xue, J. H. (2017): Reevaluation of the value of wetland ecosystem services in Chongming County, Shanghai. – Journal of Nanjing Forestry University (Natural Science Edition) 41(1): 28-34.

[5] Chandrasekar, K., Sesha Sai, M. V. R., Roy, P. S., Dwevedi, R. S. (2010): Land Surface Water Index (LSWI) response to rainfall and NDVI using the MODIS vegetation index product. – International Journal of Remote Sensing 31(15): 3987-4005.

[6] Costanza, R., Mageau, M. (1999): What is a healthy ecosystem? – Aquatic Ecology 33: 105-115.

[7] Costanza, R., d' Arge, R., de Groot, R. S., et al. (1997): The value of the world's ecosystem services and natural capital. – Nature 387: 253-260.

[8] Costanza, R., de Groot, R. S., Sutton, P., et al. (2014): Changes in the global value of ecosystem services. – Global Environmental Change 26: 152-158.

http://www.aloki.hu ● ISSN 1589 1623 (Print) ● ISSN 1785 0037 (Online)
DOI: http://dx.doi.org/10.15666/aeer/1705_1090910927

[9] Crist, E. P. (1985): A TM Tasseled Cap equivalent transformation for reflectance factor data. – Remote Sensing of Environment 17(3): 301-306.
[10] Daily, G. C. (1997): Nature's Services: Societal Dependence on Natural Eco-Systems. – Island Press, Washington, DC.
[11] Davidson, N. C. (2014): How much wetland has the world lost? Long-term and recent trends in global wetland area. – Marine and Freshwater Research 65(10): 936-941.
[12] De Groot, R. S., Wilson, M. A., Boumans, R. M. J. (2002): A typology for the classification, description and valuation of ecosystem functions, goods and services. – Ecological Economics 41(3): 393-408.
[13] Ehrenfeld, J. G. (2000): Evaluating wetlands within an urban context. – Urban Ecosystems 4(1): 69-85.
[14] Friedl, M. A., McIver, D. K., Hodges, J. C. F., Zhang, X. Y., Muchoney, D., Strahler, A. H., Woodcock, C. E., Gopal, S., Schneider, A., Cooper, A., et al. (2002): Global land cover mapping from MODIS: algorithms and early results. – Remote Sensing Environment 83: 287-302.
[15] Frohn, R. C., D'Amico, E., Lane, C., Autrey, B., Rhodus, J., Liu, H. (2012): Multi-temporal sub-pixel Landsat ETM+classification of isolated wetlands in Cuyahoga County, Ohio, USA. – Wetlands 32(2): 289-299.
[16] Fu, B., Burgher, I. (2015): Riparian vegetation NDVI dynamics and its relationship with climate, surface water and groundwater. – Journal of Arid Environment 113: 59-68.
[17] Gardner, R. C., Barchiesi, S., Beltrame, C., Finlayson, C. M., Galewski, T., Harrison, I., Paganini, M., Perennou, C., Pritchard, D. E., Rosenqvist, A., Walpole, M. (2015): State of the World's Wetlands and Their Services to People: A Compilation of Recent Analyses. – Ramsar Briefing Note No. 7. Ramsar Convention Secretariat, Gland, Switzerland.
[18] Geng, G. B. (2014): The situation of wetland protection in China is not optimistic. – Green China 3: 8-11.
[19] Jiang, H., Liu, C., Sun, X., et al. (2015): Remote sensing reversion of water depths and water management for the stopover site of Siberian cranes at Momoge, China. – Wetlands 35(2): 369-379.
[20] Jim, C. Y., Chen, W. Y. (2009): Ecosystem services and valuation of urban forests in China. – Cities 26: 187-194.
[21] Keddy, P. A. (2010): Wetland Ecology: Principles and Conservation. – Cambridge University Press, Cambridge.
[22] Kentula, M. E., Gwin, S. E., Pierson, S. M. (2004): Tracking changes in wetlands with urbanization: sixteen years of experience in Portland, Oregon, USA. – Wetlands 24(4): 734-743.
[23] LePage, B. A. (2011): Wetlands: A Multidisciplinary Perspective. – In: LePage, B. A. (ed.) Wetlands. Springer, Dordrecht.
[24] Li, H. B., Wei, N. N. (2015): Spatial transfer process of urban wetland ecosystem services—a case of estuarine wetlands Quanzhou Bay. – Wetland Science 13(1): 98-102.
[25] Li, T. Gao, X. (2016): Ecosystem services valuation of Lakeside Wetland Park beside Chaohu Lake in China. – Water 8: 301.
[26] Li, X. W., Li, M. D., Liang, C., Zhuge, H. J. (2014): On the current key issues in wetland restoration. – Journal of Natural Resources 29(7): 1257-1269.
[27] Luo, K. S., Tao, F. L. (2017): Method for wetland type extraction using remote sensing combing object-oriented and tasseled cap transformation – Transactions of the Chinese Society of Agricultural Engineering 33(3): 198-203.
[28] Ma, L., Bu, Z. H., Peng, G. L., et al. (2011): Temporal and spatial variation of soil and water loss and its control in Nanjing area from 2001 to 2008. – Acta Pedologica Sinica 48(4): 683-692.
[29] McFeeters, S. K. (1996): The use of the Normalized Difference Water Index (NDWI) in the delineation of open water features. – International Journal of Remote Sensing 17(7): 1425-1432.

http://www.aloki.hu ● ISSN 1589 1623 (Print) ● ISSN 1785 0037 (Online)
DOI: http://dx.doi.org/10.15666/aeer/1705_1090910927

[30] McPherson, E. G., Nowak, D., Heisler, G., Rowntree, R. (1997): Quantifying urban forest structure, function, and value: the Chicago urban forest project. – Urban Ecosystem 1(1): 49-61.
[31] Millennium Ecosystem Assessment (MA) (2003): Ecosystems and Human Well-Being: A Framework for Assessment. – Island Press, Washington, DC.
[32] Millennium Ecosystem Assessment (MA) (2005a): Ecosystems and Human Well-being: Wetlands and Water Synthesis. – World Resources Institute, Washington, DC.
[33] Millennium Ecosystem Assessment (MA) (2005b): Ecosystems and Human Well-Being: Current State and Trends. – Island Press, Washington, DC.
[34] Mostafiz, C., Chang, N. B. (2018): Tasseled cap transformation for assessing hurricane landfall impact on a coastal watershed. – International Journal of Applied Earth Observation and Geoinformation 73: 736-745.
[35] Nanjing Statistical Bureau (2012): Nanjing Statistical Yearbook 2011. – Phoenix Publishing House, Nanjing.
[36] Nie, Z. B. (2011): China Foodstuff Yearbook 2011 – Economic Management Press, Beijing.
[37] Niu, Z. G., Zhang, H. Y., Wang, X. W., Yao, W. B., Zhou, D. M., Zhao, K. Y., Zhao, H., Li, N. N., Huang, H. B., Li, C. C., Yang, J., Liu, C. X., Liu, S., Wang, L., Li, Z., Yang, Z. Z., Qiao, F., Zheng, Y. M., Chen, Y. L., Sheng, Y. W., Gao, X. H., Zhu, W. H., Wang, W. Q., Wang, H., Weng, Y. L., Zhuang, D. F., Liu, J. Y., Luo, Z. C., Cheng, X., Guo, Z. Q., Gong, P. (2012): Mapping wetland changes in China between 1978 and 2008. – Chinese Science Bulletin 57(22): 2813-2823.
[38] Parker, K. A., Springall, B. T., Garshong, R. A., et al. (2018): Rapid increases in bat activity and diversity after wetland construction in an urban ecosystem. – Wetlands. https://doi.org/10.1007/s13157-018-1115-5.
[39] Rao, E. M. (2015): Soil Conservation Service Changes (2000-2010) and Its Influencing Factors of China's Ecosystem. – Chinese Academy of Science, Beijing.
[40] Šabić, D, Vujadinović, S., Stojković, S., Djurdjić, S. (2018): Urban development consequences on the wetland ecosystems transformations—case study: Pančevački Rit, Serbia. – Contemporary Problems of Ecology 11(2): 227-238.
[41] Sawut, M., Eziz, M., Tiyip, T. (2013): The effects of land-use change on ecosystem service value of desert oasis: a case study in Ugan Kuqa River Delta Oasis, China. – Canadian Journal of Soil Science 93(1): 99-108.
[42] Sharma, B., Rasul, G., Chettri, N. (2015): The economic value of wetland ecosystem services: evidence from the Koshi Tappu Wildlife Reserve, Nepal. – Ecosystem Service 12: 84-93.
[43] Sica, Y. V., Quintana, R. D., Radeloff, V. C., Cavier-Pizarro, G. I. (2016): Wetland loss due to land use change in the Lower Paraná River Delta, Argentina. – Science of the Total Environment 568: 967-978.
[44] Sullivan, P. L., Gaiser, E. E., Surratt, D., Rudnick, D. T., Davis, S. E., Sklar, F. H. (2014): Wetland ecosystem response to hydrologic restoration and management: The Everglades and its urban-agricultural boundary (FL, USA). – Wetlands 34(1): 1-8.
[45] Thenkabail, P. S., Wu, Z. T. (2012): An automated cropland classification algorithm (ACCA) for Tajikistan by combining Landsat, Modis, and secondary data. – Remote Sensing 4(10): 2890-2918.
[46] Tyrväinen, L., Miettinen, A. (2000): Property prices and urban forest amenities. – Journal of Environmental Economics and Management 39: 205-223.
[47] Xie, G. D., Lu, C. X., Cheng, S. K. (2001): Progress in evaluating the global ecosystem services. – Resources Science 23(6): 2-9.
[48] Xie, G. D., Zhen, L., Lu, C. X., Xiao, Y., Chen, C. (2008): Expert knowledge based valuation method of ecosystem services in China. – Journal of Natural Resources 23(5): 911-919.

http://www.aloki.hu ● ISSN 1589 1623 (Print) ● ISSN 1785 0037 (Online)
DOI: http://dx.doi.org/10.15666/aeer/1705_1090910927

[49] Xie, G. D., Zhen, L., Lu, C. X., Xiao, Y., Li, W. H. (2010): Applying value transfer method for eco-service valuation in China. – Journal of Resources and Ecology 1(1) 51-59.
[50] Xie, G. D., Zhang, C. X., Zhang, C. S., Xiao, Y., Lu, C. X. (2015a): The value of ecosystem services in China. – Resources Science 37(9): 1740-1746.
[51] Xie, G. D., Zhang, C. X., Zhang, L. M., Chen, W. H., Li, S. M. (2015b): Improvement of the evaluation method for ecosystem service value based on per unit are. – Journal of Natural Resources 8: 1243-1254.
[52] Xue, L. L., Yuan, X. Z., Wang, Y. H., He, B. L., Liu, F. B. (2015): Evaluation and analysis of the value of wetland ecosystem service in Chongqing. – Journal of Sichuan Forestry Science and Technology 36(5): 7-10.
[53] Yang, Q., Liu, G. Y. (2018): Wetland ecosystem services assessment based on emergy: a case of Pearl River delta urban agglomeration. – Acta Scientiae Circumstantiate 38(11): 4527-4538.
[54] Yarbrough, L. D., Easson, G., Kuszmaul, J. S. (2012): Proposed workflow for improved Kauth–Thomas transform derivations. – Remote Sensing of Environment 124(2): 810-818.
[55] Zhang, X. Y., Schaaf, C. B., Friedl, M. A., Strahler, A. H., Gao, F., Hodges, J. C. F. (2002): MODIS tasseled cap transformation and its utility. – IEEE International Geoscience and Remote Sensing Symposium 2: 1063-1065.
[56] Zhang, B., Shi, Y. T., Li, Q. X., Xie, G. D. (2017a): The key ecological services and their values of wetland ecosystems in Beijing. – Journal of Natural Resources 32(8): 1311-1324.
[57] Zhang, B., Shi, Y. T., Liu, J. H., Xu, J., Xie, G. D. (2017b): Economic values and dominant providers of key ecosystem services of wetlands in Beijing, China. – Ecological Indicators 77: 48-58.
[58] Zhang, X. H., Zhang, R., Wu, J., Zhang, Y. Z., Lin, L. L., Deng, S. H., Peng, H. (2016): An emergy evaluation of the sustainability of Chinese crop production system during 2000-2010. – Ecological Indicators 60: 622-633.
[59] Zhang, Y. R., Zhou, D. M., Niu, Z. G., Xu, F. J. (2014): Valuation of lake and marsh wetlands ecosystem services in China. – Chinese Journal of Geographical Sciences 24(3): 269-278.
[60] Zhang, Y. R., Zhou, D. M., Liu, M. (2015a): Ecosystem service valuation research of Chinese inland wetlands based on case study. – Acta Ecologica Sinica 35(13): 4279-4286.
[61] Zhang, Z., Gao, J. H., Gao, Y. N. (2015b): The influences of land use changes on the value of ecosystem services in Chaohu Lake Basin, China. – Environmental Earth Sciences 74(1): 385-395.
[62] Zorrilla-Miras, P., Palomo, I., Gómez-Bagghetun, E., Martín-López, B., Lomas, P. L., Montes, C. (2014): Effects of land-use change on wetland ecosystem services: a case study in the Doñana Marshes (SW Spain). – Landscape and Urban Planning 122: 160-174.

http://www.aloki.hu ● ISSN 1589 1623 (Print) ● ISSN 1785 0037 (Online)
DOI: http://dx.doi.org/10.15666/aeer/1705_1090910927

THE EFFECT OF DIFFERENT IRRIGATION PERIODS ON GROWTH INDICATORS OF SOME WEED SPECIES

ASADI, S.* – ABADI, H. R. M. D. C. – ASGARI, A. – ZADEH, P. S.

Faculty of Agriculture, University of Mohaghegh Ardabili, Ardabil, Iran

**Corresponding author*
e-mail: behtari@live.com

(Received 25th Mar 2019; accepted 12th Jul 2019)

Abstract. Environmental conditions have a great influence on the growth and development of weeds and, consequently, on their ability to compete, and changing these conditions can be effective in weed management. For this purpose, an experiment was carried out in 2016 and 2017 in the greenhouse of the Faculty of Agriculture and Natural Resources, University of Mohaghegh Ardabili, Iran. The studied factors were four weed species Red root pigweed (*Amaranthus retroflexus)*, Jimsonweed (*Datura stramonium)*, Russian knapweed (*Acroptilon repens* L*)* and Catchweed (*Setaria verticilata*) and three irrigation periods to field capacity (irrigation daily (control), irrigation once in every three days and irrigated once every six days). Results showed that with increasing irrigation period, Leaf Area Index (LAI), Relative Growth Rate (RGR), Weed Growth Rate (WGR), Net Assimilation Rate (NAR) and Total Dry Matter (TDM) decreased. The extent of decrease in growth indices was different between weeds C3 and C4. Total dry matter of Catchweed and Red root pigweed responded to increased irrigation periods less than others. In control irrigation, Jimsonweed growth indices were higher than other weeds, but to exert stress and increasing irrigation periods, Red root pigweed was more successful and a stronger competitor.
Keywords: *weeds management, environmental conditions, growth analysis, drought stress, irrigation period*

Introduction

Weeds are a hidden foe for crop plants, interfering with their functions and suppressing their growth and development. Hence, weeds have been documented as serious plant pests since the ancient times. Environmental factors influence weed growth and composition of arable weed species, therefore need more accurate estimations of the damage potential of arable weeds to develop effective weed control strategies while maintaining crop yield (Zimdahl, 2013; Peters et al., 2014). The purpose of the study of physiological characteristics is to describe or explain how the plant reacts to environmental conditions (Beech and Norman, 2002). One of the major problems in the production of agricultural products is the competition of weeds over growth resources, especially water stored in the soil (Monaco et al., 2002). In addition to weeds competition, drought stress is another factor in reducing production. Drought is one of the most important environmental stresses that has destructive and harmful effects on different plant growth stages, organ structure and activity (Eslami et al., 2012). In different experiments, humidity and temperature are mentioned as the most influential environmental factors on the growth of weed seedlings (Benvenuti et al., 2001). Results of Chauhan and Johnson (2010) showed that with increasing drought stress, the vegetative and reproductive characteristics of barnyard grass weed (*Echinochola cruss- galli L.*) decreased. Webster and Grey (2008) reported that under drought stress the biomass of *Commelina benghalensis* decreased. In research studies on the effect of irrigation periods (1, 3, 6, 9, 12 and 15 days) on weed growth characteristics of *Echinochloa colona* and *Rottboellia cochinchinensis*, it was found that

http://www.aloki.hu ● ISSN 1589 1623 (Print) ● ISSN 1785 0037 (Online)
DOI: http://dx.doi.org/10.15666/aeer/1705_1092910940

in general, with prolonging irrigation periods, height, number of leaves, number of stems, dry weight of shoot, root dry weight and seed production of these weeds decreased (Chauhan and Johnson, 2010 and Chauhan, 2013). Since changes in weeds growth indices have been considered less than environmental conditions change, so this experiment was conducted to evaluate the effect of irrigation periods on growth indices of Red root pigweed (*Amaranthus retroflexus)*, Jimsonweed (*Datura stramonium)*, Russian knapweed (*Acroptilon repens L)* and Catchweed (*Setaria verticilata*).

Materials and methods

The experiment was carried out as a factorial experiment based on randomized complete block design with five replications in the greenhouse of the Faculty of Agriculture and Natural Resources, University of Mohaghegh Ardebili, Iran during 2016 and 2017. The studied factors were four weed species; Red root pigweed (*Amaranthus retroflexus)*, Jimsonweed (*Datura stramonium)*, Russian knapweed (*Acroptilon repens L)* and Catchweed (*Setaria verticilata*) and three irrigation periods to field capacity (irrigation daily (control), irrigation once in every three days and irrigated once every six days). Weed seeds were collected from the surrounding farms. For planting nylon 12 L pots (26 × 36 cm) were filled with agricultural soil until sufficient growth conditions were provided for the roots. The amount of soil within each pot was 10 kg. The soil characteristics are shown in *Table 1*. Weed seeds were planted at a depth of 1 cm and immediately irrigated to field capacity. Roots of the same Russian knapweed were cultivated horizontally at a depth of 4 cm. Four pots were considered for each treatment in each replication, in order to destructive sampling. After germination of seeds, different irrigation periods were performed. Sampling started from the four-leaf stage of the plants and repeated once every 10 days. For this purpose, the plants were cut from soil surface, and after measuring the leaf area and their number, they were dried in an oven for 48 h at 75 °C. The roots were also separated from the soil by washing and their weight and length were measured. The length of the root was measured by measuring the longest root length with a ruler. Also, in measuring root dry weight, the root system of the plant was washed after being placed in an oven with a numerical scale of 0.001. To exit healthy roots, the soil is poured into nylon pots, at the end of the work, the pots were placed in the water pond and the root soil was washed out. For the above characteristics, analysis of variance and comparison of mean of cultivars were performed using SAS software.

Table 1. *Soil physical and chemistry properties*

pH	EC (Ms/cm)	OM %	Soil texture	Clay	Silt	Sand
7.8	366	1.74	Clay loam	36.72	34.56	28.72

Growth analysis parameters such as Total Dry Matter (TDM), Relative Growth Rate (RGR), Weed Growth Rate (WGR), Leaf Area Index (LAI), and Net Assimilation Rate (NAR) were measured using the following relationships (Rosal et al., 1984), and the charts were drawn with the help of Excel software.

$$TDM = e^{(a1 + b1t + c1t2 + d1t3)} \quad \text{(Eq.1)}$$

http://www.aloki.hu ● ISSN 1589 1623 (Print) ● ISSN 1785 0037 (Online)
DOI: http://dx.doi.org/10.15666/aeer/1705_1092910940

where TDM, total dry matter (g/m^2), was obtained by weighing the total dry matter of the plant in square meter.

$$LAI = e^{(a2 + b2t + c2t2 + d2t3)} \quad \text{(Eq.2)}$$

where LAI: leaf area index, by measuring the leaf area with the help of the device leaf area meter, and was calculated using the formula LAI = LA / P.

$$LDW = e^{(a3 + b3t + c3t2 + d3t3)} \quad \text{(Eq.3)}$$

where LDW: Green leaf dry weight (g or mg). Weight of green leaves dried in the oven, also, whose surface was calculated, weighed and noted. The other growth indices were calculated with the help of the following values.

$$WGR = RGR \times TDM \quad \text{(Eq.4)}$$

where WGR: Weed growth rate ($g\ m^{-2}\ d^{-1}$).

Weed growth rate is the derivative function of the total dry matter in unit of time (t) or multiplication RGR in TDM.

$$WGR = (b1 + 2c_1t + 3d_1t^2)\ e^{(a1 + b1t + c1t2 + d1t3)}$$
$$RGR = TDM/CGR \quad \text{(Eq.5)}$$

where RGR: Relative growth rate ($gg^{-1}d^{-1}$). Relative growth rate is the derivative of natural logarithm function of total dry matter in unit of time (t) or the result is the division of TDM on CGR.

$$Ln\ TDM = a1 + b1t + c1t2 + d1t3$$
$$RGR = b1 + 2c1t + d1/2t3 \quad \text{(Eq.6)}$$
$$NAR = CGR/LAI$$

where NAR: net assimilation rate ($gm^{-2}\ d^{-1}$).

$$NAR = (b1 + 2c1 + 3d1t2)\ e^{(a1-a2) + (b1-b2)\ t + (c1-c2)\ t2 + (d1-d2)\ t3}$$

Results and discussion

Weeds growth rate (WGR)

The results showed that WGR was affected by irrigation periods and for all weed species was at its peak for the first irrigation periods (control) in both 2016 and 2017 years in Jimsonweed 7.5 and 8.5 $g.m^2$ d, red root pigweed 5.5 and 6.2 $g.m^2$. d, Russian knapweed 4 and 4.3 $g.m^2$. d and Catchweed 3.3 and 2.9 g.m2. d. Regarding the logical and direct relationship between LAI and WGR, these results were consistent with the results obtained for LAI and showed that drought stress affects leaves development, dry matter production and growth rate. The changes trend in the growth rate of weeds in all treatments was relatively similar (*Fig. 1*). In control irrigation, WGR collapsed after reaching its peak at (45 to 54) days after planting the examined species. But for the second irrigation period the start of WGR collapse happens on 32-40 days, and for the

http://www.aloki.hu ● ISSN 1589 1623 (Print) ● ISSN 1785 0037 (Online)
DOI: http://dx.doi.org/10.15666/aeer/1705_1092910940

third irrigation period on 30 to 32 days. It seems that weeds, under severe water shortages, take action by falling leaves to reduce evapotranspiration, before reaching their maximum growth, and thus lose their Carbohydrate factory. As can be viewed, WGR decreases in the third irrigation period earlier than another period. Investigating *Figure 1* shows that there is a difference between the four weed species in terms of WGR. In the irrigation control, Jimsonweed has a maximum growth rate. The reason for this can be pointed out the high level of leaf area index, which that caused the sunlight more and better to use. Jimsonweed retains its leaf area, it showed more ability to reach maximum WGR, because it makes more carbohydrates and receives better radiation. Whatever growth rate of the weed has, its ability is increased to compete with the crop. Because in this case, weed can more effectively overcome the canopy of the crop and maximize the use of limited resources available (Sadeghi et al., 2009). By increasing the irrigation period, the amount of CGR in weeds decreased. Nevertheless, the extent of this reduction is accompanied by some changes. As can be seen in *Figure 1,* by applying stress and increasing the irrigation period, the decrease in the growth rate of Jimsonweed and Russian knapweed weeds is greater than that is of Red root pigweed and Catchweed. In fact, it is quickly impacted by stress. This can be attributed to the fact that the two weeds are C3 plants. In fact, under conditions of water shortage and drought stress, C3 weeds have less competitive power than C4 weed (Sadeghi et al., 2009). From among the two weeds of the C4, Red root pigweed has a high resistance to stress. With regard to the direct relationship between WGR and LAI, it can be concluded that red root pigweed with a high leaf area can reach to a high WGR, because it makes more carbohydrates with the receipt of better radiation (Karim Zadeh Asl et al., 2004).

Therefore, it can be concluded that Jimsonweed can be problematic in the field under stressless conditions and continuous irrigation or regular rainfall, but if rainfall reduces or irrigation is low, the weeds flora will be changed and red root pigweed will be problematic. Also, it was found out that the weed growth rate is important at the time of applying a weed management strategy, including the use of herbicides.

$$WGR = (b1 + 2c1t + 3d1t2)\, e(a1 + b1t + c1t2 + d1t3)$$

$$WGR = RGR \times TDM$$

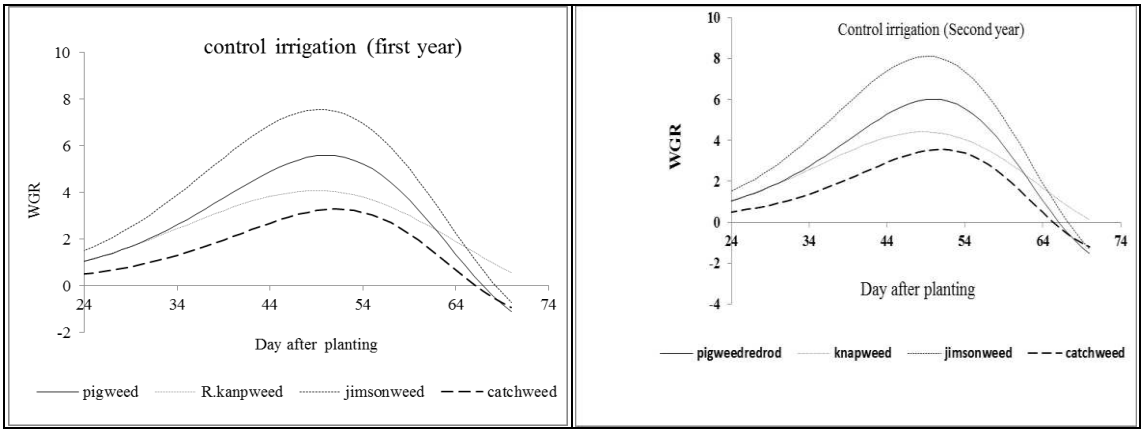

http://www.aloki.hu ● ISSN 1589 1623 (Print) ● ISSN 1785 0037 (Online)
DOI: http://dx.doi.org/10.15666/aeer/1705_1092910940

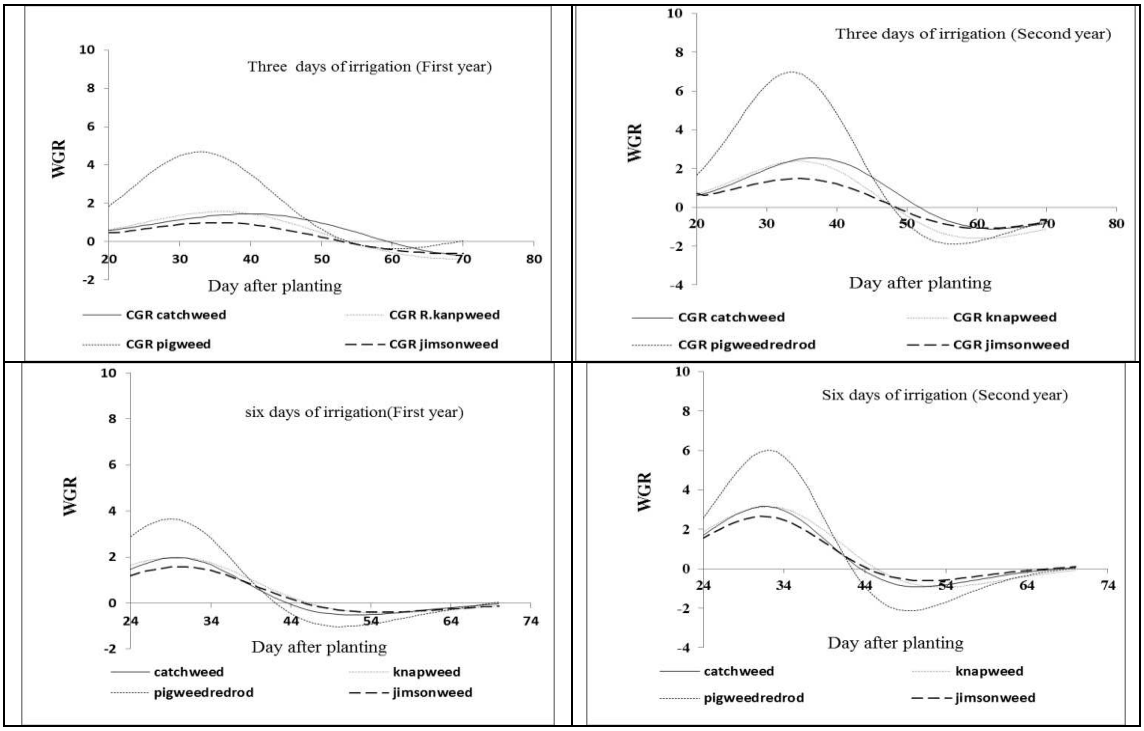

Figure 1. *The effect of irrigation period on the changes trend in weed growth rate during the growing season*

Total dry matter (TDM)

The results showed that in two years of experimentation, weed total dry matter declined with increasing irrigation period (*Fig. 2*). In all of the sampling, in the two years, Jimsonweed had the highest total dry matter (100 and 110 g per plant) in irrigation control. With increasing irrigation period (3 and 6 days) and applying drought stress and water shortage conditions, decreasing of Jimsonweed total dry matter was more intense. Catchweed and Red root pigweed total dry matter, changed less afoul and declined under stress conditions. This can be attributed to the fact that the two weeds are C4 plants. In fact, C3 weeds have less competitive power than weed C4 under conditions of water shortage and drought stress.

$$TDM = e^{(a1 + b1t + c1t2 + d1t3)}$$

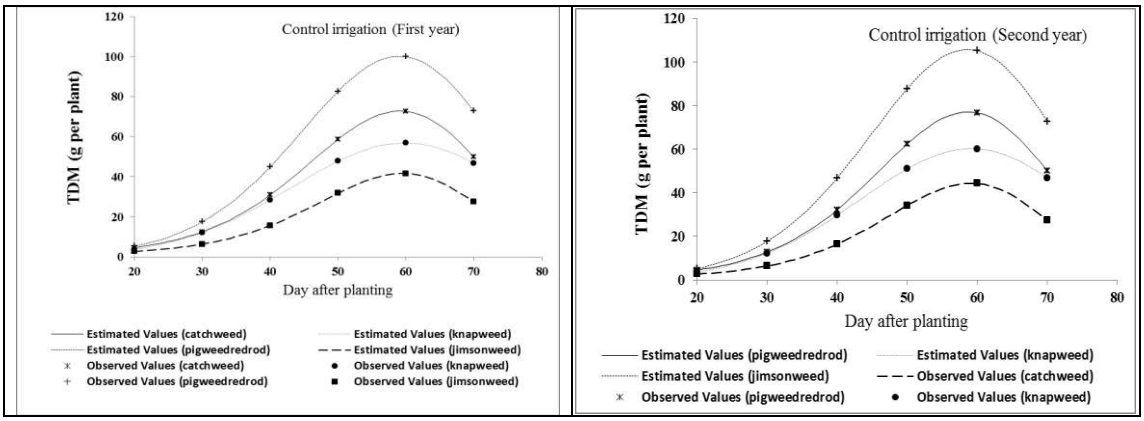

http://www.aloki.hu ● ISSN 1589 1623 (Print) ● ISSN 1785 0037 (Online)
DOI: http://dx.doi.org/10.15666/aeer/1705_1092910940

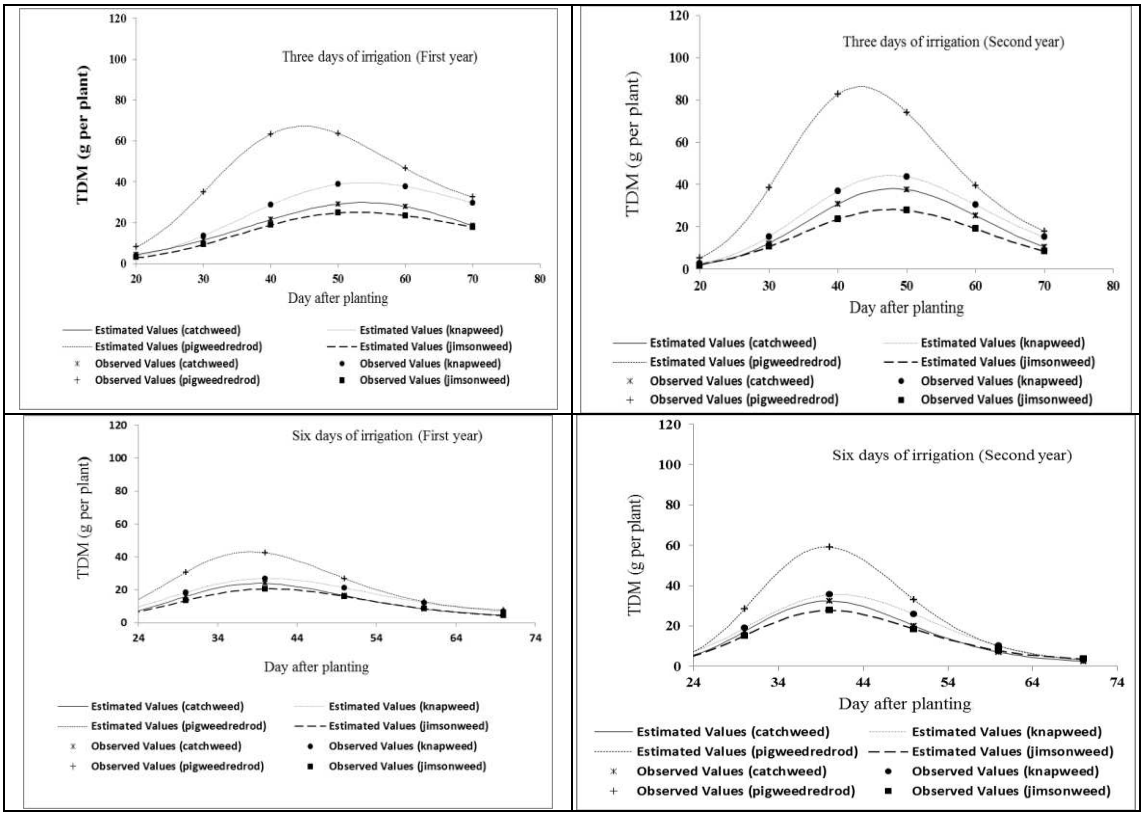

Figure 2. *The effect of irrigation period on changes trend in weed total dry matter during the growing season*

Leaf area index (LAI)

In the irrigation control, LAI is at its peak at all weeds examined. Jimsonweed (6 and 6.5), Red root pigweed (4.5 and 5), Russian knapweed (5.5 and 7.5) and Catchweed (2.3 and 2.7). In the meantime, LAI Jimsonweed is higher than other weeds. As seen in *Figure 3,* with the onset of stress and applying irrigation periods of 3 and 6 days, LAI reduced all weeds, and in 3 days, in both years, in Red root pigweed, Jimsonweed, Catchweed and Russian knapweed, it reached (3.8 and 5, 1.7 and 2, 1.5 and 2, 1.4 and 1.6) and in 6 days (2.4 and 3.2, 1.4 and 1.9, 1.9 and 2.5, 1.5 and 1.7) respectively. It is clearly that water shortage influence on plant morphology for example loss leaf number and leaf area reduction. Therefore, the results can be justified. Although the LAI begins to collapse after its peak, but it is becoming more intense with increasing irrigation periods.

Rawson and Turner (1982) concluded during the experiment that the number of leaves in sunflowers under drought stress was less than in non-stressed cultivars, also, the leaf area increased with increasing number of irrigation period. The main symptom of drought stress at the stage of growth is the reduction of the number and size of leaves. If the water shortage continues, the lower leaves fell and plant height will be significantly lower than normal.

$$LAI = e\ (a2 + b2t + c2t2 + d2t3)$$

http://www.aloki.hu ● ISSN 1589 1623 (Print) ● ISSN 1785 0037 (Online)
DOI: http://dx.doi.org/10.15666/aeer/1705_1092910940

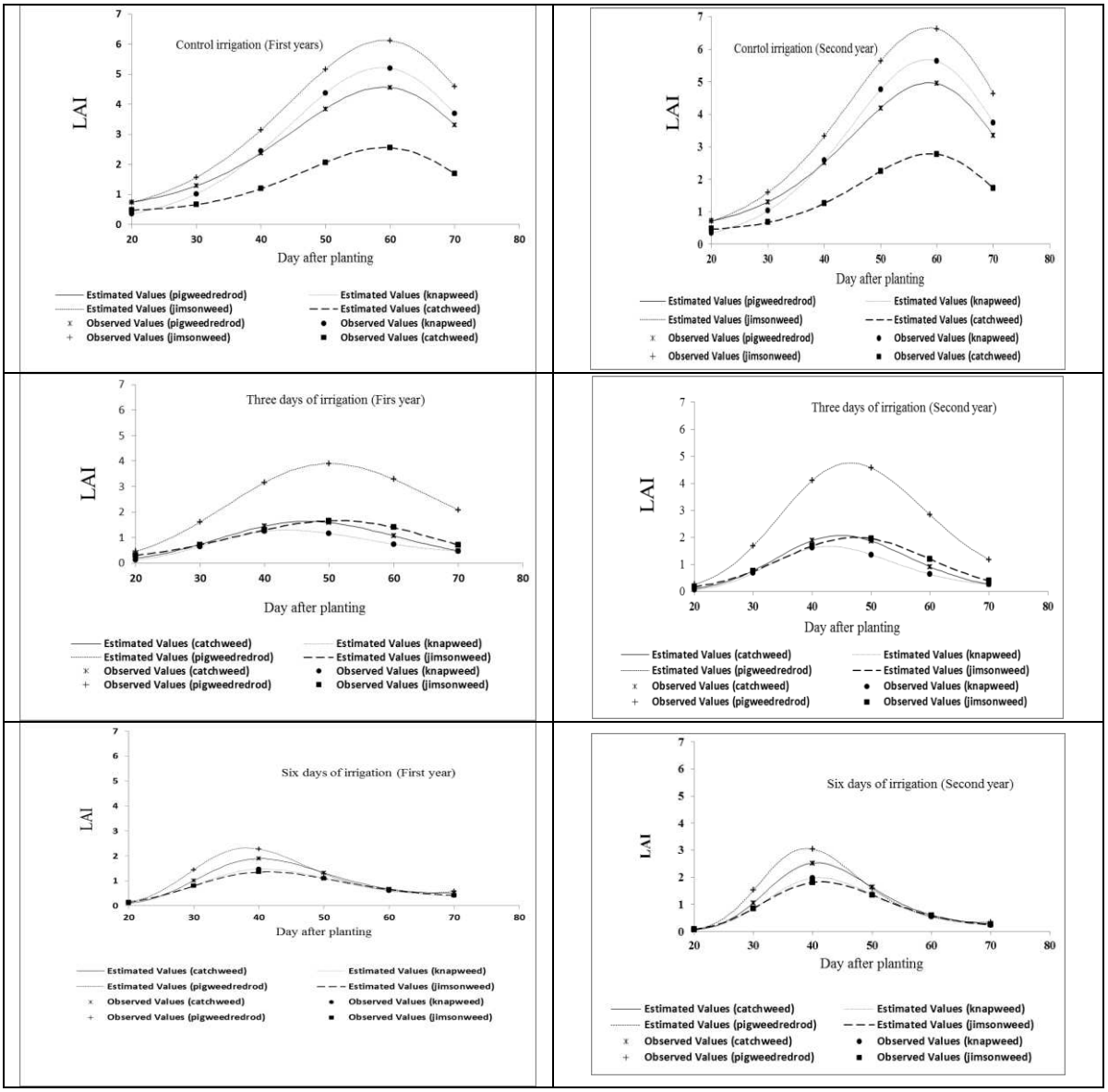

Figure 3. *The effect of irrigation period on changes trend in leaf area index during the growing season*

Figure 3 shows that Jimsonweed leaf area index is at a higher point than other weeds, but by applying irrigation periods, LAI reduction in Jimsonweed is more intense and it arrived less than the Red root pigweed leaf area index. Regarding what is seen from this curve in an environment without stress, Jimsonweed has better leaf area development and more potential for dry matter production than other weeds. Better leaf development allows the carbohydrate factory to be more productive and more competitive than other weeds. But by applying irrigation periods and increasing irrigation periods, it gives its place to the Red root pigweed.

Relative growth rate (RGR)

The results showed that in all irrigation periods, RGR was decreasing trend and with increasing irrigation periods, the rate of reduction of RGR also increased. RGR in all

http://www.aloki.hu ● ISSN 1589 1623 (Print) ● ISSN 1785 0037 (Online)
DOI: http://dx.doi.org/10.15666/aeer/1705_1092910940

weeds in the first irrigation periods at 68-73 days after planting, for the second and third irrigation periods at 50-60 and 41-44 days after planting, respectively, was zero. Six days irrigation gets zero faster than three days and control treatment (*Fig. 4*). Human et al. (1990) stated that RGR changes have decreased mode relative time, but its slope depends on environmental factors. Drought stress causes premature aging of the plant and this mechanism for that is the plant as soon as complete its growth period to escape dryness (Kochaki and Sarmadnia, 1990). Yegappan et al. (1982) has also achieved similar results. It seems with longing irrigation periods, the RGR faster reaches to zero.

$$RGR = TDM/CGR$$

$$Ln\ TDM = a1 + b1t + c1t2 + d1t3$$

$$RGR = b1 + 2c1t + d1/2t3$$

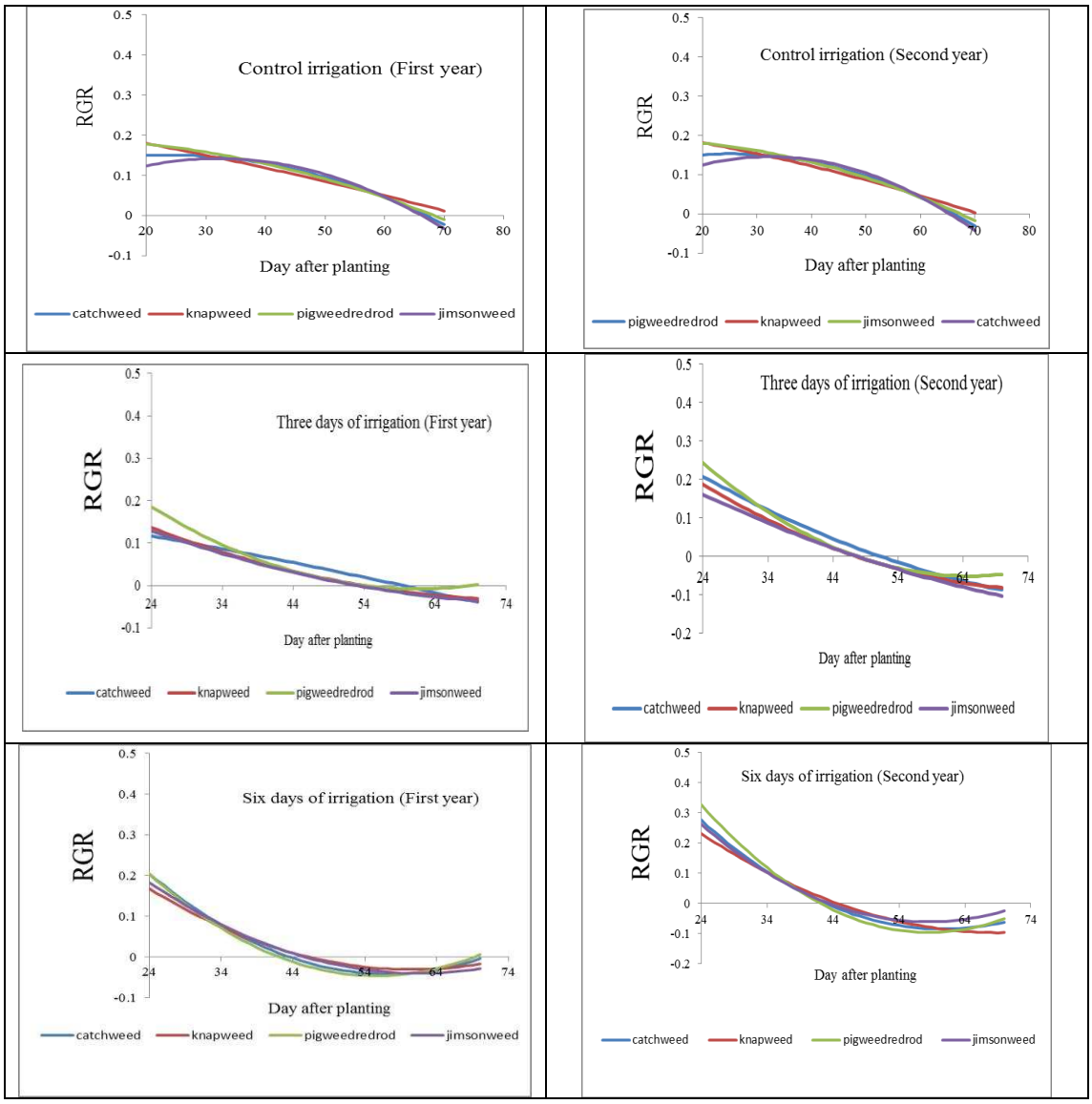

Figure 4. *The effect of irrigation period on relative growth rate of weeds*

http://www.aloki.hu ● ISSN 1589 1623 (Print) ● ISSN 1785 0037 (Online)
DOI: http://dx.doi.org/10.15666/aeer/1705_1092910940

Net assimilation rate (NAR)

NAR starts the descent trend for all periods of irrigation, however, the slope falling of NAR was slower in control than other both irrigation periods (*Fig. 5*). Given that in normal mode, Nar decreases due to shading leaves, but in treatments under stress, even though, photosynthesis capacity is reduced due to the closure of stomata as a mechanism to combat water losses, however, due to the shortage of leaves numbers and lower leaf area, little shading is observed in less irrigated treatments. This results are controversial with the results obtained for LAI. The photosynthesis restriction under the influence of irrigation shortages has a greater effect on the falling of the NAR, than the shading of leaves, and that is the cause of an intensive slope falling of the NAR in long irrigation periods. Wise et al. (2013) stated that drought stress, which causing reduces in the leaf water potential to -15bar, reduces pure photosynthesis by up to 50%, and the reason for this is the lack of stomatal conductivity due to the closure of the stomata. They also stated that cyclic and noncyclic photophosphorylation and electron transfer decrease under drought stress where the leaf water potential reaches between -10 to -11 atmospheres. However, water shortages affect enzymes of the dark reaction of photosynthesis. With the results, it can be said that in treatments under stress, with less shading leaves due to the lack of leaf area development, and photosynthesis limitation, single leaf photosynthesis is reduced and the effect of this factor is greater than that is of the shading leaves.

$$NAR = CGR/LAI$$

$$NAR = (b1 + 2c1 + 3d1t2)\, e^{(a1 - a2) + (b1 - b2)\, t + (c1 - c2)\, t2 + (d1 - d2)\, t3}$$

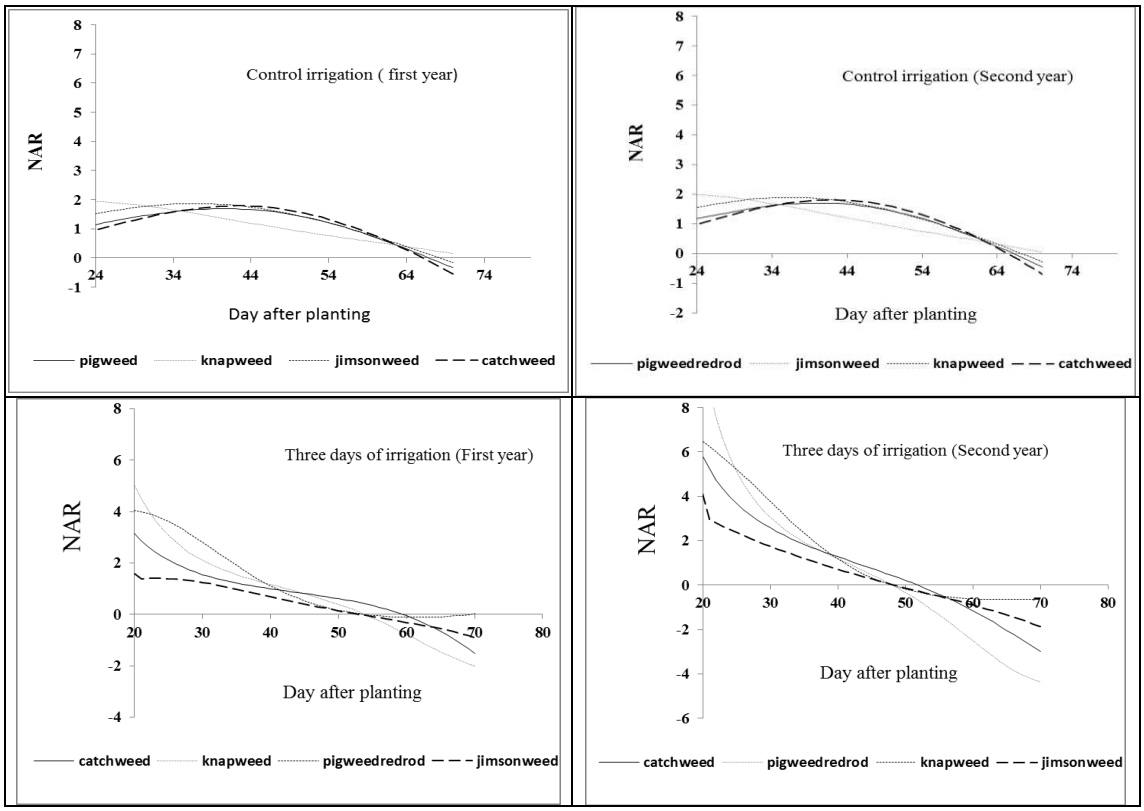

http://www.aloki.hu ● ISSN 1589 1623 (Print) ● ISSN 1785 0037 (Online)
DOI: http://dx.doi.org/10.15666/aeer/1705_1092910940

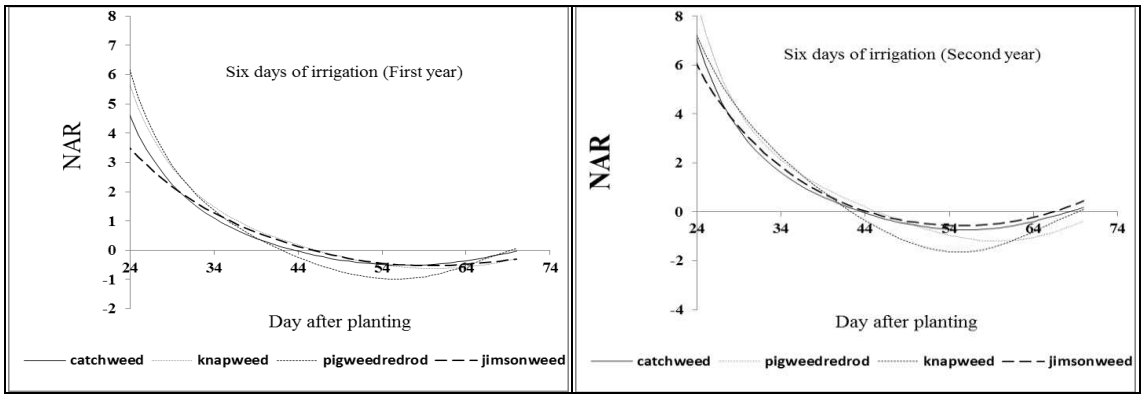

Figure 5. *The effect of irrigation period on net assimilation rate of weeds*

Related traits to root and plant height

ANOVA analysis was shown in *Table 2*. According to *Table 3* in all sampling, in both years, Jimsonweed in control irrigation, and followed that, Red root pigweed has the highest height. Russian knapweed was the shortest plant among the species. By applying drought stress and increasing irrigation periods, the height of all weeds decreased, but the decrease in Jimsonweed height was higher than the Red root pigweed. This act can be attributed to the photosynthetic system of both plants. In conditions of water shortage and drought stress, C3 weeds has less competitive power than C4 weeds. Regarding the rate of weed height increase under normal conditions, Jimsonweed is stronger than other weeds and the optimum time to control it may be short. But, in drought stress conditions, the height of the Red root pigweed is higher and the control of the Red root pigweed is in the priority. Also, in the case of root weighing traits, in all weeds, with increasing irrigation period, root dry weight decreased. Nevertheless, the root length showed an increasing trend. During drought stress, soil layers are depleted from moisture, the root system penetrates into the depths of the soil (Klepper, 1990), and root density under stress conditions is much higher than in non-stress conditions. When exposed to drought stress, the plant allocates more dry matter to the root system to increase the absorbing ability of the roots, as a result, changes in the morphological characteristics of the roots are created, such as increasing the length of the roots per unit of weight (Aerts and Chapin, 2008).

Table 2. *Analysis of variance of studied traits in different irrigation periods*

	d.f	Mean squares		
		Root dry weight	Root length	Height
Year (A)	1	0.007^{ns}	0.04^{ns}	0.022^{ns}
Error a	6	0.03^{ns}	0.10^{ns}	0.248^{ns}
Weed spices (B)	3	34.52^{**}	22.51^{**}	5.478^{**}
Irrigation (C)	2	8.63^{**}	5.37^{**}	23.623^{**}
A×B	3	0.0008^{ns}	0.07^{ns}	0.013^{ns}
A×C	2	0.001^{ns}	0.05^{ns}	0.006^{ns}
B× C	6	1.75^{**}	1.02^{**}	0.966^{**}
A×B× C	6	0.02^{ns}	0.04^{ns}	0.025^{ns}
Error B	66	0.04	0.086	0.07
%CV		11.15	6.92	5.89

ns, *,** Not significant (P > 0.05), significant at P < 0.05, and P < 0.01 respectively

http://www.aloki.hu ● ISSN 1589 1623 (Print) ● ISSN 1785 0037 (Online)
DOI: http://dx.doi.org/10.15666/aeer/1705_1092910940

Table 3. *Comparison of the mean of studied traits in different irrigation periods*

ab	Irrigation	Root dry weight (g plant^{-1})	Root length (cm)	Height (cm)
Amaranthus retroflexus	Control	23.35a	7.50f	31.55b
	3 day	12.18b	9.21ef	27.65c
	6 day	5.98c	10.28e	16.35f
Datura stramonium	Control	4.95c	24.88b	41.32a
	3 day	2.06def	19.77c	24.90d
	6 day	1.90efg	33.07a	14.74f
Setaria verticilata	Control	0.90fgh	17.89c	31.28b
	3 day	0.53gh	23.53b	20.87e
	6 day	0.32h	32.76a	15.76f
Acroptilon repens	Control	3.43d	13.52d	21.18e
	3 day	2.81de	17.33c	15.178f
	6 day	1.59efgh	17.67c	11.91g

Conclusion

The results showed that all indices decreased by increasing irrigation period. Red root pigweed showed more tolerance to long irrigation period than others. Thus in dried condition red root pigweed can be weed dominant. Unlike, Jimsonweed showed a better growth in control.

REFERENCES

[1] Aerts, R., Chapin, F. S. (2008): The mineral nutrition of wild plants revisited: reevaluation of processes and patterns. – Advances in Ecological Research 62: 26-34.
[2] Beech, D. F., Norman, M. J. T (2002): The effect of time of planting on y attributes of varieties of safflower. – Australian Journal of Basic Applied Sciences 3: 140-148.
[3] Benvenuti, S., Macchia, M., Mieles, S. (2001). Quantitative analysis of emergence of seedlings from buried weed seeds with increasing soil depth. – Weed Science 49: 528-535.
[4] Chauhan, B. S. (2013): Growth response of itchgrass (*Rottboellia cochinchinensis*) to water stress. – Weed Science 61: 98-103.
[5] Chauhan, B. S., Johnson, D. E. (2010): Growth and reproduction of Jungle rice (*Echinochloa colona*) in response to water stress. – Weed Science 58: 132-135.
[6] Eslami, R., Tajbakhsh, M., Ghafari, A., Roustaei, M., Barnousi, I. (2012): Evaluation of drought tolerance in dry lands wheat genotypes under different moisture. – Electronic Journal of Crop Production 2: 129-143.
[7] Human, J. J., Tolit, J. D., Vezuidenhout, H. D. Bryun, L. P. (1990): The influence of photosynthesis and yield of sunflower. – Agric.Res.37:542-549.
[8] Karim Zadeh Asl, K. H., Mazaheri, D., Peyghambari, S. A. (2004): Effect of four irrigation periods on seed yield and physiologyical indexes of three sunflower cultivars. – Desert (BIABAN) 9(2): 255-266.
[9] Klepper, B. (1990): Root Growth and Water Uptake. – In: Stewart, B. A., Nielsen, D. R. (eds.) Irrigation of Agricultural Crops. Agron. Monogr. 30. ASA, CSSA, and SSSA, Madison, WI, pp. 281-322.
[10] Kochaki, A., Sarmadni (1990): Plant Physiology. 2nd Ed. – Jahad University Press. Ferdosi Mashhad University.
[11] Monaco, T. J., Weller, S. C., Ashton, F. M. (2002): Weed Science: Principles and Practices. 4th Ed. – John Wiley and Sons, Inc., New York.

http://www.aloki.hu ● ISSN 1589 1623 (Print) ● ISSN 1785 0037 (Online)
DOI: http://dx.doi.org/10.15666/aeer/1705_1092910940

[12] Peters, K., Breitsameter, L., Gerowitt, B. (2014): Impact of climate change on weeds in agriculture: a review. – Agron. Sustain. Dev. 34: 707-721.
[13] Russell, M. P., Wilhelm, W. W., Olsson, R. A., Power, J. F. (1984): Growth analysis based on degree day. – Crop Sci. 24: 28-32.
[14] Rawson, H. M., Turner, N. C. (1982): Recovery from water stress in five sunflower cultivars. Effect of the timing of water application on leaf area and seed production. – Aus. Plant Physiol. 9: 437.
[15] Sadeghi, H., Bagestani, M. H., Akbari, G. A., Hejazi, A. (2009): Evaluation of soybean (*Glycine Ma*.) and some weed species growth indices under competition condition. – Entomology and Phytopathology 71: 88-106.
[16] Webster, T. M., Grey, T. L. (2008): Growth and reproduction of Benghal dayflower (Commelina benghalensis) in response to drought stress. – Weed Science 56: 561-566.
[17] Wise, R. R., Fredrick, J. R., Alm, D. M., Kramer, D. M., Hesketh, J. D., Crofts, A. R., Ort, D. R. (2013): Investigation of photosynthesis induced leaf water deficits in field grown sunflower. – Uir. of III Ineis Cell Environ 913L: 923-931.
[18] Zimdahl, R. L. (2013): Fundamentals of Weed Science. 4th Ed. – Academic Press, San. Diego, USA.

http://www.aloki.hu ● ISSN 1589 1623 (Print) ● ISSN 1785 0037 (Online)
DOI: http://dx.doi.org/10.15666/aeer/1705_1092910940

THE RELATIONSHIP BETWEEN CERTAIN MICROBIOLOGICAL AND SOME ARBUSCULAR MYCORRHIZAL PARAMETERS OF PLANTS PREVALENT AROUND AN ALUMINUM BAUXITE MINE DEPOSIT

ATMACA, E.* – ÇETIN KARACA, U.

Soil Science and Plant Nutrition Department, Agriculture Faculty, Selcuk University, Campus, Konya, Turkey
(phone: +90-332-223-2962; fax: +90-332-241-0108)

**Corresponding author*
e-mail: emelatmaca2016@gmail.com; phone: +90-332-223-2962; fax: +90-332-241-0108

(Received 25th Mar 2019; accepted 4th Jul 2019)

Abstract. The aim of our research was to study certain microorganisms living in the root areas of plants growing in stressed habitats such as mining sites. In the present study, the distributions of arbuscular mycorrhizal fungi (A.M.F.) spores in the root rhizospheres of certain plants (*Onopordum acanthium*, *Festuca glauca, Euphorbia helioscopia* L., *Plantago lanceolata* L., *Salvia officinalis*, *Mentha pulegium* L., *Verbascum thapsus* L. and *Crocus sativus* L.) that are prevalent around the Seydişehir Aluminum Plant Bauxite Deposit (SAPBD) were examined along with the infection rates of these spores in the plant roots, and the morphological definitions of these spores were presented. The highest values in the number of arbuscular mycorrhizal spores, arbuscular mycorrhizal infection rate, dehydrogenase, catalase, urease enzyme activities, the total number of bacteria, the vesicle and arbuscule rates, and also the DSE (dark septate endophyte) fungal structures were obtained from the plant *Euphorbia helioscopia* L., and the soils taken from its rhizosphere. The most prevalent spore species detected in the soils sampled from the Bauxite Mine sampling area were *Glomus* sp., *Acaulospora* sp. and *Archaeospora* sp. Fluctuations were observed in the arbuscular mycorrhizal infection rates of the roots depending on the species of the plants.
Keywords: *mycorrhizal infection rate, spore number, mine area, morphological identification, Seydişehir*

Introduction

Fungi play a central role in many microbiological and ecological processes, influencing soil fertility, decomposition, the cycling of minerals and organic matter, as well as plant health and nutrition (Finlay, 2008). Different symbiotic mycorrhizal associations between plants and fungi occur, almost ubiquitously, throughout a wide range of terrestrial ecosystems. Mycorrhizae are very common in disturbed areas, which indicates their positive role in establishing and building the plant community. There are several studies reporting the role of mycorrhizae in stressed habitats (Kumar et al., 2003). Furthermore, mycorrhizal associations are essential to the colonization of nutrient-deficient soil heaps left after mining

Soil contamination by heavy metals is an issue of major importance in industrialized areas. The detrimental effects of heavy metals on soil's biochemical and biological properties have been reported in the past and microbes are the pioneer of the living creation and play a vital role in mine restoration (Singh et al., 2011b; Li et al., 2012; Ma et al., 2016) High concentrations of metal in soil are toxic to bacteria and fungi, but the roots of most plants growing in polluted soils are colonized by A.M. fungi (Shetty et al., 1994a). This is an indication of the ability of A.M. fungi to develop tolerance to contaminants. Most studies aimed at evaluating the relationship between AMF and

http://www.aloki.hu ● ISSN 1589 1623 (Print) ● ISSN 1785 0037 (Online)
DOI: http://dx.doi.org/10.15666/aeer/1705_1094110961

plants in soil contaminated with high metals have found increased tolerance and reduced damage in mycorrhizal plants (Shaker-Koohi, 2014). The species richness of AMF in mining areas has also been reported to be inversely related to soil high metal levels. The metals Zn, Cu, and Pb (Klauberg-Filho et al., 2002); Pb and Zn (Zarei et al., 2010); and Al, As, Ba, Cd, Cr, Cu, Pb, Se, Sr, and Zn (Biró et al., 2005) are some of the metals involved in reducing the diversity of mycobionts. However, despite the apparent exclusion of species and increased dominance imposed by the environmental damage generated by mining, AMF communities are rarely composed of less than 10 species. In areas of bauxite mining in Brazil, the number of species was found to vary from six (Melloni et al., 2003) to 21 (Silva et al., 2005).

When metals are at toxic concentrations in soil, mycorrhizal rather than non-mycorrhizal host plants are able to colonize these polluted sites (Shetty et al., 1994a, b). Thus, mycorrhizal colonization may be the key to plant survival in contaminated environments by enhancing metal resistance in plants and also by improving the uptake of essential nutrients. Nevertheless, metal resistance in A.M. fungi has not been extensively investigated with respect to their host plants (Meharg and Cairney, 2000). These studies demonstrate that plants are able to adapt quickly. Arbuscular mycorrhizal fungi, which are associated with most plant species and can serve as intermediaries for the uptake of soil nutrients, might be particularly important in mine tailings (Taheri and Bever, 2010). For example, Cumming and Ning (2003) found that A.M. fungi conferred Al resistance to *Andropogon virginicus* L. reducing Al uptake and translocation in host plants. The response of plants to mycorrhizal colonization combined with toxic metal exposure varies depending on plant species, fungal community, biotic and abiotic conditions, concentration of toxins, and pH. This suggests complex interactions involving many variables (Dietterich et al., 2017; Maynard et al., 2018).

Yet, few studies have examined plant response in terms of the adaptation of their symbionts, particularly in comparison to unadapted communities (Taheri and Bever, 2010). Furthermore, the impact of A.M. fungi community on soil quality is important in that it helps us to understand the function of the ecosystems. Relevant studies can provide important guidance for maintaining the balance of the soil-plant system and the development of sustainable agriculture (Huang et al., 2014). Mycorrhizal infection can increase the absorption of various mineral nutrients by the host plants (Smith et al., 2011; Wang et al., 2011), improve the host plant's water utilization efficiency under drought conditions (Augé, 2001; Huang et al., 2011; Tian et al., 2013), improve the host plant's resistance to salinity and heavy metals (Bothe et al., 2010; Garg and Kaur, 2013) and improve the host plant's resistance to disease. (Wehner et al., 2010; Meyer et al., 2013) Since one part of the morphological structure of A.M. fungi is located in the plant roots, and the other part in the soil, its infection will inevitably affect both the host plant and soil ecology. Studies on the distribution and infection rates of mycorrhizal spores in mining areas around the world and also studies to determine the types of spores are gaining more importance with each passing day. However, there are no studies on the mycorrhizae that exist in mining areas in Turkey. So, we determined the rate of mycorrhizal colonization in the plant root, the number of mycorrhizal spores in the plant rhizosphere and conducted the morphological identification of mycorrhizal spore species in various different plants growing in the vicinity of an aluminum mineral deposit. In doing so, we endeavored to make a general contribution to knowledge about the mycorrhizal state of these particular areas.

http://www.aloki.hu ● ISSN 1589 1623 (Print) ● ISSN 1785 0037 (Online)
DOI: http://dx.doi.org/10.15666/aeer/1705_1094110961

Materials and methods

Description of the sampling site

This study was carried out in an opencast mine site at the Seydişehir Aluminum Plant Bauxite Deposit (SAPBD), in Konya, Turkey (N 12 76 53, E 40 07 27 and 1671 m). This mining area is called the "Mortaş Bauxite Deposit". The Mortaş Bauxite Deposit is one of the largest bauxite deposits in the West Taurus Mountains and is located near Keçili village (the new name of the village is Madenli) located 15 km south of Seydişehir, and it occurs along the unconformity between Lower and Upper Cretaceous limestone layers (Atabey, 1976; *Fig. 1*).

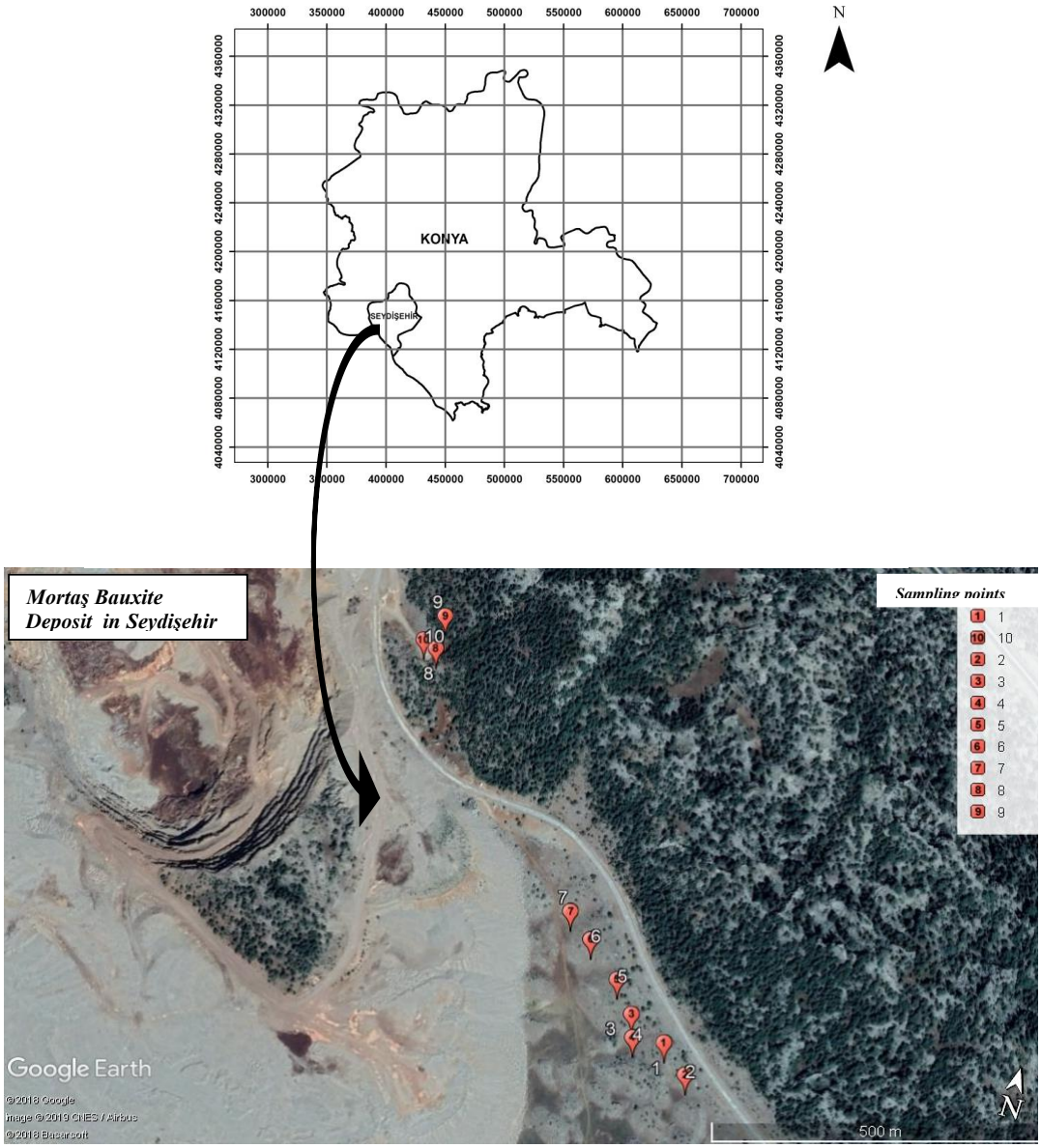

Figure 1. *Research area (Seydişehir Mortaş Bauxite Deposit) and locations of sampling points*

The Seydişehir-Akseki-Alanya district is of major economic importance and was investigated in the early 60's by A. Egger, who produced an unpublished detailed map

http://www.aloki.hu ● ISSN 1589 1623 (Print) ● ISSN 1785 0037 (Online)
DOI: http://dx.doi.org/10.15666/aeer/1705_1094110961

of the regional geology of the area. The Seydişehir deposits contain a total of 26.3 million tons of high-alumina boehmite bauxite at 55–67% Al_2O_3. Detailed exploration of the Seydisehir deposits by ETI Aluminum established a reserve of boehmitic bauxite measuring 25.8 million tons at 57–58% Al_2O_3, 6 million tons of which have already been mined (Öztürk et al., 2002).

The mean meteorological data of Seydişehir District (where the sampling area is located) for the study period (January–December 2017) were obtained from the 8th Konya Provincial Directorate of Meteorology. According to the data, the mean maximum temperature was 18.6 °C; the mean minimum temperature was 6.61 °C; the average temperature was 12.60 °C and the temperature distribution was generally around the seasonal norms throughout the year. Total annual precipitation was 746.40 mm with 53.89% of this precipitation occurring in the winter season, and 20.72% in fall. The periods of summer and spring were arid. In the locality, annual average wind velocity is 1.5 m/s. Dominant wind direction is north- northwest and average velocity of the winds blowing from this direction is 1.2 m/s. The averaged soil temperature in the locality is 16.1 °C in 5 cm depth; 15.8 °C in 10 cm depth; 15.1 °C in 20 cm depth;15.6 °C in 50 cm depth; and 15.6 °C in 100 cm depth.

Soil sampling and hosts

Soil samples were taken through random sampling in autumn in 2017. The samples were taken from soil layers at 0 to 20 cm below the surface (where the plant roots are the most extensive and thus the activities of microorganisms are the highest) using a spade to collect about 1 kg of soil. A quantity of the sampled soils was kept at +4 °C in a refrigerator so that microbiological analyses could be made. Later, the sampled soils were dried in air and passed through a 2 mm sieve in preparation for other analyses (some physical and some chemical). The number of soil samples was based on the number of the most prevalent perennial plants (The species were Asteraceae: *Onopordum acanthium subsp. acanthium* (1), Poaceae: *Festuca glauca syn F. cinerea F. ovina var glauca* (2), Euphorbiaceae: *Euphorbia helioscopia* L. (3 and 9: The same plant was sampled at a different distance to the pit), Plantaginaceae: *Plantago lanceolata* L. (4 and 8: The same plant was sampled at a different distance to the pit), Lamiaceae: *Salvia officinalis* L. *and Mentha pulegium* L. (5 and 6 respectively), Scrophulariaceae: *Verbascum thapsus* L. (7), Iridaceae: *Crocus sativus* L. (10). Samples of three of each of the aforementioned plants were taken from the sampling area, and the means of the values obtained from the three plants were used in the analyses. Plant names, localization and heights are presented in *Table 1*. The plants were described by Davis (1965-1985). In this study, the total number of plants is 10, but there are 8 different plants in these 10. Three and eight are the same, and also four and nine are the same plant varieties and they are indicated as different sample numbers since those are sampled from different locations.

Some microbiological, physical and chemical properties of the studied site soils

The taken soil samples were air dried and passed through a 2 mm sieve before being analyzed in the laboratory. The analyses were conducted to determine soil characteristics, such as electrical conductivity (EC), pH, $CaCO_3$, organic matter, and texture. The electrical conductivity (EC) and pH of the samples were determined using an electrical meter and a pH meter, respectively (Richards, 1954). $CaCO_3$ percentage

http://www.aloki.hu ● ISSN 1589 1623 (Print) ● ISSN 1785 0037 (Online)
DOI: http://dx.doi.org/10.15666/aeer/1705_1094110961

was determined according to Hızalan and Ünal (1965); organic matter according to Jackson (1958); texture according to Bouyoucos (1995) by means of the hydrometer method. Total nitrogen was determined according to Bremner (1996) using the Kjeldahl method, and available phosphorus was determined by the Olsen method (Olsen et al., 1954). Ammonium acetate solution (1 N, pH 7) was used to determine exchangeable Ca, Mg and K (Thomas, 1982). Available Fe, Cu, Mn and Zn were determined by atomic absorption spectrophotometry using DTPA extraction methods (Lindsay and Norwell, 1978). The sampled soils were subjected to microbiological analyses with their natural moisture content. The oven dry weights of the soils were determined and calculations were made according to the oven dry soil weight. Soil respiration was determined according to Isermeyer (1952); total bacteria and fungi count were determined according to the soil dilution and plate count method (Drews, 1983). The dehydrogenase activity (DHA) of the soils was determined according to Thalmann (1968); catalase activity (CA) was measured using the method by Beck (1971); urease activity was assayed using the method by Hoffmann and Teicher (1961). The percentage of root colonization was calculated by the gridline intersect method and, when the amount of roots was low by the slide method (Giovanetti and Mosse, 1980). The percentage of AM colonization was calculated as the number of segments infected out of 100 segments that were examined under a stereo microscope at 40X magnification (Giovanneti and Mosse, 1980). All the soil analyses and measurements were carried out in triplicate and the mean values were used in the statistical analysis.

Table 1. *The plants sampled around SAPBD, and the coordinates and height above sea level of the locations from where they were taken*

No	Name of plant	Coordinate	Altitude (m)
1	*Onopordum acanthium* (Asteraceae)	37°16’15.76”N, 31°53’50.61”E	1,611
2	*Festuca glauca* (Poaceae)	37°16’14.37”N, 31°53’52.53”E	1,611
3	*Euphorbia helioscopia* L. (Euphorbiaceae)	37°16’16.80”N, 31°53’48.03”E	1,607
4	*Plantago lanceolata* L. (Plantaginaceae)	37°16’15.56”N, 31°53’48.56”E	1,602
5	*Salvia officinalis* (Lamiaceae)	37°16’18.45”N, 31°53’46.46”E	1,607
6	*Mentha pulegium* L. (Lamiaceae)	37°16’20.24”N, 31°53’43.99”E	1,606
7	*Verbascum thapsus* L. (Scrophulariaceae)	37°16’21.48”N, 31°53’42.12”E	1,607
8	*Plantago lanceolata* L. (Plantaginaceae)	37°16’33.63”N, 31°53’28.22”E	1,689
9	*Euphorbia helioscopia* L. (Euphorbiaceae)	37°16’35.52”N, 31°53’28.18”E	1,698
10	*Crocus sativus* L. (Iridaceae)	37°16’33.98”N, 31°53’27.20”E	1,687

Assessment of arbuscular mycorrhizal fungi colonization and spores

The root samples were cleaned carefully with deionized water and stained using the method described by Phillips and Hayman (1970), and the percentage colonization was calculated using the gridline intersect method (Giovanneti and Mosse, 1980).

The spores were quantified and characterized according to the sieving and decanting procedure developed by Gerdeman and Nicolson (1963) and INVAM (2004). Spore quantification was examined under a stereomicroscope (Olympus SX 60 trinocular microscope) at 40X magnification. For spore observation and identification, the spores

http://www.aloki.hu ● ISSN 1589 1623 (Print) ● ISSN 1785 0037 (Online)
DOI: http://dx.doi.org/10.15666/aeer/1705_1094110961

were mounted on glass slides and identified to genus level, whenever possible, using a compound microscope (Euromex-Novex B-Series) at 100-400X magnification, based on the descriptions in Brundrett et al. (1996) and the information from the INVAM website (INVAM, 2004).

Data analysis

The data obtained were statistically analyzed using one-way analysis of variance and the means were separated by Duncan's multiple range test ($P < 0.01$ and 0.05) using Minitab 16 software. Correlation analysis was also performed. Correlation coefficient (r^2) was calculated between soil chemical features and mycorrhizal parameters (Minitab, 1997).

Results and discussion

Physical and chemical properties of the site soil

The means and standard deviations of some physical and chemical properties of the soil samples taken in three replicates from the rhizosphere soils of 10 plants (8 different plants) sampled around the SAPBD are given in *Table 2*.

Table 2. *Results of some chemical analyses and textures belonging to the soils of plants sampled around SAPBD*

Soil number	pH	EC µS/cm	Org. mat. %	$CaCO_3$ %	Texture
1	7.23 ± 0.01	160.47 ± 1.37	2.31 ± 0.04	2.62 ± 0.08	Loam
2	7.23 ± 0.01	299.33 ± 1.96	4.63 ± 0.01	4.36 ± 0.00	Silty loam
3	6.50 ± 0.26	165.40 ± 1.05	5.27 ± 0.04	1.69 ± 0.12	Loam
4	7.10 ± 0.01	140.83 ± 0.65	1.97 ± 0.01	2.68 ± 0.04	Loam
5	7.36 ± 0.04	151.97 ± 0.19	2.26 ± 0.07	3.78 ± 0.09	Loam
6	5.80 ± 0.01	145.77 ± 0.54	2.00 ± 0.04	6.05 ± 0.12	Sandy loam
7	7.17 ± 0.01	128.23 ± 0.49	1.69 ± 0.01	6.63 ± 0.08	Sandy loam
8	7.21 ± 0.01	113.73 ± 1.04	3.00 ± 0.01	50.68 ± 1.53	Sandy clay loam
9	5.77 ± 0.01	134.74 ± 1.29	4.97 ± 0.01	40.38 ± 0.99	Sandy loam
10	6.92 ± 0.06	131.26 ± 1.13	2.91 ± 0.04	26.47 ± 1.19	Sandy clay loam

Regarding the soil characteristics of the survey area: pH varied between 5.77 and 7.36, organic matter content between 1.69 and 5.27%, electrical conductivity between 113.73 and 299.33 dS/cm, and percentage of $CaCO_3$ between 1.69 and 50.68; texture classes were Loam, Silty Loam, Sandy Loam and Sandy Clay Loam (*Table 2*).

In addition, the contents of some micro and macro elements found in the soils sampled are presented in *Table 3*.

Root colonization of A.M. fungi

The roots of all 10 host plants were colonized by A.M. fungi, but the degree of colonization varied both among plant species and dependent on soil properties (*Table 5*). Typical A.M. fungal structures, i.e. arbuscules and vesicles (*Fig. 2a-c, f*) were

http://www.aloki.hu ● ISSN 1589 1623 (Print) ● ISSN 1785 0037 (Online)
DOI: http://dx.doi.org/10.15666/aeer/1705_1094110961

observed in the roots of all host plants but moniliform cell and dark septate endophytic fungal hyphea (*Fig. 2d-e*) were observed only in the roots of *Euphorbia helioscopia* L. (Euphorbiaceae). The colonization of vesicles varied from 0.00% to 83.54%, the colonization of arbuscules varied from 79.34% to 100%, and the colonization of hyphae varied from 0.00% to 60.33%. The highest vesicle and arbuscule rates were obtained from *Euphorbia helioscopia* L. (83.54%-100%), and the highest hyphae rate was obtained from *Festuca glauca* (60.33%). Statistically significant differences were observed among the rhizospheres of different plant species ($P < 0.01$ and $P < 0.05$) (*Table 4*). The mycorrhizal structures (arbuscules, vesicles and hypha) and also spore percentages were significantly higher (87.67 number/10 g soil) in the *Euphorbia helioscopia* L. compared to other plants and other rhizosphere soils.

Table 3. *Results of some macro and micro nutrient elements belonging to the soils of plants sampled around SAPBD*

Soil number	N %	P_2O_5 mg kg^{-1}	K_2O mg kg^{-1}	Ca mg kg^{-1}	Mg mg kg^{-1}	Fe mg kg^{-1}	Cu mg kg^{-1}	Zn mg kg^{-1}	Mn mg kg^{-1}
1	0.19712	13.78	198.3	6411	2050	24.52	1.336	0.388	21.81
2	0.19222	34.59	273.7	7127	3070	33.41	1.512	0.838	35.61
3	0.31892	34.59	368.7	5313	3790	32.01	1.87	0.792	22.95
4	0.26012	17.29	220.9	5981	2800	23	1.294	0.412	305
5	0.07056	16.41	239.3	6236	1980	20.39	1.026	0.332	21.46
6	0.15022	13.48	150.3	6102	2540	28.18	1.114	0.292	20.7
7	0.04536	10.26	147.7	6157	2640	23.32	0.958	0.252	15.88
8	0.04368	9.38	83.86	3848	450	11.87	1.26	1.97	14.01
9	0.09744	16.71	170.4	4374	620	27.58	0.95	0.546	16.21
10	0.0504	15.53	192.2	4511	510	9.03	0.738	1.178	8.37

Among the mycorrhizal parameters examined in plant roots, a positive correlation was found between vesicle rate and arbuscule rate at a significant level ($P < 0.01$, $r = 0.6447$), and a significant and positive correlation ($P < 0.05$, $r = 0.5009$) was also found between vesicle rate and dehydrogenase activity. In addition to the positive and significant relationship between arbuscule rate and vesicle rate ($P < 0.01$), a positive and significant relationship was again detected between arbuscule rate and the number of spores per screen opening 50-100 μm in diameter ($P < 0.01$, $r = 0.6306$), and there was also a positive and significant relationship between arbuscule rate and urease enzyme activity ($P < 0.01$, $r = 0.3932$). By contrast, a negative and significant correlation was detected between arbuscule rate and hyphae rate and between arbuscule rate and root length ($P < 0.05$, $r = -0.3784$ and $r = -0.5362$, respectively in *Table 5*).

The photographs of the different formations exhibited by arbuscular mycorrhizal and DSE fungal colonization observed in plant roots are shown in *Figure 2a-f.*

Of the mycorrhizal structures, the vesicle and arbuscule formations are shown in *Figure 2a, c* and *f,* coiled intraradical hyphae (large arrow) are shown in *Figure 2b,* moniliform cells are shown in *Figure 2d*. Mycelia of dark septate endophytes (DSE) accompanied the A.M. fungi colonization, and were observed in only one plant species (Zubek et al., 2011). Dark septate endophytic fungal hyphea are shown in *Figure 2e.* All of these formations were obtained from the roots of the plant *Euphorbia helioscopia* L.

http://www.aloki.hu ● ISSN 1589 1623 (Print) ● ISSN 1785 0037 (Online)
DOI: http://dx.doi.org/10.15666/aeer/1705_1094110961

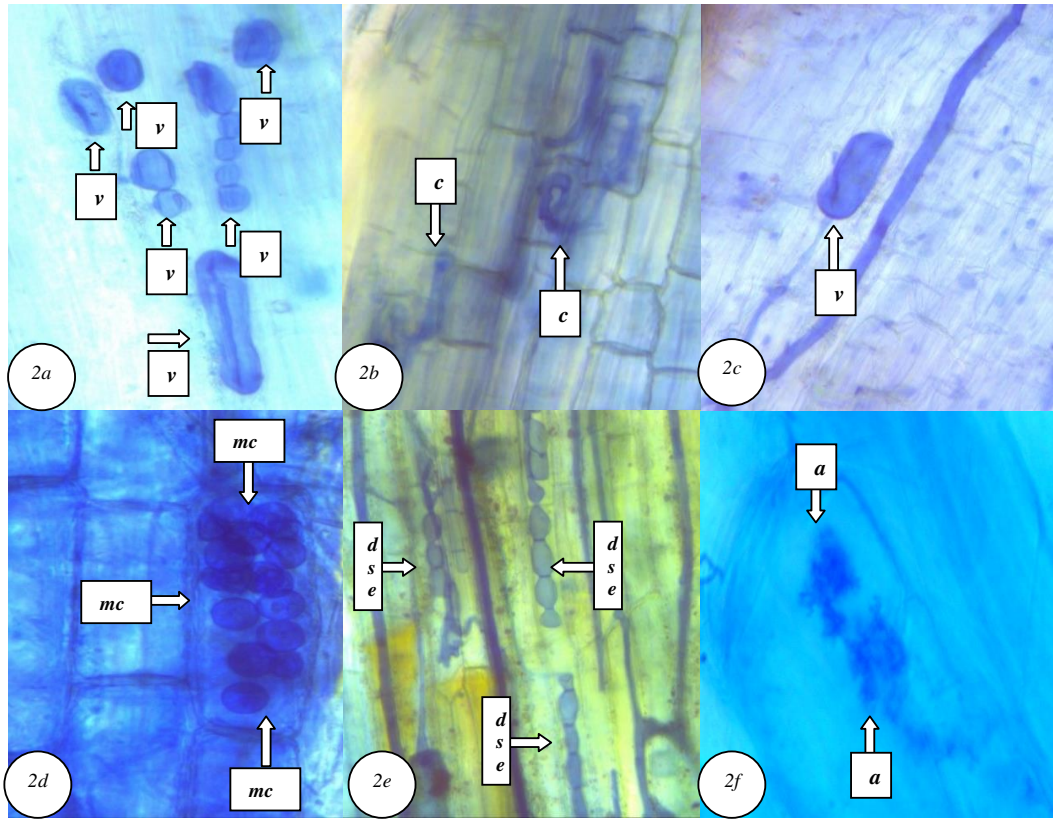

Figure 2. a *Vesicles (v) in roots of Festuca glauca (Poaceae).* ***b*** *Stained coiled (c) intraradical hyphae (large arrow) in Salvia officinalis (Lamiaceae) roots.* ***c*** *Vesicles (v) in roots of Plantago lanceolata L. (Plantaginaceae).* ***d*** *Moniliform cells (mc) in Euphorbia helioscopia L. (Euphorbiaceae).* ***e*** *Dark septate endophytic (dse) fungal hyphea in Euphorbia helioscopia L. (Euphorbiaceae) roots.* ***f*** *Arbuscules (a) in roots of Euphorbia helioscopia L. (Euphorbiaceae)*

Spore density of A.M. fungi

The total A.M. fungi spore density ranged between 24.33-87.67 count/10 g soil in the rhizosphere zone of the ten host plants. The highest A.M. fungi spore density was observed in the rhizosphere of the plant *Euphorbia helioscopia* L., and the lowest A.M. fungi spore density (24.33-26.00-26.00 count/10 g soil) was obtained in the rhizosphere of *Verbascum thapsus* L. and *Plantago lanceolata* L. (Two plants sampled). On the other hand, the distribution of spore numbers varied according to sieve size and plant variety. The highest spore counts were taken from smaller size (38-50 µm) while the lowest spore counts were taken from larger size (>250 µm) sieves.

Considering all sieve sizes, the highest spore count in the 38-50 µm sieve was found at the rhizosphere region of *Onorpodum acanthium* (46.67 number/10 g soil), the highest spore count in the 50-100 and 100-250 µm sieves was found at the rhizosphere region of *Euphoria helioscopia* L. (39.00-32.00 number/10 g soil) and the highest spore count in the > 250 µm sieve (6.67 number/10 g soil) was found at the rhizosphere region of *Mentha pulegium* L. (*Table 4*).

As can also be seen from *Table 5*, the correlation analysis carried out in the study revealed that there was a positive and significant relationship between the total number of spores and the number of spores remaining in the 30-50 µm sieve, and also between the total number of spores and the microbial respiration value and the total number of

http://www.aloki.hu ● ISSN 1589 1623 (Print) ● ISSN 1785 0037 (Online)
DOI: http://dx.doi.org/10.15666/aeer/1705_1094110961

bacteria ($P < 0.01$, $r = 0.6969$, $r = 0.7609$, $r = 0.7404$, respectively). Similarly, a positive and significant relationship was again found ($P < 0.01$) between the total number of spores and the number of spores remaining in the 100-150 μm sieve, and between catalase urease enzyme activities and the total number of fungi ($r = 0.4558$, $r = 0.5233$, $r = 0.4169$, $r = 0.5425$, respectively) (*Table 5*).

Evaluation of certain biological properties of the research area soil

Certain mycorrhizal parameters, as well as microbiological properties of the research soils, were analyzed. In this scope, the dehydrogenase, catalase and urease activities of the soils, total number of fungus, bacteria, and microbial respiration values were determined. Of the parameters mentioned above, the highest values in terms of dehydrogenase, urease and catalase activities, vesicle-arbuscule rates, and the total number of mycorrhizal spores were obtained from the root rhizosphere of the plant *Euphorbia helioscopia* L. In addition, as the result of the distribution of the total number of mycorrhizal spores with respect to sieve diameter, the highest number of spores remaining on the 50-100 μm and 100-250 μm sieves were also obtained from the rhizosphere of the same plant. Also, DSE fungal structures were determined from the root rhizosphere of the plant *Euphorbia helioscopia* L. Of the interpretations regarding the significance levels and degrees of the bilateral relationships between the analyzed biological parameters, those that are related to mycorrhizal parameters were presented above. The correlation analyses conducted on the root length data showed that there was a significant ($P = 0.05$) and positive (0.4911) relationship between root length and hypha rate; a significant ($P = 0.05$) and negative (-0.5362) relationship between root length and arbuscule rate; also, a significant ($P = 0.01$) and negative relationship between root length and the number of spores remaining on the 50-100 μm sieve. While a significant ($P < 0.05$) and positive (0.4203) correlation was determined between dehydrogenase enzyme activity and urease enzyme activity, again a positive ($r = 0.4963$) correlation was found at the same level ($P < 0.05$) between dehydrogenase activity and total number of bacteria. It was determined that there was a positive correlation ($P < 0.01$) between catalase enzyme activity and microbial respiration, and the number of spores remaining on the 35-50 μm sieve ($r = 0.7995$, $r = 0.7047$, respectively); also a positive correlation ($P < 0.05$) was found between catalase enzyme activity and the number of spores remaining on the 50-100 μm sieve, and hypha rate ($r = 0.4092$, $r = 0.4313$ respectively). From another enzyme analysis carried out in the soil, it was determined that there was a significant and positive correlation ($P < 0.05$) between urease enzyme activity and number of spores remaining on the 50-100 μm sieve, dehydrogenase enzyme activity, and total number of bacteria ($r = 0.5339$, $r = 0.4203$, $r = 0.5497$, respectively) (*Table 5*).

Determination of morphological diagnosis of A.M. fungi

Morphological identifications were made for A.M. fungi spores that were isolated from the rhizosphere zones of the plants sampled from mining areas. The A.M. fungal spores counted in the study were found to belong to three different mycorrhizal fungi genera and the counting results were compared to one another. The plants that were in symbiosis with *Acaulospora*, *Glomus* and *Scutellospora* were found as *Onopordum acanthium, Euphorbia helioscopia* L., *Plantago lanceolata* L., and *Crocus sativus* L.. The highest number of mycorrhizal spores was detected in *Glomus* sp. The present study recorded a total of three A.M. fungal genera: *Glomus* sp. (*Fig. 3a*, *3i*),

http://www.aloki.hu ● ISSN 1589 1623 (Print) ● ISSN 1785 0037 (Online)
DOI: http://dx.doi.org/10.15666/aeer/1705_1094110961

Acaulospora sp. (*Fig. 3b, 3d, 3e, 3h*) and *Entrophospora* sp. (*Fig. 3c, 3f, 3g*). *Acaulospora* sp. was the most frequently occurring genera (66.67%) followed by *Glomus* (22.22%) and *Entrophospora* sp. (11.11%).

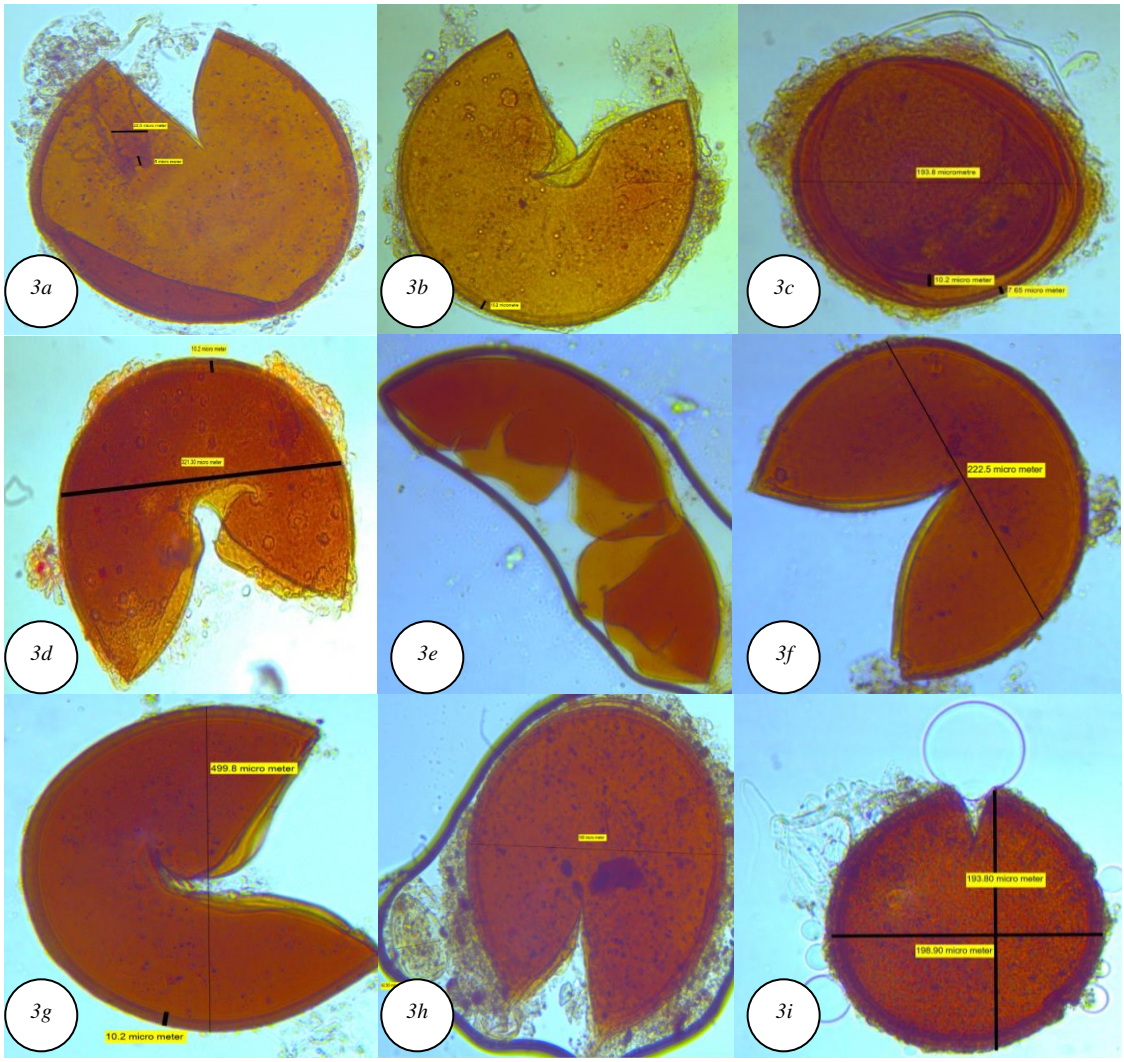

Figure 3. *Three genus of mycorrhiza spores identified in plant rhizospheres.* ***a*** *X400 in PVLG; 5-22.5 µm.* ***b*** *X200 in PVLG; 10.2 µm.* ***c*** *X200 in PVLG; 193.8 in Onopordum acanthium (Asteraceae).* ***d*** *X200 in PVLG; 321.30-10.2 µm.* ***e*** *X200 in PVLG.* ***f*** *X200 in PVLG; 222.5 µm.* ***g*** *X200 in PVLG; 499.8-10.2 µm in Plantago lanceolata L. (Plantaginaceae).* ***h*** *X400 in PVLG; 180-42.5 µm in Euphorbia helioscopia L. (Euphorbiaceae).* ***i*** *X200 in PVLG; 198.90-193.80 µm in Crocus sativus L. (Iridaceae)*

Discussion

From all of the findings, it can be said that both the distributions of mycorrhizal spores in the soil and the infection rates they formed in the plant roots may vary in the same plant and soil even in short term intervals. For this reason, the data obtained from microbiological studies in which mycorrhizal distribution and infection rates are determined can only represent the moment of collection and are valid for only a short period of time. Since microbiological parameters can be affected by various factors and the action mechanism is again a living organism system, the cycle of effective factors is both quick and fluctuated.

http://www.aloki.hu ● ISSN 1589 1623 (Print) ● ISSN 1785 0037 (Online)
DOI: http://dx.doi.org/10.15666/aeer/1705_1094110961

In addition, although the distances among the locations where the mining area plants used in our study were sampled were not very far, differences were still observed in the mycorrhizal parameters measured in the soils and the plants, and also in the results of the analyses of the activities of other microorganisms, and these differences were found to be statistically significant ($P < 0.05$), which confirms the statements explained above. As a matter of fact, the distribution of A.M. fungi in different ecological regions and their relations with soil properties and native plants have been investigated by several researchers (Cooke et al., 1993; Janardhanan, 1994; Aliasgharzadeh et al., 2001; Shi et al., 2007; Bi et al., 2019).

It is established that variations in A.M. fungi distribution, spore density and colonization with different host plant species are generated by a variety of mechanisms, including variation in host species and their phenology, mycorrhizal dependency, soil properties, host plant-mediated alteration of the soil microenvironment, or other unknown host plant traits (Eom et al., 2000; Wang et al., 2004). In addition, species and isolates of A.M. fungi differ in their tolerance to adverse physical and chemical conditions in soil (Augé, 2004; Daei et al., 2009; Barea et al., 2013). In our study, the highest values in terms of both mycorrhizal and other microbiological parameters were obtained particularly from the plant *Euphorbia helioscopia* L. This finding could be explained by the fact that this plant has a different physiology and thus a different mechanism compared to the others. Early reports revealed that plants of *Euphorbiaceae* contain many kinds of secondary metabolites, such as triterpenoids (Biesboer et al., 1982; Teresa et al., 1987), diterpenoids (Sahai et al., 1981; Yamamura et al., 1989; Öksüz et al., 1995; Madureira et al., 2004) steroids (Biesboer et al., 1982), lipids (Biesboer et al., 1982; Teresa et al., 1987), flavonoids and tannins (Durrani et al., 1987; Zhang and Guo, 2006). In addition to various medical and known properties of the plant, researchers conducted and have been continuing to carry out several studies on the use of the plant in agriculture and on its insecticide properties (Uzair et al., 2009). However, there are no studies on the potential of arbuscular mycorrhizal organisms that have a mutualistic symbiotic association with the root of *Euphorbia helioscopia* L. in the soil and their effects on the infection of mycorrhizal fungus spores in the plant root. For this reason, the data obtained in the present study could serve as a base for the future studies on similar topics.

In terms of the parameters examined in the study; although the values obtained from *Euphorbia helioscopia* L. were found to be higher compared to other plants, mycorrhizal fungus spores were observed in the root rhizospheres of all the plants examined in the study.

The spore numbers in the rhizosphere soil ranged between 24.33-87.67 spores per 10 g^{-1} dry soil. The average spore count recorded was 53.99 spores per 10 g^{-1} dry soil (*Table 4*).

In terms of the parameters examined in the study, although the values obtained from *Euphorbia helioscopia* L. were found to be higher compared to other plants, mycorrhizal fungus spores were observed in the root rhizospheres of all the plants examined in the study.

In the same way, arbuscule, vesicle, and hypha formations, which are among mycorrhizal parameters, were detected in the roots of all the plants. The A.M. fungi infection rate ranged between 0-83.54% (vesicle rate), 79.34-100% (arbuscule rate) and 0-60.33% (hypha rate) and the mean A.M. fungi infection rates recorded were 44.61-88.33-26.60% as vesicle, arbuscule and hypha rates, respectively.

http://www.aloki.hu ● ISSN 1589 1623 (Print) ● ISSN 1785 0037 (Online)
DOI: http://dx.doi.org/10.15666/aeer/1705_1094110961

In addition, as can be seen from the correlation values in *Table 5*, there is a very strict and positive interaction between the mycorrhizal spore distribution in the soil and the other microbiological parameters of the soil analyzed in the study. The effect of soil enzymes is particularly noticeable in this interaction. Soil enzyme activity has been widely used to evaluate soil management effects (Dick, 1994; Bandick and Dick, 1999; Utobo and Tewari, 2014). The application of microorganism quantity and soil enzyme activity when investigating the effects of mycorrhizal fungi on soil ecosystem functions can improve our understanding of the correlation between mycorrhizal fungi and soil ecosystem functions. Many studies have shown that mycorrhizal colonization may affect the soil microbial communities either directly or indirectly through root exudates (Nuccio et al., 2013; Zubek et al., 2013). Camprubi et al. (1995), Kieliszewska-Rokicka (2001); Nadgórska-Socha et al. (2006); Fernández et al. (2012) investigated the effects of mycorrhizal fungi on soil biological quality by observing soil enzyme activity. In this paper, vesicle, arbuscule, and hypha rates also showed a relationship particularly with soil enzymes in addition to other microbiological parameters. The interactions of vesicle, arbuscule, and hypha rates with the enzymes in the soil were found to be different from one another. That is, a positive and significant correlation ($P < 0.01$) was found between the vesicle rate determined in the plant roots and dehydrogenase enzyme activity, between arbuscule rate and urease enzyme activity, and between hypha rate and catalase enzyme activity. This interaction of mycorrhizal formations in the plant root with the presence of enzymes outside the root could be attributed to the fact that the enzymes mentioned have an effect on the existence of organic matter in the soil.

As a matter of fact, the finding that among the nine plants used in the study, the highest results for certain biological analyses were generally obtained from the root rhizosphere of the same plant could be explained by the fact that the plant has a specific structure and also that the soil in which it grows has a high content of organic matter, with this organic matter being a source of substrate for the enzymes mentioned above. Thus, urease is an extracellular enzyme that provides the hydrolysis of urea reaching the soil in various ways (plant residuals, animal tissues, and fertilizers). After these enzymes are produced by the soil microorganisms to decompose the nutrient substances, they are kept by colloids of soils such as clay and organic matter and can sustain their activities independent of the microorganism cell producing these enzymes. The distribution of urease activity in the soils in the study area is shown in *Table 4*. In the soils studied, the values of urease activity were obtained between 8.71–77.87 μg per N g dry soil^{-1} and it was seen that the highest activity occurred in the soil taken from the rhizosphere of the plant *Euphorbia helioscopia* L. (*Euphorbiaceae*) (no.9), which had the lowest pH (5.77), while the lowest activity was observed in the soil taken from the rhizosphere of the plant *Verbascum thapsus* L. (*Scrophulariaceae*). Similar values of urease activity were also obtained by Douglas and Bremner (1971), Klein and Koths (1980), Bolton et al. (1985), Kızılkaya et al. (1998a, b), and Garcia et al. (2000), Qian et al. (2012) and Bi et al. (2019).

On the other hand, dehydrogenase activity is used when assessing total microbiological activity in soils. However, this enzyme activity is not generally associated with the total number of microorganisms. Dehydrogenase activity is largely affected by environmental factors such as soil moisture and temperature, and by soil properties such as organic matter (Carpenter et al., 1995; Lipson et al., 1999). Therefore, the activity of this enzyme yields its microbiological activity at the moment when the soil sample is taken. However, the highest dehydrogenase activity was

http://www.aloki.hu ● ISSN 1589 1623 (Print) ● ISSN 1785 0037 (Online)
DOI: http://dx.doi.org/10.15666/aeer/1705_1094110961

obtained from the soil in which the highest urease enzyme activity was obtained, i.e. from the rhizosphere soil of the plant *Euphorbia helioscopia* L. (*Euphorbiaceae* (no.9) as 14.27 μg TPF per 1 g dry soil^{-1}. This rhizosphere soil had a high number of mycorrhizal spores (83 in 10 g soil^{-1}) and the highest number of bacteria (26 × 10^5 kob/ml). The distribution of dehydrogenase activity in the study area soils is shown in *Table 4*. The results obtained from dehydrogenase activity of this paper were close to Ross (1970), Bolton et al. (1985), Kızılkaya et al. (1998b, c), Garcia et al. (2000), Qian et al. (2012).

Catalase activity is a criterion used when assessing aerobic microorganisms in soils. Therefore, the catalase activity of soils indicates the desire of soil microorganisms to live in aerobic conditions. Catalase activity varies depending on the aeration condition of soils, O_2 concentration in the soil air, and the number of microorganisms (Schinner et al., 1996; Smith and Read, 2008). The distribution of catalase activity of the common plants existing in the rhizosphere soils around the SAPBD is shown in *Table 4*.

It was found that the catalase activity of the common plants in the rhizosphere soils around the SAPBD ranged between 0.6-7 ml O_2 per 5 g dry soil^{-1} and that the soil with the highest activity was that of the plant *Euphorbia helioscopia* L. (Euphorbiaceae) (no.9). It was also found that this soil had the highest organic matter content (5.27%) and the lowest $CaCO_3$ content (1.69%). In the literature Kızılkaya et al. (1998b, c), Garcia et al. (2000), Abdel Latef and Chaoxing (2011) also found their results in this range. In addition, Samuel et al. (2008) reported in their study that catalase activity was higher in the 0-20 cm part of the soil, i.e. in its top layer where there are more oxygen and more organic matter. Hence, they suggested that alternation had positive effects on the enzyme activity compared to monoculture.

The values regarding the CO_2 production of the soils sampled from the rhizosphere zones of the common plants around the SAPBD are shown in *Table 4*. Carbon dioxide production is used as an indicator of microbial activity in the soil. While heterotopic–qualified microorganisms in the soil decompose the organic matter, they produce CO_2. This process continuing in the soil is also referred to as soil respiration. Although all conditions (moisture, temperature, etc.) affecting the soil microorganisms affect the amount of CO_2, soil organic matter is the main soil property affecting the CO_2 production (Cheng, 1999). It was found that the CO_2 production in the rhizosphere soils of the prevalent plants around the SAPBD ranged between 31.62–73.06 mg CO_2 10 g dry soil^{-1}, and the soil with the highest CO_2 production was again detected in the rhizosphere soil of the plant *Euphorbia helioscopia* L. (Euphorbiaceae) (no.3), which had the highest organic matter content (5.27%) and the lowest lime content (1.69% $CaCO_3$). Kızılkaya et al. (1998c) investigated the microbiological properties of the soils of the Harran Plain and found that CO_2 production varied between 4,5–70,3 mg CO_2 per 100 g soil^{-1}, Kızılkaya et al. (1998b) found that CO_2 production varied between 15.50–68.50 mg CO_2 per 100 g soil^{-1} in the forestry soils of Samsun-Alaçam and Kohler et al. (2009), Wang et al. (2017), Papp et al. (2018) found similar results.

On the other hand, three different spore species (*Glomus* sp., *Acaulospora* sp. and *Entrophospora* sp.) belonging to A.M. fungi were identified in the rhizosphere zones of the 10 plants. In the present study, since the spores isolated from the root rhizosphere region were directly prepared as slides without performing trap culture, a very clear image could not be taken from the spores and methodologically the spores could be identified only based on genus.

http://www.aloki.hu ● ISSN 1589 1623 (Print) ● ISSN 1785 0037 (Online)
DOI: http://dx.doi.org/10.15666/aeer/1705_1094110961

Table 4. *The results of DUNCAN test applied to some biological parameters determined in the plants and soils belonging to the plants and sampled soils around SAPBD*

Soil no	Host	Microbial respiration (mg CO_2 10 g dry soil^{-1})	Dehidrogenase enzyme activity (mg TPF 10 g soil^{-1})	Catalase enzyme activity (mg O_2 5g soil^{-1})	Urease enzyme activity (µg N g dry soil^{-1})	Root length (m/g plant)	∑ Bacteria (kob/ml)	∑ Fungi (kob/ml)	% Vesicle	% Arbuscule	% Hypha	∑ spore number (number/10 g dry soil)	>38 µm	>50 µm	>100 µm	>250 µm
1	*Onopordum acanthium*	72.97a	7.06cde	4.87c	29.08b	157.72ı	15.67bc	10.00b	0.00j	79.98e	39.67c	85.33a	46.67a	31.33b	6.33e	1.00bc
2	*Festuca* glauca	71.02a	6.50cde	6.20b	18.32cde	683.11a	12.00cd	9.00bc	29.67g	79.95e	30.88d	53.33c	26.00c	10.67e	16.33c	0.33cd
3	*Euphorbia helioscopia*L.	73.06a	9.18bc	7.00a	17.91cde	193.27g	8.00ef	7.33bcd	83.54a	100.06a	60.33a	87.67a	20.00d	34.00b	32.00a	1.67b
4	*Plantago lanceolata* L.	35.68d	7.37cd	3.60e	27.24bc	190.01g	1.00g	3.67d	59.14d	92.36b	8.17g	26.00e	6.00g	15.00d	4.67e	0.33cd
5	*Salvia officinalis*	63.87ab	5.94de	3.60d	14.91de	212.89f	18.00b	19.67a	44.25e	99.87a	0.00h	64.33b	31.33b	27.67c	5.00e	0.33cd
6	*Mentha pulegium* L.	50.00c	7.73bcd	4.13f	22.32bcd	329.22d	9.67de	9.67b	39.97f	79.97e	10.00g	42.67d	23.67c	0.67g	11.67d	6.67a
7	*Verbascum thapsus* L.	42.46cd	4.21e	1.40g	8.71e	260.62e	4.67fg	6.00bcd	24.97h	83.81d	16.65f	24.33e	9.67ef	10.00e	4.67e	0.00d
8	*Plantago lanceolata* L.	31.62d	10.73b	0.60c	19.31bcd	440.82c	8.33def	4.33d	20.28ı	79.34e	19.99e	26.00e	7.67fg	6.00f	12.00d	0.33cd
9	*Euphorbia helioscopia* L.	52.92bc	14.27a	4.60g	77.87a	185.92h	26.00a	5.00cd	69.14c	100.51a	42.50b	83.00a	26.00c	39.00a	16.33c	1.67b
10	*Crocus sativus* L.	37.15d	14.25a	0.60g	12.62de	490.46b	18.33b	9.33bc	75.14b	87.44c	37.80c	47.33d	11.67e	14.00d	21.67b	0.33cd
LSD		**11.83**	**3.154**	**0.4542**	**10.49**	**4.095**	**3.672**	**4.388**	**1.689**	**1.462**	**2.149**	**4.933**	**2.764**	**2.853**	**2.053**	**0.8544**

*P<0.05, **P<0.01

http://www.aloki.hu ● ISSN 1589 1623 (Print) ● ISSN 1785 0037 (Online)
DOI: http://dx.doi.org/10.15666/aeer/1705_1094110961

Table 5. *The results of correlation test applied to some parameters determined belonging to the sampled plants and soils around SAPBD*

Properties of soil and plant	Microbial respiration (mg CO_2 10 g dry soil^{-1})	Mycorrhizal fungus spore				Total spor (number/ 10 g soil)	Rate of vesicle (%)	Rate of arbuscule (%)	Rate of hypha (%)	Root length (m/g plant)	Dehidrogenase enzyme activity (mg TPF 10 g soil^{-1})	Catalase enzyme activity (mg O_2 5g soil^{-1})	Urease enzyme activity (µg N g dry soil^{-1})	∑ Fungi number kob/ml	∑ Bacteria number kob/ml
		38µm	50 µm	100 µm	250 µm										
pH	0.0063	-0.1919	-0.0770	0.0891	-0.6250*	-0.1557	-0.4506*	-0.1370	0.0199	0.2123	-0.4098*	-0.2734	-0.5802**	0.2091	-0.2915
EC µS/cm	0.5792*	0.3582*	-0.0603	0.1028	-0.1012	0.1780	-0.1469	-0.2461	0.6547**	0.5870**	-0.2727	0.6157**	-0.1207	0.1660	0.0104
% $CaCO_3$	-0.5028*	-0.3384	-0.0338	0.1893	-0.1163	-0.1317	0.0752	-0.0463	0.0080	0.2100	0.6653**	-0.5285*	0.4146*	-0.3476	0.3652*
% Clay	0.3437	0.2015	0.1809	0.2017	-0.4388*	0.2312	0.2462	0.0118	0.6839**	0.4829*	0.2872	0.3894*	0.0032	0.0003	0.1696
% Silt	0.6732**	0.4673*	-0.0474	-0.0910	0.0884	0.1875	-0.2346	-0.1972	0.3872*	0.2504	-0.5593*	0.7478**	-0.2332	0.2529	-0.2224
% Sand	-0.6827**	-0.4683*	-0.0163	0.0315	0.0568	-0.2302	0.1371	0.1665	-0.5367*	-0.3478	0.3982*	-0.7618**	0.1920	-0.2070	0.1443
% Org. Mat.	0.4621	0.3398	0.2954	0.0457	-0.2484	0.3218	0.4101*	0.0702	0.7505**	0.3214	0.3383	0.6050**	0.3280	-0.1564	0.2989
(%) N	-0.5870*	0.4520*	0.1585	-0.5089*	0.0131	0.1334	0.2484	0.1411	0.3019	-0.2547	-0.1891	0.7979**	0.0441	-0.1469	-0.3415
P_2O_5 mg kg^{-1}	0.8144**	0.3531	0.1715	-0.0291	-0.2090	0.2408	0.3915*	0.0979	0.6543**	0.2856	-0.0512	0.7792**	-0.0484	0.0490	-0.0296
K_2O mg kg^{-1}	0.6619**	0.4071*	0.3959*	-0.0107	-0.2271	0.3901*	0.4733*	0.3352	0.4226*	-0.0812	-0.1427	0.7594**	-0.1297	0.2332	-0.0408
Ca mg kg^{-1}	0.5275*	0.3452	-0.0615	-0.0732	0.1402	0.1288	-0.3891*	-0.1457	0.0780	0.0495	-0.7482**	0.4929*	-0.3232	0.3613*	-0.2633
Mg mg kg^{-1}	0.5014*	0.2626	-0.0861	-0.4297*	0.0449	-0.0589	0.0226	-0.0117	0.1182	-0.1300	-0.6399**	0.6665**	-0.3525	0.0658	-0.5589*
Fe mg kg^{-1}	0.4812*	0.5361*	0.1864	-0.3142	0.2288	0.2776	0.0400	0.0438	0.3174	-0.1261	-0.3543*	0.8897**	0.2467	-0.0262	-0.0851
Cu mg kg^{-1}	0.5496*	0.4268*	0.0568	-0.4523*	-0.1493	0.0748	-0.0134	-0.1274	0.4113*	-0.0208	-0.2654	0.7271**	-0.1339	-0.1286	-0.3949*
Mn mg kg^{-1}	-0.3006	-0.3727*	-0.0993	-0.3337	-0.1560	-0.3696*	0.1700	0.4370*	-0.3114	-0.2319	-0.1646	0.0522	0.0364	-0.3094	-0.5200*
Zn mg kg^{-1}	-0.3578*	-0.3190	-0.2971	0.0904	-0.3342	-0.3122	0.0162	-0.3215	0.2753	0.5347*	0.4718*	-0.4061*	-0.1287	-0.2762	0.0004
Mic. Resp.	-	0.8105**	0.5016*	0.0660	0.0220	0.6969**	-0.0919	-0.0247	0.4549*	-0.1053	-0.3261	0.7995**	0.0732	0.3866*	0.2875
38µm	0.8105**	-	0.5152*	-0.0823	0.1973	0.7609**	-0.2163	-0.1766	0.4878*	-0.2418	-0.0526	0.7047**	0.2522	0.2735	0.3936*
50µm	0.5016*	0.5152*	-	0.2599	0.1192	0.1023	0.2406	0.6306**	0.0880	-0.5841**	0.1868	0.4092*	0.5339*	0.2807	0.6091**
100µm	0.0660	-0.0823	0.2599	-	0.1192	0.4558*	0.1616	0.2963	-0.1507	0.2704	0.2184	-0.1664	-0.0018	0.6772**	0.6132**
250µm	0.0220	0.1973	-0.2299	0.1192	-	0.1023	-0.0412	-0.1426	-0.3537*	-0.0946	-0.0006	0.1402	0.1328	0.2343	0.0987
Total Spor	0.6969**	0.7609**	0.8557**	0.4558*	0.1023	-	0.0688	0.3336	0.2091	-0.3404	0.1455	0.5233**	0.4169*	0.5425*	0.7404**
Rate of vesicle	-0.0919	-0.2163	0.2406	0.1616	-0.0412	0.0688	-	0.6447**	0.0333	-0.1170	0.5009**	0.1557	0.2166	-0.0896	0.1638
Rate of arbuscule	-0.0247	-0.1766	0.6306**	0.2963	-0.1426	0.3336	0.6447**	-	-0.3784*	-0.5362*	0.1910	0.1531	0.3932*	0.1277	0.2239
Rate of hypha	0.4549*	0.4878*	0.0880	-0.1507	-0.3537*	0.2091	0.0333	-0.3784*	-	0.4911*	0.2321	0.4313*	0.0758	-0.1847	0.2206
Root length	-0.1053	-0.2418	-0.5841**	0.2704	-0.0946	-0.3404	-0.1170	-0.5362*	0.4911*	-	0.0988	-0.1629	-0.3274	-0.0284	-0.0091
Dehidrog. Enz. Act.	-0.3261	-0.0526	0.1868	0.2184	-0.0006	0.1455	0.5009*	0.1910	0.2321	0.0988	-	-0.2014	0.4203*	-0.2431	0.4963*
Catalase Enz. Act.	0.7995**	0.7047**	0.4092*	-0.1664	0.1402	0.5233*	0.1557	0.1531	0.4313*	-0.1629	-0.2014	-	0.2602	0.1196	0.0696
Urease Enz. Act.	0.0732	0.2522	0.5339*	-0.0018	0.1328	0.4169*	0.2166	0.3932*	0.0758	-0.3274	0.4203*	0.2602	-	-0.3006	0.5497*
∑ Fungi numb.	0.3866*	0.2735	0.2807	0.6772**	0.2343	0.5425*	-0.0896	0.1277	-0.1847	-0.0284	-0.2431	0.1196	-0.3006	-	0.3273
∑ Bacteria numb.	0.2875	0.3936*	0.6091**	0.6132**	0.0987	0.7404**	0.1638	0.2239	0.2206	-0.0091	0.4963*	0.0696	0.5497*	0.3273	-

http://www.aloki.hu ● ISSN 1589 1623 (Print) ● ISSN 1785 0037 (Online)
DOI: http://dx.doi.org/10.15666/aeer/1705_1094110961

Conclusions

This is the first study that has attempted to describe the diversity and distribution of A.M. fungi in the mine area rhizosphere soils in Turkey. Mycorrhizal parameters (infection rate, spore count, and morphological identification) were not examined on a very large number of host plants. Only the host plants that are dominant in the sampling area and in the sampling season were collected. The plants that were sampled around mine areas are available in every season, i.e. they do not exhibit any change. The plant species that are prevalently existent around Seydişehir Aluminum Plant in the autumn period.

In conclusion, the findings of this study emphasize the need for an understanding of the ecology of A.M. fungi in various ecosystems and soils for the successful selection and introduction of A.M. fungal species and strains for particular environments. A.M. fungi spore population in the soil and spore colonization in the plant root may change depending on seasonal variation, soil properties, host plant variety and the mechanism of the host plant (He et al., 2002; Bohrer, 2004).

In the present study, significant correlations were found both among the microbial parameters in the soil and among certain properties of the soil in general. The presence of life forms in a soil and their activity are among the most important indicators of that soil's health and quality. As a matter of fact, although the present study was carried out on soil and plant samples around a mining area, the high number and activity of the microorganisms in the soil in the sampling period could be due to the prevalence of non-culture plants growing in the soil in the study area.

In addition, of the three spore genera mentioned above, *Acaulospora* in particular was found to be not only a spore genus dominant in the plant root rhizospheres, but also a spore genus with a high infection rate in the plant roots from which it was isolated.

This gives rise to the opinion that this spore genus contains spore species that are potentially important for the areas in the vicinity of bauxite deposits, and that the use of these spore species in the rehabilitation of the soils that possess similar conditions could yield useful results. For further studies, the symbiosis of plant *Euphorbia helioscopia* L. with arbuscular mycorrhiza and with other fungi should be considered in studies involving stressed environments. In addition, the authors suggest that the benefits of symbiosis for stressed environments should be investigated in detail.

REFERENCES

[1] Abdel Latef, A. A. H., Chaoxing, H. (2011): Effect of arbuscular mycorrhizal fungi on growth, mineral nutrition, antioxidant enzymes activity and fruit yield of tomato grown under salinity stres. – Scientia Horticulturae 127: 228-233.

[2] Aliasgharzadeh, N., Saleh Rastin, N., Towfighi, H., Alizadeh, A. (2001): Occurrence of arbuscular mycorrhizal fungi in saline soils of the Tabriz Plain of Iran in relation to some physical and chemical properties of soil. – Mycorrhiza 11: 119-122.

[3] Atabey, M. E. (1976): Mineralogy, chemistry and origin of the Mortas bauxite deposit, Seydisehir, Konya, Turkey. – Comite International pour I'REtude des Bauxites de l'Alumine et de l'Aluminium Travaux 13: 77-89 [Also published in Türkiye Jeoloji Kurumu Bülteni 19: 9-14 (in Turkish with English abstract)].

[4] Augé, R. M. (2001): Water relations, drought and vesicular-arbuscular mycorrhizal symbiosis. – Mycorrhiza. 11: 3-42.

http://www.aloki.hu ● ISSN 1589 1623 (Print) ● ISSN 1785 0037 (Online)
DOI: http://dx.doi.org/10.15666/aeer/1705_1094110961

[5] Augé, R. M. (2004): Arbuscular mycorrhizae and soil/plant water relations. – Can. J. Soil Sci. 84: 373-381. DOI: 10.4141/S04-002.
[6] Bandick, A. K., Dick, R. P. (1999): Field management effects on soil enzyme activities. – Soil Biol Biochem. 31: 1471-1479.
[7] Barea, J. M., Pozo, M. J., Azcón, R., Azcón-Aguilar, C. (2013): Microbial Interactions in the Rhizosphere. – In: Bruijn, F. de (ed.) Molecular Microbial Ecology of the Rhizosphere. Wiley-Blackwell, USA, pp. 29-44.
[8] Beck, T. H. (1971): Die Messung der Katalasenaktivität von Böden. – Z. Pflanzenernähr, Bodenkd. 130: 68-81.
[9] Bi, Y. L., Wang, J., Feng, Y. B., Yu, H. Y., Qin, Y. F., Yu, M. (2019): Effect of arbuscular mycorrhiza on root self-repairing action of *Amorpha fruticosa* L. in coal mining subsidence land in arid areas. – J. China Coal Soc. 8: 050.
[10] Biesboer, D. D, Amour, P. D., Wilson, S. R. Mahlberg, P. (1982): Sterols and triterpenols in latex and cultured tissues of Euphorbia pulcherrima. – Phytochemistry 21(5): 1115-1118.
[11] Biró B, Posta, K., Füzy, A., Kadar, I. (2005): Mycorrhizal functioning as part of the survival mechanisms of barley (*Hordeum vulgare* L.) at long-term heavy metal stress. – Acta Biol Szeged 49: 65-67.
[12] Bohrer, K., Friese, C. F., Amon, J. P. (2004): Seasonal dynamics of arbuscular mycorrhizal fungi in differing wetland habitats. – Mycorrhiza 14: 329-337.
[13] Bolton, H. Jr., Elliot, L. F., Papendick, R. I., Bezdicek, D. F. (1985): Soil microbial biomass and selected enzyme activities: effect of fertilization and cropping practices. – Soil Biol. Biochem. 17(3): 297-303.
[14] Bothe, H., Regvar, M., Turnau, K. (2010): Arbuscular Mycorrhiza, Heavy Metal, and Salt Tolerance. – In: Sherameti, I., Varma, A. (eds.) Soil Heavy Metals. Soil Biology. Vol. 19. Springer-Verlag, Berlin, pp. 87-111.
[15] Bouyoucos, G. J. (1995): A recalibration of the hydrometer method for making mechanical analysis of the soils. – Agronomy Journal 4(9): 434.
[16] Bremner, J. M. (1996): Nitrogen total. – In: Bartels, J. M., Bigham, J. M. (eds.) Methods of Soil Analysis. American Society of Agronomy, Madison, WI, pp. 1085-1121.
[17] Brundrett, M., Bougher, N., Dell, B., Grove, T., Malajczuk, N. (1996): Working with Mycorrhizas in Forestry and Agriculture. – ACIAR, Canberra.
[18] Camprubi, A., Calvet, C., Estaun, V. (1995): Growth enhancement of Citrus reshni after inoculation with *Glomus intraradices* and *Trichoderma aureoviride* and associated effects on microbial populations and enzyme activity in potting mixes. – Plant Soil. 173: 233-238.
[19] Carpenter-Boggs, L., Loynachan, T. E., Stahl, P. D. (1995): Spore germination of Gigaspora margarita stimulated by volatiles of soil-isolated actinomycetes. – Soil Biol Biochem. 27: 1445-1451.
[20] Cheng, W. (1999): Rhizosphere feedbacks in elevated CO_2. – Tree Physiology 19: 313-320.
[21] Cooke, J. C., Butlera, R. H., Madole, G. (1993): Some observations on the vertical distribution of vesicular arbuscular mycorrhizae in roots of salt marsh grasses growing in saturated soils. – Mycologia 85: 547-550.
[22] Cumming, J. R., Ning, J. (2003): Arbuscular mycorrhizal fungi enhance aluminium resistance of broomsedge (*Andropogon virginicus* L.). – J. Exp. Bot. 54(386): 1447-1459.
[23] Daei, G., Ardekani, M. R., Rejali, F., Teimuri, S., Miransari, M. (2009): Alleviation of salinity stress on wheat yield, yield components, and nutrient uptake using arbuscular mycorrhizal fungi under field conditions. – J. Plant Physiol. 166: 617-625. DOI: 10.1016/j.jplph.2008.09.013.
[24] Davis, P. H. (1965-1985): Flora of Turkey and the East Aegean Islands. – Edinburgh Univ. Press, Edinburg.

http://www.aloki.hu ● ISSN 1589 1623 (Print) ● ISSN 1785 0037 (Online)
DOI: http://dx.doi.org/10.15666/aeer/1705_1094110961

[25] Dick, R. P. (1994): Soil Enzyme Activities as Indicators of Soil Quality. – In: Doran, J. W., Coleman, D. C., Bezdicek, D. F., Stewart, B. A. (eds.) Defining Soil Quality for a Sustainable Environment. SSSA Special Publication. Vol 35. Soil Science Society of America, Madison, Wl, pp. 107-124.
[26] Dietterich, L. H., Gonneau, C., Casper, B. B. (2017): Arbuscular mycorrhizal colonization has little consequence for plant heavy metal uptake in contaminated field soils. – Ecological Applications 27(6): 1862-1875.
[27] Douglas, L. A., Bremner, J. M. (1971): A rapid method of evaluating different compounds as inhibitors of urease in soils. – Soil Biol Biochem. 3: 309-315.
[28] Drews, G. (1983): Mikrobiologisches Praktikum für Naturwissen-schaftler. Fourth Ed. – Springer Verlag, Berlin.
[29] Durrani, A. A., Rafiullah, M., Ikram, M. (1967): *Euphorbia helioscopia* Linn. – Pak J Sci & Ind. Res. 10(3): 167-170.
[30] Eom, A. H., Hartnett, D. C., Wilson, G. W. T. (2000): Host plant species effects on arbuscular mycorrhizal fungal communities in tallgrass prairie. – Oecologia 122: 435-444.
[31] Fernández, D. A., Roldán, A., Azcón, R., Caravaca, F., Bååth, E. (2012): Effects of water stress, organic amendment and mycorrhizal inoculation on soil microbial community structure and activity during the establishment of two heavy metal-tolerant native plant species. – Microb Ecol. 63(4): 794-803. DOI: 10.1007/s00248-011-9972-y.
[32] Finlay, R. (2008): Ecological aspects of mycorrhizal symbiosis: with special emphasis on the functional diversity of interactions involving the extraradical mycelium. – J Exp Bot. 59: 1115 1126.
[33] Garcia, C., Hernandez, T., Roldan, A., Albaladejo, J., Castillo, V. (2000): Organic amendment and mycorrhizal inoculation as a practice in afforestation of soils with *Pinus halepensis* Miller: effect on their microbial activity. – Soil Biology and Biochemistry 32(8-9)1173-1181.
[34] Garg, N., Kaur, H. (2013): Response of antioxidant enzymes, phytochelatins and glutathione production towards Cd and Zn Stresses in *Cajanus cajan* (L.) Mill sp genotypes colonized by arbuscular mycorrhizal fungi. – J Agron Crop Sci. 199: 118-133.
[35] Gerdeman, J. W., Nicolson, T. H. (1963): Spores of mychorriza endogene species. Extracted from soil by wet sieving and decanting. – Trans Brit Mycol Soc. 46: 235-244.
[36] Giovanneti, M., Mosse, B. (1980): An evaluation of techniques for measuring vesicular arbuscular mycorrhizal infection in roots. – New Phytol. 84: 489-500. http://dx.doi.org/10.1111/j.1469-8137.1980.tb04556.x.
[37] He, X., Mouratov, S., Steinberger, Y. (2002): Temporal and spatial dynamics of vesicular-arbuscular mycorrhizal fungi under the canopy of *Zygophyllum dumosum* Boiss. in the Negev Desert. – J. Arid Environ. 52: 379-387.
[38] Hızalan, E., Ünal, H. (1965): Soil Chemical Analysis. – University of Ankara Agriculture Faculty Publics, Ankara (in Turkish).
[39] Hoffmann, G. G., Teicher., K. (1961): Ein kolorimetrisches Verfahren zur Bestimmung der Urease Aktivität in Böden. – Z. Pflanzenernähr. Düng, Bodenk. 91: 55-63. (in German with English abstract).
[40] Huang, Y. Z., Zhong, M., Wu, W., Sui, L. H., Zhang, C., Hao, X. W. (2014): Effects of Arbuscular mycorrhizal fungi isolated from white clovers (*Trifolium repens* L.) on soil bacteria and fungi. – Chemistry and Ecology 30(2): 118-132.
[41] Huang, Z., Zou, Z. R., He, C. X., He, Z. Q., Zhang, Z. B., Li, J. M. (2011): Physiological and photosynthetic responses of melon (*Cucumis melo* L.) seedlings to three Glomus species under water deficit. – Plant Soil. 339: 391-399.
[42] INVAM (2004): Identification of AMF to genus level. – http://invam.caf.wvu.edu/.
[43] Isermeyer, H. (1952): Estimation of Soil Respiration in Closed Jars. – In: Alef, K., Nannipieri, P. (eds.) Method in Applied Soil Microbiology and Biochemistry. Academic Press, London, pp. 214-216.

http://www.aloki.hu ● ISSN 1589 1623 (Print) ● ISSN 1785 0037 (Online)
DOI: http://dx.doi.org/10.15666/aeer/1705_1094110961

[44] Jackson, M. L. (1958): Soil Chemical Analysis. – Prentice-Hall, Inc., Englewood Cliffs, NJ, pp. 1-498.
[45] Janardhanan, K. K., Abdul-Khaling Naushin, F., Ramaswamy, K. (1994): Vesicular arbuscular mycorrhiza in an alkaline user land ecosystem. – Current Science 67: 465-469.
[46] Kızılkaya, R., Arcak, S., Horuz, A., Karaca, A. (1998a): Çeltik tarımı yapılan topraklarda enzim aktiviteleri ile toprak özellikleri arasındaki ilişkiler. – Pamukkale Üniversitesi Mühendislik Bilimleri Dergisi 4(3): 797-804. (in Turkish with English abstract).
[47] Kızılkaya, R., Sürücü, A., Arcak, S. (1998b): Samsun, Alaçam orman topraklarının bazı biyolojik ve kimyasal özellikleri. – XIV. Ulusal Biyoloji Kongresi. 7-10 Eylül. Samsun. Cilt I., pp. 240-254 (in Turkish with English abstract).
[48] Kızılkaya, R., Kızılgöz, İ., Arcak, S., Kaptan, H., Rakıcıoğlu, S. (1998c): Microbiological properties of soils of Harran Plain. – M. Şefik Yeşilsoy International Symposium on Arid Region Soil, 21-24 September, Menemen-İzmir, Turkey, pp. 569-574.
[49] Kieliszewska-Rokicka, B. (2001): Soil Enzymes and Their Importance in Soil Microbial Activity Estimation. – In: Dahm, H., Pokojska-Burdziej, A. (eds.) Drobnoustroje środowiska glebowego. Aspekty fizjologiczne, biochemiczne, genetyczne. Wydawnictwo Adam Marszałek, Toruń, pp. 37-47 (in Polish).
[50] Klauberg-Filho, O., Siqueira, J. O., Moreira, F. M. S. (2002): Fungos micorrízicos arbusculares em solos de área poluída com metais pesados. – R Bras Ci Solo 26: 125-134.
[51] Klein, T. M., Koths, J. S. (1980): Urease, protease and acid phosphatase in soil continuously cropped to corn by conventional or no-tillage methods. – Soil Biol. Biochem. 12(3): 293-294.
[52] Kohler, J., Caravaca, F., Mar, M., Alguacil, A. R. (2009): Elevated CO_2 increases the effect of an arbuscular mycorrhizal fungus and a plant-growth-promoting rhizobacterium on structural stability of a semiarid agricultural soil under drought conditions. – Soil Biology and Biochemistry 41(8): 1710-1716.
[53] Kumar, A., Raghuwanshi, R., Upadhyay, R. S. (2003): Vesicular arbuscular mycorrhizal association in naturally revegetated coal mine spoil. – Tropical Ecology 44(2): 253-256.
[54] Li, H. Y., Li, D. W., He, C. M., Zhou, Z. P., Mei, T., Xu, H. M. (2012): Diversity and heavy metal tolerance of endophytic fungi from six dominant plant species in a Pb–Zn mine wasteland in China. – Fungal Ecol 5(3): 309-315.
[55] Lindsay, W. L., Norvell, W. A. (1978): Development of a DTPA soil test for zinc, iron, manganese and copper. – Soil Sci Soc Am J 42: 421-428.
[56] Lipson, D. A., Schadt, C. W., Schmidt, S. K., Monson, R. K. (1999): Ectomycorrhizal transfer of amino acid-nitrogen to the alpine sedge *Kobresia myosuroides*. – New Phytol. 142: 163-167.
[57] Ma, Y., Oliveira, R. S., Freitas, H., Zhang, C. (2016): Biochemical and molecular mechanisms of plant-microbe-metal interactions: relevance for phytoremediation. – Front Plant Sci 7: 918. DOI: 10.3389/fpls.2016.00918.
[58] Madureira, A. M., Duarte, M. T., Piedade, M. F. M., Ascenso, J. R., Ferreira, M. J. U. (2004): Isoprenoid compounds from Euphorbia portlandica X-ray structure of lupeportlandol, a new lupane triterpene. – J. Braz. Chem. Soc. 15(5): 742-747.
[59] Maynard, D. S., Covey, K. R., Crowther, T. W., Sokol, N. W., Morrison, E. W., Frey, S. D., van Diepen, L. T. A., Bradford, M. A. (2018): Species associations overwhelm abiotic conditions to dictate the structure and function of wood-decay fungal communities. – Ecology (Ecological Society of America) 99(4): 801-811.
[60] Meharg, A. A., Cairney, J. W. G. (2000): Co-evolution of mycorrhizal symbionts and their hosts to metal-contaminated environments. – Adv. Ecol. Res. 30: 69-112.
[61] Melloni, R., Siqueira, J. O., Moreira, F. M. S. (2003): Fungos micorrízicos arbusculares em solos de área de mineração de bauxita em reabilitação. – Pesq Agropec Bras 38: 267-276.
[62] Meyer, J. B., Song-Wilson, Y., Foetzki, A., Luginbuhl, C., Winzeler, M., Kneubuhler, Y., Matasci, C., Mascher-Frutschi, F., Kalinina, O., Boller, T., Keel, C., Maurhofer, M.

http://www.aloki.hu ● ISSN 1589 1623 (Print) ● ISSN 1785 0037 (Online)
DOI: http://dx.doi.org/10.15666/aeer/1705_1094110961

(2013): Does wheat genetically modified for disease resistance affect root colonizing pseudomonads and arbuscular mycorrhizal fungi? – PLoS One 8: e53825: 1-12.
[63] Minitab (1997): MINITAB Reference Manual. – Sowers, Lebanon, Pennsylvania.
[64] Nadgórska-Socha, A., Łukasik, I., Ciepał, R., Pomierny, S. (2006): The activity of selected enzymes in soil loaded with varied heavy metals level. – Acta Agrophysica 8(3): 713-725.
[65] Nuccio, E. E., Hodge, A., Pett-Ridge, J., Herman, D. J., Weber, P. K., Firestone, M. K. (2013): An arbuscular mycorrhizal fungus significantly modifies the soil bacterial community and nitrogen cycling during litter decomposition. – Environ Microbiol. 15: 1870-1881.
[66] Olsen, S. R., Cole, C. V., Watanabe, F. S., Dean, L. A. (1954): Estimation of Available Phosphorus in Soils by Extraction with Sodium Bicarbonate. – USDA Circular 939, US Government Printing Office, Washington, pp. 1-19.
[67] Öksüz, S., Gürek, F., Gil, R. R., Pengsuparp, T., Pezzuto, J. M., Cordell, G. A. (1995): Four diterpene esters from *Euphorbia myrsinites*. – Phytochemistry 38(6): 1457-1462.
[68] Öztürk, H., Hein, J. R., Hanilci, N. (2002): Genesis of the Dogan-kuzu and Mortas bauxite deposits, Taurides, Turkey: separation of Al, Fe, and Mn and implications for passive margin metallogeny. – Economic Geology 97: 1063-1077.
[69] Papp, M., Fóti, S., Nagy, Z., Pintér, K., Posta, K., Fekete, S., Csintalan, Z., Balogh, J. (2018): Rhizospheric, mycorrhizal and heterotrophic respiration in dry grasslands. – European Journal of Soil Biology 85: 43-52.
[70] Phillips, J. M., Hayman, D. S. (1970): Improved procedures for clearing roots and staining parasitic and vesicular arbuscular mycorrhizal fungi for rapid assessment of infection. – Trans Br Mycol Soc. 55: 158-161.
[71] Qian, K., Wang, L., Yin, N. (2012): Effects of AMF on soil enzyme activity and carbon sequestration capacity in reclaimed mine soil. – International Journal of Mining Science and Technology 22(4): 553-557.
[72] Richards, L. A. (1954): Diagnosis and Improvements Salina and Alkali Soils. – U.S. Dep. Agr. Handbook 60, Stroudsburg.
[73] Ross, D. J. (1970): Effects of storage on dehydrogenase activities of soils. – Soil Biol. Biochem. 2: 55-61.
[74] Sahai, R., Rastogi, R. P., Jakupovic, J., Bohlmann, F. (1981): A diterpene from *Euphorbia maddeni.* – Phytochemistry 20(7): 1665-1667.
[75] Samuel, A. D., Domuta, C., Ciobanu, C., Şandor, M. (2008): Field management effects on soil enzyme activities. – Romanian Agricultural Research 25: 61-68.
[76] Schinner, F., Öhlinger, R., Kandeler, E., Margesin, R. (1996): Methods in Soil Biology. – Springer Verlag, Berlin, pp. 1-426.
[77] Shaker-Koohi, S. (2014): Role of arbuscular mycorrhizal (AM) fungi in phytoremediation of soils contaminated: a review. – IJABBR 2(5): 1854-1864.
[78] Shetty, K. G., Banks, M. K., Hetrick, B. A. D., Schwab, A. P. (1994a): Biological characterization of a southeast Kansas mining site. – Water Air Soil Pollut. 78: 169-177.
[79] Shetty, K. G., Hetrick, B. A. D., Figge, D. A. H., Schwab, A. P. (1994b): Effects of mycorrhizae and other soil microbes on revegetation of heavy metal contaminated mine spoil. – Environ. Pollut. 86: 181-188.
[80] Shi, Z. Y., Zhang, L. Y., Li, X. L., Feng, G., Tian, C. Y., Christie, P. (2007): Diversity of arbuscular mycorrhizal fungi associated with desert ephemerals in plant communities of Junggar Basin, northwest China. – Applied Soil Ecology 35(1): 10-20.
[81] Silva, G. A., Trufem, S. F. B., Saggin-Júnior, O. J. (2005): Arbuscular mycorrhizal fungi in a semiarid copper mining area in Brazil. – Mycorrhiza 15: 47-53.
[82] Singh, J. S., Abhilash, P. C., Singh, H. B., Singh, R. P., Singh, D. P. (2011b): Genetically engineered bacteria: an emerging tool for environmental remediation and future research perspectives. – Gene 480(1): 1-9.

http://www.aloki.hu ● ISSN 1589 1623 (Print) ● ISSN 1785 0037 (Online)
DOI: http://dx.doi.org/10.15666/aeer/1705_1094110961

[83] Smith, S. E., Read, D. J. (2008): Mycorrhizal Symbiosis. 3rd Ed. – Academic Press, London.
[84] Smith, S. E., Jakobsen, I., Gronlund, M., Simth, F. A. (2011): Roles of arbuscular mycorrhizas in plant phosphorus nutrition: interactions between pathways of phosphorus uptake in arbuscular mycorrhizal roots have important implications for understanding and manipulating plant phosphorus acquisition. – Plant Physiol. 156: 1050-1057.
[85] Speir, T. W. (1977): Studies on climosequence of soils in tussock grasslands. II. Urease, phosphatase and sulfatase activities of top soils and their relationships with other properties including plant available sulfur. – N. Z. J. Sci. 20: 159-166.
[86] Taheri, W. I., Bever, J. D. (2010): Adaptation of plants and arbuscular mycorrhizal fungi to coal tailings in Indiana. – Appl. Soil Ecol. 45: 138-143.
[87] Teresa, J. D. P., Urones, J. G., Marcos, I. S., Basabe, P., Cuadrado, M. J. S., Moro, R. F. (1987): Triterpenes from *Euphorbia broteri*. – Phytochem. 26(6): 1767-1776.
[88] Thalmann, A. (1968): Zur Methodik der Bestimmung der Dehydrogenase Aktivität im Boden mittels Triphenyltetrazoliumchlorid. – Landw. Forsch. 21: 249-259.
[89] Thomas, G. W. (1982): Exchangeable Cations. – In: Page, D. L., (ed.) Methods of Soil Analysis. Part II. Chemical and Microbiological Properties. 2nd Ed. American Society of Agronomy, Madison, WI, pp. 159-165.
[90] Tian, Y. H., Lei, Y. B., Zheng, Y. L., Cai, Z. Q. (2013): Synergistic effect of colonization with arbuscular mycorrhizal fungi improves growth and drought tolerance of *Plukenetia volubilis* seedlings. – Acta Physiol Plant. 35: 687-696.
[91] Utobo, E. B., Tewari, L. (2014): Soil enzymes as bioindicators of soil ecosystem status. – Applied Ecology and Environmental Research 13(1): 147-169.
[92] Uzair, M., Loothar, B. A., Choudhary, B. A. (2009): Biological screening of *Euphorbia helioscopia* L.. – Pak J Pharm Sci. 22(2): 184-186.
[93] Wang, F. Y., Liu, R. J., Lin, X. G., Zhou, J. M. (2004): Arbuscular mycorrhizal status of wild plants in saline-alkaline soils of the Yellow River Delta. – Mycorrhiza 14: 133-137.
[94] Wang, H., Liu, S., Wang, J., Li, D., Shi, Z., Liu, Y., Xu, J., Hong, P., Yu, H., Zhao, Z., Ming, A., Lu, L., Cai, D. (2017): Contrasting responses of heterotrophic and root-dependent respiration to soil warming in a subtropical plantation. – Agricultural and Forest Meteorology 247: 221-228.
[95] Wang, J., Huang, Y., Jiang, X. Y. (2011): Influence of ectomycorrhizal fungi on absorption and balance of essential elements of *Pinus tabulaeformis* seedlings in saline soil. – Pedosphere 21: 400-406.
[96] Wehner, J., Antunes, P. M., Powell, J. R., Mazukatow, J., Rillig, M. C. (2010): Plant pathogen protection by arbuscular mycorrhizas: a role for fungal diversity? – Pedobiologia 53: 197-201.
[97] Yamamura, S., Shizuri, Y., Koemura, S. (1989): Diterpenes from *Euphorbia helioscopia*. – Phytochemistry 28(12): 3421-3436.
[98] Zhang, W., Guo, Y. W. (2006): Chemical studies on the constituents of the Chinese medicinal herb *Euphorbia helioscopia* L. – Chem Pharm Bull. 54(7): 1037-1039.
[99] Zarei, M., Hempel, S., Wubet, T. (2010): Molecular diversity of arbuscular mycorrhizal fungi in relation to soil chemical properties and heavy metal contamination. – Environ Pollut. 158(8): 2757-2765.
[100] Zubek, S., Nobis, M., Błaszkowski, J., Mleczko, P., Nowak, A. (2011): Fungal root endophyte associations of plants endemic to the Pamir Alay Mountains of Central Asia. – Symbiosis 54(3): 139-149.
[101] Zubek, S., Błaszkowski, J., Seidler-Łożykowska, K., Bąba, W., Mleczko, P. (2013): Arbuscular mycorrhizal fungi abundance, species richness and composition under the monocultures of five medicinal plants. – Acta Sci Pol-Hortoru. 12: 127-141.

http://www.aloki.hu ● ISSN 1589 1623 (Print) ● ISSN 1785 0037 (Online)
DOI: http://dx.doi.org/10.15666/aeer/1705_1094110961

POTENTIAL FOR NITROUS OXIDE EMISSION MITIGATION FROM SPRINKLING IRRIGATION APPLICATIONS OF CHEMICAL FERTILIZER COMPARED TO FURROW IRRIGATION IN ARID REGION AGRICULTURE

YANG, W. Z.[1, 2,3,4] – KANG, Y. H.[1,2*] – FENG, Z. W.[2] – GU, P.[3] – WEN, H. Y.[3] – LIU, L. J.[3]

[1]*Institute of Geographic Sciences and Natural Resources Research, Chinese Academy of Sciences, Beijing 100101, China*

[2]*Inner Mongolia Potato Engineering & Technology Research Center, College of Life Sciences, Inner Mongolia University, Hohhot 010021, China*

[3]*Inner Mongolia Key Laboratory of Environmental Chemistry, Inner Mongolia Normal University, Hohhot 010022, China*

[4]*College of Chemistry and Environmental Sciences, Inner Mongolia Normal University, Hohhot 010022, China*

**Corresponding author*
e-mail: doctorbachelar@yeah.net

(Received 26th Mar 2019; accepted 13th Jun 2019)

Abstract. Sprinkling water is applied in shorter irrigation intervals and lighter irrigation applications in arid areas. The water-saving irrigation is the primary method of local agricultural production. Since chemical fertilizer is the primary emission source of nitrous oxide (N_2O), it is appropriate to verify the general influence of water-saving irrigation on N_2O. Results of the study, conducted in a potato field as the experimental site for two consecutive years, using two different irrigation systems – namely, furrow (FI) and sprinkling-irrigation (SI) with a mineral N fertilizer (NF) and a control without any fertilizer (Control) are reported. The N_2O emission fluxes with NF were higher than those of the control in each irrigation system. On plots where the NF was applied, mean emissions fluxes of N_2O was 152.02 μg/(m^2 hr) in FI, 36.53μg/(m^2 hr) in SI from 2016 to 2017. The reduction of N_2O emissions from SI was due to the lower amount of water applied every time and the lower NO_3^--N and NH_4^+-N of soil associated with SI. This work showed that SI is a method that helps save water and mitigates emissions of the atmospheric N_2O pollutants compared to FI.
Keywords: *greenhouse gas, moisture, fertilization, emission factor, potato field*

Introduction

Nitrous oxide (N_2O) is one of the most significant long-lived greenhouse gases in the atmosphere. The atmospheric N_2O concentration has increased from 270 ppbv (10^{-9} volume ratio) in 1750 to 324 ppbv in 2011, resulting in an increase of 0.17 W/m^2 in radiative forcing. Especially from 2007 to 2011, N_2O concentration in the atmosphere increased linearly at an annual average rate of 6% (IPCC, 2013; Schilt et al., 2014). Agricultural production is the primary source of N_2O emission (Robertson et al., 2000). Agricultural emissions accounted for about 56% of the total anthropogenic atmospheric N_2O emissions in 2005 (US-EPA, 2006). The water strategy is one of the essential factors that affect the emissions of N_2O from agricultural soils. In irrigated soils, the amount of water used and its distribution in the soil influence moisture temporally and spatially. Consequently, different moisture content determines the processes that control

http://www.aloki.hu ● ISSN 1589 1623 (Print) ● ISSN 1785 0037 (Online)
DOI: http://dx.doi.org/10.15666/aeer/1705_1096310976

the amount of N transported, N mineralized such as NO_3^--N leaching within the soil. The changes on water and nitrogen in the soil affect the temporal and spatial distribution for various forms of nitrogen and the formation of N_2O. These irrigating systems, for instance, furrow (FI) or sprinkling irrigation (SI), significantly influence the movement of water in the soil because vertical and lateral infiltration are produced simultaneously (Auxiliadora et al., 2018; Naghedifar et al., 2018).

In arid and semiarid areas, FI is one of the most traditional surface irrigation systems because many crops that do not grow in water for long periods are suitable for this irrigation method. Under FI, water is delivered into each strip at a high amount from a head at its upper end to promote the rapid dissolution of fertilizers because of soaking in large quantities of water (Naghedifar et al., 2018). After the irrigation with long intervals and heavy application depths, water flows through the macropores, and most of the soil volume is wetted, temporarily creating the high ratio of anaerobic microsites, even if the small ratio of the ridge top may remain dry.

SI is one of the most popular methods of irrigation worldwide as an efficient and economically viable alternative (Ezequiel et al., 2018), because it offers the precise controlling of irrigation water amount and uniformity to decrease water and N losses (Lorenzo et al., 2018; José et al., 2018). Sprinkling water is applied on shorter irrigation intervals and lighter irrigation applications. Canopy induced irrigation water redistribution, which influenced the spatial and temporal variability of water in the soil. Irrigation water reaches the surface of the soil after it passes through the developed crop canopy, like precipitation. The wetted front in the soil surface moves downward under capillarity action and only a small part of the soil volume is nearly saturated due to the uniformity of irrigation (Naghedifar et al., 2018; Zapata et al., 2018). The wetted front from the soil surface advances slightly into the soil during sprinkling irrigation (Laura et al., 2008). Consequently, increasing the amount of water from different irrigation systems increases the wetted volume and shape in the soil, which mainly depends on the quantity and rate of applied water. The hydraulic properties in the irrigated soil determine the horizontal and vertical infiltration of water (Li et al., 2003; Vázquez et al., 2005). In previous studies, although the influences of moisture on crop growth have been very well recorded in SI and FI systems (Davidson, 1991; Granli and Bockman, 1994), the effects of these different wetted patterns in the soils on N_2O emissions are not known. So far, the information on N_2O emissions and the related importance do not appear in the comparison between sprinkling and furrow irrigation soils.

We assumed that the irrigation methods will influence N_2O emissions because of the different wetted forms in the furrow and sprinkling irrigation soils. In the sprinkled soil, the applied water at low water amount may be beneficial to more aerobic than anaerobic environment. The advance of the wetting front may produce pulses of N_2O from the furrow-irrigated areas, similar to those observed after irrigation when soil was dry (Diego et al., 2017). Therefore, we doubt that the differences of water distributed between SI and FI soils may occur the different states in N_2O emissions. In our studies, the objectives were to compare N_2O emissions in the soils from a potato field with furrow and sprinkling irrigation, and to assess how the two irrigation systems modulated the N_2O emissions and emission factor of N_2O. In this experiment, the results would help to develop the strategies to mitigate N_2O emissions from the soils fertilized with chemical fertilizers in irrigated agriculture.

http://www.aloki.hu ● ISSN 1589 1623 (Print) ● ISSN 1785 0037 (Online)
DOI: http://dx.doi.org/10.15666/aeer/1705_1096310976

Materials and methods

Description of the study site

The experiment was implemented during the 2016–2017 at the potato experimental farm in the suburbs of Hohhot, Inner Mongolia (latitude 40°45′34″N, longitude 111°41′56″E), in the middle of Inner Mongolia Plateau located in the hinterland of the Asian continent (*Fig. 1*). The soil was a Calcic Haploxerept with a sandy clay loam texture (Soil Survey Staff, 1992). Some physico-chemical properties in the upper (0–30 cm) horizon of the soil were: pH, 7.79; organic matter, 0.93 ± 0.2 g/kg; bulk density, 1.25 ± 0.2 g/cm^3; clay, 32%; silt, 20%; and sand, 48%; $CaCO_3$, 8.54 ± 0.1 g/kg. The mean annual precipitation is 335 mm and the mean annual temperature is 6.7 °C (averages for the previous 15 years).

Figure 1. *The experimental site and equipments used to collect gases in the potato field*

Experimental design and field management

The experiment was arranged according to a split-plot design. Two main plots (600 m^2) were selected in the experimental field with two treatments. Every main plot was divided into six subplots (5×10 m) in a randomized complete block design with three replicates. The main-plot treatments were different irrigation systems: furrow and sprinkling irrigation. Each mainplot was also split according to the fertilizer treatment applied:(i) N, P, and K compound fertilizer and urea as a chemical fertilizer (NF, 390 kg N/ha) and (ii) a control without any fertilizer (Control). The amount of applied fertilizer is the local range used by farmers for potato crops (360–410 kg N/ha). Fertilizers were applied by hand and immediately incorporated into the upper 15 cm of the soil using a rotovator. Sprinkling irrigation is often used to apply soluble fertilizers, in small amounts, as and when irrigated. Per subplot included five pressure-compensated sprinkling irrigation lines spaced 90 cm apart. Each sprinkling irrigation line was fitted with a solid set consisting of six full circle impact sprinklers (Elgo 80B2, made in Israel) with a wetting radius of 10 m, spaced 2.8 m apart, mounted on 1.30 m risers. A water meter (LXS-20C, TEFEN Manufacture, Nahsholim, Israel) was installed in the main pipe to measure sprinkling water amount in each experimental plot. This method is a popular practice in local farmers.

The experimental site for the furrow irrigation involved five furrows in each subplot, which were spaced 90 cm apart and ploughed 30 cm deep. The furrows were enclosed at the end of each experimental site, as irrigation water was intercepted to prevent it from flowing out of the field. The subplots were independent, but irrigated at the same time. The furrows were constructed using a seeding machine. The amount of used

http://www.aloki.hu ● ISSN 1589 1623 (Print) ● ISSN 1785 0037 (Online)
DOI: http://dx.doi.org/10.15666/aeer/1705_1096310976

irrigation water was recorded by water meter on each irrigated subplot after fertilizer application.

A potato crop (*Solanum tuberosum* L. *cv. Favorita*) requiring about 105 days to reach maturity was planted by potato seeder on May 25th, 2016 and May 15th, 2017. The potatoes were planted on the raised beds 0.3 m high and 0.6 m wide, with the top of 0.3 m bed wide and with a 0.20 m spacing between plants in a row and sowing rate of 2250 kg/ha. The time for potatoes to be harvested is September.

Irrigation management

The first irrigation began on May 25th, 2016 and May 15th, 2017, immediately after the potatoes were planted. Water application intensity in the first was 40 mm for sprinkling irrigation. After the potatoes revived, the sprinkling field was irrigated when the mean soil matric potential (SMP) of the 0–20 cm soil layer decreased to about −24.5 kPa. The distribution of main potato-root zones determined the irrigation duration, which was usually about 1.5 min, with about 10 mm of water each time at a pressure of 0.1 Mpa by automatic control with computer. Sprinkling irrigation was stopped 20 d before harvesting.

The date and water amount of furrow irrigation were implemented based on local irrigation practices. Irrigation was uniformly applied three times throughout the crop growing season: once when potatoes were planted and the second in the tuber set stages and third time during the tuber bulking stages. The amount of water applied at each irrigation event was about 200 mm. The total amounts of water applied for sprinkling and furrow irrigation during the study period were 200.7 and 601.8 mm in 2016, 205 and 593.7 mm in 2017, respectively. Sprinkling irrigation frequency was higher, while total irrigation water was smaller in the sprinkling-irrigated field than in the furrow irrigated field in the experimental seasons. Sprinkling irrigation always characterizes by the higher frequency with a smaller quota for each event respected to furrow irrigation. Total precipitation was less than 200 mm during the crop growing season.

Sampling and analysis of N_2O

The N_2O fluxes were measured in situ simultaneously from each sprinkling irrigation and furrow irrigation plot using a static opaque chamber method (Yang et al., 2018). The chamber headspace was a 125 l cube (50 cm × 50 cm × 50 cm). The outer layer of the chamber was covered with sponge and aluminum foil, which is used to prevent the chamber from being heated by sunlight. The chambers were placed inside the square stainless-steel rings (50 cm × 50 cm) to ensure a good seal without destroying the compactness of the soil. The square stainless-steel rings were inserted into the soil, to a depth of 15 cm. On a day before sampling the gas samples, those rings were taken in order not to disturb the water distribution during irrigation. The chambers were closed for 60 min between 8:00 a.m. and 9:00 a.m. During this time, N_2O concentrations increased linearly. At 0 min, 5 min, 10 min, 15 min, and 20 min, the gas samples (100 ml) were collected in evacuated three-part polypropylene syringes, respectively. They were taken once per week throughout the potato growing season from planting to harvesting. The air temperature inside the chambers was observed during collecting sample. Soil temperature was monitored in the field using a portable digital thermometer (JM 624, JinMing Instrument Co. Ltd., Tianjin, China) inserted into the

http://www.aloki.hu ● ISSN 1589 1623 (Print) ● ISSN 1785 0037 (Online)
DOI: http://dx.doi.org/10.15666/aeer/1705_1096310976

soil: the monitored data were stored in a data logger. The moisture of soil was measured by the TDR350-indicating instrument (SPECTRUM Inc., ST Petersburg, Florida, USA).

The N_2O in the samples were measured and analyzed within 12 h by gas chromatograph (Agilent 6820D, Agilent Corporation, Shanghai, China) that was used two detectors: an electron capture detector (ECD) and a hydrogen flame ionization detector (FID). Its configurations described by Jiao (2015) were implemented for the N_2O analysis (Jiao et al., 2015).

Soil analysis

After sampling the gas, the soil in each stainless-steel ring was simultaneously collected and soil NO_3^--N and NH_4^+-N were determined by extracting 8 g of fresh soil with 60 ml of deionized water and 50 ml of KCl (0.01 M), respectively. They were measured using a micro-Kjeldahl procedure (Aulakh et al., 2000). SOC was determined by analysing soil extracts using a TOC analyzer (Sievers 5310 C, GE Analytical Instruments, USA) (Lim and Choi, 2014). Precipitation data were collected from the portable weather station located in the potato experimental farm.

Calculation method of N_2O emissions

Fluxes of N_2O was estimated within the closed chamber from the linear increase of gas concentration over sampling time of 0 min, 5 min, 10 min, 15 min, and 20 min based on $r^2 \geq 0.90$ while providing the maximum available flux data in the analysis of gas emissions (Jiao et al., 2015). Gas concentrations were converted to mass per unit volume (μg N_2O/uL) using the Ideal Gas Law at chamber air temperature measured during each sampling event and 0.101 MPa. Fluxes of N_2O were computed as:

$$F = \frac{\Delta C}{\Delta t} \times V/A \times \propto \quad \text{(Eq.1)}$$

where F is the flux rate of N_2O (μg N_2O–N/(m^2 hr)), $\Delta C/\Delta t$ denotes the increase or decrease of gas concentration in the chamber (μg/(L h)), V is the volume of the chamber (L), A is the covered surface area (m^2), and $\propto$ is a conversion coefficient for elemental N (28/44 for N_2O) (*Eq. 1*). Gas fluxes which failed linearity test were not included in the data analysis and accounted for < 2% of the total data set, while gas fluxes that failed significance and detection tests were set to zero flux. A complete discussion of chamber flux method is described in (Adviento-Borbe and Linquist, 2016).

Data statistics and analysis

The N_2O emissions were estimated by successive linear interpolation of N_2O emissions from the soils associated with the different irrigation systems. Statistical analyses were performed using SPSS version 22.0 (SPSS Inc., Chicago, IL, USA). A one-way analysis of variance (ANOVA) was used to evaluate the differences in seasonal and annual cumulative emissions of N_2O between the different irrigation. Tukey's multiple range tests were used to determine whether significant differences occurred between the treatments at a significance level of 0.05. A two-way ANOVA was used to analyze the effects of treatments and their interactions on N_2O emissions. Data drafting was run by SigmaPlot 13 and Excel 2016.

http://www.aloki.hu ● ISSN 1589 1623 (Print) ● ISSN 1785 0037 (Online)
DOI: http://dx.doi.org/10.15666/aeer/1705_1096310976

Results

Changes in precipitation and temperatures

The frequency of rainfall in crop growing season in 2016 is higher than that in 2017. There was no significant difference in the total rainfall of the crop growing season in 2016 and 2017 ($p > 0.05$), which were 196.6 mm and 198.8 mm, respectively. The atmospheric temperature showed a consistent trend of change from May to September in 2016 and 2017. The temperature began to increase gradually in April and was higher from July to August than other months (*Fig. 2*).

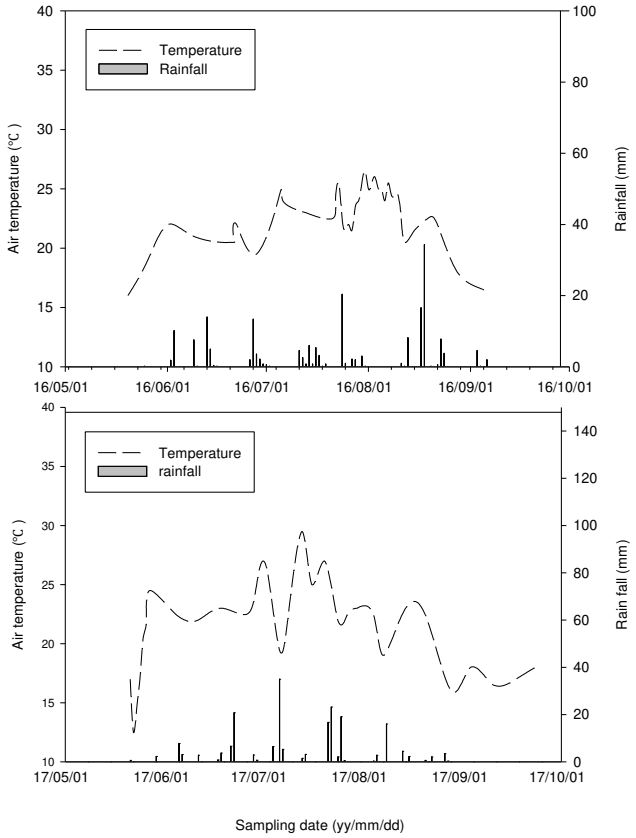

Figure 2. *Variable amount of temperature and precipitation in the potato experimental farm in 2016 and 2017*

Variation relationship between N_2O emission fluxes and the moisture or temperature in the soils of SI and FI

The potato field under four treatments from sprinkling irrigation systems and furrow irrigation systems exhibited a similar trend in N_2O emission fluxes. A significant emission peak of N_2O was detected in July and August throughout the testing stage from 2016 to 2017 (*Fig. 3*). Both the chemical fertilizer applied and the irrigation methods used affected the N_2O emission fluxes (*Fig. 3*). The NF soils from SI exhibited the highest N_2O emission fluxes, with 613.5 μg/(m^2 hr) in July 2017. The highest N_2O emission fluxes were produced with 1047.9 μg/(m^2 hr) from FI in the NF soils in July 2017. For the fertilization treatment and control under furrow irrigation system, the N_2O fluxes observed were higher than that in the sprinkling irrigation system in two crop

http://www.aloki.hu ● ISSN 1589 1623 (Print) ● ISSN 1785 0037 (Online)
DOI: http://dx.doi.org/10.15666/aeer/1705_1096310976

growing seasons, respectively. The N_2O emission fluxes of the fertilization treatment were higher than those of the control treatment in each irrigation system during the experimental period (*Fig. 3*).

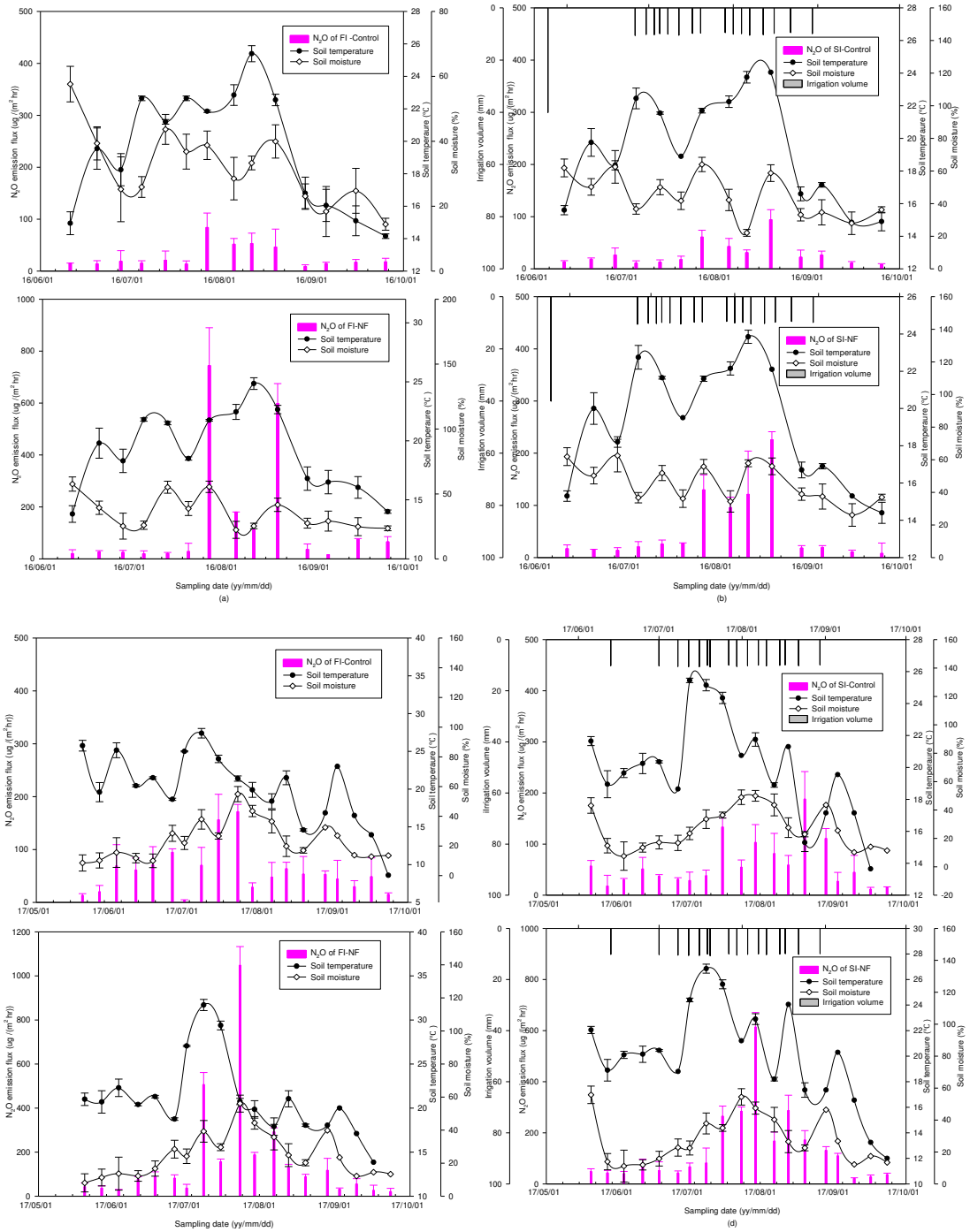

Figure 3. *Variation relationship between N_2O emission fluxes and the soil moisture or soil temperature in Control and NF in 2016 from FI (a) and SI (b), in 2017 from FI (c) and SI (d). (SI-NF and FI-NF refer to the treatment of fertilization from sprinkling irrigation and furrow irrigation. SI-Control and FI-Control refer to the treatment of no fertilization from sprinkling irrigation and furrow irrigation. Vertical bars indicate standard errors. The y-axes in the graphs (a)–(d) are on different scales)*

http://www.aloki.hu ● ISSN 1589 1623 (Print) ● ISSN 1785 0037 (Online)
DOI: http://dx.doi.org/10.15666/aeer/1705_1096310976

The variables of soil moisture and temperature exhibited generally consistent trends with N_2O emission fluxes from two irrigation systems. The soil moisture and temperature were higher, and N_2O emission fluxes of soils of two irrigation systems were higher in July and August than in May–June and in September (*Fig. 3*). During the irrigation period (from May to September), mean moisture of soil remained 45.9 and 44.5% under the furrow irrigation fertilization (NF) and furrow irrigation control (Control) system, and 39.7 and 34.3% under the sprinkling irrigation fertilization (NF) and sprinkling irrigation control (Control) system in 2016. The mean moisture of soil remained 26.1 and 26.6% under the NF and Control system from FI, and 24.6 and 23.3% under the NF and Control system from SI in 2017 (*Fig. 3*). Mean moisture was generally higher in NF and Control of FI than NF and Control plots of SI. There was no significant effect of two irrigation systems on the average daily soil temperature in the 0–30 cm soil layer from May to September ($p > 0.05$). There was no significant difference in soil temperature and moisture content for fertilized soil and soil without fertilizer of each irrigation system ($p > 0.05$).

Cumulative N_2O emissions in both irrigation systems

A significant difference in cumulative N_2O emissions of soils from the two irrigation systems was measured during the potato growing season in 2016 ($F = 13.84$, $p < 0.001$) and 2017 ($F = 6.49$, $p < 0.001$). The soils in Control of SI ($F = 47.0$, $p < 0.001$), NF of SI ($F = 7.8$, $p < 0.01$), Control of FI ($F = 57.5$, $p < 0.001$), and NF of FI ($F = 3.0$, $p < 0.05$) showed significant differences in the inter-annual cumulative N_2O emissions (*Fig. 4*). The cumulative N_2O emissions were significantly higher for NF and Control from FI than for NF and Control from SI over the annual sunflower growing season. The cumulative N_2O emissions in the fertilized soil were higher than that of the controlled soils each irrigation system. The cumulative N_2O emissions were 373.03 and 425.12 mg/m^2 for the FI with NF in 2016 and 2017. The cumulative N_2O emissions were 150.40 and 252.01 mg/m^2 for SI with NF from 2016 to 2017, respectively. The cumulative N_2O emissions from SI with NF were 59.68% and 40.72% lower than those from FI with NF for 2016 and 2017, respectively. The cumulative N_2O emissions of the Control soil from SI were 74.51 and 177.05 mg/m^2, and were 2.12% (2016) and 2.10% (2017) lower than that of the Control soil from FI in May – September during the annual potato field tested stage (*Fig. 4*). The cumulative N_2O emissions varied significantly with different irrigation systems throughout the potato experimental period. Sprinkling irrigation significantly reduced N_2O emissions.

Emission factor of N_2O

Emission factor of N_2O (EF) denotes the percentage of nitrogen lost in the form of N_2O gas in nitrogenous fertilizer, and can better evaluate the N_2O emission ratio of the fertilizers applied. EF of nitrogen fertilizer has been widely used in estimating regional and global N_2O emission inventories from farmland. The EF increased with N_2O emission due to increasing nitrogen fertilizer applied per unit area. EF from furrow irrigation and sprinkling irrigation in our study was 0.76% and 0.20% in 2016, 0.62% and 0.19% in 2017, respectively (*Fig. 5*). Compared with furrow irrigation, sprinkling irrigation can significantly reduce EF. The EF from sprinkling irrigation was 73.68% and 69.35% lower than that of furrow irrigation in 2016 and 2017. There was no significant difference in the inter-annual EF in furrow irrigation or sprinkling irrigation compared to soil air.

http://www.aloki.hu ● ISSN 1589 1623 (Print) ● ISSN 1785 0037 (Online)
DOI: http://dx.doi.org/10.15666/aeer/1705_1096310976

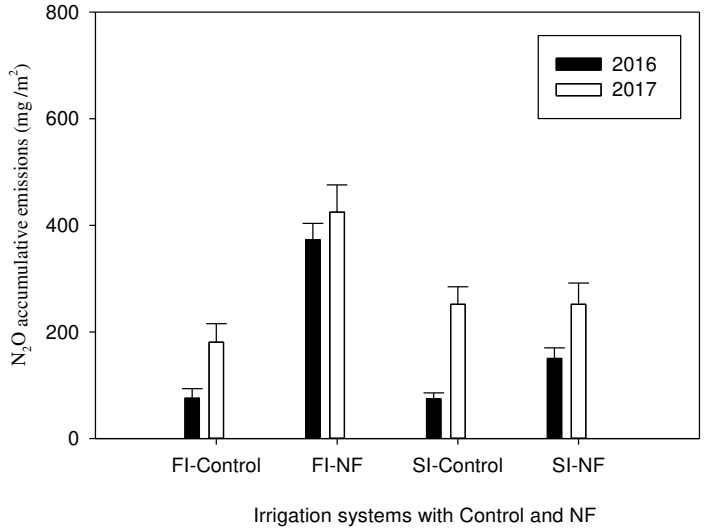

Figure 4. *Cumulative N_2O emissions varied significantly in Control and NF with FI and SI throughout the potato experimental period. (SI-NF and FI-NF refer to the treatment of fertilization from sprinkling irrigation and furrow irrigation. SI-Control and FI-Control refer to the treatment of no fertilization from sprinkling irrigation and furrow irrigation. Vertical bars indicate standard errors for each irrigation system)*

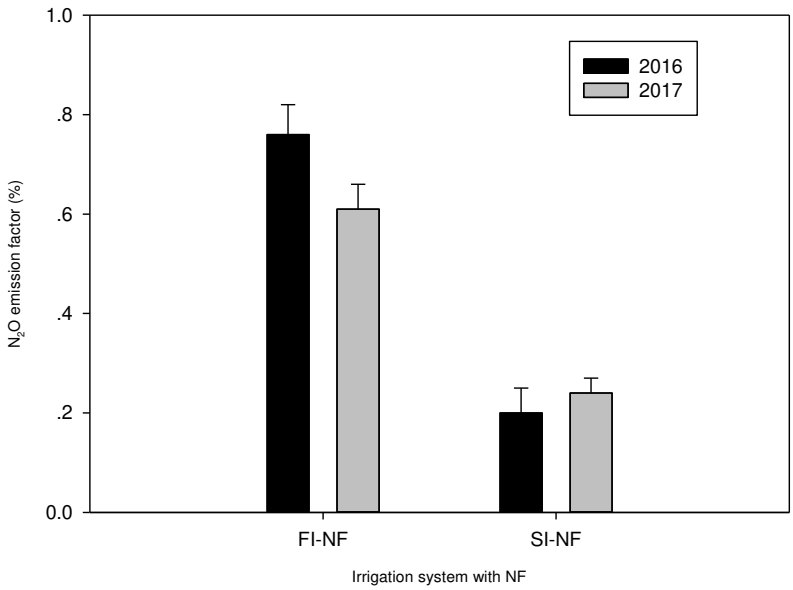

Figure 5. *Emission factor of N_2O varied between FI-NF and SI-NF in 2016 and 2017. (SI-NF and FI-NF refer to the treatment of fertilization from sprinkling irrigation and furrow irrigation. Vertical bars indicate standard errors for each irrigation system)*

Discussion

Seasonal variation of N_2O emissions in two irrigation systems

The biggest N_2O emission pulses were generated and there are higher emission rate in July and August during the season of vigorous potato growth from 2016 to 2017, in both the sprinkling irrigation and furrow irrigation treatments. Seasonal dynamics of

http://www.aloki.hu ● ISSN 1589 1623 (Print) ● ISSN 1785 0037 (Online)
DOI: http://dx.doi.org/10.15666/aeer/1705_1096310976

N_2O emissions fluxes were consistent with the changes of moisture and temperature in soil that were greater in July – August than in May–June and September–October (*Fig. 3*). These discoveries are consistent with the results of Kallenbach et al. (2010) in the soils from other arid and semiarid areas (Kallenbach et al., 2010). The production and consumption of N_2O from the soils are affected via the processes of nitrification and denitrification with microorganisms participating. These processes are all related to soil temperature and moisture (Firestone and Davidson, 1989). Soil moisture controls the biotic and abiotic processes, and operates a critical regulation function in the microbial activities of soils, for instance, N mineralization, nitrification and denitrification that are all quantitatively influenced by the applied irrigation methods (Sánchez-Martín et al., 2008). Climate and soil abiotic factors: soil temperature and moisture, can affect the dynamic changes of N_2O, with visible seasonal characteristics, in particular, in water transport.

N_2O emissions fluxes in the fertilized and control soils from sprinkling irrigation and furrow irrigation

Mean emissions fluxes of N_2O was 152.02 μg/(m^2 hr) in furrow irrigation, 36.53 μg/(m^2 hr) in sprinkling irrigation for fertilization treatment from 2016 to 2017. Change of irrigation mode affects N_2O source emission from farmland soil. In furrow irrigation, the peak value of N_2O emissions in the NF was four times higher than in sprinkling irrigation. Sprinkling irrigation compared with traditional furrow irrigation, significantly reduced N_2O emission from potato fields (*Fig. 4*). The amount of applied water in furrow irrigation was more significant than the saturated hydraulic conductivity in the soils, with furrows remaining flooded for several hours. The NH_4^+-N from the NF in the wetting soils was fleetly nitrified, increasing the concentration of NO_3^--N. In FI, the high rate of used water quickly dissolved these fertilizers and produced a great deal of NH_4^+-N and NO_3^--N on the surface layer of the soil profile. Rapidly dissolving a lot of fertilizer would partly illustrate the significantly greater ($P < 0.05$) NO_3^--N and NH_4^+-N concentration found in furrow irrigation system than in sprinkling irrigation system (*Table 1*). The essential differences between the concentration of NO_3^--N and NH_4^+-N of the soil have emerged in the decision on irrigation strategy. The process of soil nitrogen conversion is different from that of N_2O emission between sprinkling irrigation and furrow irrigation. Tensiometers controlled the sprinkling irrigation. The irrigation was triggered when SMP at 0.2 m depth directly under the sprinkling emitters reached –24.5 kPa. The irrigation was stopped when the amount of water applied to each irrigation event was about 10 mm. Values for the soil NO_3^--N and NH_4^+-N concentration in the upper 10 cm layer for the same fertilizer treatment generally remained lower on NF from SI than FI (*Table 1*). The NO_3^--N and NH_4^+-N that will not be leached were concentrated in the root zone of potato under sprinkling irrigation. The NO_3^--N and NH_4^+-N are beneficial to the uptake of potato due to the low amount of water from sprinkling irrigation. The results of Wang et al.'s (2012) research are consistent with our study (Wang et al., 2012). The concentration of NO_3^--N and NH_4^+-N in furrow irrigation soil is significantly higher than that in water-saving irrigation soil. Sprinkling irrigation reduces the concentration of NO_3^--N and NH_4^+-N, inhibits denitrification and reduces N_2O emissions. High concentrations of NO_3^--N and NH_4^+-N trigger higher N_2O emissions during nitrification and denitrification (Sánchez-Martín et al., 2008). In our study, high NO_3^--N and NH_4^+-N contents in furrow irrigation resulted in high N_2O emission.

http://www.aloki.hu ● ISSN 1589 1623 (Print) ● ISSN 1785 0037 (Online)
DOI: http://dx.doi.org/10.15666/aeer/1705_1096310976

Table 1. *Basic physical and chemical properties of soil from sprinkling irrigation and furrow irrigation*

Year	Treatments	Bulk density (g cm^{-3})	Porosity (%)	NH_4^+-N (mg kg^{-1})	NO_3^--N (mg kg^{-1})
2016	FI-NF	1.34 ± 0.07a	48.13 ± 1.40a	7.09 ± 1.10a	34.28 ± 1.25a
	SI-NF	1.21 ± 0.03b	49.86 ± 0.53b	6.46 ± 1.00b	22.98 ± 1.60b
	FI-Control	1.35 ± 0.05a	49.23 ± 0.62c	6.64 ± 1.22c	21.76 ± 1.21c
	SI-Control	1.19 ± 0.01b	52.58 ± 0.75d	6.08 ± 1.43d	16.64 ± 1.36e
2017	FI-NF	1.29 ± 0.02c	50.42 ± 2.30e	6.95 ± 1.35e	73.66 ± 2.21f
	SI-NF	1.17 ± 0.02b	55.15 ± 1.80f	6.25 ± 1.06f	37.76 ± 1.13g
	FI-Control	1.29 ± 0.01c	50.09 ± 1.20c	6.76 ± 1.40b	34.41 ± 2.05h
	SI-Control	1.21 ± 0.01b	53.17 ± 0.38d	6.21 ± 1.20d	30.47 ± 1.97i

SI-NF and FI-NF refer to the treatment of fertilization from sprinkling irrigation and furrow irrigation. SI-Control and FI-Control refer to the treatment of no fertilization from sprinkling irrigation and furrow irrigation. NH_4^+-N and NO_3^--N are seasonal mean. Bulk density and porosity are the value at the end of the growing season

Comparing sprinkling irrigation with furrow irrigation in potato field, soil bulk density under sprinkling irrigation (1.17 g/cm^3) is lower than that under furrow irrigation (1.29 g/cm^3) from 2016 to 2017 (*Table 1*). Sprinkling irrigation compared with furrow irrigation increases soil porosity, improves soil permeability. The topsoil in sprinkling irrigation fields was looser than that in furrow irrigation fields (Sun et al., 2008). Sprinkling irrigation is one of the water-saving irrigation methods widely adopted in agricultural production. The environmental conditions of soils in sprinkling irrigation were similar to that of drip irrigation (Lv et al., 2010), and favored nitrification, contributing to lower emissions of N oxides (Sánchez-Martín et al., 2008). Both the high consumption and frequency of used water in the furrow irrigation strategy produced the high moisture of soil in the plots. The high moisture in the soils resulted in the emergence of a high proportion of anaerobic environment. High soil moisture not only stimulates soil microbial activity, but also reduces the flow of oxygen in soil, leading to nitrification and denitrification. Use of furrow irrigation gave higher N_2O emission losses than drip irrigation (Sánchez-Martín et al., 2008). Different infiltration and redistribution patterns of irrigation water result in different distribution patterns of soil water in time, horizon and vertical depth, which have an important impact on the production and emission of N_2O and its spatial and temporal distribution. Under drip irrigation, as water supply is low, the process of soil N_2O production from denitrification will be limited, and the N_2O emission will be reduced (Kallenbach et al., 2010; Sánchez-Martín et al., 2010). Soil in furrow-irrigated potato fields emits more N_2O than that in sprinkling-irrigated. Sprinkling irrigation can reduce N_2O emission from farmland soil.

The used NF treatment in the potato field also had a significant impact on the results achieved. The concentration of NH_4^+-N and NO_3^--N was significantly ($P < 0.05$) greater in the fertilization treatment than in the Control for sprinkling irrigation and furrow irrigation, respectively (*Table 1*). The N_2O emissions of soils were commonly higher in the fertilization treatment than in the Control in sprinkling irrigation and furrow irrigation throughout the testing stage (*Fig. 3*). In irrigated agriculture, both the availability of water and N fertilizers has an essential effect on N_2O emissions. Higher concentrations of NH_4^+ and NO_3^- were detected in the soils of NF compared with the

http://www.aloki.hu ● ISSN 1589 1623 (Print) ● ISSN 1785 0037 (Online)
DOI: http://dx.doi.org/10.15666/aeer/1705_1096310976

soil of no fertilizer (Vallejo et al., 2005). The effect of the ions from nitrification and denitrification processes caused higher N_2O emissions in the soils with chemical fertilizer compared with the soils of no fertilizer in drip irrigation and furrow irrigation systems (Sánchez-Martín et al., 2008).

Emission factor of N_2O in two irrigation systems

In our study, mean emission factor of N_2O from nitrogenous fertilizer for two-year growth period in potato fields is 0.20 and 0.69 % in sprinkling irrigation and furrow irrigation, respectively. Statistics such as Xu et al. (2016) show that the N_2O emission factor of nitrogen fertilizer is 0.50%~0.82% during the growth period of summer maize, 0.61%~1.13% in a vegetable field in the arid area (Xu et al., 2016). The EF of N_2O from the potato field of furrow irrigation in our study is in the range of EF from Xu et al. (2016) in the upland field. The EF of N_2O in potato field from sprinkling irrigation was significantly lower than that in the soils of the upland field, and it was 61% lower than the lowest EF (0.61%) of N_2O in vegetable soil and 81% lower than the highest EF (1.13%) of N_2O. Sprinkling irrigation significantly reduces N_2O emissions.

Kang and Eltahir (2018) use the Massachusetts Institute of Technology (MIT) Regional Climate Model (MRCM) to perform simulations for the historical period (1975–2005), as well as future climate (2070–2100) assuming two scenarios of GHG emissions with furrow irrigation which cools surface temperature and moistens surface air, but boosts integrated measures of temperature and humidity, and hence enhances intensity of heatwaves. China is currently one of the largest contributors to the emissions of greenhouse gases, with potentially serious implications to its population (Kang and Eltahir, 2018). Sprinkling irrigation in China is widely used to reduce these greenhouse gas emissions.

The irrigation strategy had an important impact on the pattern of N_2O emissions. The choice of an irrigation system is regarded as a critical way of saving water in arid and semiarid regions and maintaining optimal crop yield. In this experiment, sprinkling irrigation has been demonstrated that it can also be used as a tool for mitigating emissions of N_2O. To date, no results have been published comparing sprinkling and furrow irrigation. Although our results indicate that the N_2O emission pattern of sprinkling irrigation contributed to lower emissions on N_2O, many studies will be essential to assess the effect of some parameters related to sprinkling irrigation. These parameters include soil characteristics, especially hydraulic conductivity of affecting water distribution. Moreover, as sprinkling irrigation is frequently combined with applied chemical fertilizer, further work is needed to assess the influence of frequency, rate and type of N fertilized on N_2O emissions via sprinkling irrigation.

Conclusions

This study demonstrated that the choice of irrigation strategy had a significant effect on N_2O emissions. Sprinkling irrigation saves water and also helps to reduce the production of N_2O. Therefore, it can be regarded as an effective method for mitigating the gas loss in the soils of agroecosystems in arid and semiarid areas. Nevertheless, more field studies are needed to assess the influence of the new irrigation technologies on N_2O emissions and the comprehensive influence of using both water and N.

http://www.aloki.hu ● ISSN 1589 1623 (Print) ● ISSN 1785 0037 (Online)
DOI: http://dx.doi.org/10.15666/aeer/1705_1096310976

Acknowledgements. The National Natural Science Foundation of China under grant number 41765010, the National Key Research and Development Program of China under grant number 2016YFC0400105, the Inner Mongolia Youth Innovative Talent Training Program of the Prairie Excellence Project 2016 funded this research and Program for Young Talents of Science and Technology in Universities of Inner Mongolia Autonomous Region.

REFERENCES

[1] Adviento-Borbe, M. A. A., Linquist, B. (2016): Assessing fertilizer N placement on CH_4 and N_2O emissions in irrigated rice systems. – Geoderma 266: 40-45.

[2] Aulakh, M. S., Khera, T. S., Doran, J. W. (2000): Yields and nitrogen dynamics in a rice–wheat system using green manure and inorganic fertilizer. – Soil Science Society America Journal 64: 1867-1876.

[3] Auxiliadora, C., Juan, H., Jesús, A. B., Glen, R. (2018): Sensor-based assessment of soil salinity during the first years of transition from flood to sprinkler irrigation. – Sensors 616: 1-18.

[4] Davidson, E. A. (1991): Fluxes of Nitrous Oxide and Nitric Oxide from Terrestrial Ecosystems. – In: Rogers, J. E., Whitman, W. B. (eds.) Microbial Production and Consumption of Greenhouse Gases: Methane, Nitrous Oxides and Halomethanes. American Society for Microbiology, Washington, pp. 219-235.

[5] Diego, A., Alberto, S. C., Gemma, A., Antonio, V. (2017): Rainfall amount and distribution regulate DMPP effects on nitrous oxide emissions under semiarid Mediterranean conditions. – Agriculture Ecosystems & Environment 238: 36-45.

[6] Ezequiel, S., Antonio, P. D. C., Tarlei, A. B., José, A. F., Richard, K., Bruno, M. (2018): Test methods for characterising the water distribution from irrigation sprinklers: Design, evaluation and uncertainty analysis of an automated system. – Biosystems Engineering 169: 42-56.

[7] Firestone, M. K., Davidson, E. A. (1989): Microbial Basin of NO and N_2O Production and Consumption in Soil. – In: Andreae, M. O., Schimel, D. S. (eds.) Exchange of Trace Gases between Terrestrial Ecosystem and the Atmosphere. Wiley, London, pp. 7-21.

[8] Granli, T., Bockman, O. C. (1994): Nitrogen oxide from agriculture. – Norwegian Journal of Agricultural Sciences 12: 7-127.

[9] IPCC (2013): Climate Change 2013: The Physical Science Basis. – In: Stocker, T. F., Qin, D., Plattner, G. K., Tignor, M., Allen, S. K., Boschung, J., Nauels, A., Xia, Y., Bex, V., Midgley, P. M. (eds.) Contribution of Working Group I to the Fifth Assessment Report of the Intergovernmental Panel on Climate Change. Cambridge University Press, New York.

[10] Jiao, Y., Hou, J. H., Zhao, J. H., Yang, W. Z. (2015): Cropland age from grassland conversion to cropland affects nitrous oxide emission. – Acta Agriculturae Scandinavica, Section B -Soil & Plant Science 65: 566-574.

[11] José, C., Eva, T. M., Francisco, M. (2018): Sprinkler irrigation frequency affects maize yield depending on irrigation time. – Agronomy Journal 110: 1862-1873.

[12] Kallenbach, C. M., Rolston, D. E., Horwath, W. R. (2010): Cover cropping affects soil N_2O and CO_2 emissions differently depending on type of irrigation. – Agriculture Ecosystems & Environment 137: 251-260.

[13] Kang, S. C., Eltahir, E. A. B. (2018): North China Plain threatened by deadly heatwaves due to climate change and irrigation. – Nature Communications 9: 2894.

[14] Laura, S. M., Augusto, A., Alejandro, B., Lourdes, G. T., Antonio, V. (2008): Influence of drip and furrow irrigation systems on nitrogen oxide emissions from a horticultural crop. – Soil Biology & Biochemistry 40: 1698-1706.

[15] Li, J., Zhang, J., Ren, L. (2003): Water and nitrogen distribution as affected by fertigation of ammonium nitrate from a point source. – Irrigation Science 22: 19-30.

http://www.aloki.hu ● ISSN 1589 1623 (Print) ● ISSN 1785 0037 (Online)
DOI: http://dx.doi.org/10.15666/aeer/1705_1096310976

[16] Lim, S. S., Choi, W. J. (2014): Changes in microbial biomass, CH_4 and CO_2 emissions, and soil carbon content by fly ash co-applied with organic inputs with contrasting substrate quality under changing water regimes. – Soil Biology & Biochemistry 68: 494-502.
[17] Lorenzo, D. M., Martina, M., Alex, C. B., Tiago, A. K., Cleber, M. A. (2018): Classification of rice grains of lowland cultivars grown under flood irrigation and sprinkler irrigation. – Engenharia Agrícola 38: 599-605.
[18] Lv, G. H., Kang, Y. H., Li, L., Wan, S. Q. (2010): Effect of irrigation methods on root development and profile soil water uptake in winter wheat. – Irrigation Science 28: 387-398.
[19] Naghedifar, S. M., Ziaei, A. N., Ansari, H. (2018): Simulation of irrigation return flow from a Triticale farm under sprinkler and furrow irrigation systems using experimental data: A case study in arid region. – Agricultural Water Management 210: 185-197.
[20] Robertson, G. P., Paul, E. A., Harwood, R. R. (2000): Greenhouse gases in intensive agriculture: Contributions of individual gases to the radiative forcing of the atmosphere. – Science 289: 1922-1925.
[21] Sánchez-Martín, L., Vallejo, A., Dick, J., Skiba, U. M. (2008): The influence of soluble carbon and fertilizer nitrogen on nitric oxide and nitrous oxide emissions from two contrasting agricultural soils. – Soil Biology & Biochemistry 40: 142-151.
[22] Sánchez-Martín, L., Meijide, A., Garcia-Torres, L., Vallejo, A. (2010): Combination of drip irrigation and organic fertilizer for mitigating emissions of nitrogen oxides in semiarid climate. – Agriculture Ecosystems & Environment 137: 99-107.
[23] Schilt, A., Brook, E. J., Bauska, T. K., Baggenstos, D., Fischer, H., Joos, F., Petrenko, V. V., Schaefer, H., Schmitt, J., Severinghaus, J. P., Spahni, R., Stocker, T. F. (2014): Isotopic constraints on marine and terrestrial N_2O emissions during the last deglaciation. – Nature 516: 234-237.
[24] Soil Survey Staff. (1992): Keys to Soil Taxonomy. Sixth Ed. – USDA, Washington DC.
[25] Sun, Z. Q., Kang, Y. H., Jiang, S. F. (2008): Effects of water application intensity, drop size and water application amount on the characteristics of topsoil pores under sprinkler irrigation. – Agricultural Water Management 95: 869-876.
[26] US-EPA (2006): Global Anthropogenic Non-CO_2 Greenhouse Gas Emissions, 1990-2020. – United States Environmental Protection Agency, EPA 430-R-06-003, June 2006, Washington DC, USA. Accessed 26 March 2007.
[27] Vázquez, N., Pardo, A., Suso, M. L., Quemada, M. (2005): A methodology for measuring drainage and nitrate leaching in unevenly irrigated vegetable crops. – Plant and Soil 269: 297-308.
[28] Vallejo, A., Garcıa-Torres, L., Diez, J. A., Arce, A., Lopez-Fernandez, S. (2005): Comparison of N losses (NO_3, N_2O, NO) from surface applied, injected or amended (DCD) pig slurry of an irrigated soil in a Mediterranean climate. – Plant and Soil 272: 313-325.
[29] Wang, X. J., Wei, C. Z., Zhang, J., Dong, P., Wang, J., Zhu, Q. C., Wang, J. X. (2012): Effects of irrigation mode and N application rate on cotton field fertilizer N use efficiency and N losses. – Chinese Journal of Applied Ecology 23: 2751-2758.
[30] Xu, Y. X., Guo, L. P., Xie, L. Y., Yun, A. P., Li, Y. C., Zhang, X., Zhao, X., Diao, T. T. (2016): Characteristics of background emissions and emission factors of N_2O from major upland fields in China. – Scientia Agricultura Sinica 49: 1729-1743.
[31] Yang, W. Z., Yang, M. D., Wen, H. Y., Jiao, Y. (2018): Global Warming Potential of CH_4 uptake and N_2O emissions in saline–alkaline soils. – Atmospheric Environment 191: 172-180.
[32] Zapata, N., Robles, O., Playán, E., Paniagua, P., Romano, C., Salvadorb, R., Montoya, F. (2018): Low-pressure sprinkler irrigation in maize: differences in water distribution above and below the crop canopy. – Agricultural Water Management 203: 353-365.

http://www.aloki.hu ● ISSN 1589 1623 (Print) ● ISSN 1785 0037 (Online)
DOI: http://dx.doi.org/10.15666/aeer/1705_1096310976

DROUGHT TOLERANCE AND SUSCEPTIBILITY OF MAIZE (*ZEA MAYS* L.) USING YIELD RESPONSE FACTOR AND TOLERANCE INDICES

HAMA, B. M. – MOHAMMED, A. A.*

Crop Science Department, College of Agricultural Sciences, University of Sulaimani, Sulaimani, Kurdistan Region, Iraq
(e-mail: bekhal.mustafa@univsul.edu.iq; phone: +964-770-190-0487)

**Corresponding author*
e-mail: aram.muhammed@univsul.edu.iq; phone: +964-770-157-6760

(Received 26th Mar 2019; accepted 13th Jun 2019)

Abstract. In order to evaluate the drought tolerance and susceptibility of six maize hybrids under water deficit conditions, an investigation was conducted during the growing season of 2016 at the Qlyasan Research station- University of Sulaimani. The field experiment was implemented according to the split plot design with three replications, four different irrigation levels were allocated in main plots, while six maize (*Zea mays* L.) hybrids were cultivated in the sub-plots. The yield response factor (Ky) was estimated through calculating adjusted crop coefficient (Ks) as well as adjusted Crop evapotranspiration (ETc adj.) in growth stages, including initial, rapid growth, mid-season, and the late season, revealing Ks values lower than that obtained by FAO paper No.33, (0.49, 0.6, 0.528, and 0.204) respectively. Four stress tolerance indices, including stress tolerance index (STI), stress tolerance (TOL), mean productivity (MP),) and geometric mean productivity (GMP) were used in this study. Data analysis demonstrated that the indices STI, TOL, MP, and GMP were more effective in defining the high yielding hybrids under different growing conditions. The results of the cluster analysis, yield response factor (Ky) and stress indices corresponded due to tolerance and susceptibility of maize hybrids.
Keywords: *water deficit, resistance, sensibility, maize hybrid*

Introduction

Maize (*Zea mays* L.) is considered as the third most important cereal crop after wheat and rice around the world, it covers 4.8% of the total cropped area and attributes 3.5% of the global agricultural crop output (Ahmad et al., 2011; Deryng et al., 2014). Some of the challenges that influence the productivity and the expansion of the maize cultivation in a semiarid region are caused by water deficit and shortage in water availability, the yield of different crops reaches the maximum value with evapotranspiration (ETm), therefore an actual yield (Ya) matches with an actual evapotranspiration (ETa) (Nacharchi et al., 2011). Drought tolerance consists of ability of crop for growth and production under water deficit conditions. A long-term drought stress effects on plant metabolic reactions associates with, plant growth stage, water storage capacity of the soil and physiological aspects of plant. Crop response to the limited water condition is important for adjusting the relationship between grain yield and efficient irrigation systems to evaluate crop performance under water deficit condition (Carvalho et al., 2016; Irandoust and Bijanzadeh, 2017).

The yield response factor (Ky) is a factor that describes the reduction in relative yield according to the reduction in ETc caused by a soil water shortage, the response of a crop to its soil moisture environment is quantified through Ky (Greaves and Wang, 2017), the values of Ky are crop specific and may vary over the growing season (Steduto et al., 2012). Usually, the decrease in yield due to water deficit during the vegetative and

http://www.aloki.hu ● ISSN 1589 1623 (Print) ● ISSN 1785 0037 (Online)
DOI: http://dx.doi.org/10.15666/aeer/1705_1097710988

ripening period is relatively small, while during the flowering and yield formation periods it will be large. Values for Ky for individual growth periods and for the complete growing season have been included in the FAO Irrigation and Drainage Paper No 33. The importance of the yield response factor is to determine the efficiency of water use and crop productivity, which is founded on the relative yield loss of any crop to the relative reduction of water requirements, differences in actual evapotranspiration and the crop response factor which usually vary according to crop growing conditions. The average Ky value founded by previous researchers (Najarchi et al., 2011) was higher than the previous reported values, thus, the reductions in yield under effect of deficit irrigation are higher than those reported by FAO (Doorenbos and Kassam, 1979). Enormous distinction of Ky value for maize resulted from variation in environmental effects and growth patterns were represented in the previous research, there was deviation from finding of Doorenbos and Kassam (1979), whom they determined ky value for maize 1.25, while other researchers documented 2.15 for sensitive genotypes and 1.56 for water deficit resistance genotypes, as well the different values of ky 1.58 and 1.50 were showed with stress condition at tasseling or silking and post silking stage, however the ky value for those growing stages were 0.40, 1.50, and 0.50 found by Doorenbos and Kassam (1979).

Drought indices clarify the effect of drought on the yield forfeiture comparing with the yield under no stress condition has been used for drought tolerance checking (Mitra,2001). To evaluate response of plant genotypes to drought stress, some selection indices based on a mathematical relation between stress- and optimum conditions has been proposed. Moghaddam et al. (2002) found Stress Tolerant Index (STI) was more useful in order to select favourable corn cultivars under stressful and stress-free conditions, however the greater TOL value indicate to larger grain yield reduction under stress condition, whereas lowest TOL indicate to lower grain yield reduction under stress condition. Khalili et al. (2004) showed that based on Geometric Mean Productivity (GMP) and STI indices, corn hybrids with high yield in both stress and non-stress environments can be selected. Talebi et al. (2009) concluded that GMP and STI were able to discriminate tolerant genotypes under stress conditions, their results indicated that there was a positive and significant correlation among Yp and (MP, GMP and STI) and Ys and (MP, GMP and STI) and they hence were better predictors of Yp and Ys than TOL. There was indication of significant correlation between MP, STI, and GMP with the yield at both non-stress and stress conditions (Zare, 2012).

Thus, the objective of this study was the evaluation of yield response factor and the efficiency and profitability of different selection indices in the identification of maize hybrids, which are compatible with stressful and optimal conditions, to achieve hybrids that can tolerate water deficit condition especially at sensitive growth stages.

Materials and methods

Six maize hybrids were evaluated in the investigation includes Medium 791, Btaris, Cantabpis, Fajr 260, Es-Solito 655, and Dhqan. All hybrids were produced from College of Agriculture, the University of Kurdistan, Sianandaj-Iran. The study was conducted during the summer season of 2016 at the Qlyasan Research Station, College of Agricultural Sciences, University of Sulaimani/KRG-Iraq (35° 34’ 19” N 45° 22’ 1.6” E with altitude of 754 m.a.s.l). The experiment was laid out in a split plot design in which water deficit levels will be in the main plots and each treatment was replicated

http://www.aloki.hu ● ISSN 1589 1623 (Print) ● ISSN 1785 0037 (Online)
DOI: http://dx.doi.org/10.15666/aeer/1705_1097710988

three times. Each replication was divided into four main plots with different schedules irrigation. The six hybrids were randomly distributed within the sub-plots. Four irrigation treatments were used as well Irrigation (I_1), deficit irrigation during the vegetative period (I_2), reproductive period (I_3) and both of them (I_4). A net plot size of 4 m × 10.2 m was kept. The crop was sown during the first week of Jully in rows 70 cm apart and 25 cm between plants. In order to prevent the lateral spread of water plots a distance of 2 m between plots was left bare. Phosphorus fertilizer, as triple super phosphate, was applied before sowing time with rate of 150 kg ha^{-1}. The nitrogen fertilizer, as urea 46% N, was applied by two doses, the first one was applied at the seedling stage and the second application was on tasseling stage. All other agricultural practices were behaving as required. The yield response factor (Ky) was calculated, for determining the responses of maize hybrids to the effect of water deficit, a simple, linear crop-water production function was introduced in the FAO Irrigation and Drainage Paper No 33 (Steduto et al., 2012) to predict the reduction in crop yield when crop stress was caused by a shortage of soil water:

$$[1-\frac{Ya}{Ym}]=Ky[1-(\frac{ETc\,adj}{ETc})] \quad \text{(Eq.1)}$$

Where: Ya = actual yield of the crop [ton ha^{-1}], Ym = maximum (expected) yield in the absence of environmental or water stress [ton ha^{-1}], Ky = a yield response factor [-], ETc adj = adjusted (actual) crop evapotranspiration [mm d^{-1}], ETc = crop evapotranspiration for standard conditions (no water stress) [mm d^{-1}].

In the crop coefficient approach the crop evapotranspiration, ETc, is calculated by multiplying the reference crop evapotranspiration, ETo, by a crop coefficient, Kc The adjusted Crop Coefficient, or stress, crop coefficient (Ks) which describes the effect of water stress on crop transpiration was quantified for determining the exact effect of the soil water stress on the crop transpiration in water deficit treatments, the incorporation of the effect of water stress into crop coefficient (Kc) was determined as:

$$ETc\ adj = Ks \times Etc \quad \text{(Eq.2)}$$

Where is the = stress, crop coefficient [dimensionless], Etc = crop evapotranspiration [mm d^{-1}].

$$ETc = Kc \times ETo \quad \text{(Eq.3)}$$

Where Kc = crop coefficient [dimensionless], ETo = reference evapotranspiration [mm^{-1}].

$$ETo = P(0.46 \times Tmean + 8) \quad \text{(Eq.4)}$$

$$Ks = (TAW - Dr) / (TAW - RAW) \quad \text{(Eq.5)}$$

Where TAW = the total available soil water in the root zone [mm], RAW = the readily available soil water in the root zone [mm], Dr = root zone depletion [mm].

$$TAW = 1000\ (\theta F.C - \theta W.P)Zr \quad \text{(Eq.6)}$$

http://www.aloki.hu ● ISSN 1589 1623 (Print) ● ISSN 1785 0037 (Online)
DOI: http://dx.doi.org/10.15666/aeer/1705_1097710988

Where θF. C = the water content at field capacity [m^3 m^{-3}], θW.P = the water content at wilting point [m^3 m^{-3}], Zr = the rooting depth [m].

$$Dr = 1000\ (\theta F.C - \theta i - 1)Zr \quad \text{(Eq.7)}$$

Where θi – 1 = the average soil, water content for the effective root zone [mm].

$$RAW = p \times TAW \quad \text{(Eq.8)}$$

Where p = average fraction of Total Available Soil Water (TAW) that can be depleted from the root zone before moisture stress.

The studied drought resistance indices were calculated by using the following relationships in *Table 1*:

Table 1. *The computing relations of the parameters studied in the experiment*

Parameters	Formula	Reference
Stress Tolerance Index (STI)	STI = Ypi × YsiYp²	Fernandez, 1992
Tolerance Index (TOL)	TOL = Ypi – Ysi	Rosielle and Hamblin, 1981
Geometric Mean Productivity (GMP)	GMP = Ypi × Ysi	Fernandez, 1992
Mean Productivity (MP)	MP = Ypi + Ysi2	Rosielle and Hamblin, 1981

Ysi = yield of hybrid in stress condition, Ypi = yield of hybrid in normal condition And SI that is stress intensity, where: SI = [1 – YsYp]. Ys = total yield mean in stress condition, Yp = total yield mean in normal condition

The software JMP version 13 and XLSTAT version 16 were used for statistical analysis like one-way analysis of variance and LSD test at the 5% level. The principal component analysis (PCA) Eriksson et al. (1999) was determined to assess the relationship between the variables. Depending on the means of stress indices characters, the dendrogram was produced by using the Euclidean distances and unweighted pair-group method with the arithmetic mean (UPGMA) analysis method.

Results and discussion

Water stress may be induced under the effect of lower water supply and the evapotranspiration will drop below the standard crop evapotranspiration, ETc., The reduction in the value of crop coefficients under water deficit conditions is determined using the stress crop coefficient Ks (calculated with *Eq. 5*). *Table 1* demonstrates the adjusted crop evapotranspiration ETc adj. (Calculated with the *Eq. 2*) For water deficit treatments include I_2, I_3, and I_4 as well adjusted crop coefficient (Ks x Kc), because the modification of vegetation and ground cover mean that the crop coefficient Kc varies during the growing period as well with influence of water deficit levels (Payero et al., 2008; Allen et al., 2017). In order to determining the yield response factor of maize hybrids under influence of well irrigation as well water deficit levels, the adjusted evapotranspiration was used, the stress crop coefficient that calculated for different growth stages of six maize hybrids were declined from 0.7, to 0.49, for irrigation levels, I_2, I_3, and I_4 respectively during initial stage, and from 1.2, to 0.6, for rapid growth stage and from 1.2, to 0.528, for mid season stage and for the late season stage it declined from 0.6 to 0.204. The calculation of adjusted evapotranspiration was done in

http://www.aloki.hu ● ISSN 1589 1623 (Print) ● ISSN 1785 0037 (Online)
DOI: http://dx.doi.org/10.15666/aeer/1705_1097710988

accordance with adjusted Kc (Kc x Ks). The adjusted crop evapotranspirations were used in calculating the yield response factor Ky of the maize hybrids in different growth stages and demonstrated in *Table 2*, the variation between adjusted evapotranspiration and actual evapotranspiration has created under influence of higher reference evapotranspiration, similar results were documented by (Kuscu et al., 2013).

Table 2. *Adjusted crop coefficient and adjusted crop evapotranspiration in different growth stages*

Growth stages	I. T.	T. min	T. max	T. mean	ETo	Kc	ETc	TAW	RAW	Dr	Kc × Ks	ETc adj.
Initial	I1	35.6	43.63	39.615	8.39	0.7	5.873	32.04	17.622	12.93	0.7	5.873
	I2									21.72	0.49	4.1111
	I3									12.93	0.7	5.873
	I4									21.72	0.49	4.1111
Rapid growth	I1	35.62	43.88	39.75	7.62	1.2	9.144	75.25	22.575	22.54	1.2	9.144
	I2									48.37	0.6	4.572
	I3									22.54	1.2	9.144
	I4									48.37	0.6	4.572
Mid-season	I1	24.72	33.24	28.98	5.65	1.2	6.78	134.4	73.91	70.25	1.2	6.78
	I2									70.25	1.2	6.78
	I3									107.25	0.528	2.9832
	I4									107.25	0.528	2.9832
Late-season	I1	17.34	26.13	21.74	4.14	0.6	2.484	134.4	73.91	73.625	0.6	2.484
	I2									73.625	0.6	2.484
	I3									113.625	0.204	0.8446
	I4									113.625	0.204	0.8446

I.T.: irrigation treatment, T.min: minimum temperature, T.max: maximum temperature, T.mean: mean of temperature, ETo: reference evapotranspiration, Kc: crop coefficient, ETc: crop evapotranspiration, TAW: total available soil water in the root zone, RAW: readily available soil water in the root zone, Dr = root zone depletion, Ks: stress crop coefficient, ETc adj: adjusted crop evapotranspiration

Yield response factor (Ky)

The effect of water deficit levels represented as I_1, I_2, I_3, and I_4 on the kernel yield of six maize hybrids indicated to decrease in yield with decreasing the water availability, there were variation in the values of yield response factor Ky which indicate to the sensitivity of maize to water stress, and there were differences in the effect of water deficit between the growth stages across the growing season (Dijaman et al., 2013). *Table 3* demonstrate the values of Ky of six maize hybrids in four growth stages include initial stage, rapid growth stage, mid-season stage, and the late season stage, the schedule of the water deficit treatments was varied according to the severity of the water shortage as well the sensitivity of the growth stages, the water deficit treatment during the initial and rapid growth stages were with I_2 and I_4 only, the response of all maize hybrids through Ky values under effect of I_2 were greater than 1 except the hybrids H_3 and H_4 showing (0.843 and 0.616) respectively, demonstrating less sensitivity to water deficit decrease, while Ky of all hybrids were indicated to greater values with the influence of I_4 than that was obtained with the effect of I_2 by (24.226%, 30.8%, 44.5%, 42.6%, 28.8%, and 28.8%) for (H_1, H2, H3, H_4, H_5, and H_6) respectively, demonstrating the greater effect of the water deficit condition created with

http://www.aloki.hu ● ISSN 1589 1623 (Print) ● ISSN 1785 0037 (Online)
DOI: http://dx.doi.org/10.15666/aeer/1705_1097710988

the effect of I_4 due to decreasing in the kernel yield of six maize hybrids, the most sensitive hybrid in initial and rapid growth stages was shown with response of H_5, showed Ky value of 1.653 and 2.32. The Ky value of all hybrids during the mid season with the influence of the levels I_3 and I_4, the comparative between the Ky value in this stage of tasseling and silking which is sensitive to stress and that obtained by FAO was greater with variation between maize hybrids that expanded from 0.472 of H_3 to 1.306 for H6, Ky values of all hybrids in the late season under the impact of the I_4 level revealed a higher sensitivity of maize hybrids except the hybrid H_4, in the late season the lower values of Ky were taken out for all hybrids with the effect of I_3 and I_4 with specificity to H_3 and H_4 that they manifested Ky values (0.4, 0.65 and 0.469, 0.487) respectively, the results of late season were close to the finding of Doorenbos and Kassam (1979). The higher water potential of the air during the growing season of maize in the region resulted the differences of Ky value in comparison with the finding of previous researchers include that obtained by FAO are in agreement with results of Doorenbos and Kassam (1994), Dagdelen et al. (2005), Mengu and Ozgurel (2008) and Najrachi et al. (2011).

Table 3. *Yield response fractions for six hybrids in four growth stages under stress and non-stress conditions*

Growth stages	Hybrids	I_1	I_2	I_3	I_4
Initial growth stage I_1 & I_3: no stress I_2 & I_4: stress	H_1	-	1.47	-	1.94
	H_2	-	1.323	-	1.913
	H_3	-	0.843	-	1.52
	H_4	-	0.616	-	1.073
	H_5	-	1.653	-	2.32
	H_6	-	1.443	-	2.026
Rapid growth stage I_1 & I_3: no stress I_2 & I_4: stress	H_1	-	0.882	-	1.164
	H_2	-	0.794	-	1.148
	H_3	-	0.506	-	0.912
	H_4	-	0.37	-	0.644
	H_5	-	0.992	-	1.392
	H_6	-	0.866	-	1.216
Mid-season growth stage I_1 & I_2: no stress I_3 & I_4: stress	H_1	-	-	0.896	1.041
	H_2	-	-	0.862	1.026
	H_3	-	-	0.472	0.815
	H_4	-	-	0.767	0.576
	H_5	-	-	1.017	1.245
	H_6	-	-	1.305	1.087
Late-season growth stage I_1 & I_2: no stress I_3 & I_4: stress	H_1	-	-	0.759	0.881
	H_2	-	-	0.73	0.869
	H_3	-	-	0.4	0.69
	H_4	-	-	0.65	0.487
	H_5			0.862	1.054
	H_6			1.106	0.921

According to the irrigation schedule used in the study, the I_1 represented well irrigation in all growth stages, I_3 performed water stress in reproductive stage only (mid and late season), while I_2 caused water stress during the initial and rapid stages, and I_4 exemplified water stress in all growth stages

http://www.aloki.hu ● ISSN 1589 1623 (Print) ● ISSN 1785 0037 (Online)
DOI: http://dx.doi.org/10.15666/aeer/1705_1097710988

Stress indices

The results of analyses of variance demonstrated significant differences among maize hybrids for kernel yield under well irrigation and water stress conditions (YPi and Ysi) and for the investigated drought related indices which were presented in *Table 4*. High yield value in non-stress (Ypi) and stress conditions (Ysi) was exhibited by hybrid Medium 791, displaying (7.267 ton ha^{-1}) and (4.058 ton ha^{-1}) respectively. While low yield value in non-stress and stress conditions was exhibited by hybrids Fajr 260 with (2.748 ton ha^{-1}) and Dhqan (1.044 ton ha^{-1}) respectively. The maximum value of STI (1.633), MP (5.662) and GMP (5.370) indices was by hybrid Medium 791. In addition, the highest value for TOL (3.641 ton ha^{-1}) was from hybrid Medium 791. Thus, the hybrid Medium 791 had a desirable yield in all conditions and hence it is recommendable in a semiarid conditions, results are similar to that obtained by previous researchers as Rosielle and Humblin (1981), Fernandez (1992) and Dijaman et al. (2013).

Table 4. *Means and selection indices for grain yield (ton ha^{-1}) of six maize hybrids evaluated under stress and non-stress condition*

Hybrids	Ypi	Ysi1	Ysi2	Ysi3	STI	TOL	MP	GMP
	7.27	4.058			1.633	3.208	5.662	5.37
Medium 791			3.625		1.451	3.641	5.445	4.916
				3.035	1.193	4.231	5.15	4.448
	4.36	2.629			0.642	1.733	3.495	3.305
Btaris			2.256		0.559	2.105	4.519	3.048
				1.856	0.425	2.505	3.109	2.641
	2.88	2.152			0.347	0.728	2.516	2.482
Cantabpis			2.118		0.341	0.762	2.499	2.463
				1.567	0.25	1.314	2.223	2.083
	2.75	2.237			0.342	0.51	2.492	2.475
Fajr 260			1.568		0.236	1.18	2.158	2.074
				1.861	0.285	0.887	2.304	2.253
	4.44	2.527			0.644	1.913	3.483	3.315
Es-Solito 655			1.912		0.481	2.528	3.176	2.899
				1.347	0.319	3.093	2.893	2.381
	3.87	2.192			0.481	1.675	3.028	2.854
Dhqan			1.044		0.217	2.822	2.455	1.977
				1.513	0.314	2.353	2.689	2.314

Ypi: Yield of a given hybrid in optimal conditions. Ysi1: Yield of a given hybrid in stress conditions (in vegetative period). Ysi2: Yield of a given hybrid in stress conditions (in reproductive period). Ysi3: Yield of a given hybrid in stress conditions (in vegetative & reproductive period). STI: stress tolerance index. TOL: tolerance index. MP: mean productivity. GMP: geometric mean productivity

The results of analyses of variance for the investigated drought related indices were presented in *Table 5*. Significant differences were found for all stress indices, The performance of six maize hybrids with stress indices showed significant differences among all hybrids that evaluated under stress and non-stress conditions. The H_1 showed the highest value of STI with 1.426 indicating to high yield potential and higher stress tolerance, and minimum value of H_4 Fajr260 was 0.288, the highest value of TOL was obtained by H_1 (medium 791) revealing 3.694 demonstrating greater reduction in grain yield under water deficit condition, while the minimum value of TOL manifested with

http://www.aloki.hu ● ISSN 1589 1623 (Print) ● ISSN 1785 0037 (Online)
DOI: http://dx.doi.org/10.15666/aeer/1705_1097710988

H_3 and H4 (0.935 and 0.859) indicating to a lesser reduction in grain yield. The higher values of MP and GMP showed by H_1 demonstrate high correlation between these indices and the yield. The results were similar to that documented by Papathanasiou et al. (2015).

Table 5. *Mean value for selection indices of six maize hybrids evaluated under stress and non-stress condition*

Hybrids	STI	TOL	MP	GMP
Medium 791	1.426	3.694	5.419	4.911
Btaris	0.542	2.114	3.707	2.998
Cantabpis	0.313	0.935	2.413	2.343
Fajr 260	0.288	0.859	2.318	2.267
Es-Solito 655	0.481	2.511	3.184	2.865
Dhqan	0.337	2.283	2.724	2.381
LSD ($P \leq 0.05$)	0.297	0.949	0.689	0.656

The biplot analysis (*Fig. 1*) is required to identify the best performance hybrids for both stress and non-stress conditions. The principle component analysis (PCA) converts the variables to the independent combinations. These principle components formed 100% of the total variation among maize hybrids. The two principal components PC1 and PC2 revealed 99.40% of the original phenotypic variation. The value of the contribution of first and second components was 94.29 and 5.11%, respectively. Regarding the distribution of indices and hybrids on PCA plot, the indices or hybrids that were subsisting away from the centre of the plot in the positive trends of distinct traits demonstrated their best performance, whereas; the indices or hybrids that were out most from the centre of the plot in the negative orientation of traits displayed their weak performance (*Fig. 1*). The most important component, PC1, was positively and negatively influenced by indices: STI, MP, GMP, and TOL. The second PCA accounted for 5.11% of all variations. The maize hybrids showed a wide variability in phenotypic traits among them. Four groups of maize hybrids with different genetic constituents were highlighted on scatter plot: the first group composed of H_1. The second group included H_2 and the third group composed H_3 and H_4, whereas the fourth groups contained H_5 and H_6, respectively. On the other hand, the results of some stress indices (STI, GMP, MP, and YI) for H_1 hybrid were opposite to those recorded for H_6 hybrid. As shown in PCA biplot, the highest values of GMP, MP, STI and YI were recorded by H_1 hybrid signalizing that genotypes with larger PCA1 and lower PCA2 scores gave high yields (Darvishzadeh et al., 2010; Khodarahmpour et al., 2011). This result indicates that H_1 hybrid was the most tolerant hybrid, whereas, the hybrids: H_5 and H_6 were the most susceptible hybrids. H_3 and H_4 hybrids shared common indices.

Cluster analysis for the six maize hybrids was behaving to identify a cluster grouping based on kernel yield under effect of water deficit and full irrigation, the results manifested four major groups of maize hybrids with different genetic constituents were highlighted in the scatter plot, the first group was implicated the hybrid (Medium 791), however the second group included Btaris only. The third group composed of (Cantabpis and Fajr 260), whereas the last group composed of two different hybrids (Es-Solito 655 and Dhqan) (*Fig. 2*). The results displayed the existence of variability among the maize hybrids involved in the study, On the other hand, the results of drought resistance indices variation of some traits of Medium 791 hybrid were inversely related

http://www.aloki.hu ● ISSN 1589 1623 (Print) ● ISSN 1785 0037 (Online)
DOI: http://dx.doi.org/10.15666/aeer/1705_1097710988

to those recorded for Dhqan hybrid, our results are in agreement with those of Bouslama and Schapaugh (1984), Anwer et al. (2011) and Khalili et al. (2012). The results of the cluster analysis, and yield response factor (Ky) and stress indices of six maize hybrids were corresponded due to maize hybrid performance.

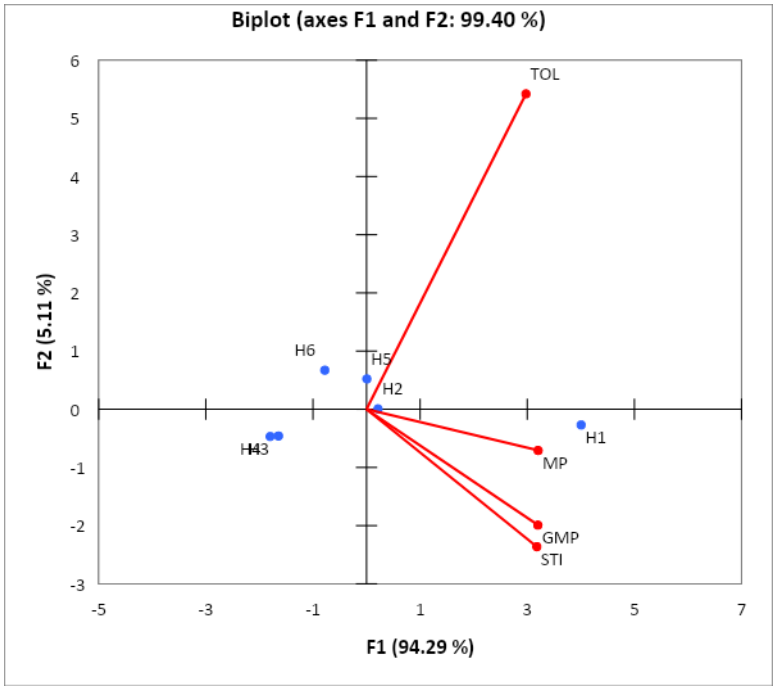

Figure 1. *The biplot display of yield in four drought tolerance indices*

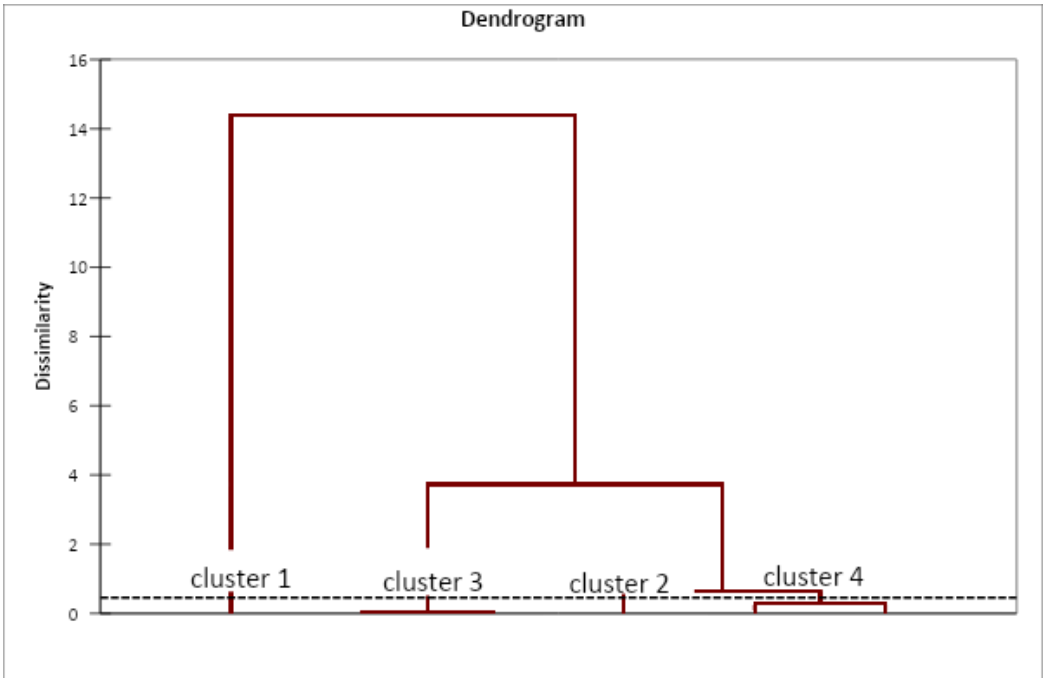

Figure 2. *Cluster analysis of maize hybrids depending on drought tolerance indices characters using Euclidean distance and unweighted pair-group method average (UPGMA)*

http://www.aloki.hu ● ISSN 1589 1623 (Print) ● ISSN 1785 0037 (Online)
DOI: http://dx.doi.org/10.15666/aeer/1705_1097710988

Conclusions

The higher means of seasonal evapotranspiration were imperative to the necessity of determining of the yield response factor (Ky) more accurately in different growth stages, included initial, rapid growth, mid season, and late season stages through calculating of adjusted crop coefficient, as well adjusted crop evapotranspiration. The results of Ky in all growth stages were varied with that was reported by FAO no.33. The results of the correlation coefficient between the yield of maize hybrids and stress indices manifested significant correlation with the water stress conditions created with second and third levels of irrigations, furthermore with indices STI, TOL, MP, and GMP. The results of the cluster analysis displayed the existence of variability among the maize hybrids through four major groups of maize hybrids with different genetic constituents were highlighted in the scatter plot, indicating to the (Medium 791) hybrid as a most tolerant hybrid, whereas, the hybrids Es-Solito 655, and Dhqan were the most susceptible hybrids. Although the hybrid Medium 791 with a desirable yield in all conditions is recommendable in a semiarid conditions, further research may be required to be conducted for evaluating the tolerance and susceptibility of maize hybrids.

REFERENCES

[1] Ahmad, S. Q., Khan, S., Ghaffar, M., Ahmad, F. (2011): Genetic diversity analysis for yield and other parameters in maize (Zea mays L.) genotypes. – Asian J. Agri. Sci. 3(5): 385-388.

[2] Allen, R. G., Pereira, L., Raes, D., Smith, M. (2017): FAO Irrigation and Drainge Paper No.56. Crop Evapotranspiration (guidelines for computing crop water requirements). – FAO, Rome.

[3] Anwar, J., Subhani, G. M., Hussain, M., Ahmad, J., Hussain, M., Munir, M. (2011): Drought tolerance indices and thier correlation with yield in exotic wheat genotypes. – Pak. J. Bot. 43: 1527-1530.

[4] Bouslama, M., Schapaugh, W. T. (1984): Stress tolerance in soybean. Part 1: Evaluation of three screening techniques for heat and drought tolerance. – Crop Sci J 24: 933-937.

[5] Carvalho, D. F., Neto, D. H. O., Felix, L. F., Guerra, J. G. M., Salvador, C. A. (2016): Yield, water use efficiency, and yield response factor in carrot crop under different irrigation depths. – Ciência Rural, Santa Maria. http://dx.doi.org/10.1590/0103-8478cr20150363.

[6] Dagdelen, N., Yilmaz, E., Sezgin, F., Gurbuz, T. (2005): Water yield relation and water use efficiency of cotton (Gossypium hirsutum l.) and second crop corn (Zea mays L.) in western Turkey. – Agricultural Water Management. DOI: 10.1016/j.agwat.2005.05.006.

[7] Darvishzadeh, R., Pirzad, A., Hatami-Maleki, H., Kiani, S. P., Sarrafi, A. (2010): Evaluation of the reaction of sunflower inbred lines and their F1 hybrids to drought conditions using various stress tolerance indices. – Spanish Journal of Agricultural Research 8(4): 1037-1046.

[8] Deryng, D., Conway, D., Kutty, N. R., Price, J., Warren, R. (2014): Global crop yield response to extreme heat stress under multiple climate change futures. – Environ. Res. Lett. 9: 034011.

[9] Dijaman, K., Irmak, S., Rathje, W. R., Martin, D. L., Eisenhauer, D. E. (2013): Maize evapotranspiration, yield production functions, biomass, grain yield, harvest index, and yield response factors under full and limited irrigation. – American Society of Agricultural and Biological Engineers 56(2): 273-293.

[10] Doorenbos, J., Kassam, A. H. (1979): Yield Response to Water. – FAO Irrigation and Drainage paper No. 33. FAO, Rome.

http://www.aloki.hu ● ISSN 1589 1623 (Print) ● ISSN 1785 0037 (Online)
DOI: http://dx.doi.org/10.15666/aeer/1705_1097710988

[11] Doorenbos, J., Kassam, A. H. (1994): Yield Response Factor to water. – FAO Irrigation and Drainage paper no. 33. FAO, Rome.
[12] Eriksson, L., Johansson, E., Kettaneh-Wold, N., Wold, S. (1999): Introduction to Multi- and Megavariate Data Analysis Using Projection Methods (PCA & PLS). – Umetri AB, Umea, Sweden.
[13] Fernandez, G. J. (1992): Effective selection criteria for assessing plant stress tolerance. – Proceeding of the International Symposium on Adaptation of Vegetables and other Food Crops in Temperature and Water Stress, Aug 13-16, Taiwan, pp. 257-270.
[14] Greaves, G. E., Wang, Y. (2017): Yield response, water productivity, and seasonal water production functions for maize under deficit irrigation water management in southern Taiwan. – Plant Production Science 20(4): 353-365.
[15] Irandoust, T., Bijanzadeh, E. (2017): Crop water stress index and canopy temperature changes of triticale (X Triticosecale Wittmack) cultivars under irrigation scheduling. – Jordan Journal of Agricultural Sciences 13: 745-755.
[16] Khalili, M., Kazemi, M., Moghaddam, A., Shakiba, M. (2004): Evaluation of drought tolerance indices at different growth stages of late-maturing corn genotypes. – Proceedings of the 8th Iranian Congress of Crop Science and Breeding, Rasht, Iran, pp. 298.
[17] Khalili, M., Naghavi, M. R., Aboughadareh, A. P., Talebzadeh, S. J. (2012): Evaluating of drought stress tolerance based on selection indices in spring canola cultivars (Brassica napus L.). – Journal of Agricultural Science 4(11).
[18] Khodarahmpour, Z., Choukan, R., Bihamta, M. R. Hervan, E. M. (2011): Determination of the best heat stress tolerance indices in maize (Zea mays L.) inbred lines and hybrids under khuzestan province conditions. – J. Agr. Sci. Tech.13: 111-121.
[19] Kuscu, H., Karasu, A., Ozi, M., Demir, A. O., Turgut, I. (2013): Effect of irrigation amounts applied with drip irrigation on maze evapotranspiration, yield, water use efficiency, and net rreturn in a subhuimed climate. – Turkish Journal of Field Crops 18: 13-19.
[20] Mengu, G. P., Ozgorel, M. (2008): An evaluation of water yield relations in maize (Zea mays L.) in Turkey. – Pakistan J. Biol. Sci. 11: 517-524.
[21] Mitra, J. (2001): Genetics and Genetic improvement of drought resistance in crop plants. – Curr.Sci.80: 758-762.
[22] Moghaddam, A., Hadizadeh, M. H. (2002): Response of corn hybrids and their parental lines to drought using different stress tolerant indices. – Iranian J. Seed and Seedling 18: 255-272.
[23] Nacharchi, M., Kaveh, F., Babazadeh, H., Manshouri, M. (2011): Determination of the yield response factor for field crop deficit irrigation. – African Journal of Agricultural Research 6: 3700-3705.
[24] Papathanasioua, F., Dordasb, C., Gekasb, F., Pankoub, C., Ninoub, E., Mylonasb, I., Tsantarmasc, K., Sistanisa, I., Sinapidouc, E., Lithourgidisd, A., Petrevskaa, J., Papadopoulosa, I., Zouliamise, P., Kargiotidouc, A., Tokatlidisc, I. (2015): The use of stress tolerance indices for the selection of tolerant inbred lines and their correspondent hybrids under normal and water-stress conditions. – Procedia Environmental Sciences 29: 274-275.
[25] Payero, J. O., Tarkalson, D. D., Irmak, S., Davison, D., Petersen, J. L. (2008): Effect of irrigation amounts applied with subsurface drip irrigation on corn evapotranspiration, yield, water use efficiency, and dry matter production in a semiarid climate. – Agricultural Water Management 95(8): 895-908.
[26] Rosielle, A. A., Hamblin, J. (1981): Theoretical aspects of selection for yield in stress and non-stress environments. – Crop Sci 21: 943-946.
[27] Steduto, P., Hsiao, T. C., Fereres, E., Raes, D. (2012): Crop Yield Response to Water. – FAO, Rome.

http://www.aloki.hu ● ISSN 1589 1623 (Print) ● ISSN 1785 0037 (Online)
DOI: http://dx.doi.org/10.15666/aeer/1705_1097710988

[28] Talebi, R., Fayaz, F., Naji, A. M. (2009): Effective selection criteria for assessing drought stress tolerance in durum wheat (Triticum durum Des). – General and Applied Pl. Physio. 35: 64-74.
[29] Zare, M. (2012): Evaluation of drought tolerance indices for the selection of Iranian barley (Hordeum vulgare) cultivars. – African Journal of Biotechnology 11(93): 15975-15981.

http://www.aloki.hu ● ISSN 1589 1623 (Print) ● ISSN 1785 0037 (Online)
DOI: http://dx.doi.org/10.15666/aeer/1705_1097710988

ANTHROPOGENIC, BIOGENIC AND PYROGENIC EMISSION SOURCES AND ATMOSPHERIC FORMALDEHYDE (HCHO) AND NITROGEN DIOXIDE (NO_2) COLUMNS OVER DIFFERENT LANDUSE/LANDCOVERS OF SOUTH ASIA

RANA, A. D.[1] – PARVEZ, S.[1] – UL-HAQ, Z.[1*] – BATOOL, S. A.[1] – CHAUDHARY, M. N.[2] – MAHMOOD, K.[1] – TARIQ, S.[1]

[1]*Remote Sensing and GIS Group, Department of Space Science, University of the Punjab, Lahore, Pakistan*

[2]*Institute of Geology, University of the Punjab, Lahore, Pakistan*

**Corresponding author*
e-mail: zia.spsc@yahoo.com; phone: + 92-301-435-2543

(Received 27th Mar 2019; accepted 2nd Jul 2019)

Abstract. This study presents spatiotemporal variability of two important air pollutants, Formaldehyde (HCHO) and Nitrogen dioxide (NO_2), concomitant to underlying anthropogenic, biogenic and pyrogenic emission sources from different landuse/landcovers over South Asia, from 2005-2016, using OMI sensor onboard Aura satellite. Annual and seasonal spatial distributions for both the gases reveal that trends of change are linked with landuse/landcovers of different geographical regions of South Asia. Annual distribution of NO_2 shows a negative trend from 2012-2016, with annual decrease of ~1.06% in comparison to a rise, from 2005-2011 at a rate of ~1.86%/year. Analyzing seven study zones, distinctively identifies higher-emissions for both the gases from anthropogenic sources, in zones, 2,3,4 and 6, highlighting, emissions from megacities of Pakistan (Lahore, Faisalabad), India (Delhi, Kolkata, Lucknow) and Bangladesh (Dhaka), mainly due to urbanization, power-generation plants and mining-activities. Episodes of pyrogenic-emissions dominate seasonally in zones2 and 4, due to crop residue burning from Punjab plains of Pakistan and India and zone5 from Bangladesh and Myanmar. Isoprene, a precursor to HCHO is one of its main biogenic sources and higher emissions of HCHO dominate in zones3 and 7 with deciduous forests of lower Himalayas in northwest and Western Ghats in southwest India. In zones 4,5 HCHO emissions are dictated by isoprene emissions from Sundarbans in Bangladesh and palm-oil-plantations in Myanmar.
Keywords: *trace gases, OMI, spatiotemporal analysis, isoprene, remote sensing*

Abbreviations: ACCMIP: Atmospheric Chemistry and Climate Model Intercomparison Project; BVOCs: Biogenic Volatile Organic Compounds; CH_4: Methane; CityZEN: megaCITY- Zoom for the Environment; CO: Carbon Monoxide; ECCAD: Emissions of atmospheric Compounds & Compilation of Ancillary Data; GOME: Global Ozone Monitoring Experiment; HCHO: Formaldehyde; IGB: Indo-Gangetic Basin; MACCity: Monitoring Atmospheric Composition and Climate/CityZEN EU projects; MODIS: Moderate Resolution Imaging Spectroradiometer; NASA: National Aeronautics and Space Administration; NCEP: National Centers for Environmental Prediction; NDVI: Normalized Difference Vegetation Index; NMVOCs: Non-Methane Volatile Organic Compounds; NOx: Nitrogen Oxides; NO_2: Nitrogen Dioxide; O_3: Ozone; OH: Hydroxyl Radicals; OMI: Ozone Monitoring Instrument; SAARC: South Asian Association for Regional Cooperation; SCIAMACHY SCanning Imaging Absorption spectroMeter for Atmospheric CHartographY; Terra: Earth observing satellite system Launched by NASA; UV: Ultra Violet; UV-Vis: Ultraviolet to Visible; VOCs: Volatile Organic Compounds

Introduction

In the troposphere, Formaldehyde (HCHO) exists everywhere as a short-lived indoor and outdoor pollutant with a lifetime of few hours during the daylight (Sander et al., 2006). It is a carcinogenic pollutant, affecting the tropospheric photochemistry (Hassan

http://www.aloki.hu ● ISSN 1589 1623 (Print) ● ISSN 1785 0037 (Online)
DOI: http://dx.doi.org/10.15666/aeer/1705_1098911015

et al., 2018) and U.S. Environmental Protection Agency has declared, HCHO as the most important carcinogen in the outdoor air and is identified amongst the 187 hazardous air pollutants (Zhu et al., 2017; Zhang et al., 2018) Main source of tropospheric HCHO is oxidation of methane (CH_4) by Hydroxyl (OH) radicals. Whereas, short lived Non-Methane Volatile Organic Compounds (NMVOC) like alkanes, alkenes, aromatic hydrocarbons, and isoprene as a source of oxidation, dominate Methane in the continental boundary layer and contribute significantly to tropospheric HCHO concentrations. Ecologically, predictable and broadly defined trends for the isoprene dominance have been established as a Biogenic Volatile Organic Compounds (BVOC) over monoterpene. Isoprene as one of the BVOC after oxidation produces HCHO as a major product, and describes the temperature variations as a dominant variable at ecosystem level (Harrison et al., 2013). These temperature variations in the bigger context of climate change also affect the natural emissions of Volatile Organic Compounds (VOCs), like the emission of isoprene from vegetation (US-EPA, 2009). HCHO in the atmosphere is also contributed by vegetation (Lathiere et al., 2006), biomass burning processes and fuel combustion (Lee et al., 1998) in lesser content than oxidation. In midlatitude and forest cover of tropical regions, Isoprene as a VOC is the major precursor of HCHO (Palmer et al., 2003, 2006; Barkley et al., 2008; Curci et al., 2010).

Atmospheric oxidation of VOCs produces HCHO in large amounts, that can be detected through space as a total column by solar UV backscatter (Chance et al., 2000). Monitoring and recording of observations for HCHO columns from space started with the launch of the Global Ozone Monitoring Experiment (GOME) instrument in 1995 (Chance et al., 2000). Detection of HCHO columns using remote sensing data have been successfully used as a proxy for the identification of biogenic repositories and emissions of VOCs from the underlying sources (Palmer et al., 2003; Millet et al., 2008; Stavrakou et al., 2009; Marais et al., 2012; Barkley et al., 2013; Bauwens et al., 2016), pyrogenic sources (Shim et al., 2005; Gonzi et al., 2011) and anthropogenic sources (Fu et al., 2007; Marais et al., 2014; Zhu et al., 2014; Souri et al., 2017). Long term trends of HCHO column data have been analyzed by (De Smedt et al., 2010, 2015) with the help of GOME instrument and with the succeeding satellites like GOME-2, Ozone Monitoring Instrument (OMI) and Scanning Imaging Absorption Spectrometer for Atmospheric Cartography (SCIAMACHY).

In a recent study by (Zhu et al., 2018) using Ozone Monitoring Instrument (OMI) onboard Aura satellite, observing HCHO concentration over china for a period of 2005-2015, have observed strong seasonal pattern existing for high concentrations of HCHO in the summer season. At regional scale, increase has also been observed in the HCHO column for a period of 2005 to 2010 while, a decrease has been observed from 2010-2015. In addition to this, (Zhu et al., 2018) have also found that urban areas exhibit higher concentrations of HCHO column and increase has been observed for the emissions from industrial sources along with the similar emissions from residential sources. In summer times it has been concluded, that, anthropogenic VOCs contribute to high emissions along with the isoprene emissions.

In the atmosphere, nitrogen dioxide (NO_2) is considered as a highly reactive gas (US-EPA, 1998). Nitrogen oxides ($NO_x = NO + NO_2$), especially NO_2 in the atmosphere, has been observed to have adverse impacts on both, the human health and on the natural environment (Case et al., 1979; Barck et al., 2005). Another important aspect of the presence of NO_x in the atmosphere is that these gases and hydrocarbons are correlated

http://www.aloki.hu ● ISSN 1589 1623 (Print) ● ISSN 1785 0037 (Online)
DOI: http://dx.doi.org/10.15666/aeer/1705_1098911015

with the surface level ozone (Varotsos et al., 1992). The tropospheric NO_2 pollution is greatly influenced by the spatial patterns of socio-economic conditions of certain geographical regions as well as it is affected by the changes in meteorological conditions, and also can be attributed to the topographic attributes, defined by the elevation, land use and land cover of the area under investigation (Parra et al., 2009). Emissions of NO_2 along with the other trace gases in Indo-Gangetic Plain (IGP) can be specifically associated with the agricultural landuse/landcover. As, significant emissions of NO_2, CO, CO_2, CH_4, and aerosol have been observed from the crop residue burning of both rice, wheat and from rice paddies as well (Ali et al., 2014; ul-Haq et al., 2014; Tariq and Ali, 2015). Keeping in view the environmental perspective, in South Asia, Pakistan is facing severe environmental problems due to rapid urbanization, with the need for more industrialization and motorization, energy crises and deforestation, leading to raised emissions of NO_2 (ul-Haq et al., 2017, 2018).

Atmospheric NO_2 and HCHO both have spectral absorption signatures in Ultraviolet to Visible (UV-Vis) regions of electromagnetic spectrum and are observed through the satellite sensors like OMI. These two pollutants have become of central importance and core data products, even for the future satellite-based programs for monitoring air quality (Nowlaqn et al., 2018). In a study, by (Zhu et al., 2017), emissions of HCHO produced through the oxidation of biogenically produced isoprene are linked with the concentrations of ($NO_x \equiv NO + NO_2$) in the atmosphere. Another important linkage, observed in the study by (Zhu et al., 2017), is between the absence of anthropogenic emissions of NO_x and a reduction observed in the emissions of HCHO. Presence of these two gases as indoor and outdoor pollutants has also been established as a health risk, and in a study by (Maroziene and Grazuleviciene, 2002), low birth weight and preterm births have been observed to have some linkage with the maternal exposures during first trimester to ambient HCHO and NO_2 exposures respectively. According to a study, controlling the emissions of NO_2 is beneficial to both, environment and human health, as it improves the quality of the air with ozone and also reduces the risks of cancer related to HCHO emissions (Zhu et al., 2017).

The objectives of this study are to analyze spatiotemporal trends of tropospheric HCHO and NO_2 columns over South Asia for a temporal window of 12 years, from 2005-2016, with the help of remote sensing data from Ozone Monitoring Instrument (OMI) aboard the NASA Aura spacecraft. Interannual variability and seasonal trend analyses with spatial landuse/landcover pockets in varying scales and diversity of the landforms, influencing and modeling the local columns of HCHO and NO_2 will be analyzed. Some of the major biogenic activities on the global scale are affecting biogenic emissions of VOCs, as tropical deforestation has resulted in 29% decrease in isoprene emissions (Lathière et al., 2006). Assessment of the emission of the subject trace gases, affected by the underlying landuse/landcover in connection with anthropogenic, biogenic and pyrogenic activities is important to understand the atmospheric processes and photochemistry shaping up the overall atmospheric profile in this part of the world. For an in-depth analysis, to analyze the impact and trends of change on local HCHO and NO_2 columns, seven study zones will be analyzed for the assessment of emissions from different landuse/landcover directly or indirectly impacting tropospheric columns of HCHO and NO_2.

http://www.aloki.hu ● ISSN 1589 1623 (Print) ● ISSN 1785 0037 (Online)
DOI: http://dx.doi.org/10.15666/aeer/1705_1098911015

Material and methods

Geography and meteorology of study area

South Asia refers to the Southern region of the Asian continent with the most densely populated countries of the world, comprising of sub-Himalayan member states of South Asian Association for Regional Cooperation (SAARC), including Pakistan, India, Bhutan, Maldives, Sri Lanka, Afghanistan, Bangladesh and Nepal (Joshi, 2015) shown in *Figure 1a*. This region is marked in North by three gigantic mountain ranges of Himalaya, Hindukush and Karakoram, with emanating thickly populated, major river basins of Indus, Ganges, Brahmaputra, and Meghna extending from Pakistan to Bangladesh. The driest and deserted Baluchistan plateau located in Afghanistan and Pakistan, while the Peninsular India, consisting of Deccan plateau and the island countries of Sri Lanka and Maldives (Seligman, 2008; UNEP, 2008).

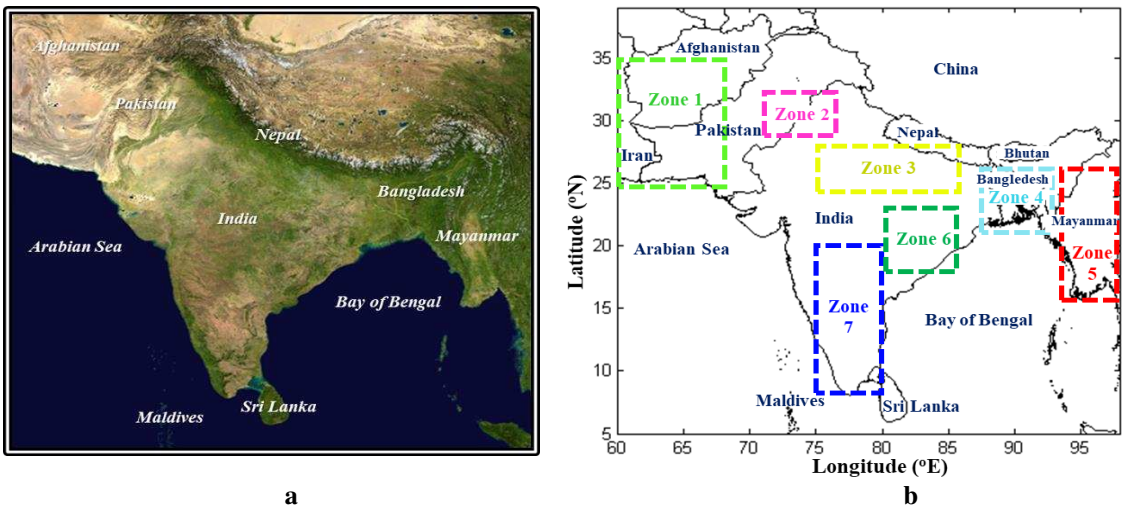

Figure 1. *(a) Satellite image map of South Asia showing landuse/landcover of world's most densely populated region. (Source: https://upload.wikimedia.org/wikipedia/commons/2/2a/Asia_satellite_orthographic.jpg), (b) Map of South Asia showing country boundaries and selected seven study zones shown in different colors*

South Asian climate is quite variant, dictated by highest mountains of the world, exhibiting arctic temperatures, transitioning in temperate regions in lower Himalayas to the tropical scenarios in Deccan plateau in the central India. Alternating wet and dry weather sessions brought by the monsoons control the overall climate of South Asia. Wet monsoons are caused by the moist winds from the sea in summertime, while in winter the dry monsoon is associated with the dry winds blowing out from land areas (UNEP, 2008; Joshi, 2015). For an in-depth analysis and investigation of HCHO and NO_2 along with the processes, South Asian region has been further investigated in seven study zones (*Fig. 1b*), from zone-1 to zone-7, comprising of regions with different landuse/landcovers, representatives of anthropogenic, biogenic and pyrogenic activities and emissions taking place at different scales. These seven study zones with corresponding geographic locations and possible/prominent sources of HCHO and NO_2 emissions from different landuse/landcovers and related activities have been detailed in *Table 1*.

http://www.aloki.hu ● ISSN 1589 1623 (Print) ● ISSN 1785 0037 (Online)
DOI: http://dx.doi.org/10.15666/aeer/1705_1098911015

Table 1. *Study zones with geographical locations and prominent landuse/landcover sources of emissions of HCHO and NO_2. (Source: Lathière et al., 2010; Tariq et al., 2015; Sippo et al., 2016)*

Study zones	Geographical bounding	Prominent landuse/landcover sources of NO_2	Prominent landuse/landcover sources of HCHO
Zone-1	25-35 °N, 60-68 °E	Karachi, Gawadar and Chahbhar Ports activities, fossil fuel burning, urban (megacity Karachi)	Karachi, Gawadar and Chahbhar Ports activities, fossil fuel burning, urban (megacity Karachi), Shipping activity and emissions
Zone-2	28-32 °N, 72-77 °E	Large scale crop-residue burning, (post-monsoon and pre-monsoon pyrogenic emissions), Agricultural Landuse/Landcover, urban (megacities Lahore, Delhi, Faisalabad), industries, home heating, brick kilns, power plants	Large scale crop-residue burning (post-monsoon and pre-monsoon), urban (megacities Lahore, Delhi, Faisalabad), industries, home heating, brick kilns, power plants, deciduous forests in lower Himalayas in North Western parts of India (Biogenic emissions)
Zone-3	24-28 °N, 75-87 °E	Crop-residue burning (post-monsoon and pre-monsoon pyrogenic emissions), industries, home heating, brick kilns, power plants	Crop-residue burning (post-monsoon and pre-monsoon pyrogenic emissions), industries, home heating, brick kilns, power plants. Deciduous forests in sub-Himalayan Siwalik ranges in India and Nepal
Zone-4	20-26 °N, 87-92 °E	Large scale crop-residue burning (pre-monsoon pyrogenic emissions), Mining activities, power plants, industries, brick kilns, urban (megacities Dhaka, Kolkata, Anthropogenic emissions)	Large scale crop-residue burning (pre-monsoon), Mining activities, power plants, industries, brick kilns, urban (megacities Dhaka, Kolkata) Biogenic emissions from the mangroves of Sundarbans in Bangladesh
Zone-5	15-26 °N, 93-98 °E	Large scale crop-residue burning (pre-monsoon), fossil fuel burning, home heating	Large scale crop-residue burning (pre-monsoon), fossil fuel burning, home heating, Biogenic emissions from Palm oil plantations in Myanmar
Zone-6	18-23 °N, 80-85°E	Major coal powered energy production plants and the largest coal mining region of India	Major coal powered energy production plants and the largest coal mining region of India
Zone-7	08-20°N, 75-80 °E	South Western Ghats of India, Anthropogenic emissions from the mega city of Bengaluru	South Western Ghats of India with deciduous montane rain forests in Kerala, and Karnataka states of India, Anthropogenic emissions from the mega city of Bengaluru

Maps of relative humidity at 925 mb, surface precipitation, wind vector at 925 mb and surface air temperature for South Asia for study period from 2005 to 2016 have been shown in *Figure 2*. These maps of selected meteorological parameters show the variations captured for four seasons i.e. winter season, comprising of the months of December, January and February, Pre-monsoon, described by March, April and May, Monsoon season, studied for the months of June, July and August, and Post-monsoon season consisting of the months of September, October and November. These

http://www.aloki.hu ● ISSN 1589 1623 (Print) ● ISSN 1785 0037 (Online)
DOI: http://dx.doi.org/10.15666/aeer/1705_1098911015

parameters have been mapped using records from NCEP–Reanalysis data from NOAA/OAR/ESRL PSD, Boulder, Colorado, USA. *http://www.esrl.noaa.gov/psd/.*

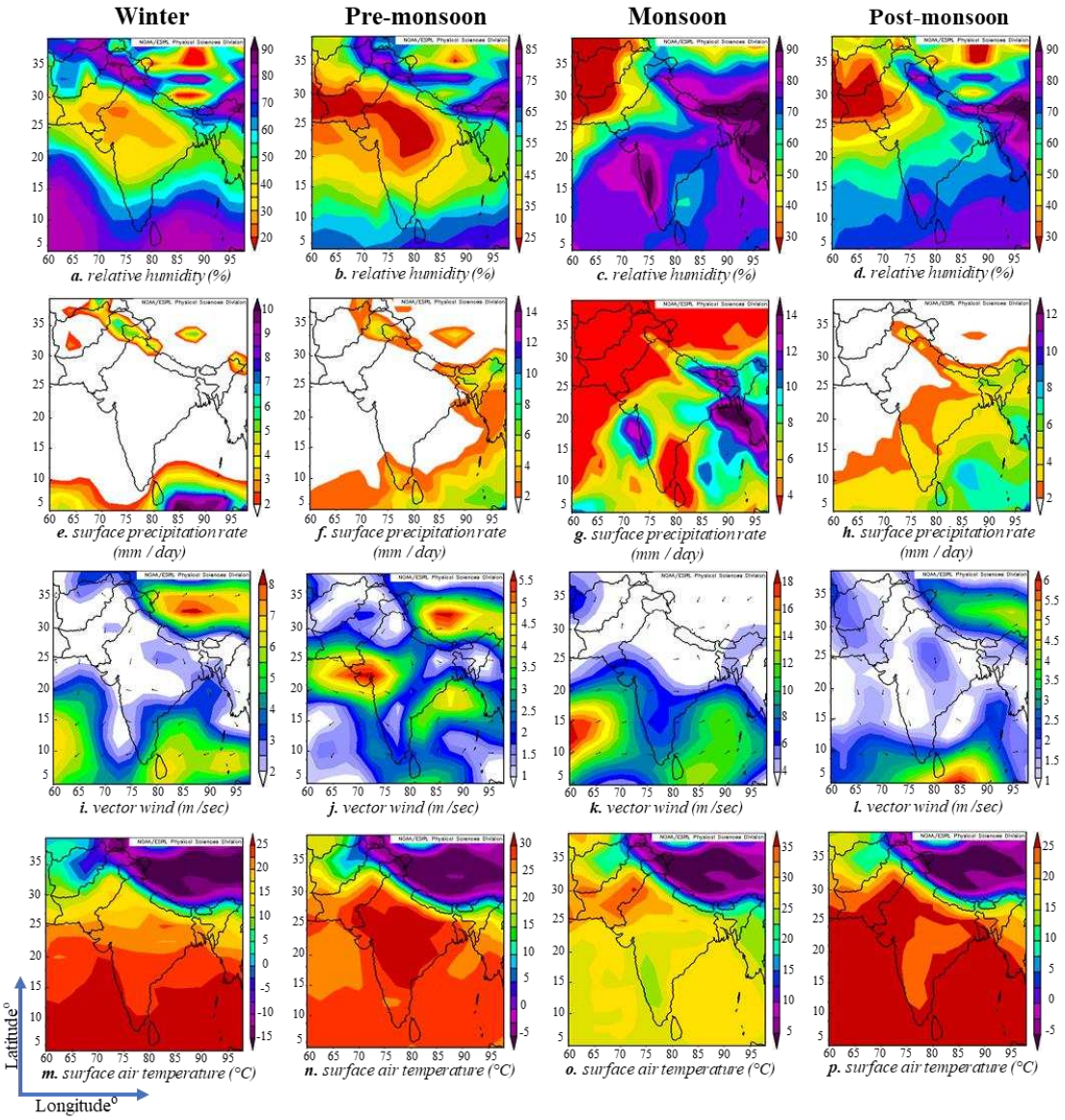

Figure 2. *Maps showing seasonal composite means for the study period (2005-2016) of relative humidity (%) at 925 mb (a–d), surface precipitation rate (mm/day) (e–h), vector wind (m s-1) at 925 mb (i–l), and surface air temperature (°C) (m–p) over South Asia. Source: NOAA/ESRL Physical Sciences Division, Boulder Colorado from their Web site at http://www.esrl.noaa.gov/psd/*

Maps show the highest relative humidity in monsoon season for most of South Asia, especially on the Eastern regions, comprising of Bangladesh, Myanmar and central India along with the coastal belt in the Southeastern parts of India besides the Western Ghats. However, the winter season has been found dry over South Asia for having the minimum relative humidity for the study period. Monsoon season also dominates the

http://www.aloki.hu ● ISSN 1589 1623 (Print) ● ISSN 1785 0037 (Online)
DOI: http://dx.doi.org/10.15666/aeer/1705_1098911015

surface precipitation over South Asia, with few pockets of precipitations observed over the Himalayas in the winter season.

Pre-monsoon season highlights the high content of winds, especially in the mid latitude areas of South Asia, rising from the Runn of Kutch along the India Pakistan coastal border and in the Rajhistan desert. High wind vectors are also observed in Tibetan plateau in the pre-monsoon season. A consistent cold pattern can be observed all along the Himalayas, throughout the year in all four seasons in the maps showing the low surface air temperatures for the study period. Whereas, pre-monsoon and post-monsoon seasons exhibit high temperatures in mid latitudes to the southern parts of South Asia. Changes observed in the concentrations of tropospheric NO_2 column over South Asia could possibly be linked to the shifts in meteorological regimes controlled by the meteorological phenomenon, which result in the changes in the rates of chemical reactions in the troposphere (Voulgarakis et al., 2010).

NCEP/NCAR reanalysis data

In 1991, a reanalysis1 project between National Center for Environmental Prediction (NCEP) and National Center for Atmospheric Research (NCAR) started to expand the National Meteorological Center (NMC)'s Climate Data Assimilation System (CDAS) project capacity. Objective of the CDAS project was to improve the forecasts by NMC operational Global Data Assimilation System (GDAS) over the last decade for the apparent climate change. In this reanalysis project a frozen state-of-the-art analysis and forecast system is used for the assimilation of the past data to perform reanalysis from 1957 to present. For the futuristic development in CDAS, same frozen state-of-the-art analysis/forecast system will be used to assess the anomalies in the current climate in the context of long reanalysis with the same data assimilation system (Kalnay et al., 1996). An improved version of reanalysis 1(R1) has been developed by NCEP/NCAR as Reanalysis 2 (R2). Improvements in R1 include updates in the model with better parameterization, inclusion of additional data and fixing the errors in assorted data assimilation. Data from NCEP/NCAR can be downloaded for more than 80 meteorological variables like, Surface temperature, Relative humidity, geopotential height, u-and v- wind components etc. Data from these sources are gridded and archived at the grid interval of 2.5° × 2.5° providing global data and is available from https://www.esrl.noaa.gov/psd/data/reanalysis/reanalysis.shtml.

OMI data for NO_2 and HCHO

Ozone Monitoring Instrument (OMI) is a joint venture of Dutch-Finnish collaboration (Levelt et al., 2006) onboard NASA's EOS Aura satellite, launched in July 2004. OMI is a push-broom near-UV/Visible spectrometer orbiting in a sun-synchronous orbit with an ascending node, crossing the equator at 13:40 local time. OMI sensor captures data of various trace gases including NO_2 and HCHO. OMI scanner consists of two 2-dimensional Charged Coupled Devices (CCD) detectors (Dobber et al., 2006). To sync the spectral and spatial registration, one of the two CCDs, i.e. CCD1 captures the UV1 (264-311 nm) and UV2 (264-311 nm), while CCD2 captures the VIS (349-504 nm) spectral bands. Spectral features of NO_2 are more prominent in the later channel, while UV2 spectral channel is used for HCHO slant column densities (SCDs) (Zara et al., 2018). OMI sensor captures the global data daily with spatial resolutions of 13 × 24 km^2 to ~25 × 105 km^2 in nadir and to the outermost

http://www.aloki.hu ● ISSN 1589 1623 (Print) ● ISSN 1785 0037 (Online)
DOI: http://dx.doi.org/10.15666/aeer/1705_1098911015

swath-angle, respectively with a swath of 2600 km at every given exposure in the orbit (De Graaf et al., 2016; Krotkov et al., 2016).

OMI tropospheric HCHO data

OMI sensor has been in orbit for more than a decade, and its long-term observations of tropospheric HCHO column has provided valuable information regarding this important trace gas carcinogen. HCHO column data used in this study has a grid interval of 0.25° latitude by 0.25° longitude, retrieved through Differential Optical Absorption Spectroscopy (DOAS) algorithm and an Intermediate Model of the Global and Annual Evolution of Species (IMAGES) as a priori information (Kaczorowski and Perelli, 2004). OMI sensor also provides a valuable difference in time window, providing a complimentary early afternoon data of tropospheric HCHO column at 13:40 local solar time (Kurosu, 2008; Millet et al., 2008) as compared to the other satellites, like GOME-2 at 9:30 and SCIAMACHY at 10:00 local solar time providing the HCHO column data at mid-morning (Chance et al., 2000; Palmer et al., 2001; De Smedt et al., 2008). The Royal Belgian Institute for Space Aeronomy (BIRA-IASB), in the previous version addressed the instrumental degradation and the striping effect by employing row-dependent background normalization (De Smedt et al., 2015). Several improvements in the product also include accounting for more accurately the absorption of O_2-O_2. For this purpose, interactive DOAS algorithm involving three fitting intervals was used. In order to reduce the degradation, radiances in remote equatorial Pacific were used (De Smedt et al., 2015). In the previous products, some of the main reasons of uncertainty, ranging from 30 to 40% in the tropospheric HCHO column include, errors in retrieval of the SCD and errors in estimation of Air Mass Factor (AMF) (De Smedt et al., 2008), where AMF has been defined as the ratio of SCD and VCD (Millet et al., 2006). Therefore, the HCHO products available on (TEMIS) are highly applicable for the spatial and temporal assessment of HCHO distributions over South Asia in the context of regional landuse/landcover. In this study, daily, global, gridded (OMHCHOd) Level-3 data for tropospheric HCHO Vertical Column Density (VCD) has been used for the study period of twelve years, i.e. 2005-2016, obtained from Tropospheric Emission Monitoring Internet Service (TEMIS) (http://h2co.aeronomie.be/).

OMI tropospheric NO_2 data

NASA's EOS Aura satellite with OMI sensor was launched in July 2004, and provides a daily, global gridded coverage of tropospheric concentrations of NO_2. For retrievals of NO_2 the cloud conditions used, have taken into account the cloud cover to be clear and up to 30% in Air Mass Factor (AMF), that uses the Lambertian Cloud Model with an assumed albedo of 0.8 to develop a simulated profile of NO_2 (Stammes et al., 2008). Radiative transfer models are used to calculate the AMFs, which considers the parameters like, surface albedo, cloud and aerosol properties, optical geometry, vertical distribution of absorbing trace gas and atmospheric scattering by air molecules (Bucsela et al., 2006; Stammes et al., 2008; Boersma et al., 2011). For the estimation of NO_2 Slant Column Densities (SCDs) to retrieve the vertical NO_2 column, Differential Optical Absorption Spectroscopy (DOAS) spectral fitting, with radiance in the range of 405-465 nm has been used. In order to get the Vertical Column Density (VCD) of a gas, SCD, depending upon density of the gas and various other parameters is divided by the

http://www.aloki.hu ● ISSN 1589 1623 (Print) ● ISSN 1785 0037 (Online)
DOI: http://dx.doi.org/10.15666/aeer/1705_1098911015

AMF. Improvement in NO_2 retrievals can be achieved by curtailing the errors introduced in calculating AMF, due to surface albedo, presence of clouds and NO_2 profile as the dominant anomalous factors, affecting the accurate tropospheric NO_2 retrievals over areas with enhanced NO_2 (Boersma et al., 2004). Uncertainties in surface albedo contribute 20-30%, while, for cloud fraction it may contribute as high as 20-50% errors for the estimation of NO_2 column (Boersma et al., 2004). Another factor contributing to the inaccurate estimates of NO_2 are aerosols, that can indirectly affect the calculations for the AMF, as they introduce uncertainties in the cloud fraction calculations (Boersma et al., 2008, 2009). A comparison of ground-based in-situ measurements and the data retrieved from OMI sensor suggests that the data from OMI sensor is 0-30% biased (Lamsal et al., 2010). In this study, OMI sensor product (OMNO2d v003) for tropospheric NO_2 column prepared at level-3, providing the data in gridded form at a grid interval of 0.25° latitude by 0.25° longitude is used and downloaded from Giovanni, https://giovanni.gsfc.nasa.gov/.

MACCity emissions data

MACCity is a joint data product contributed by two projects namely, Monitoring Atmospheric Composition and Climate (MACC) and megaCITY–Zoom for the Environment (CityZEN). MACCity products deliver emission data for various atmospheric gasses for the last about sixty years, from 1960 to 2020 and is provided by Emissions of atmospheric Compounds & Compilation of Ancillary Data (ECCAD). MACCity anthropogenic emission datasets are based on Representative Concentration Pathways (RCPs, 8.5, van Vuuren et al., 2011) and Atmospheric Chemistry and Climate Model Inter-comparison Project ACCMIP, (Lamarque et al., 2010). For the futuristic projections of emissions for different scenarios used in the IPCC AR5 report (van Vuuren et al., 2011), starting point for the development of the RCPs is based on the ACCMIP emissions in year, 2000. Whereas, anthropogenic emissions inventoried through ACCMIP rely on various emission database inventories combined and synchronized together, including RETRO, EDGAR, EMEP, EPA, REAS, GICC and GFEDv2, which are based on emission estimates due to anthropogenic activities, historical emissions databases, modelled studies and satellite observations. Many modelers name the MACCity as A2-ACCMIP for having some minor differences between A2-ACCMIP (AeroCom Phase II-ACCMIP) and MACCity (Diehl et al., 2012). MACCity anthropogenic emission datasets are available for download from Ether/ECCAD databases, provided at *http://www.eccad.sedoo.fr.*

In this study, MACCity data for HCHO and NO_x emissions gridded at 0.5° latitude by 0.5° longitude (Granier et al., 2011) have been analyzed for the study period of 12 years, i.e. from 2005 to 2016, generated through six different anthropogenic emission sectors, including industrial sector (for both non-combustion and combustion), waste burning from agricultural fields, residential emissions, energy production sector, transportation sector and an overall sumsector (Amnuaylojaroen et al., 2014).

Analysis and discussion

MACCity HCHO emissions

Spatial distributions of MACCity HCHO emission data from different emission sectors for South Asia spanning over a period of 12 years, from 2005 to 2016 are shown

http://www.aloki.hu ● ISSN 1589 1623 (Print) ● ISSN 1785 0037 (Online)
DOI: http://dx.doi.org/10.15666/aeer/1705_1098911015

in *Figure 3*. Spatial representation of sum emissions due to anthropogenic activities contributed by some of the major emission sources are shown in *Figure 3a*. These major contributors to the sum sector include emissions from agricultural waste, residential and commercial practices, from industrial processes, transportation sector and from energy production and distribution sectors as shown in *Figure 3*.

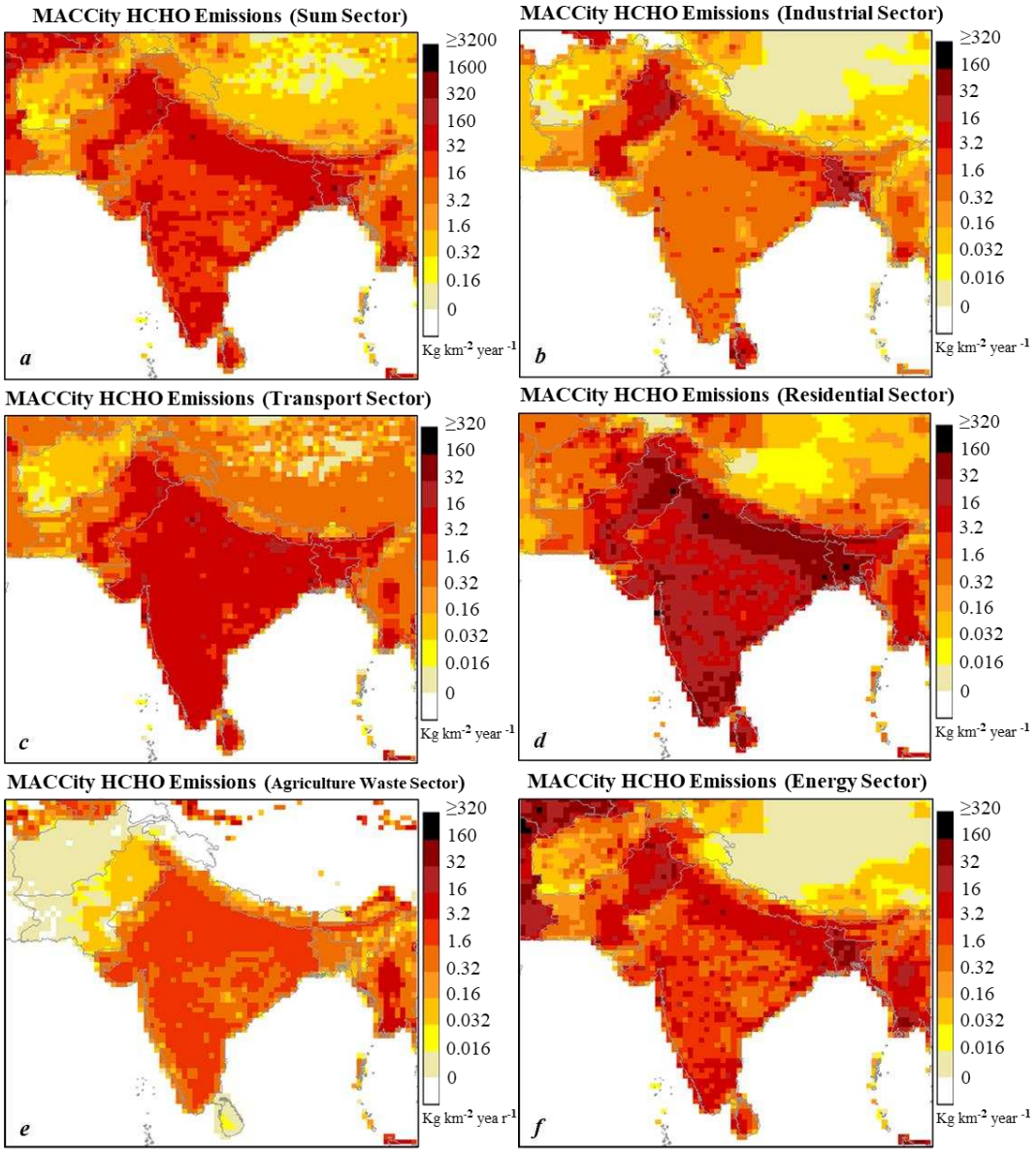

Figure 3. *MACCity based average anthropogenic HCHO emissions (kg km^{-2} year^{-1}) from (a) Sum sector (b) Industrial sector (c) Transport sector (d) Residential sector (e) Agricultural Waste sector and (f) Energy sector over South Asia during 2005-2016*

As shown in *Table 2*, MACCity HCHO anthropogenic emission datasets have shown a considerable rise in emissions from transportation sector in South Asia, raising the emissions from ~8536 kg km^{-2} year^{-1} in 2005 to ~12322 kg km^{-2} year^{-1} in 2016. A

http://www.aloki.hu ● ISSN 1589 1623 (Print) ● ISSN 1785 0037 (Online)
DOI: http://dx.doi.org/10.15666/aeer/1705_1098911015

statistical linear regression-based change analysis on annual mean data of 12 years (2005-2016), shows, ~51% rise in the emissions from transportation sector with ($R^2 = 0.74$). Like the transportation sector, residential and energy sectors also show significant rises, i.e. 13.8% and 11.5% respectively derived through regression-based trend analysis of 12 years of the study period with corresponding coefficients of determination ($R^2 = 0.72$ and 0.62) respectively. Anthropogenic emissions of HCHO are generally observed to be on a rise during the study period and overall sum sector emissions are raised by 21.6% with coefficient of determination ($R^2 = 0.86$) over South Asia. According to (Surl et al., 2018), these high emissions of HCHO from NMVOCs may be associated with the origination from the stationary combustion sources like, residential areas and also from the transportation sectors. In this study, high percentage changes observed in the transportation and residential sectors during the study period 2005-2016 are also endorsed by the observations in the foresaid study.

Table 2. *MACCity average anthropogenic emissions of HCHO in (kg km^{-2} year^{-1}), percentage change, slope of the regression equation and coefficient of determination R^2 over South Asia from January 2005 to December 2016*

Emission sectors	**Average emissions kg km^{-2} year^{-1} (2005-2016)**	**% Change (2005-2016)**	**(Slope of regression equation); (Coefficient of determination R^2)**
Sum sector	72740	21.6	(1234.2 ± 146.6); (0.86)
Agricultural waste sector	2611	7.5	(17.1 ± 5.1); (0.53)
Energy sector	17207	11.5	(169.9 ± 40.9); (0.62)
Industrial sector	4759	3.5	(14.9 ± 6.2); (0.36)
Residential sector	38909	13.8	(457.3 ± 88.4); (0.72)
Transportation sector	9397	51.1	(347.7 ± 65.2); (0.74)

MACCity NO_x emissions

Spatial distributions of MACCity NO_x emissions from different emission sources for the study region over a period of 12 years, from 2005 to 2016 are shown in *Figure 4*. Spatial representation of sum emissions due to anthropogenic activities contributed by some of the major emission sources in South Asia are shown in *Figure 4a.* Major contributors to the sum sector include emissions from residential and commercial practices, from industrial processes, from agricultural waste, transportation sector and from energy production and distribution sectors as shown in *Figure 4.*

As given in *Table 3*, MACCity NO_x anthropogenic emission datasets have shown a considerable rise in the emissions from the transportation sector in South Asia for the study period of 12 years. Emissions in this sector vary from ~ 573947 kg km^{-2} year^{-1} in year 2005 to ~ 1120025 kg km^{-2} year^{-1} in 2016, making a drastic rise in emissions to about 95.6% with a coefficient of determination ($R^2 = 0.98$), through a linear regression trend analysis. This rise is also consistent with the rise in emissions of HCHO for transportation sector showing the largest change in anthropogenic emissions with an increase of ~51% for the study period. Like the transportation sector, energy and industrial sectors also show significant rises in the emissions of NO_x, i.e. 35.3% and 20.7% respectively with the corresponding coefficient of determination ($R^2 = 0.94$ and 0.97) determined through regression analysis for the entire study period of 12 years.

http://www.aloki.hu ● ISSN 1589 1623 (Print) ● ISSN 1785 0037 (Online)
DOI: http://dx.doi.org/10.15666/aeer/1705_1098911015

Anthropogenic emissions of NO_x are generally on a rise as observed by the overall sum sector emissions raised by 42.7% having a coefficient of determination ($R^2 = 0.99$). In this study, these high emissions of NO_x may be associated with the overall high emissions recorded for the tropospheric HCHO column as well, and as reported by Surl et al. (2018).

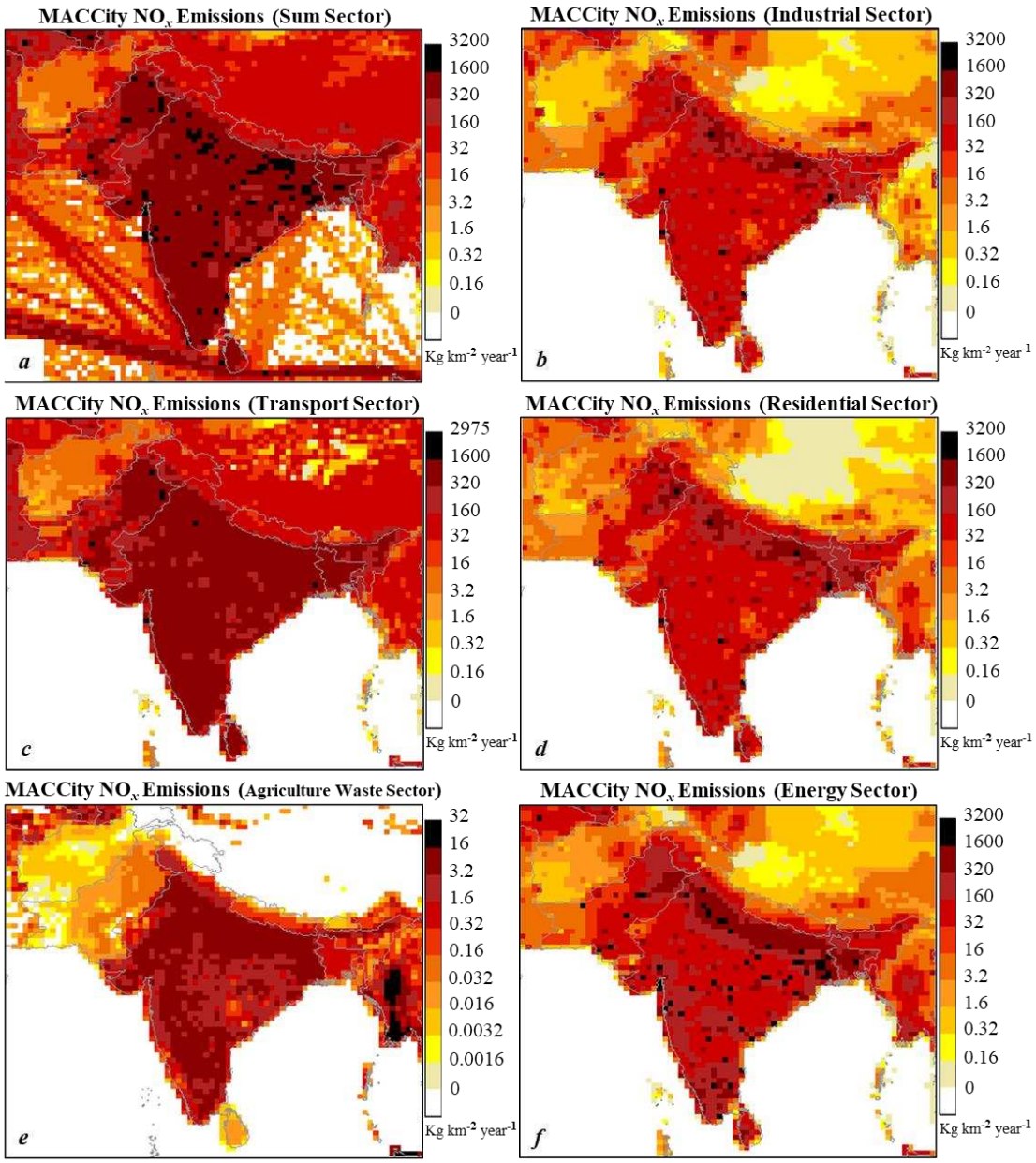

Figure 4. *MACCity based average anthropogenic NO_x emissions (kg km^{-2} $year^{-1}$) from (a) sum sector (b) industrial sector (c) transport sector (d) residential sector (e) agricultural waste sector and (f) energy sector over South Asia during 2005-2016*

http://www.aloki.hu ● ISSN 1589 1623 (Print) ● ISSN 1785 0037 (Online)
DOI: http://dx.doi.org/10.15666/aeer/1705_1098911015

Table 3. *MACCity average anthropogenic emissions of NO_x in (kg km^{-2} $year^{-1}$), Percentage change, slope of the regression equation and coefficient of determination R^2 over South Asia from January 2005 to December 2016*

Emission sectors	Average emissions kg km^{-2} $year^{-1}$ (2005-2016)	% Change (2005-2016)	(Slope of regression equation); (Coefficient of determination *R2*)
Sum sector	2291691	42.7	(73255.4 ± 2178.8); (0.99)
Agricultural waste sector	8357	5.5	(40.6 ± 12.6); (0.51)
Energy sector	697934	35.3	(19055.9 ± 1512.2); (0.94)
Industrial sector	231386	20.7	(3950.3 ± 213.9); (0.97)
Residential sector	239234	12.9	(2648.7 ± 177.9); (0.96)
Transportation sector	816925	95.6	(48034.7 ± 2017.3); (0.98)

Zonal analyses of HCHO columns

Data products from OMI sensor, for HCHO and NO_2 have been analyzed for spatiotemporal analysis of the tropospheric columns of HCHO and NO_2. Annual means values for both the gases, regression trends and percentage changes for the entire study period of 2005-2016, for South Asia and seven study zones are shown in *Table 4*.

Table 4. *Summary of annual mean OMI-HCHO (× 10^{15} molecules cm^{-2}) and OMI-NO_2 (× 10^{15} molecules cm^{-2}), parameters of linear regression analysis and percentage change over entire South Asia and seven study zones during the period of 2005-2016*

HCHO	Annual mean OMI-HCHO (× 10^{15} molec cm^{-2})	Slope of regression equation	Coefficient of determination (R^2)	% Change
Zone-1	04.22 ± 0.05	0.004 ± 0.015	0.081	01.15
Zone-2	10.12 ± 0.21	0.074 ± 0.03	0.45	08.34
Zone-3	10.08 ± 0.13	0.091 ± 0.03	0.49	10.50
Zone-4	10.20 ± 0.16	0.073 ± 0.04	0.29	08.22
Zone-5	08.12 ± 0.14	0.080 ± 0.03	0.41	11.50
Zone-6	09.88 ± 0.12	0.066 ± 0.05	0.16	07.58
Zone-7	08.50 ± 0.12	0.081 ± 0.03	0.49	11.09
South Asia	06.22 ± 0.14	0.050 ± 0.01	0.53	09.86
NO_2	**Annual mean OMI-HCHO (× 10^{15} molec cm^{-2})**	**Slope of regression equation**	**Coefficient of determination (R^2)**	**% Change**
Zone-1	0.77 ± 0.01	0.004 ± 0.002	0.27	6.61
Zone-2	2.43 ± 0.15	0.038 ± 0.009	0.67	18.91
Zone-3	1.91 ± 0.06	0.020 ± 0.003	0.85	12.11
Zone-4	1.82 ± 0.14	0.035 ± 0.006	0.76	23.64
Zone-5	0.93 ± 0.02	-0.005 ± 0.006	0.06	-5.87
Zone-6	1.81 ± 0.17	0.040 ± 0.006	0.81	27.96
Zone-7	1.32 ± 0.04	0.009 ± 0.006	0.21	7.66
South Asia	0.83 ± 0.05	0.006 ± 0.003	0.34	7.89

http://www.aloki.hu ● ISSN 1589 1623 (Print) ● ISSN 1785 0037 (Online)
DOI: http://dx.doi.org/10.15666/aeer/1705_1098911015

From *Table 4,* it is clear that the highest annual average value for tropospheric HCHO column, averaged for the entire study period of 12 years has been observed for zone-4, as $(10.20 \pm 0.16) \times 10^{15}$ molecules cm^{-2}. While, the lowest value $(4.22 \pm 0.05) \times 10^{15}$ molecules cm^{-2} for zone-1. The largest positive trend or change (ΔHCHO = 11.50%) has been observed for zone-5, while the lowest trend of change (ΔHCHO = 1.15) has been found for zone-1. This high value of change of HCHO column observed in zone-5, mainly representing the Myanmar region, can be attributed to the high rate of oil palms plantations in southern parts of Myanmar in the last decade. Oil palms have been reported to have a much stronger isoprene emission capacity (Lathière et al., 2010) than the tropical forests of South Asia (Stavrakou et al., 2014). With this plantation activity, associated changes to the landcovers and anthropogenic emissions due to urbanization and changing of natural vegetation with forest plantations have been reported to have significant impacts on the emissions of isoprene (Wiedinmyer et al., 2006) and isoprene being a linchpin for the connection between the satellite observations of tropospheric HCHO column and forested landcover (Wolf et al., 2016). Another high percentage of change in HCHO column, i.e. (ΔHCHO = 11.09%) is observed in zone-7, comprising of the major forest cover on southwestern coast of Indian state Kerala and this region is characterized as a region, where the isoprene has been observed to have the longest lifetime in air (Surl et al., 2018) which also contributes to the high concentrations observed for HCHO column using OMI data. Because of capturing data in early afternoon at 13:40 local time, providing ample time for this longest living isoprene to get converted into HCHO.

Zone-3 also exhibits a considerable change (ΔHCHO = 10.50%) over the study period. Emissions in this study zone are presented with compound influences, i.e., biogenic emissions from forested landcover regions of the states of Uttar Pradesh and Bihar in India and contributions from Nepalis forests. HCHO emissions in this zone are also contributed by the anthropogenic emissions from coal powered thermal electricity generation plants in the states of Uttar Pradesh and Bihar and cities of Jaipur and Lucknow and from the city of Katmandu from neighbouring Nepal. The weak positive trend found in zone-1 with (ΔHCHO = 1.15%) over the span of 12 years can be attributed to the arid and dry landcover, presented mostly by desert landcover, barren rocks and dry sandy soils with weak biogenic sources available for HCHO emissions and the being the least populated region of South Asia, comprising of Baluchistan province of Pakistan and parts of Southwestern Afghanistan for any considerable or noticeable anthropogenic emissions.

Among rest of the zones, i.e. zone-2 with (ΔHCHO = 8.34%) and zone-4 with (ΔHCHO = 8.22%), primarily represent the zones of high anthropogenic emissions through the megacities of Lahore, Faisalabad and Delhi in zone-2, while, Dhaka and Kolkata in zone-4. In zone-2, Pyrogenic emissions contribution comes through crop residue burning activity in the plains of irrigated belts of Punjab, on both, Indian and Pakistani sides. In zone-4, the HCHO contribution is very compound in nature, as all the three, anthropogenic, pyrogenic and biogenic sources are contributing, especially for Bangladesh. Here, contribution to the emissions through pyrogenic sources come from the crop residue burning. While, mangroves of Sundarbans emit significant amounts of isoprene which according to a study, is one of the main biogenic VOC (Barr et al., 2003; Exton et al., 2015) and is a precursor of HCHO. Emissions from zone-6 with (ΔHCHO = 7.58%) represents the regions of Indian states of Orissa and Chhattisgarh, marked with presence of extensive mining and coal powered electricity generation

http://www.aloki.hu ● ISSN 1589 1623 (Print) ● ISSN 1785 0037 (Online)
DOI: http://dx.doi.org/10.15666/aeer/1705_1098911015

power plants and therefore, high emissions through anthropogenic activities. This region is attributed for being the largest coal mining area, along with mega coal powered electricity production plants in eastern India. Mean annual change for South Asia for the study period 2005-2016, ($\Delta HCHO = 9.86\%$) can be understood well with distinct anthropogenic, biogenic and selective pyrogenic sources of emissions of HCHO for different zones of land-use/landcover, contributing to the specific emissions of the tropospheric HCHO column.

Zonal analyses of NO_2 columns

Annual means values of tropospheric NO_2 column, regression trends and percentage changes for the entire study period of 2005-2016, for South Asia and seven study zones are shown in *Table 4*. From *Table 4* tropospheric column of NO_2 for the study period 2005-2016 has been observed with the highest average annual value of $(2.43 \pm 0.15) \times 10^{15}$ molecules cm^{-2} for zone-2, while the lowest value $(0.77 \pm 0.01) \times 10^{15}$ molecules cm^{-2} is observed for zone-1. Emissions captured through OMI sensor of vertical column of NO_2 exhibits the largest positive trend of change with ($\Delta NO_2 = 27.96\%$) in zone-6, and the lowest negative trend of change has been observed for zone-5 being ($\Delta NO_2 = -5.87\%$). It is also interesting to note here, that the annual mean value for the entire study period for zone-5 being $(0.93 \pm 0.02) \times 10^{15}$ molecules cm^{-2} is higher than the annual mean value observed in zone-1 $(0.77 \pm 0.01) \times 10^{15}$ molecules $cm^{-2,}$ but still the overall change for the entire study period of 12 years for zone-5 is less than zone-1. The largest trend of change found in zone-6 can be attributed to the Eastern coal mining zone of Indian states of Chhattisgarh and Orissa, where emissions of NO_2 have increased to $50 \pm 20\%$ from 2005-2015 (Krotkov et al., 2016) and are further complemented by 16 coal fired electricity power plants with a capacity of ~18000 Mega Watts (MW) and ~330 tons of NO*x* emissions annually (Sarath and Puja, 2014).

Zone-2 with a changing trend of ($\Delta NO_2 = 18.91\%$) is characterized with anthropogenic emissions from thickly populated megacities of Delhi, and Lahore, the Industrial city of Faisalabad and also due to pyrogenic emissions from the biomass burning, which also increase the aerosol loading in the region, especially in post-monsoon and winter season (Tariq et al., 2015) from Indian and Pakistani Punjab region. This high aerosol loading may also result in underestimation of NO_2 due to shielding effect of aerosols such as PM2.5 (Jamstec, 2014). Increasing trend in this zone of (~1.58% rise per year) has been found closely consistent with the (Ghude et al., 2009) as of ($1.76 \pm 1.1\%$ per year) for the South Asian countries. This zone-2 has also been found with the highest annual mean concentrations of column of NO_2 value for the entire study period of 2005-2016, i.e. $(2.43 \pm 0.15) \times 10^{15}$ molecules cm^{-2} because of high anthropogenic activity due to rapid urbanization, increasing vehicular activity, more food requirement, high crop residue burning and high biofuel burning for heating purposes. (Azad and Kitada, 1998; Ghose et al., 2004; Badarinath et al., 2006, 2009; Ghude et al., 2008, 2009; Gurjar et al., 2008; Renuka et al., 2014; Ali et al., 2014; ul-Haq et al., 2014; Tariq and Ali, 2015; Tariq et al., 2016). Lowest Observed negative trend ($\Delta NO_2 = -5.87\%$) has been found in zone-5, with annual mean value $(0.93 \pm 0.02) \times 10^{15}$ molecules cm^{-2}, with a consistently decreasing trend after the year 2011, reversing the positively changing trend observed till 2011 to a negative or decreasing trend for zone-5. Data from annual mean values for the vertical column of NO_2 reveal that this negative trend is consistent with the overall South Asian trends observed after the year 2011 to 2016 having ($\Delta NO_2 = -5.29\%$ making it ~-1.05% per year). Similar

http://www.aloki.hu ● ISSN 1589 1623 (Print) ● ISSN 1785 0037 (Online)
DOI: http://dx.doi.org/10.15666/aeer/1705_1098911015

declining trends have also been observed over China in studies by (Richter et al., 2015; Irie et al., 2016).

Zone-4 has also been observed as one of the positively trending regions with ($\Delta NO_2 = 23.64\%$) and annual mean emissions of NO_2 for the entire study period to be $(1.82 \pm 0.14) \times 10^{15}$ molecules cm^{-2}. This region is attributed with high emissions of NO_2 due to anthropogenic activities from megacities of Kolkata and Dhaka and crop residue burning, especially in pre-monsoon seasons (ul-Haq et al., 2015). Zone-3 has also been reported with high amounts of annual mean NO_2 emissions for the study period, being $(1.91 \pm 0.06) \times 10^{15}$ molecules cm^{-2} representing the changing trend to be ($\Delta NO_2 = 12.11\%$). This region also contributes significantly enough for emissions of NO_2, due to its industrial and anthropogenic activities for having coal mining region and coal-powered electricity generation power plants in the states of Bihar and Uttar Pradesh, emissions from the Indian cities of Jaipur and Lucknow and from neighbouring city of Kathmandu in Nepal. Zone-7 exhibits the similar trend as discussed particularly for zone-5 and generally matches with the changing trends for South Asia. In this zone, a decreasing trend has also been seen for the annual mean values of NO_2 after 2011 up to 2016. This makes the overall spatial average emissions of NO_2 for the study period to be $(1.32 \pm 0.04) \times 10^{15}$ molecules cm^{-2}, with an overall changing trend as ($\Delta NO_2 = 7.66\%$), and is more closely related to what was reported by (Ghude et al., 2008). South Asian mean annual change over the study period 2005-2016, ($\Delta NO_2 = 7.89\%$) can be understood well with distinct anthropogenic, biogenic and pyrogenic sources of emissions of NO_2 for different zones of land-use/landcover, contributing and affecting to the specific emissions of the tropospheric NO_2 column.

Spatial distributions of HCHO and NO_2 columns

Mean Spatial distributions derived from the annual mean values of OMI data for tropospheric columns of HCHO and NO_2 emissions along with the changing trends over South Asia for the entire study period, from 2005 to 2016 are shown in *Figure 5*.

In *row (a), Figure 5,* Spatial distributions of annual-mean area averaged tropospheric HCHO column ($\times 10^{15}$ molecules cm^{-2}), and annual-mean area averaged tropospheric NO_2 column ($\times 10^{15}$ molecules cm^{-2}) over South Asia for the study period of 2005 to 2016 are presented, retrieved through OMI data on left and middle columns respectively. Trends of these area averaged annual mean values, both for, HCHO and NO_2 from 2005 to 2016 over South Asia are also presented in the right column of *row (a)*, *Figure 5*. A linear regression on the annual mean values of NO_2 data shows an increasing trend, with annual increase of ~0.66% and an overall increase of ~7.9% for the entire study period, with a slope of 0.006 (± 0.003), coefficient of determination ($R^2 = 0.35$) and *y*-intercept at 0.830426 (± 0.019072) $\times 10^{15}$ molecules cm^{-2}. These increasing trends of NO_2 for a period of first seven years from 2005-2011, with annual increase of ~1.86% making seven-year increase of ~13.01%, with a slope of 0.0172 ± 0.0029, coefficient of determination ($R^2 = 0.88$) and *y*-intercept at 0.7767 (± 0.013096) $\times 10^{15}$ molecules cm^{-2} have been found well in agreement with the trends presented by (Ghude et al., 2009), i.e. $1.76 \pm 1\%$ per year over south Asia. However, NO_2 retrievals from OMI data, after reaching to a peak value in year 2011 with 0.845567 (± 0.040695) $\times 10^{15}$ molecules cm^{-2} show consistently a negative change, till 2016. This decreasing trend has been observed for every two consecutive succeeding years for tropospheric NO_2 columns, showing the consistency in this declining trend. In the last five years of the study, from 2012 to 2016, the rate of change per year has been

http://www.aloki.hu ● ISSN 1589 1623 (Print) ● ISSN 1785 0037 (Online)
DOI: http://dx.doi.org/10.15666/aeer/1705_1098911015

observed to be reduced with decreasing values of NO_2 column, having an annual decrease of ~1.06% as compared to the value of change for the first seven years of the study. i.e. ~1.86%, and making an overall decrease for the last five years of ~5.29%, with a slope of -0.012 (± 0.007), coefficient of determination (R^2 = 0.50) and *y*-intercept at 0.907322 (± 0.023287) $\times 10^{15}$ molecules cm^{-2}. Similar decreasing trends of the tropospheric NO_2 column have also been reported in China after the year 2011, where this rate of decline has been reported to be ~6% year $^{-1}$(Richter et al., 2015; Irie et al., 2016). Reasons for lowering the values of the tropospheric column of NO_2 could be linked to the shift in meteorological regions, affecting. e.g., the rates of chemical reactions and air mass visibility for satellite observations in troposphere (Voulgarakis et al., 2010) and due to strategies adopted for lowering NOx emissions through technological improvements like adoption of cleaner technologies and also due to some decline in the economic activity related to NOx emissions (Hilboll et al., 2017).

Linear regression analysis performed on the area averaged annual mean values of HCHO data shows an increasing trend over South Asia, with an annual increase of ~0.74% and an overall increase of ~9.86% for the study period of twelve years, with a slope of 0.050508 (± 0.014932), coefficient of determination (R^2 = 0.53) and *y*-intercept at 6.220404 (± 0.109894) $\times 10^{15}$ molecules cm^{-2}. Such increasing trends of HCHO over countries of South Asia have also been reported in the study by (De Smedt et al., 2010). These increasing trends for HCHO emissions could also be associated with the increasing anthropogenic sources of emission in South Asia as shown by the results from the MACCity emission data sources, which indicate that for the period of 2005-2016 anthropogenic emissions have been increased to about 22% and hence the overall increase in HCHO emissions.

In *Figure 5*, *rows (b), (c), (d)* and *(e)* also represent spatial distributions of area averaged seasonal mean values of HCHO and NO_2 columns averaged from OMI monthly mean data for the entire study period of 12 years from 2005 to 2016 for Pre-Monsoon, Monsoon, Post-Monsoon and Winter seasons respectively. Seasonal spatial distributions of HCHO and NO_2 columns show the variations of emissions with the changing seasonal conditions over different landuse/landcovers. In *Figure 5*, *row (b),* HCHO column exhibits higher concentrations for pre-monsoon season, observed along the Indo-Gangetic Basin (IGB) with the forest cover, especially along the foothills of the Himalayas in northwestern India, industrial landuse and activity in the Eastern mining zone of India, biogenic emissions from the mangrove forests (Barr et al., 2003; Exton et al., 2015; Sippo et al., 2016) of Sundarbans in Bangladesh and the forest cover of western Ghats in the states of Kerala and around. Similar anthropogenic and biogenic emissions have also been observed from Myanmar. In *Figure 5*, *row (b),* the spatial distribution of tropospheric NO_2 column for pre-monsoon season retrieved through OMI also highlights the megacities of Lahore and Delhi representing the major contributions through anthropogenic emissions and from crop residue and biomass burning for heating purposes. These pre-monsoon, spring seasonal high values may be associated with the meteorological conditions as well (ul-Haq et al., 2015). Such highlighted emissions are also observed in the in the Eastern mining zone of India in the states of Chhattisgarh and Orissa, also the pre-monsoon pyrogenic emissions are also highlighted in the Bangladesh region.

http://www.aloki.hu ● ISSN 1589 1623 (Print) ● ISSN 1785 0037 (Online)
DOI: http://dx.doi.org/10.15666/aeer/1705_1098911015

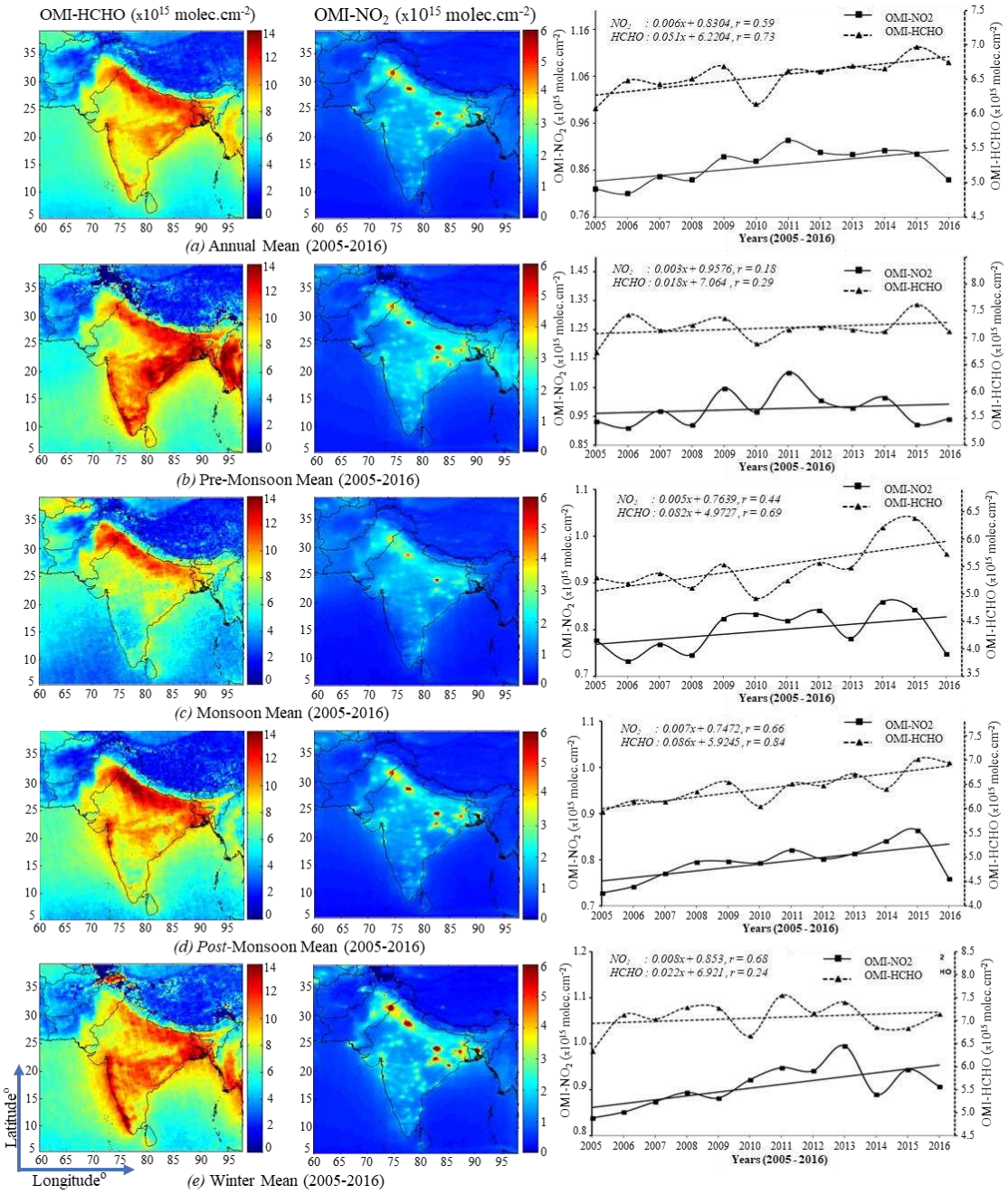

Figure 5. *Annual mean area averaged spatial distributions of tropospheric columns of HCHO and NO_2 (× 10^{15} molecules cm^{-2}) over South Asia for study period of (2005-2016) along with the varying trend for 12 years is shown in row (a), in left and middle columns respectively. Seasonal, mean area averaged spatial distributions of HCHO and NO_2 columns (× 10^{15} molecules cm^{-2}) along with the varying seasonal trend for entire study period for all the four seasons over South Asia from (2005-2016) are shown as, Pre-Monsoon in row (b), monsoon in row (c), post-monsoon in row (d) and winter in row (e), respectively*

Spatial distribution of HCHO and NO_2 columns for the monsoon season (*Fig. 5*, *row c*), exhibits relatively low activity for both NO_2 and HCHO emissions for the underlying landcovers. Lower values of HCHO column in the monsoon conditions could be

http://www.aloki.hu ● ISSN 1589 1623 (Print) ● ISSN 1785 0037 (Online)
DOI: http://dx.doi.org/10.15666/aeer/1705_1098911015

ascribed to low wind speeds, high humidity and rain driven washout of the gaseous air pollutants (Verma et al., 2015). This can also be seen from *Figure 2*, where low wind vectors are observed in monsoon season along with high precipitation resulting in this kind of washout phenomenon of pollutants. Whereas, these seasonal low values observed for NO_2 could be associated with the higher concentration of (Hydroxyl) OH ions, making an increased activity of photo-dissociation of NO_2, advection of clean air mass and due to increased solar radiation for having longer day hours (Ravindra et al., 2003; Ghude et al., 2009; Yoo et al., 2014).

Spatial distribution of HCHO column over South Asia for post monsoon season (*Fig. 5*, *row d*), shows lower concentrations and that can be associated with low biogenic emissions especially from the forested regions due to leaf phenological variations depicted by the low values of NDVI 0.379 ± 0.029, derived by MODIS onboard Terra satellite , as compared to pre-monsoon season with NDVI values to be 0.527 ± 0.018, for the months of March, April and May. These phenological changes in post monsoon season could be one of the reasons for lower values of isoprene emissions and hence the lower concentrations of HCHO column observations (Surl et al., 2018). Post-monsoon relatively higher concentrations of NO_2 column are observed due to the activity of large-scale crop waste burning (ul-Haq et al., 2014).

Spatial distribution of HCHO column over South Asia for winter season (*Fig. 5, row 5*) shows lower concentrations of HCHO, as compared to the summer season. These relatively low emissions may be connected to the lower emissions of Isoprene in winters, as the Isoprene emissions have a clear distinct seasonal cycle, showing high emissions in the summers than in winters (Malik et al., 2018). And as this isoprene is oxidized with air, it gets converted to HCHO (Palmer et al., 2003, 2006), therefore the two associated low emissions could be linked in the winter season. High emissions have been observed for NO_2 in the winter season due to more crop residue burning in the winters in the region of Indian and Pakistani Punjab, especially highlighting the regions near Lahore, and Delhi around, two mega cities with anthropogenic emissions as well. Also, the higher concentrations have been found in the eastern mining zones of India and emissions from the Bangladesh side.

Conclusion

In this study a spatiotemporal assessment of two important atmospheric air pollutants, i.e. HCHO and NO_2 has been carried out over South Asia, being the most thickly populated region of the world, by using satellite remote sensing data from OMI sensor onboard Aura satellite. This study spans over a period of 12 years, from 2005 to 2016. Different analysis on the remote sensing data for these gases, help in identifying three distinct types of sources of emissions for these atmospheric pollutants, i.e. emissions through anthropogenic activities, emissions through pyrogenic activities and emissions through nature or biogenic sources. Further, these three distinct sources have very specific associations with the different landuse/landcovers. These associations are explained and analyzed in seven different study zones, selected at different geographical locations of South Asia, representing different landuse/landcovers ranging from the arid desert like areas, to thickly populated areas, to mountainous forested landcovers, to the mangroves forest cover, to the mining regions and to the agricultural belts defining the main landcovers of the region. Analyses of the annual spatial data for both the gases for a period from 2005 to 2016 show an overall increasing trend for anthropogenic NO_2

http://www.aloki.hu ● ISSN 1589 1623 (Print) ● ISSN 1785 0037 (Online)
DOI: http://dx.doi.org/10.15666/aeer/1705_1098911015

emissions. A linear regression on the annual mean values of NO_2 data shows this trend with annual increase of ~0.66% and an overall increase of ~7.9% for the entire study period, with a slope of 0.006 (± 0.003), coefficient of determination (R^2 = 0.35) and *y*-intercept at 0.830426 (± 0.019072) $\times 10^{15}$ molecules cm^{-2}. An important finding in this trend analysis is that for the first seven years of the study, i.e. from 2005 to 2011, NO_2 emissions are increasing with a faster rate of about ~1.86% per year but in the last six years, i.e. from 2012 to 2016 this rate has been observed to be reduced to ~1.06% annually, making this rising trend to check. Reasons for lowering the values of the tropospheric column of NO_2 could be linked to the shift in meteorological regions, affecting, e.g., the rates of chemical reactions and air mass visibility for satellite observations in troposphere, and due to strategies adopted for lowering NO_x emissions through technological improvements like adoption of cleaner technologies and also due to some decline in the economic activity related to NOx emissions. Similar increasing trends have been observed for HCHO emissions for South Asia. Linear regression analysis performed on the area averaged annual mean values of HCHO data shows this increasing trend over South Asia, with annual increase of ~0.74% and an overall increase of ~9.86% for the study period of 12 years, with a slope of 0.050508 (± 0.014932), coefficient of determination (R^2 = 0.53) and *y*-intercept at 6.220404 (± 0.109894) $\times 10^{15}$ molecules cm^{-2}. These increasing trends for HCHO emissions could also be associated with the increasing anthropogenic sources of emission in South Asia as shown by the results from the MACCity emission data sources, which indicate that, for the period of 2005-2016 anthropogenic emissions have been increased to about 22% and hence the overall increase in HCHO emissions. Seasonality has been observed in the emission trends of HCHO and NO_2 over South Asia as, the effects of seasonal changes are associated sometimes with anthropogenic activities and sometimes with the biogenic and pyrogenic activities, resulting the corresponding impacts on the emissions of these gases in atmosphere. For further localized analysis, seven study zones have been analyzed, representing some of the available representative variations of landuse and landcovers. These zones have been typically observed in the context of anthropogenic, natural or biogenic and pyrogenic sources of emissions.

REFERENCES

[1] Ali, M., Tariq, S., Mahmood, K., Daud, A., Batool, A., ul-Haq, Z. (2014): A study of aerosol properties over Lahore (Pakistan) by using AERONET data. – Asia-Pacific J Atmos Sci 50: 153-162.

[2] Amnuaylojaroen, T., Barth, M. C., Emmons, L. K., Carmichael, G. R., Kreasuwun, J., Prasitwattanaseree, S., Chantara, S. (2014): Effect of different emission inventories on modeled ozone and carbon monoxide in Southeast Asia. – Atmos. Chem. Phys. 14: 12983-13012. http://dx. doi.org/10.5194/acp-14-12983-2014.

[3] Azad, A. K., Kitada, T. (1998): Characteristics of the air pollution in the city of Dhaka, Bangladesh in winter. – Atmos Environ 32(11): 1991-2005.

[4] Badarinath, K. V. S., Chand, K. T. R., Prasad, K. V. (2006): Agriculture crop residue burning in the Indo-Gangetic Plains—a study using IRSP6 AWiFS satellite data. – Curr Sci 91: 1085-1089.

[5] Badarinath, K. V. S., Kharol, S. K., Sharma, A. R., Prasad, V. K. (2009): Analysis of aerosol and carbon monoxide characteristics over Arabian Sea during crop residue burning period in the Indo-Gangetic Plains using multi-satellite remote sensing datasets. – J Atmos Solar Terr Phys 71: 1267-1276.

http://www.aloki.hu ● ISSN 1589 1623 (Print) ● ISSN 1785 0037 (Online)
DOI: http://dx.doi.org/10.15666/aeer/1705_1098911015

[6] Barck, C., Lundahl, J., Halldén, G., Bylin, G. (2005): Brief exposures to NO_2 augment the allergic inflammation in asthmatics. – Environmental Research 97: 58-66.

[7] Barkley, M. P., Palmer, P. I., Kuhn, U., Kesselmeier, J., Chance, K., Kurosu, T. P., Martin, R. V., Helmig, D., Guenther, A. (2008): Net ecosystem fluxes of isoprene over tropical South America inferred from Global Ozone Monitoring Experiment (GOME) observations of HCHO columns. – J. Geophys. Res.-Atmos. 113: d20304. https://doi.org/10.1029/2008JD009863.

[8] Barkley, M. P., Smedt, I. D., Van Roozendael, M., Kurosu, T. P., Chance, K., Arneth, A., Hagberg, D., Guenther, A., Paulot, F., Marais, E. (2013): Top-down isoprene emissions over tropical south America inferred from SCIAMACHY and OMI formaldehyde columns. – J Geophys Res Atmos 118(12): 6849-6868. https://doi.org/10.1002/jgrd.50552.

[9] Barr, J. G. J. D., Fuentes, N., Wang, Y., Edmonds, J. C., Zieman, B. P., Hayden, D. L., Childers. (2003): Red mangroves emit hydrocarbons. – Southeast. Nat. 2: 499-510.

[10] Bauwens, M. T., Stavrakou, J. F., Müller, I., De Smedt, M., Van Roozendael, G. R., van der Werf, C., Wiedinmyer, J. W., Kaiser, K., Sindelarova, Guenther, A. (2016): Nine years of global hydrocarbon emissions based on source inversion of OMI formaldehyde observations. – Atmos. Chem. Phys. 16: 10,133-10,158. DOI: 10.5194/acp-16-10133-2016.

[11] Boersma, F., Bucsela, E., Brinksma, E., Gleason, J. F. (2002): NO_2. – In: Chance, K. (ed.) OMI Algorithm Theoretical Basis Document. OMI Trace Gas Algorithms. – Smithsonian Astrophysical Observatory, Cambridge, Vol. IV, pp 13-36.

[12] Boersma, K. F., Eskes, H. J., Brinksma, E. J. (2004): Error analysis for tropospheric NO_2 retrieval from space. – J Geophys Res Atmos 109(D4).

[13] Boersma, K. F., Jacob, D. J., Bucsela, E. J., Perring, A. E., Dirksen, R., Yantosca, R. M., Cohen, R. C. (2008): Validation of OMI tropospheric NO_2 observations during INTEX-B and application to constrain NOx emissions over the eastern United States and Mexico. – Atmos Environ 42(19): 4480-4497.

[14] Boersma, K. F., Jacob, D. J., Trainic, M., Rudich, Y., De Smedt, I., Dirksen, R., Eskes, H. J. (2009): Validation of urban NO_2 concentrations and their diurnal and seasonal variations observed from the SCIAMACHY and OMI sensors using in situ surface measurements in Israeli cities. – Atmos Chem Phys 9: 3867-3879. DOI: 10. 5194/acp-9-3867-2009.

[15] Boersma, K. F., Eskes, H. J., Dirksen, R. J., van der A, R. J., Veefkind, J. P., Stammes, P., Huijnen, V., Kleipool, Q. L., Sneep, M., Claas, J., Leitao, J., Richter, A., Zhou, Y., Brunner, D. (2011): An improved tropospheric NO_2 column retrieval algorithm for the Ozone Monitoring Instrument. – Atmos Meas Tech 4: 1905-1928.

[16] Bucsela, E. J., Celarier, E. A., Wenig, M. O., Gleason, J. F., Veefkind, J. P., Boersma, K, F., Brinksma, E. J. (2006): Algorithm for NO_2 vertical column retrieval from the Ozone Monitoring Instrument. – IEEE Trans Geosci Remote Sens 44: 1245-1258.

[17] Case, G. D., Dixon, J. S., Schooley, J. C. (1979): Interactions of blood metalloproteins with nitrogen oxides and oxidant air pollutants. – Environmental Research 20: 43-65.

[18] Chance, K., Palmer, P. I., Spurr, R. J. D., Martin, R. V., Kurosu, T. P., Jacob, D. J. (2000): Satellite observations of formaldehyde over North America from GOME. – Geophys. Res. Lett. 27: 3461-3464. DOI: 10.1029/2000GL011857.

[19] Curci, G., Palmer, P. I., Kurosu, T. P., Chance, K., Visconti, G. (2010): Estimating European volatile organic compound emissions using satellite observations of formaldehyde from the Ozone Monitoring Instrument. – Atmos. Chem. Phys. 10: 11501-11517. https://doi.org/10.5194/acp-10-11501-2010.

[20] De Graaf, M., Sihler, H., Tilstra, L. G., Stammes, P. (2016): How big is an OMI pixel? – Atmos. Meas. Tech. 9: 3607-3618. DOI: 10.5194/amt-9- 3607-2016.

[21] De Smedt, I., Müller, J. F., Stavrakou, T., van der A, R., Eskes, H., Van Roozendael, M. (2008): Twelve years of global observations of formaldehyde in the troposphere using

http://www.aloki.hu ● ISSN 1589 1623 (Print) ● ISSN 1785 0037 (Online)
DOI: http://dx.doi.org/10.15666/aeer/1705_1098911015

GOME and SCIAMACHY sensors. – Atmos. Chem. Phys. 8: 4947-4963. DOI: 10.5194/acp-8-4947-2008.

[22] De Smedt, T., Stavrakou, J.-F., Müller, R. J., van der, A., Roozendael, M. V. (2010): Trend detection in satellite observations of formaldehyde tropospheric columns. – Geophysical Research Letters 37: L18808. DOI: 10.1029/2010GL044245.

[23] De Smedt, I., Stavrakou, T., Hendrick, F., Danckaert, T., Vlemmix, T., Pinardi, G., Theys, N., Lerot, C., Gielen, C., Vigouroux, C., et al. (2015): Diurnal, seasonal and long-term variations of global formaldehyde columns inferred from combined OMI and GOME-2 observations. – Atmos. Chem. Phys 15: 12,519-12,545. DOI: 10.5194/acp-15-12519-2015.

[24] Diehl, T., Heil, A., Chin, M., Pan, X., Streets, D., Schultz, M., Kinne, S. (2012): Anthropogenic, biomass burning, and volcanic emissions of black carbon, organic carbon, and SO2 from 1980 to 2010 for hindcast model experiments. – Atmos. Chem. Phys. Discuss. 12: 24895-24954. http://dx.doi.org/10.5194/acpd-12-24895-2012.

[25] Dobber, M. R., Dirksen, R. J., Levelt, P. F., van den Oord, G. H. J., Voors, R. H. M., Kleipool, Q., Jaross, G., Kowalewski, M., Hilsenrath, E., Leppelmeier, G. W., de Vries, J., Dierrsen, W., Rozemeijer, N. C. (2006): Ozone Monitoring Instrument calibration. – IEEE Trans. Geosci. Remote Sens. 44: 1209. DOI: 10.1109/TGRS.2006.869987.

[26] Exton, D. A., McGenity, T. J., Steinke, M., Smith, D. J. Suggett, D. J. (2015): Uncovering the volatile nature of tropical coastal marine ecosystems in a changing world. – Glob. Change Biol. 21: 1383-1394. DOI: 10.1111/gcb.12764.

[27] Fu, T.-M., Jacob, D. J., Palmer, P. I., Chance, K., Wang, Y. X., Barletta, B., Blake, D. R., Stanton, J. C., Pilling, M. J. (2007): Space-based formaldehyde measurements as constraints on volatile organic compound emissions in east and south Asia and implications for ozone. – J. Geophys. Res. 112: D06312. DOI: 10.1029/2006JD007853.

[28] Ghose, M. K., Paul, R., Banerjee, S. K. (2004): Assessment of the impacts of vehicular emissions on urban air quality and its management in Indian context: the case of Kolkata (Calcutta). – Environ Sci Policy 7: 345-351.

[29] Ghude, S. D., Fadnavis, S., Beig, G., Polade, S. D., van der A, R. J. (2008): Detection of surface emission hot spots, trends, and seasonal cycle from satellite-retrieved NO_2 over India. – J Geophys Res Atmos 113. DOI: 10.1029/2007JD009615.

[30] Ghude, S. D., Van der A, R. J., Beig, G., Fadnavis, S., Polade, S. D. (2009): Satellite derived trends in NO_2 over the major global hotspot regions during the past decade and their intercomparison. – Environ Pollut 157: 1873-1878.

[31] Gonzi, S., Palmer, P. I., Barkley, M. P., De Smedt, I., Van Roozendael, M. (2011): Biomass burning emission estimates inferred from satellite column measurements of HCHO: Sensitivity to co-emitted aerosol and injection height. – Geophys. Res. Lett. 38: L14807. DOI: 10.1029/ 2011GL047890.

[32] Granier, C., Bessagnet, B., Bond, T., D'Angiola, A., van der Gon, D. H., Frost, G. J., Heil, A., Kaiser, J. W., Kinne, S., Klimont, Z., Kloster, S., Lamarque, J.-F., Liousse, C., Masui, T., Meleux, F., Mieville, A., Ohara, T., Raut, J., Riahi, K., Schultz, M. G., Smith, S. J., Thompson, A., van Aardenne, J., van der Werf, G. R., van Vuuren, D. P. (2011): Evolution of anthropogenic and biomass burning emissions of air pollutants at global and regional scales during the 1980-2010 period. – Clim. Change 109 (1-2): 163-190. http://dx.doi.org/10.1007/s10584- 011-0154-1.

[33] Gurjar, B. R., Butler, T. M., Lawrence, M. G., Lelieveld, J. (2008): Evaluation of emissions and air quality in megacities. – Atmos Environ 42: 1593-1606.

[34] Hassan, S. K., El-Abssawy, A. A., Khoder, M. I. (2018): Effect of seasonal variation on the levels and behaviors of formaldehyde in the atmosphere of a suburban area in Cairo, Egypt. – Asian Journal of Atmospheric Environment 12(4): 356-368.

[35] Harrison, S. P., Morfopoulos, C., Dani, K. G. S., Prentice, I. C., Arneth, A., Atwell, B. J., Michael, P., Barkley, M. P., Leishman, M. R., Loreto, F., Belinda, E., Medlyn, B. E., Niinemets, U., Possell, M., Pe-uelas, J., Wright, I. J. (2013): Volatile isoprenoid

http://www.aloki.hu ● ISSN 1589 1623 (Print) ● ISSN 1785 0037 (Online)
DOI: http://dx.doi.org/10.15666/aeer/1705_1098911015

emissions from plastid to planet. – New Phytologist 197: 49-57. DOI: 10.1111/nph.12021.

[36] Hilboll, A., Richter, A., Burrows, J. P. (2017): NO_2 pollution over India observed from space — the impact of rapid economic growth, and a recent decline. – Atmos. Chem. Phys. Discuss. DOI: 10.5194/acp-2017-101: 2017.

[37] Irie, H., Muto, T., Itahashi, S., Kurokawa, J., Uno, I. (2016): Turnaround of tropospheric nitrogen dioxide pollution trends in China, Japan, and South Korea. – Sola 12: 170-174. DOI: 10.2151/sola.2016-035. 2016.

[38] JAMSTEC (2014): JAMSTEC 2014 Annual Report. – http://www.godac.jamstec.go.jp/catalog/data/doc_catalog/media/AR_2014_all.pdf (accessed on 17 May 2019).

[39] Joshi, R. M. (2015): Education in South Asia. – In: Smelser, N. J., Baltes, P. B. (eds.) International Encyclopedia of the Social & Behavioral Sciences, 2nd Ed.. Elsevier, Amsterdam, pp. 194-197.

[40] Kalnay, E., Kanamitsu, M., Kistler, R., Collins, W., Deaven, D., Gandin, L., Iredell, M., Saha, S., White, G., Woollen, J., Zhu, Y., Chelliah, M., Ebisuzaki, W., Higgins, W., Janowiak, J., Mo, K. C., Ropelewski, C., Wang, J., Leetmaa, A., Reynolds, R., Jenne, R., Joseph, D. (1996): The NCEP/NCAR 40-year reanalysis project. – Bull. Am. Meteorol. Soc. 77: 437-471.

[41] Kaczorowski, J., Perelli, A. (2004): Inversion of CO and NO_x emissions using the adjoint of the IMAGES model. – Atmos. Chem. Phys. Discuss. 4: 7985-8068.

[42] Krotkov, N. A., McLinden, C. A., Li, C., Lamsal, L. N., Celarier, E. A., Marchenko, S. V., Swartz, W. H., Bucsela, E. J., Joiner, J., Duncan, B. N., Boersma, K. F., Veefkind, J. P., Levelt, P. F., Fioletov, V. E., Dickerson, R. R., He, H., Lu, Z., Streets, D. G. (2016): Aura OMI observations of regional SO_2 and NO_2 pollution changes from 2005 to 2015. – Atmos. Chem. Phys. 16: 4605-4629. https://doi.org/10.5194/acp-16-4605-2016.

[43] Kurosu, T. P. (2008): OMHCHO README FILE. – https://www.cfa.harvard.edu/atmosphere/Instruments/OMI/PGEReleases/READMEs/OMHCHO_README.pdf (accessed on 12 May 2019).

[44] Lamarque, J., Bond, T. C., Eyring, V., Granier, C., Heil, A., Klimont, Z., Lee, D., Liousse, C., Mieville, A., Owen, B., Schultz, M. G., Shindell, D., Smith, S. J., Stehfest, E., Van Aardenne, J., Cooper, O. R., Kainuma, M., Mahowald, N., McConnell, J. R., Naik, V., Riahi, K., van Vuuren, D. P. (2010): Historical (1850-2000) gridded anthropogenic and biomass burning emissions of reactive gases and aerosols: methodology and application. – Atmos. Chem. Phys. 10: 7017-7039. http://dx.doi.org/10.5194/acp-10-7017-2010.

[45] Lamsal, L. N., Martin, R. V., van Donkelaar, A., Celarier, E. A., Bucsela, E. J., Boersma, K. F., Dirksen, R., Luo, C., Wang, Y. (2010): Indirect validation of tropospheric nitrogen dioxide retrieved from the OMI satellite instrument: insight into the seasonal variation of nitrogen oxides at northern midlatitudes. – J Geophys Res 115: D05302. DOI: 10.1029/2009JD013351.

[46] Lathière, J., Hauglustaine, D. A., Friend, A. D., De Noblet-Ducoudré, N., Viovy, N., Folberth, G. A. (2006): Impact of climate variability and land use changes on global biogenic volatile organic compound emissions. – Atmos. Chem. Phys. 6: 2129-2146. https://doi.org/10.5194/acp-6-2129-2006.

[47] Lathière, J., Hewitt, C. N., Beerling, D. J. (2010): Sensitivity of isoprene emissions from the terrestrial biosphere to 20th century changes in atmospheric CO 2 concentration, climate, and land use. – Global Biogeochemical Cycles - Global Biogeochem Cycle 24. DOI: 10.1029/2009GB003548.

[48] Lee, Y.-N., Zhou, X., Kleinman, L. I., Nunnermacker, L. J. Springston, S., Daum, P., Newman, L., Keigley, W. G., Holdren, M. W., Spicer, C., Young, V., Fu, B., Parrish, D., Holloway, J., Williams, J., Roberts, J., Ryerson, T. B., Fehsenfeld, F. (1998): Atmospheric chemistry and distribution of formaldehyde and several multioxygenated

http://www.aloki.hu ● ISSN 1589 1623 (Print) ● ISSN 1785 0037 (Online)
DOI: http://dx.doi.org/10.15666/aeer/1705_1098911015

carbonyl compounds during the 1995 Nashville/Middle Tennessee Ozone Study – J. Geophys. Res. 103: 22,449-22,462.

[49] Levelt, P. F., Van den Oord, G. H. J., Dobber, M. R., Mälkki, A., Visser, H., De Vries, J., Stammes, P., Lundell, J. O. V., Saari, H. (2006): The Ozone Monitoring Instrument. – IEEE Transaction on Geoscience and Remote Sensing 44(5): 1093-1101.

[50] Malik, T. G., Gajbhiye, T., Pandey, S. K. (2018): Seasonality in emission patterns of isoprene from two dominant tree species of Central India: implications on terrestrial carbon emission and climate change. – Proceedings of the International Academy of Ecology and Environmental Sciences 8(4): 204-212.

[51] Marais, E. A., Jacob, D. J., Kurosu, T. P., Chance, K., Murphy, J. G., Reeves, C., Mills, G., Casadio, S., Millet, D. B., Barkley, M. P., Paulot, F., Mao, J. (2012): Isoprene emissions in Africa inferred from OMI observations of formaldehyde columns. – Atmos. Chem. Phys. 12: 6219-6235, https://doi.org/10.5194/acp-12-6219.

[52] Marais, E. A., Jacob, D. J., Wecht, K., Lerot, C., Zhang, L., Yu, K., Kurosu, T. P., Chance, K., Sauvage, B. (2014): Anthropogenic emissions in Nigeria and implications for ozone air quality: A view from space. – Atmos. Environ. 99: 32-40. DOI: 10.1016/j.atmosenv.2014.09.055.

[53] Maroziene, L., Grazuleviciene, R. (2002): Maternal exposure to low-level air pollution and pregnancy outcomes: a population-based study. – Environ Health 9: 1: 6.

[54] Millet, D. B., Jacob, D. J., Turquety, S., Hudman, C. R., Wu, S., Fried, A., James Walega, J., Heikes, B. G., Blake, D. R., Singh, H. B., Anderson, B. E., Clarke, A. D. (2006): Formaldehyde distribution over North America: Implications for satellite retrievals of formaldehyde columns and isoprene emission. – Journal of Geophysical Research 111: D24S02.

[55] Millet, D. B., Jacob, D. J., Boersma, K. F., Fu, T. M., Kurosu, T. P., Chance, K., Heald, C. L., Guenther, A. (2008): Spatial distribution of isoprene emissions from North America derived from formaldehyde column measurements by the OMI satellite sensor. – J. Geophys. Res. 113: D02307. DOI: 10.1029/2007JD008950.

[56] Nowlan, C. R., Liu, X., Janz, S. J., Kowalewski, M. G., Chance, K., Follette-Cook, M. B., Fried, A., González Abad, G., Herman, J. R., Judd, L. M., Kwon, H.-A., Loughner, C. P., Pickering, K. E., Richter, D., Spinei, E., Walega, J., Weibring, P., Weinheimer, A. J. (2018): Nitrogen dioxide and formaldehyde measurements from the GEOstationary Coastal and Air Pollution Events (GEO-CAPE) airborne simulator over Houston, Texas. – Atmos. Meas. Tech. 11: 5941-5964. https://doi.org/10.5194/amt-11-5941-2018.

[57] Palmer, P. I., Jacob, D. J., Chance, K. V., Martin, R. V. D. R. J., Kurosu, T. P., Bey, I., Yantosca, R. M., Fiore, A. M. (2001): Air mass factor formulation for spectroscopic measurements from satellites: Application to formaldehyde retrievals from the Global Ozone Monitoring Experiment. – J. Geophys. Res. 106: 14539- 14550. DOI: 10.1029/2000JD900772.

[58] Palmer, P. I., Jacob, D. J., Fiore, A. M., Martin, R. V., Chance, K., Kurosu, T. P. (2003): Mapping isoprene emissions over North America using formaldehyde column observations from space. – J. Geophys. Res.-Atmos. 108: 4180. https://doi.org/10.1029/2002JD002153. 2003.

[59] Palmer, P. I., Abbot, D. S., Fu, T.-M., Jacob, D. J., Chance, K., Kurosu, T. P., Guenther, A., Wiedinmyer, C., Stanton, J. C., Pilling, M. J., Pressley, S. N., Lamb, B., Sumner, A. L. (2006): Quantifying the seasonal and interannual variability of North American isoprene emissions using satellite observations of the formaldehyde column. – J. Geophys. Res.-Atmos. 111: D12315. https://doi.org/10.1029/2005JD006689. 2006.

[60] Parra, M. A., Elustondo, D., Bermejo, R., Santamaria, J. M. (2009): Ambient air levels of volatile organic compounds (VOC) and nitrogen dioxide (NO_2) in a medium size city in Northern Spain. – Science of the Total Environment 407: 999-1009.

http://www.aloki.hu ● ISSN 1589 1623 (Print) ● ISSN 1785 0037 (Online)
DOI: http://dx.doi.org/10.15666/aeer/1705_1098911015

[61] Ravindra, K., Mor S., Ameena, A., Kamyotra, J. S., Kaushik, C. P. (2003): Variation in spatial pattern of criteria air pollutants before and during initial rain of monsoon. – Environ Monit Assess 87: 145-153.

[62] Renuka, K., Gadhavi, H., Jayaraman, A., Lal, S.., Naja, M., Rao, S. V. B. (2014): Study of ozone and NO_2 over Gadanki—a rural site in South India. – J Atmos Chem 71: 95-112.

[63] Richter, A., Hilboll, A., Burrows, J. P. (2015): Revisiting satellite derived tropospheric NO_2 trends. – http://presentations.copernicus.org/EGU2015-10674_presentation.pdf.

[64] Sander, S. P., Finalyson-Pitts, B. J., Friedl, R. R., Golden, D. M., Huie, R. E., Keller-Rudeck, H., Kolb, C. E., Kurylo, M. J., Molina, M. J., Moortgat, G. K., Orkin, L. V., Ravishankara, A. R., Wine, P. H.(2006): Chemical Kinetics and Photochemical Data for Use in Atmospheric Studies. Evaluation number 15, NASA Panel for Data Evaluation. – JPM Publication 06-2, Jet Propulsion Laboratory, Pasadena.

[65] Sarath, K., Guttikunda, P. J. (2014): Atmospheric emissions and pollution from the coal-fired thermal power plants in India. – Atmospheric Environment 92: 449-460.

[66] Ghude, S. D., Van der A, R. J., Beig, S., Fadnavis, Polade, S. D. (2009): "Satellite derived trends in NO_2 over the major global hotspot regions during the past decade and their inter-comparison". – Environmental Pollution 157(6): 1873-1878.

[67] Seligman, D. (2008): World's Major Rivers. An Introduction to International Water Law with Case Studies. – Colorado River Commission of Nevada, Las Vegas, Nevada. http://crc.nv.gov.

[68] Shim, C., Wang, Y., Choi, Y., Palmer, P. I., Abbot, D. S., Chance, K. (2005): Constraining global isoprene emissions with Global Ozone Monitoring Experiment (GOME) formaldehyde column measurements. – J. Geophys. Res. 110: D24301. DOI: 10.1029/2004JD005629.

[69] Sippo, J. Z., Maher, D. T., Tait, D. R., Ruiz-Halpern, S., Sanders, C. J., Santos, I. R. (2016): Mangrove out welling is a significant source of oceanic exchangeable organic carbon. – Limnology and Oceanography Letters 2(1): 1-8.

[70] Souri, A. H., Choi, Y., Jeon, W., Woo, J.-H., Zhang, Q., J.-i. Kurokawa. (2017): Remote sensing evidence of decadal changes in major tropospheric ozone precursors over East Asia. – J. Geophys. Res. Atmos. 122: 2474-2492. DOI: 10.1002/2016JD025663.

[71] Stammes, P., Sneep, M., de Haan, J. F., Veefkind, J. P., Wang, P., Levelt, P. F. (2008): Effective cloud fractions from the ozone monitoring instrument: theoretical framework and validation. – J Geophy Res 113: D16S38. DOI: 10.1029/2007JD008820.

[72] Stavrakou, T., Müller, J.-F., Smedt, I. De., Van Roozendael, M., van der Werf, G. R., Giglio, L., Guenther, A. (2009): Global emissions of nonmethane hydrocarbons deduced from SCIAMACHY formaldehyde columns through 2003-2006 – Atmos. Chem. Phys. 9: 3663-3679. DOI: 10.5194/acp-9-3663-2009.

[73] Stavrakou, T., Müller, J.-F., Bauwens, M., De Smedt, I., Van Roozendael, M., Guenther, A., Wild, M., Xia, X. (2014): Isoprene emissions over Asia 1979-2012: impact of climate and land-use changes. – Atmos. Chem. Phys. 14: 4587-4605. 2014 www.atmos-chem-phys.net/14/4587/2014/. DOI: 10.5194/acp-14-4587-2014.

[74] Surl, L., Palmer, P. I., González Abad, G. (2018): Which processes drive observed variations of HCHO columns over India? – Atmos. Chem. Phys. 18: 4549-4566. https://doi.org/10.5194/acp-18-4549-2018.

[75] Tariq, S., Ali, M. (2015): Spatio-temporal distribution of absorbing aerosols over Pakistan retrieved from OMI Onboard Aura Satellite. – Atmos Pollut Res. DOI: 10.5094/APR.2015.030.

[76] Tariq, S., ul-Haq, Z., Ali, M. (2015): Analysis of optical and physical properties of aerosols during crop residue burning event of October 2010 over Lahore, Pakistan. – Atmos Pollut Res. DOI: 10.1016/j.apr.2015.05.002.

[77] Tariq, S., ul-Haq, Z., Ali, M. (2016): Satellite and ground-based remote sensing of aerosols during intense haze event of October 2013 over Lahore, Pakistan. – Asia-Pac J Atmos Sci. DOI: 10.1007/ s13143-015-0084-3.

http://www.aloki.hu ● ISSN 1589 1623 (Print) ● ISSN 1785 0037 (Online)
DOI: http://dx.doi.org/10.15666/aeer/1705_1098911015

[78] ul-Haq, Z., Tariq, S., Ali, M., Mahmood, K., Batool, S. A., Rana, A. D. (2014): A study of tropospheric NO_2 variability over Pakistan using OMI data. – Atmospheric Pollution Research 5: 709-720. DOI: 10.5094/APR.2014.080.

[79] ul-Haq, Z., Tariq, S., Rana, A. D., Ali, M., Mahmood, K., Shahid, P. (2015): Satellite remote sensing of total ozone column (TOC) over Pakistan and neighbouring regions. – International Journal of Remote Sensing 36(4): 1038-1054. DOI: 10.1080/01431161.2015.1007255.

[80] ul-Haq, Z., Tariq, S., Ali, M., Rana, A. D., Mahmood, K. (2017): Satellite sensed tropospheric NO_2 patterns and anomalies over Indus, Ganges, Brahmaputra and Meghna river basins. – International Journal of Remote Sensing 38(5): 1423-1450. DOI: 10.1080/01431161.2017.1283071.

[81] ul-Haq, Z., Rana, A. D., Tariq, S., Mahmood, K., Ali, M., Bashir, I. (2018): Modeling of tropospheric NO_2 column over different climatic zones and land use/land cover types in South Asia. – Journal of Atmospheric and Solar-Terrestrial Physics 168: 80-99.

[82] UNEP (2008): United Nations Environment Programme and Development Alternatives. – South Asia Environment Outlook 2009: UNEP, SAARC and DA. United Nations Environment Programme (UNEP).

[83] US-EPA (2009): Assessment of the Impacts of Global Change on Regional U.S. Air Quality: A Synthesis of Climate Change Impacts on Ground-Level Ozone. – US EPA, Washington, DC.

[84] van Vuuren, D. P., Edmonds, J., Kainuma, M., Riahi, K., Thomson, A., Hibbard, K., Hurtt, G. C., Kram, T., Krey, V., Lamarque, J.-F., Masui, T., Meinshausen, M., Nakicenovic, N., Smith, S. J., Rose, S. K. (2011): The representative concentration pathways: an overview. – Clim. Change 109: 5-31.

[85] Varotsos, C., Cartalis, C., Feidas, C., Gerasi, E., Asimakopoulos, D. N. (1992): Relationship of ozone and its precursors in the West Coast Air Basin of Athens: a statistical model for the assessment of air quality in an urban area. – Atmos. Res. 28: 41-47.

[86] Verma, A. K., Saxena, A., Khan, A. H., Sharma, G. D. (2015): Air pollution problems in Lucknow City, India: a review. – J. Environ. Res. Develop. 9(4): April-June.

[87] Voulgarakis, A., Savage, N. H., Wild, O., Braesicke, P., Young, P. J., Carver, G. D., Pyle, J. A. (2010): Interannual variability of tropospheric composition: the influence of changes in emissions, meteorology and clouds – Atmos. Chem. Phys. 10: 2491-2506. DOI: 10.5194/acp-10- 2491-2010.

[88] Wiedinmyer, C., Tie, X., Guenther, A., Neilson, R., Granier. C. (2006): Future changes in biogenic isoprene emissions: how might they affect regional and global atmospheric chemistry? – Earth Interactions 10: 3.

[89] Wolfe, G. M., Kaiser, J., Hanisco, T. F., Keutsch, F. N., de Gouw, J. A., Gilman, J. B., Graus, M., Hatch, C. D., Holloway, J., Horowitz, L. W., Lee, B. H., Lerner, B. M., Lopez-Hilifiker, F., Mao, J., Marvin, M. R., Peischl, J., Pollack, I. B., Roberts, J. M., Ryerson, T. B., Thornton, J. A., Veres, P. R., Warneke, C. (2016): Formaldehyde production from isoprene oxidation across NO_x regimes, – Atmos. Chem. Phys. 16: 2597-2610.

[90] Yoo, J-M., Lee, Y. R., Kim, D., Jeong, M-J., Stockwell, W., Kundu, K., Prasun., Soo-Min, O., Dong-Bin, S., Lee, Suk-Jo, L. (2014): New indices for wet scavenging of air pollutants (O3, CO, NO2, SO2, and PM10) by summertime rain. – Atmospheric Environment 82. 226-237. 10.1016/j.atmosenv.2013.10.022.

[91] Zara, M., Boersma, K. F., De Smedt, I., Richter, A., Peters, E., van Geffen, J. H. G. M., Beirle, S., Wagner, T., Van Roozendael, M., Marchenko, S., Lamsal, L. N., Eskes, H. J. (2018): Improved slant column density retrieval of nitrogen dioxide and formaldehyde for OMI and GOME-2A from QA4ECV: intercomparison, uncertainty characterisation, and trends. – Atmos. Meas. Tech. 11: 4033-4058. https://doi.org/10.5194/amt-11-4033-2018.

http://www.aloki.hu ● ISSN 1589 1623 (Print) ● ISSN 1785 0037 (Online)
DOI: http://dx.doi.org/10.15666/aeer/1705_1098911015

[92] Zhang, J., Song, F., Tao, J., Zhang, Z., Shi, S. Q. (2018): Research Progress on Formaldehyde. Emission of Wood-Based Panel. – International Journal of Polymer Science Art. ID 9349721. https://doi.org/10.1155/2018/9349721.

[93] Zhu, L., Jacob, D. J., Mickley, L. J., Marais, E. A., Cohan, D. S., Yoshida, Y., Duncan, B. N., Abad, G. G., Chance, K. V. (2014): Anthropogenic emissions of highly reactive volatile organic compounds in eastern Texas inferred from oversampling of satellite (OMI) measurements of HCHO columns – Environ. Res. Lett. 9: 114004. DOI: 10.1088/1748-9326/9/11/114004.

[94] Zhu, L., Jacob, D. J., Kim, P. S., Fisher, J. A., Yu, K., Travis, K. R., Olfe, G. M. (2016): Observing atmospheric formaldehyde (HCHO) from space: validation and intercomparison of six retrievals from four satellites (OMI, GOME2A, GOME2B, OMPS) with SEAC^{4}RS aircraft observations over the Southeast US. – Atmospheric chemistry and physics 16(21): 13477-13490. DOI: 10.5194/acp-16-13477-2016.

[95] Zhu, L., Jacob, D. J., Keutsch, F. N., Mickley, L. J., Scheffe, R., Strum, M., Abad, G. G., Chance, K., Yang, K., Rappenglück, B., Millet, D. B., Baasandorj, M., Jaeglé, L., Shah, V. (2017): Formaldehyde (HCHO) As a hazardous air pollutant: mapping surface air concentrations from satellite and inferring cancer risks in the United States. – Environmental Science & Technology 51(10): 5650-5657. DOI: 10.1021/acs.est.7b01356.

[96] Zhu, S., Li, X., Yu, C., Wang, H., Wang, Y., Miao, J. (2018): Spatiotemporal variations in satellite-based formaldehyde (HCHO) in the Beijing-Tianjin-Hebei Region in China from 2005 to 2015. – Atmosphere 9: 5.

http://www.aloki.hu ● ISSN 1589 1623 (Print) ● ISSN 1785 0037 (Online)
DOI: http://dx.doi.org/10.15666/aeer/1705_1098911015

COMPARISON OF HPAIV INFECTIVITY BETWEEN ADULTS AND JUVENILES DOMESTIC DUCKS AFTER NASAL INSTILLATION OF H5N6 VIRUS

PARK, J. E. – KIM, J. S. – HONG, Y. J. – SON, K. – KIL, J. – JHEONG, W. – KWON, J. T.*

Biosafety Research Team, Environmental Health Research Department
National Institute of Environmental Research, Incheon 404-708, Republic of Korea

**Corresponding author*
e-mail: inhtox@gmail.com; phone:+82-32-560-7144; fax:+82-32-568-2038

(Received 28th Mar 2019; accepted 13th Jun 2019)

Abstract. Highly pathogenic avian influenza viruses (HPAIVs) can cause serious damage to wild birds and poultry. In this study, HPAIVs were administered via intranasal instillation to juvenile and adult domestic ducks, consisting of inoculation and contact groups, for comparative contagiousness. Oropharyngeal (OP) and cloacal (CL) swab analysis showed the overall virus shedding to be higher in OP than in CL. In addition, OP virus titer was higher in adults than in juveniles in the contact group. Our results indicate that adult susceptibility to AIV infection was greater than juvenile susceptibility, in case of samples from inoculated OP swab 2 days past inoculation (dpi) and contact OP swab 7 dpi. AIV distribution in the pancreas in juveniles was higher than that in adults; however, the virus was not detected in the trachea of either adults or juveniles. In conclusion, the results of this study suggest that differences in infectivity and prevalence of viruses in adults and juveniles may be influenced by the species of birds and neuraminidase enzymatic activity of the virus.
Keywords: *highly pathogenic avian influenza virus, contact, inoculation, distribution, birds*

Introduction

Avian Influenza virus (AIV), an influenza virus A of the family Orthomyxoviridae, is a single-stranded RNA virus with sixteen hemagglutinin (HA) subtypes (H1 to H16) and nine neuraminidase (NA) subtypes (N1 to N9) (Woo et al., 2017). Based on its pathogenicity, it is classified as either highly pathogenic AIV (HPAIV) or low pathogenic AIV (LPAIV). HPAIVs include H5 and H7, which are responsible for considerable illness or death in wild birds (Jeong et al., 2014).

In 1997, H5N1 HPAI outbreak occurred in chicken farms and live bird markets in Hong Kong, and the first case of chicken to human direct transmission of H5 was reported. Officially, H5N1 HPAIVs had emerged in 53 countries and human infections had occurred in 15 countries between 2003 and March 2014 (WHO).

In wildlife, the first HPAIV to cause the death of waterfowl was A/tern/South Africa/61 (H5N3) of H5 (Becker, 1966), following which H5N1 HPAIV appeared in many wild birds in Hong Kong (during 2002) and western China (Lake Qinghai; during 2005) (Ellis et al., 2004; Liu et al., 2005). Recently, HPAIVs have occurred throughout Asia, Europe, the Middle East, and several African countries linked to flyways (Olsen et al., 2006). Since wild birds, especially waterfowls, move their breeding site and wintering site, every winter, around 100,000–200,000 mallards arrive in Korea for spending the winter in various environments such as bird sanctuaries, inland small rivers, and lakes. In the spring, the waterfowls migrate for breeding; they pass through the east coast of North Korea after spanning North-eastern China (Kang et al., 2016).

http://www.aloki.hu ● ISSN 1589 1623 (Print) ● ISSN 1785 0037 (Online)
DOI: http://dx.doi.org/10.15666/aeer/1705_1101711022

Since 2010, China has reported subtypes of Clade 2.3.4.4 H5 HPAIV in ducks (including H5N2, H5N5, H5N6, and H5N8) (Zhao et al., 2013; Su et al., 2015). The first report of Group C H5N6, clade 2.3.4.4, was from Korea and Japan, in fall 2016. After that, group C of H5N6 had been frequently detected in Korea during 2017 (Jeong et al., 2017; Woo et al., 2017). Despite reports of several types of H5 HPAIVs and comparison across the different subtypes, understanding of infection susceptibility across adults and juveniles is still lacking. Infection susceptibility is important to understand for the prevalence and management of diseases. Especially, comparison between adults and juveniles will be useful for understanding epidemiological consequences. In many wildlife diseases, juveniles have driven the spread of diseases (Ashby and Bruns, 2018). Therefore, in this study, we evaluated the susceptibility of H5N6 as a HPAIV (A/Whooper swan/Korea/Gangjin/W49-1/2016) at both adult and juvenile stages of ducks, and compared the infection sensitivity between the two.

Materials and Methods

Experimental design

The experimental groups consisted of 12 domestic ducks, each including a control group (*Table 1*). Animals confirmed negative for avian influenza virus infection in ELISA test (IDVet, Grabels, France, ID Screen Influenza A antibody Competition Multi-Species) prior to the experiment. Each control group (n = 4) was instilled with 0.2 ml of phosphate-buffered saline (PBS) via the same exposure route. Five ducks were inoculated with H5N6 viruses via the choanal cleft using 0.2 ml of 106.5 50% egg infectious dose (EID50)/100 µl in adult and juvenile, separately. After 8 h, three healthy animals were cohoused with virus-injected animals for infectivity studies. All animal experiments were performed according to the Guidelines for Care and Use of the National Institute of Environmental Research (NIER 18-3) at biosafety level 3 (ABL3, KCDC-15-3-05) and were approved by Institutional Biosafety Committee (NIER-2018-IBC-01).

Table 1. *Group of animals used in the experiments*

Group		**Adult**	**Juvenile**
		Number of Animals	
Control		4	4
Test	Inoculation	5	5
	Contact	5	3

Swab samples from the trachea and cloaca at days 1, 2, 3, 4, 5, 7, 10, and 14 were collected using transport tubes (Universal Viral Transport Standard Kit, BD). Samples were serially diluted 10-fold and titrated using specific pathogens free (SPF) eggs to determine EID50/0.1 ml. After 3 days post inoculation (dpi), two animals each of injection group and control group were euthanized, tissue and organ samples collected (such as trachea, lung, kidney, spleen, caecal tonsil, liver, intestine, pancreas, and proventriculus), and viral replication evaluated by real-time RT-PCR. RNA was isolated from 100 mg of each tissue using a Maxwell RSC simpleRNA Tissue KIT (Promega, Madison) that was discovered using PowerCheck™ Influenza A Real-Time PCR Kit

http://www.aloki.hu ● ISSN 1589 1623 (Print) ● ISSN 1785 0037 (Online)
DOI: http://dx.doi.org/10.15666/aeer/1705_1101711022

(Avian Influenza Virus Real-time PCR Kit, JSB-VT-023, JS Biotech, Korea) for nucleoprotein (NP) genes. Statistical analysis was performed using PRISM 5 software and two-way ANOVA (considering mean and standard deviation (SD)).

Results and Discussion

Comparison of infectivity

H5N6 virus from oropharyngeal (OP) and cloacal (CL) swab (A/Whooper swan/Korea/Gangjin/W49-1/2016/[H5N6]) of both adults and juveniles was isolated from 1–5 dpi and 7 dpi, and the overall viral shedding was confirmed to be higher in OP swab samples than in CL ones (*Figure 1*). In inoculated individuals, OP swab samples were also used to compare shedding between adults and juveniles. The first isolated virus at 2 dpi in adult samples showed the highest titer value (105.17 EID50/0.1 ml) of shedding. In addition, OP virus titer was higher in adults than in juveniles in the contact group (*Figure 1*). In inoculation and contact groups, results of OP swab samples at 2 dpi and 7 dpi were statistically significant *($P < 0.01$)*.

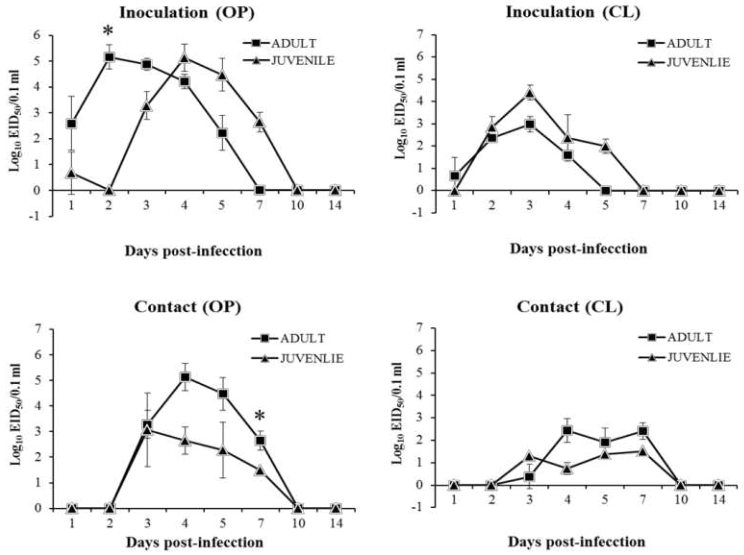

Figure 1. *Comparison between adults and juveniles for the virus isolated from oropharyngeal (OP) and cloacal (CL) swab of animals inoculated with 106.5 EID50/0.1 ml A/Whooper swan/Korea/Gangjin/W49-1/2016/[H5N6], and those non-inoculated but co-housed (Contact) with inoculated ones. Data were analyzed by two-way ANOVA with Bonferroni post-test, using Prism 5 statistics software and calculating the mean and standard deviation (SD) (n = 3, *$P < 0.01$)*

According to previous studies, immunity in juveniles is lower than that in adults, due to which, AIV infection is consistently higher in juveniles than in adults (Ip et al., 2008; Pybus et al., 2012). However, our results showed that adult susceptibility to AIV infection was greater than juvenile susceptibility, in case of samples from inoculated OP swab on 2 dpi and contact OP swab on 7 dpi (*Figure 1*). According to the seroprevalence study on wild waterfowl in Alaska, AIV antibodies in 11 species of wild waterfowls were higher in adults than in juveniles (Wilson et al., 2013), which was

http://www.aloki.hu ● ISSN 1589 1623 (Print) ● ISSN 1785 0037 (Online)
DOI: http://dx.doi.org/10.15666/aeer/1705_1101711022

probably because the virus susceptibility depends on the exposure of AIV to the species. Same pattern had also been shown in pink-footed geese (*Anser brachyrhynchus*) and Bewick's swans (*Cygnus columbiannus bewickii*) (Hoye et al., 2011a, b).

Moreover, reproduction might also affect influenza host susceptibility (van Dijk et al., 2018). During breeding season, most animals, including birds, use lots of energy in reproduction, hence showing relatively lower immunity than in non-breeding season. Adult individuals in our study were 22-week-old, and since ducks generally breed during May–July, their testicles were found enlarged upon autopsy (Blums et al., 2002; Ashby and Bruns, 2018). Therefore, we suspect that reproduction activity promotes higher infection susceptibility in adult than in juveniles.

The tissue from animals occurred in most of the internal organs of both adult and juvenile from H5N6, except for the trachea, caecal tonsil, intestine, proventriculus, brain, and muscle. AIV distribution in the pancreas from juveniles was higher than that from adults; however, the virus was not detected in the trachea from either adults or juveniles (*Table 2*). Although trachea is one of the main organs for detecting AI virus, almost no virus was detected in our study, which might be explained based on the report by Das et al. (2008), which showed that tracheal swab is less sensitive for detecting AIV in preclinical chickens.

Table 2. *AIV distribution in tissues of infected duck (both adult and juvenile)*

Age	Tra[a]	Lung	Kid	Spl	CT	Liv	Int	Pan	Pro	Brain	Mus
Adult1	-[b]	+	++	++	-	+	-	++	-	+	-
Adult2	-	-	-	-	-	+	-	++	-	-	-
Juvenile1	-	+	++	-	-	-	-	+++	-	-	-
Juvenile2	+	++	+++	++	-	+	+	+++	-	+	-
Control (PBS)	-	-	-	-	-	-	-	-	-	-	-

[a]Tra; Trachea, Kid; Kidney, Spl; Spleen, CT; Caecal Tonsil, Liv; Liver, Int; Intestine, Pan; Pancreas, Pro; Proventriculus, Mus; Muscle
[b]+++; 20 < CT < 25, ++; 25 < CT < 30, +; 30 < CT < 35, -; CT < 35

Mucin secretion is an important factor for the prevention of influenza virus infection in the airway (Burnet, 1948; Zanin et al., 2016). Especially, between influenza virus NA enzyme activity and mucus barrier may be affection in infectivity (Cohen et al., 2013; Zanin et al., 2015). Previous study had reported no H5N6 virus infectivity due to aerosol diffusion in ferret model (Sun et al., 2016). In the present study, our results demonstrated that the H5N6 virus is spread by direct contact between individuals and that the infectivity depends on the NA enzyme activity in duck model.

Conclusion

Our results suggest that differences in infectivity and prevalence of virus in adults and juveniles may be influenced by the species of birds, breeding season and NA enzymatic activity of the virus. This information may be helpful in further study to understand age-dependent infection sensitivity of avian species and affection of reproduction and these reasons should be considering when monitoring AIV.

http://www.aloki.hu ● ISSN 1589 1623 (Print) ● ISSN 1785 0037 (Online)
DOI: http://dx.doi.org/10.15666/aeer/1705_1101711022

Acknowledgements. This work was supported by a grant from the National Institute of Environment Research (NIER), funded by the Ministry of Environment (MOE) of the Republic of Korea (NIER-RP2018-114).

REFERENCES

[1] Ashby, B., Bruns, E. (2018): The evolution of juvenile susceptibility to infectious disease. – Proc. R. Soc. B 285(1881): 20180844.

[2] Becker, W. B. (1966): The isolation and classification of tern virus: Influenza Virus A/Tern/South Africa/1961. – The Journal of Hygiene 64(3): 309-320.

[3] Blums, P., Nichols, J. D., Hines, J. E., Mednis, A. (2002): Sources of variation in survival and breeding site fidelity in three species of European ducks. – Journal of Animal Ecology 71(3): 438-450.

[4] Burnet, F. M. (1948): Mucins and mucoids in relation to influenza virus action: v. The destruction of "francis inhibitor" activity in a purified mucoid by virus action. – Australian Journal of Experimental Biology and Medical Science 26(5): 389-402.

[5] Cohen, M., Zhang, X.-Q., Senaati, H. P., Chen, H.-W., Varki, N. M., Schooley, R. T., Gagneux, P. (2013): Influenza A penetrates host mucus by cleaving sialic acids with neuraminidase. – Virology journal 10(1): 321.

[6] Das, A., Spackman, E., Thomas, C., Swayne, D. E., Suarez, D. L. (2008): Detection of H5N1 high-pathogenicity avian influenza virus in meat and tracheal samples from experimentally infected chickens. – Avian diseases 52(1): 40-48.

[7] Ellis, T. M., Barry Bousfield, R., Bissett, L. A., Dyrting, K. C., Luk, G. S., Tsim, S., Sturm-Ramirez, K., Webster, R. G., Guan, Y., Peiris, J. M. (2004): Investigation of outbreaks of highly pathogenic H5N1 avian influenza in waterfowl and wild birds in Hong Kong in late 2002. – Avian Pathology 33(5): 492-505.

[8] Hoye, B. J., Fouchier, R. A., Klaassen, M. (2011a): Host behaviour and physiology underpin individual variation in avian influenza virus infection in migratory Bewick's swans. – Proceedings of the Royal Society B: Biological Sciences 279(1728): 529-534.

[9] Hoye, B. J., Munster, V. J., Nishiura, H., Fouchier, R. A., Madsen, J., Klaassen, M. (2011b): Reconstructing an annual cycle of interaction: natural infection and antibody dynamics to avian influenza along a migratory flyway. – Oikos 120(5): 748-755.

[10] Ip, H. S., Flint, P. L., Franson, J. C., Dusek, R. J., Derksen, D. V., Gill, R. E., Ely, C. R., Pearce, J. M., Lanctot, R. B., Matsuoka, S. M. (2008): Prevalence of influenza A viruses in wild migratory birds in Alaska: patterns of variation in detection at a crossroads of intercontinental flyways. – Virology journal 5(1): 71.

[11] Jeong, J., Kang, H.-M., Lee, E.-K., Song, B.-M., Kwon, Y.-K., Kim, H.-R., Choi, K.-S., Kim, J.-Y., Lee, H.-J., Moon, O.-K. (2014): Highly pathogenic avian influenza virus (H5N8) in domestic poultry and its relationship with migratory birds in South Korea during 2014. – Veterinary microbiology 173(3-4): 249-257.

[12] Jeong, J., Woo, C., Ip, H. S., An, I., Kim, Y., Lee, K., Jo, S.-D., Son, K., Lee, S., Oem, J.-K. (2017): Identification of Two novel reassortant avian influenza a (H5N6) viruses in whooper swans in Korea, 2016. – Virology journal 14(1): 60.

[13] Kang, T., Kang, Y.-M., Jeong, W., Moon, O.-K., Yoon, H., Choi, J., Lee, H. (2016): Spring migration of mallards (Anas platyrhynchos) tracked with wild-trackers in East Asia. – Journal of Asia-Pacific Biodiversity 9(3): 323-327.

[14] Liu, J., Xiao, H., Lei, F., Zhu, Q., Qin, K., Zhang, X.-W., Zhang, X.-l., Zhao, D., Wang, G., Feng, Y. (2005): Highly pathogenic H5N1 influenza virus infection in migratory birds. – Science 309(5738): 1206-1206.

[15] Olsen, B., Munster, V. J., Wallensten, A., Waldenström, J., Osterhaus, A. D., Fouchier, R. A. (2006): Global patterns of influenza A virus in wild birds. – Science 312(5772): 384-388.

http://www.aloki.hu ● ISSN 1589 1623 (Print) ● ISSN 1785 0037 (Online)
DOI: http://dx.doi.org/10.15666/aeer/1705_1101711022

[16] Pybus, O., Perrins, C., Choudhury, B., Manvell, R., Nunez, A., Schulenburg, B., Sheldon, B., Brown, I. (2012): The ecology and age structure of a highly pathogenic avian influenza virus outbreak in wild mute swans. – Parasitology 139(14): 1914-1923.
[17] Su, S., Bi, Y., Wong, G., Gray, G. C., Gao, G. F., Li, S. (2015): Epidemiology, evolution, and recent outbreaks of avian influenza virus in China. – Journal of virology 89(17): 8671-8676.
[18] Sun, H., Pu, J., Wei, Y., Sun, Y., Hu, J., Liu, L., Xu, G., Gao, W., Li, C., Zhang, X. (2016): Highly pathogenic avian influenza H5N6 viruses exhibit enhanced affinity for human type sialic acid receptor and in-contact transmission in model ferrets. – Journal of virology: JVI. 00127-16.
[19] van Dijk, J. G., Verhagen, J. H., Wille, M., Waldenström, J. (2018): Host and virus ecology as determinants of influenza A virus transmission in wild birds. – Current opinion in virology 28: 26-36.
[20] WHO: Available online: https://www.who.int/influenza/human_animal_interface/en/.
[21] Wilson, H. M., Hall, J. S., Flint, P. L., Franson, J. C., Ely, C. R., Schmutz, J. A., Samuel, M. D. (2013): High seroprevalence of antibodies to avian influenza viruses among wild waterfowl in Alaska: implications for surveillance. – PLoS One 8(3): e58308.
[22] Woo, C., Kwon, J.-H., Lee, D.-H., Kim, Y., Lee, K., Jo, S.-D., Dong Son, K., Oem, J.-K., Wang, S.-J., Kim, Y. (2017): Novel reassortant clade 2.3. 4.4 avian influenza A (H5N8) virus in a grey heron in South Korea in 2017. – Archives of virology 162(12): 3887-3891.
[23] Zanin, M., Marathe, B., Wong, S.-S., Yoon, S.-W., Collin, E., Oshansky, C., Jones, J., Hause, B., Webby, R. (2015): Pandemic swine H1N1 influenza viruses with almost undetectable neuraminidase activity do not transmit via aerosols in ferrets and are inhibited by human mucus, but not swine mucus. – Journal of virology: JVI. 02537-14.
[24] Zanin, M., Baviskar, P., Webster, R., Webby, R. (2016): The interaction between respiratory pathogens and mucus. – Cell host & microbe 19(2): 159-168.
[25] Zhao, K., Gu, M., Zhong, L., Duan, Z., Zhang, Y., Zhu, Y., Zhao, G., Zhao, M., Chen, Z., Hu, S. (2013): Characterization of three H5N5 and one H5N8 highly pathogenic avian influenza viruses in China. – Veterinary microbiology 163(3-4): 351-357.

http://www.aloki.hu ● ISSN 1589 1623 (Print) ● ISSN 1785 0037 (Online)
DOI: http://dx.doi.org/10.15666/aeer/1705_1101711022

Eurovir Hygiene-Labor GmbH
Im Biotechnologiepark TGZ I
D-14943 Luckenwalde

Eurovir® Hygiene-Labor
Antivirale Validierung & Rabies

Virucidal activity of

„PMF-concentrate“

against the *Transmissible Gastroenteritis Virus of Swine (TGEV)*

(used as a model virus for the
Middle East Respiratory Syndrome Coronavirus (MERS-CoV)

<u>Short report</u> of the screening test S3

by

PD Dr. Olaf Thraenhart and Dr. Christian Jursch

Study time: in March 2015

Principal: PMF Natural Products company
Arab Republic of Egypt

Product: ***PMF-concentrate***
[Lot-no.: not specified; product sample as arrived; Arrival: 01.08.2014, Storage at 2-8°C]

Parameter of test:

- 0,75 g of PMF-concentrate solved within 2,95 mL of A. bidest (25,42% [w/v])
- T = 37° C and 60 and 240 min. of exposure

Test system:

- Transmissible Gastroenteritis Virus of Swine (TGEV); Strain: Toyama
  (Origin: Virusbank of the Bundesforschungsanstalt f. Viruskrankheiten der Tiere; Friedrich Löffler-Institut, Insel Riems, Germany)
- ST75/2 cells (foetal testis cells of swine)
  (Origin: Robert Koch-Institute, Berlin, Germany)

Test method:

- The testing was performed following the guideline of the DVV and the Robert Koch-Institute (DVV/RKI-guideline [*Bundesgesundhbl. (2008); 51 (8):937-945*]): for the quantitative virucidal suspension test (QST).
- With this testing virus titration of the main samples was performed according to *Lycke's* methodolgy *(Arch Ges Virusforsch (1957); 7:483-493).*

Tab. 1: ***Dosage of product*** *(solvent: A. bidest)*

Set	Product(s)	Conc. in Test *(1x)*	Working sol. *(x 1,25)*	Dosage	pH of working sol.
#1	PMF-concentrate	20,34%	25,42%	0,75 g in 2,95 mL	pH 9,54 *(in test: pH 9,52)*

Tab. 2: Results of virus inactivation

Samples	1a + 1b	2a + 2b
	Virus inactivation	
Exposure time	t = 60 min.	t = 240 min.
Virus input [1] *(per test volume)*	6,11 ± 0,34	5,50 ± 0,32
Detection limit *(cytotoxicity level)*	< 1 ID_{50} *(0,0 lg ID_{50})*	
Residual virus [1] (log ID_{50} ± K [95%])	1,80 ± 0,34 *(43/480 virus positive cell culture units)*	< 1 ID_{50} *(0,0 lg ID_{50})* *(0/480 virus positive cell culture units)*
Reduction [2] (log ID_{50} ± K [95%])	**4,31 ± 0,48**	**> 5,50 ± 0,45**

[1] = Calculation of 95% confidential interval of virus titer as well as virus reduction following DVV/RKI-Guideline.
[2] = Virus reduction: titer of virus control minus titer of sample (lg ID_{50}).

Results: (cf. Tab. 2)

Control tests

- With S3 the amount of input virus at 37° C was estimated to lg ID_{50} = 6,13 ± 0,34 after 60 min.
- After 240 min. of incubation at 37° C virus titer was declined to lg ID_{50} = 5,52 ± 0,32 due to the influence of temperature (Δ virus titer = 0,61 ± 0,46).
- With the *Lycke's* method a sample dilution was done (VF = 1000). With that dilution no cytotoxicity was visible and the susceptibility of the detection cells was given (Δ titer = 0,18 ± 0,47).

Virus inactivation

- With 20,34% of PMF (final test concentration) and after 60 min. the virus reduction factor was estimated to **RF = 4,31 ± 0,48.**
- After the exposure time was prolonged to 240 min. no residual virus could be detected. The corresponding virus reduction factor was estimated to **RF > 5,50 ± 0,45**.

Conclusions:

- Prolongation of the exposure at 37° C from 60 to 240 min. was associated with only a minor reduction of input virus (Δ virus titer = 0,61 ± 0,46). The test virus was sufficiently stable at the test temperature over the observation period.
- After 60 min. at 37° C the tested product PMF-concentrate in its 20,34% dilution (final concentration) inactivated *TGEV* by RF = 4,31 ± 0,48 or by 99,995% under the test conditions. After 240 min. a virus reduction factor of RF > 5,5 ± 0,45 was observed, correspondent to a virus reduction of 99,999%.

Luckenwalde, 18th of March 2015

Dr. Christian Jursch
(Laboratory manager and Managing Director of Eurovir)

Inactivation of *TGEV* (a model virus for MERS-CoV) by *PMF-concentrate*
- testing with the quantitative virucidal supension test at T = 37 °C -

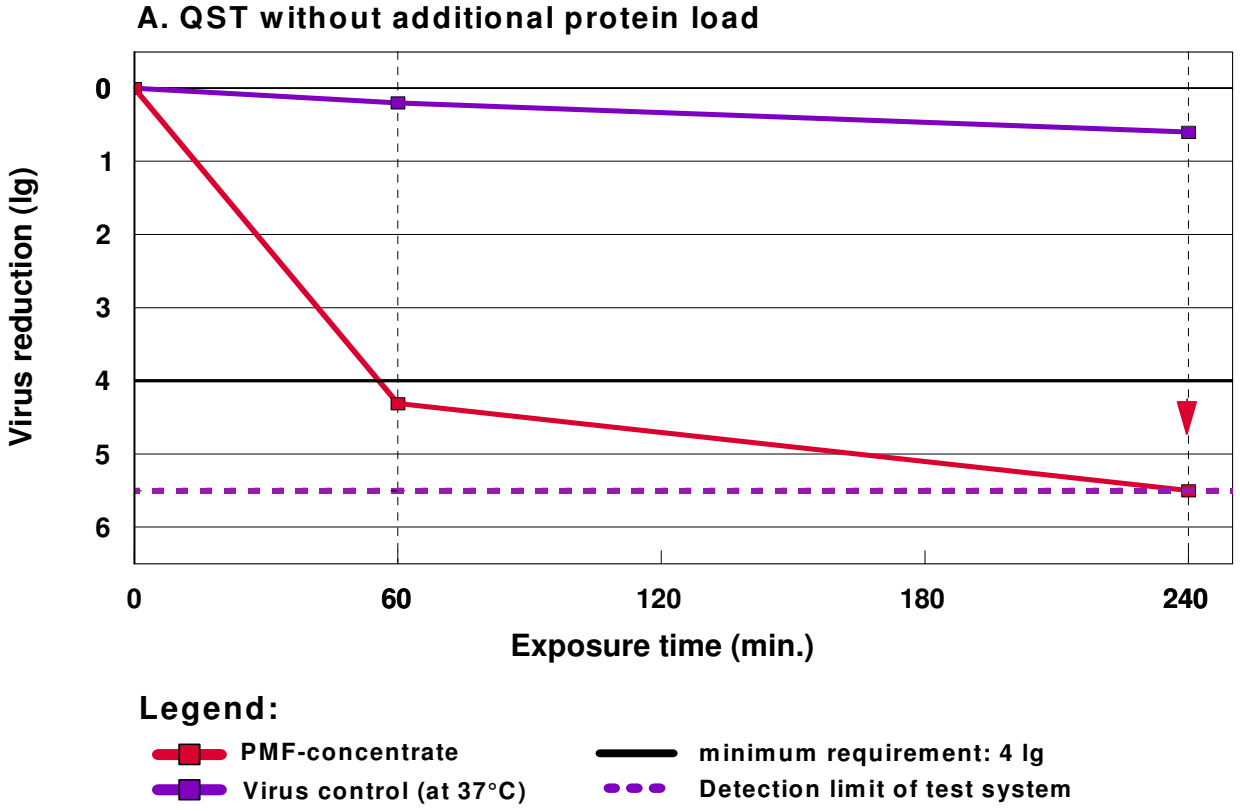

Fig. 1

- Attachment: Experimental protocols -

- Virucidal activity of the product *PMF-concentrate* - Experiment S3 at T = 37° C / testing in the *quantitative suspension test (QST)* using the methodology of *Lycke* for virus titration of the main samples.

  The testing was performed with the *Transmissible Gastroenteritis Virus of Swine (TGEV)* which served as a model virus for the *Middle East Respiratory Syndrome Coronavirus (MERS-CoV).*

Information about the testing

Principal:	PMF Natural Products company	*Test run:*	S3
Product(s):	PMF-concentrate	*Test date:*	12.03.2015
Test system:	TGEV *(Toyama)* + ST75/2-cells	*Analysis:*	18.03.2015 *(6 p.i.)*

Test methodology and test parameters

Test method: quantitative virucidal suspensions test according to DVV/RKI-guideline *(Version 08/08)*
Test mixture: 1 VT protein load + 1 VT virus suspension + 8 VT 1,25fold working solution
Protein load: no additional protein load *(PBS)*
Parameter: test temperature: 37° C with the exposure time(s) of: 60 and 240 min.

Tested product sample(s)

1st product: PMF-concentrate *[Product sample: as received (designation: PMF), Arrival: 01.08.2014, Storage at 2-8° C]*

Tab. 1: Weight of content

Set	Product(s)	Conc. in Test *(1x)*	Working sol. *(x 1,25)*	Dosage	pH of working sol.
#1	PMF-concentrate	20,34%	25,42%	0,75 g in 2,95 mL	pH 9,71 *(in test: pH 9,69)*

Tab. 2: Content of samples

Samples	1a	1b	2a	2b
	Virus inactivation			
	Set #1 / 60 min.		Set #1 / 240 min.	
PBS	15µL	15µL	15µL	15µL
TGEV	15µL	15µL	15µL	15µL
PMF / Sol.	120µL	120µL	120µL	120µL
Titration	*Lycke (VF = 1000)*		*Lycke (VF = 1000)*	

Samples	3a	3b	4a	4b	5
	Virus control / 60 Min.		Virus control / 240 Min.		Cytotoxicity
	w/o		w/o		Set #1/240 min.
PBS	15µL	15µL	15µL	15µL	15µL
TGEV	15µL	15µL	15µL	15µL	
Medium					15µL
PBS	120µL	120µL	120µL	120µL	
PMF / Sol.					120µL
Titration	S&K *(VF = 5)*		S&K *(VF = 5)*		*Lycke (VF = 1000)*

Performing of the test

1. Preparation of the product solution: (in the specified sequence)

- ***0,75 g PMF-concentrate*** was solved with agitation and warming to 37°C in 2,95 mL A. bidest.

2. Preparation of the test samples

- Per test point (concentration/exposure time) 2 redundant test samples were prepared.
- Test mixture: 1 vol. PBS + 1 vol. virus suspension + 8 vol. PMF-working solution (1,25-fold)

3. Dilution of the test sample and estimation of virus titer

- ***Termination of virus inactivation:*** after exposure the test samples were diluted with medium *(cf. virus titration).*
- With the ***virus control*** the virus titer was estimated using the methodology of *Spearman & Kärber* with VF = 5 from 113 µL (out of 150 µL of the test sample).
- With the ***virus inactivation samples*** the virus titer was estimated using the methodology of *Lycke.* For each of the test samples (a and b) 48 µL was added to 96 mL Medium, corresponding to a dilution of VF = 1000. All of the 96 mL were then transferred to cell cultures with 200 µL per well (480 wells).

4. Susceptibility control

- Sample 5 (cytotoxicity sample) was diluted 1000fold and was then distributed to cell cultures (cf. virus inactivation). Afterwards a virus dilution serie (VK/E) was transferred to these cells.

5. Judgement of the cells / virus detection

- At day 6 p.i. the cell cultures were examined visually using a microscope (magnification: 100fold). The virus positive cell cultures were identified by the virus induced CPE).

Tab. 3.1: Virus control + Susceptibility control *(virus titration: according to Spearman & Kärber)*

Samples	3a	3b	Ø	4a	4b	Ø	5	VK/E
	Virus control / 60 min.			Virus control / 240 min.			Susceptibility Control	
1 / -0,7	4/4 [1]	4/4	**8/8**	4/4 [1]	4/4	**8/8**	8/8	8/8
2 / -1,4	4/4	4/4	**8/8**	4/4	4/4	**8/8**	8/8	8/8
3 / -2,1	4/4	4/4	**8/8**	4/4	4/4	**8/8**	8/8	8/8
4 / -2,8	4/4	4/4	**8/8**	4/4	4/4	**8/8**	8/8	8/8
5 / -3,5	4/4	4/4	**8/8**	4/4	4/4	**8/8**	8/8	8/8
6 / -4,2	4/4	4/4	**8/8**	4/4	4/4	**8/8**	8/8	8/8
7 / -4,9	4/4	4/4	**8/8**	4/4	3/4	**7/8**	8/8	8/8
8 / -5,6	3/4	4/4	**7/8**	2/4	2/4	**4/8**	4/8	3/8
9 / -6,3	1/4	1/4	**2/8**	0/4	0/4	**0/8**	0/8	2/8
10 / -7,0	1/4	0/4	**1/8**					1/8
11 / -7,7	0/4		**0/8**					0/8
ZK	0/4	0/4	**0/8**	0/4	0/4	**0/8**	0/8	0/8
Titer/test vol. ($lg\ ID_{50}$)	6,13	6,13	**6,13**	5,6	5,43	**5,52**	5,78 ± 0,39	5,60 ± 0,26
Average ± CI (95%) [2]	6,13 ± 0,34 per 100 µL *(≃6,11 lg ID_{50} pro 96 µL)*			5,52 ± 0,32 per 100 µL *(≃5,50 lg ID_{50} pro 96 µL)*			RF = 0,18 ± 0,47	
Reduction [3] lg ID_{50} ± CI [95%]	-			**0,61 ± 0,46**			**cells susceptible: yes [2]**	

[1] = number of virus positive cell culture units to total number of cell culture units
[2] = Calculation of 95% confidental intervall of virus titer as well as virus reduction following DVV/RKI-Guideline.
[3] = Virus reduction: titer of virus control minus titer of sample ($lg\ ID_{50}$).
[4] = Susceptibility of the detection cells is to be assumed when Δ virus titer is ≤ lg 0,5 [DVV/RKI-Guideline].

Tab. 3.2:Virus inactivation *(virus titration: according to Lycke)*

Samples	1a + 1b	2a + 2b
	Virus inactivation *(VF = 1000)*	
	Set #1 / 60 min.	Set #1 / 240 min.
analysed sample vol.	2 x 48 = 96 µL	2 x 48 = 96 µL
Cell culture units	480	480
Virus positive	43	0
Ratio p [2]	0,0896	0,0
Residual virus *(lg ID_{50} per 96 µL)*	1,80 ± 0,34	< 1 ID_{50} *(0,0 lg ID_{50})*
Virus input *(lg ID_{50} per 96 µL)*	6,11 ± 0,34	5,50 ± 0,32
Reduction [3] ***(lg ID_{50} ±CI [95%])***	**4,31 ± 0,48**	**> 5,50 ± 0,45**

[1] = sample volume transferred onto cell cultures: 48 µL from test mix a. plus 48 µL from test mix b. resulting in 2 x 48 = 96 µL
[2] = ratio of virus positive cell culture units to total number of cell cultures.
[3] = Virus reduction: titer of virus control (cf. Tab. 3.1) minus titer of sample (lg ID_{50})

Estimation of virus titer by LYCKE´s method (Arch Ges Virusforsch (1957); 7:483-493)

Calculation of virus titer by using the following formula:

$- ID_{50} = [1{,}4 \times \ln (1-p)]$ p = ratio of positive cell cultures to total number of cell cultures

- ***Example:*** 51 out of 100 cell culture units was virus positive → p = 51/100 = 0,51

p put into formula: $- ID_{50} = [1{,}4 \times \ln (1- 0{,}51)]$

with ln (0,49): $- ID_{50} = 1{,}4 \times -0{,}71$

resulting in: $- ID_{50} = -0{,}998$ or $ID_{50} = 0{,}998$

That means that per single cell culture unit 0,998 or 1 ID_{50} of residual virus was present.

When this content of virus was multiplied with the number of cell culture units (= 100) the complete amount of residual virus was obtained: 1,0 ID_{50} x 100 = 100 ID_{50} or lg ID_{50} = 2,0

Result of the example: the total quantity of residual virus which was present in the examined sample of liquid was estimated to **lg ID_{50} = 2,0**

Materials and reagents used:

- ***Testvirus***

Test virus	Transmissible Gastroenteritis Virus of Swine (TGEV)
Strain	Toyama 36
Origin	Virusbank der BFA f. Viruskrankheiten der Tiere; Friedrich Löffler-Institut, Insel Riems Virus (lyophilisate) v. 05/2003; kindly provided by Dr. M. Dauber (Virus passage FLI +0)
Virus material used in test	Supernatant from infected cell culture, Virus propagation TGEV-12 v. 16.02.2015; Set #1 Virus passage: FLI +12;

- ***Cells***

Cells	ST75/2 cells (foetal testis cells of swine)
Origin	Robert Koch-Institut, Berlin Cells reveived 03/2002 in frozen condition (1 Ampoule; v. 13.02.1996); corresponding to cell passage RKI +0
Cell passage used in test	RKI + 3 / + 15

- ***Additional material and reagents***

Material	*Supplier*	*Order No.*	*Lot*	*Expiry date*
DMEM	Biochrom	F 0435	1006 C	11/2015
Glutamine	Biochrom	K 0283	0978 B	08/2016
Pen./Strept.	Biochrom	A 2213	0627 C	05/2017
FCS	Biochrom	S 0210	0677 B	06/2019
PBS	Biochrom	L 1820	0743 C	07/2017
Trypsin	Invitrogen	25300-096	1437736	09/2015

- ***Performing of the experiment and responsibilities***

Part of experiment	Performed by (position)
Supervision	Dr. Ch. Jursch (Laborleiter)
Control of product input	Fr. S. Sachs (Biologielaborantin) und Dr. Ch. Jursch (Laborleiter)
Performing the test	Fr. S. Sachs (Biologielaborantin)
Cell culturing	Fr. S. Sachs (Biologielaborantin)
Reading of cells & Raw data	Dr. Ch. Jursch (Laborleiter)
Data input & Analysis	Dr. Ch. Jursch (Laborleiter)
Protocol preparation	Dr. Ch. Jursch (Laborleiter)

Eurovir Hygiene-Labor GmbH
Im Biotechnologiepark TGZ I
D-14943 Luckenwalde

Eurovir® Hygiene-Labor
Antivirale Validierung & Rabies

Virucidal activity of

„PMF-concentrate“

against the Influenza A Virus (H1N1)

Short report of the screening tests S1 and S2

by

PD Dr. Olaf Thraenhart and Dr. Christian Jursch

Study time: August - September 2014

Principal: PMF Natural Products company
Arab Republik of Egypt

Product: ***PMF-concentrate***
[Lot-no.: not specified; product sample as arrived; Arrival: 01.08.2014, Storage at 2-8°C]

Parameter of test:

- 0,75 g of PMF-concentrate solved within 2,95 mL of A. bidest (25,42% [w/v])
- T = 37° C and 60 and 240 min. of exposure

Test system:

- Influenza A Virus (H1N1); Strain: New Caledonia
(Origin: Chiron Behring, Marburg/Lahn, Germany)
- Madin Darby Canine Kidney Cells (MDCK)
(Origin: Robert Koch-Institute, Berlin, Germany)

Test method:

- The testing was performed following the guideline of the DVV and the Robert Koch-Institute (DVV/RKI-guideline [*Bundesgesundhbl. (2008); 51 (8):937-945*]): for the quantitative virucidal suspension test (QST).
- With test S1 the *Spearman & Kärber's* method for virus titration of the main samples was used (cf. DVV/RKI-guideline).
- With test S2 virus titration of the main samples was performed according to *Lycke's* methodolgy *(Arch Ges Virusforsch (1957); 7:483-493).*

Tab. 1: ***Dosage of product*** *(solvent: A. bidest)*

Set	Product(s)	Conc. in Test *(1x)*	Working sol. *(x 1,25)*	Dosage	pH of working sol.
#1	PMF-concentrate	20,34%	25,42%	0,75 g in 2,95 mL	pH 9,54 *(in test: pH 9,52)*

Tab. 2: Results of virus inactivation

Samples	1a + 1b	2a + 2b	1a + 1b	2a + 2b
	Screening test S1 *(virus titration: Spearman & Kärber)*		***Screening test S2*** *(virus titration: acc. Lycke*	
Exposure time	t = 60 min.	t = 240 min.	t = 60 min.	t = 240 min.
Virus input [1] *(per test volume)*	4,47 ± 0,36	4,38 ± 0,23	4,88 ± 0,26	4,88 ± 0,39
Detection limit *(cytotoxicity level)*	2,45		< 1 ID_{50} *(0,0 lg ID_{50})*	
Residual virus [1] (log ID_{50} ± K [95%])	2,19 ± 0,32	≤ 2,45	3,26 ± 0,26	< 1 ID_{50} *(0,0 lg ID_{50})*
Reduction [2] (log ID_{50} ± K [95%])	**2,28 ± 0,48**	**≥ 1,93 ± 0,23**	**1,62 ± 0,37**	**> 4,88 ± 0,55**

[1] = Calculation of 95% confidential interval of virus titer as well as virus reduction following DVV/RKI-Guideline.
[2] = Virus reduction: titer of virus control minus titer of sample (lg ID_{50}).

Results: (cf. Tab. 2)

Control tests

Screening test S1:

- The pH of the 1,25fold concentrated working solution were measured to pH 9,54.
- In the test sample this pH changed only slightly to pH 9,52.
- With S1 the amount of input virus at 37° C was estimated to lg ID_{50} = 4,47 ± 0,36 after 60 min. and to lg ID_{50} = 4,38 ± 0,23 after 240 min. (Δ virus titer = 0,10 ± 0,42).
- Using the *Spearman & Kärber's* titration method a cytotoxicity titer of lg TD_{50} = 2,45 was recorded for the test samples. This is equivalent with the detection limit of screening test S1.

Screening test S2:

- With S2 the amount of input virus at 37° C was estimated to lg ID_{50} = 4,88 ± 0,26 after 60 min. and to lg ID_{50} = 4,88 ± 0,39 after 240 min. (Δ virus titer = 0,0 ± 0,47).
- With the *Lycke's* method a sample dilution was done (VF = 1000). With that dilution no cytotoxicity was visible and the susceptibility of the detection cells was given (Δ titer = 0,18 ± 0,53). In addition, the detection limit of screening test S2 could be improved by 2,45 Log.

Virus inactivation

Screening test S1:

- With 20,34% of PMF (final test concentration) and after 60 min. the virus reduction factor was estimated to **RF = 2,28 ± 0,48.** After 240 min. no residual virus could be detected (test virus below detection limit, due to product associated cytotoxicity [lg TD_{50} = 2,45]). The corresponding virus reduction factor was estimated to **RF ≥ 1,93 ± 0,23**.

Screening test S2:

- With 20,34% of PMF (final test concentration) and after 60 min. the virus reduction factor was estimated to **RF = 1,62 ± 0,37.** After 240 min. no residual virus could be detected. The corresponding virus reduction factor was estimated to **RF > 4,88 ± 0,55**.

Conclusions:

- Prolongation of the exposure at 37° C from 60 to 240 min. was not associated with a reduction of input virus. The test virus was stable at the test temperature over the observation period.
- Using the *Lycke's* method of virus titration the results from the first screening test (S1) could be significantly improved.
- After 60 min. at 37° C 20,34% PMF (final concentration) inactivated influenza virus by RF = 1,95 ± 0,30 *(average from S1 and S2)* or by 98,9% under the test conditions. After 240 min. a virus reduction factor of RF > 4,88 ± 0,55 was observed, correspondent to a virus reduction of 99,998%.

Luckenwalde, 12th of November 2014

Dr. Christian Jursch
(Laboratory manager and Managing Director of Eurovir)

Inactivation of influenza A virus by *PMF-concentrate*
- testing with the quantitative virucidal supension test at T = 37 °C -

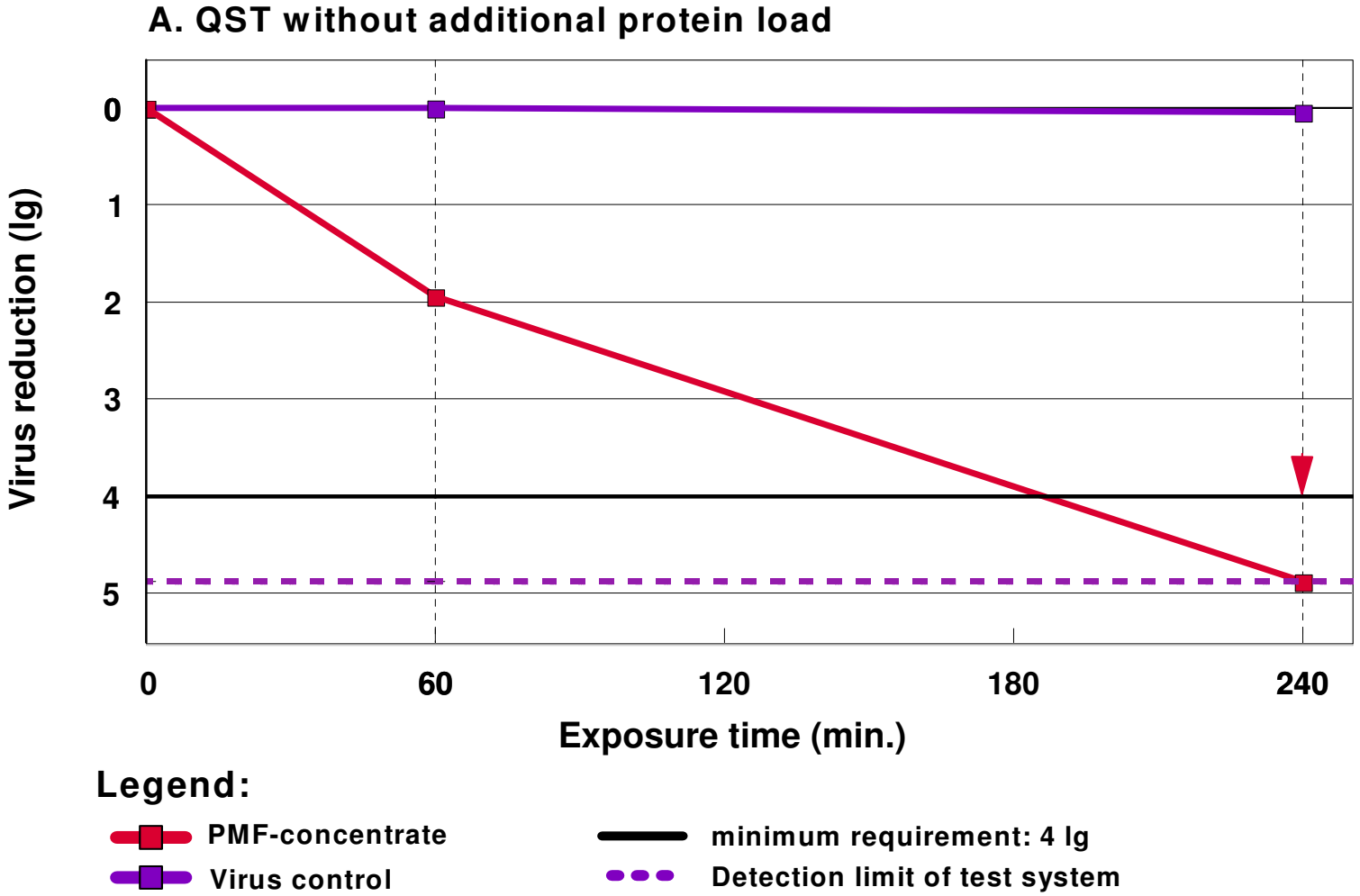

Fig. 1

- Attachment: Experimental protocols -

- Virucidal activity of the product *PMF-concentrate* - Experiment S1 at T = 37° C / testing in the *quantitative suspension test (QST)* against *influenza A virus* using *Spearman & Kärber's* method for virus titration of the main samples.

- Virucidal activity of the product *PMF-concentrate* - Experiment S2 at T = 37° C / testing in the *quantitative suspension test (QST)* against *influenza A virus* using the methodology of *Lycke* for virus titration of the main samples.

Information about the testing

Principal:	PMF Natural Products company	*Test run:*	S1
Product(s):	PMF-concentrate	*Test date:*	26.08.2014
Test system:	Influenza *(H1N1)* + MDCK-cells	*Analysis:*	01.09.2014 *(6 p.i.)*

Test methodology and test parameters

Test method: quantitative virucidal suspensions test according to DVV/RKI-guideline *(Version 08/08)*
Test mixture: 1 VT protein load + 1 VT virus suspension + 8 VT 1,25fold working solution
Protein load: no additional protein load *(PBS)*
Parameter: test temperature: 37° C with the exposure time(s) of: 60 and 240 min.

Tested product sample(s)

1st product: PMF-concentrate *[Product sample: as received (designation: PMF), Arrival: 01.08.2014, Storage at 2-8° C]*

Tab. 1: Weight of content

Set	Product(s)	Conc. in Test *(1x)*	Working sol. *(x 1,25)*	Dosage	pH of working sol.
#1	PMF-concentrate	20,34%	25,42%	0,75 g in 2,95 mL	pH 9,54 *(in test: pH 9,52)*

Tab. 2: Content of samples

Samples	1a	1b	2a	2b
	Virus inactivation			
	Set #1 / 60 min.		Set #1 / 240 min.	
PBS	15µL	15µL	15µL	15µL
Influenza	15µL	15µL	15µL	15µL
PMF / Sol.	120µL	120µL	120µL	120µL
Titration	S&K *(VF = 5)*		S&K *(VF = 5)*	

Samples	3a	3b	4a	4b	5
	Virus control / 60 Min.		Virus control / 240 Min.		Cytotoxicity
	w/o		w/o		Set #1/240 min.
PBS	15µL	15µL	15µL	15µL	15µL
Influenza	15µL	15µL	15µL	15µL	
Medium					15µL
PBS	120µL	120µL	120µL	120µL	
PMF / Sol.					120µL
Titration	S&K *(VF = 5)*		S&K *(VF = 5)*		S&K *(VF = 5)*

Performing of the test

1. Preparation of the product solution: (in the specified sequence)

- ***0,75 g PMF-concentrate*** was solved with agitation and warming to 37°C in 2,95 mL A. bidest.

2. Preparation of the test samples

- Per test point (concentration/exposure time) 2 redundant test samples were prepared.
- Test mixture: 1 vol. PBS + 1 vol. virus suspension + 8 vol. PMF-working solution (1,25-fold)

3. Dilution of the test sample and estimation of virus titer

- ***Termination of virus inactivation:*** after exposure the test samples were diluted with medium *(cf. virus titration).*
- With the ***virus control*** the virus titer was estimated using the methodology of *Spearman & Kärber* with VF = 5 from 113 µL (out of 150 µL of the test sample).
- With the ***virus inactivation samples*** the virus titer was estimated using the methodology of *Spearman & Kärber* with VF = 5 from 113 µL (out of 150 µL of the test sample).

4. Judgement of the cells / virus detection

- At day 6 p.i. supernatant of the cell cultures were tested with the HA-test (haemagglutination).

Tab. 3.1: Virus control *(virus titration: according to Spearman & Kärber)*

Samples	3a	3b	Ø	4a	4b	Ø	5
	Virus control / 60 min.			Virus control / 240 min.			Cytotoxicity
	w/o			w/o			Set #1
1 / -0,7	4/4 [1]	4/4	**8/8**	4/4 [1]	4/4	**8/8**	4/4
2 / -1,4	4/4	4/4	**8/8**	4/4	4/4	**8/8**	4/4
3 / -2,1	4/4	4/4	**8/8**	4/4	4/4	**8/8**	4/4
4 / -2,8	4/4	4/4	**8/8**	4/4	4/4	**8/8**	0/4
5 / -3,5	4/4	4/4	**8/8**	4/4	4/4	**8/8**	
6 / -4,2	4/4	1/4	**5/8**	3/4	3/4	**6/8**	
7 / -4,9	1/4	0/4	**1/8**	0/4	0/4	**0/8**	
8 / -5,6	1/4		**1/8**				
9 / -6,3	0/4		**0/8**				
10 / -7,0							
11 / -7,7							
ZK	0/4	0/4	**0/8**	0/4	0/4	**0/8**	0/4
Titer/test vol. ($lg\ ID_{50}$)	4,9	4,03	**4,47**	4,38	4,38	**4,38**	2,45
Average ± CI (95%) [2]	4,47 ± 0,36 per 100 µL			4,38 ± 0,23 per 100 µL			-
Reduction [3] $lg\ ID_{50}$ ± CI [95%]	-			**0,10 ± 0,42**			-

[1] = number of virus positive cell culture units to total number of cell culture units
[2] = Calculation of 95% confidental intervall of virus titer as well as virus reduction following DVV/RKI-Guideline.
[3] = Virus reduction: titer of virus control minus titer of sample ($lg\ ID_{50}$).

Tab. 3.2:Virus inactivation *(virus titration: according to Lycke)*

Samples	1a	1b	Ø	2a	2b	Ø
	Virus inactivation / 60 min.			Virus inactivation / 240 min.		
	Set #1			Set #1		
1 / -0,7	tox	tox	**tox**	tox	tox	**tox**
2 / -1,4	tox	tox	**tox**	tox	tox	**tox**
3 / -2,1	0/4 [1]	1/4	**1/8**	tox	tox	**tox**
4 / -2,8	2/4	2/4	**4/8**	0/4	0/4	**0/8**
5 / -3,5	0/4	0/4	**0/8**			
6 / -4,2						
7 / -4,9						
8 / -5,6						
9 / -6,3						
10 / -7,0						
11 / -7,7						
ZK	0/4	0/4	**0/8**	0/4	0/4	**0/8**
Titer/test vol. ($lg\ ID_{50}$)	2,1	2,28	**2,19**	≤ 2,45	≤ 2,45	**≤ 2,45**
Average ± CI (95%) [2]	2,19 ± 0,32 per 100 µL			≤ 2,45 per 100 µL		
Reduction [3] $lg\ ID_{50}$ ± CI [95%]	**2,28 ± 0,48**			**≥ 1,93 ± 0,23**		

[1] = number of virus positive cell culture units to total number of cell culture units
[2] = Calculation of 95% confidental intervall of virus titer as well as virus reduction following DVV/RKI-Guideline.
[3] = Virus reduction: titer of virus control minus titer of sample ($lg\ ID_{50}$).

Materials and reagents used:

- ***Testvirus***

Test virus	Influenza A Virus, subtype H1N1
Strain	A/New Caledonia/20/99, IVR-116
Origin	Chiron Behring; Marburg, Germany
Test virus	Seet virus material; Ch.-Bez.: A 04/03; arrived at Eurovir at 18.03.2003 Virus Passage: original virus; Chiron Behring +0 Original seet virus was 10fold diluted with MEM; stored at -80° C

- ***Cells***

Cells	MDCK/63 (Madin Darby canine kidney cells)
Origin	Nationales Referenzzentrum für Influenza; Robert Koch-Institut, Berlin, Germany cells received in living condition with 73th passage at 09.07.2001 (= RKI +0)
Cell passage used	RKI +3 / + 9 / + 28

- ***Additional material and reagents***

Material	*Supplier*	*Order No.*	*Lot*	*Expiry date*
DMEM	Biochrom	F 0435	1272 B	11/2015
Glutamine	Biochrom	K 0283	0978 B	08/2016
Pen./Strept.	Biochrom	A 2213	0018 C	01/2017
FCS	Biochrom	S 0210	0338 T	04/2015
PBS	Biochrom	L 1820	0123 C	01/2017
Trypsine	Invitrogen	25300-096	1437736	09/2015
Hens erythrocytes	Labor Dr. Merk	E-200	E200/1435	03.09.2014

- ***Performing of the experiment and responsibilities***

Part of experiment	Performed by (position)
Supervision	Dr. Ch. Jursch (Laborleiter)
Control of product input	Fr. S. Sachs (Biologielaborantin) und Dr. Ch. Jursch (Laborleiter)
Performing the test	Fr. S. Sachs (Biologielaborantin)
Cell culturing	Fr. S. Sachs (Biologielaborantin)
indirect virus detection / HA-test	Fr. S. Sachs (Biologielaborantin)
Reading of cells & Raw data	Fr. S. Sachs (Biologielaborantin)
Data input & Analysis	Dr. Ch. Jursch (Laborleiter)
Protocol preparation	Dr. Ch. Jursch (Laborleiter)

Information about the testing

Principal:	PMF Natural Products company	*Test run:*	S2
Product(s):	PMF-concentrate	*Test date:*	19.09.2014
Test system:	Influenza *(H1N1)* + MDCK-cells	*Analysis:*	25.09.2014 *(6 p.i.)*

Test methodology and test parameters

Test method: quantitative virucidal suspensions test according to DVV/RKI-guideline *(Version 08/08)*
Test mixture: 1 VT protein load + 1 VT virus suspension + 8 VT 1,25fold working solution
Protein load: no additional protein load *(PBS)*
Parameter: test temperature: 37° C with the exposure time(s) of: 60 and 240 min.

Tested product sample(s)

1st product: PMF-concentrate *[Product sample: as received (designation: PMF), Arrival: 01.08.2014, Storage at 2-8° C]*

Tab. 1: Weight of content

Set	Product(s)	Conc. in Test *(1x)*	Working sol. *(x 1,25)*	Dosage	pH of working sol.
#1	PMF-concentrate	20,34%	25,42%	0,75 g in 2,95 mL	pH 9,54 *(in test: pH 9,52)*

Tab. 2: Content of samples

Samples	1a	1b	2a	2b
	Virus inactivation			
	Set #1 / 60 min.		Set #1 / 240 min.	
PBS	15µL	15µL	15µL	15µL
Influenza	15µL	15µL	15µL	15µL
PMF / Sol.	120µL	120µL	120µL	120µL
Titration	*Lycke (VF = 1000)*		*Lycke (VF = 1000)*	

Samples	3a	3b	4a	4b	5
	Virus control / 60 Min.		Virus control / 240 Min.		Cytotoxicity
	w/o		w/o		Set #1/240 min.
PBS	15µL	15µL	15µL	15µL	15µL
Influenza	15µL	15µL	15µL	15µL	
Medium					15µL
PBS	120µL	120µL	120µL	120µL	
PMF / Sol.					120µL
Titration	S&K *(VF = 5)*		S&K *(VF = 5)*		*Lycke (VF = 1000)*

Performing of the test

1. Preparation of the product solution: (in the specified sequence)

- ***0,75 g PMF-concentrate*** was solved with agitation and warming to 37°C in 2,95 mL A. bidest.

2. Preparation of the test samples

- Per test point (concentration/exposure time) 2 redundant test samples were prepared.
- Test mixture: 1 vol. PBS + 1 vol. virus suspension + 8 vol. PMF-working solution (1,25-fold)

3. Dilution of the test sample and estimation of virus titer

- ***Termination of virus inactivation:*** after exposure the test samples were diluted with medium *(cf. virus titration).*
- With the ***virus control*** the virus titer was estimated using the methodology of *Spearman & Kärber* with VF = 5 from 113 µL (out of 150 µL of the test sample).
- With the ***virus inactivation samples*** the virus titer was estimated using the methodology of *Lycke.* For each of the test samples (a and b) 48 µL was added to 96 mL Medium, corresponding to a dilution of VF = 1000. All of the 96 mL were then transferred to cell cultures with 200 µL per well (480 wells).

4. Susceptibility control

- Sample 5 (cytotoxicity sample) was diluted 1000fold and was then distributed to cell cultures (cf. virus inactivation). Afterwards a virus dilution serie (VK/E) was transferred to these cells.

5. Judgement of the cells / virus detection

- At day 6 p.i. supernatant of the cell cultures were tested with the HA-test (haemagglutination).

Tab. 3.1: Virus control + Susceptibility control *(virus titration: according to Spearman & Kärber)*

Samples	3a	3b	Ø	4a	4b	Ø	5	VK/E
	Virus control / 60 min.			Virus control / 240 min.			Susceptibility Control	
1 / -0,7	4/4 [1]	4/4	**8/8**	4/4 [1]	4/4	**8/8**	8/8	8/8
2 / -1,4	4/4	4/4	**8/8**	4/4	4/4	**8/8**	8/8	8/8
3 / -2,1	4/4	4/4	**8/8**	4/4	4/4	**8/8**	8/8	8/8
4 / -2,8	4/4	4/4	**8/8**	4/4	4/4	**8/8**	8/8	8/8
5 / -3,5	4/4	4/4	**8/8**	4/4	4/4	**8/8**	8/8	8/8
6 / -4,2	4/4	4/4	**8/8**	3/4	4/4	**7/8**	7/8	8/8
7 / -4,9	2/4	2/4	**4/8**	1/4	2/4	**3/8**	3/8	3/8
8 / -5,6	0/4	0/4	**0/8**	1/4	1/4	**2/8**	2/8	3/8
9 / -6,3				0/4	0/4	**0/8**	0/8	0/8
10 / -7,0								
11 / -7,7								
ZK	0/4	0/4	**0/8**	0/4	0/4	**0/8**	0/8	0/8
Titer/test vol. ($lg\ ID_{50}$)	4,9	4,9	**4,9**	4,73	5,08	**4,9**	4,91 ± 0,39	5,08 ± 0,23
Average ± CI (95%) [2]	4,90 ± 0,26 per 100 µL *(≃4,88 lg ID_{50} pro 96 µL)*			4,90 ± 0,39 per 100 µL *(≃4,88 lg ID_{50} pro 96 µL)*			Δ titer = 0,18 ± 0,53	
Reduction [3] lg ID_{50} ± CI [95%]	-			**0,0 ± 0,47**			**cells susceptible: yes [2]**	

[1] = number of virus positive cell culture units to total number of cell culture units
[2] = Calculation of 95% confidental intervall of virus titer as well as virus reduction following DVV/RKI-Guideline.
[3] = Virus reduction: titer of virus control minus titer of sample ($lg\ ID_{50}$).
[4] = Susceptibility of the detection cells is to be assumed when Δ virus titer is ≤ lg 0,5 [DVV/RKI-Guideline].

Tab. 3.2:Virus inactivation *(virus titration: according to Lycke)*

Samples	1a + 1b	2a + 2b
	Virus inactivation *(VF = 1000)*	
	Set #1 / 60 min.	Set #1 / 240 min.
analysed sample vol.	2 x 48 = 96 µL	2 x 48 = 96 µL
Cell culture units	480	480
Virus positive	448	0
Ratio p [2]	0,9333	0,0
Residual virus *(lg ID_{50} per 96 µL)*	3,26 ± 0,26	< 1 ID_{50} *(0,0 lg ID_{50})*
Virus input *(lg ID_{50} per 96 µL)*	4,88 ± 0,26	4,88 ± 0,39
Reduction [3] ***(lg ID_{50} ± CI [95%])***	**1,62 ± 0,37**	**> 4,88 ± 0,55**

[1] = sample volume transferred onto cell cultures: 48 µL from test mix a. plus 48 µL from test mix b. resulting in 2 x 48 = 96 µL
[2] = ratio of virus positive cell culture units to total number of cell cultures.
[3] = Virus reduction: titer of virus control (cf. Tab. 3.1) minus titer of sample (lg ID_{50})

Estimation of virus titer by LYCKE´s method (Arch Ges Virusforsch (1957); 7:483-493)

Calculation of virus titer by using the following formula:

$- ID_{50} = [1,4 \times \ln (1-p)]$ p = ratio of positive cell cultures to total number of cell cultures

- ***Example:*** 51 out of 100 cell culture units was virus positive → p = 51/100 = 0,51

p put into formula: $- ID_{50} = [1,4 \times \ln (1- 0,51)]$

with ln (0,49): $- ID_{50} = 1,4 \times -0,71$

resulting in: $- ID_{50} = -0,998$ or $ID_{50} = 0,998$

That means that per single cell culture unit 0,998 or 1 ID_{50} of residual virus was present.

When this content of virus was multiplied with the number of cell culture units (= 100) the complete amount of residual virus was obtained: 1,0 ID_{50} x 100 = 100 ID_{50} or lg ID_{50} = 2,0

Result of the example: the total quantity of residual virus which was present in the examined sample of liquid was estimated to **lg ID_{50} = 2,0**

Materials and reagents used:

- ***Testvirus***

Test virus	Influenza A Virus, subtype H1N1
Strain	A/New Caledonia/20/99, IVR-116
Origin	Chiron Behring; Marburg, Germany
Test virus	Seet virus material; Ch.-Bez.: A 04/03; arrived at Eurovir at 18.03.2003 Virus Passage: original virus; Chiron Behring +0 Original seet virus was 10fold diluted with MEM; stored at -80° C

- ***Cells***

Cells	MDCK/63 (Madin Darby canine kidney cells)
Origin	Nationales Referenzzentrum für Influenza; Robert Koch-Institut, Berlin, Germany cells received in living condition with 73th passage at 09.07.2001 (= RKI +0)
Cell passage used	RKI +3 / + 9 / + 35

- ***Additional material and reagents***

Material	*Supplier*	*Order No.*	*Lot*	*Expiry date*
DMEM	Biochrom	F 0435	1272 B	11/2015
Glutamine	Biochrom	K 0283	0978 B	08/2016
Pen./Strept.	Biochrom	A 2213	0018 C	01/2017
FCS	Biochrom	S 0210	0338 T	04/2015
PBS	Biochrom	L 1820	0123 C	01/2017
Trypsine	Invitrogen	25300-096	1437736	09/2015
Hens erythrocytes	Labor Dr. Merk	E-200	E200/1439	01.10.2014

- ***Performing of the experiment and responsibilities***

Part of experiment	Performed by (position)
Supervision	Dr. Ch. Jursch (Laborleiter)
Control of product input	Fr. S. Sachs (Biologielaborantin) und Dr. Ch. Jursch (Laborleiter)
Performing the test	Fr. S. Sachs (Biologielaborantin)
Cell culturing	Fr. S. Sachs (Biologielaborantin)
indirect virus detection / HA-test	Fr. S. Sachs (Biologielaborantin)
Reading of cells & Raw data	Fr. S. Sachs (Biologielaborantin)
Data input & Analysis	Dr. Ch. Jursch (Laborleiter)
Protocol preparation	Dr. Ch. Jursch (Laborleiter)

ANTIVIRAL ACTIVITY OF EXTRACTED FRACTION FROM CAMEL URINE AGAINST CORONA AND INFLUENZA A (H1N1) VIRUSES

AL ATTAS, S. A.[1] – KHORSHID, F. A.[1] – KAO, M.[2] – BAHIELDIN, A.[1*]

[1]*Department of Biological Sciences, Faculty of Science, King Abdulaziz University Jeddah 21589, Saudi Arabia*

[2]*Fachtierarzt für Mikrobiologie Fachgebiet II.3 virologische und serologische Diagnostik Landesbetrieb Hessisches Landeslabor (LHL), Druseltalstraße 67- 34131 Kassel, Germany*

[*]*Corresponding author*
e-mail: abmahmed@kau.edu.sa; phone: +966-506-32-9922
ORCID ID: 0000-0002-6496-7881

(Received 30th Mar 2019; accepted 1st Jul 2019)

Abstract. PMF (a camel urine or PM 701 fraction), is a traditional treatment for many human diseases. Demands for developing clinical treatments against dangerous viruses are increasing. This study aimed to investigate the effects of PMF as a novel pharmaceutical drug *in vitro* in inducing antiviral and/or virostatic activity against MERS-CoV and influenza A (H1N1) viruses. Infectivity assay was determined by end point dilution titration, infective dose was calculated and PMF virucidal activity was evaluated as a reduction factor. Quantitative virucidal suspension test was performed using TGEV virus, as a model for MERS-CoV, and H1N1 virus. The results indicated that PMF concentration of 20.34% inactivated 99.5% of the TGEV virus after 60 min, and 99.9% after 240 min. The results also indicated that the same PMF concentration inactivated H1N1 virus on Madin Darby canine kidney cells (MDCK/63) by 98.90% and 99.99% after 60 and 240 min, respectively. We speculate that copper and zinc elements in PMF might vitally contribute to the antiviral and virostatic activity. In conclusion, PMF was proven to induce antiviral *in vitro* activity against both viruses, hence, is recommended to use as a therapeutic antiviral agent in the future.
Keywords: *PMF, MERS-CoV, TGEV, H1N1, virostatic activity*

Introduction

Corona viruses (CoVs) cause a wide range of respiratory and gastric diseases. Most CoVs are RNA viruses, which replicate in epithelial cells of respiratory and digestive tracts (van der Hoek et al., 2004). These viruses enter the cell by viral spike (S) proteins that bind to cellular receptors and facilitate virus-cell membrane fusions. Du et al. (2017) indicated that spike protein is a key target as antiviral mechanism against CoVs. Lin et al. (2017) were able to induce antiviral activity against the virus by resveratrol treatment. Müller et al. (2017) also indicated the successful usage of binase in inhibiting virus genome replication. The diversity of CoVs is reflected in S protein variability, which is involved in different receptor interactions and respond to different environmental conditions (Belouzard et al., 2012). A new corona virus was identified during summer of 2012 in Saudi Arabia (Zaki et al., 2012) and named Middle East respiratory syndrome corona virus (MERS-CoV) by International Committee on Taxonomy of Viruses (de Groot et al., 2013). The Middle East respiratory syndrome is a pneumonic illness caused by a novel lineage C betacoronavirus (CoV). In 2014, a total of 178 MERS cases were confirmed in humans, which resulted in 76 deaths (WHO, 2014). Infection with MERS-CoV can also cause abdominal pain, diarrhea, fever and renal failure (Assiri et al., 2013).

http://www.aloki.hu ● ISSN 1589 1623 (Print) ● ISSN 1785 0037 (Online)
DOI: http://dx.doi.org/10.15666/aeer/1705_1102311031

The virus was found mostly in the lower respiratory tract samples, while low concentrations were found in stool, urine, and blood samples (Drosten et al., 2013). Limited human-to-human transmission has resulted in clusters of cases; the remaining sporadic cases in humans are of zoonotic origin (Assiri et al., 2013). Up to date, both reservoir and intermediate hosts remain unidentified, delaying any success on controlling the virus. MERS-CoV had been spread into eleven countries of the Middle East, North Africa, South Korean and Europe. Therefore, there are global concerns over security, but the Economist report announced that "Concern over security must not slow urgent work, studying a deadly virus is risky; not studying it is riskier" (Economist.com, 2014). The demand for developing clinical treatment against MERS-CoV is increasing, but the strict limitations for using strains of new deadly virus is still slowing down and retards scientific investigations. In this study, we used TGEV virus as a model for MERS-CoV, as both are corona viruses. Transmissible Gastroenteritis Virus (TGEV) belongs to corona viridae family, genus *Alphacoronavirus*, species Alphacoronavirus (Frieman, 2014). It is an enveloped virus with a positive single stranded RNA genome. TGEV infects pigs and rarely humans. In pigs, mortality rate is close to 100%. The pathology of TGEV is similar to that of other corona viruses. They enter the host by attaching to cell membrane using spike glycoprotein and multiplies in cell lining of small intestine resulting in loss of absorptive cells and shortening of villi. The infected host then loses the ability for digesting food and dies from dehydration (Frieman, 2014).

H1N1 is the subtype of influenza A virus causing swine and human flu (Lim and Mahmood, 2011; Kong et al., 2015). It is an orthomyxovirus harboring the two glycoproteins haemagglutinin and neuraminidase (Du et al., 2017). Up to 2015, more than 40 million people died due to the infection with H1N1 (Kong et al., 2015). Cloning and sequencing of the eight virus genes revealed that human influenza virus is closely related to avian influenza virus with regard to their coding sequences (Taubenberger et al., 2005; Morens and Fauci, 2007; Taubenberger et al., 2007).

Natural products are important source for novel drug therapies of efficient compounds with diverse biological activities and unique chemical structures. Camel urine is known as a traditional treatment of many diseases in Arabs countries (Alghamdi and Khorshid, 2012; Mahboub et al., 2015). The relative density of mature camel urine ranges from 1.02 to 1.07 g/dL; pH varied between acidic or alkaline; urea level ranged from 18-36 g/dL and creatinine level ranged from 0.2-0.5 g/L (Al-Bashan, 2011). Chemical and microscopic examination showed the presence of phosphorus, calcium oxalate and ammonium urate and some epithelial and granular cells (Al-Bashan, 2011). PMF (a camel urine or PM 701 fraction) is a novel pharmaceutical drug that was extracted from PM 701 (lyophilized camel urine) that is able to selectively inhibit the proliferation of cancer cells significantly without affecting normal cells at human cell culture level and animal models (Khorshid, 2008, 2009; Khorshid et al., 2005, 2009, 2011; El-Shahawy et al., 2010). Prospects of the use of therapeutic nanoparticles, nanobodies and nanorods from this natural product was recently explored for cancer therapy (Getachew Alebie et al., 2017).

New treatments cannot be tested directly on humans because they could be potentially dangerous and experiment can be costly. Alternatively, human cell culture and animal models are used traditionally for testing and developing safe dose and working mechanisms of innovative therapies. In this study, we detected the influence of PMF in terms of antiviral activity on TGEV as a model virus on fetal testis cells of swine (ST75/2) and H1N1 virus utilizing Madin Darby canine kidney cell line (MDCK/63).

http://www.aloki.hu ● ISSN 1589 1623 (Print) ● ISSN 1785 0037 (Online)
DOI: http://dx.doi.org/10.15666/aeer/1705_1102311031

Materials and Methods

Extraction of PMF

PMF was extracted at the laboratory of King Fahad Medical Research Center, King Abdulaziz University (KAU) in Jeddah, Saudi Arabia as previously described (Khorshid et al., 2009). Then, PMF was transported in IATA-compliant container from Saudi Arabia to Eurovir Institute in Luckenwalde, Germany. The fraction was stored at 2-8°C prior testing for virucidal activity against TGEV and H1N1 viruses. The PMF product was tested as a working solution of 25.42% (w/v) and pH of 9.71 (0.75 g of PMF-concentrate was solved with agitation and warming to 37ºC in 2.95 mL of aqua bidest). In the test sample, PMF working solution was diluted with a factor of 1:25 due to addition of TGEV or H1N1 suspensions and interfering phosphate-buffered saline substance (PBS).

TGEV and H1N1 virus suspensions

TGEV strain Toyama was obtained from virus bank of the Bundesforschungsanstalt f. Viruskrankheiten der Tiere; Friedrich Löffler-Institut, InselRiems, Germany, as a model virus for MERS-CoV. Influenza A virus subtype (H1N1) the commonest cause of human influenza (flu) and seasonal Influenza, New Caledonia /20/99, IVR-116 Strain was obtained from virus bank of the Chiron Behring, Marburg/Lahn, Germany. Originally obtained viruses were 10-fold diluted with MEM; then stored at -80°C until use.

Experimental cells

ST75/2 cells; fetal testis cells of swine obtained from Robert Koch-Institute, Berlin/ Germany, were used as a target for MERS-CoV virus. They were inspected regularly for morphological alterations and mycoplasmas contamination in which none were detected. For maintenance and growing of the cells, media involved Eagle's minimum essential medium (EMEM), Lot.Nr., glutamine, penicillin/streptomycin, fetal calf serum, PBS and trypsin.

Madin Darby canine kidney reporter cell line MDCK/63; obtained from National reference center for influenza, Robert Koch-Institute, Berlin/Germany, were used as a target for H1N1 virus. Cells survived in living condition with 73th passage of RKI +3/+9/+35 at 09.07.2001 (= RKI +0). These cells are highly permissive for influenza virus replication and provide a highly specific and sensitive approach for simultaneous detection and isolation of influenza viruses.

Infectivity assay

To prepare TGEV or H1N1 test virus suspensions, ST75/2 and MDCK/63 cells, that had been cultured with EMEM and 10% fetal calf serum (FCS), were inoculated with TGEV or H1N1, respectively, in 25 cm^2 cell culture flasks. After 48 hours and after induction of cytopathic effect, freezing and thawing were carried out once. Cell debris was removed by centrifugation at 3000 rpm for 10 min at 4°C and supernatant was recovered as test virus suspension and stored in aliquots at -80°C.

Infectivity was determined by virus titration of end point dilution titration using microliter process. One hundred µl aliquots of samples were serially diluted with cold EMEM and transferred to four wells of polystyrol 24-well microliter plate with

http://www.aloki.hu ● ISSN 1589 1623 (Print) ● ISSN 1785 0037 (Online)
DOI: http://dx.doi.org/10.15666/aeer/1705_1102311031

performed monolayer of ST75/2 or MDCK cells (placed in each well on the previous day with 100 µl aliquots including approx. $1.5x10^4$ cells). Infective dose ($TCID_{50}$) and their 95% confidence intervals were calculated with Spearman-Karber method (Khorshid et al., 2009). The main samples virus titration was performed and the corresponding virus titer was calculated as previously indicated (Khorshid et al., 2011). The virucidal activity of PMF was evaluated by calculating the decrease in titers in comparison with control untreated titration. The difference is given as a reduction factor (RF). Quantitative virucidal suspension test (QST) was performed following the guideline of DVV and Robert Koch-Institute. Control and virus inactivation screening tests were performed as recently indicated (Al Attas et al., in preparation).

Statistical analysis

Data were expressed as numbers or means +/- standard deviation or numbers as appropriate using SPSS software version 20.0.

Results and Discussion

The results for the influence of PMF on the MERS-CoV virus is shown in *Figure 1* and *Supplementary file S1*. The analysis included one control test in which the amount of input virus at 37°C was estimated to be lg ID50 = 6.13 ± 0.34 after 60 min. After 240 min, virus titer was declined to lg ID50 = 5.52 ± 0.32 due to the influence of temperature (Δ virus titer = 0.61 ± 0.46). With the *Lycke's* method, a sample dilution was done (VF = 1000). With that dilution, no cytotoxicity was visible and the susceptibility of the detection cells was given (Δ titer = 0.18 ± 0.47). With PMF final test concentration of 20.34%, the virus reduction factor (RF) was estimated to be 4.31 ± 0.48 after 60 min. After the exposure time was prolonged to 240 min, no residual virus could be detected. The corresponding virus reduction factor was estimated to be > 5.50 ± 0.45 corresponding to a virus reduction of 99.999% (*Supplementary file S1*).

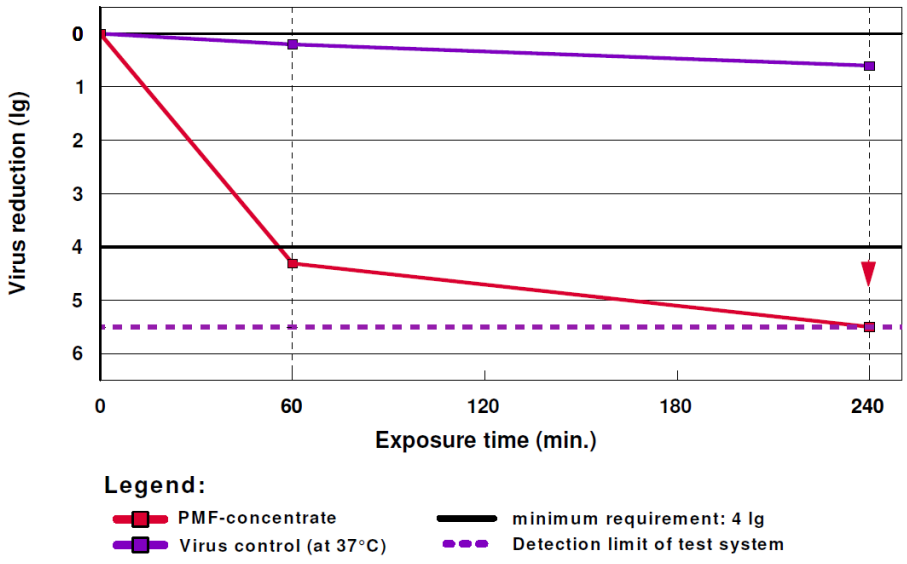

Figure 1. *MERS-CoV virus reduction (lg) as affected by the treatment of camel urine fraction (PMF) and measured after 60 and 240 min. Virus reduction = titer of virus control minus titer of sample (lg ID_{50})*

http://www.aloki.hu ● ISSN 1589 1623 (Print) ● ISSN 1785 0037 (Online)
DOI: http://dx.doi.org/10.15666/aeer/1705_1102311031

The results for the influence of PMF on the H1N1 virus is shown in *Figure 2* and *Supplementary file S2*. The analysis included two control tests. Screening test S1 indicated that the pH of the 1.25 fold concentrated working solution were measured to pH 9.54, which was changed only slightly to pH 9.52. The amount of input virus at 37°C was estimated to be lg ID50 = 4.47 ± 0.36 after 60 min and to lg ID50 = 4.38 ± 0.23 after 240 min (Δ virus titer = 0.10 ± 0.42). Using the Spearman & Kärber's titration method, a cytotoxicity titer of lg TD50 = 2.45 was recorded for the test samples. This is equivalent with the detection limit of this screening test. Screening test S2 indicated that the amount of input virus at 37°C was estimated to be lg ID50 = 4.88 ± 0.26 after 60 min and to lg ID50 = 4.88 ± 0.39 after 240 min (Δ virus titer = 0). With the *Lycke's* method, a sample dilution was done (VF = 1000). With that dilution, no cytotoxicity was visible and the susceptibility of the detection cells was given (Δ titer = 0.18 ± 0.53). In addition, the detection limit of this screening test could be improved by 2.45 Log. Virus inactivation in this screening test indicated that 20.34% of PMF (final test concentration) resulted in virus reduction factor of 2.28 ± 0.48 after 60 min. After 240 min, no residual virus could be detected (test virus below detection limit, due to product associated cytotoxicity [lg TD50 = 2.45]). The corresponding virus reduction factor was estimated to be 1.93 ± 0.23. For the second screening test, 20.34% of PMF (final test concentration) resulted in the virus reduction factor of 1.62 ± 0.37 after 60 min.

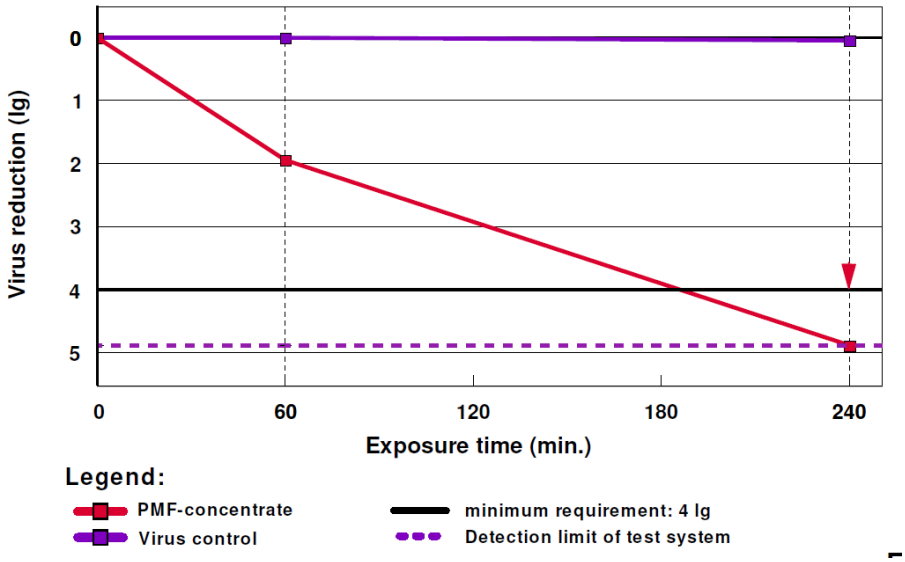

Figure 2. *H1N1 virus reduction (lg) as affected by the treatment of camel urine fraction (PMF) and measured after 60 and 240 min. Virus reduction = titer of virus control minus titer of sample (lg ID_{50})*

After 240 min, no residual virus could be detected. The corresponding virus reduction factor was estimated to be > 4.88 ± 0.55 corresponding to a virus reduction of 99.998% (*Supplementary file S2*).

The overall results indicated that PMF is a promising bio-product derived from camel urine with antiviral potentials. However, the mechanism of action is yet to be deciphered. Many viral diseases have associated with high morbidities and mortalities, and new approaches should be presented to find a cure. Many identified antiviral drugs

http://www.aloki.hu ● ISSN 1589 1623 (Print) ● ISSN 1785 0037 (Online)
DOI: http://dx.doi.org/10.15666/aeer/1705_1102311031

have also been used as anticancer agents in which drugs are effective in preventing DNA synthesis. The lyophilized PM701 extracted fraction from camel urine at 150 mg/g inhibited cancer cells proliferation without damaging normal cells at cell culture level (Khorshid et al., 2011; Mahboub et al., 2015). The MDCK reporter cell line established in this study is highly permissive for influenza virus replication and provides a highly specific and sensitive approach for simultaneous detection and isolation of influenza viruses (Hossain et al., 2010). Yao and coworkers (2014) had described that anti-herpes simplex virus drug (acyclovir) is an effective agent for cancer treatment. Camel urine was proven to induce cytotoxic influence in major types of human cancer cell lines (El-Shahawy et al., 2010; Al-Yousef et al., 2012). It was evident that the anticancer properties of camel's urine can be performed as antiviral properties. Anticancer properties were not attributed to a given compound in the camel's urine, such as zinc, copper and amino acids (Khorshid et al., 2009; Raouf et al., 2009; Ahmed et al., 2010; Ali et al., 2011). Jannah and coworkers also described that zinc and copper are the two key elements in PMF that delivers its antimicrobial effect (Jannah et al., 2013). Zinc has been proven to have antiviral activities against TGEV by viral multiplication within cells via inhibiting protein but it has no effect on cell infection (Weia et al., 2012). Sunada and colleagues conducted their study on bacteriophages and concluded that copper ion reduced infectious ability of phages (Sunada et al., 2012). Therefore, both copper and zinc are thought to have a vital role in antiviral and virostatic activity of PMF used in the present study. The high antimicrobial effect of crude extracts of camel urine was speculated to be due to its high osmolarity, high levels of proteins and potassium metallic ions (Stankova et al., 2009; Khorshid et al., 2011). Khorshid and coworkers (El-Shahawy et al., 2010; Khorshid et al., 2011; Mahboub et al., 2015) recorded that camel urine had cytotoxicity only against various human cancer cell lines, with negligible effect on non-tumorigenic epithelial and fibroblast cells (Khorshid et al., 2005, 2015). Several studies have also successfully proven the anticancer, antibacterial and antifungal effects of PMF (Khorshid et al., 2011, 2015; Mahboub et al., 2015).

Up to date, there are no effective treatments against human coronaviruses infections that has high mortality rate of up to 40% (Feikin et al., 2015). The American Academy of Pediatrics (2017-2018) indicated the recommendations for prevention and control of N1H1 by the use of trivalent, rather than the quadrivalent live attenuated influenza vaccine, containing the A/Michigan/45/2015 (H1N1) pdm09-like virus. The report indicated that antiviral medication in children can be important in controlling the disease, but this cannot be a substitute for vaccination. Our results indicate that PMF might be used solely as a potential alternative cure of the disease.

The present study highlighted the virucidal activity of PMF against the two viruses with no observed effects on the control. These results suggested that PMF treatment has an *in vitro* powerful effect on the virus replication process at the cellular level. The antiviral activity mode of action of camel urine fraction PMF has not been identified. Therefore, more investigations are needed concerning gene expression profiling to investigate the apoptotic activity of PMF. The antiviral activity of PMF should be enhanced for fast promising therapy using a wide range of DNA and RNA virus models as well as cancer inducing viruses.

http://www.aloki.hu ● ISSN 1589 1623 (Print) ● ISSN 1785 0037 (Online)
DOI: http://dx.doi.org/10.15666/aeer/1705_1102311031

Conclusion

The MERS-CoV and H1N1 viral infections, identified in the Middle East, have global concerns because of their associated high morbidity and mortality. The results of *in-vitro* PMF treatment showed a significant reduction in the titers of the two viruses across time indicating that PMF has potential antiviral activities. More studies are recommended to fractionate and monitor the antiviral activity of PMF compositions and to determine molecular mechanisms of action.

Acknowledgments. The authors acknowledge GCC patents office for granted this project GCC Patent No. GC0002755 and European patent office for granted Europe patent No. 2263681. The authors also acknowledge Engineer Musab Alyasin for pear for the cost of transporting and testing of PMF; Professor Enas A Hamed, Professor of Physiology, Faculty of Medicine, Assiut University, Assiut, Egypt for critical reading of the manuscript.

REFERENCES

[1] Ahmed, G. A., Khorshid, F. A., Kumosani, T. A. (2010): FT-IR spectroscopy of A549 cells treated with PMF: structural changes in DNA and cell membrane. – J. Thoracic Onco. 5: 46S.

[2] Al-Bashan, M. M. (2011): *In vitro* assessment of the antimicrobial activity and biochemical properties of camel's urine against some human pathogenic microbes. – Middle-East J. Sci. Res. 7: 947-958.

[3] Alghamdi, Z., Khorshid, F. A. (2012): Cytotoxicity of the urine of different camel breeds on the proliferation of lung cancer cells, A549. – J. Nat. Sci. Res. 2: 9-16.

[4] Ali, A., Khorshid, F. A., Aboarky, H., Osman, A. M. (2011): Tumor lung cancer model for assessing anti-neoplastic effect of PMF in rodents: histopathological study. – Trends in Appl. Sci. Res. 6: 1214-1221.

[5] Al-Yousef, N., Gaafar, A., Al-Otaibi, B., Al-Jammaz, I., Al-Hussein, K., Aboussekhra, A. (2012): Camel urine components display anti-cancer properties in vitro. – J. Ethnopharmacol. 143: 819-825.

[6] American Academy of Pediatrics: Recommendations for prevention and control of influenza in children (2017-2018). – Pediatirics 140: e20172550.

[7] Assiri, A., McGeer, A., Perl, T. M., Price, C. S., Al Rabeeah, A. A., Cummings, D. A. T., Alabdullatif, Z. N., Assad, M., Almulhim, A., Makhdoom, H., Madani, H., Alhakeem, R. (2013): Hospital outbreak of Middle East respiratory syndrome coronavirus. – N. Engl. J. Med. 369: 407-416.

[8] Belouzard, S., Millet, J. K., Licitra, B. N., Whittaker, G. R. (2012): Mechanisms of coronavirus cell entry mediated by the viral spike protein. – Viruses 4: 1011-1033.

[9] de Groot, R. J., Baker, S. C., Baric R. S., Brown, C. S., Drosten, C., Enjuanes, L., Fouchier, R. A. M., Galiano, M., Gorbalenya, A. E., Memish, Z. A., Perlman, S., Poon, L. L. M., Snijder, E. J., Stephens, G. M., Woo, P. C. Y., Zaki, A. M., Zambon, M., Ziebuhr, J. (2013): Middle East respiratory syndrome coronavirus (MERS-CoV): announcement of the coronavirus study group. – J. Virol. 87: 7790-7792.

[10] Drosten, C., Seilmaier, M., Corman, V. M., Hartmann, W., Scheible, G., Sack, S., Guggemos, W., Kallies, R., Muth, D., Junglen, S., Müller, M. A., Haas, W., Guberina, H., Röhnisch, T., Schmid-Wendtner, M., Aldabbagh, S., Dittmer, U., Gold, H., Graf, P., Bonin, F., Rambaut, A., Wendtner, C. M. (2013): Clinical features and virological analysis of a case of Middle East respiratory syndrome coronavirus infection. – Lancet Infect. Dis. 13: 745-751.

http://www.aloki.hu ● ISSN 1589 1623 (Print) ● ISSN 1785 0037 (Online)
DOI: http://dx.doi.org/10.15666/aeer/1705_1102311031

[11] Du, L., Yang, Y., Zhou, Y., Lu, L., Li, F., Jiang, S. (2017): MERS-CoV spike protein: a key target for antivirals. – Expert Opin. Ther. Targets 21: 131-143.
[12] El-Shahawy, A., Elsawi, N. M., Baker, W. S., Khorshid, F. A., Neveen, A., Geweely, N. (2010): Spectral analysis, molecular orbital calculations and antimicrobial activity of PMF-G fraction extracted from PM-701. – Int. J. Pharma. Biosci. 1: 1-19.
[13] Feikin, D. R., Alraddadi, B., Qutub, M., Shabouni, O., Curns, A., Oboho, I. K., Tomczyk, S. M., Wolff, B., Watson, J. T., Madani, T. A. (2015): Association of higher MERS-CoV virus load with severe disease and death, Saudi Arabia, 2014. – Emerg. Infect. Dis. 21: 2029-2035.
[14] Frieman, M. (2014): The art of war: battles between virus and host. – Curr. Opin. Virol. 6: 76-77.
[15] Getachew Alebie, G., Yohannes, S., Worku, A. (2017): Therapeutic applications of camel's Milk and urine against cancer: current development efforts and future perspectives. – J. Cancer Sci. Therapy 9: 5.
[16] Hossain, M. J., Perez, S., Guo, Z., Chen, L. M., Donis, R. O. (2010): Establishment and characterization of a Madin-Darby canine kindey reported cell for influenza A virus assays. – J. Clin. Microbiol. 48: 2515-2523.
[17] Jannah, H., Ali, A. S., Efat, M. M., Khorshid, F. A. (2013): An ointment contains pmf showed promising results for treatment of psoriasis in human. – Intl. J. Med. Appl. Sci. 2: 15-20.
[18] Khorshid, F. A., Moshref, S. S., Heffny, N. (2005): An ideal selective anticancer agent in vitro, I- tissue culture study of human lung cancer cells A549. – JKAU- Med. Sci 12: 3-18.
[19] Khorshid, F. A. (2008): Preclinical evaluation of PM 701 in experimental animals. – Intl. J. Pharmacol. 1: 443-451.
[20] Khorshid, F. A. (2009): Potential anticancer natural product against human lung cancer cells. – Trends in Med. Res. 4: 9-15.
[21] Khorshid, F. A., Osman, A. A., Abdulsattar, E. (2009): Cytotoxicity of bioactive fractions from PM 701. – EJEAFChe 8: 1091-1098.
[22] Khorshid, F. A., Rahimaldeen, S. A., Alameri, J. S. (2011): Apoptosis study on the effect of PMF on different cancer cells. – Intl. J. Biol. Chem. 5: 150-155.
[23] Khorshid, F. A., Rabah, S., As, A., Noor, S. O., Alkabkaby, H. (2015): Safety of oral administration of PMF a fraction derived from camel urine: acute study on mice. – Intl. J. Emerg. Technol. Adv. Engineer. 6: 365-370.
[24] Kong, W., Wang, F., Dong, B., Ou, C., Meng, D., Liu, J., Fan, Z. C. (2015): Novel reassortant influenza viruses between pandemic (H1N1) 2009 and other influenza viruses pose a risk to public health. – Microb. Pathog. 89: 62-72.
[25] Lim, B. H., Mahmood, T. A. (2011): Influenza A H1N1 2009 (Swine Flu) and pregnancy. – J. Obstet. Gynaecol. 61: 386-393.
[26] Lin, S. C., Ho, C. T., Chuo, W. H., Li, S., Wang, T. T., Lin, C. C. (2017): Effective inhibition of MERS-CoV infection by resveratrol. – BMC Infect. Dis. 17: 144.
[27] Mahboub, F. A., Khorshid, F. A., Emwas, A. M. (2015): The cytotoxic effect of small and large molecules of PMF fraction extracted from camel urine on cancer cells. – British J. Med. Med. Res. 6: 384-396.
[28] Morens, D. M., Fauci, A. S. (2007): The 1918 influenza pandemic: insights for the 21st century. – J. Infect. Dis. 195: 1018-1028.
[29] Müller, C., Ulyanova, V., Ilinskaya, O., Pleschka, S., Mahmud, R. S. (2017): A Novel antiviral strategy against MERS-CoV and HCoV-229E using Binase to target viral genome replication. – BioNanoScience 7: 294-299.
[30] Raouf, G. A., Khorshid, F. A., Kumosani, T. (2009): FT-IR spectroscopy as a tool for identification of apoptosis-induced structural changes in A549 cells dry samples treated with PM 701. – Intl. J. Nano Biomaterials 2: 396-408.

http://www.aloki.hu ● ISSN 1589 1623 (Print) ● ISSN 1785 0037 (Online)
DOI: http://dx.doi.org/10.15666/aeer/1705_1102311031

[31] Stankova, I., Chuchkov, K., Shishkov, S., Kostova, K., Mukova, L., Galabov, A. S. (2009): Synthesis, antioxidative and antiviral activity of hydroxycinnamic acid amides of thiazole containing amino acid. – Amino Acids 37: 383-388.
[32] Sunada, K., Minoshima, M., Hashimoto K. (2012): Highly efficient antiviral and antibacterial activities of solid-state cuprous compounds. – J. Hazard, Mater. 235-236: 265-270.
[33] Taubenberger, J. K., Reid, A. H., Lourens, R. M., Wang, R., Jin, G., Fanning, T. G. (2005): Characterization of the 1918 influenza virus polymerase genes. – Nature 437: 889-893.
[34] Taubenberger, J. K., Hultin, J. V., Morens, D. M. (2007): Discovery and characterization of the 1918 pandemic influenza virus in historical context. – Antivir. Ther. 12: 581-591.
[35] The Economist (2014): Livestock insurance in Kenya: no risk, no reward. – Economist.com.
[36] van der Hoek, L., Pyrc, K., Jebbink, M. F., Vermeulen-Oost, W., Berkhout, R. J., Wolthers, K. C., Wertheim-van Dillen, P. M., Kaandorp, J., Spaargaren, J., Berkhout, B. (2004): Identification of a new human coronavirus. – Nature Med. 10: 368-373.
[37] Wei, Z., Burwinkel, M., Palissa, C., Ephraim, E., Schmidt, M. F. (2012): Antiviral activity of zinc salts against transmissible gastroenteritis virus in vitro. – Veterinary Microbiol. 160: 468-472.
[38] World Health Organization (WHO) (2014): Middle East respiratory syndrome coronavirus (MERS-CoV) summary and literature update—as of 20 January 2014. – [cited 2014 Feb 20]. http://www.who.int/csr/disease/coronavirusinfections/ MERS CoV 2014.
[39] Yao, J., Zhang, Y., Ramishetti, S., Wang, Y., Huang, L. (2014): Turning an antiviral into an anticancer drug: Nanoparticle delivery of acyclovir monophosphate. – J. Controlled Release 170: 414-420.
[40] Zaki, A. M., van Boheemen, S., Bestebroer, T. M., Osterhaus, A. D., Fouchier, R. A. (2012): Isolation of a novel coronavirus from a man with pneumonia in Saudi Arabia. – New Engl. J. Med. 367: 1814-1820.

http://www.aloki.hu ● ISSN 1589 1623 (Print) ● ISSN 1785 0037 (Online)
DOI: http://dx.doi.org/10.15666/aeer/1705_1102311031

EVALUATION OF WATER FOOTPRINT OF SELECTED CROP CONSUMPTION IN TEHRAN PROVINCE

REZAEI KALVANI, S.[1] – SHARAAI, A.[1*] – MANAF, L.[1] – HAMIDIAN, A.[2]

[1]*Faculty of Environmental Studies, Universiti Putra Malaysia, 43400 UPM Serdang, Selangor, Malaysia*

[2]*Department of Environmental Science and Engineering, Faculty of Natural Resources, University of Tehran, Karaj, Iran*

**Corresponding author*
e-mail: amirsharaai@upm.edu.my; phone: +60-3-8946-8031; fax: +60-3-8946-7468

(Received 30th Mar 2019; accepted 13th Jun 2019)

Abstract. The sharp increase in water consumption poses a risk of increasing water scarcity in developing countries. The aim of this study is to the quantify variability of per capita Water Footprint (WF) of consumption of selected crops in Tehran province from 2008–2014. Blue and green WF were computed using WF approach. Besides, per capita WF of crop consumption was evaluated using bottom-up approach. The result illustrated the external water footprint had the largest contribution in total WF of crops consumption in the Tehran province (2008-2014). The total water footprint of crop consumption decreased because the population and per capita WF also decreased. Besides, wheat and rice had the largest per capita WF. This study discloses that it is essential to have appropriate water management to reduce water stress originating from agricultural sector in future. The consumption of wheat in Iran is high, more precisely 2 times larger than global average. It is recommended to reduce the consumption of wheat in Tehran or replace it with other crops. Besides that, decision makers in agricultural sector should reduce water lost, with declining production of cherry, pear, and peach. Furthermore, reducing water footprint of crops and efficient agricultural water management are recommended.
Keywords: *per capita water footprint, water consumption, agricultural water management, CROPWAT model, virtual water*

Introduction

Water footprint is identified as a strong tool to evaluate water consumption through the supply chain of products because it has multidimensional indicator which is able to evaluate direct and indirect water consumption. Besides, water footprint contains information about the types of water used including ground and surface water footprint (blue WF) and irrigation water footprint (green WF) (Hoekstra et al., 2011). The WF method is able to evaluate water consumption in a variety of scale from city (Wu, 2014) to global scale (Hoekstra and Chapagain, 2007). Water footprint of provinces is calculated by summing up the internal and external WFs (Hoekstra and Chapagain, 2007). Virtual water trade plays an important role in mitigating water shortages in water-stressed areas (Qian et al., 2018). However, exporting crops from water-stressed regions can increase water scarcity. Iran is facing severe water scarcity due to population growth, economic growth, inefficiency of agricultural water usage, and inappropriate water management (Madani, 2014). Besides, Iran has the largest blue water consumption and blue water footprint per capita (Hoekstra and Mekonnen, 2011).

In spite of existing vast number of literature, there has been lack of attention to the annual changes of water footprint of crop consumption and the associated water loss and saving at provincial scale. Besides, most of the studies have evaluated water

http://www.aloki.hu ● ISSN 1589 1623 (Print) ● ISSN 1785 0037 (Online)
DOI: http://dx.doi.org/10.15666/aeer/1705_1103311044

footprint at country scale (Gephart et al., 2016; Ge et al., 2011; Zhuo, Mekonnen, and Hoekstra, 2016; Feng et al., 2015). It is important to know how much water is consumed due to crop use and how human consumption pattern impacts inter-provincial and international water dependencies. Very few studies have been done on the water footprint of Iran's crop consumption (Hoekstra and Mekonnen, 2011; Hoekstra and Chapagain, 2007; Karandish and Hoekstra, 2017); on water footprint of cereal crops throughout different provinces in Iran (Ababaei and Etedali, 2016); on water footprint of the cement industry in western Iran (Hosseinian and Nezamoleslami, 2018) and on the virtual water trade in Iran (Yousefi et al., 2017; Faramarzi et al., 2010). Besides, there has been lack of attention on the provincial water footprint and water saving assessment. Okadera et al. (2015) applied the "top-down" approach to evaluate the WF of energy supplies in one of China's provinces. Besides that, Zhao et al. (2018) and Chen et al. (2017) have assessed water footprints in all the provinces of China.

The objective of this research is to evaluate and analyze water footprint of 14 important crops in Tehran province and to assess water savings and losses from 2007 to 2014.

Materials and methods

Area of study

Tehran province is located in the northern central plateau of Iran with population of more than 13 million people in 2014. It accommodates approximately 18% of Iran population (Statistical Centre of Iran). It is the richest province in Iran which contributes approximately 29% of overall GDP. The area of Tehran province spans 18,909 km^2. The climate in the northern part of Tehran is alpine whereas in the southern part, it is arid and semi-arid. The total average rainfall is around 200 mm annually. The sum of precipitation with minimum and maximum temperature in Tehran in 2008 is illustrated in *Figure 1*.

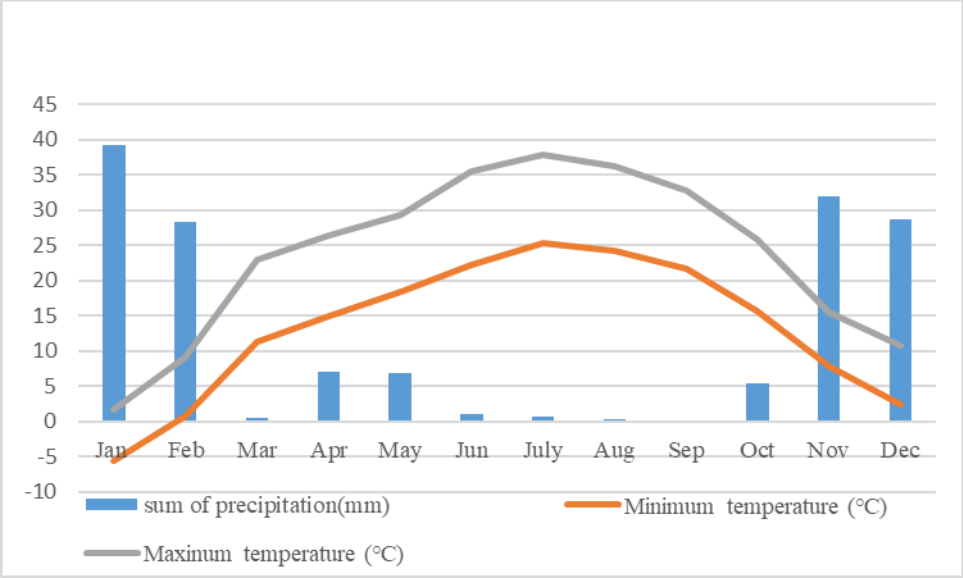

Figure 1. *The plot of minimum and maximum temperature and sum of precipitation (2008)*

http://www.aloki.hu ● ISSN 1589 1623 (Print) ● ISSN 1785 0037 (Online)
DOI: http://dx.doi.org/10.15666/aeer/1705_1103311044

The nation water footprint has two components: internal and external. Internal WF is the water footprint of crops that are produced within the border of Tehran for domestic consumption. On the other hand, external WF refers to WF of crops produced outside of (imported to) Tehran and consumed within Tehran. The WF in Tehran province is evaluated by summing up internal and external WF (*Fig. 2*). Besides, it is important to distinguish between WF of production and WF of consumption. WF of production is defined as the volume of WF that is used from domestic water resources for production of goods and services. However, consumptive WF refers to the volume of WF that is used from domestic and foreign water resources for domestic consumption (Hoekstra and Mekonnen, 2011).

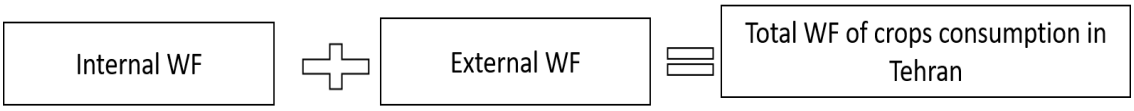

Figure 2. *National water footprint accounting framework based on Hoektra method (Hoekstra and Chapagain, 2007)*

First of all, the water footprint of crop production in Tehran province was evaluated. It was calculated based on Hoekstra method (Hoekstra et al., 2011). Secondly, WF of crops that are produced outside Tehran and consumed within Tehran (Hamedan, Lorestan, Ahvaz, Mazandaran, Qazvin, and Kermanshah provinces); also known as external WF was evaluated. Finally, per capita WF of crops, water saving, and water loss in Tehran were assessed.

Internal and external water footprint of crops in Tehran province

The WF of cultivated crops in Tehran, as well as imported crops from other provinces to Tehran were evaluated. For this research, the most important crops were selected including wheat, barley, maize, peaches, potatoes, rice, onions, tomatoes, grapes, oranges, cherries, peas, and apples. Water footprints of these crops were computed based on Hoekstra approach. The CROPWAT software was used to compute evapotranspiration of each growing crop.

Water footprint assessment methodology

The blue and green WF for each crop and each year were evaluated for each province based on Hoekstra approach. The blue WF was calculated by dividing blue Crop Water Use CWU_{blue} (m^3/ha) by the yield (Y) (ton/ha) – *Equation 1* (Hoekstra et al., 2011). The green water footprint was computed using similar method – *Equation 2* (Hoekstra et al., 2011).

$$WF_{blue} = \frac{CWU_{blue}}{Y} \quad \text{(Eq.1)}$$

$$WF_{green} = \frac{CWU_{green}}{Y} \quad \text{(Eq.2)}$$

http://www.aloki.hu ● ISSN 1589 1623 (Print) ● ISSN 1785 0037 (Online)
DOI: http://dx.doi.org/10.15666/aeer/1705_1103311044

Crop water use (CWU_{blue} and CWU_{green}) were derived by multiplying 10 with ET_{blue} and ET_{green}, respectively – *Equations 3* and *4* (Hoekstra et al., 2011). Ten is used to convert the unit of millimetre, mm to m^3.

$$CWU_{blue} = 10\sum_{d}^{lg\ p} ET_{blue} \quad \text{(Eq.3)}$$

$$CWU_{green} = 10\sum_{d}^{lg\ p} ET_{green} \quad \text{(Eq.4)}$$

Measurement of ET is laborious and time-consuming, hence CROPWAT model was used to simulate ET for each crop by using climate data and crop parameters based on Allen method (Allen, 1998).

Water footprint of crop consumption

The blue and green WF of each crop were evaluated (m^3/year) using bottom-up method (Hoekstra et al., 2011). The water footprint for each crop was estimated by multiplying the volume of crop consumption by water footprint of crops. The WF of crops was calculated using *Equation 5.*

$$WF_{cons,indir} = \sum_{p}^{n} (c[p] \times WF_{P[P]}) \quad \text{(Eq.5)}$$

where $C[P]$ refers to the volume of crop consumption of product p within Tehran (ton/year) and $WF_{pro[p]}$ is WF of crop production from originating region (m^3/ton).

Water saving and loss

Water saving through international crop trade was evaluated based on Champaign et al. method (2006). It was calculated by multiplying the volume of import of crops (ton y^{-1}) by the WF of the crops (m^3 $year^{-1}$) within Tehran. The inter-provincial water saving through inter-provincial trades was assessed using similar method. The water footprints of imported crops from abroad were obtained from Mekommen and Hoekstra (2011). The blue and green water losses were accounted as the water footprints of extra production exported to other regions.

Data

The volume of crop yield and crop production in Tehran and other provinces were obtained from the Ministry of Agriculture, Jahad, in Tehran. The climate data including minimum and maximum temperature, rainfall, sunshine, humidity, and wind speed were obtained from Mehrabad weather station. Rooting depth, critical depletion, yield response, crop height is obtained from OPTIWAT which were local data. Data for the volume of crop consumption and trade were obtained from Tehran's chambers of commerce, industries, mines and agriculture.

http://www.aloki.hu ● ISSN 1589 1623 (Print) ● ISSN 1785 0037 (Online)
DOI: http://dx.doi.org/10.15666/aeer/1705_1103311044

Results

Per capita (green and blue) WF of different crop consumption is shown in *Figure 3*. The per capita water footprint of wheat in 2010 had increased due to the increase in the volume of production within the Tehran province which held large volume of WF as compared to the external WF. Besides, WF of wheat consumption showed reduction trend due to the decrease of per capita wheat consumption. WF of rice consumption showed fluctuating trend as it depends on the volume of consumption which was fluctuating too. Besides that, rice consumption per person had decreased from 35 kg/cap in 2008 to 34 kg/cap in 2014.

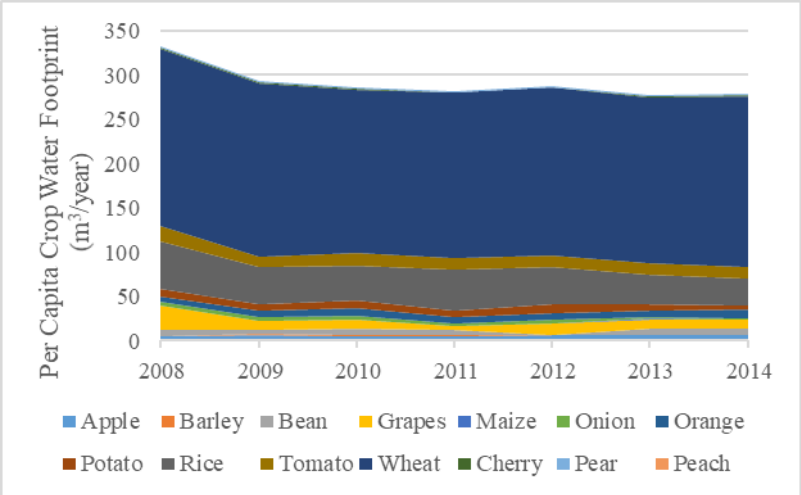

Figure 3. *Per capita water footprint of crop consumption (2008–2014)*

Figure 4 illustrates the total WF of crop consumption in Tehran province (2008–2014). It shows a declining trend in 2010 due to the decrease in the population of Tehran ever since Alborz province was separated from Tehran during the same year. Besides that, the per capita consumption of wheat and rice had also decreased.

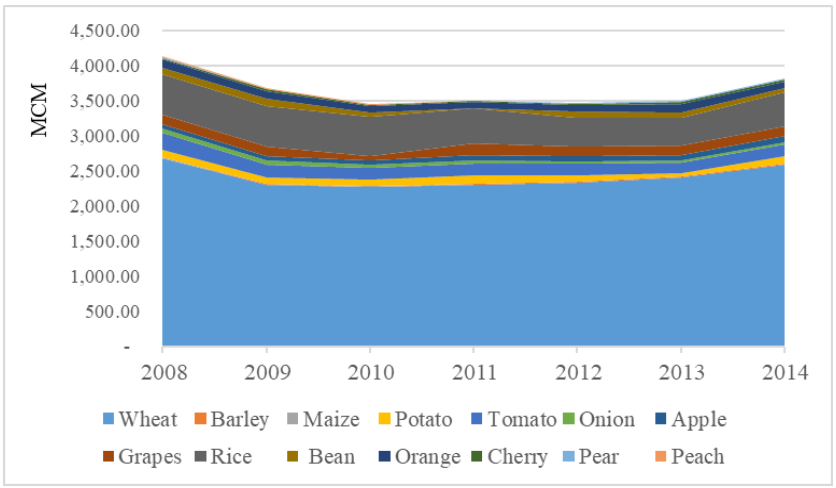

Figure 4. *The total WF of crop consumption in Tehran province (2008–2014)*

http://www.aloki.hu ● ISSN 1589 1623 (Print) ● ISSN 1785 0037 (Online)
DOI: http://dx.doi.org/10.15666/aeer/1705_1103311044

Figure 5 shows the internal and external WF of different crops in the Tehran province. Tehran province is independent of external WF in the production of apples, pears, peaches, and cherries. This means, Tehran province produced and consumed all of the produce. Besides, Tehran imported 2,848 billion m^3 of virtual water and consumed 377 million m^3 of internal water footprint in 2008. Tehran saved water resources by importing crops from other provinces and abroad. For example, most of the wheat consumption within Tehran is imported from the USA. Wheat and rice have the largest WF of consumption in Tehran province since both of them are consumed at a large scale.

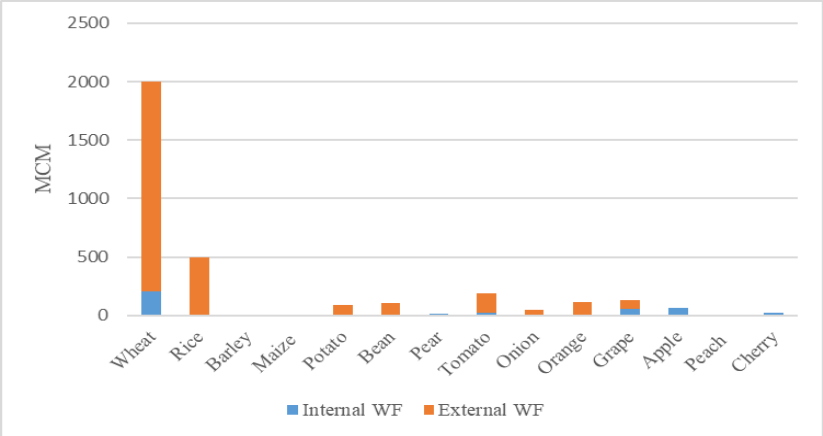

Figure 5. *Internal and external WF of crop consumption in Tehran province*

Figure 6 shows the average per capita WF of crop consumption in Tehran province. Wheat had the largest per capita WF (blue and green) amounting to 189 m^3/cap/year from 2008 to 2014. Next to wheat, rice had the largest per capita WF amounting to 46 m^3/cap/year. These were followed by tomatoes, potatoes, oranges, beans, apples, and grapes respectively. Cherries, pears, barley, peaches, and maize had low per capita WF.

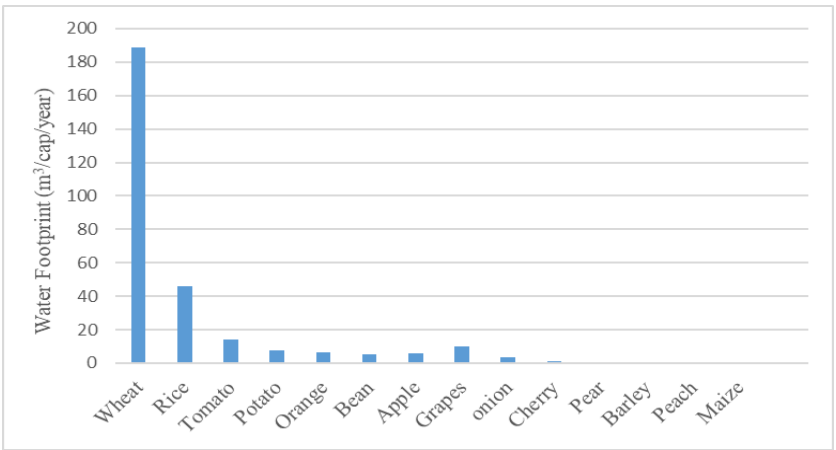

Figure 6. *The average per capita WF of different crops (2008–2014)*

http://www.aloki.hu ● ISSN 1589 1623 (Print) ● ISSN 1785 0037 (Online)
DOI: http://dx.doi.org/10.15666/aeer/1705_1103311044

Internal and external water footprint trend (2008–2014) is illustrated in *Figure 7*. Dependency on external WF had increased in 2010 when Alborz had separated from Tehran. Internal water footprint was a bit higher in 2014 which means water footprint in 2014 had increased. The external water footprint in 2014 was higher than 2008 because consumption of wheat had decreased.

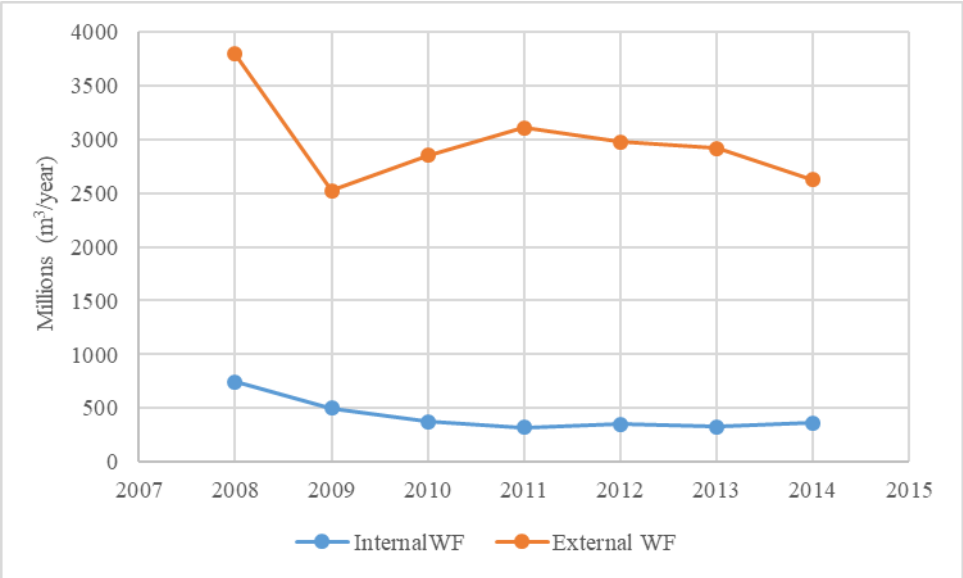

Figure 7. *The internal and external WF trend (2008–2014)*

Figure 8 shows the proportion of internal and external WF in Tehran province. Only 10% of Tehran's WF is attributed to internal WF. Most of the crops are produced outside of Tehran and exported into the Tehran province.

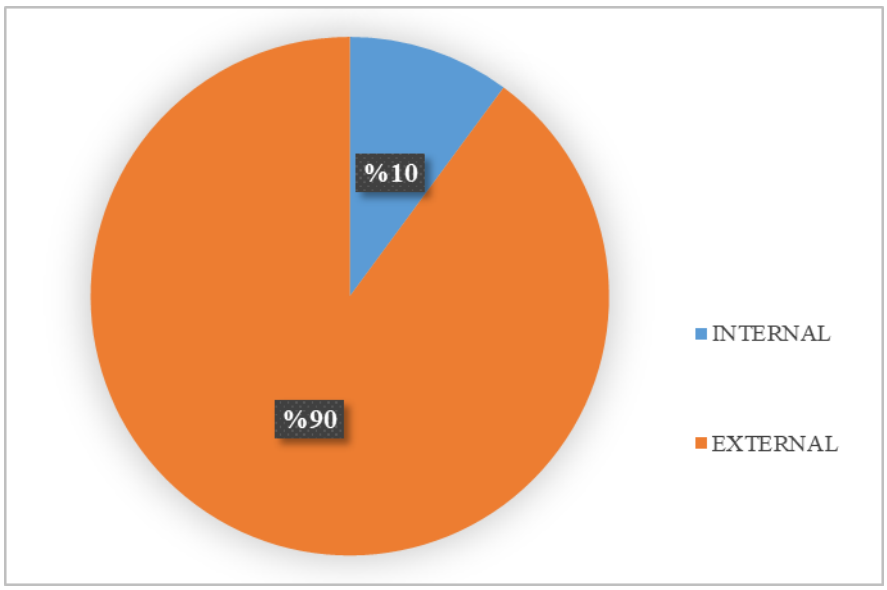

Figure 8. *The contribution of internal and external WF in Tehran's total WF*

http://www.aloki.hu ● ISSN 1589 1623 (Print) ● ISSN 1785 0037 (Online)
DOI: http://dx.doi.org/10.15666/aeer/1705_1103311044

Figure 9 shows the total water footprint of Tehran province in agricultural sector for selected crops; derived by summing up the internal and external WF. The internal and external WF amounted to 377 million m^3/year, and 2,848 billion m^3/year respectively. The total water consumption was 3,225 billion m^3/year. Blue WF accounted for the largest contribution of internal WF while green WF was the largest shareholder of external WF. By importing crops externally, there will be more saving for Tehran's blue WF.

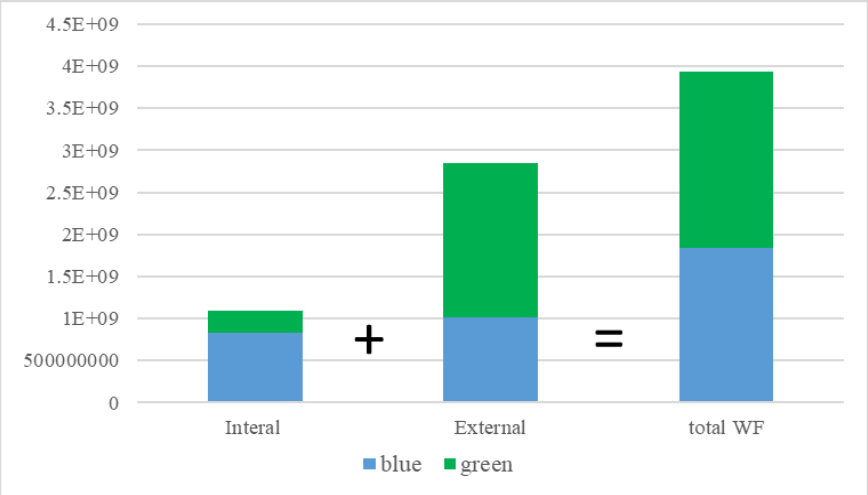

Figure 9. *The total WF in Tehran province*

Figure 10 shows the total blue and green water savings (WS) as a result of international and inter-provincial trades which have fluctuations. The blue water saving resulting from international trade had increased from 1.79 billion m^3 in 2010 to 1.9 billion in 2014 due to the increase in dependency on external WF. The total blue water saving from both international and inter-provincial crops had increased from 3,161 billion in 2008 to 3,234 billion m^3 in 2014.

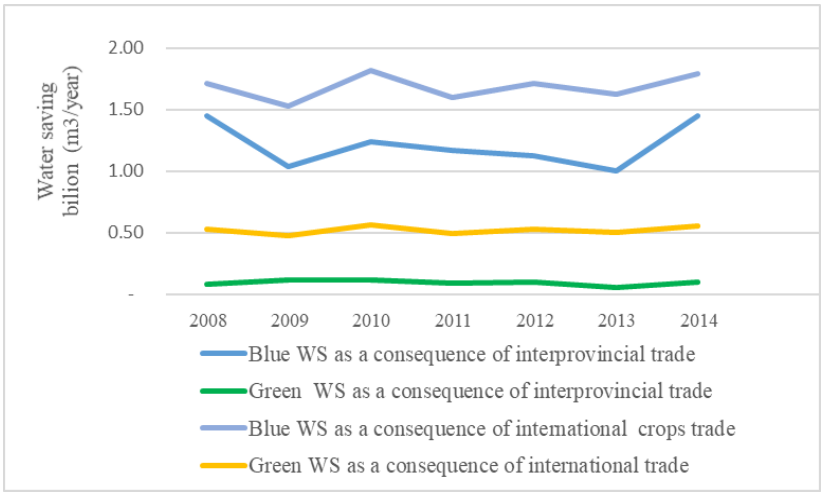

Figure 10. *Blue and green water saving as a result of international and inter provincial trade in Tehran (2008–2014)*

http://www.aloki.hu ● ISSN 1589 1623 (Print) ● ISSN 1785 0037 (Online)
DOI: http://dx.doi.org/10.15666/aeer/1705_1103311044

Blue WF per ton of crops in exporting countries are lower than Tehran as it has arid climate with high evapotranspiration. Blue water saving is increased as a result of international trade. On the other hand, green water saving is low because crop production within Tehran is mostly related to blue water footprint. Besides, green water footprint within the exporting region for all crops is larger than Tehran. Moreover, inter-provincial and international crop trades contribute to overall blue water saving.

Table 1 illustrates water savings from both international and national crop trades in 2008 and 2014. It shows that WS for wheat, potatoes, and onions in 2008 is lower than 2014 as the production of these crops within Tehran had increased. While WS for rice had decreased due to decline in the volume of rice consumption in 2014.

Table 1. *The water saving as a result of crops trade in Tehran Province (2008 and 2014)*

	WS as a result of crops trade (m^3/year)	**WS as a result of crops trade (m^3/year)**
	2008	**2014**
Wheat	2,237,927,587.50	2,343,328,030
Rice	1,111,524,117	993,982,416
Potato	83,311,520	103,726,320
Tomato	108,496,382	91,565,460
Onion	8,120,862	9927648
Grapes	219,463,024	147,818,440

Blue and green water losses in Tehran

Fig. 11 shows total blue water loss in Tehran province from 2008 to 2014. The total blue water loss had declined from 100 million m^3 in 2008 to 28 million m^3 in 2009 due to the reduction in production amount. Total green water loss had also decreased from 9 million m^3 in 2008 to 4 million m^3 in 2009. Moreover, Alborz province had been separated from Tehran during this time and most of the extra production came from pears and peaches of this province (2008). Then, blue water loss showed a fluctuating trend from 2009 to 2014 as it relies on the volume of extra production and the blue WF amount which are not stable. Blue water loss was larger than green water loss as the production of crops in Tehran relies on blue WF.

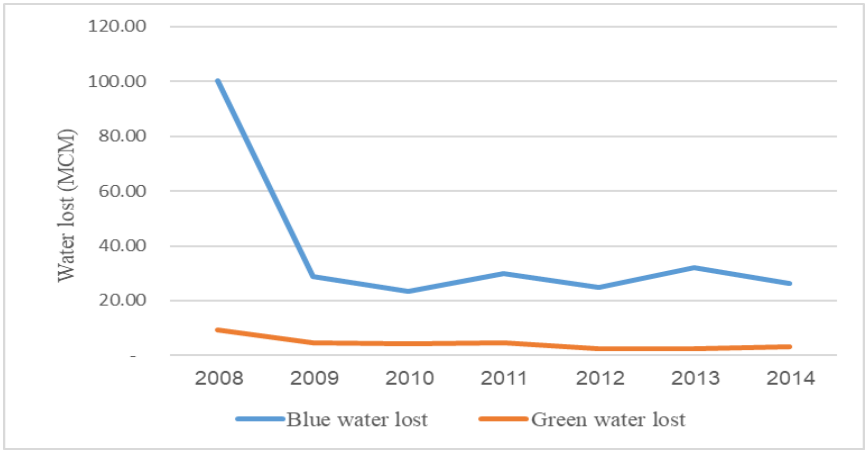

Figure 11. *The blue and green water lost (2008-2014)*

http://www.aloki.hu ● ISSN 1589 1623 (Print) ● ISSN 1785 0037 (Online)
DOI: http://dx.doi.org/10.15666/aeer/1705_1103311044

Discussion

Water footprint accounts for the volume of actual water consumption by humans. It is identified as an appropriate indicator for computing the impact of human activities on water resources. According to current research, there are four major factors impacting water footprint of crop consumption: (1) Population, (2) the volume of crop consumption, (3) the volume of internal production, (4) the external WF per ton of crop production. Besides that, water footprint of crop consumption in Tehran showed a reduction trend due to the increase in external WF. In the current study, per capita WF for wheat in Tehran was larger than evaluated by Hoekstra who has evaluated per capita WF at global scale. However, our result is different because this assessment is done at local scale. Besides, most of the wheat consumed in Tehran are imported from the USA which has low WF. Additionally, other studies have evaluated that water footprint of cereal crops in arid region of Iran was 397 m^3/capita/year which are relatively similar to our result (Karandish and Hoekstra, 2017).

The result indicates that crop production in Tehran has the largest WF compared to other countries, similar to Hoekstra's result who claims that water footprint of Iran is high due to low productivity and high evapotranspiration (Hoekstra and Chapagain, 2007; Fader et al., 2011).

The WF of crop consumption shows a reduction trend which disagrees with the result of Karandish who claims that WF of crop consumption for all provinces of Iran has increased because of population growth and increase in crop consumption (Karandish and Hoekstra, 2017). The WF consumption had decreased from 2008 to 2014 in Tehran province due to the increase in dependency on external WF and decrease in population. The reason for population decrease was Alborz separation from Tehran province in 2010**.**

Conclusion

This study shows Tehran's water self-sufficiency had decreased from 2008 to 2014. Furthermore, per capita WF of crop consumption had decreased due to the increase in dependency on external WF and decrease in population from 2008 to 2014. WF per ton of imported crop production was lower than Tehran because of climate condition. Besides, WF of crop consumption within Tehran is more strongly reliant on external WF. Tehran province has produced only 10 per cent of its crop consumption; it has been under severe water scarcity due to population and climate condition. Moreover, Tehran province can save water resources by importing crops from water-abundant areas. Tehran saved 3.23 billion m^3 of internal water resources through inter-provincial and international crop trade in 2014.

Total blue and green water losses had decreased from 2008 to 2014 due to reduction in the volume of extra production when Alborz was separated from Tehran province. Water loss depends on extra production that is exported to other regions. The decision makers should reduce the production of fruits for export purposes such as pears, peaches, and cherries because Tehran is under high groundwater stress with moderate surface water scarcity (Rezaei Kalvani et al., 2019). Additionally, production of cereal crops should be reduced as these crops consume high volume of blue water in Tehran due to climate condition.

Water footprint assessment can contribute to enhance water use efficiency in agricultural sector by providing useful information for decision makers. Besides, it is

http://www.aloki.hu ● ISSN 1589 1623 (Print) ● ISSN 1785 0037 (Online)
DOI: http://dx.doi.org/10.15666/aeer/1705_1103311044

crucial to apply developed technology and appropriate water management in order to enhance water use efficiency and lower water footprint per ton of crops to reduce per capita water footprint in Tehran.

The consumption of wheat in Iran is high; two times higher than global average. Change in food consumption habits contributes to increased food security at regional scale. It is recommended to reduce the consumption of wheat in Tehran or replace it with other crops. Besides, changing food consumption habits contributes to increase food security at a regional scale. It would also be helpful to assess the per capita water footprint of different dietary changes in the future water footprint assessment.

Acknowledgements. The authors would like to gratefully acknowledge Universiti Putra Malaysia (GP/2018/9592300) for supporting this research project.

REFERENCES

[1] Ababaei, B., Etedali, H. R. (2017): Water footprint assessment of main cereals In Iran. – Agricultural Water Management 179: 401-411.
[2] Allen, R. G. et al. (1998): Crop Evaporation Guideline for Computing Crop Water Requirements. – FAO Irrigation and Drainage Paper 56, FAO, Rome.
[3] Chen, W. et al. (2017): China's water footprint by province, and inter-provincial transfer of virtual water. – Ecological Indicators 74: 321-333.
[4] Fader, M. et al. (2011): Internal and external green-blue agricultural water footprints of nations, and related water and land savings through trade. – 1641-1660.
[5] Faramarzi, M. et al. (2010): Analysis of intra-country virtual water trade strategy to alleviate water scarcity in Iran. – Hydrology & Earth System Sciences Discussions 7(2): 1417-1433.
[6] Feng, L. et al. (2015): The driving force of water footprint under the rapid urbanization process: a structural decomposition analysis for Zhangye City in China. – Journal of Cleaner Production 163: S322-S328.
[7] Ge, L. et al. (2011): An Evaluation of China's Water Footprint. – Water Resources Management 25(10): 2633-2647.
[8] Gephart, J. A. et al. (2016): The environmental cost of subsistence: optimizing diets to minimize footprints. – Science of the Total Environment 553: 120-127.
[9] Hoekstra, A. Y. et al. (2011): The Water Footprint Assessment Manual. Setting the Global Standard. – Earthscan, London.
[10] Hoekstra, A. Y., Chapagain, A. K. (2007): Water footprints of nations: water use by people as a function of their consumption pattern. – Water Resources Management 21(1): 35-48.
[11] Hoekstra, A. Y., Mekonnen, M. M. (2011): The water footprint of humanity. – Proceedings of the National Academy of Sciences 109(9): 3232-3237.
[12] Hosseinian, S. M. and Nezamoleslami, R. (2018): Water footprint and virtual water assessment in cement industry : a case study in Iran. – Journal of Cleaner Production 172: 2454-2463.
[13] Karandish, F., Hoekstra, A. Y. (2017): Informing national food and water security policy through water footprint assessment : the case of Iran. – Water 9(11): 831.
[14] Madani, K. (2014): Water management in Iran: what is causing the looming crisis? – Journal of Environmental Studies and Sciences 4: 315-328.
[15] Okadera, T. et al. (2015): Evaluating the water footprint of the energy supply of Liaoning Province, China: a regional input-output analysis approach. – Energy Policy 78: 148-157.

http://www.aloki.hu ● ISSN 1589 1623 (Print) ● ISSN 1785 0037 (Online)
DOI: http://dx.doi.org/10.15666/aeer/1705_1103311044

[16] Qian, Y. et al. (2018): Water footprint characteristic of less developed water-rich regions: Case of Yunnan, China. – Water Research 141: 208-216.
[17] Rezaei Kalvani, S. et al. (2019): Assessing ground and surface water scarcity indices using ground and surface water footprints in the Tehran province of Iran. – Applied Ecology and Environmental Research 17(2): 4985-4997.
[18] Wu, L. (2014): Analysis of water sustainable utilization in Changsha city based on water footprint theory. – Applied Mechanics and Materials 694: 532-535.
[19] Yousefi, H. et al. (2017): Virtual water evaluation for grains products in Iran. Case study: pea and bean. – Journal of Water and Land Development 35(1): 275- 280.
[20] Zhao, G. et al. (2018): Provincial water footprint in China and its critical path. – Ecological Indicators 105: 634-644.
[21] Zhuo, L., Mekonnen, M. M., Hoekstra, A. Y. (2016): Consumptive water footprint and virtual water trade scenarios for China - with a focus on crop production, consumption and trade. – Environment International 94: 211-223.

http://www.aloki.hu ● ISSN 1589 1623 (Print) ● ISSN 1785 0037 (Online)
DOI: http://dx.doi.org/10.15666/aeer/1705_1103311044

ECOLOGICAL AGRICULTURE DEVELOPMENT AND SPATIAL AND TEMPORAL CHARACTERISTICS OF CARBON EMISSIONS OF LAND USE

SUN, Q. – LIAO, B. – TAO, Q. Y.*

Management College, Beijing Union University, Beijing 100101, China

**Corresponding author*
e-mail: qytaomail@163.com

(Received 1st Apr 2019; accepted 13th Jun 2019)

Abstract. With the continuous development of society, the agricultural economy has shown a good development trend, but at the same time it has produced more and more carbon emissions, and the greenhouse effect has increased, posing a threat to the ecological environment. Agricultural carbon emissions are important factors. Therefore, studying the temporal and spatial characteristics of agricultural carbon emissions is an urgent task. This paper focused on agricultural carbon emissions from land use and tested and predicted future carbon emissions based on three types of carbon source factors using the auto regressive integrating moving average (ARIMA) model. The spatial and temporal characteristics of agricultural carbon emissions were analyzed from the dimension of time and space. According to the results, the total agricultural carbon emission and intensity of the eastern region ranked the first, followed by the middle region; the total agricultural carbon emission of different regions increased, but slower; the agricultural carbon emission intensity of different regions decreased, and overall decreased faster. This study effectively verifies the deep influence of the development of ecological agriculture on the spatial and temporal characteristics of carbon emission of land use.
Keywords: *ecological environment, carbon source factor, temporal sequence prediction, economic system, temporal and spatial characteristics*

Introduction

In the process of agricultural economic development, the impact of land use change on greenhouse gas emissions has become a core issue in today's carbon cycle research. With the emergence of these phenomena, a series of social and environmental problems have arisen, and the situation of agricultural development is very worrying. Therefore, research on the temporal and spatial characteristics of carbon emissions of land use is extremely urgent (Simmons and Matthews, 2016). In response to this problem, many experts and scholars have put forward their own opinions. Zhang and Fang (2013) effectively assessed and predicted agricultural carbon emissions based on six relevant aspects of agricultural carbon sources, put forward the research method of decomposition factor based on kaya model, and found that the rapid development of agricultural economy increased carbon emission. Liu et al. (2014) proposed a model which was composed of gray model (GM) (1,1) model, auto regressive integrating moving average (ARIMA) model and second order polynomial regression (SOPR) model to predict and analyze the carbon emission intensity of carbon dioxide. Han et al. (2018) believed that there was an inevitable connection between agricultural carbon emissions and agricultural economic growth and put forward the study of the coupling and decoupling effects of agricultural carbon emissions and their driving factors. Chuai et al. (2015) believed that the change of land use type would not only directly affect the carbon stocks in terrestrial ecosystems, but also had an indirect impact on the frequent occurrence of anthropogenic carbon emissions in coastal areas. Therefore, a linear

http://www.aloki.hu ● ISSN 1589 1623 (Print) ● ISSN 1785 0037 (Online)
DOI: http://dx.doi.org/10.15666/aeer/1705_1104511053

programming model was proposed to improve the land use structure and achieve the goal of low carbon emissions. Gong and Chen (2011) analyzed the status of carbon emissions and proposed suggestions of land use regulation based on low-carbon emissions: setting up and optimizing land ecological compensation mechanisms, etc., which is conducive to promoting carbon emission reduction and protecting the ecological environment. In this study, the agricultural carbon emission was analyzed and predicted based on the three kinds of carbon source factors of agricultural carbon emission and ARIMA model, and the spatiotemporal distribution characteristics of agricultural carbon emissions were clearly illustrated. This work provides a reference for the development of ecological agriculture in China.

Materials and methods

Development of ecological agriculture

Agriculture is the foundation of a country's foothold, which realizes the basic material data needs of human beings by converting biology into solar energy. While the efficiency of agricultural production is constantly improving, the ecological environment has been sacrificed, which has caused great threats to human beings. In order to slow down the severity of this phenomenon, a scientific and standardized ecological agriculture has been emerged. Ecological agriculture refers to a modern agricultural development mode which combines systematic engineering methods with modern scientific achievements, strictly follows the growth law of ecological economy, is based on the basic principles of ecology, and has the intention of protecting and improving agricultural ecological environment (Wu et al., 2015). It is a project involving multiple aspects, such as economic science and natural science (Onofrei et al., 2016).

The most important feature of eco-agricultural production is ecological character, in which the effect of protecting the ecological environment is significant, but the production efficiency is not very high when the input cost is high. The purpose of eco-agriculture development include protecting the ecological environment and promoting high-productivity and high-ecological double harvest. Therefore, a sustainable, scientific and efficient agricultural development model was developed by combining ecological agriculture with China's national conditions and using modern scientific management tools, and moreover the advantages of every area are taken as the emphatically developed agricultural projects to implement regional eco-agricultural construction, which can effectively protect ecological environment while obtaining large economic benefits and promote the harmonious development of society.

Carbon emissions of land use

Applying land to different application areas, such as planting crops, raising livestock, developing waters, and building high-rise buildings, will result in different types of land use, and changes in land use will have different carbon emission effects. The so-called land-use carbon emissions refers to the carbon dioxide released by changes in the field of land application and people on the land in their production and life (Fu et al., 2017), in a direct or indirect way. Direct carbon emissions represents carbon emissions from changes in land use cover and land management concepts and methods; indirect carbon emissions represents carbon emissions of human activities in different types of land use

http://www.aloki.hu ● ISSN 1589 1623 (Print) ● ISSN 1785 0037 (Online)
DOI: http://dx.doi.org/10.15666/aeer/1705_1104511053

(Kato and Yamagata, 2014). Carbon emission of land use is expressed as E *(t)*, the carbon emission of type a land use is expressed as e_a *(t)*, the area of type a land use is expressed as S_a *(hm^2)*, and the carbon emission coefficient of type a land use *(t/hm^2)* is expressed as δ_a. Then the computational formula of carbon emission of different types of land use is:

$$E = \sum e_a = \sum S_a \delta_a \quad \text{(Eq.1)}$$

Agricultural carbon emission is an important part of carbon emission of land use. Therefore, this study investigated carbon emission of land use by focusing on agricultural carbon emission. Agricultural carbon emission is mainly analyzed through three types of carbon source factors, including carbon emission of agricultural land use, carbon emission of paddy fields, and carbon emission of livestock farming (Han et al., 2018). The carbon emission of agricultural land use mainly include carbon emission of chemical products such as pesticides, agricultural film and chemical fertilizers, organic carbon emission produced by the damage of ploughing activities to soil organic carbon pool, and carbon emission produced by electric energy loss and loss of energy such as diesel during farming by agricultural machinery. Specific carbon sources include pesticide inputs and their changes, fertilizer inputs and their changes, agricultural irrigation inputs and their changes, agricultural land cultivation methods and their changes, and agricultural machinery products inputs and changes (Ismael et al., 2018). Carbon emissions from paddy field planting mainly include carbon emission from rice planting in different growth cycles, early rice, late rice and mid-season rice. The main carbon sources in livestock farming are intestinal fermentation of livestock and poultry and livestock manure (Asumadu-Sarkodie and Owusu, 2017).

Spatial distribution

Through the collection and sorting of relevant data on agricultural carbon emissions, the agricultural carbon emission areas are generally divided into four levels, including low agricultural carbon emission areas, medium agricultural carbon emission areas, slightly high agricultural carbon emission areas and high agricultural carbon emission areas. It can be seen from *Fig. 1* that the high agricultural carbon emission areas are mainly distributed in provinces such as Sichuan, Shandong, Jiangsu, Anhui, Hunan and Hubei, the slightly high agricultural carbon emission areas are mainly distributed in provinces such as Inner Mongolia, Heilongjiang, Yunnan, Guangdong and Jiangxi, the medium agricultural carbon emission areas are mainly distributed in provinces such as Gansu, Shaanxi, Zhejiang, Fujian, Jilin and Liaoning, and the low agricultural carbon emission areas are mainly distributed in provinces such as Qinghai, Shanxi and Hainan (Pang and Zhao, 2013). The agricultural carbon emissions of the eastern region account for a large proportion, followed by the central region and western region, which has a great relationship with factors such as climate, economy and environment. The change of every factor will produce different agricultural phenomena and development effects. As the eastern region has good climatic conditions, excellent economic environment and fast agricultural development, the proportion of the agricultural carbon emission of the eastern region is larger than that of the other two regions.

Relevant data on agricultural carbon emissions in the eastern, central and western regions in 2015 were collected and sorted, and experimental results were obtained based

http://www.aloki.hu ● ISSN 1589 1623 (Print) ● ISSN 1785 0037 (Online)
DOI: http://dx.doi.org/10.15666/aeer/1705_1104511053

on the algorithm of agricultural carbon emissions. The experimental data mainly consisted of carbon emissions generated by different chemical products in agricultural land use, carbon emissions generated by the rice planting process in different periods, carbon emissions generated by livestock breeding and total agricultural carbon emission. Moreover deep study was carried out to analyze the spatial difference characteristics of different regions in the dimension of space, and corresponding experimental conclusions were obtained.

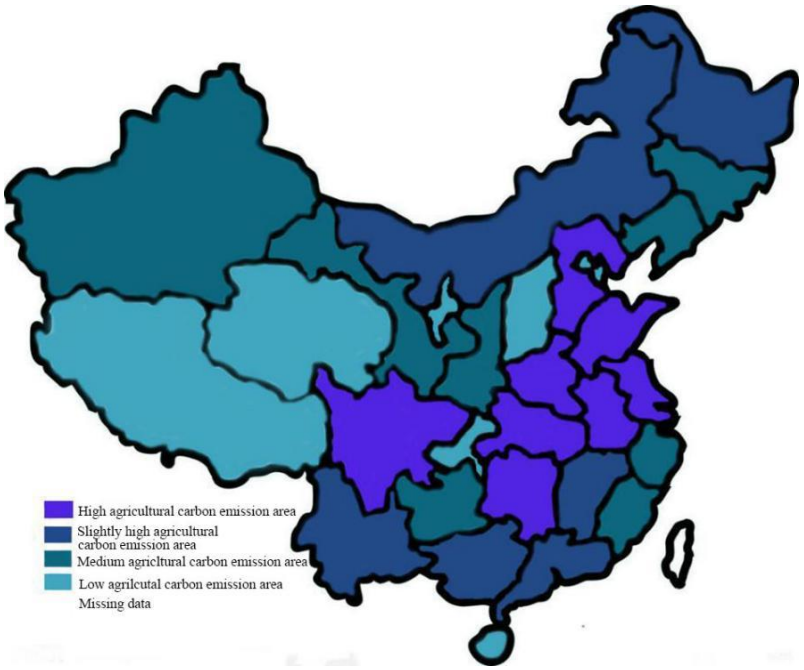

Figure 1. *Spatial distribution characteristics of China's agricultural carbon emissions*

Temporal distribution

Methods for analyzing the temporal sequence characteristics of agricultural carbon emissions

With the rapid development of the agricultural economy, China's agricultural carbon emissions are generally on the rise, and the government's agricultural policy has always placed food security as a top priority to meet China's demand for food. In 2004, the relevant government departments promulgated a number of policies conducive to the agricultural economy and did not forget to promote the development of agriculture while making rapid progress in society. In 2006, the government completely abolished the agricultural tax to promote the enthusiasm of farmers. However, in the environment of rapid development of agriculture and with the continuous improvement of production efficiency, a series of negative phenomena have emerged, such as the sacrifice of the ecological environment; hence the government has paid more and more attention to the protection of the ecological environment. In 2007, the 17th National Congress of the Communist Party of China was fully convened, and the importance of protecting the ecological environment was strongly emphasized. So far, ecological agriculture has continued to develop, and the business philosophy has been moving closer to scientific and normative. The various factors will affect the changes in agricultural carbon

http://www.aloki.hu ● ISSN 1589 1623 (Print) ● ISSN 1785 0037 (Online)
DOI: http://dx.doi.org/10.15666/aeer/1705_1104511053

emissions, mainly reflected in the characteristics of time distribution. Therefore, this paper studied the temporal and spatial sequence characteristics of agricultural carbon emissions from the total amount and intensity of agricultural carbon emissions.

Data on agricultural carbon emissions in the eastern, central and western regions from 2012 to 2018 were collected and sorted, and the corresponding calculation was made to obtain experimental results. Moreover, the simulation experiment of prediction was made using EViews9.0. The corresponding ARIMA model was established. A time series was established and tested. Then the relevant parameters of the model were compared, diagnostic test was made, and the total amount and intensity of agricultural carbon emissions from 2019 to 2025 was predicted. The corresponding verification results were obtained, and the temporal distribution characteristics of agricultural carbon emissions in the eastern, central and western regions were analyzed, and the corresponding experimental conclusions were obtained for reference.

Prediction of agricultural carbon emissions

Agricultural carbon emissions in the eastern, central and western regions from 2019 to 2025 were predicted using ARIMA model. The model can be used for time series prediction. It is established by transforming the non-stationary time series into the stationary time series, regressing the lag value, and implementing the regression operation on the present value and the lag value of the random error term. In ARIMA(p,d,q), p is autoregressive item, q is the number of moving average items, d is the number of differences made when the time series is converted to be stationary, ε_t is a stationary time series, and u_t is the residual white noise sequence, and ϕ_m and θ_m $(i = 1,2,\cdots, p, m = 1,2,3,\cdots, q)$ are ε_t and the parameter of ε_t. The calculation formula is:

$$\varepsilon_t = c + \phi\varepsilon_{t-1} + \phi\varepsilon_{t-2} + \cdots + \phi_p\varepsilon_{t-p} + u_t + \theta_1 u_{t-1} + \theta_2 u_{t-2} + \cdots + \theta_q u_{t-q} \qquad \text{(Eq.2)}$$

The prediction steps are as follows. Firstly, the original sequence *ADF* was tested and verified. If there was a unit root, then in order to make it meet the stability conditions, *d*-order differential operation was made on the initial sequence. Then the correlation study was made on the characteristics of sequence after differential operation. Moreover the values of p and q were obtained through the autocorrelation function and partial autocorrelation function graphs of sequence. Dependent variable *AR(p)* and *MA(q)* were estimated by least square estimation or maximum likelihood estimation. Diagnostic test was performed on the residual of the mode. Finally the data of agricultural carbon emission was predicted.

Results

Analysis of spatial characteristics of carbon emission

The spatial characteristics of agricultural carbon emissions in the eastern, central and western regions in 2015 were analyzed, and the results are shown in *Table 1* (unit: tens of tons).

It can be seen from *Table 2* that the carbon emissions of agricultural land use in the eastern and central regions accounted for the largest proportion, followed by the carbon emission of paddy field planting and livestock breeding. The carbon emission of

http://www.aloki.hu ● ISSN 1589 1623 (Print) ● ISSN 1785 0037 (Online)
DOI: http://dx.doi.org/10.15666/aeer/1705_1104511053

livestock farming in the western region accounted for the largest proportion, followed by the carbon emission of agricultural land use and paddy field planting. In general, there were differences between regions. The eastern and central regions have high land utilization rate because of the large area of plains, and the climatic conditions for rice planting are good; therefore the carbon emissions of agricultural land use and paddy field planting were high. The western region has low land utilization rate because of the high altitude. Moreover the climate conditions for rice planting are bad. But the broad meadow resources are suitable for the breeding of livestock such as cattle and sheep. Therefore the carbon emissions of livestock breeding in the western region was high.

Table 1. *Spatial differences in agricultural carbon emissions in the eastern, central and western regions*

	Carbon emission of agricultural land use	Carbon emission of paddy field planting	Carbon emission of livestock breeding	Total agricultural carbon emission
The eastern region	12078.36	7512.98	3498.35	23089.69
The central region	8102.98	5236.12	3857.26	17196.36
The western region	5423.78	3012.56	7932.84	16369.18

Table 2. *Temporal differences of agricultural carbon emissions in the eastern, central and western regions*

Year	Total of eastern	Total of central	Total of western	Intensity of eastern	Intensity of central	Intensity of western
2012	10023.69	8523.56	7123.89	57.98	53.98	47.26
2013	15756.19	12619.55	12036.25	56.78	52.19	46.96
2014	20523.56	16169.63	15369.36	55.78	51.06	45.02
2015	23089.69	17196.36	16369.18	54.06	50.97	43.46
2016	23965.36	18636.78	16987.16	49.87	47.56	40.12
2017	24579.63	19369.43	17693.98	45.99	43.99	37.98
2018	25969.36	20869.58	18996.78	37.02	36.09	32.13

In 2015, the total amount of agricultural carbon emissions in the eastern region ranked the first, followed by the central region. The total amount of agricultural carbon emission in the western region was the smallest compared with the other two regions, and the differences between the regions were large. The eastern region, compared with the central and western regions, has superior economic environment, larger scale of agriculture and higher modern technology level, which makes agricultural carbon emissions increase; therefore, the total amount of agricultural carbon emissions was the largest. In comparison, the western region had the poorest condition in those aspects; hence the total agricultural carbon emission was the smallest.

Analysis of temporal characteristics of carbon emission

The temporal characteristics of agricultural carbon emissions in the eastern, central and western regions from 2012 to 2018 were analyzed, and the results are shown in *Table 2* (unit of the total carbon emission: ten thousand tons; unit of carbon emission intensity: kg/mu).

http://www.aloki.hu ● ISSN 1589 1623 (Print) ● ISSN 1785 0037 (Online)
DOI: http://dx.doi.org/10.15666/aeer/1705_1104511053

It can be seen from *Table 2* that the total amount of agricultural carbon emissions in the eastern, central and western regions was generally on the rise from 2012 to 2018, because the scale of agriculture in each region was expanding and the industrial technology was effectively improved. However, the growth rate of the total carbon emissions has slowed down, and the phenomenon of agricultural carbon emission has improved, which is because that China's agricultural policy is constantly adjusted, the popularization rate of ecological agriculture management concept has been greatly improved, and the development mechanism of ecological agriculture has been continuously optimized and improved.

From 2012 to 2018, the carbon emission intensity in the eastern, central and western regions showed a downward trend. Moreover, it can be seen that the decline amplitude in carbon intensity in different regions became larger, which is because that the government tends to pay more attention to environmental protection and release low-carbon agriculture related policies and the mechanism of ecological agriculture becomes more and more scientific.

Prediction of agricultural carbon emissions

A simulation experiment was conducted on the total amount and intensity of agricultural carbon emissions in the eastern, central and western regions from 2019 to 2025, and the results are shown in *Table 3* (unit of the total carbon emission: ten thousand tons; unit of carbon emission intensity: kg/mu).

As can be seen from *Table 3*, from 2019 to 2025, the total amount of agricultural carbon emissions in the eastern, central and western regions increased, but the magnitude tended to be gentle. The gentle increase is because that the continuous development of ecological agriculture has promoted the development of low-carbon economy, and the agricultural management concept is moving closer to the new mode of low input and high production. But the pace of developing the agricultural economy cannot be stopped; therefore, the agricultural carbon emissions has an increase.

Table 3. *Prediction of agricultural carbon emissions in the eastern, central and western regions*

Year	Total of eastern	Total of central	Total of western	Intensity of eastern	Intensity of central	Intensity of western
2019	26001.36	22009.39	20012.96	37.01	35.94	32.06
2020	27098.35	24005.98	22080.45	36.96	35.69	31.96
2021	28809.36	25065.12	23601.78	36.75	35.36	31.65
2022	29500.96	25956.45	24806.95	36.19	35.02	31.08
2023	29769.36	26963.47	25102.69	35.32	34.01	30.56
2024	30002.23	27965.15	25672.63	34.59	33.09	29.56
2025	30400.79	28137.65	26012.73	32.01	31.01	28.46

The intensity of agricultural carbon emissions in the eastern, central and western regions generally declined, and the decline amplitude became larger. The reason is that the change of agricultural policy has made the concept of eco-agriculture economy more and more popular and more and more attention is paid to the protection of the ecological environment during the development of agricultural economy, which makes the intensity of agricultural carbon emission low.

http://www.aloki.hu ● ISSN 1589 1623 (Print) ● ISSN 1785 0037 (Online)
DOI: http://dx.doi.org/10.15666/aeer/1705_1104511053

Generally speaking, with the rapid development of China's eco-agriculture and the high popularity of the concept of protecting the ecological environment, the severe phenomenon of China's agricultural carbon emissions will continue to improve, especially in the aspects of agricultural carbon emission amount and intensity. The improvement of agricultural carbon emissions will affect the carbon emissions of land use, and moreover the ecological agricultural economic system will continue to be optimized to promote the healthy development of agriculture.

Conclusion

With the rapid development of the agricultural economy, the ecological environment has deteriorated and the carbon emissions of agriculture have increased. Therefore, the research on the temporal and spatial characteristics of land use carbon emissions has developed into an important research topic. Studying this topic can grasp the temporal and spatial characteristics of agricultural carbon emissions in various regions and help effectively optimize and improve the relevant mechanisms of agricultural carbon emissions. This paper mainly focused on agricultural carbon emissions among carbon emissions of land use, compared and analyzed the three types of carbon source factors based on agricultural carbon emissions, analyzed the spatial and temporal characteristics of agricultural carbon emissions in the eastern, central and western regions, and established an ARIMA model. The total amount and intensity of agricultural carbon emissions in the western, central and middle regions were predicted and analyzed. It was found that the total carbon emission amount and intensity in the eastern region were the highest, followed by the central region, the total agricultural carbon emissions of all the regions increased, but in a gentle amplitude, and the agricultural carbon emission intensity of all the regions decreased in a fast speed. The study of the spatial and temporal characteristics of carbon emissions of land use is conducive to promoting the efficient development of ecological agriculture in the future.

REFERENCES

[1] Asumadu-Sarkodie, S., Owusu, P. A. (2017): The causal nexus between carbon dioxide emissions and agricultural ecosystem–an econometric approach. – Environ Sci Pollut Res Int 24(2): 1608-1618.

[2] Chuai, X., Huang, X., Wang, W., Zhao, R., Zhang, M., Wu, C. (2015): Land use, total carbon emissions change and low carbon land management in Coastal Jiangsu, China. – Journal of Cleaner Production 103: 77-86.

[3] Fu, B., Wu, M., Che, Y., Yang, K. (2017): Effects of land-use changes on city-level net carbon emissions based on a coupled model. – Carbon Management 1-18.

[4] Gong, B., Chen, B. (2011): The Regulation Analysis of Low-Carbon Orientation for China Land Use. – Computer & Computing Technologies in Agriculture IV: 602-609.

[5] Han, H., Zhong, Z., Guo, Y., Xi, F., Liu, S. (2018): Coupling and decoupling effects of agricultural carbon emissions in China and their driving factors. – Environmental Science & Pollution Research International 2018(9): 1-14.

[6] Ismael, M., Srouji, F., Boutabba, M. A. (2018): Agricultural technologies and carbon emissions: evidence from Jordanian economy. – Environmental Science and Pollution Research 25(11): 10867-10877.

http://www.aloki.hu ● ISSN 1589 1623 (Print) ● ISSN 1785 0037 (Online)
DOI: http://dx.doi.org/10.15666/aeer/1705_1104511053

[7] Kato, E., Yamagata, Y. (2014): BECCS capability of dedicated bioenergy crops under a future land-use scenario targeting net negative carbon emission. – Earth's Future 2(9): 421-439.
[8] Liu, L., Zong, H., Zhao, E., Chen, C., Wang, J. (2014): Can China realize its carbon emission reduction goal in 2020: From the perspective of thermal power development. – Applied Energy 124: 199-212.
[9] Onofrei, V., Teliban, G. C., Balan, C. B., Ropotoaia, I., Buburuz, A. A., Clinciu-Rad, R. A., Robu, T. (2016): Necessity, Desirability and Importance of Ecological Agriculture in the Context of Medicinal Plants Cultivation. – Bulletin of University of Agricultural Sciences and Veterinary Medicine Cluj-Napoca. Agriculture 73(1).
[10] Pang, L., Zhao, J. (2013): An Empirical Study on China's Regional Carbon Emissions of Agriculture. – International Journal of Asian Business and Information Management (IJABIM) 4.
[11] Simmons, C. T., Matthews, H. D. (2016): Assessing the implications of human land-use change for the transient climate response to cumulative carbon emissions. – Environmental Research Letters 11(3): 035001.
[12] Wu, H., Zhang, Y., Yuan, Z., Gao, L. (2015): A review of phosphorus management through the food system: identifying the roadmap to ecological agriculture. – Journal of Cleaner Production S095965261501001X.
[13] Zhang, Y., Fang, G. (2013): Research on Spatial-Temporal Characteristics and Affecting Factors Decomposition of Agricultural Carbon Emission in Suzhou City, Anhui Province, China. – Applied Mechanics and Materials 291-294: 1385-1388.

http://www.aloki.hu ● ISSN 1589 1623 (Print) ● ISSN 1785 0037 (Online)
DOI: http://dx.doi.org/10.15666/aeer/1705_1104511053

CHINESE FIR (*CUNNINGHAMIA LANCEOLATA*) A GREEN GOLD OF CHINA WITH CONTINUES DECLINE IN ITS PRODUCTIVITY OVER THE SUCCESSIVE ROTATIONS: A REVIEW

FAROOQ, T. H.[1,2,3] – YAN, W.[3] – RASHID, M. H. U.[1,2] – TIGABU, M.[4] – GILANI, M.M.[1,2] – ZOU, X. H.[1,2] – WU, P.F.[1,2*]

[1]*Forestry College, Fujian Agriculture and Forestry University, Fuzhou, 350002 Fujian Province, PR China*

[2]*Fujian Provincial Colleges and University Engineering Research Center of Plantation Sustainable Management, Fuzhou, 350002 Fujian Province, PR China*

[3]*National Engineering Laboratory for Applied Technology of Forestry and Ecology in South China, Central South University of Forestry and Technology, Changsha, 410000 Hunan Province, PR China*

[4]*Southern Swedish Forest Research Center, Faculty of Forest Science, Swedish University of Agricultural Sciences, PO Box 49, SE-230 53 Alnarp, Sweden*

**Corresponding author*
e-mail: fjwupengfei@126.com, fjwupengfei@fafu.edu.cn; phone/fax: + 86-591-8378-0261

(Received 1st Apr 2019; accepted 19th Jun 2019)

Abstract. Chinese fir (*Cunninghamia lanceolata*) is a prized timber species, which is grown in China from more than a thousand years. According to 8th national forest inventory data, Chinese fir plantations area expanded over an area of 11 million hectares, which occupies almost 18.2% area of all plantations in China principally in southern China. Successive rotations with clear cutting have become a common practice for Chinese fir plantations. These management practices on continues bases have led to a declining in yield production. Therefore, a serious concern has been raised on the Chinese fir plantations less yield and long-term productivity decline, particularly about the current rotation regime. In this review, we discussed the general causes of Chinese fir productivity decline and their effective solution. In forest conservation, the decline in soil quality is a serious ecological problem and recalcitrant litter, monoculture planting has aggravated the mechanism of soil degradation in Chinese fir plantations. The deteriorated soil properties in Chinese fir plantations were well mirrored in the reduction of plantation growth. Traditional plantation method of successive rotation without the period of fallow and management system of clear cutting, complete ploughing, burning of site and residues removal could be blamed for site degradation resulting in the poor growth and productivity decline of Chinese fir plantations. Complete burning and clear-cutting can lead to soil degradation by the loss of nutrients and organic matter. Therefore, a comprehensive knowledge of Chinese fir in terms of low productivity causes and solutions will allow us better forest management strategies and better development of plantation and afforestation throughout China.
Keywords: *productivity, soil quality, soil degradation, forest conservation, Chinese fir, China*

Introduction

Plantation forests are the significant part of the forest ecosystems of China (*Fig. 1*), and Chinese fir (*Cunninghamia lanceolata* (Lamb) Hook) is one of most planted species in these plantation forests. It is a typical evergreen sub-tropical conifer with high timber yield, excellent timber quality, and fast growth. It is the third most commonly planted species in plantation forests worldwide (State Forestry Administration, 2010). Chinese fir is often used in the provision of the ecosystem as well as inorganic matter storage. It

http://www.aloki.hu ● ISSN 1589 1623 (Print) ● ISSN 1785 0037 (Online)
DOI: http://dx.doi.org/10.15666/aeer/1705_1105511067

is characterized by its fast growth rate when grown in a monoculture plantation, producing volumes of up to 450 m^3/ha after 25 years (Wang et al., 2014). Its timber accounts for 24% of China's national commercial timber production (FAO, 2007). Fast growing species, along with the quick economic returns also provide the opportunity to mitigate the climate change by sucking the big carbon emissions, which had a significant impact on global climate (Yang et al., 2005). Since 1949, due to afforestation policies area under Chinese fir plantations increased nearly tripled (Li et al., 2013).

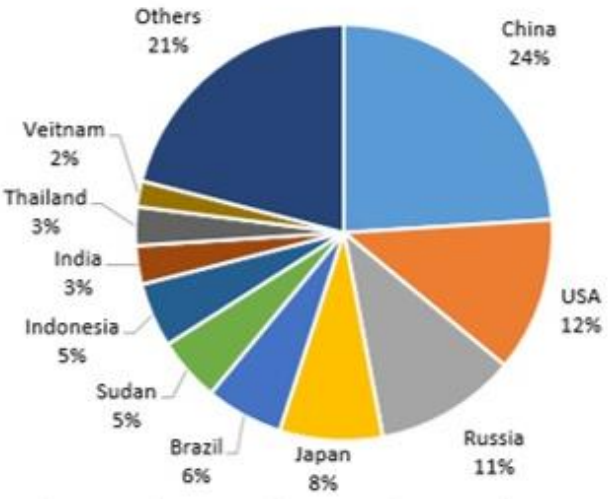

Figure 1. *Distribution of plantations forests worldwide (FAO, 2007)*

As one of the most important subtropical coniferous species, Chinese fir plantations have been using across China for more than one thousand years, especially in southern China (Wu, 1984). China gradually increased its area under plantations since the 1970s (Yu, 1997) and southern China have the highest percentage (54.3%) of forests primarily the plantations (Wang et al., 2014). According to 8th national forest inventory, data indicates that Chinese fir plantations expand over an area of 11 million hectares which occupies almost 18.2% area of all plantations in China and 6% worldwide (FAO, 2015; State Forestry Administration, 2014).

Since the 1980s, the cultivated area under Chinese fir plantations has been expanded from disconnected patches to large plantations (hills to high mountains) to meet the growing need (Ma et al., 2002). Majority of the Chinese fir plantations are monoculture and increasing timber demand resulted in shorter rotations (15 years) without the period of fallow (Bi et al., 2007; Tian et al., 2011). Successive rotations with clear cutting have become a common practice (Hu et al., 2014; Ma et al., 2007). These management practices on continues bases have led to declining in yield production along with soil degradation due to below-ground resources loss (nutrient loss) and accumulation of toxic substances (Chen et al., 2013; Hu et al., 2014). Shorter rotations have led to a high nutrient loss in foliage and biomass per tree component decreased as compare to longer rotations especially in the branches per unit biomass (Fang, 1987; Ma et al., 2007; Zhou et al., 2015). Therefore, a serious concern has been raised on the Chinese fir plantations less yield and long-term productivity decline (Bi et al., 2007; Zhao et al., 2013), particularly about the current rotation regime. Therefore, we have reviewed various aspects of Chinese fir related to short rotations regime, which are directly involved in

http://www.aloki.hu ● ISSN 1589 1623 (Print) ● ISSN 1785 0037 (Online)
DOI: http://dx.doi.org/10.15666/aeer/1705_1105511067

Chinese fir productivity decline like nutrient availability, nutrient cycling, soil microbes and their biochemical activities etc. We try to uncover the basic problems in the Chinese fir decline over successive rotations and possible effective solutions provided by the various previous studies. This study would provide a reference for future researches.

Chinese fir description

The genus "Cunninghamia" is an evergreen coniferous specie in the cypress family Cupressaceae. Traditionally, it is said that this genus contains two species, Chinese fir (*Cunninghamia lanceolata* Lamb) Hook) and Taiwan fir (*Cunninghamia konishii),* but genetic obedience suggested them as the same species which is usually known as "Chinese fir".

They are native to China, Taiwan, Northern Vietnam, and Laos. Distribution of Chinese fir in China is shown in (*Fig. 2).* They may reach a height of 50 m, generally with the conical shape with tiered and horizontal branches, which often somewhat pendulous toward the tips. Chinese fir has green needle-like leaves, which are softly spun, leathery and stiff (*Fig. 3*). Needles spiral around the stem in an upward arch. Chinese Fir is a valued species in China which is vital because of its fast growth and high-quality timber wood (i.e., straight and decay resistant), along with its historical value and significant culture it is used as an ornamental tree.

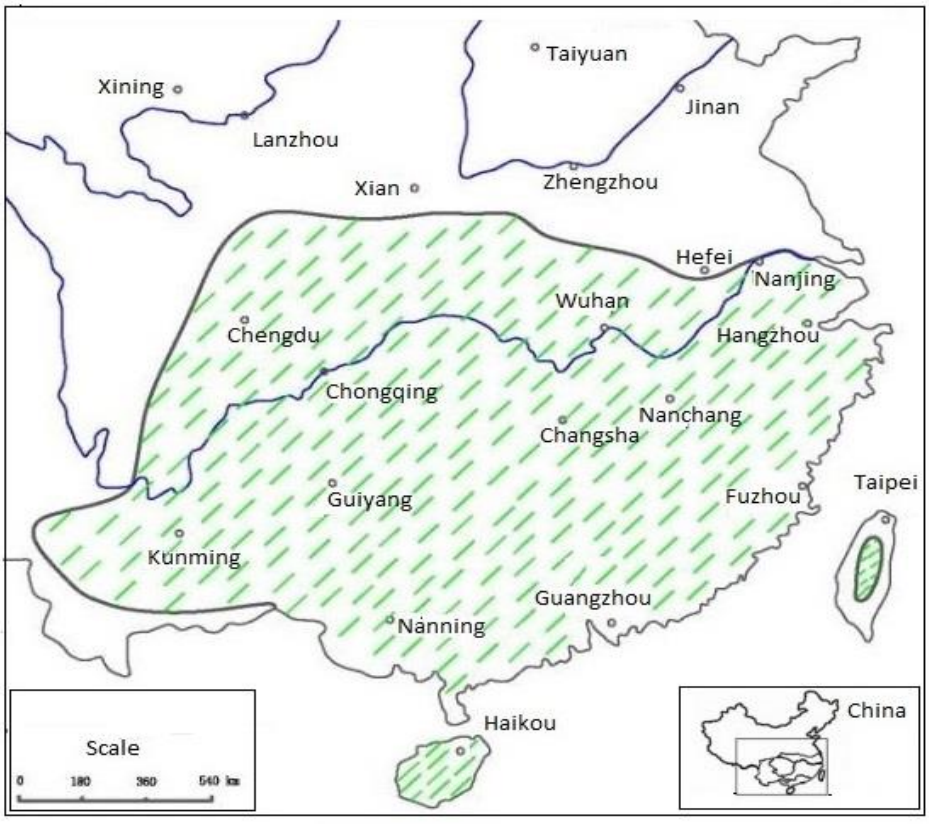

Figure 2. *Distribution of Chinese fir (Cunninghamia lanceolata) in China mainly spread in southern China (Wang et al., 2012)*

http://www.aloki.hu ● ISSN 1589 1623 (Print) ● ISSN 1785 0037 (Online)
DOI: http://dx.doi.org/10.15666/aeer/1705_1105511067

Figure 3. *Description of Chinese fir (Cunninghamia lanceolata (Lamb) Hook) tree*

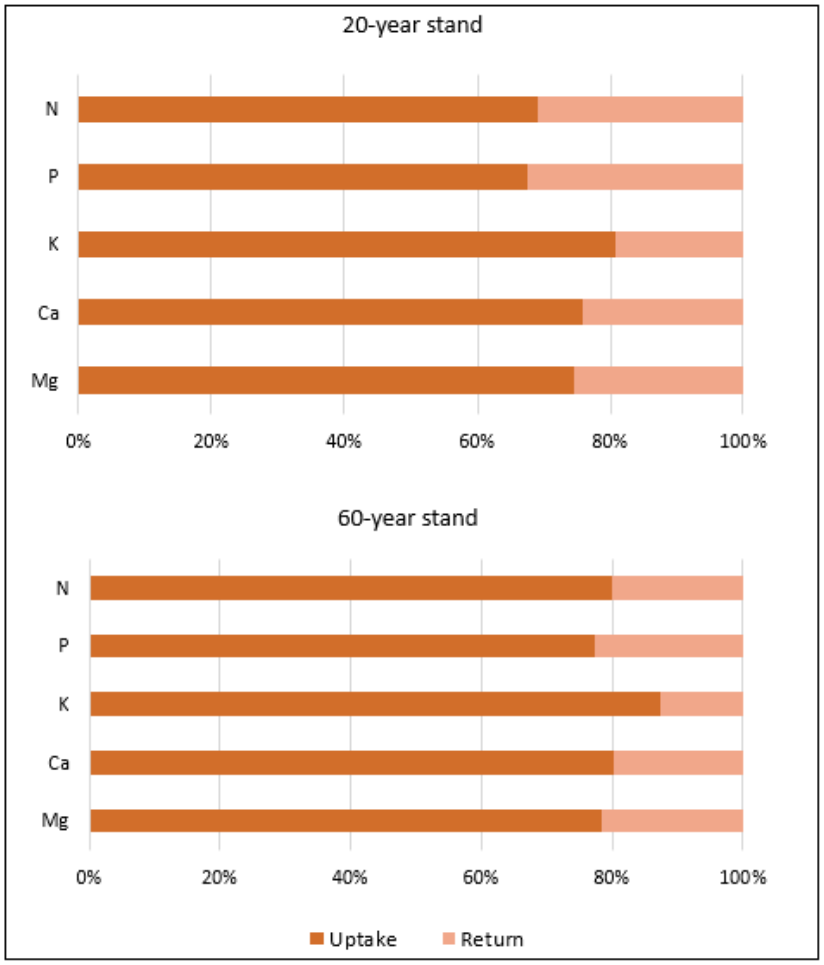

Figure 4. *Nutrient uptake, return and uptake/return ratio Chinese fir plantations of different ages (kg.hm^{-2} a^{-1})*

http://www.aloki.hu ● ISSN 1589 1623 (Print) ● ISSN 1785 0037 (Online)
DOI: http://dx.doi.org/10.15666/aeer/1705_1105511067

Stand development can be the key factors in the nutrient distribution and cycling as well as in biomass production (Li, 1996; Ma et al., 2002, 2007; Zhao et al., 2013). Different factors influence the nutrient absorption of the trees, which include growth rate, nutrient use efficiency and stand nutrient demand (Hobbie, 2015). Climatic as well as physical and chemical factors also affect the nutrient contents and nutrient use efficiency (Piao et al., 2010). According to Ma et al. (2007), annual nutrient uptake and nutrient use efficiency in Chinese fir plantations increased while the nutrient return decreased with stand development. Soil microbes are also the key ingredients in maintaining good soil structure by gas exchange and good drainage, which keeps soil healthy (Bhardwaj et al., 2014).

Data in the *Table 1* showed fungal population firstly increased from 1-year-old plantation to 20-year-old plantation but decreased in 40-year-old plantations. Bacterial population decreased from 1-year-old plantation to 20-year-old but again increase from 20-year-old to the 40-year-old plantation. Overall, microbial population decreased in 20-year-old plantation due to the decrease in bacterial population.

Table 1. *Soil microbial population in different aged Chinese fir (Cunninghamia lanceolata) plantations (10^3.g^{-1} soil)*

Soil microbes	Plantation age		
	1 yr.	20 yr.	40 yr.
Fungi	74	468	199
Bacteria	16900	13660	15760
Total microbes	16974	14218	15959

Nutrient contents and biochemical activity of soil microbes

Chinese fir plantations consume a large number of nutrients because of its fast growth (Farooq et al., 2019a), and due to short rotation periods, nutrient contents availability decreased significantly over the successive rotations. In Chinese fir plantations, soil nutrient contents decreased drastically as the rotation increased (Fang, 1987; Chen et al., 1990). Data in *Table 2* showed that soil humus carbon (SHC) was 37.6 gkg^{-1}, 33.8 $gkg^{-1,}$ and 32.4 gkg^{-1} in first, second and third rotation respectively during Chinese fir plantation. Soil total nitrogen (TN) was 4.28 gkg^{-1}, 3.91 gkg^{-1} and 3.36 gkg^{-1} in first, second and third rotation respectively while total phosphorous (TP) was 0.27 gkg^{-1}, 0.23 gkg^{-1} and 0.14 gkg^{-1}. In first rotation soil total Potassium (TK) was 19.7 gkg^{-1}, moreover, in the second and third rotation, it was 16.5 gkg^{-1} and 14.3 gkg^{-1} (*Table 2*). SHC decreased up to 15.7% in the second rotation while TN, TP, and TK decreased up to 18.4%, 9.6%, and 2.4%, respectively.

In terms of third rotation, SHC decreased up to 32% from the first to third rotation while the TN, TP, and TK decreased up to 36%, 61.2%, and 11.4%, respectively. As the soil depth got deeper, the contents of all the elements declined over successive rotations (Zhang et al., 2004). Plant available contents also decreased from first to the third rotation. When the Chinese fir plantation was regenerated from the site of first rotation, available nitrogen (N_A), available phosphorous (P_A) and available potassium (K_A) decreased significantly by 42.4%, 44.1%, and 37.5% respectively while on the site of second rotation, $N_{A,}$ P_A and K_A decreased by 24.2%, and 47.8% and 5.9% (*Table 2*). When the plantations start getting mature (18-20 years), the nutrient content availability

http://www.aloki.hu ● ISSN 1589 1623 (Print) ● ISSN 1785 0037 (Online)
DOI: http://dx.doi.org/10.15666/aeer/1705_1105511067

in the soil surface layer (0-20 cm) was only 50.8%, 14.1% and 36.6% for N, P and K, respectively. In the 20-40 cm and 40-60 cm soil layers' nutrient contents also decreased markedly. Due to the low rate of litter-fall decomposition, this cause imbalance between nutrient uptake and return (Liao et al., 2000). During a study in south China, Yang et al. (2005) described that in surface soil layer (0-20 cm) hydrolysable nitrogen content declined in the second and third rotations by 3% and 18%, respectively, as compared to first rotation while available phosphorus decreased 7% and 20% under Chinese fir stands.

Soil nutrients decline over the successive rotations could be reflected in soil microbial population and in their biochemical activities (Bhardwaj et al., 2014). In Chinese fir plantations, when continuous cropping took place over successive rotations biochemical activity of soil microbes decline significantly (Chen et al., 2015; Wu et al., 2017). Nitrogen fixation was 13.2% in the first rotation while it decreased up to 11.4% and 5.9% in second and third rotation respectively. Ammonification also declined by 82%, ranging from 1.6 mg $N.g^{-1}$ soil to 0.4 mg $N.g^{-1}$ soil from first to third rotation. Fiber decomposition was 3.3 CO_2 mg. g^{-1} soil, 0.8 CO_2 mg. g^{-1} soil and 1.4 CO_2 mg. g^{-1} soil in the first, second and third rotation while respiration was 1.6%, 1.1%, and 0.8% respectively. Nitrogen fixation, fiber decomposition, and respiration decreased by 54.1%, 59.2%, and 39.8% when continuous cropping of Chinese fir plantation took place for twice (*Table 3*).

Table 2. *Variation in the soil total nutrient contents, available nutrient contents, soil microbe's biochemical activity, and productivity over the successive rotations in Cunninghamia lanceolata plantations*

Nutrient contents	1st rotation	2nd rotation	3rd rotation
Total nitrogen (gkg^{-1})	4.28	3.91	3.36
Total phosphorus (gkg^{-1})	0.271	0.238	0.14
Total potassium (gkg^{-1})	19.7	16.5	14.3
Humus carbon (gkg^{-1})	37.6	33.8	32.4
Hydrolysable nitrogen ($mgkg^{-1}$)	105.3	95.3	73.2
Available phosphorus ($mgkg^{-1}$)	58.7	52.3	28.7
Available potassium ($mgkg^{-1}$)	101.5	59.6	53.2

Table 3. *Variation in the biochemical activity of soil microbes over the successive rotations in Cunninghamia lanceolata plantations*

Biochemical activity	1st rotation	2nd rotation	3rd rotation
Nitrogen fixation (%)	13.2	11.4	5.9
Ammonification (mg N. g^{-1}soil)	1.6	0.9	0.4
Fiber decomposition (CO_2 mg.g^{-1} soil)	3.3	0.8	1.4
Respiration (%)	1.6	1.1	0.8

Chinese fir growth and productivity

Chinese fir growth and production decreased over the successive rotations (Selvaraj et al., 2017). In productive Chinese fir stands (25-year-old), 280 t ha^{-1} biomass was reported with about 80% of total biomass allocated to the tree stem, which decreased

http://www.aloki.hu ● ISSN 1589 1623 (Print) ● ISSN 1785 0037 (Online)
DOI: http://dx.doi.org/10.15666/aeer/1705_1105511067

over the successive rotations (Zhao and Zhou, 2005). The high soil nutrition consumption due to continuous cropping cause a negative impact on the tree growth of Chinese fir plantations. A decline reported in annual increment in diameter at breast height (DBH) (Farooq et al. (2019b), height and volume in Chinese fir plantations of the same age but with different rotations (Zhou et al., 2016a). Diameter at breast height (DBH) decreased from 14.1 cm to 11.5 cm from first to third rotation (Tang et al., 2016). Plant height also decreased from 15.5 m to 10.8 m from first to the third rotation. Tree volume was 378.5 $m^3.hm^{-2}$, 268.8 $m^3.hm^{-2}$ and 176.4 $m^3.hm^{-2}$ respectively in first, second and third rotation (*Table 4*). The average height, DBH, and volume declined by 14.2%, 12.1%, and 32.3%, respectively in the second rotation and 22.8%, 36.5% and 53.2%, respectively for the third rotation. Higher tree mortality reported in third rotation as compared to the first and second rotation. It was 11.2%, 17.5%, and 21.6% respectively in the first, second and third rotation (*Fig. 5*).

Table 4. *Variation in the growth and productivity over the successive rotations in Cunninghamia lanceolata plantations*

Growth and productivity	1st rotation	2nd rotation	3rd rotation
DBH (cm)	14.1	12.8	11.5
Height (m)	15.4	13.6	10.8
Volume ($m^3.hm^{-2}$)	378.5	268.8	176.4
Tree mortality (%)	11.2	17.5	21.6

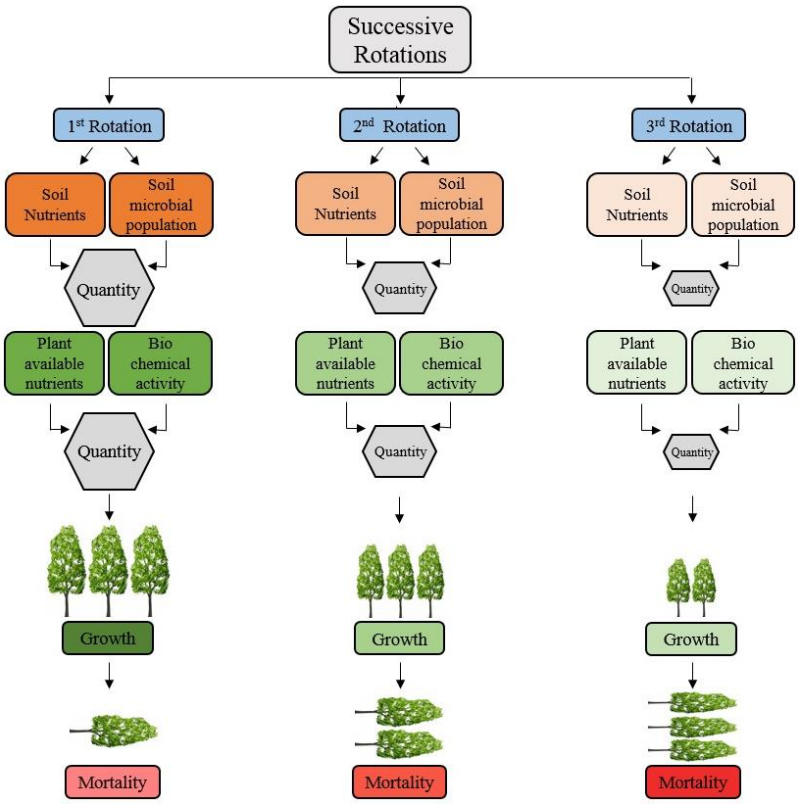

Figure 5. *Graphical summary of soil quality decline affecting the Chinese fir plantations growth and productivity over the successive rotations. (Decrease in the shade of colours of boxes shows decrease in nutrients availability, biochemical activity and growth)*

http://www.aloki.hu ● ISSN 1589 1623 (Print) ● ISSN 1785 0037 (Online)
DOI: http://dx.doi.org/10.15666/aeer/1705_1105511067

Discussion

Due to its soft and adorable timber, Chinese fir is an important species of China, which is in use for manufacturing of buildings, temples, furniture, and coffins, as well as an ornamental tree. Additionally, it also used as biomass energy and pulp production (Ma et al., 2002a, b; Wood et al., 2009). Nutrient cycling and biomass production are the important components of forest productivity (Tian et al., 2011; Farooq et al., 2018) which can vary with stand age, development and different silvicultural techniques (Hou et al., 2009; Zhao et al., 2013). Chinese fir productivity decreased over the years, and current management practices and short rotation policy are highly criticized for being a reason for less productivity (Chen et al., 2004). In Chinese fir plantations, these characteristics have been described in various previous studies in different regions of China (Li, 1996; Liao et al., 2000; Chen et al., 2004; Zhang et al., 2004; Zhao and Zhou, 2005; Ma et al., 2007; Wu et al., 2011; Chen et al., 2013; Zhao et al., 2013; Tang et al., 2016; Zhou et al., 2016b; Selvaraj et al., 2017). From the last one thousand years' traditional plantation method and management system of clear-cutting, complete ploughing, burning of the site and residues removal are under-used which is blamed for site degradation resulting in the poor growth and less production of Chinese fir plantations (Zhou et al., 2016c). Complete burning is the cause of organic matter and some nutrient loss; furthermore, minerals are lost due to rainfall (Wenhua, 2004; You et al., 2015). Soil erosion increased significantly due to complete ploughing while clear cutting resulted in soil and water loss (Dias et al., 2015). Conventional management practice effects tree morphology and biomass production. Morphological characteristics such as survival rate, average diameter at breast height, average height and biomass production were lower in stands where plantations were established with clear cutting and complete burning irrespective of rotation time (Bhardwaj et al., 2014).

Monoculture plantations are also the reason for productivity decline as monoculture system has low resistance and more suspected to pest attack due to the less biodiversity and bad stability (Liu et al., 2018). Non-development of understory vegetation and no proper thinning are the critical issues in the less productivity and poor growth because understory vegetation can markedly improve the soil nutrient and enhanced the biochemical activity (Chen et al., 2004; Zhou et al., 2016b). The decline in productivity is also associated with the non-use of fertilizers as in this era fertilizers are vital for crop development especially in the rotations without a period of fellows (Havlin et al., 2016). However, some experiments by different research teams in different areas showed contradictory results regarding the benefits of fertilizers. In a research on the 5-year old plantation, Li et al. (1991) reported that fertilizer applications of P and K could increase stand growth while Liao et al. (2000) found that P application increased stand growth only at the beginning while N fertilizers showed no effect moreover K fertilizer effects negatively.

The conventional Chinese fir plantation management system has to be replaced with the recently science based and rational management system, which is multi-culturing, includes clear cutting but of small area and mild site preparation. Cutting leftovers should be buried rather than burned. Pure plantation should be avoided and gradually replaced with agroforestry (Chinese fir mixed plantation) such as planting different herbs and shrubs. This could enforce higher productivity with the increase of the timber production and improve the soil physical and chemical properties to certain degrees as herbs and shrubs are easy to decompose and are rich in nutrients. Hence, it will enrich the soil resources. In nutrient-poor soils, direct approach of nutrient inputting should be

http://www.aloki.hu ● ISSN 1589 1623 (Print) ● ISSN 1785 0037 (Online)
DOI: http://dx.doi.org/10.15666/aeer/1705_1105511067

used by applying fertilizers especially the compound fertilizer containing P can have a huge impact on plant growth especially in south china where the sites are mostly P-deficient.

In plantation ecosystem soil microbes are the important decomposers, they are the good indicator of the soil quality and habitat change because they play an important role in nutrient transformations (Chen et al., 2015; Wu et al., 2017). Soil contains a different type of bacteria, algae, fungi, and earthworms. The optimum amount of soil microbial population increases the efficiency of fertilizer and irrigation application (Paul, 2014). Furthermore, it releases essential nutrients N, P, K, and hydrogen back to the soil. On the other hand, excessive soil organic matter can be a problem also as it encourages the growth of unwanted herbs and shrubs, moreover, it also decreases the efficiency of irrigation and fertilizer application (Brevik et al., 2015). These are some of the benefits and disadvantages that soil microbial population can provide to plantation ecosystem (Jacobsen et al., 2014). For soil microbial benefits, an optimum environment that favours soil microbial growth is necessary to build a healthy soil microbial population. Organic based fertilizers can be an excellent way to provide them a healthy environment in which they can thrive in (Hartmann et al., 2015; Hudson, 2015). General causes of productivity decline in Chinese fir plantations and their effective solutions are described in *Table 5*.

Table 5. *Reasons of Chinese fir productivity decline and effective solutions*

General causes of less productivity	Effective solutions	References
Traditional plantation method and management system that creates site degradation	Replacing conventional Chinese fir plantation management system with recently science based multicultural and rational management system	Minghe and Ritchie, 1999; Hu et al., 2006
Short rotation pattern and establishing a plantation on infertile lands	Rotation lengths should be increased and plantation establishment on infertile lands should be discouraged	Ma et al., 2000a; Ma et al. 2007; Slevaraj et al. 2017
Decline in soil fertility due to slash burning and residual removal	Avoid the activities that soil compromise soil fertility. Cutting leftovers should be buried rather than burned	Xiong, 2008; Ma et al., 2000b; Zhijun et al. 2018
Clearcutting and complete plowing before the plantation establishment	Clear cutting but of small area and mild site perpetration	Farooq et al., 2019a; Ma et al., 2002
Introduction of monoculture Chinese fir plantations	Introduction of mixture plantation like agroforestry system should be encouraged and monoculture should be discouraged	Hu et al., 2006; Xiong, 2008; Wang et al., 2008; You et al., 2015
Even aged plantations, non-development of understory vegetation and no proper thinning	Introduction of multi-layering and multi-aged plantations	Lin et al., 2001; Ma et al., 2002; Chen, 2007; Zhou et al., 2015
The decline in the soil microbial population and biochemical activities of soil microbes over the successive rotations	Organic based fertilizers can be an excellent way to provide soil microbes a healthy environment in which they can thrive in	Wang et al., 2008; Zhang et al., 2017
Non-use of fertilizers and organic manure	Essential use of compost and fertilizers	Chen et al., 1990; Liao et al., 2000

http://www.aloki.hu ● ISSN 1589 1623 (Print) ● ISSN 1785 0037 (Online)
DOI: http://dx.doi.org/10.15666/aeer/1705_1105511067

Acknowledgments. This study was financially supported by the National Natural Science Foundation of China (31600502 and 31870614), the Science and Technology Major Project of Fujian Province, China (2018NZ0001-1) and the Special Technology Innovation Foundation of Fujian Agriculture and Forestry University (CXZX2016059).

Conflict of interests. The authors declare no conflict of interests exists.

REFERENCES

[1] Bhardwaj, D., Ansari, M. W., Sahoo, R. K., Tuteja, N. (2014): Biofertilizers function as key player in sustainable agriculture by improving soil fertility, plant tolerance and crop productivity. – Microbial Cell Factories 13(1). DOI: 10.1186/1475-2859-13-66.

[2] Bi, J., Blanco, J. A., Seely, B., Kimmins, J. P., Ding, Y., Welham, C. (2007): Yield decline in Chinese-fir plantations: a simulation investigation with implications for model complexity. – Canadian Journal of Forest Research 37(9): 1615-1630.

[3] Brevik, E. C., Cerdà, A., Mataix-Solera, J., Pereg, L., Quinton, J. N., Six, J., Van Oost, K. (2015): The interdisciplinary nature of soil. – Soil 1(1): 117-129.

[4] Chen, C., Zhang, J., Zhou, C., Zheng, H. (1990): Researches on improving the quality of forest land and the productivity of artificial *Cunninghamia lanceolata* stands. – Chinese Journal of Applied Ecology 1(2): 97-106 (in Chinese with English abstract).

[5] Chen, L., Wang, S., Chen, C. (2004): Degradation mechanism of Chinese fir plantation. – Chinese Journal of Applied Ecology 15(10): 1953-1957 (in Chinese with English abstract).

[6] Chen, L. (2007): Management model of multi-storied Chinese fir plantation. – Subtropical Agriculture Research 3(2): 87-90 (in Chinese with English abstract).

[7] Chen, G. S., Yang, Z. J., Gao, R., Xie, J. S., Guo, J. F., Huang, Z. Q., Yang, Y. S. (2013): Carbon storage in a chronosequence of Chinese fir plantations in southern China. – Forest Ecology and Management 300: 68-76.

[8] Chen, X. L., Wang, D., Chen, X., Wang, J., Diao, J. J., Zhang, J. Y., Guan, Q. W. (2015): Soil microbial functional diversity and biomass as affected by different thinning intensities in a Chinese fir plantation. – Applied Soil Ecology 92: 35-44.

[9] Dias, T., Dukes, A., Antunes, P. M. (2015): Accounting for soil biotic effects on soil health and crop productivity in the design of crop rotations. – Journal of the Science of Food and Agriculture 95(3): 447-454.

[10] Fang, Q. (1987): Effect of replanted Chinese fir plantation on soil fertility and its growth. – Scientia Silvae Sinicae 23(4): 389-397 (in Chinese with English abstract).

[11] FAO (2007): State of the World's Forests. – Food and Agriculture Organization of the United Nations, Rome, pp. 88-90.

[12] FAO (2015): Global Forest Resources Assessment. – FAO, Rome. http://www.fao.org/forestresources-assessment/en/ (accessed on 20 December 2018).

[13] Farooq, T. H., Tigabu, M., Ma, X., Zou, X., Liu, A., Odén, P. C., Wu, P. (2018): Nutrient uptake, allocation and biochemical changes in two Chinese fir cuttings under heterogeneous phosphorus supply. – iForest-Biogeosciences and Forestry 11(3): 411-417.

[14] Farooq, T. H., Ma, X., Rashid, M. H. U., Wu, W., Xu, J., Tarin, M. W. K., He, Z., Wu, P. (2019a): Impact of stand density on soil quality in Chinese fir (*Cunninghamia lanceolata)* monoculture. – Applied Ecology and Environmental Research 17(2): 3553-3566.

[15] Farooq, T. H., Wu, W., Tigabu, M., Ma, X., He, Z., Rashid, M. H. U., Gilani, M. M., Wu, P. (2019b): Growth, Biomass Production and Root Development of Chinese fir in Relation to Initial Planting Density. – Forests 10(3): 236.

[16] Hartmann, M., Frey, B., Mayer, J., Mäder, P., Widmer, F. (2015): Distinct soil microbial diversity under long-term organic and conventional farming. – The ISME Journal 9(5): 1177.

http://www.aloki.hu ● ISSN 1589 1623 (Print) ● ISSN 1785 0037 (Online)
DOI: http://dx.doi.org/10.15666/aeer/1705_1105511067

[17] Havlin, J. L., Tisdale, S. L., Nelson, W. L., Beaton, J. D. (2016): Soil Fertility and Fertilizers. – Pearson Education, India.
[18] Hobbie, S. E. (2015): Plant species effects on nutrient cycling: revisiting litter feedbacks. – Trends in Ecology and Evolution 30(6): 357-363.
[19] Hu, Y. L., Wang, S. L., Zeng, D. H. (2006): Effects of single Chinese fir and mixed leaf litters on soil chemical, microbial properties and soil enzyme activities. – Plant and Soil 282: 379-386.
[20] Hu, Z., He, Z., Huang, Z., Fan, S., Yu, Z., Wang, M., Zhuo, X., Fang, C. (2014): Effects of harvest residue management on soil carbon and nitrogen processes in a Chinese fir plantation. – Forest Ecology and Management 326: 163-170.
[21] Hudson, N. (2015): Soil Conservation: Fully Revised and Updated. – New India Publishing Agency, Delhi.
[22] Jacobsen, C. S., Hjelmsø, M. H. (2014): Agricultural soils, pesticides and microbial diversity. – Current Opinion in Biotechnology 27: 15-20.
[23] Li, Y. Q., Xu, Q. Y., Liu, Z. J. (1991): Early five years' effect of fertilization on young Chinese fir plantation. – Chinese Journal of Soil Science 22(11): 28-32 (in Chinese with English abstract).
[24] Li, W. H., Li, F. (1996): Research of Forest Resources in China. – China Forestry Publishing House, Beijing, China, pp. 39-53 (in Chinese with English abstract).
[25] Li, J., Chen, X., Zhu, N., Tan, Y., Yan, Y., Gao, Z., Zhang, Y. (2013): Study on selection of main fuel-wood forest tree species in South China and combustion characteristics of wood pellets of fuel-wood trees. – Journal of Central South University of Forest and Technology 33: 126-129.
[26] Liao, L. P., Ma, Y. Q., Wang, S. L., Gao, H., Yu, X. J. (2000): Decomposition of leaf litter of Chinese fir in mixture with major associated broad-leaved plantation species. – Acta Phytoecological Sinica 24(1): 27-33 (in Chinese with English abstract).
[27] Lin, K., Yu, X. T., Huang, B. L., He, Z. Y. (2001): Dynamical characteristics of undergrowth plant diversity in Chinese fir plantations. – Chinese Journal of Applied and Environmental Biology 7(1): 13-19 (in Chinese with English abstract).
[28] Liu, B., Liu, Q., Daryanto, S., Guo, S., Huang, Z., Wang, Z., Wang, L., Ma, X. (2018): Responses of Chinese fir and Schima superba seedlings to light gradients: Implications for the restoration of mixed broadleaf-conifer forests from Chinese fir monocultures. – Forest Ecology and Management 419: 51-57.
[29] Ma, X., Liu, A., Ma, Z., Fan, S. (2000a): A comparative study on nutrient accumulation and distribution of different generations of Chinese fir plantations. – Chinese Journal of Applied Ecology 11(4): 501-506 (in Chinese with English abstract).
[30] Ma, X., Ye, S., Chen, S. (2000b): Effects of rotation on site productivity maintenance of Chinese fir plantation. – Science Silvae Sinica 36(6): 47-52 (in Chinese with English abstract).
[31] Ma, X., Liu, C., Hannu, I., Westman, C. J., Liu, A. (2002): Biomass, litterfall and the nutrient fluxes in Chinese fir stands of different age in subtropical China. – Journal of Forestry Research 13(3): 165-170.
[32] Ma, X., Heal, K., Liu, A., Jarvis, P. G. (2007): Nutrient cycling and distribution in different-aged plantations of Chinese fir in southern China. – Forest Ecology and Management 243(1): 61-74.
[33] Minghe, L., Ritchie, G. A. (1999): Eight hundred years of clonal forestry in China: I. traditional afforestation with Chinese fir (*Cunninghamia lanceolata* (Lamb.) Hook.). – New Forests 18(2): 131-142.
[34] Paul, E. A. (2014): Soil microbiology, ecology and biochemistry. – Academic Press.
[35] Piao, S., Ciais, P., Huang, Y., Shen, Z., Peng, S., Li, J., Zhou, L., Liu, H., Ma, Y., Ding, Y., Friedlingstein, P. (2010): The impacts of climate change on water resources and agriculture in China. – Nature 467(7311): 43.

http://www.aloki.hu ● ISSN 1589 1623 (Print) ● ISSN 1785 0037 (Online)
DOI: http://dx.doi.org/10.15666/aeer/1705_1105511067

[36] Selvaraj, S., Duraisamy, V., Huang, Z., Guo, F., Ma, X. (2017): Influence of long-term successive rotations and stand age of Chinese fir (*Cunninghamia lanceolata)* plantations on soil properties. – Geoderma 306: 127-134.
[37] State Forestry Administration (2014): General Situation of Forest Resources in China - The 8th National Forest Inventory. – State Forestry Administration, Beijing.
[38] Tang, X., Lu, Y., Fehrmann, L., Forrester, D. I., Guisasola-Rodríguez, R., Pérez-Cruzado, C., Kleinn, C. (2016): Estimation of stand-level aboveground biomass dynamics using tree ring analysis in a Chinese fir plantation in Shitai County, Anhui Province, China. – New Forests 47(2): 319-332.
[39] Tian, D., Xiang, W., Chen, X., Yan, W., Fang, X., Kang, W., Dan, X., Peng, C., Peng, Y. (2011): A long-term evaluation of biomass production in first and second rotations of Chinese fir plantations at the same site. – Forestry 84(4): 411-418.
[40] Wang, Q. K., Wang, S. L. (2008): Soil microbial properties and nutrients in pure and mixed Chinese fir plantations. – Journal of Forestry Research 19(2): 131-135.
[41] Wang, B., Wei, W., Xing, Z., You, W., Niu, X., Ren, X., Liu, C. (2012): Biomass carbon pools of Cunninghamia lanceolata (Lamb.) Hook. forests in subtropical China: Characteristics and potential. – Scandinavian Journal of Forest Research 27(6): 545-560.
[42] Wang, L., Zhang, Y., Berninger, F., Duan, B. (2014): Net primary production of Chinese fir plantation ecosystems and its relationship to climate. – Biogeosciences Discussions 11(4). DOI: 10.5194/bgd-11-5639-2014.
[43] Wenhua, L. (2004): Degradation and restoration of forest ecosystems in China. – Forest Ecology and Management 201(1): 33-41.
[44] Wood, T. E., Lawrence, D., Clark, D. A., Chadzon, R. L. (2009): Rain forest nutrient cycling and productivity in response to large-scale litter manipulation. – Ecology 90(1): 109-121.
[45] Wu, Z. L. (1984): Chinese fir. – Forestry of China Publications, Beijing.
[46] Wu, P., Ma, X., Tigabu, M., Wang, C., Liu, A., Oden, P. C. (2011): Root morphological plasticity and biomass production of two Chinese fir clones with high phosphorus efficiency under low phosphorus stress. – Canadian Journal of Forest Research 41(2): 228-234.
[47] Wu, Z., Li, J., Zheng, J., Liu, J., Liu, S., Lin, W., Wu, C. (2017): Soil microbial community structure and catabolic activity are significantly degenerated in successive rotations of Chinese fir plantations. – Scientific Reports 7(1): 6691.
[48] Xiong, H. (2008): Study on variation of the properties of soil in multi-storied Chinese fir plantation. – Subtropical Agriculture Research 4(4): 283-286 (in Chinese with English abstract).
[49] Yang, Y. S., Guo, J., Chen, G., Xie, J., Gao, R., Li, Z., Jin, Z. (2005): Carbon and nitrogen pools in Chinese fir and evergreen broadleaved forests and changes associated with felling and burning in mid-subtropical China. – Forest Ecology and Management 216(1-3): 216-226.
[50] You, C., Jiang, L., Xi, F., Wang, W., Li, M., Xu, Z., Gu, L., Wang, F., Zhang, Z. (2015): Comparative evaluation of different types of soil conditioners with respect to their ability to remediate consecutive tobacco monoculture soil. – International Journal of Agriculture and Biology 17(5). DOI: 10.17957/IJAB/15.0017.
[51] Yu, X. (1997): Silviculture of Chinese Fir. – Science and Technology Press of Fujian, Fuzhou.
[52] Zhang, X., Kirschbaum, M. U., Hou, Z., Guo, Z. (2004): Carbon stock changes in successive rotations of Chinese fir (*Cunninghamia lanceolata* (lamb) hook) plantations. – Forest Ecology and Management 202(1-3): 131-147.
[53] Zhang, W., Lu, Z., Yang, K., Zhu, J. (2017): Impacts of conversion from secondary forests to larch plantations on the structure and function of microbial communities. – Applied Soil Ecology 111: 73-83.

http://www.aloki.hu ● ISSN 1589 1623 (Print) ● ISSN 1785 0037 (Online)
DOI: http://dx.doi.org/10.15666/aeer/1705_1105511067

[54] Zhao, M., Zhou, G.-S. (2005): Estimation of biomass and net primary productivity of major planted forests in China based on forest inventory data. – Forest Ecology and Management 207(3): 295-313.
[55] Zhao, M., Xiang, W., Tian, D., Deng, X., Huang, Z., Zhou, X., Peng, C. (2013): Effects of increased nitrogen deposition and rotation length on long-term productivity of *Cunningham lanceolata* in Southern China. – PLoS One 8(2): 55376.
[56] Zhijun, H., Selvalakshmi, S., Vasu, D., Liu, Q., Cheng, H., Guo, F., Ma, X. (2018): Identification of indicators for evaluating and monitoring the effects of Chinese fir monoculture plantations on soil quality. – Ecological Indicators 93: 547-554.
[57] Zhou, L., Addo-Danso, S. D., Wu, P., Li, S., Ma, X. (2015): Litterfall production and nutrient return in different-aged Chinese (*Cunningham lanceolata*) plantations in South China. – Journal of Forestry Research 26(1): 79-89.
[58] Zhou, H., Meng, S., Liu, Q. (2016a): Diameter Growth, Biological Rotation Age and Biomass of Chinese Fir in Burning and Clearing Site Preparations in Subtropical China. – Forests 7(8): 177.
[59] Zhou, L., Cai, L., He, Z., Wang, R., Wu, P., Ma, X. (2016b): Thinning increases understory diversity and biomass, and improves soil properties without decreasing growth of Chinese fir in southern China. – Environmental Science and Pollution Research 23(23): 24135-24150.
[60] Zhou, L., Shalom, A. D. D., Wu, P., He, Z., Liu, C., Ma, X. (2016c): Biomass production, nutrient cycling and distribution in age-sequence Chinese fir (*Cunninghamia lanceolate*) plantations in subtropical China. – Journal of Forestry Research 27(2): 357-368.

http://www.aloki.hu ● ISSN 1589 1623 (Print) ● ISSN 1785 0037 (Online)
DOI: http://dx.doi.org/10.15666/aeer/1705_1105511067

STUDY ON THE COUPLING AND COORDINATION DEGREE OF HIGH-QUALITY ECONOMIC DEVELOPMENT AND ECOLOGICAL ENVIRONMET IN BEIJING-TIANJIN-HEBEI REGION

LIAO, M. L.[1] – CHEN, Y.[1] – WANG, Y. J.[2*] – LIN, M. S.[3*]

[1]*Institute for Urban and Environmental Studies, Chinese Academy of Social Sciences*
No. 28 Shuguangxili, Chaoyang District, Beijing, China

[2]*School of Economics and Management, University of Chinese Academy of Sciences*
No.19(A) Yuquan Road, Shijingshan District, Beijing, China

[3]*College of Tourism, Fujian Normal University*
No. 1 Science and Technology Road, Minhou University Town, Fuzhou, China
(phone: +86-10-8268-0673; fax: +86-10-8268-0673)

[*]*Corresponding authors*
e-mail: wangyj@ucas.ac.cn; fax +86-10-8268-0673
e-mail: linms@fjnu.edu.cn; fax +86-0591-2286-8726

(Received 2nd Apr 2019; accepted 11th Jul 2019)

Abstract. With the rapid development of urbanization and industrialization in China, the issue of high-quality economic development and ecological environment has arisen. Taking the Beijing-Tianjin-Hebei region as the research subject, this paper measured the comprehensive scores of economic development and ecological environment, and analyzed the coupling degree of these two systems from 2000 to 2018. According to the four degrees of coupling and coordination, this paper defined the degree of coupling and coordination between the economic development and ecological environment in Beijing-Tianjin-Hebei region, and put forward some policy suggestions. The result shows that, between 2000 and 2018, (1) the coupling degree of economic development and ecological environment in Beijing-Tianjin-Hebei region is $C \in [0.2, 1]$, which is changing with time, and has gone through all stages of coupling; the coordination degree of economic development and ecological environment in Beijing-Tianjin-Hebei region is $D \in [0.1, 0.5]$, which is in the low-middle stage. (2) The coupling degree of economic development and ecological environment in Beijing-Tianjin-Hebei region shows a trend of increasing first and then decreasing, while the coordination degree shows a rising trend, and remains more or less flat compared to the coupling degree.
Keywords: *high-quality development, ecological development, coupling degree, coordination degree, Beijing-Tianjin-Hebei Region*

Introduction

China's economic construction has achieved remarkable results since the reform and opening up, with an average growth rate of 9.78% from 1978 to 2011. Affected by the global economic crisis in 2012, China's economic growth has slowed down, with an average growth rate of 7.2% from 2012 to 2017. It has become a new norm for China's economic growth to shift from high-speed to medium-high speed. A basic feature of the new era for China's economic development is the transition from a phase of rapid growth to a stage of high-quality development, and the promotion of high-quality economic development is an essential requirement for the new normal in economic development (Cheng and Qiu, 2018).

http://www.aloki.hu ● ISSN 1589 1623 (Print) ● ISSN 1785 0037 (Online)
DOI: http://dx.doi.org/10.15666/aeer/1705_1106911083

In 1978, China's urbanization level was only 17.9%, while by the end of 2018, it was up to 59.58%. According to The Report on Chinese Industrialization issued by the Chinese Academy of Social Sciences, China has entered the second stage of the late-industrialization since 2015, with an overall industrialization level index of 84. What's more, with the industrialization level index of 95, 76 and 71, respectively, all the eastern, central and western regions in China have entered the stage of the late-industrialization (Hu, 2017). The economic growth in the middle and late stages of industrialization mainly depends on the growth of the secondary industry, that is, China's economic development relies heavily on industries with high energy consumption and high pollution. The rapid development of China's economy and the promotion of urbanization and industrialization have caused serious damage to the ecological environment, and the destruction of the ecological environment has also inhibited the economic growth (Liao and Wang, 2019). Since 2016, many cities in China have been affected by haze, especially cities in the Beijing-Tianjin-Hebei Region. Within the Bohai Economic Circle, the Beijing-Tianjin-Hebei Region is not only the largest and most sophisticated economic zone in Northern China, but also an important political and cultural center of China. However, since the economic development in the Beijing-Tianjin-Hebei Region is dependent on high-energy-consumption and high-pollution industries, there have been serious environmental problems in the Beijing-Tianjin-Hebei Region. And the economic development in this region has transformed to the coordination between high-quality economic development and the development of ecological environment. Therefore, this paper analyzed the characteristics of each stage of the economic and environmental development based on the measurement of the coupling degree between the economic development and the ecological environment system in the Beijing-Tianjin-Hebei region, and provided a basis for the high-quality economic development there.

Literature Review

At the 19th National Congress of the Communist Party of China, president Xi Jinping declared that "China's economy has been transitioning from a phase of rapid growth to a stage of high-quality development. This is a pivotal stage for transforming our growth model, improving our economic structure, and fostering new drivers of growth." The transformation of China's economy from a phase of rapid growth to a stage of high-quality development is the essential requirement for the new normal in economic development (Sheng, 2018). In the fundamental economic theories, high-quality development can be expressed as the mode, structure and momentum of economic development living up to its real nature, which is to satisfy people's growing needs for a better life (Jin, 2018). Shi et al. (2018) measured the high-quality economic development index based on the two dimensions of economic growth fundamentals and social achievements. The results show that time span of China's inter-provincial economic growth quality fluctuation cycle has been widening gradually, the distribution of economic growth in the Eastern, central and Western China is unbalanced and difficult to close in short term, and the quality of economy growth of China will enter a long-term uptrend channel. The high-quality economic development refers to the economic development stressing both quantity and quality of economic growth, and lay emphasis on the quality of economic growth. The existing researches on economic development have been mainly conducted from the

http://www.aloki.hu ● ISSN 1589 1623 (Print) ● ISSN 1785 0037 (Online)
DOI: http://dx.doi.org/10.15666/aeer/1705_1106911083

perspectives of sources of economic growth, reasons for slow-speed development of economy and the evaluation of low-carbon or green economy. According to the study of Shen et al. (2011), though the development model oriented by manufacturing and service industries, with urbanization as space carrier and marketization as system, can promote the sustainable and high-speed economic growth in China, the restraints on this model is increasing. Nie et al. (2011) found there has been misallocation of resources in state-owned enterprises, and almost no reallocation of resources within the industries, which contributed to the inefficiency of China's manufacturing industry. Zhuang et al. (2014) evaluated the low-carbon development of several cities in China and made comparisons with that of international cities. Chen et al. (2018) analyzed the relationship between the governance of haze pollution and high-quality economic development, and believed that the improvement of economic development quality is the premise of the transformation of economic development mode, and the governance of haze pollution can help improve the quality of the atmospheric environment and economic development, and promote the high-quality development of economy in return.

"Coupling" is a concept derived from the mechanical nexus between two parts of something. From the perspective of ecology, "coupling" refers to the interaction, transition and development of two or more system elements or subsystems (Zhang et al., 2016). The elements in a coupling system are closely related, and their cooperation can improve the productivity and ecological function of the system. The coupling construction of the ecosystem is actually the development process of the ecosystem from disorder to order (Liu, 2016). Since urbanization involves a series of coupling processes, coupling simulation and optimization are widely applied in solving planning problems and rapid development of regional economy (Li et al., 2011). Using the panel data of Lianyungang, Li et al. (2012) analyzed the challenges of rapid urbanization in coastal cities with a coupling and coordination degree model focusing on the degree of coordination between urbanization and the environment, and found that the dynamic of coordination between urbanization and environment showed a U-shaped curve. Lei et al. (2015) investigated the relationship between urbanization and air environment from the perspective of coupling coordination theory, and found that the degree of coordinated coupling between urbanization and air environment exhibited an S-shaped curve, indicating that the slightly unbalanced development of Wuhan has turned into the barely balanced development, and has entered a period of superiorly balanced development, with the air environment lagging. Wang et al. (2014) conducted a quantitative analysis of the coupling relation between urbanization and ecological environment in Nanchang and Jiujiang urban belts, and the results showed that the coordination degree of Nanchang rises at a faster speed, reaching a moderate balance level, while that of Jiujiang remains at a low level. Therefore, Nanchang and Jiujiang urban belts should further transform its economic growth model, optimize the industrial structure, improve its technology and embark on a new-urbanization path featuring resource-saving, low carbon emission, environmental-friendly and cost effective. You (2016) assessed the coordinated degree of urbanization by quantifying four involved processes (demographic, social, economic and spatial) in Shanghai from 1952 to 2012, and found that the demographic urbanization advanced continuously and roughly presented a U-shaped trend. Guo et al. (2015) examined the coupling relationship between urbanization and environment in the Huaihe River Basin from both exploratory and analytical perspectives. The

http://www.aloki.hu ● ISSN 1589 1623 (Print) ● ISSN 1785 0037 (Online)
DOI: http://dx.doi.org/10.15666/aeer/1705_1106911083

results showed the degree of coupling and the degree of policy coordination appeared to fluctuate over time.

The existing researches on the coupling relationship between high-quality economic development and eco-environmental protection are mainly conducted in the Yangtze River delta, farming-pastoral zones in northern China and mountainous areas, with the coupling coordination degree model and qualitative analysis. Zhang et al. (2015) analyzed the coupling and coordination relationship between economic development and ecological environment system from 1999 to 2003 in the extensive Yangtze River delta with the coupling coordination degree model, and found that the coupling of economic development and ecological environment was in the running-in stage, while the coordination degree of economic development and ecological environment was moderate. Based on the analysis of coupling relationship between regional economy and ecological environment, Jiang et al. (2010) established a dynamic coupling model of coordinated development of the regional economy and ecological environment, and studied the coordinated development of economy and ecological environment in Jiangsu Province. The results showed that, between 1995 and 2007, the economic development index of Jiangsu Province showed a rapid growth trend, while the index of ecological environment system showed a slow growth trend with several fluctuations, the economy and ecological environment of Jiangsu Province were developing harmoniously. Zhang et al. (2010) predicted the coordinated development of economy and ecological environment of farming-pastoral zone in northern China in the future ten years with a variety of methods. Hu et al. (2012) studied the coupling modes and implementation forms of the coordinated development of economy and ecological environment in the lake basins of Yunnan Plateau. Wang et al. (2013) estimated the coupling and coordination degree of tourism economic development and ecological environment of the forest parks in Shanxi Province. Fang et al. (2016) analyzed the theoretical framework and methodology of the interactive coupled effects between urbanization and eco-environment in mega-urban agglomerations with the method of qualitative analysis. In addition, some scholars have studied the response of ecological environment to marine economy development and its influencing factors in Bohai Bay Rim Area (Li et al., 2017; Li and Gao, 2017), explored the coupling relationship between economic development and ecological environment in poverty-stricken areas (Cao et al., 2016; Liu et al., 2007), and analyzed the coupling relationship between the benefit of economic development and ecological environment quality along the Silk Road Economic Belt (Wang, 2018).

It can be seen that, although there are many researches on the relationship between economic development and ecological environment, few of them were conducted in the Beijing-Tianjin-Hebei region, and even fewer from the perspective of high-quality economic development. What's more, the existing researches mainly focus on the economic growth, while this paper tends to take a comprehensive consideration of the scale, level and potential of the economic development, that is, study the coupling relationship between economic development and environmental protection from the perspective of high-quality economic development. The economic growth in China has entered a period of transformation with quality as its first priority, and the economic growth in Beijing-Tianjin-Hebei Region is crucial to China's economic growth. After a long term high-speed economic development in the Beijing-Tianjin-Hebei Region, problems such as the singularization of industrial structure, exhaustion

http://www.aloki.hu ● ISSN 1589 1623 (Print) ● ISSN 1785 0037 (Online)
DOI: http://dx.doi.org/10.15666/aeer/1705_1106911083

of resources and deterioration of ecological environment have been emerging, and the "crowding-out effect" of backward production capacity in the core area is getting more and more serious, leading to an outward flow of core industries. Therefore, this paper conducted the research on the coupling relationship between economic growth and ecological environment in the Beijing-Tianjin-Hebei Region from the perspective of high-quality economic development, supplemented the coupling theory of economy and ecological environment with the concept of high-quality development, and provided guidance for coordinating the economic development and eco-environmental protection in the Beijing-Tianjin-Hebei Region.

Materials and Methods

Research Method

Improved entropy method

The entropy method is a method for determining the weight of index according to the amount of information transmitted by each index to the decision maker, which excludes the influence of subjective factors on weighting and the overlap of information brought by multiple index. In order to avoid the shortcomings of the traditional entropy method, it is necessary to process the original data of the index, that is the improved entropy method. It can be calculated as follows:

Standardize

As there is a dimension between the economic system and the ecological environment system, the index should be standardized.

$$u_{ij} = \frac{x_{ij} - \min(x_{ij})}{\max(x_{ij}) - \min(x_{ij})} \quad \text{(Eq.1)}$$

uij is the positive index;

$$u_{ij} = \frac{\max(x_{ij}) - x_{ij}}{\max(x_{ij}) - \min(x_{ij})} \quad \text{(Eq.2)}$$

uij is the negative index;

uij refers to the j-th index in the i-th system, and the value of uij is xij (i=1,2; j=1, 2, …n), with max(xij) refers to the maximum value and min(xij) the minimum value of xij.

Calculate

Calculate the proportion of index uij:

$$\mathrm{R}_{ij} = \frac{u_{ij}}{\sum_{i=1}^{m} u_{ij}} \quad \text{(Eq.3)}$$

http://www.aloki.hu ● ISSN 1589 1623 (Print) ● ISSN 1785 0037 (Online)
DOI: http://dx.doi.org/10.15666/aeer/1705_1106911083

Measure the entropy of each index:

$$e_j = \frac{-1}{\ln m * \sum_{i=1}^{m} R_{ij} \ln R_{ij}} \quad \text{(Eq.4)}$$

Calculate the difference coefficient of each index:

$$g_j = 1 - e_j \quad \text{(Eq.5)}$$

The larger the value of gj is, the more important the index is in the evaluation system.

Calculate the weight of each index:

$$w_{ij} = (1 - e_j) / (n - \sum_{j=1}^{n} e_j) \qquad \text{j=1, 2, …n} \qquad \text{(Eq.6)}$$

Calculate the synthetical value of the system:

$$V_j = \sum_{j=1}^{n} w_j R_{ij} \qquad \text{j=1, 2, …n} \qquad \text{(Eq.7)}$$

The Coupling and Coordination Degree Model

The coupling degree is used to describe the degree of influence among the system or elements (Liu et al., 2011), while the coordination degree is the degree of harmony between systems or elements of the system in the process of development, which reflects the tendency of a system from disorder to order (Wu et al., 1997). It can be seen that, the coupling degree and coordination degree are two different indicators, with the coupling degree reflects the strength of interaction between two parties, regardless of advantages or disadvantages; and the coordination degree is the degree of good coupling in the interaction, reflecting the quality of coordination. Therefore, the research has been conducted from the following two aspects:

Coupling degree function

Construct a coupling degree function of high-quality economic development and eco-environmental protection, that is:

$$C = \sqrt{U_1 U_2} / (U_1 + U_2) \quad \text{(Eq.8)}$$

Among them, the value of C is between 0 and 1. C=0 indicates that there is no coupling relationship between high-quality economic development and eco-environmental protection, and C=1 indicates that there is a good coupling between high-quality economic development and eco-environmental protection.

Coupling and coordination degree function

The coupling and coordination degree function of high-quality economic development and eco-environment protection is:

http://www.aloki.hu ● ISSN 1589 1623 (Print) ● ISSN 1785 0037 (Online)
DOI: http://dx.doi.org/10.15666/aeer/1705_1106911083

$$D = \sqrt{C \cdot T} \quad \text{(Eq.9)}$$

$$T = \alpha U_1 + \beta U_2 \quad \text{(Eq.10)}$$

where D is the coupling and coordination degree, and T is the comprehensive coordination index of high-quality economic development and eco-environmental protection, representing the coordination index of high-quality economic development and eco-environmental protection at each coupling level. α and β represent the contribution rate of each system, that is, the contribution coefficient of high-quality economic development and eco-environmental protection. Since there is an interaction between high-quality economic development and eco-environmental protection, both α and β are 0.5. Similar to the coupling degree, the coordination degree can also be divided into 4 levels (see *Table 1*).

Table 1. *The level of coupling and coordination degree*

Value of coupling degree	Phase of coupling	Value of coupling and coordination degree	Type of coupling and coordination	Phase of coordination
0<C≤0.3	Separation phase	0<D≤0.3	Low coupling and coordination degree	Separation phase with low coordination
0.3<C≤0.5	Antagonistic phase	0.3<D≤0.5	Medium coupling and coordination degree	Antagonistic phase with medium coordination
0.5<C≤0.8	Running-in phase	0.5<D≤0.8	High coupling and coordination degree	Running-in phase with high coordination
0.8<C≤1	Coupling phase	0.8<D≤1	Extremely high coupling and coordination degree	Coupling phase with extremely high coordination

Index Selection

Due to the wide variety of influencing factors involved in urban economic development and ecological environment, as well as the complex interaction mechanism among them, their development status and impacts cannot be reflected with only one indicator. Therefore, we would like to select indicators and construct an indicator system based on existing researches (see *Table 2*).

Results

With the improved entropy method, we standardized the raw data of the Beijing-Tianjin-Hebei region from 2000 to 2018, and calculated the entropy and weight of each indictor in the economic development and ecological environment system of Beijing, Tianjin and Hebei. The synthesis scores of economic development and ecological environment systems in the Beijing-Tianjin-Hebei Region are shown in *Table 3*.

It can be seen from *Table 3* that:

(1) From the perspective of economic development, there is an uptrend in synthesis scores of the economic development in the Beijing-Tianjin-Hebei region from 2000 to 2018, with Beijing developed the fastest in 2003-2011, followed by Tianjin and Hebei. By the year of 2011, Tianjin ranked the first in economic development, followed by Hebei and Beijing. It can be explained by Beijing's high-speed economic development in the preceding years brought by regulatory policies and convenient transportation.

http://www.aloki.hu ● ISSN 1589 1623 (Print) ● ISSN 1785 0037 (Online)
DOI: http://dx.doi.org/10.15666/aeer/1705_1106911083

Table 2. *The index system and weight of index of the coupling and coordination degree model of economic development and ecological environment*

System	Target	Index	Weight
Economic development system	Scale of economic development	GDP (100 million yuan)	0.066
		Fiscal revenue (100 million yuan)	0.084
		Total fixed assets investment (100 million yuan)	0.086
		Gross industrial production (100 million yuan)	0.065
	Level of economic development	Per capita GDP (10 thousand yuan)	0.061
		Rural per capita net income (yuan)	0.067
		Urban per capita disposable income (yuan)	0.069
	Potential of economic development	Local fiscal revenue in GDP (%)	0.072
		Per capita expenditure on science, education, culture, health and other undertakings (yuan)	0.043
		The number of people receiving undergraduate or junior college education (10 thousand people)	0.024
		The number of the employed in urban area (10 thousand people)	0.105
Ecological environment system	Ecological environment pollution	SO_2 emission (10 thousand tons)	0.015
		Pollutant discharge_chemical oxygen demand (COD) (10 thousand tons)	0.042
		Production of industrial solid waste (10 thousand tons)	0.052
	Ecological environment management	Green coverage rate in urban built-up areas (%)	0.030
		Disposal of industrial solid waste (10 thousand tons)	0.077
		Sewage treatment capacity in urban areas (10 thousand cubic meters per day)	0.043

Table 3. *Synthesis scores of economic development and ecological environment systems in the Beijing-Tianjin-Hebei Region from 2000 to 2018*

Year	Beijing Economic development	Beijing Ecological environment	Tianjin Economic development	Tianjin Ecological environment	Hebei Economic development	Hebei Ecological environment
2000	0.02	0.03	0.01	0.14	0.07	0.09
2001	0.03	0.06	0.02	0.14	0.07	0.09
2002	0.06	0.08	0.03	0.12	0.07	0.09
2003	0.08	0.11	0.05	0.16	0.04	0.10
2004	0.12	0.09	0.07	0.14	0.06	0.10
2005	0.16	0.13	0.10	0.12	0.10	0.11
2006	0.19	0.16	0.13	0.12	0.13	0.11
2007	0.24	0.18	0.18	0.11	0.17	0.12
2008	0.28	0.21	0.22	0.12	0.22	0.14
2009	0.32	0.21	0.26	0.11	0.25	0.15
2010	0.37	0.21	0.33	0.11	0.32	0.18
2011	0.44	0.13	0.44	0.07	0.41	0.10
2012	0.49	0.12	0.52	0.07	0.51	0.10
2013	0.54	0.13	0.57	0.09	0.57	0.16
2014	0.57	0.14	0.62	0.09	0.61	0.17
2015	0.63	0.17	0.66	0.13	0.66	0.16
2016	0.67	0.24	0.68	0.19	0.71	0.22
2017	0.65	0.20	0.70	0.17	0.70	0.19
2018	0.66	0.15	0.73	0.19	0.75	0.16

Data sources: Calculated according to the China City Statistical Yearbook

(2) From the perspective of ecological environment, the low scores of ecological environment system in the Beijing-Tianjin-Hebei Region may be due to the economic development mode and the rapid pace of development, which has caused serious damages to the ecological environment, and the ecological environment destruction, in

http://www.aloki.hu ● ISSN 1589 1623 (Print) ● ISSN 1785 0037 (Online)
DOI: http://dx.doi.org/10.15666/aeer/1705_1106911083

turn, has restricted the economic development over time. The significant fluctuation in synthesis scores of ecological environment systems after 2010 can be explained by the impact of high-speed of economic development and urbanization on ecological environment, which has led to the energy resources depletion, environmental pollution and ecological imbalance. However, the improvement of synthesis scores of ecological environment systems after 2013 may be related to the economic regulatory policies which laid more emphasis on quality rather than speed of economic development.

(3) Through the comparison of the economic development and ecological environment in the Beijing-Tianjin-Hebei region, we can see that the score of economic development was lower than that of ecological environment from 2000 to 2018. What's more, during the study period, the score of economic development continued to rise, while that of the ecological environment continued to decline, indicating that there is a negative correlation between economic development and ecological environment in Beijing-Tianjin-Hebei region.

Discussion

Characteristics of time variation

The coupling degree (C) and the coordination degree (D) of the Beijing-Tianjin-Hebei region from 2000 to 2018 have been calculated according to the formula (see *Figure 1*).

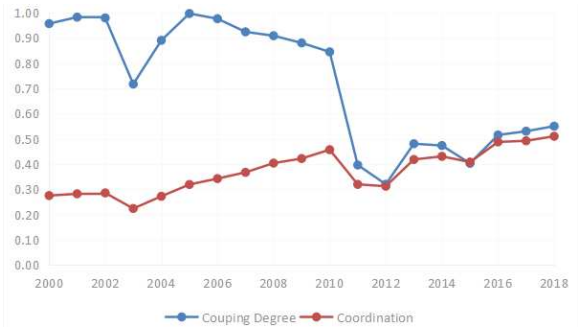

Figure 1. *Mean value of the coupling and coordination degree between economic development and ecological environment system in the Beijing-Tianjin-Hebei Region in 2000-2018*

It can be seen from *Figure 1* that, the coupling and coordination degree between economic development and ecological environment system in Beijing-Tianjin-Hebei Region in 2000-2018 fluctuated greatly. The years from 2000 to 2002 can be seen as the coupling phase and the year of 2003 as the running-in phase, which can ben explained as the lagged effect of China's accession to the WTO in 2001 on the economic development in Beijing-Tianjin-Hebei Region. With the years from 2004 to 2010 as another coupling phase, the years from 2000 to 2010 can be taken as the coupling phase on the whole. During this period, China's economy has been developing rapidly and the environmental problems have not yet emerged, but the coupling degree between economic development and ecological environment in the Beijing-Tianjin-Hebei region has shown a downward trend. In 2011, the coupling degree dropped to 0.4 suddenly and has not exceed 0.5 until 2018. The years of 2011-2018 is the antagonistic phase of the coupling relationship between economic development and ecological environment in

http://www.aloki.hu ● ISSN 1589 1623 (Print) ● ISSN 1785 0037 (Online)
DOI: http://dx.doi.org/10.15666/aeer/1705_1106911083

Beijing-Tianjin-Hebei region. It is in line with the reality that China's economic development has entered a new normal of medium-to-high-speed growth and is accompanied by the frequent occurrence of environmental pollution problems such as haze. In order to resolve the contradiction between economic development and environmental protection, the coordinated development in the Beijing-Tianjin-Hebei region should be strengthened and the integration of industrial layout should be promoted. What's more, the development of the Circum-Bohai Sea Economic Zone can be promoted by exploring the effective path of ecological civilization construction, strengthening the complementary advantages of Beijing, Tianjin and Hebei, and enhancing the coordination of population, economy, resources and environment in the Beijing-Tianjin-Hebei region.

The analysis of coordination degree shows that, from 2000 to 2018, the coordination degree of Beijing-Tianjin-Hebei Region has been increasing steadily with sight fluctuations, which is at a low-to-moderate level. This can be explained by the high level of urbanization and the continuous optimization of industrial structure, which are not in line with the environmental protection.

From 2000 to 2011, there was a great difference between the coupling degree and coordination degree of economic development and eco-environmental protection. It can be explained by the damage to the ecological environment brought by the rapid development of economy. Since 2011, the gap between coupling degree and coordination degree has been narrowed because of the adjustment of industrial structure and the transformation or upgrading of economy, which has taken the ecological civilization construction and economic development into full consideration.

Characteristics of spatial pattern

The coupling and coordination degrees between economic development and ecological environment of Beijing, Tianjin and Hebei have been calculated by SPSS (see *Table 4*). It can be seen from *Table 4* that, there were large fluctuations in both coupling and coordination degree of Beijing, Tianjin and Hebei after 2010. The coupling relationship between economic development and ecological environment in Beijing has experienced the coupling phase of 2000-2010, the antagonistic phase of 2011-2015, and the running-in phase of 2016-2018. This can be explained by the high-speed economic development and the good environmental condition in 2000-2010. Since 2011, the economic development has slowed down and the problems of environmental pollution has emerged. At present, with the goal of high-quality economic development, Beijing has made more efforts to protect the environment, and the coupling relationship between economic development and ecological environment has been optimizing. The coordination degree between economic development and ecological environment in Beijing has been increasing steadily with slight fluctuations, which is moderate in general. There has been a drastic fluctuation in the coupling degree of Tianjin from 2000 to 2018, with the years of 2004-2008 as the coupling phase. It can be explained by the economic transition and upgrade, or the interaction between various influencing factors of the two systems and the unbalanced economic development. The coupling relationship between economic development and ecological environment of Hebei showed the same trend as that of Beijing, but its coupling degree is lower than that of Beijing, which can be explained by the unbalanced economic and social development, the unreasonable industrial structure, and the serious impact of external factors.

http://www.aloki.hu ● ISSN 1589 1623 (Print) ● ISSN 1785 0037 (Online)
DOI: http://dx.doi.org/10.15666/aeer/1705_1106911083

Table 4. *Coupling and coordination degree of economic development and ecological environment in the Beijing-Tianjin-Hebei Region from 2000 to 2018*

Year	Coupling degree of Beijing	Coordination degree of Beijing	Coupling degree of Tianjin	Coordination degree of Tianjin	Coupling degree of Hebei	Coordination degree of Hebei
2000	0.97	0.15	0.12	0.10	0.96	0.28
2001	0.76	0.18	0.25	0.14	0.98	0.28
2002	0.93	0.25	0.38	0.17	0.98	0.29
2003	0.96	0.31	0.50	0.23	0.72	0.22
2004	0.97	0.32	0.80	0.29	0.89	0.27
2005	0.98	0.37	0.98	0.33	1.00	0.32
2006	0.98	0.41	0.99	0.35	0.98	0.34
2007	0.96	0.45	0.88	0.35	0.92	0.37
2008	0.96	0.48	0.82	0.37	0.91	0.40
2009	0.91	0.49	0.72	0.37	0.88	0.42
2010	0.86	0.50	0.56	0.35	0.84	0.46
2011	0.49	0.37	0.20	0.23	0.40	0.32
2012	0.41	0.35	0.17	0.22	0.32	0.31
2013	0.37	0.35	0.22	0.27	0.48	0.42
2014	0.39	0.37	0.19	0.26	0.47	0.43
2015	0.46	0.43	0.30	0.34	0.40	0.41
2016	0.60	0.52	0.47	0.45	0.52	0.49
2017	0.64	0.55	0.49	0.50	0.52	0.55
2018	0.67	0.53	0.53	0.52	0.55	0.55
均值	0.75	0.39	0.50	0.31	0.72	0.38

Data sources: Calculated according to the China City Statistical Yearbook

On the whole, the coordination degree of economic development and ecological environment in Beijing-Tianjin-Hebei region shows an upward trend with some slight fluctuations. However, the coordination degrees of economic development and ecological environment in Beijing, Tianjin and Hebei are all at the coupling phase with low and medium coordination, which indicates that, though the advantages in ecological environment have not been fully transformed into advantages in economic development, there has already been a virtuous circle between economic development and ecological environment.

Types of urban development

According to the coupling and coordination degree of urban economic development and ecological environment, the cities can be divided into four types: high coupling & high coordination degree, high coupling & low coordination degree, low coupling & high coordination degree, low coupling & low coordination degree. In cities with high coupling & high coordination degree, the development of economy and ecological environment are promoted together, so that, the emphasis should be laid on the cultivation of talents, transformation of development mode, optimization of industrial structure, protection of ecological environment and improvement of treatment efficiency of municipal waste and pollutants, forming a pattern of synchronous development of economy and ecological environment. The high coupling & low coordination degree indicates that although the economy is developing rapidly, the development of ecological environment is restricted by the local environmental carrying capacity. Therefore, the development mode should be transformed immediately so as to coordinated the development of economy and ecological environment, that is, enhancing the protection of ecological environment, giving full play to the advantages

http://www.aloki.hu ● ISSN 1589 1623 (Print) ● ISSN 1785 0037 (Online)
DOI: http://dx.doi.org/10.15666/aeer/1705_1106911083

of local resource endowment, developing the industries with local characteristics, adjusting the industrial structure, replacing the extensive development modes with green and high-efficient ones, and laying a solid foundation for the sustainable development in the future. Cities with low coupling & high coordination degree should be developed in a low energy-consumption, green and low-carbon development mode, which lays more emphasis on publicizing the advantages of local ecological environment, attracting foreign investment, developing industries with local characteristics and accelerating the economic development. Low coupling & low coordination degree may be resulted from the restrictions of historical and natural conditions. With the backward economic development and the crying need for eco-environmental protection, the extensive development mode have to be adjusted, the protection and modification of ecological environment have to be strengthened, the development of economy and ecological environment have to be coordinated through reasonable planning and implementation of various preferential policies for talent introduction.

The distributions of the mean values of coupling and coordination degree between economic development and ecological environment in the Beijing-Tianjin-Hebei Region from 2000 to 2016 are shown in *Figure 2*. It can be seen that, Beijing, Tianjin and Hebei are all regions with high coupling & low coordination degree, which indicates that though the degrees of urbanization and industrialization in these three regions are relatively high, and the economy is developing rapidly as well, the ecological environment has been damaged severely.

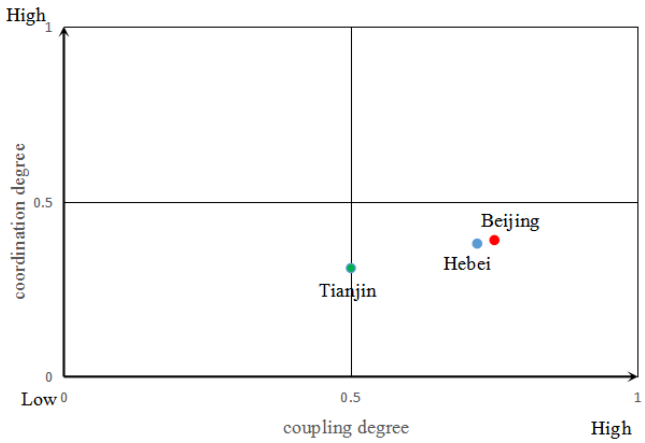

Figure 2. *Distribution of coupling and coordination degree in the Beijing-Tianjin-Hebei Region*

Conclusions and policy recommendations

Conclusions

Taking the Beijing-Tianjin-Hebei region as the research object, this paper measured the comprehensive scores of economic development and ecological environment, and analyzed the coupling degree of these two systems from 2000 to 2018. According to the four degrees of coupling and coordination, this paper defined the the degree of coupling and coordination between the economic development and ecological environment in Beijing-Tianjin-Hebei region, and put forward some policy suggestions. The result shows that, between 2000 and 2018, (1) the coupling degree of economic development and ecological environment in Beijing-Tianjin-Hebei region is C∈[0.2, 1], which is

http://www.aloki.hu ● ISSN 1589 1623 (Print) ● ISSN 1785 0037 (Online)
DOI: http://dx.doi.org/10.15666/aeer/1705_1106911083

changing with time, and has gone through all stages of coupling; the coordination degree of economic development and ecological environment in Beijing-Tianjin-Hebei region is D∈[0.1, 0.5], which is in the low-middle stage. (2) The coupling degree of economic development and ecological environment in Beijing-Tianjin-Hebei region shows a trend of increasing first and then decreasing, while the coordination degree shows a rising trend, and remains about flat compared with the coupling degree.

Policy recommendations

Since the reform and opening up, with the dependence on the secondary industry, the relationship between economic development and ecological environment in the Beijing-Tianjin-Hebei region is characterized by high coupling and low coordination. In order to build a world-class urban agglomeration with strong international competitiveness and promote the high-quality development driven by national innovation, the relationship between economic growth and environmental protection in the Beijing-Tianjin-Hebei region should be coordinated, and the high-quality development in coordination should be promoted by constructing a sophisticated economic structure.

First of all, the industrial integration in the Beijing-Tianjin-Hebei Region should be promoted to narrow the gap between industrial base and industrial advantages. By giving priority to the development of the tertiary industry, upgrading the structure of manufacturing and service industries, cultivating high-tech industries, and exploring new patterns for industrial development, the quality and efficiency of the economic development in the Beijing-Tianjin-Hebei region will be improved.

Second, the concept of green development should be established. In the process of high-quality economic development in the Beijing-Tianjin-Hebei region, it is necessary to bear the goal of energy conservation and increasing the resource utilization rate in mind, so as to promote the development of green cities continuously and integrate the concept of green development into the economic and social development.

Third, implement the innovation-driven development strategy vigorously. The innovation-driven development strategy is the inevitable requirement for promoting the transformation of economic development mode and the switch of growth momentum in Beijing-Tianjin-Hebei region. It is necessary to build a high-tech and advanced economic structure and give full play to the leading role of Beijing. Promote the organic unity and coordination of the industry chain, value chain, innovation chain and service chain by improving the industry chain, enhancing the value chain, optimizing the innovation chain and expanding the service chain.

Finally, promote the coordinated development of population in Beijing-Tianjin-Hebei region. As the main migration destinations in the Beijing-Tianjin-Hebei region, the pressure on resources and environment carrying capacity in Beijing and Tianjin has been increasing with the growth of population. Therefore, the intellectual and information resources of urban development should be coordinated to promote the high-quality economic development in the Beijing-Tianjin-Hebei region. Taking the opportunity of the construction of the Xiong'an New Area, confine the rapid growth of population in Beijing and transfer the population to Hebei orderly. Promote the rational allocation of human resources and other high-end resources in Beijing-Tianjin-Hebei region, contribute to the coordinated development of industries and promote the industrial upgrading of other regions of the country.

http://www.aloki.hu ● ISSN 1589 1623 (Print) ● ISSN 1785 0037 (Online)
DOI: http://dx.doi.org/10.15666/aeer/1705_1106911083

Acknowledgements. The study was funded by the Program for Risk Assessment of Climate Change and Adaptive Mode of Production, Livelihood and Eco-environment in Xiongan New Area of the Ministry of Science and Technology of China (2018YFA0606304); Program for National Conditions Survey of CASS Thinktank for Eco-civilization Studies (STWM2019C001); Program for Fujian Natural Science Foundation Project (2019J01430).

REFERENCES

[1] Cao, S., Wang, Y., Duan, F., Zhao, W. J., Wang, Z. H., Fang, N. (2016): Coupling between ecological vulnerability and economic poverty in contiguous destitute areas, China: Empirical analysis of 714 poverty-stricken counties. – Chinese Journal of Applied Ecology 27(8): 2614-2622.

[2] Chen, S., Chen, D. (2018): Air Pollution, Government Regulations and High-quality Economic Development. – Economic Research Journal 2: 20-34.

[3] Cheng, C. P., Qiu, Y. T. (2018): The Theory and Practice for Sustained High Growth of China's Economy Since the Reform and Opening-up. – China Soft Science 2: 160-167.

[4] Fang, C., Zhou, C., Gu, C., Chen, L., Li, S. (2016): Theoretical analysis of interactive coupled effects between urbanization and eco-environment in mega-urban agglomerations. – Acta Geographica Sinica 71: 531-550.

[5] Guo, Y., Wang, H., Nijkamp, P., Xu, J. (2015): Space-time changes in interdependent urban-environmental systems: A policy study on the Huai River Basin in China. – Habitat International 45: 135-146.

[6] Hu, Y., Yang, R. (2012): Study on the coupling mode of economy and eco-environment of the lake basins in plateau. – Inquiry into Economic Issues (5): 173-178.

[7] Hu, A. G. (2017): China Entering Post-industrial Era. – Journal of Beijing Jiaotong University 16(1): 1-16.

[8] Jiang, H., He, J. (2010): The Dynamic Coupling Model of Coordinated Development between Regional Economic and Ecological Environment Systems Based on Jiangsu Province. – Soft Science 24(3): 63-68.

[9] Jin, B. (2018): Study on the "High-Quality Development" Economics. – China Industrial Economics: 5-18.

[10] Lei, D., Zhao, W., Huang, Y., Cheng, S., Liu, C. (2015): Research on the Coupling Coordination Relationship between Urbanization and the Air Environment: A Case Study of the Area of Wuhan. – Atmosphere 6(10): 1539-1558.

[11] Li, X., Shi, X., He, J., Liu, X. (2011): Coupling Simulation and Optimization to Solve Planning Problems in a Fast-Developing Area. – Annals of the Association of American Geographers 101(5): 1032-1048.

[12] Li, Y., Li, Y., Zhou, Y., Shi, Y., Zhu, X. (2012): Investigation of a coupling model of coordination between urbanization and the environment. – Journal of Environmental Management 98(1): 127-133.

[13] Li, H., Gao, Q. (2017): Scientific and Technological Progress, Marine Economic Development and Ecological Environmental Change. – East China Economic Management (31): 100-107.

[14] Li, H., Gao, Q., Wu, F. (2017): Ecological environment response to marine economy development and the influence factors in Bohai Bay Rim Area. – China Population, Resources and Environment 27: 36-43.

[15] Liao, M., Wang, Y. (2019): China's Energy Consumption Rebound Effect Analysis Based on the Perspective of Technological Progress. – Sustainability 11: 1461.

[16] Liu, G., Shen, L., Liu, X. (2007): Harmonious Interactions between Economic Development and Ecological Environment Conservation in Resource-Rich and Economy-Poor Regions: A Case in Yulin City, Shaanxi Province. – Resources Science 4: 18-24.

http://www.aloki.hu ● ISSN 1589 1623 (Print) ● ISSN 1785 0037 (Online)
DOI: http://dx.doi.org/10.15666/aeer/1705_1106911083

[17] Liu, D., Yang, Y. (2011): Coupling coordinative degree of regional economy-tourism-ecological environment: a case of Anhui Province. – Resources & Environment in the Yangtze Basin 20(7): 892-896.
[18] Liu, J. (2016): Framing sustainability in a telecoupled world. – Acta Ecologica Sinica (23): 7870-7885.
[19] Nie, H., Jia, R. (2011): The Productivity and Misallocation of Resources of Manufacturing Enterprises in China. – The Journal of World Economy (7): 27-42.
[20] Shen, K., Li, Z. (2011): The Driving Force and Restraints on China's Economic Growth. – Economic Perspectives 1: 26-32.
[21] Sheng, Y. (2018): Construct the modern economic system and promote the high-quality economic development - the essential characteristic of China's economic development in the new era. – Qiushi.
[22] Shi, B., Ren, B. (2018): A Measurement of China's Provincial Economic High Quality Development. – On Economic Problems 4: 1-6.
[23] Wang, L., Su, J., Huang, X. (2013): Analysis on the coupling and coordination degree between economic development and ecological environment of the forest park in Shanxi province. – Journal of Agrotechnical Economics 8: 98-104.
[24] Wang, Y. (2018): Study on the coupling relationship between the efficiency of economic development and the quality of ecological environment along the Silk Road Economic Belt. – Statistics & Decision 1: 141-144.
[25] Wu, M., Lang, D. (1997): Research On the Coordination Degree of Environment-Economy System. – Environmental Pollution & Control 19(2): 20-23.
[26] Yongxiang (2014): Empirical Study of the Coupling Coordination Relationship of urbanization and ecological environment in Nanchang and Jiujiang urban belts. – Journal of Interdisciplinary Mathematics 17: 16.
[27] You, H. (2016): Quantifying the coordinated degree of urbanization in Shanghai, China. – Quality & Quantity 50(3): 1273-1283.
[28] Zhang, P., Hu, Y., Zhao, M. (2010): The Coordinated Perspective of Economic Development and Eco-environment in Northen Agriculture and Stock Raising Interlace Area. – China Population, Resources and Environment 20: 150-154.
[29] Zhang, R., Jiao, H. (2015): Coupling and Coordinating between Economic Development and Ecological Environment in the Pan Yangtze River Delta. – Resources and Environment in the Yangtze Basin 24: 719-727.
[30] Zhang, X., Xie, Y. (2016): County Urbanization: Ecological Notion, Coupling Mechanism and Realization Path. – Journal of Agro-Forestry Economics and Management 15(6): 727-734.
[31] Zhuang, G., Zhu, S., Yuan, L., Tan, X. (2014): Ranking of Low-carbon Development Level of Chinese Cities and International Comparative Study. – Journal of China University of Geosciences (Social Sciences Edition) 14: 17-23, 138.

http://www.aloki.hu ● ISSN 1589 1623 (Print) ● ISSN 1785 0037 (Online)
DOI: http://dx.doi.org/10.15666/aeer/1705_1106911083

RELATIONSHIP BETWEEN GEOLOGIC PARENT MATERIAL AND GROWTH OF FOREST TREES IN THE GÖLHISAR BASIN IN SW ANATOLIA, TURKEY

ALTUNBAS, S.[1*] – ATALAY, I.[2] – SILER, M.[3]

[1]*Deprtment of Soil Science and Plant Nutriment, Akdeniz University, Antalya, Turkey*

[2]*Department of Geography, Karabük University, Karabük, Turkey*

[3]*Department of Geography, Fırat University, Elazığ, Turkey*

**Corresponding author*
e-mail: saltunbas@akdeniz.edu.tr

(Received 3rd Apr 2019; accepted 20thAug 2019)

Abstract. Gölhisar Basin which is located in the southern part of Lakes Region, in SW of Turkey contains four main geologic parent materials composed of serpentine-peridotite, Mesozoic limestone, Neogene marl deposit and Quaternary colluvial deposit on which Calabrian pine (*Pinus brutia*) and Anatolian black pine (*Pinus nigra* subsp. *pallasiana*) grow. Tree productivity and/or growth rate is considerably different on these parent materials. This is mainly related to the weathering degree of serpentine-peridotite, stratification and compactness of marl deposit and the crack structure of limestone. For example, the productive Calabrian pine (*Pinus brutia*) trees grow on the deeply weathered serpentine-peridotite parent material in the Gölhisar basin. Draft appearances of Calabrian pines are found on exposed peridotite-serpentine in sloping areas. Besides, tree biomass is low on compact marl deposit due to the fact that taproot development of trees is mostly prevented by the compact marl deposit and horizontal marl layers. The productivity of Calabrian pine and black pine (*Pinus brutia*) trees on the limestone is higher than on the marl deposit and low weathered serpentine in the study area, in general. The aim of this study is to illustrate the importance of parent materials containing serpentine-peridotite, limestone, marl and colluvial deposits on the growth of *Pinus brutia* and *Pinus nigra* trees in the Gölhisar Basin.
Keywords: *tree growth, serpentine weathering, biome classification*

Introduction

Forest trees mostly grow on exposed parent materials occurring most of sloping areas. Here the chemical and physical composition of the parent materials and their weathering degrees play very important roles in the growth of trees. Especially the weathering of the parent materials mostly contributes to the release of the plant nutrients and weathered parent materials form a soft ground to develop of the plant root system, in general. For this reason, there is close relationship between the weathering degree of the parent materials and biomass of trees and/or tree growth rate. According to studies carried out relating to the importance of the tree biomass in Turkey, the good/high site index (site quality class) stands and trees occur on the deeply weathered parent materials; whereas, the poor stands are found on the semi weathered and low weathered parent materials. For example, good site index black pine forests were established on the deep weathered serpentine in the Karsanti locality in east of Mediterranean Taurus Mountains, Dirgine locality and Yenice Basin in NW of Anatolia; while, poor site index forests appear on the low weathered and unweathered serpentine in the Datça Peninsula, Kemer locality, west of Antalya Gulf (Atalay and Efe, (2010a), (2014); Atalay, (2016a).

http://www.aloki.hu ● ISSN 1589 1623 (Print) ● ISSN 1785 0037 (Online)
DOI: http://dx.doi.org/10.15666/aeer/1705_1108511106

In serpentine area of Kemer locality, CEC of soil in the poor stand is 8-10 $cmol_c\ kg^{-1}$, while this figure is about 38 $cmol_c\ kg^{-1}$ in good stand (Atalay, 2014). According to the study made on the parent material and biomass of the forest trees in the western part of Mediterranean Region, the highest productive forests are found on cracked limestone, the lowest one exists on the bare land of serpentine (Tetik and Yeşilkaya, 1997). It can be said that unweathered serpentine in the various parts of Anatolia is generally seen as bare land notably on the sloping area. Herbaceous plants only grow on the stabilized slopes on serpentine with thin soil cover.

On the other hand, different vegetation communities were established on the drift-derived soil and bedrock-derived soil in Keen of Hamar in the Shetland (Carter, 1987). In the study to be made in Central Coastal range of California showed that plant available Mg and Ca in serpentine soils exceed values assessed in chert soils. Magnesium is nearly 3 times more abundant than Ca in the serpentine soils and ion uptake discrimination and ion suppression in the roots are major mechanisms for serpentine vegetation to tolerate the chemistry of serpentine soils (Oze et al., 2008). The vegetation of serpentines presents a wide range of appearances. Biologists have concentrated on the situations where serpentine vegetation is in sharp contrast with that of the surroundings (Proctor et al., 1975). Serpentine soils are extreme habitats for plants. These extreme habitat conditions are rich with floristic diversity, especially endemic and rare taxa. The species which are specialist for serpentine habitats can survive by developing adaptations toward these intense stress conditions (Going et al., 2009). The ecology of serpentine systems has a significant importance for the sustainability of biodiversity and preservation of species (Özdeniz et al., 2017).

As to limestone, cracked limestone having high content of clay on the sloping area contributes a good habitat for the growth of forest trees due to the fact that three roots easily develop toward the deep parts along the cracks of limestone. On the other hand, especially red Mediterranean soil (Alfisol/Luvisol) with clayey in texture and its CEC more than 40 $cmol_c\ kg^{-1}$ that developed along the thin cracks and voids and among the bedding surface of limestones also form suitable conditions for the growth of cedar (*Cedrus libani*), black pine (*Pinus nigra*) and Taurus fir (*Abies cilicica*) trees in the Taurus Mountains (Atalay, 1987, 1997, 2014; Atalay and Efe, 2014).

The stratification situation, particularly the inclination of the layer and compactness of marl deposits forms different environments in terms of the tree growth. Namely, good site index of forests are found on soft marl deposits, while poor site index stand occurs on the compact and horizontal layered marl deposit because tree root development is considerably prevented by compact and horizontal layers (Atalay and Efe, 2014; Gregorich et al., 2001). Vertical cracks and thin soft zone in the marl deposit support taproot development of tree roots in the marl deposit. For this reason, the high growth rate trees and forests are commonly seen in these areas. Marl deposit on the sloping areas is very vulnerable for erosion and sensitive land degradation (Cerda, 1999; Atalay et al., 2019a).

Deep weathered gneiss and micaschist producing sandy soil supports to grow of productive forest; while outcropped gneiss and micaschist appearing as a rocky land on the steep slope is generally absent from the forest. Volcanic sand and tuff deposit, and thick sandy soil developed on the granite and gneiss create a good habitat for the growth scots pine (*Pinus sylvestris*) under cold and subhumid climate and stone pine (*Pinus pinea*) in the Mediterranean climate in Anatolia (Atalay, 2014, 2016b).

http://www.aloki.hu ● ISSN 1589 1623 (Print) ● ISSN 1785 0037 (Online)
DOI: http://dx.doi.org/10.15666/aeer/1705_1108511106

The importance of parent materials on the growth of plants is briefly mentioned some textbooks (Cunningham and Saigo, 1999; Foth, 1990; Smith and Smith, 2003).

The select of Gölhisar Basin as study area is related to display different parent material properties and forests. In this study our aim is to elucidate of the parent material effects on the three growths in the Gölhisar Basin which is located in the Lakes Region of SW Anatolia in Turkey (*Fig. 1*).

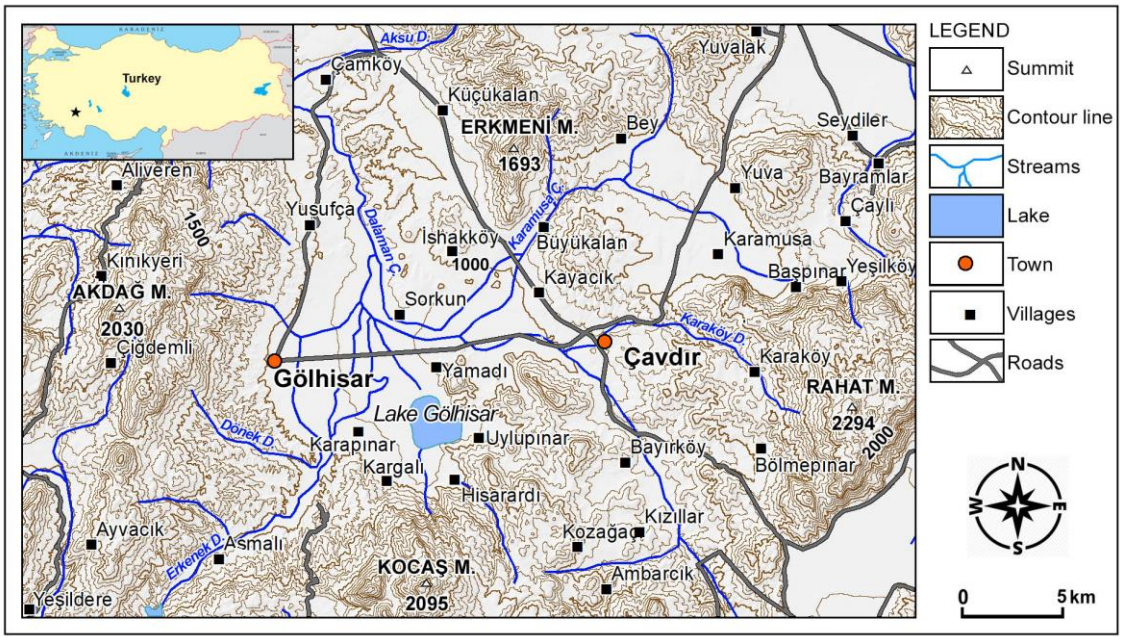

Figure 1. *Location and topographic map of the study area*

Materials and methods

General physical properties like the formation of geologic parent materials, topographic traits, climate, soil and vegetation, notably forest belts of the study area were briefly mentioned. The existence of different parent material and various forest clusters were taken into consideration in the selected experimental sites. Generally, in the selected experimental sites forest cluster and individual tree occurrence change sharply depending on parent material spreading. These areas are clearly seen in the sloping areas of Gölhisar Basin, because they have many parent materials composed of peridotite-serpentine, limestone, marl and colluvial deposit, and two main forest vegetation belts composed of Calabrian pine (*Pinus brutia*) and Anatolian black pine (*Pinus nigra* subsp. *pallasiana*). On the other hand, the main aim of the study is to reveal the growth rate of *Pinus brutia* and *Pinus nigra* on the different parent materials especially serpentine, limestone and marl deposit in the selected sites. Measurements of trees and collecting parent materials and soil samples were carried out in the summer season of 2018 in the study area (*Figs. 1* and *2*).

Pinus brutia experimental sites were selected on the different weathered serpentine-peridotite, limestone; horizontal and inclined layers of marl deposit and colluvial deposit; *Pinus nigra* experiment sites were selected on serpentine and limestone in the Gölhisar Basin. In the selection of trees in the experimental sites the different weathering stages of parent materials were taken into consideration. The figures and

http://www.aloki.hu ● ISSN 1589 1623 (Print) ● ISSN 1785 0037 (Online)
DOI: http://dx.doi.org/10.15666/aeer/1705_1108511106

graphs of trees showing the relationships among the age, diameter and height, and the parent material properties were prepared. Thus, the relationship between weathering situation of parent materials and the tree growth in the selected experimental sites was assessed. Relationship between tree growth and cation exchange capacity of the parent materials mainly indicating the weathering stages and plant nutriment capacity was explained. Special attendance was focused on significance of serpentine weathering on the vegetation growth and relating examples with serpentine were given not only experimental sites but also other places of the study area. Besides water allocation and surface erosion observations were made to explain the relationship between water and weathering properties of parent materials in the field. According to archaeological and historical knowledge human impact on the destruction of vegetation especially forest cover and its effect on the tree growth was mentioned. Lastly, statistical evaluation between tree growth and parent material was made.

On the other hand, to show the distribution of the forest trees and geologic parent material a profile and geologic parent material map were drawn. Topographic maps in the scale of 1/25 000 and modified geologic map in the scale of 1/100 000 were also used. The general geologic, geomorphic evolution and pedogeomorphology of the study area was used from the previous studies (Atalay, 2017; Atalay et al., 2017, 2019b; Altunbas, 2018).

The samples of the soil and semiweathered parent materials of the experimental sites were taken to determine of texture, pH, $CaCO_3$, organic matter and CEC (Cation exchange capacity). Their determinations were made at the Soil Laboratory of Soil Science and Plant Nutriment of Agricultural Faculty, Akdeniz University. Texture of soil samples determined based on Bouyoucos hydrometer method Bouyoucos (1955) and organic material was made Walkley-Black (Black, 1965), $CaCO_3$ determined Jackson (1967), Exchangeable Cations determined according to 1N ammonium acetate method Kacar (1995), Cation Exchange Capacity (CEC) determined According to sodium acetate method USDA (1969) and Kacar (1995), respectively.

Results

Geologic setting and the formation of parent materials

Gölhisar Basin which is located in the southern part of Lake Subregion in the north-western part of the Mediterranean geographical Region of Turkey contains Mesozoic submarine ultramafic volcanic rocks, Mesozoic limestone-marble, neogene sedimentary deposit mostly containing marl and Quaternary fluvio-limnic, alluvial and colluvial deposit (*Figs. 1* and *2*). The basement of the study area is mainly composed of ultramafic rocks especially peridotite-serpentine rocks or parent materials that formed with the eruption of lava erupted from the mid-oceanic ridge and spread on the bottom of the Tethys Ocean occupying the present-day Taurus Mountain belt during the Lower Mesozoic period. The deposited mud composed of carbonates and clay materials on the bottom of Tethys Ocean was converted into limestones with folding and uplifting tectonic movements occurred during the end of Mesozoic Era. Present-day Gölhisar Basin collapsed by the faulting movements was occupied by the Neogene Lake in which clayey and calcareous materials were deposited. Neogene (Pliocene) marly deposits containing marl, sandy clay, calcareous siltstone and sandstone, and clayey layers intercalations are widespread in the southern part of Gölhisar Basin. Thick colluvial and fluvio-limnic deposits are found on the edge of the highlands encircled the Gölhisar

http://www.aloki.hu ● ISSN 1589 1623 (Print) ● ISSN 1785 0037 (Online)
DOI: http://dx.doi.org/10.15666/aeer/1705_1108511106

Basin (Altunbas, 2018; Atalay, 2017; Atalay et al., 2017, 2019a). Alluvions occur on the bottom land of Gölhisar Basin (*Figs. 2* and *3*).

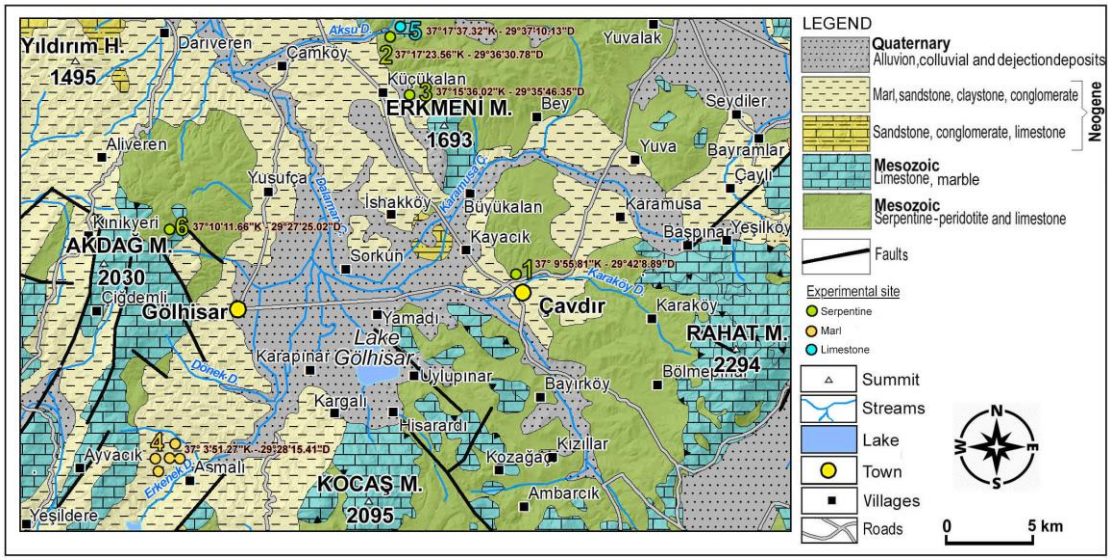

Figure 2. *Geologic parent materials and experimental sites of the study area*

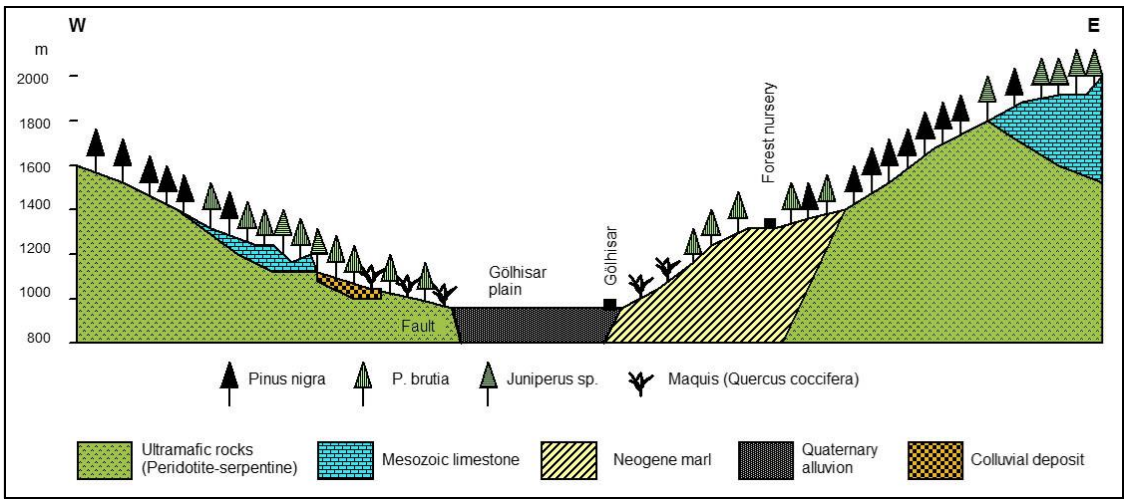

Figure 3. *Geologic cross-section and forest trees distribution in the Gölhisar Basin*

Geomorphic-topographic setting

Present-day topography of Gölhisar Basin was formed by the vertical tectonic movements occurred during the Neogene and Early Quaternary periods (Atalay et al., 2017). Main topographic-geomorphologic units and their formations are shortly explained below:

Mountainous areas

These areas encircling high mountainous areas of the basin were formed by the vertical faulting movements; the relative altitude between the collapsed Gölhisar Basin

http://www.aloki.hu ● ISSN 1589 1623 (Print) ● ISSN 1785 0037 (Online)
DOI: http://dx.doi.org/10.15666/aeer/1705_1108511106

and its encircling highlands is more than 1000 m. Thus, the highlands have been deeply dissected by the streams flowing into the basin. The slope inclination on fault scarps is over 80% especially on the mountain slopes facing Gölhisar town in the west of study area.

Gully landforms

Neogene Lake occupying the Gölhisar Basin was captured by the Dalaman River flowing in to Mediterranean Sea. Thus, emerging the Neogene Lake deposits have been also incised by the streams that established on the neogene deposit surface. Gully landform resembling bedland topography has been formed. The erosion on the marly deposits is commonly seen on the steep slopes of the valley in the southern part of the basin.

Colluvial deposits

Thick colluvial deposits that formed as the result of accumulation of the eroded materials derived from the upland areas are common on the edge of the mountainous areas. There is some close relationship between the topographic-geomorphological units and the growth rate of the trees in the study area, in general.

Physical geography setting

Climate

The climate of the study area is the transitional climate, characterized with a somewhat mild and rainy winters, a moderate hot and rainless summers, between the Mediterranean climate and continental climate of Central Anatolia according to climatic types of Turkey (Atalay, 2012). According to data obtained from the meteorological stations in the study area, mean annual temperature which is 12 °C at the Gölhisar town decreases continually toward the highlands. The mean annual precipitation which is c. 500 mm rises up to 700-800 m in the highlands. In the spreading areas of Calabrian pine (*Pinus brutia*) clusters the mean annual temperature is about 11-12 °C, mean winter temperature is above freezing point, and mean annual precipitation changes between 300 mm and 600 mm. In the *Pinus nigra* occurrence areas, mean annual temperature is nearly 8-9 °C and mean annual precipitation is over 500 mm.

Soil

In the study area, solum horizon is rarely seen due to the active erosion occurring in the sloping area. Most of soils belong to intrazonal soils reflecting the physical and chemical properties of parent materials in the study area (Atalay et al., 2019b). Indeed, lithosol/entisol containing serpentine particles is common at the all serpentine experimental sites. Clayey and calcareous soil is common on the steep slopes of marl deposit. Only thin A horizon of Rendoll subordo of Mollisol ordo or Rendzic Leptosol with clayey loam in texture and alkaline reaction occurs on the flat land of marl deposit. Red Mediterranean soil/Luvisol which is clayey in texture is found along the cracks of limestone at experimental site 5. Colluvial soil containing sandy and gravelly materials is common on the lower edge of hilly area as is found at experimental site 3. Plant nutriment capacity and texture of the soil/parent material depends on the weathering stage of parent materials, in general.

http://www.aloki.hu ● ISSN 1589 1623 (Print) ● ISSN 1785 0037 (Online)
DOI: http://dx.doi.org/10.15666/aeer/1705_1108511106

Vegetation

Two main forest belts are found in the study area: *Pinus brutia* and *Pinus nigra*. The ecological properties of these forests in Mediterranean climatic region of Turkey and the study area are summarized below.

In Turkey, native occurrences areas of Calabrian pine (*Pinus brutia* Ten.) forests beginning seashore climb up to 1500 m on the south facing slopes of Taurus Mountains and cover the lower forest belt of the Mediterranean climatic region of Turkey. Mean annual temperature ranges from 12 to 18 °C and mean January temperature is continually over 0 °C. Mean yearly precipitation changes 400 and 2400 mm most of which fall during the winter season in the optimum growing areas of Calabrian pine forests that are very resistant against drought. It grows all parent materials. The highest productive areas were established summer rainy area and on flysch parent material composed of alternation of sandy, silty, clayey limestone layers in Adana Province (Atalay et al., 1998).

In the study area Calabrian pine (*Pinus brutia*) forest belt generally lies between 1000 and 1200 m and its vertical distribution considerable changes depending on aspect factors (*Fig. 3*). Indeed, the upper limit of the Calabrian pine climb up to 1500 m on the south facing slopes of mountains. Maquis vegetation composed of mainly *Quercus coccifera* which is the lowerstory vegetation of Calabrian pine forest is widespread where Calabrian pine forests have been destroyed.

In Turkey, native occurrence areas of Anatolian *Pinus nigra* subsp. *pallasiana* (Lamb.) Holmboe forests are found between the subhumid-cold climate and subhumid-semiarid continental climate of Turkey and their optimum growing areas cover inland part of the Northern Anatolian Region and oro-Mediterranean forest belt of Taurus Mountains. *P. nigra* forests commence at an elevation of 1000 m in the western inland part of the Northern Anatolia and climb up to 2400 m in the Kahramanmaras Province in the eastern part of Mediterranean Region. In the optimum growing areas the mean annual temperature is about 8 °C, January temperature below the freezing point. The mean annual precipitation is over 600 mm. Good site index of *P. nigra* forests appear backward region of western Black Sea Region, inland part of West Anatolia and oro-regions of Aegean and Mediterranean Mountains (Atalay and Efe, 2010; Atalay, 2014).

In the study area, Anatolian black pine (*Pinus nigra*) forests begin on the upper level of the Calabrian forest belt mostly in the southern highland of the study area and climb up to 2000 m. Some of *Pinus nigra* native occurrence areas are replaced by poor juniper communities composed of *Juniperus oxycedrus, J. foetidissima* and J. *excelsa* in places where *P. nigra* forests have been degenerated and destroyed (*Fig. 3*).

Growth rate of trees at the experimental sites

Experimental sites were selected to determine the growth rate of Calabrian pine (*Pinus brutia*) and Anatolian black pine *P. nigra* on the different parent materials in the Gölhisar Basin. Four experimental sites were selected on the serpentine which is a product of hydrous alternation of ultramafic rocks mostly peridotite in the bottom of ocean covers a large area in the study area (*Figs. 2* and *3*).

The growth of Calabrian pine (Pinus brutia Ten.) experimental sites

To reveal the growth rate of the Calabrian pine (*Pinus brutia*) two experimental sites were selected on the serpentine, one site on the colluvial deposit, and one site on the

http://www.aloki.hu ● ISSN 1589 1623 (Print) ● ISSN 1785 0037 (Online)
DOI: http://dx.doi.org/10.15666/aeer/1705_1108511106

marl deposit; totally four sites belong to the Calabrian pine cluster (*Fig. 2*). General description sites and the measurement of age, height and diameter of *Pinus brutia* at the experimental sites are introduced below.

Experimental site 1

Located near the highway between Burdur-Gölhisar.

General description of the site: Experimental site is located near the Gölhisar-Burdur road, 10 km NE of Gölhisar, at an elevation of 1100 m, 37°9'55.81"N-29°42'8.89"E. Undulating topography is dominant; serpentine is exposed in most part of the area due to the intense erosion. The height and diameter of *Pinus brutia* trees changes frequently depending on weathering degree of the serpentine; the highest height of *P. brutia* is found on the bottom of valley due to the collection of water and weathered serpentine; while, *P. brutia* trees which are in chaparral appearance are found on the exposed unweathered serpentine (*Table 1*; *Fig. 4*). Shirking aspect of this site it to show great changes on the height, diameter and age of *Pinus brutia* trees depending on different weathering stage of serpentine.

Table 1. *The height, diameter and age of Pinus brutia on serpentine experimental site at an elevation of 1110 m in the 10 km NE of Gölhisar town, 37°9'55.81"N-29°42'8.89"E*

Weathering degree of serpentine	Location of trees	Height (m)	Diameter (cm)	Age (year)
Good weathered	1. Bottom of small valley	14	38	45
Exposed serpentine	2. The upper part of hill slope	1.2	4	30
Semi weathered	3. Top of the hill	3.5	37	16
Weathered	4. Top of hill	3.2	14	37
Weathered	5. Top of hill	8	26	36
Semi weathered	6. Top of hill	4	26	36

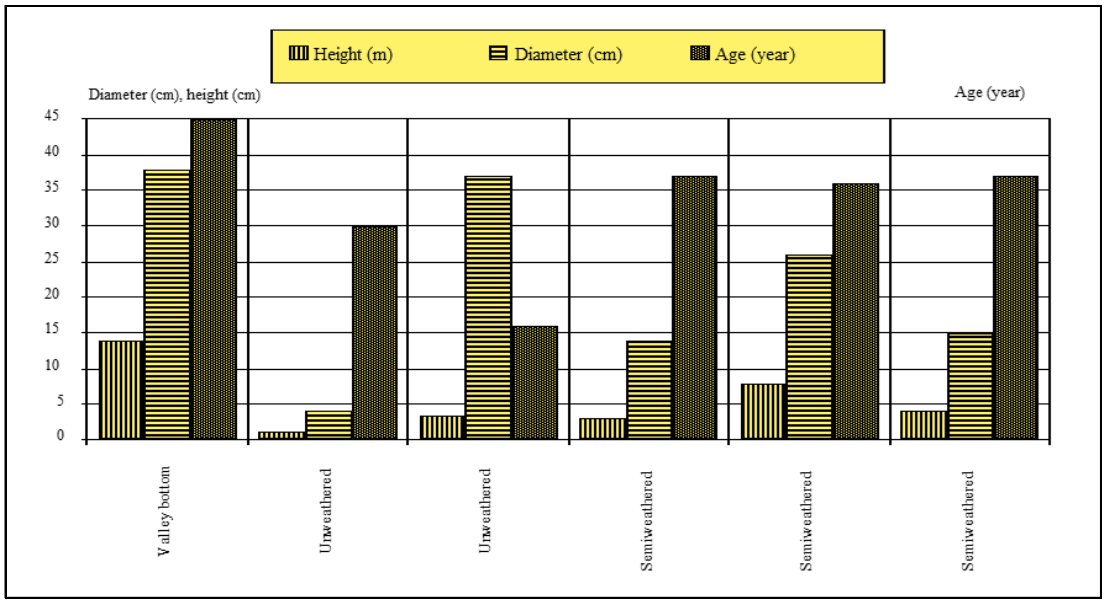

Figure 4. *The graph illustrating the relationships among height, diameter and age of Pinus brutia at the experimental site 1*

http://www.aloki.hu ● ISSN 1589 1623 (Print) ● ISSN 1785 0037 (Online)
DOI: http://dx.doi.org/10.15666/aeer/1705_1108511106

Experimental site 2

Located on the western aspect of the valley in the c. 30 km north of Gölhisar, 37°17'23.56"N-29°36'30.78"E.

General description of the site: Serpentine parent material is common. The weathering degree changes frequently depending of the slope inclination and erosion process. Semi weathered serpentine is widespread on the slightly inclined surface, but unweathered serpentine is exposed on steep slopes of valley. The dissected topography is common; slightly surfaces are found upper parts of the hills.

In this site great differences in the growth of *Pinus brutia* are seen to have depended on weathering of the serpentine. Indeed, the lowest growth rate was established on the active erosion place of steep slopes of valley on which unweathered serpentine was outcropped. There no great differences among the height of *P. brutia* on the slightly inclination area (*Table 2; Fig. 5*).

Table 2. *The height, diameter and age of Pinus brutia on weathered serpentine experimental site at an elevation of 1100 m near road in 25 km NNE of Gölhisar, 37°17'23.56"N-29°36'30.78"E*

Weathering degree of serpentine	Location of tree	Height (m)	Diameter (cm)	Age (year)
Weathered serpentine	The slope inclination low	16	34	85
Weathered serpentine	The slope inclination low	21	42	98
Low weathered serpentine	Inside of valley, active erosion	6	9	50

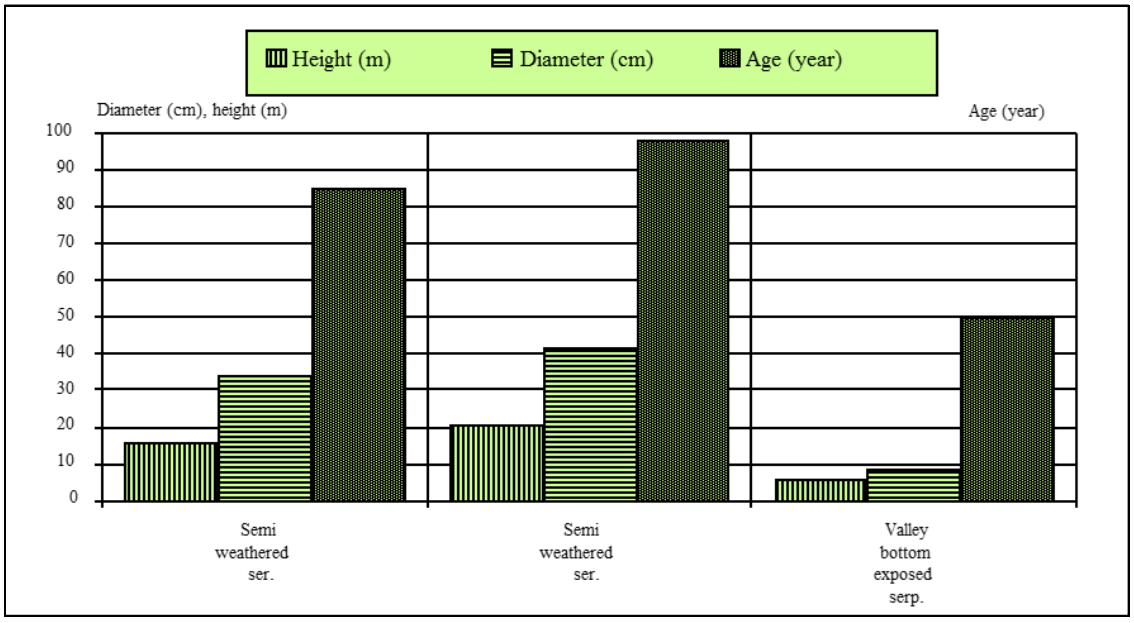

Figure 5. *The graph showing the relationships among height, diameter and age of Pinus brutia at the experimental site 2 on serpentine*

http://www.aloki.hu ● ISSN 1589 1623 (Print) ● ISSN 1785 0037 (Online)
DOI: http://dx.doi.org/10.15666/aeer/1705_1108511106

Experimental site 3

Located on the colluvial deposit in the Gölova Forest Directory, near forest fire observation tower, at an elevation of 1150 m, 37°15'36.02"N- 29°35'46.35"E.

General description of the site: Topographically this site is found on slightly inclined area lying on the edge of hilly area. The colluvial deposit has been formed with the accumulation of the small gravels, sands and silts transported by the running water derived from the serpentine area. The reddish colour of the colluvial deposit clearly reflects a good oxidation process.

Thick colluvial deposit creates a good habitat for the growth of *Pinus brutia*. Because both horizontal and taproot development of root structure clearly show the existence of good ecological conditions on colluvial deposit. For this reason, there is no great difference among the height of trees in terms of height, diameter and age (*Table 3; Fig. 6*). The productive *P. brutia* trees are only found on the colluvial deposit when compared to other sites.

Table 3. *Calabrian pine cluster on the colluvial gravelly deposit in Gölova forest directory of Gölhisar, 37°15'36.02"N-29°35'46.35"E*

Parent material	Topography	Height (m)	Diameter (cm)	Age (year)
Very thick gravelly, sandy colluvial deposit	Slightly inclined surface of colluvial deposit	12.5	32	57
Same	Same	16	39	53
Same	Same	17	40	58

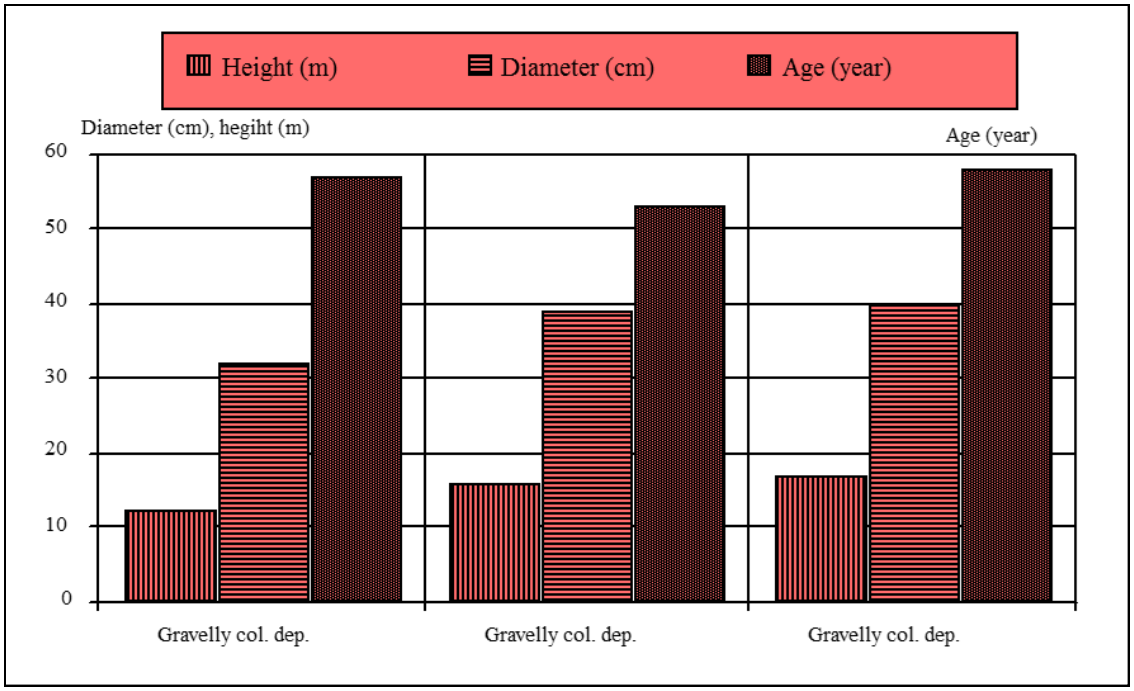

Figure 6. *The graph showing the relationships among height, diameter and age of Pinus brutia on the colluvial deposit*

http://www.aloki.hu ● ISSN 1589 1623 (Print) ● ISSN 1785 0037 (Online)
DOI: http://dx.doi.org/10.15666/aeer/1705_1108511106

Experimental site 4

Located on the neogene marl deposit in the eastern part of the Gölhisar town at an elevation of 1100 m, 37° 3'51.27"N, 29°28'15.41"E.

General description of site: Parent material is composed of marl deposits; it contains both horizontal and inclined calcareous sandstone, siltstone layers and gravelly lenses belonging to fluvial deposit. Marl deposit has been dissected by the tributaries of the main stream flowing into Gölhisar Plain. Small flatlands are seen on the horizontal layer among the upper parts of valleys. The debris flows occur on the steep slopes of valley. Entisol is common on the sloping areas; thin A horizon with rich organic content belonging to rendzina (Rendoll, Rendzic leptosol) is only seen on the flat land. *P. brutia* clusters occur everywhere of the area. But productive *P. brutia* is found on the soft marly deposit and inclined layers. A somewhat productive *P. brutia* trees appear on the marl horizontal layers with soft and crack structure supporting the taproot development, while compact marl creates a poor habitat for the growth of *Pinus brutia*. Besides the high sun radiation somewhat prevents the productivity of *Pinus nigra* on the slopes facing-south due to summer aridity. The growth rate of the Calabrian pine on the marl deposit is generally good as compared with the serpentine parent materials (*Table 4; Fig. 7*).

The growth of Anatolian black pine (Pinus nigra subsp. pallasiana) experimental sites

Anatolian black pine (*P. nigra*) forests appearing upper boundary of the Calabrian pine (*P. brutia*) belt are found only small cluster in the N of Gölhisar and mountainous areas rising 2000 m of elevation in the southern part of the Gölhisar town. To reveal the growth rate of the Anatolian black pine on the limestone and serpentine two experimental sites were selected. General description sites and the measurement results of these experimental sites are introduced below.

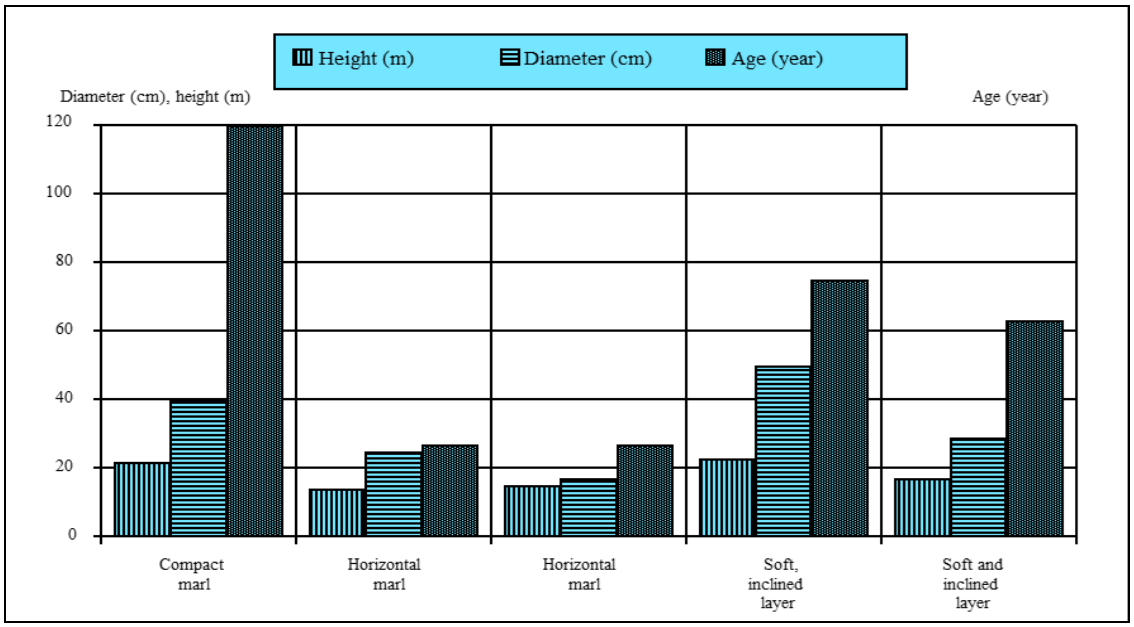

Figure 7. *The graph showing relationships among height, diameter and age of Pinus brutia at the experimental site 4 on the marl deposit*

http://www.aloki.hu ● ISSN 1589 1623 (Print) ● ISSN 1785 0037 (Online)
DOI: http://dx.doi.org/10.15666/aeer/1705_1108511106

Table 4. *Calabrian pine growing on the neogene marl deposit in the north of Gölhisar town*

Properties of neogene deposits	Location	Height (m)	Diameter (cm)	Age (year)
Horizontal hard layers	Almost flat land near road	21.5	40	120
Horizontal layers	Flat and radiation intensity high	14	25	27
Horizontal marl layer	Flat and low radiation intensity	15	17	27
Soft and inclined marly layer	Upper part of the hill near Gölhisar road	23	50	75
Soft and inclined marly layer	Lower part of the hill near Gölhisar road	17	29	63

Experimental site 5

Located near the highway between Burdur-Gölhisar, at an elevation of 1200 m, 37°17'37.32"N-29°37'10.13"E.

General description of site: Located in the 30 km NNW of Gölhisar town. Cracked and crystallized limestone is common on the serpentine. The slope inclination is very low. Most of the *Pinus nigra* trees have been destroyed to obtain timber; thick litter cover appears under the of *Pinus nigra* cluster on the limestone. There is no surface erosion due to the rainfall easily infiltrates along the limestone cracks. There are no notably differences among *P. nigra* trees in terms of the height, diameter and age, in general (*Table 5; Fig. 8*). Cracked limestones containing low content of clay create a suitable condition for the growth of *P. nigra*; because of the roots of *P. nigra* easily develop toward the deeper part along the cracks of limestone.

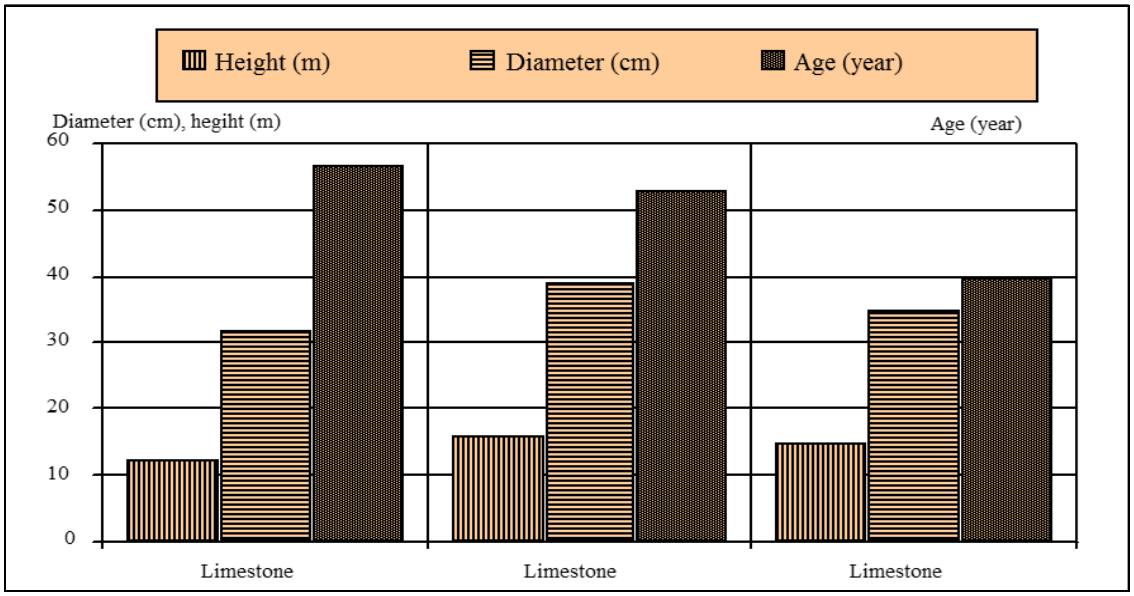

Figure 8. *Relationships among height, diameter and age of Pinus brutia at the experimental site 5 on the limestone*

http://www.aloki.hu ● ISSN 1589 1623 (Print) ● ISSN 1785 0037 (Online)
DOI: http://dx.doi.org/10.15666/aeer/1705_1108511106

Table 5. *Anatolian black pine cluster on the limestone, near the road, 25 km NNW of Gölhisar, 37°17'37.32"N, 29°37'10.13"E*

Parent material	Topography	Height (m)	Diameter (cm)	Age (year)
Cracked Mesozoic limestone	Hill edge slightly inclination	17	41	48
Cracked limestone	Limestone blocks	14	30	38
Cracked limestone	Limestone blocks	15	35	40

Experimental site 6

Güdük Hill locality on Ak Mountain, far from 30 km in the west of Gölhisar town, 1600-1700 m, 37°10'11.66"N-29°27'25.02"E.

Description of the site: Güdüktepe locality is found at an elevation of 1600-1700 m on the east facing slopes of the Ak Mountain in the western part of Gölhisar town (*Fig. 1* and *2*). Parent material is composed of cracked and unweathered serpentine. Inclination of the slope is more than 60%, and its elevation is about 1600-1700 m. Güdük Hill is one of the main spreading areas of *P. nigra* forests. Here lithosol/entisol is common due to intense erosion. Lithosol and over grazing activity prevents considerably the regeneration of *P. nigra*. That is why; *P. nigra* seedlings that are rarely seen indicate presence of low native regeneration.

In this experimental site, *P. nigra* grows within the cracks and the partly weathered vertical zone of serpentine. The highest *P. nigra* is found on the cracked serpentine; because the roots of the *P. nigra* easily follow deeply along the cracks of serpentine. Shrinking aspect of this area, weathered serpentine particles have been transported by the runoff due to high inclination of the slope. It can be said that the site index of the *P. nigra* is in poor quality on the exposed serpentine. The growth rate of *P. nigra* is tend to increase from the steep slope to the upper part of the hill and wide bottom of valley, in general. However, there is no direct relationship between the diameter and height of *P. nigra* trees, but considerable differences of *Pinus nigra* age imply the weathering process occurring along the cracks of serpentine, especially in the root zone (*Table 6; Fig. 9*).

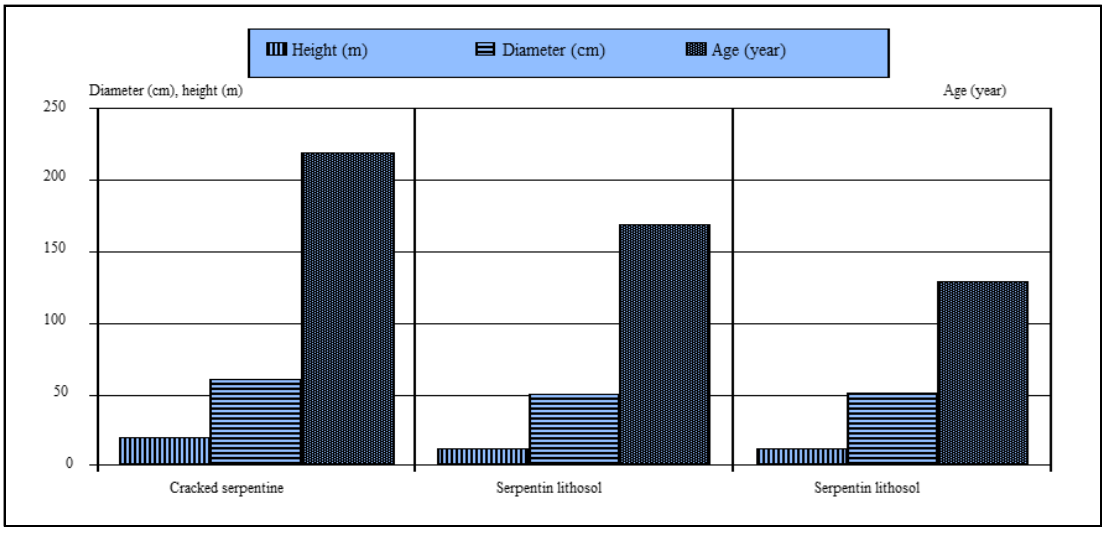

Figure 9. *Relationships among height, diameter and age of Pinus nigra at the experimental site 6 on the serpentine in the Göktepe locality, Ak Mountain*

http://www.aloki.hu ● ISSN 1589 1623 (Print) ● ISSN 1785 0037 (Online)
DOI: http://dx.doi.org/10.15666/aeer/1705_1108511106

Table 6. *Relationships among height, diameter and age of Pinus nigra at the experimental site 6 on the serpentine*

Parent material	Topography	Height (m)	Diameter (cm)	Age (year)
Cracked serpentine rock	Slightly inclined surface	21	62	220
Lithosol	Near top of hill	13	51	170
Lithosol	Lower slope of valley	13	52	130

Relationship between growth rate of vegetation and physical and chemical properties of parent materials

According to field observations and the data of laboratory analysis of soils and parent materials in the study area there is close relationship between the growth rate of vegetation and weathering degree and/or stage of serpentine. As is seen experimental site 1, the highest height Calabrian pine tree is found on good and deeply weathered serpentine with CEC (Cation exchange capacity) 33 $cmol_c\ kg^{-1}$, this figure is c. 13 $cmol_c\ kg^{-1}$ at the site of the lowest height of Calabrian pine (*Table 7*). Poor stand forest in appearance of dwarf trees and shrubs are common on the low weathered and exposed serpentine which is in green colour. One of these areas notably preventing factor to grow of herbaceous vegetation is found at the Taşpınar locality in the SW of Lake Ak. Here CEC of low weathered and exposed serpentine is about 2 $cmol_c\ kg^{-1}$. In this place other preventing factor is the presence of thin sandy soil with very low field capacity and dissecting with rills that are formed with the transportation of sandy particles by runoff (*Table 8*). The presence of a few *Pinus brutia* trees are not related the low CEC on the sandy soil because the growth of *P. brutia* depends on the weathering process in the root zone. In other words, the release of the plant nutriments on the serpentine surface determine only the growth of seedlings and herbaceous vegetation but the growth rate and/or productivity of trees is mainly related to the weathering degree of the root zone (*Table 7*). Organic material of all sites is less than 1%.

Table 7. *Some physical and chemical properties of serpentine at experimental site 1*

Parent material properties	Sand (%)	Clay (%)	Silt (%)	Texture class	$CaCO_3$ (%)	K ($cmol_c\ kg^{-1}$)	Ca ($cmol_c\ kg^{-1}$)	Mg ($cmol_c\ kg^{-1}$)	Na ($cmol_c\ kg^{-1}$)	CEC ($cmol_c\ kg^{-1}$)
Upper part of weathered serpentine	59	21	20	SCL	13.7	1	51	4.3	0.26	24.3
Lower part of weathered serpentine	79	7	14	LS	5.1	0.2	60	12	0.5	33
Less weathered serpentine	71	13	16	SL	6.7	0.1	39.4	3.4	12	12.9
Sand of serpentine	73	7	20	SL	1.5	0.04	3.2	3.4	12	20

On the other hand, release of the $CaCO_3$, clay contents and cations mainly of Ca^{++} and Mg^{++} are higher on the deeply weathered serpentine than on low weathered serpentine. This is responsible for the increase of CEC in the weathered serpentine (*Tables 8–10; Fig. 10*).

http://www.aloki.hu ● ISSN 1589 1623 (Print) ● ISSN 1785 0037 (Online)
DOI: http://dx.doi.org/10.15666/aeer/1705_1108511106

Table 8. *Some physical and chemical analysis of exposed serpentine at Taşpınar locality, 37°38'38.13"N-29°45'33.46"E in the SW of Lake Ak locality, north of Gölhisar Basin*

Parent material properties	Sand (%)	Clay (%)	Silt (%)	Texture class	$CaCO_3$ (%)	K ($cmol_c\ kg^{-1}$)	Ca ($cmol_c\ kg^{-1}$)	Mg ($cmol_c\ kg^{-1}$)	Na ($cmol_c\ kg^{-1}$)	CEC ($cmol_c\ kg^{-1}$)
Exposed soft serp. with rill	67	6	27	SL	14.8	0.1	10	9.7	0.1	1.8
Low weathered bare serp.	67	6	27	SL	2.9	0.1	10	9.7	0.11	2.0
Low weathered bare serp.	71	13	16	SL	6.7	0.1	39.4	3.4	12	12.9
Partly weathered serp. with herb	65	9	26	SL	2	0.8	21	5.7	0.14	14.5

Table 9. *Some physical and chemical data of serpentine melange area at 2 km northwest of Yeşilova town, 37°31'13.34"N-29°46'39.32"E, Burdur province*

Parent material properties	Sand (%)	Clay (%)	Silt (%)	Texture class	$CaCO_3$ (%)	K ($cmol_c\ kg^{-1}$)	Ca ($cmol_c\ kg^{-1}$)	Mg ($cmol_c\ kg^{-1}$)	Na ($cmol_c\ kg^{-1}$)	CEC ($cmol_c\ kg^{-1}$)
Deeply weathered serpentine	46	25	29	L	33	0.3	36.3	13.5	0.12	34.4
Deeply weathered reddish serpentine	37	29	24	CL	23	0.4	37.5	14.7	0.13	43.8
Less weathered serpentine	79	9	12	LS	33.7	0.05	20.8	2.8	0.03	13.8

Table 10. *Some physical and chemical analysis of marl deposits in the south of Gölhisar town*

Parent material properties	Sand (%)	Clay (%)	Silt (%)	Texture class	$CaCO_3$ (%)	K ($cmol_c\ kg^{-1}$)	Ca ($cmol_c\ kg^{-1}$)	Mg ($cmol_c\ kg^{-1}$)	Na ($cmol_c\ kg^{-1}$)	CEC ($cmol_c\ kg^{-1}$)
Marl deposit in S of Gölhisar	17	27	56	SiL	53.7	0.8	49.6	15.3	0.29	23.8
Marl deposit	11	47	42	SiC	48	1.3	40.7	18.7	0.28	33.7
Compact marl deposit	21	23	56	SiC	40.5	0.4	34.4	8.7	0.15	10.48

The weathering process in melange area that is composed of the mixture limestone and serpentine frequently changes. In such area, the amounts of CEC of the serpentine depend on the weathering and oxidation process. For instance, in the melange area at the 2 km northwest of the Gölhisar town CEC changes between 12.8 and 43.8 $cmol_c\ kg^{-1}$ (*Table 9*). The fertile agricultural fields are common on the flat land of melange areas of the study area in general. On the other hand, the cracks of serpentine contribute to develop deeply of root system, and chemical and physical weathering processes occurring along the root

http://www.aloki.hu ● ISSN 1589 1623 (Print) ● ISSN 1785 0037 (Online)
DOI: http://dx.doi.org/10.15666/aeer/1705_1108511106

and crack zones contribute tend to increase the releases of the abundant plant nutriments. This situation produces a good habitat for the growth of trees. In fact, cracked serpentine and deeply developed root system support to increase of the biomass productivity of all trees.

CEC of the soil developed on the serpentine changing between 35 and 50 $cmol_c\ kg^{-1}$ forms fertile agricultural lands in the Gölhisar Basin. Soft marl deposit containing sand particles is generally responsible for the growth of forest due to deeply root development of trees. While compact marl deposit and horizontal compact layers mostly prevent to form good stand of forest because taproot development of trees is very hard and CEC is less than the soft marl deposit (*Table 10*).

General relationships among the height, diameter and age of the trees

There are great differences among the height, diameter and ages of the trees at most of the experimental sites. The highest differences are seen in *P. brutia* sparse cluster on the different weathered serpentine at experimental site 1. Here, the ranges of the height 1.2 m to 8 m, diameter 4 to 37 cm, and age 16 to 45 years. This is mainly related to the weathering stages of serpentine. There is no considerable difference among the *P. brutia* trees on serpentine colluvial deposit at experimental site 3 and *P. nigra* trees at experimental site 5 on the limestone. These last two sites can be regarded as productive forest cluster (*Fig. 10*).

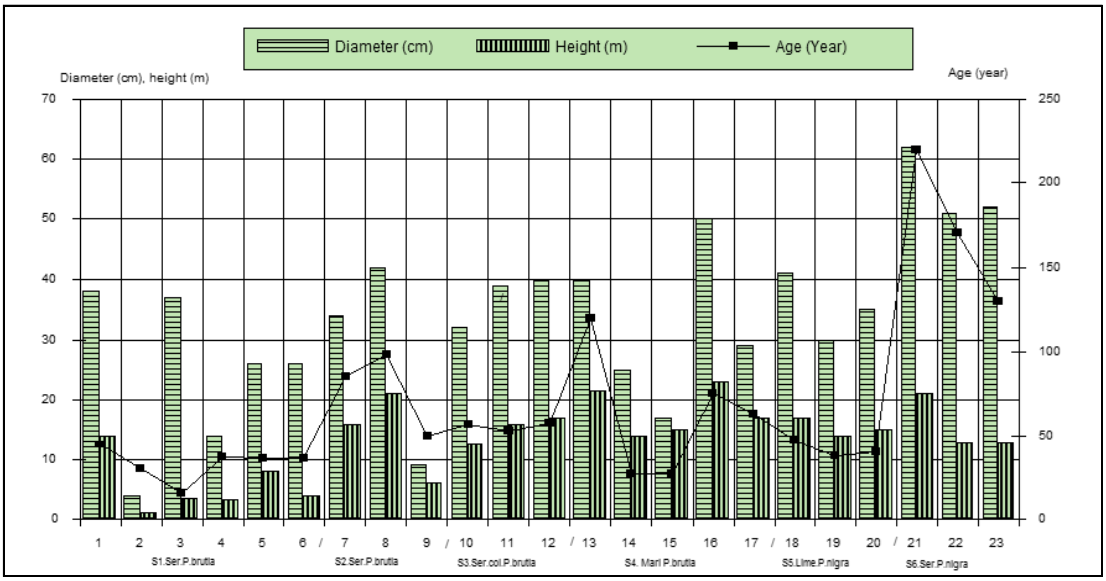

Figure 10. *The graph showing relationships among the age, diameter and height of the individual trees at the experimental sites reveals the importance of the tree growth notably depending on parent materials. "/" indicates between the boundary of experimental sites. (Abbreviations: S1, 2, 3... experimental sites. Ser. serpentine. Ser. col. Serpentine colluvial deposit)*

General relationship between height and age

Relationship between height and age is one of the indicators of the productivity in uniform ecological environment. In the productive habitats there are very little differences between the height and diameter of trees (Saatcioglu, 1976). Very little

http://www.aloki.hu ● ISSN 1589 1623 (Print) ● ISSN 1785 0037 (Online)
DOI: http://dx.doi.org/10.15666/aeer/1705_1108511106

differences between height and age are found among the *P. nigra* trees growing on the limestone at experimental site 5 and among the *P. brutia* trees growing on the serpentine colluvial deposit at site 3. Here parent materials are in uniform properties. The increase of the differences among the trees indicates clearly the existence of different parent materials and their weathering stages. The existence of great difference between the height and age may relate to the inclination of layer and compactness of marl deposit at the experimental site 5 (*Fig. 11*).

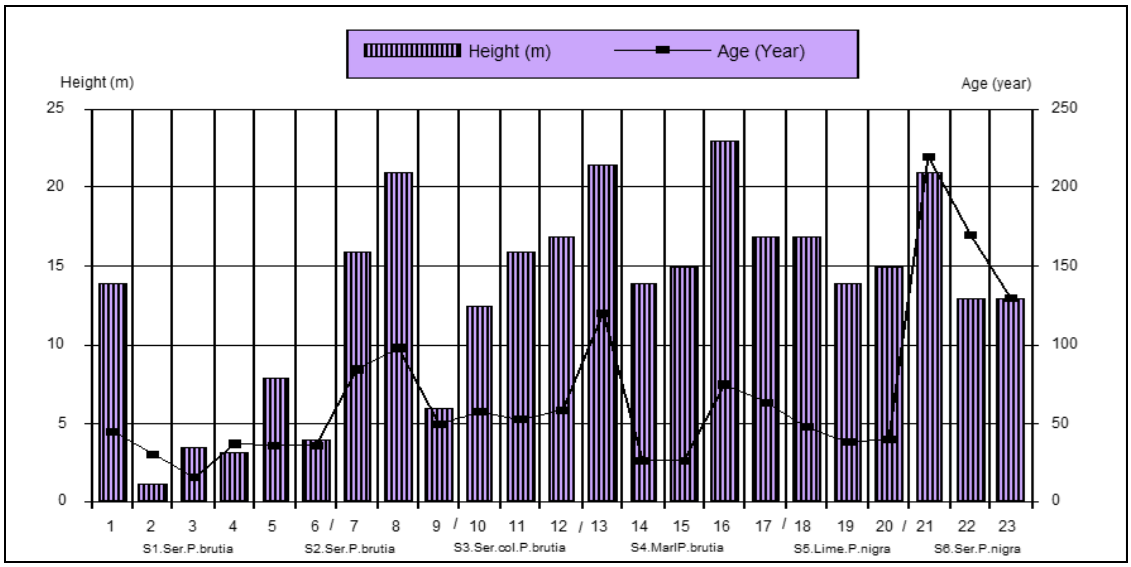

Figure 11. *The relationship between height and age of trees in the experimental sites*

The general relationship between age and diameter

As a general rule, the thickness of diameter continually increases toward the end of felling cycle (rotation, length) of trees and diameter thickness is the best indicator of the annual increment of trees. There is irregular relationship between age and thickness of diameter of most of trees in the study area. Indeed, the great changes are found between the age and diameter at experimental sites 1, 2, 4 and 6; this is related to the different weathering process of the parent materials, while the reasonable relationship between diameter and age is found on the serpentine colluvial deposit at site 3 and on the limestone at site 5 (*Fig. 12*).

Available water effects on the tree growth

Available water capacity of the soil and parent material is generally low due to high inclination surface and sandy and sandy loam texture of soil. Most of the atmospheric water flow as runoff/overland flow on the serpentine and marl deposit occurring on the inclined surface. Here available water of trees depends on the amount of infiltration capacity of water through the cracks and collection of water in the root zone. In the karstic/limestone area almost all atmospheric water easily infiltrates via the cracks of limestone; thus, tree roots take available water from the soil that is developed along the cracks. For this reason, the tree growth rate is higher on the karstic land occurring in the study area, especially at site 5. Meanwhile, that tree productivity is high on colluvial deposit as is the site 3 is related to the accumulation of the water. Individual tree growth also depends on the available water

http://www.aloki.hu ● ISSN 1589 1623 (Print) ● ISSN 1785 0037 (Online)
DOI: http://dx.doi.org/10.15666/aeer/1705_1108511106

content in the root zone. For example, at the experimental site 1 the lowest growth rate of *Pinus brutia* tree is found on the steep slopes, while highest growth rate of *Pinus brutia* is found on the bottom of the small valley due to water collection (*Table 1; Fig. 4*). Field capacity is very low on the sandy material on the serpentine occurring sloping area especially in the vicinity of Taşpınar village. Here the occurrence of the rill erosion and absence of herbaceous vegetation is mainly related to the transportation of mostly sandy particles by runoff and low field capacity of sandy soil.

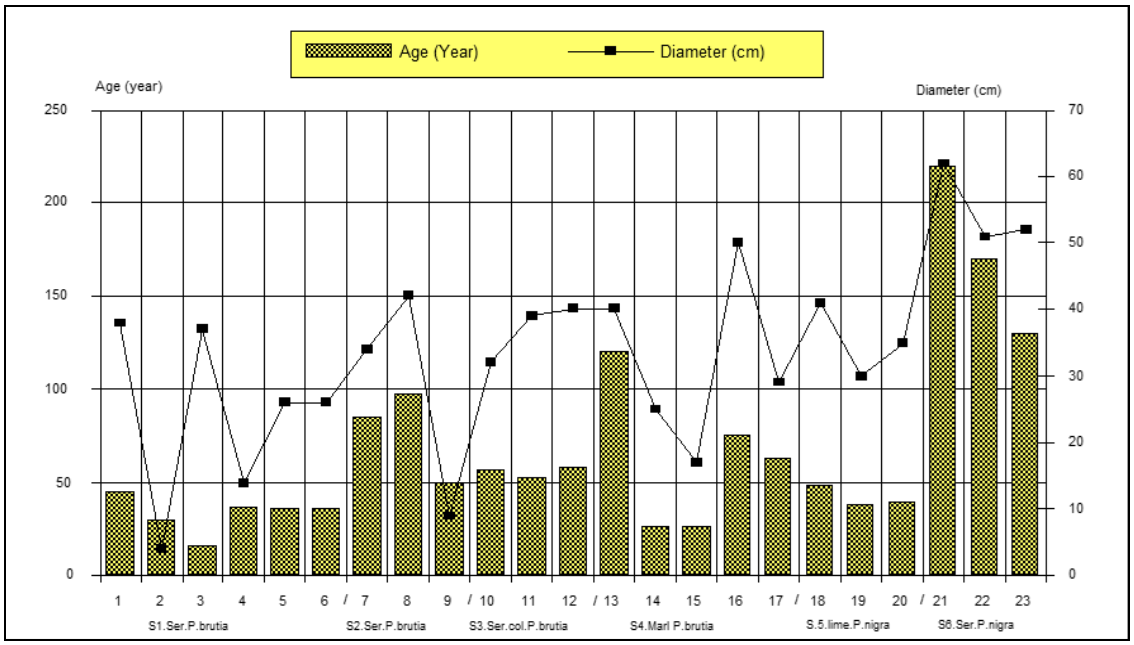

Figure 12. *The relationships between age and diameter at the experimental sites*

Human impact on the growth of trees

The settlement history of Gölhisar basin back to Neolithic period dated at least 7000 year BP (Roberts, 1990; Atalay, 1992). The vegetation especially forest destruction was probably commenced during the Roman period. At that time the famous historical city Kibyra (UNECO heritage city) was located on the crossroads of Phrygian, Carian, Lycian and Pisidian cultures and of commercial routes running east-west and north-south directions on the lower slope of the Ak Mountain in 1 km south of present-day Gölhisar town. Up to present time, most of the forests have been destroyed and degenerate to obtain timber and agricultural land. With the degeneration of the forest, soil and parent material erosion has been started on the sloping area. Thus, parent materials have been outcropped in the various parts of Gölhisar depression. As mentioned before, outcropped parent materials have been led to decrease the growth rate of the trees at most of the experimental sites. It can be said that forest destruction is one of the main reasons of tree growth on parent materials exposed on the degenerated forest area of Gölhisar Basin.

Statistical evaluation

According to statistical evaluation depending on the height, diameter and age of the trees, one-way ANOVA test for *Pinus brutia*, no significant correlation was found in the data range ($P < 0.05$).

http://www.aloki.hu ● ISSN 1589 1623 (Print) ● ISSN 1785 0037 (Online)
DOI: http://dx.doi.org/10.15666/aeer/1705_1108511106

As a result of the independent T-test for Pinus nigra, a significant correlation was found on the age and diameter of the trees ($P < 0.05$) of different parent material. A difference in the tree heights of different parent materials ($P < 0.05$) was not found.

Discussion

Vegetation growth and its productivity depend on not only climatic conditions but also physical and chemical properties of the parent materials. In the flat and slightly undulating areas of same climatic region parent material effects on the tree growth is very little. In these areas site index of forest is found in same category. But growth rate and/or productivity of forest changes considerably depending on the weathering process of the parent materials. In Turkey, the site index of forests shows great difference in terms of timber quality and biomass productivity. For example, the low site index Calabrian pine occurs on the siliceous parent material in north of Foca in the north of Aegean Sea shore, trachyte in south of the Lake Tortum, low weathered serpentine in western coastal belt of Antalya Gulf, Datça peninsula in the south-western part of Anatolia and horizontal marl deposits (Çukur, 1999; Çukur and Atalay, 2004; Atalay, 2014; Atalay and Efe, 2014).

On the other hand, the parent material effects on the tree growth are one of the significant procedures in the silvicultural application and reforestation and afforestation activities. For example, the seedlings to be planted on compact marl deposit have been subjected to dry during one and three year period, because the vertical development of seedlings' roots has been prevented by the horizontal layered and compact marl deposit (Atalay et al., 2014). To make successful reforestation and afforestation marl deposit should be deeply ploughed to plant the seedlings. Unweathered and low weathered serpentine forming hard surface also mostly prevents the natural regeneration. As a matter of fact, the cedar (*Cedrus libani*) plantation to be carried out on the marl deposit and serpentine is not appropriate application since the ecology of the cedar is taken into consideration in the Burdur-Gölhisar Basin. First time, the CEC of the serpentine depending on weathering process and marl deposit on the growth of trees are explained in our study. Stone pine (*Pinus pinea*) reforestation to be carried out on the serpentine is inappropriate application, because this pine only grows on the sand dunes and sandy soil developed on the granite and gneiss under the Mediterranean climatic conditions (Atalay, 2014). In the forest management planning and the classification of forest stand index, the importance of parent material effects have been not sufficiently used in Turkey.

The importance of serpentine, marl and limestone forming lithobiome is detailed explained on the tree growth and the response to the land degradation process. Indeed, in the study area, the exposed unweathered serpentine and marl deposit on the forest destroyed sloping areas can be regarded as vulnerable areas for the formation of land degradation.

To establish the productivity and/or site index and to select the species of trees in the reforestation and afforestation activities it is necessary to classify the natural environment according to lithobiomes and pedobiomes (Bailey, 1995a, b, 1998; Atalay, 2014). These biomes form a distinct habitat on which flora and fauna is different than that other biomes. To classify of given natural environment as biomes can be regarded the one of fundamental principles of sustainable planning of the plant especially forest growth, site index and productivity. On the other hand, these classifications will

http://www.aloki.hu ● ISSN 1589 1623 (Print) ● ISSN 1785 0037 (Online)
DOI: http://dx.doi.org/10.15666/aeer/1705_1108511106

contribute the selection of tree species in the reforestation and afforestation activities and silvicultural applications. However, similar studies relating to forestry have not been conducted except for "Ecoregions of Turkey (Atalay, 2014).

Conclusion

The parent material effects on the growth rate and/or productivity of trees in the sloping areas is one of leading issues in the determination of forest products, silvicultural applications and reforestation activities. In the study first time we analyzed the importance of the serpentine, limestone, marl and colluvial deposits on the growth of *Pinus brutia* and *Pinus nigra* trees. In the further studies the lithobiomes and pedobiomes should be used in the assessment of the natural environment and tree growth, and similar studies should be carried out. These studies are necessary to sustainable planning on the forest production and maintain the natural equilibrium.

Acknowledgements. We would like to offer our gratitude to Forest Engineer Oktay Demirci for measurements of the height, diameter and age of the trees and Emrah Ramazanoglu for statistical evaluation of trees. We would like special thanks to Bekir Karacabey, General Director of Forest of the General Forest Directory, Ministry of Agriculture and Forest, Kenan Akduman, Isparta Regional Director of Forest and Celal Korkmaz Burdur Forest Operation Manager for their supports and helps the project named "Ecology, ecosystem and Rehabilitation of Marble Quarries in the Burdur-Gölhisar Basin", prepared by I. Atalay, S. Altunbas and M. Siler.

REFERENCES

[1] Altunbas, S. (2018): Pedogeomorphology of the Burdur-Gölhisar Basin, SW Anatolia, Turkey. – Fresenius Environmental Bul. 28(1-2): 139-149.
[2] Atalay, İ. (1987): Sedir (*Cedrus libani* A. Rich) General Ecological Properties of the Natural Occurrence Areas of Cedar (*Cedrus libani* A. Rich) and Regioning of Seed Transfer of Cedar in Turkey. – Publications of General Directorate of Forestry 663/61, Ankara.
[3] Atalay, İ. (1992): The Paleogeograhy of the Neareast (From Late Pleistocene to Early Holocene) and Human Impact. – Aegean University Press, Bornova, Izmir, Turkey.
[4] Atalay, İ. (1997): Red Mediterranean soils in some karstic regions of Taurus Mountains, Turkey. – Catena 28: 247-260.
[5] Atalay, İ. (2012): Applied Climatology. – Meta Press, İzmir.
[6] Atalay, İ. (2014): Ecoregions of Turkey (2nd Ed.). – Meta Press, İzmir.
[7] Atalay, İ. (2016a): Applied Geomorphology (in Turkish). – Meta Press, İzmir.
[8] Atalay, İ. (2016b): Soil Formation, Classification and Geography (in Turkish). – Meta Press, İzmir.
[9] Atalay, İ. (2017): Geomophology of Turkey (in Turkish). – Meta Press, İzmir.
[10] Atalay, İ., Efe, R. (2010a): Structural and distributional evaluation of forest ecosystems in Turkey. – Journal of Environmental Biology 31: 61-70.
[11] Atalay, İ., Efe, R. (2010b): Ecology of the Anatolian Black Pine (*Pinus nigra* subsp. *pallasiana* (Lamb.) Holmboe) and Its Dividing into Regions In Terms Of Seed Transfer. – Publications of Ministry of Environment and Forestry No. 424, Publications of Seed Breeding Research Directorate No. 37.
[12] Atalay, İ., Efe, R. (2014): The Factors Determining of Forest Productivity in the Western Part of Taurus Mountains (SW Anatolia). – In: Efe, R., Öztürk, M. (eds.) Tourism -

http://www.aloki.hu ● ISSN 1589 1623 (Print) ● ISSN 1785 0037 (Online)
DOI: http://dx.doi.org/10.15666/aeer/1705_1108511106

Environment and Ecology in the Mediterranean Region II. Chap. 8. Cambridge Scholars Publishing, Cambridge, UK, pp. 111-128.

[13] Atalay, İ., Sezer, L. İ., Çukur, H. (1998): Kızılçam (Pinus brutia Ten.) Ecology of Red Pine (Pinus brutia Ten.) Forests and Their Dividing into Regions in Terms of Seed Transfer. – Publications of Forest Trees and Seed Breeding Research Directorate, No: 6.

[14] Atalay, İ., Adıgüzel, H., Dal, N. (2017): Geomorphological evolution of the Gölhisar depression, SW Anatolia, Turkey. – In: Tonbul, S. Şengün, T., Siler, M., Canpolat, A. (eds.) Proceeding Book of the International Symposium on Geomorphology, 12-14 October 2017, pp. 137-145.

[15] Atalay, İ., Altunbas, S., Siler, M., Dal, N. (2019a): Ecology, Ecosystem and Rehabilitation of Marble Quarries in the Burdur-Gölhisar Basin, SW Anatolia. – General Directorate of Forestry, Ankara (in press).

[16] Atalay, İ., Altunbas, S., Siler, M. S. (2019b): The Importance of Marl Deposits on the Soil Formation, Land-Use and Land Degradation in Turkey. – In: Namlı, A. et al. (eds.) Proc. of 10th International Soil Congress, Successful Transformation toward Land Degradation Neutrality: Future Perspective, Akça, pp. 82-89.

[17] Black, C. A. (1965): Soil-Plant Relationships. – John Wiley and Sons, Inc., New York.

[18] Bouyoucos, G. J. (1955): A reclamation of the hydrometer method for making mechanical analysis of the soils. – Agronomy Journal 4(9): 434.

[19] Bailey, R. G. (1995a): Description of the Ecoregions of the United States. – United States Department of Agriculture Forest Service, Pub No. 1391, Washington, DC.

[20] Bailey, R. G. (1995b): Ecosystem Geography. – Springer, New York.

[21] Bailey, R. G. (1998): Ecoregions. The Ecosystem Geography of the Oceans and Continents. – Springer, New York.

[22] Carter, S. P., Proctor, J., Slingsby, D. R. (1987): Soil and vegetation of the Keen of Hamar serpentine, Shetland. – Journal of Ecology 75: 21-42.

[23] Cerda, A. (1999): Parent material and vegetation affect soil erosion in Eastern Spain. – Soil Science Soc. of America 63(2): 362-368.

[24] Cukur, H. (1999): Ecosystems of Aegean Region. – Unpublished Doctorate Thesis, Educational Sciences Institute, Dokuz Eylul University, Izmir.

[25] Cukur, H., Atalay, İ. (2004): The Effects of the Parent Material on the Natural Environment of Turkey. – Ielenicz, M., Popescu, N., Baltearu, D., Atalay, İ. (eds.) Environmental Change and Sustainable Development Proc. of Second Romanian-Turkish Workshop of Geography. Editura Universitara, Bucharest, pp. 145-154.

[26] Cunningham, W. P., Saigo, B. W. (1999): Environmental Science. – WCB, McGraw-Hill.

[27] Foth, H. D. (1990): Fundamentals of Soil Science. – John Wiley and Sons, New York.

[28] Going, B. M., Hillerislambers, J., Levine, J. M. (2009): Abiotic and biotic resistance to grass invasion in serpentine annual plant communities. – Oecologia 159(4): 839-847).

[29] Gregorich, E. G., Turchenek, L. W., Carter, M. R., Angers, D. A. (2001): Soil and Environmental Science Dictionary. – CRC Press, Boca Raton, FL.

[30] Jackson, M. C. (1967): Soil Chemical Analysis. – Prentice Hall of India Private Limited, New Delhi.

[31] Kacar, B. (1995): Chemical Analyses of Soil and Plant. III. Soil Analyses. – Ankara University, Agricultural Faculty, Ankara.

[32] Özdeniz, E., Özbey. B. G., Kurt, L and Bölükbaşı, A. (2017): Serpentine ecology and contributions to the serpentine flora of Turkey. – Journal of Soil Science and Plant Nutrition 5(1): 22-33).

[33] Oze, C., Skinner, C., Robert, W. S., Coleman, G. (2008): Growing up green on serpentine soils: Biogeochemistry of serpentine vegetation in the Central Coast Range of California. – Applied Geochemistry 23(12): 3391-3403.

http://www.aloki.hu ● ISSN 1589 1623 (Print) ● ISSN 1785 0037 (Online)
DOI: http://dx.doi.org/10.15666/aeer/1705_1108511106

[34] Proctor, J., Woodell, R. J. (1975): The ecology of Serpentine soils. – Advances in Ecological Research 9: 255-366.

[35] Roberts, N. (1990): Human-Induced Landscape Change in the South and Southwest Turkey during the Late Holocene. – In: Bottema, S., Entjes-Nieborg, G., Van Zeist, W. (eds.) Man's role in the shaping of the East Mediterranean Landscape. A. A. Balkema, Rotterdam/Brookfield, pp. 53-68.

[36] Saatçioglu, F. (1976): Biological Fundamentals and Principles of Silviculture. – İstanbul Univ. Faculty of Forest Pub. 222, İstanbul.

[37] Smith, R. L., Smith, T. M. (2003): Elements of Ecology. 5th Ed. – Benjamin Cumming, San Francisco.

[38] Tetik, M., Yeşilkaya, Y. (1997): Relationships Bedrock-Soil and Bonitet-Soil in the Pine Forest of Antalya Region. – Western Mediterranean Forestry Research Directorate, No 6.

[39] USDA (1969): Soil Taxonomy - A. Basic System of Soil Classification for Making and Interpreting Soil Surveys. Agriculture Handbook, No: 436. – Soil Con. Serv., Washington, DC.

http://www.aloki.hu ● ISSN 1589 1623 (Print) ● ISSN 1785 0037 (Online)
DOI: http://dx.doi.org/10.15666/aeer/1705_1108511106

EFFECTS OF DIFFERENT BIOCHARS AMMENDMENTS ON PHYSIOCHEMICAL PROPERTIES OF SOIL AND ROOT MORPHOLOGICAL ATTRIBUTES OF *FOKENIA HODGINSII* (FUJIAN CYPRESS)

TARIN, M. W. K.[1] – FAN, L. L.[1] – SHEN, L.[1] – LAI, J. L.[1] – TAYYAB, M.[2] – SARFRAZ, R.[2] – CHEN, L. Y.[3] –YE, J.[3]– HE, T. Y.[3] – RONG, J. D.[1] – CHEN, L.G. [1]– ZHENG, Y. S.[1,3*]

[1]*College of Forestry, Fujian Agriculture and Forestry University Fuzhou, Fujian 350002, People's Republic of China*

[2]*Fujian Agriculture and Forestry University, Fuzhou 350002, China*

[3]*College of Arts & College of Landscape Architecture, Fujian Agriculture and Forestry University, Fuzhou, Fujian 350002, People's Republic of China*

[*]*Corresponding author*
e-mail: zys1960@163.com; phone: +86-50-397-265

(Received 4th Apr 2019; accepted 13th Jun 2019)

Abstract. Biochar (BC) is the carbon-rich material, increasingly as a soil additive for carbon sequestration and soil improvement. Various studies have shown that BC have a profound effect on root morphological traits on agricultural systems, however the effect of BC amendments on the root traits of forest species is scant. The current study attempts to evaluate the effects of different BCs as a soil amendment on the growth and root morphological traits of *Fokienia hodginsii.* For that reason, three different types of BCs; bamboo (BB), hardwood (BH), and rice straw (BR) with four levels (0, 5, 20, and 80 g $kg^{-1}$of soil) collectively ten treatment combination including control (Bo) were incorporated to soil and seedlings were allowed to grow in pots in greenhouse for one year. After one year uprooted seedlings roots were scanned and analyzed by using WinRHIZO software for comparison. Bamboo and rice straw BC amendments were found to significantly improve root traits particularly root volume, average diameter, and root length compared to Bo. Additionally, the seedlings treated with BR80, BB80, and BH80 attained 36%, 29%, and 25% biomass, respectively compared to Control (Bo). Soil physiochemical properties particularly soil pH also varied between different BCs types and levels. Consequently, BC alkalinity is an important feature to correct soil acidity and improve soil fertility by altering soil nutrient content. Root establishment in acidic soils can be enhanced by BC amendments but selection of BC and soil is crucial to maximizing soil improvement and seedlings roots traits.
Keywords: *Fokienia hodginsii, root traits, biomass, winRHIZO, alkalinity, soil improvement*

Introduction

Fokenia hodginsii (Fujian cypress) is an important conifer; native to China and Vietnam. Currently, on the basis of its distribution, this conifer is globally threatened, protected species (B2/second degree) in China, and as vulnerable in red list of threatened species; generated by international union for conservation of nature (IUCN) (Luu and Thomas, 2000; Ding et al., 2017; Tarin et al., 2019). Timber of this conifer is valuable because of its straight grain and different aroma and is also being exported to Europe and elsewhere in Asia (Osborn, 2004). Moreover, siam-wood essential oil or pemou oil is extracted from its stumps and roots which contains high sesquiterpene content; which can sanitize and purify the air, kill bacteria, and resist insects. Furthermore, extract oil can be used to improve emotional balance and the mental clarity in aromatherapy (Paluch, 2009). As a result of, certain increase in human

http://www.aloki.hu ● ISSN 1589 1623 (Print) ● ISSN 1785 0037 (Online)
DOI: http://dx.doi.org/10.15666/aeer/1705_1110711120

population has put enormous pressure on this conifer community by over logging for utilization of timber wood (Nguyen et al., 2015; Tarin et al., 2017). These anthropogenic (human activities) and pedogenic or natural factors (parent material) has resulted infertile soils (Lal, 2015). Consequently, high rates of deforestation, rise in global temperature (approximately 0.85± 0.20°C) during last 130 years will lead to unfavorable and harsh conditions for plants such as drought and flood etc. globally (Alexander et al., 2006; Tarin et al., 2019) Additionally, intensive forest management for conversion of natural forests into artificial plantations has been shown to deteriorate the soil physical health, like, reducing pH and porosity, and increasing bulk density (Tonks et al., 2017).

Global climate change and intensive forest management both have adversely affected the features of forest soils via decrease in soil organic carbon, acidification, biological properties, and biodiversity (Li et al., 2018). Vast areas of tropical and subtropical regions of Southern China, soils are acidic where; soil fertility is the major constraint to plant growth (Haynes and Mokolobate, 2001; Baquy et al., 2017). However, mineral lime has been conventionally used to raise the soil pH (Adams, 1984) nevertheless, because of its high costs, much attention has been given to replacements like incorporation of crop straw in soil which also can increase soil pH (Xu and Coventry, 2003). Besides, direct addition of such plant residues into the soils do not stay longer because of decomposition (Yuan and Xu, 2011). Recently, biochar (BC) has received much attention as an alternate to these soil organic amendments and is considered as a potential fertilizer due to partial combustion of several organic components. It has mostly alkaline nature subject to pyrolysis temperature over 400°C (Gaskin et al., 2008) and can raise the pH of acidic soils by decreasing exchangeable Al from soil (Chan et al., 2008b). Its amendments into the soil can improve soil fertility (Topoliantz et al., 2005), stimulate the plant growth (Jeffery et al., 2011a) and enhance the sequestration of CO_2 from the atmosphere (Lehmann et al., 2006).

Numerous studies on agriculture and horticulral system have been shown to examine, how BC effects on plant growth and root morphological parameters. Inappropriately, research on effects of BCs amendments on growth of trees particularly on root morphological parameters is rare. BC application into the soil has significant effects on growth and root morphology as plant roots contact directly to its particles for uptake of soil nutrients and water (Prendergast-Miller et al., 2014). Therefore, measurement of roots morphological parameters, such as root length, root diameters etc. are essential to understand plant physiological functions. It is necessary to determine how root morphological traits respond to different BC application under multiple levels for better management of forest species.

In the context of previous studies, responses of root traits like root morphology and biomass (Brennan et al., 2014; Keith et al., 2015), root-associated microbes, and nutrient concentration (Rillig et al., 2010; Vanek and Lehmann, 2015) can be influenced by incorporation of BCs. Moreover, root morphological traits play diversified roles in plant growth and development (Nie et al., 2013). For instance, root length is possibly one of the important parameter, mainly because of general indicator of plant response to environmental factors and also controls the acquisition of nutrients or water (Clothier and Green, 1997; Edwards et al., 2004) whereas for the biomass increase, root diameter is considered as beneficial (Eissenstat and Yanai, 1997). To date, BC effects on root morphological traits are highly variable and controversial. For instance, because of various factors, root biomass remains relatively stable, decrease or increase under BCs

http://www.aloki.hu ● ISSN 1589 1623 (Print) ● ISSN 1785 0037 (Online)
DOI: http://dx.doi.org/10.15666/aeer/1705_1110711120

application (Macdonald et al., 2014; Prendergast-Miller et al., 2014; van de Voorde et al., 2014). The BC type (different materials or pyrolysis temperature) is an important factor because it varies significantly in chemical composition and pH (Lehmann et al., 2011). Consequently, the variation in characteristics of BCs and their application rate may also influence the soil physiochemical properties and ultimately alter the root morphological traits (Reibe et al., 2015; Reverchon et al., 2014). For that reason, it is important to know how root traits respond under different BCs application. In the current study, it was hypothesized that addition of BC into the soil may affect the biomass and root traits of the *F. hodginsii* seedlings by improving the soil physiochemical properties. Therefore, one year pot experiment was conducted to examine the effects of three different BCs under four levels (i) to identify the effects of different BCs on the physiochemical properties of soil, (ii) to investigate the effects of different BCs on growth (biomass) of *F. hodginsii* seedlings, and root morphological traits.

Material and methods

Study area and design

The present study was started in March, 2017 at Bamboo Institute of Fujian Agriculture and Forestry University Fuzhou, Fujian Province, P. R. China (lat. 26° 5' N, long. 119° 13' E, elevation 12 m; *Fig. 1*).

Figure 1. *Boundary of Fujian Agriculture and Forestry University (Bamboo Institute), experimental design and order*

The metrological informations of the study site during the entire experiment period are presented in *App. 1*. Three different types of commercial biochars (BCs); bamboo

http://www.aloki.hu ● ISSN 1589 1623 (Print) ● ISSN 1785 0037 (Online)
DOI: http://dx.doi.org/10.15666/aeer/1705_1110711120

biochar (BB, produced at 450°C), hardwood biochar (BH, produced at 420°C), and rice straw biochar (BR, produced at 500°C) were used; which were purchased from Nanjing Qinfeng Straw Technology Co. Ltd. China. Before application to soil the physiochemical characteristics of these BCs and basic soil were determined (*Table 1*).

Table 1. *Physiochemical properties of BCs and soil used in the experiment, BB: bamboo biochar*

Characteristics	BB	BH	BR	Basic soil
pH	9.687	5.703	9.833	4.685
EC (m Scm^{-1})	3.140	6.343	4.070	106.667
TC (g Kg^{-1})	311.220	330.530	250.053	3.358
OM (g Kg^{-1})	536.543	569.834	431.092	5.790
TN (g Kg^{-1})	6.243	8.297	5.153	0.497
AP (mg Kg^{-1})	32.381	24.318	29.076	10.245
TP(g Kg^{-1})	0.399	0.296	0.311	0.256
Ext. K (g Kg^{-1})	0.335	0.321	0.371	0.356
C:N Ratio	49.975	39.846	48.641	6.864

BB; Bamboo biochar, BH: hardwood Biochar, BR, rice straw biochar TN: total nitrogen, TC: total carbon, TP: total phosphorus, AP: available phosphorus, OM: organic matter, Ext. K: extractable potassium, C: N: carbon nitrogen ratio

These three BCs were incorporated to soil with four different levels; 0, 5, 20, and 80 g kg^{-1} of soil (Tarin et al., 2019). One-year old seedlings of *F. hodginsii* (uniform size) were collected from forest nursery (Anxi County, Fujian, China), transplanted to poly vinyl pots (height = 18 cm, top circumference = 62 cm, bottom circumference = 52 cm, d = 22 cm), and established in greenhouse in completely randomized design (four replication) for one year till the end of March, 2018. These seedlings were allowed to grow under greenhouse condition (natural light) and usual irrigation practice in order to produce healthy seedlings (Wang et al., 2014; Razaq et al., 2017). Additionally, after 15 days of establishment, all the seedlings were treated 10 g each pot with NPK fertilizer (Tarin et al., 2019). After one year; March 2018, seedlings were uprooted to determine plant fresh/dry weights and morphological parameters of roots.

Determination of physiochemical properties of soil

To determine the soil physiochemical properties, all the analysis were conducted in the Bamboo Institute, College of Forestry, Fujian Agriculture and Forestry University, China. At the start of the experiment (March, 2017), physiochemical properties of soil and all three types of BCs were assessed (*Table 1*). After one year, at the end of experiment (March, 2018), soil samples from 0-15 cm depth from each replicates were collected, mixed to produce composite samples and were sealed in clean, air-tight polythene bags. Four samples from each treatments were air-dried and then passed through a 2-mm/0.149-mm mesh to assess the physiochemical properties of soil. Soil pH (1:2.5 soil/water suspensions) was measured by using glass electrode meter as described by Tarin et al. (2019). Elemental analyzer (Thermo Scientific™, Waltham, MA, USA) was used for determination of soil Total N and C (Carbon) and then calculated as organic matter (OM), whereas for determination of total Phosphorus (TP) and available Phosphorus (AP) alkali fusion-Mo-Sb anti-colorimetry method as described by Sarfraz et al. (2019). Ammonium acetate solution was used for the measurement of extractable Potassium (ext. K) (Pansu and Gautheyrou, 2007).

http://www.aloki.hu ● ISSN 1589 1623 (Print) ● ISSN 1785 0037 (Online)
DOI: http://dx.doi.org/10.15666/aeer/1705_1110711120

Biomass and morphological parameters

Above ground morphological parameters like plant height and basal diameters of seedlings were measured by using the ordinary measuring tape (cm) and vernier caliper (mm), respectively. Whereas for biomass determination, seedlings were uprooted from pots with intensive care to avoid any damage to the roots, washed with deionized water and similarly, for roots morphological traits, root samples were carefully taken in each treatment, using the procedure described by Guo et al. (2008). The root samples were scanned with Expression 10000XL 1.0 scanner (dpi = 400; Epson Telford, Ltd., Telford, UK). Finally, the seedlings were oven dried to constant mass at 65°C, in order to determine dry mass. Later the images of roots were analyzed by using WinRHIZO (Pro2004b) software (Instruments Regent Co., Ville de Québec, QC, Canada) in order to determine the root surface area, root volume, total root length, and average root diameter.

Statistical analysis

Data was statistically analyzed with SPSS-19 statistical software. All the data were expressed as means and standard errors (SE) with four replications. Comparisons of different means were analyzed by Duncan's multiple range tests; α 0.05 probability level. For tables and figures Origin lab 8.5 and Microsoft excels were used.

Results

Effects of biochar amendments on physiochemical properties of soil

At the final harvest, soil nutrient dynamics under different BCs amended treatments were changed (*Fig. 2*). The change in soil pH after one-year under different BCs (BB, BH, and BR) incorporated samples is shown in *Figure 2a*.

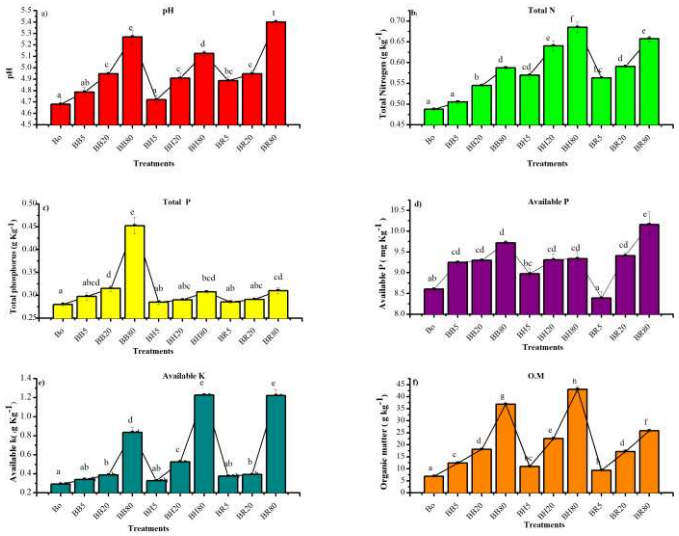

Figure 2. *Comparison of soil physiochemical properties under different biochars amendments. Treatments include; control as Bo, bamboo biochar as (BB; 5, 20 and 80 representing different doses g kg^{-1} of soil), hardwood biochar as (BH; 5, 20 and 80 representing different doses g kg^{-1} of soil), rice straw biochar as (BR; 5, 20 and 80 representing different doses g kg^{-1} of soil). Different letters indicate significant difference (P ≤ 0.05) among different treatments with error bars*

http://www.aloki.hu ● ISSN 1589 1623 (Print) ● ISSN 1785 0037 (Online)
DOI: http://dx.doi.org/10.15666/aeer/1705_1110711120

The liming effects of BB and BR were significant for rising soil pH ($P \leq 0.05$) as compared to BH. All BCs amended soil presented higher macronutrients (NPK) concentrations compared to Bo. Available P concentrations were significantly higher under BR80 compared to all other treatments, whereas total N concentration was highest in BH80. Overall, the concentrations of macro-nutrients increased under higher doses of BCs depending upon their type. Total N, Total P, available P, extractable K, and organic matter showed significant difference than that of Bo.

Effects of biochar amendments on biomass and morphological parameters of seedling

Application of BC significantly increased the morphological parameters of the seedlings. *Figure 3* shows the complete comparison of treatments combination for above and below ground attributes.

Figure 3. *Complete view of seedlings showing the above and below ground comparison of morphological traits for all the treatments.*
Treatments include; control as Bo, bamboo biochar as (BB; 5, 20 and 80 representing different doses g kg^{-1} of soil), hardwood biochar as (BH; 5, 20 and 80 representing different doses g kg^{-1} of soil), rice straw biochar as (BR; 5, 20 and 80 representing different doses g kg^{-1} of soil)

Our results showed that BCs application increased the plant height, particularly seedlings treated with BB20, BH20 and BR20 were taller and showed significant difference than that of Bo (*Fig. 4a*). Moreover, within different BCs treatments, no significant difference was observed for seedlings basal diameter except BR80 amendments (*Fig. 4b*). Under different BC amendments, biomass of seedlings, treated with BB80, BH20, BH80, BR20, and BR80 were significantly increased than that of Bo (*Fig. 4c*). Likewise, for dry weight, seedlings treated with BB20, BB80, BR20, and BR80 showed significant differences compared to Bo (*Fig. 4d*).

Effects of biochar amendments on root morphological traits

Results from the current study suggested that BC amendment promoted the morphological traits of the roots. Under different BC types and levels, the roots morphological characteristics varied in terms of root volume, surface area, diameter, and length. BC application significantly ($P \leq 0.05$) increased root volume in all the BCs

http://www.aloki.hu ● ISSN 1589 1623 (Print) ● ISSN 1785 0037 (Online)
DOI: http://dx.doi.org/10.15666/aeer/1705_1110711120

treated seedlings except BH5 and BR5 as compared to Bo. For all BCs treatment combinations, highest root volume was observed in seedlings treated with BB80 and BR80 (*Fig. 5a*).

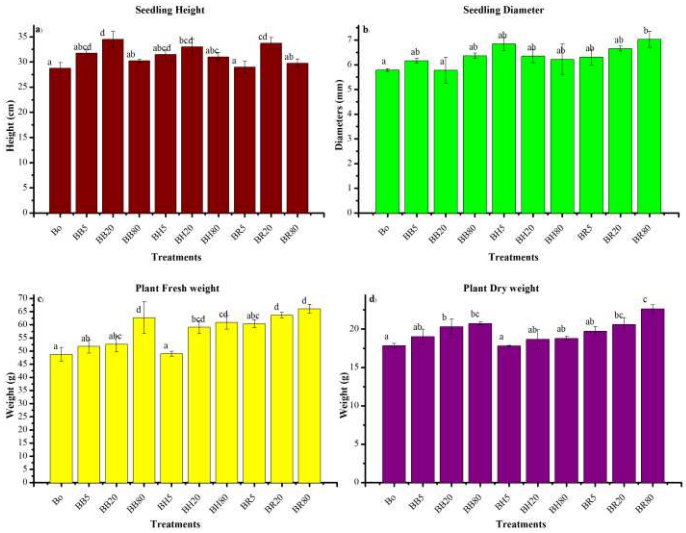

Figure 4. *Comparison of above ground parameters of seedlings treated with different biochars, a) seedling height b) seedling basal diameter, c) plant fresh weight, d) dry weight. Treatments include; control as Bo, bamboo biochar as (BB; 5, 20 and 80 representing different doses g kg^{-1} of soil), hardwood biochar as (BH; 5, 20 and 80 representing different doses g kg^{-1} of soil), rice straw biochar as (BR; 5, 20 and 80 representing different doses g kg^{-1} of soil). Different letters indicate significant difference ($P \leq 0.05$) among different treatments with error bars*

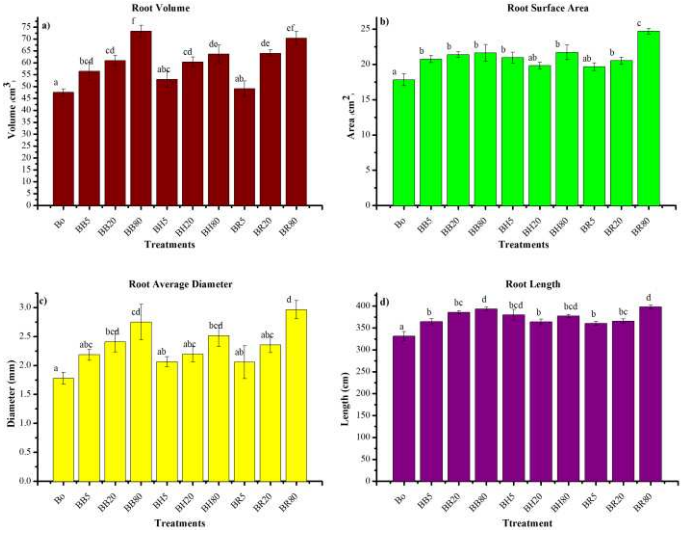

Figure 5. *Comparison of root morphological features among all BC treatments; a) Root volume (cm^3), b) Root surface area (cm^2), c) Root average diameter (mm), d) Root length (cm). Treatments include; control as Bo, bamboo biochar as (BB; 5, 20 and 80 representing different doses g Kg^{-1} of soil), hardwood biochar as (BH; 5, 20 and 80 representing different doses g Kg^{-1} of soil), rice straw biochar as (BR; 5, 20 and 80 representing different doses g Kg^{-1} of soil) Different letters indicate significant difference ($P \leq 0.05$) among different treatments with error bars*

http://www.aloki.hu ● ISSN 1589 1623 (Print) ● ISSN 1785 0037 (Online)
DOI: http://dx.doi.org/10.15666/aeer/1705_1110711120

Root surface area of the seedlings was not much influenced within the different BC ammendments, although there was significant difference among the seedlings treated with Bo, BH20 and BR5 compared to all other treatment combination with maximum value in BR80 (*Fig. 5b*). For average diameter, seedlings treated with BB5, BH5, BH20, BR5, and BR20 had no significant difference than that of Bo and under BR80 amendments, seedlings had the highest roots diameter followed by BB80 with significant difference compared to Bo (*Fig. 5c*). Similarly, BC treated seedlings significantly increased the root length compared to Bo but between different BCs treatment combinations, there was no significant difference, except BB80 and BR80 (*Fig. 5d*).

Discussion

Effects of biochars amendments on physiochemical properties of soil

Various studies have demonstrated that BC application into the soil can promotes the plant growth by improving physiochemical properties of soil like essential nutrients (NPK), pH and cation exchange capacity (Lehmann et al., 2011). Therefore, the responses of root traits to BC incorporated soil depend on soil type and BC (Macdonald et al., 2014). In addition, BC often applied with fertilizer to the soil has interactively regulated the root growth of the plants (Alburquerque et al., 2015). The incorporation of all three BCs increased soil pH, however the rise in pH was evident under higher dose of BB and BR (*Fig. 2a*) because both of these two BCs have higher pH compared to BH (*Table 1*). Alkaline nature of BCs (BB and BR) to soil has resulted increase in pH. Our results are in the line with the previous findings where incorporation of alkaline BC with higher dose raised the soil pH (Ishii and Kadoya, 1994). Moreover, the liming effect of BR was generally greater than that of other two types of BCs (BB and BH); our findings are in the agreement with the previous study on acidic soil (Wang et al., 2009). Therefore, the pH of BC must be taken into account in order to control liming effects and consequently can be applied to acidic soil to raise the soil pH. In the current study the soil pH of Bo was 4.68, consequently, lower soil pH (highly acidic) always reduces the cation exchange capacity and also the bio-availability of nutrients (Verheijen et al., 2010). The rise in soil pH from 4.68 to 5.27 and 5.40 under BB80 and BR80, respectively altered soil physiochemical properties (*Fig. 2a*) which is the agreement with numerous studies (Vaccari et al., 2011; Yuan and Xu, 2011). Our results were further justified by Yuan and Xu (2011) that incorporation of BC not ameliorates soil acidity and but also improves the soil fertility. The total Nitrogen (TN) contents were highest in BH80 compared to other types of BCs (BB and BR). A potential mechanism for increased Nitrogen retention in soils mixed with BCs is the increased nitrates recycling because of higher availability of C (Verheijen et al., 2010). The increase in SOM and total N following BC application is similar to previous findings where soil C and N were increased because of application of different types of BCs (Stavi and Lal, 2013; Angst et al., 2014). Consequently, under BB80 and BR80 treatments, greater values were observed for available P compared to BH80 (*Fig. 3d*). Nevertheless, evidence suggests that BC can increase the nitrification if applied to acidic soils (Ball et al., 2010; Nelson et al., 2011). On the contrary, as described by few researchers that incorporation of BC to agricultural system, may decrease soil N just after addition, because N demand for agriculture crops has always been higher compared to forests plants (Tammeorg et al., 2012). At the start of our experiment

http://www.aloki.hu ● ISSN 1589 1623 (Print) ● ISSN 1785 0037 (Online)
DOI: http://dx.doi.org/10.15666/aeer/1705_1110711120

(March, 2017) for better effect of BCs, we had applied minimal dose (10 g each pot) of NPK fertilizer to all treatments including Bo. In the view of this, earlier BCs studies have demonstrated that application of BC combined with fertilizers have been more effective for attaining better growth (Sarfraz et al., 2017). Besides, increased N retention under rice straw BC experiment is similar to our findings (Noguera et al., 2010). In our experiment BB80 and BR80 treatments, soil pH was relatively higher than that of other treatment combinations, rise in soil pH resulting availability of P, because pH of BH under three levels (BH5, BH20, and BH80) was not much increased. Our these findings are in the line with the previous findings, because BCs particles not only holds the soil N in the form of nitrates, but also supply P to the soil and plant but their affect varies under different feedstocks (Prendergast-Miller et al., 2014). Additionally BC incorporation increased the extractable potassium (Ext. K) under BC amendments because BC is a soil conditioner which might act like a fertilizer and it contains ash which in return adds nutrients like Potassium (K), Magnesium (Mg), and Calcium (Ca) to soil which in response raises the soil pH and provide essential nutrients to soil for better growth (Agegnehu et al., 2015).

Effects of biochars amendments on morphology and biomass

Various studies have confirmed that BC addition to soil increases the seedlings and roots growth both under natural and nursery conditions (Chan et al., 2008a; Noguera et al., 2010). Growth parameters of *F. hodginsii* seedlings under BC amended soils were improved as compared to Bo (*Fig. 3*) which is consistent with previous findings (Ali et al., 2017; Tayyab et al., 2018). Strong positive responses to BC additions were observed in biomass, resulting increase in plant fresh weight and height of (*Fig. 4a and c*), which is agreement with the previous studies (Caroline et al., 2016; Seehausen et al., 2017). Because BC is a soil conditioner which might act like a fertilizer and provide nutrients to soil for plant growth (Agegnehu et al., 2015). The availability of primary nutrients to soil for plants (Sarfraz et al., 2017) with improved water holding capacity is attributed to the BC structure (Jeffery et al., 2011). Better water retention is the consequence of BC amended soil, which increases the water use efficiency of a plant, thus enhancing plant height and fresh/dry weight (Liang et al., 2006; Uzoma et al., 2011; Younis et al., 2015). In general, seedling growth parameters (seedling height, Biomass, root traits) varied only within the BC types and with the highest doses. The results obtained from the current study suggested that BC application increased the above and below ground morphological attributes (*Figs. 4 and 5*). Although basic soil in this study was strongly acidic (pH 4.68), but the slight increase in pH by applying alkaline BCs (BB and BR) has resulted improvement in nutrient availability (or nutrient use efficiency) with successive growth which is in the line with the findings of Robertson et al. (2012). BCs application particularly under BB and BR (20 and 80 g kg^{-1} of soil) increased the root volume, surface area, total root length, and average root diameter compared to Bo (*Fig. 5*). However, under BH (5, 20, 80 g kg^{-1}) the root morphological traits had greater or no significant difference compared to Bo. Previously for conifers seedling, there is no research data to compare the BC effects on root traits but our findings are attributed to change in the physiochemical properties of soil. Under higher dose of BCs (20 and 80 g kg^{-1} of soil) the improved roots morphological traits are consistent with previous studies (Razaq et al., 2017). Similar to our findings, Guo et al. (2008) reported that BC incorporation to acidic soil has been known to influence the root surface area, length, and volume of the seedlings in acidic red soil. In another study by Ishii and Kadoya

http://www.aloki.hu ● ISSN 1589 1623 (Print) ● ISSN 1785 0037 (Online)
DOI: http://dx.doi.org/10.15666/aeer/1705_1110711120

(1994) who demonstrated that application of BC increases the plant and root biomass. Our these results were further justified by Yang et al. (2015) who confirmed at the seedling stage, incorporation of BC improves the root morphological traits because of improved water holding capacity and soil physiochemical properties ultimately effects the root growth (Piccolo et al., 1996). Even though there are only few other comparable studies like, review by Lehmann et al. (2011) has demonstrated that BC has positive effect on root growth. BC application has significant effects on morphological traits and functioning of roots because its particles contact the roots directly for uptake of nutrients. The increased root length in our experiment (*Fig. 5d*) suggests that BC application increases the plant rhizosphere enabling plants to absorb water and nutrients freely (Prendergast-Miller et al., 2014). BC addition to soil, also enhances the microbe's community, reduces soil pathogen, and boosts plant defenses which consequently improve the seedlings health with minimal damage to the environment (Elad et al., 2010). Overall, these findings demonstrate the potential of BC application for improved seedling growth.

Conclusion

Our results confirmed that positive response of *F. hodginsii* biomass and root growth was attributed to BC amendment at seedling stage because it can serve as a direct nutrient supply through addition of soluble P and biochar-N retention (Prendergast-Miller et al., 2014). But the positive effects varied under different level and BC feedstock used. The seedlings treated with BR80, BB80, and BH80 attained 36%, 29%, and 25% biomass, respectively compared to Bo. Our these findings are in consistent with previous studies suggesting increase in biomass of woody plants summarized by a meta-analysis with an average 41% increase in biomass (Thomas and Gale, 2015). This is the first report on the effect of BC application on *F. hodginsii* morphological traits of root. Biochar application improved the physiochemical properties of soil, biomass and roots morphological attributes at seedling stage in greenhouse experiment. The current experiment was focused on the influence of different BCs application on *F. hodginsii* root traits at the early stage in a pot experiment. It is suggested that further field studies are needed to assess the complete effect of BC application on root system changes, soil microbial and nutrients dynamics.

Acknowledgements. The current project was funded by Science and Technology Major Projects of Fujian Province [2018NZ0001-1], Fujian Agriculture and Forestry University Science and Technology Development Fund Project [KF2015085], and Fujian Seedling Science and Technology Research Project, P. R. China.

REFERENCES

[1] Adams, F. (1984): Crop response to lime in the southern United States. – Soil acidity liming: 211-265.

[2] Agegnehu, G., Bass, A. M., Nelson, P. N., Muirhead, B., Wright, G., Bird, M. I. (2015): Biochar and biochar-compost as soil amendments: Effects on peanut yield, soil properties and greenhouse gas emissions in tropical North Queensland, Australia. – Agric Ecosyst Environ. https://doi.org/10.1016/j.agee.2015.07.027.

http://www.aloki.hu ● ISSN 1589 1623 (Print) ● ISSN 1785 0037 (Online)
DOI: http://dx.doi.org/10.15666/aeer/1705_1110711120

[3] Alburquerque, J. A., Cabello, M., Avelino, R., Barrón, V., del Campillo, M. C., Torrent, J. (2015): Plant growth responses to biochar amendment of Mediterranean soils deficient in iron and phosphorus. – J Plant Nutr Soil Sci 178: 567-575.
[4] Alexander, L. V., Zhang, X., Peterson, T. C., Caesar, J., Gleason, B., Tank, A. M. G. K., Haylock, M., Collins, D., Trewin, B., Rahimzadeh, F. (2006): Global observed changes in daily climate extremes of temperature and precipitation. – J Geophys Res Atmos 111.
[5] Ali, S., Rizwan, M., Qayyum, M. F., Ok, Y. S., Ibrahim, M., Riaz, M., Arif, M. S., Hafeez, F., Al-Wabel, M. I., Shahzad, A. N. (2017): Biochar soil amendment on alleviation of drought and salt stress in plants: a critical review. – Environ Sci Pollut Res 24: 12700-12712. https://doi.org/10.1007/s11356-017-8904-x.
[6] Angst, T. E., Six, J., Reay, D. S., Sohi, S. P. (2014): Impact of pine chip biochar on trace greenhouse gas emissions and soil nutrient dynamics in an annual ryegrass system in California. – Agric Ecosyst Environ 191: 17-26.
[7] Ball, P. N., MacKenzie, M. D., DeLuca, T. H., Montana, W. E.(2010): Wildfire and charcoal enhance nitrification and ammonium-oxidizing bacterial abundance in dry montane forest soils. – J Environ Qual 39: 1243-1253.
[8] Baquy, M., Li, J.-Y., Xu, C.-Y., Mehmood, K., Xu, R.-K. (2017): Determination of critical pH and Al concentration of acidic Ultisols for wheat and canola crops. – Solid Earth 8: 149-159.
[9] Brennan, A., Jiménez, E. M., Puschenreiter, M., Alburquerque, J. A., Switzer, C. (2014): Effects of biochar amendment on root traits and contaminant availability of maize plants in a copper and arsenic impacted soil. – Plant Soil 379: 351-360.
[10] Caroline, A., Debode, J., Vandecasteele, B., D'Hose, T., Cremelie, P., Haegeman, A., Ruttink, T., Dawyndt, P., Maes, M. (2016): Biological, physicochemical and plant health responses in lettuce and strawberry in soil or peat amended with biochar. – Appl Soil Ecol 107: 1-12.
[11] Chan, K. Y., Van Zwieten, L., Meszaros, I., Downie, A., Joseph, S. (2008a): Using poultry litter biochars as soil amendments. – Soil Res 46: 437-444.
[12] Chan, K. Y., Van Zwieten, L., Meszaros, I., Downie, A., Joseph, S. (2008b): Agronomic values of greenwaste biochar as a soil amendment. – Soil Res 45: 629-634.
[13] Clothier, B. E., Green, S. R. (1997): Roots: the big movers of water and chemical in soil. – Soil Sci 162: 534-543.
[14] Ding, M., Meng, K., Fan, Q., Tan, W., Liao, W., Chen, S. (2017): Development and Validation of EST-SSR Markers for *Fokienia hodginsii* (Cupressaceae). – Appl Plant Sci 5: 1600152. https://doi.org/10.3732/apps.1600152.
[15] Edwards, E. J., Benham, D. G., Marland, L. A., Fitter, A. H. (2004): Root production is determined by radiation flux in a temperate grassland community. – Glob Chang Biol 10: 209-227.
[16] Eissenstat, D. M., Yanai, R. D. (1997): The ecology of root lifespan, in: Advances in Ecological Research. – Elsevier, pp. 1-60.
[17] Elad, Y., David, D. R., Harel, Y. M., Borenshtein, M., Kalifa, H. B., Silber, A., Graber, E. R. (2010): Induction of systemic resistance in plants by biochar, a soil-applied carbon sequestering agent. – Phytopathology 100: 913-921.
[18] Gaskin, J. W., Steiner, C., Harris, K., Das, K. C., Bibens, B. (2008): Effect of low-temperature pyrolysis conditions on biochar for agricultural use. – Trans ASABE 51: 2061-2069.
[19] Guo, D., Xia, M., Wei, X., Chang, W., Liu, Y., Wang, Z. (2008): Anatomical traits associated with absorption and mycorrhizal colonization are linked to root branch order in twenty-three Chinese temperate tree species. – New Phytol 180: 673-683.
[20] Haynes, R. J., Mokolobate, M. S. (2001): Amelioration of Al toxicity and P deficiency in acid soils by additions of organic residues: a critical review of the phenomenon and the mechanisms involved. – Nutr Cycl agroecosystems 59: 47-63.
[21] Ishii, T., Kadoya, K. (1994): Effects of charcoal as a soil conditioner on citrus growth and vesicular-arbuscular mycorrhizal development. – J Japanese Soc Hortic Sci 63: 529-535.
[22] Jeffery, S., Verheijen, F. G. A., van der Velde, M., Bastos, A. C. (2011): A quantitative review of the effects of biochar application to soils on crop productivity using meta-analysis. – Agric

http://www.aloki.hu ● ISSN 1589 1623 (Print) ● ISSN 1785 0037 (Online)
DOI: http://dx.doi.org/10.15666/aeer/1705_1110711120

Ecosyst Environ 144: 175-187. https://doi.org/10.1016/j.agee.2011.08.015.
[23] Keith, A., Singh, B., Dijkstra, F. A. (2015): Biochar reduces the rhizosphere priming effect on soil organic carbon. – Soil Biol Biochem 88: 372-379.
[24] Lal, R. (2015): Restoring soil quality to mitigate soil degradation. – Sustainability 7: 5875-5895.
[25] Lehmann, J., Gaunt, J., Rondon, M. (2006): Bio-char sequestration in terrestrial ecosystems–a review. – Mitig Adapt Strateg Glob Chang 11: 403-427.
[26] Lehmann, J., Rillig, M. C., Thies, J., Masiello, C. A., Hockaday, W. C., Crowley, D. (2011): Biochar effects on soil biota–a review. – Soil Biol Biochem 43: 1812-1836.
[27] Li, Y., Hu, S., Chen, J., Müller, K., Li, Y., Fu, W., Lin, Z., Wang, H. (2018): Effects of biochar application in forest ecosystems on soil properties and greenhouse gas emissions: a review. – J Soils Sediments 18: 546-563. https://doi.org/10.1007/s11368-017-1906-y.
[28] Liang, B., Lehmann, J., Solomon, D., Kinyangi, J., Grossman, J., O'neill, B., Skjemstad, J. O., Thies, J., Luizao, F. J., Petersen, J. (2006): Black carbon increases cation exchange capacity in soils. – Soil Sci Soc Am J 70: 1719-1730.
[29] Luu, N. D. T., Thomas, P. I. (2000): Conifers of Vietnam. Foreign languages pub. – Hou Hanoi.
[30] Macdonald, L. M., Farrell, M., Van Zwieten, L., Krull, E. S. (2014): Plant growth responses to biochar addition: an Australian soils perspective. – Biol Fertil soils 50: 1035-1045.
[31] Nelson, N. O., Agudelo, S. C., Yuan, W., Gan, J. (2011): Nitrogen and phosphorus availability in biochar-amended soils. – Soil Sci 176: 218-226.
[32] Nguyen, D. Q., Phan, T. P. H., Dao, V. T. (2015): Effect of storage time and pretreatment on seed germination of the threatened coniferous species Fokienia hodginsii. – Plant Species Biol 30: 291-296. https://doi.org/10.1111/1442-1984.12062.
[33] Nie, M., Lu, M., Bell, J., Raut, S., Pendall, E. (2013): Altered root traits due to elevated CO2: a meta-analysis. – Glob Ecol Biogeogr 22: 1095-1105.
[34] Noguera, D., Rondón, M., Laossi, K.-R., Hoyos, V., Lavelle, P., de Carvalho, M. H. C., Barot, S. (2010): Contrasted effect of biochar and earthworms on rice growth and resource allocation in different soils. – Soil Biol Biochem 42: 1017-1027.
[35] Osborn, T. (2004): Preparation and implementation of a strategy for the management of Fokienia hodginsii in Vietnam by 2008. – FFI, Hanoi.
[36] Paluch, G. E. (2009): Characterization of botanical terpene activity in arthropods.
[37] Pansu, M., Gautheyrou, J. (2007): Handbook of soil analysis: mineralogical, organic and inorganic methods. – Springer Science & Business Media.
[38] Piccolo, A., Pietramellara, G., Mbagwu, J. S. C. (1996): Effects of coal derived humic substances on water retention and structural stability of Mediterranean soils. – Soil Use Manag 12: 209-213.
[39] Prendergast-Miller, M. T., Duvall, M., Sohi, S. P. (2014): Biochar-root interactions are mediated by biochar nutrient content and impacts on soil nutrient availability. – Eur J Soil Sci 65: 173-185. https://doi.org/10.1111/ejss.12079.
[40] Prendergast-Miller, M. T., Duvall, M., Sohi, S. P. (2014): Biochar–root interactions are mediated by biochar nutrient content and impacts on soil nutrient availability. – Eur J Soil Sci 65: 173-185.
[41] Razaq, M., Salahuddin, Shen, H. L., Sher, H., Zhang, P. (2017): Influence of biochar and nitrogen on fine root morphology, physiology, and chemistry of Acer mono. – Sci Rep 7: 1-11. https://doi.org/10.1038/s41598-017-05721-2.
[42] Reibe, K., Götz, K.-P., Roß, C.-L., Döring, T. F., Ellmer, F., Ruess, L. (2015): Impact of quality and quantity of biochar and hydrochar on soil Collembola and growth of spring wheat. – Soil Biol Biochem 83: 84-87.
[43] Reverchon, F., Flicker, R. C., Yang, H., Yan, G., Xu, Z., Chen, C., Bai, S. H., Zhang, D. (2014): Changes in δ 15 N in a soil–plant system under different biochar feedstocks and application rates. – Biol Fertil soils 50: 275-283.

http://www.aloki.hu ● ISSN 1589 1623 (Print) ● ISSN 1785 0037 (Online)
DOI: http://dx.doi.org/10.15666/aeer/1705_1110711120

[44] Rillig, M. C., Wagner, M., Salem, M., Antunes, P. M., George, C., Ramke, H.-G., Titirici, M.-M., Antonietti, M. (2010): Material derived from hydrothermal carbonization: effects on plant growth and arbuscular mycorrhiza. – Appl Soil Ecol 45: 238-242.
[45] Robertson, S. J., Rutherford, P. M., López-Gutiérrez, J. C., Massicotte, H. B. (2012): Biochar enhances seedling growth and alters root symbioses and properties of sub-boreal forest soils. – Can J Soil Sci 92: 329-340. https://doi.org/10.4141/cjss2011-066.
[46] Sarfraz, R., Shakoor, A., Abdullah, M., Arooj, A., Hussain, A., Xing, S. (2017): Impact of integrated application of biochar and nitrogen fertilizers on maize growth and nitrogen recovery in alkaline calcareous soil. – Soil Sci Plant Nutr 63: 488-498. https://doi.org/10.1080/00380768.2017.1376225.
[47] Sarfraz, R., Li, S., Yang, W., Zhou, B., Xing, S. (2019): Assessment of physicochemical and nutritional characteristics of waste mushroom substrate biochar under various pyrolysis temperatures and times. – Sustain. 11: 1-14.
[48] Seehausen, M., Gale, N., Dranga, S., Hudson, V., Liu, N., Michener, J., Thurston, E., Williams, C., Smith, S., Thomas, S. (2017): Is There a Positive Synergistic Effect of Biochar and Compost Soil Amendments on Plant Growth and Physiological Performance? – Agronomy 7: 13. https://doi.org/10.3390/agronomy7010013.
[49] Stavi, I., Lal, R. (2013): Agroforestry and biochar to offset climate change: a review. – Agron Sustain Dev 33: 81-96.
[50] Tammeorg, P., Brandstaka, T., Simojoki, A., Helenius, J. (2012): Nitrogen mineralisation dynamics of meat bone meal and cattle manure as affected by the application of softwood chip biochar in soil. – Earth Environ Sci Trans R Soc Edinburgh 103: 19-30.
[51] Tarin, M. W., Nizami, S. M., Jundong, R., Lingyan, C., You, H., Farooq, T. H., Gilani, M. M., Ifthikar, J., Tayyab, M., Zheng, Y. (2017): Range vegetation analysis of Kherimurat Scrub Forest, Pakistan. – Int J Dev Sustain 66: 2186-8662.
[52] Tarin, M. W. K., Fan, L., Tayyab, M., Sarfraz, R., Chen, L., He, T., Rong, J., Chen, L., Zheng, Y. (2019): Effects of Bamboo Biochar Amendment on the Growth and Physiological Characteristics of Fokienia Hodginsii. – Appl Ecol Environ Res 16: 8055-8074. https://doi.org/10.15666/aeer/1606_80558074.
[53] Tayyab, M., Islam, W., Khalil, F., Ziqin, P., Caifang, Z., Arafat, Y., Hui, L., Rizwan, M., Ahmad, K., Waheed, S., Tarin, M. W. K., Hua, Z. (2018): Biochar: an efficient way to manage low water availability in plants. – Appl Ecol Environ Res 16: 2565-2583. https://doi.org/10.15666/aeer/1603_25652583.
[54] Thomas, S. C., Gale, N. (2015): Biochar and forest restoration: a review and meta-analysis of tree growth responses. – New For 46: 931-946.
[55] Tonks, A. J., Aplin, P., Beriro, D. J., Cooper, H., Evers, S., Vane, C. H., Sjögersten, S. (2017): Impacts of conversion of tropical peat swamp forest to oil palm plantation on peat organic chemistry, physical properties and carbon stocks. – Geoderma 289: 36-45.
[56] Topoliantz, S., Ponge, J.-F., Ballof, S. (2005): Manioc peel and charcoal: a potential organic amendment for sustainable soil fertility in the tropics. – Biol Fertil Soils 41: 15-21.
[57] Uzoma, K. C., Inoue, M., Andry, H., Fujimaki, H., Zahoor, A., Nishihara, E. (2011): Effect of cow manure biochar on maize productivity under sandy soil condition. – Soil use Manag 27: 205-212.
[58] Vaccari, F. P., Baronti, S., Lugato, E., Genesio, L., Castaldi, S., Fornasier, F., Miglietta, F. (2011): Biochar as a strategy to sequester carbon and increase yield in durum wheat. – Eur J Agron 34: 231-238.
[59] Van de voorde, T. F. J., van Noppen, F., Nachenius, R. W., Prins, W., Mommer, L., Van Groenigen, J.-W., Bezemer, T. M. (2014): Biochars produced from individual grassland species differ in their effect on plant growth. – Basic Appl Ecol 15: 18-25.
[60] Vanek, S. J., Lehmann, J. (2015): Phosphorus availability to beans via interactions between mycorrhizas and biochar. – Plant Soil 395: 105-123.

http://www.aloki.hu ● ISSN 1589 1623 (Print) ● ISSN 1785 0037 (Online)
DOI: http://dx.doi.org/10.15666/aeer/1705_1110711120

[61] Verheijen, F., Jeffery, S., Bastos, A. C., Van Der Velde, M., Diafas, I. (2010): Biochar application to soils: a critical review of effects on soil properties, processes and functions. – JRC Scientific and technical Report. https://doi.org/10.2788/472.
[62] Wang, N., Li, J., Xu, R. (2009): Use of agricultural by-products to study the pH effects in an acid tea garden soil. – Soil use Manag 25: 128-132.
[63] Wang, Y., Pan, F., Wang, G., Zhang, G., Wang, Y., Chen, X., Mao, Z. (2014): Effects of biochar on photosynthesis and antioxidative system of Malus hupehensis Rehd. seedlings under replant conditions. – Sci Hortic (Amsterdam) 175: 9-15. https://doi.org/10.1016/j.scienta.2014.05.029.
[64] Xu, R. K., Coventry, D. R. (2003): Soil pH changes associated with lupin and wheat plant materials incorporated in a red–brown earth soil. – Plant Soil 250: 113-119.
[65] Yang, L., Liao, F., Huang, M., Yang, L., Li, Y. (2015): Biochar improves sugarcane seedling root and soil properties under a pot experiment. – Sugar tech 17: 36-40.
[66] Younis, U., Athar, M., Malik, S. A., Raza Shah, M., Mahmood, S. (2015): Biochar impact on physiological and biochemical attributes of spinach Spinacia oleracea (L.) in nickel contaminated soil. – Glob J Environ Sci Manag 1: 245-254.
[67] Yuan, J. H., Xu, R. K. (2011): The amelioration effects of low temperature biochar generated from nine crop residues on an acidic Ultisol. – Soil Use Manag 27: 110-115. https://doi.org/10.1111/j.1475-2743.2010.00317.x.

APPENDIX

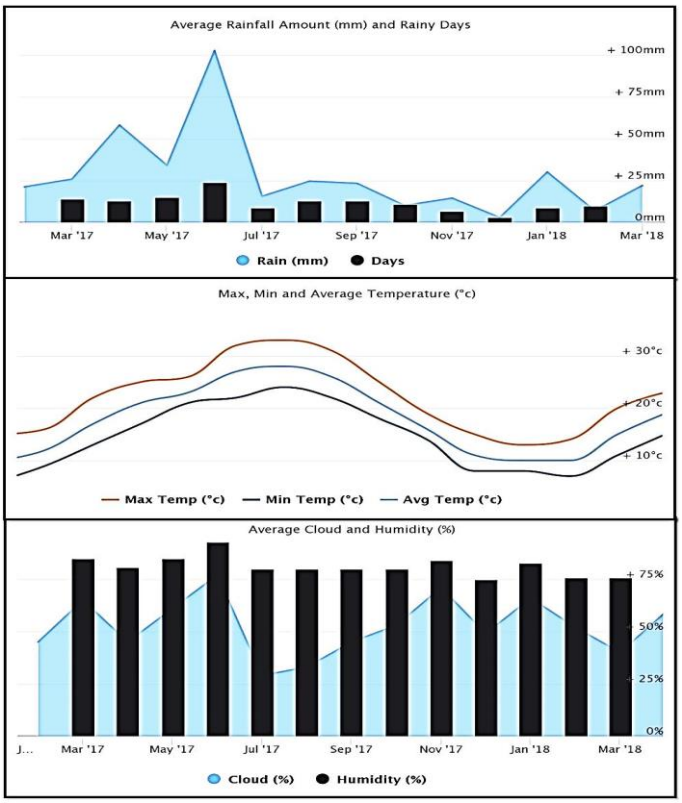

A-1. *One-year metrological information of study area, during the entire experiment period (Ref: https://www.worldweatheronline.com)*

http://www.aloki.hu ● ISSN 1589 1623 (Print) ● ISSN 1785 0037 (Online)
DOI: http://dx.doi.org/10.15666/aeer/1705_1110711120

PERFORMANCE EVALUATION OF MASS TRANSFER-BASED METHOD USING GLOBAL PERFORMANCE INDEX IN SEMI-ARID REGION, SAUDI ARABIA

ISLAM, S.[1*] – ABDULLAH, R. A. B.[1] – ALGAHTANI, A.[2,3] – IRSHAD, K.[4] – HIROL, H.[1]

[1]*Department of Civil Engineering, University Teknologi Malaysia, P.O. Box 81310, Johor Bahru, Johor, Malaysia*

[2]*Mechanical Engineering Department, College of Engineering, King Khalid University, Abha 61413, Asir, Kingdom of Saudi Arabia*

[3]*Research Centre for Advanced Materials Science (RCAMS), King Khalid University, P.O. Box 9004, Abha 61413, Asir, Kingdom of Saudi Arabia*

[4]*Center of Research Excellence in Renewable Energy (CoRERE), King Fahd University of Petroleum & Minerals, Dhahran, Saudi Arabia*

**Corresponding author*
e-mail: isaiful2@graduate.utm.my; phone: +966-59-521-9933; fax: +966-17-241-8816

(Received 4th Apr 2019; accepted 11th Jul 2019)

Abstract. The main aim of this research work is to assess the performance of the various mass transfer-based method with respect to standard FAO56-PM. Daily meteorological data from 1979 to 2018 has been used to compute reference evapotranspiration (ETo). The climatic data from 1979 to 2006 were used for the development of the calibrated equations and data from 2007 to 2018 were applied for validation purpose. The evaluated, calibrated and further validation of calibrated models were compared using statistical tools in order to ranked the models effectiveness using Global Performance Indicator (GPI) where higher GPI value shows better model. The models were then arranged using GPI and it was found that proposed model resulted with best GPI value of 5.02, 2.85 and 5.19 during evaluation, calibration and validation respectively followed by Albrecht model. The results of this study could be used by the water management system, crop cultivators, crop advisors, researchers from research centres. Moreover, it is beneficial for the decision maker in the vast field of agriculture, hydrology and environment**.** The calibration and validation of different ETo equations tend to increase their performance. Thus, the validated evapotranspiration model that used less climatic parameters can predict the ETo condition accurately for Asir region.
Keywords: *water management, calibration, validation, semi-arid condition, reference evapotranspiration model, mass transfer equation*

Introduction

Precise evaluation of reference evapotranspiration (ETo) plays a vital role for water resource management, efficient irrigation management, crop production, environmental assessment (Estevez et al., 2016). The reference evapotranspiration can be measured directly by lysimeter (Xu et al., 2013). However, measurements by lysimeter proved to be tedious work (Irmak et al., 2003). Consequently, Food and Agriculture Organization of the United Nations (FAO) recommends the standard Penman-Monteith FAO-56 PM, which was acknowledged in various parts of the world (Allen et al., 1998). Notwithstanding the aforementioned technique have shortcoming under certain unique conditions (Widmoser, 2009); however, it is still considered the standard technique for computing evapotranspiration for a reference surface (Xystrakis and Matzarakis, 2010;

http://www.aloki.hu ● ISSN 1589 1623 (Print) ● ISSN 1785 0037 (Online)
DOI: http://dx.doi.org/10.15666/aeer/1705_1112111141

Tabari et al., 2013), i.e., well-watered, actively growing grass of a height of 0.12 m with an albedo of 0.23 that uniformly covers the area and has a surface resistance of 70 s/m (Allen et al., 1998). The only shortcoming in FAO56-PM is that it requires various climatic data which are not easily available or measured. Hence keeping this shortcoming in mind many researchers have developed reference evapotranspiration equation which requires lesser input parameters that are categorized as mass transfer-, radiation-, temperature-, and pan evaporation-based methods (Sentelhas et al., 2010). However, such empirical equations need to be rectified by calibration against lysimetric or standard FAO56-PM technique at different regions. The researchers have performed various studies for simplified evapotranspiration equations against the FAO56-PM technique around the world, including Iran (Tabari et al., 2013), Southern Greece (Xystrakis and Matzarakis, 2010), Canada (Sentelhas et al., 2010), Tunisia (Jabloun and Sahli, 2008), Bulgaria (Popova et al., 2006), the Syria, the USA, Netherlands, the Philippines and Spain (Stockle et al., 2004). The past studies in saudi Arabia were basically assessed different ETo models against the FAO-56 Penman Monteith model based on the Central and Eastern region of Saudi Arabia (Salih and Sendil, 1984; Abo-Ghobar and Mohammad, 1995; Al-Omran et al., 2004; Elnesr et al., 2010; Islam et al.,2019). However very less study have been done in regards with evaluation calibration and validation of mass transfer equation. The mass transfer-based models are based on the principle of Dalton's law and employ eddy motion transfer of water vapor from an evaporating surface to the atmosphere (Singh and Xu, 2002; Tabari et al., 2013), the performance accuracy of these models reduces if aerodynamic effects have lower value as discussed by (Kiefer et al., 2017). These results provide significantly accurate result in many cases (Jensen, 1974). However, air temperature and wind speed have been measured at inconsistent heights, resulting different equations with similar or identical structure. So, the outcome resulting from input climatic condition varies from one location and or height to another and will be difficult to do with certainty (Helfrich, 1982). The mass transfer-based equation as compared to Standard FAO56-PM model have rarely been used in Southern region of Saudi Arabia. Hence, it is utmost important to carry out research based on evaluating the performance of various mass transfer reference evapotranspiration models to determine the best, or a relatively appropriate model for estimating the ETo in Semi-arid region. This can aid in recognizing the suitable method that can be used as an alternative equation to standard FAO56-PM method. The finding of the research work is helpful in reducing the error during the evapotranspiration computation. Moreover, the best-evaluated model equation the for evapotranspiration could assist in computing the evapotranspiration in future in the field of water management system, climate change studies, irrigation and water resource planning.

Study area

Site description

The research work deals with Abha mountainous region of Aseer province, Kingdom of Saudi Arabia having an area of 370 km^2 located between the latitude of 18°10′12.39″N and 18°23′33.05″N and longitude of 42°21′41.58″E and 42°39′36.09″E as shown in *Figure 1*. The zone is prone to heavy rainfall as compared to other parts of Saudi Arabia. The elevation varies from 1951 to 2991 m (msl) with average precipitation of 355 mm which mainly occurs between June and October.

http://www.aloki.hu ● ISSN 1589 1623 (Print) ● ISSN 1785 0037 (Online)
DOI: http://dx.doi.org/10.15666/aeer/1705_1112111141

Figure 1. *Location map of Abha Asir region, Kingdom of Saudi Arabia*

Data availibility

In this research work, weather parameters were collected from Abha meteorological weather station for the period between 1979 and 2018 which includes wind velocity, mean temperature, maximum and minimum temperature, mean relative humidity and solar radiation as well. The data collected were checked (Arnold and Allen, 1996). The weather data are shown in *Table 1*.

Table 1. *Characteristics of Abha weather parameters during the study period*

	Max temp (°C)	**Min temp (°C)**	**Mean temp (°C)**	**Wind velocity (m/s)**	**Humidity (%)**
Max	35.1	21.4	25.1	5.23	88
Min	20.3	-0.4	11.9	0.75	14
Mean	28.60	9.12	18.76	2.36	54.77
StDev	3.68	4.41	3.73	0.64	12.96
Kurtosis	-1.18	-1.05	-1.39	2.57	-0.66
Skewness	-0.17	-0.128	-0.06	1.14	0.043

Methodology

In this research work ETo were estimated by nine mass transfer reference evapotranspiration model and one proposed model based on available climatic data. Moreover, the reference ETo values were estimated using standardized FAO56-PM. The values evaluated from different mass transfer based equations were compared with the reference value obtained from FAO56-PM for the period between 1979 and 2018. Further, all ten equations were calibrated for the period between 1979 and 2006 then validation of calibrated equation for the period between 2007 and 2018 with respect to FAO56-PM model. The performance of equations was evaluated by utilizing ten statistical finally based on evaluation criteria the global performance index has been computed and the ranking were done in order to get most promising model which can be used alternative to FAO56-PM model. The flowchart (*Fig. 2*) described the stepwise procedure to compute most promising model among nine model to be used as alternate of FAO56-PM model.

http://www.aloki.hu ● ISSN 1589 1623 (Print) ● ISSN 1785 0037 (Online)
DOI: http://dx.doi.org/10.15666/aeer/1705_1112111141

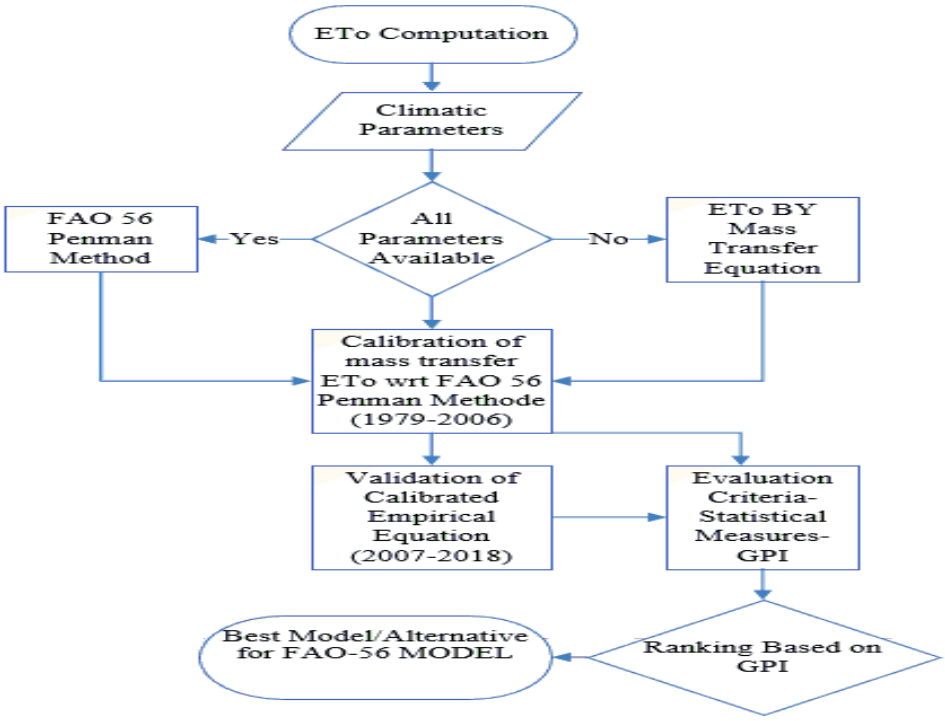

Figure 2. *Flowchart showing stepwise computation of ETo*

Reference evapotranspiration (ETo) model

This study work aims to analyze trends of the monthly ETo calculated by the Standard FAO56-PM model as given by *equation 1* in the Asir region, Kingdom of Saudi Arabia. However, the use of the FAO56-PM is restrained due to limited climatic input parameters; hence, the alternative solution is to use various mass transfer models. In this research work nine-mass transfer and one proposed alternative method for estimating ETo have been chosen for this study. The selection of methods was based on their wide acceptance, simple calculation procedure and applicability in present conditions. The models are described as *equations 2–10*.

FAO Penman-Monteith (Allen et al., 1998)

$$ETo = \frac{0.408\times\Delta\times(Rn-G)+\gamma\times\left(\frac{900}{T+273}\right)\times u_2\times(e_s-e_a)}{\Delta+\gamma\times(1+0.34u_2)} \quad \text{(Eq.1)}$$

Mass transfer based ETo model

Dalton (1802)

$$ETo = (0.3648 + 0.07223u_2) \times (e_s - e_a) \quad \text{(Eq.2)}$$

Trabert (1896)

$$ETo = 0.408 \times 0.3075 \times \sqrt{u_2} \times (e_s - e_a) \quad \text{(Eq.3)}$$

Meyer (1926)

$$ETo = (0.375 + 0.05026u_2) \times (e_s - e_a) \quad \text{(Eq.4)}$$

http://www.aloki.hu ● ISSN 1589 1623 (Print) ● ISSN 1785 0037 (Online)
DOI: http://dx.doi.org/10.15666/aeer/1705_1112111141

Rohwer (1931)

$$ETo = 0.44(1 + 0.27u_2) \times (e_s - e_a) \quad \text{(Eq.5)}$$

Penman (1948)

$$ETo = 0.35 \times (1 + 0.24u_2) \times (e_s - e_a) \quad \text{(Eq.6)}$$

Albrecht (1950)

$$ETo = (0.1005 + 0.297u_2) \times (e_s - e_a) \quad \text{(Eq.7)}$$

Brockamp (1963)

$$ETo = (0.543u_2^{0.456}) \times (e_s - e_a) \quad \text{(Eq.8)}$$

WMO (1966)

$$ETo = (0.1298 + 0.0934u_2) \times (e_s - e_a) \quad \text{(Eq.9)}$$

Mahringer (1970)

$$ETo = 0.15072 \times \sqrt{3.6u_2} \times (e_s - e_a) \quad \text{(Eq.10)}$$

where ETo = reference evapotranspiration (mm day^{-1}); Rn = net radiation at the crop surface (MJm^{-2} day^{-1}); G = soil heat flux density (MJm^{-2} day^{-1})) that is taken as zero for daily ETo estimation; u_2 = wind speed at 2 m height (m s^{-1}); e_s = saturation vapor pressure (kPa); e_a = actual vapor pressure (kPa); T = temperature at 2 m height (°C); (e_s–e_a) = vapor pressure deficit (kPa); Δ = slope of vapor pressure curve (kPa °C^{-1}); and γ = psychrometric constant (kPa °C^{-1}); T_{max} = Maximum Temperature (°C); T_{min} = Minimum Temperature (°C); T_{mean} = Mean Temperature (°C); RH_{mean} = Mean Relative Humidity (%); RH_{max} = Maximum Relative Humidity (%); RH_{min} = Minimum Relative Humidity (%)

Model development and validation

The fact that leads to model development in study area is that the previously established models for reference evapotranspiration estimation were reliable in the areas for which they were developed. However, when applied in other region it leads to larger errors. To overcome this comparative study of reference evapotranspiration model with standard FAO56-PM or by measuring instrument was performed. The basic idea of comparison was to judge which models gives better result for specific area of interest moreover it allows comparative study of all developed model for same meteorological data and for the same condition and period of time. The main shortcoming of these developed models were they have limited area of reliability as their variables involved in the equation may not be easily available and sometimes it is difficult to compare with one another due to region specific model variables. Recognizing the above concerns, an attempt is made in this research work to analyse various existing mass transfer-based method and to develop new model for Abha Asir region of Saudi Arabia. This is because the mass-transfer approaches generally are easiest to use and often are the only practical method available. The model hence developed must be simple in nature having easily measurable variable comprises of most influencing factors with acceptable accuracy. The proposed mass-transfer (aerodynamic) based methods utilize the concept of eddy motion transfer of water vapour from an evaporating surface to the atmosphere. All such methods are based on Dalton's law. It is evident that evapotranspiration

http://www.aloki.hu ● ISSN 1589 1623 (Print) ● ISSN 1785 0037 (Online)
DOI: http://dx.doi.org/10.15666/aeer/1705_1112111141

depends on heat energy and vapour pressure gradient and also depend on other factors, such as geological locations, seasons, etc.

The generalized expression which led to the formulation of proposed equation is as follows (*Eq. 11*):

$$ETo = c(e_s - e_a) = f(u)(e_s - e_a) \quad \text{(Eq.11)}$$

where ETo is reference evapotranspiration, e_s is the saturation vapour pressure, e_a is the vapour pressure in the air and C is aerodynamic conductance. The term e_a is also equal to the saturation vapour pressure at the dew point temperature it is normally assumed to be dependent on wind speed. Therefore, *equation 11* is expressed as the wind function f(u). This function depends on, among other factors, the observational heights of the wind speed and vapour pressure measurements. Although the two heights need not be the same, the same experimental layout must be used for a particular value of the function. Accuracy of the proposed model was measured with statistical indicators as described by Martins et al. (2017) based on regression analysis as given by *Equation 12:*

$$P_i(y) = a0 + b0O_i(x) \quad \text{(Eq.12)}$$

The regression equation (Eq. 12) represents FAO56-PM computed with observed data, Oi (x), and daily ETo computed with estimated variables, Pi (y). A value of b0 = 1.0 indicates that the fitted line is y = x, so that Oi and Pi are similar. A value of b0 > 1.0 suggests over-estimation and b0 < 1.0 under-estimation. The determination coefficient (R^2) regression between Oi and Pi showing value closer to one indicate good fit. Moreover the RMSE Value should also be checked for accuracy of result. Based on regression analysis new proposed equation has been formulated which is expressed as follows:

$$ETo = (0.37 + 0.72u_2) \times (e_s - e_a) \quad \text{(Eq.13)}$$

Although FAO 56 PM, found to work well in numerous locations if the required data are available. However it requires measurements of temperature, relative humidity, wind speed, and solar radiation. This data demand is the main constraint on its use in locations where climate data are limited. In high mountain environments, such as the Abha Asir region, Saudi Arabia, meteorological monitoring is limited and high-quality data are scarce. Moreover measurements of relative humidity by electronic sensors are commonly plagued by hysteresis, nonlinearity and calibration errors (Allen, 1996). In order to make the study more realistic the estimated result of FAO56-PM were compared with reference evapotranspiration value measured from Davis Vantage Pro2 weather stations installed in Abha region. The instrument is affordable, accurate, durable, and easy to use and moreover real-time data for weather conditions can be easily available. It uses air temperature, relative humidity, average wind speed, and solar radiation data to estimate ETo, which is calculated once an hour. ETo requires the optional solar radiation sensor. Also the measured values from instrument were compared with proposed equation. Validation of FAO56-PM and proposed model with measured value as represented by *Figure 3a-b*. After evaluating FAO56-PM with measure ETo the RMSE and MBE value found to be 0.154 and 0.01 mm while coefficient of determination found to be 0.988 with

http://www.aloki.hu ● ISSN 1589 1623 (Print) ● ISSN 1785 0037 (Online)
DOI: http://dx.doi.org/10.15666/aeer/1705_1112111141

slope and intercept of 1.01 and -0.03, respectively. On the other hand while evaluating proposed model ETo with measure ETo the RMSE and MBE value found to be 0.178 and -0.01 mm while coefficient of determination found to be 0.987 with slope and intercept of 1.09 and -0.249 respectively.

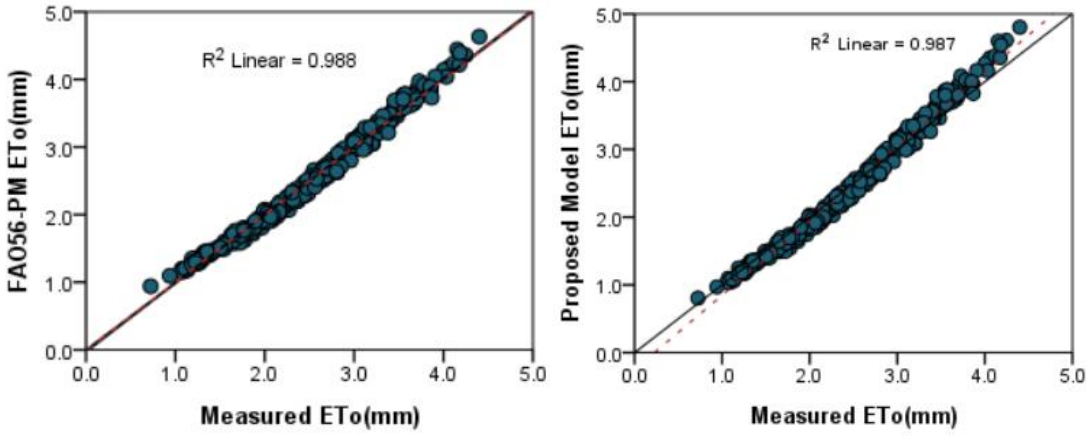

(a) (b)

Figure 3. *Validation of standard FAO56-PM ETo and proposed model ETo with measured ETo*

Calibration and validation of ET_O equations

The linear regression analysis has been performed to calibrate and validate the mass transfer empirical models against the FAO56 PM model (Allen et al., 1998). The specific expression is shown in the below equation:

$$ET_{FA056-PM} = a.ET_{EMP} + b \quad \text{(Eq.14)}$$

where $ET_{FAO56\ PM}$ shows the daily reference evapotranspiration estimated by the standard FAO56-PM model and ET_{EMP} shows the ten mass transfer models respectively. The constant a and b represent calibrated empirical coefficients in the equation. In this research work, the climatic data from 1979 to 2006 were used for the development of the calibrated equations and data from 2007 to 2018 were applied for validation purpose. This partitioning is important as more data is required for the models' training. The main objective of calibrating ETo was to make the slope equally inclined to both x and y axis and intercept reaching zero. For this purpose, a linear regression was done in between Standard PM-ETo and values were obtained through the nine ETo equations. To accomplish this, calibration coefficients need to be determined which can be obtained by applying product operation to the slope of a regression line between the FAO56-PM-ETo and ETo equation by inversing the slope. This will get a new slope so that the new equation will be closer to unity. Moreover, opposite sign value of the intercept was added to get a new intercept close to zero for new regression equation. The calibration and validation of ETo estimates were performed as suggested by (Xu et al., 2013)

Evaluation criteria and global performance index (GPI)

The GPI is computed by using ten statistical measure such as Mean Absolute Error(MAE), Root Mean Square Error (RMSE), Mean Absolute Relative Error (MARE),

http://www.aloki.hu ● ISSN 1589 1623 (Print) ● ISSN 1785 0037 (Online)
DOI: http://dx.doi.org/10.15666/aeer/1705_1112111141

Uncertainty at 95% (U95), Root mean squared relative error (RMSRE), Relative Root Mean Square Error (RRMSE), Mean Bias Error (MBE), Coefficient of determination (R^2), Maximum Absolute Relative Error (erMax) and t-statistics (Ali et al., 2019). For Coefficient of determination (R^2) the highest value (ideally equal to 1) is preferable, while for all other statistical errors ideally a value of zero is preferred. Despotovic et al. (2015) proposed the GPI by scaling the values of statistical tools in between 0 and 1, followed by subtracting the scaled values of error indicators from the corresponding medians and finally summing up the differences so obtained using the weight factors. Mathematically, for the i^{th} model,

$$GPI_i = \sum_{j=1}^{10} \alpha_j \left(\tilde{y}_j - \tilde{y}_{ij}\right) \quad \text{(Eq.15)}$$

where, α_j have a value of + 1 for statistical errors having a recommended value of 0 and a value of -1 for statistical errors that have a recommended high value of 1 (e.g. R). $\tilde{y}_j$ and $\tilde{y}_{ij}$ are the median and scaled values, respectively.

Willmott and Matsuura (2005) used MAE as statistical measure as shown by Equation 16:

Mean absolute error (MAE)

$$MAE = \frac{1}{n}\sum_{i=1}^{n}\left|ET_{O,Mi} - ET_{o,FAO56-PM}\right| \quad \text{(Eq.16)}$$

Root mean square error

$$RMSE = \left[\frac{1}{n}\sum_{i=1}^{n}\left(ET_{O,Mi} - ET_{o,FAO56-PM}\right)^2\right]^{\frac{1}{2}} \quad \text{(Eq.17)}$$

Mean absolute relative error (MARE)

$$MARE = \frac{1}{n}\sum_{i=1}^{n}\left|\frac{ET_{O,Mi} - ET_{o,FAO56-PM}}{ET_{O,Mi}}\right| \quad \text{(Eq.18)}$$

Behar et al. (2015) and Gueymard (2014) applied U_{95} in modelling of solar radiation as given by *Equation 19:*

Uncertainty at 95%

$$U_{95} = 1.96(SD^2 + RMSE^2)^{\frac{1}{2}} \quad \text{(Eq.19)}$$

Root mean squared relative error

$$RMSRE = \sqrt{\frac{1}{n}\sum_{i=1}^{n}\left(\frac{ET_{O,Mi} - ET_{o,FAO56-PM}}{ET_{O,Mi}}\right)^2} \quad \text{(Eq.20)}$$

Li et al. (2013) applied RRMSE as a statistical performance measure in the modelling of global solar radiation as given by *Equation 21:*

Relative root mean square error

http://www.aloki.hu ● ISSN 1589 1623 (Print) ● ISSN 1785 0037 (Online)
DOI: http://dx.doi.org/10.15666/aeer/1705_1112111141

$$RRMSE = 100 \times \frac{\sqrt{\frac{1}{n}\sum_{i=1}^{n}\left(ET_{O,Mi} - ET_{o,FAO56-PM}\right)^2}}{\sum_{i=1}^{n} ET_{O,Mi}} \quad \text{(Eq.21)}$$

Mean bias error

$$MBE = \frac{1}{n}\sum_{i=1}^{n}\left(ET_{O,Mi} - ET_{o,FAO56-PM}\right) \quad \text{(Eq.22)}$$

Correlation coefficient

$$R^2 = 1 - \frac{\sum_{i=1}^{n}\left(ET_{O,Mi} - ET_{o,FAO56-PM}\right)^2}{\sum_{i=1}^{n}\left(ET_{O,Mi} - ET_{O,Mi_{av}}\right)^2} \quad \text{(Eq.23)}$$

Maximum absolute relative error

$$erMAX = max\left(\left|\frac{ET_{O,Mi} - ET_{o,FAO56-PM}}{ET_{O,Mi}}\right|\right) \quad \text{(Eq.24)}$$

Stone (1993) and Mulaudzi et al. (2015) t-statistics in the evaluation of solar radiation t-statistics

$$t = \left[\frac{(n-1)MBE^2}{RMSE^2 - MBE^2}\right]^{\frac{1}{2}} \quad \text{(Eq.25)}$$

$ET_{O,Mi}$ = reference evapotranspiration by ith model; $ET_{o,FAO56-PM}$ = reference evapotranspiration by standard model 1; SD = standard deviation.

Results

The comparative study of all reference evapotranspiration equation with Standard Penman-Monteith equation is shown in *Figure 4a-j.* The plot clearly stated that the reference evapotranspiration value from all the ten equations has a high correlation with the FAO56-PM with the coefficient of determination R^2 range from 0.89 to 0.96 The highest correlation was shown by proposed model while the lowest correlation by Meyer model. The best fit of a model is measured by the linear regression line slope close to unity and the intercept to zero. The variation of slope and intercept for all models is shown in *Table 2*. While evaluating the performance of mass transfer equation against Standard FAO56-PM, the best estimates as shown in *Table 3* were obtained by proposed equation with $R^2 = 0.96$, MAE = 0.2 mm/day; RMSE = 0.23 mm/day; MARE = 0.1; U95 = 1.05%; RMSRE = 0.12; RRMSE = 0.09; MBE = 0.2 mm/day; erMax = 0.23; t-statistic = 18.47 mm/day. Moreover the GPA value shows highest score. Similarly worst outcome was shown by Trabert model. The computed GPI value during evaluation, calibration and validating the calibrated model are shown in *Tables 4–6*. The comparative study of global performance index during evaluation is shown in *Figure 5*.

The main objective of the model calibration is to improve the performance of all equations. The computed result from the year 1979 to 2006 was used to calibrate the evapotranspiration equation. From the result for calibrated model (*Fig. 6a-j*), it can be observed that the coefficient for determination improved substantially with values of R^2 ranges from 0.9 to 0.987 whereby high correlation was shown by proposed model and

http://www.aloki.hu ● ISSN 1589 1623 (Print) ● ISSN 1785 0037 (Online)
DOI: http://dx.doi.org/10.15666/aeer/1705_1112111141

lower value by Meyer method. While evaluating the performance of mass transfer equation against standard FAO56-PM after calibration the best estimates were obtained by proposed equation with high coefficient of determination $R^2 = 0.987$, MAE = 0.07 mm/day; RMSE = 0.09 mm/day; MARE = 0.03; U95 = 0.85%; RMSRE = 0.04; RRMSE = 0.04; MBE = 0.07 mm/day; erMax = 0.1; t-statistic = 13.48 mm/day as shown by *Table 3*. Moreover, the GPA Value shows that proposed highest score as shown by *Table 5*. Similarly, worst outcome was shown by Meyer model.

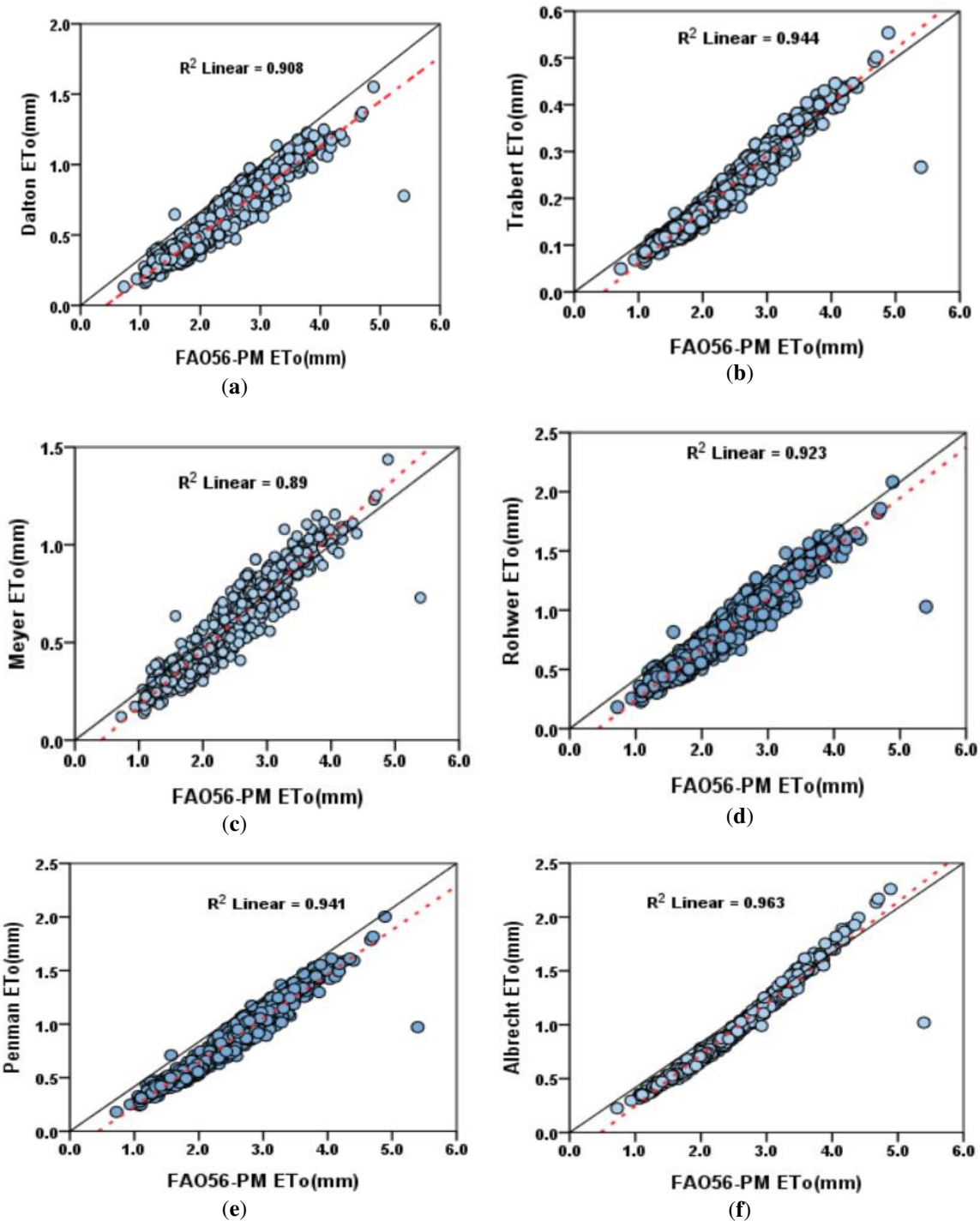

http://www.aloki.hu ● ISSN 1589 1623 (Print) ● ISSN 1785 0037 (Online)
DOI: http://dx.doi.org/10.15666/aeer/1705_1112111141

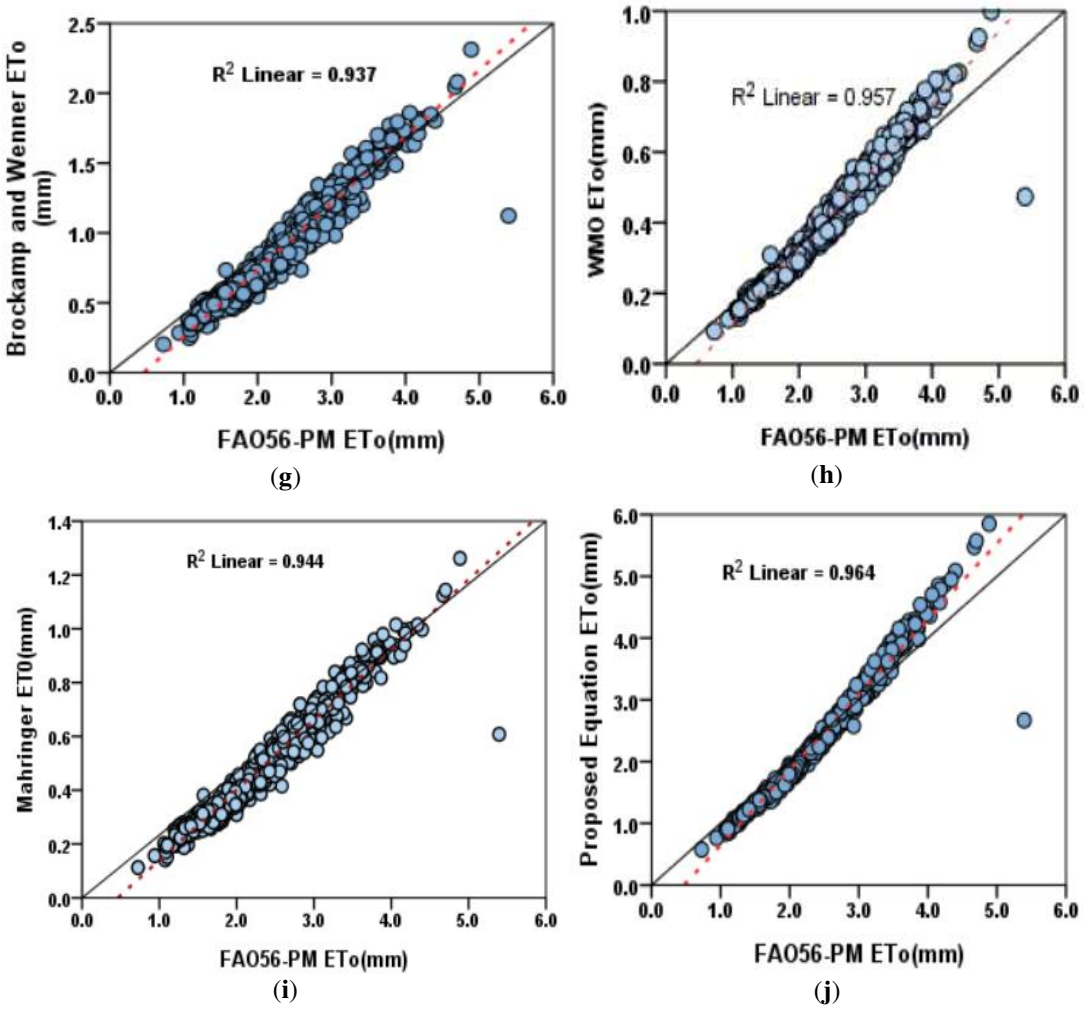

Figure 4. *Relationship between the daily ETo estimates of each method versus the FAO56-PM at Asir region for the 1979–2018 period*

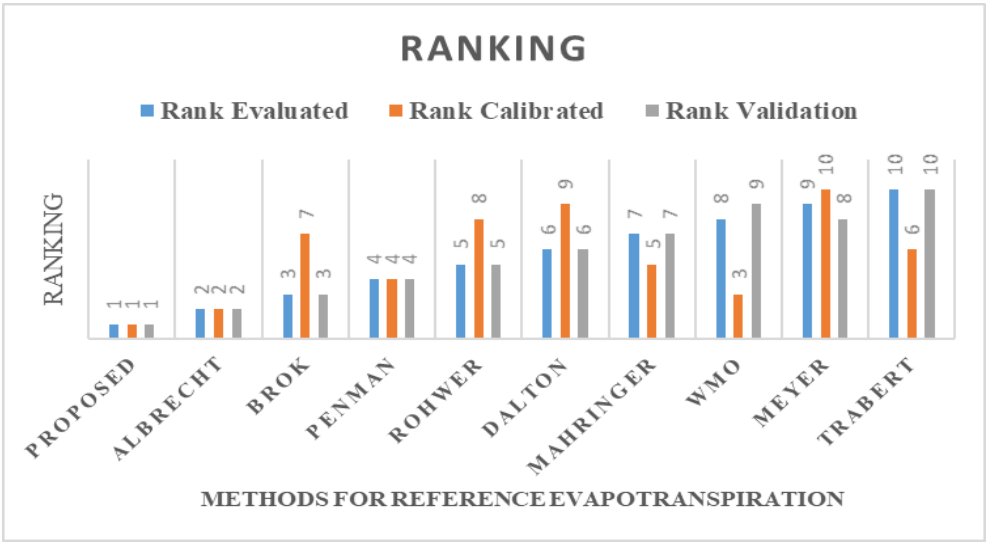

Figure 5. *Comparison of ranking of ETo estimates based on ETo equation, calibrated equation and validating the calibrated equation*

http://www.aloki.hu ● ISSN 1589 1623 (Print) ● ISSN 1785 0037 (Online)
DOI: http://dx.doi.org/10.15666/aeer/1705_1112111141

Table 2. *Slope and intercept of all model during evaluation, calibration and validation against FAO56-PM*

Sno	Evaluation		Calibration		Validation	
Method	**Slope**	**Intercept**	**Slope**	**Intercept**	**Slope**	**Intercept**
Dalton (1802)	0.316	-0.134	1.02	-0.036	0.301	-0.079
Trabert (1896)	0.114	-0.05	1.01	-0.058	0.109	0.012
Meyer (1926)	0.29	-0.122	1.02	-0.037	0.275	-0.068
Rohwer (1931)	0.426	-0.183	1.01	-0.036	0.406	-0.121
Penman (1948)	0.412	-0.181	1.01	-0.034	0.39	0.120
Albrecht (1950)	0.473	-0.225	1.01	-0.031	0.455	-0.156
Brockamp (1963)	0.476	-0.218	1.01	-0.034	0.455	-0.152
WMO (1966)	0.206	-0.09	1.01	-0.033	0.198	-0.046
Mahringer (1970)	0.261	-0.12	1.01	-0.034	0.249	-0.068
Proposed (2019)	1.22	-0.575	1.01	-0.031	1.17	-0.449

Table 3. *Statistical measures of all model during evaluation, calibration and validation against FAO56-PM*

		Dalton	**Trabert**	**Meyer**	**Rohwer**	**Penman**	**Albrecht**	**Brockamp**	**WMO**	**Mahringer**	**Proposed**
Evaluated	MAE	1.83	2.21	1.88	1.62	1.64	1.50	1.53	2.03	1.93	0.20
	RMSE	1.91	2.33	1.97	1.69	1.71	1.56	1.59	2.13	2.03	0.23
	MARE	3.30	10.80	3.72	2.17	2.23	1.73	1.85	5.35	4.18	0.10
	U95%	1.93	2.33	1.98	1.72	1.74	1.61	1.64	2.14	2.04	1.06
	RMSRE	3.37	10.91	3.81	2.22	2.27	1.75	1.89	5.39	4.23	0.12
	RRMSE	3.20	10.73	3.58	2.08	2.17	1.69	1.76	5.34	4.10	0.10
	MBE	1.83	2.21	1.88	1.62	1.64	1.50	1.53	2.03	1.93	0.20
	R^2	0.91	0.94	0.89	0.92	0.94	0.96	0.94	0.96	0.94	0.96
	erMax	5.71	16.38	6.82	3.70	3.46	2.80	3.32	7.06	6.62	0.24
	T-STAT	32.15	30.09	31.85	33.78	33.55	34.56	34.95	30.86	31.54	18.48
		Dalton	**Trabert**	**Meyer**	**Rohwer**	**Penman**	**Albrecht**	**Brockamp**	**WMO**	**Mahringer**	**Proposed**
Calibrated	MAE	0.16	0.12	0.18	0.14	0.11	0.08	0.12	0.09	0.11	0.07
	RMSE	0.20	0.15	0.22	0.18	0.14	0.10	0.16	0.11	0.15	0.09
	MARE	0.08	0.06	0.09	0.07	0.05	0.03	0.06	0.04	0.05	0.03
	U95%	0.87	0.86	0.89	0.87	0.86	0.85	0.86	0.85	0.86	0.85
	RMSRE	0.11	0.08	0.12	0.09	0.07	0.04	0.08	0.05	0.07	0.04
	RRMSE	0.09	0.07	0.10	0.08	0.06	0.04	0.07	0.05	0.06	0.04
	MBE	0.16	0.12	0.18	0.14	0.11	0.08	0.12	0.09	0.11	0.07
	R^2	0.92	0.96	0.90	0.94	0.96	0.99	0.95	0.98	0.96	0.99
	erMax	0.25	0.18	0.30	0.21	0.16	0.13	0.19	0.12	0.17	0.10
	T-STAT	12.62	11.63	13.10	12.09	11.47	13.11	11.36	13.37	11.31	13.48
		Dalton	**Trabert**	**Meyer**	**Rohwer**	**Penman**	**Albrecht**	**Brockamp**	**WMO**	**Mahringer**	**Proposed**
Validation	MAE	1.92	2.34	1.98	1.69	1.72	1.59	1.59	2.16	2.05	0.20
	RMSE	2.01	2.46	2.07	1.76	1.79	1.65	1.65	2.26	2.14	0.25
	MARE	2.82	7.79	3.16	1.88	1.97	1.60	1.60	4.65	3.60	0.08
	U95%	2.03	2.46	2.09	1.80	1.83	1.70	1.70	2.27	2.16	1.11
	RMSRE	2.86	7.82	3.21	1.91	1.99	1.61	1.63	4.67	3.63	0.10
	RRMSE	2.82	8.17	3.16	1.86	1.95	1.57	1.57	4.74	3.64	0.10
	MBE	1.92	2.34	1.98	1.69	1.72	1.59	1.59	2.16	2.05	0.20
	R^2	0.89	0.91	0.87	0.89	0.90	0.92	0.90	0.91	0.91	0.92
	erMax	3.79	9.37	4.32	2.57	2.56	2.10	2.22	5.45	4.48	0.23
	T-STAT	32.52	30.72	32.20	33.82	33.91	35.67	35.03	31.78	32.30	12.58

http://www.aloki.hu ● ISSN 1589 1623 (Print) ● ISSN 1785 0037 (Online)
DOI: http://dx.doi.org/10.15666/aeer/1705_1112111141

Table 4. *Ranking based on global performance index for various methods during evaluation period (1979-2018)*

Method	MAE	RMSE	MARE	U95%	RMSRE	RRMSE	MBE	R^2	erMax	T-STAT	GP1	Rank
Proposed	0.76	0.75	0.25	0.61	0.25	0.24	0.76	-0.29	0.28	0.82	5.02	1
Albrecht	0.12	0.12	0.10	0.18	0.10	0.09	0.12	-0.27	0.12	-0.16	1.05	2
Brockamp	0.10	0.11	0.09	0.16	0.09	0.09	0.10	0.08	0.09	-0.18	0.56	3
Penman	0.05	0.05	0.05	0.07	0.05	0.05	0.05	0.02	0.08	-0.09	0.33	4
Rohwer	0.06	0.06	0.06	0.09	0.06	0.06	0.06	0.27	0.06	-0.11	0.12	5
Dalton	-0.05	-0.05	-0.05	-0.07	-0.05	-0.05	-0.05	0.47	-0.06	-0.01	-0.91	6
Mahringer	-0.10	-0.10	-0.13	-0.16	-0.13	-0.13	-0.10	-0.02	-0.12	0.03	-0.93	7
WMO	-0.15	-0.15	-0.24	-0.23	-0.24	-0.25	-0.15	-0.18	-0.15	0.07	-1.31	8
Meyer	-0.07	-0.07	-0.09	-0.11	-0.09	-0.08	-0.07	0.71	-0.13	0.01	-1.43	9
Trabert	-0.24	-0.25	-0.75	-0.39	-0.75	-0.76	-0.24	-0.02	-0.72	0.12	-3.95	10

Table 5. *Ranking based on global performance index for various methods during calibration period (1979-2006)*

Method	MAE	RMSE	MARE	U95%	RMSRE	RRMSE	MBE	R^2	erMax	T-STAT	GP1	Rank
Proposed	0.38	0.44	0.38	0.26	0.42	0.44	0.38	-0.30	0.36	-0.52	2.85	1
Albrecht	0.34	0.40	0.36	0.21	0.39	0.41	0.34	-0.28	0.25	-0.35	2.63	2
WMO	0.24	0.31	0.26	0.26	0.31	0.30	0.24	-0.19	0.27	-0.47	1.92	3
Penman	0.04	0.04	0.05	0.09	0.06	0.04	0.04	0.02	0.08	0.41	0.82	4
Mahringer	0.04	0.03	0.04	0.04	0.04	0.04	0.04	-0.02	0.04	0.48	0.81	5
Trabert	-0.04	-0.03	-0.04	-0.07	-0.04	-0.04	-0.04	-0.02	-0.04	0.34	0.02	6
Brok	-0.06	-0.07	-0.06	-0.04	-0.07	-0.07	-0.06	0.07	-0.08	0.46	-0.12	7
Rohwer	-0.24	-0.23	-0.23	-0.16	-0.21	-0.23	-0.24	0.27	-0.19	0.12	-1.88	8
Dalton	-0.45	-0.41	-0.44	-0.36	-0.41	-0.42	-0.45	0.46	-0.39	-0.12	-3.91	9
Meyer	-0.62	-0.56	-0.62	-0.74	-0.58	-0.56	-0.62	0.70	-0.64	-0.34	-5.97	10

Table 6. *Ranking based on global performance index for various methods during validation period (2007-2018)*

Method	MAE	RMSE	MARE	U95%	RMSRE	RRMSE	MBE	R^2	erMax	T-STAT	GP1	Rank
Proposed	0.76	0.75	0.30	0.61	0.30	0.28	0.76	-0.26	0.32	0.86	5.19	1
Albrecht	0.11	0.12	0.10	0.17	0.11	0.10	0.11	-0.23	0.12	-0.14	1.02	2
Brok	0.11	0.11	0.10	0.17	0.10	0.10	0.11	0.07	0.10	-0.11	0.73	3
Penman	0.05	0.05	0.06	0.08	0.06	0.05	0.05	0.02	0.07	-0.06	0.37	4
Rohwer	0.06	0.06	0.07	0.10	0.07	0.07	0.06	0.28	0.07	-0.06	0.21	5
Dalton	-0.05	-0.05	-0.06	-0.08	-0.06	-0.05	-0.05	0.47	-0.07	0.00	-0.92	6
Mahringer	-0.11	-0.11	-0.16	-0.17	-0.16	-0.16	-0.11	-0.02	-0.14	0.00	-1.07	7
Meyer	-0.07	-0.08	-0.10	-0.12	-0.10	-0.10	-0.07	0.74	-0.13	0.01	-1.50	8
WMO	-0.16	-0.16	-0.29	-0.25	-0.29	-0.29	-0.16	-0.19	-0.25	0.03	-1.64	9
Trabert	-0.24	-0.25	-0.70	-0.39	-0.70	-0.72	-0.24	-0.02	-0.68	0.07	-3.82	10

Ten calibrated evapotranspiration equations have been validated for the period of 2007–2018 in order to show which calibrated equation perform well and can be further employed as an alternative to Standard FAO Penman Monteith model. From output of validation of calibrated equation (*Fig. 7a-i*), it can be observed that the coefficient of

http://www.aloki.hu ● ISSN 1589 1623 (Print) ● ISSN 1785 0037 (Online)
DOI: http://dx.doi.org/10.15666/aeer/1705_1112111141

determination ranges from 0.87 to 0.92 with high correlation shown by Proposed model and lower value by Meyer model. While evaluating the performance of mass transfer equation against Standard FAO56-PM during validation of calibrated equation, the best estimates were obtained by proposed equation with high determination coefficient (R^2 = 0.92; MAE = 0.19 mm/day; MSE = 0.09 mm/day; MARE = 0.03; U95 = 0.85; RMSRE = 0.04; RRMSE = 0.04; MBE = 0.07 mm/day; erMax = 0.1; t-Statistics = 13.48 mm/day as shown by *Table 3*. Moreover, the GPA Value shows highest score as shown by *Table 6*. Similarly, worst outcome was shown by Meyer model.

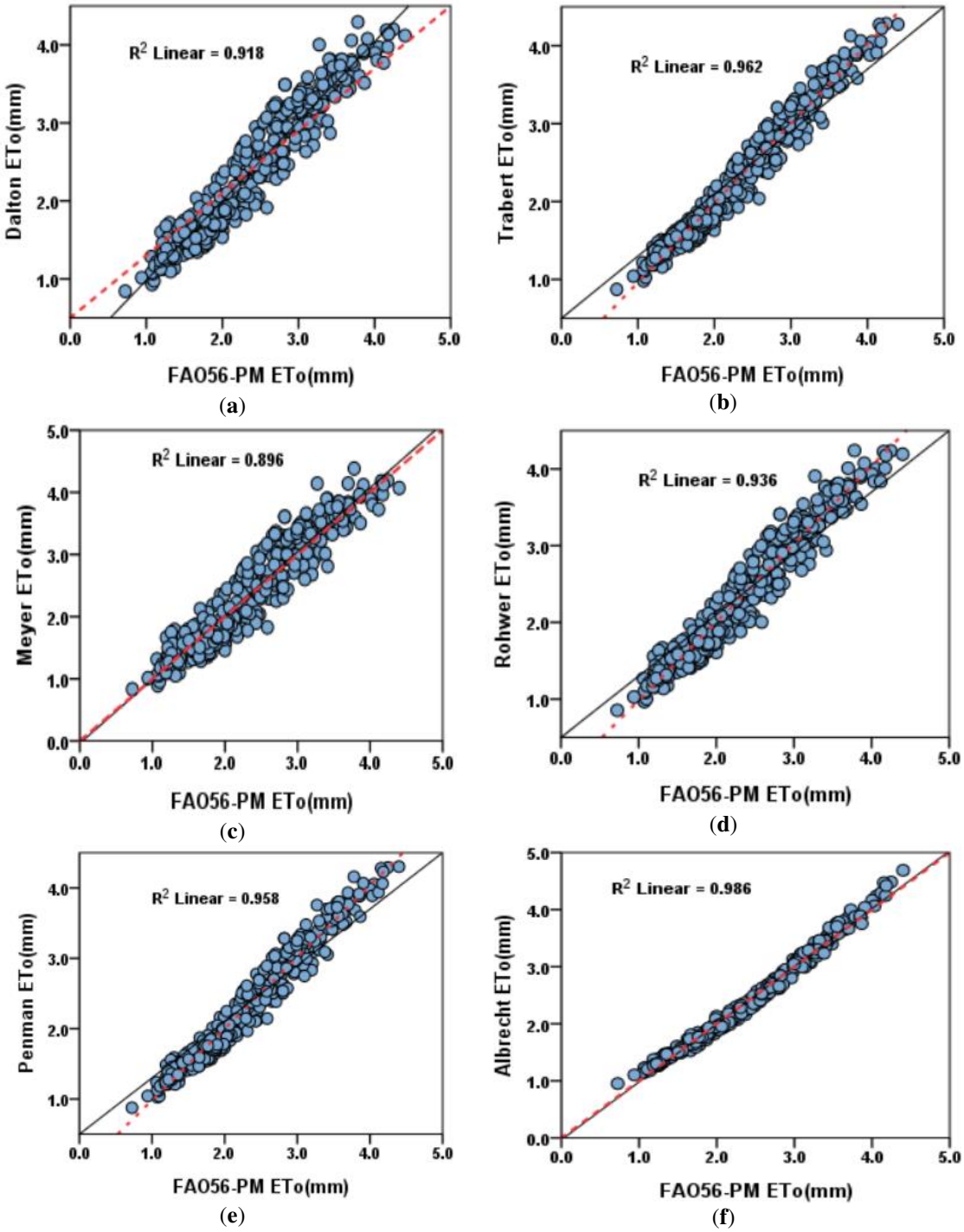

http://www.aloki.hu ● ISSN 1589 1623 (Print) ● ISSN 1785 0037 (Online)
DOI: http://dx.doi.org/10.15666/aeer/1705_1112111141

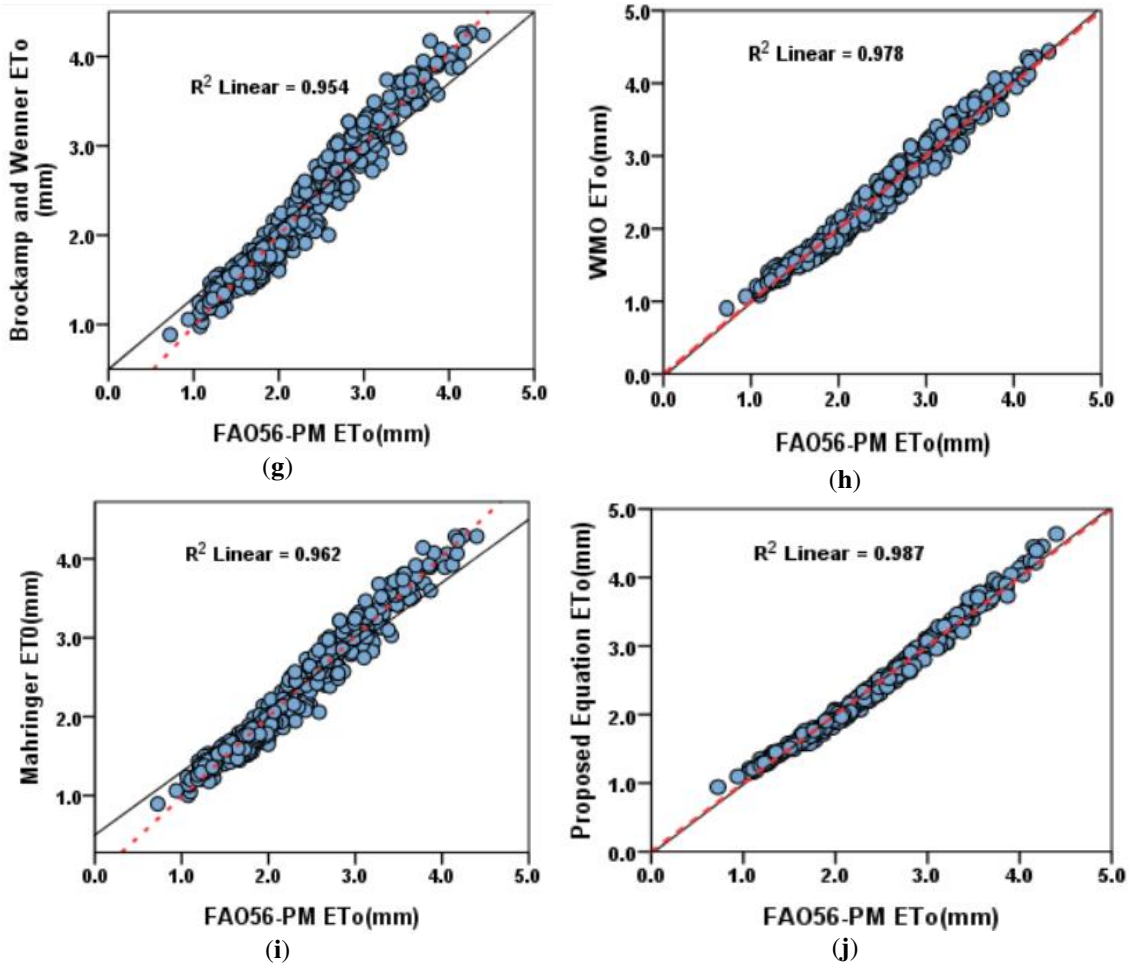

Figure 6. *Relationship between the calibrated daily ETo estimates of each method versus the FAO56-PM at Asir region for the 1979-2006 period*

Discussion

Different ETo models were used around the world to compute the reference evapotranspiration by using various climatic parameters such as mean temperature (Tm), relative humidity (RH) solar radiation (Rs) and wind speed (u)). FAO56-PM model is the most accurate model for estimating the ETo over the past few decades. But due to the constraint of limited climatic parameters, alternative equation has to be found out. Thus, to find an alternative technique of accurate prediction of ETo under climatic condition, the performance of the nine mass models and one proposed model were evaluated against the FAO56-PM model by using the ten common statistical approaches. Additionally, a linear regression model was adopted to calibrate and validate the performance of the empirical models during the 1979–2006 and 2007–2018 time periods respectively. The result evaluated from 1979 to 2018 showed that the proposed mass transfer method performed better without calibration with the highest coefficient of determination ($R^2 = 0.96$). The statistical output showed that the proposed model performed better as compared to the other model. The models are calibrated similar to the studies of Irmak et al. (2003) and Xu and Singh (2001). Valipour (2015) indicated overestimation of ETo by mass transfer-based equations, compared to the

http://www.aloki.hu ● ISSN 1589 1623 (Print) ● ISSN 1785 0037 (Online)
DOI: http://dx.doi.org/10.15666/aeer/1705_1112111141

Penman-Monteith model similar to the results reported by Winter et al. (1995). The Penman equation was the best performing equation among mass transfer equations across 15 provinces in Iran with the least ETo overestimate of 0.03 mm/day as the Papadakis equation (Valipour, 2015). The Trabert and Mahringer equations performed relatively well under the sahelian climatic conditions as reported by Djaman et al. (2015). Tabari et al. (2013) reported that Trabert and Mahringer equations underestimated ETo with average error of 26% and 31%, respectively in Iran while (Djaman et al., 2015) reported average ETo underestimation of 16% and 31% at Ndiaye (coastal area) and at Fanaye (inland area) in the Senegal River Valley and Delta, respectively. Adversely, poor performance of the Mahringer equation was reported in Poland (Bogawski and Bednorz, 2014). Singh and Xu (2002) indicated reasonable performance of the Meyer, Dalton, and Rohwer equation for free water evaporation estimation from four weather stations in north-western Ontario, Canada. The results of this study showed the specificity of each ETo equation and this might have been due to the sensitivity of the models to the climatic variables used in each model (Valipour, 2015). The performance of mass transfer empirical methods was evaluated against FAO56-PM method owing to its, rigorousness, comprehensiveness as from the work of several researchers (e.g. Ali and Shui, 2009; Tabari et al., 2013). After calibrating the empirical equation from (1979-2006), it was observed that there was a remarkable improvement in the performance of these nine equations. Additionally, the findings revealed that the calibration improved the reliability and consistency of different ET_0 equations. The correlation value significantly increased. Moreover, the statistical measures such as RMSE, SEE, MBE and PE significantly reduced for all the models.

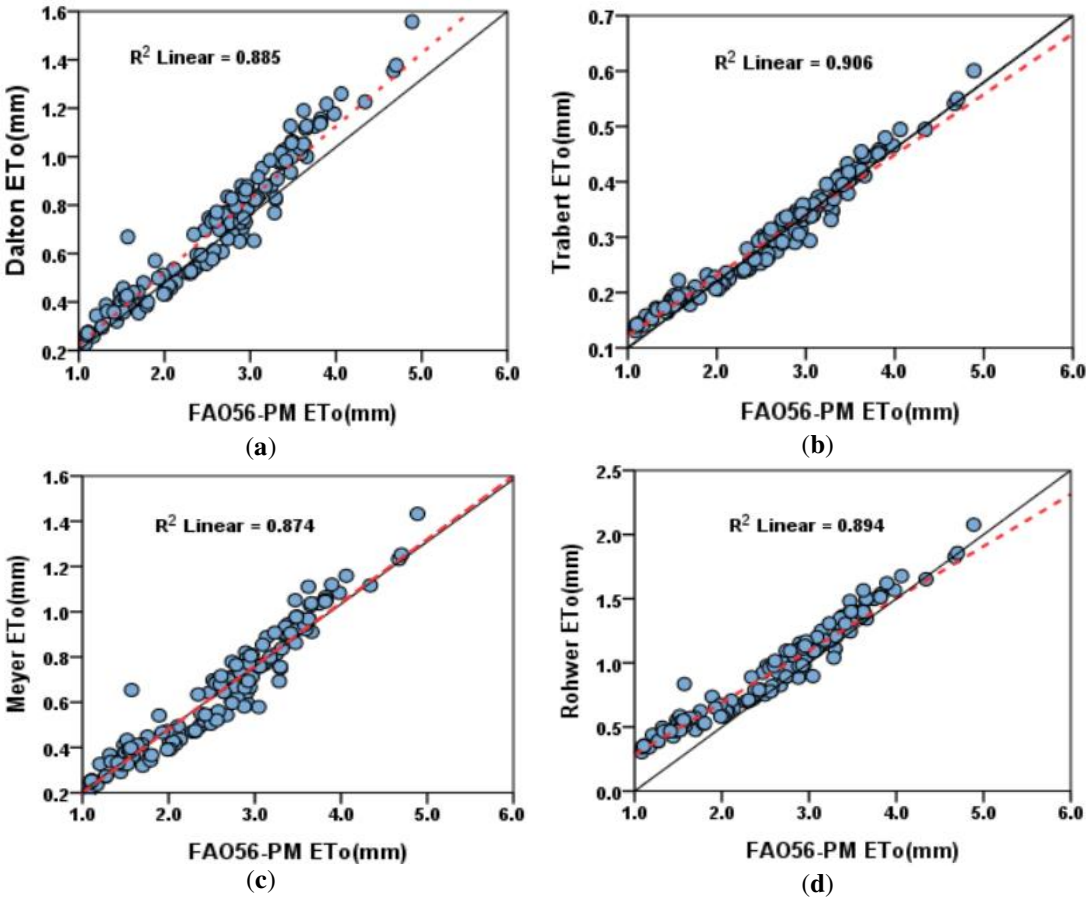

http://www.aloki.hu ● ISSN 1589 1623 (Print) ● ISSN 1785 0037 (Online)
DOI: http://dx.doi.org/10.15666/aeer/1705_1112111141

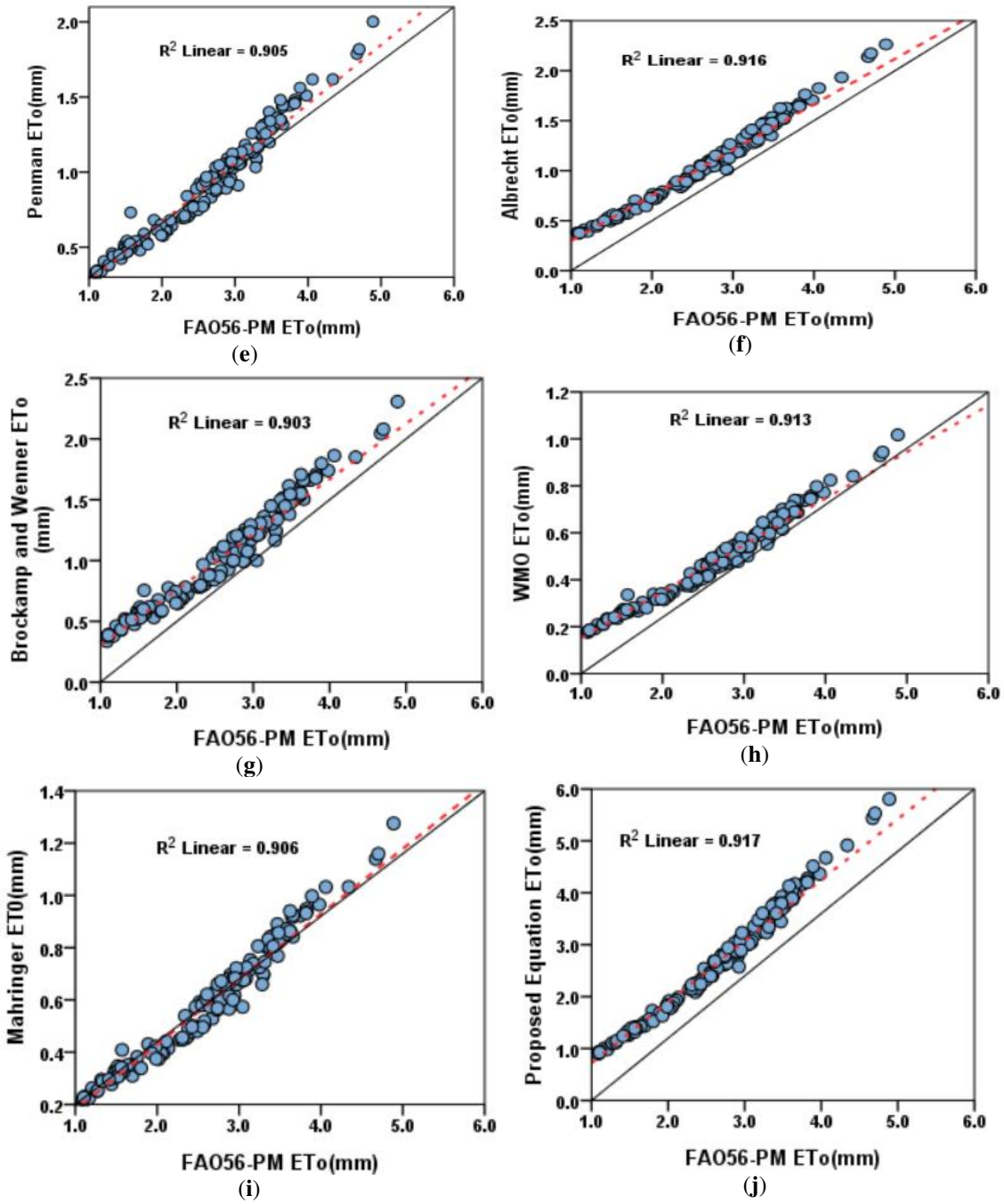

Figure 7. *Relationship between the validation of calibrated daily ETo estimates of each method versus the FAO56-PM at Asir region for the 2007-2018 period*

Valipour (2015) reported that there was an improvement in the calibrated Trabert and Mahringer equations in Iran with MBE as low as 0.02 mm/day. He indicated that the Trabert model can skip the calibration process to generate the best performance in Iran. The dependency of mass transfer equation on the vapor pressure was too small. It was reported that better performance of the Trabert and Mahringer equations were in inland area than at the coastal area in the Senegal River Valley (Djaman et al., 2015). The validation of the nine ETo equations for the 2007–2018 period is presented in *Figure 6*.

http://www.aloki.hu ● ISSN 1589 1623 (Print) ● ISSN 1785 0037 (Online)
DOI: http://dx.doi.org/10.15666/aeer/1705_1112111141

The statistical analysis showed a strong correlation between the calibrated equations to the PM estimates (*Table 4*). The findings of the research are in agreement with Kisi and Zounemat Kermani (2014). The outcomes of the study will provide meaningful guidance for agricultural production, hydrological planning and management in the vital region as well as other regions with similar climates.

Conclusions

The current study was performed with an aim to evaluate the ten reference evapotranspiration models (nine mass transfers and one proposed model) with respect to standard FAO56 PM model in the semi-arid region of Kingdom of Saudi Arabia. The ten evapotranspiration models have been successfully evaluated (period: 1979-2018), calibrated (period: 1979-2006) and further validated (period: 2007-2018). Based on the evaluation criteria, the GPI has been computed and the ranking operation was performed in order to observe the performance against the FAO56 PM equation under the available climatic conditions in Asir region. The effectiveness of the evaluated models can be judged based on the regression and statistical evaluation criteria which can be summarized as below:

- There was a remarkable improvement in the performance of calibrated equation. Moreover, the calibration approach improves the reliability and consistency of different evapotranspiration equation.
- The GPI is better to index ranking of equations as it takes into account the integrated approach of all the selected evaluation statistics.
- The ranking based on GPI of evaluated evapotranspiration models shows that the proposed model performed very well without calibration with GPI value of 5.02 and worst performance shown by Trabert.
- The ranking based on GPI of calibrated model reveals the fact that proposed model performed efficiently with the coefficient of determination up to 0.987 with GPI value of 2.85 and the worst performance shown by Meyer model
- Validation of calibrated equation shows that the proposed method was the most promising model and can be used as an alternative approach to Standard FAO-56 Penman Monteith model under the limited climatic condition followed by Albrecht model.
- The results of this study could be used by the water management system, crop cultivators, crop advisors, researchers and students from universities and research centres. Moreover, it is beneficial for the decision maker in the vast field of agriculture, hydrology and environment.

Acknowledgments. The authors would like to acknowledge the Deanship of Scientific Research (King Khalid University, Ministry of Education, Kingdom of Saudi Arabia) for providing administrative and financial support (award number R.G.P.1./74/40). The authors of current work wish to thank Universiti Tecknologi Malaysia, Johor Bahru for their facilities and Lab support. We would also like to thank general authority of the meteorological department, Abha, Asir region, Saudi Arabia for providing the weather data.

Conflict of interests: The authors declare no conflict of interests.

http://www.aloki.hu ● ISSN 1589 1623 (Print) ● ISSN 1785 0037 (Online)
DOI: http://dx.doi.org/10.15666/aeer/1705_1112111141

REFERENCES

[1] Abo-Ghobar, H. M., Mohammad, S. (1995): Evapotranspiration measurement by lysimeters in a desert climate. – Arab Gulf Journal of Scientific Research 13(1): 109-122.
[2] Albrecht, F. (1950): Die Methoden zur Bestimmung der Verdunstung der natürlichen Erdoberfläche. – Archiv für Meteorologie, Geophysik und Bioklimatologie, Serie B 2(1-2): 1-38.
[3] Ali, M., Jamil, B. (2019): Estimating diffuse solar radiation in India: performance characterization of generalized single-input empirical models. – Urban Climate 27: 314-350.
[4] Ali, M. H., Shui, L. T. (2009): Potential evapotranspiration model for Muda irrigation project, Malaysia. – Water Resources Management 23(1): 57.
[5] Allen, R. G. (1996): Assessing integrity of weather data for reference evapotranspiration estimation. – J. Irrig. and Drain. Engrg., ASCE 122(2): 97-106.
[6] Allen, R. G., Pereira, L. S., Raes, D., Smith, M. (1998): Crop Evapotranspiration-Guidelines for Computing Crop Water Requirements. – FAO Irrigation and Drainage Paper 56. FAO, Rome.
[7] Al-Omran, A. M., Al-Ghobari, H. M., Alazba, A. A. (2004): Determination of evapotranspiration of tomato and squash. – International Agricultural Engineering Journal 13(142): 27-36.
[8] Arnold, J. G., Allen, P. M. (1996): Estimating hydrologic budgets for three Illinois watersheds. – Journal of Hydrology 176(1-4): 57-77.
[9] Behar, O., Khellaf, A., Mohammedi, K. (2015): Comparison of solar radiation models and their validation under Algerian climate – the case of direct irradiance. – Energy Conversion and Management 98: 236-251.
[10] Bogawski, P., Bednorz, E. (2014): Comparison and validation of selected evapotranspiration models for conditions in Poland (Central Europe). – Water Resources Management 28(14): 5021-5038.
[11] Brockamp, B., Wenner, H. (1963): Verdunstungsmessungen auf den Steiner See bei Münster. – Dt Gewässerkundl Mitt 7: 149-154.
[12] Dalton, J. (1802): Experimental essays on the constitution of mixed gases; on the force of steam or vapor from water and other liquids in different temperatures, both in a Torricellian vacuum and in air; on evaporation and on the expansion of gases by heat. – Memoirs of the Literary and Philosophical Society of Manchester 5(2): 535-602.
[13] Despotovic, M., Nedic, V., Despotovic, D., Cvetanovic, S. (2015): Review and statistical analysis of different global solar radiation sunshine models. – Renewable and Sustainable Energy Reviews 52: 1869-1880.
[14] Djaman, K., Balde, A. B., Sow, A., Muller, B., Irmak, S., N'Diaye, M. K., ... Saito, K. (2015): Evaluation of sixteen reference evapotranspiration methods under Sahelian conditions in the Senegal River Valley. – Journal of Hydrology: Regional Studies 3: 139-159.
[15] ElNesr, M., Alazba, A., Abu-Zreig, M. (2010): Spatio-temporal variability of evapotranspiration over the Kingdom of Saudi Arabia. – Applied Engineering in Agriculture 26(5): 833-842.
[16] Estévez, J., García-Marín, A. P., Morábito, J. A., Cavagnaro, M. (2016): Quality assurance procedures for validating meteorological input variables of reference evapotranspiration in mendoza province (Argentina). – Agricultural Water Management 172: 96-109.
[17] Gueymard, C. A. (2014): A review of validation methodologies and statistical performance indicators for modeled solar radiation data: towards a better bankability of solar projects. – Renewable and Sustainable Energy Reviews 39: 1024-1034.

http://www.aloki.hu ● ISSN 1589 1623 (Print) ● ISSN 1785 0037 (Online)
DOI: http://dx.doi.org/10.15666/aeer/1705_1112111141

[18] Helfrich, K. R., Adams, E. E., Godbey, A. L., Harleman, D. R. F. (1982): Evaluation of Models for Predicting Evaporative Water Loss in Cooling Impoundments. – Final Report (No. PB-82-229725). Energy Lab, Massachusetts Inst. of Tech., Cambridge, USA.
[19] ISLAM, S., ABDULLAH, R. A. B., ALGAHTANI, A., IRSHAD, K., & HIROL, H. (2019): PERFORMANCE OF VAPOUR PRESSURE MODELS IN THE COMPUTATION OF VAPOUR PRESSURE AND EVAPOTRANSPIRATION IN ABHA, ASIR REGION, SAUDI ARABIA. –APPLIED ECOLOGY AND ENVIRONMENTAL RESEARCH 17(4): 9691-9715
[20] Irmak, S., Irmak, A., Allen, R. G., Jones, J. W. (2003): Solar and net radiation-based equations to estimate reference evapotranspiration in humid climates. – Journal of Irrigation and Drainage Engineering 129(5): 336-347.
[21] Jabloun, M. D., Sahli, A. (2008): Evaluation of FAO-56 methodology for estimating reference evapotranspiration using limited climatic data: application to Tunisia. – Agricultural Water Management 95(6): 707-715.
[22] Jensen, M. E. (1973): Consumptive Use of Water and Irrigation Water Requirements. – ASCE, New York, pp. 215-215.
[23] Jensen, M. E. (1974): Consumptive Use of Water and Irrigation Water Requirements. – ASCE, New York.
[24] Kiafar, H., Babazadeh, H., Marti, P., Kisi, O., Landeras, G., Karimi, S., Shiri, J. (2017): Evaluating the generalizability of GEP models for estimating reference evapotranspiration in distant humid and arid locations. – Theoretical and Applied Climatology 130(1-2): 377-389.
[25] Kisi, O., Zounemat-Kermani, M. (2014): Comparison of two different adaptive neuro-fuzzy inference systems in modelling daily reference evapotranspiration. – Water Resources Management 28(9): 2655-2675.
[26] Li, M. F., Tang, X. P., Wu, W., Liu, H. B. (2013): General models for estimating daily global solar radiation for different solar radiation zones in mainland China. – Energy Conversion and Management 70: 139-148.
[27] Mahringer, W. (1970: Verdunstungsstudien am Neusiedler See. – Archiv für Meteorologie, Geophysik und Bioklimatologie, Serie B 18(1): 1-20.
[28] Martins, D. S., Paredes, P., Raziei, T., Pires, C., Cadima, J., Pereira, L. S. (2017): Assessing reference evapotranspiration estimation from reanalysis weather products. An application to the Iberian Peninsula. – Int J Climatol 37(5): 2378-2397.
[29] Meyer, A. (1926): Über einige Zusammenhänge zwischen Klima und Boden in Europa. – Doctoral Dissertation, ETH, Zurich.
[30] Mulaudzi, T. S., Maluta, N. E., Sankaran, V. (2015): Evaluation of the global solar irradiance in the Vhembe district of Limpopo Province, South Africa, using different theoretical modelsEvaluation of the global solar irradiance in the Vhembe district of Limpopo Province, South Africa, using different theoretical models. – Turkish Journal of Physics 39(3): 264-271.
[31] Penman, H. L. (1948): Natural evaporation from open water, bare soil and grass. – Proceedings of the Royal Society of London. Series A. Mathematical and Physical Sciences 193(1032): 120-145.
[32] Popova, Z., Kercheva, M., Pereira, L. S. (2006): Validation of the FAO methodology for computing ETo with limited data. Application to South Bulgaria. – Irrigation and Drainage: The Journal of the International Commission on Irrigation and Drainage 55(2): 201-215.
[33] Rohwer, C. (1931): Evaporation from a Free Water Surface. – US Dept. of Agr. Tech. Bull. 271.
[34] Salih, A. M., Sendil, U. (1984): Evapotranspiration under extremely arid climates. – Journal of Irrigation and Drainage Engineering 110(3): 289-303.
[35] Sentelhas, P. C., Gillespie, T. J., Santos, E. A. (2010): Evaluation of FAO Penman–Monteith and alternative methods for estimating reference evapotranspiration with

http://www.aloki.hu ● ISSN 1589 1623 (Print) ● ISSN 1785 0037 (Online)
DOI: http://dx.doi.org/10.15666/aeer/1705_1112111141

missing data in Southern Ontario, Canada. – Agricultural Water Management 97(5): 635-644.

[36] Singh, V. P., Xu, C. Y. (1997): Evaluation and generalization of 13 mass-transfer equations for determining free water evaporation. – Hydrological Processes 11(3): 311-323.

[37] Stöckle, C. O., Kjelgaard, J., Bellocchi, G. (2004): Evaluation of estimated weather data for calculating Penman-Monteith reference crop evapotranspiration. – Irrigation Science 23(1): 39-46.

[38] Stone, R. J. (1993): Improved statistical procedure for the evaluation of solar radiation estimation models. – Solar Energy 51(4): 289-291.

[39] Tabari, H., Grismer, M. E., Trajkovic, S. (2013): Comparative analysis of 31 reference evapotranspiration methods under humid conditions. – Irrigation Science 31(2): 107-117.

[40] Trabert, W. (1896): Neue Beobachtungen über Verdampfungsgeschwindigkeiten. – Meteorol. Z. 13: 261-263.

[41] Valipour, M. (2015a): Importance of solar radiation, temperature, relative humidity, and wind speed for calculation of reference evapotranspiration. – Archives of Agronomy and Soil Science 61(2): 239-255.

[42] Valipour, M. (2015b): Investigation of Valiantzas' evapotranspiration equation in Iran. – Theoretical and Applied Climatology 121(1-2): 267-278.

[43] Widmoser, P. (2009): A discussion on and alternative to the Penman–Monteith equation. – Agricultural Water Management 96(4): 711-721.

[44] Willmott, C. J., Matsuura, K. (2005): Advantages of the mean absolute error (MAE) over the root mean square error (RMSE) in assessing average model performance. – Climate Research 30(1): 79-82.

[45] Winter, T. C., Rosenberry, D. O., Sturrock, A. M. (1995): Evaluation of 11 equations for determining evaporation for a small lake in the north central United States. – Water Resources Research 31(4): 983-993.

[46] WMO (1966): Measurement and estimation of evaporation and evapotranspiration. – Tech. Pap. (CIMO-Rep) 83, Genf.

[47] Xu, C. Y., Singh, V. P. (2001): Evaluation and generalization of temperature-based methods for calculating evaporation. – Hydrological Processes 15(2): 305-319.

[48] Xu, J., Peng, S., Ding, J., Wei, Q., Yu, Y. (2013): Evaluation and calibration of simple methods for daily reference evapotranspiration estimation in humid East China. – Archives of Agronomy and Soil Science 59(6): 845-858.

[49] Xystrakis, F., Matzarakis, A. (2010): Evaluation of 13 empirical reference potential evapotranspiration equations on the island of Crete in southern Greece. – Journal of Irrigation and Drainage Engineering 137(4): 211-222.

http://www.aloki.hu ● ISSN 1589 1623 (Print) ● ISSN 1785 0037 (Online)
DOI: http://dx.doi.org/10.15666/aeer/1705_1112111141

OIL, ENVIRONMENTAL POLLUTION AND LIFE EXPECTANCY IN NIGERIA

AGBANIKE, T. F.[1*] – NWANI, C.[1] – UWAZIE, U. I.[2] – UMA, K. E.[1] – ANOCHIWA, L. I.[1] – IGBERI, C. O.[3] – ENYOGHASIM, M. O.[1] – UWAJUMOGU, N. R.[1] – ONWUKA, K. O.[1] – OGBONNAYA, I. O.[1]

[1]Department of Economics and Development Studies, Alex Ekwueme Federal University, Ndufu-Alike, Ebonyi Sate, Nigeria
(e-mails: nwanichinaza@gmail.com – C. Nwani; kaluskyebng@yahoo.com – K. E. Uma; lanochiwa@yahoo.com – L. I. Anochiwa; mic_martserve@yahoo.com – M. O. Enyoghasim; ketchyus@yahoo.com – N. R. Uwajumogu; odulukwe@yahoo.com – K. O. Onwuka; ioogbons@yahoo. com – I. O. Ogbonnaya)

[2]Department of Economics, Michael Okpara University of Agriculture, Umudike, Abia State, Nigeria
(e-mail: ui.uwazie@yahoo.com)

[3]Department of Agriculture (Agricultural Economics and Extension Programme), Alex Ekwueme Federal University, Ndufu-Alike, Ebonyi Sate, Nigeria
(e-mail: igberitina@yahoo.com; Christiana.igberi@funai.edu.ng)

**Corresponding author*
e-mail: tobechi_agbanike@yahoo.co.uk, tobechi.agbanike@funai.edu.ng; phone: +234-90-6035-4318

(Received 4th Apr 2019; accepted 13th Jun 2019)

Abstract. This study used the autoregressive distributed lag (ARDL) bounds testing approach to cointegration to examine the dynamic relationship between environmental pollution and life expectancy in Nigeria over the period 1971 to 2014 incorporating the role of the oil sector. The ARDL estimates suggest that while oil export provides the revenue required to improve life expectancy in the country, it also generates economic conditions that accelerate environmental pollution in the country. The results show that the impact of carbon dioxide (CO_2) emissions on life expectancy in Nigeria is negative and stronger in the long run. To further the understanding of the impacts of oil production activities and CO_2 emissions on life expectancy in Nigeria, gender differences in life expectancy were considered. The results highlight the urgent need for health policy measures in Nigeria to incorporate effective mitigation and adaptation strategies to reduce the impact of the increasing role of the oil sector on health condition, wellbeing of the people and the overall goal of improving life expectancy in Nigeria.
Keywords: *export receipts, health policy, carbon dioxide (CO_2) emissions, greenhouse gases (GHG), gas flaring*

Introduction

Life expectancy, a measure of the length of life expected to be lived by an individual at birth is considered an important indicator of a nation's health condition and individual's wellbeing. Since individuals make a nation, improving life expectancy is a very important and necessary condition needed to achieve long-term sustainable economic development (Barlow and Vissandjée, 1999; Alam et al., 2016; Shahbaz et al., 2016). Recent studies show that life expectancy of a nation is reflected in the social, economic, demographic and environmental conditions (see Hertz et al., 1994; Barlow and Vissandjée, 1999; Pautrel, 2009; Bergh and Nilsson, 2010; Mariani et al., 2010; Qureshi et al., 2015; Sede and Ohemeng, 2015; Alam et al., 2016; Kim and Kim, 2016;

http://www.aloki.hu ● ISSN 1589 1623 (Print) ● ISSN 1785 0037 (Online)
DOI: http://dx.doi.org/10.15666/aeer/1705_1114311162

Shahbaz et al., 2016; Lu et al., 2017; Wu, 2017; Abbas and Awan, 2018; Bader and Ganguli, 2019). Therefore, the impacts of various economic, social and environmental factors on life expectancy for a given country have become a very important issue among policy makers. However, despite the increasing attention of studies on identifying the determinants of life expectancy, there is still no empirical study that examines how oil sector activities and the resultant environmental pollution impact on life expectancy in Nigeria. Hence, this study aims to fill this identified gap in the existing literature by investigating the dynamic relationship between oil sector activities, environmental pollution and life expectancy in Nigeria.

The threat of oil sector activities on environmental quality in Nigeria has been widely recognized and cannot be overlooked (see Ologunorisa, 2001; Ugochukwu and Ertel, 2008; Audu et al., 2016). A deteriorating environment is responsible for many adverse effects on health and well-being (Tai et al., 2015; Chaabouni et al., 2016; Marsh et al., 2016; Perera, 2018). Policymakers in Nigeria are facing pressure in ensuring sustainable health condition and wellbeing of the people. The main reason being that social, economic and environmental conditions that determine the quality of health care services and individual's wellbeing depend significantly on oil sector activities as illustrated in *Figure 1*. On one hand, fiscal spending that determines health care expenditure, quality of education, availability of employment opportunities and sanitation facilities and access to portable drinking water depends solely on the volume of crude oil receipts, which accounts for about 95% of export earnings in Nigeria. Higher volume of crude oil export could therefore be interpreted to suggest more economic resources for better health care services. On the other hand, the exploration and production activities of the oil sector in Nigeria have resulted in environmental pollution, by way of relentless flaring and venting of gas to the environment (Audu et al., 2016). There is a global acceptance that the rising level of greenhouse gases in the atmosphere is the single greatest public health threat of the 21st century. Extreme temperature and weather conditions such as heat wave, storm, drought, and flood caused by the absorption of some of the radiation emitted from the earth by greenhouse gases in the atmosphere are considered by experts as one of the major direct risks to human health (Bezirtzoglou et al., 2011; Franchini and Mannucci, 2015; Wu et al., 2016; Liang and Gong, 2017). For instance, some health issues prevalent in Nigeria including respiratory and cardiovascular diseases, diarrheal diseases in children and mosquito-borne diseases such as malaria are among diseases identified to be most sensitive to temperature and climate conditions (see Bezirtzoglou et al., 2011). With this in mind, the need to understand and control the potential consequences of the activities of the oil sector on health conditions and wellbeing of Nigerians cannot be overemphasized.

Although life expectancy in Nigeria has improved over the years, *Figure 2* shows that it is still below the average life expectancy in Low income countries and Sub-Saharan African economies. Looking at the comparative figures, the life expectancy in South Africa and Ghana is higher with over nine years in 2014. In recognition of the urgent need to improve life expectancy in Nigeria, health policy makers have set policy targets and a number of policy measures have been taken in this direction including the primary health care service intended to enhance access to quality health care, the commercialization policy designed to inject some measures of efficiency into public hospital management and the National Health Insurance Scheme designed to mitigate the cost of access to quality health care (Sede and Ohemeng, 2015). In the light of the above discussion, this study aims at offering some policy measures to the attainment of

http://www.aloki.hu ● ISSN 1589 1623 (Print) ● ISSN 1785 0037 (Online)
DOI: http://dx.doi.org/10.15666/aeer/1705_1114311162

health policy targets by examining the dynamic relationship between oil sector activities, environmental pollution (as proxied by CO_2 emissions) and life expectancy in Nigeria. This is achieved by employing the auto-regressive distributed lag (ARDL) bounds testing approach for cointegration analysis to uncover the long-run and short-run impacts of the variables including (i) the impact of oil resource as source of revenue on environmental quality and life expectancy in Nigeria (ii) the impact of crude oil production and exploration on life expectancy in Nigeria, and (iii) the impact of CO_2 emissions on life expectancy in Nigeria.

The remainder of this study is structured as follows: Section 2 presents the data and methodology of the study. Section 3 presents the empirical results. In section 4 the empirical results are discussed and some policy implications highlighted. Finally, section 5 offers some concluding remarks.

Materials and methods

Definition of variables and data description

This study uses annual data covering the period from 1971 to 2014 to examine the dynamic relationship between oil sector activities, environmental pollution and life expectancy in Nigeria. The average daily crude oil production is used to capture oil production effect while the value of oil exports is used to capture oil income effect of the activities of the oil sector. Carbon dioxide (CO_2) emissions in metric tons per capita is used to measure environmental pollution. Life expectancy is measured as the average number of years of life of the total population (female and male), male population and female population. List of all the variables and data sources are presented in *Table 1*.

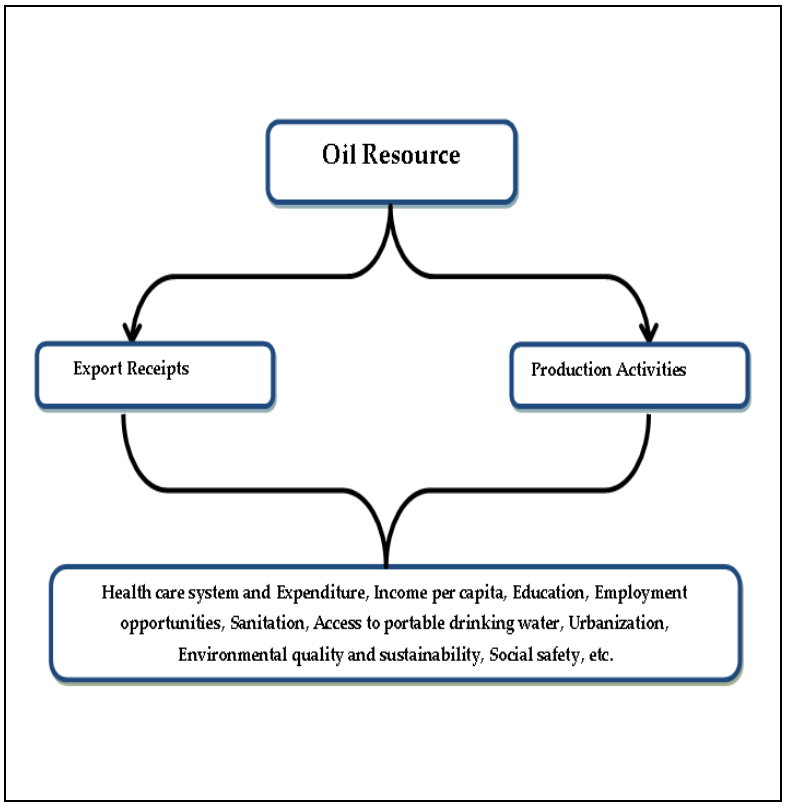

Figure 1. *Oil resource and health services*

http://www.aloki.hu ● ISSN 1589 1623 (Print) ● ISSN 1785 0037 (Online)
DOI: http://dx.doi.org/10.15666/aeer/1705_1114311162

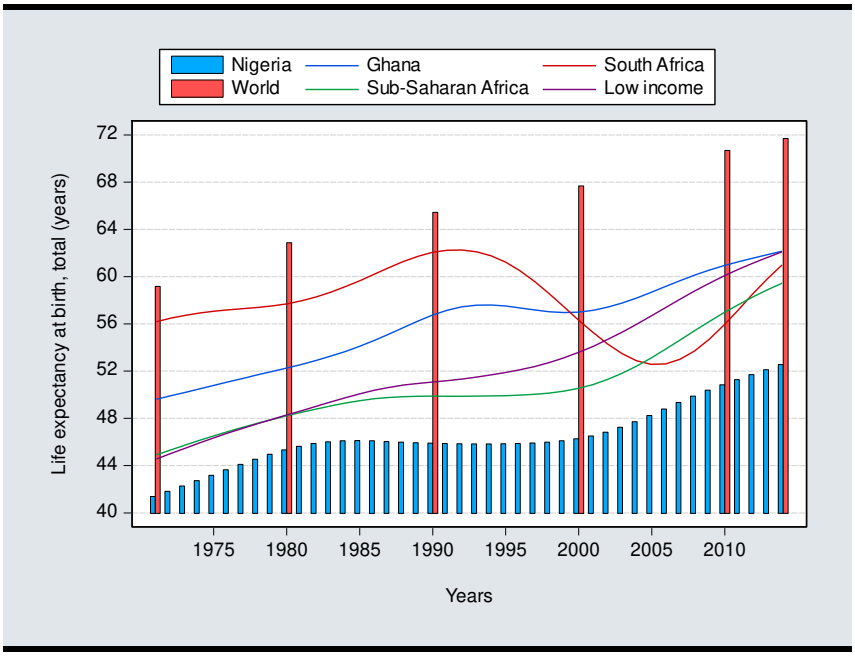

Figure 2. *Life expectancy at birth, total (years). (Data source: World Development Indicators, World Bank)*

Table 1. *Definition of variables and data description*

Variable	Definition	Source
CO2	CO_2 emissions (metric tons per capita)	World Development Indicators Database, World Bank
LifE	Life Expectancy at Birth, Total (years)	World Development Indicators Database, World Bank
LifEM	Life Expectancy at Birth, Male (years)	World Development Indicators Database, World Bank
LifEF	Life Expectancy at Birth, Female (years)	World Development Indicators Database, World Bank
Rgdpc	GDP per capita (constant 2010 US$)	World Development Indicators Database, World Bank
VPet	Values of petroleum exports (m $)	OPEC Annual Statistical Bulletin 2018 Online
Crdoilp	Daily crude oil production (average)	OPEC Annual Statistical Bulletin 2018 Online
Pcrd	Private credit by deposit money banks to GDP (%)	Global Financial Development Indicators, World Bank
Dcrd	Domestic credit to private sector (% of GDP)	World Development Indicators Database, World Bank
Popgrt	Population Growth (Annual %)	World Development Indicators Database, World Bank
Infrt	Inflation, consumer prices (annual %)	World Development Indicators Database, World Bank
Trd	Trade (Export + Import % of GDP)	World Development Indicators Database, World Bank

Empirical model and estimation method

This study empirically examines three log-linear models to uncover the relationship between oil sector activities, environmental pollution and life expectancy in Nigeria over the period 1971-2014. Model 1 and Model 2 examine the impact of oil sector activities and CO2 emissions on life expectancy in Nigeria while Model 3 examines the role of oil sector activities in explaining environmental pollution (CO_2 emissions) in Nigeria. In Model 1 specified in *Equation 1* oil sector activity is captured using value of petroleum exports per capita (oil income effect) while in Model 2 specified in *Equation 2* oil sector activity is captured using the average daily crude oil production (oil production effect). *Figure 3* summarises the three causal relationships examined in this empirical study.

http://www.aloki.hu ● ISSN 1589 1623 (Print) ● ISSN 1785 0037 (Online)
DOI: http://dx.doi.org/10.15666/aeer/1705_1114311162

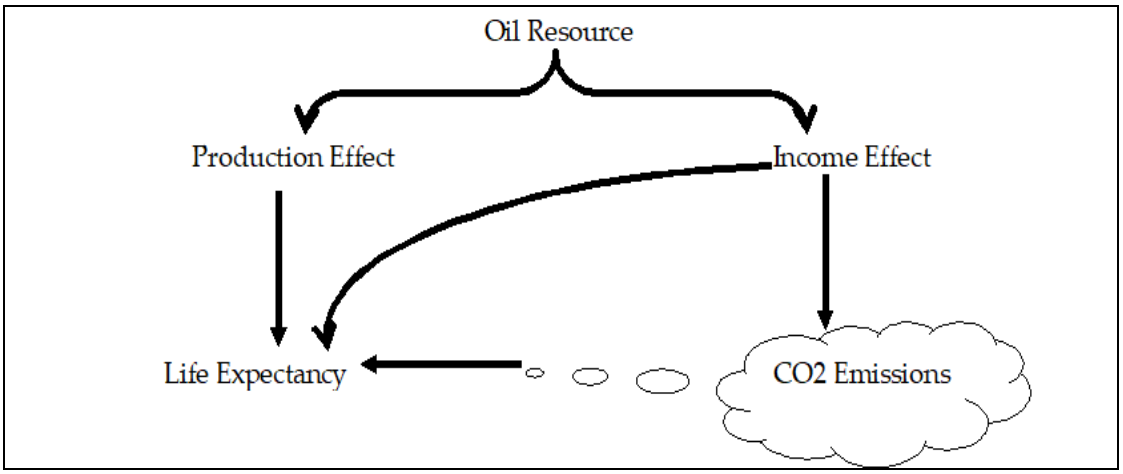

Figure 3. *Hypothesized relationship between oil sector activities, CO_2 emissions and life expectancy in Nigeria*

Model 1

$$lnLif = \alpha_0 + \alpha_1 lnRgdpc + \alpha_2 lnCO2 + \alpha_3 ln\text{Pvet} + \alpha_4 lnContrl1 + \alpha_5 Contrl2 + \alpha_5 Contrl3 + e_t \quad \text{(Eq.1)}$$

Model 2

$$lnlif = \beta_0 + \beta_1 lnRgdpc + \beta_2 lnCO2 + \beta_3 ln\text{Crdoilp} + \beta_4 lnContrl1 + \beta_5 Contrl2 + \beta_6 Contrl3 + e_t \quad \text{(Eq.2)}$$

Model 3

$$lnCO2 = \pi_0 + \pi_1 lnRgdpc + \pi_2 lnlif + \pi_3 ln\text{Pvet} + \pi_4 lnContrl1 + \pi_5 Contrl2 + \pi_5 Contrl3 + e_t \quad \text{(Eq.3)}$$

$lnLif$ represents life expectancy, measured as the average number of years of life of the total population (female and male) $lnLifE$, male population $lnLifEM$ and female population $lnLifEF$. $lnRgdpc, lnCO2, ln\text{Pvet}$ and $ln\text{Crdoilp}$ are as defined in *Table 1*. $lnContrl1, lnContrl2$ and $lnContrl3$ are used to control for the influence of other factors considered important in this empirical analysis. These factors include international trade, financial development and population growth. e_t is the error term.

Following Murthy and Okunade (2016), Shahbaz et al. (2016) and Abbas and Awan (2018) this study employs the autoregressive distributed lag (ARDL) Bounds testing approach to co-integration proposed by Pesaran et al. (2001) to investigate the log-linear empirical model specified in *Equations 1, 2* and *3*. The ARDL approach offers some desirable statistical advantages over other co-integration techniques. While other co-integration techniques require all the variables to be integrated of the same order, ARDL test procedure provides valid results whether the variables are I(0) or I(1) or mutually co-integrated, captures both short-run dynamics and long-run equilibrium adjustment of the studied process and provides very efficient and consistent test results in small and large sample sizes (see Pesaran et al., 2001). The implementation of the ARDL test for *Equations 1, 2* and *3* involves the estimation of the following models:

http://www.aloki.hu ● ISSN 1589 1623 (Print) ● ISSN 1785 0037 (Online)
DOI: http://dx.doi.org/10.15666/aeer/1705_1114311162

ARDL estimation for Model 1:

$$\Delta lnlif_t = a_0 + \sum_{i=1}^{n} a_{1i}\Delta lnlif_{t-i} + \sum_{i=0}^{n} a_{2i}\Delta lnRgdpc_{1_{t-i}} + \sum_{i=0}^{n} a_{3i}\Delta lnCO2_{2_{t-i}} + \sum_{i=0}^{n} a_{4i}\Delta lnVpet_{3_{t-i}} + \sum_{i=0}^{n} a_{5i}\Delta lnCtrl1_{4_{t-i}} + \sum_{i=0}^{n} a_{6i}\Delta lnCtrl2_{5_{t-i}} + \sum_{i=0}^{n} a_{7i}\Delta lnCtrl3_{6_{t-i}} + a_8 lnlif_{t-1} + a_9 lnRgdpc_{t-1} + a_{10} lnCO2_{t-1} + a_{11} lnVpet_{t-1} + a_{12} lnCtrl1_{t-1} + a_{13} lnCtrl2_{t-1} + a_{14} lnCtrl3_{t-1} + \varepsilon_t \quad (4) \qquad \text{(Eq.4)}$$

ARDL estimation for Model 2:

$$\Delta lnlif_t = \beta_0 + \sum_{i=1}^{n} \beta_{1i}\Delta lnlif_{t-i} + \sum_{i=0}^{n} \beta_{2i}\Delta lnRgdpc_{1_{t-i}} + \sum_{i=0}^{n} \beta_{3i}\Delta lnCO2_{2_{t-i}} + \sum_{i=0}^{n} \beta_{4i}\Delta lnCrdoilp_{3_{t-i}} + \sum_{i=0}^{n} \beta_{5i}\Delta lnCtrl1_{4_{t-i}} + \sum_{i=0}^{n} \beta_{6i}\Delta lnCtrl2_{5_{t-i}} + \sum_{i=0}^{n} \beta\,\Delta lnCtrl3_{6_{t-i}} + \beta_8 lnlif_{t-1} + \beta_9 lnRgdpc_{t-1} + \beta_{10} lnCO2_{t-1} + \beta_{11} lnCrdoilp_{t-1} + \beta_{12} lnCtrl1_{t-1} + \beta_{13} lnCtrl2_{t-1} + \beta_{14} lnCtrl3_{t-1} + \varepsilon_t \quad (5) \qquad \text{(Eq.5)}$$

ARDL estimation for Model 3:

$$\Delta lnCO2_t = \pi_0 + \sum_{i=1}^{n} \pi_{1i}\Delta lnCO2_{t-i} + \sum_{i=0}^{n} \pi_{2i}\Delta lnRgdpc_{1_{t-i}} + \sum_{i=0}^{n} \pi_{3i}\Delta lnlif_{2_{t-i}} + \sum_{i=0}^{n} \pi_{4i}\Delta lnVpet_{3_{t-i}} + \sum_{i=0}^{n} \pi_{5i}\Delta lnCtrl1_{4_{t-i}} + \sum_{i=0}^{n} \pi_{6i}\Delta lnCtrl2_{5_{t-i}} + \sum_{i=0}^{n} \pi_{7i}\Delta lnCtrl3_{6_{t-i}} + \pi_8 lnCO2_{t-1} + \pi_9 lnRgdpc_{t-1} + \pi_{10} lnlif_{t-1} + \pi_{11} lnVpet_{t-1} + \pi_{12} lnCtrl1_{t-1} + \pi_{13} lnCtrl2_{t-1} + \pi_{14} lnCtrl3_{t-1} + \varepsilon_t \quad (6) \qquad \text{(Eq.6)}$$

where Δ is the difference operator while ε_t is white noise error term. The following hypotheses are tested to investigate the existence of co-integration among the variables: the null hypothesis of no cointegration among the variables in *Equation 4* is given as $(H_o: a_8 = a_9 = a_{10} = a_{11} = a_{12} = a_{13} = a_{14} = 0)$ examined against the alternative hypothesis $(H_1: a_8 \neq a_9 \neq a_{10} \neq a_{11} \neq a_{12} \neq a_{13} \neq a_{14} \neq 0)$. In *Equation 5* the null hypothesis of no cointegration among the variables is $(H_o: \beta_8 = \beta_9 = \beta_{10} = \beta_{11} = \beta_{12} = \beta_{13} = \beta_{14} = 0)$ against the alternative hypothesis $(H_1: \beta_8 \neq \beta_9 \neq \beta_{10} \neq \beta_{11} \neq \beta_{12} \neq \beta_{13} \neq \beta_{14} \neq 0)$. In *Equation 6* the null hypothesis of no cointegration among the variables is $(H_o: \pi_8 = \pi_9 = \pi_{10} = \pi_{11} = \pi_{12} = \pi_{13} = \pi_{14} = 0)$ against the alternative hypothesis $(H_1: \pi_8 \neq \pi_9 \neq \pi_{10} \neq \pi_{11} \neq \pi_{12} \neq \pi_{13} \neq \pi_{14} \neq 0)$. The decision to reject or accept H_o (no co-integration among the variables) is based on the following conditions: if the calculated F-statistics is greater than the upper critical bound, then H_o is rejected and the variables are co-integrated, if the calculated F-statistics is less than the lower bound, then H_o is accepted and the variables are not co-integrated, but if the calculated F-statistics remains between the lower and upper critical bounds then the decision is inconclusive (Pesaran et al., 2001).

After testing for cointegration among the variables, the long-run coefficients of the variables are then estimated. The existence of cointegration between the variables implies that causality exist in at least one direction. The error correction model for the estimation of the short run relationships is specified as:

http://www.aloki.hu ● ISSN 1589 1623 (Print) ● ISSN 1785 0037 (Online)
DOI: http://dx.doi.org/10.15666/aeer/1705_1114311162

$$\Delta lnlif_t = a_0 + \sum_{i=1}^{n} a_{1i}\,\Delta lnlif_{t-i} + \sum_{i=0}^{n} a_{2i}\,\Delta lnRgdpc_{1_{t-i}} + \sum_{i=0}^{n} a_{3i}\Delta lnCO2_{2_{t-i}} + \sum_{i=0}^{n} a_{4i}\,\Delta lnVpet_{3_{t-i}} + \sum_{i=0}^{n} a_{5i}\,\Delta lnCtrl1_{4_{t-i}} + \sum_{i=0}^{n} a_{6i}\,\Delta lnCtrl2_{5_{t-i}} + \sum_{i=0}^{n} a_{7i}\,\Delta lnCtrl3_{6_{t-i}} + \lambda_1 ECM_{t-1} + u_{2t} \quad (7) \qquad \text{(Eq.7)}$$

$$\Delta lnlif_t = \beta_0 + \sum_{i=1}^{n} \beta_{1i}\,\Delta lnlif_{t-i} + \sum_{i=0}^{n} \beta_{2i}\,\Delta lnRgdpc_{1_{t-i}} + \sum_{i=0}^{n} \beta_{3i}\,\Delta lnCO2_{2_{t-i}} + \sum_{i=0}^{n} \beta_{4i}\,\Delta lnCrdoilp_{3_{t-i}} + \sum_{i=0}^{n} \beta_{5i}\,\Delta lnCtrl1_{4_{t-i}} + \sum_{i=0}^{n} \beta_{6i}\,\Delta lnCtrl2_{5_{t-i}} + \sum_{i=0}^{n} \beta\,\Delta lnCtrl3_{6_{t-i}} + \lambda_2 ECM_{t-1} + u_{2t} \quad (8) \qquad \text{(Eq.8)}$$

$$\Delta lnCO2_t = \pi_0 + \sum_{i=1}^{n} \pi_{1i}\,\Delta lnCO2_{t-i} + \sum_{i=0}^{n} \pi_{2i}\,\Delta lnRgdpc_{1_{t-i}} + \sum_{i=0}^{n} \pi_{3i}\,\Delta lnlif_{2_{t-i}} + \sum_{i=0}^{n} \pi_{4i}\,\Delta lnVpet_{3_{t-i}} + \sum_{i=0}^{n} \pi_{5i}\,\Delta lnCtrl1_{4_{t-i}} + \sum_{i=0}^{n} \pi_{6i}\,\Delta lnCtrl2_{5_{t-i}} + \sum_{i=0}^{n} \pi_{7i}\,\Delta lnCtrl3_{6_{t-i}} + \lambda_3 ECM_{t-1} + u_{3t} \quad (9) \qquad \text{(Eq.9)}$$

ECM_{t-1} is the error correction term obtained from the cointegration model. The error correction coefficients (λ_1, λ_2 and λ_3) indicate the rate at which the cointegration models correct previous period disequilibrium or speed of adjustment to restore the long-run equilibrium relationship. A negative and significant ECM_{t-1} coefficient implies that any short term movement between the dependent and explanatory variables will converge back to the long-run relationship.

This study implements the following diagnostic tests to ensure the acceptability of the empirical models: Breusch–Godfrey serial correlation LM test, ARCH test for heteroscedasticity, Jarque-Bera normality test and Ramsey RESET test for functional form. The stability of the long-run coefficients together with the short-run dynamics are tested using the cumulative sum of recursive residuals (CUSUM) and the cumulative sum of squares of recursive residuals (CUSUMSQ) tests.

Results

Figure 4 displays plots of the data series of the variables of interest. The figure shows that life expectancy in Nigeria improved from 41.4 years in 1971 to 52.5 years in 2014. CO_2 emissions which increased from 0.56 metric tons per capita in 1971 to 1.01 in 1974 decreased to 0.54 metric tons per capita in 2014. Interestingly daily crude oil production which increased from 1531.20 thousand barrels in 1971 to 2255.0 thousand in 1974 also decreased to 1807.05 thousand barrels in 2014. In the light of the observed movements in these series, it would be of great interest for health policy making to examine the dynamic relationship between oil sector activities, environmental pollution (as proxied by CO_2 emissions) and life expectancy in Nigeria. This is achieved by employing the auto-regressive distributed lag (ARDL) bounds testing approach for cointegration analysis to uncover the long-run and short-run impacts of the variables including the impact of oil resource as source of revenue on environmental quality and life expectancy in Nigeria, the impact of crude oil production and exploration on life expectancy in Nigeria, and the impact of CO_2 emissions on life expectancy in Nigeria.

http://www.aloki.hu ● ISSN 1589 1623 (Print) ● ISSN 1785 0037 (Online)
DOI: http://dx.doi.org/10.15666/aeer/1705_1114311162

Unit root tests

The ARDL-bounds cointegration testing approach allows variables to be integrated of different orders [I(0) and I(1)], but does not require any of the variables to be integrated of order 2 [I(2)] (see Pesaran et al., 2001) . It is therefore essential to examine the stationarity of the variables to ensure that none of the variables is integrated of order 2 [I(2)]. To determine the order of integration of the variables, the Augmented Dickey Fuller test for unit root is implemented. The results in *Table 2* show that inflation rate (*ln*Infr) is integrated of order zero, I(0) while other variables are integrated of order one I(1). In the presence of structural breaks however, the Augmented Dickey Fuller test and other conventional unit root tests are known to provide biased results because of their low explanatory strength to reject the null hypothesis of unit root. This is because these unit root tests do not incorporate information about structural break dates emanating from structural changes (Perron, 2006). To overcome this condition, modified augmented Dickey-Fuller test that detects unknown single structural break in a series is employed (see Vogelsang and Perron, 1998). The innovational outlier (IO) model which assumes that the break occurs gradually, with the breaks following the same dynamic path as the innovations is implemented. The results in *Table 2* show a structural break in all the series. For life expectancy (*ln*lifE), a structural break is found in the series in 1997. For CO2 emissions, a structural break exists in 1986. These results give indication that the economy has observed significant policy shocks at the selected break dates. The stationary properties show that none of the variables is integrated at second difference [I(2)]. The integration of the variables at I(0) and I(1) makes ARDL the preferred approach in this empirical analysis.

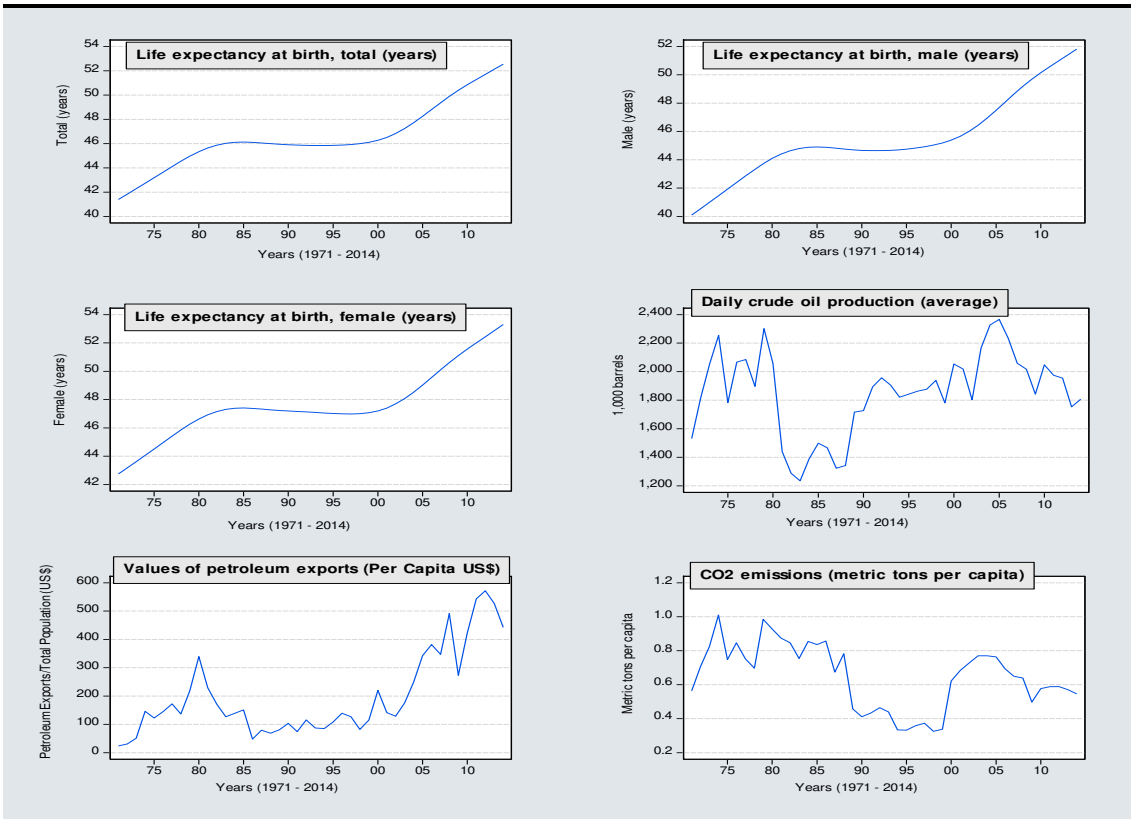

Figure 4. *Plots of the data series of the variables of interest*

http://www.aloki.hu ● ISSN 1589 1623 (Print) ● ISSN 1785 0037 (Online)
DOI: http://dx.doi.org/10.15666/aeer/1705_1114311162

Table 2. *Unit root test results*

	Augmented Dickey Fuller		Modified augmented Dickey Fuller test with structural break				Result
	Levels I(0)	First difference I(1)	Levels I(0)		First difference I(1)		
	t-statistic	t-statistic	t-statistic	Break date	t-statistic	Break date	
*ln*CO2	-1.842214 [0]	-6.859844 [0]***	-3.031649 [0]	1986	-8.087606 [0]***	2000	I(1) with break
*ln*LifE	1.515890 [4]	-3.734049 [5]***	-2.557130 [3]	1997	-5.385017 [5]***	1998	I(1) with break
*ln*LifEM	1.135337 [3]	-3.566672 [5]**	-2.557675 [3]	1997	-5.460568 [6]***	1999	I(1) with break
*ln*LifEF	1.355290 [4]	-3.497989 [5]**	-2.389715 [3]	1998	-5.393951 [6]***	1999	I(1) with break
*ln*Rgdpc	-0.043059 [0]	-5.388869 [0]***	-2.250641 [0]	2003	-7.370283 [0]***	2004	I(1) with break
*ln*VPet	-2.456715 [0]	-7.388426 [0]***	-4.153401 [0]	2003	-8.290113 [0]***	1986	I(1) with break
*ln*Crdoilp	-2.510039 [0]	-6.446855 [0]***	-3.030107 [0]	1987	-7.659908 [0]***	1981	I(1) with break
*ln*Pcrd	-2.285337 [1]	-4.724064 [0]***	-2.823542 [1]	2006	-5.836209 [2]***	1990	I(1) with break
*ln*Dcrd	-2.639002 [0]	-5.207635 [0]***	-3.308173 [2]	2006	-6.397791 [0]***	2010	I(1) with break
*ln*Popgrt	-1.859284 [3]	-4.738240 [2]***	-3.374165 [4]	1978	-8.682119 [1]***	1988	I(1) with break
*ln*Infrt	-3.706383 [0]***	-6.795280 [1]***	-5.635724 [1]***	1995	-7.645655 [0]***	1990	I(0) with break
*ln*Trd	-2.525016 [0]	-8.019394 [1]***	-3.563918 [0]	1986	-8.488151 [0]***	2001	I(1) with break

Results of ARDL co-integration test

In ARDL bounds cointegration analysis, lag length selection test is considered very important as the F-statistic required for the implementation of the model is known to be sensitive to lag order. This first step test involves examining the sequential modified LR test statistic (LR), Final prediction error (FPE), Akaike information criterion (AIC), Schwarz information criterion (SIC) and Hannan-Quinn information criterion (HQ) for the selection of appropriate lag length. The implementation of this first step test shows that 3 is suggested by all the criteria as the appropriate lag length for the implementation of the ARDL bounds cointegration test for all the specifications. Following the suggestion of Lütkepohl (2006) in small sample analysis, this study uses Akaike Information Criterion (AIC) for selecting the optimal lag length.

Given the relatively small sample size of 44 observations (1971-2014) used in this study, the critical values for the evaluation of the null hypothesis are taken from Narayan (2005). Narayan (2005) computed two sets of critical values: lower bounds I(0) and upper bounds critical I(1) for sample sizes ranging from T = 30 to 80. The results of the co-integration test based on the ARDL-bounds testing method are presented in *Table 3*. The results indicate that the F-statistic is greater than the upper critical bound from Narayan (2005) at 1% significant level for all the specifications of the ARDL models examined using restricted intercept and no trend. This study therefore rejects the null hypothesis of no cointegration among the variables. This shows that there is a long-run causal relationship between oil sector activities, environmental pollution, life expectancy at birth and other selected indicators of economic performance in Nigeria.

Long-run and short-run estimates

The estimates for all the specifications of Model 1 are presented in *Table 4*. The long-run coefficients in Panel B show that the coefficient of the oil export revenue *ln*VPet is positive and statistically significant at 1% level in specifications 1 and 3, and at 5% level in specification 2. From the long-run coefficients, a 1% increase in the value

http://www.aloki.hu ● ISSN 1589 1623 (Print) ● ISSN 1785 0037 (Online)
DOI: http://dx.doi.org/10.15666/aeer/1705_1114311162

of petroleum exports (oil revenue) significantly increases life expectancy at birth by 0.0714%. Distinguishing between male and female populations, the estimates suggest that a 1% increase in the value of petroleum exports (oil revenue) contributes more to life expectancy of the male population (0.1076%) than the female pollution (0.0457%). The coefficient of CO_2 emissions is negative and statistically significant in all the three specifications of Model 1. For the overall population, the coefficient which is significant at 1% level indicates that a one per cent increase in the level of CO_2 emissions in the Nigerian economy would cause life expectancy at birth to decrease by 0.0438%. Specifications LifEM (male population) and LifEF (female population) shows that a one per cent increase in the level of CO2 emissions in the economy affects the male population more (-0.0596) than the female population (-0.0262). The coefficient of GDP per capita is positive and statistically significant. Panel A of *Table 4* shows that the short-run coefficient of the value of petroleum exports (oil revenue) is positive and statistically significant for the overall population at 5% level. Overall the results in *Table 4* show that the long-run effects of the value of petroleum exports (oil revenue) and CO_2 emissions on life expectancy in Nigeria are stronger in the long run.

The results of Model 2 are presented in *Table 5*. Oil sector activities are captured using the average of daily crude oil production (oil production effect). The long-run estimates in Panel B show that an increase the production activities of the oil sector significantly decreases life expectancy in the country. The coefficient of -0.1276 which is statistically significant at 10% level for the overall population shows that a one per cent increase in crude oil production activities decreases life expectancy in the country by 0.1276%. The results also suggest that the long-run influence of crude oil production activities (oil production effect) on life expectancy of the female population is statistically significant at 1% level. The coefficient of CO_2 emissions is negative and statistically significant in all the specifications of Model 2, confirming the negative impact of an increase in the level of CO_2 emissions on life expectancy in Nigeria as observed from the results of Model 1. It is also observed from the results in Pane A of *Table 5* that the short-run effect of oil sector production activities on life expectancy of the female population in Nigeria is negative and statistically significant at 5% level. The long-run and short-run estimates therefore suggest that oil sector production activities exert more influence on life expectancy of the female population in Nigeria.

Table 3. *ARDL bounds cointegration test results*

Specifications	Break date	ARDL	F-statistic	Result
1. F_{LifE}(*ln*LifE|*ln*Rgdpc, *ln*CO2, ***ln***VPet, *ln*Pcrd, ***ln***Infrt, ***ln***Popgrt)	1997	(3, 3, 2, 2, 2, 2, 1)	13.7792***	Cointegration
2. F_{LifEM}(*ln*LifEM|*ln*Rgdpc, *ln*CO2, ***ln***VPet, *ln*Pcrd, ***ln***Infrt, ***ln***Popgrt)	1997	(3, 3, 2, 2, 2, 2, 1)	11.0617***	Cointegration
3. F_{LifEF}(*ln*LifEF|*ln*Rgdpc, *ln*CO2, ***ln***VPet, *ln*Pcrd, ***ln***Infrt, ***ln***Popgrt)	1998	(3, 3, 2, 3, 2, 1, 1)	14.6931***	Cointegration
4. F_{LifE}(*ln*LifE|*ln*Rgdpc, *ln*CO2, *ln*Crdoilp, *ln*Dcrd, ***ln***Infrt, ***ln***Trd)	1997	(3, 3, 2, 2, 3, 3, 0)	5.5262***	Cointegration
5. F_{LifEM}(*ln*LifE|*ln*Rgdpc, *ln*CO2, *ln*Crdoilp, *ln*Dcrd, ***ln***Infrt, ***ln***Trd)	1997	(3, 3, 2, 2, 3, 3, 0)	5.9579***	Cointegration
6. F_{LifEF}(*ln*LifEF|*ln*Rgdpc, *ln*CO2, *ln*Crdoilp, *ln*Dcrd, ***ln***Infrt, ***ln***Trd)	1998	(3, 3, 2, 1, 3, 3, 1)	13.7034***	Cointegration
7. F_{CO2}(*ln*CO2|*ln*Rgdpc, *ln*LifE, ***ln***VPet, *ln*Pcrd, ***ln***Popgrt, ***ln***InTrd)	1986	(1, 2, 3, 0, 2, 0, 0)	5.8217***	Cointegration
8. F_{CO2}(*ln*CO2|*ln*Rgdpc, *ln*LifEM, ***ln***VPet, *ln*Pcrd, ***ln***Popgrt, ***ln***InTrd)	1986	(1, 3, 3, 0, 2, 0, 0)	6.1908***	Cointegration
Critical value bounds (k = 6)		**1%**	**5%**	**10%**
I(0) bound		3.505	2.618	2.218
I(1) bound		5.121	3.863	3.314

ARDL Models selected on Akaike info criterion (AIC). *** indicates Significance at 1% level. Source of critical value bounds: Narayan (2005) Appendix: Case II Restricted intercept and no trend for

http://www.aloki.hu ● ISSN 1589 1623 (Print) ● ISSN 1785 0037 (Online)
DOI: http://dx.doi.org/10.15666/aeer/1705_1114311162

Table 4. *ARDL estimates for Model 1*

Panel A	**Short-run estimates**					
	***ln*LifE**		***ln*LifEM**		***ln*LifEF**	
Variable	**Coefficient**	**[t-Stat]**	**Coefficient**	**[t-Stat]**	**Coefficient**	**[t-Stat]**
ECM(-1)	-0.00895***	[-12.8029]	-0.006***	[-11.2961]	-0.00927***	[-13.1693]
Δ*ln*LifE(-1)	2.19941***	[86.3745]				
Δ*ln*LifE(-2)	-1.32414***	[-43.1240]				
Δ*ln*LifEM(-1)			2.14898***	[89.8460]		
Δ*ln*LifEM(-2)			-1.24116***	[-45.1255]		
Δ*ln*LifEF(-1)					2.18366***	[81.4109]
Δ*ln*LifEF(-2)					-1.33928***	[-40.7618]
Δ*ln*Rgdpc	0.00002	[0.0774]	-0.00034	[-1.3105]	0.00049	[1.7912]
Δ*ln*Rgdpc(-1)	-0.0016***	[-6.5170]	-0.00135***	[-5.3032]	-0.00194***	[-7.9689]
Δ*ln*Rgdpc(-2)	-0.00092***	[-4.3493]	-0.00119***	[-5.4785]	-0.0007***	[-3.0775]
ΔlnCO2	-0.00004	[-0.5209]	0.00007	[0.8129]	0.00008	[1.0084]
ΔlnCO2(-1)	0.00021**	[2.6974]	0.00024***	[3.0099]	0.00017**	[2.0110]
Δ*ln*VPet	0.00011**	[2.0831]	0.00003	[0.6005]	0.00009*	[1.7421]
Δ*ln*VPet(-1)	-0.00019***	[-4.5409]	-0.00025***	[-5.4566]	-0.0001**	[-2.2016]
Δ*ln*VPet(-2)					0.00008*	[1.8761]
Δ*ln*Pcrd	-0.00021**	[-2.2487]	-0.00064***	[-6.8055]	0.00001	[0.1208]
Δ*ln*Pcrd(-1)	-0.00044***	[-5.4592]	-0.00029***	[-3.3944]	-0.00033***	[-4.3163]
Δ*ln*Infrt	0.00006***	[3.0663]	0.00003	[1.2768]	0.00007***	[3.5260]
Δ*ln*Infrt(-1)	0.00007***	[3.5274]	0.00012***	[5.5420]		
Δ*ln*Popgrt	0.00764***	[11.7255]	0.00837***	[11.3105]	0.00613***	[10.0485]
Δ*ln*Brk97	0.00006	[1.0360]	0.00002	[0.3137]		
Δ*ln*Brk98					-0.00003	[-0.4369]
Panel B	**Long-run estimates**					
Variable	**Coefficient**	**t-Stat**	**Coefficient**	**t-Stat**	**Coefficient**	**t-Stat**
C	2.1408***	[8.2696]	2.2965***	[6.1960]	1.6835***	[5.0664]
*ln*Rgdpc	0.1663***	[3.5846]	0.1151	[1.5404]	0.2528***	[5.3633]
*ln*CO2	-0.0438***	[-3.3025]	-0.0596**	[-2.7076]	-0.0262*	[-1.9654]
*ln*VPet	0.0714***	[3.5289]	0.1076**	[2.4086]	0.0457***	[3.0997]
*ln*Pcrd	0.0831***	[5.5542]	0.0698**	[2.4139]	0.0912***	[5.0013]
*ln*Infrt	-0.0094	[-1.3649]	-0.0281	[-1.6682]	0.0013	[0.3077]
*ln*Popgrt	0.0069	[0.0793]	0.1176	[0.6177]	-0.0552	[-0.8611]
Brk97	0.0054	[0.4626]	0.0009	[0.0482]		
Brk98					-0.0012	[-0.0911]
Panel C	**Diagnostic tests**					
Adjusted R^2	0.9999		0.9999		0.9999	
D-W Statistic	2.0139		2.0981		1.9613	
SC x^2	0.0650	[0.7987]	0.2557	[0.6131]	0.0001	[0.9928]
Het $x^2(1)$	0.9452	[0.3309]	0.1162	[0.7332]	0.0194	[0.8893]
RESET	0.8974	[0.3568	2.0866	[0.1668]	1.0810	[0.3130]
JB	0.3083	[0.8572]	0.1852	[0.9115]	1.4504	[0.4842]

*, **, and *** indicate significance at 10%, 5% and 1% respectively. t-statistics in [ ] and p-values in ( ); Adj R2 means adjusted R-squared; SC means Breusch–Godfrey serial correlation LM test; Het is the ARCH test for heteroscedasticity; RESET is the Ramsey RESET test; JB is theJarque-Bera Normality test

http://www.aloki.hu ● ISSN 1589 1623 (Print) ● ISSN 1785 0037 (Online)
DOI: http://dx.doi.org/10.15666/aeer/1705_1114311162

Table 5. *ARDL estimates for Model 2*

Panel A	***ln*LifE**		***ln*LifEM**		***ln*LifEF**	
	Short-run estimates					
Variable	**Coefficient**	**t-Statistic**	**Coefficient**	**t-Statistic**	**Coefficient**	**t-Statistic**
ECM(-1)	-0.01054***	[-8.5459]	-0.0096***	[-8.8210]	-0.0162***	[-12.8756]
Δ*ln*LifE(-1)	2.43521***	[42.2057]				
Δ*ln*LifE(-2)	-1.5281***	[-23.6345]				
Δ*ln*LifEM(-1)			2.49034***	[40.3552]		
Δ*ln*LifEM(-2)			-1.56279***	[-23.1835]		
Δ*ln*LifEF(-1)					2.4693***	[58.3620]
Δ*ln*LifEF(-2)					-1.64432***	[-31.6522]
Δ*ln*Rgdpc	-0.00011	[-0.1898]	-0.00065	[-1.2583]	0.00115***	[2.8786]
Δ*ln*Rgdpc(-1)	-0.0024***	[-5.1392]	-0.00273***	[-5.8942]	-0.00259***	[-8.7166]
Δ*ln*Rgdpc(-2)	-0.00096**	[-2.3626]	-0.00115**	[-2.8286]	-0.00073**	[-2.4323]
ΔlnCO2	-0.00015	[-1.0112]	-0.0002	[-1.3286]	-0.00006	[-0.5325]
ΔlnCO2(-1)	0.00036**	[2.4911]	0.00029**	[2.0346]	0.00036***	[3.5183]
Δ*ln*Crdoilp	-0.00047	[-1.5370]	-0.00022	[-0.7302]	-0.00057**	[-2.6454]
Δ*ln*Crdoilp(-1)	0.0005*	[1.9325]	0.00068**	[2.6620]		
Δ*ln*Dcrd	0.00029**	[2.5952]	0.00029**	[2.6133]	0.00048***	[5.4908]
Δ*ln*Dcrd (-1)	-0.00073***	[-7.2795]	-0.00081***	[-7.7138]	-0.00088***	[-11.6511]
Δ*ln*Dcrd (-2))	-0.00067***	[-7.1648]	-0.00075***	[-7.8107]	-0.00072***	[-10.6233]
Δ*ln*Infrt	-0.00008**	[-2.1625]	-0.00016***	[-3.9734]	-0.00003	[-1.3599]
Δ*ln*Infrt(-1)	0.00015***	[4.0606]	0.00023***	[5.5851]	0.0001***	[3.6769]
Δ*ln*Infrt(-2)	0.00013***	[3.2972]	0.00015***	[3.7759]	0.00009***	[3.2091]
Δ*ln*Trd	-0.00021*	[-1.7952]	-0.00024**	[-2.0398]	-0.00029***	[-3.6283]
Δ*ln*Brk97	-0.00014	[-1.3436]	-0.00024**	[-2.3551]		
Δ*ln*Brk98					0.00027***	[3.6853]
Panel B	**Long-run estimates**					
Variable	**Coefficient**	**t-Stat**	**Coefficient**	**t-Stat**	**Coefficient**	**t-Stat**
C	2.5121***	[5.1859]	2.5707***	[5.3690]	2.1807***	[9.8739]
*ln*Rgdpc	0.3021***	[6.8741]	0.3069***	[7.0251]	0.3006***	[12.5104]
*ln*CO2	-0.0674**	[-2.4549]	-0.0784**	[-2.9980]	-0.0346***	[-2.9255]
*ln*Crdoilp	-0.1276*	[-1.9341]	-0.1426*	[-1.9763]	-0.0782***	[-3.1981]
*ln*Dcrd	0.1020***	[10.6247]	0.1151***	[11.0141]	0.0905***	[20.2187]
*ln*Infrt	-0.0261*	[-1.9435]	-0.0432**	[-2.5914]	-0.0077	[-1.5954]
*ln*Trd	-0.0283	[-1.5677]	-0.0274	[-1.5127]	-0.0304***	[-2.9735]
Brk97	-0.0019	[-0.1071]	-0.0137	[-0.7001]		
Brk98					0.0171	[1.8927]
Panel C	**Diagnostic tests**					
Adjusted R^2	0.9999		0.9999		0.9999	
D-W Statistic	1.9584		1.8673		2.0757	
SC x^2	0.0113	[0.9154]	0.1773	[0.6737]	0.4176	[0.5181]
Het $x^2(1)$	0.7166	[0.3972]	0.0373	[0.8468]	0.0273	[0.8687]
RESET	0.8774	[0.3628]	1.2712	[0.2762]	0.4684	[0.5030]
JB	0.5829	[0.7472]	0.5713	[0.7515]	0.2171	[0.8971]

*, **, and *** indicate significance at 10%, 5% and 1% respectively. t-statistics in [ ] and p-values in ( ); Adj R^2 means Adjusted R-squared; SC means Breusch–Godfrey serial correlation LM test; Het is the ARCH test for heteroscedasticity; RESET is the Ramsey RESET test; JB is the Jarque-Bera Normality test

http://www.aloki.hu ● ISSN 1589 1623 (Print) ● ISSN 1785 0037 (Online)
DOI: http://dx.doi.org/10.15666/aeer/1705_1114311162

The estimates of Model 3 are presented in *Table 6*. The dependent variable is CO_2 emissions. This model examines the influence of oil sector activities and life expectancy on CO_2 emissions in Nigeria.

Table 6. *ARDL estimates for Model 3*

Panel A	**Specification 1**		**Specification 2**	
	Short-run estimates			
Variable	**Coefficient**	**t-Statistic**	**Coefficient**	**t-Statistic**
ECM(-1)	-0.5496***	[-5.0580]	-0.5726***	[-5.1901]
Δ*ln*Rgdpc	0.3527	[0.9031]	0.7151*	[1.7929]
Δ*ln*Rgdpc(-1)	-1.6256***	[-4.3010]	-1.2373***	[-3.2567]
Δ*ln*Rgdpc(-2)			0.6689**	[2.1276]
Δ*ln*LifE	-58.6223	[-0.5934]		
Δ*ln*LifE(-1)	389.8753*	[1.7729]		
Δ*ln*LifE(-2)	-367.2620**	[-2.8167]		
Δ*ln*LifEM			145.2533	[1.4735]
Δ*ln*LifEM(-1)			12.5453	[0.0571]
Δ*ln*LifEM(-2)			-191.8012	[-1.4660]
Δ*ln*VPet	0.3960***	[5.7580]	0.4434***	[6.3971]
Δ*ln*Pcrd	0.5397***	[3.8675]	0.7801***	[4.8282]
Δ*ln*Pcrd(-1)	-0.5221***	[-4.0170]	-0.5326***	[-4.0652]
Δ*ln*Popgrt	-0.8893	[-0.9491]	-1.6198*	[-1.7329]
Δ*ln*Trd	-0.1932**	[-2.0600]	-0.1727*	[-1.8894]
ΔBrk86	0.4276***	[4.1478]	0.4129***	[4.0859]
Panel B	**Long-run estimates**			
Variable	**Coefficient**	**t-Statistic**	**Coefficient**	**t-Statistic**
C	40.2176***	[4.7902]	41.5316***	[5.5126]
*ln*Rgdpc	1.8636	[1.1692]	1.9177	[1.5217]
*ln*LifE	-14.9700***	[-3.2225]		
*ln*LifEM			-15.6707***	[-4.2039]
*ln*VPet	0.6226**	[2.8126]	0.6508***	[3.2034]
*ln*Pcrd	1.3532**	[2.7447]	1.6521***	[3.6544]
*ln*Popgrt	-1.8287	[-1.2336]	-2.3382	[-1.6742]
*ln*Trd	-0.2735	[-1.4243]	-0.2007	[-1.0920]
Panel C	**Diagnostic tests**			
Adjusted R^2	0.8623		0.8659	
D-W Statistic	1.9645		2.1762	
SC x^2	0.0001	[0.9996]	0.6645	[0.4150]
Het $x^2(1)$	0.6170	[0.4322]	0.0069	[0.9337]
RESET	1.5116	[0.2308]	2.3541	[0.1386]
JB	0.7992	[0.6706]	0.9215	[0.6308]

*, **, and *** indicate significance at 10%, 5% and 1% respectively. t-statistics in [ ] and p-values in ( ); Adj R^2 means Adjusted R-squared; SC means Breusch–Godfrey serial correlation LM test; Het is the ARCH test for heteroscedasticity; RESET is the Ramsey RESET test; JB is the Jarque-Bera Normality test

http://www.aloki.hu ● ISSN 1589 1623 (Print) ● ISSN 1785 0037 (Online)
DOI: http://dx.doi.org/10.15666/aeer/1705_1114311162

The long-run estimates in Panel B show that the coefficient of the oil income *ln*VPet is positive and statistically significant at 5% level in specifications 1, and at 1% level in specification 2. From the long-run coefficients, a one per cent increase in the value of petroleum exports (oil revenue) significantly increases CO_2 emissions in Nigeria by 0.6226% in the long-run. The long-run estimates also suggest that a significant negative relationship exists between life expectancy and CO_2 emissions in Nigeria. The short-run estimates in Panel A show that a one per cent increase in petroleum export (oil revenue) produces over 0.3960% increase in CO_2 emissions in Nigeria in the short-run. It is therefore evident from the results in *Table 6* that oil export revenue contributes significantly to environmental pollution in the long-run as well as in the short-run.
The coefficient of ECM (-1) in all the specifications of Model 1, 2 and 3 is negative and significant at 1% level indicating that the adjustment of variables towards long-run dynamics is achieved. The diagnostic test results in Panel C of *Tables 4, 5* and *6* show that there is no evidence of serial correlation, heteroscedasticity and functional form misspecification in each of the ARDL models specified. *Figures 5–12* show the cumulative sum of recursive residuals (CUSUM) and the cumulative sum of squares (CUSUMSQ) stability test results for each of the ARDL specifications. The CUSUM and CUSUMSQ are all within the critical boundaries for the 5% significance level indicating that the coefficients of the ARDL model in each of the specifications are stable.

Discussion of results and policy implications

The schematic view of the results of this empirical study is presented in *Figure 13*.

The positive relationship between the value of petroleum export and life expectancy in Nigeria suggests the dependence of health care expenditure, quality of education, employment opportunities, access to portable drinking water and other socio-economic drivers of life expectancy on oil income. This result is consistent with the findings of Bader and Ganguli (2019) for the Gulf Cooperation Council (GCC) countries. While oil export provides the income required to improve life expectancy in the country, it also generates conditions that accelerate environmental pollution in the economy. This shows that income from oil export significantly generates economic activities in the energy-intensive sectors and rapid accumulation of energy-using technologies in the economy. It is therefore expected that economic diversification policies in Nigeria would incorporate strategies encouraging firms in energy energy-intensive sectors including oil and gas firms to adopt advanced technologies that minimize environmental pollution. The income from petroleum exports could be used in the development of renewable energy sources in the economy. The development of solar and wind energy sources could increase access to clean forms of energy and lessen the level of CO_2 emissions, which threaten environmental quality and reduce life expectancy of Nigerians.

The significant negative relationship between crude oil production and life expectancy indicates that an increase in the production activities of the oil sector creates environmental conditions considered direct risk to human health (Perera, 2018). While the threat of oil sector activities on environmental quality in Nigeria has been widely recognized (see Ologunorisa, 2001; Ugochukwu and Ertel, 2008; Audu et al., 2016), this study documents that the deteriorating environment is responsible for many adverse effects on health and well-being of Nigerians and therefore suggests that health policies

http://www.aloki.hu ● ISSN 1589 1623 (Print) ● ISSN 1785 0037 (Online)
DOI: http://dx.doi.org/10.15666/aeer/1705_1114311162

targeting improvement in life expectancy will have to incorporate sound environmental measures aimed at reducing CO2 emissions from gas flaring in Nigeria's oil and gas industry. Considering gender differences in life expectancy in Nigeria, the results show that while a one per cent increase in the level of CO_2 emissions in the economy affects the life expectancy of the male population more than the female population, crude oil production activities of the oil sector have significant negative short-run and long-run effects on life expectancy of the female population in Nigeria. This empirical result highlights the complexity of the environmental impact of oil resource on life expectancy in Nigeria.

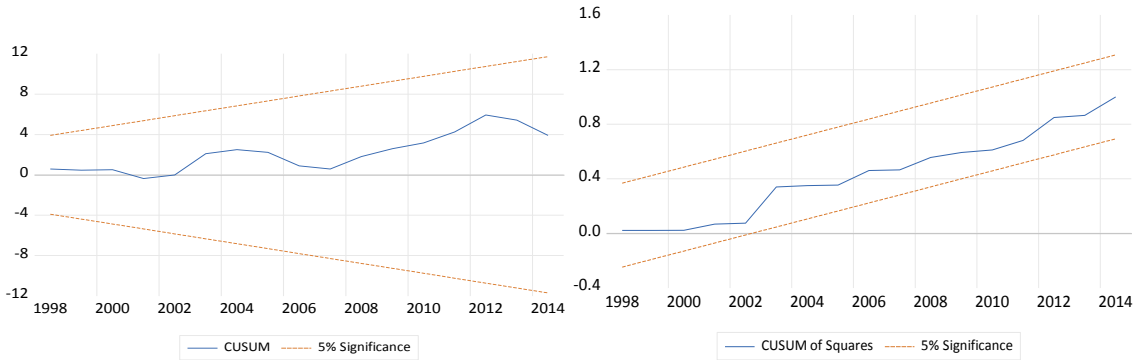

Figure 5. *CUSUM and CUSUM of squares (Model 1 specification lnLifE)*

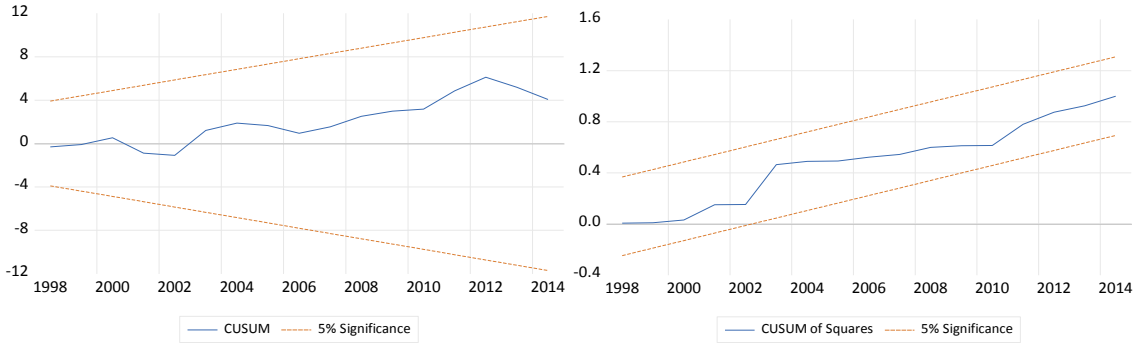

Figure 6. *CUSUM and CUSUM of squares (Model 1 specification lnLifEM)*

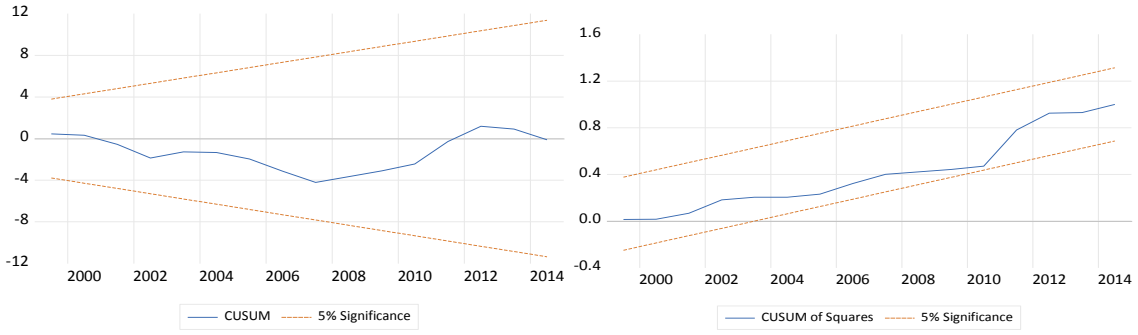

Figure 7. *CUSUM and CUSUM of squares (Model 1 specification lnLifEF)*

http://www.aloki.hu ● ISSN 1589 1623 (Print) ● ISSN 1785 0037 (Online)
DOI: http://dx.doi.org/10.15666/aeer/1705_1114311162

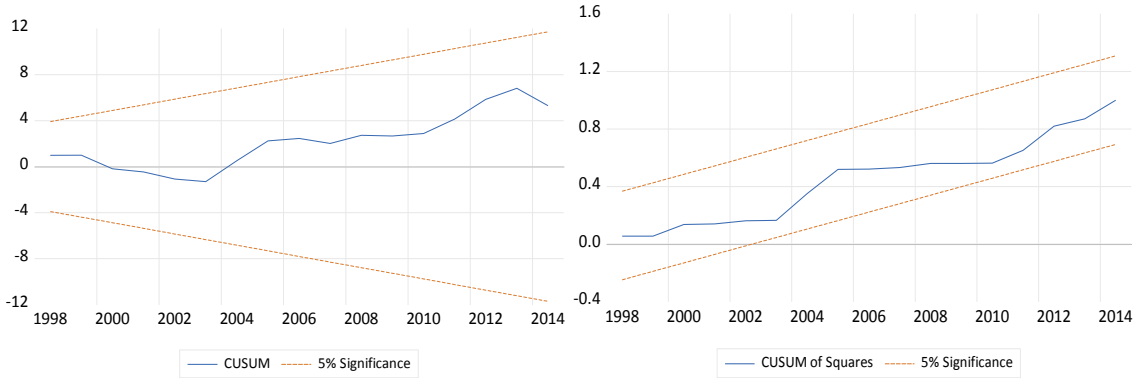

Figure 8. *CUSUM and CUSUM of squares (Model 2 specification lnLifE)*

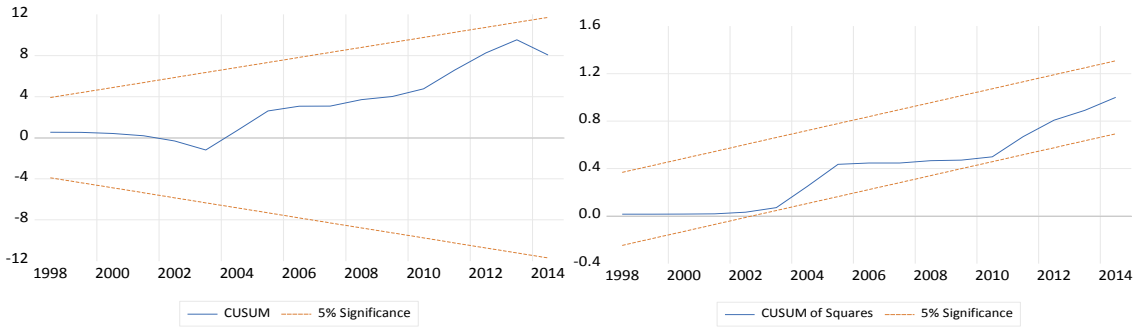

Figure 9. *CUSUM and CUSUM of squares (Model 2 specification lnLifEM)*

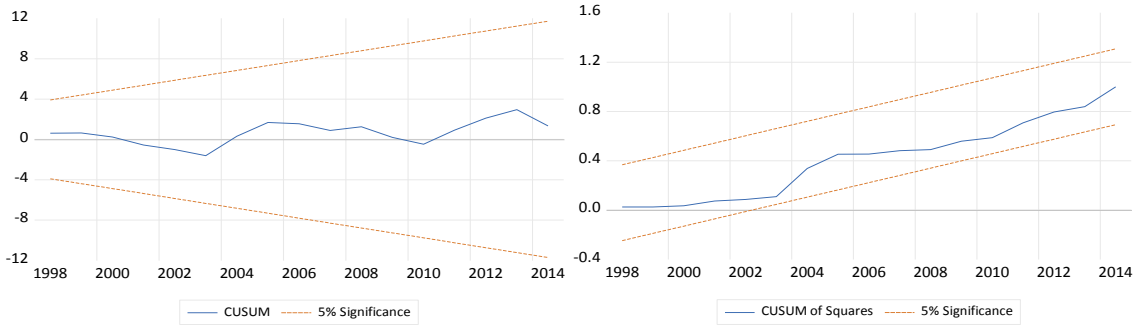

Figure 10. *CUSUM and CUSUM of squares (Model 3 specification lnLifEF)*

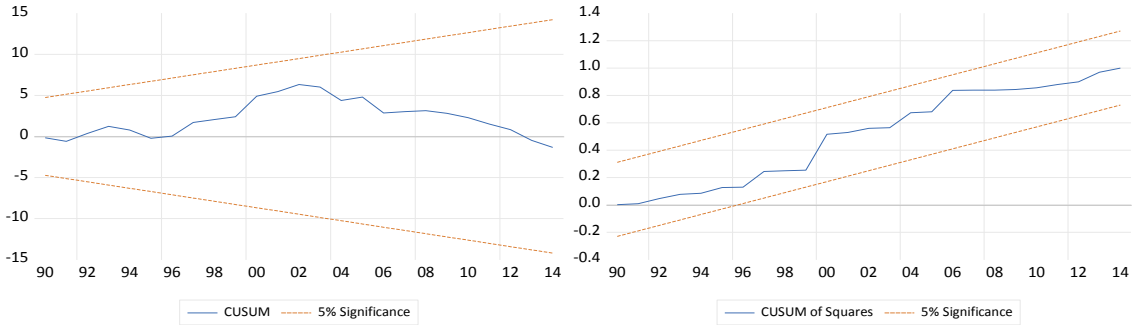

Figure 11. *CUSUM and CUSUM of squares (Model 3 specification 1)*

http://www.aloki.hu ● ISSN 1589 1623 (Print) ● ISSN 1785 0037 (Online)
DOI: http://dx.doi.org/10.15666/aeer/1705_1114311162

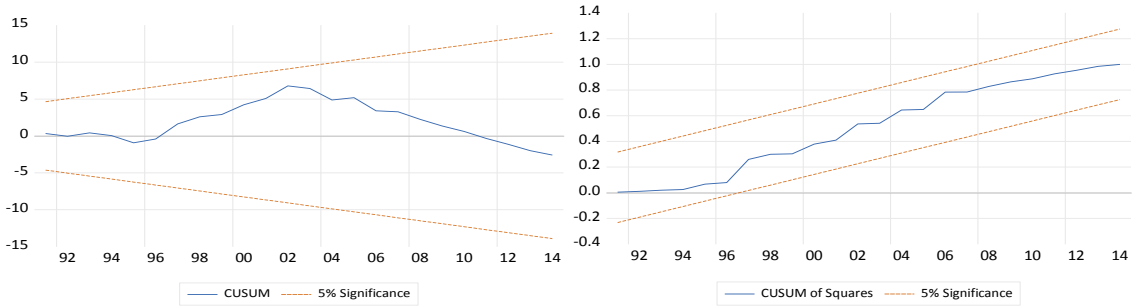

Figure 12. *CUSUM and CUSUM of squares (Model 3 specification 2)*

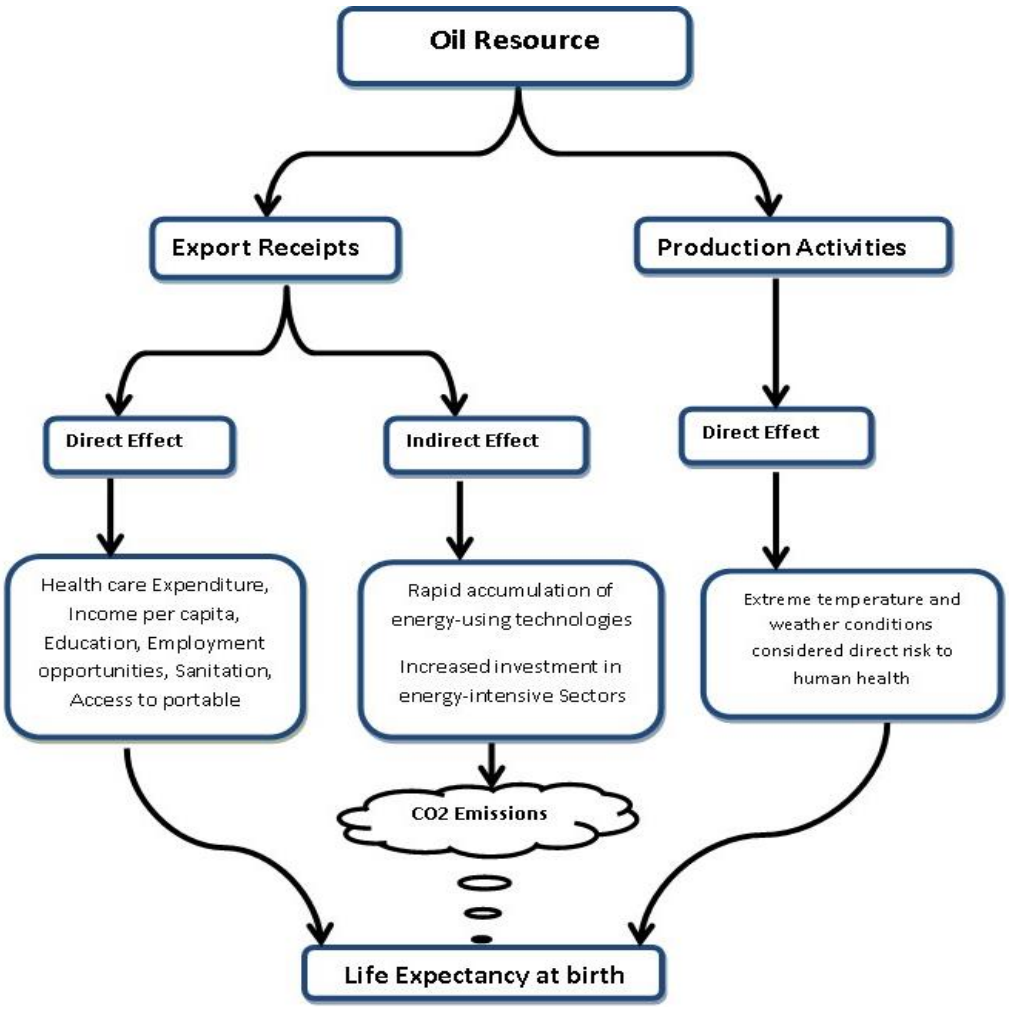

Figure 13. *Relationship between oil resource, CO_2 emissions and life expectancy in Nigeria*

From the above discussion, the health implications of the activities of the oil and gas firms in Nigeria cannot be neglected. The activities of the oil and gas sector in Nigeria generate conditions that harm the health of the people through carbon dioxide (CO_2) emissions. One of these conditions that require urgent attention is the amount of gas flared from oil and gas activities in the country. Nigeria which began the production of crude oil in 1958 still lacked sufficient infrastructure and policy measures to reduce gas

http://www.aloki.hu ● ISSN 1589 1623 (Print) ● ISSN 1785 0037 (Online)
DOI: http://dx.doi.org/10.15666/aeer/1705_1114311162

flaring, which is the most significant contributor of CO2 emission from oil and gas activities in Nigeria (Anomohanran, 2012). It may be necessary for the Nigerian government to design policy measures aimed at reducing gas flaring from the activities of oil and gas firms. Oil and gas firms operating in Nigeria have attempted to implement measures aimed at reducing gas flaring in time past. However, it is not certain if any of these efforts yielded significant level of reduction in the amount of gas flared yearly from oil and gas activities as these efforts were either not completed or facilities vandalised (Anomohanran, 2012). The schematic view of the results of this empirical study presented in *Figure 13* therefore highlights the urgent need for policy measures to consider the environmental consequences of the dependence of the economy on oil resource and its implications on health condition, well-being and quality of life of Nigerians, if the country must experience significant improvement in life expectancy.

Conclusion

This study examined the dynamic relationship between oil sector activities, environmental pollution and life expectancy in Nigeria over the period 1971 to 2014. The long-run relationship among the variables is examined using ARDL bounds testing approach to cointegration. The results provide evidence of cointegration between the variables with the incorporation of the presence of a structural break observed in the series. The ARDL estimates suggest (i) a positive relationship between oil export revenue and life expectancy (ii) a positive relationship between oil export revenue and CO_2 emissions (iii) a negative relationship between crude oil production activities and life expectancy, and (iv) a negative relationship between CO_2 emissions and life expectancy. To further the understanding of the impacts of oil production activities and CO_2 emissions on life expectancy in Nigeria, gender differences in life expectancy in Nigeria was considered. The results show that (i) a one per cent increase in the level of CO_2 emissions in the economy affects the life expectancy of the male population more than the female population (ii) a one per cent increase in the value of petroleum exports (oil revenue) contributes more to life expectancy of the male population than the female pollution, and (iii) strong empirical evidence that crude oil production activities of the oil sector have significant short-run and long-run effects on life expectancy of the female population in Nigeria. Overall the results show that the impact of CO_2 emissions on life expectancy in Nigeria is stronger in the long-run.

This study provides empirical evidence to support the urgent need for health policy measures in Nigeria to incorporate effective strategies for mitigation and adaptation meant to reduce the impact of the increasing role of the oil sector on health condition, wellbeing of the people and the overall goal of improving life expectancy in Nigeria.

REFERENCES

[1] Abbas, F., Awan, H. S. (2018): What determines health status of population in Pakistan? – Social Indicators Research 139: 1-23.

[2] Alam, M. S., Shahbaz, M., Paramati, S. R. (2016): The role of financial development and economic misery on life expectancy: evidence from post reforms in India. – Social Indicators Research 128: 481-497. DOI 10.1007/s11205-015-1040-4.

[3] Anomohanran, O. (2012): Determination of greenhouse gas emission resulting from gas flaring activities in Nigeria. – Energy Policy 45: 666-670.

http://www.aloki.hu ● ISSN 1589 1623 (Print) ● ISSN 1785 0037 (Online)
DOI: http://dx.doi.org/10.15666/aeer/1705_1114311162

[4] Audu, A., Jimoh, A., Abdulkareem, S. A., Onyeji, L. (2016): Economics and environmental impacts of oil exploration and exploitation in Nigeria. – Energy Sources, Part B: Economics, Planning and Policy 11: 251-257. DOI: 10.1080/15567249.2011.627411.
[5] Bader, Y., Ganguli, S. (2019): Analysis of the association between economic growth, environmental quality and health standards in the Gulf Cooperation Council during 1980-2012. – Management of Environmental Quality: An International Journal. https://doi.org/10.1108/ MEQ-03-2018-0061.
[6] Barlow, R., Vissandjée, B. (1999): Determinants of national life expectancy. – Canadian Journal of Development Studies 20: 9-29. DOI: 10.1080/02255189.1999.9668787.
[7] Bergh, A., Nilsson, T. (2010): Good for living? On the relationship between globalization and life expectancy. – World Development 38(9): 1191-1203.
[8] Bezirtzoglou, C., Dekas, K., Charvalos, E. (2011): Climate changes, environment and infection: facts, scenarios and growing awareness from the public health community within Europe. – Anaerobe 17: 337-340.
[9] Chaabouni, S., Zghidi, N., Mbarek, M. B. (2016): On the causal dynamics between CO_2 emissions, health expenditures and economic growth. – Sustainable Cities and Society 22: 184-191.
[10] Franchini, M., Mannucci, P. M. (2015): Impact on human health of climate changes. – European Journal of Internal Medicine 26: 1-5.
[11] Hertz, E., Hebert, J. R., Landon, J. (1994): Social and environmental factors and life expectancy, infant mortality, and maternal mortality rates: results of cross-national comparison. – Social Science and Medicine 39: 105-I 14.
[12] Kim, J. I., Kim, G. (2016): Country-level socioeconomic indicators associated with healthy life expectancy: income, urbanization, schooling, and internet users: 2000-2012. – Social Indicators Research 129: 391-402. DOI 10.1007/s11205-015-1107-2.
[13] Liang, L., Gong, P. (2017): Climate change and human infectious diseases: a synthesis of research findings from global and spatio-temporal perspectives. – Environment International 103: 99-108.
[14] Lu, Z., Chen, H., Hao, Y., Wang, J., Song, X., Mok, T. (2017): The dynamic relationship between environmental pollution, economic development and public health: evidence from China. – Journal of Cleaner Production 166: 134-147.
[15] Lütkepohl, H. (2006): Structural Vector Autoregressive Analysis for Cointegrated Variables. – In: Hübler, O., Frohn, J. (eds.) Modern Econometric Analysis. Springer, Berlin, pp. 73-86.
[16] Mariani, F., Perez-Barahona, A., Raffin, N. (2010): Life expectancy and the environment. – Journal of Economic Dynamics & Control 34: 798-815.
[17] Marsh, K, Ganz, G. L., Hsu, J., Strandberg-Larsen, M., Gonzalez, R. P., Lund, N. (2016): Expanding health technology assessments to include effects on the environment. –Value in Health 19: 249 – 254.
[18] Murthy, V. N. R., Okunade, A. A. (2016): Determinants of U.S. health expenditure: Evidence from autoregressive distributed lag (ARDL) approach to cointegration. – Economic Modelling 59: 67-73.
[19] Narayan, P. K. (2005): The saving and investment nexus for China: evidence from cointegration tests. – Applied Economics 37: 1979-1990. https://doi.org/10.1080/00036840500278103.
[20] Ologunorisa, T. E. (2001): A review of the effects of gas flaring on the Niger Delta environment. – The International Journal of Sustainable Development & World Ecology 8: 249-255. DOI: 10.1080/13504500109470082.
[21] Pautrel, X. (2009): Pollution and life expectancy: how environmental policy can promote growth. – Ecological Economics 68: 1040-1051.

http://www.aloki.hu ● ISSN 1589 1623 (Print) ● ISSN 1785 0037 (Online)
DOI: http://dx.doi.org/10.15666/aeer/1705_1114311162

[22] Perera, F. (2018): Pollution from fossil-fuel combustion is the leading environmental threat to global pediatric health and equity: solutions exist. – International Journal of Environmental Research and Public Health 15: 16. DOI: 10.3390/ijerph15010016.
[23] Perron, P. (2006): Dealing with Structural Breaks. – In: Hassani, H., Mills, T. C., Patterson, K. (eds.) Palgrave Handbook of Econometrics (1st Ed.) Palgrave Macmillan, UK.
[24] Pesaran, M. H., Shin, Y., Smith, R. J. (2001): Bounds testing approaches to the analysis of long run relationships. – Journal of Applied Econometric 16: 289-326. https://doi.org/10.1002/jae.616.
[25] Qureshi, M. I., Rasli, A. M., Awan, U., Ma, J., Ali, G., Faridullah, Alam, A., Sajjad, F., Zaman, K. (2015): Environment and air pollution: health services bequeath to grotesque menace. – Environmental Science and Pollution Research 22: 3467-3476. DOI 10.1007/s11356-014-3584-2.
[26] Sede, P. I., Ohemeng, W. (2015): Socio-economic determinants of life expectancy in Nigeria (1980-2011). – Health Economics Review 5. DOI 10.1186/s13561-014-0037-z.
[27] Shahbaz, M., Loganathan, N., Mujahid, N., Ali, A., Nawaz, A. (2016): Determinants of life expectancy and its prospects under the role of economic misery: a case of Pakistan. – Social Indicators Research 126: 1299-1316 DOI 10.1007/s11205-015-0927-4.
[28] Tai, M.; Chao, C., Hu, S. (2015): Pollution, health and economic growth. – North American Journal of Economics and Finance 32: 155-161.
[29] Ugochukwu, C. N. C., Ertel, J. (2008): Negative impacts of oil exploration on biodiversity management in the Niger De area of Nigeria. – Impact Assessment and Project Appraisal 26: 139-147.
[30] Vogelsang, T. J., Perron, P. (1998): Additional test for unit root allowing for a break in the trend function at an unknown time. – International Economic Review 39: 1073-1100.
[31] Wu, C. (2017): Human capital, life expectancy, and the environment. – The Journal of International Trade & Economic Development 26: 885-906. DOI: 10.1080/09638199.2017.1314543.
[32] Wu, X., Lu, Y., Zhou, S., Chen, F., Xu, B. (2016): Impact of climate change on human infectious diseases: empirical evidence and human adaptation. – Environment International 86*:* 14-23.

http://www.aloki.hu ● ISSN 1589 1623 (Print) ● ISSN 1785 0037 (Online)
DOI: http://dx.doi.org/10.15666/aeer/1705_1114311162

EFFECT OF ORGANIC LOADING RATE ON COPRODUCTION OF HYDROGEN AND METHANE FROM MOLASSES WASTEWATER AND ENERGY CONVERSION BY TWO-PHASE ANAEROBIC FERMENTATION

KAPUMBE, D. J.[1] – MIN, L.[1] – KISOHOLO, M. A.[2] – SUN, C. Y.[3] – YONGFENG, L.[1*]

[1]*School of Forestry, Northeast Forestry University, P.O. Box 150040 Harbin, China*

[2]*School of Forestry, Northeast Forestry University, Harbin, China; Ruwenzori State University, Butembo, Democratic Republic of Congo, P.O. Box 150040 Harbin, China*

[3]*School of Environmental and Chemical Engineering, Heilongjiang University of Science and Technology, P.O. Box 150040 Harbin, China*

[*]*Corresponding author*
e-mail: dr_lyf@163.com; phone: +86-139-0361-4476

(Received 5th Apr 2019; accepted 13th Jun 2019)

Abstract. Effect of organic loading rate on the operational performance of reactors and energy conversion efficiency by two-phase anaerobic fermentation was proposed and investigated using molasses wastewater. Hydrogen and methane production rate were determined in the hydrogenic up-flow anaerobic sludge blanket (UASB) reactor and the methanogenic UASB reactor. At analyzed optimum system organic loading rate (OLR) of 20 g COD/L $_{reactor}$·d, hydrogen was efficiently produced from the hydrogenic reactor with the highest production rate of 2.0±0.21 L/L $_{reactor}$·d and in the methanogenic reactor, methane was produced from residual organic matters and volatile fatty acids (VFAs) with a production rate of 1.9±0.3 L/L $_{reactor}$·d. Finally, the energy conversion efficiency was increased from 12.1% (hydrogen only production) to 91.2% (hydrogen and methane coproduction). The results of this study indicated that the hydrogenic reactor presented relatively low energy conversion efficiency while the methanogenic reactor presented a high one.
Keywords: *organic matter, upflow anaerobic sludge blanket, hydrogenic reactor, volatile fatty acids, methanogenic reactor*

Introduction

Hydrogen (H_2) as a renewable energy carrier can replace fossil fuels and address issues of energy shortage and environmental emissions (Lee and Chung, 2010). Hydrogen is being focused on as a promising alternative to fossil fuels because it does not discharge contaminants (Panda et al., 2016). Also, hydrogen is a promising future energy carrier because the sole byproduct of H_2 combustion is pure water that generates 2.75 times more energy (122 kJ/g) than hydrocarbon fuels (Scott, 2004). Furthermore, biological hydrogen production seems to be more attractive because organic waste materials can be used as substrate and the hydrogen-producing system can be operated under low temperature and pressure conditions (Sivagurunathan et al., 2016). The calorific value of hydrogen is three times greater than that of petrol, 3.9 times that of ethanol and 4.5 times that of coal (Fayaz et al., 2012). Among the various hydrogen production methods, hydrogen production from organic wastes by anaerobic fermentation seems to be the most promising and environmentally friendly (Siddiqui et al., 2011). Anaerobic fermentation has unique characteristics like high ecological adaptability, simple reaction conditions and low nutrient requirement

http://www.aloki.hu ● ISSN 1589 1623 (Print) ● ISSN 1785 0037 (Online)
DOI: http://dx.doi.org/10.15666/aeer/1705_1116311174

(Puyol et al., 2017) and it can use microbes through manipulating the organic matter in the biomass to extract hydrogen in an anaerobic environment (Han et al., 2012). The advantages of the two-stage fermentation process are high-energy recovery and process stability (Nualsri et al., 2016). Anaerobic digestion entails two-stage processes involving the sequential action of acid-forming and methane-forming bacteria. In the first stage, acid-forming bacteria (facultative and anaerobic bacteria) convert the complex organic compounds into simpler organics (volatile fatty acids-VFAs) and also carbon dioxide and hydrogen gases. In the second stage, the organic acids and hydrogen are converted into methane and carbon dioxide by methanogens. The efficiency of an anaerobic treatment depends on both the acidogenic and methanogenic phases (Shi et al., 2017). Hydrogen is mainly produced in the acidogenic stage of anaerobic digestion during the fermentation of organic wastes. Several factors affect the fermentative hydrogen production, including inoculum, substrate characteristics, reactor type, nitrogen and phosphate contents, temperature and pH, among others (Wang and Wan, 2009). However, the low theoretical energy efficiency of about 33.5% is the main obstacle to hydrogen production by anaerobic fermentation which significantly limits its development and industrial application (Chen et al., 2012). How to increase energy conversion efficiency from organic wastes is a challenging topic. It was found in previous studies (Carucci et al., 2005; Luo et al., 2010) that the effluents of the anaerobic fermentation process including mainly volatile fatty acids (VFAs) and alcohols can be reutilized to recover the thermal enthalpies and further produce methane, thereby dramatically increasing the energy conversion efficiency. Among the various anaerobic wastewater treatment technologies, upflow anaerobic sludge blanket (UASB) reactors have achieved considerable success and these reactors have been applied to treat a wide range of effluents such as sugar, pulp and paper, dairy, chemical, potato starch, bean balancing, soft drinks, fish processing, noodle processing, yeast production, slaughterhouse, and coffee processing industries (Metcalf and Eddy, 2003; Yetilmezsoy and Sakar, 2008; Farghaly and Tawfik, 2017). Therefore, the upfow anaerobic sludge blanket (UASB) reactor has been recognized as an essential wastewater treatment technology among anaerobic treatment methods.

Given these considerations, the present study aimed to evaluate the effect of OLRs on the hydrogen and methane production to achieve the optimum energy conversion efficiency using a two-phase anaerobic process which consisted of two up-flow anaerobic sludge blanket (UASB) reactor.

Materials and methods

Seed sludge and feeding

The seed sludge used in this study was the dewatering sludge obtained from a local municipal wastewater treatment plant (Harbin, China). For the hydrogenic UASB, the sludge was aerated for 30 days to inhibit the methane-producing bacteria activity. For the methanogenic UASB, the raw sludge was acclimatized in the reactor operated at pH 6.5, fed continuously with the molasses substrate at OLR of 4.0 g COD/L·d. After enough enrichment over 30 days, the methanogenic sludge began to be fed with the effluent of the hydrogenic UASB.

http://www.aloki.hu ● ISSN 1589 1623 (Print) ● ISSN 1785 0037 (Online)
DOI: http://dx.doi.org/10.15666/aeer/1705_1116311174

Experimental setup

Coproduction of hydrogen and methane from molasses wastewater was carried in a two-phase anaerobic process which consisted of two up-flow anaerobic sludge blanket (UASB) reactor (*Figure 1*) with the same working volume of 10 L.

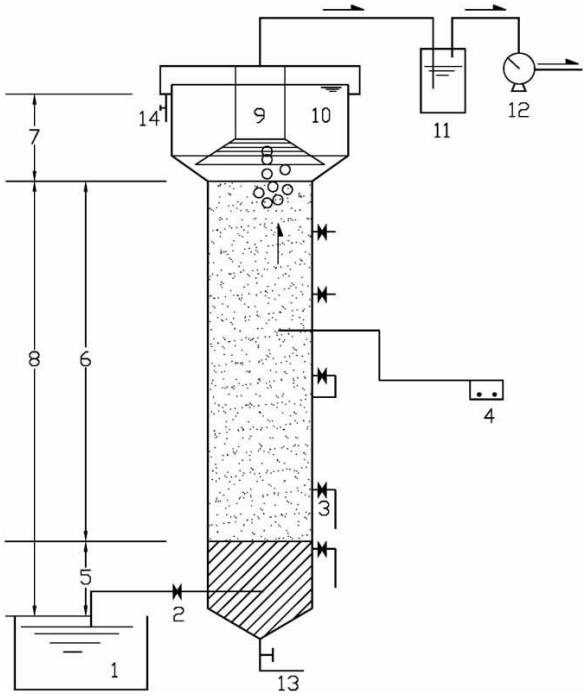

Figure 1. *Structure of the UASB reactor. 1. Raw water tank; 2.Peristaltic pump; 3. Sample connection; 4. Temperature controller; 5. Sludge bed; 6. Superposed layer; 7. Reaction zone; 8. Separating zone; 9. Three phase separation zone; 10. Precipitation area; 11. Water seal; 12. Wet gas flow meter. 13. Mud mouth; 14. Outlet*

The internal diameter was 10 cm and a height of 1.3 m for the two reactors. Operating temperature of the bioreactors was maintained through an electric jacket to 35˚C. The two reactors operated for 60 days, and the operational conditions (OLR and respective HRT) are presented in *Table 1*. The UASB reactor for hydrogen production (hydrogenic) was fed with molasses wastewater using a peristaltic pump while the UASB reactor for methane production was supplied with the effluent collected from the hydrogenic reactor. In this study, the steady-state condition was defined as the condition that the biogas varied within 5% for ten days (*Figure 2*).

Table 1. *operational conditions (OLR and respective HRT) of reactors*

Period (d)	**Hydrogenic UASB**		**Methanogenic UASB**	
	OLR (g COD/$L_{reactor}$·d)	**HRT** (h)	**OLR** (g COD/$L_{reactor}$·d)	**HRT**(h)
1-15	12	4	3.5	21
16-30	16	6	4.1	18
31-45	20	8	5.0	15
46-60	30	10	6.2	12

http://www.aloki.hu ● ISSN 1589 1623 (Print) ● ISSN 1785 0037 (Online)
DOI: http://dx.doi.org/10.15666/aeer/1705_1116311174

Analytical methods

COD, pH, and alkalinity were monitored and measured daily according to Standard methods (Apha, 1995). Hydrogen and methane were analyzed using gas chromatography (SC-7, Shandong Lunan Instrument Factory). The gas chromatograph was equipped with a thermal conductivity detector and a stainless steel column (2 m×5 mm) filled with Porapak Q (50-80 meshes). Nitrogen was used as the carrier gas at a flow rate of 40 mL/ min.

Figure 2. *Physical photo of the UASB reactor*

Conversion efficiency of energy

The conversion efficiency of energy was calculated from hydrogen and methane according to the following equation:

$$R= (V_H \cdot \beta_H + V_M \cdot \beta_M)/ (F \cdot W) \quad \text{(Eq.1)}$$

where R represents the conversion efficiency of energy in the hydrogenic and methanogenic reactor, V_H and V_M represent the volume of hydrogen and methane (L/d), respectively. β_H and β_M represent the COD equivalent of hydrogen and methane, respectively and the hydrogen and methane COD equivalents (g O_2/L H_2 and CH_4) were 0.71 and 2.86, respectively. F represents the influent rate of the hydrogenic reactor (L/d). W represents the COD concentration of molasses wastewater.

http://www.aloki.hu ● ISSN 1589 1623 (Print) ● ISSN 1785 0037 (Online)
DOI: http://dx.doi.org/10.15666/aeer/1705_1116311174

Results and discussion

Optimum system OLR for hydrogenic UASB

The UASB reactor for hydrogen production operated during 60 days under different OLR and HRT. Organic loading rate (OLR) is an essential parameter in studying bioreactors (Venetsaneas et al., 2009). To optimize a system for hydrogen production, it is necessary to define either a range of OLRs that the operation can handle effectively or an optimal OLR for a maximum hydrogen production rate. The pH variation at different OLRs and the hydrogen production and COD removal at different OLRs are respectively presented in *Figure 3* and *Figure 4*.

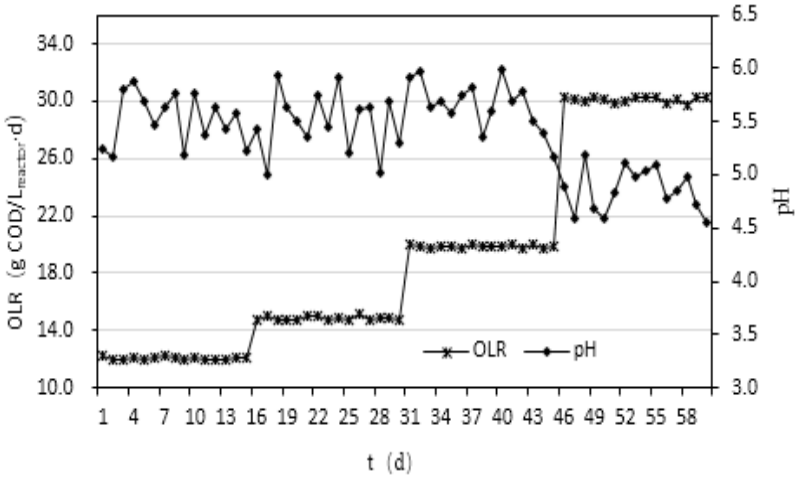

Figure 3. *The pH variation at different OLRs*

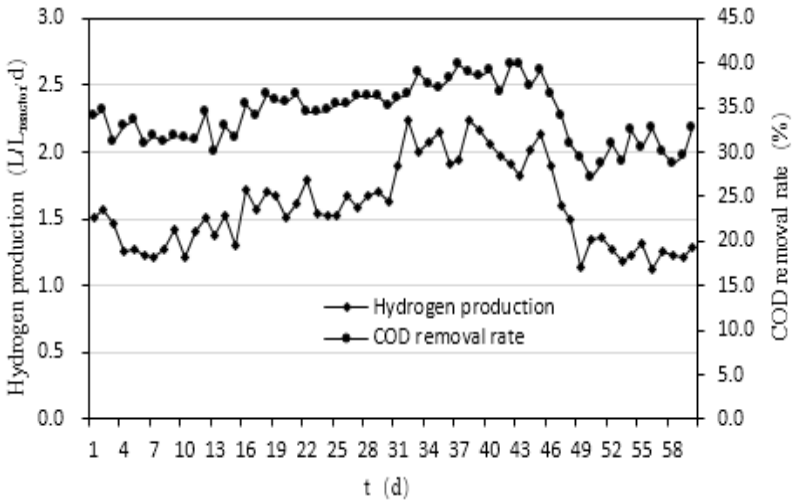

Figure 4. *The hydrogen production and COD removal at different OLRs*

The pH parameter was critical for maintaining the reliability of the hydrogenic fermentation process, and the VAFs (Ethanol, acetic acid, propionic acid and butyric acid) production resulted in a reduction of hydrogenase activity significantly. *Figure 3* shows that the hydrogenic system pH was within 4.5-6.0 range.

http://www.aloki.hu ● ISSN 1589 1623 (Print) ● ISSN 1785 0037 (Online)
DOI: http://dx.doi.org/10.15666/aeer/1705_1116311174

As indicated in *Figure 4*, the maximum hydrogen production was achieved to be 2.0±0.21 L/L $_{reactor}$·d which stated the most exuberant metabolic activities of hydrogenic microorganisms at the OLR of 20 g COD/L $_{reactor}$·d. At the same time, the COD removal rate presented by hydrogenic reactor was up to the highest level of 38.1±0.55%. The higher OLR showed a negative influence on the hydrogenic microorganisms through decreasing hydrogen production and COD removal efficiency, which was explained by the reduction of pH value caused by VFAs accumulation. These results are similar to those obtained by Krishnan et al. (2017) who observed that increased OLR is considered to indicate vigorous biomass concentration conditions that could bring toxicity to the system. The observed trends were supported by the work of Zhang et al. (2015), they found that the anaerobic digestion of food waste at OLR of 3 gVS/L/d caused VFA accumulation. Therefore, the OLR of 20 g COD/L $_{reactor}$·d was determined to be the suitable operating condition for a hydrogenic reactor with the maximum hydrogen production from molasses wastewater and COD removal efficiency. Zahedi et al. (2018) examined the effect of the increase in organic loading rates (OLRs), by reducing the solids retention time (SRT) from 20 d to 5 d, in single-phase mesophilic anaerobic co-digestion of sewage sludge with glycerine (1% v/v). They confirmed that anaerobic co-digestion of these biowastes under steady-state conditions could achieve an 85 ± 5% reduction in volatile fatty acids (VFA) at SRTs between 20 and 9 d, with a methane production yield of around 0.8 l CH_4/L/d. Decreases in the SRT not only allow the sludge stability and biogas production to be maintained but also lead to an increase in the waste that could be treated and lower operating costs.

Biase et al. (2018) tested the Bench-scale anaerobic moving bed biofilm reactors (AMBBR) at mesophilic conditions and different HRT of 24, 18, 12, 10, 8 and 6 h. They also studied temperatures of 15, 25, and 35˚C at a constant HRT of 18 h. During the HRT study, it was found that AMBBR could be operated with COD removal above 80% at all HRT and therefore OLR below 23 kg-COD $m^{-3}d^{-1}$ at 40% media fill ratio. The highest performance of 92% removal of sCOD was attained at 5.4 kg-COD $m^{-3}d^{-1}$. This corresponded to surface area loading rates (SALR) of 18 g-sCOD $m^{-2}d^{-1}$ with methane yields of 0.34 m^3-CH_4 kg-COD^{-1} removed at 35˚C. At OLR above 23 kg-COD $m^{-3}d^{-1}$, the performance decreased below 80% sCOD removal at 35˚C.

Amorim et al. (2018) evaluated the rapid startup of UASB reactors at 30˚C for the cassava wastewater treatment. The reactor was operated under eight different conditions with a hydraulic retention time (HRT) of 8 or 12 h and organic loading rates (OLR) of 12.0 or 15.5 g $COD.L^{-1}d^{-1}$. The UASB system with the best performance was that with the 8 h HRT and OLR of 12.0 g $COD .L^{-1}d^{-1}$, with COD removal rates ranging from 71 to 80 % and methane production of 0.260 L CH_4 g $^{-1}$ $COD_{removed}$.

Moreover, Corsino et al. (2018) observed that under an OLR lower than 7 kg TCOD $m^{-3}d^{-1}$ the removal efficiency of total chemical oxygen demand (TCOD) was approximately 90% in the two aerobic granular sludge sequencing batch reactors (AGSBR) investigated. In contrast, at higher OLR a significant decrease in the removal efficiency (from 90% to less than 75%) was observed in the reactor R2.

Tritt and Kang (2017) reported that the reactor performance during their investigation showed a maximum 95% COD removal efficiency at an organic loading rate (OLR) of 1 kg COD/ m^3-d with its corresponding hydraulic retention time (HRT) of 7.5 d. At a higher OLR of 4.0 kg COD/ m^3-d, the COD removal efficiency of 75% was achieved with an HRT of 2 d. No significant difference in COD removal efficiencies was found between the reactors operated in both up-flow and down-flow modes.

http://www.aloki.hu ● ISSN 1589 1623 (Print) ● ISSN 1785 0037 (Online)
DOI: http://dx.doi.org/10.15666/aeer/1705_1116311174

Methane production from hydrogenic effluent by methanogenic UASB

The UASB reactor for methane production was fed with the acidogenic effluent collected from the CSTR and operated during 60 days under different OLR and HRT. The OLR was gradually augmented by increasing the concentration of the influent and then by decreasing the HRT (*Table 1*). *Figure 5* reveals the profile of the methane production and COD removal rate of the methanogenic reactor during the operation.

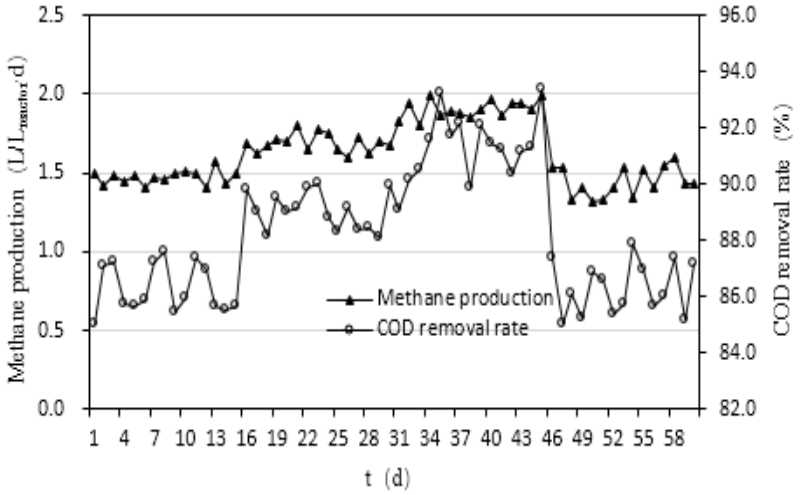

Figure 5. *The methane production and COD removal at different OLRs*

At the HRT 15 h, the OLR of 5.0 g COD/L reactor·d, the methanogenic UASB presented the optimal operation performance with the methane production of 1.9±0.3 L/L reactor·d. At HRT 12 h, the increased existence of activated sludge was detected in the methanogenic effluent caused by excessive flow velocity, so the methane production began to decrease remarkably down to 1.5±0.55 L/L reactor·d which showed that the reactor tends to go to lousy run statement. The COD removal rate has a similar variation curve with methane production, range between 85% and 93.5%, showing its high treatment efficiency and excellent process stability. In another study, Wang et al. (2009) found that increasing the HRT from 6 to 24 h, the COD of the effluent was gradually reduced from 257 to 124.4 mg/L, and the total removal rate of the COD increased from 88.1 to 95.6% in the anaerobic reactor treating starch wastewater. Besides, Colin et al. (2007) observed that the amount of biogas product (L-biogas/L.d) increased with the increase in organic loading rate. At the maximum of OLR of 18.11 g COD/L.d and HRT of 9.5 h, gas productivity of 3.7 L/ (L.d) was achieved in an anaerobic horizontal flow filter packed with bamboo peace treating starch wastewater. Moreover, Wu et al. (2018) reported in their study that the daily CH_4 production from the three treatments increased with the OLR. Results of Begum et al. (2018) disclosed that the range of methane yield in single and two-stage AD fluctuated between 0.21 and 0.34 L CH_4/(g COD removed) and 0.2 to 0.32 L CH4/(g COD removed) respectively with an overall increase of 21% in COD removal efficiencies can be achieved in two-stage AD.

Furthermore, Hu et al. (2018) related that the methane production rate increased with OLR increasing in thermophilic and mesophilic reactors. Their results indicated that

http://www.aloki.hu ● ISSN 1589 1623 (Print) ● ISSN 1785 0037 (Online)
DOI: http://dx.doi.org/10.15666/aeer/1705_1116311174

thermophilic anaerobic reactors allow higher loading rate and yield higher methane production, substrate degradation, and pathogen destruction.

Shen et al. (2018) reported in their study that the volumetric methane production rate (VMPR) of experimental and control group revealed an increasing tendency with the increment of OLR. They attributed that phenomenon to the accumulation of VFAs in the system, which further inhibited the activity of methanogens and eventually resulted in the acidification of the AD system.

Arreola-Vargas et al. (2018) reported a linear trend between methane production and OLR with the highest volumetric methane production rate of 3.03 L CH_4 $d^{-1}L^{-1}$. Wickham et al. (2018) also reported that the increase in biogas production was proportional to the increase in organic loading rate (OLR) in their study.

Increased energy conversion efficiency by two-phase UASB

During hydrogenic fermentation, the most amounts of organic matters were converted into the VFAs, and the degraded COD was just removed in the form of hydrogen. So, the hydrogenic reactor presented relative low energy conversion efficiency varying between 8.0% and 12.1%, which is shown in *Figure 6*.

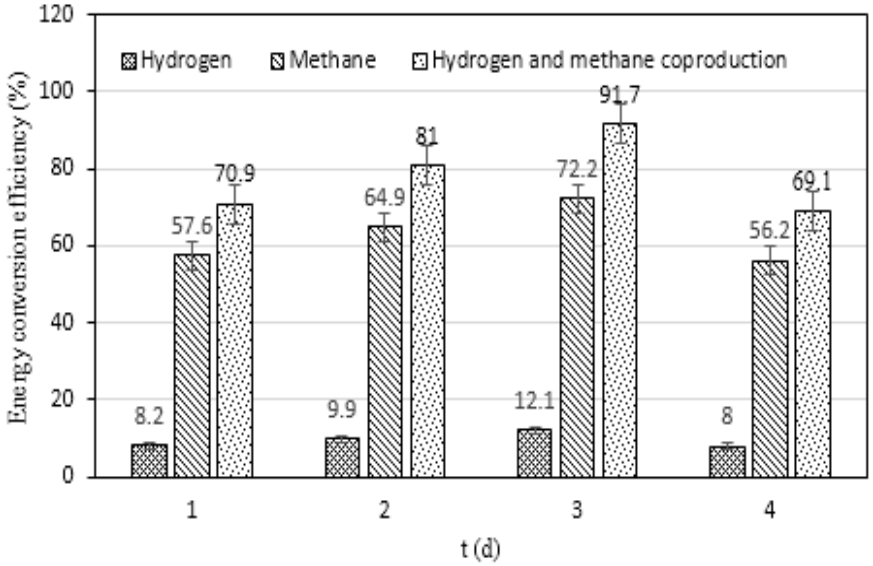

Figure 6. *The energy conversion efficiency for hydrogen and methane production*

At the operation condition of OLR 20 g COD/L $_{reactor}$·d for the hydrogenic reactor, the VFAs existed in hydrogenic effluent could be efficiently utilized by methanogenic microorganisms to produce the methane, which resulted in the high level of COD removal efficiency. The energy conversion efficiency of the methanogenic reactor reached up to the maximum value of 72.2% at OLR 5 g COD/L $_{reactor}$·d. The total energy conversion efficiency was also improved from 12.1% to 91.7% by two-phase anaerobic fermentation system. In the same way, Corona and Razo-Flores (2018) studied continuous H_2 and CH_4 production in a two-stage process to increase energy recovery from agave bagasse enzymatic-hydrolysate. The two-stage ongoing process significantly increased energy conversion efficiency (56%).

http://www.aloki.hu ● ISSN 1589 1623 (Print) ● ISSN 1785 0037 (Online)
DOI: http://dx.doi.org/10.15666/aeer/1705_1116311174

Comparison of hydrogen and methane production with other two-stage anaerobic digestion processes

Several researchers have studied the two-stage anaerobic digestion processes as shown in *Table 2*. Among the presented works, the two stages CSTR-UASB achieved the highest maximum hydrogen rate of 6.0 L/L/d and maximum methane rate of 6.4 L/L/d using agave bagasse (Corona and Razo-Flores, 2018).

Table 2. *Comparison of hydrogen and methane production with other two-stage anaerobic digestion processes*

Substrate	Reactor type	Temp.	HRT	Maximum HPR (L/L/d)	Maximum MPR (L/L/d)	Reference
Cheese whey	CSTR	35 °C	24 h	2.51	5.04	(Antonopoulou et al., 2008)
	PBR	35 °C	4.4 d			
Olive pulp	CSTR	35 °C	7.5 h	0.46	1.13	(Koutrouli et al., 2009)
	CSTR	35 °C	10 d			
Municipality Biowaste	CSTR	55 °C	5 h	0.85	1.75	(Cavinato et al., 2011)
	CSTR	55 °C	13 d			
Mixture wastewater	CSTR	37 °C	0.75 d	1.72	0.33	(Dareioti and Kornaros, 2014)
	CSTR	37 °C	25 d			
Molasses	CSTR	35 °C	5 h	3.06	2.01	(Wang et al., 2013)
	UASB	35 °C	15 h			
Molasses	PBR	35 °C	6 h	2.8	1.94	(Park et al., 2010)
	PBR	35 °C	6 d			
Pelletized Grass	CSTR	35 °C	18 h	0.65	1.4	(Massanet-Nicolau et al., 2015)
	CSTR	35 °C	270 h			
Agave bagasse	CSTR	35 ° C	6 h	6.0	6.4	(Corona and Razo-Flores, 2018)
	UASB	22–25 °C	14 h			
Molasses	UASB	35 °C	8h	2.0	1.9	This study
	UASB	35 °C	15h			

NR: data not reported; CSTR: continuous stirred-tank reactor; PBR: Packed-bed reactor; HPR: hydrogen product rate; MPR: methane product rate

Conclusion

The hydrogen and methane coproduction system containing two UASB reactors in this study were established at optimum OLR of 20 g COD/L reactor·d and 6.2 g COD/L reactor·d, respectively, for maximum biogas production from molasses wastewater. The maximum hydrogen production rate was reached at the OLR of 20 g COD/L reactor·d while the maximum methane production rate was reached at the OLR of 5.0 g COD/L reactor·d. Experimental data illustrated that the two-phase anaerobic fermentation process was a promising mean to recover energy from organic wastewater and provided the essential operation parameters guideline for the future industrial application. The feasibility of the two-phase anaerobic fermentation would need to be further studied.

http://www.aloki.hu ● ISSN 1589 1623 (Print) ● ISSN 1785 0037 (Online)
DOI: http://dx.doi.org/10.15666/aeer/1705_1116311174

Acknowledgements. This work was financially supported by Heilongjiang province natural science foundation of China (Grants No. 201354).

REFERENCES

[1] Amorim, M. C. C., de S. e Silva, P. T., Gavazza, S., Sobrinho, M. A. M. (2018): Viability of rapid startup and operation of UASB reactors for the treatment of cassava wastewater in the semi-arid region of northeastern Brazil. – The Canadian Journal of Chemical Engineering 96(5): 1036-1044.

[2] Antonopoulou, G., Stamatelatou, K., Venetsaneas, N., Kornaros, M., Lyberatos, G. (2008): Biohydrogen and methane production from cheese whey in a two-stage anaerobic process. – Industrial & Engineering Chemistry Research 47(15): 5227-5233.

[3] Apha, A. (1995): WPCF, Standard methods for the examination of water and wastewater. – American Public Health Association, Washington, DC.

[4] Arreola-Vargas, J., Snell-Castro, R., Rojo-Liera, N. M., González-Álvarez, V., Méndez-Acosta, H. O. (2018): Effect of the organic loading rate on the performance and microbial populations during the anaerobic treatment of tequila vinasses in a pilot-scale packed bed reactor. – Journal of Chemical Technology & Biotechnology 93(2): 591-599.

[5] Begum, S., Anupoju, G. R., Sridhar, S., Bhargava, S. K., Jegatheesan, V., Eshtiaghi, N. (2018): Evaluation of single and two stage anaerobic digestion of landfill leachate: Effect of pH and initial organic loading rate on volatile fatty acid (VFA) and biogas production. – Bioresource technology 251: 364-373.

[6] Carucci, G., Carrasco, F., Trifoni, K., Majone, M., Beccari, M. (2005): Anaerobic digestion of food industry wastes: effect of codigestion on methane yield. – Journal of Environmental Engineering 131(7): 1037-1045.

[7] Cavinato, C., Bolzonella, D., Fatone, F., Cecchi, F., Pavan, P. (2011): Optimization of two-phase thermophilic anaerobic digestion of biowaste for hydrogen and methane production through reject water recirculation. – Bioresource Technology 102(18): 8605-8611.

[8] Chen, C.-C., Sen, B., Chuang, Y.-S., Tsai, C.-J., Lay, C.-H. (2012): Effect of effluent recycle ratio in a continuous anaerobic biohydrogen production system. – Journal of Cleaner Production 32: 236-243.

[9] Colin, X., Farinet, J.-L., Rojas, O., Alazard, D. (2007): Anaerobic treatment of cassava starch extraction wastewater using a horizontal flow filter with bamboo as support. – Bioresource technology 98(8): 1602-1607.

[10] Corona, V. M., Razo-Flores, E. (2018): Continuous hydrogen and methane production from Agave tequilana bagasse hydrolysate by sequential process to maximize energy recovery efficiency. – Bioresource technology 249: 334-341.

[11] Corsino, S. F., Di Trapani, D., Torregrossa, M., Viviani, G. (2018): Aerobic granular sludge treating high strength citrus wastewater: Analysis of pH and organic loading rate effect on kinetics, performance and stability. – Journal of environmental management, 214: 23-35.

[12] Dareioti, M. A., Kornaros, M. (2014): Effect of hydraulic retention time (HRT) on the anaerobic co-digestion of agro-industrial wastes in a two-stage CSTR system. – Bioresource technology 167: 407-415.

[13] di Biase, A., Devlin, T., Kowalski, M., Oleszkiewicz, J. (2018): Performance and design considerations for an anaerobic moving bed biofilm reactor treating brewery wastewater: Impact of surface area loading rate and temperature. – Journal of environmental management 216: 392-398.

[14] Farghaly, A., Tawfik, A. (2017): Simultaneous hydrogen and methane production through multi-phase anaerobic digestion of paperboard mill wastewater under different operating conditions. – Applied biochemistry and biotechnology 181(1): 142-156.

http://www.aloki.hu ● ISSN 1589 1623 (Print) ● ISSN 1785 0037 (Online)
DOI: http://dx.doi.org/10.15666/aeer/1705_1116311174

[15] Fayaz, H., Saidur, R., Razali, N., Anuar, F., Saleman, A., Islam, M. (2012): An overview of hydrogen as a vehicle fuel. – Renewable and Sustainable Energy Reviews 16(8): 5511-5528.
[16] Han, W., Wang, B., Zhou, Y., Wang, D.-X., Wang, Y., Yue, L.-R., Li, Y.-F., Ren, N.-Q. (2012): Fermentative hydrogen production from molasses wastewater in a continuous mixed immobilized sludge reactor. – Bioresource technology 110: 219-223.
[17] Hu, Y., Kobayashi, T., Qi, W., Oshibe, H., Xu, K.-Q. (2018): Effect of temperature and organic loading rate on siphon-driven self-agitated anaerobic digestion performance for food waste treatment. – Waste Management 74: 150-157.
[18] Koutrouli, E. C., Kalfas, H., Gavala, H. N., Skiadas, I. V., Stamatelatou, K., Lyberatos, G. (2009): Hydrogen and methane production through two-stage mesophilic anaerobic digestion of olive pulp. – Bioresource Technology 100(15): 3718-3723.
[19] Krishnan, S., Singh, L., Sakinah, M., Thakur, S., Wahid, Z. A., Ghrayeb, O. A. (2017): Role of organic loading rate in bioenergy generation from palm oil mill effluent in a two-stage up-flow anaerobic sludge blanket continuous-stirred tank reactor. – Journal of cleaner production 142: 3044-3049.
[20] Lee, Y.-W., Chung, J. (2010): Bioproduction of hydrogen from food waste by pilot-scale combined hydrogen/methane fermentation. – International journal of hydrogen energy 35(21): 11746-11755.
[21] Luo, G., Xie, L., Zou, Z., Wang, W., Zhou, Q., Shim, H. (2010): Anaerobic treatment of cassava stillage for hydrogen and methane production in continuously stirred tank reactor (CSTR) under high organic loading rate (OLR). – International journal of hydrogen energy 35(21): 11733-11737.
[22] Massanet-Nicolau, J., Dinsdale, R., Guwy, A., Shipley, G. (2015): Utilising biohydrogen to increase methane production, energy yields and process efficiency via two stage anaerobic digestion of grass. – Bioresource technology 189: 379-383.
[23] Metcalf, E., Eddy, H. (2003): Wastewater engineering: treatment and reuse. – In: Techobanoglous, G., Burton, F. L., Stensel, H. D. (eds.) Wastewater Engineering, Treatment, Disposal and Reuse. Tata McGraw-Hill Publishing Company Limited, 4th edition. New Delhi, India.
[24] Nualsri, C., Kongjan, P., Reungsang, A. (2016): Direct integration of CSTR-UASB reactors for two-stage hydrogen and methane production from sugarcane syrup. – International Journal of Hydrogen Energy 41(40): 17884-17895.
[25] Panda, S. K., Mishra, S. S., Kayitesi, E., Ray, R. C. (2016): Microbial-processing of fruit and vegetable wastes for production of vital enzymes and organic acids: Biotechnology and scopes. – Environmental research 146: 161-172.
[26] Park, M. J., Jo, J. H., Park, D., Lee, D. S., Park, J. M. (2010): Comprehensive study on a two-stage anaerobic digestion process for the sequential production of hydrogen and methane from cost-effective molasses. – International journal of hydrogen energy 35(12): 6194-6202.
[27] Puyol, D., Batstone, D. J., Hülsen, T., Astals, S., Peces, M., Krömer, J. O. (2017): Resource recovery from wastewater by biological technologies: opportunities, challenges, and prospects. – Frontiers in microbiology 7: 2106.
[28] Scott, D. S. (2004): Hydrogen-the case for inevitability. – International journal of hydrogen energy 3(29): 225-227.
[29] Shen, F., Li, H., Wu, X., Wang, Y., Zhang, Q. (2018): Effect of organic loading rate on anaerobic co-digestion of rice straw and pig manure with or without biological pretreatment. – Bioresource technology 250: 155-162.
[30] Shi, X., Leong, K. Y., Ng, H. Y. (2017): Anaerobic treatment of pharmaceutical wastewater: a critical review. – Bioresource technology 245: 1238-1244.
[31] Siddiqui, Z., Horan, N., Salter, M. (2011): Energy optimisation from co-digested waste using a two-phase process to generate hydrogen and methane. – International journal of hydrogen energy 36(8): 4792-4799.

http://www.aloki.hu ● ISSN 1589 1623 (Print) ● ISSN 1785 0037 (Online)
DOI: http://dx.doi.org/10.15666/aeer/1705_1116311174

[32] Sivagurunathan, P., Kumar, G., Bakonyi, P., Kim, S.-H., Kobayashi, T., Xu, K. Q., Lakner, G., Tóth, G., Nemestóthy, N., Bélafi-Bakó, K. (2016): A critical review on issues and overcoming strategies for the enhancement of dark fermentative hydrogen production in continuous systems. – International journal of hydrogen energy 41(6): 3820-3836.
[33] Tritt, W. P., Kang, H. (2017): Slaughterhouse wastewater treatment in a bamboo ring anaerobic fixed-bed reactor. – Environmental Engineering Research 23(1): 70-75.
[34] Venetsaneas, N., Antonopoulou, G., Stamatelatou, K., Kornaros, M., Lyberatos, G. (2009): Using cheese whey for hydrogen and methane generation in a two-stage continuous process with alternative pH controlling approaches. – Bioresource technology 100(15): 3713-3717.
[35] Wang, J., Wan, W. (2009): Factors influencing fermentative hydrogen production: a review. – International journal of hydrogen energy 34(2): 799-811.
[36] Wang, R.-M., Wang, Y., Ma, G.-P., He, Y.-F., Zhao, Y.-Q. (2009): Efficiency of porous burnt-coke carrier on treatment of potato starch wastewater with an anaerobic–aerobic bioreactor. – Chemical Engineering Journal 148(1): 35-40.
[37] Wang, B., Li, Y., Wang, D., Liu, R., Wei, Z., Ren, N. (2013): Simultaneous coproduction of hydrogen and methane from sugary wastewater by an "ACSTRH–UASBMet" system. – International Journal of Hydrogen Energy 38(19): 7774-7779.
[38] Wickham, R., Xie, S., Galway, B., Bustamante, H., Nghiem, L. D. (2018): Anaerobic digestion of soft drink beverage waste and sewage sludge. – Bioresource technology 262: 141-147.
[39] Wu, C., Huang, Q., Yu, M., Ren, Y., Wang, Q., Sakai, K. (2018): Effects of digestate recirculation on a two-stage anaerobic digestion system, particularly focusing on metabolite correlation analysis. – Bioresource technology 251: 40-48.
[40] Yetilmezsoy, K., Sakar, S. (2008): Development of empirical models for performance evaluation of UASB reactors treating poultry manure wastewater under different operational conditions. – Journal of Hazardous materials 153(1-2): 532-543.
[41] Zahedi, S., Rivero, M., Solera, R., Perez, M. (2018): Mesophilic anaerobic co-digestion of sewage sludge with glycerine: Effect of solids retention time. – Fuel 215: 285-289.
[42] Zhang, W., Zhang, L., Li, A. (2015): Anaerobic co-digestion of food waste with MSW incineration plant fresh leachate: process performance and synergistic effects. – Chemical Engineering Journal 259: 795-805.

http://www.aloki.hu ● ISSN 1589 1623 (Print) ● ISSN 1785 0037 (Online)
DOI: http://dx.doi.org/10.15666/aeer/1705_1116311174

EFFECTS OF GA_3 AND ABA ON THE GERMINATION OF DORMANT OAT (*AVENA SATIVA* L.) SEEDS

GE, J. Y.[1,2] – ZHANG, B.[1] – KHAN, T. A.[2] – WANG, X.[1,2] – REN, Q. J.[1] – JIA, P. F.[2] – WANG, X. Y.[1] – HU, Y. G.[2*] – REN, C. Z.[3]

[1]*Zhangjiakou Academy of Agricultural Sciences, Zhangjiakou City, Hebei 075000, China*

[2]*College of Agronomy and Biotechnology, China Agricultural University, Beijing 100193, China*

[3]*Baicheng Academy of Agricultural Sciences, Baicheng City, Jilin 137000, China*

**Corresponding author*
e-mail: gejy207@163.com, huyuegao@cau.edu.cn

(Received 22nd Mar 2019; accepted 4th Jul 2019)

Abstract. The dormancy characteristics of oat seed that can germinate after one season or one year are used to build and maintain vegetation to protect soils from desertification in Northern China. The aim of this study was to estimate the effects of endogenous and exogenous GA_3 and ABA on oat seed (*Avena sativa* L. BaiYan 7) germination. The results showed that seed without peel hull had lower endogenous ABA content and the ratio of ABA/GA_3 than seeds with peel hull. The best GA_3 treatment duration for milky ripe, wax ripe, full ripe seeds were 60 min (m) or 120 m, 60 m and 30 m, respectively. Seed germination rate, germination potential and germination index all increased then decreased with the increasing of GA_3 concentrations. The best GA_3 concentration treatment was 100 mg L^{-1}, while the turning point was 200 mg L^{-1}. The dormancy rate of low temperature storage seeds was higher than those stored in room temperature at each storage time, and both decreased with the increase of the storage time. New seeds or stored for 1-2 months, had significantly enhanced germination rate by exogenous GA_3. GA3 treatment had no effect on germination rate for the seeds that had been stored for over 3 months. Germination rate decreased with the increase of ABA concentrations. The most inhibitive effect, which lead to reduction of seed germination by 37.7% and 4.0%, when the concentration of ABA was 500 mg L^{-1} and 1000 mg L^{-1}, respectively. GA_3 could decrease the inhibition effect of ABA on seed germination.
Keywords: *oat, germination rate, gibberellic acid (GA3), abscisic acid (ABA) endogenous, exogenous*

Introduction

China's desertification area is about 1.74 million km^2, accounting for 18% of the total land area, and the area is going to increase in the future (Islam et al., 2011; Cheng et al., 2018). To solve this problem, it is important to build and maintain plant biology to increase surface coverage and restore native vegetation, which is the main reason why Chinese government has set up China Agriculture Research System to support the production and study of oat (Lin et al., 2012; Qian et al., 2018). Oat (*Avena sativa L.*) is a annual herbaceous plant belonging in gramineous precocious subfamily. It has strong ability to resist wind erosion and easy to sow, and easy to build plant (Lin et al., 2012; Zang et al., 2018). Oat can be cultivated in the marginal land with less water and fertilizer requirement so well adapted in desert area (Ren et al., 2007; Rabiei et al., 2012; Zang et al., 2015; Khan et al., 2019). Li et al. (2009) proved the strong anti-erosion ability of oat than corn, sunflower and mung bean, which will help to prevent farmland from desertification. "Baiyan7", breed by Baicheng Academy of Agricultural Sciences, has dormancy characteristics. Some other researches showed the dormancy strength of "Baiyan 7" can affect the vegetation establishment. Now the studies of oat

http://www.aloki.hu ● ISSN 1589 1623 (Print) ● ISSN 1785 0037 (Online)
DOI: http://dx.doi.org/10.15666/aeer/1705_1117511189

planting have focused on breeding, cultivation, physiological and biochemical aspects, oat seed science research focuses on the germination optimum temperature, germination substrate, salinity stress and seed storage, but the researches about the effect of phytohormones on germination of dormant oat are quite few. It is an innate property of seed that defines the environmental conditions in which the seed is able to germinate. It is determined by genetics with a substantial environmental influence which is mediated, at least in part, by the plant hormones abscisic acid and gibberellins (Finch-Savage and Leubne, 2006). Many previous studies show that GA_3 is the main regulator on seed germination and it could lift the bud and seed dormancy and promote bud instead of light or low temperature (Mukhtar and Singh, 2006; Ozkaya et al., 2006; Liu et al., 2016). Other study also found that for the germination of brown rice seed, in addition to water and a certain temperature, GA_3 was a promoting substance of seed germination (Damaris et al., 2019). ABA is a phytohormone which has been shown to be involved in a wide range of plant physiology (Wilkinson and Davies, 2010; Zhang et al., 2017). ABA could inhibit seed germination requirement concentration varies.

Therefore, we aims to 1) estimate the best GA3 concentration and treat time for germination of oat seed with different maturity; 2) evaluate the oat seed germination as affected by ABA input; 3) test the combination effect of GA3 and ABA for oat seed germination.

Materials and methods

Study site and materials

The experiment was conducted at Baicheng Academy of Agricultural Sciences, Baicheng, Jilin province, China (45° 37'N, 122° 48'E, 152 m elevation). The detail information of experiment sites could be found in Zang et al., 2018 and Qian et al., 2018. Bai Yan 7 oat (*Avena sativa* L.) seed used in this experiment supplied by the Baicheng Academy of Agricultural Sciences. Part of the seeds collected immediately for germination test, and other stored at room temperature under dry conditions or at 4 °C refrigerator for later use.

Experimental design

a) The effects of GA_3 treat time on germination of oat seed with different maturity

Each different matured oat seed were soaked in 100 mg L^{-1} GA_3 for different times in order to test the germination. The treatments time were T1 = 0 m, T2 = 30 m, T3 = 60 m, T4 = 120 m, and T5 = 240 m, different maturity were S1 = milky ripe, S2 = wax ripe, and S3 = full ripe. So the experiment had 15 treatment combinations, with three biological replications, and each replicates have 200 seeds. First, the seeds soaked and disinfected in 4.0% sodium hypochlorite solution for 30 min, then washed 5-6 times with distilled water. Second, tweezers were used to put the seeds in Petri dishes lined with filter paper, each plate contained 200 seeds and were kept at sufficient distance. Third, the Petri dishes were placed in an incubator maintaining temperature 20 °C, distilled water was used to keep the filter paper moist, sprout numbers in each treatment were recorded every morning, for 10 days, and the whole process were repeated 3 times. (These materials and methods are applicable to the following experiments.)

http://www.aloki.hu ● ISSN 1589 1623 (Print) ● ISSN 1785 0037 (Online)
DOI: http://dx.doi.org/10.15666/aeer/1705_1117511189

b) The effects of GA3 concentrations on wax ripe seed germination

The wax ripe seeds were soaked in different GA_3 concentrations for 120 min, and then test the germination. Six treatments were established with increasing GA_3 concentrations as 0, 12.5, 25, 50, 100, and 200 mg L^{-1} (i.e. A1, A2, A3, A4, A5, and A6, respectively).

c) The effects of GA3 on germination of oat seed in different maturity with or without peel

Different maturities were cream ripe, wax ripe and full ripe. Each maturity seeds had four treatments: B1 = seeds with peel, B2 = seeds without peel, B3 = unpeeled seeds soaked in GA_3 for 2 h, B4 = peeled seeds soaked in GA_3 for 2 h.

d) The effects of GA_3 on germination of different matured oat seeds under low or room temperature

Oat seeds with different maturity were stored under low or room temperature. Different maturities were cream ripe, wax ripe and full ripe. Each kind of seeds had five storage durations: 0, 1, 2, 3, and 4 months (i.e. C1, C2, C3, C4, and C5).

e) The interaction effect of GA3 and ABA on germination of oat seed

GA_3 and ABA were dissolved in a small amount of ethanol, constant volume with distilled water, GA_3 preparation of 100 mg L^{-1}, the ABA 1000 mg L^{-1} as stock solution, respectively, using the GA_3 liquid and different concentrations of ABA dilution to deal with the sterilized seed, soak 30 min, remove seeds, and dry with filter paper, then do germination test. For GA_3 and ABA application, first the seed soak with different concentrations of ABA solution 30 min, after that soak with GA_3 solution for 30 min, and then start germination test. This experiment has nine treatments: D1 = 1000 mg L^{-1} ABA; D2 = 500 mg L^{-1} ABA; D3 = 250 mg L^{-1} ABA; D4 = 100 mg L^{-1} ABA; D5 = 100 mg L^{-1} GA_3 + 100 mg L^{-1} ABA; D6 = 100 mg L^{-1} GA_3 + 250 mg L^{-1} ABA; D7 = 100 mg L^{-1} GA_3 + 500 mg L^{-1} ABA; D8 = 100 mg L^{-1} GA_3 + 1000 mg L^{-1} ABA; CK use distilled water as control.

The detail experimental design of all experiment in present study also have been summarised as *Table A1* in the *Appendix*.

Determination indexes and methods

a) Seed collection standard

Oat seed development process was divided into three maturity phase. Full ripe: glumes white and open, the appearance of seed is yellowish-white, hard; wax ripe: glumes the sallow semi-open, the appearance of seed is yellow-green, slightly harder, volume reach mature state; milk ripe: glumes green and closed, the appearance of seed is green, tender, the volume does not reach mature state.

b) Determination of germination rate, germination potential, germinating, germination index and T50

Test method reference to the international seed testing and GB/T2930.4-2001.

http://www.aloki.hu ● ISSN 1589 1623 (Print) ● ISSN 1785 0037 (Online)
DOI: http://dx.doi.org/10.15666/aeer/1705_1117511189

Germinating refers to the ratio of the sum of the maximum number of germination within three days and total number of germination.

T_{50} refers to seed germination rate of the time required in half of the final germination.

$$\text{Germination rate (\%)} = (n / N) \times 100 \quad \text{(Eq.1)}$$

In this equation n refers to the seed within the specified time normal germination accumulated grains, N refers to the total number of tested seeds.

$$\text{Germination potential (\%)} = (A / N) \times 100 \quad \text{(Eq.2)}$$

In *Equation 2,* "A" refers to the cumulative germination rate of 3 d before the test.

$$\text{Germination index} = \Sigma Gt / Dt \quad \text{(Eq.3)}$$

In *Equation 3,* "Gt" refers to the number of germination of the time t, "Dt" refers to the germination days.

Statistical analyses

Experimental raw data use the Excel (2007 version) statistical software to collate, then use both SAS (8.0 version) and Mstate-C statistical software to analyse. A factorial layout within randomized complete block design with 3 replications was used to analysis the variation of GA_3 processing time effect on germination characteristics of seeds in different maturity. Seed maturity were milky ripe seed, wax ripe seed and full ripe seed. GA_3 processing times were included 0, 30, 60, 120 and 240 min. In order to determine the influence of GA_3 concentration on different experimental characteristics, a randomized complete block design with three replications were used. GA_3 concentrations were 0, 12.5, 25, 50, 100 and 200 mg L^{-1}.

Results and discussion

As shown in *Table 1*, fully ripe seeds with or without peel, had significant differences ($p < 0.05$) in endogenous GA_3, ABA and GA_3/ABA at different storage periods. Endogenous GA_3 in fully ripe seeds without peel in each storage period were significantly higher than those with peel ($p < 0.05$). With the extension of storage time, endogenous GA_3 in full ripe seeds without peel were increased by 68.7%, 121.4%, 59.2%, 18.2%, and 29.0%, respectively when compared with seeds with peel. GA_3 contents showed a tremendous increasing trend with the storage time. Endogenous ABA in full ripe seeds with peel in each storage period was significantly higher than that in the seeds without peel ($p < 0.05$), with the extension of storage time, endogenous ABA in full ripe seed with peel than seed without peel were increased by 8.4%, 49.0%, 37.7%, 74.5%, and 36.7%, respectively, which means that it contains a certain amount of ABA within the peel. The ratio of GA_3/ABA in full ripe seeds without peel in each storage period was significantly higher than that in the seeds with peel ($p < 0.05$), with the extension of storage time, the ratio of GA_3/ABA in full ripe seeds without peel than seed with peel were increased by 82.8%, 229.9%, 119.2%, 106.2%, and 76.3%, respectively (*Table 1*).

http://www.aloki.hu ● ISSN 1589 1623 (Print) ● ISSN 1785 0037 (Online)
DOI: http://dx.doi.org/10.15666/aeer/1705_1117511189

Table 1. *Full ripe seed phytohormones content at different storage periods with or without peel*

Treatment	Determination index	Storage time (month)				
		0	1	2	3	4
With peel	GA_3 (ng/g.FW)	9.25d	5.24e	11.50c	19.18b	39.95a
Without peel		15.61d	11.60e	18.31c	22.67b	52.52a
With peel	ABA (ng/g.FW)	146.18c	137.41e	148.42b	169.33a	138.01d
Without peel		134.91a	92.23e	107.81b	97.03d	100.94c
With peel	GA_3/ABA	0.06d	0.04e	0.08c	0.11b	0.29a
Without peel		0.12d	0.13d	0.17c	0.23b	0.51a

Different letters within a row indicate significant differences between the mean *($p < 0.05$)*

Table 2 showed that, wax ripe seed with or without peel, have significant differences ($p < 0.05$) in endogenous GA_3, ABA and GA_3/ABA at different storage periods. GA3 content in wax ripe seed which was stored for three months was significantly lower in the seed without peel than seed with peel ($p < 0.05$), the rest are significantly higher than wax ripe seed with peel ($p < 0.05$), with the storage time of 0 m (month), 1 m, 2 m, 4 m, and endogenous GA_3 in wax ripe seed without peel than seed with peel, the increase by 67.7%, 15.5%, 80.1%, and 59.9% was seen. Endogenous ABA in wax ripe seed with peel in each storage period are significantly higher than that without peel ($p < 0.05$), with the extension of storage time, endogenous ABA in wax ripe seed with peel than seed without peel were increased by 55.6%, 152.8%, 165.9%, 270.9%, and 72.9%, respectively; this means that it contains a certain amount of ABA within the peel. The ratio of GA_3/ABA in wax ripe seed without peel in each storage period are significantly higher than seed with peel ($p < 0.05$). Moreover, with the extension of storage time, the ratio of GA_3/ABA in full ripe seed without peel than seed with peel were increased by 161.0%, 191.9%, 378.8%, 209.9%, 176.3% (*Table 2*).

Table 2. *Wax ripe seed phytohormones content of the different storage period with or without peel*

Treatment	Determination index	Storage time (month)				
		0	1	2	3	4
With peel	GA_3 (ng/g.FW)	19.79c	20.10c	16.45d	23.12b	37.09a
Without peel		33.20b	23.20d	29.63c	19.32e	59.29a
With peel	ABA (ng/g.FW)	223.03a	158.33d	169.16c	202.80b	131.84e
Without peel		143.37a	62.63d	63.62c	54.67e	76.27b
With peel	GA_3/ABA	0.09d	0.13b	0.10cd	0.11bc	0.28a
Without peel		0.23d	0.37c	0.47b	0.35c	0.78a

Different letters within a row indicate significant differences between the mean ($p < 0.05$)

Table 3 showed that, milky ripe seed with peel or without peel, the endogenous GA_3, ABA and GA_3/ABA at different storage periods have significant differences ($p < 0.05$). Milky ripe seed without peel GA_3 content in addition to storage for four month had no significant with seed with peel ($p < 0.05$), the rest were significantly higher than seed

http://www.aloki.hu ● ISSN 1589 1623 (Print) ● ISSN 1785 0037 (Online)
DOI: http://dx.doi.org/10.15666/aeer/1705_1117511189

with peel ($p < 0.05$), with the storage time of 0 m (month), 1 m, 2 m, 3 m, endogenous GA_3 in milky ripe seed without peel than seed with peel were increased by 44.0%, 37.7%, 76.9%, and 25.7%, respectively; the endogenous ABA in milky ripe seed with peel in each storage periods are significantly higher than seed without peel ($p < 0.05$), with the extension of storage time, endogenous ABA in milky ripe seed with peel than seed without peel were increased by 38.9%, 18.8, 162.2, 107.9, 71.3%, this means it contain a certain amount of ABA within the peel. Milky ripe seed without peel the ratio of GA_3/ABA in addition to storage for 0 month had no significant difference with the seed with peel ($p < 0.05$), the rest were significant ($p < 0.05$); with the storage time of 2 m (month), 3 m, 4 m, and the ratio of GA_3/ABA in milky ripe seed without peel than seed with peel were increased by 48.2%, 65.4%, and 73.6%, respectively (*Table 3*).

Table 3. *Milky ripe seed phytohormones content of the different storage period with or without peel*

Treatment	Determination index	Storage time (month)				
		0	1	2	3	4
With peel	GA_3 (ng/g.FW)	8.62e	10.53d	16.15c	25.35b	55.07a
Without peel		5.99e	7.65d	9.13c	20.17b	55.82a
With peel	ABA (ng/g.FW)	179.97c	154.57e	211.17a	174.54d	189.59b
Without peel		129.59a	130.10a	80.53d	83.94c	110.70b
With peel	GA_3/ABA	0.05d	0.07c	0.08c	0.15b	0.29a
Without peel		0.05d	0.06d	0.11c	0.24b	0.50a

Different letters within a row indicate significant differences between the mean ($p < 0.05$)

Seed maturity has significant influence on germination potential, germination rate, germination index and T_{50}(d). Uniformity was not significantly influenced by seed maturity. Germination potential, germination rate and germination index were significantly affected by GA_3 processing time; however, this effect on uniformity and T_{50}(d). Like, seed maturity, the interaction between seed maturity and GA_3 processing time has significant effect on all experimental characteristics expect uniformity (*Table 4*).

Table 4. *Analysis variance the effect of GA3 processing time on germination characteristics of seeds in different maturity*

S.O.V	d.f.	Germination potential (%)	Germination rate (%)	Germination index	Uniformity	T_{50} (d)
Seed maturity (S)	2	0.573^{**}	0.569^{**}	3296.65^{**}	0.002	1.622^{**}
GA_3 processing time (T)	4	0.041^{**}	0.039^{**}	166.62^{**}	0.008^{ns}	0.222^{ns}
S×T	8	0.31^{**}	0.028^{**}	94.07^{*}	0.004	0.122^{ns}
Error	28	0.008	0.007	29.173	0.005	0.094

ns: non significant; *significant at 0.05 significance in F-tests; **significant at 0.001 significance in F-tests

The highest germination potential was related to full ripe seed and the lowest one was obtained by milky ripe seed, there was no significant difference between wax and

http://www.aloki.hu ● ISSN 1589 1623 (Print) ● ISSN 1785 0037 (Online)
DOI: http://dx.doi.org/10.15666/aeer/1705_1117511189

full ripe seed, but both of them have significant differences with milky ripe seed. The maximum germination rate and germination index also achieved in full ripe seeds. No significant differences were found in these two experimental traits between milky and ripe seed, but both of them had significant differences with full ripe seed. There were no significant differences among milky ripe seed, wax ripe seed and full ripe seed. Wax ripe seed has obtained the highest T_{50}, but its difference with full ripe seed was not significant. However, not only wax ripe seed, but also full ripe seed had significant difference with milky seed maturity. The maximum germination potential and germination rate was occurred in 120 and 60 min GA_3 processing time, respectively. 120 min GA_3 processing time had obtained the maximum germination index which just had significant differences with control treatment (0 min). There were no significant differences among treatments in uniformity index, furthermore, the maximum one was obtained by control treatment (0 min). On the one hand, the highest T_{50} was related to control treatment; on the other hand, the lowest one was obtained by 60, 120 and 240 min. Moreover, there were no significant differences among treatments. The results show that seeds immersed for 60 m by GA_3 had best effect to promote germination to ripe seeds, and they inhibited germination when immersed for 240 m. The maximum germination potential and germination rate was related to interaction between full ripe seed and 30 min of GA_3 processing time, and the highest germination index was achieved in full ripe seed and 120 min GA_3 processing time interaction. There were no significant differences among interaction traits in uniformity. Both, interaction between milky ripe seed and control treatment in processing time, interaction between milky ripe seed and 30 min of GA_3 processing time had obtained the highest T_{50}, which had significant differences with all other interaction (*Table 5*).

Table 5. *Mean comparison for germination characteristics*

Treatment	Germination potential (%)	Germination rate (%)	Germination index	Uniformity	T_{50} (d)
Seed maturity (S)					
Milky ripe seed (S1)	38.22b	35.47b	21.37b	0.9647a	3.60a
Wax ripe seed (S2)	49.78a	34.67b	21.72b	0.9520a	3.06b
Full ripe seed (S3)	53.33a	68.80a	47.22a	0.9767a	3.00b
GA_3 processing time (m) (T)					
0 (T1)	38c	45c	23.62b	1.00a	3.33ab
30 (T2)	49ab	52c	29.65a	0.95a	3.44a
60 (T3)	53a	53a	33.58a	0.99a	3.11b
120 (T4)	54a	43d	34.45a	0.94a	3.11b
240 (T5)	44bc	28b	29.20a	0.93a	3.11b
Seed maturity × GA_3 processing time (S × T)					
S1T1	24h	22h	12.53e	1.00a	4.00a
S1T2	29h	24gh	15.27de	1.00a	4.00a
S1T3	49defg	46def	28.31c	0.97a	3.33b
S1T4	52def	50cde	29.25c	0.96a	3.33b
S1T5	37fgh	33fgh	21.49cde	0.89a	3.33b
S2T1	21h	21h	13.33e	1.00a	3.00b

http://www.aloki.hu ● ISSN 1589 1623 (Print) ● ISSN 1785 0037 (Online)
DOI: http://dx.doi.org/10.15666/aeer/1705_1117511189

S2T2	36fgh	34fgh	21.17cde	0.93a	3.33b
S2T3	46efg	45def	28.44c	1.00a	3.00b
S2T4	33gh	33fgh	20.64cde	0.91a	3.00b
S2T5	37fgh	38efg	25.00cd	0.90a	3.00b
S3T1	69abc	68ab	45.00ab	1.00a	3.00b
S3T2	84a	78a	52.52a	0.92a	3.00b
S3T3	64bcd	64abc	44.00ab	1.00a	3.00b
S3T4	77ab	76a	53.46a	0.96a	3.00b
S3T5	57cde	57bcd	41.11b	1.00a	3.00b

Means with common letters within each column do not differ significantly. The effect of seed maturity, GA_3 processing time, and their interaction were evaluated. The treatments for seed manturity were milky ripe seed (S1), wax ripe seed (S2), and full ripe seed (S3). The treatments for GA_3 processing time were0 (T1), 30 (T2), 60 (T3), 120 (T4), and 240 m (T5)

Germination potential has positive and significant correlation with germination rate and germination index, which means that with increase of germination potential, germination rate increase significantly. However, germination potential has negative and significant correlation with T_{50} and non-significant positive correlation with uniformity. The positive significant correlation was found between germination rate and germination index. T_{50} also had negative and significant correlation with both germination rate and germination index. Furthermore, the correlation between uniformity and T_{50} was positive, but it was not significant (*Table 6*). GA_3 concentration had significant influence on germination potential, germination rate and germination index, but uniformity and T_{50} were not affected by it (*Table 7*).

Table 6. *Simple correlation among experimental characteristics in different seed maturity and GA3 processing time*

Traits	Germination potential	Germination rate	Germination index	Uniformity	T_{50}
Germination potential	1				
Germination rate	0.988^{**}	1			
Germination index	0.978^{**}	0.987^{**}	1		
Uniformity	0.009^{ns}	0.060^{ns}	0.063^{ns}	1	
T_{50}	-0.439^{**}	-0.498^{**}	-0.510^{**}	0.004^{ns}	1

ns: non significant; *significant at 0.05 significance in F-tests; **significant at 0.001 significance in F-tests

Table 7. *Analysis of variance for the influence of different GA3 concentrations on wax ripe seed germination*

S.O.V	d.f.	Germination potential	Germination rate	Germination index	Uniformity	T_{50}
Replication	2	0.006	0.006	16.98	0.012^{ns}	0.056
GA_3 concentrations	5	0.055^{**}	0.088^{**}	195.77^{**}	0.022^{ns}	0.489^{ns}
Error	10	0.008	0.007	24.89	0.008	0.182

ns, non significant; *significant at 0.05 significance in F-tests; **significant at 0.001 significance in F-tests

http://www.aloki.hu ● ISSN 1589 1623 (Print) ● ISSN 1785 0037 (Online)
DOI: http://dx.doi.org/10.15666/aeer/1705_1117511189

The highest germination potential and germination rate was related to 100 mg L^{-1} GA_3 concentration, which had significant differences with all treatments, except 200 mg L^{-1} in both experimental traits. The highest and the lowest germination rate were achieved in 100 mg L^{-1} and control treatment (0 mg L^{-1}) GA_3 concentration, which had significant difference with each other. 100 GA_3 concentration had obtained the maximum germination index, which had significant differences with 0 mg L^{-1} and 12.5 mg L^{-1}. There were no significant differences among treatments in uniformity. The highest T_{50} was related to 50 mg L^{-1} and 100 mg L^{-1}, respectively. Like uniformity, no significant difference was found among treatments (*Table 8*).

Table 8. *Mean comparison for experimental characteristics of wax ripe seed germination in different GA3 concentration*

Treatment	Germination potential (%)	Germination rate (%)	Germination index	Uniformity	T_{50} (d)
GA_3 concentration (mg L^{-1})					
0	21.3d	21.3c	13.33c	1.00a	3.00a
12.5	26.7cd	26.7c	15.99bc	1.00a	3.33ab
25	37.3bcd	49.3b	25.75a	0.82a	3.33ab
50	41.3abc	49.3b	25.01ab	0.85a	4.00a
100	57.3a	66.7a	33.98a	0.84a	4.00a
200	49.3ab	53.3ab	30.09a	0.82a	3.66ab

Means with common letters within each column do not differ significantly

Influence of different maturity seed germination by dealing with GA3

The results showed that, after manual peel out seed, the immersed with GA_3, seeds in different maturity had significantly improved germination rate, germination energy and germination index, which had significant difference with other treatments. Manual removal treatment (B2) and GA_3 treatment (B3) had significant difference with B1 in germination rate. Milky ripe seeds had significant differences in germination potential by dealing with GA_3; seeds treated by B4 were significantly higher than other treatments in germination rate, there was no significant difference between B2 and B3, but also it was significantly higher than B1; seeds treated by B4 was significantly higher than other treatments in germination index, when others have no significant difference; T_{50} of B4 and B3 is shortened one day than B2 and B1. B4 had no significant difference with B3 in the germination potential of wax ripe seed, but it was significantly higher than B2 and B1; furthermore, there was no significant difference between B3 and B2, but B3 was significantly higher than B1. There was no significant difference between B2 and B1; seed treated by B4 was significantly higher than other treatments in germination rate, there was no significant difference between B2 and B3, but they were significantly higher than B1. Seed treated by B4 was significantly higher than other treatments in germination rate, furthermore, B2 was significantly higher than B3 and B1 in germination index, and there was no significant difference between B3 and B1; T_{50} of B4 and B3 was shortened one day than B2 and B1. Full ripe seed had significant difference in germination potential. Full ripe seed had significant difference in germination rate, there was no significant difference between B4 and B1, but all of them were significantly higher than other treatments; T_{50} of B4 and B3 is shortened one day than B2 and B1 (*Table 9*).

http://www.aloki.hu ● ISSN 1589 1623 (Print) ● ISSN 1785 0037 (Online)
DOI: http://dx.doi.org/10.15666/aeer/1705_1117511189

Table 9. *Influence of different maturity seed germination by dealing with GA3*

Provenances	treatments			
	B1	**B2**	**B3**	**B4**
Milky ripe				
Germination rate (%)	0.0d	2.5c	3.2b	3.7a
Germination potential (%)	40.7c	56.0b	58.7b	65.3a
Germination index	13.3b	13.4b	12.9b	22.1a
T_{50}(d)	8	8	7	7
Geminating	0.9	1.0	1.0	0.8
Wax ripe				
Germination rate (%)	2.7c	3.0bc	3.5ab	4.0a
Germination potential (%)	42.7c	65.3b	67.3b	80.0a
Germination index	11.5c	16.8b	13.2c	22.8a
T_{50}(d)	8	8	7	7
Geminating	0.8	0.9	0.9	0.8
Full ripe				
Germination rate (%)	6.7d	8.3c	15.3b	22.7a
Germination potential (%)	75.7d	77.3c	79.3b	92.0a
Germination index	28.1a	20.6b	16.1c	29.6a
T_{50}(d)	7	7	6	6

Different letters within a row indicate significant differences between the mean ($p < 0.05$)

Influence of different maturity seed germination under low temperature and room temperature storage conditions by dealing with GA3

The results showed that using GA_3 treatment to harvest and storage one month cream ripe seed at room temperature, the germination rate were higher than comparison results, the difference reached significant level ($p < 0.05$), increasing 8 and 5.1 percentage points; using GA_3 treatment at room temperature to storage for two months, three months and four months, seed germination rate compared to the comparison was not significant. Storage at room temperature for three and four months, seed germination rate was lower than the comparison, reduced by 2 and 3 percentage points. Germination rate of the new harvest, cold storage for one and two months milk ripe seed treated by GA_3, was higher than the comparison, the difference reached significant level ($p < 0.05$), increasing 8, 6.9 and 5.5 percentage points, respectively; germination rate of cold storage two and three months milky ripe seed treated by GA_3 was lower than the comparison for 4%, the difference was not significant (*Table 10*).

Table 10. *Influence of milky ripe seed germination under room temperature and 0 °C storage conditions by dealing with GA3*

Treatment	Germination rate (%)				
	0 month	**1 month**	**2 month**	**3 month**	**4 month**
Room temperature and no GA_3	11e	35.1d	46.7c	55b	73a
Room temperature and GA_3	19d	40.2c	50.3b	53b	70a
0 °C and no GA_3	11e	30.4d	40.2c	50b	69a
0 °C and GA_3	19e	37.3d	45.7c	51b	65a

Different letters within a row indicate significant differences between the mean ($p < 0.05$)

http://www.aloki.hu ● ISSN 1589 1623 (Print) ● ISSN 1785 0037 (Online)
DOI: http://dx.doi.org/10.15666/aeer/1705_1117511189

Using GA_3 treatment to newly harvested and stored one month wax ripe seeds at room temperature, the germination rate was higher than comparison results, the difference reached significant level ($p < 0.05$), increasing by 10 and 5.5 percent; Using GA_3 treatment at room temperature and stored for two, three and four months, seed germination rate compared to the comparison was not significant, storage at room temperature for four months, seed germination rate was lower than the comparison, reducing it by 3.5%. Germination rate of the new harvest, cold storage for one and two months wax ripe seeds treated with GA_3 was higher than the comparison, the difference reached significant level, increasing by 10, 7.1 and 9.6%. Germination rate of cold storage two and three months wax ripe seeds treated by GA_3 was lower than the comparison by 2%, the difference was not significant (*Table 11*).

Table 11. *Influence of full ripe seed germination under room temperature and 0 °C storage conditions by dealing with GA3*

Treatment	Germination rate (%)				
	0 month	1 month	2 month	3 month	4 month
Room temperature and no GA3	26.3d	50.8c	82.2b	92.1a	90.3a
Room temperature and GA3	43.2c	78.5b	90.5a	90.2a	91.6a
0 °C and no GA3	26.3e	45.6d	72c	82b	88a
0 °C and GA3	43.2d	65.6c	83b	80ab	85a

Different letters within a row indicate significant differences between the mean ($p < 0.05$)

Using GA_3 treatment to harvest and storage one and two month fully mature seeds at room temperature, the germination rate was both higher than comparison results, the difference reached extremely significant level ($p < 0.01$), increasing 16.9, 27.7 and 8.3%; using GA_3 treatment at room temperature to storage for three and four months, seed germination rate compared to the comparison was not significant ($p > 0.05$), storage at room temperature for three months, seed germination rate was lower than the comparison reducing it by 1.9 percentage points; germination rate of the new harvest, cold storage a month and two months fully mature seeds treated by GA_3 had higher than the comparison, the difference reached significant level ($p < 0.05$), increasing by 16.9, 20 and 9%, respectively; germination rate of cold storage three and four months fully mature seeds treated by GA_3 was lower than the comparison by 2% and 3%, according to storage period for the sequence, the difference was not significant (*Table 12*).

Table 12. *Influence of wax ripe seed germination under room temperature and 0 °C storage conditions by dealing with GA_3*

Treatment	Germination rate (%)				
	0 month	1 month	2 month	3 month	4 month
Room temperature and no GA_3	14.4e	50.3d	69.3c	80b	85.5a
Room temperature and GA_3	24.4d	55.8c	73.3b	81a	82a
0 °C and no GA_3	14.4e	45d	60.7c	73b	82a
0 °C and GA_3	24.4e	52.1d	70.3c	74b	80a

Different letters within a row indicate significant differences between the mean ($p < 0.05$)

http://www.aloki.hu ● ISSN 1589 1623 (Print) ● ISSN 1785 0037 (Online)
DOI: http://dx.doi.org/10.15666/aeer/1705_1117511189

The results of this experiment showed that the GA_3 treatment promote seed storage at room temperature or low temperature seed germination, especially for two months, but not for three or more months or even inhibition.

GA3 and ABA interaction effects on seed germination

The test results showed the significant differences, in the germination rate of each treatment compared with CK, D5, D6, D7 ($p < 0.01$); the D8 germination rate was significantly higher than that of D4, D3, D2, D1, ($p < 0.05$). D1 and D2 were the most important treatment which inhibited seed germination compare to other treatments, seed germination in D3 and D4 were 36.0% and 24.0%, respectively; under the same concentration of ABA, the seed germination rate of ABA and GA_3 interaction treatment was higher than ABA treatment, but it was still lower than CK levels. These results suggest that ABA inhibits seed germination, and inhibition increased with the increase trend of ABA concentration; furthermore GA_3 can alleviate the inhibitory effect of ABA on seed germination and alleviating margin of D1, D2 with GA_3 is larger than the D3, D4 (*Fig. 1*).

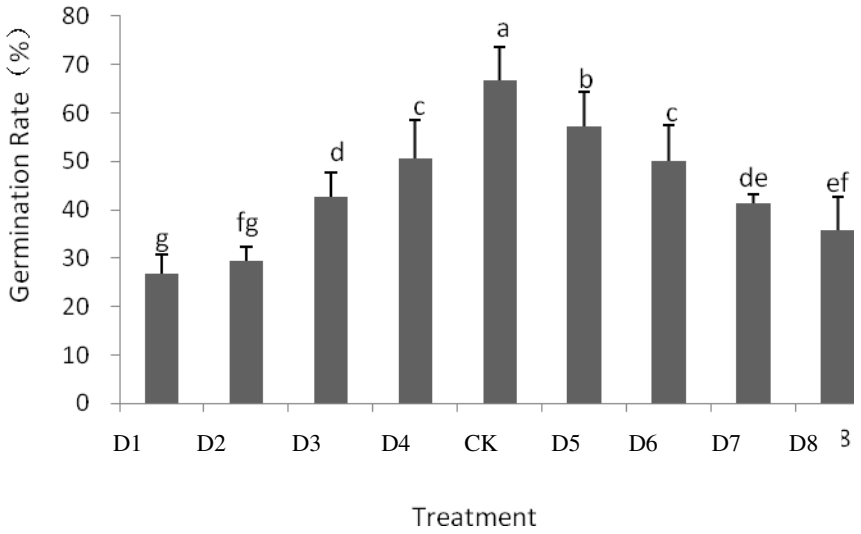

Figure 1. *GA_3 and ABA interaction effects on seed germination*

The results of this experiment showed that the endogenous GA_3 content of each maturity degree oat seed increased with the storage period, while endogenous ABA content decreased with storage time to extend. Different maturity seed GA_3/ABA ratio increase with the storage time, and this result is the same for maturity germination rate. Furthermore, GA_3 content of seed without peel were higher than those with peel at each storage time, while ABA content showed the opposite. Thus, the peel may contain more ABA and conducive to seed dormancy. This was in agree with the observed germination of wild oat with positive relationship between ABA/GA_3 ratio and seed germination, it further strongly affected the dormancy rate (Yu et al., 2016; Esashi, 2017). Zeng and Zhao (2001) indicated that the red string seed showed during seed development, the content of endogenous GA_3 showed a decreasing trend, that GA_3 content in dry seeds in room temperature and low temperature during storage have

http://www.aloki.hu ● ISSN 1589 1623 (Print) ● ISSN 1785 0037 (Online)
DOI: http://dx.doi.org/10.15666/aeer/1705_1117511189

shown pre gradually reduce, the latter has an upturn, and the content of endogenous GA_3 and no significant correlation with the seed germination rate. Seed germination rate significantly increased with storage time extended, the role of GA_3 to enhance the seed germination rate weakened. This is similar to the results of Zeng and Zhao (2001) that related to GA_3, a role on a red string seed germination. This experiment showed that when seeds are treated with different concentrations of exogenous ABA, seed germination rate decreased with the increase of ABA concentration, even when at the same time there is application of GA_3, the germination rate of seed was certain upward, but still lower than in CK. So ABA inhibited seed germination, but its inhibitory effect in a certain extent can be remission by GA_3. Wang et al. (2004) also reported the influence of ABA on the inhibition of rice seed germination results.

Conclusions

Seeds without peel had lower endogenous ABA content and the ratio of ABA/GA_3 than seeds with peel. The best GA_3 treatment time for milky ripe, wax ripe, full ripe seed were 60 min (m) or 120 m, 60 m, and 30 m, respectively. Seed germination rate, germination potential and germination index were all first increased and then decreased with increasing GA3 concentrations. The best treatment concentration of GA_3 was 100 mg L^{-1}, the turning point was 200 mg L^{-1}. The dormancy rate of low temperature storage seeds were higher than those stored in room temperature at each storage time, and both were decreased with the storage time. New seeds or stored for 1-2 months, showed significantly enhanced germination rate by exogenous GA_3. GA3 treatment had no effect on germination rate for seeds that had been stored for over 3 months. ABA inhibits the germination rate, which decreases with the increasing concentration of ABA. The most inhibitive effect, which leaded to a seed germination reduction by 37.7% and 4.0%, appeared when the concentration of ABA was 500 and 1000 mg L^{-1}. GA_3 could abate the effect which ABA inhibited seed germination.

Acknowledgements. We are grateful to the study grants from the earmarked fund for China Agriculture Research System (CARS-08-B-1). Thanks to the guidance of Laichun Guo and Chunlong Wang in the experiment, and thanks the workers in Baicheng Academy of Agricultural Sciences for their skilled technical assistant.

REFERENCES

[1] Beck, E., Ziegler, P. (1989): Biosynthesis and degradation of starch in higher plants. – Ann Rev Plant Physiol. 40: 95-117.

[2] Cheng, L., Lu, Q., Wu, B., Yin, C., Bao, Y., Gong, L. (2018): Estimation of the costs of desertification in China: a critical review. – Land Degradation & Development 29(4): 975-983.

[3] Damaris, R. N., Lin, Z., Yang, P., He, D. (2019): The Rice Alpha-Amylase, Conserved Regulator of Seed Maturation and Germination. – International Journal of Molecular Sciences 20(2): 450.

[4] Esashi, Y. (2017): Ethylene and Seed Germination. – In: Mattoo, A. K. (ed.) The Plant Hormone Ethylene. CRC Press, Boca Raton, FL, pp. 133-157.

[5] Finch-Savage, W. E., Leubner-Metzger, G. (2006): Seed dormancy and the control of germination. – New Phytologist 171(3): 501-523.

http://www.aloki.hu ● ISSN 1589 1623 (Print) ● ISSN 1785 0037 (Online)
DOI: http://dx.doi.org/10.15666/aeer/1705_1117511189

[6] Islam, M. R., Shahidul, A. M., Eneji, A. E., Ren, C. Z., Song, W. J., Hu, Y. G. (2011): Evaluation of water-saving superabsorbent polymer for forage oat (Avena sativa L.) production in arid regions of northern China. – Journal of Food, Agriculture and Environment 9(2): 514-518.
[7] Khan, T. A., Nadeem, F., Gao, Y., Yang, Y., Wang, X., Zeng, Z., Hu, Y. (2019): A larger root system in oat (*Avena nuda* L.) is coupled with enhanced biomass accumulation and hormonal alterations under low nitrogen. – Applied Ecology and Environmental Research 17(2): 4631-4653.
[8] Li, M., Hu, Y. G., Zeng, Z. H., Ren, C. Z., Mao, N., Song, W. J., Jia, P. F. (2009): Wind tunnel experiment on anti-wind erosion capacity of four crop stubbles in Horqin sandy land. – Chinese Agricultural Science Bulletin 11: 254-258 (in Chinese).
[9] Lin, Y. C., Zeng, Z. H., Ren, C. Z., Guo, L. C, Wang, C. L., Hlatshwayo, P., Hu, Y. G. (2012): Effects of different soil moisture regimes on gas exchange in response to light, growth and biomass in naked oat (Avena nuda L.) – Journal of Food, Agriculture and Environment 10(3-4): 1473-1478.
[10] Liu, X., Hu, P., Huang, M., Tang, Y., Li, Y., Li, L., Hou, X. (2016): The NF-YC–RGL2 module integrates GA and ABA signalling to regulate seed germination in Arabidopsis. – Nature Communications 7: 12768.
[11] Lou, Y. L., Feng, Z. H. (1995): Lixia River region of Jiangsu Province of wheat following rice field oats the summering law research. – Jiangsu Journal of Agricultural Sciences 11: 25-29 (in Chinese).
[12] Mukhtar, F. B., Singh, B. B. (2006): Influence of photoperiod and gibberellic acid (GA3) on the growth and flowering of cowpea (Vigna unguiculata (L.) Walp). – Journal of Food, Agriculture and Environment 4(2): 201-203.
[13] Ozkaya, O., Dundar, O., Kuden, A. (2006): Effect of preharvest gibberellic acid treatments on postharvest quality of sweet cherry. – Journal of Food, Agriculture and Environment 4(1): 189-191.
[14] Qian, X., Zang, H., Xu, H., Hu, Y., Ren, C., Guo, L., ... Zeng, Z. (2018): Relay strip intercropping of oat with maize, sunflower and mung bean in semi-arid regions of Northeast China: Yield advantages and economic benefits. – Field Crops Research 223: 33-40.
[15] Rabiei, E., Khodambashi, M., Pirbalouti, G. (2012): The study of the drought tolerance indices of oat (Avena sativa L.). – Journal of Food, Agriculture and Environment 10(2): 646-648.
[16] Ren, C. Z., Ma, B. L., Burrows, V., Zhou, J., Hu, Y. G., Guo, L., Wei, L., Sha, L., Deng, L. (2007): Evaluation of early mature naked oat varieties as a summer-seeded crop in dryland northern climate regions. – Field Crops Research 103: 248-254.
[17] Wang, X., Tao, L. X., Huang, X. L. (2004): Physiological mechanisms of exogenous ABA inhibition of germination of rice seeds. – Acta Agronomica Sinica 30: 1250-1253 (in Chinese).
[18] Wilkinson, S., Davies, W. J. (2010): Ozone ABA and ethylene: new insights from cell to plant to community. – Plant Cell Environ 33: 510-525.
[19] Yu, Y., Zhen, S., Wang, S., Wang, Y., Cao, H., Zhang, Y., ... Yan, Y. (2016): Comparative transcriptome analysis of wheat embryo and endosperm responses to ABA and H 2 O 2 stresses during seed germination. – BMC Genomics 17(1): 97.
[20] Zang, H., Qian, X., Wen, Y., Hu, Y., Ren, C., Zeng, Z., ... Wang, C. (2018): Contrasting carbon and nitrogen rhizodeposition patterns of soya bean (Glycine max L.) and oat (Avena nuda L.). – European Journal of Soil Science 69(4): 625-633.
[21] Zeng, L., Zhao, L. J. (2001): Effects of GA3 and ABA on seed development and germination of Salvia splendens. – Journal of Shanghai Jiaotong University (Agricultural Science) 4: 276-279 (in Chinese).
[22] Zhang, Q., Van Wijk, R., Shahbaz, M., Roels, W., Schooten, B. V., Vermeer, J. E., Laha, D. (2017): Arabidopsis phospholipase C3 is involved in lateral root initiation and ABA

http://www.aloki.hu ● ISSN 1589 1623 (Print) ● ISSN 1785 0037 (Online)
DOI: http://dx.doi.org/10.15666/aeer/1705_1117511189

responses in seed germination and stomatal closure. – Plant and Cell Physiology 59(3): 469-486.

APPENDIX

Table A1. *The summary of all experiments and treatments evaluated in present study*

Experiment	Treatment
a	Factor 1 (Seed maturity): S1 = milky ripe, S2 = wax ripe, and S3 = full ripe Factor 2 (GA_3 treat time): T1 = 0, T2 = 30, T3 = 60, T4 = 120, and T5 = 240 min
b	Factor 1 (GA_3 concentration): A1 = 0, A2 = 12.5, A3 = 25, A4 = 50, A5 = 100, and A6 = 200 mg L^{-1}
c	B1 = seeds with peel, B2 = seeds without peel, B3 = seeds with peel, soaked in GA3 for 2 h, and B4 = seeds without peel, soaked in GA3 for 2 h
d	Factor 1 (Seed maturity): S1 = milky ripe, S2 = wax ripe, and S3 = full ripe Factor 2 (Seed storage time): C1 = 0, C2 = 1, C3 = 2, C4 = 3, and C5 = 4 month
e	D1 = 1000 mg L^{-1} ABA; D2 = 500 mg L^{-1} ABA; D3 = 250 mg L^{-1} ABA; D4 = 100 mg L^{-1} ABA; D5 = 100 mg L^{-1} GA3 + 100 mg L^{-1} ABA; D6 = 100 mg L^{-1} GA3 + 250 mg L^{-1} ABA; D7 = 100 mg L^{-1} GA3 + 500 mg L^{-1} ABA; D8 = 100 mg L^{-1} GA3 + 1000 mg L^{-1} ABA; CK use distilled water as control

http://www.aloki.hu ● ISSN 1589 1623 (Print) ● ISSN 1785 0037 (Online)
DOI: http://dx.doi.org/10.15666/aeer/1705_1117511189

GENE FLOW FROM MAJOR GENETICALLY MODIFIED CROPS AND STRATEGIES FOR CONTAINMENT AND MITIGATION OF TRANSGENE ESCAPE: A REVIEW

RIZWAN, M.[1] – HUSSAIN, M.[2] – SHIMELIS, H.[3*] – HAMEED, M. U.[4] – ATIF, R. M.[5] – AZHAR, M. T.[5,6] – QAMAR, Z.[2] – ASIF, M.[6]

[1]*Nuclear Institute of Agriculture, Tandojam (Sindh), Pakistan*

[2]*Nuclear Institute for Agriculture and Biology, Faisalabad, Pakistan*

[3]*School of Agricultural, Earth and Environmental Sciences, African Centre for Crop Improvement, University of KwaZulu-Natal, Pietermaritzburg, South Africa*

[4]*National Agricultural Research Center, Islamabad, Pakistan*

[5]*Department of Plant Breeding and Genetics, University of Agriculture, Faisalabad, Pakistan*

[6]*School of Biological Sciences M084, The University of Western Australia, Crawley, Australia*

[7]*National Institute for Biotechnology and Genetic Engineering, Faisalabad, Pakistan*

**Corresponding author*
e-mail: shimelish@ukzn.ac.za

(Received 27th Mar 2019; accepted 19th Jun 2019)

Abstract. Recent advancements in biotechnology resulted in rapid adoption of genetically modified (GM) crops in the agriculture systems. At the same time, transgene escape has also been reported and examples reveal global dimension of the problem. Pollen mediated gene flow (PMGF) is the major pathway for transgene escape. Almost all transgenes have been escaped into their Non-GM counterpart and wild relatives. Although gene flow varies between species, crops, and ecological zones/environments but intraspecific gene flow (> 10%) is not uncommon in adjacent populations. Whereas in outcrossing species, 1% gene flow at thousand meters' isolation is not unusual, and magnitude is even higher than the mutation rate. It is well documented that transgene flow is deteriorating different production systems in agriculture and famers choice to cultivate GM, conventional and organic crops. If comprehensive policy is not implemented, then in future it will be difficult to detect and remove transgenes from the environment; if unexpected problems arise.
Keywords: *biosafety, biological containment, coexistence, genetic contamination, out-crossing, pollen dispersal, transgene flow*

Introduction

Gene flow, a natural phenomenon, changes the gene frequency in population due to outcrossing of gametes, movement of individuals across countries or groups from one place to another (Goodman and Newell, 1985; Ellstrand, 2003; Cerdeira and Duke, 2006). In the current scenario of agriculture, where 189.8 million ha of GM crops were planted in 2017 with global market value of US$ 17.2 billion (ISAAA, 2017), coexistence and identity preservation among transgenic and non-transgenic cropping systems at the field level are becoming important issues (Beckie and Hall, 2008). Concerns have been identified and raised about GM plants in new environmental conditions and in response to transgene escape into wild relatives and crop to crop has

http://www.aloki.hu ● ISSN 1589 1623 (Print) ● ISSN 1785 0037 (Online)
DOI: http://dx.doi.org/10.15666/aeer/1705_1119111208

gained much attention of plant biologists. It is not uncommon for transgenic plants to mate with their wild relatives. Spontaneous hybridization will occur among transgenic and non-transgenic plants unless the proper distances are maintained, and also the engineered plants are specifically designed to limit gene flow (Gressel, 1999; Daniell, 2002). It is not necessary that gene flow creates problem but it may enhance local genetic diversity and in part it depends on the phenotypes conferred by transgenes (Ellstrand and Hoffman, 1990; Ellstrand, 2003). Outcrossing poses negative impacts in terms of contamination in non-transgenic crops but again problem depends on new allele whether causes an increase in transgene escape or not. According to Kareiva and Marvier (2000), gene flow varies between species, within species of same crop, populations, genotypes and environments. Surprisingly, intraspecific gene flow occurs at high rate. Gene flow of more than 10% is not uncommon in adjacent populations. For outcrossing species, 1% gene flow at thousand meters isolation is not unusual and the magnitude is higher than the rate of mutation (Ellstrand, 2014). Further, adventitious mixing of GM and non-GM crops also raises the question about maintenance of different production systems in agriculture sector and famers choice to grow either GM, conventional or organic crops. Various measures have been proposed to minimize transgene escape, such as the use of refuge surrounding the GM crop in the field with barren zones, genetic methods to handicap the fitness of transgenic hybrid (Gressel, 1999; Daniell, 2002). Monitoring transgene escape has been initiated to measure the adverse impact on environment (NRC, 2002). The impact of gene flow is so high that even single gene can contaminate the population, so it is difficult to establish an effective monitoring programme (Marvier et al., 1999). This review describes the facts and thoughts behind transgene escape, sources and level of contamination in major crops, containment and mitigation strategies, their comparison, conclusion and future prospects.

Transgene escape: facts and speculations

Transgene escape is a fact and usually restricted to within species or closely related species and this is referred to as vertical gene flow. It is very rare that gene flow occurs between species, i.e. horizontal gene flow. In contrary, diagonal gene flow occurs between closely related species (Gressel, 2015). With these concerns, the genetically engineered (GE) crops have been cultivated for commercial and research purposes under some restrictions to avoid transgene escape. But after 22 years of GE crops, we failed to control gene flow in a systematic manner (Ryffel, 2014).

Convincing evidences of transgene escape have been found in cotton, maize, soybean, oilseed rape, rice, and wheat (Baltazar et al., 2015; Dong et al., 2016; Londo et al., 2011; Mizuguti et al., 2010; Ramzan et al., 2014; Serrat et al., 2013), and describes that transgene escape (*Table 1*). Transgene may not only flow in area bordering the GM field but may also happen far away. These findings are not limited to a certain region of the world instead the examples reveals global dimension of the problem. Hybridization of GM plants with their conventional parents and adventitious presence of seed has been observed as expected.

Cotton is an illustrative example, where gene flow both vertical and diagonal has been documented in several studies (*Table 1*). Transgenes in *Gossypium hirsutum* conferring insect and herbicide resistance have been escaped through pollen to conventional counterparts, *G. barbadense,* refugees and wild relatives (Heuberger et al.,

http://www.aloki.hu ● ISSN 1589 1623 (Print) ● ISSN 1785 0037 (Online)
DOI: http://dx.doi.org/10.15666/aeer/1705_1119111208

2010). Similarly, PMGF has been reported from GE maize. Similar case is reported in Mexico, where GM corn was not allowed for commercial cultivation but transgene escape was found in landraces (Mercer and Wainright, 2008). Initially these findings were controversial but dies, good evidences for the escape of transgenes were found through comprehensive experimentations (Mercer and Wainright, 2008).

Another example is from oilseed rape, in which glyphosate resistance was found in field grown glufosinate resistant oilseed rape. The fact that in several cases stacked events that were not engineered in the laboratory identified in the field. This showed the rapidity of recombining genes between varieties of an outcrossing species (*Table 1*). In case of wheat, many studies on escape of herbicide resistance genes have been documented as a part of literature. This escape is independent off whether the resistance is created by mutagenesis or transgenic. Therefore, the risk assessment should be based on the biology of a field crop, the traits, occurrence of compatible relatives and transformation method, i.e. classical breeding or genetic engineering used for trait integration.

Table 1. *Some evidences of natural transgene escape in different crops*

From	To	Transgene escaped	Trait	Type of flow	Medium of escape	Region	Reference
Cotton *Gossypium hirsutum*	Non-*Bt.* cotton	MON-531, Cry1Ac, Cry2A	Insect resistance	Vertical	Pollen and seed	Pakistan	Ramzan et al. (2014)
	Gossypium barbadense	EPSPS	Herbicide resistance	Diagonal	Pollen	USA	Van Deynze et al. (2011)
	Refuges of non-Bt cotton	Cry1Ac	Insect resistance	Vertical	Pollen and adventitious presence of seed	Arizona USA, Tolima Colombia	Heuberger et al. (2010), Rache et al. (2013)
	Non-*Bt.* cotton	Cry1Ac and CP4 EPSPS	Insect and herbicide resistance	Vertical	Pollen	Beijing China	Yan et al. (2015)
	Wild populations	Cry1Ab/Ac, Cry2A, CP4-EPSPS and PAT/ Bar	Insect and herbicide resistance	Diagonal	Pollen	Mexico	Wegier et al. (2011)
Maize *Zea mays*	Non-GM maize	MON-810	Insect resistance	Vertical	Pollen	Slovakia, Spain	Mihalčík et al. (2012), Pla et al. (2006)
	Non-GM maize	PAT, CDC2	Herbicide tolerance	Vertical	Pollen	UK	Weekes et al. (2007)
	Non-GM maize	MON-89Ø34-3, MON-88Ø17-3, MON-ØØ6Ø3-6	Insect resistance and herbicide tolerance	Vertical	Pollen	Mexico	Baltazar et al. (2015)
	Landraces	Cry1Ab/Ac, Cry9C, CP4-EPSPS	Insect and herbicide resistance	Diagonal	Pollen	Mexico	Mercer and Wainwright (2008)
Soybean *Glycine max*	Conventional soybean	EPSPS	Herbicide resistance	Vertical	Outcrossing by honeybees	Brazil	Abud et al. (2007), Chiari et al. (2011)
	Conventional soybean	EPSPS	Glyphosate tolerance	Vertical	Pollen	Japan	Yoshimura et al. (2006)
	Glycine soja	EPSPS	Glyphosate tolerance	Diagonal	Pollen	Japan	Mizuguti et al. (2010)
Oilseed rape *Brassica napus*	*B. juncea, B. carinata*	EPSP	Glyphosate resistance	Diagonal	Pollen	Canada	Song et al. (2009), Seguin-Swartz et al. (2013)
	B. juncea	EPSP, bar	Herbicide resistance	Diagonal	Pollen	China	Song et al. (2010)

http://www.aloki.hu ● ISSN 1589 1623 (Print) ● ISSN 1785 0037 (Online)
DOI: http://dx.doi.org/10.15666/aeer/1705_1119111208

	B. juncea	BtCry1Ac	Insect resistance	Diagonal	Pollen	Japan	Lei et al. (2011)
	Non-GM oilseed rape	Bar	Glufosinate resistance	Vertical	Pollen mediated	China	Cai et al. (2008)
	B. rapa *B. nigra*	CP4EPSPS, Cry1Ac	Insect and herbicide resistance	Diagonal	Glyphosate drift and selection pressure	USA	Londo et al. (2011)
Wheat *Triticum aestivum*	*Aegilops biuncialis*	Single major gene	Difenzoquat resistance	Diagonal	Hybridization	Spain	Loureiro et al. (2009)
	Aegilops cylindrica	Pch1	Disease resistance	Diagonal	Hybridization	USA	Perez- Jones et al. (2006)
	Aegilops cylindrica	ALS	Imidazolinone resistance	Diagonal	Pollen	North America	Gaines et al. (2008), Gandhi et al. (2006), Rehman et al. (2010)
	Dwarf male sterile line	Nib8	Wheat yellow mosaic virus resistance	Vertical	Pollination by wind	China	Dong et al. (2016)
	Non GM wheat	Bar and gfp	Herbicide resistance	Vertical	Pollen	Russia	Miroshnichenko et al. (2016)
Rice *Oryza sativa*	Weedy rice	ALS	Imidazolinone resistance	Vertical	Pollen	USA	Valverde (2013), Gealy (2005), Shivrain et al. (2009)
	Weedy rice	CpTI and Bt/CpT	Insect resistance	Vertical	Pollen	China	Cao et al. (2009)
	O. rufipogon	Bar	Herbicide resistance	Diagonal	Pollen	China	Wang et al. (2006)
	O. sativa F. spontanea	Bar	Herbicide resistance	Diagonal	Cross pollination	Spain	Serrat et al. (2013)

Genetically modified crops and gene flow

Cotton

Cotton is first genetically engineered crop which was commercially introduced in 1996. It is primarily a self-pollinated crop but 5-30% outcrossing may occur due to pollinators (Poehlman, 2013). Its pollen is large and sticky which makes pollinators potentially important in cross pollination (Van Deynze et al., 2005). Due to often cross pollination GM cotton is continuously contaminating its non-GM germplasm which have superior yield and fiber quality traits required for farmer and industrialist. This threatens the use of refugees and complicates the removal of transgene from the environment if unexpected problems arise. Many studies on the level of contamination in cotton are documented. In a recent study, Ramzan et al. (2014) reported highest rate of contamination (22% from Bt samples and 20% from non-Bt) from Faisalabad, the city of Pakistan where previously cotton was the major commercially grown crop. Heuberger et al. (2010) identified the potential sources of Bt contamination and demonstrated that out crossing (due to abundance of honeybees), proximity to Bt fields and human factors contribute to seed contamination in cotton. Therefore, it is necessary for cotton breeders to screen their breeding material thoroughly for the removal of genetic contamination from non-Bt. Cotton germplasm for the development of non-Bt strains in future.

Maize

In maize, gene flow occurs between all sexually compatible plant types, i.e. commercial hybrids, landraces and eventual wild relatives (Baltazar et al., 2015). The

http://www.aloki.hu ● ISSN 1589 1623 (Print) ● ISSN 1785 0037 (Online)
DOI: http://dx.doi.org/10.15666/aeer/1705_1119111208

driving sources behind transgene flow are pollen transfer between hybrids of different transgene controlling certain traits, cultivator determined seed selection and mixing. But both traits are affected by farmer's practices and agroecological circumstances.

The cultivation of open-pollinated varieties (OPVs) along with commercial hybrids also increase rate of gene flow (Sanvido et al., 2008). The synchronization of flowering in GM maize and its non-GM is important to determine the potential of pollens for gene flow by cross-hybridization (Palaudelmas et al., 2008). The role of seeds as an additional source for gene flow in maize must not be underestimated (Dyer et al., 2009). Farmers share and recycle maize seeds which increases gene flow locally but also increases the distance that transgene travel. Seed saving and sharing need to be analyzed along with PMGF to understand that what happens from local to regional, national and transnational levels, over time.

Soybean

Weeds are the major problem in soybean cultivation. To control plague a foreign gene CP4 was introduced to develop herbicide resistant soybean. Transgene flow becomes a major problem because the farmers prefer to grow conventional soybean. Cultivation of GM soybean has been increased many fold due to the introduction of glyphosate resistant soybean (Yoshimura et al., 2006). Due to more availability of transgenic cultivars, the contamination of conventional cultivars and unintended combination of transgenes through natural crossing is becoming a serious threat. Ray et al. (2003) reported 0.65 to 6.32% natural cross pollination in soybean in different experiments and highlighted the potential for transgene flow. Cross pollination in soybean is more likely facilitated by insects (Rust et al., 1980), since soybeans are predominantly self-pollinating and the flowers have anatomical features of entomophilous plant species (Erickson and Garment, 1979).

Oilseed rape

Oilseed rape (*Brassica napus* L.) has been genetically modified to tolerate broad spectrum herbicides. Due to its ability of producing large amount of pollen, it is an ideal crop to understand the implications of transgene flow. Oilseed rape is known to exhibit different levels of outcrossing. It is partially pollinated by honeybees and bumble bees and is also known to release large amounts of air-borne pollen. Timmons et al. (1995) demonstrated that cross-pollination in oilseed could vary from 5 to 55%. There are number of factors which control PMGF that includes flowering synchrony, mode of pollen dispersal (wind and insect), area density of donor, recipient plants and physical distance (Campbell, 1985).

Wheat

PMGF is main mode of transgene flow in wheat flower for disseminating transferred alien genes (Song et al., 2004). The gene flow in wheat usually occurs over very short distances and at extremely low frequencies, but measures should be taken to avoid contamination of non-GM wheat. In wheat, average cross-pollination rate is 1-2% in close proximity (Gustafson et al., 2005). Loureiro et al. (2007) demonstrated high rates of cross pollination (37 to 56%) by using emasculated wheat as pollen receptor at 0 m distance between two cultivars of *Triticum aestivum*. In another study, Loureiro et al. (2012) investigated that PMGF in transgenic wheat using three conventional wheat

http://www.aloki.hu ● ISSN 1589 1623 (Print) ● ISSN 1785 0037 (Online)
DOI: http://dx.doi.org/10.15666/aeer/1705_1119111208

species and found a maximum outcrossing of 3.5%. Currently there are no commercial GM wheat varieties but extensive research is being carried out for the development of herbicide resistance either through genetic engineering or mutagenesis. Therefore, the concern is that once transgenic is commercially released there is potential for gene flow from GM to Non-GM wheats. So, the effective methods like isolation distances or containment and mitigation strategies should be opted for preventing outcrossing and contamination between compatible genotypes.

Rice

Rice is highly self-pollinated crop but pollen mediated outcrossing occurs when flowering period of various cultivars get synchronized and/or grown in close vicinity, but frequency of gene flow is very low (< 1.0%). Previous studies found that GM rice may hybridize with traditional cultivars (Rong et al., 2005; Yuan et al., 2007), weedy rice (Chen et al., 2004; Zhang et al., 2006; Olguin et al., 2009), and wild rice (Chen et al., 2004; Yao et al., 2008). Transgene flow from GM rice to other cultivars and weedy relatives is a major risk associated with commercial release (Messeguer, 2003). Development of GM rice varieties for having various traits like herbicide tolerance (bar and EPSPs), disease resistance (Xa21) and insect resistance (Bt and CpTI genes) are in pipeline for commercialization (Xia et al., 2011; Parisi et al., 2016). These developments warn the researchers to prioritize the studies related to risk associated with transgene flow from GM to non-GM rice.

Transgene containment and mitigation strategies

While dealing with trans-gene flow one should keep in view the situations according to transgenic crops. The research work on risk assessment during gene escape can be a useful aspect while countering gene flow (Chapman and Burke, 2006). In general, there are two approaches; either we can keep the gene in original GMO or can mitigate the effects (Gressel and Al-Ahmad, 2006). The possible containment and mitigation strategies are discussed here and their comparison on the basis of positive and negative aspects is given in *Table 2*.

Transgene containment strategies

Physical containment

Usually gene flow occurs through pollen or seed, so one way to contain transgene can be preventing seeds and pollen dispersal (Linder et al., 1998). This dispersal can be prevented using isolation of GM crop by using various physical barriers in addition to careful processing of seed (Arriola, 1997). Researchers have found effective solution by using pollen barriers, stopping insect flow in crops and physical isolation. Staniland et al. (2000) limited the out-crossing up to 0.015% complimenting the results of Morris et al. (1994) where out-crossing was reduced to 0.94% in two different experiments. All of this sounds very convincing when used in experiments but when we look at ground realities different shocking cases are reported like, scientists have found traces of trans-genes in seeds from non-experimental area. Landraces of maize (*Zea maize*) in Mexico was found with tarns-genes despite of fact that GM corn was not allowed to cultivate in the country (Ortiz-Garcia et al., 2005). Similarly glyphosate resistance was found in

http://www.aloki.hu ● ISSN 1589 1623 (Print) ● ISSN 1785 0037 (Online)
DOI: http://dx.doi.org/10.15666/aeer/1705_1119111208

cultivars of *B. napus* grown in Canada, a year before cultivation of GM brassica was allowed to plant (Hall et al., 2000). A non-GM crop was found with trans-genes, this crop was cultivated (at long enough distance to reduce pollen contamination) after a GM crop carrying gene for a pharmaceutical product on a field of registered company following all the rules for isolation (Fox, 2003). More alarming situation will be faced when most of world crops will be transgenic and isolation will not be possible (Rieger et al., 2002). These situations can be addressed by more careful processing and transportation of seed from GM crops plants, isolation of cultivars having sophisticated genes with more sensitive markers.

Table 2. *Comparison of different transgene flow countermeasures for their positive and negative aspects*

Countering technique	Positive aspects	Doubts	References
Physical containments	• Easy and simple to use • Economical • Easily useable to all crops	• Not been able to contain transgene completely • It is almost impossible to stop flow through seed based products	Arriola (1997), Linder et al. (1998)
Biological/molecular containments			
Sterility	• Gain great results using complete sterility	• Male sterility fount to be leaky as it can serve as female parent • For complete sterility vegetative propagation is necessary so not possible in all crops • Farmer will not be able to produce own seed causing monopoly of seed companies	Daniell (2002), Schernthaner et al. (2003)
Clistogamy	• Biological control without use of any danger to gene pool	• Can cause inbreeding depression • Difficult to use in all crops • Some leakage has been observed	Husken et al. (2010), Gealy (2005)
Apomixes	• Good for fixing heterosis	• Difficult to attain • Can cause dispersal through pollen if not complemented by sterility	Bicknell and Kultunow (2004), Bhat et al. (2005)
Maternal transformation	• Can effectively hinders the dispersal through pollen • If complemented with female sterility it can be a good option	• Not possible in all crops due to biparental inheritance • Backcrossing of hybrid with GM crop can disperse the trait	Maliga (2004), Haider et al. (2009)
Incompatible genome	• No extra labor is required	• Can only possible in crops having multiple genomes • Compatibility with homologous genomes have been reported	Lu (2003)
Gene splitting	• It can be effective if complimented with other techniques	• Gene splitting alone can cause up to 25% gene flow in segregating generation	Dong et al. (2015), Wang et al. (2014)
Expression in virus	• Alone can contain transgene flow effectively	• Transgene will be good only for single generation	Kelloniemi et al. (2008)
GURTs	• Sound effective technique	• No evaluation yet • Issues regarding monopoly of seed companies	Swanson and Goschl (2000)
Transgenic mitigation	• It disable transgene irrespective of flow • Found good results in evaluating TM	• If transgene is not removed it can restore expression at any stage • Very minute quantity of transgene flow is still there it can slow down the process but cannot completely shut it down • Different blocking genes used can be a novel threat to biosafety	Gressel and Al-Ahmad (2006), Kuvshinov et al. (2001), Saurabh et al. (2014)

http://www.aloki.hu ● ISSN 1589 1623 (Print) ● ISSN 1785 0037 (Online)
DOI: http://dx.doi.org/10.15666/aeer/1705_1119111208

Biological and molecular containment

This sort of containment utilizes genetic manipulation to create plants with less ability to disperse transgenes usually by interference in pollination and fertilization process (Moon et al., 2011). There are different processes which are implemented to contain transgene biologically. In the following sections it is tried to explain basic principle and examples of different mechanisms.

Sterility

Most of the times transgene flow occurs through pollens so implying the trait of male sterility can cordially reduce the problem (Daniell, 2002). This system is incorporated in cytoplasmic DNA and can be restored by environmental stimuli or restorer genes in nuclear DNA (Schnable and Wise, 1998). This technology is seemed to be less viable as it is reported that in field male sterile plants are not fully sterile. In addition, if male sterile plant is used as female parent it can recover transgenic trait as a result of backcrossing (Daniell, 2002).

Another technique seems more convincing and viable if compared with male sterility, it utilizes sterility of both the sex in plants and they can still produce viable seed (Seed sterility) this process imply the use of different deleterious genes which can only trigger under specific conditions/stimuli, i.e. temporal or site specific promoters (only express in gametes) or any chemical reaction (Ryffel, 2014). Schernthaner et al. (2003) proposed a technique to produce sterile seed; they used lethal genes (lethal for seed fertility) and these are closely linked with gene of interest along with repressing genes on homologous chromosome on same loci. After hybridization the repressor gene will segregate from combo of transgene and lethal gene will cause death of plant due to having trans-gene that will lead to counter trans-gene flow.

Cleistogamy

Cleistogamy is a modification of flower structure to promote self-pollination but it avoids outcrossing in barley, soybean and rice, and is effective mean against transgene flow (Husken et al., 2010). Cleistogamy can be induced by mutations or genetic engineering. In addition, various genes have been identified, i.e. OsMADS 2, OsMADS 1, OsMADS 3 and SUPERWOMAN 1 (SPW 1) in rice (Lee et al., 2003; Xiao et al., 2003; Prasad et al., 2005; Yadav et al., 2007), and Cly1 and Cly2 genes in barley (Wang et al., 2013). But most of these genes cause sterility due to interaction with reproductive parts of flower (Agarwal et al., 2007). Out-crossing was restricted to 2-6% by transformation of these genes but sterility was in question (Gealy, 2005). To restore the fertility, a mutant of SUPERWOMAN 1 named SPW 1^{145T} was discovered (Yoshida et al., 2007).

Apomixes

The use of apomixes is most successful method to stop trans-gene flow and this is also modification in floral structure that can be propagated by asexual means (Gressel, 2015; Kwit et al., 2011). Some of crops like banana, potato and sugarcane are naturally asexually propagated but introduction of this trait in other crop plants is tedious and time consuming work without effecting the seed production and this mechanism has also a property for fixing the hybrid vigor (Bicknell and Kultunow, 2004). Different

http://www.aloki.hu ● ISSN 1589 1623 (Print) ● ISSN 1785 0037 (Online)
DOI: http://dx.doi.org/10.15666/aeer/1705_1119111208

techniques can be utilized for this purpose like apomixes, parthenogenesis and manipulating ploidy levels. As study goes on asexual reproduction it is taken that most easy and frequently considered way is using apomictic traits (Gressel, 2015; Ryffel, 2014). Apomictic plants produce seed without undergoing meiosis, but in combination with male sterility can be a more effective method for containment of unwanted gene flow (Bhat et al., 2005). According to an estimate about 400 plant species and 40 families reproduce through apomixes (Carman, 1997). So this trait can be used widely because 40 representative families are available as reference. The over-expression of various genes (*OsLEC1* and *OsLEC2)* enhances production of apomictic embryo. The gene namely *SERK* and *OsAPOSTART* are found responsible for apomixes induction in *P. pratensis* (Albertini et al., 2005). Use of apomixes as a containment strategy has been proven in GM-bahia grass where transgene flow was limited to only 0.2% (Sandhu et al., 2010).

Maternal effects

One of the few techniques for containing unwanted gene flow can be transformation of genes controlling economically important gene in plastids and mitochondria (Maliga, 2004). This method can be useful in decreasing the frequency of transgene flow but cannot be effective in traits where complete leakage is found (Gressel and Al-Ahmad, 2006). As crossing is a two way process so GM crop can also serve as female parent so with backcrossing hybrids can recover the transgene and spread it (Stewart et al., 2003). An additional problem is that some species like brassica share cytoplasm along with nucleus during meiosis (Haider et al., 2009). Some research works revealed that there is 0.4% introgression of transgene occur while using this technique (Avni and Edelman, 1991). Another experiment showed that pollens transmit cytoplasmic traits in 3×10^{-4} hybrids out of 780000 (Wang et al., 2004). Ruf et al. (2007) showed in an experiment that transmission was 1.58×10^{-5}. This small leakage can be further controlled by complimenting this trait with female sterility.

Incompatible genome

One possible option against gene flow is to incorporate the transgene in such a way that its probability to disperse through gamete is at minimum value. Some crops like wheat contain different genomes (Werner et al., 1992). By targeting the genome which is less compatible to wild and weedy relatives to incorporate the transgene will make fairly less chance for gene to escape (Lu, 2003). This technique has some practical problems; firstly it does not work for all the crops, secondly there have been reports for partial compatibility of homologous genomes (Knott et al., 1989; Snow, 2002). This partial compatibility can play role for unintended gene flow.

Gene splitting

Hirata et al. (1990) discovered a genetic structure called as intein which are capable of protein *trans*-splicing, it can combine two different DNA sequences in shape of a single protein and splice out of mature protein. Dong et al. (2015) proposed a containment strategy taking intein as major working agents, they proposed to split the gene of interest into two different sequences and place far away in genome and combine them with inteins, as far away sequences have more chances to segregate during meiosis and named it as gene splitting. Wang et al. (2014) practically perform this phenomenon

http://www.aloki.hu ● ISSN 1589 1623 (Print) ● ISSN 1785 0037 (Online)
DOI: http://dx.doi.org/10.15666/aeer/1705_1119111208

to produce GM tobacco. This technique showed no signs of transgenes into F_1 population but backcross population showed 25% plants with trans-gene.

Expression in virus

Another technique can be to use virus mediated expression of beneficial trait using shuttle vector. Successful expression has been observed using this technique (Kelloniemi et al., 2008). By this gene can be limited to virus and danger of dispersal will be minimum but problem with this technique is making transgenic every year will increase cost of seed production as GM will remain good for just a single generation (Gressel, 2015).

Genetic use restriction technology (GURT)

GURT or "terminator technology" is also one way to preventing transgene flow. This technology was developed by multinational companies to protect intellectual property rights (Swanson and Goschl, 2000). GURT can be categorize into variety based (V-GURT) and trait based (T-GURT) (Van-Acker et al., 2007). V-GURT works on principle of seed sterility while T-GURT works on limiting the exposure of a specific trait to other crops. V-GURT was found more effective as compared to T-GURT (Goeschl and Swanson, 2003). Lin et al. (2008) used RNAi mechanism to contain herbicide resistant gene in rice. RNAi gene was closely linked to glyphosate resistance gene (gene of interest) to avoid crossing over during meosis, the RNAi gene was used to silence a gene which confer resistance to another herbicide, bentazone so GM rice was resistant to glyphosate but susceptible to bentazone. By applying bentazone to following generation plants carrying escape genes were effectively abolished. Similar experiment was repeated by Liu et al. (2012) using double transgenic and found complimentary results. GURTS are more effective for transgenic with industrial products (Lee and Natesan, 2006). Major concerns about terminator technology are that it will create the monopoly of seed companies but despite that it is an effective technique (Hills et al., 2007).

Transgene mitigation strategies

Containment techniques pose a major question to counter with the problem as when they are assessed almost every technique allows a little leak (Gressel, 2015). Even a smallest leak cannot make sure the complete containment, it rather slow down the process or direct it to a single direction but ultimate results are similarly harmful even if it appears some time later, just the slightest chance to not spread trans-gene is if it have no selection advantage or unfit for spread (Ryffel, 2014). If somehow expression of transgene is limited or sequence is deleted from offspring/gamete it will be more efficient way to block unintended gene flow. Scientists have tried and still coming up with different methods to fulfill the goal, in general these techniques are termed as "transgenic mitigation (TM) techniques" (Ryffel, 2014). TM was found more efficient to deal with transgene flow for traits more beneficial to agriculture (Lee and Natesan, 2006). Gressel (1999) proposed a technique to decrease the fitness of volunteer plant by incorporation of a deleterious gene closely linked to transgene and causing negative selection pressure on volunteer plants. These genes can be for say breaking dormancy, reduce shattering and dwarfing genes. Some experiments were effectively carried out to

http://www.aloki.hu ● ISSN 1589 1623 (Print) ● ISSN 1785 0037 (Online)
DOI: http://dx.doi.org/10.15666/aeer/1705_1119111208

show the effectiveness. Al-Ahmad et al. (2004) inserted herbicide resistance gene linked with a dwarfing gene into tobacco plant. Both genes were linked close to avoid later crossing over and confirmed by PCR. Results revealed that volunteer plants and hybrids had only 17% fitness leading fewer chances for them to survive. Using same model on B. *napus* revealed only 12% fitness in the following progeny (Al-Ahmad and Gressel, 2005). Efficiency of this technique is strictly depends upon level of unfitness of trait to volunteer plants and nature of GM crops, this system can be made more effective using two or more TM genes (Gressel and Al-Ahmad, 2006). Some effectively used TM genes are; giberallic acid insensitive conferring dwarfness, abscisic acid insensitive which break seed dormancy and SHATTERPROOF confer less seed shattering (Daniell, 2002). Kuvshinov et al. (2001) described a technique named as "recoverable block of function" (can also categorize under chemical TM). They incorporate a blocking sequence and a recovering sequence along with trans-gene, recovering sequence remains active in normal conditions and stops working under chemical control. Pollen excision also works on similar principals as it excises transgene from pollen or cause complete pollen sterility by triggering RNAi mechanism. Site specific mutagenesis or recombinase is utilized for this purpose (Saurabh et al., 2014). Moon et al. (2011) use a codon optimized serine resolvase recombinase (CinH) with its recognition sites along transgene, CinH was incorporated under influence of a pollen specific promoter LAT 59 to hinder the expression of transgene into pollen and ultimately hybrids. They found less than 1% pollens expressing transgene. In additions zinc finger nucleases, TALEN, CRISPR-Cas and Ecor1 restriction endoneucleases had also found effective to deletion of transgene from pollen (Straus and Lahaye, 2013).

Conclusion

Escape of transgene from GM crop plants to non-GM and wild relatives may pose potential environment risks. Understanding of transgene escape will facilitate the sustainable and safe cultivation of GM varieties of different crops. Further, perceived food safety and identity preservation is necessary for different production systems in agriculture sector and famers choice to cultivate GM, conventional or organic crops. Therefore, to favor the GM technology, we should take into consideration the biosafety measures as well as potential techniques to contain or mitigate the transgene effect.

REFERENCES

[1] Abud, S., De Souza, P. I. M., Vianna, G. R., Leonardecz, E., Moreira, C. T., Faleiro, F. G., Júnior, J. N., Monteiro, P. M. F. O., Rech, E. L., Aragão, F. J. L. (2007): Gene flow from transgenic to non-transgenic soybean plants in the Cerrado region of Brazil. – Genetics and Molecular Research 6: 445-52.

[2] Agarwal, P., Arora, R., Ray, S., Singh, A. K., Singh, V. P., Takatsuji, H., Tyagi, A. K. (2007): Genome-wide identification of C2H2 zinc-finger gene family in rice and their phylogeny and expression analysis. – Plant Molecular Biology 65: 467-485.

[3] Al-Ahmad, H., Gressel, J. (2005): Transgene containment using cytokinin-reversible male sterility in constitutive, gibberellic acid–insensitive (Δgai) transgenic tobacco. – Journal of Plant Growth Regulation 24: 19-27.

[4] Al-Ahmad, H., Galili, S., Gressel, J. (2004): Tandem constructs to mitigate transgene persistence: tobacco as a model. – Molecular Ecology 13: 697-710.

http://www.aloki.hu ● ISSN 1589 1623 (Print) ● ISSN 1785 0037 (Online)
DOI: http://dx.doi.org/10.15666/aeer/1705_1119111208

[5] Albertini, E., Marconi, G., Reale, L., Barcaccia, G., Porceddu, A., Ferranti, F., Falcinelli, M. (2005): SERK and APOSTART. Candidate genes for apomixis in Poa pratensis. – Plant Physiology 138: 2185-2199.
[6] Arriola, P. E. (1997): Risks of escape and spread of engineered genes from transgenic crops to wild relatives. – AgBiotech News and Information 9: 157-160.
[7] Avni, A., Edelman, M. (1991): Direct selection for paternal inheritance of chloroplasts in sexual progeny of Nicotiana. – Molecular and General Genetics 225: 273-277.
[8] Baltazar, B. M., Castro, E. L., Espinoza, B. A., de la Fuente, M. J. M., Garzón, T. J. A., González, G. J. (2015): Pollen-mediated gene flow in maize: implications for isolation requirements and coexistence in Mexico, the center of origin of Maize. – PLoS ONE 10(7): e0131549. DOI: 10.1371/journal.pone.0131549.
[9] Beckie, H. J., Hall, L. M. (2008): Simple to complex: modelling crop pollen-mediated gene flow. – Plant Science 175: 615-628.
[10] Bhat, V., Dwivedi, K. K., Khurana, J. P., Sopory, S. K. (2005): Apomixis: an enigma with potential applications. – Current Science - Bangalore 89: 1879.
[11] Bicknell, R. A., Koltunow, A. M. (2004): Understanding apomixis: recent advances and remaining conundrums. – The Plant Cell 16(suppl 1): S228-S245.
[12] Cai, L., Zhou, B., Guo, X., Dong, C., Hu, X., Hou, M., Liu, S. (2008): Pollen-mediated gene flow in Chinese commercial fields of glufosinate-resistant canola (*Brassica napus*). – Chinese Science Bulletin 53: 2333-2341.
[13] Campbell, D. R. (1985): Pollen and gene dispersal: the influence of competition for pollination. – Evolution 39: 418-431.
[14] Cao, Q. J., Xia, H., Yang, X., Lu, B. R. (2009): Performance of hybrids between weedy rice and insect-resistant transgenic rice under field experiments: implication for environmental biosafety assessment. – Journal of Integrated Plant Biology 51: 1138-1148.
[15] Carman, J. G. (1997): Asynchronous expression of duplicate genes in angiosperms may cause apomixis, bispory, tetraspory, and polyembryony. – Biological Journal of the Linnean Society 61: 51-94.
[16] Cerdeira, A. L., Duke, S. O. (2006): The current status and environmental impacts of glyphosate–resistant crops: a review. – Journal of Environment Quality 35: 1633-1658.
[17] Chapman, M. A., Burke, J. M. (2006): Letting the gene out of the bottle: the population genetics of genetically modified crops. – New Phytologist 170(3): 429-443.
[18] Chen, L. J., Lee, D. S., Song, Z. P., Suh, H. S., Lu, B. R. (2004): Gene flow from cultivated rice (*Oryza sativa*) to its weedy and wild relatives. – Annals of Botany 93: 67-73.
[19] Chiari, W. C., Ruvolo-Takasusuki, M. C. C., Chambó, E. D., Arias, C. A., Hoffmann-Campo, C. B., Toledo, V. A. A. (2011): Gene Flow between Conventional and Transgenic Soybean Pollinated by Honeybees. – In: Hasaneen, M. N. (ed.) Herbicides: Mechanisms and Mode of Action. InTech, Rijeka, Croatia, pp. 137-152.
[20] Daniell, H. R. (2002): Molecular strategies for gene containment in transgenic crops. – Nature Biotechnology 20: 581-586.
[21] Dong, S., Liu, Y., Yu, C., Zhang, Z., Chen, M. Wang, C. (2016): Investigating pollen and gene flow of WYMV-resistant transgenic wheat N12-1 using a dwarf male-sterile line as the pollen receptor. – PloS One 11: e0151373.
[22] Dong, Y., Wang, X., Tang, Q., Wang, Z. (2015): Theoretical basis of gene splitting technique and its application in the control of transgene flow. – Agricultural Biotechnology 4(3): 1.
[23] Dyer, G. A., Serratos-Hernández, J. A., Perales, H. R., Gepts, P., Piñeyro-Nelson, A., Chávez, Á., Salinas-Arreortua, N., Yúnez-Naude, A., Taylor, J. E., Alvarez-Buylla, E. R. (2009): Dispersal of transgenes through maize seed systems in Mexico. – PloS One 4(5): e5734.

http://www.aloki.hu ● ISSN 1589 1623 (Print) ● ISSN 1785 0037 (Online)
DOI: http://dx.doi.org/10.15666/aeer/1705_1119111208

[24] Ellstrand, N. C. (2003): Dangerous Liaisons? When Cultivated Plants Mate with Their Wild Relatives. – Johns Hopkins University Press, Baltimore, MD.
[25] Ellstrand, N. C. (2014): Is gene flow the most important evolutionary force in plants? – American Journal of Botany 101: 737-753.
[26] Ellstrand, N. C., Hoffman, C. A. (1990): Hybridization as an avenue for escape of engineered genes. – Bioscience 40: 438-442.
[27] Erickson, E. H., Garment, M. B. (1979): Soya-bean flowers: nectary ultrastructure, nectar guides, and orientation on the flower by foraging honeybees. – Journal of Apicultural Research 18: 3−11.
[28] Fox, J. L. (2003): Puzzling industry response to ProdiGene fiasco. – Nature Biotechnology 21(1): 3-4.
[29] Gaines, T. A., Henry, W. B., Byrne, P. F., Westra, P., Nissen, S. J., Shaner, D. L. (2008): Jointed goatgrass (*Aegilops cylindrica*) by imidazolinone-resistant wheat hybridization under field conditions. – Weed Science 56: 32-36.
[30] Gandhi, H. T., Mallory-Smith, C. A., Watson, C. J. W., Vales, M. I., Zemetra, R. S., Riera-Lizarazu, O. (2006): Hybridization between wheat and jointed goatgrass (*Aegilops cylindrica*) under field conditions. – Weed Science 54: 1073-1079.
[31] Gealy, D. R. (2005): Gene Movement between Rice (*Oryza sativa*) and Weedy Rice (*Oryza sativa*): A U.S. Temperate Rice Perspective. – In: Gressel, J. (ed.) Crop Ferality and Volunteerism. – CRC Press, Boca Raton, FL, pp. 323-354.
[32] Goeschl, T., Swanson, T. (2003): The development impact of genetic use restriction technologies: a forecast based on the hybrid crop experience. – Environment and Development Economics 8(01): 149-165.
[33] Goodman, R. M., Newell, N. (1985): Genetic Engineering of Plants for Herbicide Resistance: Status and Prospects. – In: Halvorson, H., Pramer, D., Rogul, M. (eds.) Engineered Organisms in the Environment: Scientific Issues. American Society of Microbiology, Washington, DC, pp. 47-53.
[34] Gressel, J. (1999): Tandem constructs: preventing the rise of super weeds. – Trends in Biotechnology 17(9): 361-366.
[35] Gressel, J. (2015): Dealing with transgene flow of crop protection traits from crops to their relatives. – Pest Management Science 71: 658-667.
[36] Gressel, J., Al-Ahmad, H. (2006): Mitigating transgene flow from crops. – ASB News Report.
[37] Gustafson, D. I., Horak, M. J., Rempel, C. B., Metz, S. G., Gigax, D. R., Hucl, P. (2005): An empirical model for pollen-mediated gene flow in wheat. – Crop Science 45: 1286.
[38] Haider, N., Allainguillaume, J., Wilkinson, M. J. (2009): Spontaneous capture of oilseed rape (*Brassica napus*) chloroplasts by wild *B. rapa*: implications for the use of chloroplast transformation for biocontainment. – Current Genetics 55: 139-150.
[39] Hall, L., Topinka, K., Huffman, J., Davis, L., Good, A. (2000): Pollen flow between herbicide-resistant *Brassica napus* is the cause of multiple-resistant *B. napus* volunteers 1. – Weed Science 48: 688-694.
[40] Heuberger, S., Ellers-Kirk, C., Tabashnik, B. E., Carriere, Y. (2010): Pollen and seed-mediated transgene flow in commercial cotton seed production fields. – PLoS ONE 5(11): e14128. DOI: 10.1371/journal.pone.0014128.
[41] Hills, M. J., Hall, L., Arnison, P. G., Good, A. (2007): Genetic use restriction technologies (GURTs): strategies to impede transgene movement. – Trends in Plant Science 12: 177-183.
[42] Hirata, R., Ohsumk, Y., Nakano, A., Kawasaki, H., Suzuki, K., Anraku, Y. (1990): Molecular structure of a gene, VMA1, encoding the catalytic subunit of H (+)-translocating adenosine triphosphatase from vacuolar membranes of Saccharomyces cerevisiae. – Journal of Biological Chemistry 265: 6726-6733.

http://www.aloki.hu ● ISSN 1589 1623 (Print) ● ISSN 1785 0037 (Online)
DOI: http://dx.doi.org/10.15666/aeer/1705_1119111208

[43] Husken, A., Prescher, S., Schiemann, J. (2010): Evaluating biological containment strategies for pollen-mediated gene flow. – Environmental Biosafety Research 9(02): 67-73.
[44] ISAAA (2017): Global Status of Commercialized Biotech/GM Crops: 2017. – ISAAA Brief No. 53. ISAAA, Ithaca, NY.
[45] Kareiva, P., Marvier, M. (2000): An Overview of Risk Assessment Procedures Applied to Genetically Engineered Crops. – In: Proceedings of Incorporating Science, Economics, and Sociology in Developing Sanitary and Phytosanitary Standards in International Trade. National Academy Press, Washington, DC, pp. 231-238.
[46] Kelloniemi, J., Mäkinen, K., Valkonen, J. P. T. (2008): Three heterologous proteins simultaneously expressed from a chimeric potyvirus: infectivity, stability and the correlation of genome and virion lengths. – Virus Research 135(2): 282-291.
[47] Knott, V., Blake, D. J., Brownlee, G. G. (1989): Completion of the detailed restriction map of the *E. coli* genome by the isolation of overlapping cosmid clones. – Nucleic Acids Research 17(15): 5901-5912.
[48] Kuvshinov, V., Koivu, K., Kanerva, A., Pehu, E. (2001): Molecular control of transgene escape from genetically modified plants. – Plant Science 160(3): 517-522.
[49] Kwit, C., Moon, H. S., Warwick, S. I., Stewart, C. N. (2011): Transgene introgression in crop relatives: molecular evidence and mitigation strategies. – Trends in Biotechnology 29(6): 284-293.
[50] Lee, D., Natesan, E. (2006): Evaluating genetic containment strategies for transgenic plants. – Trends in Biotechnology 24: 109-114.
[51] Lee, S., Jeon, J. S., An, K., Moon, Y. H., Lee, S., Chung, Y. Y., An, G. (2003): Alteration of floral organ identity in rice through ectopic expression of OsMADS16. – Planta 217(6): 904-911.
[52] Lei, L., Stewart, C. N., Tang, Z. X., Wei, W. (2011): Dynamic expression of green fluorescent protein and Bacillus thuringienesis Cry1Ac endotoxin in interspecific hybrids and successive backcross generations (BC1 and BC2) between transgenic *Brassica napus* crop and wild *Brassica juncea*. – Annals of Applied Biology 159: 212-219.
[53] Lin, C., Fang, J., Xu, X., Zhao, T., Cheng, J., Tu, J., Shen, Z. (2008): A built-in strategy for containment of transgenic plants: creation of selectively terminable transgenic rice. – PLoS One 3(3): e1818.
[54] Linder, C. R., Taha, I., Rieseberg, L. H., Seiler, G. J., Snow, A. A. (1998): Long-term introgression of crop genes into wild sunflower populations. – Theoretical and Applied Genetics 96: 339-347.
[55] Liu, C., Li, J., Gao, J., Shen, Z., Lu, B. R., Lin, C. (2012): A built-in mechanism to mitigate the spread of insect-resistance and herbicide-tolerance transgenes into weedy rice populations. – PLoS One 7: e31625.
[56] Londo, J. P., Bollman, M. A., Sagers, C. L., Lee, E. H., Watrud, L. S. (2011): Glyphosate-drift but not herbivory alters the rate of transgene flow from single and stacked trait transgenic canola (*Brassica napus*) to non-transgenic *B. napus and B. rapa*. – New Phytologist 191(3): 840-849.
[57] Loureiro, I., Escorial, M. C., González-Andujar, J. L., García-Baudin, J. M., Chueca, M. C. (2007): Wheat pollen dispersal under semiarid field conditions: potential outcrossing with *Triticum aestivum* and *Triticum turgidum*. – Euphytica 156(1-2): 25-37.
[58] Loureiro, I., Escorial, C., Garcia-Baudin, J. M., Chueca, C. (2009): Hybridization, fertility and herbicide resistance of hybrids between wheat and *Aegilops biuncialis*. – Agronomy for Sustainable Development 29: 237-245.
[59] Loureiro, I., Escorial, M. C., Gonzalez, A., Chueca, M. C. (2012): Pollen-mediated gene flow in wheat (*Triticum aestivum* L.) in a semiarid field environment in Spain. – Transgenic Research 21(6): 1329-39.
[60] Lu, B. R. (2003): Transgene containment by molecular means- is it possible and cost effective? – Environmental Biosafety Research 2(1): 3-8.

http://www.aloki.hu ● ISSN 1589 1623 (Print) ● ISSN 1785 0037 (Online)
DOI: http://dx.doi.org/10.15666/aeer/1705_1119111208

[61] Maliga, P. (2004): Plastid transformation in higher plants. – Annual Reviews of Plant Biology 55: 289-313.
[62] Marvier, M. A., Meir, E., Kareiva, P. M. (1999): How Do the Design of Monitoring and Control Strategies Affect the Chance of Detecting and Containing Transgenic Weeds? – In: Ammann, K., Jacot, Y., Simonsen, G., Kjellsson, G. (eds.) Methods for Risk Assessment of Transgenic Plants. Vol. III. Ecological Risks and Prospects of Transgenic Plants, Where Do We Go from Here? A Dialogue between Biotech Industry and Science I. Birkhäuser Verlag, Basel, pp. 109-122.
[63] Mercer, K. L., Wainwright, J. D. (2008): Gene flow from transgenic maize to landraces in Mexico: an analysis. – Agriculture, Ecosystems & Environment 123: 109-115.
[64] Messeguer, J. (2003): Gene flow assessment in transgenic plants. – Plant Cell, Tissue and Organ Culture 73: 201-212.
[65] Mihalčík, P., Hrčková, K., Singer, M., Plačková, A., Kraic, J. (2012): Effect of MON 810 cultivation and prevention to adventitious presence in non-GM fields: a case study in Slovakia. – Plant Protection Science 48: S11–S17.
[66] Miroshnichenko, D., Pushin, A., Dolgov, S. (2016): Assessment of the pollen-mediated transgene flow from the plants of herbicide resistant wheat to conventional wheat (*Triticum aestivum* L.). – Euphytica 209: 71-84.
[67] Mizuguti, A., Ohigashi, K., Yoshimura, Y., Kaga, A., Kuroda, Y., Matsuo, K. (2010): Hybridization between GM soybean (*Glycine max* (L.) Merr.) and wild soybean (*Glycine soja* Sieb. et Zucc.) under field conditions in Japan. – Environmental Biosafety Research 9: 13-23.
[68] Moon, H. S., Abercrombie, L. L., Eda, S., Blanvillain, R. T., James, G. O., David, W., Stewart, J. C. N. (2011): Transgene excision in pollen using a codon optimized serine resolvase CinH-RS2 site-specific recombination system. – Plant Molecular Biology 75(6): 621-631.
[69] Morris, W. F., Kareiva, P. M., Raymer, P. L. (1994): Do barren zones and pollen traps reduce gene escape from transgenic crops? – Ecological Applications 4(1): 157-165.
[70] NRC (National Research Council). (2002): Environmental Effects of Transgenic Plants. – National Academy Press, Washington, DC.
[71] Olguin, E. R. S., Arrieta-Espinoza, G., Lobo, J. A., Espinoza-Esquivel, A. M. (2009): Assessment of gene flow from a herbicide-resistant indica rice (*Oryza sativa* L.) to the Costa Rican weedy rice (*Oryza sativa*) in tropical America: factors affecting hybridization rates and characterization of F1 hybrids. – Transgenic Research 18: 633-647.
[72] Ortiz-García, S., Ezcurra, E., Schoel, B., Acevedo, F., Soberón, J., Snow, A. A. (2005): Absence of detectable transgenes in local landraces of maize in Oaxaca, Mexico (2003-2004): – Proceedings of the National Academy of Sciences of the United States of America 102: 12338-12343.
[73] Palaudelmàs, M., Melé, E., Peñas, G., Pla, M., Nadal, A., Serra, J., Salvia, J., Messeguer, J. (2008): Sowing and flowering delays can be an efficient strategy to improve coexistence of genetically modified and conventional maize. – Crop Science 48: 2404-2413.
[74] Parisi, C., Tillie, P., Rodríguez-Cerezo, E. (2016): The global pipeline of GM crops out to 2020. – Nature Biotechnology 34: 31.
[75] Perez-Jones, A., Mallory-Smith, C. A., Riera-Lizarazu, O., Watson, C. J. W., Wang, Z., Rehman, M. (2006): Introgression of a straw breaker foot rot resistance gene from winter wheat into jointed goat grass. – Crop Science 46: 2155-2160.
[76] Pla, M., La Paz, J. L., Peñas, G., García, N., Palaudelmàs, M., Esteve, T., Messeguer, J., Melé, E. (2006): Assessment of real-time PCR based methods for quantification of pollen-mediated gene flow from GM to conventional maize in a field study. – Transgenic Research 15: 219-228.

http://www.aloki.hu ● ISSN 1589 1623 (Print) ● ISSN 1785 0037 (Online)
DOI: http://dx.doi.org/10.15666/aeer/1705_1119111208

[77] Poehlman, J. M. (2013): Breeding Field Crops. – Springer Science & Business Media, New York.
[78] Prasad, K., Parameswaran, S., Vijayraghavan, U. (2005): OsMADS1, a rice MADS-box factor, controls differentiation of specific cell types in the lemma and palea and is an early-acting regulator of inner floral organs. – The Plant Journal 43: 915-928.
[79] Rache, L., Mora, J., Chaparro, A. (2013): Study of gene flow from GM cotton (*Gossypium hirsutum*) varieties in "El Espinal" (Tolima, Colombia). – Acta Biologica Colombiana 18: 489-498.
[80] Ramzan, S., Rehman, M., Shaheen, T., Hussain, K., Qasim, M., Asif, M., Bukhari, S. A. (2014): Vertical flow of Bt genes in transgenic cotton (*Gossypium hirsutum L.)*. – Journal of Animal and Plant Science 24: 1904-1907.
[81] Ray, J. D., Kilen, T. C., Abel, C. A., Paris, R. L. (2003): Soybean natural cross-pollination rates under field conditions. – Environmental Biosafety Research 2: 133-138.
[82] Rehman, M., Hansen, J. L., Mallory-Smith, C. A., Hang, A., Burton, C., Zemetra, R. S. (2010): Determining the pollen parent of field-grown backcross progenies of wheat (Triticum aestivum L.) × jointed goatgrass (Aegilops cylindrica Host) hybrids using genomic in situ hybridization (GISH). – Crop Science 50: 1474-1479.
[83] Rieger, M. A., Lamond, M., Preston, C., Powles, S. B., Roush, R. T. (2002): Pollen-mediated movement of herbicide resistance between commercial canola fields. – Science 296: 2386-2388.
[84] Rong, J., Song, Z., Su, J., Xia, H., Lu, B. R., Wang, F. (2005): Low frequency of transgene flow from Bt/CpTI rice to its non-transgenic counterparts planted at close spacing. – New Phytologist 168: 559-566.
[85] Rust, R. W., Mason, C. E., Erickson, E. H. (1980): Wild bees on soybeans, *Glycine max.* – Environment Entomology 9: 230−232.
[86] Ruf, S., Karcher, D., Bock, R. (2007): Determining the transgene containment level provided by chloroplast transformation. – Proceedings of the National Academy of Sciences 104: 6998-7002.
[87] Ryffel, G. U. (2014): Transgene flow: facts, speculations and possible countermeasures. – GM Crops & Food 5: 249-258.
[88] Sandhu, S., Blount, A. R., Quesenberry, K. H., Altpeter, F. (2010): Apomixis and ploidy barrier suppress pollen-mediated gene flow in field grown transgenic turf and forage grass (Paspalum notatum Flüggé). – Theoretical and Applied Genetics 121(5): 919-929.
[89] Sanvido, O., Widmer, F., Winzeler, M., Streit, B., Szerencsits, E., Bigler, F. (2008): Definition and feasibility of isolation distances for transgenic maize cultivation. – Transgenic Research 17(3): 317-335.
[90] Saurabh, S., Vidyarthi, A. S., Prasad, D. (2014): RNA interference: concept to reality in crop improvement. – Planta 239(3): 543-564.
[91] Schernthaner, J. P., Fabijanski, S. F., Arnison, P. G., Racicot, M., Robert, L. S. (2003): Control of seed germination in transgenic plants based on the segregation of a two-component genetic system. – Proceedings of the National Academy of Sciences 100: 6855-6859.
[92] Schnable, P. S., Wise, R. P. (1998): The molecular basis of cytoplasmic male sterility and fertility restoration. – Trends in Plant Science 3: 175-180.
[93] Serrat, X., Esteban, R., Peñas, G., Català, M. M., Melé, E., Messeguer, J. (2013): Direct and reverse pollen-mediated gene flow between GM rice and red rice weed. – AoB Plants 5: 050.
[94] Seguin-Swartz, G., Beckie, H. J., Warwick, S. I., Roslinsky, V., Nettleton, J. A., Johnson, E. N. (2013): Pollen-mediated gene flow between glyphosate-resistant *Brassica napus* canola and *B. juncea* and *B. carinata* mustard crops under large-scale field conditions in Saskatchewan. – Canadian Journal of Plant Science 93: 1083-1087.

http://www.aloki.hu ● ISSN 1589 1623 (Print) ● ISSN 1785 0037 (Online)
DOI: http://dx.doi.org/10.15666/aeer/1705_1119111208

[95] Shivrain, V. K., Burgos, N. R., Sales, M. A., Mauromoustakos, A., Gealy, D. R., Smith, K. L. (2009): Factors affecting the outcrossing rate between Clearfield™ rice and red rice (*Oryza sativa*). – Weed Science 57: 394-403.
[96] Snow, A. A. (2002): Transgenic crops—why gene flow matters. – Nature biotechnology 20: 542-542.
[97] Song, X. L., Munns, K., Qiang, S., Blackshaw, R., Sharma, R. (2009): Detection and quantification of 5 enolpyruvylshikimate-3-phosphate synthase (cp4 epsps) upon *Brassica napus* × *Brassica juncea* outcrossing using real-time PCR. – European Food Research & Technology 228: 939-944.
[98] Song, X. L., Wang, Z., Zuo, J., Huangfu, C. H., Qiang, S. (2010): Potential gene flow of two herbicide-tolerant transgenes from oilseed rape to wild *B. juncea* var. gracilis. – Theoretical and Applied Genetics 120: 1501-1510.
[99] Song, Z., Lu, B. R., Chen, J. (2004): Pollen flow of cultivated rice measured under experimental conditions. – Biodiversity & Conservation 13: 579-90.
[100] Staniland, B. K., McVetty, P. B. E., Friesen, L. F., Yarrow, S., Freyssinet, G., Freyssinet, M. (2000): Effectiveness of border areas in confining the spread of transgenic Brassica napus pollen. – Canadian Journal of Plant Science 80: 521-526.
[101] Stewart, C. N., Halfhill, M. D., Warwick, S. I. (2003): Transgene introgression from genetically modified crops to their wild relatives. – Nature Reviews Genetics 4: 806-817.
[102] Straus, A., Lahaye, T. (2013): Zinc fingers, Tal effectors, or Cas9-based DNA binding proteins: what's best for targeting desired genome loci? – Molecular Plant 6: 1384-1387.
[103] Swanson, T., Goschl, T. (2000): Genetic use restriction technologies (GURTs): impacts on developing countries. – International Journal of Biotechnology 2: 56-84.
[104] Timmons, A. M., O'Brien, E. T., Charters, Y. M., Dubbels, S. J., Wilkinson, M. J. (1995): Assessing the risks of wind pollination from fields of genetically modified *Brassica napus* ssp. *oleifera*. – Euphytica 85: 417-423.
[105] Valverde, B. E. (2013): Is herbicide resistant rice the ultimate solution for controlling weedy rice? Experiences from the Americas. – Korean Journal of Weed Science 33: 11-23.
[106] Van, A., Rene, C., Szumgalski, A. R., Friesen, L. F. (2007): The potential benefits, risks and costs of genetic use restriction technologies. – Canadian Journal of Plant Science 87: 753-762.
[107] Van Deynze, A. E., Sundstrom, F. J., Bradford, K. J. (2005): Pollen-mediated gene flow in California cotton depends on pollinator activity. – Crop Science 45: 1565-1570.
[108] Van Deynze, A. E., Hutmacher, R. B., Bradford, K. J. (2011): Gene flow between *Gossypium hirsutum* L. and *Gossypium barbadense* L. is asymmetric. – Crop Science 51: 298-305.
[109] Wang, F., Yuan, Q. H., Shi, L., Qian, Q., Liu, W. G., Kuang, B. G., Zeng, D. L., Liao, Y. L., Cao, B., Jia, S. R. (2006): A large-scale field study of transgene flow from cultivated rice (*Oryza sativa*) to common wild rice (*O. rufipogon*) and barnyard grass (*Echinochloa crusgalli*). – Plant Biotechnology Journal 4: 667-676.
[110] Wang, N., Ning, S., Pourkheirandish, M., Honda, I., Komatsuda, T. (2013): An alternative mechanism for cleistogamy in barley. – Theoretical and Applied Genetics 126: 2753-2762.
[111] Wang, T., Li, Y., Shi, Y., Reboud, X., Darmency, H., Gressel, J. (2004): Low frequency transmission of a plastid-encoded trait in Setaria italica. – Theoretical and Applied Genetics 108: 315-320.
[112] Wang, X. J., Jin, X., Dun, B. Q., Kong, N., Jia, S. R., Tang, Q. L., Wang, Z. X. (2014): Gene-splitting technology: a novel approach for the containment of transgene flow in Nicotiana tabacum. – PloS One 9: e99651.
[113] Weekes, R., Allnutt, T., Boffey, C., Morgan, S., Bilton, M., Daniels, R., Henry, C. (2007): A study of crop-to-crop gene flow using farm scale sites of fodder maize (*Zea mays* L.) in the UK. – Transgenic Research 16(2): 203-211.

http://www.aloki.hu ● ISSN 1589 1623 (Print) ● ISSN 1785 0037 (Online)
DOI: http://dx.doi.org/10.15666/aeer/1705_1119111208

[114] Wegier, A., Pineyro-Nelson, A., Alarcón, J., Galvez-Mariscal, A., Álvarez-Buylla, E. R., Piñero, D. (2011): Recent long-distance transgene flow into wild populations conforms to historical patterns of gene flow in cotton (*Gossypium hirsutum*) at its center of origin. – Molecular Ecology 20: 4182-94.
[115] Werner, J. E., Endo, T. R., Gill, B. S. (1992): Toward a cytogenetically based physical map of the wheat genome. – Proceedings of the National Academy of Sciences 89: 11307-11311.
[116] Xia, H., Lu, B. R., Xu, K., Wang, W., Yang, X., Yang, C., Luo, J., Lai, F., Ye, W., Fu, Q. (2011): Enhanced yield performance of Bt rice under target-insect attacks: implications for field insect management. – Transgenic Research 20: 655-664.
[117] Xiao, H., Wang, Y., Liu, D., Wang, W., Li, X., Zhao, X., Zhu, L. (2003): Functional analysis of the rice AP3 homologue OsMADS16 by RNA interference. – Plant Molecular Biology 52: 957-966.
[118] Yadav, S. R., Prasad, K., Vijayraghavan, U. (2007): Divergent regulatory OsMADS2 functions control size, shape and differentiation of the highly derived rice floret second-whorl organ. – Genetics 176: 283-294.
[119] Yan, S., Zhu, J., Zhu, W., Li, Z., Shelton, A. M., Luo, J., Cui, J., Zhang, Q., Liu, X. (2015): Pollen-mediated gene flow from transgenic cotton under greenhouse conditions is dependent on different pollinators. – Scientific Reports 5: 15917 DOI: 10.1038/srep15917.
[120] Yao, K., Hu, N., Chen, W., Li, R., Yuan, Q., Wang, F., Qian, Q., Jia, S. (2008): Establishment of a rice transgene flow model for predicting maximum distances of gene flow in southern China. – New Phytologist 180: 217-228.
[121] Yoshida, H., Itoh, J. I., Ohmori, S., Miyoshi, K., Horigome, A., Uchida, E., Satoh, H. (2007): Superwoman1-cleistogamy, a hopeful allele for gene containment in GM rice. – Plant Biotechnology Journal 5: 835-846.
[122] Yoshimura, Y., Matsuo, K., Yasuda, K. (2006): Gene flow from GM glyphosate-tolerant to conventional soybeans under field conditions in Japan. – Environmental Biosafety Research 5: 169-173.
[123] Yuan, Q. H., Shi, L., Wang, F., Cao, B., Qian, Q., Lei, X. M., Liao, Y. L., Liu, W. G., Cheng, L., Jia, S. R. (2007): Investigation of rice transgene flow in compass sectors by using male sterile line as a pollen detector. – Theoretical and Applied Genetics 115: 549-560.
[124] Zhang, W., Linscombe, S. D., Webster, E., Tan, S., Oard, J. (2006): Risk assessment of the transfer of imazethapyr herbicide tolerance from Clearfield rice to red rice (Oryza sativa). – Euphytica 152: 75-86.

http://www.aloki.hu ● ISSN 1589 1623 (Print) ● ISSN 1785 0037 (Online)
DOI: http://dx.doi.org/10.15666/aeer/1705_1119111208

LIVELIHOOD RESILIENCE OF VEGETABLE FARMERS: EFFICACY OF ORGANIC FARMING IN DEALING WITH CLIMATE CHANGE IN JAVA, INDONESIA

FACHRISTA, I. A.[1,2] – IRHAM[3*] – MASYHURI[3] – SURYANTINI, A.[3]

[1]*Assessment Institute for Agricultural Technology of Bangka Belitung, Indonesian Agency for Agricultural Research and Development Ministry of Agriculture, Jakarta, Indonesia*

[2]*Faculty of Agriculture, Universitas Gadjah Mada, Indonesia*

[3]*Department of Agricultural Socio-Economics, Faculty of Agriculture, Universitas Gadjah Mada, Yogyakarta, Indonesia*

**Corresponding author*
e-mail: irham@ugm.ac.id

(Received 6th Apr 2019; accepted 2nd Jul 2019)

Abstract. Some researchers believe that organic farming can improving farmer's resilience in dealing with climate change. Livelihood resilience is attributed to buffer capacity, self-organization, and learning capacity. Therefore, this study aims to 1) compare buffer capacity, self-organization, and learning capacity between organic and conventional farmers, 2) compare the level of livelihood resilience between organic and conventional farmers, and 3) know important determinants that influence the livelihood resilience of farmers in the face of climate change. Data were obtained through a survey involving 112 organic farmers and 112 conventional farmers in Java, Indonesia. The t-test was used to find out the buffer capacity, self-organization and learning capacity and livelihood resilience of farmers in the face of climate change. Ordinary least square was used to find out important determinants that influence the livelihood resilience level of farmers. The analysis shows that buffer capacity and learning capacity of organic farmers are better than that of the conventional farmers. Organic farmers have better livelihood resilience than conventional farmers. Important determinants that influence the farmer's level of resilience are cooperation networks, adaptation strategies and accessibility to extension services, and climate information and training. The study recommends that policymakers need to develop organic farming and supporting institutions to increase farmer's resilience in dealing with climate change.
Keywords: *buffer capacity, learning capacity, self-organization, adaptation, vegetable farming*

Introduction

Recent climate change has adversely affected horticultural crops (Haryono and Las, 2011; Rejekiningrum et al., 2011; Surmaini et al., 2011). The various negative impacts of climate change on horticulture crops, especially vegetables, include crop failure, decreased quantity, decreased product quality, increasing number of pest attack and plant disease problems, thus making farmers at risk of unprofitable vegetable cultivation (Ayyogari et al., 2014). Reports have been made on the negative impacts of climate change on vegetable crops in Indonesia that include extreme rainfall damaging vegetable crops and decreasing agricultural production, which may eventually lead to crop failure. In addition, it was reported that extreme rain throughout 2010 caused several vegetable productions in Indonesia to decrease by 20-25% (Rejekiningrum et al., 2011).

On this account, it is noteworthy that organic farming plays a significant role in dealing with climate change. Organic farming will have higher resilience than

http://www.aloki.hu ● ISSN 1589 1623 (Print) ● ISSN 1785 0037 (Online)
DOI: http://dx.doi.org/10.15666/aeer/1705_1120911232

conventional farming (Jacobi et al., 2015). As a result, farmers with a better level of resilience will be more capable at maintaining and improving their livelihood and welfare opportunities since they are more adjustable to facing climate change disruptions. In the face of climate change, it is necessary to integrate resilience and livelihood because climate change will affect human livelihoods at greater intensity (Tanner et al., 2015). The approach on livelihood focuses on interactions between the livelihood context, livelihood assets, institutions, livelihood strategies, and the impact of livelihoods. Meanwhile, livelihood resilience in the face of climate change is characterized by a strategy carried out by actors to maintain and enhance their assets (Speranza et al., 2014).

Farmer's resilience in dealing with climate change varies between regions. There have been several studies to address the level of farmer's resilience in the face of climate change conducted in developing countries (e.g., Lal, 2014; Marseva et al., 2016; Tambo, 2016). In the face of climate change, most farmers' resilience levels are classified into the weak to moderate categories, such as farmers in Nepal (Lal, 2014) and farmers in northeast Ghana (Tambo, 2016). The research conducted by Marseva et al. (2016), also showed that in Central Java, Indonesia, farmer's resilience in the face of climate change is still relatively low. Low resilience level in dealing with climate change is attributed to the low level of human, social and physical capital owned by farmers.

There are some dimensions of measuring the level of resilience to climate change used by researchers. Some dimension used to measure resilience include: 1) based on asset (e.g., Thulstrup, 2015), 2) based on six dimension of Resilience Index Measure and Analysis (RIMA) of the Food and Agriculture Organization of the United Nations, which include income and food access, access to basic services, assets, social safety nets, stability, and adaptive capacity (e.g., FAO, 2016; Tambo, 2016; Tambo and Wünscher, 2017; Weldegebriel and Amphune, 2017). The measurement of resilience integrated with livelihoods, known as livelihood resilience, was put forward by Speranza et al. (2014). Livelihood resilience in the face of climate change is constituted of buffer capacity, self-organization, and learning capacity (Speranza et al., 2014).

As what the experts have put forward, organic farming is the right solution to increase the farmers' livelihood resilience in the face of climate change. However, there were only few researches to address the livelihood resilience of the farmers' in dealing with climate change despite its relevance to the current situation. Therefore, this study aims to 1) compare buffer capacity, self-organization, and learning capacity between organic and conventional farmers, 2) compare the level of livelihood resilience between organic and conventional farmers in dealing with climate change, and 3) know important determinant that affects the livelihood resilience of organic farmers and conventional in dealing with climate change.

Materials and methods

Research location and sampling

The research location was determined purposively in Java, especially in the Special Region of Yogyakarta and Central Java Province, considering that the two areas greatly develop organic vegetable cultivation. Some regencies of each province were selected for the research location, namely Sleman Regency (Special Region of Yogyakarta) and Magelang Regency, Boyolali Regency and Semarang Regency (Central Java) (*Fig. 1*).

http://www.aloki.hu ● ISSN 1589 1623 (Print) ● ISSN 1785 0037 (Online)
DOI: http://dx.doi.org/10.15666/aeer/1705_1120911232

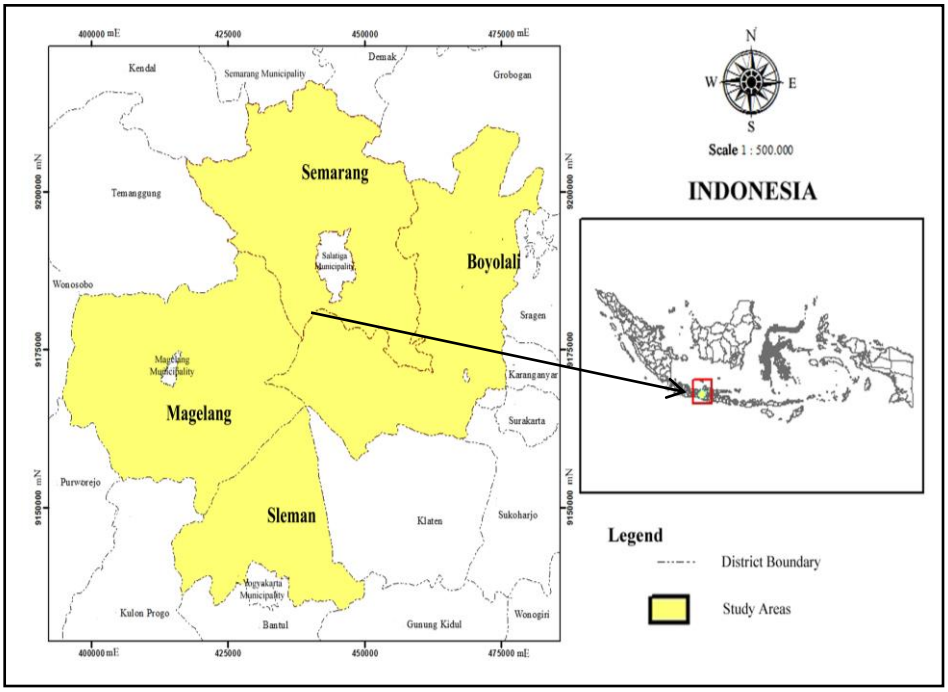

Figure 1. *Study area*

The survey was conducted in February - August 2018, by involving organic farmers and conventional farmers. Organic farmers selected by using proportionate random sampling method (*Table 1*).

Table 1. *Population and sample of organic farmers*

Regency	Population	Sample
Sleman	30	22
Magelang	24	17
Boyolali	25	18
Semarang	77	55
Total	156	112

The sample size based on Slovin's formula, is given as follows: $n = N/(1+(N.e^2)$, where n is the sample size, N is the population size and e is the margin of error (0.05). Therefore based on the formula, the sampling size in this research is 112 organic farmer, and as comparison, there are 112 conventional farmers. Conventional vegetable farmers are living nearby organic vegetable farmers with the consideration that both groups experience the negative impact of climate change and relatively have similar socioeconomic conditions.

The survey was conducted with a structured questionnaire guide. The first part of the questionnaire collects some background information such as age, household size, marketing network in selling crop yields with other parties, and accessibility to various institutions such as credit institutions, extension, access to information and climate training. The second part investigates adaptation strategies adopted by farmers to reduce

http://www.aloki.hu ● ISSN 1589 1623 (Print) ● ISSN 1785 0037 (Online)
DOI: http://dx.doi.org/10.15666/aeer/1705_1120911232

the negative impact of climate change on vegetable farming. The last section addresses farmers' livelihood resilience in dealing with climate change. This study collected 224 questionnaires for analysis.

Analytical methods

Data analysis

Data were analyzed by t-test and ordinary least square (OLS) regression analysis. The t-test was used to compare buffer capacity, self-organization and learning capacity and the level of livelihood resilience between organic vegetable farmers and conventional vegetable farmers in the face of climate change. OLS was used to find out important determinants affecting the farmers' livelihood resilience index in dealing with climate change. Important determinants that affect farmers' livelihood resilience in dealing with climate change were selected based on the previous studies, such as age (Tesso et al., 2012; Weldegebriel and Amphune, 2017), household size (Weldegebriel and Amphune, 2017), engagement in trade (Weldegebriel and Amphune, 2017), and accessibility to various institutions such as credit institutions (Keil et al., 2008; Tesso et al., 2012), extension institutions (Tesso et al., 2012), information on climate change (Keil et al., 2008), climate training and the amount of adaptation that farmers have applied to deal with climate change (Tambo and Wünscher, 2017; Uy et al., 2011). The description of each variable used in this study is presented in *Table 2.*

Table 2. *Description of variables*

Variable	Description of the variables
Livelihood resilience	Livelihood resilience in the face of climate change (index)
Age	Age of the head of the family in years
Household size	Number of family members in the household
Engagement in trade	Dummy (1 = if farmers have engagement in trade and 0 = if otherwise)
Access to credit	Dummy (1 = if farmers have access to credit institutions and 0 = if otherwise)
Access to extension services	Dummy (1 = if farmers have access to extension services and 0 = if otherwise)
Access to climate information	Dummy (1 = if farmers have access to climate information and 0 = if otherwise)
Access to climate training	Dummy (1 = if farmers have access to climate training and 0 = if otherwise)
Number of adaptation strategies	The number of adaptation strategies applied by farmers in facing climate change

Adaptation strategies adopted by farmers to reduce the negative impacts of climate change were obtained from the previous research and preliminary information, namely implementing implementing mixed cropping (Abid et al., 2016; Fosu-Mensah et al., 2012; Ichdayanti, 2014), using superior varieties (Ali and Erenstein, 2017; Ichdayanti, 2014; Milambo, 2013; Ruminta, 2015; Tambo, 2016), growing non water-intensive vegetable (Ichdayanti, 2014), implementing crop rotation (Kurniawati, 2012), adjusting planting and harvesting dates (Ali and Erenstein, 2017; Deressa et al., 2009; Fosu-Mensah et al., 2012), increasing the dose of organic matter (Irham et al., 2018; Makate et al., 2017), using mulch (Ichdayanti, 2014), using shade (Adiyoga and Lukman, 2018; Kurniawati, 2012), changing irrigation techniques (Abid et al., 2016; Tambo, 2016), using *pranata mangsa* a local technique based on regular natural events (initial information from farmer interviews).

http://www.aloki.hu ● ISSN 1589 1623 (Print) ● ISSN 1785 0037 (Online)
DOI: http://dx.doi.org/10.15666/aeer/1705_1120911232

Table 3. *Components, indicators, description and values of livelihood resilience in dealing with climate change*

Component	Indicators	Description	Units
Buffer capacity	Human capital	Duration of education	Years
		Farming experience	Years
		Other skills besides farming	Count
		Number of sick family members	Count
	Financial capital	Annual revenue of vegetable farming	USD/ha
		Livestock saving	USD
		Annual labor income	USD/year
		Dependency ratio: a ratio of members aged below 15 and above 64 to those aged 15-64	Ratio
	Social capital	Asset increase due to organization partnership	USD
		Support of workforce from the group	Man-days
		Use of group equipment	Count
	Physical capital	Machinery, equipment, buildings, farming wells	USD
	Natural capital	Weighted averaged soil fertility of the land owned by farmer	Index
Self-organization	Cooperation and network	Number of group organization followed by farmers	Count
	Trust	Trust between community members in lending and borrowing funds	Percentage
	Reliance on own resources	The closest distance needed to obtain farming inputs	Kilometer
Learning capacity	Knowledge of treat and opportunities	The ability to analyze threats to increase production over the past 12 months	Count
		Ability to analyze opportunities to increase production over the past 12 months	Count
	Shared vision	Frequency of discussion on farming development over the past 12 months	Count
	Commitment to learning	Frequency of regular meetings with counselors	Count
		Discussion frequency on the previous farming performance with counselors and other farmers	Count
		Time allocated per month to find information on technology	Minute per month
	Knowledge identification capability-monitoring	The best time to sell and buy the best product	Count
		Frequency of consultation on planning agricultural products sold	Count
		The number of technological innovations to applied by farmers in the upcoming planting season	Count
		The number of technological innovations tested by farmers in the last 12 months	Count
		Number of technological innovations adopted by farmers in the last 12 months	Count
		Number of technological innovations applied now	Count

http://www.aloki.hu ● ISSN 1589 1623 (Print) ● ISSN 1785 0037 (Online)
DOI: http://dx.doi.org/10.15666/aeer/1705_1120911232

		Frequency in discussing the problem of farming production with other actors in the group	Count
	Knowledge sharing capability	Number of farmers given new information or methods by respondent farmers	Count
	Knowledge transfer capability	The number of ideas that farmers learn from other farmers and other actors	Count
	Functioning feedback mechanism	Frequency of interaction with officers related to business production in groups	Count

Measurement of livelihood resilience

The livelihood resilience used in this study was adapted from Speranza et al. (2014), Murphy (2015), Wahyuni (2016) and based on the construction of this study. Components, indicators and measurements of farmers' livelihood resilience in dealing with climate change are presented in *Table 3*. Livelihood resilience consists of three components, namely buffer capacity, self-organization and learning capacity. Each component consists of several indicators that can represent livelihood resilience. The steps taken to measure the livelihood resilience index are:

1. Normalization

It is important to normalize each indicator to make it in the range of 0 to. 1. Normalization was done because indicators of livelihood resilience are measured on a different scale. The normalization methods were based on the Human Development Index method (UNDP, 2006). Some indicators show that if the indicator value increases, the livelihood resilience will decrease. On this basis, we use two normalization methods so that the increasing value of each indicator will increase livelihood resilience:

a) Indicators where higher values, which imply better resilience such as education time, farming experience, farming acceptance, were normalized using the following formula:

$$\tau_{norm} = \frac{\tau_{ij} - \tau_{\min}}{\tau_{\max} - \tau_{\min}} \quad \text{(Eq.1)}$$

b) Indicators with higher values, which imply lower resilience such as sick family members and dependency ratios, were normalized using the following formula:

$$\tau_{norm} = \frac{\tau_{\min} - \tau_{\max}}{\tau_{\max} - \tau_{\min}} \quad \text{(Eq.2)}$$

where:

τ_{norm} = the value of j indicator is for normalized household

τ_{ij} = the value of j indicator is for household i

http://www.aloki.hu ● ISSN 1589 1623 (Print) ● ISSN 1785 0037 (Online)
DOI: http://dx.doi.org/10.15666/aeer/1705_1120911232

τ_{max} = maximum value of sub-indicators for all households

τ_{min} = minimum value of sub-indicators for all households

2. Measuring livelihood resilience index

After normalization, the researcher calculated the livelihood resilience index using the equal-weight approach. The equal-weight approach assumes that each indicator has the same contribution to the livelihood resilience index. Measurements using this method are based on the average normalized values (Gbetibouo et al., 2010; Tambo and Wünscher, 2017). The value of each indicator was then averaged to obtain the value of each of the three indicators. The compound value was averaged to obtain the overall value of the livelihood resilience index. The farmers' livelihood resilience index in dealing with climate change resulted in the ranges from 0 to 1.

Result

Socioeconomic profile of farmers and adaptation to climate change

The socioeconomic conditions of organic vegetable farmers are better than those of conventional farmers (*Table 4*). Organic vegetable farmers have better accessibility to credit institutions, extension service, and engagement in trade than conventional farmers. Organic farmers are also younger and have more household members than conventional farmers. Young farmers will easily accept the technology, which can be used to adapt to climate change and family members can help farmers in vegetable farming. Organic farmers also implement more adaptation strategies to reduce the impact of climate change on vegetable farmer.

Table 4. *Socioeconomic profile of farmers and adaptation to climate change*

	Organic		Conventional		Difference[a]	
	Mean	Std. Dev	Mean	Std. Dev		
Age	45.214	12.836	45.455	11.527	-0.241	
Household size	4.125	1.330	3.866	1.212	0.259	
Engagement in trade	0.839	0.369	0.179	0.385	0.661	***
Access to credit	0.321	0.469	0.143	0.352	0.179	**
Access to extension services	0.634	0.484	0.500	0.723	0.134	**
Access to climate information	0.554	0.499	0.500	0.502	0.054	
Access to climate training	0.107	0.311	0.080	0.273	0.027	
Number of adaptation strategies	6.295	1.257	5.598	1.423	0.696	***

[a]Significance based on Pearson chi-square for differences in proportions between the two groups or t-test for the average difference between the two groups. ***Significant at 1% level. **Significant at 5% level

Buffer capacity, self-organization and learning capacity of organic and conventional farmers

Table 5 presents the description and indicator values of the buffer capacity. The three indicators that greatly contribute to the buffer capacity of organic vegetable farmers and

http://www.aloki.hu ● ISSN 1589 1623 (Print) ● ISSN 1785 0037 (Online)
DOI: http://dx.doi.org/10.15666/aeer/1705_1120911232

conventional vegetable farmers are natural capital, human capital and financial capital. This fact indicates that the three capitals play a significant role in increasing the buffer capacity of farmers. The significant difference from the indicators that compose the buffer capacity between organic vegetable farmers and conventional vegetable farmers lies in social capital, physical capital and natural capital. Organic farmers have higher social capital, physical capital and natural capital than conventional vegetable farmers. Organic vegetable farmers have higher social capital than conventional vegetable farmers because organic farmers get an increase in assets from group membership and support of the workforce from the group. Moreover, organic farmers also have better physical capital values as manifested through their ownership of machinery and other equipment. Natural capital such as soil fertility that owned by organic farmer higher than the conventional farmers.

On the other hand, organic vegetable farmers commonly have lower human capital and financial capital than conventional vegetable farmers. *Table 5* shows that the human capital owned by organic vegetable farmers is lower than conventional vegetable farmers because organic farmers have shorter farming experience and have a greater number of dependents and sick families than conventional vegetable farmers, although the difference between organic and conventional is not statistically significant. Organic vegetable farmers also to have lower financial capital than conventional vegetable farmers, although the difference between organic and conventional is not statistically significant. Organic farmers have greater farming and labor income than conventional vegetable farmers, but organic farmers have a lower number of livestock savings and a higher level of dependency than conventional vegetable farmers. A higher level of dependency of organic farmer than conventional vegetable farmers because organic farmers have more family members than conventional farmers.

Table 5. *Indicator values of buffer capacity component*

Indicators - description	Organic	Conventional	Difference[a]	
Human capital	0.479	0.483	-0.004	
Duration of education	0.391	0.371	0.020	
Farming experience	0.270	0.322	-0.052	
Other skills besides farming	0.281	0.249	0.032	
Number of sick family member	0.973	0.991	-0.018	
Financial capital	0.279	0.285	-0.006	
Annual income of vegetable farming	0.283	0.174	0.109	***
Livestock saving	0.048	0.079	-0.031	**
Annual labor income	0.048	0.038	0.010	
Dependency ratio	0.738	0.847	-0.109	***
Social capital	0.046	0.024	0.022	**
Asset increase due to organization partnership	0.023	0.001	0.022	**
Support of workforce from the group	0.063	0.022	0.041	**
Use of group equipment	0.053	0.049	0.004	
Physical capital	0.047	0.009	0.038	**
Machinery, equipment, buildings, farming wells	0.047	0.009	0.038	**
Natural capital	0.751	0.617	0.134	***
Weighted averaged soil fertility of the land owned by farmer	0.751	0.617	0.134	***

[a] t-test for differences in the mean of two groups. ***Significant at level 1%. **Significant at level 5%

http://www.aloki.hu ● ISSN 1589 1623 (Print) ● ISSN 1785 0037 (Online)
DOI: http://dx.doi.org/10.15666/aeer/1705_1120911232

The indicator values of the self-organization components that make up the livelihood resilience index are presented in *Table 6.* Reliance on own resources owned by organic and conventional vegetable farmers contribute greatly to the value of self-organization, followed by trust and cooperation and network. Organic and conventional vegetable farmers do not have to travel far distance to obtain inputs. In addition, the people surrounding them also trust each other in terms of lending and borrowing. However, cooperation and network of organic vegetable farmers are higher than conventional farmers, since organic vegetable farmers have established a cooperation with other parties and have better participation in organizations than conventional vegetable farmers.

Table 6. *Indicator values of the self-organization component*

Indicators - description	Organic	Conventional	Difference[a]	
Cooperation and network	0.330	0.259	0.071	**
Number of group organization followed by farmers	0.330	0.259	0.071	**
Trust	0.593	0.566	0.027	
Trust between community members in lending and borrowing funds	0.330	0.259	0.071	**
Reliance on own resources	0.754	0.747	0.007	
The closest distance needed to obtain farming inputs	0.754	0.747	0.007	

[a]t-test for different means of the two groups. **Significant at the 5% level

Table 7 presents the indicator values of the learning capacity component of conventional vegetable and organic vegetable farmers. Three indicators, namely knowledge of threat and opportunities, knowledge sharing capability, and knowledge identification capability of monitoring contribute to higher value than other indicators. This indicates that these indicators contribute highly to the learning capacity of organic and conventional vegetable farmers. Other indicators such as shared vision, commitment to learning, capability sharing and functioning feedback mechanism shared by organic and conventional vegetable farmers indicate a low value.

All description and indicator values of learning capacity of organic vegetable farmers are higher than those of conventional vegetable farmers (*Table 7*). Organic vegetable farmers have better knowledge at analyzing threats and opportunities, various visions, commitment to learning and knowledge of identification, knowledge sharing and transfer, as well as better feedback mechanism than conventional vegetable farmers. The significant difference in the indicator of the learning capacity component between organic vegetable farmers and conventional vegetable farmers lies in commitment to learning, knowledge of identification capability of monitoring, knowledge sharing capability, knowledge transfer capability, and feedback mechanism function. This indicates that organic vegetable farmers have more regular meetings with extension workers, and allocated time per month to find information on technology. Organic farmers also know better the best time to sell and buy products that conventional farmers. Furthermore, organic farmers have applied, adopted, and plan to used more technology, better ability in providing and receiving information from other actors, and more frequency of interactions with officers related to business production in groups than conventional vegetable farmers.

http://www.aloki.hu ● ISSN 1589 1623 (Print) ● ISSN 1785 0037 (Online)
DOI: http://dx.doi.org/10.15666/aeer/1705_1120911232

Table 7. *Indicator values of the learning capacity component*

Indicators - description	Organic	Conventional	Difference[a]	
Knowledge of treat and opportunities	0.593	0.566	0.027	
The ability to analyze threats	0.459	0.458	0.001	
Ability to analyze opportunities	0.727	0.673	0.054	*
Shared vision	0.099	0.074	0.025	
Frequency of discussion on farming development	0.099	0.074	0.025	
Commitment to learning	0.093	0.054	0.039	**
Frequency of regular meetings	0.103	0.060	0.043	**
Discussion frequency on the previous farming performance	0.101	0.079	0.022	
Time allocated per month to find information on technology	0.076	0.025	0.051	**
Knowledge identification capability-monitoring	0.237	0.089	0.148	***
The best time to sell and buy the best product	0.098	0.060	0.038	*
Frequency of consultation on planning agricultural products	0.670	0.321	0.349	***
The number of technological innovations to be applied by farmers in the upcoming planting season	0.065	0.016	0.049	***
The number of technological innovations tested by farmers in the last 12 months	0.084	0.034	0.050	**
Number of technological innovations adopted by farmers in the last 12 months	0.366	0.104	0.262	***
Number of technological innovations applied now	0.284	0.070	0.214	***
Frequency in discussing the problem of farming production with other actors in the group	0.089	0.015	0.074	***
Knowledge sharing capability	0.029	0.005	0.024	*
Number of farmers given new information or methods by respondent farmers	0.029	0.005	0.024	*
Knowledge transfer capability	0.423	0.274	0.149	***
The number of ideas that farmers learn from other farmers and other actors	0.423	0.274	0.149	***
Functioning feedback mechanism	0.127	0.031	0.096	***
Frequency of interaction with officers related to business production in groups.	0.127	0.031	0.096	***

[a]t-test for mean differences of the two groups. [***]Significant at level 1%. [**]Significant at level 5%. [*]Significant at level 10%

The measurement of the resilience indicator values of organic and conventional vegetable farmers' livelihoods are presented in *Figure 2*. The value of buffer capacity of organic vegetable farmers (0.321) is higher than conventional vegetable farmers (0.283), learning capacity of organic farmers (0.229) is higher than conventional vegetable farmers (0.156), and the value of organic farmers' self-organization (0.559) is higher than conventional farmers (0.524). Organic farmers have a better buffer capacity, learning capacity and self-organization in dealing with climate change than conventional vegetable farmers. Self-organizing ability of organic vegetable farmers is slightly different from conventional vegetable farmers, indicating that organic and conventional vegetable farmers are in the trustworthy community and relatively close distance in obtaining the inputs.

http://www.aloki.hu ● ISSN 1589 1623 (Print) ● ISSN 1785 0037 (Online)
DOI: http://dx.doi.org/10.15666/aeer/1705_1120911232

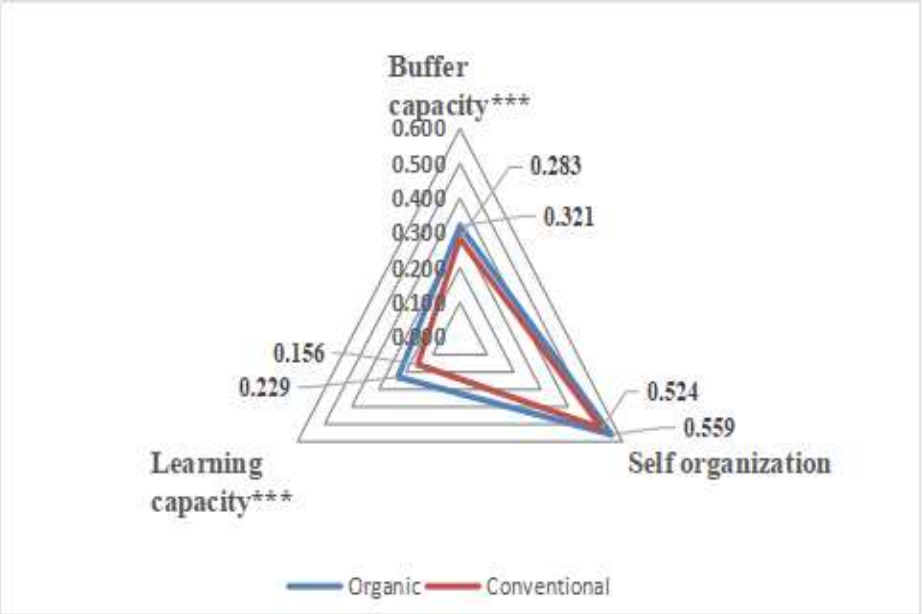

Figure 2. *Comparison between the indicator value of livelihood resilience between organic vegetable farmers and conventional vegetable farmers. (Note: the highest value of each indicator is 1; *** significant at the level of 1% based on the results of the t-test for mean differences of the two groups)*

Livelihood resilience index of organic and conventional farmers in dealing with climate change

Figure 3 showed that the value of livelihood resilience of organic vegetable farmers (0.375) in dealing with climate change was higher than that of conventional vegetable farmers (0.329). Organic vegetable farmers are more resilient to climate change than conventional vegetable farmers. *Figure 2* shows that the self-organization of organic vegetable farmer and conventional vegetable farmers contribute the most to livelihood resilience index. The second and third indicator that contributes to livelihood resilience index is buffer capacity and learning capacity.

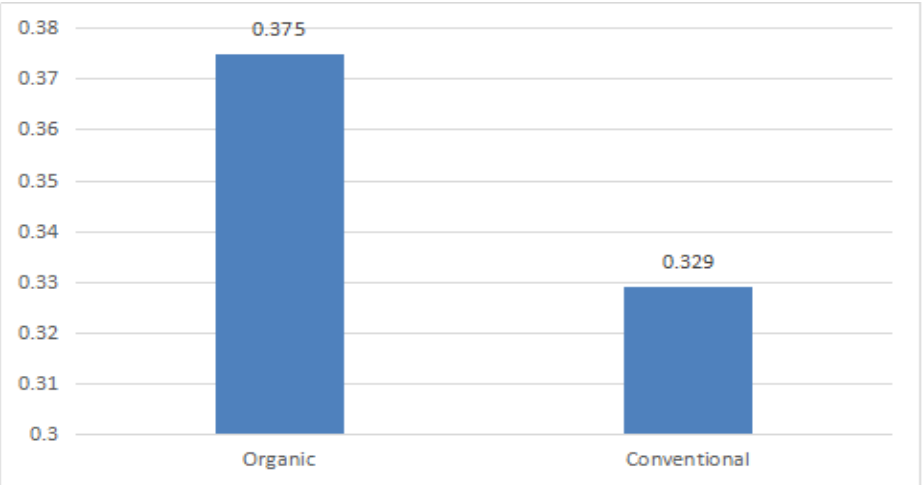

Figure 3. *Livelihood resilience index of organic and conventional vegetable farmers*

http://www.aloki.hu ● ISSN 1589 1623 (Print) ● ISSN 1785 0037 (Online)
DOI: http://dx.doi.org/10.15666/aeer/1705_1120911232

Determinants that influence the livelihood resilience of organic and conventional vegetable farmers in dealing with climate change

Important determinants that affect the livelihood resilience index of organic and conventional vegetable farmers in dealing with climate change are presented in *Table 8*. The analysis shows that the livelihood resilience index of organic vegetable farmers in dealing with climate change is influenced by household size, engagement in trade, access to extension service and the number of adaptation strategies adopted by farmers to reduce the impact of climate change. On the other hand, conventional farmers' livelihood resilience index in dealing with climate change is influenced by household size, farmers' access to climate information, access to climate training and the number of strategies adopted by conventional vegetable farmers to reduce the negative impacts of climate change. Each important determinant that influences the level of livelihood resilience of organic and conventional farmers in dealing with climate change are listed as follows:

1. Age

The age of farmers does not affect livelihood resilience index of both organic and conventional farmers in the face of climate change.

2. Household size

Household size affects the level of livelihood resilience of organic and conventional farmers. The negative household size coefficient indicates that the increase in household size of organic and conventional farmers will reduce the level of livelihood resilience of farmers in dealing with climate change. The coefficient of household size for organic and conventional farmers is 0.012 and 0.008 respectively, indicating that any increase in household size of one person will reduce the livelihood resilience index of organic farmers by 0.012 points and conventional farmers by 0.008 points.

3. Engagement in trade

Engagement in trade has a significant effect on the livelihood resilience index of organic farmers. Positive coefficients indicate that farmers who have established trading cooperation in selling farm products with other parties will have higher resilience in dealing with climate change than farmers who do not cooperate with other parties.

4. Access to credit

The access of organic and conventional farmers to credit does not affect the livelihood resilience index of farmers in the face of climate change.

5. Access to extension services

Farmer's access to extension services only has a significant effect on the livelihood resilience of organic farmers in the face of climate change. The coefficient of access to extension services with a positive sign indicates that organic farmers who have access to extension services have a better livelihood resilience in facing climate change than farmers who do not have access to extension services.

6. Access to climate information

Farmer's access to climate information influences the livelihood resilience indexes of conventional farmers in the face of climate change. The access to climate information coefficient of organic farmers having a positive sign indicates that organic farmers who have access to climate information have better livelihood resilience in dealing with climate change than farmers who do not have access to climate information.

7. Access to climate training

Farmers' access to climate training has a positive and significant effect on conventional farmers' livelihood resilience index, meaning that conventional farmers

http://www.aloki.hu ● ISSN 1589 1623 (Print) ● ISSN 1785 0037 (Online)
DOI: http://dx.doi.org/10.15666/aeer/1705_1120911232

who have access to climate training have higher resilience in dealing with climate change than farmers who do not have access to climate training.

8. Number of adaptation strategies

The number of adaptation strategies will affect the level of livelihood resilience of organic and conventional farmers in the face of climate change. The number of adaptation strategies coefficient shows a positive sign, meaning that each increase in the number of adaptation strategies implemented by organic and conventional farmers can increase the livelihoods resilience index of farmers in dealing with climate change.

Table 8. *Analysis of OLS important determinants that influence the level of livelihood resilience of organic and conventional farmers in dealing with climate change*

Explanatory variabel	Expected sign	Organic farmers		Conventional farmers	
Age	+	0.000 (0.001)		-0.001 (0.001)	
Household size	+	-0.012 (0.005)	**	-0.008 (0.005)	*
Engagement in trade	+	0.033 (0.018)	*	0.007 (0.015)	
Access to credit	+	-0.005 (0.014)		-0.022 (0.016)	
Access to extension services	+	0.023 (0.013)	*	-0.010 (0.008)	
Access to climate information	+	0.002 (0.013)		0.027 (0.012)	
Access to climate training	+	0.030 (0.021)		0.060 (0.021)	**
Number of adaptation strategies	+	0.015 (0.005)	**	0.011 (0.004)	**
Constant	+	0.289 (0.048)	***	0.313 (0.041)	***
Sig. F test		0.007		0.005	
R-Square		0.179		0.126	

The exploratory OLS model has passed all the diagnostic tests, such as multicollinearity tests, heteroscedasticity test, and diagnostic plots to check the normality and linearity assumptions. ***Significant at level 1%. **Significant at level 5%. *Significant at level 10%. The standard error in parentheses

Discussion

The study confirms that the buffer capacity, self-organization and learning capacity of organic vegetable farmers is higher than that of conventional vegetable farmers. Social capital, natural capital and physical that make up the buffer capacity of organic vegetable farmers is higher than that of conventional vegetable farmers. Organic vegetable farmers also have more fertile land and equipment to support farming activities. However, financial capital of organic vegetable farmers in the study area is lower than that of conventional farmers, although vegetable farming income received by organic farmers is higher than that received by conventional farmers. Farming income

http://www.aloki.hu ● ISSN 1589 1623 (Print) ● ISSN 1785 0037 (Online)
DOI: http://dx.doi.org/10.15666/aeer/1705_1120911232

and participation of farmers in groups can increase buffer capacity in dealing with climate change (Jacobi et al., 2015).

Organic vegetable farmers have better self-organization and learning capacity than conventional farmers. The majority of organic vegetable farmers in research locations are incorporated in farmer groups. Farmer groups can also increase learning capacity of organic vegetable farmers to be higher than that of conventional vegetable farmers. Farmers can exchange information related to cultivation, plant disease, pests, harvests, product prices and farming problems due to climate change. Farmer groups also become a key place for farmers to obtain and exchange information and technology between farmers (Bryan et al., 2013). It is noteworthy that organic vegetable farmers and their surrounding communities trust each other very well. Organic farmers can also get their farming inputs in a relatively closer distance than that of conventional farmers. For example, organic farmers can easily find the ingredients for making vegetable pesticides in their surroundings. Organic vegetable farmers receive various information from farmer groups and surrounding communities. The results of this study are in line with those of Jacobi et al. (2015), which states that organic farmers have better networks than conventional farmers.

The second analysis confirms that organic vegetable farmers in the study area are more resilient than conventional vegetable farmers, which is in line with Jacobi et al. (2015). Organic farmers are more resilient because of group membership or cooperation that can increase their adaptive capacity and buffer capacity (Jacobi et al., 2015). Resilience of organic and conventional vegetable farmers in research locations rests on self-organizations. Vegetable farmers in the face of climate change should use this self-organization ability to increase buffer capacity and learning capacity. In many developing countries, organic farming systems have the potential to maintain farmers' livelihoods when farmers are adversely affected by climate change. In addition, organic farming production and income are often the same or higher than those of conventional farmers (Scialabba, 2007). Resilience of organic farming also depends on the ability and experience of farmers in adaptation (Milestad and Darnhofer, 2003).

The third analysis confirms the important determinants that influence the level of resilience of organic and conventional vegetable farmers in the face of climate change. Important determinants affecting the livelihood resilience index of organic farmers in dealing with climate change are household size, engagement in trade, access to extension services, and the number of adaptation strategies implemented by farmers. On the contrary, conventional farmers' livelihood resilience index in dealing with climate change is affected by household size, access to climate information, access to climate training, and the number of adaptation strategies applied by conventional farmers to reduce the impact of climate change.

The household size of vegetable farmers in the study location will influence the livelihood resilience index of organic vegetable farmers and conventional vegetable farmers in the face of climate change. However, this result is not in line with the research conducted by Weldegebriel and Amphune (2017), indicating that household size does not affect the livelihood resilience of farmers in the research area. The household size of organic vegetable farmers and conventional vegetable farmers in the research location indicate the number of family members to be borne by the household. Therefore, an increase of household size would reduce the livelihood resilience of farmers in dealing with climate change. Engagement in trade is positively and significantly affected by the resilience of organic vegetable farmers in the face of

http://www.aloki.hu ● ISSN 1589 1623 (Print) ● ISSN 1785 0037 (Online)
DOI: http://dx.doi.org/10.15666/aeer/1705_1120911232

climate change. The positive relationship between engagement in trade with farmers' resilience in dealing with climate change supports the research of Jacobi et al. (2015). Most of organic vegetable farmers in the research locations have marketing network for agricultural products with other parties. This marketing network ensures certain sales and price, making organic vegetable farmers have a higher income than conventional vegetable farmers. The received income of vegetable farming can increase the buffer capacity of farmers in dealing with climate change.

Organic vegetable farmers in the study area have better access to credit and extension services. Good accessibility can improve the self-organization and learning capacity of farmers in facing climate change. On this account, Jacobi et al. (2015) state that organic farmers are more resilient because they are integrated with farmer organizations that can increase their adaptive capacity and buffer the capacity to deal with climate change. Vegetable farmers at the research location regularly hold farmer group meetings, such as every once a month. At this group meeting, farmers obtain and share information about technology to increase production and efforts made to deal with the negative impacts of climate change. Other factors that influence the livelihood resilience of farmers in dealing with climate change are farmers' access to climate-related information and climate training. The results showed that conventional vegetable farmers' access to climate information and climate training had a positive effect on livelihood resilience, meaning that farmers who had access to climate information and climate training would be more resilient than those without access.

The number of adaptation strategies applied by farmers to reduce the negative impact of climate change also has a positive effect on the level of livelihood resilience of farmers in the face of climate change. In other words, an increase in each number of adaptation strategy can increase the livelihood resilience of farmers in the face of climate change. Adaptation of farmers to climate change will help farmers reduce the adverse effects of climate change. Vegetable farmers at the research site adopted an adaptation strategy in the form of mixed cropping, using superior varieties, planting water-intensive plants, rotating crops, adjusting planting and harvesting times, increasing doses of organic matter, using mulch, using shade, changing irrigation techniques, and using prey institutions. The number of adaptation strategies implemented by farmers to reduce the impact of climate change ranges from one to nine strategies. The combination of adaptation strategies implemented by farmers aims to maintain farming production. Production continuity can increase farmers' income so that the buffer capacity of farmers in facing climate change increases. This result is in line with the research conducted by (Tambo and Wünscher, 2017; Uy et al., 2011) Improved adaptation strategies are required to reduce the negative impacts of climate change, and the government plays a key role in increasing farmers' awareness and knowledge of climate change (Korkmsz, 2018). Farmers should consider the current and future impacts of climate change to establish adaptation strategies to be implemented in the face of climate change (Nhuan et al., 2018).

Conclusions

Overall, organic vegetable farmers have a better buffer capacity, self-organization, and learning capacity than conventional vegetable farmers. These three components contribute to the higher level of livelihood resilience index, so organic vegetable farmers are more resilient in dealing with climate change than conventional vegetable

http://www.aloki.hu ● ISSN 1589 1623 (Print) ● ISSN 1785 0037 (Online)
DOI: http://dx.doi.org/10.15666/aeer/1705_1120911232

farmers. Self-organization contributes the most to improving livelihood resilience, which increases the livelihood resilience index of farmers in the face of climate change. Therefore, both organic and conventional vegetable farmers should have applied self-organization to increase learning capacity and buffer capacity. It is possible to improve the resilience level of organic vegetable farmers in dealing with climate change through engagement in trade, accessibility of organic vegetable farmers to extension services, and more number of adaptation strategies. Meanwhile, the resilience level of conventional vegetable farmers can be increased through access to climate information, climate training access, and number of farmers' adaptation strategies. This study recommends that policymakers need to develop organic farming and institutions through cooperation and climate training program to increase farmers' resilience in dealing with climate change.

Acknowledgements. We also would like to express our sincere gratitude to Indonesian Agency for Agricultural Research and Development Ministry of Agriculture. This paper is part of a Ph.D. research project at Univeristas Gadjah Mada, Yogyakarta, Indonesia. Our sincere appreciation is also extended to all parties who have provided information to complete this article.

REFERENCES

[1] Abid, M., Schneider, U. A., Scheffran, J. (2016): Adaptation to climate change and its impacts on food productivity and crop income: perspectives of farmers in rural Pakistan. – Journal Rural Studies 47: 254-266. https://doi.org/10.1016/j.jrurstud.2016.08.005.

[2] Adiyoga, W., Lukman, L. (2018): Vegetable farmers' perception on adaptation to climate change in lowland and highland areas of South Sulawesi (Persepsi dan adaptasi petani sayuran terhadap perubahan iklim di Sulawesi Selatan). – Jurnal Hortikultura 27: 279-296. https://doi.org/10.21082/jhort.v27n2.2017.p279-296.

[3] Ali, A., Erenstein, O. (2017): Assessing farmer use of climate change adaptation practices and impacts on food security and poverty in Pakistan. – Climate Risk Management 16: 183-194. https://doi.org/10.1016/j.crm.2016.12.001.

[4] Ayyogari, K., Sidhya, P., Pandit, M. K. (2014): Impact of climate change on vegetable cultivation: A Review. – International Journal of Agriculture, Environment and Biotechnology 7: 145-155. https://doi.org/10.5958/j.2230-732X.7.1.020.

[5] Bryan, E., Ringler, C., Okoba, B., Roncoli, C., Silvestri, S., Herrero, M. (2013): Adapting agriculture to climate change in Kenya: household strategies and determinants. – Journal of Environmental Management 114: 26-35. https://doi.org/10.1016/j.jenvman.2012.10.036.

[6] Deressa, T. T., Hasan, R. M., Ringler, C., Alemu, T. T., Yusuf, M., Tadesse, T., Hassan, R. M., Ringler, C., Alemu, T. T., Yesuf, M., Deressa, T. T., Hassan, R. M., Ringler, C., Alemu, T. T., Yesuf, M. (2009): Determinants of farmers' choice of adaptation methods to climate change in the Nile Basin of Ethiopia. – Global Environmental Change 19: 248-255. https://doi.org/10.1016/j.gloenvcha.2009.01.002.

[7] FAO (2016): Resilience Index Measurement and Analysis Model. – Food and Agriculture Organization of the United Nations, Rome.

[8] Fosu-Mensah, B. Y., Vlek, P. L. G., MacCarthy, D. S. (2012): Farmers' perception and adaptation to climate change: A case study of Sekyedumase district in Ghana. – Environment, Development and Sustainability 14: 495-505. https://doi.org/10.1007/s10668-012-9339-7.

http://www.aloki.hu ● ISSN 1589 1623 (Print) ● ISSN 1785 0037 (Online)
DOI: http://dx.doi.org/10.15666/aeer/1705_1120911232

[9] Gbetibouo, G. A., Ringler, C., Hassan, R. (2010): Vulnerability of the South African farming sector to climate change and variability: an indicator approach. – Natural Resources Forum 34: 175-187. https://doi.org/10.1111/j.1477-8947.2010.01302.x.
[10] Haryono, Las, I. (2011): Mitigation strategy and agricultural adaptation to global climate change impacts (Strategi mitigasi dan adaptasi pertanian terhadap dampak perubahan iklim global), in: Prosiding Seminar Nasional "Era Baru Pembangunan Pertanian: Strategi Mengatasi Masalah Pangan, Bioenergi dan Perubahan Iklim. – Pusat Sosial EKonomi Kementerian Pertanian, Bogor, pp. 1-10.
[11] Ichdayanti, L. I. (2014): Farmer's responses and adaptation to climate change (Respon petani dan adaptasinya terhadap perubahan iklim). – Jurnal Agribisnis 8: 155-170.
[12] Irham, Saito, O., Mohri, H., Wirakusuma, G., Rohmah, F., Perwitasari, H. (2018): Traditional Farmers' Adaptation Strategies on Climate Change of Different Environmental Conditions in Yogyakarta Province, Indonesia. – In: Takeuchi, K., Saito, O., Matsuda, H., Mohan, G. (eds.) Resilient Asia: Fusion of Traditional and Modern Systems for a Sustainable Future. Springer Imprint, Tokyo.
[13] Jacobi, J., Schneider, M., Mariscal, M. P., Huber, S., Weidmann, S., Bottazzi, P., Rist, S. (2015): Farm resilience in organic and nonorganic cocoa farming systems in Alto Beni, Bolivia. – Agroecology and Sustainable Food Systems 39: 798-823. https://doi.org/10.1080/21683565.2015.1039158.
[14] Keil, A., Zeller, M., Wida, A., Sanim, B., Birner, R. (2008): What determines farmers' resilience towards ENSO-related drought? An empirical assessment in Central Sulawesi, Indonesia. – Climate Change 86: 291-307. https://doi.org/10.1007/s10584-007-9326-4.
[15] Korkmsz, M. (2018): Public awareness and perception of climate change: differences in concern about climate change in the west Mediterranean region of Turkey. – Applied Ecology and Environmental Research 16: 4039-4050. https://doi.org///dx.doi.org/10.15666/aeer/1604_40394050.
[16] Kurniawati, F. (2012): Knowledge and adaptation of vegetable farmers to climate change (Pengetahuan dan adaptasi petani sayuran terhadap perubahan iklim. Studi kasus: Desa Cibodas, Kecamatan Lembang, Kabupaten Bandung Barat). – Thesis. Universitas Padjajaran, Bandung.
[17] Lal, S. S. (2014): Climate change resilience and vulnerability of farmers in Nepal. – Doctoral Dissertation. Hiroshima University, Jepang.
[18] Makate, C., Makate, M., Mango, N. (2017): Smallholder farmers' perceptions on climate change and the use of sustainable agricultural practices in the Chinyanja Triangle, Southern Africa. – Social Science 6: 1-14. https://doi.org/10.3390/socsci6010030.
[19] Marseva, A. D., Putri, E. I. K., Ismail, A. (2016): Analysis of resilience factors of farmer households in facing climate variability (Analisis faktor resiliensi rumah tangga petani dalam menghadap variabilitas iklim). – Jurnal Ekonomi dan Pembangunan Indonesia 17: 15-27.
[20] Milambo, K. H. (2013): Farmers' adaptations to rainfall related climate variability risks and their implications on food security in the semi-arid Sikonge District, Tanzania. – Thesis. Sokoine University, Marogoro.
[21] Milestad, R., Darnhofer, I. (2003): Building farm resilience : the prospects and challenges of organic farming. – Journal of Sustainable Agriculture 23: 81-97. https://doi.org/10.1300/J064v22n03_09.
[22] Murphy, A. (2015): Creating Resilient Livelihoods A Cross-sectional Study of Livestock Farmers in the Paraguayan Chaco. – Wageningen University, Netherlands.
[23] Nhuan, M. T., Tue, N. T., Quy, T. D. (2018): Enhancing Resilience to Climate Change and Disasters for Sustainable Development: Case Study of Vietnam Coastal Urban Areas. – In: Takeuchi, K., Saito, O., Matsuda, H., Mohan, G. (eds.) Resilient Asia: Fusion of Traditional and Modern Systems for a Sustainable Future. Springer Imprint, Tokyo.
[24] Rejekiningrum, P., Las, I., Amien, I., Surmaini, E., Pramudia, A., Sarvina, Y. (2011): Adaptation to climate change in the agricultural sector (Adaptasi perubahan iklim sektor

http://www.aloki.hu ● ISSN 1589 1623 (Print) ● ISSN 1785 0037 (Online)
DOI: http://dx.doi.org/10.15666/aeer/1705_1120911232

pertanian). – Badan Penelitian dan Pengembangan Kementerian Pertanian Indonesia, Jakarta.

[25] Ruminta (2015): Analysis of decreased rice production due to climate change in Bandung Regency, West Java (Analisis penurunan produksi tanaman padi akibat perubahan iklim di Kabupaten Bandung Jawa Barat). – Jurnal Kultivasi 15: 37-45.

[26] Scialabba, N. (2007): Organic agriculture and food security. – Conference on Organic Agriculture and Food Security, Rome, 3-5 May.

[27] Speranza, I. C., Wiesmann, U., Rist, S. (2014): An indicator framework for assessing livelihood resilience in the context of social-ecological dynamics. – Global Environmental Change 28: 109-119. https://doi.org/10.1016/j.gloenvcha.2014.06.005.

[28] Surmaini, E., Runtunuwu, E., Irsal, L (2011): Efforts of agricultural sector in dealing with climate change (Upaya sektor pertanian dalam menghadapi perubahan iklim). – Jurnal Litbang Pertanian 30: 1-7. https://doi.org/10.21082/JP3.V30N1.2011.P1-7.

[29] Tambo, J. A (2016): Adaptation and resilience to climate change and variability in north-east Ghana. – International Journal of Disaster Risk Reduction 17: 85-94. http://dx.doi.org/10.1016/j.ijdrr.2016.04.005.

[30] Tambo, J. A., Wünscher, T. (2017): Enhancing resilience to climate shocks through farmer innovation: evidence from northern Ghana. – Regional Environmental Change 17: 1505-1514. https://doi.org/10.1007/s10113-017-1113-9.

[31] Tanner, T., Lewis, D., Wrathall, D., Bronen, R., Cradock-Henry, N., Huq, S., Lawless, C., Nawrotzki, R., Prasad, V., Rahman, M. A., Alaniz, R., King, K., McNamara, K., Nadiruzzaman, M., Henly-Shepard, S., Thomalla, F. (2015): Livelihood resilience in the face of climate change. – Nature Climate Change 1: 1-4. https://doi.org/10.1038/nclimate2431.

[32] Tesso, G., Emana, B., Ketema, M. (2012): Analysis of vulnerability and resilience to climate change induced shocks in North Shewa, Ethiopia. – Agricultural Sciences 03: 871-888. https://doi.org/10.4236/as.2012.36106.

[33] Thulstrup, A. W. (2015): Livelihood resilience and adaptive capacity: tracing changes in household access to capital in Central Vietnam. – World Development 74: 352-362. https://doi.org/10.1016/j.worlddev.2015.05.019.

[34] UNDP (2006): Human Development Report 2006: Beyond Scarcity: Power, Poverty and the Global Water Crisis. – UNDP, New York.

[35] Uy, N., Takeuchi, Y., Shaw, R. (2011): Local adaptation for livelihood resilience in Albay, Philippines. – Environmental Hazards 10: 139-153. https://doi.org/10.1080/17477891.2011.579338.

[36] Wahyuni, K. I. (2016): Economic value and livelihood vulnerability index of farmer's household in District Timor Tengah Utara, Province East Nusa Tenggara (Penilaian ekonomi dan indeks kerentanan rumahtangga petani di Kabupaten Timor Tengah Utara, Provinsi Nusa Tenggara Timur). – Thesis. Institut Pertanian Bogor, Bogor.

[37] Weldegebriel, Z. B., Amphune, B. E. (2017): Livelihood resilience in the face of recurring floods : an empirical evidence from Northwest Ethiopia. – Geoenvironmental Disasters 4: 1-19. https://doi.org/10.1186/s40677-017-0074-0.

http://www.aloki.hu ● ISSN 1589 1623 (Print) ● ISSN 1785 0037 (Online)
DOI: http://dx.doi.org/10.15666/aeer/1705_1120911232

APPENDIX

SURVEY QUESTIONNAIRE

LIVELIHOOD RESILIENCE OF VEGETABLE FARMERS: EFFICACY OF ORGANIC FARMING IN DEALING WITH CLIMATE CHANGE IN JAVA, INDONESIA

This research survey questionnaire is purely for academic purposes with the objective **"Assessing and comparing livelihood resilience between organic and conventional farmers and it determinant".** You are assured of confidentiality of any view expressed in relation to this research. I therefore entreat you to provide information as accurate as possible for true results. Thank you for your kind co-operation.

Questionnaire number	:
Name of interviewer	:
Date of interviewer	:
Name of respondent	:
District	:
Organic/conventional	:

A. FARMERS' CHARACTERISTICS AND ACCESSIBILITY

1. Age : ..... years
2. Household size : ..... person/people

Status in family	Age (years)

3. Do you have access to cooperation in selling crops? ☐ Yes, ☐ No
4. Do you have access to credit institution? ☐ Yes, ☐ No
5. Do you have access to extension services? ☐ Yes, ☐ No
6. Do you have access to climate information? ☐ Yes, ☐ No
7. Do you have access to participate in climate training? ☐ Yes, ☐ No

B. ADAPTATION TO CLIMATE CHANGE

1. Have you made any adjustments in your farming ways in response to climate change ? ☐ Yes, ☐ No
2. What adjustments in your farming ways have you made in response to climate change?

Adjustment in farming	Yes/No
Implementing mixed cropping	
Using superior varieties	
Growing non water-intensive vegetable	
Implementing crop rotation	
Adjusting planting and harvesting dates	
Increasing the does of organic matter	

http://www.aloki.hu ● ISSN 1589 1623 (Print) ● ISSN 1785 0037 (Online)
DOI: http://dx.doi.org/10.15666/aeer/1705_1120911232

Using mulch	
Using shade	
Changing irrigation techniques	
Using *pranata mangsa*	

C. LIVELIHOOD RESILIENCE

1. BUFFER CAPACITY

a) Human Capital

1. Education : ..... years
2. Farming experience : ..... years
3. Do you have other ability beside farming? ☐ Yes, (specify)....., ☐ No
4. How many family members are permanently ill? …….. person/people

b) Financial Capital

1. Please specify the type, quantity and selling price of the vegetable products that you have produced for the past year.

Type	Quantity	Price (USD/kg)

2. Please specify the type, number of livestock and the price of livestock that you currently have.

Type (cow/goat/others)	Quantity	Price per unit (USD)

3. Please state your work, time and income for you and your family members obtained from work as a laborer in the past year.

Actor (farmer/wife/ others)	Job	Working days a month	Daily earnings	Revenue per month	Period of work per year

c) Social Capital

1. Asset increase due to organization partnership

Please specify the name of group and the income you earn from your participation in a group.

Name of group	Income (USD)

2. Support of workforce from the group

Please state the group name, number of work days and the amount of labor support that you have received from group members in vegetable farming activities during the past year.

Name of group	Farming activities	Number of work days	Amount of labor support

http://www.aloki.hu ● ISSN 1589 1623 (Print) ● ISSN 1785 0037 (Online)
DOI: http://dx.doi.org/10.15666/aeer/1705_1120911232

3. Use of group equipment

Please specify the type and number of group equipment you have used in the past year.

Name of group	Equitment	Quantity

d) Physical Capital

Do the assets that you currently have, such as machinery, buildings, equipment, water storage, remain productive?

Assets	Quantity	Price per unit (USD)
1. Machinery		
2. Water storage		
3.		
4.		

e) Natural Capital

In your opinion, what is the level of soil fertility on your vegetable farming land? Please fill in 1 if the land is very infertile, 2 if it is not fertile, 3 if it is fertile, 4 if fertile, and 5 if it is very fertile.

Plot	Land area (m^2)	Soil fetility
1		
2		

2. SELF-ORGANIZATION

a) Cooperation and network

Please specify the name of the group or association that you are following.....

.....

b) Trust

What is the level of trust of the people around you in lending and borrowing? ….. %

Questions	Number of People
For example, there are five people around you who need funds for farming, and request a loan without interest. How many people will you give a loan?	
For example, you need a loan for farming. If there are five people around you, how many people will give you a loan?	

c) Reliance on own resources

What is the closest distance between farming land and input resources? …….. meters.

3. LEARNING CAPACITY

a) Knowledge of treat and opportunities

Could you mention the characteristics of the vegetables infected with the primary disease pests such as the following:

Primary disease pests	Yes/No
1. Shrinking leaves, dry shoots curved due to aphids.	
2. The leaves are seen shiny white spots and the become brown which shows	

http://www.aloki.hu ● ISSN 1589 1623 (Print) ● ISSN 1785 0037 (Online)
DOI: http://dx.doi.org/10.15666/aeer/1705_1120911232

trips.	
3. The leaves are damaged, hollow and the remaining leaf bones are attacked by caterpillars.	
4. For vegetables that have fruit, there are black streaks on the fruit and rot, which indicates fruit flies.	
5. Wilt that occurs in all parts of the plant starting from the leaves and suddenly shows attacked by bacterial wilt.	
6. Rounded spots resembling frog eyes with brownish edges on leaves that show leaf spots.	
7. The fruit is brown and black spotted that indicate an anthracnose attack.	
8. The fruit is brown, rotten, and wet due to fruit rot.	

Do you know the technology below to increase your vegetable farming production? Please give a sign (V) if you know.

Technology	Sign (V)
1. Use of superior seeds without genetic engineering (organic), and superior commercial seeds (conventional).	
2. Seedling and sorting of seeds before moving to the field, especially for small fruiting plants such as mustard greens, tomatoes, and eggplants. Whereas, for large fruiting plants such as cucumber, long beans, and beans, can be planted directly.	
3. Use of mulch for plants such as tomatoes, eggplants, and beans.	
4. Use of roofed shade.	
5. Making beds with a width of 100-120 cm and a height of 30 cm.	
6. The land is cultivated by hoeed or plowed to a depth of 30-40 cm.	
7. The provision of manure is 2-3 tons per 1000 square meters for organic farming, and around 1.5-3 tons per hectare for conventional farming.	
8. Recommended plant spacing according to each type of vegetable crop.	
9. Supplementary fertilization according to recommendation, namely the provision of manure, urine or other organic material (organic), and fertilizer application according to recommendations per plant.	
10. Crop rotation.	
11. Irrigation and watering management.	
12. Mechanical and organic pest and disease control (organic farming), and according to the principle of Integrated Pest Mangement (conventional farming).	
13. Yields are placed in shaded places and treated with care.	

b) Shared vision and commitment to learning

1. How many regular meetings with extension agents in the previous year?.....
2. Did you allocate time to find information on technology? ☐ Yes, that is … minutes/month. ☐No.
3. How many times have you discussed the development and performance of farming with farmers, extension, or other stakeholders during the last 12 months?

Actor	Frequency of farming development discussion	Frequency of farming performance discussion
Farmer		
Extension officer		
District agricultural officer		
Researcher		
Other (specify)		

c) Knowledge identification capability-monitoring

1. In your opinion, when is the right time to sell your agricultural products for the last 12 months to get a good price?.....
2. How many times have you consulted about farming planning forecasting?.....

http://www.aloki.hu ● ISSN 1589 1623 (Print) ● ISSN 1785 0037 (Online)
DOI: http://dx.doi.org/10.15666/aeer/1705_1120911232

3. Among the following technologies, give a sign (V) if the technology is used now and in the future, and technology has been tried once and adopted for the past 12 months.

Technology	Sign (V)			
	Tested	Adopted	Applied now	Applied in the upcoming planting season
1. Use of superior seeds without genetic engineering (organic), and superior commercial seeds (conventional).				
2. Seedling and sorting of seeds before moving to the field, especially for small fruiting plants such as mustard greens, tomatoes, and eggplants. Whereas, for large fruiting plants such as cucumber, long beans, and beans, can be planted directly.				
3. Use of mulch for plants such as tomatoes, eggplants, and beans.				
4. Use of roofed shade.				
5. Making beds with a width of 100-120 cm and a height of 30 cm.				
6. The land is cultivated by hoeed or plowed to a depth of 30-40 cm.				
7. The provision of manure is 2-3 tons per 1000 square meters for organic farming, and around 1.5-3 tons per hectare for conventional farming.				
8. Recommended plant spacing according to each type of vegetable crop.				
9. Supplementary fertilization according to recommendation, namely the provision of manure, urine or other organic material (organic), and fertilizer application according to recommendations per plant.				
10. Crop rotation.				
11. Irrigation and watering management.				
12. Mechanical and organic pest and disease control (organic farming), and according to the principle of Integrated Pest Mangement (conventional farming).				
13. Yields are placed in shaded places and treated with care.				
14. Others:.....				

4. How many times have you discussed farming problems with the following actors:

Actor	Frequency of farming problems discussion
Farmer	
Extension officer	
District agricultural officer	
Researcher	
Other (specify)	

d) Knowledge sharing capability

http://www.aloki.hu ● ISSN 1589 1623 (Print) ● ISSN 1785 0037 (Online)
DOI: http://dx.doi.org/10.15666/aeer/1705_1120911232

Have you ever provided information on technology or methods to other farmers for the past 12 months? ☐ Yes, if yes please fill in the table below. ☐ No.

Teknology	Number of farmers

e) Knowledge transfer capability

Have you ever received information on technology or methods from other partiesor the past 12 months? ☐ Yes, if yes please fill in the table below. ☐ No.

Technology	Sources (Sign V)				
	Farmers	Extension officer	District agricultural officer	Researcher	Other

f) Functioning feedback mechanism

How many times have you interacted with farmers, extension, related agencies, or researchers, in a community that discussed farming production for the past 12 months? ……..... meeting time.

http://www.aloki.hu ● ISSN 1589 1623 (Print) ● ISSN 1785 0037 (Online)
DOI: http://dx.doi.org/10.15666/aeer/1705_1120911232

ASSESSMENT OF SOIL LOSS FROM LAND USE/LAND COVER CHANGE AND DISASTERS IN THE LONGMEN SHAN MOUNTAINS, CHINA

CHEN, P.[1] – FENG, Z.[1*] – MANNAN, A.[1] – CHEN, S.[1]– ULLAH, T.[2]

[1]*Beijing Key Laboratory of Precision Forestry, Beijing Forestry University, Beijing 100083, China*

[2]*School of Nature Conservation, Beijing Forestry University, Beijing 100083, China*

**Corresponding author*
e-mail: fengzhongke@126.com; phone/fax: +86-138-1030-5579

(Received 9th Apr 2019; accepted 2nd Jul 2019)

Abstract. Soil erosion is the main cause of the decline in global available land resources, and China is one of the countries suffering from severe soil erosion. In this paper, the RUSLE model and GIS were used to assess the changes in soil erosion in different ecosystems and counties. The results showed that from 2005 to 2017, the highest rate of ecosystem change was in the other ecosystems category, with an increase in mean soil loss to 4.06 $t \cdot ha^{-1} \cdot year^{-1}$. For the counties, the highest soil erosion was recorded in Maoxian County during the study period, because Maoxian County was one of the severely affected counties in the Wenchuan Earthquake. The mean soil loss in Yingjing was relatively small, as the estimates for 2005 and 2017 were 0.08 $t\ ha^{-1} \cdot year^{-1}$ and 0.09 $t \cdot ha^{-1} \cdot year^{-1}$, respectively. The areas with severe soil loss are along rivers, mainly distributed along the Minjiang and Tuojiang River basins and their tributaries. The findings of our study will be helpful for identifying high-risk zones, and developing policies to minimize human, environmental and economic losses in any disastrous event.
Keywords: *soil erosion, revised universal soil loss equation, Landsat, geo-hazards, ecosystem*

Introduction

Soil is a limited natural resource that is vital for human survival (Stefano et al., 2016; Gao and Cao, 2011). Soil erosion is one of the important reasons for the decline in global available land resources. Global soil erosion causes a loss of 2.5 to 4 billion tons of topsoil every year, directly costing $40 billion. Soil erosion also leads to a decline in crop yields, hinders global economic development, and poses a threat to food security and human welfare (FAOUN, 2015; Luca, 2015). China has long suffered from soil erosion (Xiao et al., 2016; Gao and Cao, 2011), and approximately 37.6% of its land resources are affected by soil erosion (Gao et al., 2016; Zhang et al., 2012). Soil erosion is a form of soil degradation, which refers to the process of destruction, separation and sedimentation of soil and its parent material under the external force of hydraulics, wind, freeze-thaw cycles or gravity (Meyer, 1984). Soil erosion has become a focus of global research, because of a series of associated ecological and environmental problems, such as land degradation, and soil fertility loss (Luca, 2015).

The occurrence of soil erosion is determined by natural factors and is influenced by human factors (Guo, 2010). Natural factors determine the occurrence and development of water and soil loss in the region, and human factors have the positive effect of controlling soil loss and have the negative effect of accelerating soil loss, such as land use and land cover (LULC) change (Wischmeier, 1978). Climate change and global warming caused by LULC changes directly or indirectly affect soil erosion at different

http://www.aloki.hu ● ISSN 1589 1623 (Print) ● ISSN 1785 0037 (Online)
DOI: http://dx.doi.org/10.15666/aeer/1705_1123311247

scales, accelerating the soil erosion rate (Konukcu et al., 2017; Nojarov et al., 2015). Other human activities disturb the land surfaces of the earth, thus altering the rate of natural erosion and rate of soil degradation (Rompaey et al., 2010; Sharma et al., 2007). The intensities of soil erosion are closely related to land use and are greatly affected by changes in LULC (Wang et al., 2018; Ferreira et al., 2015; Leh et al., 2013). Many previous studies have shown that changes in land use or surface vegetation accelerate soil erosion (Diyabalanage et al., 2017; Ganasri and Ramesh, 2016; Zhang et al., 2017; Balasubraman et al., 2015).

In addition, the occurrence of earthquakes and secondary geological disasters will also aggravate soil erosion (Hovius et al., 2011; Lin et al., 2006). After an earthquake, the surface soil is easily disturbed or buried by secondary geological disasters, destroying the structure of the surface soil. Secondary geological disasters caused by earthquakes, such as landslides, mudslides, and collapses, provide a large amount of loose solid matter for soil erosion under the influence of external forces such as rainfall, runoff, and earthquakes (Vittoz et al., 2001; Peng et al., 2012). The 5.12 Wenchuan Earthquake (Ms 7.9) was one of the most devastating earthquakes in China. Due to the loose soil, steep slope, surface vegetation destruction and additional rainfall after the earthquake, the soil erosion in this area was intensified. After the earthquake, preliminary statistics from the National Bureau of Statistics of China showed that soil erosion occurred in 149.2 km^2 of land, an increase of 11.03% over the previous period (Gan et al., 2018). The area of vegetation damaged by earthquakes in Sichuan Province is 32.867×10^4 ha (FDSP, 2008). After the vegetation is destroyed, the bedrock is exposed, and the "buffering" protective layer that prevents surface erosion by rainfall is lost, which aggravates the erosion rate of the loose material on the surface layer (Cui et al., 2010). Therefore, it is particularly important to quantify the effects of soil erosion and to develop effective soil protection measures (Santillan et al., 2010).

Numerical models are important methods for assessing and predicting soil erosion (Panagos et al., 2017). Various soil erosion models, including the Universal Soil Loss Equation (USLE) (Wischmeier and Smith, 1978), the Modified USLE (MUSLE) (Williams, 1975), the Revised USLE (RUSLE) (Renard et al., 1997), and the Unit Stream Power-based Erosion Deposition (USPED) (Mitasova et al., 1996), or physically-based models, such as the Water Erosion Prediction Project (WEPP) (Nearing, 1997) and the European Soil Erosion Model (EUROSEM) (Morgan et al., 2015), have been developed for estimating, analysing and predicting soil erosion. Among these models, the RUSLE is the most commonly used to estimate the long-term soil erosion rate of hillsides in large-scale studies (Rulli et al., 2013; Panagos et al., 2015; Ganasri et al., 2016; Zhao et al., 2017). This model has been proven effective for estimating soil loss in different parts of the world. An increasing number of studies combine RUSLE and USLE with 3S (GIS, RS, and global positioning system (GPS)) to detect soil erosion rates at different temporal and spatial scales, along with aerospace and computer technology (Alexakis et al., 2014; Anees et al., 2014).

The study area is in the Longmen Shan fault zone, which is the overlying zone of the Qinghai-Tibet Plateau and the Sichuan Basin. It is an important sensitive zone of China's ecological environment because of its complex geological structures and rich biodiversity. During and after the Wenchuan Earthquake (May 12, 2008) the natural environment of the area in the Longmen Shan fault zone deteriorated. Long-term effects and complex aftershocks have caused a series of environmental problems, such as disturbance of ecosystems, vegetation loss and soil degradation. The objective of this

http://www.aloki.hu ● ISSN 1589 1623 (Print) ● ISSN 1785 0037 (Online)
DOI: http://dx.doi.org/10.15666/aeer/1705_1123311247

study is to use GIS technology to quantitatively evaluate soil erosion in the Longmen Shan area in 2005, 2008, 2010 and 2017 using the RUSLE model to explore the response of soil erosion to LULC changes and the impact of earthquakes on soil erosion. Analysis of the evolution process of soil erosion provides a reference for soil and water conservation in the Longmen Shan area.

Materials and methods

Study area

The Longmen Shan fault covering an area of 55213 km^2 is extended from Luding and Tianquan in the south to Baoxing, Dujiangyan, Jiangyou and Guangyuan Cities in the northeast, and it enters the area of Ningqiang and Jixian in Shaanxi Province. The total length of the Longmen Shan fault is 500 km, and the width is 40-50 km. The peaks are undulating and the river valleys are both vertical and horizontal. The terrain is extremely complicated and is located in the transition zone between the Tibetan Plateau and Sichuan Basin. The terrain forms a natural boundary between the Chengdu Plain and the western Sichuan Plateau. The area has an elevation range of 309~7100 m (*Fig. 1*), and the overall terrain is high in the west and low in the east, with the highest point being 7100 m (Yong, 2006). The landform is mainly in the piedmont alluvial plains, mountains and plateaus (Yong, 2006). The Longmen Shan fault zone consists of four nearly parallel faults, namely, the southeastern boundary of the Longmen Shan fault zone, Guanxian-Anxian fault, central main Yingxiu-Beichuan fault, and the northwestern boundary of the Wenchuan-Maoxian and Qingchuan fault. The temperature in the Longmen Shan area decreases with increasing elevation, showing a geographical distribution of high temperatures in the east and low temperatures in the west, and the three-dimensional climate features are obvious, forming a distinct, unique and diversified vertical climate zone in the region. The mountainous areas with an elevation of 1000-2000 m belong to the humid climate zone, while the polar regions with an elevation of 2000-5000 m belong to the cold alpine climate zone (Li, 2013). The water system in the Longmen Shan fault area is dominated by horizontal rivers. The river and streams flow perpendicular to the Longmen Mountains and discharge into the Yangtze River. The study area has a rich diversity of plants and animal species, such as *Panda*, *Davidia involucrata*, *Cercidiphyllum Japonicum*, and *Ginkgo biloba* (Di et al., 2010).

Data acquisition

The satellite imageries for the years 2005, 2008, 2010 and 2017 were used for this study to see the soil erosion because of LULC changes. Landsat thematic mapping and enhanced thematic mapping (TM and ETM+) for 2005, and SPOT5 and HJ-1 for 2008, 2010, and 2017 were used to classify LULC changes in the study area. TM and ETM + have a 30 m spatial resolution. The important possible drivers of LULC change, including the expansion of farmland, massive resettlement and expansion of mechanized farming in recent years, were captured by selecting the specific periods. In addition, field surveys were carried out from July to September identify to various LULC change classes that prevail in the study area. A digital elevation model (DEM) of the study area with a 30 m resolution was also downloaded from http://www.Gscloud.cn for processing and analysing erosion parameters.

http://www.aloki.hu ● ISSN 1589 1623 (Print) ● ISSN 1785 0037 (Online)
DOI: http://dx.doi.org/10.15666/aeer/1705_1123311247

The rainfall data of Sichuan Province and its surrounding cities were taken from the China Meteorological Science Data Sharing Service Network (http://cdc.Cma.gov.cn), whereas the soil map of the area was obtained from the Nanjing Institute of Soil Science, Chinese Academy of Sciences.

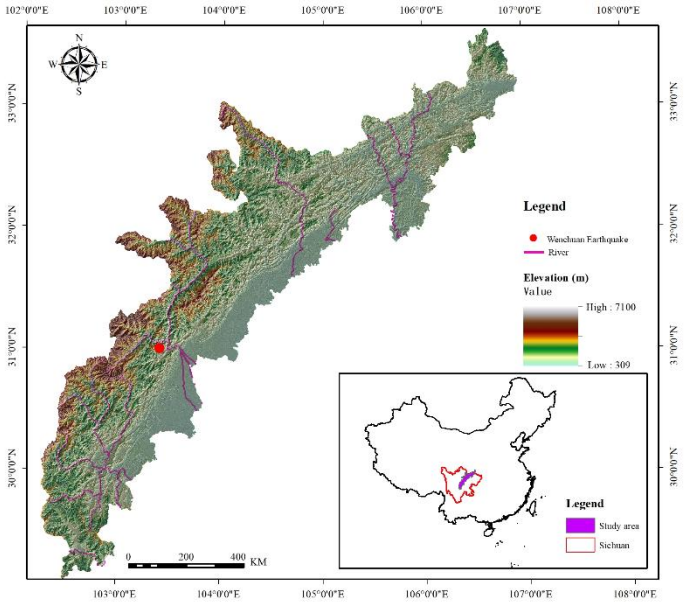

Figure 1. *Location and digital elevation model (DEM) of the study area*

Methodology

We used the RUSLE model, which is an improved version of the USLE developed by Wischmeier and Smith (1978), to estimate annual soil loss. The estimate of soil erosion generated by RUSLE, which has been widely used in soil erosion, is reliable (Anees et al., 2018; Haregeweyn et al., 2017). GIS and RUSLE widely adopted conservation-planning tools throughout the world, which are user-friendly and applicable for a basin with limited data. The RUSLE equation is expressed as follows:

$$A = R \times K \times LS \times C \times P \quad \text{(Eq.1)}$$

where A is the actual soil loss (t ha^{-1} $year^{-1}$), R is the rainfall erosivity factor (m.t.cm/ha.h.y), K is the soil erodibility factor (dimensionless), LS is the slope length and slope steepness factor (dimensionless), C is the cover management factor (dimensionless), and P is the conservation practices factor (dimensionless).

Estimation of rainfall erosivity (R-factor)

The rainfall erosivity factor reflects the erosion potential of rainfall under standard conditions. This factor is a dynamic indicator for evaluating soil stripping and handling erosion, and directly affects the prediction accuracy of the soil erosion model (Özşahin et al., 2018). The annual rainfall erosivity value (R) (Wang and Jiao, 1996) was determined by analysing annual rainfall data from 150 stations in Sichuan and its surrounding cities using *Equation 2:*

http://www.aloki.hu ● ISSN 1589 1623 (Print) ● ISSN 1785 0037 (Online)
DOI: http://dx.doi.org/10.15666/aeer/1705_1123311247

$$R = 0.207(P \cdot I_{60} / 100)^{1.205} \quad \text{(Eq.2)}$$

where R is the annual erosivity (m.t.cm/ha.h.y), I_{60}-year is the maximum 60 min rainfall (mm), and P-year is the rainfall total (mm). In this study, the R value of the rainfall station in the Longmen Shan area and surrounding provinces was calculated by the above formula (*Eq. 2*), and then, the R-value map of the Longmen Shan area was obtained by interpolation using "Kriging" in the ArcGIS platform (Diodato and Bellocchi, 2007).

Soil erodibility factor estimation (K-factor)

The soil erodibility factor (K) is a quantitative description of the intrinsic erodibility of a particular soil and an indicator of the sensitivity of soil properties to erosion (Zhai et al., 2011). The K-factor represents the relationship among annual average soil loss, hydraulic processes, and sediment transportability under ordinary soil conditions (Özşahin et al., 2018). In this study, the K-factor was estimated by combining the results of the studies (Zhujun et al., 2019; Wang et al., 2018) utilizing *Equation 3:*

$$K = \left\{0.2 + 0.3\exp\left[-0.0256 * SAN(1 - \frac{SIL}{100})\right]\right\}(\frac{SIL}{CLA + SIL})^{0.3} * (1.0 - \frac{0.25C}{C + \exp(3.72 - 2.95C)}) * (1.0 - \frac{0.25SN1}{SN1 + \exp(-5.51 + 22.9SN1)}) \quad \text{(Eq.3)}$$

$$SN1 = 1 - SAN / 100 \quad \text{(Eq.4)}$$

where SAN, SIL, and CLA are the mass fractions (%) of sand, silt and clay, respectively; and C is the mass fraction of soil organic carbon (SOC) (%). The soil type and the SOC data were captured from the soil data.

The K-factor map, obtained using the kriging spatial interpolation method in GIS, is more suitable for soil moisture spatial interpolation in the Longmen Shan region (Yao et al., 2013).

Estimation of the slope length and slope gradient factor (LS-factor)

The LS-factor in RUSLE reflects the ratio of gross soil loss under given conditions with respect to slope length (L-factor) and slope steepness (S-factor) (Renard et al., 1997). The slope length is closely related to soil erosion. On a regional scale, the factors, including the slope length (L) and slope steepness (S), were calculated by using the DEM (30 m×30 m) of the study area. The method developed by Wischmeier and Smith was adopted to calculate L using *Equation 5:*

$$\begin{cases} L = (\lambda / 22.13)^{\alpha} \\ \alpha = \beta(\beta + 1) \\ \beta = (\sin\theta / 0.089) / [3.0 \times (\sin\theta)^{0.8} + 0.56] \end{cases} \quad \text{(Eq.5)}$$

where λ is the slope length (m), 22.13 represents the slope length of the standard district (m), α is the index of the slope length calculated using the method by Renard (1997), β

http://www.aloki.hu ● ISSN 1589 1623 (Print) ● ISSN 1785 0037 (Online)
DOI: http://dx.doi.org/10.15666/aeer/1705_1123311247

indicates the ratio of rill to inter rill erosion, and θ represents the slope gradient extracted from the DEM data. The effect of slope gradient on erosion (Zhao et al., 2017) is represented by the steepness factor (S) of the slope, which is calculated using the equation established by Liu et al. (Liu et al., 2000). The greater the slope steepness factor is, the greater the possibility of soil loss and the more severe the soil erosion. The slope steepness factor is calculated as follows:

$$\begin{cases} S = 10.8 \times \sin\theta + 0.03 & \theta < 5^{\circ} \\ S = 16.8 \times \sin\theta - 0.5 & 5^{\circ} \le \theta < 10^{\circ} \\ S = 21.91 \times \sin\theta - 0.96 & \theta \ge 10^{\circ} \end{cases} \quad \text{(Eq.6)}$$

Based on the Map algebra function in ArcGIS (Version 10.2), L was calculated according to the equation. The LS value distribution is calculated by multiplying the spatial distribution of the S and L factors.

Estimation of cover management factor and support practice factor (C and P factor)

The C value reflects the impact of crop and management activities on erosion rate. The protective vegetation layer helps stabilize topsoil, thus preventing soil degradation, and plays an important role in enhancing soil impact resistance. The C value is an important indicator to evaluate the influence of vegetation factors on soil erosion capacity (Rao et al., 2013). The P value is the ratio of the amount of soil loss after soil conservation measures to the amount of soil loss without any soil conservation measures. This value reflects the inhibition of soil erosion by soil conservation measures. The C and P factors are dimensionless numbers between 0 and 1. In this study, by referring to the literature data, the C and the P values corresponding to the land use type are selected (*Table 1*), and the model automatically converts the field into a raster layer (Ran, 2015; Teng et al., 2018).

Results and discussion

The results revealed that significant LULC occurred in the Longmen Shan region (*Fig. 2*) after the Wenchuan Earthquake. The dynamic parameters (rainfall erosivity, cover management and conservation practices) were measured for 2005, 2008, 2010 and 2017. The different input parameters have the capacity to alter the rate of soil erosion (Özşahin et al., 2018). The precipitation data for 2005, 2008 and 2010 were merely used for R-factor values, and the results were 421.86 m.t.cm/ha.h.y, 392.04 m.t.cm/ha.h.y, 451.69 m.t.cm/ha.h.y and 402.37 m.t.cm/ha.h.y, respectively. The R-factor values in 2008 were lower than those in the other years. Vegetation cover is an important component of any prediction model, because it is the erosion risk variable most affected by human manipulation (Sahin and Kurum, 2002). In contrast, the C-factor values spatiotemporally varied due to LULC in the study area, such as the increase in the settlement and bare areas by 317 km^2 and 138 km^2, respectively, from 2005 to 2017. However, the LS and K factors are presented as individual maps because they do not change over time. The K-factor and a higher magnitude of the LS-factor were obtained in the Longmen Shan area.

http://www.aloki.hu ● ISSN 1589 1623 (Print) ● ISSN 1785 0037 (Online)
DOI: http://dx.doi.org/10.15666/aeer/1705_1123311247

Table 1. *Cover management factor (C) and support practice factor (P) values according to LULC classes*

Ecosystem type	Land use type	C value	P value
Forest ecosystem	Evergreen Needleleaf Forest	0.12	1
	Evergreen Broadleaf Forest	0.12	1
	Deciduous Needleleaf Forest	0.12	1
	Deciduous Broadleaf Forest	0.12	1
	Mixed Forests	0.12	1
	Shrub Forest	0.12	1
Grassland ecosystem	Meadow	0.18	1
	Barren Grassland	0.18	1
	Alpine Meadow	0.18	1
	Shrub Grassland	0.18	1
Farmland ecosystem	Paddy Field	0.25	0.15
	Irrigated Cropland	0.22	0.6
	Dryland Cropland	0.22	0.6
Settlement	Urban and Built-up	0	0
	Rural Settlement	0	0
Wetland ecosystem	Swamp	0.05	1
	Seaside Wetlands	0	0
	Water Bodies	0	0
	Bottom Land	0	0
	Ice and Snow	0	0
Others	Bare Rock	0	0
	Bare Land	1	1
	Sandy Land	1	1

LULC change

The rate of LULC change was computed from 2005 to 2017 (*Table 2*). The forest ecosystem area decreased by -181 km^2, and the rate of change in the forest ecosystem is relatively stable. The grassland and farmland ecosystem areas decreased by -336 km^2 and -334 km^2, respectively, from 2005 to 2017. The grassland ecosystem and farmland ecosystem have shown a negative rate of change for the study periods. The farmland ecosystem showed the highest rate of changes (-0.16%) in the period (2005-2017). In contrast, settlement, wetland ecosystems and other ecosystems showed a positive rate of change for both periods. Settlements and other ecosystems showed the highest rate of change (2.32% and 4%, respectively) in the period, and the areas of the settlement ecosystem and other ecosystems increased by 317 km^2 and 138 km^2, respectively.

Rapid and massive population growth, the main factor of these LULC changes, leads to overexploitation of natural resources and destruction of the ecological environment caused by the devastating May 12, 2008 Wenchuan Earthquake (Peng et al., 2012). In general, slope steepness, geology and shaking intensity are the main factors that affect the distribution of earthquake-induced landslides (Wang et al., 2007). Furthermore, Di et al. (2010) observed that the combination of elevation and slope may have contributed most to the distribution of mass landslides triggered by the Wenchuan Earthquake.

http://www.aloki.hu ● ISSN 1589 1623 (Print) ● ISSN 1785 0037 (Online)
DOI: http://dx.doi.org/10.15666/aeer/1705_1123311247

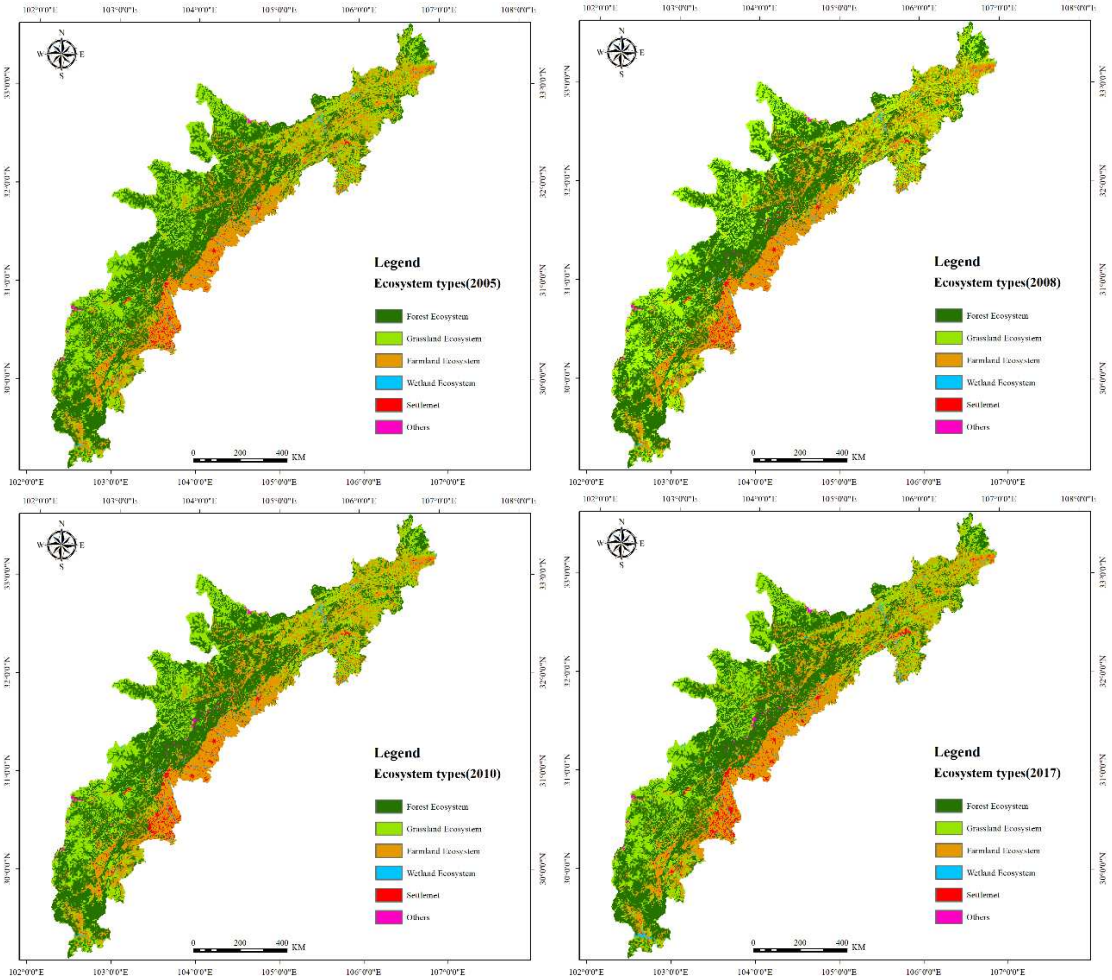

Figure 2. *Ecosystem types of 2005, 2008, 2010 and 2017 in the study area*

Table 2. *Change in land use and land cover*

Ecosystem	2005		2008		2010		2017		2005-2017 Change	
	Area (km^2)	Rate (%)	Area (km^2)	Rate (%)	Area (km^2)	Rate (%)	Area (km^2)	Rate (%)	Area (km^2)	Rate (%)
Forest	23929	41.82	24045	42.02	23979	41.90	23748	41.73	-181	-0.05
Grassland	15996	27.96	15837	27.68	15853	27.70	15660	27.52	-336	-0.14
Farmland	14009	24.48	13923	24.33	13816	24.14	13675	24.03	-334	-0.16
Settlement	780	1.36	805	1.41	911	1.59	1097	1.93	317	2.32
Wetland	390	0.68	424	0.74	424	0.74	467	0.82	77	1.21
Other	109	0.19	179	0.31	230	0.40	247	0.43	138	4.00

Soil loss of different ecological types

The soil loss was estimated by integrating the maps of the six RUSLE factors in a GIS environment. An overall increase in soil loss was observed for forest ecosystems,

http://www.aloki.hu ● ISSN 1589 1623 (Print) ● ISSN 1785 0037 (Online)
DOI: http://dx.doi.org/10.15666/aeer/1705_1123311247

grassland ecosystems, farmland ecosystems and other ecosystems from 2005 to 2010 (*Table 3*), and from 2010 to 2017, the soil loss for forest ecosystems, grassland ecosystems, farmland ecosystems and other ecosystems decreased. The total soil loss of the forest ecosystem in 2005, 2008, 2010 and 2017 was 276.88 × 10^4 t ha^{-1}·$year^{-1}$, 258.26 × 10^4 t ha^{-1}·$year^{-1}$, 295.76 × 10^4 t ha^{-1} $year^{-1}$, 152.62 × 10^4 t ha^{-1}·$year^{-1}$, respectively. The total soil loss of theg rassland ecosystem in 2005, 2008, 2010 and 2017 was 192.77 × 10^4 t ha^{-1}·$year^{-1}$, 176.48 × 10^4 t ha^{-1}·$year^{-1}$, 204.43 × 10^4 t ha^{-1}·$year^{-1}$, 156.34 × 10^4 t ha^{-1}·$year^{-1}$, respectively. The total soil loss of the farmland ecosystem in 2005, 2008, 2010 and 2017 was 129.21 × 10^4 t ha^{-1}·$year^{-1}$, 118.00 × 10^4 t ha^{-1}·$year^{-1}$, 135.34 × 10^4 t ha^{-1}·$year^{-1}$, and 111.52 × 10^4 t ha^{-1}·$year^{-1}$, respectively. The total soil loss of the other ecosystems in 2008, 2010 and 2017 was 3.36 × 10^4 t ha^{-1}·$year^{-1}$, 4.02 × 10^4 t·ha^{-1}·$year^{-1}$, and 10.03 × 10^4 t ha^{-1}·$year^{-1}$, respectively. The amount of soil loss in 2017 was lowest. From 2005 to 2017, the contribution to total soil loss of the forest ecosystem decreased by 35.45%, and that of the grassland ecosystem and farmland ecosystem increased by 36.32% and 25.9%, respectively. The total soil loss of the other ecosystems increased by 2.33%, and in 2008, it increased by 0.60% because of the Wenchuan Earthquake. Geo-hazards induced by the Wenchuan Earthquake resulted in intense surface material movement that led to the removal and destruction of a large area of vegetation. In the upper Minjiang River, forest cover decreased from 28.44% in 2005 to 24.45% in 2008 after the earthquake (Cui et al., 2009; Huang et al., 2009). In Xuanping and Yuli towns, 17.79 × 10^4 m^2 and 1.549 km^2, respectively, of farmlands and forests were submerged along the rising water level of rivers and valleys (Fan et al., 2008).

Table 3. *Soil loss of different ecological types*

Soil loss	Total soil loss (×10^4) (t·$year^{-1}$)				Mean soil loss (t·ha^{-1}·$year^{-1}$)				% Contribution to total soil loss			
	2005	2008	2010	2017	2005	2008	2010	2017	2005	2008	2010	2017
Forest	276.88	258.26	295.76	152.62	1.16	1.07	1.23	0.64	46.23	46.44	46.24	35.45
Grassland	192.77	176.48	204.43	156.34	1.21	1.11	1.29	1	32.19	31.74	31.97	36.32
Farmland	129.21	118	135.34	111.52	0.92	0.85	0.98	0.82	21.58	21.22	21.16	25.90
Settlement	0	0	0	0	0	0	0	0	0	0	0	0
Wetland	0	0	0	0	0	0	0	0	0	0	0	0
Other	0	3.36	4.02	10.03	0	1.88	1.75	4.06	0	0.6	0.63	2.33

Soil loss at the district and county scales

The areas with the highest soil erosion in the Longmen Shan area are mainly distributed in the western part of the Longmen Shan fault zone over a long, narrow area, and are mainly located in Qingchuan, northwest Pingwu, Maoxian, Wenchuan, Baoxing and Hanyuan Counties (*Fig. 3; Table 4*). Soil erosion in Maoxian County was the most devastating, with a mean soil loss value in 2005, 2008, 2010 and 2017 of 2.3 t ha^{-1}·$year^{-1}$, 2.13 t ha^{-1}·$year^{-1}$, 2.45 t ha^{-1}·$year^{-1}$, and 1.55 t·ha^{-1}·$year^{-1}$, respectively, which contributed to total soil losses of 14.77%, 14.74%,14.76%, and 13.87%, respectively. Wenchuan, Baoxing and Hanyuan Counties account for more than 10% of the total area.

http://www.aloki.hu ● ISSN 1589 1623 (Print) ● ISSN 1785 0037 (Online)
DOI: http://dx.doi.org/10.15666/aeer/1705_1123311247

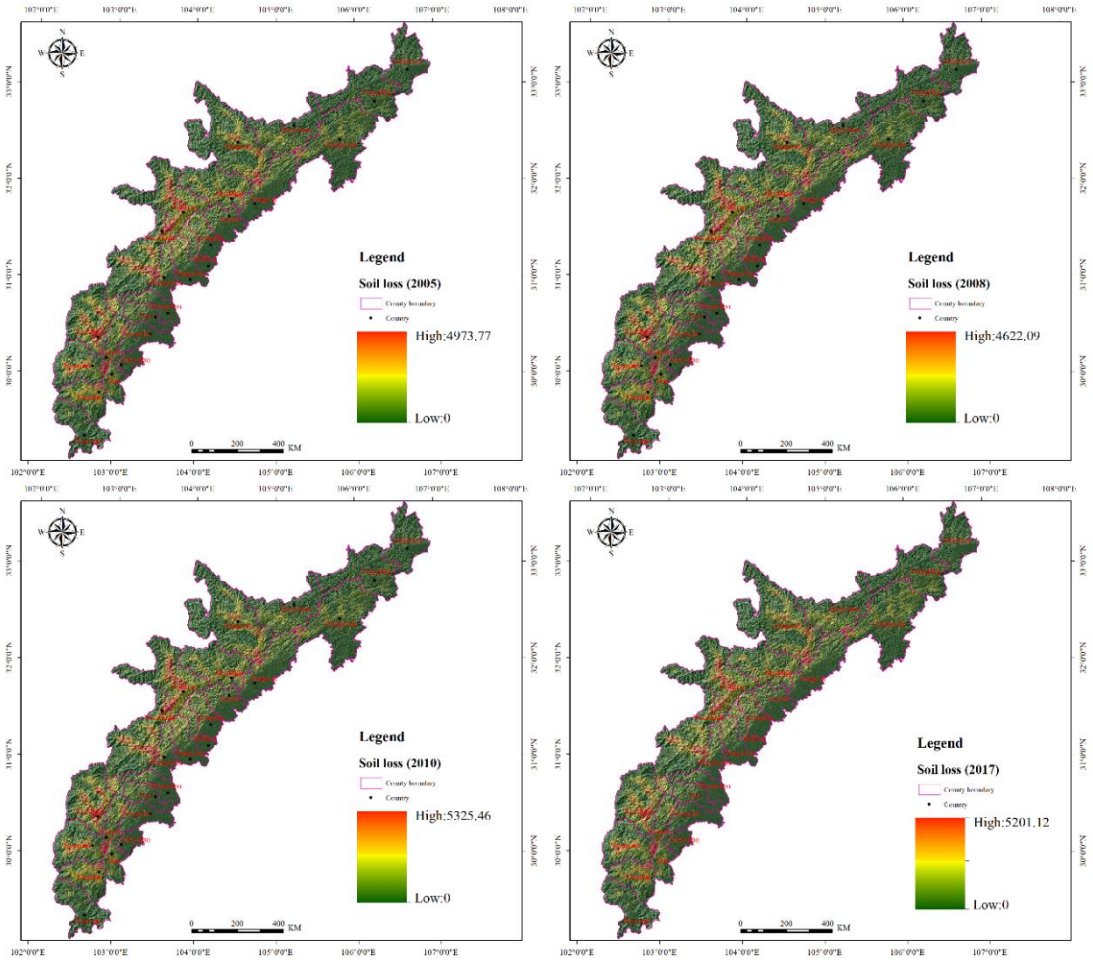

Figure 3. *Soil loss on county scale in 2005, 2008, 2010 and 2017 in the study area*

Less soil erosion was reported at lower elevations. These areas are mainly distributed in the eastern part of the Longmen Shan fault zone: Guanyuan, Jianyou, Anxian, Shifang, Mianzhu, Pengzhou, Dujiangyan, Chongzhou, Dayi, Handan, Mingshan, Yaan, etc. The soil loss of Yingjing was relatively small, with mean soil loss values in 2005, 2008, 2010 and 2017 of 0.08 t ha^{-1}·$year^{-1}$, 0.08 t ha^{-1}·$year^{-1}$, 0.09 t·ha^{-1}·$year^{-1}$, 0.09 t·ha^{-1}·$year^{-1}$, respectively, which contributed to total soil losses of 0.32%, 0.33%, 0.33%, and 0.52%, respectively.

The areas with severe soil loss are mainly distributed along the Minjiang River and its tributaries at higher elevations in the western Longmen. The 2008 Wenchuan Earthquake caused severe damage to the vegetation in the area, increased surface exposure, and caused frequent occurrences of geological disasters such as mudslides and landslides after the earthquake, resulting in an increase in soil loss in 2010. A geological survey in Sichuan Province recorded 3286 landslides and 1218 rock avalanches in the different counties after the earthquake (Li et al., 2011). A massive magnitude of denudation occurs frequently in 3 to 5 years after a strong earthquake e.g., the large debris flow disaster in 2010 after the 2008 Wenchuan Earthquake (Tang et al., 2011). Vegetation along rivers and valleys has been destroyed by debris flows, which also limit potential vegetation restoration (Cui et al., 2009). In the seven years after the

http://www.aloki.hu ● ISSN 1589 1623 (Print) ● ISSN 1785 0037 (Online)
DOI: http://dx.doi.org/10.15666/aeer/1705_1123311247

Wenchuan Earthquake, there were six large-scale debris flow disasters in the Baisha-Longxi River basin, covering an area of 188.5 km^2 (Peng et al., 2012).

Table 4. *The list of soil loss according to different ecological types*

Soil loss	Total soil loss ($\times 10^4$) ($t \cdot year^{-1}$)				Mean soil loss ($t \cdot ha^{-1} \cdot year^{-1}$)				% Contribution to total soil loss			
	2005	2008	2010	2017	2005	2008	2010	2017	2005	2008	2010	2017
Jiangyou	20.05	18.54	21.36	14.04	0.74	0.68	0.79	0.52	3.35	3.33	3.34	3.26
Maoxian	88.48	81.96	94.37	59.70	2.30	2.13	2.45	1.55	14.77	14.74	14.76	13.87
Beichuan	39.26	36.47	41.62	28.72	1.35	1.25	1.43	0.99	6.56	6.56	6.51	6.67
Wenchuan	83.59	76.79	88.63	49.48	2.04	1.87	2.16	1.21	13.96	13.81	13.86	11.49
Mianzhu	9.48	9.54	10.75	8.04	0.75	0.76	0.85	0.64	1.58	1.71	1.68	1.87
Shifang	7.29	6.97	7.85	5.16	0.85	0.81	0.91	0.60	1.22	1.25	1.23	1.20
Pengzhou	11.99	11.55	13.05	8.21	0.84	0.81	0.91	0.57	2.00	2.08	2.04	1.91
Dujiangyan	12.85	11.22	12.93	8.13	1.07	0.93	1.08	0.68	2.15	2.02	2.02	1.89
Baoxing	82.98	76.95	88.66	55.23	2.66	2.47	2.84	1.77	13.86	13.84	13.86	12.83
Chongzhou	3.57	3.32	3.81	1.93	0.32	0.30	0.35	0.18	0.60	0.60	0.60	0.45
Dayi	5.38	5.00	5.76	3.02	0.45	0.42	0.48	0.25	0.90	0.90	0.90	0.70
Lushan	25.30	23.51	27.08	16.66	2.01	1.87	2.15	1.33	4.22	4.23	4.23	3.87
Qionglai	4.09	3.81	4.38	2.30	0.30	0.28	0.32	0.17	0.68	0.68	0.69	0.54
Anxian	36.65	34.01	39.18	28.71	1.52	1.41	1.63	1.19	6.12	6.12	6.13	6.67
Pingwu	0.46	0.43	0.49	0.35	0.07	0.07	0.08	0.06	0.08	0.08	0.08	0.08
Qingchuan	11.11	10.32	11.85	8.32	1.06	0.98	1.13	0.79	1.86	1.86	1.85	1.93
Tianquan	25.41	23.61	27.16	18.92	1.44	1.34	1.54	1.07	4.24	4.25	4.25	4.39
Mingshan	5.95	6.19	7.09	4.66	0.43	0.45	0.51	0.34	0.99	1.11	1.11	1.08
Yaan	3.28	3.05	3.51	2.99	0.15	0.14	0.16	0.14	0.55	0.55	0.55	0.69
Yingjing	1.95	1.81	2.08	2.24	0.08	0.08	0.09	0.09	0.32	0.33	0.33	0.52
Hanyuan	66.00	61.30	70.62	54.22	1.12	1.04	1.20	0.92	11.02	11.02	11.04	12.60
Mianxian	6.90	6.41	7.39	7.39	0.21	0.20	0.23	0.23	1.15	1.15	1.16	1.72
Ningqiang	17.12	15.85	18.24	15.80	0.58	0.54	0.62	0.54	2.86	2.85	2.85	3.67
Guanyuan	29.73	27.50	31.66	26.31	0.60	0.55	0.64	0.53	4.96	4.95	4.95	6.11

Conclusion

In this study, LULC changes were monitored in Longmen Shan in 2005, 2008, 2010 and 2017 using remote sensing and GIS approach. The map of LULC changes illustrates positive growth in the settlement ecosystem and other ecosystems, which led to a sharp increase in industrialization and geo-hazards induced by the Wenchuan Earthquake. Negative growth has also been observed in the grassland ecosystem and farmland ecosystem due to destruction of the ecological environment. The areas with severe soil loss are mainly distributed along rivers in the high-elevation areas of the western Longmen Mountains and along the Minjiang and Tuojiang River basins and their tributaries.

Risk monitoring of heterogeneous regions in different time series can provide a timely understanding of the status of soil erosion and make reliable predictions. In future research, the erosion model can also be used to predict climate change scenarios, and thus be used for effective erosion management practices. Therefore, the results of

http://www.aloki.hu ● ISSN 1589 1623 (Print) ● ISSN 1785 0037 (Online)
DOI: http://dx.doi.org/10.15666/aeer/1705_1123311247

this study can adequately show the distribution of soil erosion in the region, and provide an important reference for decision makers to develop appropriate solutions. Finally, the ideas, modelling methods and corresponding policies used in this study are helpful for providing important references for soil erosion analysis in other regions.

Acknowledgements. The research reported in this manuscript is funded by the Fundamental Research Funds for the Central Universities (Grant No. 2015ZCQ-LX-01), the National Natural Science Foundation of China (Grant No. U1710123).

REFERENCES

[1] Alexakis, D. D., Gryllakis, M. G., Koutroulis, A. G., Agapiou, A., Themistocleous, K., Tsanis, I. K., Michaelides, S., Pashiardis, S., Demetriou, C., Aristeidou, K. (2013): GIS and remote sensing techniques for the assessment of land use change impact on flood hydrology: The case study of Yialias basin in Cyprus. – Natural Hazards Earth System Sciences Discussions 1: 4833-4869.

[2] Anees, M. T., Abdullah, K., Nawawi, M. N. M., Norulaini, N. A. N., Syakir, M. I., Omar, A. K. M. (2018): Soil erosion analysis by RUSLE and sediment yield models using remote sensing and GIS in Kelantan state, Peninsular Malaysia. – Soil Research 56(4).

[3] Anees, M. T., Javed, A., Khanday, M. Y. (2014): Spatio-temporal land cover analysis in Makhawan watershed (M.P.), India through remote sensing and GIS techniques. – Journal of Geographic Information System 6: 298-306.

[4] Balasubramani, K., Veena, M., Kumaraswamy, K., Saravanabavan, V. (2015): Estimation of soil erosion in a semi-arid watershed of Tamil Nadu (India) using revised universal soil loss equation (RUSLE) model through GIS. – Modeling Earth Systems Environment 1: 1-17.

[5] Cui, P., Zhu, Y. Y., Han, Y. S., Chen, X. Q., Zhuang, J. Q. (2009): The 12 May Wenchuan earthquake-induced landslide lakes: distribution and preliminary risk evaluation. – Landslides 6: 209-223.

[6] Cui, P., Zhuang, J. Q., Chen, X. C., Zhang, J. Q., Zhou, X. J. (2010): Characteristics and countermeasures of debris flow in Wenchuan area after the earthquake. – Journal of Sichuan University 42: 10-19.

[7] Di, B., Zeng, H., Zhang, M., Ustin, S. L., Tang, Y., Wang, Z., Chen, N., Zhang, B. (2010): Quantifying the spatial distribution of soil mass wasting processes after the 2008 earthquake in Wenchuan, China: a case study of the Longmenshan area. – Remote Sensing of Environment 114: 761-771.

[8] Diodato, N., Bellocchi, G. (2007): Estimating monthly (R)USLE climate input in a Mediterranean region using limited data. – Journal of Hydrology 345: 224-236.

[9] Diyabalanage, S., Samarakoon, K. K., Adikari, S. B., Hewawasam, T. (2017): Impact of soil and water conservation measures on soil erosion rate and sediment yields in a tropical watershed in the Central Highlands of Sri Lanka. – Applied Geography 79: 103-114.

[10] Fan, J., Tian, B., Cheng, G., Tao, H., Zhang, J., Yan, D., Fenghuan, S. U., Liu, B. (2008): Investigation on damming object induced by the earthquake of Wenchuan on May 12 based on multi-platform remote sensing. – Journal of Mountain Science 26: 257-262.

[11] Ferreira, V., Panagopoulos, T., Cakula, A., Andrade, R., Arvela, A. (2015): Predicting soil erosion after land use changes for irrigating agriculture in a large reservoir of southern Portugal. – Agriculture, Agricultural Science Procedia 4: 40-49.

[12] Food and Agriculture Organization of the United Nations (FAOUN) (2015): Status of the World's Soil Resources. – FAOUN, Washington, DC.

[13] Forestry Department of Sichuan Province (FDSP) (2008): The Report of Thematic Evaluation on Forest Loss in Wenchuan Earthquake. – FDSP, China.

http://www.aloki.hu ● ISSN 1589 1623 (Print) ● ISSN 1785 0037 (Online)
DOI: http://dx.doi.org/10.15666/aeer/1705_1123311247

[14] Gan, F., He, B., Wang, T. (2018): Water and soil loss from landslide deposits as a function of gravel content in the Wenchuan earthquake area, China, revealed by artificial rainfall simulations. – Plos One 13: e0196657.
[15] Ganasri, B. P., Ramesh, H. (2016): Assessment of soil erosion by RUSLE model using remote sensing and GIS. A case study of Nethravathi Basin. – Geoscience Frontiers 7: 953-961.
[16] Gao, H., Zhanbin, L. I., Jia, L., Li, P., Guoce, X. U., Ren, Z., Pang, G. (2016): Capacity of soil loss control in the Loess Plateau based on soil erosion control degree. – Journal of Geographical Sciences 26: 457-472.
[17] Gao, Y., Cao, S. (2011): A degradation threshold for irreversible loss of soil productivity: a long-term case study in China. – Journal of Applied Ecology 48: 1145-1154.
[18] Guo, S, Y. (2010): Theory and Method of Soil and Water Conservation Monitoring. – China Water Conservancy and Hydropower Press, Beijing, China.
[19] Haregeweyn, N., Tsunekawa, A., Poesen, J., Tsubo, M., Meshesha, D. T., Fenta, A. A., Nyssen, J., Adgo, E. (2017): Comprehensive assessment of soil erosion risk for better land use planning in river basins: case study of the Upper Blue Nile River. – Science of the Total Environment 574: 95-108.
[20] Hovius, N., Meunier, P., Lin, C. W., Chen, H., Chen, Y. G., Dadson, S., Horng, M. J., Lines, M. (2011): Prolonged seismically induced erosion and the mass balance of a large earthquake. – Earth Planetary Science Letters 304: 347-355.
[21] Huang, G. Z., Liu, X. D., He, F. 2009. Damaged vegetation conditions and reconstruction countermeasures for calamity regions in the upper reach of Minjiang River. –Journal of Sichuan Forestry Science and Technology 30 (3):95–99.
[22] Konukcu, F., Albut, S., Altürk, B. (2017): Land use/land cover change modelling of Ergene River basin in Western Turkey using CORINE land use/land cover data. – Agronomy Research 15(2): 435-443.
[23] Leh, M., Bajwa, S., Chaubey, I. (2013): Impact of land use change on erosion risk: an integrated remote sensing, geographic information system and modeling methodology. – Land Degradation Development 24: 409-421.
[24] Lin, W. T., Lin, C. Y., Chou, W. C. (2006): Assessment of vegetation recovery and soil erosion at landslides caused by a catastrophic earthquake: a case study in Central Taiwan. – Ecological Engineering 28: 79-89.
[25] Li, Y, J. (2013): Research on Geological Landscape and Suitability of Traditional Settlements in Middle North Section of Long-men Mountain. – Chengdu University of Technology, Chengdu, pp. 24-50.
[26] Li, Q. A. N., Zhang, J. F., Zhao, F. J. (2011): Extracting secondary disaster of Wenchuan earthquake: application of object-oriented image-classifying technology. – Journal of Natural Disasters 20: 160-168.
[27] Liu, B. Y., Nearing, M. A., Shi, P. J., Jia, Z. W. (2000): Slope length effects on soil loss for steep slopes. – Soil Science Society of America Journal 64: 1759-1763.
[28] Luca, M. (2015): Govern our soils. – Nature 528(7580): 32-33.
[29] Morgan, R. P. C., Quinton, J. N., Smith, R. E., Govers, G., Poesen, J. W. A., Auerswald, K., Chisci, G., Torri, D., Styczen, M. E. (2015): The EUROpean Soil Erosion Model (EUROSEM): a dynamic approach for predicting sediment transport from fields and small catchment. – Earth Surface Processes Landforms 23: 527-544.
[30] Meyer, L, D. (1984): Evaluation of the universal soil loss equation. – Soil Water Conservation 39: 99-104.
[31] Mitasova, H., Hofierka, J., Zlocha, M., Iverson, L. R. (1996): Modelling topographic potential for erosion and deposition using GIS. – International Journal of Geographical Information Systems 10: 629-641.
[32] Nearing, M. A. (1997): A single, continuous function for slope steepness influence on soil loss. – Soil Science Society of America Journal 61: 917-919.

http://www.aloki.hu ● ISSN 1589 1623 (Print) ● ISSN 1785 0037 (Online)
DOI: http://dx.doi.org/10.15666/aeer/1705_1123311247

[33] Nojarov, P. (2015): Circulation factors affecting precipitation over Bulgaria. – Theoretical Applied Climatology: 1-15.
[34] Özşahin, E., Duru, U., Eroğlu, İ. (2018): Land use and land cover changes (LULCC), a key to understand soil erosion intensities in the Maritsa Basin. – Water 10: 335-350.
[35] Panagos, P., Borrelli, P., Meusburger, K., Yu, B., Klik, A., Lim, K. J., Yang, J. E., Ni, J., Miao, C., Chattopadhyay, N. (2017): Global rainfall erosivity assessment based on high-temporal resolution rainfall records. – Scientific Reports 7: 4175.
[36] Panagos, P., Borrelli, P., Meusburger, K., Zanden, E. H. V. D., Poesen, J., Alewell, C. (2015): Modelling the effect of support practices (P-factor) on the reduction of soil erosion by water at European scale. – Environmental Science Policy 51: 23-34.
[37] Peng, C., Lin, Y. M., Chen, C. (2012): Destruction of vegetation due to geo-hazards and its environmental impacts in the Wenchuan earthquake areas. – Ecological Engineering 44: 61-69.
[38] Ran, L. I. (2015): Research on the ecological benefits of soil conservation of Yulin City based on InVEST model. – Arid Zone Research 32(5): 882-889.
[39] Rao, E., Xiao, Y., Ouyang, Z. (2013): Spatial characteristics of soil conservation service and its impact factors in Hainan Island. – Acta Ecologica Sinica 33: 746-755.
[40] Renard, K. G., Foster, G. R., Weesies, G. A., Mccool, D. K., Yoder, D. C. (1997): Predicting Soil Erosion by Water: A Guide to Conservation Planning with the Revised Universal Soil Loss Equation (RUSLE). – Agricultural Handbook. US Government Printing Office, Washington, DC.
[41] Rompaey, A. J. J. V., Govers, G., Puttemans, C. (2010): Modelling land use changes and their impact on soil erosion and sediment supply to rivers. – Earth Surface Processes Landforms 27: 481-494.
[42] Rulli, M. C., Offeddu, L., Santini, M. (2013): Modeling postfire water erosion mitigation strategies. – Hydrology and Earth System Sciences 17(6): 2323-2337.
[43] Sahin, S., Kurum, E. (2002): Erosion risk analysis by GIS in environmental impact assessments: a case study - Seyhan Köprü Dam construction. – Journal of Environmental Management 66: 239-247.
[44] Santillan, J., Makinano, M., Paringit, E. (2011): Integrated Landsat image analysis and hydrologic modeling to detect impacts of 25-year land-cover change on surface runoff in a Philippine watershed. – Remote Sensing 3: 1067-1087.
[45] Sharma, E., Bhuchar, S., Xing, M. A., Kothyari, B. P. (2007): Land use change and its impact on hydro-ecological linkages in Himalayan watersheds. – Tropical Ecology 48(2): 151-161.
[46] Stefano, C. D., Ferro, V., Burguet, M., Taguas, E. V. (2016): Testing the long term applicability of USLE-M equation at an olive orchard microcatchment in Spain. – Catena 147: 71-79.
[47] Tang, C., Zhu, J., Ding, J., Cui, X., Chen, L., Zhang, J. (2011): Catastrophic debris flows triggered by a 14 August 2010 rainfall at the epicenter of the Wenchuan earthquake. – Landslides 8: 485-497.
[48] Teng, H., Liang, Z., Chen, S., Yong, L., Rossel, R. A. V., Chappell, A., Wu, Y., Zhou, S. (2018): Current and future assessments of soil erosion by water on the Tibetan Plateau based on RUSLE and CMIP5 climate models. – Science of the Total Environment 635: 673-686.
[49] Vittoz, P., Stewart, G. H., Duncan, R. P. (2001): Earthquake impacts in old-growth Nothofagus forests in New Zealand. – Journal of Vegetation Science 12: 417-426.
[50] Wang, F. X., Wang, Z. Y., Lee, J. H. W. (2007): Acceleration of vegetation succession on eroded land by reforestation in a subtropical zone. – Ecological Engineering 31: 232-241.
[51] Wang, L., Qian, J., Qi, W. Y., Li, S. S., Chen, J. L. (2018): Changes in soil erosion and sediment transport based on the RUSLE model in Zhifanggou watershed, China. – Proc. IAHS 377: 9-18.

http://www.aloki.hu ● ISSN 1589 1623 (Print) ● ISSN 1785 0037 (Online)
DOI: http://dx.doi.org/10.15666/aeer/1705_1123311247

[52] Wang, W., Jiao, J. (1996): Quantitative evaluation on factors influencing soil erosion in China. – Bulletin of Soil Water Conservation 16(5): 1-20.
[53] Williams, J. R. (1975): Present and Prospective Technology for Predicting Sediment Yields and Sources: Proceedings of the Sediment-Yield Workshop. – U.S. Department of Agriculture, Agricultural Research Service, Washington, DC.
[54] Wischmeier, W. H., Smith, D. D. (1978): Predicting Rainfall Erosion Losses. A Guide to Conservation Planning. – Agric Handbook 537. USDA, Washington, DC.
[55] Xiao, W., Zhao, X., Zhang, Z., Ling, Y., Zuo, L., Wen, Q., Fang, L., Xu, J., Hu, S., Liu, B. (2016): Assessment of soil erosion change and its relationships with land use/cover change in China from the end of the 1980s to 2010. – Catena 137: 256-268.
[56] Yao, X. L., Bo-Jie, F. U., Yi-He, L., Sun, F. X., Guo, X. J. (2013): The soil moisture interpolation method based on GIS and statistical models in Loess Plateau region. – Journal of Soil Water Conservation 27(6): 93-102.
[57] Yong, L. I. (2006): Sedimentary responses to late cenozoic thrusting and strike-slipping of Longmen Shan along eastern margin of Tibetan Plateau. – Acta Sedimentologica Sinica 24: 153-164.
[58] Zhai, W. F., Lin-Shu, X. U. (2011): Study on the soil erodibility K-value in the typical black region of Northeast China. – Chinese Journal of Soil Science 42(5): 1209-1213.
[59] Zhang, S., Fan, W., Li, Y., Yi, Y. (2017): The influence of changes in land use and landscape patterns on soil erosion in a watershed. – Science of the Total Environment 574: 34-45.
[60] Zhang, Y., Liu, X., Li, Z., Zhu, Q. (2012): Surveying soil erosion condition in Loess Plateau using soil erosion model. – Transactions of the Chinese Society of Agricultural Engineering 28: 165-171.
[61] Zhao, G., Kondolf, G. M., Mu, X., Han, M., Zhong, H., Zan, R., Fei, W., Peng, G., Sun, W. (2017): Sediment yield reduction associated with land use changes and check dams in a catchment of the Loess Plateau, China. – Catena 148: 126-137.
[62] Zhujun, C., Lei, W., Ansheng, W., Jingbo, G., Yongli, L., Jianbin, Z. (2019): Land-use change from arable lands to orchards reduced soil erosion and increased nutrient loss in a small catchment. – Science of the Total Environment 648: 1097-1104.

http://www.aloki.hu ● ISSN 1589 1623 (Print) ● ISSN 1785 0037 (Online)
DOI: http://dx.doi.org/10.15666/aeer/1705_1123311247

COMPARISON ON THE TOLERANCE AND ACCUMULATION OF HEXAVALENT CHROMIUM BY DIFFERENT CROPS UNDER HYDROPONIC CONDITIONS

SUN, Z. Q. – QIU, Y. H. – LI, S. W. – HAN, X. M. – LI, H. L.*

School of Water Conservancy and Environment, University of Jinan, Jinan 250022, China

**Corresponding author*
e-mail: ujn_lihl@163.com

(Received 9th Apr 2019; accepted 2nd Jul 2019)

Abstract. Seedlings of six crops including wheat, radish, cucumber, Chinese cabbage, oilseed rape, and lettuce were treated with hexavalent chromium (Cr(VI)) in a hydroponic system. Root surface area, tissue biomass, the activities of superoxide dismutase (SOD) and peroxidase (POD), and chromium contents were determined to evaluate the tolerance and accumulation of Cr(VI) by these crops. The results showed that the biomass reduction of wheat was the lowest, and that of lettuce was the highest. Significant decrease in SOD activity was observed in 1 mg/L Cr(VI) treatment for Chinese cabbage and radish. While significant activation effect on the POD was observed in 1 mg/L or 5 mg/L Cr(VI) treatment for Chinese cabbage and oilseed rape. Moreover, the activities of the two antioxidant enzymes in cucumber leaves did not change significantly at the two levels of Cr(VI) concentrations. The transfer coefficient of Chinese cabbage was the highest, while that of lettuce was the lowest. In conclusion, Chinese cabbage has a certain tolerance to Cr(VI) and exhibits the highest accumulation of Cr in the edible parts. Therefore, when planting crops in low and medium Cr contaminated soil, concerns should be addressed on the food safety issues from leafy vegetables, especially Chinese cabbage.
Keywords: *crop, chromium (VI), physiological and biochemical properties, accumulation*

Introduction

Crops are one of the most important sources of human food, providing the essential energy and nutrients for the human body. There is increasing concern regarding the health risks arising from the absorption and accumulation of heavy metals by the edible parts of crops (Noli and Tsamos, 2016). Among all the heavy metals, chromium (Cr) is considered as a serious environmental contaminant for the biota (Kabata-Pendias, 2011). Consumption of contaminated foods is considered to be the most common pathway of human exposure to Cr compared to inhalation and dermal contact (Wang et al., 2011). Cr(III) and Cr(VI) are the two main forms of chromium, among which Cr(VI) has higher water solubility and thus higher bioavailability. Due to its high redox potential, Cr(VI) can interfere with photosynthesis and respiration processes, uptake of water and minerals, enzyme activity, and leads to damage on the membrane lipid and DNA, resulting in a severe decline in crop yield and quality (Singh et al., 2013). Mutagenic and carcinogenic to humans, Cr(VI) is identified as a class A carcinogen (Prado et al., 2016; Feng et al., 2004). Therefore, studying the biotoxicity of Cr(VI) is essential for the safe production of agricultural products and the protection of the environment and human health.

There are some differences on the stress response and accumulation of Cr by different crops due to the differences in external morphology, internal structure as well as physiological and biochemical mechanisms on the absorption of heavy metals. For example, Bashri et al. (2016) studied the physiological and biochemical characteristics

http://www.aloki.hu ● ISSN 1589 1623 (Print) ● ISSN 1785 0037 (Online)
DOI: http://dx.doi.org/10.15666/aeer/1705_1124911260

of two Amaranthus species, in which they found the species with higher antioxidant defense system exhibited higher tolerance to Cr(VI) stress. It was reported that members of the Brassicaceae family can absorb and transfer high concentrations of Cr into the edible parts (Singh et al., 2013; Cervantes et al., 2001). Furthermore, difference in the physiological and biochemical response and accumulation of Cr by different cultivars of the same crop was also reported. For example, Guo et al. (2015) observed that the growth of Lumai 22 (Cr tolerant wheat cultivar) was less inhibited than Zhoumai 9 (Cr sensitive wheat cultivar). Moreover, a greater proportion of Cr was accumulated in the roots and the cell walls of the aerial parts in Lumai 22 compared with those of Zhoumai 9. Gill et al. (2015) found the ultrastructural damage in leaf mesophyll and root tip cells was most pronounced in Zheda 622 cultivar among the four different cultivars of *Brassica napus* L. Plants have specific mechanisms to protect from oxidative damages, such as enzymatic antioxidants and non-enzymatic antioxidants, which scavenge the reactive oxygen species (ROS). Wang et al. (2012) studied the tolerance of three species of grasses to Cr(VI) stress, in which they found Medicago sativa was less tolerant to Cr compared with *Trifolium repens* and *Festuca arundinacea*, which is likely due to the reduced activities of peroxidase (POD) and superoxide dismutase (SOD) of *Medicago sativa* with the increase of chromium concentration. Most of the above researches focused on the comparison of different cultivars of the same crop under the Cr stress. There are still knowledge gaps with regard to the stress response and accumulation of Cr by different crops.

Therefore, in this study, two levels of Cr(VI) were used for hydroponic treatment to study the stress response and accumulation of Cr by six crops including wheat, radish, cucumber, Chinese cabbage, oilseed rape, and lettuce. It can provide theoretical support for the rational and safe cultivation of crops in low and medium Cr-contaminated soil.

Materials and methods

Materials

The seeds of six crops including wheat (Jimai 22), radish (Zheda Chang), cucumber (green cucumber), Chinese cabbage (Jiaoyan 5869), oilseed rape (Shanghai Qing), and lettuce (four seasons lettuce) were purchased from Shandong Academy of Agricultural Sciences (Jinan, China), Ma'anshan Qiutian Seed Industry (Nanjing, China), Nanjing Jinshengda Seed (Nanjing, China), Qingdao Jiaoyan Seedling (Qingdao, China), Nanjing Jinshengda Seed (Nanjing, China), and Nanjing Green Collar Seed Industry Co., Ltd (Nanjing, China), seperately.

Hydroponic experiment

The seeds were firstly sterilized with 10% H_2O_2 for 20 min, then washed thoroughly with distilled water. Subsequently, the seeds were germinated on filter paper saturated with deionized water and placed in the dark at 25 °C for 24 h. The germinated seeds were grown in plastic pots filled with quartz sand, which were placed in an artificial climate chamber with the daylight/night time of 14/10 h, daylight/night temperature of 24 ± 2 °C/18 ± 2 °C, the light intensity of 25000 lux, and the relative humidity of 75%. Wheat, radish, and cucumber were cultured for 2 weeks. Chinese cabbage, oilseed rape, and lettuce were grown to the stage of 4 leaves and 1 core. Then uniform seedlings were selected and transferred to glass containers with 400 mL of modified Hoagland nutrient

http://www.aloki.hu ● ISSN 1589 1623 (Print) ● ISSN 1785 0037 (Online)
DOI: http://dx.doi.org/10.15666/aeer/1705_1124911260

solution aerated with an air pump (4 seedlings per container). The nutrient solution (pH = 6.0) consists of 944 mg/L $Ca(NO_3)_2$, 490 mg/L $MgSO_4$, 136 mg/L KH_2PO_4, 510 mg/L KNO_3, 2.86 mg/L H_3BO_3, 1.81 mg/L $MnCl_2$, 0.22 mg/L $ZnSO_4$, 0.09 mg/L $(NH4)_6Mo_7O_{24}$, 0.08 mg/L $CuSO_4$, and 3.67 mg/L NaFe-EDTA. After 3 days of acclimatization, the crops were exposed to 0, 1 mg/L and 5 mg/L of Cr(VI) (K_2CrO_4). Each treatment had three replicates. The nutrient solution was renewed every 3 days.

Measurement of gas exchange parameters

The photosynthetic gas exchange parameters of the crops, including photosynthetic rate, stomatal conductance, and transpiration rate, were measured using a portable photosynthesis instrument (LC pro-SD, ADC, England) after 15 days of treatment.

Measurement of growth and morphological parameters

Crops were harvested and separated into roots and the aerial parts after 15 days of exposure, then washed with deionized water and dried with filter paper to measure the fresh biomass. The aerial parts were placed in an oven at 105 °C for 30 min, then dried at 70 °C. The dry biomass was weighed. The roots were first scanned using a root scanner (ScanMaker i800plus, Shanghai Zhongjing Technology Co., Ltd., China) to measure the surface area, then were dried to measure the dry biomass. The dried crop tissues were pulverized with a stainless steel pulverizer for later use.

Determination of antioxidant enzyme activity

Frozen leaves were homogenized in 6 mL pre-cooled potassium phosphate buffer (50 mM, pH = 7.8) containing 1% (w/v) polyvinylpyrrolidone (PVP) with a chilled mortar and pestle. The homogenate was centrifuged at 10,000 g for 15 min at 4 °C and the supernatant obtained was used for enzymes assay.

SOD (EC 1.15.1.1) activity was determined by the nitroblue tetrazolium (NBT) method (Gonzalez et al., 1998). The assay mixture contained 50 mM phosphate buffer (pH 7.8), 130 mM methionine, 750 μM NBT, 100 μM EDTA-Na_2, and 20 μM riboflavin. A total volume of 3.3 mL assay mixture was placed under a 4000 lx fluorescent lamp for 15-20 min and then determined using an ultraviolet visible spectrophotometer (UV-2550, Shimadzu, Japan) at 560 nm. One unit of SOD activity is the amount of enzyme that is required to cause 50% inhibition in the reduction of NBT. POD (EC 1.11.1.7) activity was determined using the guaiacol method (Zhou and Leul, 1998). The reaction mixture was comprised of 50 mM phosphate buffer (pH = 7.8), 30% H_2O_2, 20 mM guaiacol, and 100 μL enzyme extract. Activities of POD were assayed by measuring the absorbance at 436 nm with 3 mL of the mixture. One unit of POD activity was defined as the amount of enzyme catalyzing the oxidation of 1 μmol of guaiacol in 1 min.

Determination of Cr contents in the crop tissues

For determination of Cr contents, a certain amount of the roots or the aerial parts was weighed into a digestion tube. Ten milliliter digestion solution consisting of HNO_3 and H_2O (1:1, V/V) was added soaking overnight. A graphite digestion instrument (EE, USA) was used to digest the tissues for about 12 h at temperature of 105 °C. Then 1 mL of H_2O_2 was added to the remaining digestion solution and continue to digest to obtain

http://www.aloki.hu ● ISSN 1589 1623 (Print) ● ISSN 1785 0037 (Online)
DOI: http://dx.doi.org/10.15666/aeer/1705_1124911260

clear solution. The solution was made up to 50 mL using Milli-Q water. Chromium contents were measured by ICP-MS (iCAP Q, Thermo Fisher Scientific, America).

Statistical analysis

Bio-concentration factor (BCF) is the ratio of the concentration of heavy metals in the roots or the aerial parts of plants to that in soil or solution (Ding et al., 2016). The transfer factor (TF) is the percentage of Cr concentration in the aerial parts to that in the roots, indicating the ability of heavy metals to be translocated from the roots to the aerial parts (Ali et al., 2013). The tolerance index (TI) is the percentage of the biomass of crop at Cr stress to that of the control treatment (Wilkins, 1978).

Data processing and analysis were performed using Excel and SPSS 22. One-way ANOVA and the least squares deviation (LSD) test were used to compare the difference among different treatments. Statistical significance was accepted at $p < 0.05$. The figures were graphed using Origin 2017 software. The data results were expressed as mean ± standard error.

Results

Effect of Cr(VI) on the growth traits of crops

The fresh biomass and root area of the six crops showed a decreasing tendency with increasing Cr(VI) concentration (*Table 1*). For the treatments of 1 mg/L of Cr(VI), the root biomasses of wheat and Chinese cabbage were not significantly different from those of the control, while those of radish, cucumber, oilseed rape, and lettuce decreased significantly compared with those of the control, with reduction of 25%, 73%, 30%, and 71%, respectively. Treatments with 5 mg/L of Cr(VI) significantly reduced the root biomasses of all the six crops. The reduction in root biomass was the lowest for wheat (25%), followed by radish (49%), oilseed rape (59%), Chinese cabbage (68%), cucumber (76%), and lettuce (92%). The aerial biomasses of the six crops were reduced significantly under the two levels of Cr(VI) treatments. Similar to those of the roots, wheat showed the lowest reductions in the aerial biomass, which were 27% and 49%, respectively. While lettuce presented the highest reduction, which were 82% and 94%, respectively. Under 5 mg/L of Cr(VI) stress, the root and shoot TI of wheat were 75% and 51%, respectively. While the root and shoot TI of lettuce were 7% and 6%, respectively. The results indicated that wheat has stronger tolerance to Cr(VI) toxicity, while lettuce showed less tolerance compared with other crops.

Under the two levels of Cr(VI) stress, except for cucumber, the TI values for the aerial parts of the other five crops were all lower than those of the roots, indicating the biomasses of the aerial parts other than roots of these five crops are more sensitive to Cr(VI) toxicity and could be used as biomarkers.

Effect of Cr(VI) on the photosynthetic properties of crops

The photosynthetic rate and transpiration rate of the six crops responded differently under the two levels of Cr(VI) treatments (*Table 2*). Under 1 mg/L of Cr(VI) treatment, the stomatal conductance and transpiration rate of wheat, cucumber, and oilseed rape did not change significantly, while those of radish, Chinese cabbage, and lettuce decreased significantly. The stomatal conductance and transpiration rate of the six crops were significantly reduced under 5 mg/L of Cr(VI) treatment. The transpiration rates in

http://www.aloki.hu ● ISSN 1589 1623 (Print) ● ISSN 1785 0037 (Online)
DOI: http://dx.doi.org/10.15666/aeer/1705_1124911260

the leaves of wheat, radish, cucumber, Chinese cabbage, oilseed rape, and lettuce were reduced by 63%, 79%, 56%, 60%, 71%, and 87%, respectively. The stress of Cr(VI) on the transpiration rate in the leaves of wheat, cucumber, and Chinese cabbage is relatively low, which may account for the insignificant change in the leaf water contents of these three crops under Cr(VI) treatment of 1 mg/L (*Fig. 1*). The photosynthetic rates of wheat, radish, and Chinese cabbage did not change significantly, while those of cucumber, oilseed rape, and lettuce were significantly reduced under 1 mg/L of Cr(VI) treatment. Under 5 mg/L of Cr(VI) treatment, the photosynthesis rates of wheat, radish, cucumber, Chinese cabbage, oilseed rape, and lettuce decreased significantly, with reductions of 51%, 61%, 55%, 41%, 79%, and 80%, respectively. The effects of Cr(VI) on the photosynthetic rates of wheat and Chinese cabbage are less than those of other crops, while are higher than those of oilseed rape and lettuce.

Table 1. *Effect of Cr (VI) on the growth traits of crops*

Parameters	Cr(VI) (mg/L)	Wheat	Radish	Cucumber	Chinese cabbage	Oilseed rape	Lettuce
Root biomass (g per container)	0	3.20±0.23a	0.91±0.07a	8.72±1.78a	2.65±0.26a	2.47±0.71a	9.98±2.08a
	1	2.92±0.19ab	0.68±0.04b	1.94±0.32 bc	2.10±0.65ab	1.71±0.51bc	2.88±1.43bc
	5	2.41±0.10b	0.47±0.05c	1.75±0.54c	0.84±0.14b	1.02±0.19c	0.78±0.07c
Aerial biomass (g per container)	0	4.98±0.39a	15.1±0.37a	19.6±1.45a	23.7±1.33a	22.4±2.04a	63.0±9.2a
	1	3.62±0.16b	9.87±0.06b	8.61±1.55b	15.1±4.64b	12.7±1.94b	11.6±5.43bc
	5	2.56±0.03c	5.16±0.05c	5.70±0.34c	5.53±0.87c	6.63±0.59c	3.84±0.44b
Root area (cm^2)	0	99.7±4.48a	26.0±4.94a	188±19.40a	32.0±1.28a	32.2±1.46a	157±24.9a
	1	80.7±10.89b	14.6±0.44bc	36.2±8.26bc	29.8±4.70ab	21.3±2.59bc	38.3±2.93bc
	5	53.4±2.12c	12.1±1.65c	35.9±6.67c	18.8±1.12c	17.3±0.68c	18.8±0.89c
Root TI	1	91	74	22	79	69	28
	5	75	51	20	40	41	7
Shoot TI	1	72	60	43	63	49	18
	5	51	34	29	23	25	6

Values are presented as means and standard error. Different letters indicate statistically significant difference between different treatments

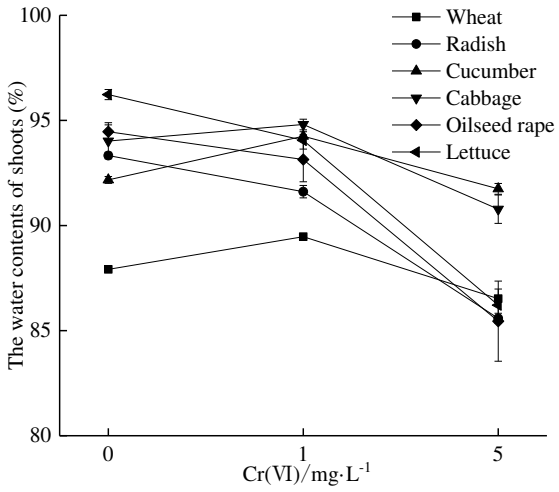

Figure 1. *Effect of Cr(VI) on the water contents (%) of the six crops. (Bars indicate standard error)*

http://www.aloki.hu ● ISSN 1589 1623 (Print) ● ISSN 1785 0037 (Online)
DOI: http://dx.doi.org/10.15666/aeer/1705_1124911260

Table 2. *Effect of Cr(VI) on the photosynthetic parameters of crops*

Parameters	Cr(VI) (mg/L)	Wheat	Radish	Cucumber	Chinese cabbage	Oilseed rape	Lettuce
Stomatal conductance ($mol/m^2/s$)	0	0.40±0.02a	0.21±0.01a	0.14±0.03a	0.42±0.19a	0.24±0.05a	0.46±0.04a
	1	0.35±0.08ab	0.10±0.02b	0.09±0.01ab	0.18±0.02bc	0.17±0.01ab	0.13±0.01b
	5	0.11±0.01c	0.03±0.01c	0.05±0.04b	0.05±0.02c	0.06±0.01bc	0.02±0.00c
Transpiration rate ($mol/m^2/s$)	0	3.14±0.44ab	2.09±0.43a	1.22±0.18ab	3.47±0.66a	2.37±0.34a	3.09±0.20a
	1	3.58±0.08a	1.20±0.1b	1.44±0.06a	2.55±0.13b	2.26±0.34ab	1.81±0.12b
	5	1.68±0.18c	0.44±0.08c	0.54±0.18c	1.00±0.36c	0.95±0.18c	0.42±0.08c
Photosynthetic rate (μmol $CO_2/m^2/s$)	0	17.3±4.42a	4.44±0.45a	3.53±0.26a	9.00±1.0a	6.68±0.11a	8.76±0.38a
	1	11.6±2.19ab	3.64±0.08ab	1.98±0.16bc	5.16±0.08b	4.87±0.26ab	7.07±0.25b
	5	8.5±1.28b	1.77±0.30c	1.61±0.15c	1.96±0.39c	3.96±0.98bc	1.89±0.11c

Values are presented as means and standard error. Different letters indicate statistically significant difference between different treatments

Effects of Cr(VI) on the activities of antioxidant enzymes

The effects of Cr(VI) on the SOD and POD activities of the six crops are shown in *Figure 2*.

As can be seen, Cr(VI) treatment of 5 mg/L significantly inhibited the SOD activity of all the crops except that of cucumber. Moreover, for Chinese cabbage and radish, significant decrease in SOD activity was observed at 1 mg/L of Cr(VI) treatment. Especially for radish, SOD activity was not detected at the two levels of Cr(VI) treatments. It is suggested that Chinese cabbage and radish are sensitive to the stress of Cr(VI). Similar to that of SOD, Cr(VI) treatment of 5 mg/L resulted in significant inhabitation on POD activity of all the crops except cucumber and oilseed rape. For Chinese cabbage and oilseed rape, significant activation effect on the POD was observed at 1 mg/L or 5 mg/L of Cr(VI) treatment. Interestingly, the SOD and POD activities of cucumber did not change significantly at the two levels of Cr(VI) treatments. This indicated that cucumber is not sensitive to the stress of Cr(VI).

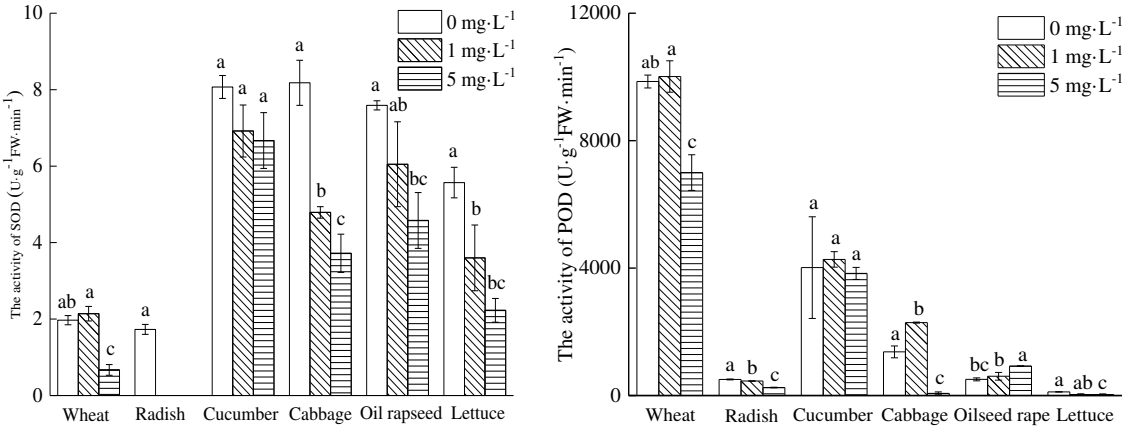

Figure 2. *Effect of Cr (VI) on the activities of antioxidant enzymes in crops. (Bars indicate standard error)*

http://www.aloki.hu ● ISSN 1589 1623 (Print) ● ISSN 1785 0037 (Online)
DOI: http://dx.doi.org/10.15666/aeer/1705_1124911260

The accumulation of Cr by crops

With the increase of Cr(VI) concentration in hydroponic solution, the Cr contents in the crop tissues increased significantly except the roots of cucumber and Chinese cabbage (*Table 3*). Under Cr(VI) treatment of 1 mg/L, the Cr content in lettuce roots is the highest (1024 μg/g), followed by oilseed rape (772 μg/g), Chinese cabbage (736 μg/g), cucumber (695 μg/g), radish (651 μg/g), and wheat (246 μg/g). For 5 mg/L of Cr(VI) treatment, the Cr content in lettuce roots is also the highest (2823 μg/g), followed by radish (1453 μg/g), oilseed rape (1161 μg/g), Chinese cabbage (876 μg/g), cucumber (700 μg/g), and wheat (427 μg/g). The Cr contents in the aerial parts of the six crops were far below those of the roots. Under Cr (VI) treatment of 1 mg/L, the Cr content in the aerial parts of Chinese cabbage is the highest (35.9 μg/g), followed by oilseed rape (19.5 μg/g), lettuce (16.2 μg/g), radish (13.4 μg/g), wheat (13.2 μg/g), and cucumber (9.00 μg/g). Under Cr(VI) treatment of 5 mg/L, the Cr contents in the aerial parts of the six crops followed the same order.

Table 3. *The uptake, accumulation, and translocation of Cr by crops*

	Cr(VI) (mg/L)	Wheat	Radish	Cucumber	Chinese cabbage	Oilseed rape	Lettuce
Cr contents in roots (μg/g DW)	1	246±22.3b	611±0.67b	695±38.9ab	736±67.3ab	772±20.9b	1024±105b
	5	427±0.29a	1453±9.20a	700±35.5a	876±55.8a	1161±60.2a	2823±260a
Cr contents in the aerial parts (μg/g DW)	1	13.2±1.38b	13.4±1.79b	9.00±0.09b	35.9±5.55b	19.5±0.32b	16.2±2.96b
	5	38.3±1.91a	38.2±3.94a	25.0±1.53a	209±3.18a	104±3.79a	63.8±10.5a
Aerial BCF	1	13.0±1.10a	13.4±1.79a	9.00±0.09a	35.9±5.55ab	19.5±0.32ab	16.2±2.96a
	5	7.66±0.38b	9.95±2.36ab	5.00±0.31b	41.8±0.64a	20.8±0.75a	15.3±2.79ab
Root BCF	1	246±22.3b	603±7.75a	784±91.2a	736±67.3a	862±90.9a	737±89.8a
	5	111±25.5a	290±1.84b	140±7.10b	210±36.1b	279±47.4b	565±52.1b
TF (%)	1	5.12±0.57b	2.06±0.16ab	1.16±0.11b	4.93±1.21b	2.48±0.26b	1.57±0.15b
	5	9.06±0.76a	3.02±0.69a	4.67±0.94a	18.6±3.51a	8.97±0.14a	2.92±0.21a

Values are presented as means and standard error. Different letters indicate statistically significant difference between different treatments

For the roots, the BCF values of the six crops decreased significantly with the increase of Cr(VI) treatment concentration. Under Cr(VI) treatment of 1 mg/L, the BCF for wheat roots was significantly lower than those of other crops. Under 5 mg/L of Cr(VI) treatment, the root BCF of lettuce was the highest, followed by radish, oilseed rape, Chinese cabbage, cucumber, and wheat. For the aerial parts, the BCF of Chinese cabbage, oilseed rape, lettuce, and radish did not change significantly at the two levels of Cr(VI) treatments, while those of wheat and cucumber decreased significantly with the increase of Cr(VI) treatment concentration. The BCF of the aerial parts of Chinese cabbage is the highest, and that of cucumber is the lowest.

Except for radish, the TF of other crops increased significantly with the increase of Cr(VI) treatment concentration. Under Cr(VI) treatment of 1 mg/L, the TF values of the six crops ranged from 1.16 to 5.12, following the order of wheat > Chinese cabbage > oilseed rape > radish > lettuce > cucumber. Under Cr(VI) treatment of 5 mg/L, the TF values of the six crops ranged from 2.92 to 18.6. Different from that of 1 mg/L

http://www.aloki.hu ● ISSN 1589 1623 (Print) ● ISSN 1785 0037 (Online)
DOI: http://dx.doi.org/10.15666/aeer/1705_1124911260

treatment, the order is Chinese cabbage > wheat > oilseed rape > cucumber > radish > lettuce.

Discussion

It has been demonstrated that Cr could inhibit the growth of plant, cause chlorosis in newly budded leaves and the decrease in root surface area. These indicators have been used to assess the responses of crops to the Cr stress (Bashri et al., 2016; Anjum et al., 2017; Liu et al., 2008; Pandey et al., 2005; Tiwari et al., 2009). In the present study, the biomasses of crop tissues decreased with the increase of Cr(VI) concentration in the nutrient solution (*Table 1*). The results are consistent with those of wheat seedlings exposed to Cr(VI) (Guo et al., 2015). All the six crops were stressed by 1 mg/L of Cr(VI), and the aerial parts of the six crops were more sensitive to Cr stress than the roots except for cucumber (*Table 1*). This may be due to the reduced root activity, which inhibits the transport of nutrients from roots to the aerial parts. The growth parameters of the six crops were significantly reduced because the crops could not acquire abundant nutrients to maintain normal physiological activity (Ali et al., 2013). The TI can be used to indicate the tolerance of crops to heavy metals, the greater the value, the stronger the tolerance of plants to heavy metals (Liu and Wang, 2002). In the present study, the growth parameters and the TI values indicated that wheat exhibited strong tolerance to Cr(VI) among the six crops, while lettuce was relatively less tolerant to Cr(VI).

The main parameters affecting crop photosynthesis and transpiration include stomatal conductance, transpiration rate, and photosynthetic rate. In this study, as the Cr(VI) treatment level increased, the stomatal conductance, transpiration rate, and photosynthetic rate of the six crops showed a decreasing tendency. The increase of chlorophyllase activity in crops resulted in the decomposition of chlorophyll under the stress of heavy metals (Hegedus and Erdei, 2001), which led to lower capacity for light-harvesting, thus the decrease in photosynthetic rate. On the other hand, the decrease of the photosynthetic rate under Cr(VI) stress may be attributed to the interference of Cr on nutrient absorption, respiration rate, and cell membrane permeability. In addition, Cr(VI) can induce chloroplast ultrastructural abnormalities, such as the alteration of thylakoid (Luisa Brito et al., 2009). The treatment of 5 mg/L Cr(VI) significantly reduced the stomatal conductance of the crop leaves. This can be explained by the damage to the stomatal guard cells of crop leaves caused by the high oxidation potential of Cr(VI) (Hayat et al., 2012). Former study has found that Cr can reduce the tracheary diameter of bean plants, thereby reducing the longitudinal movement of water (Barceló and Poschenrieder, 1990), which may bring about the reduced transpiration rate of the crops. Similar results have also been reported by Gill et al. (2015), Liu et al. (2008), and Ali et al. (2011), in which they found that high concentrations of Cr can reduce the net photosynthetic rate, stomatal conductance, and transpiration rate of oilseed rape, *Amaranthus viridis L* and barley. Heavy metal stress results in severe dehydration of plant shoots by interfering with the water transport from roots to shoots. In general, heavy metals can affect water contents through water absorption, water transformation of plastids and protoplasts, and stomatal function (Poschenrieder and Barceló, 1999). In this study, under the stress of 5 mg/L of Cr(VI), the water contents of wheat and cucumber did not change significantly, while those of radish, Chinese cabbage, oilseed rape, and lettuce decreased significantly.

http://www.aloki.hu ● ISSN 1589 1623 (Print) ● ISSN 1785 0037 (Online)
DOI: http://dx.doi.org/10.15666/aeer/1705_1124911260

Subjected to Cr stress, crops are stimulated to produce reactive oxygen species (ROS), such as H_2O_2, OH^-, O^{2-}, which bring about oxidative damage to biomolecules such as lipids, proteins, and nucleic acids. Therefore, crops control the production of peroxidative radicals by developing a complex enzymatic antioxidant system to prevent plants from being oxidatively damaged (Ashraf et al., 2015). This defense mechanism includes various antioxidant enzymes such as SOD, catalase (CAT), and POD. Crop cells increase the activity of antioxidant enzymes and eliminate excess ROS to maintain ROS balance (Gill and Tuteja, 2010). The differences in antioxidant defense mechanisms induced by heavy metals depend on the species of heavy metal and crops (Hayat et al., 2012). SOD and POD are vital enzymes in crop antioxidant defense mechanisms. SOD is the most critical substance accounting for plant stress tolerance, providing a first line of defense to reduce the toxic effects caused by elevated levels of ROS. In general, the activities of antioxidant enzymes will be promoted under low concentration of heavy metal exposure while be inhibited under high concentrations of heavy metal exposure. Huang et al. (2011) showed that 10^{-6} mol/L of Cr(VI) stress had no significant effect on SOD and POD activities in maize, while 10^{-5} mol/L of Cr(VI) stress showed significant decreases in SOD and POD activities. In this study, under the stress of Cr(VI), the antioxidant enzyme activities of different crops were very different. The SOD and POD activities of wheat, cucumber, and oilseed rape as well as the POD activity of lettuce did not change significantly when treated with 1 mg/L of Cr(VI). The activities of SOD and POD in the leaves of radish and the activity of SOD in the leaves of Chinese cabbage and lettuce significantly decreased, while the activity of POD in the leaves of Chinese cabbage significantly increased. It showed that under 1 mg/L of Cr(VI) stress, wheat was tolerant to the Cr stress, while lettuce presented its sensitivity to the Cr stress. The increase of antioxidant enzyme activity may be attributed to the blockage of electron transport chains in mitochondria induced by Cr(VI), which directly affects the production of superoxide radicals. With the increase of Cr concentration, the enzyme activity decreases, which is due to the inhibition of Cr(VI) to the enzyme system (Hayat et al., 2012). Also, Huang et al. (2011) found that the dramatic changes in antioxidant enzyme activity may be related to the expression of isoenzymes during the transformation of nutritional mode.

The six crops showed considerable differences in the absorption, translocation, and accumulation of Cr. Wang et al. (2012) have found different oil crops showed different tolerance and accumulation of Cr. In this study, Cr was mainly retained in the roots of the six crops, ranging from 2823 μg/g (lettuce) to 426.5 μg/g (wheat). However, due to the difference in the translocation of Cr by different crops, the TF of Chinese cabbage (18.6%) was the highest, which resulted in the highest content of Cr (208.8 μg/g) in the aerial parts of Chinese cabbage. The Cr contents in the aerial parts of oilseed rape and lettuce are significantly higher than those of the other three crops. It has been found that transpiration plays a vital role in the translocation of heavy metals by crops (Ji et al., 2017). In this study, there is a significant positive correlation between the TF of Cr and the transpiration rate of the six crops under Cr(VI) treatment of 1 mg/L ($R^2 = 0.75$), which was not observed under Cr(VI) treatment of 5 mg/L because of the higher toxic effect of Cr(VI) at this level.

Based on the above analysis, it can be found that wheat is more tolerant to Cr(VI) and has a weaker accumulation ability for Cr, while lettuce is more sensitive to Cr(VI) and has a stronger ability to accumulate Cr. Therefore, lettuce will bring more risks than wheat when planted in low and medium concentration Cr(VI)-contaminated soils. This

http://www.aloki.hu ● ISSN 1589 1623 (Print) ● ISSN 1785 0037 (Online)
DOI: http://dx.doi.org/10.15666/aeer/1705_1124911260

study is limited to the sensitivity and accumulation of Cr (VI) by six crops under hydroponic conditions. The treatment level of 5 mg/L Cr(VI) may be too high, which resulted in excessive toxicity and high Cr contents in crops. Although the results can reflect the tolerance of crops to Cr(VI), the tolerance, the translocation and accumulation of Cr by these six crops in soil systems remain to be further studied.

Conclusions

Under Cr(VI) stress conditions, the growth traits and photosynthetic characteristics of the six crops were more inhibited with increasing treatment concentration. Among them, wheat showed the strongest tolerance to Cr(VI), with the lowest accumulation of Cr in the shoots. Lettuce presented to be the most sensitive vegetables, with most Cr accumulated in the roots. Chinese cabbage had a certain tolerance to Cr(VI) and showed the highest accumulation of Cr in the edible parts, which may pose a threat to the safety of agricultural products if planted in Cr contaminated soils. In this study, the results on the tolerance and accumulation of Cr were based on the hydroponic conditions, the accumulation of Cr in soil systems by these crops should be further studied in the future.

Acknowledgements. This research was funded by National Key Research and Development Program of China, grant number 2016YFD0800407. The authors would like to thank Prof. Yibing Ma for his suggestions on how to improve the manuscript.

REFERENCES

[1] Ali, B., Wang, B., Ali, S., Ghani, M. A., Hayat, M. T., Yang, C., Xu, L., Zhou, W. J. (2013): 5-aminolevulinic acid ameliorates the growth, photosynthetic gas exchange capacity, and ultrastructural changes under cadmium stress in Brassica napus L. – Journal of Plant Growth Regulation 32: 604-614.

[2] Ali, S., Zeng, F., Qiu, L., Zhang, G. (2011): The effect of chromium and aluminum on growth, root morphology, photosynthetic parameters and transpiration of the two barley cultivars. – Biologia Plantarum 55: 291-296.

[3] Ali, S., Farooq, M. A., Yasmeen, T., Hussain, S., Arif, M. S., Abbas, F., Bharwana, S. A., Zhang, G. (2013): The influence of silicon on barley growth, photosynthesis and ultra-structure under chromium stress. – Ecotoxicology and Environmental Safety 89: 66-72.

[4] Anjum, S. A., Ashraf, U., Khan, I., Tanveer, M., Shahid, M., Shakoor, A., Wang, L. (2017): Phyto-toxicity of chromium in maize: oxidative damage, osmolyte accumulation, anti-oxidative defense and chromium uptake. – Pedosphere 27: 262-273.

[5] Ashraf, U., Kanu, A. S., Mo, Z., Hussain, S., Anjum, S. A., Khan, I., Abbas, R. N., Tang, X. (2015): Lead toxicity in rice: effects, mechanisms, and mitigation strategies—a mini review. – Environmental Science and Pollution Research 22: 18318-18332.

[6] Barceló, J., Poschenrieder, C. (1990): Plant water relations as affected by heavy metal stress: a review. – Journal of Plant Nutrition 13: 1-37.

[7] Bashri, G., Parihar, P., Singh, R., Singh, S., Singh, V. P., Prasad, S. M. (2016): Physiological and biochemical characterization of two Amaranthus species under Cr(VI) stress differing in Cr(VI) tolerance. – Plant Physiology and Biochemistry 108: 12-23.

[8] Cervantes, C., Campos-Garcia, J., Devars, S., Gutiérrez-Corona, F., Loza-Tavera, H., Torres-Guzmán, J. C., Moreno-Sánchez, R. (2001): Interactions of chromium with microorganisms and plants. – FEMS Microbiology Reviews 25: 335-347.

http://www.aloki.hu ● ISSN 1589 1623 (Print) ● ISSN 1785 0037 (Online)
DOI: http://dx.doi.org/10.15666/aeer/1705_1124911260

[9] Ding, H., Wang, G., Lou, L., Lv, J. (2016): Physiological responses and tolerance of kenaf (Hibiscus cannabinus L.) exposed to chromium. – Ecotoxicology and Environmental Safety 133: 509-518.
[10] Feng, X. H., Yi, S., Sridhar, B. B. M., David, L. M. (2004): Distribution, transformation and bioavailability of trivalent and hexavalent chromium in contaminated soil. – Plant and Soil 265: 243-252.
[11] Gill, R. A., Zang, L., Ali, B., Farooq, M. A., Cui, P., Yang, S., Ali, S., Zhou, W. (2015): Chromium-induced physio-chemical and ultrastructural changes in four cultivars of Brassica napus L. – Chemosphere 120: 154-164.
[12] Gill, S. S., Tuteja, N. (2010): Reactive oxygen species and antioxidant machinery in abiotic stress tolerance in crop plants. – Plant Physiology and Biochemistry 48: 909-930.
[13] Gonzalez, A., Steffen, K. L., Lynch, J. P. (1998): Light and excess manganese. Implications for oxidative stress in common bean. – Plant Physiology 118: 493-504.
[14] Guo, H. Y., Zhang, H., Tian, Z., Wang, Q., Sun, J., Dai, Y. (2015): Genotypic differences of chromium absorption and tolerance mechanism to chromium stress in wheat seedlings. – Journal of Triticeae Crops 35: 1386-1394 (in Chinese).
[15] Hayat, S., Irfan, M., Wani, A. S., Tripathi, B. N., Ahmad, A. (2012): Physiological changes induced by chromium stress in plants: an overview. – Protoplasma 249: 599-611.
[16] Hegedus, A., Erdei, S. G. (2001): Comparative studies of H_2O_2 detoxifying enzymes in green and greening barley seedlings under cadmium stress. – Plant Science 160: 1085-1093.
[17] Huang, H., Gao, X., Wang, J. (2011): The influence of Cr(VI) to the growth and antioxidant system of seedling of Zea mays L. – Journal of Agro-Environment Science 30: 633-638 (in Chinese).
[18] Ji, Y., Wan, Y., Wang, Q., Zhang, Y., Li, H. (2017): Effects of root characteristics and transpiration on cadmium uptake by cucumber seedlings under varied iron levels. – Acta Scientiae Circumstantiae 37: 1939-1946 (in Chinese).
[19] Kabata-Pendias, A. (2011): Trace Elements in Soils and Plants. 4th Ed. – CRC Press, Boca Raton, FL.
[20] Liu, D., Zou, J., Wang, M., Jiang, W. (2008): Hexavalent chromium uptake and its effects on mineral uptake, antioxidant defence system and photosynthesis in Amaranthus viridis L. – Bioresource Technology 99: 2628-2636.
[21] Liu, X., Wang, Q. (2002): Research on lead uptake and tolerance in six plants. – Acta Phytoecologica Sinica 26: 533-537 (in Chinese).
[22] Luisa Brito, P., Jurandi Gonçalves de, O., Ricardo, A. A., Douglas Rodrigues, R., Marcelo Gomes da, S., Angela, P. V. (2009): Ecophysiological responses of water hyacinth exposed to Cr^{3+} and Cr^{6+}. – Environmental and Experimental Botany 65: 403-409.
[23] Noli, F., Tsamos, P. (2016): Concentration of heavy metals and trace elements in soils, waters and vegetables and assessment of health risk in the vicinity of a lignite-fired power plant. – Science of the Total Environment 563-564: 377-385.
[24] Pandey, V., Dixit, V., Shyam, R. (2005): Antioxidative responses in relation to growth of mustard (Brassica juncea cv. Pusa Jaikisan) plants exposed to hexavalent chromium. – Chemosphere 61: 40-47.
[25] Poschenrieder, C., Barceló, J. (1999): Water Relations in Heavy Metal Stressed Plants. – In: Prasad, M. N. V. (ed.) Heavy Metal Stress in Plants. 2nd Ed., Springer, Berlin.
[26] Prado, C., Ponce, S. C., Pagano, E., Prado, F. E., Rosa, M. (2016): Differential physiological responses of two Salvinia species to hexavalent chromium at a glance. – Aquatic Toxicology 175: 213-221.
[27] Singh, H. P., Mahajan, P., Kaur, S., Batish, D. R., Kohli, R. K. (2013): Chromium toxicity and tolerance in plants. – Environmental Chemistry Letters 11: 229-254.
[28] Tiwari, K. K., Dwivedi, S., Singh, N. K., Rai, U. N., Tripathi, R. D. (2009): Chromium (VI) induced phytotoxicity and oxidative stress in pea (Pisum sativum L.): biochemical

http://www.aloki.hu ● ISSN 1589 1623 (Print) ● ISSN 1785 0037 (Online)
DOI: http://dx.doi.org/10.15666/aeer/1705_1124911260

changes and translocation of essential nutrients. – Journal of Environmental Biology 30: 389.

[29] Wang, A., Huang, S., Zhong, G., Xu, G., Liu, Z., Shen, X. (2012): Effect of Cr(VI) stress on growth of three herbaceous plants and their Cr uptake. – Environment Science 33: 2028-2037 (in Chinese).

[30] Wang, S., Lu, J. Y., Li, Y. X., Qi, J., Ye, Q. F. (2012): Chromium and lead tolerance and accumulation in several oil crops. – Journal of Agro-Environment Science 31: 1310-1316 (in Chinese).

[31] Wang, Z. X., Chen, J. Q., Chai, L. Y., Yang, Z. H., Huang, S. H., Zheng, Y. (2011): Environmental impact and site-specific human health risks of chromium in the vicinity of a ferro-alloy manufactory, China. – Journal of Hazardous Materials 190: 980-985.

[32] Wilkins, D. A. (1978): The measurement of tolerance to edaphic factors by means of root growth. – New Phytologist 80: 623-633.

[33] Zhou, W., Leul, M. (1998): Uniconazole-induced alleviation of freezing injury in relation to changes in hormonal balance, enzyme activities and lipid peroxidation in winter rape. – Plant Growth Regulation 26: 41-47.

http://www.aloki.hu ● ISSN 1589 1623 (Print) ● ISSN 1785 0037 (Online)
DOI: http://dx.doi.org/10.15666/aeer/1705_1124911260

DETERMINANTS OF ADAPTATION MEASURES ON CLIMATE CHANGE. A CASE OF SMALL-SCALE MAIZE FARMERS IN THE NORTH-WEST PROVINCE OF SOUTH AFRICA

ODUNIYI, O. S.* – ANTWI, M. A. – TEKANA, S. S.

Department of Agriculture and Animal Health, University of South Africa, Florida Campus, Florida, South Africa
(e-mails: antwima@unisa.ac.za, tekanss@unisa.ac.za)

**Corresponding author*
e-mail: sammiey2007@yahoo.com

(Received 10th Apr 2019; accepted 2nd Jul 2019)

Abstract. Adaptation to climate change varies according to regions, it could be effective in relation to people and their locations. Adaptation to climate change in sub-Saharan Africa is different from that of developed countries, as resources are limited. This study was conducted in Ngaka Modiri Molema District Municipality in North West Province of South Africa. This study examined the determinants of climate change adaptation strategies among rural farmers' households in the study area. A total number of 346 questionnaires were administered to the farmers in the district using the stratified random sampling technique. Data were captured and analyzed using SPSS and EVIEWS software. Multicollinearity analysis was first performed to remove highly correlated variables from the model followed by the use of Tobit regression analysis. The results of the analysis indicated that farm size ($p < 0.01$), gender ($p < 0.01$), type of farm ($p < 0.05$), farm ownership ($p < 0.05$), land acquisition ($p < 0.01$), source of climate change information ($p < 0.01$), support received on climate change ($p < 0.1$), and adaptation barrier were statistically significant ($p < 0.01$) and influenced climate change adaptation strategies. The study concluded that to support climate change adaptation among the rural farmers in the study area, considerable attention should be paid to understanding the socio-economic characteristics of the rural households, source of information and support received on climate change.
Keywords: *adaptive capacity, Tobit regression model, climate change, Ngaka Modiri Molema District Municipality*

Abbreviations: IPCC: Intergovernmental Panel on Climate Change, FAO: Food and Agriculture Organization, SSA: Sub Saharan Africa, LRAD: Land Redistribution for Agricultural Development, PLAS: Proactive Land Acquisition Strategy, UNDP: The United Nations Development Programme

Introduction

Climate change is real, perhaps one of the most serious environmental threats facing agriculture and rural livelihoods in Sub-Saharan Africa (SSA). Year in year out, it has become clearer that change in weather is happening at a rapid pace and it will have a profound severe negative impact on agriculture, management of natural resources and consequently on livelihood and food security. Climate change has significantly affected global agriculture in the 21st century (Ochieng et al., 2016). The effects of climate change on agricultural production and livelihood is expected to intensify over time, and to vary across countries and regions (Food and Agricultural Organization of the United Nations, FAO, 2016). Climate change could impair economic growth and other aspects of human and natural well-being (Butler, 2018).

Climate change is known to be an important challenge facing African countries. The impact is largely due to low income, greater reliance on climate-sensitive sectors such as agriculture, and weak capacity to adapt to the changing climate. Agriculture in sub-

http://www.aloki.hu ● ISSN 1589 1623 (Print) ● ISSN 1785 0037 (Online)
DOI: http://dx.doi.org/10.15666/aeer/1705_1126111272

Saharan Africa continues to suffer from climate change due to the temperature rising and rainfall frequency and intensity fluctuating (Winifred et al., 2018). Climate change has negatively impacted on SSA countries because of their low human adaptive ability to foresee increases in tremendous events resulting from widespread poverty, heavy reliance on rain-fed agriculture, lack of economic and technological resources, insufficient safety nets and educational progress (Osumanu et al., 2017). According to Adebayor (2012), the effects of climate change, economically, socially and environmentally, have been a bane on sustainable agricultural production and food security in SSA endangering the livelihood of two-thirds of the population who work within the agricultural sector. It is projected that cereal crop may decrease yield in sub-Saharan Africa due to intensifying water stress and frequent incidence of diseases, pests and weeds outbreaks (Niang et al., 2014).

Southern Africa is expected to experience an increase in temperature and disruption in rainfall patterns as well as an increased frequency of extreme climate events such as drought and floods as a result of climate change. South Africa inclusive, is vulnerable to climate change and variability due to a high increase in temperature resulting in the frequent occurrence of drought, shortage of underground water, scarcity and spatial variability of rainfall pattern (Pereira, 2017). South Africa has been experiencing an increase in warmer days and more decrease in the number of cooler days (Davis et al., 2016). According to Linus et al. (2014), it was reported that between 1960 to 2050 the air temperatures in South Africa are expected to increase by 2 °C on average, while atmospheric carbon-dioxide levels are expected to increase by about 235 ppm (from 315 to 550 ppm).

The higher temperature is expected to increase crop heat stress and evapotranspiration demand in the North West Province of South Africa. The impacts are expected to affect natural resources such as air and water, which are considered to be the most critical factor associated with climate change. A report by Kiker (2015), on climate change synthesis on vulnerability and adaptation assessment, revealed that South Africa including North West Province is experiencing climate change which affects the water and air required by crops for survival. According to Blignaut et al. (2009), North West is considerably warmer with evidence that the future temperature will increase than normal which could make the region susceptible to marked reductions in maize production.

Notably, North West Province is one of the largest maize producers in the country (The South African Agricultural Baseline, 2011). The impact of climate change on the production of maize in the study area has resulted in low maize production coupled with a shortage of food and low income. This unpleasant situation in the study area has escalated into maize importation rather than exportation that the country was known of in the past. A report by Sensako (2015), established that South Africa was compelled to import 934,000 metric tons of yellow maize, which was worth about $137 million at current international prices, from countries such as Argentina and Ukraine in 2015 spanning through the end of March 2016 as drought reduced the maize yield. Therefore, there is no gainsaying that the examination of the adaptation measures that farmers need to employ in order to cope with climate change to fully maximize the production of maize which is a staple food in North West Province of South Africa becomes necessary.

Without appropriate responses, climate change is likely to constrain economic development and poverty reduction efforts. Adaptation strategies are needed as a tool to

http://www.aloki.hu ● ISSN 1589 1623 (Print) ● ISSN 1785 0037 (Online)
DOI: http://dx.doi.org/10.15666/aeer/1705_1126111272

promote livelihood in rural communities. Adaptation is one major policy option for reducing the negative impact of climate change. Since, Sub Saharan Africa is predicted to be among the most vulnerable regions to climate change (IPCC, 2014), and because of the reliance on rainfall and other natural systems, smallholder rural households, who constitute 65% of the total population in SSA are the primary victims of climate change. Some coping mechanisms must be in place to adapt to climate change. In recent years, the determinants to climate change adaptation have been limited, and this has become a key concern to farmers, researchers, and policymakers. The available empirical evidence on the determinants of climate change adaptation among rural household farmers have been on large scale and extremely disintegrated (Osumanu et al., 2017). To ensure a better understanding of smallholder rural households' vulnerability and factors determining climate change adaptation, there is a need to investigate the factors responsible.

The objective of this study is to identify and provide a comprehensive understanding of different factors that determine adaptation to climate change among rural households in the study area. The significance of this study is that the findings will assist in directing specific and appropriate measures in combating the factors that affect climate change adaptation strategies in the study area. This would also help to provide improved supervision on appropriate interventions to enhance the resilience of agriculture-dependent households and communities.

Materials and methodology

The study was carried out in Ngaka Modiri Molema District Municipality of the North-West Province. The province lies in the north of South Africa on the Botswana border, with the Kalahari Desert to the west, Gauteng province to the east and the Free State to the south. North West province is the fourth smallest province in the country. It consists of four district municipal councils (Ngaka Modiri Molema District Municipality, Bojanala Platinum District Municipality, Dr. Ruth Segomotsi Mompati District Municipality, and Dr. Kenneth Kaunda District Municipality) which are in turn divided into 18 local municipalities. The province takes up about 8.7 percent of South Africa's land area (106 512 km²), with mining being the major contributor to the Province economy followed by farming activities in which maize is predominantly planted.

Data were collected from Ngaka Modiri Molema district municipality, which consists of 5 local municipalities as shown in *Figure 1*. The list of small and emerging maize farmers in the district comprising about 575 farmers was obtained from Department of Agriculture, Forestry and Fisheries (DAFF) and also from Grain SA. Raosoft sample size calculator was used to determine the sample size from the population of the small and emerging maize farmers in the study area. The sample size calculator took into account the confidence level, the response distribution and the margin of error as indicated below:

$$x = Z\,(^{c}/_{100})^2\, r(100-r) \quad \text{(Eq.1)}$$

$$n = {}^{N\,x}/_{(N-1)E^2 + x)} \quad \text{(Eq.2)}$$

$$E = \text{Sqrt}\,[{}^{(N\,-\,n)x}/_{n(N-1)}] \quad \text{(Eq.3)}$$

http://www.aloki.hu ● ISSN 1589 1623 (Print) ● ISSN 1785 0037 (Online)
DOI: http://dx.doi.org/10.15666/aeer/1705_1126111272

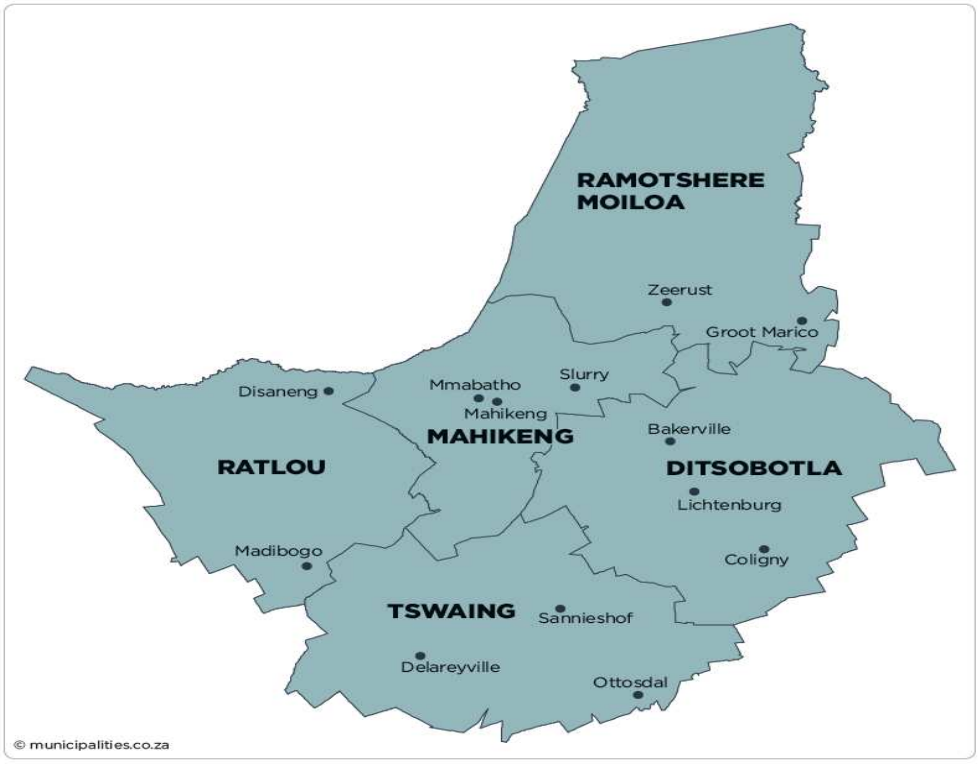

Figure 1. *Map of Ngaka Modiri Molema District Municipality. (Source: Municipal Demarcation Board, 2010)*

A total number of 346 questionnaires were administered to the farmers in the district using the stratified random sampling technique. This technique was employed to group the population of the farmers from the 5 local municipalities in the district into strata. Thereafter, random sampling was used to select from each stratum. A specific number of the sample size was selected from each stratum as shown in *Table 1*.

Table 1. *Data collection according to the selected local municipalities. (Source: author's computation, 2017)*

Stratum (local municipalities in the district)	The population of small scale maize farmers	Selected sample size
Tswaing	200	132
Ditsobotla	150	109
Mahikeng	100	80
Ratlou	15	15
Ramotshere Moiloa	10	10

The questionnaires consisted of a logical flow of questions related to household socio-economic characteristics (demography), climate change adaptation information. The questionnaires were explained to the local extension officers before the survey because they understood the farmers better and could translate the questions into the local language. Face to face interviews and focus group discussions were conducted in each local municipality where each session lasted for about 45 min.

http://www.aloki.hu ● ISSN 1589 1623 (Print) ● ISSN 1785 0037 (Online)
DOI: http://dx.doi.org/10.15666/aeer/1705_1126111272

The data were captured and analyzed using EVIEWS software. Multicollinearity analysis was employed to remove variables that are correlated to each other from the wide list of variables obtained from the questionnaires as shown in *Table 2*. A Tobit regression model was used to identify the factors that determine adaptation to climate change in the study area.

Table 2. *Multicollinearity analysis. (Source: author's computation, 2017)*

Variables	Collinearity statistics	
	Tolerance	**VIF**
Number of years of farming	0.578	1.731
Farm size	0.731	1.367
Household size	0.760	1.315
Gender	0.816	1.225
Household marital status	0.706	1.416
Education level	0.602	1.661
Farming as major income	0.567	1.763
Types of farm	0.787	1.270
Who manages the farm	0.919	1.088
Who owns the farm	0.799	1.251
Land acquisition	0.741	1.350
Climate change awareness	0.748	1.337
Source of climate change information	0.707	1.414
Climate change information through extension services	0.723	1.382
Channel of information received on climate change	0.658	1.519
Support received on climate change	0.617	1.620
Adaptation barrier	0.685	1.460
Mean VIF		1.422

The Tobit model, also called a censored regression model, was employed to estimate linear relationships among variables when there is either left or right-censoring in the dependent variable as shown in the equation below. In other words, the factors influencing climate change adaptation in the study area were estimated using Tobit regression analysis. The model was developed by Tobin (1958). Following Schwarze (2004), since the dependent variable is bounded between 0 and 1 (i.e., the variables are censored at 0.0 and 1.0), conventional regression methods fail to consider the qualitative difference between zero and continuous observations. However, the Tobit model could combine the properties of multiple regression and Probit/Logit model. Therefore, the Tobit model which was initially established for censored data was applied for the analysis. The model is specified as:

$$Y_i = \beta Xiifi^* = \beta Xi + ui > Ti \quad \text{(Eq.4)}$$

$$Y_i = \beta 0 + \beta iXi + ui \quad \text{(Eq.5)}$$

where: uí = normally distributed with zero mean and constant variance; X_i = vector of explanatory variables; βi = vector of the parameter estimates.

http://www.aloki.hu ● ISSN 1589 1623 (Print) ● ISSN 1785 0037 (Online)
DOI: http://dx.doi.org/10.15666/aeer/1705_1126111272

The model is fully estimated as follows:

$$yi^* = \beta 0 + \beta 1xi + \varepsilon i = xi'\beta + \varepsilon i,\ \varepsilon i \sim N(0,\sigma 2) \quad \text{(Eq.6)}$$

$$\text{If } yi^* > 0 => yi = \text{climate change} = yi^* = xi'\beta + \varepsilon i \quad \text{(Eq.7)}$$

$$\text{If } yi^* \leq 0 => yi = 0 (y^* \text{ can be negative, but if it is, } y = 0) \quad \text{(Eq.8)}$$

$$\text{Probability Model } --\varepsilon i \sim N(0, \sigma 2) \quad \text{(Eq.9)}$$

$$\text{Prob}(y = 0|x) = \text{Prob}(y^* \leq 0|x) = \text{Prob}\ [(y^* - X\beta)/\sigma \leq (0 - X\beta)/\sigma|x] \quad \text{(Eq.10)}$$

$$\text{Prob}[z \leq - X\beta/\sigma|x] = \Phi(-X\beta/\sigma) = 1 - \Phi(X\beta/\sigma) \quad \text{(Eq.11)}$$

$$\text{Prob}(y > 0|x) = \text{Prob}(y^* > 0|x) = 1 - \Phi(-X\beta/\sigma) = \Phi(X\beta/\sigma) \quad \text{(Eq.12)}$$

Yi = Climate change adaptation strategies index determined by dividing the number of climate change adaptation strategies used by the individual farmers by all the climate change adaptation strategies available in the study area. Thus, the value of the climate change adaptation strategies index ranges between zero (0) and one (1). Thus, the explanatory variables used in the analysis include the socioeconomic variable of the household head and information pertaining to climate change and its adaptation, which are:

X_1 = Number of years of farming (years)
X_2 = Farm size (hectares)
X_3 = Household size (number of persons in the household)
X_4 = Gender of household head (Male = 1; Female = 0)
X_5 = Age of household head (years)
X_6 = Marital status
X_7 = Household head educational level
X_8 = Household head source of income
X_9 = Type of farm
X_{10} = Who manages the farm
X_{11} = Who owns the farm
X_{12} = Land acquisition
X_{13} = Climate change awareness
X_{14} = Information receive on climate change
X_{15} = Source of climate change information
X_{16} = Climate change information through extension services
X_{17} = Channel of information on climate change
X_{18} = Support received on climate change
X_{19} = Climate change adaptation
X_{20} = Adaptation barrier

Results and discussion

The household farm size in *Table 3* was statistically significant ($p < 0.01$) and had a negative association. This suggests that the size of the farm had an influence on climate

http://www.aloki.hu ● ISSN 1589 1623 (Print) ● ISSN 1785 0037 (Online)
DOI: http://dx.doi.org/10.15666/aeer/1705_1126111272

change adaptation in the study area. Farmers with small farm size tend to ignore adaptation measures as a result low resources, however, farmers with large farm size are likely to have more capacity to try out various adaptation strategies and invest in climate risk coping strategies. This could also mean that farmers reduced their farm size in other to adapt to climate change as they have little resources to cope. The larger the farm size the more the adaptation strategies of changing crop cultivars and crop types. This result is supported by Abid et al. (2015), who reported that farmers with large farm size try more adaptation options. On the contrary, Mohammed et al. (2014) reported a negative result where a large farm size requires greater levels of investment to implement adaptive strategies to climate change. The same result was explained by Acquah and Onumah (2011) that farm size was negatively significant to climate change adaptation and its effects (*Fig. 2*).

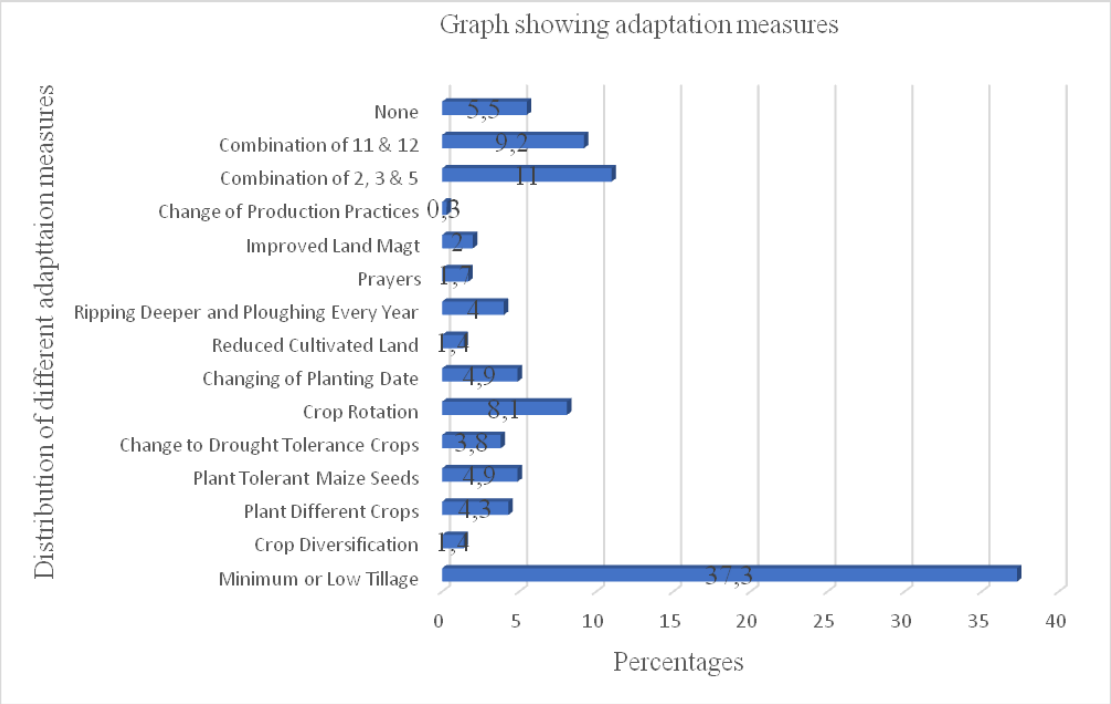

Figure 2. *Distribution of different adaptation measures in the study area*

According to *Table 3,* gender was statistically significant ($p < 0.01$) and influenced climate change adaptation. Various research has revealed that gender is an important factor affecting adoption decision among farmers. The result from the study area revealed that male farmers (84.1%) are more involved in farming and thus, adapting to climate change than women. Male farmers are more likely to perceive a change in the climatic condition unlike female farmer because male-headed households have a higher probability of acquiring information than female-headed households. This finding is supported by Ncube et al. (2016) who reported that male-headed households were more likely to perceive changes in the surrounding than female-headed households. However, Sharaunga et al. (2015) reported that empowering women in smallholder agriculture is very crucial in reducing vulnerability to climate change among rural households.

In *Table 3*, the type of farm a household head engage in has an influence on climate change adaptation. The type of farm in this regard includes individual farm, family

http://www.aloki.hu ● ISSN 1589 1623 (Print) ● ISSN 1785 0037 (Online)
DOI: http://dx.doi.org/10.15666/aeer/1705_1126111272

farm, community and tribal farm which was statistically significant ($p < 0.05$) to climate change adaptation. This suggests that individual farms adopt natural resources management and conservation practices better compare to tribal or community farm type as individual can manage information based on his or her household resources and needs.

Table 3. *Parameter estimates (model specification) of the Tobit regression analysis on factors that influence climate change adaptation. (Source: author's computation, 2017)*

Variables	Coefficient	Std. error	z- Statistic	Pr(> |z|)
Years of farming (X_1)	0.006116	0.003868	1.581138	0.1138
Farm size (X_2)	-0.013340	0.004865	-2.742015***	0.0061
Household size (X_3)	-0.005277	0.005735	-0.920130	0.3575
Gender (X_4)	-0.062083	0.016218	-3.827976***	0.0001
Marital status (X_5)	0.010947	0.006693	1.635506	0.1019
Education (X_6)	0.005051	0.005117	0.987128	0.3236
Source of income (X_7)	-0.017227	0.015601	-1.104226	0.2695
Type of farm (X_8)	-0.009591	0.004362	-2.198753**	0.0279
Manage farm (X_9)	0.003761	0.026335	0.142799	0.8864
Owns farm (X_{10})	-0.022814	0.011036	-2.067288**	0.0387
Land acquisition (X_{11})	0.009078	0.003044	2.982234***	0.0029
Climate change awareness (X_{12})	0.098297	0.066811	1.471266	0.1412
Source of climate change information (X_{13})	0.022988	0.007113	3.232000***	0.0012
Climate information through extension services (X_{14})	0.013465	0.014691	0.916559	0.3594
Channel of information on climate change (X_{15})	0.007942	0.005393	1.472588	0.1409
Support received on climate change (X_{16})	-0.005196	0.002948	-1.762625*	0.0780
Adaptation barrier (X_{17})	-0.190419	0.006259	-30.42514***	0.0000
C	0.203205	0.277651	0.731872	0.4642
Error distribution				
SCALE: C (19)	0.099657	0.003788	26.30651	0.0000
Mean dependent var	1.057803	S.D. dependent var	0.233709	
S.E. of regression	0.102511	Akaike info criterion	-1.664344	
Sum squared resid	3.436285	Schwarz criterion	-1.453124	
Log likelihood	306.9315	Hannan-Quinn criterion	-1.580235	
Avg. log likelihood	0.887085			
Wald test equation				
Test statistic	Value	df	Probability	
F-statistic	91.26040	(17, 327)	0.0000	
Chi-square	1551.427	17	0.0000	

$p < 0.1$ (*); $p < 0.05$ (**); $p < 0.01$ (***) at 10%, 5% and 1% level of significance, respectively

In the same train of thought, *Table 3* revealed that an individual who owns the farm was statistically significant ($p < 0.05$) and influence climate change adaptation strategies. This result implied that the knowledge and experience of the farm owner determine the adoption of natural resources management and conservation practices to use. Research by Habtemariam et al. (2016) reported that educated and experienced farmers are expected to have more knowledge and information about climate change

http://www.aloki.hu ● ISSN 1589 1623 (Print) ● ISSN 1785 0037 (Online)
DOI: http://dx.doi.org/10.15666/aeer/1705_1126111272

and adaptation measures to use in response to climate challenges. Theis et al. (2018) reported that land ownership individually managed, is widely believed to encourage the adoption of technologies linked to physical assets such as land and irrigation system.

The land is a fundamental factor of production. The method of acquiring land or farm by the farmers was statistically significant ($p < 0.01$) and influence climate change adaptation in the study area as shown in *Table 3.* Various methods of land acquisition as identified in the study area include; land redistribution for agricultural development (LRAD), PLAS, land affair, hire, inheritance, own finance. This result implies that adaptation strategies are linked to land acquisition method. Farmers who buy land hire or through land affair tend to adopt adaptation strategies more as they need to produce much in other to pay and make a profit to sustain a livelihood.

The sources of information received on climate change influence adaptation strategies. In *Table 3,* the information source was statistically significant ($p < 0.01$) where the majority of the respondents in the study area obtained information through media (radio). The source of information influence climate change adaptation because the information from non-reputable source might not be the right information needed to adapt in other to transform or increase food production, and different information target different environment and farming systems. In addition, the source from which information is being received determines the effectiveness and farmers' adoption. According to Akinnagbe et al. (2015), it was reported that crop farmers got their information from sources which may not be unconnected with their level of interaction in the communities. Farmers need information in which extension officers play a significant role (Gabriel et al., 2013).

According to *Table 3,* the support received by the farmers was statistically significant ($p < 0.1$). The support received includes; formal credit, insurance, farmer to farmer extension, relatives, subsidies. Adaptation to climate change becomes easier when farmers receive support on climate change. The inability of the farmers to get the necessary support and resources might hinder the farmers from adapting to climate change. According to UNDP (2018), it was emphasized that most farmers in Africa are operating under resource limitation which prevents adaptation measures. Derr (2018) reported that institutional support for climate change adaptation is needed for rural farmers in order to adapt to climate change scenario and events.

In *Table 3,* the adaptation barrier was statistically significant ($p < 0.01$) and influence climate change adaptation in the study area. Barriers to adaptation restrict people's ability to address the negative impacts of climate change. Examples of adaptation barrier in the study area are lack of knowledge and education, lack of structural and infrastructural resources, lack of capital resources and extension officers. Adaptation barriers prevent farmers from adopting various strategies and practices to cope with the impact of climate change variability and events. Farmers need resources and information to be able to adapt without which farm productivity is affected. This result was supported by Brown and Sonwa (2015), who reported that in agricultural communities, lack of financial capital is one barrier to adaptation, such as the adoption of improved crop varieties and diversification of livelihoods.

Conclusion and recommendation

The study reveals that climate change poses several challenges to the livelihoods of rural households in the study area. It also provides a comprehensive understanding of

http://www.aloki.hu ● ISSN 1589 1623 (Print) ● ISSN 1785 0037 (Online)
DOI: http://dx.doi.org/10.15666/aeer/1705_1126111272

the factors that hinders adaptation to climate change in the study area, which includes; farm size, household gender, type of farms, who owns the farm, land acquisition, source of climate change information, support received on climate change, and adaptation barrier. This study highlights that fostering climate change adaptation does not only entails scientific knowledge especially in the study area (SSA) but also community involvement and development of solutions using local approach and socio-economic characteristics of the rural household. The recommendation drawn from this study is that in attempting to support households' adaptation strategies to climate change, and develop sustainable strategies that will be culturally accepted by rural households and communities, considerable attention should be paid to understanding socio-economic factors such as farm size, household gender, type of farms, who owns the farm, land acquisition, and also information on climate change.

Acknowledgments. We like to express our sincere gratitude to the anonymous reviewers for improving the quality of this paper. We also acknowledge the support of those who have contributed to the success of this paper. We acknowledge the funding provided by the University of South Africa.

Conflict of interests. The authors declare that there is no conflict of interests.

REFERENCES

[1] Abid, M., Scheffran, J., Schneider, U. A., Ashfaq, M. (2015): Farmers' perceptions of and adaptation strategies to climate change and their determinants: the case of Punjab Province, Pakistan. – Earth System Dynamics 6(1): 225-243. doi.org/10.5194/esd-6225-2015.

[2] Acquah, H. D., Onumah, E. E. (2011): Farmers' perception and adaptation to climate change effects: A willingness to pay. – J. Sustain. Dev. Afr. 13: 150-161.

[3] Adebayor, A. A. (2012): Evidence of climate change in Taraba State: a preliminary report. – A paper presented at the Faculty of Science Seminar Series held at the Lecture Hall on 13th September 2012. Taraba State University, Jalingo, Nigeria.

[4] Akinnagbe, O. M., Attamah, C. O., Igbokwe, E. M. (2015): Sources of information on climate change among crop farmers in Enugu North Agricultural Zone, Nigeria. – International Journal of Research in Agriculture and Forestry 2(11): 27-33.

[5] Blignaut, J., Liza, U., James, A. (2009): Agriculture production's sensitivity to changes in climate in South Africa. – South African Journal of Science 105(1-2).

[6] Brown, H. C. P., Sonwa, D. J. (2015): Rural local institutions and climate change adaptation in forest communities in Cameroon. – Ecology and Society 20(2): 6: 4-8. doi.org/10.5751/ES-07327-200206.

[7] Butler, C. D. (2018): Climate change, health, and existential risks to civilization: a comprehensive review (1989⁻2013). – International Journal of Environmental Research and Public Health 15(10): 2266. DOI: 10.3390/ijerph15102266.

[8] Davis, C. L., Hoffman, M. T., Roberts, W. (2016): Recent trends in the climate of Namaqualand, a mega diverse arid region of South Africa. – S Afr J Sci 112(4): 9. doi.org/10.17159/ sajs.2016/20150217.

[9] Derr, T. (2018): Climate change perceptions and adaptation among small-scale farmers in Uganda: a community-based participatory approach. – A thesis submitted in partial fulfillment of the requirements for the degree of Master of Science in geography at The University of Utah State University Logan, Utah, pp. 22-83.

[10] Food and Agriculture Organization of the United Nations (2016): The State of Food and Agriculture. Climate Change, Agriculture and Food Security. –FAO, Rome.

http://www.aloki.hu ● ISSN 1589 1623 (Print) ● ISSN 1785 0037 (Online)
DOI: http://dx.doi.org/10.15666/aeer/1705_1126111272

[11] Gabriel, D., Sait, S. M., Kunin, W. E., Benton, T. G. (2013): Food production vs. biodiversity: comparing organic and conventional agriculture. – J Appl Ecol 50: 355-364. DOI: 10.1111/1365-2664.12035.
[12] Habtemariam, L. T., Gandorfer, M., Kassa, G. A., Heissenhuber, A., München, T. U. (2016): Reference tools. – Environmental Management. doi.org/10.1007/s00267-016-0708-0.
[13] IPCC (2014): Climate Change 2014: Impacts, Adaptation and Vulnerability. Summary for Policy Makers. – Cambridge University Press, Cambridge.
[14] Kiker, G. A. (2015): South African County Study on Climate Change Synthesis Report for the Vulnerability and Adaptation (V&A) Section of the South African Climate Change, Vulnerability and Adaptation Assessment. – School of Bioresources Engineering and Environmental Hydrology, University of Natal, Durban, South Africa..
[15] Linus, B. G., Sogbesan, O. A., Ekundayo, T. M., Kesonga, G. M. (2014): Fishing communities and fishing as livelihoods in Adamawa state. – Direct Research Journal of Agriculture and Food Science 2(11): 195-204.
[16] Mohammed, N. U., Wolfgang, B., Jason, S. E. (2014): Factors affecting farmers' adaptation strategies to environmental degradation and climate change effects: a farm level study in Bangladesh. – Climate Change 2: 223-241. DOI: 10.3390/cli2040223.
[17] Ncube, M., Madubula, N., Ngwenya, H., Zinyengere, N., Zhou, L., Francis, J., Madzivhandila, T. (2016): Climate change, household vulnerability and smart agriculture: the case of two South African provinces. – Jamba (Potchefstroom, South Africa) 8(2): 182. DOI: 10.4102/jamba.v8i2.182.
[18] Niang, I., Ruppel, O. C., Abdrabo, M. A., Essel, A., Lennard, C., Padgham, J., Urquhart, P. (2014): Africa. – In: Climate Change 2014: Impacts, Adaptation, and Vulnerability. Part B: Regional Aspects. Contribution of Working Group II to the Fifth Assessment Report of the Intergovernmental Panel on Climate Change. Cambridge University Press, Cambridge, UK.
[19] Ochieng, J., krimi, L., Mathenge, M. (2016): Effect of Climate Variability and Change on Agricultural Production: The Case of Small Scale Farmers in Kenya. – Tegemeo Institute of Agricultural Policy and Development, Egerton, Kenya. doi.org/10.1016/j.njas.2016.03.005.
[20] Osumanu, I. K., Aniah, P., Yelfaanibe, A. (2017): Determinants of adaptive capacity to climate change among smallholder rural households in the Bongo District, Ghana. – Ghana Journal of Development Studies 14(2): 143-145. doi.org/10.4314/gjds.v14i2.8.
[21] Pereira, L. (2017): Climate change impacts on agriculture across Africa. Subject: environmental issues and problems. – Agriculture and the Environment. DOI: 10.1093/acrefore/9780199389414.013.292.
[22] Schwarze, S. (2004): Determinants of Income Generating Activities of Rural Households: A Quantitative Study in the Vicinity of Love-Lindu National Park in Central Sulawesi, Indonesia. – Institute of Rural Development. University of Goettingen, Goettigen.
[23] Sharaunga, S., Mudhara, M., Bogale, A. (2015): The impact of 'women's empowerment in agriculture' on household vulnerability to food insecurity in the KwaZulu-Natal Province. – Forum for Development Studies 42(2): 195-223. doi.org/10.1080/08039410.2014.997792.
[24] Sensako (2015): South Africans forced to import maize as drought destroys crops. – http://www.sensako.co.za/NewsArticle.aspx?id=8 (accessed on 13 May 2019).
[25] South African Agricultural Baseline (2011): Maize Production. – Department of Agriculture of South Africa, Jean du Plessis, Bureau for Food and Agricultural Policy (BFAP). https://www.syngenta.co.za/maize (accessed on 10 October 2017).
[26] Theis, S., Lefore, N., Meinzen‐Dick, R., Bryan, E. (2018): What happens after technology adoption? Gendered aspects of small scale irrigation technologies in Ethiopia,

http://www.aloki.hu ● ISSN 1589 1623 (Print) ● ISSN 1785 0037 (Online)
DOI: http://dx.doi.org/10.15666/aeer/1705_1126111272

Ghana, and Tanzania. – Agriculture and Human Values 35: 671-684. doi.org/10.1007/s10460-018-9862-8.

[27] Tobin, J. (1958): Estimation of relationships for limited dependent variables. – Econometrica 26: 24 36.

[28] UNDP (2018): Climate Change Adaptation in Africa UNDP. Synthesis of Experiences and Recommendations. – UDNP, New York, pp. 6-87. https://www.thegef.org/sites/default/files/publications/CCA-Africa-Final.pdf (accessed on 13 May 2019).

[29] Winifred, C., Nancy, W., Mungai, S. S., Hillary, K., Bett, H. L. (2018): "Farmers' perspectives: impact of climate change on African indigenous vegetable production in Kenya". – International Journal of Climate Change Strategies and Management 10(4): 551-579. doi.org/10.1108/IJCCSM-07-2017-0160.

http://www.aloki.hu ● ISSN 1589 1623 (Print) ● ISSN 1785 0037 (Online)
DOI: http://dx.doi.org/10.15666/aeer/1705_1126111272

INDUCING EFFECT OF CHITOSAN ON THE PHYSIOLOGICAL AND BIOCHEMICAL INDICES OF EGGPLANT (*SOLANUM MELONGENA* L.) GENOTYPES UNDER HEAT AND HIGH IRRADIANCE

LIAQAT, A.[1*] – IHSAN, M. Z.[1] – RIZWAN, M. S.[1] – MEHMOOD, A.[2] – IJAZ, M.[3] – ALAM, M.[4] – ABDULLAH, M.[1] – WAJID, M.[5] – HUSSAIN, R.[6] – NAEEM, M.[7] – YAQUB, M. S.[6]

[1]*Cholistan Institute of Desert Studies (CIDS), The Islamia University of Bahawalpur, Bahawalpur, Pakistan*

[2]*Department of Agronomy, University of Agriculture, Faisalabad, Pakistan*

[3]*College of Agriculture, Bahauddin Zakariya University, Bahadur sub Campus, Layyah, Pakistan*

[4]*Department of Horticulture, The University of Agriculture, Peshawar, Pakistan*

[5]*Plant Physiology Division, Nuclear Institute of Agriculture, Tandojam, Sindh, Pakistan*

[6]*Department of Horticultural Sciences, UCA&ES, The Islamia University of Bahawalpur, Bahawalpur, Pakistan*

[7]*Directorate of Agriculture Extension and Adaptive Research, Government of Punjab, Lahore, Pakistan*

**Corresponding author*
e-mail: liaqatali@iub.edu.pk

(Received 11th Apr 2019; accepted 11th Jul 2019)

Abstract. Among abiotic stresses, high temperature is an obstructive factor in plant growth and physiological activities for sustainable agriculture, worldwide. Chitosan is a bio-based stimulant and may be helpful in reducing adversative effects of temperature stress. A field experiment was conducted to investigate the role of chitosan as high temperature stress regulator in two eggplant genotypes (Black boy and Sandhya) under arid environment. Temperature stress was maintained by delayed planting of eggplant as compared to its optimum planting time. Results showed that foliar application of chitosan has significantly improved the eggplant growth and yield characteristics. The effect of chitosan was more prominent on the genotype Black boy over Sandhya and recovery of plants improved with the increase in its application rate. The maximum yield was obtained in Black boy that was 42% higher to control and 14% to Sandhya at chitosan application of 175 mg L^{-1}. Application of chitosan also improved the proline content, glycinebetain, total soluble solids and total phenolics accumulation. The late season high temperature stress significantly reduced the linear electron flow and non-photochemical quenching but the application of chitosan significantly improved both these characters. The positive effect of chitosan on plant physiochemical traits was more promising on genotype Black boy over Sandhya. These findings showed that the chitosan can be used as an ecofriendly compound to enhance plants activities under stress conditions.
Keywords: *climate change, chitosan, high temperature, photosynthesis, fruit generative*

http://www.aloki.hu ● ISSN 1589 1623 (Print) ● ISSN 1785 0037 (Online)
DOI: http://dx.doi.org/10.15666/aeer/1705_1127311287

Introduction

Climate change is expected to continue increasing and poses regionally differing threats to agriculture in this World. South Asia is snowballing in the last few decades and the situation is further becoming severe in global warming scenario (IPCC, 2014). The high concentration of population in this region generally reliance on natural resources and agriculture along the coastal areas to derive their economy and development for their livelihood. Currently, declining soil productivity and extreme weather conditions; rising temperature, salinity, drought as well as deforestation have had sever affects posing a threat to throw the countries back into the poverty trap. The efforts regarding adjustment and mitigation of the source climate change such as green-house gas emissions by burning of fossils fuels, as well as deforestation and urbanization, are needed to combat this issue (Churkina, 2016; Mgbemene et al., 2016; Myers et al., 2017). Agriculture and food security is a fundamental human activity at risk by this global warming. The rising temperature is the key factor controlling the cropping patterns and water availability in coming decades (Rasul, 2016; Teixeira et al., 2013).

Temperature is the primary determinant of crop production, particularly in arid areas (Ihsan et al., 2016). Temperature controls the rate of plant metabolic processes that is ultimate source of biomass, phytonutrients, fruit development and yield of plant. The photosynthetic rates peak at about 30 °C and decreases thereafter 17% for each degree Centigrade in average (Ali et al., 2011; Lobell and Asner, 2003). High temperature affects plant physiology at both cellular and whole plant through stomatal conductance and osmotic pressure. High temperature stress reduces plant growth and development through excessive evapotranspiration effects, may lead to nutritional imbalance such as sulphur, specific ion effects as well as low turgor potential of plant (Ihsan et al., 2016). The adding effect of each of these factors can affect plant processes like lipid peroxidation, photosynthesis, energy and protein formation.

The high temperature in addition with drought spells encourage more `harmful impact on growth parameters such as plant height, the number of leaves per plant, shoot dry weight, shoot length, root length, flower induction, and ultimately the yield attributes (Ainsworth and Ort, 2010; Jiao et al., 2012; Shehata et al., 2012).

Eggplant (*Solanum melongena* L.) is a well-known vegetable, widely cultivated in central, south Asia and some African countries (Hazra et al., 2003; Ranil et al., 2017). The ideal temperature for plant growth and fruit development lies between 22ºC and 30 °C. With an unnatural weather change, temperature in south Asia is often over 35 °C, which is not suitable for growth, flower bud formation, and may cause pollen infertility (Pandit et al., 2010). Such damage is estimated to the reduced harvest and subsequently low yield. Currently, attempts to measure the potential benefits of climate mitigation actions on the agricultural sector, which have been put forward, such as heat-tolerant varieties, improving irrigation systems and certain cultivation measures. However, the use of bio-stimulants, such as chitosan or chitin could be one of the approaches to cope with the negative impact of abiotic stress such as high temperature and heat stress.

Chitosan (CTS) are polysaccharides, a derivative of chitin, obtained from the waste products of sea food is one of the most preferred biopolymers, harmless to plants, animals and, since the last decade, chitosan uses are increasing due to its non-toxicity, biodegradability, biocompatibility, and stimulant to cell activation and plant growth (Elieh-Ali-Komi and Hamblin, 2016). Previous studies reported chitosan use in

http://www.aloki.hu ● ISSN 1589 1623 (Print) ● ISSN 1785 0037 (Online)
DOI: http://dx.doi.org/10.15666/aeer/1705_1127311287

agriculture to manage abiotic stresses and to improve crop production and quality (Katiyar et al., 2015; Sharif et al., 2018).

Chitosan prevents adverse effects of the abiotic stresses in plants through regulating different mechanisms. Application of chitosan boosted photosynthesis that elicited the scavenging of reactive oxygen species under stress conditions. Chitosan involved in protecting plants from high temperature stress and photo-damage through production of heat shock proteins (Chandra et al., 2015; Landi et al., 2017). The first protein complex (PSII) is more sensitive than PSI (Allakhverdiev et al., 2008; De Ronde et al., 2004; Sonoike, 2011). High temperature stress above 40 °C inhibit PSII activity through denaturation of this protein complex and inhibiting of enzymes activity (Kehoe, 2010; Walters, 2005). The other mechanism damaged through high temperature stress in plants is the thylakoid proton conductance (Baker et al., 2007; Rochaix, 2011). In some plants these mechanisms are more chilling sensitive than high temperature stress (Sonoike, 2011).

The positive role of chitosan in various stresses management is well documented in different crops. Its role in high temperature stress management in eggplant (*Solanum melongena* L.*)* has been never studied and reported. Considering chitosan positive response in different stresses management in agriculture crops, the present study is designed to evaluate its role in PSII regulation and osmoprotectant (proline, soluble carbohydrates, and glycinebetaine) performance under high temperature stress in eggplant (*S. melongena* L.) genotypes. Moreover, the effect of chitosan will be studied on crop agronomic and fruit generative characters.

Material and methods

Experimental site and soil preparation

The field experiment was conducted in the research area of 'The Islamia University of Bahawalpur (29.35˚N, 71.69˚E)., near cholistan desert, Pakistan (*Fig. 1*). The climate of the experimental location is arid with sever hot summer and cool dry winter (*Table 1*). The experimental plots were prepared by deep ploughing, after the harvest of Maize crop. The eggplant (*Solanum melongena*) seedlings were obtained from a vegetable crops nursery near Lahore, Punjab and transplanted on 27th March 2017. In this experiment, a randomized complete block design was used with three replications. The experimental bed size was 1.5 m × 0.6 m, with plant density 7.12 plants m^{-2}. The plantation was made on the both sides of the beds. Plant to plant distance was maintained at 45 cm while row to row distance was maintained at 30 cm apart. The non-experimental area of approximately 1 meter (0.92 m) left fallowed between two blocks.

Treatments application

Two eggplant genotypes (Black boy and Sandhya) were tested against chitosan application for heat stress mitigation on somatic and generative characters. Chitosan was applied at five different levels. Chitosan levels were comprised of T0: 0 mg L^{-1}, T1: 125 mg L^{-1}, T2: 150 mg L^{-1}, T3: 175 mg L^{-1} and T4: 200 mg L^{-1} respectively (*Table 2*). Chitosan application was based into different phases, depending on plant vegetative and developmental stage. The heat stress was maintained by late planting in March that initiated flowering in the hot months of June and July.

http://www.aloki.hu ● ISSN 1589 1623 (Print) ● ISSN 1785 0037 (Online)
DOI: http://dx.doi.org/10.15666/aeer/1705_1127311287

Table 1. *Monthly temperature, relative humidity, wind speed and rainfall during the crop growing season*

Month	Temperature °C		Relative humidity (%)	Wind speed (KPH)	Rainfall (mm)
	Maximum	Minimum			
March	40	17.4	45	10	-
April	44	23.6	31	13	-
May	49	26.29	27	16	12
June	49	30	24	14	200
July	45	28.29	48	13	118
August	44	27.6	47	12	145
September	44	23.6	46	12	-
October	42	16.38	38	8	-

Observation in each column are based on monthly data means

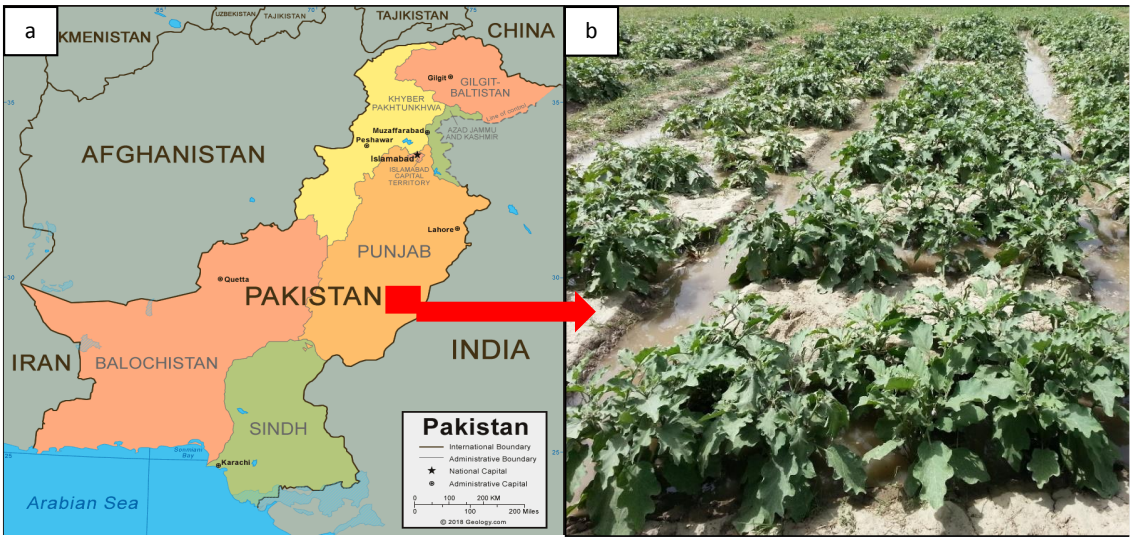

Figure 1. *Location of the experimental region (a = a map of the experimental region, b = a photo of the experimental block)*

Table 2. *Details of different chitosan treatments used in experiment of eggplant (Solanum melongena L.) genotypes under heat and high irradiance*

Parameters		Uses
Treatment	T0	Control (0 mg L^{-1})
	T1	125 mg L^{-1}
	T2	150 mg L^{-1}
	T3	175 mg L^{-1}
	T4	200 mg L^{-1}
Variety	V1	Black boy
	V2	Sandhya

The chitosan was added as fumigant. The growing season was grouped into five phases, and the application of chitosan was based on the requirement and growth of the crop stage

http://www.aloki.hu ● ISSN 1589 1623 (Print) ● ISSN 1785 0037 (Online)
DOI: http://dx.doi.org/10.15666/aeer/1705_1127311287

Data collection/sampling

The Data recording was made randomly, 5 plants from each bed, 15 plants from each block and 30 plants from each treatment. The measurements were made for number of leaves, shoot fresh weight, root fresh weight, no of flowers per plant, no of fruits per plant, shoot/root ratio and pant biomass. Chemical analysis of leaf for antioxidant enzymes, i.e., proline, glycinebetaine and total phenolics were also performed at full maturity stage. Measurements were also made for net photosynthesis, linear electron flow and Non-photochemical quenching when plants produced first fruit. Five plants for each treatment were up-rooted and washed to remove debris and soil particles. Shoot length; from hypocotyl to the tip of the shoot was measure in centimeters. Similarly, the root length was calculated from base of hypocotyl to the tip of root. Root/shoot fresh and dry weight and fruit weight were measured in grams with the help of electrical balance. Number of leaves, shoots, flowers and fruits were counted manually at maturity stage. Flower drop were measured by subtracting total number of fruits from total number of flowers.

For the extraction of total soluble sugars, lyophilized leaf samples, 0.05 g was extracted in 5 mL solvent of 80% ethanol for 24 h according to prescribed method of Schortemeyer et al. (1997). Absorbance was measured at 623 nm using a Cary 50 Bio spectrophotometer (Varian, Australia). The total phenolic contents were measured according to the Folin–Ciocalteau method modified to Dewanto et al. (2002). Absorbance was measured at 765 nm using a Cary 50 Bio spectrophotometer (Varian, Australia). Quantification was carried out by comparison against the external standard gallic acid, 3,4,5-trihydroxybenzoic acid (Sigma–Aldrich, Germany). The amount of glycinebetaine was estimated according to the method of Grieve and Grattan (1983). The absorbance for glycinebetaine (GB) was measured at 365 nm using a Varian Cary 50 spectrophotometer (Agilent Technologies Inc., USA). Proline was extracted according to the method of Bates et al. (1973), with some modifications. The absorbance was noted at 520 nm using a double beam spectrophotometer (Hitachi-120, Japan). Proline concentration was determined from a standard curve and calculated on dry weight basis.

To determine whether the tested eggplant (*S. melongena* L) plants are involved in photoinhibition and repair processes, PSII activity was measured. The dissipation of excess light energy as heat was monitored by measuring the development of NPQt. Photosynthesis and energy dissipation was measured on field-grown plants using a PhotosynQ, portable photosynthesis system (Kuhlgert et al., 2016).

Statistics

Five replicate samples were used for each factor. Data for the level of chitosan was evaluated by analysis of variance (ANOVA) followed by Tukey's studentized range test (HSD) ($P < 0.05$) using SPSS version 18.0 (SPSS Inc., Chicago, II., USA). The level of chitosan was taken as independent factor while physiological and biochemical indices as dependent factor. Descriptive analysis (SPSS Inc., Chicago, II., USA were made to reveal the differences between data. Differences were considered to be significant at $p < 0.05$.

http://www.aloki.hu ● ISSN 1589 1623 (Print) ● ISSN 1785 0037 (Online)
DOI: http://dx.doi.org/10.15666/aeer/1705_1127311287

Results

Foliar application of chitosan significantly improved the eggplant growth and yield characteristics except for number of leaves plant^{-1} and number of flowers per plant^{-1}; however, the improvement was dependent on the chitosan dose and the eggplant genotype. Generally, the increase in chitosan level increased the growth and yield of both genotypes (*Tables 3* and *4*). However, the varietal response was variable for different growth parameters to different applied levels of chitosan. The effect of chitosan was significant for, plant height, number of shoots plant^{-1}, root length, root fresh weight and root dry weight for Black boy and plant height, number of shoots plant^{-1}, root length and root dry weight (*Table 5*). Similarly, the effect of chitosan was significant for number of fruits plant^{-1}, weight of each fruit and yield plant^{-1} for Black boy. While the number of fruits per plant^{-1}, flower drop plant^{-1}, weight of each fruit, yield plant^{-1} and flower drop percentage for Sandhya genotype (*Table 6*).

Table 3. *ANOVA comparison for different levels of chitosan on the morphological traits of eggplant (Solanum melongena L.) genotypes under heat and high irradiance*

Source of variation		Var-1				Var-2			
		Replication	Treatment	Error	Total	Replication	Treatment	Error	Total
No of leaves plant^{-1}	Degree of freedom	7	4	28	39	7	4	28	39
	Mean squares		100.25				116.6		
	F-value		2.348				1.822		
	P-value		0.073 ^{NS}				0.147^{NS}		
Plant height	Degree of freedom	7	4	28	39	7	4	28	39
	Mean squares		61.562				155.855		
	F-value		5.989				9.343		
	P-value		0.001**				0.000***		
No of shoots plant^{-1}	Degree of freedom	7	4	28	39	7	4	28	39
	Mean squares		2.088				4.588		
	F-value		2.894				4.621		
	P-value		0.036*				0.004**		
Root length (cm)	Degree of freedom	7	4	28	39	7	4	28	39
	Mean squares		48.375				44.412		
	F-value		22.727				18.899		
	P-value		0.000***				0.000***		
Fresh weight root	Degree of freedom	7	4	28	39	7	4	28	39
	Mean squares		93.85				62.9		
	F-value		3.207				2.164		
	P-value		0.024*				0.094 ^{NS}		
Dry weight root	Degree of freedom	7	4	28	39	7	4	28	39
	Mean squares		15.538				40.962		
	F-value		5.149				19.44		
	P-value		0.002**				0.000***		

Probability level at 5%, P ≤ 0.001***, NS = Non-significant, Var-1 = variety 1, Var-2 = variety 2

The response of genotypes for above mentioned traits was maximum at 150 mg L^{-1} to 175 mg L^{-1} for most of the traits except for fresh weight of root (125 g) and flower drop % (62%) in Sandhya that was the highest at low concentration (125 mg L^{-1}) of chitosan. During the developmental stages, maximum plant height was recorded with chitosan dose of 175 mg L^{-1} in both of the genotypes; 73.99 cm in Black boy and 64.70

http://www.aloki.hu ● ISSN 1589 1623 (Print) ● ISSN 1785 0037 (Online)
DOI: http://dx.doi.org/10.15666/aeer/1705_1127311287

cm in Sandhya (*Table 5*). The maximum number of shoots plant^{-1} was recorded in Sandhya that was 21% higher to control and 3% to Black boy. The root length was significantly varied under chitosan treatments compared to control ($P < 0.05$). The maximum root length was noticed when treated with chitosan at 175 mg L^{-1} in both genotypes of eggplant. The root length was ranged between 17-23 cm in genotype Black boy and 16-22 cm in genotype Sandhya. The mean shoot dry weight was increased up to 22% in Sandhya and 15% in Black boy over control with the increase in chitosan dose from 150 mg L^{-1} to 175 mg L^{-1} respectively.

Table 4. *ANOVA comparison for different levels of chitosan on the yield component traits of eggplant (Solanum melongena L.) genotypes under heat and high irradiance*

Source of variation		Var-1				Var-2			
		Replication	Treatment	Error	Total	Replication	Treatment	Error	Total
No of flowers plant^{-1}	Degree of freedom	7	4	28	39	7	4	28	39
	Mean squares		57.400				21.85		
	F-value		2.415				0.691		
	P-value		0.067 ^{NS}				0.603^{NS}		
No of fruit plant^{-1}	Degree of freedom	7	4	28	39	7	4	28	39
	Mean squares		61.562				136.462		
	F-value		5.989				9.608		
	P-value		0.001**				0.000***		
Flower drop plant^{-1}	Degree of freedom	7	4	28	39	7	4	28	39
	Mean squares		5.588				225.288		
	F-value		0.285				6.709		
	P-value		0.886^{NS}				0.000***		
Weight of each fruit	Degree of freedom	7	4	28	39	7	4	28	39
	Mean squares		307.588				244.15		
	F-value		5.086				5.346		
	P-value		0.002**				0.002**		
Yield plant^{-1}	Degree of freedom	7	4	28	39	7	4	28	39
	Mean squares		0.844				1.757		
	F-value		19.362				45.625		
	P-value		0.000***				0.000***		
Flower drop (%)	Degree of freedom	7	4	28	39	7	4	28	39
	Mean squares		42.846				429.811		
	F-value		2.122				9.796		
	P-value		0.099 ^{NS}				0.000***		

Probability level at 5%, $P \leq 0.001$***, NS = Non-significant, Var-1 = variety 1, Var-2 = variety 2

Both genotypes attained almost similar amount of root fresh weight at medium dose of chitosan and that was only 7% higher to control. The effect of chitosan was non-significant for genotype Sandhya root fresh weight. The maximum root dry matter (26.87 g) was recorded in Black boy that was slightly higher than Sandhya at chitosan dose of 175 mg L^{-1} while Sandhya attained almost similar amount of root dry weight at chitosan dose of 150 mg L^{-1} (*Table 5*).

Chitosan have non-significant influence on number of flowers induced in both genotypes. The values were ranged between 61.38 to 67.88 in Black boy and 61.75 to 65.75 in Sandhya genotype (*Table 4*). At low dose of chitosan, the flower drop was maximum for Sandhya. Genotypes varied significantly in terms of fruit number. A

http://www.aloki.hu ● ISSN 1589 1623 (Print) ● ISSN 1785 0037 (Online)
DOI: http://dx.doi.org/10.15666/aeer/1705_1127311287

higher number of fruits were noted in genotype Black boy (36.75) as compared to Sandhya. Exogenous application of chitosan has also a significant influence on yield of eggplant genotypes. The maximum yield was attained at 175 mg L^{-1} in Black boy that was 42% higher to control and 14% to Sandhya at the same level of chitosan. This higher yield was due to a low flower drop and higher fruit setting at 175-200 mg L^{-1} chitosan application.

Table 5. *Effect of chitosan on the morphological traits of eggplant (Solanum melongena L.) genotypes under heat and high irradiance*

Treatment	Plant height (cm)	No of shoots plant^{-1}	Root length (cm)	Fresh weight root (g)	Dry weight root (g)
T_0V_1	62.38 ± 1.53 b	7.63 ± 0.32 b	18.63 ± 0.59 c	116.13 ± 3.06 b	23.38 ± 0.75 b
T_1V_1	69.15 ± 1.50 a	8.25 ± 0.36 ab	17.38 ± 0.26 c	120.00 ± 2.28 ab	24.75 ± 0.55 ab
T2V1	71.85 ± 1.27 a	9.00 ± 0.26 a	20.88 ± 0.69 b	125.00 ± 1.52 a	24.63 ± 0.59 ab
T_3V_1	73.99 ± 1.63 a	8.63 ± 0.26 ab	23.00 ± 0.56 a	121.25 ± 0.97 ab	26.87 ± 0.54 a
T_4V_1	70.63 ± 1.82 a	8.50 ± 0.26 ab	22.63 ± 0.32 ab	123.50 ± 0.65 ab	26.25 ± 0.59 a
T_0V_2	54.26 ± 1.49 c	7.63 ± 0.37 b	16.87 ± 0.54 c	118.00 ± 2.22 a	20.75 ± 0.45 b
T_1V_2	63.75 ± 0.92 a	8.25 ± 0.36 ab	19.00 ± 0.56 bc	125.00 ± 2.97 a	25.00 ± 0.65 a
T_2V_2	57.25 ± 1.60 bc	7.63 ± 0.37 b	19.25 ± 59 b	120.00 ± 1.16 a	26.63 ± 0.41 a
T_3V_2	64.70 ± 1.35 a	9.25 ± 0.36 a	22.63 ± 0.41 a	123.25 ± 1.11 a	24.87 ± 0.54 a
T_4V_2	61.26 ± 1.71 ab	9.00 ± 0.26 ab	22.00 ± 0.56 a	123.00 ± 1.33 a	25.75 ± 0.45 a

Mean values (± SD) for all determinants are based on n = 8. Different letters within column indicate significant differences between levels of chitosan, T0, T1, T2, T3 and T4 ($p < 0.05$). Treatment (T) 0: control; T1: 125 mg L^{-1}; T2: 150 mg L^{-1}; T3: 175 mg L^{-1}; T4: 200 mg L^{-1}

Table 6. *Effect of chitosan on the yield component traits of the eggplant (Solanum melongena L.) genotypes under heat and high irradiance*

Treatment	No of fruit plant^{-1}	Flower drop plant^{-1}	Weight of each fruit (g)	Yield plant^{-1} (kg)	Flower drop (%)
T_0V_1	29.75 ± 0.75 b	31.63 ± 1.59 a	66.88 ± 2.43 b	1.99 ± 0.06 b	51.36 a
T_1V_1	35.63 ± 1.14 a	31.00 ± 1.74 a	74.50 ± 2.87 ab	2.04 ± 0.06 b	46.38 a
T2V1	34.50 ± 1.03 a	32.75 ± 1.58 a	83.38 ± 3.12 a	2.04 ± 0.06 b	48.58 a
T_3V_1	36.75 ± 1.29 a	30.63 ± 1.19 a	79.50 ± 2.66 a	2.77 ± 0.07 a	45.44 a
T_4V_1	35.87 ± 1.34 a	32.00 ± 1.65 a	77.50 ± 2.59 ab	2.19 ± 0.09 b	47.06 a
T_0V_2	24.88 ± 1.13 b	29.50 ± 2.65 b	67.87 ± 2.74 c	1.82 ± 0.05 c	46.38 b
T_1V_2	34.13 ± 0.51 a	40.87 ± 1.44 a	78.50 ± 2.52 a	1.82 ± 0.04 c	62.02 a
T_2V_2	34.50 ± 2.11 a	31.00 ± 1.10 b	78.50 ± 2.18 a	1.84 ± 0.05 c	47.77 b
T_3V_2	34.25 ± 1.37 a	27.25 ± 2.77 b	77.75 ± 2.29 ab	2.47 ± 0.08 b	43.54 b
T_4V_2	33.37 ± 0.98 a	29.87 ± 1.71 b	68.50 ± 2.14 bc	2.83 ± 0.09 a	46.47 b

Mean values (± SD) for all determinants are based on n = 8. Different letters within column indicate significant differences between levels of chitosan, T0, T1, T2, T3 and T4 ($p < 0.05$). Treatment (T) 0: control; T1: 125 mg L^{-1}; T2: 150 mg L^{-1}; T3: 175 mg L^{-1}; T4: 200 mg L^{-1}

The effect of chitosan foliar application was also studied on plant physiological characters (*Fig. 2*). The proline content of both the genotypes increased significantly by increasing the chitosan application. There was synergistic stimulation with increased

http://www.aloki.hu ● ISSN 1589 1623 (Print) ● ISSN 1785 0037 (Online)
DOI: http://dx.doi.org/10.15666/aeer/1705_1127311287

levels of chitosan. Proline concentration in eggplant leaves were ranged between 8.12 and 10.11 umol/ml DW in Black boy and 8.30 to 9.48 umol/ml DW in Sandhya genotype. However, the highest increase was observed at chitosan concentration of 175 mg L^{-1} in both genotypes. Similarly, the maximum concentration of glycinebetain (8.53 ug/ml DW) was noticed in Black boy at the chitosan rate of 175 mg L^{-1} and that was 45% higher than control. The effect of chitosan application was also prominent on total soluble solids and total phenolics accumulation. As reported in other growth and yield traits, the highest dose of chitosan failed to produce the maximum accumulation of total soluble solids and total phenolics in both genotypes. The total phenolics in Black boy that was maximum (124 mg/g DW) at 175 mg L^{-1} of chitosan. Again, the satisfactory results were obtained at medium dose of chitosan that produced 31% higher total soluble solids and 18% higher total phenolics in Black boy and 33-16% in Sandhya.

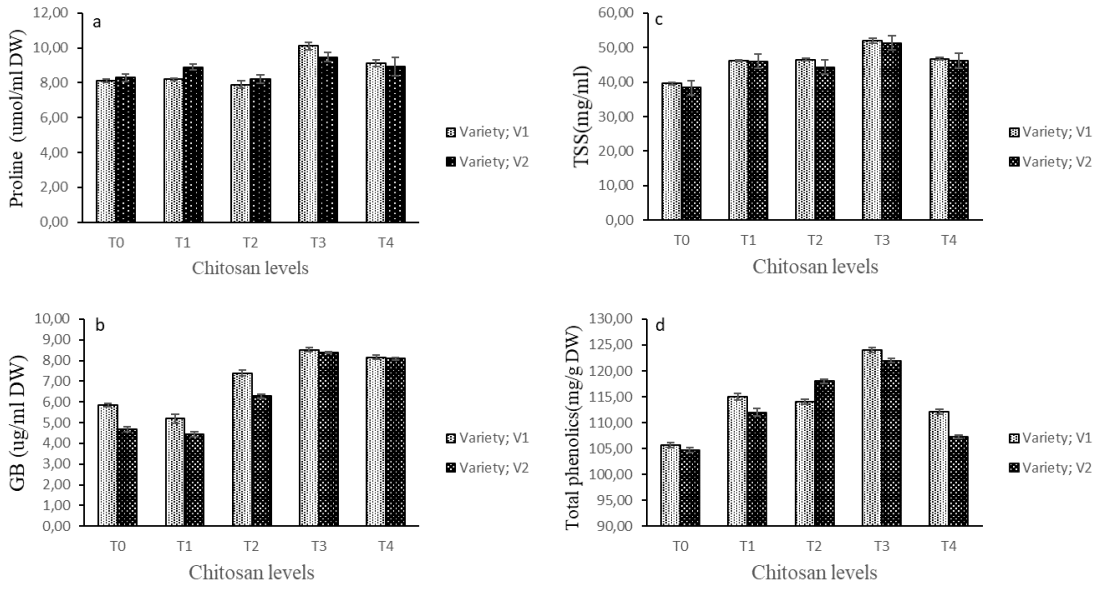

Figure 2. *Mean values for Proline (umol/ml DW ± SD), Glycinebetaine (ug//ml DW ± SD), Total soluble solids (mg/ml DW ± SD and Total phenolics (mg/g DW ± SD) of eggplant (Solanum melongena L.) genotypes subjected to different level of Chitosan (T0, T1, T2, T3, T4) under heat and high irradiance. Treatment (T) 0: control; T1: 125 mg L^{-1}; T2: 150 mg L^{-1}; T3: 175 mg L^{-1}; T4: 200 mg L^{-1}*

The linear electron flow (LEF) was measured from the matured leaves of both varieties. Constant value of LEF was noticed in Black boy for all chitosan treatments except for control that produced the significant lower value for LEF. On contrary, the LEF gradually increased with the increase in chitosan dose in Sandhya genotype (*Fig. 3*). In addition, the non-photochemical quenching (NPQt) was monitored to evaluate the excess heat energy dissipation during high irradiance. The high temperature stress induced more severe NPQt in both genotypes' seedlings. The NPQt was directly influenced to the level of the high temperature and heat stress. Genotype Black boy produced higher NPQt (0.65) as compared the Sandhya that produced slightly lower value for NPQt (0.64). The quantum yield of photosystem II (PSII) has also measured to estimate the efficiency of photosystem II under high temperature stress.

http://www.aloki.hu ● ISSN 1589 1623 (Print) ● ISSN 1785 0037 (Online)
DOI: http://dx.doi.org/10.15666/aeer/1705_1127311287

Exogenous chitosan application improved chlorophyll contents in both genotypes. The values were varied between 51.05 and 60.73 (SPAD) in Black boy and 54.75 and 60.83 (SPAD) in Sandhya during late planting high temperature stress. It was the lowest in control, gradually increased with the increase in chitosan dose level up to 175 mg L^{-1} and after that negatively responded to any increase in chitosan dose (*Fig. 3*).

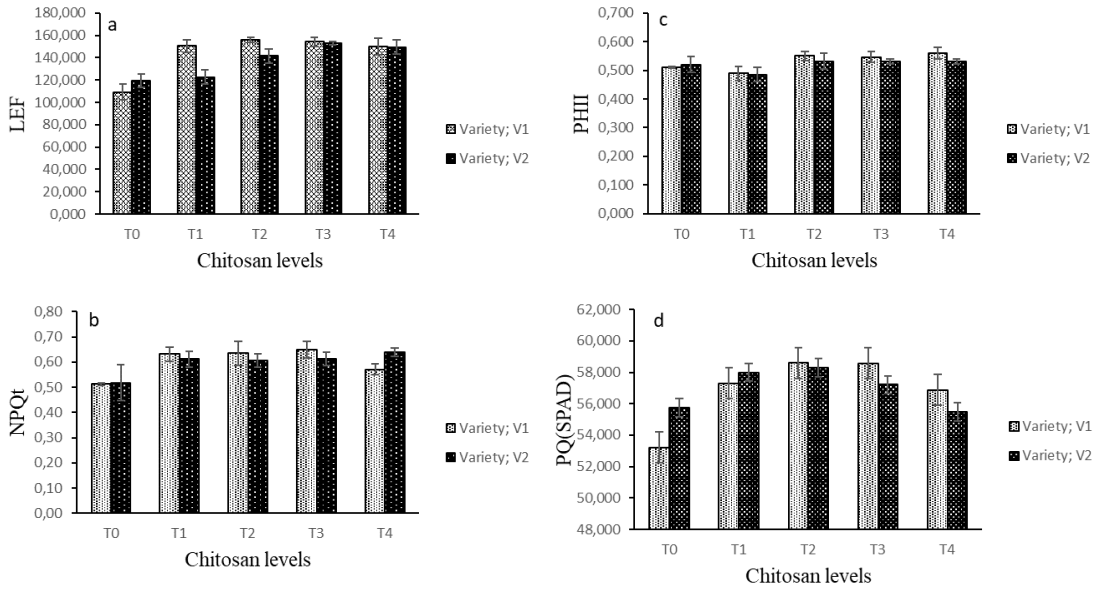

Figure 3. *Mean values (± SD) for Photosystem II, Linear electron flow, Non-photochemical quenching and PQ-spade of eggplant (Solanum melongena L.) genotypes subjected to different level of Chitosan (T0, T1, T2, T3, T4) under heat and high irradiance. Treatment (T) 0: control; T1: 125 mg L^{-1}; T2: 150 mg L^{-1}; T3: 175 mg L^{-1}; T4: 200 mg L^{-1}*

Discussion

Chitosan regulated plant growth, yield and physiological traits studied under high temperature stress. The mechanism of high temperature stress regulation is not still clearly established but however, chitosan application at different growth stages of the plants under stress stimulated the plant growth that has helped plant to withstand the adverse effects of the stress (Katiyar, 2015). The inactivation of enzymes involved in different processes of photosynthesis and the carbon flux are the major effects of high temperature stress.

Similarly, the photo inhibition was due to high light intensity, might be the other reason of plant growth inhibition (Guidi et al., 2019). Chitosan also has stimulated the activity of sucrose hydrolyzing enzymes in seedlings under stressful environment. The additive role of chitosan application has been found to synthesize plant hormones such as auxin and gibberellins by stimulating a signal related to biosynthesis and may help plant to maintain its growth and development under high temperature stress. Some studies have reported its involvement in protecting cell membrane from deterioration under abiotic stresses.

Chitosan application produced the highest shoot dry weight at a concentration of 0.01%. A number of researchers reported similar results related to plant growth and yield improvement with the application of chitosan (Amiri et al., 2015; Safikhan et al., 2018). In this experiment, high temperature stress caused stunted eggplant growth, and

http://www.aloki.hu ● ISSN 1589 1623 (Print) ● ISSN 1785 0037 (Online)
DOI: http://dx.doi.org/10.15666/aeer/1705_1127311287

this might be due to the low availability of nutrients and poor functioning of nutrient uptake mechanism due to impaired photosynthesis. Application of Chitosan improved photosynthesis through increasing leaf chlorophyll content that might has stabilized the cell membrane, detoxify the deleterious effects of antioxidant's, and helped in cell elongation and multiplication (Malerba and Cerana, 2016; Salachna and Zawadzińska, 2014). The improvement in these mechanisms ultimately resulted in significant yield improvement under high temperature stress.

It is concluded that foliar application of chitosan at vegetative stages enhance the plant growth and development (number of leaves, shoots length, pedicel length, plant height) which helped plants to secure fruiting and fruit yield in eggplant.

The physiological and biochemical responses of chitosan has been found to act as stimulator which ultimately encode a gene expression, and thereby plants treated with chitosan may be less prone to stress evoked unfavorable conditions such as high and low temperatures, drought as well as salinity (Zhao et al., 2008). Under high temperature stress, proline content, glycinebetain, total soluble sugars and total phenolics contents in leaves of eggplant genotypes decreased significantly. The application of chitosan improved the total phenolics level in both genotypes. The results are in agreement with previously investigations that reported positive role of chitosan in cell membrane permeability, concentration of soluble sugars and proline (Guan et al., 2009).

Accumulation of total free sugars and phenolic contents serves as adaptive mechanism in plants under high temperature stress. In the same manner osmolytes protect the cell membrane against adverse effects of heat stress. Accumulation of ions such as proline improves the membrane stability in plants and these ions uptake improve with the application of chitosan. Chitosan regulates stomatal closure, ion uptake and transpiration. Moreover, chitosan plays prolific role in many morphological and physiological functions of the plants (Safikhan, 2018).

Exogenous application of chitosan increased eggplant height through improvement in leaf chlorophyll content and number of leaves per plant. The growth stimulatory effects of chitosan on vegetative parts of plants especially number of leaves per plant, plant height and leaf chlorophyll content has previously reported in cucumber (Katiyar et al., 2015; Shehata et al., 2012) and safflower (Amiri et al., 2015). Chitosan foliar spray also helped to control insect pest attack, plant and fruit diseases. Chitosan is a natural, inert and cheap molecule that regulates different biological responses in plants depending upon its concentration, plant species and developmental stage.

We can measure the performance of a plant by its amount of chlorophyll content under stress condition. Chitosan application significantly increased chlorophyll content of both genotypes of eggplant. Foliar application of chitosan increased chlorophyll content of soybean (18%) and peanut (23%) (Dzung, 2005). Plants loss their chlorophyll content as a photo protection mechanism to reduce light absorbance at high temperature stress either by slow synthesis or fast breakdown of chlorophyll contents (Elsheery and Cao, 2008; Wise et al., 2004). Both eggplant genotypes showed positive response to applied chitosan spray through stabilizing the chlorophyll content and maintaining the photosynthetic rate (PSII). Involvement of chitosan has confirmed in modulating the activity of dimers and monomers during the protein synthesis (Sharif et al., 2018).

The NPQT of chlorophyll fluorescence is associated with a decrease in the rate of photosystem II. The NPQT measures the active percentage of PSII reaction center that

http://www.aloki.hu ● ISSN 1589 1623 (Print) ● ISSN 1785 0037 (Online)
DOI: http://dx.doi.org/10.15666/aeer/1705_1127311287

is capable of photochemistry and changes in PSII (Guidi et al., 2019; Malerba and Cerana, 2016). Similar changes were also noticed in this study where NPQT was slightly increased or stabilized with increased level of chitosan however, this moderate increase was statistically not significant. Consequently, the decreased demand for product of electron transport that was used for assimilation resulted in heat dissipation of light energy.

Previously, it was reported that the abiotic stress may lead to a decrease in the photochemical efficiency and electron transport activity due to the changes in the structure of the photosynthetic apparatus (Guidi, 2019; Mittal, 2012). The results in this study suggest that chitosan can modulate moderately the flow of intercellular ion transport and enhances the activity of antioxidants enzymes which helps in preventing the membrane damage in the granal and stromal thylakoids under stress conditions (Malerba and Cerana, 2016; Salachna and Zawadzińska, 2014). The results in *Figure 2a, b* regarding LEF and NPQT are in agreement with previous studies suggesting the photoinhibition through changes in protective high-energy-state by increase in NPQT (Guidi et al., 2019). Additionally, repair mechanisms such as excision repair, photoreactivation, quenching and free radical scavenging could be activated to prevent and slow down the damage caused by long exposure to high temperature stress by chitosan application (Choi et al., 2013; Zhang et al., 2008).

Conclusion

The exogenous application of chitosan has significant influence on the physiological and biochemical attributes of eggplant genotypes. Major changes were noticed in parameters affecting growth and development such as, flower induction, flower drop, fruits plant^{-1}, weight of each fruit and yield plant^{-1}. The effect was more prominent on Black boy over Sandhya cultivar. The thermostability of reaction center of PSII was also noticed, may possibly due to of less ROS accumulation, an aiding influence due to increased level of chitosan application. The chitosan application especially with concentration 175 mg L^{-1} improved the plant growth and development, increased the content of proline, glycinebetain, total soluble solids and total phenolics. The chitosan has moderated the influence of high temperature and heat stress by accelerating the antioxidant enzymes activities. The yield of the eggplant was positively changed to the level of chitosan application. The increased level of chitosan produced more yield under high temperature and heat stress. It can be concluded that chitosan may be used as an eco-friendly compound to protect and to enhance growth, development and other biochemical parameters under high temperature and heat stress.

REFERENCES

[1] Ainsworth, E. A., Ort, D. R. (2010): How do we improve crop production in a warming world? – Plant Physiology 154: 526-530.

[2] Ali, L., Svensson, B., Alsanius, B. W., Olsson, M. E. (2011): Late season harvest and storage of Rubus berries—major antioxidant and sugar levels. – Scientia Horticulturae 129: 376-381.

[3] Allakhverdiev, S., Kreslavskii, V., Klimov, V., Los, D., Carpentier, R., Mohanty, P. (2008): Heat stress: An overview of molecular responses in photosynthesis. – Photosynthesis Research 98: 541.

http://www.aloki.hu ● ISSN 1589 1623 (Print) ● ISSN 1785 0037 (Online)
DOI: http://dx.doi.org/10.15666/aeer/1705_1127311287

[4] Amiri, A., Sirousmehr, A., Esmaeilzadeh, B. S. (2015): Effect of foliar application of salicylic acid and chitosan on yield of safflower (Carthamus tinctorius L.). – Journal of Plant Research (Iranian Journal of Biology) 28(4): 712-725.
[5] Baker, N. R., Harbinson, J., Kramer, D. M. (2007): Determining the limitations and regulation of photosynthetic energy transduction in leaves. – Plant, Cell & Environment 30: 1107-1125.
[6] Bates, L. S., Waldren, R. P., Teare, I. (1973): Rapid determination of free proline for water-stress studies. – Plant and Soil 39: 205-207.
[7] Chandra, S., Chakraborty, N., Dasgupta, A., Sarkar, J., Panda, K., Acharya, K. (2015): Chitosan nanoparticles: a positive modulator of innate immune responses in plants. – Scientific Reports 5: 15195.
[8] Choi, Y.-S., Kim, Y.-M., Hwang, O.-J., Han, Y.-J., Kim, S. Y., Kim, J.-I. (2013): Overexpression of arabidopsisabf3 gene confers enhanced tolerance to drought and heat stress in creeping bentgrass. – Plant Biotechnology Reports 7: 165-173.
[9] Churkina, G. (2016): The role of urbanization in the global carbon cycle. – Frontiers in Ecology and Evolution 3: 144.
[10] De Ronde, J. A., Cress, W. A., Krüger, G. H. J., Strasser, R. J., Van Staden, J. (2004): Hotosynthetic response of transgenic soybean plants, containing an arabidopsis p5cr gene during heat and drought stress. – Journal of Plant Physiology 161: 1211-1224.
[11] Dewanto, V., Wu, X., Adom, K. K., Liu, R. H. (2002): Thermal processing enhances the nutritional value of tomatoes by increasing total antioxidant activity. – Journal of Agricultural and Food Chemistry 50: 3010-3014.
[12] Dzung, N. (2005): Application of chitin, chitosan and their derivatives for agriculture in vietnam. – Journal of Chitin Chitosan 10: 109-113.
[13] Elieh-Ali-Komi, D., Hamblin, M. R. (2016): Chitin and chitosan: production and application of versatile biomedical nanomaterials. – International Journal of Advanced Research 4: 411-427.
[14] Elsheery, N. I., Cao, K.-F. (2008): Gas exchange, chlorophyll fluorescence, and osmotic adjustment in two mango cultivars under drought stress. – Acta Physiologiae Plantarum 30: 769-777.
[15] Grieve, C., Grattan, S. (1983): Rapid assay for determination of water soluble quaternary ammonium compounds. – Plant and Soil 70: 303-307.
[16] Guan, Y.-J., Hu, J., Wang, X.-J., Shao, C.-X. (2009): seed priming with chitosan improves maize germination and seedling growth in relation to physiological changes under low temperature stress. – Journal of Zhejiang University Science 10: 427-433.
[17] Guidi, L., Lo Piccolo, E., Landi, M. (2019): Chlorophyll fluorescence, photoinhibition and abiotic stress: does it make any difference the fact to be a c3 or c4 species? – Frontiers in Plant Science 10: 174.
[18] Hazra, P., Rout, A., Roy, U., Nath, S., Roy, T., Dutta, R., Acharya, S., Mondal, A. (2003): Characterization of brinjal (Solanum melongena L.) germplasm. – Vegetable Science 30: 145-149.
[19] Ihsan, M. Z., El-Nakhlawy, F. S., Ismail, S. M., Fahad, S. (2016): Wheat phenological development and growth studies as affected by drought and late season high temperature stress under arid environment. – Frontiers in Plant Science **7**: 795.
[20] IPCC (2014): Climate Change 2014 - Impacts, Adaptation and Vulnerability: Regional Aspects. – Cambridge University Press, Cambridge, UK.
[21] Jiao, Z., Li, Y., Li, J., Xu, X., Li, H., Lu, D., Wang, J. (2012): Effects of exogenous chitosan on physiological characteristics of potato seedlings under drought stress and rehydration. – Potato Research 55: 293-301.
[22] Katiyar, D., Hemantaranjan, A., Singh, B. (2015): Chitosan as a promising natural compound to enhance potential physiological responses in plant: a review. – Indian Journal of Plant Physiology 20: 1-9.

http://www.aloki.hu ● ISSN 1589 1623 (Print) ● ISSN 1785 0037 (Online)
DOI: http://dx.doi.org/10.15666/aeer/1705_1127311287

[23] Kehoe, D. M. (2010): Chromatic adaptation and the evolution of light color sensing in cyanobacteria. – Proceedings of the National Academy of Sciences 107: 9029-9030.
[24] Kuhlgert, S., Austic, G., Zegarac, R., Osei-Bonsu, I., Hoh, D., Chilvers, M. I., Roth, M. G., Bi, K., TerAvest, D., Weebadde, P. (2016): Multispeq Beta: a tool for large-scale plant phenotyping connected to the open photosynq network. – Royal Society Open Science 3: 160592.
[25] Landi, L., De Miccolis Angelini, R. M., Pollastro, S., Feliziani, E., Faretra, F., Romanazzi, G. (2017): Global transcriptome analysis and identification of differentially expressed genes in strawberry after preharvest application of benzothiadiazole and chitosan. – Frontiers in Plant Science 8: 235.
[26] Lobell, D. B., Asner, G. P. (2003): Climate and management contributions to recent trends in U.S. agricultural yields. – Science 299: 1032.
[27] Malerba, M., Cerana, R. (2016): Chitosan effects on plant systems. – International Journal of Molecular Sciences 17: 996.
[28] Mgbemene, C. A., Nnaji, C. C., Nwozor, C. (2016): Industrialization and its backlash: focus on climate change and its consequences. – Journal of Environmental Science and Technology 9: 301-316.
[29] Myers, S. S., Smith, M. R., Guth, S., Golden, C. D., Vaitla, B., Mueller, N. D., Dangour, A. D., Huybers, P. (2017): Climate change and global food systems: potential impacts on food security and undernutrition. – Annual Review of Public Health 38: 259-277.
[30] Pandit, M., Thapa, H., Akhtar, S., Hazra, P. (2010): Evaluation of brinjal genotypes for growth and reproductive characters with seasonal variation. – Journal of Crop and Weed 6: 31-34.
[31] Ranil, R. H. G., Prohens, J., Aubriot, X., Niran, H. M. L., Plazas, M., Fonseka, R. M., Vilanova, S., Fonseka, H. H., Gramazio, P., Knapp, S. (2017): Solanum insanum L. (subgenus Leptostemonum Bitter, Solanaceae), the neglected wild progenitor of eggplant (S. melongena L.): a review of taxonomy, characteristics and uses aimed at its enhancement for improved eggplant breeding. – Genetic Resources and Crop Evolution 64: 1707-1722.
[32] Rasul, G. (2016): Managing the food, water, and energy nexus for achieving the Sustainable Development Goals in South Asia. – Environmental Development 18: 14-25.
[33] Rochaix, J.-D. (2011): Regulation of photosynthetic electron transport. – Biochimica et Biophysica Acta (BBA)-Bioenergetics 1807: 375-383.
[34] Safikhan, S., Khoshbakht, K., Chaichi, M. R., Amini, A., Motesharezadeh, B. (2018): Role of chitosan on the growth, physiological parameters and enzymatic activity of milk thistle (Silybum marianum (L.) Gaertn.) in a pot experiment. – Journal of Applied Research on Medicinal and Aromatic Plants 10: 49-58.
[35] Salachna, P., Zawadzińska, A. (2014): Effect of chitosan on plant growth, flowering and corms yield of potted freesia. – Journal of Ecological Engineering 15: 3.
[36] Schortemeyer, M., Stamp, P., Feil, B. (1997): Ammonium tolerance and carbohydrate status in maize cultivars. – Annals of Botany 79: 25-30.
[37] Sharif, R., Mujtaba, M., Ur Rahman, M., Shalmani, A., Ahmad, H., Anwar, T., Tianchan, D., Wang, X. (2018): The multifunctional role of chitosan in horticultural crops - a review. – Molecules (Basel, Switzerland) 23: 872.
[38] Shehata, S. A., Fawzy, Z., El-Ramady, H. (2012): Response of cucumber plants to foliar application of chitosan and yeast under greenhouse conditions. – Australian Journal of Basic and Applied Sciences 6: 63-71.
[39] Sonoike, K. (2011): Photoinhibition of photosystem I. – Physiologia Plantarum 142: 56-64.
[40] Teixeira, E. I., Fischer, G., van Velthuizen, H., Walter, C., Ewert, F. (2013): Global hot-spots of heat stress on agricultural crops due to climate change. – Agricultural and Forest Meteorology 170: 206-215.

http://www.aloki.hu ● ISSN 1589 1623 (Print) ● ISSN 1785 0037 (Online)
DOI: http://dx.doi.org/10.15666/aeer/1705_1127311287

[41] Walters, R. G. (2005): Towards an understanding of photosynthetic acclimation. – Journal of Experimental Botany 56: 435-447.
[42] Wise, R., Olson, A., Schrader, S., Sharkey, T. (2004): Electron transport is the functional limitation of photosynthesis in field-grown Pima coton plants at high temperature. – Plant, Cell & Environment 27: 717-724.
[43] Zhang, X., Wollenweber, B., Jiang, D., Liu, F., Zhao, J. (2008): Water deficits and heat shock effects on photosynthesis of a transgenic Arabidopsis thaliana constitutively expressing ABP9, a bZIP transcription factor. – Journal of Experimental Botany 59: 839-848.
[44] Zhao, J., Zhang, X., Wollenweber, B., Jiang, D., Liu, F. (2008): Water deficits and heat shock effects on photosynthesis of a transgenic Arabidopsis thaliana constitutively expressing ABP9, a bZIP transcription factor. – Journal of Experimental Botany 59: 839-848.

http://www.aloki.hu ● ISSN 1589 1623 (Print) ● ISSN 1785 0037 (Online)
DOI: http://dx.doi.org/10.15666/aeer/1705_1127311287

EFFECT OF BIOLOGICAL NITRIFICATION INHIBITOR ON NITROGEN FIXATION AND EMISSION REDUCTION IN STRAW AND DAIRY MANURE COMPOSTING

REN, L. T.[1,3,4] – ZHANG, X.[1] – YANG, L.[2*] – HAO, B.[4] – SHAO, Q. Q.[1] – ZHANG, C. J.[3]

[1]*Anhui Science and Technology University, Bengbu, Anhui, China*

[2]*China Institute of Standardization, Beijing, China*

[3]*Anhui Laimujia Biotechnology Co., Ltd., Bengbu, Anhui, China*

[4]*Benbu Ludu Biotechnology Co., Ltd., Bengbu, China*

**Corresponding author*

(Received 11th Apr 2019; accepted 4th Jul 2019)

Abstract. The purpose of this study was to analyze the effect of biological nitrification inhibitor MHPP on nitrogen fixation and emission reduction for straw and dairy manure composting. During the period from May to September in China, the engineering large-scale composting was performed with dark box sampling was conducted to take composting gas sample which was studied gas chromatography. The result indicated that, in relation to the control, to which no MHPP extract solution was added, the addition of 0.2%, 0.4%, 0.6% and 0.8% MHPP extract solutions reduced the methane emission by 44.52%, 56.56%, 61.93%, 59.59%, the N_2O emission by 36.24%, 39.49%, 62.39 and 55.81%, and the NH_3 emission by 23.72%, 65.61%, 65.40% and 72.61%; after the addition of biological nitrification inhibitor, the composting process slowed down; the ammonium nitrogen content was high while the nitrate nitrogen content was low; all substances thoroughly decomposed in the end. Moreover, the final ammonium nitrogen content was higher in all cases when compared to the control. The results showed that the addition of 0.6% MHPP extract solution worked the best for nitrogen fixation and emission reduction and thus is appropriate to be used extensively in production activities.
Keywords: *crop residue composting, N_2O, NH_3, CH_4, biological nitrification inhibitor*

Introduction

With the increase of grain output in China, the straw resources grew constantly to more than a billion tons; furthermore, the mushrooming of livestock and poultry feeding industry in China produced a lot of waste. Both are considered environmental difficulties of rural areas and agriculture. As one of the effective approaches of fertilization against non-point source pollution in the planting and breeding industry, high-temperature aerobic composting has aroused wide concern all over the world, and turning into a research focus in the field of eco-friendliness and environmental protection.

High-temperature composting technology that may bring about non-point source pollution is widely recognized in agriculture, but researchers argued that the emission of some harmful gases and greenhouse gases, including NH_3, CH_4 and N_2O, may cause secondary pollution to a certain extent during high-temperature composting. During composting, the degradation and nitrification and denitrification of organic nitrogen produces a certain amount of NH_3 and N_2O; the emission of N-containing gas result in a nitrogen loss that range from 16% to 76%, which not only impairs the quality of compost, but may also lead to environmental pollution (Wu et al., 2012). Moreover, ammonia is not only an important factor affecting acid rain, but is also a key component

http://www.aloki.hu ● ISSN 1589 1623 (Print) ● ISSN 1785 0037 (Online)
DOI: http://dx.doi.org/10.15666/aeer/1705_1128911301

of odor substances in composting plants; the Emission Standard for Odor Pollutants (GB14554-93) issued by China in 1993 announces ammonia as the primary odor pollutant. According to the IPPC report 2014, the 100a greenhouse effect produced by N_2O and CH_4 was 25 and 298 times that of CO_2, respectively (IPCC, 2014). From this perspective, the emission of ammonia and greenhouse gases during composting not only adversely reduced the land use value, but also resulted in odor pollution, acid rain, greenhouse effect and other new ecological and environmental problems; in addition, they may harm human and animal health. Hence, along with the growing sophistication of composting technology, how to reduce nitrogen loss and greenhouse gas emission during composting has become a research focus.

Adding chemical additives like peat, calcium superphosphate, ferric chloride, zeolite and clay (Yang et al., 2005) is considered one of the effective ways to emission realize nitrogen fixation and emission reduction. Liu et al. (2015) found that adding 3% bamboo acetic acid to compost materials helped to reduce greenhouse gas emission and improve compost quality. Works of Ren et al. (2008) showed that the nitrogen fixation rate reached 73.1–97% with the addition of phosphate and magnesium hydroxide, etc. during composting; Jiang et al. (2018) found that NH_3 volatilization was significantly reduced during aerobic degradation of pig manure and corn straws by adding calcium phosphate and phosphoric acid.

Through the research on generation and regulation of odor in pig manure composting, Luo et al. (2012) found that the addition of calcium phosphate during pig manure composting not only reduced the compost pH and the concentration of volatile NH_3, but also facilitated the transformation of NH_4^+-N into other forms of nitrogen, thereby improving nitrogen retention. Lin et al. (2008), Weng et al. (2012) and Ren et al. (2009) found that the addition of calcium phosphate helped to reduce NH_3 emission during composting and thus retain nitrogen. Jiang et al. (2016) found in his study that the addition of nitrification inhibitor dicyandiamide (DCD) based on the use of acidic nitrogen fixer reduced the total greenhouse gas emission by 78% and NH_3 emission by 53%. The added nitrification inhibitors (NIs) are a generic term of a class of chemical substances that inhibit nitrification reaction by inhibiting the activity of nitrifying bacteria, thereby reducing nitrogen loss. DCD is widely used in Europe and America as a NI, but it is seldom used for composting. Li et al. (2008) and Ji et al. (2011) found that DCD reduced CH_4 and N_2O emission of rice and wheat by over 20%. Luo et al. (2013) and Jiang et al. (2016) also confirmed that the addition of DCD during composting of pig manure and straws remarkably reduced N_2O emission. Chen et al. (2017) tried to use calcium superphosphate with DCD for sludge composting and achieved remarkable effect: The nitrogen losses were reduced by 13%, and the greenhouse gas emissions by 74.8%.

Although nitrification inhibitors are significantly effective in reducing N_2O emission, they are not extensively used in production due to their high cost and toxicity; hence, some researchers shifted their attention to lower-cost biological nitrification inhibitors. Zakir et al. (2008) identified the MHPP (methyl 3-(4-hydroxyphenyl) propionate) as a biological nitrification inhibitor from sorghum root exudate to inhibit nitrification in soil. Wei et al. and Zhu et al. (2015) studied the molecular mechanism of MHPP, but there are few reports on the application of MHPP in composting. In this study, MHPP was used for composting and is compared with DCD, the most commonly used nitrification inhibitor, to systematically study the effect of this new nitrogen fixation and emission reduction conditioner on the rule of nitrogen gas and greenhouse gas emission during fermentation of straws and dairy manure; its purpose is to provide a theoretical

http://www.aloki.hu ● ISSN 1589 1623 (Print) ● ISSN 1785 0037 (Online)
DOI: http://dx.doi.org/10.15666/aeer/1705_1128911301

basis for the selection of nitrogen fixation and emission reduction conditioner for straw and dairy manure composting.

Materials and methods

Test materials

The wheat straws for the test were taken from the Fengyang Plantation of Anhui Science and Technology University and was smashed to 8-10 cm in size. The fresh dairy manure was taken from the cattle farm of Fucheng Town, Fengyang County, Anhui Province. The initial properties of straws and dung before the test are shown in *Table 1*. The 2nd and 4th row used for calculate C/N ratio. The calcium superphosphate was purchased from Bengbu Tianyi Biological Agents Co., Ltd., and its effective component was defined as P_2O_5 (≥ 18%); the dicyandiamide was analytically pure.

Table 1. *Physical and chemical characters of raw materials*

Materials	Moisture content (%)	Total organic carbon mass fraction (g/kg)	pH	Total nitrogen (g/kg)	Total phosphorous (g/kg)	Total potassium (g/kg)	C/N
Dairy manure	62.62±0.55	398.76±0.34	7.85±0.08	24.86±0.12	30.32±0.32	11.17±0.18	16.04
Wheat Straw	12.65±0.23	489.23±0.38	7.21±0.03	8.92±0.13	3.28±0.41	79.34±0.29	54.82

Values in average ± standard deviation (n = 3)

Test design

This test was performed at the plantation test field of Anhui Science and Technology University in China between May and September 2017. It was performed on a cement floor, and the composting treatment design was as follows: Fresh weight of dairy manure: straw = 1.5:1, and the treatment details are shown in *Table 2*. the MHPP leaching liquor was added once every seven days; the calcium superphosphate was added only once, and "blank" indicates no calcium superphosphate was added; refer to *Table 2* for details. 7.5 t of dairy manure and 3t of straws were prepared; the straws were smashed into 8-10 cm in size and mixed with the dairy manure with spray water to a proportion of approx. 65%; the mixture was divided evenly into five piles (4 t per pile); the temperature was raised to above 65 °C, at which manual turning was conducted with the help of weed-grasping machine every 7days. The compost temperature was determined on a daily basis (9:00 am) during composting, and samples were taken d0, d5, d10, d15, d20, d25, d30, d35, d40 and d45, respectively. The composting was ceased when the germination rate of Chinese cabbage seeds reached over 90%.

Test items and methods

Samples of greenhouse gases (CH_4, N_2O, and CO_2) were taken with static dark boxes customized from Fenglu Building Materials Store in Xuanwu District, Nanjing; the sampling case covered with aluminum foil (PVC, L × W × H = 50 cm × 50 cm × 50 cm) was placed over the pile; we measure thecircumference of the pile when we took gas sample. We calculate area by circumference. The pile is protected from disturbance and

http://www.aloki.hu ● ISSN 1589 1623 (Print) ● ISSN 1785 0037 (Online)
DOI: http://dx.doi.org/10.15666/aeer/1705_1128911301

sealed with water; set it aside for 30 min before the sampling was started, and gas was collected with a 50 ml syringe with a three-phase valve every 10 min (3 cycles in total); the sample test was finished within 24 h; where the test was not finished within 24 h, the gas was collected with a 100 ml sampling bag. CH_4 and N_2O were analyzed with the gas chromatograph (Agilient 4890, the USA) at the same time, and the CH_4 and N_2O concentrations were determined respectively with FID (Flame Ionization Detector) and ECD (Electron Capture Detector). The ammonia sample was taken with dark box through gas collection and ventilation, and the gas was sampled with a sampling pump; 10 ml of sulfuric acid absorbent was put in the bubble sampler, where its flow rate was 1.2 L per minute; the sampling process lasted for 10 min. Determination was performed with Nessler's Reagent. Weed-grasping machine used HTZC-600 (Henan Hengtong Machinery Co., Ltd.) , sampling pump used E-Switch-MRO292-1.2L (Shanghai Shenyuan Scientific Instruments Co., Ltd.) (*Photo 1*).

Table 2. *Addition proportion of materials in each compost treatment*

Treatment	Raw materials (fresh weight)	Percentage of additives to raw materials mass/%	
		Calcium superphosphate	Nitrification inhibitor
CK	Dairy manure: Straws = 1.5:1	0%	0
T1	Dairy manure: Straws = 1.5:1	0%	1%DCD
T2	Dairy manure: Straws = 1.5:1	2%	1%DCD
T3	Dairy manure: Straws = 1.5:1	0%	1% MHPP
T4	Dairy manure: Straws = 1.5:1	2%	1% MHPP

Photo 1. *The equipment we used and experimental picture*

Results

Effect of addition of MHPP addition on the variation of compost temperature

Temperature is an important indicator indicating of whether the organic matters are degraded rapidly during composting of straws and dairy manure. The treatment-specific temperature fluctuations during composting for this test are shown in *Figure 1*. In each

http://www.aloki.hu ● ISSN 1589 1623 (Print) ● ISSN 1785 0037 (Online)
DOI: http://dx.doi.org/10.15666/aeer/1705_1128911301

treatment cycle, the mesophilic microorganisms degraded the soluble and easily degradable organic matters in straws and dairy manure at low temperature in the initial phase of composting, where a lot of heat was released, resulting in the quick rise of compost temperature within a short time; with the decrease of available organic matters, the activity intensity of microorganisms decreased progressively, and the compost temperature dropped gradually; in this process, the compost became thoroughly decomposed.

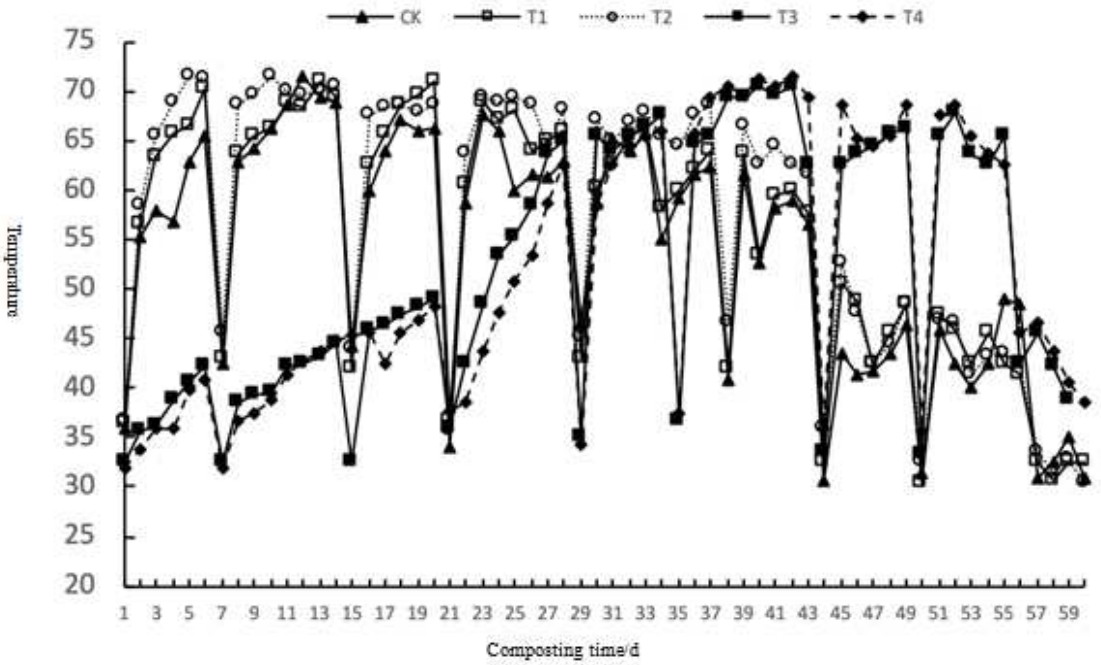

Figure 1. *Change of temperature during composting period*

Control and treatment 1 and 2 got into the high temperature period (> 50 °C) on d2 and went above 70 °C on d5; the heat-up effect was extremely obvious and higher than that of control; the high temperature lasted for approx. one month before the temperature starting to drop. The temperatures of Treatment 3 and Treatment 4 went up slowly at the beginning of composting, and reached 50 °C on d24; this may be because that the microbial activity was probably inhibited with the obvious inhibiting effect of MHPP; despite the slow rise, the high temperature lasted for approx. one month later. The high temperature period (> 50 °C) of each treatment lasted for about one month, which was much longer than 5 days for innocuous treatment according to the national regulations of China; this helps to kill pathogenic microorganisms and pathogenic eggs during composting, thus assuring the innocuous treatment of composting.

Effect of the addition of MHPP addition on emission of methane as a greenhouse gas from compost

CH_4 is a greenhouse gas produced by methane bacteria from the simple organic matters like methylamines, methyl alcohols, methyl acids and other carbon-containing compounds, as well as carbon dioxide and hydrogen in straws and dairy manure in pile. As shown in *Figure 2,* the methane emission peaks of all the four treatments occurred at

http://www.aloki.hu ● ISSN 1589 1623 (Print) ● ISSN 1785 0037 (Online)
DOI: http://dx.doi.org/10.15666/aeer/1705_1128911301

early stage of composting; the quick rise of temperature in early stage stimulated microorganisms to degrade organic matters efficiently, which consumed a lot of oxygen; as a result, the excessively low locally soluble oxygen content facilitated the production of high content of CH_4. As the composting progressed, the organic carbon available in straws and dairy manure was consumed progressively, and the microbial activity decreased, and the CH_4 emission rate went down gradually; in the end, the degradation of organic matters stopped, so CH_4 emission was hardly detected.

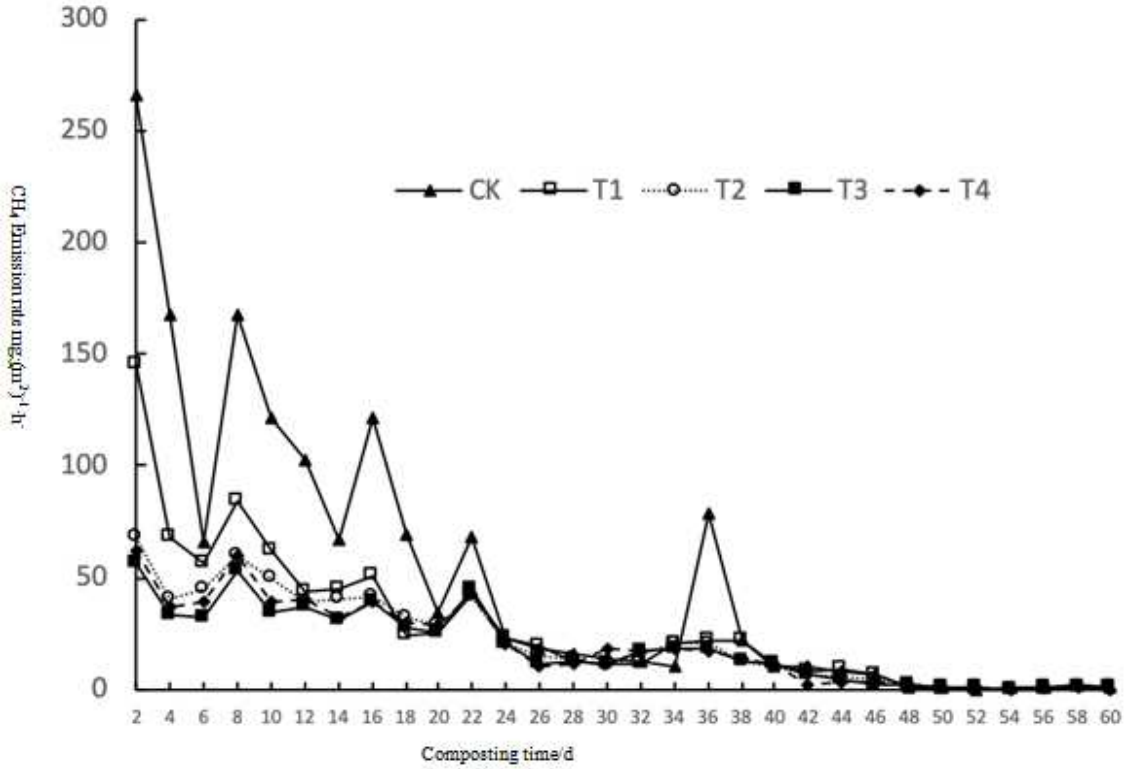

Figure 2. *CH_4 emission rate during composting*

The CH_4 emission peak was detected in CK treatment at the very beginning, where the mean emission rate was 49.52 mg/m^2/h; the T1-T4 drainage rates were lower than that of CK, indicating that the addition of DCD and MHPP played a remarkable role in reducing emission from the composting of dairy manure and straws; measurement and calculation showed that the cumulative emission from CK was approx. 71.30 g/m^2, while the emission from T1-T4 was 39.56 g/m^2, 30.98 g/m^2, 27.15 g/m^2 and 28.81 g/m^2, which indicated the emission was reduced by 44.52%, 56.56%, 61.93% and 59.59%, respectively. It is observed that the effect of DCD to which calcium superphosphate was added was more obvious, while the addition of calcium superphosphate exhibited insignificant effect on MHPP emission reduction.

That the addition of calcium superphosphate and DCD help to reduce methane emission echoed the report of Luo et al.(2012), The main reason for such reduction is because that the sulfate ions in calcium superphosphate help to reduce the pile pH, which further inhibited the activity of methane bacteria, thereby realizing in the reduction of methane emission. In addition, since sulfate reducing bacteria reduce sulfate radicals into S^{2-} with acetic acid, lactic acid and hydrogen ions as electron

http://www.aloki.hu ● ISSN 1589 1623 (Print) ● ISSN 1785 0037 (Online)
DOI: http://dx.doi.org/10.15666/aeer/1705_1128911301

donors and with sulfate radicals as electron acceptors during composting, methane bacteria could finish their own biochemical metabolism; a competitive relation existed in between; additionally, S^{2-} had certain toxic effect on methane bacteria. However, the rate of emission reduction was not enhanced after the addition of calcium superphosphate to MHPP; the principal reason may be that the acidic calcium superphosphate brought about no promoter action in the ammonium nitrogen environment of MHPP.

The addition of calcium superphosphate reduced the carbon-nitrogen ratio, indicating that the addition of calcium superphosphate facilitated the ingestion of affecting component in microorganisms during composting, thus facilitating the microbial metabolism and the decomposition of organic matters.

Effect of the addition of MHPP on emission of N_2O as a greenhouse gas from compost

Ammonium nitrogen was continuously transformed into nitrate nitrogen during composting, and N_2O was frequently produced in this nitrification process; in addition, N_2O was generated during the denitrification from nitrate nitrogen to ammonium nitrogen. As can be seen from CK in *Figure 3,* the low temperature and adequate oxygen in early stage of traditional composting promoted the generation of abundant N_2O at compost surface, which was consistent with the studies of Hao et al. (2001) and Sommer et al. (2000). In the thorough decomposition period, the substantive production of nitrate nitrogen brought about denitrification that produced N_2O. The nitrates and nitrites generated in areas where there was plenty of oxygen were carried by pile turning into the anaerobic zone, where denitrification occurred while some N_2O was emitted, which was echoed the studies of Thompson et al. (2004) and Fukumoto et al. (2003); the nitrification process oxidized ammonia into hydroxylamine with the help of catalytic effect of ammonia monooxygenase on ammonia oxidizing bacteria and ammonia-oxidizing archaea; hydroxylamine produced NO_2^- under the action of hydroxylamine oxidoreductase, while NO_2^- was the key source of N_2O, so the major way to reduce N_2O should be the alleviation of nitration and denitrification reaction; there were two key ways of blockage: First, the production of initial NH_3 could be reduced by changing the pile pH; second, the ammonia monooxygenase or hydroxylamine reductase could be inhibited through DCD nitrification inhibitors.

In the present study, calcium superphosphate was used to improve the pile pH by reducing it below 6.5, thereby considerably reducing the emission of NH_3, the precursor of N_2O. As can be seen from *Figure 3,* the addition of DCD, calcium superphosphate and MHPP to T1-T4 caused the N_2O amount to drop significantly; the N_2O emission from T1, T2, T3 and T4 were 36.24%, 39.49%, 62.39% and 55.81% respectively less than the total N_2O emission from CK. The MHPP worked better in emission reduction; the effect of DCD with calcium superphosphate added was more obvious, while the effect of MHPP with calcium superphosphate added in emission reduction was inferior to the effect of MHPP without calcium superphosphate added.

Effect of MHPP addition on emission of harmful gas NH_3 from composting

As shown in *Figure 4,* a lot of ammonia was emitted in early stage of CK during traditional composting because the temperature rise in early stage of composting resulted in constant degradation of nitrogenous organic compounds, which produced

http://www.aloki.hu ● ISSN 1589 1623 (Print) ● ISSN 1785 0037 (Online)
DOI: http://dx.doi.org/10.15666/aeer/1705_1128911301

abundant ammonium nitrogen; in the stationary phase, the reduction of degradable nitrogen and the transformation of ammonium nitrogen into nitrate nitrogen or organic nitrogen enabled ammonia to effectively fix nitrogen in the form of ammonium phosphate when calcium superphosphate is added.

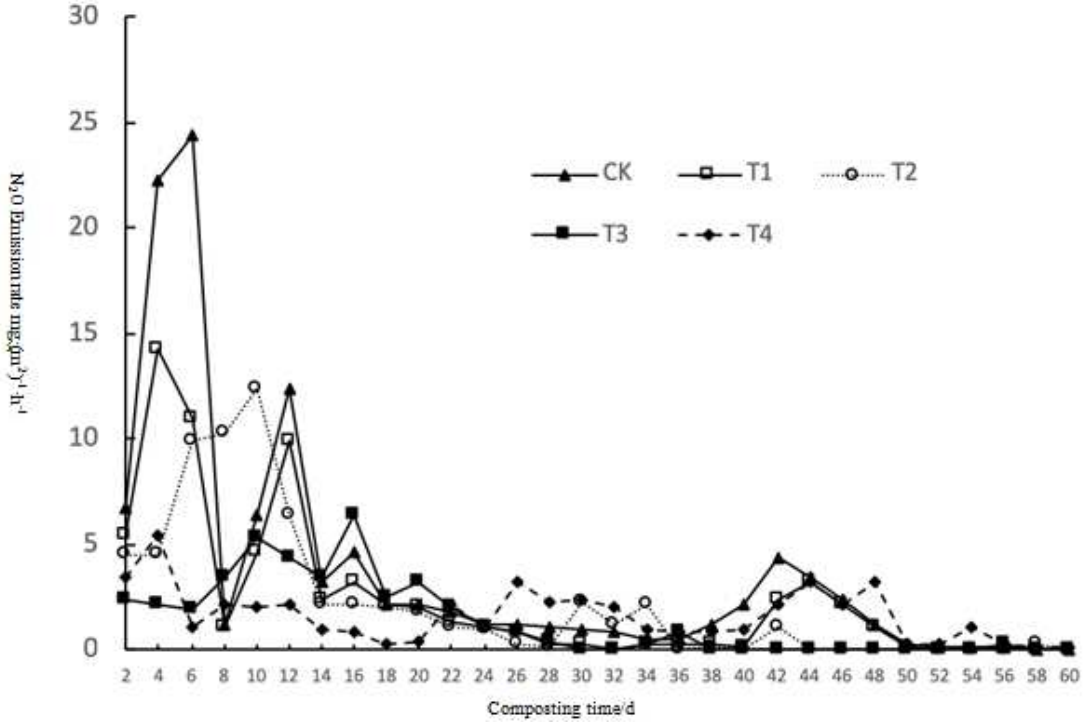

Figure 3. *N_2O emission rate during composting*

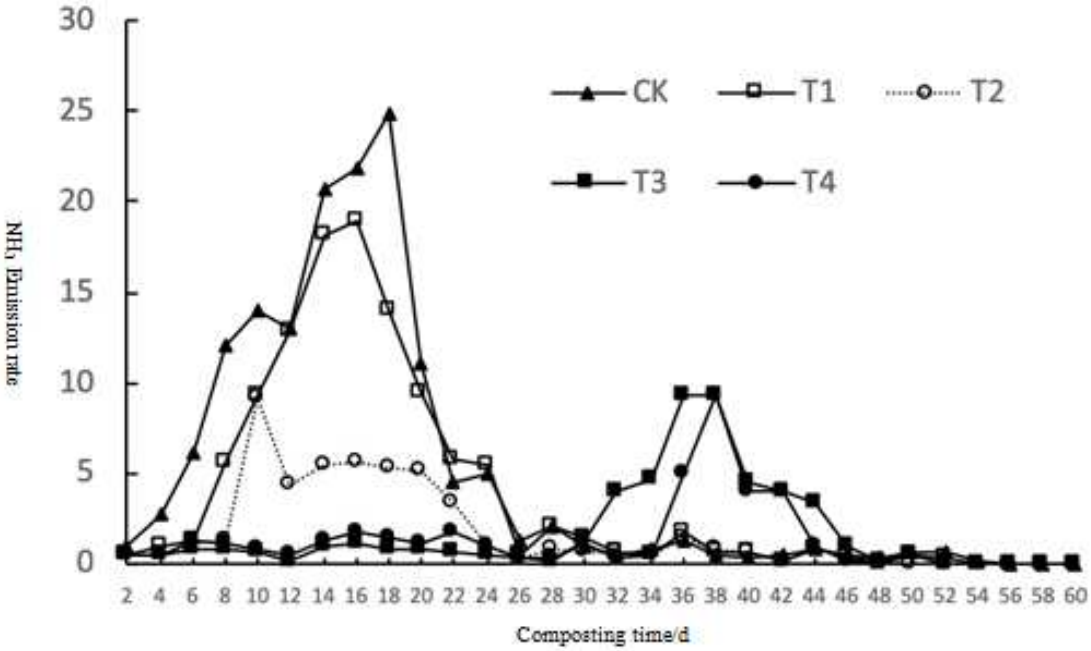

Figure 4. *NH_3 emission rate during composting*

http://www.aloki.hu ● ISSN 1589 1623 (Print) ● ISSN 1785 0037 (Online)
DOI: http://dx.doi.org/10.15666/aeer/1705_1128911301

The NH_3 emission during composting is shown in *Figure 4,* where the NH_3 emission of all the four treatments peaked during high-temperature period; nitrogenous organic compounds were substantively decomposed during high-temperature period, which produced a lot of ammonia. The ammonia emission was extremely low in the early and late stages of composting when temperatures were relatively low; throughout the stages, the emission of ammonia was reduced by T1-T4 by 23.72%, 65.61%, 65.40% and 72.61% respectively as compared with the control; the dominant mechanism was as follows: The acidic calcium superphosphate regulated the pH during composting below 6.5; as a result, N existed in the form of NH_4+, which went against the release of ammonia; in such a case, it existed in the form of ammonium acid phosphate or ammonium sulfate. The study performed by Li et al. (2008) demonstrated that the addition of calcium superphosphate reduced the ammonia emission from pig manure and rice straws by 39.39%; the value in the present study is greater than in that study, because nitrification inhibitor was added in the present study in addition to calcium superphosphate.

Variation of ammonium nitrogen (NH_4^+-N) content and nitrate nitrogen (NO_3^--N) contents

Ammonium nitrogen (NH_4^+-N) and nitrate nitrogen (NO_3^--N) content variation is considered an important indicator for determination of nitrogen circulation during composting; refer to *Figure 5* for the variation pattern during composting; with the constant degradation of organic matters at early stage of composting, the composting of each treatment reached the high-temperature period, when microbial activity intensified, and the NH_4^+-N content of each treatment rose continually; it is observed that the NH_4^+-N from CK in traditional composting dropped rapidly after 28 days, while the NO_3^--N of CK shot up after the same period, which indicated that the NH_4^+-N of control was turning into NO_3^--N, and that the decrease was greater than the increase; and that the decrease was greater than the increase; this demonstrated that part of the nitrogen was emitted from the pile in the form of gas, namely NH_3 and N_2O. Where calcium superphosphate, DCD and MHPP were added to T1-T4, the NH_4^+-N of T1 slightly decreased in approx. 28 days, while that of T2, T3 and T4 did not went down significantly, which indicated the combination of calcium superphosphate and DCD alleviated the transformation and decomposition of NH_4^+-N; only the NO_3 -N of T1 slightly increased after 28 days while that of T2-T4 exhibited no significant rise, which demonstrated that calcium superphosphate, DCD and MHPP prevented NH_4^+-N turning into NO_3^--N, because DCD and MHPP inhibited the activity of nitrifying bacteria, thereby inhibiting or event preventing the nitrification in compost.

Physico-chemical and material decomposition indicators

Germination percentage is an important indicator for evaluation of compost decomposition; it is generally agreed that thorough decomposition is realized when GI > 80%; “thorough decomposition” means the application of fertilizer to crops bring about no secondary decomposition and lead to no adverse effects. In the present study, the germination percentage was higher than 96%, much higher than 80%; the reason why the germination percentage did not reach 100% may be because that it was impossible for any seeds to realize a germination percentage of 100%. A compost conductivity greater than 4 ms/cm may cause physiological damage to field crops, so

http://www.aloki.hu ● ISSN 1589 1623 (Print) ● ISSN 1785 0037 (Online)
DOI: http://dx.doi.org/10.15666/aeer/1705_1128911301

compost conductivity is also known as an important indicator of compost safety; as shown in *Table 3*, the conductivity dropped from 3.19–3.294 ms/cm to 0.96–1.89 ms/cm, which represented the compliance with safety requirements.

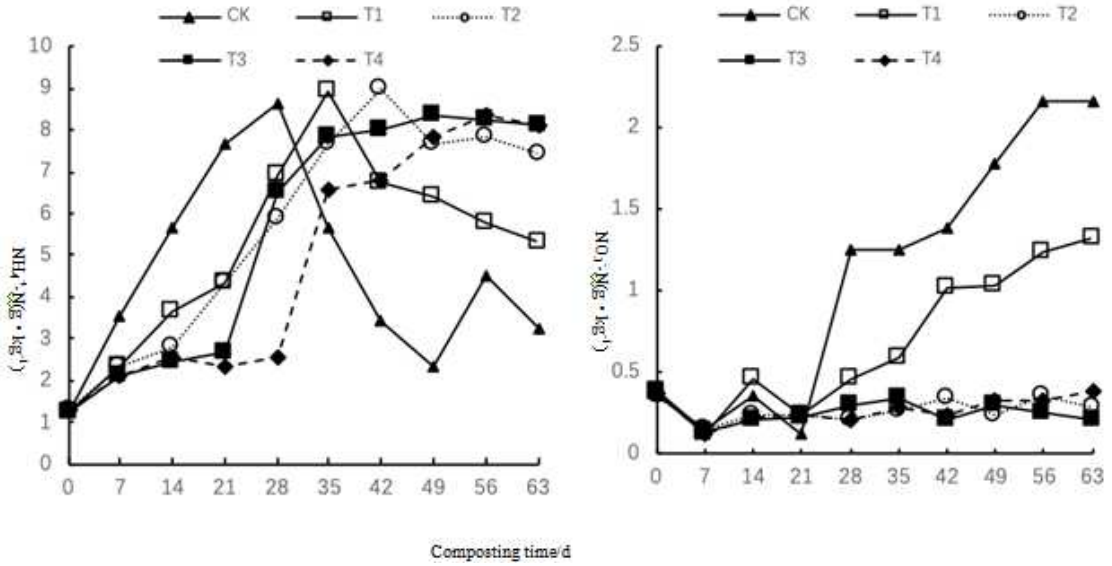

Figure 5. *Changes of NH_4^+-N and NO_3^--N content*

Table 3. *Chemical and physical characters and maturity index of composting*

Treatment	Compost Period	C/N	pH	Germination%	Electric conductivity EC/(ms·cm-1)
CK	Start	25.79a	7.85±0.08a	28.50±6.75a	3.25±0.15a
	End	10.23a	7.46±0.12b	97.75±0.25ab	0.96±0.08d
T1	Start	25.79a	7.81±0.03a	22.75±7.75d	3.29±0.21a
	End	10.09b	7.86±0.32a	98.75±0.50a	1.22±0.03c
T2	Start	25.79a	7.79±0.06a	23.25±3.50c	3.32±0.05a
	End	9.87c	7.16±0.09c	96.25±0.25b	1.68±0.08b
T3	Start	25.79a	7.19±0.03b	28.50±7.75a	3.23±0.04a
	End	10.13a	7.09±0.09d	98.75±0.75a	1.86±0.02a
T4	Start	25.79a	6.85±0.08c	25.50±5.75b	3.19±0.03a
	End	10.02b	7.12±0.09c	97.75±0.25ab	1.89±0.05a

Lower-case letters indicate significant differences at $p < 5\%$ level

Discussion

Chemically synthetic nitrification inhibitors principally include dicyandiamide (DCD), nitrapyrin and DMPP, which have been brought into production; however, these chemically synthetic inhibitors are not extensively used in agricultural production due to their high costs, their instable properties in different climates and soils (Li et al., 2008) and certain problems to be solved.

DCD, as a common nitrification inhibitor, can effectively inhibit the oxidation of ammonia, alleviate the leaching loss of nitrate nitrogen and the nitrogen loss resulting from denitrification, and improve the utilization of nitrogenous fertilizer (Moir et al.,

http://www.aloki.hu ● ISSN 1589 1623 (Print) ● ISSN 1785 0037 (Online)
DOI: http://dx.doi.org/10.15666/aeer/1705_1128911301

2010); however, there were some drawbacks with the application of DCD: The application rate of DCD had to reach 15–30 kg per Mu (666.7 square meters) so as to achieve inhibiting effect; DCD was extremely mobile in soil since it was easily soluble in water (Jacinthe et al., 1992), and the resulting spatial separation from ammonium nitrogen may impair the inhibiting effect; in the case of intense rainfall or soil with poor water retention capacity, leaching loss of DCD may frequently occur; the repeated application of DCD may cause the degradation rate to increase, thus reducing the half-time. Certain studies reported that the application of DCD may bring about toxic effects on crops (Xmb et al., 2003). The application of nitrapyrin increases the yield by 7%, reduces the nitrogen loss by 16%, and reduces the greenhouse gases emission by 51% (Woil et al., 2004); however, since nitrapyrin is a chlorinated organic matter, its long-term application may adversely affect the environment. Furthermore, nitrapyrin is prone to volatilization and photolysis, which makes it unsuitable for surface fertilization; moreover, the risk of corrosion and explosion makes it difficult to apply and keep this substance. Other studies showed that nitrapyrin exhibited certain toxicity that brought about curved and sallow leaves etc. in some plants (Maftoun et al.1981).

In contrast, the biological nitrification inhibitor MHPP produced through induction in ammonium nitrogen environment is a biological product produced by plants that are not harmful to the environment; since neither toxic nor side effect was detected during the test, MHPP is expected to be extensively generalized in composting and agricultural production. However, this substance is still under study, and the way to turn it into stable powder for extensive popularization is one of the important aspects of next step of research.

Conclusion

1. The combination of calcium superphosphate and MHPP did not cause the composting of straws and dairy manure to slow down, but improved the final compost quality; the ultimate germination percentage of each treatment was 97.5%, 98%, 98% and 97.5%, respectively.
2. The addition of calcium superphosphate and MHPP reduced the nitrogen oxide and ammonia emission during composting; the most appropriate content of MHPP was found to be 0.6%, where the emission of NH_3, N_2O and CH_4 were reduced by 65.40%, 62.39% and 61.93%, respectively.
3. Since the present test was a large engineering test featuring large mass of raw material and fermentation field, it was difficult to perform repeated tests; however, the gas sampling and chemical test indicates were repeatedly tested during the test after adequate mixing of raw materials, so the experimental data are reasonable and rational.
4. Recommendations: The compost will be used in field. We did not research how compost influence gas emission during plant growth. So further researches should be conduct on how compost influences gas emissions during using process.

Acknowledgements. The study was funded by the Science and Technology Major Projects of Anhui Province (18030701190); Natural science Research Program in Universities in Anhui (KJ2018A0527); National Key R&D Program of China (2018YFF0213502-3; 2018YFF0213501-4), Anhui Provincial Education Department's Revitalization Program for 2019 (gxyq2019061), the Dean fund project (562016Y-4686).

http://www.aloki.hu ● ISSN 1589 1623 (Print) ● ISSN 1785 0037 (Online)
DOI: http://dx.doi.org/10.15666/aeer/1705_1128911301

REFERENCES

[1] Chen, S. L., Yuan, J., Li, G. X., He, S. Zhang, B. (2017): Combination of superphosphate and dicyandiamide decreasing greenhouse gas and NH_3 emissions during sludge composting. – Transactions of the Chinese Society of Agricultural Engineering 33(6): 199-206.

[2] Fukumoto, Y., Osada, T., Hanajima, D., Haga, K. (2003): Patterns and quantities of NH_3, N_2O, and CH_4 emissions during swine manure composting without forced aeration–effect of compost pile scale. – Bioresource Technology 89(2): 109-114.

[3] Hao, X. Y., Chang, C., Larney, F., Travis, G. R. (2001): Greenhouse gas emissions during cattle feedlot manure composting. – Journal of Environmental Quality 30(2): 376-386.

[4] IPCC Core Writing Team (2014): Climate change 2014. Synthesis report: Contribution of Working Groups I, II and III to the Fifth Assessment Report of the Intergovernmental Panel on Climate Change. – IPCC, Geneva.

[5] Jacinthe, P. A., Pichtel, J. R. (1992): Interaction of Nitrapyrin and Dicyandiamide with Soil Humic Compounds. – Soil Science Society of America Journal 56(2): 465-470.

[6] Jiang, T., Ma, X. G., Tang, Q., Yang, L., Li, G. (2016): Combined use of nitrification inhibitor and struvite crystallization to reduce the NH_3, and N_2O emissions during composting. – Bioresource Technology 217: 210-218.

[7] Jiang, T., Chang, J. L., Ma, X. G., Li, G. X. (2018): Comprehensive comparison of different nitrogen in situ conservation agents during composting. – Journal of Agro-Environment Science 37(2): 369-375.

[8] Li, B., Wang, C. Q., Jiang, L. Q., Li, H. X., Yang, J., Yang, B. C. (2008): Effect of chemical amendments on NH_3 emissions and compost maturity duriong co-composting of pig manure and straw. – Journal of Agro-Environment Science 27(4): 1653-1661.

[9] Li, X. L., Ma, J., Xu, H., Cao, J. L., Cai, Z., Yagi, K. (2008): Effect of different application time of DCD on methane and nitrous oxide emissions during rice growth period. – Acta Ecologica Sinica 28(8): 3675-3681.

[10] Lin, X. F., Li, G. X., Ren, L. M., Wang, B. (2008): Effect of $FeCl_3$ and $Ca(H_2PO_4)_2$ as amendments on reducing nitrogen loss during composting. – Journal of Agro-Environment Science 27(4): 1662-1666.

[11] Liu, F., Zhou, L. (2015): Effects of cotton stalk wood vinegar on CH_4 and CO_2 emissions from cow manure composting. – Jiangsu Agricultural Sciences 43(9): 364-369.

[12] Luo, Y., Li, G., Luo, W., Schuchardt, F., Jiang, T., Xu, D. (2013): Effect of phosphogypsum and dicyandiamide as additives on NH_3, N_2O and CH_4, emissions during composting. – Biomedical and Environmental Sciences 25(7): 1338-1345.

[13] Luo, Y. M., Li, G. X., Frank, S., Wang, K., Jiang, T., Luo, M. (2012): Effects of additive superphosphate on NH_3, N_2O and CH_4 emissions during pig manure composting. – Transactions of the Chinese Society of Agricultural Engineering 28(22): 235-242.

[14] Maftoun, M., Yasrebi, J., Darbekeshti, M. (1981): Comparative phytotoxicity of nitrapyrin and ATC to several leguminous species. – Plant and soil 63(2): 303-306.

[15] Mccarty, G. W., Bremner, J. M. (1989): Inhibition of nitrification in soil by heterocyclic nitrogen compounds. – Biology & Fertility of Soils 8(3): 204-211.

[16] Ministry of Agriculture of PRC (2017): National Development and Reform Commission. – National 13th Five-Year Plan for Rural Biogas Development and Reform of Agricultural Economics 178, Beijing.

[17] Moir, J. L., Cameron, K. C., Di, H. J. (2010): Effects of the nitrification inhibitor dicyandiamide on soil mineral N, pasture yield, nutrient uptake and pasture quality in a grazed pasture system. – Soil Use & Management 23(2): 111-120.

[18] Ren. L. M. (2009): Study on Mechanism of Carbon and Nitrogen Loss and Control During Composting. – China Agricultural University, Beijing.

http://www.aloki.hu ● ISSN 1589 1623 (Print) ● ISSN 1785 0037 (Online)
DOI: http://dx.doi.org/10.15666/aeer/1705_1128911301

[19] Ren, L. M., He, Q., Li, G. X., Lu, P., Li, C. P. (2008): Effect of $Mg(OH)_2$ and H_3PO_4 amendments on nitrogen conservation during simulated aerobic composting and its benefit analyses. – Transactions of the Chinese Society of Agricultural Engineering 24(4): 225-228.
[20] Sommer, S. G., Moller, H. B. (2000): Emission of greenhouse gases during composting of deep litter from pig production-effect of straw content. – Journal of Agricultural Science 134: 327-335.
[21] Subbarao, G. V., Arango, J., Masahiro, K., Hooperd, A. M., Yoshihashia, T., Andoa, K. Y., Nakaharaa, K., DeshpandeeI, S., Ortiz-Monasterioc, M. I., Ishitanib, M., Petersb, N., Chirindab, L., Wollenbergf, J. C., Latag, B., Gerard, C. S., TobitaaI, M., Raob, H. J., Iwanagaa, M. (2017): Genetic mitigation strategies to tackle agricultural GHG emissions: The case for biological nitrification inhibition technology. – Plant Science 262: 165-168.
[22] Thompson, A. G., Wagner-Riddle, C., Fleming, R. (2004): Emissions of N_2O and CH_4 during the composting of liquid swine manure. – Environmental Monitoring and Assessment 91(1/2/3): 87-104.
[23] Wang, Y., Li, N. N., Zhu, D. W., Zhou, W. B., Chen, Y. X., Wu, Y. P. (2018): Influence of straw pretreatment on the thermophilic composting process with pig manure. – Journal of Agro-Environment Science 37(9): 2021-2028.
[24] Wei, T. J. (2015): Mechanisms of Sorghum Secreting Biological Nitrification Inhibitors and Their Effects on Soil Ammonia-oxidizing Microorganisms. – Journal of Nanjing Agricultural University, Nanjing.
[25] Weng. J. J. (2012): Nitrogen conservation of calcium superphosphate in swine manure compost. – Journal of Anhui Agricultural Science 40(8): 4528-4529.
[26] Wolt, J., D. (2004): A meta-evaluation of nitrapyrin agronomic and environmental effectiveness with emphasis on corn production in the Midwestern USA. – Nutrient Cycling in Agroecosystems 69(1): 23-41.
[27] Wu, W. X., Li, L. J., Lu, H. H., Wang, C., Deng, H. (2012): Mechanisms of nitrous oxide emission during livestock manure aerobic composting. – Chinese Journal of Applied Ecology 23(6): 1704-1712.
[28] Xie, G. H., Bao, W. Q., Liu, J. J., An, J. (2018): An overview of researches on livestock and poultry excreta resource in China. – Journal of China Agricultural University. 23(4): 75-87.
[29] Xmb, M., Del, P. A., Merino Pestavillo, J. M. (2003): Dicyandiamide and 3,4-dimethyl pyrazole phosphate decrease N_2O emissions from grassland but dicyandiamide produces deleterious effects in clover. – Journal of Plant Physiology 160(12): 1517-1523.
[30] Yang, J. I., Jia, Y. U., Jing, M. A., Xiaoping, L. I., Hua, X. U. (2011): Effect of timing of DCD application on nitrous oxide emission during wheat growing period. – Acta Ecologia Sinica 31(23): 7151-7160.
[31] Yang, Y. M, Liu, H. L., Yang, Z. F., Xi, B. D., Zhang, X. F. (2005): Methods and techniques in the control of nitrogen loss during the composting—a review. – Journal of Beijing Normal University 41(2): 213-216.
[32] Yu, Q. G., Yin, J. Z., Ma, J. W., Zou, P., Hui, L., Sun, W. C. Fu, J. R. (2014): Effects of nitrification inhibitor DMPP application in agricultural ecosystems and their influencing factors: a review. – Journal of Agro-Environment Science 33(6): 1057-1066.
[33] Zakir, H. A., Subbarao, G. V., Pearse, S. J., Gopalakrishnan, S., Ito, O., Ishikawa, T., Kawano, N., Nakahara, K., Yoshihashi, T., Ono, H., Yoshida, M. (2008): Detection, isolation and characterization of a root-exuded compound, methyl 3-(4-hydroxyphenyl) propionate, responsible for biological nitrification inhibition by sorghum (Sorghum bicolor). – New Phytologist 180(2): 442-451.

http://www.aloki.hu ● ISSN 1589 1623 (Print) ● ISSN 1785 0037 (Online)
DOI: http://dx.doi.org/10.15666/aeer/1705_1128911301

EFFICIENCY OF HIGH-STANDARD FARMLAND DEVELOPMENT BASED ON MATTER-ELEMENT EXTENSION AND TOPSIS MODELING

TIAN, J. S.[1] – JIANG, Z. H.[2] – GUO, J. C.[1*] – LIU, X.[1]

[1]*School of Science, Anhui Agricultural University, Hefei 230036, China*

[2]*Hefei Pastoral Land Planning and Mapping Company Limited, Hefei 230031, China*

**Corresponding author*
e-mail: liuxin@ahau.edu.cn

(Received 12th Apr 2019; accepted 11th Jul 2019)

Abstract. To better assess high-standard farmland development projects, this paper built an evaluation system containing three indices: soil efficiency, infrastructure efficiency as well as economic and social efficiency, which were measured after the development of high-standard farmlands. By combining the matter-element extension theory with the TOPSIS model, the authors built a high-standard farmland development evaluation system to assess the soil efficiency, infrastructure efficiency, economic and social efficiency as well as the overall efficiency after completion of a high-standard farmland development project. the authors found the weight of the index for infrastructure efficiency to be 0.46, with the degree of similarity to the optimal solution reaching 1.0, thus it is rated excellent in terms of its impact on the overall efficiency evaluation; the weight of economic and social efficiency was 0.37, with its degree of similarity being 0.29, thus rated good accordingly; while the weight of soil efficiency was 0.17, with its degree of similarity being 0.00, thus it had the least impact on overall efficiency. The sequencing result by the TOPSIS model showed that the effective depth of soil had the highest impact on soil efficiency, meanwhile the road access rate influenced infrastructure efficiency the most, and public satisfaction mattered most in terms of economic and social efficiency.
Keywords: *land development, land engineering, high-standard farmland, evaluation system, efficiency*

Introduction

High-standard farmland development projects normally involve land development, soil improvement, irrigation and water supply, rural road network building, farmland protection and ecological reservation. These projects aim to reduce or remove major restrictions on farmland development and improve their quality. As proposed in the Chinese government document "*Opinions on Accelerating Modernization of Agriculture and Building a Moderately Prosperous Society by the Central Government and State Council*", the governments at all levels should boost development of high-standard farmlands by increasing investment and integrating financial sponsorship, and governments at all levels should put this endeavour among their top priorities. Thus, development of high-standard farmlands is in fact a land development project in which the scientific evaluation of the project efficiency accounts to be a significant step.

Current Chinese domestic projects (Hwang and Yoon, 1981; Yang et al., 2013; Liu et al., 2012; Zhao and Zhu, 2010; Wu et al., 2008; Li et al., 2010; Xin et al., 2009; Gao et al., 2011) have already studied many topics in this area, including efficiency evaluation of land development projects, evaluation index systems for high-standard farmland development, arable land overall quality evaluation index systems, preliminary location selection of high-standard farmland development, basic farmland demarcation or suitability and timing of high-standard farmland development. For instance, published

http://www.aloki.hu ● ISSN 1589 1623 (Print) ● ISSN 1785 0037 (Online)
DOI: http://dx.doi.org/10.15666/aeer/1705_1130311316

studies have used the TOPSIS (Technique for Order of Preference by Similarity to Ideal Solution) model (Tsaur, 2011; Korkmaz, 2008; Jun et al., 2011; Liu et al., 2006) to analyze priorities in high-standard farmland development, and studied the potential quality of arable land based on grading factors and matter-element modeling (Zhao et al., 2017, 2018). Some of these studies have focused on location selection and division of high-standard farmland by combining the TOPSIS model with the local spatial auto-correlation method (Yang et al., 2018, 2017a, 2017b). Some others have expounded on the feasibility and spatial stability of high-standard farmland development via the TOPSIS model and used the four-quadrant method to analyze the spatial and temporal distribution in high-standard farmland development (Xue et al., 2014). Other studies have explored the time series of high-standard farmland development on the basis of land evaluation and site analysis system (Bian et al., 2016). Nevertheless, current research on the high-standard farmland post-development efficiency have been mainly carried out by way of the entropy weight method, the TOPSIS model or the entropy-weight-based matter-element extension model to analyze the efficiency (Xin et al., 2017; Cai and Li, 2014). To enrich the repository of methods for high-standard farmland development evaluation, this research proposed a new evaluation method that combines the matter-element extension model with the TOPSIS model. With the matter element as its basis, the proposed method develops a matter-element model with three post-development indices – soil efficiency, infrastructure efficiency and economic and social efficiency – to evaluate farmland development efficiency through the analysis of the respective weight of the indices in the correlation function. The weights resulting from the function are then introduced into the TOPSIS model to calculate the degree of similarity and evaluate the soil efficiency, infrastructure efficiency, economic and social efficiency as well as the overall efficiency. The result of the weight analysis by way of the correlation function is shown to be in agreement with the result of the efficiency-based similarity analysis.

Materials and methods

Research area description

This research takes the high-standard farmland development project of Shangwei Village in Shannan Town, Feixi County of Hefei in Anhui province of China as the research target to evaluate the post-development efficiency. The study area is situated at about 116° 45’ to 116° 48’ east longitude and 31° 40’ to 31° 42’ north latitude (*Fig. 1*). Located in the northwest part of Shannan Town, Shangwei covers an area of 7.9 km^2, including 260 hm^2 of farmlands and 200 hm^2 of woods. This project area, with its northern part higher than its southern part, mainly consists of hills and is divided into two sections – one in the east and the other in the west – with the County Road No. 042 as the line of demarcation. Subject to the tropical monsoon climate, the area has an average annual temperature that falls between 15 and 16 °C and an average annual precipitation between 900 and 1000. The whole development project lasted from the end of February 2017 to the beginning of August 2017. Given the actual conditions of the project area, three sampling sites were selected for soil efficiency inside a key development region, where farmlands abound.

Research data presented in this study was collected from diverse sources, including the database for land utilization of Feixi, Heifei, in 2013, the land use map of Feixi prepared in September 2016, the (updated) land use database of Feixi, Heifei, in 2016

http://www.aloki.hu ● ISSN 1589 1623 (Print) ● ISSN 1785 0037 (Online)
DOI: http://dx.doi.org/10.15666/aeer/1705_1130311316

and the overall land use planning map (2006-2020). Other research materials are also referred to, such as the surveyed landform map of the project area in 2016, the planning report for the high-standard farmland development project in 2016, the project completion landform map, the result of a questionnaire survey carried out in October 2017 and sampling research data obtained in October 2017. In the questionnaire survey, 95 questionnaires were collected from the total of 100 distributed. According to China's high-standard farmland construction standards and evaluation criteria for high-standard farmland construction, the target groups of the questionnaire survey were mainly local farmers, managers and acceptance experts. Among the participants, the ages were mainly between 30 and 60 years old, the education experience of senior high school and college were the main one.

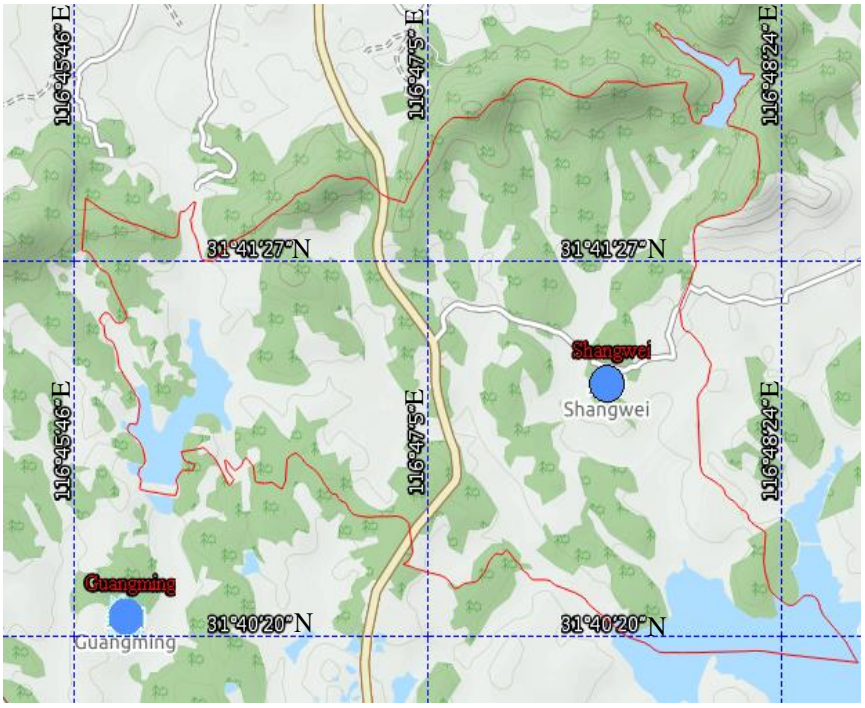

Figure 1. *Location map of research area (Feixi County of Hefei in China)*

Research methodology

The core objective of high-standard farmland development is to maximize economic and social efficiency while ensuring ecological conservation. Extenics is a subject that studies the possibility of extension of matters and explores the law and methods for innovation of the extensibility of matters through formalized models to address problems. There are diverse indicators for evaluation of high-standard farmland efficiency and results from single-index evaluation methods are usually incompatible with each other, therefore, the Extenics theory, which is applicable to such research situations, is applicable to this study. The TOPSIS method works out the degree of similarity between the calculated results and the optimal solution to evaluate the results' quality. The TOPSIS method is based on the Euclidean distance calculated between the positive ideal solution (PIS) and the negative ideal solution (NIS). As presented above, this project presents an evaluation system with three indices (soil efficiency,

http://www.aloki.hu ● ISSN 1589 1623 (Print) ● ISSN 1785 0037 (Online)
DOI: http://dx.doi.org/10.15666/aeer/1705_1130311316

infrastructure efficiency and economic and social efficiency) according to the high-standard farmland development criteria (Criterion of High Standard Farmland, 2012), establishes a weight model of correlation function index based on matter elements and analyzes the development results. The weights obtained via the correlation function are introduced into the TOPSIS model, which is then optimized to work out the degree of similarity of each index to the ideal solution. In this way, an evaluation can be made on the soil efficiency, infrastructure efficiency, economic and social efficiency as well as the overall efficiency of the high-standard farmland development project.

Evaluation index system

Based on existing studies and the actual conditions of the project area, the model presents an evaluation system of indices, assuming that the indices are representative, comparable, operable and quantitative. The efficiency of high-standard farmland development is taken as the evaluation target, with three indices – soil efficiency, infrastructure efficiency, economic and social efficiency – as the evaluation criteria. Each evaluation index includes multiple criteria with deciding factors, as shown for the index system in *Table 1*. According to domestic research publications, the degree of similarity is divided into four levels to make a qualitative evaluation. The criteria are as follows: when the degree of similarity stands between 0.80 and 1.00, the efficiency is rated "excellent"; when the number falls between 0.60 and 0.80, the efficiency is rated "good"; the efficiency is rated "moderate" when the number is between 0.30 and 0.60; while it is rated "poor" if the number stays between 0.00 and 0.30.

Table 1. *Efficiency evaluation index system*

Target	Criterion and code	Index (deciding factors) and code	Index type	Mean	Suitable value
High-standard farmland development efficiency	Soil efficiency (O_{11})	Effective depth of soil (cm) c_1	Positive	60.0	100
		Organic content of soil (g/kg) c_2	Positive	11.6	20
		pH scale c_3	Suitable	6.8	6.0-7.9
	Infrastructure efficiency (O_{21})	Agricultural mechanization level (%) c_4	Positive	75.0	100
		Irrigation water utilization coefficient c_5	Positive	0.6	1.0
		Rate of guaranteed irrigation (%) c_6	Positive	85.0	100
		Road access rate (%) c_7	Positive	90.0	100
	Economic and social efficiency (O_{31})	Agricultural production cost (10000 rmb/hm^2) c_8	Negative	1.6	0
		Static return on investment (%) c_9	Positive	7.1	100
		Degree of public satisfaction (%) c_{10}	Positive	93.0	100

(1) The indices and suitable values in the table above are identified by referring to relevant regulations for high-standard farmland development (Farmland Construction, 2016; Regulation for Gradation on Agriculture Land Quality, 2012; Cultivated Land Quality Grade, 2016) and related research publications. (2) The average score of soil efficiency is obtained from sampling of the sites, from scores of infrastructure efficiency from scoring results by experts, and from scores of the economic and social efficiency from questionnaire surveys. (3) Agricultural production cost and static return on investment refer to economic efficiency; degree of public satisfaction represents social efficiency

High-standard farmland development efficiency evaluation

The matter-element extension model and TOPSIS model are combined to evaluate the soil efficiency, infrastructure efficiency, economic and social efficiency as well as the overall efficiency of the high-standard farmland development project.

http://www.aloki.hu ● ISSN 1589 1623 (Print) ● ISSN 1785 0037 (Online)
DOI: http://dx.doi.org/10.15666/aeer/1705_1130311316

Matter-element model building

According to previous published models (Zhao and Su, 2010; Cai et al., 2008; Yang and Cai, 2008), O_{mj} is set with j levels of evaluation; c_i is the evaluation index for standard levels; V_{mji} is the range of classical field defined by the respective levels of indices; a_{mji} and b_{mji} are the upper limit and lower limit of the classical field, respectively; P is the evaluation standard; x_{pi} is the range of the segment field of P in terms of each evaluation index of c_i; a_{pi} and b_{pi} are the upper limit and lower limit of the segment field, respectively; Q represents the matter element to be evaluated (development efficiency) and x is the efficiency value of Q in terms of the evaluation index c_i. The relation between x_{pi}, the segment field value, and v_{mji}, the classical field value, is $v_{mji} \subset x_{pi}$. The classical matter element model, the segment field matter element model and the to-be-evaluated matter element model that can be built are as follows: $M_{mj} = (O_{mj},\ c_i,\ v_{mji})$, $M_p = (P,\ c_i,\ x_{pi})$, $M_q = (Q,\ c_i,\ x_i)$.

Weight model building

In the evaluation of efficiency (Zhao and Su, 2010; Cai et al., 2008; Yang and Cai, 2008), the weighing method can help measure differences among indices, but in most cases, the scoring method, which involves subjective judgements, dominates and undermines the objectivity of the result. By introducing the average score of each index into the classical field and segment field of the matter-element extension model, our model calculates the weight of each index through the correlation function to decide whether the index meets the standard, so that the result can steer clear of subjective errors and w_i, the normalized weight of c_i, can be calculated. When $x_i \in x_{pi}$ (segment field), the classical field is $v_{mji} = (a_{mji}, b_{mji})$, with $i = 1, 2, \cdots n$ (evaluation index) and $j = 1, 2, \cdots m$ (evaluation standard level), then the correlation function between the evaluation value and the classical field presents as:

$$K_{ji}(x_i, v_{mji}) = \begin{cases} \dfrac{2(x_i - a_{mji})}{b_{mji} - a_{mji}}, \text{when } x_i \le \dfrac{a_{mji} + b_{mji}}{2} \\ \dfrac{2(b_{mji} - x_i)}{b_{mji} - a_{mji}}, when x_i > \dfrac{a_{mji} + b_{mji}}{2} \end{cases} \quad \text{(Eq.1)}$$

In *Equation 1, K_{ji} (x_i, V_{mji})* refers to the simple correlation value between the actual efficiency values and corresponding standard values of evaluation indices; other symbols follow the same pattern in meaning. j stands for the level of evaluation standard. The larger j is, the larger the represented index's influence on the criteria is. The correlative weight calculation model then presents as:

$$q_i = \begin{cases} j \times (1 + \max(K_{ji}(x_i, v_{mji}))), when \max(K_{ji}(x_i, v_{mji})) \ge -\dfrac{1}{2} \\ 0.5 \times j, when \max(K_{ji}(x_i, v_{mji})) < -\dfrac{1}{2} \end{cases} \quad \text{(Eq.2)}$$

http://www.aloki.hu ● ISSN 1589 1623 (Print) ● ISSN 1785 0037 (Online)
DOI: http://dx.doi.org/10.15666/aeer/1705_1130311316

In *Equation 2, j* stands for the highest level of evaluation. On the contrary, the smaller *j* is, the smaller the corresponding index's influence on the criteria is. In this case, the correlation weight calculation model is:

$$q_i = \begin{cases} (m-j+1)\times(1+\max(K_{ji}(x_i, v_{mji}))), \text{when } \max(K_{ji}(x_i, v_{mji})) \geq -\frac{1}{2} \\ 0.5\times(m-j+1), when \max(K_{ji}(x_i, v_{mji})) < -\frac{1}{2} \end{cases} \quad \text{(Eq.3)}$$

In *Equation 3, j* stands for the lowest level of evaluation and *m* is the number of evaluation levels.

TOPSIS model

TOPSIS is a multi-criteria analysis method, which was originally proposed by Hwang and Yoon in 1981 to compare different solutions, and it is also an integrated evaluation method for multi-objective and decision-making solutions. It can not only make the best of the original data and reflect the gap between different decision-making solutions, but also describe the general condition of the objectives or specific targets in an authentic, direct and reliable way, therefore it is widely applicable. The authors assumed that there are a total of *m* objectives, each of which has *n* attributes, and the initial value of the attribute j^{th} of the objective i^{th} is x_{ij}, the initial evaluation matrix *V* is then formed. As the dimensions of indices vary, the initial matrix is normalized into the normalized matrix *V'*. By combining the weight matrix *W* obtained from the correlation function model with the normalized initial evaluation matrix *V'*, the weighted evaluation matrix *Z* is obtained.

(1) We first calculated the positive ideal solution (PIS) and negative ideal solution (NIS) of the evaluated objective through the weighted judgement matrix, then worked out the Euclidean distance that each objective has from PIS and NIS, and last the following model is built:

$$\text{Euclidean distance from PIS: } S_i^+ = \sqrt{\sum_{j=1}^{m}(f_{ij} - f_j^+)^2},\ j = 1,2,...,\ n \quad \text{(Eq.4)}$$

$$\text{Euclidean distance from NIS: } S_i^- = \sqrt{\sum_{j=1}^{m}(f_{ij} - f_j^-)^2},\ j = 1,2,...,\ n \quad \text{(Eq.5)}$$

(2) Next, the authors calculated C_i, the degree of similarity of each objective to the optimal solution (or optimal value):

$$C_i = S_i^- / (S_i^+ + S_i^-),\ \ i = 1,2,...,m \quad \text{(Eq.6)}$$

According to C_i, the scale of the similarity, the objectives can then be sequenced to create the basis for decision-making. In *Equation 6,* the larger C_i is, the closer the efficiency of the item i^{th} is to the optimal value. The values for the degree of similarity fall within the range from 0.00 to 1.00, and the closer the value is to 1.00, the better the

http://www.aloki.hu ● ISSN 1589 1623 (Print) ● ISSN 1785 0037 (Online)
DOI: http://dx.doi.org/10.15666/aeer/1705_1130311316

corresponding index's efficiency is; on the contrary, similarity closer to 0.00 means poorer efficiency.

Data analysis process

Data processing

Range identification of classical field and segment field

The correlation function in the matter-element extension model plays a pivotal role in determining the weights of indices, and it is related to the classical field and segment field in the model. The conventional methods to identify the range include work experience-based identification by experts, criteria-based identification, sampling data-based identification and others. On the basis of previous reports describing criteria for high-standard farmland development, the research presented here, by referring to data collected from sampling sites of completed projects, statistics from questionnaire surveys and consultation with experts, identifies the ranges of the classical field and the segment field at four evaluation levels for the corresponding indices, as shown in *Table 2*.

Table 2. *Range of the classical fields and the segment fields of evaluation indices*

Index code	Classical field range				Segment field range
	Poor	Moderate	Good	Excellent	
c_1	[30, 50)	[50, 60)	[60, 70)	[70, 100]	[30, 100]
c_2	[0, 5)	[5, 10)	[10, 20)	≥ 20	[0, 20]
c_3	[4.5, 5.5]	(5.5, 6.0]	(6.0, 6.5]	(6.5, 7.9]	[4.5, 7.9]
c_4	[0, 50)	[50, 60)	[60, 70]	[70, 100]	[0, 100]
c_5	[0.1, 0.5)	[0.5, 0.55)	[0.55, 0.6)	[0.6, 1.0]	[0.1, 1.0]
c_6	[10, 50)	[50, 60)	[60, 70]	[70, 100]	[10, 100]
c_7	[30, 50)	(50, 60)	(60, 80)	(80, 100)	[30, 100]
c_8	≥ 2.0	(2.0, 1.5)	(1.5, 1.0)	< 1.0	[0, 2]
c_9	[0, 5]	[5, 8]	[8, 10]	> 10	[0, 10]
c_{10}	[0, 50]	[50, 60]	[60, 75]	[75, 100]	[0, 100]

Index weight in the TOPSIS model

The standard level that an index's evaluation value belongs to is represented by *j*. A larger value of *j* means larger influence of the index on the criteria, hence deserving a larger scale of weight; on the contrary, a smaller *j* means less influence of the corresponding index on the criteria, hence deserving a smaller weight. The results are shown in *Table 3*.

Processing of data on soil efficiency, infrastructure efficiency and economic and social efficiency through the TOPSIS model

The main components of high-standard farmland development evaluation criteria include: construction task evaluation, construction quality evaluation, construction effectiveness evaluation, construction management evaluation, social impact evaluation

http://www.aloki.hu ● ISSN 1589 1623 (Print) ● ISSN 1785 0037 (Online)
DOI: http://dx.doi.org/10.15666/aeer/1705_1130311316

and comprehensive evaluation (Assessment Standard of Well-Facilitated Farmland Construction, 2016; Criterion of High Standard Farmland, 2012). The high-standard farmland development project, in planning and location selection, aims to improve the infrastructure, increase the level of agricultural automation and achieve agricultural mass production in the selected area. The infrastructure in the selected area is largely poor in quality and suffers from damages, which undermines the land productivity and the level of agricultural mechanization. Besides, irrigation-caused pit ponds and collapses of irrigation canals are rife among alluvial farm fields, casting a blight on agricultural irrigation. When the project is completed, project-acceptance experts select three sampling sites in the project area to assess the soil efficiency. According to the principles of TOPSIS modeling and given the inconsistent quantitative units of indices, the original evaluation matrix is normalized to produce and sequence the degree of similarity of the soil efficiency, infrastructure efficiency as well as economic and social efficiency, as shown in *Table 4*. The statistics for infrastructure efficiency are taken from scores by project-acceptance experts and those for economic and social efficiency are from questionnaire surveys.

Table 3. *Index weight*

Index code	Weight			
	Index correlated	**Index normalized**	**Criterion correlated**	**Criterion normalized**
c_1	12.60	0.68		
c_2	3.20	0.17	18.60	0.17
c_3	2.80	0.15		
c_4	11.00	0.21		
c_5	9.00	0.18	51.00	0.46
c_6	13.00	0.26		
c_7	18.00	0.35		
c_8	3.20	0.08		
c_9	16.80	0.40	41.60	0.37
c_{10}	21.60	0.52		

Table 4. *Efficiency index evaluation matrix and similarity degree*

Efficiency	Index	Normalized evaluation				Similarity	Ranking
Soil efficiency	c_1	0.9768	0.9762	0.9745		1.00	1
	c_2	0.1841	0.1878	0.1936		0.09	2
	c_3	0.1098	0.1085	0.1132		0.00	3
Infrastructure efficiency	c_4	0.4953	0.5009	0.4937	0.4785	0.77	3
	c_5	0.0034	0.0051	0.0042	0.0042	0.00	4
	c_6	0.5979	0.5956	0.5937	0.6035	0.94	2
	c_7	0.6302	0.6279	0.6354	0.6378	1.00	1
Economic and social efficiency	c_8	0.0164	0.0176	0.0173	0.0164	0.00	3
	c_9	0.0761	0.0774	0.0748	0.0761	0.06	2
	c_{10}	0.9970	0.9968	0.9970	0.9970	1.00	1

http://www.aloki.hu ● ISSN 1589 1623 (Print) ● ISSN 1785 0037 (Online)
DOI: http://dx.doi.org/10.15666/aeer/1705_1130311316

Processing of data on overall efficiency through the TOPSIS model

Based on data from *Tables 1–4*, our model makes use of the TOPSIS model to calculate and sequence the degree of similarity of three decision-making factors for overall efficiency, as shown in *Table 5*.

Table 5. *Overall efficiency evaluation matrix and similarity degree*

Criterion	Normalized judgement matrix			Distance from PIS	Distance from NIS	Similarity	Ranking
o_{11}	1.2722	1.2753	1.2769	0.1621	0.0001	0.00	3
o_{21}	1.7267	1.7280	1.7259	0.0001	0.1621	1.00	1
o_{31}	1.0873	1.0932	1.0900	0.1152	0.0469	0.29	2

Results analysis

In light of the leveling criteria of efficiency indices and based on the results of *Tables 3–5*, we analyze our results in two different ways: the weights of indices and the TOPSIS modeling results.

Soil efficiency analysis

(1) Analysis of index weight based on the correlation function. The results of normalized weight analysis on the criterion level after completion of the high-standard farmland development project follow the order: effective depth of soil (0.68) > Organic content of soil (0.17) > pH scale (0.15). This means that, among the factors that influence the soil efficiency, the effective depth of soil accounts for the largest indicator, hence it has the largest weight, followed by the organic content of soil and then by the pH scale. According to Jenks natural breaks method, indicators having a weight equaled or above 0.3 are important indicators, those within the range [0.1, 0.3) are secondary indicators and those smaller than 0.1 are boundary indicators. Therefore, among all the indicators for soil efficiency, the effective depth of soil is an important indicator, the organic content of soil a secondary indicator and the pH scale a boundary indicator.

(2) Analysis of the TOPSIS modeling results. The indicator effective depth of soil has the longest distance from the NIS, with a degree of similarity of 0.6177, while its distance from the optimal solution approaches 1.00, hence it is rated excellent in efficiency, which means that this indicator has the largest influence on soil efficiency; the distance of the indicator organic content of soil from PIS is 0.5603, and its distance from NIS is 0.09, so the indicator is rated poor in efficiency and plays a secondary role; the distance of the indicator pH scale from PIS is 0.6177, and its distance from the optimal solution is 0.00, so it is rated poor in efficiency and has the least influence. These indicators are ranked in the model in the following order: effective depth of soil, organic content of soil and pH scale.

Infrastructure efficiency analysis

(1) Analysis of the index weight based on the correlation function. The results of normalized weight analysis of infrastructure efficiency follow the order: road access rate (0.35) > rate of guaranteed irrigation (0.26) > agricultural mechanization level

http://www.aloki.hu ● ISSN 1589 1623 (Print) ● ISSN 1785 0037 (Online)
DOI: http://dx.doi.org/10.15666/aeer/1705_1130311316

(0.21) > irrigation water utilization rate (0.18). This means that, among the indicators for infrastructure efficiency, the road access rate plays the most important part, followed by the rate of guaranteed irrigation and then the agricultural mechanization level, with the irrigation water utilization rate having the least impact. According to Jenks natural breaks method, among the decision-making factors for infrastructure efficiency, road access rate is an important indicator, the rate of guaranteed irrigation, agricultural mechanization level and irrigation water utilization rate are secondary indicators, and there are no boundary indicators.

(2) Analysis of the TOPSIS modeling results. The indicator of road access rate has the longest distance from NIS, with a degree of similarity of 0.3273, and its distance from the optimal solution is 1.00, so it is rated excellent and has the largest influence on infrastructure efficiency. The distance of the indicator rate of guaranteed irrigation from NIS is 0.3081, and its degree of similarity to the optimal solution is 0.94, so it is rated excellent and plays a secondary role in infrastructure efficiency. The distance of agricultural mechanization level from PIS is 0.0741, and its degree of similarity to the optimal solution is 0.77, so the indicator is rated good and plays a relatively important role in infrastructure efficiency. The irrigation water utilization rate is most distant from the PIS, with a distance of 0.3273, and its degree of similarity to the optimal solution is 0.00, so it is rated poor in efficiency level and does not have much impact on infrastructure efficiency. These indicators are ranked in the model in the following order: road access rate, rate of guaranteed irrigation, agricultural mechanization level and irrigation water utilization rate.

Economic and social efficiency analysis

(1) Analysis of index weight based on the correlation function. The results of normalized weight analysis of economic and social efficiency follow the order: rate of public satisfaction (0.52) > static return on investment (0.40) > agricultural production cost (0.08). It means that among the indicators affecting economic and social efficiency, the rate of public satisfaction weighs the highest, followed by static return on investment and then by the agricultural productivity cost. According to Jenks natural breaks method, among the decision-making factors for economic and social efficiency, the indicators of rates of public satisfaction and static return on investment are important indicators, and the agricultural production cost is a boundary indicator, as the agricultural production cost is correlated with many unpredictable factors such as the environment and weather (unfavorable weather will increase the cost). The high-standard farmland development project improves the roads, achieves a general mechanization of agricultural production and reduces the workload and extra expenditures. With the cost of fertilization basically unchanged, the agricultural production cost is reduced, moreover, the static return on investment and the rate of public satisfaction would be both increased.

(2) Analysis based on the TOPSIS modeling results. The rate of public satisfaction is the most distant from the NIS, with a distance of 0.6477, and its degree of similarity to the optimal solution is 1.00, so this indicator is rated excellent in efficiency level and has the largest impact on economic and social efficiency; the indicator of static return on investment has a distance of 0.6091 from the NIS, and its degree of similarity to the optimal solution is 0.06, so it is rated poor in efficiency level and plays a secondary role in economic and social efficiency; the agricultural production cost has the longest distance from the PIS, 0.6477, and its degree of similarity to the optimal solution is

http://www.aloki.hu ● ISSN 1589 1623 (Print) ● ISSN 1785 0037 (Online)
DOI: http://dx.doi.org/10.15666/aeer/1705_1130311316

0.00, so it has the least impact on economic and social efficiency. These indicators are ranked in the model in the following order: rate of public satisfaction, static return on investment and agricultural production cost.

Overall efficiency analysis

(1) Analysis based on index weight and the correlation function. The normalized weight analysis in terms of the criteria in the high-standard farmland development project is presented in the following expression: infrastructure efficiency (0.46) > economic and social efficiency (0.37) > soil efficiency (0.17). This order indicates that, among the indices that influence the project's overall efficiency, infrastructure efficiency has the largest weight, followed by economic and social efficiency, while soil efficiency has the least impact. According to Jenks natural breaks method, the infrastructure efficiency and the economic and social efficiency are thus rated as important indicators, while soil efficiency is a secondary indicator. Infrastructure efficiency consists of one important indicator and three secondary indicators, without boundary indicators; economic and social efficiency includes two important indicators and one boundary indicator; soil efficiency involves one important indicator, one secondary and one boundary. Therefore, it can be concluded that the infrastructure efficiency is positively correlated with the overall efficiency, while soil efficiency, with a lower value, is in negative correlation with the overall efficiency.

(2) Analysis of the TOPSIS modeling results. The infrastructure efficiency is the most distant from NIS, with a distance at 0.1621, and its degree of similarity to the optimal solution is 1.00, so its efficiency level is rated excellent; in the case of economic and social efficiency, its distance from NIS is 0.0469, 0.1152 from PIS and its degree of similarity to the optimal solution is 0.29, so it is rated as poor in the efficiency level and plays a secondary role in the overall efficiency; the degree of similarity of soil efficiency to the optimal solution is 0.00, so soil efficiency is rated poor in the efficiency level and has the least impact on overall efficiency.

To summarize, the index weight analysis results based on correlation functions and those of the TOPSIS modeling are consistent. According to the mean score and suitability score of the project shown in *Table 1*, the key to the overall efficiency of high-standard farmland development is to improve infrastructure efficiency.

Conclusions

(1) The advantage of matter-element modeling is that it extends the actual evaluation indices which are not within the range of the standard values towards the standard values, with the correlation function identifying the positive field, negative field and zero field. The range of the correlation function is $(-\infty, +\infty)$, so it reflects the status of an object in a more accurate way and thus facilitates quantitative evaluation. These advantages are what the traditional fuzzy comprehensive evaluation method and analytic hierarchy process cannot provide. Meanwhile, by sequencing the weights of indices and leveling their respective impacts, the model found that infrastructure efficiency and economic and social efficiency are important indicators in the overall efficiency evaluation, while soil efficiency is a secondary indicator.

(2) The overall efficiency of the high-standard farmland development project is reflected by three indices –soil efficiency, infrastructure efficiency and economic and social efficiency. It is found that infrastructure efficiency is the most distant from the

http://www.aloki.hu ● ISSN 1589 1623 (Print) ● ISSN 1785 0037 (Online)
DOI: http://dx.doi.org/10.15666/aeer/1705_1130311316

NIS, with a distance of 0.1621, and its degree of similarity to the optimal solution is 1.00, so it is rated excellent in efficiency level while the soil efficiency has the least impact on the overall efficiency, with its degree of similarity to the optimal solution standing at 0.00.

Discussion

(1) The presented research combines matter-element extension modeling with TOPSIS modeling for high-standard farmland development efficiency evaluation. Compared with previous reported methods (Xue et al., 2014; Bian et al., 2016; Xin et al., 2017; Cai and Li, 2014; Tsaur, 2011; Korkmaz, 2008; Jun et al., 2011; Liu et al., 2006), the method used in this work has several advantages. Specifically, by constructing a matter-element model of classical and segment fields, it utilized the extensibility of matter elements to identify the evaluation objectives accurately and comprehensively; and by analyzing the correlation degree among factors in the correlation function, the model calculated the weight of each index, normalized the weight matrix and improved the weight measurement method to avoid the influence of subjective factors on the evaluation result.

(2) It is of great importance to select indices scientifically in evaluating efficiency of high-standard farmland development. The evaluation index system in this paper was built based on analysis of previous published studies, the particular situation of the project area and in consultation with project-acceptance experts. Ecological factors were not taken into account and only one indicator, public satisfaction, was included in the index of social efficiency. In this study, the authors did not compare the results with other results from different research methods, due to limitations on the overall length of the manuscript. In subsequent studies, the authors expect to improve the presented model to increase the accuracy of the research results.

Acknowledgements. These researches were financially supported by Quality Engineering (Teaching Research Project) of Anhui Agricultural University (Grant No. 2018aujyxm047) and National Natural Science Foundation of China (Grant No. 41504031).

REFERENCES

[1] Assessment Standard of Well-Facilitated Farmland Construction (2016): 2016-GB/T33130. – General Administration of Quality Supervision Inspection and Quarantine of the People's Republic of China, Beijing.
[2] Bian, Z. X., Yang, Z. J., Qian, F. K. (2016): Study on time sequence of high-standard prime farmland based on LESA. – Journal of Natural Resources 31(3): 436-446.
[3] Cai, J., Li, S. P. (2014): Social effects evaluation of high-standard primary farmland construction project based on entropy-weighted method and extension model. – China Land Sciences 28(10): 40-47.
[4] Cai, W., Yang, C. Y., Chen, W. W. (2008): Extension Set and Extension Data Mining. – The Science Publishing Company, Beijing.
[5] Criterion of High Standard Farmland (2012): 2012-NY/T 2148. – Ministry of Agriculture and Rural Affairs of the People's Republic of China, Beijing.
[6] Cultivated Land Quality Grade (2016): 2016-GB/T33469. – General Administration of Quality Supervision Inspection and Quarantine of the People's Republic of China, Beijing.

http://www.aloki.hu ● ISSN 1589 1623 (Print) ● ISSN 1785 0037 (Online)
DOI: http://dx.doi.org/10.15666/aeer/1705_1130311316

[7] Gao, M. X., Zhang, Q., Zhao, G. X. (2011): Evaluation methods and application of land consolidation. – Transactions of the Chinese Society of Agricultural Engineering 7(10): 300-307.
[8] Hwang, C. L., Yoon, K. (1981): Methods for Multiple Attribute Decision Making. – Springer, Berlin.
[9] Jun, K. S., Chung, E. S., Sung, J. Y., et al. (2011): Development of spatial water resources vulnerability index considering climate change impacts. – Science of the Total Environment 409(24): 5228-5242.
[10] Korkmaz, M. (2008): Analysis of economic efficiency at forest enterprises with TOPSIS method. – Optical Engineering 47(5): 525-534.
[11] Li, Z., Wang, J., Bai, Z. K. (2010): Method of comprehensive benefit evaluation of land consolidation based on evaluation model of matter element. – Bulletin of Soil and Water Conservation 30(6): 190-194.
[12] Liu, C., Frazier, P., Kumar, L., et al. (2006): Catchment-wide wetland assessment and prioritization using the multi-criteria decision making method TOPSIS. – Environmental Management 38(2): 316-326.
[13] Liu, L., Yu, L., Li, Z. (2012): Study on evaluation of integrated benefit of land consolidation based on ameliorated Fuzzy AHP. – Research of Soil and Water Conservation 19(3): 204-208.
[14] Regulation for Gradation on Agriculture Land Quality (2012): 2012-GB/T2845. – General Administration of Quality Supervision Inspection and Quarantine of the People's Republic of China, Beijing.
[15] Tan, X., Wang, X. R., Tang, H. Z. (2013): Evaluation index system and method on construction condition of county well-facilitated capital farmland: a case study of Mianzhu County. – Southwest China Journal of Agricultural Sciences 26(5): 1977-1983.
[16] Tsaur, R. C. (2011): Decision risk analysis for an interval TOPSIS method. – Applied Mathematics & Computation 218(8): 4295-4304.
[17] Wu, G. C., Liu, D. Z., Fu, G. H. (2008): Social benefit evaluation of land reconsolidation projects based on entropy-weighted extentic matter- element model. – China Land Science 22(5): 40-46.
[18] Xin, G. X., Yang, Q. Y., Yang, H. J. (2009): Impact assessment of land consolidation post-project. – Transactions of the Chinese Society of Agricultural Engineering 25(11): 312-317.
[19] Xin, G. X., Yang, C. X., Yang, Q. Y. (2017): Post-evaluation of well-facilitated capital farmland construction based on entropy weight method and improved TOPSIS model. – Transactions of the Chinese Society of Agricultural Engineering 33(1): 238-249.
[20] Xue, J., Han, J., Zhang, F. R. (2014): Development of evaluation model and determination of its construction sequence for well-facilitated capital farmland. – Transactions of the Chinese Society of Agricultural Engineering 30(5): 193-203.
[21] Yang, C. Y., Cai, W. (2008): Extension Engineering. – The Science Publishing Company, Beijing.
[22] Yang, J., Wang, Z. S., Jin, G. (2013): Post-benefit evaluation of land consolidation project implementation based on AHP and FUZZY comprehensive evaluation. – Resources and Environment in the Yangtze Basin 22(8): 1036-1042.
[23] Yang, J. Y., Xu, F., Liu, G. C. (2017a): Demarcation method of permanent prime cultivated land based on TOPSIS. – Transactions of the Chinese Society of Agricultural Machinery 48(8): 133-139.
[24] Yang, J. Y., Zhao, L., Xu, F. (2017b): Zoning of high standard prime farmland construction based on arable lands connectivity. – Transactions of the Chinese Society of Agricultural Machinery 48(4): 142-148.
[25] Yang, J. Y., Zhang, X., Xu, F. (2018): Designation method of permanent basic farmland based on TOPSIS and local spatial auto-correlation. – Transactions of the Chinese Society of Agricultural Machinery 49(4): 172-180.

http://www.aloki.hu ● ISSN 1589 1623 (Print) ● ISSN 1785 0037 (Online)
DOI: http://dx.doi.org/10.15666/aeer/1705_1130311316

[26] Zhao, D. L., He, S. S., Lin, S. W. (2017): Selection of high-standard farmland construction priority area based on TOPSIS and hotspot analysis. – Transactions of the Chinese Society of Agricultural Machinery 48(7): 153-158.
[27] Zhao, D. L., Lin, S. W., Yang, J. Y. (2018): Potential of cultivated land quality based on combination of grading factors and matter element analysis. – Transactions of the Chinese Society of Agricultural Machinery 49(4): 181-191.
[28] Zhao, J. R., Zhu, D. L. (2010): Emergy-based analysis of expost benefits of land exploitation and consolidation. – Transactions of the Chinese society of Agricultural Engineering 26(10): 337-344.
[29] Zhao, S. X., Niu, H. P., Zhang, H. B. (2018): Construction and application of obstacle diagnosis model based on ecological niche on well-facilitated farmland. – Transactions of the Chinese Society of Agricultural Machinery 49(1): 194-202.
[30] Zhao, Y. W., Su, N. (2010): Extension Design. – The Science Publishing Company, Beijing.

http://www.aloki.hu ● ISSN 1589 1623 (Print) ● ISSN 1785 0037 (Online)
DOI: http://dx.doi.org/10.15666/aeer/1705_1130311316

DETERMINING THE FACTORS AFFECTING REPRODUCTION OF AN ENDEMIC BLACK PINE VARIETY [*PINUS NIGRA* SUBSP. *PALLASIANA* VAR. *YALTIRIKIANA*] IN TURKEY

ORAL, D.

Istanbul University Cerrahpasa, Faculty of Forestry, Department of Forest Botany
34473 Sariyer, Istanbul, Turkey
e-mail: dilek@istanbul.edu.tr; phone: +90-212-338-2400/25322; fax: +90-212-226-1113
ORCID ID: 0000-0002-7627-5663

(Received 13th Apr 2019; accepted 16th Jul 2019)

Abstract. *Pinus nigra* subsp. *pallasiana* var. *yaltirikiana* has a very restricted spread, and is an endemic black pine variety in Turkey. This plant has a poor generative reproduction performance. It is unclear which factors are responsible for this low reproduction capacity. Therefore, objective of this study was to investigate pollen and seed characteristics of the plant. For this purpose, pollen samples were collected in the pollination period, and seed samples were collected in the cone ripening period in the natural distribution site of this plant in Black Sea Region. Pollen samples were examined whether or not they have normal shape and size. Seed samples were tested for germination percentage and seed size and soundness were also examined. Results showed that pollen samples seemed to have normal shape and size, and seeds have a germination percentage of 71. This study indicated that the conservation of *Pinus nigra* subsp. *pallasiana* var. *yaltirikiana* through in-situ and ex-situ strategies and the establishment of a seed orchard in a different area by taking grafts are important in terms of ensuring continuity of limited number individuals.
Keywords: *Pinus nigra* subsp. *pallasiana, yaltirikiana, germination, seed, pollen*

Introduction

Pinus nigra J.F.Arnold subsp. *pallasiana* (Lamb.) Holmboe, which spreads across Balkans, Southern Carpathians, Crimea, Cyprus and Syria, constitutes forests in mountainsides of Black Sea, Marmara, Aegean and Central Anatolia regions and Toros Mountains of Turkey, and rarely seen at sea level (Coode and Cullen, 1965; Akkemik et al., 2011; Kandemir and Mataracı, 2018). In accordance with the recent studies, it is accepted that there are three varieties including var. *fastigiata* Businský, var. *yaltirikiana* Alptekin and var. *pallasiana* (f. *pallasiana* and f. *seneriana* (Saatcioglu) Kandemir & Mataraci) in Turkey, and that its taxa except *pallasiana* f. *pallasiana* are endemic (Kandemir and Mataracı, 2018).

Pinus nigra J.F.Arnold subsp. *pallasiana* (Lamb.) Holmboe var. *yaltirikiana* Alptekin is distinguishable from other varieties by the fact that its cones are bigger (at least 8 cm) and leaves are longer (at least 14 cm) (Alptekin, 1987; Yaltırık, 1988; Kandemir and Mataracı, 2018; Oral and Mataraci, 2018). Alptekin (1987), who named the variety, indicated the cone sizes of *Pinus nigra* subsp. *pallasiana* var. *yaltirikiana* as 7.8 cm (max.11.19) × 3.71 cm (max.4.4).

In Oral and Mataraci (2018)'s article, in which they identified a new epitype (ISTO 37320) instead of a holotype composed of only a cone, the average female cone size was 9.16 (7.69-10.23) x 3.94 (3.55-4.31) cm, male cone size was 1.58 (1.28-2.16) x 0.54 (0.48-0.62) cm; leave size was 17.21 (13.80-20.20) x 0.18 (0.16-0.22) cm and sheath length was 0.95 (0.67-1.16) cm. In addition, it was especially emphasized that the cone and leaf length should be evaluated concomitantly for the diagnosis of taxon.

http://www.aloki.hu ● ISSN 1589 1623 (Print) ● ISSN 1785 0037 (Online)
DOI: http://dx.doi.org/10.15666/aeer/1705_1131711326

It was known that this variety was in 1985 in Karabuk-Yenice and Sinop-Boyabat (Alptekin, 1987). Oral and Mataracı (2018), during a field visit to these locations in 2017, stated that they survived owing to the fact that its individuals in Boyabat were taken under preservation. It is suggested by them that its danger catagory due to fewness of both individuals and seeds was "Critically endangered" (CR) (Ekim et al., 2000). During the field visit to Yenice, it never seen *Pinus nigra* subsp. *pallasiana* var. *yaltirikiana* even though all locations given in herbarium records were visited. There were black pines with shorter cones (5.66-8.50 cm) in these locations.

Yaman and Saribas (1999) compared pollen sizes of *Pinus nigra* subsp. *pallasiana* var. *yaltirikiana* in Karabuk-Yenice, which is its holotype location, with pollens of the other endemic black pines, which were taken from natural areas. As a result of the study, it was stated that it should be compared with the pollen samples in Sinop-Boyabat due to the fact that frequency distribution of *Pinus nigra* subsp. *pallasiana* var. *yaltirikiana*'s pollen sizes (length-L and width-l) was not normal.

In this study, it is aimed at determining vitality of the seeds of *Pinus nigra* subsp. *pallasiana* var. *yaltirikiana* in order to ensure the sustainability of the existence of its in Sinop-Boyabat. Therefore, it has been investigated number of sound seeds and germination percentage, and the morphological characteristics of its pollen to determine whether it has especially a morphological development inhibitive to fertilization.

Materials and methods

Pollen and seed samples were collected from the trees growing only in Sinop-Boyabat, Karageriş Mountain, (41°18′49,91″K, 34°34′41,15″D) at elevation of 1239 m (*Figs.1 and 2*).

Figure 1. *Individuals of Pinus nigra* subsp. *pallasiana* var. *yaltirikiana in Boyabat-Kapaklıpınar*

Only four trees were present in the site with ages of approximately between 80-100 years and height of 10-12 m. Dominant vegetation in the site includes some tree species such as *Pinus nigra* J.F.Arnold subsp. *pallasiana* (Lamb.) Holmboe var. *pallasiana, Pinus sylvestris* L. var. *hamata* Steven f. *hamata*, *Juniperus communis* L. subsp. *saxatilis* Pall. in the overstorey cover, some schrub species such as *Cistus laurifolius* L., *Rubus canescens* DC. var. *canescens*, *Rosa canina* L., *Crataegus monogyna* Jacq. subsp. *monogyna, Mespilus germanica* L. and some herbaceous plants such as *Veronica chamaedrys* L, *Dactylis glomerata* L., *Poa annua* L. in the understorey cover.

http://www.aloki.hu ● ISSN 1589 1623 (Print) ● ISSN 1785 0037 (Online)
DOI: http://dx.doi.org/10.15666/aeer/1705_1131711326

Mean annual precipitation is about 620 mm and most of it falls between September and June. The driest month is July, with 30 mm of rainfall. Most of the precipitation here falls in December, averaging 75 mm. Average annual temperature is around 12.9°C and changes between 4°C in January and 21.7°C in July (Climate-Data.org, 2019). The site has a deep soil (>80 cm) with sandy loam texture covered with mull type forest floor with 2 cm depth (GDF, 2011).

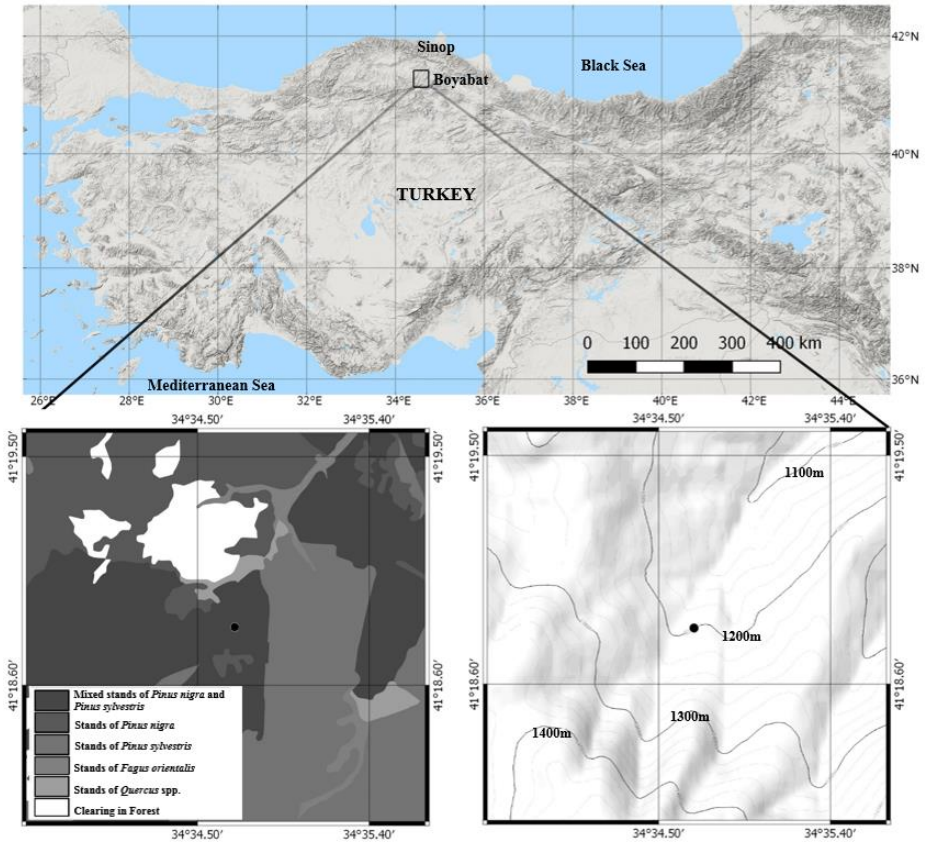

Figure 2. *The location of the sample collection area (●) and the different types of habitats in its surrounding*

Pollen samples were taken from each of four trees at the height of 3 m above soil surface in the pollination period in May 2018 and brought to Palynology Laboratory of Forest Botany Department at Istanbul University Cerrahpasa (I.U.C.) Faculty of Forestry. Then, pollen samples preparations were prepared separately for each individual tree according to the Wodehouse method (Wodehouse, 1959) and the measurements were carried out after waiting for 2 months for pollens in preparations to reach a normal form and sizes (Aytug, 1960). Then, they were examined. The measurements of pollen grains sizes in the preparations were done in the Leica DM750 light microscope (LM) as computer assisted, and 10x ocular, x40, x100 immersion objective were used. Under the light microscope, on equatorial axis of the pollen samples, length (β) and height (P) of saccus, distance from pollen to the outermost end of the saccus (p), height (h) of pollen body; on polar axis of theirs, length (L) and width (l) of pollen, length (B) and width (b) of saccus, distance from pollen to the outermost end of the saccus (be) were measured (*Fig. 3*) (Aytug, 1967).

http://www.aloki.hu ● ISSN 1589 1623 (Print) ● ISSN 1785 0037 (Online)
DOI: http://dx.doi.org/10.15666/aeer/1705_1131711326

At least 50 measurements were performed for each pollen feature in each of the 4 preparations, then the averages were taken. A part of these pollens was kept in the fridge in +4°C to examine with Scanning Electron Microscope (SEM). The size of the pollen, and ornamentation were studied by taking photos with both SEM and LM.

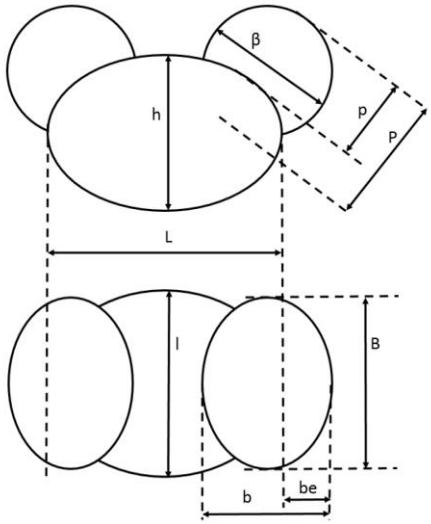

Figure 3. *Pine pollen sizes (upper: polar axis, β: length of saccus, P: height of saccus, p: distance from pollen to the outermost end of the saccus, h: height of pollen body; lower: equatorial axis, L: length of pollen, l: width of pollen, B: length of saccus, b: width of saccus, be: distance from pollen to the outermost end of the saccus)*

On December 20, 2018, cone samples were collected in order to determine the viability of the seeds in 2 years old cones of *Pinus nigra* subsp. *pallasiana* var. *yaltirikiana*. A total of 17 cones from four trees were collected from any side of canopy cover at the height of 3-6 m above soil surface. In order not to affect sustainability of its presence in the location, the number of cones was limited by also taking into account the fact that it already has a small number of individuals. The cones, which were brought to I.U.C. Faculty of Forestry, Department of Silviculture, Seed Technology and Silviculture Laboratory, were kept in drying-oven at a temperature of 46°C for 24 hours so that seeds could be taken out (Genc, 2004). Only seeds in 13 cones were counted as there were no seeds in 4 cones; seed length, width and thickness, and wing length and width were measured; and the seeds were weighed to determine their weights.

406 seeds were divided into four groups and placed on filter paper saturated with deionized water in 4 petri dishes at 20°C (±0.5°C) for germination test. The seeds were considered to be germinated when radicles showed geotropism. Seed germinations were monitored for 28 days. As the seeds germinated they removed from the petri dishes. Ungerminated seeds were checked with cutting test for soundness. Germinated seeds were planted into pots (Boydak and Çalışkan, 2014). Besides, it was ensured that they continued development in order to determine the number of cotyledon. The seeds germinated within first week of the study. Planted into pots in the nursery and monitored for seedling survival for 60 days.

In order to determine whether or not a change exists in chromosome number, mitotic chromosomes were prepared from root tips and pre-treated with α-bromo-naphthalene (ABN) at +4°C for 24 h. Roots were fixed for a minimum of 2 h in absolute ethanol:

http://www.aloki.hu ● ISSN 1589 1623 (Print) ● ISSN 1785 0037 (Online)
DOI: http://dx.doi.org/10.15666/aeer/1705_1131711326

glacial acetic acid, (3:1,v/v), hydrolysed at 60°C in 1 N HCl for 16 min and stained in Feulgen reagent. Finally, root tips were squashed in 1% aceto-orcein. Chromosomes were counted in the groups of in the preparation prepared from the crushed root tips (Altınordu et al., 2014).

Main statistical parameters were estimated and presented in the result section (Akalp, 2016).

Results and Discussion

The results of measurements made for pollen sizes are given in *Table 1* by comparison with the results of literature studies. According to the results of observations and measurements made in pollen preparations showed that pollens of *Pinus nigra* subsp. *pallasiana* var. *yaltirikiana* were not defective and that there was no obstacle for seed formation by fertilization.

Table 1. *Mean ($\bar{x}$ ±SD) measurements of pollen dimensions of Pinus nigra* subsp. *pallasiana varieties*

Measured parts (µm)		Present study	Results of previous (literature) studies			
		var. *yaltirikiana* (Boyabat-Sinop)	**var. *yaltirikiana* * (Yenice-Karabük)**	**var. *fastigiata* * (Kütahya)**	**var. *pallasiana* f. *şeneriana* * (Bolu)**	**var. *pallasiana* f. *pallasiana* ** (Muğla)**
Polar view	**L**	46.67±3.00***	46.78±6.79***	51.97±8.44***	55.13±3,68***	57.04±4.21***
	l	37.32±3.62	43.57±5.86	46.20±6.53	47.03±3.63	44.96±3.12
	B	35.18±2.09	38.37±3.60	39.45±5.19	41.17±2.23	39.80±3.01
	b	26.95±1.84	28.96±3.71	29.11±3.42	30.41±2.23	30.20±2.38
	be	10.23±1.61	10.73±2.68	10.97±2.45	11.28±2.27	10.28±2.28
Equatorial view	**h**	32.27±2.32	37.38±3.91	40.04±5.41	41.65±2.90	39.84±3.32
	β	29.46±1.68	32.74±2.32	32.39±5.21	33.56±2.83	31.48±3.21
	P	24.36±1.36	28.15±2.78	27.54±4.19	28.22±3.42	25.76±2.19
	p	16.31±1.26	14.21± 3.59	15.80±2.75	15.03±1.82	17.20±2.04
Ratios	**L/l**	1.25	1.07	1.12	1.17	1.27
	L/h	1.45	1.25	1.30	1.32	1.43
	B/b	1.31	1.32	1.36	1.35	1.32
	be/b	0.38	0.37	0.38	0.37	0.34
	β/P	1.21	1.16	1.18	1.19	1.22
	p/P	0.67	0.50	0.57	0.53	0.67

* Yaman and Sarıbaş (1999), ** Aytuğ (1967), ***SD (standard deviation)

Figure 4 shows polar and equatorial view of *Pinus nigra* subsp. *pallasiana* var. *yaltirikiana* pollens under LM and their exine surfaces under SEM. As in the other varieties (Yaman and Sarıbas, 1999), bisaccate pollens are inaperture; recesses and protrusions are apparent; pollen ornamentation is verrucate, and its structure is tectatae; saccus ornamentation is regular; it consists of small closed islets and canals (*Fig. 4*).

It is seen that sizes of pollens of all varieties of *Pinus nigra* subsp. *pallasiana* (*Table 1*) were similar; however, pollens of *Pinus nigra* subsp. *pallasiana* var. *yaltirikiana*, which were collected from both locations, were smaller than the pollens of other varieties. When *Pinus nigra* subsp. *pallasiana* var. *yaltirikiana* pollens of two locations (Boyabat and Yenice) were compared, it was found that the width (l), height (h) and saccus sizes (β, P, B, b, be) of pollens in Sinop were lower, while distance from pollen to the outermost end of the saccus (p) was higher. In contrast to pollens of

http://www.aloki.hu ● ISSN 1589 1623 (Print) ● ISSN 1785 0037 (Online)
DOI: http://dx.doi.org/10.15666/aeer/1705_1131711326

Yenice (Yaman and Sarıbas, 1999), the frequency distributions of pollen dimensions of samples collected from Boyabat were normal. When L/l and L/h ratios were compared, it can be said that pollens in Boyabat is slightly flattened in equatorial view.

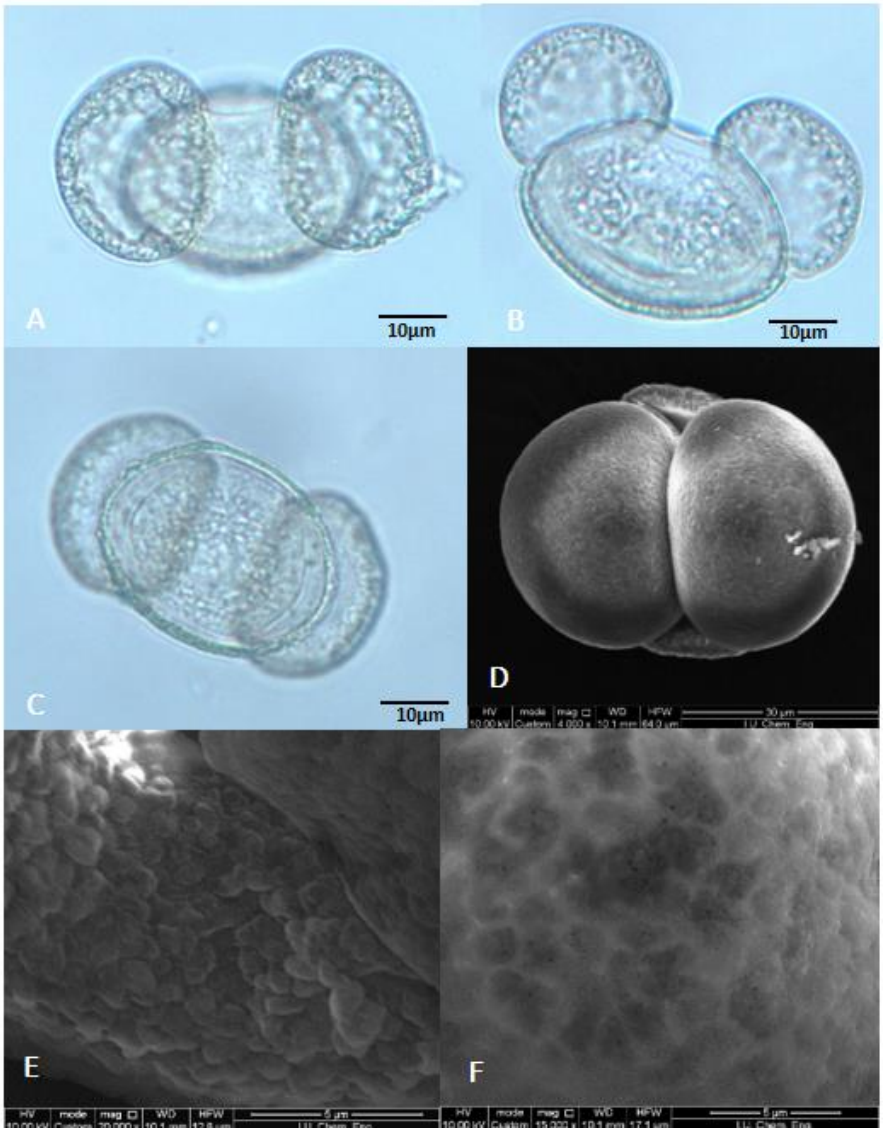

Figure 4. *Pollens of Pinus nigra* subsp. *pallasiana* var. *yaltirikiana. A-C (Light microscope-LM): A-Polar (Distal), B-Equatorial, C-Polar (Proximal) views; D-F (SEM): D-Dry pollen grain, E-Exine surface (proximal pole), F-Exine surface (saccus)*

It is shown that results of the measurements made on 406 seeds and 234 seed wings of *Pinus nigra* subsp. *pallasiana* var. *yaltirikiana* in *Table 2*. The number of seeds in the first three cones were very low. The sizes of the seeds were 7.10 x 3.83 x 2.40 mm; while the seed-wing sizes were 34.88 x 8.26 mm. In literature, the seed sizes of *Pinus nigra* subsp. *pallasiana* was given as 6.5 (4-9) x 3.71 (3-4) mm; the wing sizes of it as 24.73 x 7.7 mm (Alptekin, 1987; Kandemir and Mataracı, 2018). Accordingly, wing of *Pinus nigra* subsp. *pallasiana* var. *yaltirikiana* seed is longer.

http://www.aloki.hu ● ISSN 1589 1623 (Print) ● ISSN 1785 0037 (Online)
DOI: http://dx.doi.org/10.15666/aeer/1705_1131711326

Atay (1959) stated that average germination capability of black pine seeds was 91.3%, average germination energy was 62%, and 1000 seed weight was 22.5 g. As compared to results of previous studies about seeds of *Pinus nigra* subsp. *pallasiana* var. *yaltirikiana,* mean germination percentage was 71% on 28th day and the average germination energy was 47%, and 1000 seed weight was around 21.14 g (*Table 3*). Although the germination percentage is considered as the percentage of seeds germinated within the first 7 days, the values at days 4, 7 and 10 can also be used in some cases that require precision (Boydak and Çalışkan, 2014).

Table 2. *Some characteristics of the seeds of Pinus nigra* subsp. *pallasiana* var. *yaltirikiana*

	Number of sound seed in a cone	1000 seed weight (g)	Seed (n=406)			Seed wing (n=234)	
			Length (mm)	Width (mm)	Thickness (mm)	Seed (n=406)	Width (mm)
Mean	18	21.14	7.10	3.83	2.40	34.88	8.26
Range	0-35	11.4-35.1	4.15-8.69	2.59-4.79	0.96-3.42	25.79-41.07	5.29-10.42

Table 3. *Percentages of sound seed, germination, germination rates and number of cotyledon for each cone samples of Pinus nigra* subsp. *pallasiana* var. *yaltirikiana*

	All seeds	Sound seeds	Empty seeds	Germination seeds (for all seeds)	Germination rate (for sound seeds)					Cotyledon
					4	7	10	14	28	
Number	406	198	208	140	70	93	109	126	140	8.3 (6-10)
%	-	49	51	35	35	47	55	63	71	-

As seen from *Table 3*, almost half of the seeds were sound with a germination percentage of 71 (*Fig. 5*).

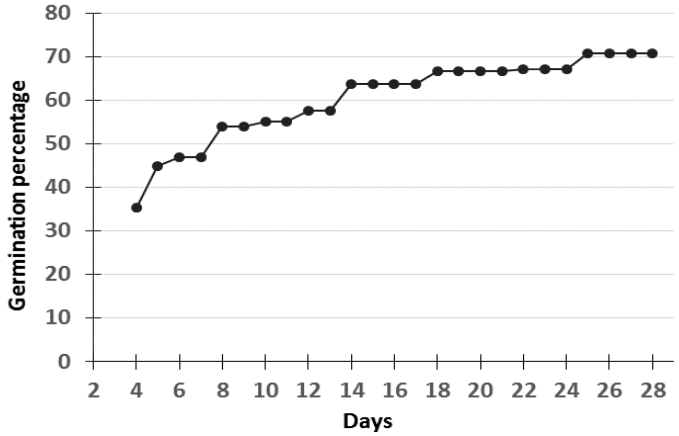

Figure 5. *Germination of Pinus nigra* subsp. *pallasiana* var. *yaltirikiana seeds under 20°C*

As compared to results of previous studies sound seed production and germination of *Pinus nigra* subsp. *pallasiana* var. *yaltirikiana* was lower when sound seeds were considered. Moreover, if all seeds including unsound ones were considered, germination percentage dropped to 35%, and 49.3% of the germination took place in the four-day period in germination chamber.

http://www.aloki.hu ● ISSN 1589 1623 (Print) ● ISSN 1785 0037 (Online)
DOI: http://dx.doi.org/10.15666/aeer/1705_1131711326

140 seeds were germinated under laboratory conditions, and germinated seeds were planted into pots. 93 out of 140 germinated seeds were planted into pots seven days after the germination and monitored for seedling survival. As seen from *Figure 6*, more than half of the seedlings (56%) died and 44% survived for 60 days.

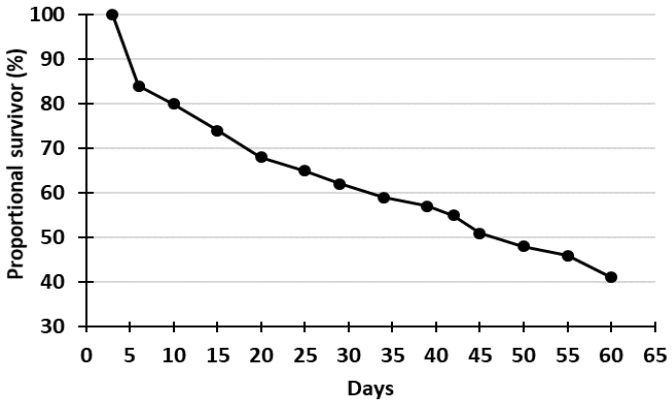

Figure 6. *Proportional survival of Pinus nigra* subsp. *pallasiana* var. *yaltirikiana seedlings*

The number of cotyledons was 8.3 (6-10). Likewise, Kaya and Temerit (1994) stated that the average number of cotyledons for 7 black pine populations they collected from Central Anatolia was 8.25.

In this study, the chromosome number of *Pinus nigra* subsp. *pallasiana* var. *yaltirikiana* was determined as 2n = 24, as known for black pines (Kaya et al., 1985; Salajova and Salaj, 1992; Hizume et al., 2002; Naydenov et al., 2003).

Ensuring the continuity of the limited number individuals of *Pinus nigra* subsp. *pallasiana* var. *yaltirikiana* in the natural distribution area is important in terms of genetic diversity and sustainability. These individuals should be taken under conservation by in-situ and ex-situ conservation strategies. As it is determined that seeds with the capacity to produce sound seeds and capability of germination can be obtained through current *Pinus nigra* subsp. *pallasiana* var. *yaltirikiana* individuals in the area, seedlings to be grown in the nursery by seeds with these characteristics can be planted around existing individuals to increase the number of theirs in this area.

In addition, seed orchard can be established in a different area by taking grafts from existing individuals, and sound seeds with the capability of germination can be obtained from these individuals. On the other hand, on the long run, observation must be performed in terms of purity of these seeds against the possibility of fertilizing female flowers of *Pinus nigra* subsp. *pallasiana* var. *yaltirikiana* individuals of the pollens of *Pinus nigra* subsp. *pallasiana* var. *pallasiana* individuals located in the same spread area.

Conclusions and Suggestions

Pinus nigra subsp. *pallasiana* var. *yaltirikiana* is an endemic variety in Turkey. The chromosome numbers of this taxon was found to be as 2n = 24. Its pollen dimensions were measured and the result showed that pollen seemed healthy with good shape. Therefore, we can conclude that there is nothing wrong with the pollens for reproduction of *Pinus nigra* subsp. *pallasiana* var. *yaltirikiana.* On the other hand, it

http://www.aloki.hu ● ISSN 1589 1623 (Print) ● ISSN 1785 0037 (Online)
DOI: http://dx.doi.org/10.15666/aeer/1705_1131711326

seemed that this plant taxon has poor cone, germinable seed production with poor seedling survival. Because 49% of the seeds were sound, and 71% of them germinated within 28th days. Additionally, only 44% of seedlings survived and more than half of the seedlings (56%) died within 60 days. These meant that seedling survival of this taxon under nursery conditions was poor. Sound seed production and their germination percentage were lower compared to the results of previous studies. These findings can be considered as an indicator of poor reproduction of *Pinus nigra* subsp. *pallasiana* var. *yaltirikiana.* As it has a limited distribution, it is possible that this taxon which is in danger of survival in the near future, can be removed successfully from the list of danger categories in the future with the protection of the habitat and protection efforts for population growth. Some additional studies are needed for better understanding for seedling survival and growth under field conditions in the second step. It is necessary to maintain the existing stand of this tree firstly to ensure the sustainability of the taxon; and then to increase the presence in the natural distribution area with the individuals to be grown from the seeds.

Acknowledgments. I would like to thank Assoc.Prof.Dr. Ilker Genc for his help in determination of chromosome number; Mr. Mustafa Diktas (Manager) and Mr. Fatih Sahin (Chief) from Sinop-Boyabat Forest Enterprice for their help in field studies.

REFERENCES

[1] Akalp, T. (2016): Statistical Methods. – Istanbul University Publication, IU number: 5219, Faculty of Forestry number: 511, Istanbul: 95-119. (in Turkish).
[2] Akkemik, U., Yılmaz, H., Oral, D., Kaya, A. (2011): Some Changes in Taxonomy of Pines (*Pinus* L.) Native to Turkey. – Forestist (JFFIU) 61(1): 63-78.
[3] Alptekin, U. (1987): Geographical Variations of Anatolian Black Pine (*Pinus nigra* Arn. subsp. *pallasiana* (Lamb.) Holmboe). – Forestist (JFFIU) Seri A 36(2): 132-154. (in Turkish).
[4] Altınordu, F., Martin, E., Hamzaoğlu, E., Çetin, Ö. (2014): New chromosome counts, karyotype analyses and asymmetry indices in some taxa of genus *Senecio* L. and related genera *Tephroseris* (Rchb.) Rchb. and *Turanecio* Hamzaoğlu belong to tribe Senecioneae (Asteraceae) from Turkey. – Plant Systematics and Evolution 300(10): 2205-2216. doi: 10.1007/s00606-014-1042-8.
[5] Atay, İ. (1959): Researches on Seed of Black Pine. – Forestist (JFFIU) A series 9(1): 48-96. (in Turkish).
[6] Aytug, B. (1960): Quelques Mensurations des pollens de *Pinus silvestris* L. – Pollen et Spores, Paris 2(2): 305-309.
[7] Aytug, B. (1967): Pollen Morphology and Palynological Investigations on Important Gymnospermae Taxa of Turkey. – Kutulmuş Press, Istanbul. (in Turkish and French).
[8] Boydak, M., Calıskan, S. (2014): "Germination rate". – In Afforestation. OGEM-VAK, 978-975-93943-8-7, Istanbul, p.118. (in Turkish).
[9] Climate-Data.org (2019): https://tr.climate-data.org/asya/tuerkiye/sinop/boyabat-19451/. – accessed on 1 February 2019.
[10] Coode, J. E., Cullen, J. (1965): *Pinus* L. – In: Davis, P. H. (ed.) Flora of Turkey and East Aegean Islands. Edinburgh Univ. Press, Edinburgh 1: 72-75.
[11] Ekim, T., Koyuncu, M., Vural, M., Duman, H., Aytaç, Z., Adıgüzel, N. (eds.) (2000): Turkey Plants Red Data Book (Pteridophyta ve Spermatophyta). – TTKD ve Van 100. Yıl University Publication, Ankara, p. 9. (in Turkish).

http://www.aloki.hu ● ISSN 1589 1623 (Print) ● ISSN 1785 0037 (Online)
DOI: http://dx.doi.org/10.15666/aeer/1705_1131711326

[12] GDF (General Directory of Forestry) (2011): Forest Management Plan for period of 2012-2020. – Kastamonu Regional Directory of Forestry, Boyabat Forest Enterprice, Turkey.
[13] Genc, M. (2004): Basic Principles of Silviculture. – Suleyman Demirel University, Forest Faculty, Publication number: 44, Isparta, p.233. (in Turkish).
[14] Hizume, M., Shibata, F., Matsusaki, Y., Garajova, Z. (2002): Chromosome identification and comparative karyotypic analyses of four *Pinus* species. – Theor Appl Genet 105: 491-497. doi: 10.1007/s00122-002-0975-4, accessed on 3 January 2019.
[15] Kandemir, A., Mataracı, T. (2018): *Pinus* L. – In: Güner, A., Kandemir, A., Menemen, Y., Yıldırım, H., Aslan, S., Ekşi, G., Güner, I., Çimen, A. Ö. (eds.) Illustrated Flora of Turkey. ANG Vakfı Nezahat Gökyiğit Botanik Bahçesi Yayınları. Istanbul, 2: 324-354. (in Turkish).
[16] Kaya, Z., Ching, K. K., Stafford, S. G. (1985): A Statistical Analysis of Karyotypes of European Black Pine (*Pinus nigra* Arnold) from Different Sources. – Silvae Genetica 34(4/5): 148-156.
[17] Kaya, Z., Temerit, A. (1994): Genetic Structure of Marginally Located *Pinus nigra* var. *pallasiana* Populations in Central Turkey. – Silvae Genetica 43(5/6): 272-277.
[18] Naydenov, K., Tremblay, F., Ganchev, P. (2003): Karyotypic Diversity in European Black Pine (*Pinus nigra* Arn.) from Bulgarian Provenances. – Phyton (Horn, Austria) 43(1): 9-28.
[19] Oral, D., Mataracı, T. (2018): A research on the presence of *Pinus nigra* J.F.Arnold subsp. *pallasiana* (Lamb.) Holmboe var. *yaltirikiana* Alptekin (Pinaceae) in Anatolia. – Bağbahçe Bilim Dergisi 5(3): 10-16. doi: 10.30796/ANGV.2018.9, accessed on 3 January 2019.
[20] Salajova, T., Salaj, J. (1992): Somatic embryogenesis in European black pine (*Pinus nigra* Arn). – Biologia Plantarum 34(3-4): 213-218.
[21] Wodehouse, R. P. (1959): Pollen Grains, Their Structure, Identification and Significance. – Science and Medicine, New York.
[22] Yaltırık, F. (1988): Dendrology Course Book I, Gymnospermae. – Istanbul Univ. Faculty of Forestry Publications 3443/386, İstanbul. (in Turkish).
[23] Yaman, B., Sarıbas, M. (1999): Pollen Morphology of Varieties of *Pinus nigra* subsp *pallasiana* Growing Naturally in Turkey. – Symposium Proceedings Book, 1st International Symposium on Protection of Natural Environment and Ehrami Karaçam, Kütahya, Turkey, 23-25th September 1999, 323-331.

http://www.aloki.hu ● ISSN 1589 1623 (Print) ● ISSN 1785 0037 (Online)
DOI: http://dx.doi.org/10.15666/aeer/1705_1131711326

CHANGES OF HEAVY METAL CONTENT IN SEDIMENTS AT HAIZHOU BAY AND RISK ASSESSMENT

ZHANG, Y. M.[1] – WANG, J.[2*] – MENG, K.[3] – QIU, Y. F.[2]

[1]*School of Environment, Nanjing Normal University, Nanjing 210023, China*

[2]*College of Marine Science and Engineering, Nanjing Normal University, Nanjing 210023, China*

[3]*Jiangsu Yunfan Testing Technology Co., Ltd., Nanjing 210023, China*

**Corresponding author*
e-mail: wangjing0108@njnu.edu.cn

(Received 15th Apr 2019; accepted 2nd Jul 2019)

Abstract. This research studied the six heavy metal contents, their distribution and the level of pollution in sediments at Haizhou Bay in 2009 and 2014. It was found that the content of cadmium (Cd), lead (Pb), zinc (Zn) and copper (Cu) accounted for the major factors in the sediments at Haizhou Bay. The content of major pollutants presented a declining trend from south to north, and the Pb-intensive area moved from the southern waters of the study area in 2009 to the northern waters of Ganyu Port in 2014. Analysis of the pollution load index shows that the study area suffers from medium-level pollution; the most polluted area was the waters around the estuary of Dragon-King River in 2009 and Ganyu Port in 2014, which meant that development of the port had significant impact on the heavy metal contents. Assessment based on the geo-accumulation index shows that Pb pollution deteriorated and Cd pollution abated slightly over the past 5 years. Analysis of comprehensive potential risk index indicates that the ecological risk of the study area from 2009 to 2014 was at the low-medium level, with Cd being the major contributor to the risks.
Keywords: *pollution assessment, spatial distribution, variation characteristics, potential ecological risk*

Introduction

A bay is a recessed area where the ocean stretches into a continent, and as an area that connects a continent with the sea, it provides a space where life and production thrive and where sediments and pollutants from rivers converge (Wang et al., 2008; Reddy et al., 2016). Heavy metal contents are toxic, durable, bio-accumulative, contributive to ecological risks and hard to decompose (Nguyen et al., 2016; Harikrishnan et al., 2017; Jahan and Strezov, 2018; Zhao et al., 2018). Due to these features, heavy metal pollution is a growing concern throughout the world, posing threats to marine ecology and human health (Rahman and Ishiga, 2012; Phillips et al., 2015; Keshavarzi et al., 2018; Wang et al., 2018). In these years, many bays across the world have suffered disproportional heavy metal pollution (Hyun et al., 2007; Qiao et al., 2013; Zhang et al., 2017; Pejman et al., 2017; Celishernandez et al., 2017; Naifar et al., 2018; Qu et al., 2018; Liang et al., 2018). Heavy metals, after finding their way into the water, adhere to and accumulate in suspended sediments before being released into the water again through complicated desorption mechanisms, so marine sediments are the "confluence" and "source" of heavy metal contents (Singh et al., 2005; Guan et al., 2016). Therefore, it is of great significance to record the heavy metal contents in sediments as an environmental indicator.

Located in the northern waters of Lianyungang in Jiangsu province of China, Haizhou Bay is the only bay-styled waters in Jiangsu and is renowned as one of the

http://www.aloki.hu ● ISSN 1589 1623 (Print) ● ISSN 1785 0037 (Online)
DOI: http://dx.doi.org/10.15666/aeer/1705_1132711339

eight largest fishing ports in China for its rich marine resources. As development of coastal regions in Jiangsu was upgraded into a national project in 2009, industrial activities along the coastline boomed and port development projects in the northern waters witnessed a rise. Previous studies on Haizhou Bay have probed into topics like the content, spatial distribution and pollution of heavy metal contents. Li and Xu (2014) researched the distribution and pollution of heavy metal contents in surface sediments; Zhang et al. (2013) researched on pollution of heavy metal contents in intertidal column sediments. At the year end of 2012, Ganyu Port in northern Haizhou Bay was put into operation, which inevitably led to ecological impacts on this area (Dobaradaran et al., 2018; Jahan and Strezov, 2018), but research in the influence of the port on Haizhou Bay is absent. In this study, the heavy metal pollution levels were assessed in surface sediments of Haizhou Bay in 2009 and 2014. The study objectives were to: (1) analyze the content and spatial distribution characteristics of six heavy metal contents in surface sediments in 2009 and 2014 and determine the main pollution factors of Haizhou Bay sediments; (2) Assess the content and distribution of heavy metal contents in sediments over the past five years and analyze the causes; (3) assess the extent of the contamination and ecological risks of the six heavy metal contents in sediments. This study analyzed the changes of sediments in the study area and the influence of human activities on sediments to provide data support and a scientific basis for ecological protection in Haizhou Bay.

Materials and methods

Introduction to the study area

Located in the northeast of Lianyungang city in Jiangsu province, China, Haizhou Bay is a half-open bay that adjoins East-West Tied-island of Lianyungang city on the north and reaches Mount Lan in Shandong province northwards. The seabed slopes to the east and presents a landform of "scouring in the north and silting in the south". Sediments in this area are diverse, with grits being the main sediment in the northern part, silt in the central part and clay in the southern part (Zhang and Feng, 2009; Liu et al., 2010), so the size of sediment particles increases from south to north. On the west of Haizhou Bay are estuaries of over ten rivers including Xiuzhen River and Dragon-King River which bring pollutants from the continent to the bay. Haizhou is a traditional fishing port which, as the port-based industries took off and the Ganyu Port area was put into operation in 2012, has risen to the focus in Jiangsu's initiative to extend the port and boost port-based economy.

Sampling and sample processing

On-site sampling was done in December 2009 and October 2014, and 10 samples of surface sediments were collected each time. The sampling sites are shown in *Figure 1*. The research targets are six types of heavy metal contents – Cd, As, Cu, Pb, Cr and Zn. Sampling and analysis performed in October 2014 were in accordance with technical standards specified in "The Specification for Marine Monitoring – Part 5: Sediment Analysis" (GB17378.5-2007). Using the grab sampler, we collected 3 to 4 sample surface sediments with a grain diameter within 5 cm and placed the samples into wide-mouthed reagent bottles and polyethylene bags for frozen storage. During analysis of the samples, we made use of atomic absorption spectrometry (AAS) to detect Cu, Pb,

http://www.aloki.hu ● ISSN 1589 1623 (Print) ● ISSN 1785 0037 (Online)
DOI: http://dx.doi.org/10.15666/aeer/1705_1132711339

Zn, Cr and Cd, and used atomic absorption spectrometry to detect As. All reagents used for analysis of heavy metal contents were guaranteed reagents and water used in experiments was ultrapure water. Meanwhile, parallel samples were used to realize quality control and the testing errors between parallel samples of these six heavy metal contents were all below 5%. The heavy metal content detection method performed is detailed in the reference by Li and Xu (2014).

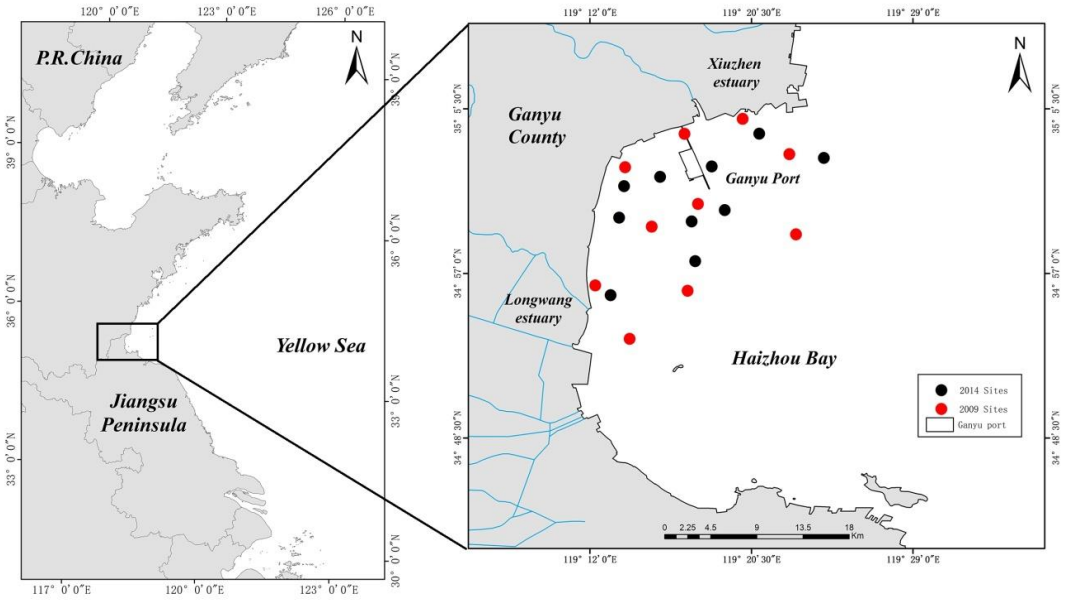

Figure 1. *Location of sample sites*

Methods

Pollution load index (PLI)

The pollution load index was first proposed by Tomlinson in 1980 to assess pollution by different chemical elements at different sites. The equations for calculation are:

$$PLI=\sqrt[n]{C_f^1 \times C_f^2 \times C_f^3 \times \ldots \times C_f^n} \quad \text{(Eq.1)}$$

$$C_f^i = C_n^i / C_0^i \quad \text{(Eq.2)}$$

where PLI refers to the pollution load index of a certain site, C_f^i the pollution index of one element, C_n^i the value obtained through actual measurement, and C_0^i the background value. The grading standard for PLI (Tomlinson et al., 1980; Zhu et al., 2013) is shown in *Table 1*.

Geo-accumulation index

Geo-accumulation Index (Igeo) was first proposed by G. Müller, a German scientist. It is a quantitative index for assessment of heavy metal contents in sediments and can be used to assess pollution caused by heavy metal contents. The calculation equation is:

http://www.aloki.hu ● ISSN 1589 1623 (Print) ● ISSN 1785 0037 (Online)
DOI: http://dx.doi.org/10.15666/aeer/1705_1132711339

$$I_{\text{geo}} = \log_2 \frac{C_n}{1.5B_n} \quad \text{(Eq.3)}$$

where Cn denotes the content of Element n in actual measurement, and Bn is the background value of this element on earth which, in this research, specifically refers to the background value of the content of the researched element in the tidal marsh of Jiangsu province measured in the 1980s by Chen et al. (1985). 1.5 is a coefficient identified by considering possible changes caused by differences of rocks in different places. The grading standard of geo-accumulation index (Müller, 1969) is also shown in *Table 1*.

Potential ecological risk index

The potential ecological risk index was first proposed by a Swedish environmentalist named Hakanson in 1980 to assess the potential ecological hazards of heavy metal contents in sediments. This method combines the ecological impact, environmental impact and toxicologic research of heavy metal contents to reflect the potential ecological risks of heavy metals. The calculation equations are:

$$C_f^i = C_{\text{n}}^i / C_0^i \quad \text{(Eq.4)}$$

$$E_r^i = T_r^t \times C_f^i \quad \text{(Eq.5)}$$

$$RI = \sum (E_{\text{r}}^i) \quad \text{(Eq.6)}$$

where *RI* is the value of comprehensive potential ecological risks, E_r^i the value of potential risks of one element. T_r^t denotes the toxicological coefficient of an element which, in this research, adopts the standard toxicological coefficients of heavy metal contents proposed by Hakanson (1980): the respective toxicological coefficients of Cd, As, Cu, Pb, Cr and Zn are 30, 10, 5, 5, 2, and 1. C^i_f is the pollution coefficient of a certain element, $C_n{}^i$ the value obtained through actual measurement and $C_0{}^i$ the background value. The grading standard for the potential ecological risk index of a given element and for the comprehensive potential ecological risk index is also presented in *Table 1*.

Results and discussion

Changes in the heavy metal contents

The heavy metal contents in surface sediments in the study area detected in 2009 and 2014 are shown in *Table 2*. The ranges of the heavy metal contents (mg/kg) at different sampling sites in 2009 were: 3.89-8.26 for As (averaged at 5.42), 10.9-29.5 for Cu (averaged at 17.85), 11.8-19.7 for Pb (averaged at 15.875), 37.4-98.8 for Zn (average at 61.96), 38.6-94.9 for Cr (averaged at 63.1) and 0.0964-0.247 for Cd (averaged at 0.144). The ranges of the heavy metal contents (mg/kg) at different sampling sites measured in 2014 were: 6.32-11.31 for As (averaged at 9.16), 11.89-30.69 for Cu (averaged at 20.97), 21.40-43.28 for Pb (averaged at 31.59), 15.6-118.70 for Zn

http://www.aloki.hu ● ISSN 1589 1623 (Print) ● ISSN 1785 0037 (Online)
DOI: http://dx.doi.org/10.15666/aeer/1705_1132711339

(averaged at 81.29), 24.74-77.01 for Cr (averaged at 47.38), 0.07-0.15 for Cd (averaged at 0.11). Compared with the data in 2009, the average content of Pb, As, Zn and Cu increased by 98.68%, 68.85% and 17.48% in 2014, while the average content of Cd and Cr declined by 23.83% and 24.90%, respectively. In comparison with the heavy metal contents in sediments obtained by studies in China and other countries (see *Table 2*), the content of Cu, Cd and Pb in sediments in Haizhou Bay exceeded that in other regions, and the content of Zn and Cr stayed at a medium level.

Table 1. *Grading standard for geo-accumulation index and potential ecological risk index of heavy metal contents*

I_{geo}	Pollution Level	*PLI*	Pollution level	E_r^i	Single-factor potential ecological risk	*RI*	Comprehensive potential ecological risk
≤ 0	No pollution	< 1	No pollution	< 40	Low	< 110	Low
0~1	Mild pollution	1~2	Medium pollution	40~80	Medium	110~220	Medium
1~2	Mild-medium pollution	2~3	Heavy pollution	80~160	Medium-high	220~440	High
2~3	Medium pollution	≥ 3	Severe pollution	160~320	High	≥ 440	Extremely high
3~4	Serious pollution			≥ 320	Extremely high		
4~5	Heavy pollution						
> 5	Severe pollution						

Table 2. *Comparison of heavy metal contents in the study area (mg/kg)*

Project (sampling time)		As	Cu	Pb	Zn	Cr	Cd	Source
Hanzhou Bay, China (2009.12)	Maximum	8.26	29.5	19.7	98.8	94.9	0.247	This study
	Minimum	3.89	10.9	11.8	37.4	38.6	0.0964	
	Mean	5.42	17.85	15.875	61.96	63.1	0.144	
Haizhou Bay, China (2014.10)	Maximum	11.31	30.69	43.28	118.70	77.01	0.15	
	Minimum	6.32	11.89	21.40	15.60	24.74	0.07	
	Mean	9.16	20.97	31.59	81.29	47.38	0.11	
Soil background value of tidal marsh in Jiangsu province		7.38	15.02	11.40	47.15	60.11	0.042	Chen et al. (1985)
Jiaozhou Bay, China		n.d.	38.8	55.2	107.4	69.9	0.42	Liang et al. (2018)
Laizhou Bay, China		4.84	6.89	14.01	n.d.	17.10	0.08	Zhang et al. (2017)
San Francisco Bay, USA		n.d.	38.6	21.8	153.2	21.1	0.2	Lu et al. (2005)
Persian Gulf, Iran		n.d.	32.1	48.3	62.5	89	0.8	Pejman et al. (2017)
Gabes Gulf, Tunisia		4.17	37	10.71	104.90	77.22	8.14	Naifar et al., 2018
Masan Bay, Korea		n.d.	43.4	44	206	67.1	1.24	Hyun et al. (2007)

n.d.: not detected

http://www.aloki.hu ● ISSN 1589 1623 (Print) ● ISSN 1785 0037 (Online)
DOI: http://dx.doi.org/10.15666/aeer/1705_1132711339

In 2009, the average content of five heavy metals – Cd, Pb, Zn, Cu and Cr, exceeded the background value of the heavy-metal content in the tidal marsh of Jiangsu province, the detected values of these five heavy metals being 3.42 times, 1.39 times, 1.31 times, 1.19 times and 1.05 times as much as the background values, so Cd, Pb, Zn and Cu are the main factors that exceeded the background value. In 2014, the average content of five heavy metals – Pb, Cd, Zn, Cu and As, exceeded the background value of heavy-metal content in the tidal marsh of Jiangsu province, with the detected values of these five metals being 2.77 times, 2.51 times, 1.72 times, 1.40 times and 1.24 times as much as the background values, so the main factors that exceeded the average value are Cd, Pb, Zn and Cu. The degree to which the content of Pb, Zn and Cu exceeded the background value increased, among which the most salient was that of Pb; though the degree to which the content of Cd exceeded the background value declined, its degree of enrichment remains salient.

Spatial distribution of major factors of high-level content

In light of results of research done in 2009 and 2014 (locations of research sites are shown in *Fig. 1*), we concluded the distribution of major factors of high-level content (Cd, Pb, Zn and Cu) in *Figure 2*.

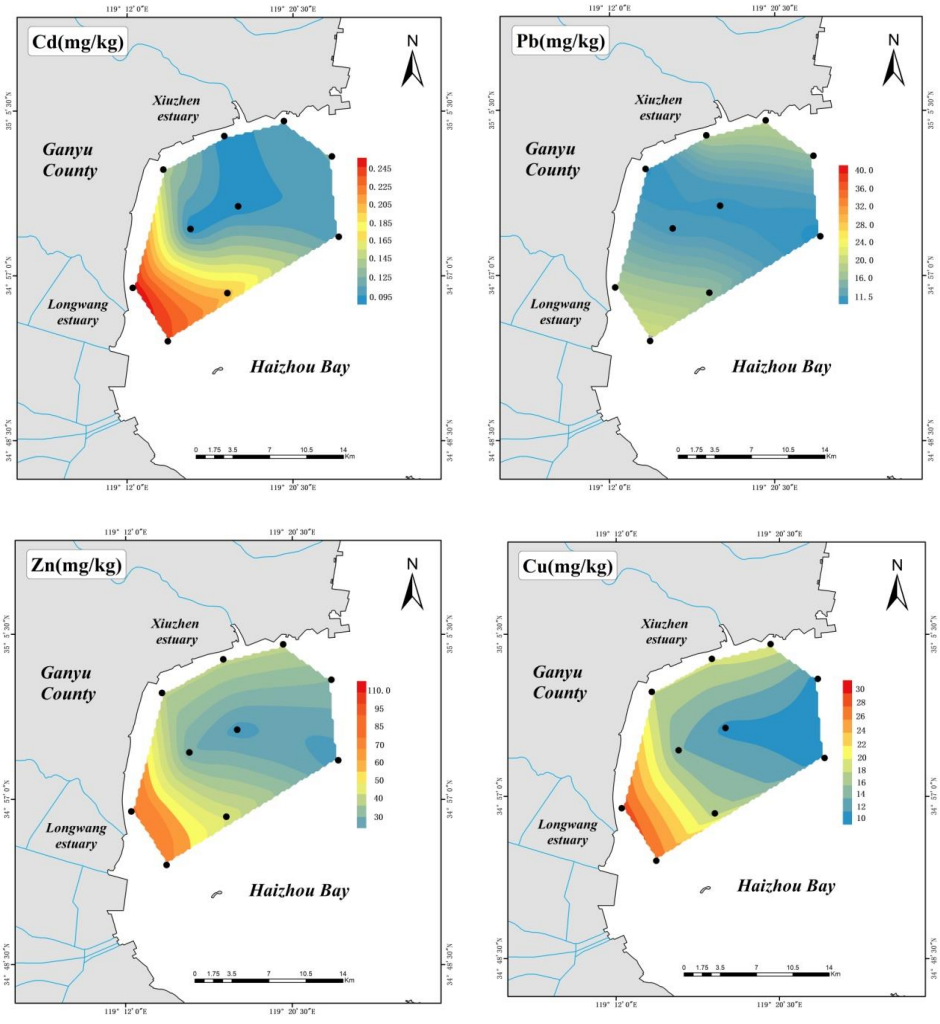

Figure 2. a *Spatial distribution of heavy metal contents in 2009*

http://www.aloki.hu ● ISSN 1589 1623 (Print) ● ISSN 1785 0037 (Online)
DOI: http://dx.doi.org/10.15666/aeer/1705_1132711339

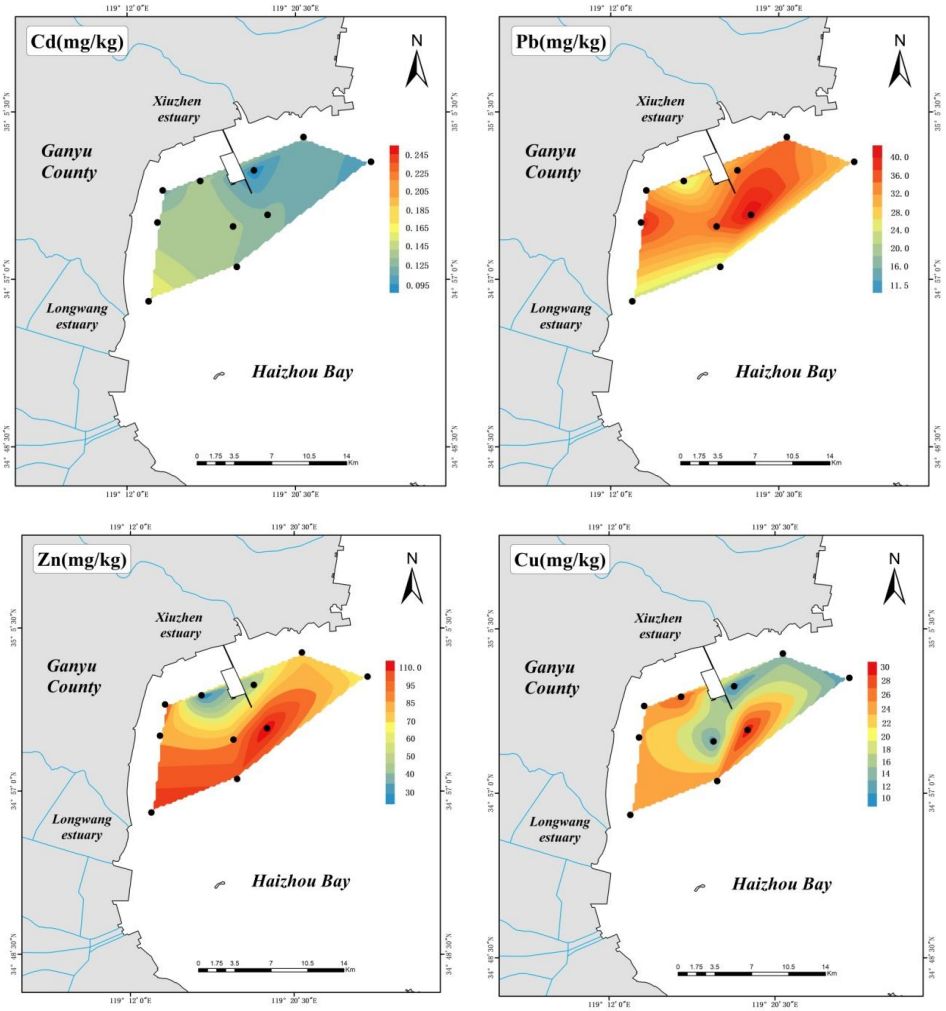

Figure 2. b *Spatial distribution of heavy metal contents in 2014*

In 2009, the content of these four heavy metal contents declined from south to north, and the distribution of Cd, Zn and Cu nearly followed the same pattern as in 2009. Like the heavy metal contents, the size of sediment particles also followed a declining trend from south to north. As proved by many previous studies, the heavy metal contents and the size of sediment particles are interrelated (Li et al., 2015): the larger the surface area of a sediment particle, the more heavy metals it absorbs, and the larger the grain size, the lower the level of enrichment of heavy metals. However, the Pb-intensive area moved from the southern waters in 2009 to the waters around Ganyu Port in 2014, which indicated that the increase of pollutants from ships due to development of Ganyu Port led to a rise of the heavy metal contents.

Characteristics of heavy-metal pollution

Table 3 shows the pollution load index (*Eqs. 1* and *2*) of heavy metal contents in surface sediments in the study area, and *Figure 3* demonstrates the distribution of the pollution load index in sampling sites. In 2009, the pollution load index at the sampling sites changes between 0.92 to 1.96, and the pollution level varies from no pollution to medium pollution. Among all the sampling sites, 80% are rated as medium pollution

http://www.aloki.hu ● ISSN 1589 1623 (Print) ● ISSN 1785 0037 (Online)
DOI: http://dx.doi.org/10.15666/aeer/1705_1132711339

and 20% rated as no pollution. In 2014, the pollution load index at the sampling sites changes between 1.12 and 2.12, and the degree of pollution varies from medium pollution to severe pollution; 10% of the sampling sites suffer from severe pollution and 90% from medium pollution. Thus, the pollution load index in 2014 is higher than that in 2009. From the map for distribution of pollution load index, the waters around the estuary of Dragon-King River had the highest pollution load index in 2009, while in 2014, both the estuary of Dragon-King River and the waters around Ganyu Port had a high pollution load index, making Ganyu Port another area of severe pollution. It indicates that development of the bay has led to tangible impacts on the sediments and hence deserves more attention.

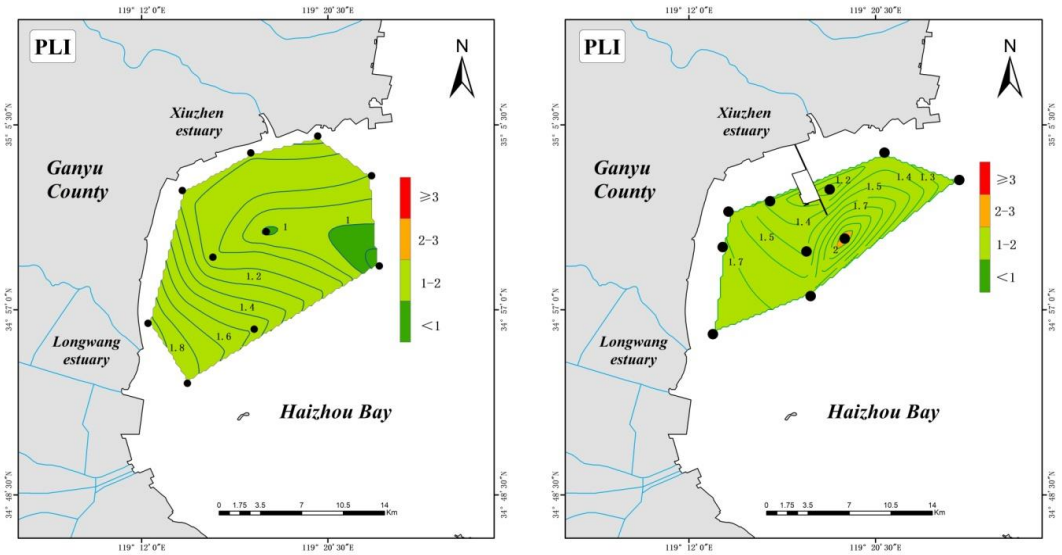

Figure 3. *The distribution of the pollution load index of heavy metals in surface sediments*

Table 3. *Pollution load index and pollution degree of heavy metals in surface sediments of the study area*

2009.12			2014.10		
Sampling site	***PLI***	**Pollution degree**	**Sampling site**	***PLI***	**Pollution degree**
1	1.85	Medium pollution	1	1.34	Medium pollution
2	1.96	Medium pollution	2	1.17	Medium pollution
3	1.59	Medium pollution	3	1.12	Medium pollution
4	1.11	Medium pollution	4	1.35	Medium pollution
5	1.24	Medium pollution	5	2.12	Severe pollution
6	0.99	No pollution	6	1.69	Medium pollution
7	0.92	No pollution	7	1.47	Medium pollution
8	1.21	Medium pollution	8	1.72	Medium pollution
9	1.28	Medium pollution	9	1.66	Medium pollution
10	1.10	Medium pollution	10	1.77	Medium pollution
Minimum	0.92		Minimum	1.12	
Maximum	1.96		Maximum	2.12	
Mean	1.34	Medium pollution	Mean	1.54	Medium pollution

http://www.aloki.hu ● ISSN 1589 1623 (Print) ● ISSN 1785 0037 (Online)
DOI: http://dx.doi.org/10.15666/aeer/1705_1132711339

Table 4 demonstrates assessment of the geo-accumulation index (*Eq. 3*). In 2009, the mean of the geo-accumulation index of the six heavy metals in surface sediments in Haizhou Bay is sequenced as Cd > Pb > Zn > Cu > Cr > As, among which Cd shows the highest level of enrichment and is rated as mild-medium pollution in terms of the level of pollution, As is rated as no pollution and the other four metals are rated as clean or mild pollution. In 2014, the mean of geo-accumulation index of the six heavy metal contents in surface sediments in Haizhou Bay is sequenced as Pb > Cd > Zn > Cu > As > Cr, among which Pb has the highest geo-accumulation index and is rated as severe pollution, followed by Cd, and the other four metals are rated as clean or no pollution in terms of the level of pollution. It can be concluded that from 2009 to 2014, the pollution of Pb witnessed a tangible increase while the pollution of Cd has been mitigated. In light of the spatial distribution of Pb in 2014, it can be seen that Pb accumulates in waters around Ganyu Port and its accumulation is closely linked to the number of ships. Relevant studies have proved that consumption of leaded gasoline would increase the content of Pb in the environment (Blake and Goulding, 2002; Wilcke et al., 1998; Lv et al., 2015). The Ganyu Port is teeming with ships and burning of leaded gasoline increases the risks of Pb pollution. Cd is a standard element in fertilizers (Lv et al., 2015). The mitigation of Cd pollution may be attributed to promotion of advanced agricultural technologies, strengthened control over fertilizers and other ecological protection measures.

Table 4. *Geo-accumulation index and potential ecological risk index of heavy metals in surface sediments of the study area*

Project (sampling time)			As	Cu	Pb	Zn	Cr	Cd
I_{geo}	2009.12	Range (mean)	-1.51~-0.42 (-1.07)	-1.05~0.39 (-0.42)	-0.54~0.2 (-0.13)	-0.92~0.48 (-0.26)	-1.22~0.07 (-0.57)	0.61~1.97 (1.10)
		Degree of pollution	Clean	Clean ~mild pollution	Clean ~mild pollution	Clean ~mild pollution	Clean ~mild pollution	Mild ~ mild-medium pollution
	2014.10	Range (mean)	-0.81~0.03 (-0.30)	-0.92~0.45 (-0.18)	0.32~1.34 (0.84)	-2.18~0.75 (0.03)	-1.88~-0.23 (-1.03)	0.21~1.22 (0.72)
		Degree of pollution	Clean-mild pollution	Clean-mild pollution	Mild ~ mild-medium pollution	Clean-mild pollution	Clean-mild pollution	Mild ~ mild-medium pollution
E_r^i	2009.12	Range (mean)	5.27~11.19 (7.35)	3.63~9.82 (5.94)	1.04~1.73 (1.39)	5.18~8.64 (6.97)	1.28~3.16 (2.10)	68.86~176.43 (102.59)
		Ecological risk	Low	Low	Low	Low	Low	Medium ~ high
	2014.10	Range (mean)	8.56~15.33 (12.41)	3.96~10.22 (6.98)	1.88~3.80 (2.77)	9.39~18.98 (13.86)	0.82~2.56 (1.58)	52.14~105.00 (75.43)
		Ecological risk	Low	Low	Low	Low	Low	Medium-relatively high
RI	2009.12	Range (mean)	90.33~208.14（126.35）					
		Ecological risk	Low ~ medium					
	2014.10	Range (mean)	83.92~141.14（113.02）					
		Ecological risk	Low ~ medium					

Assessment of potential ecological risk

According to *Table 1*, we achieved the potential ecological risk of each heavy metal (*Eqs. 4* and *5*) and the comprehensive ecological risk (*Eq. 6*) in 2009 and 2014, as shown in *Table 4*. *Figure 4* shows the distribution of the comprehensive ecological risk index. In 2009, the mean of potential ecological risk of As, Cu, Pb, Zn, Cr and Cd is 7.35, 5.94, 1.39, 6.97, 2.10 and 102.59; and when these metals are sequenced according

http://www.aloki.hu ● ISSN 1589 1623 (Print) ● ISSN 1785 0037 (Online)
DOI: http://dx.doi.org/10.15666/aeer/1705_1132711339

to the size of the mean, it is Cd > As > Zn > Cu > Cr > Pb, and the ecological risk of Cd is rated as medium ~ high. In 2014, the mean of potential ecological risks of As, Cu, Pb, Zn, Cr and Cd is 12.41, 6.98, 2.77, 13.86, 1.58 and 75.43, so the sequence changes into Cd > Zn > As > Cu > Pb > Cr, and the ecological risk of Cd is rated medium ~ relatively high. From 2009 to 2014, Cd remains the main contributor to potential ecological risks in the study area.

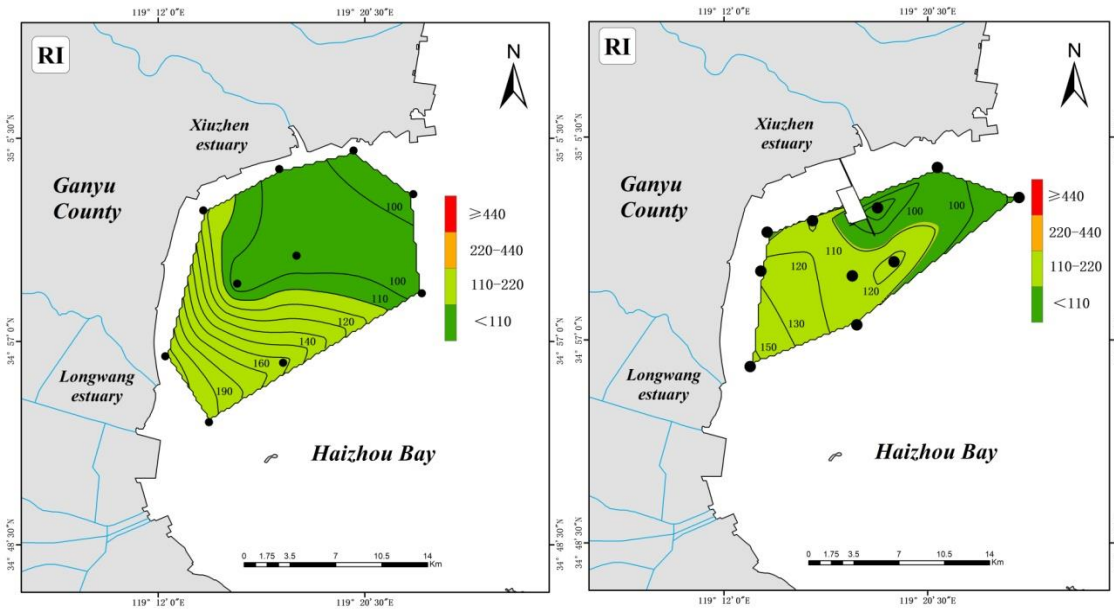

2009 **2014**

Figure 4. *The distribution of the comprehensive ecological risk index*

In 2009, the mean of RI (comprehensive potential ecological risk index) of the study area is 126.35, which falls between 90.33 and 208.14, rated low ~ medium in terms of the level of risks. In 2014, the mean of RI is 113.02, which falls between 89.92 and 141.14, rated low ~ medium in terms of the level of risks. According to the map of comprehensive potential ecological risk index distribution (*Fig. 4*), from 2009 to 2014, the comprehensive potential ecological risk index reaches the highest level in the waters around the estuary of Dragon-King River and declines northwards, which is consistent with the spatial distribution of the main pollutant – Cd. Therefore, the waters around the estuary of Dragon-King River remains a region most susceptible to ecological risks in the study area and hence deserves more attention.

Conclusion

As the result shows, in 2009, the average content of As, Cu, Pb, Zn, Cr and Cd is 5.42, 17.85, 15.875, 61.96, 63.1 and 0.144, respectively (unit: mg/kg), while in 2014, the number changes to 9.13, 21.45, 31.99, 84.80, 48.85 and 0.11 (unit: mg/kg). From 2009 to 2014, Cd, Pb and Zn account for the main factors that push the value of heavy-metal content in Haizhou Bay above the soil background value of tidal marshes in

http://www.aloki.hu ● ISSN 1589 1623 (Print) ● ISSN 1785 0037 (Online)
DOI: http://dx.doi.org/10.15666/aeer/1705_1132711339

Jiangsu province; the content of Pb, Zn and Cu rises, with Pb witnessing the largest increase; the content of Cd decreases slightly but its level of enrichment remains high.

The major pollution factors in 2009 (Cd, Pb, Zn and Cu) and those in 2014 (Cd, Zn and Cu) present a similar trend in spatial distribution, with their content declining from south to north, but the Pb-intensive area moved from the southern waters in 2009 to the waters around Ganyu Port in 2014.

Analysis of the geo-accumulation index shows that from 2009 to 2014, the pollution of Pb witnessed tangible increase while the pollution of Cd was mitigated. Analysis of the pollution load index shows that the study area suffers from medium-level pollution and the pollution increases from 2009 to 2014. In 2009, the estuary of Dragon-King River was the most polluted area, while in 2014, the waters around Ganyu Port accounted for another severely-polluted area, which reflects the obvious influence of port development on the heavy metal contents in sediments in the study area. The pollution of Cd is closely linked to the amount of pollutants brought by Dragon-King River from the continent.

Analysis of the single-factor potential ecological risk shows that the ecological risk of Cd is rated medium ~ high, while that of other heavy metals is rated low. Assessment of the comprehensive potential ecological risk shows that the ecological risk of the study area from 2009 to 2014 is rated low ~ medium, the waters around the estuary of Dragon-King River remains a region most susceptible to ecological risks and is hence worth more attention.

Cd, Pb, Zn and Cu are the main pollution factors in the sediments of the study sea area. Further attention should be paid to the changes trend of these four heavy metal contents and their influencing factors in the sediments of the study sea area in the future. Pollution from rivers and ports has affected the heavy metal contents of sediments in the study area. With the construction and development of Ganyu Port, its impact on heavy metals in sediments needs further investigation and study. In the future, we should strengthen the control of river and port discharge in the study area to reduce the impact on heavy metals in marine sediments.

REFERENCES

[1] Blake, L., Goulding, K. W. T. (2002): Effects of atmospheric deposition, soil pH and acidification on heavy metal contents in soils and vegetation of semi-natural ecosystems at Rothamsted Experimental Station, UK. – Plant and Soil 240(2): 235-251.

[2] Celishernandez, O., Rosaleshoz, L., Cundy, A. B., et al. (2017): Sedimentary heavy metal(loid) contamination in the Veracruz shelf, Gulf of Mexico: A baseline survey from a rapidly developing tropical coast. – Marine Pollution Bulletin 119(2): 204-213.

[3] Chen, B. B., Hu, R. Q., Chen, M. D. (1985): Natural background values of environmental elements in coastal soil in Jiangsu. – Journal of Nanjing Agricultural University 8(3): 54-60.

[4] Dobaradaran, S., Soleimani, F., Nabipour, I., et al. (2018): Heavy metal levels of ballast waters in commercial ships entering Bushehr port along the Persian Gulf. – Marine Pollution Bulletin 126: 74-76.

[5] Guan, Q., Wang, L., Pan, B., et al. (2016): Distribution features and controls of heavy metals in surface sediments from the riverbed of the Ningxia-Inner Mongolian reaches, Yellow River, China. – Chemosphere 144: 29-42.

[6] Hakanson, L. (1980): An ecological risk index for aquatic pollution control. A sedimentological approach. – Water Research 14(8): 975-1001.

http://www.aloki.hu ● ISSN 1589 1623 (Print) ● ISSN 1785 0037 (Online)
DOI: http://dx.doi.org/10.15666/aeer/1705_1132711339

[7] Harikrishnan, N., Ravisankar, R., Chandrasekaran, A., et al., (2017): Assessment of heavy metal contamination in marine sediments of East Coast of Tamil Nadu affected by different pollution sources. – Marine Pollution Bulletin 121: 418-424.
[8] Hyun, S., Lee, C., Lee, T., et al. (2007): Anthropogenic contributions to heavy metal distributions in the surface sediments of Masan Bay, Korea. – Marine Pollution Bulletin 54(7): 1059-1068.
[9] Jahan, S., Strezov, V. (2018): Comparison of pollution indices for the assessment of heavy metals in the sediments of seaports of NSW, Australia. – Marine Pollution Bulletin 128: 295-306.
[10] Keshavarzi, B., Hassanaghaei, M., Moore, F., et al. (2018): Heavy metal contamination and health risk assessment in three commercial fish species in the Persian Gulf. – Marine Pollution Bulletin 129(1): 245-252.
[11] Li, C., Song, C., Yin, Y., et al. (2015): Spatial distribution and risk assessment of heavy metals in sediments of Shuangtaizi estuary, China. – Marine Pollution Bulletin 98(1): 358-364.
[12] Li, F., Xu, M. (2014): Source Characteristics and Contamination Evaluation of Heavy Metals in the Surface Sediments of Haizhou Bay. – Environmental Science 35(3): 1035-1040.
[13] Liang, X., Song, J., Duan, L., et al. (2018): Source identification and risk assessment based on fractionation of heavy metals in surface sediments of Jiaozhou Bay, China. – Marine Pollution Bulletin 128: 548-556.
[14] Liu, F. C., Zhang, C. Y., Peng, J. (2010): Characteristics of spatial variability of sediment grain size in the Haizhou Bay. – Marine Sciences 34(7): 54-58.
[15] Lu, X. Q., Werner, I., Young, T. M., et al. (2005): Geochemistry and bioavailability of metals in sediments from northern San Francisco Bay. – Environment International 31(4): 593-602.
[16] Lv, J., Liu, Y., Zhang, Z., et al. (2015): Identifying the origins and spatial distributions of heavy metals in soils of Ju county (Eastern China) using multivariate and geostatistical approach. – Journal of Soils and Sediments 15(1): 163-178.
[17] Müller, G. (1969): Index of geoaccumulation in sediments of the Rhine River. – Geojournal 2(3): 108-118.
[18] Nguyen, T. T, H., Zhang, W., Li, Z., et al. (2016): Assessment of heavy metal pollution in Red River surface sediments, Vietnam. – Marine Pollution Bulletin 113(1-2): 513.
[19] Naifar, I., Pereira, F., Zmemla, R., et al. (2018): Spatial distribution and contamination assessment of heavy metals in marine sediments of the southern coast of Sfax, Gabes Gulf, Tunisia. – Marine Pollution Bulletin 131: 53-62.
[20] Pejman, A., Bidhendi, G. N., Ardestani, M., et al. (2017): Fractionation of heavy metals in sediments and assessment of their availability risk: A case study in the northwestern of Persian Gulf. – Marine Pollution Bulletin 114(2): 881-887.
[21] Phillips, D. P., Human, L. R., Adams, J. B., et al. (2015): Wetland plants as indicators of heavy metal contamination. – Marine Pollution Bulletin 92(1): 227-232.
[22] Qiao, Y., Yang, Y., Gu, J., et al. (2013): Distribution and geochemical speciation of heavy metals in sediments from coastal area suffered rapid urbanization, a case study of Shantou Bay, China. – Marine Pollution Bulletin 68(1): 140-146.
[23] Qu, B., Song, J., Yuan, H., et al. (2018): Intensive anthropogenic activities had affected Daya Bay in South China Sea since the 1980s: evidence from heavy metal contaminations. – Marine Pollution Bulletin 135: 318-331.
[24] Rahman, M. A., Ishiga, H. (2012): Trace metal concentrations in tidal flat coastal sediments, Yamaguchi Prefecture, southwest Japan. – Environmental Monitoring and Assessment 184(9): 5755-5771.
[25] Reddy, B. C., Jayaraju, N., Sreenivasulu, G., et al. (2016): Heavy metal pollution monitoring with foraminifera in the estuaries of Nellore coast, East coast of India. – Marine Pollution Bulletin 113(1): 542-551.

http://www.aloki.hu ● ISSN 1589 1623 (Print) ● ISSN 1785 0037 (Online)
DOI: http://dx.doi.org/10.15666/aeer/1705_1132711339

[26] Singh, K. P., Mohan, D., Singh, V. K., et al. (2005): Studies on distribution and fractionation of heavy metals in Gomti River sediments—a tributary of the Ganges, India. – Journal of Hydrology 312(1): 14-27.
[27] Tomlinson, D. L., Wilson, J. G., Harris, C. R., Jeffery, D. W. (1980): Problems in the assessment of heavy-metal levels in estuaries and the formation of a pollution index. – Helgoländer Meeresuntersuchungen 33: 566-575.
[28] Wang, M., Tong, Y., Chen, C., et al. (2018): Ecological risk assessment to marine organisms induced by heavy metals in China's coastal waters. – Marine Pollution Bulletin 126: 349-356.
[29] Wang, Y. S., Lou, Z. P., Sun, C. C., Sun, S. (2008): Ecological environment changes in Daya Bay, China, from1982 to 2004. – Marine Pollution Bulletin 56: 1871-1879.
[30] Wilcke, W., Muller, S., Kanchanakool, N., et al. (1998): Urban soil contamination in Bangkok: heavy metal and aluminium partitioning in topsoils. – Geoderma 86(3): 211-228.
[31] Zhang, C. Y., Feng, X. L. (2009): The spatial distribution and analysis about the grain-size of sediments in the Lianyungang nearshore sea area. – Acta Oceanologica Sinica 31(4): 120-127.
[32] Zhang, P., Hu, R., Zhu, L., et al. (2017): Distributions and contamination assessment of heavy metals in the surface sediments of western Laizhou Bay: implications for the sources and influencing factors. – Marine Pollution Bulletin 119(1): 429-438.
[33] Zhang, R., Zhou, L., Zhang, F., et al. (2013): Heavy metal pollution and assessment in the tidal flat sediments of Haizhou Bay, China. – Marine Pollution Bulletin 74(1): 403-412.
[34] Zhao, Y. F., Xu, M., Liu, Q., et al. (2018): Study of heavy metal pollution, ecological risk and source apportionment in the surface water and sediments of the Jiangsu coastal region, China: a case study of the Sheyang Estuary. – Marine Pollution Bulletin 137: 601-609.
[35] Zhu, Z. M., Li, Z. G., Bi, X. Y., Han, Z. X., Yu, G. H. (2013): Response of magnetic properties to heavy metal pollution in dust from three industrial cities in China. – Hazardous Materials 246-247: 189-198.

http://www.aloki.hu ● ISSN 1589 1623 (Print) ● ISSN 1785 0037 (Online)
DOI: http://dx.doi.org/10.15666/aeer/1705_1132711339

FISH SPECIES COMPOSITION, DISTRIBUTION AND CONSERVATION IN THE WUYI MOUNTAINS, CHINA

SHI, Z. M.[1] – HU, X. M.[1] – LIN, M. R.[1] – TANG, X. L.[1] – YANG, J. H.[1] – HU, M. L.[1,2,3*]

[1]*School of Life Sciences, Nanchang University, Nanchang, Jiangxi, P. R. China*

[2]*Ministry of Education Key Laboratory of Poyang Lake Environment and Resource Utilization, Nanchang University, Nanchang, Jiangxi, P. R. China*

[3]*Jiangxi Key Laboratory of Aquatic Animal Resource and Utilization, Nanchang University, Nanchang, Jiangxi, P. R. China*

**Corresponding author*
e-mail: humaolin@ncu.edu.cn; phone: +86-791-8525-6500

(Received 15th Apr 2019; accepted 4th Jul 2019)

Abstract. According to the fish checklist of 16 nature reserves in the Wuyi Mountains of China, a total of 126 freshwater fish species belonging to 5 orders and 17 families were present. Cypriniformes (consisting of 101 species and accounting for 69.8% of the total) was the major components of the fish fauna. And species of family Cyprinidae comprised 51.6% of the total and classified into 10 subfamilies. Overall, 72 species (57.1% of the total) were endemic to China. The comparison of species richness, endemic species richness and values of F-index, G-index and G-F index between the west and east slopes of Wuyi Mountains showed that there was a higher fish species diversity in the east slope. And among the three districts (i.e. the north, middle and south sections of Wuyi Mountains), fish species diversity was highest at the north section, good at the middle section and lowest at the south section. We divided 16 nature reserves into two regions according to geographical location and four regions according to river type through cluster analysis. Current threats to conservation of fish species diversity in the Wuyi Mountains were reviewed and management solutions were suggested.
Keywords: *freshwater fish, species diversity, nature reserve, Jiangxi Province, Fujian Province*

Introduction

The Wuyi Mountains is located in the southeast of China, and on the borderline between Jiangxi and Fujian province (*Fig. 1a*). It runs from the northeast to southwest with a length of about 540 km, and the highest peak is up to 2158 m. Therefore, the mountain range had been given "roof of the East China" (Guan, 2016). Streams in the mountain range flow into the Yangtze, Oujiang, Minjiang and Hanjiang rivers which drain into the East and South China seas (*Fig. 1b*). And the mountain range presents a subtropical humid monsoon climate with four distinct seasons. The annual average precipitation of Wuyi mountain is 1600 mm and 2000 mm, and the mean annual temperature range is from 17 to 20 °C, and annual average relative humidity was up to 78% (Guan, 2016).

In addition, the mountain range is a key area for the conservation of biodiversity in Chinese ecosystems. And it preserves the most typical, intact and largest zonal evergreen broad-leaved forest and subtropical forest ecosystems at the same latitudinal band of the world, so the mountain range had been called the "natural botanical garden", "insect world", "avian paradise" and so on (Liu et al., 2012). Fujian Wuyishan Nature Reserve (NR), the first national nature reserve, was created in 1979. By 2015, 45 nature reserves of different grades and types were established including 15 national

http://www.aloki.hu ● ISSN 1589 1623 (Print) ● ISSN 1785 0037 (Online)
DOI: http://dx.doi.org/10.15666/aeer/1705_1134111357

NRs, 14 provincial NRs, one city-level NR and 15 county-level NRs. Except for one paleontological relic reserve and seven wildlife reserves, the others are forest ecological reserves (Ministry of Ecology and Environment of the PRC, 2016). Among the 45 NRs, Tongboshan NR, Jiangxi Wuyishan NR, Yangjifeng NR, Matoushan NR, Ganjiangyuan NR, Jinpenshan NR, Lingyunshan NR, Laohunao NR, Fengyangshan NR, Fujian Wuyishan NR, Emeifeng NR, Minjiangyuan NR, Longxishan NR, Junzifeng NR, Tianbaoyan NR, and Guilongshan NR were investigated on fish species diversity. The Wuyi Mountains can be divided into two areas (east slope and west slope), the boundary between east slope and west slope is the ridge of Wuyi Mountains, not only important in physical geography, but also divided Jiangxi Province and Fujian Province. From north to south, the altitude of Wuyi Mountain ranges is getting lower, and can be divided into three regions (north section, middle section and south section) through the geographical division and the description of the location in the investigation report of the nature reserve (Zhong, 2004; Chen et al., 2009).

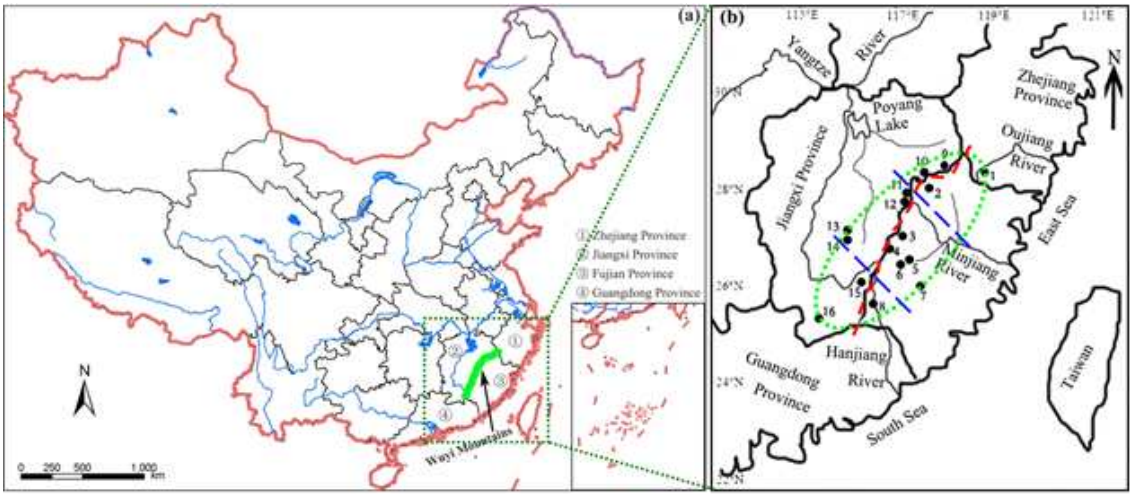

No.	Code	Nature Reserve (NR)	No.	Code	Nature Reserve (NR)	No.	Code	Nature Reserve (NR)	No.	Code	Nature Reserve (NR)
1	FNR	Fengyangshan NR	5	LoNR	Longxishan NR	9	ToNR	Tongboshan NR	13	LaNR	Laohunao NR
2	FWNR	Fujian Wuyishan NR	6	JuNR	Junzifeng NR	10	JWNR	Jiangxi Wuyishan NR	14	LiNR	Lingyunshan NR
3	ENR	Emeifeng NR	7	TiNR	Tianbaoyan NR	11	YNR	Yangjifeng NR	15	GaNR	Ganjiangyuan NR
4	MiNR	Minjiangyuan NR	8	GuNR	Guilongshan NR	12	MaNR	Matoushan NR	16	JiNR	Jinpenshan NR

Figure 1. *Maps showing the locations of Wuyi Mountains (a) and 16 nature reserves (b). In the map b, the Wuyi Mountains (the yellow elliptical region) is divided into two areas (west slope and east slope) by a dotted red line and three districts (north section, middle section and south section) by two blue broken lines*

The 16 NRs are evenly located in the east and west slopes of the Wuyi Mountains, and lie on the north, middle and south sections of the mountain range (*Fig. 1b*). And the basic information of the 16 NRs was given in (*Table 1*).

Almost all of the rivers in those NRs were characterized by shallow water depths, surrounding by mountains, narrow channel widths and relatively fast currents flowing over boulder substrate. The main rivers in NRs are: Shiwudugang River in ToNR; Yanshanhe River in JWNR; Luxihe River, Luotanghe River and Guiganghe River in YNR; Matoushanhe River, Douhuanhe River in MaNR; Guganghe River in LaNR; Linchihe River in LiNR; Shiliaohe River, Pantianhe River in GaNR; Daqiaohe River in JiNR; Haohe River in FNR; Futunxi River, Chongyangxi River in FWNR; Shanxi

http://www.aloki.hu ● ISSN 1589 1623 (Print) ● ISSN 1785 0037 (Online)
DOI: http://dx.doi.org/10.15666/aeer/1705_1134111357

River, Puxi River and Yongxingqu River in ENR; Chuxi River, Suixi River in MiNR; Yujiaxi River, Lishanxi River and Weixi River in LoNR; Xiafangxi River, Xiayangxi River, Chenglanxi River and Zhushexi River in JuNR; Sukengxi River, Guixi River and Shushaxi River in TiNR; Tongfanghe River, Jinxihe River and Chenlianhe River in GuNR.

Table 1. *Basic information of 16 nature reserves in the Wuyi Mountains, China. The nature reserve codes are the same as those in Figure 1*

Nature reserve	Geographical coordinate	Area (km^2)	Protection object	Protection type	Protection level	Stream basin
ToNR	118°12′-118°21′E 28°03′-28°15′N	108	Mid-subtropical broadleaved evergreen forests	Forest ecological	National	Yangtze River
JWNR	117°39′-117°55′E 27°48′-28°00′N	160.07	Mid-subtropical broadleaved evergreen forests, rare animals and plants	Forest ecological	National	
YNR	117°11′-117°28′E 27°51′-28°02′N	109.46	Amphibian, subtropical broadleaved evergreen forests	Wildlife	National	
MaNR	117°10′-117°18′E 27°43′-27°52′N	138.67	Subtropical broadleaved evergreen forests, rare plants	Forest ecological	National	
LaNR	115°51′-116°03′E 26°58′-27°17′N	220	South China tiger and habitats	Wildlife	Provincial	
LiNR	115°50′-116°01′E 26°50′-27°02′N	113.43	Subtropical broadleaved evergreen forests	Forest ecological	Provincial	
GaNR	116°03′-116°20′E 25°52′-26°06′N	161.01	Mid-subtropical broadleaved evergreen forests	Forest ecological	National	
JiNR	115°10′-115°15′E 25°11′-25°15′N	37.12	Subtropical broadleaved evergreen forests	Forest ecological	County	
FNR	119°03′-119°15′E 27°40′-27°58′N	260.52	forest ecosystems, rare animals and plants	Forest ecological	National	Oujiang River
FWNR	117°27′-117°51′E 27°33′-27°54′N	565.27	Mid-subtropical forest ecosystems	Forest ecological	National	Minjiang River
ENR	117°01′-117°10′E 26°52′-27°06′N	103	Rare birds, Isoetes orientalis and habitats, broadleaved deciduous forests of Fagus lucida	Wildlife	Provincial	
MiNR	116°46′-116°59′E 26°35′-26°49′N	130.22	Native populations of Bretschneidera sinensis and Taxus chinensis var mairei, unique biological community, forest vegetation of the Mingjiang river source	Wildlife	National	
LoNR	117°13′-117°21′E 26°28′-26°37′N	156.93	Mid-subtropical forest ecosystems, rare animals and plants	Forest ecological	National	
JuNR	116°47′-117°31′E 26°19′-26°39′N	180.61	Mid-subtropical broadleaved evergreen forests, Taxus chinensis var mairei	Forest ecological	National	
TiNR	117°28′-117°35′E 25°50′-26°01′N	110.15	Mid-subtropical broadleaved evergreen forests, wild orchidaceae, Tsuga longibracteata forest, Rhododendron simiarum forest, Sphagnum bog	Forest ecological	National	
GuNR	116°02′-116°40′E 25°02′-26°02′N	57.68	Mid-subtropical forest ecosystems	Forest ecological	Provincial	Hanjiang River

http://www.aloki.hu ● ISSN 1589 1623 (Print) ● ISSN 1785 0037 (Online)
DOI: http://dx.doi.org/10.15666/aeer/1705_1134111357

At present, many researchers have investigated biodiversity and distribution of the bryophytes, ferns, vascular plants, freshwater crabs and reptiles in the Wuyi Mountains (Guan, 2006; Li et al., 2006; Ye et al., 2007; Zhu, 2010; Cheng et al., 2011; Shi et al., 2012). Although many scholars have studied the biodiversity and composition of fish and published many related articles, the diversity of fish species in mountainous areas has not been comprehensively studied. In order to systematically understand the species diversity of fish in Wuyi Mountain, it is very important to comprehensively analyze the spatial distribution and composition of fish in Wuyi Mountain. The objectives of this study are to: (1) to describe the species composition and diversity of fish in 16 nature reserves; (2) analyse the biodiversity and relationship of fish in 16 nature reserves.

Materials and methods

Many papers have studied on the fish in 16 nature reserves, which is A good compilation opportunity to make a fish species list to research the Wuyi mountain's biodiversity. (Anonymity, 1981, 1997; Lin, 2002, 2004; Lin et al., 2005; Liu and Fu, 2006; Guo et al., 2011; Hu et al., 2011, 2015, 2018; Liu et al., 2012; Zeng et al., 2013; Li et al., 2015; Miao et al., 2016; Zhu et al., 2017). By re-analyze and summarize the research results of fish species diversity in nature reserves, biodiversity information can be obtained.

Nowadays, the G-F index is an important method for studying fish diversity, which is usually used to analyze species diversity of birds and mammals (Jiang and Ji, 1999; Yu et al., 2005; Li and Wu, 2006; Cai et al., 2009; Huang and Liu, 2011). Computing the diversity indexes at the genus level (G-index) and the family level (F-index); then to calculate the ratio of G-index and F-index as G-F index, the values can be either positive or negative.

(1) F-index:

$$D_F = -\sum_{k=1}^{m} D_{Fk} = -\sum_{k=1}^{m}\sum_{i=1}^{n} p_i lnpi \quad \text{(Eq.1)}$$

where n = the number of genera in family k, pi = Ski/Sk, Ski = the number of species in genus i, Sk = the number of species in family k, m = the total number of families in the class.

(2) G-index:

$$D_G = -\sum_{j=1}^{p} q_j lnq_j \quad \text{(Eq.2)}$$

where qj = Sj/S, Sj = the number of species in genus j, S = the total number of species in the class, p = the total number of genus in the class.

(3) G-F index:

$$D_{G\text{-}F} = 1 - D_G / D_F \quad \text{(Eq.3)}$$

http://www.aloki.hu ● ISSN 1589 1623 (Print) ● ISSN 1785 0037 (Online)
DOI: http://dx.doi.org/10.15666/aeer/1705_1134111357

Cluster analysis is often used to study the distribution of fish species and other community ecological problems. (Yin et al., 2016). A dataset containing all species from each site has been established to enable similarity measurements based on the presence (1) or absence (0) of each species from each site. (Huang et al., 2013). Pairwise similarities among all sites were computed in order to create a similarity coefficient matrix. The hierarchical cluster, furthest-neighbour method with pearson correlation was used for cluster analysis based on the matrix. All analyses were performed using SPSS 13.0 software.

Results

Composition of fish species

126 freshwater fish species (see Appendix 1) in the 16 NRs were recorded, belonging to five orders and 17 families. Cypriniformes (comprised of four families and 88 species, 69.8% of total species) was the dominant order followed by Siluriformes (five families and 21 species, 16.7%) and Perciformes (five families and 13 species, 10.3%), while Anguilliformes and Synbranchiformes were represented by two species respectively (*Table 2*). Species of family Cyprinidae comprised 51.6% of the total species richness and classified into 10 subfamilies (i.e. Danioninae, Leuciscinae, Cultrinae, Xenocyprinae, Hypophthalmichthyinae, Acheilognathinae, Gobioninae, Gobiobotinae, Cyprininae and Barbinae).

Table 2. *Fish diversity indices in different districts of the Wuyi Mountains, China*

District	G-index	F-index	G-F index	Species richness
West slope	1.6628	2.3287	0.2860	77
East slope	1.8365	2.9620	0.3800	100
North section	1.6261	2.9232	0.4437	91
Middle section	1.7948	3.0614	0.4137	101
South section	1.3090	1.5061	0.1309	30

Overall, 72 species (57.1% of the total species) are endemic to China, belonging to 11 families. Cyprinidae is the dominant family of endemic species (33 species) and the subdominant family was Balitoridae (16 species), and Bagridae (11 species), while Cobitidae, Amblycipitidae, Percichthyidae, Gobiidae, Sisoridae, Siluridae, Ondontobutidae and Osphronemidae were represented by only one or two species respectively (see *Appendix*).

Spatial variation of fish species diversity

Among the 16 NRs, eight reserves (including ToNR, JWNR, YNR, MaNR, LaNR, LiNR, GaNR and JiNR) are located in the west slope of the Wuyi Mountains, while other reserves (FNR, FWNR, ENR, MiNR, LoNR, JuNR, TiNR and GuNR) lie on the east slope of the mountain range. In addition, four reserves (ToNR, JWNR, FNR and FWNR) are located in the north section of the Wuyi Mountains, nine reserves (YNR, MaNR, LaNR, LiNR, ENR, MiNR, LoNR, JuNR and TiNR) in the middle section of

http://www.aloki.hu ● ISSN 1589 1623 (Print) ● ISSN 1785 0037 (Online)
DOI: http://dx.doi.org/10.15666/aeer/1705_1134111357

the mountain range, and three reserves (GaNR, JiNR and GuNR) in the south section of the mountain range (*Fig. 1b*).

A greater number of species (average: 42 vs. 21) and endemic species (19 vs. 11) were recorded from the east slope of the Wuyi Mountains compared to the west slope of the mountain range (*Fig. 2*). And the number of species and endemic species from the north section of the Wuyi Mountains was the largest (average: 36 and 20), followed by the middle section of the mountain range (35 and 15), while the average species number and endemic species number in the south section of the mountain range were only 15 and 8, respectively (*Fig. 3*).

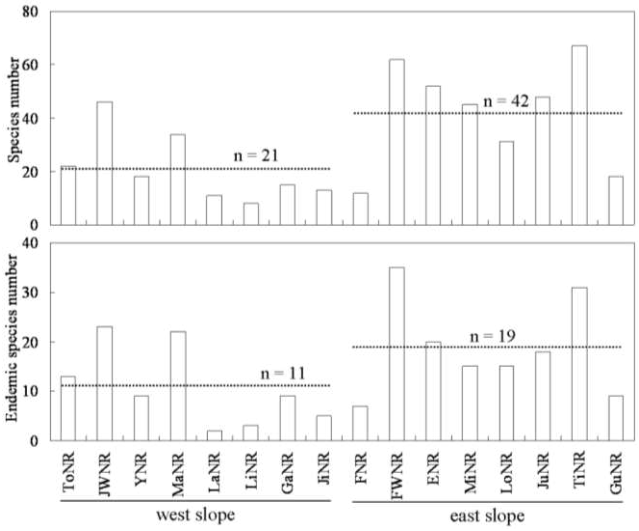

Figure 2. *Species and endemic species richness in the west and east slopes of Wuyi Mountains, China (n = average number of fish species). The nature reserve codes are the same as those in Figure 1*

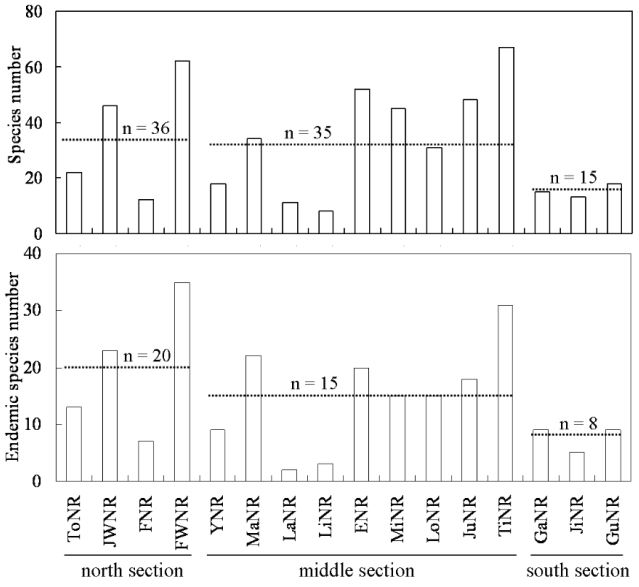

Figure 3. *Species and endemic species richness in the north, middle and south sections of Wuyi Mountains, China (n = average number of fish species). The nature reserve codes are the same as those in Figure 1*

http://www.aloki.hu ● ISSN 1589 1623 (Print) ● ISSN 1785 0037 (Online)
DOI: http://dx.doi.org/10.15666/aeer/1705_1134111357

In addition, greater values of F-index, G-index and G-F index were also obtained from the east slope of the Wuyi Mountains compared to the west slope of the mountain range. And F-index, G-index and G-F index in the north section and middle section of the mountain range were similar, while the F-index, G-index and G-F index in the south section of the mountain range were the lowest (*Table 2*). The species richness of north section, middle section have similarity. While the species richness of south section were the lowest, and the east slope's richness is higher than west slope.

Clustering analysis

By studying the presence-absence data of fish in each nature reserve in Wuyi Mountains, the fish fauna can be divided into four regions (*Fig. 4*). The first region included MiNR, ENR, JuNR, TiNR, FWNR and LoNR, their mountain streams belong to the Minjiang River Basin. The second and third regions were FNR and GuNR, their mountain streams flow into the Oujiang River or the Hanjiang River respectively. The fourth region included JWNR, LaNR, ToNR, JiNR, YNR, GaNR, LiNR and MaNR, their mountain streams belong to the Poyang Lake Basin which flows into the Yangtze River. In addition, according to the result of cluster analysis, 16 nature reserves can be divided into two faunas, the east slope and west slope of the Wuyi Mountains.

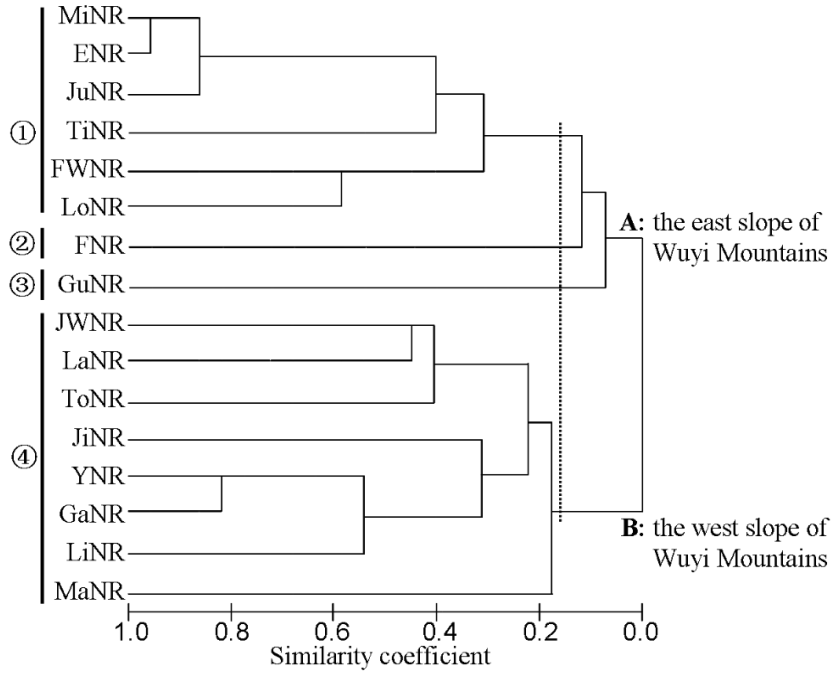

Figure 4. *The classification of 16 nature reserves in the Wuyi Mountains, China. 1: Minjiang River System; 2: Oujiang River System; 3: Hanjiang River System; 4: Yangtze River System. The nature reserve codes are the same as those in Figure 1*

Discussion

Characters of fish species diversity

A total of 1323 species and 877 endemic species of freshwater fish had been reported in China (Xing et al., 2016). The results of the existing studies on the 16 nature reserves in the Wuyi Mountains showed that a total of 126 species (9.5% of all freshwater fish

http://www.aloki.hu ● ISSN 1589 1623 (Print) ● ISSN 1785 0037 (Online)
DOI: http://dx.doi.org/10.15666/aeer/1705_1134111357

species in China) and 72 endemic species (8.2% of all freshwater endemic species in China) were found to be distributed in mountain streams. Several endangered (*Anguilla marmorata, Acrossocheilus wenchowensis, Liobagrus marginatus* and *Pseudobagrus medianalis*) and vulnerable species (*Leptobotia elongate, Siniperca obscura* and *Siniperca roulei*) were found in the Wuyi Mountains, and most of them are endemic to China. The coldwater and endemic species (e.g. *Rhynchocypris oxycephalus*) had also been found in the mountain range. In addition, endemic species of families Balitoridae and Gobiidae, the sucker structure under their bodies allows them to attach to the boundary layer matrix created by water flow at the bottom of the water so as to survive in mountain streams, and they were found in most nature reserves within the mountain range. We can conclude that the diversity and conservation of freshwater fish species (especially endemic species) are highly dependent on the mountain stream environment of Wuyi Mountains. The stability and low disturbance of habitats （such as the introduction of less exotic species） may be the reason for the collection of rich species and endemic species in the mountain range. First-third streams are widely distributed in 16 nature reserves in Wuyi Mountains. Temperatures in the mountains also rarely reach 20 °C in summer because of the high forest coverage rates in the riparian areas of the mountain range. And the content of dissolved oxygen is high, which provides suitable living conditions for these fishes (Hu et al., 2011, 2015, 2018; Guo et al., 2011; Huang et al., 2013).

As environments be different, the species composition of fish also change (Cowx, 1994). The comparison of species number, endemic species number and values of F-index, G-index and G-F index between the west and east slopes of Wuyi Mountains showed that there was a higher fish species diversity in the east slope. And among the three districts (i.e. the north, middle and south sections of Wuyi Mountains), fish species diversity was highest at the north section, good at the middle section and lowest at the south section (Fu et al., 2003; Jang et al., 2003; Yin et al., 2016; Song et al., 2017). Existing studies for bryophytes, ferns, vascular plants, freshwater crabs and reptiles in the Wuyi Mountains showed the similar variation tendency (Guan, 2006; Li et al., 2006; Ye et al., 2007; Zhu, 2010; Cheng et al., 2011; Shi et al., 2012).

Current threats

The biodiversity of the Wuyi Mountains is threatened by a wide range of anthropogenic activities, including overexploitation and habitat change. Sedentary species are also affected by hydrological alterations and tend to redistribute along the river gradient (Araújo et al., 2013). Habitat alteration and destruction as the major cause of most extinctions of freshwater fishes (Thomas., 1994). Despite being prohibited by law, unsustainable and short-term fishing practices like electro-fishing are rampant throughout China (Zhao et al., 2015), causing great damage to fish resources in various regions of the country. In the mountain range, some people catch fish for food on streams using electro-fishing, rotenone or other poisons (Guo et al., 2011; Hu et al., 2011, 2015, 2018; Liu et al., 2012; Zeng et al., 2013; Miao et al., 2016). This kind of fishing had led to over-fishing which had also caused a rapid decline in fish biodiversity.

In recent decades, agricultural activity, increased demand for drinking water, and the construction of multi-purpose dams, artificial reservoirs, and levees and weirs have led to major changes in China's streams and rivers (Fu et al., 2003). In the mountain range,

http://www.aloki.hu ● ISSN 1589 1623 (Print) ● ISSN 1785 0037 (Online)
DOI: http://dx.doi.org/10.15666/aeer/1705_1134111357

dams had been built on streams in most of nature reserves (Guo et al., 2011; Hu et al., 2011, 2015, 2018; Liu et al., 2012; Zeng et al., 2013; Miao et al., 2016). Streams with faster flow rates often slow down and transformed into wide and slow-flowing streams. These factors have impeded the efficient migration of species migrating between different river habitats. This variation means that these organisms will be replaced by species which adapted to slower streams (Hu et al., 2009). Anthropogenic hydrological changes have had a negative affect the biodiversity of fish greatly.

Conservation recommendations

The Chinese government and environmental protection agencies have taken measures to protect the biodiversity of fish in these nature reserves, but these measures have not been effective. Changes brought by human activities and facilities accelerate the deterioration of mountain river environment, so the protection measures for fish biodiversity need to be improved and strengthened.

First, an in-depth understanding of both large-scale species richness patterns and endemism patterns is an essential basis for the conservation of freshwater fish resources (Oberdorff et al., 1999). A more comprehensive assessment of the status of freshwater fish stocks can be achieved using this method. But the data need to be updated in time for the protection agency to formulate the correct protection measures. Therefore, the overall freshwater fish resource assessment of Wuyi Mountains needs to be carried out as soon as possible. In addition, the government should establish a comprehensive database to update the status and information of species.

Second, the development of effective management measures is the first step to protect the species diversity and endemism of Wuyi mountain's fish, which will effectively control and manage the integrity of the fish life cycle and the maintenance of population quantity in the river. The government needs to improve the construction of fish passage facilities so that fish can migrate smoothly between rivers and breeding (Jang et al., 2003).

Third, Penalties for illegal activities should be increased in the mountain area of Wuyi Mountains, so as to better protect fish diversity and resource quantity better. At the same time, fishing must be prohibited in mountainous areas, especially the use of poison such as rotenone. Draft legislation on wildlife buffer zones in the Wuyi Mountains, promoting sustainable agriculture to prevent pollution and limit fishing activities (Jang et al., 2003).

Conclusion

These results indicate that the freshwater fish species diversity is closely related to the environment of Wuyi mountain streams, especially for the endemic species. However, fish biodiversity in the mountain range is facing numerous threats, such as over-exploitation and habitat alteration. Thus, the conservation of fish biodiversity has become urgent, and an integrated management plan should be developed and effectively implemented.

Acknowledgements. This work was supported by the National Natural Science Foundation of China [31360118] and Innovation and Entrepreneurship Fund of Nanchang University [2018270].

Conflicts of interests. The authors declare that they have no conflicts of interests.

http://www.aloki.hu ● ISSN 1589 1623 (Print) ● ISSN 1785 0037 (Online)
DOI: http://dx.doi.org/10.15666/aeer/1705_1134111357

REFERENCES

[1] Araújo, E. S., Marques, E. E., Freitas, I. S., Neuberger, A. L., Fernandes, R., Pelicice, F. M. (2013): Changes in distance decay relationships after river regulation: similarity among fish assemblages in a large Amazonian river. – Ecology of Freshwater Fish 22: 543-552.

[2] Anonymity (1981): Report of Scientific Survey on Fengyangshan Nature Reserve. – Zhejiang Science and Technology Press, Lishui.

[3] Anonymity (1997): Report of Scientific Survey on Longxishan Nature Reserve. – Fujian Science and Technology Press, Fuzhou.

[4] Cai, D. S., Zhao, X. G., Zhu, Y., Zhou, J., Shi, J., Han, Y. Q. (2009): Investigation on fish resources and analysis of species diversity in Lijiang River. – Journal of Guangxi Normal University 27(2): 130-136.

[5] Chen, Y. L., Zhang, Q. J., Xu, H. (2009): Reptilian Fauna and Zoogeographic Division of Fujian Province. – Sichuan Journal of Zoology 28(6): 928-932.

[6] Cheng, S. L., Yuan, R. B., Mao, Y. X. (2011): Reptilian geographical distribution and G-F index in Wuyi Mountains. – Resources and Environment in the Yangtze Basin 20(Z1): 22-29.

[7] Cowx, I. G., (1994): Strategic Approach to Fishery Rehabilitation. Rehabilitation of Freshwater Fisheries. – Fishing News Books. Blackwell Science, Oxford, pp. 3-10.

[8] Fu, C. Z., Wu, J. H., Chen, J. K., Wu, Q. H., Lei, G. C. (2003): Freshwater fish biodiversity in the Yangtze River basin of China: patterns, threats and conservation. – Biodiversity and Conservation 12: 1649-1685.

[9] Guan, S. R. (2016): Studies on Biodiversity of Bryophytes in Wuyi Mountain, China. – Hangzhou Normal Univ., Hangzhou.

[10] Guo, S., Wu, Z. Q., Hu, M. L., Zhou, H. M. Li, Q. (2011): Preliminary survey of fish Yangjifeng Nature Reserve, Jiangxi Province. – Journal of Hydroecology 32(3): 142-144.

[11] Hu, M. L., Wu, Z. Q., Liu, Y. L., (2009): The fish fauna of mountain streams in the Guanshan National Nature Reserve, Jiangxi, China. – Environmental Biology of Fishes 86: 23-27.

[12] Hu, M. L., Wu, Z. Q., Li, Q., Huang, L. L. (2011): Preliminary research on fish species diversity of Ganjiangyuan Nature Reserve in Jiangxi Province. – Sichuan Journal of Zoology 30(3): 467-470.

[13] Hu, M. L., Wu, Z. Q., Ouyang, S. ,Wu, X. P. (2015): Ichthyofaunal diversity of mountain streams in the Tongboshan Nature Reserve, China. – African Journal of Agricultural Research 10(18): 1965-1970.

[14] Hu, M. L., Wang, C. Y., Zhang, X. Y., Yuan, R. B., Zhang, A. F., Wu, L. Z. Jian, S. Q. (2018): Fish species abundance and distribution in Wuyishan National Nature Reserve, Jiangxi Province, China. – eco mont-Journal on Protected Mountain Areas Research and Management 10(2): 9-16.

[15] Huang, L. L., Wu, Z. Q., Li, J. H. (2013): Fish fauna, biogeography and conservation of freshwater fish in Poyang Lake Basin, China. – Environmental Biology of Fishes 96: 1229-1243.

[16] Huang, Z. H., Liu, B. (2011): G-F index of reptiles in Jiangxi Province. – Journal of Jinggangshan University 32(3): 124-127.

[17] Jang, M. H., Lucas, M. C., Joo, G. J. (2003): The fish fauna of mountain streams in South Korean national parks and its significance to conservation of regional freshwater fish biodiversity. – Biological Conservation 114: 115-126.

[18] Jiang, Z. G., Ji, L. Q. (1999): Avian-mammalian species diversity in nine representative sites in China. – Chinese Biodiversity 7(3): 61-66.

[19] Li, Y. M., Wu, X. B. (2006): Avian diversity in Wuhu City in summer and winter. – Chinese Journal of Applied Ecology 17(2): 269-274.

[20] Li, Z. J., Lin, P., Ye, W., Chen, L. Z., Qiu, L., Chen, S. B., Liu, C. D., He, J. Y., Dai, D. S., Li, L. (2006): Diversity connectivity of vascular plants from southern to northern Wuyi Mountains. – Progress in Natural Science 16(8): 959-964.

http://www.aloki.hu ● ISSN 1589 1623 (Print) ● ISSN 1785 0037 (Online)
DOI: http://dx.doi.org/10.15666/aeer/1705_1134111357

[21] Li, Z. J., Chen, X. L., Liu, C. M., Jin, B. S. (2015): Research on Biodiversity in the Emeifeng Nature Reserve of Fujian. – Science Press, Beijing.
[22] Lin, P. (2002): Report of Scientific Survey on Tianbaoyan Nature Reserve of Fujian. – Xiamen, Xiamen University Press, Xiamen.
[23] Lin, P. (2004): Report of scientific survey on Minjiangyuan Nature Reserve of Fujian. – Xiamen, Xiamen University Press, Xiamen.
[24] Lin, P., Li, Z. J., Zhang, J. (2005): Report of Scientific Survey on Junzifeng Nature Reserve of Fujian. – Xiamen University Press, Xiamen.
[25] Liu, J. Q., Yang, Q., Xiao, G. R., Liu, C. M. (2012): Wuyi Mountain Biodiversity Research Information Platform, Fujian, China. – Science Press, Beijing [in Chinese].
[26] Liu, X. Z., Fu, Q. (2006): Scientific Survey and Study of Rare Phytocoenosium on the Matoushan Nature Reserve in Jiangxi Province. – China Forestry Press, Beijing.
[27] Miao, C., Zhu, Y. H., Yuan, R. B., Zou, Z. A. Hu, M. L., Shao, S. P., Yin, H., Yan, X. (2016): Fish species diversity in Jinpenshan Nature Reserve Zone, Jinagxi Province, in Summer. – Chinese Journal of Fisheries 29(4): 28-32.
[28] Ministry of Ecology and Environment of the PRC (2016): Writing a Research Paper. – http://www.mee.gov.cn/stbh/zrbhq/qgzrbuqml/201611/P020161125598658863 59.pdf (accessed: 8 November 2016).
[29] Oberdorff, T., Lek, S., Guegan, J. F. (1999): Patterns of endemism in riverine fish of the Northern Hemisphere. – Ecology Letters 2: 75-81.
[30] Shi, L. B., Zhang, X. Y., Zou, J. X., Wang, Y., Liu, D. R., Zhu, C. C., Zhou, X. M. (2012): Distribution pattern of the freshwater crabs among Wuyi Mountains. – Journal of Nanchang University (Natural Science) 36(6): 556-561.
[31] Song, X. J., Tang, W. Q., Zhang, Y. (2017): Freshwater fish fauna and zoogeographical divisions in the Wuyi-Xianxialing Mountains of eastern China. – Biodiversity Science 25(12): 1331-1338.
[32] Thomas, C. D. (1994): Extinction, colonisation, and metapopulations: environmental tracking by rare species. – Conservation Biology. 8: 373-378.
[33] Xing, Y. C., Zhang, C. G., Fan, E. Y., Zhao, Y. H. (2016): Freshwater fishes of China: species richness, endemism, threatened species and conservation. – Diversity and Distributions 22: 358-370.
[34] Ye, W., Li, Z. J., Benito, C. T., Chang, Y., Chen, L. Z., He, J. Y., Liu, C. D. (2007): Study on the biodiversity of ferns from southern to northern Wuyi Mountains. – Journal of Xiamen University (Natural Science) 46(3): 431-437.
[35] Yin, C., Huang, L. L., Xu, L., Huang, J., Gao, M. H. (2016): Fish diversity in nature reserves of Jiangxi Province, China. – eco mont-Journal on Protected Mountain Areas Research 8(2): 33-42.
[36] Yu, X. D., Luo, T. H., Zhou, H. Z., (2005): Large-scale patterns in species diversity of fishes in the Yangtze River Basin. – Biodiversity Science 13(6): 473-495.
[37] Zeng, Z. G., Zeng, T., Chen, J. K., Jin, B. S. (2013): Preliminary investigation of fish resources of the Guilong Mountain Provincial Nature Reserve in Fujian Province in summer. – Journal of Fujian Fisheries 35(3): 167-174.
[38] Zhao, Y., Gozlan, R. E., Zhang, C. (2015): Current State of Freshwater Fisheries in China. – In: Craig, J. F. (ed.) Freshwater Fisheries Ecology. John Wiley and Sons Ltd, Hoboken, NJ, pp. 221-229.
[39] Zhong, C. F.,(2004): Reptilian Fauna and Zoogeographic Division of Jiangxi Province. – Sichuan Journal of Zoology 23(3): 222-229.
[40] Zhu, C. C., (2010): Zoogeographical Significance of Freshwater Crabs Family Potamidae and Parathelphusidae in Wuyi Mountain Region. – NanChang, Jiangxi, China.
[41] Zhu, Y. H., Yuan, R. B., Zou, Z. A., Hu, M. L. (2017): A study on fish diversity connectivity in western Wuyi Mountains. – Transactions of Oceanology and Limnology 5: 93-101.

http://www.aloki.hu ● ISSN 1589 1623 (Print) ● ISSN 1785 0037 (Online)
DOI: http://dx.doi.org/10.15666/aeer/1705_1134111357

APPENDIX 1

The list of fish and distribution of 16 nature reserves in the Wuyi Mountains, China. The nature reserve codes are the same as those in Figure 1. (The presence-absence data of fish species are obtained from Anonymity, 1981, 1997; Lin, 2002, 2004; Lin et al., 2005; Liu and Fu, 2006; Guo et al., 2011; Hu et al., 2011, 2015, 2018; Liu et al., 2012; Zeng et al., 2013; Li et al., 2015; Miao et al., 2016; Zhu et al., 2017)

Order/family/species	ToNR	JWNR	YNR	MaNR	LaNR	LiNR	GaNR	JiNR	FNR	FWNR	ENR	MiNR	LoNR	JuNR	TiNR	GuNR
Anguilliformes																
Anguillidae																
Anguilla japonica									+	+	+	+		+	+	+
Anguilla marmorata										+	+			+	+	
Cypriniformes																
Cyprinidae																
Aphyocypris chinensis											+	+		+		
Opsariichthys bidens	+	+	+	+	+		+	+	+	+	+	+	+	+	+	+
Zacco platypus	+	+	+	+	+	+	+	+		+	+	+	+	+	+	+
Ctenopharyngodon idella		+													+	
Elopichthys bambusa											+	+				
Mylopharyngodon piceus		+														
Ochetobius elongatus											+	+		+		
**Rhynchocypris oxycephalus*	+	+		+						+						
Squaliobarbus curriculus											+	+				
Culter alburnus	+														+	
Cultrichthys erythropterus	+									+			+		+	
Hemiculter leucisculus	+	+			+					+	+	+		+	+	
**Megalobrama amblycephala*	+	+														
Megalobrama terminalis											+	+			+	
Pseudohemiculter dispar				+						+	+	+	+	+		

http://www.aloki.hu ● ISSN 1589 1623 (Print) ● ISSN 1785 0037 (Online)
DOI: http://dx.doi.org/10.15666/aeer/1705_1134111357

Pseudohemiculter hainanensis		+													+	
Pseudolaubuca sinensis		+														
**Sinibrama macrops*	+	+		+						+	+	+		+	+	
**Distoechodon compressus*											+	+		+	+	
**Distoechodon tumirostris*		+									+			+	+	+
Xenocypris argentea						+			+					+	+	
Xenocypris davidi		+														
Xenocypris microlepis															+	
**Aristichthys nobilis*		+													+	
Hypophthalmichthys molitrix		+													+	
Acheilognathus barbatulus											+	+		+		
**Acheilognathus barbatus*										+						
Acheilognathus chankaensis				+									+		+	
**Acheilognathus polylepis*				+												
Acheilognathus tonkinensis										+	+	+	+	+	+	
**Rhodeus ocellatus*		+	+				+	+					+			+
**Rhodeus sinensis*		+														
Abbottina rivularis		+								+	+	+	+	+		
**Belligobio nummifer*										+					+	
**Gnathopogon imberbis*	+	+	+				+			+			+			
**Gnathopogon taeniellus*										+					+	
Hemibarbus labeo		+									+	+	+	+	+	+
Hemibarbus maculatus		+			+			+		+					+	
**Huigobio chenhsienensis*				+												
**Huigobio chinssuensis*				+												
**Microphysogobio fukiensis*										+	+	+	+	+		
**Microphysogobio kiatingensis*		+								+						
**Pseudogobio vaillanti*		+		+						+			+	+	+	
Pseudorasbora parva		+	+		+		+			+	+	+	+	+	+	

http://www.aloki.hu ● ISSN 1589 1623 (Print) ● ISSN 1785 0037 (Online)
DOI: http://dx.doi.org/10.15666/aeer/1705_1134111357

**Rhinogobio typus*														+	+	
**Sarcocheilichthys kiangsiensis*																+
Sarcocheilichthys nigripinnis													+			
**Sarcocheilichthys parvus*				+												
**Sarcocheilichthys sinensis fukiensis*											+	+		+		
Saurogobio dabryi dabryi										+	+	+	+	+	+	
**Saurogobio gracilicaudatus*				+												
Squalidus argentatus					+					+	+	+		+	+	
**Squalidus wolterstorffi*										+			+	+		
**Gobiobotia longibarba*											+	+				
Carassius auratus auratus		+	+		+		+	+	+	+	+	+	+	+	+	+
Cyprinus carpio		+			+					+	+	+		+	+	
**Acrossocheilus hemispinus cinctus*		+		+												
**Acrossocheilus hemispinus hemispinus*										+	+	+	+	+	+	
**Acrossocheilus kreyenbergii*											+	+		+	+	
**Acrossocheilus labiatus*				+					+	+		+	+			
**Acrossocheilus parallens*	+	+	+	+	+	+	+	+		+					+	+
**Acrossocheilus spinifer*										+						
**Acrossocheilus wenchowensis*									+						+	
**Onychostoma barbatula*	+	+	+	+				+		+	+	+	+	+	+	
Spinibarbus hollandi		+		+						+	+	+		+	+	
Nemacheilidae																
Schistura fasciolata				+						+						
Cobitidae																
Cobitis sinensis										+						
Cobitis taenia				+						+	+			+	+	
Misgurnus anguillicaudatus	+	+	+		+	+	+	+	+	+	+	+	+	+	+	+

http://www.aloki.hu ● ISSN 1589 1623 (Print) ● ISSN 1785 0037 (Online)
DOI: http://dx.doi.org/10.15666/aeer/1705_1134111357

**Leptobotia elongate*											+						
**Leptobotia tientaiensis compressicauda*											+					+	
Balitoridae																	
**Formosania davidi*	+										+	+	+		+	+	
**Formosania fascicauda*										+	+						
**Formosania lacustre*											+						
**Formosania stigmata*		+					+	+			+			+		+	+
**Formosania tinkhami*										+							+
Liniparhomaloptera disparis disparis				+													
**Pseudogastromyzon changtingensis changtingensis*		+															+
**Pseudogastromyzon changtingensis tungpeiensis*	+																
**Pseudogastromyzon cheni*																	+
**Pseudogastromyzon fangi*										+							
**Pseudogastromyzon fasciatus fasciatus*		+		+							+	+	+	+	+	+	
**Vanmanenia caldwelli*											+			+		+	
**Vanmanenia gymnetrus*											+						
**Vanmanenia pingchowensis*			+			+	+										
**Vanmanenia stenosoma*	+	+		+	+												
**Vanmanenia xinyiensis*							+	+									
**Hemimyzon formosanus*										+							
Siluriformes																	
Amblycipitidae																	
**Liobagrus anguillicauda*	+	+	+							+	+	+		+	+	+	
**Liobagrus marginatus*				+													
Sisoridae																	

http://www.aloki.hu ● ISSN 1589 1623 (Print) ● ISSN 1785 0037 (Online)
DOI: http://dx.doi.org/10.15666/aeer/1705_1134111357

**Glyptothorax fukiensis*		+									+				+	+	
Glyptothorax sinensis		+															
Siluridae																	
Silurus asotus	+	+	+								+	+	+		+	+	
**Silurus meridionalis*																+	
Clariidae																	
Clarias fuscus		+	+	+			+				+	+	+	+	+	+	
Bagridae																	
**Hemibagrus macropterus*		+		+													
**Leiocassis crassilabris*											+	+	+	+	+	+	
**Leiocassis tenuifurcatus*				+							+	+	+			+	
Pelteobagrus fulvidraco			+	+							+	+	+	+	+	+	
**Pelteobagrus nitidus*																+	
Pelteobagrus vachellii																+	
**Pseudobagrus adiposalis*				+													
**Pseudobagrus albomarginatus*				+							+	+	+		+	+	
**Pseudobagrus medianalis*	+																
**Pseudobagrus ondon*		+	+			+	+										
**Pseudobagrus taiwanensis*	+																
**Pseudobagrus tenuis*											+	+		+		+	
**Pseudobagrus truncatus*		+		+							+	+		+		+	+
Pseudobagrus ussuriensis				+													
Synbranchiformes																	
Synbranchidae																	
Monopterus albus	+	+					+	+			+	+	+		+	+	+
Mastacembelidae																	
Sinobdella sinensis											+						
Perciformes																	
Percichthyidae																	

http://www.aloki.hu ● ISSN 1589 1623 (Print) ● ISSN 1785 0037 (Online)
DOI: http://dx.doi.org/10.15666/aeer/1705_1134111357

Siniperca chuatsi		+									+	+		+	+	
Siniperca knerii															+	
**Siniperca obscura*										+	+				+	
**Siniperca roulei*										+	+	+		+	+	
Siniperca scherzeri										+	+	+		+	+	
Odontobutidae																
**Micropercops swinhonis*				+												
Gobiidae																
**Rhinogobius cliffordpopei*	+	+	+	+			+									
**Rhinogobius davidi*										+					+	+
Rhinogobius giurinus	+	+	+	+		+		+		+			+		+	+
Osphronemidae																
**Macropodus chinensis*			+				+			+	+				+	
Macropodus opercularis						+					+	+		+	+	
Channidae																
Channa asiatica								+			+	+		+		
Channa maculata											+	+		+	+	+

http://www.aloki.hu ● ISSN 1589 1623 (Print) ● ISSN 1785 0037 (Online)
DOI: http://dx.doi.org/10.15666/aeer/1705_1134111357

PRELIMINARY STUDY ON BIODIVERSITY OF BUTTERFLIES IN BEYKOZ GROVE OF ISTANBUL, TURKEY

KUCUKOSMANOGLU, A.

Department of Forest Entomology and Protection, Faculty of Forestry, Istanbul University, 34473 Bahcekoy, Sariyer, Istanbul, Turkey
(e-mail: aliko@istanbul.edu.tr)

(Received 17th Apr 2019; accepted 11th Jul 2019)

Abstract. In this study, Lepidoptera species collected by sweep net in Beykoz grove, Istanbul province, Turkey during the years of 2017–2018 was evaluated. A total of 182 specimens were collected in Beykoz. According to identification results, 57 species belonging to 12 families were recorded. The family Noctuidae was represented by the highest number of species (19), followed by Geometridae (16) and Notodontidae (6).
Keywords: *sweep net, butterflies, biodiversity, fauna, Beykoz*

Introduction

Lepidoptera, butterflies and moths, are very common insects and well known because of their very attractive colours and patterns on their wings. This order is recognized as one of the largest order of insects (Romoser and Stoffolana, 1994). Adults of the majority of extant species feed on nectar, the juice of overripe fruit or other liquids. Larvae of almost all species are phytophagous, and no parts of plants remain unexploited. Because of their phytophagus habits and high reproductive rate, many species are important pests (Gillott, 2005). The ecological-faunistic complex situation of butterflies is important for biodiversity.

There are several regional studies to determine the Lepidoptera fauna in Turkey (Akbulut et al., 2003; Akkuzu et al., 2007; Avci, 1997; Beskardes, 2002; Can, 2008; Cebeci, 2003; De Lattin, 1950, 1951; Graves, 1925, 1926; Hakyemez, 1994; Hesselbarth et al., 1995; Kansu, 1963; Kaygin et al., 2009; Kornosor, 1987; Mathew, 1881; Mol, 1977; Okyar and Aktac, 1998, 1999; Rebel, 1903).

With the new records published on butterfly observation sites of Butterfly Turkish (kelebek-turk.com) by butterfly observers, the number of butterfly species in the province of Istanbul is 125. In order to determine the butterfly species diversity of Beykoz grove of Istanbul, a field study was carried out in 2017–2018.

Materials and methods

The study was conducted between the years of 2017 and 2018 in Beykoz grove located within Istanbul region (*Fig. 1*). Beykoz is a small holiday town on the Marmara Sea coasts in the city of Istanbul. Beykoz grove (located at 41° 07’ 59”N, 29° 05’ 54”E) covers in the form of deciduous forests, composed of various tree species and tall shrubs. In the forested area dominant trees are *Platanus* sp., *Quercus* spp., *Alnus glutinosa, Acer campestre, Fraxinus excelsior, Carpinus betulus, Castanea sativa, Tilia tomentosa* and *Poulus tremula.* Having rich flora and suitable climate conditions enabled Beykoz owning rich and divergent Biodiversity.

http://www.aloki.hu ● ISSN 1589 1623 (Print) ● ISSN 1785 0037 (Online)
DOI: http://dx.doi.org/10.15666/aeer/1705_1135911366

Specimens were collected using a sweep net. Captured specimens were put into tightly closed killing jars immediately and brought to the laboratory for preparation and identification. Ethyl acetate was used as a killing agent. The collecting dates and locations concerning each specimen were recorded in the field note book. Specimens were pinned using insect pins (mostly, 3 - 4 - 5 sized) and were mounted on spreading boards. For identification, different studies (Fibiger, 1993; Forster and Wohlfahrt, 1971; Marini and Trentini, 1986; NHM, 2009; Savela, 2001; Spuler, 1910) were used. The Lepidoptera collections of Forest Entomology and Protection Department of Istanbul University, Faculty of Forestry were also used.

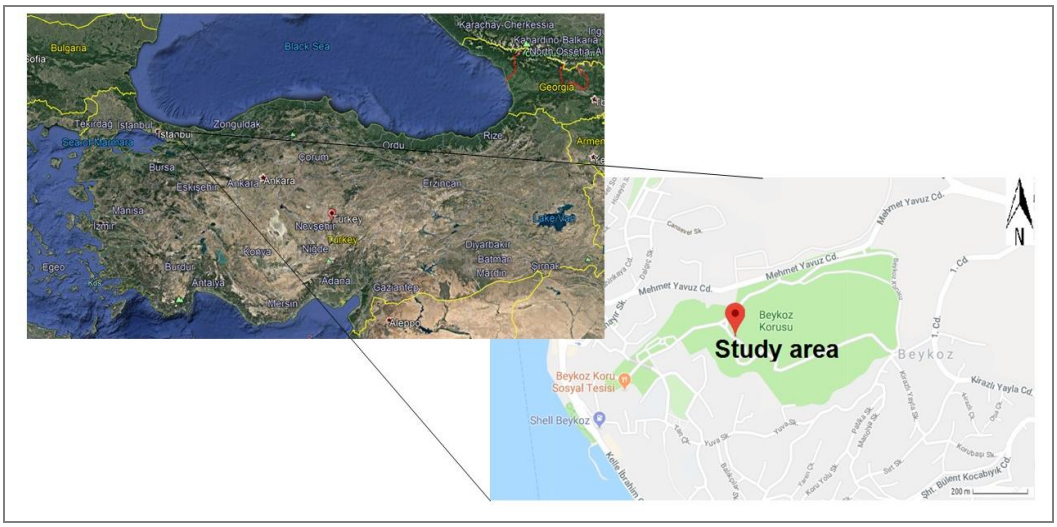

Figure 1. *Location of study area*

Results and discussion

A total of 182 specimens were collected from this location in Beykoz region of Istanbul. 57 species belonging to 12 families of the order Lepidoptera were identified and listed as follows. Family names and species in each family were listed as arranged alphabetically:

Order **LEPIDOPTERA** Linnaeus, 1758
Family **COSSIDAE** Leach, [1815]
Cossus cossus (*Linnaeus, 1758*)
Zeuzera pyrina (Linnaeus, 1761)
Family **CRAMBIDAE** Leach, [1815]
Cydalima perspectalis (Walker, 1859)
Family **TORTRICIDAE** Latreille, [1803]
Tortrix viridana (*Linnaeus, 1758*)
Family **PYRALIDAE** Latreille, 1809
Dioryctria abietella (Denis & Schiffermüller, 1775)
Nomophila noctuella (Denis & Schiffermüller, 1775)
Family **LASIOCAMPIDAE** Harris, 1841
Lasiocampa quercus (Linnaeus, 1758)
Family **SATURNIIDAE** Boisduval, 1837
Saturnia pavonia (Linnaeus, 1758)
Family **GEOMETRIDAE** Leach, [1815]

http://www.aloki.hu ● ISSN 1589 1623 (Print) ● ISSN 1785 0037 (Online)
DOI: http://dx.doi.org/10.15666/aeer/1705_1135911366

Alcis repandata (Linnaeus, 1758)
Ascotis selenaria (Denis & Schiffermüller, 1775)
Campaea margaritata (Linnaeus, 1767)
Cosmorhoe ocellata (Linnaeus, 1758)
Geometra papilionaria (Linnaeus, 1758)
Gnophos sartata (Treitschke, 1827)
Hemistola chrysoprasaria (Esper, 1795)
Hemithea aestivaria (Hübner, 1789)
Idaea aversata (Linnaeus, 1758)
Idaea ochrata (Scopoli, 1763)
Melanthia procellata (Denis & Schiffermüller, 1775)
Opisthograptis luteolata (Linnaeus, 1758)
Peribatodes rhomboidaria (Denis & Schiffermüller, 1775)
Plagodis dolabraria (Linnaeus, 1767)
Scopula nigropunctata (Hufnagel, 1767)
Selenia lunaria (Hübner, 1788)
Family **NOTODONTIDAE** Stephens, 1828
Drymonia dodonaea (Denis & Schiffermüller, 1775)
Phalera bucephala (Linnaeus, 1758)
Pheosia tremula (Clerck, 1759)]
Pterostoma palpina (Clerck, 1759)
Spatalia argentina (Denis & Schiffermüller, 1775)
Stauropus fagi (Linnaeus, 1758)
Family **THAUMETOPOEIDAE** Aurivillus, 1889
Thaumetopoea pityocampa (Denis & Schiffermüller, 1775)
Family **LYMANTRIIDAE** Hampson, [1893]
Calliteara pudibunda (Linnaeus, 1758)
Euproctis chrysorrhoea (Linnaeus, 1758)
Lymantria dispar (Linnaeus, 1758)
Family **ARCTIIDAE** Leach, [1815]
Arctia villica (Linnaeus, 1758)
Miltochrista miniata (Forster, 1771)
Phragmatobia fuliginosa (Linnaeus, 1758)
Spilosoma lubricipeda (Linnaeus, 1758)
Family **NOCTUIDAE (**Latreille, 1809)
Agrotis cinerea (Denis & Schiffermüller, 1775)
Agrotis ipsilon (Hufnagel, 1766)
Amphipyra pyramidea (*Linnaeus, 1758*)
Autographa gamma (*Linnaeus, 1758*)
Callopistria juventina (Stoll, 1782)
Chersotis margaritacea (Villers, 1789)
Chloantha hyperici (Denis & Schiffermüller, 1775)
Conistra rubiginea (Denis & Schiffermüller, 1775)
Dysgonia algira (Linnaeus, 1758)
Emmelia trabealis (Scopoli, 1763)
Epilecta linogrisea (Denis & Schiffermüller, 1775)
Euplexia lucipara (Linnaeus, 1758)
Heliothis peltigera (Denis & Schiffermüller, 1775)

http://www.aloki.hu ● ISSN 1589 1623 (Print) ● ISSN 1785 0037 (Online)
DOI: http://dx.doi.org/10.15666/aeer/1705_1135911366

Herminia tarsipennalis Treitschke, 1835
Melanchra persicariae (Linnaeus, 1761)
Mythimna vitellina (*Hübner, 1808*)
Noctua orbona (Hufnagel, 1766)
Noctua pronuba (Linnaeus, 1758)
Xestia castanea (Esper, 1798)

A total of 182 individuals with 57 species belonging to 12 families were identified in Beykoz grove. Nymphalidae family was dominant, whereas Riodinidae had the least number of individuals. The highest number of species belongs to Noctuidae (19, 33.3%), followed by Geometridae (16, 28.1%) and Notodontidae (6, 10%). The number of species in each family (*Figs. 2* and *3*) and their ratios to the families were given in *Table 1*. In *Table 2,* the data concerning the capturing dates and the collecting locations about each specimen were given.

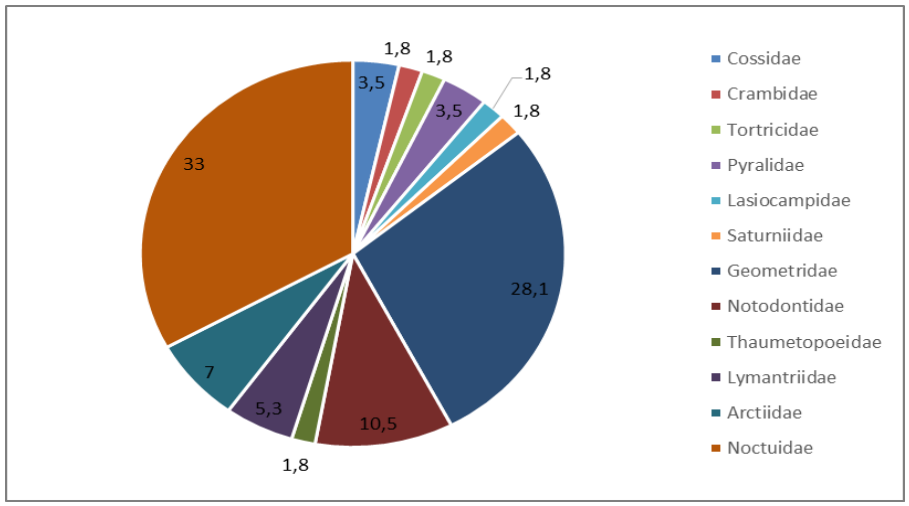

Figure 2. *Percentage of species into each family*

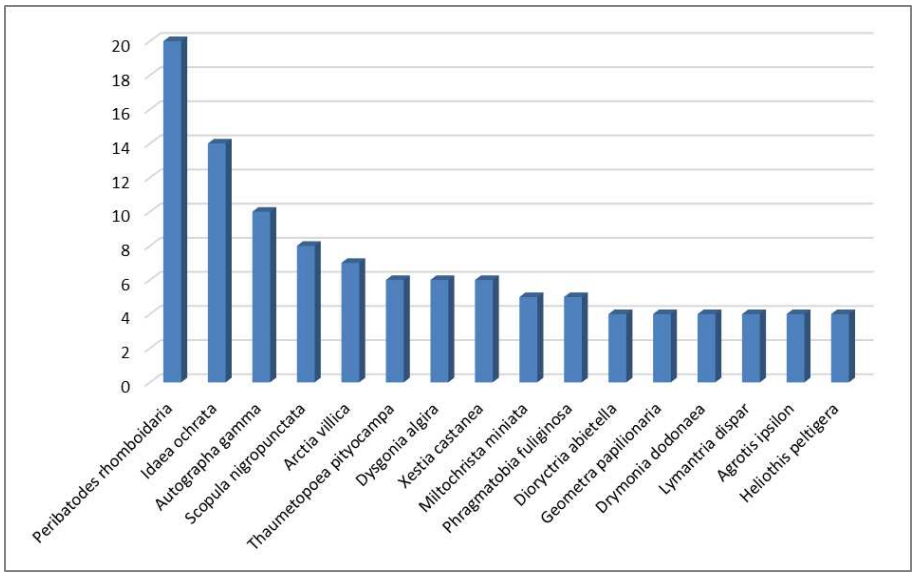

Figure 3. *The total number of collected species*

http://www.aloki.hu ● ISSN 1589 1623 (Print) ● ISSN 1785 0037 (Online)
DOI: http://dx.doi.org/10.15666/aeer/1705_1135911366

Table 1. *Number of species and rates of families*

Family	Number of species	Rate (%)
Cossidae	2	3.5
Crambidae	1	1.8
Tortricidae	1	1.8
Pyralidae	2	3.5
Lasiocampidae	1	1.8
Saturniidae	1	1.8
Geometridae	16	28.1
Notodontidae	6	10.5
Thaumetopoeidae	1	1.8
Lymantriidae	3	5.3
Arctiidae	4	7.0
Noctuidae	19	33.0
Total	57	100

Table 2. *The capturing dates about each specimen in Beykoz region*

Species	Date
Cossus cossus	10.06.2017 (3). Totally 3 specimens
Zeuzera pyrina	14.07.2017 (2); 28.06.2018 (1). Totally 3 specimens
Tortrix viridana	20.07.2018 (1). Totally 1 specimen
Dioryctria abietella	17.06.2018 (2); 19.06.2018 (2). Totally 4 specimens
Nomophila noctuella	20.06.2017 (1). Totally 1 specimen
Lasiocampa quercus	13.08.2018 (3). Totally 3 specimens
Saturnia pavonia	20.04.2018 (2). Totally 2 specimens
Alcis repandata	17.06.2017 (2). Totally 2 specimens
Ascotis selenaria	25.08.2018 (1). Totally 1 specimen
Campaea margaritata	20.07.2017 (1); 28.07.2017 (2). Totally 3 specimens
Cosmorhoe ocellata	18.07.2017 (1). Totally 1 specimen
Geometra papilionaria	15.06.2017 (4). Totally 4 specimens
Gnophos sartata	07.08.2018 (3). Totally 3 specimens
Hemistola chrysoprasaria	08.06.2018 (1). Totally 1 specimen
Hemithea aestivaria	28.06.2017 (1); 06.07.2018 (1). Totally 2 specimens
Idaea aversata	29.06.2017 (1). Totally 1 specimen
Idaea ochrata	29.06.2017 (2); 17.07.2017 (2); 15.07.2018 (3); 23.07.2018 (3). Totally 14 specimens
Melanthia procellata	22.06.2017 (1). Totally 1 specimen
Opisthograptis luteolata	24.05.2017 (1). Totally 1 specimen
Peribatodes rhomboidaria	10.05.2017 (4); 16.06.2017 (5); 22.06.2017 (2); 25.07.2018 (4); 22.06.2018 (2); 23.06.2018 (3). Totally 20 specimens
Plagodis dolabraria	19.05.2017 (1); 15.06.2017 (1); 18.06.2018 (1). Totally 3 specimens
Scopula nigropunctata	14.06.2017 (2); 17.06.2017 (1); 22.06.2018 (1); 17.07.2018 (1); 05.08.2018 (3). Totally 8 specimens
Selenia lunaria	28.05.2017 (1). Totally 1 specimen
Drymonia dodonaea	20.05.2018 (1); 22.05.2018 (1); 24.05.2018 (2). Totally 4 specimens
Phalera bucephala	28.06.2017 (3). Totally 3 specimens
Pheosia tremula	25.09.2018 (1). Totally 1 specimen
Pterostoma palpina	30.08.2018 (3). Totally 3 specimens
Spatalia argentina	30.06.2018 (3). Totally 3 specimens
Stauropus fagi	20.08.2018 (2); 23.08.2018 (1). Totally 3 specimens
Thaumetopoea pityocampa	18.07.2017 (6). Totally 6 specimens
Calliteara pudibunda	16.05.2017 (2). Totally 2 specimens
Euproctis chrysorrhoea	03.07.2017 (1). Totally 1 specimen
Lymantria dispar	03.08.2018 Avcikoru (4). Totally 4 specimens
Arctia villica	17.06.2017 (2); 09.05.2018 (2); 15.06.2018 (3). Totally 7 specimens

http://www.aloki.hu ● ISSN 1589 1623 (Print) ● ISSN 1785 0037 (Online)
DOI: http://dx.doi.org/10.15666/aeer/1705_1135911366

Miltochrista miniata	17.07.2017 (3); 18.07.2017 (2). Totally 5 specimens
Phragmatobia fuliginosa	20.07.2017 (3); 27.07.2017 (2). Totally 5 specimens
Spilosoma lubricipeda	28.06.2017 (2). Totally 2 specimens
Agrotis cinerea	10.08.2018 (1). Totally 1 specimen
Agrotis ipsilon	05.08.2018 (1); 10.08.2018 (2); 15.08.2018 (1)). Totally 4 specimens
Amphipyra pyramidea	15.07.2018 (1) Totally 1 specimen
Autographa gamma	13.06.2017 (1); 17.06.2017 (2); 10.08.2018 (2); 12.08.2018 (2); 14.08.2018 (3). Totally 10 specimens
Callopistria juventina	10.06.2017 (2). Totally 2 specimens
Chersotis margaritacea	23.05.2017 (1). Totally 1 specimen
Chloantha hyperici	22.06.2017 (1). Totally 1 specimen
Conistra rubiginea	10.08.2017 (1). Totally 1 specimen
Dysgonia algira	17.06.2017 (2); 05.07.2017 (4). Totally 6 specimens
Emmelia trabealis	07.07.2017 (1). Totally 1 specimens
Epilecta linogrisea	23.07.2017 (1). Totally 1 specimen
Euplexia lucipara	20.08.2018 (1). Totally 1 specimen
Heliothis peltigera	10.05.2017 (1); 12.06.2017 (2); 15.08.2018 (1).
Herminia tarsipennalis	15.06.2017 (1). Totally 1 specimen
Lacanobia w-latinum	02.07.2018 (1). Totally 1 specimen
Melanchra persicariae	20.06.2017 (1). Totally 1 specimen
Mythimna vitellina	20.07.2018 (1). Totally 1 specimens
Noctua orbona	05.08.2018 (3). Totally 3 specimens
Noctua pronuba	10.06.2017 (1); 22.06.2018 (2). Totally 3 specimens
Xestia castanea	10.07.2017 (2); 15.08.2018 (4). Totally 6 specimens
Totally 57 species	**Totally 182 specimens**

Conclusions

In this research, 57 species belonging to 12 families of suborder Heterocera were captured and identified in Beykoz region of Istanbul. Most of the species were from three families: Noctuidae (19, 33.0%), followed by Geometridae (16, 28.1%) and Notodontidae (6, 10.5%). Among the lepidopteran species collected, 33 were considered pests for forest trees: *C. cossus*, *Z. pyrina, T. viridana, D. abietella, L. quercus, S. pavonia, A. repandata, C. margaritata, G. papilionaria, H. aestivaria, P. dolabraria, S. lunaria, H. pyritoides, D. dodonaea, P. bucephala, P. tremula, P. palpina, S. argentina, S. fagi, T. processionea, C. pudibunda, E. chrysorrhoea, L. dispar, L. monacha*, *P. fuliginosa, S. lubricipeda, A. psi, A. pyramidea, B. bicolorana, C. rubiginea, L. w-latinum, M. lunaris* and *M. alpium* (Kimber, 2009; Savela, 2001). Oak (*Quercus* spp.) is the dominant tree in the region and according to the literature (Kimber, 2009; Savela, 2001), *C. cossus*, *T. viridana, L. quercus, S. pavonia, C. margaritata, H. aestivaria, S. lunaria, D. dodonaea, P. bucephala, S. argentina, T. processionea, C. pudibunda, E. chrysorrhoea, L. dispar, L. monacha, A. psi, A. pyramidea, B. bicolorana, C. rubiginea, L. w-latinum, M. lunaris* and *M. alpium* caterpillars prefer oak leaves as their food plants.

Z. pyrina differs from these species as its larvae food regimes. The adults of *Z. pyrina* fly during June and July were collected in the end of July and in the beginning of August. L. monacha adults are different from L. dispar adults by means of morphological appearances. They often show traces of bright pink colour on the body, especially the abdomen, which however is normally concealed when at rest. L. monacha was regarded as the first record for the region.

http://www.aloki.hu ● ISSN 1589 1623 (Print) ● ISSN 1785 0037 (Online)
DOI: http://dx.doi.org/10.15666/aeer/1705_1135911366

Most of the species obtained were collected in summer months. This was because summer is the most suitable season for the mating and regeneration activities of Lepidopteran adults.

As Kaygin et al. (2009) said: the habitats, where the butterfly and moth species have been abundantly observed should be protected and these particular locations should be preserved as butterfly protection areas. Beykoz is one of the potential butterfly protection areas.

REFERENCES

[1] Akbulut, S., Yuksel, B., Keten, A. (2003): The Lepidoptera (Insecta) Fauna of Duzce Province, Turkey. – Turk. J. Zool. 27(5): 257-268.
[2] Akkuzu, E., Ayberk, H., Inac, S. (2007): Hawk Moths (Lepidoptera: Sphingidae) of Turkey and their zoogeographical distribution. – J. Environ. Biol. 28(4): 723-730.
[3] Avci, M. (1997): Tortricidae Fauna in forests of Marmara Region. – Ph.D. Thesis, Istanbul University, Forestry Faculty, Istanbul.
[4] Beskardes, V. (2002): The butterfly and moth (Lepidoptera) species living in Istanbul Catalca Administration Forests. – M.Sc. Thesis, Istanbul University, Forestry Faculty, Istanbul.
[5] Can, F. (2008): The geometrid moths (Lepidoptera) from the Middle and Eastern Black Sea Regions of Turkey. – Turk J. Zool. 32: 351-358.
[6] Cebeci, H. H. (2003): Entomological problems in Istanbul Regional Directorate. – Ph.D. Thesis, Istanbul University, Forestry Faculty, Istanbul.
[7] Coulson, R. N., Witter, J. A. (1984): Forest Entomology (Ecology and Management). – John Wiley and Sons, New York.
[8] De Lattin, G. (1950): Türkische Lepidopteren I. – Istanbul University Journal 15(4): 301-328.
[9] De Lattin, G. (1951): Türkische Lepidopteren II. – Istanbul University Journal 16(1): 45-73.
[10] Fibiger, M. (1993): Noctuidae Europaeae. – Entomological Press, Soro.
[11] Forster, W., Wohlfahrt, A. (1971): Die Schmetterlinge Mitteleuropas, Eulen (Noctuidae), Band IV. – Franckhsche Verlagshandlung Stuttgart.
[12] Gillott, C. (2005): Entomology. – Springer, Dordrecht.
[13] Graves, P. P. (1925): Lepidoptera of the Constantinople. – Entomologist 63: 191-194.
[14] Graves, P. P. (1926): Heterocera from Macedonia, Gallipoli and Central Greece. – Entomologist's Rec. J. Var. 38: 152-158, 165-170.
[15] Hakyemez, A. (1994): The Forest Noctuidae species of Zonguldak Regional Directorate. – Review of Faculty of Forestry, Istanbul University 44(2): 111-133.
[16] Hesselbarth, G., Van Oorschot, H., Wagener, S. (1995): Die Tagfalter der Türkei, 3 Band. – Selbstverlag Sigbert Wagener, Bocholt.
[17] Kansu, A. (1963): The list for Turkish Lepidoptera: V. – Plant Prot. Bull. 3(3): 208-223.
[18] Kaygin, A. T., Yildiz, Y., Avci, M. (2009): Lepidoptera fauna in Bartin province, in western Black Sea region of Turkey. – Afr. J. Agric. Res. 4(9): 815-822.
[19] Kimber, I. (2009): UK moths web page. – http://www.ukmoths.org.uk/ (accessed: 23 November 2009].
[20] Kornosor, S. (1987): Distribution and systematics of Noctuinae and Plusiinae (Lep. Noctuidae) species in South and Southeast Region of Turkey. – Turk. Entomol. Congress, October 13-16, İzmir, Turkey, pp. 649-659.
[21] Marini, M., Trentini, M. (1986): I Macrolepidotteri dell'appennino lucchese. – Universita degli Studi di Bologna, Instituto e Museo di Zoologia, Bologna.

http://www.aloki.hu ● ISSN 1589 1623 (Print) ● ISSN 1785 0037 (Online)
DOI: http://dx.doi.org/10.15666/aeer/1705_1135911366

[22] Mathew, G. F. (1881): List of Lepidoptera observed in the neighbourhood of Gallipoli Turkey in 1878. – Entomologist's Mon. Mag. 18: 10-13, 29-32, 92-100.
[23] Mol, T. (1977): Gometridae species living in Marmara and Eagean Regional Forests. – Rev. of the Faculty of Forestry, University of Istanbul 2329(234): 125.
[24] NHM (2009): Natural History Museum web page. – http://www.nhm.ac.uk/jdsml/researchcuration/research/projects/lepindex/index.dsml (accessed: 23 November 2009).
[25] Okyar, Z., Aktac, N. (1998): Additives to Heterocera (Lepidoptera) fauna of Thracian Region. – Turk. J. Entomol. 22(1): 47-56.
[26] Okyar, Z., Aktac, N. (1999): Faunistic and Taxonomic studies on the Geometridae species of Turkish Thrace. – Turk. J. Zool. 23: 99-132.
[27] Rebel, H. (1903): Studien über die Lepidopterenfauna der Balkanlander I. (Bulgarien, Ostrumelien). – Annln. Naturh. Mus. (Wien) 18: 123-347.
[28] Romoser, S. W., Stoffolano, G. J. (1994): The Science of Entomology. – Wm. C. Brown Communications Inc., Iowa.
[29] Savela, M. (2001): Klepidoptera web page. – http://www.funet.fi/pub/sci/bio/life/insecta/lepidoptera/index.htm (accessed: 23 November 2009).
[30] Spuler, A. (1910): Die Schmetterlinge Europas. – E. Schweizerbartsche Verlagsbuchhandlung, Stuttgart.

http://www.aloki.hu ● ISSN 1589 1623 (Print) ● ISSN 1785 0037 (Online)
DOI: http://dx.doi.org/10.15666/aeer/1705_1135911366

THE IMPACT OF THE POLLUTION OF THE AQUATIC ENVIRONMENT OF MARINE FISHERIES ON THE FISH PRODUCTION OF SAUDI ARABIA

GHANEM, A. – ALNAFISSA, M.*

College of Food and Agriculture Sciences, King Saud University, P. O. Box 2460, Riyadh 11451 Kingdom of Saudi Arabia

**Corresponding author*
e-mail: malnafissa@ksu.edu.sa

(Received 18th Apr 2019; accepted 11th Jul 2019)

Abstract. The research aimed to measure the impact of pollution of the aquatic environment of marine fisheries on fish production in Saudi Arabia. This study achieves its objectives based on published secondary data and the estimation of the recursive model by ordinary least squares (OLS) method during the 1995-2017 period. The results of the study show the decline of the productivity of fishing vessels due to overfishing and failure to keep pace with the biological growth rate. The proportion of fish stocks within a biologically sustainable level declined from 87% in 2013 to 54% in 2017. The major factor of the decline of fish stocks and the productivity of fishing vessels is the environmental pollution of marine fisheries such as untreated sewage. The 10% increase of untreated sewage leads to a decrease in marine fish production by 20.9%.
Keywords: *productivity, overfishing, wastewater, recursive model, Red Sea, Arabian Gulf*

Introduction

The coast of Saudi Arabia extends over 2,900 km of the Red Sea and Arabian Gulf. The number of fishermen and fishing workers in the Kingdom is around 28.04 thousand, reaching 0.86% of the total population of 32.55 million in 2017 (Ministry of Environment, Water and Agriculture, 2017). Even with the expansion of the fishing water area and the increase in the number of fishermen and fishing vessels, fish production does not meet the increasing consumption needs. Therefore, there is an increase in the import of fish to the country. The total quantity of fish imports reached 163.85 thousand tons, valued at SR 1315.26 million of the total value of imports of agricultural and animal products which is 27303 million riyals in 2017 (General Authority for Statistics, 2017).

Due to the rapid development of the petrochemical industry in Saudi Arabia, the amount of waste, whether oil, industrial, or carbon ash waste from fuel combustion, in power generation and desalination plants has increased. The Kingdom's solid waste is estimated at about 12 million metric tons annually from the petrochemical, cement and oil refining industries. Heavy materials are thrown into the sea or buried in the soil, desert. Besides the impact of heavy fuel oil waste used in power plants and saltwater desalination on Saudi's marine environment, there is an effect of overfishing of fish stocks in the Red Sea and Arabian Gulf (Alnashwan and Ghanem, 2010). There are several studies have addressed the environmental problems of different fisheries.

Basaham et al. (2009) study showed that although Jeddah's sewage estuary has been moved to the edge of the coral reef towards the open sea, pollution remains widespread, endangering coastal environments and posing a threat to public health. This was evidenced by the heavy growth of algae and the increased concentration of heavy

http://www.aloki.hu ● ISSN 1589 1623 (Print) ● ISSN 1785 0037 (Online)
DOI: http://dx.doi.org/10.15666/aeer/1705_1136711374

elements in sediments. Al-Najjar (2015) estimated some heavy elements in the Chirocentrus dorab fish caught from the Iraqi coast. The results showed the total concentration of elements (lead, iron, nickel, cobalt, and copper) was 6590.26 μg/g dry weight for fish. Bouazem and Wennon (2015) estimated the revenues and costs of seawater desalination for Saudi Arabia during the period 2000-2014. In terms of cost, the cost of energy is one of the depleted natural resources, as well as the environmental costs summarized by the volume of emissions and saline solution from the stations. The cost of pollution from desalination plants, especially CO_2, is estimated at 19.4 $ per ton.

Qubartai's (2016) study addressed the environmental impact assessment of desalination technology and its relationship to pre-treatment levels. The saline water desalination results in a brine solution that increases salt content in the water. Additive chemicals also increase pollution. The environmental impact of desalination plants depends on both the physic-chemical properties of the discharged water and the hydrographic and biological properties of the aquatic environment. The other study by Alamin and Guthi (2017) dealt with marine environmental pollution through international law. The study showed that the marine environment is part of the global ecosystem. International law guarantees a set of rules for the protection of the marine environment, the obligations of States and measures that States must apply to their domestic legal systems with a view to protecting the marine environment from pollution.

Qamra et al. (2018) studied the economic effects of Lake Mariout pollution on agricultural production during the period 1990-2015. This study shows the increase of the total quantity of industrial and agricultural waste and the drainage of Alexandria Governorate by 10% leads to a decrease in the production of fish of Mariout Lake by 12.9%. Finally, the Ministry of Environment, Water and Agriculture of the Kingdom of Saudi Arabia (2018) prepared a national strategy for the environment, in view of the increasing pressures on the environment and natural resources in the Kingdom during the past decades. The strategy explained the increasing consumption of non-renewable water and the growing sources of water pollution.

This study aimed to analyze the effect of pollution of the aquatic environment on fish production in Saudi Arabia during the period 1995-2017 by studying the following objectives:

1. The current status of fish production and productivity of vessels operating in Saudi Arabia's marine fisheries.
2. Problems of the aquatic environment of marine fisheries (the Red Sea and the Arabian Gulf).
3. Measuring the impact of pollution of the aquatic environment on the quantity and value of fish production in Saudi Arabia.

Definitions

Through the study there are several research concepts, the most important of which are the following:

Environmental pollution. Pollution is defined as the state of the environment itself or the resultant changes in it and causes the person a direct or indirect disturbance, damage, disease or death. Pollution is also defined as any quantitative or qualitative change in the components of the living or non-living environment, and environmental systems cannot absorb it without changing its balance. Quantitative change results in the addition of toxic substances that are deadly in their natural concentrations such as

http://www.aloki.hu ● ISSN 1589 1623 (Print) ● ISSN 1785 0037 (Online)
DOI: http://dx.doi.org/10.15666/aeer/1705_1136711374

mercury, carbon oxide, and derived substances, while qualitative variation results from the addition of artificial compounds to natural ecosystems (Alnashwan and Ghanem, 2010).

Modern boats (commercial vessels). Boats with a length of more than nine meters, and contain modern equipment such as the discovery of places of gathering fish, electronic navigation equipment and modern communications devices, in addition to the winch and fishing equipment of high efficiency.

Traditional boats. Boats that are between 5 and 20 meters long and do not contain the equipment included in the modern boats, except for the winch and the bottom trawling of the shrimp fishing in the Arabian Gulf.

Fishermen could be called for traditional fishermen, investors, and fishermen for temporary periods. A traditional fisherman is a citizen who works himself in a fishing craft on a boat he owns. An investor is a citizen who invests part or all of his money in marine fisheries and owns modern fishing boats. The temporary fisherman refers to the children of fishermen who work with their parents in the marine fisheries sector and are under the age of 18 years. In addition, the other citizen fisherman who does the fishing but does not own boats or fishing boats (Ghanem and Al-Obaid, 2002).

Materials and methods

The study based on the secondary data presented in the statistical yearbook issued by the Ministry of Environment, Water, and Agriculture, in addition to the Bulletin of Export and Import Statistics published by the General Authority for Statistics. The proposed model of this study to analyze the impact of pollution of the aquatic environment on fish production during the period 1995-2017 through Recursive model consists of two behavioral equations (*Eq. 1* and *2*) and an indicative equation (*Eq. 3*). These equations are as follows:

$$Y_{1t} = a_0 + a_1 X_{1t} + a_2 X_{2t} + a_3 X_{3t} + e_{1t} \quad \text{(Eq.1)}$$

$$Y_{2t} = b_0 + b_1 \hat{Y}_{1t} + b_2 X_{4t} + e_{2t} \quad \text{(Eq.2)}$$

$$Y_{3t} = \hat{Y}_{2t} \times X_{5t} \quad \text{(Eq.3)}$$

These equations of the model include the following variables: (1) Endogenous Variables: there are three variables which are the fish production of the Red Sea and Arabian Gulf in thousand tons (Y_{1t}), the total fish production of Saudi fisheries per thousand tons (Y_{2t}), and the value of fish production in billion riyals (Y_{3t}); and (2) Exogenous Variables: there are five variables which are the number of fishing boats (X_{1t}), number of licensed fishermen (X_{2t}), total untreated wastewater in million cubic meters (X_{3t}), the total production of the rest of Saudi fisheries in thousand tons (X_{4t}), and the average wholesale price of fish by thousand riyals/ton (X_{5t}). It is clear from the proposed model that the fish production of the Red Sea and Arabian Gulf affects the total fish production of Saudi fisheries and thus affects the value of fish production. Thus, the causality is carried in one direction and not in the other. Models that follow this pattern are called the Recursive Model (Abdelkader, 1990).

http://www.aloki.hu ● ISSN 1589 1623 (Print) ● ISSN 1785 0037 (Online)
DOI: http://dx.doi.org/10.15666/aeer/1705_1136711374

Results

Current status of fish production and productivity of vessels

By following the change in fish production and the productivity of vessels operating in Saudi Arabia's marine fisheries during the period 1995-2017 (*Table 1*), it is clear that most of the vessels engaged in marine fisheries (the Red Sea and Arabian Gulf) are traditional. Fishing vessels are concentrated in the Red Sea, whereas 80.22% of the total number of vessels is employed, while only 19.78% in the Arabian Gulf during the study period. Even though the fisheries of Arabian Gulf dominated fish production, with the average production reach to 34.28 thousand tons that represent 45.34% of the average total fish production, followed by Red Sea fisheries by 31.7%, followed by fish farms and international waters by 22.16% and 1.07% respectively.

Table 1. *Statistical analysis of the evolution of the number of boats, fishermen, fish production and the production of fishing boats in the Red Sea and Arabian Gulf (1995-2017). (Source: collected and calculated from Statistical Yearbook, Ministry of Environment, Water and Agriculture, Statistics and Information Department, several editions, 1995-2017)*

List	Minimum	Maximum	Average	Standard deviation	Coefficient of variation%
The number of fishing boats in the Red Sea					
Traditional	5055	10102	8110	1762.71	21.74
Modern	108	169	150	16.91	11.31
The number of fishing boats in Arabian Gulf					
Traditional	1799	3768	2012	403.56	20.06
Modern	5	45	26	13.57	53.10
Total number of vessels in marine fisheries	7157	12195	10297	1689.23	16.40
Numbers of fishermen and fishing workers					
Fishermen	1000	10270	8275	2117.6	25.59
Saudi fishing workers	1647	2964	1990	289.64	14.55
Non Saudi fishing workers	11772	17112	15111	1860.69	12.31
Total numbers of fishermen and fishing workers	20239	29715	25767	3269.16	12.69
Production of vessels operating in the Red Sea in thousand tons					
Traditional	13.24	18.68	16.77	1.50	8.95
Modern	5.12	9.21	7.20	1.35	18.81
Total	20.45	27.51	23.97	1.98	8.27
Production of vessels operating in Arabian Gulf in thousand tons					
Traditional	18.44	45.19	33.88	8.88	26.20
Modern	0.04	2.06	0.40	0.62	153.73
Total	19.58	45.26	34.28	8.45	24.65
International water production per thousand tons	0	3.91	0.81	1.33	164.55
Production of fish farms in thousand tons	2.69	55.00	16.75	13.57	80.97
Total fish production per thousand tons	48.39	121.40	75.61	20.64	27.29

http://www.aloki.hu ● ISSN 1589 1623 (Print) ● ISSN 1785 0037 (Online)
DOI: http://dx.doi.org/10.15666/aeer/1705_1136711374

Average productivity of vessels operating in the Red Sea per ton/vessel					
Traditional	1.32	3.21	2.18	0.56	25.81
Modern	32.07	64.69	48.60	9.74	20.04
Average productivity of vessels operating in the Arabian Gulf per ton/vessel					
Traditional	9.66	22.97	17.02	4.33	25.42
Modern	1.43	45.78	13.40	13.38	99.85

The average productivity of traditional vessels in Red Sea fisheries decreased from 2.95 tons/vessel in 1995 to 2.58 tons/vessel in 2017. By taking the same period of time, the productivity of modern vessels in Red Sea fisheries also decreased from 63.79 to 33.18 tons/vessel. The average productivity of modern vessels in Arabian Gulf fisheries decreased from 25.33 to 10.0 tons/vessel during the same period of time.

The impact of pollution of the aquatic environment on the quantity and value of fish production

To study the economic effects of the pollution of the aquatic environment on quantity and value of Saudi Arabia's fish production, the equations of the proposed model were estimated by the ordinary least squares (OLS) method during the period 1995-2017. The result from a model analysis in *Table 2* shows the increase of untreated sewage waste in Saudi Arabia by 10% leads to a decrease of 20.9% in fish production of marine fisheries. The increase in the estimated of production of marine fisheries by 10% leads to an increase in total fish production of Saudi Arabia by 0.8%, while an increase of 10% for the production of the rest of Saudi fisheries leads to an increase in total fish production by 9.9%. The significance of this estimation is at 1%. According to the Breusch-GodFrey serial correlation LM Test, there is no autocorrelation in the errors in an estimated regression model. Also, there is no autocorrelation in the squared series, according to the Arch Test. In addition, the estimated equations are well represented in the data used in this estimation according to the efficiency indicators of the model such as U Theil's inequality coefficient, which is close to zero (*Table 3*).

Table 2. *An estimated model of the impact of pollution on the quantity and value of fish production of Saudi Arabia (1995-2017). (Source: Computed from Statistical Yearbook, Ministry of Environment, Water and Agriculture, 1995-2017)*

List	Equation
Production of marine fisheries	$\begin{gathered} \mathrm{Ln}\hat{Y}_1 = -16.028 + 0.06\,\mathrm{Ln}\,X_1 - 0.209\,\mathrm{Ln}\,X_3 + 0.69AR(1) \\ (-2.22)^{*}\ (1.96)^{*}\quad (-2.43)^{*}\quad (5.77)^{**} \\ R^2 = 0.82\quad F = 31.37\quad D.W = 1.67 \\ LM\ test = 0.17\quad Arch\ test = 0.06 \end{gathered}$
Total fish production	$\begin{gathered} \mathrm{Ln}\hat{Y}_2 = 0.05 + 0.008\,\mathrm{Ln}\,\hat{Y}_1 + 0.099\,\mathrm{Ln}\,X_4 + 0.62\,AR(1) \\ (5.29)^{**}\quad (2.07)^{*}\quad (449.77)^{**}\quad (2.80)^{**} \\ R^2 = 0.99\quad F = 1859763\quad D.W = 1.39 \\ LM\ test = 0.44\quad Arch\ test = 0.70 \end{gathered}$
Total value of fish production	$Y_3 = \hat{Y}_2 * X_2$

**Statistically significant at level 1%. *Statistically significant level 5%

http://www.aloki.hu ● ISSN 1589 1623 (Print) ● ISSN 1785 0037 (Online)
DOI: http://dx.doi.org/10.15666/aeer/1705_1136711374

Table 3. *Indicators for measuring the efficiency of the estimated model (1995-2017). (Source: Compiled and calculated from the behavioral equations of the estimated model in Table 3)*

Indicator	Behavioral equation	
	First	Second
The root mean square error (RMSE)	0.19	0.001
Mean absolute error (MAE)	0.15	0.0009
Mean absolute percentage error (MAPE)	9.40	0.01
(U) Theil: Theil inequality coefficient	0.06	0.00008

Discussion

In general, it is clear the degradation of the productivity of vessels in Saudi fishery marines during the period of study. This could be caused by different factors such as:

- The continuous increase in the number of fishermen and traditional and modern vessels in the Red Sea and Arabian Gulf regions. Whereas increasing the number of boats in a fishing area means increasing the number of fishing trips on the same fishing area. This phenomenon is known as overfishing, which leads to a failure to keep pace with the rate of biological growth of the fish catch rate, and thus to affect the fish stocks of those.
- The ability of most fishing vessels operating in marine fisheries is less than 100 mechanic horses. Therefore, these vessels cannot sail long distances at sea and approach the continental slope. Since there is a direct relationship between the power of the motor or the engine and sailing long distances in Sea, stand the weather conditions is appropriate, and stay longer in the sea.

Problems of the aquatic environment of Saudi marine fisheries

The marine fisheries of Saudi Arabia have been exposed to several environmental problems, the most important of which is pollution and the phenomenon of overfishing. The pollution of the aquatic environment of Saudi marine fisheries is attributed to several factors: (1) the movement of oil tankers and commercial vessels between East and West, which makes marine fisheries vulnerable to pollution during loading and unloading operations, ship refueling and waste disposal, (2) discharge of untreated sewage and waste of industrial facilities located on the coast of Red Sea and Arabian Gulf, (3) port clearance and ship maintenance and painting, (4) seawater desalination companies, (5) oil and mineral exploration in marine waters, (6) the management of maritime ports and oil companies may have to use chemicals to disperse spots Oily resulting from some accidental accidents and spills, and (7) oil spill resulting from the military operations. Whereas there was an oil spill from Nowruz Field that lasted for eight months during the Iran-Iraq war in 1983. The amount of oil spilled ranged from 200 to 500 thousand tons. Also, the amount of oil leaking was about one million tons during the war of the liberation of Kuwait in 1991. Despite efforts to contain this massive oil spill, it was a major cause of the destruction of at least 300 km from the eastern coast of Saudi Arabia and the deaths of many marine organisms and birds. Because of the pollution of the aquatic environment of marine fisheries and overfishing, the rate of biological growth of the fishing rate has not kept up with a fishing rate. The

http://www.aloki.hu ● ISSN 1589 1623 (Print) ● ISSN 1785 0037 (Online)
DOI: http://dx.doi.org/10.15666/aeer/1705_1136711374

data in *Table 4* show that the percentage of fish stocks within a biologically sustainable level has decreased from 87% in 2013 to 54% in 2017.

Therefore, the pollution of the aquatic environment of marine fisheries is one of the main reasons to decrease the rate of biological growth of the fish that leads to a decrease in the percentage of fish stocks within a biologically sustainable level. This reason confirms by the result of data analysis through this study which there is an inverse relationship between untreated sewage waste and fish production of marine fisheries in Saudi Arabia.

Table 4. *Evolution of the size and proportion of fish stocks within the biologically sustainable level (2010-2017). (Source: Statistical Yearbook, Ministry of Environment, Water and Agriculture, 2017)*

Year	Size of fish stocks within the biologically sustainable level by 1,000 tons	Percentage of fish stocks within a biologically sustainable level %
2010	65.07	71
2011	63.17	79
2012	71.39	80
2013	61.77	87
2014	67.99	74
2015	64.88	62
2016	66.54	62
2017	66.40	54

Conclusion

Pollution sources of marine fisheries (the Red Sea and Arabian Gulf) are abundant in the territorial waters of Saudi Arabia which have negative impacts on fish production, health, and human well-being. Shows the increase of untreated sewage waste in Saudi Arabia by 10% leads to a decrease of 20.9% in fish production of marine fisheries. In order to protect marine fisheries from pollution, the study recommends the following: (1) Raise awareness about the importance of preserving the marine environment through research and regulation of fishing rules such as length of fishhook, number of fishing trips, minimum and maximum size of fish, the amount of fishing, the prohibited fishing seasons and prohibited fishing sites, (2) develop fishing boats and increase their ability to sail long distances in the Red Sea and Arabian Gulf, so the phenomenon of overfishing can be eliminated and the preservation of fish stocks, (3) tighten control over all facilities and plants that discharge their wastes in marine waters, (4) improve the primary treatment of sewage, (5) implement more research to study the effect of pollution to damages the marine natural resources in Saudi Arabia and analysis the effective policy tools to improve aquatic environment, and (6) Cooperation among the Gulf Cooperation Council (GCC) countries on the establishment of a network to monitor and control pollution. This may require aerial and night monitoring and surveillance to detect expected violations.

Acknowledgements. The authors extend their sincere appreciation to the Deanship of Scientific Research at King Saud University for supporting the work through the College of Food and Agricultural Sciences Research Center. Furthermore, the authors thank the Deanship of Scientific Research at King Saud University for their technical support.

http://www.aloki.hu ● ISSN 1589 1623 (Print) ● ISSN 1785 0037 (Online)
DOI: http://dx.doi.org/10.15666/aeer/1705_1136711374

REFERENCES

[1] Abdelkader, A. (1990): Methods of Measuring Economic Relations with Computer Applications. – Egyptian Universities House, Alexandria.
[2] Alamin, M., Guthi, Q. (2017): Marine environmental pollution in light of international law. – Journal of Scientific Research in International Legislation 5(9): 429-439.
[3] Al-Najjar, G. (2015): The accumulation of some heavy metals in the chiocentrus dorab fish caught from Iraqi coasts. – Journal of King Saud University, Agricultural Sciences 26(2): 127-143.
[4] Alnashwan, O., Ghanem, A. (2010): Environmental Economic Policies and Measurements - Applied Study in Saudi Arabia and Egypt. First Ed. – Al-Moayad Publishing and Distribution House, Saudi Arabia.
[5] Basaham, A., Rifaat, A., El-Mamoney, M., El Sayed, M. (2009): Re-evaluation of the impact of sewage disposal on coastal sediments of the southern Corniche, Jeddah, Saudi Arabia. – Journal of King Abdulaziz University, Marine Sciences 20(1): 109-126.
[6] Bouazem, K., Wennon, A. (2015): Desalination of seawater in Saudi Arabia: realized revenues and costs incurred during the period (2000-2014). – Arab Economic Research Journal 71: 21-42
[7] General Organization for Statistics (2017): Import Statistics. – Riyadh, Saudi Arabia.
[8] Ghanem, A., Al-Obaid, A. (2002): The economic dimension of fish production and consumption in Saudi Arabia. – Journal of King Saud University, Agricultural Sciences 14(2): 191-198.
[9] Ministry of Environment, Water and Agriculture (1995-2017): Statistical Yearbook (several editions). – Statistics and Information Department, Riyadh, Saudi Arabia.
[10] Ministry of Environment, Water and Agriculture (2017): Executive Summary of the National Environmental Strategy. – Riyadh, Saudi Arabia.
[11] Qamra, S., Jamila, A., Hassan, G. (2018): Study of the economic impacts of Lake Mariout pollution on agricultural production. – Egyptian Journal of Agricultural Economics 29(3) September: 110-145.
[12] Qubartai, S. (2016): Environmental impact assessment of desalination technology and its relation to pre-treatment quantities. – Journal of Environmental Research and Sustainable Development 145(1): 145-163.

http://www.aloki.hu ● ISSN 1589 1623 (Print) ● ISSN 1785 0037 (Online)
DOI: http://dx.doi.org/10.15666/aeer/1705_1136711374

SPATIAL AND TEMPORAL VARIATION AND PROBABILITY CHARACTERISTICS OF EXTREME PRECIPITATION EVENTS IN THE MIN RIVER BASIN FROM 1961 TO 2016

CHEN, T.[1,2] – AO, T. Q.[1*] – ZHANG, X.[1,3,4] – LI, X. D.[1] – ZHOU, L.[1] – LI, M. R.[1] –YANG, K. B.[1]

[1]*State Key Laboratory of Hydraulics and Mountain River Engineering, College of Water Resource and Hydropower, Sichuan University, Chengdu/610065, China*

[2]*Heavy Rain and Drought-Flood Disasters in Plateau and Basin Key Laboratory of Sichuan Province, Chengdu/610072, China*

[3]*State Key Laboratory of Hydrology-Water Resources and Hydraulic Engineering Nanjing Hydraulic Research Institute, Nanjing/210029, China*

[4]*Research Center for Climate Change, Ministry of Water Resources, Nanjing/210029, China*

[*]*Corresponding author*
e-mail: aotianqi@scu.edu.cn

(Received 18th Apr 2019; accepted 11th Jul 2019)

Abstract. Based on the daily precipitation data of 25 national meteorological stations in the Min River Basin (the MRB), the temporal and spatial variation trends of extreme precipitation events from 1961 to 2016 were analyzed using multiple extreme precipitation indices and the Mann-Kendall trend analysis. The extreme precipitation in different recurrence periods was calculated by using the regional frequency analysis combined with the spatial distribution characteristics of extreme precipitation events. The spatial distribution of the extreme precipitation index in the MRB varies considerably. The average characteristics of extreme precipitation are changing from short-term extreme precipitation to sustained extreme precipitation. The main reasons for this change are the significant increases in wet days and consecutive wet days, particularly the number of heavy precipitation days (R10mm). On this basis, the Min River is divided into four hydro-climatically consistent regions and the maxima of RX1DAY's and RX5DAY's 20-year and 100-year recurrence periods are found. The traditional at-site hydrological frequency analysis averaged the spatial differences within the basin and underestimated the extreme precipitation in the middle reaches. This indicates that the regional frequency analysis has some reference significance for solving the problem of neglecting the uneven spatial distribution of extreme precipitation in precipitation estimation.
Keywords: *climate change, extreme precipitation indices, regional frequency analysis, precipitation estimation, Mann-Kendall trend analysis*

Introduction

The IPCC Fifth Assessment Report pointed out that the global average surface temperature increased by 0.85°C between 1880 and 2012 (IPCC, 2013), and global warming has become an indisputable fact. In the context of global warming, extreme events such as floods, droughts, typhoons, high temperatures, low temperatures and freezing rain and snow often occur (Changnon et al., 2000; Zengxin, 2011; Fu et al., 2013; Tian et al., 2016). As an important part of the water cycle, precipitation directly

http://www.aloki.hu ● ISSN 1589 1623 (Print) ●ISSN1785 0037 (Online)
DOI: http://dx.doi.org/10.15666/aeer/1705_113751394

affects the hydrological process of runoff and increases the frequency of flooding disasters (Wang et al., 2004; Kampata et al., 2008; Millett et al., 2009; Chen et al., 2009; Xu et al., 2010; Zhang et al., 2012).

The IPCC report also points out that the land surface temperature in China has risen by 1.38°C in the past 60 years, 0.23°C every 10 years, which is higher than the global average. The climate change is likely to develop further. Many scholars have analyzed the extreme precipitation in different regions of China: the studies have shown that there are obvious regional differences in the extreme precipitation and precipitation frequency in different regions of Qinling-Huaihe River North of Henan (Liet al., 2015), Pearl River Basin (Huang et al., 2014), and Yellow River Basin (He et al., 2014), indicating that there are obvious spatial differences in the distribution of extreme precipitation events.

Though the analysis of the characteristics of extreme precipitation over time in different regions, it is also found that there are spatial differences in the temporal variation of extreme precipitation events (Chu et al., 2012; Li et al., 2012; Bai et al., 2015; Tian et al., 2016). Zhai et al. (2005) found that there was no obvious change trend in annual precipitation and the intensity of precipitation was on the rise. However, the trend of extreme precipitation events showed obvious spatial differences. Influenced by East Asian monsoon activities, China was extremely vulnerable to large-scale flood disasters, especially in the Yangtze River Basin (YRB). Yu et al. (2004) pointed out that while the precipitation in northern China was decreasing, the precipitation in mainland China took the form of "flooding in the South and drought in the North". The probability of flood disasters in the YRB was much greater than that in other regions of China. Zhai (1999) showed that the annual precipitation in the YRB showed a significant upward trend. The extreme precipitation in the middle and lower reaches of the YRB showed a significant upward trend, and the change trend in the upper reaches of the YRB was not obvious. Pan et al. (2017) used the methods of trend and catastrophe analysis, R/S analysis and hydrological frequency analysis to study the temporal and spatial evolution characteristics and future trends of extreme precipitation in the YRB. The results show that the regional extreme precipitation index in the YRB shows an upward trend, and the annual changes of the extreme precipitation index in the middle and lower reaches are greater than in the upper reaches. Wu (2016) used the Mann-Kendall (MK) test to study the changes of extreme precipitation in 11 regions of China, and concluded that the flood disaster in the upper reaches of the YRB had an obvious increasing trend. Bai (2015) used Logistic regression model to study the characteristics of extreme precipitation in the YRB. The results show that the frequency of extreme precipitation in the upper and middle reaches has a significant non-linear increasing trend, but the variation trend of extreme precipitation frequency in the Sichuan Basin located in the upper reaches of the YRB is not obvious. Qian (2005) found that the intensity of extreme precipitation and the frequency of persistent rainy days in the upper reaches of the YRB showed a downward trend. Zhang (2006) simulated extreme precipitation in the YRB through PRECIS climate model simulation and concluded that extreme precipitation events in the middle

http://www.aloki.hu ● ISSN 1589 1623 (Print) ●ISSN1785 0037 (Online)
DOI: http://dx.doi.org/10.15666/aeer/1705_113751394

and lower reaches had an overall upward trend, but the upstream trend was not obvious. Chen et al. (2017) predicted that extreme precipitation in China would increase significantly in the lower reaches of the YRB in the 21st century by using the IPCC AR4 model and coupling it with the atmospheric circulation model.

From the above conclusions, we can see that the study of the YRB shows that there is an increasing trend in extreme precipitation in the YRB (Zhai et al., 1999; Yu, 2004; Pan et al., 2017), but there are also obvious regional differences there. The consistent conclusion for the middle and lower reaches of the YRB is that the extreme precipitation in the middle and lower reaches shows an upward trend (Zhai et al., 1999; Zhang et al., 2006; Pan et al., 2017; Chen et al., 2017), which is also the main contribution of the overall extreme precipitation in the YRB. At the same time, the conclusions of the upper reaches of the YRB are not entirely unified. Some studies of the upper reaches show an upward trend, but the upward trend is lower than that of the middle and lower reaches of the YRB (Xu et al., 2016; Pan et al., 2017). Other studies show that the extreme precipitation in the upper reaches of the YRB has not changed significantly with time and may even have shown a downward trend (Zhai et al., 1999; Qian et al., 2005; Zhang et al., 2006; Luyao et al., 2015). The conclusion of extreme precipitation variation in the upper reaches of the YRB is not entirely uniform, which may be related to the incomplete data periods, different methods and incomplete definitions of extreme precipitation indices used. When the data period used is not exactly the same, because of the quasi-periodic oscillation of precipitation in the YRB (Chen et al., 2017), the trend of extreme precipitation in the analysis results is related to the length of the time series used in the analysis. When different research methods are used, the results may be different (Qian et al., 2005; Luyao et al., 2015). The methods of extreme precipitation research are mainly divided into two categories. One is statistical analysis of precipitation data, such as using MK trend test, MK mutation analysis, wavelet analysis and other statistical methods (Karl et al., 1998; Bonsal et al., 2001; Pal et al., 2011; Tramblay et al., 2012; Yang et al., 2012; Croitoru et al., 2013). Because statistical methods depend heavily on the length of observation data and the selected site data, the results of different research periods or sites in the same region may vary greatly. The other is to simulate the characteristics of extreme precipitation using models. Because the current climate models cannot accurately simulate the temporal and spatial changes of future extreme climate events, the prediction of future extreme precipitation by multi-model sets also has a series of problems of accuracy and deviation, such as the error of a single model may affect the whole prediction conclusion, and multimodal ensemble forecasting results may smooth some extreme weather events (Li et al., 2012). At the same time, different indicators of extreme precipitation will also affect the results. The indicators of extreme precipitation were proposed by the World Meteorological Organization (WMO) Meteorological Committee (CCL) and Climate Variability and Predictability Research Program (CLLVAR) in 2006. The recommended extreme precipitation indicators can point out the characteristics of extreme precipitation, including intensity, frequency, and duration.

http://www.aloki.hu ● ISSN 1589 1623 (Print) ●ISSN1785 0037 (Online)
DOI: http://dx.doi.org/10.15666/aeer/1705_113751394

Before that, the extreme precipitation indices used were not perfect (Zhai et al., 1999; Qian et al., 2005; Su et al., 2006).

In addition to the above three reasons, which have an impact on the research results of extreme precipitation in the YRB, there is also a reason for the spatial differences of regional changes in the YRB. When the study area is large (for example, dividing the YRB into upper, middle and lower reaches), it will be difficult to reflect the spatial and temporal variations of extreme precipitation in different regions of the basin, because the overall study of the region will smooth out the regional characteristics of extreme precipitation. At the same time, if its trend keeps rising in the future, it will be difficult to reflect the temporal and spatial variation trend by using the entire dataset. The predictions of precipitation estimated by using the whole data will be more uncertain. Moreover, the significance of the trend and changes in the extreme precipitation index in the predictions of precipitation also has not been given sufficient attention. Therefore, the Min River Basin (the MRB), which belongs to the upper reaches of the YRB and is the largest tributary of the upper reaches of the Yangtze River, is selected as the study area for the current study. The MRB is in the transition area from the high-altitude area to the basin on the eastern side of the Qinghai-Tibet Plateau. There are great differences in altitude, topography and climate conditions in this area. The study of extreme precipitation variation in the MRB is of great significance to the analysis of extreme precipitation variation trends in the Yangtze River and the upper reaches of the Yangtze River. Previous research on the precipitation characteristics of the MRB has concentrated on the lower reaches of the MRB, and has mainly focused on the general characteristics of precipitation in the MRB. In the context of global warming, the MRB shows different regional response characteristics, which will have a huge impact on regional environmental ecology. Therefore, on the basis of previous research work, this paper focuses on the MRB, using the daily precipitation data of 26 meteorological stations in the MRB from 1961 to 2016, using MK trend analysis, to analyze the temporal and spatial variation of extreme precipitation in the MRB. Considering the significant changes of extreme precipitation in different regions, the MRB was divided into climatic consistent regions and the estimated precipitation of the basin was calculated by using the regional frequency analysis.

Materials and Methods

The Min River (*Fig. 1*) is the largest tributary of runoff in the Yangtze River. The total drop of the Min River is 3560 meters, and the basin area is 135 881 square kilometers. It is an important area for hydropower development in Southwest China. According to the geographical characteristics of the main river, the upper reaches extend from the source to Dujiangyan City, the middle reaches from Dujiangyan City to Leshan City, and the lower reaches from Leshan City to Yibin City.

http://www.aloki.hu ● ISSN 1589 1623 (Print) ●ISSN1785 0037 (Online)
DOI: http://dx.doi.org/10.15666/aeer/1705_113751394

Precipitation Data

The daily precipitation data of 25 stations (*Table 1*) from 1961 to 2016 is provided by the China Meteorological Administration. Relevant station data is available at http://data.cma.cn/. The precipitation data have been qualitatively controlled.

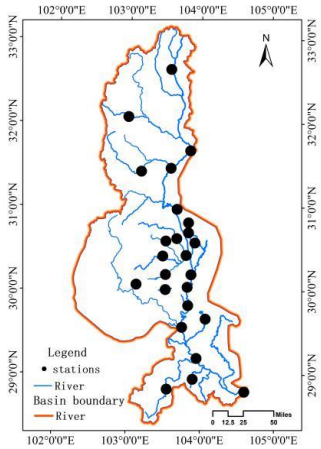

Figure 1. *Min River drainage map*

Table 1. *The basic information of the meteorological stations in the MRB*

Station number	Longitude (°E)	Latitude (°N)	Altitude (m)	Station name	Station class
the upper reaches					
56182	103.57	32.65	2850	Songpan	base station
56185	102.98	32.08	2400	Heishui	general stations
56180	103.85	31.68	1591	Maoxian	general stations
56183	103.58	31.47	1326	Wenchuan	general stations
56184	103.17	31.43	1885	Lixian	general stations
the middle reaches					
56188	103.67	30.98	699	Dujiangyan	base station
56189	103.93	30.98	582	Pengzhou	general stations
56187	103.83	30.7	539	Wenjiang	base station
56288	103.92	30.58	495	Shuangliu	general stations
56181	103.67	30.63	534	Chongzhou	general stations
56272	103.83	30.82	559	Pixian	general stations
56276	103.8	30.43	468	Xinjin	general stations
56285	103.52	30.6	524	Dayi	general stations
56284	103.48	30.42	501	Qionglai	general stations
56281	103.52	30.2	511	Pujiang	general stations
56391	103.82	30.05	415	Meishan	general stations
56289	103.87	30.2	437	Pengshan	general stations
56381	103.52	30.02	496	Dangling	general stations
56383	103.83	29.83	455	Qingshen	general stations
56386	103.75	29.57	424	Leshan	base station
the lower reaches					
56390	104.07	29.67	404	Jingyan	general stations
56389	103.95	29.2	388	Qianwei	general stations
56480	103.55	28.83	541	Mabian	general stations
56490	103.9	28.95	397	Muchuan	general stations
56492	104.6	28.8	341	Yibin	base station

http://www.aloki.hu ● ISSN 1589 1623 (Print) ●ISSN1785 0037 (Online)
DOI: http://dx.doi.org/10.15666/aeer/1705_113751394

Extreme Precipitation Index

Twelve extreme precipitation indices are used in this study. They are recommended by the World Meteorological Organization (WMO) Meteorological Committee (CCL) and Climate Variability and Predictability Research Program (CLLVAR) (Alexander et al., 2006). These indicators have been applied to analyze the characteristics of extreme precipitation (Wu et al., 2016). In this article, three supplementary indices (SPIs) are added to describe the variation trend of precipitation in the MRB. Detailed descriptions of ETIs and SPIs are presented in *Table 2*.

Table 2. *Definitions of extreme precipitation indices employed in the study*

ETIs			
CWD	Consecutive wet days	Maximum number of consecutive days with RR≥1mm	days
R10mm	Number of heavy precipitation days	Annual count of days when RR≥10mm	days
R25mm	Number of very heavy precipitation days	Annual count of days when RR≥25mm	days
RX1DAY	Maximum 1-day precipitation	Annual maximum 1-day precipitation	mm
RX5DAY	Maximum 5-day precipitation	Annual maximum 5-day precipitation	mm
R95T	very wet day precipitation	Annual total precipitation when RR≥95th percentile of 1961-2016 daily precipitation	mm
R99T	Extremely wet day precipitation	Annual total precipitation when RR≥99th percentile of 1961-2016 daily precipitation	mm
PRCPTOT	Annual total wet day precipitation	Annual total precipitation in wet days (RR≥1mm)	mm
SDII	Simple daily intensity index	Annual total precipitation divided by the number of wet days in the year	mm/day
SPIs			
R95PT	Precipitation fraction due to very wet days	Ratio between R95T and PRCPTOT	%
R99PT	Precipitation fraction due to extremely wet days	Ratio between R99T and PRCPTOT	%
WD	Wet days	Annual count of days when RR≥1mm	days

Note: RR denotes daily precipitation

Methods

MK Trend Test

A MK test is a non-parametric test recommended and widely used by the WMO. A MK test does not require samples to follow a certain distribution, nor is it disturbed by a few abnormal values. A MK trend test was used to analyze the trend change of time series of precipitation, runoff, temperature, and water quality (Mann, 1945; Kendall, 1945; Vijay et al., 2010; Wu et al., 2016). It is suitable for non-normal distribution data such as hydrology and meteorology and is easy to calculate (Xu et al., 2007; Burn et al., 2008; Wu et al., 2008; Zhang et al., 2008; Wang, 2009). The calculation formula of the MK test can be found in Reference (Mann, 1945).

http://www.aloki.hu ● ISSN 1589 1623 (Print) ●ISSN1785 0037 (Online)
DOI: http://dx.doi.org/10.15666/aeer/1705_113751394

Regional Frequency Analysis

The regional frequency analysis combines linear moment with regional analysis method, avoids the limitation of traditional at-site frequency analysis method, improves the unbiasedness and robustness of parameter estimation, improves the accuracy of frequency design value (Lin et al., 2006), and effectively improves the accuracy and reliability of hydrological frequency analysis. At present, it has been widely used in hydrological frequency analysis (Li et al., 2015; Shao et al., 2016; Yang et al., 2009).

Firstly, this study chooses the indicators which can reflect the obvious spatial differences in extreme precipitation. Combining with the longitude, latitude, elevation and linear moment parameters of each station, all stations are preliminarily divided by clustering analysis method, and the discordance detection and heterogeneity detection (Xiong et al., 2004) are used to test whether each zone is a reasonable hydrometeorological consistency region.

On this basis, in view of the divided hydrometeorological consistent region, this study assumes that the stations in the hydrometeorological consistent region conform to Kappa distribution. Monte Carlo simulation is used to simulate the study area N_{sim} times, each time generating the same length of historical rainfall data series corresponding to each site. Furthermore, Monte Carlo simulation test is used to determine the optimal frequency distribution for each hydrometeorological consistency region in the five three-parameter frequency distribution patterns (Chen, 2014): generalized Pareto distribution (GPA), generalized extreme value distribution (GEV), generalized logistic distribution (GLO), generalized normal distribution (GNO) and Pearson III distribution (PE3). Finally, using the index flood method (Cunnane, 1989) and the optimal frequency distribution line, the design values of rainstorm frequencies for different recurrence periods of each station are calculated.

The calculation formula of the discordance detection is as follows:

$$D_i = \frac{1}{3} N (u_i - \bar{u})^T A^{-1} (u_i - \bar{u}) \quad \text{(Eq.1)}$$

In the formula: $u_i = [t^i, t_3^i, t_4^i]^T$ (i = 1, 2, 3... N) is a three-dimensional vector consisting of three linear moment coefficients: linear deviation coefficient L-Cv, linear deviation coefficient L-Cs and linear kurtosis coefficient L-Ck.

$$\bar{u} = N^{-1} \sum_{i=1}^{N} u_i \quad \text{(Eq.2)}$$

$$A = \sum_{i=1}^{N} (u_i - \bar{u})(u_i - \bar{u})^T \quad \text{(Eq.3)}$$

http://www.aloki.hu ● ISSN 1589 1623 (Print) ●ISSN1785 0037 (Online)
DOI: http://dx.doi.org/10.15666/aeer/1705_113751394

If the discordance coefficient $D_i \leq \frac{N-1}{3}$, there is no singularity in the region. If $D_i > \frac{N-1}{3}$, it is considered that the site is a discordance point. It is necessary to further check the rationality and reliability of the site data and make a correct trade-off.

The formula of the heterogeneity detection is as follows:

$$H_1 = \frac{(V_1 - \mu_v)}{\sigma_v} \quad \text{(Eq.4)}$$

Among them,

$$V_1 = \left\{ \sum_{i=1}^{N} n_i (t^i - t^R)^2 / \sum_{i=1}^{N} n_i \right\}^{\frac{1}{2}} \quad \text{(Eq.5)}$$

$$t^R = \sum_{i=1}^{N} n_i t^i / \sum_{i=1}^{N} n_i \quad \text{(Eq.6)}$$

where n_i is the length of rainfall data series of the *i-th* station in the consistent area, t^i is the linear potential coefficient L-Cv at the *i-th* station in the consistent area, N is the total number of stations in the consistent area. μ_v and σ_v are the mean and mean square deviation of V_1 calculated by Monte Carlo simulation.

If $H_1 < 1$ the area is acceptably consistent, if $1 \leq H_1 < 2$ the area is possibly heterogeneous, and if $H_1 \geq 2$ the area is heterogeneous. The stations in the area need to be adjusted when $H_1 \geq 1$ is acceptable until they meet the criteria.

Results Analysis

Spatial Distribution

As can be seen from *Figure 2*, the maximum number of consecutive wet days (CWD) in the MRB was relatively uniform. The frequency of extreme precipitation events (R10mm and R25mm) in the lower and middle reaches of the MRB was significantly higher than that in the upper reaches. The spatial distribution of RX1DAY and RX5DAY were similar, showing a gradual increase in the upper and middle reaches of the basin, and a decrease in the lower reaches. The results show that the intensity of extreme

http://www.aloki.hu ● ISSN 1589 1623 (Print) ●ISSN1785 0037 (Online)
DOI: http://dx.doi.org/10.15666/aeer/1705_113751394

precipitation events in the MRB was largest in the middle reaches, especially in the continuous extreme precipitation, followed by the lower reaches, and lowest in the upper reaches. The percentile index of extreme precipitation events (R95T, R99T, R95PT and R99PT) were larger in the middle and lower reaches than in the upper reaches of the MRB.

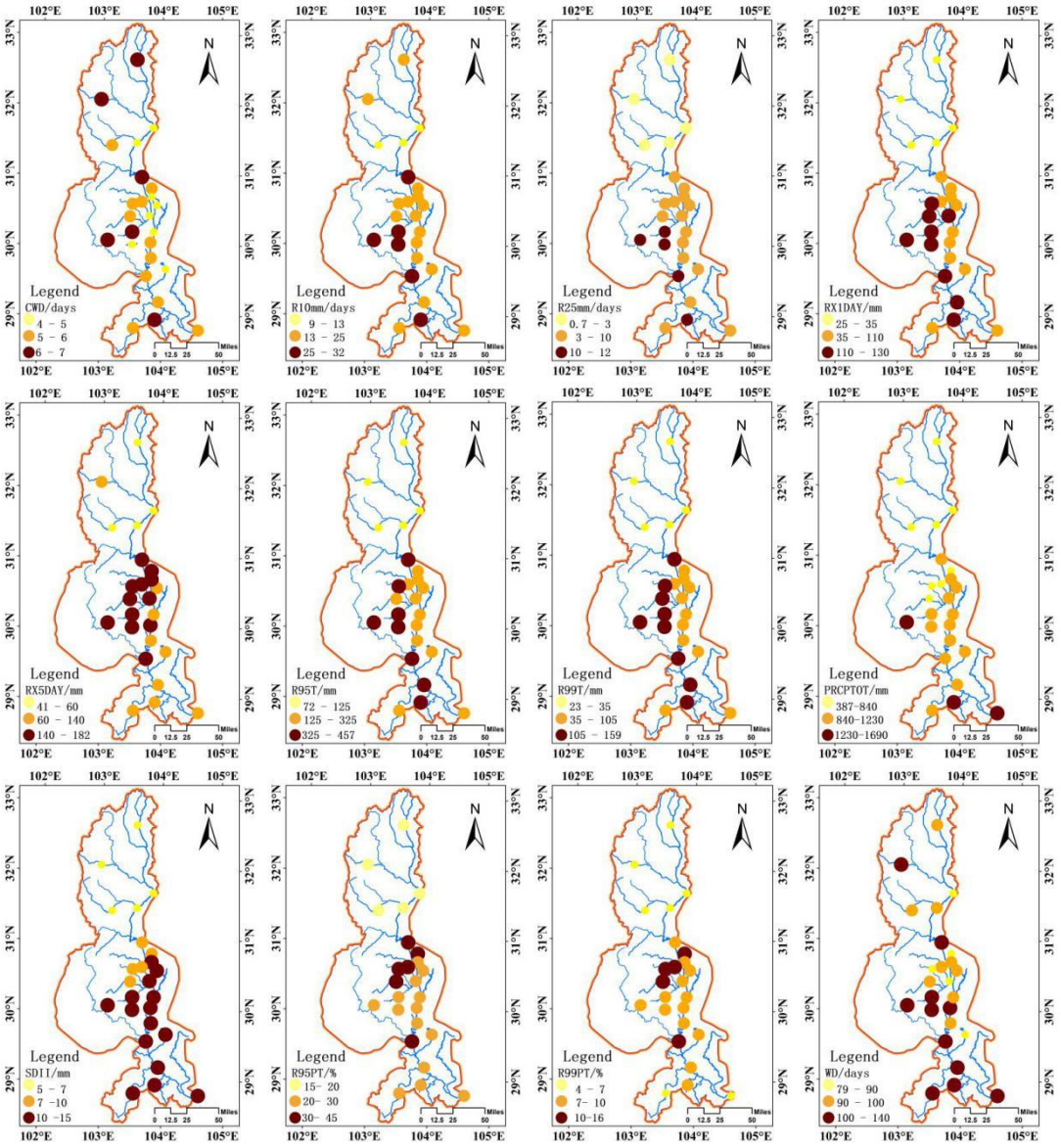

Figure 2. *Spatial Distribution of Extreme Precipitation Index in the MRB*

The PRCPTOT, the WD and the SDII in the MRB were higher in the lower reaches than in the middle reaches, and higher in the middle reaches than in the upper reaches. In a word, the main manifestation is that the high value of extreme precipitation index mainly appears in the middle and lower reaches of the basin, in which there is a high value

http://www.aloki.hu ● ISSN 1589 1623 (Print) ●ISSN1785 0037 (Online)
DOI: http://dx.doi.org/10.15666/aeer/1705_113751394

center of extreme precipitation intensity in the middle reaches of the basin, while the low value appears in the upper reaches of the basin.

Trends of Spatial Change

As can be seen from *Figure 3*, the CWD shows an upward trend in the whole basin.

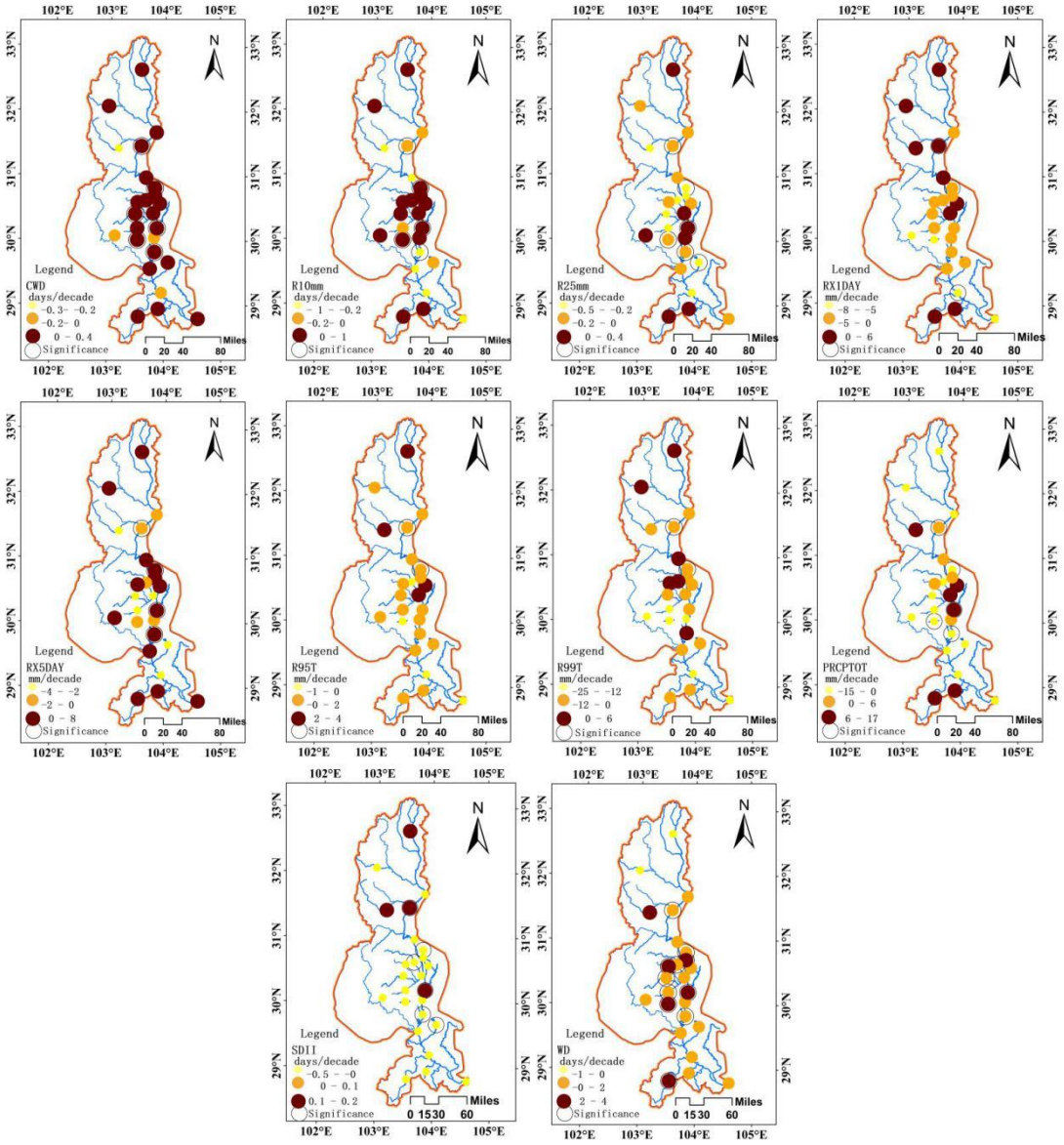

Figure 3. *Spatial distribution of extreme precipitation index in the MRB*

The frequency of R10 mm in the upper reaches of the basin decreases while that in the middle and in the lower reaches increases, while the frequency of R25mm mainly decreases in the whole basin. There are some regional differences in the spatial distribution of the RX1DAY change trend (*Fig. 3*).

http://www.aloki.hu ● ISSN 1589 1623 (Print) ●ISSN1785 0037 (Online)
DOI: http://dx.doi.org/10.15666/aeer/1705_113751394

The upper reaches of the basin show a weak growth trend. The weak decrease trend is dominant in the middle and lower reaches. RX5DAY shows a downward trend in the upper reaches of the river basin. The results show that the spatial distribution difference of short-term extreme precipitation decreases and the spatial distribution difference of continuous extreme precipitation increases. The spatial pattern of extreme precipitation ratio (R95T and R99T) shows a decreasing trend. From the PRCPOT of each station in the basin, the middle reaches of the basin show an upward trend, while the upstream and downstream of the basin show a downward trend. The trend of SD II was mainly downward in the basin, and the trend of WD is mainly upward in the basin. In a word, the average characteristics of extreme precipitation in the middle and lower reaches of the MRB are changing from short-term extreme precipitation to sustained extreme precipitation, while the upper reaches of the MRB show the trend of increasing short-term rainfall intensity.

Time Trend

In this paper, the Tyson polygon method was used to assign different weight coefficients to each station in the basin. The temporal variation trend of extreme precipitation index in the basin was calculated using the MK trend test (*Table 3*) and the linear trend method (*Table 3* and *Fig. 4*).

Table 3. *Temporal trends of the ETIs in the MRB*

Index	CWD	R10mm	R25mm	RX1DAY	RX5DAY	R95T	R99T	PRCPTOT	SDII	WD
MK	**2.14**	0.77	0.20	-0.72	1.53	-0.72	-1.37	0.614	-0.67	**1.66**
T	0.15	0.29	0.015	-0.63	2.4	-3.4	-3.8	5.6	-0.021	1.6

Notes: MK denotes MK statistics. T denotes trends (decade^{-1}). Values for the trends at the 0.05 significance level are shown in bold

The CWD of the MRB shows a significant upward trend. The R10mm shows a non-significant upward trend, while the R25mm shows a slightly upward trend. The RX1DAY shows a non-significant downward trend, while RX5DAY shows a non-significant upward trend. It shows that the characteristics of precipitation have changed from short-term heavy precipitation to persistent heavy precipitation. The R95T, R99T, R95PT and R99PT show non-significant downward trends. The results show that the proportion of one-day extreme precipitation to total precipitation has been weakening in recent years. The PRCPTOT showed no significant upward trend, SDII showed non-significant downward trend, WD showed a significant upward trend. In a word, the average characteristics of extreme precipitation in the MRB have changed from short-term extreme precipitation to persistent extreme precipitation. The main reasons for this change are the significant increase of the WD, the CWD and the R10mm, especially the increase of the R10mm.

http://www.aloki.hu ● ISSN 1589 1623 (Print) ●ISSN1785 0037 (Online)
DOI: http://dx.doi.org/10.15666/aeer/1705_113751394

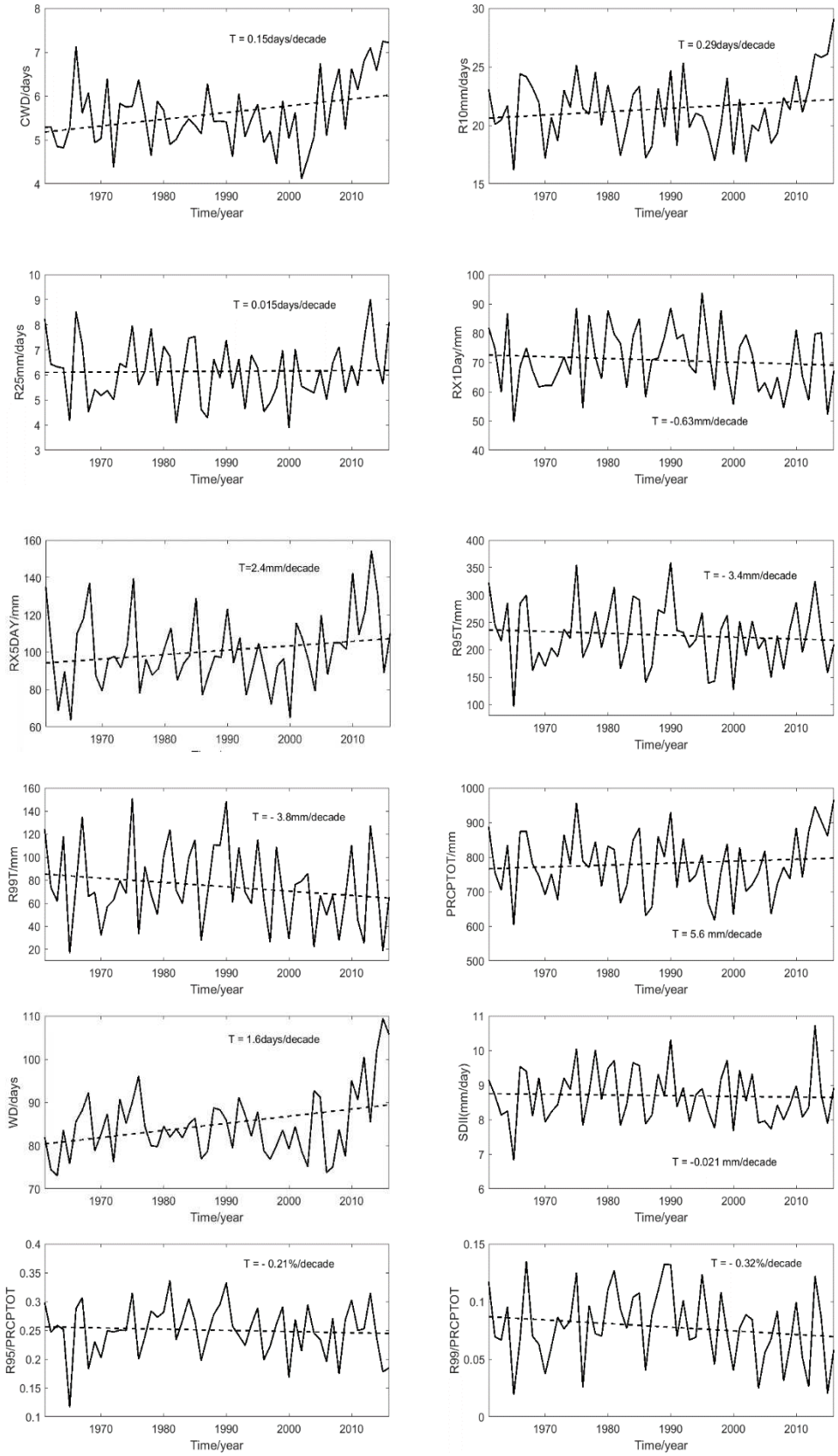

Figure 4. *Interannual variation of extreme precipitation index in the MRB*

http://www.aloki.hu ● ISSN 1589 1623 (Print) ●ISSN1785 0037 (Online)
DOI: http://dx.doi.org/10.15666/aeer/1705_113751394

Estimated Precipitation in the MRB Calculated by Regional Frequency Analysis

According to the analysis above, it is concluded that there are large spatial variations in extreme precipitation in the Min River. Extreme precipitation has the spatial difference of persistent extreme precipitation (RX5DAY), while short-term extreme precipitation (RX1DAY) decreases. On this basis, the regional frequency analysis, which combines the linear moments with the regional analysis method, is used to calculate the estimated precipitation for RX5DAY reflecting persistent extreme precipitation and RX1DAY reflecting short-term extreme precipitation.

Hydrometeorological Consistency Zone

The Cluster analysis is used to classify the precipitation by considering latitude, elevation, and the first order linear distance of the average value of RX1DAY or RX5DAY. The results of the classification are tested for discordance and heterogeneity. *Table 4* shows that the zoning results for RX1DAY and RX5DAY are acceptable according to the discordance test and heterogeneity test.

The Selection of Optimal Frequency Distribution Line

According to the hydrometeorological consistency region of the MRB, the optimal frequency distribution pattern of each hydrometeorological consistency region is determined by the Monte Carlo simulation test. The results (*Table 5*) show that the optimal linear distribution of RX1DAY in the four climate-consistent regions of the MRB was generalized logical distribution (GLO). The optimal linear distribution of RX5DAY in region 1 and region 2 of the MRB was generalized logical distribution (GLO). The optimal linear distribution of RX5DAY in region 3 was generalized extreme value distribution (GEV) and in region 4 was generalized normal distribution (GNO).

Calculation of Estimated Precipitation

According to the distribution function parameters of RX1DAY and RX5DAY precipitation series estimated by L-moments, combined with quantile formula, the precipitation of each station at the level of 1-100a recurrence period was estimated. According to the results of Monte Carlo test, the optimal distribution of RX1DAY and RX5DAY series at different stations in the MRB was selected, and the precipitation extremes at different recurrence periods were calculated by using the optimal distribution.

From the results of regional frequency analysis (*a1-d1 in Figure 5*), it can be seen that the maximum value of the 20-year and the 100-year recurring precipitation was concentrated in the middle reaches of the Min River. The 20-year recurrence period of RX1DAY was 230 mm in Leshan area and the 100-year recurrence period of RX1DAY was 340 mm. The 20-year recurrence period of RX5DAY was 330 mm in Mingshan and the 100-year recurrence period of RX5DAY was 420 mm in Mingshan.

http://www.aloki.hu ● ISSN 1589 1623 (Print) ●ISSN1785 0037 (Online)
DOI: http://dx.doi.org/10.15666/aeer/1705_113751394

Table 4. *The results of discordance detection and heterogeneity test in three hydrometeorological consistent regions of the MRB*

Region	Station number (RX1DAY)	Di (RX1DAY)	Critical Value of Di	H1 (RX1DAY)	Station number (RX5DAY)	Di (RX5DAY)	Critical Value of Di	H1 (RX5DAY)
region1	2	Songpa (1.00) Heishui (1.00)	1.333	-0.6	2	Songpan (1.00) Heishui (1.00)	1.33	0.8
region2	3	Maoxian (1.00) Wenchuan (1.00) Lixian (1.00)	1.333	-0.29	3	Maoxian (1.00) Wenchuan (1.00) Lixian (1.00)	1.33	0.30
region3	15	Shuangliu (0.58) Xinjin (0.12) Dujiangyan (2.14) Pengzhou (0.95) Wenjiang (0.99) Chongzhou (0.22) Dayi (0.51) Qionglai (0.97) Pujiang (1.78) Minshan (1.53) Meishan (0.14) Pengshan (1.60) Dangling (1.54) Qingshen (0.72) Leshan (1.22)	3	-0.09	13	Shuangliu (0.52) Xinjin (0.06) Dujiangyan (1.83) Pengzhou (0.89) Wenjiang (0.86) Chongzhou (0.15) Dayi (0.62) Qionglai (0.97） Pujiang (1.20) Minshan (1.87) Meishan (1.41) Dangling (2.01) Leshan (1.07)	3	-0.03
region4	5	Jingyan (0.99) Qianwei (1.28) Mabian (1.31) Muchuan (1.08) Yibin (0.33)	1.333	-0.13	7	Pengshan (1.31) Qingshen (0.35) Jingyan (1.16) Qianwei (1.62) Mabian (0.94) Muchuan (1.15) Yibin (0.46)	1.333	0.82

http://www.aloki.hu ● ISSN 1589 1623 (Print) ●ISSN1785 0037 (Online)
DOI: http://dx.doi.org/10.15666/aeer/1705_113751394

Table 5. *Monte Carlo simulation results of distribution lines in four hydrometeorological consistent regions of the MRB*

index	linearity	Region1		Region2		Region3		Region4	
		RX1DAY	RX5DAY	RX1DAY	RX5DAY	RX1DAY	RX5DAY	RX1DAY	RX5DAY
Z	GLO	-0.81	0.34	-0.02	0.02	1.30	1.76	.20	1.38
	GEV	-1.86	-1.43	-0.82	-0.82	-1.62	-0.96	-1.19	-1.25
	GNO	-1.88	-0.99	-0.98	-0.98	-1.80	-1.25	-1.48	-1.03
	PE3	-2.10	-1.00	-1.35	-1.88	-1.35	-2.11	-2.10	-1.31
	GPD	-4.08	-4.64	-2.70	-5.45	-7.87	-6.78	-4.34	-6.52
Optimal Distribution Linearity		GLO	GLO	GLO	GLO	GLO	GEV	GLO	GNO

The traditional at-site hydrological frequency analysis (*a2-d2 in Figure 5*) refers to the calculation of all stations using the same frequency function instead of zoning the stations. It can be seen that the 20-year and 100-year maximum distribution of RX1DAY and RX5DAY was mainly distributed in the middle of the Min River, followed by the lower reaches of the basin, and the upper reaches of the basin were relatively small. The spatial distribution was consistent with the results of regional frequency analysis.

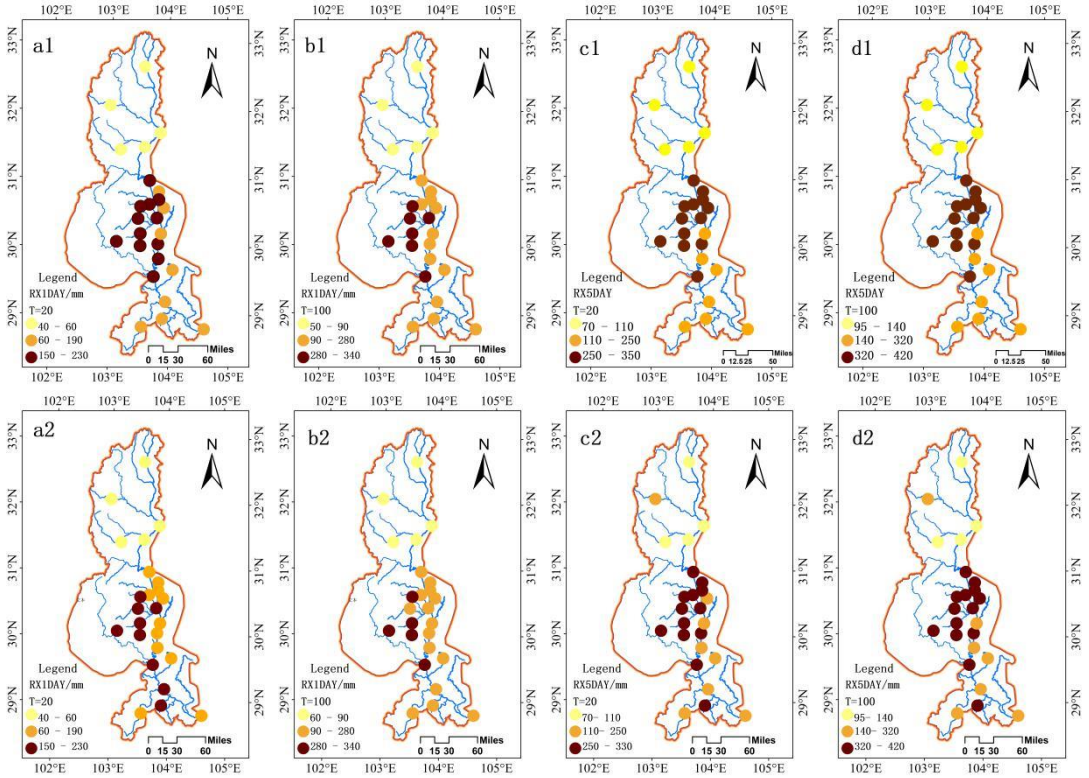

Figure 5. *Spatial distribution of estimated precipitation with RX1DAY and RX5DAY recurrence periods of 20 and 100 years*

http://www.aloki.hu ● ISSN 1589 1623 (Print) ●ISSN1785 0037 (Online)
DOI: http://dx.doi.org/10.15666/aeer/1705_113751394

By comparing the estimated precipitation calculated by the two methods, the extreme precipitation in the middle reaches of the basin by traditional at-site hydrological frequency analysis was lower than that by regional frequency analysis, and slightly higher than that by regional frequency analysis in the lower reaches of the basin. To a certain extent, the difference between the upper, middle, and lower reaches of the basin was reduced, the spatial difference was averaged, and the extreme precipitation in the middle reaches of the basin was underestimated. It is unsafe to estimate the estimated precipitation based on the spatial distribution of extreme precipitation. The regional frequency analysis can effectively avoid the problem that the estimated precipitation estimated by the overall data neglects the spatial distribution of the overall internal changes in the context of climate change.

Discussion

The MRB is located in the transition zone between the Qinghai-Tibet Plateau terrain and the eastern plain of China. The upper reaches of the basin are characterized by low humidity and less external water vapor transport. The middle and lower reaches of the basin are affected by tropical monsoon, subtropical monsoon, and plateau monsoon. The complex climate and special geographical location provide conditions for the uneven spatial distribution of extreme precipitation events. The frequency of extreme precipitation events in the lower and middle reaches of the MRB is significantly higher than that in the upper reaches. This may be related to the fact that the upper reaches of the MRB have low humidity and low water vapor transport due to the high altitude. Meanwhile, the intensity of extreme precipitation events in the MRB is the largest in the middle reaches, especially in the continuous extreme precipitation. The intensity of extreme precipitation events in the lower reaches is larger than that in the upper reaches. This is mainly because the middle reaches of the MRB is located in the rainstorm area in the northwest of the basin, which is affected by the eastern side of the Qinghai-Tibet Plateau and is a rainstorm area far from the ocean in China, resulting in the intensity of extreme precipitation events in the middle reaches of the MRB (Peng et al., 1985; Li et al., 2011).

The spatial distribution of extreme precipitation index in the MRB is quite different. The spatial variation trend of extreme precipitation in the MRB was that the spatial difference of RX5DAY increases, while the spatial difference of RX1DAY decreases. The main factors affecting the spatial variation of extreme precipitation were the spatial variation of R10mm and WD.

According to the trend analysis, the average characteristics of extreme precipitation in the MRB have changed from short-term extreme precipitation to persistent extreme precipitation. The main reasons for this change are the increase of the WD, the CWD and the R10mm, especially the increase of the R10mm.

http://www.aloki.hu ● ISSN 1589 1623 (Print) ●ISSN1785 0037 (Online)
DOI: http://dx.doi.org/10.15666/aeer/1705_113751394

At the same time, with the development of urbanization, Dujiangyan, Meishan and Leshan in the middle reaches of the MRB and Yibin Station in the lower reaches of the MRB are affected by the urban heat island effect, which further makes the distribution of precipitation uneven, thus affecting the distribution of extreme precipitation (Shou et al., 2012; Zhao et al., 2019).

In addition, the analysis methods used in this paper are uncertain, and it is necessary to further study the characteristics of extreme precipitation from different perspectives by various methods. Based on the results of this study, the relationship between extreme precipitation and atmospheric circulation needs to be further verified. At the same time, correlation analysis can be used to find out which factors are related to extreme precipitation.

Acknowledgements. This research was financially supported by National Natural Science Foundation of China (No. 50979062); Sichuan Key Laboratory of Rainstorm, Drought and Flood Disasters in Plateau and Basin (No. Provincial Heavy Laboratory 2018-Youth-09); Sichuan Science and Technology Department's Key Research and Development Project (No. 2018SZ0343); Sichuan Meteorological Service Center Project (No. SCQF2019007).

REFERENCES

[1] Croitoru, A-E., Chiotoroiu, B-C., Todorova, V. I., Torica, V. (2013): Changes in precipitation extremes on the Black Sea Western Coast. – Global and Planetary Change 10-19.

[2] Alexander, L. V., Zhang, X., Peterson, T. C., Gleason, B., Klein Tank, A. M. G., Haylock, M., Collins, D., Trewin, B., Rahimzadeh, F., Tagipour, A., Kumar, K. R., Revadekar, J. (2006): Global observed changes in daily climate extremes of temperature and precipitation. – Journal of Geophysical Research 111(D5): D05109.

[3] Bai, L. Y., Rong, Y. S. (2015): Reanalysis of the characteristics of extreme rainfall in the Yangtze River basin during recent 50 years. – Journal of Water Resources Research 4(1): 88-100.

[4] Bonsal, B. R., Zhang, X. B., Vincent, L. A., Hogg, W. D. (2001): Characteristic of daily and exreme temperature over Canada. – Climate 4(9): 1959-1976.

[5] Burn, D. H. (2008): Climatic influences on stream flow timing in the headwaters of the Mackenzie River Basin. – J. Hydrol. 352: 225-238.

[6] Changnon, S. A., Pielk, R. A., Changnon, D., Sylves, L. T., Pulwarty, R. (2000): Human factors explain the increased losses from weather and climate extremes. – Bulletin of the American Meteorological Society 81(3): 437-442.

[7] Chen, Y., Xu, C., Hao, X., Li, W., Chen, Y., Zhu, C., Ye, Z. (2009): Fifty-year climate change and its effect on annual runoff in the Tarim River Basin, China. – Quaternary International 208(1-2): 53-61.

http://www.aloki.hu ● ISSN 1589 1623 (Print) ●ISSN1785 0037 (Online)
DOI: http://dx.doi.org/10.15666/aeer/1705_113751394

[8] Chen, H., Sun, J., Chen, X., Zhou, W. (2012): CGCM projections of heavy rainfall events in China. – International Journal of Climatology 32(3): 441-450.

[9] Chen, X. (2014): Study on high-risk regionalization of heavy rainfall based on regional linear moment method and its application in Guangxi. – Nanjing University of Information Science and Technology, Nanjing.

[10] Chu, H. J., Pan, T. Y., Liu, J. J. (2012): Change-point detection of long-duration extreme precipitation and the effect on hydrologic design: a case study of south Taiwan. – Stochastic Environmental Research and Risk Assessment 2626(8): 1123-1130.

[11] Cunnane, C. (1989): Statistical distributions for flood frequency analysis. – Operational Hydrology Report 44(11): 369-369.

[12] Fu, G., Yu, J., Yu, X., Ouyang, R., Zhang, Y., Wang, P., Liu, W., Min, L. (2013): Temporal variation of extreme rainfall events in China, 1961-2009. – Journal of Hydrology 487: 48-59.

[13] He, Z., He, J. (2014): Temporal and spatial variation of extreme precipitation in the Yellow River basin from 1960 to 2012. – Resources Science 3: 490-501.

[14] Huang, Q., Chen, Z. (2014): Regional study on the trends of extreme temperature and precipitation events in the Pearl River basin. – Advances in Earth Science 8: 956-967.

[15] IPCC. (2013): Climate Change 2013: The Physical Science Basis. – In: Stocker, T. F., Qin, D., Plattner, G. K., Tignor, M., Allen, S. K., Boschung, J., Nauels, A., Xia, Y., Bex, V., Midgley, P. M. (eds.) Contribution of Working Group I to the Fifth Assessment Report of the Intergovernmental Panel on Climate Change. Cambridge University Press, Cambridge, United Kingdom and New York.

[16] Kampata, J. M., Parida, B. P., Moalafhi, D. B. (2008): Trend analysis of rainfall in the head streams of the Zambezi River Basin in Zambia. – Phys. Chem. Earth 33: 621-625.

[17] Karl, T. R., Knight, R. W. (1998): Secular trends of precipitation amount, frequency, and intensity in the USA. – Bull Am Met Soc 79: 231-241.

[18] Kendall, M. G. (1970): Rank Correlation Methods. – Griffin, London.

[19] Li, Y. Q., Zhang, X. C. (2011): Main Advances in the Research of "Yaan Sky Leakage". – Torrential Rain and Disasters 30(4): 289-295.

[20] Li, X. Z., Liu, X. D. (2012): Numerical simulations of extreme precipitation in eastern China under A1B scenario. – Journal of Tropical Meteorology 28(3): 379-391.

[21] Li, Z., Zheng, F. L., Liu, W. Z., Jiang, D. (2012): Spatially downscaling GCMs outputs to project changes in extreme precipitation and temperature events on the Loess Plateau of China during the 21st Century. – Global and Planetary Change 82-83: 65-73.

[22] Li, M., Lin, B. Z., Shao, Y. H. (2015): Study on Spatial Continuity of Precipitation Quantile Estimates Based on Regional L-moments Analysis. – Journal of China Hydrology 35(4): 14-19.

[23] Li, S., Yang, S., Liu, X. (2015): Spatiotemporal variability of extreme precipitation in north and South of the Qinling-Huaihe region and influencing factors during 1960-2013. – Progress in Geography 3: 354-363.

http://www.aloki.hu ● ISSN 1589 1623 (Print) ●ISSN1785 0037 (Online)
DOI: http://dx.doi.org/10.15666/aeer/1705_113751394

[24] Lin, B., Bonnin, G. M., Martin, D. L. (2006): Regional Frequency Studies of Annual Extreme Precipitation in the United States Based on Regional L-Moments Analysis. – ASCE Proceedings, Omaha, NE, USA.

[25] Luyao, B., Yanshu, R. (2015): Reanalysis of the Characteristics of Extreme Rainfall in the Yangtze River Basin during Recent 50 Years. – Journal of Water Resources Research 2015(4): 88-100.

[26] Mann, H. B. (1945): Non-parametric tests against trend. – Econometrica 13: 245-259.

[27] Millett, B., Johnson, W. C., Guntenspergen, G. W. (2009): Climate trends of the North American prairie pothole region 1906-2000. – Climatic Change 93: 243-267.

[28] Pal, I., Al-Tabbaa, A. (2011): Monsoon rainfall extreme indices and tendencies from 1954-2003 in Kerala, India. – Climatic Change 106(3): 407-419.

[29] Pan, X., Yin, Y. X., Wang, X. J. (2017): Spatio-temporal characteristics and future trend of extreme precipitation in the Yangtze river basin during 1960 to 2010. – Resources and Environment in the Yangtze Basin 26(3): 436-444.

[30] Peng, G. K., Li, Z. Y., Chai, F. X. (1985): The relationship between topography and precipitation in ya'an district. – Plateau Meteorology 4(3): 230-240.

[31] Qian, W., Lin, X. (2005): Regional trends in recent precipitation indices in China. – Meteorology and Atmospheric Physics 90(30): 193-207.

[32] Qing, T. (2016): Precipitation and temperature changes in the major Chinese river basins during 1957-2013 and links to sea surface temperature. – Journal of Hydrology 536: 208-221.

[33] Shao, Y. H., Wu, J. M., Li, M. (2016): Frequency Analysis of Extreme Precipitation in Huaihe River Basin Based on Hydrometeorological Regional L-moments Method. – Journal of China Hydrology 36(6): 16-23.

[34] Shou, Y. X., Zhang, D. (2012): Recent advances in understanding urban heat island effects with some future prospects. – Acta Meteorologica Sinica 70(3): 338-353.

[35] Su, B. D., Jiang, T. G. Y., Chen, Z. H. (2006): Observed trends of precipitation extremes in the Yangtze River basin during 1960 to 2004. – Advances in Climate Change Research 2(1): 9-14.

[36] Tian, Q., Prange, M., Merkel, U. (2016): Precipitation and temperature changes in the major Chinese river basins during 1957-2013 and links to sea surface temperature. – Journal of Hydrology 536: 208-221.

[37] Tramblay, Y., Badi, W., Driouech, F., Adlouni, S. E., Neppel, L., Servat, E. (2012): Climate change impacts on extreme precipitation in morocco. – Global and Planetary Change 82-83: 1-114.

[38] Vijay, K., Sharad, K. J. (2010): Trends in seasonal and annual rainfall and rainy days in Kashmir Valley in the last century. – Quat. Int. 212: 64-69.

[39] Wang, Z., Ding, Y., He, J. (2004): An updating analysis of the climate change in China in recent 50 years. – Acta Meteorological Sinica 62(2): 228-236.

[40] Wang, S. J. (2009): Changing pattern of the temperature, precipitation and runoff in Chuanjiang Section of the Yangtze River. – Resour. Sci. 31: 1142-1149.

http://www.aloki.hu ● ISSN 1589 1623 (Print) ●ISSN1785 0037 (Online)
DOI: http://dx.doi.org/10.15666/aeer/1705_113751394

[41] Wu, H., Soh, L. K., Samal, A., Chen, X. H. (2008): Trend analysis of streamflow drought events in Nebraska. – Water Resour. Manage. 22: 145-164.

[42] Wu, X., Wang, Z., Zhou, X., Lai, C., Lin, W., Chen, X. (2016): Observed changes in precipitation extremes across 11 basins in China during 1961-2013. – Int. J. Climatol 36: 2866-2885.

[43] Xiong, L. H., Guo, S. L., Wang, C. J. (2004): Advance in regional flood frequency analysis from abroad. – Advances in Water Science 2: 2.

[44] Xu, Z. X., Li, J. Y., Liu, C. M. (2007): Long-term trend analysis for major climate variables in the Yellow River basin. – Hydrol. Processes 21: 1935-1948.

[45] Xu, Z., Liu, Z., Fu, G., Chen, Y. (2010): Trends of major hydroclimatic variables in the tarim river basin during the past 50 years. – Journal of Arid Environments 74(2): 1-267.

[46] Yang, T., Chen, X., Yang, H. W., Xie, H. W. (2009): Regional flood frequency analysis in Pearl River Delta region based on L-moments approach. – Journal of Hohai University (Natural Sciences) 37(6): 615-619.

[47] Yang, T., Hao, X., Shao, Q., Xu, C., Zhao, C., Chen, X., Wang, W. (2012): Multi-model ensemble projections in temperature and precipitation extremes of the Tibetan Plateau in the 21st century. – Global and Planetary Change 80-81: 1-13.

[48] Yu, R. C. (2004): Tropospheric cooling and summer monsoon weakening trend over East Asia. – Geophysical Research Letters 31(22): L22212.

[49] Zengxin, Z. (2011): Evaluating the non-stationary relationship between precipitation and stream flow in nine major basins of China during the past 50 years. – Journal of Hydrology 409: 81-93.

[50] Zhai, P. M., Ren, F. M., Zhang, Q. (1999): Detection of trends in China's precipitation extremes. – Acta Meteorologica Sinica 52(2): 208-216.

[51] Zhai, P., Zhang, X., Wan, H., Pan, X. (2005): Trends in total precipitation and frequency of daily precipitation extremes over china. – Journal of Climate 18(7): 1096-1108.

[52] Zhang, Y., Xu, Y., Dong, W. (2006): A future climate scenario of regional changes in extreme climate events over China using the PRECIS climate model. – Geophysical Research Letters 33(24): L24702.

[53] Zhang, Y., Du, X. R. (2008): Analysis of temperature and precipitation change over last 50 years in Leshan City. – Plateau Mt. Meteor. Res. 28(3): 68-71.

[54] Zhang, M., Wei, X., Sun, P., Liu, S. (2012): The effect of forest harvesting and climatic variability on runoff in a large watershed: the case study in the upper Minjiang river of Yangtze river basin. – Journal of Hydrology (Amsterdam): 464-465.

[55] Zhao, C. P., Zhou, J. H., Li, Z. (2019) Influence of Urbanization on the Change of Rainstorm in Taiyuan. – Journal of Arid Meteorology 37(1): 109-118.

http://www.aloki.hu ● ISSN 1589 1623 (Print) ●ISSN1785 0037 (Online)
DOI: http://dx.doi.org/10.15666/aeer/1705_113751394

MODELING AND SIMULATION OF MEMBRANE BIOREACTOR MODEL BASED ON ASM3 FOR DOMESTIC WASTEWATER TREATMENT

KAPUMBE, D. J.[1] – MIN, L.[1] – ZHANG, X.[1] – KISOHOLO, M. A.[1] – YONGFENG, L.[1*]

[1]*School of Forestry, Northeast Forestry University, Harbin 150040, Heilongjiang, China*

**Corresponding author*
e-mail: dr_lyf@163.com; phone: +86-139-0361-4476

(Received 18th Apr 2019; accepted 11th Jul 2019)

Abstract. Membrane bioreactor (MBR) is a water treatment system with a combination of the membrane separation unit and the bioreactor. The Activated Sludge Model (ASM) developed by the International Water Association offer a valuable instrument for designing, optimizing, and operation of the MBR. In this research, the MBR process based on the Activated Sludge Model No. 3 (ASM3) was compiled by the use of MATLAB/Simulink platform which can be applied to the water quality analysis of the MBR reactor effluent. The visual ASM3-MBR sewage processing simulation system was developed and had the advantages of an intuitive interface, clear meaning, easy data input, etc. After the model establishment, the division of model components, sensitivity analysis, and model calibration and verification, ASM3-MBR was amended and improved in this study.
Keywords: *activated sludge, MATLAB/Simulink, modelling, water quality, separation unit*

Introduction

The membrane bioreactor (MBR) is a system that combines biological treatment with membrane filtration into a single process. MBR is one of the most tent potent domestic/industrial wastewater treatment and reuse technologies currently (Ng and Kim, 2007). Also, this efficient and reliable technology has become a legitimate alternative to conventional activated sludge processes due to its perfect retention of biomass, pathogens removal, higher process performance and system stability (Castelo-Grande et al., 2010). The membrane bioreactors achieve perfect organics; chemical oxygen demand (COD), biochemical oxygen demand (BOD), and nutrient (nitrogen, phosphorus) removal as well as perfect retention of suspended solids.

Recently, MBR, especially submerged MBR, has been gaining a lot of attention for wastewater treatment in the aspects of high-quality effluent and a small footprint (Braak et al., 2011). The MBR process combines the biodegradation by the activated sludge process and the solid-liquid separation by the membrane filtration (Chang et al., 2006). It is, therefore, reasonable to use Activated Sludge Models to characterize the biomass dynamics in an MBR system. Mathematical modelling of MBR technology may help in providing insight into the factors that play a crucial role in the MBR process (Lee et al., 2002). At the same time, it can provide invaluable data for the design, forecast, and control of MBR technology.

Up to this day, mathematical model simulation of activated sludge processes have been used for the design of structures and control of operations in wastewater plants in most parts of the world. Since the publication of the first Activated Sludge Model (ASM) in 1986 (Liwarska-Bizukojc et al., 2011), the Activated Sludge Model No. 1 (ASM1) and its successors have become increasingly more popular. ASM1 was developed to model BOD and nitrogen removal, but it did not adequately describe all

http://www.aloki.hu ● ISSN 1589 1623 (Print) ● ISSN 1785 0037 (Online)
DOI: http://dx.doi.org/10.15666/aeer/1705_1139511407

nutrients removal. Therefore Activated Sludge Model No. 2 (ASM2) was designed to incorporate biological nutrient removal of nitrogen and phosphorus (Gujer et al., 1995). However, ASM2 was far more complex, which created model operational difficulties. Activated Sludge Model No. 3 (ASM3) aimed to correct the defects of ASM1 and presented a new standard for ASM based modelling (Gujer et al., 1999).

The ASM3 model can effectively simulate the operation of the MBR. With the ASM3 model, the dimensions of various structures of the MBR are determined, and the appropriate process flow can be accurately selected. The key operating parameters of the MBR can also be predicted and determined; therefore, using the ASM3 model to simulate the MBR can optimize the operation and management of the MBR. The factors that affect the process of the MBR can be analyzed and evaluated.

Although the ASM series of models have gained widespread recognition from water treatment workers, due to the complexity of the model structure and parameters, it is still difficult to directly use them in reactor design, and many scholars are based on such models. At the expense of the universality of the model, many simplified models have been created, and proper monitoring and control results have been achieved. Using MATLAB/Simulink as the simulation software, the ASM3-based simulation of the MBR process can more intuitively reflect the effect of the reactor operation and can use the program to make a right prediction of the effluent outcome of the MBR (Gao et al., 2018).

Indeed, recently Li et al. (2009) applied a hybrid ASM model and showed the hybrid ASM model was calibrated and validated through a submerged MBR system under the reference condition. Mannina et al. (2011) presented an integrated MBR features and the calibration model protocol was illustrated with a pilot MBR plant in submerged configuration based on ASM1.

The major problem in the simulation of MBR is that the port has not been visualized. Only the programmers who are familiar with the structure can operate it flexible. Hence, through a concise and structured overview of past developments, this paper studied the effects of submerged MBR's wastewater treatment. This paper explored ASM3 based on modelling applied to MBR processes; ASM3 was chosen as the simulator and used the Simulink Toolbox in MATLAB7.0 to build a visual simulated program. The operation was done to predict the variation tendency of the effluent quality under the changing situation of inflow and outflow water quality when the reactor was in operation. This paper searches for the optimal operating parameters and will provide the basis for engineering design.

Materials and methods

Experimental set-up

An integrated MBR was used in the test. The test device diagram is shown in *Figure 1*. The temperature of the reactor 4 was adjusted to 25 °C by the heater 7, 5 is a hollow fiber membrane module, and the membrane material was polyacrylamide, hollow fiber filament. The diameter was about 0.6 mm, the inner diameter was about 0.3 mm, the membrane pore size was 0.05 μm, the length of the membrane module was 0.5 m, the membrane molecular weight cut-off was 10000 Dalton, and the surface area of the membrane was 1 m^2. The device used a micro-porous aerator for aeration, and the amount of aeration can be adjusted by the air flow meter 3. The liquid level of the reactor was controlled by the balance tank. The float valve automatically controls the

http://www.aloki.hu ● ISSN 1589 1623 (Print) ● ISSN 1785 0037 (Online)
DOI: http://dx.doi.org/10.15666/aeer/1705_1139511407

liquid level with the flow rate of the discharge water. With the change of the flow rate of the discharge water, the float valve was automatically controlled to maintain the balance between the discharge flow and the inflow. The hydrodynamic power was provided by the net head pressure difference. After the new membrane was placed in the reactor, water was pumped out using a glass water injector. The reactor had a sufficient volume of 18 L. The aeration intensity of the device was very large, dissolved oxygen (DO) was maintained at about 8 mg/L. After the commissioning operation was stable, the HRT of the control system was 5 h, during which no sludge was discharged. When the system was operating stably, the concentration of incoming and outgoing water was measured.

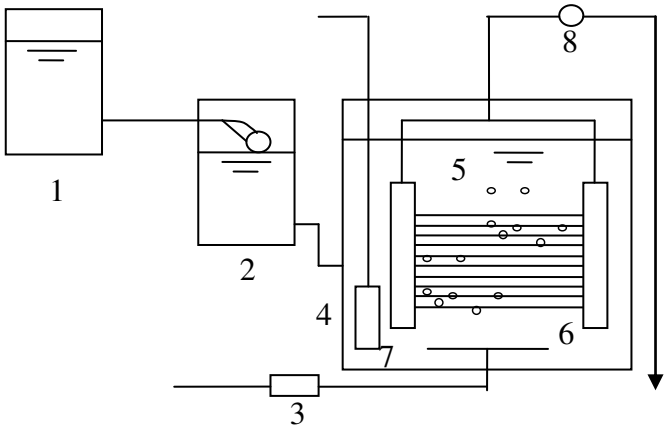

Figure 1. *Schematic diagram of the test. (1 elevated tank, 2 balance tank, 3 air flow meter, 4 reactor, 5 hollow fiber membrane,6 aeration device, 7 heater, 8 vacuum table)*

Mass balance and removal rates

The biological reaction rate of a component (i), at the time (t), r_i was obtained according to the following equation (Mannina et al., 2011):

$$r_i = \sum_j \upsilon_{ij} \rho_j \qquad \text{(Eq.1)}$$

Where υ is the stoichiometric matrix, ρ is the kinetic rate, i and j are respectively the state variables and the biological processes. Meanwhile, the differential equations for all state variables were obtained from *Equations 2, 3* and *4* by the mass balance:

$$\frac{dS_i}{d_t} = \frac{Q_{in}S_{i,0} - Q_o S_i + Q_w S_i}{V} + r_i \qquad \text{(Eq.2)}$$

$$\frac{dX_i}{dt} = \frac{Q_{in}X_{i,0} - Q_w X_i}{V} + r_i \qquad \text{(Eq.3)}$$

$$Q_o = Qf \qquad \text{(Eq.4)}$$

http://www.aloki.hu ● ISSN 1589 1623 (Print) ● ISSN 1785 0037 (Online)
DOI: http://dx.doi.org/10.15666/aeer/1705_1139511407

where Q_{in} is the influent flow-rate, Q_o is the effluent flow-rate, Q_w is the wasted sludge flow-rate, V is the volume of the MBR $S_{i,0}$ and S_i are the concentration of soluble substrates in the influent and supernatant respectively, $X_{i,0}$ and X_i are the concentration of particulate substrate in the influent and reactor, respectively, f is the coefficient of membrane interception.

In consideration of the heterotrophic bacteria and nitrifying bacteria in water in an amount negligible, these two components of this differential equation are simplified:

$$\frac{dX_H}{dt} = r_H \tag{Eq.5}$$

$$\frac{dX_A}{dt} = r_A \tag{Eq.6}$$

The purpose of the sensitivity analysis of the model parameters was to study the influence of the size of the model parameter's error on the system's prediction (Wang et al., 2016). In the simulation, those parameters with higher sensitivity in the model need to be corrected. For parameters with lower sensitivity, the typical default values given by ASM3 can be directly used for simulation.

The sensitivity analysis method was used to analyze the simulated results of the ASM3-MBR model, and the dynamic parameter values and stoichiometric coefficients in the model were increased by 10% based on initial costs (Lee et al., 2002) and changed under the condition of keeping other parameters unchanged. The sensitivity value of a parameter was calculated according to the equation below:

$$\sigma_{j,i} = \frac{\dfrac{C_{i,1} - C_{i,0}}{C_{i,0}}}{\dfrac{\tau_{j,1} - \tau_{j,0}}{\tau_{j,0}}} = \frac{\dfrac{\Delta C_i}{C_{i,0}}}{\dfrac{\Delta \tau_j}{\tau_{j,0}}} \tag{Eq.7}$$

Where $\tau_{j,0}$ is the initial value of the parameter, $\tau_{j,1}$ is the parameter values after the change, $C_{i,0}$ and $C_{i,1}$ are a concentration of effluent indicator before and after the parameter change indicator. After an increase of 10% based on the initial values, the corresponding sensitivity values of parameters are positive and negative points. The positive value indicates that the increase of the parameter makes the effluent concentration of the component rise, and the negative value indicates that the increase of the parameter causes the effluent concentration of the component to decrease.

Modelling

The simulated program establishes its flow chart based on the parameter of the integrated MBR technology and design. ASM3 was chosen as a simulator, and the Simulink Toolbox in MATLAB7.0 was used to build a visual simulated program. The simulation model includes an influent module, the reaction module, and effluent combination module. The reaction module processing corresponding reactions, the

http://www.aloki.hu ● ISSN 1589 1623 (Print) ● ISSN 1785 0037 (Online)
DOI: http://dx.doi.org/10.15666/aeer/1705_1139511407

influent module will feed components distribution in 13 kinds of parts according to specific rules. And effluent combination module is just the opposite; it is a combination of 13 types of component indicators need to detect the effluent, such as COD, Ammonia, total nitrogen (TN), as the basis for process analysis.

The establishment of the model starts with the basic sub-processes rate equation. The other components of the reaction rate equation are built by the mathematical operation. One or several parts of the kinetic equation can be used to describe a sub-process.

In the established model system, all the 13 sub-process can be built with the process. The basic rate equation is multiplied by a sub-process component in a stoichiometric coefficient of the sub-process. The sum of the parts in each sub-process of the reaction rate is the component of the total reaction rate of all sub-processes in which it participates. Such as X_I generated in the sub-process 6, 7, 11, and 12; therefore, X_I's total kinetic equation for the four sub-process reaction rate sums. We have:

$$(dX_I / d_t)_T = f_I[(dX_I / d_t)_6 + (dX_I / d_t)_7 + (dX_I / d_t)_{11} + (dX_I / d_t)_{12}] \quad \text{(Eq.8)}$$

In the MBR, a component of the quality in total rate equation of the ASM3 is the total reaction rate equation and the "one into one out" sum.

To X_I, for example, the total rate equation is:

$$\frac{dX_I}{d_t} = \frac{Q_{in}X_{I,0} - Q_o X_I}{V} \pm \sum \left(\frac{dX_I}{d_t} \right)_R \quad \text{(Eq.9)}$$

According to the method, the 13 component of the ASM3 corresponding model (S_{O2}, S_I, S_S, S_{NH2}, S_{N2}, S_{NOX}, S_{ALK}, X_I, X_S, X_H, X_{STO}, X_A and X_{SS}) is established, and finally the simultaneous integration and then encapsulated.

After the model package, can be entered ASM3 as parameters in the parameter input box, these parameters can be adjusted as needed. In the first time of simulation, the input is the default reference values given by the International Water Association (IWA).

Data conversion is an essential factor in the model simulations. The data conversion floor is the measured data to the component data of ASM3 model transform process. Because the actual test data is not entirely of model constituents and therefore fall under the restriction of various conditions, it is difficult to measure constituents by using experiment. Hence, this concerns the problem of how to transform data into the model. This step is essential, whether the transformation is appropriate or not directly determines the success of the application of the model. In this test, the value influent COD, total nitrogen (TN), and ammonia were measured.

Finally, a visual interface of the ASM3-MBR was established. Simulated program debugs through static data, first carries out a sensitivity analysis for the model parameter and then corrects the parameter, control the error between system prediction's result and the actual measured results of the water within 5%.

Figure 2 shows the simulation program of ASM3-MBR where TCOD represents the total influent COD, V represents the reactor volume, HRT represents hydraulic retention time, Q_w is the wasted sludge flow-rate, SNH4, 0 represents the influent ammonia content, SN2, 0 represents the total influent nitrogen, TN means influent TN content,

http://www.aloki.hu ● ISSN 1589 1623 (Print) ● ISSN 1785 0037 (Online)
DOI: http://dx.doi.org/10.15666/aeer/1705_1139511407

SALK, 0 represents influent alkalinity, XSS, 0 indicates influent suspended solids content. After clicking the left of each window to run the input data can be observed on the right side of each window after the simulation of COD, ammonia nitrogen, TN results.

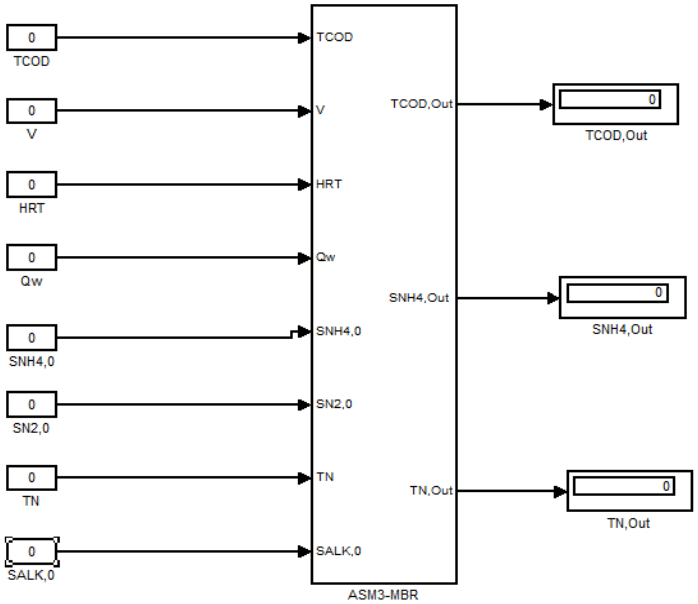

Figure 2. *The simulation program of ASM3-MBR*

The bottom floor of the simulation program is the basic rate equation. The second floor is the encapsulation of the relevant rate equations. The third floor is the encapsulation of a component of the overall reaction rate equation package. The fourth floor is the encapsulation of the integral simultaneous component of the total rate equation. The fifth floor is the input floor of the ASM3 model parameters, is the encapsulation of the entire rate equation integration module, parameter module, initial of points, and influent quality. Enter ASM3 typical kinetic parameter values. The simulation program uses the International Water Association (IWA) recommended default value (20 °C) (Henze et al., 2000).

Results and discussion

Sensitivity analysis

According to *Equation 7, Table 1* shows ASM3 model sensitivity analysis results. From the parameter sensitivity analysis in *Table 1* we can see that:

1. Some parameters have almost no effect on all the simulation results, such as the yield in the endogenous respiration, the rate of hypoxia based respiration, and the significant influence on the simulation results, such as the ratio of the hydrolysates, the maximum rate of growth. For these parameters with high sensitivity, parameter correction must be carried out in the simulation process to meet the precision requirements of the model. For the parameters with low sensitivity, the parameters cannot be corrected in the simulation, and the typical default values of the ASM3 model can be used directly.

http://www.aloki.hu ● ISSN 1589 1623 (Print) ● ISSN 1785 0037 (Online)
DOI: http://dx.doi.org/10.15666/aeer/1705_1139511407

2. The higher sensitivity of the effluent COD simulation value to the parameter change from high to low is proportion in the hydrolysate, hydrolysis saturation constant, hydrolysis rate constant, aerobic yield per unit stock, aerobic endogenous respiration rate, the aerobic yield of heterotrophic bacteria, maximum specific growth rate.
3. The higher sensitivity of the effluent NH_3-N simulation value to the parameter change from high to low is: the maximum specific growth rate, the ammonia nitrogen saturation coefficient, the aerobic endogenous respiration rate, the aerobic yield of heterotrophic bacteria, the aerobic yield, the maximum specific growth rate, and the saturation constant for the unit stock.
4. The higher sensitivity of the effluent TN simulation value to the parameter change is from the highest to the lowest: the unit nitrate yield, aerobic endogenous respiration rate, heterotrophic aerobic yield, and unit stock aerobic yield, maximum specific growth rate, hydrolysis saturation constant, storage rate regular.

Parameter calibration

The sensitivity analysis method is used to adjust the parameters with high sensitivity, and some settings with low sensitivity are set according to reference or typical values. The model parameter correction is performed on the MATLAB/Simulink platform. The differential equations involved in the model are solved in MATLAB using the established ASM3-MBR model (Song et al., 2012). After studying most of the literature, it was discovered that the process of correcting the model using data from dynamic inflows requires more computational time than static influx, and it has been proved in practice that static influent water is used to simulate the resulting information of the system (Bournazou et al., 2010). It will not be less than that obtained when using dynamic flood simulation (Wang et al., 2016). Therefore, the average value of the actual inlet and outlet water and water quality characteristics of the integrated MBR is used as the steady-state inlet and outlet water values to correct the parameters of the ASM3-MBR model. Because of the average water value, the parameters that make the relative residual difference between the benefits of the simulated values of COD, NH_3-N, TN, and the measured values are minimal.

In the process of model calibration, the following principles need to be followed:

1. Most parameters should not be changed during the calibration process.
2. For each correction, only one parameter is changed. This is because there are usually substantial interactions between parameters in the model, so it is difficult to estimate the combined effects of several parameters, and changing multiple parameters during correction can lead to difficulties in calibration. Therefore, for the two parameters of the interaction, only the one that has a high more significant influence on the simulation result can be changed.
3. If the sensitivity of a parameter is low, this parameter does not need to be modified. However, if for some reason, the parameter must be modified, it must be adjusted according to the logic operation rules.

The model correction mainly adjusts the following four parameters: f_{SI} adjusted to -0.45, μ_A adjusted to 0.8, Y_A adjusted to 0.27, k_H adjusted to 3.1. Other parameters

http://www.aloki.hu ● ISSN 1589 1623 (Print) ● ISSN 1785 0037 (Online)
DOI: http://dx.doi.org/10.15666/aeer/1705_1139511407

were fine-tuned only for those with relatively high sensitivity. Simulation results after adjustment parameters are shown in *Table 2*.

Table 1. *ASM3 model sensitivity analysis results*

Symbol	Characterization	Sensitivity		
		COD	**Ammonia**	**TN**
k_H	Hydrolysis rate constant	-0.1116	-0.0008	0.0373
K_X	Hydrolysis saturation constant	0.1302	-0.0649	0.1056
k_{STO}	Storage rate constant	0.0009	-0.0852	0.0994
η_{NO_x}	Anoxic reduction factor	0.0009	-0.0325	0.0373
K_{O_2}	Saturation constant for S_{O_2}	0.0009	-0.073	0.0186
K_{NO_x}	Saturation constant for S_{NO_x}	0.0009	-0.0892	0.0373
K_S	Saturation constant for substrate SS S_S	0.0009	-0.0243	0.0248
K_{STO}	Saturation constant for X_{STO}	-0.0009	-0.0122	0.0186
μ_H	Maximum specific growth rate of X_H	0.0279	-0.1095	0.1304
K_{NH_4}	Saturation constant for ammonium, S_{NH_4}	0.0009	-0.0284	0.0373
K_{ALK}	Alkalinity saturation constant for X_H	0.0009	-0.0284	0.0373
b_{H,O_2}	Aerobic endogenous respiration rate for X_H	0.0372	-0.0365	0.2547
b_{H,NO_x}	Anoxic endogenous respiration rate for X_H	0.0009	-0.0243	0.0373
b_{STO,O_2}	Aerobic respiration rate of X_{STO}	0	-0.0446	0.0559
b_{STO,NO_x}	Anoxic respiration rate for X_{STO}	0	-0.0162	0.0248
μ_A	Maximum specific growth rate of X_A	0	-1.144	0.0311
K_{A,NH_4}	Ammonium substrate saturation for X_A	0.0009	0.9736	0.0373
K_{A,O_2}	Oxygen saturation for nitrifiers	0.0009	-0.0892	0.0373
$K_{A,ALK}$	Bicarbonate saturation for nitrifiers	0.0009	0.0649	0.0373
b_{A,O_2}	Aerobic endogenous respiration rate of X_A	0.0009	0.7911	0.0497
b_{A,NO_x}	Anoxic endogenous respiration rate of X_A	0.0009	-0.0365	0.0435
f_{SI}	Production of S_I in Hydrolysis	0.1571	0	0.0123
Y_{STO,O_2}	The aerobic yield of stored product per S_S	0.0465	0.1095	-0.1925
Y_{STO,NO_x}	The anoxic yield of stored product per S_S	0.0009	-0.0406	0.0373
Y_{H,O_2}	Aerobic yield of heterotrophic biomass	0.0372	0.1136	-0.1988
Y_{H,NO_x}	Anoxic yield of heterotrophic biomass	0.0009	-0.0284	0.0311
Y_A	Yield of autotrophic biomass per NO_3-N	0.0009	-0.0649	-1.5217
f_{X_I}	Endogenous respiration in the yield	0	0	0

http://www.aloki.hu ● ISSN 1589 1623 (Print) ● ISSN 1785 0037 (Online)
DOI: http://dx.doi.org/10.15666/aeer/1705_1139511407

Table 2. *Simulation results after adjustment parameters*

Constituent	COD	Ammonia	TN
The average of influent	460.29	19.71	20.6
Measured value of effluent	17.62	0.31	11.97
Typical simulation results	24.29	0.2465	15.27
Simulation results of parameter correction	17.74	0.3118	11.94
Typical error of simulation results	3.79%	20.48%	37.57%
Correction parameter of simulation results	0.07%	0.06%	0.03%

It can be seen from *Table 2* that the error of the simulated values of the effluent COD, NH_3-N, and TN after correction is 0.07%, 0.06%, and 0.03% respectively. The simulated values are in good agreement with the measured values, and the simulation is ideal. Therefore, the validated ASM3-MBR model can be used to simulate and predict the effluent index of the reactor.

Zhou et al. (2013) in their research reported that the simulated results fitted very well with the experimental data. After 30 days of simulation, the fluctuations in effluent COD concentrations over the intervals were less than 0.3%. The goodness of fit of the COD between the measured and simulated values was 99.7%. The difference between the simulated and measured NH_4-N values was less than 0.8%, implying a right model prediction for ammonia removal. Overall, the modified ASM3 model obtained a right first prediction concerning the long-term behaviour of effluent COD and NH_4-N concentrations. Also, Blomberg et al. (2018) observed that the ammonia oxidation was directly linked to all of the main nitrogen conversion reactions in the activated sludge process (ASP). The model was able to reproduce the measured NH_4 peaks in the effluent of the ASP throughout the simulation. During the calibration period, the modelled peaks were able to reach the measured values throughout the simulation. Consistently, the model was able to reproduce the measured peaks during the validation phase. Elawwad et al. (2017) reported that the ASM3 provided good representation for WWTP performance. The modelled effluent COD was consistent with the measured COD values.

Comparison of simulation results of ASM3 model under different influent water quality

The MBR reactor in this test did not discharge mud during the test. The sludge concentration in the reactor was about 2000 mg/L when the device was started. The temperature of the reactor was maintained at 24 °C and the hydraulic retention time was 5 h during operation, the aeration intensity was maintained at a relatively broad level to ensure the dissolved oxygen concentration in the reactor fully. The DO was maintained at about 8 mg/L.

The measured and simulated values of the integrated MBR effluent COD and the residual analysis diagram are shown in *Figures 3* and *4.*

From *Figures 3* and *4,* it can be seen that the integrated MBR has a good removal effect on the COD, the effluent COD was very low, and the total COD removal rate was high. The overall impact of the ASM3-MBR model on the simulation of COD effluent was good, except for some points, the simulation values and the measured values were in good agreement. After calculation, the simulated relative error of COD was from

http://www.aloki.hu ● ISSN 1589 1623 (Print) ● ISSN 1785 0037 (Online)
DOI: http://dx.doi.org/10.15666/aeer/1705_1139511407

0.46 to 23.66%, and the average relative error was 3.88%. Wu et al. (2016) observed an average absolute relative error between the measured and simulated values of 16.8% for the COD effluent while simulating and optimizing a practical cooking wastewater treatment plant (CWTP). Their results revealed that the ASM3 model had been successfully established to simulate the biological process of the CWTP.

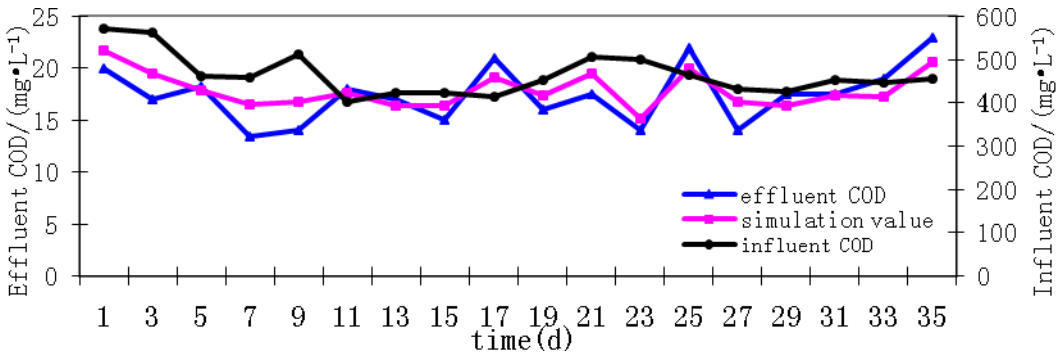

Figure 3. *The measured and simulated values of the integrated MBR effluent COD*

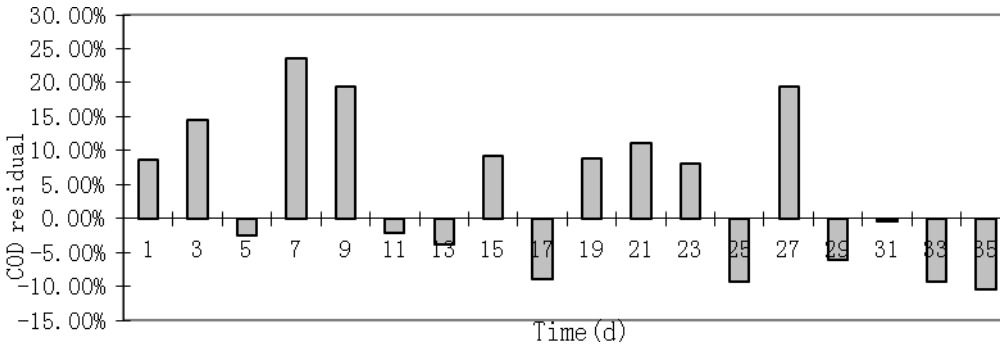

Figure 4. *The residual analysis diagram of the integrated MBR effluent COD.*

The measured and simulated values of the integrated MBR effluent NH_3-N and the residual analysis diagram are shown in *Figures 5* and *6*.

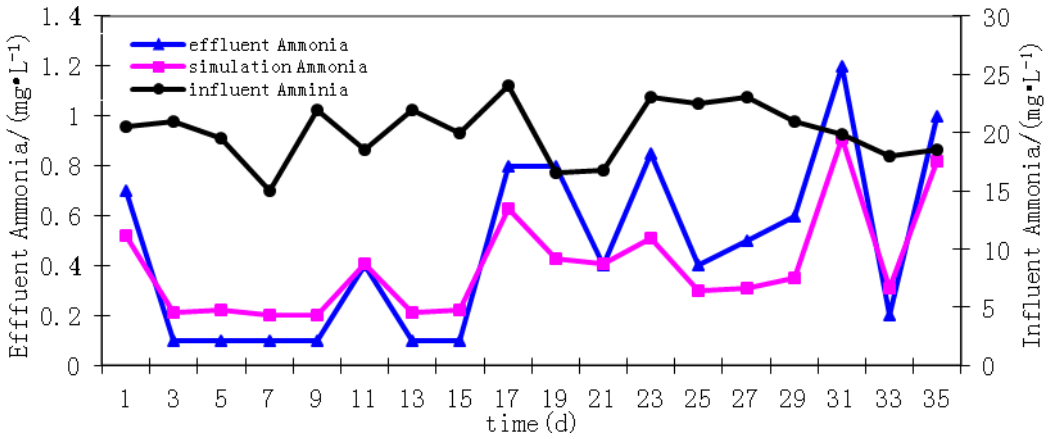

Figure 5. *The measured and simulated values of the integrated MBR effluent NH_3-N*

http://www.aloki.hu ● ISSN 1589 1623 (Print) ● ISSN 1785 0037 (Online)
DOI: http://dx.doi.org/10.15666/aeer/1705_1139511407

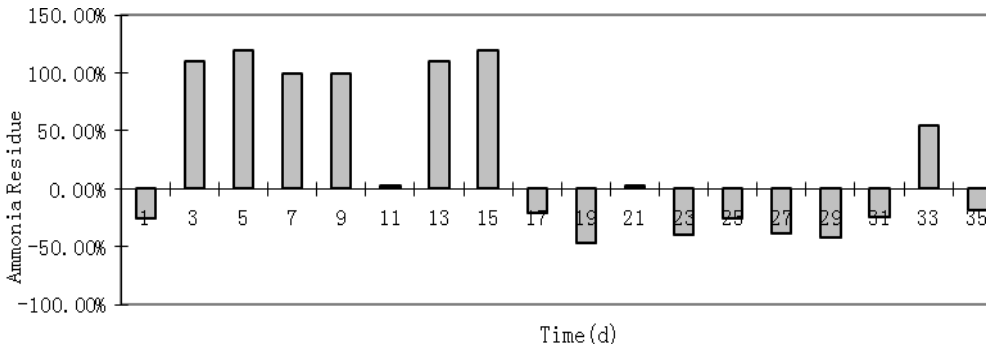

Figure 6. *The residual analysis diagram of the integrated MBR effluent NH_3-N*

As seen in *Figure 5,* the integrated MBR process worked well with NH_3-N. In MBR, since the correlation between the influent NH_3-N value and the effluent NH_3-N value was relatively weak, the simulated value of the effluent NH_3-N during the simulation of the ASM3 model was between the NH_3-N values of the influent. There is a close correlation. Therefore, when using the ASM3-MBR model established based on ASM3 to simulate MBR, there will be some errors between the effluent NH_3-N simulated value and the effluent NH_3-N measured value. However, because the concentration of NH_3-N in the effluent was deficient, and the effluent standard was fully met, and the prediction of total effluent nitrogen was not substantially affected, the prediction could be considered as reasonable. From *Figures 5* and *6,* the relative error of NH_3-N simulation was from 2.5 to 120%, and the average relative error was about 24.44%. However, Wu et al. (2016) observed an average absolute relative error between the measured and simulated values of 15% for NH_4-N effluent and a good agreement in the benefits from the model prediction, and practical measurement was observed.

Figures 7 and *8* show the measured and simulated values of the integrated MBR effluent TN and the residual analysis diagram of the integrated MBR effluent TN.

From *Figures 7* and *8,* the overall effect of the ASM3-MBR model for effluent simulation of TN was good, except for some points, the simulation values and the measured values were in good agreement. After calculation, the relative error of TN simulation was from 0.18 to 27.43%, and the average relative error was 5.39%.

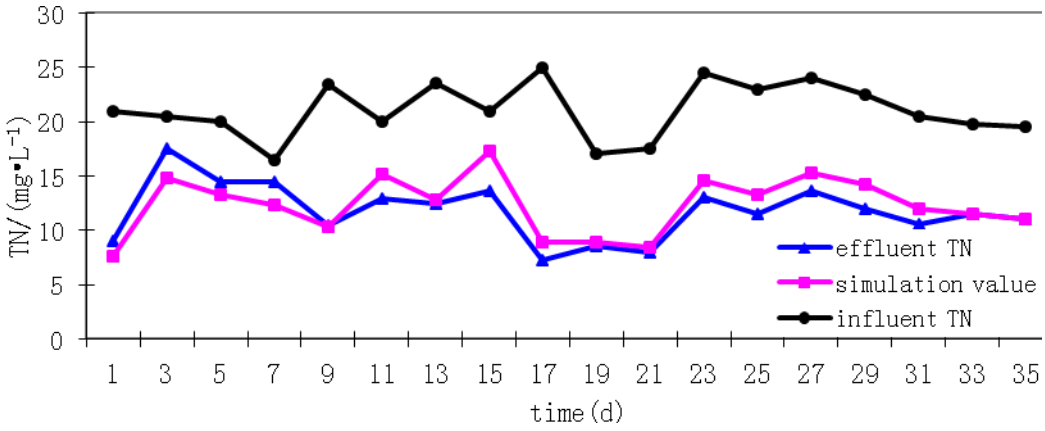

Figure 7. *The measured and simulated values of the integrated MBR effluent TN*

http://www.aloki.hu ● ISSN 1589 1623 (Print) ● ISSN 1785 0037 (Online)
DOI: http://dx.doi.org/10.15666/aeer/1705_1139511407

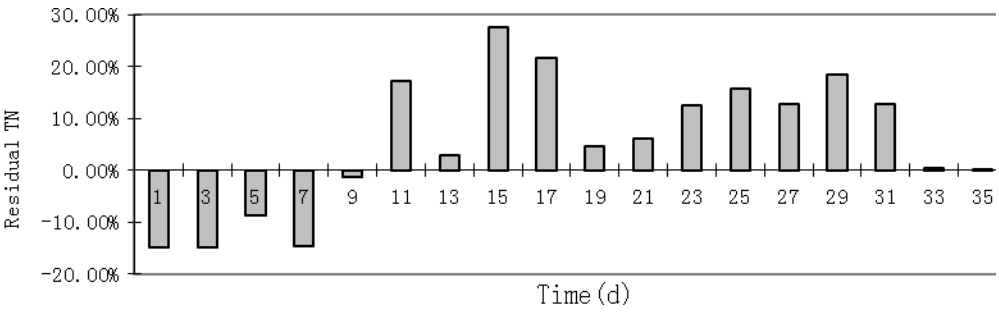

Figure 8. *The residual analysis diagram of the integrated MBR effluent TN*

Conclusion

In this research, the established ASM3-MBR model simulation system was used to simulate the steady-state and dynamics of the integrated MBR. The simulation results of the ASM3-MBR model for the effluent COD, NH_3-N, and TN were analyzed. In general, the self-developed simulation system was more consistent with the simulated and measured values of the effluent COD and TN of the MBR system, thus validating the effectiveness and practicality of the ASM3-MBR model. The simulation results also showed that the error between the simulated value and the measured value was unavoidable. The ASM3-MBR model can more accurately simulate the treatment effect of the integrated MBR and the changing rules of various pollutants. This has a significant supporting role in understanding the contaminant removal mechanism of the integrated MBR, optimizing the operational control of the reactor, and predicting the outflow indicators.

It can be concluded that, a precise adjustment and optimization of the simulation program ASM3-MBR can be used to predict the effluent quality of the MBR process sewage treatment plant, and the operation management of the sewage treatment plant can be optimized. More research is, however, required to optimize ASM3-MBR model performance, especially the effluent quality, and reduction of error between the simulated value and the measured value.

This optimization will make ASM3-MBR model more attractive for use as a preferred remediation strategy in wastewater treatment, considering the significant of contaminant removal mechanism of the integrated MBR.

Acknowledgements. This research has been supported by the Heilongjiang Province Natural Science Foundation of China (E201354).

REFERENCES

[1] Blomberg, K., Kosse, P., Mikola, A., Kuokkanen, A., Fred, T., Heinonen, M., Mulas, M., Lübken, M., Wichern, M., Vahala, R. (2018): Development of an extended ASM3 model for predicting the nitrous oxide emissions in a full-scale wastewater treatment plant. – Environmental Science & Technology 52(10): 5803-5811.

[2] Bournazou, M. C., Arellano-Garcia, H., Wozny, G., Lyberatos, G., Kravaris, C. (2010): Model reduction of the ASM3 extended for two-step nitrification. – IFAC Proceedings 43(6): 60-65.

http://www.aloki.hu ● ISSN 1589 1623 (Print) ● ISSN 1785 0037 (Online)
DOI: http://dx.doi.org/10.15666/aeer/1705_1139511407

[3] Braak, E., Alliet, M., Schetrite, S., Albasi, C. (2011): Aeration and hydrodynamics in submerged membrane bioreactors. – Journal of Membrane Science 379(1-2): 1-18.
[4] Castelo-Grande, T., Augusto, P. A., Monteiro, P., Barbosa, D. (2010): Design and application of a membrane bioreactor unit to upgrade and enhance the required performance of an installed wastewater treatment plant. – Asia-Pacific Journal of Chemical Engineering 5(1): 73-82.
[5] Chang, C.-Y., Chang, J.-S., Lin, Y.-W., Erdei, L., Vigneswaran, S. (2006): Quantification of air stripping and biodegradation of organic removal in acrylonitrile-butadiene-styrene (ABS) industry wastewater during submerged membrane bioreactor operation. – Desalination 191(1-3): 162-168.
[6] Elawwad, A., Zaghloul, M., Abdel-Halim, H. (2017): Simulation of municipal-industrial full scale WWTP in an arid climate by application of ASM3. – Journal of Water Reuse and Desalination 7(1): 37-44.
[7] Gao, F., Nan, J., Li, S., Wang, Y. (2018): Modeling and simulation of a biological process for treating different COD: N ratio wastewater using an extended ASM1 model. – Chemical Engineering Journal 332: 671-681.
[8] Gujer, W., Henze, M., Mino, T., Matsuo, T., Wentzel, M., Marais, G. (1995): The activated sludge model No. 2: biological phosphorus removal. – Water Science and Technology 31(2): 1-11.
[9] Gujer, W., Henze, M., Mino, T., Van Loosdrecht, M. (1999): Activated sludge model no. 3. – Water Science and Technology 39(1): 183-193.
[10] Henze, M., Gujer, W., Mino, T., van Loosdrecht, M. C. (2000): Activated sludge models ASM1, ASM2, ASM2d and ASM3. – IWA Publishing, London.
[11] Lee, Y., Cho, J., Seo, Y., Lee, J. W., Ahn, K.-H. (2002): Modeling of submerged membrane bioreactor process for wastewater treatment. – Desalination 146(1-3): 451-457.
[12] Li, F., Behrendt, J., Wichmann, K., Otterpohl, R. (2009): Evaluation of factors influencing soluble microbial product in submerged MBR through hybrid ASM model. – Frontiers of Environmental Science & Engineering in China 3(2): 226-235.
[13] Liwarska-Bizukojc, E., Olejnik, D., Biernacki, R., Ledakowicz, S. (2011): Calibration of a complex activated sludge model for the full-scale wastewater treatment plant. – Bioprocess and Biosystems Engineering 34(6): 659-670.
[14] Mannina, G., Di Bella, G., Viviani, G. (2011): An integrated model for biological and physical process simulation in membrane bioreactors (MBRs). – Journal of Membrane Science 376(1-2): 56-69.
[15] Ng, A. N., Kim, A. S. (2007): A mini-review of modeling studies on membrane bioreactor (MBR) treatment for municipal wastewaters. – Desalination 212(1-3): 261-281.
[16] Song, Y.-j., Xie, Y.-b., Yudianto, D. (2012): Extended activated sludge model no. 1 (ASM1) for simulating biodegradation process using bacterial technology. – Water Science and Engineering 5(3): 278-290.
[17] Wang, H.-C., Cheng, H.-Y., Wang, S.-S., Cui, D., Han, J.-L., Hu, Y.-P., Su, S.-G., Wang, A.-J. (2016): Efficient treatment of azo dye containing wastewater in a hybrid acidogenic bioreactor stimulated by biocatalyzed electrolysis. – Journal of Environmental Sciences 39: 198-207.
[18] Wu, X., Yang, Y., Wu, G., Mao, J., Zhou, T. (2016): Simulation and optimization of a coking wastewater biological treatment process by activated sludge models (ASM). – Journal of Environmental Management 165: 235-242.
[19] Zhou, M., Gong, J., Yang, C., Pu, W. (2013): Simulation of the performance of aerobic granular sludge SBR using modified ASM3 model. – Bioresource Technology 127: 473-481.

http://www.aloki.hu ● ISSN 1589 1623 (Print) ● ISSN 1785 0037 (Online)
DOI: http://dx.doi.org/10.15666/aeer/1705_1139511407

IN SILICO DETECTION OF SPECIES- AND ORDER-SPECIFIC MARKERS BASED ON VIRTUAL PCR-RFLP OF THE *COI* GENE IN INSECT

SABIR, J. S. M.[1] – RABAH, S.[1] – YACOUB, H.[2] – HAJRAH, N. H.[1] – ATEF, A.[1] – HALL, N.[1,3] – BAHIELDIN, A.[1,4*]

[1]*Department of Biological Sciences, Faculty of Science, King Abdulaziz University (KAU), P.O. Box 80141, Jeddah 21589, Saudi Arabia*

[2]*Department of Biological Sciences, Faculty of Science, University of Jeddah, Dahaban 23881, Saudi Arabia*

[3]*The Genome Analysis Center, Norwich Research Park, Norwich, NR4 7UH, UK*

[4]*Department of Genetics, Faculty of Agriculture, Ain Shams University, Cairo, Egypt*

**Corresponding author*
e-mail: abmahmed@kau.edu.sa; phone: +966-50-632-9922

(Received 18th Apr 2019; accepted 1st Jul 2019)

Abstract. COI is the first subunit of the mitochondrial cytochrome C oxidase gene that is commonly used for barcoding via sequencing and molecular identification of insect orders and species. However, fast and cheap data analysis might still be required for the detection of insect orders and species to replace sequencing in large populations. The latter can be emphasized by detecting restriction enzyme site polymorphisms in COI sequences of insect orders and species. In the present study, we have utilized an in silico approach for detecting species- and order-specific molecular markers in insects collected from Saudi Arabia based on the new non-traditional open source tool, namely C*is*SERS. A number of 237 restriction enzymes were checked for the presence of their recognition sites within the *COI* gene sequence of the different insect species. Generated data was displayed in predicted agarose gels as virtual PCR-RFLP patterns. The results indicated the occurrence of 14 species-specific and three order-specific molecular markers representing 10 species and two orders of insect. The highest number of species-specific markers (3 markers) was generated for *Idolus picipennis* (Order: Coleoptera), followed by the two hemipteran *Macrosteles* sp. and *Osbornellus auronitens* (two markers each). Three order-specific markers were generated for orders Lepidoptera (two markers) and Diptera (one marker). The overall results demonstrated that C*is*SERS efficiently allowed for the detection of species- and order-specific markers that can further be utilized in screening large insect populations.
Keywords: *PCR-RFLP, CisSERS, genetic characterization*

Introduction

Subunit I (658 nt) of the mitochondrial cytochrome C oxidase (COX) gene (namely *COI*) started in 2003 to be the most universal marker for species identification in animal (Hebert et al., 2003, 2004). Recent concerns were raised for the insufficiency of insect biodiversity data in Saharo-Arabian region including Saudi Arabia and the lack of conducted traditional surveys (Ashfaq et al., 2018). The latter makes it vital to gain insights on such a virgin area in terms of insect classification and biodiversity.

Our recent study (Ashfaq et al., 2018) proved the feasibility and efficiency of utilizing *COI* gene in barcoding insects collected from Saudi Arabia. In the present study, we further utilized virtual PCR-RFLP based on the barcode sequences targeting the recovery of fast and cheap approach for characterizing insect orders and species in

http://www.aloki.hu ● ISSN 1589 1623 (Print) ● ISSN 1785 0037 (Online)
DOI: http://dx.doi.org/10.15666/aeer/1705_1140911418

large populations. Methods based on restriction enzyme digestion (ex., PCR-RFLP) are easy to perform, reproducible, and cost-effective and require less equipment and expertise (Agarwal et al., 2008). In the past, restriction enzyme-based molecular markers were commonly employed, but with the emergence of high-throughput sequencing technologies, they facilitated more in-depth genomic analysis and characterization. PCR-based restriction fragment length polymorphic markers (or PCR-RFLP) are used for gene mapping and molecular breeding (Shu et al., 2011). To detect the efficacy of re-utilizing PCR-RFLP for molecular characterization, we were required to use efficient in silico tools suitable for analyzing large genomic datasets towards the recovery of a fast and cost-effective approach in characterizing large insect populations in the future.

Access to computational tools that processes massive amounts of DNA sequence information from multiple samples is useful for addressing difficult biological questions. Several current restriction site analysis tools were designed to handle only few sequences for targeted analysis (Neff et al., 2002; Vincze et al., 2003; Ilic et al., 2004; Thiel et al., 2004; Zhang et al., 2005; Taylor and Provart, 2006; Chang et al., 2010). *Cis*SERS (or customizable in silico sequence evaluation for restriction sites) tools were designed specifically for PCR-RFLP marker detection (Sharpe et al., 2016). Such a new graphical user interface helps in detecting enzyme restriction sites in large DNA sequence datasets and enables high-throughput analysis of multiple sequences for restriction sites with a possibly embedded dynamic visualization functionality. It can predict places the enzyme cuts during gel electrophoresis and save time and effort of running unrequired several enzymatically-digested DNA samples. Such information can help in deciding which enzymes to be selected in digesting DNA for restriction-site associated DNA (or RAD) sequencing libraries and further cloning. C*is*SERS can also be utilized in detecting methylated DNAs as the original PCR-RFLP will vary from the virtual pattern for any methylation susceptible restriction enzyme site. C*is*SERS is expected to pave the way between sequence acquisition and implementation of diverse wet-lab approaches to solve biological questions more easily.

In this work, we utilized the COI subunit for specimens of six insect orders collected from Saudi Arabia to detect species- and order-specific molecular markers based on the use of C*is*SERS surface tools in order to generate virtual PCR-RFLP. This information will be useful in the future analysis of large insect populations via PCR-RFLP.

Materials and methods

For sample collection, a Malaise trap (Hutcheson and Jones, 1999; Hill et al., 2005) was installed at Hada Al-Sham station, King Abdulaziz University (KAU) located in the western region (near Makkah) of Saudi Arabia (21.795°N, 39.711°E). Sample collection, morphological classification up to Sanger sequencing were done as indicated in our most recent study (Ashfaq et al., 2018).

C*is*SERS was used to develop fasta files for restriction site analysis and generate predicted gel images as described (Sharpe et al., 2016). Outputs describe the cut counts and locations for each restriction site and dynamically created predicted gel images. The master list of enzymes (237 in the present study) is retrieved from the REbase database (Vincze et al., 2003). A set of formulas used via C*is*SERS is retrieved in order to produce fragment size (Neff et al., 2002; Ilic et al., 2004; Agarwal et al., 2008; Shu et

http://www.aloki.hu ● ISSN 1589 1623 (Print) ● ISSN 1785 0037 (Online)
DOI: http://dx.doi.org/10.15666/aeer/1705_1140911418

al., 2011). The motif detection feature of C*is*SERS was previously validated using *Nostoc* and *ATPC1* genes (Sharpe et al., 2016).

For validating the in silico datasets, DNAs from the different 30 insect species were isolated and subjected to PCR to recover the *COI* gene fragment (634 bp). Restriction analysis including five selected restriction enzymes was done following standard protocols to validate five species-specific markers of four insect species. The products of restriction analysis were detected using electrophoresis on agarose gels (1.2% in 1x TBE buffer), stained with ethidium bromide (0.3 ug/ml), then visually examined with UV transilluminator and photographed using a CCD camera (UVP, UK).

Results and discussion

Generating a DNA barcode based on the common *COI* gene fragment involves sequencing, then BLAST towards the identification of sequence homology down to the species level. Conventional DNA sequencing is time-consuming and costly, which makes it difficult to be universally utilized. The latter approach generates no particular species- or order-specific markers that can be solely used in preliminary screening of any insect population. In PCR-RFLP, the restriction sites are identified in the target gene fragment (e.g., *COI*), and polymorphism is based on the number and sizes of the cleaved fragment of any given species. This method is simple, cheap and time-saving, thus meets many applications (Liu et al., 2001, 2003; Um et al., 2001; Ding et al., 2003; Wang et al., 2005, 2007; Ying et al., 2007).

In our previous study, *COI* barcodes were analyzed at the DNA level for a number of 560 insect samples collected during four-week time course in Saudi Arabia. Recovered sequences were trimmed to 634 nucleotides and number of samples was narrowed to 175 representing 30 species of six insect orders. Sequences of these species were utilized in generating the virtual PCR-RFLP patterns via C*is*SERS surface tools. A number of 237 restriction enzymes were checked for the presence of recognition sites within the *COI* gene sequence (634 bp) of the different insect species. The consensus sequences of the 30 insect species were fed to the program and restriction sites for enzymes that either uniquely cut DNA of one single species or resulted in the occurrence of a DNA fragment specific to a single insect order are shown in *Figure A1* in the *Appendix*. The figure indicates the positions of the 17 selected enzymes that cut within the COI sequence that meet the above mentioned criterion. Interestingly, no restriction sites were shown in the first 181 nt of the gene (*Fig. A1*; *Table 1*). All selected restriction sites are located downwards. The resulted species- and order-specific markers are shown in the virtual PCR-RFLP patterns shown in *Figures 1* and *2*, respectively, while summarized in *Figure 3*. Species-specific markers were recovered for 10 out of the 30 insect species. The largest number of species-specific markers are shown for *Idolus picipennis* (3 markers) of order Coleoptera, followed by *Macrosteles sp.* and *Osbornellus auronitens* (2 markers each) of order Hemiptera (*Fig. 1*). The single species-specific markers were detected for seven other species, e.g., *Monomorium junodi*, *Camponotus maculatus*, *Balta vilis*, *Belenois aurota*, *Ephysteris subdiminutella*, *Carpomya vesuviana* and *Tabanus striatus*. Numbers of 2, 4, 1, 2, 3 and 1 species-specific markers were shown for orders Hymenoptera, Hemiptera, Blattodae, Lepidoptera, Coleoptera and Diptera, respectively (*Figs. 1* and *A1*). The results at the order level indicate the recovery of three order-specific markers.

http://www.aloki.hu ● ISSN 1589 1623 (Print) ● ISSN 1785 0037 (Online)
DOI: http://dx.doi.org/10.15666/aeer/1705_1140911418

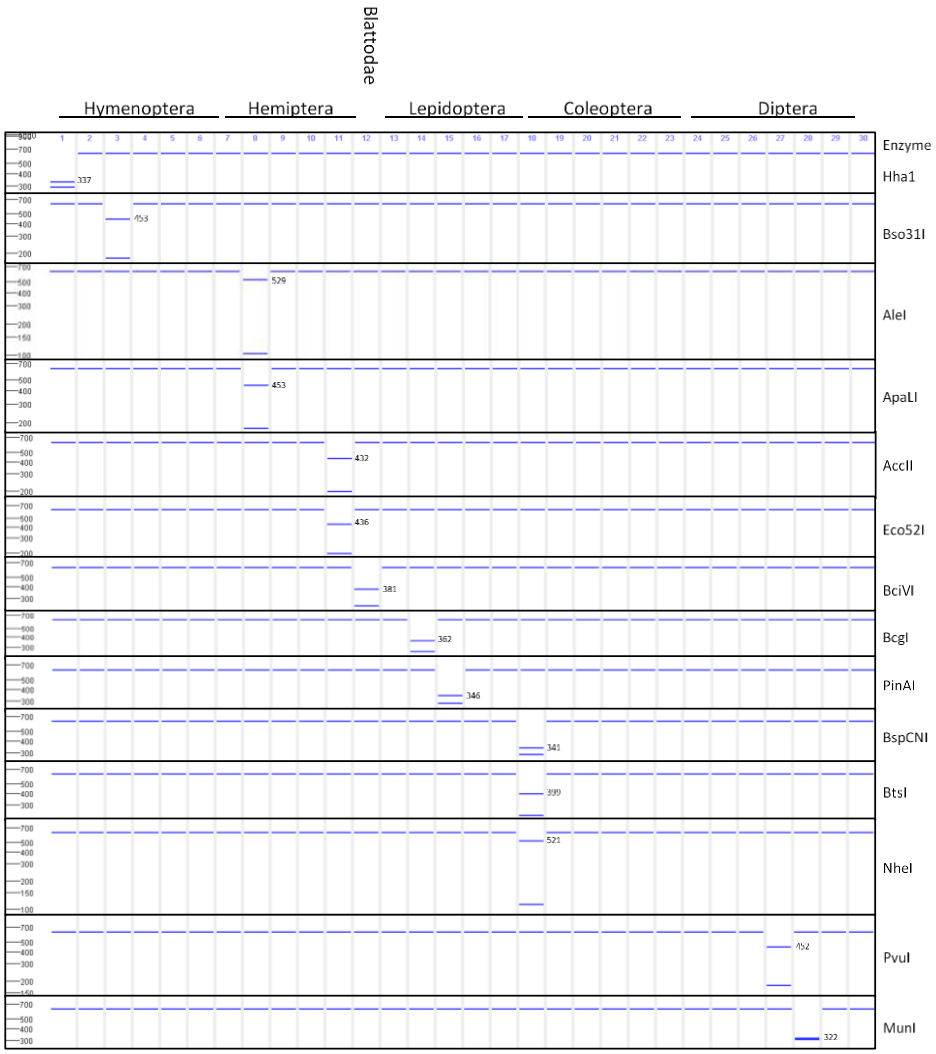

Figure 1. *Virsual electrophregrams generated from CisSERS tools to describe specific PCR-RFLP markers in COI gene in 10 insect species belonging to six insect orders. Based on ach restriction enzyme has a unique site in the gene for a given insect species. Species numbers (1-30) refer to insect species shown in Table 1*

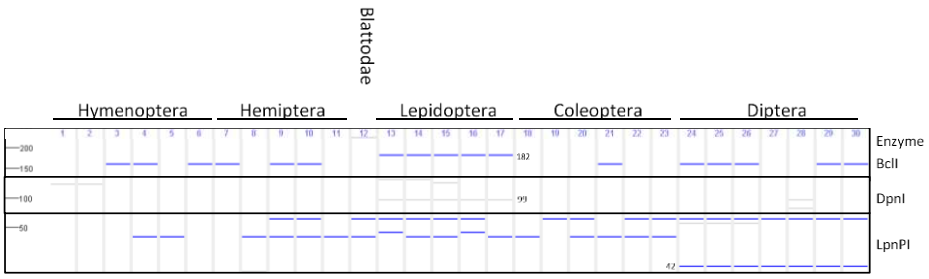

Figure 2. *Virsual electrophregrams generated from CisSERS tools to describe specific PCR-RFLP markers in COI gene in two out of six insect orders. Each restriction enzyme has multiple recogintion sites in the gene for the different insect species and orders. One fragment for each of the enzymes BclI (182 bp), DpnI (99 bp) are specific for order Lepidoptera, while one fragmente of the enzyme LpnPI (42) is specific for order Diptera. Species numbers (1-30) refer to insect species shown in Table 1*

http://www.aloki.hu ● ISSN 1589 1623 (Print) ● ISSN 1785 0037 (Online)
DOI: http://dx.doi.org/10.15666/aeer/1705_1140911418

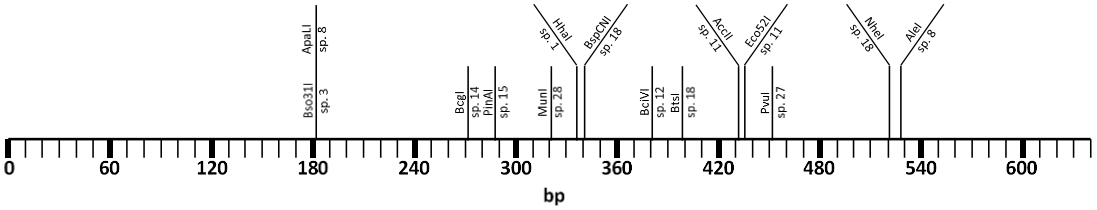

Figure 3. *Restriction map for the enzymes uniquely cut the COI gene in a given insect species. The map involves 14 enzymes specific for 10 species of the six insect orders. Species numbers refer to insect species shown in Table 1*

Table 1. *List of insect species and orders along with restriction enzymes with recognition sites within COI gene*

No.	Species	Enzyme	Species-specific marker (bp) 5`…….3`	Order	Enzyme	Order-specific marker (bp)
1	*Monomorium junodi*	HhaI	337//297	Hymenoptera	-	-
2	*Cataglyphis ibericus*	-	-			
3	*Camponotus maculatus*	Bso31I	181//453			
4	*Hymenoptera sp.*	-	-			
5	*Nomioides facilis*	-	-			
6	*Tachytes crassus*	-	-			
7	*Batracomorphus angustatus*	-	-	Hemiptera	-	-
8	*Macrosteles sp.*	AleI, ApaLI	529//105, 181//453			
9	*Colladonus tahotus*	-	-			
10	*Sacphytopius vaccinium*	-	-			
11	*Osbornellus auronitens*	AccII, Eco52I	202//432, 436//198			
12	*Balta vilis*	BciVI	381//253	Blattodae	-	-
13	*Tarucus theophrastus*	-	-	Lepidoptera	BclI DpnI	182 99
14	*Belenois aurota*	BcgI	242//362			
15	*Ephysteris subdiminutella*	PinAI	288//346			
16	*Tuta absoluta*	-	-			
17	*Batrachedra amydraula*	-	-			
18	*Idolus picipennis*	BspCNI, BtsI, NheI	341//293, 399//235, 521//113	Coleoptera	-	-
19	*Melanotus villosus*	-	-			
20	*Algarobius prosopis*	-	-			
21	*Exomala pallidipennis*	-	-			
22	*Xylotrupes siamensis*	-	-			
23	*Copris tripartitus*	-	-			
24	*Lispe albitarsis*	-	-	Diptera	LpnPI	42
25	*Chrysomya chani*	-	-			
26	*Anthomyiopsis nigrisquamata*	-	-			
27	*Carpomya vesuviana*	PvuI	452//182			
28	*Tabanus striatus*	MunI	322//312			
29	*Leptogaster cylindrica*	-	-			
30	*Asyndetus sp.*	-	-			

Two of which are shown for order Lepidoptera and one is shown for order Diptera (*Fig. 2*). Exact position of each marker is shown in *Figure A1*. Sizes of these markers are 182 and 99 nt for order Lepidoptera and 42 for order Diptera. Enzymes that generated these markers are BclI, DpnI and LpnPI, respectively. Interestingly, DpnI

http://www.aloki.hu ● ISSN 1589 1623 (Print) ● ISSN 1785 0037 (Online)
DOI: http://dx.doi.org/10.15666/aeer/1705_1140911418

enzyme has a 4-nt recognition site (GATC) that exists within the 6-nt recognition site (TGATCA) of BclI enzyme. The TGATCA site is located at 453 nt, therefore, the two enzymes cut DNA at this site. DpnI has another site at 552 nt, which is located 99 nt downstream the first, while BclI has no further sites downstream the first (*Fig. A1*). Accordingly, the cut with BclI resulted in the occurrence of 182 nt marker, while the cut with DpnI enzyme resulted in the occurrence of 99 nt marker. The results generated from *Cis*SERS tools were validated via the restriction analysis of PCR products involving five randomly selected species-specific markers and electrophoregram results supported those generated by *Cis*SERS tools (*Fig. A2*). Concerns on the reproducibility of PCR were repeatedly raised. Besides, dry-lab restriction analysis requires validation via wet-lab experimentation. Therefore, we consider the data shown in *Fig. A2* can validate both the PCR approach as such as well as the utility of *Cis*SERS tools. Other universal markers, ex., 16S rRNA gene, were successfully utilized in detecting PCR-RFLP patterns of the causative bacteria of neonatal sepsis, e.g., *Staphylococcus aureus* and *Klebsiella* spp. (Rohit et al., 2016). The results indicated that PCR-RFLP is useful for the early diagnosis of culture negative neonatal sepsis in human.

There are many restriction site analysis tools designed to handle only few/short sequences (Neff et al., 2002; Vincze et al., 2003; Ilic et al., 2004; Thiel et al., 2004; Zhang et al., 2005; Taylor and Provart, 2006; Chang et al., 2010). Of which, NEBcutter handles a less than 300 kb, besides, it is not set up for multiple sequence analysis (Vincze et al., 2003). The other tools are web-server based with limited functionality for high-throughput analysis. However, *Cis*SERS was developed to enable high-throughput analysis of multiple/long sequences for restriction sites. In addition, *Cis*SERS solely allows for custom motif detection to identify conserved sites, e.g., *cis*- and *trans*-acting element binding sites. Sharpe et al. (2016) indicated the effectiveness and multiple distinctive functionalities of *Cis*SERS in analyzing mature sequence data of *cfq* gene. They also indicated that utilizing *Cis*SERS in transcriptomic or genomic analysis enables a guidance during subsequent restriction enzyme-based experimentation. PCR-based approaches could make identification of insect at species level easier, faster and more accurate compared with traditional morphological approaches. We think this work in the first of its kind in detecting species- or order-specific molecular markers in insects as well as in the utility of *Cis*SERS in discriminating insect orders and species. In conclusion, *Cis*SERS is a fast, cost-effective surface tools enable bridging the gap between sequence acquisition and implementation of wet-lab approaches towards addressing important biological clues.

Conclusion

Data generated in the present study from virtual PCR-RFLP via *Cis*SERS provided useful information. Firstly, it narrows the number of restriction enzymes to be used in the future in studying any insect population. Second, it supports the utility of the wet-lab PCR-RFLP as a fast, cheap, requires less equipment and cost-effective approach for characterizing insect populations. Third, it provides species- and order-specific markers that can be used as a first layer of detection at the species or order levels. Such an approach can be adopted for other types of universal markers in prokaryotic as well as eukaryotic organisms.

http://www.aloki.hu ● ISSN 1589 1623 (Print) ● ISSN 1785 0037 (Online)
DOI: http://dx.doi.org/10.15666/aeer/1705_1140911418

Acknowledgments. This project was funded by the Deanship of Scientific Research (DSR), King Abdulaziz University, Jeddah, under Grant no. (99-130-35-HiCi). The authors, therefore, acknowledge with thanks DSR technical and financial support.

Author contributions. All authors have read and approved this manuscript. Conceived and designed the experiments: JS, SR, NH, AB. Performed the experiments: HY, NH, AA. Analyzed the data: HY, NH, AA, KA. Wrote the paper: JS, KA, NH, AB.

Conflict of interests. The authors declare that they have no conflict of interests.

Data availability. Authors declare no unavailable data generated through or related to the course of this research.

REFERENCES

[1] Agarwal, M., Shrivastava, N., Padh, H. (2008): Advances in molecular marker techniques and their applications in plant sciences. – Plant Cell Rep. 27: 617-631.
[2] Ashfaq, M., Sabir, J. S. M., El-Ansary, H. O., et al. (2018): Insect diversity in the Saharo-Arabian region: Revealing a little-studied fauna by DNA barcoding. – PLoS ONE 13: e0199965.
[3] Chang, H. W., Cheng, Y. H., Chuang, L. Y., et al. (2010): SNP-RFLPing 2: an updated and integrated PCR-RFLP tool for SNP genotyping. – Bmc Bioinformatics 11: Artn 173. DOI: 10.1186/1471-2105-11-173.
[4] Ding, X. Y., Wang, Z. T., Zhou, K. Y., et al. (2003): Allele-specific primers for diagnostic PCR authentication of *Dendrobium officinale*. – Planta Medica 69: 587-588.
[5] Hebert, P. D. N., Cywinska, A., Ball, S. L., et al. (2003): Biological identifications through DNA barcodes. – Proc. Biol. Sci. 270: 313-321.
[6] Hebert, P. D. N., Penton, E. H., Burns, J. M., et al. (2004): Ten species in one: DNA barcoding reveals cryptic species in the neotropical skipper butterfly *Astraptes fulgerator*. – Proc. Natl. Acad. Sci. USA 101: 14812-14817.
[7] Hill, D., Fasham, M., Tucker, G., et al. (2005): Handbook of Biodiversity Methods: Survey, Evaluation and Monitoring. – Cambridge University Press, Cambridge.
[8] Hutcheson, J., Jones, D. (1999): Spatial variability of insect communities in a homogenous system: Measuring biodiversity using Malaise trapped beetles in a *Pinus radiata* plantation in New Zealand. – Forest Ecol. Manag. 118: 93-105.
[9] Ilic, K., Berleth, T., Provart, N. J. (2004): BlastDigester—a web-based program for efficient CAPS marker design. – Trends in Genet. 20: 280-283.
[10] Liu, X. H., Wang, Y. Q., Zhou, K. Y., et al. (2003): Study on allele-specific diagnostic PCR of the traditional Chinese medicines of the deers. – Acta Pharmaceutica Sinica 36: 634-635.
[11] Liu, Z., Wang, Y. Q., Zhou, K., et al. (2001): Authentication of Chinese crude drug, Gecko, by allele-specific diagnostic PCR. – Planta Medica 67: 385-387.
[12] Neff, M. M., Turk, E., Kalishman, M. (2002): Web-based primer design for single nucleotide polymorphism analysis. – Trends in Genet. 18: 613-615.
[13] Rohit, A., Maiti, B., Shenoy, S., et al. (2016): Polymerase chain reaction-restriction fragment length polymorphism (PCR-RFLP) for rapid diagnosis of neonatal sepsis. – Indian J. Med. Res. 143: 72-78.
[14] Sharpe, R. M., Koepke, T., Harper, A., et al. (2016): CisSERS: Customizable *in silico* sequence Evaluation for restriction sites. – PLoS ONE 11: e0152404.
[15] Shu, Y. J., Li, Y., Zhu, Z. L., et al. (2011): SNPs discovery and CAPS marker conversion in soybean. – Mol. Biol. Rep. 38: 1841-1846.
[16] Taylor, J., Provart, N. J. (2006): CapsID: a web-based tool for developing parsimonious sets of CAPS molecular markers for genotyping. – BMC Genet. 7: Artn 27.

http://www.aloki.hu ● ISSN 1589 1623 (Print) ● ISSN 1785 0037 (Online)
DOI: http://dx.doi.org/10.15666/aeer/1705_1140911418

[17] Thiel, T., Kota, R., Grosse, I., et al. (2004): SNP2CAPS: a SNP and INDEL analysis tool for CAPS marker development. – Nucleic Acids Res. 32: ARTN e5.
[18] Um, J. Y., Chung, H. S., Kim, M. S., et al. (2011): Molecular authentication of Panax ginseng species by RAPD analysis and PCR-RFLP. – Biol. Pharma. Bull. 24: 872-875.
[19] Vincze, T., Posfai, J., Roberts, R. J. (2003): NEBcutter: a program to cleave DNA with restriction enzymes. – Nucleic Acids Res. 31: 3688-3691.
[20] Wang, C. Z., Li, P., Ding, J. Y., et al. (2005): Identification of *Fritillaria pallidiflora* using diagnostic PCR and PCR-RFLP based on nuclear ribosomal DNA internal transcribed spacer sequences. – Planta Medica 71: 384-386.
[21] Wang, C. Z., Li, P., Ding, J. Y., et al. (2007): Simultaneous identification of *Bulbus Fritillariae cirrhosae* using PCR-RFLP analysis. – Phytomedicine 14: 628-632.
[22] Ying, Y., Xu, H., Wang, Z. T. (2007): Allele-specific diagnostic PCR authentication of *Dendrobium thyrsiflorum*. – Acta Pharmaceutica Sinica 42: 98-103.
[23] Zhang, R. F., Zhu, Z. H., Zhu, H. M., et al. (2005): NP Cutter: a comprehensive tool for SNPPCR-RFLP assay design. – Nucl. Acids Res. 33: W489-W92.

APPENDIX

Figure A1. *(See next page) Consensus GOI nucleotide sequences of the 30 insect species describing the recognition sites of the 17 restriction enzymes used in detecting PCR-RFLP markers at the species (14 markers) and order (3 markers) levels. Blue and red boxes indicate BclI (182 bp) DpnI (99 bp) fragments specific for Lepidopteran species, while green box indicates the LpnPI (42 bp) fragment specific for dipteran species*

http://www.aloki.hu ● ISSN 1589 1623 (Print) ● ISSN 1785 0037 (Online)
DOI: http://dx.doi.org/10.15666/aeer/1705_1140911418

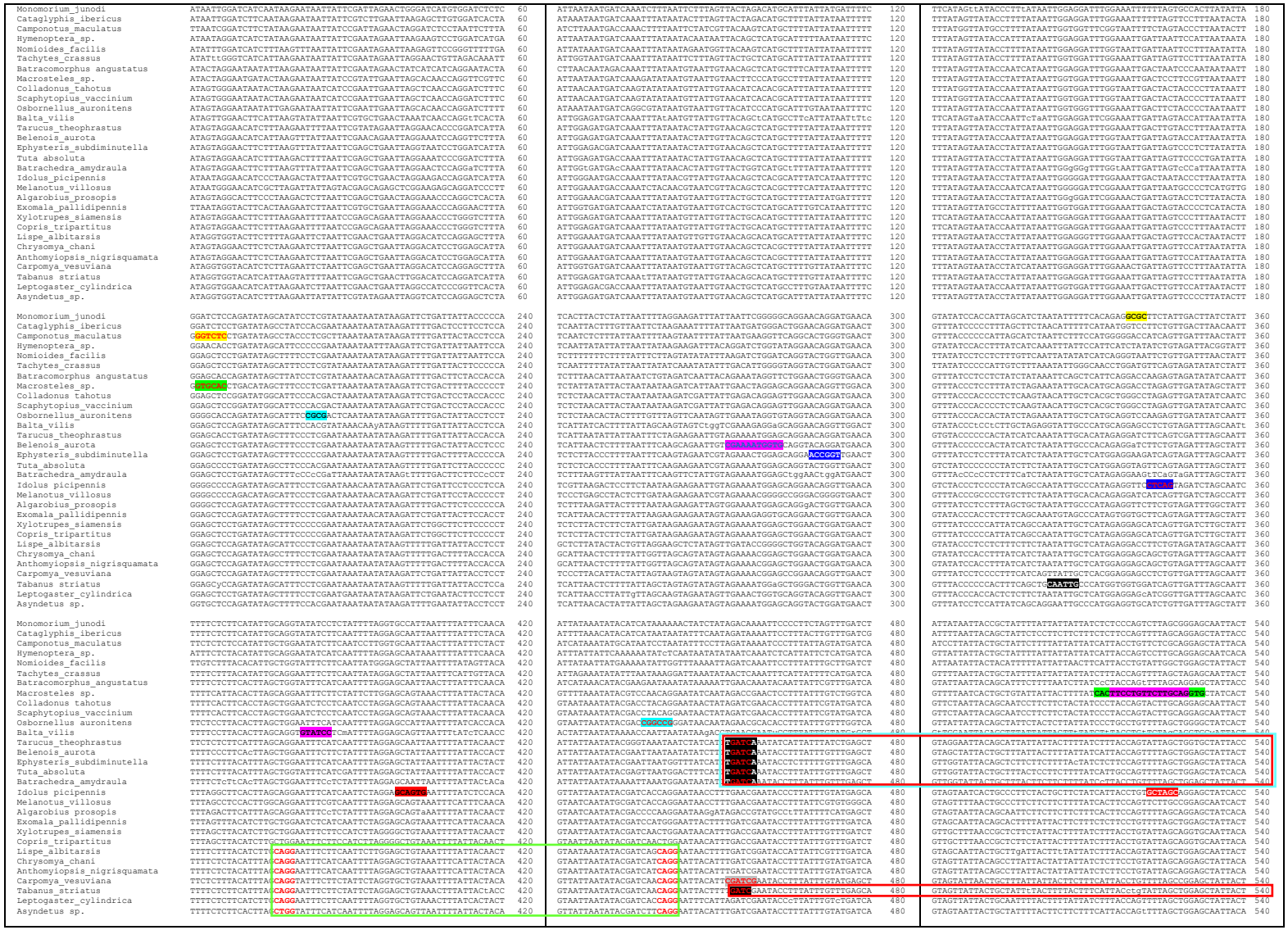

APPLIED ECOLOGY AND ENVIRONMENTAL RESEARCH 17(5):11409-11418.
http://www.aloki.hu ● ISSN 1589 1623 (Print) ● ISSN 1785 0037 (Online)
DOI: http://dx.doi.org/10.15666/aeer/1705_1140911418

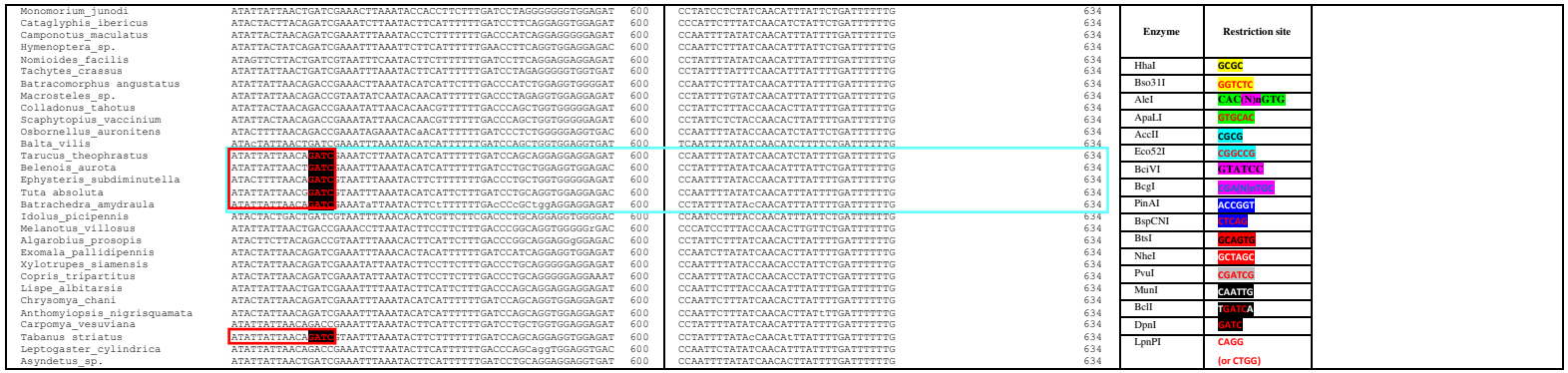

Monomorium_junodi	ATATTATTAACTGATCGAAACTTAAATACCACCTTCTTTGATCCTAGGGGGGGTGGAGAT	600	CCTATCCTCTATCAACATTTATTCTGATTTTTTG	634
Cataglyphis_ibericus	ATACTACTTAACAGATCGAAATCTTAATACTTCATTTTTTGATCCTTCAGGAGGTGGAGAT	600	CCCATTCTTTATCAACATCTATTCTGATTTTTTG	634
Camponotus_maculatus	ATATTACTAACAGATCGAAATTTAAATACCTCTTTTTTTGACCCATCAGGAGGGGGAGAT	600	CCAATTTTATATCAACATTTATTTTGATTTTTTG	634
Hymenoptera_sp.	ATATTACTATCAGATCGAAATTTAAATTCTTCATTTTTTGAACCTTCAGGTGGAGGAGAC	600	CCAATTCTTTATCAACATTTATTCTGATTTTTTG	634
Nomioides_facilis	ATAGTTCTTACTGATCGTAAATTCAATACTTCTTTTTTTGATCCTTCAGGAGGAGGAGAT	600	CCTATTTTATATCAACATTTATTTTGATTTTTTG	634
Tachytes_crassus	ATATTATTAACTGATCGAAATTTAAATACTTCATTTTTTGATCCTAGAGGGGGTGGTGAT	600	CCTATTTTATTTCAACATTTATTTTGATTTTTTG	634
Batracomorphus_angustatus	ATATTATTAACAGACCGAAACTTAAATACATCATTCTTTGACCCATCTGGAGGTGGGGAT	600	CCAATTCTTTATCAACATTTATTTTGATTTTTTG	634
Macrosteles_sp.	ATATTATTAACAGACCGTAATATCAATACAACATTTTTTGACCCTAGAGGTGGAGGAGAT	600	CCTATTTTGTATCAACATTTATTTTGATTTTTTG	634
Colladonus_tahotus	ATATTACTAACAGACCGAAATATTAACACAACGTTTTTTGACCCAGCTGGTGGGGGAGAT	600	CCTATTCTTTACCAACACTTATTTTGATTTTTTG	634
Scaphytopius_vaccinium	ATATTACTAACAGACCGAAATATTAACACAACGTTTTTTGACCCAGCTGGTGGGGGAGAT	600	CCTATTCTCTACCAACACTTATTTTGATTTTTTG	634
Osbornellus_auronitens	ATACTTTTAACAGACCGAAATAGAAATACaACATTTTTTGATCCCTCTGGGGGAGGTGAC	600	CCAATTTTATACCAACATCTATTCTGATTTTTTG	634
Balta_vilis	ATACTATTAACTGATCGAAATTTAAATACATCATTTTTTGATCCAGCTGGTGGAGGTGAT	600	TCAATTTTATATCAACATCTTTCTGATTTTTTG	634
Tarucus_theophrastus	ATATTATTAACAGATCGAAATCTTAATACATCATTTTTTGATCCAGCAGGAGGAGGAGAT	600	CCAATTTTATATCAACATCTATTTTGATTTTTTG	634
Belenois_aurota	ATATTATTAACTGATCGAAATTTAAATACATCATTTTTTGATCCTGCTGGAGGTGGAGAC	600	CCTATTTTATATCAACATTTATTCTGATTTTTTG	634
Ephyseria_subdiminutella	ATACTTTTAACAGATCGTAATTTAAATACTTCTTTTTTTGACCCTGCTGGTGGGGGAGAT	600	CCAATTTTATACCAACATTTATTTTGATTTTTTG	634
Tuta_absoluta	ATATTATTAACGGATCGTAATTTAAATACATCATTCTTTGATCCCTGCAGGTGGAGGAGAC	600	CCAATTTTATATCAACATTTATTTTGATTTTTTG	634
Batrachedra_amydraula	ATATTATTAACAGATCGAAATaTTAATACTTCtTTTTTTGAcCCcGCtggAGGAGGAGAT	600	CCTATTTTATAcCAACATTTATTTTGATTTTTTG	634
Idolus_picipennis	ATACTACTGACTGATCGTAATTTAAACACATCGTTCTTCGACCCTGCAGGAGGTGGGGAC	600	CCAATCCTTTACCAACATTTATTCTGATTTTTTG	634
Melanotus_villosus	ATATTTATTAACTGACCGAAACCTTAATACTTCCTTCTTTGACCCGGCAGGTGGGGGrGAC	600	CCCATCCTTTACCAACACTTGTTCTGATTTTTTG	634
Algarobius_prosopis	ATACTTCTTACAGACCGTAATTTAAACACTTCATTCTTTGACCCGGCAGGAGGGGAGAC	600	CCTATTCTTTATCAACACTTATTTTGATTTTTTG	634
Exomala_pallidipennis	ATACTATTAACAGATCGAAATTTAAACACTACATTTTTTGATCCATCAGGAGGTGGAGAT	600	CCAATCTTATATCAACACTTATTTTGATTTTTTG	634
Xylotrupes_siamensis	ATACTATTAACAGATCGAAATTTAAACACTTCCTTTTTTGACCCTGCAGGTGGAGGAGAT	600	CCAATTTTATTATCAACACCTATTCTGATTTTTTG	634
Copris_tripartitus	ATACTATTAACAGATCGAAATATTAATACTTCCTTCTTTGACCCTGCAGGGGGAGGAAAT	600	CCAATTTTATACCAACACCTATTCTGATTTTTTG	634
Lispe_albitarsis	ATATTTATTAACTGATCGAAATTTTAATACTTCATTCTTTGACCCAGCAGGAGGAGGAGAT	600	CCAATTCTTTACCAACATTTATTTTGATTTTTTG	634
Chrysomya_chani	ATACTATTAACAGATCGAAATTTAAATACATCATTTTTTGATCCAGCAGGTGGAGGAGAT	600	CCAATTCTTTATCAACACTTATTTTGATTTTTTG	634
Anthomyiopsis_nigrisquamata	ATACTATTAACAGATCGAAATTAAATACATCATTTTTTGATCCAGCAGGTGGAGGAGAT	600	CCAATTCTTTATCAACACTTATtTTGATTTTTTG	634
Carpomya_vesuviana	ATATTATTAACAGACCGAAATTTAAATACTTCATTCTTTGATCCTGCTGGTGGAGGAGAT	600	CCTATTTTATATCAACATTTATTTTGATTTTTTG	634
Tabanus_striatus	ATATTATTAACAGATCGTAATTTAAATACTTCTTTTTTTGATCCAGCAGGAGGTGGAGAT	600	CCTATTTTATAcCAACAtTATTTTGATTTTTTG	634
Leptogaster_cylindrica	ATATTATTAACAGACCGAAATCTTAATACTTCATTTTTTGACCCAGCaggTGGAGGTGAC	600	CCAATTCTATATCAACATTTATTTTGATTTTTTG	634
Asyndetus_sp.	ATATTATTAACTGATCGAAATTTAAATACTTCATTTTTTGATCCTGCAGGAGGAGGTGAT	600	CCAATTTTATATCAACACTTATTTTGATTTTTTG	634

Enzyme	Restriction site
HhaI	GCGC
Bso31I	GGTCTC
AleI	CAC(N)$_4$GTG
ApaLI	GTGCAC
AccII	CGCG
Eco52I	CGGCCG
BciVI	GTATCC
BcgI	CGA(N)$_6$TGC
PinAI	ACCGGT
BspCNI	CTCAG
BtsI	GCAGTG
NheI	GCTAGC
PvuI	CGATCG
MunI	CAATTG
BclI	TGATCA
DpnI	GATC
LpnPI	CAGG (or CTGG)

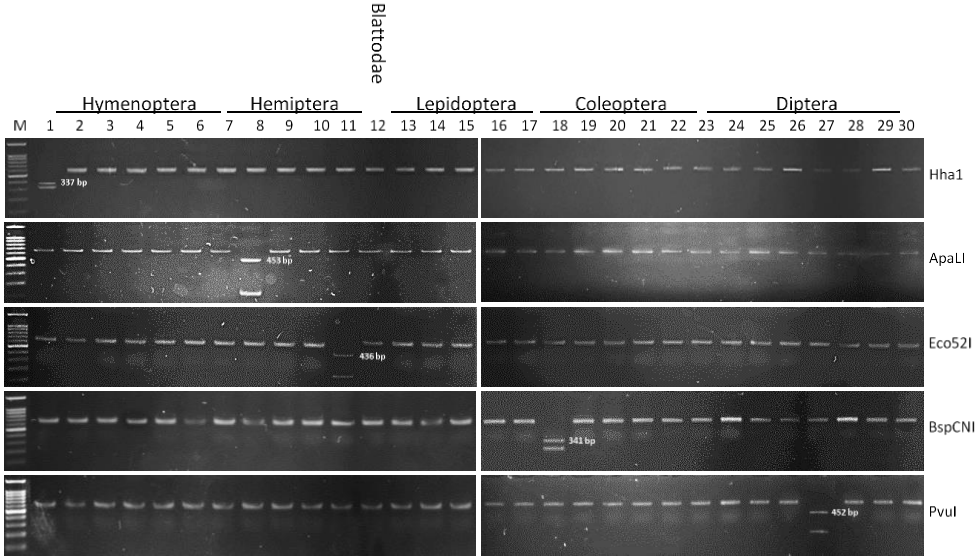

Figure A2. *Electrophregrams describing specific PCR-RFLP markers in COI gene in five insect species belonging to four insect orders used for validating restriction sites resulted from CisSERS tools. Each restriction enzyme has a unique site in the gene for a given insect species. Species numbers (1-30) refer to insect species shown in Table 1*

http://www.aloki.hu ● ISSN 1589 1623 (Print) ● ISSN 1785 0037 (Online)
DOI: http://dx.doi.org/10.15666/aeer/1705_1140911418

EFFECT OF COBALT ON THE ENVIRONMENT AND LIVING ORGANISMS - A REVIEW

KOSIOREK, M. – WYSZKOWSKI, M.*

Department of Environmental Chemistry, University of Warmia and Mazury in Olsztyn, Łódzki Square 4, 10-727 Olsztyn, Poland
(phone: +48-89-523-3976)

**Corresponding author*
e-mail: miroslaw.wyszkowski@uwm.edu.pl

(Received 18th Apr 2019; accepted 12th Jul 2019)

Abstract. This literature review presents a summary of papers related to the determination of the sources of cobalt compound presence in the environment and the resulting pollution of water and land. Their properties, determining their toxicity to living organisms, have been specified, with sections devoted to their effect on microorganisms and plants. The influence (negative and positive) of cobalt on living organisms in water and soil environments, including the biological balance of the soil (the number of microorganisms, enzymatic activity) and plant growth and development, and the possibilities of their use in the phyto- and bioremediation of areas polluted with cobalt have been described. Particular emphasis has been placed on the presentation of the effect of cobalt on animals and man.
Keywords: *cobalt, contamination, environment, microorganisms, plants, animals, human*

Introduction

Throughout history, human activity has contributed to environmental transformation. Over time, substantial population growth has significantly influenced the introduction of innovations in the world of technology which, in turn, have caused increasing interference of some processes in the environment (Guzmán-Morales et al., 2011). The development of industry, electric appliances, transport and the use of growing amounts of chemicals, mainly in the construction, chemical and agricultural sectors, has led to the appearance of different kinds of pollutants in the environment (Page and Feller, 2005; Murtaza et al., 2008; Dhaneesh et al., 2012; Wyszkowski and Sivitskaya, 2012; Modrzewska and Wyszkowski, 2014).

Heavy metals are the most common group of pollutants reducing the natural regeneration ability of the environment (Malik and Zeb, 2009; Mansouri et al., 2012). Many heavy metals are necessary for the proper functioning of living organisms. Some others, however, exert a negative effect on their development (Wyszkowska and Wyszkowski, 2002, 2003; Ciećko et al., 2005; Wyszkowski and Wyszkowska, 2009; Chmielowska-Bąk et al., 2014) and it should be remembered that the toxicity of a given chemical compound is determined by the dose introduced into the organism in a unit of time (Dhaneesh et al., 2012; Dobrowolski and Otto, 2012; Bezerra et al., 2014).

In environmental protection, the greatest focus is on such heavy metals as cadmium, lead and mercury, although other micronutrients also deserve attention due to the possibility of significant soil loading (Page and Feller, 2005). Among the elements present in amounts exceeding trace values in the soil, water, and air environments, cobalt (not yet fully known as a trace element) has attracted special attention (Fermoso et al., 2010). The diversified use of this metal in different branches of industry has caused growing demand in the world market (Lefebvre et al., 2008; Malik and Zeb,

http://www.aloki.hu ● ISSN 1589 1623 (Print) ● ISSN 1785 0037 (Online)
DOI: http://dx.doi.org/10.15666/aeer/1705_1141911449

2009; Sytschev et al., 2009; Biswas et al., 2013; Huang et al., 2013). This contributed to the emergence of numerous companies involved in the production of this element. Production of cobalt by major companies worldwide in the recent years has been on a significant increase. The total production of cobalt by major companies in 2008 amounted to 28,901 tonnes (Elliot and Litzinger, 2015), while by 2015, it increased to 220 000 tonnes (Sun et al., 2019).

With the growing demand for this raw material (Liu and Erhan, 2002; Pathak and Choppin, 2009; Fermoso et al., 2010; Banks et al., 2012; Hong et al., 2012; Esther et al., 2013) the problem of its excessive accumulation in the environment began to appear and also started to have a significant effect not only on plants (Akbar et al., 2013) and animal organisms, but also on humans (Balestrazzi et al., 2009; Koigoora et al., 2013; Devi et al., 2014).

The aim of this paper is to present the sources of cobalt occurrence in the natural environment and its effect on the functioning of selected groups of living organisms. The influence of cobalt on environment, living organisms in water and soil environments, including the biological balance of the soil (the number of microorganisms, enzymatic activity) and plant growth and development, animals and man was presented. The possibilities of use of microorganisms and plants in the phyto- and bioremediation of areas polluted with cobalt have been described.

Sources and forms of cobalt presence in the environment

In the periodic table of elements, cobalt is classified as a transition metal (Koch et al., 2007). It has both chalcophile, siderophile and lithophile properties. Its chalcophility manifests itself mainly in the fact that it can occur in the form of sulfides in the lowest parts of the Earth's mantle (Lock et al., 2006), while cobalt siderophility is related to its low affinity to oxygen and sulfur, which makes this metal soluble in liquid nitrogen and able to occur in the Earth's core. Cobalt also occurs in the silicate layer of the Earth's crust, which indicates litophile properties. It is assumed that the natural cobalt content in the Earth's crust does not exceed 12 $mg \cdot kg^{-1}$ (Sheppard et al., 2007). Alkaline igneous rocks are the largest cobalt accumulators. They contain up to 200 $mg \cdot kg^{-1}$ of this element, while the same igneous rocks, but with an acidic character, contain no more than 15 $mg \cdot kg^{-1}$. Small cobalt contents are also found in sedimentary rocks, where its concentration is highest in mudstones (around 20 $mgkg^{-1}$) and lowest in limestones (around 3 $mg \cdot kg^{-1}$). Minerals are also a source of cobalt, which include CoAsS (cobaltite), $CoCO_3$ (spherocobaltite), Co_3S_4 (linnaeite), $Co(Ni)As_3$ (smaltite) and $CoAs_2$ (safflorite) (Luo et al., 2010). The contamination of soil with cobalt have the effect on other trace elements in soil, e.g. they may be increased the content of lead, chromium, nickel and zinc in soil (Kosiorek and Wyszkowski, 2019c).

Cobalt is released during the weathering process in the oxidation state of +2 and is then strongly bound by the mineral and organic-mineral complex in a readily- and slowly- exchangeable form (Swarnalatha et al., 2013). Due to ion exchange and chemical processes, cobalt is adsorbed by clay minerals, which results in the formation of complex compounds on their surface (Li et al., 2009). Special importance in this respect is attributed to montmorillonite, whose sorption capacity (also including for cobalt) is significantly higher than other clay minerals. The adsorption of this element by manganic minerals is also possible. The most frequent form of cobalt presence in the soil is Co^{2+} (ionic form), Co^{3+} (coordination compounds) as well as $CoOH^{+}$

http://www.aloki.hu ● ISSN 1589 1623 (Print) ● ISSN 1785 0037 (Online)
DOI: http://dx.doi.org/10.15666/aeer/1705_1141911449

and$Co(OH)_3^-$. Moreover, small amounts of readily-soluble cobalt in the form of $Co(OH)_2^0$ occur in the soil solution, whose amount compared to the total content is no higher than 5%. Organic fertilization causes a small increase in the amounts of cobalt in a soluble form in the soil (Faucon et al., 2007). A naturally high soil cobalt level is closely linked to manganese and iron presence as well as organic soils. This is due to the high susceptibility of the oxides of these metals to binding and adsorbing the cations of divalent and trivalent cobalt, as well as easy sorption by organic matter (Dávila-Rangel and Solache-Ríos, 2006). It is assumed that loamy and alluvial soils have naturally high cobalt contents of up to 12 $mg \cdot kg^{-1}$, and podsolic and silty soils have the lowest, with a mean cobalt content of only 5.5 $mg \cdot kg^{-1}$. Compared to the average cobalt content in the world's soils, this value is not much higher than the lowest cobalt content in sandy and silty soils, where it is 8 $mg \cdot kg^{-1}$. However, soils formed from bedrock with a high cobalt content can contain up to 500 $mg \cdot kg^{-1}$ of this element (Tappero et al., 2007).

Cobalt mobility in soils is low (Fujikawa and Fukui, 2001; Edwards et al., 2012). It is assumed that over 95% of cobalt after prior introduction into the soil does not move and it remains in the soil down to a depth of around 5 cm. Increasing the acidity and anaerobic soil conditions causes the cobalt mobility to increase (Narendrula et al., 2012). The main cause of this tendency is the inhibition of valence bonds with Fe and Mn. However, since divalent cobalt and manganese ions do not have strong complex formation abilities, the outer hydration shell is not destroyed during their binding (Lalah et al., 2009). The presence of cobalt in the form of chelates also contributes to increasing the soil mobility of this element. The main causes of increasing the soil cobalt content include improper fertilizer management (Saaltink et al., 2014), use of some pesticides (Defarge et al., 2018) as well as inappropriately-used sludge from municipal sewage treatment plants (Ebrahimi et al., 2009; Ben-Fredj et al., 2014; Li et al., 2014; Zupančič and Skobe, 2014). Application of different substances (e.g. manure, zeolite, calcium oxide) to soil reduced the content of cobalt and other trace elements in soil (Kosiorek and Wyszkowski, 2019c). These materials (especially manure) have a positive effect on the available forms of phosphorus, potassium and magnesium, total nitrogen and other properties of soil (Kosiorek and Wyszkowski, 2019b).

Significant importance is also attributed to cobalt compounds emitted to the air, mainly during the combustion of hard coal and petroleum, which are especially transferred to the soil environment during intensive precipitation (Biswas et al., 2013; Singh and Cameotra, 2013). The extraction of different kinds of raw materials, particularly metallic, also leads to soil pollution with this element (Narendrula et al., 2012; Huang et al., 2013). Transport also causes a rise in cobalt content in the environment (Kuoppamäki et al., 2014; Werkenthin et al., 2014).

In Poland, the soil cobalt content limits are set out in the Regulation of the Polish Minister of the Environment of 1 September (2016) on soil quality standards and land quality standards. For protected areas and land which is part of a protected area and in the surface soil layer (down to 30 cm) of agricultural land, the permissible cobalt content should not be higher than 20-50 $mg \cdot kg^{-1}$ of soil dry matter and in the soil layer in industrial areas, surface mining land in use and communication areas, it may not exceed 200 $mg \cdot kg^{-1}$ of soil dry matter.

Both in surface waters and groundwaters, cobalt occurs in the oxidation state of +2 and +3. Moreover, it can also occur in the form of complex compounds, which it forms with cyanides, ammonia and edetic and nitrilotriacetic acid, most often present in

http://www.aloki.hu ● ISSN 1589 1623 (Print) ● ISSN 1785 0037 (Online)
DOI: http://dx.doi.org/10.15666/aeer/1705_1141911449

different kinds of detergents (Ghassabzadeh et al., 2010). The natural cobalt concentration in fresh surface waters does not exceed 0.2 $\mu g \cdot dm^{-3}$ and in drinking water it is 0.03 $\mu g \cdot dm^{-3}$. Salt groundwaters, compared to fresh waters, are characterized by its lowest natural content - 0.02 $\mu g \cdot dm^{-3}$ (Qiu and Zheng, 2009). Cobalt solubility mainly depends on the pH of the water environment and on its concentration (Ochieng et al., 2009). The content of cobalt in surface waters is various (*Table 1*).

Due to rapid cobalt binding by organic matter, all kinds of clay minerals and iron and manganese in an oxide form, cobalt in an oxidized form does not persist very long in water. The result is substantial cobalt accumulation in the bottom sediments of both fresh and salt waters (Sukdeo et al., 2012; Ghandour et al., 2014), where its content in the sediments of flowing surface waters is around 13 $mg \cdot kg^{-1}$. According to Jayasiri et al. (2014) the cobalt sedimentation rate is affected by climatic conditions and seasonal fluctuations (Mohiuddin et al., 2012). The mobility and solubility of this element in bottom sediments is determined mainly by its form (Wu et al., 2012) and sorption processes occurring between cobalt ions and negatively-charged sediment molecules (Jayasiri et al., 2014). As a result of changing physicochemical conditions, cobalt in sediments may be re-released to water (Sukdeo et al., 2012; Zamani-Hargalani et al., 2014).

Table 1. *The content of cobalt in fresh and salty waters worldwide*

Place, country	Cobalt content in water	Source
Rivers		
Tsurumi, Yokohama, Japan	14000-75000 $\mu g \cdot dm^{-3}$	Mohiuddin et al. (2012)
Ramisi, Kenya	3.70-8.30 $\mu g \cdot dm^{-3}$	Ochieng et al. (2009)
Amazon, South America	0.006-0.011 $\mu g \cdot dm^{-3}$	Yabuki et al. (2014)
Ho Chi Minh City (Saigon), Vietnam	1 $\mu g \cdot dm^{-3}$	Chanpiwat and Sthiannopkao (2014)
Lakes		
Respomuso, Pyrenees, Spain	0.08 $\mu g \cdot dm^{-3}$	Zaharescu et al. (2009)
Nasser, Egypt	185 $\mu g \cdot dm^{-3}$	Rashed (2001)
Malta, Poland	10-20 $\mu g \cdot dm^{-3}$	Rzymski et al. (2014)
Khanphur, Pakistan	81-848 $\mu g \cdot dm^{-3}$	Iqbal et al. (2012)
Kanyaboli, Kenya	5.56-6.30 $\mu g \cdot dm^{-3}$	Ochieng et al. (2008)
Sea		
Red Sea, Jemen coast	0.05-0.75 $\mu g \cdot dm^{-3}$	Al-Shiwafi et al. (2005)
Baltic Sea, Poland	0.45 $\mu g \cdot dm^{-3}$	Kabata-Pendias and Pendias (2001)

The metals and ceramic industries are most responsible for cobalt introduction into surface waters. Due to the wide-ranging application of this metal, particularly in the petrochemical, aviation or power industries, the amount of introduced wastewater with substantial cobalt contents has a negative effect not only on the condition of surface waters, but also on the condition of groundwaters (Wang et al., 2007; Abdel-Razek et al., 2009; Ebrahimi et al., 2009; Abd-Alla et al., 2014; Chanpiwat and Sthiannopkao, 2014). Additionally, pollutants also present in the air, which travel with waste to a given body of water (Mohiuddin et al., 2012; Sandergaard, 2013) and tourist activity (Koigoora et al., 2013) can contribute to this situation. In groundwaters, cobalt content depends mainly on the well location and on the water extraction technique. The main

http://www.aloki.hu ● ISSN 1589 1623 (Print) ● ISSN 1785 0037 (Online)
DOI: http://dx.doi.org/10.15666/aeer/1705_1141911449

factors which can cause an increase in its content in groundwaters are: contamination of unconfined groundwaters from bedrocks containing the water-bearing layer (Obiri, 2007) and anthropogenic activities (Upadhyaya et al., 2014).

The permissible cobalt concentration for class I and II of uniform parts of surface waters is set out at ≤ 0.05 mg·dm^{-3} (Regulation of the Polish Minister of the Environment of 21 July, 2016). The permissible cobalt concentration in groundwaters is: class I (very good) - 0.02 mg·dm^{-3}, class II (good) - 0.05 mg·dm^{-3}, class III (satisfactory) - 0.2 mg·dm^{-3}, class IV (unsatisfactory) - 1 mg·dm^{-3}, class V (poor) > 1 mg·dm^{-3} (Regulation of the Polish Minister of the Environment of 21 December, 2015). Cobalt content in surface waters largely depends on the treated wastewater introduced into them. According to the Regulation of the Polish Minister of the Environment of 18 November (2014) the permitted cobalt concentration in treated wastewater from the ceramic industry should not be higher than 0.1 mg·dm^{-3} and less than 1 mg·dm^{-3} in the other wastewater types.

Apart from cobalt presence in soils and waters, this element is also in the air in an oxidized and insoluble form in dust (Pietrodangelo et al., 2014). Its natural content in the air is low. It is assumed that this value ranges from 0.0005 to 0.005 ng·dm^{-3}. Excessive levels of the natural cobalt air content are found only over urbanized areas (Albayrak and Mor, 2011; Canepari et al., 2014; Dos Anjos-Paulino et al., 2014). This relationship is presented in *Table 2* which provides the contents of cobalt in the air in certain parts of the world.

Table 2. *The content of cobalt in the air in selected places in the world*

Place, country	Cobalt content in air	Source
Łódź, Poland	0.31 ng·m^{-3}	Bem et al. (2003)
Cap Ferrat, south-west coast of France	0.10-0.28 ng·m^{-3}	Heimbürger et al. (2010)
South-East Sea of Japan, Japan	0.31-0.41 ng·m^{-3}	Kang et al. (2009)
Milan, Italy	2.10 ng·m^{-3}	Rizzio et al. (2001)
Rio de Janeiro, Brazil	0.40 ng·m^{-3}	Miranda and Tomaz (2008)
Beijing, China	7.90 ng·m^{-3}	Wang et al. (2001)
Frankfurt am Main, Germany	0.08 ng·m^{-3}	Zereini et al. (2005)

The most frequent sources of air pollution with this element are hard coal-fired power plants and road transport (Mahapatra et al., 2013). An increased air cobalt content is caused by: wind erosion (Singh et al., 2013; Canepari et al., 2014), metal industry activity (Sheppard et al., 2007) and the presence of dust rising from storage sites for different kinds of stored waste and hydrothermal particles (Sheppard et al., 2007; Antony et al., 2011; Singh et al., 2013). Seasonal variation of a given area affects the air cobalt concentration (Canepari et al., 2014).

In Polish legislation, the permissible reference values for cobalt are contained in the Regulation of the Polish Minister of the Environment of 26 January (2010) on reference values for various substances in the air. The permissible reference value for cobalt, expressed as the sum of this metal and its compounds in PM_{10} dust, averaged for the time of 1 h, is 5 μg Co·dm^{-3} and for the whole calendar year this value should not exceed 0.4 μg Co·dm^{-3}. EU law sets out the average emission limit values for 10 heavy metals in total, including cobalt and its compounds (expressed as cobalt - Co) at 0.5

http://www.aloki.hu ● ISSN 1589 1623 (Print) ● ISSN 1785 0037 (Online)
DOI: http://dx.doi.org/10.15666/aeer/1705_1141911449

$mgN \cdot dm^{-3}$ over a sampling period of a minimum of 30 min and a maximum of 8 h (Directive 2010/75/EU).

Cobalt also occurs in the natural environment in the form of the ^{55}Co, ^{56}Co, ^{57}Co, ^{58}Co, ^{60}Co isotopes, resulting from human activity (Tappero et al., 2007; Antony et al., 2011). They are characterized by radioactive properties, due to which they can emit beta and gamma radiation to the environment. Beta and gamma particles are charged positively or uncharged, respectively. Their formation is the result of numerous nuclear reactions. The radioactive half-life of cobalt ranges from several dozen days to thousands of years (Mollah and Begum, 2001). Cobalt isotopes have very wide application. An example can be ^{60}Co, which serves both for human radiotherapy and also for cold pasteurization of different seasonings and food products. Despite their positive use, cobalt isotopes are also a by-product of nuclear processes (Nagpal, 2004). Their negative environmental impact is associated with their high mobility, which mainly depends on the chelate effect of the radioactive cobalt compound and on its oxidation state. Its decomposition in the soil is a very long process and can be accelerated only by decay if it is organic pollution. In the water environment, radioactive cobalt occurs in the oxidation state of +2 and +3 (Tappero et al., 2007). Cobalt in the oxidation state of +3 is both stable and mobile in the water environment. Cobalt presence in a divalent form allows easier adsorption of free ions of this element on the surface of iron occurring in an oxide form. The cobalt(II) form is not as stable as cobalt(III), which is caused by the absence of ligands responsible for its persistence in water (Hau et al., 2008).

In Polish legislation, there are no set out radioactive cobalt limits and in international law the content limit for this form of cobalt present in surface waters is set out by USEPA (2000 after 56 FR 33121, Appendix B 000), where for ^{57}Co this level is 4870 $pCi \cdot dm^{-3}$, for ^{58}Co - 1590 $pCi \cdot dm^{-3}$ and for ^{60}Co - 218 $pCi \cdot dm^{-3}$.

As it results from the review of the above literature, the main cause for the contamination of the environment with cobalt has become the development of civilisation, and the inextricably linked development of industry. The elevated contents of this element taken up from the soil, water or the air by living organisms have been introduced into the food chain, at the same time creating a risk to their lives and proper functioning (*Fig. 1*).

Cobalt is not biodegradable as after its introduction to the environment, it constantly circulates within it, with only its form being transformed. With the introduction of cobalt into higher and higher links of the food chain, however, the excessive accumulation thereof occurs. Therefore, it creates the greatest risk to the final link of the food chain, namely the human (Biesalski and Grimm, 2012).

Effect of cobalt on microorganisms

The soil is inhabited in the greatest numbers by viruses, bacteria, fungi, algae and protozoa. Due to organic matter decomposition, they expand their biomass and contribute to increasing humus in the soil. Proper microorganism development depends on different kinds of factors, such as: light, humidity, temperature or nutrient availability. Among the many compounds affecting the course of microbiological processes, special importance is attributed to trace elements, which include cobalt (Wang et al., 2007; Abdel-Razek et al., 2009; Hlima et al., 2012). Maintaining its optimal content in microorganism cells can assist metabolic processes or increase their

http://www.aloki.hu ● ISSN 1589 1623 (Print) ● ISSN 1785 0037 (Online)
DOI: http://dx.doi.org/10.15666/aeer/1705_1141911449

content of vitamin B_{12} assisting growth processes (Marrero et al., 2007; Kun-Tai et al., 2008; Abskharon et al., 2010). As shown by the results of the study by Hlima et al. (2012), cobalt presence in xylose isomerase ensures the proper course of sugar metabolism in microorganisms. Cobalt is part of the coenzymes of the genus *Rhizobium* bacteria or the free-living *Azotobacter* bacteria responsible for binding nitrogen from the air (Rancelis et al., 2012) because vitamin B_{12} synthesis is necessary for the course of redox processes and nucleoprotein synthesis (Pulgarín et al., 2013; Abd-Alla et al., 2014).

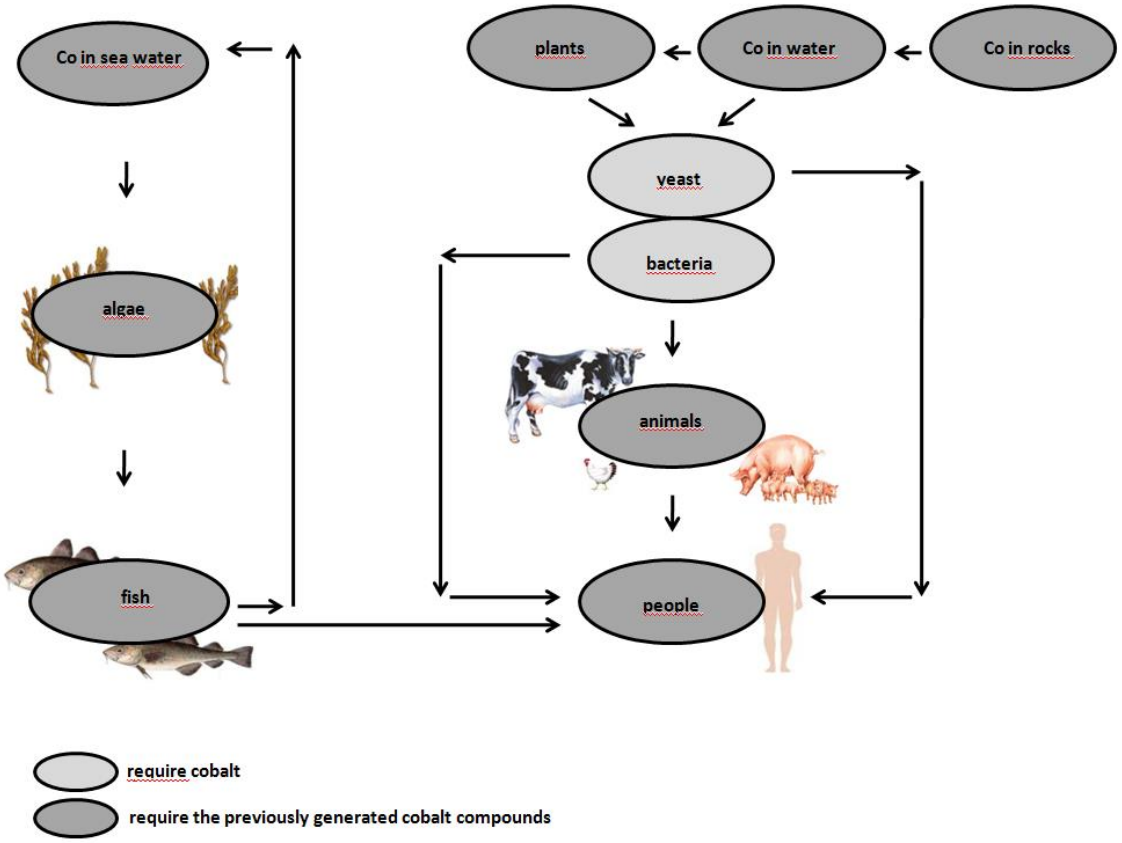

Figure 1. *Cobalt cycle in the environment. (Source: own work based on Biesalski and Grimm, 2012)*

Proper cobalt content in microorganisms is also important due to the initiation of many enzymatic reactions (Minamihata et al., 2012; Elleuche et al., 2014), protein absorption and decomposition (Antony et al., 2011). This is particularly visible for papilionaceous plants, due to their symbiosis with nodule bacteria. In these bacteria, cobalt is the activator of the urease enzyme, which is the catalyst in the urea decomposition reaction (Witte et al., 2002). Apart from carbon dioxide and water, the main product of this reaction is ammonia, which is also the final product of ammonification and enables the initiation of nitrification, where this compound will be oxidized to nitrites and nitrates (Guo et al., 2014). Nitrification is one of the major processes characterizing soil quality. Cobalt has a crucial effect on nitrification rate, but its excessive content in the soil may inhibit the process (Wyszkowska et al., 2006). In a study by Wyszkowska et al. (2006) in soil with a neutral reaction, this process was

http://www.aloki.hu ● ISSN 1589 1623 (Print) ● ISSN 1785 0037 (Online)
DOI: http://dx.doi.org/10.15666/aeer/1705_1141911449

inhibited to a small degree by cobalt, applied at a lower dose (200 $mg \cdot kg^{-1}$ soil), regardless of the testing date. Under a higher cobalt dose (400 $mg \cdot kg^{-1}$ soil), nitrification decreased twofold-threefold. This adverse effect disappeared completely on the 60th day of soil incubation. An excessive soil cobalt content may cause a decrease in the mineral nitrogen content ($N\text{-}NH_4^+ + N\text{-}NO_3^-$). According to Welp (1999) cobalt acts more weakly in the soil than other heavy metals on the activity of dehydrogenases: $Hg > Cu > Cr^{6+} > Cr^{3+} > Cd^{2+} > Ni^{2+} > Zn^{2+} > As^{3+} > Co^{2+} > Pb^{2+}$ and, in the view of Nowak et al. (2003) also on the activity of acid phosphatase: $Cu^{2+} > Al^{3+} > Cd^{2+} > Zn^{2+} > Fe^{3+} > Ni^{2+} > Pb^{2+} > Sn^{2+} > Fe^{2+} > Co^{2+}$ and alkaline phosphatase: $Cd^{2+} > Al^{3+} > Zn^{2+} > Fe^{3+} > Cu^{2+} > Pb^{2+} > Ni^{2+} > Fe^{2+} > Se^{2+} > Co^{2+}$.

According to Wang et al. (2010) cobalt has an average effect on soil microorganisms in the heavy metal toxicity series (Cr > Pb > As > Co > Zn > Cd > Cu). Exceeding the threshold levels may, however, have a negative effect on the proper course of life processes (Maguire and Collins, 2001). The result may be disturbance of the course of redox reactions, inhibition of biopolymer hydrolysis processes or the slowing of enzymatichydrolysis (Abd-Alla et al., 2014; Hu et al., 2014). Radicals and unstable products of enzymatic reactions, causing cell growth, begin to appear in these organisms. The cell wall bursts as a result of increased osmotic pressure. Another result of an excessive cobalt content in microorganism cells may be the inhibition or acceleration of cell division (Antony et al., 2011).

Apart from microorganisms reacting negatively to high cobalt doses, there are also those which have the ability to remove it. The reduced cobalt harmfulness to these organisms is the result of their having cell systems affecting accumulation, excretion or enzymatic changes, which can reduce its harmfulness (Hoffman et al., 2010). There are also typically specialized groups of microorganisms with specific regenerative abilities enabling the accumulation of excessive cobalt amounts from the soil (Peca et al., 2008; Abskharon et al., 2010).

The analyzed literature shows that a high ability to remove cobalt from the soil characterizes such bacteria as: *Pseudomonas denitrificans* (Rong et al., 2008), *Pectobacterium antrosepticum* (Elleuche et al., 2014), *Escherichia coli* (Freeman et al., 2005), *Cellulosimicrobium cellulans* and yeasts: *Schizosaccharomyces pombe* or *Saccharomyces cerevisiae* (Ruta et al., 2010; Ryuko et al., 2012). Organisms more sensitive to increased cobalt contents include, among others, the bacteria *Rhizobium tibeticum* (Abd-Alla et al., 2014) or *Serratia marcescens* (Marrero et al., 2007). Harmful effects are also visible in fungi, for example, *Aspergillus oryzae* and *Aspergillus niger* (Biswas et al., 2013; Li et al., 2014). Abdel-Razek et al. (2009) also found a high resistance of some fungi from the genera *Paecilomyces, Rhizopus, Penicillium, Trichoderma* and *Pythium* to excessive cobalt contents. Wang et al. (2007) confirmed the negative effects of cobalt on nematodes (*Caenorhabditis elegans*). Earthworms are also at risk due to the accumulation of the part of cobalt which is not excreted (Ashfaq et al., 2009).

Some groups of microorganisms, due to the production of biosurfactants, have the ability to remove cobalt. They mainly include bacteria, fungi and yeasts. One of the many microorganisms able to produce surface active agents in the form of lipopeptides is the bacterium *Bacillus subtilis*. Singh and Cameotra (2013) report that the ability to remove cobalt resulting from the application of this biosurfactant is over 35%.

Maintaining proper growth conditions for a given group of microorganisms to increase pollutant removal efficiency also has a special effect on the initiation of the

http://www.aloki.hu ● ISSN 1589 1623 (Print) ● ISSN 1785 0037 (Online)
DOI: http://dx.doi.org/10.15666/aeer/1705_1141911449

above processes (Abdel-Razek et al., 2009). According to Amir and Pineau (2003) acceleration of cobalt cleanup from the soil by heterotrophic bacteria can be affected by a slightly acid soil reaction. Maintaining the pH at this level creates ideal conditions for faster release of this element in the soil, due to which it becomes more available to these microorganisms. Cobalt biosorption rate is also affected by the ambient temperature at which microorganisms live (Biswas et al., 2013). The higher it is, the more efficient this process is. This relationship was also confirmed by Abdel-Razek et al. (2009) who found raising the temperature by 10 °C led to an increase in cobalt accumulation by around 10%. Soil microorganisms are also able to remove radioactive cobalt, which is confirmed by Sassman et al. (2007).

Cobalt is also present in salt and fresh surface waters and in groundwaters. Its proper amount, not exceeding the limit values, is necessary for the course of growth processes in water microorganisms, as well as for soil microorganisms (Elleuche et al., 2014). Microorganisms present in water are also able to reduce cobalt content under conditions of its excessive accumulation (Amir and Pineau, 2003). These processes include extracellular secretion, biotransformation and intracellular absorption and its precipitation outside the cleaning organism. Apart from naturally-occurring water microorganisms able to absorb cobalt, there are also those which are characterized by a higher biosorptive ability. Bacteria present in sea water can also contribute to cobalt content reduction (Amir and Pineau, 2003; Antony et al., 2011). These organisms include, among others, *Cunninghamella elegans* (Abdel-Razek et al., 2009) as well as *Shewanella*, which reduces the pollution of waters with radioactive cobalt (Hau et al., 2008).

Effect of cobalt on plants

Cobalt is the trace element which have a strong effect on growth and development of plants. The negative effect of soil contamination with cobalt on plants depends on many other factors e.g. soil reaction, content of organic matter, clay and other macronutrients and micronutrients in soil. The result of cobalt presence in the soil is its accumulation in plants, also including in their fruits (Soylak et al., 2013). It is absorbed by plant roots in the form of a cation in the oxidation state of +2 and chelate compounds (Karuppanapandian and Kim, 2013). Cobalt availability to plants largely depends on the soil conditions (Jonnalagadda et al., 2008; Agbenin et al., 2009; Wendling et al., 2009). This was confirmed in a study by Edwards et al. (2012) where the application of drainage in pasture soil accelerated the weathering of minerals and increased cobalt absorption by grasses. The accumulation rate for aquatic plants mainly depends on such factors as temperature, salinity and water oxygen concentration (Chatterjee and Dube, 2005). The necessity of cobalt for marine flora was confirmed by Antony et al. (2011) in a study conducted on marine phytoplankton.

Because of the cobalt presence in the coenzyme of nodule bacteria, it plays a significant role in papilionaceous plants (Tappero et al., 2007; Collins and Kinsela, 2011). Due to flavonoid secretion by plant roots, gene expression by genus *Rhizobium* microorganisms is induced. The genes encoding enzymes in nodules cause the infection of root hairs and then the formation of nitrogen-binding nodules. This is also the reason for the presence of substantial cobalt contents in these plants (Abd-Alla et al., 2014). Cobalt presence in plants also allows the proper course of metabolic and growth processes to be maintained (Page and Feller, 2005; Ashraf and Mian, 2008; Rong et al.,

http://www.aloki.hu ● ISSN 1589 1623 (Print) ● ISSN 1785 0037 (Online)
DOI: http://dx.doi.org/10.15666/aeer/1705_1141911449

2008; Collins and Kinsela, 2011; Soylak et al., 2012). According to Trejo-Tapia et al. (2001) cobalt content in plants has a positive effect on the production of betalains and secondary metabolites and cobalt is also responsible for leaf pigmentation in leguminous plants (Rancelis et al., 2012). It also plays a significant role during ethylene synthesis inhibition in sunflower, which was confirmed by Benlloch-González et al. (2010). Additionally, it serves as a catalyst in many enzymatic processes (Tappero et al., 2007; Dong Cho et al., 2012; Karuppanapandian and Kim, 2013).

Cobalt content varies depending on plant organ type. Murtaza et al. (2008) found that this content is higher in leaves than in the other parts of vegetables. This was also confirmed in a study by Chatterjee and Dube (2005) where cobalt was accumulated in greater amounts in the aboveground parts of cauliflower and cabbage than in their roots. For cereals, as Page and Feller (2005) reported that a similar tendency was obtained in wheat, but younger leaves have a much higher requirement for this element than older ones.

Cobalt toxicity is closely related with the acidity of the soil. In alkaline soil the toxic effect of cobalt contamination on plant development is smaller than in acid soil. For higher plants, no effect of cobalt on their growth and development has been shown (Tappero et al., 2007; Rancelis et al., 2012; Rognerud et al., 2013). However, to meet the nutritional requirements, cobalt content in their tissues should not be lower than 0.08 mg/kg. Among papilionaceous plants, clovers have the greatest accumulative abilities and among cereals, wheats have the highest. In vegetables, cabbage and lettuce are characterized by the highest cobalt contents (Nirmal-Kumar et al., 2007). Application of different sorbents to soil (e.g. manure, calcium oxide, etc.) is effective in reducing the negative effect of contamination of cobalt on plants (*Figs. 2* and *3*). They reduced the content of cobalt and its bioconcentration and translocation in plants.

As a result of exceeding the limit values for cobalt, iron assimilability is blocked, which causes the appearance of toxic symptoms (Chatterjee and Chatterjee, 2002; Tappero et al., 2007). Increased cobalt contents in plants can cause disturbances of physiological, biochemical and metabolic processes (Wendling et al., 2009). According to Abd-Alla et al. (2014) these contents can also contribute to stopping the growth of nodules on the roots of papilionaceous plants and thus reduce their nitrogen assimilability (Jain and Nainawatee, 2000). The consequence of exceeding the permissible dose in plants is stopping growth processes and the appearance of disease symptoms, such as chlorosis, necrosis or tissue death (Chatterjee and Chatterjee, 2002; Chatterjee and Dube, 2005; Wyszkowski et al., 2009). Photosynthesis is disturbed, the intercellular spaces become smaller and the chloroplast structure disintegrates (Chatterjee and Chatterjee, 2002; Chaudhari et al., 2017).

These disturbances can also delay the maturation of flowers which, in turn, reduces their productivity and decreases plant yield significantly (Keeling et al., 2003; Chatterjee et al., 2006; Wyszkowski and Wyszkowska, 2007; Chaudhari et al., 2017; Muthaura et al., 2017; Jadoon and Malik, 2018). Moreover, much lower amounts of poor quality seeds are produced and the production of sugars, protein or starch deteriorates considerably. Some enzymes, such as peroxidase or acid phosphatase, increase their activity (Chatterjee et al., 2006). The plants growth on soil with the highest contamination of cobalt was halted, because water and nutrients uptake from soil by plants is decreased.

http://www.aloki.hu ● ISSN 1589 1623 (Print) ● ISSN 1785 0037 (Online)
DOI: http://dx.doi.org/10.15666/aeer/1705_1141911449

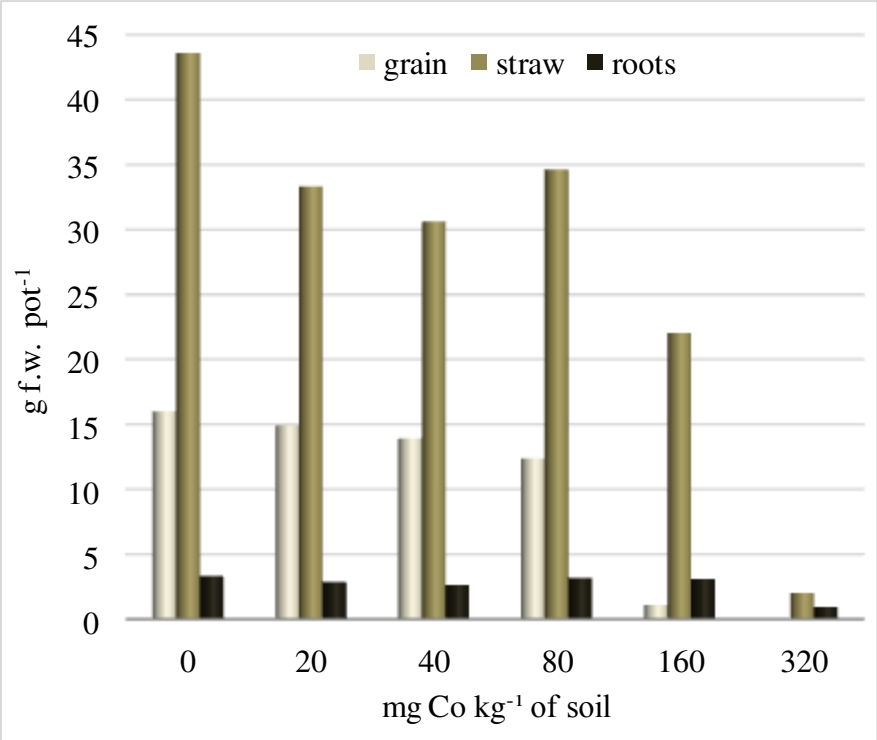

Figure 2. *Effect of cobalt contamination on oats mass*

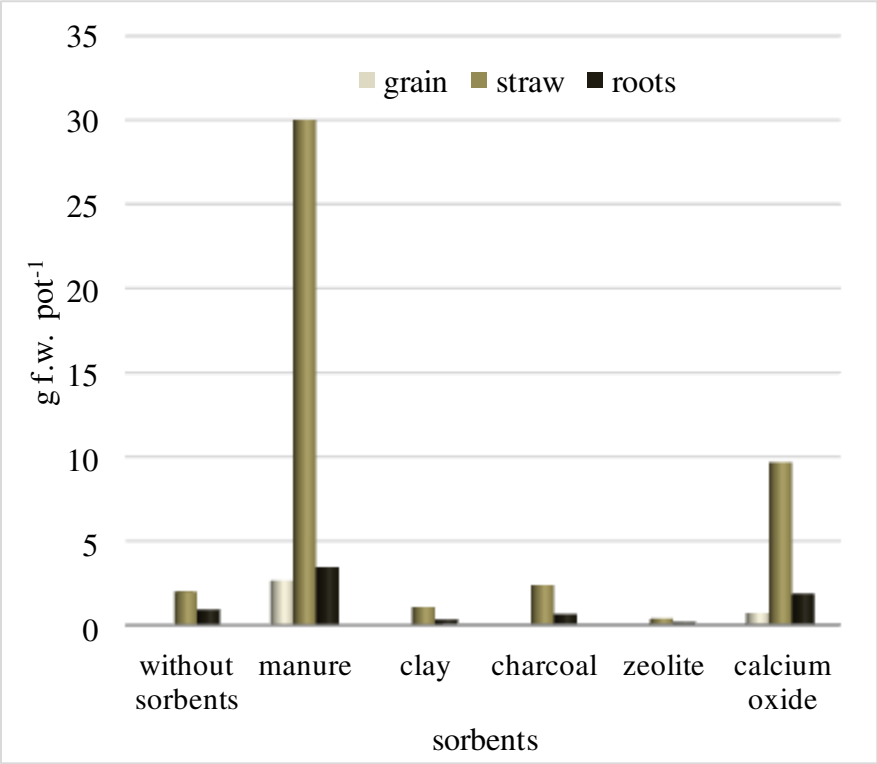

Figure 3. *Effect of sorbents on oats mass in objects contaminated with 320 mg Co kg^{-1} of soil*

http://www.aloki.hu ● ISSN 1589 1623 (Print) ● ISSN 1785 0037 (Online)
DOI: http://dx.doi.org/10.15666/aeer/1705_1141911449

Apart from the above plants, there are also those which do not show symptoms of toxicity associated with excessive cobalt accumulation (McLeod and Ciravolo, 2007). Cobalt content can range in them from 1.000 to even 50.000 $mg \cdot kg^{-1}$ (Faucon et al., 2009). Examples of such plants are: *Alyssum murale, Alyssum corsicum* (Collins and Kinsela, 2011), *Bulbostylis pseudoperennis* (Saad et al., 2012), *Crepidorhopalon perennis, Crepidorhopalon tenuis* (Faucon et al., 2009), *Nyssa sylvatica* (Kukier et al., 2004; Chatterjee et al., 2006; McLeod and Ciravolo, 2007; Tappero et al., 2007; Van der Ent et al., 2013), *Sopubia neptunii, Crotalaria cobalticola* (Saad et al., 2012), *Lemna minor* (Hu et al., 2019).

Both terrestrial and aquatic plants have these abilities (Chatterjee and Dube, 2005). Cobalt presence in the tissues of these plants, called hyperaccumulators, mainly depends on soil, water and air pollution (Guzman-Morales et al., 2011; Saad et al., 2012; Cheruiyot et al., 2013). The soil pH also has a significant effect: the lower it is, the higher the cobalt absorption is by the plants (Tappero et al., 2007; Collins and Kinsela, 2011).

Cobalt accumulation in hyperaccumulators is different in every plant organ. According to Kukier et al. (2004) and Tappero et al. (2007) cobalt contents are much higher in aboveground parts than in roots, but over time this content increases. Such a tendency was confirmed by Tappero et al. (2007) who observed much higher cobalt content in older leaves of *Alyssum murale* than in younger ones. McLeod and Ciravolo (2007) on *Nyssa sylvatica* and *Nyssa aquatica* shows the opposite tendency. The highest cobalt concentration is observed near leaf margins, close to leaf trichomes. Apart from the cobalt presence in leaf tissues, it can also be adsorbed on its surface. The soil contamination with cobalt increased the content of this trace element in plants and the translocation coefficient and decreased the coefficients of the bioconcentration and transfer (Kosiorek and Wyszkowski, 2019d). The stress of cobalt increased the production of some amino and organic acids (Hu et al., 2019). The increased cobalt content in the plants characterized by high abilities for its accumulation usually causes them to have lower amounts of nutrients, such as calcium, potassium or magnesium (Faucon et al., 2009). These plants also have limited water absorption ability (Karuppanapandian and Kim, 2013).

An excessive soil cobalt content, apart from reducing plant growth and development, can affect the absorption of other elements by plants. In a study by Wyszkowski et al. (2009) soil contamination with cobalt caused a decrease content of potassium, phosphorus, sodium, magnesium and especially calcium in the aboveground parts of oats. In another experiment by Wyszkowski and Wyszkowska (2007) low cobalt doses (10-20 mg $Co \cdot kg^{-1}$ soil) had a small effect on macronutrient content in spring barley. Its very high doses (320 mg $Co \cdot kg^{-1}$ soil) caused increased contents of all macronutrients, especially calcium, sodium and nitrogen, in the aboveground parts of this plant. In experiment by Kosiorek and Wyszkowski (2019a) the contamination of soil with cobalt increased the concentration of nitrogen, phosphorus, sodium, calcium in all organs of oat (grain, straw and roots). Chatterjee and Chatterjee (2003) point out a high increase in phosphorus content and Gopal et al. (2003) a decrease in phosphorus and protein and non-protein nitrogen in plants under the influence of cobalt.

http://www.aloki.hu ● ISSN 1589 1623 (Print) ● ISSN 1785 0037 (Online)
DOI: http://dx.doi.org/10.15666/aeer/1705_1141911449

Effect of cobalt on animals

Cobalt is included among elements commonly present in the cells of animal organisms. Its content depends on the feed type consumed by a given animal and on the state of environmental pollution at the place where it lives (Söyüt and Beydemir, 2011). Vitamin B_{12} and cyanocobalamin is the most frequent form of cobalt presence inside the body of animals, both terrestrial and aquatic. Cobalt content in these compounds is over 6%. The presence of vitamin B_{12} enables the regulation of erythrocyte production as well as of the metabolism of proteins and nucleic acids (Stangl et al., 2000; Antony et al., 2011). This compound also participates in many enzymatic redox processes as the activator. Only those microorganisms that live in the soil, water environment and in an animal's alimentary tract are capable of its synthesis (Mukherjee and Kaviraj, 2011).

The effect of cobalt on aquatic animals is particularly important due to assisting enzymatic and metabolic processes (Mukherjee and Kaviraj, 2011; Söyüt and Beydemir, 2011). It is absorbed via the respiratory tract, adsorption or as a result of the consumption of vegetable and animal food (Klavins et al., 2009; Malik and Zeb, 2009; Dhaneesh et al., 2012; De Jesus et al., 2014). Cobalt absorption depends on many environmental factors. The state of water environment pollution and the amount of organic matter in a given body of water are included among them most often (Malik and Zeb, 2009). According to Klavins et al. (2009) cobalt accumulation in aquatic animal organs is lower with a higher organic matter content in the water habitat. Numerous studies by researchers (Klavins et al., 2009; Malik and Zeb, 2009; Waheed et al., 2014) also confirm the effect of differences in the age, sex, species and diet of aquatic animals on cobalt assimilation.

Increased cobalt absorption by aquatic animals is also affected by the amount of mobile forms of this element accumulated in the bottom sediments of lakes, rivers and seas (Mohiuddin et al., 2012; Rognerud et al., 2013; Swarnalatha et al., 2013; Jayasiri et al., 2014; Ramani et al., 2014). A particular risk to these animals is posed by sediments near highly populated places or places impacted by different industry branches and on the edge of water bodies (Swarnalatha et al., 2013; Chanpiwat and Sthiannopkao, 2014; Ghandour et al., 2014; Rzymski et al., 2014). A change in physicochemical water conditions is an additional factor causing increased cobalt release to waters (Ochieng et al., 2008; Sukdeo et al., 2012; Wu et al., 2012; Hierro et al., 2014; Zamani-Hargalani et al., 2014). The state of the pollution of coral reefs, which, apart from being a refuge for many animals, accumulate substantial amounts of pollutants, is also included among these factors (Koigoora et al., 2013; Briand et al., 2014). Studies by Malik and Zeb (2009), Chanpiwat and Sthiannopkao (2014) and Jayasiri et al. (2014) also include seasonality, which leads to changes in water parameters.

A high cobalt concentration, both in fresh and salt waters, leads to its excessive accumulation in the internal organs of the animals inhabiting them (Söyüt and Beydemir, 2011; Iqbal et al., 2012). Fish are the most studied aquatic animals in waters polluted with heavy metals, including cobalt. According to De Jesus et al. (2014) and Waheed et al. (2014) cobalt accumulates mainly in the inedible fish parts, which include gills, intestines, kidneys and liver. This was also confirmed by Klavins et al. (2009) and Türkmen et al. (2011). According to Malik and Zeb (2009) among the organs listed above, liver and kidneys stand out for their high abilities for the accumulation and detoxification of this metal. Cobalt also accumulates in the edible parts, such as flesh or skin, with its content much lower than in the above-listed organs (Malik and Zeb, 2009; Schmitt et al., 2009; Tepe, 2009). Waheed et al. (2014) found that cobalt content is

http://www.aloki.hu ● ISSN 1589 1623 (Print) ● ISSN 1785 0037 (Online)
DOI: http://dx.doi.org/10.15666/aeer/1705_1141911449

higher in the muscles and gills of herbivorous fish than in carnivorous fish. Cobalt accumulation in fish organs leads to changes in the course of genetic, cytological or metabolic processes which are the cause of many diseases (Rzymski et al., 2014). Cobalt also affects the other animals inhabiting aquatic ecosystems, which was confirmed by many studies (Cavet et al., 2003; Türkmen et al., 2011; Lavoie et al., 2012; Abdallah, 2013; Alquezar and Anastasi, 2013; Holland et al., 2013; Sandergaard, 2013) where a high cobalt content was recorded in bivalves, shrimps, blue-green algae and algae inhabiting fresh waters. For salt bodies, excessively high cobalt doses showed a negative effect on scorpions, blue-green algae and sponges (Padovan et al., 2012; Alquezar and Anastasi, 2013; Batista et al., 2014).

High cobalt amounts accumulate in the successive links of the food chain, which are terrestrial and aerial animals (Klavins et al., 2009; Malik and Zeb, 2009; Albayrak and Mor, 2011; Söyüt and Beydemir, 2011; Mansouri et al., 2012; Sandergaard, 2013). In the body of terrestrial animals, cobalt is important due to its participation in the formation of vitamin B_{12} (Stangl et al., 2000). In ruminants, it is produced in the rumen (Agbenin, 2002; Tiffany and Spears, 2005; Bishehsari et al., 2010) and the amount of this vitamin is highest in muscles, liver, kidneys and the heart. Animal products such as eggs, cheeses or milk can also contain substantial amounts of cobalt (Tiffany and Spears, 2005).

Cobalt content within the optimal amount is necessary for the course of proper life processes in every organism living on land. The youngest animals have the highest requirement for this element (Kadim et al., 2006; Ceacero et al., 2009). Older animals have a lower cobalt requirement, but its content rises over time as a result of accumulation. Cobalt also plays an important role as the catalyst of many enzymatic processes (Swarup et al., 2006). Kadim et al. (2006) found that the injection of 350 pg dm^{-3} of cobalt ensures the proper course of growth processes. The appropriate cobalt level in insects inhibits caspase production, due to which the intestinal epithelium is not damaged (Cheruiyot et al., 2013).

Both a deficiency and excess of cobalt can result in the appearance of disease symptoms. Sheep are particularly sensitive to cobalt deficiency, as reported by Bishehsari et al. (2010). An excessively low cobalt dose in the feed of these animals becomes the cause of anemia, reduced plasma homocysteine concentration (Stangl et al., 2000; Taugbol et al., 2010) and decreased weight gain leading to anorexia. Symptoms of reduced body mass and shape in goats resulting from cobalt deficiency are confirmed by Kadim et al. (2006). A higher resistance of goats than sheep to low amounts of cobalt present in their body was also found in their study. Another symptom was discolorations appearing on the wool produced by these animals and a characteristic discharge from the ears and eyes. Reduced absorption of nutrients and necessary trace metals, such as copper, iron or nickel, also leads to a decreased quality of meat from these animals (Stangl et al., 2000). According to Taugbol et al. (2010) an excessively high amount of cobalt present in the blood of dairy cows can lead to a reduced level of fatty acid desaturation products in milk and in blood. Excess cobalt can also cause a reduced flow of divalent metals, such as iron and zinc, to udders and disrupt enzymatic activity in the mammary gland cells. Negative effects of cobalt accumulation have also been observed in the organisms of forest animals, e.g on growth processes in wild boar. Yarsan et al. (2014) found that excessively high doses lead to circulatory and nervous system disorders and bone diseases. According to Ceacero et al.

http://www.aloki.hu ● ISSN 1589 1623 (Print) ● ISSN 1785 0037 (Online)
DOI: http://dx.doi.org/10.15666/aeer/1705_1141911449

(2009) deer are among the forest mammals which are best able to regulate cobalt absorption.

Other symptoms of the effect of cobalt include lower animal weight gain and a higher mortality of the born progeny. The surviving progeny can inherit the same defects as parental organisms. Due to the carcinogenic effect of cobalt compounds, it can also lead to the inhibition of DNA repair processes, change gene expression patterns or generate oxygen and nitrogen in a reactive form. It can significantly affect the FAS signal and the caspase pathways similar to this signal, thus contributing to the induction of apoptosis (Wang et al., 2007; Cheruiyot et al., 2013).

The presence of different kinds of cobalt compounds in the air and food can significantly contribute to their excessive accumulation in bird organs. Albayrak and Mor (2011) report that these compounds accumulate in similar amounts in the organs of both sparrow sexes. The only exception is female kidneys, where much higher cobalt contents were found than in male kidneys. These differences are the result of the metabolism of cobalt participating in the activity of sex hormones. Females can contain much higher cobalt contents than males due to an increased amount of feed consumed during egg formation. After eggs are laid, cobalt content in female organisms decreases (Norouzi et al., 2012). A study by Mansouri et al. (2012) on cobalt content in the organs of seabirds shows the opposite tendency, which is affected by moulting. It was also found that cobalt content in the organs of migratory birds was higher than in the organs of sedentary birds, which is significantly affected by the quality of the consumed feed.

Increased cobalt contents can also accumulate in bird feathers as a result of interstitial excretion from their internal organs (Norouzi et al., 2012). Determining the cobalt content in young feathers allows its concentration in blood to be determined, while in older feathers it is not possible due to blood flow changes (Malik and Zeb, 2009). Another animal organism sensitive to cobalt contamination are the larvae of the silkworm *Antheraea assama* (Devi et al., 2014). Excessive cobalt concentration in its body prevents it reaching the stage at which it is able to produce silk and may cause death.

Effect of cobalt on the human body

Cobalt in the human body, as in animals, performs an important role in the formation of vitamin B_{12} (Dobrowolski and Otto, 2012). According to ATSDR (2004) 0.1 μmol of cobalt in the form of vitamin B_{12} supplies a necessary amount of cobalt to the human body. The highest cobalt intake which does not cause negative effects is 1800 μmol. Vitamin B_{12} deficiency is supplemented, apart from its supply in plant and animal products to the human body, also by the application of drugs (Ulusoy et al., 2012). Its deficiency in the human body leads to the appearance of anemia, resulting from a low amount of produced vitamin B_{12}. Another manifestation of a cobalt deficiency in the human body is disturbed functioning of the alimentary, nervous and osseous systems (Jonnalagadda et al., 2008; Soylak et al., 2012).

The disease symptoms resulting from exceeding the permissible dose include, among others, allergic reactions, lung and heart diseases (Basu et al., 2010; Díaz-Rizo et al., 2012; Dobrowolski and Otto, 2012; Ryuko et al., 2012; Ulusoy et al., 2012; Devi et al., 2014). Intensification of the above symptoms is most often encountered in industrial plants, where exposure to the harmful effect of this element is much higher than in other places with a human presence (Benderli-Cihan et al., 2011; Pietrodangelo et al., 2014).

http://www.aloki.hu ● ISSN 1589 1623 (Print) ● ISSN 1785 0037 (Online)
DOI: http://dx.doi.org/10.15666/aeer/1705_1141911449

Basu et al. (2010) and Ryuko et al. (2012) report that the most frequent symptoms of potassium excess are skin inflammations and asthma. Frequent use of tools which contain cobalt admixtures, as well as the presence in industrial plants, significantly affects the induction of allergic reactions, mainly on the skin of the hands. The occupations particularly exposed to such risks are carpenters and metal workers (Thyssen et al., 2011).

The harmful effect of cobalt can also be the result of absorbing its too high dose with food and drinking water (Obiri, 2007; Upadhyaya et al., 2014). This is particularly important for pregnant women who, depending on the type of consumed food, can accumulate substantial amounts of cobalt in their bodies, which also affects the developing fetus. This was confirmed by Chan-Hon-Tong et al. (2013) who found that a group of tested pregnant women eating mainly fish had a higher blood cobalt content than the women consuming sweets, fruit, milk products and soups. A study by Foster et al. (2012) did not find, however, differences in the blood cobalt content of pregnant women depending on consumed food. Due to genotoxic properties, it is important that the cobalt limit is not exceeded (Chan-Hon-Tong et al., 2013). A low cobalt content present in alcoholic beverages can cause the appearance of disease symptoms. This was confirmed in a study by Ulusoy et al. (2012) where it was found that the consumption of beer with a content of cobalt chloride from 1 to 2 $mgdm^{-3}$ caused changes in the nails of palms and feet, called dyshidrosis. Other symptoms include frequent vomiting and diarrhea, blood pressure changes or headaches. High cobalt contents also lead to damage to the immunological system (Bezerra et al., 2014; Valera et al., 2014). Another symptom of exceeding the permissible dose is damage to DNA and disruption of its repair. Cobalt toxicity has a stronger effect in the presence of iron, to which it is linked by similar atomic properties (Ryuko et al., 2012).

Due to its quite high solubility in systemic fluids, it becomes more mobile and also more harmful to all internal organs. Benderli-Cihan et al. (2011) found much higher cobalt contents in the hair of women with breast cancer than in healthy women, as well as the possibility of cobalt accumulation in nails and teeth. The defense reaction of the body to the presence of an excessively high cobalt dose involves physiological processes. Therefore, its amounts are highest in kidneys and liver (Ulusoy et al., 2012). Cobalt harmfulness in the human body is also associated with the radiation of isotopes of this element, which are the cause of many short- and long-term diseases. An excessively high cobalt isotope accumulation also leads to an increased cancer risk (Bezerra et al., 2014).

Summary

Apart from natural cobalt contents in the environment, pollution with this element has begun to increase in recent years. The main cause of this is the growing extraction and manifold application of cobalt in different branches of industry (Biswas et al., 2013). The appearance of cobalt levels exceeding the environmental threshold levels has led, however, to disturbances in the proper functioning of living organisms. Not only animals or plants which are the first component of the food chain are at risk, but also the subsequent trophic levels, where accumulated cobalt contents show signs of toxicity (Maguire and Collins, 2001; Basu et al., 2010). The application of sorbents to soil (especially organic matter and calcium oxide) reduce the effect of cobalt on soil organisms and plants. A very important role in the removal of cobalt from soil plays

http://www.aloki.hu ● ISSN 1589 1623 (Print) ● ISSN 1785 0037 (Online)
DOI: http://dx.doi.org/10.15666/aeer/1705_1141911449

phytoremediation by plant hyperaccumulators. High cobalt doses are not, however, the only cause of its negative influence on living organisms. The presented literature review shows that cobalt is also an indispensable dietary micronutrient for living organisms, from microorganisms to the human body. Cobalt deficiencies cause many diseases, whose treatment is a long-lasting process requiring, in most cases, diet adjustment to the dietary needs of a given organism (Soylak et al., 2013).

Focusing on the elements included in the group of heavy metals is useful in assessing environmental pollution. However, it would also be advisable to systematically monitor cobalt content in the environment (especially the soil environment), which affects the quality of produced feed and food, which consequently directly affects the absorption of optimal cobalt amounts by living organisms.

Acknowledgements. This study was supported by the Ministry of Science and Higher Education funds for statutory activity.

REFERENCES

[1] Abd-Alla, M. H., Bagy, M. K., Wahab, A., Bashandy, S. R. (2014): Activation of *Rhizobium tibeticum* with flavonoids anhances nodulation, nitrogen fixation and growth of fenugreek (*Trigonella foenum-graecum* L.) grown in cobalt polluted soil. – Archives of Environmental Contamination & Toxicology 66(2): 303-315. https://doi.org/10.1007/s00244-013-9980-7.

[2] Abdallah, M. A. (2013): Bioaccumulation of heavy metals in mollusca species and assessment of potential risks to human health. – Bulletin of Environmental Contamination & Toxicology 90(5): 552-557. https://doi.org/10.1007/s00128-013-0959-x.

[3] Abdel-Razek, A. S., Abdel Ghany, T. M., Mahmoud, S. A., El Sheikh, H. H., Mahmoud, M. S. (2009): The use of free and immobilized *Cunninghamella elegans* for removing cobalt ions from aqueous waste solutions. – World Journal of Microbiology & Biotechnology 25(12): 2137-2145. https://doi.org/10.1007/s11274-009-0118-z.

[4] Abskharon, R. N. N., Hassan, S. H. A., Kabir, M. H., Qadir, S. A., Gad El Rab, S. M. F., Wang, M. H. (2010): The role of antioxidants enzymes of *E. coli* ASU3, a tolerant strain to heavy metals toxicity, in combating oxidative stress of copper. – World Journal of Microbiology & Biotechnology 26(2): 241-247. https://doi.org/10.1007/s11274-009-0166-4.

[5] Agbenin, J. O. (2002): The impact of long-term cultivation and management history on the status and dynamics of cobalt in a savanna Alfisol in Nigeria. – European Journal of Soil Science 53(2): 169-174. https://doi.org/10.1046/j.1365-2389.2002.00433.x.

[6] Agbenin, J. O., Danko, M., Welp, G. (2009): Soil and vegetable compositional relationships of eight potentially toxic metals in urban garden fields from northern Nigeria. – Journal of the Science of Food & Agriculture 89(1): 49-54. https://doi.org/10.1002/jsfa.3409.

[7] Akbar, F. M., Zafar, M., Hamid, A., Ahmed, M., Khaliq, A., Khan, M. R., Rehman, Z. (2013): Interactive effect of cobalt and nitrogen on growth, nodulation, yield and protein content of field grown pea. – Horticulture Environment & Biotechnology 54(6): 465-474. https://doi.org/10.1007/s13580-013-0001-6.

[8] Albayrak, T., Mor, F. (2011): Comparative tissue distribution of heavy metals in House Sparrow (Passer domesticus, Aves) in polluted and reference sites in Turkey. – Bulletin of Environmental Contamination & Toxicology 87(4): 457-462. https://doi.org/10.1007/s00128-011-0364-2.

http://www.aloki.hu ● ISSN 1589 1623 (Print) ● ISSN 1785 0037 (Online)
DOI: http://dx.doi.org/10.15666/aeer/1705_1141911449

[9] Alquezar, R., Anastasi, A. (2013): The use of the cyanobacteria, *Cyanobium* sp., as a suitable organism for toxicity testing by flow cytometry. – Bulletin of Environmental Contamination & Toxicology 90(6): 684-690. https://doi.org/10.1007/s00128-013-09778.
[10] Al-Shiwafi, N., Rushdi, A. I., Ba-Issa, A. (2005): Trace metals in surface seawaters and sediments from various habitats of the Red Sea coast of Yemen. – Environmental Geology 48(4-5): 590-598. https://doi.org/10.1007/s00254-005-1315-1.
[11] Amir, H., Pineau, R. (2003): Release of Ni and Co by microbial activity in New Caledonian ultramafic soils. – Canadian Journal of Microbiology 49(4): 288-293. https://doi.org/10.1139/W03-039.
[12] Antony, R., Sujith, P. P., Fernandes, S. O., Verma, P., Khedekar, V. D., Loka Bharathi, P. A. (2011): Cobalt immobilization by manganese oxidizing bacteria from the Indian Ridge System. – Current Microbiology 62(3): 840-849. https://doi.org/10.1007/s00284-010-9784-1.
[13] Ashfaq, M., Ali, S., Hanif, M. A. (2009): Bioaccumulation of cobalt in silkworm (*Bombyx mori* L.) in relation to mulberry, soil and wastewater metal concentrations. – Process Biochemistry 44(10): 1179-1184. https://doi.org/ 10.1016/j.procbio.2009.05.006.
[14] Ashraf, W., Mian, A. A. (2008): Levels of selected heavy metals in black tea varieties consumed in Saudi Arabia. – Bulletin of Environmental Contamination & Toxicology 81(1): 101-104. https://doi.org/10.1007/s00128-008-9402-0.
[15] ATSDR (2004): Toxicological profile for cobalt. –gency for Toxic Substances and Disease Registry. U.S. Department of Health and Human Services, Public Health Service, Atlanta, GA.
[16] Balestrazzi, A., Bonadei, M., Quattrini, E., Carbonera, D. (2009): Occurrence of multiple metal-resistance in bacterial isolates associated with transgenic white poplars (*Populus alba* L.). – Annals of Microbiology 59(1): 17-23. https://doi.org/10.1007/BF03175593.
[17] Banks, C. J., Zang, Y., Jiang, Y., Heaven, S. (2012): Trace element requirements for stable food waste digestion at elevated ammonia concentration. – Bioresource Technology 104: 127-135. https://doi.org/10.1016/j.biortech.2011.10.068.
[18] Basu, N., Abare, M., Buchanan, S., Cryderman, D., Nam, D. H., Sirkin, S., Schmitt, S., Hu, H. (2010): A combined ecological and epidemiologic investigation of metal exposures amongst Indigenous peoples near the Marlin Mine in Western Guatemala. – Science of the Total Environment 409(1): 70-77. https://doi.org/10.1016/j.scitotenv.2010.09.041.
[19] Batista, D., Muricy, G., Rocha, R. C., Miekeley, N. F. (2014): Marine sponges with contrasting life histories can be complementary biomonitors of heavy metal pollution in coastal ecosystems. – Environmental Science & Pollution Research 21(9): 5785-5794. https://doi.org/10.1007/s11356-014-2530-7.
[20] Bem, H., Gallorini, M., Rizzio, E., Krzemińska, M. (2003): Comparative studies on the concentrations of some elements in the urban air particulate matter in Łodź City of Poland and in Milan, Italy. – Environment International 29(4): 423-428. https://doi.org/ 10.1016/S0160-4120(02)00190-3.
[21] Benderli-Cihan, Y., Sözen, S., Oztürk-Yildirim, S. (2011): Trace elements and heavy metals in hair of stage III breast cancer patients. – Biological Trace Element Research 144(1-3): 360-379. https://doi.org/10.1007/s12011-011-9104-z.
[22] Ben-Fredj, F., Wali, A., Khadhraoui, M., Han, J., Funamizu, N., Ksibi, M., Isoda, H. (2014): Risk assessment of heavy metal toxicity of soil irrigated with treated wastewater using heat shock proteins stress responses: case of El Hajeb, Sfax, Tunisia. – Environmental Science & Pollution Research 21(6): 4716-4726. https://doi.org/10.1007/s11356-013-2411-5.
[23] Benlloch-González, M., Romera, J., Cristescu, S., Harren, F., Fournier, J. M., Benlloch, M. (2010): K^+ starvation inhibits water-stress-induced stomatal closure via ethylene synthesis in sunflower plants. – Journal of Experimental Botany 61(4): 1139-1145. https://doi.org/10.1093/jxb/erp379.

http://www.aloki.hu ● ISSN 1589 1623 (Print) ● ISSN 1785 0037 (Online)
DOI: http://dx.doi.org/10.15666/aeer/1705_1141911449

[24] Bezerra, J. D., Santos-Amaral, R., Santos-Júnior, J. A., Genezini, F. A., Menezes, R. S., De Oliviera, I. A. (2014): Characterization of heavy metals in a uranium ore region of the state of Pernambuco, Brazil. – Bulletin of Environmental Contamination & Toxicology 92(3): 270-273. https://doi.org/10.1007/s00128-013-1183-4.
[25] Biesalski, H. K., Grimm, P. (2012): Żywienie. Atlas i podręcznik. Wyd. I. – Elsevier, Amsterdam.
[26] Bishehsari, S., Mehdi-Tabatabaei, M., Aliarabi, H., Alipour, D., Zamani, P., Ahmadi, A. (2010): Effect of dietary cobalt supplementation on plasma and rumen metabolites in Mehraban lambs. – Small Ruminant Research 90(1-3): 170-173. https://doi.org/10.1016/j.smallrumres.2010.02.010.
[27] Biswas, S., Dey, R., Mukherjee, S., Banerjee, P. C. (2013): Bioleaching of nickel and cobalt from lateritic chromite overburden using the culture filtrate of *Aspergillus niger*. – Applied Biochemistry & Biotechnology 170(7): 1547-1559. https://doi.org/10.1007/s12010-013-0289-9.
[28] Briand, M. J., Letourneur, Y., Bonnet, X., Wafo, E., Fauvel, T., Brischoux, F., Guillou, G., Bustamante, P. (2014): Spatial variability of metallic and organic contamination of anguilliform fish in New Caledonia. – Environmental Science & Pollution Research 21(6): 4576-4591. https://doi.org/10.1007/s11356-013-2327-0 .
[29] Canepari, S., Astolfi, M. L., Farao, C., Maretto, M., Frasca, D., Marcoccia, M., Perrino, C. (2014): Seasonal variations in the chemical composition of particulate matter: a case study in the Po Valley. Part II: concentration and solubility of micro- and trace-elements. – Environmental Science & Pollution Research 21(6): 4010-4022. https://doi.org/10.1007/s11356-013-2298-1.
[30] Cavet, J. S., Borrelly, G. P., Robinson, N. J. (2003): Zn, Cu and Co in cyanobacteria: selective control of metal availability. – FEMS Microbiology Reviews 27(2-3): 165-181.
[31] Ceacero, F., Landete-Castillejos, T., García, A. J., Estévez, J. A., Martinez, A., Calatayud, A., Gaspar-López, E., Gallego, L. (2009): Free-choice mineral consumption in Iberian red deer (*Cervus elaphus hispanicus*) response to diet deficiencies. – Livestock Science 122(2-3): 345-348. https://doi.org/10.1016/j.livsci.2008.08.002.
[32] Chan-Hon-Tong, A., Charles, M. A., Forhan, A., Heude, B., Sirot, V. (2013): Exposure to food contaminants during pregnancy. – Science of the Total Environment 458-460: 27-35. https://doi.org/10.1016/j.scitotenv.2013.03.100.
[33] Chanpiwat, P., Sthiannopkao, S. (2014): Status of metal levels and their potential sources of contamination in Southeast Asian rivers. – Environmental Science & Pollution Research 21(1): 220-233. https://doi.org/10.1007/s11356-013-1858-8.
[34] Chatterjee, C., Dube, B. K. (2005): Impact of pollutant elements on vegetables growing in sewage-sludge-treated soils. – Journal of Plant Nutrition 28(10): 1811-1820. https://doi.org/10.1080/01904160500251175.
[35] Chatterjee, C., Gopal, R., Dube, B. K. (2006): Physiological and biochemical responses of French bean to excess cobalt. – Journal of Plant Nutrition 29(1): 127-136. https://doi.org/10.1080/01904160500416513.
[36] Chatterjee, J., Chatterjee, C. (2002): Amelioration of phytotoxicity of cobalt by high phosphorus and its withdrawal in tomato. – Journal of Plant Nutrition 25(12): 2731-2743. https://doi.org/10.1081/PLN-120015535.
[37] Chatterjee, J., Chatterjee, C. (2003): Management of phytotoxicity of cobalt in tomato by chemical measures. – Plant Science 164(5): 793-801. https://doi.org/10.1016/S0168-9452(03)00066-9.
[38] Chaudhari, B. H., Parmar, J. K., Mali, R. H., Bumbadiya, N. H. (2017): Effect of Co level and FYM on growth and yield of fodder maize. – International Journal of Chemical Studies 5(1): 327-329.
[39] Cheruiyot, D. J., Boyd, R. S., Moar, W. J. (2013): Exploring lower limits of plant elemental defense by cobalt, copper, nickel, and zinc. – Journal of Chemical Ecology 39(5): 666-674. https://doi.org/10.1007/s10886-013-0279-y.

http://www.aloki.hu ● ISSN 1589 1623 (Print) ● ISSN 1785 0037 (Online)
DOI: http://dx.doi.org/10.15666/aeer/1705_1141911449

[40] Chmielowska-Bąk, J., Lefèvre, I., Lutts, S., Kulik, A., Deckert, J. (2014): Effect of cobalt chloride on soybean seedlings subjected to cadmium stress. – Acta Societatis Botanicorum Poloniae 83(3): 201-207. https://doi.org/10.5586/asbp.2014.027.
[41] Ciećko, Z., Kalembasa, S., Wyszkowski, M., Rolka, E. (2005): The magnesium content in plants on soil contaminated with cadmium. – Polish Journal of Environmental Studies 14(3): 365-370.
[42] Collins, R. N., Kinsela, A. S. (2011): Pedogenic factors and measurements of the plant uptake of cobalt. – Plant & Soil 339(1): 499-512. https://doi.org/10.1007/s11104-010-0584-y.
[43] Dávila-Rangel, J. I., Solache-Ríos, M. (2006): Sorption of cobalt by two Mexican clinoptilolite rich tuffs zeolitic rocks and kaolinite. – Journal of Radioanalytical & Nuclear Chemistry 270(2): 465-471.
[44] Defarge, N., Spiroux de Vendômois, J., Séralinia, G. E. (2018): Toxicity of formulants and heavy metals in glyphosate-based herbicides and other pesticides. – Toxicology Reports 5: 156-163. https://doi.org/10.1016/j.toxrep.2017.12.025.
[45] de Jesus, I. S., da Silva-Medeiros, R. L., Cestari, M. M., de Almeida-Bezerra, M., de Mello-Affonso, P. R. (2014): Analysis of metal contamination and bioindicator potential of predatory fish species along Contas River basin in northeastern Brazil. – Bulletin of Environmental Contamination & Toxicology 92(5): 551-556. https://doi.org/10.1007/s00128-013-1188-z.
[46] Devi, G., Gopal-Bhattacharyya, K., Mahanta, L. B., Devi, A. (2014): Trace metal composition of PM2.5, soil, and Machilus bombycina leaves and the effects on Antheraea assama silk worm rearing in the oil field area of northeastern India. – Water Air & Soil Pollution 225: 1884-1897. https://doi.org/10.1007/s11270-014-1884-2.
[47] Dhaneesh, K. V., Gopi, M., Noushad, K. M., Ganeshamurthy, R., Kumar, T. T., Balasubramanian, T. (2012): Determination of metal levels in thirteen fish species from Lakshadweep Sea. – Bulletin of Environmental Contamination & Toxicology 88(1): 69-73. https://doi.org/10.1007/s00128-011-0459-9.
[48] Díaz-Rizo, O., Hernández-Merlo, M., Echeverría-Castillo, F., Arado-López, J. O. (2012): Assessment of metal pollution in soils from a former Havana (Cuba) solid waste open dump. – Bulletin of Environmental Contamination & Toxicology 88(2): 182-186. https://doi.org/10.1007/s00128-011-0505-7.
[49] Directive 2010/75/EU of the European Parliament and of the Council of 24 November (2010): On industrial emissions (integrated pollution prevention and control). – Official Journal of the European Union L 334/17-119.
[50] Dobrowolski, R., Otto, M. (2012): Determination of nickel and cobalt in reference plant materials by carbon slurry sampling GFAAS technique after their simultaneous preconcentration onto modified activated carbon. – Journal of Food Composition & Analysis 26(1-2): 58-65. https://doi.org/10.1016/j.jfca.2012.03.002.
[51] Dong Cho, Y., Kim, J., Chung Kim, D. (2012): Cobalt-requiring 5′-deoxy-5′-methylthioadenosine nucleosidase from soybean (*Glycine max*) cotyledon. – Journal of Plant Biochemistry & Biotechnology 21(1): 113-116. https://doi.org/10.1007/s13562-11-0061-6.
[52] Dos Anjos-Paulino, S., Oliveira, R. L., Loyola, J., Minho, A. S., Arbilla, G., Quiterio, S. L., Escaleira, V. (2014): Trace metals in PM10 and PM 2,5 samples collected in a highly industrialized chemical/petrochemical area and its urbanized surroundings. – Bulletin of Environmental Contamination & Toxicology 92(5): 590-595. https://doi.org/10.1007/s00128-014-1219-4.
[53] Ebrahimi, M., Panahi, R., Dabbagh, R. (2009): Evaluation of native and chemically modified Sargassum glaucescens for continous biosorption of Co(II). – Applied Biochemistry & Biotechnology 158(3): 736-746. https://doi.org/10.1007M2010-008-8389-7.

http://www.aloki.hu ● ISSN 1589 1623 (Print) ● ISSN 1785 0037 (Online)
DOI: http://dx.doi.org/10.15666/aeer/1705_1141911449

[54] Edwards, A. C., Coull, M., Sinclair, A. H., Walker, R. L., Watsun, C. A. (2012): Elemental status (Cu, Mo, Co, B, S and Zn) of Scottish agricultural soils compared with a soil-based risk assessment. – Soil Use & Management 28(2): 167-176. https://doi.org/10.1111/j.1475-2743.2012.00408.x.

[55] Elleuche, S., Fodor, K., von der Heyde, A., Klippel, B., Wilmanns, M., Antranikian, G. (2014): Group III alcohol dehydrogenase from Pectobacterium atrosepticum: insights into enzymatic activity and organization of the metal ion-containing region. – Applied Microbiology & Biotechnology 98(9): 4041-4051. https://doi.org/10.1007/s00253-013-5374-z.

[56] Elliot, D., Litzinger, T. (2015): 2014 Production Statistics. – Cobalt News 15/2: 1-8.

[57] Esther, J., Panda, S., Behera, S. K., Sukula, L. B., Pradhan, N., Mishra, B. K. (2013): Effect of dissimilatory Fe(III) reducers on bio-reduction and nickel-cobalt recovery from Sukinda chromite-overburden. – Bioresource Technology 146: 762-766. https://doi.org/10.1016/j.biortech.2013.07.103.

[58] Faucon, M. P., Ngoy-Shutcha, M., Meerts, P. (2007): Revisiting copper and cobalt concentrations in supposed hyperaccumulators from SC Africa: influence of washing and metal concentrations in soil. – Plant & Soil 301: 29-36. https://doi.org/10.1007/s11104-007-9405-3.

[59] Faucon, M. P., Colinet, G., Mhay, G., Ngongo-Luhembwe, M., Verburggen, N., Meerts, P. (2009): Soil influence on Cu and Co uptake and plant size in the cuprophytes *Crepidorhopalon perennis* and *C. tenuis* (*Scrophulariaceae*) in SC Africa. – Plant & Soil 317: 201-212. https://doi.org/10.1007/s11104-008-9801-3.

[60] Fermoso, F. G., Bartecek, J., Lens, P. N. (2010): Effect of vitamin B12 pulse addition on the performance of cobalt deprived anaerobic granular sludge bioreactors. – Bioresource Technology 101(14): 5201-5205. https://doi.org/10.1016/j.biortech.2010.02.047.

[61] Foster, W. G., Cheung, A. P., Davis, K., Graves, G., Jarrell, J., Leblanc, A., Liang, C. L., Leech, T., Walker, M., Weber, J. P., Von Oostdam, J. (2012): Circulating metals and persistent organic pollutant concentrations in Canadian and non-Canadian born primiparous women from five Canadian centres: results of a pilot biomonitoring study. – Science of the Total Environment 435-436: 326-336 https://doi.org/10.1016/j.scitotenv.2012.06.070.

[62] Freeman, J. L., Persans, M. W., Nieman, K., Salt, D. E. (2005): Nickel and cobalt resistance engineered in Escherichia coli by overexpression of serine acetyltransferase from the nickel hyperaccumulator plant Thlaspi goesingense. – Applied & Environmental Microbiology 71(12): 8627-8633. https://doi.org/10.1128/AEM.71.12.8627-8633.2005.

[63] Fujikawa, Y., Fukui, M. (2001): Vertical distribution of trace metals in natural soil horizons from Japan. Part 2. Effects of organic components in soil. – Water, Air & Soil Pollution 131(1-4): 305-328. https://doi.org/10.1023/A:1011927802703.

[64] Ghandour, I. M., Basaham, S., Al-Washmi, A., Masuda, H. (2014): Natural and anthropogenic controls on sediment composition of an arid coastal environment: Sharm Obhur, Red Sea, Saudi Arabia. – Environmental Monitoring & Assessment 186(3): 1465-1484. https://doi.org/10.1007/s10661-013-3467-x.

[65] Ghassabzadeh, H., Torab-Mostaedi, M., Mohaddespour, A., Ghannadi, M. M., Ahmadi, S. J., Zaheri, P. (2010): Characterizations of Co (II) and Pb (II) removal process from aqueous solutions using expanded per-lite. – Desalination 261(1-2): 73-79. https://doi.org/10.1016/j.desal.2010.05.028.

[66] Gopal, R., Dube, B. K., Sinha, P., Chatterjee, C. (2003): Cobalt toxicity effects on growth and metabolism of tomato. – Communications in Soil Science & Plant Analysis 34(5-6): 619-628. https://doi.org/10.1081/CSS-120018963.

[67] Guo, Y. J., Di, H. J., Cameron, K. C., Li, B. (2014): Effect of application rate of a nitrification inhibitor, dicyandiamide (DCD), on nitrification rate, and ammonia-oxidizing bacteria and archaea growth in a grazed pasture soil: an incubation study. –

http://www.aloki.hu ● ISSN 1589 1623 (Print) ● ISSN 1785 0037 (Online)
DOI: http://dx.doi.org/10.15666/aeer/1705_1141911449

Journal of Soils & Sediments 14(5): 897-903. https://doi.org/10.1007/s11368-013-0843-7.

[68] Guzmán-Morales, J., Morton-Bermea, O., Hernández-Álvarez, E., Rodríguez-Salazar, M. T., García-Arreola, M. E., Tapia-Cruz, V. (2011): Assessment of atmospheric metal pollution in the urban area of Mexico City, using *Ficus benjamina* as biomonitor. – Bulletin of Environmental Contamination & Toxicology 86(5): 495-500. https://doi.org/10.1007/s00128-011-0252-9.

[69] Hau, H. H., Gibert, A., Coursolle, D., Gralnick, J. A. (2008): Mechanism and Consequences of anaerobic respiration of cobalt by *Shewanella oneidensis* strain MR-1. – Applied & Environmental Microbiology 74(22): 6880-6886. https://doi.org/10.1128/AEM.00840-08.

[70] Heimbürger, L. E., Migon, C., Dufour, A., Chiffoleau, J. F., Cossa, D. (2010): Trace metal concentrations in the North-western Mediterranean atmospheric aerosol between 1986 and 2008: Seasonal patterns and decadal trends. – Science of the Total Environment 408(13): 2629-2638. https://doi.org/10.1016/j.scitotenv.2010.02.042.

[71] Hierro, A., Olías, M., Ketterer, M. E., Vaca, F., Borrego, J., Cánovas, C. R., Bolivar, J. P. (2014): Geochemical behavior of metals and metalloids in an estuary affected by acid mine drainage (AMD). – Environmental Science & Pollution Research 21(4): 2611-2627. https://doi.org/10.1007/s11356-013-2189-5.

[72] Hlima, H. B., Aghajari, N., Ali, M. B., Haser, R., Bejar, S. (2012): Engineered glucose isomerase from Streptomyces sp. SK is resistant to Ca^{2+} inhibition and Co^{2+} independent. – Journal of Industrial Microbiology & Biotechnology 39(4): 537-546. https://doi.org/10.1007/s10295-011-1061-1.

[73] Hoffman, D. R., Anderson, P. P., Schubert, C. M., Gault, M. B., Blanford, W. J., Sandrin, T. R. (2010): Carboxymethyl-beta-cyclodextrin mitigates toxicity of cadmium, cobalt, and copper during naphthalene biodegradation. – Bioresource Technology 101(8): 2672-2677. https://doi.org/10.1016/j.biortech.2009.10.073.

[74] Holland, A., Duivenvoorden, L. J., Kinnear, S. H. W. (2013): Humic substances increase survival of freshwater shrimp *Caridina* sp. D to acid mine drainage. – Archives of Environmental Contamination & Toxicology 64(2): 263-272. https://doi.org/10.1007/s00244-012-9823-y.

[75] Hong, Q., Dong-Li, L., Yu-You, L. (2012): High-solid mesophilic methane fermentation of food waste with an emphasis on iron, cobalt, and nickel requirements. – Bioresource Technology 103(1): 20-27. https://doi.org/10.1016/j.biortech.2011.09.036.

[76] Hu, D., Cheng, M., Hu, K., Zhang, W., Yang, Y., Xu, Q. (2019): Evaluation of cobalt hyperaccumulation and tolerance potential of the duckweed (*Lemna minor* L.). – Ecotoxicology & Environmental Safety 179: 79-87. https://doi.org/10.1016/j.ecoenv.2019.04.058.

[77] Hu, X., Wang, C., Wang, L., Zhang, R., Chen, H. (2014): Influence of temperature, pH and metal ions on guaiacol oxidation of purifield laccase from *Leptographium qinlingensis*. – World Journal of Microbiology & Biotechnology 30(4): 1285-1290. https://doi.org/10.1007/s11274-013-1554-3.

[78] Huang, L., Li, T., Liu, C., Quan, X., Chen, L., Wang, A., Chen, G. (2013): Synergetic interactions improve cobalt leaching from lithium cobalt oxide in microbial fuel cells. – Bioresource Technology 128: 539-546. https://doi.org/10.1016/j.biotech.2012.11.011.

[79] Iqbal, J., Tirmizi, S. A., Shah, M. H. (2012): Non-carcinogenic health risk assessment and source apportionment of selected metals in source freshwater Khanpur Lake, Pakistan. – Bulletin of Environmental Contamination & Toxicology 88: 177-181. https://doi.org/10.1007/s00128-011-0480-z.

[80] Jadoon, S., Malik, A. (2018): A Review of formation, toxicity of reactive oxygen species by heavy metals and tolerance in plants. – International Journal of Biochemistry Research & Review 21(2): 1-12. https://doi.org/10.9734/IJBCRR/2018/38670.

http://www.aloki.hu ● ISSN 1589 1623 (Print) ● ISSN 1785 0037 (Online)
DOI: http://dx.doi.org/10.15666/aeer/1705_1141911449

[81] Jain, V., Nainawatee, H. S. (2000): Cobalt reduces nitrate inhibition of nodulation in mungbean (*Vigna radiata*). – Biology & Fertility of Soils 31(6): 522-524. https://doi.org/10.1007/s003740000203.

[82] Jayasiri, H. B., Vennila, A., Purushothaman, C. S. (2014): Spatial and temporal variability of metals in inter-tidal beach sediment of Mumbai, India. – Environmental Monitoring & Assessment 186(2): 1101-1111. https://doi.org/10.1007/s10661-013-3441-7.

[83] Jonnalagadda, S. B., Kindeness, A., Kubayi, S., Cele, M. N. (2008): Macro, minor and toxic elemental uptake and distribution in *Hypoxis hemerocallidea*, "the African Potato"-an edible medicinal plant. – Journal of Environmental Science & Health, B 43(3): 271-280. https://doi.org/10.1080/03601230701771461.

[84] Kabata-Pendias, A., Pendias, H. (2001): Trace Elements in Soils and Plants. Third Ed. – CRC Press, Boca Raton, FL.

[85] Kadim, I. T., Mahgoub, O., Al-Ajmi, D., Al-Habsi, K. R., Johnson, E. H. (2006): Comparative effects of low levels of dietary cobalt and parenteral injections of vitamin B_{12} on body dimensions in different breeds of Omani goats. – Small Ruminant Research 66(1-3): 244-252. https://doi.org/10.1016/j.smallrumres.2005.09.018.

[86] Kang, J., Choi, M. S., Lee, C. B. (2009): Atmospheric metal and phosphorus concentrations, inputs, and their biogeochemical significances in the Japan/East Sea. – Science of the Total Environment 407(7): 2270-2284. https://doi.org/10.1016/j.scitotenv.2008.11.047.

[87] Karuppanapandian, T., Kim, W. (2013): Cobalt-induced oxidative stress causes growth inhibition associated with enhanced lipid peroxidation and activates antioxidant responses in Indian mustard (*Brassica juncea* L.) leaves. – Acta Physiologiae Plantarum 35(8): 2429-2443. https://doi.org/10.1007/s11738-0131277-y.

[88] Keeling, S. M., Stewart, R. B., Anderson, C. W. N., Robinson, B. H. (2003): Nickel and cobalt phytoextraction by the hyperaccumulator Berkheya coddii: implications for polymetallic phytomining and phytoremediation. – International Journal of Phytoremediation 5(3): 235-244. https://doi.org/10.1080/16226510390255689.

[89] Klavins, M., Potapovics, O., Rodinov, V. (2009): Heavy metals in fish from lakes in Lativia: concentrations and trends of changes. – Bulletin of Environmental Contamination & Toxicology 82(1): 96-100. https://doi.org/10.1007/s00128-008-9510-x.

[90] Koch, D., Nies, D. H., Grass, G. (2007): The RcnRA (YohLM) system of Escherichia coli: a contection between nickel, cobalt and iron homeostasis. – Biometals 20(5): 759-771. https://doi.org/10.1007/s10534-006-9039-6.

[91] Koigoora, S., Ahmad, I., Pallela, R., Janapala, V. R. (2013): Spatial variation of potentially toxic elements in different grain size fractions of marine sediments from Gulf of Mannar, India. – Environmental Monitoring & Assessment 185(9): 7581-7589. https://doi.org/10.1007M0661-013-3120-8.

[92] Kosiorek, M., Wyszkowski, M. (2019a): Content of macronutrients in oat (*Avena sativa* L.) after remediation of soil polluted with cobalt. – Environmental Monitoring & Assessment 191(389): 1-15. https://doi.org/10.1007/s10661-019-7529-6.

[93] Kosiorek, M., Wyszkowski, M. (2019b): Effect of neutralising substances on reducing influence of cobalt on the content of selected elements in soil. – International Agrophysics 33(2): 153-159. https://doi.org/10.31545/intagr/104618.

[94] Kosiorek, M., Wyszkowski, M. (2019c): Effect of neutralizing substances on the content of trace elements in soil contaminated with cobalt. – Environment Protection Engineering 45(1): 45-55. https://doi.org/10.5277/epe190104.

[95] Kosiorek, M., Wyszkowski, M. (2019d): Remediation of cobalt polluted soil after application of selected substances and using oat (*Avena sativa* L.). – Environmental Science & Pollution Research 26: 16762-16780. https://doi.org/10.1007/s11356-019-05052-x.

http://www.aloki.hu ● ISSN 1589 1623 (Print) ● ISSN 1785 0037 (Online)
DOI: http://dx.doi.org/10.15666/aeer/1705_1141911449

[96] Kukier, U., Peters, C. A., Chaney, R., Angle, J. S., Roserberg, R. (2004): The effect of pH on metal accumulation in two *Alyssum* species. – Journal of Environmental Quality 33(6): 2090-2102.

[97] Kun-Tai, L., Dong-Hong, L., Ying-Ping, Z., Yong-Hong, W., Ju, C., Si-Liang, Z. (2008): Influence of Zn^{2+}, Co^{2+} and dimethylbenzimidazole on vitamin B_{12} biosynthesis by *Pseudomonas denitrificans*. – World Journal of Microbiology & Biotechnology 24: 2525-2530. https://doi.org/10.1007/s11274-008-0770-y.

[98] Kuoppamäki, K., Setälä, H., Rantalainen, A. L., Kotze, D. J. (2014): Urban snow indicates pollution originating from road traffic. – Environmental Pollution 195: 56-63. https://doi.org/10.1016/j.envpol.2014.08.019.

[99] Lalah, J. O., Njogu, S. N., Wandiga, S. O. (2009): The effects of Mn^{2+}, Ni^{2+}, Cu^{2+}, Co^{2+} and Zn^{2+} ions on pecticide adsorption and mobility in a topical soil. – Bulletin of Environmental Contamination & Toxicology 83(3): 352-358. https://doi.org/10.1007/s00128-009-9746-0.

[100] Lavoie, M., Fortin, C., Campbell, P. G. C. (2012): Influence of essential elements on cadmium uptake and toxicity in a unicellular green alga: the protective effect of trace zinc and cobalt concentrations. – Environmental Toxicology & Chemistry 31(7): 1445-1452. https://doi.org/10.1002/ect.1855.

[101] Lefebvre, O., Al-Mamun, A., Ooi, W. K., Tang, Z., Chua, D. H., Ng, H. Y. (2008): An insight into cathode options for microbial fuel cells. – Water Science & Technology 57(12): 2031-2035 https://doi.org/10.2166/wst.2008.611.

[102] Li, X. L., Chen, C. L., Chang, P. P., Yu, S. M., Wu, W. S., Wang, X. K. (2009): Comparative studies of cobalt sorption and desorption on bentonite, alumina and silica: effect of pH and fulvic acid. – Desalination 244(1-3): 283-292. https://doi.org/10.1016/j.desal.2008.04.045.

[103] Li, Z., Feng, X., Bi, X., Li, G., Lin, Y., Sun, G. (2014): Probing the distribution and contamination levels of 10 trace metal/metalloids in soil near a Pb/Zn smelter in Middle China. – Environmental Science & Pollution Research 21(6): 4149-4162. https://doi.org/10.1007/s11356-013-2407-1.

[104] Liu, Z. S., Erhan, S. Z. (2002): Conversion of soybean oil into ion exchange resins: Removal of copper (II), nickel (II) and cobalt (II) ions from dilute aqueous solution using cocarboxylate-containing resin. – Journal of Applied Polymer Science 84: 2386-2396. https://doi.org/10.1002/app.10504.

[105] Lock, K., De Schamphelaere, K. A. C., Because, S., Criel, P., Van Eeckhout, H., Janssen, C. R. (2006): Development and validation of an acute biotic ligand model (BLM) predicting cobalt toxicity in soil to the potworm *Enchytraeus albidus*. – Soil Biology & Biochemistry 38(7): 1924-1932. https://doi.org/10.1016/j.soilbio.2005.12.014.

[106] Luo, D., Zheng, H., Chen, Y., Wang, G., Fenghua, D. (2010): Transfer characteristics of cobalt from soil to crops in the suburban areas of Fujian Province, Southeast China. – Journal of Environmental Management 91(11): 2248-2253. https://doi.org/10.1016/j.jenvman.2010.06.001.

[107] Maguire, J. L., Collins, R. A. (2001): Effects of cobalt hexammine on folding and self-cleavage of the Neurospora VS Ribozyme. – Journal of Molecular Biology 309: 45-56. https://doi.org/10.1006/jmbi.2001.4625.

[108] Mahapatra, P. S., Ray, S., Das, N., Mohanty, A., Ramulu, T. S., Das, T., Chaudhury, G. R., Das, S. N. (2013): Urban air-quality assessment and source apportionment studies for Bhubaneshwar, Odisha. – Theoretical & Applied Climatology 112(1): 243-251. https://doi.org/10.1007/s00704-012-0732-9.

[109] Malik, R. N., Zeb, N. (2009): Assessment of environmental contamination using feathers of Bubulcus ibis L., as a biomonitor of heavy metal pollution, Pakistan. – Ecotoxicology 18(5): 522-536. https://doi.org/10.1007/s10646-009-0310-9.

[110] Mansouri, B., Pourkhabbaz, A., Babaei, H., Hoshyari, E., Khodaparast, S. H., Mirzajani, A. (2012): Assessment of trace-metal concentrations in Western Reef heron (*Egretta*

http://www.aloki.hu ● ISSN 1589 1623 (Print) ● ISSN 1785 0037 (Online)
DOI: http://dx.doi.org/10.15666/aeer/1705_1141911449

gularis) and Siberian gull (*Larus heuglini*) from southern Iran. – Archives of Environmental Contamination & Toxicology 63(2): 280-287. https://doi.org/10.1007/s00244-012-9762-7.

[111] Marrero, J., Auling, G., Coto, O., Nies, D. H. (2007): High- level resistance to cobalt and nickel but probably no transenvelope efflux: metal resistance in the Cuban Serratia marcescens Strain C-1. – Microbial Ecology 53(1): 123-133. https://doi.org/10.1007/s00248-006-9152-7.

[112] Muthaura, C., Mucheru-Muna, M., Zingore, S., Kihara, J., Muthamia, J. (2017): Effect of application of different nutrients on growth and yield parameters of maize (Zea mays), case of Kandara Murang'a County. – ARPN Journal of Agricultural & Biological Science 12(1): 19-33.

[113] McLeod, K. W., Ciravolo, T. (2007): Cobalt uptake by *Nyssa aquatica*, Nyssa sylvatica var. *Biflora* and *Taxodium distichum* seedlings. – Wetlands 27(1): 40-43. https://doi.org/10.1672/0277-5212(2007)27[40:CUBNAN]2.0.CO;2.

[114] Minamihata, K., Goto, M., Kamiya, N. (2012): Activation of *Pyrococcus furiosus* alkaline phosphatase by divalent metal ions. – Biotechnology Letters 34(11): 2055-2060. https://doi.org/10.1007/s10529-012-0998-0.

[115] Miranda, R. M., Tomaz, E. (2008): Characterization of urban aerosol in Campinas, São Paulo, Brazil. – Atmospheric Research 87(2): 147-157. https://doi.org/10.1016/j.atmosres.2007.08.002.

[116] Modrzewska, B., Wyszkowski, M. (2014): Trace metals content in soils along the State Road 51 (northeastern Poland). – Environmental Monitoring & Assessment 186(4): 2589-2597. https://doi.org/10.1007/s10661-013-3562-z.

[117] Mohiuddin, K. M., Otomo, K., Ogawa, Y., Shikazono, N. (2012): Seasonal and spatial distribution of trace elements in the water and sediments of the Tsurumi River in Japan. – Environmental Monitoring & Assessment 184(1): 265-279. https://doi.org/10.1007/s10661-011-1966-1.

[118] Mollah, A. S., Begum, A. (2001): A study on transfer factors of Co-60 and Zn-65 from soil to plants in the tropical environment of Bangladesh. – Environmental Monitoring & Assessment 68(1): 91-97. https://doi.org/10.1023/A:1010791007732.

[119] Mukherjee, S., Kaviraj, A. (2011): Ecotoxicological assessment of cobalt used as supplement in the diet of common carp *Cyprinus carpio*. – Bulletin of Environmental Contamination & Toxicology 87(5): 527-530. https://doi.org/10.1007/s00128-011-0384-y.

[120] Murtaza, G., Ghafoor, A., Qadir, M. (2008): Accumulation and implications cadmium, cobalt and manganese in soils and vegetables irrigated with city effluent. – Journal of the Science of Food & Agriculture 88(1): 100-107. https://doi.org/10.1002/jsfa.

[121] Nagpal, N. K. (2004): Water Quality Guidelines for Cobalt. – Ministry of Water, Land and Air Protection, Water Protection Section, Water, Air and Climate Change Branch, Victoria.

[122] Narendrula, R., Nkongolo, K. K., Beckett, P. (2012): Comparative soil metal analyses in Sudbury (Ontario, Canada) and Lubumbashi (Katanga, DR-Kongo). – Bulletin of Environmental Contamination & Toxicology 88(2): 187-192. https://doi.org/10.1007/s00128-011-0485-7.

[123] Nirmal-Kumar, J. I., Soni, H., Kumar, R. N. (2007): Characterization of heavy metals in vegetables using inductive coupled plasma analyzer (ICPA). – Journal of Environmental Science & Management 11(3): 75-79. https://doi.org/10.4314/jasem.v11i3.55131.

[124] Norouzi, M., Mansouri, B., Hamidian, A. H., Ebrahimi, T., Kardoni, F. (2012): Comparison of the metal concentrations in the feathers of three bird species from southern Iran. – Bulletin of Environmental Contamination & Toxicology 89(5): 1082-1086. https://doi.org/10.1007/s00128-012-0798-1.

http://www.aloki.hu ● ISSN 1589 1623 (Print) ● ISSN 1785 0037 (Online)
DOI: http://dx.doi.org/10.15666/aeer/1705_1141911449

[125] Nowak, J., Szymczak, J., Słobodzian, T. (2003): The test of qualification 50% threshold of toxicity of doses different heavy metals for soil phosphatases. – Zeszyty Problemowe Postępów Nauk Rolniczych 492: 241-248.
[126] Obiri, S. (2007): Determination of heavy metals in water from boreholes in Dumasi in the Wassa West District of western region of Republic of Ghana. – Environmental Monitoring & Assessment 130(1-3): 455-463. https://doi.org/10.1007/s10661-006-9435-y.
[127] Ochieng, E. Z., Lalah, J. O., Wandiga, S. O. (2008): Water quality and trace metal distribution in a pristine Lake in the Lake basin in Kenya. – Bulletin of Environmental Contamination & Toxicology 80(4): 362-368. https://doi.org/10.1007/s00128-008-9372-2.
[128] Ochieng, E. Z., Lalah, J. O., Wandiga, S. O. (2009): Anthropogenic sources of heavy metals in the Indian Ocean coast of Kenya. – Bulletin of Environmental Contamination & Toxicology 83(4): 600-607. https://doi.org/10.1007/s00128-009-9807-4.
[129] Padovan, A., Munksgaard, N., Alvarez, B., McGuinness, K., Parry, D., Gibb, K. (2012): Trace metal concentrations in the tropical sponge Spheciospongia vagabunda at a sewage outfall: synchrotron X-ray imaging reveals the micron-scale distribution of accumulated metals. – Hydrobiologia 687(1): 275-288. https://doi.org/10.1007/s10750-011-0916-9.
[130] Page, V., Feller, U. (2005): Selective transport of zinc, manganese, nickel, cobalt and cadmium in the root system and transfer to the leaves in young wheat plants. – Annals of Botany 96(3): 425-434. https://doi.org/10.1093/aob/mci189.
[131] Pathak, P. N., Choppin, G. R. (2009): Effects of pH, ionic strength, temperature and complexing anions on the sorption behaviour of cobalt on hydrous silica. – Soil & Sediment Contamination 5(18): 590-602. https://doi.org/10.1080/15320380903085709.
[132] Peca, L., Kós, P. B., Máté, Z., Farsang, A., Vass, I. (2008): Construction of bioluminescent cyanobacterial reporter strains for detection of nickel, cobalt and zinc. – FEMS Microbiology Letters 289(2): 258-264. https://doi.org/ 10.1111/j.1574-6968.2008.01393.x.
[133] Pietrodangelo, A., Pareti, S., Perrino, C. (2014): Improved identification of transition metals in airborne aerosols by SEM-EDX combined backscattered and secondary electron microanalysis. – Environmental Science & Pollution Research 21(6): 4023-4031. https://doi.org/10.1007/s11356-013-2261-1.
[134] Pulgarín, J. A., Bermejo, L. F., Durán, A. C. (2013): Fast simultaneous determination of traces of Cu(II) and Co(II) in soils and sediments with the luminol/perborate chemiluminescent system. – Environmental Monitoring & Assessment 185(1): 573-580. https://doi.org/10.1007M0661-012-2576-2.
[135] Qiu, W., Zheng, Y. (2009): Removal of lead, copper, nickel, cobalt, and zinc from water by a cancrinite-type zeolite synthesized from fly ash. – Chemical Engineering Journal 145: 483-488. https://doi.org/10.1016/j.cej.2008.05.001.
[136] Ramani, S., Dragun, Z., Kapetanović, D., Kostov, V., Jordanova, M., Erk, M., Hajrulai-Musliu, Z. (2014): Surface water characterization of three rivers in the lead/zinc mining region of northeastern Macedonia. – Archives of Environmental Contamination & Toxicology 66(4): 514-528. https://doi.org/10.1007/s00244-014-0012-z.
[137] Rancelis, V., Cesniene, T., Kleizaite, V., Zvingila, D., Balciuniene, L. (2012): Influence of cobalt uptake by Vicia faba seeds on chlorophyll morphosis induction, SOD polymorphism, and DNA methylation. – Environmental Toxicology 27(1): 32-41. https://doi.org/10.1002/tox.20609.
[138] Rashed, M. N. (2001): Monitoring of environmental heavy metals in fish from Nasser Lake. – Environment International 27(1): 27-33. https://doi.org/10.1016/S0160-4120(01)00050-2.
[139] Regulation of the Polish Minister of the Environment of 26 January (2010): On the on reference values for various substances in the air. – Dziennik Ustaw (Official Journal) 16 poz. 87.

http://www.aloki.hu ● ISSN 1589 1623 (Print) ● ISSN 1785 0037 (Online)
DOI: http://dx.doi.org/10.15666/aeer/1705_1141911449

[140] Regulation of the Polish Minister of the Environment of 18 November (2014): On the conditions to be met when sewage into water or soil and on substances particularly harmful to the aquatic environment (as amended). – Dziennik Ustaw (Official Journal) poz. 1800.
[141] Regulation of the Polish Minister of the Environment of 21 December (2015): On the criteria and method of evaluation of groundwater. – Dziennik Ustaw (Official Journal) poz. 85.
[142] Regulation of the Polish Minister of the Environment of 21 July (2016): On the classification of the status of surface waters and environmental quality standards for priority substances. – Dziennik Ustaw (Official Journal) poz. 1187.
[143] Regulation of the Polish Minister of the Environment of 1 September (2016): On the manner of conducting the assessment of contamination of the surface of the earth. – Dziennik Ustaw (Official Journal) poz. 1395.
[144] Rizzio, E., Bergamaschi, G., Profumo, A., Gallorini, M. (2001): The use of neutron activation analysis for particle size fractionation and chemical characterization of trace elements in urban air particulate matter. – Journal of Radioanalytical and Nuclear Chemistry 248(1): 21-28. https://doi.org/10.1023/A: 1010605519848.
[145] Rognerud, S., Dauvalter, V. A., Fjeld, E., Skjelkvåle, B. L., Christensen, G., Kashulin, N. (2013): Spatial trends of trace-element contamination in recently deposited lake sediment around the Ni-Cu smelter at nikel, Kola Peninsula, Russian Arctic. – AMBIO 42(6): 724-736. https://doi.org/10.1007/s13280-013-0384-8.
[146] Rong, L., Xun-Liu, H., Zi-Tao, J. (2008): Determination of trace amounts of cobalt in foods by polymer-phase fluorophotometry with thiamine. – European Food Research & Technology 227(1): 111-116. https://doi.org/10.1007/s00217-007-0699-4.
[147] Ruta, L., Paraschivescu, C., Matache, M., Avramescu, S., Farcasanu, I. C. (2010): Removing heavy metals from synthetic effluents using "kamikaze" *Saccharomyces cerevisiae* cells. – Applied Microbiology & Biotechnology 85(3): 763-771. https://doi.org/10.1007/s00253-009-2266-3.
[148] Ryuko, S., Ma, Y., Ma, N., Sakaue, M., Kuno, T. (2012): Genome-wide screen reveals novel mechanisms for regulating cobalt uptake and detoxification in fission yeast. – Molecular Genetics & Genomics 287(8): 651-662. https://doi.org/10.1007/s00438-012-0705-9.
[149] Rzymski, P., Niedzielski, P., Klimaszyk, P., Poniedziałek, B. (2014): Bioaccumulation of selected metals in bivalves (Unionidae) and *Phragmites australis* inhabiting a municipal water reservoir. – Environmental Monitoring & Assessment 186(5): 3199-3212. https://doi.org/10.1007M0661-013-3610-8.
[150] Saad, L., Parmentier, I., Colinet, G., Malaisse, F., Faucon, M. P., Meerts, P., Mahy, G. (2012): Investigating the vegetation-soil relationships on the copper-cobalt rock outcrops of Katanga (D. R. Congo), an essential step in a biodiversity conservation plan. – Restoration Ecology 20(3): 405-415. https://doi.org/10.1111/j.1526-100X.2011.00786.x.
[151] Saaltink, R., Griffioen, J., Mol, G., Birke, M. (2014): Geogenic and agricultural controls on the geochemical composition of European agricultural soils. – Journal of Soils & Sediments 14(1): 121-137. https://doi.org/10.1007/s11368-013-0779-y.
[152] Sandergaard, J. (2013): Dispersion and bioaccumulation of elements from an open-pit olivine mine in Southwest Greenland assessed using lichens, seaweeds, mussels and fish. – Environmental Monitoring & Assessment 185(5): 7025-7035. https://doi.org/10.1007/s10661-013-3082-x.
[153] Sassman, S. A., Sarmah, A. K., Lee, L. S. (2007): Sorption of tylosin A, D, and A-aldol and degradation of tylosin A in soils. – Environmental Toxicology & Chemistry 26(8): 1629-1635.
[154] Schmitt, C. J., Brumbaugh, W. G., May, T. W. (2009): Concentrations of cadmium, cobalt, lead, nickel, and zinc in blood and fillets of northern hog sucker (*Hypentelium nigricans*) from streams contaminated by lead-zinc mining: implications for monitoring.

http://www.aloki.hu ● ISSN 1589 1623 (Print) ● ISSN 1785 0037 (Online)
DOI: http://dx.doi.org/10.15666/aeer/1705_1141911449

– Archives of Environmental Contamination & Toxicology 56(3): 509-524. https://doi.org/10.1007/s00244-009-9288-9.

[155] Sheppard, P. R., Speakman, R. J., Ridenour, G., Glascock, M. D., Farris, C., Witten, M. L. (2007): Spatial patterns of tungsten and cobalt in surface dust of Fallon, Nevada. – Environmental Geochemistry & Health 29(5): 405-412. https://doi.org/10.1007/s10653-007-9085-1.

[156] Singh, A. K., Cameotra, S. S. (2013): Efficiency of lipopeptide biosurfactants in removal of petroleum hydrocarbons and heavy metals from contaminated soil. – Environmental Science & Pollution Research 20(10): 7367-7376. https://doi.org/10.1007/s113556-013-1752-4.

[157] Singh, S. M., Sharma, J., Gawas Sakhalkar, P., Upadhyay, A. K., Naik, S., Pedneker, S. M., Ravindra, R. (2013): Atmospheric deposition studies of heavy metals in Arctic by comparative analysis of lichens and cryoconite. – Environmental Monitoring & Assessment 185(2): 1367-1376. https://doi.org/10.1007/s10661-012-2638-5.

[158] Soylak, M., Cihan, Z., Yilmaz, E. (2012): Evaluation of trace element contents of some herbal plants and spices retailed in Kayseri, Turkey. – Environmental Monitoring & Assessment 184(6): 3455-3461. https://doi.org/10.1007/s10661-011-2199-z.

[159] Soylak, M., Cihan, Z., Yilmaz, E. (2013): Heavy metal contents of organically produced, harvested, and dried fruit samples from Kayseri, Turkey. – Environmental Monitoring & Assessment 185(3): 2577-2583. https://doi.org/10.1007M0661-012-2741-7.

[160] Söyüt, H., Beydemir, S. (2011): The impact of heavy metals on the activity of carbonic anhydrase from rainbow trout (*Oncorhynchus mykiss*) kidney. – Toxicology and Industrial Health 28(4): 296-305. https://doi.org/10.1177/0748233711410914.

[161] Stangl, G. I., Roth Maier, D. A., Kirchgessner, M. (2000): Vitamin B-12 deficiency and hyperhomocysteinemia are partly ameliorated by cobalt and nickel supplementation in pigs. – Journal of Nutrition 130(12): 3038-3044. https://doi.org/10.1093/jn/130.12.3038.

[162] Sukdeo, P., Pillay, S., Bissessur, A. (2012): A geochemical assessment of the middle and lower Mvoti river system, KwaZulu-Natal, South Africa. – Environmental Earth Sciences 66(2): 481-487. https://doi.org/10.1007/s12665-011-1256-9.

[163] Sun, X., Hao, H., Liu, Z., Zhao, F., Song, J. (2019): Tracing global cobalt flow: 1995-2015. – Resources, Conservation & Recycling 149: 45-55. https://doi.org/10.1016/j.resconrec.2019.05.009.

[164] Swarnalatha, K., Letha, J., Ayoob, S. (2013): An investigation into the heavy metal burden of Akkulam-Veli Lake in south India. – Environmental Earth Sciences 68(3): 795-806. https://doi.org/10.1007/s12665-012-1780-2.

[165] Swarup, D., Patra, R. C., Naresh, R., Kumar, P., Shekhar, P., Balagangatharathilagar, M. (2006): Lowered blood copper and cobalt contents in goats reared around lead–zinc smelter. – Small Ruminant Research 63(3): 309-313. https://doi.org/10.1016/j.smallrumres.2005.03.011.

[166] Sytschev, A. E., Vadchenko, S. G., Kamynina, O. K., Balikhina, E. N., Plashichina, I. G., Krylova, E. A., Grigor'yan, A. S., Toporkova, K., Konovalov, A. N., Selezneva, I. I. (2009): Porous materials from titanium-cobalt alloys for hybrid implants. – Bulletin of Experimental Biology & Medicine 147(1): 52-58. https://doi.org/10.1007/s10517-009-0428-z.

[167] Tappero, R., Peltier, E., Gräfe, M., Heidel, K., Ginder-Vogel, M., Livi, K. J. T., Rivers, M. L., Marcus, M. A., Chaney, R. L., Sparks, D. L. (2007): Hyperaccumulator *Alyssum murale* relies on a different metal storage mechanism for cobalt than for nickel. – New Phytologist 175(4): 641-654. https://doi.org/10.1111/j.1469-8137.2007.02134.x.

[168] Taugbol, O., Karlengen, I. J., Salbu, B., Aastveit, A. H., Harstad, O. M. (2010): Intravenous injections of cobalt reduce fatty acid desaturation products in milk and blood of lactating cows. – Journal of Animal Physiology & Animal Nutrition 94(5): 635-640. https://doi.org/10.1111/j.1439-0396.2009.00950.x.

http://www.aloki.hu ● ISSN 1589 1623 (Print) ● ISSN 1785 0037 (Online)
DOI: http://dx.doi.org/10.15666/aeer/1705_1141911449

[169] Tepe, Y. (2009): Metal concentrations in eight fish species from Aegean and Mediterranean Seas. – Environmental Monitoring & Assessment 159(1-4): 501-509. https://doi.org/10.1007/s10661-008-0646-2.
[170] Thyssen, J. P., Jensen, P., Lidén, C., Julander, A., Jellesen, M. S., Menné, T., Johansen, J. D. (2011): Assessment of nickel and cobalt release from 200 unused hand-held work tools for sale in Denmark-Sources of occupational metal contact dermatitis? – Science of the Total Environment 409(22): 4663-4666. https://doi.org/10.1016/j.scitotenv.2011.07.056.
[171] Tiffany, M. E., Spears, J. W. (2005): Differential responses to dietary cobalt in finishing steers fed corn-versus barley-based diets. – Journal of Animal Science 83(11): 2580-2589. https://doi.org/10.2527/2005.83112580x.
[172] Trejo-Tapia, G., Jimenez-Aparicio, A., Rodriguesz-Monroy, M., De Jesus-Sanchez, A., Gutierrez-Lopez, G. (2001): Influence of cobalt and other microelements on the production of betalains and the growth of suspension cultures of *Beta vulgaris*. – Plant Cell Tissue & Organ Culture 67(1): 19-23. https://doi.org/10.1023/A:1011684619614.
[173] Türkmen, M., Türkmen, A., Tepe, Y. (2011): Comparison of metals in tissues of fish from Paradeniz Lagoon in the coastal area of northern east Mediterranean. – Bulletin of Environmental Contamination & Toxicology 87(4): 381-385. https://doi.org/10.1007/s00128-011-0381-1.
[174] Ulusoy, H. I., Gürkan, R., Demir, Ö., Ulusoy, S. (2012): Micelle-mediated extraction and flame atomic absorption spectrometric method for determination of trace cobalt ions in beverage samples. – Food Analytical Methods 5(3): 454-463. https://doi.org/10.1007/s12161-011-9268-3.
[175] Upadhyaya, D., Survaiya, M. D., Basha, S., Mandal, S. K., Thorat, R. B., Haldar, S., Goel, S., Dave, H., Baxi, K., Trivedi, R. H., Mody, K. H. (2014): Occurrence and distribution of selected heavy metals and boron in groundwater of the Gulf of Khambhat region, Gujarat, India. – Environmental Science & Pollution Research 21(5): 3880-3890. https://doi.org/10.1007/s11356-013-2376-4.
[176] USEPA (2000): Radionuclides Notice of Data Availability Technical Support Document. Targeting and Analysis Branch Standards and Risk Management Division Office of Ground Water and Drinking Water United States Environmental Protection Agency. – USEPA Office of Ground Water and Drinking Water in collaboration with USEPA Office of Indoor Air and Radiation United States Geological Survey. http://www.epa.gov/ogwdw/radionuclides/pdfs/regulation_radionuclides_rulemaking_techsupportdoc.pdf.
[177] Valera, P., Zavattari, P., Albanese, S., Cicchella, D., Dinelli, E., Lima, A., De Vivo, B. (2014): A correlation study between multiple sclerosis and type 1 diabetes incidences and geochemical data in Europe. – Environmental Geochemistry & Health 36(1): 79-98. https://doi.org/10.100i/s10653-013-9520-4.
[178] Van der Ent, A., Baker, A. J. M., Reeves, R. D., Pollard, A. J., Schat, H. (2013): Hyperaccumulators of metal and metalloid trace elements: Facts and fiction. – Plant & Soil 362(1): 319-334. https://doi.org/10.1007/s11104-012-1287-3.
[179] Waheed, S., Kamal, A., Malik, R. N. (2014): Human health risk from organ-specific accumulation of toxic metals and response of antioxidants in edible fish species from Chenab River, Pakistan. – Environmental Science & Pollution Research 21(6): 4409-4417. https://doi.org/10.1007/s11356-013-2385-3.
[180] Wang, C. X., Zhu, W., Peng, A., Guichreit, R. (2001): Comparative studies on the concentration of rare earth elements and heavy metals in the atmospheric particulate matter in Beijing, China, and in Delft, the Netherlands. – Environment International 26(5-6): 309-313. https://doi.org/10.1016/S0160-4120(01)00005-8.
[181] Wang, F., Yao, J., Si, Y., Chen, H., Russel, M., Chen, K., Qian, Y., Zaray, G., Bramanti, E. (2010): Short-time effect of heavy metals upon microbial community activity. – Journal of Hazardous Materials 173(1-3): 510-516. DOI: 10.1016/j.jhazmat.2009.08.114.

http://www.aloki.hu ● ISSN 1589 1623 (Print) ● ISSN 1785 0037 (Online)
DOI: http://dx.doi.org/10.15666/aeer/1705_1141911449

[182] Wang, Y., Xie, W., Wang, D. (2007): Transferable properties of multi-biological toxicity caused by cobalt exposure in Caenorhabditis elegans. – Environmental Toxicology & Chemistry 26(11): 2405-2412. https://doi.org/10.1897/06-646R1.1.
[183] Welp, G. (1999): Inhibitory effects of the total and water-soluble concentrations of nine different metals on the dehydrogenase activity of a loess soil. – Biology & Fertility of Soils 30(1): 132-139. https://doi.org/10.1007/s003740050599.
[184] Wendling, L. A., Kirby, J. K., McLaughlin, M. J. (2009): Aging effects on cobalt availability in soils. – Environmental Toxicology & Chemistry 28(8): 1609-1617. https://doi.org/10.1897/08-544.1.
[185] Werkenthin, M., Kluge, B., Wessolek, G. (2014): Metals in European roadside soils and soil solution - a review. – Environmental Pollution 189: 98-110. https://doi.org/10.1016/j.envpol.2014.02.025.
[186] Witte, C. P., Tiller, S. A., Taylor, M. A., Davies, H. V. (2002): Addition of nickel to Murashige and Skoog medium in plant tissue culture activates urease and may reduce metabolic stress. – Plant Cell Tissue & Organ Culture 68(1): 103-104. https://doi.org/10.1023/A:1012966218478.
[187] Wu, Z., He, M., Lin, C. (2012): Environmental impacts of heavy metals (Co, Cu, Pb, Zn) in surficial sediments of estuary in Daliao River and Yingkou Bay (northeast China): concentration level and chemical fraction. – Environmental Earth Sciences 66(8): 2417-2430. https://doi.org/10.1007/s12665-011-1466-1.
[188] Wyszkowska, J., Wyszkowski, M. (2002): Effect of cadmium and magnesium on microbiological activity in soil. – Polish Journal of Environmental Studies 5(11): 585-591.
[189] Wyszkowska, J., Wyszkowski, M. (2003): Effect of cadmium and magnesium on enzymatic activity in soil. – Polish Journal of Environmental Studies 12(4): 479-485.
[190] Wyszkowska, J., Kucharski, J., Kucharski, M. (2006): Nitrification process in soil contaminated with cobalt. – Polish Journal of Natural Science 20(1): 101-110.
[191] Wyszkowski, M., Sivitskaya, V. (2012): Changes in the content of organic carbon and available forms of macronutrients in soil under the influence of soil contamination with fuel oil and application of different substances. – Journal of Elementology 17(1): 139-148. https://doi.org/10.5601/jelem.2012.17.1.12.
[192] Wyszkowski, M., Wyszkowska, J. (2007): The content of macroelements in spring barley (Hordeum vulgare L.) and thiers relations with the enzymatic activity of cobalt contaminated soil. – Proceeding of SECOTOX Conference and the International Conference on Environmental Management, Engineering, Planning and Economics 1: 181-186.
[193] Wyszkowski, M., Wyszkowska, J. (2009): The effect of contamination with cadmium on spring barley (*Hordeum vulgare* L.) and its relationship with the enzymatic activity of soil. – Fresenius Environmental Bulletin 18(7): 1046-1053.
[194] Wyszkowski, M., Wyszkowska, J., Radziemska, M. (2009): Macroelement content in field of oats (*Avena sativa* L.) cultivated on soils contaminated with copper, zinc, tin, cobalt and manganese. – Ecological Chemistry and Engineering, A 16(10): 1387-1394.
[195] Yabuki, L. N. M., Colaço, C. D., Menegário, A. A., Domingos, R. N., Kiang, C. H., Pascoaloto, D. (2014): Evaluation of diffusive gradients in thin films technique (DGT) for measuring Al, Cd, Co, Cu, Mn, Ni, and Zn in Amazonian rivers. – Environmental Monitoring & Assessment 186(2): 961-969. https://doi.org/10.1007/s10661-013-3430-x.
[196] Yarsan, E., Yipel, M., Dikmen, B., Altintas, L., Ekici, H., Köksal, A. (2014): Concentrations of essential and non-essential toxic trace elements in wild boar (Sus. Scrofa L., 1758) tissues from Southern Turkey. – Bulletin of Environmental Contamination & Toxicology 92(1): 10-14. https://doi.org/10.1007/s00128-013-1134-0.
[197] Zaharescu, D. G., Hooda, P. S., Soler, A. P., Fernandez, J., Burghelea, C. I. (2009): Trace metals and their source in the catchment of the high altitude Lake Respomuso, Central

http://www.aloki.hu ● ISSN 1589 1623 (Print) ● ISSN 1785 0037 (Online)
DOI: http://dx.doi.org/10.15666/aeer/1705_1141911449

Pyrenees. – Science of the Total Environment 407(11): 3546-3553. https://doi.org/10.1016/j.scitotenv.2009.02.026.

[198] Zamani-Hargalani, F., Karbassi, A., Monavari, S. M., Abroomand Azar, P. (2014): A novel pollution index based on the bioavailability of elements: a study on Anzali wetland bed sediments. – Environmental Monitoring & Assessment 186(4): 2329-2348. https://doi.org/10.1007/s10661-013-3541-4.

[199] Zereini, F., Alt, F., Messerschmidt, J., Wiseman, C., Feldmann, I., von Bohlen, A., Müller, J., Liebl, K., Püttmann, W. (2005): Concentration and distribution of heavy metals in urban airborne particulate matter in Frankfurt am Main, Germany. – Environmental Science & Technology 39(9): 2983-2989. https://doi.org/10.1021/es040040t.

[200] Zupančič, N., Skobe, S. (2014): Anthropogenic environmental impact in the Mediterranean coastal area of Koper/Capodistria, Slovenia. – Journal of Soils & Sediments 14(1): 67-77. https://doi.org/10.1007M1368-013-0770-7.

http://www.aloki.hu ● ISSN 1589 1623 (Print) ● ISSN 1785 0037 (Online)
DOI: http://dx.doi.org/10.15666/aeer/1705_1141911449

STUDY ON THE INTERACTION MECHANISM OF FLOW AND SEDIMENT IN AN OPEN CHANNEL CONTAINING VEGETATION

QU, G.* – ZHAO, Z. C. – YAO, S. M. – ZHU, Y. H. – CHEN, D.

Changjiang River Scientific Research Institute, Wuhan, Hubei 430010, China

**Corresponding author*
e-mail: qugeng0516@163.com

(Received 19th Apr 2019; accepted 11th Jul 2019)

Abstract. The understanding of the effect of vegetation on the flow and sediment transport is extremely important for modern river management and water ecological restoration. In this study, the laboratory experiments are carried out to study the 3D flow velocity, turbulence and sediment transport affected by 3 types of flexible vegetation. The results show that the submerged and emergent vegetation generates an obvious flow resistance and significantly alters the vertical distributions of the flow velocity, especially in the vegetated and downstream regions. Due to the influence of vegetation, the flow in downstream generates many vortices with different sizes. Compared with the submerged vegetation, the emergent vegetation has a more obvious influence on the vortex flow. Vegetation also results in a nearly constant fine suspended sediment concentration in the water column for all cases, while the large flow resistance has a stronger filtration effect on the coarse sediment, which leads the coarse sediment to be deposited and the total sediment along the vegetated channel to be gradually refined. The experiment also analyzes the influence of the transverse flow on the suspended sediment transport and the interaction mechanism of flow and sediment.

Keywords: *vegetation, flow velocity, turbulence, sediment transport, vortex flow, diffusion coefficient*

Introduction

Vegetation can be found in abundance in the shore and shallow water region of rivers and plays an important role in influencing the turbulent flow field in a river channel. At present, as people pay more and more attention to the ecological protection of rivers, the research on the problems of flow and sediment transport in vegetated rivers has become one of the hottest topics in river dynamics. For a river, the vegetation tends to increase the flow resistance during the flood periods, increase the water level and thus reduce its overcurrent capacity. Besides, with the growth of vegetation and the increasing resistance, it will change the local flow and the distribution of sediment transport. Therefore, it is important to carry out research on the characteristics of flow and sediment transport in vegetated rivers. The open channel flow movement is usually a boundary layer turbulence. Under certain channel profile conditions (e.g. straight and shallow channel), it can be considered as a two-dimensional flow (Wang and Li, 2002). While affected by the physical and distribution characteristics of vegetation, the flow in

http://www.aloki.hu ● ISSN 1589 1623 (Print) ● ISSN 1785 0037 (Online)
DOI: http://dx.doi.org/10.15666/aeer/1705_1145111473

the vegetated open channel has strong properties of three-dimensional motion. The main differences in the characteristics of the two flow motions are the distribution of flow characteristic parameters, such as flow velocity, turbulence intensity, Reynolds stress, etc. (Stephan and Gutknecht, 2002; Carollo, 2002; Tang et al., 2007. The distribution of the vegetated flow has two or three divisions of the zone in the vertical direction, and the whole distribution in vertical direction does not follow the logarithmic distribution any more. Ikeda and Kanazawa (1996) conducted laboratory experiments on the flow characteristics of flexible vegetation and found that eddies and flow velocity changed significantly near the vegetation. Nezu and Onitsuka (2001) studied the turbulent flow structure in the vegetated open channel and found that the horizontal vortex near free surface was caused by the increase of Froude number and vegetation density. In terms of the maximum turbulence intensity of the flow Ikeda and Kanazawa (1996) found that the maximum turbulence intensity appeared at the top of vegetation, which was consistent with some experimental and numerical simulations. However, some researchers demonstrated that the maximum turbulence intensity of the vegetated flow was generated at the junction of the vegetation's top and non-vegetation zone (Su and Li, 2002). Wilson et al. (2003) proposed that the position of maximum turbulence tends to move toward the free surface with the increase of submergence, for the flexible vegetation with leaves. Sediment transported in the vegetated open channel has also drawn the attention of many researchers. Shi and Cao (2000) found that the presence of vegetation led to a decrease of the coefficient of turbulent diffusion and a significant increase of gravitation. In his opinion, the vegetation can not only block the bed-load transport effectively but also intercept the suspended sediment movement. However, experimental studies by Elliott (2000) on the effects of sedimentation rate by vegetation show that compared with non-vegetation, the presence of vegetation reduced sedimentation rate and made sediment more easily suspended. Lu (2008) investigated the suspended sediment transport in the rigid vegetated open channel and analyzed the influence of vegetation factors on the distribution of turbulence and sediment concentration. Jordanova and James (2003) established an empirical formula for the rate of bed-load transport in non-submerged rigid vegetated open channel by using the analogy of the equation of bed-load transport rate in non-vegetated rivers and his experimental data. Li and Shen (1973) found that compared with the parallel arrangement of vegetation in the open channel, the plum blossom staggered arrangement could obstruct the flow more efficiently and the amount of sediment transport was also relatively small. Therefore, when considering flood control and soil conservation of rivers, the vegetation arrangement in the channel should be reasonably designed.

There is plenty of research on the characteristics of flow and sediment transport in the vegetated open channels at present. Due to the complexity of vegetation morphology and the difficulties of using numerical simulation methods, there are relatively more studies using the experimental flumes. However, there are some problems that still need to be further studied: (1) There are many kinds of aquatic vegetation in river ecosystem, but at present, most of the research mainly focuses on specific types of vegetation, and

http://www.aloki.hu ● ISSN 1589 1623 (Print) ● ISSN 1785 0037 (Online)
DOI: http://dx.doi.org/10.15666/aeer/1705_1145111473

there are few research results on both submerged and emergent vegetation. Therefore, systematic research needs to be strengthened. (2) The research on the turbulent structure of three-dimensional flow in the vegetated open channel has been very thorough, but it is limited to the problems of sediment sample collections and measurement equipment. There is little research on the characteristics of flow and sediment transport within the upstream and downstream region in the partly vegetated open channel. In this paper, three representative submerged and emergent artificial flexible vegetation is used to carry out experimental studies on the characteristics of flow and sediment transport in a partly vegetated open channel. The three-dimensional distribution of flow movement, suspended sediment transport in the partly vegetated open channel is obtained. Based on these, the mechanism of interaction between flow and sediment transport in the partly vegetated open channel is further discussed. These research results aim at further enriching the understanding of the regularity of flow and sediment transport in the vegetated channel and lay a foundation for further research.

Material and Methods

Experimental equipment

All the experiments are conducted in the Hydraulics Laboratory in Changjiang River Scientific Research Institute, Wuhan, China. The experimental apparatus is mainly composed of three pumps, an inlet section to generate fully developed turbulent flow, a test section with a rectangle flume to operate interaction between flow and vegetation, an automatic control system installed at the inlet of the rectangle flume to control the amount of sediment. The re-circulating flume is 0.5 m wide, 0.5 m high and 28 m long, with glass sidewalls and bottom (*Figure 1*). The range of the flume slope is 0‰-5‰. Thin plastic board is laid on the bottom of the flume, on which the simulated vegetation is planted. In order to decrease the inlet turbulence and maintain the uniform flow, a wave dissipation board is set at the inlet of the flume. An automatic water level control system located at the outlet of the flume is used to accurately control the water level. Preliminary experiments are carried out to ensure there is no flow turbulence effect due to the thin plastic board within the measurement region. It is long enough far from the inlet to ensure that the flow through the vegetation is smooth and the measurement data is accurate. A three dimensional Macro-Acoustic Doppler Velocimetry (ADV) (SonTek, San Diego, CA, USA) is used to measure the flow velocity and turbulence at a frequency of 25 Hz with 30 second (s) sampling time. From the initial control experimental run, it is revealed that the sampling frequency is enough to obtain accurate velocity and turbulence characteristics (Li et al., 2015). Thus, 750 data measurements are collected at every location and with post-processing software (WinADV), and an average velocity value is obtained. Measurements at 5 cm below the free surface can not be taken due to ADV limitations. For more information about the application of ADV on flow measurement in a flume, refer to (Qu, 2014). The measuring equipment used in the experiment include electromagnetic flowmeter, the ADV three-dimensional

http://www.aloki.hu ● ISSN 1589 1623 (Print) ● ISSN 1785 0037 (Online)
DOI: http://dx.doi.org/10.15666/aeer/1705_1145111473

flowmeter, the automatic water level meter, Sediment sampler (The instrument uses the siphon principle for sediment sampling), Malvern Mastersizer 2000 particle size analyzer (The instrument uses laser diffraction technology to measure particle size of sediment) and the electronic balance.

(a) Flume (b) Sediment Suppler

(c) Sediment Collector (d) Particle Sizer Analysis System

Figure 1. *Experimental equipment and instruments*

Experimental program

The experiment investigates the affection of the effects on the flow and sediment transport in the open channel, based on the acquired laboratory data conducted using three artificial flexible vegetation (two kinds of submerged flexible vegetation, and one kind of emergent flexible vegetation). The three kinds of artificial vegetation use the same flexible plastic material (the material proportion is 1.35 g/cm^3, the elastic modulus is 0.03×10^5 Mpa). This kind of plastic vegetation has foliage and flexibility characteristics like true plants, which are representative of the vegetation in the riparian zone of rivers, and can simulate nature vegetation drag force in open channel (*Figure 2, Figure 3*). The three kinds of vegetation are used in the experiments with the same arrangement, and ten measured sections are arranged in the partly vegetated open channel (*Figure 4*). The flow and sediment of experimental conditions are as follows: The inlet discharge of the flume is 30 L/s. The outlet water level of the flume is 35 cm, and the amount of sediment at the inlet of the flume is 5.0 g/s. The sediment using in the experiment is a kind of plastic synthetic sand, its wet and dry density is 1.38 t/m^3, 0.67 t/m^3, respectively (Sun and Wei, 2005). *Figure 5a* shows the grading curves of the artificial sediment used for all cases and they follow a similar composition with a median particle size (D_{50}) of 0.18 mm. The maximum slope of the flume using in this experiment is 5/1000. All the experiments are controlled according to the standard of

http://www.aloki.hu ● ISSN 1589 1623 (Print) ● ISSN 1785 0037 (Online)
DOI: http://dx.doi.org/10.15666/aeer/1705_1145111473

uniform flow (the slopes of flume and water surface are the same). In order to obtain the approximately uniform flow if the slope of the water surface in the vegetated area is always larger than the maximum slope of the flume, then the flume is adjusted according to the maximum slope of 5/1000. The experimental results show that the slope of the water surface in upstream and downstream of the vegetated region is less than that in the vegetated region (*Figure 5b*), so the slope of the water surface in upstream and downstream region is less than the slope of the flume. The flow in the upstream and downstream region is the decelerating flow (Yang and Lee, 2007).

Vegetation P1 Vegetation P2 Vegetation P3

Figure 2. *Image of artificial different vegetation*

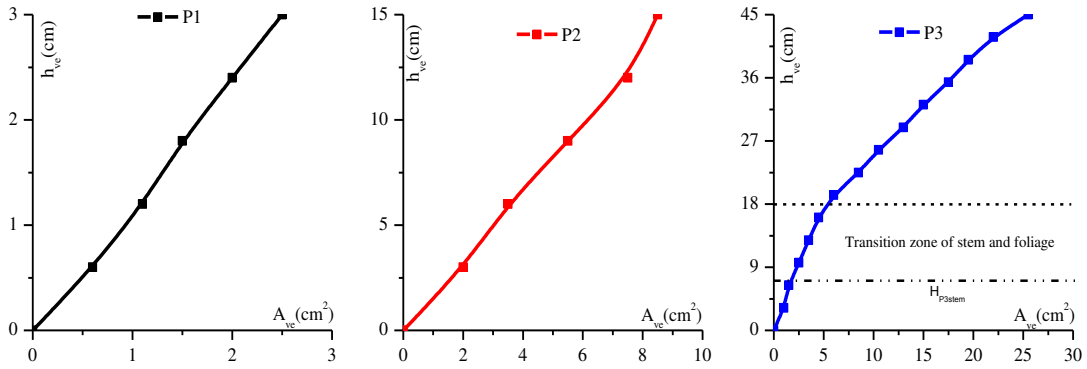

Figure 3. *Profile of the variation of the vegetation cumulative area with respect to the height of vegetation*

There are two points to note in this paper. (1) The flow pattern is different along the stream-wise in the partly vegetated open channel, however, the main research is on the effect of the flow and sediment transport in the partly vegetated channel. (2) The preliminary experiment shows that the sediment transport is basically balanced (the concentration of sediment at inlet and outlet of the open channel is basically the same) in the non-vegetated open channel under the experimental condition of *Table 1* (Case 1). In order to facilitate the comparison with the flow and sediment transport in the open

http://www.aloki.hu ● ISSN 1589 1623 (Print) ● ISSN 1785 0037 (Online)
DOI: http://dx.doi.org/10.15666/aeer/1705_1145111473

channel under different types of vegetation, the flow patterns in the upstream and downstream regions are approximately regarded as a uniform flow.

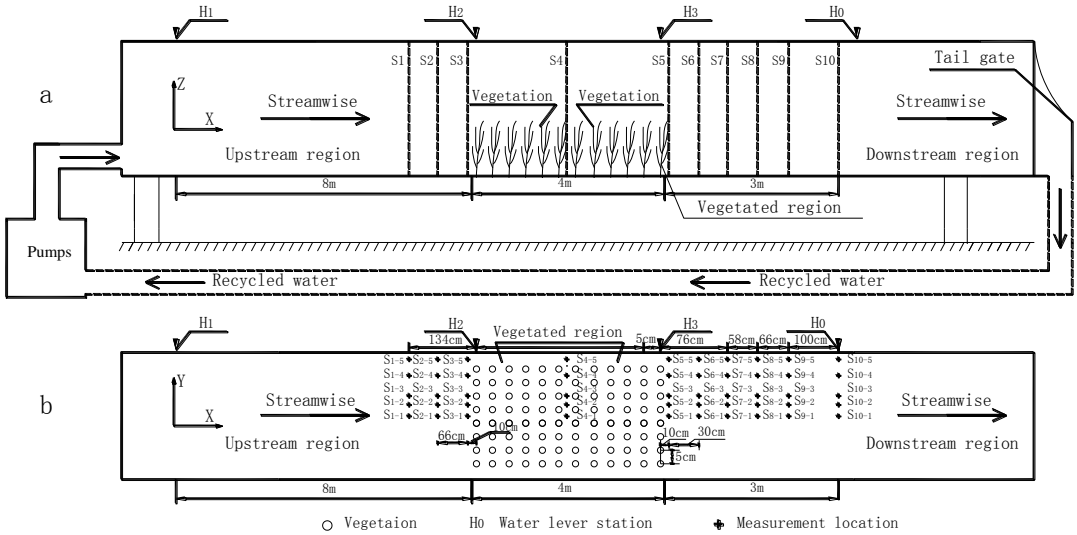

Figure 4. *Schematic diagram of the experimental flume: (a) Side view; (b) Top view (not to scale)*

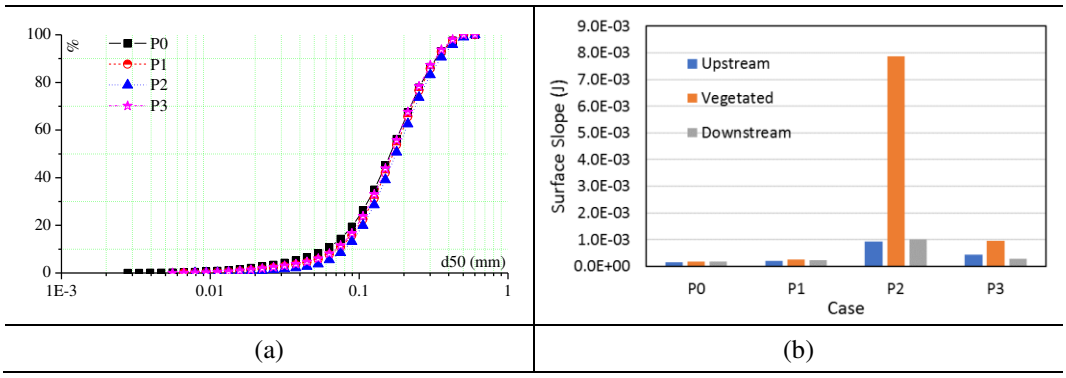

Figure 5. *The grading curves of sediment used and slope of water surface in different regions under different conditions of vegetation*

Table 1. *The conditions of flow and sediment*

Case	Type	Q (L/s)	H_O (cm)	Sa (g/s)	Ua (cm/s)	J (1/1000)	S_L (1/1000)	Remark
1	P0	30	35	5.0	17.15	0.18	0.18	Uniform flow
2	P1	30	35	5.0	17.16	0.30	0.30	Uniform flow
3	P2	30	35	5.0	17.23	0.97	0.97	Uniform flow
4	P3	30	35	5.0	17.31	8.58	5.00	Approximately uniform flow

http://www.aloki.hu ● ISSN 1589 1623 (Print) ● ISSN 1785 0037 (Online)
DOI: http://dx.doi.org/10.15666/aeer/1705_1145111473

Results

Flow velocity characteristic

Longitudinal flow velocity

(1) Flow velocity along stream-wise

To highlight the effect of artificial vegetation on the flow characteristics along the stream-wise, the longitudinal velocity data has been processed and plotted at different positions in the open channel. *Figure 6* represents the vertical distribution of the u-velocity component normalized by Ua at different longitudinal positions in the midline of the open channel. For P0, the vertical distribution of longitudinal flow velocity from S1 to S10 cross-sections basically complies with the logarithmic distribution.

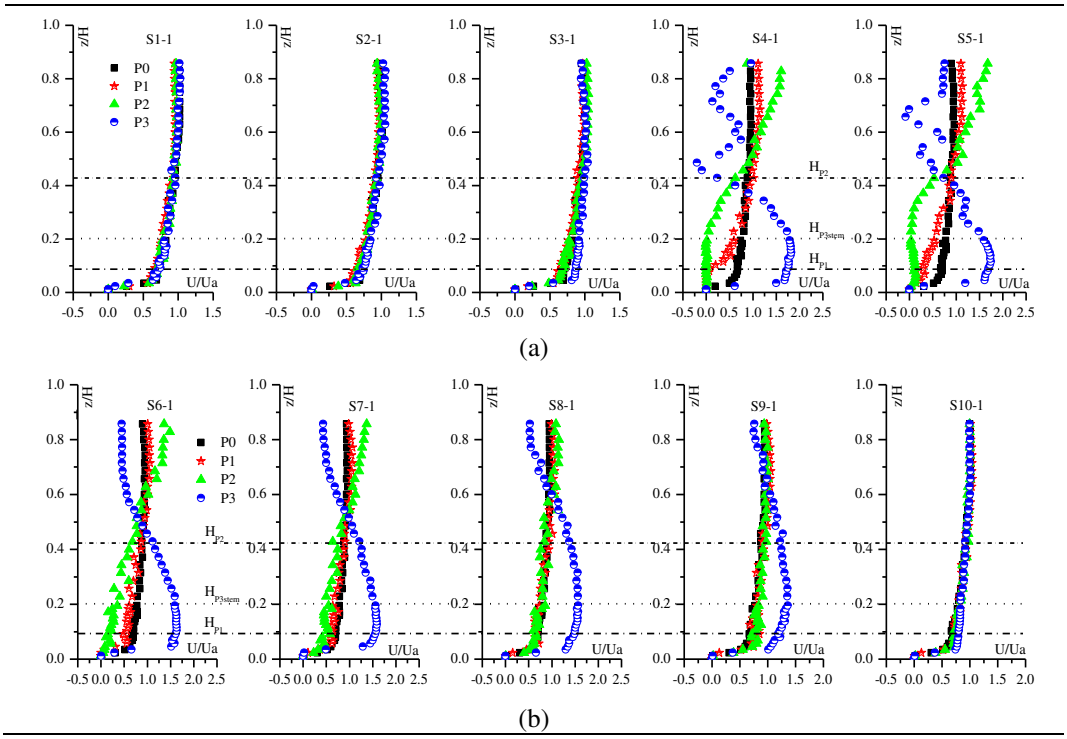

Figure 6. *The vertical distribution of the normalized velocity u/ua changed along the stream-wise in the vegetated open channel (a) from S1-1 to S5-1, (b) from S6-1 to S10-1*

For P1, in upstream region (S1-1 to S3-1), the vertical distribution of longitudinal flow velocity is basically similar to that of P0; in the vegetation region (S4-1), the flow velocity in the zone below the height of 0.2 z/H is smaller than that of P0, however, the flow velocity in the zone above the height of 0.2 z/H is larger than that of P0. The vertical distribution of flow velocity in longitudinal direction basically satisfies the logarithmic distribution from the top of P1 to the free surface (above 0.1 z/H). In the downstream region (at S5-1), the flow velocity in the zone below the height of 0.3 z/H reduces obviously. Since then, the more toward the downstream of the open channel, the flow velocity gradually approaches to that of P0, and is similar to P0 at S7-1. For

http://www.aloki.hu ● ISSN 1589 1623 (Print) ● ISSN 1785 0037 (Online)
DOI: http://dx.doi.org/10.15666/aeer/1705_1145111473

P2, the change characteristics of longitudinal flow velocity in the open channel are similar to that of P1. Since the height of P2 is significantly larger than that of P1, the change of flow velocity is not only greater than that of P1, but also the recovery distance in downstream region is significantly longer than that of P1. For the emergent vegetation (P3), the longitudinal velocity in the zone below the height of 0.3 z/H along the stream-wise is all increase to some extent compared with that of P0, especially that of at S4-1. Due to different types of vegetation with P1 and P2, the recovery distance of P3 is also significantly longer than that of P1 and P2, and not yet been fully approached to that of P0 at S10-1.

There are different vertical distributions of longitudinal flow velocity along the stream-wise in the different types of vegetated channel. For submerged vegetation, the flow velocity decreases obviously in the zone under the top of vegetation due to its strong flow resistance, while the flow velocity in the zone above the top of vegetation is increased obviously and basically complies with the logarithmic distribution. Affected by the exchange of water fluxes in different vertical zones of the downstream region, the flow is restructured and gradually restored. For emergent vegetation, the whole flow resistance is significantly higher than that of submerged vegetation due to its higher height. However, the emergent vegetation is generally composed of stem and foliage. Because the water blocking area of the stem is significantly smaller than that of the foliage, the flow velocity in the zone below the height of stem in the open channel will increase obviously, Meanwhile, the flow velocity will decrease significantly in zone of foliage, and the more closely to the vegetated region, the greater variation of flow velocity in the two vertical zones will be. The flow will undergo vigorous momentum mixing exchange in the two vertical zones, result in obvious secondary flow, and gradually return to the flow pattern of non-vegetation along the stream-wise in the downstream region.

(2) Flow velocity in transverse direction

In order to study the distribution of flow velocity in transverse direction of the partly vegetated channel, cross-section S1, S3, S4, S6, S8 and S10 are selected. Since the cross-sections and the arrangement of vegetation are strictly symmetrical along the midline of the flume, hence only half of the cross-sections of the open channel are measured. Five vertical measurement lines are arranged on each measured section, and the transverse distance of the measurement lines from the midline of the flume is 0 cm, 4 cm, 8 cm, 15 cm, 21 cm (*Figure 4*). As shown in *Figure 7*, the transverse distribution of flow velocity of every cross-section in the different types of the partly vegetated channel is basically similar. Normally, the flow velocity in transverse direction decreases gradually as approaching from the midline to sidewall of flume, which mainly due to the relatively large flow resistance on the sidewall of the flume. However, for P3, due to its larger flow resistance, near the sidewall, the flow velocity in some vertical zones (0-0.4 z/H) is greater than that of in the middle of the flume. There is no vegetation in the downstream region, where the resistance of the sidewall is the main part of the whole flow resistance, since the flow velocity at different transverse positions is affected differently by the sidewall of the flume, which results in the

http://www.aloki.hu ● ISSN 1589 1623 (Print) ● ISSN 1785 0037 (Online)
DOI: http://dx.doi.org/10.15666/aeer/1705_1145111473

significantly different recovery of flow velocity at different transverse positions. For example, when the velocity of vegetated flow is greater than that of non-vegetated flow, the distribution of velocity near the sidewall recovers more rapidly. In contrast, when the velocity of vegetated flow is smaller than that of non-vegetated flow, the distribution of velocity near the sidewall recovers more slowly.

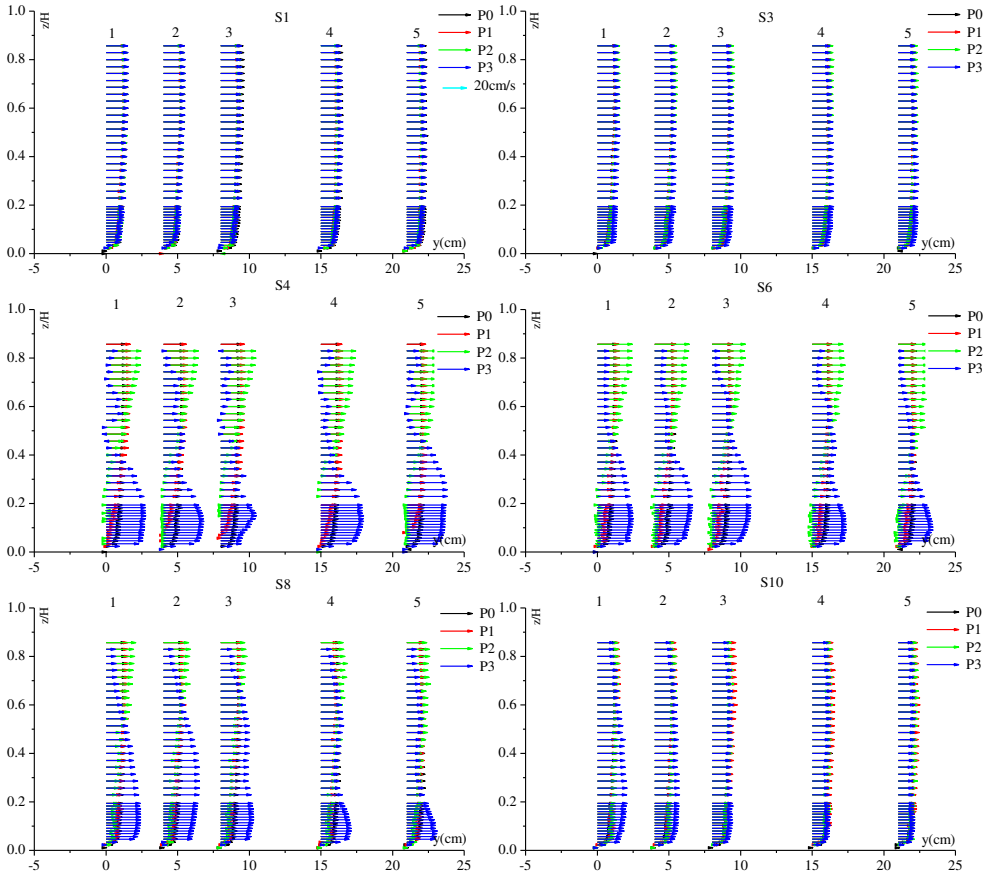

Figure 7. *The distribution of flow velocity at different transverse positions in the vegetated open channel*

(3) The regularity of influence

According to the experimental data of ten measured cross-sections, the regular influence on flow by different types of vegetation is analyzed. Considering that the regular influence of the flow characteristic at different vertical positions maybe not the same, three positions in the vertical direction are selected to be analyzed in this paper, which represent the bottom flow, the middle flow and the surface flow respectively. As shown in *Figure 8*, in terms of the range of influence, the influence on flow by different types of vegetation is greater in the downstream region than that in the upstream region. In terms of the degree of influence, all types of vegetation have great effects on the flow at the bottom position, followed by the surface position, and then the middle position.

http://www.aloki.hu ● ISSN 1589 1623 (Print) ● ISSN 1785 0037 (Online)
DOI: http://dx.doi.org/10.15666/aeer/1705_1145111473

The relative flow velocity of different types of vegetation is (P*-P0) /P0 (*represented the type of vegetation), the variation range of which near bottom, the surface and the middle is -116%-161%, -85%-68% and -73%-56%, respectively. The middle zone is the main place where the flow from bottom and surface mix intensively. Therefore, the distribution of relative flow velocity in the middle zone is more uniform than that in the other two zones. For different types of vegetation, the submerged and emergent vegetation have completely opposite effects on the bottom flow and the surface flow. Relative to submerged vegetation, emergent vegetation has a greater influence on flow and longer influenced distance.

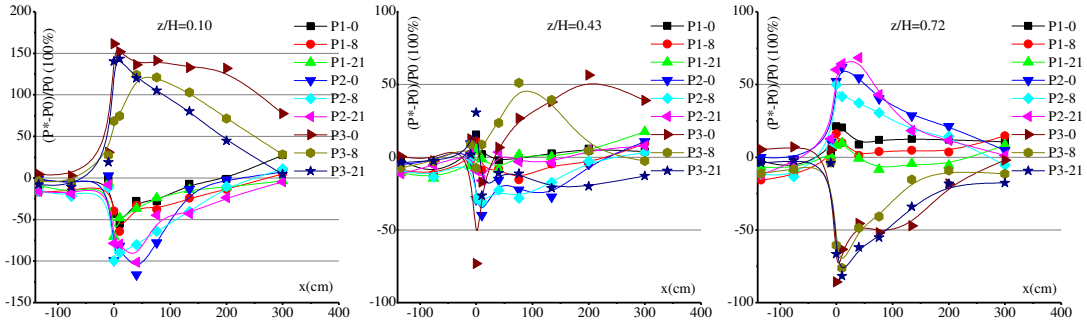

Figure 8. *The regular influence on the flow in the different vegetated open channel*

Secondary flow

The secondary flow is a relatively minor flow superimposed on the primary flow; however, it plays a crucial role in the sediment transport of the open channel. In this section, the secondary flow in the different types of the vegetated open channel is still investigated.

As can be seen from *Figure 9*, the secondary flow propagates from left sidewall to the centre of the flume at section S1 (left half of the flow) under different types of vegetation. Since the flume is strictly symmetrical with respect to the central line, the right half of the flow should propagate from right sidewall to the centre of the flume. The velocity of the secondary flow of section S1 in the vegetated open channel is larger than that of in non-vegetated open channel. Although there is a significant effect of vegetation on the secondary flow in section S1, the movement characteristic of the secondary flow does not change fundamentally.

In section S3, for the submerged vegetation (P1 and P2), because of its large flow resistance in the bottom and middle parts of the section (a place full of vegetation), the vertical distribution of secondary flow obviously propagates from the bottom to the free surface. For the emergent vegetation (P3), the vertical distribution of secondary flow obviously propagates from the free surface to the bottom for its large flow resistance in the middle and upper part of the section (a place full of foliage). However, in the bottom part of the section S3 (a place full of stem), the transverse flow of P3 is clearly shifted

http://www.aloki.hu ● ISSN 1589 1623 (Print) ● ISSN 1785 0037 (Online)
DOI: http://dx.doi.org/10.15666/aeer/1705_1145111473

towards both sides of the plant stems, which is similar to the flow movement of the cylindrical spoiler (*Figure 10*), and the similar phenomenon we still can get from Graf and Yulistiyanto, 1998.

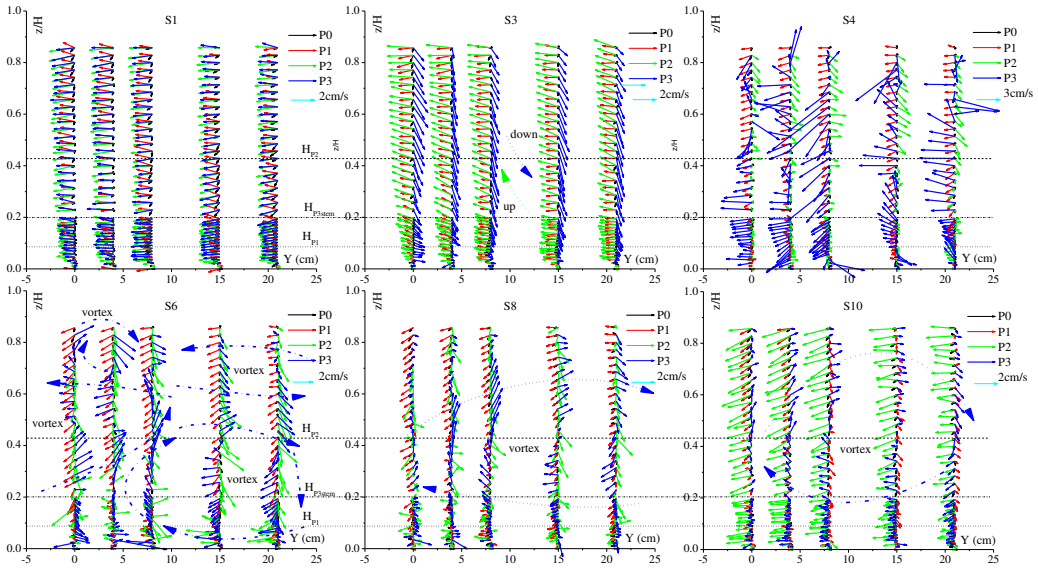

Figure 9. *The vertical distribution of secondary flow in the vegetated open channel*

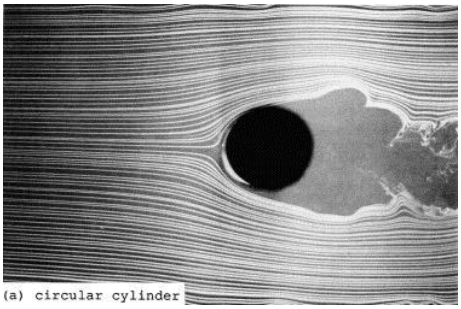

Figure 10. *The flow pattern around circular cylinder at Re=3×10^4, reprinted from Yoon & Ettema (1993)*

In section S4, where the vertical distribution secondary flow becomes more complicated due to the strong influence. For submerged vegetation (P2), the velocity of secondary flow in the zone under the height of 0.8 HP2 is small, whereas the velocity in the zone above the height of 0.8 HP2 is obviously increased. At the same time, the transverse direction of secondary flow in these two zones is not strictly consistent, which may be the result of the exchange of flow momentum and the shear layer near the canopy of submerged vegetation (*Figure 11*). For emergent vegetation (P2), its flow resistance is significantly different in the zones of stems and foliage. In the zone of foliage, the secondary flow is more significant mutations scattered and occurred in some

http://www.aloki.hu ● ISSN 1589 1623 (Print) ● ISSN 1785 0037 (Online)
DOI: http://dx.doi.org/10.15666/aeer/1705_1145111473

local positions. However, in the zone of stems, the secondary flow is less influenced and has a regular flow pattern. Furthermore, the secondary flow of P3 propagates from left sidewall to centre of the flume at the majority positions in section S4, whose direction is opposite to that in the section S3. The reason for this phenomenon might be related to the vortex flow generated in the vegetation area (see *Figure 12b*).

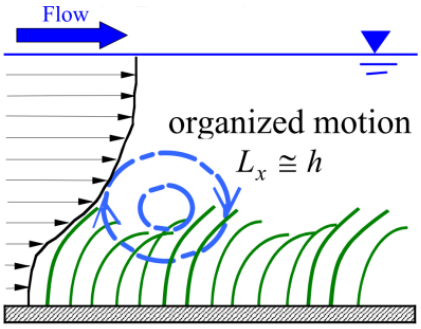

Figure 11. *The flow patterns in dense flexible vegetation (Okamoto & Nezu 2010)*

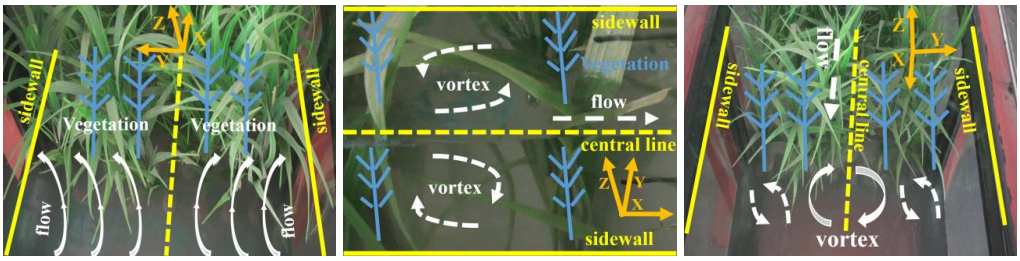

(a) S3 (b) S4 (c) S6

Figure 12. *The characteristic of secondary flow of different region under the condition of P3*

In the downstream region (S5-S10), due to the influence of vegetation, there is a significant momentum exchange among the water masses in different vertical positions and significant vortex flow is generated. In order to further analyze the characteristics of vortex flow in the downstream region, this paper selects three sections (S6, S8 and S10) and calculates the measured data by *Equation (1)*, finally obtains the vertical distribution of vortex flow in the longitudinal direction. For the purpose of making the result clearer and more intuitive, more significant distribution of vorticity is taken as an example (vegetation P3). As shown in *Figure 13*, six vortices are generated in the flow field of section S6, which indicates that there are some strong vertical exchanges of flow momentum. Obviously, in the case of sediment, this condition of flow is conducive to sediment diffusion in the three-dimensional direction and makes sediment concentration consistent in the whole section. With the mix of flow in the downstream region, the energy of flow gradually decreases, and the flow converges and merges into two vortices in section S8. Finally, there is only one large vortex in section S10 and the vorticity intensity is further weakened.

http://www.aloki.hu ● ISSN 1589 1623 (Print) ● ISSN 1785 0037 (Online)
DOI: http://dx.doi.org/10.15666/aeer/1705_1145111473

$$\Omega_x = \frac{\partial w}{\partial y} - \frac{\partial v}{\partial z} \quad \text{(Eq.1)}$$

As previously analyzed, due to the influence of vegetation, the flow in the downstream region generates many significant vortices. Compared to the submerged vegetation, emergent vegetation has more obvious influence on the flow in the downstream region. Therefore, in terms of ecological rivers, the presence of intense vortex flow in downstream of emergent vegetation region will make the substances in rivers fully diffused, which is obviously conducive to the survival and propagation of aquatic organisms.

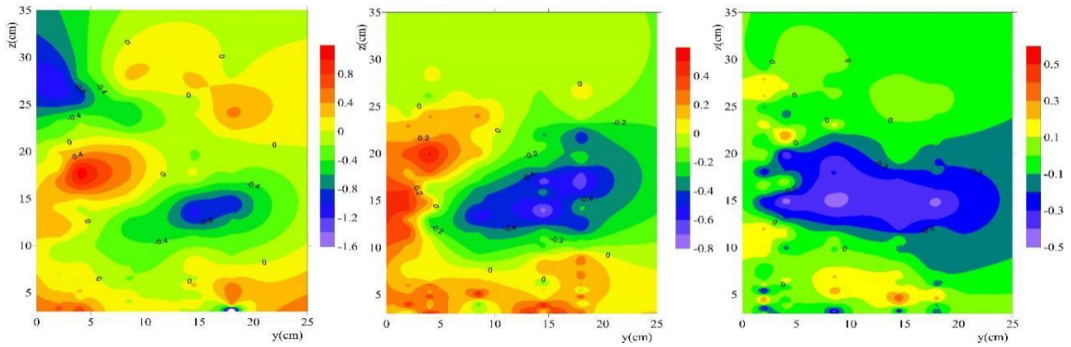

(a) S6 (b) S8 (c) S10

Figure 13. *The vertical distribution of vortex flow in longitudinal direction under the condition of P3*

Sediment transport

According to the analysis of the data measured by rivers and laboratory experiments, Hu and Hui (1995) considered that the vertical distribution of sediment concentration in open channel usually had three types. Type I distribution is that the sediment concentration increases gradually from the free surface to the riverbed, and when it reaches a maximum value at a certain vertical position, then it will decrease. Type II distribution is that the sediment concentration monotonically increases from the free surface to the riverbed, with the maximum concentration near the riverbed. Type III distribution is that the sediment concentration increases gradually from the free surface to the riverbed, with the maximum concentration still near the riverbed, and yet the sediment gradient will vary significantly at one vertical position. Ni et al. (1991) considered that the vertical pulsating flow velocity was the fundamental reason for the existence of suspended sediment in a turbulent flow. If the sediment concentration is not very large, there will be more opportunity for Type I distribution when the bed is smooth with the uniform particle size of sediment. On the contrary, there will be more opportunity for Type II distribution.

http://www.aloki.hu ● ISSN 1589 1623 (Print) ● ISSN 1785 0037 (Online)
DOI: http://dx.doi.org/10.15666/aeer/1705_1145111473

Hu and Hui (1995) considered that the appearance of Type I distribution could not be explained by only the vertical pulsatile flow velocity distribution. Whether Type I distribution occures in flow with a higher concentration depends on the ratio of particle size to flow depth, and if the ratio exceeds the critical value the flow may appear Type I distribution. The formation condition of Type II distribution is that the suspension index is large and the gravity plays a dominant role, while the formation condition of Type III distribution is that the suspension index is small and the turbulent diffusion plays a dominant role. In order to study the vertical distribution of suspended sediment transport in the different vegetated open channel, laboratory experiments are carried out. The experimental conditions are shown in *Table 1*. The median diameter of experimental sediment ranges from 0.16 mm to 0.18 mm, and the sedimentation velocity is calculated by Zhang Ruijin formula (Qian and Wan, 1986). Experimental samples are obtained by sediment sampler (*Figure 1*). The Samples are taken twice from every measured position by 1000 ml graduated cylinders, filtered and dried, and then are weighed by an electronic balance. Finally, the sediment concentration of the sample is calculated and the average of two results in the same position is taken as the sediment concentration of the measured position.

Suspended sediment concentration

According to the experimental data in three vertical lines of S1-1, S4-1 and S8-1, the vertical distribution of the suspended sediment concentration in the different types of the vegetated open channel is analyzed. As shown in *Figure 14*, the vertical distribution of the suspended sediment concentration under different types of vegetation in the upstream region (at S1-1) is basically satisfies Type I and Type II distribution, which is similar to that of in the middle reaches of Changjiang River (Cross-section JM01, Time 24 June 2016, Discharge 17900 m^3/s, Water depth 14.5 m, Depth-averaged velocity 1.47 m/s). In the vegetated region (H_2-H_3), due to the influence by vegetation, the vertical distribution of the suspended sediment concentration changes greatly relative to that in the upstream region. The value of vertical sediment concentration under conditions of P2 and P3 decreases significantly and vertical change characteristic satisfies Type III distribution. In downstream region (at S8-1), the vertical concentration of suspended sediment under different types of vegetation is distributed more evenly.

The vertical distribution of suspended sediment gradient is an important factor that represents the variation of suspended sediment transport. Since the distribution of suspended sediment concentration is more scattered than that of flow velocity, the vertical distribution of suspended sediment concentration will not be simulated in this paper, instead of being obtained by differentiating the experimental data (*Figure 15*). As shown in *Figure 15*, the sediment gradient in the zone under the height of 0.2 z/H is relatively large under the condition of vegetation, while the value of suspended sediment gradient in the zone above the height of 0.2 z/H gradually decreases and is basically negative. For P1, the vertical distribution of suspended sediment gradient in

http://www.aloki.hu ● ISSN 1589 1623 (Print) ● ISSN 1785 0037 (Online)
DOI: http://dx.doi.org/10.15666/aeer/1705_1145111473

the vegetated open channel is basically the same as that of P0, which indicates that the vegetation (P1) has a relatively slight influence on the suspended sediment transport.

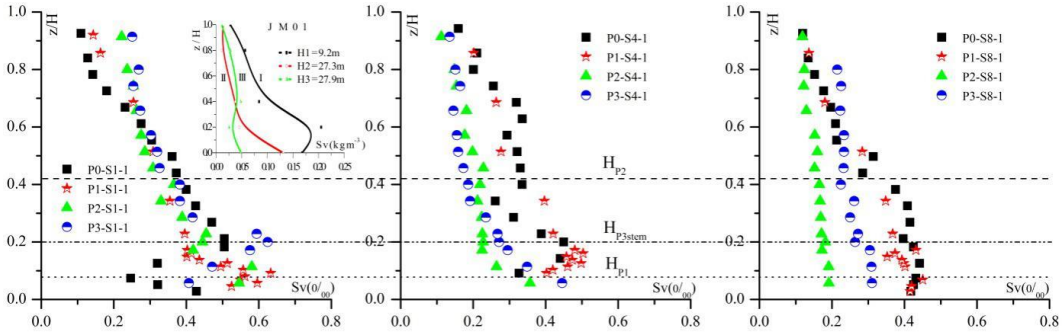

Figure 14. *The vertical distribution of the suspended sediment concentration in the different types of the vegetated open channel*

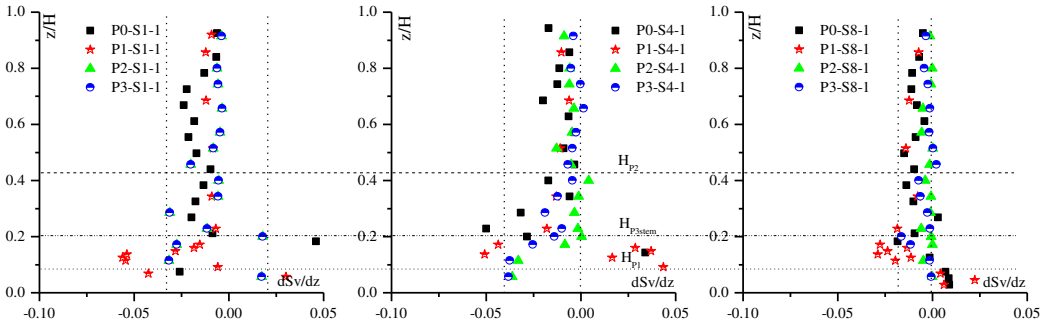

Figure 15. *The vertical distribution of the suspended sediment gradient in the different types of the vegetated open channel*

However, for P2 and P3, the vertical distribution of suspended sediment gradient gradually decreases along the stream-wise, that is to say, the vertical distribution of suspended sediment concentration tends to be consistent at S4-1 and S8-1. There are two possible reasons to explain the significant change of characteristics under conditions of P2 and P3. First, influenced by the water blocking of vegetation (P2 and P3), the large particles of suspended sediment are largely deposited in the upstream and vegetated region and the particle size of suspended sediment along the stream-wise becomes smaller and smaller, which will be conducive to the sediment suspension in the flow. Second, for P2 and P3, the turbulent diffusion of flow at S4-1 and S8-1 is significantly stronger than that of P0, which will be beneficial to the diffusion of suspended sediment in the flow.

http://www.aloki.hu ● ISSN 1589 1623 (Print) ● ISSN 1785 0037 (Online)
DOI: http://dx.doi.org/10.15666/aeer/1705_1145111473

Particle size of sediment

Malvern Mastersizer 2000 particle size analyzer is used to analyze the particle size of suspended sediment, and then the vertical distribution about different particle size of suspended sediment (less than 0.1 mm fine sediment particles and more than 0.1 mm coarse sediment particles) is analyzed. As shown in *Figure 16*, the size of suspended sediment median particles gradually diminishes from bottom to free surface. However, for P2 and P3, the vertical distribution about the size of suspended sediment median particles at S3-1 does not have significant changes, which should be related to their greater turbulence intensity of the flow in the downstream region.

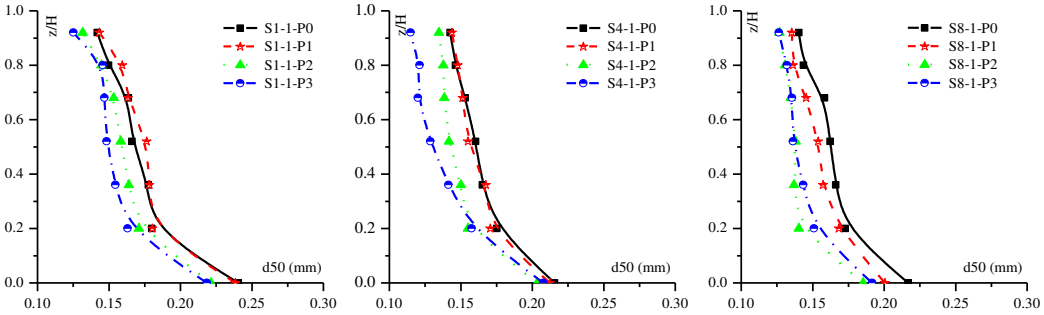

Figure 16. *The vertical distribution of suspended sediment median particles size (d_{50})*

As can be seen from *Figure 17*, the concentration of fine sediment particles does not change obviously along with the water depth. Therefore, the vertical distribution of fine sediment particles is not related to the type of vegetation and the location of the vegetated open channel.

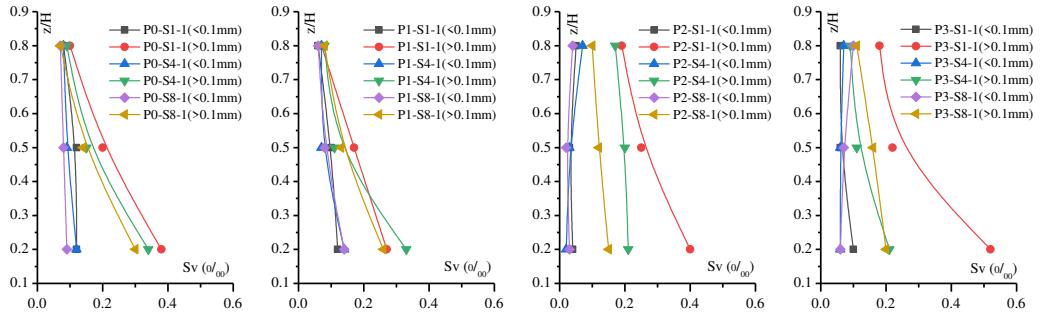

Figure 17. *The vertical distribution about concentration of different suspended sediment particles size*

On the contrary, for coarse sediment particles, the concentration decreases obviously along with the water depth. Taking P2 and P3 for example, the coarse sediment at S1-1 rapidly decreases with the increase of water depth, yet slowly decreases at S2-1 and S3-1. There are two possible reasons to explain the different changes of coarse sediment.

http://www.aloki.hu ● ISSN 1589 1623 (Print) ● ISSN 1785 0037 (Online)
DOI: http://dx.doi.org/10.15666/aeer/1705_1145111473

First, coarse sediment is largely deposited in the upstream and vegetated region due to the water blocking the impact of the vegetation. Second, the turbulence of flow in the two regions is strong and the vertical dispersion of suspended sediment is very significant. Experiments show that vegetation has a weak filtration effect on fine sediment in the open channel, but has a strong filtration effect on the coarse sediment. The proportion of fine sediment in a total load along the stream-wise gradually increases, in contrast, the proportion of coarse sediment in a total load along the stream-wise decreases gradually. As a result, the suspended sediment along the stream-wise in the vegetated open channel is gradually refined.

Discussion

Flow and sediment diffusion coefficient

Due to the turbulent characteristics of the flow, sediment transport is actually bi-directional in the process of turbulent diffusion. Under certain conditions, the total amount of sediment entering the lower concentration zone is equal to the total amount of sediment entering the higher concentration zone, at which time the distribution of sediment concentration reaches equilibrium. The reason for this balance is that the upward turbulence force of sediment is equal to the downward gravity (Ni, 1991). The sediment diffusion coefficient and flow diffusion coefficient are important indicators of flow and sediment diffusion intensity. This paper attempts to study the mechanism of interaction between flow and sediment in the partly vegetated open channel through the analysis of flow diffusion and sediment diffusion coefficient. According to the momentum transfer theory of turbulence (Ni et al., 1991) and diffusion equation of two-dimensional constant uniform flow under equilibrium conditions, formulas for calculating momentum diffusion coefficient (ε_m) and sediment diffusion coefficient can be derived (ε_s).

As shown in *Figure 18*, the vertical distribution of flow momentum diffusion coefficient increases firstly and then decreases in different types of the vegetated open channel. At S1-1, the greater flow resistance of vegetation is, the smaller value of flow momentum diffusion coefficient along the water depth is. For P2 and P3, the value of flow momentum diffusion coefficient is obviously smaller than that of P0 and P1. *Table 2* shows the correlations of flow momentum diffusion coefficient under different types of vegetation. The correlations between P0 and P1, P2, P3 are 0.81, 0.58 and 0.90, respectively. Obviously, the correlation between P0 and P2 is very low, which indicates that vegetation P2 has the greatest influence on the flow momentum diffusion coefficient in the upstream region. In the vegetated region (H_2-H_3), due to the effect of vegetation P2 and P3, the values of flow momentum diffusion coefficient in some vertical zones are significantly larger than those in upstream. The correlation between P0 and P3 also significantly reduces compared with those in upstream (*Table 2*). In the

http://www.aloki.hu ● ISSN 1589 1623 (Print) ● ISSN 1785 0037 (Online)
DOI: http://dx.doi.org/10.15666/aeer/1705_1145111473

downstream region (at S8-1), for P2 and P3, the vertical distribution of flow momentum diffusion coefficient is basically similar to that of P0, however, the maximum value along the water depth is obviously larger than that of P0, and the correlation between P0 and P2 also increases significantly relative to that in the vegetated region, yet the correlation between P0 and P3 is still small. The above change indicates that the influence on flow in the submerged vegetated open channel is mainly in the upstream and vegetated region, while that in the submerged vegetated open channel is mainly in the vegetated and downstream region.

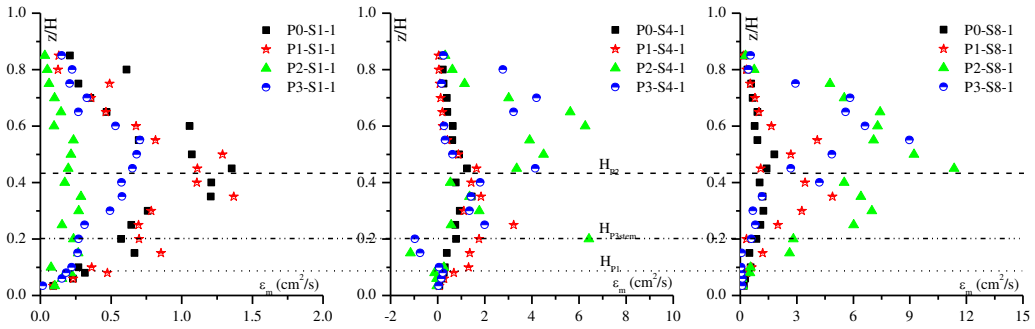

Figure 18. *The vertical distribution of momentum diffusion coefficient along the stream-wise*

Table 2. *The Correlation of flow and sediment diffusion under different types of vegetation*

Position factor		Correlation of flow diffusion coefficient			Correlation of Sediment diffusion coefficient			Correlation of flow and sediment diffusion in every case			
		P0-P1	P0-P2	P0-P3	P0-P1	P0-P2	P0-P3	P0-P0	P1-P1	P2-P2	P3-P3
S1-1	Corr	0.81	0.58	0.90	0.64	0.22	-0.19	0.55	0.76	-0.13	0.39
	Sig	2.6E-05	9.7E-03	1.5E-07	7.1E-03	4.1E-01	4.7E-01	2.6E-02	5.8E-04	6.3E-01	1.3E-01
S4-1	Corr	0.75	0.60	0.40	0.89	0.82	-0.41	0.84	0.56	0.38	0.24
	Sig	1.9E-04	6.6E-03	8.7E-02	3.2E-06	8.5E-05	1.1E-01	5.0E-05	2.3E-02	1.4E-01	3.7E-01
S8-1	Corr	0.86	0.88	0.58	0.88	-0.26	-0.54	0.63	0.58	0.15	0.45
	Sig	2.6E-06	5.1E-07	8.6E-03	5.7E-06	3.2E-01	3.1E-02	8.7E-03	1.7E-02	5.7E-01	8.1E-02

As shown in *Figure 19* and *Table 2*, the vertical distribution of sediment diffusion coefficients is obviously more complex than that of the flow momentum diffusion coefficient in different types of the vegetated open channel. For P1, the vertical distribution of sediment diffusion coefficients along the stream-wise have a high correlation with that of P0. For P2, the vertical distribution of sediment diffusion coefficients has a high correlation with that of P0 in the vegetated region (H_2-H_3). However, the correlation between P2 and P0 in the upstream and downstream regions are significantly low. For P3, the vertical distribution of sediment diffusion coefficients in the whole open channel has a low correlation with that of P0, and all of the correlations are negatively correlated.

http://www.aloki.hu ● ISSN 1589 1623 (Print) ● ISSN 1785 0037 (Online)
DOI: http://dx.doi.org/10.15666/aeer/1705_1145111473

Mechanism of interaction between flow and sediment

The reason why suspended sediment can move forward with the flow is mainly due to the contrast between the turbulent diffusion of flow and the gravity of sediment (Hu and Hui, 1995). The process of suspended sediment transport is the process of the interaction between turbulent diffusion and sediment gravity. The experimental analysis also shows that there is a medium to the high degree of correlation between the momentum and sediment diffusion coefficients in the non-vegetated open channel (*Table 2*). The mechanism of the interaction between flow and sediment in open vegetated channel is very complex. When the morphology of vegetation is relatively small, it has little effect on the process of flow and sediment transport in the open channel.

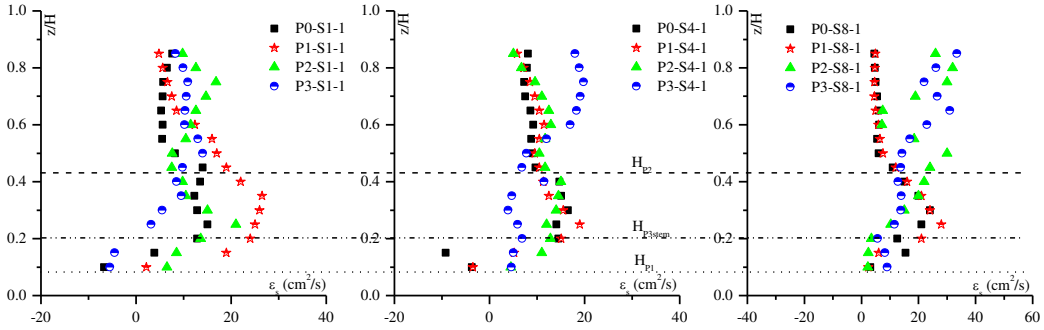

Figure 19. *The vertical distribution of sediment diffusion coefficient along the stream-wise*

However, when the morphology of vegetation is relatively large, its influence on the process of flow and sediment transport in the open channel is greater. At this time, the correlation between the flow and sediment transport is significantly reduced and even negative correlation occurs. With the increased volume of the vegetation, the area of water blocking in the cross-section gradually increases and the turbulence intensity of flow also significantly increases in the open channel, which leads to the obvious three-dimensional vortex flow in some zones. The existence of three-dimensional vortex flow is conducive to the diffusion of sediment in different directions. Since the calculated flow diffusion coefficient in this paper does not consider the influence of transverse flow in the open channel, yet the distribution of sediment concentration in the vegetated open channel is caused by the three-dimensional movement of the flow, so the correlations between the flow momentum diffusion coefficient and the sediment diffusion coefficient in some areas are low or not relevant. All these analyses show that the movement of transverse flow in the partly vegetated open channel has a crucial impact on suspended sediment transport.

http://www.aloki.hu ● ISSN 1589 1623 (Print) ● ISSN 1785 0037 (Online)
DOI: http://dx.doi.org/10.15666/aeer/1705_1145111473

Conclusions

Experiments are conducted on characteristics of the flow in the partly vegetated channel. For submerged vegetation, the flow velocity decreases obviously in the zone under the top of vegetation due to its strong flow resistance, while the flow velocity in the zone above the top of vegetation increases obviously and basically complies with the logarithmic distribution. The place slightly below the top of submerged vegetation can be regarded as the "riverbed", and is called "vegetation-equivalent riverbed". For emergent vegetation, the place where the vertical distribution of the longitudinal flow velocity fluctuates strongly is the transition zone between the stem and foliage, therefore, the upper edge of the transition zone can be regarded as the "equivalent riverbed" for the emergent vegetated channel.

The regular influence on flow in the partly vegetated open channel is analyzed. In terms of the range of influence, the influence on the flow of different types of vegetation is greater in the downstream region than that in the upstream region. In terms of the degree of influence, all types of vegetation have a great effect on the flow at the bottom position, followed by the surface position, and then the middle position. For different types of vegetation, the submerged and emergent vegetation has completely opposite effect on the bottom flow and the surface flow. Relative to submerged vegetation, emergent vegetation has a greater influence on flow and longer influenced distance.

Due to the influence of vegetation, the flow in the downstream region generates many significant vortices. Compared with the submerged vegetation, emergent vegetation has a more significant influence on the flow in the downstream region. Therefore, in terms of ecological rivers, the presence of intense vortex flow in the downstream region will make the substances in rivers fully diffused, which is obviously conducive to the survival and propagation of aquatic organisms.

The vertical distribution of suspended sediment in the partly vegetated channel becomes more and more uniform along the stream-wise. Besides, the vertical variation of the suspended sediment gradient decreases gradually along the stream-wise. Vegetation has a weak filtration effect on fine sediment in the open channel but has a strong filtration effect on the coarse sediment. The proportion of fine sediment in a total load along the stream-wise gradually increases; in contrast, the proportion of coarse sediment in a total load along the stream-wise decreases gradually. As a result, the suspended sediment along the stream-wise in the partly vegetated open channel is gradually refined.

The mechanism of the interaction between flow and sediment in the partly vegetated channel is very complex. When the morphology of vegetation is relatively small, it has little effect on the process of flow and sediment transport in the open channel. However, when the morphology of vegetation is relatively large, its influence on the process of flow and sediment transport in the open channel is greater. At this time, the correlation between the flow and sediment movement is significantly reduced and even negative correlation occurs. These show that the movement of transverse flow in the vegetated open channel has a crucial impact on suspended sediment transport.

http://www.aloki.hu ● ISSN 1589 1623 (Print) ● ISSN 1785 0037 (Online)
DOI: http://dx.doi.org/10.15666/aeer/1705_1145111473

In this paper, the vegetation is made by flexible plastics. Although the plastic vegetation has some flexibility, it is still different from natural aquatic vegetation in stiffness. To further improve the research, it is necessary to use real aquatic vegetation to carry out future experiments. For future experiments, the aquatic vegetation can be planted in the flume in advance. The effects on the flow and sediment transport can be studied separately according to the different growth stages of aquatic vegetation.

Acknowledgements. The research is supported by National Key Research and Development Program of China (under Grant No. 2016YFC0402310, No. 2016YFC0402105), National Natural Science Foundation of China (under Grant No. 51679011, No. 51309022, No. 51579172).

REFERENCES

[1] Carollo, F. G., Ferro, V., Termini, D. (2002): Flow velocity measurements in vegetated channels. – Journal of Hydraulic Engineering 128: 664-673.

[2] Elliott, A. (2000): Settling of fine sediment in a channel with emergent vegetation. – Journal of Hydraulic Engineering 126: 570-577.

[3] Graf, W. H., Yulistiyanto, B. (1998): Experiments on flow around a cylinder; the velocity and vorticity fields. – Journal of Hydraulic Research 34: 637-653.

[4] Hu, C., Hui, Y. (1995): Mechanisms and statistical laws of flow and sediment movement in open channel. – Science Press, Beijing, China.

[5] Ikeda, S., Kanazawa, M. (1996): Three-Dimensional Organized Vortices above Flexible Water Plants. – Journal of Hydraulic Engineering 122: 634-640.

[6] Jordanova, A. A., James, C. S. (2003): Experimental Study of Bed Load Transport through Emergent Vegetation. – Journal of Hydraulic Engineering 129: 474-478.

[7] Li, R. M., Shen, H. W. (1973): Effect of Tall Vegetations on Flow and Sediment. – Journal of Hydraulic Division 99: 793-814.

[8] Li, Y., Du, Wei., Yu, Z. (2015): Impact of flexible emergent vegetation on the flow turbulence and kinetic energy characteristics in a flume experiment. – Journal of Hydro-environment Research 9: 354-367.

[9] Lu, S. (2008): Experimental Study on Suspended Sediment Distribution in Flow with Rigid Vegetation. – Hohai University, Nanjing, China.

[10] Nezu, I., Onitsuka, K. (2001): Turbulent structures in partly vegetated open-channel flows with LDA and PIV measurements. – Journal of Hydraulic Research 39: 629-642.

[11] Ni, J., Wang, G., Zhang, H. (1991): The theory of sediment and flow transport and the newest applications. – Science Press, Beijing, China.

[12] Okamoto, T., Nezu, I. (2010): Flow resistance law in open-channel flows with rigid and flexible vegetation. – Bundesanstalt für Wasserbau, Karlsruhe, Germany.

[13] Qian, N., Wan, Z. (1986): Sediment movement mechanics. – Science Press, Beijing, China.

[14] Qu, G. (2014): Experimental Study on Water and Sediment Transport in Open Channel Flow with Vegetation. – Wuhan University, Wuhan, China.

http://www.aloki.hu ● ISSN 1589 1623 (Print) ● ISSN 1785 0037 (Online)
DOI: http://dx.doi.org/10.15666/aeer/1705_1145111473

[15] Shi, B., Cao, S. (2000): The Control Sand Dynamics Using Vegetation. – Ocean University of China Press, Qingdao, China.
[16] Stephan, U., Gutknecht, D. (2002): Hydraulic resistance of submerged flexible vegetation. – Journal of Hydrology 269: 27-43.
[17] Su, X., Li, C. (2002): Large eddy simulation of free surface turbulent flow in partly vegetated open channels. – International Journal for Numerical Methods in Fluids 39: 919-937.
[18] Sun, G., Wei, G. (2005): The study on model sediment experiment in Changjiang River flood control model. – Changjiang River Scientific Research Institute, Wuhan, China.
[19] Tang, H., Yan, J., Lu, S. (2007): Advances in research on flows with vegetation in river management. – Advances in Water Science 18: 785-792.
[20] Wang, X., Shao, X., Li, D. (2002): The Basis of River Dynamics. – China Water & Power Press, Beijing, China.
[21] Wilson, C., Stoesser, T., Pinzen, B. (2003): Open channel flow through different forms of submerged flexible vegetation. – Journal of Hydraulic Engineering 129: 847-853.
[22] Yang, S., Lee, J. (2007): Reynolds shear stress distributions in a gradually varied flow in a roughened channel. – Journal of Hydraulic Research 45: 462-471.
[23] Yoon, B., Ettema, R. (1993): Droplet trajectories and icing-collision efficiencies for cylinders determined using LDV. – Cold Regions Science and Technology 21: 381-397.

GLOSSARY

The following symbols are used in this paper:

A_{ve}:Cumulative area of the whole plant (cm^2)
d_{50}:Median diameter of experimental sand (mm)
Fr:Froude number
g:Gravitational constant (m/s^2)
H:Water depth (cm)
H_0:Water level control at the outlet of the flume (cm)
H_{P1}:Height of vegetation P1 (cm)
H_{P2}:Height of vegetation P2 (cm)
H_{P3}:Height of vegetation P3 (cm)
H_{P3stem}:Height of stem of vegetation P3 (cm)
h_{ve}:Different height of vegetation (cm)
J:Water surface slope
Q:Flow discharge (L/s)
Re:Reynolds number (-)
Sa:Amount of sediment at inlet of the rectangle flume (g/s)
S_L:Flume slope
S_v:Sediment volume concentration (1/1000)

u:Flow velocity of point z (cm/s)

http://www.aloki.hu ● ISSN 1589 1623 (Print) ● ISSN 1785 0037 (Online)
DOI: http://dx.doi.org/10.15666/aeer/1705_1145111473

u_a:Time-averaged stream-wise velocity (cm/s)

u_{max}:Maximum flow velocity in the depth direction (cm/s)

u_{rms}:Turbulence intensity (cm/s)

u_*:Shear velocity (cm/s)

u': Mean velocity components in longitudinal direction (cm/s)

v':Mean velocity components in transverse directions (cm/s)

w':Mean velocity components in vertical directions (cm/s)

$v'w'$: Mean velocity components in longitudinal, transverse and vertical directions, respectively (cm/s)

$-u'v'$: Reynolds stress in vertical direction (z) on plane perpendicular to stream-wise direction (cm^2/s^2)

X: Longitudinal direction
x: Distance to the vegetation region in longitudinal direction (cm)
Y: Transverse direction
y: Distance to the left sidewall of the flume (cm)
Z: Vertical direction
z: Distance to the riverbed (cm)

Greek symbols

ε_m:Momentum diffusion coefficient

ω: Settling velocity of sediment (cm/s)

κ: Von Karman's turbulence coefficient

ρ:Fluid density

ε_s:Sediment diffusion coefficient

Ω_x: Vortex rotation in longitudinal direction.

http://www.aloki.hu ● ISSN 1589 1623 (Print) ● ISSN 1785 0037 (Online)
DOI: http://dx.doi.org/10.15666/aeer/1705_1145111473

SOIL ORGANIC CONTENT OF STANDS OF DIFFERENT AGES IN A SUBTROPICAL CHIR PINE (*PINUS ROXBURGHII*) FOREST OF PAKISTAN

AMIR, M.[1] – SAEED, S.[2] – LIU, X. D.[1*] – MANNAN, A.[3] – KHAN, A.[4] – LI, Z. Z.[2] – MUNEER, M. A.[2]

[1]*Beijing Key Laboratory for Forest Resources and Ecosystem Process, College of Forestry, Beijing Forestry University, 100083 Beijing, China*

[2]*School of Forestry, Beijing Forestry University, Beijing, China*

[3]*Punjab Forest Department Government of Punjab, Lahore 54000, Pakistan*

[4]*School of Soil and Water Conservation, Beijing Forestry University, Beijing 100083, China*

[*]*Corresponding author*
e-mail: xd_liu@bjfu.edu.cn; phone: +86-134-3921-2063

(Received 19th Apr 2019; accepted 4th Jul 2019)

Abstract. Soil organic carbon (SOC) storage in forest ecosystems plays a major role in the global carbon cycle. Soil carbon across an age sequence may vary of Chir pine forest. In this study, based on the silvicultural shelterwood management system, forest area was classified into stands of three different age groups, including young stand, mature stand, and over-mature stand. Soil carbon density was assessed in each stand at three depths (0-20, 20-40, and 40-60 cm) by Walkley Black method. The results showed that SOC was higher in different stand ages at a depth of 0-20 cm as compared to the 20-40, and 40-60 cm depth. Altogether, the average potential of soil carbon density at a depth of 0-60 cm in young, mature and over-mature stand ages of Chir Pine forest was 70.96 (Mg C ha^{-1}), 68.96 (Mg C ha^{-1}) and 61.02 (Mg C ha^{-1}), respectively. The result indicates that soil carbon stock decreases with increasing forest stand ages. The results confirm that-- current management operations such as cutting, thinning, tending, may affect the soil carbon. Moreover, we recommended the regular periodic survey of soil and permanent sample plot establishment is necessary for the accurate soil carbon measurement in different stand ages of Chir pine forest.
Keywords: *shelterwood system, management operation, soil bulk density, soil depths, Murree Hill*

Introduction

Soil carbon storage is one of the most essential and significant carbon sinks in the terrestrial ecosystems, which facilitates carbon sequestration. Monitoring and assessment of soil carbon in forests are critical for the mitigation of climate change. The soil is an important sink for carbon storage (Ahmad et al., 2018; Mannan et al., 2019; Saeed et al., 2019a). Among various forest carbon pools, the estimation of soil organic carbon (SOC) is essential, because the soil is the world's largest terrestrial carbon pools, which plays a vital role in the global carbon budget (Saeed et al., 2019b). Therefore, a slight change in the soil carbon storage can have large impacts on the global carbon cycle (Johnson et al., 2007). The increasing emission of carbon dioxide from the soil is reinforced by the rising of temperature and climate change (Yang et al., 2010). SOC stored in the world's soils is approximately 1100–1600 Pg (petagrams), more than twice the carbon stored in the living vegetation, which is 750 Pg (Sundquist, 1993). Soil releases carbon to the atmosphere through deforestation and other anthropogenic activities may significantly

http://www.aloki.hu ● ISSN 1589 1623 (Print) ● ISSN 1785 0037 (Online)
DOI: http://dx.doi.org/10.15666/aeer/1705_114751487

increase the greenhouse gases concentration (Watson et al., 2000). The potential capability and assessment of soil are essential for the mitigation of CO_2 emission, improvement of surface water quality, soil physical properties, enhancement of forest production and stability, as well as decreasing of soil erosion (Lal, 2004; Lal et al., 2007).

Stand age is an essential factor affecting storage of carbon in various forest components such as in upper-story vegetation, understory vegetation, deadwood, and soil (Martin et al., 2005; Zerva et al., 2005; Peichl and Arain, 2006). Moreover, stand age is a reliable predictor of the structure and function of a forest ecosystem which may affect the carbon density among carbon pools (Bradford and Kastendick, 2010). Furthermore, various carbon pools of a forest respond differently to stand age (Zhu et al., 2010). Therefore, it is essential to understand the relationship of stand age with soil carbon and sequestration rate (Cheng et al., 2014). Some studies underlined that the potential of soil carbon sequestration is age-independent (Song et al., 2018). Some studies showed that soil carbon increase with the increase in stand age (Cao et al., 2012; Zhao et al., 2014). The soil carbon inconsistency may be depending on many other factors such as forest types, climate, previous land use and soil properties (Taylor et al., 2007).

In Pakistan, the researchers focused on the forest carbon stock such as temperate forest (Ahmad et al., 2015, 2018; Ahmad and Nizami, 2015), subtropical forest (Nizami, 2012), and in the planted forest (Saeed et al., 2016). However, no up-to-date studies have been conducted on the soil carbon allocation concerning stand age. Therefore, the current study was carried out in subtropical Chir pine (*Pinus roxburghii*) forest. This species is widely distributed in the Murree, Swat, Dir, and Azad Kashmir. The height of *Pinus roxburghii* is 120 ft, and girth is 7 to 8 ft with the whole of the top canopy. The Chir pine canopy tends to be even-aged over a compact area. The heavy needle falls, and burning reduces the growth of shrubs. Only a few of the species of grasses and herbs are noticeable, the fire virtually immune the older trees from damage and seedling show resistant after the first year while rootstock persists and new shoots appears (Champion et al., 1965). A forest fire is a common behavior of Subtropical Chir pine forest. Regularly, the forest fire incidents took place from April to June during the summer season. The falling of dry needle of Chir pine acts as fuel for forest fire (Nafees and Asghar, 2009). This species is easily cultivated and naturally regenerated in the northern area of Punjab and Khyber Pakhtunkhwa province. *Pinus roxburghii* considered as relatively short-lived and fast-growing species. Because of its longevity and fast growth, seems a suitable species for wood production. *Pinus roxburghii* is a valuable species for forestation, afforestation, and reforestation of denuded areas of Pakistan (Sheikh, 1993; Amir et al., 2018).

Under the shelterwood management system, the Chir pine forest is managed. According to this system, the forest area is divided into various blocks on the base of age, following different management operations. Felling and cutting activities are concentrated on over-mature blocks. In the mature block, thinning operations are carried out. In the young stand, cleaning operations are carried out. These different management operations in each stand age block may influence the soil carbon. Therefore, the study was designed to assess soil carbon of *Pinus roxburghii* forest ecosystem in age-sequence and to outline, the effect of management operations practices on carbon stock in different stand age classes. Moreover, to provide necessary information on carbon storage potential for the reporting of the Kyoto protocol to provide future recommendations for suitable forest management and making policy decisions. Here, our objective of the study was to investigate SOC stocks in age-sequence along various soil depths.

http://www.aloki.hu ● ISSN 1589 1623 (Print) ● ISSN 1785 0037 (Online)
DOI: http://dx.doi.org/10.15666/aeer/1705_114751487

Materials and Methods

Study site

The present study was conducted in Murree Hill of Pakistan. The latitude and longitude of the study site were ranged from 33º 47'15" to 33º 54' 47" N and 73º 16' 54" to 73º 29' 18" E. The elevations of the Chir Pine forest from sea level are range from 939 to1873 m. The mean precipitation ranges from 500 to 1200 mm while the temperature of the studied forest varies from -5ºC in winter to 40ºC in summer. The sedimentary rocks are comprised of shales, limestone sandstones, and marls. The soil was loamy with a proportion of silt, clay, and sand (Sheikh, 1993). The study area is the natural zone of Chir Pine forest that is managed under a shelterwood system. The dominant tree species of the study area is Chir Pine. The major associated tree species are *Pinus wallichiana* (kail), *Pyrus pashia* (batangi), and *Quercus incana* (rhin). The associated understory flora consists of *Carissa spinarum* (granda), *Myrsine africana* (khukhal), *Dodonea viscosa* (sanatha), *Berberis lycium* spp. (sumblu), *Capparis decidua* (karir), *Cannabus sativa* (Bang) and *Adhatoda vasica* (Bahekar). The map shows the location of the study area (*Fig. 1*).

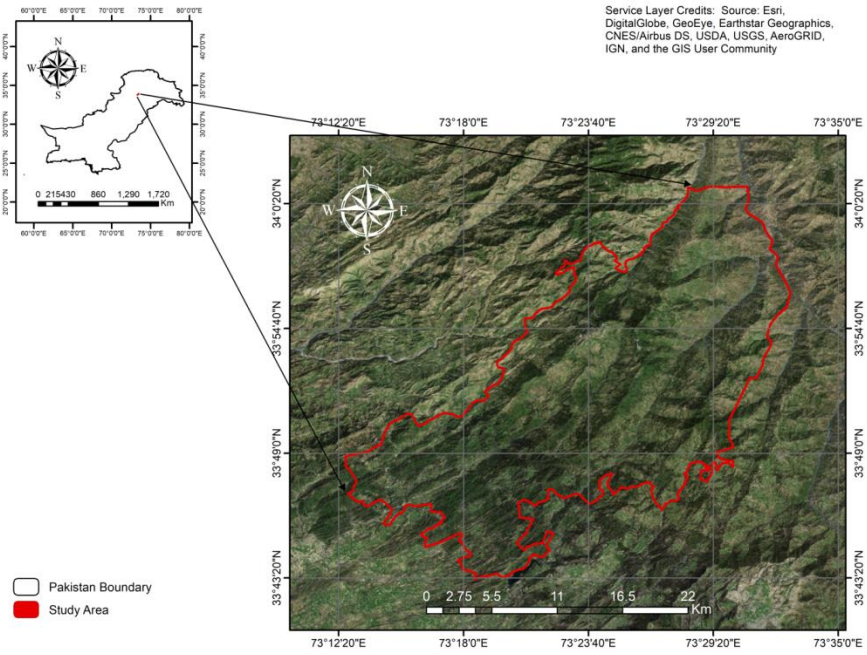

Figure 1. *Range of study area, Murree Hill*

Research design

Pinus roxburghii forest was managed under a shelterwood system. Based on uniform shelterwood silvicultural management system, the Chir Pine forest consists of four periodic blocks (PBI, PBII, PBIII, PBIV) with rotation age (100 years) and regeneration period (25 years), which followed stands of four ages (1-25, 26-50, 51-75 and 76-100 years) (*Table 1*). According to the system, regeneration felling is carried out in PBIV, but some prescribed numbers of trees are retained for seed production. After the establishment of regeneration, then seed bearer is removed for the development of new trees. The duration between regeneration and final felling take 25 years. In PBIII, the

http://www.aloki.hu ● ISSN 1589 1623 (Print) ● ISSN 1785 0037 (Online)
DOI: http://dx.doi.org/10.15666/aeer/1705_114751487

thinning operations are carried out in PBIII for growth enhancement. The study area was classified into three age classes on the base of current forest structure and accurate measurement, PBI and PBII representing young age class (1-50 years), PBIII representing the mature stand (50-75 years) and PBIV representing over the mature stand (>75 years). Moreover, the comparison of SOC with growing stock and biomass of the *Pinus roxburghii* forest, information has mentioned in *Table 2* (Amir et al., 2018).

Table 1. *Sketch of the uniform shelterwood system*

Periodic Blocks	Age at the time of formation	Age at the end of the regeneration period
PBI	1-25	76-100
PBII	26-50	51-75
PBIII	51-75	26-50
PBIV	76-100	1-25

Table 2. *Characteristics of Chir Pine forest. Superscripts in each column show significant differences at α=0.1 and p= <0.0001)*

Age group	Mean Basal Area (m^2ha^{-1})	Mean Stand Density (trees ha^{-1})	Mean Stand Volume (m^3ha^{-1})	Mean total tree biomass (t ha^{-1})
Young	15.5±1.6 ^{B}	636.6±93.7 ^{A}	83.0±12.9 ^{C}	80.0±12.4 ^{C}
Mature	35.5±18.0 ^{A}	267±115.7 ^{B}	356.0±105.9 ^{B}	343.1±167.6^{B}
Over Mature	45.9±15.1 ^{A}	147.6±56.7 ^{C}	549.4±107.1 ^{A}	529.5±176.8 ^{A}
Mean	32.3	350.4	329.4	338.3

Soil samples collection and treatment

The area maps and topographic sheets were taken from the respective forest department. GPS determined coordinates and elevation (m) of each sample area. The stratified random sampling method was done in each block. The soil samples were collected from the subplot of (1×1 m^2) within quadrate at a depth of 0-20 cm, 20-40 cm, and 40-60 cm. In each stand, eight sample plots were taken with three replicate plots. The soil samples were collected by using the Soil Augur. The volume of the soil core was 198.24 cm^3 with 5.9 cm diameter and 7.25 cm height dimension. After weighing and packing of the labeled soil samples were brought into the laboratory to keep it in the oven for 48 hours at 72ºC for further analysis and the soil bulk density was determined from air-dried soil samples. The air-dried sample was ground with a pestle and passed through 0.5 mm sieve manually for SOC determination, as mentioned by Lu (1999).

Soil bulk density calculation

For the determination of total soil carbon, the soil bulk density of samples in each age group was determined from the weight of soil sample and known volume of soil core according to given *Equation (1).*

$$SBD\ (g/cm^3) = \frac{WS}{VS} \qquad \text{(Eq.1)}$$

where SBD = soil bulk density (g/cm^3), WS = weight of soil sample (g) and VS = volume soil core (cm^3).

http://www.aloki.hu ● ISSN 1589 1623 (Print) ● ISSN 1785 0037 (Online)
DOI: http://dx.doi.org/10.15666/aeer/1705_114751487

Soil carbon measurement

Soil carbon density was determined by using the oxidizable organic carbon method (Walkley and Black, 1934; Rayment and Higginson, 1992; Anderson and Ingram, 1994; Ahmad and Nizami, 2015). In this method, the Potassium dichromate solution was prepared by drying in an oven at 105ºC for two hours and cooled it. Then distilled water was added into the 49.09 gm of dried potassium dichromate to dissolve and took one volume of solution from it. 196 gm of distilled water was added into the ferrous ammonium sulfate solution and to dissolve and prepared to one-liter volume. 5 ml sulfuric acid was taken and mixed with it and brought to one volume of solution. One gram of diphenylamine indicator was dissolve and added into the concentrated H_2SO_4. One gram of soil was taken in 500 ml beaker with 10 ml Potassium dichromate solution. 200 ml of concentrated H_2SO_4 was added, and the mixture was kept for 30 minutes, and then 10 ml of H_3PO_4 and 10 ml of water was added to the mixture, then the mixture was kept to cool for ten minutes, and 10-15 drops of Diphenylamine indicator was added to this mixture. When the mixture changes the color from violet-blue to green by the titration of 0.5 ferrous ammonium sulfate solution and then reading was noted. The total organic carbon was calculated by the given *Equation (2)*.

$$Oxidable\ organic\ carbon\ \% = \frac{blank\ volume - actual\ volume \times 0.3 \times M}{Weight\ of\ air-dry\ soil\ (gm)} \quad \text{(Eq.2)}$$

where M = Molarity of ferrous ammonium sulfate, $0.3=31\times0^{-3}\times100$, here 3 shows equivalent to the weight of carbon, Av = volume of Ferrous ammonium sulfate to titrate with sample and Bv = Ferrous ammonium sulfate solution volume to titrate it with the blank solution.

Soil carbon (Mg C ha^{-1}) calculation

Soil carbon (Mg C ha^{-1}) was calculated from the soil organic carbon (SOC %), soil bulk density (g/cm^3) and thickness of horizon (cm). Soil carbon (Mg C ha^{-1}) was calculated from the following equation (Pearson et al., 2007; Nizami, 2012; Ahmad et al., 2015).

$$Soil\ carbon\ (Mg\ C\ ha^{-1}) = SBD\ (g/cm^3) \times SOC\ (\%) \times SHT\ (cm) \times 100 \quad \text{(Eq.3)}$$

where SBD = Soil bulk density (g/cm^3), SOC = Soil organic content (%) and SHT = Soil horizon thickness (cm).

Statistical analysis

Sigmaplot (12.5 version) and Statistics (8.1 version) software were used for statistical analysis. Mean, standard deviation and standard error were calculated. Analysis of variance (One-way ANOVA) along with all pairwise comparison and least significance difference (LSD) test was performed to test the significant difference of the means values of the soil bulk density and soil carbon.

http://www.aloki.hu ● ISSN 1589 1623 (Print) ● ISSN 1785 0037 (Online)
DOI: http://dx.doi.org/10.15666/aeer/1705_114751487

Results

SOC was higher in young stand ages at a depth of 0-20 cm as compared to the 20-40, and 40-60 cm depth (*Fig. 2*). The average SOC in the young stand at a depth of 0-20, 20-40 and 40-60 cm was 36.49, 17.43 and 17.04 Mg C ha^{-1}, respectively. Moreover, the significant differences found between different stand ages at a depth of 0-20 cm, F (2, 14) = 71.70, p = 0.0000. The higher SOC was found at a depth of 0-20 cm in the mature stand age. The mean SOC in the mature stand at a depth of 0-20, 20-40 and 40-60 cm was 37.43, 17.22, and 13.31 Mg C ha^{-1}, respectively.

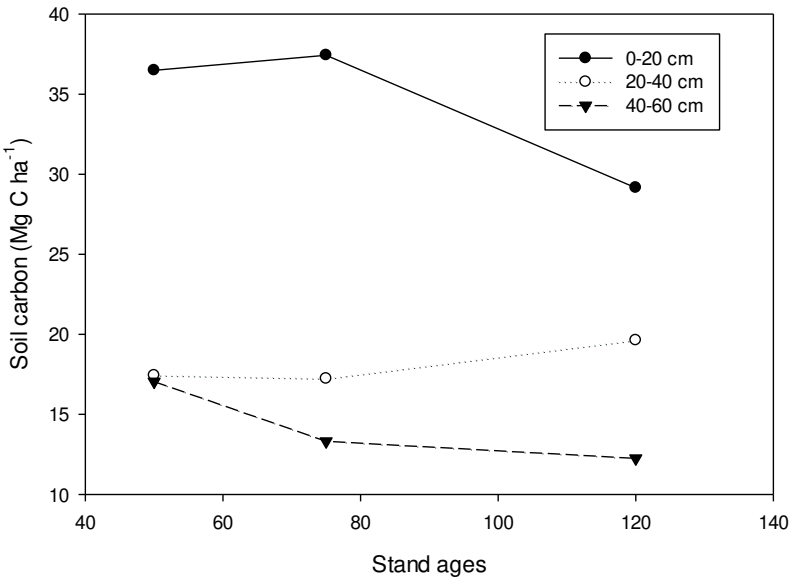

Figure 2. *Soil carbon stock of different stand ages at various soil depths*

The results showed significant differences at the top layer of the mature stand, F (2, 14) = 30.09, p = 0.0000. SOC was higher in over-mature stand ages at a depth of 0-20 cm as compared to 20-40, and 40-60cm depth. The mean SOC in over-mature stand at the depth of 0-20, 20-40 and 40-60 cm was 29.15, 19.62 and 12.25 Mg C ha^{-1}, respectively, with a significant difference, F (2, 14) = 10.14, p = 0.0019 (*Table 3 Table 4*).

Table 3. *SOC in young, mature and over-mature stand at various soil depths*

Soil depths	Young	Mature	Over-mature
0-20 cm	36.49 ± 3.98^{A}	37.43 ± 2.92^{A}	29.154 ± 3.3^{A}
20-40 cm	17.43 ± 4.23^{B}	17.22 ± 7.84^{B}	19.627 ± 6.81^{B}
40-60 cm	17.04 ± 4.06^{B}	13.31 ± 7.81^{B}	12.250 ± 8.11^{B}

Table 4. *Relationship type, equation and R^2 value of the Pinus roxburghii stands*

Soil depths	Parameters	Relationship type	Equation	R^2 Value
0-20 cm	SA & SC	Polynomial, linear	y = -0.1132x + 43.454	0.83
0-40 cm	SA & SC	Polynomial, linear	y = 0.0339x + 15.32	0.81
40-60 cm	SA & SC	Polynomial, linear	y = -0.0631x + 19.351	0.79

SA= Stand ages (<50, 50-75, >120 years old stands) and SC = Soil carbon (Mg C ha^{-1})

http://www.aloki.hu ● ISSN 1589 1623 (Print) ● ISSN 1785 0037 (Online)
DOI: http://dx.doi.org/10.15666/aeer/1705_114751487

SOC was higher in different stand ages at a depth of 0-20 cm as compared to the 20-40, and 40-60 cm depth. The average SOC in young, mature and over-mature stands were 36.493, 37.44 and 29. 15 (Mg C ha^{-1}), respectively. Moreover, the significant differences found between different stand ages at a depth of 0-20 cm, F (2, 21) = 14, $p = 0.0001$. While, the non-significant differences found at the depth of 20-40 cm (F (2, 21) = 0.34, $p = 0.72$), and 40-60 cm (F (2, 21) = 1.04, $p = 0.36$) for different stand ages. The average SOC for young, mature and over-mature stands were 17.43, 17.22, 19.62 Mg C ha^{-1} at a depth of 20-40 cm, while at a depth of 40-60 cm, there were 17.05, 13.31, 12.25 Mg C ha^{-1}, respectively (*Fig. 3*).

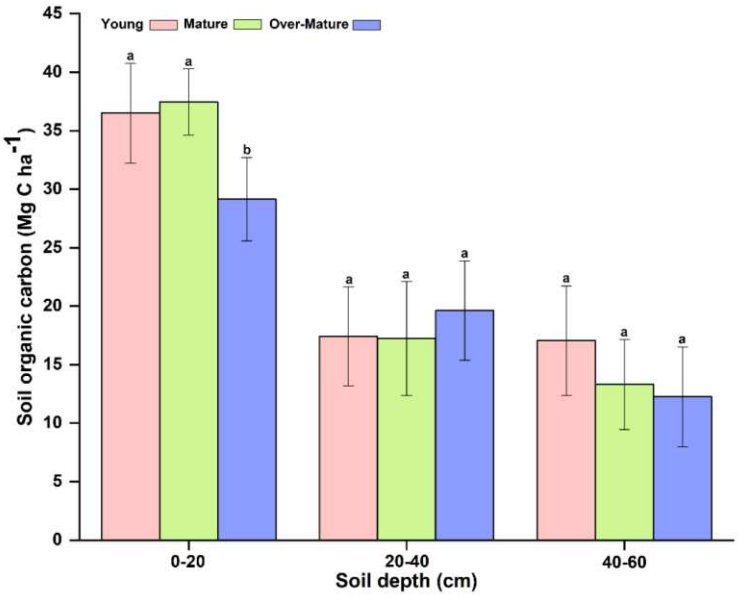

Figure 3. *Soil organic carbon contents. SOC in young, mature, and over-mature stand at various depths. The different letters on the bar are showing significant differences while the same letters are showing the non-significant different between different classes of stand ages. Alphabets on the top of each bar are showing the* $LSD_{0.05}$ *difference*

The soil organic matter (SOM) in the young stand at a depth of 0-20, 20-40 and 40-60 cm was 2.95, 1.68 and 1.38%, respectively. The SOM in the mature stand at a depth of 0-20, 20-40 and 40-40 cm was 2.88, 1.35 and 0.98%, respectively. SOM in the over-mature stand at a depth of 0-20, 20-40 and 40-60 cm was 2.76, 1.68 and 0.96%, respectively. The resulted that higher SOM was found at the 0-20 cm soil depth and following the decreasing trend from upper to lower soil depth in each stand. Soil Bulk density (SBD) results showed almost similar values in different stand ages at each depth. The mean SBD in young, mature and over-mature stands at a depth of 0-20 cm were 1.09, 1.04 and 0.93 (g/cm^3), respectively. Moreover, the significant differences found between different stand ages at a depth of 0-20 cm, F (2, 21) = 9.51, $p = 0.0011$. The average SBD in young, mature and over-mature stands at a depth of 20-40 cm were 1.13, 1.10 and 1.04 (g/cm^3), respectively. The significant difference observed at a depth of 20-40 cm in young stand ages, F (2, 21) = 4.34, $p = 0.0265$. The mean SBD in young, mature and over-mature stands at a depth of 40-60 cm were 1.15, 1.08 and 1.06 (g/cm^3),

http://www.aloki.hu ● ISSN 1589 1623 (Print) ● ISSN 1785 0037 (Online)
DOI: http://dx.doi.org/10.15666/aeer/1705_114751487

respectively. Meanwhile, the significant difference found in different stand ages $F(2, 21) = 3.64$, $p = 0.0440$ (*Fig. 4*).

Generally, the results of soil carbon analysis showed a decreasing trend with increasing stand age. Soil carbon showed decreased with increasing at different soil depth in each stand. This decreasing trend in soil may be attributed to the soil disturbance during the felling operations in the over-mature stand and decrease in the natural thinning with the stand age. Additionally, there was an inverse relationship between soil carbon and soil bulk density. Soil bulk density increased with a decrease in soil organic carbon at various depths. The higher degree of soil organic matter (SOM) showed a lower degree of bulk density. The SOM and SBD are inversely proportional to each other, which indicate higher infiltration and, proper aeration and granulation. The soil bulk densities in each stand age showed significant variation.

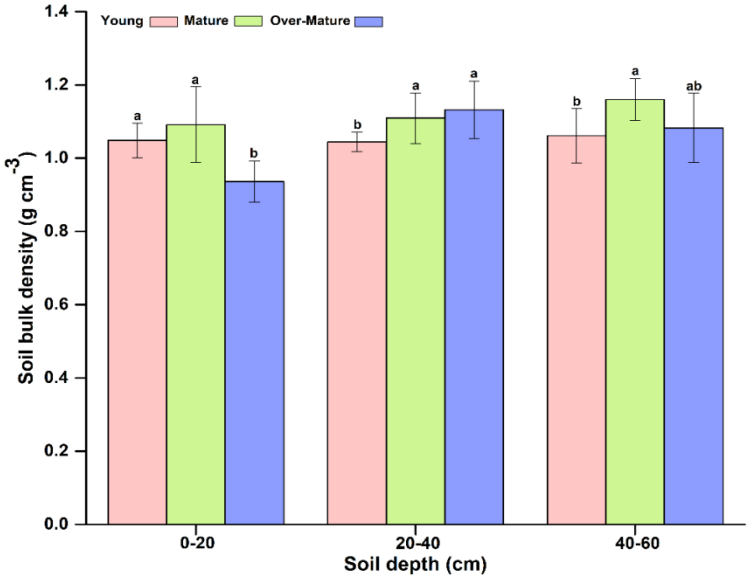

Figure 4. *Soil Bulk density. SBD in young, mature, and over-mature stand at various depths. The different letters on the bar are showing significant differences while the same letters are showing the non-significant different between different classes of stand ages. Alphabets on the top of each bar are showing the* $LSD_{0.05}$ *difference*

Discussion

It is quite difficult to compared SOC with forest biomass (Teklay and Chang, 2008; Laganiere et al., 2010), because SOC may be affected by various factors, such as stand age, tree species, forest type, climate, and soil chemical and physical properties (Richter et al., 1999; Guo and Gifford, 2002; Paul et al., 2002; Peichl and Arain, 2006; Mora et al., 2014; Wang et al., 2014). Soil organic carbon across stand age has been widely carried out with different results. In many studies, SOC stock increases with the forest stand age (Smal and Olszewska, 2008; Berthrong et al., 2009) while the opposite result was also found after afforestation (Teklay and Chang, 2008; Mao et al., 2010). Afforestation and reforestation have been considered to be essential to reduce atmospheric CO_2 emission by sequestering carbon in soils (Richter et al., 1999; Smal and Olszewska, 2008). Therefore, SOC in surface soil layer could be affected by the changes of the upperstory, understory, litter, shrub and herb biomass, and soil

http://www.aloki.hu ● ISSN 1589 1623 (Print) ● ISSN 1785 0037 (Online)
DOI: http://dx.doi.org/10.15666/aeer/1705_114751487

characteristics with stand age sequence (Six et al., 2002; Noh et al., 2010). Many studies found that the SOC content declines firstly and then increases with the increasing of stand age (Chen et al., 2005; Mao et al., 2010). The mean soil carbon showed decreased with respective stand age as well as with soil depth. The soil carbon was recorded higher in the topsoil of each stand as compared to deeper soil. It may be due to producing of SOC by the decomposition of the root system and litter, which entered into topsoil first near the ground as demonstrated by other studies (Peichl and Arain, 2006; Tian et al., 2010; Zhang et al., 2012). The current study showed carbon content of soil layer showed a decreasing trend with stand age while other study showed increasing of soil carbon with stand age due to the availability litter productivity in high older stands (Ming et al., 2014).

Soil carbon depends on the forest stand age, forest types, forest productivity, the chemical and physical properties, and litter decomposition rate of the soil (Gower, 2003; Kang et al., 2006; Jandl et al., 2007; He et al., 2013). Our study showed a decreasing trend with stand age. The proportion of soil carbon stock should need focus during any management activities for the enhancement of future soil carbon sequestration of *Pinus roxburghii* forest ecosystem.

The SOC exists different debates on whether or not SOC potential could change with respect to forest stand ages (Farley et al., 2004; Lemma et al., 2006). Some previous researches showed that soil carbon stock is not increasing with increasing stand ages significantly (Farley et al., 2004; Cheng et al., 2013), while some other researches showed that SOC increasing with increasing forest stand age (Hooker and Compton, 2003; Pregitzer and Euskirchen, 2004; Lemma et al., 2006). The difference may be due to various factors such as soil factor climatic factor and forest type (Peichl and Arain, 2006). However, generally, SOC increases with stand age in conifer forest, due to the accumulation of organic matter in older stages (Zerva et al., 2005; Li et al., 2013). However, in the case of the present study, the soil carbon decreases with increasing stand age, may be due to the result of management operations such as felling and thinning activates. During these operations, the top layer of the soil exposed to rainfall and wind, wash out the soil surface, which may lead to reducing of soil carbon.

Conclusion

The soil carbon density decreased with the increase of forest stand ages and decreased with increasing soil depths in different stand ages. However, the soil carbon showed gradually decreasing trend from young to over-mature stand. Furthermore, our results showed the effects of management operations on soil carbon. The decreasing of soil carbon value with respect to stand ages may be is the result of soil disturbances during management operations. Therefore, we suggest different protection measures such as reduced impact logging, soil conservation through mulching, maintaining understory vegetation and forest cover through regeneration, control grazing and effective management of forest fire should be considered. The appropriate management of forest could allow the importance of forest soil in the regional carbon budget.

Furthermore, the results highlighted that regeneration and afforestation of Chir Pine could promote the potential capability of SOC and provide necessary data for estimating the carbon stocks of Chir Pine forest ecosystem. The present results highlighted the importance of stand age in assessing forest soil carbon measurement for policymakers when modeling climate scenarios.

http://www.aloki.hu ● ISSN 1589 1623 (Print) ● ISSN 1785 0037 (Online)
DOI: http://dx.doi.org/10.15666/aeer/1705_114751487

Acknowledgements. The research was supported by the Beijing Forestry University Innovation Program Project (BLRW200939) and National Key Research and Development Project of China (2017YFD0600106).

REFERENCES

[1] Ahmad, A., Nizami, S. M. (2015): Carbon stocks of different land uses in the Kumrat Valley, Hindu Kush Region of Pakistan. – Journal of forestry research 26(1): 57-64.
[2] Ahmad, A., Nizami, S., Marwat, K., Muhammad, J. (2015): Annual Accumulation of Carbon in the Coniferous Forest of Dir Kohistan: An Inventory based Estimate. – Pakistan Journal of Botany 47: 115-118.
[3] Ahmad, A., Liu, Q. J., Nizami, S., Mannan, A., Saeed, S. (2018): Carbon emission from deforestation, forest degradation and wood harvest in the temperate region of Hindukush Himalaya, Pakistan between 1994 and 2016. – Land use policy 78: 781-790.
[4] Amir, M., Liu, X., Ahmad, A., Saeed, S., Mannan, A., Atif Muneer, M. (2018): Patterns of Biomass and Carbon Allocation across Chronosequence of Chir Pine (*Pinus roxburghii*) Forest in Pakistan: Inventory-Based Estimate. – Advances in Meteorology Article ID 3095891, 8 pages, https://doi.org/10.1155/2018/3095891.
[5] Anderson, J. M., Ingram, J. (1994): Tropical soil biology and fertility: a handbook of methods. – Soil Science 157(4): 265.
[6] Berthrong, S. T., Jobbágy, E. G., Jackson, R. B. (2009): A global meta-analysis of soil exchangeable cations, pH, carbon, and nitrogen with afforestation. – Ecological Applications 19(8): 2228-2241.
[7] Bradford, J. B., Kastendick, D. N. (2010): Age-related patterns of forest complexity and carbon storage in pine and aspen–birch ecosystems of northern Minnesota, USA. – Canadian Journal of Forest Research 40(3): 401-409.
[8] Cao, J., Wang, X., Tian, Y., Wen, Z., Zha, T. (2012): Pattern of carbon allocation across three different stages of stand development of a Chinese pine (*Pinus tabulaeformis*) forest. – Ecological Research 27(5): 883-892.
[9] Champion, S. H., Seth, S. K., Khattak, G. (1965): Forest types of Pakistan.
[10] Chen, X., Hutley, L. B., Eamus, D. (2005): Soil organic carbon content at a range of north Australian tropical savannas with contrasting site histories. – Plant and Soil 268(1): 161-171.
[11] Cheng, X., Han, H., Kang, F., Song, Y., Liu, K. (2013): Variation in biomass and carbon storage by stand age in pine (*Pinus tabulaeformis*) planted ecosystem in Mt. Taiyue, Shanxi, China. – Journal of Plant Interactions 9(1): 521-528. doi:10.1080/17429145.2013.862360.
[12] Farley, K. A., Kelly, E. F., Hofstede, R. G. (2004): Soil organic carbon and water retention after conversion of grasslands to pine plantations in the Ecuadorian Andes. – Ecosystems 7(7): 729-739.
[13] Gower, S. T. (2003): Patterns and mechanisms of the forest carbon cycle. – Annual Review of Environment and Resources 28(1): 169-204.
[14] Guo, L. B., Gifford, R. (2002): Soil carbon stocks and land use change: a meta-analysis. – Global change biology 8(4): 345-360.
[15] He, Y., Qin, L., Li, Z., Liang, X., Shao, M., Tan, L. (2013): Carbon storage capacity of monoculture and mixed-species plantations in subtropical China. – Forest ecology and management 295: 193-198.
[16] Hooker, T. D., Compton, J. E. (2003): Forest ecosystem carbon and nitrogen accumulation during the first century after agricultural abandonment. – Ecological Applications 13(2): 299-313.

http://www.aloki.hu ● ISSN 1589 1623 (Print) ● ISSN 1785 0037 (Online)
DOI: http://dx.doi.org/10.15666/aeer/1705_114751487

[17] Jandl, R., Lindner, M., Vesterdal, L., Bauwens, B., Baritz, R., Hagedorn, F., Byrne, K. A. (2007): How strongly can forest management influence soil carbon sequestration? – Geoderma 137(3-4): 253-268.
[18] Johnson, D., Todd, D., Trettin, C., Sedinger, J. (2007): Soil carbon and nitrogen changes in forests of Walker Branch watershed, 1972 to 2004. – Soil Science Society of America Journal 71(5): 1639-1646.
[19] Kang, B., Liu, S., Zhang, G., Chang, J., Wen, Y., Ma, J., Hao, W. (2006): Carbon accumulation and distribution in *Pinus massoniana* and *Cunninghamia lanceolata* mixed forest ecosystem in Daqingshan, Guangxi, China. – Acta Ecologica Sinica 26(5): 1320-1327.
[20] Laganiere, J., Angers, D. A., Pare, D. (2010): Carbon accumulation in agricultural soils after afforestation: a meta-analysis. – Global change biology 16(1): 439-453.
[21] Lal, R. (2004): Soil carbon sequestration impacts on global climate change and food security. – Science 304(5677): 1623-1627.
[22] Lal, R., Kimble, J. M., Rice, C. W., Reed, D., Mooney, S., Follett, R. F. (2007): Soil carbon management: economic, environmental and societal benefits. – CRC press.
[23] Lemma, B., Kleja, D. B., Nilsson, I., Olsson, M. (2006). Soil carbon sequestration under different exotic tree species in the southwestern highlands of Ethiopia. – Geoderma 136(3-4): 886-898.
[24] Li, C., Zha, T., Liu, J., Jia, X. (2013): Carbon and nitrogen distribution across a chronosequence of secondary lacebark pine in China. – The Forestry Chronicle 89(2): 192-198.
[25] Lu, R. (1999): Analytical methods of soil agrochemistry. – China Agricultural Science and Technology Publishing House, Beijing, China, pp. 18-99.
[26] Manan, A., Feng, Z., Ahmad, A., Liu, J., Saeed, A., Mukete, B. (2018): Carbon Dynamic Shifts with Land Use Change in Margallah Hills National Park, Islamabad (Pakistan) from 1990 to 2017. – Applied Ecology and Environmental Research 16(3): 3197-3214.
[27] Mannan, A., Liu, J., Zhongke, F., Khan, T. U., Mukete, B., ChaoYong, S. (2019): Application of land-use/land cover changes in monitoring and projecting forest biomass carbon loss in Pakistan. – Global Ecology and Conservation: e00535.
[28] Mao, R., Zeng, D.-H., Hu, Y.-L., Li, L. J., Yang, D. (2010): Soil organic carbon and nitrogen stocks in an age-sequence of poplar stands planted on marginal agricultural land in Northeast China. – Plant and Soil 332(1-2): 277-287.
[29] Martin, J. L., Gower, S. T., Plaut, J., Holmes, B. (2005): Carbon pools in a boreal mixed wood logging chronosequence. – Global Change Biology 11(11): 1883-1894.
[30] Ming, A., Jia, H., Zhao, J., Tao, Y., Li, Y. (2014): Above-and below-ground carbon stocks in an indigenous tree (*Mytilaria laosensis*) plantation chronosequence in subtropical China. – PloS one 9(10): e109730.
[31] Mora, J., Guerra, J., Armas-Herrera, C., Arbelo, C., Rodríguez-Rodríguez, A. (2014): Storage and depth distribution of organic carbon in volcanic soils as affected by environmental and pedological factors. – Catena 123: 163-175.
[32] Nafees, M., Asghar, A. (2009): Forest fire events in Swat valley, Pakistan. – Pak J. Plant Sci 15(1): 31-37.
[33] Nizami, S. M., Mirza, S. N., Livesley, S., Arndt, S., Fox, J. C., Khan, I. A. (2009): Estimating carbon stocks in sub-tropical pine (*Pinus roxburghii*) forests of Pakistan. – Pakistan Journal of Agricultural Sciences 46(4): 266-270.
[34] Nizami, S. M. (2012): The inventory of the carbon stocks in sub-tropical forests of Pakistan for reporting under the Kyoto Protocol. – Journal of forestry research 23(3): 377-384.
[35] Noh, N. J., Son, Y., Lee, S. K., Seo, K. W., Heo, S. J., Yi, M. J., Lee, K.-H. (2010): Carbon and nitrogen storage in an age-sequence of Pinus densiflora stands in Korea. – Science China Life Sciences 53(7): 822-830.

http://www.aloki.hu ● ISSN 1589 1623 (Print) ● ISSN 1785 0037 (Online)
DOI: http://dx.doi.org/10.15666/aeer/1705_114751487

[36] Paul, K. I., Polglase, P. J., Nyakuengama, J., Khanna, P. (2002): Change in soil carbon following afforestation. – Forest ecology and management 168(1-3): 241-257.
[37] Pearson, T. R., Brown, S. L., Birdsey, R. A. (2007): Measurement guidelines for the sequestration of forest carbon. – Gen. Tech. Rep. NRS-18. Newtown Square, PA: US Department of Agriculture, Forest Service, Northern Research Station. 42 pp18.
[38] Peichl, M., Arain, M. A. (2006): Above-and belowground ecosystem biomass and carbon pools in an age-sequence of temperate pine plantation forests. – Agricultural and Forest Meteorology 140(1-4): 51-63.
[39] Peichl, M., Arain, M. A. (2007): Allometry and partitioning of above-and belowground tree biomass in an age-sequence of white pine forests. – Forest Ecology and Management 253(1): 68-80.
[40] Pregitzer, K. S., Euskirchen, E. S. (2004): Carbon cycling and storage in world forests: biome patterns related to forest age. – Global change biology 10(12): 2052-2077.
[41] Rayment, G., Higginson, F. R. (1992): Australian laboratory handbook of soil and water chemical methods. – Inkata Press Pty Ltd.
[42] Richter, D. D., Markewitz, D., Trumbore, S. E., Wells, C. G. (1999): Rapid accumulation and turnover of soil carbon in a re-establishing forest. – Nature 400(6739): 56.
[43] Saeed, S., Ashraf, M. I., Ahmad, A., Rahman, Z. (2016): The Bela Forest ecosystem of District Jhelum. A potential carbon sink. – Pakistan Journal of Botany 48(1): 121-129.
[44] Saeed, S., Yujun, S., Beckline, M., Chen, L., Zhang, B., Ahmad, A., Iqbal, A. (2019a): Forest edge effect on biomass carbon along altitudinal gradients in Chinese Fir (*Cunninghamia lanceolata*): A study from Southeastern China. – Carbon Management 10(1): 11-22. doi:10.1080/17583004.2018.1537517.
[45] Saeed, S., Sun, Y., Beckline, M., Chen, L., Lai, Z., Mannan, A., Ullah, T. (2019b): Altitudinal Gradients And Forest Edge Effect On Soil Organic Carbon In Chinese Fir (*Cunninghamia Lanceolata*): A Study From Southeastern China. – Applied Ecology And Environmental Research 17(1): 745-757.
[46] Sheikh, M. I. (1993): Trees of Pakistan. – Pictoral Printers, Islamabad, Pakistan, vol. 110.
[47] Six, J., Callewaert, P., Lenders, S., De Gryze, S., Morris, S., Gregorich, E., Paustian, K. (2002): Measuring and understanding carbon storage in afforested soils by physical fractionation. – Soil science society of America journal 66(6): 1981-1987.
[48] Smal, H., Olszewska, M. (2008): The effect of afforestation with Scots pine (*Pinus silvestris* L.) of sandy post-arable soils on their selected properties. II. Reaction, carbon, nitrogen and phosphorus. – Plant and Soil 305(1-2): 171-187.
[49] Song, L., Zhu, J., Li, M., Zhang, J., Zheng, X., Wang, K. (2018): Canopy transpiration of *Pinus sylvestris* var. *mongolica* in a sparse wood grassland in the semiarid sandy region of Northeast China. – Agric. For. Meteorol 250-251: 192-201.
[50] Sundquist, E. T. (1993): The global carbon dioxide budget. – Science 934-941.
[51] Taylor, A. R., Wang, J. R., Chen, H. Y. (2007): Carbon storage in a chronosequence of red spruce (*Picea rubens*) forests in central Nova Scotia, Canada. – Canadian Journal of Forest Research 37(11): 2260-2269.
[52] Teklay, T., Chang, S. X. (2008): Temporal changes in soil carbon and nitrogen storage in a hybrid poplar chronosequence in northern Alberta. – Geoderma 144(3-4): 613-619.
[53] Tian, D., Yin, G., Fang, X., Yan, W. (2010): Carbon density, storage and spatial distribution under different 'Grain for Green'patterns in Huitong, Hunan province. – Acta Ecological Sinica 30: 6297-6308.
[54] Walkley, A., Black, I. A. (1934): An examination of the Degtjareff method for determining soil organic matter, and a proposed modification of the chromic acid titration method. – Soil Science 37(1): 29-38.
[55] Wang, D., Wang, B., Niu, X. (2014): Forest carbon sequestration in China and its benefits. – Scandinavian journal of forest research 29(1): 51-59.

http://www.aloki.hu ● ISSN 1589 1623 (Print) ● ISSN 1785 0037 (Online)
DOI: http://dx.doi.org/10.15666/aeer/1705_114751487

[56] Watson, R. T., Noble, I. R., Bolin, B., Ravindranath, N., Verardo, D. J., Dokken, D. J. (2000): Land use, land-use change and forestry: a special report of the Intergovernmental Panel on Climate Change. – Cambridge University Press.
[57] Yang, Y., Fang, J., Ma, W., Smith, P., Mohammat, A., Wang, S. (2010): Soil carbon stock and its changes in northern China's grasslands from 1980s to 2000s. – Global Change Biology 16(11): 3036-3047.
[58] Zerva, A., Ball, T., Smith, K. A., Mencuccini, M. (2005): Soil carbon dynamics in a Sitka spruce (*Picea sitchensis* Bong.) chronosequence on a peaty gley. – Forest Ecology and Management 205(1-3): 227-240.
[59] Zhang, H., Guan, D., Song, M. (2012): Biomass and carbon storage of Eucalyptus and Acacia plantations in the Pearl River Delta, South China. – Forest ecology and management 277: 90-97.
[60] Zhao, J., Kang, F., Wang, L., Yu, X., Zhao, W., Song, X. (2014): Patterns of biomass and carbon distribution across a chronosequence of Chinese pine (*Pinus tabulaeformis*) forests. – PLoS one 9(4): e94966.
[61] Zhu, B., Wang, X., Fang, J., Piao, S., Shen, H., Zhao, S. (2010): Altitudinal changes in carbon storage of temperate forests on Mt Changbai, Northeast China. – Journal of plant research 123(4): 439-452.

http://www.aloki.hu ● ISSN 1589 1623 (Print) ● ISSN 1785 0037 (Online)
DOI: http://dx.doi.org/10.15666/aeer/1705_114751487

PHYSIOLOGICAL RESPONSE OF LOCAL POPULATIONS OF SPECIES *CYCLAMEN PURPURASCENS* MILL. TO FOREST GAPS

RAVNJAK, B.[1*] – BAVCON, J.[1] – OSTERC, G.[2]

[1]*Department of Biology, Biotechnical Faculty, University Botanic Gardens Ljubljana, Ižanska cesta 15, 1000 Ljubljana, Slovenia*
(phone: +386-14-271-280)

[2]*Department of Agronomy, Biotechnical Faculty, University of Ljubljana, Jamnikarjeva 101, 1000 Ljubljana, Slovenia*

**Corresponding author*
e-mail: blanka.ravnjak@bf.uni-lj.si; phone: +386-31-336-507

(Received 20th Apr 2019; accepted 11th Jul 2019)

Abstract. Aspect of forest dynamics is also the formation of forest gaps. Certain plant species typical for understory, still persists in newly formed forest gaps. For such species, environmental conditions change significantly. In research the physiological response of local populations of *Cyclamen purpurascens* Mill. in forest gaps, depending on time of their formation was examined. The physiological response was measured as anthocyanin and quercetin content in cyclamen leaves, depending on forest gap and season. It was found that anthocyanin content in leaves from all gaps was statistically higher in autumn than in spring. A comparison of anthocyanin content between leaves from different gaps has shown that leaves from the youngest gap in the spring contained a statistically lowest quantity of anthocyanin malvidin 3-rutinoside, malvidin 3-glucoside, and peonidin 3-O-neoheseridoside. There were no differences between other locations. For quercetins, it was found that leaves from the youngest gap in the spring contained the highest amount of myricetin-3-rhamnoside. Conclusion is that cyclamen leaves on the youngest gap have not yet completely adapted to increased solar radiation. Quercetins represent first and immediate response to increased UV-B radiation. Leaves on youngest gap in the spring do not yet have sufficient anthocyanin to protect them against radiation.
Keywords: *anthocyanin, forest dynamics, light stress, quercetin, temperature stress*

Introduction

Forests are one of the most common type of vegetation on the Earth. The layers, from top to ground, are as follows: canopy, understory, shrub layer, and herbaceous layer. A consequence of this stratification are also microclimatic conditions in individual layers. Moisture is thus highest by the forest floor due to evaporation from the ground, and the lowest slightly above the canopy, as air circulation is more intensive there (Smith and Smith, 2001). In terms of temperature, the highest is in the canopy layer, where solar radiation is the most intensive. Temperature then drops towards the floor. Another characteristic is the day and night cycle (generally, the temperature is lowest during the night) and the seasonal cycle in deciduous forests of the warm temperate climate. During spring months in such forests, the temperature is higher also in the organic layer, since canopies lack the leaves, allowing sufficient solar radiation to reach the floor. Increased temperature along the floor in the spring thus facilitates quick growth of spring geophytes (Smith and Smith, 2001; Schultze et al., 2005). Like the temperature, light intensity is also decreasing from top to bottom. In deciduous forests, only 5% of total solar light thus reaches the floor (Chazdon and Pearcy, 1991).

http://www.aloki.hu ● ISSN 1589 1623 (Print) ● ISSN 1785 0037 (Online)
DOI: http://dx.doi.org/10.15666/aeer/1705_1148911508

Considering the lower exposure to light, plants of the herbaceous layer have various adaptations that enable efficient photosynthesis. They are capable of photosynthesis with the lowest solar radiation, utilising the light of longer wave lengths. While investing less energy into growing above-ground segments, they store more reserve food in underground plant organs, which in spring act as an additional source of food for the start of their growth (Whittaker, 1975). In plants that grow in the herbaceous layer while the canopy is leafed, photosynthetic activity mostly depends on sunflecks on the forest floor (Chazdon and Pearcy, 1991). Their leaf surfaces are larger, leaves are thinner, and have a poorly developed mesophyll tissue. They have only one layer of palisade tissue and a lower number of chloroplasts per surface unit, even though the quantity of chlorophyll in chloroplasts is higher than in leaves of plants growing in the sun. Thus, plants growing in the shade utilise to the highest possible degree the light reaching the undergrowth. Furthermore, they capture additional light with hypodermis and epidermis cells (Schultze et al., 2005; Lambers et al., 2008).

A forest gap caused by disturbances can lead tremendous stress as the sudden exposure to solar radiation for understory plants. Forest gaps are otherwise a normal occurrence and are part of the forest dynamic (Peterken, 1996). Compared to surrounding forest, temperature of floor and air, light intensity, and atmospheric humidity change to a greater extend in the area of a forest gap. Maximum light intensity in a gap is reached between 10 AM and 2 PM, and is highest at the centre of the gap. Floor temperature is positively correlated to light intensity, growing from morning to evening in large gaps. In small and medium-sized gaps, floor temperature is the highest between 12 noon and 2 PM (Buajan et al., 2016). Due to the high quantity of sunlight, all plant species that lacked sufficient light for successful growth in the understory under the canopy cannot start to grow in such locations. Generally, the number of herbaceous species is higher on forest gaps than in understorey, and is positively correlated to the size of the gap (Collins and Pickett, 1988; Mihók, 2007). Furthermore, forest gaps represent a chance for forest stand regeneration. Individual trees that only stagnated in the herbaceous layer due to lack of light can accelerate their growth when a forest gap forms (Peterken, 1996).

The larger the forest gap, the greater the effect on local populations of plant species. At the same time, a formation of a forest gaps greatly affects understory plants that are otherwise adapted to weaker sunlight intensity under the canopy. Plants of the understory can respond to the formation of a forest gap, which for them represents stress, either as stress tolerant plants or by avoiding such stress. Shady plants have a lower response plasticity to the stress factor (Middleton, 2001). The adaptation can also manifest in a population reduction of a specific shady species, with only individual specimens thriving in microenvironments, where they are still somewhat protected by the shade of other plants. For instance, when studying the species turnover in forest gap formation, the population of species *Galium odoratum* Scop. was found to be smaller on a gap than in the forest. However, some species (*Viola sylvestris* Lam., *Mercurialis perennis* L.) have adapted to the changed environmental factors (Kelemen et al., 2012).

Substances that protect the plant against permanent damage and death are flavonoids. Their synthesis is induced by UV-B radiation through phytochrome (Caldwell et al., 1983). Flavonoids include anthocyanins, water-soluble pigments present in all plant tissues. Anthocyanins have a key role in protecting tissues against

http://www.aloki.hu ● ISSN 1589 1623 (Print) ● ISSN 1785 0037 (Online)
DOI: http://dx.doi.org/10.15666/aeer/1705_1148911508

photo-inhibition and photo-oxidation (Chalker-Scott, 1999; Cooper-Driver, 2001; Gould et al., 2002; Ishizaka et al., 2002; Hughes et al., 2005, 2007; Hughes, 2011). They act as anti-oxidants that bind free radicals. This forms an anthocyanin-peroxidase system that provides protection against oxidation damage (Yamasuki, 1997; Steyn et al., 2002). Anthocyanins are located in or just under the epidermis. Located closer to the upper side of the leaf, they act as a filter, reducing the level of inbound solar radiation. Anthocyanins thus protect the internal parts of the leaf – primarily chloroplasts – against damage (Gould et al., 2000; Timmins et al., 2002). For this reason, they are – in this case – located above the chloroplasts. Plants growing in locations exposed to strong sunlight contain higher quantities of anthocyanins in leaves, stems, and flowers, compared to shady plants (Wheldale, 1916). In shady plants, they also accumulate in the lower epidermis, thus additionally participating in capturing sunlight (Chalker-Scott, 1999; Steyn et al., 2002). Anthocyanin synthesis is also light-induced; however, as opposed to other flavonoids, anthocyanins absorb sunlight in the visible part of the spectrum and less in the UV-B part (Caldwell et al., 1983; Mendez et al., 1999). Low temperatures under 25 °C accelerate anthocyanin biosynthesis, while high temperatures over 35 °C cause their degradation and inhibit their accumulation (He et al., 2010). Furthermore, excessive UV-B radiation inhibits anthocyanin synthesis, likely due to DNA damage (Chalker-Scott, 1999). In addition to anthocyanins, quercetins are also very effective in binding reactive oxygen compounds. Their synthesis increases both in low and high radiation (Agati et al., 2012; Mierziak et al., 2014). The quantity of anthocyanins and quercetins can therefore act as an indicator whether or not a plant experienced light stress (was suddenly exposed to increased solar radiation), or if it has already adapted to increased solar radiation.

In our study, the physiological response of local populations of common cyclamen (*Cyclamen purpurascens* Mill.) in Dinaric fir-beech forest to increased exposure with solar radiation, as a result of forest gap formation, was examined. The common cyclamen as the subject of our study was chosen because it is one of the typical representatives of understory. Furthermore, it is a perennial plant, allowing us to measure the response of specific specimens to forest gaps, depending on the time from the gap formation, when they were exposed to increased solar radiation. By measuring anthocyanin and quercetin quantity in common cyclamen leaves, the response of specimens in local population was determined. A higher anthocyanin content in specimens of populations growing on older forest gaps, where plants have been exposed to a strong solar radiation for a longer period was predicted. Regardless of the location (forest gap), we predicted a lower anthocyanin quantity in leaves of all common cyclamen specimens during the spring, and higher quantity during late summer and autumn. Quercetin content was examined with the same purpose. A higher quercetin quantity in leaves of specimens growing on older forest gaps was predicted.

Material and methods

Experiment design

In the study 6 sampling locations were included, where five represented forest gaps in Dinaric fir-beech forests (*Omphalodo-Fagetum*) that naturally formed at different times and one sampling location that represented juvenile phase of beech forest. All

http://www.aloki.hu ● ISSN 1589 1623 (Print) ● ISSN 1785 0037 (Online)
DOI: http://dx.doi.org/10.15666/aeer/1705_1148911508

sampling locations were located in the Dinaric biogeographic macro-region in the southern part of Slovenia (Kočevska Region) (Wraber, 1969) (*Figs. 1* and *2; Table 1*).

Figure 1. *Research area in Kočevska region (marked with red square), with detailed map of 6 sampling locations (forest gaps in Dinaric fir-beech forests)*

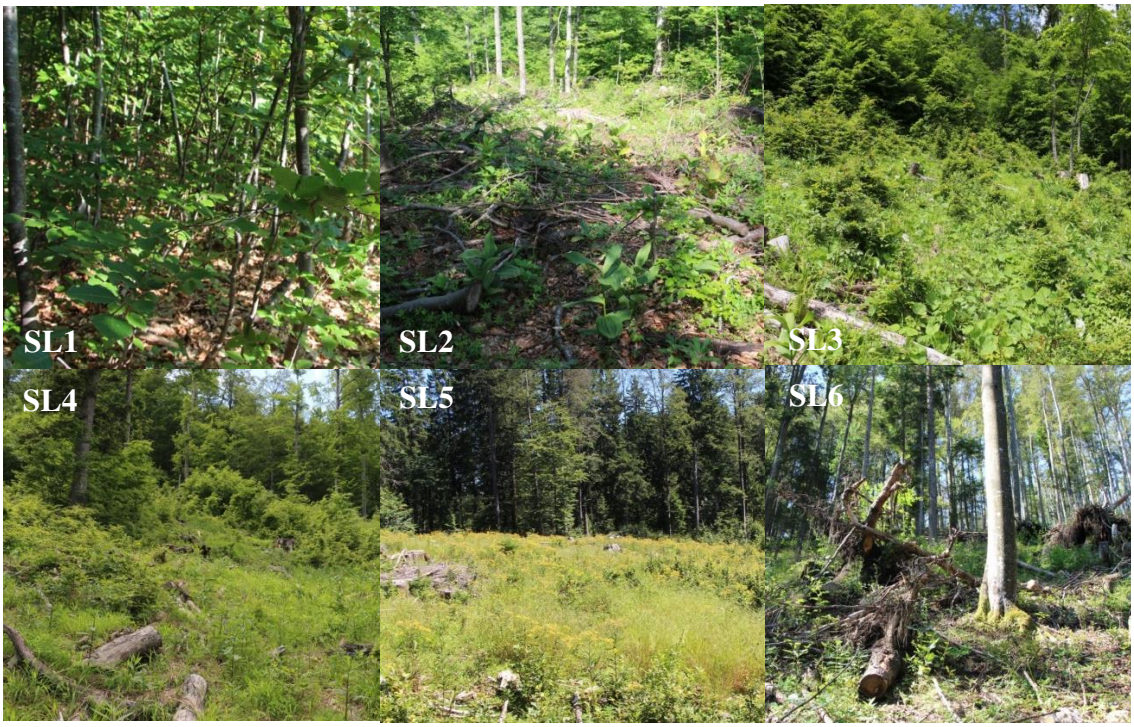

Figure 2. *Photographs of all sampling locations (SL1 – Kamen zid, SL2 – Below Barnikom, SL3 – Above Barnikom, SL4 – Below Goteniški Snežnik, SL5 – Goteniška gora, SL6 – Above Draga)*

http://www.aloki.hu ● ISSN 1589 1623 (Print) ● ISSN 1785 0037 (Online)
DOI: http://dx.doi.org/10.15666/aeer/1705_1148911508

Table 1. *Sampling locations and their features (coordinates, UTM quadrant, altitude, exposure, substrate, soil). The sampling location marked * contains juvenile phase of beech forest*

Sampling location	Coordinates	UTM	Altit.	Exp.	Surface	Substrate	Soil
SL1 (Kamen Zid)*	Y: 5479575 X: 5052223	VL75	1068 m	SE	175 m^2	Limestone	Rendzina
SL2 (Below Barnik)	Y: 5478774 X: 5051499	VL75	1132 m	SW	600 m^2	Dolomite	Rendzina
SL3 (Above Barnik)	Y: 5478904 X: 5051210	VL75	1161 m	SE	1400 m^2	Limestone, dolomite	Rendzina
SL4 (Below Goteniški Snežnik)	Y: 5480085 X: 5049403	VL74	1205 m	E	1300 m^2	Limestone, dolomite	Rendzina
SL5 (Goteniška gora)	X: 5055948 Y: 5476338	VL5	1100 m	SE	3200 m^2	Limestone, dolomite	Rendzina
SL6 (Above Draga)	Y: 5473400 X: 5052341	VL5	954 m	E	1480 m^2	Dolomite	Rendzina

This biogeographic region is characterised by the contact of Sub-Mediterranean climate and the temperate continental climate of western and southern Slovenia, resulting in large quantities of precipitation in this region (between 1,400 and 3,500 mm) (*Fig. 3*), with a distinct autumn maximum and indistinct spring maximum (Kordiš, 1993). A thick snow cover is also characteristic, and can persist long into spring due to low temperatures. Average annual temperatures in the region are between 5 °C and 8 °C (*Fig. 4*). Temperature decreases with altitude, with characteristic temperature inversion in certain areas. Beside the data for whole area we also made temperature measurements at the biggest sampling location (Goteniška gora) from May to end of December in year 2016 (*Fig. 5*). At the end of July (because of the peak of year radiation) on sunny day measurements of UV-B radiation at all sampling sites between 9:00 and 15:00 were done. Radiation was measured in transect in the middle of localities (forest gaps) and at two opposite edges (on junctures with forest). Measurements were done by Digital Ultraviolet Radiometer Model 6.2. UVB by Solarmeter USA (*Fig. 6*).

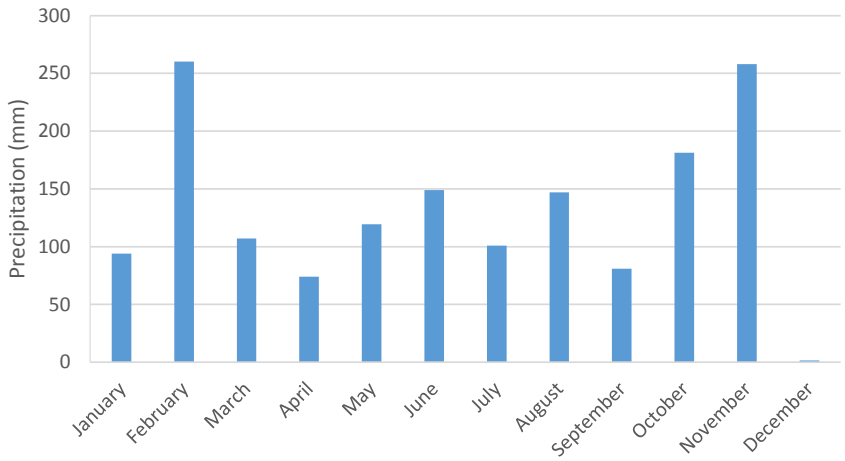

Figure 3. *Mean month precipitation for Kočevska region, measured at climatic station. (Data source: Slovenian Environment Agency - ARSO)*

http://www.aloki.hu ● ISSN 1589 1623 (Print) ● ISSN 1785 0037 (Online)
DOI: http://dx.doi.org/10.15666/aeer/1705_1148911508

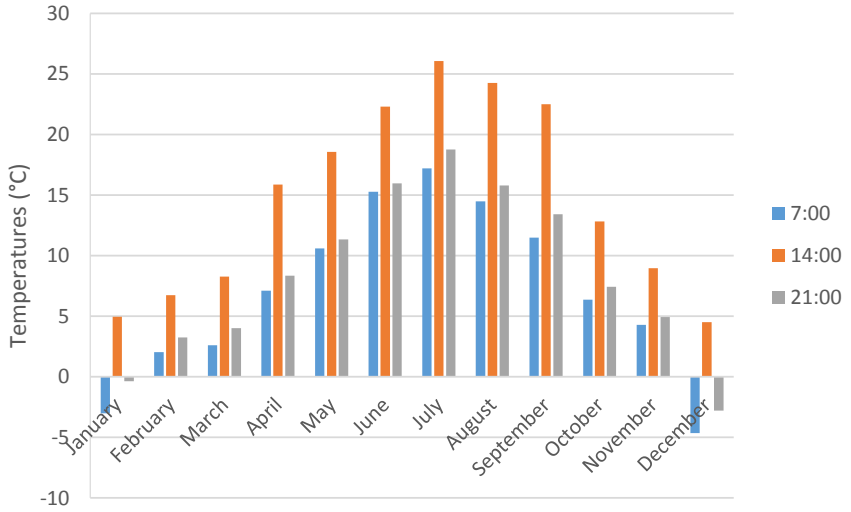

Figure 4. *Mean month temperatures for Kočevska region (measurement times at 7:00, 14:00 and 21:00), measured at climatic station. (Data source: Slovenian Environment Agency - ARSO)*

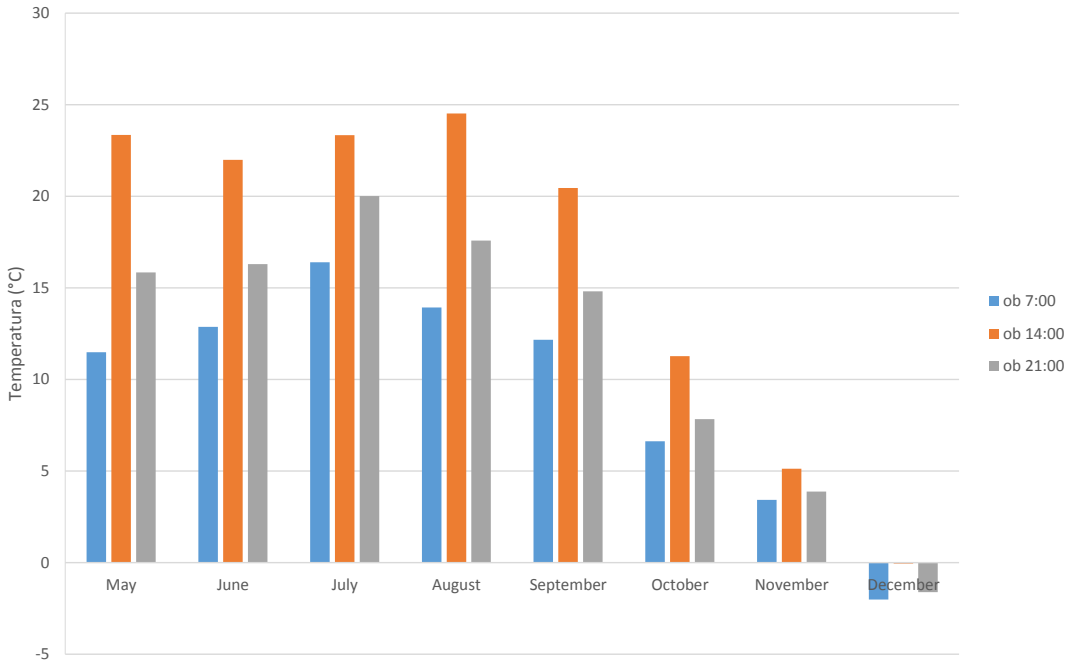

Figure 5. *Mean month temperatures measured at location Goteniška gora in year 2016 (measurement times at 7:00, 14:00 and 21:00)*

Leaf sampling for anthocyanin and quercetin analyses

The common cyclamen is a widespread species in Slovenia (Bavcon, 2009). It is a geophyte representative, as it has an underground tuber that represents a food storage tissue (Grey-Wilson, 2002). Its leaves are evergreen and whither in summer months before flowering. After flowering, new leaves begin growing (Bavcon, 2009). Leaves contain anthocyanins on their abaxial side, which in most cases give leaves a purple

http://www.aloki.hu ● ISSN 1589 1623 (Print) ● ISSN 1785 0037 (Online)
DOI: http://dx.doi.org/10.15666/aeer/1705_1148911508

colour (Grey-Wilson, 2002). Common cyclamen specimens that grow in the shade have a more intensely coloured purple leaves (Kerner, 1894). An even more intense purple colour can be found on leaves of specimens growing in locations with strong solar radiation exposure (Grey-Wilson, 1988, 2002; Mathew, 2013).

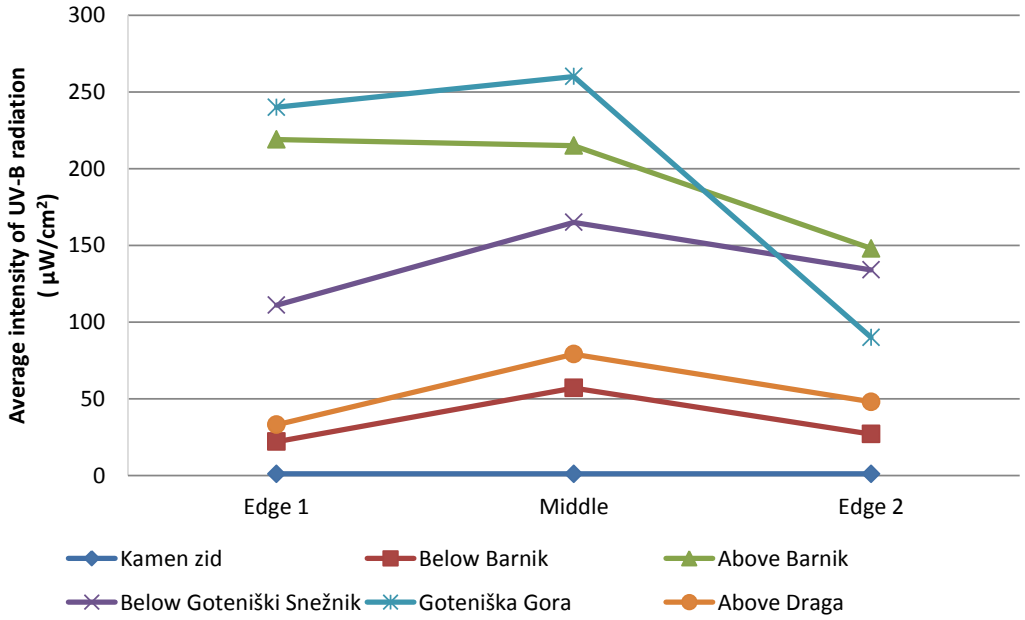

Figure 6. *Average intensity of UV-B radiation at sampling localities, measured at the end of July 2016 (Middle – middle of the gap/locality, Edge 1 – first edge of the gap/locality, Edge 2 – second edge of gap/locality)*

In year 2016 all leaves from three to six plants from all 6 sampling locations (depending on the abundance of specimens in the local populations) were removed, put in plastic bags, and stored in a portable cooling container. During spring, we did not find any common cyclamen leaves in sampling locations Goteniška gora and Below Goteniški Snežnik, because leaves had died of hard conditions during winter. During late summer, only one cyclamen leaf at the sampling location Above Barnik was found, in which we measured the anthocyanin content. This sample was not included in further statistical analysis. The leaves taken in spring were not from the same specimens then leaves taken in late summer. Cyclamen leaves were then frozen until further processing in a freezer at -18 °C. Cyclamen leaves were collected in April and then once again in late August (*Table 2*).

Anthocyanin and quercetin content measurements

Each leaf was ground in liquid nitrogen before the powder was mixed with 2 ml of extraction solution (3% formic acid + % methanol), and the anthocyanins were extracted for 1 h in an ice ultrasonic bath. The samples were then centrifuged for 7 min at 12.000 × g, filtered through Chromafil AO-20/25 polyamide filters into vials, and stored until HPLC-MS analyses in the freezer at -20 °C (Osterc et al., 2014).

Phenolic compounds were analysed on a Thermo Finnigan Surveyor HPLC system (Thermo Scientific, San Jose, USA) with a diode array detector at 350 nm (flavonols) and 530 nm (anthocyanins). Spectra of the compounds were recorded between 200 and

http://www.aloki.hu ● ISSN 1589 1623 (Print) ● ISSN 1785 0037 (Online)
DOI: http://dx.doi.org/10.15666/aeer/1705_1148911508

600 nm. The column was a Gemini C18 (150 mm×4.6 mm 3 µm; Phenomenex, Torrance, USA) operated at 25 °C. The elution solvents were aqueous 0.1% formic acid in double distilled water (A) and 0.1% formic acid in acetonitrile (B). Samples were eluted according to a linear gradient from 5% to 20% B in the first 15 min, followed by a linear gradient from 20% to 30% B for 5 min, then an isocratic mixture for 5 min, followed by a linear gradient from 30% to 90% B for 5 min, and then an isocratic mixture for 15 min before returning to the initial conditions. The injection amount was 20 µl and flow rate 0.6 mL min^{-1} (Osterc et al., 2014).

Table 2. *Numbers of samples taken per one location in each of two seasons*

Sampling location	No. of samples (spring)	No. of samples (late summer)
SL1 (Kamen Zid)	8	0
SL2 (Below Barnik)	15	13
SL3 (Above Barnik)	9	1
SL4 (Below Goteniški Snežnik)	0	15
SL5 (Goteniška gora)	0	10
SL6 (Above Draga)	18	18

All phenolic compounds were identified by a HPLC-Finnigan MS detector and an LCQ Deca XP MAX (Thermo Finigan, San Jose, CA) instrument with electrospray interface (ESI) operating in positive (for anthocyanins) and negative (other phenolic groups) ion mode. The analyses were carried out using full scan data-dependent MS^n scanning from *m/z* 110 to 1500. Column and chromatographic conditions were identical to those used for the HPLC-DAD analyses. The injection volume was 10 µL and the flow rate maintained at 0.6 mL min^{-1}. The capillary temperature was 250 °C, the sheath gas and auxiliary gas were 60 and 15 units, respectively; the source voltage was 3 kV for negative ionisation and 4 kV for positive ionisation and normalised collision energy was between 20 and 35%. Spectral data were elaborated using the Excalibur software (Thermo Scientific). The identification of compounds was confirmed by comparing retention times and their spectra as well as by adding the standard solution to the sample and by fragmentation.

Content of the following anthocyanins and quercetins was determined:
Anth1 = Malvidin-3, 5-diglucoside, **Anth2** = Cyanidin-3-neohesperidoside, **Anth3** = Malvidin-3-rutinoside, **Anth4** = Malvidin-3-glucoside, **Anth5** = Peonidin-3-O-neoheseridoside
Comp1 = Quercetin di rhamnosyl hexoside1 expressed as Quercetin-3-rutinoside, **Comp2** = Quercetin di rhamnosyl hexoside2 expressed as Quercetin-3-rutinoside, **Comp3** = Myricetin-3-rutinoside expressed as Myricetin-3-rhamnnoside, **Comp4** = Myricetin-hexoside expressed as Myricetin-3-rhamnoside, **Comp5** = Kaempferol dirhamnosyl hexoside expressed as Kaempferol-glucoside, **Comp6** = Quercetin-3-rutinoside, **Comp7** = Laricitin-3-O-rutinoside expressed as Quercetin-galaktoside, **Comp8** = Myricetin-3-rhamnoside, **Comp9** = Quercetin-3-galactoside, **Comp10** = Kaempferol 3-rutinoside expressed as Kaempferol-glucoside, **Comp11** = Isorhamnetin-3-rutinoside expressed as Isorhamnetin-glucoside, **Comp12** = Quercetin-3-rhamnoside, **Comp13** = Neohesperidoside expressed as Quercetin-3-galactoside

http://www.aloki.hu ● ISSN 1589 1623 (Print) ● ISSN 1785 0037 (Online)
DOI: http://dx.doi.org/10.15666/aeer/1705_1148911508

Statistical analysis

The effects of location and time were assessed by Two-way ANOVA followed by Duncan's multiple range test with a 95% confidence interval for the comparison of the mean values of anthocyanin and quercetin contents. We used the statistical programme Statgraphics-Plus. Uneven sample size was handled by automatic approximation of statistical program.

Results

Anthocyanins

Higher quantities of all anthocyanins of leaves collected in late summer compared to leaves collected in spring (*Fig. 7*) was found. Of leaves collected in spring, the highest anthocyanin content was measured in those collected at locations Kamen Zid and Above Barnik. In terms of anthocyanin quantity in the spring, leaves from all locations combined had the higher quantities of malvidin-3,5-diglucoside (196.6 ± 122.8 μg g^{-1}) and malvidin 3-rutinoside (69.7 ± 74.5 μg g^{-1}) (*Fig. 7*). When comparing anthocyanin content quantities in cyclamen leaves from different locations, no statistically significant differences were found for malvidin-3,5-diglucoside and cyaniding-3-neohesperidoside. For anthocyanins malvidin-3-rutinoside, malvidin-3-glucoside, and peonidin-3-O-neoheseridoside, there were statistically significant differences in content quantities for all three compounds between locations Above Barnik (*Fig. 8*) and Above Draga, as well as Above Draga and Kamen Zid. In both cases, leaves collected at location Above Draga contained significantly lower quantity of anthocyanins compared to leaves collected at the other two locations (*Fig. 8; Table 3*).

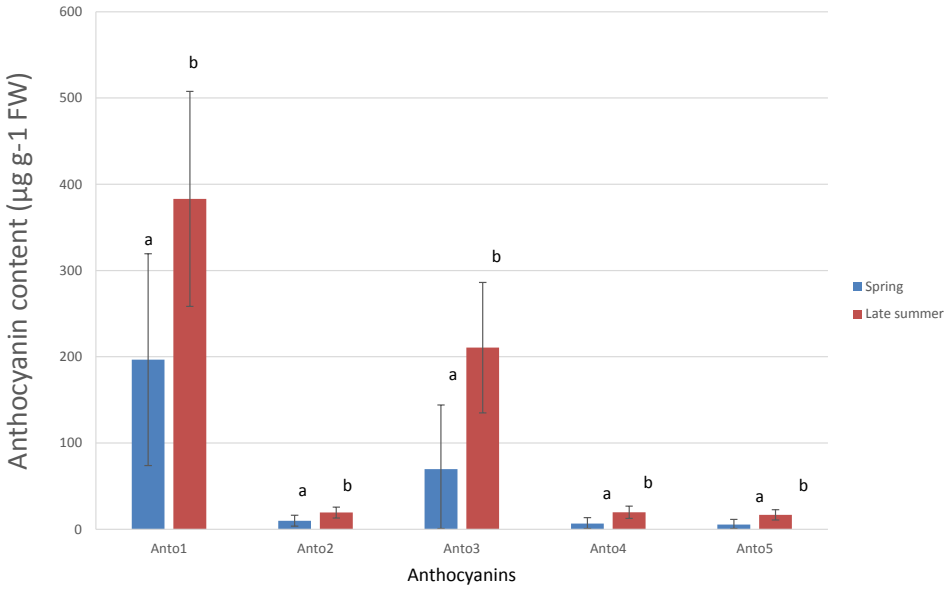

Figure 7. *Mean values, upper and lower anthocyanin content limits in cyclamen leaves collected in spring and late summer. With a 95% confidence interval and $P \leq 0.05$. Characters a and b are used to mark statistically significant differences in content of specific anthocyanins between spring and late summer samples (**Anth1** = Malvidin-3,5-diglucoside, **Anth2** = Cyanidin-3-neohesperidoside, **Anth3** = Malvidin-3-rutinoside, **Anth4** = Malvidin-3-glucoside, **Anth5** = Peonidin-3-O-neoheseridoside)*

http://www.aloki.hu ● ISSN 1589 1623 (Print) ● ISSN 1785 0037 (Online)
DOI: http://dx.doi.org/10.15666/aeer/1705_1148911508

Table 3. *Mean values, upper and lower anthocyanin content limits in cyclamen leaves collected in spring (Sp.) and late summer (Su.) at 6 locations (SL1 = Goteniška gora, SL2 = Above Barnik, 3 = Below Barnik, 4 = Above Draga, 5 = Below Goteniški Snežnik, SL6 = Kamen zid)*

Locality		SL1		SL2		SL3		SL4		SL5		SL6	
		Sp.	**Su.**	**Sp.**	**Su.**	**Sp.**	**Su.**	**Sp.**	**Su.**	**Sp.**	**Su.**	**Sp.**	**Su.**
Anth1	Upp.	/	955.6	292.3	683.6	133.9	521.1	135.4	549.5	/	557.9	213.8	/
	Mean	**/**	**641.4**	**171.8**	**308.7**	**92.7**	**236.4**	**100.5**	**340.4**	**/**	**300.4**	**153.7**	**/**
	Low.	/	327.3	51.2		51.5		65.7	131.2	/	42.9	93.6	/
Anth2	Upp.	/	48.3	14.8	34.6	6.8	26.4	6.8	27.8	/	28.3	10.8	/
	Mean	**/**	**32.4**	**8.7**	**15.6**	**4.7**	**11.9**	**5.1**	**17.2**	**/**	**15.2**	**7.8**	**/**
	Low.	/	16.6	2.6	0	2.6	0	3.3	6.6	/	2.2	4.7	/
Anth3	Upp.	/	509.8	140.7	454.3	58.0	308.0	43.4	329.3	/	294.3	108.9	/
	Mean	**/**	**328.1**	**79.3**	**119.7**	**37.0**	**143.4**	**25.6**	**208.3**	**/**	**145.3**	**78.3**	**/**
	Low.	/	146.3	17.8	0	16.0	0	7.9	87.3	/	0	47.6	/
Anth4	Upp.	/	47.9	13.2	42.7	5.6	28.9	4.1	30.9	/	27.6	10.2	/
	Mean	**/**	**30.8**	**7.5**	**11.3**	**3.5**	**13.5**	**2.4**	**19.6**	**/**	**13.7**	**7.4**	**/**
	Low.	/	13.8	1.7	0	1.6	0	0.7	8.2	/	0	4.5	/
Anth5	Upp.	/	40.4	11.1	35.9	4.6	24.4	3.4	26.1	/	23.3	8.6	/
	Mean	**/**	**25.9**	**6.3**	**9.5**	**2.9**	**11.3**	**2.0**	**16.5**	**/**	**11.5**	**6.2**	**/**
	Low.	/	11.6	1.4	0	1.3	0	0.6	6.9	/	0	3.8	/

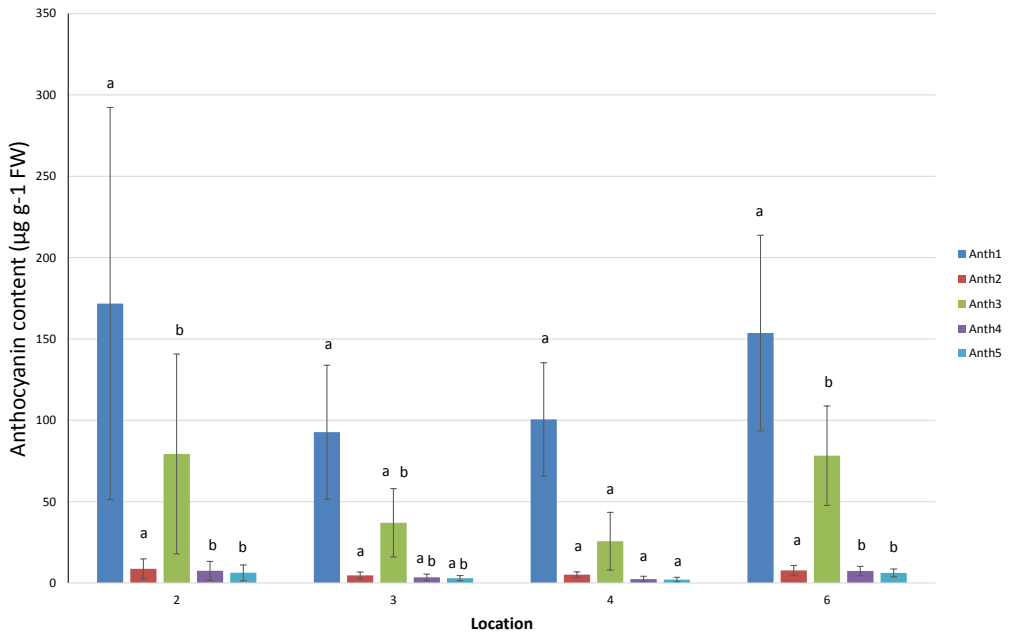

Figure 8. *Mean values, upper and lower anthocyanin content limits in cyclamen leaves collected in spring at various sampling locations (2 = Above Barnik, 3 = Below Barnik, 4 = Above Draga, 6 = Kamen Zid). With a 95% confidence interval and $P \leq 0.05$. Characters a and b are used to mark statistically significant differences in anthocyanin content of between individual locations (**Anth1** = Malvidin 3,5-diglucoside, **Anth2** = Cyanidin 3-neohesperidoside, **Anth3** = Malvidin 3-rutinoside, **Anth4** = Malvidin 3-glucoside, **Anth5** = Peonidin 3-O-neoheseridoside)*

http://www.aloki.hu ● ISSN 1589 1623 (Print) ● ISSN 1785 0037 (Online)
DOI: http://dx.doi.org/10.15666/aeer/1705_1148911508

During late summer, the highest anthocyanin content was of leaves collected at location Goteniška gora and the lowest in those collected at location Below Barnik. Even in late summer, malvidin-3, 5-diglucoside (383.1 ± 124.7 µg g^{-1}) and malvidin-3-rutinoside (210.6 ± 75.6 µg g^{-1}) were predominant for all locations combined *(Fig. 9)*. When comparing anthocyanin content in leaves from various locations, a statistically significant difference in late summer samples for anthocyanins malvidin-3, 5-diglucoside and cyanidin-3-neohesperidoside, specifically only between locations Goteniška gora and Below Barnik (*Fig. 9*) was found. So, statistically significant differences were between Goteniška gora as a oldest and largest forest gap on which temperature fluctuation are the highest (*Fig. 4*), and Below Barnik as smallest forest gap where the effect of forest edge was expressed (shading and slipstream because of trees).

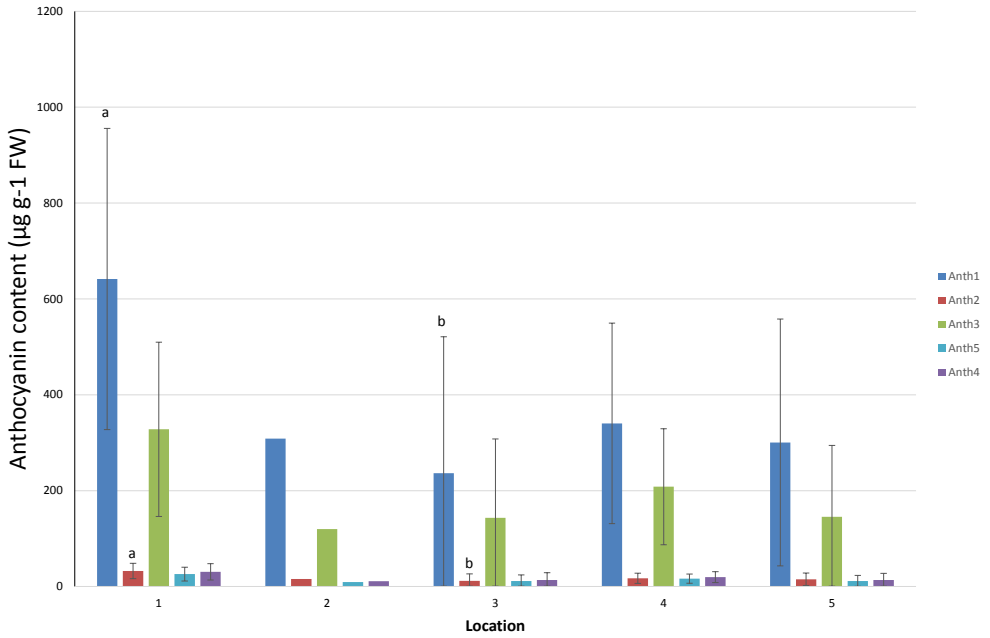

Figure 9. *Mean values, upper and lower anthocyanin content limits in cyclamen leaves collected in late summer at various sampling locations (1 = Goteniška gora, 2 = Above Barnik, 3 = Below Barnik, 4 = Above Draga, 5 = Below Goteniški Snežnik). With a 95% confidence interval and P ≤ 0.05. Character a and b is used to mark statistically significant differences in anthocyanin content between individual locations (**Anth1** = Malvidin 3,5-diglucoside, **Anth2** = Cyanidin 3-neohesperidoside, **Anth3** = Malvidin 3-rutinoside, **Anth4** = Malvidin 3-glucoside, **Anth5** = Peonidin 3-O-neoheseridoside)*

Quercetins

A comparison of quercetin content between spring and late summer cyclamen leaves showed a statistically significant higher content in late summer leaves for the following quercetins: quercetin di rhamnosyl hexoside2, quercetin-3-rutinoside, laricitin-3-O-rutinoside, myricetin-3-rhamnoside, and quercetin-3-galactoside. For quercetin di rhamnosyl hexoside and Myricetin-3-rutinoside content was higher in spring, but there were no statistically significant differences in content between seasons for the rest of the quercetins. When analysing the late summer quercetin content in cyclamen leaves from various locations, we measured the highest content in all leaves for quercetin-di-rhamnosyl hexoside2 (4050.5 ± 2413.9 µg g^{-1}), quercetin-3-rutinoside

http://www.aloki.hu ● ISSN 1589 1623 (Print) ● ISSN 1785 0037 (Online)
DOI: http://dx.doi.org/10.15666/aeer/1705_1148911508

(6129.7 ± 2961.2 µg g^{-1}), and myricetin-3-rhamnoside (1721.6 ± 1014.6 µg g^{-1}) (*Figs. 8* and *9*). Statistically significant difference in quercetin content in leaves for as many as eight quercetins between locations Above Barnik and Below Barnik was found. Quercetin quantity in leaves collected Above Barnik most often differed from other locations; in addition to the abovementioned, also from locations Above Draga (yungest gap) and Kamen Zid (juvenile beech forest). Quercetin quantities kaempferol dirhamnosyl hexoside and neohesperidoside most often differed with a statistical significance between locations Above Barnik and Below Barnik, Above Barnik and Above Draga, Above Barnik and Kamen Zid, and Below Barnik and Kamen Zid. While quercentin contents for quercetin-3-galactoside in kaempferol 3-rutinoside differed with a statistical significance between the following locations: Above Barnik and Below Barnik, Above Barnik and Kamen Zid, Below Barnik and Above Draga, and Below Barnik and Kamen Zid, contents of laricitin-3-O-rutinoside and myricetin-3-rhamnoside differed with a statistical significance between locations Above Barnik and Above Draga, Below Barnik and Above Draga, and Above Draga and Kamen Zid. In spring samples, no statistically significant differences based on sampling location for quercetin di rhamnosyl hexoside2 and quercetin-3-rhamnoside (*Figs. 10* and *11; Table 4*) was found.

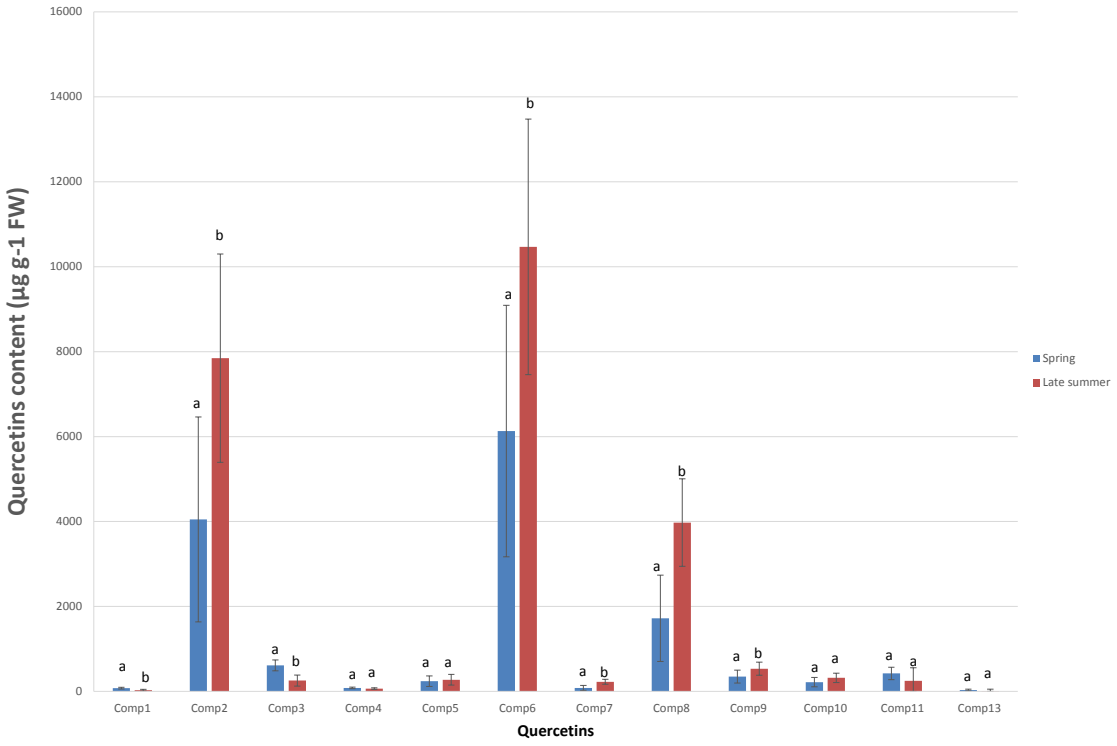

Figure 10. *Mean values, upper and lower quercetin content limits in cyclamen leaves collected in spring and late summer. With a 95% confidence interval and P ≤ 0.05. Characters a and b are used to mark statistically significant differences in content of specific quercetins between spring and late summer samples (**Comp1** = Quercetin di rhamnosyl hexoside, **Comp2** = Quercetin di rhamnosyl hexoside2, **Comp3** = Myricetin-3-rutinoside, **Comp4** = Myricetin-hexoside, **Comp5** = Kaempferol dirhamnosyl hexoside, **Comp6** = Quercetin-3-rutinoside, **Comp7** = Laricitin-3-O-rutinoside, **Comp8** = Myricetin-3-rhamnoside, **Comp9** = Quercetin-3-galactoside, **Comp10** = Kaempferol 3-rutinoside, **Comp11** = Isorhamnetin-3-rutinoside, **Comp13** = Neohesperidoside)*

http://www.aloki.hu ● ISSN 1589 1623 (Print) ● ISSN 1785 0037 (Online)
DOI: http://dx.doi.org/10.15666/aeer/1705_1148911508

Table 4. *Mean values, upper and lower quercetin content limits in cyclamen leaves collected in spring (Sp.) and late summer (Su.) at 6 locations (SL1 = Goteniška gora, SL2 = Above Barnik, 3 = Below Barnik, 4 = Above Draga, 5 = Below Goteniški Snežnik, SL6 = Kamen zid)*

Locality		SL1		SL2		SL3		SL4		SL5		SL6	
		Sp.	**Su.**	**Sp.**	**Su.**	**Sp.**	**Su.**	**Sp.**	**Su.**	**Sp.**	**Su.**	**Sp.**	**Su.**
Comp1	Upp.	/	63.6	59.1	/	101.1	53.2	77.0	48.2	/	78.0	85.6	/
	Mean.	**/**	**26.1**	**36.7**	**/**	**83.8**	**17.4**	**61.6**	**22.1**	**/**	**45.4**	**60.2**	**/**
	Low.	/	0.0	14.3	/	66.5	0.0	46.2	0.0	/	12.7	34.9	/
Comp2	Upp.	/	18002.5	/	/	/	12107.4	/	11902.5	/	14388.6	/	/
	Mean.	**/**	**11526.8**	**/**	**/**	**/**	**5922.0**	**/**	**7406.7**	**/**	**8752.8**	**/**	**/**
	Low.	/	5051.2	/	/	/	0.0	/	2910.9	/	3117.0	/	/
Comp3	Upp.	/	689.4	472.9	/	682.2	340.0	566.4	427.7	/	313.6	714.4	/
	Mean.	**/**	**416.8**	**353.5**	**/**	**589.8**	**79.7**	**484.4**	**238.4**	**/**	**76.4**	**579.2**	**/**
	Low.	/	144.2	234.2	/	497.4	0.0	402.3	49.2	/	0.0	443.9	/
Comp4	Upp.	/	123.9	69.6	/	90.8	80.8	76.9	94.5	/	93.5	87.4	/
	Mean.	**/**	**79.6**	**56.3**	**/**	**80.5**	**38.5**	**67.8**	**63.7**	**/**	**55.0**	**72.4**	**/**
	Low.	/	35.3	43.0	/	70.2	0.0	58.6	33.0	/	16.4	57.3	/
Comp5	Upp.	/	856.5	147.5	/	282.1	516.3	231.1	543.2	/	471.9	219.6	/
	Mean.	**/**	**506.7**	**105.1**	**/**	**249.3**	**182.2**	**201.9**	**300.3**	**/**	**167.4**	**171.5**	**/**
	Low.	/	156.9	62.6	/	216.4	0.0	172.7	57.5	/	0.0	123.4	/
Comp6	Upp.	/	25208.0	5252.7	/	7003.2	14270.6	4620.7	15700.3	/	13729.4	6506.5	/
	Mean.	**/**	**16953.7**	**3965.9**	**/**	**6007.2**	**6386.2**	**3735.8**	**9969.7**	**/**	**6545.6**	**5048.5**	**/**
	Low.	/	8699.4	2679.2	/	5011.1	0.0	2850.8	4239.0	/	0.0	3590.4	/
Comp7	Upp.	/	451.6	85.9	/	76.4	258.8	49.0	353.5	/	324.0	91.5	/
	Mean.	**/**	**282.9**	**71.4**	**/**	**65.2**	**97.7**	**39.1**	**236.4**	**/**	**177.2**	**75.1**	**/**
	Low.	/	114.2	56.9	/	54.0	0.0	29.2	119.3	/	30.4	58.7	/
Comp8	Upp.	/	8590.8	1617.5	/	1438.7	4934.0	923.9	5672.9	/	6099.7	1723.0	/
	Mean.	**/**	**5681.3**	**1345.2**	**/**	**1227.9**	**2154.8**	**736.7**	**3652.9**	**/**	**3567.5**	**1414.5**	**/**
	Low.	/	2771.7	1072.9	/	1017.1	0.0	549.4	1632.9	/	1035.3	1106.0	/
Comp9	Upp.	/	1112.9	267.4	/	541.5	664.9	272.4	912.5	/	651.6	376.7	/
	Mean.	**/**	**710.9**	**199.3**	**/**	**488.9**	**280.9**	**225.6**	**633.4**	**/**	**301.7**	**299.7**	**/**
	Low.	/	308.8	131.3	/	436.2	0.0	178.8	354.3	/	0.0	222.6	/
Comp10	Upp.	/	892.3	162.2	/	228.4	502.1	158.2	504.6	/	502.5	245.5	/
	Mean.	**/**	**579.9**	**119.8**	**/**	**195.6**	**203.7**	**129.0**	**287.7**	**/**	**230.6**	**197.5**	**/**
	Low.	/	267.5	77.4	/	162.8	0.0	99.8	70.9	/	0.0	149.4	/
Comp11	Upp.	/	725.3	99.6	/	102.5	484.6	75.3	511.8	/	484.2	68.5	/
	Mean.	**/**	**488.1**	**82.1**	**/**	**88.9**	**258.1**	**63.2**	**347.1**	**/**	**277.8**	**48.6**	**/**
	Low.	/	250.9	64.5	/	75.3	31.5	51.2	182.5	/	71.4	28.7	/
Comp12	Upp.	/	1147.6	/	/	/	749.4	/	871.1	/	850.1	/	/
	Mean.	**/**	**684.8**	**/**	**/**	**/**	**307.3**	**/**	**549.8**	**/**	**447.3**	**/**	**/**
	Low.	/	221.9	/	/	/	0.0	/	228.5	/	44.5	/	/
Comp13	Upp.	/	79.4	13.7	/	26.2	47.9	21.4	50.4	/	43.8	20.4	/
	Mean.	**/**	**47.0**	**9.7**	**/**	**23.1**	**16.9**	**18.7**	**27.9**	**/**	**15.5**	**15.9**	**/**
	Low.	/	14.5	64.5	/	75.3	0.0	51.2	5.3	/	0.0	28.7	/

http://www.aloki.hu ● ISSN 1589 1623 (Print) ● ISSN 1785 0037 (Online)
DOI: http://dx.doi.org/10.15666/aeer/1705_1148911508

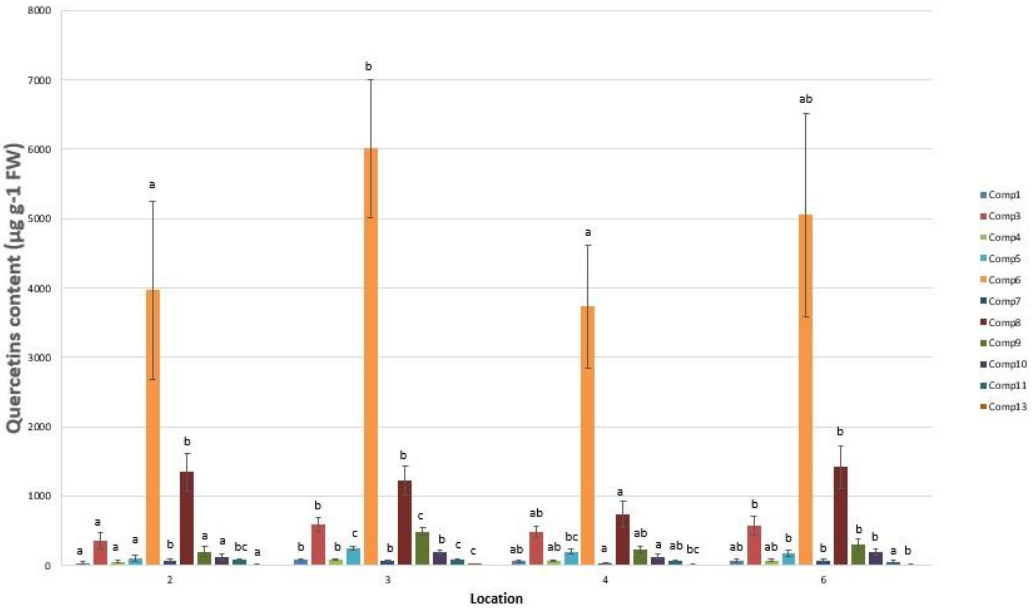

Figure 11. *Mean values, upper and lower quercetin content limits in cyclamen leaves collected in spring at various sampling locations (2 = Above Barnik, 3 = Below Barnik, 4 = Above Draga, 6 = Kamen zid). With a 95% confidence interval and P ≤ 0.05. Characters a, b and c are used to mark statistically significant differences in quercetin content between individual locations (**Comp1** = Quercetin di rhamnosyl hexoside, **Comp3** = Myricetin-3-rutinoside, **Comp4** = Myricetin-hexoside, **Comp5** = Kaempferol dirhamnosyl hexoside, **Comp6** = Quercetin-3-rutinoside, **Comp7** = Laricitin-3-O-rutinoside, **Comp8** = Myricetin-3-rhamnoside, **Comp9** = Quercetin-3-galactoside, **Comp10** = Kaempferol 3-rutinoside, **Comp11** = Isorhamnetin-3-rutinoside, **Comp13** = Neohesperidoside)*

In late summer cyclamen leaves collected at different locations, the predominant compounds by quantity in all locations were quercetin di rhamnosyl hexoside2 (7846.6 ± 2951.2 µg g^{-1}), quercetin-3-rutinoside (10467.4 ± 3006.9 µg g^{-1}), and myricetin-3-rhamnoside (3974.9 ± 1030.2 µg g^{-1}). A comparison of specific quercetin content based on location of leaf collection showed statistically significant differences only for myricetin-3-rutinoside and quercetin-3-rutinoside, specifically for the former between locations Goteniška gora and Below Barnik, Goteniška gora and Above Draga, and for the later between locations Goteniška gora and Below Barnik, and Goteniška gora and Goteniški Snežnik (*Fig. 12*).

Discussion

Anthocyanin synthesis represents an immediate reaction to increased sunlight intensity, since they act as protection against harmful UV-B radiation (Gould et al., 2002; Steyn et al., 2002; Huges et al., 2007; Huges, 2011). Anthocyanin content can therefore be a good indicator of the level of adaptation or response of originally shady plants to increased radiation intensity, which can be the result of forest gap formation.

In present study, the results confirmed the assumption that spring cyclamen leaves from all sampling locations contain lower anthocyanin quantities than late summer leaves. Plants on forest gaps are not yet exposed to such strong solar radiation during spring than in late summer (Turton, 1991; Brown et al., 1994). Higher anthocyanin

http://www.aloki.hu ● ISSN 1589 1623 (Print) ● ISSN 1785 0037 (Online)
DOI: http://dx.doi.org/10.15666/aeer/1705_1148911508

quantity in late summer probably leads to protection against increased radiation in late summer. In terms of specific anthocyanin content, leaves collected on gaps in spring and late summer contained the highest quantity of anthocyanin malvidin-3,5-diglucoside, as confirmed to be the predominant anthocyanin of *C. purpurascens* regardless of season and population (Osterc et al., 2014, 2017). The low anthocyanin content in leaves from Above Draga (youngest gap) could be explained by the fact that this forest gap is youngest, and that plants are not yet completely adapted to the increased radiation intensity, in comparison to plants that have been growing in open surfaces for some time, such as those at location Above Barnik. The latter is also facing SE and therefore distinctly exposed to strong solar radiation for most of the day. The local cyclamen population Above Draga is the most abundant in comparison to other locations. At other locations, populations are smaller, with individual cyclamen specimens growing only occasionally. As early as spring, these rare specimens already have a higher anthocyanin content and are optimally adapted to solar radiation exposure. We can thus suggest that specimens adapted from the time of forest gap formation to the time of sampling by increased anthocyanin synthesis, or that the specimens whose leaves were collected for sampling are in fact offspring of those exposed to increased solar radiation at the time of forest gap formation. Most likely, only the offspring with already higher anthocyanin content, which protect the leaf against excessively strong solar radiation, managed to survive. The latter statement seems more likely, since the study (Osterc et al., 2017) comparing anthocyanin content in wild specimens of common cyclamen, brought and grown further in culture, found unchanged anthocyanin content. Regardless of the changed environmental factors during the move to a new location, with all relocated specimens equal, cyclamen leaves collected at sunny locations contained higher quantities of malvidin-3,5-diglucoside in comparison to cyclamen specimens collected in shady habitats. Therefore, synthesis of specific quantity of anthocyanin persisted for 10 to 12 years after replanting (Osterc et al., 2017). Based on the development and ecology of the common cyclamen, we can suggest that local populations on older forests gaps are in fact not the same specimens that grew there at the time of forest gap formation. Increased anthocyanin quantity thus ensures easier survival with increased solar radiation, which was also proven with two corn genotypes (HOPI and W22) (Pietrini et al., 2002). Genotype HOPI, containing anthocyanins in leaves, could be exposed to higher light intensity with no photo-oxidation processes detected, as opposed to genotype W22.

With much higher anthocyanin quantity compared with other locations, no differences were shown between leaves collected from Kamen Zid (juvenile phase of beech forest) and on gap Above Barnik, despite the environmental differences of the two locations. One of the reason could lie in the fact that in spring, before beech trees grew leaves (beech tree leaves in this location only developed after sampling), cyclamen leaves on location Kamen Zid were exposed to increased solar radiation (comparing to season with developed beech leaves), and had increased anthocyanin synthesis for protection (Huges et al., 2005; Klančnik et al., 2016). Nevertheless, the young trees on this location are quite dense, and probably the solar radiation is still not so strong; the reason for such anthocyanin content could therefore also be lack of light, with anthocyanins additionally absorbing solar radiation (Chalker-Scott, 1999). Anthocyanin synthesis as a result of low solar radiation is common primarily in tropical understory plants, where the lack of light is more prominent and sun flecks are rarer (Wheldale, 1916; Lee et al., 1979). Species *Episcia lilacina* Hanst. was found to contain

http://www.aloki.hu ● ISSN 1589 1623 (Print) ● ISSN 1785 0037 (Online)
DOI: http://dx.doi.org/10.15666/aeer/1705_1148911508

anthocyanins primarily in the spongy tissue next to palisade tissue, which as such cannot act as protection, but can only contribute to additional light absorption (Rauch, 2009). To confirm thus hypothesis in our samples – leaves of *C. purpurascens* – additional leaves of specimens from location Kamen Zid should be collected. Using microscopic slides, we could precisely determine the location of anthocyanin accumulation in leaves. In the analysis of late summer samples, differences in content quantities of anthocyanins malvidin-3,5-diglucoside and cyaniding-3-neohesperidoside, specifically only between locations Goteniška gora (oldest gap) and Below Barnik were found. There were no differences for these two anthocyanins in spring samples, based on a comparison with the other three anthocyanins, which only showed differences in spring samples. Therefore two groups of anthocyanins could be observed: the first, with statistically significant differences in content during spring between the youngest gap (Above Draga) and the other two (Above Barnik, Below Barnik); and the second group of anthocyanins, with statistically significant differences during late summer, specifically only between the gaps Goteniška gora and Above Barnik. The leaves collected at Goteniška gora contained twice as much anthocyanins malvidin-3,5-diglucoside and cyaniding-3-neohesperidoside. The difference in content between the leaves from these two forests gaps likely is not a results of exposure duration (considering the gap formation) to increased radiation, since the gaps do not differ significantly in terms of formation time. Furthermore, they also do not differ significantly in terms of anthocyanin content during spring. We therefore assume that the late summer differences in contents of malvidin-3,5-diglucoside and cyanidin 3-neohesperidoside are the result of temperature fluctuations and high exposure to UV-B radiation (*Fig. 4*). Anthocyanins in plants also have a protective role against low temperatures and frost (Wheldale, 1916; Mendez et al., 1999). These two anthocyanins could be the ones in *C. purpurascens* leaves that act as protection against low temperatures, since differences in content occurred only in late summer, specifically between locations that differ significantly in size and exposure. The location of Goteniška gora has the largest and most exposed gap, with consequently greater temperature fluctuations (Buajan et al., 2016), which can be noticed there already in late summer, when early mornings can be quite cold (*Fig. 2*). The gap Below Barnik is the smallest, with lower temperature fluctuations due to the surrounding forest stand. At the latter location, cyclamen leaves have not yet been exposed to such low temperatures that would require protection.

Three quercetins, quercetin-di-rhamnosyl hexoside2, quercetin-3-rutinoside, and myricetin-3-rhamnoside, with much higher contents among all quercetins in *C. purpurascens* leaves taken both in spring and late summer were found. Similar results also were reported by Osterc et al. (2014, 2017). Although all five anthocyanin contents were higher in late summer than those in spring, not all quercetin showed differences between spring and late summer. Based on this we can conclude that all quercetins do not have the same function in cyclamen leaves, as was already determined for other plants, where they for example act as a protection against insects and other pathogens (Mierziak et al., 2014). Also in cyclamen leaves probably some of them do not directly participate in the protection of the leaf against increased UV radiation. In spring, statistically significant differences in content for as many as 8 quercetins (quercetin di rhamnosyl hexoside1, myricetin-3-rutinoside, myricetin-hexoside, kaempferol dirhamnosyl hexoside, quercetin-3-rutinoside, quercetin-3-galactoside, kaempferol 3-rutinoside, neohesperidoside) between locations Above Barnik and Below Barnik was

http://www.aloki.hu ● ISSN 1589 1623 (Print) ● ISSN 1785 0037 (Online)
DOI: http://dx.doi.org/10.15666/aeer/1705_1148911508

found. Based on analyses conducted, there is no explanation what causes such differences. Statistically significant differences between other locations were also found, but were quite varied based on the type of quercetin. In spring the leaves from location Above Draga contained a higher quantity of quercetin myricetin-3-rhamnoside than the leaves from locations Above Barnik, Below Barnik, and Kamen zid. Quercetins represent the immediate response and also the main protection against UV-B radiation (Mierziak et al., 2014). This specific quercetin probably provides specific quercetin provides the first protection against radiation for *C. purpurascens* leaves in spring, since the leaves at this location in spring contain the lowest quantity of anthocyanins, compared to leaves from other locations.

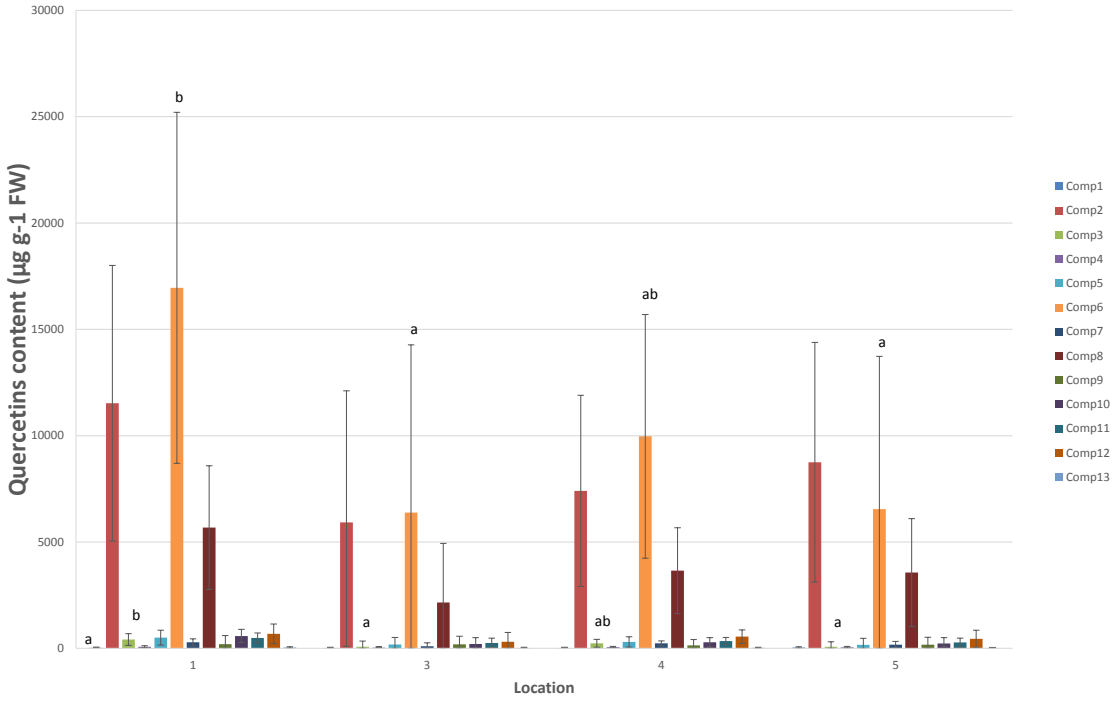

Figure 12. *Mean values, upper and lower quercetin content limits in cyclamen leaves collected in late summer at various sampling locations (1 = Goteniška gora, 3 = Below Barnik, 4 = Above Draga, 5 = Below Goteniški Snežnik). With a 95% confidence interval and $P \leq 0.05$. Character a and b is used to mark statistically significant differences in quercetin content between individual locations (**Comp1** = Quercetin di rhamnosyl hexoside, **Comp2** = Quercetin di rhamnosyl hexoside2, **Comp3** = Myricetin-3-rutinoside, **Comp4** = Myricetin-hexoside, **Comp5** = Kaempferol dirhamnosyl hexoside, **Comp6** = Quercetin-3-rutinoside, **Comp7** = Laricitin-3-O-rutinoside, **Comp8** = Myricetin-3-rhamnoside, **Comp9** = Quercetin-3-galactoside, **Comp10** = Kaempferol 3-rutinoside, **Comp11** = Isorhamnetin-3-rutinoside, **Comp12** = Quercetin-3-rhamnoside, **Comp13** = Neohesperidoside)*

A 60-min exposure to UV-B radiation is enough to activate intensive quercetin synthesis (Shourie et al., 2014). Our results from location Kamen zid confirm this characteristic of quercetins. Leaves from these locations contained a statistically significant lower quantity of eight quercetins, compared to the leaves collected at other locations. Location Kamen zid is characterised as a juvenile phase of beech forest, and is therefore the shadiest location. Because UV-B radiation is lower there (*Fig. 4*), the

http://www.aloki.hu ● ISSN 1589 1623 (Print) ● ISSN 1785 0037 (Online)
DOI: http://dx.doi.org/10.15666/aeer/1705_1148911508

leaves do not require immediate protection, and the quercetin content is therefore lower. In late summer, results showed an interesting turnaround in statistically significant differences of quercetin content. Only for two quercetins (myricetin-3-rutinoside and quercetin-3-rutinoside) the differences were measured, where the leaves from Goteniška gora contained the highest quantity of the two quercetins, which significantly differed from content in leaves from locations Below Barnik, Above Barnik, and Goteniški Snežnik. The highest content of the two quercetins in leaves from this location could be explained by their synthesis being indirectly dependant on the accumulated UV-B radiation (Sullivan and Teramura, 1988), as this gap is the largest and most exposed to solar radiation (*Fig. 1*). Quercetins therefore additionally protect the leaves on this location against radiation.

Conclusion

The cyclamens from at Above Draga have yet adapted to the increased radiation intensity due to the pretty recent formation of forest gap, as shown from their lower anthocyanin content in spring but not in summer, comparing with other locations. In the study, a wide range of anthocyanin functions was confirmed. In addition to protecting the plant against strong solar radiation, they can assist in additional absorption of light in shady plants. This was established with the statistically significant higher anthocyanin content in spring cyclamen leaves from location Kamen Zid – juvenile phase of beech forest. This is actually the shadiest location (and actually the oldest forest gap). Furthermore, the function of anthocyanins as protection against low temperatures was confirmed, specifically in cyclamen leaves at the largest and most exposed gap Goteniška gora. At this location, leaves in late summer contained a statistically significant higher quantity of anthocyanins than leaves on the smallest, less exposed gap. Higher quercetin content at the youngest gap (Above Draga), with leaves not adapted to permanent sun exposure, indicates that quercetin acts as the first immediate protection against UV-B. In late summer, the quercetin content that stands out is the one in leaves from the largest gap, which is most exposed to solar radiation for the longest duration. The reason for this is increased synthesis of anthocyanin and quercetin due to UV-B radiation accumulation. Based on study results, it is confirmed that local populations of common cyclamen were capable of surviving in forest gaps only because of increased anthocyanin and quercetin content, which protect plants against strong solar radiation. For a more detailed examination of anthocyanin accumulation in common cyclamen leaf tissues, microscopic slides would have to be prepared in the future.

REFERENCES

[1] Agati, G., Azzarello, E., Pollastri, S., Tattini, M. (2012): Flavonoids as antioxidants in plants: location and functional significance. – Plant Science 196: 67-76.

[2] Bavcon, J. (2009): Common Cyclamen (*Cyclamen purpurascens* Mill.) and Its Diversity in Slovenia. – Botanic Garden, Department of Biology, Biotechnical Faculty, Ljubljana.

[3] Brown, M. J., Parker, G. G., Posner, N. E. (1994): A survey of ultraviolet-B radiation in forest. – Journal of Ecology 82: 843-854.

[4] Buajan, S., Jinfu, L., Zhongsheng, H., Xueping, F., Muhammad, A., Farooq, T. H. (2016): Effect of gap size on the dynamic of micro environments during the daytime at

http://www.aloki.hu ● ISSN 1589 1623 (Print) ● ISSN 1785 0037 (Online)
DOI: http://dx.doi.org/10.15666/aeer/1705_1148911508

Castanopsis kawakamii Natural Reserve Forest, Sanming City, China. – Environment and Natural Resources Journal 14(2): 30-34.
[5] Caldwell, M. M., Robberecht, R., Flint, S. D. (1983): Internal filters: prospects for UV-acclimation in higher plants. – Physiologia Plantarum 58(3): 445-450.
[6] Chalker-Scott, L. (1999): Environmental significance of anthocyanins in plant stress responses. – Photochemistry and Photobiology 70(1): 1-9.
[7] Chazdon, R. L., Pearcy, R. W. (1991): The importance of sunflecks for forest understory plants. – Bioscience 41(11): 760-766.
[8] Collins, B., Pickett, S. T. A. (1988): Demographic responses of herb layer species to experimental canopy gaps in a northern hardwoods forests. – Journal of Ecology 76: 437-450.
[9] Cooper-Driver, G. A. (2001): Contributions of Jeffery Harborne and co-workers to the study of anthocyanins. – Photochemistry 56: 229-236.
[10] Gould, K. S., Markham, K. R., Smith, R. H., Goris, J. J (2000): Functional role of anthocyanins in the leaves of *Quintinia serrata* A. Cunn. – Journal of Experimental Botany 51: 1107-1115.
[11] Gould, K. S., McKelvie, J., Markham, K. R. (2002): Do anthocyanins function as antioxidants in leaves? Imaging of H_2O_2 in red and green leaves after mechanical injury. – Plant, Cell and Environment 25: 1261-1269.
[12] Grey-Wilson, C. (1988): The Genus *Cyclamen*. A Kew Magazine Monography. – Chritopher Helm/Timber, London.
[13] Grey-Wilson, C. (2002): *Cyclamen*: A Guide for Gardeners, Horticulturists and Botanists. New Edition. – BT Batsford, London.
[14] He, F., Mu, L., Yan, G.-L., Liang, N.-N., Pan, Q.-H., Wang, J., Reeves, M. J., Duan, C.-Q. (2010): Biosynthesis of anthocyanins and their regulation in colored grapes. – Molecules 15: 9057-9091.
[15] Hughes, N. M. (2011): Winter leaf reddening in 'evergreen' species. – New Phytologist 190: 573-581.
[16] Hughes, N. M., Neufeld, H. S., Burkey, K. O. (2005): Functional role of anthocyanins in high-light winter leaves of the evergreen herb *Galax urceolata*. – New Phytologist 168: 575-587.
[17] Hughes, N. M., Morley, C. B., Smith, W. K. (2007): Coordination of anthocyanin decline and photosynthetic maturation in juvenile leaves of three deciduous tree species. – New Phytologist 175(4): 675-585.
[18] Ishizaka, H., Yamada, H., Sasaki, K. (2002): Volatile compounds in the flowers of *Cyclamen persicum*, *C. purpurascens* and their hybrids. – Scientia Horticulturae 94: 125-135.
[19] Kelemen, K., Mihók, B., Gálhidy, L. (2012): Dynamic response of herbaceous vegetation to gap opening in a central European beech stand. – Silva Fennica 46: 53-65.
[20] Kerner, V. M. (1894): The Natural History of Plants. – Blackie & Son, London.
[21] Klančnik, K., Levpušček, M., Gaberščik, A. (2016): Variegation and red abaxial epidermis define the leaf optical properties of *Cyclamen purpurascens*. – Flora 224: 87-95.
[22] Kordiš, F. (1993): Dinaric Beech-Fir Forests in Slovenia. – Department of Forestry, Biotechnical Faculty, Ljubljana.
[23] Lambers, H., Chapin III, F. S., Pons, T. L. (2008): Plant Physiological Ecology, Second Edition. – Springer Science + Business Media, New York.
[24] Lee, D. W., Lowry, J. B., Stone, B. C. (1979): Abaxial anhocyanin layer in leaves of tropical rain forest plants: enhancer of light capture in deep shade. – Biotropica 11(1): 70-77.
[25] Matthew, B. (2013): Genus *Cyclamen* in Science, Cultivation, Art and Culture. – Royal Botanic Gardens Kew, Richmond.

http://www.aloki.hu ● ISSN 1589 1623 (Print) ● ISSN 1785 0037 (Online)
DOI: http://dx.doi.org/10.15666/aeer/1705_1148911508

[26] Mendez, M., Gwynn Jones, D., Manetas, Y. (1999): Enhanced UV-B radiation under filed conditions increases anthocyanin and reduces the risk of photoinhibition but does not affect growth in the carnivorous plant *Pinguicula vulgaris.* – New Phytologist 144: 275-282.
[27] Middleton, L. (2001): Shade-tolerant flowering plants: adaptations and horticultural implications. – Acta Horticulturae 552: 95-102.
[28] Mierziak, J., Kostyn, K., Kulma, A. (2014): Flavonoids as important molecules of plant interactions with the environment. – Molecules 19: 16240-16265.
[29] Mihók, B., Gálhidy, L., Kenderes, K., Standovár, T. (2007): Gap regeneration patterns in a semi-natural beech forest stand in Hungary. – Acta Silvatica & Lignaria Hungarica 3: 31-45.
[30] Osterc, G., Cunja, V., Mikulič Petkovšek, M., Schmitzer, V., Štampar, F., Bavcon, J. (2014): Foliage identification of different autochthonous common cyclamen genotypes (*Cyclamen purpurascens* Mill.) using various biochemical parameters. – Scientia Horticulturae 173: 37-44.
[31] Osterc, G., Mikulič Petkovšek, M., Štampar, F., Ravnjak, B., Bavcon, J. (2017): Impact of specific environmental characteristics of the site origin (shady, sunny) on anthocyanin and flavonol contents of replanted plants at common cyclamen (*Cylamen purpurascens* Mill.). – Acta Physiologiae Plantarum 39(64): 1-10.
[32] Peterken, G. F. (1996): Natural Woodland, Ecology and Conservation in Northern Temperate Regions. – Cambridge University Press, New York.
[33] Pietrini, F., Iannelli, M. A., Massacci, A. (2002): Anthocyanin accumulation in the illuminated surface of maize leaves enhances protection from photo-inhibitory risks at low temperature, without further limitation to photosynthesis. – Plant, Cell & Environment 25(10): 1251-1295.
[34] Podani, J. (2006): Braun-Blanquet's legacy and data analysis in vegetation science. – Journal of Vegetation Science 17: 113-117.
[35] Rauch, A. (2009): Leaf colour patterns, vegetative and sexual reproduction of *Episcia lilacina* (Gesneriaceae). – Diplomarbeit, Universität Wien, Wien.
[36] Schultze, E.-D., Beck, E., Müller-Hohenstein, K. (2005): Plant Ecology. – Springer Verlag, Berlin.
[37] Shourie, A., Tomar, P., Srivastava, D., Chauhan, R. (2014): Enhanced biosynthesis of quercetin occurs as a photoprotective measure in *Lycopersicum esculentum* Mill. under acute UV-B exposure. – Brazilian Archives of Biology and Technology 57(3): 317-325.
[38] Smith, R. L., Smith, T. M. (2001): Ecology & Field Biology. – Benjamin Cummings, San Francisco.
[39] Sullivan, J. H., Teramura, A. H. (1988): Effects of ultraviolet-B irradiation on seedling growth in the Pinaceae. – American Journal of Botany 75: 225-230.
[40] Steyn, W. J., Wand, S. J. E., Holcroft, D. M., Jacobs, G. (2002): Anthocyanins in vegetative tissues: a proposed unified function in photoprotection. – New Phytologist 155: 349-361.
[41] Timmins, G. S., Holbrook, N. M., Field, T. S. (2002): Le Rouge et le Noir: Are Anthocyanins Plant Melanins? – In: Gould, K. S., Lee, D. W. (eds.) Anthocyanins in Leaves. Advances in Botanical Research 37. Academic Press, Amsterdam, pp. 18-35.
[42] Turton, S. M. (1991): Solar Radiation Regimes in Rainforest Understoreys, Gaps and Clearings, with Special Reference to Northeast Queensland. Vol. 1. PhD Thesis. – James Cook University, New Queensland.
[43] Wheldale, M. (1916): The Antocyanin Pigments. – Cambridge University, Merton.
[44] Whittaker, R. H. (1975): Communities and Ecosystems. – Macmillan Publishing, New York.
[45] Wraber, M. (1969): Pflanzengeographische Stellung und Gliederung Sloveniens. – Acta Geobotanica 176-199.
[46] Yamasaki, H. (1997): A function of color. – Trends in Plant Sciences 2: 2-7.

http://www.aloki.hu ● ISSN 1589 1623 (Print) ● ISSN 1785 0037 (Online)
DOI: http://dx.doi.org/10.15666/aeer/1705_1148911508

A STUDY ON THE QUALITIES THAT AFFECT PREFERENCE OF RURAL RECREATION AREAS

SARI, D.

Department of Landscape Architecture, Faculty of Art and Design, Artvin Çoruh University
08000 Arhavi, Artvin, Turkey
(e-mail: deryasari@artvin.edu.tr; phone: +90-466-215-1092; fax: +90-466-215-1093)

(Received 21st Apr 2019; accepted 4th Jul 2019)

Abstract. Individuals, who struggle due to various stress factors in urban areas, travel to recreation areas to spend their leisure time, to relax, to make contact with nature and to replenish their energy. Rural recreation areas meet these requirements and offer the best natural environment for urban residents. However, the sustainability of recreation areas and recreational activities are important due to the increasing demand and diverse visitor objectives. Thus, sustainable plans for rural recreation areas should include a balance between human preferences and demands and preservation of the nature. The aim of the present study was to determine the qualities that affect the preferences of individuals for rural recreation areas. In this context, the quality preferences of potential visitors in Artvin province (Turkey) were determined based on a survey that investigated 21 qualities in detail. In the study, correlations between participant attributes and preference rates were analyzed with t-test and analysis of variance. The cluster analysis conducted based on the mean preference scores demonstrated that 8 qualities were most effective on preferences. Concurrently, significant differences were determined between occupant attributes and preference scores. The present study was conducted to contribute to future planning strategies for decision makers and further comprehensive studies.
Keywords: *visitor preferences, rural recreation, survey, quality preferences, nature tourism*

Introduction

Most recreational activities are conducted in natural environments (Kraus, 1971), and today, rural recreation areas are among the spaces where individuals predominantly fulfill their recreational needs. Due to their natural integrity and richness, rural recreation areas offer renewal and leisure opportunities for urban dwellers.

Outdoor recreation refers to the activities that individuals conduct in spaces that allow access to nature or green areas as part of their daily or weekend routines. Nature tourism is a term that includes the activities that individuals conduct to have fun during holidays and focus on nature and generally involve overnight accommodations. This usually means traveling to national parks, forests, lakes, seashores or rural areas and participating in activities that are compatible with the natural qualities of these spaces (Bell et al., 2007).

Outdoor recreation, conducted in natural and semi-natural environments, often referred to as green and blue spaces, plays a crucial role in physical and mental health, as well as wellbeing and social outcomes, and contributes significantly to human health (Hartig et al., 2014; Korpela et al., 2014; Triguero-Mas et al., 2015; Cox et al., 2017; Schirpke et al., 2018). Increasing involvement in outdoor recreation activities can be considered as beneficial for both the individual and the society at large (Eriksson and Nordlund, 2013).

The pressures on individuals to live under negative living conditions in residential areas that are not adequate for their mental and physical requirements, technological advances, transportation facilities and the increase in per capita leisure time improved

http://www.aloki.hu ● ISSN 1589 1623 (Print) ● ISSN 1785 0037 (Online)
DOI: http://dx.doi.org/10.15666/aeer/1705_1150911523

the interest of individuals living in metropolitan cities and high income areas in rural areas (Guo et al., 2010; Sahbaz and Altinay, 2015; Yang, 2017; Schirpke et al., 2018).

Urban parks and green spaces offer physical activity, entertainment, natural experience and social interaction opportunities for urban residents (McCormack et al., 2010; Andkjær and Arvidsen, 2015). For example, ancient trees in these spaces attract visitors and contribute to the urban ecological, aesthetic and functional quality (Jim and Zhang, 2013). However, the activities that individuals could conduct in these spaces, which are part of the urban everyday landscape, are limited. Thus, rural areas play an important role in active outdoor recreation activities for individuals. For example, the main goal in visiting forests is the increasing interest in relaxation, getting away from the daily routine, to exercise and conduct sports activities in the forest (Hansen-Moller and Oustrup, 2004; Andkjær and Arvidsen, 2015).

Nature-based recreation provides visitors the opportunity to meet their recreational needs, while maintaining the diversity and richness of regional natural, cultural and historical resources. Recreational visitors search for natural spaces to meet their recreational needs and often go to remote areas for recreation. This leads to a high demand for natural areas and resources (Shrestha et al., 2007).

As a result of the increase in recreational activities, individuals started to change their recreational space preferences. Thus, the demand for national parks that are rich in natural and cultural values, has increased. Several countries transformed these trends into an advantage, inviting tourists to preservation areas such as national and nature parks (Şahbaz and Altınay, 2015).

The results of surveys conducted in the United States indicated that more than 206 million people aged 15 and over participate in outdoor recreation activities every year, and several outdoor activity participants preferred forests, parks and preservation areas. Visitors visited natural spaces to participate in nature-based recreational activities such as hiking, having fun with family and friends, picnicking and watching natural landscapes, which are among the most popular outdoor activities conducted in the USA (Cordell et al., 2002; Shrestha et al., 2007).

Participation of individuals in recreational activities may vary based on their lifestyles and how they would like to spend their time. The diversity in participation varies based on the country, the social structure, the cultural level and the modern life habits of the population (Tekin et al., 2012). However, several factors such as age, gender, occupation, income level, etc. could be effective on individual recreational preferences. Today, the participation in leisure and recreational activities became a rapid growth industry and the activities offered to masses became a significant market (Tekin et al., 2012).

The extensive literature on outdoor recreation often targeted special natural areas, that include the following elements (De Valck et al., 2017): Forests, mountains, lakes, rivers, coastal areas, protected areas, and national parks. Furthermore, despite the extensive literature on destination attractions (Lee et al., 2010), there is a gap in the literature about studies on the decision-making processes involved in recreational destination preferences for the use of nature (De Valck et al., 2017).

Thus, determination of the factors that affect the demands for nature-human interaction would guide future planners and managers to identify the adequacy, content and adequacy of future recreational activities. The aim of the present study was to determine the qualities that were effective on the selection of rural recreational areas by individuals.

http://www.aloki.hu ● ISSN 1589 1623 (Print) ● ISSN 1785 0037 (Online)
DOI: http://dx.doi.org/10.15666/aeer/1705_1150911523

Materials and methods

In order to determine the qualities that are effective on rural recreational area preferences, initially, a literature review was conducted. Several studies were found in the literature on nature-based tourism activities. Most accessed research were based on surveys and focused on recreation potential (Plieninger et al., 2013; De Valck et al., 2016) or conducted with proxy-based methods (Paracchini et al., 2014; Grêt-Regamey et al., 2015). Fewer studies emphasized demand based on participant approaches (Beeco et al., 2014; Zoderer et al., 2016) and economic evaluation techniques such as willingness-to-pay (WTP) (Nielsen et al., 2007; Rosenberger et al., 2012) or travel-cost method (Fleming and Cook, 2008; Schirpke et al., 2018). Furthermore, personal interviews with experts and SWOT analysis were also used as an instrument to measure the problems of sustainable tourism in the theoretical framework and to collect qualitative data (e.g. Sanagustin Fons et al., 2011).

The recreational services available in the market were determined based on consumer preferences, that were expressed through demand patterns (Tribe, 2011). Thus, 21 qualities were identified in order to determine the potential visitor expectations from rural recreation areas and the qualities the potential visitors considered more important. The preferences of these qualities were determined with a questionnaire.

The survey was conducted with 448 individuals who were the residents of Artvin province located in northeastern Turkey on the Black Sea coast, Artvin Çoruh University staff and students. In the province of Artvin, there are several rural recreation areas, including 2 National Parks, 3 Nature Preservation Areas, 2 Nature Parks, 2 Natural Monuments, 1 Wildlife Development Area and 1 Biosphere Reserve Area. Furthermore, there are 8 Forest Recreation Areas and 1 Urban Forest (Eminağaoğlu and Beğen, 2015). Due to these characteristics, the survey was conducted in the city of Artvin.

Survey participants were randomly selected and initially, participant demographics such as gender, age, education, profession and income level were determined (Torkildsen, 2005). In the second section of the questionnaire, participants were asked to answer the question "When deciding to visit a rural recreation area, rate your preference for each quality listed below." In the questionnaire, 21 qualities were scored based on a 5-point Likert-type scale. Accordingly, the scoring was as follows: 1 = I do not prefer at all, 2 = I prefer less, 3 = I prefer a little, 4 = I prefer a lot, 5 = I prefer the most. To improve the comprehensibility of the questions, descriptions (explanations) were provided for Recreation and Rural Recreation Activity terms in the questionnaire form.

Participant demographics and classification were determined with frequency analysis. Mean preference score (MPS) and significance (effectiveness) were determined for each question. For the included qualities, the MPS was classified as follows:

- $1 \leq MPS < 2$: the quality is least effective in rural recreation area preference.
- $2 \leq MPS < 3$: the quality has moderate effect.
- $3 \leq MPS < 4$: the quality is effective.
- $4 \leq MPS \leq 5$: the quality is highly effective.

Cluster analysis was conducted for 21 qualities based on the MPS values. Thus, a dendrogram, where the most preferred qualities were categorized based on the similarities, was created. PAST (Paleontological Statistics) software was used in cluster

http://www.aloki.hu ● ISSN 1589 1623 (Print) ● ISSN 1785 0037 (Online)
DOI: http://dx.doi.org/10.15666/aeer/1705_1150911523

analysis and the dendrogram. The t-test (for gender) and One-Way ANOVA were conducted to determine the significant differences between participant demographics and preferences. The data are presented as a summary table to facilitate the interpretation of the statistical findings. SPSS 19.0 statistics software was used for the analyzes.

Results

After the survey was conducted, faulty and inconsistent forms were excluded and the answers in the remaining 448 questionnaires were converted into Excel worksheets. Thus, the final 238 participants were male and 210 were female. The distribution and frequencies of the participants based on age (4 categories), education (3 categories), occupation (4 categories) and income (6 categories) are presented in *Table 1*.

Table 1. *Survey participant demographics (n=448)*

Participants		Percentage (%)	Frequency
Gender	Male	53.1	238
	Female	46.9	210
Age	16-25	41.7	187
	26-35	31.7	142
	36-45	19.9	89
	> 45	6.7	30
Education	Middle and High school	14.1	63
	University	63.8	286
	Postgraduate	22.1	99
Occupation (Job)	Student	33.9	152
	Civil servant	29.5	132
	Self-employment/Private sector employee	17.0	76
	Other (unemployed, worker, retired, etc.)	19.6	88
Income* (TL)	No income	33.5	150
	500-1500	11.6	52
	1600-2500	11.4	51
	2600-3500	11.8	53
	3600-4500	16.5	74
	≥ 4600 and over	15.2	68

*1 Turkish lira (TL)= 0.16 EUR= 0.18 USD, The cross exchange rate is based on the date 18.03. 2019

Based on the survey data, where 21 effective qualities on rural recreational area preferences of individuals were questioned, arithmetic mean of preference scores was determined for each question (*Table 2*). The general study findings demonstrated that the four most preferred qualities were "being in contact with the nature, facilities to rest, relaxation, and to have a peace of mind" (Q3, MPS = 4.68), "Recreation area has beautiful landscapes" (Q4, MPS = 4.58), "The recreational area is clean and natural" (Q11, MPS = 4.58), and "The recreation area is safe" (Q20, MPS = 4.49). The three least preferred qualities were "availability of activities such as festivals, concerts etc. in

http://www.aloki.hu ● ISSN 1589 1623 (Print) ● ISSN 1785 0037 (Online)
DOI: http://dx.doi.org/10.15666/aeer/1705_1150911523

the recreation area" (Q18, MPS = 3.12), "Presence of various geological formations in the recreation area" (Q15, MPS = 3.60) and "a space I have experienced and enjoyed before" (Q21, MPS = 3.78).

Table 2. *The qualities that were effective on rural recreational area preferences and mean preference scores (MPS)*

Questions/qualities	Qualities that affect rural recreational area preferences	MPS
Q1	Easy access to the recreation area	3.98
Q2	Inexpensive recreational area	3.94
Q3	Being in contact with the nature, facilities to rest, relaxation, and to have a peace of mind	4.68
Q4	Recreation area has beautiful landscapes	4.58
Q5	The area allows the visitors to leave with good memories	4.40
Q6	The area provides entertainment facilities	3.96
Q7	The area makes the visitors feel renewed physically and psychologically	4.43
Q8	Recreation area facilities that allow the visitors to spend time with family and friends	4.42
Q9	Availability of facilities that allow to spend alone time in the recreational area	3.83
Q10	The area provides different landscapes in summer, winter and fall	4.29
Q11	The recreational area is clean and natural	4.58
Q12	The area provides food-beverage and picnic facilities	4.08
Q13	The area provides facilities for sports activities (such as skiing, swimming, trekking, mountain biking, etc.)	3.90
Q14	Availability of moving or still water in the recreation area (such as lake, sea or stream)	4.03
Q15	Presence of various geological formations in the recreation area (such as valleys, canyons, and cliffs)	3.60
Q16	Presence of a forest in the recreation area	4.10
Q17	Calm and non-crowded recreation area	4.05
Q18	Organization of activities such as festivals, festivities, concerts, etc. in the recreational area	3.12
Q19	Facilities to experience adventures and discoveries	3.90
Q20	Safety in the recreation area	4.49
Q21	Previously experienced and satisfactory recreational area	3.78

The groups formed as a result of the cluster analysis, where the preferred qualities were classified based on similarity, are presented in *Figure 1*.

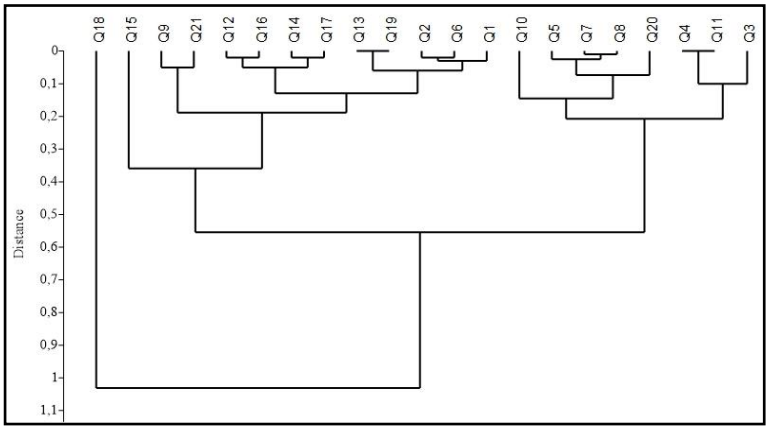

Figure 1. *Cluster analys dendrogram for qualities (Similarity measure: Euclidean)*

http://www.aloki.hu ● ISSN 1589 1623 (Print) ● ISSN 1785 0037 (Online)
DOI: http://dx.doi.org/10.15666/aeer/1705_1150911523

Thus, the most effective qualities about rural recreation area preferences were grouped as follows:

- Q3: "Being in contact with the nature, facilities to rest, relaxation, and to have a peace of mind".
- Q11: "The recreational area is clean and natural".
- Q4: "Recreation area has beautiful landscapes".
- Q20: "The recreation area is safe".
- Q8: "Recreation area facilities that allow the visitors to spend time with family and friends".
- Q7: "The area makes the visitors feel renewed physically and psychologically".
- Q5: "The area allows the visitors to leave with good memories".
- Q10: "The area provides different landscapes in summer, winter and fall".

T-test and analysis of variance were used to determine whether there were significant differences based on gender, age, education, occupation and income. It was determined that there were significant differences between preference scores of Q1, Q3, Q4, Q5, Q6, Q7, Q8, Q9, Q11, Q20 based on gender (*Table 3*), Q2, Q3, Q6, Q9, Q16, Q18, Q19 based on age (*Table 4*), Q2, Q3, Q4, Q6, Q7, Q8, Q9, Q12, Q16, Q18 based on education level (*Table 5*), Q2, Q5, Q9, Q13 based on occupation (*Table 6*), and Q2, Q5, Q6, Q7, Q9, Q12, Q16, Q18, Q21 based on income level (*Table 7*).

Table 3. *Mean preference and significance levels of questioned qualities based on participant gender*

Qualities	Gender			
	Male	Female	F	Sig.
Q1	3.88 a	4.10 b	0.923	0.035
Q2	3.86a	4.04 a	4.515	0.055
Q3	4.61 a	4.76 b	16.756	0.015
Q4	4.47 a	4.70 b	24.832	0.001
Q5	4.27 a	4.54 b	8.86	0
Q6	3.82 a	4.11 b	0.461	0.003
Q7	4.29 a	4.58 b	15.819	0
Q8	4.32 a	4.52 b	3.793	0.011
Q9	3.72 a	3.95 b	1.939	0.028
Q10	4.22 a	4.36 a	1.431	0.095
Q11	4.52 a	4.65 b	11.27	0.048
Q12	4.04 a	4.13 a	0.007	0.318
Q13	3.86 a	3.94 a	0.429	0.423
Q14	3.99 a	4.07 a	0.503	0.416
Q15	3.66 a	3.54 a	0.386	0.255
Q16	4.11 a	4.09 a	0.002	0.753
Q17	4.02 a	4.08 a	1.342	0.57
Q18	3.03 a	3.23 a	0.032	0.105
Q19	3.85 a	3.95 a	0.019	0.367
Q20	4.34 a	4.66 b	26.217	0
Q21	3.71 a	3.85 a	2.438	0.162

Letters a, b denote similarities and differences based on t-test. Same letter denotes similarity, different letters denote difference

http://www.aloki.hu ● ISSN 1589 1623 (Print) ● ISSN 1785 0037 (Online)
DOI: http://dx.doi.org/10.15666/aeer/1705_1150911523

Table 4. *Mean preference and significance levels of questioned qualities based on participant age*

Qualities	Age					
	16-25	**26-35**	**36-45**	**> 45**	**F**	**Sig.**
Q1	4.01 a	4.06 a	3.80 a	3.97 a	1.211	0.305
Q2	4.22 c	3.87 b	3.48 a	3.93 bc	11.677	0
Q3	4.71ab	4.77 b	4.49 a	4.67 ab	3.543	0.015
Q4	4.55 a	4.62 a	4.58 a	4.53 a	0.314	0.815
Q5	4.48 a	4.35 a	4.35 a	4.27 a	1.195	0.311
Q6	4.15 b	3.89 ab	3.69 a	3.90 ab	4.582	0.004
Q7	4.42 a	4.51 a	4.35 a	4.27 a	1.238	0.295
Q8	4.41 a	4.46 a	4.33 a	4.50 a	0.59	0.622
Q9	3.89 ab	3.66 a	3.85 ab	4.17 b	2.137	0.095
Q10	4.32 a	4.23 a	4.18 a	4.70 b	3.01	0.03
Q11	4.56 a	4.59 a	4.56 a	4.67 a	0.221	0.882
Q12	4.14 a	4.03 a	4.01 a	4.13 a	0.601	0.615
Q13	4.03 a	3.77 a	3.75 a	4.03 a	2.351	0.072
Q14	4.07 a	3.97 a	3.97 a	4.17 a	0.622	0.601
Q15	3.56 a	3.58 a	3.63 a	3.90 a	0.872	0.455
Q16	4.03 a	4.12 ab	4.12 ab	4.40 b	1.473	0.221
Q17	4.00 a	4.04 a	4.11 a	4.17 a	0.387	0.762
Q18	3.40 c	3.12 bc	2.67 a	2.77 ab	7.383	0
Q19	4.06 b	3.87 ab	3.61 a	3.83 ab	3.58	0.014
Q20	4.48 a	4.46 a	4.55 a	4.57 a	0.318	0.812
Q21	3.81 a	3.67 a	3.90 a	3.70 a	0.981	0.401

Letters a, b, c denote similarities and differences based on variance analysis. Same letter denotes similarity, different letters denote difference (Post Hoc Test, Duncan, alpha 0.05)

Table 5. *Mean preference and significance levels of questioned qualities based on participant education*

Qualities	Education				
	Middle and High school	**University**	**Postgraduate**	**F**	**Sig.**
Q1	4.05 a	3.97 a	3.97 a	0.138	0.871
Q2	4.19 b	4.01 b	3.61 a	7.949	0
Q3	4.54 a	4.66 ab	4.83 b	4.133	0.017
Q4	4.59 ab	4.51 a	4.75 b	3.799	0.023
Q5	4.38 a	4.37 a	4.47 a	0.64	0.528
Q6	4.17 b	3.95 ab	3.83 a	2.182	0.114
Q7	4.43 ab	4.36 a	4.63 b	4.185	0.016
Q8	4.62 b	4.35 a	4.48 ab	3.099	0.046
Q9	4.10 b	3.81 ab	3.70 a	2.476	0.085
Q10	4.19 a	4.30 a	4.31 a	0.456	0.634
Q11	4.56 a	4.55 a	4.68 a	1.23	0.293
Q12	4.27 b	4.07 ab	3.99 a	1.692	0.185
Q13	3.78 a	3.96 a	3.78 a	1.54	0.216
Q14	4.00 a	4.02 a	4.07 a	0.137	0.872
Q15	3.60 a	3.61 a	3.60 a	0.005	0.995
Q16	4.35 b	4.02 a	4.16 ab	3.461	0.032
Q17	4.11 a	3.97 a	4.22 a	2.347	0.097
Q18	3.41 b	3.15 ab	2.85 a	3.929	0.02
Q19	3.86 a	3.88 a	3.97 a	0.283	0.754
Q20	4.57 a	4.44 a	4.60 a	1.632	0.197
Q21	4.02 a	3.74 a	3.73 a	1.829	0.162

Letters a, b denote similarities and differences based on variance analysis. Same letter denotes similarity, different letters denote difference (Post Hoc Test, Duncan, alpha 0.05)

http://www.aloki.hu ● ISSN 1589 1623 (Print) ● ISSN 1785 0037 (Online)
DOI: http://dx.doi.org/10.15666/aeer/1705_1150911523

Table 6. *Mean preference and significance levels of questioned qualities based on participant occupation*

Qualities	Occupation					
	Student	**Civil servant**	**Self emp./Private sector employee**	**Others**	**F**	**Sig.**
Q1	3.98 a	3.93 a	3.96 a	4.08 a	0.352	0.788
Q2	4.22 b	3.78 a	3.70 a	3.93 a	6.387	0
Q3	4.67 a	4.67 a	4.68 a	4.73 a	0.178	0.911
Q4	4.52 a	4.58 a	4.62 a	4.63 a	0.519	0.67
Q5	4.46 ab	4.31 a	4.54 b	4.28 a	2.262	0.081
Q6	4.08 a	3.88 a	3.82 a	3.99 a	1.466	0.223
Q7	4.41 a	4.34 a	4.50 a	4.51 a	1.047	0.372
Q8	4.38 a	4.48 a	4.36 a	4.44 a	0.501	0.682
Q9	3.89 ab	3.67 a	4.08 b	3.74 a	2.546	0.056
Q10	4.32 a	4.30 a	4.28 a	4.23 a	0.224	0.88
Q11	4.54 a	4.60 a	4.57 a	4.63 a	0.32	0.811
Q12	4.14 a	4.11 a	3.95 a	4.05 a	0.762	0.516
Q13	4.07 b	3.81 ab	3.75 a	3.84 ab	2.241	0.083
Q14	4.05 a	4.03 a	4.04 a	3.97 a	0.154	0.927
Q15	3.53 a	3.58 a	3.72 a	3.67 a	0.666	0.574
Q16	4.01 a	4.18 a	4.14 a	4.10 a	0.91	0.436
Q17	4.04 a	4.09 a	4.00 a	4.03 a	0.14	0.936
Q18	3.35 a	2.98 a	3.05 a	3.00 a	2.399	0.067
Q19	4.06 a	3.73 a	3.86 a	3.90 a	2.085	0.101
Q20	4.45 a	4.51 a	4.50 a	4.53 a	0.229	0.876
Q21	3.78 a	3.71 a	3.83 a	3.83 a	0.289	0.834

Letters a, b denote similarities and differences based on variance analysis. Same letter denotes similarity, different letters denote difference (Post Hoc Test, Duncan, alpha 0.05)

Table 7. *Mean preference and significance levels of questioned qualities based on participant income*

Qualities	Income (TL)							
	No income	**500-1500**	**1600-2500**	**2600-3500**	**3600-4500**	**> 4600**	**F**	**Sig.**
Q1	4.09 a	3.90 a	4.06 a	3.96 a	3.95 a	3.81 a	0.776	0.568
Q2	4.19 c	4.10 c	4.12 c	3.94 bc	3.68 ab	3.46 a	6.674	0
Q3	4.66 ab	4.63 ab	4.82 b	4.53 a	4.77 ab	4.69 ab	1.432	0.211
Q4	4.55 a	4.52 a	4.67 a	4.70 a	4.49 a	4.60 a	0.781	0.564
Q5	4.42 b	4.50 b	4.49 b	4.55 b	4.08 a	4.41 b	3.126	0.009
Q6	4.05 bc	4.29 c	4.02 bc	3.98 bc	3.81 ab	3.60 a	3.324	0.006
Q7	4.38 ab	4.56 b	4.53 b	4.60 b	4.19 a	4.47 ab	2.423	0.035
Q8	4.35 a	4.54 a	4.51 a	4.57 a	4.35 a	4.34 a	1.027	0.401
Q9	3.87 ab	4.00 b	3.73 ab	4.06 b	3.55 a	3.79 ab	1.712	0.131
Q10	4.30 a	4.31 a	4.29 a	4.43 a	4.27 a	4.15 a	0.656	0.657
Q11	4.59 a	4.42 a	4.63 a	4.62 a	4.59 a	4.57 a	0.607	0.695
Q12	4.08 abc	4.29 c	4.22 abc	4.26 bc	3.86 a	3.91 ab	2.282	0.046
Q13	3.99 a	4.00 a	3.92 a	3.91 a	3.70 a	3.78 a	1.005	0.414
Q14	4.03 a	4.06 a	3.98 a	4.13 a	3.99 a	4.00 a	0.192	0.966
Q15	3.49 a	3.60 a	3.82 a	3.64 a	3.68 a	3.59 a	0.81	0.543
Q16	3.94 a	3.94 a	4.45 c	4.36 bc	4.05 ab	4.16 abc	3.662	0.003
Q17	3.99 a	4.06 a	4.00 a	4.19 a	3.95 a	4.21 a	0.797	0.552
Q18	3.11 ab	3.79 c	3.33 b	3.06 ab	2.97 ab	2.69 a	4.962	0
Q19	3.99 a	4.06 a	3.80 a	3.89 a	3.78 a	3.76 a	0.868	0.503
Q20	4.50 a	4.52 a	4.47 a	4.66 a	4.45 a	4.38 a	0.71	0.616
Q21	3.82 ab	3.85 ab	3.84 ab	4.09 b	3.54 a	3.59 a	2.223	0.051

Letters a, b, c denote similarities and differences based on variance analysis. Same letter denotes similarity, different letters denote difference (Post Hoc Test, Duncan, alpha 0.05)

http://www.aloki.hu ● ISSN 1589 1623 (Print) ● ISSN 1785 0037 (Online)
DOI: http://dx.doi.org/10.15666/aeer/1705_1150911523

Discussion and conclusions

Schirpke et al. (2018) reported that social preferences could be explained by landscaping properties and tourism infrastructure. In fact, the primary aim of the present study was to determine the correlation between individual preferences for rural recreation areas and the landscape qualities. Several studies were conducted on the expectations/preferences of individuals about recreation areas (e.g., Cheung and Jim, 2013; Chiu et al., 2016; Heagney et al., 2018). The present study is not a field study, but it is about the qualities that determined the rural recreational area preferences of the individuals.

The way individuals spend leisure time is, above all, closely associated with certain demographics. Thus, participants' gender, age, occupation, education and income level data were scrutinized in the study.

The rural recreation area satisfaction factors vary based on occupant demographics. In a study conducted by Uzun and Müderrisoğlu (2010), it was partially confirmed that rural recreation area satisfaction factors varied based on user demographics and the user demographics such as age, education level, time spent in the area, visit frequency and group size were effective on rural recreation area satisfaction. In the present study, analysis of participant preference scores for 21 qualities demonstrated that the highest difference (significant difference) was based on differences in gender, education and income levels (for 10 qualities). This was followed by age (7 qualities) and occupation (4 qualities). Participant demographics also affected the preference rankings.

In certain studies conducted with couples, it was found that there was no significant difference between the leisure satisfaction levels based on gender (e.g., Siegenthaller and O'Dell, 2000; Di Bona, 2000; Berg et al., 2001). In the present study, it was determined that there was a significant difference between 10 quality scores.

The most preferred experiences include enjoying the natural scenery, peace and quiet. These qualities are preferred preferably near the home of the visitors; however, these are increasingly found only in rural and suburban areas (Bell et al., 2007). In the present study, it was observed that the most important quality for the potential visitors was "being in contact with the nature, facilities to rest, relaxation, and to have a peace of mind" (Q3).

Previous studies in the literature reported that besides the natural characteristics of rural recreation areas (such as unique landscapes and locations), other factors that affect the visitor demand include weather conditions (Humpel et al., 2002; Suminski et al., 2008; Nasir et al., 2012), accessibility (Humpel et al., 2002; Neuvonen et al., 2007; Bestard and Font, 2009; Paracchini et al., 2014; Ala-Hulkko et al., 2016), facilities, price and quality of services (Sava, 2015), accommodation and periodical lodging facilities (Humpel et al., 2002), peer recommendation, advertising-promotions (Sava, 2015), and security and aesthetic features (Humpel et al., 2002). Furthermore, Folmer et al. (2016) investigated the reasons for attractiveness and participant descriptions for the most attractive green spaces. In conclusion, it was determined that qualities such as large green areas, silence, naturalness, water (attractive water surface, river, lake or sea), panoramic and open views, good recreational opportunities, diversity (diverse plant species, land use and seasons), non-urban characteristics, personal bond, historical characteristics, wildlife and flora, harmony (of the landscape), farming (the landscape used by farmers) were effective on occupant preferences. The qualities scrutinized in the present study are consistent with previous study findings.

http://www.aloki.hu ● ISSN 1589 1623 (Print) ● ISSN 1785 0037 (Online)
DOI: http://dx.doi.org/10.15666/aeer/1705_1150911523

Recreational and aesthetic values generally overlap and these are usually discussed together (Van Zanten et al., 2016). For example, a beautiful landscape is an important factor in tourism destination and nature-based recreation preferences (Scolozzi et al., 2014). The high landscape quality and unspoiled nature in rural recreation areas are among the most sought-after qualities by potential visitors, as demonstrated by Q4, Q10 and Q11.

On the other hand, urbanization and high number of visitors negatively affect recreation quality (Scolozzi et al., 2014). The present study findings demonstrated that festivals, festivities, concerts, etc. organized in the recreation area were moderately or relatively effective (Q18, MPS: 3.12) on visitor preferences. However, the calmness of the recreation area, the lack of crowds (Q17, MPS: 4.05) were more effective factors on preference.

Certain studies reported that cultural preferences might affect park occupancy (Tu et al., 2015; Chow et al., 2016). Public spaces and recreation facilities offer a variety of facilities for children, adults and families, however activity preferences in parks depend on the occupant age and gender (Cohen et al., 2007; Kaczynski et al., 2011; Moore et al., 2017). Thus, alternatives should be designed based on different user requirements, or thematic approaches should be preferred in plans.

Accessible infrastructure determines the occupancy of a suitable recreational area and proximity to residential areas is a crucial factor for recreational area occupancy (Weyland and Laterra, 2014; Peña et al., 2015; Ala- Hulkko et al., 2016; Schirpke et al., 2018). Certain studies demonstrated that there was a correlation between the distance to the recreation area and the number of visits to the recreation area; the number of visits decreased with an increase in the distance to the recreation area or the nearest forest (Roovers et al., 2002; Neuvonen et al., 2007). However, it was observed that one of the most significant preference factors was proximity to home parameter (e.g. Sava, 2015). Furthermore, there was a significant correlation between accessibility, facilities, and aesthetic attributes and physical activity (Neuvonen et al., 2007). However, the present study findings demonstrated that "easy access to the recreation area" (Q1, MPS = 3.98) was an effective quality and among the most preferred 8 qualities. This may be due to availability of natural resources in the city of the participants' residence, personal preferences and other factors.

Individuals prefer forests, bodies of water and natural mountain landscapes for wildlife observation, hiking and trekking activities (Bell et al., 2007; Pastorella et al., 2017). Most rural recreation areas include forests. The presence of recreational facilities such as picnic areas, training paths and parking lots could affect the recreational preferences in forests (Tapsuwan et al., 2012; Agimass et al., 2018). Furthermore, the presence of various landscape characteristics in or near the recreation areas (such as different landscapes, water and coastal areas) increases the value of the area for complementary recreational activities. Previous studies demonstrated that the presence of water leads to high landscape preference scores (Kaltenborn and Bjerke, 2002; Dramstad et al., 2006). Kaplan and Kaplan (1989) reported that this preference may be due to the evolutionary adaptation of humankind (De Valck et al., 2017). In fact, it was determined that Q14 was "very effective" (MPS = 4.03) on rural recreation area preference.

In visitor decision-making processes, peer recommendations are more effective when compared to mass media promotion of services (Sava, 2015). It was determined that previous experiences and satisfaction were an effective factor on repeat visits in these

http://www.aloki.hu ● ISSN 1589 1623 (Print) ● ISSN 1785 0037 (Online)
DOI: http://dx.doi.org/10.15666/aeer/1705_1150911523

areas (Q21, MPS = 3.78). On the other hand, the fact that the facilities available in the recreation area that allow the visitors to spend time with family and friends (Q8, MPS = 4.42) was preferred more when compared the ability to spend personal time (Q9, MPS = 3.83). This may be due to the personal or cultural traits of the participants.

The present study findings were relatively parallel to the findings of similar studies conducted in various countries. However, the present study findings demonstrated that the 8 qualities were more effective on visitor preferences about a rural recreation area. These qualities were also the most influential qualities for a rural recreation area to attract visitors. On the other hand, it was noted that there were significant differences between the preference scores based on participant demographics.

Unspoiled rural landscape without human intervention and related natural beauties decrease every day and the importance of these areas increase gradually. Thus, sustainability of natural resources is one of the important targets for nature-based tourism destinations. It is important to understand the expectations of the occupants and to take management decisions accordingly (Lime et al., 2004). In order to achieve a broader perspective in the measurement of the demand for recreation areas, it is necessary to investigate the factors that affect the preferences and tendencies of potential visitors with a multidimensional approach (such as social and cultural traits, service providers, local administrations). It was observed that the qualities discussed in the present study had significant effects on rural recreation preferences. Therefore, the present study could contribute to the future planning strategies of the decision-makers and further comprehensive studies.

Acknowledgements. The author would like to thank Artvin Coruh University for their consent and all participants for their contribution to the study. The experimental section of the present study was previously presented in the XI. European Conference on Social and Behavioral Sciences (2016, Rome, Italy).

REFERENCES

[1] Agimass, F., Lundhede, T., Panduro, T. E., Jacobsen, J. B. (2018): The choice of forest site for recreation: A revealed preference analysis using spatial data. – Ecosystem Services 31(C): 445-454.

[2] Ala-Hulkko, T., Kotavaara, O., Alahuhta, J., Helle, P., Hjort, J. (2016): Introducing accessibility analysis in mapping cultural ecosystem services. – Ecological Indicators 66: 416-427.

[3] Andkjær, S., Arvidsen, J. (2015): Places for active outdoor recreation – a scoping review. – Journal of Outdoor Recreation and Tourism 12: 25-46.

[4] Beeco, J. A., Hallo, J. C., Brownlee, M. T. (2014): GPS visitor tracking and recreation suitability mapping: tools for understanding and managing visitor use. – Landscape and Urban Planning 127: 136-145.

[5] Bell, S., Tyrväinen, L., Sievänen, T., Pröbstl, U., Simpson, M. (2007): Outdoor recreation and nature tourism: a European perspective. – Living Reviews in Landscape Research 1(2): 1-46.

[6] Berg, E., Trost, M., Schneider, I. E., Allison, M. T. (2001): Dyadic exploration of the relationship of leisure satisfaction, leisure time, and gender to relationship satisfaction. – Leisure Sciences 23: 35-46.

[7] Bestard, A. B., Font, A. R. (2009): Environmental diversity in recreational choice modeling. – Ecological Economics 68: 2743-2750.

http://www.aloki.hu ● ISSN 1589 1623 (Print) ● ISSN 1785 0037 (Online)
DOI: http://dx.doi.org/10.15666/aeer/1705_1150911523

[8] Cheung, L. T. O., Jim, C. Y. (2013): Ecotourism service preference andmanagement in Hong Kong. – International Journal of Sustainable Development and World Ecology 20(2): 182-194.
[9] Chiu, H. Y., Chan, C. S., Marafa, L. M. (2016): Local perception and preferences in nature tourism in Hong Kong. – Tourism Management Perspectives 20: 87-97.
[10] Chow, B. C., McKenzie, T. L., Sit, C. H. P. (2016): Public parks in Hong Kong: characteristics of physical activity areas and their users. – International Journal of Environmental Research and Public Health 13(7): 639.
[11] Cohen, D. A., McKenzie, T. L., Sehgal, A., Williamson, S., Golinelli, D., Lurie, N. (2007): Contribution of public parks to physical activity. – American Journal of Public Health 97(3): 509-514.
[12] Cordell, H. K., Betz, C. J., Green, G. T. (2002): Recreation and the environment as cultural dimensions in contemporary American society. – Leisure Science 24: 13-41.
[13] Cox, D. T. C., Shanahan, D. F., Hudson, H. L., Plummer, K. E, Siriwardena, G. M., Fuller, R. A., Anderson, K., Hancock, S., Gaston, K. J. (2017): Doses of neighborhood nature: The benefits for mental health of living with nature. – BioScience 67(2): 147-155.
[14] De Valck, J., Broekx, S., Liekens, I., De Nocker, L., Van Orshoven, J., Vranken, L. (2016): Contrasting collective preferences for outdoor recreation and substitutability of nature areas using hot spot mapping. – Landscape and Urban Planning 151: 64-78.
[15] De Valck, J., Landuyt, D., Broekx, S., Liekens, I., De Nocker, L., Vranken, L. (2017): Outdoor recreation in various landscapes: Which site characteristics really matter? – Land Use Policy 65: 186-197.
[16] Di Bona, L. (2000): What are the benefits of leisure? An exploration using the leisure satisfaction scale. – British Journal of Occupational Therapy 63(2): 50-58.
[17] Dramstad, W. E., Tveit, M. S., Fjellstad, W. J., Fry, G. L. A. (2006): Relationships between visual landscape preferences and map-based indicators of landscape structure. – Landscape and Urban Planning 78(4): 465-474.
[18] Eminağaoğlu, Ö., Beğen, H. A. (2015): Artvin'de Önemli Hassas Alanlar. – In: Eminağaoğlu, Ö. (ed.) Artvin'in Bitkileri, Promat Basın Yayın San. ve Tic. A.Ş., İstanbul.
[19] Eriksson, L., Nordlund, A. (2013): How is setting preference related to intention to engage in forest recreation activities? – Urban Forestry & Urban Greening 12: 481-489.
[20] Fleming, C. M., Cook, A. (2008): The recreational value of Lake McKenzie, Fraser Island: An application of the travel cost method. – Tourism Management 29: 1197-1205.
[21] Folmer, A., Haartsen, T., Buijs, A., Huigen, P. P. P. (2016): Wildlife, flora, and the perceived attractiveness of green places: a comparison between local and national green places. – Journal of Outdoor Recreation and Tourism 16: 16-23.
[22] Grêt-Regamey, A., Weibel, B., Kienast, F., Rabe, S., Zulian, G. (2015): A tiered approach for mapping ecosystem services. – Ecosystems Services 13: 16-27.
[23] Guo, Z., Zhang, L., Li, Y. (2010): Increased dependence of humans on ecosystem services and biodiversity. – PloSOne 5(10): e13113.
[24] Hansen-Moller, J., Oustrup, L. (2004): Emotional, physical/ functional and symbolic aspects of an urban forest in Denmark to nearby residents. – Scandinavian Journal of Forest Research 19: 56-64.
[25] Hartig, T., Mitchell, R., de Vries, S., Frumkin, H. (2014): Nature and health. – Annual Review of Public Health 35: 207-228.
[26] Heagney, E. C., Rose, J. M., Ardeshiri, A., Kovac, M. (2018): Optimising recreation services from protected areas: Understanding the role of natural values, built infrastructure and contextual factors. – Ecosystem Services 31: 358-370.
[27] Humpel, N., Owen, N., Leslie, E. (2002): Environmental factors associated with adults' participation in physical activity: a review. – American Journal of Preventive Medicine 22: 188-199.

http://www.aloki.hu ● ISSN 1589 1623 (Print) ● ISSN 1785 0037 (Online)
DOI: http://dx.doi.org/10.15666/aeer/1705_1150911523

[28] Jim, C. Y., Zhang, H. (2013): Species diversity and spatial differentiation of old-valuable trees in urban Hong Kong. – Urban Forestry & Urban Greening 12: 171-182.
[29] Kaczynski, A. T., Wilhelm Stanis, S. A., Hastmann, T. J., Besenyi, G. M. (2011): Variations in observed park physical activity intensity level by gender, race, and age: individual and joint effects. – Journal of Physical Activity & Health 8(2): 151-160.
[30] Kaltenborn, B. P., Bjerke, T. (2002): Associations between environmental value orientations and landscape preferences. – Landscape and Urban Planing 59(1): 1-11.
[31] Kaplan, R., Kaplan, S. (1989): The Experience of Nature: A Psychological Perspective. – Cambridge University Press, Cambridge, UK.
[32] Korpela, K., Borodulin, K., Neuvonen, M., Paronen, O., Tyrväinen, L. (2014): Analyzing the mediators between nature-based outdoor recreation and emotional well-being. – Journal of Environmental Psychology 37: 1-7.
[33] Kraus, R. (1971): Recreation and Leisure in Modern Society. – TACC, USA.
[34] Lee, C. F., Huang, H. I., Yeh, H. R. (2010): Developing an evaluation model for destination attractiveness: Sustainable forest recreation tourism in Taiwan. – Journal of Sustainable Tourism 18(6): 811-828.
[35] Lime, D. W., Anderson, D. H., Thompson, J. L. (2004): Identifying and Monitoring Indicators of Visitor Experience and Resource Quality: A Handbook for Recreation Resource Managers. – University of Minnesota, Department of Forest Resources, St Paul, Minnesota.
[36] McCormack, G. R., Rock, M., Toohey, A. M., Hignell, D. (2010): Characteristics of urban parks associated with park use and physical activity: are view of qualitative research. – Health & Place 16(4): 712-726.
[37] Moore, J. B., Cook, A., Schuller, K., Lub, Y., Yuan, Z., Maddock, J. E. (2017): Physical activity and park use of youth in Nanchang, China. – Preventive Medicine Reports 8: 256-260.
[38] Nasir, R. A., Anuar, A. N. A., Md Darus, F., Jaini, N., Salleh, S. A., (2012): The climatology effects on outdoor recreation perception and activity in Shah Alam. – Procedia Social and Behavioral Sciences 49: 193-201.
[39] Neuvonen, M., Sievänen, T., Tönnes, S., Koskela, T. (2007): Access to green areas and the frequency of visits: a case study in Helsinki. – Urban Forestry and Urban Greening 6: 235-247.
[40] Nielsen, A. B., Olsen, S. B., Lundhede, T. (2007): An economic valuation of the recreational benefits associated with nature-based forest management practices. – Landscape and Urban Planning 80: 63-71.
[41] Paracchini, M. L., Zulian, G., Kopperoinen, L., Maes, J., Schägner, J. P., Termansen, M., Zandersen, M., Perez-Soba, M., Scholefield, P. A., Bidoglio, G. (2014): Mapping cultural ecosystem services: A framework to assess the potential for outdoor recreation across the EU. – Ecological Indicators 45: 371-385.
[42] Pastorella, F., Giacovelli, G., De Meo, I., Paletto, A. (2017): People's preferences for Alpine forest landscapes: results of an internet-based survey. – Jornal of Forest Research 22(1): 36-43.
[43] Peña, L., Casado-Arzuaga, I., Onaindia, M. (2015): Mapping recreation supply and demand using an ecological and a social evaluation approach. – Ecosystem Services 13: 108-118.
[44] Plieninger, T., Dijks, S., Oteros-Rozas, E., Bieling, C. (2013): Assessing, mapping, and quantifying cultural ecosystem services at community level. – Land Use Policy 33: 118-129.
[45] Roovers, P., Hermy, M., Gulick, H. (2002): Visitor profile, perceptions and expectations in forests from a gradient of increasing urbanization in Belgium. – Landscape and Urban Planning 59: 129-145.

http://www.aloki.hu ● ISSN 1589 1623 (Print) ● ISSN 1785 0037 (Online)
DOI: http://dx.doi.org/10.15666/aeer/1705_1150911523

[46] Rosenberger, R. S., Needham, M. D., Morzillo, A. T., Moehrke, C. (2012): Attitudes, willingness to pay, and stated values for recreation use fees at an urban proximate forest. – Journal of Forest Economics 18: 271-281.
[47] Şahbaz, R. P., Altınay, M. (2015): Türkiye'deki milli parkların rekreasyon faaliyetleri açısından değerlendirilmesi. – Journal of Tourism and Gastronomy Studies 3(3): 125-135.
[48] Sanagustin Fons, M. V., Moseñe Fierro, J. A., Gómez y Patiño, M. (2011): Rural tourism: A sustainable alternative. – Applied Energy 88: 551-557.
[49] Sava, A. M. (2015): Factors affecting the choice of recreation providers: a conceptual model. – Procedia Economics and Finance 23: 622-627.
[50] Schirpke, U., Meisch, C., Marsoner, T., Tappeiner, U. (2018): Revealing spatial and temporal patterns of outdoor recreation in the European Alps and their surroundings. – Ecosystem Services 31: 336-350.
[51] Scolozzi, R., Schirpke, U., Detassis, C., Abdullah, S., Gretter, A. (2014): Mapping alpine landscape values and related threats as perceived by tourists. – Landscape Research 40(4): 1-15.
[52] Shrestha, R. K., Stein, T. V., Clark, J. (2007): Valuing nature-based recreation in public natural areas of the Apalachicola River region, Florida. – Journal of Environmental Management 85: 977-985.
[53] Siegenthaller, K. L., O'Dell, I. (2000): Leisure attitude, leisure satisfaction and perceived freedom in leisure within family dyads. – Leisure Sciences 22: 281-295.
[54] Suminski, R., Poston, W., Market, P., Hyder, M., Sara, P. (2008): Meteorological conditions are associated with physical activities performed in open-air settings. – International Journal of Biometeorology 52(3): 189-197.
[55] Tapsuwan, S., Macdonald, D. H., King, D., Poudyal, N. (2012): A combined site proximity and recreation index approach to value natural amenities: an example from a natural resource management region of Murray-Darling Basin. – Journal of Environmental Management 94(1): 69-77.
[56] Tekin, M., Devecioglu, S., Yarar, D. N. (2012): Examination of recreation levels of university students with regard to various variables. – Procedia, Social and Behavioral Sciences 46: 320-325.
[57] Torkildsen, G. (2005): Leisure and Recreation Management. – (5th ed.), NY: Routledge, New York.
[58] Tribe, J. (2011): The Economics of Recreation, Leisure and Tourism. – (4th ed.), Oxford, Elsevier.
[59] Triguero-Mas, M., Dadvand, P., Cirach, M., Martínez, D., Medina, A., Mompart, A., Basagaña, X., Gražulevičienė, R., Nieuwenhuijsen, M. J. (2015): Natural outdoor environments and mental and physical health: relationships and mechanisms. – Environment International 77: 35-41.
[60] Tu, H., Liao, X., Schuller, K., Cook, A., Fan, S., Lan, G., Lu, Y., Yuan, Z., Moore, J. B., Maddock, J. E. (2015): Insights from an observational assessment of park-based physical activity in Nanchang, China. – Preventive Medicine Reports 2: 930-934.
[61] Uzun, S., Müderrisoğlu, H. (2010): Kırsal rekreasyon alanlarında kullanıcı memnuniyeti: Bolu Gölcük ormaniçi dinlenme yeri örneği. – Süleyman Demirel Üniversitesi Orman Fakültesi Dergisi 1: 67-82.
[62] van Zanten, B. T., Zasada, I., Koetse, M. J., Ungaro, F., Häfner, K., Verburg, P. H. (2016): A comparative approach to assess the contribution of landscape features to aesthetic and recreational values in agricultural landscapes. – Ecosystem Services 17: 87-98.
[63] Weyland, F., Laterra, P. (2014): Recreation potential assessment at large spatial scales: a method based in the ecosystem services approach and landscape metrics. – Ecological Indicators 39: 34-43.
[64] Yang, Y. (2017): The practice and exploration of Shanghai recreational trail system planning. – Procedia Engineering 198: 127-138.

http://www.aloki.hu ● ISSN 1589 1623 (Print) ● ISSN 1785 0037 (Online)
DOI: http://dx.doi.org/10.15666/aeer/1705_1150911523

[65] Zoderer, B. M., Tasser, E., Erb, K., Stanghellini, P. S. L., Tappeiner, U. (2016): Identifying and mapping the tourists' perception of cultural ecosystem services: A case study from an Alpine region. – Land Use Policy 56: 251-261.

http://www.aloki.hu ● ISSN 1589 1623 (Print) ● ISSN 1785 0037 (Online)
DOI: http://dx.doi.org/10.15666/aeer/1705_1150911523

IDENTIFICATION OF DIFFERENTIALLY EXPRESSED GENES OF SORGHUM [*SORGHUM BICOLOR* (L.) MOENCH] SEEDLINGS UNDER NITROGEN STRESS BY RNA-SEQ

YANG, G. D.[1,3] – ZHOU, Y. F.[1*] – HUANG, R. D.[1] – LIN, F.[2] – HU, Z. Y.[3] – HAO, Z. Y.[3] – LIANG, C. B.[4] – WANG, Q.[5] – MENG, X. X.[5] – DONG, L. D.[6]

[1]*College of Agronomy, Shenyang Agricultural University*
No.120 Dongling Road, Shenyang 110866 Liaoning, China

[2]*College of Bioscience and Biotechnology, Shenyang Agricultural University*
No.120 Dongling Road, Shenyang 110866 Liaoning, China

[3]*Keshan Branch of Heilongjiang Academy of Agricultural Sciences*
161005 Heilongjiang, China

[4]*Industrial Crops Institute of Heilongjiang Academy of Agricultural Sciences*
150086 Heilongjiang, China

[5]*Crop Resources Institute of Heilongjiang Academy of Agricultural Sciences*
150086 Heilongjiang, China

[6]*School of Life Sciences, Guangzhou University, 510006 Guangzhou, China*

[*]*Corresponding author*
e-mail: zhouyufei2002@aliyun.com; zhouyufei@syau.edu.cn

(Received 22nd Apr 2019; accepted 16th Jul 2019)

Abstract. Sorghum [Sorghum bicolor (L.) Moench] is an important cereal crop with high nitrogen utilization efficiency. In order to analyze the mechanisms of different sorghum genotypes to low-N tolerance and provide the theoretical basis for the breeding of low nitrogen tolerant sorghum varieties, two materials (KZ15 and SZ7) with different tolerance to low-N were treated with nitrogen by hydroponics, the phenotypes were observed, physiological indexes were measured and transcripts were analyzed in this study. Compared to SZ7, KZ15 showed significantly higher capacity of low-N tolerance. The results showed that the change of KZ15 chlorophyll content was lower than that of SZ7 under low-N stress. The activity of nitrate reductase (NR) and glutamine synthetase (GS) had a smaller reduction in KZ15 than SZ7 under low-N stress. High-throughput sequencing revealed several common differentially expressed genes (DEGs) between KZ15 and SZ7, including nitrogen transport and nitrate assimilation genes. In the tolerant genotype KZ15, there were more transcripts related to high affinity nitrate transporters (NRT2.4, NRT3.1 and NRT4.5), suggesting an improved uptake efficiency of inorganic and organic forms of nitrogen. In addition, an abundance of certain transcription factors in the tolerant genotype KZ15 suggests that they may play roles in regulating the response to N-stress. This study will enable us to discover candidate genes potentially useful in improving the resistance to low nitrogen stress by genetic engineering technology and provide theoretical basis for the breeding of low nitrogen tolerant sorghum varieties.
Keywords: *sorghum, N tolerance, chlorophyll, transcriptome, differentially expressed genes, candidate genes*

Introduction

Nitrogen is a necessary major element for the growth and development of higher plants, which takes part in a series of physiological and biochemical reactions,

http://www.aloki.hu ● ISSN 1589 1623 (Print) ● ISSN 1785 0037 (Online)
DOI: http://dx.doi.org/10.15666/aeer/1705_1152511536

involving various metabolic pathways (Kraiser et al., 2011). There are two mechanisms for obtaining nitrogen in plants: one is to absorb nitrogen nutrition by nodular nitrogenase, which is mainly in leguminous plants. The other is to absorb $NH4^+$, $NO3^-$, and other mineral ions from the soil by root transporters. Sorghum mainly absorbs nitrogen through the second mechanism. Studies of nitrogen stress by quantitative trait loci analysis have mainly focused on maize (Gallais et al., 2004), rice (Obara et al., 2004), Arabidopsis (Loudet et al., 2003a,b) and sorghum (Gelli et al., 2017). At present, the study in low nitrogen tolerance of sorghum has lagged behind other grain crops (Rosa et al., 2014). Few studies of the answers of the molecular response mechanisms of growth and development to nitrogen deficiency of sorghum have been reported.

In this study, the phenotypic and transcriptomic responses of two sorghum varieties, KZ15 and SZ7, under low nitrogen stress and control were investigated. Unraveling mechanisms underlying low nitrogen tolerance of sorghum may provide useful information to genetic engineering and improve the low nitrogen tolerance of sorghum. Such knowledge can also be useful for increasing nitrogen use efficiency for sustainable agriculture.

Materials and methods

Plant materials and growth conditions

Two sorghum varieties, Keza15 (KZ15, tolerant to nitrogen starvation) and Suiza7 (SZ7, sensitive to nitrogen starvation), were used for this study, which were provided by the Keshan branch of the Heilongjiang Academy of Agricultural Sciences.

This experiment was conducted in the greenhouse of Keshan Branch of Heilongjiang Academy of Agricultural Sciences in China. Uniform and plump-eared sorghum seeds were selected and germinated under dark conditions after disinfection, and then sown in vermiculite.

Stress treatments and sample preparations

Trifoliate seedlings were moved into foam boxes wrapped in black plastic film and then cultured with Hoagland nutrient solution. The average temperature and light-dark period were 25°C/20°C and 14 h/10 h. $CaCl_2$ was added to supplement Ca^{2+}. Control plants (in the solution of 4 mmol/L $Ca(NO_3)_2$) were grown in parallel and collected at the same time points. The pH value was adjusted to 5.8 (Ma, 2014). KA, SA, KB and SB indicated the seedlings of KZ15 and SZ7 in low nitrogen treatment and control, respectively. The process was repeated in triplicate. Leaves of seedling which treated for seven days were taken as samples.

The method of the determination of chlorophyll content was referred to the modified method cited by Wang et al. (2006). The following formulas were used to calculate the content of photosynthetic pigments, in which V and W indicated the volume of extracting liquid (ml) and the weight of material (g).

$$\text{Chlorophyll a (Ca) / mg·g-1= (12.21A663-2.81A646) V/ (1000 ×W)} \quad \text{(Eq.1)}$$

$$\text{Chlorophyll b (Cb) / mg·g-1= (20.13A646-5.03A663) V / (1000× W)} \quad \text{(Eq.2)}$$

http://www.aloki.hu ● ISSN 1589 1623 (Print) ● ISSN 1785 0037 (Online)
DOI: http://dx.doi.org/10.15666/aeer/1705_1152511536

The method of nitrate reductase determination was referred to Rajasekhar et al. (1986). The determination of glutamine synthase (GS) was referred to the method of Ding et al. (2006).

The experiment was performed using three biological replicates, and differences were statistically analyzed using Student's t-test ($^{*}P<0.05$, $^{**}P<0.01$). Bars indicate standard error of the mean. Microsoft Excel 2010 and SPSS 18.0 software are employed for data collation and analysis.

RNA seq analysis

Total RNA was isolated from each sample. Quality and quantity evaluation of total RNA, library constructing, and Illumina sequencing were performed in the Beijing Genome Institute (BGI, Shenzhen, China).

Transcript data analysis

TopHat 2 (Kim et al., 2015) was used to compare transcripts with reference genomes. After genome comparison, the StringTie tool was used to identify exonic regions, and then the transcript was reconstructed. The transcript was reconstructed by the DeNovo assembly method. The actual transcripts were screened out, and the low expression transcripts were filtered by the TPM value (filtering criteria: TPM > 0.5 in at least one sample).

Differential expressed genes between samples were defined by DESeq using two separate models (Anders and Huber, 2010), based on fold change >2 and false discovery rate–adjusted P value < 0.05.

According to the result of GO annotation, DEGs were classified to GO terms according to official classification. Phyper was used to perform GO functional enrichment. The p-value calculating formula in hyper geometric test was:

$$P = 1 - \sum_{i=0}^{m-1} \frac{\binom{M}{i}\binom{N-M}{n-i}}{\binom{N}{n}} \quad \text{(Eq.3)}$$

Then, false discovery rate (FDR) was calculated for each p-value. In general, the term FDR <= 0.01 was defined as significantly enriched.

Results

Phenotypic investigation of KZ15 and SZ7 under low-N stress

To evaluate the impact of low-N stress on sorghum, seedlings were planted in an intelligent greenhouse with low-N stress (0 mmol/L) and under control conditions (4 mmol/L). Under low-N stress, the seedlings of SZ7 leaves turned pale yellow, but the seedlings of KZ15 leaves did not significantly change (*Fig. 1A and 1B*). Subsequently, chlorophyll content, activity of nitrate reductase (NR) and glutamine synthetase (GS) were measured in both KZ15 and SZ7 of the low-N treatment and control. The results showed that the seedlings of SZ7 have a 28.77% average decrease in total chlorophyll content, but the seedlings of KZ15 only have 12.39% average decrease (*Fig. 1C*).

http://www.aloki.hu ● ISSN 1589 1623 (Print) ● ISSN 1785 0037 (Online)
DOI: http://dx.doi.org/10.15666/aeer/1705_1152511536

Compared to the control, the content of chlorophyll a and chlorophyll b in SZ7 showed a 27.32% and 33.66% decrease, respectively. But the content of that in KZ15 was 8.86% and 22.71%, respectively (*Fig. 1D, 1E*). These results demonstrate that the change of KZ15 chlorophyll content was lower than that of SZ7 under low-N stress, and chlorophyll b content was more sensitive under low-N stress than the content of chlorophyll a. In addition, the activity of NR and GS was significantly reduced in SZ7 under low-N stress, but the activity of NR and GS exhibited little change in KZ15 under low-N stress (*Fig. 1F, 1G*). These results demonstrate that KZ15 is more N-stress tolerant compared with SZ7.

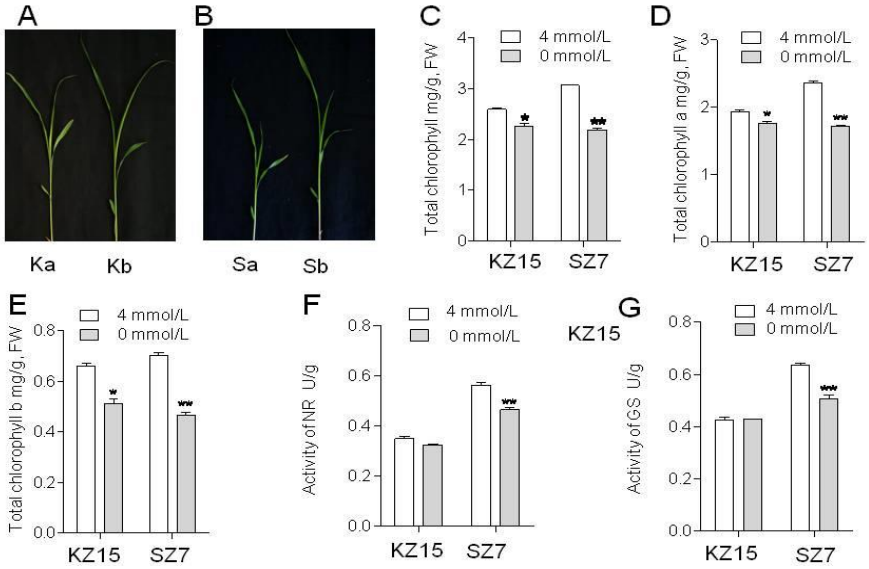

Figure 1. *Morphological performance of KZ15 and SZ7 measured under low-N treatment and non-stress concrol nitrogen concentration treatment. (A, B) Phenotype of KZ15 and SZ7 under low-N treatment. (C) Total chlorophyll content. (D) Chlorophyll a content. (E) Chlorophyll b content. (F) Activity of NR. (G) Activity of GS. (*P <0.05; **P <0.01). The experiment was performed using three biological replicates, and differences were statistically analyzed using Student's t-test (*P<0.05, **P<0.01). Bars indicate standard error of the mean*

Summary of transcriptomic profiling sequencing

Both full-N and low-N treatments were used to analyze the response of sorghum seedlings to nitrogen stress. Twelve libraries were constructed and sequenced. After removing low-quality reads, an average of 24.09 Mb (range of 24.04 to 24.11 Mb) clean reads were obtained in each library, in which more than 86.27% of clean reads per library could be mapped to the reference sorghum genome (*Table 1*). The Q30 values were higher than 90%, which indicated that the sequencing quality was good. The GC content of 12 samples ranged from 52.11% to 55.24%. This result indicated that the sequencing data could be used for further analysis.

Special and common low-N-responsive DEGs between KZ15 and SZ7

To examine the special and common DEGs between KZ15 and SZ7 under low-N treatment, a Venn diagram were constructed. Many common DEGs were identified in KZ15 and SZ7. In total, 793 DEGs were common low-N-responsive genes (*Fig. 2A*),

http://www.aloki.hu ● ISSN 1589 1623 (Print) ● ISSN 1785 0037 (Online)
DOI: http://dx.doi.org/10.15666/aeer/1705_1152511536

among which 277 were upregulated (*Fig. 2B*) and 486 were downregulated (*Fig. 2C*). Under low-N treatment, 404 DEGs were found specifically upregulated in KZ15 and 762 DEGs were specifically upregulated in SZ7. In addition, 642 and 1132 DEGs were specifically downregulated in KZ15 and SZ7, respectively (*Fig. 2A, 2B*).

Table 1. *Categorization and abundance of transcripts detected with RNA-seq*

Sample	Total Raw Reads (Mb)	Total Clean Reads (Mb)	Clean Reads Q30 (%)	Mapping Ratio to genome	Mapping Ratio to genes	GC (%)
ka_1	24.14	24.11	90.34	94.58%	86.57%	53.21
ka_2	24.14	24.10	90.95	94.64%	86.58%	53.47
ka_3	24.14	24.11	90.88	94.37%	86.27%	52.11
kb_1	24.14	24.07	91.42	94.70%	86.99%	54.23
kb_2	24.14	24.11	91.28	94.83%	87.26%	53.85
kb_3	24.14	24.11	91.52	94.88%	87.35%	53.75
sa_1	24.14	24.11	91.08	94.96%	86.91%	53.11
sa_2	24.14	24.11	90.73	95.20%	87.28%	52.95
sa_3	24.14	24.04	90.71	94.96%	86.91%	55.24
sb_1	24.14	24.07	91	94.83%	86.75%	54.73
sb_2	24.14	24.08	90.79	95.20%	87.14%	55.31
sb_3	24.14	24.08	90.7	94.75%	86.51%	54.53

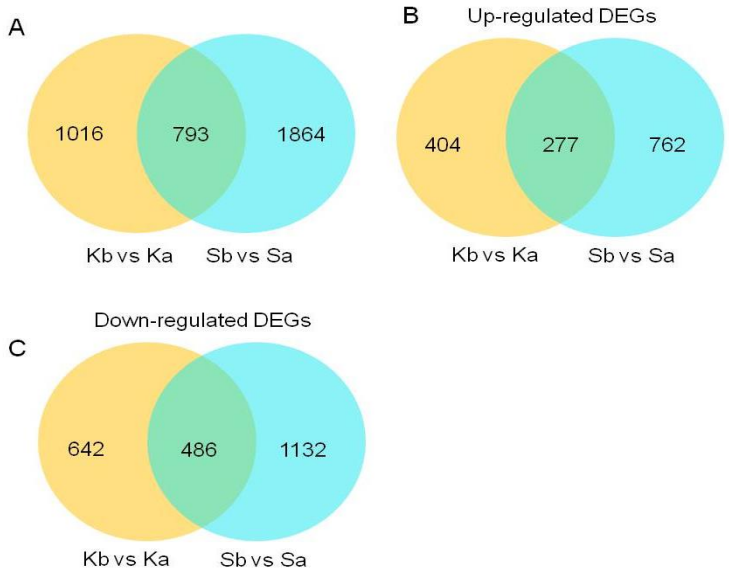

Figure 2. *Venn diagrams of differentially expressed genes (DEGs) after nitrogen deficiency., (A).Venn diagram showing the common DEGs between KZ15 and SZ7., (B).Venn diagram showing the special and common up-regulated DEGs between KZ15 and SZ7., (C).Venn diagram showing the special and common down-regulated DEGs between KZ15 and SZ7*

GO enrichment of DEGs

The DEGs were categorized into 46 functional groups in KZ15 and SZ7. According to the significance and reliability, GO entries with significant enrichment were screened and simplified. Twenty-six GO entries with the highest enrichment significance were screened out in KZ15 (*Table 2*), and 11 GO items with the highest significance were selected in SZ7 (*Table 3*). In biological process, GO terms related to metabolic process were the most enriched both in tolerant cultivar KZ15 (513) and sensitive cultivar KZ15

http://www.aloki.hu ● ISSN 1589 1623 (Print) ● ISSN 1785 0037 (Online)
DOI: http://dx.doi.org/10.15666/aeer/1705_1152511536

(731). DEG transcripts associated with stress responses included drug decomposition process in sensitive genotypes. DEGs associated with the metabolic process of pigmentation and glutathione were enriched in tolerant genotypes.

Table 2. *GO analysis of genes specifically expressed in KZ15 after N-starvation*

GO term	Ontology	Description	Gene Number	P-value
GO:0009522	C	Photosynthetic system I	10 of 720	0.00022
GO:0005576	C	Extracellular domain	64 of 720	0.00025
GO:0009521	C	Photosynthetic system	11 of 720	0.0439
GO:0016491	F	Oxidoreductase activity	179 of 944	1.97E-11
GO:0003824	F	Catalytic activity	663 of 944	6.69E-06
GO:0048037	F	Cofactor binding	114 of 944	9.42E-06
GO:0046527	F	Glucose transferase activity	38 of 944	2.51E-05
GO:0080043	F	3- Quercetin Glucosyl transferase activity	27 of 944	2.92E-05
GO:0080044	F	7- Quercetin Glucosyltransferase activity	27 of 944	2.92E-05
GO:0046906	F	Tetrapyrrol binding	62 of 944	0.00015
GO:0035251	F	UDP- Glucose transferase activity	31 of 944	0.00049
GO:0016168	F	Chlorophyll binding	8 of 944	0.00787
GO:0020037	F	Heme binding	54 of 944	0.01346
GO:0004364	F	Glutathione transferase activity	17 of 944	0.02068
GO:0042440	P	Pigment Metabolism	18 of 715	6.47E-05
GO:0019748	P	Secondary metabolic process	40 of 715	0.00027
GO:0015994	P	Metabolism of chlorophyll	11 of 715	0.00087
GO:0006778	P	Metabolism of Porphyrin-containing Compounds	14 of 715	0.00251
GO:0051186	P	Cofactor metabolic process	60 of 715	0.00625
GO:0006749	P	Glutathione Metabolism	18 of 715	0.01025
GO:0033013	P	Tetrapyrrol Metabolism	14 of 715	0.01182
GO:0009765	P	Photosynthesis, Light Harvest	9 of 715	0.01922
GO:0018298	P	Protein chromophore linkage	8 of 715	0.02056
GO:0009407	P	Toxin decomposition process	11 of 715	0.02232
GO:0090487	P	Secondary metabolite decomposition process	11 of 715	0.02232
GO:0046148	P	Pigment biosynthesis process	12 of 715	0.02666

C: Cellular component; P: Biological process; F: Molecular function

Table 3. *GO analysis of genes specifically expressed in SZ7 after N-starvation*

GO term	Ontology	Description	Gene Number	p-value
GO:0005576	C	Extracellular domain	87 of 1111	0.00114
GO:0009522	C	Photosynthetic system I	11 of 1111	0.00263
GO:0009521	C	Photosynthetic system	16 of 1111	0.00485
GO:0016491	F	Oxidoreductase activity	239 of 1407	3.12E-10
GO:0046906	F	Tetrapyrrol binding	90 of 1407	8.89E-07
GO:0048037	F	Cofactor binding	156 of 1407	9.07E-06
GO:0020037	F	Heme binding	83 of 1407	2.19E-05
GO:0003824	F	catalytic activity	951 of 1407	0.00074
GO:0004497	F	Monooxygenase activity	55 of 1407	0.02333
GO:0042737	P	Drug decomposition process	47 of 1019	0.00837
GO:0051187	P	Cofactor catabolism	35 of 1019	0.01595

C: Cellular component; P: Biological process; F: Molecular function

In molecular function ontology, catalytic activity was the term which was enriched and most abundant in both KZ15 (633) and SZ7 (951). The terms oxidoreductase activity, cofactor binding, tetrapyrrole binding and heme binding were found in both KZ15 and SZ7. GO terms belonging to molecular functions such as glutathione transferase activity, chlorophyll binding, glucose transferase activity, 3-quercetin

http://www.aloki.hu ● ISSN 1589 1623 (Print) ● ISSN 1785 0037 (Online)
DOI: http://dx.doi.org/10.15666/aeer/1705_1152511536

glucosyl transferase activity, and UDP-glucose transferase activity were enriched in KZ15. With respect to cellular component ontology, 64 genes were enriched in the extracellular region, followed by the photosynthetic pathway, suggesting that genes differentially expressed in the photosynthetic system and extracellular region of KZ15 may play an important role in low nitrogen tolerance. In SZ7, the most significant Go term was extracellular domain (87 genes). The other two GO terms (Photosynthetic system I and photosynthetic system) were related to the photosynthetic system.

Functional enrichment of significant genes

In this study, KEGG pathway enrichment analysis of DEGs of KZ15 and SZ7 under nitrogen starvation were carried out. In KZ15, a total of 1526 genes were found to be enriched in 124 pathways, which were divided into five branches: cell process, genetic information processing, environmental information processing, metabolism, and biological system. The results showed that nitrogen starvation had certain effects on the biosynthesis of secondary metabolites, carbohydrates, amino acids, lipids, terpenoids, ketones, cofactors, vitamins, plant signal transduction, membrane transport, protein folding, sorting, degradation, and DNA transcription. In addition, there were 125 DEGs that were related to environmental adaptation. In this study, the top ten pathways with the highest enrichment level were analyzed (*Table 4*). We found that the difference of nitrogen treatments caused changes of genes related to secondary metabolites biosynthesis, porphyrin metabolism, chlorophyll metabolism, photosynthetic antenna protein pathways, and other pathways, suggesting that these substances may be related to the absorption or metabolism of nitrogen in KZ15.

Table 4. *Top 10 KEGG pathway in KZ15 after N-starvation*

No.	Pathway ID	Pathway	DEGs genes	Pvalue	Qvalue
1	ko01110	Secondary Metabolites Biosynthesis	283	6.83E-15	8.47E-13
2	ko00860	Porphyrin and chlorophyll metabolism	19	2.70E-07	1.67E-05
3	ko00196	Photosynthetic antenna protein	8	9.05E-06	3.74E-04
4	ko01100	Metabolic pathway	380	1.65E-05	4.31E-04
5	ko00250	Metabolism of alanine, aspartic acid and glutamic acid	16	1.74E-05	4.31E-04
6	ko00220	Arginine biosynthesis	15	2.15E-05	4.44E-04
7	ko00941	flavonoid biosynthesis	22	6.12E-05	1.08E-03
8	ko04712	Plant rhythm	31	0.000188563	2.92E-03
9	ko00350	Tyrosine metabolism	15	0.000289618	3.67E-03
10	ko00908	Zeatin biosynthesis	10	0.000301345	3.67E-03

In SZ7, a total of 1694 genes were found to be enriched in 119 pathways. The results showed that nitrogen treatment had certain effects on the metabolism of carbohydrates, secondary metabolites, amino acids, lipids, terpenoids, ketones, cofactors, microorganisms, plant signal transduction, membrane transport, and DNA transcription and translation. A total of 161 DEGs were related to environmental adaptation. In this study, the top ten pathways with the highest enrichment level were analyzed (*Table 5*). We found that the difference of nitrogen level in SZ7 caused the different expression of genes related to the biosynthesis of secondary metabolites, monoterpenes, carotenoids, content of amino acids, starch, and sucrose, suggesting that these substances might be related to the metabolism of nitrogen uptake of SZ7.

http://www.aloki.hu ● ISSN 1589 1623 (Print) ● ISSN 1785 0037 (Online)
DOI: http://dx.doi.org/10.15666/aeer/1705_1152511536

Table 5. *Top 10 KEGG pathway in SZ7 after N-starvation*

No.	Pathway ID	Pathway	DEGs genes	Pvalue	Qvalue
1	ko01110	Secondary Metabolites Biosynthesis	344	5.12E-07	6.46E-05
2	ko00902	Monoterpene biosynthesis	9	7.72E-05	4.86E-03
3	ko00906	carotenoid biosynthesis	18	0.000176	7.40E-03
4	ko00904	Diterpenoid biosynthesis	18	0.000853	2.15E-02
5	ko00350	Tyrosine metabolism	18	0.000853	2.15E-02
6	ko00250	Metabolism of alanine, aspartic acid and glutamic acid	16	0.001541	3.24E-02
7	ko00500	Starch and Sucrose Metabolism	67	0.002004	3.34E-02
8	ko01100	Metabolic pathway	519	0.002124	3.34E-02
9	ko00950	Biosynthesis of Isoquinoline Alkaloids	13	0.003257	4.56E-02
10	ko00909	Biosynthesis of sesquiterpenes and triterpenes	11	0.00804	1.01E-01

Genes involved in nitrogen metabolism and glutathione metabolism

The results of GO enrichment analysis indicated the common low-N responses on nitrogen metabolism and the processes of glutathione metabolism in both KZ15 and SZ7. Nitrogen metabolism was composed of nitrogen transport and nitrate assimilation. In total, 16 genes participated in nitrogen metabolism, including nitrate reductase, ferredoxin-nitrite reductase, ureide permease 2, chloride channel protein and the NRT1/ PTR FAMILY (NRT2.2, NRT2.3, NRT3.1, NRT4.3, NRT4.4, and NRT6.3), which were all upregulated in both KZ15 and SZ7 under N-starvation. Only five genes (IN2-1, NRT4.3, NRT6.3, NRT8.3, and NRT8.5) encoding nitrate transport proteins were downregulated after N-starvation (*Figure 3A*).

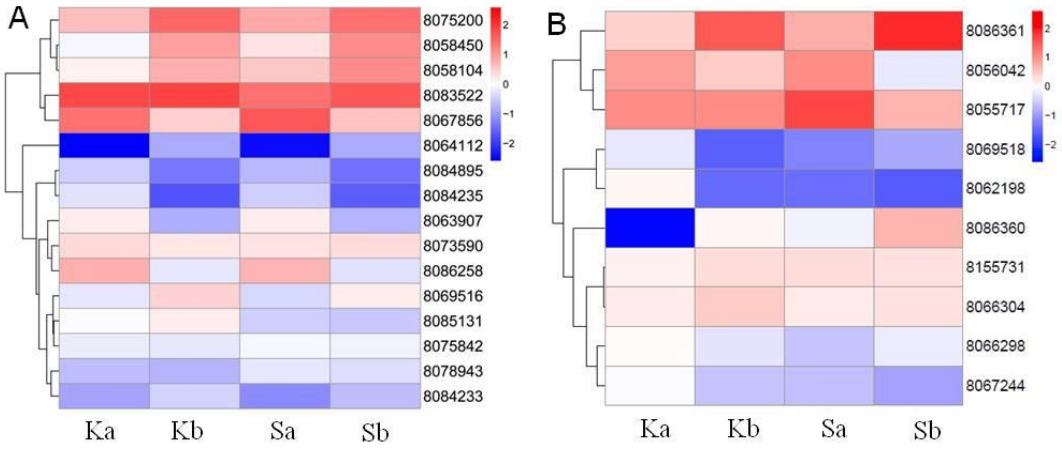

Figure 3. *Heatmap of differentially expressed genes (DEGs) related to Nitrogen metabolism (A) and Glutathione metabolic (B) in KZ15 and SZ7 under N-starvation*

Although similar expression pattern of genes involved in nitrogen metabolism existed in both varieties under N-starvation, the gene expression pattern in cell redox homeostasis was distinct. Among these, eight DEGs mapped to the cell redox homeostasis pathway and glutathione metabolism was found to be upregulated in KZ15 and SZ7 under N-starvation. Only two DEGs had the opposite expression (*Figure 3B*).

http://www.aloki.hu ● ISSN 1589 1623 (Print) ● ISSN 1785 0037 (Online)
DOI: http://dx.doi.org/10.15666/aeer/1705_1152511536

DEG transcripts abundant in KZ15 under N-starvation

Genes that are differentially expressed in only one variety should be important for the phenotypic differences between KZ15 and SZ7 under N-starvation. A total of 389 genes that were especially up-regulated in KZ15 were functionally involved in low-N tolerance. The expression of DEGs related to nitrogen metabolism and defense response was identified, which included genes associated with nitrate uptake and assimilation, transcriptional regulation, hormone-signaling, and oxidative stress. The results of RNA-seq for known nitrogen transport and assimilation genes indicated that N-stress may increase the abundance of genes encoding high affinity nitrate transporters in tolerant cultivars KZ15. For example, genes encoding the nitrate transporters NRT2.4, NRT3.1, and NRT4.5 were more abundant in the tolerant genotype KZ15 than SZ7 (*Figure 4A*).

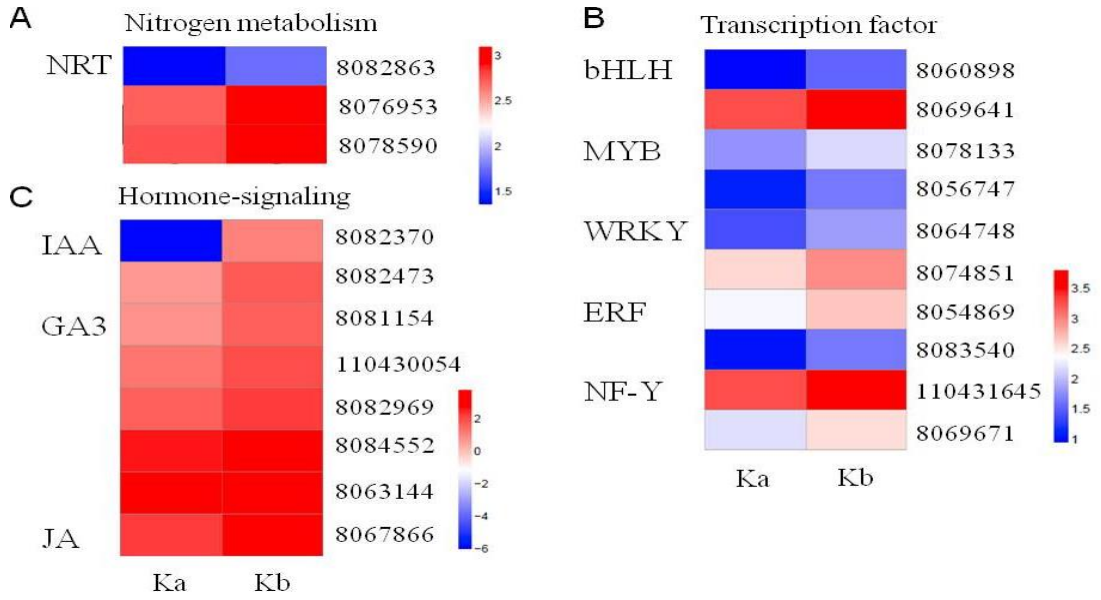

Figure 4. *Heatmap of differentially expressed genes(DEGs) related to low-N tolerance responses in KZ15. (A) Nitrogen metabolism. (B) Transcription factors*

Transcription factors are important in molecular mechanisms regulating growth, developmental processes, and responses to biotic or abiotic stress. In this study, a total of ten transcription factor (TF) encoding genes were especially upregulated in KZ15 under N-starvation. These transcription factors included the WRKY, MYB(myeloblastosis), bHLH(b helix–loop–helix) , ERF (ethylene responsive factor), and NF-Y(nuclear factor-Y) transcription factor families (*Figure 4B*). In addition, several genes associated with hormone-signaling pathways were upregulated in the tolerant genotype KZ15 under N-starvation, such as auxin responsive GH3(Gretchen Hagen 3) gene, auxin-responsive protein IAA30, gibberellin receptor GID1(Gibberellin insensitive dwarf 1), gibberellin 2-oxidase, and jasmonate ZIM (Zinc finger gene) domain-containing protein (*Figure 4C*). DEGs involved in oxidative stress response and flavonoid metabolites were also upregulated in KZ15 under N-stress.

http://www.aloki.hu ● ISSN 1589 1623 (Print) ● ISSN 1785 0037 (Online)
DOI: http://dx.doi.org/10.15666/aeer/1705_1152511536

Discussion

Changes of physiology and expressing genes in sorghum under low-N stress

The results of this study showed that the DEGs in chloroplast of SZ7 were significantly more abundant than that of KZ15. When nitrogen was deficient, physiological analysis also showed that the chlorophyll content of SZ7 was significantly lower than that of the normal nitrogen application, while the chlorophyll content of KZ15 did not change significantly under different nitrogen treatments. The activity of NR and GS decreased under low nitrogen, but the decrease of KZ15 was lower than that of SZ7. The decrease of low nitrogen tolerance sorghum was lower than that of low nitrogen sensitivity sorghum. The results of this study are consistent with previous studies on maize (Presterl et al., 2010), wheat (Han et al., 2007; Xiong et al., 2016), and rice (Zeng et al., 2007).

The results of RNA-sequencing revealed a series of DEGs between KZ15 and SZ7. To understand the molecular mechanisms of these two sorghum cultivars with significantly different nitrogen uptake levels, we found that 681 genes and 1039 genes were upregulated in KZ15 and SZ7 without nitrogen application, respectively, and the number of downregulated genes were 1128 and 1618, respectively. As an N^+ starvation sensitive genotype, the results showed that the DEGs of SZ7 were significantly more abundant than those of KZ15 in the process of organic nitrogen biosynthesis and nitrogen metabolism, which is similar to previous studies in maize and Arabidopsis thaliana (Gallais and Hirel, 2004). We also found that both cultivars were involved in photosynthesis and protein differential expression. Similar phenomena have been found in the gene expression profile of Arabidopsis thaliana (Himanen et al., 2004).

Special and common Low-N-responsive DEGs in sorghum under low-N stress

In this study, many DEGs were identified in both sorghum varieties which may be a response to low-N stress. Previous studies have shown that many DEGs associated with high affinity nitrate transporters (NRT2.2, NRT2.3, NRT2.5, and NRT2.6) were identified in low-N tolerant sorghum varieties (Gelli et al., 2014). Consistent with this, we found that the transcript encoding nitrate transporters NRT2.4, NRT3.1, and NRT4.5 were abundant in the tolerant genotype KZ15 compared to SZ7. We also found that the NRT1/ PTR family (NRT2.2, NRT2.3, NRT3.1, NRT4.3, NRT4.4, and NRT6.3) was upregulated in both KZ15 and SZ7 under N-starvation.

It has been reported that SiMYB3 takes part in the growth and development of lateral roots and elongation of main roots mediated by low nutritional stress in millet; it also plays an important regulatory role in the signaling pathways of nitrogen, phosphorus, and potassium (Hu et al., 2015). A total of 235 MYB transcription factors were found in this study. Two MYB transcription factors were especially upregulated in KZ15 under different nitrogen treatments, indicating that MYB transcription factors may play an important role in the process of low-nitrogen stress response in sorghum.

Conclusion

To analyze the molecular mechanism of sorghum response to low nitrogen, the phenotypic and transcript profiling of different resistant varieties were studied. The results showed that the content of chlorophyll and the activity of NR and GS of SZ7

http://www.aloki.hu ● ISSN 1589 1623 (Print) ● ISSN 1785 0037 (Online)
DOI: http://dx.doi.org/10.15666/aeer/1705_1152511536

were more sensitive than that of KZ15 under low-N stress. A total of 1809 and 2657 DEGs were identified from KZ15 and SZ7.

We suggest that MYB transcription factors may play an important role in regulating the expression of genes related to nitrogen stress response. The ERF, bHLH, WRKY, and NF-Y families of transcription factors could also be involved in the response to low nitrogen tolerance in sorghum. In the tolerant cultivar KZ15, 389 upregulated genes were found functionally involved in low-N tolerance. These 389 genes are mainly involved in nitrogen metabolism, defense response, oxidative stress response, and flavonoid metabolism. We speculate that three nitrate transporter genes (NRT2.4, NRT3.1, and NRT4.5) and ten transcription factors may play an important role in improving the nitrogen use efficiency of sorghum. Overexpression of these genes may improve the tolerance of sensitive sorghum genotypes to nitrogen starvation. The expression patterns and regulation mechanisms of these genes associated with the tolerance to low nitrogen will be analyzed in future. These genes can also be used as candidate genes for improving sorghum tolerance to low nitrogen by genetic engineering, and lay a foundation for the breeding of new sorghum varieties with low nitrogen tolerance.

REFERENCES

[1] Anders, S., Huber, W. (2010): Differential expression analysis for sequence count data. – Genome biology 11(10): R106.

[2] Ding, Y., Luo, W., Xu, G. (2006): Characterisation of magnesium nutrition and interaction of magnesium and potassium in rice. – Annals of Applied Biology 149(2): 111-123.

[3] Gallais, A., Hirel, B. (2004): An approach to the genetics of nitrogen use efficiency in maize. – Journal of Experimental Botany 55: 295-306.

[4] Gelli, M., Konda, A. R., Liu, K., Zhang, C., Clemente, T. E., Holding, D. R., Dweikat, I. M. (2017): Validation of QTL mapping and transcriptome profiling for identification of candidate genes associated with nitrogen stress tolerance in sorghum. – BMC Plant Biol. 17: 123.

[5] Han, S. F., Li, S. W., Wu, L. Q., Wen, H. D., Xiao, K. (2007): Responses and corresponding physiological mechanisms of different wheat varieties in their nitrogen efficiency and nitrogen uptake to nitrogen supply. – Chinese Journal of Applied Ecology 18(4): 807-812.

[6] Himanen, K., Vuylsteke, M., Vanneste, S., Vercruysse, S., Boucheron, E., Alard, P., Chriqui, D., Montagu, M. V., Inze, D., Beeckman, T. (2004): Transcript profiling of early lateral root initiation. – Proc Natl Acad Sci USA 101: 5146-5151.

[7] Hu, L. (2015): Transcriptome analysis of Foxtail millet (Setaria italic) under low nitrogen stress and characteristics and functional identification of SiMYB3. – Master dissertation of Chinese Academy of Agricultural Sciences (in Chinese with English Abstract).

[8] Kim, D., Langmead, B. (2015): HISAT: a fast spliced aligner with low memory requirements. – Nat. Methods 12: 357-360.

[9] Kraiser, T., Gras, D. E., Gutierrez, A. G., Gonzalez, B., Gutierrez, R. A. (2011): A holistic view of nitrogen acquisition in plants. – J Exp Bot 62: 1455-66.

[10] Loudet, O., Chaillou, S., Merigour, P., Talbotec, J., Daniel, V. F. (2003a): Quantitative Trait Loci Analysis of nitrogen use efficiency in Arabidopsis. – Plant Physilology 131: 345-358.

http://www.aloki.hu ● ISSN 1589 1623 (Print) ● ISSN 1785 0037 (Online)
DOI: http://dx.doi.org/10.15666/aeer/1705_1152511536

[11] Loudet, O., Chaillou, S., Krapp, A., Daniel, V. F. (2003b): Quantitative Trait Loci analysis of water and anion contents in interaction with nitrogen availability in Arabidopsis thaliana. – Genetics 163: 711-722.
[12] Ma, J. (2014): The morphological and physiological characteristics of sorghum under low phosphorus and nitrogen, and the study of sorghum microRNA under low nitrogen stress. – Ph.D. dissertation of Shanxi Agricultural University (in Chinese with English Abstract).
[13] Obara, M., Sato, T., Sasaki, S., Kashiba, K., Nagano, A., Nakamura, I., Ebitani, T., Yano, M., Yamaya, T. (2004): Identification and characterization of a QTL on chromosome 2 for cytosolic glutamine synthetase content and panicle number in rice. – Theor Appl Genet 110: 1-11.
[14] Presterl, T., Groh, S., Landbeck, M., Seitz, G., Schmidt, W., Geiger, H. H. (2010): Nitrogen uptake and utilization efficiency of European maize hybrids developed under conditions of low and high nitrogen input. – Plant Breeding 121(6): 480-486.
[15] Rajasekhar, V. K., Mohr, H. (1986): Appearance of nitrite reductase incotyledons of the mustard (Sinapis alba L.) seedling as affected by nitrate, phytochrome and photooxidative damage of plastids. – Planta 168(3): 369-376.
[16] Rosa, R. M., Rosa, Y., Rosa, J. J., Rosa Jr, E. J., Silva, E. F., Martinez, M. A., Rosa, D. B. C. J., Soares, J. S. (2014): Influence of nitrogen, potassium and phosphate fertilizers on quality and longevity of gladiolus. – Revista Brasileira de Horticultura Ornamental 20(2): 143-153.
[17] Wang, X. K. (2006): Principles and Techniques of Plant Physiology and Biochemistry Experiments. – Higher Education Press, Beijing.
[18] Xiong, S. P., Wu, K. Y., Wang, X. C., Zhang, J., Du, P., Wu, X., Ma, X. M. (2016): Analysis of root absorption characteristics and nitrogen utilization of wheat genotypes with different N efficiency. – Scientia Agricultura Sinica 49(12): 2267-2279.
[19] Zeng, J. M., Cui, K. H., Huang, J. L., He, F., Peng, S. B. (2007): Responses of physio-biochemical properties to N-fertilizer application and its relationship with nitrogen use efficiency in rice (Oryza sativa L.). – Acta Agronomica Sinica 33(7): 1168-1176.

http://www.aloki.hu ● ISSN 1589 1623 (Print) ● ISSN 1785 0037 (Online)
DOI: http://dx.doi.org/10.15666/aeer/1705_1152511536

PHYLOGENETIC ANALYSIS OF ENOLASE GENE FAMILY IN DIFFERENT SPECIES

LIU, K. C. [1] – LIU, C.[1] – FAN, M. X.[2] – ZHANG, C. Y.[1] – CAI, F. C.[1] – LI, Q. Y.[1] – CHEN, M. M.[1] – JIANG, Y.[1] – HU, W. B.[1] – LIN, F.[1*]

[1]*College of Bioscience and Biotechnology, Shenyang Agricultural University, No. 120 Dongling Road, Shenyang, 110866 Liaoning, China*

[2]*Liaoning Key Laboratory of Urban Integrated Pest Management and Ecological Security, College of Life Science and Bioengineering, Shenyang University, Shenyang 110044, China*

**Corresponding author*
e-mail: fenglinsn@126.com

(Received 22nd Apr 2019; accepted 16th Jul 2019)

Abstract. Enolase is involved in the glycolytic pathway of many organisms and is a key rate-limiting enzyme, which plays an important role in the growth and development of various species. In this study, the enolase gene sequences and amino acid sequences of more than 40 species were first downloaded, and phylogenetic analysis and molecular evolution studies were performed using bioinformatics methods. The phylogenetic tree was constructed to predict the conserved type of enolase evolution and the enolase evolution relationship of each species. It was found that the enolase of each species was very conservative during the evolution process. In addition to studying the evolutionary relationship of enolase of various species, the protein structure was predicted, and the secondary structure of enolase protein was predicted. The results showed that the secondary structure was very similar. The homology modeling method was used to predict the tertiary structure of enolase, and it was found that although there were slight differences, they were similar. In addition, statistical comparison analysis of the introns of each species enolase found that the gap between the number of introns and the locus was small, suggesting their close evolutionary relationship. It is predicted that a variety of plant and animal enolase catalytic kinase-specific phosphorylation sites, the results show that the kinase domain sequence contains three phosphorylation sites: serine (Ser), threonine (Thr) and tyrosine (Tyr). The amount of serine is the highest and the degree of similarity is high. The Ka/Ks ratio of most species is greater than 1. This indicates that enolase is mainly influenced by positive selection in evolution. Our results will help provide insights into the evolution of enolase and provide a theoretical basis for subsequent experiments.
Keywords: *enolase, glycolysis pathway, evolution, phosphorylation, intron*

Introduction

Enolase, originally discovered by Lohman and Meyerhof in 1934, is a rate-limiting enzyme in the glycolysis pathway. Enolase not only catalyzes the dehydration reaction from 2-phospho-D-glycerate (2-PGA) to phospho-enolpyruvate (PEP) in glycolysis metabolism, but also catalyzes the phospho-enolpyruvate hydratase reaction to convert PEP to 2-PGA (Lohman and Meyerhof, 1934; Armand et al., 2016) (*Fig. 1*). Further studies have demonstrated some divalent metal ions (Mg^{2+}, Mn^{2+}, Zn^{2+}, Ca^{2+}, Co^{2+} and Ni^{2+}) have activation effect on enolase activity, especially Mg^{2+} which is the strongest natural activator of enolase (Warburg et al., 1942; Mizuno et al., 2007). Enolase has long been considered as an ancient enzyme with only catalytic function. In addition to glycolytic pathways, enolase is also plays an important role in some physiological and pathological processes in organisms, such as ithe regulation of transcription, apoptosis, and cell differentiation (Straeten et al., 1991; Ucker et al., 2016).

http://www.aloki.hu ● ISSN 1589 1623 (Print) ● ISSN 1785 0037 (Online)
DOI: http://dx.doi.org/10.15666/aeer/1705_1153711550

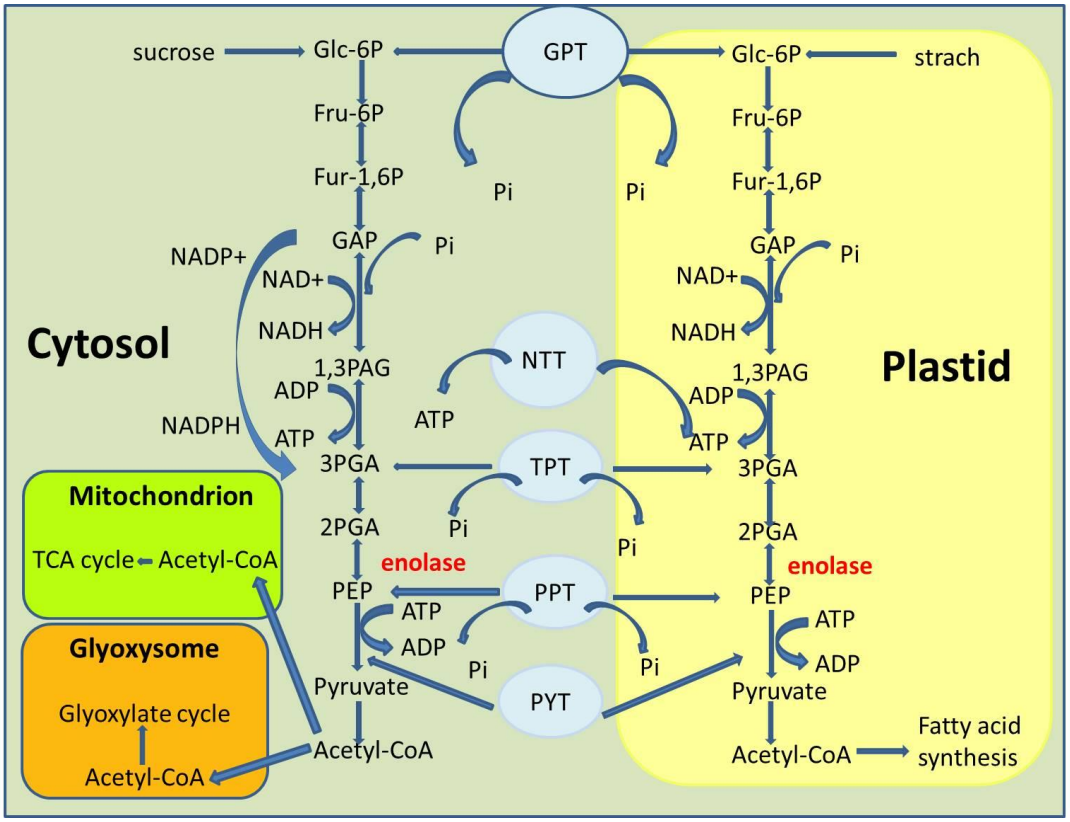

Figure 1. *Glycolysis pathway (PYT: pyruvate translocator; GPT: glucose phosphate/Pi translocator; PPT: phosphoenolpyruvate/Pi translocator; TPT: triose phosphate/Pi translocator; Fru-1, 6P: fructose 1,6 bisphosphate; Fru-6P: fructose 6 phosphate; GAP: glyceraldehyde-3-phosphate; Glc-6P: glucose 6 phosphate; PEP: phosphoenolpyruvate; 1,3-PGA: 1,3-bisphosphoglycerate;2-PGA: 2-phosphoglycerate; 3-PGA: 3-phosphoglycerate)*

Enolase occupies an important position in the fermentation metabolic pathway, especially in the glycolytic pathway. This enzyme is widely present in almost all the species. The gene sequences of enolases are highly conserved. The enolase is evolutionarily affiliated tothe enolase superfamily, which includes the MR (mandelate racemase) family, the MLE (muconate lactonizing enzyme) family, and the enolase family (Gerlt et al., 2012).

The crystal structures of enolase from some prokaryotes and eukaryotes have been resolved. The main structure of the enolase consists of two anti-parallel identical subunits. Each of these subunits contains a relatively long C-terminus and a relatively short N-terminal domain. The former domain is folded into a $\beta_2\alpha_2(\beta\alpha)_6$ topology, and the latter domain is folded into a $\beta_3\alpha_4$ topology (Lebioda et al., 1988). The activity center of enolase is located in the folded cavity of the C-terminal domain. Unlike the high degree of structural conservation and similarity, the aggregation state of enolase varies widely among different species.

Enolase is recognized as a multifunctional protein. In addition to the glycolysis function in metabolic pathway, enolase is also expressed as a receptor for plasminogen on the surface of many types of cells to ensure that plasminogen hydrolyzing activity is concentrated on the cell surface. This causes hydrolase cleavage of plasmin, which leads to the growth of tumor cell invasion and the associated inflammatory response

http://www.aloki.hu ● ISSN 1589 1623 (Print) ● ISSN 1785 0037 (Online)
DOI: http://dx.doi.org/10.15666/aeer/1705_1153711550

(Perconti et al., 2017). By removing the function of its plasminogen receptor and its catalytic function in glycolysis, enolase also exhibits other intracellular localization and cellular functions, all of which are well known for its glycolysis function. This suggests that it may play a role in cell recognition and invasion, vacuole formation and development, and transcriptional processes (Pal et al., 2009). In addition, differential expression of enolase is also thought to be associated with some pathophysiological states, such as cancer, Alzheimer's disease, rheumatoid arthritis. For example, a large number of studies have generally shown that the enzymatic enzyme's glycolysis function is significantly enhanced in tumor cells and is used as a marker for cancer progression (Song et al., 2014; Reev et al., 1986). Therefore, enolase is considered as a hallmark of many diseases. In plants studies about enolase have shown that the enolase gene expression and enzyme activity will change under high temperature, anaerobic, high salt, dry early, low temperature and other stress conditions (Barkla et al., 2009; Iida et al., 1985; Grondin et al., 2015). Under stress conditions, plants produce large amounts of free radicals that cause damage to the photosynthetic system. This stress response of enolase can provide energy for its repair. Enolase is a glycolytic enzyme that is consistent with its primary function in the cytoplasm. In the cytoplasm, enolase can be free, and other glycolytic enzymes in the cytoskeleton. Interaction occurs in combination (Subramanian et al., 2000). For example, pyruvate kinase, phosphoglycerate mutase and aldolase. The first two enzymes are closely adjacent to the enolase in the glycolytic pathway, and aldolase interacts with some of the cytoskeletal proteins (Aaronson et al., 1995). Studies have shown that α-enolase has a certain effect on hypoxia tolerance through non-glycolytic pathways. Under hypoxic conditions, the expression of α-enolase may be enhanced in cells. Protection under anaerobic conditions (Straeten et al., 1991).

We will carry out evolutionary cluster analysis of each species enolase, and analyze the protein secondary structure, tertiary structure, phosphorylation site, number of introns, and ka/ks value to prove the conservation of enolase. Through the research results of this paper, we can better analyze the evolutionary relationship between enolase in various species, and provide theoretical basis for subsequent research in molecular biology.

Materials and methods

Identification of enolase genes

In this study, the genes which encode enolase from 50 species were collected from databases and related articles, The relevant enolase sequences were obtained from phytozome database (available) online: (https://phytozome.jgi.doe.gov/pz/portal.html) and NCBI:(https://www.ncbi.nlm.nih.gov) results are merged and the extra sequences are removed. For genes with more than one predicted isotype, we only analyzed the longest peptide sequence for each gene.

Prediction of enolase structure

The amino acid sequences of enolase from 42 species were input into the SOPMA online software (https;//npsaprabi.ibcp.fr/cgi-bin) to predict the secondary structure of the enolase protein. And draw the obtained data into a table. Use SWISS-MODEL

http://www.aloki.hu ● ISSN 1589 1623 (Print) ● ISSN 1785 0037 (Online)
DOI: http://dx.doi.org/10.15666/aeer/1705_1153711550

(https://swissmodel.expasy.org/) online software to predict and build a tertiary structural model of enolase

The phylogram and selection of enolase

All enolase amino acid sequences in 50 species including maize, wheat, rice, Arabidopsis, mouse, orangutan were aligned by ClustalX v1.83 (Higgins et al., 1992). Use the default parameters. MEGA 6.0 (Tamura et al., 2011) using the NJ method was used to generate a phylogenetic tree. The enolase gene intron information for maize, wheat, rice, Arabidopsis, mice, orangutans, etc. is from Ensembl Genomes (Available online: http://ensemblgenomes.org/). The value of Ka/Ks was very important since it could estimate the changes of encoded amino acid sequences and gene functions, further estimate gene evolution. Each Ka and Ks value can be calculated by DnaSPv5.0 software (available online: http://www.ub.edu/dnasp/).

Phosphorylation analysis of enolase

KinasePhos (http://kinasephos.mbc.nctu.edu.tw/) was used to predict the kinase specific phosphorylation site in which enolase catalyzes. The software has high sensitivity and specificity, categorizing known phosphorylation sites by substrate sequences and their associated protein kinase classification.

The enolase gene intron information for 30 species including maize, rice, Arabidopsis, orangutan, and mouse is from Ensembl Genomes (available online at http://ensemblgenomes.org/).

Results

Conservative evolution of enolase

To investigate the gene evolutionary relationship, a total of 51 enolases from 50 species were aligned using MEGA software. The clustering analysis result showed that amino acid sequence levels in monkeys, bonobos, Sumatran orangutans, beluga whales, tilapia, rainbow trout, pigeons, ducks, birds, yeast, staphylococcus, staphylococcus, and streptococci. The enolase of 50 species was subjected to cluster analysis at the amino acid sequence level and merged with the system evolution, and the calibration parameters were repeated 1000 times (*Fig. 2*). The gymnosperms Araucaria and Selaginella are clustered together. Monocotyledonous corn, wheat, sorghum, and rice are clustered together, while most dicotyledonous plants such as peanuts, soybeans, pumpkins, and bitter gourds are clustered together, but peppers and tobacco. Gathering together as one, Arabidopsis and mulberry are clustered together. It may be that enolase has some differences in evolution among these species, which is worthy of our subsequent analysis. Enolase generally has the characteristics of closer evolution of the plant within the family. In mammals, mammals such as beluga whales, orangutans, monkeys, and horses are grouped together, rainbow trout in fish, tilapia are grouped together, mosquitoes, fruit flies, and silkworms are grouped together. Staphylococcus, streptococcus, and heatococcus are grouped together. Further analysis found that the similarity of several major crops such as wheat, corn, rice and sorghum was more than 54%, and the sequence similarity of beluga whales, horses, bonobos, red marmosets and Sumatran orangutans reached over 98%. This indicates that the enolase gene is evolutionarily conservative.

http://www.aloki.hu ● ISSN 1589 1623 (Print) ● ISSN 1785 0037 (Online)
DOI: http://dx.doi.org/10.15666/aeer/1705_1153711550

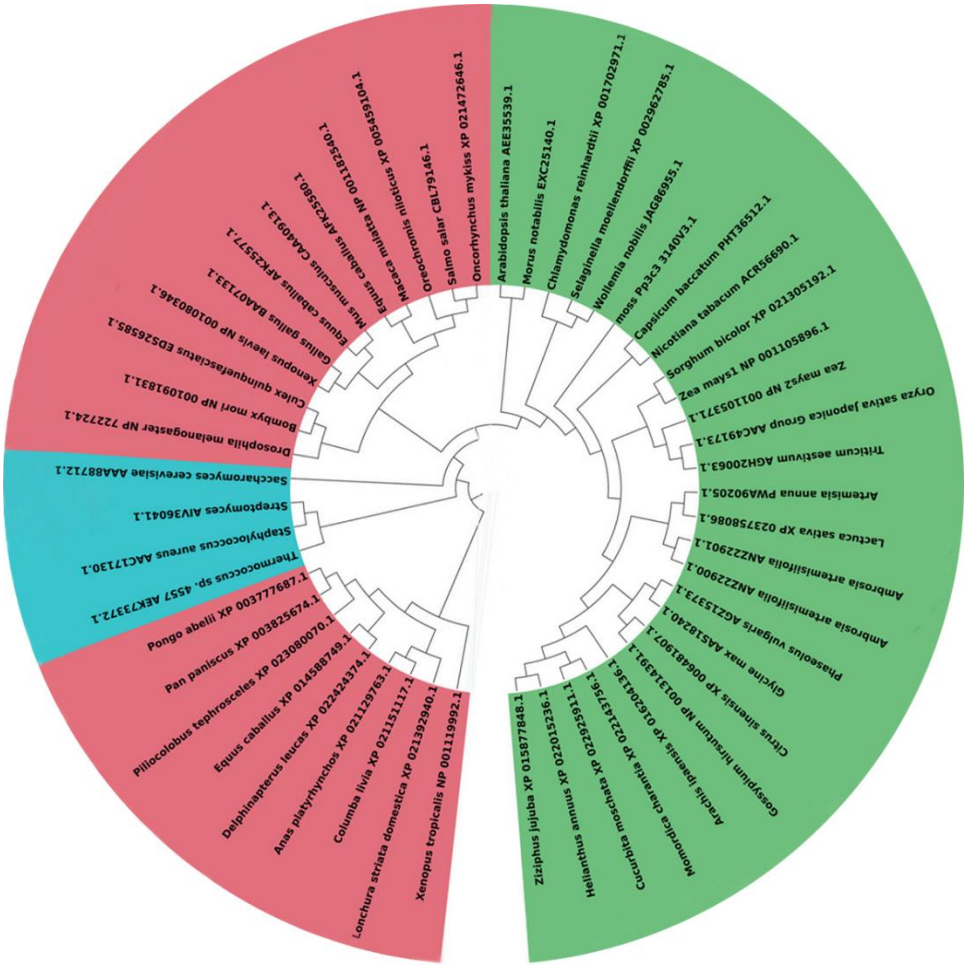

Figure 2. *Evolutionary analysis of the enolase amino acid sequence. (Note: Phylogenetic tree of enolase in 50 species including maize, rice, Arabidopsis, orangutan, and mouse. Green represents plants, pink represents animals, and blue represents fungi)*

Enolase protein structure analysis

The high-order structure formed by folding and winding of amino acid residues by van der Waals force, hydrogen bonding, etc. is called protein secondary structure, and mainly includes α-helix, β-sheet, random coil and extended chain. The secondary structure of 42 species of enolase protein was analyzed online using SOPMA software. The results showed that the enolase protein contained the above secondary structure, α-helix and random. Curl is the most frequently occurring structure, while the elongation chain and β-sheet appear less *(Schedule 1)*. The number of sputum-helix in plants is between 182 and 235, accounting for 39.96% to 46.53%. The number of "random" curls is between 143 and 171, accounting for 32.13% to 35.65%. In animals, the number of sputum-helix is between 184 and 292, accounting for 40.66% to 47%. The number of "random" curls is between 138 and 244, accounting for 31.8% to 40%. In the fungi, the number of α-helix is between 184 and 1945, accounting for 42.99%~44.7%. The number of "random" curls is between 136 and 143, accounting for 31.34% to 33.41%. The SWISS-MODEL uses the online tool SWISS-MODEL to model the tertiary structure of 42 species of enolase protein. After homologous modeling of 42 species of

http://www.aloki.hu ● ISSN 1589 1623 (Print) ● ISSN 1785 0037 (Online)
DOI: http://dx.doi.org/10.15666/aeer/1705_1153711550

enolase protein, it was found that the proteins are highly similar in spatial structure, and the proteins of each species have highly conserved structural features, so we constructed a tertiary structure of corn, orangutan, and thermococci enolase protein. The figures are representative of plants, animals, and bacteria (*Fig. 3a, b* and *c*). The results show that the tertiary structure of the enolase proteins of the three species is very similar. Both are bilaterally symmetric structures, and the positions of the active centers are also the same. And it can be seen intuitively that the α-helix, β-sheet, "random" curl, the number of extension chains and the sections are similar. However, the number of secondary structures of animal enolase is much higher than that of plants and fungi. Using Swiss-Pdb Viewer to analyze the results of homology modeling, the predicted dihedral angle of the protein residue is located in the yellow core region, indicating that its spatial structure is stable. PyMOL is used to process and analyze the modeling results, and the Ramachandran diagram is obtained. Ramachandran diagrams are mainly divided into permitted areas, maximum allowed areas, and disallowed areas. In general, the ratio of the amino acid of the model to the allowable region and the maximum allowable region is more than 90% of the total protein. The spatial structure conformation of the protein conforms to the rule of stereochemistry. As shown in *Figure 3d, e* and *f*, more than 90% of the dihedral angles of the enolase protein residues were detected in the allowable zone and the maximum allowable zone, indicating that it has a stable spatial conformation. In *Figure 3d, e* and *f* can be intuitively seen that the distribution of the secondary structure of the three representative species in the tertiary structure is concentrated in three main regions, and the representative species of the animal, in addition to the main three regions, are also distributed in other regions. This is different from the representatives of plants and fungi.

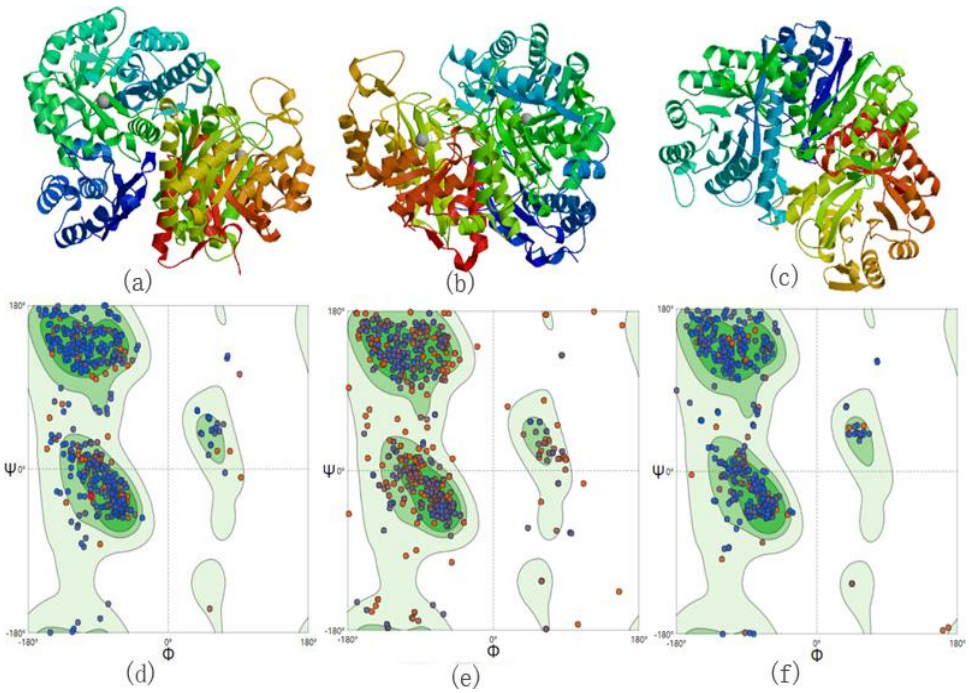

Figure 3. *Enolase tertiary structure diagram.* ***a*** *The tertiary structure of corn enolase,* ***b*** *the tertiary structure of the orangutan enolase, and* ***c*** *the tertiary structure of the thermococcal enolase.* ***d*** *A PyMOL map representing the tertiary structure of corn enolase,* ***e*** *a PyMOL map representing the tertiary structure of the orangutan enolase, and* ***f*** *a PyMOL map representing the tertiary structure of the thermococcal enolase*

http://www.aloki.hu ● ISSN 1589 1623 (Print) ● ISSN 1785 0037 (Online)
DOI: http://dx.doi.org/10.15666/aeer/1705_1153711550

Enolase phosphorylation site analysis

Phosphorylation of proteins is one of the important covalent modifications in organisms. About one-third of proteins are hyperphosphorylated during mammalian cell life cycle; 5% of genes in vertebrate genomes The encoded protein is a protein kinase and phosphoenzyme involved in the phosphorylation and dephosphorylation processes. Plants are grown in the soil and cannot move away from biological or abiotic stresses like animals. Therefore, plant cells usually use receptors on the cell surface to sense environmental changes, transmit signals through various signaling pathways in the body, and finally respond appropriately to various external stimuli (Morris and Walker, 2003). The protein phosphorylation sites of eukaryotic cells mainly occur on the hydroxyl groups of the serine (Ser), threonine (Thr) and tyrosine (Tyr) residues, and different protein kinases can recognize and modify the difference of different proteins Site. Kinase Phos (http://kinasephos.mbc.nctu.edu.tw/) was used to predict the kinase-specific phosphorylation sites that 14 plants and 11 animal enolase catalyze. The software is highly sensitive and specific, categorizing known phosphorylation sites by substrate sequences and their associated protein kinase classification. According to the prediction results of phosphorylation sites (*Fig. 4a* and *b*), the amino acid sites with a predicted score of 0.5 or more were recorded. The results showed that the kinase domain sequence contains three phosphorylation sites: serine, serine (Thr) and tyrosine (Tyr). Among them, the potential of serine phosphorylation sites is the highest in animals. Plants have the highest levels of potential serine phosphorylation sites and tyrosine phosphorylation sites. There are 6 phosphorylation sites in rice, wheat and jujube. Maize, citrus, kidney bean, sorghum and peanut contain 5 phosphorylation sites, and corn, rice, wheat, sorghum, jujube and citrus contain Thr47 and Thr59 phosphate. Chemical site. Peanut, kidney bean, soybean, and bitter gourd all contain Thr46 and Thr58 phosphorylation sites, and tobacco contains Thr46 phosphorylation site. Rice, wheat and jujube contain Ser277 phosphorylation sites, citrus, peanuts, and Ser276 phosphorylation sites, and bitter melon and soybean contain Ser275 phosphorylation sites. Kidney beans, soybeans, and bitter gourd contain Ser382 phosphorylation sites, citrus, peanuts, and Ser383 phosphorylation sites, and corn, sorghum, and jujube contain Ser384 phosphorylation sites. Sumatra orangutans, horses, monkeys, and beluga contain Ser289, Ser527, and Thr189 phosphorylation sites.

Enolase intron number analysis

An intron is a non-coding sequence of a break gene that can be transcribed but is cleaved off during mRNA processing, so there is no intron coding sequence on the mature mRNA. In eukaryotes, most genes are interrupted by one or more introns, which may contain “old codes”, which are part of the gene that loses its function during evolution. It may be a key event in the conservative evolution of gene structure. Because the intron is meaningless to the structure of the translation product and is not subject to the pressure of natural selection, it has more mutations than the exon accumulation. In addition, there is growing evidence that loss or increase in introns may be an important factor in the progressive diversity and complexity of genes. We downloaded the enolase genes from 30 species and counted the number of introns. The results are shown in *Figure 5*. Among them, the main crops of maize, rice, sorghum, soybean, and wheat enolase genes had 16 introns. The number of animal introns is mainly concentrated in 11, 13, and 14.

http://www.aloki.hu ● ISSN 1589 1623 (Print) ● ISSN 1785 0037 (Online)
DOI: http://dx.doi.org/10.15666/aeer/1705_1153711550

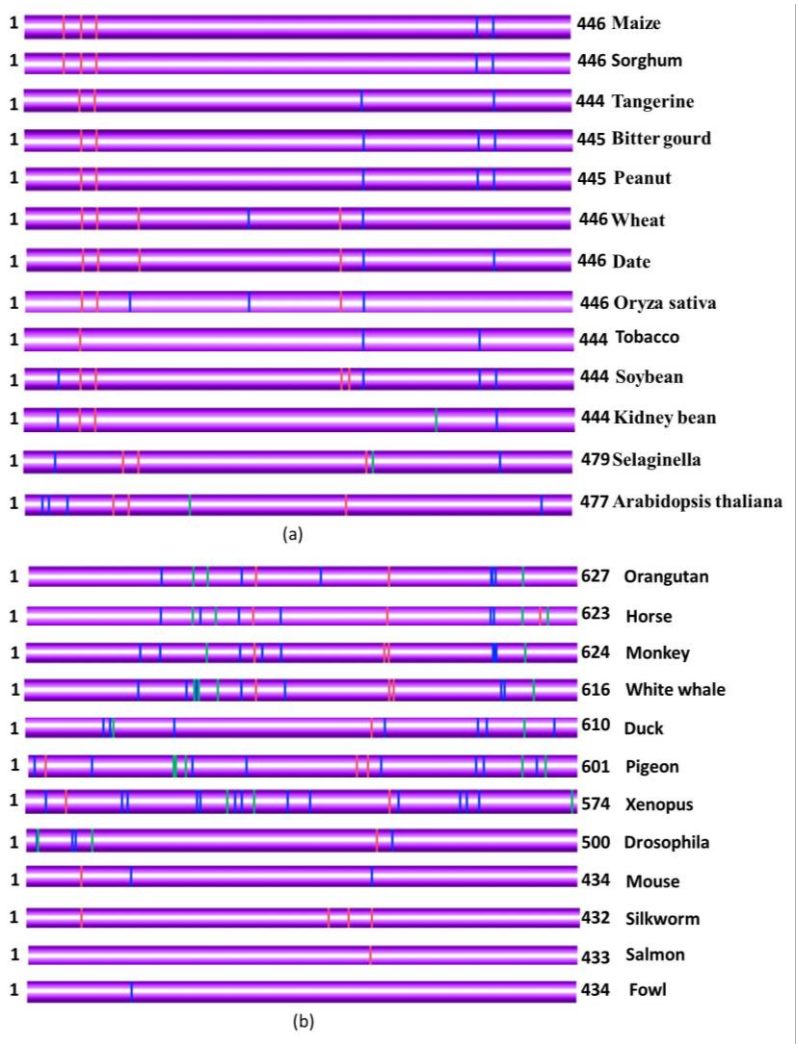

Figure 4. *Enolase phosphorylation site analysis. (Note: Phosphorylation sites of enolase in 24 species such as maize, rice, Arabidopsis, orangutan, and mouse. Red represents serine, green represents threonine, and blue represents tyrosine.* ***a*** *The position and number of phosphorylation sites of plant enolase, and* ***b*** *the location and number of phosphorylation sites of animal enolase)*

The evolution selection of enolase

In genetics, Ka/Ks or dN/dS represents the ratio between the heterosexual substitution (Ka) and the synonymous substitution (Ks). This ratio can be used to determine if there is a selective pressure on this protein-coding gene. Nucleotide variants that do not result in amino acid changes are referred to as synonymous mutations, and vice versa. It is generally believed that synonymous mutations are not naturally selected, while non-synonymous mutations are naturally selected. Because synonymous substitutions cause amino acid changes that may alter the conformation and function of the protein, and thus cause adaptive changes that result in advantages or disadvantages of natural selection (generally disadvantages). Non-synonymous substitutions do not alter the composition of the protein and are therefore unaffected by natural selection, so Ks can reflect the background base substitution rate of the evolutionary process. The ratio of Ka/Ks can indicate which choice the gene is. In

http://www.aloki.hu ● ISSN 1589 1623 (Print) ● ISSN 1785 0037 (Online)
DOI: http://dx.doi.org/10.15666/aeer/1705_1153711550

evolutionary analysis, it is meaningful to understand the rate at which synonymous and non-synonymous mutations occur. Commonly used parameters are the following: synonymous mutation frequency (Ks), non-synonymous mutation frequency (Ka), ratio of non-synonymous mutation rate to synonymous mutation rate (Ka/Ks). If Ka/Ks > 1, then a positive selection effect is considered. If Ka / Ks = 1, then a neutral choice is considered to exist. If Ka/Ks < 1, then a purification selection effect is considered (Baumgarten et al., 2003). The frequency of enolase Ka/Ks in plants is mainly between 1.2 and 1.4, and all Ka/Ks are almost > 1 (*Fig. 6a* and *b*). The frequency of enolase Ka/Ks in animals is mainly between 1.0 and 1.2. Although most of the Ka/Ks are > 1, there are certain ratios between 0.8 and 1.0 indicating (*Fig. 6c* and *d*) that the enolase gene is mainly influenced by the positive selection effect in evolution. The enolase in plants is almost always influenced by the positive selection effect in evolution. The enolase in animals is influenced by the positive selection effect in evolution, but some are also affected by negative selection.

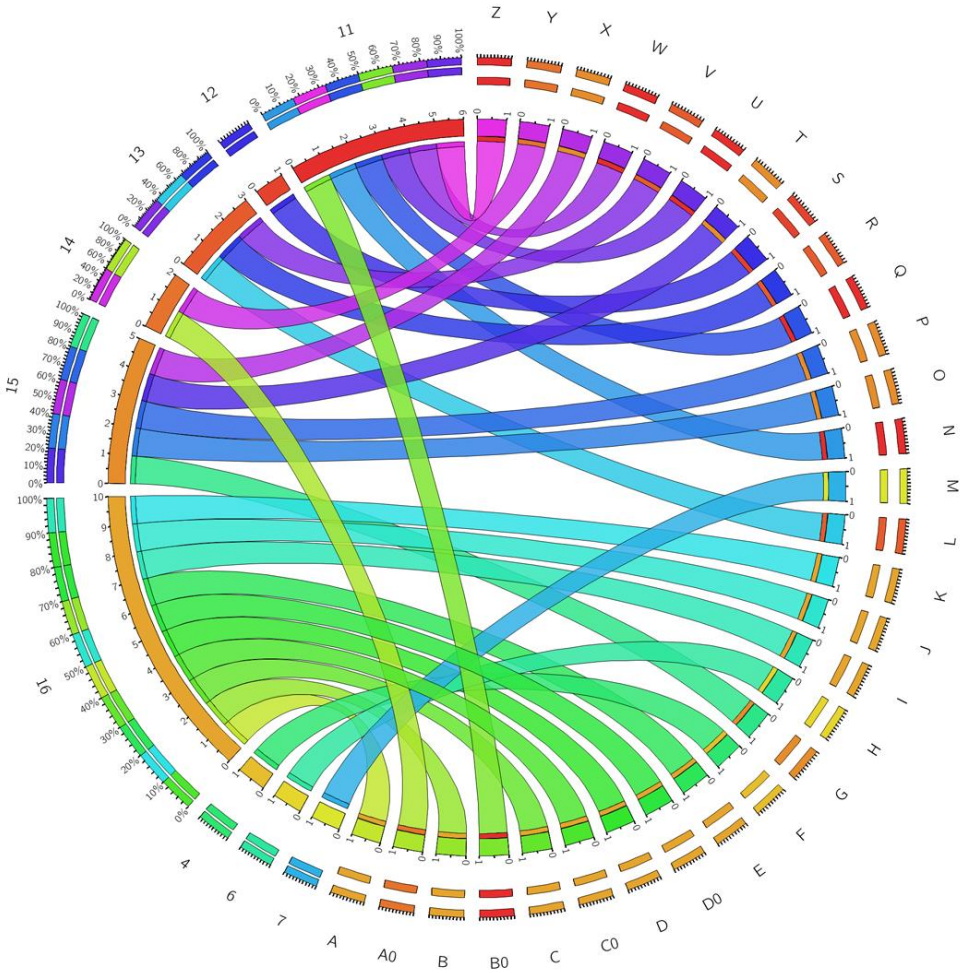

Figure 5. *Enolase intron analysis. (Note: Circos map of the enolase gene in 30 species including maize, rice and Arabidopsis. The number on the left represents the number of introns, the letter on the right is the code of the species. A: corn, B: corn, c: soybean, D: sorghum, E: peanut, F: yeast, G: cotton, H: Arabidopsis, I: rice, J: wheat, K: tobacco, L: orangutan, M: silkworm, N: Xenopus laevis, O: citrus, P: pigeon, Q: squid, R: monkey, S: Selaginella, T: bitter gourd, U: tilapia, V: duck, W: horse, X: Pumpkin, Y: Sumatran orangutan, Z: Lettuce, A0: Sunflower, B0: Mouse, CO: Jujube, D0: Sesame)*

http://www.aloki.hu ● ISSN 1589 1623 (Print) ● ISSN 1785 0037 (Online)
DOI: http://dx.doi.org/10.15666/aeer/1705_1153711550

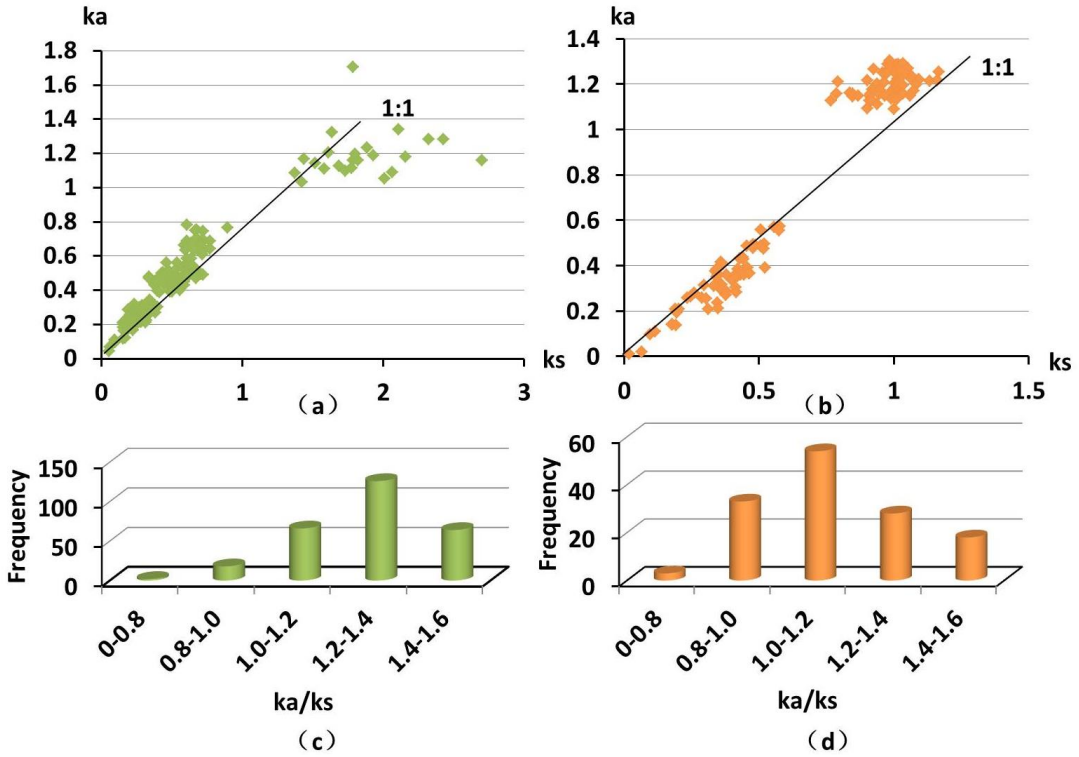

Figure 6. *The distribution and frequency of Ka/Ks values. (Note: The orange and green colors represent the animal and plant respectively.* ***a, b*** *The Ka/Ks distribution. The line in black is the boundary of Ka/Ks = 1.* ***c, d*** *The frequency distribution of Ka/Ks)*

Discussion

As one of the key enzymes in the glycolytic pathway, Enolase catalyzes the conversion of 2-phosphoglycerate to phosphoenolpyruvate during glycolysis, which is essential for cell anabolism and energy production (Pancholi et al., 2001). The enolase gene of multiple species was studied, and the genetic evolution relationship, molecular structure and protein function expressed by these genes were analyzed based on bioinformatics methods. It was found that the enolase candidate amino acid sequences of 50 species have high similarity, some even higher than 99%, indicating that they are highly conserved during evolution. From the constructed phylogenetic tree (*Fig. 2*), it can be seen that the gymnosperms are clustered into one, the monocotyledons are clustered into one, and most of the dicotyledons are also clustered into one, but the dicotyledonous plants of pepper and tobacco are gathered together as one. The Arabidopsis and mulberry trees are clustered together and do not cluster with other dicotyledonous plants, probably due to the evolutionary evolution of the enolase genes in these four plants to the rest of the plants. However, in general, enolase has the characteristics of closer evolution of the plant. Animals are divided into two branches, each containing mammals, one of which includes fruit fly, mouse, horse, fish and fungal branches are relatively close, presumably due to the more conservative enolase gene in each species There is little difference within the long process, and only slight changes in the long evolutionary process, so the molecular evolution trend of animal enolase is inconsistent with the evolutionary trend of species. This situation has also appeared in the evolution of other genes. The evolutionary distance of the miR166 gene family is

http://www.aloki.hu ● ISSN 1589 1623 (Print) ● ISSN 1785 0037 (Online)
DOI: http://dx.doi.org/10.15666/aeer/1705_1153711550

not related to the genetic relationship between the species itself (Xu-Yao et al., 2014) speculate that the gene may evolve in different ways and speeds. The similarity of the enolase amino acid sequence of each species is very high. The similarity between the bean and soybean, sorghum and corn in the plant reaches 100%, the similarity between bitter gourd and pumpkin reaches 99%, and the beluga whale, horse, bonobo, red marmoset in the animal. The sequence similarity of Sumatra orangutans reached over 98%, and the similarity of other animals was above 80%. This indicates that enolase is highly conserved in evolution. Next, we analyze the introns of the enolase gene of each species. Generally, the number of introns is similar, and the intron position and phase between genes with closer evolution are more similar. The number of introns of the enolase gene in most species is concentrated in 11-16 (*Fig. 3*). It shows that the evolutionary relationship of enolase is very close in different species. It is worth noting and discussing that only six of the introns in the Arabidopsis enolase gene are the same as the other species. Enolase is not expressed in the leaves of Arabidopsis, and if silenced, it affects the development of Arabidopsis sporozoites and gametophytes (Prabhakar et al., 2010) and the absence of enolase also affects the root development of Arabidopsis (Prabhakar et al., 2009). The Arabidopsis enolase structure has a pair of disulfide bonds formed by Cys residues, which can undergo redox regulation. The enolase in corn, tomato and ramie does not contain this pair of Cys residues. It seems possible that enolase is redox-regulated by a Cytosolic thioredoxin system in a limited number of plant species including ice plant and Arabidopsis (Anderson et al., 1998). We can later study what kind of particularity the enolase has in its structure and evolution with other plants. The enolase phosphorylation site of each species was predicted to have the highest number of serines and high similarity (*Fig. 4*). The eight phosphorylation sites of Thr46, Thr47, Thr58, Ser275, Ser276, Ser277, Ser382 and Ser383 appeared most frequently in plants. The three phosphorylation sites of Ser289, Ser527 and Thr189 appeared most frequently in animals. The phosphorylation sites of plant enolase are more conservative in evolution than animals, both in number and in location. The similarity of phosphorylation sites in animals is not very high. There are only three phosphorylation sites at high frequencies, and the phosphorylation sites of similar genetically related species are still very similar, such as mammalian orangutans and beluga whales, horse. Most protein interactions are carried out through the activation of phosphating sites, which provides a basis for the subsequent interaction of enolase with its upstream and downstream related proteins. Secondary structure analysis of 42 species of enolase showed that α-helix and “random” crimp were conserved structures, while α-helix and “random” curls were the most numerous, so α-helix and “Random” curl plays an important role in the formation of advanced structures of enolase. The prediction of secondary structure indicates that the secondary structure of protein determines its tertiary structure, which is closely related to the function of protein expression. Based on the similarity of secondary structure of enolase of each species, its functional similarity is predicted. Very conservative, the difference is not big. It can be seen from the (*Fig. 5*) that the tertiary structure of the enolase of each species is also very similar. It is generally accepted that a case where a nucleotide variation does not cause an amino acid change is called a synonymous mutation (Ks), and a phenomenon in which a nucleotide mutation also causes an amino acid change is called a non-synonymous mutation (Ka). Usually, under natural selection, synonymous mutations are not affected, but synonymous mutations are affected by natural selection (Yang et al., 2006). Their ratio Ka/Ks is a molecular evolutionary parameter that weighs

http://www.aloki.hu ● ISSN 1589 1623 (Print) ● ISSN 1785 0037 (Online)
DOI: http://dx.doi.org/10.15666/aeer/1705_1153711550

the pressure of selection to determine whether there is a selective pressure on the gene-encoded gene (Shiu et al., 2004). As shown in (*Fig. 6*), it is not that there are positive selection sites for most enolase genes in plants or animals. Some of them have a positive selection site, but their Ka/Ks values are close to 1, indicating positive selection and natural selection for enolase. Genetic evolution affects key roles. Such genes are genes that are rapidly evolving in the near future and are very important for the evolution of species. In summary, we conducted a comparative study on the enolase genes of different species by bioinformatics methods, and found that the enolase gene evolution is very conservative and similar in function. Since enolase is a key rate-limiting enzyme in the glycolytic pathway, the results of this study can provide an analytical basis for subsequent molecular experiments, and are highly versatile in terms of increased yield, resistance to stress, cancer intervention, and treatment in GM crops prospects (Altenberg et al., 2004; Pu et al., 2007).

Acknowledgements. This research was supported by the National Natural Science Foundation of China (grant Nos. 31571672 and 31671707).

REFERENCES

[1] Aaronson, R. M. (1995): Non-neuronal enolase is an endothelial hypoxic stress protein. – Journal of Biological Chemistry 270(46): 27752-7.
[2] Altenberg, B., Greulich, K. O. (2004): Genes of glycolysis are ubiquitously overexpressed in 24 cancer classes. – Genomics 84(6): 1014-1020.
[3] Anderson, L. E., Li, A. D., Stevens, F. J. (1998): The enolases of ice plant and arabidopsis contain a potential disulphide and are redox sensitive. – Phytochemistry 47(5): 707-13.
[4] Armand, D. A., Flores-Tornero, M., Rosa-Telléz, S., Muñoz-Bertomeu, J., Segura, J., Ros, R. (2016): The specific role of plastidial glycolysis in photosynthetic and heterotrophic cells under scrutiny through the study of glyceraldehyde-3-phosphate dehydrogenase. – Plant Signal. Behavior 11: e1128614.
[5] Barkla, B. J., Vera-Estrella, R., Hernandez-Coronado, M., Pantoja, O. (2009): Quantitative proteomics of the tonoplast reveals a role for glycolytic enzymes in salt tolerance. – The Plant Cell 21(12): 4044-4058.
[6] Baumgarten, A., Cannon, S., Sprangler, R., May, G. (2003): Genome-level evolution of resistance genes in Arabidopsis thaliana. – Genetics 165(1): 309-319.
[7] Gerlt, J. A., Babbitt, P. C., Jacobson, M. P., Almo, S. C. (2012): Divergent evolution in enolase superfamily: strategies for assigning functions. – Journal of Biological Chemistry 287(1): 29-34.
[8] Grondin, M., Chow-Shi-Yée, M., Ouellet, F., Averill-Bates, D. A. (2015): Wheat enolase demonstrates potential as a non-toxic cryopreservation agent for liver and pancreatic cells. – Biotechnology Journal 10(5): 801-810.
[9] Higgins, D. G., Bleasby, A. J., Fuchs, R. (1992): Clustal v: improved software for multiple sequence alignment. – Comput Appl Biosci 8(2): 189-191.
[10] Iida, H., Yahara, I. (1985): Yeast heat-shock protein of mr 48,000 is an isoprotein of enolase. – Nature 315(6021): 688-690.
[11] Lebioda, L., Stec, B. (1988): Crystal structure of enolase indicates that enolase and pyruvate kinase evolved from a common ancestor. – Nature 333(6174): 683-686.
[12] Lohman, K., Meyerhof, O. (1934): Über die enzymatische Umwandlung von Phosphoglyzerinsäure in Brenztraubensäure und Phosphorsäure (Enzymatic

http://www.aloki.hu ● ISSN 1589 1623 (Print) ● ISSN 1785 0037 (Online)
DOI: http://dx.doi.org/10.15666/aeer/1705_1153711550

transformation of phosphoglyceric acid into pyruvic and phosphoric acid). – Biochem. Z. 273: 60-72.

[13] Pal Bhowmick, I., Kumar, N., Sharma, S., Coppens, I., Jarori, G. K. (2009): Plasmodium falciparumenolase: stage-specific expression and sub-cellular localization. – Malaria Journal 8(1): 179.

[14] Pancholi, V. (2001): Multifunctional α-enolase: its role in diseases. – Cellular & Molecular Life Sciences Cmls 58(7): 902-920.

[15] Perconti, G., Maranto, C., Romancino, D. P., Rubino, P., Feo, S., Bongiovanni, A., et al. (2017): Pro-invasive stimuli and the interacting protein hsp70 favour the route of alpha-enolase to the cell surface. – Scientific Reports 7(1): 3841.

[16] Piast, M., Kustrzeba-Wójcicka, I., Matusiewicz, M., Banaś, T. (2005): Molecular evolution of enolase. – Acta Biochimica Polonica 52(2): 507-13.

[17] Prabhakar, V., Löttgert, T., Gigolashvili, T., Bell, K., Ulf-Ingo Flügge, Häusler, R. E. (2009): Molecular and functional characterization of the plastid-localized phosphoenolpyruvate enolase (eno1) from Arabidopsis thaliana. – FEBS letters 583(6): 983-991.

[18] Prabhakar, V., Löttgert, T., Geimer, S., Dörmann, P., Krüger, S., Vijayakumar, V., et al. (2010): Phosphoenolpyruvate provision to plastids is essential for gametophyte and sporophyte development in Arabidopsis thaliana. – Plant Cell 22(8): 2594-2617.

[19] Pu, L. J., Huang, S. M., Liu, F. (2007): Effects of losartan on expressions of plasminogen activator and plasminogen activator inhibitor-1 of rat proximal tubular epithelial cells cultured with high glucose. – Medical science edition 38(5): 813.

[20] Reeve, J. G., Stewart, J., Watson, J. V., Wulfrank, D., Twentyman, P. R., Bleehen, N. M. (1986): Neuron specific enolase expression in carcinoma of the lung. – British Journal of Cancer 53(4): 519-528.

[21] Song, Y., Luo, Q., Long, H., Hu, Z., Que, T., Xi'an Zhang, et al. (2014): Erratum to: alpha-enolase as a potential cancer prognostic marker promotes cell growth, migration, and invasion in glioma. – Molecular Cancer 13(1): 235.

[22] Straeten, D. V. D., Rodrigues-Pousada, R. A., Montagu, G. M. V. (1991): Plant enolase: gene structure, expression, and evolution. – The Plant Cell 3(7): 719-735.

[23] Subramanian, A. (2000): Structural analysis of alpha -enolase. Mapping the functional domains involved in down-regulation of the c-myc protooncogene. – Journal of Biological Chemistry 275(8): 5958-5965.

[24] Tamura, K., Peterson, D., Peterson, N., Stecher, G., Nei, M., Kumar, S. (2011): MEGA5: Molecular evolutionary genetics analysis using maximum likelihood, evolutionary distance, and maximum parsimony methods. – Mol. Biol. Evol. 28: 2731-2739.

[25] Ucker, S. D. (2016): Exploiting death: apoptotic immunity in microbial pathogenesis. – Cell Death and Differentiation 23: 990-996.

[26] Walker, T., Morris, J., Threlfall, R., Main, G. (2003): Analysis of wine components in cynthiana and syrah wines. – Journal of Agricultural & Food Chemistry 51(6): 1543.

[27] Warburg, O., Christian, W. (1942): Isolation and crystallization of enolase. – Biochim. Z. 310: 384-421.

[28] Xu-Yao, Z., Si-Yun, C., Lei, Z., et al. (2003): Evolution of MIR166 gene family in land plants. – Plant Diversity and Resources 36(3): 331-341.

http://www.aloki.hu ● ISSN 1589 1623 (Print) ● ISSN 1785 0037 (Online)
DOI: http://dx.doi.org/10.15666/aeer/1705_1153711550

APPENDIX

	Alpha helix (%)		Beta turn (%)		Random coil (%)		Extended strand (%)	
Glycine max	191	43.02%	34	7.66%	149	33.56%	70	15.77%
Citrus sinens	193	43.37%	40	8.99%	143	32.13%	69	15.51%
Sorghum bicolor	185	41.48%	33	7.40%	159	35.65%	69	15.47%
Arach ipaens	191	42.92%	36	8.09%	149	33.48%	69	15.51%
Saccharomyces cereviae	190	43.48%	36	8.24%	147	33.64%	64	14.65%
Selaginella moellendorffii	222	46.35%	31	6.47%	155	32.36%	71	14.82%
Momordica charantia	193	43.47%	40	9.01%	143	32.21%	68	15.32%
Capsicum baccatum	235	45.11%	33	6.33%	171	32.82%	82	15.74%
Chlamydomonas reinhardtii	218	45.70%	33	6.92%	159	33.33%	67	14.05%
Gossypium hirsutum	190	42.70%	37	8.31%	150	33.71%	68	15.28%
Cucurbita moschata	195	43.92%	39	8.78%	140	31.53%	70	15.77%
Arabidops thaliana	205	42.98%	37	7.76%	154	32.29%	81	16.98%
Artemia annua	191	43.02%	39	8.78%	150	33.78%	64	14.41%
Morus notabil	215	39.96%	37	6.88%	201	37.36%	85	15.80%
Oryza sativa	192	43.05%	35	7.85%	152	34.08%	67	15.02%
Ambrosia artemiifolia	184	42.69%	35	8.12%	147	34.11%	65	15.08%
Culex quinquefasciatus	182	42.03%	30	6.93%	153	35.33%	68	15.70%
Lactuca sativa	186	41.89%	36	8.11%	148	33.33%	74	16.67%
Triticum aestivum	197	44.17%	33	7.40%	154	34.53%	62	13.90%
Nicotiana tabacum	189	42.57%	38	8.56%	151	34.01%	66	14.86%
Zea mays	192	43.05%	36	8.07%	146	32.74%	72	16.14%
Moss	196	44.04%	36	8.09%	149	33.48%	64	14.38%
Ziziphus jujuba	191	42.83%	35	7.85%	153	34.30%	67	15.02%
Pan pancus	292	46.57%	26	4.15%	241	38.44%	68	15.02%
Delphinapterus leucas	288	46.75%	34	5.52%	230	37.34%	64	10.39%
Xenopustropical	273	47.56%	35	6.10%	211	36.76%	55	9.58%
Pongo abelii	288	46.08%	35	5.60%	238	38.08%	64	10.24%
Equus caballus	184	42.40%	32	7.37%	153	35.25%	65	14.98%
Piliocolobus tephrosceles	274	43.91%	45	7.21%	228	36.54%	77	12.34%
Mus musculus	184	42.40%	31	7.14%	147	33.87%	72	16.59%
Lonchura striata domestica	234	43.82%	41	7.68%	190	35.58%	69	12.92%
Anas platyrhynchos	248	40.66%	42	6.89%	244	40.00%	76	12.46%
Gallus gallus	190	43.78%	33	7.60%	143	32.95%	68	15.67%
Columba livia	263	43.76%	30	4.99%	245	40.77%	63	10.48%
Oreochrom niloticus	192	44.24%	35	8.06%	138	31.80%	69	15.90%
Salmo salar	189	43.75%	32	7.41%	140	32.41%	71	16.44%
Drosophila melanogaster	200	40.00%	35	7.00%	181	36.20%	84	16.80%
Bombyx mori	189	43.65%	35	8.08%	145	33.49%	64	14.78%
Streptomyces	184	42.99%	34	7.94%	143	33.41%	67	15.65%
Staphylococcus aureus	194	44.70%	38	8.76%	136	31.34%	66	15.21%
Thermococcus	187	43.49%	34	7.91%	140	32.56%	69	16.05%

http://www.aloki.hu ● ISSN 1589 1623 (Print) ● ISSN 1785 0037 (Online)
DOI: http://dx.doi.org/10.15666/aeer/1705_1153711550

VOLATILE SOLID KINETIC DEGRADATION OF EFB BIOWASTE COMPOSTING PROCESS

ALKARIMIAH, R.[1*] – SUJA', F.[2]

[1]*School of Civil Engineering, Universiti Sains Malaysia, 14300 Pulau Pinang, Malaysia*

[2]*Faculty of Engineering and Built Environment, Universiti Kebangsaan Malaysia, 43600 Bangi, Selangor, Malaysia*
(phone: +60-38-911-8364/8911/8354; fax: +60-38-911-8355)

**Corresponding author*
e-mail: cerosnani@usm.my; phone: +60-45-996-264; fax: +60-45-996-906

(Received 22nd Apr 2019; accepted 11th Jul 2019)

Abstract. Volatile Solid (VS) parameters are used to study kinetic changes in compost materials. The Michaelis-Menten model is used in determining the volatile kinetics of the process. The composting materials used only are shredded empty fruit bunches (EFB) and palm oil mill effluent (POME) sludges obtained from the palm oil mill plantation. All the composting processes carried out in this study were performed in the rotary drum reactor. This experiment is conducted with 4 different runs. Run A used 10 kg EFB ratio: 1 kg sludge: 5 kg recycle compost, Run B with 5 kg EFB: 0.5 kg sludge: 2.5 kg recycle compost and Run C at 5 kg ratio EFB: 2.0 kg sludge: 0.5 kg recycle compost. The highest temperature achieved is 55°C (Run A), 43 C (Run B) and 53.3°C (Run C). For the final C/N ratios for Run A, B, C and D are 20.61, 17.54, 13.06 and 14.51 respectively. Based on the results of the four Runs that have been done, it is found that the kinetic change in Run has the best mathematical expression $y=103.31^{-0.015x}$ with R-square value of 0.9097 and derived K_1 value of this study is 106.0117 and K_2 is 0.012.
Keywords: *Michaelis-Menten model, shredded EFB, POME sludge, rotary drum reactor*

Introduction

Composting is a biochemical degradation process of organic substances that are converted into a cleaner material and a more stable humus. The main factors in controlling the composting process include the parameters of the environment such as temperature, moisture content, pH and ventilation as well as natural parameters of the substrate material such as C/N ratio, particle size and nutrient content. In determining the degradation and creating useful measurements in the loss of organic matter during the composting process, it is necessary to determine the kinetic process using the data obtained from experimental studies under controlled conditions. According to Levenspiel (1999), kinetics is generally a study of the rate or speed of a reaction. Substrate degradation models play a key role in the mathematical modelling of temperature, moisture and oxygen profiles in the composting process. In relation to temperature prediction, mathematical models have been shown to be mainly successful in simulating the basic shape of composting temperature profiles However, less precise in forecasting peak temperature, and the time required to reach it (Mason, 2009).

Most kinetic parameters are usually used to describe the nature of maturity of compost materials. The nature of maturity of composting materials that is often used is the properties of physico-chemical changes such as C/N ratio, ash and cation capacity change (Planas and Pelaez, 2001). However, there are also studies using enzyme activity measurement as an indicator of composting activity (Pelaez et al., 2004). In general, studies on kinetic changes in composting process are important to obtain a

http://www.aloki.hu ● ISSN 1589 1623 (Print) ● ISSN 1785 0037 (Online)
DOI: http://dx.doi.org/10.15666/aeer/1705_1155111566

chemical change pattern on the nature of the reaction system, and it is also an important basis for the theory in the combustion and dissolution process which then provides a method for studies involving heat conversion and mass. Knowledge of kinetic reaction changes will also help in the design of a composting system (Manu et al., 2016).

Researchers have studied the determination of decomposition in the composting process. Various parameters have been studied such as the use of oxygen content (Pressel and Bidling Maier, 1981), carbon mineralization rates (Bernal et al., 1998), carbon fractions (Whang and Meenaghan, 1980; Gilmour et al., 1996), biodegradation of lignocellulose (Vikman et al., 2002), biodegradation of polyatic acid (PLA) (Stloukal et al., 2015), biodegradable volatile solid degradation (Mason, 2008; Zhang et al., 2010), organic matter degradation (Kulikowska, 2016; Ge et al., 2015; Manu et al., 2016; Petric et al., 2012; Bustamante et al., 2008), thermal decomposition reaction (Giwa et al., 2018). Tiqua et al. (1996) have studied the changes in microbial characteristics including heterotrophic aerobic population, oxygen consumption rate, dehrogenic activity and C/N microbial mass during pine-stool composting process and wood dust straw. Yamada and Kawase (2006) also reviewed kinetic analysis for microbiological and oxygen use reactions for activated sludge aerobic composting process. In their study, microbiological responses are represented by the Monod equation.

Whang and Meenaghan (1980), Seng (1999) and Tweib et al. (2014) have studied the characteristics of the kinetic composting process. They have measured carbon fractions by using CHN analyzer tools as early as 6-8 days of composting process. They have discovered the characteristics of the composting process using the Michaelis-Menten model. From the study, they have concluded that the constant Michaelis-Menten, K_1 is a constant representing the description of a system used. This study aims to evaluate the rate of kinetic change of volatile substance in the rotary drum reactor. The analysis steps developed in this study can be used to obtain K_1 and K_2 values in a step to increase the composting scale to pilot scale by using Michaelis-Menten model.

Methodology

Raw material and reactor design

The main raw materials used in this study are palm oil mill effluent (POME) sludge and empty fruit bunches (EFB). Shredded fresh empty fruit bunches (EFB) used for compost materials were obtained from Sri Ulu Langat Palm Oil Processing Factory, Dengkil, Selangor, Malaysia. Meanwhile, POME sludge for this study is gathered from conventional aerobic pond treatment from same factory. Recycle compost also used in the mixing of fresh sample for this experiment. The recycle compost is obtained from EFB and POME composting process that is more than 1 year old from previous experiments. *Figures 1* and *2* show the shredded EFB and POME sludge from conventional aerobic pond treatment gathered for this study. While, *Table 1* shows the chemical and physical characteristics of the raw materials and recycle compost that used in this experiment.

Rotary drum reactor system that used in this study facilitated with 3 phase motors. The rotary drum reactor is made from stainless steel measuring 3 m long with a diameter of 0.6 m and an initial active volume of 0.4 m^3. The rotary drum reactor works with the support of a 3-phase motor system with a maximum 2 rotation per minute. There are 8 inner blades with length of 5 cm each in order to enhance the mixing in the

http://www.aloki.hu ● ISSN 1589 1623 (Print) ● ISSN 1785 0037 (Online)
DOI: http://dx.doi.org/10.15666/aeer/1705_1155111566

reactor. Mixing of palm oil mill effluents (POME) and empty fruit bunches (EFB) insert through the feeding part. *Figure 3* shows the schematic diagram of the rotary drum reactor used in this study.

Figure 1. *Shredded fresh empty fruit bunches (EFB)*

Figure 2. *Palm oil mill effluent (POME) sludge gathered from conventional aerobic pond treatment*

http://www.aloki.hu ● ISSN 1589 1623 (Print) ● ISSN 1785 0037 (Online)
DOI: http://dx.doi.org/10.15666/aeer/1705_1155111566

Table 1. *The chemical and physical properties of the raw materials*

Parameter	Fresh empty fruit bunches (EFB)	Aerobic palm oil mill effluent (POME) sludge	Recycle compost
Moisture Content, %	24 ±5.8	94 ± 3.3	80 ± 0.5
pH	6.7 ± 0.2	7.5 ± 0.5	7.59 ± 0.3
Total organic carbon (TOC), % dry weight	53 ± 1.5	19.0 ± 1.6	12.43 ± 1.5
Total Kjedahl nitrogen (TKN), % dry weight	0.9 ± 0.1	2.3 ± 0.2	1.21 ± 0.9
C/N	58.9	8.3	10.3

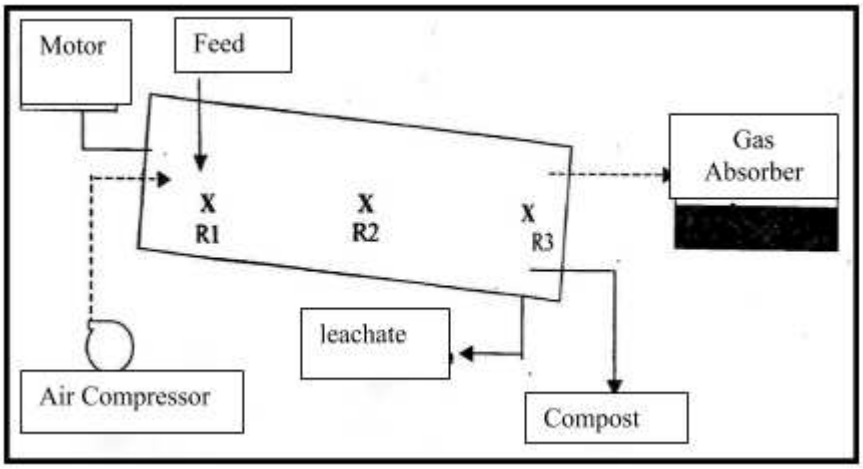

Figure 3. *Schematic diagram of rotary drum reactor*

Temperature profile observation

The temperature of the compost in the reactor is obtained by using the thermometer probe (Digital Thermometer, Thermocouple Thermometer Type K, Nicety® DT804, US). *Figure 4* shows the digital thermometer used to indicate the temperature reading throughout the composting process. The length of this probe thermometer is 1 m. Therefore, temperature readings on composting materials within the reactor can be taken up to 1 meter from the input section (at point R2 referring to *Fig. 3*). The temperature reading of this study is taken twice daily, i.e. in the morning and in the evening. The probe thermometer embedded into the compost heap is left for 5-10 min until the reading on the digital display of the thermometer starts stable.

Preparation of compost mixture

In this experiment, fresh and shredded EFB has been mixed with POME sludge. On average, the length of EFB fiber size taken fresh from the plant used in this phase is within 3-13 cm. In general, smaller particles of organic matter particles will provide sufficient surface area for bacterial and microorganisms reactions. EFB mixtures and POME sludge are mixed manually outside the reactor before being added into a rotary drum. For Run A, as much as 10 kg EFB, 5 kg of recycle compost and 2 kg of POME sludge is manually mixed before being put into a rotary drum reactor every day. For Run B 5 kg EFB, 2.5 kg of recycle compost and 2 kg of POME sludge added daily into

http://www.aloki.hu ● ISSN 1589 1623 (Print) ● ISSN 1785 0037 (Online)
DOI: http://dx.doi.org/10.15666/aeer/1705_1155111566

the reactor. Meanwhile for Run C, 5 kg of EFB, 0.5 kg of recycle compost and 2.0 kg of POME sludge added daily. For this experiment runs, only one-time replicate has been carried out of each mixture. *Table 2* shows the mixing ratio of this experimental runs.

Figure 4. *Thermometer digital and thermocouple Type K (Nicety ® DT804)*

The process of adding compost materials of each Runs into a rotary drum is done on daily basis until the content of the drum reactor reaches 90% full. In total, 150 kg of EFB fiber (a mixture of fresh EFB fiber and recycle compost) and 30 kg of POME sludge have been used for each Runs in this study. From the observations on Run A, the compost product reached at the outlet section on the day 11th. Meanwhile, for Run B and Run C the compost product resulted at the outlet section on the day 16th.

The compost products that comes out at the outlet section will then be restored into the rotary drum reactor in the feed section until the composting process is completed. For sampling purposes for pH parameters, moisture content, fiber length, nutrient content and C/N ratio, 200 g of compost was gathered. The sampling process for the above parameters is taken every 3 days. For the temperature parameter, the reading is taken every day in the morning and in the evening. All the compost samples taken were then stored in the frozen room at 4°C before being analyzed.

Table 2. *Weight and mixing ratio between empty fruit bunches (EFB), palm oil mill effluent (POME) sludge and recycle compost on each experimental runs*

Run	EFB (kg)	POME sludge (kg)	Recycle compost (kg)	Mixing ratio	Operational period (days)
A	10	1	5	10:1:5	43
B	5	0.5	2.5	5:0.5:2.5	23
C	5	2.0	0.5	5:2:0.5	29

http://www.aloki.hu ● ISSN 1589 1623 (Print) ● ISSN 1785 0037 (Online)
DOI: http://dx.doi.org/10.15666/aeer/1705_1155111566

Volatile solid and carbon content

To analyze the carbon content, the ash method was used is. Sub-samples of dried compost from moisture content analysis were then burned in the furnace for 4 hours at 550°C. Volatile solid computations are shown in *Equation 1* below:

$$\%\ Volatile\ Solid = \frac{X1 - X2}{X1 - M} \times 100 \quad \text{(Eq.1)}$$

where X1 = Initial sample weight and crucible before furnaced, X2 = Final sample weight and crucible after furnaced, M = Crucible weight.

Organic matter is estimated to be equivalent to volatile matter/solid (Hoyos et al., 2002). Therefore, the amount of organic carbon can be determined using the formula as shown in *Equations 2* and *3* according to Hoyos et al. (2002).

$$\%\ Carbon\ C = \frac{\%Organic\ matter}{1.8} \quad \text{(Eq.2)}$$

$$= \frac{\%\ Volatile\ solid}{1.8} \quad \text{(Eq.3)}$$

whereby 1.8 is constant.

Kinetic study

The Michaelis Menten model is a widely used kinetic model in the study of biochemical enzyme reactions that estimate the formation of complex mixtures simultaneously under quasi-equilibrium conditions. Whang and Meenaghan (1980), Seng (1999) and Tweib et al. (2014) have adapted this model in their composting studies. Conceptual reaction mechanisms are interpreted by the following stoichiometric schemes, where the equation rates have been simplified and mathematically manipulated to achieve satisfactory results in the graphic attempts as shown in the following *Equation 4*. *Figure 5* shows how the kinetic study was carried out using the Michaelis-Menten model in this study

$$C + X \leftrightarrow CX \rightarrow X + P \quad \text{(Eq.4)}$$

where C=Substrate, X=Free organism, CX=Activated substrate-organic complex, P=Product from endogenous reaction.

The second estimate made is an endogenous reaction is irreversible based on practical view. Mass stability equations for activated complex substrate microbes, CX can be described as *Equation 5* below:

$$\frac{D(CX)}{D_t} = k_1(C)(X) - (k_{-1} + k_2)(CX) \quad \text{(Eq.5)}$$

http://www.aloki.hu ● ISSN 1589 1623 (Print) ● ISSN 1785 0037 (Online)
DOI: http://dx.doi.org/10.15666/aeer/1705_1155111566

where K_1=the reaction rate constant of the forward reaction by converting substrate (C) and free organism (X) to the active complex organism substrate (CX), k_{-1}=the reaction rate constant of the inverse reaction by converting substrate (C) and free organism (X) to the active complex organism substrate (CX), k_2=the reaction rate constant of the forward reaction by converting the complex organism substrate (CX) to the free organism (X) and the product (P).

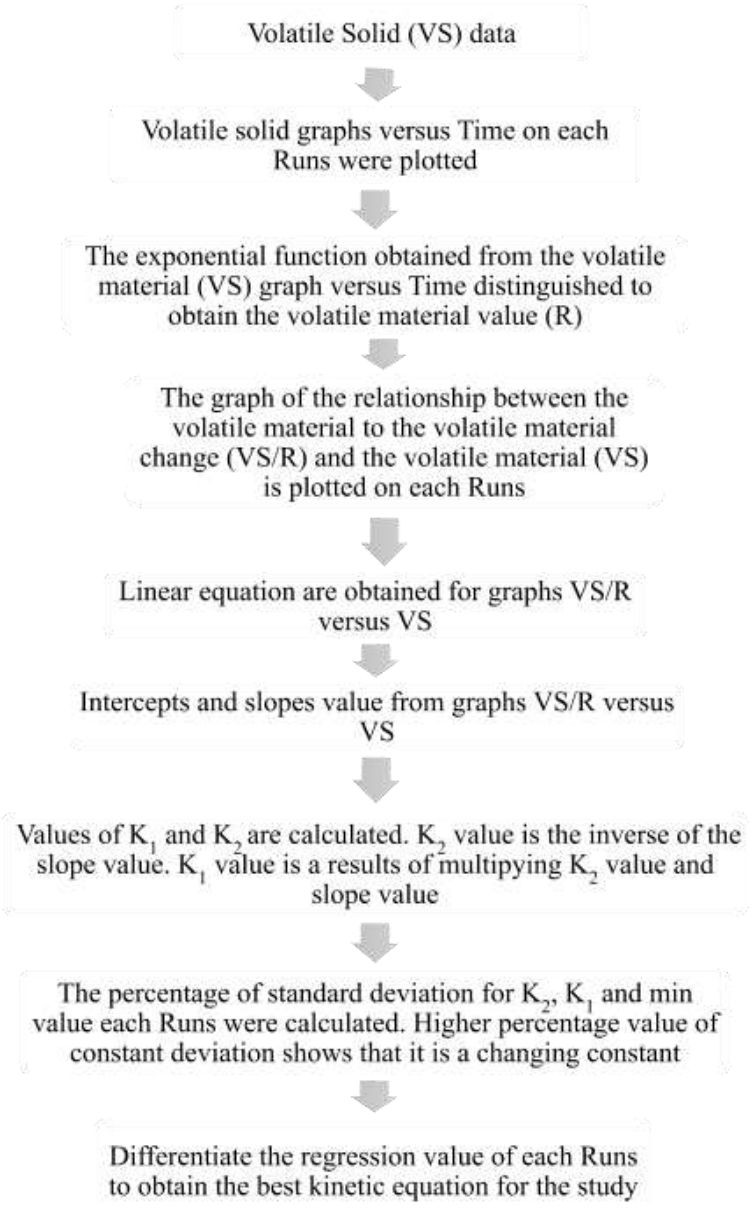

Figure 5. *Michaelis-Menten model kinetic study procedure*

The estimation for an indirect quasi-equilibrium state as *Equation 6:*

$$\frac{D(CX)}{dt} = 0 \qquad \text{(Eq.6)}$$

Therefore, *Equation 5* becomes *Equation 7* as follows:

http://www.aloki.hu ● ISSN 1589 1623 (Print) ● ISSN 1785 0037 (Online)
DOI: http://dx.doi.org/10.15666/aeer/1705_1155111566

$$(CX) = \frac{(C)(X)}{K_1} \quad \text{(Eq.7)}$$

where k_1 is obtained from *Equation 8,*

$$K_1 = \frac{K - 1 + k_2}{k_1} \quad \text{(Eq.8)}$$

Product production rate (P) is equal to the substrate rate estimate. Therefore *Equation 9* is,

$$\frac{d(P)}{dt} = R = k_2(CX) \quad \text{(Eq.9)}$$

where, R=substrate estimation rate.

In the meantime, the concentration of microorganisms, XT, can be expressed as *Equation 10* as below:

$$X_t = X + CX \quad \text{(Eq.10)}$$

By completing the *Equation 10* and replacing it in *Equation 11:*

$$CX = \frac{(C)(X_T)}{K_1 + C} \quad \text{(Eq.11)}$$

From *Equations 10* and *11,* the R value is obtained by using *Equation 12:*

$$R = \frac{K_2(C)}{K_1 + (C)} \quad \text{(Eq.12)}$$

Where the calculated value of K_2 is obtained from *Equation 13:*

$$K_2 = k_2(X_T) \quad \text{(Eq.13)}$$

Therefore, *Equation 13* is the kinetic equation for the composting process.

Results and discussion

Temperature profile

Temperature gives a huge impact on microbiological processes. Important responses and other elements of composting processes are also affected by temperature changes. Time-temperature relationship affects the rate of decomposition of organic matter and therefore it is important to produce stable and mature compost products for application of plants. In this study, the temperature reading is taken before the compost material is added (morning time), and after the compost material is added (evening time) into the

http://www.aloki.hu ● ISSN 1589 1623 (Print) ● ISSN 1785 0037 (Online)
DOI: http://dx.doi.org/10.15666/aeer/1705_1155111566

rotary drum reactor. The composting process of Run A is run for 43 days. The initial temperature of the Run A compost mixture is 31.8°C.

At Run A, the highest temperature reached was 55°C on the 10th day of composting process, after composting was added. Temperatures within the range 40–55°C remain for 24 days on the Run A composting process. On day 35 the temperature of the composting process began to show a decrease to the range of 32.1–38.1 C until the end of the composting process. The increase in temperature to the thermophilic phase between 50-70°C during composting is indispensable for the destruction of pathogens and parasites.

Meanwhile, the initial temperature of Run B composting material is 32°C. The increase in temperature on Run B is seen evenly, i.e. from 32°C (initial temperature) to 39.9°C on day 3. On day 4, the temperature starts to reach 40°C range. On Run B, compost temperature remains in the range 40–43°C (the highest temperature reached on the 11^{th} day). The final day of composting, the temperature value before the sample was entered and after the sample was entered has decreased to 37°C and 39.6 C respectively. The compost temperature of this mixture is seen to not achieve optimum temperature of 45°C. This may be due to a 5 kg mix EFB: 2.5 kg recycled compost: 1 kg of POME sludge is not an ideal mix for the optimal development of microbes in compost heap.

The initial temperature of compost material on Run C was 25.5°C. The observed temperature increases gradually in this run. The temperature within the range 30°C lasts for 8 days at the beginning of the composting process. Starting from day 9, the temperature starts to raise into the range 40°C until day 22. On day 23, Run D composting temperature increases to 53.3°C. Temperatures within the range of 50°C to 53°C are seen to last for only 4 days. On 27th day the temperature began to decline again with the final temperature of 36.7°C before the addition of composting material and 45.8 C after composting material was added.

From the three mixtures, the mesophilic phase begins in the first 3-8 days of the composting process. The abundance of organic substances at present has encouraged the activity of microorganisms and subsequently generating heat energy which causes temperature rise to occur. When temperatures rise above 45°C, thermophilic microorganisms will dominate the compost mass. *Figure 6* shows the temperature profile for Run A, B and C.

Volatile solid degradation

In this study, the degradation kinetics of the volatile material were used to study the kinetic changes of compost materials. The Michaelis-Menten model is used in determining the kinetic content of volatile composting samples. All the data from the experiments obtained are appropriate to the exponential function. *Figures 7–9* show graphs of volatile material against time for each Run.

Table 3 shows the exponential function obtained from the experimental runs along with the regression factor for the volatile solids compost material against the time of the study conducted.

The exponential function obtained as described in the table above is then differentiate. The differential equations obtained from the above exponential function represent the volatile solid change (R) in the compost material. The differential equation of the all Runs as shown in *Equations 14–16* below.

http://www.aloki.hu ● ISSN 1589 1623 (Print) ● ISSN 1785 0037 (Online)
DOI: http://dx.doi.org/10.15666/aeer/1705_1155111566

$$Run\ A: R = \frac{dx}{dy} = 0.674x^{-1.007} \quad \text{(Eq.14)}$$

$$Run\ B: R = \frac{dx}{dy} = 1.5497x^{-1.015} \quad \text{(Eq.15)}$$

$$Run\ C: R = \frac{dx}{dy} = 1.1859x^{-1.012} \quad \text{(Eq.16)}$$

Table 3. *Exponential function and regression factor for volatile solid*

Run	Exponential function	Regression factor
A	Y=96.366 $^{(-0.007x)}$	0.724
B	Y=103.31 $^{(-0.015x)}$	0.909
C	Y=98.828 $^{(-0.012x)}$	0.785

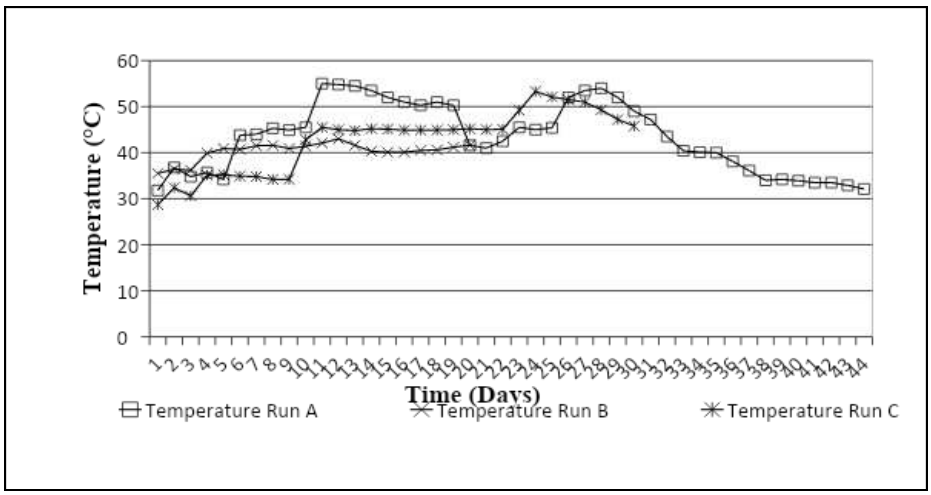

Figure 6. *Temperature profile for Run B to Run C*

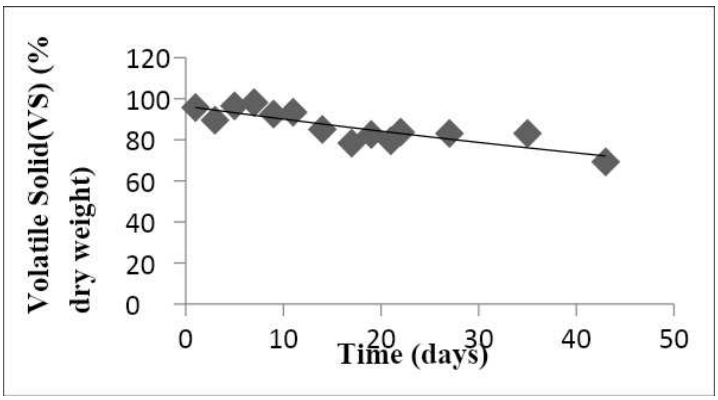

Figure 7. *Volatile solid changes on Run A*

http://www.aloki.hu ● ISSN 1589 1623 (Print) ● ISSN 1785 0037 (Online)
DOI: http://dx.doi.org/10.15666/aeer/1705_1155111566

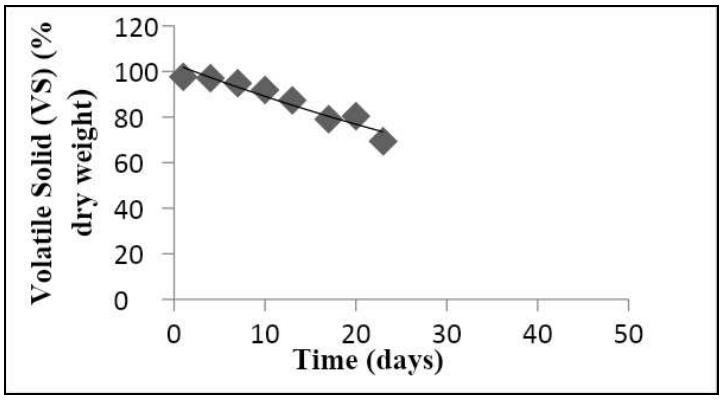

Figure 8. *Volatile solid changes on Run B*

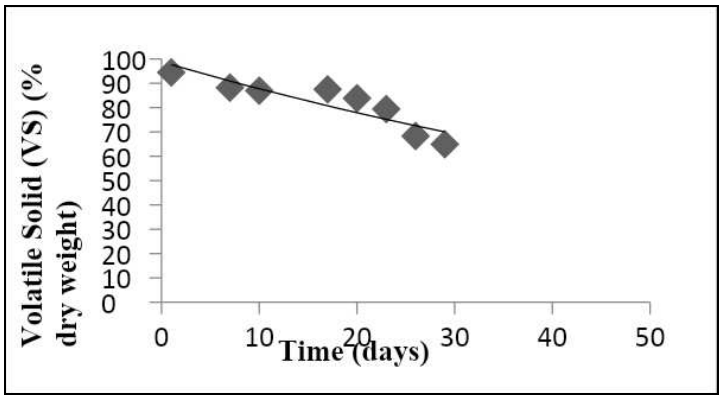

Figure 9. *Volatile solid changes on Run C*

From the volatile solid value (VS) and the volatile solid change value (R), the relationship between the volatile solid to the volatile solid change (VS/R) and volatile solid (VS) can be correlated graphically. The relationship between volatile solid to volatile solid change (VS/R) and volatile solid (VS) is most suitable for linear equations. The VS/R graph against VS on each Runs is shown in *Figures 10–12*.

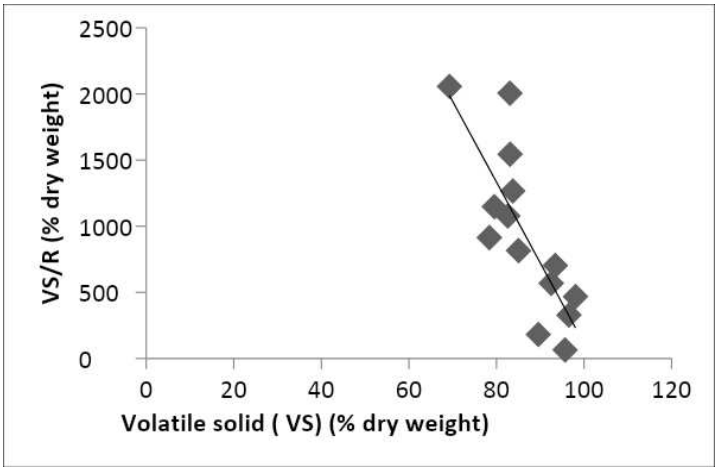

Figure 10. *VS/R against VS for Run A*

http://www.aloki.hu ● ISSN 1589 1623 (Print) ● ISSN 1785 0037 (Online)
DOI: http://dx.doi.org/10.15666/aeer/1705_1155111566

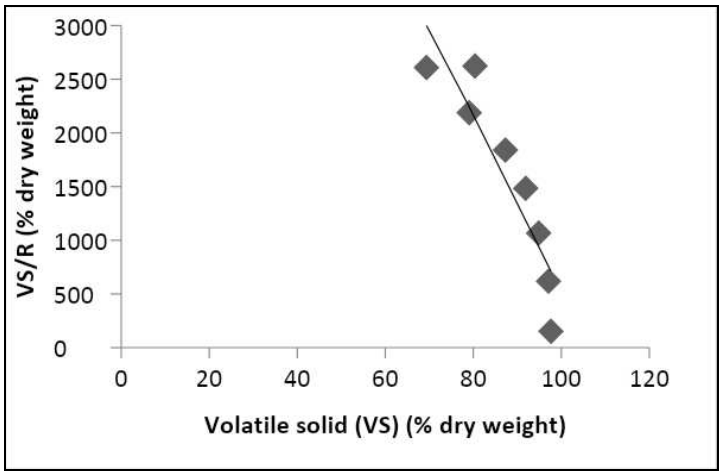

Figure 11. *VS/R against VS for Run B*

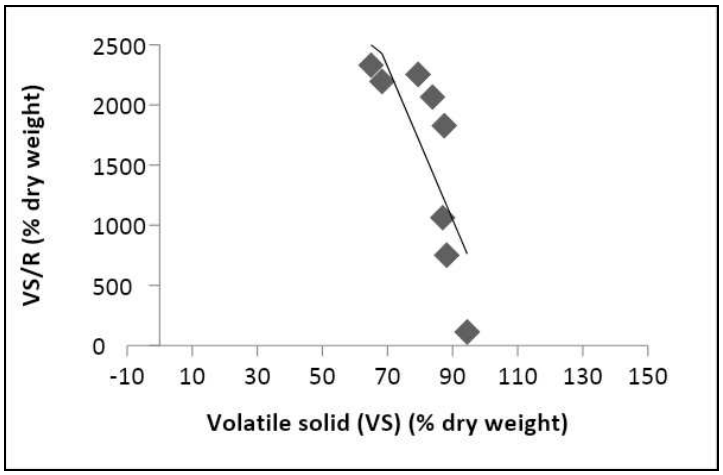

Figure 12. *VS/R against VS for Run C*

The formula for linear equations obtained from the VS/R graph against VS and the regression factor as shown in *Table 4*.

Table 4. *Linear equation for VS/R graph against VS and regression factor*

Run	Liner equation	Regression factor
A	Y = -61.042x + 6216.9	0.6423
B	Y = -82.443x + 8761.3	0.8378
C	Y = - 63.575x + 6769.3	0.6195

Based on regression factor value obtained from exponential function and linear function, it is found that Run B composting process is best in terms of volatile solids degradation process (VS). Therefore, linear function for Run B has been selected as kinetic mode for Phase composting process. The intercept and slope values obtained from the above linear equations are then considered for K_1 and K_2 values. The value of

http://www.aloki.hu ● ISSN 1589 1623 (Print) ● ISSN 1785 0037 (Online)
DOI: http://dx.doi.org/10.15666/aeer/1705_1155111566

K_2 is calculated by inverting the value of the slope. Whereas the value of K_1 is obtained by multiplying the value of K_2 with the intercept value from the linear equation above. The conclusions on the values of slope, intercept, K_1 and K_2 are shown in *Table 5*.

Table 5. *Slope, intercept and K_1 and K_2 value*

Run	Slope	Intercept	K_1	K_2
A	61.042	6216.9	101.9572	0.0164
B	82.443	8761.3	106.0117	0.0121
C	63.575	6769.3	106.2780	0.0157
Mean			103.7517	0.0142

From *Table 5*, the value of K_1 obtained is within the range 101.957–106.2780, whereas the value of K_2 is in the range of 0.0121–0.0164. The mean values of K_1 and K_2 are 103.7517 and 0.0142 respectively. Then, the percent of error of each constant obtained is also calculated. The result of the percent of error and standard deviation as shown in *Table 6.*

Table 6*. The percent of error, mean and standard deviation of K_1 and K_2 on each run*

Run/mean/standard deviation	K_2	Percent of error K_2 (%)	K_1	Percent of error K_1 (%)
A	0.0164	15.49	101.957	1.73
B	0.0121	14.79	106.0117	2.18
C	0.0157	10.56	106.2780	2.43
Mean	0.0142	13.0275	103.7517	2.305
Standard deviation	0.00216	2.4730	2.8084	0.4805

From the results obtained in *Table 6*, it is found that the percent of error for the K_2 constant is within the range of 10.56 - 15.49% with a mean value of 13.0275%. Whereas, the maximum percent of error for the K_1 constant is 2.43% and the minimum value is 1.73% with a mean value of 2.305%. If compared to the mean values of K_1 and K_2 each recorded at 2.305% and 13.0275% respectively, it is found that the K_2 constant value is higher than K_1 and this indicates that the value of K_2 is a variable independent. This is consistent with the Michaelis Menten model, while the K_1 value is dissociation constant for a system. Meanwhile, K_2 is the variable dependent on composting system towards the microbial population found in the compost material.

The constants obtained from this experiment are also compared with previous earlier study by Whang and Meenaghan (1980), Seng (1999) and Tweib et al. (2014). K_1 and K_2 value obtained from Whang and Meenaghan (1980) study are 1.2243 and 0.0325, resepectively. The value of K_1 and K_2 from Seng (1999) study are 80.515 and 0.9029, respectively. Meanwhile K_1 and K_2 value from Tweib et al. (2014) are 81.64 and 1.0301, respectively. The value of K_1 and K_2 from this study shows a big difference compared to the value obtained from Whang and Meenaghan (1980). This difference is due to the different experiments performed. Whang and Meenaghan (1980) have used carbon fraction as a limitation indicator by using a unit of weight of carbon (gram) per weight of ash (gram) which finally the result found is dimensionless (g/g). While this study uses volatile material (VS) as an indicator parameter, expressed as a percentage unit (%) per dry weight sample. However, the similarities between this study and the

http://www.aloki.hu ● ISSN 1589 1623 (Print) ● ISSN 1785 0037 (Online)
DOI: http://dx.doi.org/10.15666/aeer/1705_1155111566

studies conducted by Seng (1999) and Tweib et al. (2014) are using volatile material (VS) as indicator parameters, which are expressed in percentages (%) per dry weight sample. In addition, the K_1 constant value is equal to the initial value of the indicator parameter which is the percentage of volatile material. Thus, the magnitude of K_1 values in the results of this study and the study conducted by Seng (1999) and Tweib et al. (2014) is in two digits (in percent value), while the results of the study by Whang and Meenaghan (1980) are in the form of one digit.

The value of K_2 is the system variable as defined in the Michaelis-Menten Model, where this value depends on the number of microbial populations and the second stage constant reaction, k_2. Due to the function of the relationship between the total microbial population and the operating system, the K_2 value indirectly serves as an indicator of the efficiency of a composting system. Found that K_2 constant value for this study and the research done by Whang and Meenaghan (1980) is almost identical. Whang and Meenaghan (1980) have used a mixture of cow and wood dust as a compost material while this study uses EFB and POME as compost materials and carried out on a large scale. Whereas, studies conducted by Seng (1999) and Tweib et al. (1999) were conducted on a small scale, hence the value of K_2 in both studies was greater compared to this study and Whang and Meenaghan (1980) because the composting process on the laboratory scale was easier to control than the large-scale composting/pilot scale

Based on the results of the 3 Runs that have been done, it is found that the kinetic change in this study has the best mathematical expression is in Run B as *Equations 17* and *18* below:

$$y = 103.31^{-0.015x} \qquad r^2 = 0.9097 \qquad \text{(Eq.17)}$$

where y = Volatile solid material, x = time.

After *Equation 17* above is obtained, plot VS/R against VS for model is also done to get linear equations:

$$y = -82.443x + 8761.3 \quad r^2 = 0.8378 \qquad \text{(Eq.18)}$$

The K_1 value for Run B is 106.0117 and K_2 is 0.012. From the volatile kinetic results obtained from this study, two assumptions can be made i.e., the formation of simple complex mixtures and endogenous reactions are irreversible.

Conclusion

The production of sludge and solid materials in the palm oil plant, as well as the need to address the increasingly expensive disposal problems as well as the current disposal methods that potentially create contaminants and their own sludge potential as soil adapters are the contributing factors and the stimulants in the production and use of composting methods. In the composting process, optimization is an important step in obtaining an effective process and good compost quality. On average, 150 kg of EFB fibers have been used in each Runs in this experimental study. The maximum temperature (thermophilic temperature) achieved at Run A, B, C is 55°C, 43°C and 53.3°C, respectively. For the final C/N ratios of Run A, B and C respectively are 20.61, 13.06 and 14.51 respectively. Based on the C/N final value reading at each run, it can be

http://www.aloki.hu ● ISSN 1589 1623 (Print) ● ISSN 1785 0037 (Online)
DOI: http://dx.doi.org/10.15666/aeer/1705_1155111566

concluded that all runs achieve the optimum C/N ratio. However, the lowest C/N ratio is obtained in Run B. This is compounded by the mixture in Run B using more recycle compost as well as assisting in the process of decomposition of fresh compost. Recycle compost used in this study contains a low C/N ratio of 10.3 and has matured over 1 year. In kinetic studies, volatile changes in Run B experiments are also seen to be more stable. In the determination of volatile solid kinetic for the composting process, it was found that the Michaelis Menten model was appropriate. Overall, it can be concluded that the composting process is one of the alternatives to solving the problem of solid waste dumping in palm oil plantation in an integrated solid waste management system. This method has the potential to conserve and retrieve beneficial ingredients compost with many positive features. The resulting compost is also the final product that can be used as a soil enhancer or plant fertilizer.

REFERENCES

[1] Bernal, M. P., Paredes, C., Sanchez-Monedero, M. A., Roig, A. (1998): Carbon mineralization from organik waste at different composting stages during their incubation with soil. – Agr. Ecosyst. Environ. 69: 175-189.

[2] Bustamante, M. A., Paredes, C., Marhuenda-Egea, F. C., Pérez-Espinosa, A., Bernal, M. P., Moral, R. (2008): Co-composting of distillery wastes with animal manures: Carbon and nitrogen transformations in the evaluation of compost stability. – Chemosphere 72: 551-557.

[3] Ge, J., Huang, G., Huang, J., Zeng, J., Han, L. (2015): Mechanism and kinetics of organic matter degradation based on particle structure variation during pig manure aerobic composting. – Journal of Hazardous Materials 292: 19-26.

[4] Gilmour, J. T., Clark, M. D., Mark, D., Daniel, S. M. (1996): Predicting long-term decomposition of biosolids with a seven-day test. – Journal of Environmental Quality 25(4): 766-770.

[5] Giwa, A. S., Heng Xu, H., Wu, J., Li, Y., Chang, F., Zhang, X., Jin, Z., Huang, B., Wang, K. (2018): Sustainable recycling of residues from the food waste (FW) composting plant via pyrolysis: thermal characterization and kinetic studies. – Journal of Cleaner Production 180: 43-49.

[6] Hoyos, S. E. G., Juarez, J. V., Ramonet, C. A., Lopez, J. G., Rios, A. A., Uribe, E. G. (2002): Aerobic thermophilic composting of waste sludge from gelatin-grenetine industry. – Resourcers Conservation and Recycling 34: 161-173.

[7] Kulikowska, D. (2016): Kinetics of organic matter removal and humification progress during sewage sludge composting. – Waste Management 49: 196-203.

[8] Levenspiel, O. (1999): Chemical Reaction Engineering (3rd Ed.). – John Wiley, New York.

[9] Manu, M. K., Kumar, R., Garg, A. (2016): Drum composting of food waste: a kinetic study. – Procedia Environmental Sciences 35: 456-463.

[10] Mason, I. G. (2009): Predicting biodegradable volatile solids degradation profiles in the composting process. – Waste Management 29: 559-569.

[11] Peláez, C., Mejıa, A., Planas, A. (2004): Development of a solid phase kinetic assay for determination of enzyme activities during composting. – Process Biochemistry 39: 971-975.

[12] Petric, I., Helic, A., Avdic, E. A. (2012): Evolution of process parameters and determination of kinetics for co-composting of organic fraction of municipal solid waste with poultry manure. – Bioresource Technology 117: 107-116.

[13] Planas, A. Pelaez, C. A. (2001): Composting of cattle and agriculture waste: variables and processes. – Afinidad 58: 93-104.

http://www.aloki.hu ● ISSN 1589 1623 (Print) ● ISSN 1785 0037 (Online)
DOI: http://dx.doi.org/10.15666/aeer/1705_1155111566

[14] Pressel, F., Bidlingmaier, W. (1981): Analyzing decay rate of composting. – Biocycle 22(5): 50-51.
[15] Seng, N. H. (1999): Kinetic study of laboratory scale composting process. – Tesis M. Eng, Universiti Putra Malaysia, Selangor, pp. 1-88.
[16] Stloukal, P., Pekarová, S., Kalendova, A., Mattausch, H., Laske, S., Holzer, C., Chitu, L., Bodner, S., Maier, G., Slouf, M., Koutny, M. (2015): Kinetics and mechanism of the biodegradation of PLA/clay nanocomposites during thermophilic phase of composting process. – Waste Management 42: 31-40.
[17] Tiquia, S. M., Tam, N. F. Y., Hodgkis, I. J. (1996): Microbial activities during composting of spent manure sawdust litter at different moisture content. – Bioresource Technology 55: 201-205.
[18] Tweib, S. A., Abd Rahman, R., Khalil, M. S. (2014): Determination of kinetics of co composting of organic fraction of municipal solid waste with palm oil mill sludge (POMS). – Journal of Solid Waste Technology and Management 40 (2): 136-147.
[19] Vikman, M., S. Karjomaa, S., Kapanen, A., Wallenius, K., Itävaara, M. (2002): The influence of lignin content and temperature on the biodegradation of lignocellulose in composting conditions. – Appl Microbiol Biotechnol. 59: 591-598.
[20] Whang, D. S., Meenaghan, G. F. (1980): Kinetic model of composting process. – Compost Sci./Land Utiliz. 21: 44-46.
[21] Yamada, Y., Kawase, Y. (2006): Aerobic composting of waste activated sludge: kinetic analysis for microbiological reaction and oxygen consumption. – Waste Management 26: 49-61.
[22] Zhang, J., Gao, D., Chen, T. B., Zheng, G. D., Jun Chen, J., Maa, C., Guo, S. L., Du, W. (2010): Simulation of substrate degradation in composting of sewage sludge. – Waste Management 30: 1931-1938.

http://www.aloki.hu ● ISSN 1589 1623 (Print) ● ISSN 1785 0037 (Online)
DOI: http://dx.doi.org/10.15666/aeer/1705_1155111566

A CONSTITUTIVE MODEL FOR THE DEBRIS FLOW EROSION OF SLOPE SOIL

ZHAO, J.-K.* – WANG, D. – SONG, W.-B.

College of Engineering, Nanjing Agricultural University, Nanjing 210031, China

**Corresponding author*
e-mail: jikunzhao_2006@163.com

(Received 22nd Apr 2019; accepted 11th Jul 2019)

Abstract. In this study, a constitutive model for debris flow erosion of slope soil under the influence of barriers was derived and established based on the Bingham Model theory. The upper reaches of the Laoshan were used as a study case to build an indoor slope model and simulate the debris flow erosion of slopes. Debris flow velocity, soil erosion patterns and extent of accumulation were analyzed. The results indicated that without a barrier, debris flows maintained an accelerated motion, and loose particles moved under the action of shearing strength and subsequent slope surface erosion. Accumulation was observed as overlapping stacked slices. Under the influence of barriers, debris flows were separated and blocked, which resulted in the reduction of the velocity and quality of the moving body with two symmetrical bodies formed in the accumulation area. When the barrier was placed in a high position, debris flows were distributed early and the new velocities and impacts were smaller. Furthermore, the solids carrying capacity decreased and the slope soil depths in the most in-depth sections of the erosion pit were less variable. Therefore, the erosion competency was relatively weak, which provided better protection to the downstream slope soil.
Keywords: *Laoshan area, shearing strength, barrier, soil erosion depths, slope surface*

Introduction

Debris flows are very destructive geological disasters. Due to their shearing strength, loose materials also move, which creates secondary disasters induced by erosion. Construction projects are often destroyed. Moreover, people's lives and property safety are threatened. Therefore, it is necessary to research the mechanisms of rainfall-induced debris flows, which can facilitate a better understanding of these disasters. These models can be used to forecast, prevent, and mitigate disasters. Thus far, research on debris flow processes have focused on numerical simulations and experiments.

International scholars have established a dynamic model for debris flows based on the SH theory. For example, the DAN calculation model was proposed by Hungr and McDougall (Hungr, 2008; Hungr and McDougall, 2009), which assumes that resistance includes internal and slope resistance and considers internal forces and erosion. The model represents different motion states and the simplified model has been verified with multiple inversion analysis. He et al. (2007) studied the initiation mechanisms for corroding to a ditch using numerical simulations. The authors also discussed the influence of factors on initial velocities, such as gravity, falling gradient, and soil strength. Fan et al. (2010) simulated dynamic entrainment processes, and they found that entrainment could increase the volume of debris flow motion, making debris flows more destructive. Based on Bingham rheological theory, Zhang et al. (2012) built a debris flow model and simulated gully bed evolution to explore bed erosion deposition processes. Wang (2001) established an energy theory for debris flow movement. He also derived a theoretical formula to determine average velocity,

http://www.aloki.hu ● ISSN 1589 1623 (Print) ● ISSN 1785 0037 (Online)
DOI: http://dx.doi.org/10.15666/aeer/1705_1156711585

which was verified by experiments. Based on small flume experiments, Liu (2006) found that under specific experimental parameters, the regression equations for velocity and range resulted in both velocity and deposition range ratios. Lin et al. (2013) used experiments to explore debris flow deposition laws over erodible beds with changes in debris flow intensity, the total amount of debris flow, channel slope, and bed material density. Han et al. (2012) examined the Lian Hua-xin and Niujuan gullies to discuss the erosion and development and evolution features of slope and gully debris flows, respectively.

Setting barriers can be an effective measure to control debris flow processes. Based on simulations and experiments, many scholars (Ma et al., 2007; Fan et al., 2010; Huang and Lu, 2013; Prieto et al., 2018) discussed barrier effects on debris flow motion. Zhou et al. (2013) conducted model tests to explore the effect of anchor-slope protection in preventing slope debris flows and macro-meso mechanisms of soil deformation. Zhao et al. (2015) studied slope sliding and debris flow evolution with and without barriers. Those studies suggest that bank erosion increases the mass and density of the debris flow.

Many studies have found that debris flows separate when passing through a barrier (Langhans et al., 2017; Zhang et al., 2018; Lee and Jeong, 2018; Ugelvig and Egholm, 2018). The barrier position and rotation angle could change the deposition areas. When the rotation angle is equal to the critical value or exceeds it, parts of debris flow are blocked, and deposition areas drastically decrease. However, most researchers have focused on the deposition process and have rarely considered the barrier effect on velocity and slope soil erosion depths. Deposition areas are often centralized places where people live in mountainous areas. The deposition range is an important parameter to categorize dangerous areas. However, research that combines deposition range and the characterization of parameters such as velocity and erosion depths in slope soil is limited. Therefore, it is challenging to analyse disaster mechanisms and risks from debris flows systematically.

At present, most experimental studies are strongly empirical, and the applicable scope of the regression formula needs further validation, which is a challenge because of their complexity in composition and variability of dynamical processes. In addition, studies combining constitutive theories on the erosion process with laboratory experiments are few.

This study derived and established a constitutive model for the evolution of debris flows with and without barriers based on the Bingham Model theory. An indoor slope model was built to experimentally simulate debris flow erosion of slope soil. The constitutive model was validated using the experimental results gathered through inversion analysis.

Material and Methods

The model includes the viscous force, turbulence intensity within the slurry, and friction and collision force between the particles during energy transfer. Slurry and slope properties, including the roughness of soil surface, are incorporated. The turbulence power of the debris flow can be ignored because of its significant viscosity. The simplified Bingham model is adopted:

http://www.aloki.hu ● ISSN 1589 1623 (Print) ● ISSN 1785 0037 (Online)
DOI: http://dx.doi.org/10.15666/aeer/1705_1156711585

$$\tau = \tau_B + \eta \frac{dv}{dy} \quad \text{(Eq.1)}$$

where, τ is shearing strength, τ_B is yield shearing strength, η is the coefficient of viscosity, and dv/dy is the velocity gradient in the y direction.

Influencing factors, such as the concentration of debris flow, distribution of particle size, and slope, are considered. The Manning equation is used in the velocity equation; the starting velocity is expressed as follows (Shu and Fei, 2003):

$$v_0 = 1.62\left[\frac{S_v(1-S_v)}{d_{10}}\right]^{\frac{2}{3}} h^{\frac{1}{3}} J^{\frac{1}{6}} = 1.62Bh^{\frac{1}{3}} J^{\frac{1}{6}} \quad \text{(Eq.2)}$$

where, S_v is the volume concentration of debris flow, d_{10} is the lower limit of particle size, h is the depth of mud, and J is the slope. *Eq. (2)* has been verified using measured data from Jiangjia Gully and Hunshui Gully.

Constitutive model of debris flow erosion on soils without barriers

Debris flows are influenced by the friction resistance from the slope surface and internal viscous forces as they start to move. The slope surface resistance and quality of the landslide body from t_{i-1} to t_i can be expressed as:

$$\begin{cases} f_i = \mu_0\left(m_{i-1} + \dfrac{dm}{dt}\Delta t\right) g\cos\beta \\ m_i = m_{i-1} + \dfrac{dm}{dt}\Delta t \\ \Delta t = t_i - t_{i-1} \end{cases} \quad \text{(Eq.3)}$$

where, μ_0 is the friction coefficient of the slope surface, β is the slope of the flowing area, dm/dt is the velocity of the quality change, g is gravitational accelerations, f_i and m_i are resistance from slope surface and quality of debris flow at time ti, respectively. Moreover, Δt is the time that the debris flow is moving, i=1,2,3….

From t_{i-1} to t_i, the laws of conservation of energy are:

$$\begin{cases} \dfrac{1}{2}m_{i-1}v_{i-1}^2 + m_{i-1}g(Y - y_{i-1}) - m_i g(Y - y_i) - \dfrac{1}{2}m_i v_i^2 = W_f(t_{i-1} \sim t_i) + W_S(t_{i-1} \sim t_i) \\ W_f(t_{i-1} \sim t_i) = \mu_0 g\cos\beta \int_{t_{i-1}}^{t_i}\left(m_{i-1} + \dfrac{dm}{dt}t\right)dt \end{cases} \quad \text{(Eq.4)}$$

where, v_i is the velocity at time ti, Y is the initial height of the debris flow, $W_f(t_{i-1} \sim t_i)$ and $W_S(t_{i-1} \sim t_i)$ are energy consumptions to overcome resistance and

http://www.aloki.hu ● ISSN 1589 1623 (Print) ● ISSN 1785 0037 (Online)
DOI: http://dx.doi.org/10.15666/aeer/1705_1156711585

viscous forces from the slope surface, respectively. The formula is the typical expression of the work of cohesion from t_{i-1} to t_i.

According to another expression of energy (Huang and Lu, 2013):

$$E_i = h_{ci} + \frac{v_i^2}{2g} \quad \text{(Eq.5)}$$

The energy consumption of debris flow from t_{i-1} to t_i is:

$$\Delta E = h_{ci-1} - h_{ci} + \frac{v_{i-1}^2 - v_i^2}{2g} \quad \text{(Eq.6)}$$

where, h_{ci} is the height of center of mass of debris flow at time and ΔE is energy consumption.

After combining *Eq. (4)* with *(6), Eq.(7)* is the recursive expression about v_i^2:

$$v_i^2 = \frac{v_{i-1}^2(m_{i-1}g - 1) + Am_{i-1} + B \cdot \frac{dm}{dt}\Delta t + C}{m_{i-1}g + g \cdot \frac{dm}{dt}\Delta t - 1} \quad \text{(Eq.7)}$$

where, A, B, and C are expressed as $2g^2(y_i - y_{i-1})$, $2g^2(y_i - Y)$, and $2g(h_{ci} - c_{i-1})$, respectively.

When i=1, the common expression for v_t^2 can be obtained:

$$v_t^2 = \frac{v_0^2(m_0 g - 1) + 2m_0 g^2 y + 2g^2(y - Y)\frac{dm}{dt} \cdot t + C_1}{m_0 g + g \cdot \frac{dm}{dt} \cdot t - 1} \quad \text{(Eq.8)}$$

where, C_1 is $2g(h_{ct} - h_{c0})$, t is time, and y is the y intercept.

A new equation for shearing strength can be obtained by substituting the derivation of *Eq. (8)* into *Eq. (1)*:

$$\tau = \tau_B + \eta \frac{m_t g^2}{(m_t g - 1)v_t} \quad \text{(Eq.9)}$$

where, m_t and v_t are the quality and velocity of debris flow at time t, respectively.

Similarly, the cohesion power from 0 to t can be obtained from the law of conservation of energy:

$$W_S(0 \sim t) = \frac{1}{2}m_0 v_0^2 + m_0 g Y - m_t g(Y - y) - \frac{1}{2}m_t v_t^2 - \mu_0 g \cos\beta \int_0^t (m_0 + \frac{dm}{dt} \cdot t)dt \quad \text{(Eq.10)}$$

http://www.aloki.hu ● ISSN 1589 1623 (Print) ● ISSN 1785 0037 (Online)
DOI: http://dx.doi.org/10.15666/aeer/1705_1156711585

Constitutive model of debris flow erosion on soils with barriers

The barrier is designed as an equilateral triangular prism to simplify the calculation. The length of the waist and bottom sides are l_0 and l_1, respectively. The safety height is H, regardless of the displacement and overflow over the barrier under the impact of the debris flow.

The barrier is fixed on the central axis of the slope (*Figure 1*) to reduce the variables' interference on the constitutive model based on the barrier position. The distance from the barrier to the side of the plat is x_1 (note: the physical quantities without vector symbols are scalars, such as t_1 and x_1). The energy consumption to overcome the friction from the barrier is ignored, because the roles for shunting and obstructing are stronger than the buffering role.

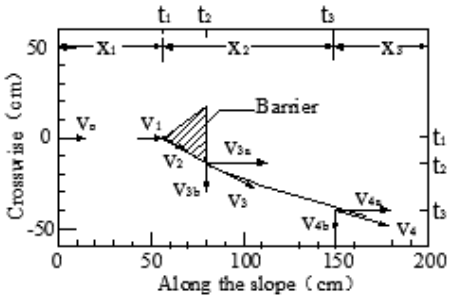

Figure 1. *Velocity diagram for a barrier on the axis of the slope*

The movement before a debris flow contacts the barrier is the first phase, followed successively by movement along the barrier and after separating from it.

According to the decomposition principle for velocity, v_1 is decomposed into two symmetrical components at time t_1 (*Figure 2a*):

$$v_2 = \frac{v_1}{2\cos\frac{\theta}{2}} \tag{Eq.11}$$

where, θ is the apical angle of the triangle.

Similarly, the quality has an equal distribution:

$$m_2 = \frac{1}{2}m_1 \tag{Eq.12}$$

From t_1 to t_2, the law of conservation of energy can be expressed as follows:

$$\begin{cases} \frac{1}{2}m_2{v_2}^2 + m_2 g(Y - y_2) - \frac{1}{2}m_3{v_3}^2 - m_3 g(Y - y_3) = W_f(t_1 \sim t_2) + W_S(t_1 \sim t_2) \\ m_3 = m_2 + \frac{dm}{dt}(t_2 - t_1) \\ W_f(t_1 \sim t_2) = \mu_0 g \cos\beta \int_{t_1}^{t_2} (m2 + \frac{dm}{dt}t)dt \end{cases} \tag{Eq.13}$$

http://www.aloki.hu ● ISSN 1589 1623 (Print) ● ISSN 1785 0037 (Online)
DOI: http://dx.doi.org/10.15666/aeer/1705_1156711585

where, v_j, m_j and y_j are velocity, quality and y intercept after separating from the barrier at time t_{j-1}, respectively. Wherein, j=2, 3…..

$$v_3^2 = \frac{v_2^2(m_2 g - 1) + Am_2 + B \cdot \frac{dm}{dt}(t_2 - t_1) + C}{m_2 g + g \cdot \frac{dm}{dt}(t_2 - t_1) - 1} \quad \text{(Eq.14)}$$

where, A, B and C are expressed as $2g^2(y_3 - y_2)$, $2g^2(y_3 - Y)$, and $2g(hc_3 - h_{c2})$, respectively; h_{cj} is the height of the center of mass of debris flow at time t_{j-1}.

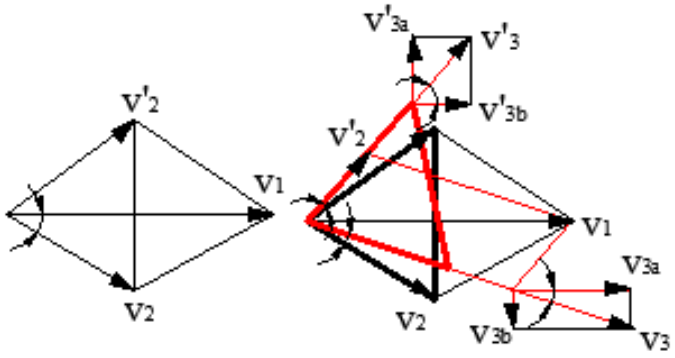

(a) (b)

Figure 2. *Velocity diagrams for a barrier on the slope: (a) along the axial; (b) Rotated* ϕ

From t_2 to t_3, the trajectory of the debris flow is approximately a parabola. The slope surface resistance consists of resistance on the slope axis direction and lateral resistance. The law of conservation of energy can be expressed as follows:

$$\begin{cases} \frac{1}{2}m_3 v_3^2 + m_3 g(Y - y_3) - \frac{1}{2}m_4 v_4^2 - m_4 g(Y - y_4) = W_f(t_2 \sim t_3) + W_S(t_2 \sim t_3) \\ m_4 = m_3 + \frac{dm}{dt}(t_3 - t_2) \\ W_f(t_2 \sim t_3) = (\mu_0 + \mu_1) g \cos\beta \int_{t_2}^{t_3} \left(m_3 + \frac{dm}{dt} t \right) dt \end{cases} \quad \text{(Eq.15)}$$

where, μ_1 is coefficient of friction of lateral resistance.

The velocity after separating from the barrier at time t_3 can be obtained by combining *Eq. (14)* with *Eq. (15)*:

$$v_4^2 = \frac{v_3^2(m_3 g - 1) + Am_3 + B \cdot \frac{dm}{dt}(t_3 - t_2) + C}{m_3 g + g \cdot \frac{dm}{dt}(t_3 - t_2) - 1} \quad \text{(Eq.16)}$$

http://www.aloki.hu ● ISSN 1589 1623 (Print) ● ISSN 1785 0037 (Online)
DOI: http://dx.doi.org/10.15666/aeer/1705_1156711585

where, A, B, and C are expressed as $2g^2(y_4-y_3)$, $2g^2(y_4-Y)$, and $2g^2(y_4-Y)$, respectively.

Higher values of θ result in longer lateral distances. Thus, the scope of the 'Not erosion zone' is large, which means that the protected areas in the middle and lower reaches are broad.

A new equation for shearing strength when debris flow passes the barrier can be obtained after substituting the derivation of *Eq. (16)* into *Eq. (1)*:

$$\tau = \tau_B + \eta \frac{m_P g^2}{(m_P g - 1)v} \quad \text{(Eq.17)}$$

where, m_P and v are the quality and velocity of the debris flow at t, respectively; wherein, m_P can be expressed as $m_0/2 + (t3 - t_1/2)\,dm/dt$.

Based on these equations, the change in the barrier position and rotation angle can be quantified (*Figure 3*).

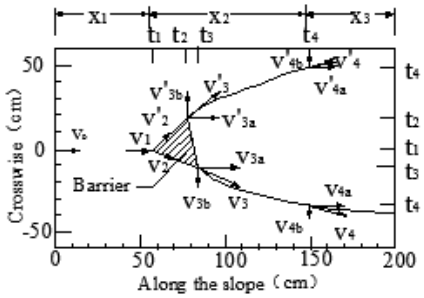

Figure 3. *Velocity diagram for a barrier rotating ϕ degrees*

Assuming that the distance from plat to the vertex of barrier is fixed (x_1), the degrees of counterclockwise rotation that centers the barrier vertex is ϕ. The velocity will be decomposed into v_2 and v'_2 when the debris flow contacts the barrier according to the sine theorem:

$$\frac{v_1}{|\sin(\pi-\theta)|} = \frac{v_2}{\left|\sin(\frac{\theta}{2}+\phi)\right|} = \frac{v'_2}{\left|\sin(\frac{\theta}{2}-\phi)\right|} \quad \text{(Eq.18)}$$

The quality of the moving body on the left is not equal to the right under the influence of rotation. The volume is expressed as $V = \int dV = \iiint da \times db \times dh$, and the qualities of moving body on both sides at time t_1 are:

$$\begin{cases} m_2 = (m_1 - D)/2 \\ m'_2 = (m_1 + D)/2 \end{cases} \quad \text{(Eq.19)}$$

http://www.aloki.hu ● ISSN 1589 1623 (Print) ● ISSN 1785 0037 (Online)
DOI: http://dx.doi.org/10.15666/aeer/1705_1156711585

where, D is $\rho \tan\phi \iiint db \times db \times dh$.

According to the law of conservation of energy, a left moving body from t_1 to t_3 and from t_3 to t_4 can be expressed as follows, respectively:

$$\begin{cases} \frac{1}{2} m_2 v_2^2 + m_2 g(Y - y_2) - \frac{1}{2} m_3 v_3^2 - m_3 g(Y - y_3) = W_f(t_1 \sim t_3) + W_3(t_1 \sim t_3) \\ m_3 = m_2 + \frac{dm}{dt}(t_3 - t_1) \\ W_f(t_1 \sim t_3) = \mu_0 \cos\beta \int_{t_1}^{t_3} \left(m_2 + \frac{dm}{dt} t \right) dt \end{cases} \quad \text{(Eq.20)}$$

$$\begin{cases} \frac{1}{2} m_3 v_3^2 + m_3 g(Y - y_3) - \frac{1}{2} m_4 v_4^2 - m_4 g(Y - y_4) = W_f(t_3 \sim t_4) + W_S(t_3 \sim t_4) \\ m_4 = m_3 + \frac{dm}{dt}(t_4 - t_3) \\ W_f(t_3 \sim t_4) = (\mu_0 + \mu_{1)} \cos\beta \int_{t_3}^{t_4} \left(m_3 + \frac{dm}{dt} t \right) dt \end{cases} \quad \text{(Eq.21)}$$

The velocity of the left body at time t_4 after separation from the barrier can be obtained by combining *Eq. (20)* with *Eq. (21)*.

$$v_4^2 = \frac{v_3^2(m_3 g - 1) + A m_3 + B \frac{dm}{dt}(t_4 - t_3) + C}{m_3 g + g \cdot \frac{dm}{dt}(t_4 - t_3) - 1} \quad \text{(Eq.22)}$$

where, A, B, and C are expressed as $2g^2(y_4 - y_3)$, $2g^2(y_4 - Y)$, and $2g(h_{c4} - h_{c3})$, respectively.

Identically, a new formula for the shearing strength of the left moving body at time t can be expressed as follows:

$$\tau = \tau_B + \eta \frac{m_1 g^2}{(m_1 g - 1) v} \quad \text{(Eq.23)}$$

where, m_l is $(m_0 - D)/2 + (dm/dt)(t - t_1/2)$.

Similarly, the velocity of the right body at the same time is:

$$v'^2_4 = \frac{v'^2_3(m'_3 g - 1) + A m'_3 + B \frac{dm}{dt}(t_4 - t_2) + C}{m'_3 g + g \cdot \frac{dm}{dt}(t_4 - t_2) - 1} \quad \text{(Eq.24)}$$

where, A, B, and C are expressed as $2g^2(y'_4 - y'_3)$, $2g^2(y'_4 - Y)$, and $2g(h'_{c4} - h'_{c3})$, respectively.

http://www.aloki.hu ● ISSN 1589 1623 (Print) ● ISSN 1785 0037 (Online)
DOI: http://dx.doi.org/10.15666/aeer/1705_1156711585

The shearing strength of the right moving body at the same time is:

$$\tau = \tau_B + \eta \frac{m_r g^2}{(m_r g - 1)v} \quad \text{(Eq.25)}$$

where, m_r can be expressed as: $(m_1 + D)/2 + (dm/dt)(t - t_1)$

The adjusted rheological model under the influence of a barrier is identical to the condition without it. Therefore, the shearing strength can be expressed as:

$$\tau = \tau_B + \eta \frac{mg^2}{(mg - 1)v} \quad \text{(Eq.26)}$$

The qualities with the three conditions can be deduced as followings:

$$m = \begin{cases} m_0 + \dfrac{dm}{dt} t & (without\ barrier) \\ \dfrac{m_0}{2} + \dfrac{dm}{dt}(t_3 - \dfrac{t_1}{2}) & (barrier\ rotates\ along\ axies) \\ \dfrac{m_0 - D}{2} + \dfrac{dm}{dt}(t - \dfrac{t_1}{2}) & (body\ on\ left\ side) \\ \dfrac{m_0 + D}{2} + \dfrac{dm}{dt}(t - t_1) & (body\ on\ right\ side) \end{cases} \quad \text{(Eq.27)}$$

Without a barrier, debris flows accelerate motion under the resultant force. According to *Eq. (8)*, the impact force increases along with the ever-increasing quality, and the capacity to erode slope soil increases. However, the overall shearing strength decreases as a result of weak liquidity. As a result, the erosion depths shallow. After setting a barrier, debris flows will be separated as they make contact with it. Comparing *Eq. (8)* with *Eq. (22)*, the velocity with a barrier is much smaller than others. The acceleration decreases along with a decrease in quality, and the impact decreases. Eventually, slope soil erosion downstream weakens.

Results

Figure 4 shows a plan view map of the Laoshan area in Nanjing, China, the study area. It locates at 32°07'3.55"N and 118°37'42.30"E. The area of interest trend is from southwest to northeast and the western section is higher and steeper than other areas. As shown in *Figure 5*, the mountain profile consists of bed rock on the bottom, the gravel layer and the soil layer. The layer thickness ration is about 3:2:9. Most area of the slope are steep, from 30 to 60. It has a high incidence of debris flow under rainfall that will clog roads and other construction facilities.

Configuring the indoor soil model

A 2.1 m long, 4 m wide, and 2 m high slope soil model was built inside (*Figure 6*). The reduced scale represents the natural proportions of the soil structure. A 30-cm-thick bevel face with a gradient of 5° was built on the bottom as the bedrock using cement

http://www.aloki.hu ● ISSN 1589 1623 (Print) ● ISSN 1785 0037 (Online)
DOI: http://dx.doi.org/10.15666/aeer/1705_1156711585

mortar. The model soil slope was composed of a 20-cm-deep sand stratum with an overlying 90-cm-deep soil stratum. There is a flat crest at the top and flat base near the toe of the slope. The flat base is fully open. In addition, a 1.93 m long, 0.5 m wide, and 0.4 m high storage tank was placed on the flat crest. The storage tank had a 30° slope inside which could accommodate 0.386 m^3 slurry that could be released all at once. When the door opened, the slurry flowed along the ramp way.

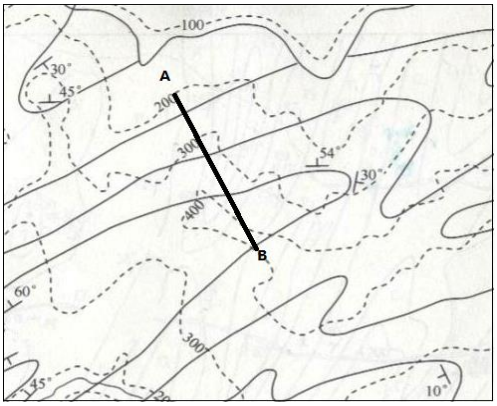

Figure 4. *Plan view map of the study area (1:25000)*

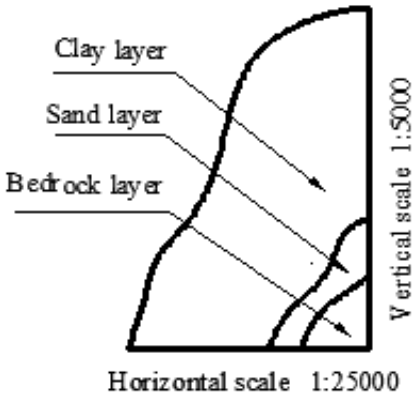

Figure 5. *Exploration section line map*

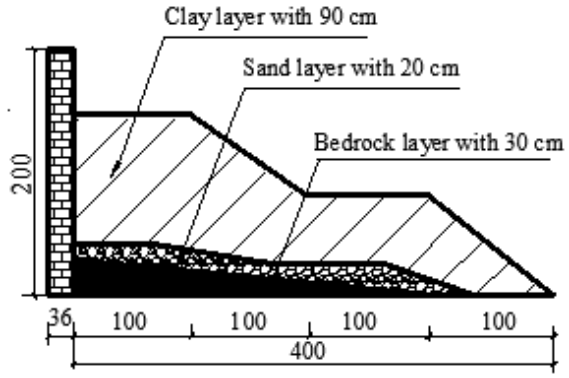

Figure 6. *Cross-section of the model slope indicating the thicknesses of each stratum*

The model slope was fully consolidated under natural conditions in order that the soil was returned to the pre-disturbance state. The soils used in the model experiments were collected from the research area to maintain natural conditions. Before each test, various monitoring indicators were measured. Experiments began once each index indicated essential stability. And embedded probes were placed at eight monitoring locations on the upper and lower layers, as shown in *Figure 7*. Points 1 and 4 were on the middle of the platform; points 2 and 5 were on the side edges; points 3 and 6 were in the middle of the slope; and points 7 and 8 were near the toe.

After scaling, soils from the corresponding locations in the study area were collected to test the mechanical properties. Slope sliding and the debris flow detection system was determined to measure the shearing strength of the experimental and undisturbed soils (*Figure 8*). The shearing strength of the undisturbed soils in the upper layer was higher

http://www.aloki.hu ● ISSN 1589 1623 (Print) ● ISSN 1785 0037 (Online)
DOI: http://dx.doi.org/10.15666/aeer/1705_1156711585

than that in the lower layer. According to *Figure 8*, the shearing strength at monitoring points 1, 2, 3, and 8 plotted along line. Based on these results, the shearing strengths of experimental soils were close to those of the undisturbed soils. Therefore, the accuracy of the model was guaranteed.

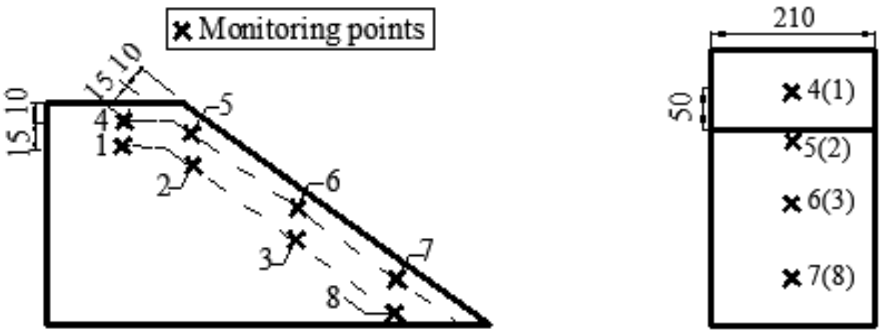

Figure 7. *Locations of monitoring points:(a) side view; (b) top view*

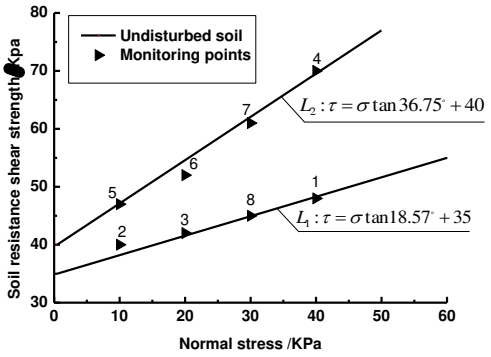

Figure 8. *Lines of shear strength*

Based on soil thickness and the maximum erosion depth without a barrier, a 30-cm-high barrier to form a 'Not erosion zone' was used in the experiments. Along the bottom, each side was 30 cm long and it was buried 10 cm deep in the soils. The barrier positions and rotation angles on the model slope are shown in *Figure 9*.

Figure 10 shows the coordinates used in the experiments. The debris flow process induced by rainfall on a 200-cm-long slope with a 45° slope was studied. The slope was 140 cm high and 140 cm wide (horizontal), with observation points at 7 cm intervals starting at 0 on the Y coordinate axis.

The density of slurry was 20.1 kN/m^3. A 45° slope was used for the movement area. The barriers were placed at L/3 and L/2 (L is the length of slope) along the slope, and barriers' rotation angles of 0° and 15° along axis were considered. Several trials were performed under these four conditions. *Table 1* shows the set of variables for each condition category.

Analysis of debris flow evolution

In the experiment, debris flows began with a nonzero initial velocity, and the velocity along the slope was faster than other directions, as shown in *Figure 11*. The gravity,

http://www.aloki.hu ● ISSN 1589 1623 (Print) ● ISSN 1785 0037 (Online)
DOI: http://dx.doi.org/10.15666/aeer/1705_1156711585

slope friction and internal viscous force changed as the amount of solid material carried along the slope increased. Particle separation was generated during the process due to the incorporation of large particles, which hindered an increase of velocity. This resulted in a nonlinear acceleration curve and overall change in shearing strength of the debris flow.

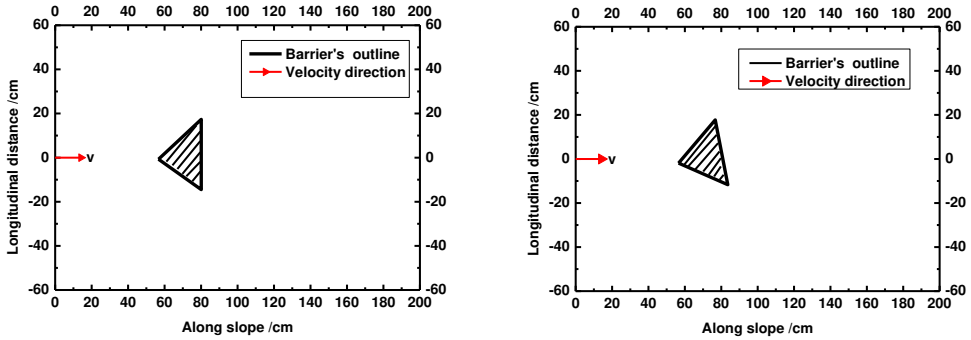

Figure 9. *Schematic diagram of the barrier positions and rotation angles:(a) barrier without rotation; (b) barrier rotated* ϕ

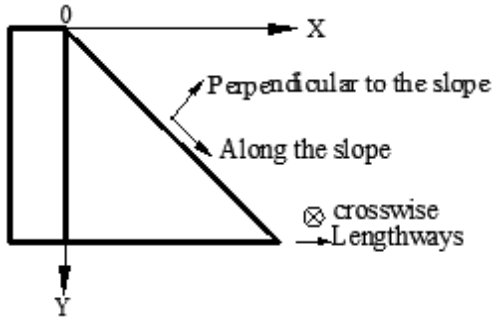

Figure 10. *Schematic diagram showing the coordinate directions*

Table 1. *Variables for each condition*

Conditions	Density (kN/m^3)	Slope (°)	Barrier	
			Position	Angle (°)
Condition Ⅰ	20.1	45	no	no
Condition Ⅱ	20.1	45	L/3	no
Condition Ⅲ	20.1	45	L/3	15
Condition Ⅳ	20.1	45	L/2	0

According to the experimental and calculated results, curves showing the relationships between velocity and time were generated, as shown in *Figure 12*. Conditions (II), (III), and (IV) were used to evaluate the right side of the flow surface. Based on the $v-t$ curve and calculations, the relationship between shearing strength and time is shown in *Figure 13*.

http://www.aloki.hu ● ISSN 1589 1623 (Print) ● ISSN 1785 0037 (Online)
DOI: http://dx.doi.org/10.15666/aeer/1705_1156711585

Figure 11. *Debris flow patterns*

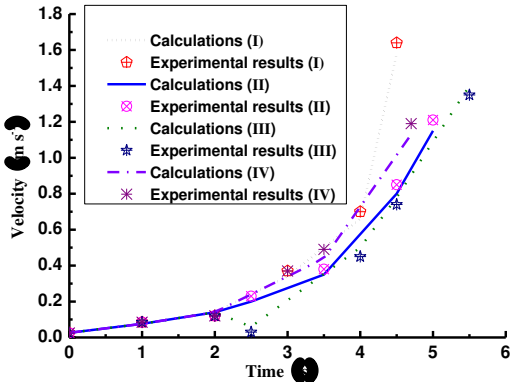

Figure 12. *Velocity-time curves for different conditions*

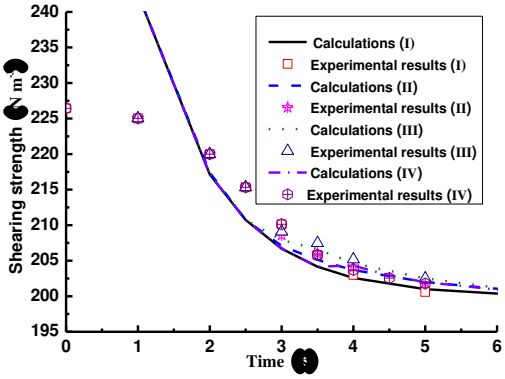

Figure 13. *Shearing strength-time curves for different conditions*

Figure 12 shows that under Condition (I), the debris flows showed accelerated motion with a nonzero initial velocity, with 2 s and 4 s as significant turning points. Loose material was carried by shearing strength along the slope surface, with an increasing impact force. The erosion capacity was enhanced and the velocity reached a peak of 1.6 m/s, when the debris flow arrived at the toe of the slope at 4.5 s. Comparing Conditions (I), (II) and (III) in *Figure 13*, after contacted with the barrier at 2 s, the velocity decreased. The velocity of Condition (II) was almost constant at 2.5 s, because

http://www.aloki.hu ● ISSN 1589 1623 (Print) ● ISSN 1785 0037 (Online)
DOI: http://dx.doi.org/10.15666/aeer/1705_1156711585

the decomposition generated it under a force equal to the fundamental force. However, the acceleration decreased with a reduction in quality, reaching a lower velocity at the same time as Condition (I). Under Condition (III), the barrier diversion decreased the velocity 0.1 m/s at 2.5 s, and velocity of rotation (right side) was significantly faster than the other side (*Figure 2b*). Simultaneously, the quality also changed so that it was more extensive on the right side. The slower the 'initial velocity', the lower the kinetic energy, and weak soil erosion was confirmed in both the calculations and experimental results.

Comparing Conditions (II) and (IV) in *Figure 12*, when the barrier was close to the toe of slope, the original movement pattern was maintained longer and contact with the barrier was later. Under condition (II), the debris flow began a new accelerated motion when it made contact with the barrier at 2 s. The velocity under Condition (I) was the same as under Condition (IV) and both were greater than the acceleration under Condition (II) from 2 s to 3.5 s. The velocity under Condition (IV) reached 0.5 m/s at 3.5 s. This velocity was unchanged at contact with the barrier, and then accelerated along it. At this point, the maximum numerical difference in velocity between Conditions (II) and (IV) was 0.1 m/s. Subsequently, Condition (IV) was greater than Condition (II). Therefore, the impact force upstream of L/3~L/2 under Condition (IV) was greater than that under condition (II), and soil erosion in the region was significant, indicating that the protective effect of the downstream region was weaker than that in Condition (II). These conclusions were the same in both the calculations and experimental results.

Figure 13 shows a non-linear negative correlation between shearing strength and time. Comparing *Figure 12* with *Figure 13*, four conditions reached a maximum shearing strength at 1 s. As the debris flow process advanced, loose particles increased. In spite of the increasing velocity, the overall shearing strength decreased. The curve under Condition (I) flattened after 4 s and the head of the debris flow was close to the slope toe. As the liquidity worsened, the overall shearing strength weakened and approached the yield stress. Influenced by the barrier position, the velocities at the head both decreased after 2.5 s and 3.5 s under Conditions (II) and (III). The overall shearing strength declined, flattened out after 5 s and 6 s, and consistently approached the yield stress. The curve of the shearing strength under Condition (III) was gentler than that under Condition (II). The overall energy consumption was large and the shearing strength decreased under the influence of the barrier. Both the ability to carry loose particles and erosion weakened. Therefore, variations in velocity and shearing strength under Condition (III) were moderate.

In summary, debris flows slowed after contact with the barrier. With quality deallocation, the impact force weakened and the surface erosion in the downstream area decreased. When the barrier was in the high position, the weakening effect was clear.

Furthermore, a greater rotation angle resulted in the experimental results were in agreement with calculations.

Analysis of soil erosion depths after debris flows

To explore the soil erosion effect on erosion depths, the right side was evaluated under Conditions (IV), (V) and (VI). *Figure 14* shows the cross-sectioned positions. Based on the experimental data, variations in slope surface erosion patterns under different conditions are shown in *Figure 15*, which were similar under all the evaluated conditions. The upper part of the model slope was shallow, while the center at 56 cm

http://www.aloki.hu ● ISSN 1589 1623 (Print) ● ISSN 1785 0037 (Online)
DOI: http://dx.doi.org/10.15666/aeer/1705_1156711585

appeared deeper than other areas. Erosion depths shallowed in the lower part of the slope. The slopes differed between the upper and lower segments: steep in the upper (49.3°) and more moderate in the lower (36.5°). Debris flows were in a state of accelerated motion in the movement area. Loose material on the pathway surface moved under the influence of shearing strength, which resulted in the surface erosion. The mechanism for erosion was an increase in the capacity of carrying solids at a certain velocity. This erosion was also associated with a reduction in overall moisture content and higher viscosity. Turbulent flow was unusual at high viscosity but could carry more surface materials away. Therefore, the erosion ability would weaken after an increase in density.

Figure 14. *Cutting positions for different conditions: (a) with barrier; (b) without barrier*

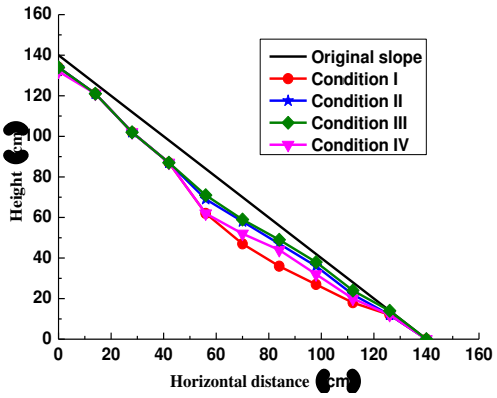

Figure 15. *Variations in slope surface erosion depths for different conditions*

Within the horizontal distance from 0 to 56 cm, the depth variations were consistent for the four conditions. Soils were 5 cm deep from approximately 0 to 40 cm after erosion, and gradually deepened from 40 to 56 cm. Depth variations under Conditions (I) and (II) were consistent and more precise than that under the other conditions. Variations were moderate under Condition (II) and most gentle under Condition (III). At a horizontal distance of 40 cm, debris flows had a resolvable velocity and earlier quality distribution under the influence of the barrier compared to Condition (II).

http://www.aloki.hu ● ISSN 1589 1623 (Print) ● ISSN 1785 0037 (Online)
DOI: http://dx.doi.org/10.15666/aeer/1705_1156711585

Subsequently, on both sides of the moving body, new erosion was initiated with the weak force. The overall shearing strength was small under Condition (II). Therefore erosion depths were significantly less than that under Conditions (I) and (IV). Comparing Conditions (III) and (II), the areas affected on the sides were different, induced by the barrier rotation. As a result, distributions in quality and velocity were also unequal. Although the quality under Condition (III) was greater than that under Condition (II), the overall kinetic energy was smaller. Therefore, the shearing strength was smaller and the ability to carry solid material was weaker under Condition (III). This result is shallower in the curve of erosion depths under Condition (III) than under Condition (II). In the horizontal distance from 56 to 140 cm, the debris flow separated under the influence of the barrier under Condition (IV). Its initial kinetic energy was small and erosion ability was weak, so that the soil depths were shallower than those under Condition (I). The velocity under Condition (IV) was much larger than that under Conditions (II) and (III), hence the curve of the slope surface erosion patterns under Condition (IV) was lower than that under Conditions (II) and (III).

Based on the comparative analysis, the following conclusions were reached: a greater rotation angle resulted in a smaller 'initial kinetic energy' on the side of rotation, weaker overall shearing strength, and capacity for carrying soil. Therefore, appropriate position placement and rotation angle of the barrier will help protect downstream areas. More broadly, the slope line becomes gentle after erosion. A comparison of the experimental results with calculations is provided in *Figure 12*.

Analysis of deposition range after erosion

The head of the debris flow decelerates after arriving at the horizontal plane, while the tail maintains acceleration. However, the tail decelerated rapidly after reaching the ramp exit. *Figure 12* shows the deposition range under different conditions.

When the head of the debris flow reached the slope toe, the velocity peaked. Deposition began when the slope decreased. Influenced by strong friction from the ground, the power components decreased, and longitudinal velocity declined. Because the ground was flat, the boundary constraints in the horizontal direction disappeared and a transverse circulation was generated. The slurry spread and fan bodies fully developed because the flow was unobstructed. In addition, because of complex transverse momentum, the internal resistance of the slurry increased. Eventually, deposition formed under the influence of the viscous force and ground friction.

Figure 16 shows that the depositions all formed lap alluvial fans. Two alluvial fans developed under Conditions (II), (III), and (IV). When the barrier was on the centerline of the slope, this was the point of debris flow contact, which resulted in symmetric split-flows. Moreover, the deposition bodies under Conditions (II) and (IV) were approximately symmetrical.

Discussion

Comparing Conditions (II) and (IV), the single alluvial fan was narrow and long under Condition (IV), but wide and short under Condition (II). The maximum length, width, and thickness of the deposition were 52 cm, 40 cm, and 12 cm under Condition (IV), respectively. The corresponding values were 86.5%, 125%, and 142% of that under Condition (II). The deposition points of the maximum thickness under Conditions (IV) and (II) were located at the leading edge, at 28 cm and 35 cm, respectively. A low

http://www.aloki.hu ● ISSN 1589 1623 (Print) ● ISSN 1785 0037 (Online)
DOI: http://dx.doi.org/10.15666/aeer/1705_1156711585

barrier position resulted in a long acceleration time. Therefore, when it reached the horizontal plane, the vertical velocity was large, and the fan could develop fully. Therefore, the position of the maximum deposition thickness was far from the exit ramp.

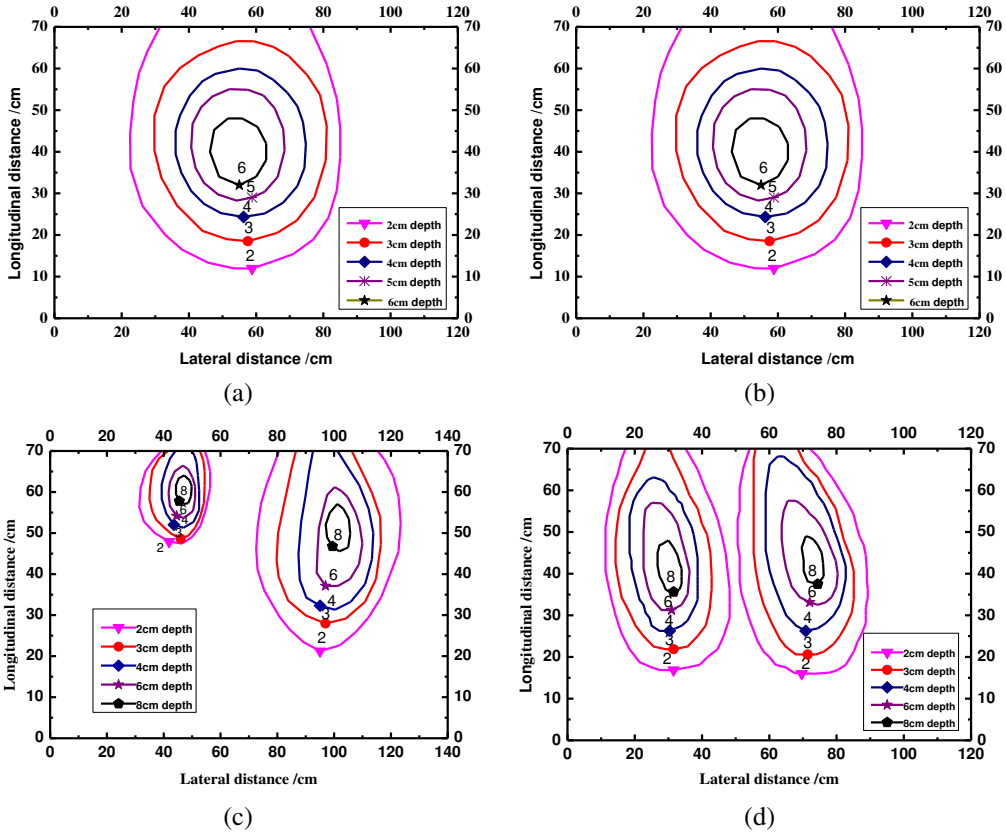

Figure 16. *Accumulation under different conditions: (a) condition (I), (b) condition (II), (c) condition (III), and (d) condition (IV)*

Comparing Conditions (II) and (III), the barrier rotated counterclockwise along the axis was examined. The effective contact area and quality on the right side were larger than that on the left side. The proportional change was approximately 1:2. The maximum length and width of deposition on the left under Condition (III) were 20 cm and 25 cm, respectively. On the right side, the corresponding values were 5/2 and 8/5 times than that on the left. The deposition area was twice as large as that of the left, in agreement with the calculated values. Thus, a greater angle resulted in a more significant quality of the right moving body. The high lateral velocity component resulted in longer movement time in the lateral direction. As a result, the space between the deposition bodies was large and the quality (on the right side) of the deposition body on the rotating direction (reverse) was high. The results also showed that the deposition area ratio was approximately equal to the quality ratio between the left and right for the moving body.

http://www.aloki.hu ● ISSN 1589 1623 (Print) ● ISSN 1785 0037 (Online)
DOI: http://dx.doi.org/10.15666/aeer/1705_1156711585

Conclusions

This study derived and established a constitutive model for slope soil erosion due to the debris flow with and without barriers based on the Bingham Model theory. This constitutive model was established based on Bingham Model velocities and equations under Conditions of different barrier positions and rotations. Equations for the modified Bingham Model were provided under three Conditions.

The upper reaches of the Laoshan was used as the study case to build an indoor slope model and simulate debris flow erosion processes. The experimental results were in agreement with calculations. Based on the constitutive equations, predictions of the soil erosion depths and deposition range after erosion were more accurate. Expressions for the shearing strength were also verified through experiments.

The buffering effect improved as the barrier and edge of platform were moved closer. In these Conditions, the shearing strength weakened, and then the damage in the downstream region due to soil erosion also decreased. A greater rotation angle also weakened the damage in the direction of rotation. Therefore, interception facilities should be built on the upstream slope and the rotation angle based on the characteristics of the active region downstream should be considered. These efforts will result in the optimal interception, diversion, and weakening of slope erosion.

In future research, we will focus on the secondary disasters of debris flow because debris flow is a very destructive geological disaster. Loose material moves in response to debris flow's shearing force, thereby creating a secondary disaster induced by erosion. Rainfall is the main reason for slope instability, which leads to large-scale landslides.

Acknowledgements. The study was supported by the Special Fund of Basic Scientific Research Operations of Central Universities of China (Grant No. KYZ201664) and by the Natural Science Foundation of Jiangsu Province (Grant No. BK2010457). Their financial support is gratefully acknowledged. We thank the Associate Editor and anonymous reviewers for their helpful and insightful comments.

REFERENCES

[1] Fan, Y. Y., Wang, S. J., Wang, E. Z., Liu, X. L. (2010): Simulation analysis of dynamic process of entrainment of path material by debris flow. – Chinese Journal of Rock Mechanics and Engineering 29(S2): 4146-4152.

[2] Han, Y. S., Huang, P., Zhu, Y. Y., Hu, K. H. (2012): Field monitoring and erosion-deposition sediment of flash-flood debris flow in suffered areas-a case study at Lianhuaxin Gully. – Journal of Hydraulic Engineering 43(S2): 133-138.

[3] He, S. M., Wu, Y., Li, X. P. (2007): Research on eroded start mechanism of channel debris flow. – Rock and Soil Mechanics 28(S1): 155-159.

[4] Huang, J. Y., Lu, T. H. (2013): Research and application of permeable arch dam in preventing projects for debris flow. – Journal of Water Resources and Architectural Engineering 11(1): 166-169.

[5] Hungr, O. (2008): Simplified models of spreading flow of dry granular material. – Canadian Geotechnical Journal 45(8): 1156-1168.

[6] Hungr, O., McDougall, S. (2009): Two numerical models for landslide dynamic analysis. – Computers and Geosciences 35(5): 978-992.

[7] Langhans, C., Nyman, P., Noske, P. J., Van der Sant, R. E. (2017): Post-fire hillslope debris flows: Evidence of a distinct erosion process. – Geomorphology 295(10): 55-75.

http://www.aloki.hu ● ISSN 1589 1623 (Print) ● ISSN 1785 0037 (Online)
DOI: http://dx.doi.org/10.15666/aeer/1705_1156711585

[8] Lee, K., Jeong., S. (2018): Large deformation FE analysis of a debris flow with entrainment of the soil layer. – Computes and Geotechnics 96(4): 258-268.
[9] Lin, X. P., You, Y., Liu, J. F., Zhao, Y. B., Liu, S. L. (2013): Experiment study on channel deposition of viscous debris flow over erodible beds. – Journal of Mountain Science 31(3): 327-333.
[10] Liu, J. F., Ou, G. Q., You, Y. (2006): Experimental research on velocity and deposition mode of debris flow. – Research of Soil and Water Conservation 13(1): 120-121.
[11] Ma, Z. Y., Zhang, J., Liao, H. J. (2007): Numerical simulation of viscous debris flow block engineering. – Rock and Soil Mechanics 28(S1): 389-392.
[12] Prieto, J. A., Journeay, M., Acevedo, A. B., Arbelaez, J. D., Ulmi., M. (2018): Development of structural debris flow fragility curves (debris flow buildings resistance) using momentum flux rate as a hazard parameter. – Engineering Geology 239(18): 144-157.
[13] Shu, A. P., Fei, X. J. (2003): Calculation for velocity and discharge of the viscous debris flow. – Journal of Sediment Research 47(3): 3-11.
[14] Ugelvig, S. V., Egholm, D. L. (2018): The influence of basal-ice debris on patterns and rates of glacial erosion. – Earth and Planetary Science Letters 490(5): 110-121.
[15] Wang, Z. Y. (2001): Experimental study on debris flow head and the energy theory. – Journal of Hydraulic Engineering 45(3): 18-26.
[16] Zhang, W. S., Zhao, Y. X., Cui, P., Peng, H., Chen, X. J. (2012): Two-dimensional numerical model for debris flow motion and gully bed evolution. – Science of Soil and Water Conservation 10(1): 1-5.
[17] Zhang, N. T., Matsushima. (2018): Numerical investigation of debris materials prior to debris flow hazards using satellite images. – Geomorphology 308(5): 54-63.
[18] Zhao, J. K., Wang, D., Chen, J. H. (2015): Experimental study on slope sliding and debris flow evolution with and without barrier. – Water Science and Engineering 8(1): 68-77.
[19] Zhou, J., Li, Y. X., Zhang, J., Jia, M. C. (2013): Macro-Meso Research of soil deformation mechanism of debris flow on slope prevention. – Chinese Journal of Rock Mechanics and Engineering 32(5): 1001-1008.

http://www.aloki.hu ● ISSN 1589 1623 (Print) ● ISSN 1785 0037 (Online)
DOI: http://dx.doi.org/10.15666/aeer/1705_1156711585

ECOLOGICAL RESTORATION STATUS INDEX FOR EVALUATING THE RESTORED COAL GANGUE PILE: A CHRONOSEQUENCE STUDY BASED ON THE PLANT-SOIL SYSTEM IN THE SHANXI MINING AREA, CHINA

HAO, J.[1] – GUO, D. G.[2] – LI, H. Y.[1*] – MENG, W. Q.[3]

[1]*College of Environmental Science and Engineering, Nankai University, 38 Tong Yan Road, Jinnan District, Tianjin 300350, China*
(e-mail: haojing1987.happy@163.com; phone: +86-178-2201-5686)

[2]*College of Environment and Resource, Shanxi University, 92 Wu Cheng Road, Xiaodian District, Taiyuan 030006, China*

[3]*College of Urban and Environmental Science, Tianjin Normal University, 393 Binshui West Road, Xiqing District, Tianjin 300387, China*

**Corresponding author*
e-mail: eialee@nankai.edu.cn

(Received 22nd Apr 2019; accepted 12th Jul 2019)

Abstract. This study was carried out to evaluate ecological restoration status of restored coal gangue pile in Shanxi Province, China, using ecological restoration status index (ERSI) based on a dynamic plant-soil system. ERSI was a unitless value that indicated the status of ecological restoration in the restored site. Five-year dynamics of the plant-soil system were monitored in the restored coal gangue pile at Sima Coal Mine of Lu'an Group, Changzhi, Shanxi, China, from 2009 to 2013. The fixed plots were established based on the chronosequence (space-for-time). The natural secondary community was selected as the reference site. The parameter system for evaluation of ecological restoration status was established on the basic characteristics of the plant community and soil physicochemical properties. Principal component analysis (PCA) was employed to derive ERSI. The first year was taken as the benchmark year. Except for year 2, the ecological restoration status in years 3 to 5 of the recovery and reference site were better than that in the benchmark year. Overall, the ERSI value increased with recovery age during the early stage of recovery. With recovery age, the uncertainty of ERSI showed decreased trend by Monte Carlo simulation (MCS).
Keywords: *ecological restoration status index, soil property, plant community, Monte Carlo, early stage*

Introduction

Soil properties and plant community characteristics are two critical milestones of any restoration plan (Orozco-Aceves et al., 2017; Li and Liber, 2017). In a plant-soil system, plants and soil are interdependent (Krumins et al., 2015). Soil development is necessary to support plant growth (Orozco-Aceves et al., 2017). In turn, plant growth can improve the soil properties (Ahirwal et al., 2017; Li and Liber, 2017). Therefore, it is essential to evaluate the ecological restoration status through both aspects of plant and soil. How should the parameter system of ecological restoration status evaluation based on a plant-soil system be established for a restored site? How should the restoration status of a restored site in every year of recovery be scientifically evaluated? These questions are still debated by researchers of restoration ecology. Thus, many current situation evaluations of ecological restoration status (Rossini-Oliva et al., 2016) have been reported, but they are insufficient dynamic evaluations of ecological restoration

http://www.aloki.hu ● ISSN 1589 1623 (Print) ● ISSN 1785 0037 (Online)
DOI: http://dx.doi.org/10.15666/aeer/1705_1158711604

status base on chronosequence. Moreover, these current situation evaluations have mostly focused on a particular aspect of the plant-soil system, such as plant community characteristics or soil physical or chemical properties (Gomez-Ros et al., 2013) but are insufficient when aiming at the plant-soil system.

Many evaluation parameters including qualitative parameters (e.g., habitat complexity) and quantitative parameters (e.g., vegetation coverage) have been presented. There are some recognized evaluation parameters, such as species diversity, plant biomass, vegetation coverage, soil density, total porosity, field capacity, organic matter content, TN, available nitrogen, total phosphorus, AP, and pH (Ott and Van Aarde, 2014; Licina et al., 2013; Parraga-Aguado et al., 2013; Anawar et al., 2013; Bodlák et al., 2012). However, the parameters of basic plant community characteristics (such as the index of growth and decline of species, community similarity, and community stability) are insufficient for ecological restoration status evaluation. The parameter system of evaluation for ecological restoration status is still not systemic (Liu, 2011).

Evaluation methods are varied. Single evaluation methods and combination evaluation methods are usually used for evaluations. The analytic hierarchy process (AHP), fuzzy comprehensive evaluation method (FCE), principal component analysis (PCA), clustering analysis and gray correlation evaluation, among others (Gomez-Ros et al., 2013), are single evaluation methods. AHP-FCE, PCA-AHP, and PCA-TOPSIS (Hao et al., 2016; Zhao et al., 2014; Bouzon et al., 2016) are combination evaluation methods. Based on the way of determining the weight of parameters, these methods are divided into three categories: subjective assignment value (e.g., experts scoring method, AHP), objective assignment value (e.g., PCA, entropy value method), and comprehensive assignment value (e.g., FCE). These methods include the following three features in selecting recovery goals for ecological restoration status evaluation.

Take existing standards as the recovery goal. Zhang et al. (2007) took the figure of 1/100 land resources in the People's Republic of China as a grading standard. The soil suitability evaluation hierarchy of vegetation restoration in a coal gangue pile was divided into 4 levels: very suitable, suitable, barely suitable, and temporarily not suitable. By referring to the degree of land desertification, soil wind erosion intensity grading and the secondary general survey of soil data, Yao and Yang (2014) divided the degree of mine ecological restoration status into four levels: perfect, fine, average, and low.

Take a certain ideal status as the recovery goal. Zhao et al. (2014) set evaluation grades with a relatively proximity degree between soil quality and the worst state. The closer the value was to 1, the closer to the ideal evaluation object and the higher the evaluation grade were, but the lower the evaluation level was.

Take natural secondary communities or communities without human disturbance as the main recovery goal. Lacking long-term dynamic monitoring and mechanism research of the plant-soil system (Tripathi et al., 2016), these recovery goals are unscientific to some extent (Mark et al., 2012). Whether these recovery goals are optimal is usually questionable.

The evaluation of ecological restoration status based on plant-soil systems is important to estimate the restoration status of restored sites, so establishing a parameter system for the ecological restoration status is essential (Pietrzykowski and Chodak, 2014). In the present research, the parameter system was established on the basic plant community characteristics and soil physicochemical properties. Based on the parameter

http://www.aloki.hu ● ISSN 1589 1623 (Print) ● ISSN 1785 0037 (Online)
DOI: http://dx.doi.org/10.15666/aeer/1705_1158711604

system, an integrated 'ecological restoration status index (ERSI)' could be developed by principal component analysis and used to evaluate the ecological restoration status quantitatively based on the chronosequence in a restored coal gangue pile. Moreover, the first year was taken as the benchmark year, the recovery goal was not specifically selected. It will be expected that if the ERSI value in one year is below that of the benchmark year, the ecological restoration status in this year is worse than the benchmark. Conversely, if the ERSI value in another year is above that of the benchmark year, the ecological restoration status in this year is better than the benchmark (Mukhopadhyay et al., 2014). It was predicted that the ERSI value would increase with recovery age in the early stage of recovery (Mukhopadhyay et al., 2014; Orozco-Aceves et al., 2017; Hao et al., 2015). This study was carried out to evaluate ecological restoration status of restored coal gangue pile in Shanxi Province, China, using ERSI based on a dynamic plant-soil system.

Material and methods

Study site

The study site is representative ecological restoration area in north of China. The study was conducted in the restored coal gangue pile at Sima Coal Mine of Lu'an Group, Changzhi, Shanxi, China, from 2009 to 2013 (*Fig. 1a*). The climate is temperate, with a 9 °C mean and a -29 °C minimal annual temperature. The frost-free period is 160 days. The annual rainfall is approximately 340 mm to 833 mm, and the annual evaporation capacity is approximately 1,558 mm. The original soil type was loess-like calcareous soil. The soil erosion modulus was from 500 to 1,000 $t \cdot (km^2 \cdot a)^{-1}$. The original landforms were mainly ravines covered by native secondary plants, such as *Bothriochloa ischaemum*, *Artemisia lavandulaefolia,* and *Melilotus officinalis* (*Fig. 1b*).

The fixed plots were established based on the chronosequence (space-for-time) (Mudrák et al., 2016; Alvey et al., 2003; Elgersma, 1998; Hao et al., 2016). The restored coal gangue pile consisted of three platforms with a stair-step shape established in 2009, 2010 and 2011 (*Fig. 1c*). The area of each platform was 1,500 m^2 (50 m long, 30 m wide). The total area of the three platforms was 4,500 m^2. The altitude difference between adjoining platforms was 10 m. The restoration procedure included forming and leveling the surface of each platform. During the forming process, the coal gangue layer and soil layer were alternated in stacking. Above each coal gangue layer, there was a soil layer. The thickness of each coal gangue layer was 3 m. The thickness of each soil layer was 50 cm. The last layer was the soil layer with a thickness of 80 cm. The soil was taken from the surrounding loess-like calcareous soil. After leveling the surface of each platform, *Populus tomentosa* (no canopy, 3.5 m height) was grown on each platform. The distances between the arbors and rowledges were 1.5 m and 2 m, respectively. Herbs maintained spontaneous recovery after trees were planted.

There were three sample plots. Each sample plot (400 m^2) consisted of 16 tree subsamples (area of each tree subsample = 25 m^2) established at the middle of each platform (*Fig. 1d*). 48 tree subsamples were set. An area of 1 m^2 was set at the left corner of each subsample for the herb sample. Each sample plot consisted of 16 herb samples. 48 herb samples were set. The reference site was a native secondary community with dominate species *Artemisia brachyloba*. The distance between the reference site and the restored coal gangue pile was approximately 1,000 m. Six samples (area of each sample = 25 m^2) were in the reference site on the north of the coal

http://www.aloki.hu ● ISSN 1589 1623 (Print) ● ISSN 1785 0037 (Online)
DOI: http://dx.doi.org/10.15666/aeer/1705_1158711604

gangue pile using GPS. The contents of investigation including basic plant community characteristics, soil physical properties and soil chemical properties in each sampling unit were repeated each year during the summer (August) from 2011 to 2013.

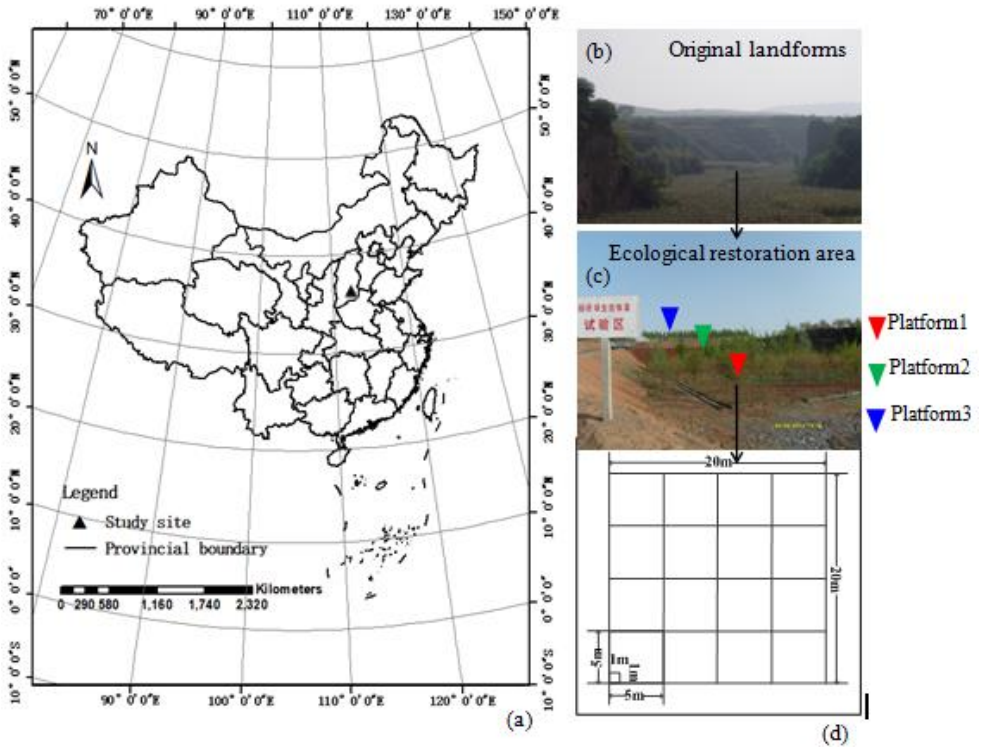

Figure 1. *Locations and design of experimental plots. (a) Location of study site in China. (b) Original landforms of study site. (c) Ecological restoration area. Red triangle: platform1 established in 2009. Green triangle: platform2 established in 2010. Blue triangle: platform3 established in 2011. (d) Design of experimental plots in each platform*

Plant community

The basic characteristics of the plant community, including the diameter at breast height (DBH) of trees, plant species, height, canopy, and coverage, were investigated. Twelve typical sampling units (area of each typical sample = 1 m^2) were set on each platform and the reference site to obtain the herbal biomass. All herbal bodies were harvested, placed in sealed bags, cleaned, and dried to a constant weight at 80 °C in the incubator. The dry weights of the herb were determined by electronic scales (accuracy 0.01).

The integrity of the vertical structure (IVS) was assigned 1, 2 and 3: 1 means the vertical structure has only one layer; 2 means the vertical structure has two layers; and 3 means the vertical structure has three layers.

The species richness index (SRI) was assigned a value according to the species evenness and dominance of a community (*Table 1*).

The index of the growth and decline of species (IGDS) indicates the dynamic of immigration and emigration of plant species in a community. If the index of growth and decline of species is close to 1.00, growth and decline maintain a dynamic balance. In the present study, taking the first year as the benchmark, the index of growth and

http://www.aloki.hu ● ISSN 1589 1623 (Print) ● ISSN 1785 0037 (Online)
DOI: http://dx.doi.org/10.15666/aeer/1705_1158711604

decline of species was determined by the net immigration rate in year 1 and is set equal to 100 (*Eqs. 1-3*).

$$IGDS_j = I_j/E_j(j = 2,3,4,5)(If\ j = 1, C_1 = 100) \quad \text{(Eq.1)}$$

$$I_j = \frac{N_{Ij}}{N_1} \times 100\%\ (j = 2,3,4,5) \quad \text{(Eq.2)}$$

$$E_j = \frac{N_{Ej}}{N_1} \times 100\%\ (j = 2,3,4,5) \quad \text{(Eq.3)}$$

where j is a plant community, $IGDS_j$ is the index of growth and decline of species for community j, I_j is the net immigration rate of community j compared to the benchmark, E_j is the net emigration rate of community j compared to the benchmark, N_{Ij} is the number of immigration species of community j compared to the benchmark, N_{Ej} is the number of emigration species of community j compared to the benchmark, and N_1 is the number of species of the benchmark year (year 1).

Table 1. *The assignment and implication for index of species richness*

Assignment	Implication
1	Obvious dominant species, worse species evenness
2	Obvious dominant species, better species evenness
3	Unobvious dominant species, worse species evenness
4	Unobvious dominant species, better species evenness

Index of species evenness < 0.95 means worse species evenness; > 0.95 means better species evenness

The value of community similarity (VCS) was determined by the Jaccard similarity index, which means the similarity of species between community *A* and community *B* (*Eq. 4*).

$$VCS = \frac{c}{(a+b-c)} \times 100\% \quad \text{(Eq.4)}$$

where a is the number of species for community *A*, b is the number of species for community *B*, and c is the number of species in common between communities *A* and *B*.

The index of community stability (ICS) was determined by M. Godron's stability determination method (Godron, 1972).

Soil property

In each platform, eight big samples (25 m^2) were selected and located by GPS. Three typical samples of topsoil (0-20 cm) were collected after clearing away the surface litter in each big sample. Each typical sample consisted of three subsamples (area of each subsample = 0.04 m^2). The subsamples were in the typical sample point approximately 20 cm and mixed thoroughly. There were eight replicates in each platform. The sampling was carried out each year from 2011 to 2013 during the summer. Moreover, in the summer of 2011, three typical contrasted sampling units were established in every big sample at the reference site. Each typical sample consisted of three subsamples (area

http://www.aloki.hu ● ISSN 1589 1623 (Print) ● ISSN 1785 0037 (Online)
DOI: http://dx.doi.org/10.15666/aeer/1705_1158711604

of each subsample = 0.04 m^2). Eight replicates were carried out in each platform. These typical soil samples were air-dried and used for physical and chemical analysis. Soil moisture (SM) content, soil field capacity (SFC), and soil density (SD) were determined according to Xie et al. (2012). Soil total porosity (STP) was calculated according to Zhang (2006). The contents of soil total organic carbon (STOC), soil organic matter (SOM), readily oxidized organic carbon (ROOC), particulate organic carbon (POC), total nitrogen (TN), available phosphorus (AP), available potassium (AK), and soil pH were determined according to Su (2010).

Ecological restoration status index (ERSI)

In this research, Principal component analysis (PCA) was used to calculate the weight of each parameter and select the major parameters. Principal components (PCs) that had an eigenvalue ≥ 1 and that explained at least 5% of the variation of the data were selected. On each particular principal component (PC), the highly weighted parameters (absolute value) were considered very important and chosen for the ecological restoration status index (ERSI). ERSI was a unitless value (from 0 to 1) that indicated the status of ecological restoration in the coal gangue pile (Mukhopadhyay et al., 2014). It is expected that if the ERSI value is higher, the ecological restoration status is superior (Mukhopadhyay et al., 2014). In this study, the first year of recovery was taken as the benchmark year. By comparing the ERSI value in every year of recovery to that in the benchmark year, the ecological restoration status was evaluated. The final ERSI equation is as follows (*Eq. 5*):

$$ERSI = \sum_{i=1}^{n} W_i S_i \quad \text{(Eq.5)}$$

where i is the number of parameters, W_i is the normalized weight value (w_i) of parameter i, $\sum_{i=1}^{n} W_i = 1$, S_i is the normalized value of parameter i, and $W_i S_i$ is the contribution of parameter i on the calculated ERSI.

The W_i equation is as follows (*Eq. 6*):

$$W_i = w_i / \sum_{i=1}^{n} w_i \quad \text{(Eq.6)}$$

where w_i is the weight value of parameter i by PCA, and $\sum_{i=1}^{n} w_i$ is the total weight value of the major parameters selected by PCA; this W_i equation was used to normalize the weight value of parameter i.

The S_i equation is as follows (*Eq. 7*):

$$S_i = a/[1 + (x_i/x_{i0})^b] \quad \text{(Eq.7)}$$

This S_i equation was used to convert the real values of the ecological restoration status parameters into unitless scores (from 0 to 1), where x_i is the real value of parameter i, x_{io} is the mean value of parameter i with all stages of recovery, and a is the maximal score of the ecological restoration status property and is set equal to 1.00. In the real value range of each parameter (from minimum to maximum of the real value), the lower the value of the parameter, the better the development of the parameter, thus, b was set equal to 2.5. In turn, b was set equal to -2.5 (Mukhopadhyay et al., 2014). The similar method described by Mukhopadhyay et al. (2014) aimed at mine soil quality and derived a mine soil quality index (MSQI). MSQI was derived based on the mine soil

http://www.aloki.hu ● ISSN 1589 1623 (Print) ● ISSN 1785 0037 (Online)
DOI: http://dx.doi.org/10.15666/aeer/1705_1158711604

physical, chemical and biological parameters without the parameters of the plant community. In the process of mine ecological restoration, the interaction between mine soil and plant community always exists. ERSI involves not only the parameters of the mine soil physicochemical properties but also the parameters of basic characteristics of plant communities. The dynamic development of a mine plant-soil system could be expressed by ERSI.

Monte Carlo simulation (MCS)

Monte Carlo simulation (MCS) is a method to estimate uncertainty with the aid of computer software. This methodology provides an uncertainty value without any approximations or shortcuts (Zeng et al., 2018). In this research, MCS was used to analyze the uncertainty of the ERSI. Firstly, the means and standard deviations of parameters in each recovery age were calculated. Based on the current sample data and experiences, the distribution functions of parameters were defined. Then, ERSI was defined by the function of define forecast according to *Equation 5*. Finally, using the function of run preference, the number of simulation and sensitivity analysis were operated. ERSI values of each period were obtained. In this paper, 10000 simulations were conducted. The confidence level was 95%.

Statistical analysis

PCA was completed by using Microsoft Excel and SPSS 11.5. The correlations and differences between variables were calculated according to Pearson's coefficient and Least-significant difference (LSD), respectively (Hao et al., 2015). A probability level of 0.05 was always used as the threshold for significance. MCS and sensitivity analysis were conducted by Crystal Ball software.

Results

Plant community

The dominant species of the herbal community were *Artemisia lavandulaefolia* (years 1 and 2), *Puccinellia distans* (year 3), *Leymus chinensis* (years 4 and 5), and *Artemisia brachyloba* (reference site). The coverage of the community achieved 80% in years 4 and 5. In previous research (Hao et al., 2016), overall, the average DBH of trees (ADT) (from 4.89 to 11.85 cm), coverage of the herb layer (CHL) (from 35 to 80%) and coverage of the community (CC) (from 40 to 80%) increased with recovery age. The average ratio height and canopy of trees fluctuated due to the growth characteristics of *Populus tomentosa.* The average height of the herb layer (AHHL), total biomass of the herb layer (TBHL) and index of species diversity (ISD) also fluctuated due to the differences of dominant species and species components, which were expressed by the dynamics of immigration and emigration of plant species in a community. In years 4 and 5, IGDS maintained a dynamic balance (from 1.0 to 1.1). The community stability was worse. The vertical structure of the community always had two layers (tree and herb) from years 1 to 5. From years 3 to 5, the index of species richness mainly remained 1, and the change of VCS mainly remained within 0.688-0.710. It was indicated that in years 1 to 2, the species component changed significantly. However, in later years, the species component changed slightly with the promoted soil properties.

http://www.aloki.hu ● ISSN 1589 1623 (Print) ● ISSN 1785 0037 (Online)
DOI: http://dx.doi.org/10.15666/aeer/1705_1158711604

Soil physicochemical properties

In previous research (Hao et al., 2015), overall, SM (from 4.095 to 2.860%) and SD (1.603 to 1.243 g/cm^3) decreased with recovery age due partly to the worse water retaining capacity of the mine soil. Partly because the weathering of coal gangue strengthened gradually, STP, STOC, SOM, TN, AP, and AK increased (Sena et al., 2015). In addition, SFC deceased (from 21.2% to 20.2%) in years 1 to 3 but increased (21.5%) in later years. POC contents decreased in year 2 and were 0.011-0.012 g/kg in later years. The soil was alkaline due to aluminum ion exchanged through the weathering of coal gangue; pH values ranged from 8.50 to 8.03 and decreased with recovery age due to aluminum ion loss by rainfall. Significant differences of soil properties were shown between year 5 of recovery and the reference site ($P < 0.05$) (Hao et al., 2015).

Correlation between plant and soil

During the early stage of ecological restoration in the coal gangue pile, significantly negative correlation was shown between ADT and SM content ($P < 0.05$) (*Table 2*). CHL was significantly negatively correlated ($P < 0.05$) with SD. ISD was significantly positively correlated with POC ($P < 0.05$). IGDS was significantly negatively correlated with STP ($P < 0.05$).

Table 2. *Correlation between basic plant community characteristics and soil properties*

Parameter	ADT	CHL	CC	ISD	IGDS
SM	-0.921*	-	-	-	-
SD	-	-0.822*	-	-	-
STP	-	-	-	-	-0.812*
STOC	0.940*	0.903*	0.875*	-	-
ROOC	0.938*	0.930**	0.903*	-	-
POC	-	-	-	0.850*	-
pH	-.923*	-0.852*	-0.814*	-	-
AP	0.916*	0.852*	0.832*	-	-
AK	0.951*	0.974**	0.970**	-	-

The average DBH of trees (ADT), coverage of the herb layer (CHL), coverage of the community (CC), index of species diversity (ISD), the index of the growth and decline of species (IGDS), soil moisture (SM), soil density (SD), soil total porosity (STP), soil total organic carbon (STOC), readily oxidized organic carbon (ROOC), particulate organic carbon (POC), soil pH (pH), available phosphorus (AP) and available potassium (AK)
Note:* Correlation is significant at the 0.05 level (2-tailed). ** Correlation is significant at the 0.01 level (2-tailed).

Ecological restoration status index (ERSI)

Through principal component analysis, eigenvalues were above 1.0 in the first four principal components (PCs) (*Table 3*). Significant positive correlations were shown between principal component-1 (PC-1) and STOC, ROOC, TN, and AP (*Fig. 2*). The significant negative correlation was shown between PC-1 and pH. STOC and ROOC, pH and TN were significant positively ($P < 0.01$) and negatively ($P < 0.05$) correlated,

http://www.aloki.hu ● ISSN 1589 1623 (Print) ● ISSN 1785 0037 (Online)
DOI: http://dx.doi.org/10.15666/aeer/1705_1158711604

respectively. It was indicated that PC-1 represented the soil chemical properties. Under PC-2, ADT was highly weighted. ISD was highly weighted in PC-3. TBHL and SOM were highly weighted in PC-4. Given adequate time, the rich herb biomass can supply SOM. However, in this research, neither parameter showed significant correlation due to the limit of the recovery age (only five years). The percentage of cumulative explanation was 97.6% by nine parameters (ADT, TBHL, ISD, SOM, STOC, ROOC, pH, TN, AP). Thus, the nine parameters would be used to derive ERSI.

The parameters of *Equation 7* are presented in *Table 4*. ERSI in every year is as follows (*Eq. 8*):

$$ERSI = \sum_{i=1}^{n} W_i S_i \ (n = 9) = W_1 \times S_1 + W_2 \times S_2 + W_3 \times S_3 + W_4 \times S_4 + W_5 \times S_5 + W_6 \times S_6 + W_7 \times S_7 + W_8 \times S_8 + W_9 \times S_9 = 0.13270 \times S_1 + 0.13270 \times S_2 + 0.13270 \times S_3 + 0.13270 \times S_4 + 0.26540 \times S_5 + 0.10060 \times S_6 + 0.05379 \times S_7 + 0.02470 \times S_8 + 0.02470 \times S_9 \quad \text{(Eq.8)}$$

Table 3. *Total explaining variances of ecological restoration status in restored coal gangue pile*

Component	Initial eigenvalues			Extraction sums of squared loadings		
	Total	Variance %	Cumulative %	Total	Variance %	Cumulative %
1	13.984	58.269	58.269	13.984	58.269	58.269
2	5.301	22.086	80.354	5.301	22.086	80.354
3	2.834	11.810	92.164	2.834	11.810	92.164
4	1.301	5.422	97.587	1.301	5.422	97.587
5	.579	2.413	100.000			
6	2.693E-15	1.122E-14	100.000			
7	1.429E-15	5.953E-15	100.000			
8	1.045E-15	4.353E-15	100.000			
9	4.972E-16	2.072E-15	100.000			
10	3.766E-16	1.569E-15	100.000			
11	3.218E-16	1.341E-15	100.000			
12	2.446E-16	1.019E-15	100.000			
13	1.874E-16	7.807E-16	100.000			
14	2.787E-17	1.161E-16	100.000			
15	6.636E-18	2.765E-17	100.000			
16	-6.925E-17	-2.885E-16	100.000			
17	-1.408E-16	-5.866E-16	100.000			
18	-1.929E-16	-8.039E-16	100.000			
19	-2.460E-16	-1.025E-15	100.000			
20	-2.949E-16	-1.229E-15	100.000			
21	-3.195E-16	-1.331E-15	100.000			
22	-5.491E-16	-2.288E-15	100.000			
23	-5.760E-16	-2.400E-15	100.000			
24	-7.019E-16	-2.925E-15	100.000			

http://www.aloki.hu ● ISSN 1589 1623 (Print) ● ISSN 1785 0037 (Online)
DOI: http://dx.doi.org/10.15666/aeer/1705_1158711604

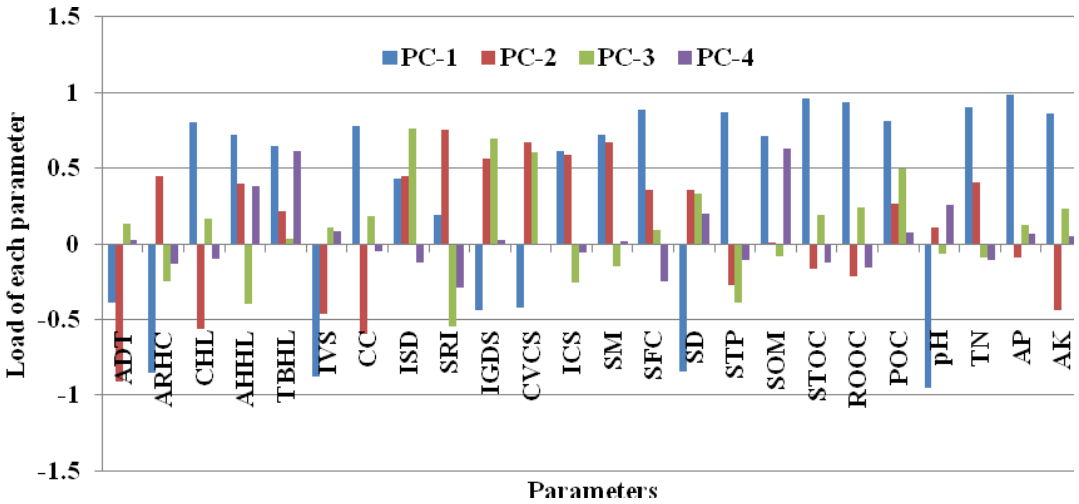

Figure 2. *Load of each parameter on PC-1, PC-2, PC-3 and PC-4, respectively. Abbreviations: The average DBH of trees (ADT), average the ratio height and canopy of trees (ARHC), coverage of the herb layer (CHL), the average height of the herb layer (AHHL), total biomass of the herb layer (TBHL), the integrity of the vertical structure (IVS), coverage of the community (CC), index of species diversity (ISD), the species richness index (SRI), the index of the growth and decline of species (IGDS), change of value of community similarity (CVCS), the index of community stability (ICS), soil moisture (SM), soil field capacity (SFC), soil density (SD), soil total porosity (STP), soil organic matter (SOM), soil total organic carbon (STOC), readily oxidized organic carbon (ROOC), particulate organic carbon (POC), soil pH (pH), total nitrogen (TN), available phosphorus (AP) and available potassium (AK)*

Table 4. *The values of parameters in Equation 7 for ecological restoration status in restored coal gangue pile*

Parameters	i	Rang	Type	b	Mean (x_{i0})
STOC	1	5.979-20.021	More is better	-2.5	12.437
ROOC	2	0.011-0.037	More is better	-2.5	0.024
pH	3	7.80-8.50	Less is better	2.5	8.230
TN	4	0.042-1.016	More is better	-2.5	0.230
AP	5	3.850-8.300	More is better	-2.5	5.815
ADT	6	4.89-11.85	More is better	-2.5	7.08
ISD	7	2.535-2.902	More is better	-2.5	2.728
TBHL	8	390.50-621.08	More is better	-2.5	499.55
SOM	9	23.440-46.360	More is better	-2.5	33.125

Soil total organic carbon (STOC), readily oxidized organic carbon (ROOC), soil pH (pH), total nitrogen (TN), available phosphorus (AP), the average DBH of trees (ADT), index of species diversity (ISD), total biomass of the herb layer (TBHL) and soil organic matter (SOM)
The value range: The value range of each parameter is from the minimum to maximum real values

Using the PCA, the contribution of each ecological restoration status parameter to the calculated ERSI in every year is shown in *Figure 3*. Comparing to other parameters, the contribution of AP was largest in every year and was 0.10, 0.07, 0.14, 0.13 and 0.14, respectively. The contribution of pH ranged from 0.06 to 0.07. The contributions of STOC and ROOC increased with recovery age (from 0.02 in year 2 to 0.08 in year 5).

http://www.aloki.hu ● ISSN 1589 1623 (Print) ● ISSN 1785 0037 (Online)
DOI: http://dx.doi.org/10.15666/aeer/1705_1158711604

The first year was taken as the benchmark year. The ERSI value (0.25) was lower in year 2 of recovery than that in the benchmark year. ERSI then increased from 0.45 in year 3 to 0.53 in year 5, more than that in the benchmark year. A significant difference was shown between year 5 and the other years ($P < 0.05$). ERSI of the reference site was the highest (0.65) in *Figure 3*. A significant difference was shown between the reference site and other years ($P < 0.05$). It was indicated that the ecological restoration status of the restored site would take more time to reach the level of the reference site. A quadratic curve ($R^2 = 0.7892$) between ERSI and recovery age is shown in *Figure 4*. Overall, ERSI increased with recovery age during the early stage of recovery (the first five years) (*Fig. 5*).

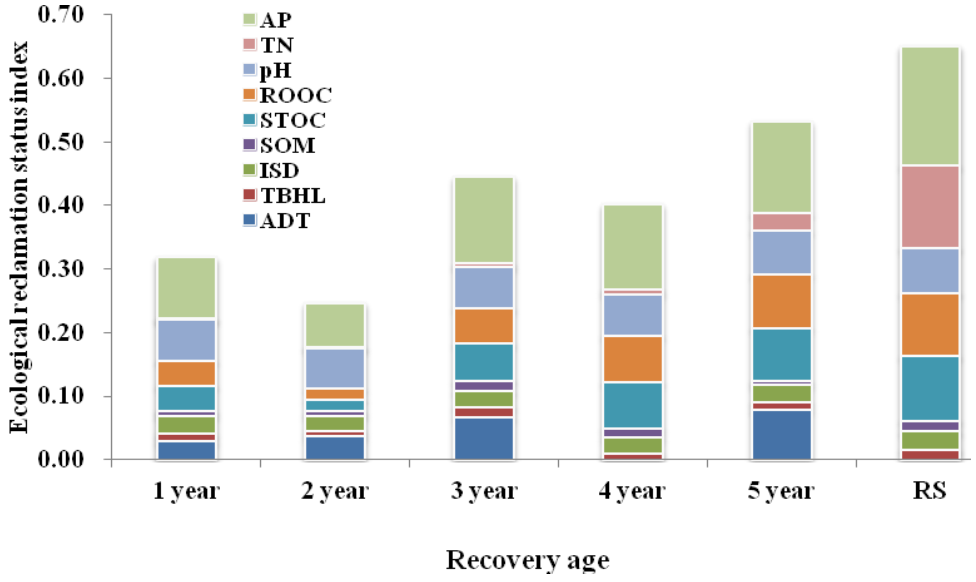

Figure 3. *Contribution of each parameter on calculated ERSI. Abbreviations: Soil organic matter (SOM), soil total organic carbon (STOC), readily oxidized organic carbon (ROOC), soil pH (pH), total nitrogen (TN), available phosphorus (AP), average DBH of trees (ADT), index of species diversity (ISD) and total biomass of the herb layer (TBHL). Reference site (RS)*

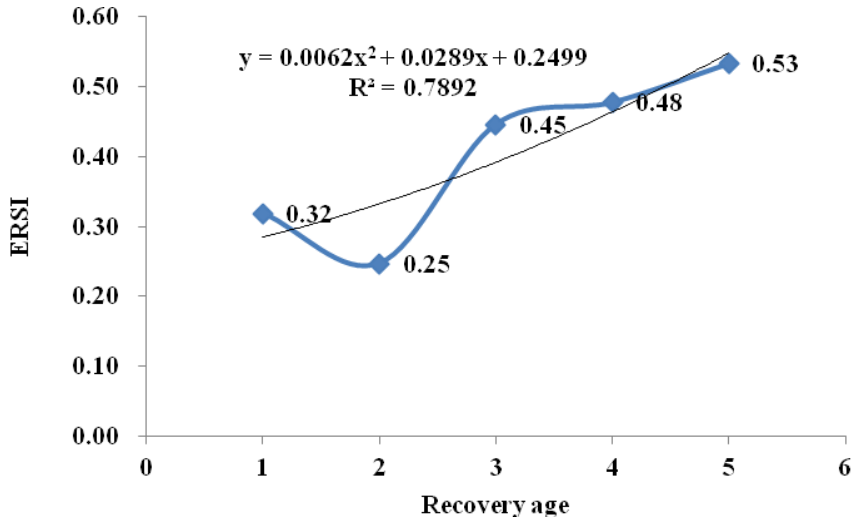

Figure 4. *Correlation between recovery age and ERSI*

http://www.aloki.hu ● ISSN 1589 1623 (Print) ● ISSN 1785 0037 (Online)
DOI: http://dx.doi.org/10.15666/aeer/1705_1158711604

Figure 5. *Ecological restoration in every recovery year and RS. Reference site (RS)*

Uncertainty analysis of the ERSI by MCS

To analyze the uncertainty of the ERSI, the study introduced MCS. Based on the distribution function, mean and standard deviation of each parameter in every recovery age in *Table 5*, 10000 simulations were carried out. 10000 random values of each parameter were generated in every stage. Then based on the *Equation 8,* 10000 simulations of ERSI were conducted in every stage (*Table 6*). The uncertainty in 2 year was maximum (± 4.00%), the largest uncertainty contribution came from the SOM (*Table 5*). In later years of recovery, the uncertainty became lower. The uncertainty in 5 year was minimum (± 1.89%). In RS, the uncertainty was ± 3.08%.

Table 5. *Distributions, means and standard deviations of the parameters in the estimation of ERSI using the MCS*

Parameter	Distribution	1 year		2 year		3 year		4 year		5 year		RS	
		Mean	Standard deviation	Mean	Standard deviation	Mean	Standard deviation	Mean	Standard deviation	Mean	Standard deviation	Mean	Standard deviation
STOC	Normal	8.74	0.4704	5.98	0.9426	11.27	0.8169	13.37	0.9428	15.25	0.0008	20.02	2.2314
ROOC	Normal	0.01	0.0014	0.01	0.0008	0.01	0.0022	0.01	0.0009	0.01	0.0005	0.02	0.0024
pH	Normal	8.46	0.0812	8.50	0.1227	8.35	0.0821	8.24	0.1513	8.03	0.0476	7.80	0.1071
TN	Normal	0.05	0.0087	0.04	0.0087	0.07	0.0062	0.08	0.0083	0.14	0.0291	0.86	0.0212
AP	Normal	4.64	0.0801	3.85	0.0962	5.97	0.1235	5.87	0.0952	6.26	0.0423	8.30	0.1742
ADT	Logistic	4.89	0.4125	5.63	0.5472	9.29	1.5489	10.80	2.2351	11.85	3.1470	-	-
ISD	Normal	2.90	0.0532	2.54	0.0470	2.62	0.0748	2.74	0.0750	2.69	0.0936	2.88	0.0576
TBHL	Logistic	482.51	1.6778	398.14	0.8990	621.08	3.4943	390.50	2.0306	484.95	1.2511	620.13	2.4446
SOM	Normal	15.20	0.8870	10.31	1.0221	19.24	0.4876	23.46	1.2110	25.37	1.2871	36.90	0.7151

Soil total organic carbon (STOC), readily oxidized organic carbon (ROOC), soil pH (pH), total nitrogen (TN), available phosphorus (AP), the average DBH of trees (ADT), index of species diversity (ISD), total biomass of the herb layer (TBHL) and soil organic matter (SOM). Reference site (RS)

http://www.aloki.hu ● ISSN 1589 1623 (Print) ● ISSN 1785 0037 (Online)
DOI: http://dx.doi.org/10.15666/aeer/1705_1158711604

Table 6. *The ERSI in each recovery age using MCS*

Recovery age	Mean	Uncertainty/%	95% Coverage interval
1 year	0.32	± 3.13	0.28-0.36
2 year	0.25	± 4.00	0.20-0.29
3 year	0.45	± 2.22	0.40-0.48
4 year	0.48	± 2.08	0.43-0.51
5 year	0.53	± 1.89	0.49-0.59
RS	0.65	± 3.08	0.54-0.69

Uncertainty: the standard deviation of ERSI value from MCS divided by the arithmetic mean of it. Reference site (RS)

During the different period, the sensitivity of each parameter to ERSI was different (*Fig. 6*). In years 1 and 2 of recovery, STOC was main influencing factor to ERSI, the sensitivity coefficient of STOC was 0.570 and 0.402, respectively. In years 3 and 4 of recovery, ROOC was main influencing factor to ERSI, the sensitivity coefficient of ROOC was 0.516 and 0.573, respectively. The sensitivity coefficient of TN was highest (0.684) in year 5. SOM (0.449) was the most sensitivity factor in RS. It was indicated that at the early stage of recovery, STOC, ROOC and TN played important roles in improving ecological restoration status in coal gangue pile. With the restored area becoming near-nature in adequate time, SOM will play an important role in ecological restoration. It was suggested reasonably supplying STOC, ROOC and TN content will promote ecological restoration process at early stage of recovery.

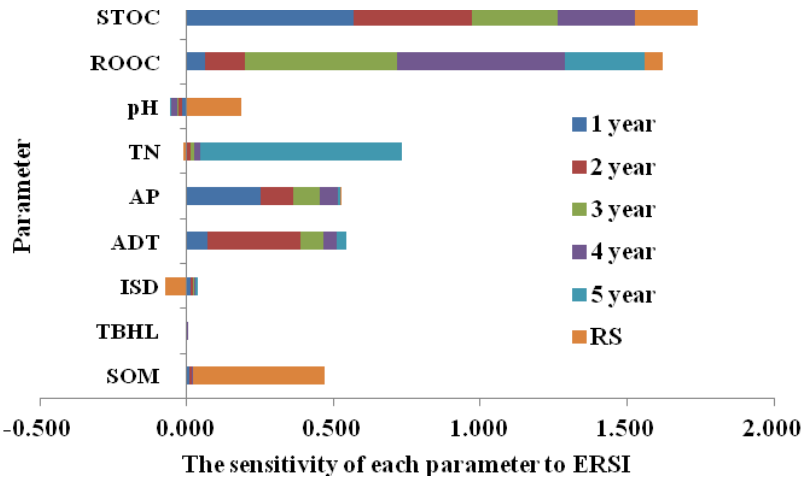

Figure 6. *The sensitivity of each parameter to ERSI. Abbreviations: Soil organic matter (SOM), soil total organic carbon (STOC), readily oxidized organic carbon (ROOC), soil pH (pH), total nitrogen (TN), available phosphorus (AP), average DBH of trees (ADT), index of species diversity (ISD) and total biomass of the herb layer (TBHL). Reference site (RS)*

Discussion

Correlation between plant and soil

During the early stage of ecological restoration in the coal gangue pile, significantly negative correlation was shown between ADT and SM content because the growth of

http://www.aloki.hu ● ISSN 1589 1623 (Print) ● ISSN 1785 0037 (Online)
DOI: http://dx.doi.org/10.15666/aeer/1705_1158711604

Populus tomentosa consumed more soil moisture. CHL was significantly negatively correlated with SD because herbal roots and litters improved soil porosity. With increasing ADT, CHL and CC, STOC, ROOC, AP and AK increased significantly due partly to heavy litters falling from trees (*Populus tomentosa*), and herbs decomposed to improve the soil organic carbon, phosphorus and potassium (Sorenson et al., 2011; Mukhopadhyay et al., 2016). It was indicated that *Populus tomentosa* can be the pioneer species to achieve quick recovery in mining areas (Li and Liber, 2017). ISD was significantly positively correlated with POC, which is probably because dead species bodies improved the POC content (Hao et al., 2015). IGDS was significantly negatively correlated with STP. This was probably because in the benchmark year (year 1), the plant species was the net immigration species, the penetration of plant roots was limited, and STP was low. In the later years, immigration and emigration of species maintained the dynamic balance, IGDS was 1.0-1.1, and STP increased with increasing penetration strength of plant roots (Mukhopadhyay et al., 2016). Lower SM content, better gas porosity and permeability, rich STOC, AP and AK were beneficial to the biomass accumulation of *Leymus chinensis* and *Setaria viridis*. Increasing SOM, POC, AP and AK caused an adverse effect on the biomass accumulation of *Artemisia lavandulaefolia* and *Melilotus officinalis*. In turn, the accumulation of herb biomass also supplied SOM content in adequate time. Leguminous plants, such as *Melilotus officinalis,* immigrated and fixed nitrogen to increase TN content (Hao et al., 2015).

Ecological restoration status index (ERSI)

The parameters system of evaluation comprised six parameters of soil chemical properties and three parameters of basic plant community characteristics. It was suggested that soil chemical properties play a very important role in mine ecological restoration status. The growth of a plant community depends on improved soil chemical properties, such as rich soil nitrogen and organic matter. In turn, the nitrogen fixing capacities of leguminous plants increase TN content. The biomass of plants supplies organic matter to the soil. The basic characteristics of plant community in the restored area as the important parameters that should be included in the ecological evaluation of the recovery status. Mukhopadhyay et al. (2014) also determined six soil parameters, but they were soil physical (2, number of parameters), chemical (2) and biological (2) parameters. Only STOC was a common parameter. The difference of initial parameters resulted in the differences of the other five parameters in both experiments.

Although ADT increased, the total declining content of AP, ROOC, STOC, ISD and TBHL were greater than the increasing content. AP, ROOC and STOC supported rich plant species during the first year. In turn, ISD and TBHL decreased due to the number of species decreasing in year 2 of recovery. A lower score also existed in year 2 of restoration in Mukhopadhyay et al. (2014). It was suggested that the ecological restoration status in year 2 was lower than that in the benchmark year. Trees and herbs grew rapidly with recovery age. Species diversity and community stability were enhanced gradually. Nitrogen fixation of leguminous plants, such as *Melilotus officinalis,* increased TN content. The total organic carbon increased with the accumulation of vegetation litter and biomass. Moreover, plant roots enriched SOM in the rhizosphere (Montiel-Rozas et al., 2015). AP content also increased from gradual weathering. In turn, the biomass of the herb layer also increased based on the increasing species diversity and soil nutrition with recovery age (Lv and Zheng, 2009). It was suggested that the ecological restoration status in years 3 to 5 was better than that in the

http://www.aloki.hu ● ISSN 1589 1623 (Print) ● ISSN 1785 0037 (Online)
DOI: http://dx.doi.org/10.15666/aeer/1705_1158711604

benchmark year. In Mukhopadhyay et al. (2014), the mine soil quality index (MSQI) reflected the soil properties. In this research, ERSI reflected the results of the interaction between the mine soil and plant community. Their interaction revealed the internal cause of development in mine ecological restoration status.

This time for disturbed mine soil could be at least 20 years based on proper restoration strategy, as reported by Anderson et al. (2008). Orozco-Aceves et al. (2017) suggested that in 22 years, soil physicochemical and key biological properties after restoration still were not recovered to the conditions of the reference soil. In addition, if the restoration method is unsuitable, the restored mining site may remain polluted even 30 years later (Gomez-Ros et al., 2013). The restoration statuses are different in different study sites, climate and restoration methods, etc. However, the reference site was not the final recovery goal. For example, the reference site (natural secondary community) was not the optimal recovery goal in Li (2010). With increasing recovery age, the ecological restoration status in the coal gangue pile would be better than at the reference site (Hao et al., 2016).

We found that a quadratic curve is showed between ERSI and recovery age. It was reported that a positive liner correlation was shown between the mine soil quality index and recovery age (Mukhopadhyay et al., 2014). The different type of correlation might result from the differences of the parameter system and study site. Overall, ERSI increased with recovery age during the early stage of recovery (the first five years). It was indicated that ecological restoration status had a promoted trend during the early stage of recovery (Orozco-Aceves et al., 2017; Mukhopadhyay et al., 2014). This suggested that the functions of the plant-soil system gradually improved with recovery age. However, Li (2010) found that the evaluation result of the ecological restoration status was as follows: year 5 > year 4 > year 3 > reference site > year 1 > year 2. The conclusion was different from this study. The causes of this difference were the differences of artificial planting species and the parameter system. For example, in Li (2010), the dominant species of the tree layer was *Crataegus pinnatifida*, and the parameter system involved soil heavy metal content. In the present research, the dominant species of the tree layer was *Populus tomentosa*, and soil heavy metal content was uninvolved in the parameter system.

Ecological restoration and natural succession are dynamic processes. At present, artificial vs. natural recovery is controversial for the restoration of coal gangue piles (Woziwoda and Kopec, 2014). This study suggested that artificial recovery (establishing trees) in the first year of recovery, followed by natural herbal recovery in later years, could achieve quick ecological restoration during the early stage of recovery in the mining area. It was suggested that a rapid recovery process could be achieved by reasonable artificial imitation or appropriate interference (Burton et al., 2006; Mudrák et al., 2016). However, it is noteworthy that if invasive alien species are planted in the process of artificial restoration in the mining area, the opposite effect may occur (Holl, 2002). Thus, considering the magnitude of the problem and developing each restoration method are essential steps to evaluate the status of ecological restoration at restored sites (Gomez-Ros et al., 2013).

ERSI was developed based on the plant-soil system of a restored coal gangue pile in the first five years of recovery. The first year was taken as the benchmark year. By comparing the ERSI value in every year of recovery to that in the benchmark year, the ecological restoration status was evaluated. Long-term monitoring the plant-soil system

http://www.aloki.hu ● ISSN 1589 1623 (Print) ● ISSN 1785 0037 (Online)
DOI: http://dx.doi.org/10.15666/aeer/1705_1158711604

will be the focus of further research. ERSI could play a positive demonstration and radiation role in the future evaluation of ecological restoration status in mining areas.

Conclusions

The parameter system for evaluation of ecological restoration status in restored coal gangue piles was established on the basic plant community characteristics and soil physicochemical properties. Principal component analysis (PCA) was employed to derive an ecological restoration status index (ERSI). ERSI was developed based on the parameter system of the plant-soil system in a restored coal gangue pile during the early stage of recovery (the first five years of recovery). The first year was taken as the benchmark year. By comparing the ERSI value in every year of recovery to that in the benchmark year, the ecological restoration status was evaluated. Except for year 2, the ecological restoration status in years 3 to 5 of recovery and the reference site were better than that in the benchmark year. ERSI reflected the results of the interaction between the mine soil and plant community. Overall, ERSI increased with recovery age during the early stage of recovery.

With recovery age, the uncertainty of ERSI showed decreased trend by MCS, and the sensitivity of each parameter to ERSI was different. At the early stage of recovery, STOC, ROOC and TN played important roles in improving ecological restoration status in coal gangue pile.

Acknowledgments. This work was supported by the Project of Tianjin Science and Technology Planning of China (grant no. 18ZXSZSF00200), the Research and Development Project by Lu'an Mining Group Limited Liability Company of China (grant no. 1103100301), and the Technology Special Commissioner Project of Tianjin Natural Science Fund of China (grant no. 16JCTPJC53900). The authors thank all the assistors for their kind help.

Conflict of interests. The authors declare that they have no conflict of interests.

REFERENCES

[1] Ahirwal, J., Maiti, S. K., Reddy, M. S. (2017): Development of carbon, nitrogen and phosphate stocks of reclaimed coal mine soil within 8 years after forestation with Prosopis juli ora (Sw.) Dc. – Catena 156: 42-50.

[2] Alvey, S., Yang, C. H., Buerkert, A., Crowley, D. E. (2003): Cereal/legume rotation effects on rhizosphere bacterial community structure in West African soils. – Biology and Fertility of Soils 37: 73-82.

[3] Anawar, H. M., Hossain, M., Canha, N., Santa-Regina, I., Freitas, M. C. (2013): Adaptation, tolerance, and evolution of plant species in a pyrite mine in response to contamination level and properties of mine tailings: sustainable rehabilitation. – Journal of Soils and Sediments 13: 730-741.

[4] Anderson, J. D., Ingram, L. J., Stahl, P. D. (2008): Influence of reclamation management practices on microbial biomass carbon and soil organic carbon accumulation in semiarid mine lands of Wyoming. – Applied Soil Ecology 40: 387-397.

[5] Bodlák, L., Křováková, K., Nedbal, V., Pechar, L. (2012): Assessment of landscape functionality changes as one aspect of reclamation quality - the case of Velká podkrušnohorská dump, Czech Republic. – Ecological Engineering 43: 19-25.

http://www.aloki.hu ● ISSN 1589 1623 (Print) ● ISSN 1785 0037 (Online)
DOI: http://dx.doi.org/10.15666/aeer/1705_1158711604

[6] Bouzon, M., Govindan, K., Rodriguez, C. M. T., Campos, L. M. S. (2016): Identification and analysis of reverse logistics barriers using fuzzy Delphi method and AHP. – Resources Conservation and Recycling 108: 182-197.
[7] Burton, C. M., Burton, P. J., Hebda, R., Tumer, N. J. (2006): Determining the optimal sowing density for mixture of native plants used to revegetate degraded ecosystems. – Restoration Ecology 14: 379-390.
[8] Elgersma, A. M. (1998): Primary forest succession on poor sandy soils as related to site factors. – Biodiversity and Conservation 7: 193-206.
[9] Godron, M. (1972): Some aspects of heterogeneity in grasslands of Cantal. – Statistical Ecology 3: 397-415.
[10] Gomez-Ros, J. M., Garcia, G., Penas, J. M. (2013): Assessment of restoration success of former mental mining areas after 30 years in a highly polluted Mediterranean mining area: Gartagena-La Union. – Ecological Engineering 57: 393-402.
[11] Hao, J., Guo, D. G., Shangguan, T. L., Zhang, J., Liu, W. H., Zhang, P. P. (2015): Changes in soil factors at early stage of spontaneous herbal recovery in a Coal Gangue Yard. – Bangladesh Journal of Botany 44(5): 689-697.
[12] Hao, J., Guo, D. G., Shangguan, T. L., Liu, W. H., Zhang, J., Zhang, P. P. (2016): Ecological performance assessment on early plant reclamation in coal gangue yard. – Acta Ecologica Sinica 36: 1946-1958.
[13] Holl, K. D. (2002): Long-term vegetation recovery on reclaimed coal surface mines in the eastern USA. – Journal of Applied Ecology 39: 960-970.
[14] Krumins, J. A., Goodey, N. M., Gallagher, F. (2015): Plant-soil interactions in metal contaminated soils. – Soil Biology & Biochemistry 80: 224-231.
[15] Li, J. F. (2010): Study on Quality assessment of ecological restoration in mine Derelict land in Beijing. – Doctorate Dissertation, Beijing Forestry University, Beijing.
[16] Li, S. Q., Liber, K. (2017): Influence of different revegetation choices on plant community and soil development nine years after initial planting on a reclaimed coal gob pile in the Shanxi mining area, China. – Science of the Total Environment. https://doi.org/10.1016/j.scitotenv.2017.09.252.
[17] Licina, V., Aksic, M. F., Colic, S., Zec, G. (2013): A bioassessment of soil nickel genotoxic effect in orchard planted on rehabilitated coalmine overburden. – Ecotoxicology and Environmental Safety 98: 374-382.
[18] Liu, Y. G. (2011): Evaluation of artificial restoration effect of the abandoned mines in Beijing. – Doctorate Dissertation. Beijing Forestry University, Beijing.
[19] Lv, C. H., Zheng, F. L. (2009): Evaluation of soil quality during vegetation restoration in the Ziwuling Area of Loess Plateau. – Science of Soil and Water Conservation 7: 12-18.
[20] Mark, T., David, M., Patrick, A. (2012): Recent advances in restoration ecology: Examining the modern Australian agro-ecological and post-mining landscapes. – Agriculture Ecosystems & Environment 163: 1-2.
[21] Montiel-Rozas, M. M., Madejón, E., Madejón, P. (2015): Evaluation of phytostabilizer ability of three ruderal plants in mining soils restored by application of organic amendments. – Ecological Engineering 83: 431-436.
[22] Mudrák, O., Doležal, J., Frouz, J. (2016): Initial species composition predicts the progress in the sonptaneous succession on post-mining sites. – Ecological Engineering 95: 665-670.
[23] Mukhopadhyay, S., Maiti. S. K., Masto, R. E. (2014): Development of mine soil quality index (MSQI) for evaluation of reclamation success: a chronosequence study. – Ecological Engineering 71: 10-20.
[24] Mukhopadhyay, S., Masto, R. E., Yadav, A., George, J., Ram, L. C., Shukla, S. P. (2016): Soil quality index for evaluation of reclaimed coal mine spoil. – Science of the Total Environment 542: 540-550.

http://www.aloki.hu ● ISSN 1589 1623 (Print) ● ISSN 1785 0037 (Online)
DOI: http://dx.doi.org/10.15666/aeer/1705_1158711604

[25] Orozco-Aceves, M., Tibbett, M., Standish, R. J. (2017): Correlation between soil development and native plant growth in forest restoration after surface mining. – Ecological Engineering 106: 209-218.
[26] Ott, T., Van Aarde R. J. (2014): Coastal dune topography as a determinant of abiotic conditions and biological community restoration in northern KwaZulu-Natal, South Africa. – Landscape & Ecological Engineering Official 10: 17-28.
[27] Parraga-Aguado, I., Gonzalez-Alcaraz, M. N., Alvarez-Rogel, J., Jimenez-Carceles, F. J., Conesa, H. M. (2013): The importance of edaphic niches and pioneer plant species succession for the phytomanagement of mine tailings. – Environmental Pollution 176: 134-143.
[28] Pietrzykowski, M., Chodak, M. (2014): Near infrared spectroscopy-A tool for chemical properties and organic matter assessment of afforested mine soils. – Ecological Engineering 62: 115-122.
[29] Rossini-Oliva, S., Mingorance, M. D., Monaci, F., Valdés, B. (2016): Ecophysiological indicators of native *Cistus ladanifer* L. at Riotinto mine tailings (SW Spain) for assessing its potential use for rehabilitation. – Ecological Engineering 91: 93-100.
[30] Sena, K., Barton, C., Hall, S., Angel, P., Agouridis, C., Warner, R. (2015): Influence of spoil type on afforestation success and natural vegetative recolonization on a surface coal mine in Appalachia, United States. – Restoration Ecology 23: 131-138.
[31] Sorenson, P. T., Quideau, S. A., Mackenzie, M. D., Landhäusser, S. M., Oh, S. W. (2011): Forest floor development and biochemical properties in reconstructed boreal forest soils. – Applied Soil Ecology 49: 139-147.
[32] Su, M. (2010): Test study on soil nutrient cycling of coal mining subsidence area and its impact on the ecological environment. – Master Dissertation. Hebei University of Engineering, Handan.
[33] Tripathi, N., Singh, R. S., Hills, C. D. (2016): Soil carbon development in rejuvenated Indian coal mine spoil. – Ecological Engineering 90: 482-490.
[34] Woziwoda, B., Kopec, D. (2014): Afforestation or natural succession? Looking for the best way to manage abandoned cut-over peatlands for biodiversity conservation. – Ecological Engineering 63: 143-152.
[35] Xie, Y. G., Che, J. X., Sun, W. B., Peng, X. (2012): Comparison study of mining subsidence years on soil physical properties of in mining area. – Research of Soil & Water Conservation 19(4): 26-29.
[36] Yao, G. Z., Yang, T. T. (2014): Research on ecological evaluation system of environment governance in mining area. – Western Resources 2: 173-175.
[37] Zeng, Y. H., Liu, L. M., Zhang, H., Do, D. D., Nicholson, D. (2018): A Monte Carlo study of adsorption-induced deformation in wedge-shaped graphitic micropores. – Chemical Engineering Journal 346: 672-681.
[38] Zhang, C. X., Xu, L., Zhou, X. D. (2007): Land suitability assessment f vegetation restoration of the coal gangue pile of Fuxin mine area. – Research of Soil & Water Conservation 14: 246-248.
[39] Zhang, X. W. (2006): Researches on the succession order of the soil and vegetation in the abandoned field of the mining area in the semi-arid region. – Master Dissertation. Liaoning Technical University, Fuxin.
[40] Zhao, X. W., Jia, S. H., Li, M., Liu, Y., Su, T. C. (2014): Soil quality assessment by TOPSIS method based on PCA in the afforested coal gangue area. – Journal of Northeast Forestry University 2: 98-102.

http://www.aloki.hu ● ISSN 1589 1623 (Print) ● ISSN 1785 0037 (Online)
DOI: http://dx.doi.org/10.15666/aeer/1705_1158711604

STUDY ON A SINGLE INTERPOLATION FUSION ALGORITHM FOR MULTISOURCE REMOTE SENSING DATA OF SOIL MOISTURE

YU, J. S.[1] – CHEN, J. P.[1#] – LI, X. J.[2#] – LIU, Y. M.[1#] – YAO, X. L.[1,2*]

[1]*College of Water Sciences, Beijing Normal University, No. 19 Xinjiekouwai Street, Beijing 100875, China*

[2]*College of Resource Environment and Tourism, Capital Normal University, No. 105 XiSanhuan North Road, Beijing 100048, China*

[#]*These authors contributed equally to this work*

**Corresponding author*
e-mail: yaoxiaolei87@163.com; phone: +86-10-6225-1121

(Received 22nd Apr 2019; accepted 12th Jul 2019)

Abstract. Remote sensing of soil moisture can provide important data for monitoring large-scale agricultural drought. Due to differences between the various sensors and inversion methods, remote sensing data from different sources are unsuitable for direct comparison and analysis. Data fusion has become an area of active research regarding the application of remote sensing data. Based on the principle of cumulative distribution function matching, this study proposed a continuous relationship establishment algorithm for multisource remote sensing soil moisture data. Using this new algorithm, soil Moisture and Ocean Salinity (SMOS) and Climate Change Initiative (CCI) satellite data from the Songnen Plain as test data were fused to a long time series product of real-time remote sensing soil moisture data. This application validation of this new method to SMOS and CCI indicated that this Lagrange interpolation continuous fusion algorithm could improve the fusion accuracy of multisource remote sensing soil moisture data significantly. The low-value region of the cumulative probability distribution curve is a crucial data segment for characterization of agricultural drought. Through implementation of the proposed continuous fusion algorithm, fused SMOS and CCI data were found to have high coincidence at each quantile in the low-value region of the curve.
Keywords: *agricultural drought, continuous fusion, Songnen Plain, SMOS, CCI*

Introduction

Remote sensing of soil moisture has been used in simulation, monitoring and analysis of drought characteristics (Atlas, 1993; Su, 2003; Sheffield and Wood, 2007; Bolten et al., 2010). It is effective for quickly detecting change in large-scale agricultural droughts. However, such remote sensing data can have different spatial and temporal resolutions and various time series lengths due to the variety of platforms, sensors and inversion methods available. Satellite data of the same terrestrial object released by different sources cannot be used directly for continuous analysis and the absolute value cannot be compared directly. To overcome this problem, remote sensing data fusion is proposed as an effective means of integrating multisource satellite-derived ground object information (Schmitt and Zhu, 2007, 2016).

Data fusion is defined as a multilevel integration process for detection, association, analysis and a combination of sensors designed to produce a single signal of higher quality and reliability (Waltz and Llinas, 1990; Sportouche et al., 2011; Li et al., 1995). Due to the resource complementarity of multiple sensors, multisource fusion can

http://www.aloki.hu ● ISSN 1589 1623 (Print) ● ISSN 1785 0037 (Online)
DOI: http://dx.doi.org/10.15666/aeer/1705_1160511617

provide information that is more comprehensive than obtained from a single sensor (Khaleghi, 2013). The data fusion principle is the cumulative distribution function (CDF) matching method. The CDF principle was first proposed by Calheiros in 1987 (2010), and it has since been used for the correction of radar remote sensing precipitation data (Atlas et al., 1990; Anagnostou et al., 2010). In recent years, this CDF matching principle is widely used to reduce the systematic biases between the original data and the reference data by rescaling the target data to the direction of the reference data (Reichle, 2004; Drusch, 2005; Brocca et al., 2011; Lee and Im, 2015).

In the implementation of the CDF principle based on some reliable data, the fusion of remote sensing data from other sources can be used to improve the spatiotemporal resolution of the data or to extend the length of the data time series. Fused remote sensing data can improve its quality and reliability and enable its maximal utilization (Li et al., 1995). Previous studies that have used this principle to conduct fusion research on different remote sensing data groups have reported reduced remote sensing data bias and improved time series lengths for single data sources (Reichle and Koster, 2004; Liu et al., 2009). Based on this principle, the same basic data can be used to correct the fusion of multiple remote sensing datasets from different sources (Liu et al., 2010). In recent years, this principle has also been applied to the data fusion of multiple remote sensing soil moisture products (Lee et al., 2017). The CDF principle can maintain the original relative change mode of remote sensing data (Liu et al., 2010) and adjust the data scope to be close to the real value, which can improve the accuracy of remote sensing soil moisture data for characterization of surface features. However, the above calculation algorithm of fusion is simplistic and the fusion precision needs to be improved. The piecewise linear regression method is generally used to establish the relationship between the cumulative distribution curves of data from different sources. This method sets the same section for different cumulative distribution curves, and it obtains the linear equation of the two data correlations in that section to realize the fusion of one set of data to the other on the same quantile. The main disadvantage of subsection fusion is that the subsection properties will lead to a certain fitting error of the curve in the subsection, irrespective of the subsection density.

Given the increasing levels of research into remote sensing products and their application, the demands for data in terms of time series length and real-time update speed have increased. Improvement of the accuracy of multisource remote sensing data fusion is one of the most important scientific problems to be overcome in relation to research of remote sensing applications. Based on the CDF matching theory, this study constructed a new continuous fusion algorithm to address the problem of low accuracy in the piecewise linear fusion method, to improve the fusion accuracy in the low-value region of the cumulative probability distribution curve (i.e., this critical stage related to impending or emerging drought). The fusion effect of this proposed algorithm was verified by SMOS and CCI data in the Songnen Plain (Northeast China).

Data and study area

Soil moisture and ocean salinity (SMOS) data

The Soil Moisture and Ocean Salinity (SMOS) satellite designed specifically for monitoring global soil moisture content and ocean salinity. The L-band, which is insensitive to surface roughness and vegetation coverage, is very suitable for soil moisture inversion. The SMOS soil moisture data are obtained using a radiative transfer

http://www.aloki.hu ● ISSN 1589 1623 (Print) ● ISSN 1785 0037 (Online)
DOI: http://dx.doi.org/10.15666/aeer/1705_1160511617

model using luminance temperature data (Calvet et al., 2011; Ramirez-Beltran et al., 2010). Related study has proven that the SMOS soil moisture data has high inversion accuracy and signification advantage over other remote sensing data in areas with high vegetation coverage (Al-Yaari et al., 2014). The daily SMOS Level-3 volumetric ($m^3 m^{-3}$) soil moisture data (January 2010 to March 2016) used in this study were obtained from the expert center in Barcelona, Spain (http://www.smos-bec.icm.csic.es/smos_products). For SMOS data, radio frequency interference (RFI) is revealed to be an important source of noise (Anterrieu, 2011). This dataset discarded some data which do not meet the quality requirement in the processing of RFI. The Level-3 data in this dataset is remapped to an Equal Area Scalable Earth grid of 25 km × 25 km. According to the data analysis, during the main growth stage of crops from April to October, this dataset still has a high coverage in Northeast China. This daily SMOS dataset is a near real-time soil moisture data (delay one day). In the management of agricultural drought resistance, timeliness is important for the evaluation of agricultural drought. But this data cannot be used to perform frequency and evolution analysis due to the short length of the time series.

Climate change initiative (CCI) data

The European Space Agency (ESA) launched the Climate Change Initiative (CCI) program in 2010 to generate a dataset of global soil moisture based on passive, active and fused products (Dorigo et al., 2017). This program was designed to produce complete and consistent global soil moisture dataset by several active and passive remote sensing data. The long time series CCI dataset, which comprises a variety of integrated multisatellite soil moisture products, provides the possibility for long-term dynamic analysis of global soil moisture (Hollmann et al., 2013). This dataset has been widely adopted since its release, and it has been verified and applied in many regions of the world (González-Zamora et al., 2018; Jian et al., 2018; Wang et al., 2018; Siyu et al., 2017). As reprocessing data, real-time drought evaluation cannot be undertaken using this dataset. This study uses daily CCI (version 02.2) volumetric ($m^3 m^{-3}$) combined data (1978-2014) to carry out the algorithm validation. These daily soil moisture products have a grid resolution of 0.25° (Chakravorty et al., 2016).

The fusion calculation algorithm proposed in this study can extent the time series of remote sensing data. And it will have another significant advantage if the new fusion data has the property of near real-time update at the same time. Therefore, in this study CCI data is the basic data in fusion calculation. Through fusion calculation, the real-time update SMOS data has been rescaled to CCI to produce the new fusion data, which has the property of both long time series and real-time update. Before fusion, both SMOS and CCI data have been rescaled to the same spatial and temporal resolution.

Study area

This study verified the proposed continuous algorithm by application to an area of the Songnen Plain (43°36′–49°45′N, 121°27′–128°12′E), which is one of the main bases for grain production in Northeast China (Wang et al., 2004). The Songnen Plain has a temperate semihumid-semiarid continental monsoon climate (Zheng et al., 2015). Mean annual precipitation is 350–600 mm with 70–80% of precipitation occurring in June–September. The typical zonal soils are black soil and chernozem. The Songnen Plain is within the drainage area of the Songhua River. The Second

http://www.aloki.hu ● ISSN 1589 1623 (Print) ● ISSN 1785 0037 (Online)
DOI: http://dx.doi.org/10.15666/aeer/1705_1160511617

Songhua River and the Nen River merge in the center of the area to form the Songhua River. In recent years, mean precipitation on the Songnen Plain has declined and the area has suffered frequent drought disasters, especially in western regions. Due to its flat terrain, simple underlying surface type and wide distribution of farmland, this region is ideal for research on remote sensing evaluation of drought. The elevation of the Songnen Plain is 200– 250 m above sea level. The soil in this region is fertile with vast farmland and few hills. Black soil, meadow soil, dark-brown soil and chernozem are widely distributed in there (Jiang et al., 2016).

Methodology

Data fusion in this study is to rescale one data against another basic data by the relationship obtained from data for the overlapping period. The CDF matching method is the principle of establishing relationship by cumulative distribution curves in data fusion. The calculation error of fusion in the process of establishing the relationship between two curves is very important because it determines the accuracy of the data produced for subsequent application. Currently, the relationship establish algorithm is piecewise linear regression. The relational fitting curve constructed by piecewise might lead to large error in the fusion result. To reduce error and improve fusion accuracy, this study proposed a continuous relationship establish method in fusion of multisource remote sensing soil moisture data based on the CDF principle. By using this new continuous algorithm, the overlapping period (2010-2013) data can be used to establish the relationship between CCI and SMOS in each quantile of the cumulative probability distribution curve. In the absence of CCI soil moisture data, the relationship of each quantile can rescale real-time SMOS to CCI, consequently to produce a new fusion data with the property of long time series and real-time update.

Cumulative distribution function (CDF)

The CDF is the sum of the probabilities that a random variable falls within a certain interval in the sample space, and it is the integral of the probability density function. When plotting the integral distribution function, it is often defined as the integral of the histogram distribution because the real probability distribution function is unknown. The objective of this study is to derive an algorithm by using CDF principle to fuse real-time SMOS data to the benchmark long time series CCI remote sensing soil moisture data. This new algorithm can make the SMOS and CCI data having the similar distribution curves. Subsequently, a set of real-time updated and long-term remote sensing soil moisture data could be synthesized.

The fusion process of soil moisture data can be expressed as follows:

$$cdf_c(x') = cdf_s(x) \quad \text{(Eq.1)}$$

where cdf_c is the CDF of the CCI soil moisture, cdf_s is the CDF of the SMOS soil moisture, x is the soil moisture of the SMOS product and x' is the fused SMOS soil moisture. In fusion computing, the closer the match of the two curves, the better the fusion precision and the effect.

http://www.aloki.hu ● ISSN 1589 1623 (Print) ● ISSN 1785 0037 (Online)
DOI: http://dx.doi.org/10.15666/aeer/1705_1160511617

Piecewise linear algorithm

Piecewise linear regression is the commonly used correlation calculation method in fusion and its calculation process is shown in *Figure 1*. As an example, the cumulative probability distribution curves of the SMOS and CCI datasets were divided into 10 segments: 0%, 10%, 20%, 30%, 40%, 50%, 60%, 70%, 80%, 90% and 100%. The correlation between their respective cumulative probability distribution curves can be obtained based on the linear equation of these two datasets in each segment.

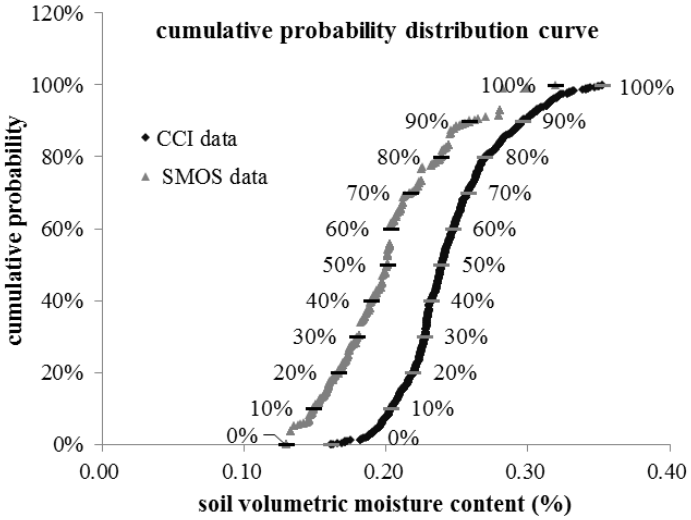

Figure 1. *Schematic of piecewise linear fusion between SMOS and CCI soil moisture*

Lagrange continuous algorithm

To improve fusion accuracy, correlation calculation algorithms of cumulative probability distribution curve between different data need to be further improved. This study proposed a Lagrange continuous algorithm to establish the relationship between the SMOS and CCI cumulative probability distribution curves. Between the cumulative probability distribution curves of the SMOS and CCI datasets, each SMOS value has a corresponding probability distribution value *P*. On the CCI curve, if a CCI value corresponds to this probability value *P*, this CCI value is used as the fused SMOS value. If the probability value *P* has no corresponding CCI value, an appropriate value is calculated using an interpolation method. The Lagrange equidistant interpolation continuous algorithm can realize continuous fusion of the SMOS and CCI data in each quantile on the probability distribution curve.

Interpolation refers to the interpolation of discrete data to the continuous function, such that the continuous function curve passes through all data points. Interpolation can be used to estimate an approximation of the function at other points based on the value of the function at a finite point. Unary interpolation can calculate the approximate value at interpolation point t using the function when given the value at n equidistant nodes. The Lagrange interpolation polynomial was first published by Waring in 1779, rediscovered by Euler, and published by Lagrange in 1795 (Meyer et al., 2008; Jeffreys and Jeffreys, 1988). Lagrange interpolation polynomial can be expressed as follows:

http://www.aloki.hu ● ISSN 1589 1623 (Print) ● ISSN 1785 0037 (Online)
DOI: http://dx.doi.org/10.15666/aeer/1705_1160511617

$$L(x) = \sum_{j=0}^{k} y_j \ell_j(x) \quad \text{(Eq.2)}$$

where, $l_j(x)$ is the Lagrange basic polynomial (also called the interpolation basis function), which can be expressed as

$$\ell_j(x) = \prod_{i=0, i\neq j}^{k} \frac{x - x_i}{x_j - x_i} = \frac{(x - x_0)}{(x_j - x_0)} \cdots \frac{(x - x_{j-1})}{(x_j - x_{j-1})} \frac{(x - x_{j+1})}{(x_j - x_{j+1})} \cdots \frac{(x - x_k)}{(x_j - x_k)} \quad \text{(Eq.3)}$$

Through Lagrange interpolation, each SMOS data element has a corresponding CCI value, and the CCI value obtained using this interpolation method has minimal deviation on the cumulative probability curve. *Figure 2* shows the cumulative distribution curve schematic of SMOS and CCI, together with the fused SMOS (labeled SMOS' in the figure) obtained using the proposed Lagrange interpolation continuous algorithm. It can be seen that the cumulative distribution curve of the SMOS' data almost overlaps with the curve of CCI data.

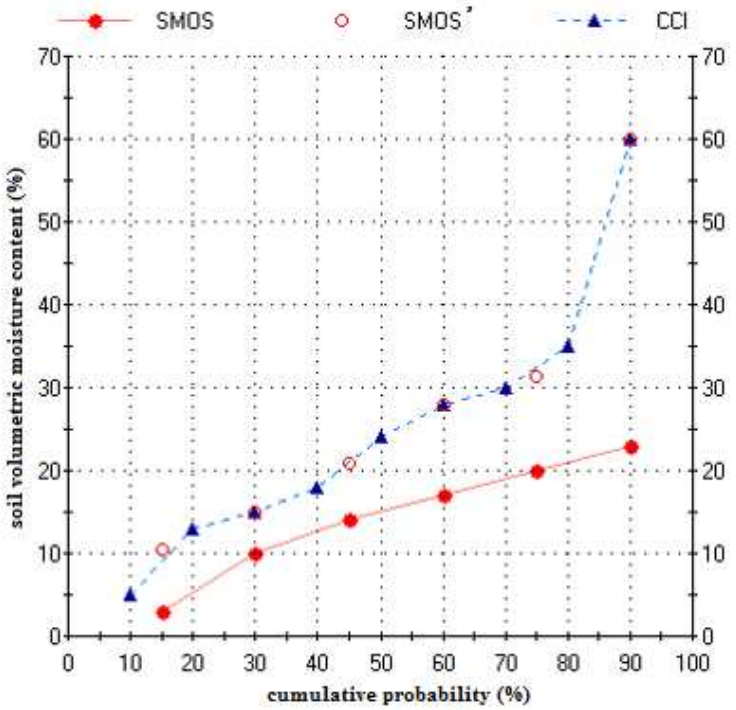

Figure 2. *Schematic of Lagrange continuous fusion between SMOS and CCI soil moisture*

Continuous fusion algorithm results analysis

Analysis of fusion data time series

Comparison of time series of remote sensing soil moisture data before and after fusion can illuminate the change of scope of the remote sensing data manifest by the fusion algorithm. As an example, the comparison of Shuangcheng in Songnen Plain is presented in *Figure 3*.

http://www.aloki.hu ● ISSN 1589 1623 (Print) ● ISSN 1785 0037 (Online)
DOI: http://dx.doi.org/10.15666/aeer/1705_1160511617

Following the fusion process, the fused SMOS data (labeled SMOS' in *Fig. 3*) are clearly closer to the CCI data distribution. The values of the SMOS data time series before fusion are generally lower than the CCI data values. After fusion, the soil water content of the SMOS data is increased, especially in months with low soil water content. The SMOS' data maintain the change characteristics of the original data time series. And the range of data values is adjusted to a certain extent, enhancing the degree of similarity with the CCI data range. In the case of Shuangcheng, the SMOS data range of Shuangcheng changed from 13–30% to 19–35% through fusion.

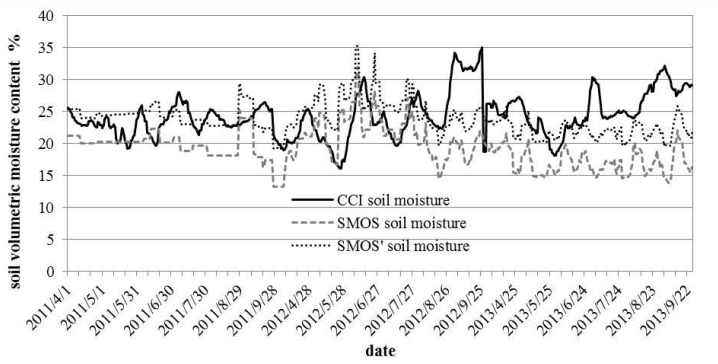

Figure 3. *Soil moisture time series of SMOS, CCI and fusion SMOS data in Shuangcheng*

Comparison of cumulative probability distributions between the two fusion methods

According to the CDF matching principle, the closer the curve of the target data to the cumulative probability distribution curve, the higher the fusion accuracy. Here, the result of the fusion of SMOS and CCI data of Shuangcheng (in Songnen Plain) is taken as an example for comparative analysis. The relationship between the cumulative probability distribution curves of the fused SMOS (labeled SMOS' in *Fig. 3*) and CCI data fused by piecewise linear algorithm and the Lagrange continuous algorithm is shown in *Figure 4a* and *b,* respectively.

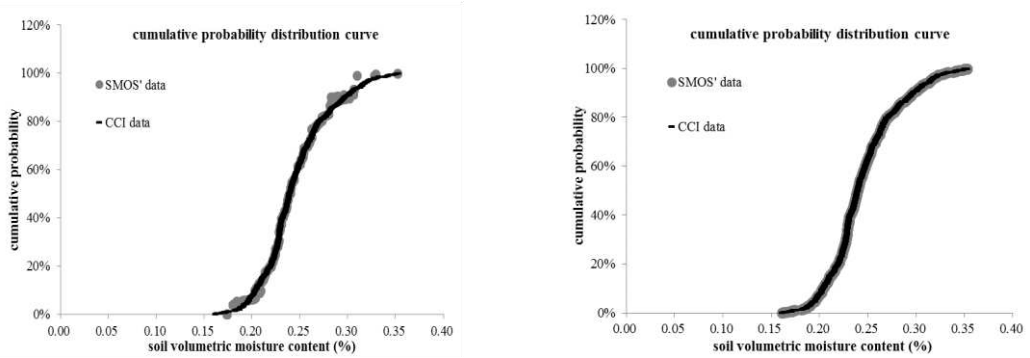

a. Piecewise linear fusion method **b. Lagrange interpolation fusion method**

Figure 4. *Cumulative probability distributions derived using (a) piecewise linear algorithm and (b) Lagrange continuous algorithm in Shuangcheng*

The result of the piecewise linear fusion shows certain error in SMOS' data, especially in the low-value region that is indicative of drought. This error would cause

http://www.aloki.hu ● ISSN 1589 1623 (Print) ● ISSN 1785 0037 (Online)
DOI: http://dx.doi.org/10.15666/aeer/1705_1160511617

loss of accuracy in real-time drought evaluation based on this fused soil moisture. The correlation established using the linear equation in each segment is the cause of this error. The result of the Lagrange continuous fusion shows the cumulative probability distribution curves of the SMOS' data (fused data) and CCI data (target data) coincide almost exactly (*Fig. 4b*). The two curves retain a high degree of coincidence in the low-value region of the curve. In terms of the cumulative probability distribution curve, the Lagrange continuous algorithm has higher fusion accuracy than the piecewise linear algorithm in fusion calculation.

The fusion precision of the two algorithms is also assessed quantitatively assessed by determining the coefficient of correlation (R^2) and the Nash efficiency coefficient (E_{NS}). The Nash efficiency coefficient can be calculated as follows:

$$E_{ns} = 1 - \frac{\sum_{i=1}^{n} (O_i - P_i)^2}{\sum_{i=1}^{n} \left(O_i - \overline{O}\right)^2} \quad \text{(Eq.4)}$$

where O_i and P_i represent the CCI and SMOS' data, respectively, and $\bar{O}$ is the average of the CCI data. The closer the value of E_{NS} to 1, the better the degree of coincidence between the two results.

The values of R^2 and E_{NS} of the two curves obtained using the piecewise linear algorithm were 0.98 and 0.97, respectively. And the R^2 and E_{NS} values in the low-value region were 0.73 and 0.52, respectively. The values of R^2 and E_{NS} of the two curves obtained using the Lagrange continuous algorithm were 0.99 and 0.99, respectively. And the R^2 and E_{NS} values in the low-value region were also 0.99 and 0.99, respectively. Therefore, it is evident that the Lagrange continuous algorithm improves the fusion precision significantly in the low-value region which be used for the characterization of drought.

Verification of remote sensing soil moisture by drought event

The fused SMOS data (SMOS' data), SMOS and CCI data were also evaluated for accuracy of drought expression. Site observation data from six stations within the study area were used as the basis for quantitative evaluation of the degree of consistency between the remote sensing data and the site observation data in the expression of drought events. The in situ data comes from China crop growth and development data set in China meteorological data network. This dataset contains moisture data per ten-day for 7 soil depths at each site. The surface 10 cm data was compared with the remote sensing data for verification. Here, as quantitative evaluation indices, hit rate (*H*), false alarm rate (*F*) and equitable threat score (*ETS*) are used to reflect the level of agreement of remote sensing of soil moisture with drought events (Grayson and Western, 1998). The higher the *ETS* value, higher the *H* value and lower the *F* value, the closer the level of agreement between the remote sensing data and drought events. The cumulative probability distribution of 30% is used as the threshold of the occurrence of drought both for remote sensing data and in situ data.

These evaluation indices define *a* as the number of events when drought is shown to occur in both the in situ observations and the fused SMOS data, *b* is when drought occurs in the fused SMOS data but not in the in situ observations, *c* is when drought occurs in the in situ observations but not in the fused SMOS data and *d* is when drought

http://www.aloki.hu ● ISSN 1589 1623 (Print) ● ISSN 1785 0037 (Online)
DOI: http://dx.doi.org/10.15666/aeer/1705_1160511617

does not occur in either the fused SMOS data or the in situ observations. Then, *H* can be expressed as follows:

$$H = \frac{a}{a + b} \quad \text{(Eq.5)}$$

where the range of values of *H* is 0–1(1 being the best); *F* can be written as

$$F = \frac{b}{b + d} \quad \text{(Eq.6)}$$

where the range of values of *F* is 0–1 (0 being the best) and *ETS* can be expressed as

$$ETS = \frac{a - a_{ref}}{a - a_{ref} + b + c} \quad \text{(Eq.7)}$$

where the range of values of *ETS* is -1/3 to 1 (1 being the best). Here, a_{ref} is expressed as

$$a_{ref} = \frac{(a + b)(a + c)}{(a + b + c + d)} \quad \text{(Eq.8)}$$

The drought verification of SMOS, CCI and SMOS' data for the six sites in the study area is shown in *Table 1*. CCI (version 02.2) dataset produced by several active and passive remote sensing data has integrally highest hit rate and equitable threat score. SMOS data as a single data source has integrally lowest hit rate and equitable threat score. SMOS' data is a combination of CCI and SMOS, with real-time update feature as with SMOS, and has significantly more accurate results for drought events verification than SMOS. The fused SMOS data has the characteristics of long time series and real-time update, which achieves the purpose of fusion research in this paper. In terms of drought event validation, SMOS' has a better validation effect than SMOS, indicating that this SMOS' dataset can be applied to drought evaluation research.

Table 1. *Drought verification by in situ data*

Site	Hit rate *H*			False alarm *F*			Equitable threat score *ETS* (10^{-2})		
	SMOS	CCI	SMOS'	SMOS	CCI	SMOS'	SMOS	CCI	SMOS'
Keshan	0.31	0.69	0.38	0.27	0.14	0.26	2.26	38.16	6.00
Fuyu	0.11	0.64	0.69	0.37	0.16	0.13	-11.28	31.08	38.82
Hailun	0.58	0.33	0.53	0.18	0.27	0.21	25.09	3.26	19.16
Tailai	0.33	0.57	0.43	0.07	0.19	0.23	18.6	23	11.11
Anda	0.4	0.57	0.35	0.24	0.2	0.27	8.41	20.91	4.42
Changling	0.35	0.5	0.25	0.28	0.22	0.31	3.67	15.88	-2.93
Meihekou	0.18	0.55	0.36	0.33	0.19	0.28	-7.04	21.97	4.36

http://www.aloki.hu ● ISSN 1589 1623 (Print) ● ISSN 1785 0037 (Online)
DOI: http://dx.doi.org/10.15666/aeer/1705_1160511617

Comparison of CCI data between version 02.2 and version 04.2

The latest version of CCI soil moisture product (v04.2) has already included the SMOS soil moisture. *Figure 5* shows the time series comparison of two different version of CCI data in a county in the study area. The new version of CCI data that incorporates SMOS is more similar in scope to SMOS data. The time series of CCI (v04.2) combined dataset is form 1978 to 2016, and the timeliness limited the application in real-time evaluation. The fusion method proposed in this paper can generate near-real-time, long-sequence data products that can reflect real drought events more accurately than SMOS.

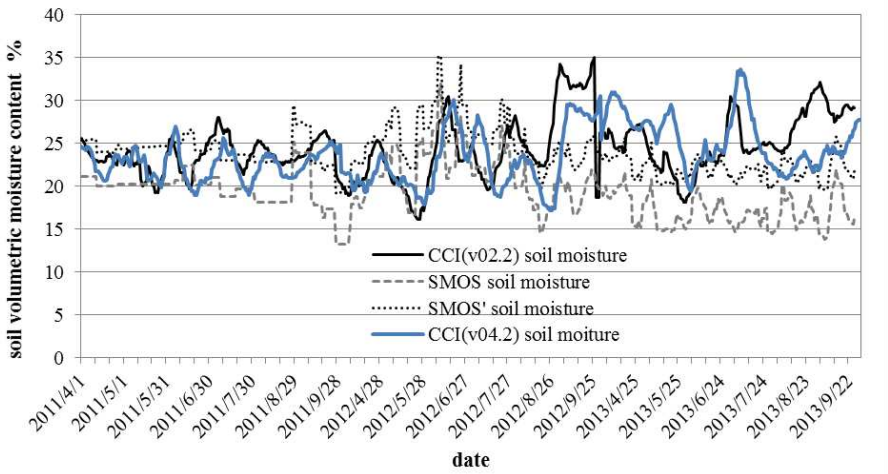

Figure 5. *Soil moisture time series of CCI(v02.2), CCI(v04.2), SMOS, and SMOS' data in Shuangcheng*

Discussion and conclusion

The efficacy of the application of remote sensing soil moisture data to the evaluation of agricultural drought is reflected mainly in the validity and accuracy of the remote sensing data when soil moisture is low (i.e., impending or emerging drought). Remote sensing data fusion technology that uses one dataset to extend a time series or to improve the update speed of another dataset is an important method with which to improve the performance of remote sensing data application. Fusion precision and the fusion algorithm are the primary problems associated with the application of such techniques to remote sensing datasets.

The existing piecewise linear fusion method can produce certain deviation, especially in the low-value region of a soil moisture curve that represents the stage of impending or emerging drought. Such deviation could easily lead to large errors in fused data used in drought forecasting, which could result in the misreporting or omission of agricultural drought events. Adopting the fusion principle of cumulative distribution function matching, this study constructed a continuous fusion algorithm, based on which analysis of the precision of the fusion of Soil Moisture and Ocean Salinity (SMOS) satellite data with Climate Change Initiative (CCI) satellite data was conducted at county level on the Songnen Plain (Northeast China). It was demonstrated that the proposed Lagrange continuous fusion algorithm could improve the fusion precision of

http://www.aloki.hu ● ISSN 1589 1623 (Print) ● ISSN 1785 0037 (Online)
DOI: http://dx.doi.org/10.15666/aeer/1705_1160511617

multisource remote sensing data and enhance the sensitivity of remote sensing soil moisture data in the characterization of drought.

Through application of the fusion algorithm, a fused CCI–SMOS remote sensing soil water product was generated at the county level for the Songnen Plain area. Through analysis of time series data before and after the fusion process, it was revealed that the fused SMOS data range was closer to the CCI data range than the original data, while the relative change mode of the original data was retained. After the in situ data verification, fused SMOS data has a better validation effect than SMOS. The systematic deviation of the fused remote sensing soil water product was reduced, while displaying the advantages of a long time sequence and near real-time features. The results of this study could provide data support for further real-time evaluation and frequency analysis of large-scale agricultural drought on the regional scale. Validation analysis studies between the other different data sources and in other regions are needed to further verify the availability of this new fusion method.

Acknowledgments. This study was supported by the National Natural Science Foundation of China (Grant No. 51779007, 41671018), National Key Research and Development Program of China (Grant No. 2016YFC0401308), and Project funded by China Postdoctoral Science Foundation (2018M631707).

REFERENCES

[1] Al-Yaari, A., Wigneron, J. P., Ducharne, A., et al. (2014): Global-scale comparison of passive (SMOS) and active (ASCAT) satellite based microwave soil moisture retrievals with soil moisture simulations (MERRA-Land). – Remote Sensing of Environment 152: 614-626.

[2] Anagnostou, E. N., Negri, A. J., Adler, R. F. (2010): Statistical adjustment of satellite microwave monthly rainfall estimates over Amazonia. – Journal of Applied Meteorology 38(11): 1590-1598.

[3] Anterrieu, E. (2011): On the detection and quantification of RFI in L1a signals provided by SMOS. – IEEE Transactions on Geoscience and Remote Sensing 49(10): 3986-3992.

[4] Atlas, D., Rosenfeld, D., Wolff, D. B. (1990): Climatologically tuned reflectivity-rain rate relations and links to area-time integrals. – Journal of Applied Meteorology 29(11): 1120-1135.

[5] Atlas, R., Woldson, N., Terry, J. (1993): The effect of SST and soil moisture anomalies on GLA model simulations of the 1988 U.S. summer drought. – J. Clim. 6: 2034-2048.

[6] Bolten, J. D., Crow, W. T., Zhan, X., et al. (2010): Evaluating the Utility of Remotely Sensed Soil Moisture Retrievals for Operational Agricultural Drought Monitoring. – IEEE Journal of Selected Topics in Applied Earth Observations & Remote Sensing 3(1): 57-66.

[7] Brocca, L., Hasenauer, S., Lacava, T., et al. (2011): Soil moisture estimation through ASCAT and AMSR-E sensors: An intercomparison and validation study across Europe. – Remote Sensing of Environment 115(12): 3390-3408.

[8] Calheiros, R. V., Zawadzki, I. (2010): Reflectivity-rain rate relationships for radar hydrology in Brazil. – Journal of Applied Meteorology 26(1): 118-132.

[9] Calvet, J. C., Wigneron, J. P., Walker, J., et al. (2011): Sensitivity of passive microwave observations to soil moisture and vegetation water content: L-band to W-band. – IEEE Transactions on Geoscience & Remote Sensing 49(4): 1190-1199.

[10] Chakravorty, A., Chahar, B. R., Sharma, O. P., et al. (2016): A regional scale performance evaluation of SMOS and ESA-CCI soil moisture products over India with

http://www.aloki.hu ● ISSN 1589 1623 (Print) ● ISSN 1785 0037 (Online)
DOI: http://dx.doi.org/10.15666/aeer/1705_1160511617

simulated soil moisture from MERRA-Land. – Remote Sensing of Environment 186: 514-527.

[11] Dorigo, W., Wagner, W., Albergel, C., et al. (2017): ESA CCI soil moisture for improved Earth system understanding: state-of-the art and future directions. – Remote Sensing of Environment S0034425717303061.

[12] Drusch, M. (2005): Observation operators for the direct assimilation of TRMM microwave imager retrieved soil moisture. – Geophysical Research Letters 32(15):L15403.

[13] González-Zamora, Á., Sánchez, N., Pablos, M., et al. (2018): CCI soil moisture assessment with SMOS soil moisture and, in situ, data under different environmental conditions and spatial scales in Spain. – Remote Sensing of Environment S0034425718300166.

[14] Grayson, R. B., Western, A. W. (1998): Towards areal estimation of soil water content from point measurements: time and space stability of mean response. – Journal of Hydrology 207(1-2): 68-82.

[15] Sportouche, H., Tupin, F., Denise, L. (2011): Extraction and three-dimensional reconstruction of isolated buildings in urban scenes from high-resolution optical and SAR spaceborne images. – IEEE Transactions on Geoscience and Remote Sensing 49(10): 3932-3946.

[16] Hollmann, R., Merchant, C., Saunders, R., et al. (2013): The ESA Climate Change Initiative: satellite data records for essential climate variables. – Bulletin of the American Meteorological Society 94(10): 1541-1552.

[17] Jeffreys, H., Jeffreys, B. S. (1988): Lagrange's Interpolation Formula. – In: Jeffrey, H., Jeffreys, B. S. Methods of Mathematical Physics. Third Ed. – Cambridge University Press, Cambridge.

[18] Jian, K., Rui, J., Xin, L., et al. (2018): Spatial upscaling of sparse soil moisture observations based on ridge regression. – Remote Sensing 10(2): 192-202.

[19] Khaleghi, B., Khamis, A., Karray, F. O., et al. (2013): Multisensor data fusion: a review of the state-of-the-art. – Information Fusion 14(1): 28-44.

[20] Lanqi, J., Lijuan, Z., Shuying, Z., et al. (2016): Accuracy assessment of approaches to spatially explicit reconstruction of historical cropland in Songnen Plain, Northeast China. – Journal of Geographical Sciences 26(2): 219-229.

[21] Lee, C. S., Park, J. D., Shin, J., et al. (2017): Improvement of AMSR2 soil moisture products over South Korea. – IEEE Journal of Selected Topics in Applied Earth Observations & Remote Sensing 99: 1-11.

[22] Lee, J. H., Im, J. A. (2015): Novel bias correction method for soil moisture and ocean salinity (SMOS) soil moisture: retrieval ensembles. – Remote Sensing 7(12): 16045-16061.

[23] Li, N. H., Manjunath, B. S., Mitra, S. K. (1995): Multisensor image fusion using the wavelet transform. – Graphical Model and Image Processing 57(3): 235-245.

[24] Liu, Y. Y., Parinussa, R. M., Dorigo, W. A., et al. (2010): Developing an improved soil moisture dataset by blending passive and active microwave satellite-based retrievals. – Hydrology & Earth System Sciences Discussions 15(2): 425-436.

[25] Liu, Y. Y., Van Dijk, A. I. J. M., De Jeu, R. A. M., et al. (2009): An analysis of spatiotemporal variations of soil and vegetation moisture from a 29-year satellite-derived data set over mainland Australia. – Water Resources Research 45(7): 4542-4548.

[26] Meyer, R., Bo, C., Perron, F. (2008): Adaptive rejection Metropolis sampling using Lagrange interpolation polynomials of degree 2. – Computational Statistics & Data Analysis 52(7): 3408-3423.

[27] Ramirez-Beltran, N. D., Calderon-Arteaga, C., Harmsen, E., et al. (2010): An algorithm to estimate soil moisture over vegetated areas based on in situ and remote sensing information. – International Journal of Remote Sensing 31(10): 2655-2679.

http://www.aloki.hu ● ISSN 1589 1623 (Print) ● ISSN 1785 0037 (Online)
DOI: http://dx.doi.org/10.15666/aeer/1705_1160511617

[28] Reichle, R. H., Koster, R. D. (2004): Bias reduction in short records of satellite soil moisture. – Geophysical Research Letter 31(19): 187-206.
[29] Schmitt, M., Zhu, X. X. (2016): Data Fusion and Remote Sensing: an ever-growing relationship. – IEEE Geoscience and Remote Sensing Magazine 4(4): 6-23.
[30] Sheffield, J., Wood, E. F. (2007): Characteristics of global and regional drought, 1950–2000: Analysis of soil moisture data from off-line simulation of the terrestrial hydrologic cycle. – Journal of Geophysical Research 112(D17):D17115.
[31] Siyu, M., Qianxin, W., Jie, W., et al. (2017): Temporal evolution of regional drought detected from GRACE TWSA and CCI SM in Yunnan Province, China. – Remote Sensing 9(11): 1124-1138.
[32] Su, Z. (2003): Assessing relative soil moisture with remote sensing data: theory, experimental validation, and application to drought monitoring over the North China Plain. – Physics & Chemistry of the Earth 28(1): 89-101.
[33] Waltz, E., Llinas, J. (1990): Multisensor Data Fusion. – Artech House Inc., Norwood, MA, pp. 245-253.
[34] Wang, H. X., Wan, Z. J., Yu, S. P., et al. (2004): Catastrophic eco-environmental change in the Songnen Plain, northeastern China since 1900s. – Chinese Geographical Science 14(2): 179-185.
[35] Wang, S., Mo, X., Hu, S., et al. (2018): Assessment of droughts and wheat yield loss on the North China Plain with an aggregate drought index (ADI) approach. – Ecological Indicators 87: 107-116.
[36] Zheng, S. H., Qin, Z. H., Zhang, W. B. (2015): Drought variation in Songnen Plain and its response to climate change. – Chinese Journal of Agrometeorology 36(5): 640-649.

http://www.aloki.hu ● ISSN 1589 1623 (Print) ● ISSN 1785 0037 (Online)
DOI: http://dx.doi.org/10.15666/aeer/1705_1160511617

CHANGE OF NUTRIENTS AND HUMUS IN THE COMPOSTING PROCESS USING DIFFERENT LIVESTOCK MANURES

FENG, L.[1] – YU, Q.[1] – ZHEN, Q.[2*] – DONG, H.[2] – ZHENG, J.[3] – WANG, Y.[3]

[1]*Liaoning Province Clean Energy Key Laboratory, Shenyang Aerospace University, Shenyang Daoyi Street 37, Shenyang 110136, China*
(phone: +86-180-4003-8889)

[2]*School of New Energy and Power Engineering, Lanzhou Jiaotong University, No. 88, Anning West Road, Anning District, Lanzhou 730070, China*
(phone: +86-139-1930-2012)

[3]*School of Energy and Power Engineering, Lanzhou University of Technology, No. 287, Langongping Road, Qilihe District, Lanzhou 730050, China*
(phone: +86-139-1925-7393)

**Corresponding author*
e-mail: zxf283386515@163.com; phone: +86-139-1930-2012

(Received 22nd Apr 2019; accepted 12th Jul 2019)

Abstract. Aerobic manure composting was carried out using raw materials of like fresh manure of cattle, pig and chicken, and 10% corn stalk as a raising agent. The changing trend of the composting parameters in the composting process of different livestock manures including temperature, pH, water content, nutrients and humus were studied mainly. The results showed that the organic carbon content continued to decrease during composting. At the end of the composting, the total carbon content of the composting R2 (pig manure) was highest with a value of 294.7 ± 19.15 $g \cdot kg^{-1}$, whereas the total carbon content of the R3 (chicken manure) was the lowest with the value of 284.57 ± 11.78 $g \cdot kg^{-1}$. The contents of the total nitrogen, phosphorus and potassium showed an increasing trend during livestock manure composting process. The total nitrogen and total phosphorus were found to be highest in the R2, while total potassium was the highest in R3 with values of 2.25 ± 0.18%, 2.41 ± 0.15% and 0.78 ± 0.19%, respectively. The contents of total humic acid and free humic acid demonstrated an initial decreasing trend, and later showed an increasing trend. The contents of the total and free humic acid were found to be highest R3, with values of 29.84 ± 1.98 and 25.84 ± 1.25%.
Keywords: *fecal treatment, humic acid, organic carbon, composting system, resource utilization*

Introduction

The gradual increase in the number of extensive and intensive livestock and poultry farms satisfied the human needs for the livestock and poultry products. However, the casual stacking and inefficient treatment of the large amounts of livestock manure makes a significant burden on the environment (Liang et al., 2013). Nowadays, the livestock manure, industrial waste water and domestic waste water have been considered as the three paralleling pollution sources. Livestock manure has been an important factor that impedes the healthy development of the breeding industry. Besides, it also wastes the precious nutrient resources in large amounts (Xi et al., 2016). Currently, the livestock manure is increasing in its production with a speed of 10% each year. In 2014, the total amount of livestock manure was 6 billion t, which contained 60 million t of the nutrient resource, and equaled the quantity of the main fertilizer used in China in that year (Wang et al., 2013; Finstein et al., 2016; Guo et al., 2016). On one hand, these solid wastes contribute a certain extent of pollution to

http://www.aloki.hu ● ISSN 1589 1623 (Print) ● ISSN 1785 0037 (Online)
DOI: http://dx.doi.org/10.15666/aeer/1705_1161911628

the environment. On the other hand, these wastes contain high quantities of organic matter and essential nutrient such as nitrogen, phosphorus, potassium and the biomass which is vital for the plants (Zhou et al., 2014). Thus, the application of the organic fertilizers prepared from the livestock manures on farmlands can not only effectively decrease the quantity of fertilizers and decrease the input cost of fertilizers, but also increase the organic matter content of soil and the soil fertility, thus promoting the sustainable utilization of farmland (Warker, 2001). In 2015, the Chinese government proposed "the activity of zero increase of the pesticide application quantity", thereby providing an unprecedented opportunity for development of organic fertilizers.

The humus produced in the composting process is a lignan derivative produced by the oxidation of the side chain of the lignan by microorganisms, which forms the key core and the skeleton of humus. This is one of the most important formation pathways of the humus (Ktilcia et al., 2014; Smars et al., 2002). In the composting process, the index of humification is related to the water-soluble carbohydrate and phenolic structure. It demonstrates the inverse relationship between the phenolic compounds and the humification index in the composting process, which confirms that the phenolic compounds are the principle materials of humus. The generation of humus with smaller molecular weight, less hydroxyl groups and minimal functional group occurs very rapidly in composting than in soil. There are many enzymes involved in the composting process, mainly including the hydrolase and redoxase. The mineralization extent of composting is mainly affected by the change in the enzyme activity of the hydrolase, while the extent and intensity of humification are affected by the change in the enzyme activity of the redoxase (Gao et al., 2010; Bernal et al., 2010). The species of the inducible enzyme dominates the composing process. Thus, the enzyme activity can demonstrate the change in the organic matter in different stages of the composting reaction (Bolta et al., 2003). Abdennaceur et al. (2011) showed that the transformation in the aromatic organic compounds in composting humus could be characterized by the enzyme activity of polyphenol oxidase, with an inverse relationship to the maturity of composting. Currently, many studies have been conducted on the microflora in aerobic composting with materials of single livestock manure; however, there are scarce reports on the comparison of the change of humus and nutrients in the composting process with raw materials of different livestock manures. In this study, the changes of material composition of heap in the composting with different livestock manures were studied using the raw materials of three livestock manure of cattle, pig and chicken, focus on change rule of TN, TP, TK, humus and free humus content in the composting process, which could provide a theoretical evidence and technical support for local enterprises.

Materials and methods

Experiment materials

Cattle manure, pig manure and chicken manure used in the composting process with livestock manures were procured from the breeding farm near Shenyang Aerospace University in Shenbei New District, Shenyang, Liaoning. Corn stalks were also provided by the same breeding farm. Corn stalks were cut into pieces of 2-4 cm by the knife mill before use. The physicochemical properties of composting materials are shown in *Table 1*.

http://www.aloki.hu ● ISSN 1589 1623 (Print) ● ISSN 1785 0037 (Online)
DOI: http://dx.doi.org/10.15666/aeer/1705_1161911628

Table 1. *Agrochemical characters of different compost materials*

Raw materials	Water content (%)	pH	Total carbon (%)	Total nitrogen (%)	Total potassium (K_2O%)	Total phosphorus (P_2O_5%)	C/N
Cattle manure	68.9	7.64	38.32	1.78	1.48	1.45	21.53
Pig manure	73.4	7.35	39.41	1.80	1.58	1.78	21.89
Chicken manure	70.8	7.28	41.15	2.99	1.52	2.98	13.76
Corn stalk	21.5	7.19	54.82	1.04	0.98	0.46	52.71

Experimental method

An aerobic static composting was conducted using the composting materials of three livestock manures, including cattle manure (R1), pig manure (R2) and chicken manure (R3). The 21 d composting reaction was conducted with 6 self-designed aerobic composting boxes among which 2 composing boxes were considered as a group to contain single type of livestock manure.

The results of every parameter data in the experiments were taken as an average. The porosity and organic matter content of the livestock manure were adjusted by additives of 10% corn stalk. In the whole composting process, different parameters like temperature, oxygen concentration, carbon dioxide concentration, density, etc. was monitored. Besides, the stink gas produced during the composting process was treated using a bio-filter (as shown in *Fig. 1*). The changes in the aforementioned parameters in the composting process were compared and the pile nutrients (the content of C-N-P-K) in the composing process in different livestock manure, humus and free humus were mainly analyzed.

Experiment apparatus

The self-designed composting box was used in the composting experiment. The experiment apparatus of the composting is shown in *Figure 1*.

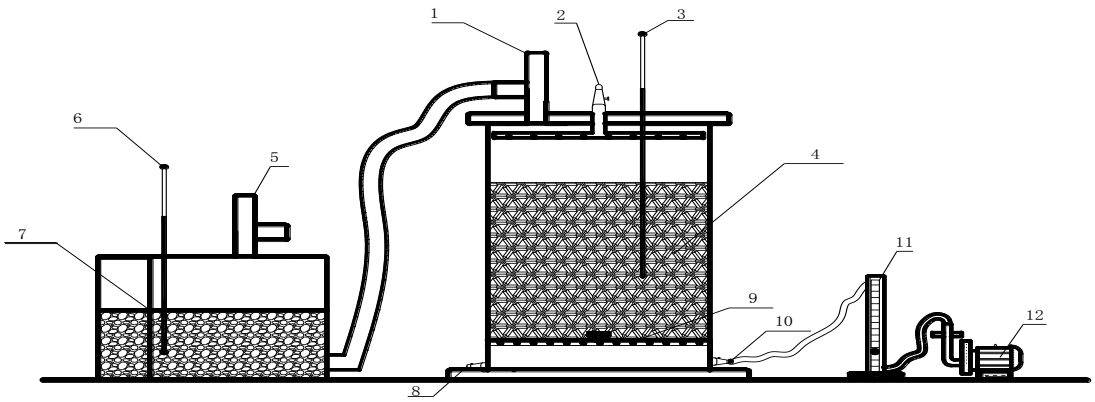

Figure 1. *Experimental apparatus used in the aerobic composting with livestock manures. 1. Vent of the composting box 2. Back-ejecta nozzle of leachate 3. Thermometer 4. Composting box 5. Gas outlet of bio-filter 6. Thermometer 7. Bio-filter 8. Discharge pipe of leachate 9. Grid plate 10. Inlet pipe 11. Flow meter 12. Fan*

http://www.aloki.hu ● ISSN 1589 1623 (Print) ● ISSN 1785 0037 (Online)
DOI: http://dx.doi.org/10.15666/aeer/1705_1161911628

Results and discussion

Changes in C-N-P-K content in the composting with different livestock manures

Change in total carbon content in the composting with different livestock manures

Figure 2 shows the changes in the total carbon content in the composting process with different livestock manures. It was seen that the total carbon contents in the pile were in the following order at the initial stage of the composting process: R3 (chicken manure) > R1 (cattle manure) > R2 (pig manure), with corresponding values of 378.45 ± 25.45 g·kg^{-1}, 366.28 ± 18.18 g·kg^{-1} and 358.24 ± 24.18 g·kg^{-1}, respectively. With the process of the composting of the livestock manures, the organic carbon source was transformed to carbon dioxide due to the decomposition of the organic carbon by microorganisms. Thus, the organic carbon content in the pile exhibited a decreasing trend. At the end of the composting, total carbon content was in the following order: R2 (pig manure) > R1 (cattle manure) > R3 (chicken manure), with corresponding values of 294.7 ± 19.15 g·kg^{-1}, 290.45 ± 13.14 g·kg^{-1} and 284.57 ± 11.78 g·kg^{-1}, respectively. The decreasing amplitude of the total organic carbon in the composting piles with different livestock manures of R1, R2 and R3 were different with a degradation rate of the organic carbon of 20.7%, 17.7% and 24.8%, respectively. The decreasing amplitude of R3 (chicken manure) was the largest, whereas the decreasing amplitude of R2 (pig manure) was the smallest. In the whole composting process, the change of the total carbon content showed a decreasing trend due to the transformation of the carbon, which was the main component of energy material of microorganisms and cells to yield carbon dioxide and humus by the decomposition and utilization of microorganisms in the composting process. The loss of carbon due to the emission of the carbon dioxide resulted in the gradual decrease of the organic carbon during the composting process. At the end of the composting, the total carbon content of R2 (pig manure) was the highest, whereas the total carbon content of R3 (chicken manure) was the lowest (Khalil, et al., 2011; Guo et al., 2016).

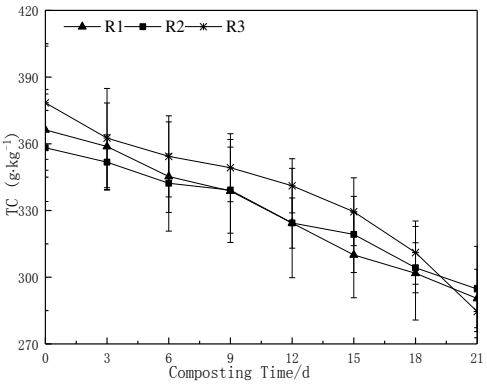

Figure 2. *Change of TC in three kinds of livestock dung composting*

Change in total nitrogen content in the composting with different livestock manure

Figure 3 shows the change in the total nitrogen content in the composting process with different livestock manures. It was seen that the total nitrogen content in the initial composting process was in the order of: R2 (pig manure) > R3 (chicken manure) > R1 (cattle manure), with corresponding values of 1.57 ± 0.11, 1.41 ± 0.08 and

http://www.aloki.hu ● ISSN 1589 1623 (Print) ● ISSN 1785 0037 (Online)
DOI: http://dx.doi.org/10.15666/aeer/1705_1161911628

1.28 ± 0.18%, respectively. With the process of the composting reaction, the total nitrogen percent content in all the composting piles with livestock manures showed an increasing trend, mainly because both the organic carbon and the organic nitrogen were assimilated and catabolized by microorganisms in the composting process. The need of organic carbon in the microorganisms was higher than the need of organic nitrogen, with the general need ratio of carbon to nitrogen as 25:1. The degradation velocity of organic carbon was higher than that of organic nitrogen in the composting degradation process, resulting in the lower attrition rate of organic nitrogen than that of organic carbon in the composting process. Thus, the percent content of total nitrogen in all the composting piles with livestock manures demonstrated an increasing trend. At the end of the composting, the total nitrogen content in R1, R2 and R3 composting increased, with the corresponding increasing amplitude of 50.78%, 43.33% and 51.77%, respectively, among which the increasing amplitude of R3 (chicken manure) was the largest, while the increasing amplitude of R2 (pig manure) was the smallest.

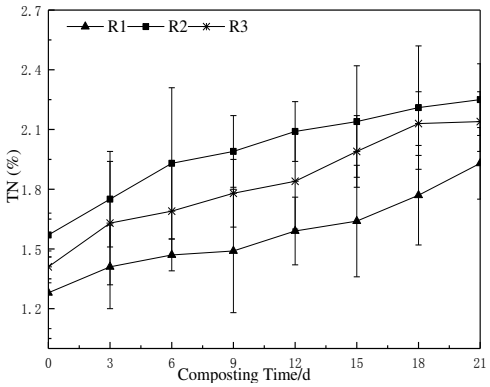

Figure 3. *Change of TN in three kinds of livestock dung composting*

Change in total phosphorus content in the composting with different livestock manure

Figure 4 shows the change of the total phosphorus content in the composting process with different livestock manures. It was observed that the total nitrogen content in the initial composting process in different piles was in the following order: R2 (pig manure) > R3 (chicken manure) > R1 (cattle manure), with corresponding values of 1.80 ± 0.12, 1.64 ± 0.17 and 1.25 ± 0.15%, respectively. The percentage content of total phosphorus in all the composting pile with livestock manures demonstrated an increasing trend with the process of the composting reaction. This was mainly due to the assimilation and catabolism of organic carbon, organic nitrogen and organic phosphorus by microorganisms in the composting process with livestock manures. The need of organic carbon for microorganisms was higher than that of the organic nitrogen and organic phosphorus. And the general need ratio of C:N:P was 100:5:1. The degradation velocity of the organic carbon in the composting degradation process was higher than that of organic phosphorus, resulting in the lower attrition rate of organic phosphorus than that of the organic carbon and organic nitrogen in the composting process. Thus, the percent content of total phosphorus in the composting piles with livestock manures demonstrated an increasing trend. At the end of the composting, the total phosphorus contents of R1, R2 and R3 composting increased by 25.61%, 33.38% and 11.58%, respectively, among which the increasing amplitude of R2 (pig manure) was largest,

http://www.aloki.hu ● ISSN 1589 1623 (Print) ● ISSN 1785 0037 (Online)
DOI: http://dx.doi.org/10.15666/aeer/1705_1161911628

whereas the increasing amplitude of R3 (chicken manure) was smallest. There was neither any production of leachate nor any loss of phosphorus. Thus, the evaporation loss of the total phosphorus in the composting was relatively small.

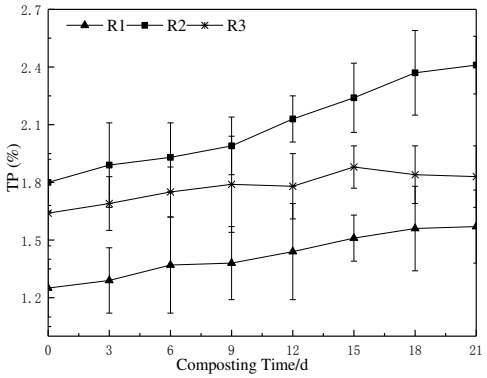

Figure 4. *Change of TP in three kinds of livestock dung composting*

Change in total potassium content in the composting with different livestock manures

Figure 5 shows the change in the total potassium content in composting process with different livestock manures. It was seen that the total potassium content in the initial composting process in the piles was in the following order: R3 (chicken manure) > R1 (cattle manure) > R2 (pig manure), with corresponding vales of 1.21 ± 0.12, 1.14 ± 0.12 and 1.03 ± 0.22%, respectively. The total potassium percentage content in all the composting piles with livestock manures demonstrated an increasing trend with the process of composting reaction due to the low adsorption and utilization rate of potassium. In the composting process with livestock manures, the organic carbon, organic nitrogen and organic phosphorus were all assimilated and catabolized by microorganisms. The need of organic carbon, organic nitrogen and organic phosphorus of microorganisms were higher than that of organic potassium. There was almost no loss of potassium in the composting process. Thus, the total potassium percentage content in the composting pile with all different livestock manures demonstrated an increasing trend. At the end of the composting, the total potassium content of R1, R2 and R3 composting increased by 35.88%, 62.13% and 47.07%, respectively, among which the increasing amplitude of R2 (pig manure) was largest, whereas the increasing amplitude of R1 (cattle manure) was smallest.

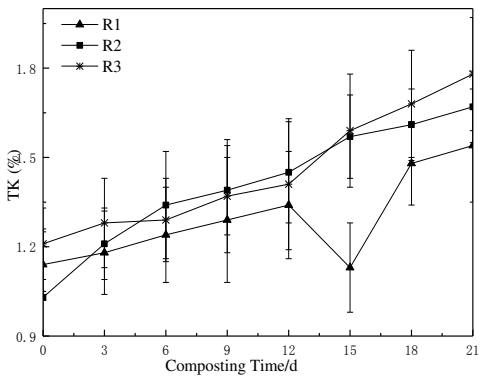

Figure 5. *Change of TK in three kinds of livestock dung composting*

http://www.aloki.hu ● ISSN 1589 1623 (Print) ● ISSN 1785 0037 (Online)
DOI: http://dx.doi.org/10.15666/aeer/1705_1161911628

Change of humus content in the composting process with livestock manures

The humus content is the key index describing the quality of organic fertilizer, which can enhance the soil fertility, change the formation of aggregate structure, adjust the soil porosity, and increase the ability of ventilation and water-retaining of soil. Furthermore, the growth of crops can be promoted by the changing of metabolism in plants influenced by the changing of enzyme activity.

Change in total humic acid content in the composting process with livestock manures

Figure 6 shows the change in the total humic acid content in the composting process with livestock manures. It was seen that the total humic acid content in the initial composting process in the piles was in following order: R3 (chicken manure) > R1 (cattle manure) > R2 (pig manure), with corresponding values of 37.82 ± 2.45, 36.84 ± 1.25 and 32.18 ± 1.58%, respectively. With the process of the composting reaction, the total humic acid content in the pile demonstrated an initial decrease, followed by an increase in all the piles. In the 0-15 d period of the reaction, the total humic acid in the initial period of R1, R2 and R3 was 36.84 ± 1.25, 32.18 ± 1.58 and 37.82 ± 2.45%, respectively, that decreased after 15 d to 14.87 ± 1.98, 13.64 ± 1.78 and 18.45 ± 2.40, respectively, with a corresponding decreasing amplitude of 59.63, 57.61 and 51.21%, respectively. This was due to the decomposition of the unstable humic acid generated in the degradation of the susceptible organic matters by the thermophilic bacteria in the high temperature period. The content of total humic acid reached the minimum at 15 d, and then increased. At the end of the reaction, the total humic acid content of R1, R2 and R3 were 25.12 ± 1.77, 24.21 ± 1.89 and 29.84 ± 1.98%, respectively. The increase of the total humic acid content in the late stage of the reaction was due to the decrease of the temperature and the enhancement of the microorganism activities, which was beneficial for the stability of humus structure and properties. The organic matter that was difficult to degrade was transformed to humic acid by the microorganisms. Thus, the total humic acid content in the product was found to be increased, thereby enhancing the quality of the composting product.

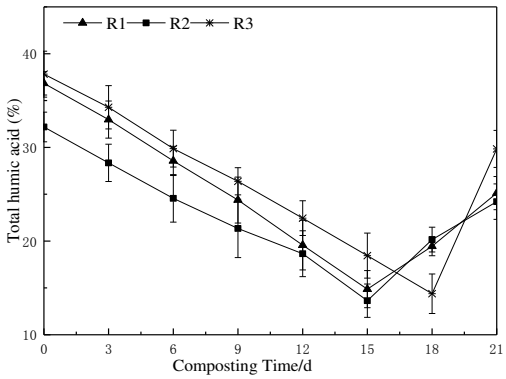

Figure 6. *Change of total humic acid in three kinds of livestock dung composting*

Change in free humic acid content in the composting with different livestock manures

Figure 7 shows the change in the free humic acid content in the composting process with different livestock manures. It was seen that the changing trends of the free and

http://www.aloki.hu ● ISSN 1589 1623 (Print) ● ISSN 1785 0037 (Online)
DOI: http://dx.doi.org/10.15666/aeer/1705_1161911628

total humic acid were similar. The free humic acid content was in a descending order: R3 (chicken manure) > R1 (cattle manure) > R2 (pig manure) in the initial stage of composting reaction with livestock manures with corresponding values of 26.84 ± 1.87, 19.87 ± 1.23 and 18.53 ± 1.29%, respectively. With the process of the composting reaction, the free humic acid content in the pile demonstrated a trend of initial decrease, with a subsequent increase. In the 0-15 d period of the reaction, the free humic acid content in the initial stage of R1, R2 and R3 piles was 19.87 ± 1.23, 18.53 ± 1.29 and 26.84 ± 1.87, respectively, which decreased to 16.88 ± 1.99, 15.98 ± 1.98 and 20.18 ± 1.27, respectively, at 15 d, with corresponding decreasing amplitudes of 15.04, 13.76 and 24.81%, respectively. This was due to the decomposition of the unstable humic acid and the even more unstable free humic acid by the thermophilic bacteria. The content of free humic acid reached the minimum at 15 d and then increased. At the end of the reaction, the free humic acid content of R1, R2 and R3 was 24.84 ± 1.87, 23.45 ± 1.56 and 25.84 ± 1.25, respectively. The increase of the free humic acid content in the late stage of reaction was due to the decrease in the temperature and the enhancement of microorganism activities, which were beneficial for the stability of humus structure and properties. The organic matter which was difficult to degrade was transformed to total humic acid by the microorganisms. Thus, the total humic acid content in the product was increased, thereby enhancing the quality of the composting product.

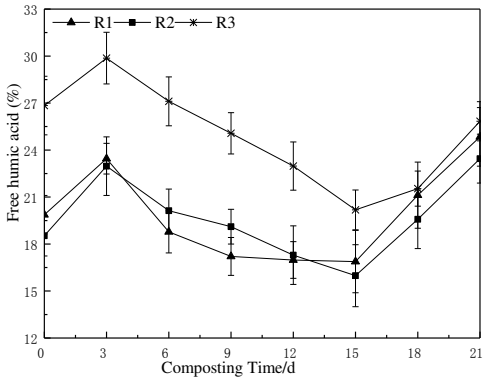

Figure 7. *Change of free humic acid in three kinds of livestock dung composting*

The results of the variance analysis showed that the discrimination of free humic acid content in the composting piles with R1, R2 and R3 livestock manures was not significant with a descending order of R3 (chicken manure) > R1 (cattle manure) > R2 (pig manure).

Humic acid in the composting was transformed from newborn and original humic acid in the materials. The composting time, raw materials, composting technologies, and the environment conditions can be factors limiting the formation of humic acid in composting (Xiao et al., 2011). Besides, microorganisms are also known to greatly influence the formation of humic acid, e.g. mesophilic microorganisms in the composting process can promote the formation of humic acid (Kinney et al., 2012; He et al., 2004; Malifiska et al., 2014).

The experimental results showed that the contents of total and free humic acid in all the composting piles with livestock manures increased dramatically in the late stage of the composting, accompanied by a decrease in temperature. The decrease of

http://www.aloki.hu ● ISSN 1589 1623 (Print) ● ISSN 1785 0037 (Online)
DOI: http://dx.doi.org/10.15666/aeer/1705_1161911628

temperature and maturity could promote the increase of the content of total humic acid and thus enhance the composting quality. At the end of the composting, the contents of total and free humic acid in the composting with chicken manure were highest.

Conclusions

1) The organic carbon content in the composting with livestock manures gradually decreased. At the end of the composting, the total carbon content of R2 (pig manure) composting was highest with the value of 294.7 ± 19.15 $g \cdot kg^{-1}$, whereas the total carbon content of R3 (chicken manure) composting was lowest with the value of 284.57 ± 11.78 $g \cdot kg^{-1}$.

2) Total nitrogen, total phosphorus and total potassium in all the composing process with livestock manures demonstrated an increasing trend. At the end of the composting, the contents of total nitrogen, total phosphorus and total potassium were highest in R2 (pig manure), R2 (pig manure) and R3 (chicken manure), respectively, with corresponding values of 2.25 ± 0.18, 2.41 ± 0.15 and 1.78 ± 0.19%, respectively.

3) The contents of total and free humic acid in all the composting process with livestock manures demonstrated a trend of an initial decrease, followed by an increasing trend. At the end of the composting, the contents of total and free humic acid in R3 (chicken manure) were highest with corresponding values of 29.84 ± 1.98 and 25.84 ± 1.25%, respectively.

This article mainly writes the use of pig manure, chicken manure and cow dung for composting, to explore the trend of physical and chemical indicators such as temperature and humus during composting. In this experiment, only a single livestock manure is used for composting. Next, I will choose different livestock manures mixed compost, or livestock manure and straw mixed compost will be selected for scientific guidance of agricultural and livestock waste composting quality control.

Acknowledgements. This work was funded by the National Natural Science Foundation project (51509122), and Gansu Provincial Higher Education Science and Technology Achievements Transformation Project (2018D-04), Gansu Natural Science Foundation (18JR3RA154), 2018 Yangling Demonstration Zone Collaborative Innovation Major Project (2018CXY-14).

REFERENCES

[1] Abdennaceur, H., Kaouala, B., Naceur, J. (2011): Microbial characterization during composting of municipal solid waste. – Bioresource Technology 80(3): 217-225.

[2] Bernal, M. P., Alburquerque, J. A., Moral, R. (2010): Composting of animal manures and chemical criteria for compost maturity assessment. A review. – Bioresource Technology 100(3): 5444-5453.

[3] Bolta, S., Mihelic, R., Lobnik, F., et al. (2003): Microbial community structure during composting with and without massinocula. – Compost Science and Utilization 11(1): 6-15.

[4] Finstein, M. S., Morris, M. L. (1975): Microbiology of municipal solid waste composting. – Advances in Applied Microbiology 19: 113-151.

[5] Gao, M., Liang, F., Yu, A., Li, B. (2010): Evaluation of stability and maturity during forced-aeration composting of chicken manure and sawdust at different C/N ratios. – Chemosphere 78: 614-619.

http://www.aloki.hu ● ISSN 1589 1623 (Print) ● ISSN 1785 0037 (Online)
DOI: http://dx.doi.org/10.15666/aeer/1705_1161911628

[6] Guo, X., Huang, J., Lu, Y., et al. (2016a): The influence of flue gas desulphurization gypsum additive on characteristics and evolution of humic substance during co-composting of dairy manure and sugarcane pressmud. – Bioresource Technology 219(3): 169-174.
[7] Guo, X., Lu, Y., Li, Q. (2016b): Effect of adding flue gas desulphurization gypsum on the transformation and fate of nitrogen during composting. – Compost Science & Utilization 24(4): 230-237.
[8] He, Z., Griffin, T. S., Honeycutt, C. W. (2004): Phosphorus distribution in dairy manures. – Journal of Environmental Quality 33(4): 1528-1534.
[9] Khalil, A. I., Beheary, M. S., Salem, E. M. (2011): Monitoring of microbial population and their cellulolytic activities during the composting of municipal solid waste. – World Journal of Microbiology and Biotechnology 17(1): 155-161.
[10] Kinney, T., Masiello, C., Dugan, B., et al. (2012): Hydrologic properties of biochars produced at different temperatures. – Biomass & Bioenergy 41(5): 34-43.
[11] Ktilcia, R., Yaldiz, O. (2014): The composting of agricultural wastes and the new parameter for the assessment of the process. – Ecological Engineering 69(4): 220-225.
[12] Liang, C., Das, K. C., McClendon, R. W. (2013): The influence of temperature and moisture contents regimes on the aerobicmicrobial activity of a biosolids composting blend. – Bioresource Technology 86(2): 131-137.
[13] Malifiska, K., Zabochnicka-Switek, M., Dach, J. (2014): Effects of biochar amendment on ammonia emission during composting of sewage sludge. – Ecological Engineering 7(1): 474-478.
[14] Smars, S., Gustafsson, L., Bech-Friis, B., et al. (2002): Improvement of the composting time for household waste during an initial low pH phase by mesophilic temperature control. – Bioresource Technology 84(2): 237-241.
[15] Wang, K., Li, W., Gong, X., et al. (2013): Spectral study of dissolved organic matter in biosolid during the composting process using inorganic bulking agent: UV-vis, GPC, FTIR and EEM. – International Biodeterioration & Biodegradation 85(3): 617-623.
[16] Warker, J. F. (2001): Methods to evaluate maturity of compost. – Compost Science 12(1): 33-55.
[17] Xi, B., Zhao, X., He, X., et al. (2016): Successions and diversity of humic-reducing microorganisms and their association with physical-chemical parameters during composting. – Bioresource Technology 219: 204-21 1.
[18] Xiao, Y., Zeng, G. M. (2011): Changes in the actinomycetal communities during continuous thermophilic composting as revealed by denaturing gradient gel electrophoresis and quantitative PCR. – Bioresour Technol 102(4): 1383-1388.
[19] Zhou, Y., Selvam, A., Wong, J. (2014): Evaluation of humic substances during co-composting of food waste, sawdust and Chinese medicinal herbal residues. – Bioresource Technology 168(5): 229-234.

http://www.aloki.hu ● ISSN 1589 1623 (Print) ● ISSN 1785 0037 (Online)
DOI: http://dx.doi.org/10.15666/aeer/1705_1161911628

EFFECTS OF DIFFERENT TYPES OF MULCHING FILMS ON SOIL EVAPORATION AND TEMPERATURE

SUN, S. J.[1] – ZHU, Z. C.[1] – CHEN, Z. J.[1] – WANG, W.[1,2] – YIN, G. H.[2] – DONG, K. B.[1*]

[1]*College of Water Conservancy, Shenyang Agricultural University, Shenyang 110866, China*

[2]*Institute of Applied Ecology, Chinese Academy of Sciences, Shenyang 110016, China*

**Corresponding author*
e-mail: dongkebao@126.com

(Received 22nd Apr 2019; accepted 12th Jul 2019)

Abstract. Biodegradable plastic films, which are alternatives to traditional polyethylene plastic films and have similar functions, are incorporated into the soil after the crop season, and could, therefore, increase grain yield and decrease film-residues. In this study, we investigated the effect of three types of biodegradable films mulched (liquid film (LF), multi-functional paper film (MPF), and powder film (PF)), conventional plastic film mulched (PE) and unmulched (CK) on soil water and temperature in pots without crops. The results showed that cumulative temperature increased markedly under LF, PF, PE, and MPF by 20.3, 19.3, 24.4, and 22.7 °C, respectively, compared to CK. The greatest reduction in total evaporation compared to CK was observed under PE (43.9 mm). Soil evaporation was reduced the most under PE (36.5mm); however, the MPF and PF treatments significantly decreased total soil evaporation by 2.7 mm and 3.1 mm, respectively, compared to CK. Our results indicated that biodegradable films improved the average soil temperature at a depth of 10 cm and reduced soil evaporation, under MPF and PF resulting in the greatest overall improvement. We concluded that multi-functional paper film and powder film can be alternatives to traditional polyethylene plastic film.
Keywords: *water saving in agriculture, biodegradable films, crop yields, green agriculture, environmental pollution*

Introduction

In recent decades, plastic film mulching has been one of the most important agronomic practices impacting crop yields worldwide (Zhang et al., 2016). Many earlier studies have shown that plastic film mulching offers considerable advantages, such as increasing soil temperature, reducing evaporation, improving crop quality and yield, controlling salinity accumulation, and reducing the leaching of fertilizer (Wang et al., 2016; Xu et al., 2006). For these reasons, the utilization of plastic film has increased substantially; similarly, the area mulched has also increased. Previous studies have shown that the worldwide consumption of plastic film has reached 0.5–1.5 million tons per year (Yang et al., 2015). Consumption of plastic film in China accounts for 60% of the world plastic film demand, making China the largest market in the world for these products (Yang et al., 2015). However, from the environment's perspective, plastic film mulching can cause several environmental issues because of its non-degradable nature. After crop harvesting, the plastic film progressively breaks down into pieces that remain and accumulate in the field (Briassoulis et al., 2013, 2015). Moreover, these residual films have been shown to decrease soil permeability, hinder crop root development, reduce nutrient and moisture absorption by crops, and inevitably result in crop production losses (Yan et al., 2006). Many measures have been undertaken to counter these problems, including burning and recycling of plastic films or disposal in landfills (Kyrikou and Briassoulis, 2007). In China, however, the recovery rate of plastic films from the fields was very low because of high labor costs and

http://www.aloki.hu ● ISSN 1589 1623 (Print) ● ISSN 1785 0037 (Online)
DOI: http://dx.doi.org/10.15666/aeer/1705_1162911638

poor efficiency of the recovery machinery (Zhang et al., 2016). Thus, an increasing number of studies have been conducted to develop eco-friendly alternative mulch products that satisfy all the desired functional properties of plastic films (Touchaleaume et al., 2016). Alternative mulching products such as biodegradable films, which have properties similar to conventional plastics but are decomposed and catabolized by microorganisms into carbon dioxide and water over time, are being increasingly used for crop production as they represent a sustainable agronomic solution (Costa et al., 2014). Studies have indicated that biodegradable film can theoretically reduce disposal and labor costs markedly by becoming incorporated directly into the soil rather than requiring disposal by burning or landfill use (Kasirajan and Ngouajio, 2013). Additionally, the biodegradable film had considerable beneficial effects on soil temperature and water content by reducing heat loss and evaporation (Ren et al., 2016). However, different biodegradable films have different functional properties. Studies have shown that some biodegradable films do not have a significant influence on soil water content and temperature because of their short lifespan. Moreover, it has also been suggested that the degradation rate of some biodegradable films is low, causing more serious problems than residual films. Taken together, these results suggest that the development of new types of biodegradable films is required to consistently improve their performance in the field.

In this study, three new types of biodegradable films and their effect on soil water content and temperature were investigated. The first film was a liquid mulching film; this is a new kind of agricultural product that is mainly manufactured from organic polymer materials. It is sprayed or poured onto the soil surface and dries to form a durable, permeable film that connects with soil particles to form a special soil membrane structure; this allows the plant to breathe and water to penetrate, thereby aiding moisture retention and prevention of scattering of solid fertilizers (Yin et al., 2013). The second film was a powder mulching film (humic acid-degradable film) that is mainly manufactured from the raw material humic acid. It can also be sprayed onto the fields to form a durable and biodegradable black film that helps retain moisture and improve soil conditions (Tian et al., 2008). The third film was a multi-functional paper film that not only has good mechanical strength, light transmission, water penetration, and water and heat preservation properties, but also can degrade naturally over a certain period of time (Zhou and Zhu, 2002); this film is produced from plant paper pulp and annexing agents such as wet strength and transparent agents.

In this study, these three different types of degradable mulching films were used as soil mulch to compare their effects with common plastic films and a non-mulching control. The effects and characteristics of the different mulch films on soil moisture and temperature were determined. The results of this study will be useful for farmers in selecting more suitable field mulch films, and for smallholders in improving their products and increasing the yield in future.

Materials and methods

The experiments were conducted from 7 September to 15 November 2014 in the rain-protection shed of the Liaoning Province Key Laboratory of Water Saving (Institute of Applied Ecology, Chinese Academy of Sciences) that is located in Shenyang city, Liaoning Province. It is situated at 41°10′N–42°12′N latitude and 123°20′E–123°45′E longitude at a height of 44.7 m above sea level. This area is characterized by temperate semi-humid continental climate, with a daily average of 6 h of sunshine.

http://www.aloki.hu ● ISSN 1589 1623 (Print) ● ISSN 1785 0037 (Online)
DOI: http://dx.doi.org/10.15666/aeer/1705_1162911638

The soil was collected from Fuxin Mongolian autonomous county of Liaoning province. The type of soil is brown earth and the texture is sandy loam. Prior to the experiment, the soil was dried and ground through a 5-mm sieve.

We used the following films: polyethylene plastic film (width of 200 mm, thickness of 0.01 mm); powder film (fully degradable plastic powder); liquid membrane (fully degradable liquid mulch film); and multi-functional paper film.

In this experiment, five treatments were used: mulching with (a) polyethylene plastic film (PE), (b) liquid film (LF), (c) multi-functional paper film (MPF), or (d) powder film (PF), and (e) an unmulched control (CK) (*Fig. 1*). The experiment was conducted in a randomized complete design and each treatment repeated three times. Each pot was filled with 10 kg of soil to which 3.6 kg of water was added to achieve an average soil moisture content of 28%. The pot height is 30 cm and the upper and lower inner diameters are 26 cm and 18 cm, respectively and the height of soil in pot is 25 cm.

(a) (b) (c) (d) (e)

Figure 1. *The different treatments used in this experiment*

The weight of each pot was measured at 9:00 A.M. on the first day using an electronic balance with an accuracy of 0.005 g. The pots were weighed daily for the first 20 d after the films were mulched, every 2 d from 20 to 40 d, and every 5 d from 40 d to 70 d. The amount of evaporation between two time-points was calculated as the difference between the weight of the pots at those two time-points. For each treatment, the cumulative soil evaporation was the difference between the weight of the first pot and the weight of the last pot and then it was converted to expressed in millimeters.

Soil temperature was measured at depths of 5 and 10 cm using a geothermometer at 9:00 A.M every 3 d from the first day to the last day of the experiment. For each treatment, the cumulative soil temperature was the sum of all recorded temperatures.

The liquid membrane was observed using a Quanta 250 environmental scanning electron microscope at half a month and four months respectively after it was mulched

SPSS software (version 20) was used for statistical analysis of the experimental results. The effects of the treatments on the measured parameters (soil evaporation and soil temperature) were evaluated using one-way analysis of variance (ANOVA). Least significant differences (LSD) were used to analyze the differences between the means of treatments. The differences were considered statistically significant with a threshold of $p \leq 0.05$.

Results and discussion

Effect of different treatments on soil moisture

Differing patterns of soil evaporation (soil water change) were observed under different mulch treatments from 7 September to 15 November 2014. This is consistent with the different materials having different effects on evaporation (*Fig. 2*). *Figure 2* shows that

http://www.aloki.hu ● ISSN 1589 1623 (Print) ● ISSN 1785 0037 (Online)
DOI: http://dx.doi.org/10.15666/aeer/1705_1162911638

mean soil evaporation of MPF, PF, LF and CK during the experiment period were 1.1, 1.1, 1.2 and 1.2 mm, respectively, which are significantly higher than that of PE (0.2 mm). In addition, soil water evaporation fluctuated more under the biodegradable film treatments (MPF, PF, and LF) and the control (CK), which coefficient of variance were 89%, 83%,87% and 82% respectively, than the PE treatment (47%). These results indicated that the polyethylene plastic film was able to better prevent evaporation than the biodegradable films; this is consistent with previously reported results (Ren et al., 2016). Costa et al. (2014) also reported that the average soil water content under the PE treatment was markedly higher than that under the biodegradable film mulching treatments. Marked variations in soil water evaporation under the biodegradable film mulching treatments and CK were recorded in first twenty days mainly because of the higher air temperature and longer lighting time in September; this seasonal pattern also likely explains that greater fluctuation in evaporation observed in September than after September. *Figure 3* shows that although evaporation under PE was lower than that under the three biodegradable film mulching treatments, the MPF and PF treatments greatly improved moisture retention in comparison with CK. This result is consistent with the results of Ren et al. (2016), who found that the use of biodegradable films considerably reduced soil water evaporation and enhanced the retention of soil moisture, and those of Wang et al. (2016), who reported that the use of biodegradable films resulted in soil water storage values between 90.4%–95.4% of those obtained under the PE treatment. Taken together, these results indicate that biodegradable films are acceptable substitutes for plastic film in terms of moisture retention.

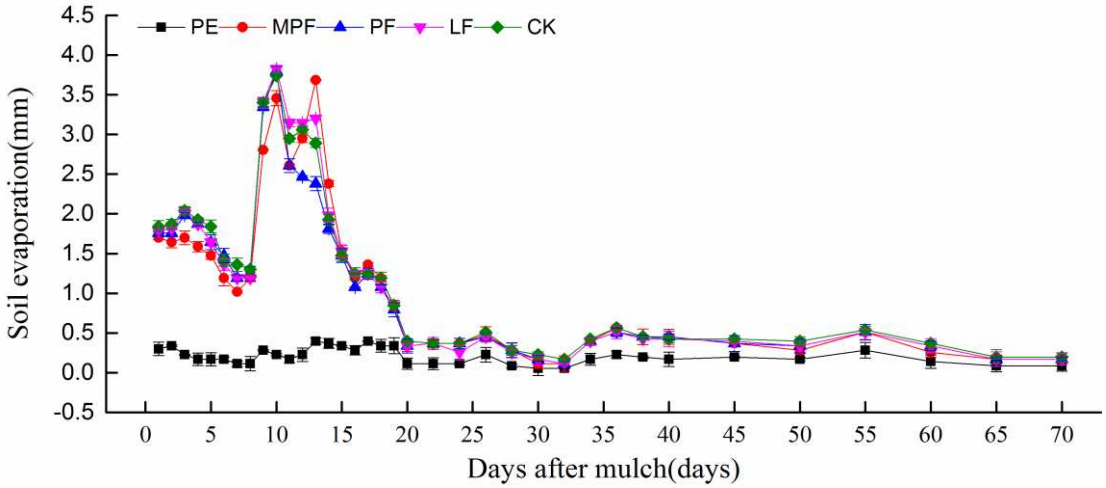

Figure 2. *Changes in soil moisture under different treatments*

The total evaporation for different mulching treatments are illustrated in *Figure 3*. Generally, the total amount of soil evaporation under the mulching treatments was significant less than for CK. Compared to CK, the, LF, PF, PE, and MPF treatments reduced the total evaporation by, 0.7, 3.1, 36.5 and 2.7 mm, representing 1.6%, 7.1%, 83.0%, and 6.0% of the evaporation observed under CK, respectively. Overall, the total soil moisture evaporation was the lowest under PE and higher under PF, MPF, and LF in that order. This was similar to the results of a four-year field study in semi-arid areas, such as the Loess Plateau, conducted by Ren et al. (2016), who found that the PE treatment showed markedly higher soil moisture than the liquid film mulching and non-mulching treatments.

http://www.aloki.hu ● ISSN 1589 1623 (Print) ● ISSN 1785 0037 (Online)
DOI: http://dx.doi.org/10.15666/aeer/1705_1162911638

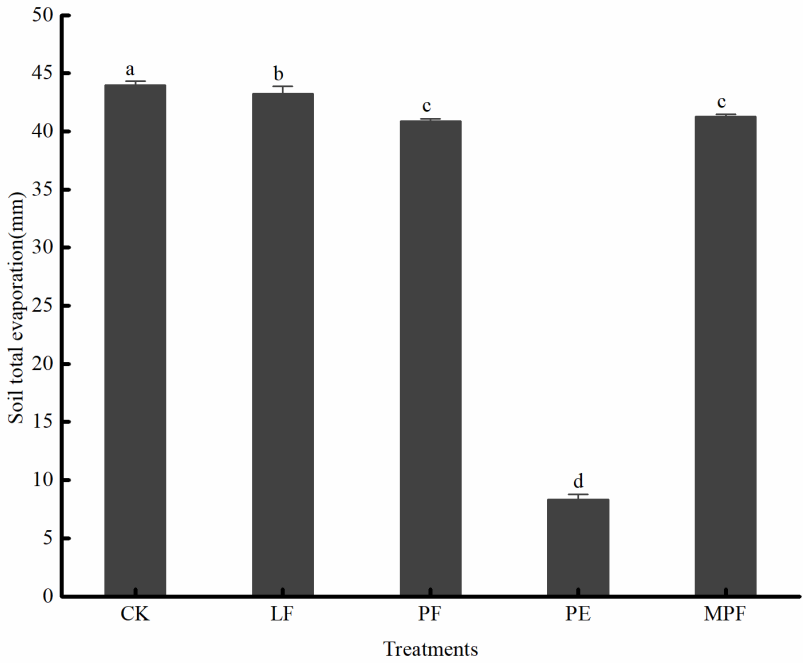

Figure 3. *Total evaporation under different treatments. (Different lowercases in a group indicate significant differences at p = 0.05 level among different treatments)*

Effect of different treatments on soil temperature

The trends in soil temperature were almost identical under the five treatments, likely because of the effects of air temperature. Many previous studies have suggested that topsoil temperature is affected considerably by air temperature (Bai et al., 2015). Consistent with these, we also found that average soil temperature at the depth of 10 cm was generally significantly affected by mulching ($p < 0.05$) (*Fig. 4*). The experimental results showed that mean soil temperature under the four mulching treatments was significantly higher than under CK. This result is consistent with a previous study that showed mean soil temperature was effectively enhanced by mulching with plastic films and biodegradable films (Ren et al., 2016). *Figure 4* also illustrates that at different stages of the experiment, the warming effects of different mulching materials differed. From 25 d to 50 d after the start of the experiment, the soil temperature was the highest under PE, indicating that PE has a stronger effect on soil temperature. This result is in agreement with those of previous studies (Costa et al., 2014; Ren et al., 2016). In the first 25 d of the experiment, however, the soil temperature under LF and MPF was higher that under PE, probably because in the first 25 d of the experiment, stable structures formed under MPF and LF were more useful in early stage. In the last 20 d of the experiment, although the soil temperature increased with air temperature about 55 d after mulching, there were no significant differences in soil temperature between the four mulching treatments. The reason is that in the last mulching period (in November), the air temperature was relative low and had not significant influence on soil.

The cumulative soil temperatures under different treatments are shown in *Figure 5*. For the mulching treatments, all the cumulative mean soil temperatures were markedly higher than for CK. Compared to CK, the cumulative temperatures under LF, PF, PE, and MPF were increased by 20.3, 19.3, 24.4, and 22.6 °C, representing 5.0%, 4.8%,

http://www.aloki.hu ● ISSN 1589 1623 (Print) ● ISSN 1785 0037 (Online)
DOI: http://dx.doi.org/10.15666/aeer/1705_1162911638

6.0%, and 5.6% of the cumulative temperature of CK. These findings are consistent with the results of other studies (Bai et al., 2015; Li et al., 2012). Liu (2012) reported that there were significant warming effects under biodegradable film treatments compared to CK. Moreover, Hu (2015) demonstrated that the use of biodegradable film in maize cultivation considerably improved the soil temperature at the depth of 10 cm. Notably, *Figure 5* illustrates that the cumulative temperature was the highest under PE, being 4.1, 5.1, and 1.7 °C higher than that under LF, PF, and MPF, respectively. This is consistent with the results of Bai et al. (2015), who found that the mean temperature at the depth of 25 cm was increased by 1.0 °C under PE, compared to biodegradable film. Although the cumulative temperature was lower under LF, PF, and MPF than under PE, these three treatments still had considerably higher cumulative temperatures than CK. A similar result was obtained by Costa et al. (2014) who reported that biodegradable film mulching improved soil warming and provided highly favorable conditions for crop growth. Taken together, these results indicate that biodegradable polymers, because of the warming effects of the biodegradable film, are sustainable alternatives to PE films in some agricultural production systems.

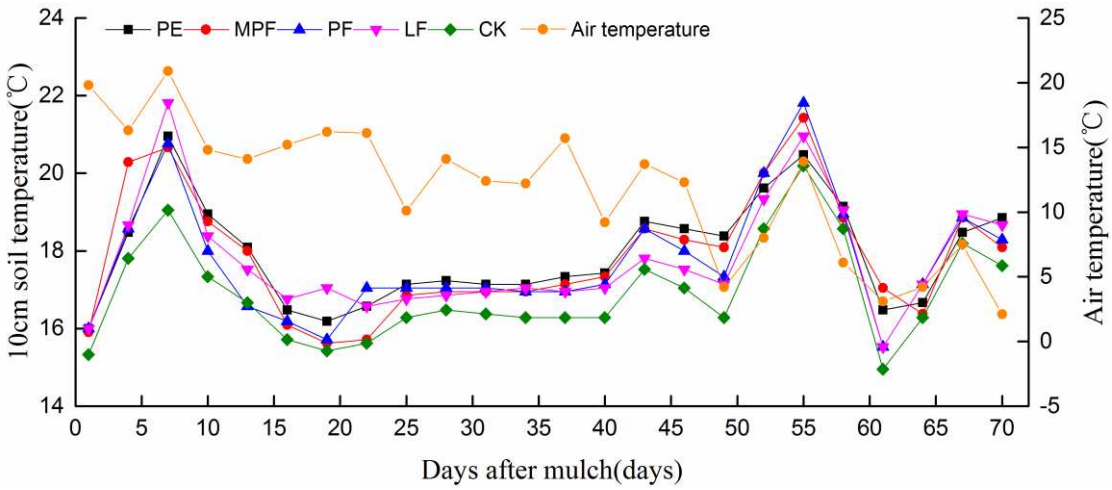

Figure 4. *Soil temperature at the depth of 10 cm under different treatments*

Modelling the effects of time spent mulched by film and soil temperature on total soil evaporation

Soil moisture is an important factor affecting crop growth; film mulching could reduce excessive soil moisture evaporation and improve soil temperature. Therefore, evaluation of the effects of different film mulching treatments on soil evaporation may provide useful information regarding selecting mulching planting technologies. The time spent mulched by a film and the soil temperature were chosen as independent variables that affect changes in soil moisture content, and the total variation in total evaporation under different treatments was chosen as the dependent variable to establish a regression model using SPSS 20.0; this model was used to analyze the effects of film-mulched time and soil temperature on total soil evaporation. The results are shown in *Table 1*.

Table 1 shows that the least adjusted R-square of all treatments was 0.69 at $p < 0.05$; this indicates that the linear equations effectively and adequately represent the

http://www.aloki.hu ● ISSN 1589 1623 (Print) ● ISSN 1785 0037 (Online)
DOI: http://dx.doi.org/10.15666/aeer/1705_1162911638

relationship between soil evaporation, soil temperature and mulching time. A negative relationship between evaporation and mulching time was obtained from the linear equations of LF, PF, MPF, and PE. This suggests that a long film- mulched time would reduce the total evaporation of soil moisture. In contrast, a higher soil temperature would result in increased evaporation.

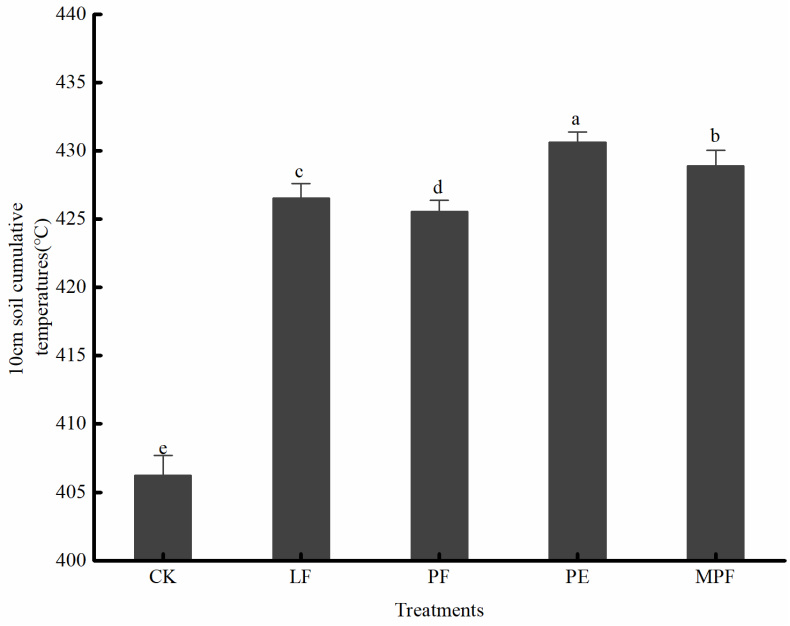

Figure 5. *Cumulative soil temperature under different treatments. (Different lowercases in a group indicate significant differences at p = 0.05 level among different treatments)*

Table 1. *Soil moisture model under different treatments*

Treatment	Linear relationship	Adjusted R Square	Sig.
Liquid film	Evaporation = 0.001-t*0.002 + 0.004*T	0.746	.000[b]
Powder film	Evaporation = 0.007-t*0.002 + 0.003*T	0.826	.000[b]
Paper film	Evaporation = 0.025-t*0.002 + 0.002*T	0.694	.000[b]
Plastic film	Evaporation = 0.008-t*0.002 + 0.04*T	0.718	.000[b]

t: time spent mulched; T: cumulative temperature

Microscopic effects of liquid film on soil structure

Combination of liquid film and soil particles

Microscopic analysis of the effects of liquid film on soil structure is shown in *Figure 6.* The results show that many small particles are combined into large particles on the soil surface by sticky flocculated colloid. Between these large particles, there were many fabric couplings that were similar to the chemical bonding that occurs in molecular structures. These couplings could connect two or more of the soil particles, allowing them to form a stable structure. In addition, these fabric couplings have a strong bonding force that makes soil particles connect in a lattice frame rather than "point to point".

http://www.aloki.hu ● ISSN 1589 1623 (Print) ● ISSN 1785 0037 (Online)
DOI: http://dx.doi.org/10.15666/aeer/1705_1162911638

When soil particles were mulched by the liquid film, the physical and chemical properties of soil improved and the accumulation of organic matter contributed to the formation of soil membrane structure that enhanced the stability of the soil surface.

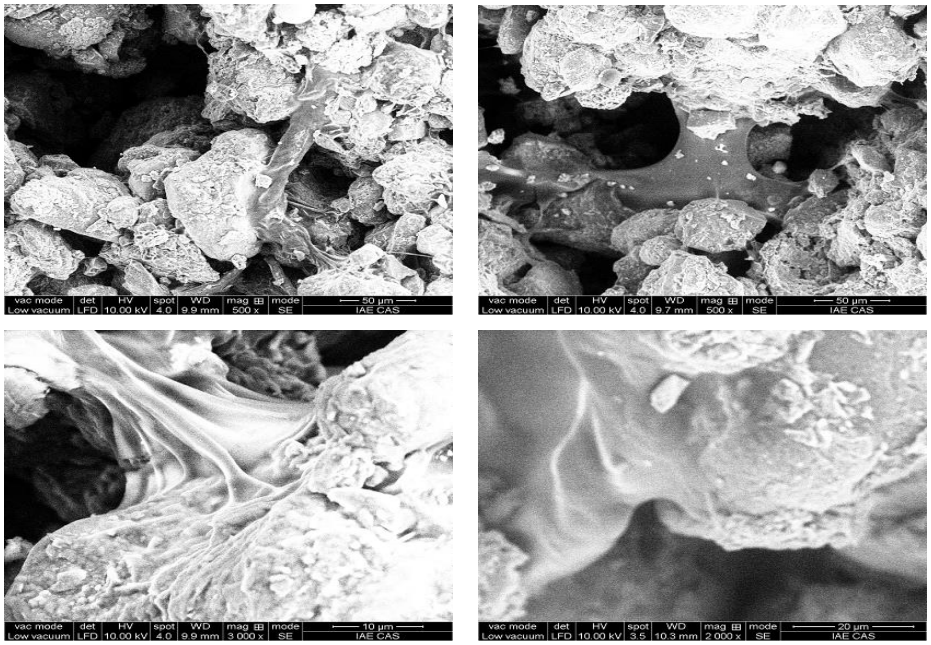

Figure 6. *Connection of the liquid film with soil particles*

Surface tension of the membrane structure

Surface tension of the membrane structure is illustrated in *Figure 7*. These images show that even with the irregular size of soil particles and the irregular size of the pores between particles, the membrane can make a tight connection between rough soil particles through the surface tension of the liquid membrane. Regardless, the surface tension of the liquid membrane on the surface of soil particles was easily broken. As shown in *Figure 7*, the liquid membrane between the soil particles was prone to damage, thereby reducing the films moisture-retaining effects. This likely explains why evaporation was higher under LF than under the other two biodegradable film mulching treatments (*Fig. 3*).

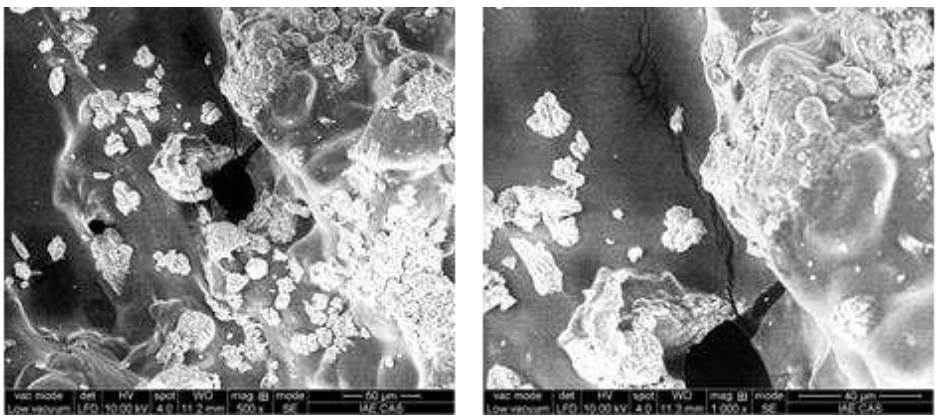

Figure 7. *The surface tension of the membrane structure*

http://www.aloki.hu ● ISSN 1589 1623 (Print) ● ISSN 1785 0037 (Online)
DOI: http://dx.doi.org/10.15666/aeer/1705_1162911638

Conclusion

Three biodegradable mulching films (liquid film, powder film, and multi-functional paper film) were used in this study and compared with the common plastic film and an untreated, unmulched control. Significantly less evaporation was observed under powder film, multi-functional paper film, and polyethylene plastic film treatments relative to CK. In terms of water retention, plastic mulch film was the best, followed by powder film and multi-functional paper film, with the liquid mulch having the lowest water retention of the tested films.

Soil warming was enhanced by mulching with plastic and biodegradable films. Moreover, soil temperature was the highest under the plastic film, followed by multi-functional paper film, powder film, and finally liquid film. The increase in cumulative soil temperature was significantly higher in the early stages of the experiment than in the later stages.

Scanning of the soil microstructure using an electron microscope showed that the correct spraying of liquid membrane could effectively cement soil particles together and reduce moisture evaporation. However, the stable structure formed by the liquid film degraded easily, accounting for the reduced moisture-retaining and warming effects that were observed under the liquid film compared to the other biodegradable film treatments.

The results of this study indicate that, currently, the effects of biodegradable films on water retention and conservation of soil temperature are still inferior to plastic films. Biodegradable film producers should, therefore, further improve their products to meet future agricultural development needs.

Acknowledgements. This work was supported by the China Special Fund for Agro-scientific Research in the Public Interest (No. 201303125), the Natural Science Foundation of Liaoning Province, China (No. 20180550617), the Scholarship of China Scholarship Council (No. 201308210026).

REFERENCES

[1] Bai, Y. S., Jia, S. H., Huang, C. X., Luo, T. F. (2015): Effect of biodegradable film on soil temperature, moisture and yield of spring wheat in dryland. – Journal of Triticeae Crop 35(11): 1558-1563 (in Chinese).

[2] Briassoulis, D., Babou, E., Hiskakis, M., Scarascia, G., Picuno, P., Guarde, D., Dejean, C. (2013): Review, mapping and analysis of the agricultural plastic waste generation and consolidation in Europe. – Waste Management & Research the Journal of the International Solid Wastes & Public Cleansing Association Iswa 31(12): 1262-1278.

[3] Briassoulis, D., Babou, E., Hiskakis, M., Kyrikou, L. (2015): Analysis of long-term degradation behaviour of polyethylene mulching films with pro-oxidants under real cultivation and soil burial conditions. – Environmental Science and Pollution Research 22(4): 2584-2598.

[4] Costa, R., Saraiva, A., Carvalho, L., Duarte, E. (2014): The use of biodegradable mulch films on strawberry crop in Portugal. – Scientia Horticulturae 173: 65-70.

[5] Hu, H. L. (2015): Studies on Yield Effects, Degradation Properties of Biodegradable Mulch Film and Its Field Demonstration. – Zhejiang University, Zhejiang (in Chinese).

[6] Kasirajan, S., Ngouajio, M. (2013): Erratum to: Polyethylene and biodegradable mulches for agricultural applications: a review. – Agronomy for Sustainable Development 33(2): 443-443.

http://www.aloki.hu ● ISSN 1589 1623 (Print) ● ISSN 1785 0037 (Online)
DOI: http://dx.doi.org/10.15666/aeer/1705_1162911638

[7] Kyrikou, I., Briassoulis, D. (2007): Biodegradation of agricultural plastic films: a critical review. – Journal of Polymers and the Environment 15(2): 125-150.
[8] Li, R., Wang, M., Jia, Z. K., Hou, X. Q., Yang, B. P., Han, Q. F., Nie, J. F., Zhang, R. (2012): Effects of different mulching patterns on soil temperature, moisture water and yield of spring maize in Weibei Highland. – Transactions of the Chinese Society of Agricultural Engineering 28(2): 106-113 (in Chinese).
[9] Liu, Q. (2012): Degradation of Biodegradable Mulch Film and Its Effect on Growth and Yield of Maize. – Northwest A&F University, Shanxi (in Chinese).
[10] Ren, X. L., Zhang, P., Chen, X. L., Guo, J. J., Jia, Z. K. (2016): Effect of Different Mulches under Rainfall Concentration System on Corn Production in the Semi-Arid Areas of the Loess Plateau. – Scientific Reports 6: 19019.
[11] Tian, Y. Y., Qiao, Y. Y., Guo, S. Y. (2008): Humic acid multifunctional degradable film (powder) standard draft. – Humic Acid 3: 47-50.
[12] Touchaleaume, F., Martin-Closas, L., Angellier-Coussy, H., Chevillard, A., Cesar, G., Gontard, N., Gastaldi, E. (2016): Performance and environmental impact of biodegradable polymers as agricultural mulching films. – Chemosphere 144: 433-439.
[13] Wang, S. Y., Fan, T. L., Li, S. Z., Zhang, J. J., Zhao, G., Wang, L., Dang, Y., Jiang, X. F. (2016): Property of biodegradable film degradation, water-retention and increasing soil temperature and its impact on maize growth and development process. – Agricultural Research in the Arid Areas 34(1): 127-133 (in Chinese).
[14] Xu, X. C., Wang, C. Y. (2006): The status and development trend of cultivation mulch film at home and abroad. – Plant Fibers and Products 28(1): 6-11.
[15] Yan, C. G., Mei, X. R., He, W. Q., Zheng, S. H. (2006): Present situation of residue pollution of mulching plastic film and controlling measures. – Transactions of the Chinese Society of Agricultural Engineering 22(11): 269-272 (in Chinese).
[16] Yang, N., Sun, Z. X., Feng, L. S., Zheng, M. Z., Chi, D. C., Meng, W. Z., Hou. Z. Y., Bai, W., Li, K. Y. (2015): Plastic film mulching for water-efficient agricultural applications and degradable films materials development research. – Advanced Manufacturing Processes 30(2): 143-154.
[17] Yin, G. H., Hao, L., Zhao, Y. H., Gu, J., Liu, Z. X. (2013): Effects of hydromulching on soil water availability. – Chinese Journal of Ecology 32(6): 1405-1411 (in Chinese).
[18] Zhang, D., Liu, H. B., Hu, W. L., Qin, X. H., Ma, X. W., Yan, C. R., Wang, H. Y. (2016): The status and distribution characteristics of residual mulching film in Xinjiang, China. – Journal of Integrative Agriculture 15(11): 2639-2646.
[19] Zhou, J. H., Zhu, H. G. (2002): Research and application of paper film. – China Pulp and Paper 5: 56-58 (in Chinese).

http://www.aloki.hu ● ISSN 1589 1623 (Print) ● ISSN 1785 0037 (Online)
DOI: http://dx.doi.org/10.15666/aeer/1705_1162911638

A BIBLIOGRAPHIC ANALYSIS OF WATER EFFICIENCY AMONG GREEN BUILDING RATING TOOLS: LEED AND ESGB

ZHOU, W. W.[1,2] – WU, D. J.[1*] – CHENG, X. X.[1*] – LUO, C. W.[1] – TAN, F. X.[1] – ZHANG, Z. L.[2]

[1]*School of Municipal and Environmental Engineering, Shandong Jianzhu University, Jinan, 250101 Shandong, China*
(phone/fax: +86-531-8636-7291)

[2]*Shandong Urban Construction Vocational College, Jinan, 250103 Shandong, China*
(phone/fax: +86-531-8970-9958)

**Corresponding authors*
e-mail: wdj@sdjzu.edu.cn, chengxiaoxiang18@sdjzu.edu.cn; phone/fax: +86-531-8636-7291

(Received 22nd Apr 2019; accepted 12th Jul 2019)

Abstract. The green building rating tools can be used to evaluate, and promote the building industry's sustainability, but previous relevant research on the comparative analysis were mainly conducted at the general, category or criteria level, very little research has been done from the indicator level via statistical analysis. Especially, research on the comparison of water efficiency is rare. To this end, this paper will focus on a thorough and comprehensive comparison of the water efficiency between Leadership in Environmental and Energy Design (LEED, US) and Evaluation Standard of Green Building (ESGB, China). The comparison of the specific terms includes six aspects, i.e. macroscopic, building water use, landscape water use, heat and cooling system use water, nontraditional water source utilization and water monitoring system. The similarities and differences of water efficiency standards are described. In the end, the development direction of domestic water efficiency technology is pointed out and meanwhile, a more reasonable water efficiency standard in China is suggested. The LEED is also suggested to use the detailed items of the non-traditional water source utilization from ESGB for reference. The research results would serve as a useful reference for both industry practitioners and academics that are interested in green buildings.
Keywords: *building certification systems, water, sustainability, green rating systems, comparative analysis, research review*

Introduction

The building industry gives great contribution in creating monetary values and jobs, and makes profound influence on the economy and society (Kang et al., 2016; Lin and Liu, 2015; Liu and Lin, 2016; Marjaba and Chidiac, 2016). However, the development of building industry causes more consumption on the natural resources and energy, simultaneously creates more social problems with carbon emissions, environmental degradation and global warming, etc. According to the World Business Council for Sustainable Development, building block production accounts for approximately 40% of total energy consumption (WBCSD, 2008), 30% of greenhouse gas (GHG) emission (UNEP SBCI, 2008), 17% of fresh water consumption, 25% of the harvested wood (Smith, 2005; Say and Wood, 2012), and produces 45%-65% of disposal waste in landfills (Yudelson, 2008). Hence, the industry is controversial. As a consequence, how to reduce the adverse environment impacts of the building industry becomes a hot point issue.

A Green Building Rating System (GBRS), defined by Nguyen and Atlan (2011), is a tool that can be used to evaluate and promote the sustainability of building industry.

http://www.aloki.hu ● ISSN 1589 1623 (Print) ● ISSN 1785 0037 (Online)
DOI: http://dx.doi.org/10.15666/aeer/1705_1163911653

With the guidance and better insights into sustainability through information analysis, valuation and comparisons, the GBRS can provide the following suggestions on the green buildings:

i. Minimize environment impact of the buildings
ii. Measure buildings' effect on the environment
iii. Objectively evaluate and judge buildings' development (Awadh, 2017)

Many GBRSs have been put into practice in the worldwide (Haapio and Viitaniemi, 2008; Kyvelou and Sinou, 2013; He et al., 2018; Ding et al., 2018), such as Building Research Establishment Environmental Assessment Method (BREEAM, United Kingdom) (BREEAM, 2016), Leadership in Environmental and Energy Design (LEED, the United States) (LEED, 2013), Evaluation Standard for Green Building (ESGB, China) (ESGB, 2014), Green Mark (GM, Singapore) (Green Mark, 2013), Comprehensive Assessment System for Building Environmental Efficiency (CASBEE, Japan) (CASBEE,2014), Green Star (GS, Australia) (Green Star,2015) and ITACA (Italy) (ITACA, 2015). Due to the fact that the GBRSs can promote sustainable practices and play an important role to the development of sustainable buildings, an increasing number of researchers have focused on the comparison the methods and tools used to evaluate the environmental performance of different kinds of buildings (US Green Building Council, 2018).

In the past years, more researchers focused on the development of the assessment standards and the refinement of the existing ones to reduce the environmental impact of the green buildings (Cole, 2006; Ding, 2008; Wang et al., 2012). For example, Mattoni et al. (2018) analyzed the five well known GBRSs (i.e. CASBEE, GS, BREEAM, LEED and ITACA) in detail to find their differences and similarities on six macro-areas (site, water, energy, comfort and safety, materials and outdoor quality), and further explored which issues exhibited more influence on the final performance rate of each systems. Lee (2013) compared the five representative assessment schemes (i.e. BREEAM, LEED, CASBEE, BEAM Plus (Hong Kong) and ESGB) and found that the BREEAM and LEED are the most comprehensive, two-phase certification method is preferable of LEED, CASBEE and BEAM plus, and the weighting coefficients adopted by ESGB were the most representative. Feng and Hewage (2014) took the energy saving performance of green vegetation on LEED certified buildings into consideration and found the green vegetation is not cost-effective in winter months or cold climatic regions due to low energy saving performance, and hence, recommend to improve overall energy performance in green buildings. Li et al. (2017) conducted a systematic review of the existing literature on green building assessment methods through comparative analysis and found the main contributing authors and represented countries, the number of comparative assessment methods, and the current topic is focused on the general comparison and the category comparison. The future research should be developed to the indicator comparison. However, there is no literature that does comprehensive comparisons on water efficiency among GBRSs in detail. Therefore, the objective of this paper is to carry out a comparative analysis on the indicator of water efficiency between LEED and ESGB from six aspects, i.e. macroscopic, building water use, landscape water use, heat and cooling system use water, nontraditional water source utilization and water monitoring system.

This paper begins with the background review of LEED and ESGB, followed by the research methodology for statistical analysis among the paper samples to present the

http://www.aloki.hu ● ISSN 1589 1623 (Print) ● ISSN 1785 0037 (Online)
DOI: http://dx.doi.org/10.15666/aeer/1705_1163911653

evidence of the basis on the topic selected. Then, the six detailed aspects are compared within the water efficiency indicator. Finally the current research focuses are presented; with future development direction is suggested. The results of the systematic review in this paper will serve as a useful reference for both industry practitioners and academics that are interested in the water efficiency of green buildings.

Overview of LEED and ESGB

LEED

LEED was developed by the US Green Building Council (USGBC) for the US Development of Energy (Wu et al., 2016; Hu et al., 2017; Schwartz and Raslan, 2013), and has become the most widely used GBRS in the world. Available for virtually all buildings, communities and home project types, LEED assessments have been carried out in 41 countries, including Canada, Brazil, Mexico, India and China (Lee, 2013; Gelowitz and McArthurand, 2018; Kern et al., 2016; Chen and Lee, 2013). LEED provides a frame work to create healthy, highly efficient and cost-saving green buildings. LEED certification is a globally recognized symbol of sustainability achievement. Now more than 2.2 million square feet is LEED certified every day with more than 92,000 projects using LEED. LEED buildings can save energy, water, resources, generate less waste and support human health. The LEED 1.0 of new construction was first launched at USGBC in 1998 (Altomonte and Schiavon, 2013; Wu et al., 2017), and LEED 2.0 based on modifications made during the pilot period was released. Then the LEED continued to be modified to respond to the needs of the market, and has been expanded to cover different kinds of buildings types. The detailed development of LEED can be seen in *Figure 1* (Doan et al., 2017).

Figure 1. *LEED development history*

Currently, LEED v4 is the newest version. It focuses on materials to get a better understanding of what is in them, and the effect of those components on human health and the environment. A stronger and performance-based approach is used to indoor environmental quality for better occupant comfort. In addition, it brings the benefits of

http://www.aloki.hu ● ISSN 1589 1623 (Print) ● ISSN 1785 0037 (Online)
DOI: http://dx.doi.org/10.15666/aeer/1705_1163911653

smart grid thinking to the forefront with a credit that rewards projects for participating in demand response programs and provides a clear picture of water efficiency by evaluating total building water use.

As *Table 1* illustrated, there are seven categories that cover (maximum number of points for each category in parentheses): location and transportation (32), sustainable sites (10), energy and atmosphere (33), water efficiency (11), materials and resources (13), indoor environmental quality (16), regional priority (4) and innovation (6); the maximum possible total score is 125 points. For example, location and transportation category includes eight indicators (maximum number of points for each indicator): neighborhood development location (16), sensible land protection (1), high-priority site (2), surrounding density and diverse uses (5), access to quality transit (5), bicycle facilities (1), reduced parking footprint (1), green vehicles (1). Each category has the prerequisites condition, which means that the criteria must be included before a project can be evaluated and the core credits given for meeting or exceeding the requirements in the categories (Alyami and Rezgui, 2012). As shown in *Table 2*, the LEED buildings awarded points for individual aspects of assessment are summed and compared against a rating scale to yield an overall grade, which may be certified (40-49 points), silver (50-59 points), gold (60-79 points) or platinum (> 80 points).

Table 1. *The comparison of LEED and ESGB on categories*

GBRS (maximum number of the points for each category)	LEED V4 (125)	ESGB 2014 (110)
Category (maximum points)	Location and transportation (32)	Sustainable site and outdoor environment (21)
	Sustainable sites (10)	Energy use (24)
	Energy and atmosphere (33)	Water saving (20)
	Water efficiency (11)	Material use (17)
	Materials and resources (13)	Indoor environmental quality (18)
	Indoor environmental quality (16)	Innovation (10)
	Regional priority (4)	------
	Innovation (6)	------

Table 2. *The comparison of LEED and ESGB on certified grade*

GBRS	**Grade**	**Credits**
LEED	Certified	40~49
	Silver	50~59
	Gold	60~79
	Platinum	> 80
ESGB	1-star	50~60
	2-star	60~80
	3-star	> 80

ESGB

In China, with the rapid increasing for building industry, the green building began to be explored in the early 1980s in response to the increasing energy use of the residential sector, especially for air-conditioning and heating (Lee, 2013). In March 2006, the first

http://www.aloki.hu ● ISSN 1589 1623 (Print) ● ISSN 1785 0037 (Online)
DOI: http://dx.doi.org/10.15666/aeer/1705_1163911653

Evaluation Standard of Green Building (GB/T 50378-2006) was promulgated by the Ministry of Construction (Lee, 2012). Then it was updated in 2014 with the second version ESGB (GB/T 50378-2014) (ESGB, 2014). From the beginning of 2008 to the end of 2015, the green building certification review system was implemented in China. There were 4071 certified projects with the total area of 472 million square meters for green building, among which 3859 projects with the area of 444 million square meters were green design, and 212 projects with the area of 28 million square meters were green operation (Ding et al., 2018).

There are six categories that cover (maximum number of points for each category in parentheses): Sustainable site and outdoor environment (21), Energy use (24), Water saving (20), Material use (17), Indoor environmental quality (18) and Innovation (10); the maximum possible total score is 110 points. For example, sustainable site and outdoor environment category includes four indicators (maximum number of points for each indicator): land saving (7.14), outdoor environment (3.78), transportation and public service (5.04), site design and ecology (5.04). The score were evaluated by both prerequisites condition and the core credits system. As is shown in *Table 2,* the overall grade of ESGB buildings is on a scale of 1-star (50 - 60 points), 2-star (60-80 points) and 3-star (above 80 points).

Research methodology

Three stages research methodology

Due to the fact that so many researchers have made fully comparisons between different GBRSs from different directions, the three stages was practiced in this review to find a new direction to conduct the analysis.

In stage 1, a thorough search was implemented in the three major data bases: Science Direct, Engineering Village, and Scopus with the key words: LEED, ESGB, green building, assessment methods, sustainable building, energy efficiency, water efficiency, environment protection, indoor environment quality, sustainable site. These reviews mainly cover papers published from 2001 to 2017. After careful reviews of paper contents and removal of duplicates, a total of 73 articles were identified for the next analysis.

During stage 2, the statistical analysis of these 73 articles was carried out to find and identify the research direction from the following aspects:

(i) The statistical number of papers in each year, as illustrated in *Figure 2*. From 2013, more and more researchers focused on the GBRSs innovation and comparison, because the GBRSs are the principle and tool to promote the development of green buildings. Based on these researches so many countries began to implement their own GBRS according to the local condition.

(ii) The statistical number of papers in each country based on the first author's nationality, as explained by *Figure 3*. Currently, green building development in China is still at its initial stage (Zhu et al., 2017; Borong et al., 2016). The BREEAM and LEED are still occupying the dominant position in the green building evaluation market with their mature experience of the green building development in UK and the US. So the papers from Chinese researchers get the main percentage for nearly about 19%. As a developing country, Chinese researchers still has a long way to explore the green building development in theory and practice.

http://www.aloki.hu ● ISSN 1589 1623 (Print) ● ISSN 1785 0037 (Online)
DOI: http://dx.doi.org/10.15666/aeer/1705_1163911653

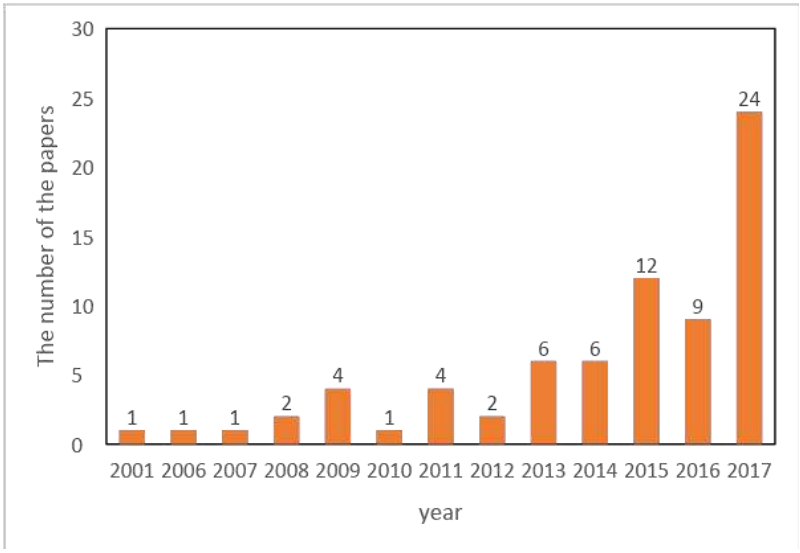

Figure 2. *The number of papers in each year of the selected articles*

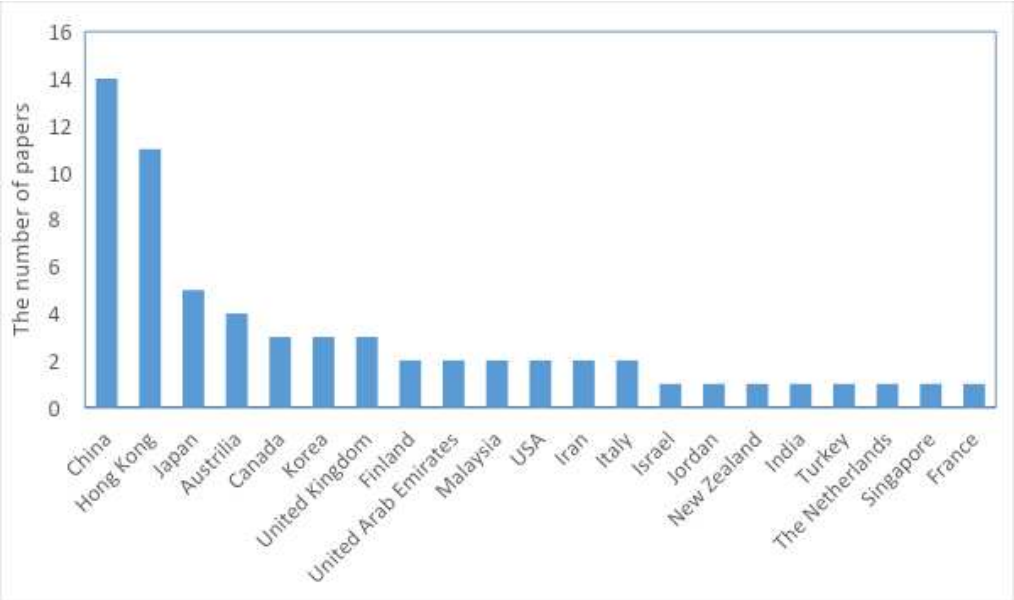

Figure 3. *The number and the percentage of the papers in each country of the selected papers*

(iii) The result to determine the main contributing authors. The formula proposed by Howard for determining the contribution of authors to a multi-authored article was adopted (Howard et al., 1987). The formula is shown in *Equation 1:*

$$\text{Score} = \frac{1.5^{\text{n-1}}}{\sum_{i=1}^{n} 1.5^{\text{n-i}}} \qquad \text{(Eq.1)}$$

where *n* denotes the number of authors of the paper and *i* is the order of each author. As indicated in *Table 3*, Lee from the Hong Kong Polytechnic University is the most active

http://www.aloki.hu ● ISSN 1589 1623 (Print) ● ISSN 1785 0037 (Online)
DOI: http://dx.doi.org/10.15666/aeer/1705_1163911653

author by far. The research from Lee focused on the comprehensive comparison of the GBRSs and the indicator of energy use from different assessment methods. Sharifi focused on the topic of the neighborhood sustainability assessment with different GBRSs (Sharifi, 2016; Sharifi and Yamagata, 2016; Sharifi and Murayama, 2013, 2014).

Table 3. *Main contributing authors*

Author	Number of papers	Score point	Affiliation
Lee W. L.	6	3.92	Hong Kong Polytechnic University
Sharifi Ayyoob	4	2.80	Nagoya University
Ann T. W. Yu	4	1.84	Hong Kong Polytechnic University
Haapio Appu	2	1.60	Helsinki University of Technology
Jian Zuo	2	1.39	University of Adelaide
Illankoon I. M. C. S.	2	0.89	Western Sydney University

(iv) Four levels comparison of the GBRSs of the selected articles. A comprehensive analysis of the selected papers is mainly compared at four levels as is shown in *Table 4:* (a) general comparison (80%); (b) category comparison (71%); (c) criterion comparison (51%); (d) indicator comparison (31%). This result is similar with the investigation result from Li et al. (2017). Thus it can be seen that the indicator comparison is still at a low level for their complicated characteristic in a very detailed sector. Among these indicators, the water efficiency comparison gets the lowest percentage (1%). At the same time, more researchers focused on the comparison on the energy use (11%) and environment (11%) etc. This phenomenon can be explained by the following reasons: (a) The experts in the water utilization sector focused on the development of the water treatment process, chemistry and material, and little relevant experts focused on the green buildings' demand. (b) Water efficiency get relatively lower points from the total scheme, which is easy to be ignored by the auditors and the owners. (c) It is difficult for the building to get more points from water efficiency indicator even after doing some improvements, but it is much easier to be optimised from the energy sector etc. So in this paper, the water efficiency indicator in LEED and ESGB is chosen to make a comparison in order to give a useful reference for both industry practitioners and academics that are interested in the GBRSs.

Table 4. *Four levels of the comparison*

Comparison topics	Sub-topics	Percentage of papers
Level 1: general comparison	• History • Certification levels • Schemes available	80%
Level 2: category comparison	• Weighting or points	71%
Level 3: criterion comparison	• Mandatory criteria • Prerequisite • Minimum points	51%
Level 4: indicator comparison	• Energy (11%) • Environment (11%) • Materials and waste (4%) • Project management (4%) • Water efficiency (1%)	31%

http://www.aloki.hu ● ISSN 1589 1623 (Print) ● ISSN 1785 0037 (Online)
DOI: http://dx.doi.org/10.15666/aeer/1705_1163911653

In terms of stage 3, the comparison of the water efficiency is analyzed from six aspects, i.e. macroscopic, building water use, landscape water use, heat and cooling system use water, nontraditional water source utilization and water monitoring system. Detailed discussions of these comparisons are shown below.

Methodology roadmap

The methodology roadmap of this review is illustrated in *Figure 4*.

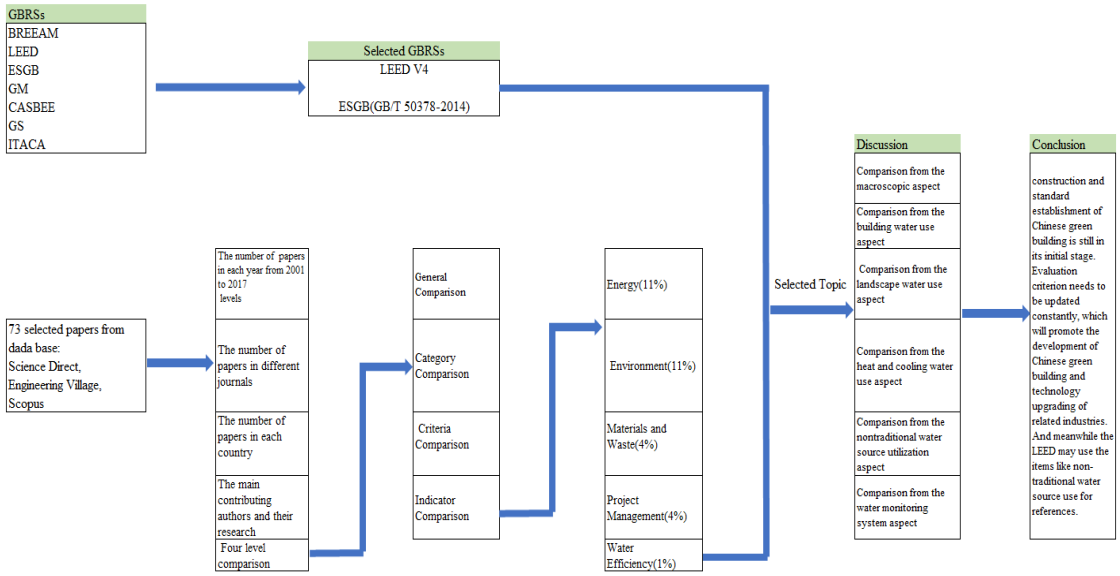

Figure 4. *Methodology roadmap*

Discussion

In this section, comparison analysis results focused on the water efficiency of the LEED and ESGB are carried out from six aspects, i.e. macroscopic, building water use, landscape water use, heat and cooling system water use, nontraditional water source utilization and water monitoring system. The differences between LEED and ESGB are related but not limited to (Awadh, 2017):

i. Considering various and interrelated categories
ii. Prioritizing and weighting concerns

Macroscopic aspect

From the macroscopic point of view, we can clearly find that:

(1) The water efficiency standards of ESGB and LEED are both composed of prerequisites items and credits items (Chen et al., 2015). The differences on prerequisites items are shown as follows:

(i) ESGB prerequisites items mainly focuses on the planning and designing of the whole water system, using water efficiency implements and setting up reasonable and thorough water system, but without any specific quantity indexes. LEED prerequisites items mainly focus on specific and measurable indexes, e.g. reducing the project's landscape water requirement by 30% from the maximum daily water requirement in this region, reducing building water consumption by 20% from the baseline and the basic

http://www.aloki.hu ● ISSN 1589 1623 (Print) ● ISSN 1785 0037 (Online)
DOI: http://dx.doi.org/10.15666/aeer/1705_1163911653

requirements of water efficiency devices, which are detailed into the energy level as well as adoptive energy-saving and water-saving methods.

(ii) Water meter measurement and installation is regarded as a credit item in ESGB but a prerequisites item in LEED.

(2) The water saving standards of ESGB and LEED both focus on building water saving, landscape water saving and condensate water systems (Joustra and Yeh, 2009). They both suggest non-traditional water resource utilization and landscape plants without irrigation required. But their concerns are obviously different. ESGB concerns about daily water consumption, pipe leakage and safety in the whole contestant area; LEED water-saving percentage concerns about each tool, such as faucet, toilet, urinal, dishwasher and clothes washer, etc.

Building water use aspect

Inclusive contents, prerequisites items indexes, water-saving instruments baseline requirements are compared to analyze the similarities and differences of ESGB and LEED.

(1) Inclusive contents

From *Table 5,* we can see that ESGB covers more comprehensive contents. Besides water meter settings and sanitary devices of water-saving requirements, ESGB also concerns water saving and using quota, pipe network leakage, with or without overpressure outflow and the conditions of public bathroom, of which the water saving and using quota standard is Civil Building Water Saving Design Standard GB50555-2010. Valve devices with tight sealing, grading measuring water meter installation are adopted to reduce pipe network leakage. With less than 0.3 MPa water supply pressures of water use spot, points of without overpressure outflow can be gotten. Showers with thermostatic control and temperature display function, user fees are promoted in public lavatory. Public water-saving consciousness is improved by connecting fees with water use. LEED does not have special requirements to public lavatory, but requires controlling the discharge water temperature and gives concrete measures, such as using back-fire arrangement, adding heat collecting system or recycling steam to boiler.

Table 5. *Comparison table of LEED and ESGB on building water-saving contents*

Items	LEED	ESGB
Water saving and consumption quota	×	√
Pipe network leakage	×	√
With or without overpressure outflow	×	√
Water monitoring system	√	√
Public bathroom	×	√
Water-saving requirements of sanitary instruments	√	√

(2) Prerequisites items indexes

ESGB prerequisites items indexes are mainly about macro-direction, which require setting out water resource utilization program, setting reasonable water supply and drainage system and selecting water-saving instruments. LEED requires specific and quantitative indexes, which includes:

http://www.aloki.hu ● ISSN 1589 1623 (Print) ● ISSN 1785 0037 (Online)
DOI: http://dx.doi.org/10.15666/aeer/1705_1163911653

(i) Building water use: the total water-saving amount of toilets, urinals, towers, kitchen faucets etc reduces 20% by the baseline.

(ii) Clothes washers, dish washers, ice machine are all qualified of "Energy Star", and water amount of spray valve is no more than 0.082 L/s.

(iii) Regulating limiting value of maximum water amount to dish washers, food steamers and combination stove.

(iv) Water meter statistics can be checked for at least five years. LEED has more concrete prerequisites item indexes and is more difficult than ESGB to get points.

(3) Water-saving instruments baseline requirements

From the basic requirements of water-saving instruments in China and the US in *Table 6,* LEED water-saving instruments have better water-saving effect than ESGB in most cases. LEED has more strict water-saving efficiency requirements. For example, LEED requires 6 L/flush in toilets and ESGB single grade toilets require 6.5 L/flush. Urinal requirement is 3.8 L/flush in LEED and 4 L/flush in ESGB. The faucet flow seems to be the same, but LEED requires higher water flow than ESGB. Consequently, LEED has more strict requirements, which means China has quite a lot to do to improve on instruments using water-saving technology.

Table 6. *Water-saving requirements baseline requirements*

Items	LEED	ESGB
Toilet	6 L/flush	According to the limit value and GB25502-2010 level of toilets water-use efficiency, the minimum requirements of scoring are 3 grades: single grade 6.5 L/flush, double/big grade 6.5 L/flush, small grade 4.2 L/flush and the average value is 5.0 L/flush
Urinal	3.8 L/flush	According to the limit value and GB28377-2012 level of urinals water-use efficiency, the minimum requirements of scoring are 3 grades, namely 4 L/flush
Faucet	Under 0.415 MPa, public lavatory faucets	According to the limit value and GB25501-2010 level of faucets water-use efficiency, the minimum requirements of scoring are 3 grades, namely 0.15 L/s (0.1 ± 0.01 MPa)
	0.03 L/s, private lavatory faucets	
	0.14 L/s, kitchen faucets 0.14 L/s	
Showerhead	Under 0.55 MPa, the flow is 0.16 L/s	Under 0.1 ± 0.01 MPa, the flow is 0.15 L/s

Landscape water use aspect

ESGB and LEED both suggest growing plants without permanent irrigation requirements. LEED requires reducing 30% landscape water by maximum daily water consumption in the prerequisites item. More than 50% water saving percentage equals 1 point, and 100% water saving percentage equals 2 points. ESGB suggests adopting water-saving irritation system, setting up soil humidity sensor, and closing device on rainy days, etc. In a word, ESGB standard concerns whether there is corresponding measures, whereas LEED pays more attention on the ultimate water-saving effect and gives specific quantitative indexes.

ESGB encourages concerning rain utilization facilities. To be specific, during the stage of the landscape design, it is highly suggested that more than 60% of the

http://www.aloki.hu ● ISSN 1589 1623 (Print) ● ISSN 1785 0037 (Online)
DOI: http://dx.doi.org/10.15666/aeer/1705_1163911653

landscape water amount should be derived from rain water. Besides, it requires using non-point source pollution controlling facilities to purify rain in landscape water and encourages using aquatic animals and plants to purify water.

Heat and cooling system water use aspect

LEED prerequisites items have regulations on cooling tower and evaporative condenser: water meter, conductance controller, overflow warning, valid drift canceller (controlling the maximum water drifting to 0.002% of recycling water in counter-current tower and 0.005% of recycling water in disposable water quality) are needed. The requirements in credit item are:

(i) Disposable water quality analysis of cooling tower and evaporative condenser have to include Ca^{2+}, total alkalinity, SiO_2, Cl^- and conductivity.

(ii) 1 point can be gained if the maximum cycle index of cooling tower reaches 10. Whether improving supplementary water quality to 10 minimum cycle index, or using 20% non-drinking water source on the basis of 1 point can get 2 points.

ESGB suggests setting water-treatment facilities to water reuse system, such as enlarging water catching tray, setting balance tube or water tank, requiring more than 80% evaporation water consumption of water supplement in the cooling tower, or using non-evaporating cooling water consumption technology. ESGB approves utilizing non-traditional water source in cooling water supplementary system. The higher the percentage of non-traditional water source use is, the higher the points are.

In terms of similarity, both of LEED and ESGB put forward concrete and quantitative indexes to specific water-saving methods, process controlling and obtained results.

Non-traditional water source utilization aspect

LEED regulates that on the basis of control items 20% water-saving percentage, the additional water-saving percentage can be acquired by the alternative water source: the additional saving of 25% = 1 point, 30% = 2 points, 35% = 3 points, 40% = 4 points, 45% = 5 points, and 50% = 6 points (Alawneh et al., 2018).

ESGB points out that reclaimed water, rainwater and sea water etc. are included in non-traditional water source. Different points come from different building types. Quantitative criteria and non-traditional water source approving use direction are definite. ESGB approves and guides non-traditional water source to flush the indoor toilet, which can gain higher points. ESGB also approves using non-traditional water source as supplementary cooling water and landscape water and gives certain points according to the proportion.

As shown in *Equation 2,* the ratio of non-traditional water source use (NWSU)

$$= \frac{\text{The total quantity of the NWSU}}{\text{The total quantity of the wateruse}} * 100\% \quad \text{(Eq.2)}$$

The NWSU includes the reuse water use, the rain water use, the sea water use and other types of NWSU. For the purpose to get the same score, the NWSU ratio requirement with the municipal reuse system (MRS) is higher than without MRS. For the new construction building, the NWSU is suggested to be used for outdoor greening, road watering and car washing. But if the project wants to get a higher score, the

http://www.aloki.hu ● ISSN 1589 1623 (Print) ● ISSN 1785 0037 (Online)
DOI: http://dx.doi.org/10.15666/aeer/1705_1163911653

NWSU should take the indoor toilet flushing into consideration in order to increase the NWSU ratio. Because the latter need stricter water quality and deeper water treatment process.

From this point of view, the ESGB has a bit more detailed direction to guide the NWSU and help the owner to get more score. This item may be used by LEED for references.

Water monitoring system aspect

LEED and ESGB both approve setting water monitoring system to the kitchen, lavatory, greening, air conditioning system, swimming pool, and landscape, respectively, according to the purpose. LEED regards the water meter monitoring system as a control item and requires 5 years' water quantity record. 80% measurable water quantity of the total quantity is required in the credit item (Kern et al., 2016). While in ESGB, water monitoring system is only a credit item. But additional points can be gained by setting water measurement devices to measure water quantity according to fees and administrative units, respectively. The arrangements will help searching leakage and venting points of the pipe and reducing the leakage of water quantity.

Conclusion

In this review, a statistic analysis from the relevant papers of different GBRSs comparison has been carried out. It is clear that some existing GBRSs from the general, category and criteria levels have been compared in the past research efforts.. But little work has been done on the comparison of water efficiency. A thorough review of comparison on water efficiency between LEED and ESGB is carried out due to their similar structure and international repercussions. Six aspects including macroscopic, building water use, landscape water use, heat and cooling system use water, nontraditional water source utilization and water monitoring system are relatively compared in detail. In terms of their similarities, ESGB and LEED are both composed of control and scoring items. Moreover, both of the two standards concern building water-saving, landscape water-saving and condensate water systems, and approve non-traditional water source utilization and landscape plants without irrigation requirement. As for their differences, ESGB mainly concerns the planning and designing of the whole water system, using water-saving instruments, setting reasonable and thorough water system, without specific and detailed quantity indexes; whereas LEED mainly concerns specific and measurable indexes. Through contrastive analysis, a lot of work still needs to be done to improve the indexes control of instruments on water-saving efficiency for China. Relating to improve non-traditional water source use ratio, more effective and feasible measures, such as cooling water supplement, rainwater utilization in landscape water, indoor toilets flushing of non-traditional water source, are put forward. In conclusion, construction and standard establishment of Chinese green building is still in its initial stage. Evaluation criterion needs to be updated constantly, which will promote the development of Chinese green building and technology upgrading of related industries. And meanwhile the LEED may use the items like non-traditional water source use for references.

http://www.aloki.hu ● ISSN 1589 1623 (Print) ● ISSN 1785 0037 (Online)
DOI: http://dx.doi.org/10.15666/aeer/1705_1163911653

Acknowledgements. This research was jointly supported by National Key Research and Development Program of China (2017YFF0209903, 2017YFF0209904), National Natural Science Foundation of China (51908334, 51908335), Shandong Provincial Natural Science Foundation (ZR2019BEE058, ZR2018BEE036), China Postdoctoral Science Foundation (2019M652427), and Doctoral Research Fund of Shandong Jianzhu University (XNBS1806, XNBS1822).

REFERENCES

[1] Alawneh, R., Mohamed Ghazali, F. E., Ali, H., et al. (2018): Assessing the contribution of water and energy efficiency in green buildings to achieve United Nations Sustainable Development Goals in Jordan. – Building and Environment 146: 119-132.
[2] Altomonte, S., Schiavon, S. (2013): Occupant satisfaction in LEED and non-LEED certified buildings. – Building and Environment 68: 66-76.
[3] Alyami, S. H., Rezgui, Y. (2012): Sustainable building assessment tool development approach. – Sustainable Cities and Society 5: 52-62.
[4] Awadh, O. (2017): Sustainability and green building rating systems: LEED, BREEAM, GSAS and Estidama critical analysis. – Journal of Building Engineering 11: 25-29.
[5] BREEAM (2016): What is BREEAM? – E-newsletter. https://www.breeam.com.
[6] CASBEE (2014): CASBEE information. – E-newsletter. http://www.ibec.or.jp/CASBEE/english/#.
[7] Chen, H., Lee, W. L. (2013): Energy assessment of office buildings in China using LEED 2.2 and BEAM Plus 1.1. – Energy and Buildings 63: 129-137.
[8] Chen, X., Yang, H., Lu, L. (2015): A comprehensive review on passive design approaches in green building rating tools. – Renewable and Sustainable Energy Reviews 50: 1425-1436.
[9] Cole, R. J. (2006): Shared markets: coexisting building environmental assessment methods. – Building Research & Information 34: 357-371.
[10] Ding, G. K. (2008): Sustainable construction--the role of environmental assessment tools. – Journal of Environmental Management 86: 451-64.
[11] Ding, Z., Fan, Z., Tam, V. W. Y., et al. (2018): Green building evaluation system implementation. – Building and Environment 133: 32-40.
[12] Doan, D. T., Ghaffarianhoseini, A., Naismith, N., et al. (2017): A critical comparison of green building rating systems. – Building and Environment 123: 243-260.
[13] ESGB (2014): Evaluation Standard for Green Building. The Ministry of Housing and Urban-Rural Development announced the issuance of the national standard "Evaluation Standard for Green Building". – http://www.mohurd.gov.cn/wjfb/201508/t20150829_224219.html.
[14] Feng, H., Hewage, K. (2014): Energy saving performance of green vegetation on LEED certified buildings. – Energy and Buildings 75: 281-289.
[15] Gelowitz, M. D. C., Mcarthur, J. J. (2018): Insights on environmental product declaration use from Canada's first LEED v4 platinum commercial project. – Resources, Conservation and Recycling 136: 436-444.
[16] Green Mark (2013): About BCA Green Mark Scheme. – https://www.bca.gov.sg/GreenMark/green_mark_buildings.html.
[17] Green Star (2015): Green Star Buildings. – https://new.gbca.org.au/green-star/.
[18] Gurgun, A. P., Komurlu, R., Arditi, D. (2015): Review of the LEED Category in Materials and Resources for Developing Countries. – Procedia Engineering 118: 1145-1152.
[19] Haapio, A., Viitaniemi, P. (2008): A critical review of building environmental assessment tools. – Environ. Impact Assess. Rev. 28: 469-482.
[20] He, Y., Kvan, T., Liu, M., et al. (2018): How green building rating systems affect designing green. – Building and Environment 133: 19-31.

http://www.aloki.hu ● ISSN 1589 1623 (Print) ● ISSN 1785 0037 (Online)
DOI: http://dx.doi.org/10.15666/aeer/1705_1163911653

[21] Howard, G. S., Cole, D. A., Maxwell, S. E. (1987): Research productivity in psychology based on publication in the journals of the American Psychological Association. – American Psychologist 42: 975-986.
[22] Hu, M., Peter, C., Sarah, G. (2017): Sustainable design rating system comparison using a life-cycle methodology. – Building and Environment 126: 410-421.
[23] ITACA (2015): ITACA Protocol. – http://www.itaca.org.
[24] Joustra, C., Yeh, D. H. (2009): Water conservation and wastewater reuse in a green building: an integrated approach towards LEED. – Proceedings of the Water Environment Federation 5: 2063-2086(24).
[25] Kang, H., Lee, Y., Kim, S. (2016): Sustainable building assessment tool for project decision makers and its development process. – Environmental Impact Assessment Review 58: 34-47.
[26] Kern, A. P., Antoniolli, C. B., Wander, P. R., et al. (2016): Energy and water consumption during the post-occupancy phase and the users' perception of a commercial building certified by Leadership in Energy and Environmental Design (LEED). – Journal of Cleaner Production 133: 826-834.
[27] Kyvelou, S., Sinou, M. (2013): Present and future of building performance assessment tools. – Management of Environmental Quality. An International Journal 17: 570-586.
[28] Lee, W. L (2012): Benchmarking energy use of building environmental assessment schemes. – Energy and Buildings 45: 326-334.
[29] Lee, W. L. (2013): A comprehensive review of metrics of building environmental assessment schemes. – Energy and Buildings 62(3): 403-413.
[30] LEED (2013): LEED is green building. – E-newsletter. https://new.usgbc.org/leed.
[31] Li, Y., Chen, X., Wang, X., et al. (2017): A review of studies on green building assessment methods by comparative analysis. – Energy and Buildings 146: 152-159.
[32] Lin, B., Liu, H. (2015): CO_2 mitigation potential in China's building construction industry: a comparison of energy performance. – Building and Environment 94: 239-251.
[33] Liu, H., Lin, B. (2016): Energy substitution, efficiency, and the effects of carbon taxation: Evidence from China's building construction industry. – Journal of Cleaner Production 141: 1134-1144.
[34] Marjaba, G. E., Chidiac, S. E. (2016): Sustainability and resiliency metrics for buildings. Critical review. – Building and Environment 101: 116-125.
[35] Mattoni, B., Guattari, C., Evangelisti, L., et al. (2018): Critical review and methodological approach to evaluate the differences among international green building rating tools. – Renewable & Sustainable Energy Reviews 82: 950-960.
[36] Nguyen, B. K., Altan, H. (2011): Comparative review of five sustainable rating systems. – Pore. Eng. 21: 376-386.
[37] Say, C., Wood, A. (2012): Sustainability rating systems around the world. – Council on Tall Buildings and Urban Habitat - Review 18-29: 759-888.
[38] Schwartz, Y., Raslan, R. (2013): Variations in results of building energy simulation tools, and their impact on BREEAM and LEED ratings: a case study. – Energy and Buildings 62: 350-359.
[39] Sharifi, A. (2016): A critical review of selected tools for assessing community resilience. – Ecological Indicators 69: 629-647.
[40] Sharifi, A., Murayama, A. (2013): A critical review of seven selected neighborhood sustainability assessment tools. – Environmental Impact Assessment Review 38: 73-87.
[41] Sharifi, A., Murayama, A. (2014): Neighborhood sustainability assessment in action: Cross-evaluation of three assessment systems and their cases from the US, the UK, and Japan. – Building and Environment 72: 243-258.
[42] Sharifi, A., Yamagata, Y. (2016): Principles and criteria for assessing urban energy resilience: a literature review. – Renewable and Sustainable Energy Reviews 60: 1654-1677.

http://www.aloki.hu ● ISSN 1589 1623 (Print) ● ISSN 1785 0037 (Online)
DOI: http://dx.doi.org/10.15666/aeer/1705_1163911653

[43] Smith, P. (2005): Architecture in a Climate of Change: A Guidance to Sustainable Design. – Architectural Press, Oxford.
[44] U. S. Green Building Council (2018): USGBC. – usgbc.org.
[45] UNEP SBCI (2008): Buildings and Climate Change. – United Nations Environment Programme, Nairobi.
[46] Wang, B. Y., et al. (2016): Measured energy use and indoor environment quality in green office buildings in China. – Energy and Buildings 129: 9-18.
[47] Wang, S., Yan, C., Xiao, F. (2012): Quantitative energy performance assessment methods for existing buildings. – Energy and Buildings 55: 873-888.
[48] WBCSD (2008): Energy Efficiency in Buildings, Business Realities and Opportunities. – The World Business Council for Sustainable Development, Geneva.
[49] Wu, P., Mao, C., Wang, J., et al. (2016): A decade review of the credits obtained by LEED v2.2 certified green building projects. – Building & Environment 102: 167-178.
[50] Wu, P., Song, Y., Shou, W., et al. (2017): A comprehensive analysis of the credits obtained by LEED 2009 certified green buildings. – Renewable & Sustainable Energy Reviews 68: 370-379.
[51] Yudelson, J. (2008): The green building revolution. – Heating/Piping/Air Condition. Eng. 80: 8.
[52] Zhu, H., Hong, J., Shen, G. Q., et al. (2017): The exploration of the life-cycle energy saving potential for using prefabrication in residential buildings in China. – Energy and Buildings 166: 561-570.

http://www.aloki.hu ● ISSN 1589 1623 (Print) ● ISSN 1785 0037 (Online)
DOI: http://dx.doi.org/10.15666/aeer/1705_1163911653

ANALYSIS OF CHANGES IN SHELTERBELT LANDSCAPE IN NORTHEAST CHINA

DENG, R. X.[1] – WANG, W. J.[2*] – LI, Y.[3] – SHI, X. L.[4] – WEI, Y. C.[1] – HAO, L. J.[1] – LI, C. J.[1] – LIU, W. Y.[1]

[1]*College of Surveying and Geo-informatics, North China University of Water Resources and Electric Power, Zhengzhou 450046, China*

[2]*College of Resources and Environment, Henan University of Economics and Law, Zhengzhou 450002, China*

[3]*Northeast Institute of Geography and Agroecology, Chinese Academy of Sciences, Changchun 130102, China*

[4]*College of Geomatics, Xi'an University of Science and Technology, Xi'an 710054, China*

**Corresponding author*
e-mail: wenjuan110@163.com; phone: +86-185-0388-6306

(Received 22nd Apr 2019; accepted 12th Jul 2019)

Abstract. Understanding the shelterbelt development in northeast China over the past 30 years will provide a scientific decision support for its management in future. In this paper, Landsat images were selected to extract shelterbelt information covering three points in time (1990, 2000 and 2010). Shelterbelt density and landscape indexes (ratio of belt to patch, connectivity, and dominance) were introduced to analyze changes in landscape. Farmland landscape indexes (ratio of farmland to zone and fragmentation) were used to analyze the effect of farmland on shelterbelt distribution and change. The result showed that: (1) shelterbelt density had considerable spatial variation. These changes were strong correlated with land-use type. Farmland fragmentation was a main index which significantly affected the connectivity and evenness of shelterbelt, especially on connectivity; (2) shelterbelt density increased about 10% over the 30 years. This modest increase included two contrasting trends, an increase by 13.2% from 1990 to 2000 followed by a 2.8% reduction by 2010. Even the quantity reduced over 2000-2010, the qualities including connectivity and evenness were getting better overall. The temporal changes of shelterbelt density had little relationship with farmland changes. This research can provide valuable information for decision makers to guide and develop future policies.
Keywords: *shelterbelt structure, landscape index, geographic information system, remote sensing*

Introduction

In 1978, the Central Committee of the Communist Party of China launched an afforestation project known as the "Three Norths" (or 3N, referring to the North West, the North and the North East of China). The 3N is one of China's most important projects at a national level (Moodre and Russell, 1990).

Objectives of the 3N project are to control wind and sand erosion, enhance soil and water conservation, improve ecological environments, and produce multiple forest products. This project is acclaimed as China's "green great wall" and "world's best ecological project". Based on an investigation of the State Forestry Administration of China, the 3N framework was configured during past 30 years and the eco-environmental benefits have begun to appear in wind reduction, soil and water conservation, farmland protection, and sand dune fixation (Wang and Zhou, 2003).

http://www.aloki.hu ● ISSN 1589 1623 (Print) ● ISSN 1785 0037 (Online)
DOI: http://dx.doi.org/10.15666/aeer/1705_1165511668

The Northeast shelterbelt is a part of the 3N project. Since the 1980s, China has invested substantial money and energy into its construction. The construction of eco-economic shelterbelts was popular in the late 1980s (Shan et al., 2018). By now, the third phase of 3N project has been completed, and the fourth phase is nearing completion. Researching and clarifying the development of the shelterbelt over the past 30 years can help identify problems of this area and provide a scientific decision support for shelterbelt management in the next phase.

Shelterbelts are used to reduce wind speed. They can help to control wind erosion, provide habitat for wildlife, protect crops and homes, and enhance the agricultural landscape (Brandle et al., 2004). The shelterbelts are in a network state on the agricultural landscape, the role of one shelterbelt is like a barrier, which is an important element in the landscape (Ding et al., 1993).

Because of their importance in the agricultural landscape, shelterbelt construction develops very rapidly. The studies were mainly focused on their structure, function and management (Fan et al., 2002). As researches expanding from field scale to landscape scale, geographic information system (GIS) and remote sensing (RS) technologies were widely used in shelterbelt research (Wiseman et al., 2009; Czerepowicz et al., 2012; Deng et al., 2013, 2017; Zheng et al., 2016). Using the principle of the landscape ecology and combining GIS and RS, landscape structure can be analyzed to accurately evaluate development and status at landscape scale. Zhou and Sun (1994) introduced landscape indexes (ratio of belt to patch, connectivity, circuitry, and dominance) to shelterbelt landscape research. These indexes were widely used to evaluate shelterbelt structure at landscape scale (Sun et al., 1997; Li et al., 2003; Guan et al., 2004; Yang et al., 2017). Based on these researches, Shi et al. (2011) developed a method evaluating the spatial heterogeneity of shelterbelts distribution at landscape scale. These researches well measured and evaluated the spatial distribution and heterogeneity in landscape, but they did not analyze the reasons behind these results. Kristensen and Caspersen (2002) analyzed the changes of shelterbelt network density, discussed the farmers' motives for shelterbelt planting in central Jutland. The results of this research provided insight into the driving forces behind shelterbelt planting and removal.

We found that, at landscape scale, the studies were mainly focused on evaluating the spatial distribution, there was few paper existed to study the changes of them, and further to regard the driving forces behind these distributions and changes. Shelterbelts are commonly planted on the farmland in the agricultural landscape. The changes of farmland may be one important factor to affect their changes. Therefore, the purpose of this paper is to research the temporal and spatial dynamics of shelterbelt planting in northeastern China, and analyze how the farmland affects the distributions and changes of them. Therefore, this paper investigates the changes of shelterbelt density and landscape indexes at three points in time (1990, 2000 and 2010). These times were chosen to cover the period of major shifts in shelterbelt planting strategies. The results provide insight into the spatial distribution and temporal changes of shelterbelt density, connectivity and distribution evenness across the study area, and understand the relationship of distributions and changes between shelterbelt and farmland. We suppose this analysis can provide valuable information for decision makers to guide and develop future shelterbelt planting policies.

http://www.aloki.hu ● ISSN 1589 1623 (Print) ● ISSN 1785 0037 (Online)
DOI: http://dx.doi.org/10.15666/aeer/1705_1165511668

Materials and methods

Study area

The boundary of northeast shelterbelt protection zone was determined by Three North Shelterbelts Construction Bureau of the State Forestry Administration of China. The area is about 584152 km^2. This zone is in eastern Inner Mongolia Autonomous Region and western Northeast China, and embraces Heilongjiang, Jilin and Liaoning provinces. Its extent is 115°–130°E and 40°–50°N (*Fig. 1*). There are very cold and long winter and hot and rainy summer. Agricultural disaster is mainly caused by windstorms and sandstorms, as well as droughts and floods. Winds from the southwest often reach 15–20 m/s in spring. Crop types are mainly maize, soybean, millet and sorghum (Zhu et al., 2010).

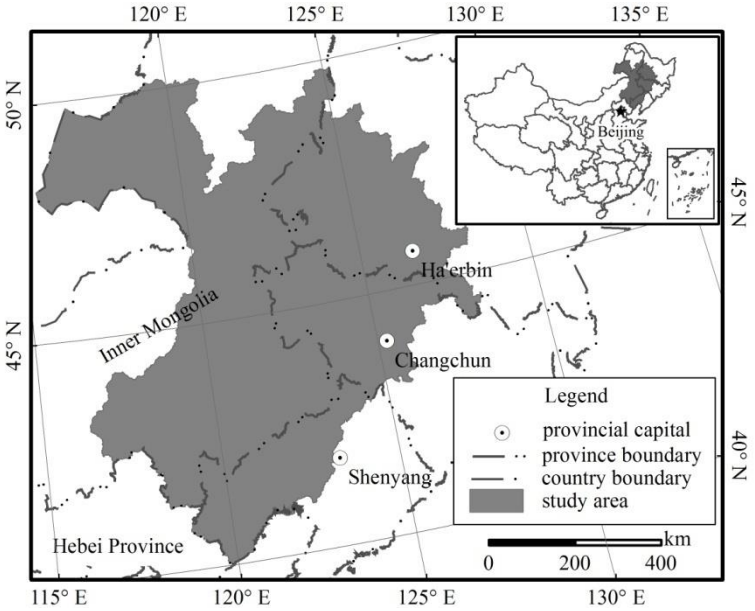

Figure 1. *The location of study area*

Data source

Shelterbelt data

Landsat series images of 30 m × 30 m spatial resolution were selected to extract shelterbelt information. Specifically, the 1990 images were acquired from Landsat-5 Thematic Mapper (TM) data, the 2000 images from Landsat-5 TM and Landsat-7 Enhanced TM (ETM) data, and the 2010 images from Landsat-5 TM data. For each time, it needed about 48 images to cover the whole study area. In order to accurately extract the information, optimal acquisition dates for images were in May, early and mid-June; second best were in early and mid-October. Considering the atmospheric difference of the images at different times, the atmospheric radiation was made based on each actual condition. Atmospheric radiation and geometric corrections were made for images with ENVI 4.8 software, and the estimated total root mean square error was less than one pixel.

Shelterbelt features in the Landsat images were sufficiently clear because of the moderate resolution and appropriate dates. Vector data were obtained as linear features

http://www.aloki.hu ● ISSN 1589 1623 (Print) ● ISSN 1785 0037 (Online)
DOI: http://dx.doi.org/10.15666/aeer/1705_1165511668

through manual interpretation via a computer interface with ArcMap 10.0 software. The result can be seen in *Figure 2*. Results were validated by field measurement and accuracy was greater than 95%.

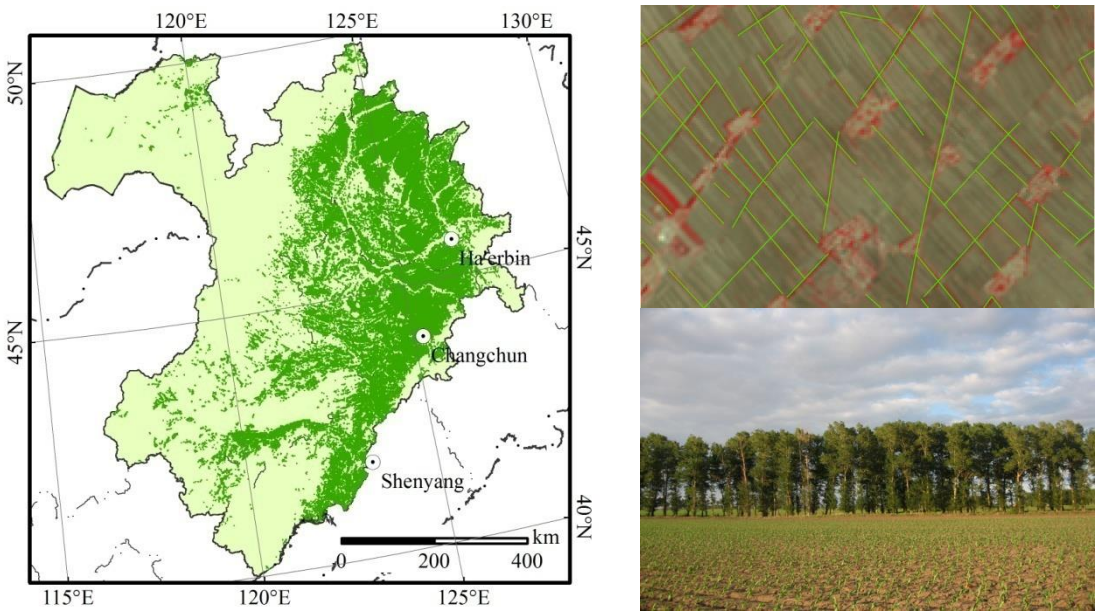

Figure 2. *The distribution of the shelterbelts, taken the shelterbelts in 2010 as example. Bottom right: the shelterbelt photographed in field. Top right: the shelterbelt in Landsat image. Left: the extracting result of shelterbelts in 2010*

Land use data

The indicators of land use interpretation were established according to the characteristics of the images, the second Chinese land investigation interpretation standard, expert knowledge, and other related geographic maps. The images were interpreted using the ArcMap 10.0 and the human-computer interactive method. Finally, land uses were classed into six types: farmland, grassland, forest, built-up land, water bodies and marsh. Data accuracy was validated by field surveys: 10% of the patches were chosen to perform accuracy assessment, the total precision was 90%, the precision of the farmland was more than 95%.

Zoning

The shelterbelt spatial distribution was related to site conditions. Therefore, we analyzed changes of the objects by the zoning method. Based on regionalization of Chinese agricultural natural resources and consideration of differences in topographic features, air temperature and precipitation, we separated the study area into seven zones. The result is shown in *Figure 3* and *Table 1*.

Landscape index of shelterbelt

The shelterbelts are in a network state in agricultural fields. Each shelterbelt interconnects and forms a network system. In the system, the junction of two or more belts or the end point of single belt are nodes. The connected edges between nodes are

http://www.aloki.hu ● ISSN 1589 1623 (Print) ● ISSN 1785 0037 (Online)
DOI: http://dx.doi.org/10.15666/aeer/1705_1165511668

belts. Ratio of belt to patch (*P*), connectivity (*Q*), and dominance (*D*) are introduced to estimate the landscape structure at regional scale (Zhou and Sun, 1994; Guan et al., 2004). We calculated these three landscape indexes to describe changes of the network in the study area between 1990 and 2010.

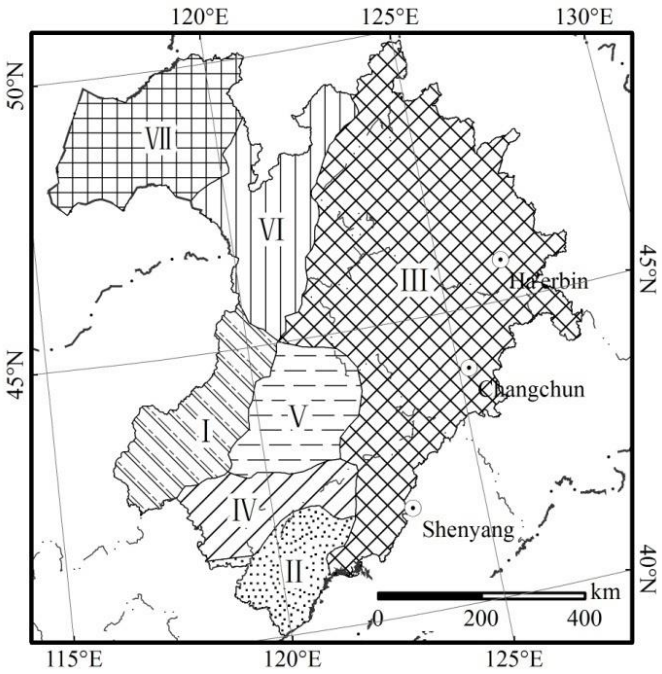

Figure 3. *Zones within the study area*

Table 1. *Description of site conditions in each zone*

Zone	Regionalization of agricultural natural resource	Topographic feature	Temperature condition	Precipitation condition
I	Pastoral and agricultural region in eastern Inner Mongolia Plateau	Medium-low mountain	Medium	Semi-arid
II	Agricultural, pastoral and forest region in Songliao Plain	Medium-low mountain	Warm	Semi-humid
III	Agricultural region in Songliao Plain	Flatland	Medium	Semi-humid
IV	Agricultural and pastoral region in eastern Inner Mongolia Plateau	Medium-low mountain	Medium	Semi-humid
V	Agricultural and pastoral region in eastern Inner Mongolia Plateau	Flatland	Medium	Semi-arid
VI	forest region in eastern Inner Mongolia Plateau	Medium-low mountain	Medium	Semi-humid
VII	Pastoral region in eastern Inner Mongolia Plateau	Upland plain	Medium	Semi-arid

(1) Ratio of belt to patch

This index is used to describe the abundance extent with aspects of area and number of networks, and measure the number of forest networks. The index is expressed as:

http://www.aloki.hu ● ISSN 1589 1623 (Print) ● ISSN 1785 0037 (Online)
DOI: http://dx.doi.org/10.15666/aeer/1705_1165511668

$$P = \frac{S_b}{A} \quad \text{(Eq.1)}$$

where S_b is a reasonable area of the shelterbelt networks (km^2) and A is patch area which should to be protected in this state (km^2).

(2) Connectivity

This index is used to measure the formed condition. It is expressed as:

$$Q = \frac{N_a - (n-1)}{L_{MAX}(V)} \quad \text{(Eq.2)}$$

where $L_{MAX}(V)$ is the maximum number of belts; V is a reasonable node number; N_a is the sum of main and assistant shelterbelts; n is the number of patches that should to be protected.

(3) Dominance of forest network

This index is used to measure the occupied area, the number and the distribution evenness within the networks. Larger values of this index indicate a larger occupied ratio and vice versa. In other words, a smaller dominance index shows that the number of forest networks is insufficient or that its distribution is not uniform. The index is expressed as

$$D = \frac{1}{2} \cdot \left(\frac{R_d + R_f}{2} + R_c \right) \quad \text{(Eq.3)}$$

where R_d represents relative abundance in the network, R_f represents frequency in the network, and R_c represents coverage in the network.

Landscape index of farmland

The farmland area was extracted from land use data by GIS method. Ratio of farmland to zone (*PF*) and fragmentation (*CF*) are chosen to estimate the landscape structure of farmland in this paper. We calculated these two landscape indexes to describe distributions and changes of the farmland in the study area between 1990 and 2010.

(1) Ratio of farmland to zone

This index is used to describe the quantity or density of farmland in the zone, which is expressed as

$$PF = \frac{S_f}{S} \quad \text{(Eq.4)}$$

where S_f is the area of farmland in the zone, and S is the area of zone that farmland located in.

http://www.aloki.hu ● ISSN 1589 1623 (Print) ● ISSN 1785 0037 (Online)
DOI: http://dx.doi.org/10.15666/aeer/1705_1165511668

(2) Fragmentation of farmland

This index is used to describe the degree of farmland fragmentation in the zone, which is expressed as

$$CF = \frac{N}{S_f} \quad \text{(Eq.5)}$$

where N is the number of farmland patches in the zone.

Results and discussion

Spatial distribution of shelterbelt density and landscape indexes

Shelterbelt density, expressed as shelterbelt length divided by zone area, is used to analyze spatial distribution in the study area. The results indicated that the spatial distribution at each time was similar, but shelterbelt density varied considerably by zone (*Fig. 4*).

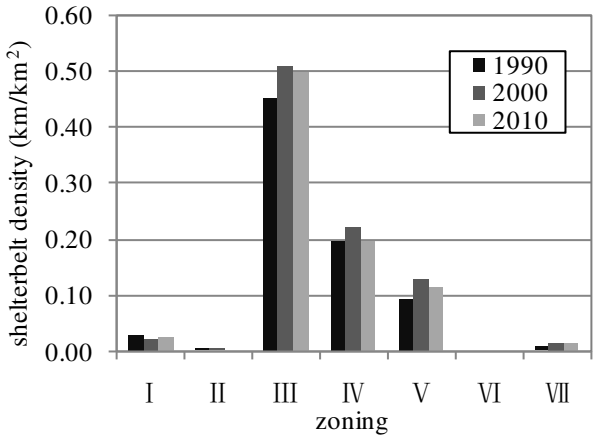

Figure 4. *Shelterbelt density in each zone*

Comparing shelterbelt density with site conditions in each zone, we found strong correlation between density and land-use type in the study area. The greatest shelterbelt density was in zone III, an agricultural region, it also had the largest area and the most shelterbelt length than other area. This was followed by zones IV and V, which were agricultural and pastoral regions. Then came zone I and VII, a pastoral or pastoral and agricultural region. Finally, with the smallest shelterbelt densities, zones II and VI, both were forest regions. We conclude that shelterbelt density decreased as land-use type transferred from agriculture to pastoral and then forest. This result is related to the shelterbelt protection function. That is, the main role of shelterbelt is to protect homes, crops and livestock by reducing wind speed, and the main land-use type is agriculture across the study area. In forest regions, windstorms and sandstorms are less frequent than the other regions, and lower shelterbelt densities there are reasonable.

Figure 5 showed the distribution of changes in landscape index between 1990 and 2010. Landscape distributions were similar in zones III, IV and V. We can see that *P*

http://www.aloki.hu ● ISSN 1589 1623 (Print) ● ISSN 1785 0037 (Online)
DOI: http://dx.doi.org/10.15666/aeer/1705_1165511668

and *D* values in III were obvious higher than other zones, the seconds were IV and V, but *Q* was almost equal to IV and V, although it was still larger than other zones. The result indicated that, the numbers of shelterbelt were larger, the shelterbelt connectivity were better, and the shelterbelt distributions were more uniform in these three zones.

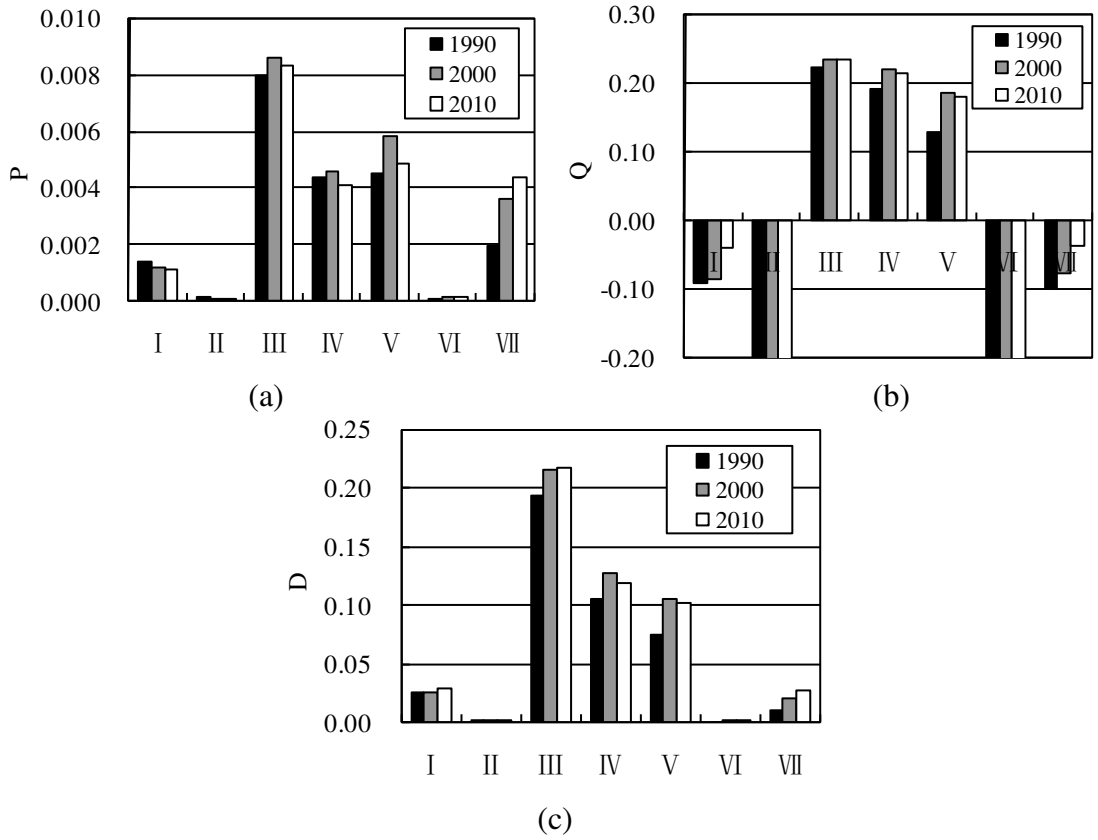

Figure 5. *The landscape indexes in each zone*

Compared with *Figures 4* and *5a*, they showed that *P* values in I and VII were higher than shelterbelt density in these zones. But they were still lower than III, IV and V. the reason for the lower landscape indexes in I, II, VI and VII was that forest or pastoral land was the dominant land-use type. Moreover, cropland was scattered in these zones, so shelterbelts in such land were fragmented.

Relationship of landscape indexes between shelterbelt and farmland

Shelterbelts are generally planted in the farmland, which may affect the shelterbelt landscape index. *PF* and *CF* were chosen as farmland indexes to analyze their relation with shelterbelt indexes. By calculating the mean value of each index in each zone, the relationship between landscape indexes of shelterbelt and *PF* showed in *Figure 6*. We can see that, the farmland density mainly affected the shelterbelt evenness (the coefficient of determination (R^2) was 0.638 between *D* and *PF*). The relationship between farmland density and shelterbelt number was not as obvious as we thought (R^2 was 0.364 between *P* and *PF*). By analyzed these two indexes in each zone, we found that two zones had opposite trend: in zone II, the *PF* value was high, which was the third one for all zones. But *P* value in this zone was the last. That because this zone

http://www.aloki.hu ● ISSN 1589 1623 (Print) ● ISSN 1785 0037 (Online)
DOI: http://dx.doi.org/10.15666/aeer/1705_1165511668

belonged to the agriculture, pastoral and forest transitional region, where land use type was more fragmental. Farmland fragmentation was a main factor to affect the *P* in this zone; the other was in zone VII, which had the smallest farmland density, the *P* value was up to the forth for all zone. This zone belonged to pastoral region and upland plain, where was more frequently affected by wind damage. For this reason, it may result that the shelterbelt spacing distance was closer than other areas. If we discarded these two zones, the relationship between these two indexes was increased to 0.775. Therefore, farmland density had some influences on shelterbelt number, but the main reason may be farmland fragmentation or site conditions.

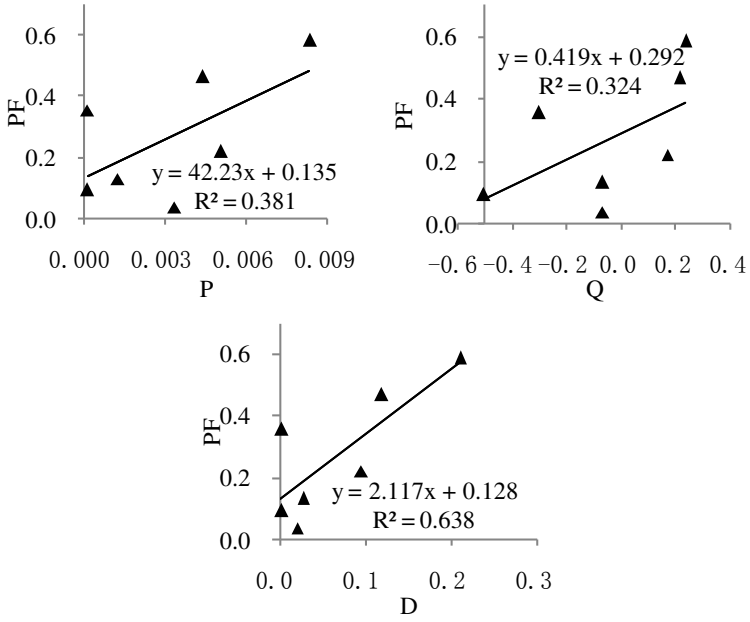

Figure 6. *The relationships between landscape indexes of shelterbelt and PF*

The relationship between landscape indexes of shelterbelt and *CF* showed in *Figure 7*. We can see that, R^2 was 0.568 between *P* and *CF*, which indicated that farmland fragmentation could affect the shelterbelt number. R^2 was 0.773 between *Q* and *CF*, and was 0.679 between *D* and *CF*, which indicated that farmland fragmentation could significantly affect the connectivity and evenness of shelterbelt, especially on connectivity. The result revealed that farmland fragmentation was a main index to affect the landscape pattern of shelterbelt. The lower of the farmland fragmentation, the higher connectivity and evenness of shelterbelt, and that may cause larger shelterbelt numbers.

Temporal change of shelterbelts density

Shelterbelt density increased by about 10% in the last 30 years, revealing that the number of shelterbelts were relatively stable over this period. The modest increase included two contrasting trends during the period: an increase by 13.2% from 1990 to 2000 followed by a 2.8% reduction by 2010. As a result of these changes, the density increased from 0.238 km/km^2 around 1990 to 0.269 km/km^2 around 2000. This then decreased to 0.262 km/km^2 around 2010. The changes of the density between 1990 and 2000, and between 2000 and 2010 can be seen from *Table 2*, the value was calculated

http://www.aloki.hu ● ISSN 1589 1623 (Print) ● ISSN 1785 0037 (Online)
DOI: http://dx.doi.org/10.15666/aeer/1705_1165511668

by shelterbelt lengths divided into total lengths in each zone. Such changes of the density were closely related to the 3N project. The first phase of this project was from 1978 to 1985. One of the main objectives in this phase was to plant more trees. The second phase from 1986 to 1996 aimed at strengthening gains made during the first phase (Moodre and Russell, 2003). For this reason, the shelterbelt density increased between 1990 and 2000. After 2000, many shelterbelts developed into over-mature forests and, because of destruction by humans, plant disease and insect pests, many shelterbelts were lost and the construction of the agro-forestry system entered updating phase. In this phase, many shelterbelts were updated, and sometimes they were too young to be recognized by remote sensing. Therefore, the density decreased between 2000 and 2010.

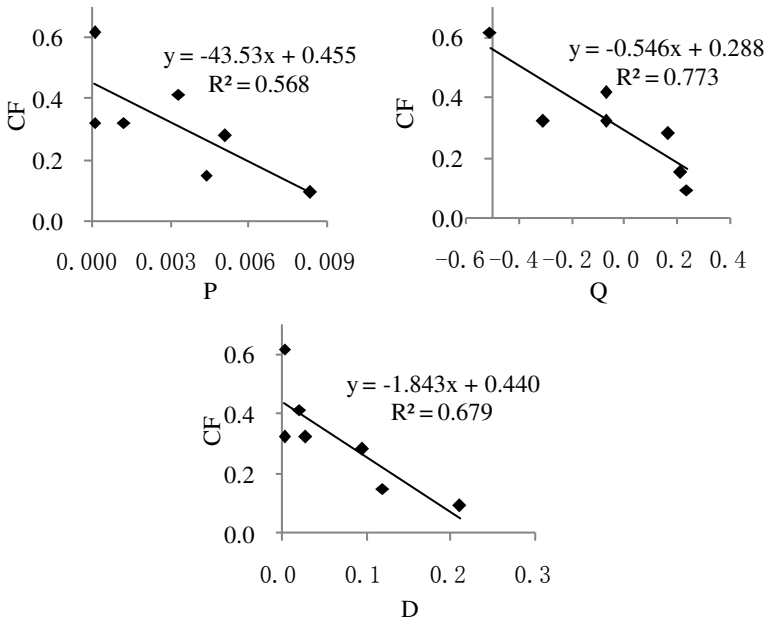

Figure 7. *The relationships between landscape indexes of shelterbelt and CF*

Table 2. *Shelterbelt changes from 1990 to 2000 and from 2000 to 2010*

Zone	Changes between 1990 and 2000			Changes between 2000 and 2010		
	Added (%)	Reduced (%)	Added in total (%)	Added (%)	Reduced (%)	Added in total (%)
I	28.7	52.4	-23.7	49.7	30.7	19.0
II	27.7	70.3	-42.6	20.4	39.3	-18.9
III	24.1	11.6	12.5	14.8	17.1	-2.3
IV	39.7	27.1	12.6	9.7	21.0	-11.3
V	48.8	10.6	38.2	12.5	23.5	-11.0
VI	50.6	18.9	31.7	63.3	44.2	19.1
VII	140.9	53.9	87.0	30.7	13.2	17.5
Average	26.3	13.1	13.2	14.8	17.7	-2.8

Added means new planted shelterbelts during this period; reduced means disappeared shelterbelts during this period; added in total means added minus reduced shelterbelts, "-" means reduced in total. The average value of the last row is calculated by changed divided total shelterbelts, not the average value of the seven zones

http://www.aloki.hu ● ISSN 1589 1623 (Print) ● ISSN 1785 0037 (Online)
DOI: http://dx.doi.org/10.15666/aeer/1705_1165511668

From *Table 2*, we can also find that between 1990 and 2000, the percent of the new planted shelterbelts was 26.3%, the fastest increased area was zone VII. The first reason was the shelterbelt density in 1990 was low in this area, and the second reason was that more shelterbelts were planted compared to the past time of this area. But we also seen that the reduced percent in VII was more faster, only second to II, the third was I. These three zones reduced faster than other areas obviously, which may be related to the site conditions. Between 2000 and 2010, the percent of new planted shelterbelts was lower than the first phase, but the disappeared shelterbelts more higher. The higher percent of added shelterbelts were in I, VI and VII, these areas were mostly belonged to pastoral or forest region. This means that the shelterbelt construction had been strengthened in these areas. Instead, Zones III, IV and V, had better shelterbelt density, the added percent was totally reduced, the shelterbelts needed to be timely updated in these areas.

The change of farmland area was produced by overlapping method. The result can be used to analyze the relationship between the changes of shelterbelt density and farmland. If the new planted shelterbelts were in the new added farmland, we considered the added shelterbelts were related to farmland, if not, there were other reasons. The same as the reduced shelterbelts. The results were shown in *Figures 8* and *9*.

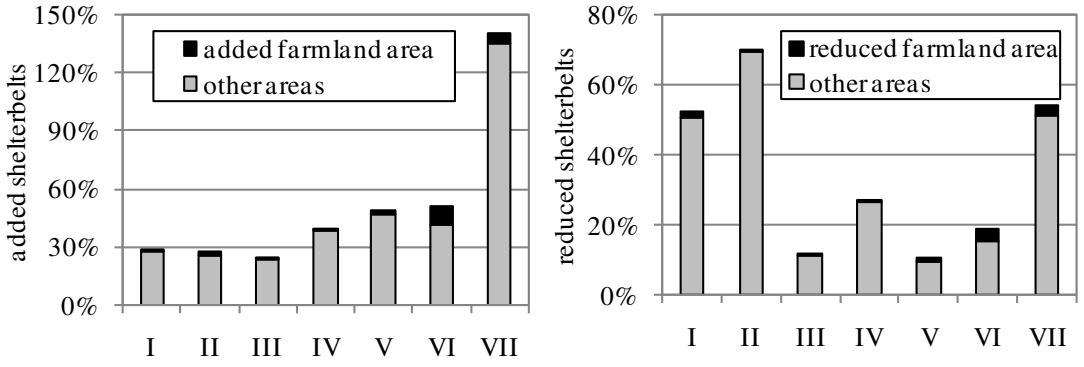

Figure 8. *The comparison between the changes of shelterbelt density and farmland from 1990 to 2000*

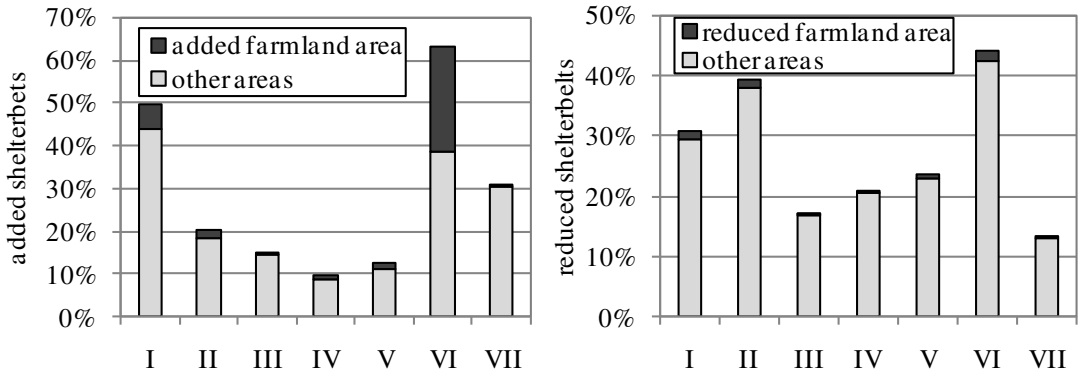

Figure 9. *The comparison between the changes of shelterbelt density and farmland from 2000 to 2010*

http://www.aloki.hu ● ISSN 1589 1623 (Print) ● ISSN 1785 0037 (Online)
DOI: http://dx.doi.org/10.15666/aeer/1705_1165511668

Figure 8 showed that the changes of shelterbelts density had little relationship with farmland changes. The new planted percent was 26.3% between 1990 and 2000, only 0.9% of them were added in new added farmlands, the other 99.1% were added by other reasons. The reduced percent was 13.1% between 1990 and 2000, only 1.6% of them were reduced in reduced farmlands, the other 98.4% were reduced by other reasons. The similar results appeared between 2000 and 2010 (seen in *Fig. 9*), the added shelterbelts in new added farmlands were 2.5% for total added shelterbelts, and the reduced were 0.7%. We can conclude that the farmland changes were not the main factor to affect the changes of shelterbelt densities. The added shelterbelts were mainly related to the shelterbelt construction by managers. The reduced shelterbelts may be mainly caused by site conditions, or human destruction, which we did not discuss in this paper, and will be done in the future work.

Change analysis of landscape indexes of shelterbelt

The changes of landscape indexes of shelterbelt and farmland between 1990 and 2010 can be seen in *Table 3*. It indicated that between 1990 and 2010, the landscape indexes were increased totally. Although the *P* value reduced from 2000 to 2010, the change was not obvious. The most important was, the *Q* and *D* were more and more better during this period, which means that, even the quantity of the shelterbelt reduced between 2000 and 2010, the qualities including connectivity and distribution evenness were more better. This means that, after decades of construction, the landscape pattern of shelterbelt had been improved. But compared to the optimized network, it had many more harder works to do.

Table 3. *The landscape index changes of shelterbelt and farmland between 1990 and 2010*

	Shelterbelt	***P***	***Q***	***D***	**Farmland**	***PF***	***CF***
1990		0.0066	0.205	0.136		0.358	0.192
2000		0.0071	0.223	0.159		0.375	0.129
2010		0.0068	0.224	0.160		0.381	0.118

Table 3 also showed that the landscape indexes of farmland were more and more better. Farmland area was increased, and fragmentation was reduced. In order to understand the relationship of landscape indexes between shelterbelt and farmland, we calculated the changed of each index from 1990 to 2000 and from 2000 to 2010 in each zone respectively, and then analyzed the relationship of the landscape index changes between shelterbelt and farmland. The result showed that, there was no significant relationship between landscape index changes of shelterbelt and farmland during these periods.

Conclusion

The following conclusions are drawn from the analysis.

Shelterbelt densities varied considerably by zone. There is a close correlation between shelterbelt density and land-use type in the study area, with that density decreasing as the type transitioned from agriculture to pastoral and then forest.

http://www.aloki.hu ● ISSN 1589 1623 (Print) ● ISSN 1785 0037 (Online)
DOI: http://dx.doi.org/10.15666/aeer/1705_1165511668

Distributions of shelterbelt in landscape index between 1990 and 2010 showed two opposing trends in seven zones. The reason for these results appeared closely connected to land-use type. Farmland fragmentation was a main index which had significantly effect on the connectivity and evenness of shelterbelt, especially on connectivity. Farmland density mainly affected the shelterbelt evenness. The shelterbelt numbers were affected by many factors, including farmland density, fragmentation and site conditions.

Shelterbelt density increased by about 10% over the last 30 years. After decades years of construction, the landscape pattern of shelterbelt had been improved. These changes of shelterbelt density had little relationship with farmland changes. The added shelterbelts were mainly related to the construction by managers. The reduced shelterbelts may be mainly caused by site conditions, or human destruction.

During the research, we found that the distribution and change shelterbelts were also closed related with the site conditions, like soil type, elevation, temperature and precipitation, which we did not discuss in this paper. In the future work, we will study the effect of site conditions on the changes of shelterbelt.

Acknowledgements. This work was supported by the National Natural Science Foundation of China under Grant number 31971723; the Key Technologies Research and Development Program of Henan Province under Grant number 192102110122.

REFERENCES

[1] Brandle, J. R., Hodges, L., Zhou, X. H. (2004): Windbreaks in North American agricultural systems. – Agrofor. Syst. 61: 65-78.

[2] Czerepowicz, L., Case, B. S., Doscher, C. (2012): Using satellite image data to estimate aboveground shelterbelt carbon stocks across an agricultural landscape. – Agric. Ecosyst. Environ. 156: 142-150.

[3] Deng, R. X., Li, Y., Wang, W. J., Zhang, S. W. (2013): Recognition of shelterbelt continuity using remote sensing and waveform recognition. – Agrofor. Syst. 87: 827-834.

[4] Deng, R. X., Li, Y., Xu, X. L., Wang, W. J., Wei, Y. C.(2017): Remote estimation of shelterbelt width from SPOT5 imagery. – Agrofor. Syst. 91: 161-172.

[5] Ding, Y. X., Jiang, S. R., Luan, Y. L., Hu, Y. Q., Cai, F. (1993): Landscape ecological analyses on the special structure of shelterbelt. – J. Nanjing For. Univ. 17(2): 7-12.

[6] Fan, Z. P., Zeng, D. H., Zhu, J. J., Jiang, F. Q., Yu, X. X. (2002): Advance in characteristics of ecological effects of farmland shelterbelts. – J. Soil Water Conserv. 16(4): 130-133.

[7] Guan, W. B., Li, C. P., Fang, X. Z. Zhao, T. N., Chen, J. G., Sun, B. P. (2004): Evaluation of landscape ecology of shelterbelt system of Beizang Town, Daxing County, Beijing. – J. Beijing For. Univ. 26(2): 25-30.

[8] Kristensen, S. P., Caspersen, O. H. (2002): Analysis of changes in a shelterbelt network landscape in central Jutland, Denmark. – J. Environ. Manage. 66: 171-183.

[9] Li, C. P., Guan, W. B., Fan, X. Z., Zhao, T. N., Chen, J. G., Sun, B. P. (2003): Assessment of landscape ecology of agricultural protection forestsystem at Beizang Town, Daxing County, Beijing. – J. For. Res. 14(2), 135-140.

[10] Moodre, R., Russell, R.(1990): The 'Three Norths' forest protection system - China. – Agrofor. Syst.10: 71-88.

[11] Shan, Q. H., Zhang, J. F., Sun, S. Y., Chen, G. C., Zhang, H. D., Shen, L. M.(2018): Construction of coastline shelterbelts and assessment of their environmental effects in Yuyao, China. – Land Degrad. Dev. 29(8): 2428-2437.

http://www.aloki.hu ● ISSN 1589 1623 (Print) ● ISSN 1785 0037 (Online)
DOI: http://dx.doi.org/10.15666/aeer/1705_1165511668

[12] Shi, X. L., Li, Y., Deng, R. X. (2011): A method for spatial heterogeneity evaluation on landscape pattern of farmland shelterbelt networks: A case study in midwest of Jilin province, China. – Chin. Geogr. Sci. 21(1): 48-56.
[13] Sun, B. P., Yue, D. P., Zhao, T. P., Cheng, T. R. (1997): The Evaluation of the spatial landscape pattern of farmland shelterbelt networks in BeizangTown, Daxing County, Beijing. – J. Beijing For. Univ. 19(1): 45-50.
[14] Wang, H. J., Zhou, H.(2003): A simulation study on the eco-environmental effects of 3N Shelterbelt in North China. – Glob. Planet. Change 37: 231-246.
[15] Wiseman, G., Kortb, J., Walker, D. (2009): Quantification of shelterbelt characteristics using high-resolution imagery. – Agric. Ecosyst. Environ. 131: 111-117.
[16] Yang, S. Y., Yang, H. J., Liu, L. J., Li, X. Y. (2017): Evaluating the landscape pattern of the farmland windbreaks in the Manas River Basin oasis. – Chin. J. Ecol. 36(6): 1690-1698.
[17] Zheng, X., Zhu, J. J., Xing, Z. F. (2016): Assessment of the effects of shelterbelts on crop yields at the regional scale in Northeast China. – Agric. Syst. 143: 49-60.
[18] Zhou, X. H., Sun, Z. W.(1994): On measuring and evaluating the spatial pattern of shelterbelt networks in landscape. – Acta Ecol. Sin. 14(1): 24-31.
[19] Zhu, J. Z., He, K. N., Wei, T. X. (2010): Science of Farmland Shelterbelt. 2nd Ed. – Chinese Forestry Press, Beijing, pp. 45-46.

http://www.aloki.hu ● ISSN 1589 1623 (Print) ● ISSN 1785 0037 (Online)
DOI: http://dx.doi.org/10.15666/aeer/1705_1165511668

CATFISH-EFFECT MULTI-OBJECTIVE PARTICLE SWARM OPTIMIZATION FOR COORDINATED DISPATCHMENT OF WATER AND SEDIMENT IN A RESERVOIR

PENG, Y.* – JI, C. M. – SHI, Y. L.

School of Renewable Energy, North China Electric Power University, Beijing 102206, China

**Corresponding author*
e-mail: pengyang@ncepu.edu.cn; phone: +86-136-9102-9633; fax: +86-10-6177-2234

(Received 22nd Apr 2019; accepted 12th Jul 2019)

Abstract. In this paper, a catfish-effect multi-objective particle swarm optimization algorithm (CE-MOPSO) is proposed for optimizing the coordinative flow-sediment scheduling in a reservoir. In the proposed CE-MOPSO, the driven effect of catfish particles is introduced to improve the convergence and diversity of solutions. The performance of the proposed CE-MOPSO was verified using a classical bi-objective test function (ZDT3), and it was found that compared with MOPSO and Sigma-MOPSO algorithms, the CE-MOPSO showed better convergence to the true Pareto optimal fronts, and provided better diversity and uniformity for the Pareto frons with smaller values of convergence index and diversity index. After the successful validations in simulation studies, the proposed approach was then applied to a real case study in the Three Gorges Reservoir in China. Our results showed that the obtained Pareto solution set effectively approximated the true Pareto optimal frontier during the process of evolution. The scheduling results of CE-MOPSO revealed the relationship between power generation and sediment deposition in ten years and can be used to develop reservoir operation policies and plan sediment trapping and flow operations in real time. These results suggest that the proposed CE-MOPSO approach is efficient and effective in managing multi-objective water resources and hydrologic problems.
Keywords: *flow-sediment optimal scheduling, particle swarm optimization, catfish's driven, Pareto optimal solution*

Introduction

Reservoir comprehensive utilization and sediment sluicing are contradictory in reservoir operation and management. Sediment deposition can reduce reservoir storage capacity, and subsequently cause decreases in the efficiency of flood control, hydropower generation, and navigation (Yoon, 1992; Yang, 2003). Therefore, the coordinated flow-sediment regulation is very important for effective and successful reservoir operation (Zhu, 1997; Han, 2003; Peng et al., 2014).

The aim of coordinated flow-sediment regulation in a reservoir is to seek maximum comprehensive benefits under the minimum sediment deposition. This can be considered as a multi-objective optimization problem (MOOP) with characteristics such as being multidimensional, dynamic, strong coupling, and nonlinear. In most previous studies, this multi-objective problem was usually solved by being transformed into a single-objective problem using vector optimization technologies, such as weighted method (Lian et al., 2004; Xiao et al., 2013), constraint method (Zhang and Feng, 1988; Xiang et al., 2010), Bayesian model averaging method (Duan et al., 2007; Yan and Moradkhani, 2014; Yan and Moradkhani, 2016), decomposition-polymerization method (Peng et al., 2004, 2014) and so on. However, the values of weight coefficients and constraint thresholds should be set subjectively in advance during the process of solving the model. A single set of fixed weights or constraint thresholds may result in only local optimum on the Pareto front. To obtain the global Pareto optimum, we need to run a

http://www.aloki.hu ● ISSN 1589 1623 (Print) ● ISSN 1785 0037 (Online)
DOI: http://dx.doi.org/10.15666/aeer/1705_1166911686

good number of simulations to examine all the weight combinations or constraint threshold (Reddy and Kumar, 2009).

As an alternative, multi-objective particle swarm optimization algorithm (MOPSO) has been shown as a useful tool for solving large and complex MOOPs, due to its stochastic and implicitly parallel properties to search for multiple local optimal solutions and consequently, to obtain the Pareto optimal solutions set. However, the algorithm of MOPSO has some disadvantages including premature convergence, reduced individual diversity, and enmeshed local optimum (Reyes-Sierra and Coello, 2006). To overcome these issues, several improved MOPSO have been proposed. For instance, Mostaghim and Teich (2003) used a Sigma method in MOPSO for searching the best local guides to speed up the convergence towards the true Pareto front with better distribution. Coello et al. (2004) used a constraint-handling mechanism and a special mutation operator to enhance exploration capability of MOPSO. Reyes-Sierra and Coello (2005) improved the MOPSO with the use of the Pareto dominance and a crowding factor to select the leaders. Leong and Yen (2006) suggested to use an adaptive local archive to promote swarm's diversity and incorporated an adjusted population size to promote swarm's competition. Branke and Mostaghim (2006) proposed a few strategies for the selection of global guides. Abido (2008) employed a clustering technique to adjust the optimal Pareto set size. Recently, the MOPSO has been increasingly applied in the field of water resources. Reddy and Kumar (2007, 2009) presented an elitist-mutation MOPSO approach for solving optimal multipurpose reservoir operation problems. Azadnia and Zahraie (Azadnia and Zahraie, 2010) used non-domination sorting and crowding distance techniques in MOPSO and applied it to optimize reservoir operation with two objectives including water supply and sediment removal. Li and Lian (2008) improved the MOPSO with self-adjusting inertia weights and Pareto-optimal archive for optimizing the coordinate reservoir deposition and power generation in reservoir operation. Despite the advances in these studies, there is still room to improve the efficiency of MOPSO, and the application of MOPSO to the coordinative flow-sediment scheduling in a reservoir has remained a challenge.

To further enhance the robustness of MOPSO, we propose a catfish-effect MOPSO algorithm (CE-MOPSO) in this paper. The catfish effect introduces a driven effect of catfish particles on individuals (i.e. the sardine particles), which was studied in the PSO algorithm and proven that the introduced catfish particle can improve the performance of the PSO (Chuang et al., 2008, 2011; Ji et al., 2011; De Souza et al., 2014). By taking advantage of such catfish effect, this paper incorporates catfish effect mechanism into the MOPSO algorithm. Different from the work in references (Chuang et al., 2008, 2011; De Souza et al., 2014), in which catfish particles were added at the extreme points of the search region and replaced 10% of original sardine particles having the smallest fitness value, this paper suggests another way to generate catfish particles and a different way that catfish particles work. The proposed algorithm was applied to optimize the coordinative flow-sediment scheduling in a real reservoir. In summary, the main contributions of the proposed CE-MOPSO algorithm are as follows.

(1) In the CE-MOPSO, the catfish particles are generated from the external archive, which is used to store the intermediate non-inferior solutions (i.e., elite particles with greater fitness value during the optimization process). Thus, the generated catfish particles have greater vigor and competitiveness than sardine particles. When the diversity of particle swarm is less than a defined threshold, catfish particles are added into the search region. The added catfish particles have driven effect on sardine

http://www.aloki.hu ● ISSN 1589 1623 (Print) ● ISSN 1785 0037 (Online)
DOI: http://dx.doi.org/10.15666/aeer/1705_1166911686

particles, which make the sardine particles escape from them. Thus, the sardine particles may jump out of the "locked" status and be guided to moving towards new area of the search space. This helps the MOPSO algorithm improve the diversity of the population, and converge fast towards true Pareto fronts in further generations.

(2) The global optimal value of the sardine particle driven-influenced by catfish particles, is decided by the Sigma value of catfish particle, which is the second close to the Sigma value of sardine particle instead of the closest one. This contributes the CE-MOPSO avoid trapping in the local optimal solutions caused by the Sigma method and finding the global optimal solution with deeper search and increased convergence speed.

(3) The proposed CE-MOPSO performance is first compared with MOPSO (Coello et al., 2004) and Sigma-MOPSO (Mostaghim and Teich, 2003) algorithms through an optimization test with a bi-objective test function (ZDT3). The results show that the CE-MOPSO have better performance in convergence and diversity. Then, the proposed algorithm is applied to solving the optimization of reservoir flow-sediment regulation in a case study. Results show that the proposed CE-MOPSO is able to obtain a well-distributed Pareto optimal front, which can reflect the relationship between power generation and reservoir deposition.

The remaining sections are organized as follows. In Section 2, we establish a reservoir flow-sediment optimal dispatching model. The proposed CE-MOPSO algorithm is elaborated in Section 3 and its performance is verified in Section 4 by comparing it with the MOPSO and Sigma-MOPSO algorithms. A case study of using the CE-MOPSO is presented in Section 5. Finally, we conclude the paper in Section 6.

Materials and methods

Materials

The Three Gorges Reservoir (TGR) in China is taken up as a case study for analyzing non-inferior relationship between hydropower generation and sediment deposition. The Three Gorges dam is located in the upper reach of the Yangtze River, as shown in *Figure 1*. The TGR is the largest multi-purpose hydropower project in China, which has great benefits of flood controlling, power generation, navigation improving, water supply, etc. The TGR began to impound water on 1 June 2003, and was in full operation in 2009. The main features of the reservoir are given in *Table 1*.

The storage capacity of TGR is 393×10^8 m^3, and every 1 m increase in water head will bring TGR great benefit of power generation. Meanwhile, reservoir sedimentation is a serious issue in TGR operation and management, because it reduces TGR storage capacity and causes decreasing capability in flood control, hydropower generation, and navigation. Increasing power generation requires increasing the water head, which result in increase in sediment deposition. Power generation and reservoir sedimentation are contradictory in the TGR operation and management. Therefore, relationship between power generation and sediment trapping need to be revealed for effective reservoir operations.

The hydropower generation and sedimentation of TGR were calculated based on the 1961~1970 hydrological series. The time interval for the scheduling calculation is ten days in June to September and one month in other months. Therefore, the total number of time intervals is 20 in a year and 200 in ten years. The range of sedimentation calculation of the TGR was from Jiangjin to the dam site of the TGR, with the total

http://www.aloki.hu ● ISSN 1589 1623 (Print) ● ISSN 1785 0037 (Online)
DOI: http://dx.doi.org/10.15666/aeer/1705_1166911686

length of 689.2 km. 210 sections were set with average section spacing of about 3,280 m. The typical cross-sections are also shown in *Figure 1*.

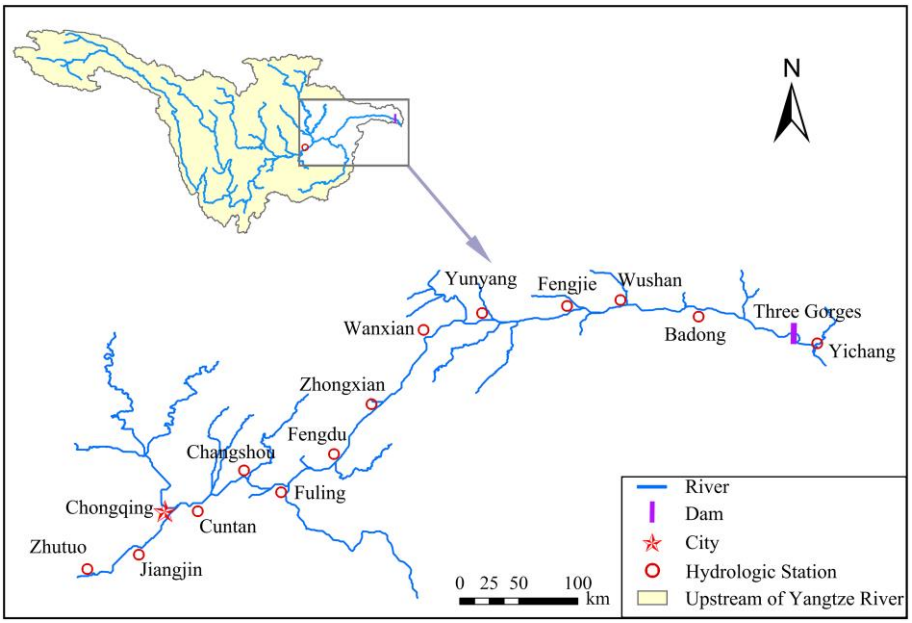

Figure 1. *Location of the studied area*

Table 1. *Primary features of the Three Gorges Reservoir*

Reservoir parameters	Quantity
Total reservoir capacity (10^8 m^3)	393
Active capacity (10^8 m^3)	165
Flood control capacity (10^8 m^3)	221.5
Dam crest elevation (m)	185
Normal water level (m)	175
Flood limited water level (m)	145
Lowest drawdown water level in dry season (m)	155
Installed capacity (10^6 kW)	22.40
Mean annual power generation (10^9 kW·h)	847

Model formulation for reservoir flow-sediment optimal scheduling

In this study, the flow-sediment optimal scheduling model takes into account the non-inferior relationships between hydropower generation and sediment siltation, with the consideration of the constraints including reservoir flood control and navigation. The developed optimization model is generalized as follows.

Objective function

The optimal regulation model includes two objectives: maximize hydropower generation and minimize sediment deposition in reservoir. The mathematical functions of the objectives are expressed as follows (Peng et al., 2004; Yoo, 2009):

http://www.aloki.hu ● ISSN 1589 1623 (Print) ● ISSN 1785 0037 (Online)
DOI: http://dx.doi.org/10.15666/aeer/1705_1166911686

$$\max E = max\sum_{t=1}^{T}\eta H_t Q_t \Delta t / 3600 = f_1(\boldsymbol{X}) \quad \text{(Eq.1)}$$

$$\min V_s = min\sum_{t=1}^{T} V_{st} = f_2(\boldsymbol{X}) \quad \text{(Eq.2)}$$

where E and V_s denote hydropower generation and sediment that deposited in the effective capacity of reservoir for all scheduling intervals; T is the total number of intervals over the scheduling horizon; $f_1(\boldsymbol{X})$ and $f_2(\boldsymbol{X})$ are functions of the objectives E and V_s; $\boldsymbol{X}$ is an independent variable decided by reservoir operation mode; η represents power coefficient; Δt is duration of an scheduling interval; H_t and Q_t are hydraulic head and release passing turbines of hydropower plant in the tth scheduling interval; V_{st} is sediment deposited in a reservoir in the tth scheduling interval.

Reservoir sedimentation calculation

In the present study, the V_{st} is calculated by a one-dimensional mathematical model for unsteady flow and nonuniform sediment transport in a reservoir (Peng and Zhang, 2006). The governing equations are described as follows:

Flow continuity equation (van Rijn, 1993)

$$\frac{\partial A}{\partial t} + \frac{\partial Q}{\partial x} = q_i \quad \text{(Eq.3)}$$

Flow momentum equation (van Rijn, 1993)

$$\frac{\partial Q}{\partial t} + \frac{\partial}{\partial x}\left(\alpha_1 \frac{Q^2}{A}\right) + gA\frac{\partial Z}{\partial x} + g\frac{n^2 Q|Q|}{AR^{4/3}} = 0 \quad \text{(Eq.4)}$$

Nonequilibrium transport equation for suspended load (Han and He, 2015)

$$\frac{\partial(AS_k)}{\partial t} + \frac{\partial(QS_k)}{\partial x} = \alpha_k \omega_k B(S_{*k} - S_k) \quad \text{(Eq.5)}$$

Sediment carrying capacity equation for suspended load (Yang, 1993)

$$S_* = S_*(U, H, \omega, \cdots) \quad \text{(Eq.6)}$$

Sediment transport rate equation for bed load (Yang, 1993)

$$g_{bk} = g_{b*k}(U, H, d, \cdots) \quad \text{(Eq.7)}$$

Total bed deformation equation (Yang, 1993)

$$\rho' \frac{\partial Z_d}{\partial t} = \sum_{k=1}^{N_s} \alpha_k \omega_k (S_k - S_{*k}) - \sum_{k=N_s+1}^{N} \frac{\partial g_{bk}}{\partial x} \quad \text{(Eq.8)}$$

http://www.aloki.hu ● ISSN 1589 1623 (Print) ● ISSN 1785 0037 (Online)
DOI: http://dx.doi.org/10.15666/aeer/1705_1166911686

where t and x are temporal and spatial axes; Q is streamflow discharge; q_l is discharge of lateral flow; A, B and H are cross-sectional area, width and depth of streamflow, respectively; Z is water level; U is cross-sectional average velocity of streamflow; R is hydraulic radius; n is Manning's roughness coefficient; S_k is suspended sediment concentration of size group k, written as $S_k = p_k S$ in which p_k and S are size distribution and sediment concentration of suspended load; S_{*k} is suspended sediment-carrying capacity of the kth group, expressed as $S_{*k} = p_{*k} S_*$ in which S_* sediment-carrying capacity of suspended load, and p_{*k} is size distribution of S_*; α_k is saturation recovery coefficient for nonequilibrium suspended load transportation of kth size group; ω_k is settling velocity of kth size group of suspended load; g_{b*k} is the actual bed load transport rate of kth size group, written as $g_{b*k} = g_b\left(d_k\right) * p_k$ in which $g_b(d_k)$ is bed load transport capacity of kth size group, and d_k is particle size of kth size group; Z_k is depth of bed deposition; g is gravitational acceleration; ρ_s' is dry density of deposits or bed material; d is particle diameter of bed material, N_s is number of size groups of suspended load; N is number of size groups of total load.

Equations 3–8 can be solved by finite difference method. Solution process consists of two steps: Flow *Equations 3* and *4* were solved firstly, and sediment *Equations* 5 and *8* secondly. For details of the solution process, the readers are referred to (Peng and Zhang, 2006). The V_{st} in *Equation 2* can be calculated based on the computed result of Z_d in *Equation 8.*

Constraints

Water volume balance constraint

The water volume balance equation is expressed as

$$V_{t+1} - V_t = \left(Q_t - q_t - S_t\right)\Delta t \qquad \text{(Eq.9)}$$

where V_{t+1} and V_t are reservoir storages at the end and beginning of the tth interval, respectively; Q_t and q_t are inflow and outflow discharges during the tth interval; S_t is discharge of loss water in a reservoir during the tth interval.

Flood control constraints of reservoir

The flood control constraints of reservoir are expressed as

$$\mathrm{Z}_t \le Z_{\max}, q_t \le q_{\max} \qquad \text{(Eq.10)}$$

where Z_t is water level of reservoir at the end of the tth interval; Z_{max} is reservoir flood limiting water level; q_{max} is permissible discharge of streamflow at flood control point downstream of reservoir.

Navigation constraints

The navigation constraints of reservoir are expressed as

http://www.aloki.hu ● ISSN 1589 1623 (Print) ● ISSN 1785 0037 (Online)
DOI: http://dx.doi.org/10.15666/aeer/1705_1166911686

$$Z_t \geq Z_{\min}, q_t \geq q_{t\min} \quad \text{(Eq.11)}$$

where Z_{min} is navigable water stage in reservoir area; q_{tmin} is minimum discharge flow that meets the needs of navigation downstream of reservoir during interval t.

Water release ability limit of dam

The outflow discharging from reservoir is restrained by the maximum discharge capacity of dam discharge structure, which can be expressed as

$$q_t \leq q(Z_t) \quad \text{(Eq.12)}$$

where $q(Z_t)$ is flood peak discharge ability limit of dam at level Z_t.

Power constraints of station

The power constraints of station are expressed as

$$N_{t,\min} \leq \eta H_t Q_t \leq N_{t,\max} \quad \text{(Eq.13)}$$

where $N_{t,\min}$ and $N_{t,\max}$ are the upper and lower limits of plant power during interval t, respectively.

The proposed catfish-effect MOPSO algorithm

Catfish effect mechanism

The catfish effect originates from an effect observed by Norwegian fishermen when they introduced catfish into a holding tank for caught sardines. The added catfishes would stimulate the movement of sardines, thus making the sardines alive and fresh longer (Hu, 2004).

The catfish effect in this study is applied to the MOPSO algorithm and this method is called catfish-effect MOPSO algorithm (CE-MOPSO). At the early evolutionary stage of particle group, particles are treated as sardine's particles, and the Sigma method (Mostaghim and Teich, 2003) is used to search the space of solution with a fast convergence rate. When sardines group are trapped in a local optimum because of poor diversity, the catfish particles will be produced from the non-inferior solutions and be put into sardine particles. The generated catfish particles will trigger the driven influence on sardine particles, and guide sardine particles towards a new search region to improve the diversity in the population.

Implementation of CE-MOPSO

The detailed steps of the proposed CE-MOPSO algorithm are given below.

Step 1: Set the parameters including swarm population size N, maximum number of iteration K, and external archive size M. The external archive is used to store the generated non-inferior solutions that can be used to guide the search. The size of external archive determines the number of non-inferior solutions.

http://www.aloki.hu ● ISSN 1589 1623 (Print) ● ISSN 1785 0037 (Online)
DOI: http://dx.doi.org/10.15666/aeer/1705_1166911686

Step 2: Initialize the population. Treat particles as sardine particles, and initialize particles in the population with random positions and velocities that meet the constrains. Initialize *M/2* non-inferior solutions and set them as the individuals in external archive.

Step 3: Calculate the fitness of each particle, and maintain the external archive based on the crowding distance of each non-inferior solution.

The equation used for computing the fitness of each particle with two-objective fitness function was expressed as follows:

$$\begin{cases} \mathrm{Fit}(f_1(\mathbf{x})) = \sum_{t=1}^{T} \eta H_t Q_t \Delta t / 3600 - M \sum_{l=1}^{L} W_l \\ \mathrm{Fit}(f_2(\mathbf{x})) = 1/\{\sum_{t=1}^{T} V_{st} - M \sum_{l=1}^{L} W_l\} \end{cases} \quad \text{(Eq.14)}$$

where M is penalty factor; W_l is the value that the tth constraint is violated; L is total number of constraints.

Generate non-inferior solutions according to the calculated fitness values of particles, and store the generated non-inferior solutions per iteration in external archive. If the number of non-inferior solutions in external archive exceeds the M, retain the individuals with larger crowding distance, thus maintain the diversity of non-inferior solutions. The crowding distance (d_j) of individual j in external archive was computed as follows (Reddy and Kumar, 2007):

$$d_j = \sum_{ob=1}^{O} \frac{|f_{ob}(j+1) - f_{ob}(j-1)|}{f_{ob}^{\max} - f_{ob}^{\min}} \quad \text{(Eq.15)}$$

where ob denotes the objective index; O is the total number of objectives; $f_{ob}^{\max}$ and $f_{ob}^{\min}$ denote the max and min values of objective function, respectively; $f_{ob}(j + 1)$ and $f_{ob}(j\text{-}1)$ are the values of objective function for individuals j-1 and j + 1, which are the two nearest to individual j.

Step 4: Determine the best value of each particle in population, and calculate the Sigma value of each individual in both population and external file as follows (Mostaghim and Teich, 2003):

$$\delta = \frac{f_1^2 - f_2^2}{f_1^2 + f_2^2} \quad \text{(Eq.16)}$$

where f_1 and f_2 denote the two objective functions' values of particle.

Step 5: Calculate the diversity of particle swarm at the kth iteration ($\xi(k)$) as follows:

$$\begin{cases} \xi(k) = \dfrac{div(k)}{div(0)} \\ div(k) = \sqrt{\dfrac{1}{Nm} \sum_{j=1}^{N} \sum_{i=1}^{m} \left[\dfrac{(x_i^j(k) - x_i^{j,gbest}(k))}{(Bu_i - Bd_i)} \right]^2} \end{cases} \quad \text{(Eq.17)}$$

http://www.aloki.hu ● ISSN 1589 1623 (Print) ● ISSN 1785 0037 (Online)
DOI: http://dx.doi.org/10.15666/aeer/1705_1166911686

where k is iteration number; j is serial number of particle; x_i^j is position in the ith dimension of particle j; $x_i^{j,gbest}$ is global best position in the ith dimension of particle j which exists in external archive, and its Sigma value is the second closest to the Sigma value of particle j; Bu_i and Bd_i denote the upper and lower limits of x_i^j.

Check whether the $\xi(k)$ is less than the scheduled threshold ξ_0. If $\xi(k) > \xi_0$, go to step 6, otherwise go to step 7.

Step 6: Determine the global optimal value of each particle using Sigma method (Mostaghim and Teich, 2003). If the sigma value of a particle in population is closest to the sigma value of an individual in external archive, the individual in external archive will be selected as the particle's global best position. Update the velocity and position of the jth particle as follows (Kennedy and Eberhart, 1995):

$$v_i^j(k+1) = \omega \times v_i^j(k) + c_1 \times r_1(x_i^{j,pbest}(k) - x_i^j(k)) + c_2 \times r_2(x_i^{gbest}(k) - x_i^j(k)) \quad \text{(Eq.18)}$$

$$x_i^j(k+1) = x_i^j(k) + v_i^j(k+1) \quad \text{(Eq.19)}$$

where ω is coefficient of inertia weight, which controls the influence of the particle previous velocity on its current one; c_1 and c_2 are learning factors; r_1 and r_2 are independent random numbers uniformly distributed in the interval [0,1]; v_i^j is the ith dimension velocity of particle j; $x_i^{j,pbest}$ is the jth particle's best position in the ith dimension.

Step 7: Generate catfish particles to promote the diversity of swarm particles.

Let C be the maximal number of catfish particles. If the number of non-inferior solutions is less than C, set all the non-inferior solutions as catfish particles. Otherwise, select C non-inferior solutions with larger crowding distance as catfish particles. The catfish particles are put into the sardine particle swarm as external competitive individuals. The added catfish particles, which act only at the current iteration and will be "dead" and removed from the particle swarm at next iteration, will trigger the driven influence on sardine particles. Thus, the search of solutions is affected by not only the guidance of global optimal value and individual optimal value, but also the driving of catfish particle. The renewed velocity of the jth particle is updated as follows:

$$\begin{aligned} v_i^j(k+1) = {} & \omega \times v_i^j(k) + c_1 \times r_1(x_i^{j,pbest}(k) - x_i^j(k)) + c_2 \times r_2(x_i^{j,gbest}(k) - x_i^j(k)) - \\ & Sat \times P \times sign(x_{Ci}^I(k) - x_i^j(k)) \times \exp\left\{-Q \times \left|x_{Ci}^I(k) - x_i^j(k)\right|\right\} \end{aligned} \quad \text{(Eq.20)}$$

where subscript C denotes catfish particle index; superscript I is a serial number of catfish particle which is closest to sardine particle j in dimension i, and is calculated as:

$$I = \left\{ l \,|\, \min_l \left(\left| x_{Ci}^I(k) - x_i^j(k) \right| \right) \right\} \quad \text{(Eq.21)}$$

Thus, the catfish particle nearest to each sardine particle in each dimension can be chosen at each iteration.

http://www.aloki.hu ● ISSN 1589 1623 (Print) ● ISSN 1785 0037 (Online)
DOI: http://dx.doi.org/10.15666/aeer/1705_1166911686

Note that the fourth item in *Equation 20* is called the driven effect item. *Sat* is a binary variable, 0 or 1 stochastically that decides if sardine particles are driven-influenced by catfish particles, which can be expressed as:

$$Sat = \begin{cases} 0 & F_I^{k+1} > F_I^k \\ 1 & F_I^{k+1} \le F_I^k \end{cases} \quad \text{(Eq.22)}$$

where F_I^k is the fitness of catfish particle *I* at the *k*th iteration.

Parameters *P* and *Q* in *Equation 20* decide how hard catfish particles drive sardine particles. The nearer the distance between catfish particle and sardine particle is, the greater driven effect of catfish particle on sardine particle is. Consequently, sardine particles keep escaping from catfish particles, and catfish particles occupy around global best position rapidly.

It can be seen that the catfish effect mechanism described in *Equation 20* has two key points: (1) Global optimal value of sardine particle is decided by the Sigma value of catfish particle, which is the second close to Sigma value of sardine particle instead of the closest one. It prevents sardine particles from trapping into the local optimal solutions caused by the Sigma method and helps sardine particles find the global optimal solution with local depth search and increased convergence speed. (2) Including the guidance of global optimal value and individual optimal value, the search of solution was also affected by the driven effect of catfish particles. This makes sardine particles escape from catfish particles generated from non-inferior solutions, which can avoid the solution search concentrating near non-inferior solutions and falling into a "locked" status. Thus, the searching space is broadened and the diversity of solution is improved.

Step 8: Generate the newer particle according to the computed velocity and position.

Step 9: Take the maximum number of iteration as terminal condition of the algorithm. If the number of iteration is less than the maximum iteration, then go to step 3; otherwise end the search and output the non-dominated solution set from external files.

The flowchart of the CE-MOPSO is exhibited in *Figure 2*.

Results and discussion

Efficiency of CE-MOPSO algorithm

Before applying to a real case study, we first demonstrated the efficiency of the proposed CE-MOPSO algorithm through a bi-objective test function (ZDT3). We compared this algorithm with MOPSO (Coello et al., 2004) and Sigma-MOPSO algorithms (Mostaghim and Teich, 2003), and used two performance metrics to assess their performance.

Performance measures

Convergence index (γ) measures the distance of the obtained non-dominated solutions to the true Pareto front, which is written as (Tripathi, 2007):

http://www.aloki.hu ● ISSN 1589 1623 (Print) ● ISSN 1785 0037 (Online)
DOI: http://dx.doi.org/10.15666/aeer/1705_1166911686

$$\gamma = \frac{1}{n}\sqrt{\sum_{i=1}^{n} d_i^2} \qquad \text{(Eq.23)}$$

where n denotes the number of members in non-dominated solutions; d_i is the Euclidean distance between the ith member in non-dominated solutions and its nearest member in the true Pareto front. A smaller value of γ reflects better convergence toward the true Pareto front.

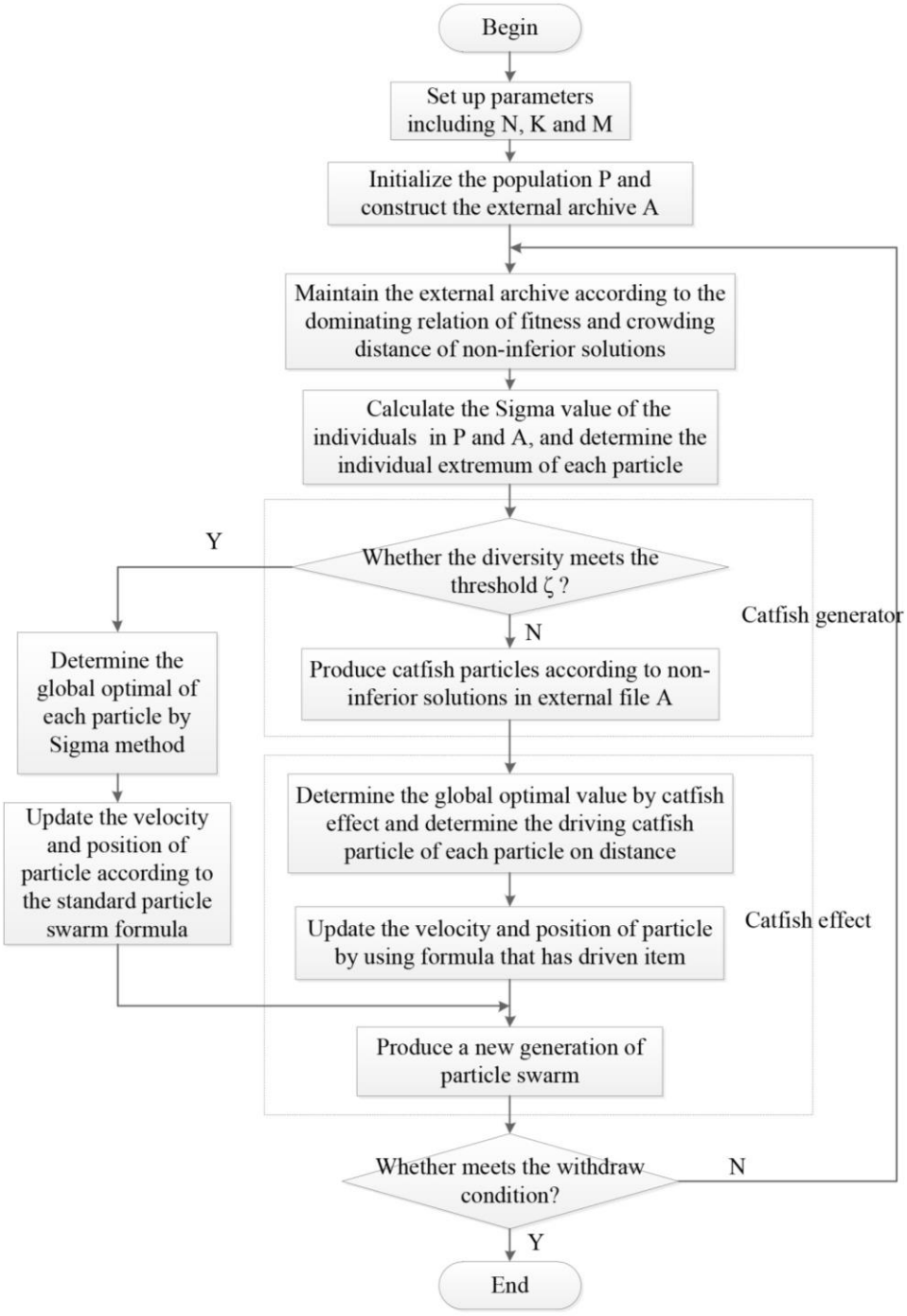

Figure 2. *The flowchart of the catfish-effect multi-objective particle swarm algorithm*

http://www.aloki.hu ● ISSN 1589 1623 (Print) ● ISSN 1785 0037 (Online)
DOI: http://dx.doi.org/10.15666/aeer/1705_1166911686

Diversity index (Δ) indicates the spread along the non-dominated solutions, which is written as (Tripathi, 2007):

$$\Delta = \frac{d_f + d_l + \sum_{i=1}^{n-1} \left| d_i - \bar{d} \right|}{d_f + d_l + (n-1) \times \bar{d}} \quad \text{(Eq.24)}$$

where d_i is the Euclidean distance between adjacent solutions in the obtained non-dominated solutions set, and $\bar{d}$ is the average of all the d_i, which is expressed as $\bar{d} = \sum_{i=1}^{n-1} d_i / (n-1)$; d_f and d_l are the Euclidean distances between the extreme solutions and the boundary solutions of the obtained non-dominated set. The smaller the value of Δ, the more uniform the distribution of the non-dominated solutions.

Discussion of results

The following parameters were chosen for the three algorithms: population size $N = 50$, archive size $M = 100$, maximum number of iteration $K = 500$, learning factors $c_1 = c_2 = 2$, inertia weight $\omega = 0.9\text{-}0.5\ k/K$, in which k is the current iteration number. Relative diversity threshold of CE-MOPSO algorithm was set to $\xi_0 = 0.45$ (The calculated results showed that the evolution of the population stabilized in the vicinity of this value and the diversity of the population needed to be promoted).

Twenty independent runs are performed for each algorithm on ZDT3, and their average and variance values of the two metrics (γ and Δ) are presented in *Table 2*. It can be seen that the proposed CE-MOPSO algorithm outperforms MOPSO and Sigma-MOPSO algorithms for ZDT3 test problem, with the lowest average and variance values of the γ. It indicates that the CE-MOPSO achieves a faster convergence rate to the true Pareto optimal fronts than MOPSO and Sigma-MOPSO algorithms. Also, our proposed CE-MOPSO algorithm obtained the best results with respect to the Δ, with the smallest average and variance values of the Δ. This shows that the proposed CE-MOPSO can to attain a better distribution of solutions than the other two algorithms for ZDT3 test problem. Therefore, it can be concluded that the solutions obtained by CE-MOPSO have better performance in convergence and diversity. It should be mentioned that the CE-MOPSO consumes much more computation time than MOPSO and Sigma-MOPSO algorithms, because the catfish's driven effect makes sardine particles explore a deeper search space to promote the diversity in population, which will consume more time.

Table 2. *Results for ZDT3: γ, Δ, and the time required per iteration*

Test function	Index	MOPSO	Sigma-MOPSO	CE-MOPSO
ZDT3	γ (average)	0.00418	0.10205	0.00311
	γ (variance)	0.00000	0.00238	0.00000
	Δ (average)	0.83195	0.76016	0.33004
	Δ (variance)	0.00892	0.00349	0.00007
	Time (sec)	16.78	19.35	71.49

The resulting Pareto fronts produced by the three algorithms for ZDT3 function are presented in *Figure 3*. It is seen that compared with MOPSO algorithm, the solutions of

http://www.aloki.hu ● ISSN 1589 1623 (Print) ● ISSN 1785 0037 (Online)
DOI: http://dx.doi.org/10.15666/aeer/1705_1166911686

Sigma-MOPSO had better convergence at two ends, but the distribution in the middle was rather dispersed with several gaps (*Fig. 3b*). The solutions of MOPSO algorithm were scattered at two ends, but the distribution in the middle was relatively continuous and uniform (*Fig. 3a*). Thus, the Sigma-MOPSO algorithm paid more attention to the convergence at two ends, but ignored the convergence quality and diversity of solution. Compared with the MOPSO and Sigma-MOPSO algorithms, the CE-MOPSO in *Figure 3c* can converge faster towards the true Pareto front, and produce the true Pareto front with better spread both at two ends and in the middle on this function. This also demonstrates that the proposed CE-MOPSO has obvious advantages in convergence and spread of solutions for ZDT3 test problem.

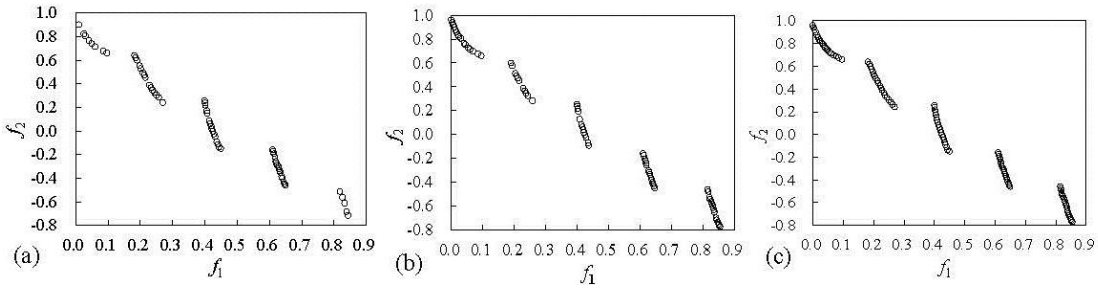

Figure 3. *Obtained Pareto fronts using (a) MOPSO, (b) Sigma-MOPSO and (c) CE-MOPSO on test function ZDT3*

Application

Case study

The one-dimensional numerical model for reservoir sedimentation was validated with other numerical results. The comparison of the computed sediment deposition for 10 years operation of the TGR was presented in *Table 3*. It is shown that the calculated sedimentation in TGR agreed well with the results calculated by Yangtze River Scientific Research Institute, the maximum relative error is 8.584% in the reach of Cuntan-Jiangjin. This indicated that the one-dimensional numerical model was accurate enough to model the sedimentation in the TGR.

Table 3*. Computed sediment deposition for 10 years operation of the TGR*

River reach	V_1 (10^8 m^3)	V_2 (10^8 m^3)	Relative error (%)
From the dam site to Fengdu	26.32	26.3	0.076
From Fengdu to Fuling	2.291	2.31	0.822
From Fuling to Changshou	1.146	1.2	4.500
From Changshou to Cuntan	0.327	0.337	2.967
From Cuntan to Jiangjin	0.213	0.233	8.584
From the dam site to Jiangjin	30.297	30.38	0.273

V_1 denotes the computed results by using the one-dimensional numerical model in the paper; V_2 denotes the computed results of Yangtze River Scientific Research Institute

Based on the designed operation scheduling of GTR, the main constraints were set as following: (1) Requirements of sediment flushing and constraints of flood control:

http://www.aloki.hu ● ISSN 1589 1623 (Print) ● ISSN 1785 0037 (Online)
DOI: http://dx.doi.org/10.15666/aeer/1705_1166911686

considering improvement of flood forecast techniques and requirement of sediment flushing, limited water level of flood control is varied between 140 m and 145 m, maximum release discharge reservoir is 55,000 m^3/s. (2) Restrictions of minimum power and navigation: minimum power of plants in dry season is 4.99 million kilowatts (kW), water level controlled by navigation upstream of TGR in dry season is 155 m.

Select water level of TGR at each time step as decision variable, and one particle represents one of operation scheduling strategies of reservoir. Thus, each particle is expressed as:

$$X^j = (x_1^j, x_2^j, \cdots, x_t^j, \cdots, x_T^j) \quad \text{(Eq.25)}$$

in which x_t^j is the water level of reservoir during period t; superscript j denotes the serial number of particles; T denote total number of time step.

Results analysis

Ten independent runs were performed for optimizing the coordinative flow-sediment scheduling operation in the TGR by using the proposed CE-MOPSO. *Figure 4* shows the obtained optimal frontier of Pareto and its evolution process through 50, 100, 300, and 500 iterations of CE-MOPSO algorithm. It is shown that the non-inferior solution set is renewed during the process of evolution, and the obtained Pareto set effectively approximate to the true Pareto frontier. Comparing the obtained Pareto frontier result of 500 iterations with that of 300 iterations, it is basically the same in the central section of B-C and A-B area, but the distribution of the non-inferior solutions near A point of 500 iterative times are better than the result of 300 iterative times. The non-inferior solutions near B point has formed a more continuous uniform distribution than those of 300 iterative times. This indicates that the diversity of non-inferior solution set is improved with iterations by catfish effect mechanism, especially the non-inferior solutions are well-distributed at each end and inflection point of the optimal frontier.

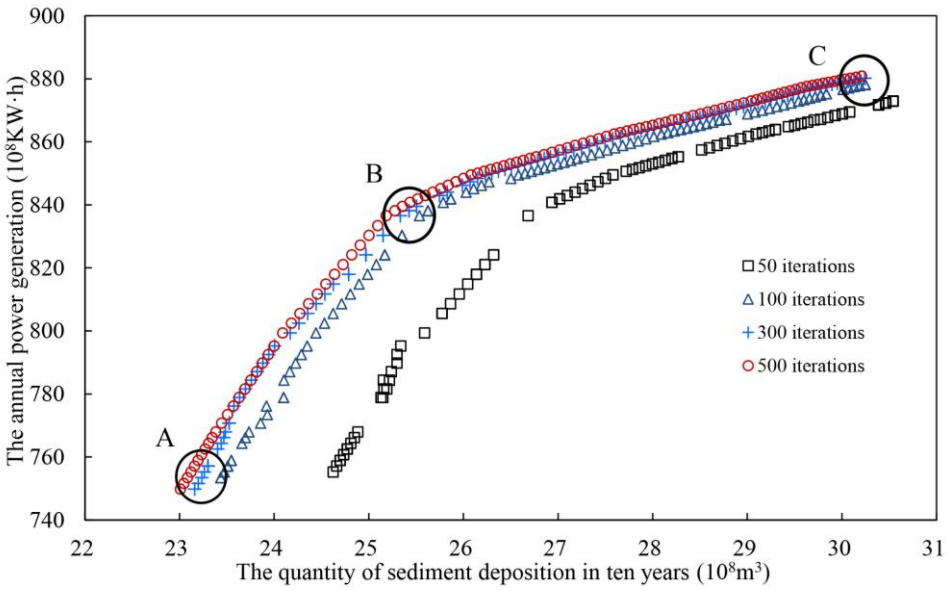

Figure 4. *The optimal frontier of Pareto and evolution process of the sedimentation in ten year and the annual average power generation*

http://www.aloki.hu ● ISSN 1589 1623 (Print) ● ISSN 1785 0037 (Online)
DOI: http://dx.doi.org/10.15666/aeer/1705_1166911686

The Pareto optimal frontier shown in *Figure 4* also reflected the relationship between annual average power generation and sediment deposition in ten years. An increased hydropower generation resulted in an increased deposition in reservoir. The targets of increasing hydropower generation and decreasing reservoir sediment deposition are in contradictory ways. B point is an inflection point of the relationship between hydropower generation and sediment deposition of the TGR. In the section of A-B area, the rate of increasing power generation is greater than the rate of increasing siltation, while the rate of increasing power generation is smaller than the rate of increasing siltation in the section of B-C area. The inflection point B is very important for the selection of a non-inferior scheme in the TGR operation. For the schemes is in A-B area, increasing 1×10^8 kW·h power generation results in 0.025×10^8 m^3 sediment silting in the reservoir. For the schemes is in B-C area, increasing 1×10^8 kW·h power generation results in 1.08×10^8 m^3 sediment silting in the reservoir.

Figure 5 shows the non-inferior reservoir operation water level processes of the schemes corresponding to points A, B and C. In A scheme, since reservoir water level was lowered in flood season and did not reach the normal storage water level at the end of flood season that affects the power generation dispatch in non-flood season, both sediment deposition and power generation is the minimum in A scheme. In C scheme, due to the high water level operation in flood season, its power generation and sediment deposition is the maximum. The operation water level of B scheme in flood season is between A and C, which not only makes full use of lowering water level for sediment reduction in flood season, but also raising the water level to the normal storage level to ensure the power generation dispatch in non-flood season, so its power generation and sediment deposition is in the middle. This operation mode is different from traditional single-objective dispatch, which belongs to of multi-objective optimization of the coordinative water-sediment dispatch.

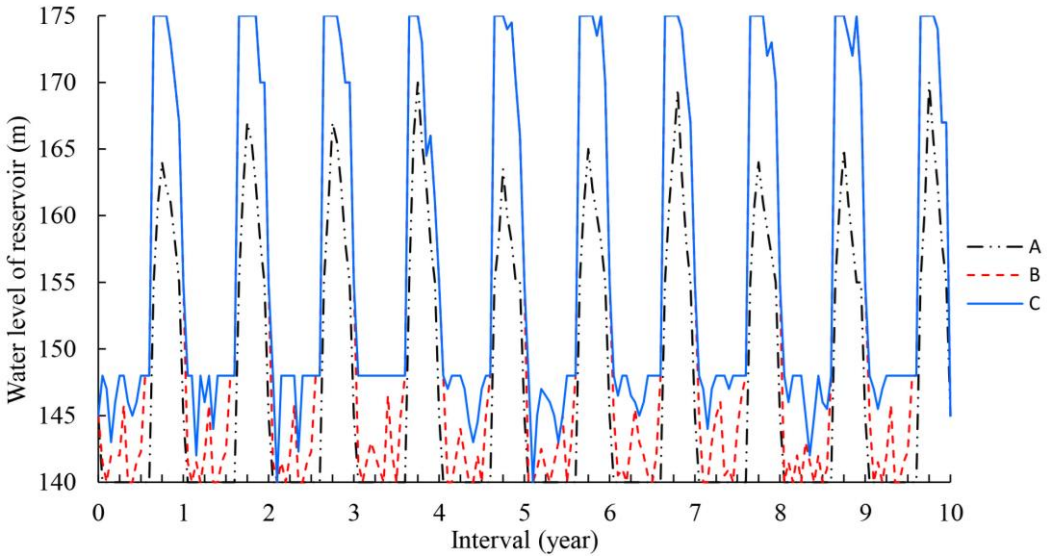

Figure 5. *Non-inferior reservoir operation level process of A, B and C schemes*

The mean annual power benefits and sedimentation represent short-term benefit and long-term benefits of the reservoir, respectively. If reservoir managers or decision makers focus on the life of reservoir that could play a long-term comprehensive

http://www.aloki.hu ● ISSN 1589 1623 (Print) ● ISSN 1785 0037 (Online)
DOI: http://dx.doi.org/10.15666/aeer/1705_1166911686

utilization benefit, the corresponding reservoir water level need to be lowed, such as scheme A. If decision makers focus on the short-term benefits of reservoir, the corresponding reservoir water level need to be raised, such as scheme C. The optimal scheme has better balance between power generation and reservoir sedimentation, and the obtained the non-inferior solutions can be used to formulate reservoir operation policies in practice. These policies can also be used to plan sediment trapping and flow operations.

Conclusion

In this paper, a catfish-effect multi-objective particle swarm optimization (CE-MOPSO) algorithm is proposed for optimizing the coordinated dispatch of water and sediment in a reservoir. Catfish particles, generated from the individuals in external archive, have greater vigor and more competitiveness than sardine particles. When added into sardine particles, the catfish particles have driven effect on sardine particles, which makes the sardine particles escape from them. By this, the sardine particles may jump out of the "locked" status, explore the search region, and improve the diversity of population. This helps the MOPSO algorithm to effectively guide the search towards the true Pareto front in further generations. In addition, the global optimal value of particle is second close to its Sigma value instead of the closest one. This prevents sardine particles from trapping into the local optimal solutions caused by the Sigma method, and helps sardine particles find the global optimal solution with local deeper search and increased convergence speed. The performance of CE-MOPSO in nonlinear numerical function optimization was first investigated with a test of classical bi-objective test function (ZDT3). The results were encouraging and promising in both computational efficiency and search efficiency when compared with the MOPSO and Sigma-MOPSO. The proposed CE-MOPSO was then applied to a multi-objective optimization of the coordinative flow-sediment regulation in the Three Gorges Reservoir. The obtained Pareto set effectively approximated the true Pareto frontier during the process of evolution. The scheduling results of CE-MOPSO reflected the tradeoff between power generation and sediment deposition in ten years, which is useful for making reservoir operation policies of sediment trapping and flow operations in practice. These results demonstrate that the proposed CE-MOPSO can provide efficient and effective solutions for the optimization of the coordinative flow-sediment scheduling in a reservoir.

However, in CE-MOPSO, we need to define the maximal number of catfish particles, which has some subjective. In the future, a better approach for selecting the maximal number of catfish particles is desired to make a balance between computation time and performance of the algorithm. In addition, we would like to compare CE-MOPSO with some other evolutionary algorithms and apply CE-MOPSO for solving higher dimensional optimization problems.

Acknowledgments. This work is funded by the Project of National Key Research and Development Program (2016YFC0402308) and the National Natural Science Foundation of China (51679088).

http://www.aloki.hu ● ISSN 1589 1623 (Print) ● ISSN 1785 0037 (Online)
DOI: http://dx.doi.org/10.15666/aeer/1705_1166911686

REFERENCES

[1] Abido, M. A. (2008): Multiobjective particle swarm optimization for optimal power flow problem. – 12th International Middle-East Power System Conf. IEEE Industrial Electronic Society, Aswan, pp. 392-396.
[2] Azadnia, A., Zahraie, B. (2010): Application of multi-objective particle swarm optimization in operation management of reservoirs with sediment problems. – World Environmental and Water Resources Congress: Challenges of Change, American Society of Civil Engineers, Rhode Island, pp. 2260-2268.
[3] Branke, J., Mostaghim, S. (2006): About selecting the personal best in multi-objective particle swarm optimization. – Parallel Problem Solving from Nature-PPSN IX, Reykjavik, pp. 523-532.
[4] Chuang, L. Y., Tsai, S. W., Yang, C. H. (2008): Catfish particle swarm optimization. – Swarm Intelligence Symposium IEEE, St. Louis, MO.
[5] Chuang, L. Y., Tsai, S. W., Yang, C. H. (2011): Improved binary particle swarm optimization using catfish effect for feature selection. – Expert Systems with Applications 38(10): 12699-12707.
[6] Coello, C. A. C., Pulido, G. T., Lechuga, M. S. (2004): Handling multiple objectives with particle swarm optimization. – IEEE Transactions on evolutionary computation 8(3): 256-79.
[7] De Souza, L., Ricardo, S., Prudêncio, B. C., Barros, F. de A. (2014): Multi-Objective Test Case Selection: A study of the influence of the Catfish effect on PSO based strategies. – Anais do XV Workshop de Testes e Tolerância a Falhas-WTF, pp. 3-16.
[8] Duan, Q., Ajami, N. K., Gao, X., Sorooshian, S. (2007): Multi-model ensemble hydrologic prediction using Bayesian model averaging. – Advance Water Resource 30(5): 1371-1386.
[9] Han, Q. (2003): Reservoir Sedimentation. – Science Press, Beijing (in Chinese).
[10] Han, Q., He, M. (2015): Mathematic Modelling of Non-Equilibrium Suspended Load Transport, Reservoir Sedimentation, and Fluvial Processes. – In: Yang, C. T., Wang, L. K. Advances in Water Resources Engineering. Springer, New York.
[11] Hu, B. (2004): Breaking Grounds. – Homa & Sekey Books, Paramus, NJ.
[12] Ji, C., Liu, F., Zhang, X. (2011): Particle swarm optimization based on catfish effect for flood optimal operation of reservoir. – Seventh International Conference on Natural Computation, IEEE, Shanghai, pp. 1197-1201.
[13] Kennedy, J., Eberhart, R. (1995): Particle swarm optimization. – Proceedings of the IEEE International Conference on Neural Networks 4: 1942-1948.
[14] Leong, W. F., Yen, G. G. (2006): Dynamic population size in PSO-based multiobjective optimization. – 2006 IEEE Congress on Evolutionary Computation, IEEE Industrial Electronic Society, Vancouver, pp. 6182-6189.
[15] Li, H., Lian, J. (2008): Multi-objective optimization of water-sedimentation-power in reservoir based on Pareto-optimal solution. – Transactions of Tianjin University 14: 282-288.
[16] Lian, J., Hu, M., Liu, Y. (2004): Research of multi-objective operation of water and sand in reservoir on sandy river. – Journal of Hydroelectric Engineering 23(2): 12-16 (in Chinese).
[17] Mostaghim, S., Teich, J. (2003): Strategies for finding good local guides in multi-objective particle swarm optimization. – Proceedings of the Institute of Electrical and Electronics Engineers (IEEE) Swarm Intelligence Symposium Institute of Electrical and Electronics Engineers, Indianapolis, pp. 26-33.
[18] Peng, Y., Zhang, H. (2006): 1-D numerical simulation of unsteady flow and sedimentation transport at the Three Gorges Reservoir (TGR). – Journal of Hydrodynamics A 21(3): 285-292 (in Chinese).

http://www.aloki.hu ● ISSN 1589 1623 (Print) ● ISSN 1785 0037 (Online)
DOI: http://dx.doi.org/10.15666/aeer/1705_1166911686

[19] Peng, Y., Li, Y. T., Zhang, H. W. (2004): Multi-objective decision-making model for coordinative dispatch of water and sediment in reservoir. – Journal of Hydraulic Engineering 4: 1-7 (in Chinese).
[20] Peng, Y., Ji, C., Gu, R. (2014): A multi-objective optimization model for coordinated regulation of flow and sediment in cascade reservoirs. – Water Resources Management 28: 4019-4033.
[21] Reddy, M. J., Kumar, D. N. (2007): Multi-objective particle swarm optimization for generating optimal trade-offs in reservoir operation. – Hydrological Processes 21(21): 2897-909.
[22] Reddy, M. J., Kumar, D. N. (2009): Performance evaluation of elitist-mutated multi-objective particle swarm optimization for integrated water resources management. – Journal of Hydroinformatics 11(1): 79-88.
[23] Reyes-Sierra, M., Coello, C. A. C. (2005): Improving PSO-based multi-objective optimization using crowding, mutation and ε-dominance. – Proc. of Evolutionary Multi-Criterion Optimization Conf. Guanajuato, pp. 505-519.
[24] Reyes-Sierra, M., Coello, C. A. C. (2006): Multi-objective particle swarm optimizers: a survey of the state-of-the-art. – International Journal of Computational Intelligence Research 2(3): 297-308.
[25] Tripathi, P. K., Bandyopadhyay, S., Pal, S. K. (2007): Adaptive multi-objective particle swarm optimization algorithm. – Proceedings of the Institute of Electrical and Electronics Engineers (IEEE) Congress on Evolutionary Computation, Singapore, pp. 2281-2288.
[26] van Rijn, L. C. (1993): Principles of Sediment Transport in Rivers, Estuaries and Coastal Seas. – Aqua Publication, Amsterdam, Netherland.
[27] Xiang, B., Ji, C. M., Peng, Y., Zhou, T. (2010): Study of water-sediment operating model based on immune particle swarm algorithm. – Journal of Hydroelectric Engineering 29(1): 97-101 (in Chinese).
[28] Xiao, Y., Peng, Y., Wang. T. (2013): Water-sediment coordinated optimized dispatch model of reservoir based on genetic algorithm and neural network. – Advances in Science and Technology of Water Resources 33(2): 9-13 (in Chinese).
[29] Yan, H., Moradkhani, H. (2014): Bayesian model averaging for flood frequency analysis. – World Environmental and Water Resources Congress, American Society of Civil Engineers, Portland, pp. 1886-1895.
[30] Yan, H., Moradkhani, H. (2016): Toward more robust extreme flood prediction by Bayesian hierarchical and multimodeling. – Natural Hazards 81: 203-225.
[31] Yang, G. L. (1993): River Mathematic Modelling. – China Ocean Press, Beijing (in Chinese).
[32] Yang, X. (2003): Manual on Sediment Management and Measurement. – Secretariat of the World Meteorological Organization, Geneva.
[33] Yoo, J. H. (2009): Maximization of hydropower generation through the application of a linear programming model. – Journal of Hydrology 376(1-2): 182-187.
[34] Yoon, Y. N. (1992): The state and the perspective of the direct sediment removal methods from reservoirs. – International Journal of Sediment Research 7(20): 99-115.
[35] Zhang, Y. X., Feng, S. Y. (1988): Multi-objective programming model in reservoir operation and its application. – Journal of Hydraulic Engineering 9: 19-27 (in Chinese).
[36] Zhu, J. (1997): Main measures that control the sedimentation in a reservoir: sediment operation. – Sichuan Water Conservancy 18(3): 6-10 (in Chinese).

http://www.aloki.hu ● ISSN 1589 1623 (Print) ● ISSN 1785 0037 (Online)
DOI: http://dx.doi.org/10.15666/aeer/1705_1166911686

RELATIONSHIPS BETWEEN TEMPORAL AND SPATIAL VARIATIONS OF WATER QUALITY AND WATER LEVEL CHANGES IN POYANG LAKE BASED ON 5 CONSECUTIVE YEARS' MONITORING

ZHENG, L.[1] – WANG, H. P.[1] – HUANG, M. S.[2] – LIU, Y.[1,3*]

[1]*College of Water Sciences, Beijing Normal University, 100875 Beijing, China*

[2]*Beijing Capital Co., Ltd., 100028 Beijing, China*

[3]*Chinese Research Academy of Environmental Sciences, 100012 Beijing, China*

**Corresponding author*
e-mail: liuyan@craes.org.cn

(Received 22nd Apr 2019; accepted 12th Jul 2019)

Abstract. Quarterly water quality monitoring data from 15 monitoring sites in Poyang Lake and the water level data from the Xingzi monitoring station in Poyang Lake from 2012 to 2016 were analyzed to determine (1) how the water quality changed both spatially and temporally and (2) how the changes of the water quality and eutrophication were related to variations in the water level. The results indicated that there were seasonal and interannual variations in the water quality of Poyang Lake. Dissolved Oxygen (DO) and Total Nitrogen (TN) reached maximum and minimum values in winter and summer, respectively. The maximum and minimum concentrations of Total Phosphorus (TP) were found in spring and summer, respectively. Chemical oxygen demand (COD) was slightly lower in spring and summer than in autumn and winter. Over the entire sampling period, the concentrations of ammonia nitrogen (NH_4-N), TP, and TN were highest in 2015. COD concentrations varied little interannually. Chlorophyll a concentrations were relatively uniform and did not show obvious seasonal variation. There was little spatial variation in the NH_4-N concentrations in spring and summer, but there was considerable variation between sites in autumn and winter; COD varied considerably between sites in spring and winter. COD and TP were not significantly correlated, but NH_4-N, TN, and the degree of eutrophication were negatively correlated, with water level changes in Poyang Lake.
Keywords: *Poyang lake, temporal, spatial, water level changes, TLI, eutrophication*

Introduction

Poyang Lake is the largest freshwater lake in China. Its drainage area, which extends over 16.22 × 104 km^2, accounts for about 9% of the Yangtze River Basin. It has an average annual runoff of 144 × 109 m^3, which accounts for about 15.5% of the Yangtze River's average annual runoff (Duan et al., 2016). Poyang Lake makes a significant contribution to the ecological functioning, ecological integrity, and regional management of the water resources of the Yangtze River Basin (Liu et al., 2016). The lake water quality can be recorded by examining the physical, chemical, and biological characteristics of the lake (Van Houtven et al., 2014). It is important to assess the quality of the lake water as it directly affects the safety of the water used by people living close to the lake and the quality of the groundwater. As the largest of all the lakes that are connected to the Yangtze River, its water quality will influence the ecological integrity and ecological functioning in the middle and lower reaches of the Yangtze River.

http://www.aloki.hu ● ISSN 1589 1623 (Print) ● ISSN 1785 0037 (Online)
DOI: http://dx.doi.org/10.15666/aeer/1705_1168711699

Poyang Lake has multiple functions; for example, it provides water for irrigation and domestic needs, is a source of aquatic products, and is an important shipping route (Wu et al., 2017). In recent years, the water quality has been affected by industrial discharges, agricultural effluent, and domestic sewage, to the point and that the ecological function of the wetland has been compromised, with consequences for the water supply capacity of the lake. More pollutants from upstream and the lower water levels in the dry season together indicate that eutrophication will increase in Poyang Lake. In recent years, many researchers have studied spatial and temporal changes in the water environment and the trophic status in Poyang Lake. For example, Hu et al. (2010) using the Nimero index, found that the conditions in Poyang Lake were eutrophic because of excessive nitrogen and phosphorus in 2010. Wu et al. (2011) found that water quality of Poyang Lake has already undergone great changes after 2003, and it is showing a deterioration trend, while Gao et al. (2010) found that in 2010, the main pollutants affecting the water quality of the lake were TP and TN. The water level in Poyang Lake is affected by climatic conditions and human activities and, because it is directly connected to the Yangtze River, the seasonal fluctuations in the water level are quite pronounced. Therefore, the relationship between water level changes and eutrophication has definite implications for water resources management (Coops et al., 2003). In their study, Wu et al. (2014) used water quality indicators to examine the temporal and spatial changes in the water quality of Poyang Lake in 2017 and also examined how these changes were related to the water level. Wang et al. (2015) used SWAT and GIS to quantitatively estimate how the exchanges between the river and lake influenced the dissolved nutrient loads in Poyang Lake and also the spatial and temporal changes in the wetland vegetation in 2015. Liu et al. (2013) collected samples of surface water from the main part of Poyang Lake, the entrance of five rivers to Poyang Lake, and the dish-shaped sub-lake, and it was found that there was serious eutrophication in 2013. Ma et al. (2013) analyzed the changes in the water quality in Poyang Lake from 2008 to 2010 and used the load analysis method to determine the main sources of the pollution in the lake in 2013. Du et al. (2015) quantitatively analyzed the relationships between the water quality of Poyang Lake and the water levels during the wet and dry seasons in 2015. They found that the water supply was increasingly inadequate to meet the demands of the gradually more intensive industries and livestock and poultry breeding activities in the Poyang Lake area, that the surrounding environment had been destroyed, and the water quality in the lake had deteriorated rapidly. The spatial and temporal variations in the water quality of Poyang Lake and the trophic status of the lake have been intensively studied. However, few studies have focused on the relationship between water quality and the water levels in Poyang Lake, and very few studies have systematically analyzed how water levels influence the water environment.

In this study, five years continuum water quality monitoring data of Poyang Lake were analyzed and the trophic status was evaluated to find out how the water quality in the lake varied both spatially and temporally over recent years. The effects of water level changes on the spatial and temporal changes in the water quality and eutrophication in different seasons and at a range of spatial scales were also examined. The results of this study will provide useful information about how the water quality in Poyang Lake varies both spatially and temporally and how the water quality is related to the water level. This study will also provide support for making scientifically robust decisions about how to implement tools to control the pollution in the lake, restore the aquatic ecosystems, allocate and protect water resources in an effective way.

http://www.aloki.hu ● ISSN 1589 1623 (Print) ● ISSN 1785 0037 (Online)
DOI: http://dx.doi.org/10.15666/aeer/1705_1168711699

Materials and methods

Study area

Poyang Lake is in the northern part of Jiangxi Province, at the southern end of the middle to lower reaches of the Yangtze River. Poyang Lake has five main inflows (including the Raohe River, Ganjiang River, Fuhe River, Xinjiang River, and the Xiushui River) and drains into the Yangtze River from its northern end. Most of the lake's water area (97%) (Lai et al., 2014) is in Jiangxi Province. With Songmen Mountain as its boundary, the main body of the lake is to the south, while the channel that connects with the Yangtze River is at the northern end. Poyang Lake is 173 km long from north to south. It is between 3 and 74 km wide from east to west with an average width of 16.90 km. The lake basin slopes from the southeast to the northwest and the shoreline is approximately 1200 km long (Yao et al., 2018). The average water level in Poyang Lake is between 14 and 15 m (Liu et al., 2016) and there are considerable seasonal and interannual variations in the water level. Records show maximum annual variations between 9.59 and 15.36 m, and minimum annual variations between 3.80 and 9.79 m (Dai et al., 2016). The water level changes seasonally in Poyang Lake. During the dry season, the water level drops, and the beach is exposed; it then rises during the wet season and the landscape is very different from that in the dry season (Yuan et al., 2015). The water level in the lake is generally highest between June and August, and lowest between December to February (Lan, 2014).

Data sources

In this study, 15 monitoring stations were specifically chosen to account for the lake's unique hydrological conditions, shape, and different functional areas were set up in Poyang Lake, as shown in *Figure 1*. Samples were collected in January, April, July, and October of each year from January 2012 to December 2016. Data for the water level were obtained from the Jiangxi Provincial Hydrographic Bureau. Water level from January, April, July, and October at the Xingzi Monitoring Station from 2012 to 2016 were used to represent the average condition in Poyang Lake. The spatial distribution pattern of water quality is demonstrated using the data of 2012.

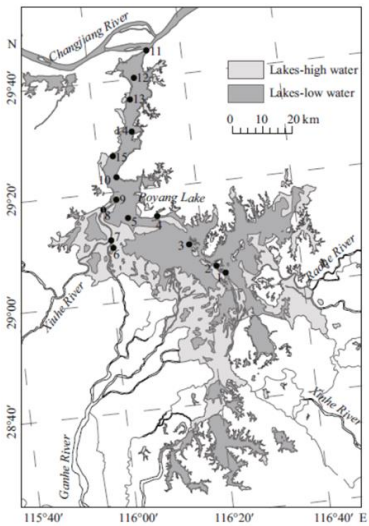

Figure 1. *Location and sampling point distribution of Poyang Lake*

http://www.aloki.hu ● ISSN 1589 1623 (Print) ● ISSN 1785 0037 (Online)
DOI: http://dx.doi.org/10.15666/aeer/1705_1168711699

Water sample analysis

Lake surveys were conducted following the procedures outlined in The Lake Ecosystem Observation Method. The transparency was determined with a Secchi Disc (SD), chemical oxygen demand (COD_{MN}) was determined by acid potassium permanganate titration, TN concentrations were determined by ultraviolet spectrophotometry after digestion with alkaline potassium persulfate, TP concentrations were determined by ammonium molybdate spectrophotometry, and chlorophyll a (Chla) was determined after hot ethanol extraction.

Lake eutrophication evaluation method

The nutrient status of the lake was determined with the trophic level index (TLI), based on Chla, TP, TN, SD, and COD_{MN} (El-Serehy et al., 2018; Napiórkowska-Krzebietke et al., 2013; Trolle et al., 2014).

The numerical values of the trophic level index (TLI) for the Poyang Lake water were calculated using the following equation:

$$TLI(\Sigma) = \sum_{j=1}^{m} W_j \cdot TLI(j) \quad \text{(Eq.1)}$$

In which TLI = trophic level index; W_j = weight of the TLI parameter; m = Number of parameters participating in the evaluation.

$$W_j = r_{ij}{}^2 \left(\sum_{j=1}^{m} r_{ij}{}^2\right)^{-1} \quad \text{(Eq.2)}$$

In which r_{ij} = Correlation coefficient between each parameter and Chla parameter. The values are shown in *Table 1*.

Table 1. *A certain lake's parameter correlated* r_{ij} *and* $r_{ij}{}^2$ *of Chla**

Parameter	Chla	TP	TN	SD	COD_{MN}
r_{ij}	1	0.84	0.82	-0.83	0.83
$r_{ij}{}^2$	1	0.7056	0.6724	0.6889	0.6889

*From the calculation results of 26 major Chinese lake survey data

$$TLI(Chl) = 10(2.5 + 1.086 ln Chl) \quad \text{(Eq.3)}$$

$$TLI(TP) = 10(9.436 + 1.624 ln TP) \quad \text{(Eq.4)}$$

$$TLI(TN) = 10(5.453 + 1.694 ln TN) \quad \text{(Eq.5)}$$

$$TLI(SD) = 10(5.118 - 1.94 ln SD) \quad \text{(Eq.6)}$$

$$TLI(COD_{MN}) = 10(0.109 + 2.661 ln\, COD_{MN}) \quad \text{(Eq.7)}$$

When the TLI was less than 30, the lake was oligotrophic; TLI values of between 30 and 50 indicated oligotrophic/mesotrophic conditions; TLI values of between 50 and 60

http://www.aloki.hu ● ISSN 1589 1623 (Print) ● ISSN 1785 0037 (Online)
DOI: http://dx.doi.org/10.15666/aeer/1705_1168711699

indicated mild eutrophication; values between 60 and 70 indicate moderate eutrophication, while values greater than 70 indicate severe eutrophication.

Result and discussion

Temporal variations in the water quality in Poyang Lake

Information about seasonal variations in the various water quality indicators in Poyang Lake from 2012 to 2016 is presented in *Figure 2*. The concentrations and data for the four quarters indicate seasonal differences. The patterns in the concentrations of DO and TN were the same. DO and TN concentrations were lowest in summer (July) and highest in winter (January). The DO concentrations were 6.59 and 12.72 mg/L, while the TN concentrations were 1.50 and 2.40 mg/L in summer (July) and winter (January), respectively. The concentrations in spring (April) and autumn (October) showed little variation and fell between the maximum winter values and minimum summer values. The NH_4-N concentrations varied widely over the year and ranged from 0.16 to 0.51 mg/L. They were low in spring and summer and high in autumn and winter.

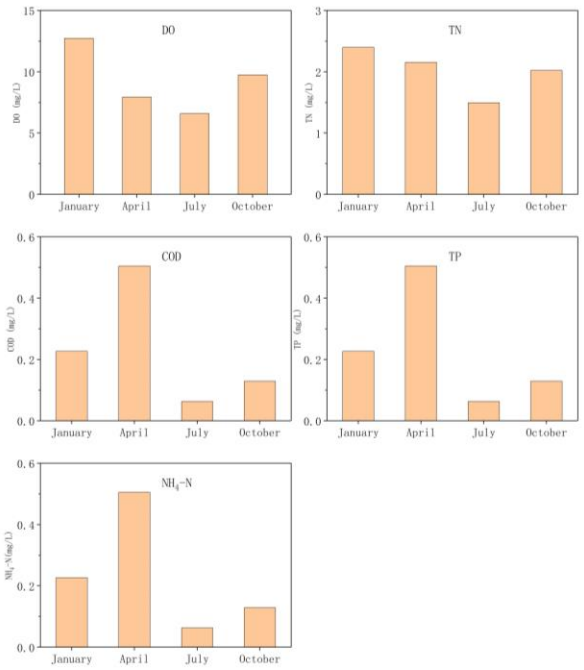

Figure 2. *Summary information about seasonal variations in the water quality indicators during the year*

There was considerable interannual variation in the various water quality indicators in Poyang Lake from 2012 to 2016, as shown in *Figure 3*. The concentrations of NH_4-N, TP, and TN reached maximum values of 0.56, 1.30, and 4.25 mg/L, respectively, in 2015 and these concentrations were considerably higher than those in the other years. The concentrations of these indicators were similar in the other years. The concentrations of NH_4-N and TN were about 50% higher in 2015 than those in the other years, while, compared to 2015, the concentrations of TP were much lower in the other

http://www.aloki.hu ● ISSN 1589 1623 (Print) ● ISSN 1785 0037 (Online)
DOI: http://dx.doi.org/10.15666/aeer/1705_1168711699

years and were generally below 0.3 mg/L. Concentrations of COD ranged from 2.24 to 3.15 mg/L and showed little between-year variation.

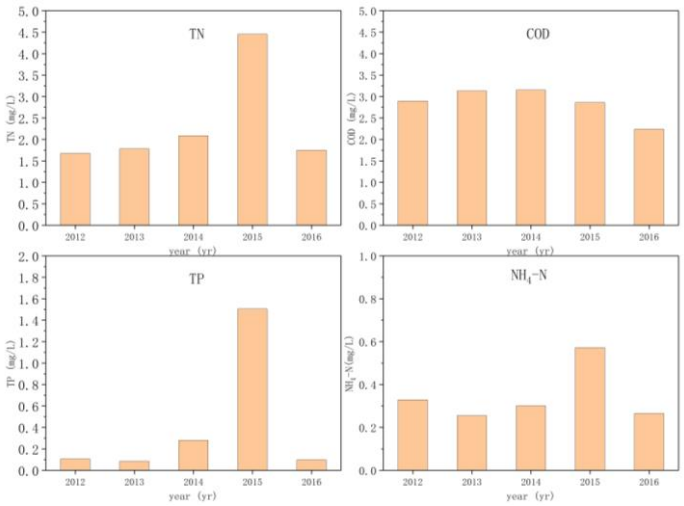

Figure 3. *Inter-annual variation in the water quality indicators*

Spatial variations in the water quality in Poyang Lake

The TN concentrations in Poyang Lake were high in autumn and winter and low in summer and autumn (*Fig. 4*). In winter (January), the TN concentration exceeded 2.0 mg/L across all of Poyang Lake, and did not differ significantly between the sampling sites. The TN concentration ranged from a minimum of about 1.8 mg/L in the western part of the lake and reached a maximum of about 3.0 mg/L in the southeastern part of the lake. In spring (April), the average TN concentration in the whole lake was relatively low and, at about 1.5 mg/L, did not differ significantly across the whole lake. In the northern part of the lake, the TN concentration reached a maximum of about 1.9 mg/L. The TN concentrations in summer and spring across the whole lake were similar. The average concentration in summer was about 1.5 mg/L and did not differ much across the whole lake, with high concentrations of up to 2.0 mg/L in only a few northern and central areas. In autumn (October), the TN concentrations were high in the south and low in the north. They were relatively low in the northern part (about 1.5 mg/L) in the channel that connected the lake to the river, and were relatively high (up to 2.0 mg/L) in the southern part of the lake.

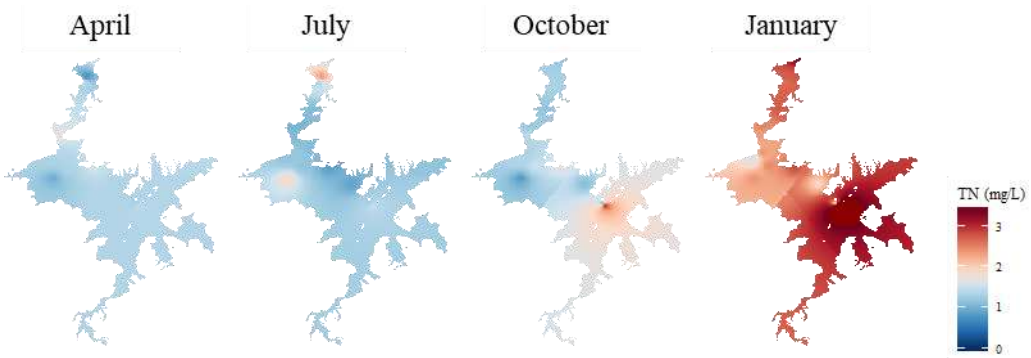

Figure 4. *Temporal and spatial distribution of TN in Poyang Lake*

http://www.aloki.hu ● ISSN 1589 1623 (Print) ● ISSN 1785 0037 (Online)
DOI: http://dx.doi.org/10.15666/aeer/1705_1168711699

Similar to TN, the TP concentrations were high in autumn and winter and low in spring and summer (*Fig. 5*). In winter (January), the TP concentrations were higher in the southern part and lower in the northern part. The TP concentration reached 0.2 mg/L in the southern lake area, and was only 0.1 mg/L in the channel that connects the lake with the river in the north. In spring (April), the TP concentration showed little variation and was low across the whole lake (0.08 mg/L). The patterns in spring and summer (July) were similar. In summer, the concentrations were low (about 0.1 mg/L) and were relatively uniform across most of the lake, but were slightly higher (0.15 mg/L) in some areas, such as in the channel that connects the lake to the river in the north. The TP concentrations were highest in autumn (October) across the whole lake. The distribution of the TP concentrations in autumn and winter were similar, and were high in the south and low in the north. The TP concentrations in the lake were much higher in autumn than in winter, and exceeded 0.2 mg/L in most of the southern part of the lake, with concentrations greater than 0.3 mg/L in some places.

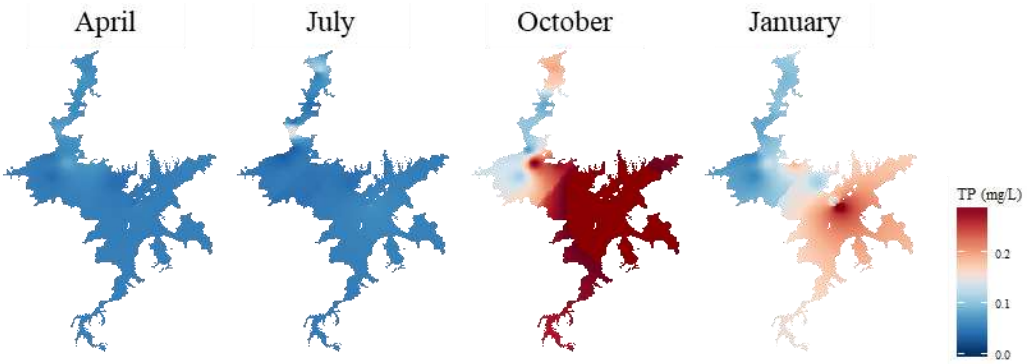

Figure 5. *Temporal and spatial distribution of TP in Poyang Lake*

Chlorophyll a was uniformly distributed in the lake both spatially and temporally (*Fig. 6*). The concentrations of Chla in the lake were lower in winter than in the other seasons, and were lower than 3.0 mg/L across the whole lake during the season. The concentrations of Chla were highest in the northwestern part of the lake. In summer (July), the Chla concentration reached a maximum value of about 15.0 mg/L at a monitoring station near Wucheng Town. The high values may attribute to the higher water consumption during summer in tourist towns, which results in higher pollutant loads, worse water quality, and causes algae to proliferate in the lake.

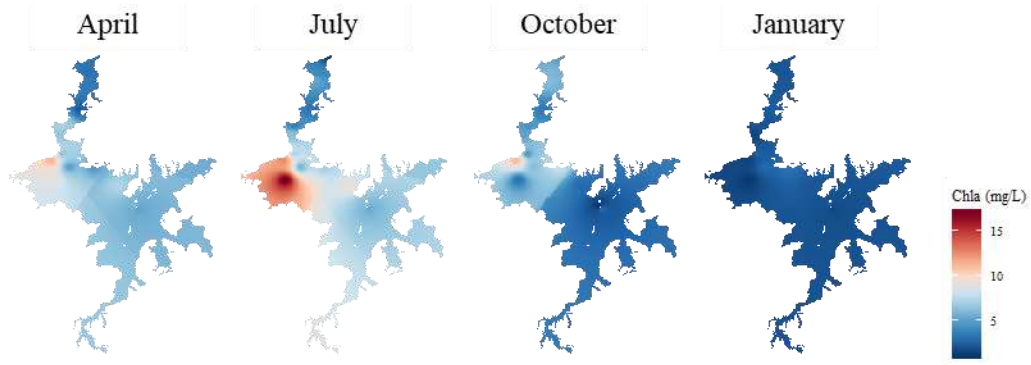

Figure 6. *Temporal and spatial distribution of Chla in Poyang Lake*

http://www.aloki.hu ● ISSN 1589 1623 (Print) ● ISSN 1785 0037 (Online)
DOI: http://dx.doi.org/10.15666/aeer/1705_1168711699

The NH_4-N concentrations in Poyang Lake demonstrated little variation in spring and summer, and large variations in autumn and winter (*Fig. 7*). In spring, the NH_4-N concentrations were generally low, with an average of about 0.2 mg/L, and were relatively uniform across the lake. The spring and summer situations were similar. In summer, the NH_4-N concentrations were relatively uniform across the whole lake and averaged about 0.1 mg/L. In the autumn, the NH_4-N concentrations varied considerably across the lake and were high in the south and low in the north. The NH_4-N concentration was about 0.5 mg/L in the channel that connects the northern part to the river, and was about 1.2 mg/L in the southern part of the lake. By contrast in autumn, the concentrations were high in the north and low in the south in the winter. The concentrations reached a maximum of about 1.0 mg/L in the northern part of the lake, but were only about 0.5 mg/L in most of the southern part of the lake.

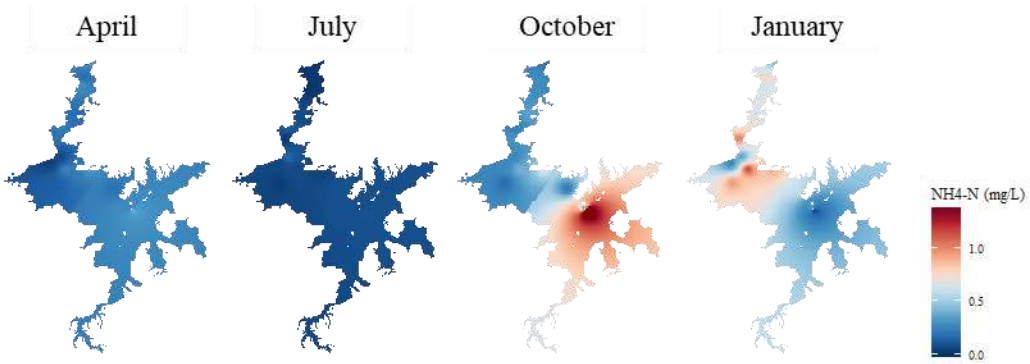

Figure 7. *Temporal and spatial distribution of NH_4-N in Poyang Lake*

The COD_{MN} in Poyang Lake showed considerable variation in spring and winter but varied little across the lake in summer and autumn (*Fig. 8*). In spring, the COD_{MN} was high in the north and low in the south. The COD_{MN} was high, up to 4.0 mg/L, in the channel that connects with the river channel in the north, but was about 3.5 mg/L in most of the southern lake. The COD_{MN} did not vary much throughout the lake in summer and autumn, and remained about 2.0 mg/L. Similar to the spring distributions, the concentrations were high in the north and low in the south in winter. The COD_{MN} reached 5.0 mg/L in the north where the lake was connected with the river channel, but was mainly between 3.0 and 3.5 mg/L in the southern part.

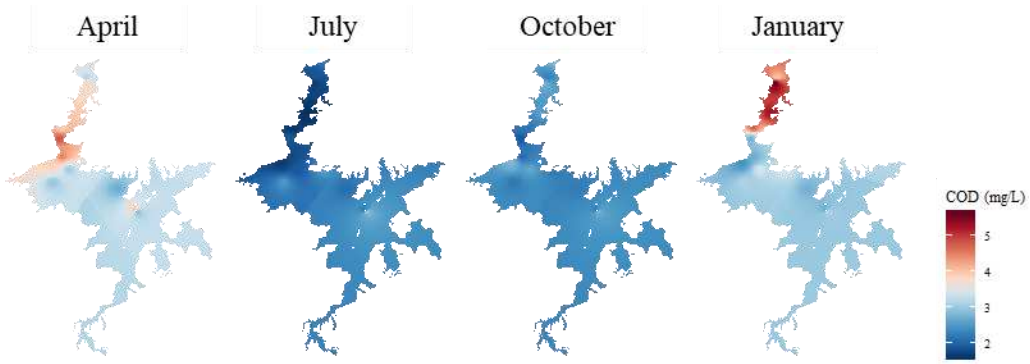

Figure 8. *Temporal and spatial distribution of COD_{MN} in Poyang Lake*

http://www.aloki.hu ● ISSN 1589 1623 (Print) ● ISSN 1785 0037 (Online)
DOI: http://dx.doi.org/10.15666/aeer/1705_1168711699

The influence of changes in the water level on the water quality of Poyang Lake

The correlations between the concentrations of COD_{MN}, NH_4-N, TN, and TP concentrations and the water level in Poyang Lake at the Xingzi Hydrological Station are shown in *Figure 9*. There were no significant correlations between COD_{MN} and TP and the changes in the water level. The concentrations of NH_4-N and TN were strongly and negatively correlated with the changes in the water level, with correlation coefficients of 0.31 and 0.19, respectively ($p < 0.05$); the concentrations of NH_4-N and TN in the lake were affected by the water level, and the concentrations gradually decreased as the water level increased.

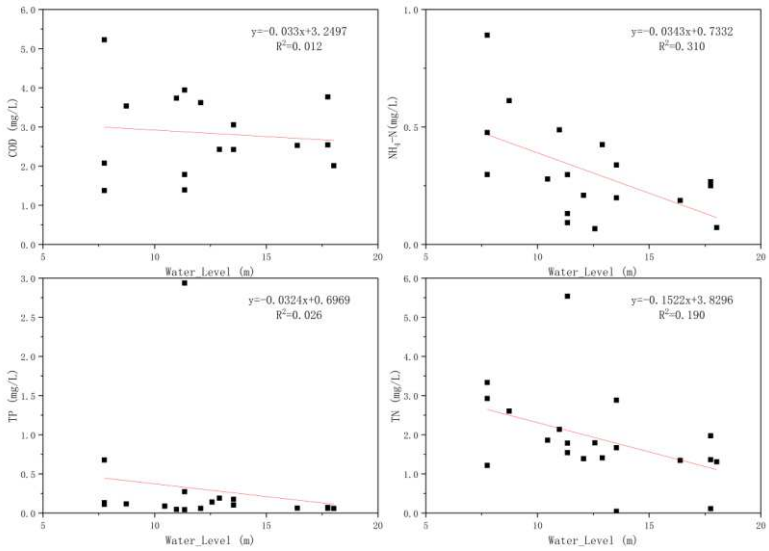

Figure 9. *Correlations between the water quality indicators and the water level*

The influence of changes in the water level in Poyang Lake on the degree of eutrophication

The average TLI in Poyang Lake was 48.35, which indicates mesotrophic conditions. There was little variation in the overall trophic status of the lake (*Fig. 10*). At Site 1, on the central/eastern part of the lake, the TLI reached a maximum of 50.20. At Site 7, on the northwestern/central part of the lake, the nutrient TLI was lowest at 45.65. The conditions at Site 1 and Site 5, which accounted for 13% of the sites, were mildly eutrophic, while the conditions at the remaining sites, or 87%, were mesotrophic. Poyang Lake is generally mesotrophic, and the trophic status does not show much spatial variation.

The TLI was negatively correlated with the water level ($R^2 = -0.62$), so that as the water level increased, the TLI, and also the degree of eutrophication, decreased accordingly. The TLI (Chla) and the water level ($R^2 = 0.24$) were weakly and positively correlated, but the TLI (TP), TLI (SD), and TLI (COD_{MN}) were negatively correlated with the water level ($R^2 = -0.52$, $R^2 = -0.41$, and $R^2 = -0.35$). As shown in *Figure 11,* there was a strong negative correlation between the TLI (TN) and the water level ($R^2 = -0.75$), so that, as the water level increased, the TLI decreased.

As the water level increased, the TLI decreased in areas affected by TN, TP, transparency, and COD_{MN}. Conversely, as the water level decreased, the TLI increased in areas affected by TN, TP, transparency, and COD_{MN}. In general, the TLI was negatively

http://www.aloki.hu ● ISSN 1589 1623 (Print) ● ISSN 1785 0037 (Online)
DOI: http://dx.doi.org/10.15666/aeer/1705_1168711699

correlated with the water level of Poyang Lake. The TLI was also negatively correlated with the water level. As the water level increased, the TLI decreased and vice verse.

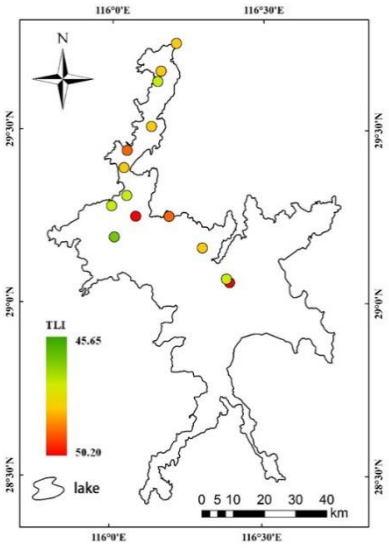

Figure 10. *Spatial distribution of the TLI in Poyang Lake*

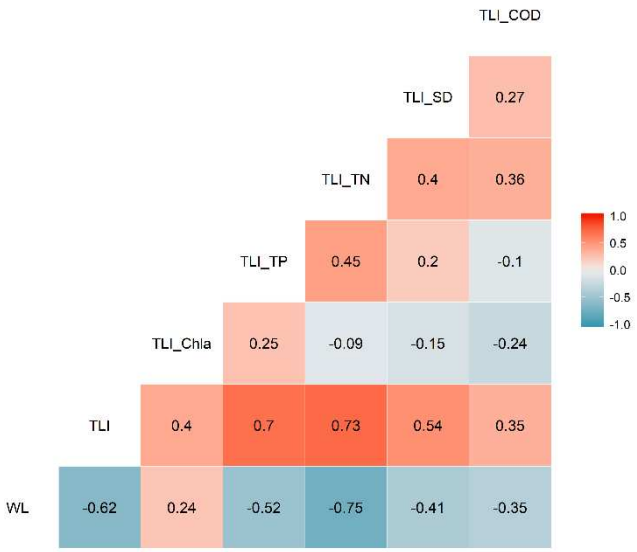

Figure 11. *The relationships between the TLI and various water quality indicators and water level (WL) in Poyang Lake*

Factors influencing temporal and spatial variations in the water quality in Poyang Lake

The water level regulates the structure and function of natural lake ecosystems. The water levels in lakes connecting with the Yangtze River change quite considerably over the course of a year. The large fluctuations in the water level of Poyang Lake will therefore affect the hydraulic retention time, the time taken for water to exchange, and the growth and energy exchange of phytoplankton. We found that, on an annual time

http://www.aloki.hu ● ISSN 1589 1623 (Print) ● ISSN 1785 0037 (Online)
DOI: http://dx.doi.org/10.15666/aeer/1705_1168711699

scale, the water level in Poyang Lake was highest in summer, the TLI was negatively correlated with the water level, and the fluctuation in the water level had the most important influence on TN. In the study of Poyang Lake from 2009 to 2014, Wu et al. (2017) found that the nutrients in the lake would be diluted in 2017 because of seasonal increases in the water level, thereby reducing the eutrophication in the lake. In the study of Poyang Lake from 2008 to 2012, Liu et al. (2014) confirmed that the trophic level was lower at higher water levels than at lower water levels in 2014. However, as the lake level and water volume decrease, sediment will be resuspended and nutrients will be released. The water level in Poyang Lake is higher in summer than in winter, so more sediment will be resuspended in winter than in summer, resulting in more serious eutrophication in winter than in summer. As shown in numerous previous studies, higher water levels will decrease eutrophication by Mao et al. (2014). In addition, Poyang Lake is connected to the Yangtze River. When the water level is high in summer, water is exchanged rapidly between them, so the degree of eutrophication is low. In winter, the water level is lower and it takes longer for the water to exchange, so the degree of eutrophication is higher. The change in the degree of eutrophication in the lake area following temporal changes in the water level can be explained by dilution of nutrients as the water level rises during precipitation, resuspension of sediments and release of nutrients when the water levels are low, and the time taken for water to turn over. The changes in the water level were correlated with the TLI for TN, TP, transparency, and COD_{MN}, and the factors that influenced the changes are consistent with those that influenced the TLI. The content of Chla is not related to changes in the water level, mainly because Chla is influenced by the water temperature, algal biomass, light, and suspended matter. The water level can, however, affect the light and the concentrations of suspended matter what is limited for shallow lakes.

The changes in the water level have little effect on how the trophic state varies spatially, and previous studies have not shown that the water level was related to the spatial distribution of the trophic state by Wang et al. (2013). The results of this study show that spatial variations in the trophic state of Poyang Lake are mainly affected by the pollutants transported into the lake from urban and industrial areas. There is no clear relationship between the water level of Poyang Lake and its trophic status. Some of the sampling points were in the main channel that connected the lake with the river. At these points, the water exchange is faster than in the main body of the lake and the self-purification ability is strong, so the pollutants gradually dilute and degrade; the degree of eutrophication is low and is only weakly related to the water level. Other monitoring points are polluted by agricultural, industrial, and domestic activities.

Conclusions

The water quality of Poyang Lake showed seasonal changes at the annual scale. The concentrations of DO and TN were lowest in summer and highest in winter, with little difference in spring and autumn. The concentrations of TP reached maximum and minimum values in spring and summer, respectively. COD was slightly lower in spring and summer than in autumn and winter. Concentrations of NH_4-N were low in spring and summer, and high in autumn and winter. The water quality of Poyang Lake also varied inter annually. Concentrations of NH_4-N, TP, and TN reached maximum values of 0.56, 1.30, and 4.25 mg/L, respectively, in 2015, but did not vary much in the other years. Concentrations of NH_4-N and TN were about 50% higher in 2015 than in other

http://www.aloki.hu ● ISSN 1589 1623 (Print) ● ISSN 1785 0037 (Online)
DOI: http://dx.doi.org/10.15666/aeer/1705_1168711699

years; TP concentrations were much higher in 2015 than in the other years, when they remained below 0.3 mg/L. The COD concentrations did not vary much between years.

There were seasonal spatial variations in the water quality in Poyang Lake. The TN concentrations across the whole lake in winter generally exceeded 2.0 mg/L, while in the spring and summer, the TN concentrations were about 1.5 mg/L. In the autumn, the TN concentrations were high in the south and low in the north. In winter, the TP concentrations were high in the south and low in the north. The concentrations of TP were low across the entire lake in the spring and summer. In autumn, the TP concentrations were much higher than in the winter, and were high in the south and low in the north. The NH_4-N concentrations in Poyang Lake were generally low at 0.2 mg/L, and showed little spatial variation across the whole lake. The NH_4-N concentrations across the whole lake were low in summer. In the autumn and winter, the NH_4-N concentrations in the lake were high in the south and low in the north, and high in the north and low in the south, respectively. In the autumn, NH_4-N concentrations were high in the south and low in the north, while the pattern was the opposite in winter. COD_{MN} in the lake in spring and winter was high in the north and low in the south. COD_{MN} did not vary significantly on the spatial scale in summer and autumn and was generally low.

Poyang Lake was mesotrophic, and the trophic status was relatively uniform. The TLI of Poyang Lake were negatively correlated with the water level. Of the water quality indicators, TN was most affected by the changes in the water level of Poyang Lake. On the temporal scale, the TLI of Poyang Lake was negatively correlated with the water level. The trophic status of Poyang Lake was spatially heterogeneous and was not affected much by the water level.

Acknowledgements. We are grateful to all staff that collected and processed samples for the monitoring program from the Poyang Lake Laboratory for Wetland Ecosystem Research (PLWER).

REFERENCES

[1] Coops, H., Beklioglu, M., Crisman, T. L. (2003): The role of water-level fluctuations in shallow lake ecosystems - workshop conclusions. – Hydrobiologia 506-509(1-3): 23-27.
[2] Dai, X., Wan, R., Yang, G., et al. (2016): Responses of wetland vegetation in Poyang Lake, China to water-level fluctuations. – Hydrobiologia 773(1): 1-13.
[3] Du, Y., Zhou, H., Peng, W., et al. (2015): Hydrodynamic and water quality characteristics simulation of Poyang lake under the influence of changes in river basins and rivers in the past 10 years. – Journal of Environmental Science 35(5): 1274-1284.
[4] Duan, W., He, B., Nover, D., et al. (2016): Water quality assessment and pollution source identification of the Eastern Poyang Lake basin using multivariate statistical methods. – Sustainability 8(2): 133.
[5] El-Serehy, H. A., Abdallah, H. S., Al-Misned, F. A., et al. (2018): Assessing water quality and classifying trophic status for scientifically based managing the water resources of the Lake Timsah, the lake with salinity stratification along the Suez Canal. – Saudi Journal of Biological Sciences 25(7): 1247-1256.
[6] Gao, G., Ruan, Z., Qiulin, O. (2010): Water quality status and changing trend in Poyang Lake. – Journal of Nanchang Institute of Technology 29(4): 50-53.
[7] Hu, C., Zhou, W., Xiao, H., et al. (2010): Eutrophication state and normal distribution features of Poyang Lake. – Yangtze River 41(19): 64-68.

http://www.aloki.hu ● ISSN 1589 1623 (Print) ● ISSN 1785 0037 (Online)
DOI: http://dx.doi.org/10.15666/aeer/1705_1168711699

[8] Lai, X., Shankman, D., Huber, C., et al. (2014): Sand mining and increasing Poyang Lake's discharge ability: a reassessment of causes for lake decline in China. – Journal of Hydrology 519: 1698-1706.
[9] Lan, Y. (2014): Forecasting performance of support vector machine for the Poyang Lake's water level. – Water Science 70(9): 1488.
[10] Liu, F., Li, M., Guo, Y. (2014): Quantitative analysis of time-space changes of water quality in Poyang lake and the impact of water level. – Journal of China Hydrology 34(4): 37-43.
[11] Liu, Q., Yu, C., Zhang, J., et al. (2013): Water quality variations in Poyang Lake. – Journal of Agro-Environment Science 32(6): 1232-1237.
[12] Liu, X., Li, Y., Liu, B., et al. (2016): Cyanobacteria in the complex river-connected Poyang Lake: horizontal distribution and transport. – Hydrobiologia 768(1): 95-110.
[13] Ma, H., Xiao, Y., Liang, Y. (2013): Water quality assessment and treatment countermeasures analysis of Poyang Lake. – Journal of Anhui Agricultural Sciences 41(30): 12129-12131.
[14] Mao, Y., Zhou, X., Wang, M. (2014): Study on the eutrophication status in Poyang lake during lower water period. – Journal of Nanchang University (Natural Science) 38(6): 596-599.
[15] Napiórkowska-Krzebietke, A., Stawecki, K., Pyka, J. P., et al. (2013): Phytoplankton in relation to water quality of a mesotrophic lake. – Polish Journal of Environmental Studies 22(3): 793-800.
[16] Trolle, D., Spigel, B., Hamilton, D. P., et al. (2014): Application of a three-dimensional water quality model as a decision support tool for the management of land-use changes in the catchment of an oligotrophic lake. – Environmental Management 54(3): 479-493.
[17] Van Houtven, G., Mansfield, C., Phaneuf, D. J., et al. (2014): Combining expert elicitation and stated preference methods to value ecosystem services from improved lake water quality. – Ecological Economics 99: 40-52.
[18] Wang, S., Shu, J., Ni, Z., et al. (2013): Investigation on pollution situation and countermeasures in Poyang Lake. – Acta Scientiae Circumstantiae 3(04): 342-349.
[19] Wang, S., Ni, Z., Chu, Z., et al. (2015): Studies on the change of the river-lake relationship and its impact on water environment in Poyang Lake. – Acta Scientiae Circumstantiae 35(5): 1259-1264.
[20] Wu, L., Li, M., Guo, Y., et al. (2011): Influence of three gorges project on water quality of Poyang Lake. – Procedia Environmental Sciences 10: 1496-1501.
[21] Wu, Z., Lai, X., Zhang, L., et al. (2014): Phytoplankton chlorophyll a in Lake Poyang and its tributaries during dry, mid-dry and wet seasons: a 4-year study. – Knowledge Management of Aquatic Ecosystems 136(412): 06.
[22] Wu, Z., Zhang, D., Cai, Y., et al. (2017): Water quality assessment based on the water quality index method in Lake Poyang: the largest freshwater lake in China. – Scientific reports 7(1): 17999.
[23] Yao, J., Zhang, Q., Ye, X., et al. (2018): Quantifying the impact of bathymetric changes on the hydrological regimes in a large floodplain lake: Poyang Lake. – Journal of Hydrology (561): 711-723.
[24] Yuan, Y., Zeng, G., Liang, J., et al. (2015): Variation of water level in Dongting Lake over a 50-year period: Implications for the impacts of anthropogenic and climatic factors. – Journal of Hydrology 525(10): 450-456.

http://www.aloki.hu ● ISSN 1589 1623 (Print) ● ISSN 1785 0037 (Online)
DOI: http://dx.doi.org/10.15666/aeer/1705_1168711699

RESEARCH ON ECOSYSTEM HEALTH ASSESSMENT INDICES AND THRESHOLDS OF A LARGE YANGTZE-CONNECTED LAKE, POYANG LAKE

ZHANG, Y. H.[1,2] – YANG, G. S.[2,3*] – WAN, R. R.[2,3*] – ZHU, H. Y.[1]

[1]*Nanjing Xiaozhuang University, Nanjing 211171, P. R. China*

[2]*Key Laboratory of Watershed Geographic Sciences, Nanjing Institute of Geography and Limnology, Chinese Academy of Sciences, Nanjing 210008, P. R. China*

[3]*University of Chinese Academy of Sciences, Beijing 100049, P. R. China*

**Corresponding authors*
e-mail: gsyang@niglas.ac.cn; rrwan@126.com

(Received 22nd Apr 2019; accepted 12th Jul 2019)

Abstract. Assessing the aquatic ecosystem health status of lakes has been the focus of lake studies for domestic and overseas researchers and water resource managers. Poyang Lake, which is one of the only two remaining large Yangtze-connected lakes in the middle reaches of Yangtze River in China, provides considerable ecosystem service functions, such as flood water storage, water supply for industrial and agricultural production, maintenance of the unique and diverse biota of the entire Yangtze floodplain ecosystem, maintenance of regional ecological balance and so on. However, due to the impact of climate change and human activities, Poyang Lake has experienced drastic hydrological changes, water quality decline and aquatic ecological function degradation in recent years. An assessment of the aquatic ecosystem health of Poyang Lake is of great importance. On the basis of the index system construction principles and a meta-analysis of previous research, this paper puts forward the index system for the ecosystem health assessment of Poyang Lake. The indices contains the three element layers of aquatic organisms, hydrologic characteristics and trophic status and the five indicators of ratio of cyanobacteria biomass to diatom biomass (CB/DB), diversity index of macrozoobenthos, lowest water level anomaly during the dry season, mean water level anomaly during rising season and trophic state index (TLI). Then, the thresholds of indicators are determined using empirical study, frequency analysis, standard specification and so on. Aquatic ecosystem health status is categorised into three groups: 'good', 'moderate' and 'poor'. The study could provide theoretical basis for identifying the causes of the lake aquatic ecosystem health degeneration and protecting the environment of Poyang Lake. This present study provides an attempt to quantify the aquatic ecosystem health in a large floodplain lake with dramatic hydrological variations and will give some impetus for floodplain ecosystem assessment and management worldwide.

Keywords: *aquatic ecosystem health, physical-chemical-biological index, hydrologic indicators, ratio of cyanobacteria biomass to diatom biomass, thresholds, large Yangtze-connected lakes, Poyang Lake*

Introduction

The global ecosystem has become increasingly destroyed since the 1960s, and human society is facing immense challenges concerning survival and development (Zeng et al., 1999). Ecologists have begun to pay attention to the issue of ecosystem health. In 1988, Schaeffer proposed the concept of ecosystem health measurement (Schaeffer et al., 1988), and domestic and foreign scholars have since initiated substantial research on the concept of ecosystem health and related concerns (Costanza et al., 1992; Rapport and Whitford, 1999). Ecosystem health assessments are common in the research fields of forests, rivers, oceans, wetlands and so on (Cui and Yang, 2002; Borja and Dauer, 2008; Davies et al., 2011). Lakes, as a crucial part of the terrestrial

http://www.aloki.hu ● ISSN 1589 1623 (Print) ● ISSN 1785 0037 (Online)
DOI: http://dx.doi.org/10.15666/aeer/1705_1170111716

surface system, serve as vital freshwater reservoirs and help conserve species gene pools on earth; they are also known for their ecological functions, including maintaining ecological balance of basins, supplying production and living water, and providing rich aquatic products, and thus have great ecological and economic significance to regional development (Yang et al., 1988). Since the introduction of the ecosystem health concept in the 1980s, the health assessment of lake aquatic ecosystems, as a key part of lake ecosystem management, has gradually become the focus of scholars, resource managers and environment managers at home and abroad (Xu et al., 2001, 2012; Kane et al., 2009). Ecosystem health assessment provides the theoretical basis for analysing the causes of lake ecosystem health degradation and the protection of lake water environment, which is also closely linked with the achievement of the virtuous cycle of lake ecosystems.

Many scholars at home and abroad have performed studies regarding the construction of the assessment index system and the determination of thresholds because they are crucial in the health assessment of lake aquatic ecosystems. The selected assessment indices mainly include two aspects. The first aspect on biological components, e.g. biomass, species, diversity indices, etc. (Xu et al., 2001; Jeppesen et al., 2011; Umi et al., 2018); Phytoplankton and macrozoobenthos are commonly selected for ecosystem health assessment (Lyche-Solheim et al., 2013; Sreeja, 2018). Eutrophication responses are mainly evaluated on phytoplankton, macrozoobenthos and large aquatic plants, whilst pH response is mainly assessed by macrobenthos and fish (Solheim et al., 2008); Large aquatic plants (Mjelde et al., 2013; Keto et al., 2006), macrozoobenthos (Baumgärtner et al., 2008), and fish (Sutela and Vehanen, 2008)) have been used to describe responses to hydromorphological alterations. The second aspect represents the systematic indices, which are constructed from aquatic biological components, such as eco-exergy, structural eco-exergy, ecological buffer capacity, entropy, etc. (Ludovisi, 2006; Ludovisi and Poletti, 2003; Kane et al., 2009). The primary assessment approaches include the comprehensive health indices (Xu, 2005; Shuai and Li, 2014) generated by index system weighting or algorithmic derivation and the water quality model-based method (Xu et al., 2013; Zhang et al., 2010; Banerjee et al., 2017; Qi et al., 2018). Poyang Lake is one of the only two remaining large Yangtze-connected lakes in the middle reaches of Yangtze River in China. Its ecosystem development is affected not only by pollutants and sediments within the lake but also by seasonal hydrological fluctuations, particularly the annual amplitudes of water levels that reach 8 m (Zhao and Tong, 2013), which can significantly affect lake structures and functions (Coops et al., 2003). In recent years, Poyang Lake has also been affected by ecological and environmental issues related to human activities. Water quality has declined and eutrophication has gradually increased, and these phenomena resulted in ecological problems such as potential hazards of cyanobacterial bloom breakout (Yang, 2012; Cheng and Li, 2006; Xu et al., 2012; Li et al., 2017; Zhang et al., 2018). Therefore, constructing a lake aquatic health assessment index system suitable for the hydrological variation characterisation of Poyang Lake and large Yangtze-connected lakes, scientifically determining assessment indicator thresholds, and evaluating lake aquatic ecosystem health are of great theoretical and practical significance. On the basis of the analysis of the ecological system and evolution characteristics of Poyang Lake, this study combines observed and acquired data to construct a preliminary aquatic ecosystem health assessment index for large Yangtze-connected lakes. Then, the aquatic ecosystem health assessment thresholds are determined by adopting the special value

http://www.aloki.hu ● ISSN 1589 1623 (Print) ● ISSN 1785 0037 (Online)
DOI: http://dx.doi.org/10.15666/aeer/1705_1170111716

method, frequency analysis method, normative standards and analogies, reference mode method and so on.

Materials and methods

Study area and data

Physical, chemical and biological variables were measured in Poyang Lake from 1984 to 2013. Data from 2007 to 2013 were supplied by the Lake Poyang Laboratory for Wetland Ecosystem Research of the Chinese Ecosystem Research Network, whilst other less and reference data were collected from previous studies (Committee, 1993; Xie et al., 2000). Water level data from 1951 to 2011 were collected from the Changjiang (Yangtze River) Water Resources Commission. The details of these datasets are shown in *Table 1* and *Figure 1*.

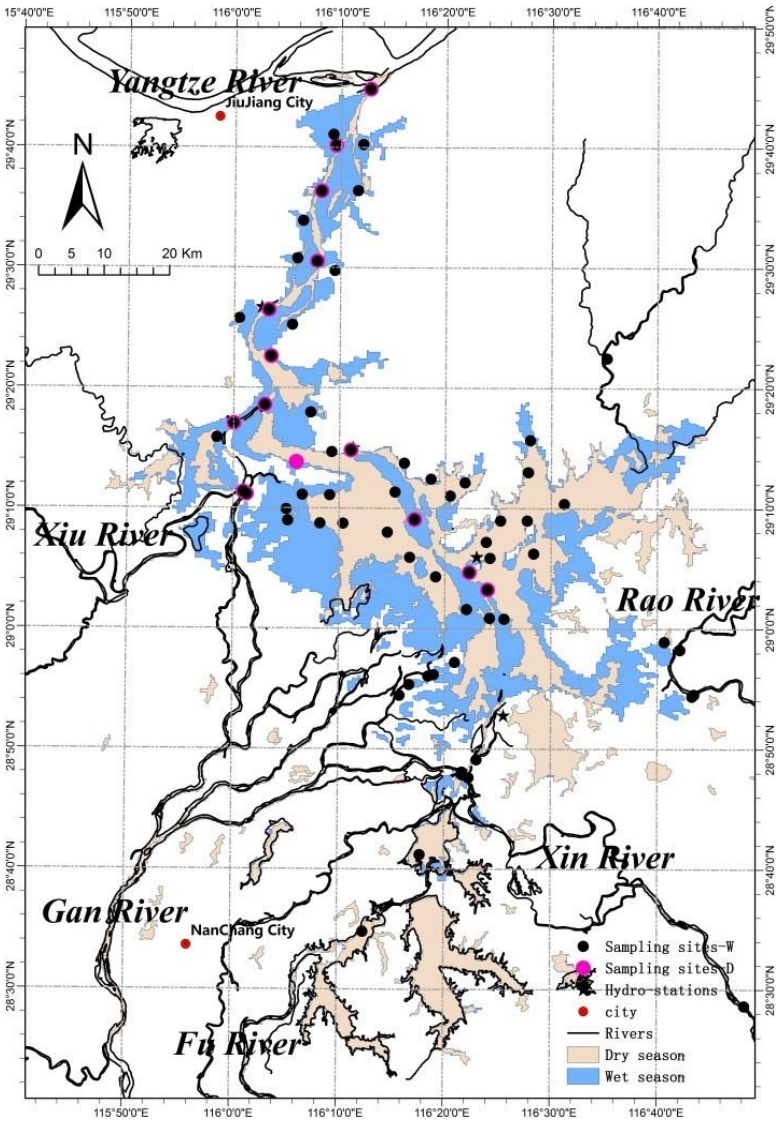

Figure 1. *Location and sampling sites of Poyang Lake*

Notes: Sampling sites-D: sampling sites in dry season, Sampling sites-W: sampling sites in wet season

http://www.aloki.hu ● ISSN 1589 1623 (Print) ● ISSN 1785 0037 (Online)
DOI: http://dx.doi.org/10.15666/aeer/1705_1170111716

Table 1. *Summary of variables and number of sites sampled in a given month and year in Poyang Lake*

Year	Month and sites	Data
1984, 1987–1993	Details shown in previous studies (Committee, 1993; Xie et al., 2000)	Biological variables (density of phytoplankton, etc.)
2007	October, 24 sites	Physical, chemical and biological variables (SD, TN, TP, COD_{mn}, Chl-a, biomass and density of phytoplankton, macrozoobenthic)
2008	June, 35 sites	
2009–2011	January, April, July and October, 15 sites	
2012	January, April and October, 15 sites July, 97 sites	Physical, chemical and biological variables (SD, TN, TP, COD_{mn}, Chl-a, biomass and density of phytoplankton, macrozoobenthic)
2013	July, 106 sites	
1951–2011	January–December, seven sites (Xingzi, Duchang, Hukou, Kangshan, Wucheng, Tangyin and Boyang)	Water level

SD: Secchi disk depth (water transparency); TN: total nitrogen; TP: total phosphorus; COD_{mn}: chemical oxygen demand; Chl-a: chlorophyll a

Methods

The construction of the aquatic ecosystem health assessment index system for in this study was mainly determined on the basis of literature research and theoretical analysis. The primary approaches for determining the index thresholds can be divided into two categories, namely, through statistical analysis approaches, such as the frequency analysis method and the special value method, direct observation of reference state and the adoption of normative standards. All statistical analyses were performed with the Statistical Program for Social Sciences (SPSS-IBM, New York, NY) 13.0 software.

Results and discussion

Construction of aquatic ecosystem health assessment index system for Poyang Lake

Many studies have demonstrated that the health status of lake aquatic ecosystems of water bodies should be assessed from the perspective of biological elements and supporting hydro-morphological and physico-chemical elements, especially water level-related indices (Mjelde et al., 2013), and not only on the basis of some specific biological, physical or chemical indices (Xie et al., 2013; Xu et al., 2013; Ghosh et al., 2018). Therefore, as a large-scale Yangtze-connected lake, the construction of an aquatic ecosystem health assessment index system for Poyang Lake must also consider the status of biological elements and supporting hydromorphological and physico-chemical elements.

1. Biological indicators

Lake ecosystems mainly include aquatic organisms such as planktons, benthic organisms, large aquatic plants and fish, etc. The indicators most widely used are biomass, quantity, species structure, and so on. On the basis of the response of various aquatic organisms to stress and the aquatic characteristics of Poyang Lake, phytoplankton and macrozoobenthos are selected to characterise the lake's aquatic ecosystem health.

http://www.aloki.hu ● ISSN 1589 1623 (Print) ● ISSN 1785 0037 (Online)
DOI: http://dx.doi.org/10.15666/aeer/1705_1170111716

(1) Phytoplankton: Phytoplankton is a critical indicator for the health assessment of lake aquatic ecosystems. Changes in algal species structure can reveal variations in the water environment (eutrophication, etc.) and lake ecosystems (Vanni, 1987; Paerl et al., 2013). The hydrological regime will affect the biomass, species composition, diversity and succession of phytoplankton (Wu and Guo, 2001). Lotic ecosystems are dominated by diatoms, whereas lentic ecosystems are dominated by cyanobacteria (De Emiliani, 2001). Relative to Taihu Lake, the phytoplankton characteristics in Poyang Lake are dominated by diatoms in the aspects of biomass and quantity, not cyanobacteria (Xu, 2013; Wu et al., 2013). But cyanobacteria bloom was also found at the centre part of the lake in 2011 (Xu, 2013). Dam construction in Poyang Lake has become controversial in recent years because of its adverse effects to water level fluctuations, and consequently, to the structure of phytoplankton (Liu et al., 2015). Many scholars have predicted the outbreak of cyanobacteria bloom after dam construction. Algal structural changes, particularly variation tendency in cyanobacteria proportion, are the primary focus of aquatic ecosystem health assessments for Poyang Lake. Constructing the ratio of cyanobacteria biomass (CB) to diatoms biomass (DB) can help determine the water environment of Poyang Lake and its aquatic ecosystem health characteristics.

(2) Macrozoobenthos: Macrozoobenthos are essential indicator organisms for monitoring human disturbance and lake pollution and thus ideal as natural monitors. The diversity index of macrozoobenthos has been widely adopted for the water pollution assessment of lakes and rivers (Shuai and Li, 2014; Xiong et al., 2003; Miler et al., 2013). The EU Water Framework Directive uses macrozoobenthos to monitor and evaluate the ecological health of lakes, as they are sensitive to water level amplitudes (i.e. water levels affect the abundance of macrozoobenthos) (Aroviita and Amalainen, 2008). The density of macrozoobenthos in Poyang Lake has drastically changed in recent years, as evidenced by the obvious decrease of molluscs (Cai et al., 2014), whilst the increased number of large animals have negatively affected the abundance of small marsh and long-horned snails (Ou et al., 2009). Large-scale sand mining and river scouring have also altered the macrozoobenthos habitat and influenced their community structures in recent years. Therefore, macrozoobenthos characterisation has been prioritised in the aquatic ecosystem assessment of Poyang Lake, and the diversity index of macrozoobenthos has been selected as the biological indicator.

Large aquatic plants and fish are also vital indicator species of aquatic ecosystem changes in Poyang Lake. However, large aquatic plants only appear in few branch areas of the lakes during the summer flooding season (Jian et al., 2015), and for the structure of fish species, there are certain similarities between Poyang Lake and Yangtze River Basin and the whole country (Hu, 2009). Hence, in this paper, we will not include large aquatic plant and fish species, considering their representativeness and substantial data availability.

2. Hydrological indicators

Habitat is commonly characterised on the basis of the following aspects: hydrology, water environment, lake morphology, and human activity or interference. The hydrological elements of Poyang Lake are relatively unique. For instance, water-level fluctuations are significant during the year, which greatly impact the lake's ecological environment. Subsequently, wetland area and distribution are directly affected, whilst the growth of aquatic organisms (e.g. phytoplankton and fish) are either directly or

http://www.aloki.hu ● ISSN 1589 1623 (Print) ● ISSN 1785 0037 (Online)
DOI: http://dx.doi.org/10.15666/aeer/1705_1170111716

indirectly affected. Therefore, hydrological element is selected as one of the habitat indicators for the aquatic ecosystem health assessment of Poyang Lake.

Previous studies have proposed that the indices for water level fluctuations include winter water level amplitude and spring flood amplitude (Hellsten, 2001; Keto et al., 2006, 2008; Mjelde et al., 2013), as they affect the species abundance of large aquatic plants (Keto et al., 2006), macrobenthos (Aroviita and Amalainen, 2006) and fish (Sutela and Vehanen, 2006). The communities of *carex–polygonum criopolitanum*, *carex–Phalaris arundinacea* and *Phalaris arundinacea–carex* in Poyang Lake are relatively sensitive to changes in water level conditions and largely affected by water level amplitudes (Zhang et al., 2012), and they have low tolerance to changes in hydrological conditions. The seasonal droughts in spring (rising season) and winter (dry season) over Poyang Lake in recent years have caused serious impacts on the wetlands and aquatic ecosystems of the lake (Yang, 2012). For instance, spring drought is disastrous to fish, as they lay eggs in large quantities due to the simulation of gonads by flowing water and aquatic plants. If the aquatic plants are exposed to non-water areas during April and May, fish reproduction will be seriously affected. The lowest water level during the dry season directly impacts the growth and distribution of wetland plants and the succession of vegetation belts, thus affecting the different ecosystem functions (e.g. wetland ecological function and migratory bird habitat function) of Poyang Lake (Hu et al., 2012). The lowest water level during the dry season will also influence the habitat of migratory birds, and its occurrence is averse to their protection (Qi and Zhang, 2014). Characterising the lowest water level in the spring drought and dry seasons of Poyang Lake is critical in evaluating the aquatic ecosystem health of the lake. Hence, the lowest water level anomalies during the dry season and the mean water level anomalies during the rising season are determined to characterise the lowest water level (dry season) and spring drought (rising season) of Poyang Lake.

Poyang Lake begins to recede in October and rise in April, as the flood season starts in June (Hu et al., 2007) whilst the dry season occurs from December to March the following year. The lowest water level anomaly during the dry season is expressed by the difference between the lowest water level of the dry season (December–March) and the mean value of the lowest water level of the dry season over multiple years. Meanwhile, the rising season anomaly is expressed by the difference between the mean water level of the rising season (April–May) and the mean of mean water level of the rising season over multiple years.

3. Water environment indicators

As discussed in the previous section (2. Hydrological indicators), water environment is one of the four elements of habitat, as its condition can directly impact the growth of aquatic organisms. Therefore, water environment is selected as another indicator of habitat. In the 1980s, Poyang Lake has entered the mesotrophic stage (Cheng and Li, 2006); at present, it is in light eutrophic stage (as reported by Environmental Bulletin in 2013). Water quality has gradually deteriorated because total nitrogen and total phosphorus have both exceeded the standard values. Eutrophication is one of the key issues of Poyang Lake and hence an important aspect of aquatic ecosystem health assessment. Here, the comprehensive nutrition state index (labelled as TLI) is selected as the indicator for the nutrition status in the aquatic ecosystem health assessment index of Poyang Lake.

http://www.aloki.hu ● ISSN 1589 1623 (Print) ● ISSN 1785 0037 (Online)
DOI: http://dx.doi.org/10.15666/aeer/1705_1170111716

In summary, the aquatic ecosystem health assessment index system of Poyang Lake is constructed from three perspectives, namely, aquatic organism elements, hydrological elements and water environment elements (*Table 2*).

Table 2. *Aquatic ecosystem assessment index of Poyang Lake*

Objective layer	Element layer	Index layer	Index explanation	Index calculation method	Determination method of index thresholds
Health assessment of Yangtze-connected lake ecosystems	Aquatic organism elements	Ratio of cyanobacteria biomass to diatom biomass (CB/DB)	Characterise the primary productivity status of lakes and ecosystem succession	Measure, calculate	Reference mode method, frequency analysis method
		Diversity index of macrozoobenthos (DI)	Characterise the features of macrozoobenthos and reveal the changes of ecosystem	$DI = \sum_{j=1}^{m} ({}^{N_i}/_{N}) \log(\frac{N_i}{N}, 2)$	Normative standards and analogies
	Hydrological elements	Lowest water level anomaly during dry season (LWLa-D)	Evaluate the characteristics of lowest water level during dry season	Difference between lowest water level in December–March and mean of lowest water level over multiple years during dry season	Special value method, frequency analysis method
		Mean water level anomaly during rising season (MWLa-R)	Evaluate the characteristics of water level during rainy season (spring drought or not)	Difference between mean water level in April–May and the mean of mean water level over multiple years during rising season	Special value method, frequency analysis method
	Water environment elements	Trophic state index (TLI)	Characterise the state of nutrition of lakes	Reference (Wang et al., 2002)	Normative standards and analogies

TLI: Trophic state index; CB/DB: Ratio of cyanobacteria biomass to diatom biomass; DI: Diversity index of macrozoobenthos; LWLa-D: Lowest water level anomaly during dry season; MWLa-R: Mean water level anomaly during rising season

Determining the aquatic ecosystem health assessment thresholds of Poyang Lake

The threshold proposed by Robert in the 1970s (May, 1997) refers to the set of thresholds and breakpoints of multiple stable states based on the characteristics and functions of the ecosystem. The methods to determine thresholds include normative standards and analogies, special value methods, statistical models, mathematical models, physical models, etc. The threshold determination methods for specific indicators are shown in *Table 2*.

1. Ratio of cyanobacteria biomass to diatom biomass

Few related researches on the indicator exist at present. In this study, health assessment thresholds are determined by performing the time reference mode method and the frequency method. *Figure 2* shows the CB/DB ratio from 1984 to 2013. The values have increased year by year, and the ratio in 2013 is larger than that in 2012. By taking the state of Poyang Lake in 1984 as the reference state of 'good' (maximum value 1.22, minimum value 0.004, average value 0.16, median value 0.04), and combined with the histogram of the CB/DB ratio in the past 30 years (*Fig. 3*), the thresholds are determined to be as follows: 'poor' (> 0.6), 'moderate' (0.4–0.6) and 'good' (< 0.4).

2. Diversity index of macrozoobenthos

The diversity index of macrozoobenthos has been widely used in water quality assessments (Lu, 1985; Lv et al., 2009; Miler et al., 2013; Xiong et al., 2003).

http://www.aloki.hu ● ISSN 1589 1623 (Print) ● ISSN 1785 0037 (Online)
DOI: http://dx.doi.org/10.15666/aeer/1705_1170111716

According to the Aquatic Biomonitoring Manual (State Environmental Protection Agency, 1993), the relationship between ecosystem health status and the macrozoobenthos Shannon diversity index can be divided into four pollution categories: H = 0 for 'severe pollution', 0 < H < 1 for 'heavy pollution', H = 1–2 for 'medium pollution' , H = 2–3 for 'light pollution' and H > 3 represents 'clean'. As shown in *Figure 4,* the diversity index of macrozoobenthos has a normal distribution, and the index with relatively high frequency is 0.8–2. The aquatic ecosystem health thresholds, which are determined on the basis of existing evaluation criteria and frequency methods, are as follows: 'poor' (0–1), 'moderate' (1–2) and 'good' (> 2).

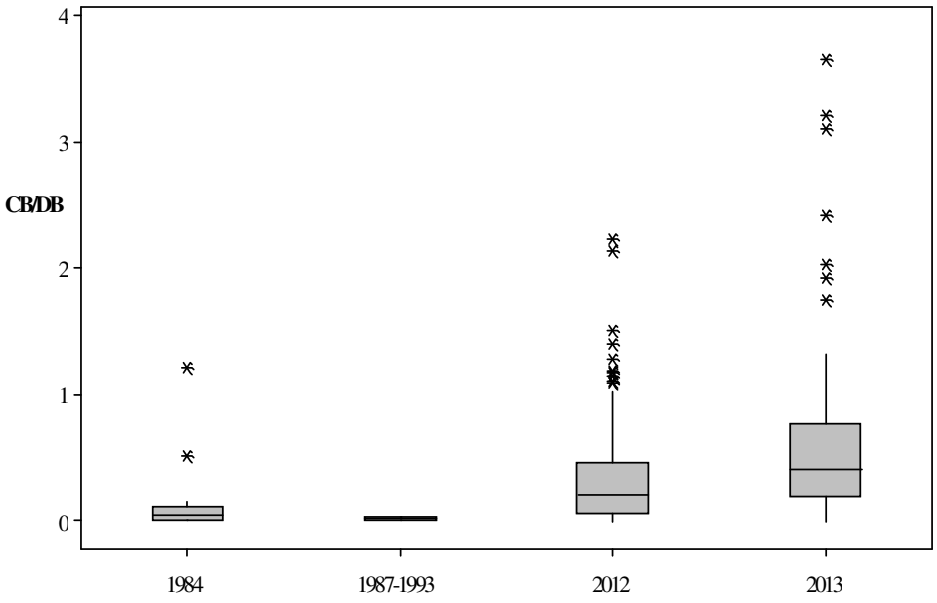

Figure 2. *Box-plot of CB/DB ratios of Poyang Lake in the recent 30 years (some data from previous studies (Committee, 1993; Xie et al., 2000))*

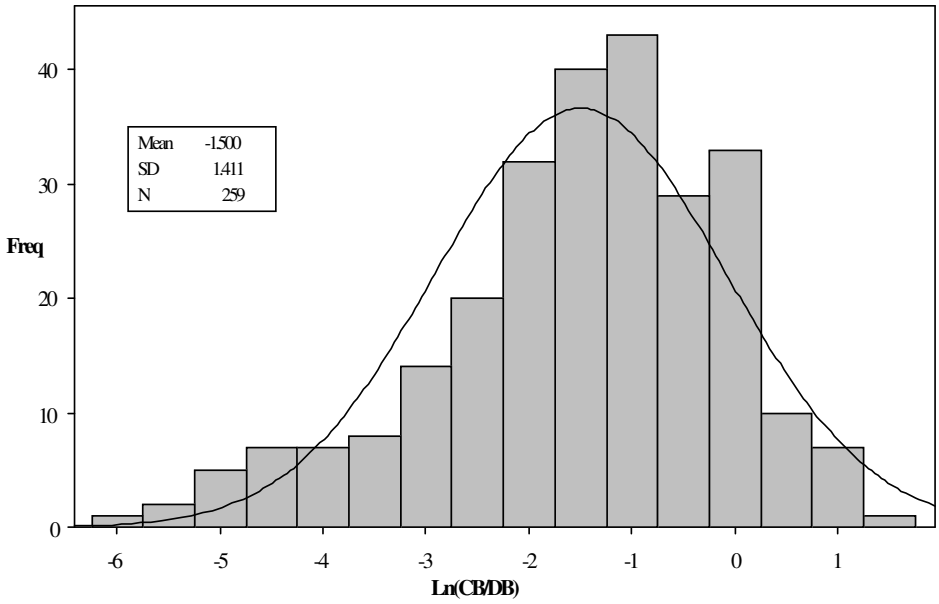

Figure 3. *Histogram of CB/DB ratios of Poyang Lake in the recent 30 years*

http://www.aloki.hu ● ISSN 1589 1623 (Print) ● ISSN 1785 0037 (Online)
DOI: http://dx.doi.org/10.15666/aeer/1705_1170111716

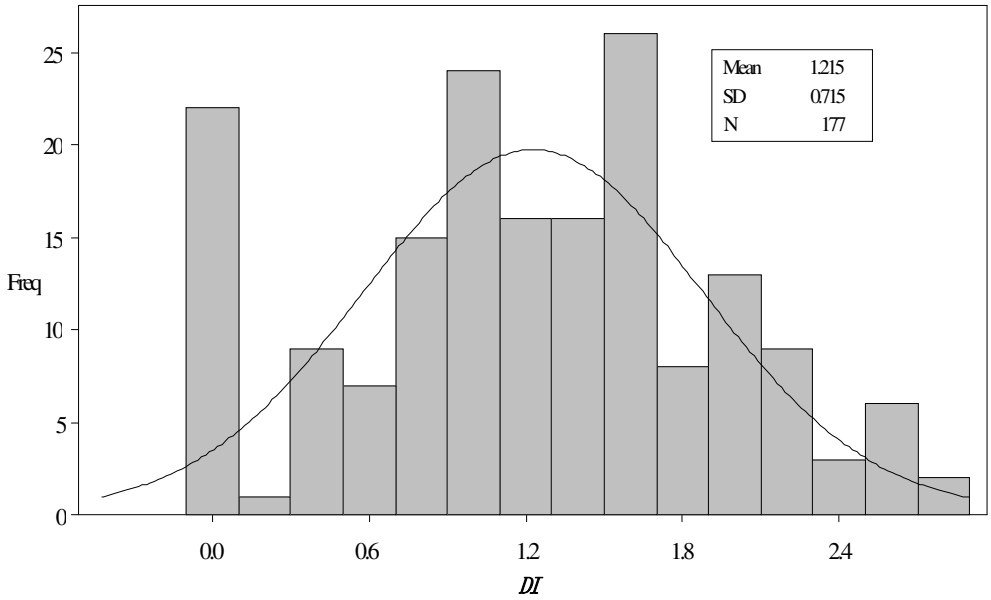

Figure 4. *Histogram of diversity index of macrozoobenthos of Poyang Lake in 2012–2013*

3. Lowest water level anomaly during the dry season

A statistical analysis of water level amplitudes during the dry season of Hukou, Xingzi, Duchang, Wucheng, Tangyin, Kangshan and Boyang stations for Poyang Lake from 1950 to 2011 was conducted. The amplitude variations of the seven stations are not significant, which is in accordance with the normal distribution. The average value is 0, the standard deviation is 0.7644 m, and the 5% and 95% tantiles are 1.34 m and −1.18 m, respectively (*Fig. 5*). In actual situations, the extremes of lowest water level during the dry season affect exposure time and area of wetlands. Exposure time directly affects the development of vegetation on the beach; it may be conducive to vegetative growth and may even result in the growth of new species of wetland ecological vegetation, but wetland degradation may occur if exposure time is too long (Ge et al., 2010). However, an extremely short exposure time over a small exposure area is unfavourable to the growth of wetland plants (Hu et al., 2010) and this will cause a series of ecological problems. Therefore, the extremes of lowest water level anomalies during the dry season signify an unhealthy state. In addition, the water level in Xingzi Station in 2008 was low with amplitude of −0.95 m during the dry season. The water levels in Duchang Station in 2008 and 2009 were low (e.g. 7.99 m in 2009, the lowest in history) with amplitudes of −1.49 m and −1.55 m during the dry season, respectively. In summary, the range of 1× standard deviation is determined to be from −0.5 to 0.5 m ('good'). The 5% and 95% tantiles (i.e. based on short plate effect, taking the minimum of absolute value) of 1× standard deviation is from 0.5 to 1.18 m and from −0.5 to −1.18 m ('moderate') and 'poor' if the value is less than −1.18 m or greater than 1.18 m, respectively.

4. Mean water level anomaly during the rising season

A statistical analysis on mean water level anomaly during the rising season of Xingzi, Duchang, Hukou, Kangshan, Tangyin, Wucheng and Boyang Stations was conducted. The findings, which accord with normal distribution, show a mean value

http://www.aloki.hu ● ISSN 1589 1623 (Print) ● ISSN 1785 0037 (Online)
DOI: http://dx.doi.org/10.15666/aeer/1705_1170111716

of 0.014 m and a standard deviation of 1.042 m (*Fig. 6*). The 5% and 95% tantiles are 1.80 m and −1.50 m, respectively. In actual situations, spring drought will affect fish breeding and wetland vegetation. The larger the MWLa-R is, the unhealthier the state will be. In the past 60 years, spring drought occurred five times since 2000, particularly in 2004, 2005, 2008, 2009 and 2011. The mean water level anomalies during the rising season in Xingzi Station for the abovementioned years are −1.44, −1.08, −1.53, −0.95 and −4.2 m. In Hukou Station, the corresponding anomalies are −1.35, −1.02, −1.34, −0.67 and −3.94 m. In Duchang Station, the corresponding values are −1.21, −0.80, −1.62, −1.15 and −3.24 m. In Wucheng Station, the corresponding values are −1.01, −1.25, −1.43, −1.12 and −3.73 m. In summary, the range of 1× standard deviation is determined to be from −1.03 to 1.06 m ('good'). The 5% and 95% tantiles (i.e. based on short plate effect, taking the minimum of absolute value) of 1× standard deviation is from 1.06 to 1.5 m and from −1.50 to −1.03 m ('moderate') and 'poor' if the value is less than −1.5 m or greater than 1.5 m, respectively.

5. Comprehensive nutrition state index

The comprehensive nutrition index is used to evaluate the nutritional status of water bodies, and it includes the five variables of Chl-a, TN, TP, COD_{mn} and SD. According to the literature (Wang et al., 2002), a TLI of < 30 means 'oligotrophic', 30–50 means 'medium nutrition', and > 50 means 'eutrophication'. The thresholds are determined on the basis of the histogram of the comprehensive nutritional status of Poyang Lake in the past six years (*Fig. 7*). The thresholds can be determined as follows: 'poor' (> 50), 'moderate' (40–50) and 'good' (< 40).

In summary, the evaluation thresholds for the aquatic ecosystem health assessment index system of Poyang Lake can be divided into the following three levels: 'good', 'moderate' (sub-healthy) and 'poor' (*Table 3*).

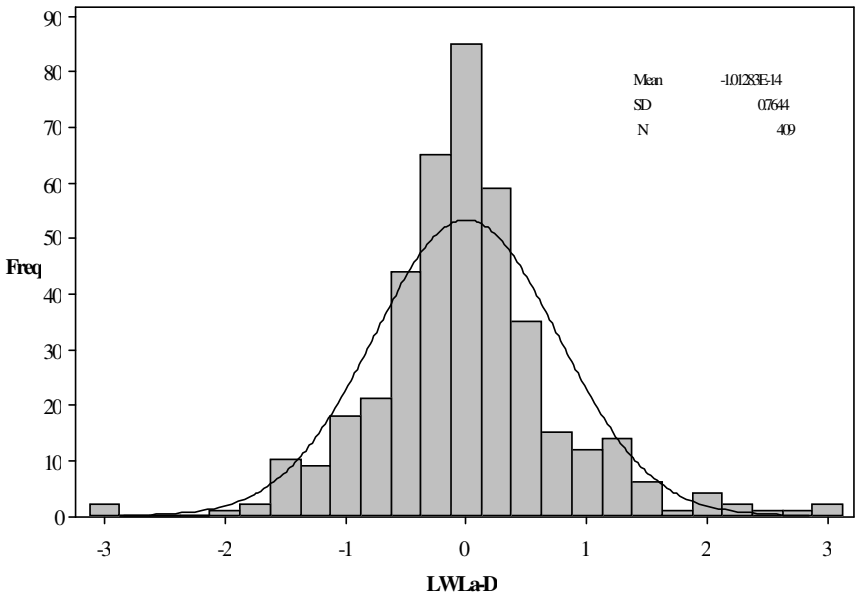

Figure 5. *Histogram of lowest water level anomaly during dry season in Hukou, Xingzi, Duchang, Tangyin, Wucheng, Kangshan and Boyang Stations*

http://www.aloki.hu ● ISSN 1589 1623 (Print) ● ISSN 1785 0037 (Online)
DOI: http://dx.doi.org/10.15666/aeer/1705_1170111716

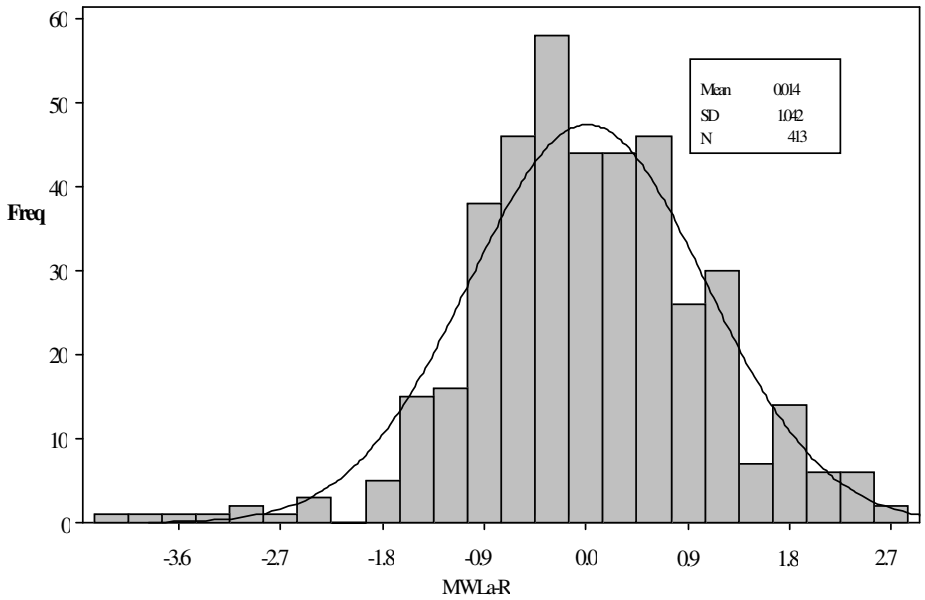

Figure 6. *Histogram of mean water level anomaly during rising season in Hukou, Xingzi, Duchang, Tangyin, Wucheng, Kangshan and Boyang Stations*

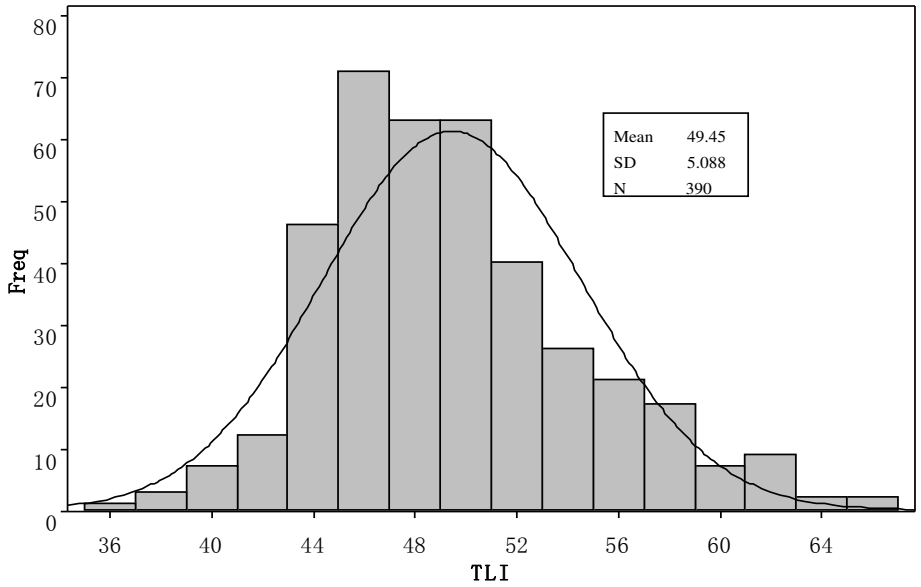

Figure 7. *Histogram of TLI of Poyang Lake in 2007–2012*

Table 3. *Threshold of indicators for Poyang Lake*

Indicators/health status	Good	Moderate (sub-healthy)	Poor
CB/DB	≤ 0.4	0.4 to 0.6	≥ 0.6
DI	≥ 2	1 to 2	0 to 1
LWLa-D (m)	−0.76 to 0.76	0.76 to 1.18, −0.76 to −1.18	< −1.18, > 1.18
MWLa-R (m)	−1.03 to 1.05	1.05 to 1.52, −1.50 to −1.03	< −1.50, > 1.52
TLI	≤ 40	40 to 50	≥ 50

http://www.aloki.hu ● ISSN 1589 1623 (Print) ● ISSN 1785 0037 (Online)
DOI: http://dx.doi.org/10.15666/aeer/1705_1170111716

Conclusions and prospects

The assessment index system for Poyang Lake presented in this paper comprises the following elements: CB/DB ratio and diversity index of macrozoobenthos for the aquatic organism index; lowest water level anomaly during the dry season and mean water level anomaly during the rising season; and the comprehensive nutrition state index with three habitat indicators. The frequency analysis method was conducted, normative standards and analogies were considered, and the special value method was performed to initially determine the thresholds for the health assessment of Poyang Lake's aquatic ecosystem. The three grades ('good', 'moderate' and 'poor') can help provide the research basis for further evaluating the aquatic ecosystem health of the large Yangtze-connected lakes, such as Poyang Lake.

This work is a preliminary study on the index system and the thresholds for the aquatic ecosystem health assessment of large-scale Yangtze-connected lakes. Thus, optimisation and adjustment are still needed. Only the indicators of phytoplankton, macrozoobenthos, and habitat (hydrology and water environment) were considered. In the future, ecological indicators (e.g. migratory fish) and thermodynamic oriented ecological indicators (e.g. ecological energy and structural ecological energy) shall also be covered. Considering that large proportions of fish in these lakes have similar ecological compositions, excluded; however, this approach may have affected the comprehensive assessment of aquatic ecosystem health of Poyang Lake in this study. Moreover, due to the hydrological rhythm ('ample flow, short water') in Poyang Lake, and large aquatic plants mainly appear in few branch area of the lake during the rising season, they are not easily accessible. That is to say, the related data are hardly got. Thus, this study did not consider aquatic plants for the time being, but future research will be conducted to improve this limitation. The indicators on hydrologic elements were determined on the basis of existing data, and further in-depth research and screening can be performed to construct more appropriate indicators. The thresholds of indices were determined on the basis of available data, but some of the important information, especially biological data, was limited. Having access to a wealth of information can help optimise this aspect of the research. In addition, the values of the indicators for Poyang Lake vary greatly with the seasons. Thus, this study only determined the mean threshold value. A further deepening of the research scope is needed for the large Yangtze-connected lakes, such as Poyang Lake, considering their obvious seasonal differences.

Acknowledgements. This study was financially supported by the National Scientific Foundation of China (Grant 41701097), the Key Research Program of the Chinese Academy of Sciences (Grant No. KFZD-SW-318), the National Scientific Foundation of China (Grant 41571107, 41801092) and Natural Science Foundation of Jiangsu province (Grant BK20161118). Special thanks go to the Lake Poyang Laboratory for Wetland Ecosystem Research (PLWER) for providing the data for this study.

REFERENCES

[1] Aroviita, J. H., Amalainen, H. (2008): The impact of water-level regulation on littoral macroinvertebrate assemblages in boreal lakes. – Hydrobiologia 613: 45-56.

[2] Banerjee, A., Chakrabarty, M., Rakshit, N., Mukherjee, J., Ray, S. (2017): Indicators and assessment of ecosystem health of Bakreswar reservoir, India: an approach through network analysis. – Ecological Indicators 80: 163-173.

http://www.aloki.hu ● ISSN 1589 1623 (Print) ● ISSN 1785 0037 (Online)
DOI: http://dx.doi.org/10.15666/aeer/1705_1170111716

[3] Baumgärtner, D., Mörtl, M., Rothhaupt, K. O. (2008): Effects of water-depth and water-level fluctuations on the macroinvertebrate community structure in the littoral zone of Lake Constance. – Hydrobiologia 613(1): 97-107.
[4] Borja, A., Dauer, D. M. (2008): Assessing the environmental quality status in estuarine and coastal systems: comparing methodologies and indices. – Ecological Indicators 8(4): 331-337.
[5] Cai, Y. J., Lu, Y. J., Wu, Z. S., Chen, Y. W., Zhang, L., Lu, Y. (2014): Community structure and decadal changes in macrozoobenthic assemblages in Lake Poyang, the largest freshwater lake in China. – Knowledge and Management of Aquatic Ecosystems 414(09).
[6] Cheng, X. Y., Li, S. J. (2006): An analysis on the evolvement processes of lake eutrophication and their characteristics of the typical lakes in the middle and lower reaches of Yangtze River. – Chinese Science Bulletin 51: 1603-1613.
[7] Committee, C. (1993): Atlas of Poyang Lake. – Science Press, Beijing, China.
[8] Coops, H., Beklioglu, M., Crisman, T. L. (2003): The role of water-level fluctuations in shallow lake ecosystems–workshop conclusions. – Hydrobiologia 506(1-3): 23-27.
[9] Costanza, R., Norton, B. G., Haskell, B. D. (1992): Ecosystem Health: New Goals for Environmental Management. – Island Press, Washington, DC.
[10] Cui, B. S., Yang, Z. F. (2002): Establishing an indicator system for ecosystem health evaluation on wetlands, I. A theoretical framework. – Acta Ecologica Sinica 22(7): l.
[11] Davies, P. E., Harris, J. H., Hillman, T. J., Walker, K. F. (2010): The Sustainable Rivers Audit: assessing river ecosystem health in the Murray-Darling Basin, Australia. – Marine and Freshwater Research 61(7): 764-777.
[12] De Emiliani, M. O. G. (1997): Effects of water level fluctuations on phytoplankton in a river-floodplain lake system (Paraná River, Argentina). – Hydrobiologia 357(1-3): 1-15.
[13] Ge, G., Ji, W. T., Liu, C. L., Xiong, S., Wu, Z. Q. (2010): Hydraulic project and wetland ecological protection in Poyang Lake. – Resources and Environment in the Yangtze Basin 19(6): 606-613.
[14] Ghosh, D., Biswas, J. K. (2018); Aquatic health indicators: holistic evaluation tools for sustainable management of a tropical oxbow lake ecosystem. – Indian Journal of Fisheries 65(4): 81-92.
[15] Hellsten, S. K. (2001): Effects of lake water level regulation on aquatic macrophyte stands in northern Finland and options to predict these impacts under varying conditions. – Acta Botanica Fennica 171: 1-47.
[16] Hu, M. L. (2009): Charaeteristics of Water Level, Water Environment and Effects on Fish Communication and Migration in the Hukou Area of Poyang Lake. – Nanchang University, Nanchang.
[17] Hu, Q., Feng, S., Guo, H., Chen, G., Jiang, T. (2007): Interactions of the Yangtze river flow and hydrologic processes of the Poyang Lake, China. – Journal of Hydrology 347(1): 90-100.
[18] Hu, Z. P., Ge, G., Liu, C. L., Chen, F. S., Li, S. (2010): Structure of Poyang Lake wetland plants ecosystem and influence of lake water level for the structure. – Resources and Environment in the Yangtze Basin 19(6): 597-605.
[19] Jeppesen, E., Nõges, P., Davidson, T. A., Haberman, J., Nõges, T., Blank, K., ... & Johansson, L. S. (2011): Zooplankton as indicators in lakes: a scientific-based plea for including zooplankton in the ecological quality assessment of lakes according to the European Water Framework Directive (WFD). – Hydrobiologia 676(1): 279-297.
[20] Jian, M. F., Jian, M. F., Li, L. Y., Wang, S. C., Yu, H. P., Yu, G. J. (2015): Distribution pattern of submerged plants in tropical wetlands of Poyang Lake and its influencing factors of water environment. – Resources and Environment in the Yangtze Basin 24(5): 765-772.

http://www.aloki.hu ● ISSN 1589 1623 (Print) ● ISSN 1785 0037 (Online)
DOI: http://dx.doi.org/10.15666/aeer/1705_1170111716

[21] Kane, D. D., Gordon, S. I., Munawar, M., Charlton, M. N., Culver, D. A. (2009): The Planktonic Index of Biotic Integrity (P-IBI): an approach for assessing lake ecosystem health. – Ecological Indicators 9(6): 1234-1247.
[22] Keto, A., Tarvainen, A., Hellsten, S. (2006): The effect of water level regulation on species richness and abundance of aquatic macrophytes in Finnish lakes. – International Association of Theoretical and Applied Limnology, Proceedings 29: 2103-2108.
[23] Keto, A., Tarvainen, A., Marttunen, M., Hellsten, S. (2008): Use of the water-level fluctuation analysis tool (Regcel) in hydrological status assessment of Finnish lakes. – Hydrobiologia 613: 133-142.
[24] Li, B., Yang, G. S., Wan, R. R., Hörmann, G., Huang, J. C., Fohrer, N., Zhang, L. (2017): Combining multivariate statistical techniques and random forests model to assess and diagnose the trophic status of Poyang Lake in China. – Ecological Indicators 83: 74-83.
[25] Liu, X., Qian, K. M., Chen, Y. W. (2015): Effects of water level fluctuations on phytoplankton in a Changjiang River floodplain lake (Poyang Lake): implications for dam operations. – Journal of Great Lakes Research 41(3): 770-779.
[26] Lu, G. Q. (1985): Bio-assessment of Dongting Lake using benthic macroinvertebrates Community Structure. – Environmental Sciences 6(2): 59-63.
[27] Ludovisi, A. (2006): Use of thermodynamic indices as ecological indicators of the development state of lake ecosystems: Specific dissipation. – Ecological Indicators 6(1): 30-42.
[28] Ludovisi, A., Poletti, A. (2003): Use of thermodynamic indices as ecological indicators of the development state of lake ecosystems. 1. Entropy production indices. – Ecological Modelling 159(2-3): 203-222.
[29] Lv, G. J., Xiong, B. X., Liu, M., et al. (2009): The community structure of macrozoobenthos and water quality assessment on different trophic types of reservoirs. – Acta Ecologica Sinica 29(10): 5339-5349.
[30] Lyche-Solheim, A., Feld, C. K., Birk, S., Phillips, G., Carvalho, L., Morabito, G., ... Kolada, A. (2013): Ecological status assessment of European lakes: a comparison of metrics for phytoplankton, macrophytes, benthic invertebrates and fish. – Hydrobiologia 704(1): 57-74.
[31] May, R. M. (1977): Thresholds and breakpoints in ecosystems with a multiplicity of stable states. – Nature 269(5628): 471-477.
[32] Miler, O., Porst, G., McGoff, E., Pilotto, F., Donohue, L., Jurca, T., ... Clarke, R. (2013): Morphological alterations of lake shores in Europe: a multimetric ecological assessment approach using benthic macroinvertebrates. – Ecological Indicators 34: 398-410.
[33] Mjelde, M., Hellsten, S., Ecke, F. (2013): A water level drawdown index for aquatic macrophytes in Nordic lakes. – Hydrobiologia 704(1): 141-151.
[34] Ou, Y. S., Zhan, C., Chen, T. H., Wu, H. L., Wu, X. P. (2009): Species diversity and resource assessment of macrozoobenthos in Poyang Lake. – Journal of Nanchang University (Engineering & Technology) 31(1): 9-13.
[35] Paerl, H. W., Valdes, L. M., Pinckney, J. L., Piehler, M. F., Dyble, J., Moisander, P. H. (2003): Phytoplankton photopigments as indicators of estuarine and coastal eutrophication. – BioScience 53(10): 953-964.
[36] Qi, L. Y., Huang, J. C., Huang, Q., Gao, J. F., Wang, S. G., Guo, Y. Y. (2018): Assessing aquatic ecological health for Lake Poyang, China: Part II index application. – Water 10(7): 909.
[37] Qi, S. H., Zhang, Q. M., Jiang, F., Liao, F. Q. (2014): Study on the effects on the landscape spatial pattern of the wintering birds' habitat from lake level in Poyang Lake Wetland. – Journal of Natural Resources 29(8).
[38] Rapport, D. J., Whitford, W. G. (1999): How ecosystems respond to stress common properties of arid and aquatic systems. – BioScience 49(3): 193-203.
[39] Schaeffer, D., Herricks, E., Kerster, H. (1988): Ecosystem health: I. Measuring ecosystem health. – Environmental Management 12(4): 445-455.

http://www.aloki.hu ● ISSN 1589 1623 (Print) ● ISSN 1785 0037 (Online)
DOI: http://dx.doi.org/10.15666/aeer/1705_1170111716

[40] Shuai, H., Li, J. B. (2014): Assessment and analysis of comprehensive health in typical years of Dongting Lake System. – Scientia Geographica Sinica 34(2): 170-177.
[41] Solheim, A. L., Rekolainen, S., Moe, S. J., Carvalho, L., Phillips, G., Ptacnik, R., ... Hesthagen, T. (2008): Ecological threshold responses in European lakes and their applicability for the Water Framework Directive (WFD) implementation: synthesis of lakes results from the REBECCA project. – Aquatic Ecology 42(2): 317-334.
[42] Sreeja, J. (2018): Biomonitoring of Paravur Lake in Kerala Using Macro-Invertebrates. – In: Rahul, A. K. et al. (eds.) Environmental Pollution. Springer, Singapore, pp. 477-485.
[43] State Environmental Protection Agency (1993): Aquatic Biological Monitoring Manual. – Southeast University Press, Nanjing.
[44] Sutela, T., Vehanen, T. (2008): Effects of water-level regulation on the nearshore fish community in boreal lakes. – Hydrobiologia 613(1): 13-20.
[45] Umi, W. A. D., Yusoff, F. M., Aris, A. Z., Sharip, Z. (2018): Rotifer community structure in tropical lakes with different environmental characteristics related to ecosystem health. – Journal of Environmental Biology 39(5): 795-807.
[46] Vanni, M. J. (1987): Effects of nutrients and zooplankton size on the structure of a phytoplankton community. – Ecology 68(3): 624-635.
[47] Wang, M. C., Liu, X. Q., Zhang, J. H. (2002): Evaluate method and classification standard on lake eutrophication. – Environmental Monitoring in China 18: 47-49.
[48] Wu, H. J., Guo, S. L. (2001): The Effect of Hydrological Regime on Phytoplankton Community. – Advances in Water Science 12: 51-55.
[49] Wu, Z., Cai, Y., Liu, X., Xu, C. P., Chen, Y., Zhang, L. (2013): Temporal and spatial variability of phytoplankton in Lake Poyang: the largest freshwater lake in China. – Journal of Great Lakes Research 39(3): 476-483.
[50] Xie, Q. M., Li, C. C., Peng, C. L. (2000): primary studies on community ecology of floating algae in Poyang Lake. – Jiangxi Science 18: 162-166.
[51] Xiong, J. L., Mei, X. G., Hu, C. L. (2003): Comparative study on the community structure and biodiversity of zoobenthos in lakes of different pollution states. – Journal of Lake Sciences 15(2): 160-168.
[52] Xu, C. P. (2013): Study on Phytoplankton Community Structure in Lake Poyang. – Nanjing Institute of Geography and Limnology, Chinese Academy of Sciences, Nanjing.
[53] Xu, C. P., Li, S. C., Chai, W. B., Chen, Y. W. (2012): A newly recorded cyanobacterial species in water blooms occurred in Lake Poyang—Merismperdia convoluta Breb. Kützing. – Journal of Lake Sciences 24(4): 643-646.
[54] Xu, F., Yang, Z. F., Chen, B., Zhao, Y. W. (2012): Ecosystem health assessment of Baiyangdian Lake based on thermodynamic indicators. – Procedia Environmental Sciences 13: 2402-2413.
[55] Xu, F., Yang, Z. F., Chen, B., Zhao, Y. W. (2013): Development of a structurally dynamic model for ecosystem health prognosis of Baiyangdian Lake, China. – Ecological Indicators 29: 398-410.
[56] Xu, F. L., Dawson, R. W., Tao, S., Cao, J., Li, B. G. (2001): A method for lake ecosystem health assessment: an Ecological Modeling Method (EMM) and its application. – Hydrobiologia 443(1-3): 159-175.
[57] Xu, F. L., Zhao, Z. Y., Zhan, W., Zhao, S. S., Dawson, R. W., Tao, S. (2005): An ecosystem health index methodology (EHIM) for lake ecosystem health assessment. – Ecological Modelling 188(2-4): 327-339.
[58] Yang, G. S. (2012): Water issues in the Yangtze River and its formation causes and controling strategies. – Resources and Environment in the Yangtze Basin 21: 821-830.
[59] Yang, G. S., Ma, R. H., Zhang, L., et al. (2010): Lake status, major problems and protection strategy in China. – J. Lake Sci. 22: 799-810.
[60] Zeng, D. H., Jiang, F. Q., Fan, Z. P., et al. (1999): Ecosystem health and sustainable development for human. – Chinese Journal of Applied Ecology 10(6): 751-756.

http://www.aloki.hu ● ISSN 1589 1623 (Print) ● ISSN 1785 0037 (Online)
DOI: http://dx.doi.org/10.15666/aeer/1705_1170111716

[61] Zhang, J. J., Gurkan, Z., Jorgensen, S. E. (2010): Application of eco-exergy for assessment of ecosystem health and development of structurally dynamic models. – Ecological Modelling 221(4): 693-702.
[62] Zhang, L., Liu, J. T., Zhang, D. W., Luo, L. G., Liao, Q. G., Yuan, L. J., Wu, N. C. (2018): Seasonal and spatial variations of microcystins in Poyang Lake, the largest freshwater lake in China. – Environmental Science and Pollution Research 25(7): 6300-6307.
[63] Zhang, L. L., Yin, J. X., Jiang, Y. Z., Wang, H. (2012): Relationship between hydrological conditions and vegetation communities in Poyang Lake national nature reserve of China. – Advance in Water Science 23(6): 768-775.
[64] Zhao, X. F., Tong, P. H. (2013): Ecosystem services valuation based on land use change in a typical waterfront town, Poyang Lake basin, China. – Progress in Environmental Protection and Processing of Resource 295: 722-725.

http://www.aloki.hu ● ISSN 1589 1623 (Print) ● ISSN 1785 0037 (Online)
DOI: http://dx.doi.org/10.15666/aeer/1705_1170111716

WATER QUALITY EVALUATION AND TREND ANALYSIS OF HUNHE RIVER BASIN IN THE UPSTREAM OF DAHUOFANG RESERVOIR

YAN, B.* – LIU, Y. T. – WANG, T. L. – JIANG, X. H.

Shenyang Agricultural University, No. 120, Dongling Road, Shenhe District, Shenyang 110866, Liaoning Province, China

**Corresponding author*
e-mail: 1993500019@syau.edu.cn; phone: +86-158-0246-3828; fax: +86-024-8848-7134

(Received 22nd Apr 2019; accepted 12th Jul 2019)

Abstract. Dahuofang Reservoir is an important drinking water source. Hunhe, Suzihe and Shehe are three main input rivers, the water quality of which directly affects the water safety. Traditional water quality analysis often adopts a single analysis method, which can only judge the rising or falling trend and trend degree of a certain parameter. The calculation process of multi-section and multi-index trend analysis is quite complicated with a large workload. Thus, in this paper, Nemerow index evaluation method was used to evaluate the water quality, 24 indicators being screened to 8, greatly reducing calculating workload. Then, trend analysis was made by seasonal Kendall test method. The results show that the Nemerow indices of TN in the three river sections were 6.94, 6.68 and 6.30, exceeding 38.8%, 33.6% and 26% of serious pollution standard (5.0) respectively, and with a highly significant upward trend. Those of fecal coliform were 17.42, 3.12 and 2.79 respectively. Beizamu section was seriously polluted, exceeding 248.4% of serious pollution standard (5.0). Gulou section belonged to heavy pollution, exceeding 4% of standard (3.0). Taigou section was also polluted, exceeding 39.5% of standard (2.0). Therefore, effective measures should be taken to control TN and fecal coliform concentrations in the three sections.
Keywords: *water pollution, indicator screening, Nemerow index evaluation, seasonal Kendall test*

Introduction

According to the Chinese Water Resources Bulletin 2017, the per capita water resource amounts to only 2300 m^3 in China, only a quarter of the world average, belonging to water shortage country. With the development of industry, acceleration of urbanization and the expansion of population, China face with a very severe environmental situation. Class I to III water quality section of the main watershed of the country accounts for 67%, while inferior V accounts for 12.9%. Among which, the Haihe River Basin is a serious pollution, and the Yellow River, Huaihe and Liaohe Basins are moderately polluted (Ministry of Water Resources, 2017).

In the 1960s, under rapid industrial development, China ignored the protection of the ecological environment, causing different levels of environmental pollution and ecological damage, resulting in frequent occurrence of water pollution accidents. The obvious increasing trend of water pollution accidents is a direct threat to the security of drinking water supply. Water pollution has become a major obstacle on the road of sustainable development in China. In the 19th National Congress of CPC, it was clearly pointed out that we should strengthen the construction of water resources and other infrastructure, adhere to the construction of ecological civilization, create a good living environment for the people, and contribute to the global ecological security. River water quality assessment is the most important basic work in the process of water environment management and improvement. Therefore, the evaluation of river water quality and the

http://www.aloki.hu ● ISSN 1589 1623 (Print) ● ISSN 1785 0037 (Online)
DOI: http://dx.doi.org/10.15666/aeer/1705_1171711729

analysis of the trend of water quality are of great significance to the control of water environmental pollution, the construction of ecological civilization and the guarantee of ecological security.

At present, the commonly used water quality evaluation methods include single factor evaluation method, index evaluation method, fuzzy evaluation method, artificial neural network evaluation method, grey clustering method and so on. The single factor evaluation method is to evaluate each water quality monitoring indicators in the water separately, and determine the comprehensive water quality level in the measured area according to the level of the worst individual water quality indicators. The evaluation method is simple to operate (Yin, 2008). The index evaluation method is generally divided into Nemerow index method, comprehensive pollution index evaluation method, water pollution index method and so on (Liu, 2010). The index evaluation method selects the indexes and evaluation criteria according to the use of water, so as to obtain the index value of a single water quality indicator. If a comprehensive evaluation is required, the weight of each indicator needs to be determined to calculate the water quality index, and the water quality evaluation is performed (Liu, 2016). The fuzzy evaluation method is to convert the qualitative analysis into quantitative calculation by the membership degree theory of fuzzy mathematics, and evaluate the water quality grade. This method combines different weight determination methods to avoid the subjectivity of the selection of weight coefficients, making the evaluation results more reasonable, but the calculation process is more complicated (Pan, 2002). Artificial neural network is a complex nonlinear science. It is introduced into the field of water quality assessment, which can fully utilize the high-speed computing power, learning ability and fault tolerance of neural networks, improve the accuracy of water quality evaluation, and avoid human factors in weight selection. However, this method requires a large amount of complete data, and the more complete the data, the higher the accuracy. The gray clustering method is based on the whitening function possessed by the clustering index of different clusters, and the clustering objects are summarized to find the maximum clustering coefficient. The clustering sample level is the water quality level. This method is used for clustering weighting by judging the grey, whitening degree of the system and the comprehensive influence of various pollution indicators, to make the weight determination method more reasonable (Yuan, 2003).

Huang (2013) and Ma (2014) evaluated the water quality of Dahuofang Reservoir in Liaoning Province by using fuzzy evaluation method and BP neural network method respectively, and drew the conclusion that the water quality in the reservoir area was class II level, while in Hunhe River and Suzihe River were all class III level and there was a certain eutrophication risk. It is mainly caused by livestock and poultry breeding, fertilizer use and sewage discharge. Zhou (2015) used the grey clustering evaluation method based on index transformation value to evaluate the water quality of the study area, which overcomes the shortcomings of randomness, ambiguity and uncertainty due to multi-index coupling in the calculation process. After verification, the results are reasonable and accurate. But in the verification process, this method only focuses on the water quality of the study area. Whether it can be popularized or applied remains to be verified. Luo and Wu (2016) put forward the improved Nemerow index evaluation method, in addition to considering the weight of each pollution index; we also pay special attention to the monitoring factors with higher weight to make comprehensive evaluation of water quality. The Nemerow index method has a simple mathematical process and is easy to calculate. It can be used to understand whether the water quality

http://www.aloki.hu ● ISSN 1589 1623 (Print) ● ISSN 1785 0037 (Online)
DOI: http://dx.doi.org/10.15666/aeer/1705_1171711729

meets the requirements. Therefore, the Nemerow index method is widely used in water quality evaluation. However, there are still some shortcomings in the classification of water quality, such as being affected by human factors, and no strict corresponding relationship between this division standard and the national standard level. Guan (2017) proposed pollution index method based on the CRITIC weight, and built a water quality evaluation model. Using CRITIC method to determine the weight takes into account the difference and conflict between the indicators on the weight, is an improvement of the entropy weight method, can objectively determine the weight value. This method overcomes the one-sided problem of single factor evaluation, and the calculation process of weight determination is relatively simple. But the method is more dependent on water quality monitoring results.

For water quality trend analysis, the commonly used statistical test methods include seasonal Kendall test, Daniel test, Spearman rank correlation coefficient method, etc. (Gao, 2013). The seasonal Kendall test is a generalization of the Mann-Kendall test (Mann, 1945; Kendall, 1975). In recent years, its calculation process has been gradually improved and applied to the trend analysis of water quality of major rivers. The results are scientific and reasonable. Although this method can determine the rise and fall tendency and trend degree of water quality parameters, it cannot reflect the result of water quality evaluation. Meng (2015) used the seasonal Kendall test to analyze the trend of water quality in the main stream of Minjiang River, pointed out the change trend of the four indicators of chemical oxygen demand (COD), five days biochemical oxygen demand (BOD_5), total phosphorus (TP) and ammonia nitrogen, analyzed the reasons, and proposed corresponding treatment measures. However, the reasons for selecting these four indicators for analysis were not explained. Pang (2017) analyzed the variation trend of groundwater quality in Guanghua Basin using the Spearman rank correlation coefficient method. This method is relatively mature at present, but it can only judge the variation trend from the past to the present and cannot represent the real change of the pollution factor in the future period. Guo (2017) used Daniel test method to analyze the trend of water quality of Nanhai reservoir in Zhangwu. The rank correlation coefficient for statistical tests was compared with Spearman rank correlation coefficient to analyze the variation trend. However, this method requires sufficient available data, while the seasonal Kendall test is not affected by missing measured values. At present, for the study of water quality analysis, people often only pay attention to unilateral water quality evaluation or trend analysis, ignoring the shortcomings of the multi-section and multi-index trend analysis process. Therefore, in this paper we combined water quality evaluation with seasonal Kendall test method. According to the evaluation results, the indexes to be evaluated were selected, which greatly reduced the calculation amount, made up for the deficiency that seasonal Kendall test cannot reflect the evaluation results, and reflected the changing trend of river water quality more intuitively.

Materials and methods

Materials

Dahuofang Reservoir is an important drinking water source of Shenyang, Fushun, Anshan, Liaoyang and some other central cities. It belongs to zonal-valley-type reservoir, about 35 km long in west-east direction, 4 km wide at its widest point, and 0.3 km wide at its narrowest point at the water surface. The project is a large-type

http://www.aloki.hu ● ISSN 1589 1623 (Print) ● ISSN 1785 0037 (Online)
DOI: http://dx.doi.org/10.15666/aeer/1705_1171711729

reservoir with a maximum depth of 37 m, maximum water storage area of 114 km^2, and a maximum storage capacity of 2.268×10^9 m^3. The annual average water evaporation in the basin is about 1100~1600 mm (according to the 20 cm scale evaporative dish). The average annual inflow is about 789.36 m^3/s, and its wet season is from April to September. The basin above Dahuofang Reservoir belongs to Hunhe River Basin, Suzihe River Basin and Shehe River Basin, and belongs to the mixed area of agriculture and forestry. In Hunhe River Basin, there are 3.45×10^5 population in Qingyuan County and 3.94×10^4 hm^2 cultivated area. The domestic sewage reaches 1.74×10^4 t/d, due to the existence of chemical mines such as Qingyuan Limestone Mine, lead to the industrial sewage reaches 1.32×10^4 t/d, and the total amount of sewage in the county is 3.06×10^4 t/d. The annual application amount of chemical fertilizer in Qingyuan County is 1.8×10^4 t, pesticide application amount is 280 t, and the dosage of film is 200 t, which caused the loss of most of the chemical substances and thus polluted the water environment. In Suzihe River Basin, there are 3.08×10^5 population in Xinbin County and 5.10×10^4 hm^2 cultivated area. The sewage can be basically treated by a sewage treatment plant. The domestic sewage treatment capacity reaches 1.61×10^4 t/d. In this basin, the pesticide application amount is 2.55 kg/hm^2, lower than the national standard. In Shehe River Basin, there are3.83×10^4 population and 4.78×10^3 hm^2 cultivated area. It is a river with the best water quality in the upstream rivers since there is no large-scale enterprise. The three rivers upstream of Dahuofang Reservoir are the main water sources of the reservoir, with Hunhe River accounting for 52.7% of the water storage, Suzihe River accounting for 37.1%, and Shehe River accounting for 10.2% (Dahuofang Reservoir Chronicles, 2006). The location map of Dahuofang Reservoir and upstream watershed is shown in *Figure 1*.

Figure 1. *Location map of Dahuofang Reservoir and upstream watershed*

In this study, the Beizamu section on Hunhe River, the Gulou section on Suzihe River and the Taigou section on Shehe River were taken as the main monitoring sections on the three input rivers upstream of Dahuofang Reservoir. The water quality monitoring data from 2003 to 2015 were analyzed. The original data were obtained from the monthly average water quality monitoring data of the three monitoring sections from April 23, 2003 to December 7, 2015 provided by the Fushun Hydrology Bureau of Liaoning Province.

The water quality of the three sections ranged from good to bad: Taigou section > Gulou section > Beizamu section. In 2015, there are six indicators that exceed the standard of the national surface water class II in Beizamu section: total nitrogen

http://www.aloki.hu ● ISSN 1589 1623 (Print) ● ISSN 1785 0037 (Online)
DOI: http://dx.doi.org/10.15666/aeer/1705_1171711729

(TN) 100%, fecal coliform count 100%, dissolved oxygen (DO) 23.3%, ammonia nitrogen 22%, five-day biochemical oxygen demand (BOD_5) 16.7%, total phosphorus (TP) 10%. There are two indicators that surpass the standard of the national surface water class II in Gulou section: total nitrogen (TN) 100%, fecal coliform count 5%. There are two indicators that exceed the standard of the national surface water class II in the Taigou section: total nitrogen (TN) 100%, dissolved oxygen (DO) 1.7%. The National Surface Water Quality (NSWQ) classification standards (Ministry of Environmental Protection, 2002) are presented in *Table 1*.

Table 1. *Chinese national surface water quality classification standards (GB3838-2002)*

Indicators	Classification				
	I	II	III	IV	V
DO ≥ (mgL^{-1})	7.5	6	5	3	2
Permanganate ≤ (mgL^{-1})	2	4	6	10	15
BOD_5 ≤ (mgL^{-1})	3	3	4	6	10
COD ≤ (mgL^{-1})	15	15	20	30	40
Ammonia Nitrogen ≤ (mgL^{-1})	0.15	0.5	1.0	1.5	2.0
TN ≤ (mgL^{-1})	0.2	0.5	1.0	1.5	2.0
TP ≤ (mgL^{-1})	0.02	0.1	0.2	0.3	0.4
Fecal Coliform Count ≤ (10^{-1} mpn 100 mL^{-1})	200	2000	10,000	20,000	40,000

Methods

In the study of water quality trend analysis, people often use only a certain trend analysis method to analyze the water quality of a river, and then get the trend of water quality change. However, in this paper, the trend of water quality in 3 sections of three rivers in the upstream of Dahuofang Reservoir will be analyzed. There are 8 indicators to be evaluated for each section, altogether 24 indexes. If the seasonal Kendall test method is used alone, the calculation amount will be large. The Nemerow index method is simple in calculation and widely used in water quality assessment. Therefore, the Nemerow index evaluation method was used to evaluate the water quality. According to the evaluation results, the polluted indicators were screened out. The seasonal Kendall test was applied to the selected indicators, which reduced the amount of calculation and made up for the shortcomings of seasonal Kendall test method which can not reflect the evaluation results. Thus, the trend analysis results were obtained, which was also the innovation of this paper.

Nemerow index evaluation method

The Nemerow index evaluation method is based on the single factor index evaluation method to evaluate water quality. The single factor index evaluation method is a method to determine the water quality category by comparing the measured concentration of a certain pollution index with the evaluation standard of the pollution index. Each water quality monitoring indicator is evaluated separately, and the category of the worst single water quality index is selected to determine the comprehensive water quality category of the measured area. The main pollution factors in river water could be determined by single factor index evaluation. The evaluation index F_i is calculated as follows:

http://www.aloki.hu ● ISSN 1589 1623 (Print) ● ISSN 1785 0037 (Online)
DOI: http://dx.doi.org/10.15666/aeer/1705_1171711729

(1) For the water quality factors whose evaluation criteria are constant values, the evaluation index is calculated by *Equation 1*.

$$F_i = \frac{C_i}{C_0} \quad \text{(Eq.1)}$$

where F_i is the evaluation index of monitoring indicator i in river water, C_i is the measured concentration of indicator i (mg L^{-1}), and C_0 is the evaluation criteria of indicator i.

(2) For the water quality factors whose evaluation standards are interval values (such as PH value), the evaluation index is calculated by *Equations 2* and *3*.

$$P_{pH} = \frac{7.0 - pH}{7.0 - pH_{sd}} \quad \text{If } pH \le 7.0 \quad \text{(Eq.2)}$$

$$P_{pH} = \frac{pH - 7.0}{pH_{su} - 7.0} \quad \text{If } pH \ge 7.0 \quad \text{(Eq.3)}$$

Herein, P_{pH} is the evaluation index of pH, dimensionless; pH is the measured value; pH_{sd} is the lower limit value of the standard; pH_{su} is the upper limit value of the standard.

When Fi is less than 1, it means the river water body is not polluted. When F_i is greater than 1, it means the river water body has been polluted. The greater the F_i is, the more serious the pollution is (Luo and Zhang, 2016). In particular, the situation of dissolved oxygen (DO) is just the opposite.

For Nemerow index method, firstly, a series of Fi values of indicators were calculated by single-factor evaluation method based on the ratio of measured concentration and standard value of selected water quality indicators; then Nemerow pollution index was obtained according to the maximum and average value of Fi. Compared with the corresponding grade standard index (Luo and Wu, 2016), the evaluation grade can be determined to judge the pollution situation. The calculation method is shown in *Equation 4*.

$$P = \left[\frac{(F_{\max})^2 + \left(\bar{F}\right)^2}{2} \right]^{1/2} \quad \bar{F} = \frac{1}{n}\sum_{i=1}^{n} F_i \quad \text{(Eq.4)}$$

where P is the Nemerow index of river water quality monitoring indicators; F_{max} is the maximum F_i value of indicator i; and $\bar{F}$ is the average of F_i of indicator i. Particularly, for DO concentration index, the F_{max} in the formula should be changed to F_{min}, that is, the minimum F_i value of indicator i.

It can be seen that Nemerow index is a comprehensive evaluation of river water quality based on the single-factor index method, which is different from the traditional single-factor index method. On the premise of judging pollution according to the

http://www.aloki.hu ● ISSN 1589 1623 (Print) ● ISSN 1785 0037 (Online)
DOI: http://dx.doi.org/10.15666/aeer/1705_1171711729

NSWQ, the possible pollution indicators are evaluated, so that the number of water pollution indicators can be effectively deleted to reduce the calculation workload of the seasonal Kendall test.

Seasonal Kendall test

The seasonal Kendall test is a method based on the Mann-Kendall test, which is used to analyze the variation trend of water quality over the years with incomplete measured water quality data, low accuracy of data or regularly changing values with seasons (Onoz, 2003). The test statistic (S) is calculated by *Equations 5* and *6*.

$$\mathrm{sgn}(x_j - x_i) = \begin{cases} 1 & x_j - x_i > 0 \\ 0 & x_j - x_i = 0 \\ -1 & x_j - x_i < 0 \end{cases} \quad \text{(Eq.5)}$$

$$S_p = \sum_{i=1}^{n-1} \sum_{j=i+1}^{n} \mathrm{sgn}(x_j - x_i) \quad \text{(Eq.6)}$$

Herein, x_i and x_j are the measured values of pollutant concentration in month p each year; S_p is the S value in month p, p = 1, 2, ...12.

The null hypothesis H_0 of seasonal Kendall test is a random variable, independent of each other in time. Assuming that the water quality data over 12 months have the same probability distribution, S_p approximately obeys the normal distribution under zero assumption. The expression of its mean and variance are shown in *Equations 7* and *8*.

$$\mathrm{E}(S_\mathrm{p}) = 0 \quad \text{(Eq.7)}$$

$$Var(S_p) = \frac{n_p(n_p - 1)(2n_p + 5) - t_p(t_p - 1)(2t_p + 5)}{18} \quad \text{(Eq.8)}$$

where n_p and t_p are the number of measured values and missed values at month p, respectively.

For the whole p months, $S = \sum_{p=1}^{12} S_p$, $Var(S) = \sum_{p=1}^{12} Var(S_p)$. If n is no less than 10, and S satisfies the normal distribution feature, then its standardized variance Z is described as *Equation 9*.

$$Z = \begin{cases} \dfrac{S-1}{[Var(S)]^{1/2}}, S > 0 \\ 0, S = 0 \\ \dfrac{S+1}{[Var(S)]^{1/2}}, S < 0 \end{cases} \quad \text{(Eq.9)}$$

http://www.aloki.hu ● ISSN 1589 1623 (Print) ● ISSN 1785 0037 (Online)
DOI: http://dx.doi.org/10.15666/aeer/1705_1171711729

The calculated Z value is compared with the standard normal distribution table with two-sided confidence levels. If $|Z| \le Z_{\alpha/2}$ at the α level of significance, H_0 should be accepted. According to the relevant research results (Robert, 1984), the critical value of significance level α is 0.1 and 0.01. If $\alpha \le 0.01$, $|Z| \ge Z_{\alpha/2}$, the test is highly significant; if $0.01 \le \alpha \le 0.1$, $|Z| \ge Z_{\alpha/2}$, the test is significant. If S > 0, it shows a significant upward trend; if $S < 0$, it shows a significant downward trend; if $S = 0$, there is no obvious variation trend.

Results

Results of Nemerow index evaluation

The data of the main monitoring sections of three rivers in the upstream of Dahuofang Reservoir from 2003 to 2015 were analyzed. Compared with the NSWQ (GB3838-2002), according to the grade II water quality standard, 8 major pollution indicators per section were screened out, which were DO, permanganate index, BOD_5, Chemical oxygen demand (COD), ammonia nitrogen, TN, TP and fecal coliform. Therefore, there are 24 indicators to be evaluated for the three monitoring sections. According to the measured concentration of each indicator, the F_i value of the corresponding year was obtained, and its average value and maximum value was calculated, thus the Nemerow pollution index was obtained. The results are shown in *Table 2*.

Table 2. *Nemerow pollution index*

Indicators	Beizamu section			Gulou section			Taigou section		
	$\bar{F}$	F_{max}	P	$\bar{F}$	F_{max}	P	$\bar{F}$	F_{max}	P
DO	1.53	1.72	1.63	1.60	1.88	1.75	1.59	1.87	1.73
Permanganate	0.86	1.31	1.11	0.65	1.05	0.87	0.53	0.82	0.69
BOD_5	0.60	1.05	0.86	0.47	0.69	0.59	0.39	0.51	0.45
COD	0.84	0.93	0.89	0.77	0.94	0.86	0.72	0.82	0.77
Ammonia nitrogen	0.76	1.34	1.09	0.47	1.28	0.96	0.41	0.85	0.67
TN	6.05	7.73	6.94	5.25	7.85	6.68	5.17	7.27	6.30
TP	0.44	0.98	0.76	0.35	0.93	0.70	0.29	0.55	0.44
Fecal coliform	5.89	23.93	17.42	1.62	4.11	3.12	1.40	3.69	2.79

If the P value of DO is greater than 1, it is indicated that dissolved oxygen is a clean index. By comparing with the classification criteria for pollution grade of Nemerow water quality index (see *Table 3*), the clean indicators were excluded, the indicators belonging to different degrees of pollution were retained, and the pollution indicators of the three sections was reduced from 24 to 8 (see *Table 4*).

Table 3. *Classification criteria for pollution grade of Nemerow water quality index*

P	< 1	1-2	2-3	3-5	> 5
Water quality level	Clean	Light pollution	Pollution	Heavy pollution	Serious pollution

http://www.aloki.hu ● ISSN 1589 1623 (Print) ● ISSN 1785 0037 (Online)
DOI: http://dx.doi.org/10.15666/aeer/1705_1171711729

Table 4. *Screened indicators and pollution levels*

Sections	Indicators	P Value	Pollution Level
Beizamu	Permanganate	1.11	Light pollution
	Ammonia nitrogen	1.09	Light pollution
	TN	6.94	Serious pollution
	Fecal coliform	17.42	Serious pollution
Gulou	TN	6.68	Serious pollution
	Fecal coliform	3.12	Heavy pollution
Taigou	TN	6.30	Serious pollution
	Fecal coliform	2.79	Pollution

It is obvious that:

(1) In Beizamu section, the Nemerow indexes of TN and fecal coliform were 6.94 and 17.42, respectively, which belonged to serious pollution. The Nemerow indexes of permanganate index and ammonia nitrogen were 1.11 and 1.09, respectively, which belonged to light pollution. Other indicators were all clean indicators;

(2) In Gulou section, the Nemerow index of TN was 6.68, which belonged to serious pollution. The Nemerow index of fecal coliform was 3.12, which was a heavy pollution. Others were all clean indicators;

(3) In Taigou section, the Nemerow index of TN was 6.30, which was a serious pollution. The Nemerow index of fecal coliform was 2.79, belonging to pollution. Others were all clean indicators.

In order to further verify the variation trend of the above pollution indicators, the seasonal Kendall test was conducted on the selected 8 indicators.

Results of seasonal Kendall test

According to the evaluation results of Nemerow index method, seasonal Kendall test was performed on the following indicators: permanganate index, ammonia nitrogen concentration, TN and fecal coliform in Beizamu section; TN and fecal coliformt in Gulou section; TN and fecal coliform in Taigou section. The test results are shown in *Table 5*.

The test results showed that Z values of TN in the three sections were 2.945, 4.951 and 5.133, respectively, with a highly significant upward trend, while the other indicators showed no significant variation trend.

Discussion

The above analysis results reveal that:

(1) TN and fecal coliform in Beizamu section belong to serious pollution, exceeding the pollution standards (the minimum standard index is 5.0) by 38.8% and 248.4%, respectively. Permanganate index and ammonia nitrogen are light pollution, exceeding 31% and 34% of the minimum pollution standards (1.0), respectively. These four pollution indicators are consistent with the main pollution indicators determined by Huang (2013) using the fuzzy evaluation method. Firstly, the Hunhe River Basin where the Beizamu section is located has a large population (3.45×10^5 people), and a large amount of domestic sewage (1.74×10^4 t/d), which leads to the excessive number of

http://www.aloki.hu ● ISSN 1589 1623 (Print) ● ISSN 1785 0037 (Online)
DOI: http://dx.doi.org/10.15666/aeer/1705_1171711729

fecal coliform bacteria. Secondly, the upstream industrial mines (e. g. Qingyuan Limestone Mine) still exist, and the industrial wastewater discharge is large (1.32×10^4 t/d) and the treatment is not timely, resulting in slight pollution of permanganate index and ammonia nitrogen. Pang (2017) also mentioned the reason why the ammonia nitrogen concentration exceeded the standard in the analysis of groundwater quality in Guanghua Basin. Thirdly, the cultivated land area of Hunhe River Basin is relatively large (3.94×10^4 hm^2). Due to the large use of pesticides and fertilizers, the TN exceeds the limit, which leads to the risk of eutrophication in water.

Table 5. *Seasonal Kendall test results*

Sections	**Indicators**	**S**	**VarS**	**Z**	α **= 0.1** $Z_{\alpha/2}$=1.645	α **= 0.01** $Z_{\alpha/2}$=2.576	**Water quality trends**
Beizamu	Permanganate	28	1878.0	0.62	<	<	No trend
	Ammonia nitrogen	-61	1414.0	-1.596	<	<	No trend
	TN	114	1472.7	2.945	>	>	Highly significant increase
	Fecal coliform	43	1766.0	0.999	<	<	No trend
Gulou	TN	191	1472.7	4.951	>	>	Highly significant increase
	Fecal coliform	-69	1766.0	-1.618	<	<	No trend
Taigou	TN	198	1472.7	5.133	>	>	Highly significant increase
	Fecal coliform	-41	1822.0	-0.937	<	<	No trend

(2) TN in Gulou section belongs to serious pollution, exceeding the pollution standard (the minimum standard index is 5.0) by 33.6%. Fecal coliform belongs to heavy pollution, exceeding 4% of the minimum pollution standard (3.0). This is due to the fact that the Suzi River Basin, where the Gulou section is located, has a large population (3.08×10^5 people) and a large amount of domestic sewage (1.6×10^4 t/d). However, there are sewage treatment plants in the area, which can discharge domestic sewage after treatment. Therefore, the quantity of fecal coliform is significantly less than that of Beizamu section, but there is still a certain degree of pollution. The number of fecal coliforms in the Aibihu Lake Wetland Nature Reserve has also shown a significant downward trend after the establishment of sewage treatment plants and the treatment of domestic sewage to meet the discharge standards (Ren, 2011). In addition, the cultivated land area in the Suzi River Basin (5.1×10^4 hm^2) is larger than in the Hunhe River Basin, and the application of pesticides and fertilizers is more, resulting in serious pollution of TN.

(3) TN in Taigou section belongs to serious pollution, exceeding the pollution standard (the minimum standard index is 5.0) by 26%. Fecal coliform belongs to pollution, exceeding 39.5% of the minimum pollution standard (2.0). This is due to the population of Shehe River Basin where the Taigou section is located is small (38,381 people), the cultivated land area is also small (4776.5 hm^2), and there is no

http://www.aloki.hu ● ISSN 1589 1623 (Print) ● ISSN 1785 0037 (Online)
DOI: http://dx.doi.org/10.15666/aeer/1705_1171711729

large-scale industrial enterprise in the upstream. Therefore, compared with the Hunhe River Basin and the Suzi River Basin, the water quality is better. This conclusion is consistent with the research result of Shi (2004). However, because of the discharge of domestic sewage and the use of pesticides and fertilizers, the TN and fecal coliforms are still polluted to varying degrees.

(4) TN concentration in the three sections of Beizamu, Gulou, Taigou all show a highly significant upward trend, while the other indicators show no significant change trend. Fang (2017) analyzed the change trend of TN concentration in the Beizamu section of Hunhe River and drew the same conclusion. This change is associated with the large-scale application of chemical fertilizers in the upstream farmland. Among the fertilizers applied in the study area, the nitrogen content accounts for 49.5% of the total content (Tang, 2016). The large amount of chemical fertilizers has resulted in nitrogen residue in soil, and with the surface runoff flowing into rivers. The TN concentration has a highly significant upward trend due to the long-term excess of nitrogen. The interannual variation curves of the TN concentration in the three sections from 2003 to 2015 (*Fig. 2*) also shows a significant upward trend, which is consistent with the above analysis conclusion.

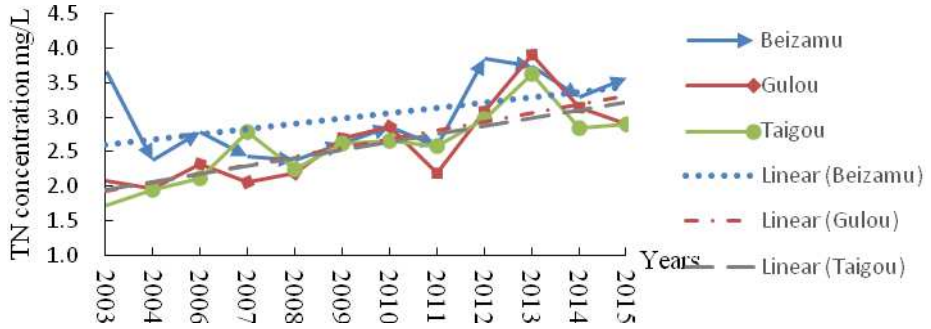

Figure 2. *Interannual variation curves and linear analysis of total nitrogen concentration in three sections from 2003 to 2015*

Conclusions

Based on the monitoring data of water quality in the upstream of Dahuofang Reservoir from 2003 to 2015 and according to the NSWQ, the water quality evaluation and water quality variation trend analysis were carried out to Hunhe River, Suzihe River and Shehe River, the three major rivers upstream of Dahuofang Reservoir. The Nemerow index method was used to preliminarily evaluate the river water quality at the three sections of Beizamu, Gulou and Taigou. 8 indicators of each section, totaling 24 indicators, were compared with the pollution grade classification standard of Nemerow water quality index. Among the original 24 pollution indicators, according to the evaluation results, the clean indicators were eliminated, the pollution indicators of different degrees were retained, and the indicators were reduced from 24 to 8. Then seasonal Kendall test method was applied to test the 8 indicators, and to predict the variation trend of water quality.

The results show that the order of water quality of the three sections is: Taigou section > Gulou section > Beizamu section. The TN concentrations in the three sections

http://www.aloki.hu ● ISSN 1589 1623 (Print) ● ISSN 1785 0037 (Online)
DOI: http://dx.doi.org/10.15666/aeer/1705_1171711729

belong to serious pollution and have a highly significant upward trend. The fecal coliform floras of the three sections are polluted to varying degrees, and the pollution in Beizamu section is the most serious. Therefore, the application of pesticides and fertilizers should be reduced as far as possible, non-point source pollution should be controlled, and eutrophication of water body should be prevented. At the same time, effective measures must be taken to ensure that domestic sewage treatment meets the discharge standards.

REFERENCES

[1] Dahuofang Reservoir Chronicles (2006): The Authority of Dahuofang Reservoir in Liaoning Province. – China Water & Power Press, Beijing.
[2] Fang, X. (2017): Research on water quality change trend based on seasonal Kendall testing method. – Heilongjiang Water Resources 3(2): 55-58.
[3] Gao, W., Chen, Y., Xu, M. (2013): Trend and driving factors of water quality change in lake Fuxian (1980-2011). – Journal of Lake Sciences 25(5): 635-642.
[4] Guan, X. J., Liu, W. K., Hu, D. (2017): Application of CRITIC-based pollution index in water quality assessment of Qingyi River. – Water Resources and Power 35(8): 49-52.
[5] Guo, X. S. (2017): Analysis of water quality trend of Zhanwu South China Sea reservoir from 2010 to 2016. – Haihe River Water Conservancy 4: 17-19.
[6] Huang, R., Han, L. X., Zhang, H. (2013): Water quality evaluation of Dahuofang Reservoir based on fuzzy evaluation and AHP method. – Yellow River 35(4): 32-34.
[7] Kendall, M. G. (1975): Rank Correlation Methods. 4th Ed. – Charles Griffin, London.
[8] Liu, C. H., Xu, L. G., Gao, H. Y. (2010): River water quality assessment methods and their research progress. – Journal of Hohai University 38(2): 290-293.
[9] Liu, L. H., Wu, L. X., Wu, J. P. (2016): Review on surface water quality index assessment method in foreign countries. – Water Resources Protection 32(1): 86-90.
[10] Luo, F., Wu, G. R., Wang, C. (2016): Application of Nemerow Pollution Index Method and single-factor evaluation method in water quality evaluation. – Environment and Sustainable development 5: 87-89.
[11] Luo, X. Q., Zhang, Q., Chen, L. Y., Meng, Q. X. (2016): Comprehensive water quality assessment of upper Nanminghe River in Guiyang based on single-factor index method. – Groundwater 38(1): 80-82.
[12] Ma, L. L., Zhou, L. F., Wang, T. L. (2014): Water quality evaluation of Dahuofang Reservoir based on BP neural network. – Journal of Shenyang Agricultural University 45(5): 637-640.
[13] Mann, H. B.(1945): Nonparametric tests against trend. – Econometrica 13(3): 245-259.
[14] Meng, C. X., Wang, X. B., Huang, Y.(2015): Analysis of water quality tendency of the mainstream of Minjiang river with Seasonal Kendall Method. – Sichuan Environment 34(06): 87-93.
[15] Ministry of Environmental Protection (2002): Environmental Quality Standards for Surface Water, GB3838-2002, P.R.C. – China Environmental Science Press, Beijing.
[16] Ministry of Water Resources of the People's Republic of China (2017): China Water Resources Bulletin. – Ministry of Water Resources Information Center, Beijing.
[17] Onoz, B., Bayazit, M. (2003): The power of statistical tests for trend detection. – Turkish Journal of Engineering and Environmental Sciences 27: 247-251.
[18] Pan, F., Fu, Q., Liang, C. (2002): Application research of fuzzy comprehensive evaluation in comprehensive evaluation of water environment quality. – Environmental Engineering 20(2): 58-61.
[19] Pang, Y., Zhang, M. Z., Pang, Z. Y. (2017): Analysis and evaluation of groundwater quality in Guanghua basin. – Water Resources and Power 35(11): 40-43+35.

http://www.aloki.hu ● ISSN 1589 1623 (Print) ● ISSN 1785 0037 (Online)
DOI: http://dx.doi.org/10.15666/aeer/1705_1171711729

[20] Ren, J. L., Jing, H. L. (2011): Analysis and evaluation of water quality of Aibihu Lake Wetland Nature Reserve. – Journal of Arid land resources and Environment 25(5): 154-157.
[21] Robert, M. H., Slack, J. R. (1984): A nonparametric trend test for seasonal date with serial dependence. – Water Resources Research 20(6): 727-732.
[22] Shi, Y. Q., Sun, X. Y. (2004): Study on Water Quality Ecology of Dahuofang Reservoir in Liaoning Province. – Chinese Society of Environmental Sciences, Shenyang.
[23] Tang, X. N. (2016): Analysis on the Source of Water Pollution in the Upper River of Dahuofang Reservoir. – Beijing University of Science and Technology, Beijing.
[24] Yin, H. L., Xu, Z. X. (2008): Comparative study of river water quality assessment methods. – Resources and Environment in the Yangtze Basin 17(5): 729-733.
[25] Yuan, D., Fu, D. Y. (2003): Application of cluster analysis to water environment quality assessment. – Journal of Sichuan Institute of Light Industry and Chemical Technology 16(3): 50-55.
[26] Zhou, Y. C., Li, H. (2015): Application of grey clustering method based on index transformation value in water quality evaluation. – Gansu Water Resources and Hydropower Technology 1: 6-8.

http://www.aloki.hu ● ISSN 1589 1623 (Print) ● ISSN 1785 0037 (Online)
DOI: http://dx.doi.org/10.15666/aeer/1705_1171711729

FRACTIONS AND TEMPORAL AND SPATIAL DISTRIBUTION OF PHOSPHORUS IN THE SEDIMENTS OF SANCHA LAKE

LI, Y.[1*] – ZHANG, J. Q.[1] – GONG, Z. L.[2] – FU, W. L.[3] – WU, D. M.[3]

[1]*Faculty of Geosciences and Environmental Engineering, Southwest Jiaotong University, No. 111 North 1st Section, Erhuan Road, Chengdu, China (phone: +86-135-1810-8466; fax: +86-028-8763-4616)*

[2]*School of Food and Biological Engineering, Xihua University, Chengdu 610039, China*

[3]*Jianyang Environmental Monitor Station, Jianyang, Sichuan 641400, China*

**Corresponding author*
e-mail: liyong@swjtu.edu.cn

(Received 22nd Apr 2019; accepted 12th Jul 2019)

Abstract. The fraction and distribution characteristics of phosphorus in the sediments of Sancha Lake were studied using the SMT Phosphorus fraction method and its influencing factors were discussed. According to the research results, total phosphorus (TP) content in the sediments was 270.00-3,722.80 $\mu g \cdot g^{-1}$, the organophosphorus (OP) content was 64.00-774.43 $\mu g \cdot g^{-1}$, the inorganic phosphorus (IP) content, a main phosphorus fraction, was 164.00-3,006.99 $\mu g \cdot g^{-1}$, accounting for about 69.32% of TP, the HCl-P content, a main phosphorus fraction of IP, was 125.00-2,474.04 $\mu g \cdot g^{-1}$, accounting for about 69.19% of IP, and the NaOH-P content was less, i.e. 51.00-689.72 $\mu g \cdot g^{-1}$, accounting for about 30.73% of IP. Different phosphorus fractions had obvious temporal and spatial variation; all the sampling sites showed a general trend where the phosphorus fraction content was higher in winter and lower in summer, similar in spring and autumn. The content of organic matter in the sediments had significant correlation with OP, NaOH-P had significant correlation with Fe in the sediments, between HCl-P in the sediments had significant correlation with Ca, APA had significant positive correlation with OP. However, the pH, TN, dissolved oxygen and temperature had no significant correlation with various phosphorus fractions.
Keywords: *phosphorus fractions, spatial and temporal distribution, sediment, Sancha Lake, eutrophication*

Introduction

Phosphorus is the main restrictive factor (Zhang et al., 2012) of Lake Eutrophication, and most phosphorus nutrient salt entering into lakes will eventually be stored in the sediments under various conditions, forming endogenous pollution (Zhu et al., 2004). The fraction of phosphorus in the sediment has an important effect on its migration and transformation mechanism (Fan et al., 2010; Hupfer et al., 1995; Chuai et al., 2014; Li et al., 2014). The distribution characteristics of phosphorus in the sediments have already been confirmed to have a direct relation to the internal load of the lake, and different fractions and contents of phosphorus in the sediments play different roles in Lake Eutrophication (Yang et al., 2013; Zhou et al., 2013). Therefore, the analysis of different fractions of phosphorus in the sediments of a lake and their temporal and spatial distribution characteristics is of great significance to further research Lake Eutrophication. This paper mainly studied the fractions, contents, temporal and spatial distribution of phosphorus in the sediments of Sancha Lake, and discussed the factors influencing the content distribution of each phosphorus fraction, so as to provide data and theoretical support for further research on the mechanisms of lake eutrophication of Sancha Lake.

http://www.aloki.hu ● ISSN 1589 1623 (Print) ● ISSN 1785 0037 (Online)
DOI: http://dx.doi.org/10.15666/aeer/1705_1173111743

Materials and methods

Brief introduction to study area

Sancha Lake is located in Tianfu New Area of Sichuan Province, east longitude 104°11′16″ to 104°17′16″, north latitude 30°13′08″ to 30°19′56″, its average depth is 8.3 m, and the maximum depth is 32.5 m. The area is under subtropical moist monsoon climate, the annual average temperature is 15.2 to 16.9 °C, and the annual average rainfall is 786.5 mm. Sancha Lake water mainly derives from the Minjiang River which accounts for about 80%, and the rest of about 20% comes from the rainfall and two streams (Tiaodeng River and Longyun River). The drainage area above the dam site is 161.25 km^2, the average runoff depth is 275.1 mm, and the average sediment discharge through surface runoff is 200,000 t. Sancha Lake and its surrounding are an important part of "International Tourism Culture Area with Two Lakes and One Mountain" in Tianfu New Area. Sancha Lake is the source of drinking water for population in Sancha Town. Moreover, it can maintain biodiversity, store water, prevent and control flood, and adjust surface runoff and climate. According to the characteristics of lake and different human activities, Sancha Lake is divided into five functional areas as shown in *Figure 1*: (I) Main runoff area of lake; (II) Highly dense area of original cage culture; (III) Adjacent human activity intensive area; (IV) Relatively dense area of enclosure culture of Dahu Lake; (V) Tail water area of reservoir. According to the monitoring results of many years, the COD_{Cr} and BOD_5 of the waters of Sancha Lake decline year by year, while TN and TP have been rising, the corresponding chlorophyll increases year by year while transparency declines year by year, showing that the eutrophication has been formed in Sancha Lake (Li, et al., 2019).

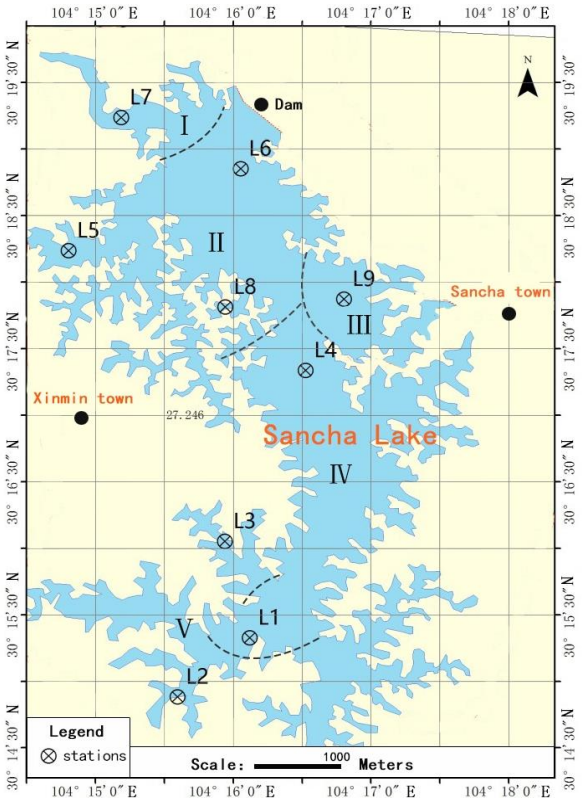

Figure 1. *Sampling sites in the Sancha Lake*

http://www.aloki.hu ● ISSN 1589 1623 (Print) ● ISSN 1785 0037 (Online)
DOI: http://dx.doi.org/10.15666/aeer/1705_1173111743

Sample collection and pretreatment

According to the distribution characteristics of the sediments of Sancha Lake and eutrophication status (Jia et al., 2013), 9 sampling sites as shown in *Figure 1* were selected, and the latitude and longitude of sampling sites were determined by GPS. In January (winter), April (spring), August (summer) and November (autumn) of 2016, the surface sediment at the bottom of Sanch Lake at each sampling site was collected using a grab bucket, then the surface sediment (0-5 cm) was collected using a organic glass column and placed in a clean sealed polyethylene bag. Three parallel samples of each sampling site were collected and mixed as the representative sample of such sampling site, and then they were stored in an ice box at 4 °C and brought back to the lab. One part of the sediment samples was immediately used for isolation of microbes and counting cultivation experiment, and the other part was grinded using a 100-mesh screen after freeze drying, and then packed in a sealed bag for the determination of phosphorus fraction and its physicochemical properties. Meanwhile, the overlying water at the bottom of the sediments of each sampling site was collected using an airtight water sampler for analysis of the index of water environment.

Determination method

The various fractions of phosphorus in the sediments were determined using the SMT chemical continuous extraction method (Ruban et al., 1999, 2001) recommended by European Standards Committee. The contents of TP, IP, OP, NaOH-P and HCl-P in the sediments were determined using the ammonium molybdate spectrophotometric method (Huang et al., 2003) Three parallel samples were determined for each fraction and then their average value was selected. Alkaline phosphatase activity (APA) was determined using the Anupama method (Anupama et al., 2008). The alkaline phosphatase can catalyze and hydrolyze p-nitrophenyl phosphate (p – NPP) to produce steady yellow p-nitrophenol (PNP). Therefore, the production rate of PNP was measured using the colorimetric method, as an index of alkaline phosphatase activity (APA). The specific methods were as follows: Firstly, about 0.5 g of wet sediments was selected and placed in a sterilized reaction tube, then 10 ml of Tris-HCl buffer with the pH of 8.4 and 0.5 $mol \cdot L^{-1}$ concentration was added to the tube and blended well at 37 °C for 1h of reaction, then 2 ml of NaOH solution with 1 mol/L concentration was added to terminate the reaction, supernatant was filtered by centrifugation, 600 nm of solution was selected for colorimetric determination and the result was converted into the activity of dried mud of unit mass, and the PNP solution with different concentration was used to made the standard curve.

Total organic carbon (TOC) in the sediments was determined as per the regulations of On the Determination of Total Organic Carbon in Sediments issued by Chinese GB/T 19145-2003 (General Administration of Quality Supervision, Inspection and Quarantine of China, 2003). The Fe, Al and Ca were determined as per the regulations of Monitoring and Distinguishing Method for Water and Wastewater issued by National Environmental Protection Bureau (State Environmental Protection Administration of China, 2002). The moisture content was determined using the weight-loss method, namely the sediment was put at 105 °C and dried to constant weight. The pH, temperature and electrical conductivity of the overlying water were determined using an HI991301 portable multi-parameter temperature meter, and the dissolved oxygen was determined using an HQ3OD portable dissolved oxygen meter.

http://www.aloki.hu ● ISSN 1589 1623 (Print) ● ISSN 1785 0037 (Online)
DOI: http://dx.doi.org/10.15666/aeer/1705_1173111743

Data analysis

Data analysis was conducted by Excel 2003 software and SPSS19.0. Correlation analysis was conducted using the Pearson correlation analysis to determine the relationship between fractions of phosphorus in the sediments and physicochemical properties.

Results

Physicochemical properties of the sediments and overlying water

The pH of the overlying water ranged from 7.15 to 8.73, averaging 7.53, 7.25, 7.91 and 8.54 in spring, summer, autumn and winter, respectively, alkaline in winter and weakly alkaline in spring, summer and autumn; the temperature ranged from 11.1 °C to 27.6 °C, averaging 18.90 °C, 26.0 °C, 20.9 °C and 13.2 °C in spring, summer, autumn and winter, respectively, with a temperature difference of about 13 °C in winter and summer, and not obvious temperature difference in spring and autumn; the DO ranged from 4.10 to 9.90 $mg \cdot L^{-1}$, averaging 6.57 $mg \cdot L^{-1}$, 4.60 $mg \cdot L^{-1}$, 6.45 $mg \cdot L^{-1}$ and 9.42 $mg \cdot L^{-1}$ in spring, summer, autumn and winter, respectively, like temperature, it had huge temperature difference in winter and summer, and not obvious temperature difference in spring and autumn. The content of moisture in the sediments ranged from 55.47% to 82.7%, averaging 73.48%, 70.42%, 73.14% and 73.46% in spring, summer, autumn and winter, respectively, changing slightly in the four seasons; the TOC in the sediments ranged from 13.7 to 36.3 $mg \cdot g^{-1}$, averaging 23.3 $mg \cdot g^{-1}$, 27.68 $mg \cdot g^{-1}$, 23.71 $mg \cdot g^{-1}$ and 22.4 $mg \cdot g^{-1}$ in spring, summer, autumn and winter, respectively, higher in summer and lower in winter, similar in spring and autumn; the TN in the sediments ranged from 1.2 to 3.1 $mg \cdot g^{-1}$, averaging 1.92 $mg \cdot g^{-1}$, 2.57 $mg \cdot g^{-1}$, 2.04 $mg \cdot g^{-1}$ and 1.73 $mg \cdot g^{-1}$ in spring, summer, autumn and winter, respectively, as with the variation laws of the TOC, it was higher in summer and lower in winter, similar in spring and autumn; the Fe in the sediments ranged from 25 to 128.4 $mg \cdot g^{-1}$, averaging 43.93 $mg \cdot g^{-1}$, 37.98 $mg \cdot g^{-1}$, 47.33 $mg \cdot g^{-1}$ and 61.46 $mg \cdot g^{-1}$ in spring, summer, autumn and winter, respectively; the Al in the sediments ranged from 4.72 to 21.67 $mg \cdot g^{-1}$, averaging 10.94 $mg \cdot g^{-1}$, 10.38 $mg \cdot g^{-1}$, 11.22 $mg \cdot g^{-1}$ and 13.43 $mg \cdot g^{-1}$ in spring, summer, autumn and winter, respectively; the Ca in the sediments ranged from 7.20 to 59.9 $mg \cdot g^{-1}$, averaging 32.74 $mg \cdot g^{-1}$, 32.86 $mg \cdot g^{-1}$, 37.34 $mg \cdot g^{-1}$ and 35.39 $mg \cdot g^{-1}$ in spring, summer, autumn and winter, respectively. From the seasonal variation of contents of Fe, Al, Ca in the sediments, it can be seen that the Fe content varied significantly in summer compared with winter, while the Al and Ca contents did not vary significantly with the seasons.

Temporal and spatial variation of content of phosphorus in the sediments

Content and distribution characteristics of TP in the sediments

As shown in *Table 1*, the content of TP in the sediments averaged 504.00-2,380.00 $\mu g \cdot g^{-1}$, 270.00-1,376.00 $\mu g \cdot g^{-1}$, 543.00-2,436.00 $\mu g \cdot g^{-1}$ b and 688.70-3722.80 $\mu g \cdot g^{-1}$ in spring, summer, autumn and winter, respectively, highest in winter, followed by spring and autumn, and lowest in winter, which was higher than Poyang Lake (689.34 $\mu g \cdot g^{-1}$), Yao Lake (987.93 $\mu g \cdot g^{-1}$) and Guanting Reservoir (1,268.93 $\mu g \cdot g^{-1}$) (Xiang et al., 2010; Jiang et al., 2016; Li et al., 2005), and higher when compared with

http://www.aloki.hu ● ISSN 1589 1623 (Print) ● ISSN 1785 0037 (Online)
DOI: http://dx.doi.org/10.15666/aeer/1705_1173111743

other similar lakes. From *Figure 2* it can be seen that different sampling sites had significantly different TP content and the same sampling site had significantly different TP content in different seasons, all the sampling sites showed a general trend where the phosphorus fraction content was higher in winter and lower in summer, similar in spring and autumn, which was due to the fact that vigorous growth of plankton of the waters had great demand for phosphorus in summer and the plankton of the waters conducted excessive decomposition of phosphorus in the sediments in the absence of phosphorus of the waters (Xie et al., 2003). The content of TP in L8, L6 and L5 of the highly dense area of original cage culture and L9 of the adjacent human activity intensive area was high, of which, it was highest in L8 and L9, reaching 3,723 $\mu g \cdot g^{-1}$ in L8 in winter; the content of TP in L4 and L1 of the relatively dense area of enclosure culture of Dahu Lake was relatively high, reaching 1,200 $\mu g \cdot g^{-1}$ in winter; the content of TP in L7 of the main runoff area of lake and L2 and L3 of the tail water area of reservoir was low compared with other sampling sites, of which, the content of TP averaged 643 $\mu g \cdot g^{-1}$ in L2, a sampling site with minimum pollution, which belongs to a moderately polluted area in accordance with EPA standard.

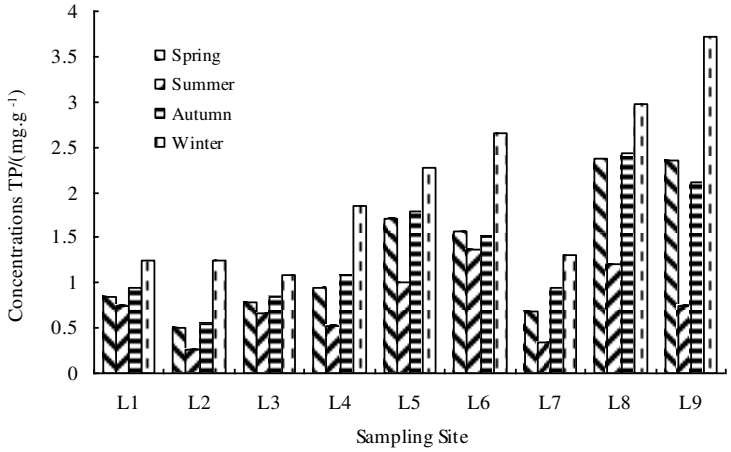

Figure 2. *Seasonal variation of content of TP in different sampling sites*

Content and distribution characteristics of IP in the sediments

As shown in *Table 1*, the IP content was 431.00-1,627.00 $\mu g \cdot g^{-1}$, 164.00-900.00 $\mu g \cdot g^{-1}$, 291.00-1, 568.00 $\mu g \cdot g^{-1}$ and 531.95-3, 006.99 $\mu g \cdot g^{-1}$ in spring, summer, autumn and winter, respectively, accounting for about 69.32% of TP, thus IP was the main factor influencing the TP variation. IP mainly included two phosphorus fractions namely NaOH-P and HCl-P, presenting HCl-P > NaOH-P in spring, summer, autumn and winter, showing that HCl-P was the main factor influencing the IP variation. As shown in *Table 2*, the correlation analysis indicated that there was significant correlation between IP and TP ($P < 0.01$). As shown in *Figure 3*, the spatial distribution of IP in spring, summer, autumn and winter was similar to that of TP, with basically same high value point, except for L5 and L6 in which the IP content of L5 was higher than that of L6. *Table 1* showed that the NaOH-P content was 144.00-592.00 $\mu g \cdot g^{-1}$, 51.00-371.00 $\mu g \cdot g^{-1}$, 168.00-504.00 $\mu g \cdot g^{-1}$ and 197.02-689.72 $\mu g \cdot g^{-1}$ in spring, summer, autumn and winter, respectively, averaging 32.84%, 38.64%, 36.44% and 27.00% of IP, respectively, changing slightly in summer and autumn, and low in winter may be due to

http://www.aloki.hu ● ISSN 1589 1623 (Print) ● ISSN 1785 0037 (Online)
DOI: http://dx.doi.org/10.15666/aeer/1705_1173111743

the fact that weak reduction condition was favorable for NaOH-P to release to the overlying water on account of low oxygen content in the waters. In the spatial distribution, as shown in *Figure 3*, the content of NaOH-P in the sediments of L9 of the adjacent human activity intensive area was high, followed by L8, L6 and L5 of the highly dense area of original cage culture, and similar to TP in spatial distribution in other sampling sites in spring, summer, autumn and winter. The HCl-P content was 234.00-1,433.00 $\mu g \cdot g^{-1}$, 125.00-545.00 $\mu g \cdot g^{-1}$, 278.00-1,063.00 $\mu g \cdot g^{-1}$ and 330.98-2,474.04 $\mu g \cdot g^{-1}$ in spring, summer, autumn and winter, respectively, averaging 71.33.00%, 63.17%, 69.52% and 76.74% of IP, respectively, thus HCl-P was the main constituent of IP, changing slightly in summer and autumn, highest in winter, and low in summer may be due to the fact that the microorganism activity was highly favorable for HCl-P to release to the overlying water, showing the characteristics (Lau et al., 2002) of the sediments in eutrophic lakes. As shown in spatial distribution diagram 5, the HCl-P content was similar to TP in spatial distribution in spring, summer, autumn and winter, with basically same high value point.

Table 1. *Variation of phosphorus fractions in the sediments*

	Spring			**Summer**		
	Variation range ($\mu g \cdot g^{-1}$)	**Average value±standard deviation ($\mu g \cdot g^{-1}$)**	**Variation factor ($\mu g \cdot g^{-1}$)**	**Variation range ($\mu g \cdot g^{-1}$)**	**Average value±standard deviation ($\mu g \cdot g^{-1}$)**	**Variation factor ($\mu g \cdot g^{-1}$)**
TP	504.00-2380.00	1304.39± 720.85	0.55	270.00-1376.00	762.01± 377.15	0.49
IP	431.00-1627.00	903.72±455.50	0.50	164.00-900.00	533.01±269.50	0.51
OP	110.00-848.00	399.26±245.48	0.61	64.00-360.00	230.00±113.09	0.49
NaOH-P	144.00-592.00	296.61±154.20	0.52	51.00-371.00	205.98±110.45	0.54
HCl-P	234.00-1433.00	644.69±381.63	0.59	125.00-545.00	336.69±159.98	0.48
	Autumn			**Winter**		
	Variation range ($\mu g \cdot g^{-1}$)	**Average value±standard deviation ($\mu g \cdot g^{-1}$)**	**Variation factor ($\mu g \cdot g^{-1}$)**	**Variation range ($\mu g \cdot g^{-1}$)**	**Average value±standard deviation ($\mu g \cdot g^{-1}$)**	**Variation factor ($\mu g \cdot g^{-1}$)**
TP	543.00-2436.00	1352..88±638.53	0.47	688.70-3722.80	1977.31±1003.71	0.51
IP	291.00-1568.00	866.12±452.74	0.52	531.95-3006.99	1449.53±840.60	0.58
OP	172.00-868.00	437.63±264.26	0.60	177.15-774.43	525.56±202.36	0.38
NaOH-P	168.00-504.00	315.61±141.87	0.45	197.02-689.72	393.15±193.08	0.49
HCl-P	278.00-1063.00	602.42±296.86	0.49	330.98-2474.04	1112.07±698.38	0.54

Table 2. *Coefficients of correlation between different phosphorus fractions in the sediments (n = 36)*

	TP	**OP**	**IP**	**HCl-P**	**NaOH-P**
TP	1				
OP	0.906**	1			
IP	0.598**	-0.542**	1		
HCl-P	0.435*	-0.364*	0.462**	1	
NaOH-P	0.414*	-0.202	0.282	-0.722**	1

*$P < 0.05$; **$P < 0.01$

http://www.aloki.hu ● ISSN 1589 1623 (Print) ● ISSN 1785 0037 (Online)
DOI: http://dx.doi.org/10.15666/aeer/1705_1173111743

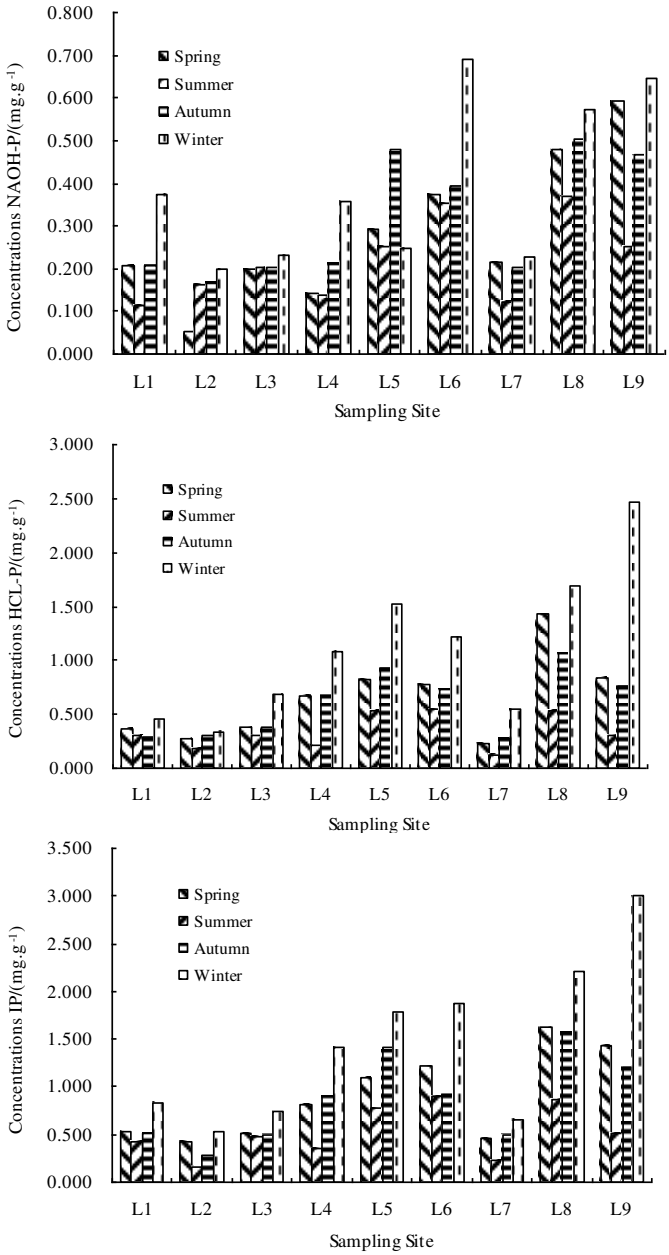

Figure 3. *Seasonal variation of contents of NaOH-P, HCl-P and IP in the sediments in different sampling sites*

Content and distribution characteristics of OP in the sediments

As shown in *Table 1*, the OP content was 110.00-848.00 $\mu g \cdot g^{-1}$, 64.00-360.00 $\mu g \cdot g^{-1}$, 172.00-868.00 $\mu g \cdot g^{-1}$ and 177.15-774.43 $\mu g \cdot g^{-1}$ in spring, summer, autumn and winter, respectively, averaging 32.84%, 38.64%, 36.44% and 27.00% of TP, respectively, lower than IP of TP, however, the content of OP in the sediments was rich, higher than that of the same type of lakes such as Taihu, Chaohu and Longgan Lake (Fan, et al., 2007). As shown in spatial distribution *Figure 4*, in terms of OP content, L8 of the highly dense area of original cage culture and L9 of the adjacent human activity intensive area were high, L6 and L5 of the highly dense area of original cage culture were lower than that of L8 in the same area, L7 of the main runoff area of lake was higher than L4 of the

http://www.aloki.hu ● ISSN 1589 1623 (Print) ● ISSN 1785 0037 (Online)
DOI: http://dx.doi.org/10.15666/aeer/1705_1173111743

relatively dense area of enclosure culture of Dahu Lake, which may be due to the fact that the organic matter was deposited in this area, and L2 and L3 of the tail water area of reservoir were the lowest. Furthermore, like TP, all the sampling sites showed a general trend where the phosphorus fraction content was higher in winter and lower in summer, similar in spring and autumn.

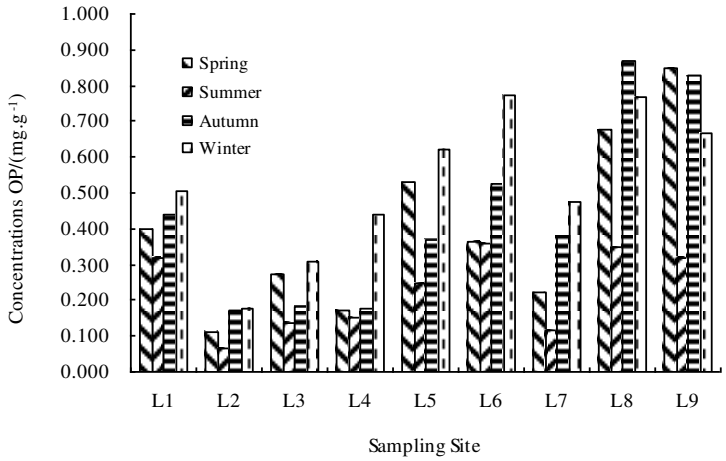

Figure 4. *Seasonal variation of content of OP in the sediments in different sampling sites*

Temporal and spatial variation of alkaline phosphatase in the sediments

The alkaline phosphatase (APA) in the sediments ranged from 1.40 to 9.80 μmol·g^{-1}·h^{-1}, averaging 5.63 μmol·g^{-1}·h^{-1}, 6.86 μmol·g^{-1}·h^{-1}, 5.89 μmol·g^{-1}·h^{-1} and 4.17 μmol·g^{-1}·h^{-1} in spring and summer autumn and winter, respectively. From *Figure 5*, it can be seen that the APA of different sampling sites in summer was higher than that in winter, and similar in spring and autumn. The study showed that the enzyme activity was high in summer due to high temperature and low in winter due to low temperature (Wilczek et al., 2005), and the temperature increase can increase the affinity between enzyme and substrate, thus leading to enzyme catalytic rate increase (Chróst and Rai, 1993); in addition, the metabolic rate of microorganism will increase with the increase of temperature and then induce the microorganism to produce more enzyme (Wallenstein et al., 2010), therefore, the APA in the study area showed obvious seasonal variation. In the spatial distribution of APA, like OP, L8, L6 and L5 of the highly dense area of original cage culture and L9 of the adjacent human activity intensive area were high, followed by L1 of the relatively dense area of enclosure culture, L7 of the main runoff area of lake was higher than L4 of the relatively dense area of enclosure culture of Dahu Lake, and L2 and L3 of the tail water area of reservoir were the lowest. It can be seen that the high APA of the highly dense area of original cage culture and the adjacent human activity intensive area indicated that the APA was closely related to the input of pollutants (Zhang et al., 2007), in culture dosing and human activity area, the more nutrients input, the more organic phosphorus or enzymatic hydrolysis phosphorus increase, thus inducing the higher APA, such a mechanism was known as the substrate inducing mechanism (Li et al., 2007). Therefore, APA can be used as an indicator of the degree of sediment pollution to a certain extent (Huang et al., 2013). By correlation analysis, it can be seen that the APA had a significant correlation ($P < 0.05$) with OP only in winter, while poor correlation with other phosphorus fractions.

http://www.aloki.hu ● ISSN 1589 1623 (Print) ● ISSN 1785 0037 (Online)
DOI: http://dx.doi.org/10.15666/aeer/1705_1173111743

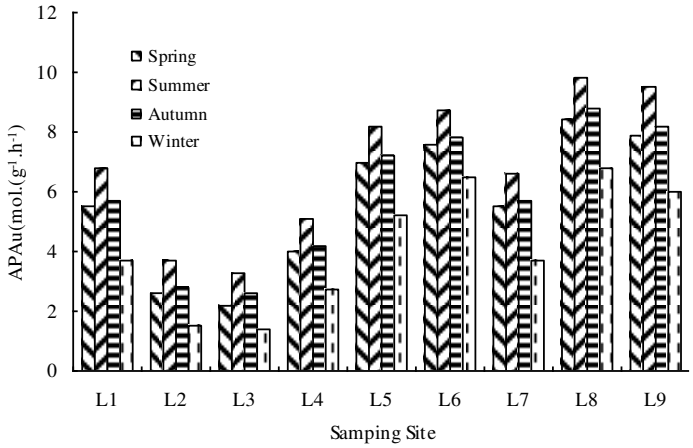

Figure 5. *Seasonal variation of content of APA in the sediments in different sampling sites*

Discussion

Distribution characteristics of different phosphorus fractions in the sediments of Sancha Lake

The phosphorus fractions in the sediments are closely related to the migration process of phosphorus to the overlying water, therefore, comprehending the distribution characteristics of different phosphorus fractions in the sediments has important practical significance to control the internal source pollution and reduce the endogenous phosphorus release. In this study, 9 sampling sites were selected as the representative samples of the sediments, and statistical analysis was conducted for the composition of different phosphorus fractions. The OP, NaOH-P and HCl-P in the sediments of Sancha Lake averaged 30%, 20.5% and 49.5% of TP, respectively, suggesting that HCl-P was the main constituent of phosphorus, followed by OP, while NaOH-P, mostly easily to release and with most biological activity, was the lowest. The decomposition of NaOH-P was closely related to the environmental conditions such as oxidation-reduction potential, while the morphological transformation and release process of HCl-P and OP were mostly related to the microorganism. Previous studies have indicated that microorganism dissolves HCL-P by secretion of organic acid, while phosphatase secreted by microorganism is an indispensable mediator of OP degradation pathway (Wu and Zhou, 2005). Therefore, in the sediments of Sancha Lake that are rich in HCl-P and OP, microorganism should play an important role in the migration and transformation process of phosphorus. The distribution characteristics of phosphorus fractions of different sampling sites were different, L8 of the highly dense area of original cage culture had high OP content, accounting for approximately 49% of TP, which was significantly higher than the average level of the whole lake, L9 of the adjacent human activity intensive area had high NaOH-P content, accounting for approximately 36% of TP, L6 and L5 of the highly dense area of original cage culture also had high OP content, averaging close to 40%, L1 and L4 of the relatively dense area of enclosure culture of Dahu Lake had low OP and NaOH-P contents, but high absolute content of HCl-P, which may be due to the fact that the fish of the upper water consumed and absorbed the phosphorus of the waters in the growth process, thus promoting the release of OP and NaOH-P in the sediments, and L2 and L3 of the tail water area of reservoir had low OP, NaOH-P and HCl-P contents on account of little

http://www.aloki.hu ● ISSN 1589 1623 (Print) ● ISSN 1785 0037 (Online)
DOI: http://dx.doi.org/10.15666/aeer/1705_1173111743

water flow and low pollution. Since OP and NaOH-P were phosphorus with release potential, so L8 and L9 had the most endogenous phosphorus release potential, meanwhile, L6, L5, L4 and L1 could exhibit strong phosphorus release capability under appropriate environmental conditions such as high temperature and hypoxia.

Correlation between different phosphorus fractions in the sediments of Sancha Lake

Correlation between different phosphorus fractions in the sediments of Sancha Lake was as shown in *Table 2*. TP had significant correlation with four phosphorus fractions, among which, the coefficient of correlation between TP and OP was higher, presenting extremely significant correlation, suggesting that the variation of content of TP in the sediments of Sancha Lake was closely related to OP fluctuation. IP had extremely significant correlation with HCl-P and positive correlation with NaOH-P, but not significant correlation, which may be due to the fact that the microbial activity was highly favorable for HCl-P to release to overlying water. IP had extremely significant negative correlation with OP, suggesting a presence of mutual transformation between IP and OP. HCl-P had significant negative correlation with OP, suggesting that the orthophosphate released from decomposition of these two phosphorus fractions may transform towards fraction of each other under suitable environmental conditions. Furthermore, there was significant negative correlation between HCl-P and NaOH-P, two main phosphorus fractions of IP.

Correlation between different phosphorus fractions in the sediments of Sancha Lake and physiochemical factors

Correlation between different phosphorus fractions in the sediments of Sancha Lake and physiochemical factors was shown in *Table 3*. Based on isothermy, Zhou et al. (2005) discovered, after investigating the sediments of Taihu Lake, that the influence of pH on phosphorus adsorption was an inverted "U" shape, and positive correlation on phosphorus analysis. the pH of the sediments of Sancha Lake was neutral leaning alkalinity, i.e. weakly alkaline in the four seasons, and had significant correlation with HCl-P phosphorus fractions, while the content of organic matter in the sediments had significant correlation with OP, such similar laws were also found by Huang et al. (2005) in studies on lake and reservoir. NaOH-P had significant correlation with the content of Fe in the sediments, whose formation was closely related to the adsorption and binding of iron and aluminum compounds, HCl-P in the sediments had extremely significant correlation with Ca. APA had extremely significant positive correlation with TP and OP and significant positive correlation with IP, which was basically in agreement with the results of a study by Jiang et al. (2011), who concluded that the APA had significant correlation with TP, IP and OP in the sediments. Other studies have suggested a complex relationship between APA and OP, and Xue et al. (1995) suggested that if the IP produced by enzymolysis of ALP was used by the biological organisms in the sediments, then the APA had positive correlation with OP; if the IP produced by enzymolysis of ALP moved upward into the overlying water, then the APA had negative correlation with OP. While Huang and Huang (1999) pointed out that the dissolved IP and small molecule OP concentration were the main factors influencing the APA variation because the APA jumped to high value when the dissolved IP or small molecule OP were almost depleted. Therefore, the relationship between the APA

http://www.aloki.hu ● ISSN 1589 1623 (Print) ● ISSN 1785 0037 (Online)
DOI: http://dx.doi.org/10.15666/aeer/1705_1173111743

and phosphorus was uncertain, which may be associated with the biological effect, physicochemical conditions of the sedimentation and nutrient content.

In addition, the TN, dissolved oxygen, temperature will also have an impact on the phosphorus fractions and phosphorus content, but their correlation was not significant, which may be related to water power, environmental media conditions and biological effect.

Table 3. *Coefficients of correlation between different phosphorus fractions in the sediments and physicochemical properties (n = 36)*

	TN	TOC	Fe	Al	Ca	PH	O2	T	APA
TP	-0.201	-0.338	0.345	0.284	0.403*	0.020	-0.131	-0.147	0.466**
OP	0.047	0.382*	0.331	0.196	0.291	0.051	0.184	-0.37	0.596**
IP	0.247	0.245	0.157	0.257	0.462**	-0.098	-0.038	-0.117	0.344*
HCl-P	-0.236	-0.082	0.282	0.185	0.749**	-0.023*	0.072	-0.089	0.0586
NaOH-P	-0.200	0.012	0.430*	0.46*	0.281	0.133	0.256	-0.269	0.054

*$P < 0.05$; **$p < 0.01$

Conclusions

(1) The content of TP in the sediments of Sancha Lake ranged from 504.00 to 2,380.00 $\mu g \cdot g^{-1}$, 270.00 to 1,376.00 $\mu g \cdot g^{-1}$, 543.00 to 2,436.00 $\mu g \cdot g^{-1}$ and 688.70 to 3,722.80 $\mu g \cdot g^{-1}$ in spring, summer, autumn and winter, respectively. The contents of all phosphorus fractions were highest in winter, followed by spring and autumn, and smallest in winter. In the four seasons IP was the main phosphorus fraction of TP, averaging about 69.52% of TP, in which HCl-P was the main phosphorus fraction, averaging 71.8% of IP, and OP averaged about 29.50% of TP.

(2) In the spatial distribution, different sampling sites had significantly different phosphorus fraction content and the same sampling site had significantly different phosphorus fraction content in different seasons, all the sampling sites showed a general trend where the phosphorus fraction content was higher in winter and lower in summer, similar in spring and autumn. The contents of all phosphorus fractions were basically same, high in the highly dense area of original cage culture and adjacent human activity intensive area, relatively high in the relatively dense area of enclosure culture of Dahu Lake, and low in the main runoff area of lake and tail water area of reservoir.

(3) Correlation analysis showed that the content distribution of phosphorus in the sediments was influenced by many factors in the sedimentary environment, exhibiting different correlation in different seasons. TP had extremely significant correlation with APA and significant correlation with Ca, OP had extremely significant correlation with APA and significant correlation with TOC, HCl-P had extremely significant correlation with Ca, NaOH-P had significant correlation with Ca and Al, IP had significant correlation with Ca, and pH, TN as well as dissolved oxygen and temperature of the overlying water will also influence the phosphorus fractions and phosphorus contents, but their correlation was not significant.

Acknowledgements. This research was funded by the Sichuan science and technology support project (2018GZ0416).

http://www.aloki.hu ● ISSN 1589 1623 (Print) ● ISSN 1785 0037 (Online)
DOI: http://dx.doi.org/10.15666/aeer/1705_1173111743

REFERENCES

[1] Anupama, V. N., Amrutha, P. N., Chitra, G. S. (2008): Phosphatase activity in anaerobic bioreactors for wastewater treatment. – Water Research 42: 2796-2802.

[2] Chróst, R. J., Rai, H. (1993): Ectoenzyme activity and bacterial secondary production in nutrient-impoverished nutrient-enriched freshwater mesocosms. – Microbial Ecology 25(2): 131-150.

[3] Chuai, X., Yang, L., Cheng, S. (2014): Characteristics and influencing factors of phosphorus adsorption on sediment in Lake Taihu and Lake Hulun. – Environmental Science 35(3): 951-957.

[4] Fan, C. X., Wang, C. X. (2007): Lake Environmental Geochemistry and Eutrophication in Middle and Lower Yangtze River. – Science Press Publishing, Beijing, China.

[5] Fan, J., Wang, D., Zhang, K. (2010): Experimental study on a dynamic contaminant release into overlying water-body across sediment-water interface. – Journal of Hydrodynamics, Series B 22(5): 354-357.

[6] General Administration of Quality Supervision, Inspection and Quarantine of the People's Republic of China (AQSIQ) (2003): GB/T19145-2003 Determination of Total Organic Carbon in Sedimentary Rock. – Standards Press of China, Beijing.

[7] Huang, B., Huang, S. (1999): Regulation of dissolved phosphorus in the variety of alkaline phosphatase activity of marine microalgae. – Acta Oceanologica Sinica 21(1): 55-60.

[8] Huang, Q. H., Wang, D. H., Wang, C. X. (2003): Relation between phosphorus forms in the sediments and lake eutrophication. – China Environmental Science 23(6): 583-586.

[9] Huang, Q. H., Wang, Z. J., Wang, D. H., Wang, C. X., Ma, M., Jin, X. C. (2005): Origins and mobility of phosphorus forms in the sediments of lakes Taihu and Chaohu, China. – Journal of Environmental Science and Health, Part A 40: 91-102.

[10] Huang, R., Wang, S., Zhao, H. (2013): Study on temporal and spatial variation of alkaline phosphatase activity in the surface sediments of Erhai Lake. – Research of Environmental Sciences 26(3): 250-255.

[11] Hupfer, H., Gachter, R., Giovanoli, R. (1995): Transformation of phosphorus species in settling seston and during early sediment diagenesis. – Aquatic Sciences 57(4): 305-324.

[12] Jia, B. Y., Tang, Y., Fu, W. L. (2013): Relationship among sediment characteristics, eutrophication process and human activities in the Sancha Lake. – China Environ. Sci. 33: 1638-1644.

[13] Jiang, J. M., Zhao, H., Shen, M. N. (2011): Distribution and impact factor of alkaline phosphatase activity in the intertidal surface sediments of the Yangtze Estuary. – Acta Scientiae Circumstantiae 31(10): 2233-2239.

[14] Jiang, L., Guan, G., Liao, C. (2016): Occurrence and spatial distribution of phosphorus in the sediments of the Yao Chi. – Chinese Journal of Environmental Engineering 10(5): 2756-2760.

[15] Lau, S. S. S., Lane, S. N. (2002): Biological and chemical factors influencing shallow lake eutrophication: a long-term study. – Science of the Total Environment 288: 167-181.

[16] Li, C., Yuan, H., Huang, H. (2005): The vertical distribution characteristics of phosphorus solubilizing bacteria in the sediment of Guanting Reservoir. – Science of China series D. Geoscience 35(Supplementary issue): 241-248.

[17] Li, C., Lu, J., Li, H. (2007): The landward changes of soil enzyme activities in a tidal flat wetland of the Yangtze River estuary and correlations with physico-chemical factors. – Acta Ecologica Sinica 27(9): 3663-3669.

[18] Li, Q., Yin, J., Xi, B. (2014): Characteristics of organic phosphorus fractions in sediments of inflow rivers of Lake Chaohu, China. – Chinese Journal of Environmental Engineering 8(2): 441-447.

http://www.aloki.hu ● ISSN 1589 1623 (Print) ● ISSN 1785 0037 (Online)
DOI: http://dx.doi.org/10.15666/aeer/1705_1173111743

[19] Li, Y., Zhang, J. Q., Gong, Z. L.(2019): Gcd gene diversity of quinoprotein glucose dehydrogenase in the sediment of Sancha Lake and its response to the environment. – Int. J. Environ. Res. Public Health 16: 1-18.
[20] Ruban, V., Srigault, S., Demare, D., Philippe, A. M. (1999): An investigation of the origin and mobility of phosphorus in freshwater sediments from Bort-Les-Orgues Reservoir, France. – Journal of Environmental Monitoring 1: 403-407.
[21] Ruban, V., López-Sánchez, J. F., Pardo, P. (2001): Harmonized protocol and certified reference material for the determination of extractable contents of phosphorus in freshwaer sediments. A synthesis of recent works. – Fresenius Journal of Analytical Chemistry 370(2/3): 224-228.
[22] State Environmental Protection Administration of China (2002): Water and Wastewater Monitoring and Analysis Method. – China Environmental Science Press, Beijing.
[23] Wallenstein, M., Allison, S. D., Ernakovich, J. (2010): Controls on the temperature sensitivity of soil enzymes: a key driver of in situ enzyme activity rates. – Soil Enzymology 22: 245-258.
[24] Wilczek, S., Fischer, H., Pusch, M. T. (2005): Regulation and seasonal dynamics of extracellular enzyme activities in the sediments of a large lowland river. – Microbial Ecology 50(2): 253-267.
[25] Wu, G. F., Zhou, X. P. (2005): Characterization of phosphorus-releasing bacteria in a small eutrophic shallow, eastern lake. – Water Research 39: 4623-4632.
[26] Xiang, S., Zhou, W. (2010): Occurrence and distribution of phosphorus in sediments of Poyang Lake. – Journal of Lake Science 22(5): 649-654.
[27] Xie, L. Q., Xie, P., Li, S. X., Tang, H. J. (2003): The low TN: TP ratio, a cause or a result of Microcystis blooms. – Water Research 37: 2073-2080.
[28] Xue, X., Hong, H., Huang, B. (1995): Distribution and dynamics of alkaline phosphatase activity and their relationship with various forms of phosphorus in the sediments of the Western sea of Xiamen. – Acta Oceanologica Sinica 17(5): 81-87.
[29] Yang, L., Tang, Z., Hao, Y. (2013): Morphometry of phosphorus in the lake sediments of Taihu by chemical sequential extraction method. – Global Geology 32(3): 634-639.
[30] Zhang, T., Wang, X., Jin, X. (2007): Vertical variation of alkaline phosphatase activity and phosphorus forms in the Taihu Lake sediment and the relationship between them. – Journal of Agro-Environment Science 26(1): 36-40.
[31] Zhang, Z., Wang, Z., Holden, J. (2012): The release of phosphorus from sediment into water in subtropical wetlands: A warming microcosm experiment. – Hydrological Processes 26(1): 15-26.
[32] Zhou, A., Tang, H., Wang, D. (2005): Phosphorus adsorption on natural sediments: modeling and effects of pH and sediment composition. – Water Research 39(7): 1245-1254.
[33] Zhou, X., Guo, H., Zhang, J. (2013): Simulated study on phosphorus release from sediment in Changshou Lake influenced by environmental factors. – Chinese Journal of Environmental Engineer-ring 7(5): 1671-1675.
[34] Zhu, G., Qin, B., Gao, G. (2004): Fractionation of phosphorus in sediments and its relation with soluble phosphorus contents in shallow lakes located in the middle and lower reaches of Changjiang River, China. – Acta Scientiae Circumstantiae 24(3): 381-388.

http://www.aloki.hu ● ISSN 1589 1623 (Print) ● ISSN 1785 0037 (Online)
DOI: http://dx.doi.org/10.15666/aeer/1705_1173111743

THE EFFECTS OF DIFFERENT ROOTSTOCKS ON AROMA VOLATILE CONSTITUENTS IN THE FRUITS OF 'FUJI' APPLES (*MALUS DOMESTICA* BORKH.)

GUR, E.

Canakkale Onsekiz Mart University, Faculty of Agriculture, Department of Horticulture
17020 Canakkale, Turkey
(e-mail: engingur@comu.edu.tr; phone: +90-(286)-218-00-18)

(Received 22nd Apr 2019; accepted 4th Jul 2019)

Abstract. Five-year-old 'Fuji' (*Malus domestica* Borkh.) apple trees grafted on MM-106, M-9, M-26, and MM-111 in a commercial orchard in Çanakkale (Turkey), were used for determination of fruit quality and aroma volatiles. Fruits were sampled at the commercial harvesting stage at the end of September in 2015 and 2016. Fruit quality characteristics and aroma volatiles changed significantly in apples grown on four different rootstocks. The largest fruits (212.2 g) with highest total soluble solids (18.40%) were obtained from the trees on M9 rootstock. According to chromatography analysis, a total of 51 volatiles were detected in 'Fuji' fruits. Ester compounds were a major part of total volatiles in the fruits. The highest total ester content was obtained from the trees on M9 rootstock, whereas the lowest was from MM106 rootstock. 2-Methylbutyl acetate and ethyl 2-methylbutanoate were the main ester compounds in the fruits considering all volatiles. The total ester concentration in the total volatile compounds in the 'Fuji' apples grafted on the M9 rootstock was 95.52%. This rate was 91.28% for the M26 rootstock, 91.04% for the MM111 rootstock and 88.30% for the MM106 rootstock. The study concluded that the M9 rootstock enhances the aroma content of 'Fuji' apples.
Keywords: *pomology, quality, chromatography, ester compounds, SPME*

Introduction

The total world apple production for 2016 was 89,329,179 metric tons. China, USA, Poland, Turkey, Iran and Italy had the greatest shares of apple production. In Turkey, apples are grown in almost all parts of the country, and there was a total 3,032,164 metric tons of apple production in 2017 (FAOSTAT, 2018). The most widely-grown varieties of apples in Turkey are 'Starking Delicious', 'Golden Delicious', 'Amasya', 'Jonathan', 'Granny Smith', 'Red Chief', 'Braeburn', 'Pink Lady', 'Gala' and 'Fuji' (Özçağıran, 2005). 'Fuji' apples are one of the popular apple varieties frequently grown mostly in China, Japan, Brazil, USA, New Zealand and Spain. Besides its high fruit quality, 'Fuji' apples are long-lasting fruits. It is reported that the significant aroma compounds in 'Fuji' fruits are ethyl 2-methylbutanoate, 2-methylbutyl acetate and hexyl acetate (Echeverría et al., 2004). Aroma has been known since ancient times (Vicentini et al., 2018). Aroma is of capital importance for quality characteristics in apples. Aroma is the foremost characteristic that influences the purchase decision of a consumer about apples. There are numerous studies on volatile compounds that contribute to the flavour of an apple and more than 300 volatile compounds have been identified through chromatography techniques (Dimick and Hoskin, 1983). One of these techniques, GC-MS, helps to investigate phenolic and polyphenolic compounds in plant species (Zishan et al., 2017). Ester compounds are the main components of apple flavour (Paillard, 1990).

The selection and use of rootstock is vital. It has great impact on the characteristics of the apple variety grafted on the rootstock. It also affects yield, biotic and abiotic

http://www.aloki.hu ● ISSN 1589 1623 (Print) ● ISSN 1785 0037 (Online)
DOI: http://dx.doi.org/10.15666/aeer/1705_1174511756

stress conditions, and quality characteristics of fruits. Many researchers have examined and published several studies on the impact of rootstocks on yield and fruit quality in apples. The most widely used rootstocks in the world are M9, MM106, MM111, and M26 (Jackson, 2003). The M9 rootstock is the most commonly used dwarf rootstock for high density planting. Apple seedling rootstocks produce trees about 35 to 40 percent larger.

According to the literature, there is no specific research concerning the comparison of aroma compounds for different widely-used apple rootstocks. This study was performed in 2015-2016 and seeks to compare the aroma volatile compounds that contribute to the flavour of 'Fuji' variety grafted on different rootstocks.

Materials and Methods

The 'Fuji' orchard was established with a row and intra-row spacing of 3 meters to 1.5 meters for the M9 rootstock, 3 meters to 2 meters for the M26 rootstock, 4 meters to 3 meters for the MM106 rootstock and 6 meters to 5 meters for the MM111 rootstock in 2010. The orchards where the fruit samples were collected, are located in the district of Lapseki, Çanakkale, Turkey (*Fig. 1*).

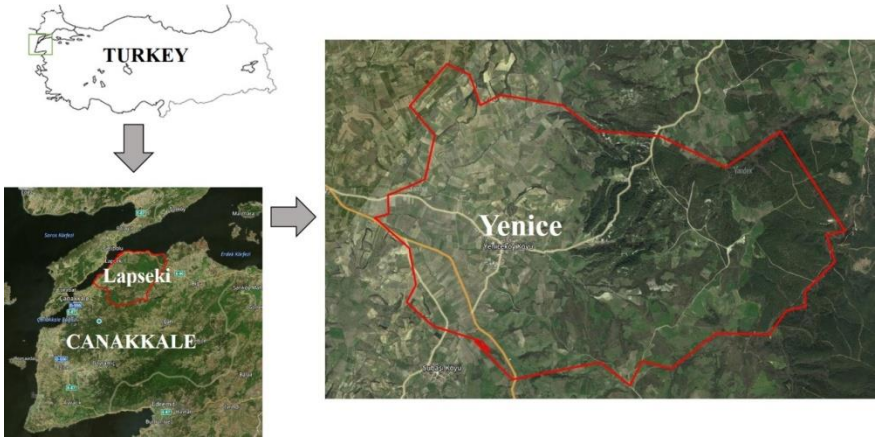

Figure 1. *Study area*

The region is well known for high quality pome fruits and stone fruits production and located at the nortwest of Turkey. In this region annual apple production is approxmately 115.000 tons. Different planting distances are used for commercial apple production due to rootstock effects on tree sizes. Application of fertilizers, pesticides, irrigation schedule were arranged according to the Global GAP certification programme for apple producers in Lapseki-Çanakkale. All the applications were made at the same time and same concentrations. The soil texture was generally clay-loamy and the reaction was slightly alkaline (pH 7.2). GPS coordinates of experimental site is 40º19'48'' N, 26º43'47'' E and elevation is 49 m above sea level.

Collection of fruit samples

The fruits of the 'Fuji' trees grafted on different rootstocks were collected in 30 September, in accordance with commercial harvest criteria. The fruits were sampled during 2015 and 2016 harvesting seasons. The fruits collected did not have any harmful

http://www.aloki.hu ● ISSN 1589 1623 (Print) ● ISSN 1785 0037 (Online)
DOI: http://dx.doi.org/10.15666/aeer/1705_1174511756

symptoms or suffer from any disease. These fruits were then transferred to the laboratories and prepared for pomological and chromatography analyses. Five trees from each rootstock / Fuji combinations were used for fruit sampling and 20 fruits from each trees were harvested for further analyses. So, one hundred fruits were used for each rootstock / Fuji combinations.

Evaluation of fruit quality characteristics

Fruit weight of 'Fuji' apples (g) was calculated considering the average value of 20 fruits by individual weighing with a 0.01 g precision digital balance (Model 612, Sartorius). Flesh firmness was measured on two paired sides of each fruit by removing a 1 mm thick disk of skin from each side of the fruit using a penetrometer (Model FT-327, Effegi). Total soluble solids (TSS) in the fruit juice were measured with a digital refractometer (PR-101, Atago) and expressed as °Brix. Titratable acidity (TA) was determined by using a sample of the juice from 20 fruits. The juice samples were diluted with distilled water (1:2) and titrated to pH 8.2 with a benchtop pH meter (InoLab pH 7110, WTW) with 0.1 N NaOH. The results were expressed as g malic acid/100 g fresh weight (FW).

Volatile extraction and GC/MS conditions

For headspace sampling, SPME fibres coated with polydimethylsiloxane–divinylbenzene (Supelco Co., Bellefonte, PA, USA) were used as described before by Wang et al. (2009). The fibre was activated according to the manufacturer's instructions. The headspace solid phase microextraction method was used for the isolation and concentration of volatiles. For each extraction, 2 g of the pulp and 0.6 g NaCl were placed in a 4 ml capped vial. The vial was placed in a 45°C water bath with a magnetic stirrer to warm to constant temperature, and the SPME fibre was exposed to the headspace of the sample to adsorb the analyses for 30 min. The fibre was then introduced into the heated chromatograph injector port.

The identification and quantification of volatile compounds in the samples were performed on a Shimadzu QP2010 Plus GC-MS (*Fig. 2*) using the method described by Wang et al. (2009) with a slight modification.

Figure 2. *Shimadzu QP 2010 Plus GS-MS system for chromatography analyses of volatiles*

http://www.aloki.hu ● ISSN 1589 1623 (Print) ● ISSN 1785 0037 (Online)
DOI: http://dx.doi.org/10.15666/aeer/1705_1174511756

Separations were done with a DB-WAX column (60 m × 0.2 mm, i.d., and 0.25 µm, film thickness; J & W, USA), which was preconditioned at 250°C for a period of 2 hours. Helium was used as the carrier gas (3 ml/min). The analysis was conducted following the program at 40°C for 2 min, 40-150°C (3°C/min), then 150-220°C (10°C/min), and 250°C (5 min). The temperature of the injector was 250°C. The interface between GC and MS was at 250°C. Electron impact ionization was at 70 eV, EI mode, and the filament current was 0.25 mA. The ion-source temperature was 200°C. The scan range was 35-425 aMU.

Statistical analysis

Differences between strains were evaluated with analysis of variance using the SAS General Linear Model procedure: PROC GLM procedure of SAS (version 6.12; SAS Institute, Cary NC) (SAS, 1997). When this analysis was statistically significant (Ftest), mean separation was performed using the Tukey Test.

Results

The 'Fuji' apple trees budded in mid-March under the ecological conditions where the study was performed, and came into full bloom by April 20th. The harvest was gathered on September 30th in both years. The total number of days between full bloom and the harvest date was 152 to 158 days. *Table 1* and *Fig. 3* present the results from the pomological analysis of the fruit samples obtained in both years.

Table 1. *Quality characteristics of the 'Fuji' apple fruits grafted on different rootstocks (average values of two years)*

	Fruit weight (g)	Fruit width (mm)	Fruit length (mm)	Fruit firmness	Total soluble solids (%)	pH	Total titratable acidity (%)
M9	212.20 ±4.26	82.43 ±9.15	67.59 ±8.45	4.96 ±0.62	18.40 ±1.63	4.20 ±0.05	0.48 ±0.02
M26	188.60 ±8.54	78.30 ±5.55	54.65 ±6.35	6.75 ±0.65	14.70 ±1.14	4.10 ±0.03	0.63 ±0.02
MM106	157.33 ±9.35	71.74 ±7.25	49.59 ±7.65	7.00 ±0.54	12.50 ±1.21	4.70 ±0.08	0.88 ±0.03
MM111	145.82 ±11.75	68.43 ±8.35	47.19 ±8.75	4.96 ±0.57	12.40 ±0.88	3.80 ±0.09	0.90 ±0.05
$LSD_{\%5}$	8.1	4.4	4.7	1.2	1.7	0.2	0.06

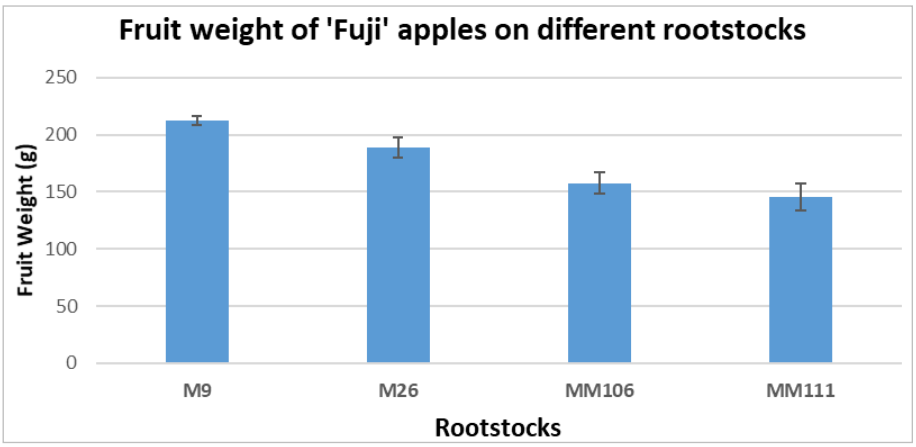

Figure 3. *Comparison of fruit weight of 'Fuji' apples grafted on different rootstocks*

http://www.aloki.hu ● ISSN 1589 1623 (Print) ● ISSN 1785 0037 (Online)
DOI: http://dx.doi.org/10.15666/aeer/1705_1174511756

Among the 'Fuji' apple varieties grafted on different rootstocks, the fruits grafted on M9 were 212.20 grams in weight, which was the highest fruit weight. The apples with the highest fruit width were 82.43 mm grafted on M9, whereas those with the lowest fruit width were the ones grafted on MM111. Further, the apples with the highest fruit length were 67.59 mm grafted on M9, while those with lowest fruit length were 47.19 mm grafted on MM111. The fruits grafted on MM106 had the highest fruit firmness of 7.00; on the other hand, the fruits grafted on M9 and MM111 had lowest fruit firmness of 4.96. The fruits with the highest amount of soluble solids were grafted on the M9 rootstock with 18.40%, while the fruits with the lowest amount of soluble solids were grafted on MM111 with 12.40%. The highest pH value in the fruits was 4.70 grafted on MM106, while the lowest pH value in the fruits was 3.80 grafted on the MM111. The apples with the highest total acidity values were grafted on MM111 of 0.90%, while the apples with the lowest total acidity values were grafted on M9 of 0.48%.

The 'Fuji' apples grafted on M9 have an average fruit weight of 283.96 grams, fruit width of 84 mm, fruit length of 73.6 mm, 12.96% soluble solids, 0.59% total acidity and pH of 3.91 (Baytekin and Akca, 2011). Another study found that the 'Fuji' variety grafted on the M9 rootstock had a fruit weight of 197.33 grams and 16% soluble solids (Ünivar and Pırlak, 2016). Various researchers have reported the positive effects of the M9 rootstock on fruit weight (Nicolai, 1998; Brown and Wolfe, 1999; Autio and Krupa, 2001; Marini, 2002).

Volatile aroma compounds

The chromatography analyses of the fruit samples obtained from the apple trees grafted on different rootstocks successfully revealed the volatile compounds. *Table 2* presents the results for the volatile compounds and amounts of the samples from 2015. *Table 3* shows the results of the samples from 2016; *Table 4* presents the average results for both years.

Based on the results from 2015 and 2016, there were a total of 51 volatile compounds identified in both years. The aroma profiles in 2015 and 2016 were similar since the climate conditions in these two years were similar. The analyses concluded that 22 of the compounds were ester compounds; 17 of them were alcohol compounds; 7 of them were acid compounds and 5 were aldehyde compounds.

The total aroma amount of the fruits examined in the year 2015 varied between 275.13 µg/kg and 559.58 µg/kg. The aroma compounds in the 'Fuji' apples on the M9 rootstock were 2.03 times more than those on the MM106 rootstock (*Table 2*). The total ester content in the 'Fuji' fruits on the M9 rootstock was 535.02 µg/kg, whereas the MM106 rootstock had the lowest ester content of 242.29 µg/kg. This was also the case for 2016 (*Table 3*). In 2016, the total volatile compounds from M9 amounted to 542.05 µg/kg, while the total volatile compounds from MM106 amounted to 300.92 µg/kg. As for the ester compounds, those from M9 were 517.34 µg/kg and those from MM106 were 266.49 µg/kg. Considering the average values, the total volatile compounds in the 'Fuji' fruits on the M9 rootstock amounted to 550.89 µg/kg. The M9 rootstock was followed by MM111 (409.16 µg/kg), M26 (352.00 µg/kg), and MM106 (288.15 µg/kg) (*Table 4*). That being said, it can be argued that compared to other rootstocks, the M9 rootstock has an enhancing effect on the aroma content of the 'Fuji' fruits (*Fig. 4*).

http://www.aloki.hu ● ISSN 1589 1623 (Print) ● ISSN 1785 0037 (Online)
DOI: http://dx.doi.org/10.15666/aeer/1705_1174511756

Table 2. *Volatile compounds of the 'Fuji' apple variety grafted on different rootstocks (µg/kg FW) (2015)*

		Rootstocks			
Esters		**M9**	**M26**	**MM106**	**MM111**
1	Ethyl acetate	4.50	13.11	14.46	15.36
2	Propyl acetate	2.43	2.14	4.23	1.66
3	2-Methylpropyl acetate	0.02	0.07	0.07	0.08
4	Butyl acetate	1.29	1.70	1.32	1.99
5	2-Methylbutyl acetate	243.34	125.54	96.56	132.54
6	Pentyl acetate	2.66	1.18	1.54	2.43
7	Butyl butanoate	2.34	1.76	0.97	2.67
8	Hexyl acetate	27.54	11.30	6.45	20.14
9	Hexyl butanoate	4.56	3.11	2.76	3.50
10	Hexyl-2-methylbutanoate	5.34	3.64	1.75	7.80
11	Hexyl hexanoate	0.03	0.03	0.02	0.04
12	Ethyl formate	0.28	0.86	1.12	1.07
13	Ethyl propanoate	0.02	0.07	0.01	0.05
14	Tert-Butyl propanoate	0.02	0.03	0.02	0.04
15	Butyl propanoate	22.12	12.54	3.54	18.80
16	Hexyl propanoate	13.34	8.90	5.76	20.45
17	Ethyl butanoate	0.01	0.01	0.02	0.04
18	Hexyl butanoate	3.36	2.16	3.34	4.43
19	Ethyl 2-methylbutanoate	185.45	125.76	90.45	124.78
20	Butyl 2-methylbutanoate	7.75	5.14	3.75	8.80
21	Ethyl hexanoate	2.24	1.16	0.45	3.67
22	Butyl hexanoate	6.38	5.60	3.70	7.30
	TOTAL ESTERS	**535.02**	**325.81**	**242.29**	**377.64**
Alcohols					
23	2-Propanol	1.03	1.16	0.64	0.19
24	Ethanol	4.17	3.54	4.30	5.63
25	2-Butanol	0.03	0.09	0.08	0.11
26	2-Methyl-1-propanol	0.16	0.35	0.35	0.41
27	3-Pentanol	0.02	0.09	0.13	0.11
28	2-Pentanol	0.07	0.27	0.4	0.32
29	Butanol	6.73	8.10	6.62	9.47
30	2-Methyl-1-butanol	1.23	3.67	2.47	4.30
31	Pentanol	0.20	0.26	0.25	0.30
32	Hexanol	2.39	2.93	2.83	3.42
33	[Z]-3-hexen-1-ol	0.02	0.03	0.04	0.04
34	[E]-2-hexen-1-ol	0.09	0.09	0.20	0.11
35	2-Methyl-1-phenyl-1-propanol	0.06	0.18	0.26	0.21
36	Farnesol	0.12	0.11	0.19	0.13
37	Tetradecanol	0.04	0.09	0.06	0.11
38	6-Methyl-5-hepten-2-ol	0.07	0.05	0.14	0.06
39	2-Ethyl-1-hexanol	0.10	0.32	0.37	0.37
	TOTAL ALCOHOLS	**16.53**	**21.33**	**19.33**	**25.29**
Acids					
40	Acetic acid	0.31	1.20	1.39	1.40
41	Hexanoic acid	0.28	0.42	0.67	0.49
42	[E]-2-Hexenoic acid	0.03	0.08	0.05	0.09
43	Octanoic acid	0.02	0.07	0.08	0.08
44	Nonanoic acid	0.02	0.07	0.04	0.08
45	Dodecanoic acid	0.01	0.01	0.01	0.01
46	Tridecanoic acid	0.07	0.10	0.02	0.12
	TOTAL ACIDS	**0.74**	**1.95**	**2.26**	**2.27**
Aldehydes					
47	Hexanal	4.07	3.88	6.03	4.53
48	[E]-2-hexenal	3.01	3.37	4.84	3.94
49	2-Methyl-4-pentenal	0.06	0.07	0.11	0.08
50	Butanal	0.07	0.19	0.16	0.22
51	[Z]-3-hexenal	0.08	0.09	0.11	0.11
	TOTAL ALDEHYDES	**7.29**	**7.60**	**11.25**	**8.88**
	TOTAL VOLATILES	**559.58**	**356.69**	**275.13**	**414.08**

http://www.aloki.hu ● ISSN 1589 1623 (Print) ● ISSN 1785 0037 (Online)
DOI: http://dx.doi.org/10.15666/aeer/1705_1174511756

Table 3. *Volatile compounds of the 'Fuji' apple variety grafted on different rootstocks (µg/kg FW) (2016)*

		Rootstocks			
Esters		**M9**	**M26**	**MM106**	**MM111**
1	Ethyl acetate	4.19	11.93	14.03	14.44
2	Propyl acetate	2.28	1.95	4.10	1.56
3	2-Methylpropyl acetate	0.02	0.06	0.07	0.08
4	Butyl acetate	1.33	1.72	1.41	1.87
5	2-Methylbutyl acetate	250.64	126.8	113.32	124.59
6	Pentyl acetate	2.74	1.19	1.65	2.50
7	Butyl butanoate	2.41	1.78	1.04	2.75
8	Hexyl acetate	28.37	11.41	6.50	20.74
9	Hexyl butanoate	4.70	3.14	2.85	3.61
10	Hexyl-2-methylbutanoate	5.50	3.68	1.87	8.03
11	Hexyl hexanoate	0.03	0.03	0.02	0.04
12	Ethyl formate	0.29	0.87	1.20	1.10
13	Ethyl propanoate	0.02	0.07	0.01	0.05
14	Tert-Butyl propanoate	0.02	0.03	0.02	0.04
15	Butyl propanoate	20.57	12.67	3.79	19.36
16	Hexyl propanoate	13.41	8.10	6.16	21.06
17	Ethyl butanoate	0.01	0.01	0.02	0.04
18	Hexyl butanoate	3.12	1.97	3.57	4.56
19	Ethyl 2-methylbutanoate	162.47	118.44	96.78	121.52
20	Butyl 2-methylbutanoate	7.21	4.68	4.01	9.06
21	Ethyl hexanoate	2.08	1.06	0.48	3.45
22	Butyl hexanoate	5.93	5.10	3.59	6.86
	TOTAL ESTERS	**517.34**	**316.69**	**266.49**	**367.31**
Alcohols					
23	2-Propanol	0.96	1.06	0.62	0.18
24	Ethanol	3.92	3.22	4.17	5.29
25	2-Butanol	0.03	0.08	0.08	0.10
26	2-Methyl-1-propanol	0.16	0.35	0.37	0.39
27	3-Pentanol	0.02	0.09	0.14	0.10
28	2-Pentanol	0.07	0.27	0.43	0.33
29	Butanol	6.93	8.18	7.08	9.75
30	2-Methyl-1-butanol	1.27	3.71	2.64	4.43
31	Pentanol	0.21	0.26	0.27	0.31
32	Hexanol	2.46	2.96	3.03	3.52
33	[Z]-3-hexen-1-ol	0.02	0.03	0.04	0.04
34	[E]-2-hexen-1-ol	0.09	0.09	0.21	0.11
35	2-Methyl-1-phenyl-1-propanol	0.06	0.18	0.28	0.22
36	Farnesol	0.11	0.11	0.20	0.13
37	Tetradecanol	0.04	0.09	0.06	0.11
38	6-Methyl-5-hepten-2-ol	0.07	0.05	0.15	0.06
39	2-Ethyl-1-hexanol	0.09	0.29	0.40	0.38
	TOTAL ALCOHOLS	**16.51**	**21.02**	**20.17**	**25.45**
Acids					
40	Acetic acid	0.29	1.09	1.35	1.32
41	Hexanoic acid	0.26	0.38	0.65	0.46
42	[E]-2-Hexenoic acid	0.03	0.07	0.05	0.08
43	Octanoic acid	0.02	0.07	0.09	0.08
44	Nonanoic acid	0.02	0.07	0.04	0.08
45	Dodecanoic acid	0.01	0.01	0.02	0.01
46	Tridecanoic acid	0.07	0.10	0.02	0.12
	TOTAL ACIDS	**0.7**	**1.79**	**2.22**	**2.15**
Aldehydes					
47	Hexanal	4.19	3.92	6.45	4.67
48	[E]-2-hexenal	3.10	3.4	5.18	4.06
49	2-Methyl-4-pentenal	0.06	0.07	0.12	0.08
50	Butanal	0.07	0.19	0.17	0.23
51	[Z]-3-hexenal	0.08	0.09	0.12	0.11
	TOTAL ALDEHYDES	**7.5**	**7.67**	**12.04**	**9.15**
	TOTAL VOLATILES	**542.05**	**347.17**	**300.92**	**404.06**

http://www.aloki.hu ● ISSN 1589 1623 (Print) ● ISSN 1785 0037 (Online)
DOI: http://dx.doi.org/10.15666/aeer/1705_1174511756

Table 4. *Volatile compounds of the 'Fuji' apple variety grafted on different rootstocks (µg/kg FW) (Average)*

		Rootstocks				
Esters		**M9**	**M26**	**MM106**	**MM111**	**MSD***
1	Ethyl acetate	4.35 c*	12.52 b	14.25 a	14.90 a	1.422
2	Propyl acetate	2.36 b	2.05 c	4.17 a	1.61 d	0.262
3	2-Methylpropyl acetate	0.02 c	0.07 b	0.07 ab	0.08 a	0.010
4	Butyl acetate	1.31 c	1.71 b	1.37 c	1.93 a	0.140
5	2-Methylbutyl acetate	246.99 a	126.17 b	104.94 c	128.57 b	17.886
6	Pentyl acetate	2.70 a	1.19 d	1.60 c	2.47 b	0.138
7	Butyl butanoate	2.38 b	1.77 c	1.01 d	2.71 a	0.116
8	Hexyl acetate	27.96 a	11.36 c	6.48 d	20.44 b	0.924
9	Hexyl butanoate	4.63 a	3.13 c	2.81 d	3.56 b	0.181
10	Hexyl-2-methylbutanoate	5.42 b	3.66 c	1.81 d	7.92 a	0.275
11	Hexyl hexanoate	0.03	0.03	0.02	0.04	NS
12	Ethyl formate	0.29 c	0.87 b	1.16 a	1.09 a	0.078
13	Ethyl propanoate	0.02	0.07	0.01	0.05	NS
14	Tert-Butyl propanoate	0.02	0.03	0.02	0.04	NS
15	Butyl propanoate	21.35 a	12.61 c	3.67 d	19.08 b	1.497
16	Hexyl propanoate	13.38 b	8.50 c	5.96 d	20.76 a	0.972
17	Ethyl butanoate	0.01	0.01	0.02	0.04	NS
18	Hexyl butanoate	3.24 b	2.07 c	3.46 b	4.50 a	0.362
19	Ethyl 2-methylbutanoate	173.96 a	122.10 b	93.62 c	123.15 b	22.518
20	Butyl 2-methylbutanoate	7.48 b	4.91 c	3.88 d	8.93 a	0.716
21	Ethyl hexanoate	2.16 b	1.11 c	0.47 d	3.56 a	0.261
22	Butyl hexanoate	6.16 b	5.35 c	3.65 d	7.08 a	0.727
	TOTAL ESTERS	**526.22 a**	**321.29 c**	**254.45 d**	**372.51 b**	**29.538**
Alcohols						
23	2-Propanol	1.00 b	1.11 a	0.63 c	0.19 d	0.111
24	Ethanol	4.05 b	3.38 c	4.24 b	5.46 a	0.488
25	2-Butanol	0.03 b	0.09 ab	0.08 ab	0.11 a	0.075
26	2-Methyl-1-propanol	0.16 b	0.35 a	0.36 a	0.40 a	0.147
27	3-Pentanol	0.02 b	0.09 a	0.14 a	0.11 a	0.057
28	2-Pentanol	0.07 b	0.27 ab	0.42 a	0.33 a	0.214
29	Butanol	6.83 c	8.14 b	6.85 c	9.61 a	0.519
30	2-Methyl-1-butanol	1.25 d	3.69 b	2.56 c	4.37 a	0.198
31	Pentanol	0.21	0.26	0.26	0.31	NS
32	Hexanol	2.43 c	2.95 b	2.93 b	3.47 a	0.212
33	[Z]-3-hexen-1-ol	0.02	0.03	0.04	0.04	NS
34	[E]-2-hexen-1-ol	0.09 b	0.09 b	0.21 a	0.11 b	0.079
35	2-Methyl-1-phenyl-1-propanol	0.06 c	0.18 b	0.27 a	0.22 ab	0.081
36	Farnesol	0.12 b	0.11 b	0.20 a	0.13 b	0.059
37	Tetradecanol	0.04	0.09	0.06	0.11	NS
38	6-Methyl-5-hepten-2-ol	0.07	0.05	0.15	0.06	NS
39	2-Ethyl-1-hexanol	0.10 c	0.31 b	0.39 a	0.38 a	0.041
	TOTAL ALCOHOLS	**16.55 d**	**21.19 b**	**19.79 c**	**25.41 a**	**0.815**
Acids						
40	Acetic acid	0.30 c	1.15 b	1.37 a	1.36 a	0.128
41	Hexanoic acid	0.27 d	0.40 c	0.66 a	0.48 b	0.052
42	[E]-2-Hexenoic acid	0.03	0.08	0.05	0.09	NS
43	Octanoic acid	0.02 b	0.07 ab	0.09 a	0.08 a	0.055
44	Nonanoic acid	0.02	0.07	0.04	0.08	NS
45	Dodecanoic acid	0.01	0.01	0.02	0.01	NS
46	Tridecanoic acid	0.07 ab	0.10 ab	0.02 b	0.12 a	0.081
	TOTAL ACIDS	**0.72 c**	**1.88 b**	**2.25 a**	**2.22 a**	**0.186**
Aldehydes						
47	Hexanal	4.13 c	3.90 c	6.24 a	4.60 b	0.412
48	[E]-2-hexenal	3.06 c	3.39 c	5.01 a	4.00 b	0.334
49	2-Methyl-4-pentenal	0.06 b	0.07 b	0.12 a	0.08 ab	0.045
50	Butanal	0.07 b	0.19 a	0.17 a	0.23 a	0.066
51	[Z]-3-hexenal	0.08	0.09	0.12	0.11	NS
	TOTAL ALDEHYDES	**7.40 c**	**7.64 c**	**11.66 a**	**9.02 b**	**0.773**
	TOTAL VOLATILES	**550.89 a**	**352.00 c**	**288.15 d**	**409.16 b**	**30.544**

*MSD: Minimum Significant Difference on Tukey multiple range test by $p<0.01$, NS: Non-Significant

http://www.aloki.hu ● ISSN 1589 1623 (Print) ● ISSN 1785 0037 (Online)
DOI: http://dx.doi.org/10.15666/aeer/1705_1174511756

The total ester concentration in the total volatile compounds of the 'Fuji' apples grafted on the M9 rootstock was 95.52%. This rate was 91.28% for the M26 rootstock, 91.04% for the MM111 rootstock and 88.30% for the MM106 rootstock. Ester compounds are the main components of apple flavours and constitute 85 to 95% of the total volatile compounds (Paillard, 1990). Isoleucine, an amino acid, plays an important role in the synthesis of ester compounds. A greater availability of isoleucine amino acid increases the concentration of ester compounds (Sugimoto et al., 2011). Thus, it seems that the dwarf M9 rootstock has an increasing effect on the amount of isoleucine.

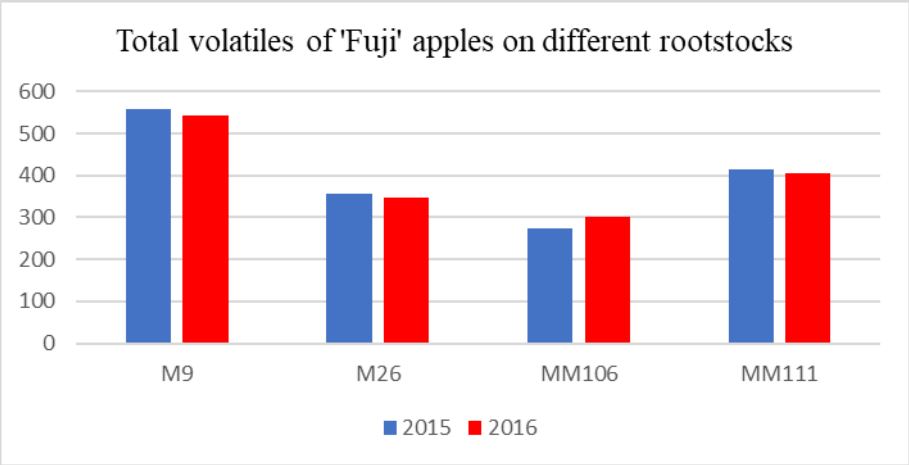

Figure 4. *Total volatiles of 'Fuji' apples on different rootstocks in two years*

In the year 2015, the ratio of 2-methylbutyl acetate compound in the 'Fuji' varieties grafted on M9 was 45.48% in all ester compounds and 43.49% in all volatile compounds; in 2016, this rate was 48.45% in all ester compounds and 46.24% in all volatile compounds. Further, in the year 2015, the ratio of 2-methylbutyl acetate compound in the 'Fuji' varieties grafted on M26 was 38.53% in all ester compounds and 35.20% in all volatile compounds; in 2016, this rate was 40.04% in all ester compounds and 36.52% in all volatile compounds. As for the MM106 rootstock, the ratio was 39.85% in all ester compounds and 35.10% in all volatile compounds in 2015, and it was 45.52% in all ester compounds and 37.66% in all volatile compounds in 2016. Lastly, for the MM111 rootstock, the ratio was 35.10% in all ester compounds and 32.01% in all volatile compounds in 2015, and it was 33.92% in all ester compounds and 30.83% in all volatile compounds in 2016. The other important ester compound in the 'Fuji' apples was ethyl 2-methylbutanoate. In the fruit samples obtained in 2015, the amount of this compound was 185.45 µg/kg for the M9 rootstock, 125.76 µg/kg for the M26 rootstock, 124.78 µg/kg for the MM111 rootstock, and 90.45 µg/kg for the MM106 rootstock (*Table 2*). In 2016, the amount was 162.47 µg/kg for the M9 rootstock, 121.52 µg/kg for the MM111 rootstock, 118.44 µg/kg for the M26 rootstock, and 96.78 µg/kg for the MM106 rootstock (*Table 3*). In the year 2015, the ratio of ethyl 2-methylbutanoate in the 'Fuji' varieties grafted on M9 was 34.66% in all ester compounds and 33.14% in all volatile compounds; in 2016, this rate was 31.40% in all ester compounds and 29.97% in all volatile compounds. Further, in the year 2015, the ratio of ethyl 2-methylbutanoate compound in the 'Fuji' varieties grafted on MM106, where the compound was found at the lowest amount, was 37.33% in all ester

http://www.aloki.hu ● ISSN 1589 1623 (Print) ● ISSN 1785 0037 (Online)
DOI: http://dx.doi.org/10.15666/aeer/1705_1174511756

compounds and 32.88% in all volatile compounds; in 2016, this rate was 36.32% in all ester compounds and 32.16% in all volatile compounds. The average amount of the compound was 173.96 µg/kg for the M9 rootstock, 123.15 µg/kg for the MM111 rootstock, 122.10 µg/kg for the M26 rootstock and 93.62 µg/kg for the MM106 rootstock (*Fig. 5*).

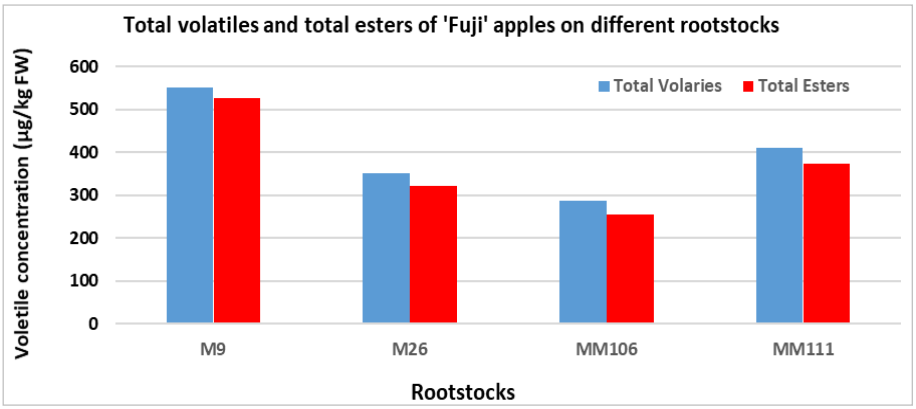

Figure 5. *Comparison of total volatiles and total ester concentrations of 'Fuji' apples grafted on different rootstocks in two years*

Besides, hexyl acetate and butyl propanoate are also notable among the ester compounds. Based on the average amount of these compounds, the 'Fuji' fruits obtained from the M9 rootstock yielded different results compared to other rootstocks (*Table 4*). Several researchers reported that esters are the main component groups of apple flavour (Echeverría et al., 2004; Mannucci et al., 2017). A study by Qin et al. (2017) identified 64 compounds based on the aroma profile of 'Fuji' apples gathered from 43 different regions in China. The researchers identified 43 ester compounds and the proportion of ester compounds in the total aroma compounds was 89.9%. As for the total amount of alcohol, the fruits collected from the MM111 rootstock had the highest amount of alcohol in both years (25.29 and 25.45 µg/kg). The M9 rootstock had the lowest amount of alcohol, which was 16.53 µg/kg and 16.51 µg/kg, respectively (*Table 2* and *Table 3*). Lower amounts of acidic compounds, which are among volatile compounds, were obtained compared to the amounts of the other main compound groups. In terms of the total acidic compounds, acetic acid identified in the MM111 rootstock was highest (*Table 4*). The amount of acetic acid in this rootstock was 1.40 µg/kg in 2015 and 1.32 µg/kg in 2016 (*Table 2* and *Table 3*).

Following esters and alcohols, aldehydes were the volatile compound group with the next highest level. Hexanal and [E]-2-hexanal were the compounds with the highest values in this group. The MM106 rootstock had the highest average value in terms of the total amount of aldehyde compounds (11.66 µg/kg). The lowest amount of aldehyde was found in the fruits on the M9 rootstock (7.40 µg/kg) (*Table 4*).

The results of this two-year study showed that the M9 rootstock has positive impact on the aroma profile of the 'Fuji' apples. It is remarkable that the M9 rootstock considerably increases the amount of ester compounds particularly.

http://www.aloki.hu ● ISSN 1589 1623 (Print) ● ISSN 1785 0037 (Online)
DOI: http://dx.doi.org/10.15666/aeer/1705_1174511756

Discussion

Wang et al. (2005) analysed the volatile compounds of conventional and organically cultivated 'Fuji' apple varieties on GC-MS using SPME method. As a result, 64 compounds were found in organic system and 51 compounds were found in control fruits. Tao et al. (2011) used the GC-MS with SPME method to determine the aroma components in eight apple varieties. As a result, 28 esters, 3 alcohols and 2 alkane compounds were determined. A study by Kviklys et al. (2014) revealed that the total phenol content of the M9 rootstock was higher than the M26 rootstock. However, they reported that there was no distinctive difference between different rootstocks in terms of the total phenol content. Unlike the total phenolic compounds, the amount of volatile compounds varied between rootstocks.

Although the effect of rootstocks on the quality characteristics of fruits has been analysed in different varieties, the studies about their impact on aroma profile are extremely low in number. Seker et al. (2017) reported the positive effects of the 'GF677' rootstock on the aroma profile of 'Cresthaven', a peach variety. Further studies may focus on the effect of rootstocks on aroma profile in different apple varieties.

Conclusion

Rootstocks may have great effect on aroma compound formation due to different carbohydrate and fatty acid metabolism pathways. So, utilization of different rootstocks should be considered for specific aroma compound improvements in apples.

REFERENCES

[1] Autio, W. R., Krupa, J. (2001): Rootstock effects on ginger gold apple trees. – Fruit Notes 66: 50-52.

[2] Baytekin, S., Akca, Y. (2011): Determination of performance different apple cultivars on M9 apple rootstock. – Journal of Agricultural Faculty of Gaziosmanpasa University 28(1): 45-51.

[3] Brown, G. R., Wolfe, D. (1999): Rootstock and interstem effects on pome and stone fruit trees. – In: Rowell, B. (ed.) Fruit and Vegetable Crops Research Reports. Kentucky Agricultural Experiment Station, University of Kentucky College of Agriculture Department of Horticulture Lexington, p: 14-18.

[4] Dimick, P. S., Hoskin, J. C. (1983): Review of apple flavor-state of the art. – CRC Critical Reviews in Food Science and Nutrition 18: 387-409.

[5] Echeverría, G., Graell, J., López, M. L., Lara, I. (2004): Volatile production, quality and aroma-related enzyme activities during maturation of 'Fuji' apples. – Postharvest Biology and Technology 31(3): 217-227. doi:10.1016/j.postharvbio.2003.09.003.

[6] FAOSTAT. (2018): Food and Agricultural Organization of the United Nations, Statistical Data. – Available at : http://www.fao.org/faostat/en/#data/PP.

[7] Jackson, J. E. (2003): Biology of apples and pears. – Cambridge University Press.

[8] Kvikly, D., Liaudanskas, M., Janulis, V., Viskelis, P., Rubinskiene, M., Lanauskas, J., Uselis, N. (2014): Rootstock genotype determines phenol content in apple fruits. – Plant, Soil and Environment 60(5): 234-240.

[9] Mannucci, A., Serra, A., Remorini, D., Castagna, A., Mele, M., Scartazza, A., Ranieri, A. (2017): Aroma profile of Fuji apples treated with gelatin edible coating during their storage. – LWT-Food Science and Techology 85: 28-36.

http://www.aloki.hu ● ISSN 1589 1623 (Print) ● ISSN 1785 0037 (Online)
DOI: http://dx.doi.org/10.15666/aeer/1705_1174511756

[10] Marini, R. P. (2002): Does rootstock influence apple fruit size? – Compact Fruit Tree 35(1): 8-10.
[11] Nicolai, J. (1998): European trends in apple tree density, Rootstocks and Tree Training. – 41th Annual IDFTA Conference, February 21-25, Pasco, Washington.
[12] Özçağıran, R., Ünal, A., Özeker, E., İsfendiyaroğlu, M. (2005): Apple. Temperate Climate Fruit Types, Pome Fruits, Vol: II. – Ege University Faculty of Agriculture Publications, Bornova, İzmir, No: 556.
[13] Paillard, N. M. M. (1990): The flavour of apples, pears and quinces. – In: Morton, I. D., Macleod, A. J. (eds.) Food flavours, Part C. The flavour of fruits. Elsevier, Amsterdam, The Netherlands, p. 1-41.
[14] Qin, L., Wei, Q. P., Kang, W. H., Zhang, Q., Sun, J., Liu, S. Z. (2017): Comparison of volatile compounds in 'Fuji' apples in the different regions in China. – Food Science and Technology Research 23(1): 79-89.
[15] SAS Institute. (1997): SAS/STAT Guide for Personal Computers. – SAS Institute Inc., Cary, USA.
[16] Seker, M., Ekinci, N., Gur, E. (2017): Effects of different rootstocks on aroma volatile constituents in the fruits of peach (Prunus persica L. Batsch cv. 'Cresthaven'). – New Zealand Crop and Horticultural Science 45(1): 1-13.
[17] Sugimoto, N., Jones, A. D., Beaudry, R. (2011): Changes in free amino acid content in 'Jonagold' apple fruit as related to branched-chain ester production, ripening, and senescence. – J. Amer. Soc. Hort. Sci.
[18] Tao, C., Wang, D., Yang, X., Luo, Y. (2011): Determination of aroma components of 8 cultivars of apple fruit by SPME and GC-MS. – Journal of Gansu Agricultural University 2011-01.
[19] Ünüvar, G., Pırlak, L. (2016): Determination of phenological and pomological characters of some apple cultivars grafted on M9 rootstock at Karaman ecological conditions. – Nevsehir Journal of Science And Technology, TARGİD, Special Number: 96-106. DOI: 10.17100/nevbiltek.210971.
[20] Vicentini, C. B., Buldrini, F., Bosi, G., Romagnoli, C. (2018): "Spigo nardo": from the Erbario Estense a possible solution for its taxonomical attribution. – Rendiconti Lincei, Scienze Fisiche e Naturali 29(4): 909-921.
[21] Wang, X., Shi, D., Şarkı, Y., Zhai, H. (2005): GC-MS analysis of fruit aroma components of organic 'Fuji' apple. – Journal of Fruit Science 2005-6.
[22] Wang, Y. J., Yang, C. X., Li, S. H., Yang, L., Wang, Y. N., Zhao, J. B., Jiang, Q. (2009): Volatile characteristics of 50 peaches and nectarines evaluated by HP-SPME with GC–MS. – Food Chem. 116: 356-364.
[23] Zishan, A., Anwar, S., Shiwali, S. (2017): Evaluation of in vitro antioxidant activity, HPLC and GC–MS analysis along with chemoprofiling of Decalepis arayalpathra: a critically endangered plant of Western Ghats, India. – Rendiconti Lincei 28(4): 711-720.

http://www.aloki.hu ● ISSN 1589 1623 (Print) ● ISSN 1785 0037 (Online)
DOI: http://dx.doi.org/10.15666/aeer/1705_1174511756

MINERAL PROFILE OF THE WINTER WHEAT GRAIN: EFFECTS OF SOIL TILLAGE SYSTEMS AND NITROGEN FERTILIZATION

DOLIJANOVIĆ, Ž.[1] – ROLJEVIĆ NIKOLIĆ, S.[2*] – KOVAČEVIĆ, D.[1] – DJURDJIĆ, S.[3] – MIODRAGOVIĆ, R.[3] – JOVANOVIĆ TODOROVIĆ, M.[2] – POPOVIĆ DJORDJEVIĆ, J.[4*]

[1]Department of Field and Vegetable Crops, Faculty of Agriculture, University of Belgrade, St. Nemanjina 6, 11080, Belgrade, Serbia (phone: +381-11-441-3321)

[2]Institute of Agricultural Economics, Belgrade, St. Volgina 15, 11060 Belgrade, Serbia (phone: +381-11-697-2842, fax: +381-11-697-2848)

[3]Department for Agricultural Engineering, Faculty of Agriculture, University of Belgrade, St. Nemanjina 6, 11080, Beograd, Serbia (phone: +381-11-441-3449)

[4]Department of Food Technology and Biochemistry, Faculty of Agriculture, University of Belgrade, St. Nemanjina 6, 11080, Belgrade, Serbia (phone: +381-11-441-3142)

**Corresponding authors*
e-mail: svetlana_r@iep.bg.ac.rs (S. Roljević Nikolić, ORCID ID: 0000-0002-3139-0289); jelenadj@agrif.bg.ac.rs (J. Popović Djordjević, ORCID ID: 0000-0003-4057-3826)

(Received 22nd Apr 2019; accepted 12th Jul 2019)

Abstract. The aim of this study was to analyze the impact of various systems of soil tillage and nitrogen doses on the mineral composition of the grain of the common winter wheat cultivar (*Triticum aestivum* ssp. *vulgare*), cv. Azra selected for the conventional intensive production. The field experiment was conducted on luvic chernozem in completely randomized blocks. Wheat was grown under three soil tillage systems: conventional tillage, mulch tillage and no-tillage, and the experiment included two doses of N fertilization (60 and 120 kg ha^{-1}). Concentrations of eighteen elements (As, Al, Ba, Ca, Co, Cr, Cu, Fe, Hg, K, Mg, Mn, Ni, S, Sr, P, V and Zn) in wheat grain samples were determined by means of inductively coupled plasma with optical emission spectrometry (ICP–OES). The results indicated that concentrations of the studied elements in the wheat grain were significantly affected by the tillage systems and fertilization rates ($p < 0.001$), as well as by the interaction of these two factors. A smaller dose of nitrogen fertilizer (60 kg ha^{-1}) had a significantly better impact on the concentration of macro- and microelements in the wheat grain than the dose of 120 kg N ha^{-1}. The reduced tillage systems and lower nitrogen rates in nutrition had a better effect on the increase of the content of the studied elements in the wheat grain than the conventional cultivation which applied higher nitrogen rates.
Keywords: *wheat grain, production system, fertilization, macroelements, microelements, ICP-OES*

Introduction

Wheat (*Triticum aestivum* L.) is one of the most significant cultivated species and the staple food for more than 50% of the global population (Rizwan et al., 2016). The average per capita consumption of wheat in developed countries and developing countries amounts to 95 kg and 61 kg, respectively (FAO, 2016). In Serbia, the average per capita consumption of wheat is 180 kg, which is significantly higher than the consumption rates in most European countries (USDA, 2017). Due to its high global

http://www.aloki.hu ● ISSN 1589 1623 (Print) ● ISSN 1785 0037 (Online)
DOI: http://dx.doi.org/10.15666/aeer/1705_1175711771

consumption in the form of different food products, wheat is considered to be an important source of minerals in the everyday human nutrition.

The bioavailability of microelements in cereals is generally low (Kan, 2015; Dapkekar et al., 2018) and the concentrations of trace elements that are valuable for human nutrition steadily decrease with an increase in yield, which has adverse consequences, including 'hidden hunger' (Cakmak et al., 2010). Approximately half of the global population has zinc deficiency, and anaemia induced by iron deficiency is the most common phenomenon in Europe (Kan, 2015; Winiarska-Mieczan et al., 2019). In this context, the increase of micronutrient concentrations such as Fe and Zn in cereal grain has become a high-priority research area (Cakmak et al., 2010; Kutlu, 2018). Certain heavy metals (Zn, Cu and Ni) are necessary for biological processes in the human organism and they represent integral and catalytic components of proteins and enzymes, but they can be toxic in an overdose (Tiwari and Lata, 2018). On the other hand, toxic or non-essential elements such as As, Cd, Cr and Pb have no biological function in the human body and can be harmful for human health even in extremely low concentrations in case of long-term exposure (Lei et al., 2015; Zhang et al., 2019). What is more, these metals are responsible for the depletion of certain essential elements (Abbas et al., 2017).

The optimal application of fertilizers is an important factor for obtaining high yield and high quality products. Among the elements of mineral nutrition, nitrogen has the most important role in forming the yield (Litke et al., 2018), quality and utilizable value of the wheat grain (Blandino et al., 2016). Numerous studies have shown that the application of nitrogen fertilizer can promote the accumulation of certain microelements in the wheat grain, such as Fe and Zn (Kutman et al., 2011; Singh et al., 2018). This effect is explained by the fact that the sufficient supply of nitrogen increases the content of proteins in the grain, and the proteins are where Fe and Zn are accumulated (Barunawati et al., 2013). Similarly, previous research has shown that the concentration of Fe and Zn has a significant positive correlation with the content of proteins and P in the wheat grain (Zhao et al., 2009).

There has recently been an increasing interest in reduced soil tillage, stimulated by ecological and economic reasons (Sharma et al., 2011). According to some authors, the methods of reduced soil tillage increase soil density and inadequate distribution of nitrogen, phosphorus and microelements (Klikocka and Marks, 2018), which can consequently affect the uptake of mineral matter and thus influence the yield and crop quality. However, Stanislawska-Glubiak and Korzeniowska (2012) did not determine significant differences between various tillage systems regarding the content of microelements in wheat plants, except in respect of P and Mg in the early growth phases when the concentration of these elements was higher in the NT and MT systems than in CT. A similar study indicated that the NT system did not lead to the impairment of the quality of wheat and maize grains in terms of the primary mineral content, which is extremely significant for the nutritional value of the wheat grain (Stanisławska-Glubiak and Korzeniowska, 2012).

Scientific literature is still deficient in information regarding the impact of tillage on the chemical content of the wheat grain. Thus, the aim of this research was to determine the impact that tillage systems and different fertilization rates, within the applied cultivation technology, had on the differences in the content of the studied elements in the wheat grain of the cultivar Azra.

http://www.aloki.hu ● ISSN 1589 1623 (Print) ● ISSN 1785 0037 (Online)
DOI: http://dx.doi.org/10.15666/aeer/1705_1175711771

Materials and methods

Field experiment

The examination of the effects of different tillage systems and fertilization rates on the content of macro- and microelements in the wheat grain was conducted at the research field "Radmilovac" that belongs to the Faculty of Agriculture (44°45' N, 20°35' E, Serbia) in the growing season of 2016-2017. The soil type was luvic chernozem (WRB, 2014), with the following characteristics: $pH_{(H2O)}$ 8.04, total content of N 13%, available forms of phosphorus 22.18 mg P_2O_5 100 g^{-1} dry weight and potassium 19.10 mg K_2O 100 g^{-1} dw, content of humus in the topsoil layer 2.45%.

The study used the winter cultivar of common wheat (*Triticum aestivum* ssp. *vulgare*), cv. Azra, selected for the conventional intensive production. Cv. Azra is a winter hardy cultivar of medium late maturity. It is very well-resistant to *Erysiphe graminis* DC. and well-resistant to *Puccinia striiformis* f. sp. *tritici* (*Pst*). Its hectolitre weight amounts to 80 - 85 kg, protein content is 11.5 - 13.0%, and it belongs to the B1-B2 quality group. The previous crop was maize (*Zea mays* L.).

A two-factor field trial was arranged using split plot design in three replications, with the area of the elementary plot amounting to 6 m^2. The examined factors were tillage and fertilization. Three different tillage systems were used and two levels of fertilization were applied (*Fig. 1*).

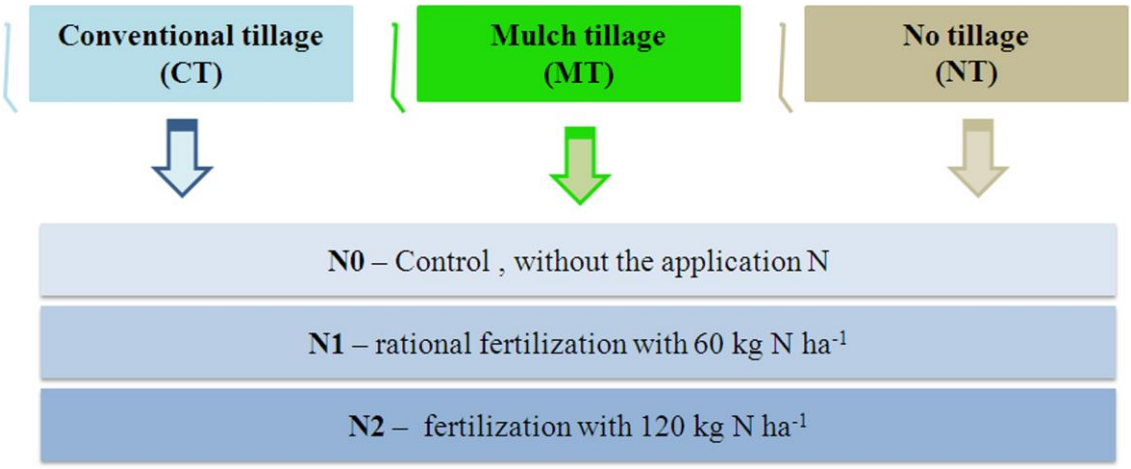

Figure 1. *Experiment design*

1. Conventional tillage (CT) - ploughing using a mouldboard plough at 25 cm and pre-sowing tillage using a disc harrow and a harrow,
2. Mulch tillage (MT) - tillage performed using a chisel plough at 25 cm with more than 30% of maize crop residues on the soil surface and the pre-sowing tillage using a disc harrow and a harrow,
3. No tillage (NT) - seeds were sown directly into unploughed soil, with the complete maize crop residues left on the surface.

Basic fertilization by NPK fertilizers was conducted during the autumn in the same quantity for all treatments. Spring fertilization was performed in the tillering phase using the KAN mineral fertilizer (25-27% N) and it differed in terms of pure nitrogen

http://www.aloki.hu ● ISSN 1589 1623 (Print) ● ISSN 1785 0037 (Online)
DOI: http://dx.doi.org/10.15666/aeer/1705_1175711771

quantities. Sowing was conducted on October 28th, 2016 with the crop density of 650 seeds m^{-2}. Standard cultivation measures in wheat production were applied and harvest was performed on June 29th, 2017.

Grain sample preparation for chemical analysis

In the grain of Azra cultivar, concentrations of macroelements: calcium (Ca), potassium (K), magnesium (Mg), phosphorus (P) and sulphur (S), as well as microelements: aluminium (Al), arsenic (As), barium (Ba), cobalt (Co), chromium (Cr), copper (Cu), iron (Fe), mercury (Hg), manganese (Mn), nickel (Ni), strontium (Sr), vanadium (V) and zinc (Zn) were determined.

The representative samples were made using a random square method as described by Korunović and Stojanović (1989). The wheat grain samples were ground in the laboratory mill SJ-500 (producer "Metron"), and then prepared for the chemical analysis. Both soil and grain samples were subjected to the process of "wet digestion" as described in our previous work (Popović-Djordjević et al., 2019).

The determination of the content of the elements was performed using the inductively coupled plasma-optical emission spectroscopy (ICP–OES) analysis. The analysis was conducted using the instrument Thermo Scientific iCAP 6500 Duo ICP (Thermo Fisher Scientific, Cambridge, UK). The calibration of the instrument was performed by means of two certified multielement ICO-OES standards: Multi–Element Plasma Standard Solution 4, Specpure® (Alfa Aesar GmbH & Co KG, Germany) and SS–Low Level Elements ICV Stock (10 mg L–1K) (VHG Labs, Inc–Part of LGC Standards, Manchester, NH 03103 USA). The analytic process was verified by the certified reference material EPA Method 200.7 LPC Solution (ULTRA Scientific, USA). The correlation of the measured concentrations with the certified values amounted to 96-104%.

Statistical analysis

Data processing was performed in the SPSS statistical package. The method for analyzing the variance (*F test*) for dual factor examination was used, and the significance of differences between the treatments was tested with the LSD test at the significance level of $p < 0.05$. Statistical data are given in *Table A1* in the *Appendix*.

Results

Concentration of macroelements in the wheat grain

The total content of the examined macroelements, as well as their average values are presented in *Table 1*. The total content of macroelements detected in the NT system (9968.11 mg kg^{-1}) was higher ($p < 0.05$) than in the MT and CT systems, by 1.7% and 5.3%, respectively. Differences in the treatment by means of nitrogen fertilization were also significant, where the content of macroelements in the control (9968.11 mg kg^{-1}) was higher by 2.3 and 3.2% than at the N1 and N2 levels, respectively.

The concentration of the examined macroelements, expressed in mg kg^{-1}, was in the following order: P (4058.89) > K (3350.33) > Mg (1169.55) > S (996.89) > Ca (171.33). The analysis of variance showed the statistically significant variability of macroelement concentrations among the studied tillage systems, as well as among the rates of nitrogen fertilization (*Table A1*). Considering the differences in the tillage

http://www.aloki.hu ● ISSN 1589 1623 (Print) ● ISSN 1785 0037 (Online)
DOI: http://dx.doi.org/10.15666/aeer/1705_1175711771

systems, the results indicate that the lowest concentration of all studied macroelements was detected in the CT system. The highest concentration of Ca (178.67 mg kg^{-1}), K (3410.33 mg kg^{-1}), Mg (1236.33 mg kg^{-1}) and P (4167.00 mg kg^{-1}) was detected in the NT system, while the highest concentration of S (1016.33 mg kg^{-1}) was found in the MT system.

Table 1. *Concentration of macroelements (mg kg^{-1}) in the wheat grain, cv. Azra*

Tillage	N Rate	Ca	K	Mg	P	S	Total content of macroelements
CT	N0	164 ± 2	3652 ± 34	1300 ± 7	4470 ± 14	1031 ± 1	10617.00
	N1	173 ± 4	3244 ± 24	1094 ± 14	3917 ± 12	965 ± 6	9393.00
	N2	141 ± 2	2926 ± 22	942 ± 26	3388 ± 17	983 ± 6	8380.00
MT	N0	165 ± 3	3287 ± 32	1139 ± 27	3973 ± 22	981 ± 6	9545.00
	N1	177 ± 3	3462 ± 34	1180 ± 27	4180 ± 19	1040 ± 5	10039.00
	N2	186 ± 2	3351 ± 11	1162 ± 23	4101 ± 4	1028 ± 3	9828.00
NT	N0	189 ± 4	3271 ± 26	1192 ± 11	4007 ± 17	954 ± 3	9613.00
	N1	178 ± 3	3333 ± 33	1158 ± 6	4023 ± 10	979 ± 2	9671.00
	N2	169 ± 3	3627 ± 11	1359 ± 4	4471 ± 9	1011 ± 2	10637.00
Tillage	CT	159.33	3274.00	1112.00	3925.00	993.00	9463.33
	MT	176.00	3366.67	1160.33	4084.67	1016.33	9804.00
	NT	178.67	3410.33	1236.33	4167.00	981.33	9968.11
N Rate	N0	172.67	3403.33	1210.33	4150.00	988.67	9925.00
	N1	176.00	3346.33	1144.00	4040.00	994.67	9701.00
	N2	165.33	3301.33	1154.33	3986.67	1007.33	9615.00

Data are expressed as mean ± standard deviation (n = 3)

The concentration of macroelements in the grain significantly varied depending on different levels of nitrogen fertilization (*Tables 1* and *A1*). In the control group, there was a significantly higher concentration of P (4150.00 mg kg^{-1}), K (3403.33 mg kg^{-1}) and Mg (1210.33 mg kg^{-1}) than in the N1 and N2 variant. The highest concentration of Ca (176.00 mg kg^{-1}) was in the cases when the dose of 60 kg N ha^{-1} was applied, while the sulphur concentration in N2 (1007.33 mg kg^{-1}) was higher by approximately 2% than in the N0 and N1 variants (*Fig. 2*).

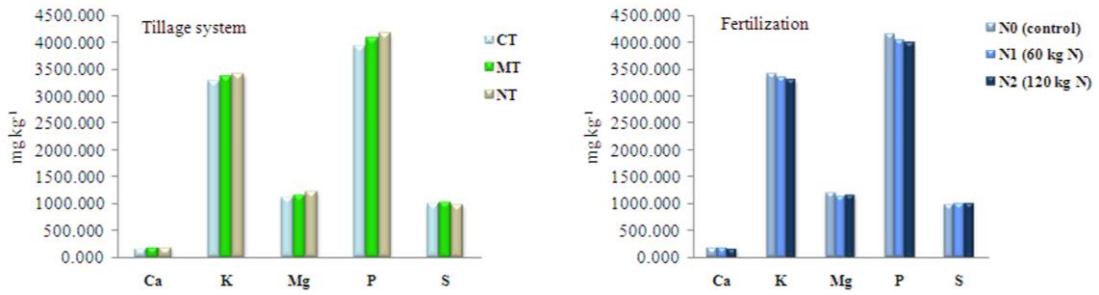

Figure 2. *Changes of macroelement concentration (mg kg^{-1}) in the grain within different tillage systems and levels of fertilization*

http://www.aloki.hu ● ISSN 1589 1623 (Print) ● ISSN 1785 0037 (Online)
DOI: http://dx.doi.org/10.15666/aeer/1705_1175711771

Observing the interaction between the tillage systems and the levels of nitrogen fertilization, it can be noticed that the highest average value of Ca (189 ± 4 mg kg^{-1}) was recorded in the NT system with the N0 variant, and it was significantly higher than in other tillage systems and levels of nitrogen fertilization. It is interesting that the differences in the K concentration were not significant between the CT system with the N0 variant (3652 ± 34 mg kg^{-1}) and the NT system with the N2 variant (3627 ± 11 mg kg^{-1}). On the other hand, the concentrations of Mg (1300 ± 7 mg kg^{-1}), P (4470 ± 14 mg kg^{-1}) and S (1031.0 ± 1.0 mg kg^{-1}) in the CT system with the variant N0 were significantly higher than in other tillage systems and fertilization levels. The obtained results indicate that the reduced tillage and/or application of lower nitrogen rates do not decrease the macroelement contents in the wheat grain (*Fig. 2*).

Concentration of microelements in the wheat grain

The total content of microelements in the wheat grain and their average concentrations are presented in *Table 2*. The research results showed that the microelement content in the grain was affected by the tillage system and fertilization rate, as well as by the interaction of these factors (*Table A1*). There is a small but significant difference regarding the microelement content between the CT system (103.691 mg kg^{-1}) and NT system (102.048 mg kg^{-1}). Considering the differences between the rates of nitrogen fertilization, it can be noticed that the total content of microelements in the N2 variant (76.096 mg kg^{-1}) is significantly lower than in N1 (108.229 mg kg^{-1}) and N0 (104.880 mg kg^{-1}).

The concentrations of Al, Cr and Hg were below the limit of detection (LOD) in all studied grain samples of Azra cultivar. The concentrations of detected microelements, expressed in mg kg^{-1}, were in the following order: Fe (38.10) > Zn (27.90) > Mn (22.26) > Cu (3.87) > Ba (2.65) > Sr (0.83) > V (0.35) > Ni (0.29) > As (0.11) > Co (0.06).

The content of Fe detected in the NT system (46.170 mg kg^{-1}) was significantly higher than in the MT (23.390 mg kg^{-1}) and CT system (44.740 mg kg^{-1}). The highest concentration of Fe in the amount of 47.330 mg kg^{-1} was detected in the variant of fertilization with the smaller dose of nitrogen (60 kg ha^{-1}), while the lowest concentration (20.200 mg kg^{-1}) was detected in the application of nitrogen at the rate of 120 kg ha^{-1} (*Fig. 3*). The interaction of the examined factors indicates that the highest Fe concentration (101.3 ± 1.0 mg kg^{-1}) was obtained in the NT system with the N0 variant, and it was significantly higher than in other tillage systems and fertilization levels (*Table 2*).

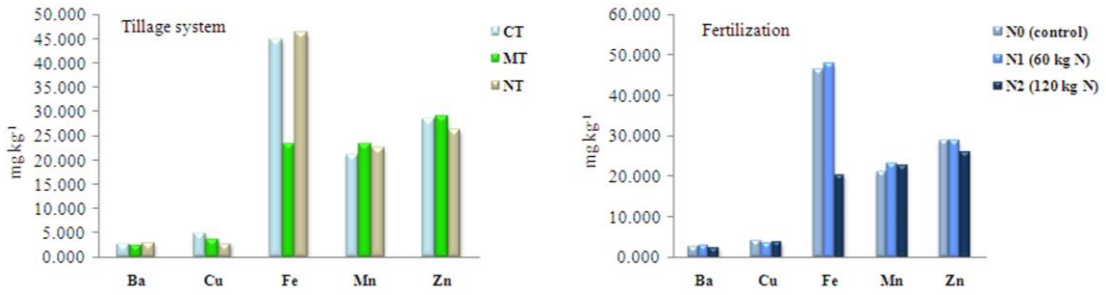

Figure 3. *Changes of Ba, Cu, Fe, Mn and Zn concentration (mg kg^{-1}) in the grain within different tillage systems and levels of fertilization*

http://www.aloki.hu ● ISSN 1589 1623 (Print) ● ISSN 1785 0037 (Online)
DOI: http://dx.doi.org/10.15666/aeer/1705_1175711771

Table 2. *Concentration of microelements (mg kg^{-1}) in the wheat grain, cv. Azra*

Tillage	N rate	As	Ba	Co	Cu	Fe	Mn	Ni	Sr	V	Zn	Total content of microelements
CT	N0	<LOD	2.32±0.02	0.06±0.02	6.61±0.06	21.12±0.07	21.4±0.3	1.30±0.09	0.688±0.005	0.284±0.002	34.21±0.06	87.992
	N1	0.013±0.003	2.68±0.02	0.25±0.02	2.61±0.05	96.7±0.8	22.6±0.4	0.36±0.06	0.697±0.003	0.53±0.05	29.0±0.2	155.440
	N2	<LOD	2.97±0.03	<LOD	5.98±0.07	16.4±0.3	19.3±0.3	<LOD	0.79±0.02	<LOD	22.2±0.2	67.640
MT	N0	0.177±0.004	2.94±0.05	0.012±0.003	2.06±0.06	16.57±0.09	21.0±0.4	<LOD	0.909±0.008	0.164±0.003	27.47±0.10	71.302
	N1	<LOD	3.66±0.02	0.018±0.003	6.52±0.07	28.3±0.3	24.9±0.4	0.5±0.2	0.878±0.003	0.78±0.02	31.95±0.02	97.506
	N2	<LOD	0.62±0.03	0.084±0.010	2.60±0.05	25.3±0.4	23.8±0.3	0.023±0.004	0.855±0.004	0.65±0.04	27.66±0.07	81.592
NT	N0	0.24±0.02	2.459±0.008	0.050±0.009	3.84±0.05	101.3±1.0	20.8±0.3	0.171±0.02	0.905±0.007	0.38±0.02	25.2±0.2	155.345
	N1	0.34±0.03	2.56±0.02	0.041±0.006	1.93±0.05	18.3±0.2	22.1±0.2	0.068±0.002	0.793±0.004	0.320±0.005	25.29±0.05	71.742
	N2	0.19±0.05	3.66±0.02	0.018±0.002	2.67±0.07	18.9±0.4	24.4±0.2	0.17±0.03	0.908±0.004	<LOD	28.14±0.10	79.056
Tillage	CT	0.004	2.657	0.103	5.066	44.740	21.100	0.553	0.725	0.271	28.470	103.691
	MT	0.059	2.407	0.038	3.727	23.390	23.233	0.174	0.881	0.531	29.027	83.467
	NT	0.257	2.893	0.036	2.813	46.170	22.433	0.136	0.869	0.233	26.210	102.048
N Rate	N0	0.139	2.573	0.041	4.170	46.330	21.067	0.490	0.834	0.276	28.960	104.880
	N1	0.118	2.967	0.103	3.687	47.770	23.200	0.309	0.789	0.543	28.747	108.229
	N2	0.063	2.417	0.034	3.750	20.200	22.500	0.064	0.851	0.217	26.000	76.096

Al, Cr and Hg were below LOD; Data are expressed as mean ± standard deviation (n = 3)

http://www.aloki.hu ● ISSN 1589 1623 (Print) ● ISSN 1785 0037 (Online)
DOI: http://dx.doi.org/10.15666/aeer/1705_1175711771

Significant differences between the tillage systems were also detected regarding the concentration of Zn. In the NT system (26.210 mg kg^{-1}) it was lower by 9.7% and 7.9% than in the MT and CT systems, respectively. Considering the variants of nitrogen fertilization, Zn concentration was significantly lower than in the control, particularly in the N2 variant (10.2%). Observing the interaction of the examined factors, it can be noticed that the highest Zn concentration was detected in the CT system with the control variant (34.21 ± 0.06 mg kg^{-1}), in the MT system with the N1 variant (31.95 ± 0.02 mg kg^{-1}), and in the NT system with the N2 variant (28.14 ± 0.10 mg kg^{-1}) (*Table 2*).

When it comes to Mn, there were also significant differences regarding the tillage system and fertilization rate. The highest Mn concentration was detected in the MT system (23.233 mg kg^{-1}), and it was higher than in the CT and NT systems by 10.1% and 3.6%, respectively. The Mn concentration in the N1 variant (23.200 mg kg^{-1}) was higher than in the N0 and N2 variants by 10.1% and 3.2%, respectively.

The application of the conventional tillage system resulted in the significantly higher concentrations of Cu (5.066 mg kg^{-1}), Ni (0.553 mg kg^{-1}) and Co (0.103 mg kg^{-1}) than in the NT and MT systems, while there were no significant differences regarding nickel and cobalt between the NT and MT systems. It was also noticed that the concentrations of Cu and Ni in the grain decreased with the increased rate of nitrogen fertilization. Therefore, the highest concentrations of these microelements were detected in the variant N0 (4.170 mg kg^{-1} and 0.490 mg kg^{-1}). The concentration of Co in the wheat grain was the highest when the application of nitrogen was at the rate of 60 kg ha^{-1} and the differences between the variants N0 (0.041 mg kg^{-1}) and N2 (0.034 mg kg^{-1}) were not significant.

The highest Ba concentration was detected in the NT system (2.893 mg kg^{-1}), which was higher ($p < 0.05$) by 20.2% and 8.9% than in the MT and CT systems, respectively. Significant differences were also obtained at different fertilization rates. The Ba concentration in the N2 variant (2.417 mg kg^{-1}) was lower by 6.1% and 18.5% than in the control and N1 variant, respectively.

The content of Sr in plants is highly variable. The research results showed that the Sr concentration in the grain was the lowest in the CT system (0.725 mg kg^{-1}), and it was lower than in the MT and NT system by 17.7% and 16.5%, respectively. When it comes to the differences in fertilization rates, the lowest Sr concentration (0.789 mg kg^{-1}) in the grain was detected when applying the dose of 60 kg N ha^{-1}, while its concentration was the highest (0.851 mg kg^{-1}) at the rate of 120 kg N ha^{-1}.

The highest concentrations of V were detected in the MT system (0.531 mg kg^{-1}) and at the nitrogen application at a rate of 60 kg ha^{-1} (0.543 mg kg^{-1}). The intensity of soil tillage had an impact on the increase of As content, while the application of N fertilizers decreased the concentration of this trace element in the wheat grain (*Fig. 4*).

Discussion

A high yield of good quality is based on the proper use of agro-technical measures, primarily on the appropriate soil tillage and adapted crop fertilization. In modern agriculture, it is important to understand the effects of these measures since they can affect the product quality (Klikocka and Marks, 2018), and also contribute to the protection and preservation of soil fertility.

http://www.aloki.hu ● ISSN 1589 1623 (Print) ● ISSN 1785 0037 (Online)
DOI: http://dx.doi.org/10.15666/aeer/1705_1175711771

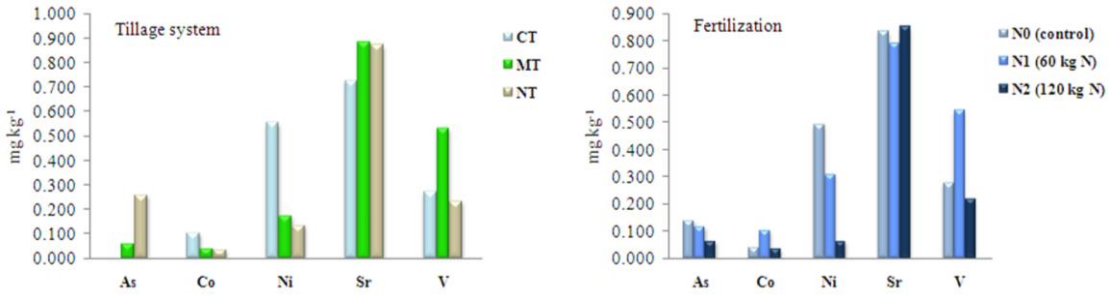

Figure 4. *Changes of As, Co, Ni, Sr and V concentration (mg kg^{-1}) in the grain within different tillage systems and levels of fertilization*

It was determined that the mineral content in the wheat grain, cv. Azra, differed significantly depending on the tillage system. The grain originating from the NT system had a significantly higher content of macroelements than in the MT system (1.7%) and CT system (5.3%). The highest concentrations of Ca (178.67 mg kg^{-1}), K (3410.33 mg kg^{-1}), Mg (1236.33 mg kg^{-1}) and P (4167.00 mg kg^{-1}) were detected in the NT system ($p < 0.001$), while the highest S concentration (1016.33 mg kg^{-1}) was found in the wheat grain cultivated in the MT system ($p < 0.05$). The obtained results suggest that the reduced tillage systems can have a positive effect on the concentration of macroelements in the wheat grain. According to De Vita et al. (2007), the NT system is more efficient than the CT in arid environments since it decreases the evaporation of moisture from soil surface, which ensures its better availability to plants. Furthermore, Wozniak (2010) states that the reduced tillage and lowered rates of N fertilizers increase the content of minerals in the wheat grain.

Nitrogen has a crucial role in the vegetative growth and crop quality (Faizy et al., 2017; Litke et al., 2018). However, the intensive application of mineral fertilizers has different local and global effects on the environment and human health. The research results have shown that the lowest average concentrations of Ca (165.33 mg kg^{-1}), K (3301.33 mg kg^{-1}) and P (3986.67 mg kg^{-1}) were detected in the variant with the highest rate of nitrogen fertilization (120 kg ha^{-1}). Studying the nitrogen application in protected areas, Bar-Tal et al. (2001) concluded that the application of larger doses of nitrogen decreased the assimilation of Ca, which is probably a consequence of the increased concentration of NH_4^+. Other studies showed that higher rates of N fertilizer application increased the content of phosphorus and potassium in the wheat grain (Gaj and Gorski, 2014; Faizy et al., 2017), which can be affected by numerous factors such as assortment, crop maturity, soil type and content, fertilizer type and rate (Jākobsone et al., 2015; Kan, 2015). In this study, fertilizer application did not have a positive effect on the increase of Mg concentration in the wheat grain. Nutrition treatment at the N rates of 60 and 120 kg ha^{-1} had similar values of Mg content, and they were significantly lower than in the control treatment (1210.33 mg kg^{-1}). Considering the studied macroelements, only S had a detected rise of concentration connected to the increase of N fertilizer dose. Similarly, Jamal et al. (2010) stated that there was a high positive correlation between the nitrogen and sulphur contents in wheat.

The analysis of variance of the obtained results showed that tillage had a statistically significant effect on concentration of microelements in the grain of cv. Azra. The highest ($p < 0.05$) concentrations of Fe (46.170 mg kg^{-1}), Ba (2.893 mg kg^{-1}) and As (0.257 mg kg^{-1}) were detected in NT, while the concentrations of Zn (29.027 mg kg^{-1}),

http://www.aloki.hu ● ISSN 1589 1623 (Print) ● ISSN 1785 0037 (Online)
DOI: http://dx.doi.org/10.15666/aeer/1705_1175711771

Mn (23.233 mg kg^{-1}), Sr (0.881 mg kg^{-1}) and V (0.531 mg kg^{-1}) in the MT system were significantly higher than in the CT and NT systems (*Figs. 3* and *4*). Arsenic is an environmental and food-chain contaminant, and inorganic As is a class-one carcinogen (Zhao et al., 2010). Wozniak and Makarski (2012) underline that the availability of microelements in well aerated soils is lower than in the less aerated ones, so it can be concluded that the multiple aeration of ground in the ploughing system depresses the availability of Zn and Cu, unlike in the ploughless tillage. The assimilation of Fe, Cu, Mn and Zn in the reduced tillage systems is easier not only for wheat but also for weeds in the calcareous soil (Taghizadeh et al. 2014). In addition, Santiago et al. (2008) found out that there was a higher concentration of Mn, Cu and Zn in the plants cultivated in the NT system than in the ones from CT and MT systems. Higher concentration of Mn in the conditions of reduced tillage (23.233 mg kg^{-1} and 22.433 mg kg^{-1}) than in the case of conventional tillage (21.100 mg kg^{-1}) can be explained by the better moisture content in the soil in MT and NT systems, which was confirmed by other studies (Wozniak and Makarski, 2012). The decrease of mineral content in the food is considered to be related to the intensive agricultural practices which can result in their depletion from the soil (Kan, 2015).

Reduced tillage increases the content of organic matter and preserves soil fertility more than the conventional management practices (De Sanctis et al., 2012). Rizwan et al. (2016) say that organic amendments could be used to reduce the uptake of toxic trace elements by crop plants. The research results have shown that the lowest concentrations of microelements such as Co (0.036 mg kg^{-1}), Cu (2.813 mg kg^{-1}) and Ni (0.136 mg kg^{-1}) were detected in the NT system (*Figs. 3* and *4*). Other authors also underlined the tendency of heavy metals to make stable compounds with the organic matter and thus lower their bioavailability (Kabata Pendias, 2011).

Understanding the interactions between nitrogen and other elements is the key for the improvement of the efficiency of fertilizer application (Domagała-Świątkiewicz and Gąstoł, 2013). The highest total content of microelements (108.229 mg kg^{-1}) was recorded with the nitrogen application at a dose of 60 kg ha^{-1}, while the lowest (76.096 mg kg^{-1}) was detected when the dose of 120 kg ha^{-1} was applied. Also, the lowest concentrations of Ba (2.417 mg kg^{-1}), Co (0.034 mg kg^{-1}), Ni (0.064 mg kg^{-1}), V (0.217 mg kg^{-1}), Zn (26.000 mg kg^{-1}) and Fe (20.200 mg kg^{-1}) were detected when applying the highest nitrogen dose (*Figs. 3* and *4*). The average Ba concentration in plant tissues ranges between 2 and 13 mg kg^{-1} and the higher concentrations of Ba are found in the plants from aridic zones (Kabata Pendias, 2011), whereas V is relatively easily taken up from acid soil, and some studies show that it is related to the process of biological nitrogen fixation (Bjekić, 2014). Fe availability to plants is dictated by the redox potential and pH soil reaction. In soils of higher pH, Fe is oxidized and is mostly in the form of insoluble ferric oxides which are less available to plants (Morrissey and Guerinot, 2009). In this case, the nitrate form of nitrogen (brought by a higher fertilization rate) probably increased pH and thus lowered the Fe uptake by plants. Zhao et al. (2009) underlined that Zn and Fe concentrations were significantly and positively correlated with P content, which was confirmed in this study since the lowest values of all three elements were detected in the N2 variant.

On the other hand, numerous authors state that larger doses of N fertilizer increase the microelement content in wheat, and some of the studies include the combined application of nitrogen and certain microelements (Klikocka and Marks, 2018; Kutman et al., 2011). Years-long research has shown that the application of higher nitrogen rates

http://www.aloki.hu ● ISSN 1589 1623 (Print) ● ISSN 1785 0037 (Online)
DOI: http://dx.doi.org/10.15666/aeer/1705_1175711771

leads to the increase in Fe, Zn and Cu concentrations, but it does not affect Mn concentration in the wheat grain (Shi et al., 2010). Later studies showed that the applied forms of N fertilizer had different effects on Mn content in plants (Klikocka and Marks, 2018). Svećnjak et al. (2013) reported that the content of trace elements depended primarily on the bioavailability of the minerals, but that different wheat cultivars could absorb different element levels from the soil, and that the same wheat cultivar could absorb different mineral levels from different soils.

The results have shown that Ni concentration (0.064 mg kg^{-1}) in the grain was the lowest in the variant with the highest rate of nitrogen application (*Fig. 4*), which can be the consequence of soil acidity, organic matter content and sorption capacity (Shaheen et al., 2017; Wlasniewski et al., 2019). The study of Wlasniewski et al. (2019) did not record a significant impact of mineral nutrition on the varying of nickel quantities in the wheat and barley grain, but it noticed a certain tendency of reducing the content of this metal in the wheat grain with the increase of NPK dose (Wlasniewski et al., 2019).

Conclusion

The results of the research have shown that the tillage system and level of nitrogen fertilization in top dressing, as well as the interaction between these two factors had an important effect on the content of macro- and microelements in the grain of winter wheat cultivar Azra. The lowest content of the examined macroelements, as well as the highest concentration of microelements Co, Cu and Ni, was observed in the grain produced in the CT system. On the other hand, the highest concentrations of microelements Fe, Ba and As were detected in the grain produced in the NT system. In the grain from the MT system, the concentrations of Mn, Sr, V and Zn were the highest in comparison with two other tillage systems. Significant differences in concentrations of macro- and microelements were detected in the grain produced with different levels of nitrogen fertilization. The highest total content of macroelements, as well as highest concentrations of Mg, K and P, was detected in the control. In the grain treated with a smaller dose of nitrogen (60 kg ha^{-1}), the highest total content of microelements, as well as the highest concentrations of Co, Ba, Fe, Mn and V, was detected. The obtained results indicated that reduced tillage and/or reduced nitrogen fertilization did not cause the reduction in macroelement content in the grain. Moreover, it had a positive effect on the content of nutritionally important minerals (Ca, Cu, Fe, K, Mg, Mn, P and Zn) in respect to the conventional tillage system with higher levels of nitrogen applied.

Acknowledgements. This work was supported by the Ministry of Education, Science and Technological Development of the Republic of Serbia (Research grants Nos. 31066, 46006 and 46009).

REFERENCES

[1] Abbas, Q., Yousaf, B., Liu, G., Zia-ur-Rehman, M., Ali, M. U., Munir, M. A. M., Hussain, S. A. (2017): Evaluating the health risks of potentially toxic elements through wheat consumption in multi-industrial metropolis of Faisalabad, Pakistan. – Environmental Science and Pollution Research 24(34): 26646-26657.

[2] Bar-Tal, A., Aloni, B., Karni, L., Rosenberg, R. (2001): Nitrogen nutrition of greenhouse pepper. II. Effects of nitrogen concentration and NO3: NH4 ratio on growth, transpiration, and nutrient uptake. – HortScience 36(7): 1252-1259.

http://www.aloki.hu ● ISSN 1589 1623 (Print) ● ISSN 1785 0037 (Online)
DOI: http://dx.doi.org/10.15666/aeer/1705_1175711771

[3] Barunawati, N., Hettwer Giehl, R. F., Bauer, B., Von Wirén, N. (2013): The influence of inorganic nitrogen fertilizer forms on micronutrient retranslocation and accumulation in grains of winter wheat. – Frontiers in Plant Science 4: 320.
[4] Bjekić, D. (2014): Characterization and effectiveness of plant growth promoting bacteria isolated from the rhizosphere of maize. – PhD Thesis, University of Novi Sad Faculty of Agriculture (in Serbian).
[5] Blandino, M., Marinaccio, F., Reyneri, A. (2016): Effect of late-season nitrogen fertilization on grain yield and on flour rheological quality and stability in common wheat, under different production situations. – Italian Journal of Agronomy 11(745): 107-113.
[6] Cakmak, I., Pfeiffer, W. H., McClafferty, B. (2010): Biofortification of durum wheat with zinc and iron. – Cereal Chemistry 87: 10-20.
[7] Dapkekar, A., Deshpande, P., Oak, M. D., Paknikar, K. M., Rajwade, J. M. (2018): Zinc use efficiency is enhanced in wheat through nanofertilization. – Scientific Reports 8(1): 6832.
[8] De Sanctis, G., Roggero, P. P., Seddaiu, G., Orsini, R., Porter, C. H., Jones, J. W. (2012): Long-term no tillage increased soil organic carbon content of rain-fed cereal systems in a Mediterranean area. – European Journal of Agronomy 40: 18-27.
[9] De Vita, P., Di Paolo, E., Fecondo, G., Di Fonzo, N., Pisante, M. (2007): No-tillage and conventional tillage effects on durum wheat yield, grain quality and soil moisture content in southern Italy. – Soil and Tillage Research 92(1-2): 69-78.
[10] Domagała-Świątkiewicz, I., Gąstoł, M. (2013): Effect of nitrogen fertilization on the content of trace elements in cv. *Bianca grapevine* (*Vitis* sp.). – Journal of Elementology 18(1): 39-53.
[11] Faizy, S. E. D., Mashali, S. A., Youssef, S. M., Elmahdy, M. S. (2017): Study of wheat response to nitrogen fertilization, micronutrients and their effects on some soil available macronutrients. – Journal of Sustainable Agricultural Sciences 43(1): 55-64.
[12] Food and Agriculture Organization of the United Nations (2016): Statistical Yearbook of the Food and Agriculture Organization: Feeding the World. – www.fao.org/docrep/018/i3107e/i3107e03.pdf.
[13] Gaj, R., Gorski, D. (2014): Effects of different phosphorus and potassium fertilization on contents and uptake of macronutrients (N, P, K, Ca, Mg) in winter wheat. – Journal of Central European Agriculture 15(4): 169-187.
[14] Jākobsone, I., Kantāne, I., Zute, S., Jansone, I., Bartkevičs, V. (2015): Macro-elements and trace elements in cereal grains cultivated in Latvia. – Proceedings of the Latvian Academy of Sciences. Section B. Natural, Exact and Applied Sciences 69(4): 152-157.
[15] Jamal, A., Moon, Y. S., Abdin, M. Z. (2010): Sulphur - a general overview and interaction with nitrogen. – Australian Journal of Crop Science 4(7): 523-529.
[16] Kabata-Pendias, A. (2011): Trace Elements in Soils and Plants. Fourth Ed. – CRC, Boca Raton, FL.
[17] Kan, A. (2015): Characterization of the fatty acid and mineral compositions of selected cereal cultivars from Turkey. – Records of Natural Products 9(1): 124.
[18] Klikocka, H., Marx, M. (2018): Sulphur and nitrogen fertilization as a potential means of agronomic biofortification to improve the content and uptake of microelements in spring wheat grain DM. – Journal of Chemistry 2018: 1-12.
[19] Korunović, R., Stojanović, S. (1989): Praktikum iz pedologije. – Poljoprivredni Fakultet, Beograd.
[20] Kutlu, I. (2018): Heritability of end-use quality and biofortification characteristics in line x tester bread wheat (*Triticum aestivum* L.) crosses. – Applied Ecology and Environmental Research 16(5): 7305-7326.
[21] Kutman, U. B., Yildiz, B., Cakmak, I. (2011): Effect of nitrogen on uptake, remobilization and partitioning of zinc and iron throughout the development of durum wheat. – Plant Soil 342: 149-164.

http://www.aloki.hu ● ISSN 1589 1623 (Print) ● ISSN 1785 0037 (Online)
DOI: http://dx.doi.org/10.15666/aeer/1705_1175711771

[22] Lei, M., Tie, B. Q., Song, Z. G., Liao, B. H., Lepo, J. E., Huang, Y. Z. (2015): Heavy metal pollution and potential health risk assessment of white rice around mine areas in Hunan Province, China. – Food Security 7: 45-54.
[23] Litke, L., Gaile, Z., Ruža, A. (2018): Effect of nitrogen fertilization on winter wheat yield and yield quality. – Agronomy Research 16(2): 500-509.
[24] Morrissey, J., Guerinot, M. L. (2009): Iron uptake and transport in plants: the good, the bad, and the ionome. – Chemical Reviews 109(10): 4553-4567.
[25] Popović Djordjević, J., Marjanović, Ž. S., Gršić, N., Adžić, T., Popović, B., Bogosavljević, J., Brčeski, I. (2019): Essential elements as a distinguishing factor between mycorrhizal potentials of two cohabiting truffle species in riparian forest habitat in Serbia. – Chemistry and Biodiversity. https://doi.org/10.1002/cbdv.201800693.
[26] Rizwan, M., Ali, S., Abbas, T., Zia-ur-Rehman, M., Hannan, F., Keller, C., ... and Ok, Y. S. (2016): Cadmium minimization in wheat: a critical review. – Ecotoxicology and Environmental Safety 130: 43-53.
[27] Santiago, A. D., Quintero, J. M., Delgado, A. (2008): Long-term effects of tillage on the availability of iron, copper, manganese, and zinc in a Spanish vertisol. – Soil and Tillage Research 98(2): 200-207.
[28] Shaheen, S. M., Antić-Mladenović, S., Wang, S. L., Niazi, N. K., Tsadilas, C. D., Ok, Y. S., Rinklebe, J. (2017): Nickel Mobilization/Immobilization and Phytoavailability in Soils as Affected by Organic and Inorganic Amendments. – In: Tsadilas, C., Rinklebe, J., Selim, J. (eds.) Nickel in Soils and Plants. CRC Press, Boca Raton, FL, pp. 283-310.
[29] Sharma, P., Abrol, V., Sharma, R. K. (2011): Impact of tillage and mulch management on economics, energy requirement and crop performance in maize–wheat rotation in rainfed subhumid inceptisols, India. – European Journal of Agronomy 34(1): 46-51.
[30] Shi, R., Zhang, Y., Chen, X. et al. (2010): Influence of long-term nitrogen fertilization on micronutrient density in grain of winter wheat (*Triticum aestivum* L.). – Journal of Cereal Science 51(1): 165-170.
[31] Singh, B. R., Timsina, Y. N., Lind, O. C., Cagno, S., Janssens, K. (2018): Zinc and iron concentration as affected by nitrogen fertilization and their localization in wheat grain. – Frontiers in Plant Science 9: 307.
[32] Stanislawska-Glubiak, E., Korzeniowska, J. (2012): Effect of soil tillage systems on nutrient concentration in winter wheat plants. – Journal of Food, Agriculture & Environment 10(2): 1353-1355.
[33] Svećnjak, Z., Jenel, M., Bujan, M., Vitali, D., Dragojević, I. V. (2013): Trace element concentrations in the grain of wheat cultivars as affected by nitrogen fertilization. – Agricultural and Food Science 22(4): 445-451.
[34] Taghizadeh, M. S., Najafi-Ghiri, M., Omidi, S. (2014): Effect of tillage system and nitrogen on micronutrient uptake by wheat and weeds grown in a calcareous soil. 19th Australasian Weeds Conference. – Science, Community and Food Security: the Weed Challenge. Baker, M., Hobart (ed.), Tasmania, Australia, 1-4 September, pp. 434-436.
[35] Tiwari, S., Lata, C. (2018): Heavy metal stress, signaling and tolerance due to plant-associated microbes: an overview. – Frontiers in Plant Science 9: 1-12.
[36] USDA (2017): Serbia: Grain and Feed Annual. – https://gain.fas.usda.gov/Recent%20GAIN%20Publications/Grain%20and%20Feed%20Annual_Belgrade_Serbia_3-31-2017.pdf.
[37] Winiarska-Mieczan, A., Kowalczuk-Vasilev, E., Kwiatkowska, K., Kwiecień, M., Baranowska-Wójcik, E., Kiczorowska, B., ... Samolińska, W. (2019): Dietary intake and content of Cu, Mn, Fe, and Zn in selected cereal products marketed in Poland. – Biological Trace Element Research 187(2): 568-578.
[38] Wlasniewski, S., Nazarkiewicz, M., Hajduk, E., Marchel, M., Kaniuczak, J. (2019): Nickel content in grain of winter wheat (*Triticum aestivum* L.) and spring barley (*Hordeum vulgare* L.) cultivated on loessial soil, depending on liming and mineral fertilization. – Journal of Elementology 24(1): 257-266.

http://www.aloki.hu ● ISSN 1589 1623 (Print) ● ISSN 1785 0037 (Online)
DOI: http://dx.doi.org/10.15666/aeer/1705_1175711771

[39] Wozniak, A. (2010): Effect of chemical plant protection on grain quality of spring wheat. – Progr. Plant Protect 50(2): 1010-1013. (in Polish).
[40] Wozniak, A., Makarski, B. (2012): Content of minerals in grain of spring wheat cv. Koksa depending on cultivation conditions. – Journal of Elementology 17(3).
[41] Zhang, W. P., Qian, J., Xu, G. J., Zhang, D. M., Kang, C., Feng, D. X., Shi, L., Zhang, C. L., Guo, Z. Y., Ma, J. H., Zhang, C. S (2019): Characterization and evaluation of heavy metal pollution in soil-wheat system around coal mines in Pingdingshan, China. – Applied Ecology and Environmental Research 17(3): 5435-5447.
[42] Zhao, F. J., Stroud, J. L., Eagling, T., Dunham, S. J., McGrath, S. P., Shewry, P. R. (2010): Accumulation, distribution, and speciation of arsenic in wheat grain. – Environmental Science & Technology 44: 5464-5468.
[43] Zhao, F. J., Su, Y. H., Dunham, S. J., Rakszegi, M., Bedo, Z., McGrath, S. P., Shewry, P. R. (2009): Variation in mineral micronutrient concentrations in grain of wheat lines of diverse origin. – Journal of Cereal Science 49(2): 290-295.

APPENDIX

Table A1. *Statistical analysis of element concentration in the grain of the winter wheat cv. Azra*

Source	Element	df	Mean square	F	Sig.	LSD 0.05
Tillage	As	2	0.154	362.664	0.000	0.020
	Ba	2	0.532	752.796	0.000	0.026
	Co	2	0.013	117.656	0.000	0.011
	Cu	2	11.561	3261.705	0.000	0.059
	Mn	2	10.453	102.261	0.000	0.317
	Ni	2	0.522	88.627	0.000	0.076
	V	2	0.194	354.068	0.000	0.023
	Zn	2	19.942	1198.658	0.000	0.128
	Sr	2	0.068	1006.157	0.000	0.008
	Ca	2	988.000	111.150	0.000	2.951
	Fe	2	1464.952	6012.113	0.000	0.489
	K	2	121440.704	6.194	0.009	26.405
	Mg	2	35356.333	103.280	0.000	18.316
	P	2	136254.333	625.658	0.000	14.609
	S	2	2858.333	160.781	0.000	4.174
	Total content of microelements	2	1135.636	1022.625	0.000	1.043
	Total content of macroelements	2	607921.000	146.041	0.000	63.87
N_rate	As	2	0.013	30.723	0.000	0.020
	Ba	2	0.723	1022.287	0.000	0.026
	Co	2	0.013	116.592	0.000	0.011
	Cu	2	0.621	175.213	0.000	0.059
	Mn	2	10.643	104.120	0.000	0.317
	Ni	2	0.408	69.313	0.000	0.076
	V	2	0.219	399.735	0.000	0.023
	Zn	2	24.569	1476.780	0.000	0.128

http://www.aloki.hu ● ISSN 1589 1623 (Print) ● ISSN 1785 0037 (Online)
DOI: http://dx.doi.org/10.15666/aeer/1705_1175711771

	Sr	2	0.009	136.048	0.000	0.008
	Ca	2	268.000	30.150	0.000	2.951
	Fe	2	2167.143	8893.884	0.000	0.489
	K	2	80891.370	4.126	0.033	26.405
	Mg	2	11464.333	33.489	0.000	18.316
	P	2	62433.333	286.684	0.000	14.609
	S	2	817.333	45.975	0.000	4.174
	Total content of microelements	2	2808.550	2529.061	0.000	1.043
	Total content of macroelements	2	230508.000	55.375	0.000	63.87
Tillage * N_rate	As	4	0.017	40.107	0.000	0.035
	Ba	4	4.249	6008.766	0.000	0.045
	Co	4	0.021	190.516	0.000	0.018
	Cu	4	16.906	4769.854	0.000	0.102
	Mn	4	9.913	96.978	0.000	0.548
	Ni	4	0.506	85.937	0.000	0.132
	V	4	0.162	296.055	0.000	0.04
	Zn	4	55.920	3361.161	0.000	0.222
	Sr	4	0.008	115.694	0.000	0.014
	Ca	4	591.500	66.544	0.000	5.112
	Fe	4	5437.586	22315.675	0.000	0.846
	K	4	385470.370	19.661	0.000	45.735
	Mg	4	60688.833	177.280	0.000	31.725
	P	4	528309.333	2425.910	0.000	25.303
	S	4	4020.333	226.144	0.000	7.23
	Total content of microelements	4	5241.089	4719.530	0.000	1.807
	Total content of macroelements	4	2355310	565.818	0.000	110.627

http://www.aloki.hu ● ISSN 1589 1623 (Print) ● ISSN 1785 0037 (Online)
DOI: http://dx.doi.org/10.15666/aeer/1705_1175711771

RELATIONSHIPS BETWEEN MACROINVERTEBRATE COMMUNITIES AND ENVIRONMENTAL PARAMETERS OF THE HU-LAN ESTUARY NATURAL WETLAND RESERVE AND ITS SURROUNDING WATERS, NORTHEAST CHINA

SHABANI, I. E.[1,2,3] – LIU, M. H.[1*] – YU, H. X.[1*] – MUHIGWA, J.-B. B.[2] – KANKONDA, B. A.[3] – EKOKO, W. A.[1,3] – CUI, X. B.[4] – WANG, G. X.[4]

[1]*Laboratory of Hydrobiology, College of Wildlife and Protected Area, Northeast Forestry University, Harbin P.O. Box 150040, China*

[2]*Université Officielle de Bukavu, P.O. Box 570-Bukavu, République Démocratique du Congo*

[3]*University of Kisangani, P.O. Box 2012 - Kisangani, République Démocratique du Congo*

[4]*Naoli River National Nature Reserve of Heilongjiang, Shuangyashan P.O. Box 155811, China*

[*]*Corresponding authors*
e-mail: manhong@nefu.edu.cn; china.yhx@163.com

(Received 22nd Apr 2019; accepted 4th Jul 2019)

Abstract. This study analyzed the relationships between environmental parameters and benthic macroinvertebrate faunas. Invertebrate richness, Shannon-Wiener diversity, functional-group and CCA were used to evaluate conditions of waterbodies of the Hu-lan Estuary Natural Wetland Reserve and its hinterlands. We measured 10 physicochemical variables and collected 165 species belonging to 6 functional feeding groups (FFGs) during spring, summer and autumn. Some of the physicochemical factors changed with seasons. Nitrate nitrogen, total nitrogen and total phosphate significantly varied with seasons ($p < 0.05$), unlike water temperature, depth, pH, dissolved oxygen, chemical oxygen demand, Ammonia nitrogen and electronic conductivity ($p > 0.05$). The taxa richness of benthic macroinvertebrates did not vary significantly within the sites ($p = 0.508$); while the Shannon-Wiener diversity showed significantly difference ($p < 0.01$) within the sites over these three seasons. Gathering-collectors were the most abundant macroinvertebrate FFG assemblages all over the sites, though there's no significant difference in the total abundance of 6 functional feeding groups identified among the sites during spring, summer and autumn ($p = 0.677$, $p = 0.681$, $p = 0.302$, respectively). Our CCA results indicated positive correlations of macroinvertebrate community compositions with environmental variables in the Hu-lan Estuary Natural Wetland Reserve and its surrounding waters.
Keywords: *taxa richness, Shannon-Wiener diversity, functional feeding groups, water parameters, canonical correspondence analysis*

Introduction

Wetlands suffer from anthropogenic pressure and therefore are altered with respect to their physicochemical composition and species diversity (Rivera-Usme et al., 2015). They are essential for the maintenance of biodiversity that depends on the wetlands for their water supply. These aquatic systems are fragile because of high population densities subsequent to accelerated urban development that seriously threatens most of its wetlands (Rivera-Usme et al., 2015). Anthropogenic activities have severely affected the condition of wetlands worldwide (Wilkins et al., 2015; Tan and Beh, 2016). Physical alteration, habitat loss, water withdrawal, pollution (Cao et al., 1997; Morse et al., 2007), overexploitation and the introduction of exotic species all contribute to the decline in freshwater species and water quality as well (Tan and Beh, 2016). The stream

http://www.aloki.hu ● ISSN 1589 1623 (Print) ● ISSN 1785 0037 (Online)
DOI: http://dx.doi.org/10.15666/aeer/1705_1177311788

community structure is a result of both long-term environmental factors and short-term critical conditions of short duration (Morse et al., 2007); and an experienced stream biologist with good knowledge of normal and stressed stream community structures often can evaluate the water quality of a stream with considerable accuracy just after a few minutes' examination of its fauna (Hilsenhoff, 1977).

Benthic macroinvertebrates are an important component of the aquatic ecosystem and reflect a multitude of physical, chemical, and biological stream features allowing them to be excellent indicators of stream health (Hilsenhoff, 1977; Allan, 2004); i.e, the impacts of stressors such as organic pollution, toxins, and physical habitat alterations or foodweb links at higher trophic levels such as fish and birds (Cummins, 1992). Among members of the aquatic environments, they are probably best suited because they are numerous in almost every stream, and they are readily collected and identified, and they are not very mobile, and generally have life cycles of a year or more (Hilsenhoff, 1977). Monitoring wetland ecosystems using aquatic macroinvertebrates has been an effective tool for documenting changes in community health (Lenat, 1987; Plafkin et al., 1989). Some macroinvertebrate indices of stream health have been identified as most useful and efficacious. These include the EPT taxa richness-Ephemeroptera, Plecoptera, Trichoptera- (Lenat and Penrose, 1996), and total benthic macroinvertebrate taxa richness (Plafkin et al., 1989). The effective use of EPT or taxa richness measures for monitoring water quality in China requires richness rating systems to be developed by biologists (Lenat, 1994). However, physicochemical monitoring tools are usually expensive and can only be used at limited site number and they are, thus, unable to achieve computation of distribution patterns (Swaminathan, 2003). Hence, biological monitoring is considered one of the alternatives which is a useful as a rapid assessment instrument to check up the status of water quality (Tan and Beh, 2016). Changes in benthic macroinvertebrate fauna with water pollution (Morse et al., 2007), have been documented and measured in several instances using various aspects including biomass, density and composition (Cao, 1997).

Benthic macroinvertebrate functional feeding-group analyses were developed initially for streams (Cummins, 1973, 1974) as key components of the river continuum concept (Vannote et al., 1980). Various ratios of the functional groups have been successfully used as surrogates for ecosystem attributes to assess the ecological condition of flowing water environments (Masese et al., 2014; Fu et al., 2016; Shabani et al., 2019). The evaluation is based on easily observed morphological and behavioral attributes associated with feeding (functional-feeding groups, FFGs) and modes of attachment, concealment, and locomotion (functional-habit groups, FHGs), together with life history patterns and drift propensity (Merritt et al., 2002).

In this paper, we determined the functional group composition of benthic macroinvertebrate fauna and modeled relationships between benthic macroinvertebrate metrics and environmental factors in the Hu-lan Estuary Natural Wetland Reserve and its surrounding waters to evaluate the effects of environmental characteristics on benthic macroinvertebrate assemblages.

Materials and methods

Study area

The Hu-lan Estuary Natural Wetland Reserve is located in the southern part of Hu lan district, Harbin city in Heilongjiang Province, Northeast China (*Fig. 1*); and extends

http://www.aloki.hu ● ISSN 1589 1623 (Print) ● ISSN 1785 0037 (Online)
DOI: http://dx.doi.org/10.15666/aeer/1705_1177311788

along of the north bank of Songhua River from East to West band. The Hu-lan River enters the estuary of Songhua River and reaches the Dadingshan dam. The natural reserve extends between 45°53'44" and 46°54'04" N latitude and between 126°41'00" and 127°15'00" E longitude. The length of the reserve from East to West is 63.5 km, with a width of 21.3 km from North to South (Liu, 2012). It covers around 192.62 km^2. The annual temperature average is 3.3°C, with mean annual precipitations of 500.4 mm (Liu, 2012). The Hu lan Estuary Natural Wetland Reserve was created in 2008 and mainly aims to protect wetland ecosystems and endangered waterfowls. The wetland is rich in biological resources with more than 465 species of plants and 348 species of vertebrates, including fishes, amphibians, reptiles, birds and mammals (Liu, 2012). According to the Classification Criteria of Nature Reserve Types and Grades of the People's Republic of China (GB/T15629-93), the Hu-lan Estuary Natural Wetland Nature Reserve belongs to the inland wetland type and natural ecosystem category. Ashihe River is an important tributary of Harbin section of Songhua River in Hu-lan Estuary. The upper reaches of Ashihe River are alpine forest streams and the middle reaches of the river pass through a large area of farmland to reach the Harbin city and join the Songhua River (Liu, 2012).

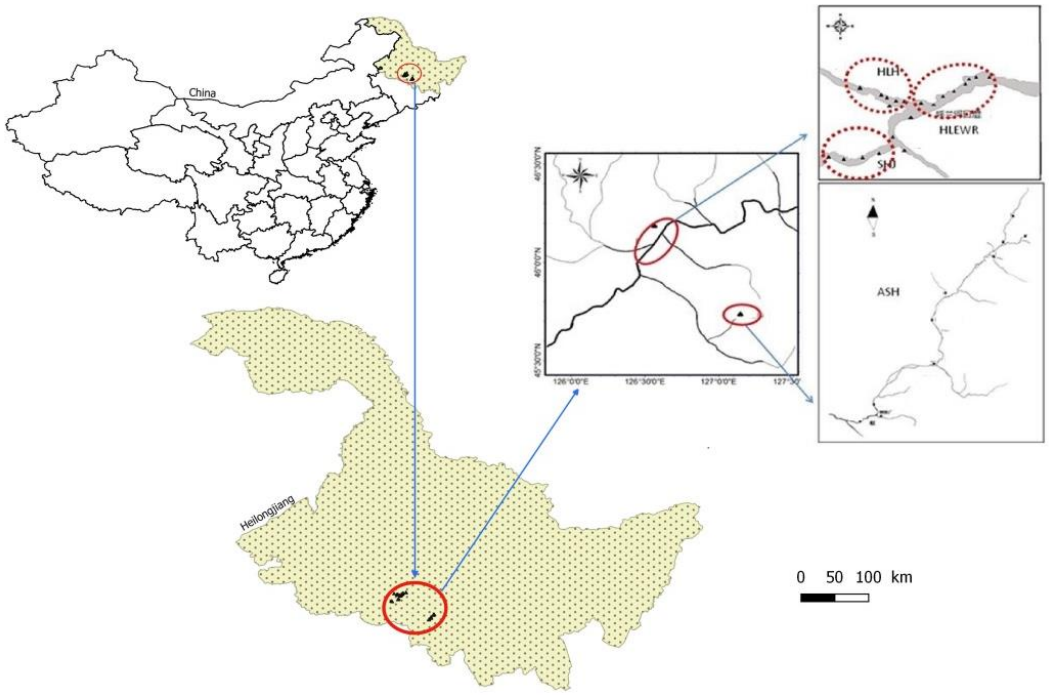

Figure 1. *Map of study site with the sampling locations in China*

Sampling of physical and chemical parameters

Four sampling locations were selected, including the Songhua River along Harbin (SHJ: N45°45'29.2″ and E126°45′10.4″, sites 1-3, 13-14), the Ashihe River upstream (ASH: N45°16′38.7″and E127°39′23.1″, sites 4-12), the Hu-lan river downstream (HLE: N45°55′33.1″ and E126°46′35.8″, sites 15-22) and the Hu-lan estuary wetland reserve (HLEWR: N45°55′31.3″ and E126°55′53.3″, sites 23-30). Physicochemical water conditions were determined in spring, summer and autumn in 2009. Water temperature

http://www.aloki.hu ● ISSN 1589 1623 (Print) ● ISSN 1785 0037 (Online)
DOI: http://dx.doi.org/10.15666/aeer/1705_1177311788

(WT, °C), pH, electronic conductivity (EC, mS/m) and dissolved oxygen (DO, mg/l) were measured in situ with a multiparameter probe. Water depth (m) was measured using Secchi disk and longline method when biological samples were collected. 500 ml of water were sampled at each site per season and put in labelled plastic containers, and then taken to the Laboratory of Hydrobiology, where nitrate nitrogen (NO_3^--N, mg/l), Ammonia nitrogen (NH_3-N, mg/l), total phosphate (TP, mg/l), total nitrogen (TN, mg/l) and chemical oxygen demand with permanganate index (COD_{Mn}, mg/l) were determined following the Chinese national water quality standards method GB3838-2002.

Benthic macroinvertebrate sampling

Several qualitative and quantitative sampling tools are designed to sample benthic macroinvertebrates (Barbour et al., 1999; Merritt et al., 2008). In this study, we used qualitative (D-frame net and handle net) and quantitative (Surber sampler: 0.09 m^2 and Petersen grab sampler: 1/16 m^2) sampling tools to collect the benthic macroinvertebrates from each of the four sampling locations. We used 500-μm mesh D-net and handle-net type devices at each site, the nets were dragged against the water flow over an area of 1 m^2 while large substrates were gently rubbed or kicked for 3-5 minutes with hands or feet, respectively, to dislodge free-living and burrowing macroinvertebrates from benthic substrates. Surber type sampling devices of 30 cm wide × 30 cm long with 0.09 m^2 catching area and a net of 500 μm in mesh size were placed along the river substrate to catch any organisms dislodged initially and carried downstream at low velocities; and the animals were subsequently swept by the water and caught in the net. We also used the Petersen sampler in wetland sites to collect macroscopic macroinvertebrates in sand, gravel, marl, or clay.

All samples were transferred into labelled plastic bags and preserved in 95% ethanol. Taxonomic determinations were conducted in the Laboratory of Hydrobiology using identification keys of Thorp and Covich (1991), Morse et al. (1994), Merritt et al. (1996), Tong (1996), and Dudgeon (1999). Each taxon was assigned to a general functional group according to their trophic specializations, as categorized by Cummins and Klug (1979), Morse et al. (1994), Vannote et al. (1980), Merritt et al. (1996), and Barbour et al. (1999). The FFGs identified were scrapers (SC), that are herbivores and feed on periphyton; shredders (SH), that feed on coarse particulate organic matter (CPOM); gatherers/collectors (GC), that consume fine particulate organic matter (FPOM); filterers/collector (FC), which filter FPOM in the water column; omnivores (OM), or those which simply do not fit neatly into the other categories; and predators (PR) that feed on other living organisms (Rivera-Usme et al., 2015).

Data analysis

The benthic macroinvertebrate taxa richness and Shannon-Wiener diversity were computed for each site and sampling season using PAST software (Hammer et al., 2001; Hammer and Ryan, 2008). Differences in benthic macroinvertebrate taxa richness and Shannon-Wiener diversity among sampling sites during spring, summer and autumn were tested using the ANOVA or Kruskal-Wallis tests in R software, and tests were considered significant at the $p < 0.05$ level. Canonical correspondence analysis was performed using CANOCO 4.5 software and Pearson correlation test (SPSS, version 16.0) to model on the correlation between benthic macroinvertebrate metrics and environmental factors. For data which fitted to the normal distribution, one-way

http://www.aloki.hu ● ISSN 1589 1623 (Print) ● ISSN 1785 0037 (Online)
DOI: http://dx.doi.org/10.15666/aeer/1705_1177311788

ANOVA and Tukey's honestly significant difference (HSD) tests, followed by Levene's test of homogeneity of variance were performed for multiple comparisons. On the other hand, data which did not fit to the normal distribution were submitted to the non-parametric Kruskal-Wallis test to evaluate the relationships between water quality variables and macroinvertebrate community metrics among sites over three seasons.

Results and discussion

Environmental variables

Table 1 shows the mean values of ten water parameters measured in the Hu-lan estuary wetland sites and its surrounding waters. Some of the physicochemical factors changed among seasons. Nitrate nitrogen (NO_3^--N), total nitrogen (TN) and total phosphate (TP) significantly varied with seasons (Kruskal-Wallis test, $p < 0.05$); unlike water temperature (WT), depth, pH, dissolved oxygen (DO), chemical oxygen demand with permanganate index (COD_{Mn}), Ammonia nitrogen (NH_3-N) and electronic conductivity (EC) which did not vary significantly (Kruskal-Wallis test, $p > 0.05$). Shabani et al. (2019) also found NO_3^--N, TN and TP concentrations significantly varied with seasons in the waterbodies of Sanjiang plain wetlands. Maloney and Feminella (2006) also recorded the highest mean value of water temperature in summer in the Southeastern plains ecoregion of central western Georgia, USA. Ortiz and Puig (2007) also found the highest mean value of water temperature in summer at the downstream reach in a Mediterranean stream. Shabani et al. (2019) also reported the highest mean value of water temperature in summer in the Sanjiang plain wetlands, obviously as the warmest season.

Table 1. *Seasonal dynamics of environmental parameters (Mean±SE).* WT = *Water temperature, DO = dissolved oxygen,* COD_{Mn} *= chemical oxygen demand,* NH_3-N = *Ammonia nitrogen,* NO_3^--N = *nitrate nitrogen, EC = electronic conductivity, TN = total nitrogen, TP = total phosphate*

Environmental parameters	Spring	Summer	Autumn
WT (°C)	12.95±0.70[a]	21.20±0.78[c]	16.31±0.96[b]
Depth (m)	6.24±1.02 [a]	6.93±1.09 [a]	5.05±0.85 [a]
pH	7.39±0.10 [ab]	7.31±0.06 [a]	7.62±0.08 [b]
DO (mg/l)	7.67±0.39 [a]	7.38±0.31 [a]	6.29±0.45 [a]
COD_{Mn} (mg/l)	3.32±0.44 [a]	8.74±0.83 [c]	5.31±0.28 [b]
NH_3-N (mg/l)	0.54±0.15 [a]	0.41±0.15 [a]	0.57±0.27 [a]
NO_3^--N (mg/l)	0.68±0.14 [a]	1.24±0.12 [a]	0.75±0.07 [b]
EC (mS/m)	15.73±1.67 [a]	17.12±1.95 [a]	15.39±1.94 [a]
TN (mg/l)	3.41±0.27 [b]	1.80±0.16 [a]	1.51±0.42 [a]
TP (mg/l)	0.11±0.03 [a]	0.05±0.002 [a]	0.30±0.06 [b]

Benthic macroinvertebrate communities

A total of 165 benthic macroinvertebrate species belonging to 16 orders were recorded during the study period (*Appendix 1*, *Table 2*). Insects were the most species-rich group, with 8 orders (Trichoptera, Ephemeroptera, Plecoptera, Diptera, Heteroptera, Odonata, Coleoptera and Neuroptera), and 41.8% of the species belonged to order of Dipterans (*Table 2*). Limnodrilus hoffmeisteri (Tubificida) was considerably abundant in the Hu-lan estuary wetland and the surrounding Waters. 78 species were

http://www.aloki.hu ● ISSN 1589 1623 (Print) ● ISSN 1785 0037 (Online)
DOI: http://dx.doi.org/10.15666/aeer/1705_1177311788

collected in the Hu-lan river downstream (HLE) followed by the Ashihe River upstream (ASH) with 71 species, the Songhua River along Harbin (SHJ) with 59 species and the Hu-lan estuary wetland reserves (HLEWR) with 52 species (*Appendix 1*). The benthic macroinvertebrate taxa richness of in these four regions did not vary significantly during the three seasons (ANOVA results, $p = 0.5081$; *Fig. 2a*). While the Shannon-Wiener diversity showed high significant difference (Kruskal-Wallis test, $p = 0.0019$, *Fig. 2b*) within the sampling zones during these three seasons.

Table 2. *Orders and number of families and species of benthic macroinvertebrates*

Order	Family number	%	Species number	%
Arhynchobdellida	1	2.63	2	1.21
Coleoptera	1	2.63	2	1.21
Decapoda	1	2.63	2	1.21
Diptera	5	13.2	69	41.80
Ephemeroptera	6	15.80	13	7.88
Heteroptera	2	5.26	6	3.64
Heterostropha	1	2.63	2	1.21
Hygrophila	2	5.26	10	6.06
Neuroptera	1	2.63	1	0.61
Odonata	2	5.26	2	1.21
Plecoptera	3	7.89	6	3.64
Rhynchobdellida	1	2.63	3	1.82
Trichoptera	8	21.10	20	12.10
Tubificida	2	5.26	22	13.30
Unionoida	1	2.63	3	1.82
Veneroida	1	2.63	2	1.21
Total	38	100.00	165	100.00

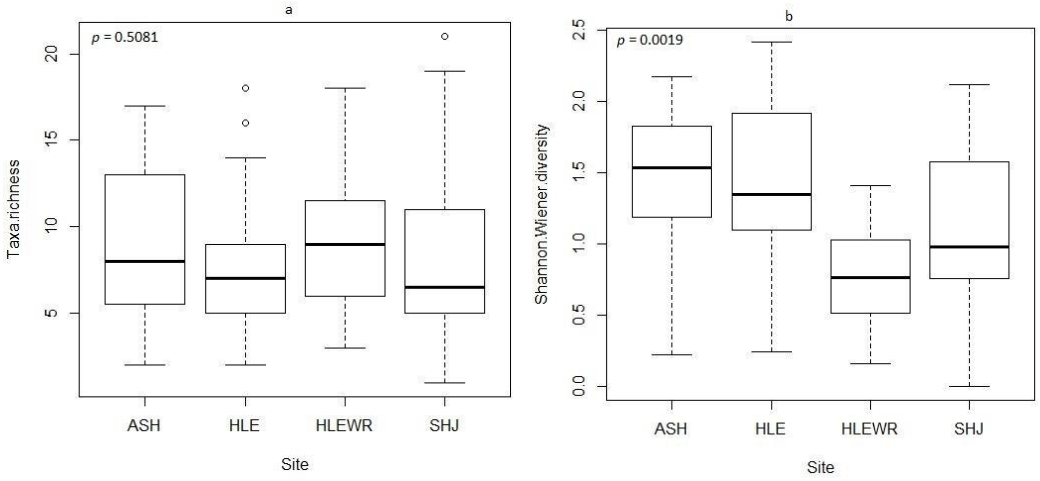

Figure 2. *Comparison of mean values of macroinvertebrate taxa richness (a) and Shannon-Wiener diversity (b) at sampling sites. ASH = Ashihe River upstream, HLE = Hu-lan river downstream, HLEWR = Hu-lan estuary wetland reserve, SHJ = Songhua River along Harbin*

Our results contracted with those of Šporka et al. (2006) in the stream of the Carpathian Mountains of central Europe; Wang et al. (2007) in Taihu lake watershed, Changzhou area; Zhao et al. (2012) in the bed sediment of the Yellow River; Pan et al.

http://www.aloki.hu ● ISSN 1589 1623 (Print) ● ISSN 1785 0037 (Online)
DOI: http://dx.doi.org/10.15666/aeer/1705_1177311788

(2013) in the Upper Yellow and Yangtze Rivers; Zhang et al. (2014) in streams and rivers of lake Taihu Basin; Pham (2017) in Saigon river and its tributaries, Vietnam; Rosser and Pearson (2018) in tropical streams; Shabani et al. (2019) in the wetlands of the Sanjiang plain, who reported that aquatic insects were the most species-rich group and occurred in almost all of the sites. Their dominance may depend on the availability of allochthonous organic detritus from riparian structure (Vannote et al., 1980).

Benthic macroinvertebrate functional feeding groups

Figure 3a,b,c report the percentage contributions of the various benthic macroinvertebrate FFGs at the sites during the three seasons. Gathering-collectors (GC) were the most dominant benthic macroinvertebrate FFG assemblages within all sites in spring and autumn. They also dominated the benthic communities in the HLEWR and SHJ in summer. Filtering-collectors (FC) and predators were the most abundant in the ASH and HLE, respectively in summer. It appeared that there's no significant difference in the total abundance of these six functional feeding groups among the sites during spring, summer and autumn (Kruskal-Wallis rank sum test, p = 0.677, p = 0.681, p = 0.302, respectively). Pan et al. (2013) also found that gathering-collectors were the predominant macroinvertebrate FFGs in the source region of the Yangtze River. Fogelman et al. (2018) also reported that the gathering-collectors were the most dominant in the macroinvertebrate collection from the Susquehanna River, USA.

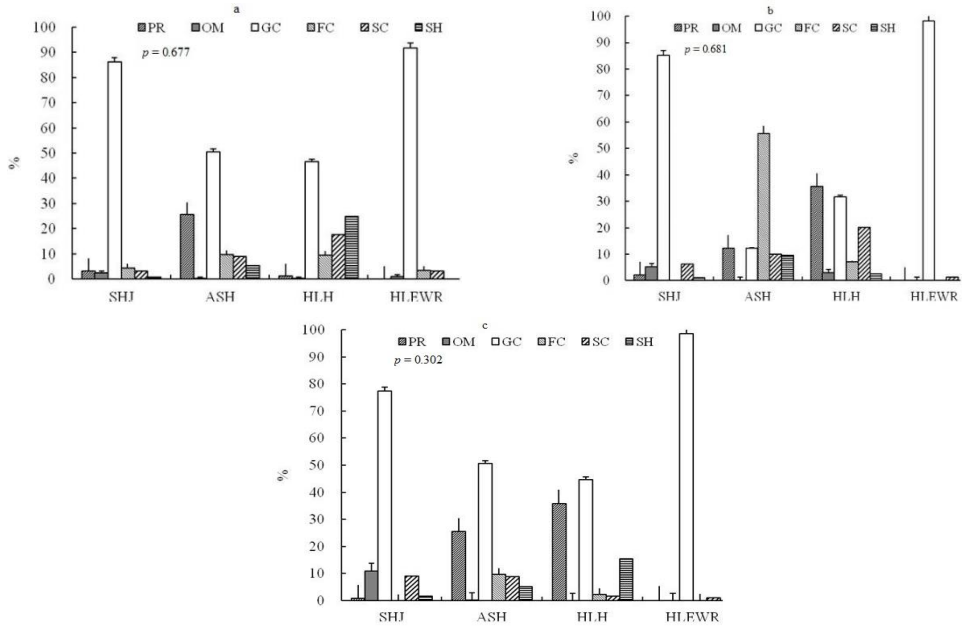

Figure 3. *Percentages of macroinvertebrate FFGs in spring (a), summer (b) and autumn (c), SH = shredders, SC = scrapers, FC = filtering-collectors, GC = gathering-collectors, PR = predators, SHJ = Songhua River along Harbin, ASH = Ashihe River upstream, HLE = Hu-lan river downstream, HLEWR = Hu-lan estuary wetland reserve*

Relationships between physicochemical variables and benthic macroinvertebrates

Figure 4 shows the CCA ordinations during the three seasons. During the spring period, the first two axes respectively explained 18.90 and 36.60% of benthic

http://www.aloki.hu ● ISSN 1589 1623 (Print) ● ISSN 1785 0037 (Online)
DOI: http://dx.doi.org/10.15666/aeer/1705_1177311788

macroinvertebrate variances, with eigenvalues of 0.964 and 0.907. Biotic data as *Chironomus pallidivittatue*, *C. okinawanus*, *C. plumosus, Limnodrilus hoffmeisteri*, *Branchiura sowerbyi*, *Ephemera shengmi* and *Polypylis hemisphaerula* exhibited high positive relationships with water temperature ($r = 0.93$) and COD_{Mn} ($r = 0.94$) at sites 1, 2, 3, 21, 23, 25, 26, 27, 28, 29 and 30 on the first axe. CCA indicated that *Nippotipula* spp., *Ameletus* spp., *Iron* spp., *Heptagenia* spp., *Ephemera sachalinensis*, *Serratella* spp., *Ephemerella fusongensis*, *Leptophlebia* spp., *Paraleptophlebia* spp., *Corixa substriata*, *Hesperocorixa distanti*, *Gyraulus convexiuculus*, *Galba truncatula*, *Galba pervia*, *Radix auricularia*, *Valvata piscinalis*, *Stenopsyche marmorata*, *Hydropsyche nakaharai*, *Hydropsyche* spp., *Polycentropus* spp. and *Alloperla sapporoensis* were positively correlated with TN and DO at sites 5, 7, 8, 10 and 11 on the second axis (*Fig. 4a,b*).

In summer season, the first two axes explained 55.40% of total variances, with eigenvalues of 0.915 and 0.958, respectively. There were positive significant correlations of *Tipulidae* spp., *Cryptochironomus defectus*, *Stictochironomus maculipennis*, *Chironomus okinawanus*, *Pentaneurella katterjokki*, *Glyptotendipes pallens*, *Ephemera shengmi*, *Unio douglasiae*, *Viviparus chui*, *Limnodrilus helveticus*, *Teneridrilus mastix*, *Limnodrilus hoffmeisteri* with electronic conductivity ($r = 0.78$), depth ($r = 0.69$), water temperature ($r = 0.94$), TN ($r = 0.71$), NO_3^--N ($r = 0.87$) and pH ($r = 0.76$) at sites 1, 2, 3, 20, 24, 25, 26, 27, 28, 29, and 30 on the first axis. While *Tabanus* spp., *Nippotipula* spp., *Cricotopus sylvestris*, *Eukiefferiella gracei*, *Ameletus* spp., *Iron* spp., *Heptagenia* spp., *Baetis* spp., *Ephemerella* spp., *Nais* spp., *Limnodrilus claparedeianus*, *Alloperla sapporoensis*, *Alloperla nikkoensis*, *Alloperla* spp., *Haploperla* spp., *Stenophylax ondakesis*, *Stenophylax koizumii* and *Astenophylax grammicus* were associated with DO and TP at sites 5, 6, 7, 8, 9 and 10 on the second axis (*Fig. 4c,d*).

During autumn, the first two CCA axes respectively explained 20.60 and 41.00% of total variances, with eigenvalues of 0.958 and 0.954. Axis 1 showed positive correlations of water temperature, TP, TN, depth, NH_3-N, electronic conductivity, COD_{Mn} and NH_3-N on *Unio douglasiae*, *Polypylis hemisphaerula*, *Viviparus chui*, *Galba pervia*, *Radix swinhoei*, *Cipangopaludina chinensis*, *Limnodrilus helveticus*, *Limnodrilus hoffmeisteri*, *Branchiura sowerbyi*, *Tubifex tubifex*, *Nais communis*, *Dero* spp. While the second axis revealed that pH and DO were the most important variables to impact the distribution of *Tabanus* spp., *Nippotipula* spp., *Holorusia* spp., *Procladius choreus*, *Stictochironomus akizukii*, *Ameletus* spp., *Iron* spp., *Heptagenia* spp., *Baetis* spp., *Baetis* spp., *Ephemera sachalinensis*, *Serratella* spp., *Ephemerella* spp., *Ephemerella fusongensis*, *Leptophlebia* spp., *Paraleptophlebia* spp., *Ephemera nigroptera*, *Corixa substriata*, *Hesperocorixa distanti*, *Sphaerium lacustre*, *Gyraulus convexiuculus*, *Radix auricularia, Radix ovata*, *Valvata piscinalis*, *Protohermes grandis*, *Parastenopsyche* spp., *Stenopsyche marmorata*, *Goera ramosa*, *Goera japonica*, *Goera kyotonis*, *Stenophylax ondakesis*, *Stenophylax koizumii*, *Astenophylax grammicus*, *Glyphotaelius admorsus*, *Hydropsyche nakaharai*, *Hydropsyche* spp., *Oecetis morii*, *Ganonema* spp. and *Polycentropus* spp at sites 4, 5, 6, 7, 8, 9, 10, 11 and 12 (*Fig. 4e,f*).

Understanding the relative importance of environmental conditions is critical for understanding how to preserve generate benefits to aquatic macroinvertebrate communities (Wilkins et al., 2015). Our modeling demonstrated that benthic macroinvertebrate species richness values were strongly associated with physical and

http://www.aloki.hu ● ISSN 1589 1623 (Print) ● ISSN 1785 0037 (Online)
DOI: http://dx.doi.org/10.15666/aeer/1705_1177311788

chemical conditions in the Hu-lan Estuary Natural Wetland Reserve and its surrounding waters. Environmental parameters as measured were very influential on macroinvertebrate diversity in freshwater habitats of this reserve. Moreover, several studies have demonstrated that differences in physical and chemical characteristics are detected anytime and with strong influence on aquatic community composition (Bertaso et al., 2015). Habitat quality was second important factor, implying that macroinvertebrate diversity also benefited from improved environmental conditions (Wilkins et al., 2015). Palmer et al. (1997), and Harper et al. (1998) argued that habitat heterogeneity can promote biotic recovery and biodiversity in aquatic environment and is often a goal of environment restoration.

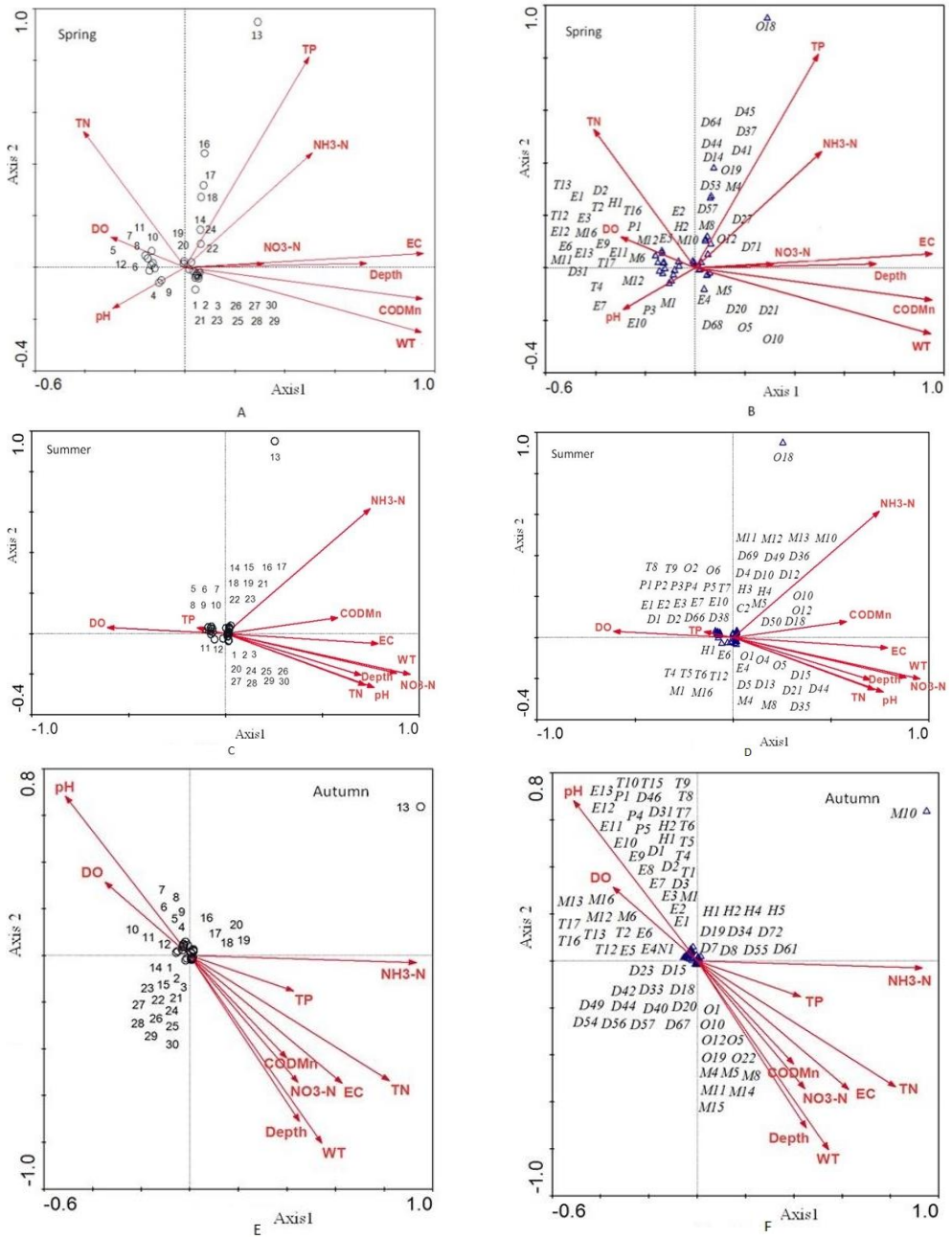

Figure 4. *CCA plots relating the benthic macroinvertebrates associated with physicochemical variables in spring (A, B), summer (C, D) and autumn (E, F)*

http://www.aloki.hu ● ISSN 1589 1623 (Print) ● ISSN 1785 0037 (Online)
DOI: http://dx.doi.org/10.15666/aeer/1705_1177311788

In our study, we recorded pollution-sensitive taxa, including Ephemeroptera, Plecoptera, Trichoptera and Odonata (EPTO) and benthic communities characterized by pollution-tolerant taxa, such as Diptera, Heterostropha, Hygrophila and Tubificida. Luo et al. (2017) also collected sensitive species (e.g., EPT taxa) and less diverse communities with dominance of tolerant species (e.g., Tubificids, Chironomids, and Physids) in the Liangjiang New Area. Although some taxa (e.g. EPTO) are sensitive to aquatic environment conditions (Barbour et al., 1992), many species in these orders are of conservation interest (Wilkins et al., 2015).

Conclusion

Our findings demonstrated the positive of benthic macroinvertebrate community compositions with environmental parameters. We found that Gathering-collectors were the most dominant benthic macroinvertebrate FFG assemblages, and recorded more sensitive and tolerant species in the Hu-lan Estuary Natural Wetland Reserve and its surrounding waters. In order to reach the conservation status assessment of species, we suggest that local faunas should be inventoried and described (many species remain unknown). Tolerance values for macroinvertebrates should be determined. More research teams using benthic macroinvertebrates to assess water quality should operate in this reserve. Wetland conservation efforts, such as planting aquatic vegetation in a watershed, can also help to improve water quality and restore natural flow regimes, and then may structure macroinvertebrate populations.

Acknowledgements. The financial support received from The Key Research and Development Program of China (Fund NO. 2016YFC0500406) for this research is gratefully acknowledged. We express also our gratitude to the staff of the Laboratory of Hydrobiology for the achievement of this work.

REFERENCES

[1] Allan, J. D. (2004): Landscapes and Riverscapes: The Influence of Land Use on Stream Ecosystems. – Annu. Rev. Ecol. Syst. 35: 257-284.
[2] Barbour, M. T., Graves, C. G., Plafkin, J. L., Wisseman, R. W., Bradley, B. P. (1992): Evaluation of EPA's Rapid Bioassessment Benthic Metrics: Metric Redundancy and Variability among Reference Stream Sites. – Environ Toxicol Chem. 11: 437-449.
[3] Barbour, M. T., Gerritsen, J., Snyder, B. D., Stribling, J. B. (1999): Rapid Bioassessment Protocols for Use in Streams and Wadeable Rivers. – In: Periphyton, Benthic Macroinvertebrates and Fish. ed. In US Environmental Protection Agency (USEPA). Washington DC: Office of Water, USEPA.
[4] Bertaso, T. R. N., Spies, M. R., Kotzian, C. B., Flores, M. L. T. (2015): Effects of forest conversion on the assemblages' structure of aquatic insects in subtropical regions. – Revista Brasileira de Entomologia 59: 43-49.
[5] Cao, Y., Bark, A. W., Williams, W. P. (1997): Analysing Benthic Macroinvertebrate Community Changes along a Pollution Gradient: A Framework for the Development of Biotic Indices. – Wat. Res. 31(4): 884-92.
[6] Cummins, K. W. (1973): Trophic Relations of Aquatic Insects. – Annual Review of Entomology 18: 183-206.
[7] Cummins, K. W. (1974): Structure and Function of Stream Ecosystems. – Bio Science 24(11): 631-641.

http://www.aloki.hu ● ISSN 1589 1623 (Print) ● ISSN 1785 0037 (Online)
DOI: http://dx.doi.org/10.15666/aeer/1705_1177311788

[8] Cummins, K. W., Klug, M. J. (1979): Feeding Ecology of Stream Invertebrates. – Annual Review of Ecology and Systematics 10: 147-72.
[9] Cummins, K. W. (1992): Invertebrates. – In: Calow, G. E., Petts, P. (eds.) The Rivers Handbook: Hydrological and Ecological Principles. Blackwell Scientific, London, UK, Pages 234-250.
[10] Dudgeon, D. (1999): Tropical Asian Streams: Zoobenthos, Ecology and Conservation. – Hong Kong Universty Press.
[11] Fogelman, K. J., Bilger, M. D., Holt, J. R., Matlaga, D. P. (2018): Decomposition and Benthic Macroinvertebrate Communities of Exotic Japanese Knotweed (*Fallopia japonica*) and American Sycamore (*Platanus occidentalus*) Detritus within the Susquehanna River. – Journal of Freshwater Ecology 33(1): 299-310.
[12] Fu, L., Jiang, Y., Ding, J., Liu, Q., Peng, Q. Z., Kang, M. Y. (2016): Impacts of Land Use and Environmental Factors on Macroinvertebrate Functional Feeding Groups in the Dongjiang River Basin, Southeast China. – Journal of Freshwater Ecology 31(1): 21-35.
[13] Hammer, O., Harper, D., Ryan, P. (2001): PAST: Paleontological Statistics Software Package for Education and Data Analysis. – Palaeontol Electronica 4: 1-9.
[14] Hammer, O., Ryan, P. (2008): PAST. – Paleontological Statistics, Ver. 1. 77.
[15] Harper, D., Ebrahimnexhad, M., Climent, I., Cot, F. (1998): Artificial Rifles in River Rehabilitation: Setting the Goals and Measuring the Successes. – Aquat Conserv Mar Freshwat Ecosyst 8: 5-16.
[16] Hilsenhoff, W. L. (1977): Use of Arthropods to Evaluate Water Quality of Streams. – Technical Bulletin No. 100, Department of Natural Resources, Madison.
[17] Lenat, D. R. (1987): The Macroinvertebrate Fauna of the Little River, North Carolina: Taxa List and Seasonal Trends. – Arch. Hydrobiol. 110(1): 19-43.
[18] Lenat, D. R. (1994): Using Aquatic Insect to Monitor Water Quality. – In: Lixin, T., Morse, J. C., Liantang, Y. (eds.) Aquatic Insects of China Useful for Monitoring Water Quality. Hohai Uniyersity Press, Nanjing, People's Republic of China.
[19] Lenat, D. R., Penrose, D. L. (1996): History of the EPT Taxa Richness Metric. – Bulletin North American Benthological Society 13: 305-7.
[20] Liu, M. H. (2012): The Ecological Monitoring and Health Assessment of Aquatic Animals Community in Hulan Estuary Natural Reserves. – Northeast Forestry University.
[21] Luo, K., Hu, X., He, Q., Wu, Z., Cheng, H., Hu, Z., Mazumder, A. (2017): Impacts of Rapid Urbanization on the Water Quality and Macroinvertebrate Communities of Streams: A Case Study in Liangjiang New Area, China. – Science of the Total Environment 621: 1601-1614.
[22] Maloney, K., Feminella, J. (2006): Evaluation of Single- and Multi-Metric Benthic Macroinvertebrate Indicators of Catchment Disturbance over Time at the Fort Benning Military Installation, Georgia, USA. – Ecological Indicators 6(3): 469-484.
[23] Masese, F. O., Nzula, K., Kipkembo, J., Gettel, G. M., Irvine, K., McClain, M. E. (2014): Macroinvertebrate Functional Feeding Groups in Kenyan Highland Streams: Evidence for a Diverse Shredder Guild. – Freshwater Science 33(2): 435-450.
[24] Merritt, R. W., Cummins, K. W., Berg, M. B. (1996): An Introduction to the Aquatic Insects of North America. Third Edit. – Kendall/Hunt Publishing Company, Dubuque, USA.
[25] Merritt, R. W., Cummins, K. W., Berg, M. B., Novak, J. A., Higgins, M. J., Wessell, K. J., Lessard, J. L. (2002): Development and Application of a Macroinvertebrate Functional-Group Approach to the Bioassessment of Remnant River Oxbows in Southwest Florida. – Journal of the North American Benthological Society 21(2): 290-310.
[26] Merritt, R. W., Cummins, K. W., Berg, M. B. (2008): An Introduction to the Aquatic Insects of North America. 4th ed. – Iowa, USA: Kendall/Hunt Publishing Company.
[27] Morse, J., Yang, L., Tian, L. (1994): Aquatic Insects of China Useful for Monitoring Water Quality. – Hohai University Press, Nanjing, People's Republic of China.

http://www.aloki.hu ● ISSN 1589 1623 (Print) ● ISSN 1785 0037 (Online)
DOI: http://dx.doi.org/10.15666/aeer/1705_1177311788

[28] Morse, J. C., Bae, Y. J., Munkhjargal, G., Sangpradub, N., Tanida, K., Vshivkova, T. S., Wang, B., Yang, L., Yule, C. M. (2007): Freshwater Biomonitoring with Macroinvertebrates in East Asia. – Front Ecol Environ 52(1): 33-4.
[29] Ortiz, J. D., Puig, M. A. (2007): Point Source Effects on Density, Biomass and Diversity of Benthic Macroinvertebrates in a Mediterranean Stream. – River Research and Applications: 170(2): 155-70.
[30] Palmer, M. A., Hakenkamp, C. C., Nelson-Baker, K. (1997): Ecological Heterogeneity in Streams: Why Variance Matters. – Journal of the North American Benthological Society 16(1): 189-202.
[31] Pan, B., Wang, Z., Li, Z., Yu, G., Xu, M., Zhao, N., Brierley, G. (2013): An Exploratory Analysis of Benthic Macroinvertebrates as Indicators of the Ecological Status of the Upper Yellow and Yangtze Rivers. – Journal of Geographical Sciences 23(5): 871-882.
[32] Pham, A. D. (2017): Linking Benthic Macroinvertebrates and Physicochemical Variables for Water Quality Assessment in Saigon River and Its Tributaries, Vietnam. – IOP Conf. Series: Earth and Environmental Science 92: 012053.
[33] Plafkin, J. L., Barbour, M. T., Porter, K. D., Gross, S. K., Hughes, R. M. (1989): Rapid Bioassessment Protocols for Use in Streams and Rivers: Benthic Macroinvertebrates and Fish. – USEPA, EPA/44/4-89-001.
[34] Rivera-Usme, J., Pinilla, G., Rangel-Churio, J., Castro, M., Camacho-Pinzón, D. (2015): Biomass of Macroinvertebrates and Physicochemical Characteristics of Water in an Andean Urban Wetland of Colombia. – Brazilian Journal of Biology 75(1): 180-190.
[35] Rosser, Z. C., Pearson, R. G. (2018): Hydrology, Hydraulics and Scale Influence Macroinvertebrate Responses to Disturbance in Tropical Streams Responses to Disturbance in Tropical Streams. – Journal of Freshwater Ecology 33(1): 1-17.
[36] Shabani, I. E., Liu, M. H., Yu, H. X., Muhigwa, J.-B. B., Geng, F. F. (2019): Benthic Macroinvertebrate Diversity and Functional Feeding Groups in Relation to Physicochemical Factors in Sanjiang Plain Wetlands, Northeast China. – Applied Ecology and Environmental Research 17(2): 3387-3402.
[37] Šporka, F., Vlek, H. E., Bulánková, E., Krno, I. (2006): Influence of Seasonal Variation on Bioassessment of Streams Using Macroinvertebrates. – Hydrobiologia 566(1): 543-555.
[38] Swaminathan, M. S. M. (2003): Bio-Diversity: An Effective Safety Net against Environmental Pollution. – Environmental Pollution 126(3): 287-291.
[39] Tan, K. W., Beh, W. C. (2016): Evaluation of Water Quality and Benthic Macrointervebrates Fauna Relationship Using Principal Component Analysis (PCA): A Case Study of Cameron Highlands Malaysia. – Environmental Management and Sustainable Development 5(1): 187-208.
[40] Thorp, J. H., Covich, A. P. (1991): Ecology and Classification of North American Freshwater Invertebrates. – Academic Press.
[41] Tong, Y. (1996): Annelida, Hirudinae. Fauna Sinica. Natural Science Foundation of China in the Period of the Eighth Five-Year Plan. – Science Press, Beijing.
[42] Vannote, R. L., Minshall, G. W., Cummins, K. W., Sedell, J. R., Cushing, C. E. (1980): The River Continuum Concept. – Canadian Journal of Fisheries and Aquatic Sciences 37(1): 130-137.
[43] Wang, B., Xu, D., Yang, L., Shen, L., Yu, H. (2007): Characteristics of Benthic Macroinvertebrates Communities in Relation to Environment in Upper Reaches of the Taihu Lake Watershed in Changzhou Area. – J Ecol Rural Environ. 23: 47-51.
[44] Wilkins, P. M., Cao, Y., Heske, E. J., Levengood, J. M. (2015): Influence of a Forest Preserve on Aquatic Macroinvertebrates, Habitat Quality , and Water Quality in an Urban Stream. – Urban Ecosyst. 18: 989-1006.
[45] Zhang, Y., Liu, L., Cheng, L., Cai, Y., Yin, H., Gao, J., Gao, Y. (2014): Macroinvertebrate Assemblages in Streams and Rivers of a Highly Developed Region (Lake Taihu Basin, China). – Aquatic Biology 23: 15-28.

http://www.aloki.hu ● ISSN 1589 1623 (Print) ● ISSN 1785 0037 (Online)
DOI: http://dx.doi.org/10.15666/aeer/1705_1177311788

[46] Zhao, W., Wang, H., Hongzhu, W., Close, P. G. (2012): Macroinvertebrates in the Bed Sediment of the Yellow River. – International Journal of Sediment Research 26(3): 255-68.

APPENDIX

Appendix 1. *Benthic macroinvertebrate taxa list in the Hu-lan Estuary Natural Wetland Reserve and its surrounding waters. FFG= functional feeding groups, ASH = Ashihe River upstream, SHJ = Songhua River along Harbin, HLE = Hu-lan river downstream, HLEWR = Hu-lan estuary wetland reserve, SH = shredders, SC = scrapers, FC = filtering-collectors, GC = gathering-collectors, PR = predators*

Taxon	Code	FFG	ASH	HLE	HLEWR	SHJ
ARHYNCHOBDELLIDA						
Whitmania spp.	H3	PR	1			1
Erpobdella octoculata	H5	PR				
COLEOPTERA						
Chlaenius spp.	C1	PR	1			
Sialis rotunda	C2	PR	1	1		
DECAPODA						
Leander modestus	N3	OM		1		
Palaemon sinensis	N4	OM		1	1	1
DIPTERA						
Tabanus spp.	D1	PR	1	1		
Nippotipula spp.	D2	SH	1	1		
Holorusia spp.	D3	SH	1			
Antocha spp.	D4	GC	1	1		
Tipulidae spp.	D5	SH		1		1
Pilaria spp.	D6	PR	1			
Cryptochironomus digitatus	D7	PR				1
Limonia spp.	D8	SH	1			
Chaoborus spp.	D10	PR	1	1		
Chironomus lugubris	D11	GC				1
Harnischia fuscimana	D12	GC		1		1
Cryptochironomus defectus	D13	PR		1		1
Polypedilum albicorne	D14	SH		1		
Stictochironomus maculipennis	D15	OM				1
Tanypus punctipennis	D16	OM			1	
Stictochironomus spp.	D17	OM				1
Chironomus dorsalis	D18	GC		1	1	1
Polypedilum pedestre	D19	SH		1		
Chironomus pallidivittatue	D20	GC		1	1	1
Chironomus okinawanus	D21	GC		1	1	1
Dicrotendipes pelochloris	D23	GC			1	
Polypedilum cultellatum	D24	SH				1
Glyptotendipes tokunagai	D25	FC			1	1
Glyptotendipes gripekoveni	D26	FC			1	
Cladotanytarsus vanderwulpi	D27	GC		1		
Acricotopus lucens	D28	GC				1
Cryptochironomus fulvus	D29	PR				1
Smittia aterrima	D30	GC	1	1	1	
Procladius choreus	D31	PR	1		1	
Polypedilum flavum	D32	SH		1		
Chironomus flaviplumus	D33	GC		1		1
Tanytarsus mendex	D34	FC		1		
Pentaneurella katterjokki	D35	_	1			1
Cricotopus sylvestris	D36	SH		1	1	1

http://www.aloki.hu ● ISSN 1589 1623 (Print) ● ISSN 1785 0037 (Online)
DOI: http://dx.doi.org/10.15666/aeer/1705_1177311788

Taxon	Code	FFG	ASH	HLE	HLEWR	SHJ
Hydrobaenus lugubris	D37	SC		1		
Cricotopus annulator	D38	SH	1			
Tanypus villipennis	D39	PR		1		
Chironomus anthracinus	D40	GC			1	1
Polypedilum sordens	D41	SH		1		
Demicryptochironomus spp.	D42	GC		1		
Procladius spp.	D43	PR				1
Glyptotendipes pallens	D44	FC		1	1	1
Polypedilum asakawanense	D45	SH		1		
Stictochironomus akizukii	D46	OM	1		1	
Demicryptochironomus vulneratus	D47	GC		1		
Chironomus circumdatus	D48	GC		1	1	
Lipiniella sekunada	D49	GC		1	1	
Cricotopus trifasciatus	D50	SH		1		
Dicrotendipes tritomus	D51	GC		1		
Endochironomus tendens	D52	SH		1		
Diplocladius spp.	D53	GC		1		1
Hexatoma bicolor	D54	PR		1		
Dicrotendipes tamaviridis	D55	GC		1		
Polypedilum scalaenum	D56	SH			1	1
Orthocladius thienemanni	D57	GC		1		1
Orthocladius vaillanti	D58	GC		1		
Cryptotendipes spp.	D59	GC				1
Parachironomus arcuatus	D60	PR		1		
Cryptochironomus ussouriensis	D61	PR		1	1	
Chironomus riparius	D62	OM				1
Chironomus salinarius	D63	OM			1	
Polypedilum surugense	D64	SH		1		1
Chironomus attenuatus	D65	OM			1	
Eukiefferiella gracei	D66	GC	1			
Polypedilum nubeculosum	D67	SH		1	1	1
Chironomus plumosus	D68	OM				1
Macropelopia nebulosa	D69	PR		1	1	1
Paracladopelma undine	D70	GC	1			
Acricotopus longipalpus	D71	GC		1		
EPHEMEROPTERA						
Ameletus spp.	E1	GC	1	1		
Iron spp.	E2	FC	1	1	1	
Heptagenia spp.	E3	SC	1			
Ephemera shengmi	E4	GC	1	1	1	1
Ephemera nigroptera	E5	GC	1			
Ephemera sachalinensis	E6	GC	1			1
Baetis spp.	E7	GC	1			
Baetiell spp.	E8	GC	1			
Serratella spp.	E9	GC	1			
Ephemerella spp.	E10	GC	1			
Ephemerella fusongensis	E11	GC	1			
Leptophlebia spp.	E12	GC	1			
Paraleptophlebia spp.	E13	GC	1			
HETEROPTERA						
Corixa substriata	H1	PR	1	1		
Hesperocorixa distanti	H2	PR		1		
Hesperocorixa kirkaldy	H3	PR		1		
Sigra distanti	H4	PR		1		
Ranatra chinensis	H5	PR	1			
Hesperocorixa valgaris	H6	PR		1		
HETEROSTROPHA						
Cipangopaludina chinensis	M15	SC			1	

http://www.aloki.hu ● ISSN 1589 1623 (Print) ● ISSN 1785 0037 (Online)
DOI: http://dx.doi.org/10.15666/aeer/1705_1177311788

Taxon	Code	FFG	ASH	HLE	HLEWR	SHJ
Valvata piscinalis	M16	SC	1		1	1
HYGROPHILA						
Polypylis hemisphaerula	M5	SC		1	1	
Gyraulus convexiuculus	M6	SC	1		1	
Hippeutis cantori	M7	SC		1		
Viviparus chui	M8	SC		1	1	1
Semisulcospira amurensis	M9	SC	1		1	1
Galba truncatula	M10	SC		1		1
Galba pervia	M11	SC		1	1	1
Radix auricularia	M12	SC	1	1	1	1
Radix ovata	M13	SC	1	1	1	1
Radix swinhoei	M14	SC	1	1	1	
NEUROPTERA						
Protohermes grandis	N1	PR		1		
ODONATA						
Ictinogomphus spp.	Od1	PR		1		1
Macromidae spp.	Od2	PR	1			
PLECOPTERA						
Alloperla sapporoensis	P1	PR	1	1		
Alloperla nikkoensis	P2	PR	1			
Alloperla spp.	P3	PR	1			
Haploperla spp.	P5	PR	1			
Cyamia spp.	P6	PR	1			
Doddsia iaponica	P7	SH	1			
RHYNCHOBDELLIDA						
Parabdella quadrioculata	H1	PR	1			
Glossiphonia lata	H2	PR	1	1		1
Helobdella stagnalis	H4	PR		1		
TRICHOPTERA						
Parastenopsyche spp.	T1	GC	1			
Stenopsyche marmorata	T2	PR	1			
Parastenopsyche sauteri	T3	GC	1			
Goera ramosa	T4	SC	1			
Goera japonica	T5	SC	1			
Goera kyotonis	T6	SC	1			
Stenophylax ondakesis	T7	SH	1			
Stenophylax koizumii	T8	SH	1			
Astenophylax grammicus	T9	SH	1			
Glyphotaelius spp.	T10	SH	1			
Apatania spp.	T11	SC	1			
Hydropsyche nakaharai	T12	FC	1	1		
Hydropsyche spp.	T13	FC	1			
Ptllocolepus spp.	T14	GC	1			
Oecetis morii	T15	GC	1			
Ganonema spp.	T16	SH	1			
Polycentropus spp.	T17	FC	1			
Hydroptila spp.	T18	SC	1			
Goera spp.	T19	SC	1			
Astenophylax spp.	T20	SH	1			
TUBIFICIDA						
Limnodrilus helveticus	O1	GC		1		1
Nais spp.	O2	GC			1	1
Limnodrilus udekemianus	O3	GC		1	1	1
Teneridrilus mastix	O4	GC				1
Limnodrilus hoffmeisteri	O5	GC	1	1	1	1
Limnodrilus claparedeianus	O6	GC	1			
Spirosperma nikolskyi	O7	GC				1
Aulodrilus pigueti	O8	GC		1	1	

http://www.aloki.hu ● ISSN 1589 1623 (Print) ● ISSN 1785 0037 (Online)
DOI: http://dx.doi.org/10.15666/aeer/1705_1177311788

Taxon	Code	FFG	ASH	HLE	HLEWR	SHJ
Aulodrilus japonicus	O9	GC		1	1	
Branchiura sowerbyi	O10	GC		1	1	1
Chaetogaster diaphanus	O11	GC		1	1	1
Tubifex tubifex	O12	GC		1	1	1
Nais bretscheri	O13	GC			1	1
Nais pseudobtusa	O14	GC				1
Paranais frici	O15	GC			1	1
Pristinella acuminata	O16	GC			1	
Nais simplex	O17	GC			1	
Slavina spp.	O18	GC			1	1
Nais communis	O19	GC		1	1	1
Uncinais uncinata	O20	GC		1		
Dero spp.	O22	GC			1	
Dero digitata	O23	GC				1
UNIONOIDA						
Corbicula nittens	M2	FC			1	
Lanceolaria grayana	M3	FC				1
Unio douglasiae	M4	FC		1	1	1
VENEROIDA						
Sphaerium lacustre	M1	FC	1			
Sphaerium spp.	N2	FC	1	1	1	
Total			71	78	52	59

[1] = present

http://www.aloki.hu ● ISSN 1589 1623 (Print) ● ISSN 1785 0037 (Online)
DOI: http://dx.doi.org/10.15666/aeer/1705_1177311788

AGROBACTERIUM-MEDIATED GENE TRANSFORMATION OF POLLEN SPECIFIC GENE STK1 IN MAIZE (*ZEA MAYS*)

JAVEED, A.[1#] – WU, S.[3#] – HUANG, S.[1] – AHMED, M.[2] – SIKANDAR, A.[2] – IQBAL, M. F.[1] – DOGAR, U. F.[4] – ZHANG, C.[1] – CHEN, M.[1] – LIU, C.[1] – HUSSAIN, K.[4] – FENG, L.[1*]

[1]*College of Bioscience and Biotechnology, Shenyang Agricultural University, Shenyang, Liaoning, China*

[2]*College of Plant protection, Shenyang Agricultural University, Shenyang, Liaoning, China*

[3]*College of Science Institute, Shenyang Agricultural University Shenyang, Liaoning, China*

[4]*Department of Botany, University of Gujrat, Hafiz Hayat Campus, Gujrat, Pakistan*

[#]*These authors have equal contribution to this paper.*

**Corresponding author*
e-mail: fenglinsn@126.com; phone: +86-248-848-7086; fax: +86-248-848-7416

(Received 22nd Apr 2019; accepted 4th Jul 2019)

Abstract. Maize is a major food, feed and fodder crop, grown extensively all over the world. Genetic engineering has a unique role in crop improvement. Serine-Threonine-Kinase1 (*ZmSTK1*) is a gene-based enzyme, which due to its biochemical action in maize pollen grains, lowers the survival capability and affects pollination. Out of different methods of genes transfer into the genome of the target cell, Agrobacterium-mediated gene transformation is an easy and convenient method in which required gene is insert into the Agrobacterium, which after multiplication carry foreign genes into the host cell's genome. In this research, a simple and easy *Agrobacterium tumefaciens*-mediated method used to establish the genetic transformation system of *zmstk1* into maize germinating embryo as receptor system. Transgenic plants obtained successfully through this method and the complicated culture process not needed. The expression of *zmstk1* in the tissue was determined by observing the histochemical localization of *zmstk1* in order to elucidate the expression of *zmstk1* in mature tassel or pollen.
Keywords: *agrobacterium tumefaciens, gene editing, gene mutation, pollen viability, transgenetic maize*

Introduction

Maize is a major crop found all over the world and used extensively for food, feed and fodder. Because of its consumption at large scale, some high yielding varieties have to be selected to meet the requirement. Naturally, dominant and vigorous varieties also play an important role in production of healthy and disease free food but for high production of maize, some controlled experiments on cellular and molecular level are required. Public and government affiliated institutions of agriculture research are investigating reasons related to adjustment of maize plant for biotic and environmental stresses. Transfer of genes of cold regions maize varieties to increase production and to improve quality, breeders focus on the improvement of new varieties by using these techniques. One of the major hurdles in functional use of this technique to temperate varieties of maize is the selection of germplasm responsible for its renaissance in tissue culture and inoculation by Agrobacterium (Souza et al., 2017). There are many ways to enhance the ability of an organism to produce the required yield of product such as natural hybridization, cellular metabolism enhancement, quantitative trait loci, molecular and genetic recombination and gene transformation into the cell. For different

http://www.aloki.hu ● ISSN 1589 1623 (Print) ● ISSN 1785 0037 (Online)
DOI: http://dx.doi.org/10.15666/aeer/1705_1178911802

purposes, different methods and ways are used. One of the best and advanced research in genetic and molecular experiments is to transfer a specific target gene into the vegetative cells of plants. For this purpose, some experiments held in Shenyang Agricultural University Shenyang, Liaoning, China.

Agrobacterium-mediated transformation is a fast and more accurate method for gene transfer with high frequency and time saving approaches (Que et al., 2014). This method is more extensively adapted now days by both civil and private institutions, however, capability of transformation varies highly from lab to lab for the same plant genotype. Here, advanced Agrobacterium-mediated transformation technique in maize by using a simple form of binary vectors exemplified. This method uses undeveloped embryos as fundamental explants and the bar gene as a selectable marker together with bialaphos as a selective agent in maize (Shrawat and Good, 2011), rice (Hei and Komari, 2008) and in switchgrass (Xi et al., 2009). Development based on genetic transfer varies, in which gene can be inserted into plants more effectively which depend on the species or variety, or the genetic marker being used (Binka et al., 2012). In recent times, a CRISPR/Cas9 toolkit used for multiplex genomic editing in different host plants based on the pGreen and in pCambia backbone (Xing et al., 2014). Genetic changes in plants which effect pollen development can be easily observed by the unusual isolation of markers linked to it (Vasal et al., 2006) and in plants where the genetic changes are due to transposons that present a phenotype are by the abnormal isolation of responsible transposon itself (Lalanne et al., 2004; Boavida et al., 2009).

Serine threonine kinase1 (STK1) and serine threonine kinase2 (STK2) are closely related to paralogous genes of maize predicted to encode serine/threonine protein kinases. Those pollens, which have mutations of *ZmSTK1* or *ZmSTK2*, can compete poorly with wild pollens, indicating to an abnormality in germination or growth of pollen tube. Both genes show their expression only in pollens but not in most of other parts of plants. In medium of germination, *ZmSTK1* and *ZmSTK2* fluorescent fusion proteins are located in the cell membrane of the somatic cell of plant. RNA-sequencing experiments indicated 534 genes, which expressed differentially in *zmstk1* mutant pollens as compared to wild type. Gene ontology molecular functional analysis revealed many differently expressed genes with supposed ribosome initiation and elongation functions, signifying that *zmstk1* may show effect on function of ribosomes. Of these two mutant forms, *zmstk1* may show a more imperative role in pollen development as compared to *zmstk2*, as mutations of *zmstk2* have a smaller transmission effect in pollen development. However, *zmstk2* acts as a booster of *zmstk1* expression because the combination of double mutation shows that pollens are too weak to survive until fertilization as compared to wild and single mutants. Therefore, it is analyzed that the *ZmSTK* paralogs play an important role in pollen development (Huang et al., 2017).

New requirements need to develop some techniques for low copy transfer of genes into the target cell by *A. tumefaciens* (Sivamani et al., 2015*)*. In these experiments, *ZmSTK1* gene transferred into the cells of maize embryo during its initial growth time. For transformation of gene there are different ways used in the bio-scientific field, out of these methods Agrobacterium-mediated method of transformation was found as an easy and best way to transform the target gene into the maize embryo cells (Yadava et al., 2017). In this experiment, *Agrobacterium tumefaciens* used as a vector for multiplication to carry the gene *ZmSTK1* into the target embryo cells and insert the gene into the genome of maize cells.

http://www.aloki.hu ● ISSN 1589 1623 (Print) ● ISSN 1785 0037 (Online)
DOI: http://dx.doi.org/10.15666/aeer/1705_1178911802

Materials and methods

Plant material

Wild-type McC and mutant *zmstk1* provided by Dr. Dooner, Rutgers University, USA. The *pMD18-T-pSTK1* recombinant plasmid and the *pCAMBIA1301* plasmid provided by the laboratory from the College of Bioscience and Biotechnology in Shenyang Agricultural University, China.

Instruments and equipment

Test thermostat incubator, PCR machine, refrigerated centrifuge, electrophoresis tank, gel electrophoresis, autoclave, water bath, gel imager, horizontal electrophoresis tank, DC power supply, shaker, 50 ml centrifuge tube, tweezers, scalpel, and 2.0 ml centrifuge tubes.

Major reagents

To make 1% Rifampicin, 0.1 g rifampicin dissolved in 10 ml methanol, sterilized after filtration and stored at -20 °C. To make 5% kanamycin, 1.0 g kanamycin dissolved in 20 ml distilled water, filtered, sterilized and preserved at -20 °C. To make 50 g/l ampicillin, 2 g ampicillin dissolved in 40 ml distilled water, sterilized after filtration and stored at -20 °C. For Acetosyringone solution, dimethyl sulfoxide dissolved in acetosyringone, 200 mmol/l solution was prepared, diluted with distilled water to make 100 mmol/l, filtered and stored at -20 °C. In addition, for 5% sodium hypochlorite solution, 50 ml of pure sodium hypochlorite dissolved in sufficient amount of distilled water, raised the volume to 1 L and stored at room temperature. 70% ethanol was prepared by adding 70 ml of pure ethanol, with the sufficient amount of distilled water and raised the volume 0.1 L. To make YEB medium, 10 g tryptone, yeast 10 g extract and 0.5 g $MgSO_4$.$7H_2O$ mixed with distilled water to raise the volume 1000 ml and stored at pH 7.2. LB medium prepared by dissolving 10 g tryptone, 5 g yeast extract, 10 g NaCl in distilled water, raised the volume to 1 L, and stored at pH 7.0. For sodium phosphate buffer (100 mmol/l, pH 7.0), Solution A (6.55 g NaH_2PO_4 .$2H_2O$ dissolved in 50 ml of distilled water) and Solution B (1.83 g Na_2HPO_4 .$12H_2O$ dissolved in 50 ml of distilled water) mixed and volume raised to 200 ml at pH 7.0. X-Gluc prepared using (5-bromo-4chloro-3 indolylglucuronide) and mother liquor (0.5 mg/ml). 0.025 g of X-Gluc dissolved in 1 ml of N-N-dimethyl amide (DMF) and stored at -20 °C. For X-Gluc base solution (10 mmol/l), 0.1 g of $K_3Fe(CN)_6$ potassium ferricyanide (1 mmol/l) and 0.13 g of $K_4Fe(CN)_6$ were mixed in 200 ml of sodium phosphate buffer, followed by the addition of 300 ul 0.1% Triton X-100, 1.12 g Na_2EDTA Potassium ferricyanide (1 mmol/l) and completely dissolved to make 250 ml.

Construction of maize ZmSTK1 expression vector

First competent cells of *E. coli*were prepared by making LB medium, which used to flatten to activate Escherichia coli DH5a single colonies, stored overnight at 37 °C. Then pre-activated single colony was selected, inoculated in 5 ml LB liquid medium and culture was shacked for 12 h at 37 °C. After that 500 µl bacteria inoculated to absorb in 50 ml LB liquid medium, shacked it at 37 °C and bacterial suspension placed in the already cooled 1.5 ml centrifuge tube and ice bathed for 15 min. The cooled suspension centrifuged for 1 min at 4 °C at 8000 rpm. Supernatant discarded after

http://www.aloki.hu ● ISSN 1589 1623 (Print) ● ISSN 1785 0037 (Online)
DOI: http://dx.doi.org/10.15666/aeer/1705_1178911802

removing the net residue of the culture medium and preserved in ice bath. Then suspended bacteria in a pre-cooled $CaCl_2$ solution (0.1 mol/l) at 4 °C and centrifuged for 1 min at 8000 rpm. Then 0.1 mol/l suspension of bacteria centrifuged for 1 min at 8000 rpm at 4 °C and supernatant removed by using 0.1 mol/l $CaCl_2$ solution. Supernatant discarded, net residual culture medium removed and 2 ml pre-cooled $CaCl_2$ solution (0.1 mol/l) added for bacterial suspension. After that, 80% of the volume of glycerol added, mixed, and stored at -80 °C in refrigerator for further use.

Double digestion reaction

The recombinant plasmids *pMD18-T-pSTK1* and *pCAMBIA1301* plasmids digested with restriction endonuclease *HindIII* and *NcoI*. *Table 1* shows the reaction system.

Table 1. *Composition of system used for digestion*

System composition	Consumption
pMD18-T-p*STK1*	15 uL
Hind Ⅲ	1 uL
NcoI	1 uL
10*buffer (Enzyme digestion buffer)	2 uL
Double distilled H_2O	1 uL
Total	20 uL

Recycled digested product

The enzyme digested with the kit and the digested product of *pMD18-T-pSTK1* digested about 1000 bp and named *HindIII-pSTK1-NcoI* and *pCAMBIA1301*. The large fragment digested product named *HindIII-pCAMBIA1301-NcoI*.

Binding with the expression vector

HindIII-pSTK1-NcoI ligated with the vector *HindIII-pCAMBIA1301-NcoI*, and the binding system incubated at 14 °C for 14 h under the conditions of *Table 2*.

Table 2. *Components of enzymatic systems*

System composition	Consumption
T4 DNA Ligase	2.0 uL
T4 Ligase buffer solution	2.0 uL
Hind Ⅲ- pCAMBIA1301-*NcoI*	4.0 uL
Hind Ⅲ-p*STK1-NcoI*	12 uL
Total	20 uL

Conversion

Thawed E. coli competent cells to complete melting drew 100 μl into a new sterile centrifuge tube and immediately placed in ice. Then 5-μl ligase enzyme added, mixed and placed in ice for 30 min followed by putting it in a hot water bath at 42 °C for 90 s and quickly placed in ice for 5 min. Then 1-l LB liquid medium added, mixed and shacked at 37 °C for 1.5 h and centrifuged for 1 min at 8000 rpm, discarded the centrifugal supernatant and added 100 μl LB liquid medium. The bacterial liquid

http://www.aloki.hu ● ISSN 1589 1623 (Print) ● ISSN 1785 0037 (Online)
DOI: http://dx.doi.org/10.15666/aeer/1705_1178911802

coated on LB solid medium containing 50 g/l of ampicillin and the surface placed up to the bacterial solution, completely absorbed by the culture medium and cultured at 37 °C for 16 to 24 h. Then a single colony picked and used PCR kit to mention the plasmid. After a double enzyme digestion, electrophoresis detection of recombinant plasmid used and digestion products tested in the positive plasmid named *pCAMBIA1301-pSTK1-GUS*saved in refrigerator at -80 °C.

Preparation of agrobacterium competent cells

Agrobacterium tumefaciens EHA105 cultured on YEB solid medium containing 1% rifampicin and cultured at 28 °C for 48 h. Activated single colony selected, inoculated with 1 ml liquid medium containing 1% rifampicin YEB and shacked at 28 °C overnight. 250 µl of the bacterial solution was taken and incubated in 25 ml of YEB liquid medium containing 1% rifampicin and shook at 28 °C until OD600 = 0.5. Next, took the bacterial suspension, ice bathed for 15 min and centrifuged in a high speed centrifugal machine for 10 min at 5000 rpm and supernatant was discarded. 5 ml 0.15 mol/l NaCl suspension of bacteria was prepared, ice bathed for 15 min and centrifuged at 5000 rpm for 10 min. Then 2 ml 0.1 mol/l pre-cooled $CaCl_2$ solution was prepared with cell suspension, 80% glycerol added and refrigerated at -80 °C.

Transformation of agrobacterium competent cells

Thawing agrobacterium competent cells

Ten ul of *pCAMBIA1301-pSTK1-GUS* added into 100 ul competent cells, mixed and ice bathed for 30 min. Next, placed in liquid nitrogen for 5 min and immediately transferred it to a 37 °C water bath for 5 min. Then 1 ml of YEB added, shook for 5 h at 28 °C, centrifuged at 220 rpm and supernatant removed. 200-µl YEB liquid medium of bacterial suspension added centrifuged at 5000 rpm for 2 min and supernatant removed. YEB solid medium containing 1% rifampicin and 5% kanamycin added and cultured at 28 °C for 48 h. Finally, a single colony picked and PCR used to identify the positive results.

Genetic transformation of maize germination embryos

Strain activation

After preparation, YEB solid medium (1-l YEB medium + 7 g agar powder) placed in a high-pressure sterilization chamber of a steam sterilizer. Petri dishes, gun, gun head, a sealing film, an inoculation ring and other tools were also placed in ultraviolet radiation chamber for sterilization and then in autoclave chamber. Bacterial culture taken out of the refrigerator for 30 min for defrosting. When the medium temperature was moderate, 1% rifampicin and 5% kanamycin added in the ultraclean working medium and poured on a flat plate. When the medium solidified, the inoculation ring burned to red with alcohol lamps, and the front of the rod fixed about 7 cm. The outer ring heated for 10 s, and inoculated ring completely cooled. The positive colonies stained with rings, and the culture medium divided into three zones. After the completion of the inoculation, the inoculation ring placed on the alcohol lamp for burning and cooled. After inoculation on the edge of the line, the area crossed again to make two areas. At the end, the third area also inoculated in the same method as it inoculated into other areas. The inoculation completed after burning the inoculation

http://www.aloki.hu ● ISSN 1589 1623 (Print) ● ISSN 1785 0037 (Online)
DOI: http://dx.doi.org/10.15666/aeer/1705_1178911802

ring. After cooling, the metal ring removed and the petri dishes closed with sealing film. Next, placed the petri dish in the incubator in a dark chamber at 28 °Cfor 48 h.

Preparation of bacteria

A single colony of *Agrobacterium tumefaciens* EHA105 containing *pCAMBIA1301-pSTK1* recombinant expression plasmid transferred on the plate with a sterilized gun tip. Seeded in YEB liquid medium containing 1% rifampicin (7.5 µl) and 5% kanamycin (1.5 µl) in a centrifuge tube (size: 2.0 ml) of 1.5 ml, shacked overnight on a 200 rpm speed in a constant temperature shaker at 28 °C and found positive results as shown in *Tables 3* and *4*. Bacterial solution transferred into the 50 ml centrifuge tube, 25 ml of YEB liquid medium, 1% rifampicin 125 µl and 5% kanamycin, 25 µl of mixture added and culture shacked well at a constant temperature. The determined OD value was in the range of 0.4-1.2. The material saved at 4 °C for further use.

Table 3. *Primers for GUS*

Name of primer	Primer sequence
Upstream primers: GUS—F	5`-GCAACTGGACAAGGCACT-3`
Downstream primers: GUS—P	5`-GAGCGTCGCAGAACATTACA-3`

Table 4. *Reaction components of bacterial culture medium for PCR*

System composition	Consumption
PCR Master Mix	5.0 uL
GUS—F	0.5 uL
GUS—P	0.5 uL
bacterial fluid	4.0 uL
Total	10.0 uL

Seed sterilization

Healthy seeds selected with no damage, soaked into 70% ethanol for sterilization for 30 s; seeds transferred to 5% sodium hypochlorite for disinfection for 45 min and rinsed the seeds 5 to 7 times with sterile water. Finally, seeds packed into a sterilized jar (200 tablets), sterilized water added and shaken with the help of a shaker at 90 rpm and soaked overnight. The next day, tubes centrifuged at 4000 rpm for 10 min, supernatant removed and precipitate transferred to the sterile jar. Fresh 1% rifampicin 125 µl, 5% kanamycin 20 ml, YEB liquid medium 25 µl, 15% 5 µl of acetosyringone and agar added as transformation and growth medium. Tip of the sterilized blade used to scrape the embryo growth point and placed in the jar. Labeled flasks placed in a thermostatic shaker and incubated at 28 °C and 90 rpm for 12 h. After those 12 h, the seeds transferred into the nutrient rich soil containing vermiculite and perlite and cultured for T° plant stage. Then set different gradients of OD value to 0.4, 0.6, 0.8, 1.0 and 1.2 and acetyl acetone (AS) with concentration gradient of 50 mmol/l, 100 mmol/l, 150 mmol/l, 200 mmol/l and the conversion rate of maize plants was calculated.

http://www.aloki.hu ● ISSN 1589 1623 (Print) ● ISSN 1785 0037 (Online)
DOI: http://dx.doi.org/10.15666/aeer/1705_1178911802

DNA extraction and identification of plant genetic transformation

When the plant reached the three-leaf stage, 1-2 cm of blade was cut and put into the centrifuge tube containing 200 µl of NaOH 0.25 mol/l and the tube was centrifuged for 30 s at 100 °C constant temperature. 200 ul of 0.25 mol/l HCl and 100 ul of 0.5 mol/l of Tris-HCl (pH 8.0, NP-40 0.25%) added to the centrifuge tube. The tube again incubated in boiling water for 2 min. About 2 mm² of the leaves was picked up after few steps treatment of acid and alkali and this sample used as a template for PCR amplification. The PCR amplification reaction conditions shown in *Table 5* and the reaction system components shown in *Table 6*.

Table 5. *PCR amplification reaction conditions*

Temperature	Duration
94 °C (Pre-denaturation)	2 min
94 °C (Denaturation)	90 s 35 cycles
57 °C (Annealing)	1 min
72 °C	2 min
72 °C	5 min
4 °C	Saved permanently

Table 6. *PCR reaction system components*

System components	Consumption
GUS-F	2.5 µL
GUS-R	2.5 µL
PCR Master Mix	7.3 µL
Blade	≤ 2 mm²
Double distilled H_20	37.7 µL
Total	50.0 µL

Gel electrophoresis machine used to separate different sized DNA fragments. For the preparation of 10* TBE buffer, 108 g Tris, 7.44 g Na_2EDTA .$2H_2O$ and 55 g of boric acid was taken in a beaker and 800 ml distilled water was added to the beaker stirred to fully dissolved, volume was raised to 1 L with addition of distilled water and stored at room temperature. 0.5* TBE buffer was prepared by mixing 25 ml 10* TBE and 475 ml distilled water and stored at room temperature. 5 mg/ml ethidium bromide(EB)aqueous solution was prepared and agarose gel plates were prepared by mixing 0.2 g agarose and 20 ml 0.5* TBE in a conical flask by flushing liquid in it. After mixing, the flask placed in the microwave for heating for 1 min to dissolve fully and then cooled to 60 °C to add EB drop by drop. After shaking the sample, the combs were fixed, the solution was poured into the sealed gel tank (thickness 3-5 mm) and air bubbles between the comb teeth discharged. Combs taken out after cooling and glue solidification, then gel plate placed into a horizontal electrophoresis tank containing 0.5* TBE buffer until the plane thickness of submerged glue became 2 mm. Further, ten to fifteen µl marker sample added in marked gel hole and input of 180 voltage, 100 mA current to the gel electrophoresis tank provided and samples were run in the gel. Power turned off; gel bands removed from the electrophoresis tank and placed in the gel imager to check the imaging results. To perform GUS

http://www.aloki.hu ● ISSN 1589 1623 (Print) ● ISSN 1785 0037 (Online)
DOI: http://dx.doi.org/10.15666/aeer/1705_1178911802

staining of transgenic plants the configured X-Gluc mother liquor and X-Gluc base solution completely mixed to a volume of 300 ml. T° genetically modified transgenic plants and wild-type plants immature and mature roots, young leaves, mature leaves, immature anthers and mature anthers placed in fixed solution of 90% acetone for 15 min. Rinsed with buffer three times, put into the GUS staining solution, vacuumed and placed in the incubator at 37 °C in the dark overnight. Next day, samples rinsed three times with 70% alcohol for decolorization, observed under the microscope, pictures taken and differences analyzed.

Results

The construction of expression vector

The digestion of recombinant plasmid *pMD18-T-pSTK1* and plasmid *pCAMBIA1301* done by Hind III and NcoI restriction enzymes. The digested *Hind III-pSTK1-NcoI* promoter and *Hind III pCAMBIA1301-NcoI* connected with *CaMV35S* promoter instead of *pCAMBIA1301* in the vector. The recombinant plasmid expressing *pCAMBIA1301-pSTK1* transferred into *Escherichia coli* competent cells. After successful transformation, plasmids extracted and transferred into the susceptible state of *Agrobacterium tumefaciens*. The screening of samples performed and selected colonies used for PCR. The results are shown in *Figure 1,* Lane 3, Lane 4 and Lane 5 in 1000 bp band.

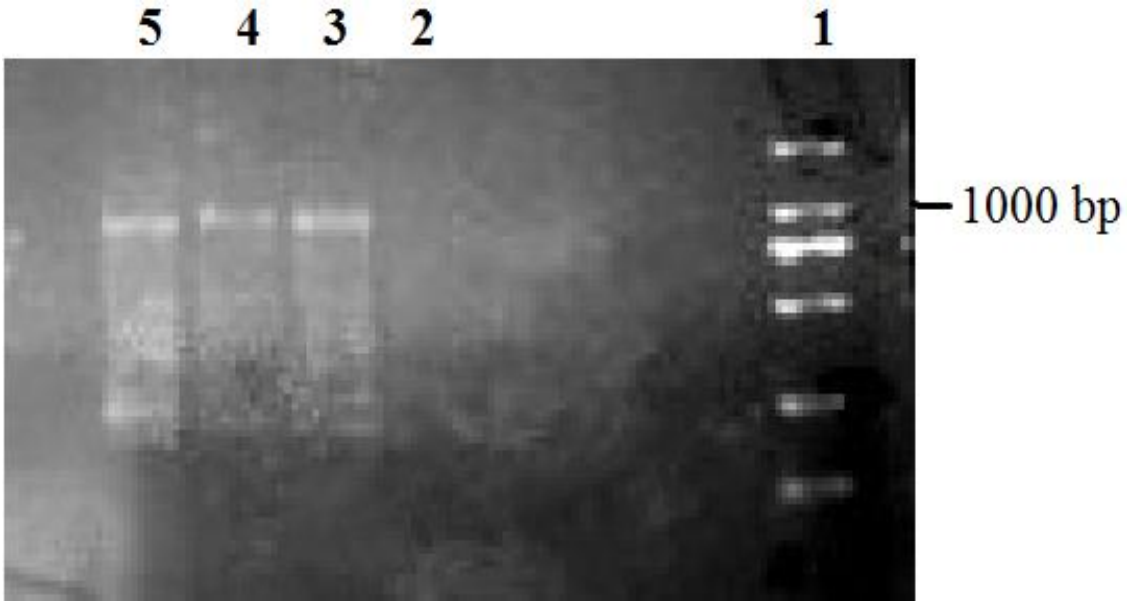

Figure 1. *PCR detection of pCAMBIA1301-pSTK1-GUS. (Note: Lane 1 is 2000 marker; Lane 2 is control carrier pCAMBIA1301; Lane 3-5 are the product to be tested)*

Identification of active colonies

Active colonies identified by their activities in PCR amplification and detection through agarose gel electrophoresis. The detection results are shown in *Figure 2,* Lane 2 and Lane 3 in about 750 bp.

http://www.aloki.hu ● ISSN 1589 1623 (Print) ● ISSN 1785 0037 (Online)
DOI: http://dx.doi.org/10.15666/aeer/1705_1178911802

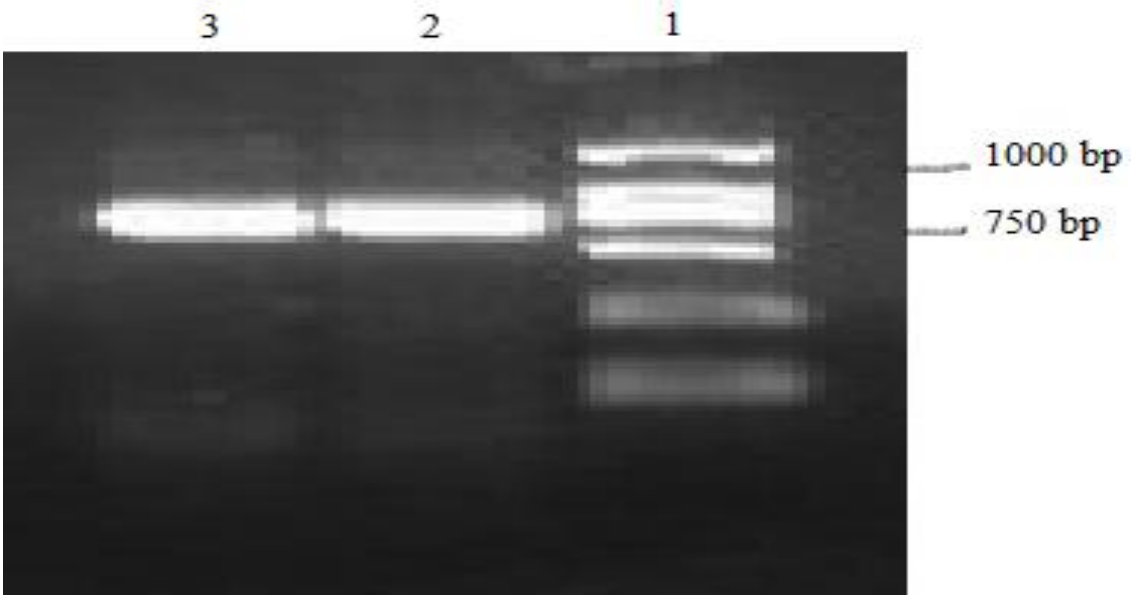

Figure 2. *Detection of bacterial liquid PCR. (Note: Lane 1 is 2000 marker; Lane 2, 3 are colonies to be tested)*

Optimization of transformation conditions

Acetosyringone AS can induce the activation of virulent gene in *Agrobacterium tumefaciens*, and promote the integration of foreign genes. The addition of AS can improve the conversion rate. The maize seeds were treated with different concentrations (OD value were 0.4, 0.6, 0.8, 1 and 1.2) of the bacteria by adding 0.1 mmol/l acetosyringone (AS) and cultivated at constant temperature of 28 °C. The results showed that different concentrations of bacteria had little effect on seed germination (around 20%) but affected the seed conversion rate. When the concentration of bacteria was up to 0.8 OD and acetosyringone concentration was 0.1 mol/l, the transformation rate was maximum.

Regeneration of germinating embryo by genetic transformation

The inoculated corn seeds cultured in nutrient rich soil containing vermiculite and perlite and 150 grains were sown in each pot (15 × 10) as shown in *Figure 3*.

Total 4000 seeds (200 per plot) incubated into germinating embryos and 807 seeds germinated after Incubation. Only three plants successfully transformed as shown in *Figure 4*. The *pstk-1* transgenic plants of T° generation obtained by Agrobacterium-mediated method. The results showed that when OD value was at 0.8 and concentration of AS was 100 mmol/l, the transformation rate was the best. The germination rate was 20.2%, and the conversion rate was 0.075%.

Transgenic plant testing

After DNA extraction, PCR amplification and detection from the transgenic plants results showed that there were bands in the samples and detected at around 750 bp. The PCR results showed that three seeds out of 4000 seeds successfully transformed (*Fig. 5*).

http://www.aloki.hu ● ISSN 1589 1623 (Print) ● ISSN 1785 0037 (Online)
DOI: http://dx.doi.org/10.15666/aeer/1705_1178911802

Figure 3. *Screening of positive plants*

Figure 4. *Transgenetic regeneration of positive plants*

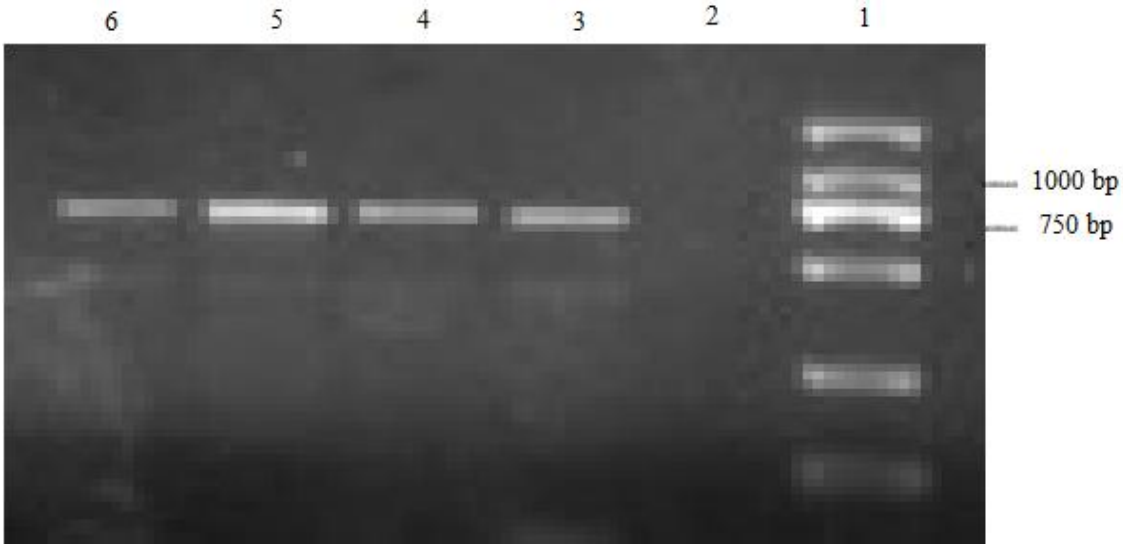

Figure 5. *PCR detection of transgenic plants. (Note: Lane 1 is 2000 marker; Lane 2 is non-transgenic plants; Lane 3 is bacterial liquid; Lanes 4-6 are the transgenic plants to be tested)*

http://www.aloki.hu ● ISSN 1589 1623 (Print) ● ISSN 1785 0037 (Online)
DOI: http://dx.doi.org/10.15666/aeer/1705_1178911802

GUS staining of regenerated plants

In GUS staining of non-transgenic plants and *PSTK1-GUS* plants parts such as immature roots, immature leaves and immature anthers, mature root, mature leaves and mature anthers and mature pollen performed. The results showed that all parts of the non-transgenic plants showed no GUS signal. *PSTK1-GUS* transgenic plant immature roots, mature roots, immature leaves, mature leaves and immature anthers also showed no GUS signal but the mature anthers and mature pollens showed GUS signal in the form of dark spots as shown in *Figure 6*.

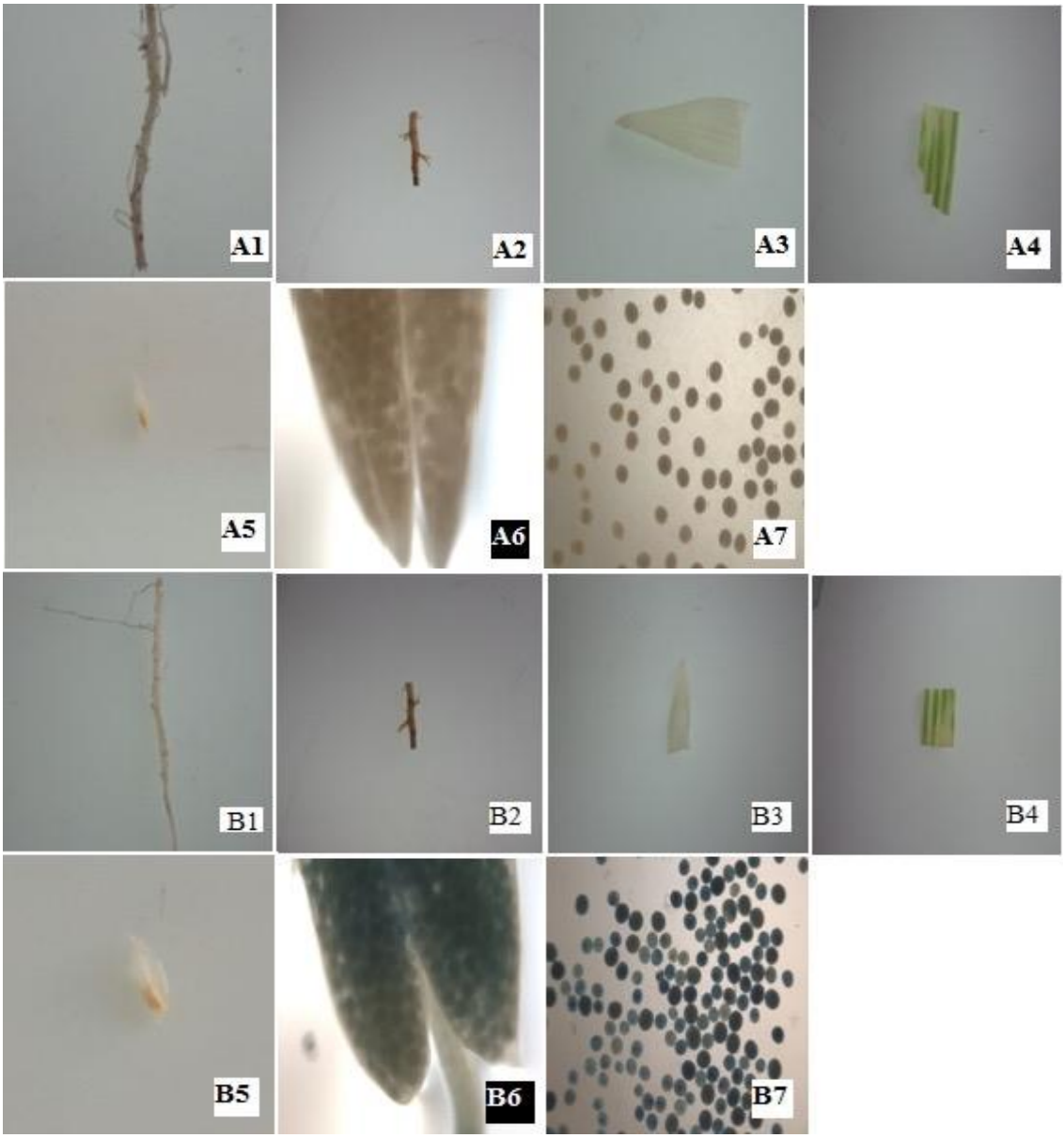

Figure 6. *GUS staining for the non-transgenic and PSTK1-GUS plant parts. (Note: A1-A7 are non-transgenic plants; B1-B7 are PSTK1-GUS plants; A1 and B1 are radicles; A2 and B2 are mature roots; A3 and B3 are immature leaves; A4 and B4 are mature leaves; A5 and B5 are immature anther; A6 and B6 are mature anther; A7 and B7 are mature pollen)*

http://www.aloki.hu ● ISSN 1589 1623 (Print) ● ISSN 1785 0037 (Online)
DOI: http://dx.doi.org/10.15666/aeer/1705_1178911802

Discussion

Genetic transformation is an effective way to increase crop yield and improve quality. With the progress of technology, the method of transgenic maize is continuously improved. In maize, there is a variety of transformation methods, such as electroporation, pollen tube pathway, gene gun, polyethylene glycol, and Agrobacterium-mediated transformation. The receptor of electroporation and polyethylene glycol (PEG) is through protoplast, which is very strict to the preparation and operation of receptor, so it cannot be widely used. The complete pollen tube transformation process is done by natural pollination, without tedious preparation work, breeding required time is short and used directly. Sometimes growing season and flowering stage can affect it. It is also affected by environmental conditions such as temperature, wind, light, rain and more. The bombardment carried out by using the tiny metal particles containing DNA to target the receptor, and DNA injected into the recipient cells by a bilayer lipid membrane. Without host restriction, biolistic method transforms into a variety of plants and improves the plant transformation rate. Moreover, receptor-mediated no-gene type restrictions can be applied to different species and different varieties. It can applied to different organelles with high degree of controllability. However, because the bombardment is random and the conversion rate is relatively low, so multiple copies of the gene are inserted in genome during rearrangement. Prone to a variety of ways, the homologous sequence can be RNA-RNA, DNA-DNA, or DNA-RNA with each other, causing transcription or posttranscriptional level gene silencing. According to various methods, Agrobacterium-mediated transformation has the advantages of relatively stable inheritance, simple operation and high conversion rate. This transformation experiment using *Agrobacterium tumefaciens*-mediated transformation of maize germinating embryo was time saving, strong repeatability and no need of the corn growing season constraints. It also does not depend on tissue culture can also be done without the process of tissue culture transformation. The receptor of this study, and the concentration conditions of bacteria and AS optimized was also corn-germinating embryo.

After acid and leaf treatment, PCR amplification used to screen the positive plants, which was simple and effective. This method does not need to extract the detected leaf DNA according to traditional procedure, shortened the testing time, only needs leaf area of not more than 2 mm. At the same time, in this method, plant leaf injury is relatively low and the cost is decreased. Therefore, this method has the advantages of less time consumption and high detection efficiency.

GUS detection method is fast, simple and stable. The GUS gene is beta-D-glucuronidase (Gus) gene, X-Gluc can be hydrolyzed into blue material and staining of tissues showed blue spots with GUS activity (visible), so gene expression of GUS detected in specific tissues at exogenous gene site. This is not reported in other gene transfer method. In this study, the *PSTK1-GUS* gene of T° transgenic plants only had GUS signal in mature anthers and mature pollens, which showed that *stk1* promoter only had transcriptional activity in mature pollen. However, for T° transgenic plants, it is not possible to determine whether the inserted fragments are integrated successfully into the genomic DNA or not and further experiments are needed to verify them.

http://www.aloki.hu ● ISSN 1589 1623 (Print) ● ISSN 1785 0037 (Online)
DOI: http://dx.doi.org/10.15666/aeer/1705_1178911802

Conclusion

The results suggested that the transformation rate to obtain transgenic plants was very low. The GUS staining of non-transgenic and transgenic *PSTK1-GUS* plants showed no GUS signal. However, mature anthers and pollens showed GUS signal in the form of dark spots, which indicated *ZmSTK1* only influences during pollen development and germination. Agrobacterium-mediated gene transformation method is advance and easy for genetic researchers to solve the mysteries behind gene mutation and function at a specific stage.

Acknowledgments. The National Natural Science Foundation of China (grant numbers. 31571672 and 31671707) supported this research.

Ethical approval. This article does not contain any studies with human participants or animals performed by any of the authors.

Conflict of interests. All authors declare that there is no conflict of interests.

REFERENCES

[1] Bińka, A., Orczyk, W., Nadolska-Orczyk, A. (2012): The Agrobacterium-mediated transformation of common wheat (Triticum aestivum L.) and triticale (x Triticosecale Wittmack): role of the binary vector system and selection cassettes. – Journal of Applied Genetics 53: 1-8.

[2] Boavida, L. C., Shuai, B., Yu, H. J., Pagnussat, G. C., Sundaresan, V., McCormick, S. (2009): A collection of Ds insertional mutants associated with defects in male gametophyte development and function in Arabidopsis thaliana. – Genetics 181: 1369-1385.

[3] Brittain, C., Kremen, C., Klein, A. M. (2013): Biodiversity buffers pollination from changes in environmental conditions. – Global Change Biology 19: 540-547.

[4] De Carvalho, C. H. S., Zehr, U. B., Gunaratna, N. S., Anderson, J. M., Kononowicz, H., Hodges, T. K. (2004): Agrobacterium-mediated transformation of sorghum: factors that affect transformation efficiency. – Genetic and Molecular Biology 27: 259-269.

[5] Gittins, J. R., Pellny, T. K., Biricolti, S., Hiles, E. R., Passey, A. J., James, D. J. (2003): Transgene expression in the vegetative tissues of apple driven by the vascular-specific rolC and CoYMV promoters. – Transgenic Research 12: 391-402.

[6] Hiei, Y., Komari, T. (2008): Agrobacterium-mediated transformation of rice using immature embryos or calli induced from mature seed. – Nature Protocol 3: 824-834.

[7] Hiei, Y., Ohta, S., Komari, T., Kumashiro, T. (1994): Efficient transformation of rice (Oryza sativa L.) mediated by Agrobacterium and sequence analysis of the boundaries of the T-DNA. – The Plant Journal 6: 271-282.

[8] Huang, J. T., Wang, Q., Park, W., Feng, Y., Kumar, D., Meeley, R. (2017): Competitive ability of maize pollen grains require paralogous serine threonine protein kinases STK1 and STK2. – Genetics: 300358.302017.

[9] Jefferson, R. A., Kavanagh, T. A., Bevan, M. W. (1987): GUS fusions: beta-glucuronidase as a sensitive and versatile gene fusion marker in higher plants. – The EMBO Journal 6: 3901.

[10] Lalanne, E., Michaelidis, C., Moore, J. M., Gagliano, W., Johnson, A., Patel, R. (2004): Analysis of transposon insertion mutants highlights the diversity of mechanisms underlying male progamic development in Arabidopsis. – Genetics1 6: 1975-1986.

http://www.aloki.hu ● ISSN 1589 1623 (Print) ● ISSN 1785 0037 (Online)
DOI: http://dx.doi.org/10.15666/aeer/1705_1178911802

[11] Que, Q., Elumalai, S., Li, X., Zhong, H., Nalapalli. S., Schweiner, M. (2014): Maize transformation technology development for commercial event generation. – Frontiers in Plant Science 5: 379.
[12] Shimoda, N., Toyoda-Yamamoto, A., Nagamine, J., Usami, S., Katayama, M., Sakagami, Y. (1990): Control of expression of Agrobacterium vir genes by synergistic actions of phenolic signal molecules and monosaccharides. – Proceeding of Natural Academy of Science 87: 6684-6688.
[13] Shrawat, A. K., Good, A. G. (2011): Agrobacterium tumefaciens-mediated genetic transformation of cereals using immature embryos. – Plant Embryo Culture: Methods and Protocols 710: 355-372.
[14] Sivamani, E., Li, X., Nalapalli, S., Barron, Y., Prairie, A., Bradley, D. (2015): Strategies to improve low copy transgenic events in Agrobacterium-mediated transformation of maize. – Transgenic Research 24: 1017-1027.
[15] Souza, R. A. V., Alves, M. C., Carneiro, N. P., Barros, B. A., Borém, A., Carneiro, A. A. (2017): Agrobacterium-mediated genetic transformation of a tropical elite maize line. – Crop Breeding and Applied Biotechnology 17: 133-140.
[16] Vasal, S. K., Riera-Lizarazu, O., Jauhar, P. P. (2006): Genetic enhancement of maize by cytogenetic manipulation, and breeding for yield, stress tolerance, and high protein quality. – Genetic Resources, Chromosomal Engineering and Crop Improvement 2: 159-197.
[17] Waines, J., Hegde, S. (2003): Intraspecific gene flow in bread wheat as affected by reproductive biology and pollination ecology of wheat flowers. – Crop Science 43: 451-463.
[18] Xi, Y., Ge, Y., Wang, Z. Y. (2009): Genetic transformation of switchgrass. – Biofuels: Methods and Protocols 581: 53-59.
[19] Xing, H. L., Dong, L., Wang, Z. P., Zhang, H. Y., Han, C. Y., Liu, B. (2014): A CRISPR/Cas9 toolkit for multiplex genome editing in plants. – BMC plant Biology 14: 327.
[20] Yadava, P., Abhishek, A., Singh, R., Singh, I., Kaul, T., Pattanayak, A. (2017): Advances in maize transformation technologies and development of transgenic maize. – Front. in Plant Science 7: 1949.
[21] Yang, L., Wang, H., Liu, J., Li, L., Fan, Y., Wang, X. (2008): A simple and effective system for foreign gene expression in plants via root absorption of agrobacterial suspension. – Journal of Biotechnology 134: 320-324.

http://www.aloki.hu ● ISSN 1589 1623 (Print) ● ISSN 1785 0037 (Online)
DOI: http://dx.doi.org/10.15666/aeer/1705_1178911802

ASSESSMENT OF GENETIC DIVERSITY BASED ON ISSR MARKERS IN NEOPESTALOTIOPSIS SPECIES COLLECTED FROM GUAVA (*PSIDIUM GUAJAVA* L.) PLANTS AFFECTED WITH CANKER DISEASE IN PAKISTAN

UL HAQ, I.[1*] – IJAZ, S.[2]

[1]*Department of Plant Pathology, University of Agriculture, University Road Faisalabad, Pakistan*

[2]*Centre of Agricultural Biochemistry and Biotechnology (CABB), University of Agriculture University Road, Faisalabad, Pakistan*

[*]*Corresponding author*
e-mail: imran_1614@yahoo.com

(Received 23rd Apr 2019; accepted 16th Jul 2019)

Abstract. Guava is susceptible to various phytopathogenic fungi that could be associated with canker diseases. In Pakistan, farmer's economy is heavily affected by this devastating disease. One of the several strategies to managing it is to develop canker disease resistant guava varieties. For the complete understanding of the associated pathogen and its detailed characterization are required. In this study, Neopestalotiopsis spp accessions of Fungal Molecular Biology Culture Collection UAF (FMB-CC-UAF) isolated from canker affected guava plants were investigated to find genetic diversity among them based on ISSR markers. Eleven (11) ISSR primers were used to analyze eight (8) Neopestalotiopsis accessions. Genetic variation among these fungal accessions were estimated using unweighted pair group method with arithmetic mean (UPGMA) based genetic diversity analysis and Nei's genetic diversity. Among them FMB-Guv-JF2 and FMB-Guv-JF7 showed 13.01% genetic difference to each other. However, the maximum genetic distance was estimated to be 82.32% between FMB-Guv-B2A and FMB-Guv-B1. Generated dendrogram revealed the grouping of investigated fungal accessions into distinct clusters with considerable genetic diversity. It is also supported by principal coordinate analysis (PCoA) which showed dispersed pattern of these fungal accessions indicating diverse genetic base.
Keywords: *fruit crop, plant pathogen, biodiversity, characterization*

Introduction

Guava (Psidium guajava L.) originating from tropical America belongs to the genus Psidium, family Myrtaceae. Its cultivars vary in size and vigor but it's usually a small tree or shrub having 3 to 10 m height with shallow root system, (Malo and Campbell, 1994; Yadava, 1996; Gutiérrez et al., 2008). Guava is now cultivated in many tropical and subtropical countries worldwide. Guava has potential to grow in a variety of soils having different textures, wide pH range (usually 4.4-9.4), drainage, even in poor soil and can tolerate dry and humid climatic conditions (Keith et al., 2006). Guava fruits have spherical to pear shape with penetrating aroma. The fruit is a great source of nutrition having vitamin A, C, B complex, iron, calcium, and phosphorus (Pachanawan et al., 2008). Pakistan ranks fourth among guava producers in the world after India, China and Thailand. In Pakistan guava is at third position in terms of area while at fourth position in terms of production (Pervaiz et al., 2008). In Pakistan guava is cultivated on 665 thousand ha with yield 31.79 t/ha (FAO, 2011), annual production is reduced from 509 to 495 thousand tons during 2015-2016 (Pakistan Bureau of Statistics, 2016). Actual yield is less than potential yields as (10-12 t/ha) (Ul-Haq et al., 2013).

http://www.aloki.hu ● ISSN 1589 1623 (Print) ● ISSN 1785 0037 (Online)
DOI: http://dx.doi.org/10.15666/aeer/1705_1180311811

Worldwide growth and production of Guava is stressed by different biotic and abiotic factors. Among the biotic factors diseases are the major production constraint of Guava. So far, 177 pathogens found to be associated with different plant parts of guava. Out of these 167 are fungal pathogens. In Pakistan twenty-one fungal pathogens have been reported so far, which to infect guava plant (Abbas et al., 2016). Twenty-one (21) fungi have been reported to infect guava plants in Pakistan *Phytopthora parasitica*, *Capnodium* sp., *Glomerella cingulate*, *Alternaria alternate*, *Alternaria tenuissima*, *Cladosporium*, *Curvularia* sp., *Fusarium solani*, *Fusarium solani* f. f. sp. Psidii, *Fusarium oxysporum*, *Fusarium oxysporum* f. f. sp. Psidi, *Penicillium* sp. on tree bark in Pattoki and Sharqpur, *Pestalotiopsis brevista*, *Phoma psidii*, *Diplodia psidii*, *Stagnopsis psidii*, *Pestalotia psidii*, *Lasiodiplodia undulate*, *Botryodiplodia theobromae*, *Polyporus* sp. Among the important fungal destructive diseases of Guava in Pakistan, Anthracnose, Wilt, Dieback/decline, fruit canker and scab are of great importance.

While conducting to document the data regarding disease incidence and severity of Guava Anthracnose, dieback and fruit canker and sampling for to detect the association of fungal pathogens with the disease affected plants, the research team of "Fungal Molecular Biology Laboratory" Department of Plant pathology, University of agriculture Faisalabad, Pakistan has identified different isolates as Neopestalotiopsis associated with guava plants. However, evolution results in continuous changes to genetic background of phytopathogens, which ultimately brings new races from them elite cultivars have become susceptible (Malathi et al., 2010). Therefore, unequivocal characterization of newly emerged pathogens is crucial for disease control (Saksena et al., 2013). ISSR marker based genetic analysis for determining and assessing the genetic variation among fungal isolates has become more reliable and efficient approach. Therefore, in this study, genetic diversity among Neopestalotiopsis species accessions of Fungal Molecular Biology Laboratory Culture Collection University of agriculture Faisalabad, Pakistan (FMB-CC-UAF), collected from canker affected guava plants were investigated using ISSR markers.

Materials and methods

Fungal accessions

Eight accessions of Neopestalotiopsis species (*Table 1*) isolated from canker infected branches, leaves and fruits of guava plants were used in this study. These fungal isolates were collected from different regions of Pakistan. Pure culture of each isolate were made by single spore technique and were maintained on Potato Dextrose Agar (PDA) medium. However, the list of potential pathogens associated to guava canker disease is given in the *Table 2*.

Table 1. *Detail of Neopestalotiopsis spp. accessions of guava plant collected from different regions of Pakistan for genetic diversity analysis*

Sr. #	Isolate code	Strain number
1	FMB-Guv-B3	FMB0026
2	FMB-Guv-C4	FMB0027
3	FMB-Guv-MB	FMB0028
4	FMB-Guv-JF2	FMB0127
5	FMB-Guv-JF7	FMB0128
6	FMB-Guv-L2A	FMB0129
7	FMB-Guv-B2A	FMB0130
8	FMB-Guv-B1	FMB0013

http://www.aloki.hu ● ISSN 1589 1623 (Print) ● ISSN 1785 0037 (Online)
DOI: http://dx.doi.org/10.15666/aeer/1705_1180311811

Table 2. *Fungal pathogen(s) associated with Psidium guajava*

Sr. No.	Pathogen	Symptom(s)	Reference	Country	Disease
1	Fusarium solani f. f. sp. Psidii	Chlorosis, wilting of branches and twigs, browning of internal tissues	Bokhari et al., 2008 and Gupta et al., 2010,	Pakistan, India	Wilt, decline
2	Fusarium oxysporum f. sp. Psidii	Infected seedlings wilt and die at seedling stage, Older plants show vein clearing, leaf epinasty, yellowing of lower leaves, stunting and defoliation. In case of severe decline quick wilting of leaves giving out burning appearance	Prasad et al., 1952; Pandey and Dwivedi, 1985; Ansar et al., 1994 and Lim and Manicom, 2003	India, Australia, Pakistan	Wilt, decline
3	Phytophthora parasitica	Reported to be associated with guava	Safdar et al., 2015	Pakistan	----------
4	Curvularia lunata	Reported to be associated with guava	Safdar et al., 2015	Pakistan	----------
5	Glomerella cingulate/ Colletotrichum gloeosporioide/	Twigs began to die back, twig blight, formation of brown which turns silvery grey on lateral stages, wither tip, bark splitting and roots began to rot at basal region	Ansar et al., 1994; Tandon and Agarwal, 1954; Lim and Manicom, 2003 and ul haq et al., 2013	All guava growing regions	Wilt, dieback and Decline
6	Pestalotiopsis psidii/ Pestalotia psidii	Symptoms appeared as small necrotic spots of blackish gray and brittle usually appeared on leaf apices. Formation of brown spots and corky lesions on fruit epidermis with elevated margin	Lim and Manicom, 2003; Misra and Prakash, 1986 and Rahman et al., 2003	Australia, India. Burma, Malaysia, Venezuela, Zambia. Bangladesh	Fruit canker and scab
7	Gloeosporium psidii/ Colletotrichum gloeosporioides	Numerous small, water soaked and shallow lesions are produced on ripened fruits, later on these lesions become enlarged and dispersed and fuse with each other to form larger spots which are irregular in shape	Srivastava and Tandon, 1969a	India	Anthracnose or Fruit rot
8	Botryodiplodia theobromae	Infection starts as brown discoloration that usually begins at the stem end and moves downwards in irregular way	Srivastava and Tandon, 1969b	India	Soft watery rot
9	Aspergillus awamori, A. wentii and A .niger	Formation of small sized, round water soaked spots, rotted portion ooze that gives out fermented smell, fruit shrinks and reduction in fruit size occur and blackish mass cover the whole fruit surface	(Gupta et al., 1979 and Lal et al., 1980	India	Aspergillus soft rot
10	Pestalotia psidii/ Pestalotiopsis psidii	Dark brown to grey colored spots appeared on leaf margins or tips. On the upper surface of leaves fruiting pustules may also develops	Bilgrami and Purohit 1971	India	Leaf spot
11	Puccnia psidii	Formation of rust pustules on leaves, shoots, flower and fruits	Misra, 2004	Brazil	Guava rust
12	Rhizopus stolonifer	On infected fruits develop oily and water soaked lesions that are slightly sunken with distinct lesion margins	Ooka, 1980	Hawaii	Rhizopus fruit rot
13	Mucor haemalis	Development of water soaked lesions on infected portion, yellow and fuzzy mass of the fungus may cover the whole fruit surface and finally rotted fruits give off yeast like smell	Kunimoto et al., 1977	India	Mucor fruit rot
13	Rhizoctonia solani	Water soaked discoloration of infected seeds as well as seedlings during pre-emergence stage. During post emergence upper leaves develops yellow to brown color, move downward and cause rotting. Finally, seedlings hands down and eventually die	Gupta, 1978	India	Damping off of seedlings/ seedling blight
14	Curvularia siddiquii	Leaves develop dark brown spots that are restricted to leaf tips and margins at initial stage that covers the whole leaf and eventually defoliate	Srivastava, 1963.	India	Leaf spot
15	Phytophthora parasitica/ Phytophthora citricola/ Phytophthora anicotianae	Infected portion develops greyish brown, water soaked lesions with a greyish black centre, internal fruit surface becomes soft that emits unpleasant smell	Mitra 1929; Gupta et al., 1978 and Ko et al.,1982		Phytophthora fruit rot

http://www.aloki.hu ● ISSN 1589 1623 (Print) ● ISSN 1785 0037 (Online)
DOI: http://dx.doi.org/10.15666/aeer/1705_1180311811

Sr. No.	Pathogen	Symptom(s)	Reference	Country	Disease
16	Alternaria tenuissima	Reported to be associated with guava	Abbas et al., 2016	Pakistan	----------
17	B. theobromae	Yellowing of leaves, wilting and complete defoliation, infected trees bears no fruits or few fruits, fruits may become dry and wrinkled	Safdar et al., 2015	Pakistan	Guava decline
18	Phoma psidii	Small circular spots having dark brown center with reddish margin. In advance stage of the disease these spots enlarge and coalesce causing necrotic patches and blighted appearance	Sridhar and Ullasa, 1978	India	Leaf blight
19	Phomopsis destructum	Formation of small lesions of dark brown color and increase to 2 cm diameter. Infected tissues become soft and entire fruit becomes rotted within few days	Rao et al., 1976	India	Phomopsis rot

Genomic DNA isolation

Genomic DNA of these studied fungal accessions was extracted from the mycelia grown on PDA media. Mycelium was ground in liquid nitrogen to turn into fine powder. The fine powder of each sample was treated by CTAB method with some modifications, for genomic DNA isolation. The quality and quantity of extracted DNA was analyzed using agarose gel electrophoresis and spectrophotometer (8000 Spectrophotometer, Thermoscientific.) respectively. Purified DNA of each sample was stored at 4°C for further analysis.

PCR analysis

PCR analysis was performed in 96 well Veriti^{TM} thermalcycler (Applied Biosystem). For genetic analysis of Neopestalotiopsis spp accessions, eleven (11) ISSR primers (*Table 3*) were used. PCR for ISSR was carried out in 25 µl reaction tubes containing primers, dNTPs, 10X *Taq* PCR buffer, Taq polymerase and genomic DNA. PCR products were separated on 2% high resolution agarose (ACTGene), visualized under Gel documentation System (BioRad) and photographs were saved.

Table 3. *List of ISSR primers and statistical data obtained by ISSR primers among Neopestalotiopsis spp accessions*

Sr.#	Primer code	Sequence (5'-3')	Total Loci	Monomorphic Loci	Polymorphic Loci	percent polymorphism	number of bands or alleles produced per primer	PIC
1	ISSR807	$(AG)_8T$	6	2	4	66.7	30	1.3037
2	ISSR823	$(TC)_8C$	5	0	5	100	22	1.7021
3	ISSR830	$(TG)_8G$	4	2	2	50	21	0.6635
4	ISSR845	$(CT)_8$ RG	5	1	4	80	19	1.3432
5	ISSR848	$(CA)_8$ RG	4	1	3	75	19	0.8745
6	ISSR857	$(AC)_8$ YG	3	0	3	100	13	1.1088
7	ISSR860	$(TG)_8$ RA	3	0	3	100	10	0.9287
8	ISSR4	$(AGC)_5$ GC	3	0	3	100	13	0.8745
9	ISSR12	$(GT)_8$	3	0	3	100	11	1.1088
10	ISSR15	$(GT)_7$ AT	3	0	3	100	14	0.8583
11	ISSR19	GC (AG)7A	2	1	1	50	15	0.1948
Total			41	7	34	----	187	----
Average			----	----	----	----	----	0.996445

http://www.aloki.hu ● ISSN 1589 1623 (Print) ● ISSN 1785 0037 (Online)
DOI: http://dx.doi.org/10.15666/aeer/1705_1180311811

Data analysis

DNA bands were counted from DNA banding profiles of each ISSR primer and scored as, "1" for presence and "0" for absence. The data were analyzed using different software packages such as; PAST v.3.16 for dendrogram based on unweighted pair group method with arithmetic mean (UPGMA) algorithm, PopGen32 v. 1.32 for similarity matrix, DARwin6 v. 6.0 software for Principal Coordinate analysis (PCoA), Power marker v. 3.25 for computing polymorphic information content (PIC).

Results

DNA markers are used to assess genetic variability among different individuals. This study was carried out with eight different neopestalotiopsis spp accessions to detect genetic variation among them. PCR amplification using eleven (11) ISSR primers yielded total 41 scorable loci of which 7 were monomorphic loci (*Table 2*). The number of scorable loci varied from 2 (ISSR19) to 6 (ISSR807). However, maximum number of alleles or bands (30) was obtained from primer ISSR807, while only 10 bands or alleles were produced by ISSR860. Of these 11 (eleven) ISSR markers, six primers (ISSR823, ISSR857, ISSR860, ISSR4, ISSR12, ISSR15) showed 100% polymorphism. The highest value of polymorphic information content (PIC) was 1.7021 of primer ISSR823, whereas the lowest value 0.1948 was from primer ISSR19 with average PIC value per primer was 0.996445.

The dendrogram clearly indicated the two clusters, of which cluster I comprising of four fungal accession, FMB-Guv-B3, FMB-Guv-MB, FMB-Guv-C4 and FMB-Guv-B1. However, cluster II was possessing four accessions viz., FMB-Guv-JF2, FMB-Guv-JF7, FMB-Guv-L2A and FMB-Guv-B2A (*Fig. 1*). This dendrogram showed that these all accessions are diverse and distinct to each other. The fungal accession FMB-Guv-B2A was shown to be highly diverse to FMB-Guv-B1 by scoring the 0.8232 that revealed they are 82.32% dissimilar followed by FMB-Guv-C4 to whom FMB-Guv-B2A is 76.91% dissimilar (*Table 4*). While fungal accessions FMB-Guv-JF2 and FMB-Guv-JF7 are closely related as compared to others with similarity co-efficient 0.1301, which showed, they have 13.01% dissimilarity, so they are more close to each other. Principal Co-ordinate analysis (PCoA) showed comparable results that were obtained in UPGMA based dendrogram (*Fig. 2*) and indicating considerable genetic variability among Neopestalotiopsis spp accessions. Principal coordinate analysis (PCoA) also indicated dispersed pattern of these fungal accessions demonstrating diverse genetic base.

Discussion

Studies at the genomic level are necessary and crucial to understand population genetics and genetic diversity and relationships among individual. There is no report for molecular marker assisted characterization of species of Neopestalotiopsis genus. Therefore, in this study, we have attempted the characterization of different isolates of Neopestalotiopsis spp collected from canker affected guava plants using ISSR molecular marker. Fungal Molecular Biology Culture Collection, University of Agriculture Faisalabad Pakistan, has accessioned these Neopestalotiopsis spp isolates. For identification of polymorphism in terms of genetic diversity among these studied fungal isolates, ISSR markers were used to assess intrapopulation genetic variation in

http://www.aloki.hu ● ISSN 1589 1623 (Print) ● ISSN 1785 0037 (Online)
DOI: http://dx.doi.org/10.15666/aeer/1705_1180311811

Neopestalotiopsis spp accessions collected from different region of Pakistan. The inherent genetic variation in this study on Neopestalotiopsis spp isolates revealed their genetic distinctness unambiguously. Dendrogram based on UPGMA, Nei's original measures and principal Coordinate analysis (PCoA) showed that they all are genetically diverse. These markers yielded percent polymorphism ranged from 50% to 100%, which is in accordance to the findings of Patel et al. (2018). In this study average polymorphic information content (PIC) values was 0.996445 that indicating the discriminating power and potential of these selected ISSR primers to determine genetic diversity among these fungal accessions. This finding is also similar to the findings of Ijaz et al. (2018 and 2019) and Patel et al. (2018).

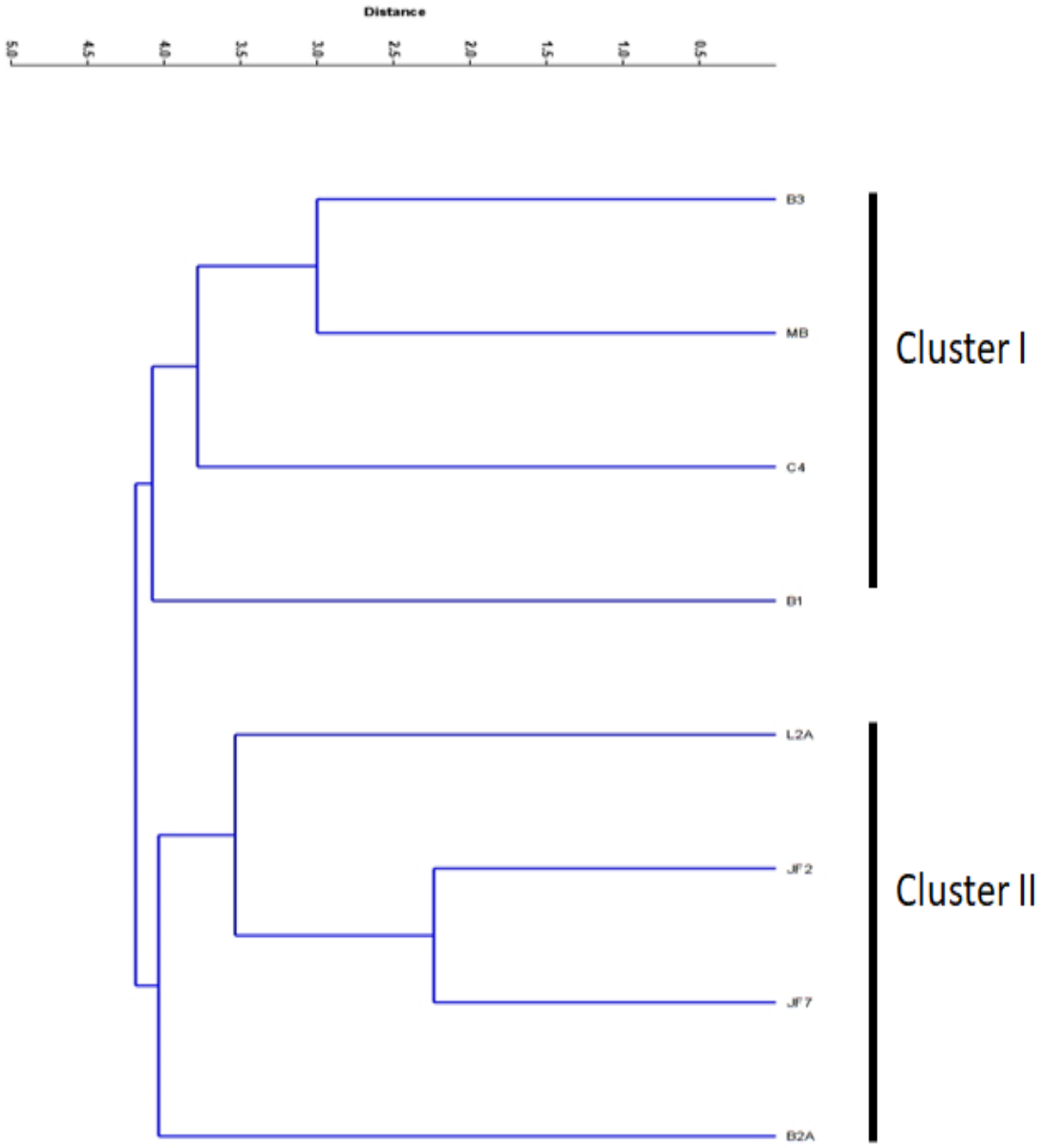

Figure 1. *Unweighted Pair Group Method with Arithmetic Mean (UPGMA) based dendrogram of eight Neopestalotiopsis spp accessions collected from canker affected guava plants*

http://www.aloki.hu ● ISSN 1589 1623 (Print) ● ISSN 1785 0037 (Online)
DOI: http://dx.doi.org/10.15666/aeer/1705_1180311811

Table 4. *Similarity Matrix table based on Nei's original measures: Nei's genetic identity (above diagonal) and genetic distance (below diagonal)*

Pop ID	B2A	L2A	JF2	JF7	B3	MB	C4	B1
B2A	****	0.6098	0.5366	0.6585	0.6585	0.6341	0.4634	0.4390
L2A	0.4947	****	0.6829	0.7073	0.6098	0.5366	0.6098	0.5366
JF2	0.6225	0.3814	****	0.8780	0.5366	0.6098	0.6829	0.5610
JF7	0.4177	0.3463	0.1301	****	0.4634	0.5854	0.6098	0.5854
B3	0.4177	0.4947	0.6225	0.7691	****	0.7805	0.5610	0.5366
MB	0.4555	0.6225	0.4947	0.5355	0.2478	****	0.7317	0.6098
C4	0.7691	0.4947	0.3814	0.4947	0.5781	0.3124	****	0.6341
B1	0.8232	0.6225	0.5781	0.5355	0.6225	0.4947	0.4555	****

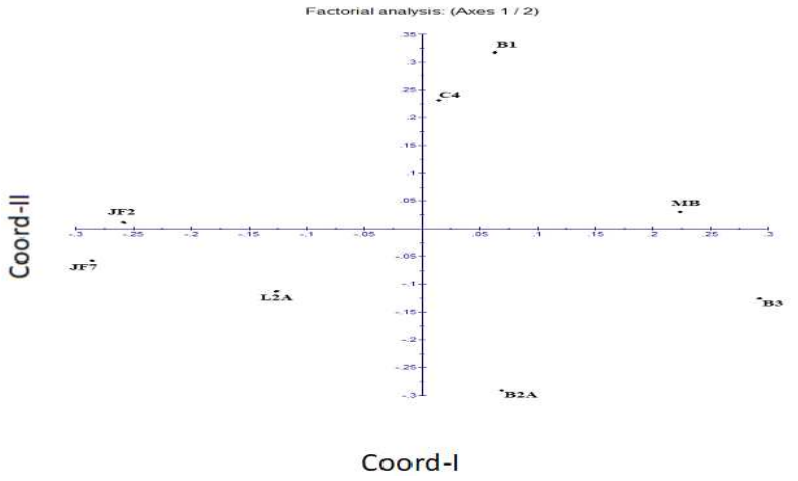

Figure 2. *Two-dimensional plot of eight Neopestalotiopsis spp accessions collected from canker affected guava plants using Principal Coordinate analysis (PCoA)*

Conclusions

This research study was based on the investigation of neopestalotiopsis species collected from canker affected guava tree. By considering these fungal isolates belonging to neopestalotiopsis species, to be an associated pathogen of canker disease in guava. We determined their genetic diversity. The genetic diversity analysis revealed that these subjects are of diverse in their genetic background, though, FMB-Guv-JF2 and FMB-Guv-JF7 showed close relatedness to each other. These results suggested that FMB-Guv-JF2 and FMB-Guv-JF7 could be as monophyletic group in phylogenetic hierarchy. However, remaining isolates were shown as genetically diverse background. The maximum genetic diversity was observed between FMB-Guv-B2A and FMB-Guv-B1 neopestalotiopsis species fungal accessions. Further experimentation to undertaking their molecular taxonomy would be an imperative step to resolve the species boundaries of theses studied isolates.

REFERENCES

[1] Abbas, S. Q., Niaz, M., Iftakhar, T., Perveen, A., Abbas, A., Riaz, S. (2016): New Fungal Records on Guava (Psidium guajava) from Pakistan. – Pakistan Academy of Sciences, p.121.

http://www.aloki.hu ● ISSN 1589 1623 (Print) ● ISSN 1785 0037 (Online)
DOI: http://dx.doi.org/10.15666/aeer/1705_1180311811

[2] Ansar, M., Saleem, A., Iqbal, A. (1994): Cause and control of guava decline in the Punjab (Pakistan). – Pakistan Journal of Phytopathology 6(1): 41-44.
[3] Bilgrami, K. S., Purohit, D. K. (1971): New pathogenic species of Pestalotia. – Indian phytopathology 24: 211-213.
[4] Bokhari, A. A., Sahi, S. T., Khan, M. A., Ahmad, R., Din, I. U. (2008): In vitro studies on the biological and chemical control of guava decline caused by different soil borne pathogens. – Pak. J. Agri. Sci. 45: 54-56.
[5] F.A.O. (2011): Food and Agriculture Organization of the United Nations statistical databases. – Accessible online at: http://faostat. fao. org.
[6] Gupta, J. H. (1978): Damping off, a new disease of guava. – Indian Journal of Mycology and Plant Pathology 8: 224.
[7] Gupta, P. C., Madaan, R. L., Suhag, L. S. (1978): Varietal reaction of guava fruits to Phytophthora nicotianae var. parasitica [India]. – Indian Journal of Mycology and Plant Pathology.
[8] Gupta, V. K., Misra, A. K., Gaur, R. K., Jain, P. K., Gaur, D., Sharma, S. (2010): Current status of Fusarium wilt disease of guava (Psidium guajava L.) in India. – Biotechnology 9(2): 176-195.
[9] Gupta, Y. K., Roy, A. N., Yadav, S., Gupta, M. N. (1980): Investigations on post-harvest diseases of guava fruits [India]. – Indian Phytopathology.
[10] Gutiérrez, R. M. P., Mitchell, S., Solis, R. V. (2008): Psidium guajava: a review of its traditional uses, phytochemistry and pharmacology. – Journal of ethnopharmacology 117(1): 1-27.
[11] Ijaz, S., Razzaq, H. A., Babar, M., Haq, I. (2018): Assessment of population genetics of shisham (*Dalbergia sissoo*) based on genetic structure and diversity analysis. – International Journal of Biosciences 13(3): 209-222.
[12] Ijaz, S., Ul Haq, I., Razzaq, H. A., Nasir, B., Babar, M. (2019): ISSR-based population genetics study for tagging a diverse population of shisham (*Dalbergia sissoo*) in Pakistan. – Applied Ecology and Environmental Research 17(3): 5851-586.
[13] Keith, L. M., Velasquez, M. E., Zee, F. T. (2006): Identification and characterization of Pestalotiopsis spp. causing scab disease of guava, Psidium guajava, in Hawaii. – Plant Disease 90(1): 16-23.
[14] Ko, W. H., Kunimoto, R. K., Nishijima, W. T. (1982): Fruit rot of guava caused by Phytophthora citricola [Psidium guajava, Hawaii]. – Plant Diseases.
[15] Kunimoto, R. K., Ito, P. J., Ko, W. H. (1977): Mucor rot of guava fruits caused by Mucor hiemalis. – Tropical Agriculture 54(2): 185-187.
[16] Lal, B., Rai, R. N., Arya, A., Tewari, D. K. (1980): A new soft rot of guava. – National Academy Science Letters 3(9): 259-260.
[17] Lim, T. K., Manicomz, B. Q. (2003): 12 Diseases of Guava. – Diseases of Tropical Fruit Crops 275.
[18] Lim, T. K., Manicom, B. A. (2003): Diseases of guava. – In: Ploetz, R. C. (ed.) Diseases of tropical fruit crops. pp. 275-289. Pub. CABI, Wallingford, U.K.
[19] Malathi, P., Viswanathan, R., Sundar, A. R., Prakasam, N., Padmanaban, P., Jothi, R., Devi, S. R., Poongothai, M. (2010): Variability among Colletotrichum falcatum pathotypes used for screening red rot resistance in sugarcane. – Sugar Cane International 28(2): 47-52.
[20] Malo, S. E., Campbell, C. W. (1994): The Guava. IFAS Extension. – Bulletin, University of Florida, USA.
[21] Misra, A. K. (2004): Guava diseases—their symptoms, causes and management. – In: Diseases of Fruits and Vegetables: Volume II (pp. 81-119). Springer, Dordrecht.
[22] Misra, A. K., Prakash, O. (1987): Studies on diseases of fruit crops. – Annual Report, CIHNP, Lucknow, pp.124-125.

http://www.aloki.hu ● ISSN 1589 1623 (Print) ● ISSN 1785 0037 (Online)
DOI: http://dx.doi.org/10.15666/aeer/1705_1180311811

[23] Mitra, M. (1929): Phytophthora parasitica dast. Causing 'damping off'disease of cotton seedlingsand 'fruit-rot'of Guava in India. – Transactions of the British Mycological Society 14(3-4): 249-254.
[24] Ooka, J. J. (1980): Guava fruit rot caused by Rhizopus stolonifer in Hawaii. – Plant Disease 64(4): 412-413.
[25] Pachanawan, A., Phumkhachorn, P., Rattanachaikunsopon, P. (2008): Potential of Psidium guajava supplemented fish diets in controlling Aeromonas hydrophila infection in tilapia (Oreochromis niloticus). – Journal of bioscience and bioengineering 106(5): 419-424.
[26] Pandey, R. R., Dwivedi, R. S. (1985): Fusarium oxysporum f. sp. psidii as a pathogen causing wilt of guava in Varanasi district, India. – Journal of Phytopathology 114(3): 243-248.
[27] Pandey, R. R., Dwivedi, R. S. (1985): Fusarium oxysporum f. sp. psidii as a pathogen causing wilt of guava in Varanasi district, India. – Phytopathologische Z. 114: 243-248.
[28] Patel, P., Rajkumar, B. K., Parmar, P., Shah, R., Krishnamurthy, R. (2018): Assessment of genetic diversity in Colletotrichum falcatum Went accessions based on RAPD and ISSR markers. – Journal of Genetic Engineering and Biotechnology 16(1): 153-159.
[29] Pervaiz, U., Khan, A., Javed, R., Zeb, J. (2008): Production constraints of guava in district Kohat. – Sarhad J. Agric 24(3): 549-554.
[30] Prasad, N., Mehta, P. R., Lal, S. B. (1952): Fusarium wilt of guava (Psidium guyava L.) in Uttar Pradesh, India. – Nature 169(4305): 753.
[31] Rahman, M. A., Ansari, T. H., Meah, M. B., Yoshida, T. (2003): Prevalence and pathogenicity of guava anthracnose with special emphasis on varietal reaction. – Pak J Bio Sci 6(3): 234-241.
[32] Rao, D. P. C., Agarwal, S. C. (1976): Efficacy of antibiotics against Phomopsis destructum causing fruit rot of guava. – Hindustan Antibiotic Bulletin 18: 108-110.
[33] Safdar, A., Khan, S. A., Safdar, M. A. (2015): Pathogenic association and management of Botryodiplodia theobromae in guava orchards at Sheikhupura district, Pakistan. – International Journal of Agriculture and Biology 17(2).
[34] Saksena, P., Vishwakarma, S. K., Tiwari, A. K., Singh, A., Kumar, A. (2013): Pathological and molecular variation in Colletotrichum falcatum went isolates causing red rot of sugarcane in the Northwest Zone of India. – Journal of plant protection research 53(1): 37-41.
[35] Sridhar, T. S., Ullasa, B. A. (1978): Leaf blight of guava-a new record. – Current Science 47(12).
[36] Srivastava, H. P. (1963): Some leaf spot fungi. – Proceedings of the National Academy of Sciences 34(3): 188-198.
[37] Srivastava, M. P., Tandon, R. N. (1969b): Studies on Botryodiplodia rot of guava. – Indian Forest Rec NS Forest Pathol.
[38] Srivastava, M. P., Tandon, R. N. (1969a): Postharvest diseases of Guava in India. – Plant Disease Reporter 53(3): 206-208.
[39] Tandon, R. N., Agarwala, R. K. (1954): Pathological studies ofGlœosporium psidii causing die-back of guavas. – Proceedings: Plant Sciences 40(4): 102-109.
[40] Ul-Haq, I. M. S., Khan, S. A., Jaskani, M. J., Ullah, Z. (2013): Occurrence of guava anthracnose in Punjab (Pakistan) and its integrated management. – Pak. J. Agri. Sci 50(4): 707-710.
[41] Yadava, U. L. (1996): Guava production in Georgia under cold-protection structure. – Progress in new crops. ASHS Press, Arlington, VA, 451-457.

http://www.aloki.hu ● ISSN 1589 1623 (Print) ● ISSN 1785 0037 (Online)
DOI: http://dx.doi.org/10.15666/aeer/1705_1180311811

UV-B TOLERANT MUTANT *ARABIDOPSIS RCD1-1* EXHIBITS HIGHER PHOTOSYNTHETIC ACTIVITY AND LESS OXIDATIVE DAMAGE

LYU, G. Z. – LI, D. B. – LIU, X. L. – LI, S. S.*

Key Laboratory of Ecology and Environmental Science in Guangdong Higher Education, School of Life Science, South China Normal University, Guangzhou 510631, China

**Corresponding author*
e-mail: lishsh@scnu.edu.cn; fax: +86-20-8521-2669

(Received 23rd Apr 2019; accepted 11th Jul 2019)

Abstract. UV-B radiation has diverse biological effects on plants. The tolerance of *rcd1-1* mutant to UV-B radiation was studied in the present research. Leaves of the wild type under UV-B exhibited chlorosis, curling, and necrotic lesions, but these phenomena were not observed in the *rcd1-1* mutant. The *rcd1-1* mutant accumulated less H_2O_2 and O_2^- under UV-B radiation, and had higher activity of anti-oxidative enzymes. UV-B radiation led to accumulation of UV-B absorbing compounds as flavonoids, and anthocyanins. The *rcd1-1* mutant under UV-B radiation had higher maximum quantum efficiency of primary photochemistry and exhibited less of a decrease of effective quantum yield of photochemical energy conversion in PS II and photochemical quenching of variable chlorophyll fluorescence yield. The *rcd1-1* mutant also showed higher non-photochemical quenching, indicating that it could dissipate excess energy. The *psbA* gene were more highly expressed in the *rcd1-1* mutant, while *ANAC013* and *UNE10* genes were negatively regulated. This may explain why the mutant had a higher photosynthetic capability under UV-B radiation. It can be confirmed that the tolerant *Arabidopsis rcd1-1* mutant under UV-B radiation exhibits higher photosynthetic activity and less oxidative damage than the wild type.
Keywords: *rcd1-1 mutant, UV-B, flavonoids, anthocyanins, gene expression*

Abbreviations: Chl *a* + *b*: chlorophyll *a* and chlorophyll *b*; Fm: maximal fluorescence of a dark-adapted sample; Fo: initial fluorescence of a dark-adapted sample; Fm': maximal fluorescence of an illuminated sample; Fs: minimal fluorescence of an illuminated sample; PSI: photosystem I; PSII: photosystem II; UV-A: ultraviolet-A radiation (315–400 nm); UV-B: ultraviolet-B radiation (280–315 nm); UV-C: ultraviolet-C radiation (wavelength < 280 nm)

Introduction

Ultraviolet radiation from sunlight is divided into three spectral regions: UV-A, UV-B and UV-C. In a natural environment, plants are exposed to 10–100 times more UV-A (315–400 nm) photons than they are to UV-B (280–315 nm) photons (Verdaguer et al., 2017). UV-B radiation has received most attention because it is strongly absorbed by ozone. UV-C, with wavelength shorter than 280 nm, does not reach ground. The decrease of the ozone layer led to a significant increase in UV-B radiation from 1970 till about 1995 and shifts in the spectral UV-composition reaching the Earth surface at mid- and high latitudes. Until now little is known about the mechanism by which the *rcd1-1* mutant tolerates UV-B radiation. In the present research, we explore the UV-B resistance of the *rcd1-1* mutant by morphological and physiological properties, and gene expression. The results may explain why the mutant is tolerant to UV-B, which could enrich our understanding of the regulation mechanism of UV-B response.

http://www.aloki.hu ● ISSN 1589 1623 (Print) ● ISSN 1785 0037 (Online)
DOI: http://dx.doi.org/10.15666/aeer/1705_1181311833

Review of literature

Plants are inevitably exposed to UV-B, as they need sunlight. High doses of UV-B radiation can cause stress and damage in plant, including DNA, protein and plasma membrane damage, production and accumulation of reactive oxygen species, cell cycle arrest, chlorophyll degradation, photosynthesis inhibition, and affect various cell processes (Ulm and Jenkins, 2015; Biever and Gardner, 2016). However, UV-B not only has adverse effects on plants, but also can activate the repair mechanism in vivo, especially for plants with insufficient or no UV-B in facility culture. UV-B regulates gene expression related to physiological processes such as metabolism, morphogenesis, photosynthesis and pest resistance (Jenkins, 2014). It also regulates leaf development, regulates clock rhythm, improves plant heat tolerance, cold tolerance, drought resistance and delays flowering time (Yin and Ulm, 2017; Dotto et al., 2018).

Exposure of plants to UV-B induces photomorphogenetic as well as physiological and genetic changes, mostly injurious but sometimes beneficial. Enhanced UV-B in solar radiation could potentially induce DNA damage and radical oxygen species (ROS) production in living cells (He and Häder, 2002; Zlatev et al., 2012). On the other hand, plants have evolved a wide range of protective and repair mechanisms against UV-B stress, such as the formation of surface wax, polyamines and specific alkaloids, flavonoid biosynthesis, DNA repair and changes in metabolism (Ulm and Nagy, 2005; Fujibe et al., 2004; Frohnmeyer and Staiger, 2003). Enhanced UV-B radiation to may also result in lower photosynthesis and leads to a decrease in crop yields. Therefore, understanding how plants protect themselves against UV-B radiation is of utmost importance for agricultural production.

In recent years the model plant *Arabidopsis thaliana* has gained the much attention in research on the effects of UV, because many research tools (such as genetic, molecular biology and bioinformatics tools) could be applied to it. The intervals of *rcd1-1* on BACs F3C3 and F27G20 containing seven open reading frames were determined by genetic mapping. Six of them matched the published genome sequence of *Arabidopsis*. At1g32230 gene has a typical C-T to ethyl methylsulfonate mutation in the antisense chain, which results in G-A transition at the GT splicing site of the third exon-intron connection. RT-PCR showed that the splicing of RCD1 intron in wild type Col-0 was consistent with the predicted structure of At1g32230 and the published full-length cDNAs of CEO1 and RIKEN. In *rcd1-1*, two transcriptional types were identified by RT-PCR amplification and sequence analysis. The 2.7-kb transcript represents mRNA, in which the next (GT) in intron III downstream of the mutant shear acceptor site is used for splicing of intron III. The misspliced *rcd1-1* mRNA was only 11 bp longer than that of wild type. In *rcd1-1*, the expression level of the shorter 1.4-kb transcript was approximately the same as that of the 2.7-kb transcript. In the 1.4-kb transcript, intron splicing occurs from the 5' end of exon IV into exon III, so exon III is completely missing. Both misspliced *rcd1-1* transcript types lead to frame loss and premature termination of codons. In wild col-0, RCD1 was expressed in stem, leaf, bud and young flower, while siliques and root transcription were lower in old flower. In *rcd1-1*, compared with wild type, gene expression increased slightly, and also in old flowers and roots compared with Col-0. In siliques of *rcd1-1*, only the shorter transcripts existed at lower abundance (Ahlfors et al., 2004).

http://www.aloki.hu ● ISSN 1589 1623 (Print) ● ISSN 1785 0037 (Online)
DOI: http://dx.doi.org/10.15666/aeer/1705_1181311833

Radical-induced cell death1 (RCD1) protein is an important regulator of stress and hormonal and developmental responses in *Arabidopsis thaliana* (Jaspers et al., 2009). CEO1, also called RCD1, is a protein from *Arabidopsis thaliana* that protects yeast against oxidative damage (Belles-Boix et al., 2000; Ahlfors et al., 2004; He et al., 2012). It contains two conserved globular protein domains: the WWE domain and a poly (ADP-ribose) polymerase (PARP)-like ADP-ribose transferase catalytic domain, the former mediated by specific protein-protein interaction (Jaspers et al., 2010). When the RCD1 protein is expressed in yeast, the yeast is protected from oxidative damage induced by *tert*–butylhydroperoxide, peroxide and diamide (Belles-Boix et al., 2000). The results from gene chip research indicate that a large number of abiotic stress related genes have reduced expression in the *Arabidopsis rcd1-1* mutant (Ahlfors et al., 2004).

Thus RCD1 may be an important regulator of the oxidative stress response, and may also be involved in other abiotic stress responses in plants (Kragelund et al., 2012). This is suggested by a number of key findings. The *Arabidopsis rcd1-1* mutant has proved to be sensitive to ozone and apoplastic superoxide (Fujibe et al., 2004; Moldau et al., 2011). Forward genetic screens for ozone sensitivity and paraquat tolerance led to the isolation of *Arabidopsis rcd1-1* and *rcd1-2* mutants (Jaspers et al., 2009; Fujibe et al., 2004; Overmyer et al., 2000). The *rcd1-2* mutant is tolerant than the wild type (Fujibe et al., 2004), as is the *rcd1-1* allele (Jaspers et al., 2010; Jiang et al., 2009). The *rcd1-2* mutant is resistant to methyl viologen, and sensitive to UV-B. The *rcd1-1* mutant is sensitive to ozone and tolerant to short-term UV-B radiation. In addition, the *rcd1-1* mutant has lower sensitivity to abscisic acid, ethylene and methyl jasmonate than the wild type. Exogenous methyl ester of jasmonic acid (MeJA) inhibits the spread of cell death in *rcd1-1* mutant (Overmyer et al., 2000). By using the gene microarray technology, the expression of a large number of abiotic stress related genes were reduced in the *rcd1-1* mutant (Ahlfors et al., 2004). The *rcd1-2* mutant was resistant to a short period of UV-B radiation and exhibited higher activity of SOD and *APX* gene expression level than the wild type (Fujibe et al., 2004).

Materials and methods

Plant materials, growth conditions and UV treatment

Wild type and mutant *Arabidopsis thaliana* used in this study were all of the ecotype Columbia-0 (Col-0) background. Seeds were vernalizated at 4 °C for 3 d before sowing (Jiang et al., 2009). Seeds were surface sterilized and sown on Murashige and Skoog medium (Murashige and Skoog, 1962) containing 3% sucrose for germination and grew for 14 days under appropriate light conditions at 22 °C. White light was provided by cool white fluorescent lamps (Philips TLD30W/865 tubes, 80 W m^{-2}). Conditions for UV-B irradiation were the same as described by Jiang (Jiang et al., 2009). Radiation (hereafter referred to as UV-B) from the UV-B tubes (Philips PLS9W/01, 1.8 W m^{-2}) was filtered through cellulose acetate film (95 μm; Kunststoff-Folien-Vertrieb GmbH, Hamburg, Germany), which transmitted both UV-A and UV-B, but blocked UV-C. Radiation for control plants (hereinafter referred to as UV-A) was filtered through Mylar film, which removed both UV-B and UV-C. The spectral irradiance from the UV lamps was determined with an iHR550 spectroradiometer (HoribaJobinYvon, Japan). The spectral irradiance was weighted with the generalized plant response action spectrum, normalized to unity at 300 nm to obtain UV-B.

http://www.aloki.hu ● ISSN 1589 1623 (Print) ● ISSN 1785 0037 (Online)
DOI: http://dx.doi.org/10.15666/aeer/1705_1181311833

Root length and dry biomass

The seeds of *Arabidopsis thaliana* were planted on MS solid medium after vernalization at low temperature and surface disinfection. The culture dishes were placed vertically. The germination and seedling growth of Arabidopsis thaliana seeds were observed 2, 4, 6, 8, 10 and 12 days after sowing, and the root growth of seedlings was measured by Image J software.

Arabidopsis thaliana seedlings were harvested 14 days after sowing. The adherent MS solid medium was washed with EDTA-Na_2 and deionized water. The fresh weight was measured. Then the fresh weight was put into 65 °C oven until the constant weight, and then the dry weight was measured.

Measurement of cell membrane permeability

The membrane permeability of the wild type and *Arabidopsis rcd1* mutant was evaluated by Evans blue staining and conductivity measurement. Evans blue staining was conducted as described with some improvement. Briefly, samples were evacuated for 5 min and then infiltrated for 20 min with 0.1% Evans blue solution. The process was repeated three times, and each repetition is the average of 10 values. The samples were then boiled for 5-10 min in a mixture of 95% ethanol and lactophenol (2:1) and stored in 5% ethanol for observation. Electrical conductivity measurements were carried out with a conductivity meter (FE330, Mettler-Toledo). The first value (R1) was obtained after the clean leaves and roots were immersed in deionized water for 2 h at room temperature. After immersion for 20 min in boiling water the samples were cooled to room temperature and then measured for a second value (R2). The relative electrical conductivities were determined according to (R1/R2) × 100%.

Location of O_2^- in the leaves, location and concentration of H_2O_2 in the leaves

Generation of O_2^- in *Arabidopsis* leaves in response to UV treatment was detected by the Nitro Blue Tetrazolium (NBT) technique (Uy et al., 2011). *Arabidopsis* leaves were bathed in 0.1 mg mL^{-1} NBT solution and, following evacuation by pumping for 10 min infiltrated under dark conditions until translucent, and then placed at room temperature for 2 h. They were then boiled in 90% ethanol until the chlorophyll was completely removed. At last, the leaves were scanned and observed by Mahalingam et al. (2006). To determine H_2O_2 in the leaves, they were infiltrated as before, but with 0.3 mg mL^{-1} 2-amino benzidine (DAB) solution after UV-B treatment. They were placed in the dark for 8 h, followed by light for 2 h and then harvested and boiled in 90% ethanol until the chlorophyll was completely removed. Finally, the leaves were scanned and observed by Ma et al. (2012). H_2O_2 analysis was assayed as described by Cheeseman (2006).

Measurements of SOD, CAT and POD activity

Frozen plant leaves (1 g) were homogenized in 50 mM sodium phosphate buffer (pH 7.0) containing 0.1 mM EDTA, 0.1%(m/v) phenylmethylsulfonyl fluoride, 1% (m/v) polyvinylpyrrolidone, 0.1% (v/v) TritonX-100 and 50 mM ascorbic acid. The extract was centrifuged at 12,000 × g for 15 min and the supernatant was used for enzymatic assays. In this study, the superoxide dismutase (SOD) activity was measured by the xanthine oxidase method with SOD Activity Assay Kit (Jiancheng Bioengineering Institute, Nanjing, China). Catalase (CAT) and polyphenol oxidase (POD) activities

http://www.aloki.hu ● ISSN 1589 1623 (Print) ● ISSN 1785 0037 (Online)
DOI: http://dx.doi.org/10.15666/aeer/1705_1181311833

were measured as described by Ma et al. (2012). For SOD, the enzyme quantity that inhibits the self-oxidation rate of the reaction solution by 50% per ml under certain conditions is defined as 1 enzyme activity unit (U). For CAT, a decrease of 0.1 in A240 per minute was defined as 1 enzyme activity unit (U). For POD, a decrease of 0.01 in A470 per minute was defined as 1 enzyme activity unit (U).

Pigment, anthocyanin, flavonoid and malondialdehyde (MDA) measurements

Total chlorophyll (Chl *a* + *b)* content in plant leaves was measured by the method of Arnon (1949). The absorbance of the extract was recorded at 663 nm and 645 nm. The concentrations of chlorophyll *a*, chlorophyll *b* and total chlorophyll were calculated using the following equation:

$$\text{Chl } a = 0.0127\ \text{A663} - 0.00269\ \text{A645}$$
$$\text{Chl } b = 0.0229\ \text{A645} - 0.00468\ \text{A663}$$
$$\text{total Chl } a+b = 0.0202\ \text{A645} + 0.00802\ \text{A663}$$

Anthocyanin content was determined as described by Noh and Spalding (1998). For flavonoid measurement, 14-day old seedlings were frozen in liquid nitrogen, flavonoids were extracted and quantified as described by Kucera et al. (2003). MDA was measured with Malondialdehyde (MDA) Assay Kit (Jiancheng Bioengineering Institute, Nanjing, China) according to the manufacturer's instruction.

Photochemical activity measurements

Photochemical efficiency was evaluated from the chlorophyll *a* fluorescence of photosystem II, using a modulated fluorometer (Heinz Walz GmbH, Effeltrich, Germany) including optimal quantum yield (Fv/Fm), effective quantum yield (ΦPSII) and non-photochemical quenching (NPQ). Optimal quantum yield was defined as (Fm-Fo)/Fm, where Fm represents maximal and Fo initial fluorescence of a dark-adapted sample. Effective quantum yield is defined as (Fm'-Fs)/Fm', where Fm' represents the maximal and Fs minimal fluorescence of an illuminated sample (Sedej and Gaberščik, 2008). NPQ-values were determined according to the Stern-Volmer equation:

$$\text{NPQ} = (\text{Fm} - \text{Fm}')/\text{Fm}'$$

RNA extraction and quantitative real-time PCR

Total RNA was extracted from seedlings by using E.Z.N.A. Plant RNA Kit (Omega, USA) according to its protocol, then digested with DNAse I (Promega, USA) to eliminate genomic DNA contamination. First-strand cDNAs were synthesized from using PrimeScript 1st strand cDNA synthesis kit (Takara Biotechnology, China) according to the manufacturer's instructions.

The quantitative PCR (q-PCR) assays were performed with the ABI PRISM 7500 Real-time PCR system (Applied Biosystems, USA) using Power SYBR Green Master Mix (Applied Biosystems, USA) following the recommended conditions (50 °C for 2 min, then 95 °C for 10 min, followed by 40 cycles of 95 °C for 15 s and 60 °C for 1 min). Sepcific Primer 5.0 software was used to design the primers for the experiment (*Table 1*).

http://www.aloki.hu ● ISSN 1589 1623 (Print) ● ISSN 1785 0037 (Online)
DOI: http://dx.doi.org/10.15666/aeer/1705_1181311833

Table 1. *The nucleotide sequences of the primers used in qPCR*

No.	Gene	Primer (5'→3')
X16077.1	*18S rRNA*	F: CGTCCCTGCCCTTTGTACAC R: CGAACACTTCACCGGATCATT
NM_103021.3	*ANAC013*	F: AGGGAAGGATAGAGTCATTCATTGT R: AGTCCGTTCGCCATTAGGTG
X79898.1	*psbA*	F: GGTGCCATTATTCCTACTTCTGC R: GTTCATAAGGACCGCCGTTGT
NM_116222.3	*UNE10*	F: TTCCATCATCGCTCCTCCAG R: GTACGACCATCGCTACATGACC

The dissociation curve was used to check for the presence of a unique PCR product and the amplification curves was analyzed to estimate the primer pair efficiencies with the LinReg software (Czechowski et al., 2005). The average efficiency of all reactions on a plate (which was always > 1.95) was used in calculations. All reactions were carried out in three technical replicates. To normalize the qPCR data, a reference gene (18sRNA) was used for detecting gene expression in the wild type and the *rcd1-1* mutant (Jiang et al., 2009).

Statistical analysis

The GraphPad Prism 8 was used for statistical analysis and drawing. For comparing results of different treatments, Variance analysis is followed by a post-hoc test in order to determine pairwise differences. Differences were considered significant for $P < 0.05$.

Results

The rcd1-1 mutant is not sensitive to UV-B radiation

After growing for 8 days in white light condition, the *rcd1-1* mutant was significantly smaller than the wild type. The *rcd1-1* mutant had slower root growth (*Fig. 1a*) and accumulated less biomass (*Fig. 1b*). Also root growth was significantly inhibited (*Fig. 1c*). The ANOVA table for the data of *Figure 1c* (Two-way ANOVA, Sidak's multiple comparisons test) was displayed in *Table A1* in the *Appendix*. Under UV-B radiation, the wild type leaves showed chlorosis, curl, and necrotic lesions. However the *rcd1-1* mutant showed less changes under UV-B radiation (*Fig. 1d*).

The rcd1-1 mutant showed less cell membrane damage after UV-B exposure

Membrane permeability (Evans Blue Stain) correlated positively with duration of UV-B irradiation, and the stain of the wild type was deeper than that of the *rcd1-1* mutant (*Fig. 2a*). The electrical conductivity of the cell membrane exhibited a highly significant increase after UV-B radiation compared to the control. Although the electrical conductivity of the wild type was significantly less than that of the *rcd1-1* mutant before UV-B irradiation, it had a rising trend with increasing irradiation time, and was largest after UV-B irradiation for 6 h (*Fig. 2b*). The ANOVA table for the data of *Figure 2b* (Two-way ANOVA, Tukey's multiple comparisons test) was displayed in *Table A2*. These results indicated that the cell membrane damage of the wild type was more serious than that of the *rcd1-1* mutant after UV-B exposure.

http://www.aloki.hu ● ISSN 1589 1623 (Print) ● ISSN 1785 0037 (Online)
DOI: http://dx.doi.org/10.15666/aeer/1705_1181311833

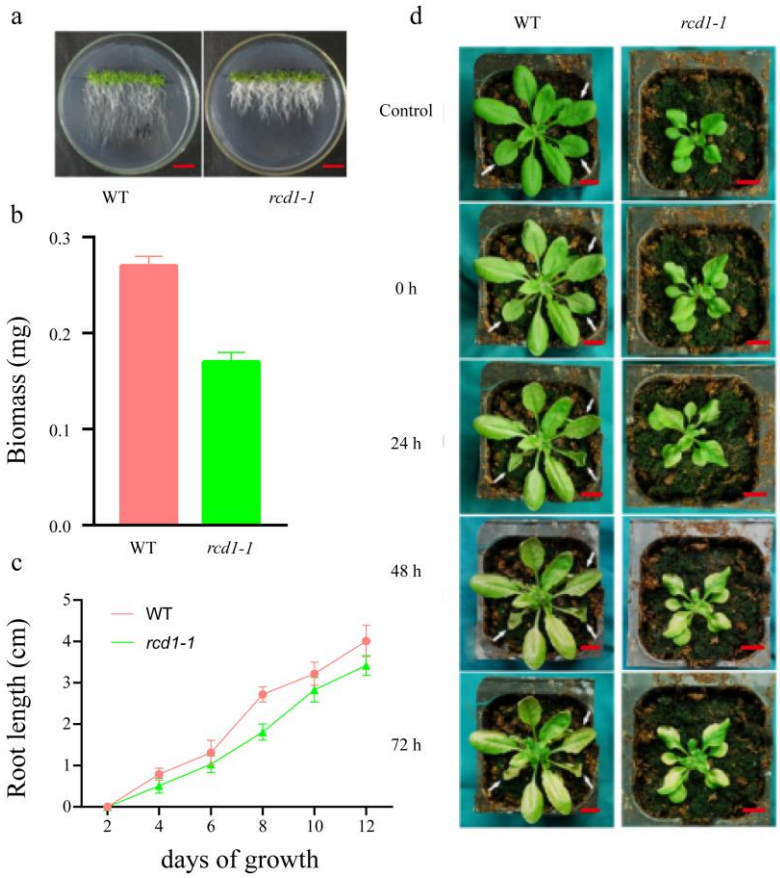

Figure 1. *The growth of Arabidopsis seedlings in normal growth condition and after UV-B radiation.* ***a*** *Seedlings of 10-day-old wild type and rcd1-1 mutant Arabidopsis.* ***b*** *Dry biomass of 10-day-old wild type and rcd1-1 mutant Arabidopsis.* ***c*** *Root length of the wild type and rcd1-1 mutant.* ***d*** *Three-week-old wild-type and rcd1-1 mutant plants were exposed to UV-B for 16 h and then allowed to recover for different time under fluorescent light before being photographed. Data are expressed as mean values ± standard errors from three replicates and error bars represent standard errors. The bar value is 10 mm*

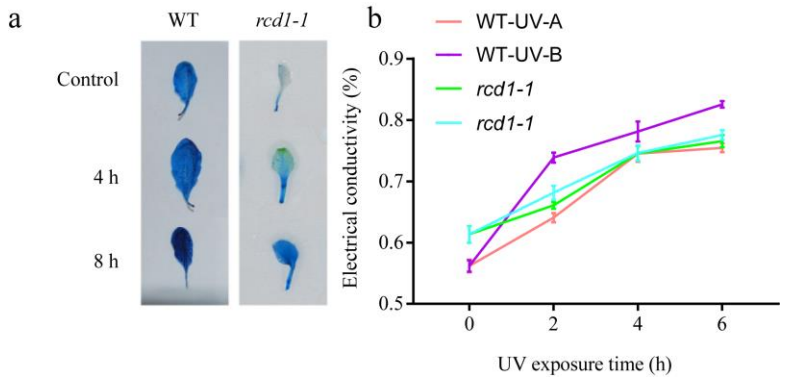

Figure 2. *Effects of enhanced UV-B radiation on cell membrane permeability of leaves. Three-week-old wild-type and rcd1-1 mutant were exposed to UV-B for 4 h and 8 h, after which the leaves were immediately harvested.* ***a*** *Leaves of the wild type and rcd1-1 mutant treated with UV-B for 0 h, 4 h and 8 h were stained with Evans blue.* ***b*** *After UV radiation, permeability of the leaves was measured with the conductivity meter. Data are expressed as mean values ± standard errors from three replicates and error bars represent standard errors*

http://www.aloki.hu ● ISSN 1589 1623 (Print) ● ISSN 1785 0037 (Online)
DOI: http://dx.doi.org/10.15666/aeer/1705_1181311833

The rcd1-1 mutant showed less content of MDA, O_2^- and H_2O_2 after UV-B exposure

To further investigate the effects of enhanced UV-B radiation on *Arabidopsis*, malondialdehyde (MDA), H_2O_2 and O_2^- productions were analyzed. The level of MDA production was significantly higher in the wild type than that in *rcd1-1* mutant after exposure for 8 h (*Fig. 3a*). The ANOVA table for the data of *Figure 3a* (Two-way ANOVA, Tukey's multiple comparisons test) was displayed in *Table A3a*. Similarly, enhanced UV-B radiation elevated H_2O_2 production considerably in the leaves after exposure for 8 h (*Fig. 3c*). The ANOVA table for the data of *Figure 3c* (Two-way ANOVA, Tukey's multiple comparisons test) was displayed in *Table A3b*. This was also shown by the DAB staining test (*Fig. 3d*). The NBT staining test showed that there was a positive correlation between accumulation of O_2^- in leaves and UV-B exposure time (*Fig. 3b*). More specifically, there was little blue precipitate in the leaves of the wild type and *rcd1-1* mutant before UV treatment and both had nearly the same light color. However, more and more blue precipitate appeared along with increasing duration of UV-B exposure, indicating that O_2^- in leaves increased. The blue precipitate in *rcd1-1* mutant leaves was less than that in the wild type at any testing time point in the whole UV-B radiation treatment process, indicating that the accumulation of O_2^- in the wild type was higher than that in *rcd1-1* mutant after UV-B radiation. In the control group (UV-A radiation treatment) the accumulation of O_2^- in the leaves was also stimulated, but the accumulation was significantly lower than for UV-B radiation. These results suggest that the damage caused by the short-term enhanced UV-B radiation to the *rcd1-1* mutant was less than that to the wild type.

Effects of antioxidant enzymatic activity of the leaves in the rcd1-1 mutant after UV-B exposure

The superoxide dismutase (SOD), peroxidase (POD) and CAT activities were assayed to investigate the effects of enhanced UV-B radiation on the antioxidative system. The SOD activity of the wild type exposed to UV-B radiation showed a slightly increasing trend, while the *rcd1-1* mutant maintained a rapid upward trend except for a decline at 4 h. The SOD activities of both genotypes were elevated after UV-B radiation for 8 h, which significantly increased from 1146 U to 1187 U in the wild type, while from 1152 U to 1299 U in *rcd1-1* mutant (*Fig. 4a*). The ANOVA table for the data of *Figure 4a* (Two-way ANOVA, Tukey's multiple comparisons test) was displayed in *Table A4a*.

The POD activity had a similar trend with the SOD activity, which showed an overall upward trend in leaves of the two genotypes with increasing duration of UV-B radiation. The difference between them was that the POD activity of *rcd1-1* mutant had always showed upward trend, while the wild type reached the highest value at the point of 6 h exposure and reduced a little at 8h. Although the POD activities of the two genotypes were almost identical under normal conditions, which increased up to 60.4% in the *rcd1-1* mutant and 41.0% in the wild type after UV-B radiation for 8 h. However, the POD enzyme activities of the two control groups treated with UV-A only increased slightly (*Fig. 4b*). The ANOVA table for the data of *Figure 4b* (Two-way ANOVA, Tukey's multiple comparisons test) was displayed in *Table A4b*.

The CAT activities differed between *rcd1-1* mutant and the wild type. The CAT activity of *rcd1-1* mutant ascended immediately under both UV-A and UV-B radiation. However, the CAT activity of the wild type fluctuated within a narrow range and finally

http://www.aloki.hu ● ISSN 1589 1623 (Print) ● ISSN 1785 0037 (Online)
DOI: http://dx.doi.org/10.15666/aeer/1705_1181311833

declined (*Fig. 4c*). The ANOVA table for the data of *Figure 4c* (Two-way ANOVA, Tukey's multiple comparisons test) was displayed in *Table A4c*. In general, the CAT activity of *rcd1-1* mutant had far higher levels than that of the wild type after UV-B radiation.

Flavonoid and anthocyanin content after UV-B exposure

As ultraviolet absorbing compounds in *Arabidopsis*, flavonoid and anthocyanin could be effectively induced when the leaves were exposed to UV-B radiation. UV exposure resulted in the accumulation of flavonoids and anthocyanin both in *rcd1-1* mutant and the wild type, but in the *rcd1-1* mutant the contents were significantly higher than in the wild type (*Fig. 5*). The ANOVA table for the data of *Figure 5b* (Two-way ANOVA, Tukey's multiple comparisons test) was displayed in *Table A5*.

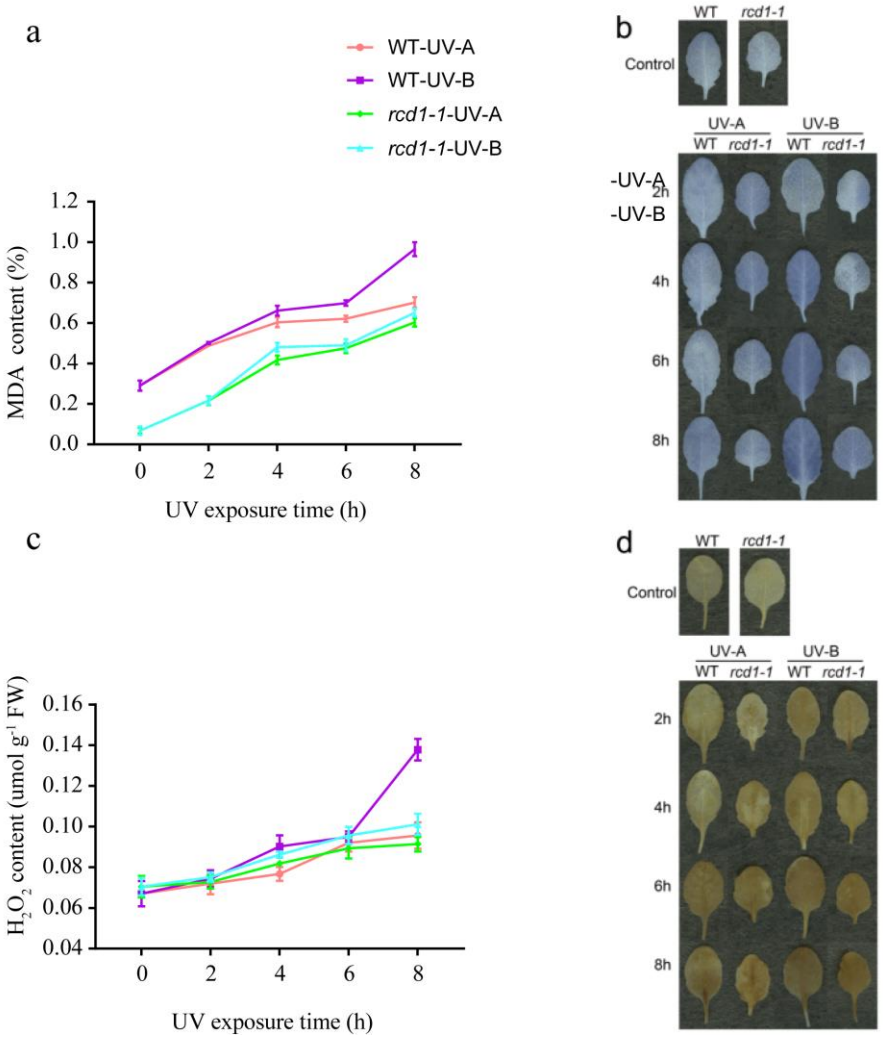

Figure 3. *Effects of enhanced UV-B radiation on the accumulation of MDA, O_2^- and H_2O_2. After UV-B radiation, the leaves were harvested.* ***a*** *MDA was measured with Malondialdehyde Assay Kit according to the manufacturer's instruction.* ***b*** *Location of O_2^- in leaves were detected by NBT staining method.* ***c*** *The concentration of H_2O_2 was measured by peroxidase coupling method.* ***d*** *Location of H_2O_2 in leaves in were detected by DAB staining method. Data are expressed as mean values ± standard errors from three replicates and error bars represent standard errors*

http://www.aloki.hu ● ISSN 1589 1623 (Print) ● ISSN 1785 0037 (Online)
DOI: http://dx.doi.org/10.15666/aeer/1705_1181311833

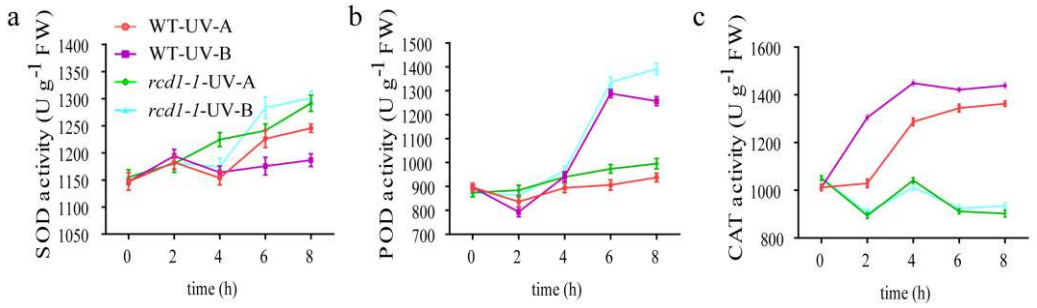

Figure 4. *Effects of enhanced UV-B radiation on the activities of antioxidant enzymes.* ***a*** *SOD;* ***b*** *POD;* ***c*** *CAT. The activity of SOD was assayed by the xanthine oxidase method, the activity of POD was detected o-methoxyphenol method and the activity of CAT was measured by spectrophotometrically. Data are expressed as mean values ± standard errors from three replicates and error bars represent standard errors*

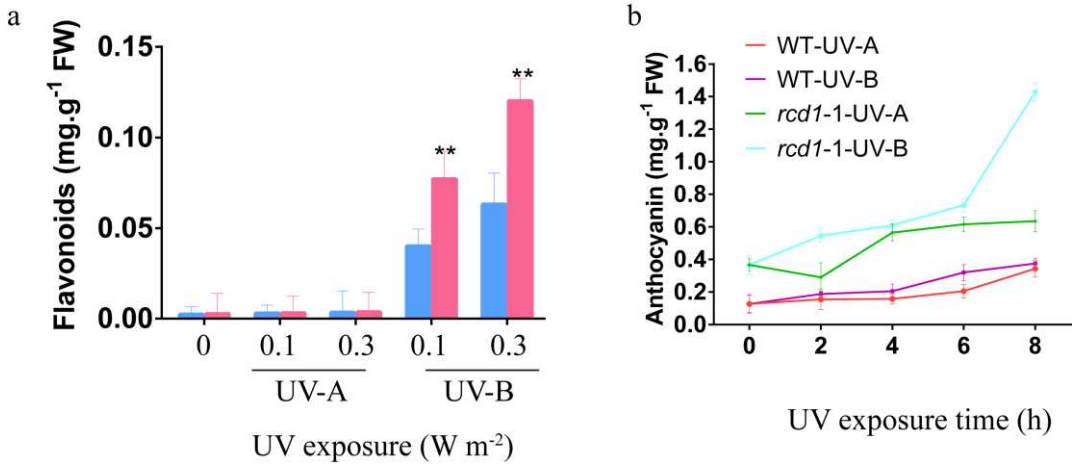

Figure 5. *Enhanced UV-B induced accumulation of UV-B absorbing compounds.* ***a*** *After UV treatment, fourteen-day-old seedlings were frozen in liquid nitrogen, flavonoids were extracted and then quantified spectrophotometrically. The symbol '*' indicates statistically differences $P < 0.05$ and the symbol '**'indicates statistically differences $P < 0.01$ (Two-way ANOVA, Tukey's multiple comparisons test).* ***b*** *Anthocyanin content in the wild type and the rcd1-1 mutant was measured spectrophotometrically. Data are expressed as mean values ± standard errors from three replicates and error bars represent standard errors*

The chlorophyll content and chlorophyll fluorescence of leaves in rcd1-1 mutant after UV-B exposure

One of the important kinds of damage of UV-B radiation to plants is the inhibition of chlorophyll synthesis. Phenotypic analysis found that the loss of green colour under UV-B radiation of the *rcd1-1* mutant was lower than that of the wild type (*Fig. 6a*). The ANOVA table for the data of *Figure 6a* (Two-way ANOVA, Tukey's multiple comparisons test) was displayed in *Table A6a*. The changes of chlorophyll content in the *rcd1-1* mutant and the wild type were measured. The downward trend of total chlorophyll in both genotypes after UV-B radiation is displayed in *Figure 6c*.

http://www.aloki.hu ● ISSN 1589 1623 (Print) ● ISSN 1785 0037 (Online)
DOI: http://dx.doi.org/10.15666/aeer/1705_1181311833

More specifically, the total chlorophyll content in both genotypes declined rapidly over the first two hours of exposure. After that, the chlorophyll content in the wild type continued to decline, while the *rcd1-1* mutant recovered transiently and chlorophyll content fell again after 8 h. After irradiation for 8 h, the total chlorophyll content in the wild type decreased by 21% while in the *rcd1-1* mutant it significantly decreased only by 15%; the total chlorophyll content of the UV-irradiated *rcd1-1* mutant was 12% higher than that of the wild type. The control group of UV-A treatment suffered only a slight decline of chlorophyll, irrespective of genotype. The trend for chlorophyll *a* was similar to that for total chlorophyll. The degradation rate of chlorophyll *a* in the wild type was significantly higher than that in *rcd1-1* mutant after UV-B radiation (*Fig. 6b*). The ANOVA table for the data of *Figure 6b* (Two-way ANOVA, Tukey's multiple comparisons test) was displayed in *Table A6b*. However, there were no differences of the degradation rate of chlorophyll *b* in the wild type and the *rcd1-1* mutant after UV-B radiation (*Fig. 6c*). The ANOVA table for the data of *Figure 6c* (Two-way ANOVA, Tukey's multiple comparisons test) was displayed in *Table A6c*.

To study the effects of enhanced UV-B radiation on photosynthesis, the chlorophyll fluorescence parameters (Fv/Fm, ϕPSII, qP and NPQ) were determined. Fluorescence values were converted to colour by chlorophyll fluorescence imager (*Fig. 7*).

The effects of enhanced UV-B radiation on the maximal efficiency of PSII photochemistry in the wild type and the *rcd1-1* mutant were reflected in the value of Fv/Fm (*Fig. 8a*). The ANOVA table for the data of *Figure 8a* (Two-way ANOVA, Tukey's multiple comparisons test) was displayed in *Table A7a*. After UV-A radiation, Fv/Fm of the wild type and *rcd1-1* mutant exhibited a slight decline -14.7% and 5% respectively. The value of Fv/Fm showed a sharp decrease from 0.79 to 0.22 (72% decrease) in the wild type under UV-B radiation, but only from 0.80 to 0.59 (26% decrease) in the *rcd1-1* mutant. The results showed that *rcd1-1* was more resistant to UV-B radiation than the wild type with respect to PSII integrity.

The quantum yield (ϕPSII) of the PSII electron transport was used to detrmine the PSII photochemical efficiency (*Fig. 8b*). The ANOVA table for the data of *Figure 8b* (Two-way ANOVA, Tukey's multiple comparisons test) was displayed in *Table A7b*. ϕPSII showed declining trends in both genotypes, but with less decline in *rcd1-1*, and none in the first two hours. Finally, ϕPSII decreased from 0.425 to 0.340 in the *rcd1-1* mutant, and from 0.420 to 0.286 in the wild type.

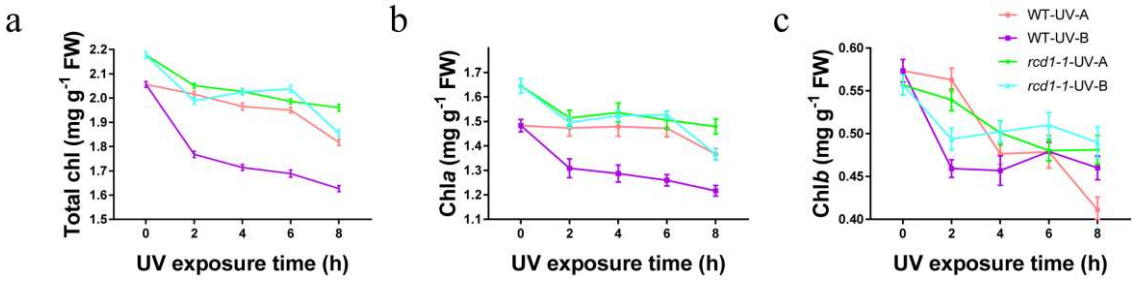

Figure 6. *Effects of enhanced UV-B radiation on chlorophyll content. After UV treatment, about 0.2 g leaves were harvested, ground in 80% (v/v) acetone solution, stored at -20 °C overnight, centrifuged and then measured OD value by spectrophotometer. Total chlorophyll content (**a**), the chl a content (**b**) and the chl b content (**c**) in the wild-type and rcd1-1 mutant were measured. Data are expressed as mean values ± standard errors from three replicates and error bars represent standard errors*

http://www.aloki.hu ● ISSN 1589 1623 (Print) ● ISSN 1785 0037 (Online)
DOI: http://dx.doi.org/10.15666/aeer/1705_1181311833

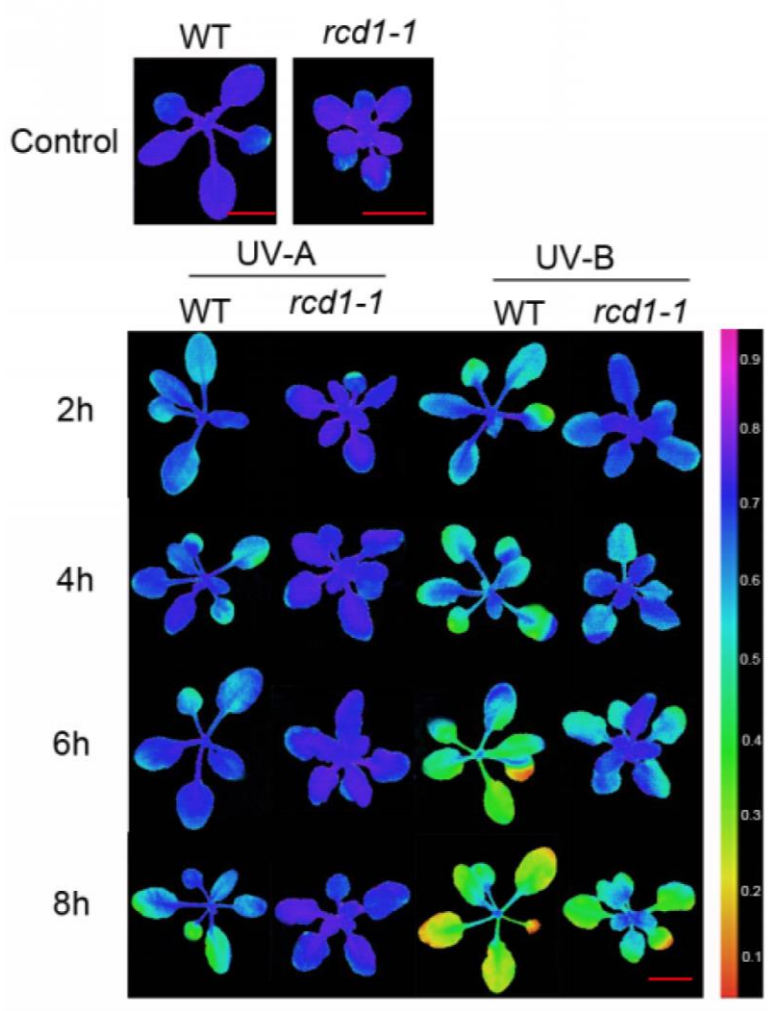

Figure 7. *Changes in fluorescence images of Fv/Fm in the wild type and rcd1-1 mutant leaves: 0 (black) to 1.0 (purple) in chlorophyll fluorescence was represented by color from black to purple. Three-week-old wild type and rcd1-1 mutants were exposed to 0.4 W m^{-2} UV for different hours and measured with Imaging-PAMM-series instrument. The bar value is 10 mm*

UV-B stress changed chlorophyll fluorescence. qP of both the wild type and *rcd1-1* mutant declined with increasing time of UV-A and UV-B exposure (*Fig. 8c*). The ANOVA table for the data of *Figure 8c* (Two-way ANOVA, Tukey's multiple comparisons test) was displayed in *Table A7c*. At the beginning of UV radiation, the qP of the wild type fell by 14.5% while that of the *rcd1-1* mutant dropped by 8%. Finally, after UV-B radiation for 8 h, the qP value of the wild type decreased by 22.6%, while that of the *rcd1-1* mutant had significantly decreased by 15%. Under normal growth condition, the non-photochemical quenching (NPQ) values of the wild type and *rcd1-1* mutant were almost the same, but at the beginning of UV-B exposure the value of NPQ of both genotypes increased slightly (*Fig. 8d*), indicating that the function of the *Arabidopsis* heat dissipation had been enhanced during this period. The ANOVA table for the data of *Figure 8d* (Two-way ANOVA, Tukey's multiple comparisons test) was displayed in *Table A7d*. After UV-B radiation for 4 h, the heat dissipation of the wild type began to decline while that of the *rcd1-1* mutant continued to rise. When plants were exposed to UV-B radiation for 6 h, the heat dissipation of the wild type was only

http://www.aloki.hu ● ISSN 1589 1623 (Print) ● ISSN 1785 0037 (Online)
DOI: http://dx.doi.org/10.15666/aeer/1705_1181311833

67.4% of that of *rcd1-1* mutant. Finally, the NPQ value decreased from 0.288 to 0.140 for the wild type, while it decreased from 0.298 to 0.193 for the *rcd1-1* mutant. The results suggested that the longer UV-B exposure impaired the PS II reaction center activity.

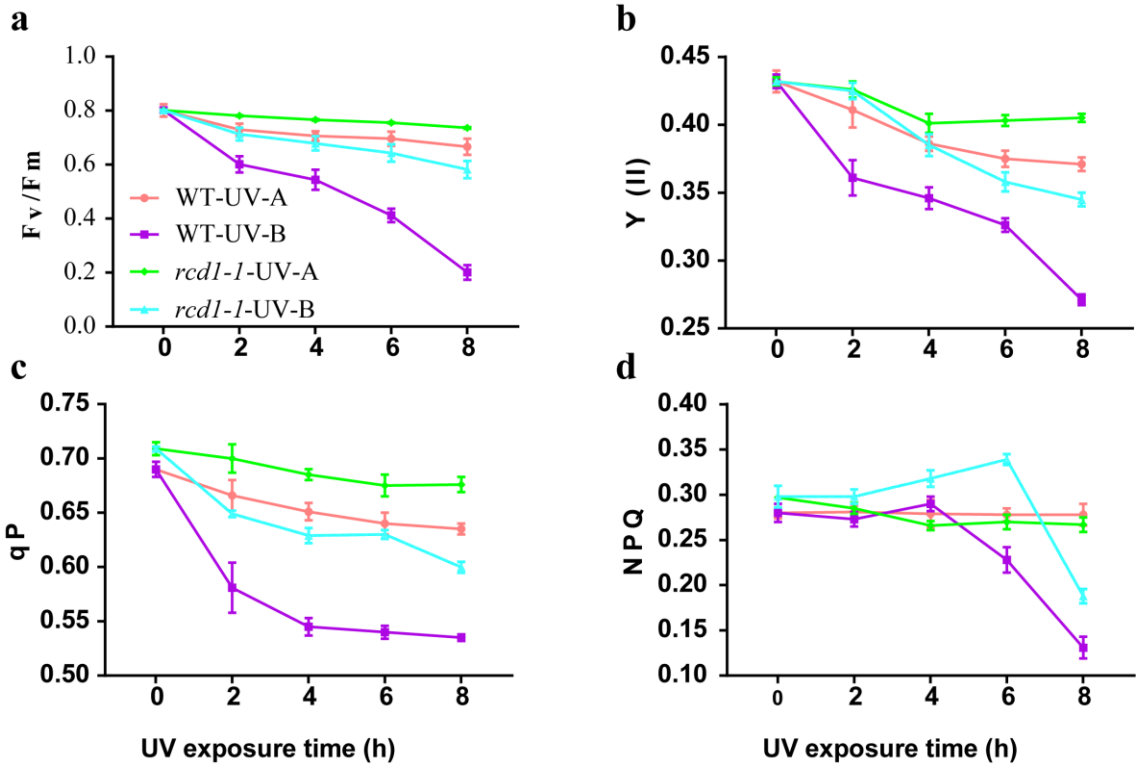

Figure 8. *Effects of enhanced UV-B radiation photosynthetic system II. After UV treatment, the maximal efficiency of PSII photochemistry (Fv/Fm) (**a**), the actual PS II efficiency (ϕPSII) (**b**), qP (**c**) and NPQ (**d**) of the wild type and rcd1-1 mutant were measured with Imaging-PAMM-series instrument. Data are expressed as mean values ± standard errors from three replicates and error bars represent standard errors*

Expression profile of psbA, ANAC013 and UNE10 gene in rcd1-1 mutant after UV-B exposure

Recent progress in the genetics of *Aribodopsis* has revealed that gene expression was regulated by UV-B radiation. In the present study, UV-B modulated the expression of *psbA*, *ANAC013* and *UNE10* genes at transcription level. The expression of the *psbA* gene of the photosystem II showed no consistent difference between plants of different genotypes after 6 h of UV-A treatment. The expression of *psbA* gene in *rcd1-1* mutant was higher than that in the wild type under UV-B radiation (*Fig. 9*). Although the expression of *ANAC013* gene in the two genotypes was significantly elevated both under UV-A and UV-B treatments, it was more highly expressed under UV-B treatment. On the other hand, the *ANAC013* gene was more highly expressed in the *rcd1-1* mutant than in the wild type under the same UV treatment (*Fig. 9*). The expression of the *UNE10* gene in the wild type increased under both UV-A and UV-B treatments, but most under UV-A treatment. In contrast, the expression of the *UNE10* gene in the *rcd1-1* mutant decreased under both UV-A and UV-B treatments (*Fig. 9*).

http://www.aloki.hu ● ISSN 1589 1623 (Print) ● ISSN 1785 0037 (Online)
DOI: http://dx.doi.org/10.15666/aeer/1705_1181311833

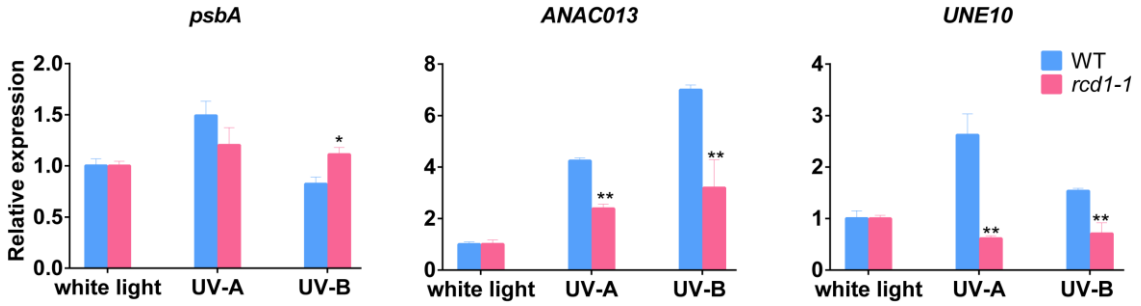

Figure 9. *UV-B-induced expression changes of light response related genes. After supplementary UV-B treatment or control UV-A treatment for 6 h, leaves of Arabidopsis wild type and rcd1-1 mutant were harvested. Relative expression of psbA, ANAC013 and UNE10 genes in the wild type and rcd1-1 mutant detected by real-time PCR. All the data shown are means ± SEM of three independent replications. Data are expressed as mean values ± standard errors from three replicates and error bars represent standard errors. The symbol '*' indicates statistically differences P < 0.05 and the symbol '**'indicates statistically differences P < 0.01 (Two-way ANOVA, Tukey's multiple comparisons test)*

Discussion

It has been reported that *rcd1-1* mutant is sensitive to ozone fumigation and apoplastic superoxide, but tolerant to methylviologen. However, the mechanisms of *rcd1-1* mutant responses to UV-B have remained to be elucidated. In the present research, we studied the effects of UV-B radiation on morphology, cellular membrane permeability, oxidative stress, antioxidant enzymatic activity, photosynthetic and sunscreen pigments, photosynthesis and photosynthetic genes expression of *Arabidopsis*. The *rcd1-1* mutant appears to be more resistant to UV-B radiation than the wild type, and the mechanism for this can now be understood.

Under ordinary growth condition, the wild type grew faster and had more biomass compared with *rcd1-1* mutant (*Fig. 1a-c*); but after UV-B radiation, the wild type exhibited chlorosis, curl, and necrotic lesions (*Fig. 1d*), while the growth of the mutant was much less affected. This was consistent with the result of changes in the chlorophyll content of leaves after UV-B radiation. Compared with the wild type, *rcd1-1* mutant showed a smaller decline in chlorophyll content when exposed to UV-B radiation (*Fig. 6*). UV-B radiation can affect the pigment concentrations in *Arabidopsis* cells by inducing photodegradation of light-absorbing pigments (Prasad and Zeeshan, 2004), resulting in loss of photosynthetic capacity. The present investigation showed that UV-B radiation significantly decreased chlorophyll *a* and *b* contents of both genotypes, but they decreased more in the wild type.

These findings prompted us to further test whether the *rcd1-1* mutant was more tolerant to UV-B radiation. The *rcd1-1* mutant suffered less serious leaf necrosis than the wild type after UV-B treatment. To further understand the extent of damage of UV-B radiation to cell membranes, the electrolyte leakage of leaves was considered, which is a classic assessment index to estimate the effects of UV-B on plasma membranes. The electrical conductivity of *rcd1-1* mutant was lower than that of the wild type after UV-B treatment. Because the higher the electrical conductivity, the more serious the injury to cell membranes; the cell membranes of *rcd1-1* mutant were less damaged than the wild type, which verified the result of Shi et al. (2005) using Evans blue staining.

http://www.aloki.hu ● ISSN 1589 1623 (Print) ● ISSN 1785 0037 (Online)
DOI: http://dx.doi.org/10.15666/aeer/1705_1181311833

Previous studies have shown that UV-B radiation induces the production of cellular reactive oxygen species (ROS), leading to oxidative stress, which in turn damages the photosynthetic apparatus (Liebel et al., 2012; Yannarelli et al., 2006). ROS accumulation induced membrane lipid peroxidation, assayed as malondialdehyde (MDA). In this present study, ROS level of the two genotypes increased in short-term enhanced UV-B treatment, revealing that UV-B radiation did induce oxidative stress. The *rcd1-1* mutant exhibited lower H_2O_2 and O_2^- accumulation levels and higher MDA level than the wild type after UV-B treatment, indicating it suffered from less oxidative stress under UV-B radiation. This might provide an explanation as to why *rcd1-1* mutant has smaller cell membrane damage than the wild type. On the other hand, antioxidant enzymes play a significant part in reactive oxygen scavenging and antioxidant defense systems. The present study showed that *rcd1-1* mutant exhibited higher activities of SOD, POD and CAT than the wild type after UV-B treatment, which explained the oxidative stress results above.

UV-B absorbing compounds, flavonoids and anthocyanin in *Arabidopsis* leaves have an important protective function reducing the transmittance of UV photons through leaf tissue (Yao and Liu, 2006). Anthocyanin production is the predominant mechanism of protection of the young plant. In the present study, *rcd1-1* mutant accumulated more flavonoids and anthocyanin than the wild type, which was similar to *rcd1-2* mutant that also accumulated more sunscreen pigments than the wild type (Ahlfors et al., 2004; Overmyer et al., 2000; Morales et al., 2015). These were evidences that *rcd1-1* mutant was more tolerant to UV-B radiation than the wild type.

Studies with artificial UV-B sources have shown that UV-B radiation may strongly affected PSII, whereas PSI appeared to be relatively insensitive (Sedej and Gaberščik, 2008). If the light energy absorbed by the plant is in excess what is needed for photosynthes, it may lead to a reduction in the potential efficiency of PSII. In the present study, *rcd1-1* mutant exhibited higher maximum quantum efficiency of primary photochemistry (Fv/Fm) than the wild type after UV-B radiation. Meanwhile, the mutant exhibited more slowly decreasing rates of effective quantum yield of photochemical energy conversion in PS II (ϕPSII) and photochemical quenching of variable chlorophyll fluorescence yield (qP). Interestingly, the *rcd1-1* mutant showed higher non-photochemical quenching (NPQ) than the wild type, so the possibility that the *rcd1-1* could release exceeded energy from UV-B by means of this process cannot be excluded. These results show that the *rcd1-1* mutant had a higher photosynthetic capability after UV-B radiation than the wild type.

RCD1 protects plant cells from running into reactive oxygen species (ROS)-triggered cell programs, including cell death, activation of pathogen-responsive genes (PR genes) and extra-plastidic antioxidant enzymes, which could support the induction of the chloroplast antioxidant system (Hiltscher et al., 2014). That the *rcd1-1* mutant exhibited higher photosynthetic capability than the wild type can be explained from the following three aspects. First, the *rcd1-1* mutant accumulated less ROS than the wild type after UV-B radiation, so its photosynthetic apparatus suffered less injury. It is known that excessive O_2^- and H_2O_2 may result in damage of PSII through their effects on the composition and structure of the light harvesting complex which lead to a disturbance in the chloroplast structure. Second, chlorophyll contents in *rcd1-1* mutant dropped less than that of the wild type after UV-B radiation. Third, the *rcd1-1* mutant had higher value of NPQ, which could release excess energy from UV-B by the process of releasing more heat than the wild type.

http://www.aloki.hu ● ISSN 1589 1623 (Print) ● ISSN 1785 0037 (Online)
DOI: http://dx.doi.org/10.15666/aeer/1705_1181311833

The two important targets of UV-B radiation in the plant are the genome and the photosynthetic machinery (Fujibe et al., 2004). One of the earliest effects of UV-B irradiation is the change of gene expression. In the present study, we have investigated changes in expression of genes of *psbA*, *ANAC013* and *UNE10*, which play important parts in photosynthesis, to further investigate the molecular mechanisms of *Arabidopsis* underlying UV-B radiation (Jaspers et al., 2009).

RCD1 is an important regulator of stress and hormonal and developmental responses in *Arabidopsis*, which might negatively regulate a wide range of stress-related down-stream genes (Jaspers et al., 2009; Fujibe et al., 2004). Previous research revealed that *RCD1* interacts with a large number of transcription factors belonging to several protein families, such as AP2/ERF, NAC and basic helix–loop–helix (bHLH) (Jaspers et al., 2009). *ANAC013* and *UNE10* belong to NAC family and basic helix–loop–helix family respectively. These results in the present research showed that *ANAC013* and *UNE10* genes are expressed to a lower extent in the mutant, which proved that *RCD1* gene negatively regulate a wide range of stress-related down-stream genes. The RCD1 functions mainly include ozone sensitivity, paraquat and UV-B tolerance and the ability to interact with different transcription factors (TFs) which could responsible for the unique functions of RCD1 (Jaspers et al., 2009). Several RCD1-interacting TFs (PIF5, PIF7, COL9, COL10 and STO) were known to play a part in light responses (Indorf et al., 2007; Castillon et al., 2007). This suggested that *RCD1* could be involved in signal transduction (Jaspers et al., 2009). *ANAC013* is regulated mainly at transcriptional level under UV-B and partly independent of *COP1*, *UVR8* and *HY5* (Jiang et al., 2012; Safrany et al., 2008). Moreover, it is also modulated by the plant hormone ABA and different abiotic stress. *UNE10* is one of light response genes and similar to *PIF7*, including MYB and BHLH domain, which play an important role in the signal path of the UV-B (Paila et al., 2008). RCD1 interacts in vivo and suppresses the activity of the transcription factors ANAC013 and ANAC017, which mediate a ROS-related retrograde signal originating from mitochondrial complex III (Shapiguzov et al., 2019). Inactivation of RCD1 leads to increased expression of mitochondrial dysfunction stimulon (MDS) genes regulated by ANAC013 and ANAC017.

The *psbA* gene is located in the chloroplast genome and encodes for the D1 protein, a core component of Photosystem II. The results in the present study revealed that the *psbA* gene of photosynthetic system II was expressed to a greater degree in *rcd1-1* mutant than the wild type, which meant photosystem II suffered less damage under UV-B. The result was in accordance with the phenomenon that the photosynthetic capability of the mutant was higher than that of the wild type. Therefore, the *RCD1* gene could be an important genetic resource to improve plant function against UV-B radiation, which may be an interested topic to provide an incentive for further scientific contributions in the near future.

Conclusion

The present research revealed that RCD-1 is sensitive to UV-B radiation in *Arabidopsis.* The *rcd1-1* mutant is more resistant to UV-B probably because of higher flavonoids and anthocyanins in the mutants. *RCD-1* gene may negatively regulate the expression of *ANAC013* and *UNE10*. More work is needed to explore the molecular mechanism of *RCD1*-mediated response to UV-B regulation.

http://www.aloki.hu ● ISSN 1589 1623 (Print) ● ISSN 1785 0037 (Online)
DOI: http://dx.doi.org/10.15666/aeer/1705_1181311833

Acknowledgements. We sincerely thank Professor Lars Olof Björn from Lund University, Sweden for his great help and critical suggestions on the research. This work was supported by the National Natural Science Foundation of China (grant NO. 31670266), the Leading Scientists Project of Guangdong Province, the Guangdong Pearl River Scholar Funded Scheme (2012), the Natural Science Foundation of Guangdong Province (grant No. 2017A030313115) and the Innovation Project of Graduate School of South China Normal University (grant NO. 2016lkxm10). We are extremely grateful to Prof. Paul Giller, School of Biological, Earth and Environmental Sciences, University College Cork, Ireland for editing the English of the manuscript. Shaoshan Li designed the research; Xianla Liu performed the experiment; Guizhen Lyu and Dongbing Li drafted the manuscript; Guizhen Lyu, Dongbing Li and Shaoshan Li read and approved the final manuscript. Conflict of interests. The authors state no conflict of interests.

REFERENCES

[1] Ahlfors, R., Lang, S., Overmyer, K., Jaspers, P., Brosch, M., Tauriainen, A. A., Kollist, H., Tuominen, H., Bellesboix, E., Piippo, M. (2004): *Arabidopsis* RADICAL-INDUCED CELL DEATH1 belongs to the WWE protein–protein interaction domain protein family and modulates abscisic acid, ethylene, and methyl jasmonate responses. – The Plant Cell 16: 1925-1937.

[2] Arnon, D. I. (1949): Copper enzymes in isolated chloroplasts, polyphenoxidase in Beta vulgaris. – Plant Physiology 24: 1-15.

[3] Belles-Boix, E., Babiychuk, E., van Montagu, M., Inze, D., Kushnir, S. (2000): CEO1, a new protein from *Arabidopsis thaliana*, protects yeast against oxidative damage. – FEBS Letters 482: 19-24.

[4] Biever, J. J., Gardner, G. (2016): The relationship between multiple UV-B perception mechanisms and DNA repair pathways in plants. – Environmental and Experimental Botany 124: 89-99.

[5] Castillon, A., Shen, H., Huq, E. (2007): Phytochrome interacting factors: central players in phytochrome-mediated light signaling networks. – Trends in Plant Science 12: 514-521.

[6] Cheeseman, J. M. (2006): Hydrogen peroxide concentrations in leaves under natural conditions. – Journal of Experimental Botany 57: 2435-2444.

[7] Czechowski, T., Stitt, M., Altmann, T., Udvardi, M. K., Scheible, W. (2005): Genome-wide identification and testing of superior reference genes for transcript normalization in *Arabidopsis*. – Plant Physiology 139: 5-17.

[8] Dotto, M., G Mez, M. S., Soto, M. S., Casati, P. (2018): UV-B radiation delays flowering time through changes in the PRC2 complex activity and miR156 levels in Arabidopsis thaliana. – Plant, Cell, Environment 41: 1394-1406.

[9] Frohnmeyer, H., Staiger, D. (2003): Ultraviolet-B radiation-mediated responses in plants. balancing damage and protection. – Plant Physiology 133: 1420-1428.

[10] Fujibe, T., Saji, H., Arakawa, K., Yabe, N., Takeuchi, Y., Yamamoto, K. T. (2004): A methyl viologen-resistant mutant of *Arabidopsis*, which is allelic to ozone-sensitive rcd1, is tolerant to supplemental ultraviolet-B irradiation. – Plant Physiology 134: 275-285.

[11] He, F., Tsuda, K., Takahashi, M., Kuwasako, K., Terada, T., Shirouzu, M., Watanabe, S., Kigawa, T., Kobayashi, N., Guntert, P. (2012): Structural insight into the interaction of ADP-ribose with the PARP WWE domains. – FEBS Letters 586: 3858-3864.

[12] He, Y., H Der, D. (2002): UV-B-induced formation of reactive oxygen species and oxidative damage of the cyanobacterium *Anabaena sp.*: protective effects of ascorbic acid and N-acetyl-l-cysteine. – Journal of Photochemistry and Photobiology B-biology 66: 115-124.

[13] Hiltscher, H., Rudnik, R., Shaikhali, J., Heiber, I., Mellenthin, M., Duarte, I. M., Schuster, G. N., Kahmann, U., Baier, M. (2014): The radical induced cell death protein 1 (RCD1) supports transcriptional activation of genes for chloroplast antioxidant enzymes. – Frontiers in Plant Science 5: 475-475.

http://www.aloki.hu ● ISSN 1589 1623 (Print) ● ISSN 1785 0037 (Online)
DOI: http://dx.doi.org/10.15666/aeer/1705_1181311833

[14] Indorf, M., Cordero, J., Neuhaus, G., Rodriguezfranco, M. (2007): Salt tolerance (STO), a stress-related protein, has a major role in light signalling. – Plant Journal 51: 563-574.
[15] Jaspers, P., Blomster, T., Brosch, M., Salojarvi, J., Ahlfors, R., Vainonen, J. P., Reddy, R. A., Immink, R. G. H., Angenent, G. C., Turck, F. (2009): Unequally redundant RCD1 and SRO1 mediate stress and developmental responses and interact with transcription factors. – Plant Journal 60: 268-279.
[16] Jaspers, P., Brosch, M., Overmyer, K., Kangasjarvi, J. (2010): The transcription factor interacting protein RCD1 contains a novel conserved domain. – Plant Signaling, Behavior 5: 78-80.
[17] Jenkins, G. I. (2014): Structure and function of the UV-B photoreceptor UVR8. – Current Opinion in Structural Biology 29: 52-57.
[18] Jiang, L., Wang, Y., Björn, L. O., Li, S. (2009): *Arabidopsis* RADICAL-INDUCED CELL DEATH1 is involved in UV-B signaling. – Photochemical and Photobiological Sciences 8: 838-846.
[19] Jiang, L., Wang, Y., Li, Q., Björn, L. O., He, J., Li, S. (2012): Arabidopsis STO/BBX24 negatively regulates UV-B signaling by interacting with COP1 and repressing HY5 transcriptional activity. – Cell Research 22: 1046-1057.
[20] Kragelund, B. B., Jensen, M. K., Skriver, K. (2012): Order by disorder in plant signaling. – Trends in Plant Science 17: 625-632.
[21] Kucera, B., Leubnermetzger, G., Wellmann, E. (2003): Distinct ultraviolet-signaling pathways in bean leaves. DNA damage is associated with β-1,3-glucanase gene induction, but not with flavonoid formation. – Plant Physiology 133: 1445-1452.
[22] Liebel, F., Kaur, S., Ruvolo, E., Kollias, N., Southall, M. (2012): Irradiation of skin with visible light induces reactive oxygen species and matrix-degrading enzymes. – Journal of Investigative Dermatology 132: 1901-1907.
[23] Ma, B., Gao, L., Zhang, H., Cui, J., Shen, Z. (2012): Aluminum-induced oxidative stress and changes in antioxidant defenses in the roots of rice varieties differing in Al tolerance. – Plant Cell Reports 31: 687-696.
[24] Mahalingam, R., Jambunathan, N., Gunjan, S., Faustin, E., Weng, H., Ayoubi, P. (2006): Analysis of oxidative signalling induced by ozone in *Arabidopsis* thaliana. – Plant Cell and Environment 29: 1357-1371.
[25] Moldau, H., Vahisalu, T., Kollist, H. (2011): Rapid stomatal closure triggered by a short ozone pulse is followed by reopening to overshooting values. – Plant Signaling & Behavior 6: 311-313.
[26] Morales, L. O., Brosche, M., Vainonen, J. P., Sipari, N., Lindfors, A., Strid, A., Aphalo, P. J. (2015): Are solar UV-B- and UV-A-dependent gene expression and metabolite accumulation in Arabidopsis mediated by the stress response regulator RADICAL-INDUCED CELL DEATH1? – Plant Cell and Environment 38: 878-891.
[27] Murashige, T., Skoog, F. (1962): A revised medium for rapid growth and bio assays with tobacco tissue cultures. – Physiologia Plantarum 15: 473-497.
[28] Noh, B., Spalding, E. P. (1998): Anion Channels and the Stimulation of Anthocyanin Accumulation by Blue Light in *Arabidopsis* Seedlings. – Plant Physiology 116: 503-509.
[29] Overmyer, K., Tuominen, H., Kettunen, R., Betz, C., Langebartels, C., Sandermann, H., Kangasjarvi, J. (2000): Ozone-sensitive *Arabidopsis* rcd1 mutant reveals opposite roles for ethylene and jasmonate signaling pathways in regulating superoxide-dependent cell death. – The Plant Cell 12: 1849-1862.
[30] Paila, U., Kondam, R., Ranjan, A. (2008): Genome bias influences amino acid choices: analysis of amino acid substitution and re-compilation of substitution matrices exclusive to an AT-biased genome. – Nucleic Acids Research 36: 6664-6675.
[31] Prasad, S. M., Zeeshan, M. (2004): Effect of UV-B and monocrotophos, singly and in combination, on photosynthetic activity and growth of non-heterocystous cyanobacterium *Plectonema boryanum*. – Environmental and Experimental Botany 52: 175-184.

http://www.aloki.hu ● ISSN 1589 1623 (Print) ● ISSN 1785 0037 (Online)
DOI: http://dx.doi.org/10.15666/aeer/1705_1181311833

[32] Safrany, J., Haasz, V., Mate, Z., Ciolfi, A., Feher, B., Oravecz, A., Stec, A., Dallmann, G., Morelli, G., Ulm, R. (2008): Identification of a novel CIS-regulatory element for UV-B-induced transcription in *Arabidopsis*. – Plant Journal 54: 402-414.
[33] Sedej, T. T., Gaberščik, A. (2008): The effects of enhanced UV-B radiation on physiological activity and growth of Norway spruce planted outdoors over 5 years. – Trees-Structure and Function 22: 423-435.
[34] Shapiguzov, A., Vainonen, J. P., Hunter, K., Tossavainen, H., Tiwari, A., Jarvi, S., Hellman, M., Aarabi, F., Alseekh, S., Wybouw, B. (2019): *Arabidopsis* RCD1 coordinates chloroplast and mitochondrial functions through interaction with ANAC transcription factors. – eLife 8: e43284.
[35] Shi, S., Wang, G., Wang, Y., Zhang, L., Zhang, L. (2005): Protective effect of nitric oxide against oxidative stress under ultraviolet-B radiation. – Nitric Oxide 13: 1-9.
[36] Ulm, R., Jenkins, G. I. (2015): Q&A: How do plants sense and respond to UV-B radiation? – BMC Biology 13: 45-50.
[37] Ulm, R., Nagy, F. (2005): Signalling and gene regulation in response to ultraviolet light. – Current Opinion in Plant Biology 8: 477-482.
[38] Uy, B., Mcglashan, S. R., Shaikh, S. (2011): Measurement of reactive oxygen species in the culture media using acridan lumigen PS-3 assay. – Journal of Biomolecular Techniques 22: 95-107.
[39] Verdaguer, D., Jansen, M. A. K., Llorens, L., Morales, L. O., Neugart, S. (2017): UV-A radiation effects on higher plants: Exploring the known unknown. – Plant Science 255: 72-81.
[40] Yannarelli, G. G., Noriega, G. O., Batlle, A., Tomaro, M. L. (2006): Heme oxygenase up-regulation in ultraviolet-B irradiated soybean plants involves reactive oxygen species. – Planta 224: 1154-1162.
[41] Yao, X., Liu, Q. (2006): Changes in morphological, photosynthetic and physiological responses of Mono Maple seedlings to enhanced UV-B and to nitrogen addition. – Plant Growth Regulation 50: 165-177.
[42] Yin, R., Ulm, R. (2017): How plants cope with UV-B: from perception to response. – Current Opinion in Plant Biology 37: 42-48.
[43] Zlatev, Z., Lidon, F. C., Kaimakanova, M. (2012): Plant physiological responses to UV-B radiation. – Emirates Journal of Food and Agriculture 24: 481-501.

APPENDIX

Table A1. *ANOVA table for the data of Figure 1c (two-way ANOVA, Sidak's multiple comparisons test)*

ANOVA table	SS	DF	MS	F (DFn, DFd)	P value
Interaction	0.7270	5	0.1454	F (5, 24) = 81.87	P < 0.0001
Row factor	62.06	5	12.41	F (5, 24) = 6989	P < 0.0001
Column factor	1.501	1	1.501	F (1, 24) = 845.0	P < 0.0001
Residual	0.04262	24	0.001776		

Table A2. *ANOVA table for the data of Figure 2b (two-way ANOVA, Tukey's multiple comparisons test)*

ANOVA table	SS	DF	MS	F (DFn, DFd)	P value
Interaction	0.01963	9	0.002181	F (9, 32) = 6.436	P < 0.0001
Row factor	0.2691	3	0.08971	F (3, 32) = 264.7	P < 0.0001
Column factor	0.01614	3	0.005381	F (3, 32) = 15.88	P < 0.0001
Residual	0.01085	32	0.0003389		

http://www.aloki.hu ● ISSN 1589 1623 (Print) ● ISSN 1785 0037 (Online)
DOI: http://dx.doi.org/10.15666/aeer/1705_1181311833

Table A3. *ANOVA table for the data of Figure 3 (two-way ANOVA, Tukey's multiple comparisons test).* ***a*** *ANOVA table for the data of Figure 3a.* ***b*** *ANOVA table for the data of Figure 3c*

(a)

ANOVA table	SS	DF	MS	F (DFn, DFd)	P value
Interaction	0.09175	12	0.007646	F (12, 40) = 5.299	P < 0.0001
Row factor	2.170	4	0.5425	F (4, 40) = 376.0	P < 0.0001
Column factor	0.7387	3	0.2462	F (3, 40) = 170.6	P < 0.0001
Residual	0.05772	40	0.001443		

(b)

ANOVA table	SS	DF	MS	F (DFn, DFd)	P value
Interaction	0.003056	12	0.0002547	F (12, 40) = 4.154	P = 0.0003
Row factor	0.01108	4	0.002771	F (4, 40) = 45.21	P < 0.0001
Column factor	0.001442	3	0.0004806	F (3, 40) = 7.841	P = 0.0003
Residual	0.002452	40	6.130e-005		

Table A4. *ANOVA table for the data of Figure 4 (two-way ANOVA, Tukey's multiple comparisons test).* ***a*** *ANOVA table for the data of Figure 4a.* ***b*** *ANOVA table for the data of Figure 4b.* ***c*** *ANOVA table for the data of Figure 4c*

(a)

ANOVA table	SS	DF	MS	F (DFn, DFd)	P value
Interaction	29590	12	2466	F (12, 40) = 12.24	P < 0.0001
Row factor	86828	4	21707	F (4, 40) = 107.7	P < 0.0001
Column factor	22413	3	7471	F (3, 40) = 37.07	P < 0.0001
Residual	8061	40	201.5		

(b)

ANOVA table	SS	DF	MS	F (DFn, DFd)	P value
Interaction	511109	12	42592	F (12, 40) = 111.4	P < 0.0001
Row factor	934451	4	233613	F (4, 40) = 611.0	P < 0.0001
Column factor	354056	3	118019	F (3, 40) = 308.7	P < 0.0001
Residual	15293	40	382.3		

(c)

ANOVA table	SS	DF	MS	F (DFn, DFd)	P value
Interaction	604397	12	50366	F (12, 40) = 294.5	P < 0.0001
Row factor	284652	4	71163	F (4, 40) = 416.1	P < 0.0001
Column factor	1485984	3	495328	F (3, 40) = 2896	P < 0.0001
Residual	6841	40	171.0		

Table A5. *ANOVA table for the data of Figure 5b (two-way ANOVA, Tukey's multiple comparisons test)*

ANOVA table	SS	DF	MS	F (DFn, DFd)	P value
Interaction	1.007	12	0.08394	F (12, 40) = 33.73	P < 0.0001
Row factor	1.502	4	0.3756	F (4, 40) = 151.0	P < 0.0001
Column factor	2.798	3	0.9328	F (3, 40) = 374.9	P < 0.0001
Residual	0.09953	40	0.002488		

http://www.aloki.hu ● ISSN 1589 1623 (Print) ● ISSN 1785 0037 (Online)
DOI: http://dx.doi.org/10.15666/aeer/1705_1181311833

Table A6. *ANOVA table for the data of Figure 6 (two-way ANOVA, Tukey's multiple comparisons test).* ***a*** *ANOVA table for the data of Figure 6a.* ***b*** *ANOVA table for the data of Figure 6b.* ***c*** *ANOVA table for the data of Figure 6c*

(a)

ANOVA table	SS	DF	MS	F (DFn, DFd)	P value
Interaction	0.1097	12	0.009143	F (12, 40) = 18.28	P < 0.0001
Row factor	0.5708	4	0.1427	F (4, 40) = 285.3	P < 0.0001
Column factor	0.6734	3	0.2245	F (3, 40) = 448.9	P < 0.0001
Residual	0.02000	40	0.0005001		

(b)

ANOVA table	SS	DF	MS	F (DFn, DFd)	P value
Interaction	0.06287	12	0.005239	F (12, 40) = 1.970	P = 0.0542
Row factor	0.2621	4	0.06552	F (4, 40) = 24.64	P < 0.0001
Column factor	0.4580	3	0.1527	F (3, 40) = 57.40	P < 0.0001
Residual	0.1064	40	0.002659		

(c)

ANOVA table	SS	DF	MS	F (DFn, DFd)	P value
Interaction	0.06287	12	0.002607	F (12, 40) = 4.434	P = 0.0002
Row factor	0.2621	4	0.01916	F (4, 40) = 32.59	P < 0.0001
Column factor	0.4580	3	0.02172	F (3, 40) = 3.694	P = 0.0194
Residual	0.1064	40	0.0005879		

Table A7. *ANOVA table for the data of Figure 8 (two-way ANOVA, Tukey's multiple comparisons test).* ***a*** *ANOVA table for the data of Figure 8a.* ***b*** *ANOVA table for the data of Figure 8b.* ***c*** *ANOVA table for the data of Figure 8c.* ***d*** *ANOVA table for the data of Figure 8d*

(a)

ANOVA table	SS	DF	MS	F (DFn, DFd)	P value
Interaction	0.2876	12	0.02396	F (12, 40) = 16.21	P < 0.0001
Row factor	0.4283	4	0.1071	F (4, 40) = 72.45	P < 0.0001
Column factor	0.5588	3	0.1863	F (3, 40) = 126.0	P < 0.0001
Residual	0.05912	40	0.001478		

(b)

ANOVA table	SS	DF	MS	F (DFn, DFd)	P value
Interaction	0.01670	12	0.001392	F (12, 40) = 10.10	P < 0.0001
Row factor	0.05295	4	0.01324	F (4, 40) = 96.12	P < 0.0001
Column factor	0.03519	3	0.01173	F (3, 40) = 85.18	P < 0.0001
Residual	0.005509	40	0.0001377		

(c)

ANOVA table	SS	DF	MS	F (DFn, DFd)	P value
Interaction	0.02015	12	0.001679	F (12, 40) = 7.184	P < 0.0001
Row factor	0.05911	4	0.01478	F (4, 40) = 63.23	P < 0.0001
Column factor	0.09733	3	0.03244	F (3, 40) = 138.8	P < 0.0001
Residual	0.009348	40	0.0002337		

(d)

ANOVA table	SS	DF	MS	F (DFn, DFd)	P value
Interaction	0.04849	12	0.004041	F (12, 40) = 16.25	P < 0.0001
Row factor	0.04648	4	0.01162	F (4, 40) = 46.72	P < 0.0001
Column factor	0.02003	3	0.006676	F (3, 40) = 26.85	P < 0.0001
Residual	0.009948	40	0.0002487		

http://www.aloki.hu ● ISSN 1589 1623 (Print) ● ISSN 1785 0037 (Online)
DOI: http://dx.doi.org/10.15666/aeer/1705_1181311833

ASSESSING THE EFFICIENCY OF JING-JIN-JI COLLABORATIVE DEVELOPMENT IN DIFFERENT LOW CARBON ECONOMY STRATEGIES AROUND XIONGAN WITH SD AND FRACTAL MODEL

XU, W.-B.[1] – ZHANG, X.-H.[1*] – WANG, X.-S.[1] – ZHANG, B.-A.[2*]

[1]*Institute of Environmental Economics, Tianjin Polytechnic University, Tianjin 300387, China*

[2]*Hebei Environment Engineering University, Qinhuangdao City 006112, China*

**Corresponding authors*
e-mail: xuehua671231@163.com (X.-H. Zhang), 15033529696@126.com (B.-A. Zhang)

(Received 23rd Apr 2019; accepted 4th Jul 2019)

Abstract. The paper presents a new method to evaluate the impact of Xiongan's construction on the collaborative development of Jing-Jin-Ji (JJJ) Urban Agglomeration under different development strategies. Firstly, the SD model of each urban node of JJJ Urban Agglomeration is constructed by using parallel calibration system, and it is applied to simulate the development trend of target system. Then, the paper sets up a fractal model base on gravitational theorem which takes population, GDP and full carbon emissions as main factors to be evaluated with the Low Carbon Economic Linkage Strength. The evaluation results show that: (1) Xiongan as a radiation center can significantly promote the collaborative development of urban agglomeration; (2) On the basis of the existing trend, improving the low-carbon level of Xiongan alone has no significant effect on the low-carbon development, while the effect is significant when Beijing, Tianjin and Xiongan low-carbon levels are improved at the same time; (3) There will be a delay in the transmission of low-carbon economic development capacity from high to low gradient, but this delay does not affect the radiation effect of high gradient cities on low gradient cities, nor does it affect the coordinated development of urban agglomerations.
Keywords: *low-carbon economic strategy, fractal dimension, JJJ Urban Agglomeration, scenario analysis*

Introduction

The Nineteenth Congress of the Communist Party of China pointed out that the main contradiction in the current Chinese society is the contradiction between the people's pursuit of a better life and the insufficient balance of development (Pan et al., 2009). The contradiction of imbalanced development is particularly prominent in Jing-Jin-Ji (JJJ) Urban Agglomeration.

The JJJ Urban Agglomeration includes Beijing, Tianjin, Xiongan New District, Shijiazhuang, Tangshan, Baoding, Langfang, Handan, Zhangjiakou, Chengde, Qinhuangdao, Cangzhou, Xingtai and Hengshui. The total area of the JJJ Urban Agglomeration is 216,000 km^2. It is dominated by plain landforms and belongs to temperate monsoon climate and semi-humid area. As one of China's important economic growth pole, the JJJ Urban Agglomeration is confronted with challenges to achieve sustainable development. The main challenge is facing two significant gradient differences (Li et al., 2013). One is the social-economic gradient, the other is the resource-environment gradient. Beijing and Tianjin show the high gradient of social economy, while the node cities in Hebei show the high gradient of resources and environment. These two kinds of gradient differences make JJJ Urban Agglomeration become the most acute contradiction area in China.

http://www.aloki.hu ● ISSN 1589 1623 (Print) ● ISSN 1785 0037 (Online)
DOI: http://dx.doi.org/10.15666/aeer/1705_1183511849

In this context, JJJ Urban Agglomeration is expected to become a model of urban agglomeration collaborative development and play a leading role in China's low-carbon development. As a newly rising radiation center of JJJ Urban Agglomeration, Xiongan has attracted much attention at home and aboard, which includes the influence of Xiongan's geographical location and different development modes on JJJ Urban Agglomeration.

The study of urban agglomeration has a long history, including both micro-scale and macro-scale research. The research involves in exploring the driving forces for the development of urban agglomerations with different focusing modes by comparing the frontiers of total factor productivity among urban agglomeration (Jia et al., 2018), sharing, matching, and learning mechanisms within urban agglomeration (Duranton et al., 2003), the dynamic mechanism of the growth of cities and urban agglomerations (Cao et al., 2012; White et al., 1994), urban location and boundary delimitation (Tannier et al., 2011), and political policies and their impact on the development of urban agglomerations (Jefferson et al., 2013). Fractal is the most commonly used method in urban agglomerations' research. Factual theory and method have been applied to analyze morphological boundaries of urban agglomerations and characterize boundary shapes (Tannier et al., 2013), and discovery the difference between planned patterns and less planned ones in morphological features of urban agglomerations (Frankhauser, 1998).

With the increasingly prominent environmental problems, it has become a worldwide concern for economists, as is witnessed by many theories and methods which aims at driving the economy towards a sustainable economy (Camagni et al., 1998). The research on urban agglomerations are gradually expanding from the economic system to environmental-economic complex system, such as the heat island effect of high-density urban agglomerations (Zhou et al., 2018), the driving force of low-carbon development (Kang et al., 2018), the evaluation of sustainable development level of urban agglomerations with multiple resource and environmental indicators (Yu et al., 2010).

Different environments co-exist in a city including the natural, the economic production and the social activation. Each of them generates positive and negative externalities for the city, since each of them represents `use advantages' and `use costs' for a city. For social activation, these externalities are manifested in energy consumption and food consumption (biomass resource consumption) and waste discharge in the daily life of clothing, food, shelter and transportation. For economic production, these externalities are finally measured in terms of resource and energy input, positive output (GDP) and negative output (waste emissions). While all the supply of natural resources and degradation of environmental pollutants are related to urban land area. Therefore city's quality of life and environmental concerns undermine all advantages associated with agglomeration economies.

SD model is a useful tool to analyze and forecast urban or city environmental economic system, which is widely used in the system simulation of homogeneous regions and the systematic analysis (Wu et al., 2018), as well as the study of expansion to the periphery of the target city (Rich et al., 2016; Yu et al., 2018). In the research of scenario analysis and strategy selection, the socio-economic plan of the target system is always one of the most important bases for scenario design, especially in carbon emission reduction (Du et al., 2018) and effective utilization of natural resources (Zhang et al., 2008). However, due to the differences of natural conditions and development patterns in heterogeneous regions, the study of urban agglomerations

http://www.aloki.hu ● ISSN 1589 1623 (Print) ● ISSN 1785 0037 (Online)
DOI: http://dx.doi.org/10.15666/aeer/1705_1183511849

focusing on these regions is very rare at present. Furthermore, there is another bottleneck problem, that is, how to normalize multiple resources and environmental factors in SD model.

There is no doubt that the dynamics of cities can be best captured by looking at them as complex systems governed by freedom, interacting on different space and time scales in a non-linear fashion (Albeverio et al., 2008). The evolution of cities often depends on the interaction of internal factors (such as decision-making of institutions and individuals) and external factors (radiation between cities and social progress). Therefore, the combination of SD model based on urban metabolic analysis and input-output flow can better solve the obvious heterogeneity in urban agglomeration system simulation and improve the integrity evaluation of urban agglomeration (Elliot et al., 2018).

In addition, the research on low carbon is developing rapidly from the initial concern of carbon emissions accounting of energy consumption to potential carbon environmental capacity of waste emissions and biomass resources consumption. The potential carbon environmental capacity occupancy of waste emissions involves both production (Tan et al., 2018) and living areas (Sun et al., 2018). While the potential carbon environmental capacity occupancy of biomass resources mainly involves living areas, whose theoretical basis is that the more land resources occupied by human demand for food, the less land resources used for the growth of high carbon-fixing vegetation (Timothy et al., 2018). The above research lays a foundation for the proposal of carbon accounting and the solution of the problem of resource and environment normalization in SD model.

Based on the analysis of system dynamics, this paper applies fractal theory and method to analyze the influence of Xiongan New District on the coordinated development of JJJ Urban Agglomeration from the perspective of low-carbon economic analysis, aiming to analyze the Xiongan New District to the promotion of low-carbon development of JJJ urban agglomeration. And this research provides a scientific basis for relevant departments to make decisions.

Materials and methods

Each node city in JJJ Urban Agglomeration has distinct heterogeneity. There are not only huge economic gradients, but also huge resource and environment gradients. In order to objectively evaluate the role of Xiongan in the low-carbon coordinated development of JJJ Urban Agglomeration and the impact of different strategies on the role, this paper proposed an integrated method which combined the system dynamics with the fractal analysis. The proposed method integrated progress and the paper following structure as: (1) analyzing JJJ Urban Agglomeration' system and identifying the Key Factors (KFs) that affect the low-carbon development; (2) setting up the framework of full carbon emission calculation cored in KFs; (3) establishing a SD model of social-economic-environmental complex system for each city in JJJ Urban Agglomeration to predict the development tendency cored in KFs; (4) based on the gravity theory, setting up the fractal model of low-carbon economic linkages strength of urban agglomerations cored in KFs; (5) designing different low-carbon scenario strategies according to system development trend prediction and relevant plan and evaluating the efficiency of JJJ collaborative development under different low carbon economy strategies around Xiongan.

http://www.aloki.hu ● ISSN 1589 1623 (Print) ● ISSN 1785 0037 (Online)
DOI: http://dx.doi.org/10.15666/aeer/1705_1183511849

The material of this paper comes from multi-source data of each node in JJJ Urban Agglomeration, including data of social and economic development, data of resource consumption and data of pollution emission.

System analysis and KFs identification

Analysis of heterogeneity of JJJ

Land is the carrier of human activities in production and life, and the carrying capacity of natural resources and environment are closely related to urban land area. Thus in this paper, the heterogeneity of JJJ Urban Agglomeration is explored based on the analysis of the density of GDP, the density of population, the intensity of biological resources consumption, the energy consumption intensity, and the intensity of pollutant emission. The degrees of various indicators above are shown in *Figure 1*.

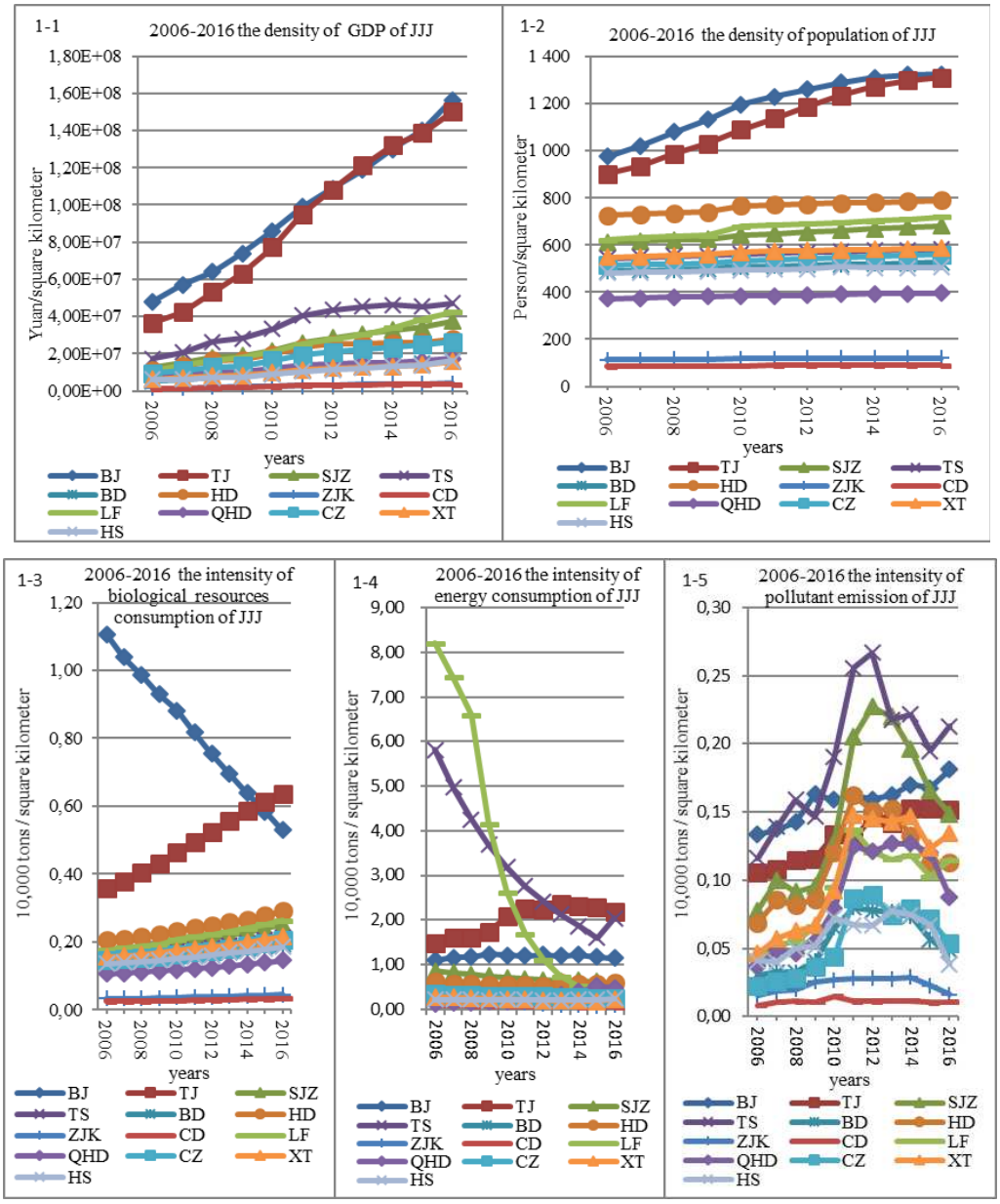

Figure 1. *The level or intensity of social economy and resource environment of JJJ*

http://www.aloki.hu ● ISSN 1589 1623 (Print) ● ISSN 1785 0037 (Online)
DOI: http://dx.doi.org/10.15666/aeer/1705_1183511849

It can be seen from *Figure 1-1* that Beijing and Tianjin are in a high gradient from the perspective of GDP density, while the other node cities of JJJ Urban Agglomeration are in low gradient, and there is a significant gradient difference in Beijing and Tianjin.

It can be seen from *Figure 1-2* that Beijing and Tianjin are still in a high gradient in terms of population density, while Langfang, Shijiazhuang, Xingtai, Baoding, Tangshan, Zhangzhou, Hengshui and Qinhuangdao are in the middle gradient group, and meanwhile Zhangjiakou and Chengde are at a low level. The gradient difference between the above high, medium and low gradients is also very obvious.

It can be seen from *Figure 1-3* that Beijing and Tianjin are high gradient from the perspective of biological resources consumption intensity (corresponding to the biomass resources output per unit area), while Shijiazhuang, Tangshan, Baoding, Handan, Langfang, Qinhuangdao, Cangzhou, Xingtai and Hengshui are in the middle gradient group, and meanwhile Zhangjiakou and Chengde are at a low level. Among them, there is a huge gradient difference between high gradient and middle gradient.

It can be seen from *Figure 1-4* that Langfang gradually decreases from a high gradient to a low gradient in terms of energy consumption intensity, while Tangshan gradually reduced from the second highest gradient to the same level in Beijing. From the distribution of gradient after 2012, Tianjin is always in the high gradient, followed by Tangshan and Beijing. The above three cities together constitute a high gradient of energy consumption, while the rest has much less gradient of energy consumption.

It can be seen from *Figure 1-5* that Tangshan is always at the highest gradient in terms of pollutant emission, while Shijiazhuang has a large fluctuation, ranging from middle gradient to high gradient. And in recent years, Shijiazhuang has a drop trend. Beijing and Tianjin are relatively stable. At the same time, Cangzhou, Hengshui and Baoding are in the middle-low gradient, while Chengde and Zhangjiakou are in low gradient.

As can be seen from the above analysis, the conclusions can be drawn that the heterogeneity of social economic, resource and environmental of the cities and towns of the JJJ Urban Agglomeration are extremely clear. Therefore, system development predictions and kinetic models for such urban agglomerations need to be built under the same input and output dynamics framework.

Identifying the KFs of JJJ based on urban metabolism

The main input of the urban system is all kinds of resources that can be provided by nature (including water environmental capacity, atmospheric environmental capacity, carbon storage capacity generated by forest resources, and various types of energy, etc.), and some of these resources are consumed through human economic activities. It is converted into products and waste, and the other part is consumed or converted into waste through human production activities. With the increase of waste discharge, the demand for environmental capacity increases accordingly. In order to control waste emissions within naturally available environmental capacity, it is necessary to treat waste generated during human production and life to reduce its emissions. Meanwhile, the process also consumes resources and energy, resulting in a carbon footprint. Therefore, waste emissions should be included in the potential carbon environmental capacity account. In addition, the biomass resources consumed in human life are rising, and the land available for growing high carbonaceous plants is declining. Therefore, biomass resource consumption should be included in the potential carbon environmental capacity occupancy account. The products formed during the production process

http://www.aloki.hu ● ISSN 1589 1623 (Print) ● ISSN 1785 0037 (Online)
DOI: http://dx.doi.org/10.15666/aeer/1705_1183511849

(measured in terms of GDP) enter the next circulation area, or as an input enter the next activity, which is either consumed in the activity or a new product is formed. Then, they go to the next activity or become a waste into the environment. The analysis of the metabolic process of the above cities shows that human consumption of biomass resources and waste emissions (including CO_2 and other emissions in the process of energy consumption, wastewater emissions and solid waste emissions) are integrated into the carbon emission accounting system, which can fully reflect the impact of urban production and living processes on the environment.

Therefore, the KFs affecting the low-carbon economy can be identified as follows: population, GDP, waste, energy and biomass resources. Of course, the population as one of the KFs is a subsystem, which is determined by the density of urban employment, the proportion of the population receiving higher education, the natural growth rate and the urbanization rate. GDP, one of the KFs, can also constitute a subsystem, which is composed of per capita GDP, economic density and per capita investment in fixed assets. Waste gas, wastewater and solid waste can form a waste discharge subsystem, which produces the amount of behavior, the amount of treatment (or treatment rate), and the impact of social and economic activities related to it. Energy consumption will also lead to the corresponding carbon emissions. As this part of the emissions is relatively large and has been the concern for a long time, it also becomes a subsystem. The consumption of biomass resources corresponds to the land occupation. The more biomass resources consumed by human life, the more land occupied for the production of these biomass resources, and the less land used for carbon sequestration (planting high carbon sequestration plants). Therefore, the consumption of biomass resources is also a KF. Accordingly, urban greening plays a role of beautifying life and absorbing carbon, so it is also one of the KFs.

Construction the calculation framework of "full carbon emission"

The "full carbon emission" account is set up cored in KFs based on the energy analysis theory and the energy conversion law (Zhang et al., 2015). The account consists of two sub-accounts, which are direct carbon emissions caused by energy consumption and potential carbon consumption caused by waste carbon emissions as well as biomass resources. Different types of substances are normalized by converting into CO_2 emissions to characterize the impact of the emissions on the green low-carbon development of urban agglomerations. Considering the contribution of different sub-items to direct and potential emissions account as well as the availability of data, the two sub-accounts are divided into several sub-sub accounts as shown in *Figure 2*.

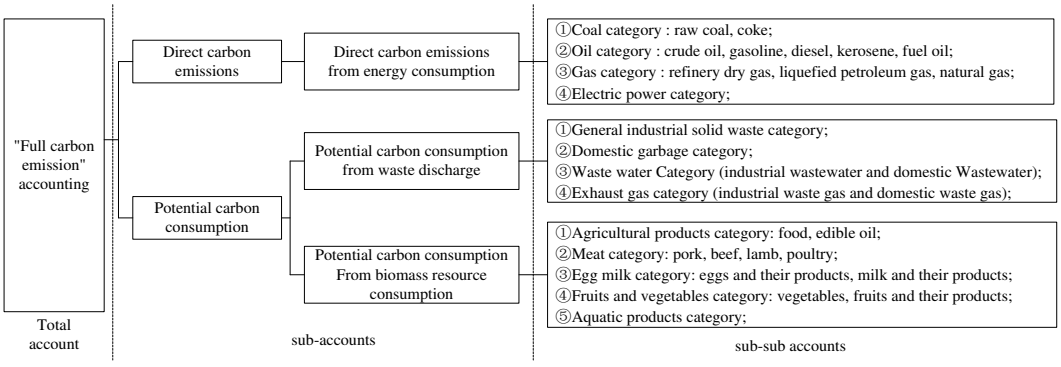

Figure 2. *The framework of the full carbon accounting account*

http://www.aloki.hu ● ISSN 1589 1623 (Print) ● ISSN 1785 0037 (Online)
DOI: http://dx.doi.org/10.15666/aeer/1705_1183511849

According to *Figure 2,* the "full carbon emission" accounting is performed. Among them, the traditional energy consumption carbon emission conversion coefficient method (Wang et al., 2018) is applied in the calculation of the direct CO_2 emission caused by energy consumption, while the potential CO_2 emissions caused by waste discharge and biomass resource consumption are converted by emergy value conversion and its corresponding with CO_2 emissions. The specific formula is as follows:

$$T_{CO_2} = T_{CO_{2e}} + T_{CO_{2w}} + T_{CO_{2b}} = \sum_{k=1}^{11} CO_{2ek} + \sum_{n=1}^{4} CO_{2wn} + \sum_{m=1}^{11} CO_{2bm}$$
$$= \sum_{k=1}^{11} (V_k \cdot \lambda_k) + \sum_{n=1}^{4} \frac{P_n \cdot \alpha_n \cdot \beta_n}{\gamma} \cdot \frac{0.8856}{3600000} + \sum_{m=1}^{11} \frac{U_m \cdot \alpha_m \cdot \beta_m}{\gamma} \cdot \frac{0.8856}{3600000} \quad \text{(Eq.1)}$$

where: T_{CO_2} is the full CO_2 emission of a certain city (full carbon emission); $T_{CO_{2e}}$ is direct carbon emissions caused by energy consumption; $T_{CO_{2w}}$ is potential carbon consumption caused by waste discharge; $T_{CO_{2b}}$ is potential carbon consumption caused by biomass resource consumption; *k* is different categories of energy consumption for direct carbon emissions (such as raw coal, coke, crude oil, gasoline, diesel, kerosene, fuel oil, refinery dry gas, liquefied petroleum gas, natural gas and electricity); CO_{2ek} is the direct CO_2 emissions consumed in category *k*; *n* is different categories of waste emissions (such as industrial solid waste, domestic garbage, industrial wastewater, domestic wastewater, industrial waste gas and domestic waste gas) which will causing potential CO_2 emissions; CO_{2wn} is potential CO_2 emissions from category *n* waste; *b* is biomass resource consumption which will causes potential CO_2 emissions; CO_{2bm} is the potential CO_2 emissions caused by the *m* type biomass resources consumption; V_k is the raw data of the *k* type energy consumption; λ_k is the CO_2 emission factor of the *k* energy consumption; P_n is the raw data of the *n* type waste discharge; α_n is the *n* type emergy conversion factor of waste; β_n is emergy conversion rate of the *n* type of waste; U_m is the raw data of the *m* type biomass resource; α_m is the emergy conversion coefficient of the *m* type biomass resource, and β_m is the emergy conversion rate of the *m* type biomass resources; γ is the emergy conversion rate of electric energy (1.05×105 sej/J), 1 kWh = 3600000 J, and the power supply per kilowatt hour is 0.8856 kg CO_2 (Odum et al., 1955).

Construction of SD model

The SD model of JJJ Urban Agglomeration economic environmental complex system account is set up cored in KFs. The relationships of the factors in the target system are shown in *Figure 3*.

Variables representing flows of information and initials, arising as results of system activities and producing the related consequences are named as level variables which described as ▭ in the flow diagram, while the rate variables are described as ⧖. Auxiliary variable means the detailed steps by which information associated with current levels are transformed into rates to bring about future changes. In addition, the symbol ☁ represents the sinks or sources.

In *Figure 3,* there are four main level variables: total population of the city, annual GDP output, total energy consumption, total water use (because JJJ Urban Agglomeration is located in water scarce areas, so the indicator is selected). In addition, there is an important system output variable-total carbon emission. All the four main

http://www.aloki.hu ● ISSN 1589 1623 (Print) ● ISSN 1785 0037 (Online)
DOI: http://dx.doi.org/10.15666/aeer/1705_1183511849

level variables and the one important output variable is described as ▭. The other variables follow the expression principle of system dynamics flow chart.

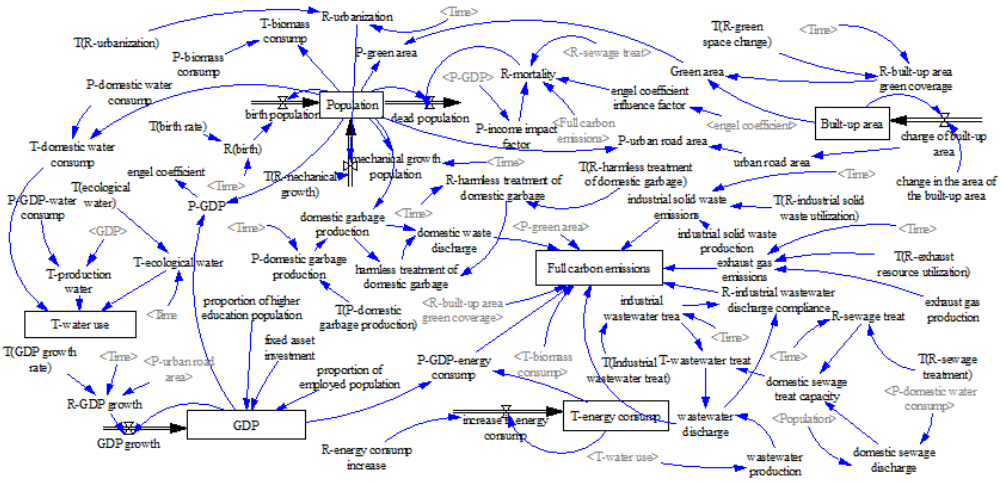

Figure 3. *the flow chart of JJJ Urban Agglomeration*

The SD model takes certain steps along the time axis in the simulation process. At the end of each step, the system variables denoting the state of the system are updated to represent the consequences resulting from the previous simulation step (Zhang et al., 2008). Initial conditions are needed in the first time step. According *Figure 3* and the above principle, we can compile the system dynamics equations of each node city of JJJ Urban Agglomeration one by one based on collecting, collating and analyzing the historical data of the system.

After SD model construction, it is necessary to identify whether the model can be in line with the real situations by the validity test and sensitivity analysis. Accordingly, parameters and relevance can be modified and confirmed until the SD model has good robustness and can reflect the real system in different scenarios.

Construction low-carbon economic linkages strength model

Based on the gravitational model, this paper combines the traditional economic linkages strength model with the "full carbon emission" model to construct the low-carbon economic linkages strength model as follows:

$$R_{ij} = \frac{\sqrt[3]{\frac{P_i}{T_{CO_{2i}}} \cdot \frac{G_i}{T_{CO_{2i}}} \cdot \frac{S_i}{T_{CO_{2i}}}}}{D_{ij}} \cdot \frac{\sqrt[3]{\frac{P_j}{T_{CO_{2j}}} \cdot \frac{G_j}{T_{CO_{2j}}} \cdot \frac{S_j}{T_{CO_{2j}}}}}{D_{ij}} \cdot M_1 \cdot M_2 \cdot M_3 \quad \text{(Eq.2)}$$

where: i and j are the central city and the irradiated city and R_{ij} is the low-carbon economic linkages strength of the central city i accepted by the radiated city j; P_i and P_j are the population size of the i and j cities respectively; G_i and G_j are the regional gross domestic product (GDP) of cities i and j respectively; S_i and S_j are the road areas of cities i and j respectively; $T_{CO_{2i}}$ and $T_{CO_{2j}}$ are cities of i and j annual CO_2 emissions respectively; D_{ij} is the distance between cities i and j; M_1 is the human resources adjustment coefficient,

http://www.aloki.hu ● ISSN 1589 1623 (Print) ● ISSN 1785 0037 (Online)
DOI: http://dx.doi.org/10.15666/aeer/1705_1183511849

which is affected by factors such as the proportion of urban employment density, the proportion of people receiving higher education (the proportion of the number of undergraduates who are over 6 years old in the permanent population of the city), the influence of natural growth rate and urbanization level; M_2 is the economic resource adjustment coefficient, which is affected by factors such as per capita GDP, economic density and per capita fixed assets investment; M_3 is the natural resource adjustment coefficient, which is affected by factors such as the population per square kilometer, per capita domestic water consumption and urban per capita green area.

According to the principle of pressure superposition, the strength of economic connection from a single source centered on a single city is calculated, and the source superposition formula is used to superpose the low-carbon economic linkages strength of two-source (two central cities) or three-source (three central cities). The formula is as follows:

$$R_j = 10 \cdot \lg(10^{\wedge 0.1 R_{i_1 j}} + 10^{\wedge 0.1 R_{i_2 j}} + 10^{\wedge 0.1 R_{i_3 j}}) \quad \text{(Eq.3)}$$

where: R_j is the low-carbon economic linkages strength of the radiated city j after accepting the superposition of two or three sources of radiation; $R_{i_1 j}$, $R_{i_2 j}$ and $R_{i_3 j}$ are different central cities i_1, i_2 and i_3 radiate the low-carbon economic linkages strength radiation of the same radiated city j ($R_{i_3 j}$ is not included when the two sources are superimposed).

After calculation of the low-carbon economic linkages strength, the distribution of social economic resources and environment in urban agglomerations can be judged by fractal dimension. The fractal dimension can be calculated as:

$$K \propto R_{(\mathrm{K})}^{-D} \quad \text{(Eq.4)}$$

where: K is the number of cities in the region; R is the intensity of low-carbon economic linkages strength between cities; D is the fractal dimension. Take the logarithm of the two sides of *Equation 3,* we can get:

$$\ln R_{(k)} = A - \frac{1}{D} \ln k \quad \text{(Eq.5)}$$

where: k is the number of cities (counties) low-carbon economic connection gravity ranking sequences, and A is an equal constant.

The basic criteria for judging rationality are as follows:

When $D = 1$, the urban agglomeration is a constrained order-scale distribution, which means that the radiation received by cities in urban agglomerations from central cities is an absolute average, not a gradient circle. It is impossible to form a high-to-low order transmission and radiation of the internal energy of the urban agglomeration (low-carbon economic linkages strength) and the radiation efficiency is not optimal.

When $D > 1$, the central city in the urban agglomeration has lost the advantage of high gradient, which is not conducive to its overall development of the urban agglomeration.

When $D < 1$, there is a difference in the distribution of economic linkages strength. From the above analysis, the best fractal dimension is $D < 1$.

http://www.aloki.hu ● ISSN 1589 1623 (Print) ● ISSN 1785 0037 (Online)
DOI: http://dx.doi.org/10.15666/aeer/1705_1183511849

Li et al. (1992) used the golden section principle and the Fibonacci sequence to derive a judgment that can be used as a reasonable distribution of the network system. That is the golden section 0.618 as the reasonable fractal dimension judgment point. According this judgment, when $D = 0.618$, the urban agglomeration is in the optimal connection gravity of the urban agglomeration.

Results

Data sources

The data of the scenarios analysis are derived from the 2007-2018 China Statistical Yearbook and the statistical yearbooks of relevant cities, the China Energy Statistical Yearbook and the relevant cities' energy statistics yearbooks and the China Environmental Statistics Yearbook. Meanwhile, some of the data are derived from the iFind. The data in this paper covers the economic development status, social development status, environmental quality and resource utilization of cities in the study.

Scenarios design

In this paper, five scenarios are carried out to analyze the strength and dimension of urban low-carbon economic linkages for analyzing the efficiency of JJJ collaborative development under different low carbon economy strategies around Xiongan. And the scenarios designed of this paper is based on the following basic hypothesis: (1) The development of JJJ Urban Agglomeration follows the relevant national and local planning, which does not cover areas and relevant indicators follow the current development trend (based on the prediction of SD model); (2) In the current scenario, Xiongan has the same economic density, population density and carbon emissions intensity as Beijing.

The five scenarios are designed as follows:

Scenario 1: "Beijing-Tianjin" dual source radiation under inertial scenarios. This paper selects the data from 2006 to 2017 as the historical data of the JJJ Urban Agglomeration. Based on the JJJ Urban Agglomeration eco-economic development system dynamics model (Wang et al., 2013), it predicts the carbon emissions and related indicators of cities in the JJJ Urban Agglomeration from 2018 to 2030.

Scenario 2: "Beijing-Tianjin-Xiongan" three-source radiation under inertia scenario. The operational data is the same as scenario 1, except that Xiongan is listed as a radiation source.

Scenario 3: Xiongan achieves carbon peaks ahead of schedule in 2018, and after reaching the peak, carbon emissions are reduced by 0.5% per year on the basis of scenario 1. Meanwhile the development trends and carbon emissions of other cities remain unchanged.

Scenario 4: On the basis of Scenario 3, Beijing and Tianjin are also used as radiation sources, and the development trend remains unchanged. The amount of carbon emissions is reduced by 0.5% per year on the basis of Scenario 1, and other cities remain unchanged.

Scenario 5: Based on Scenario 4, the development trend of other cities remains unchanged, and carbon emissions are reduced by 0.5% per year on the basis of Scenario 1.

http://www.aloki.hu ● ISSN 1589 1623 (Print) ● ISSN 1785 0037 (Online)
DOI: http://dx.doi.org/10.15666/aeer/1705_1183511849

Results analysis

Based on the above five scenarios, this part applied *Equation 1* to calculate the total carbon emissions, *Equation 2* to calculate the low-carbon economic linkages strength of single-center sources, *Equation 3* to superpose the low-carbon economic linkages strength of multi-center sources, and *Equations 4* and *5* to calculate the fractal dimension value. The calculation results are shown in *Figure 4*.

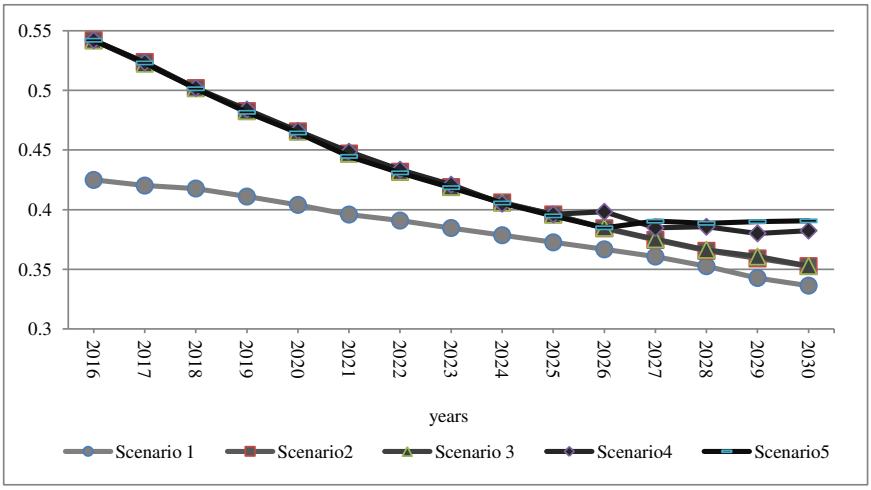

Figure 4. *2016-2030 JJJ Urban Agglomeration low-carbon economic linkages strength fractal dimension*

Building Xiongan as a radiation center of JJJ multi-center urban agglomeration can significantly promote the collaborative development of urban agglomeration

It can be seen from *Figure 4* that from 2016 to 2030, the fractal dimension of the low-carbon economic linkages strength of Scenario 2 is generally higher than the fractal dimension of Scenario 1, which indicates that "Beijing-Tianjin-Xiongan" as the radiation center is better than the "Beijing-Tianjin" dual source as the radiation center.

Synchronized upgrading of multicenter source level can better promote the development of JJJ Urban Agglomeration

From 2016 to 2025, the low-carbon economic linkages strength fractal dimension from Scenario 3 to Scenario 5 is basically equal. By 2026, there will be a divergence except for individual years, the fractal dimension of scenario 4 and scenario 5 increased steadily, while the fractal dimension of scenario 3 decreased steadily. The above comparison results show that improving the low-carbon level of Xiongan alone could not influence on the low-carbon development of JJJ Urban Agglomeration, while the effect is significant when Beijing, Tianjin and Xiongan low-carbon level is improved at the same time.

The delay of radiation from high-gradient to low-gradient will not affect the low-carbon coordinated development of JJJ Urban Agglomeration

There will be a delay in the transmission of low-carbon economic development capacity from high to low gradient. *Figure 4* shows that from 2016 to 2028, the fractal

http://www.aloki.hu ● ISSN 1589 1623 (Print) ● ISSN 1785 0037 (Online)
DOI: http://dx.doi.org/10.15666/aeer/1705_1183511849

dimension values of scenario 4 and scenario 5 were basically same. Until 2029, scenario 4 and scenario 5 developed differently. The fractal dimension of scenario 5 began to be higher than scenario 4. The above comparison shows that the delay of low-carbon development capability radiation will not affect the radiation effect of high gradient cities (central source cities) on low gradient cities, nor does it affect the coordinated development of urban agglomerations.

Discussion and conclusions

Discussion

There two points needed to be discussed:

(1) Based on the systematic analysis of the city, this paper studies the effect of Xiongan on the coordinated development of JJJ Urban Agglomeration under different scenarios from the perspective of low-carbon economy. In this paper, the source superposition method is used to measure the low-carbon economic linkages between cities in urban agglomeration under the dual-source and triple-source scenarios. This method is more realistic in describing the radiation situation of the central city to the surrounding cities in space. It has universality and generalization, and can be applied to different urban agglomerations. The difference from this paper is that you need to adjust the source superposition formula according to the number of radiation sources in urban agglomerations.

(2) In order to analyze the radiation effects of low-carbon economy under different carbon emission conditions, five schemes are established according to different total carbon emissions. Since scenario 1 and scenario 2 have the same total carbon emissions, we only choose scenarios 2, 3, 4 and 5 for analysis. The full carbon emissions of JJJ Urban Agglomeration under scenarios 2, 3, 4 and 5 are shown in *Table 1*.

Table 1. *Full carbon emissions of JJJ Urban Agglomeration under different scenarios*

Years	Scenario 2	Scenario 3	Scenario 4	Scenario 5
2016	17.5603	17.5603	17.5426	17.5426
2017	16.4905	16.4887	16.4562	16.4081
2018	16.4260	16.4241	16.3912	16.3438
2018	16.4795	16.4738	16.4400	16.3931
2020	16.6840	16.6735	16.6389	16.5920
2021	16.8278	16.8260	16.7914	16.7437
2022	17.0700	17.0683	17.0335	16.9847
2023	17.4918	17.4901	17.4548	17.4043
2024	17.9335	17.9319	17.8963	17.8438
2025	18.5864	18.5848	18.5485	18.4935
2026	19.0421	19.0406	19.0051	18.9469
2027	19.6471	19.6456	19.6110	19.5489
2028	20.4149	20.4135	20.3798	20.3129
2029	21.0656	21.0642	21.0317	20.9602
2030	22.1694	22.1681	22.1369	22.0586

http://www.aloki.hu ● ISSN 1589 1623 (Print) ● ISSN 1785 0037 (Online)
DOI: http://dx.doi.org/10.15666/aeer/1705_1183511849

As can be seen from *Table 1*, Scenario 5 has the strongest carbon reduction compared with Scenario 4, but the increase of fractal dimension is not obvious. On the contrary, scenario 4 has less carbon reduction than scenario 5, but its fractal dimension has been greatly improved. The greater the carbon reduction is, the higher the cost to be borne. Therefore, scenario 5 is much higher than scenario 4 in terms of carbon emission reduction costs, but the radiation effect has not been greatly improved. In summary, there is the most obvious carbon reduction effect in Scenario 4. So if the central cities reduce carbon in advance and grasp the key points of urban agglomeration development, they can achieve better results with less investment, which also validates conclusion 3.

Conclusions

The above fractal dimension analysis of of JJJ Urban Agglomeration show:

(1) As one radiation center of JJJ Urban Agglomeration, Xiongan can significantly promote the collaborative development of the area;

(2) For the development of the whole area, the effect of improving the low-carbon level of Xiongan alone is much less than improving the low-carbon level of Beijing, Tianjin and Xiongan at the same time;

(3) The delay which comes from the transmission from high to low gradient will not affect the radiation on the coordinated development of urban agglomerations.

In the process of low-carbon development and construction of JJJ Urban Agglomeration, it is necessary to pay attention to Xiongan's construction as a high-gradient radiation center, and improve the low-carbon level of all radiation centers in the urban agglomeration at the same time. In the near future, the low-carbon coordinated development of JJJ Urban Agglomeration will be realized at the lowest possible cost.

Acknowledgements. The authors acknowledge the National Social Science Fund of China (18BJY079) and Tianjin Philosophy and Social Science Planning Project (TJLJ15-008).

REFERENCES

[1] Albeverio, S., et al. (2008): The Dynamics of Complex Urban Systems. – Physica-Verlag, Heidelberg.

[2] Camagni, R., Capello, R., Nijkamp, P. (1998): Towards sustainable city policy: an economy-environment technology nexus. – Ecological Economics 24(1): 103-118.

[3] Cao, Y., Wei, L., Yu, H. (2012): Optimization study of provincial urban agglomeration logistics alliance system based on the SD model. – Journal of Chongqing Jiaotong University 30(2): 334-339.

[4] Duranton, G., Puga, D. (2003): Micro-foundations of urban agglomeration economies. – Social Science Electronic Publishing 4(4): 2063-2117.

[5] Du, L., Li, X., Zhao, H., et al. (2018): System dynamic modeling of urban carbon emissions based on the regional national economy and social development plan: a case study of Shanghai city. – Journal of Cleaner Production 172: 1501-1513.

[6] Elliot, T., Rugani, B., BabíAlmenar, J., et al. (2018): A proposal to integrate system dynamics and carbon metabolism for urban planning. – Procedia Cirp. 69: 78-82.

[7] Frankhauser, P. (1998): European cities - insights on outskirts. – Report Cost Action 10: 79-105.

http://www.aloki.hu ● ISSN 1589 1623 (Print) ● ISSN 1785 0037 (Online)
DOI: http://dx.doi.org/10.15666/aeer/1705_1183511849

[8] Jia, P., Li, K., Shao, S. (2018): Choice of technological change for China's low-carbon development: evidence from three urban agglomerations. – Journal of Environmental Management 206: 1308-1319.
[9] Jefferson, J., B. (2013): Dark side of the planet: hidden dimensions of urban agglomeration. – Urban Geography 39(10): 1-8.
[10] Kang, Z. Y., Li, K., Qu, J. (2018): The path of technological progress for China's low-carbon development: evidence from three urban agglomerations. – Journal of Cleaner Production 178: 644-654.
[11] Li, X., Wang, L., Ji, D., et al. (2013): Characterization of the size-segregated water-soluble inorganic ions in the Jing-Jin-Ji urban agglomeration: Spatial/temporal variability, size distribution and sources. – Atmospheric Environment 77(7): 250-259.
[12] Lu, S., Minoru, F., Tomohiro, T., et al. (2018): Improving waste to energy rate by promoting an integrated municipal solid-waste management system. – Resources, Conservation and Recycling 136: 289-296.
[13] Li, H., Ai, N. (1992): Market network with golden section features and fractal properties. – Journal of Economic Geography (4): 1-5.
[14] Odum, H. T., Odum, E. P. (1955): Trophic structure and productivity of a windward coral reef community on Eniwetok Atoll. – Ecological Monographs 25(3): 291-320.
[15] Pan, X., Zhang, Y., Xu, L., et al. (2009): An analysis of farmers' perception of the new cooperative medical system in Liaoning Province, China. – BMC Health Services Research 9(1): 1-8.
[16] Rich, K. M., Rich, M., Dizyee, K. (2016): Participatory systems approaches for urban and peri-urban agriculture planning: the role of system dynamics and spatial group model building. – Agricultural Systems 160: 110-123.
[17] Tan, R. R., Aviso, K. T., Foo, D. C. Y. (2018): Carbon emissions pinch analysis of economic systems. – Journal of Cleaner Production 182: 863-871.
[18] Tannier, C., Thomas, I. (2013): Defining and characterizing urban boundaries: a fractal analysis of theoretical cities and Belgian cities. – Computers, Environment and Urban Systems 41: 234-248.
[19] Tannier, C., Thomas, I., Vuidel, G., et al. (2011): A fractal approach to identifying urban boundaries. – Geographical Analysis 43(2): 211-227.
[20] Timothy, D., Searchinger, S., Wirsenius, T., Beringer, P. D. (2018): Assessing the efficiency of changes in land use for mitigating climate change. – Nature 564(7735): 249-264.
[21] Wu, D., Ning, S. (2018): Dynamic assessment of urban economy-environment-energy system using system dynamics model: a case study in Beijing. – Environmental Research 164(7): 70-84.
[22] White, R. (1994): Urban systems dynamics and cellular automata: fractal structures between order and chaos. – Chaos, Solitons & Fractals 4(4): 563-583.
[23] Wang, S., Su, Y., Zhao, Y. (2018): Regional inequality, spatial spillover effects and influencing factors of China's city-level energy-related carbon emissions. – Journal of Geographical Sciences 73(3): 414-428.
[24] Wang, X. (2013): Research on Regional Ecological Economic Evaluation Based on System Dynamics Method. – Tianjin Polytechnic University, Xiqing.
[25] Yu, Y., Wen, Z. (2010): Evaluating China's urban environmental sustainability with data envelopment analysis. – Ecological Economics 69(9): 1748-1755.
[26] Yu, Y., He, J., Tang, W., et al. (2018): Modeling urban collaborative growth dynamics using a multiscale simulation model for the Wuhan urban agglomeration Area, China. – ISPRS International Journal of Geo-Information 7(5): 176-188.
[27] Zhou, D., Bonafoni, S., Zhang, L., et al. (2018): Remote sensing of the urban heat island effect in a highly populated urban agglomeration area in east China. – Science of the Total Environment 628: 415-429.

http://www.aloki.hu ● ISSN 1589 1623 (Print) ● ISSN 1785 0037 (Online)
DOI: http://dx.doi.org/10.15666/aeer/1705_1183511849

[28] Zhang, X. H., Zhang, H. W., Chen, B., et al. (2008): Water resources planning based on complex system dynamics: a case study of Tianjin city. – Communications in Nonlinear Science and Numerical Simulation 13(10): 2328-2336.
[29] Zhang, X., Li, X., Ye, W., Zhang, B. (2015): Calculation of full carbon emission and evaluation of carbon emission performance. – Acta Scientiarum Naturalium Universitatis Pekinensis 51(4): 639-646.

http://www.aloki.hu ● ISSN 1589 1623 (Print) ● ISSN 1785 0037 (Online)
DOI: http://dx.doi.org/10.15666/aeer/1705_1183511849

PARAMETER UNCERTAINTY ANALYSIS IN ENVIRONMENTAL RISK ASSESSMENT CAUSED BY HAZARDOUS CHEMICAL ACCIDENT

LIU, H. L.[1,2] – LIU, N.[3] – SHEN, F.[1] – MA, J. J.[1*]

[1]*College of Territorial Resources and Tourism, AnHui Normal University, Wuhu 241000, China*

[2]*College of Computer Science and Engineering, AnHui University of Science and Technology, HuaiNan 232001, China*

[3]*School of Foreign Languages, AnHui University of Science and Technology, HuaiNan 232001, China*

**Corresponding author*
e-mail: jinjima@mail.ahnu.edu.cn, liuhl@aust.edu.cn; phone: +86-554-666-8604

(Received 23rd Apr 2019; accepted 4th Jul 2019)

Abstract. Environmental risk assessment is an important part of environmental management research. However, due to uncertainties in the environmental risk system, assessment results may be partially incomplete. This study takes the leakage accident of liquid ammonia as a typical case. By combining the method of Morris parameter sensitivity analysis with the Latin Hypercube Sampling, the probability sampling analysis is conducted on a group of parameters that have the greatest impact on the output of the accident consequence calculation model, as well as a set of radius values for lethal range caused by toxic gas and its probability distribution function are obtained. based on the probability distribution, the author took advantage of the GIS tool to conduct a comprehensive analysis, thereby calculating the indexes that characterize the status of regional environmental risk. The research ideas proposed in this paper have effectively improved the rationality of the selection of the parameters in the uncertainty analysis. Furthermore, the assessment results based on the uncertainty analysis can cover all possible accident scenarios, which not only comprehensively reflects the risk status of emergency environmental accidents, but also provides more scientific and reliable information for environmental management.
Keywords: *ammonia leakage accident, Latin Hypercube Sampling, Morris sensitivity analysis, individual risk, social risk*

Introduction

Potential hazardous chemical accidents pose serious threat to surrounding area. With the enhancement of public awareness of environmental protection, people realize that it is necessary to establish a scientific methodology system of "environmental risk assessment" for potential accident areas, so that environmental disasters can be effectively prevented (Shao et al., 2013; Hahn et al., 2010). In a broad sense, environmental risk assessment refers to the process of management and decision-making based on the assessment of possible losses to the hazards (including natural disasters) caused or triggered by various social economic activity to human health, social economy, and ecosystem and so on. In a narrow sense, environmental risk assessment usually refers to the probability estimation to the impact degree of toxic and harmful substances (including chemicals and radioactive substances) on human health and ecosystem, and puts forward plans and countermeasures for reducing environmental risk (Lu et al., 1999; Hansen et al., 2016; Chen et al., 2012; Tang et al., 2016).

http://www.aloki.hu ● ISSN 1589 1623 (Print) ● ISSN 1785 0037 (Online)
DOI: http://dx.doi.org/10.15666/aeer/1705_1185111867

In the process of environmental risk assessment, the inaccuracy of data, randomness of risk and subjectivity of researchers will lead to a certain degree of bias in the assessment results, which is the uncertainty in environmental risk assessment (Xing et al., 2006; Xu et al., 2009; García-Díaz et al., 2012). The current studies show that the existence of uncertainty makes it impossible to obtain the best estimation of the consequences in a given environmental accident, or the results obtained from analysis are not necessarily the best results. However, the existence of uncertainty does not mean that the risk assessment cannot be carried out; on the contrary, the analysis of uncertainty is an indispensable part of environmental risk system. The uncertainty reflects the integrity of risk information to some extent. There are complex causes of the uncertainty in environmental risk assessment, only by effective screening and classifying, can the corresponding treatment methods be founded out. According to one of the widely recognized classification standard, the uncertainty in environmental risk assessment can be divided into three categories: parameter uncertainty, model uncertainty and the integrity uncertainty (Abrahamsson, 2002). Among them, parameter uncertainty refers to the randomness of the valuing of the parameter; or if the specific value cannot be determined under the given conditions, then the probability distribution interval can be represented. Parameter uncertainty is the main reason for researchers' cognitive bias towards risk results. How to deal with this uncertainty correctly is becoming a hot topic in this research field, and the analysis method based on probabilistic statistics theory is a common research method at present.

The core idea of probabilistic analysis method is to assume that uncertainties are originated from randomness, and by using the probability distribution of one or more variables in the risk system, the uncertainty and variability of the results can be quantified (Maxwell et al., 1999; Abdo et al., 2017). Xu et al. constructed a conceptual model for the evaluation of pollution site exposure process, proposed to characterize the uncertainty of site pollution parameters with probability distribution function, and used Monte Carlo method to assess the contribution of parameter uncertainty to the uncertainty of exposure concentration, thus the probability distribution function of pollutant concentration at exposure points can be established (Xu et al., 2014). As for soil pollution, Labieniec et al. use probability distribution function to describe the uncertainty when estimating the exposure risk of people on the contaminated land. They assessed the uncertainty of carcinogenic risk in contaminated soil due to the uncertainty of geographical characteristics, material destination and migration process (Labieniec et al., 2007).

Through the interpretation of previous research literature, it can be found that it can directly express the transfer process of "Parameter→Model→Result" by using probabilistic analysis method to deal with the problem of parameter uncertainty (Abrahamsson, 2002; Betrie et al., 2015); but it is noteworthy that the environmental models currently used to realize the quantitative description of pollutant migration is becoming more and more complex, this kind of models often need a lot of input parameters. When using the probability analysis method to carry out the uncertainty analysis, the researchers usually adopt the empirical method and subjective to determine which parameters needed to be involved in probabilistic sampling analysis, and do not consider the contribution of the parameters to the overall uncertainty of the model's output, which would affect the accuracy of the uncertainty analysis results. The flaw of this approach to some extent limit the application and development of uncertainty analysis technology used in environmental risk assessment. So in this paper, we tries to

http://www.aloki.hu ● ISSN 1589 1623 (Print) ● ISSN 1785 0037 (Online)
DOI: http://dx.doi.org/10.15666/aeer/1705_1185111867

introduce sensitivity analysis method to objectively screen out the parameters that have high contribution to the uncertainty of the model calculation result, on this basis, the probability sampling method is used to evaluate the influence of parameter uncertainty on the result of risk assessment so as to provide environmental risk management more scientific and reliable technical support.

Methods

In order to design a complete environmental risk assessment scheme based on parameter uncertainty analysis, taking the leakage accident of liquid ammonia as a case, the research work in this paper will be carried out in three steps: (1) parameter sensitivity analysis; (2) uncertainty analysis; (3) risk characterization. As shown in *Figure 1,* firstly, the parameters with statistical characteristic in the accident consequence model are identified, and the parameters' sensitivity analysis are carried out by Morris method so as to screen out a group of parameters that contributed significantly to the uncertainty of the model output; then, these selected parameters are sampled by Latin Hypercube Sampling (LHS) method, the sample data are inputted into the model to simulate, then the probability distribution result of the lethal range values of toxic gas is obtained. Finally, based on the results of uncertainty analysis and the geographic data within the study area, the risk assessment result can be obtained after excuting the spatial analysis in the GIS software.

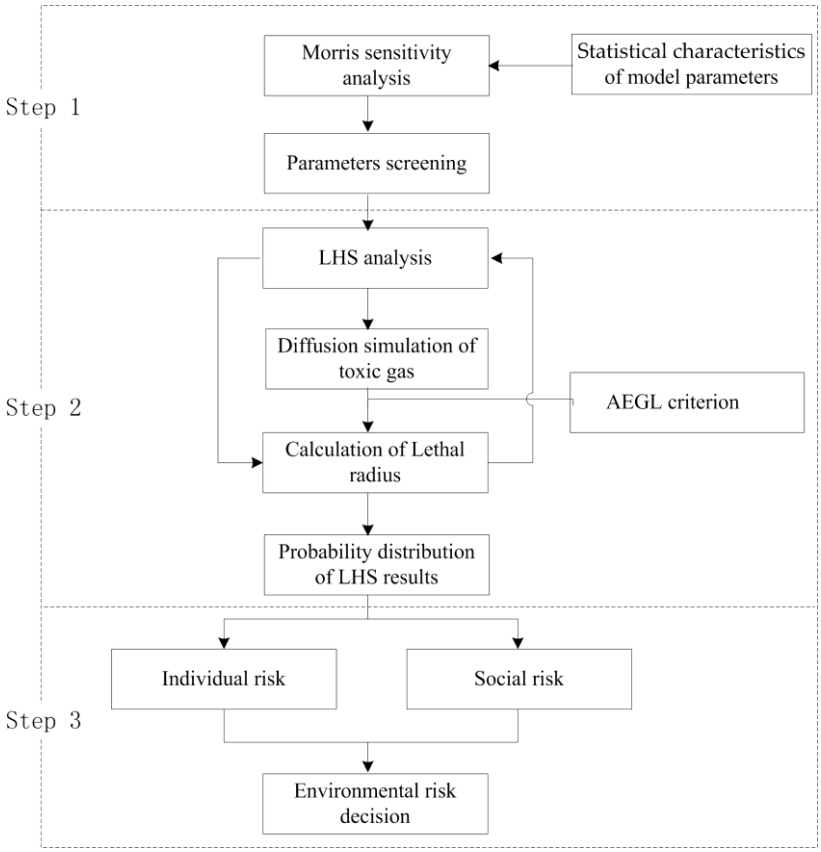

Figure 1. *The research scheme of environment risk assessment based on the uncertainty analysis (step 1: parameter sensitivity analysis; step 2: uncertainty analysis; step 3: risk characterization)*

http://www.aloki.hu ● ISSN 1589 1623 (Print) ● ISSN 1785 0037 (Online)
DOI: http://dx.doi.org/10.15666/aeer/1705_1185111867

Sensitivity analysis of model parameters

Accident consequence model and uncertainty parameters identification

There are many mathematical-physical models that can be used for calculating the harmful effect of hazardous chemical accident, among which, The Process Hazard Analysis Software Tool (PHAST) developed by Det Norske Veritas (DNV) is a very effective software package for quantitative calculation of chemical accident consequence. This software package can simulate the effect degree and spread range of gas leakage, fire and explosion by inputting parameters related at the scene of the accident. The Unified Dispersion Model (UDM) integrated in the PHAST can simulate the diffusion process of gaseous substances. And this model is very complex, which is established on the basis of many classic models including BM model, P-G model (Hanna et al., 2008). PHAST provides the interface with "batch mode", through the Matlab's control program, the repetitive execution of the calculation process can be realized, which provides possibility for subsequent sensitivity analysis and uncertainty analysis (Pandya et al., 2012).

The input parameters of UDM model involve various aspects such as leakage source status, leakage mode, diffusion field parameters and meteorological conditions. By referring to the study of Pandy et al., the parameters with uncertainty in UDM model are identified, the statistical characteristics (probability distribution type and value scope) of these parameters are shown in *Table l,* among which, the parameters' statistical characteristics of leakage source status and leakage mode can be got according to the assumption on the basis of on-site investigation data; the meteorological parameters can be gained based on the statistical analysis to the meteorological data from 2007~2017 of study area, the diffusion field parameter is derived from the expert experience after the users applied PHAST.

Table 1. *Statistical characteristics of parameters in PHAST*

Parameter name	Meaning/unit	Distribution form
T_{st}	Storage temperature/K	Triangular(263.15, 283.15, 273.15)
P_{st}	Storage pressure/Pa	Uniform(0.473e06,0.49e06)
L_h	Liquid height/m	Uniform(12.75, 17.25)
T_a	Atmospheric temperature/K	Normal(251, 10.5)
P_a	Atmospheric pressure/Pa	Uniform(0.99e05, 1.035e05)
H_a	Relative atmospheric humidity/-	Normal (68, 10)
u_a	Wind speed/$m \cdot s^{-1}$	Normal(3.4, 1.3)
D_O	Release orifice diameter/m	Triangular(0.16, 0.18, 0.20)
Z_R	Release height above ground/m	Uniform(1, 20)
Z_0	Surface roughness length/m	Uniform(0.5, 1.5)
S_{flux}	Solar radiation flux/$W \cdot m^{-2}$	Triangular(0, 1000, 500)
α_1	Jet entrainment parameter	Normal(0.17, 0.0085)
α_2	Cross-wind entrainment parameter	Normal(0.35, 0.0175)
C_E	Cross-wind spreading parameter	Normal（1.15, 0.0575）
e_{pas}	Near-field passive entrainment parameter	Normal(1, 0.05)
C_{Da}	Drag coefficient of plume in air	Exponential(69.2)
γ	Dense cloud side entrainment parameter	Exponential(34.6)
Ent_{poo}	Pool vaporisation entrainment parameter	Normal(1.5, 0.075)
r_u^{pas}	Max cloud/ambient velocity parameter	Normal(0.1, 0.005)

http://www.aloki.hu ● ISSN 1589 1623 (Print) ● ISSN 1785 0037 (Online)
DOI: http://dx.doi.org/10.15666/aeer/1705_1185111867

Morris sensitivity analysis method

Sensitivity analysis is used to assess the effect caused by model input parameter on the output result (Xu et al., 2004; King et al., 2013). The qualitative global sensitivity analysis is also called factor screening sensitivity analysis, whose purpose is to gain the rank of each input parameter sensitivity degree in the model through lower computational cost, so that some inessential parameters can be ruled out and the subsequent uncertainty analysis calculation load can be reduced. Morris method was proposed in 1991 by Max D. Morris, which can effectively identify and sort the importance of model parameters. The main idea is to assume that the "Elementary Effect"(EE), which measures the sensitivity of the parameter, is subject to a certain distribution form, and then the global parameter sensitivity can be determined by measuring the mean value and standard deviation value of the distribution (Morris, 1991).

The model contains k parameters and assumes that the variation range of these parameters is [0,1]. Morris sampling method is used to randomly generate a set of initial parameter vectors $X = (x_1, x_2, \ldots, x_k)$, where the value of x_i is randomly selected from $\{0, 1/p\text{-}1, 2/p\text{-}1, \ldots 1\text{-}\Delta\}$, p is the number of sampling points, Δ is the pre-set variable quantity, then the value of Δ is $\Delta = 1/p\text{-}1$, then the ith parameter's calculation equation of EE are as follows:

$$EE_{1i} = \frac{Y(x_1, \cdots, x_i + \Delta, \cdots, x_k) - Y(X)}{\Delta} \quad \text{(Eq.1)}$$

where Y(X) is the model output corresponding to the initial parameter vector, $Y(x_1, \ldots, x_{i-1}, x_i + \Delta, \ldots, x_k)$ is the model output corresponding to the variable quantity Δ formed by the ith parameter of the initial parameter vector. For the remaining k-1 parameters, repeat the above operation, and calculate the elementary effects of the remaining k-1 parameters respectively and randomly generate n initial vectors. Repeat the above process, then the n EE of k parameters can be represented as EE_{ij}, where j = 1, 2,…, n, i = 1, 2,…, k. The mean value and standard deviation of the EE of each parameter can be expressed as:

$$\mu_i = \sum_{j=1}^{n} EE_{ij} / n \quad \text{(Eq.2)}$$

$$\sigma_i = \sqrt{\sum_{j=1}^{n} (EE_{ij} - \mu_i)^2 / n} \quad \text{(Eq.3)}$$

The screening of parameters

The mean value and standard deviation of each parameter can be calculated by Morris method, if the parameter xi corresponds greater mean value μ, then this means it would cause larger influence on the model output value; the larger the value of variance element is, then the larger the interaction is between this parameter and other parameters when affecting the output of the model, or namely, the influence of this parameter to the output of the model is non-linear. Taking these two indexs into

http://www.aloki.hu ● ISSN 1589 1623 (Print) ● ISSN 1785 0037 (Online)
DOI: http://dx.doi.org/10.15666/aeer/1705_1185111867

consideration, m parameters involved in the subsequent sampling analysis of uncertainty can be screened out.

Uncertainty analysis

In order to realize the quantitative recognition of the uncertainty of parameters, that is, to describe the risk system by exact numerical value extracted from the conceptual uncertain risk system, the currently most widely used Monte Carlo method can be adopted (Milazzo et al., 2015), which is a kind of calculation method by random sampling statistics to estimate the probability distribution function. Due to Monte Carlo sampling may "collapse" in some sample points and lead to low sampling efficiency, so if the ideal sampling effect wants to be achieved, it requires a large number of sampling test, because of the complexity of the calculation model integrated in PHAST, this process can often take long time with huge calculation resources.

Latin hypercube sampling

On the basis of Monte Carlo method, Latin Hypercube Sampling (LHS) introduces the idea of multi-dimensional stratified sampling (Hoshino et al., 2000; Wu et al., 2015), that is, n samples are extracted from m-dimensional vector space. The steps are as follows: each dimension is divided into n intervals that do not overlap each other so that each interval has the same probability; a sample point is randomly selected from each interval in each dimension; then randomly select points from the previous step from each dimension and form them into vectors. As a more efficient sampling method, LHS has greater advantages in both sampling efficiency and running time (due to less number of iterations). Therefore, in this study, LHS is selected as the tool for uncertainty analysis of model parameters. The detailed implementation process in this study is as follows:

l) According to the results of sensitivity analysis (parameters screening), confirm m uncertain input parameters needed considering and their probability distributions.

2) According to the required sample size n, divide the value range of each input parameter X_i (i = 1, 2, … , m) into n sub-ranges.

3) Randomly select one value in each sub-range from each parameter, in this way, n samples of this input parameter can be obtained. N samples of m input parameters are randomly combined to form an n × m matrix, where j (j = 1, 2..., n) row represents the input parameters value required for the jth simulation. By substituting the input parameter value matrix into the model, n output results can be obtained.

Conversion to lethal radius

The PHAST simulation result represents the concentration distribution of diffused toxic gas, while the environmental risk assessment focuses on the impact of toxic substances leakage on human health; Therefore, the concentration result needs to be transformed into the human health effect with the help of the "Toxic dose--Response" reference criteria to get the data needed for environmental risk assessment. In this study, the risk result is shown as the magnitude of risk receptor deaths toll caused by the exposure to the risk area. The minimum lethal dose in the toxicity criteria is selected as the threshold to demarcate the radius of lethal area (hereinafter referred to as "lethal radius"), and the toxic gas diffused range is divided into the lethal area and the non-lethal area. The lethal radius is determined by the short-term exposure guidelines-Acute

http://www.aloki.hu ● ISSN 1589 1623 (Print) ● ISSN 1785 0037 (Online)
DOI: http://dx.doi.org/10.15666/aeer/1705_1185111867

Exposure Guideline Levels (AEGL) developed by National Advisory Committee (NAC) of U.S.

Statistical analysis of LHS result

After n times of repeated simulation, and the conversion of the simulation results through AEGL criterion, n lethal radius values can be obtained. By statistical analysis to the simulation results, the Probability Distribution Function (PDF) and Complementary Cumulative Distribution Function (CCDF) can be obtained, which are important bases of risk characterization.

Risk characterization

Risk characterization is a process to obtain the final quantitative risk assessment results through spatial analysis in geographic information system, it takes the analysis result of LHS analysis as the base and comprehensively takes into account the factors not involved in LHS analysis, including wind direction probability, accident occurrence probability and population distribution, etc. At present, the regional environmental risk assessment is mainly based on the geographical information system to realize the refined segmentation of the study areas so as to endow the environmental risk with geospatial attributes (Wu et al., 2006; Di Domenico et al., 2014). For the convenience of calculation, the target study area is gridded in the geographic information system platform, and the grid layer of environmental risk source, environmental risk receptor and LHS analysis results included in the risk system is established. According to all types of risk factors, every grid is given an value assignment, so the individual risk and social risk can be calculated respectively with the grid as the calculation unit.

Individual risk

It refers to the probability of death (or a specific level of injury) to an unprotected risk receptor in a specific location of the risk area for a relatively longer time. Individual risk is usually expressed as the risk contour line, and its calculation method is to calculate the individual risk in each grid center generated by each risk source in the study area. Overlay analysis would be done in the individual risk of each risk source, then the total individual risk value in a single grid can be obtained. The calculation process is shown in *Equation 4*.

$$IR_{(x,y)} = \sum_{i=1}^{M} f_i \times p_i^W \times p_i^L \times v_i \quad \text{(Eq.4)}$$

where (x, y) represents the coordinate of each grid center, f_i is the probability of an accident occurring in the risk source i, p_i^W is the probability of wind direction that would locate at (x, y), p_i^L is the LHS analysis result of the ith risk source that would locate at (x, y), v_i is the individual death probability caused by accident happening at (x, y), M is the number of risk sources in this area.

Social risk

Social risk is on the basis of individual risk to consider the regional population density, and its practical significance is to calculate the probability of a potential

http://www.aloki.hu ● ISSN 1589 1623 (Print) ● ISSN 1785 0037 (Online)
DOI: http://dx.doi.org/10.15666/aeer/1705_1185111867

accident causing more than or equal to a specified number of deaths. The social risk is usually represented by F-N curve, N stands for death toll in the abscissa, the ordinate is the probability F of occurring N or more death toll. The calculation method is shown in *Equation 5,* and the calculation result is expressed in the form of F-N curve (Hou et al., 2016; Trbojevic et al., 2000).

$$F = \sum_{y=1}^{S} \sum_{x=1}^{T} IR_{(x,y)} \qquad N_d \geq N \tag{Eq.5}$$

where S is the row number of grid in the study area, T is the column number of grid, and Nd is the death toll. From the equation, it can be seen that CCDF is need to be used in the calculation process of social risk.

Results and discussion

Study area

Wuhu is an important city and shipping hub in the middle reach of Yangtze River. The warehouse storage of Sinopec is built in Tianmenshan Street, Jinghu district along the Yangtze River. Various hazardous substances such as chemical raw materials and intermediate products make this place become a high potential hazard-formative risk source; and its adjacent area is the urban densely-populated district, so this kind of adverse condition will increase the risk degree of accidental chemical disaster. This study takes the leakage accident of liquid ammonia storage tank in this warehouse as an example to carry out the environmental risk assessment. The spatial layout of the study area is shown in *Figure* 2.

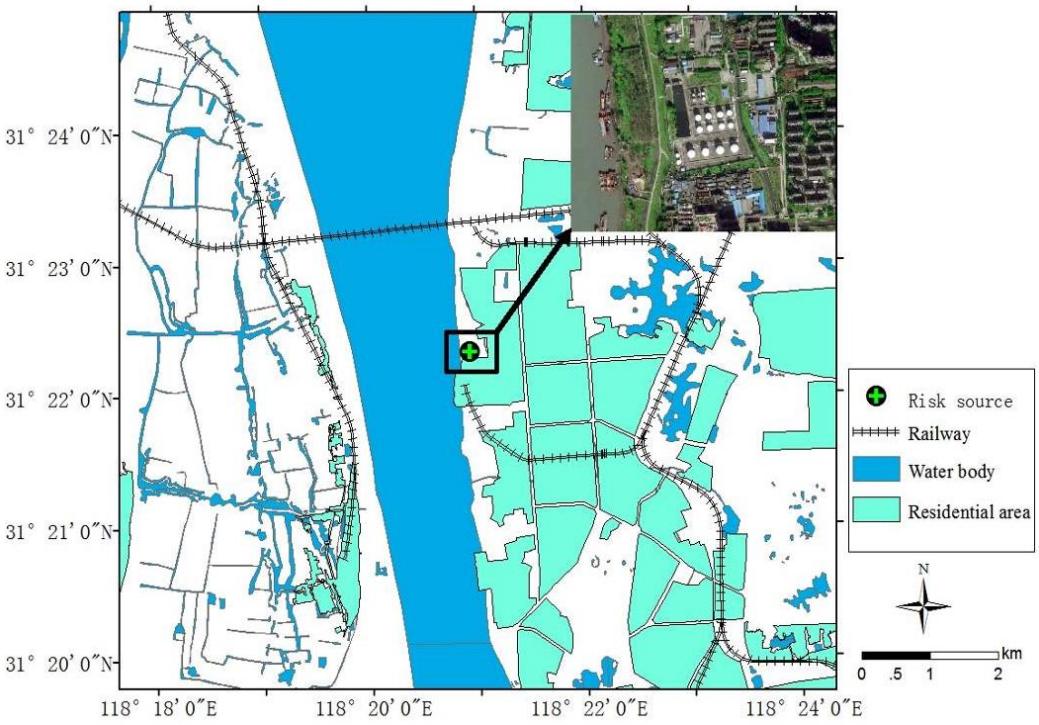

Figure 2. *Spatial layout of study area*

http://www.aloki.hu ● ISSN 1589 1623 (Print) ● ISSN 1785 0037 (Online)
DOI: http://dx.doi.org/10.15666/aeer/1705_1185111867

Parameters sensitivity analysis

Ammonia is widely used in industry. It is usually stored in the liquid phase in pressurized vessel. After its emission, a two-phase flow occurs forming an ammonia cloud composed of vapor and very fine droplets that do not fall to the ground. The droplets evaporate quickly, cooling the air. It results a cold mixture of air and ammonia, denser than the ambient air, even though pure gaseous ammonia is lighter than air at ambient temperature (vapor density of 0.73 at 288.15 K). For NH_3 releases, all the dispersion phases normally occur. Based on the analysis of historical data on leakage accident of liquid ammonia, in research work performed by this paper, the leakage mode is set as "continuous leakage", atmospheric stability class is set as D, with the duration time of 1 h, and the leakage angle is set as horizontal orientation.

According to the principle of Morris method, the sampling of the parameters involved in *Table 1* was carried out in 15 orbits and 8 sampling levels, in this way, 120 groups of samples were generated, which were inputted into the PHAST for calculation, and then the ground level ammonia concentration values at 100 m, 800 m and 3000 m downwind distance under each group of parameter conditions were respectively calculated, based on which the sensitivity index μ and σ for each parameter are calculated. In order to facilitate the comparison of each parameter's influence degree to ouput result, the scatter diagram shown in *Figure 3a, b* and *c* were drawn after taking the normalized values and absolute values of μ and σ.

According to the results shown in the scatter diagram, although the sensitivity index of each parameter varies with the downwind distance, on the whole, the parameters which have the highest sensibility are D_O (release orifice diameter) and Z_R (release height above ground). But for the parameters α_1 and α_2, the μ value is higher in the near-field diffusion. This indicates that the effect of jet velocity on ammonia diffusion is higher than wind speed in near-field, while the effect is gradually weakened in far-field diffusion. It can also be seen from the scatter diagram that the μ value of the parameter is large and the corresponding σ value is large generally, this indicates when a parameter has a greater influence on the output of the model, it tends to interact more with other parameters. Here, the μ values of the parameters corresponding to the three kinds of downwind distances are averaged and ranked. The result is shown in *Figure 3d.* It can be seen that the sensitivity of parameters D_O, Z_R, u_a, α_1, α_2, Z_0, P_a, T_a have order of magnitudes difference with the remaining parameters in *Table 1*. Therefore, they can be considered as parameters that have a greater influence on the output of the model, while other parameters have a very limited influence on the output of the model. Based on this, these 8 parameters are selected to participate in the subsequent uncertainty analysis.

LHS analysis

LHS is performed on the 8 selected parameters. By referring to the research of Kong et al.(Kong et al., 2011), the sampling times of LHS were set to 1000, and the obtained 1000 groups of parameters value are inputtted into PHAST for simulation, 1,000 simulation results and the PDF of the lethal radius of leakage gas are obtained, CCDF of the lethal radius is also obtained. The detailed results are shown in *Figure 4.*

http://www.aloki.hu ● ISSN 1589 1623 (Print) ● ISSN 1785 0037 (Online)
DOI: http://dx.doi.org/10.15666/aeer/1705_1185111867

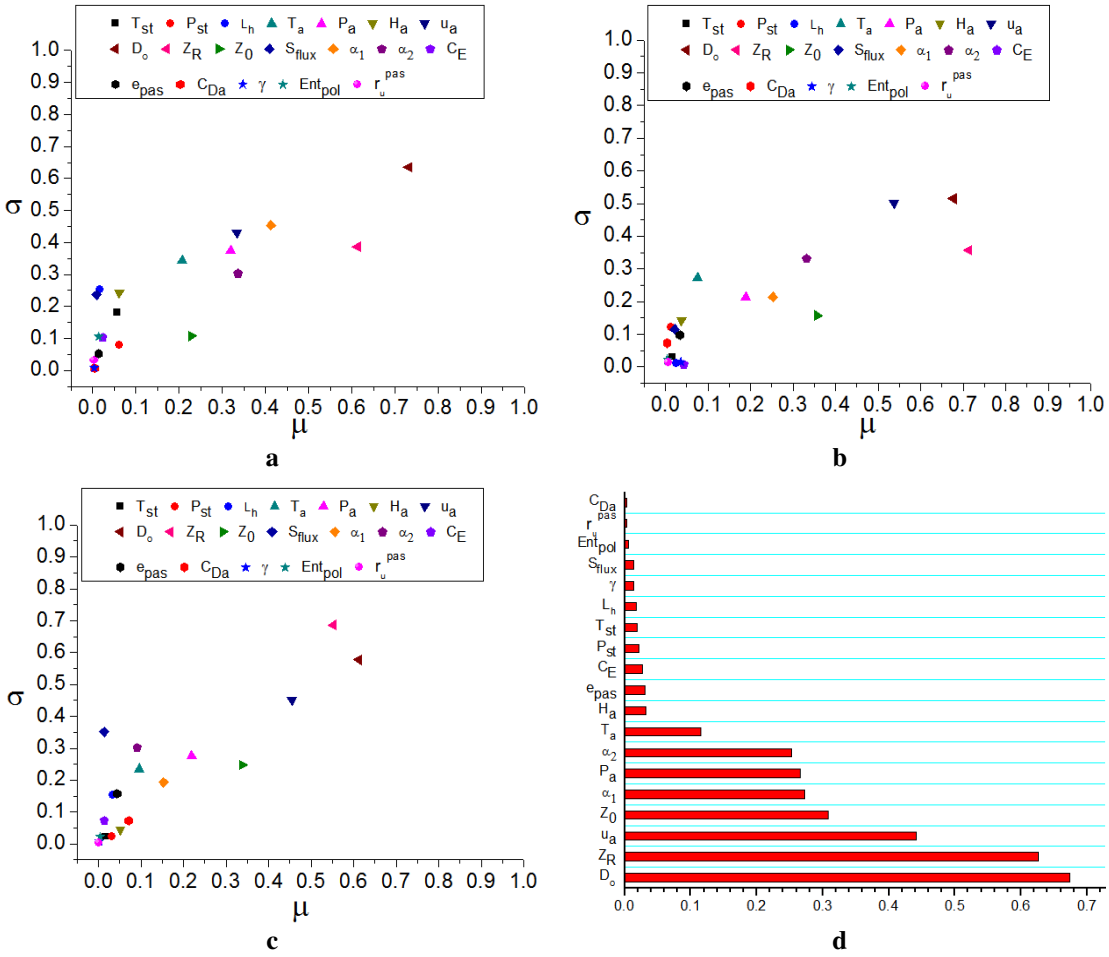

Figure 3. *Result of parameters sensitivity analysis: (a) Sensitivity index μ and σ at 100 m downwind distance; (b) Sensitivity index μ and σ at 800 m downwind distance; (c) Sensitivity index μ and σ at 3000 m downwind distance; (d) Mean value of μ for all parameters corresponding to the three kinds of downwind distances*

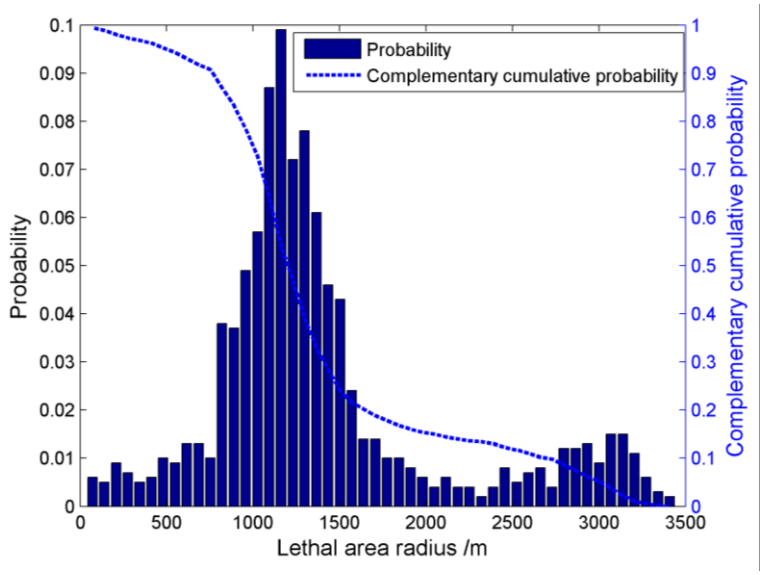

Figure 4. *Result of LHS analysis*

http://www.aloki.hu ● ISSN 1589 1623 (Print) ● ISSN 1785 0037 (Online)
DOI: http://dx.doi.org/10.15666/aeer/1705_1185111867

As the probability distribution results shown in *Figure 4,* the lethal radius of liquid ammonia leakage ranges considerably within 100 m~3500 m under the combined action of 8 independent uncertainty variables in the risk system, among them, the lethal radius around 1300 m owns greater probability than the ends of this distribution range, which can differ an orders of magnitude. From the analysis results of LHS, two conclusions can be drawn: Firstly, the environmental risk nearly about 1.3 km distant from the leakage source is relatively high, and the environmental risk beyond 1.3 km decreases with the increase of distance. Here, the magnitude of environmental risk is only a relative concept based on the LHS results, and the magnitude and acceptability of environmental risk should be evaluated by further introducing other elements in the risk system. Secondly, from the perspective of the lethal concentration distribution, the previously risk assessment research for a single and specific accident scenario is not scientific and reliable enough and would provide incomplete and even wrong information to the researchers.

Risk characterization

In order to balance the contradiction between the resolution requirement and computational efficiency of risk characterization, the grid scale is set as 50 m × 50 m in study case considering the actual situation of the study area. The grid partition is carried out in ArcGIS 10.1 to creat the LHS analysis results layer and wind direction probability layer within the study area. The results are shown in *Figure 5*. The population density of the study area is as shown in the *Figure 6*. As the grid is used as the calculation unit for environmental risk analysis, all layer files are saved as raster format.

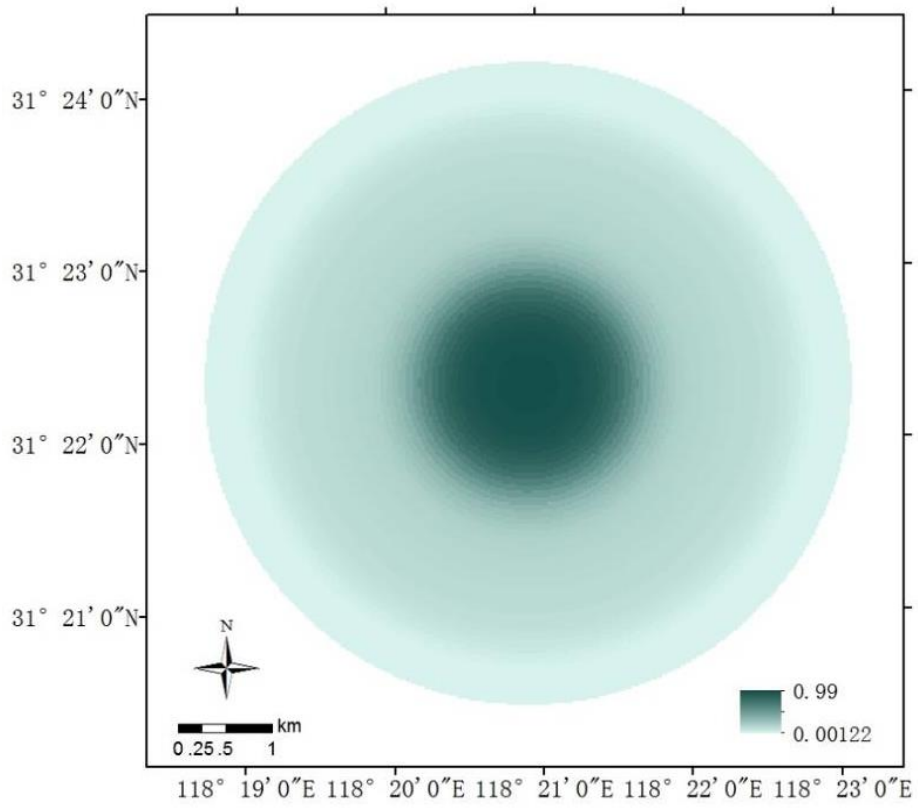

a

http://www.aloki.hu ● ISSN 1589 1623 (Print) ● ISSN 1785 0037 (Online)
DOI: http://dx.doi.org/10.15666/aeer/1705_1185111867

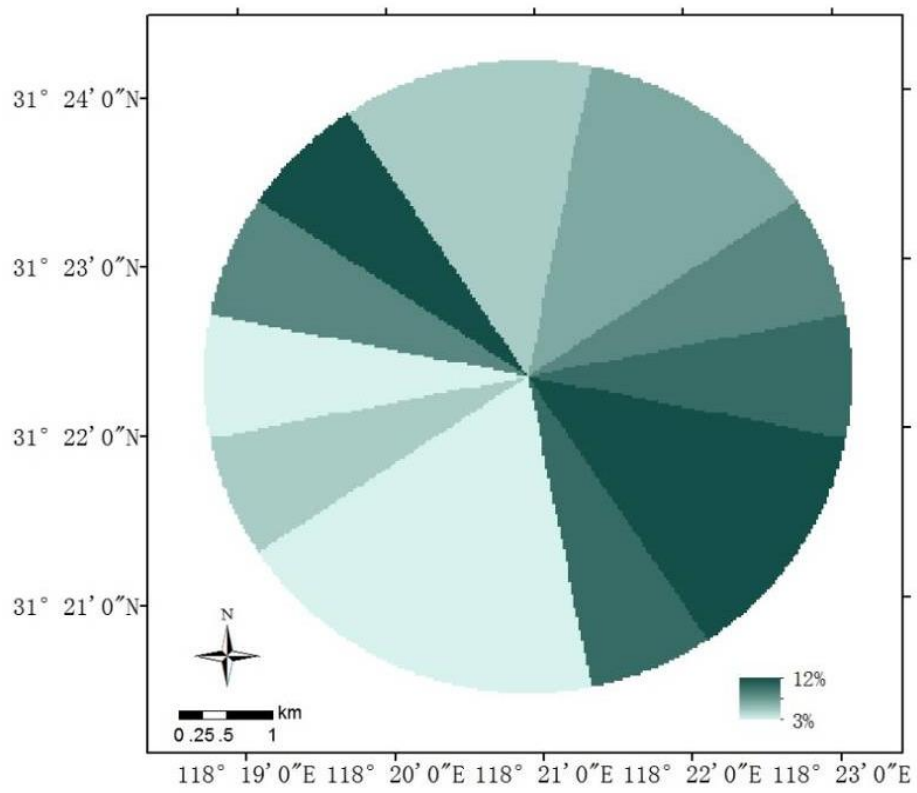

b

Figure 5. *Raster layer used in environmental risk assessment.* ***a.*** *Result of LHS analysis.* ***b*** *Wind direction probability*

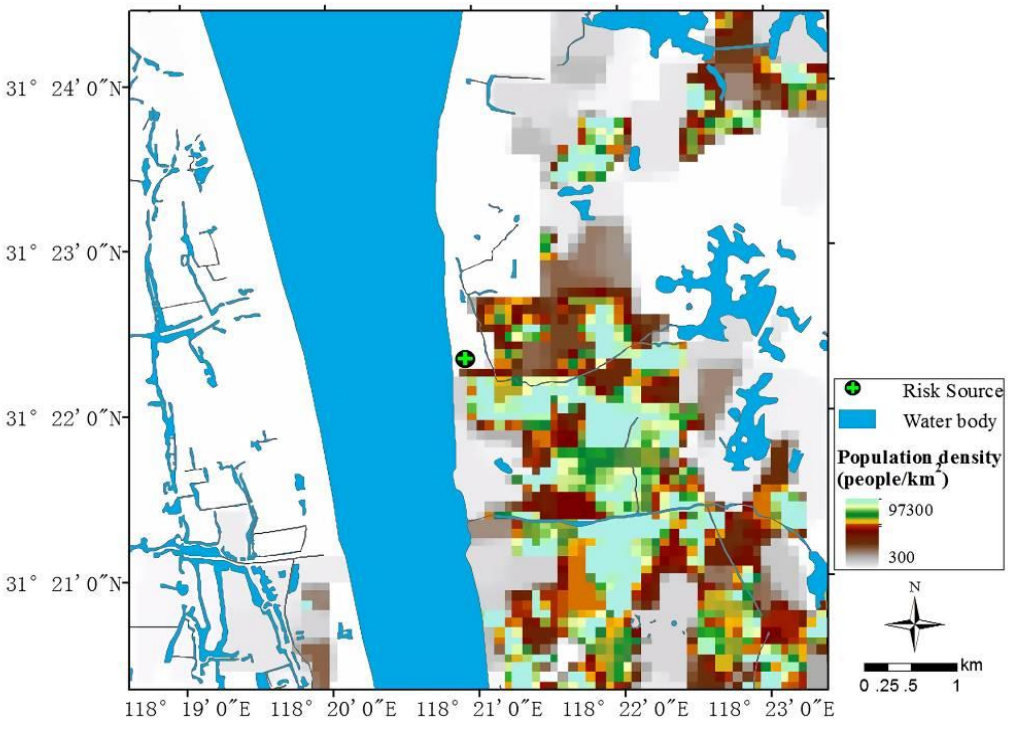

Figure 6. *Raster data of population density in study area*

http://www.aloki.hu ● ISSN 1589 1623 (Print) ● ISSN 1785 0037 (Online)
DOI: http://dx.doi.org/10.15666/aeer/1705_1185111867

Individual risk

According to the statistical analysis of the liquid-ammonia leakage accident involving more than one fatality in China over the past 20 years, the occurrence probability f in *Equation 4* is about 1.61×10^{-3}. The CCDF of the lethal radius obtained from the probability sampling analysis is used as the data source of the LHS result layer in ArcGIS. The wind direction probability is obtained through the statistical analysis of historical meteorological data from 2007~2017 in the study area. Since the toxicity criteria used is lethal concentration, so *v* is set to 1. On the basis of the discrete results in each grid, the contour lines of individual risk at different levels in the study region can be depicted through grid calculation and extraction analysis in ArcGIS.

After obtaining the assessment results of individual risk, appropriate measure standard should be selected to evaluate the acceptability of risk, which would be used as the basis of environmental risk decision (Meng et al., 2014; Liu et al., 2012). For individual risk, what are now widely recognized standard is As Low As Reasonable Practicable (ALARP) guidelines, set by Health and Safety Executive (HSE) of UK, which also have two kinds of thresholds for individual risk: acceptable risk and negligible risk. This study refers to the HSE standards, also considering the actual construction situation of Chinese hazardous chemical facilities and the socioeconomic performance of assessment object, the threshold of negligible risk level is determined as 10^{-6}/year, the threshold of acceptable risk level is 10^{-4}/year. *Figure 7* shows the individual risk contour lines of these two kinds of thresholds in case study.

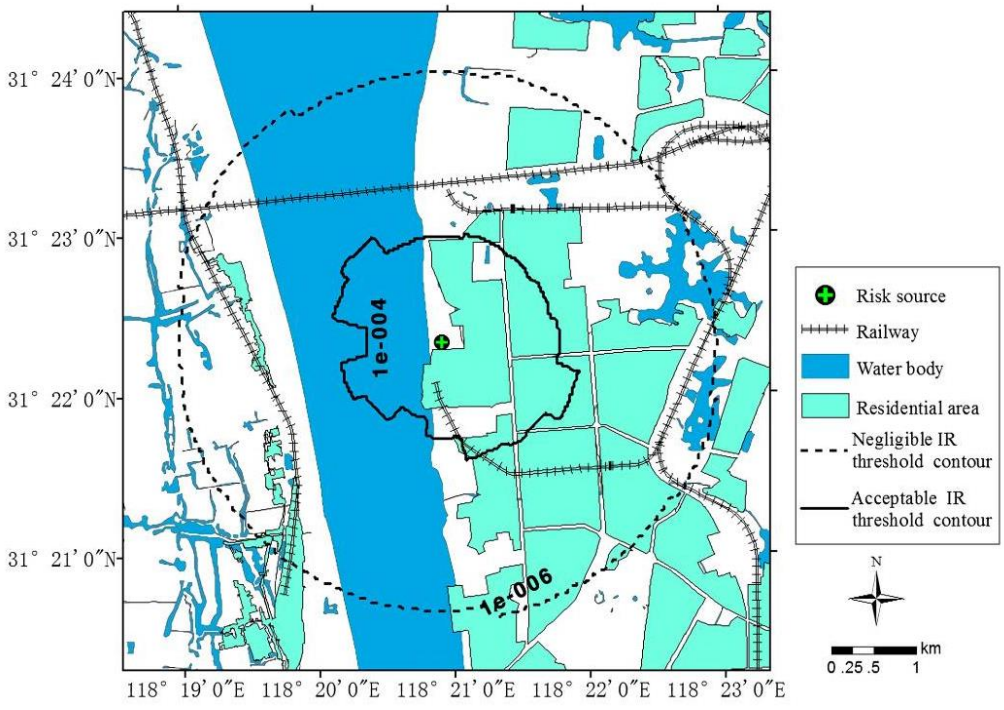

Figure 7. *Individual risk assessment result of case study*

Social risk

Social risk is by taking the analysis results of individual risk as the base to calculate the number of risk receptors within the range of individual risk field so as to obtain the

http://www.aloki.hu ● ISSN 1589 1623 (Print) ● ISSN 1785 0037 (Online)
DOI: http://dx.doi.org/10.15666/aeer/1705_1185111867

integrated risk assessment conclusion, and it also follows ALARP criterion. By referring to the measure standard of social risk acceptability in UK and the Netherlands and considering the relatively serious loss of toxic gas leakage accident consequence, the line slope of social risk assessment standard selected in this study is n = -2, namely, the risk assessment personnel holds averse attitude; the acceptable line for feature points is determined as (l, 10^{-2}) linear and the negligible line for feature points is determined as (l, 10^{-4}) linear.

The population data of study area is as shown in the *Figure 6,* hereby, the risk receptor number of each lethal radius can be calculated in ArcGIS, and so the death toll and the corresponding probability can be got. Then according to the calculation results of social risk equation, F-N curve can be depicted and the probability of death toll (≥N) can be obtained. The details can be seen in the *Figure 8*.

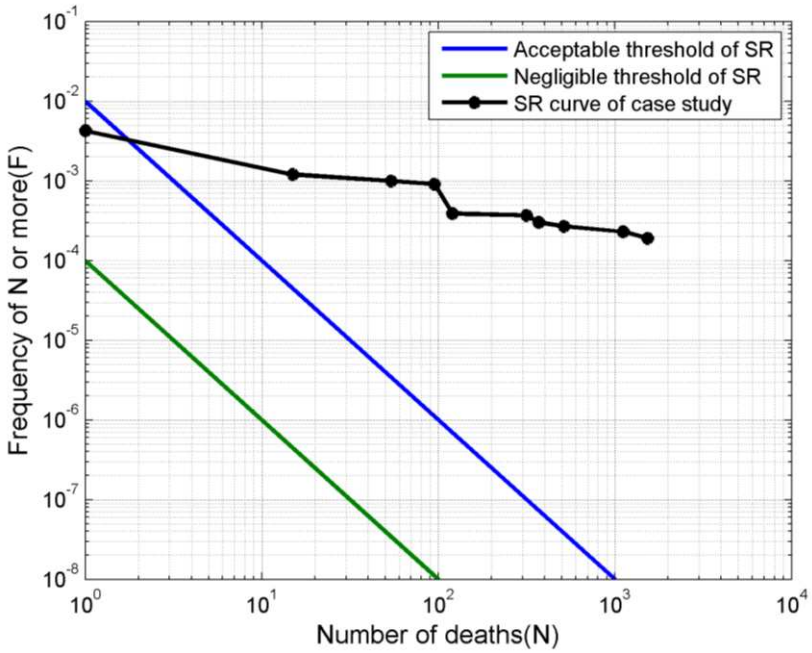

Figure 8. *Social risk assessment result of case study*

Discussion of environmental risk assessment results

According to the description of above two sections, the acceptability threshold values of individual risk and social risk are all determined, and based on which we can make some analysis about the environmental risk assessment result.

It can be seen from the individual risk contour line that some residential areas are not in the acceptable range. Through on-site investigation, there are schools and other sensitive public places in the non-ALARP area. Once an accident happens, this part of the population is vulnerable with poor self-rescue ability. According to the principle of ALARP, the relevant departments should take compulsory measures to design and plan this non-ALARP area to reduce the risk level. For people in ALARP area, the government need to further calculate the economic reasonableness before deciding whether to take further measures to reduce the individual risk value in ALARP area.

The F-N curve of case study is mostly above the acceptable level, so the social risk is not acceptable. The highly concentrated residential area near the chemical hazardous

http://www.aloki.hu ● ISSN 1589 1623 (Print) ● ISSN 1785 0037 (Online)
DOI: http://dx.doi.org/10.15666/aeer/1705_1185111867

source is the main reason for this status, namely the unreasonable land use patterns generates higher social risk. This study result also demonstrated a direct relationship between social risk and regional population distribution.

Conclusions

1) Through the results of parameter sensitivity analysis, it can be found that different input parameters in PHAST would generate different effects on the output results, and some even have magnitude-class differences. The method based on sensitivity sequencing can avoid the subjectivity and blindness of parameter selection in uncertainty analysis. The variability presented of LHS analysis results in this study, in fact, is the expression of the uncertainty of environmental risk system in the reality. Probability sampling method can effectively deal with the uncertainty problems contained in the environmental risk system. The all possible random events can be simulated and finally the probability distribution of the simulation results can be obtained, which become the basis of all potential accident scenarios simulation and more all-sided environmental risk assessment.

2) Based on the uncertainty analysis, individual risk and social risk are used to assess the regional environmental risk level, and the results show that these two kinds of assessment indexes are able to scientifically quantify the environmental risk level as well as visually show the risk level in ArcGIS platform, which contributes to the understanding of the risk decision-makers and provides a reference of risk management for the environmental department. The research results of the liquid ammonia leakage accident show that the individual risk and social risk in the study area are on the high side, which exceed the acceptable threshold. Therefore, corresponding risk management measures should be taken by the chemical enterprise and government to reduce the risk level.

3) It is a common issue concerned by the government and public about the environmental hazard source how to have safe and reasonable layout plan and decide the regional development scale according to the regional environmental risk tolerance in the urban area. In this study, regional environment risk state was evaluated from the aspect of short-term toxic harm for the personnel. Moreover, planning and adjustment suggestions were proposed to the residential area. The follow-up research work can also be in consideration of the long-term impact resulted by environmental accident to soil, water and air. With the combination of uncertainty analysis method proposed in this paper, synthetic judgment was conducted to the environmental risk tolerance for the peripheral zone of environmental hazard source.

Acknowledgements. This study is supported by the “Natural Science Foundation of China” (no. 41671352), “Philosophy Social Sciences Planning Project Of Anhui Province” (no. AHSKY2015D72), and “Science and Technology Planning Project of Huainan, Anhui Province” (no. 2018A361). I would like to thank the anonymous reviewers who have helped to improve the paper.

REFERENCES

[1] Abdo, H., Flaus, J., Masse, F. (2017): Uncertainty quantification in risk assessment - representation, propagation and treatment approaches: application to atmospheric dispersion modeling. – Journal of Loss Prevention in the Process Industries 49: 551-571.

http://www.aloki.hu ● ISSN 1589 1623 (Print) ● ISSN 1785 0037 (Online)
DOI: http://dx.doi.org/10.15666/aeer/1705_1185111867

[2] Abrahamsson, M. (2002): Uncertainty in Quantitative Risk Analysis-Characterisation and Methods of Treatment. – Rep 1024. Lund University Press, Lund, Sweden.
[3] Betrie, G. D., Sadiq, R., Nichol, C., et al. (2015): Environmental risk assessment of acid rock drainage under uncertainty: the probability bounds and PHREEQC approaches. – Journal of Hazardous Materials 301: 187-196.
[4] Chen, Y., Song, G. B., Yang, F. L., et al. (2012): Risk assessment and hierarchical risk management of enterprises in chemical industrial parks based on catastrophe theory. – International Journal of Environmental Research and Public Health 9: 4386-4402.
[5] Di Domenico, J., Vaz, C. A., de Souza, M. B. (2014): Quantitative risk assessment integrated with process simulator for a new technology of methanol production plant using recycled CO_2. – Journal of Hazardous Materials 274: 164-172.
[6] García-Díaz, J. C., Gozalvez-Zafrilla, J. M. (2012): Uncertainty and sensitive analysis of environmental model for risk assessments: an industrial case study. – Reliability Engineering and System Safety 107: 16-22.
[7] Hahn, T., Stauber, J., Dobson, S., et al. (2010): Reducing uncertainty in environmental risk assessment (ERA): clearly defining acute and chronic toxicity tests. – Integrated Environmental Assessment & Management 5: 175-177.
[8] Hanna, S., Dharmavaram, S, Zhang, J., et al. (2008): Comparison of six widely-used dense gas dispersion models for three recent chlorine railcar accidents. – Process Safety Progress 27: 248-259.
[9] Hansen, S. F. (2016): Environmental risk assessment of chemicals and nanomaterials. – Science of the Total Environment 541: 784-794.
[10] Hoshino, N., Takemura, A. (2000): On reduction of finite sample variance by extended Latin hypercube sample. – Bernoulli 6: 1035-1050.
[11] Hou, Z. Q., Zeng, Y. M. (2016): Research on risk assessment technology of the major hazard in harbor engineering. – Procedia Engineering 137: 843-848.
[12] King, D. M., Perera, B. J. C. (2013): Morris method of sensitivity analysis applied to assess the importance of input variables on urban water supply yield - a case study. – Journal of Hydrology 477: 17-32.
[13] Kong, D. P., Lu, S. X., Feng, L., et al. (2012): Uncertainty and sensitivity analysis of available safety egress time based on Latin Hypercube Sampling. – Journal of Safety & Environment 11: 176-179.
[14] Labieniec, P. A., Dzombak, D. A., Siegrist, R. L. (2007): Evaluation of uncertainty in a site-specific risk assessment. – Journal of Environmental Engineering 123: 234-243.
[15] Liu, A. H., Wu, C., Peng, X. (2012): Research on area risk assessment for chemical park based on domino effect model. – Procedia Engineering 45: 47-52.
[16] Lu, Y. S. (1999): Environmental Risk Assessment. – Tongji University Publishing Company, Shanghai.
[17] Maxwell, R. M., Kastenberg, W. E. (1999): Stochastic environmental risk analysis: an integrated methodology for predicting cancer risk from contaminated groundwater. – Stochastic Environmental Research Risk Assessment 13: 27-47.
[18] Meng, X. J., Zhang, Y., Yu, X, et al. (2014): Regional environmental risk assessment for the Nanjing Chemical Industry Park: an analysis based on information-diffusion theory. – Stochastic Environmental Research and Risk Assessment 28: 2217-2233.
[19] Milazzo, M. F., Vianello, C., Maschio, G. (2015): Uncertainties in QRA: analysis of losses of containment from piping and implications on risk prevention and mitigation. – Journal of Loss Prevention in the Process Industries 36: 98-107.
[20] Morris, M. D. (1991): Factorial sampling plans for preliminary computational experiments. – Technometrics 33: 161-174.
[21] Pandya, N., Gabas, N., Marsden, E. (2012): Sensitivity analysis of Phast's atmospheric dispersion model for three toxic materials (nitric oxide, ammonia, chlorine). – Journal of Loss Prevention in the Process Industries 25: 20-32.

http://www.aloki.hu ● ISSN 1589 1623 (Print) ● ISSN 1785 0037 (Online)
DOI: http://dx.doi.org/10.15666/aeer/1705_1185111867

[22] Shao, C. F., Yang, J., Tian, X. G., et al. (2013): Integrated environmental risk assessment and whole-process management system in chemical industry parks. – International Journal of Environmental Research and Public Health 10: 1609-1630.
[23] Tang, C., Yi, Y., Yang, Z., Sun, J. (2016): Risk analysis of emergent water pollution accidents based on a Bayesian network. – Journal of Environmental Management 165: 199-205.
[24] Trbojevic, V. M., Carr, B. J. (2000): Risk based methodology for safety improvements in ports. – Journal of Hazardous Materials 71: 467-480.
[25] Wu, G. J., Chen, W. Z., Tan, X. J., Yang, D. S. (2015): Program development of finite element reliability method and its application based on Latin hypercube sampling. – Rock & Soil Mechanics 36: 550-554.
[26] Wu, Z. Z., Duo, Y. Q., Wei, L. J., et al. (2006): Quantitative area risk assessment method and its application in land use safety planning for major hazard installations. – Engineering Science 8: 46-49.
[27] Xing, K. X., Guo, H. C. (2006): Uncertainty analysis methods in environment model. – Environmental Science & Technology 29: 112-114.
[28] Xu, C. G., Hu, Y., Chang, Y., Jiang, Y., Li, X., Bu, R., et al. (2004): Sensitivity analysis in ecological modeling. – Chinese Journal of Applied Ecology 15: 1056-1062.
[29] Xu, H. (2009): Advances of the strategies for addressing uncertainty in environmental risk assessment. – Environmental Science & Management 11: 266-273.
[30] Xu, Y., Liu, J. C., Liu, Y. Q., Neng, C. X., Dong, L. (2014): Quantification of uncertainty in evaluating the health risk of a contaminated site based on Monte Carlo method. – Acta Scientiae Circumstantiae 34: 1579-1584.

http://www.aloki.hu ● ISSN 1589 1623 (Print) ● ISSN 1785 0037 (Online)
DOI: http://dx.doi.org/10.15666/aeer/1705_1185111867

TEMPORAL AND SPATIAL CHARACTERISTICS OF EXTREME TEMPERATURE IN THE MIDDLE REACH OF THE YELLOW RIVER, CHINA

FENG, K. P.[1,2,3] – TIAN, J. C.[1,2,3*] – WANG, Z. P.[4]

[1]*School of Civil and Hydraulic Engineering, Ningxia University, Yinchuan, China*

[2]*Engineering Research Center for Efficient Utilization of Water Resources in Modern Agriculture in Arid Regions, Yinchuan, China*

[3]*Ningxia Research Center of Technology on Water-Saving Irrigation and Water Resources Regulation, Yinchuan, China*

[4]*School of Mathematics and Statistics, Ningxia University, Yinchuan 750021, China*

**Corresponding author*
e-mail: slxtjc@163.com

(Received 23rd Apr 2019; accepted 4th Jul 2019)

Abstract. the middle reach of Yellow River is a production area for main grain crops in China and is also an emerging industrial cluster. this study adopts meteorological data from 1951 to 2014 provided by 73 national ordinary stations in the study area, combines Kendall-tau non-parametric test method, Sen's slope estimation method and Savitzky-Golay smoothing filtering method based on sub-regions divided by fuzzy clustering method and analyzes the variation trend of extreme temperature indexes. The results show that: (1) in the middle reach of Yellow River, the variation trend of extreme temperature events is basically similar, but the intensity is different, and the spatial distribution is inconsistent. (2) On time scale, an upward trend has been found in extreme temperature events in the past 60 years. (3) On spatial scale, the change rate of multiple indexes in the arid sub-region is greater than that of those in the humid sub-region; the proportion of meteorological stations with significant index changes in the arid region is higher than that in the humid sub-region. Some indexes have different trends in small areas, which may be caused by local microclimates in urban heat islands and hilly areas, but further analysis and verification is also required.
Keywords: *fuzzy clustering, Kendall-tau, Sen's slope estimation, Savitzky-Golay smoothing filtering, extreme temperature*

Introduction

More than half a century in the past, scholars at home and abroad have conducted a lot of research work on extreme climate events in different regions of the world and have achieved research results of different depths. In early 2014, *Science* published 7 papers in a row to discuss the "the Challenge of Climate Science" and elaborate on some core issues of current climate and hydrology sciences, including the issue of "regional climate and extreme events". The paper believed that an important trend of warming research is to reflect global warming in the research on regional climate and extreme events, but the research needs to be further developed, where great difficulties also exist (Wang et al., 2014a; Horton et al., 2015). At present, domestic and international researches focus mainly on the observational facts of extreme climate. The fifth assessment report of the UN Intergovernmental Panel on Climate Change (IPCC) has summed up the observations and research findings of extreme temperature and precipitation events in full length. Many studies show that extreme precipitation events

http://www.aloki.hu ● ISSN 1589 1623 (Print) ● ISSN 1785 0037 (Online)
DOI: http://dx.doi.org/10.15666/aeer/1705_1186911885

are very sensitive to the global climate change, and minor changes in the climate may cause greater changes in the frequency and intensity of extreme weather events (Alexander, 2016; Diffenbaugh et al., 2017; Mooshammer et al., 2017; Grotjahn et al., 2016; Ma et al., 2015).

The middle reach of Yellow River is located in the confluence of the Loess Plateau, Ordos Plateau and Inner Mongolia Plateau; where plains, deserts, mountains, platforms, lakes and wetlands are intertwined, topography and landform are complex, terrain changes greatly and the structure of the underlying surface is complex. The area is a major producing area of main gain crops and industrial crops in China and is also an emerging industrial cluster. Extreme temperature events may have an impact on industrial and agricultural production and urban development in the area (Nie et al., 2015). In recent years, researchers have conducted a research on temporal and spatial variation characteristics, variation trends and cases of formation of extreme temperature events in mainland China (Zhou et al., 2010), northern and southern China (Zhai et al., 2003; Tang et al., 2014), certain watersheds (Wang et al., 2013) and certain provinces (Shen et al., 2012; Chen et al., 2012, 2011; Zhang et al., 2014; Li et al., 2015; Wang et al., 2016, 2012), respectively. However, the research on extreme temperature events in the middle reach of Yellow River is still insufficient so far.

Based on previous researches, this study adopts the daily temperature data of 73 meteorological stations and uses the internationally used extreme temperature event indexes to conduct an in-depth research on the temporal and spatial changes in extreme temperature events in the middle reach of Yellow River, reveal the change characteristics and trends, hoping to provide a reference for water circulation, water resource management, ecological vulnerability assessment and hydrogeological hazard warning and other researches in the area under extreme climate conditions.

Data and methodology

Data

This study adopts the temperature data from 1951 to 2014 of 73 national ordinary stations in the middle reach of Yellow River provided by China Meteorological Data Network (http://data.cma.cn/, China Surface Dataset Daily Value Dataset V3.0). The meteorological data selected has passed quality control, including inspection of climate threshold value or allowable value); inspection of extreme value of station; internal consistency inspection of set value, daily average and daily extremum; temporal and spatial consistency inspection and other measures. In addition, the distribution of meteorological stations is shown in *Figure 1*.

Research method

Definition and calculation of extreme temperature indexes

The definition of extreme temperature indexes in this research is based on the "climate change detection and indexes" determined by CCI, WCRP, CLIVAR and ETCCDMI. These indexes and their calculation methods have been widely used in the world, and the research results also reflect that these indexes are characterized by good regional adaptability, low noise, low extremity and strong significance (Li et al., 2012; Zhao et al., 2015). There are 29 indexes in this series, including temperature and precipitation. This paper selects 18 temperature indexes to analyze the extreme

http://www.aloki.hu ● ISSN 1589 1623 (Print) ● ISSN 1785 0037 (Online)
DOI: http://dx.doi.org/10.15666/aeer/1705_1186911885

temperature events in the middle reach of Yellow River, and specific indexes and definitions are shown in *Table 1*. The indexes are calculated using RClimDex1.1 software. In the process of calculation, quality inspection and control are conducted on the said meteorological data including outliers and error values. Meanwhile, this paper also adopts new international climate change benchmarks (Zhang et al., 2014).

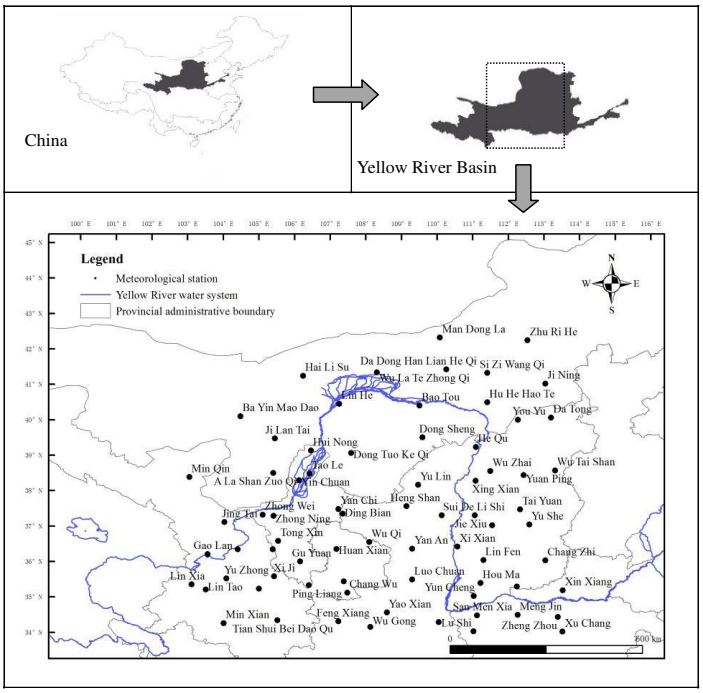

Figure 1. *Meteorological stations in the middle reach of Yellow River*

Table 1. *Definitions of extreme temperature indexes*

Abbreviation of index	Definition	Unit
DTR	Difference between daily maximum temperature and daily minimum temperature	°C
TMAXmean	Average value of annual/monthly/daily maximum temperature	°C
TMINmean	Average value of annual/monthly/daily minimum temperature	°C
TNn	Minimum value of annual/monthly/daily minimum temperature	°C
TNx	Maximum value of annual/monthly/daily minimum temperature	°C
TXn	Minimum value of annual/monthly/daily maximum temperature	°C
TXx	Maximum value of annual/monthly/daily maximum temperature	°C
FD0	Number of days in a year whose minimum temperature is below 0 °C	d
ID0	Number of days in a year whose maximum temperature is below 0 °C	d
SU25	Number of days whose daily maximum temperature is above 25 °C	d
TN10p	Number of days whose daily minimum temperature is below 10% tantile	d
TN90p	Number of days whose daily minimum temperature is above 90% tantile	d
TR20	Number of days in a year whose daily minimum temperature is above 20 °C	d
TX10p	Number of days whose daily maximum temperature is below 10% tantile	d
TX90p	Number of days whose daily maximum temperature is above 90% tantile	d
WSDI	Number of days whose maximum temperature is 90% tantile for 6 days in a row	d
CSDI	Number of days whose minimum temperature is 10% tantile for 6 days in a row	d
GSL	Time span during which the temperature is above or below 5 °C for 6 days in a row	d

http://www.aloki.hu ● ISSN 1589 1623 (Print) ● ISSN 1785 0037 (Online)
DOI: http://dx.doi.org/10.15666/aeer/1705_1186911885

Fuzzy clustering analysis

Clustering analysis is a multivariate statistical analysis method, which classifies individuals based on their several characteristics, so that individuals of the same category have a higher homogeneity while individuals of different categories have a higher heterogeneity. When it comes to dealing with actual classification problems, varying degrees of fuzziness is always seen because the boundaries of individual categories are not always clear and exact. When clustering involves fuzzy boundaries between individuals, a fuzzy clustering analysis method is usually used, which is established on fuzzy mathematics. Fuzzy C-Means (FCM for short) was proposed by Bezkek in 1981. The impact of different number of categories c on classification results is highly significant. To evaluate the classification effect under different c values in a scientific way, the predecessors have done a lot of research work and defined a number of evaluation indexes (see *Eqs. 1–4*) to guide the specific classification process. Assuming that different c values are determined according to those indexes (*Eqs. 1–4*), the smaller c value shall prevail if different c values have similar classification effect (Qi et al., 2015).

Partition coefficient (PC):

$$PC(c) = \frac{1}{N}\sum_{i=1}^{c}\sum_{j=1}^{N} u_{ij} \quad \text{(Eq.1)}$$

Classification entropy (CE):

$$CE(c) = \frac{1}{N}\sum_{i=1}^{c}\sum_{j=1}^{N} u_{ij} \log(u_{ij}) \quad \text{(Eq.2)}$$

Partition index (SC):

$$SC(c) = \sum_{i=1}^{c} \frac{\sum_{k=1}^{N}(u_{ij})^{m}\left\|x_j - v_i\right\|^2}{N_i\sum_{k=1}^{c}\left\|v_k - v_i\right\|^2} \quad \text{(Eq.3)}$$

Separation index (S):

$$S(c) = \frac{\sum_{i=1}^{c}\sum_{k=1}^{N}(u_{ij})^{2}\left\|x_j - v_i\right\|^2}{N\min_{ij}\left\|v_k - v_i\right\|^2} \quad \text{(Eq.4)}$$

Analysis method of variation trend of extreme temperature indexes

Meteorological data belongs to time series. For the trend analysis of time series, a linear regression method is usually used, but such method directly calculates the slope based on the actual data value, which is greatly affected by the abnormal value. Sen's slope estimation algorithm has strong anti-noise performance, but it cannot be used to make a significant judgment of sequence trend. The Kendall-tau non-parametric test

http://www.aloki.hu ● ISSN 1589 1623 (Print) ● ISSN 1785 0037 (Online)
DOI: http://dx.doi.org/10.15666/aeer/1705_1186911885

method does not require the sample to follow a certain distribution, allows the existence of missing values and can achieve significant judgments, but it cannot be used to obtain the slope of the sequence (ZHAI et al., 2003). Therefore, Kendall-tau non-parametric test method and Sen's slope estimation method are combined in this paper to make full use of their respective advantages, so that they can better serve the analysis of changes in extreme temperature indexes.

Savitzky-Golay smoothing filtering method

To more clearly extract and demonstrate the variation trend of extreme temperature indexes, the Savitzky-Golay smoothing filtering method is used in this paper. The method was proposed by Savitzky and Golay in 1964, which is a filtering method based on local polynomial least squares fitting in the time domain, whose prominent advantage is that it can ensure that signal shape and width remains unchanged at the time of simple and rapid filtering of noise (Cai et al., 2011;). In addition, the Savitzky-Golay smoothing filter in this study uses 7 points 2 times as the polynomial parameter.

Results and analysis

FCM-based climate division

To facilitate the analysis of the overall situation of the extreme temperature indexes in the middle reach of Yellow River on time scale, it is required to summarize 73 meteorological stations as specific climate regions. As mentioned before, the middle reach of Yellow River is located in the confluence of three major plateaus, where the terrain is complex as well as the structure of the underlying surface. It is obviously inappropriate to directly average 73 meteorological stations above and generalize the entire the middle reach of Yellow River as one region. Therefore, proper zoning is required. There are actually a lot of methods for climate zoning, the fuzzy clustering method (FCM) is used in this paper.

Combined with the natural conditions of the geographical location of the research area, latitude and longitude, altitude, average temperature and maximum and minimum temperature of the meteorological stations are regarded as characteristic values to perform clustering analysis on 73 meteorological stations in the middle reach of Yellow River. The number of divisions is preliminarily estimated to be $c = 2$ or $c = 3$. By selecting different c values, FCM can obtain corresponding membership matrix. According to the relationship reflected in the matrix, the classification results shall be plotted when $c = 2$ or $c = 3$ (see *Fig. 2*). On this basis, the most reasonable number of divisions shall be analyzed in combination with 7 different indexes listed in *Table 3*. In addition, it can be seen from *Figure 2* that more stations are not classified in the middle reach of Yellow River when $c = 3$; while the classification shows good results when $c = 2$.

To more intuitively express the FCM climate divisions in the middle reach of Yellow River, the classification results are represented in a map (see *Fig. 3*). It can be clearly observed that 73 stations are classified into 2 different climate divisions along the line of "Yuanping—Xing County—Suide—Yan'an—Pingliang—Tianshui", and the line is very close to China's 400 mm equivalent precipitation line and "HuHuanYong Line", which also fully indicates that it is reliable and reasonable to apply the fuzzy clustering algorithm to climate division in this paper. By referring to the significance of the

http://www.aloki.hu ● ISSN 1589 1623 (Print) ● ISSN 1785 0037 (Online)
DOI: http://dx.doi.org/10.15666/aeer/1705_1186911885

400 mm equivalent precipitation line, this paper defines 2 different climate divisions in the middle reach of Yellow River obtained by FCM clustering analysis as "arid and semi-arid sub-region" and "humid and semi-humid sub-region", respectively. For the purpose of conciseness, they are referred to as "arid sub-region" and "humid sub-region", respectively.

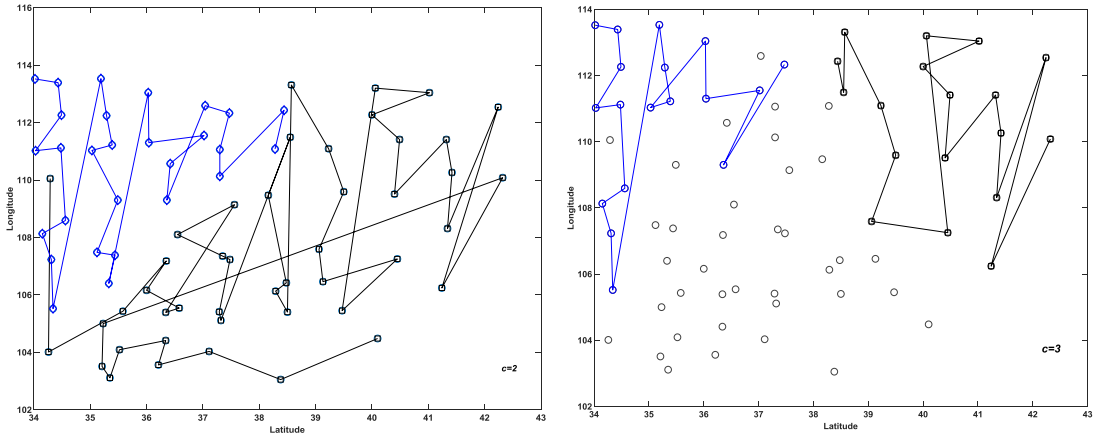

Figure 2. *FCM analysis of meteorological stations*

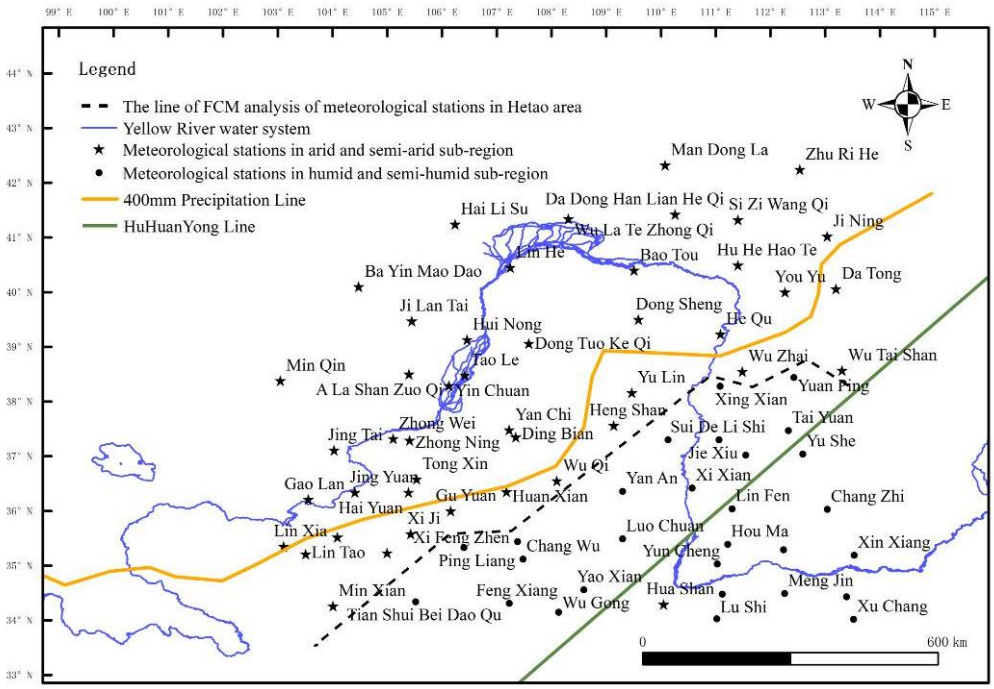

Figure 3. *FCM analysis results of meteorological stations in the middle reach of Yellow River*

Temporal and spatial variation of extreme temperature indexes

Variation of DTR, TMAXmean, TMINmean, TNn, TNx, TXn and TXx indexes

In the past 60 years, the daily temperature range (DTR) has dropped significantly, while the average maximum temperature TMAXmean and average minimum

http://www.aloki.hu ● ISSN 1589 1623 (Print) ● ISSN 1785 0037 (Online)
DOI: http://dx.doi.org/10.15666/aeer/1705_1186911885

temperature TMINmean have increased significantly, and shown an obvious stage (see *Fig. 4a, c* and *e*). DTR continued to decline around 1951-2000, TMAXmean and TMINmean continued to rise, but the variation trend of indexes began to slow down after 2000. These three indexes had the same rate of change in the arid and humid sub-regions, reaching 0.1 °C/10a, 0.2 °C/10a, and 0.3 °C/10a, respectively (see *Table 3*). The rate of increase of average minimum temperature is higher than that of average maximum temperature, which is the primary reason for the significant decrease in daily temperature range. Viewed from spatial distribution, DTR shows a significant downward trend in most meteorological stations, and the average maximum temperature and average minimum temperature show an obvious upward trend in the entire the middle reach of Yellow River (see *Fig. 4b*, *d* and *f*).

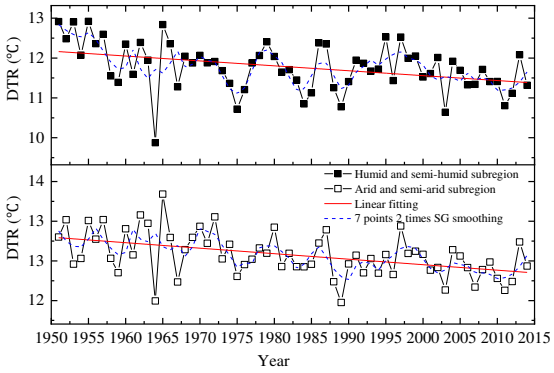

(a) Interannual variation of DTR index

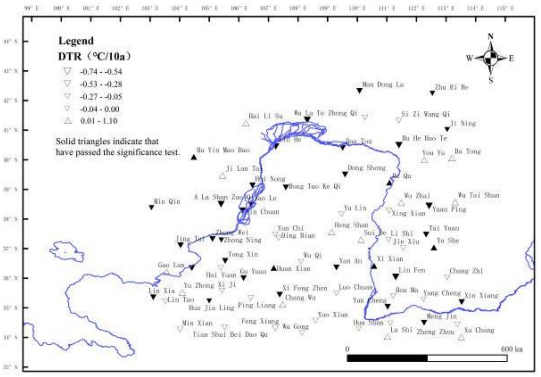

(b) Space variation of DTR index

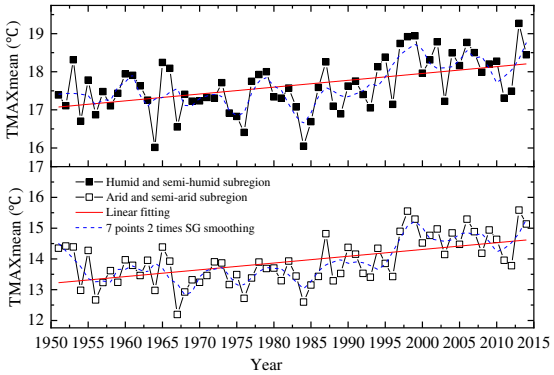

(c) Interannual variation of TMAXmean index

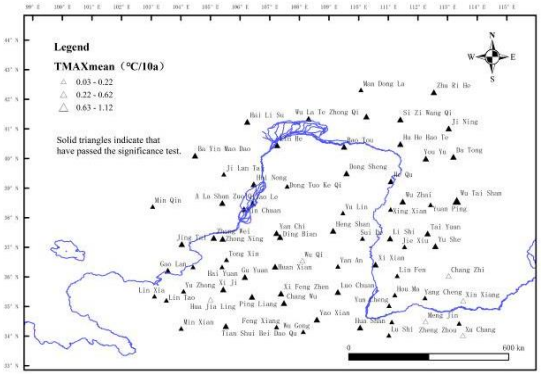

(d) Space variation of TMAXmean index

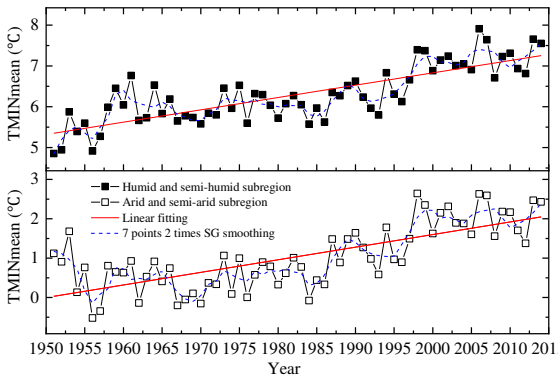

(e) Interannual variation of TMINmean index

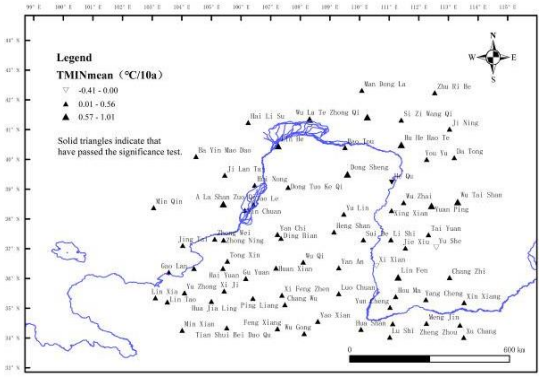

(f) Space variation of TMINmean index

Figure 4. *Temporal and spatial variation of DTR, TMAXmean and TMINmean indexes*

http://www.aloki.hu ● ISSN 1589 1623 (Print) ● ISSN 1785 0037 (Online)
DOI: http://dx.doi.org/10.15666/aeer/1705_1186911885

It can be seen from *Table 2* that the maximum values (including the extremely high value TNx of minimum temperature and extremely high value TXx of daily maximum temperature) and minimum values (including extremely low value TNn of daily minimum temperature and extremely low value TXn of daily maximum temperature) of extreme temperature show an upward trend. The minimum values have a higher rate of rise and TNx reaches the highest rate of rise in humid sub-region, that is, 0.6 °C/10a. However, the rate of rise of TXx is 0.1 °C/10a only, making it fail to pass the confidence level test.

Table 2. *Variation trend (1) of extreme temperature indexes from 1951 to 2014*

Index name	Arid sub-region	Humid sub-region
	Rate of change (°C/10a)	Rate of change (°C/10a)
DTR	-0.1**	-0.1**
TMAXmean	0.2**	0.2**
TMINmean	0.3**	0.3**
TNn	0.4**	0.6**
TNx	0.3**	0.1**
TXn	0.3*	0.4**
TXx	0.2*	0.1 n.s.

**It passed the 99% confidence level test. *It passed the 95% confidence level test. n.s. means that the variation trend is not significant

On time scale, it can be observed from 7 points 2 times SG smoothing line that TNn index tends to be upward on the whole except the decrease from 1951 to 1955 (see *Fig. 5a*); TNx index has risen significantly since 1951 and reached a peak in 1960, then went down around 1983 (more significant in humid sub-region) and showed a significant upward trend after 1983 (see *Fig. 5c*); TXn index decreased from 1951 to 1957, and then rose wavelike and showed a moderate upward trend after 2000 (see *Fig. 5e*). TXx index rose significantly around the period of 1951-1973, showed a moderate upward trend around the period of 1973-1989, then rose significantly from 1990 to 2000 and then regained a moderate upward trend after 2000 (see *Fig. 5g*).

From the perspective of spatial distribution, TNn and TNx indexes showed an upward trend in most regions, with a significant upward trend in northeastern Gansu, Ningxia, Linhe, Baotou and Hohhot, Inner Mongolia and Shanxi (see *Fig. 5b* and *d*). TXn index showed a significant upward trend in the entire the middle reach of Yellow River with a larger range (see *Fig. 5f*). TXx index rose significantly in some areas such as northeastern Gansu, Inner Mongolia Bayinmaodao, Hohhot, Yuncheng, Shanxi and other areas, with a small range (see *Fig. 5h*).

As mentioned above, average maximum temperature and minimum temperature in the middle reach of Yellow River show a significant upward trend, the rate of rise of minimum is higher than that of maximum and daily temperature range shows a significant downward trend. Seeing from Interannual variation, TNx, TNx, TXn and TXx indexes in this area tends to be upward on the whole, but they are in stages: showed a downward trend around the period of 1951-1955, rapidly rose from 1956 to 2000 and slowed down after 2000. In addition to TNN index, the rate of change of other three indexes in the arid sub-region is higher than that in the humid sub-region.

http://www.aloki.hu ● ISSN 1589 1623 (Print) ● ISSN 1785 0037 (Online)
DOI: http://dx.doi.org/10.15666/aeer/1705_1186911885

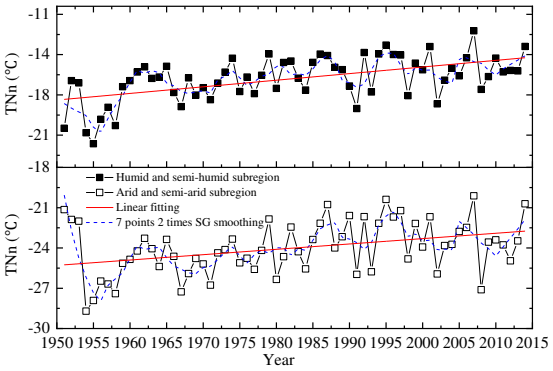

(a) Interannual variation of TNn index

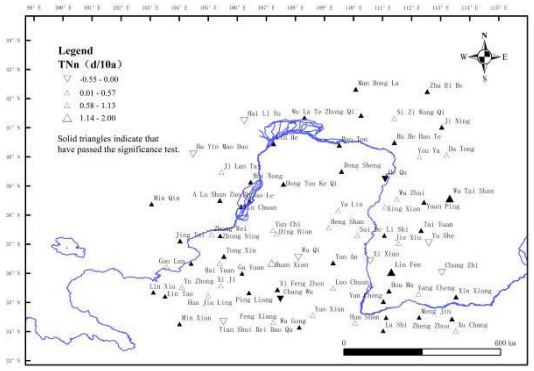

(b) Space variation of TNn index

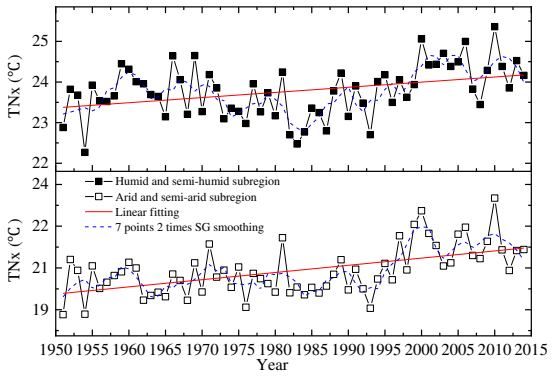

(c) Interannual variation of TNx index

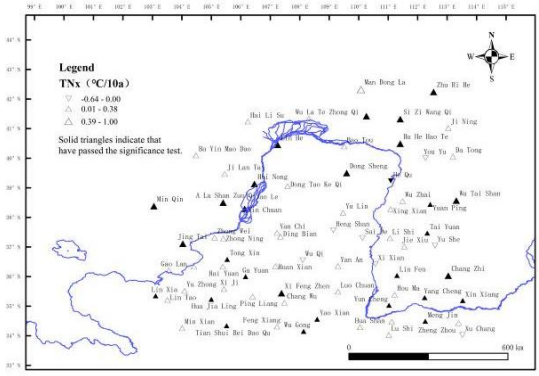

(d) Space variation of TNx index

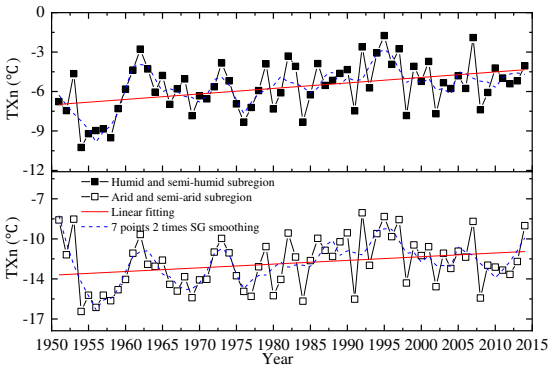

(e) Interannual variation of TXn index

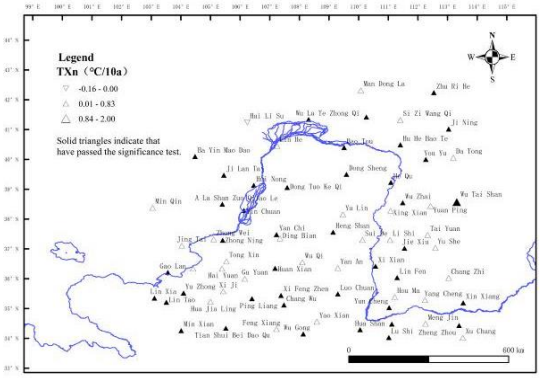

(f) Space variation of TXn index

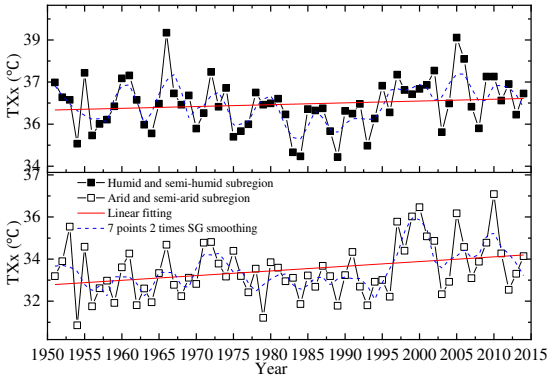

(g) Interannual variation of TXx index

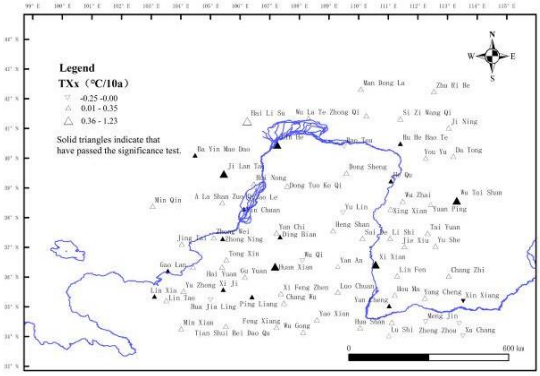

(h) Space variation of TXx index

Figure 5. *Temporal and spatial variation of TNn, TNx, TXn and TXn indexes*

http://www.aloki.hu ● ISSN 1589 1623 (Print) ● ISSN 1785 0037 (Online)
DOI: http://dx.doi.org/10.15666/aeer/1705_1186911885

It is worth noting that the variation trend of 7 indexes analyzed above slowed down around 2000, which may be related to the slowdown of global warming. In addition, the timing of the slowdown analyzed in this paper is basically consistent with relevant research conclusions (Wang et al., 2014b, c, 2005; Chen et al., 2014).

Variation of FD0, ID0, SU25, TN10p, TX10p, TR20, TN90p and TX90p indexes

From time scale, the index FD0 number of frost days in the past 60 years and the index ID0 number of frozen days show a highly significant downward trend, of which the downward rate in humid sub-region is higher than that in arid sub-region. The downward rate of FD0 and ID0 indexes in humid sub-region is -3.3d/10a and -1.9d/10a, respectively; while that in arid sub-region is -2.6d/10a and -1.5d/10a, respectively (see *Fig. 6a* and *c* and *Table 4*). It is also noted that the index number of frozen days in arid sub-region showed an upward trend while a downward trend in humid sub-region from 1951 to 1963. The index SU25 number of days in summer shows a significant upward trend, and the rate of change in arid sub-region and humid sub-region reaches up to 2.5d/10a and 1.3d/10a, respectively, which indicates that the number of days in arid sub-region whose daily maximum temperature is above 25 °C increases significantly, and the number of days in summer from a climate sense is on the rise (see *Fig. 6e*).

On spatial scale, the index FD0 number of frost days has been reduced by a large margin, the rate of change varied from -10.47 to 0 d/10a and 90% of stations have passed the significance test. The index FD0 showed a slightly upward trend in only two stations, Yushe and Xixian, which may be individual abnormal stations, which cannot negate the overall upward variation trend of FD0 index in the middle reach of Yellow River. The index ID0 number of frozen days has also been reduced by a large margin, that is, -9.62~0d/10a, and 78% of stations have passed the significance test (see *Fig. 6b* and *d*). The index SU25 number of days in summer at all meteorological stations showed an upward trend, of which 67% of stations showed a significant trend, mainly centralized in arid sub-region; while those stations without significant trend are centralized in humid sub-region. The analysis combined with *Table 3* indicates that the upward trend of the index SU25 in humid sub-region is smaller (see *Fig. 6f*).

Table 3. *Variation trend (2) of extreme temperature indexes from 1951 to 2014*

Index name	Arid sub-region	Humid sub-region
	Rate of change (d/10a)	Rate of change (d/10a)
FD0	-2.6**	-3.3**
ID0	-1.5*	-1.9**
SU25	2.5**	1.3*
TN10p	-2.2**	-2.0**
TX10p	-1.0**	-0.8**
TN90p	1.4**	1.4**
TR20	0.8**	1.2**
TX90p	0.9**	0.6*

**It passed the 99% confidence level test. *It passed the 95% confidence level test. n.s. means that the variation trend is not significant

http://www.aloki.hu ● ISSN 1589 1623 (Print) ● ISSN 1785 0037 (Online)
DOI: http://dx.doi.org/10.15666/aeer/1705_1186911885

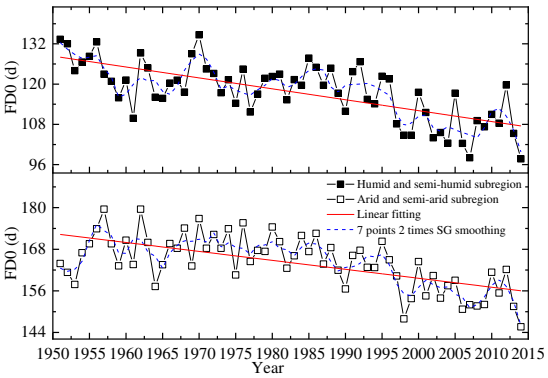

(a) Interannual variation of FD0 index

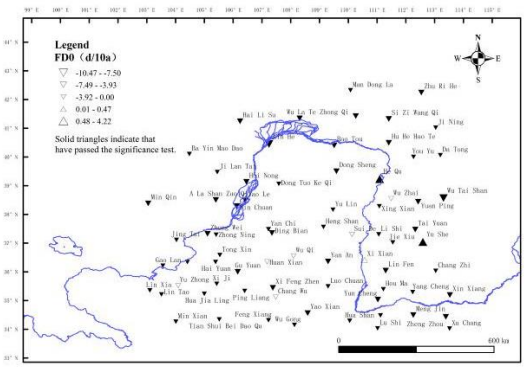

(b) Space variation of FD0 index

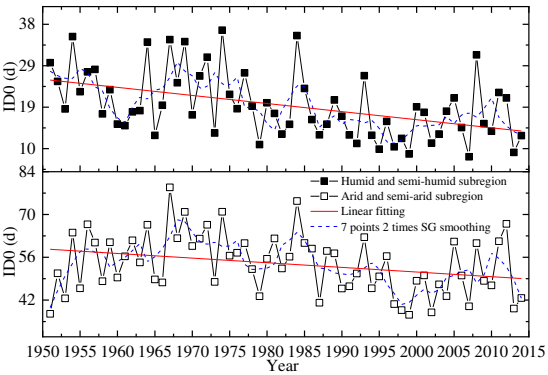

(c) Interannual variation of ID0 index

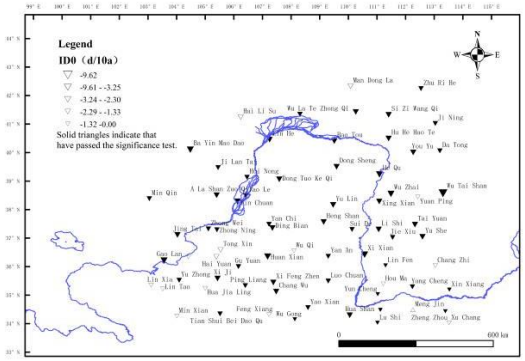

(d) Space variation of ID0 index

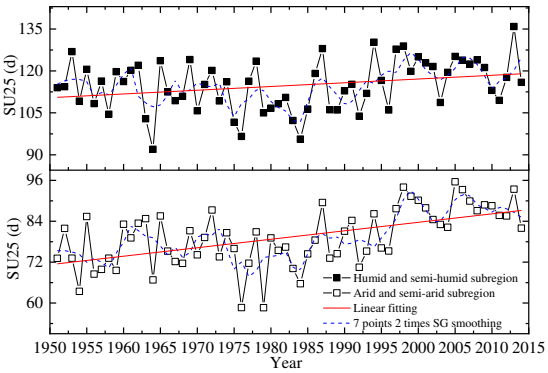

(e) Interannual variation of SU25 index

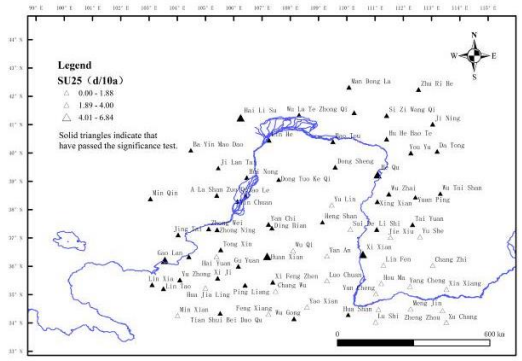

(f) Space variation of SU25 index

Figure 6. *Temporal and spatial variation of FD0, ID0 and SU25 indexes*

On time scale, number of days with cold night TN10P and number of days with cold day TX10P showed a significant wavelike downward trend, and the rate in arid sub-region is higher than that in humid sub-region (see *Fig. 7a* and *c*). Number of days with warm night TN90P, number of days with hot night TR20 and number of days with warm day TX90P showed a significant upward trend, and corresponding indexes in both arid and humid sub-regions have basically the same rate of change, but that is more significant in arid sub-region than humid sub-region, and the three indexes above have passed 99% confidence test. From 7 points 2 times SG smoothing curve, it can be seen that TN90P, TR20 and TX90P indexes tend to rise in stages: The 3 indexes showed a extremely gentle upward trend from 1951 to 1985, but later showed a sharp upward trend (see *Fig. 7e*, *g*, *i* and *Table 3*).

http://www.aloki.hu ● ISSN 1589 1623 (Print) ● ISSN 1785 0037 (Online)
DOI: http://dx.doi.org/10.15666/aeer/1705_1186911885

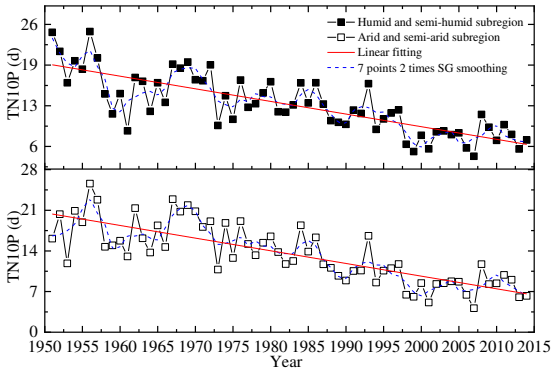

(a) Interannual variation of TN10P index

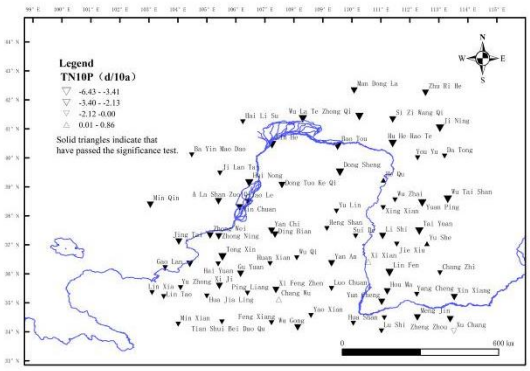

(b) Space variation of TN10P index

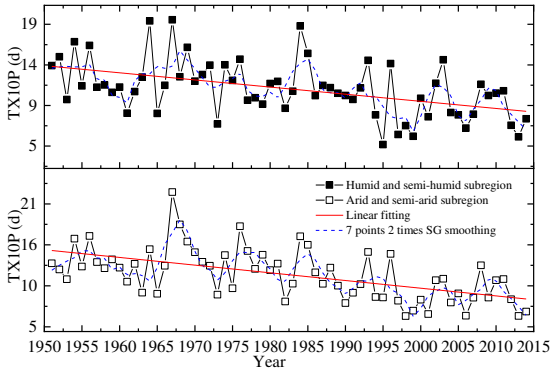

(c) Interannual variation of TX10P index

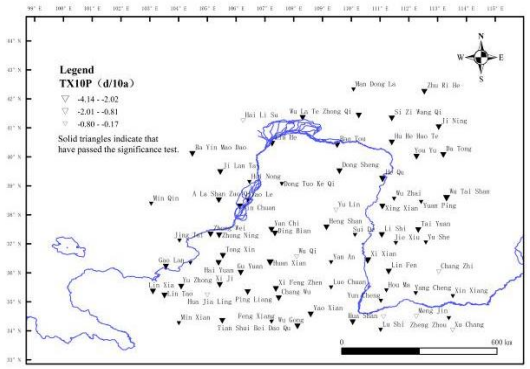

(d) Space variation of TX10P index

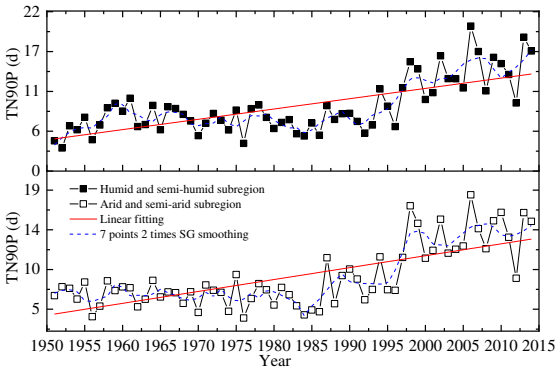

(e) Interannual variation of TN90P index

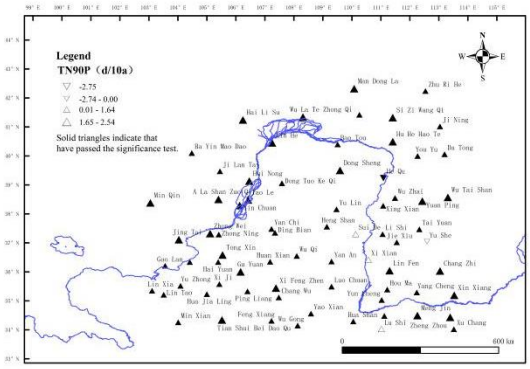

(f) Space variation of TN90P index

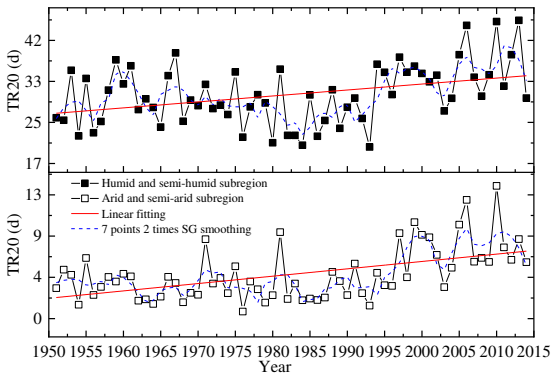

(g) Interannual variation of TR20 index

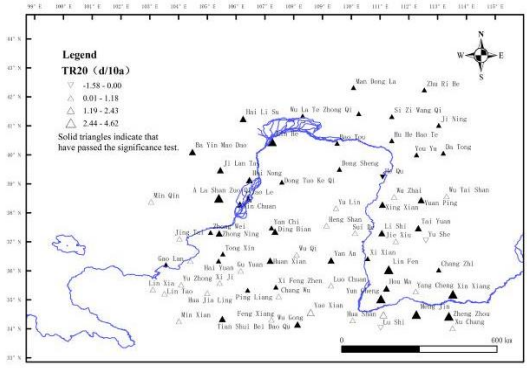

(h) Space variation of TR20 index

http://www.aloki.hu ● ISSN 1589 1623 (Print) ● ISSN 1785 0037 (Online)
DOI: http://dx.doi.org/10.15666/aeer/1705_1186911885

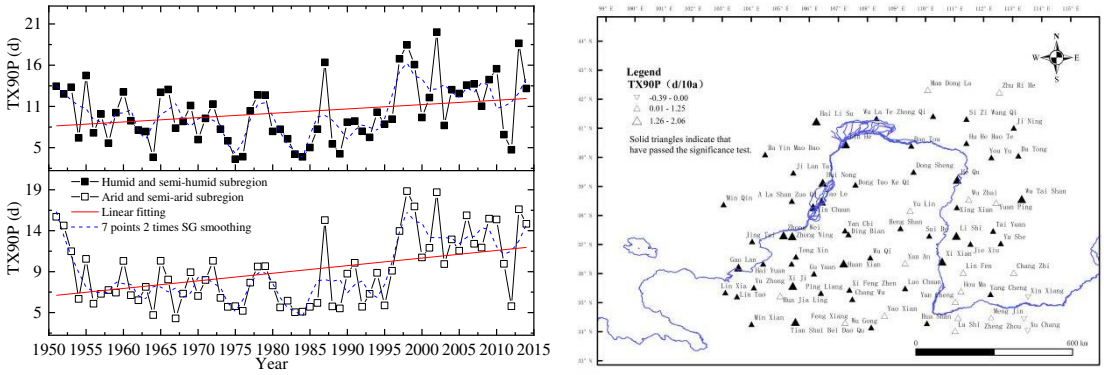

(i) Interannual variation of TX90P index (j) Space variation of TX90P index

Figure 7. *Temporal and spatial variation of TN10p, TX10p, TR20, TN90p and TX90p indexes*

On spatial scale, TN10P and TX10P indexes decreased significantly, reaching -6.43 - 0 d/10a and -1.44 - 0 d/10a, respectively, and the proportion of stations passing the significance test reached 96% and 89%, respectively. It shows that the number of days with cold night and number of days with cold day in the entire the middle reach of Yellow River has the consistent downward trend on spatial scale, but the variation is still more significant in arid sub-region than humid sub-region (see *Fig. 7b* and *d*). TN90P index showed a significant upward trend, 95% of the stations passed the significance test and only two stations in Hequ and Yushe showed a downward trend. TX90P index showed a significant upward trend in most areas of the middle reach of Yellow River, and the proportion of significant stations reached up to 74%, mainly centralized in arid sub-region; Zhengzhou, Xinxiang, Mengjin and Xuchang in humid sub-region showed a downward trend. The space variation is inconsistent in the index TR20 number of days with hot night, and a significant upward trend has been found in northeastern Gansu, north-central part of Ningia, most parts of northern Shaanxi, Linhe, Baotou and Hohhot, Inner Mongolia, most parts of Shanxi and Zhengzhou, Henan. However, a downward trend can also be found in southeastern Gansu, southern Ningxia, Huashan in central Shaanxi, Siziwangqi and Jining, Inner Mongolia (see *Fig. 7f*, *h* and *g*).

Variation of WSDI, CSDI and GSL indexes

Observed from time scale, the index of hot persistence WSDI increased significantly in arid sub-region with an increase rate of 0.7d/10a, but the wavelike upward variation trend was not significant in humid sub-region (not passed the significance test). The index of cold persistence CSDI showed a downward trend, and the downward rate was similar in both arid and humid sub-regions, that is, -2.0d/10a and -1.9d/10a, respectively, which indicates from different angles that the warming is significant in the middle reach of Yellow River. The index GSL crop growth period showed a significant upward trend on the whole, and the rate of rise in humid sub-region is much higher than that in arid sub-region, which is 2.6d/10a (see *Fig. 8a*, *c*, *e* and *Table 4*).

Observed from spatial scale, WSDI index showed an overall upward trend, and 53% of the stations passed the significance test. However, WSDI index showed a downward trend in Minxian County and Huajialing, Gansu, Guyuan and Haiyuan,

http://www.aloki.hu ● ISSN 1589 1623 (Print) ● ISSN 1785 0037 (Online)
DOI: http://dx.doi.org/10.15666/aeer/1705_1186911885

Ningxia, Zhengzhou, Xinxiang and Xuchang, Henan, which may be caused by local microclimate and other factors, but the specific reasons need to be further studied (see *Fig. 8b*). CSDI index showed a consistent downward trend on the whole in space, but the downward rate varied from 09.74 to 0d/10a, and 71% of the stations passed the significance test (see *Fig. 8d*). GSL index showed a consistent upward trend on the whole in space, but the rate varied from 0.1 to 14.04d/10a, and 78% of the stations passed the significance test. In addition, Yushe is the only station where showed a downward trend, which was not significant (see *Fig. 8f*).

Table 4. *Variation trend (3) of extreme temperature indexes from 1951 to 2014*

Index name	Arid sub-region	Humid sub-region
	Rate of change (d/10a)	Rate of change (d/10a)
WSDI	0.7**	0.6 n.s.
CSDI	-2.0**	-1.9**
GSL	2.6**	6.8**

**It passed the 99% confidence level test. *It passed the 95% confidence level test. n.s. means that the variation trend is not significant

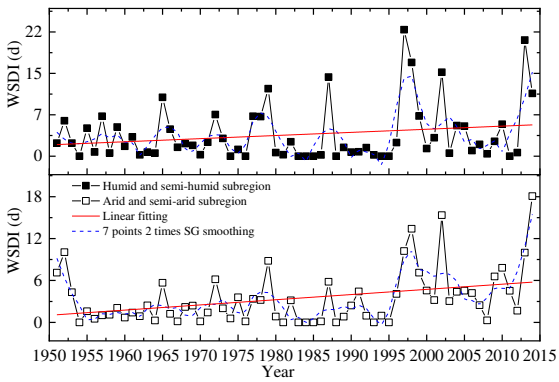

(a) Interannual variation of WSDI index

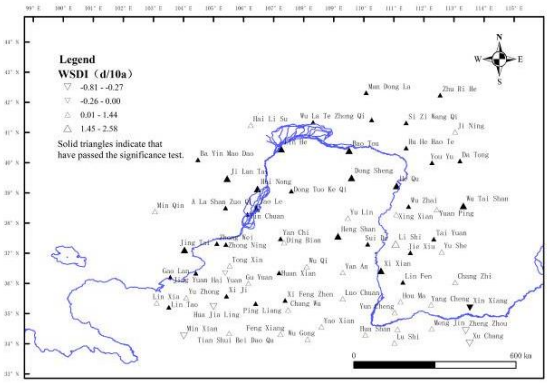

(b) Space variation of WSDI index

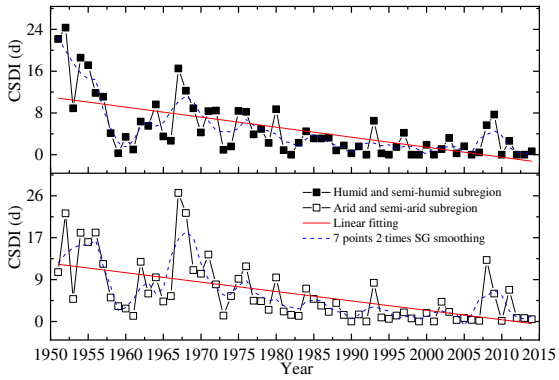

(c) Interannual variation of CSDI index

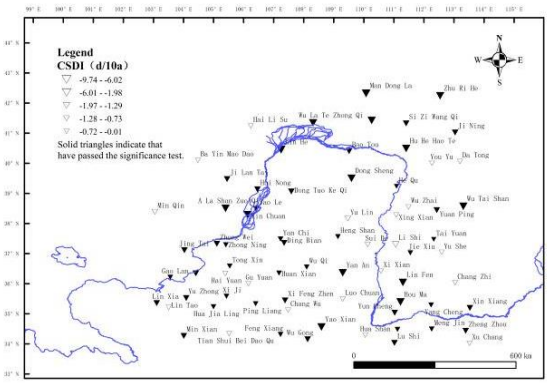

(d) Space variation of CSDI index

http://www.aloki.hu ● ISSN 1589 1623 (Print) ● ISSN 1785 0037 (Online)
DOI: http://dx.doi.org/10.15666/aeer/1705_1186911885

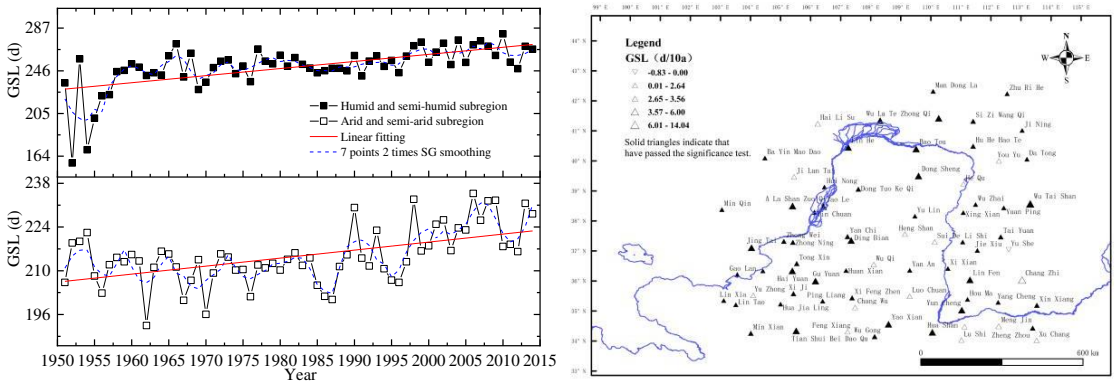

(e) Interannual variation of GSL index (f) Space variation of GSL index

Figure 8. *Temporal and spatial variation of WDSI, CSDI and GSL indexes*

Conclusion

This study analyzes the spatial-temporal scale of 18 extreme temperature indexes in the middle reach of Yellow River from 1951 to 2014, and draws the following conclusions:

(1) The middle reach of Yellow River is located in the transitional zone of arid and semi-arid and humid and semi-humid climate in China. The arid and semi-arid sub-region (located in the upper reaches of the Yellow River) and humid and semi-humid sub-region (located in the middle and lower reaches of the Yellow River) in the middle reach of Yellow River have basically similar variation trend in terms of extreme temperature events, but the intensity is different and spatial distribution is inconsistent.

(2) On time scale, it is found through the analysis of 18 extreme temperature indexes that the extreme temperature events have shown an upward trend in the past 60 years. On spatial scale, the distributional difference of each index is significant. The variation rate of multiple indexes in arid sub-region is greater than that in humid sub-region. The proportion of meteorological stations with significant variation of each index in arid sub-region is higher than that in humid sub-region. In addition, some indexes such as DTR, TNx, TNx, TXx, WSDI and TX90p has a different variation trend from the entire the middle reach of Yellow River in individual small areas, which may be caused by local microclimates in urban heat islands and hilly areas, but further analysis and verification is also required.

(3) The variation trend of indexes such as DTR, TMAXmean, TMINmean, TNn, TNx, TXx and TXx began to slow down around 2000, which may be related to the slowdown of global warming (hiatus phenomenon). The time of slowdown analyzed in this paper is basically consistent with the conclusions of relevant researches. Regarding the impact of the slowdown of global warming on extreme temperature events, the changes in extreme temperature events around the slowdown of global warming may also be further studies.

Compared with the research results of the approximate region (Zhou et al., 2011; Ma et al., 2003; Li et al., 2010; Ren et al., 2014), this study believes that the extreme temperature events in the middle reaches of the Yellow River are on the rise. This may be the product of global climate change in recent decades. Therefore, changes in extreme temperature events may have many adverse effects on the development of the

http://www.aloki.hu ● ISSN 1589 1623 (Print) ● ISSN 1785 0037 (Online)
DOI: http://dx.doi.org/10.15666/aeer/1705_1186911885

region, and appropriate measures should be considered to protect future ecological and agricultural sustainability, as well as human security.

Acknowledgements. This study was funded by "Major Innovation Projects for Building First-class Universities in China's Western Region"(Grant No. ZKZD2017002); the university first-class discipline construction project of Ningxia, China. (Grant No. NXYLXK2017A03); the Natural Science Foundation of Ningxia, China (Grant No. 2019AAC03049); the scientific research project of Ningxia Colleges and Universities (Grant No. NGY2017026) and the China Scholarship Council (Grant No. 201708645016).

REFERENCES

[1] Alexander, L. V. (2016): Global observed long-term changes in temperature and precipitation extremes: a review of progress and limitations in IPCC assessments and beyond. – Weather and Climate Extremes 11: 4-16.
[2] Cai, T., Tang, H. (2011): A survey of least squares fitting principles for smoothing filters: Savitzky-Golay. – Digital Communication 01: 63-68 + 82.
[3] Chen, L., Wang, S., Shang, K., et al. (2011): Atmospheric circulation anomalies of large-scale extreme high temperature events in Northwest China. – Journal of Desert Research 04: 1052-1058.
[4] Chen, S., Wang, J., Guo, J., et al. (2012): Evolution characteristics of the extreme high temperature event in Northwest China from 1961 to 2009. – Journal of Natural Resources 05: 832-844.
[5] Chen, X., Cai, Y., Tan, J., et al. (2014): Research progress on hiatus in the process of global warming. – Advances in Earth Science (08): 947-955.
[6] Diffenbaugh, N. S., Singh, D., Mankin, et al. (2017): Quantifying the influence of global warming on unprecedented extreme climate events. – Proceedings of the National Academy of Sciences 114(19): 4881-4886.
[7] Grotjahn, R., Black, R., Leung, R., et al. (2016): North American extreme temperature events and related large scale meteorological patterns: a review of statistical methods, dynamics, modeling, and trends. – Climate Dynamics 46(3-4): 1151-1184.
[8] Horton, D. E., Johnson, N. C., Singh, D., et al. (2015): Contribution of changes in atmospheric circulation patterns to extreme temperature trends. – Nature 522(7557): 465.
[9] Li, Y., He, D., Hu, J., et al. (2012): Spatial and temporal variations of extreme precipitation events in the Red River Basin during 1960-2007. – Journal of Natural Resources (11): 1908-1917.
[10] Li, Z., Zheng, F. L., Liu, W. Z., et al. (2010): Spatial distribution and temporal trends of extreme temperature and precipitation events on the Loess Plateau of China during 1961-2007. – Quaternary International 226(1-2): 92-100.
[11] Li, Z., Li, C., Song, J., et al. (2015): An analysis of the characteristics and causes of extremely high temperature days in the Yangtze–Huaihe River basins in summer 1960–2011. – Climatic and Environmental Research 20(5): 511−522.
[12] Mooshammer, M., Hofhansl, F., Frank, A. H., et al. (2017): Decoupling of microbial carbon, nitrogen, and phosphorus cycling in response to extreme temperature events. – Science Advances 3(5): e1602781.
[13] Ma, G., Rudolf, V. H., Ma, C. S. (2015): Extreme temperature events alter demographic rates, relative fitness, and community structure. – Global Change Biology 21(5): 1794-1808.
[14] Ma, Z. G., Fu, C. B., Ren, X. B., et al. (2003): Trend of annual extreme temperature and its relationship to regional warming in northern China. – Acta Geographica Sinica 58(Supplement 1): 11-20.

http://www.aloki.hu ● ISSN 1589 1623 (Print) ● ISSN 1785 0037 (Online)
DOI: http://dx.doi.org/10.15666/aeer/1705_1186911885

[15] Nie, J., Stevens, T., Rittner, M., Stockli, D., Garzanti, E., Limonta, M., ... Lu, H. (2015): Loess plateau storage of northeastern Tibetan plateau-derived Yellow River sediment. – Nature Communications 6: 8511.
[16] Qi, T., Zhang, Q., Wang, Y., et al. (2015): Spatiotemporal patterns of pan evaporation in spatiotemporal patterns of pan evaporation in 1960--2005 in China: changing properties and possible causes in China. – Scientia Geographica Sinica 12: 1599-1606.
[17] Ren, G., Zhou, Y. (2014): Urbanization effect on trends of extreme temperature indices of national stations over Mainland China, 1961–2008. – Journal of Climate 27(6): 2340-2360.
[18] Shen, H., Ma, M., Wang, J., et al. (2012): Variation characteristics of extreme air temperature events in Qinghai Province. – Journal of Glaciology and Geocryology 06: 1371-1379.
[19] Tang, T., Jin, R., Peng, X., et al. (2014): Analysis on extremely high temperature over southern China in summer 2013. – Meteorological Monthly 10: 1207-1215.
[20] Wang, L., Liu, T., Ding, Y., et al. (2016): Characteristics and tendency of climate change in the Hetao irrigation district in the past 50 years. – Journal of Beijing Normal University (Natural Science) 03: 402-407.
[21] Wang, Q., Zhang, M., Wang, S., et al. (2013): Extreme temperature events in Yangtze River Basin during 1962-2011. – Acta Geographica Sinica 05: 611-625.
[22] Wang, S., Luo, Y., Zhao, Z., et al. (2005): Controversy about climate warming. – Progress in Natural Science 08: 917-922.
[23] Wang, S., Luo, Y., Zhao, Z., et al. (2014a). Climate science challenges. – Advances in Climate Change Research 04: 306-309.
[24] Wang, S., Luo, Y., Zhao, Z., et al. (2014b). How long will the pause of global warming stay again? – Progressus Inquisitiones de Mutatione Climatis (06): 465-468.
[25] Wang, S., Luo, Y., Zhao, Z., et al. (2014c). Pause for thought. – Progressus Inquisitiones de Mutatione Climatis (04): 303-306.
[26] Wang, Y., Tan, D., Zhao, H. (2012): Characteristics of extreme high temperature in gansu in recent 50 Years. – Journal of Arid Meteorology 03: 410-414.
[27] Zhai, P., Pan, X. (2003): Change in extreme temperature and precipitation over Northern China during the second half of the 20th century. – Acta Geographica Sinica (S1): 1-10.
[28] Zhao, C., Chen, Y., Wang, W., et al. (2015): Temporal and spatial variation of extreme precipitation indexes of the Yellow River Basin in recent 50 years. – Yellow River 01: 18-22.
[29] Zhang, S. (2014): A new international climate change benchmark was officially opened in 2015. – Advances in Earth Science 08: 967.
[30] Zhang, Z., Chen, Y., Zhou, H. (2014): Spatiotemporal features of extreme high temperature in summer half year in Hetao and its vicinity. – Journal of Natural Disasters 02: 190-197.
[31] Zhou, Y., Ren, G. (2010): Variation characteristics of extreme temperature indices in mainland China during 1956-2008. – Climatic and Environmental Research 15(4): 405-417.
[32] Zhou, Y., Ren, G. (2011): Change in extreme temperature event frequency over mainland China, 1961−2008. – Climate Research 50(2-3): 125-139.

http://www.aloki.hu ● ISSN 1589 1623 (Print) ● ISSN 1785 0037 (Online)
DOI: http://dx.doi.org/10.15666/aeer/1705_1186911885

ANALYSIS OF REMOTE SENSING TECHNOLOGY APPLIED ON HYDROLOGY AND WATER RESOURCES –TAKING WEIHE'S ECOLOGY AS AN EXAMPLE

ZHAO, Z.* – LI, A. L. – MA, Y. M. – LIAN, H. D. – ZHANG, L.

School of Water Conservancy, North China University of Water Resources and Electric Power
136 Jinshui East Road, Zhengzhou City, 450045 Henan Province, China

**Corresponding author*
e-mail: zhaozhao@ncwu.edu.cn

(Received 23rd Apr 2019; accepted 4th Jul 2019)

Abstract. In order to study the water resources of Weihe and to maintain its ecological environment, remote sensing technology is used to study the local water resources (monitoring water quality and quantity). Weihe is not only the political and cultural center of Shaanxi Province, but also an economically active zone. It has become an important part of hydrology and water resources work in Shaanxi Province to keep abreast of the relevant situation of Weihe waters at any time, and also a prerequisite for maintaining the ecological environment of Weihe. Remote sensing technology is a high-resolution tool for obtaining target information, information transmission and comprehensive utilization of information. Especially for the dynamic subject of hydrology and water resources, the depth of Weihe waters is obtained by remote sensing technology, and the pollutant concentration data are obtained according to the characteristics of pollutants. Therefore, remote sensing technology is used to monitor the water quantity and water quality of Weihe waters and to obtain effective information on Weihe waters, which provides a basis for other studies of Weihe waters, and also has a certain supporting role in the management of relevant institutions, and ultimately realizes the sustainable ecological environment of Weihe.
Keywords: *economically active zone, information transmission, the pollutant concentration data, water quantity, the sustainable ecological environment*

Introduction

With the rapid development of social economy, environmental problems are becoming more and more serious. One of the most closely related problems is water resources (Cheng et al., 2018). People's daily life cannot do without water resources. Therefore, water quality and water quantity have become the focus of national attention. By means of administration, law and advanced science and technology, the State coordinates the relationship between social and economic development and water resources, and effectively controls pollutants entering the water body in order to maintain the balanced development of the water body and meet various needs (Xu et al., 2018). As the largest tributary of the Yellow River flowing through Shaanxi Province, Weihe needs to bear the vast majority of living and production sewage in Shaanxi Province. With the rapid economic development in Shaanxi Province and the growing urban population, it seriously threatens the ecological environment of the Weihe waters, greatly affecting the agricultural production of the surrounding farmland and the daily life of the surrounding residents, as well as the lives of the downstream residents. It poses a certain threat. Shaanxi government has issued a series of planning and renovation schemes to control the water environment of Weihe (Triegel and Guo, 1994; Mohammady et al., 2018). It can dynamically monitor the water volume and pollutant concentration of Weihe in an all-round way, so that the water volume can be guaranteed

http://www.aloki.hu ● ISSN 1589 1623 (Print) ● ISSN 1785 0037 (Online)
DOI: http://dx.doi.org/10.15666/aeer/1705_1188711899

to a certain extent and the pollutants in the water can be kept within a certain range, so as to realize the self-purification of the water area.

Remote sensing technology is a comprehensive detection technology, which has been widely used in agriculture, address, meteorology, ocean, hydrology, environmental protection and military investigation. Especially in hydrology and water resources work, the use of remote sensing technology provides an important technology for the study of hydrology and water resources (Vikesland, 2018). With the continuous development of science and technology, the application of remote sensing technology in hydrology and water resources is becoming more and more extensive. It not only can accurately provide people with relevant data, and to a large extent, save human and time costs, improve work efficiency, and provide technical support for the related work of hydrology and water resources (Cavalagli et al., 2018). At the same time, because it is not affected by geographical location, and the bad weather and environment have less interference on remote sensing technology, remote sensing technology can achieve all-weather and all-round information collection, saving the time and cost of manual monitoring.

In this form, how to use remote sensing technology to monitor water quality in an all-round and dynamic way has become an important part of local government's environmental protection and water resources protection (Mace et al., 2018). As an important water source for crop growth in Guanzhong Plain, it is necessary to monitor the water quantity and water quality of Weihe to ensure that farmers' production and life are not affected, to ensure the sustainable development of Weihe, and to achieve ecological green and sustainable development.

Therefore, remote sensing technology is used to monitor the water quantity and quality of Weihe waters (Wang et al., 2018). It can acquire and process the water quantity and quality data at a relatively fast speed and in a relatively short period, which is conducive to the acquisition of water resources-related data, thus ensuring the water quantity and improving the water quality, providing a basis for other aspects of Weihe waters research (Liu et al., 2018). It also has certain reference significance in monitoring and improving the situation of water quantity and quality of related rivers, as well as the management of relevant departments and water conservancy construction in Shaanxi Province.

Literature review

With the rapid development of the world economy, environmental pollution has become a key issue of global ecological development. Water resources are the source of human survival, and production and life are inseparable from water. The total amount of water resources per capita in China accounts for only one quarter of the world's per capita water volume, and is considered to be one of the countries lacking water resources. How to control water volume and control rivers has also become the key contents that scholars discuss. Jiang pointed out in his paper that with the increasing water demand, serious shortages of surface water and groundwater appeared in Northwest China and North China (Maggiori et al., 2017). Cai et al. found that over-exploitation of water resources led to land subsidence and ecosystem degradation in many places through the study of water resources in recent years (Nogueira et al., 2017). Jin Shuquan pointed out in the study that the water quality of the Yellow River, Huaihe and Liaohe has been affected to varying degrees in recent years. Among the 47

http://www.aloki.hu ● ISSN 1589 1623 (Print) ● ISSN 1785 0037 (Online)
DOI: http://dx.doi.org/10.15666/aeer/1705_1188711899

key cities studied, the water quality standard rate of less than 80% is up to 30% (Kussul et al., 2017).

Shi Xiaoliang, Zhou Zhenghui and Wang Xinshuang retrieved soil water content by using multi-dimensional geospatial data and long time series remote sensing images. Combined with relevant data, a groundwater monitoring model was constructed. The increasing trend of groundwater burial data in more than ten years was verified by an example, and its distribution characteristics were obtained (Zhu et al., 2017). Wang Jie and Wang Liang elaborated the basic principles and advantages of remote sensing technology, and monitored water resources. In the case of combining professional manual survey with remote sensing technology monitoring, they selected better data to ensure the effectiveness of technology and the correctness of results (Jucker et al., 2017).

Ma Qie and Hu Kun, through the comprehensive discussion on the application of remote sensing technology in hydrology and water resources, found a tool for the efficient utilization of water resources for the study of hydrology and water resources in China, and laid a foundation for their development and research (Lu et al., 2017). Fu Guobin and Liu Changming elaborated in detail the monitoring model of water area, precipitation, evaporation, soil moisture and the application and progress of remote sensing technology in the actual dynamic monitoring process from two aspects, and put forward the method of combining remote sensing technology with geographic information system (Gu et al., 2017).

Methods

Remote sensing technology

Remote sensing technology is a comprehensive earth observation science and technology. It uses sensors to receive electromagnetic wave characteristics of target objects or non-target objects, and through information transmission, storage, correction and identification of target objects, ultimately realizes the timing, positioning, quantitative and qualitative research of target objects. Remote sensing was first applied in the field of aviation, and then with the development of aerial photography technology, it gradually developed into a more practical space exploration technology (Mohanty et al., 2017).

The realization of remote sensing technology requires the participation and cooperation of many disciplines as well as a set of precise technical equipment. Therefore, the implementation of remote sensing is a relatively complex system engineering, which mainly consists of four parts (*Fig. 1*).

The information source refers to the object that needs to be detected. Because any target has the characteristics of absorbing, reflecting, transmitting and radiating electromagnetic waves, when the target encounters electromagnetic waves, they will form specific electromagnetic waves of the target. Information acquisition refers to the process of receiving and recording specific electromagnetic waves of objects by using a series of technical equipment, mainly relying on remote sensing platform and sensor equipment. Information processing mainly uses optical instruments and computer equipment to correct, analyze and interpret the information charts, words and data acquired by remote sensing, so that users can get the error of original information, and get the effective information needed by extracting the impact characteristics of the target object through sorting out and summarizing. Finally, it comes to information

http://www.aloki.hu ● ISSN 1589 1623 (Print) ● ISSN 1785 0037 (Online)
DOI: http://dx.doi.org/10.15666/aeer/1705_1188711899

application. People use remote sensing technology in different fields and purposes, and they get different information. The information data obtained are mainly for the convenience of users in the inquiry, statistics and analysis of relevant content in the research field.

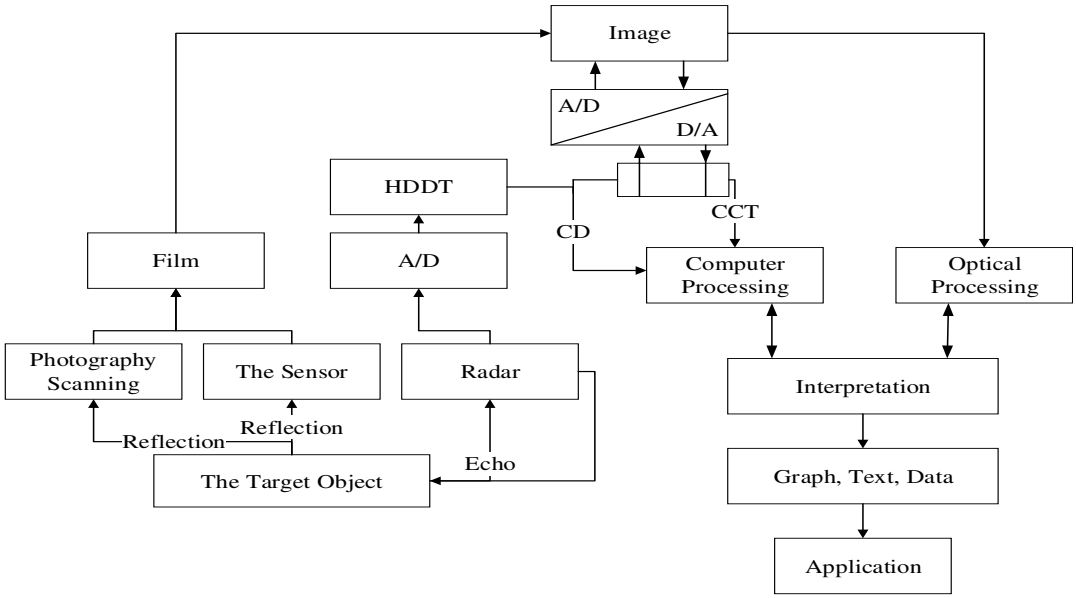

Figure 1. *Composition map of remote sensing system*

The reason why remote sensing technology can be widely used in different fields is that it is different from other technical means. There are three main aspects: firstly, the detection range is wide, the data acquisition speed is fast, and the cycle is short. It can observe the object in a relatively short period of time in a wide range, so as to obtain valuable data, which broadens people's horizons, enables people to study things from the whole, and provides valuable resources for later exploration of the rule of things (Audebert et al., 2018). Secondly, remote sensing technology can dynamically monitor the change of the object and obtain the periodic change of the object in order to predict the weather, disasters and environmental conditions. Thirdly, the data acquired by remote sensing technology is more comprehensive. It can centrally reflect the shape of objective things in each time period, truly reflect the characteristics of various things, and reflect the relevance of many things, as well as the situation for a period of time, which is conducive to the analysis of the causes of certain factors in each time period.

In hydrology and water resources work, remote sensing technology can be used to detect and remote sensing precipitation, evaporation, runoff, groundwater and sediment. When using remote sensing technology to measure precipitation, precipitation is usually indirectly judged by measuring cloud top brightness and cloud top temperature. When measuring evaporation, water evaporation and plant transpiration can be calculated by combining hydrological model. The remote sensing is used to monitor water quality mainly through the spectral analysis of water quality to classify the water quality indicators, and empirical model is used to combine the spectral characteristics of water quality and specific parameters of water body, to obtain relevant data and to provide effective data for the next step. Empirical model method requires effective combination of specific parameters of water quality and spectral characteristics of water body.

http://www.aloki.hu ● ISSN 1589 1623 (Print) ● ISSN 1785 0037 (Online)
DOI: http://dx.doi.org/10.15666/aeer/1705_1188711899

$$Y = A + BX \quad \text{or} \quad Y = AB^X \qquad \text{(Eq.1)}$$

Represents the measured value of remote sensing, Y represents the water quality parameters of objects to be estimated (ElMekawy et al., 2018), and A and B are the undetermined coefficients (*Eq. 1*).

Overview of Weihe

Weihe is the largest tributary of the Yellow River basin, with the largest amount of water. It originated from Niaoshu mountain, Weiyuan County, Dingxi City, Gansu Province. It flows into Shaanxi after Tianshui, Gansu Province, and finally into Tongguan County. The main stream of the Weihe runs 502.4 km in Shaanxi Province, with an area of 671,000 km^2 and an average runoff of 5.38 billion m^3. With the acceleration of industrialization and the continuous development of economy and society, environmental problems are becoming more and more serious, especially water pollution. Weihe is regarded as the life river of Shaanxi in Guanzhong area of Shaanxi Province. Therefore, the water quality of Weihe is closely related to the social and economic development of the area. Moreover, on the one hand, the extreme shortage of water resources in Weihe is due to the decrease of water entering Shaanxi Province year by year (Cassidy et al., 2018); on the other hand, the rapid development of economy, the continuous expansion of cities and the rapid expansion of population make the water consumption for production and living increase sharply. Most of the areas along Weihe are the production areas of crops. Irrigation water demand is large and groundwater has to be collected. This also leads to the decrease of the flow of the river recharged by groundwater, and the decrease of groundwater level also needs to be supplemented by the water in the river. This repeated impact makes the lives of people around the groundwater as a source of living water threatened. The distribution of residential areas and factories along Weihe is relatively concentrated. The demand of sewage discharged from production and living and agricultural production for Weihe water is increasing year by year. The view of Weihe Basin (*Fig. 2)* and the main cities flowed by the Weihe Basin (*Fig. 3*) are shown.

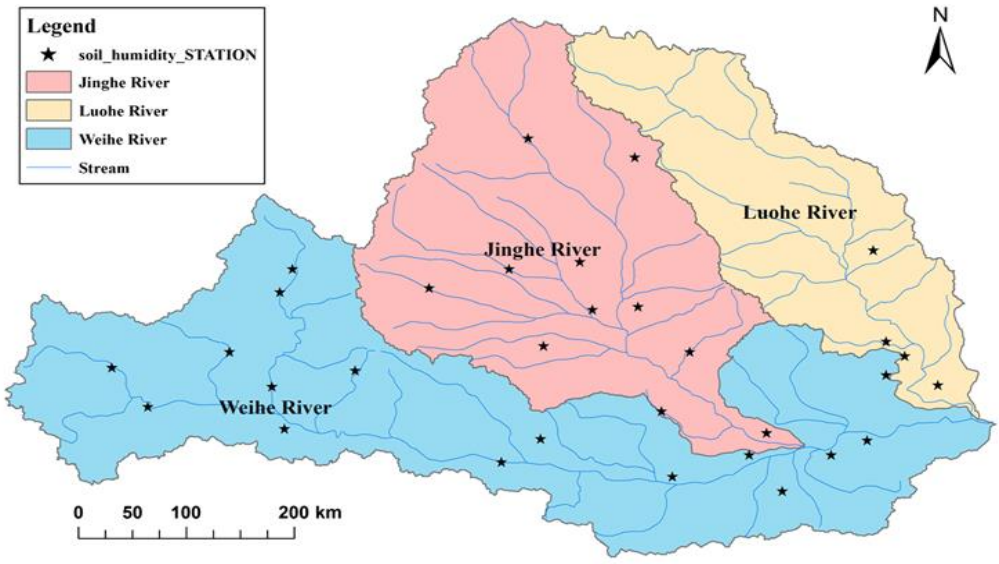

Figure 2. *View of Weihe Basin*

http://www.aloki.hu ● ISSN 1589 1623 (Print) ● ISSN 1785 0037 (Online)
DOI: http://dx.doi.org/10.15666/aeer/1705_1188711899

Figure 3. *Major cities in the Weihe Basin*

The relevant government departments have also formulated a series of treatment programs, and relevant enterprises have formulated sewage treatment measures, but the concentration of pollutants in river water is still high, so that river water cannot rely on its own purification capacity to maintain ecological balance. Therefore, in view of the problem of water pollution in Weihe, it is very important to quickly establish an effective method to detect the water quality of Weihe.

When monitoring water quantity, a zero-dimensional water quality model is adopted, and a river section is assumed to be a fully mixed reactor. When the sewage with Q_0 and C_0 inflow enters the reactor, due to stirring, the pollutants can be completely uniformly distributed in the tank (Chen et al., 2018). Thus, the equilibrium equation between water quality (*Eq. 2*) and flow rate (*Eq. 3*) is established when the water quality and flow rate are not stable.

$$\frac{dV_c}{dt} = \left(Q_0 c - Q_1 c\right) + \sum S^{'}\left(c,t\right) \quad \text{(Eq.2)}$$

$$\frac{dV}{dt} = Q_0 - Q_1 + q \quad \text{(Eq.3)}$$

When V is constant (*Eq. 4*):

$$\frac{dc}{dv} = \frac{Q_0}{V} c_0 - \frac{Q_1}{V} c + \sum S\left(c,t\right) \quad \text{(Eq.4)}$$

http://www.aloki.hu ● ISSN 1589 1623 (Print) ● ISSN 1785 0037 (Online)
DOI: http://dx.doi.org/10.15666/aeer/1705_1188711899

C is the concentration of pollutants in the tank (unit: ML-3); Q_1 is the flow rate at the time of outflow (unit: L3T-1); V is the volume of water in the tank (unit: L3); $\sum S(c,t)$ is the flow rate of source and leakage in the tank (unit: ML-3T-1); and q is the flow rate of element leakage (unit: L3T-1). As a result, there is:

$$c = \frac{1}{\left(1+\frac{Vk}{Q_1}\right)}\left(\frac{Q_0}{Q_1}\right)c_0 + \frac{1}{\left(1+\frac{Vk}{Q_1}\right)}\left(\frac{q}{Q_1}\right)c^* \quad \text{(Eq.5)}$$

c* denotes the inflow of source and drain terms, and k is the reaction rate coefficient of pollutant attenuation (*Eq. 5*).

The precipitation and evaporation of water flow are related to the balance of water flow. Therefore, it is required to control the water flow in a certain river section and keep the balance in a period of time.

$$\frac{\partial A}{\partial t} + \frac{\partial Q}{\partial x} = q \quad \text{(Eq.6)}$$

A represents the river bed area, Q is the discharge, q is the input discharge, t represents the time, and X represents the length of the river section.

Water quality monitoring is mainly to detect the types of pollutants, concentrations and changes of various pollutants in different monitoring points, so as to judge the water quality. The testing items mainly include two kinds of indicators reflecting water quality and toxic and harmful substances. The items that must be determined in water quality indexes are water temperature, suspended matter, total hardness, pH value, conductivity, dissolved oxygen, chemical oxygen consumption, ammonia nitrogen, nitrite nitrogen, nitrate nitrogen, volatile phenol, cyanide, arsenic, mercury, hexavalent chromium, lead, cadmium, petroleum, etc. (Liu et al., 2018). They can be used for sulphide, fluoride, chloride, organochlorine pesticides, organophosphorus pesticides, total chromium, copper, zinc, intestinal flora, uranium, radium and so on. The concentration of COD and NH-N_3 is studied only.

Sampling points should be determined according to water depth (*Table 1*), sampling time and sampling frequency (*Table 2*).

Results and discussion

The water quality and quantity of Xi'an, Baoji, Xianyang and Weinan along Weihe are studied. The data of these four regions are collected. The number of sewage outlets in each city (*Fig. 4*) and the data of pollutant concentration in 2007 (*Table 3*) are shown.

Table 1. *Determining sampling points according to water depth*

Water depth	Number	Position
Smaller than 5 m	1	0.3-0.5 m under the water
5-10 m	2	0.3-0.5 m under the water, and 0.5 m above the bottom
10-50 m	3	Half water depth, 0.3-0.5 m under the water, about 0.5 m above the river bottom
Larger than 50 m	Increase sampling points as appropriate	

http://www.aloki.hu ● ISSN 1589 1623 (Print) ● ISSN 1785 0037 (Online)
DOI: http://dx.doi.org/10.15666/aeer/1705_1188711899

Table 2. *Sampling time and frequency*

Objects	Sampling time and frequency
Main stream of larger river system and small and medium rivers	Sampling is not less than 6 times in a year, in rich, dry and peaceful seasons, usually twice in each period
Running through urban industrial zones, polluted rivers, browsing waters, drinking water sources, etc.	Samples are taken at least 12 times a year and at least once a month
Understand changes in water quality in a day or a few days	Sample in 24 h or in 3 days at different equal parts of time. In case of special circumstances, the number of sampling times will be increased
Background section	Sampling once a year

Table 3. *Concentration of pollutants in the sewage outlet of Weihe, Guanzhong City*

Town	Chemical oxygen demand (COD) (unit: 10,000 tons/year)	NH-N3 (unit: 10,000 tons/year)	Subtotal (unit: 10,000 tons/year)
Xi'an	9.3515	0.8319	4.4676
Baoji	1.993	0.2048	0.9396
Xianyang	2.896	0.217	1.0299
Yangling	0.018	0.009	0.0798
Weinan	2.5203	0.1735	1.0282

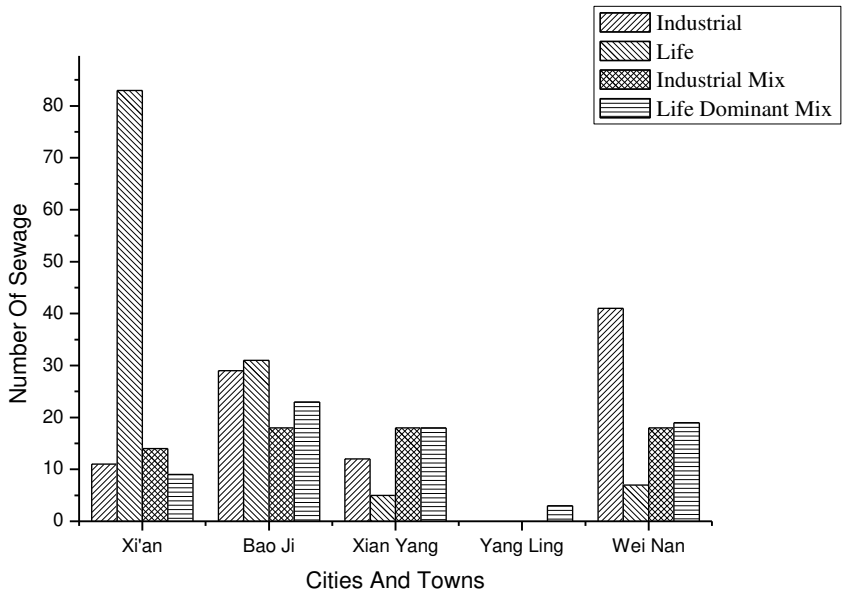

Figure 4. *Number of urban sewage outlets in the middle section of Weihe*

According to the data obtained by remote sensing technology, the discharge of wastewater is 79344 million tons per year, of which COD is 153.351 thousand tons per year and NH-N_3 is 135.68 thousand tons per year. The discharge of urban wastewater is 75.422 thousand tons per year, of which COD is 167.766 thousand tons per year and NH-N_3 is 143.62 thousand tons per year. The monitoring data (*Fig. 5*) are shown below.

http://www.aloki.hu ● ISSN 1589 1623 (Print) ● ISSN 1785 0037 (Online)
DOI: http://dx.doi.org/10.15666/aeer/1705_1188711899

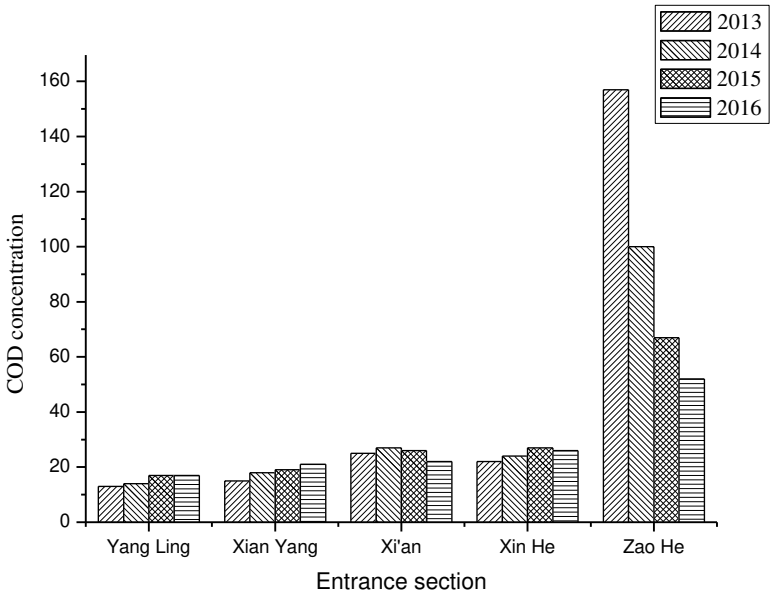

Figure 5. *Monitoring data of COD concentration (mg/L) in different sections from 2013 to 2016*

The annual total runoff variation map measured at Weinan Station is shown in (*Fig. 6*) and the relationship between precipitation and surface water resources in Weihe Basin (*Fig. 7*) are shown below.

The water balance relationship between snowfall and evaporation is calculated by water balance model, and water balance map of Weihe Basin (*Fig. 8*) is obtained.

The natural reasons for the change of water quantity in the Weihe are mainly caused by precipitation and man-made factors. There will be more precipitation in Yangling, Baoji and Weinan, less water in Xi'an and Xianyang, and higher vegetation coverage in Yangling. Therefore, the precipitation and annual runoff are less. This is because the increase of vegetation coverage increases evapotranspiration in the region. Additionally, the amount of water is affected to a certain extent, and the amount of water is reduced.

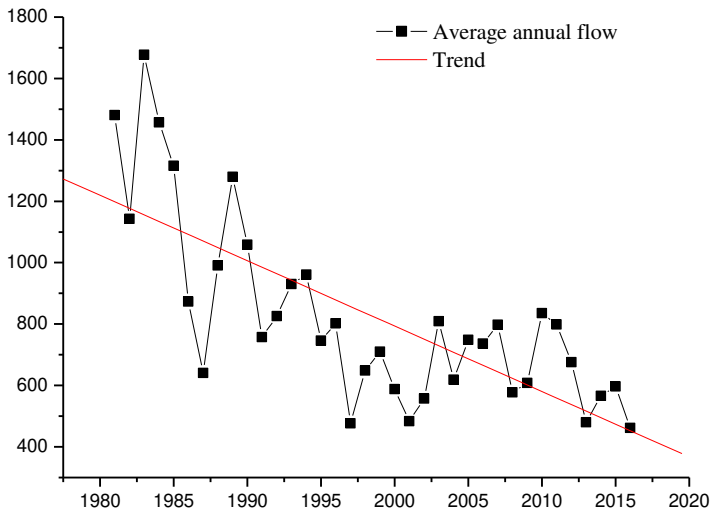

Figure 6. *Annual runoff variation map of Weinan Station from 1980 to 2017*

http://www.aloki.hu ● ISSN 1589 1623 (Print) ● ISSN 1785 0037 (Online)
DOI: http://dx.doi.org/10.15666/aeer/1705_1188711899

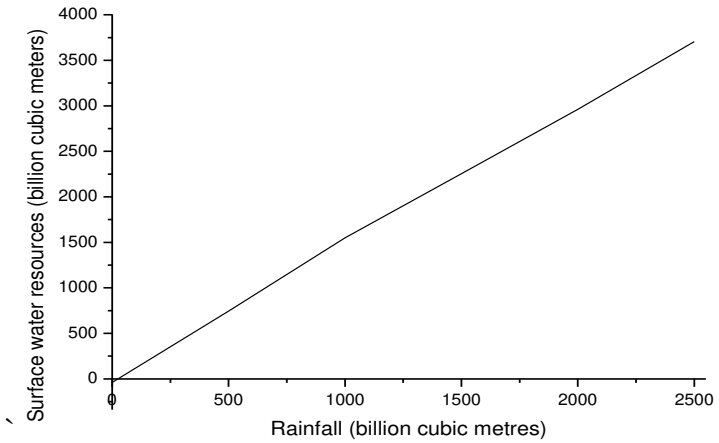

Figure 7. *The relation map between rainfall and surface water resources in Weihe Basin*

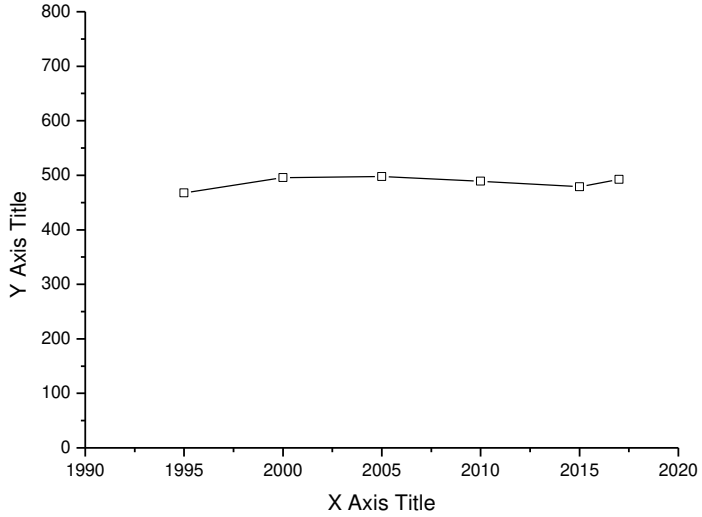

Figure 8. *Water balance map of Weihe Basin*

Moreover, because of the uneven distribution of precipitation in Weihe Basin, its tributaries are unevenly distributed and may even dry up. According to statistics, the actual runoff in the 1970s, 1980s and 1990s was 2.378 billion m^3, 2.333 billion m^3 and 2.231 billion m^3, respectively. Compared with the actual runoff, it increased by 17.0 mm, 16. 3 mm and 15.3 mm, respectively.

Using remote sensing technology to monitor precipitation can greatly improve the accuracy of monitoring, that is, to predict precipitation through cloud top brightness and cloud top temperature, which provides a reliable basis for hydrological departments to predict. The evaporation is monitored by physical methods, and the layered model is used to distinguish soil conditions, while the evaporation is measured. At present, there are also computer models for evapotranspiration, which realize the calculation of evapotranspiration and evapotranspiration on non-uniform ground. For the river runoff, it is monitored by remote sensing technology, which combines this part of data with hydrometeorological station data to survey the river runoff, and calculates the relevant data through hydrological model, which is transformed into effective information, and

http://www.aloki.hu ● ISSN 1589 1623 (Print) ● ISSN 1785 0037 (Online)
DOI: http://dx.doi.org/10.15666/aeer/1705_1188711899

then estimates the precipitation, evaporation and groundwater, finally obtains the relevant results of the river runoff. Because of this, the water volume of Weihe has been kept within a certain range in recent years, the surrounding agriculture also has a sufficient amount of irrigation water, and people's living water has been guaranteed, maintaining the sustainable development of Weihe Basin.

It can be seen that with the expansion of cities, people's living and industrial water consumption increases, while sewage discharge increases accordingly, but it is found that the discharge of COD and NH-N_3 decreases. On the one hand, it is because natural water has a certain self-purification capacity. When pollutants enter the water body, their pollutant concentration does not exceed the maximum bearing capacity of the water body. Through a series of biological and physical factors to purify the water, the concentration of pollutants in the water is reduced. On the other hand, related units of hydrology and water resources pay more attention to the water pollution and effectively treat the sewage. Using remote sensing technology to obtain relevant data, the sewage treatment rate is constantly improving.

At present, the application of remote sensing technology in hydrology and water resources is mostly qualitative research. Taking Weihe as an example, this paper studies its water quantity and water quality, lays a foundation for the protection of ecological environment in Weihe Basin, and provides ideas and methods for the study of soil water content along Weihe. However, due to the current use of remote sensing technology to obtain information, the process of interpreting information is more complex and consumes. Because of its high cost and large demand for professionals, remote sensing technology has not yet brought its energy efficiency into full play, which also has a certain guiding significance for enterprises and universities to cultivate talents.

Conclusion

Traditional hydrology and water resources research work is inefficient and has poor quality. The discovery of remote sensing technology provides technical support for hydrology and water resources related work, and largely solves the problem of low efficiency and poor quality of research work. As the "mother river" and "life river" in Shaanxi, Weihe affects the production of crops and people's lives. Therefore, the water quantity and quality of Weihe are closely related to the lives of the people around it. It is also closely related to the environment and ecology of Weihe and its coastal areas. It requires the relevant government departments to devote more energy to the governance of Weihe. Therefore, when using remote sensing technology to study the hydrology and water resources of Weihe Basin, the monitoring and remote sensing of precipitation, evaporation, runoff, COD and ammonia nitrogen (NH-N_3) in water quality are mainly applied, so as to obtain the relevant data of Weihe waters, which is conducive to improving the work efficiency of managers and maintaining the ecological environment of Weihe waters. It provides a technical branch for controlling the water quality and quantity of Weihe waters later. It also provides ideas for the water quality and quantity of other basins in Shaanxi Province, and provides a theoretical basis for relevant units to control water source problems.

Limited by the conditions, this paper inevitably produces errors in data monitoring. It is hoped that the impact of other factors on the accuracy of monitoring data can be reduced and more accurate data can be obtained in the future research process.

http://www.aloki.hu ● ISSN 1589 1623 (Print) ● ISSN 1785 0037 (Online)
DOI: http://dx.doi.org/10.15666/aeer/1705_1188711899

Acknowledgements. This work was supported by Innovation Fund for Doctoral Students of North China University of Water Resources and Electric Power.

REFERENCES

[1] Audebert, N., Le Saux, B., Lefèvre, S. (2018): Beyond RGB: very high resolution urban remote sensing with multimodal deep networks. – ISPRS Journal of Photogrammetry and Remote Sensing 140: 20-32.
[2] Cassidy, R., Jordan, P., Bechmann, M. (2018): Assessments of composite and discrete sampling approaches for water quality monitoring. – Water Resources Management 32(9): 3103-3118.
[3] Cavalagli, N., Comanducci, G., Ubertini, F. (2018): Earthquake-induced damage detection in a monumental masonry bell-tower using long-term dynamic monitoring data. – Journal of Earthquake Engineering 22(sup1): 96-119.
[4] Chen, B., Chen, L., Huang, B. (2018): Dynamic monitoring of the Poyang Lake wetland by integrating Landsat and MODIS observations. – ISPRS Journal of Photogrammetry and Remote Sensing 139: 75-87.
[5] Cheng, G., Yang, C., Yao, X. (2018): When deep learning meets metric learning: remote sensing image scene classification via learning discriminative CNNs. – IEEE Transactions on Geoscience and Remote Sensing 56(5): 2811-2821.
[6] ElMekawy, A., Hegab, H. M., Pant, D. (2018): Bio-analytical applications of microbial fuel cell–based biosensors for onsite water quality monitoring. – Journal of Applied Microbiology 124(1): 302-313.
[7] Gu, W., Lv, Z., Hao, M. (2017): Change detection method for remote sensing images based on an improved Markov random field. – Multimedia Tools and Applications 76(17): 17719-17734.
[8] Jucker, T., Caspersen, J., Chave, J. (2017): Allometric equations for integrating remote sensing imagery into forest monitoring programmes. – Global Change Biology 23(1): 177-190.
[9] Kussul, N., Lavreniuk, M., Skakun, S. (2017): Deep learning classification of land cover and crop types using remote sensing data. – IEEE Geoscience and Remote Sensing Letters 14(5): 778-782.
[10] Liu, X., Lu, Z., Yang, W. (2018): Dynamic monitoring and vibration analysis of ancient bridges by ground-based microwave interferometry and the ESMD method. – Remote Sensing 10(5): 770.
[11] Liu, Y., Hallberg, R., Sergienko, O. (2018): Climate response to the meltwater runoff from Greenland ice sheet: evolving sensitivity to discharging locations. – Climate Dynamics 51(5-6): 1-19.
[12] Lu, X., Zheng, X., Yuan, Y. (2017): Remote sensing scene classification by unsupervised representation learning. – IEEE Transactions on Geoscience and Remote Sensing 55(9): 5148-5157.
[13] Mace, J., Roelke, R., Fonseca, R. (2018): Pivot tracing: Dynamic causal monitoring for distributed systems. – ACM Transactions on Computer Systems (TOCS) 35(4): 11.
[14] Maggiori, E., Tarabalka, Y., Charpiat, G. (2017): Convolutional neural networks for large-scale remote-sensing image classification. – IEEE Transactions on Geoscience and Remote Sensing 55(2): 645-657.
[15] Mohammady, M., Moradi, H. R., Zeinivand, H. (2018): Modeling and assessing the effects of land use changes on runoff generation with the CLUE-s and WetSpa models. – Theoretical and Applied Climatology 133(1-2): 1-13.
[16] Mohanty, B. P., Cosh, M. H., Lakshmi, V. (2017): Soil moisture remote sensing: State-of-the-science. – Vadose Zone Journal 16(1). DOI: 10.2136/vzj2016.10.0105.

http://www.aloki.hu ● ISSN 1589 1623 (Print) ● ISSN 1785 0037 (Online)
DOI: http://dx.doi.org/10.15666/aeer/1705_1188711899

[17] Nogueira, K., Penatti, O. A. B., dos Santos, J. A. (2017): Towards better exploiting convolutional neural networks for remote sensing scene classification. – Pattern Recognition 61: 539-556.
[18] Triegel, E. K., Guo, L. (1994): Overview of the Fate of Pesticides in the Environment, Water Balance; Runoff vs. Leaching. – In: Honeycutt, R. C., Schabacker, D. J. (eds.) Mechanisms of Pesticide Movement into Ground Water. Lewis Publishers, Boca Raton, FL, pp. 1–13.
[19] Vikesland, P. J. (2018): Nanosensors for water quality monitoring. – Nature Nanotechnology 13(8): 651.
[20] Wang, K. N., Chao, X. J., Liu, B. (2018): Red fluorescent probes for real-time imaging of the cell cycle by dynamic monitoring of the nucleolus and chromosome. – Chemical Communications 54(21): 2635-2638.
[21] Xu, X., Li, W., Ran, Q. (2018): Multisource remote sensing data classification based on convolutional neural network. – IEEE Transactions on Geoscience and Remote Sensing 56(2): 937-949.
[22] Zhu, X. X., Tuia, D., Mou, L. (2017): Deep learning in remote sensing: A comprehensive review and list of resources. – IEEE Geoscience and Remote Sensing Magazine 5(4): 8-36.

http://www.aloki.hu ● ISSN 1589 1623 (Print) ● ISSN 1785 0037 (Online)
DOI: http://dx.doi.org/10.15666/aeer/1705_1188711899

A SIMPLIFIED ASSESSMENT MODEL OF ENVIRONMENTAL GEOLOGY SUITABILITY COMBINED WITH IN-SITU INFILTRATION TEST FOR STORMWATER MANAGEMENT AND APPLICATION

WANG, J. J. – WANG, S.W. – WANG, X.Y. – SUN, L.*

The Institute of Hydrogeology and Environmental Geology
No. 268, Zhonghua North Road, Shijiazhuang 050061, Hebei, China

**Corresponding author*
e-mail: Tairan_W@163.com

(Received 23rd Apr 2019; accepted 4th Jul 2019)

Abstract. Stormwater management is the core of sponge city construction whose essence is to solve the urban water problem by means of seepage, storage, purification, utilization and drainage. From the environmental geology point of view, this paper mainly consider the geological properties of sponge capacity in the construction of sponge city. Based on a large number of in-situ water infiltration tests and boreholes, two indexes that sponge infiltration and sponge storage are put forward to study and analyze the maximum depth of rainfall infiltration and the infiltration velocity of surface soil under the original sponge geological conditions. These two indexes can directly and effectively represent and summarize the environmental geological suitability in the construction of sponge cities. Moreover, these two indexes are easy to understand, have a strong universality, and easy to promote. Finally, taking Xinxiang city in central China as an example, the environmental geological suitability of Xinxiang sponge city construction is evaluated.
Keywords: *rainfall-runoff; sponge infiltration capacity; sponge storage capacity; stability evaluation*

Introduction

Based on China's national conditions, China is experiencing and will continue to experience a period of rapid urbanization. Urbanization promotes the modernization of the country and the rapid development of the economy. At the same time, the immaturity of the development of urbanization also bring a series of "urban diseases" (Burns, 2012; Carter, 2007; Che, 2015), such as urban water logging, water shortage, water pollution and water ecological degradation. Due to the fact that urban water problem is very complex and still in its infancy, many standards such as construction principle, development mode and index system of sponge city have not been perfected (Wang et al., 2017; Zhang et al., 2016; Yu et al., 2015; Wu et al., 2016; Qiu, 2015; Hu et al., 2015; Hu et al., 2015a, b; Wang et al., 2015; Song et al., 2007), and are still in the process of exploration.

In the 1970s, the United States was the earliest to adopt rainwater flood detention and control measures for urban water problems. However, this measure not only failed to solve the problem of rainwater flood, but also destroyed the urban water ecological balance and polluted the urban water environment due to human engineering activities. By the early 1990s, Maryland (US EPA, 2000a) was the first to propose the concept of "Low Impact Development" (LID). The main connotation is: in the process of land development, the rainfall runoff is controlled by the site to reduce the runoff and rainwater pollution load (Benedict, 2000; US EPA, 2012b). The concept was quickly accepted and developed by Australia, New Zealand and some European countries

http://www.aloki.hu ● ISSN 1589 1623 (Print) ● ISSN 1785 0037 (Online)
DOI: http://dx.doi.org/10.15666/aeer/1705_1190111910

(2015) by whom natural and harmonious new urban planning concepts such as "Water-Sensitive Urban Planning" (Hoyer et al., 2011) and "Sustainable Drainage System" (D'Arcy et al., 2000; CIRIA, 2015) were put forward on the basis of LID. Relevant German institutions classified (Ministerium fuer Umwelt, 2001) the runoff water quality of different catchments based on different geographical factors, environmental conditions, geological conditions, etc. (Council, 2008; Dong, 2011; Wanielista, 1993), used GIS technology to plan and design the rainwater treatment plan, combined the water quality conditions and disposal purposes of each city, and decided the final disposal facility (Geiger, 2001; Gantner, 2003). North American scholars (Ji, 2014) proposed the study of rainwater micro-management based on the existing natural system, retaining important hydrological characteristics and functions, adopting the favorable conditions and constraints of rainwater management at the basin scale so as to mitigate the damage to the hydrological ecological environment and restore the regional hydroecological environment as much as possible. The "Optimal Management Practices for Rainwater" research conducted by Sweden and Denmark (Martin, 2011; Revit, 2003) combines hydrological characteristics, landscape design, environmental control, and management systems to comprehensively manage rainwater and flood control. This model is widely accepted because of its low processing cost and good processing effect. It can also be practiced in small and medium-sized cities in China as one of the directions to explore the current stage of urban rainwater management in China.

Different from the traditional "fast-draining" rainwater model, many experts and scholars in China have made new explanations on the nature of sponge cities and put forward new construction concepts (Che et al., 2002). Among the local laws and regulations, Beijing, Nanning and other cities require that new construction, reconstruction and expansion projects in various regions have guiding design patterns and engineering requirements for rainwater utilization in the construction of sponge cities, and formulate many measures for urban rainwater resource utilization (Wang et al., 2017).

The essence of the sponge city construction is to solve the problem of urban water. It is not only the rationality and validity of the measures of seepage, station, storage, purification and drainage should be considered, but also the physical properties of the sponge bearing body (rock and soil), as well as the danger of storing rainwater (including environmental geological problems) should be taken into account. The core content is closely related to environmental geology and hydrology. At present, domestic and foreign scholars still have different opinions on the construction model, essential connotation and viewpoins of the sponge city. They mostly study the "engineering measures" of the construction methods and technical modes (Du, 1996; Taylor, 2005; Wang, 1999), and overlooked the geological properties of the sponge capacity in the construction of sponge cities. They do not consider the overall evaluation of the environmental geological suitability of the construction area or planning area of sponge cities. Moreover, because of the lack of funds, most studies only stay in the theoretical research stage (Keller, 1999; Lloyd, 2002; Eslami, 1995), and have not been put into practice.

Therefore, in order to evaluate the suitability of sponge city construction, we should mainly consider the underground environmental bearing capacity and evaluate the original sponge environmental geological suitability from the geological point of view. This evaluation can effectively save the construction cost of sponge city and minimize

http://www.aloki.hu ● ISSN 1589 1623 (Print) ● ISSN 1785 0037 (Online)
DOI: http://dx.doi.org/10.15666/aeer/1705_1190111910

the workload of sponge city, and have a definite object in view to achieve the goal of spongy city construction.

Materials and methods

The environmental geological suitability evaluation of sponge city construction is the premise of sponge city construction. The sponge capacity of geological body in sponge city construction directly affects the difficulty and complexity of city planning, scheme design and site construction. From the point of view of hydrogeology and environment geology, this paper mainly consider the bearing capacity of underground environment (Knödel, 2007; Argent, 2008; Rooijen, 2010). Based on a large number of in-situ water infiltration tests and boreholes, two indexes that sponge infiltration and sponge storage are put forward to study and analyze the maximum depth of rainfall infiltration and the infiltration velocity of surface soil under the original sponge geological conditions. These two indexes can directly and effectively represent and summarize the environmental geological suitability in the construction of sponge cities. They are easy to get and understand, have strong universality and are easy to popularize. Completing the evaluation of environmental geology suitability in sponge city construction can reduce the difficulty and workload of urban planning investigation, design and construction, and provide ideas and reference for urban agglomeration sponge city construction planning and design.

Sponge infiltration capacity

Sponge infiltration refers to the capacity of urban "sponge body" to infiltrate rainfall (rainfall infiltration coefficient): Assuming under an ideal condition (an atmospheric pressure, a hydraulic gradient of one, only vertical infiltration is considered) and during the whole rainfall infiltration process (*Figs. 1* and *2*), the water seepage speed during the complete infiltration process of different soil layers is V_i:

$$V_i = \frac{Q}{t_i} \quad \text{(Eq.1)}$$

V_i: Water seepage velocity in different soil layers; t_i: Complete infiltration time in different soil layers.

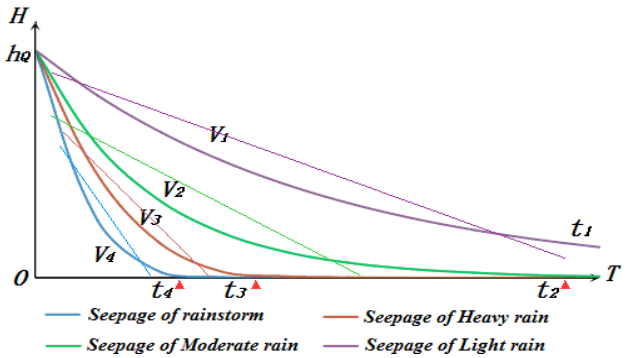

Figure 1. *Rainfall infiltration curves in different soil formations*

http://www.aloki.hu ● ISSN 1589 1623 (Print) ● ISSN 1785 0037 (Online)
DOI: http://dx.doi.org/10.15666/aeer/1705_1190111910

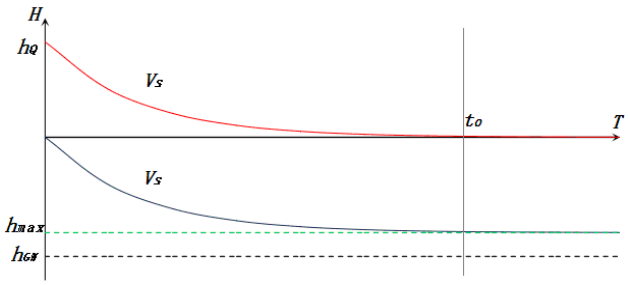

Figure 2. *Schematic diagram of rainfall infiltration curve. (A: The area of the region; Q: Maximum rainfall in 30 years; V_s: Rainwater infiltration rate; h_{max}: Maximum infiltration depth of rainfall; h_{GW}: Depth of groundwater; t_0: The time required for total infiltration of rainfall; n: Weighted effective porosity in penetration depth; h_Q: The height of the rainfall within the area)*

Sponge storage capacity

In the construction of the sponge city, the capacity of the sponge storage refers to the ability of the city "sponge body" to store rainwater (the size of aquifer storage space) and to solve urban water problems effectively (with the water supply capacity of phreatic layer).

Assuming an ideal state (an atmospheric pressure, a hydraulic gradient of 1, considering only vertical infiltration), the time required for complete rainfall infiltration is t_0, and the maximum depth of infiltration is $h_{\max}$:

$$h_{\max} = \frac{Q}{A \square n} \qquad \text{(Eq.2)}$$

Due to equal water permeability, the seepage on the ground is equal to the seepage in the aeration zone.

The sponge capacity P should be defined as: $P = \frac{h_{GW}}{h_{\max}}$

When $P > 1$, $h_{GW} > h_Q$. This indicates that the geological environment (the thickness of the aerated zone) can fully withstand the maximum rainfall Q in 30 years. It means that the city "sponge body" has sufficient rainfall storage capacity and water release capacity;

When $P=1$, $h_{GW} = h_Q$. This indicates that the geological environment just can withstand rainfall Q, and this is a critical state. To construct the sponge city, it is necessary to maintain the natural geological environment or take slight measures;

When $P < 1$, $h_{GW} < h_Q$. This indicates that geological environment cannot withstand rainfall Q. It means that the city "sponge body" has enough rainfall storage capacity and water release capacity.

Case study

Study area

Xinxiang City is located in the north of Henan Province, China. It belongs to the North China Plate. It is located in the Yellow River and Haihe River Basins. The terrain

http://www.aloki.hu ● ISSN 1589 1623 (Print) ● ISSN 1785 0037 (Online)
DOI: http://dx.doi.org/10.15666/aeer/1705_1190111910

is high in the north and low in the south. The northern part is mainly the Taihang Mountain and hilly land. The south is the alluvial fan plain of the Yellow River. The plains occupy 78% of the total land area of the city. The annual average precipitation is 573.4 mm, of which precipitation is the most from June to September, accounting for 72% of the annual precipitation, and the annual evaporation is 1748.4 mm. Xinxiang City has three national-level development zones and two provincial-level development zones, which are in a period of rapid urbanization and development.

A total of 123 sets of drilling points and 163 Investigation points information were obtained from the ground survey. The groundwater level in dry season and indoor seepage test data in the study area were collected, and 50 sets of field in-situ water seepage tests were carried out. The location distribution is presented in *Figure 3*.

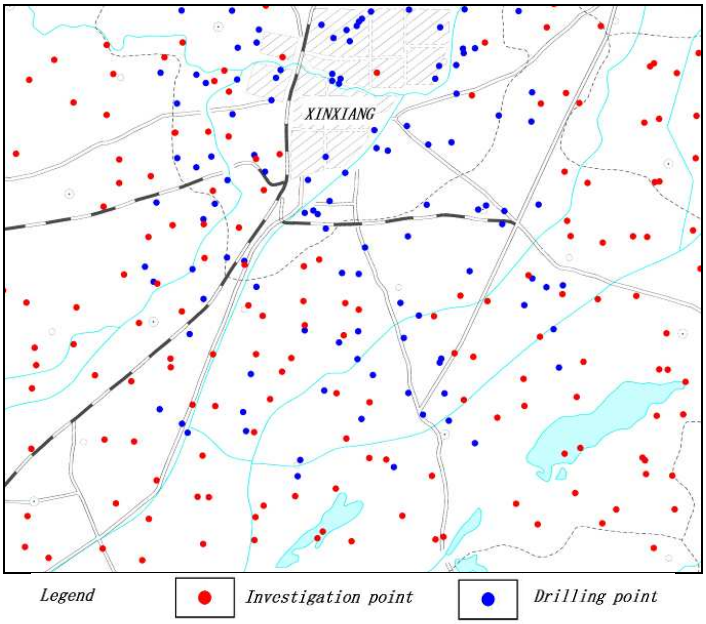

Figure 3. *Distribution of research points*

Results and discussion

Though a large number of field water seepage tests, a table (*Table 1*) of infiltration test results and their correspondent rainfall levels was obtained (*Fig. 4*).

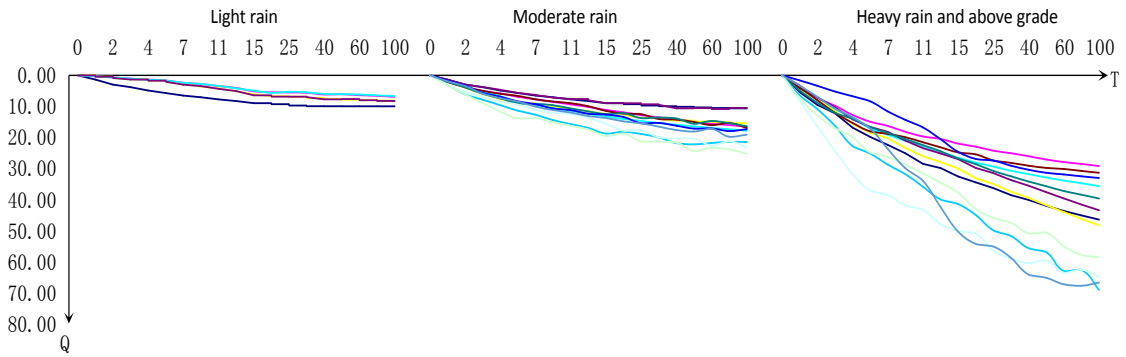

Figure 4. *Infiltration curves corresponding to different rainfall levels*

http://www.aloki.hu ● ISSN 1589 1623 (Print) ● ISSN 1785 0037 (Online)
DOI: http://dx.doi.org/10.15666/aeer/1705_1190111910

The critical value of the corresponding seepage velocity is determined by the rainfall level in *Table 1*.

Table 1. *Infiltration test results and their correspondent rainfall levels (rainfall does not produce runoff)*

Name of soil	Water seepage speed mm/d	Permeability coefficient cm/s^{-1}	Absorptive rainfall intensity	Rainfall level description (mm/d)	
Clay	4.12	< $1.2*10^{-6}$	Light rain	Light rain	0.1–9.9
Powder sticky	5.18	1.2×10^{-6}-$6.0*10^{-5}$	Light rain	Light rain	0.1–9.9
Floury soil	6.61	$6.0*10^{-5}$-$6.0*10^{-4}$	Light rain	Light rain	0.1–9.9
Loess	6.73	$3.0*10^{-4}$-$6.0*10^{-4}$	Light rain	Light rain	0.1–9.9
Silt	18.36	$6.0*10^{-4}$-$1.2*10^{-3}$	Moderate rain	Moderate rain	10–24.9
Fine sand	22.75–31.76	$1.2*10^{-3}$-$6.0*10^{-3}$	Heavy rain	Heavy rain	25–49.9
Medium sand	57.86–81.32	$6.0*10^{-3}$-$2.4*10^{-2}$	Rainstorm	Rainstorm	50–99.9
Coarse sand	87.46–125.23	$2.4*10^{-2}$-$6.0*10^{-2}$	Downpour	Downpour	100–249.9
Gravel	289.26–342.32	$6.0*10^{-2}$-$1.8*10^{-1}$	Heavy downpour	Heavy downpour	> 250

When $V < 6.0*10^{-4}$, the surface soil layer can only accept the precipitation of light rain;

When $6.0*10^{-4} < V < 1.2*10^{-3}$, the surface soil layer can only accept moderate rainfall;

When $1.2*10^{-3} < V < 6.0*10^{-3}$, the surface soil layer can accept heavy rain;

When $6.0*10^{-3} < V$, the surface water can accept the precipitation above the level of the heavy rain;

Based on the measured data and experimental results, the sponge seepage capacity and the P results of sponge storage capacity of Xinxiang sponge city is divided:

Figure 5 shows that the evaluation of sponge seepage capacity is poor in the study area, only 3% of the area infiltration rate reaches the level of heavy rain in the region, rainwater can directly infiltrate the surface aerated zone to recharge the shallow aquifer in rainy season. Rainwater does not generate rainfall-runoff, causing surface water. This area can be directly used for the water seepage construction of sponge cities. About 26.5% of the area with medium-rainfall infiltration capacity is distributed in the southwest and central part of the region. Rainfall can not fully infiltrate the surface aerated zone to recharge the shallow aquifer in rainy season. Surface runoff and surface water will be formed. In the initial stage of the construction of sponge city, it is necessary to carry out the water seepage construction of sponge city after the improvement of the sponge seepage capacity by paving with water permeability or adding engineering facilities such as grass planting ditch and vegetation buffer zone. 70% of the area only reaches the level of light rain, poor infiltration capacity, when rainwater conditions will form a large number of rainfall-runoff and lead to surface water. The intervention of artificial conditions and high cost of engineering construction, it is not appropriate to directly or selectively carry out the water seepage construction of sponge cities.

http://www.aloki.hu ● ISSN 1589 1623 (Print) ● ISSN 1785 0037 (Online)
DOI: http://dx.doi.org/10.15666/aeer/1705_1190111910

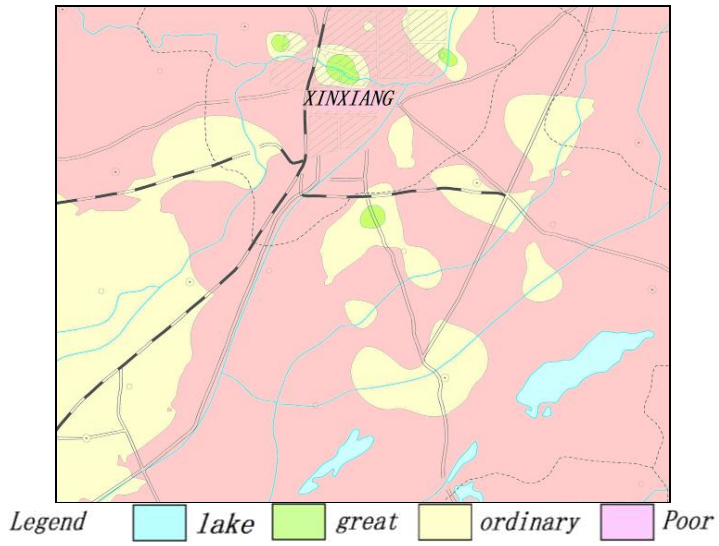

Figure 5. *The V results of sponge seepage capacity in Xinxiang sponge City*

Figure 6 shows that the evaluation of sponge storage capacity is preferably in the study area, 62% of the area can meet the annual rainfall. In rainy season, the water storage capacity of the surface aerated zone is enough to withstand rainfall infiltration and will not produce surface water. This area can be directly used for water storage construction of sponge city. In rainy season, 35.5% of the surface aerated zone in the region is in the critical range of water storage capacity, and some low-lying areas may produce surface water. In the early stage of the construction of sponge city, slope drainage should be carried out, or additional engineering facilities such as reservoirs and artificial lakes should be installed to improve the water storage capacity of sponge city. 2.5% of the area in the region has poor water storage capacity, can not withstand rainfall when rainwater conditions lead to surface water, and the intervention of artificial conditions and high cost of Engineering construction, it is not appropriate to directly or selectively carry out the water storage construction of sponge cities.

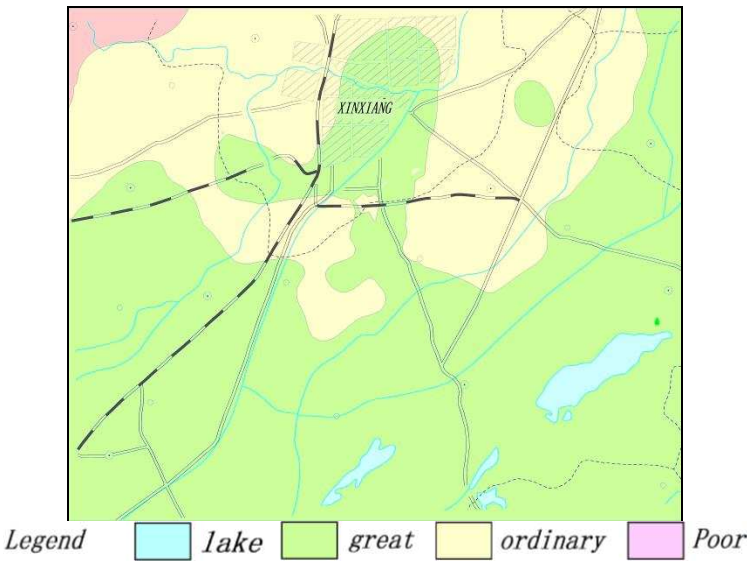

Figure 6. *The P results of sponge storage capacity in Xinxiang sponge City*

http://www.aloki.hu ● ISSN 1589 1623 (Print) ● ISSN 1785 0037 (Online)
DOI: http://dx.doi.org/10.15666/aeer/1705_1190111910

Conclusions and future work

The environmental geological suitability evaluation of sponge city construction is the premise of sponge city construction. The sponge capacity of geological body in sponge city construction directly affects the difficulty and complexity of city planning, scheme design and site construction. From the point of view of hydrogeology and environment geology, this paper mainly consider the geological properties of sponge capacity in the construction of sponge city. Based on a large number of in-situ water infiltration tests and boreholes, two indexes that sponge infiltration and sponge storage are put forward to study and analyze the maximum depth of rainfall infiltration and the infiltration velocity of surface soil under the original sponge geological conditions. These two indexes can directly and effectively represent and summarize the environmental geological suitability in the construction of sponge cities. They are easy to get and understand, have strong universality and are easy to popularize. Completing the evaluation of environmental geology suitability in sponge city construction can reduce the difficulty and workload of urban planning investigation, design and construction, and provide ideas and reference for urban agglomeration sponge city construction planning and design.

According to the sponge seepage ability and the sponge water storage ability, the environmental geological suitability of Xinxiang sponge city was evaluated by two indexes. The sponge seepage ability in the study area was obviously superior to the sponge seepage ability, which was consistent with the field investigation results. In addition, some suggestions on the construction of sponge cities are given for the regions with insufficient infiltration and storage capacity to digest the maximum rainfall.

In this paper, the ideal state hypothesis is made in the environmental suitability index of sponge city construction, and the sponge purification capacity is also an important link in the construction of sponge city. Which are insufficient and slightly rough. Besides the sponge seepage and the sponge water storage capacity should be considered simultaneously, which should be the direction and focus of further research.

Acknowledgements. This paper was supported by the National key R & D projects of China (No 2018YFC1803302) and National Nature Fund of China (No 41602261; No 41807231; No 41272301), Basic research projects of CAGS (YYWF201628).

REFERENCES

[1] Argent, N., Rolley, F., Walmsley, J. (2008): The sponge city hypothesis: does it hold water? – Australian Geographer 39(2): 109-130.

[2] Benedict, M. A. (2000): Green Infrastructure: A Strategic Approach to Land Conservation. PAS Memo. – American Planning Association, Chicago, IL.

[3] Burns, M. J., Fletcher, T. D., Walsh, C. J., et al. (2012): Hydrologic shortcomings of conventional urban stormwater management and opportunities for reform. – Landscape & Urban Planning 105(3): 230-240.

[4] Carter, T., Jackson, C. R. (2007): Vegetated roofs for stormwater management at multiple spatial scales. – Landscape & Urban Planning 80(1): 84-94.

[5] Che, S. Q., Xie, C. K., Chen, D., et al. (2015): Development and Constructive Approaches for Theories and Technologies of Sponge City System. – Chinese Landscape Architecture 31(6): 11-15.

http://www.aloki.hu ● ISSN 1589 1623 (Print) ● ISSN 1785 0037 (Online)
DOI: http://dx.doi.org/10.15666/aeer/1705_1190111910

[6] Che, W., Li, J. Q. (2002): Recent status and prospect of urban rainwater utilization. – Water Waste Eng 3: 12-14.
[7] CIRIA (2005): SUDS: Sustainable Drainage Systems: Promoting Good Practice - A CIRIA Initiative. – CIRIA, London.
[8] Council, N. R. (2008): Urban stormwater management in the United States. – National Research Council, Washington, DC.
[9] Dong, S., Han, Z. (2011): Study on planning an "eco-sponge city" for rainwater utilization. – Urban Studies 18: 37-41.
[10] Du, S. (1996): Geologic radar and its application in environmental geology. – Geophysical & Geochemical Exploration 1996.
[11] Eslami, M. R., Mahbadi, H. (1995): Some problems of ecological environmental geology in arid and semiarid areas of China. – Environmental Geology 26(1): 64-67.
[12] Gantner, K. (2003): Nachhaltigkeit urbaner Regenwasserbewirtschaftungsmethoden - Teil 1: Grundlagen. – GWF Wasser und Abwasser 3: 240-247.
[13] Geiger, W., Dreiseitl, H. (2001): Neue Wege für das Regenwasser: Handbuch zum Rückhalt und zur Versickerung von Regenwasser in Baugebieten. – München Oldenbourg Industry Verlag GmbH, Muenchen.
[14] Hoyer, J. (2011): Water Sensitive Urban Design - Principles and Inspiration for Sustainable Stormwater Management in the City of the Future. – Jovis Publishing Co., Berlin, pp. 79-87.
[15] Hu, C. W. (2015):"Sponge city" reconstructing urban water ecology. – Ecol Econ. 31(7): 10-13.
[16] Hu, N., Li, X., Ge, X. Y. (2015): Change with water—the rational cognition of sponge city system from the perspective of urban green space system. – Chinese Landscape Architecture 31(6): 21-25.
[17] Jayasooriya, V. M. (2014): Tools for modeling of stormwater management and economics of green infrastructure practices: a review. – Water Air Soil Poll 225(8): 2055.
[18] Ji, L. Y. (2014): Rainstorm management strategy and site planning practice for low impact development: an empirical analysis of North American countries. – Proceedings of the Conference on Urban Development and Planning. NC University of Technology.
[19] Keller, E. A. (1999): Introduction to Environmental Geology (4th Ed.). – Prentice Hall, Upper Saddle River, NJ.
[20] Knödel, K., Lange, G., Voigt, H. (2007): Environmental Geology: Handbook of Field Methods and Case Studies. – Springer, Heidelberg, pp. 25-33.
[21] Lloyd, S. D., Wong, T. H., Porter, B. (2002): The planning and construction of an urban stormwater management scheme. – Water Science & Technology 45(7): 1.
[22] Martin, P. (2001): Sustainable Urban Drainage Systems: Best Practice Manual for England, Scotland, Wales and Northern Ireland. – Constr Ing Res & Inf Assoc, London.
[23] Ministerium für Umwelt und Naturschutz, Landwirtschaft und Verbraucherschutz des Landes Nordrhein-Westfalen (2001): Naturnahe Regenwasserbewirtschaftung. – WAZ, Duisburg.
[24] Qiu, B. X. (2015): The connotation, ways and prospects of Spongy City (LID). – Constr S&T, (7): 11-18.
[25] Revit, M. (2003): Report 5.1: Review of the Use of Storm Water BMPs in Europe. – EVKl-CT-2002-00111.
[26] Romnée, A. (2015): Methodology for a stormwater sensitive urban watershed design. – J Hydrol 530: 87-102.
[27] Rooijen, D. J. V., Turral, H., Biggs, T. W. (2010): Sponge city: water balance of mega-city water use and wastewater use in Hyderabad, India. – Irrigation & Drainage 54(S1): S81-S91.
[28] Roy, A. H., Wenger, S. J., Fletcher, T. D., et al. (2008): Impediments and solutions to sustainable, watershed-scale urban stormwater management: lessons from Australia and the United States. – Environmental Management 42(2): 344-359.

http://www.aloki.hu ● ISSN 1589 1623 (Print) ● ISSN 1785 0037 (Online)
DOI: http://dx.doi.org/10.15666/aeer/1705_1190111910

[29] Song, Y., Yu, K. J. (2007): The landscape planning approach to construct administration system of city storm water: a case study of Weihai City. – Urban Problems 2007(8): 64-70.
[30] Taylor, G. D, Fletcher, T. D., Wong, T. H. F., et al. (2005): Nitrogen composition in urban runoff--implications for stormwater management. – Water Research 39(10): 1982-1989.
[31] US EPA (United States Environmental Protection Agency) (2000a): Low Impact Development (LID): A literature review. – EPA-841-B-00-005, Office of Water, Washington, D.C.
[32] US EPA (United States Environmental Protection Agency) (2000b): Terminology of Low Impact Development. – EPA-841-N-12-003B, Office of Water, Washington, D.C.
[33] Wang, H., Mei, C., Liu, J. H. (2017): Systematic construction pattern of the sponge city. – J Hydraul Eng 48(9): 1009-1014.
[34] Wang, J. B., Zhao, J. S., Shen, Z. Y. (2017): Discussion about the two rainfall control approaches in Sponge City Construction. – J Hydraul Eng 48(12): 1490-1498.
[35] Wang, L., Ma, C. (1999): A study on the environmental geology of the Middle Route Project of the South–North water transfer. – Engineering Geology 51(3): 153-165.
[36] Wang, N., Wu, L. F. (2015): Practice and thinking of compiling sponge city construction plan in Xiamen. – Water Waste Eng 6: 28-32.
[37] Wanielista, M. P., Yousef, Y. A. (1993): Stormwater Management. – Elsevier, Amsterdam.
[38] Wu, D. J., Zhan, S. Z., Li, Y. H. (2016): New trends and practical research on the sponge cities with Chinese characteristics. – China Soft Science (1): 79-97.
[39] Yu, K. J., Li, D. H., Yuan, H. (2015): "Sponge City": theory and practice. – City Planning Review 39(6): 26-36.
[40] Zhang, J. Y., Wang, Y. T., Hu, Q. F. (2016): Discussion and views on some issues of the sponge city construction in China. – Adv Wat Sci 27(6): 793-799.
[41] Zou, Y. X., Yi, Q., Qiu, C. H. (2015): The research on sponge city construction in southern hilly area–a case study of Ningxiang County in Hunan Province. – Econ Geogr 35(9): 65-71.

http://www.aloki.hu ● ISSN 1589 1623 (Print) ● ISSN 1785 0037 (Online)
DOI: http://dx.doi.org/10.15666/aeer/1705_1190111910

ANALYSIS OF THE CELL MEMBRANE FATTY ACIDS AND CHARACTERIZATION OF THE PSYCHROTOLERANT *SERRATIA MARCESCENS* HI6 ISOLATED FROM HOPAR (BUALTAR) GLACIER, PAKISTAN

HASSAN, N.[1] – UDDIN, S.[1] – RAFIQ, M.[1,2] – UR REHMAN, H.[1] – HALEEM, A.[1] – HAYAT, M.[1] – KHAN, M.[1] – JAMIL, S. U. U.[1,3] – HASAN, F.[1*]

[1]*Applied, Environmental and Geomicrobiology Laboratory, Department of Microbiology Quaid–i–Azam University, Islamabad 45320, Pakistan*

[2]*Bristol Glaciology Centre, School of Geographical Sciences, Faculty of Science University of Bristol, Bristol, BS8 1SS, United Kingdom*

[3]*Department of Earth and Environmental Sciences, Bahria University, Islamabad, Pakistan*

[*]*Corresponding author*
e-mail: farihahasan@yahoo.com; phone: +92-51-9064-3065

(Received 23rd Apr 2019; accepted 2nd Jul 2019)

Abstract. In this study, the bacterial isolate HI6 was recovered from the ice of the Hopar (Bualtar) glacier, Karakoram Mountain Range, Pakistan. Isolate HI6 was identified as *Serratia marcescens* through microscopic and molecular analysis (16S rRNA sequencing). *Serratia marcescens* HI6 was analyzed for different physiological characteristics including temperature, pH and culture media. *Serratia marcescens* HI6 showed best growth at 25°C, on LB medium and pH 7. In addition, the Fatty acid methyl ester (FAME) was extracted and subjected to Fourier Transform infrared (FTIR) and Gas chromatography/mass spectroscopy (GC/MS) analysis. FTIR and GC/MS analysis has revealed that cell membrane of *Serratia marcescens* HI6 contains various types of fatty acids (FA). *i*–C16:1 (35.3% out of total cell membrane fatty acids) was found most predominantly followed by *i*–C15:1 (18.5%) and *n*-C16 (13.2%). Moreover, branched fatty acids (62%) including monounsaturated fatty acids (MUFA) (e.g. *i*–C15:1 and *i*–C16:1) and saturated fatty acids (SFA) were the dominant types of fatty acids in the cell membrane. A polyunsaturated fatty acid (PUFA), C18:2(*cis*–9) (known as linoleic acid) was also detected among analyzed fatty acids.
Keywords: *16S rRNA, Fatty acid methyl ester, Fourier Transform infrared, Gas chromatography / mass spectroscopy*

Introduction

Genus *Serratia* belonging to family Enterobacteriaceae and species of genus *Serratia* share very close genotypic and phenotypic characteristics with each other (Grimont and Grimont, 2006; Karkey et al., 2018). A bacterium with ability to produce red pigments was first observed on polenta by Bizio (1823), which was later identified and named as *Serratia marcescens* (Martinec and Kocur, 1961a). Williams and Qadri (1980) have observed many strains of *Serratia marcescens* that were producing a non-diffusible red pigment prodigiosin. The prodigiosin (red colour pigment) produced by these strains appeared akin to a blood stain with quite devastating consequences on various human consumable items such as consecrated wafers, bread, and polenta (Grimont and Grimont, 2006). In this perspective, many researchers had linked the genus *Serratia*'s history, hundreds of years back (Harrison, 1924; Gaughran, 1969; Reid, 1982). Although, prodigiosin or prodigiosin–like pigments or various types of pigments with red colour, have also been observed

http://www.aloki.hu ● ISSN 1589 1623 (Print) ● ISSN 1785 0037 (Online)
DOI: http://dx.doi.org/10.15666/aeer/1705_1191111924

produced by some bacterial species other than *Serratia* (Williams and Qadri, 1980), thus characteristics of microbes concerning these prominent phenomena can only be deduced.

Serratia marcescens, an Enterobacteriaceae family member, is a Gram–negative rod that inhabits soil and water (Szewzyk et al., 1993; Sandner-Miranda et al., 2018; Yeung et al., 2018). It is a saprophytic bacterium, and has been identified in food, notably in starchy variants which offer a marvelous growth environment. Previously it was known as *Chromobacterium prodigiosum* (Wheat et al., 1951; Sleigh, 1983; Ghaith et al., 2018), Bizio proposed the name *Serratia marcescens* in 1823, which was later used by Gaughran, in 1969. Some environmental isolates were reported to produce characteristic red pigment prodigiosin, and formerly it was confused with fresh blood (Gaughran, 1969). It is an omnipresent bacterium and widely found in natural habitats such as soil, honeybee gut, water, air, plants and animals (Grimont and Grimont, 1984; Raymann et al., 2017; Dhar–Purkayastha et al., 2018; Yeung et al., 2018). The biosynthesis of prodigiosin is an important attribute of *Serratia marcescens* (Grimont and Grimont, 1984). Over past few years, it has been known as main causative agent of hospital acquired infections (Mahlen, 2011; Montagnani et al., 2015).

Membrane lipid homeostasis has been shown to play a significant role in bacterial physiology. *Escherichia coli* was used as a study model bacterium for research in lipid biosynthesis for ages (Parsons and Rock, 2013). Biosynthesis of unsaturated fatty acids is a key factor in bacterial membrane homeostasis (Zhang and Rock, 2008). Combination of fatty acids with different melting points was integrated into phospholipids. Bacteria cope with low temperature by increasing the degree of unsaturation of fatty acids incorporated in phospholipids, which leads to high membrane fluidity (Parsons and Rock, 2013). In addition, in order to maintain membrane fluidity at lower temperatures, bacteria integrate fatty acids with lower melting points into lipid bilayer with decrease of outer temperatures that help bacteria to keep balance the order-disorder transition of temperature of the membranes (Suutari and Laakso, 1994; Annous et al., 1997; Bajerski et al., 2017). It is evident from previous studies that high temperature leads to high membrane rigidity, which can be handle by decrease in degree of unsaturation of fatty acids (Ganzert et al., 2011; Bakermans et al., 2012; Bajerski and Wagner, 2013).

A variety of mechanisms are used by bacteria to sustain membrane integrity to cope with temperature changes (Parsons and Rock, 2013). In previous studies, *Serratia marcescens* has been well documented for occurrence of fatty acids in its general cell structure but not specifically in the cell membrane (Bishop and Still, 1963; Bergan et al., 1983). Bermingham et al. (1971) has reported stimulation of growth and production of pigments at temperatures higher than normal by long–chain unsaturated fatty acids in *Serratia marcescens*. The current research work was aimed to study and characterize cell membrane fatty acid profile of psychrotolerant bacterial isolate from Hopar glacier also known as Bualtar glacier in Pakistan.

Materials and Methods

Selection of the isolate HI6

Isolate HI6 (Hopar ice) (selected for this study) was previously isolated from glacial ice, Hopar glacier (36°12'54.77 N, 74°46'9.49 E) using Luria Bertani (LB) agar (*Table 1*) and incubated at 15ºC. After initial isolation, the isolate HI6 was preserved in 30% glycerol using Luria Bertani broth (LB) (*Table 1*) as culture medium and stored at –20°C for future use.

http://www.aloki.hu ● ISSN 1589 1623 (Print) ● ISSN 1785 0037 (Online)
DOI: http://dx.doi.org/10.15666/aeer/1705_1191111924

Morphology of the isolate HI6

The colony morphology of the isolate HI6 was observed and recorded in terms of shape, production of pigments, size, opacity, margin, elevation and texture. Gram staining of the isolate HI6 was done following the protocol described by Beveridge (2001) and microscopic features were recorded using Laxco™ LMC–3000 Series Bright field Compound Microscope System.

Table 1. *The composition of the applied culture mediums in detail*

Composition of Luria Bertani (g l^{-1})	
Luria Bertani Agar (LBA)	
Tryptone	10
Sodium chloride	5
Yeast extract	5
Agar	15
Luria Bertani Broth (LBB)	
Tryptone	10
Sodium chloride	5
Yeast extract	5

Molecular identification of the isolate HI6

DNA extraction, PCR amplification

The DNA of the isolate HI6 was extracted using the protocol described by Zhou et al. (1996). The extracted DNA was amplified using the thermocycler (T100^{TM} Thermal cycler, Bio–Rad Laboratories, Inc.). The universal bacterial primers 27F (5′-AGAGTTTGATCMTGGCTCAG3–′) and 1492R (5'-GGTTACCTTGTTACGACTT–3') were used for amplification purposes. Cycling conditions was used as initial denaturation at 94ºC for 1 min following by 30 cycles at 94ºC for 1 min, 55ºC for 1 min and 72ºC followed by final elongation at 72ºC for 7 min. Finally, 2% agarose gel electrophoresis was performed to confirm PCR amplification.

Sequencing and phylogenetic analysis

Sequencing (16S rRNA) of amplified PCR product of the isolate HI6 was done by Macrogen Inc. Seoul, Korea. Trimming and filtering of obtained sequences was done using BioEdit (v7.0.5). The trimmed sequences was used to find the homologous bacterial strain by searching in the National Centre for Biotechnology Information (NCBI) (Thompson et al., 1994). Tamura–Nei model (Tamura and Nei, 1993) was used to construct the evolutionary history of the isolate HI6. MEGA 6.0 software was used to construct phylogenetic tree at the bootstrap value of 1000.

Characterization of physiological parameters of the isolate HI6

Effect of different pH, media and temperature on growth of the isolate HI6 was evaluated in this study. Four different temperature, 5, 15, 25 and 35°C, five different media, Minimal salt medium (MSM), Luria Bertani (LB), Nutrient broth (NB), Peptone–yeast–meat extracts (PYM) and Artificial salt media (ASM) as well as five different pH, 3, 5, 7, 9 and 11 were selected for this experiment. Nutrient broth was used as culture medium for all temperature and pH experiments, whereas, 15°C as incubation temperature was used for pH research work. 7 days old culture of the isolate

http://www.aloki.hu ● ISSN 1589 1623 (Print) ● ISSN 1785 0037 (Online)
DOI: http://dx.doi.org/10.15666/aeer/1705_1191111924

HI6 was inoculated in 250 mL Erlenmeyer flask containing 100 mL of broth medium and incubated in shaking incubator with 120 rpm for 7 days. To check the growth, optical density (600 nm) of the isolate HI6 was recorded after every 24 hrs via spectrophotometer (Shimadzu). In addition, two-way ANOVA was applied to find the statistical significant of this experiment.

Cell membrane fatty acids analysis

Fatty acids methyl ester preparation (FAME)

The isolate HI6 was grown in LB broth and incubated at 15°C for seven days. About 100 mg culture of the isolate HI6 was taken in 20 mL glass vial and subjected to FAME extraction. Added 2 mL of 5% methanolic HCl to glass vial containing bacterial culture and heated at 70°C for 2 hours. After heating, glass vial was placed at room temperature for 30 minutes to cool down. In next step, distilled water (1 mL) was added and then vortexed well. For extraction of FAME, 1 mL of hexane was poured and vigorously vortexed for about 10 minutes. After formation of two layers in glass tube, upper layer was transferred to new 2 mL clean glass vail and stored under nitrogen at –20°C.

Fourier Transform infrared (FTIR) spectroscopy

The extracted FAME extracted from the isolate HI6 was analysed through by FTIR spectrophotometer (Bruker Tensor 27, equipped with ZnSe ATR) along with the standard obtained through (The Vitamin Company USA). The spectra of FAME from the isolate HI6 were evaluated and recorded by keeping the range in between 4000-600 cm^{-1}. About 35 µL (in triplicate) of extracted FAME was placed on the FTIR spectrophotometer tray and recorded infrared spectrum of sample. The software Opus 65 was used to compare spectrum of extracted FAME with the spectrum of known compounds present in library.

Gas chromatography/mass spectroscopy (GC/MS) analysis

FAMEs analysis was done via GC (Agilent 7890A GC) linked to MS (Agilent 5975C MSD) and controlled by a HP Compaq computer using ChemStation software by following protocol described by Abd El Razak et al. (2014). Helium used as a carrier gas (flow rate of 1 ml/min, initial pressure of 50 kPa, split at 10 ml/min). Moreover, an auto–sampler (HP7683B) was used for injecting about 1 µL of sample in hexane. In addition, FAMEs separation was carried with column (30 m× 0.25 mm) (An Agilent–fused silica capillary column) coated with 0.25 µm dimethyl poly–siloxane (HP–5). The temperature of GC was set initially from 30 to 130°C at 5°C/min then to 300°C at 20°C/min and final temperature held for 5 min. FAME Mix (C4–C24) (Sigma–Aldrich) was used to identify the resultant peaks by comparing mass spectra and R_t (retention time).

Results

Morphology and molecular identification

The isolate HI6 produced red pigment, with round, smooth, convex (3–6 mm in diameter) colonies (*Fig. 1*). Microscopic analysis showed the isolate HI6 as Gram negative short rod (0.7–2.3 µm in length and 0.3–0.8 µm in diameter).

http://www.aloki.hu ● ISSN 1589 1623 (Print) ● ISSN 1785 0037 (Online)
DOI: http://dx.doi.org/10.15666/aeer/1705_1191111924

Based on 16S rRNA sequencing, the bacterial isolate HI6 was identified as *Serratia marcescens* [GenBank accession number MG641443]. In addition, the isolate HI6 showed 100% similarity with *Serratia marcescens* after searching in National Centre for Biotechnology Information database. Phylogenetic analysis on basis of partial 16S gene sequence, clearly shows that *Serratia marcescens* HI6 grouped within clusters of closely related species of *Serratia marcescens* in phylogenetic tree (*Fig. 2*).

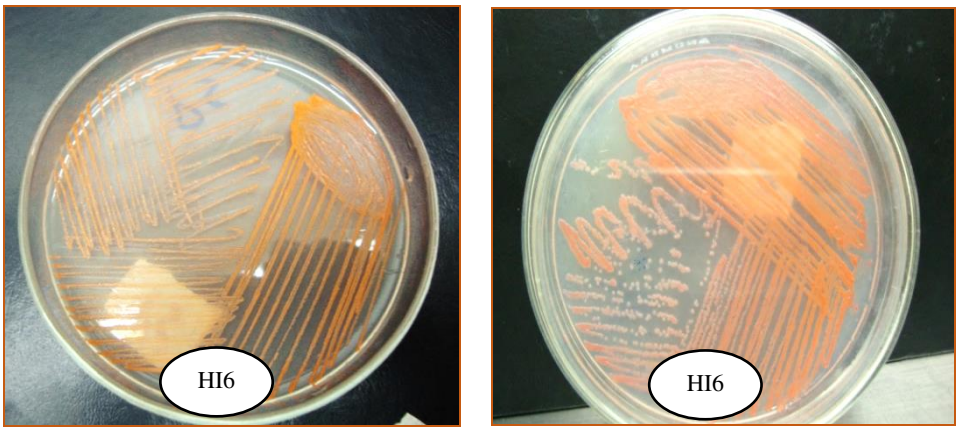

Figure 1. *The colony morphology of the isolate HI6 with production of red pigment*

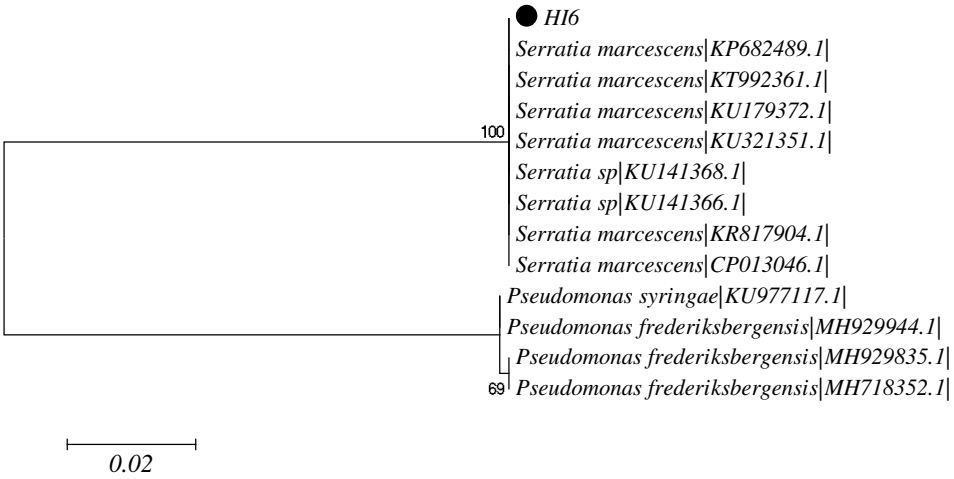

Figure 2. *Analysis of evolutionary relationship and relatedness of Serratia marcescens HI6 based on partial 16S gene sequences with closely related species by Maximum Likelihood method. Bootstrap values (1000 replicates) for node values from 50% are indicated. The species belonging to genus Pseudomonas were used as an outgroup*

Physiological characteristics

Serratia marcescens HI6 responded differently to various physiological parameters. In this experiment, it has been found that *Serratia marcescens* HI6 grow optimally at 25°C and pH 7 in LB broth (*Table 2*). The *Serratia marcescens* HI6 showed decline in its growth after 120 hrs of initial incubation in about all physiological parameters. It seemed that it has entered in exponential growth phase after 48 hrs of its starting incubation. *Serratia marcescens* HI6 was unable to show any growth at pH 3 and 45°C.

http://www.aloki.hu ● ISSN 1589 1623 (Print) ● ISSN 1785 0037 (Online)
DOI: http://dx.doi.org/10.15666/aeer/1705_1191111924

The LB broth was reported as best growth medium followed by PYM, ASW, MSM and NA. In addition, optimum growth was at pH 7 followed by pH 9, 11 and 5. Moreover, best growth was observed at 25°C followed by 35, 15 and 5°C. Based on these results, *Serratia marcescens* HI6 had the capabilities to grow at wide range of extreme physiological parameters.

Table 2. *Growth characteristics of the Serratia marcescens HI6 on different physiological parameters*

Isolate	Physiological parameters								
	Temp (°C)	**Time of incubation in hrs and OD[1]**							
		0	**24**	**48**	**72**	**96**	**120**	**144**	**168**
	5	0.243	0.578	0.710	0.989	1.219	1.487	1.398	1.387
	15	0.123	0.256	0.794	1.091	1.883	1.980	2.106	1.970
	25	0.473	0.869	1.420	1.756	1.999	2.209	2.439	2.429
	35	0.490	0.898	1.321	1.580	1.784	1.985	2.001	1.973
	45	0.123	0.077	–	–	–	–	–	–
	pH	**Time of incubation in hrs and OD**							
		0	**24**	**48**	**72**	**96**	**120**	**144**	**168**
	3	0.143	0.131	–	–	–	–	–	–
HI6	5	0.113	0.148	0.213	0.199	0.0722	0.063	0.060	0.058
	7	0.123	0.256	0.794	1.091	1.883	1.980	2.106	1.970
	9	0.134	0.230	0.753	0.963	1.352	1.103	1.102	1.090
	11	0.135	0.174	0.213	0.219	0.190	0.179	0.169	0.157
	Media	**Time of incubation in hrs and OD**							
		0	**24**	**48**	**72**	**96**	**120**	**144**	**168**
	ASW	0.020	0.0311	1.092	1.568	1.578	1.597	1.558	1.497
	LB	0.123	0.256	0.794	1.091	1.883	1.980	2.106	1.970
	MSM	0.041	0.052	0.059	0.890	1.480	1.501	1.450	1.399
	NA	0.023	0.032	0.052	1.129	1.068	1.204	1.189	1.179
	PYM	0.146	0.246	0.240	0.994	1.758	1.854	1.869	1.778

Keys: [1]Optical density, **p* value for the pH and media experiment was >0.05, **p* value for the temperature experiment was <0.05

Fourier Transform infrared (FTIR) analysis

Results of FTIR analysis revealed different functional groups present in the FAME extracted from *Serratia marcescens* HI6 (*Fig. 3*). The spectrum of the analysed FAME was compared with already online available databases as well as with standard and found that typical functional groups that are exist in fatty acids (FA) (such as saturated FA, monounsaturated FA and polyunsaturated FA), have also been presented in analysed FAME. For example, peak value 2812–3012 cm^{-1} region (which represent =C–H stretching vibration bond), 1710–1766 cm^{-1} (associated with C=O carbonyl bond) and multiple C=C double bond at 1400–1600 cm^{-1}, have clearly indicated that *Serratia marcescens* HI6 had various types of saturated FA, monounsaturated FA and polyunsaturated FA in its cell membrane (*Fig. 3*).

Gas chromatography/mass spectroscopy (GC/MS) analysis

The results of GC/MS has revealed that most copious types of fatty acids were branched fatty acids followed by monounsaturated fatty acids, n–chain saturated fatty acids, hydroxyl fatty acids and polyunsaturated fatty acids (*Fig. 4a,b*) (*Table 3*). In addition, *i*–C16:1 was found most abundant type of fatty acid followed by *i*–C15:1, n-C18:2(*cis*–9), n–C16, *ai*–C17:0, 3–OH–C14:0, n–C12, n–C14, *i*–C17:0, n–C18, n-C18:1(*trans*–9), C18:2(*cis*–9), n–C15 and n–C17 (*Table 3*).

http://www.aloki.hu ● ISSN 1589 1623 (Print) ● ISSN 1785 0037 (Online)
DOI: http://dx.doi.org/10.15666/aeer/1705_1191111924

Moreover, *Serratia marcescens* HI6 was able to produce only one type of polyunsaturated fatty acids, n–C18:2(*cis*–9) (also known as linoleic acid). Overall, branched fatty acids (62%) and *i*–C16:1 (35.2% out of total membrane fatty acids) were the main types of fatty acids produced by *Serratia marcescens* HI6 predominantly.

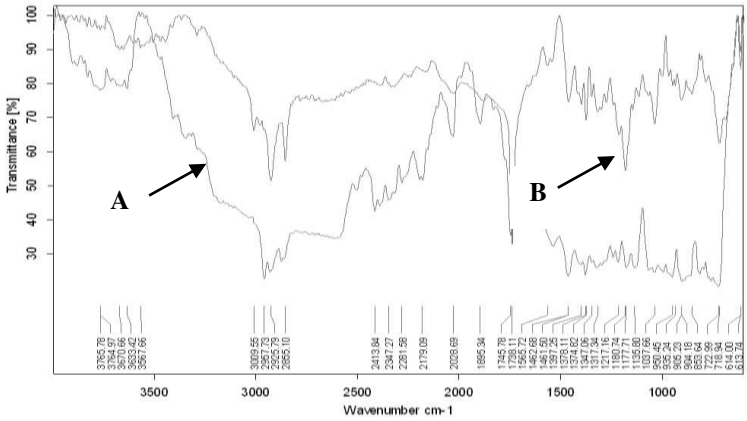

Figure 3. *Fourier Transform infrared (FTIR) spectrum of FAME extracted from the Serratia marcescens HI6. (A) Extracted FAME of the Serratia marcescens HI6 (B) Standard*

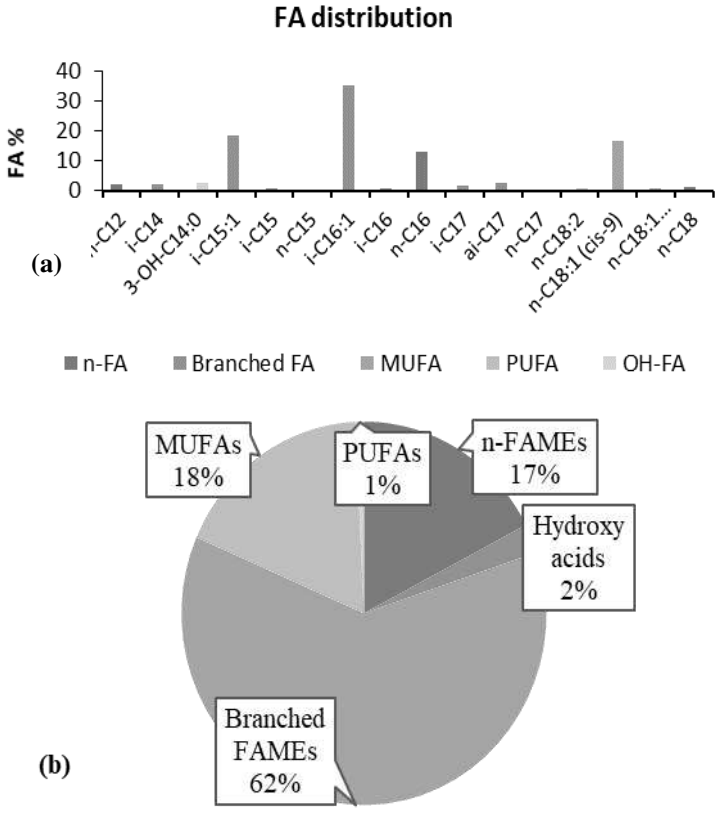

Figure 4a,b. *(a) Distribution of individual fatty acids in the cell membrane of Serratia marcescens HI6 (b) Percentage of the main types of fatty acids in the cell membrane of Serratia marcescens HI6*

http://www.aloki.hu ● ISSN 1589 1623 (Print) ● ISSN 1785 0037 (Online)
DOI: http://dx.doi.org/10.15666/aeer/1705_1191111924

Table 3. *Distribution and percentage of fatty acids in the cell membrane of the Serratia marcescens HI6*

Isolate	Carbon Chain length	Retention time	IUPIC names	%/total CM fatty acids
***Serratia marcescens* HI6**	*n*–C12	16.34	Dodecanoate	2.1
	i–C14:0	20.72	(Z)–tetradec–9–enoate	2.0
	3–OH–C14:0	25.18	3–Hydroxytetradecanoate	2.46
	i–C15:1	20.46	*iso*–10–Pentadecenoate	18.5
	i–C15:0	23.20	*iso*–Pentadecanoate	0.6
	n–C15	24.08	Pentadecanoate	0.5
	i–C16:1	24.89	(Z)–hexadec–9–enoate	35.2
	i–C16:0	25.67	*iso*–Hexadecanoate	1.0
	n–C16	26.57	Hexadecanoate	13.2
	i–C17:0	27.28	*iso*–Heptadecanoate	1.6
	ai–C17:0	28.05	*anteiso*–Heptadecanoate	2.7
	n–C17	28.85	Heptadecanoate	0.5
	C18:2(*cis*–9)	30.43	(9Z,12Z)–octadeca–9,12–dienoate	0.76
	C18:1(*cis*–9)	30.45	(Z)–octadec–9–enoate	16.8
	C18:1(*trans*–9)	30.59	(E)–octadec–9–enoate	1.0
	n–C18	31.15	Octadecanoate	1.1

Keys: *i*= iso, *ai*=anteiso, CM= cell membrane, IUPIC= International Union of Pure and Applied Chemistry

Discussion

This study was aimed to characterize physiological parameters and analyzed cell membrane fatty acids of the bacterium isolate *Serratia marcescens* HI6. In our knowledge, we are reporting for the first time *Serratia marcescens* from any glacial environment of Pakistan. Although in one study, it has been studied for laccase production isolated from glacial site in Indian Himalayan Region (IHR) (Kaira et al., 2015). *Serratia marcescens* has been known for its abilities to infect insects and spoils various types of food (Flyg and Xanthopoulos, 1983; Abdour, 2003; Bahar and Demirbag, 2007). In addition, its association with promotion of plant growth by combating with plant pathogens has also been observed (Kloepper et al., 1993). Moreover, *Serratia marcescens* has been found to fertile soils by producing phosphatases and unfriendly substances for plant pathogens (de Queiroz and de Melo, 2006; Tripura et al., 2007). Likewise, Pares (1964) has observed in soil that *Serratia marcescens* had role in the nutrient recycling by solubilizing organic iron and dissolving gold and copper. In another research, Janota–Bassalik (1963) has reported mineralization role of psychrotolerant *Serratia marcescens* accompanying by low–moor peat.

The genus *Serratia* is usually found widely in water, plants, mammals and hospitalized human patients (Grimont and Grimont, 2006) but studies about its presence and activities in both Polar and Non–polar cold regions are very rare. The primary habitat for genus *Serratia* is water as plenty of species belonged to *Serratia* has been reported from water (Grimont and Grimont, 2006). Gavini et al. (1979) has isolated *Serratia fonticola* well waters and springs. In another study conducted by Grimont and Grimont (2006), a total of 150 bacterial species belonged to genus *Serratia* including *Serratia marcescens* were reported from river water. In addition, Groscop and Brent (1964) has observed toxicity of non–diffusible red pigment prodigiosin to protozoa, produced by genus *Serratia*, which perhaps a promising factor important for its survival

http://www.aloki.hu ● ISSN 1589 1623 (Print) ● ISSN 1785 0037 (Online)
DOI: http://dx.doi.org/10.15666/aeer/1705_1191111924

in water and soil habitats. Based on such research, Grimont and Grimont (2006) has concluded that *Serratia* sp. with pigmentation abilities are existed in non–polluted rather than from polluted water.

Tolerance of *Serratia marcescens* HI6 to different extreme temperature, pH and media was assessed. *Serratia marcescens* HI6 was able to grow on temperature between 5–35°C (25°C optimum growth temp), pH between 5–11 (7 optimum growth pH) as well as on various media including ASW, LB, MSM, NB and PYM (LB optimum growth medium). Recently, Kaira et al. (2015) has reported similar findings for *Serratia marcescens* isolated from glacial site in Indian Himalayan Region (IHR). They observed psychrotolerant *Serratia marcescens* to show optimum growth at 25°C. Many other researchers have also used various temperature (5–37°C) for the growth of *Serratia marcescens* and they have found that it had the abilities to grow over a wide range of temperature (Bishop and Still, 1963; Selvakumar et al., 2008). In our knowledge, none of study has been carried out relating to tolerance of *Serratia marcescens* to extreme pH and various media.

In the present study, the fatty acids present in the cell membrane of *Serratia marcescens* HI6 were assessed using Fourier Transform Infrared (FTIR) spectroscopy. FTIR has the efficiency to recognize major parts of biological material (nucleic acids, proteins, lipids and carbohydrates) in any solution (Forfang et al., 2017). Basically, specific absorbance frequencies of FTIR are central to detect fatty acids (Forfang et al., 2017). In our study, the bands between 1710–1766 cm^{-1} were observed after analysis of extracted FAMEs by FTIR indicating the presence of C=O that associated with fatty acids. According to Dean et al. (2010), presence of the band at 1740 cm^{-1} indicated existence of C=O of ester groups, principally from FA. Moreover, Shurvell (2002) and Maquelin et al. (2002) has described the bands obtained from lipids after Fourier Transform Infrared spectroscopy analysis in detail. According to them, the lipid content present in any sample can easily detected by getting peaks associated to C-O–C stretching in esters (1070–1250 cm^{-1}), CH_2 bending (1460 cm^{-1}), C=O stretching in esters (1745 cm^{-1}), C–H stretching vibrations (=C–H stretch at 3010 cm^{-1}). The FTIR has been used by several researcher to identify the lipids and fatty acids content in many microbes such as *Chlamydomonas reinhardti*, *Scenedesmus subspicatus*, *Mucor plumbeus*, *Mucor hiemalis*, *Mucor circinelloides*, *Mortierella alpine* (Dean et al., 2010; Shapaval et al., 2014; Forfang et al., 2017).

Furthermore, the fatty acids profile of cell membrane of the isolate *Serratia marcescens* HI6 was properly studied using Gas chromatography/mass spectroscopy (GC/MS) in the current study. Findings of this analysis showed that C16:1 was present abundantly in cell membrane of *Serratia marcescens* HI6. None of such study has been carried out in past. Although Bergan et al. (1983) and Bishop and Still (1963) have analyzed the whole cell fatty acids of *Serratia marcescens*, whereas, current study is focused on cell membrane fatty acids of *Serratia marcescens*, so it is very challenging to exactly compare and discuss current study (cell membrane fatty acids analysis) with previous studies (whole cell fatty acids analysis) of *Serratia marcescens* because whole cell fatty acids could significantly differ in type and function from fatty acids present in cell membrane. As distribution of various types of fatty acids in cell membrane play significant role in bacterial adaptability in cold habitats, therefore, present research work specifically focused on it rather than to study whole cell fatty acids. However, current study has generally been discussed with other related bacterial strains of *Serratia marcescens* (Jantzen et al., 1974a, b, 1975). Our

http://www.aloki.hu ● ISSN 1589 1623 (Print) ● ISSN 1785 0037 (Online)
DOI: http://dx.doi.org/10.15666/aeer/1705_1191111924

results has supported by research work of many other researchers that observed foremost amount of C16:0, C16:1 and C18:1 in some strains of *Serratia marcescens* (Kates et al., 1964; Kates and Hagen, 1964). Although the contribution of the two last-mentioned fatty acids may also be small from the same strain Kates and Hagen (1964) has reported that amount of C16:1 and C18:1 varied depending upon culture conditions of growth of *Serratia marcescens*. It has been observed by many researcher that gram negative bacterial species possessed higher quantities of C16:0, C16:1 and C18:1 than gram positive bacteria in their cell membranes (Jantzen et al., 1974a,b, 1975; Zhao et al., 2011). Moreover, Bergan et al. (1983) has observed that family Enterobacteriaceae had high amount of C16:0 than C16:1 in their cells and has also reported in few *Acinetobacter* strains (Jantzen et al., 1975).

Likewise, the branched fatty acids were witnessed predominately in cell membrane the isolate *Serratia marcescens* HI6. The branched *iso* and *anteiso* pattern was observed in both saturated fatty acids and monounsaturated fatty acids in the current results. The incorporation of *iso* and *anteiso* branches in the fatty acids chains of cell membrane, is perhaps a strategy to cope with devastating effects of low temperature by maintaining the fluidity of cell membrane (Bajerski et al., 2013, 2017). In few studies, it has been shown that *anteiso* branches pattern of fatty acids of cell membranes in psychrotolerant bacterial species (such as *Chryseobacterium frigidum* and *Chryseobacterium haifense*) reduced the melting temperature of the plasma membrane increasing motion capability and made it possible to freely move molecules across the cell membrane (Hantsis-Zacharov and Halpern, 2007; Kim et al., 2016).

Conclusion

In conclusion, the bacterium isolate HI6 was identified as *Serratia marcescens* after 16S rRNA sequencing. The bacterium isolate *Serratia marcescens* HI6 showed a good potential to grow over a wide range of extreme physiological conditions. Results of FTIR and GC/MS has showed that the isolate HI6 had the ability to produce and accumulate various types of fatty acids in its cell membrane but predominantly *i*–C16:1 and other branched chain fatty acids. This study is important because it gives a clear idea about Fatty acids distribution in the cell membrane of *Serratia marcescens* and their possible role in adaptation in glacial habitats. In addition, this study would be helpful to understand the maintenance of cell membrane fluidity in glacial environments by *Serratia marcescens*. Finally, the bacterium isolate *Serratia marcescens*–HI6 would be used as source of polyunsaturated fatty acids (e.g. linoleic acid) as alternative to the conventional plant sources of PUFA, thus would be helpful to prevent deforestation.

Conflict of interests. The authors declare that the research was conducted in the absence of any commercial or financial relationships that could be construed as a potential conflict of interests.

Author contributions. All authors have made an equal contributions to the research work and writing of this manuscript.

http://www.aloki.hu ● ISSN 1589 1623 (Print) ● ISSN 1785 0037 (Online)
DOI: http://dx.doi.org/10.15666/aeer/1705_1191111924

REFERENCES

[1] Abd El Razak, A., Ward, A. C., Glassey, J. (2014): Screening of Marine Bacterial Producers of Polyunsaturated Fatty Acids and Optimisation of Production. – Microb Ecol 67: 454-464.

[2] Abdour, A. M. (2003): Purification and partial characterization of psychrotrophic *Serratia marcescens* lipase. – Journal of Dairy Science 86: 127-132.

[3] Annous, B. A., Becker, L. A., Bayles, D. O., Labeda, D. P., Wilkinson, B. J. (1997): Critical role of anteiso–C15:0 fatty acid in the growth of *Listeria monocytogenes* at low temperatures. – Applied Environmental Microbiology 63: 3887-3894.

[4] Bahar, A. A., Demirbag, Z. (2007): Isolation of pathogenic bacteria from *Oberea linearis* (Coleoptera: Cerambycidae). – Biology 62: 13-18.

[5] Bajerski, F., Wagner, D. (2013): Bacterial succession in Antarctic soils of two glacier forefields on Larsemann Hills, East Antarctica. – FEMS Microbiology Ecology 85: 128-142.

[6] Bajerski, F., Ganzert, L., Mangelsdorf, K., Padur, L., Lipski, A., Wagner, D. (2013): *Chryseobacterium frigidisoli* sp. nov., a psychrotolerant species of the family Flavobacteriaceae isolated from sandy permafrost from a glacier forefield. – International Journal of Systematic and Evolutionary Microbiology 63: 2666-2671.

[7] Bajerski, F., Wagner, D., Mangelsdorf, K. (2017): Cell Membrane Fatty Acid Composition of *Chryseobacterium frigidisoli* PB4T, Isolated from Antarctic Glacier Forefield Soils, in Response to Changing Temperature and pH Conditions. – Frontiers in Microbiology 8: 677.

[8] Bakermans, C., Bergholz, P. W., Rodrigues, D. F., Vishnivetskaya, T. A., Ayaladel-Rio, H. L., Tiedje, J. M. (2012): Genomic and expression analyses of cold-adapted microorganisms. – In: Miller, R. V., Whyte, L. G. (eds.) Polar Microbiology. Life in a Deep Freeze, Washington, DC, ASM Press, p. 126-155.

[9] Bergan, T., Grimont, P. A. D., Grimont, F. (1983): Fatty Acids of *Serratia* Determined by Gas Chromatography. – Current Microbiology 8: 7-11.

[10] Bermingham, M. A., Deol, B. S., Still, J. L. (1971): The relationship between prodigiosin biosynthesis and cyclic depsipeptides in *Serratia marcescens*. – Journal of General Microbiology 67(3): 319-24.

[11] Beveridge, T. J. (2001): Use of the Gram stain in microbiology. – Biotechnic and Histochemistry 76: 111-118.

[12] Bishop, D. G., Still, J. L. (1963): Fatty acid metabolism in *Serratia marcescens*: IV. The effect of temperature on fatty acid composition. – Journal of Lipid Research 4: 87-90.

[13] Bizio, B. (1823): Lettera di Bartolomeo Bizio al chiarissimo canonico Angelo Bellani sopra il fenomeno della polenta porporina. Biblioteca Italiana o sia Giornale di Letteratura. – Scienze a Arti 30: 275-295.

[14] de Queiroz, B. P. V., de Melo, I. S. (2006): Antagonism of *Serratia marcescens* towards *Phytophthora parasitica* and its effects in promoting the growth of citrus. – Brazilian Journal of Microbiology 37: 448-450.

[15] Dean, A. P., Sigee, D. C., Estrada, B., Pittman, J. K. (2010): Using FTIR spectroscopy for rapid determination of lipid accumulation in response to nitrogen limitation in freshwater microalgae. – Bioresource Technology 101: 4499-507.

[16] Dhar–Purkayastha, G., Mangar, P., Saha, A., Saha, D. (2018): Evaluation of the biocontrol efficacy of a *Serratia marcescens* strain indigenous to tea rhizosphere for the management of root rot disease in tea. – PLoS ONE 13(2): e0191761. doi.org/10.1371/journal.pone.0191761.

[17] Flyg, C., Xanthopoulos, K. G. (1983): Insect pathogenic properties of *Serratia marcescens*, passive and active resistance to insect immunity studied with protease deficient and phage–resistant mutants. – Journal of General Microbiology 129: 453-464.

http://www.aloki.hu ● ISSN 1589 1623 (Print) ● ISSN 1785 0037 (Online)
DOI: http://dx.doi.org/10.15666/aeer/1705_1191111924

[18] Forfang, K., Zimmermann, B., Kosa, G., Kohler, A., Shapaval, V. (2017): FTIR Spectroscopy for Evaluation and Monitoring of Lipid Extraction Efficiency for Oleaginous Fungi. – PLOS ONE 12.
[19] Ganzert, L., Lipski, A., Hubberten, H. W., Wagner, D. (2011): The impact of different soil parameters on the community structure of dominant bacteria from nine different soils located on Livingston Island, South Shetland Archipelago, Antarctica. – FEMS Microbiology Ecology 76: 476-491.
[20] Gaughran, E. R. L. (1969): From superstition to science: The history of a bacterium. – Transactions of the New York Academy of Sciences 31: 3-24.
[21] Gavini, F., Ferragut, C., Izard, D., Trinel, P. A., Leclerc, H., Lefebvre, B., Mossel, D. A. A. (1979): *Serratia fonticola*, a new species from water. – International journal of systematic bacteriology 29: 92-101.
[22] Ghaith, D. M., Zafer, M. M., Ismail, D. K., Al-Agamy, M. H., Bohol, M., Al-Qahtani, A., Mostafa, I. Y. (2018): First reported nosocomial outbreak of *Serratia marcescens* harboring blaIMP-4 and blaVIM-2 in a neonatal intensive care unit in Cairo, Egypt. – Infection and drug resistance 11: 2211-2217.
[23] Grimont, P. A. D., Grimont, F. (1984): Genus VIII. *Serratia*. – In: Krieg, N. R., Holt, J. G. (eds.) Bergey's Manual of systematic bacteriology. Williams and Wilkins, Baltimore, p. 477-484.
[24] Grimont, F., Grimont, P. A. D. (2006): The Genus *Serratia*. – Prokaryotes 6: 219-244.
[25] Groscop, J. A., Brent, M. M. (1964): The effects of selected strains of pigmented microorganisms on small free living amoebae. – Canadian Journal Microbiology 10: 579-584.
[26] Hantsis–Zacharov, E., Halpern, M. (2007): *Chryseobacterium haifense* sp. nov., a psychrotolerant bacterium isolated from raw milk. – International Journal of Systematic and Evolutionary Microbiology 57: 2344-2348.
[27] Harrison, F. C. (1924): The "miraculous" microorganism. – Transactions of the Royal Society of Canada 18: 1-17.
[28] Janota–Bassalik, L. (1963): Psychrophiles in low–moor peat. – Acta Microbiologica Polonica 12: 25-40.
[29] Jantzen, E., Bergan, T., Bovre, K. (1974a): Gas chromatography of bacteria whole cell methanolysates. VI. Fatty acid composition of strains within Micrococcaeeae. – Acta Pathologicae et Microbiologicae Scandinavicae 82(B): 785-798.
[30] Jantzen, E., Bryn, K., Bergan, T., Bovre, K. (1974b): Gas chromatography of bacterial whole cell methanolysates. V. Fatty acid composition of Neisseriae and Moraxellae. – Acta Pathologicae et Microbiologicae Scandinavicae 82(B): 767-779.
[31] Jantzen, E., Bryn, K., Bergan, T., Bovre, K. (1975): Gas chromatography of bacterial whole cell methanolysates. VII. Fatty acid composition of *Aeinetobacter* in relation to the taxonomy of *Neisseriaceae*. – Acta Pathologicae et Microbiologicae Scandinavicae 83(B): 569-580.
[32] Kaira, G. S., Dhakar, K., Pandey, A. (2015): A psychrotolerant strain of *Serratia marcescens* (MTCC 4822) produces laccase at wide temperature and pH range. – AMB Express 5.
[33] Karkey, A., Joshi, N., Chalise, S., Joshi, S., Shrestha, S., Nguyen, T. N. T., Dongol, S., Basnyat, B., Baker, S., Boinett, C. J. (2018): Outbreaks of *Serratia marcescens* and *Serratia rubidaea* bacteremia in a central Kathmandu hospital following the 2015 earthquakes. – Transactions of the Royal Society of Tropical Medicine and Hygiene 112(10): 467-472.
[34] Kates, M., Hagen, P. O. (1964): Influence of temperature on fatty acid composition of psychrophilic and mesophilic *Serratia* species. – Canadian Journal Biochemistry 42: 481-488.
[35] Kates, M., Adams, G. A., Martin, S. M. (1964): Lipids of *Serratia marcescens*. – Canadian Journal Biochemistry 42: 461-479.

http://www.aloki.hu ● ISSN 1589 1623 (Print) ● ISSN 1785 0037 (Online)
DOI: http://dx.doi.org/10.15666/aeer/1705_1191111924

[36] Kim, T., Kim, M., Kang, O., Jiang, F., Chang, X., Liu, P., Zhang, Y., Da, X., Zheng, C., Fang, C., Peng, F. (2016): *Chryseobacterium frigidum* sp. nov., isolated from high–Arctic tundra soil, and emended descriptions of *Chryseobacterium bernardetii* and *Chryseobacterium taklimakanense*. – International Journal of Systematic and Evolutionary Microbiology 66: 609-615.

[37] Kloepper, J. W., Tuzun, S., Liu, L., Wei, G. (1993): Plant growth–promoting rhizobacteria as inducers of systemic disease resistance. – In: Lumsden, R. D., Waughn, J. (eds.) Pest Management: Biologically Based Technologies. DC: American Chemical Society Books, Washington, p. 156-165.

[38] Mahlen, S. D. (2011): *Serratia* infections: from military experiments to current practice. – Clinical Microbiology Reviews 24: 755-791.

[39] Maquelin, K., Choo–Smith, L. P., Kirschner, C., Ngo–Thi, N. A., Naumann, D., Puppels, G. J. (2002): Vibrational Spectroscopic Studies of Microorganisms. – In: Chalmers, J. M., Griffiths, P. R. (eds.) Handbook of Vibrational Spectroscopy. John Wiley and Sons, Chichester, United Kingdom.

[40] Martinec, T., Kocur, M. (1961a): The taxonomic status of *Serratia marcescens* Bizio. – International Bulletin of Bacteriological Nomenclature and Taxonomy 11: 7-12.

[41] Montagnani, C., Cocchi, P., Lega, L., Campana, S., Biermann, K. P., Braggion, C., Pecile, P., Chiappini, E., de Martino, M., Galli, L. (2015): *Serratia marcescens* outbreak in a neonatal intensive care unit: crucial role of implementing hand hygiene among external consultants. – BMC Infectious Diseases 15:11. doi.org/10.1186/s12879-014-0734-6.

[42] Pares, Y. (1964): Action de *Serratia marcescens* dans le cycle biologique des métaux. – Annales de l'Institut Pasteur 107: 136-141.

[43] Parsons, J. B., Rock, C. O. (2013): Bacterial lipids: Metabolism and membrane homeostasis. – Progress in Lipid Research 52: 249-276.

[44] Raymann, K., Shaffer, Z., Moran, N. A. (2017): Antibiotic exposure perturbs the gut microbiota and elevates mortality in honeybees. – PLoS Biol 15:e2001861. doi:10.1371/journal.pbio.2001861.

[45] Reid, J. D., Stoufer, S. D., Ogrydziak, D. M. (1982): Efficient transformation of *Serratia marcescens* with pBR322 plasmid DNA. – Gene 17: 107-112.

[46] Sandner–Miranda, L., Vinuesa, P., Cravioto, A., Morales–Espinosa, R. (2018): The Genomic Basis of Intrinsic and Acquired Antibiotic Resistance in the Genus *Serratia*. – Frontiers in Microbiology 9: 828. doi:10.3389/fmicb.2018.00828.

[47] Selvakumar, G., Mohan, M., Kundu, S., Gupta, A. D., Joshi, P., Nazim, S., Gupta, H. S. (2008): Cold tolerance and plant growth promotion potential of *Serratia marcescens* strain SRM (MTCC 8708) isolated from flowers of summer squash (Cucurbita pepo). – Letters of Applied Microbiology 46: 171-175.

[48] Shapaval, V., Afseth, N. K., Vogt, G., Kohler, A. (2014): Fourier transform infrared spectroscopy for the prediction of fatty acid profiles in Mucor fungi grown in media with different carbon sources. – Microbial Cell Factories 13: 86.

[49] Shurvell, H. F. (2002): Spectra–Structure Correlations in the Mid– and Far–Infrared. – In: Chalmers, J. M., Griffiths, P. R. (eds.) Handbook of Vibrational Spectroscopy. John Wiley & Sons, Ltd, Chichester, United Kingdom.

[50] Sleigh, J. D. (1983): Antibiotic resistance in *Serratia marcescens*. – BMJ 287: 1651-1653.

[51] Suutari, M., Laakso, S. (1994): Microbial fatty acids and thermal adaptation. – Critical Reviews in Microbiology 20: 285-328.

[52] Szewzyk, U., Szewzyk, R., Stenström, T. A. (1993): Growth and survival of *Serratia marcescens* under aerobic and anaerobic conditions in the presence of materials from blood bags. – Journal of Clinical Microbiology 31: 1826-1830.

http://www.aloki.hu ● ISSN 1589 1623 (Print) ● ISSN 1785 0037 (Online)
DOI: http://dx.doi.org/10.15666/aeer/1705_1191111924

[53] Tamura, K., Nei, M. (1993): Estimation of the number of nucleotide substitutions in the control region of mitochondrial DNA in humans and Chimpanzees. – Molecular Biology and Evolution 10: 512-526.
[54] Thompson, J. D., Higgins, D. G., Gibson, T. J. (1994): CLUSTAL W: Improving the sensitivity of progressive multiple sequence alignment through sequence weighting, position–specific gap penalties and weight matrix choice. – Nucleic Acids Research 22: 4673-4680.
[55] Tripura, C., Sashidhar, B., Podile, A. R. (2007): Ethyl methanesulphonate mutagenesis enhanced mineral phosphate solubilization by groundnut–associated *Serratia marcescens* GPS–5. – Current Microbiology 54: 79-84.
[56] Wheat, R. P., Zuckerman, A., Rank, L. A. (1951): Infection due to Chromobacteria: report of eleven cases. – Archives of Internal Medicine 88: 461-466.
[57] Williams, R. P., Qadri, S. M. H. (1980): The pigment of *Serratia*. – In: von Graevenitz, A., Rubin, S. J. (eds.) The genus *Serratia*. CRC Press, Boca Raton, p. 31-79.
[58] Yeung, H., Chavarria, B., Shahsavari, D. (2018): A Complicated Case of *Serratia marcescens* Infective Endocarditis in the Era of the Current Opioid Epidemic. – Case Reports in Infectious Diseases. doi.org/10.1155/2018/5903589.
[59] Zhang, Y. M., Rock, C. O. (2008): Membrane lipid homeostasis in bacteria. – Nature Reviews Microbiology 6: 222-33.
[60] Zhao, Q., Bai, Y., Zhang, G., Zhu, S., Sheng, H., Sun, Y. (2011): *Chryseobacterium xinjiangense* sp. nov., isolated from alpine permafrost. – International Journal of Systematic and Evolutionary Microbiology 61: 1397-1401.
[61] Zhou, J. Z., Bruns, M. A., Tiedje, J. M. (1996): DNA recovery from soils of diverse composition. – Applied Environmental Microbiology 62: 316-322.

http://www.aloki.hu ● ISSN 1589 1623 (Print) ● ISSN 1785 0037 (Online)
DOI: http://dx.doi.org/10.15666/aeer/1705_1191111924

CONTENT OF THE SELECTED MACRO-ELEMENTS IN POTATO TUBERS *(SOLANUM TUBEROSUM* L.*)* TREATED WITH BIOSTIMULATORS

GUGAŁA, M.[1] – MYSTKOWSKA, I.[2*] – ROGÓŻ-MATYSZCZAK, A.[3] – ZARZECKA, K.[1] – SIKORSKA, A.[4]

[1]*Department of Agrotechnology, Siedlce University of Natural Sciences and Humanities, Prusa 14, 08-110 Siedlce, Poland*
(e-mail: gugala@uph.edu.pl, kzarzecka@uph.edu.pl)

[2]*Department of Agriculture, Pope John Paul II State School of Higher Education in Biala Podlaska, Sidorska 95/97, 21-500 Biała Podlaska, Poland*

[3]*Laboratory of Environmental Analyzes EKO-AGRO-TECH, Pope John Paul II State School of Higher Education in Biala Podlaska, Sidorska 95/97, 21-500 Biała Podlaska, Poland*

[4]*Department of Agriculture, The State Higher School of Vocational Education in Ciechanów, 06-400 Ciechanów, Poland*
(e-mail: aniasikorska6@wp.pl)

**Corresponding author*
e-mail: imystkowska@op.pl

(Received 23rd Apr 2019; accepted 11th Jul 2019)

Abstract. The objective of research was to assess the selected mineral components (phosphorus, calcium and magnesium) in the tubers of edible potato. Field research was carried out in the years 2015-2017 with an application of biostimulators in individual farms in the town of Międzyrzec Podlaski (51°59' N and 22°47' E), Poland. The experiment was led by means of a split-plot method. The impact of two factors was tested. The first order factor were the three varieties of edible potato: Honorata, Jelly, Tajfun, while of the second order - four variants of applying biostimulators: Kelpak SL, Titanit, GreenOk, BrunatneBio Złoto and a control variant (potato plants sprayed with distilled water). Potato plants were treated with biostimulators three times (beginning of flowering, full flowering and after plant flowering). Within the presented research the applied biostimulators increased the content of selected mineral components in the tubers of tested varieties. Tubers of plants treated with BrunatneBio Złoto preparation were characterized by the largest content of phosphorus, calcium and magnesium in comparison to the plants from control object. The content of microelements in the tubers varied significantly depending on the genotype of the variety. The greatest concentration of phosphorus was noted in the tubers of Tajfun variety, while in case of magnesium - Honorata variety. Large amount of rainfall in 2017 contributed to the occurrence of an increase of the content of phosphorus, calcium and magnesium in potato tubers. Average content of phosphorus amount to, on average: 3.4 $g \cdot kg^{-1}$, calcium 0.73 $g \cdot kg^{-1}$, and magnesium 1.36 $g \cdot kg^{-1}$.
Keywords: *variant, variety, phosphorus, calcium, magnesium*

Introduction

The nutritional value of potatoes (*Solanum tuberosum* L.), apart from carbohydrates, protein and vitamins, is determined by the content of mineral components (Leszczyński, 2012; Wójcik –Stopczyńska et al., 2012). The following are of particular importance: phosphorus, calcium, magnesium – having alkali-forming actions, their presence in food neutralizes the acidifying meat, fish and cereal product properties (Tajner-Czopek, 2006). These elements perform mainly the building and physiological functions in a plant, further to deciding about its dietetic values (Leszczyński, 2012; Wierzbicka,

http://www.aloki.hu ● ISSN 1589 1623 (Print) ● ISSN 1785 0037 (Online)
DOI: http://dx.doi.org/10.15666/aeer/1705_1192511933

2012). Phosphorus is the key component of compounds which are decisive for the energetic processes. It forms part of specific proteins and participates in the metabolism of carbohydrates. Within the national research the content of phosphorus in potato tubers was shaped at the level of 1.8-3.9 $g \cdot kg^{-1}$ (Zarzecka and Mystkowska, 2004; Wierzbicka, 2012; Zarzecka et al., 2015; Wierzbowska et al., 2016), and in the foreign research it was usually greater and amounted to 2.2-4.9 $g \cdot kg^{-1}$ (Elfaki and Abbsher, 2010; Jarvan and Edesi, 2009; Mahamud et al., 2015). Calcium is considered as an element that conditions the correct growth and development of plants. The content of calcium in tubers, within the national research, was within the limits of 0.30-0.69 $g \cdot kg^{-1}$ (Kołodziejczyk and Szmigiel, 2005; Wierzbicka and Trawczyński, 2011; Wierzbicka, 2012; Zarzecka et al., 2015), and in the foreign ones 0.2-1.4 $g \cdot kg^{-1}$ (Ekin, 2011; Mahamud et al., 2015). Magnesium is a crucial component of potato tubers. Its presence in a plant is determined by the basic processes of metabolism and energy conversion. Magnesium not only participates in approx. 300 enzymatic reactions, but it also constitute an active centre for the chlorophyll molecule. The content of magnesium in dry mass of potato tubers in research carried out by Zarzecka et al. (2006), Wierzbicka and Trawczyński (2011), Wierzbicka (2012) amounted to 0.8-1.3 $g \cdot kg^{-1}$, and in foreign researches it reached the level of 3.3 $g \cdot kg^{-1}$ (Muhamud et al., 2015). Consumption of 200 g of potatoes covers between 10-14% for phosphorus, 8-17% for magnesium.

Environmental and genetic factors have an impact on the concentration of the mineral components in potato tubers (Horvat et al., 2014; Wierzbowska et al., 2015a, b). The chemical content may change in terms of agrotechnical factors, including biostimulators. Many authors indicated a beneficial impact of biostimulators on the chemical content of potato tubers (Bienia et al., 2018; Trawczyński, 2014; Wierzbowska et al., 2016). Applying biostimulators allows correcting the bad state of nutrition of plants (Fageriai et al., 2009; Fernandez et al., 2013; Singh et al., 2013). The most crucial function performed by biostimulators is the supplementation of a deficiency of components in the period of vegetation, caused by various factors, such as intense plant development, drought, agrotechnical errors. Thus, the objective of research was to specify the impact of the selected biostimulators on the content of phosphorus, calcium and magnesium of three varieties of edible potato.

Materials and methods

The experimental site

Potato tubers from the field experiment realized in the years 2015–2017 on an individual farm within the village of Międyrzec Podlaski, Lubelskie voivodeship (51°59' N and 22°47' E), Poland constituted research material (*Fig. 1*). The experiment was conducted in three repetitions with the use of split-plot method, on soil regarded as a rye complex, very good, class IVa. In individual years of research, soils differed in the content of organic matter and available macro-elements. In 2015 and 2016, the soil was characterized by slightly acidic reaction, and in the last year of research, alkaline. The content of organic matter ranged from 15.0 to 18.7 $g \cdot kg^{-1}$. The content of available phosphorus (P) was from high to very high, potassium (K) from medium to very high, and magnesium (Mg) was high. The first factor was three moderately early varieties of edible potato: Honorata, Jelly and Tajfun, and the second one, four types of biostimulators used in three dates (beginning of flowering, fully flowering and after flowering of plants):

http://www.aloki.hu ● ISSN 1589 1623 (Print) ● ISSN 1785 0037 (Online)
DOI: http://dx.doi.org/10.15666/aeer/1705_1192511933

1. Control variant – without the use of biostimulators spraying with distilled water
2. Biostimulator Kelpak®SL (active substance - *Ecklonia maxima* algae extract), containing plant hormones: auxin - 11 $mg \cdot l^{-1}$ and cytokinin – 0.031 $mg \cdot l^{-1}$, at a dose of 0.20 $l \cdot ha^{-1}$
3. Biostimulator Tytanit® (active substance – titanium) at a dose of 0.20 $l \cdot ha^{-1}$
4. Biostimulator GreenOk® (active substance – humus substances 20 $g \cdot l^{-1}$) at a dose of 0.20 $l \cdot ha^{-1}$
5. Biostimulator BrunatneBio Złoto (active substances – plant hormones: auxin – 0.06 $mg \cdot l^{-1}$ and cytokinin - 12 $mg \cdot l^{-1}$) at a dose of 0.20 $l \cdot ha^{-1}$

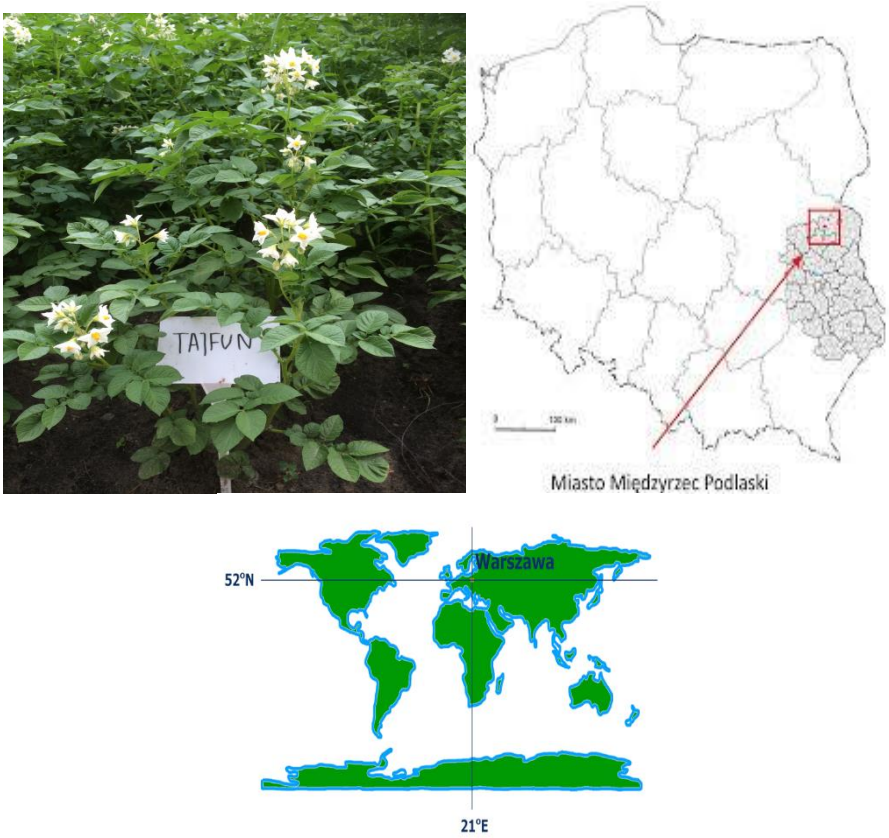

Figure 1. *Location of the experiment*

The forecrop for potato in particular years of research was winter wheat. After harvesting the forecrop, a team of post-harvest crops was made. In autumn, each year preceding planting, organic fertilization in the form of manure in the amount of 25.0 $t \cdot ha^{-1}$ and mineral fertilization with phosphorus-potassium in the amount of P – 44.0 (100 $P_2O_5 \cdot 0.44$) $kg \cdot ha^{-1}$ (lubofos for potatoes 7%) and K – 124.5 (150 $K_2O \cdot 0.83$) $kg \cdot ha^{-1}$ (lubofos for potatoes 25%) was applied. These fertilizers were plowed pre-season plowing. Nitrogen fertilizers were applied in the spring in an amount of N 100 kg/ha (nitro-chalk 27%) and mixed with the soil using a cultivator. Potatoes were planted manually under the marker at a spacing of 67.5 x 37 cm, in the third decade of April (2015, 2016, 2017). Each plot with an area of 15 m^2 accounted for five ridges. Cultivation and care treatments were carried out in accordance with the requirements of

http://www.aloki.hu ● ISSN 1589 1623 (Print) ● ISSN 1785 0037 (Online)
DOI: http://dx.doi.org/10.15666/aeer/1705_1192511933

correct. During the growing season, the potato plantation was protected with the following incidences: Actara 25 WG (thiametoksam) at the rate of 0.08 kg·ha^{-1} and Caliypso 480 SC (thiacloprid) at the rate of 0.1 l·ha^{-1}, and fungicides: Copper Max New 50 WP at the rate of 2.0 kg·ha^{-1} and Dithane Neo Tec 75 WG the rate of 2.0 kg·ha^{-1}. Samples of potato tubers (50 tubers) were taken from each of the plots during harvest in the first decade of September and stored at 10-12 °C, for 8-10 days. Chemical analyses were performed using dry material from 10 representative tubers in three replications.

Chemical analysis methods

Weight of about 0.2-0.3 g of sample was transferred to vessel and HNO_3 and HCL was added, 3:1 respectively. The vessels were placed in the rotor and loaded to the microwave.

Mineralized samples were transferred to the 50 ml flasks through filtering paper and diluted with ultra-pure water.

Samples were examined with SpectroBlue ICP OES spectrometer at the Regional Research Center for Environment, Agricultural and Innovative Technologies, Pope John II State School of Higher Education in Biała Podlaska. Analytical curves were built by diluting Bernd Kraft Der Standard Spectro Genesis ICAL Solutions and VHG SM68-1-500 Element Multi Standard 1 in 5% HNO_3. Operating parameters for ICP OES instrument: coolant flow: 12 l/min; auxiliary flow: 0.90 l/min; nebulizer flow: 0.78 l/min.; pump speed: 30 Rpm; number of measurements: 3.

Meteorological conditions

Meteorological conditions in the years of potato vegetation have been presented in *Table 1* by means of the sum of rainfall and average air temperatures. Vegetation season of 2015 turned out to be the average air temperature of 15.2 °C, higher by 0.2 °C from the average long-term and rainfall at the level of 295.1 mm. The highest average temperature of air was noted in 2016 and amounted to 15.8 °C, was higher from the average long-term one by 0.8 °C, whilst that year was characterized by the lowest volume of rainfall – 200.9 mm, lower by 134.5 mm from the long-term sum. The highest number of rainfall was noted in the vegetation season of 2017–325.4 mm and the lowest air temperature –14.6 °C (*Table 1*).

Results and discussion

Both genetic and environmental factors have an impact on the concentration of mineral elements in tubers. Many authors indicated that the volume of macro-elements in tubers depended on the particular variety (Wierzbicka and Trawczyński, 2011; Żołnowski, 2013; Muhamud et al., 2015; Wierzbowska et al., 2014, 2016).

The conducted research revealed that the genetic factor had a significant impact on the content of phosphorus in potato tubers (*Table 2*). The variety which contained the greatest volume of this component was Tajfun variety, followed by Jelly and Honorata varieties. The impact of different properties on the content of phosphorus are underlined by Wierzbowska et al. (2016), Żołnowski (2013). All the applied biostimulators in the presented studies increased the content of phosphorus in the tubers of the tested varieties. The largest average content of phosphorus was obtained after applying BrunatneBio Złoto biostimulator. The experiment conducted by Wierzbowska et al.

http://www.aloki.hu ● ISSN 1589 1623 (Print) ● ISSN 1785 0037 (Online)
DOI: http://dx.doi.org/10.15666/aeer/1705_1192511933

(2016) might be the confirmation of the obtained results, whereby the authors noted an increase of concentration of phosphorus after spraying the plants with Asahi SL, whilst other growth regulators (Bio-Algeen S90, Kelpak SL) did not change the content of phosphorus. Farouk (2015) reported an increase in the content of phosphorus in the tubers after applying biostimulators from the seaweed and potassium humus with respect of the control tubers. Biostimulators (Trifender WP, Asahi SL, Kepak SL, Bio-Algeen S90) used in the experiences of Głosek-Sobieraj et al. (2019) did not alter the content of phosphorus. The factor which also significantly modified the content of the analysed element were the hydrothermal conditions appearing in the years of researches. High content of phosphorus was noted in the tubers gathered in 2017, whereby the total rainfall volume was, respectively by 124 and 30 mm higher than in the years 2016 and 2015 (*Table 1*).

Table 1. *Weather conditions during of potato vegetation*

Years	Months						April-September
	April	May	June	July	August	September	
Air temperature (°C)							
2015	8.2	12.3	16.5	18.7	21.0	14.5	15.2
2016	9.1	15.1	18.4	19.1	18.0	14.9	15.8
2017	6.9	13.9	17.8	16.9	18.4	13.9	14.6
Multiyear mean 1996-2010	8.0	13.5	17.0	19.7	18.5	13.5	15.0
Rainfall (mm)							
2015	30.0	100.2	43.3	62.6	11.9	47.1	295.1
2016	28.7	54.8	36.9	35.2	31.7	13.6	200.9
2017	59.6	49.5	57.9	23.6	54.7	80.1	325.4
Multiyear sum (1996-2010)	33.6	58.3	59.6	57.5	59.9	42.3	335.4

Table 2. *Content of phosphorus in tubers of potatoes depending on the biostimulant used (g kg^{-1} dry matter)*

Variants	Cultivars			Years			Mean
	Honorata	Jelly	Tajfun	2015	2016	2017	
1. Control variant	3.112	3.261	3.321	3.221	3.261	3.417	3.265d
2. Kelpak SL	3.261	3.268	3.456	3.222	3.310	3.422	3.323cd
3. Tytanit	3.187	3.364	3.461	3.268	3.367	3.458	3.350bc
4. GreenOk	3.281	3.411	3.467	3.393	3.450	3.466	3.411ab
5. BrunatneBio Złoto	3.371	3.485	3.512	3.473	3.471	3.567	3.479a
Mean	3.242c	3.358b	3.443a	3.315b	3.372b	3.466a	3.366

The means marked by the same letter do not differ significantly

Phosphorus decides about the processing value of potatoes; its content in tubers amounts to an average of 57 mg·100 g^{-1}. Phosphorus is a mineral that occurs in the greatest concentration in human organisms. Upon the recommended standard of 700 mg

http://www.aloki.hu ● ISSN 1589 1623 (Print) ● ISSN 1785 0037 (Online)
DOI: http://dx.doi.org/10.15666/aeer/1705_1192511933

phosphorus per day, 100 g of potato covers the daily demand of a person for this element in 8% (Wierzbicka, 2012).

Another important element *Solanum tuberosum* is calcium, considered as the element which conditions the correct growth and development of an organism and, along with the collagen, it constitute the key building material of the skeletal system (Zarzecka et al., 2015). In an adult human organism, 99% of calcium occurs in the skeletal system (Friedrich et al., 2002; Miles and Buchman, 2009; Wierzbicka, 2012). The greatest average content of calcium was noted in Tajfun and Honorata varieties, which were in these terms homogeneous, while Jelly variety contained significantly less calcium (*Table 3*). The applied in the experiment biostimulators increased the content of calcium in the tubers, while the greatest value of calcium was obtained upon the use of BrunatneBio Złoto biostimulator. High content of calcium was indicated in the tubers gathered in 2017 in which the sum of rainfall was higher than in 2016 and 2015 (*Table 1*). The applied biostimulators reacted to the meteorological conditions in the years of researches causing a significant increase of the content of calcium in 2017, which was characterised by a beneficial distribution of temperatures and rainfall during vegetation period for potatoes (*Table 3*). All three varieties reacted in a specific manner to the thermal and humidity conditions in place in the years of cultivation, as per the indicated interaction variety x years (*Table 4*). Wierzbowska e al. (2016) within the presented research, having analysed the impact of Asahi Sl, Bio-Algen S90 and Kelpak SL biostimulators, they indicated that the content of calcium in tubers was significantly modified solely by the Asahi Sl biostimulator.

Table 3. *Content of calcium in tubers of potatoes depending on the biostimulant used (g kg^{-1} dry matter)*

Variants	Cultivars			Years			Mean
	Honorata	Jelly	Tajfun	2015	2016	2017	
1. Control variant	0.712	0.659	0.698	0.612D	0.687C	0.734BC	0.684d
2. Kelpak SL	0.734	0.665	0.723	0.678CD	0.696C	0.745B	0.707d
3. Tytanit	0.745	0.674	0.767	0.741B	0.734BC	0.789AB	0.742bc
4. GreenOk	0.754	0.679	0.773	0.787B	0.779B	0.791A	0.760ab
5. BrunatneBio Złoto	0.779	0.686	0.779	0.798A	0.834A	0.799A	0.779a
Mean	0.745a	0.673b	0.748a	0.723c	0.746b	0.772a	0.734

The means marked by the same letter do not differ significantly

Table 4. *Calcium content depending on the cultivars and years of research (g ha^{-1})*

Cultivars	Years		
	2015	2016	2017
Honorata	0.799A	0.765B	0.769AB
Jelly	0.676D	0.645D	0.765B
Tajfun	0.773A	0.713C	0.754B

The means marked by the same letter do not differ significantly

A significant component of potato tubers is magnesium the content of which in the tubers depends significantly on the varieties, types of biostimulators and weather conditions in the years of research. Honorata variety gathered the greatest volume of

http://www.aloki.hu ● ISSN 1589 1623 (Print) ● ISSN 1785 0037 (Online)
DOI: http://dx.doi.org/10.15666/aeer/1705_1192511933

magnesium, while Jelly the smallest. Biostimulators caused an increase in the concentration of magnesium with regards to the tubers gathered from the control object. The most mineral components were contained in the tubers after application of BrunatneBio Złoto biostimulator, which allows believing that BrunatneBio Złoto is an agent which acts in a stimulating manner on the gathering of phosphorus, calcium and magnesium. In light of the presented research one must note that the content of magnesium in the tubers depends on the hydrothermal conditions. The largest content of this element was present in the tubers gathered in 2017 (*Table 5*) which was characterized by excessive rainfall in comparison to the average long-term sum and was the coldest in comparison to the other vegetation periods.

Table 5. *Content of magnesium in tubers of potatoes depending on the biostimulant used (g kg^{-1} dry matter)*

Variants	Cultivars			Years			Mean
	Honorata	Jelly	Tajfun	2015	2016	2017	
1. Control variant	1.234	1.213	1.324	1.294D	1.324C	1.412B	1.300c
2. Kelpak SL	1.325	1.245	1.345	1.312C	1.334C	1.423AB	1.330bc
3. Tytanit	1.398	1.255	1.356	1.345C	1.411B	1.435A	1.367ab
4. GreenOk	1.457	1.278	1.366	1.356C	1.423AB	1.456A	1.389a
5. BrunatneBio Złoto	1.487	1.289	1.412	1.345C	1.445A	1.467A	1.407a
Mean	1.380a	1.263b	1.361a	1.330c	1.387b	1.439a	1.360

The mean marked by the same letter do not differ significantly

Conclusions

The content of phosphorus, calcium and magnesium in potato tubers was substantially diversified by the variety genotype. The largest concentration of phosphorus and calcium was noted in the tubers of Tajfun variety, while magnesium in the tubers of Honorata variety. Tubers of plants treated with BrunatneBio Złoto preparation were characterized by the greatest content of the selected mineral components. Meteorological conditions, especially large volume of rainfall in 2017, contributed to an increase of tested macro-elements (phosphorus, calcium and magnesium) in potato tubers of three edible potato varieties.

Acknowledgements. The results of the research carried out under the research theme NO. 363/S/13 were financed from the science grant granted by the Ministry of Science and Higher Education.

REFERENCES

[1] Bienia, B., Sawicka, B., Krochmal-Marczak, B. (2018): Influence of foliar fertilization with macro- and microelement fertilizers on the yield and yield structure of several potato varieties. – Fragm. Agron. 35(1): 17-28.

[2] Ekin, Z. (2011): Some analytical quality characteristics for evaluating the utilization and consumption of potato (*Solanum tuberosum* L.) tubers. – Afr. J. Biotech. 10(32): 6001-6010.

[3] Elfaki, A. E., Abbsher, A. M. (2010): Nutritional situation of potato subjected to Sudanese cooking methods. – J. Appl. Sci. Res. 6(8): 880-924.

http://www.aloki.hu ● ISSN 1589 1623 (Print) ● ISSN 1785 0037 (Online)
DOI: http://dx.doi.org/10.15666/aeer/1705_1192511933

[4] Fageria, N. K., Filho, B. M. P., Moreira, A., Guimarães, C. M. (2009): Foliar fertilization of crop plants. – J. Plant Nutrition 32: 1044-1064.
[5] Farouk, S. (2015): Imroving growth and productivity of potato (*Solanum tuberosum* L.) by some biostimulants and lithovit with or without boron. – J. Plant Prod., Mansoura Univ. 6(12): 2187-2206.
[6] Fernandez, V., Sotiropoulos, T., Brown, P. (2013): Foliar Fertilization. Scientific Principles and Field Practices. – International Fertilizer Industry Association (IFA), Paris.
[7] Friedrich, M., Jankowiak, D., Ożgo, M., Skrzypczak, W. F., Stepanowska, K. (2002): Mineral Components in Human and Animal Nutrition. – Wyd. Akademii Rolniczej, Szczecin (in Polish).
[8] Głosek-Sobieraj, M., Cwalina-Ambroziak, B., Wierzbowska, J., Waśkiewicz, A. (2018): The influence of biostimulants on the microelement content of tubers in selected potato cultivars. – Acta Sci. Pol. Hortorum Cultus 17(6): 37-48.
[9] Horvat, T., Poljak, M., Lazarević, B., Svećnjak, Z., Hanaćek, K. (2014): Effect of foliar fertilizers on physiological characteristics of potato. – Rom. Agric. Res. 31: 159-165.
[10] Jarvan, M., Edesi, L. (2009): The effect of cultivation methods on the yield and biological quality of potato. – Agron. Res. 7(Special Issue I): 289-299.
[11] Kołodziejczyk, M., Szmigiel, A. (2005): Contents of macronutrients in edible potato tubers depending on the soil complex, variety and fertilization. – Fragm. Agron. 22(1): 436-445.
[12] Leszczyński, W. (2012): Nutritional value of potato and potato products (literature review). – Biul. Ins. Hod. Aklim. Rośl. 266: 5-20 (in Polish).
[13] Mahamud, M. A., Chowdhury, M. A. H., Rahim, M. A., Mohiuddin, K. M. (2015): Mineral nutrient contents of some potato accessions of USA and Bangladesh. – J. Bangladesh Agril. Univ. 13(2): 207-214.
[14] Miles, G. P., Buchman, J. L. (2009): Impact of zebra chip disease on the mineral content of potato tubers. – American Journal of Potato Research 86 481-489.
[15] Singh, J., Singh, M., Jain, A., Bhardwaj, S., Singh, A., Singh, D. K., Bhushan, B., Dubey, S. K. (2013): An Introduction of Plant Nutrients and Foliar Fertilization: A Review. – In: Ram, T. et al. (eds.) Precision Farming: A New Approach. Daya Publishing Company, New Delhi, pp. 252-320.
[16] Tajner-Czopek, A. (2006): Methodology for determining the technological value and quality of potato consumption. – Zesz. Probl. Post. Nauk. Roln. 511: 03-95.
[17] Trawczyński, C. (2014): The influence of amino acid biostimulators - tecamin - on the yield and quality of potatoes. – Ziemn. Pol. 3: 29-34 (in Polish).
[18] Wierzbicka, A. (2012): Mineral content of potato tubers grown in the organic system their nutritional value and interaction. – J. of Research and Applications in Agricultural Engineering 57(4): 188-192 (in Polish).
[19] Wierzbicka, A., Trawczyński, C. (2011): Influence of irrigation and soil microorganisms on the content of macro and micronutrients in organic potato tubers. – Fragm. Agron. 28(4): 139-148.
[20] Wierzbowska, J., Cwalina-Ambroziak, B., Sienkiewicz, S., Głosek, M. (2014): The content of minerals in potato tubers treated with bioregulators. – J. Elementol. 19(2) Suppl. June: 71-72 (in Polish).
[21] Wierzbowska, J., Cwalina-Ambroziak, B., Głosek, M., Sienkiewicz, S. (2015a): Effect of biostimulators on yield and selected chemical properties of potato tubers. – J. Elem. 20(3): 757-768.
[22] Wierzbowska, J., Cwalina-Ambroziak, B., Bowszyc, T., Głosek-Sobieraj, M., Mackiweicz-Walec, E. (2015b): Content of microelements in tubers of potato treated with biostimulators. – Pol. J. Natur. Sc. 30(3): 225-234.
[23] Wierzbowska, J., Cwalina-Ambroziak, B., Głosek-Sobieraj, M., Sienkiewicz, S. (2016): Conttent of minerals in tubers of potato plants treated with bioregulators. – Rom. Agric. Res. 33: 291-298.

http://www.aloki.hu ● ISSN 1589 1623 (Print) ● ISSN 1785 0037 (Online)
DOI: http://dx.doi.org/10.15666/aeer/1705_1192511933

[24] Wójcik-Stopczyńska, B., Grzeszczuk, M., Jakubowska, B. (2012): The content of some nutrients and potentially harmful in edible potatoes from the commercial network. – Rocz. Państ. Zak. Hig. 63(3): 207-212 (in Polish).
[25] Zarzecka, K., Mystkowska, I. (2004): Influence of selected herbicides on the content of potassium and phosphorus in potato tubers. –J. Elem. 9(2): 175-182.
[26] Zarzecka, K., Gugała, M., Gąsiorowska, B., Makarewicz, A. (2006): Magnesium and calcium fluctuations in potato tubers influenced by the use of herbicides and their mixtures. – J. Elem. 7: 309-315.
[27] Zarzecka, K., Gugała, M., Mystkowska, I., Baranowska, A., Zarzecka, M. (2015): The comparison of selected mineral content in edible potato tubers. – Zesz. Probl. Post. Nauk Rol. 583: 133-140 (in Polish).
[28] Żołnowski, A. C. (2013): Studies on the Variability of the Yield and Quality of Table Potato (Solanum tuberosum L.) Grown under Varied Levels of Mineral Fertilization. – UWM, Olsztyn (Dissertations and Monographs), pp. 191-259 (in Polish).

http://www.aloki.hu ● ISSN 1589 1623 (Print) ● ISSN 1785 0037 (Online)
DOI: http://dx.doi.org/10.15666/aeer/1705_1192511933

CHARACTERISTICS OF THE ULTRAPHYTOPLANKTON COMMUNITY STRUCTURE AND ITS ENVIRONMENTAL RESPONSE IN THE THREE GORGES RESERVOIR (CHINA) IN 2014

LIU, M.-Q.[1,2] – LIU, Z.-X.[1] – HOU, Y.-Y.[1] – LIU, K.-S.[1] – LIU, X.-L.[1] – CHEN, Q.[1] – LIU, X.-X.[1] – LI, Y.-T.[1] – HOU, J.-J.[1*] – BI, Y.-H.[3*]

[1]*Hubei Key Laboratory of Edible Wild Plants Conservation and Utilization, Hubei Normal University, Huangshi 435002, China*

[2]*Zhejiang Normal University, College of Chemistry and Life Sciences, Jinhua 321004, China*

[3]*State Key Laboratory of Freshwater Ecology and Biotechnology, Institute of Hydrobiology, the Chinese Academy of Sciences, Wuhan 430072, China*

**Corresponding authors*
e-mail/phone: jjhou@hbnu.edu.cn/+86-71-4651-1613 (J.-J. Hou); biyh@ihb.ac.cn/+86-27-6878-0016 (Y.-H. Bi)

(Received 24th Apr 2019; accepted 12th Jul 2019)

Abstract. To characterize the ultraphytoplankton community structure and understand its succession and its relationship with environmental factors, High Performance Liquid Chromatography (HPLC-CHEMTAX) was used to analyze the photosynthetic pigment concentration and the algae composition. Algal phyla composition and their abundance were determined based on the presence of pigments, and environmental parameters were synchronously tested in the Three Gorges Reservoir in China. High-performance liquid chromatography (HPLC) analysis showed that there were eight characteristic photosynthetic pigments in the Three Gorges reservoir area: alloxanthin, chlorophyll b, chlorophyll a, fucoxanthin, lutein, neoxanthin, violaxanthin, and zeaxanthin. Among them, fucoxanthin, allophycocyanin, zeaxanthin, and chlorophyll b were the most important photosynthetic pigments in the Three Gorges reservoir area. There were significant differences in the time scale of the eight photosynthetic pigments ($P < 0.05$), but no significant difference in the seven phyla ($P > 0.05$). The calculation of the matrix factorization program chemical taxonomy (CHEMTAX) showed that the ultraphytoplankton community was composed of 7 phyla: *Euglenophytes*, *Chrysophytes*, *Cyanophytes, Cryptophytes*, *Chlorophytes*, *Diatoms*, and *Dinoflagellates*. Redundancy analysis (RDA) revealed that the key environmental factors that affected the structure of the ultraphytoplankton community were light intensity, total phosphorus, and water temperature. The results provided a basis and data support for the biodiversity of phytoplankton in the Three Gorges Reservoir and its relationship with environmental factors and environmental monitoring.
Keywords: *photosynthetic pigment, HPLC, CHEMTAX, total biomass, environmental factor*

Introduction

Ultraphytoplankton include all picoplankton (0.2~2 μm) and 2~5 μm microplankton (< 20 μm) (Ning, 1997). Ultraphytoplankton are light-dependent self-sustaining creatures that consist of prokaryotes and eukaryotes (Sieburth et al., 1978). Ultraphytoplankton are an important source of gross primary productivity and are distributed around the world, some in extreme conditions, such as high temperatures in tropical and subtropical regions, the frigid Antarctic, as well as oceans and lakes under a variety of nutrient conditions. Currently, the prokaryotes cyanobacteria, such as Synechococcus and Prochlorococcus, are a familiar subject in marine

http://www.aloki.hu ● ISSN 1589 1623 (Print) ● ISSN 1785 0037 (Online)
DOI: http://dx.doi.org/10.15666/aeer/1705_1193511952

ultraphytoplankton research (Coclet et al., 2017; Chen et al., 2011; Glove et al., 1988), while there are very few studies in fresh water.

As the world's largest deep-water reservoir, the Three Gorges Reservoir of China has huge economic benefits in terms of flood control, shipping and power generation. However, after the damming of the Yangtze River, it underwent tremendous changes in the hydrological situation and water environment (Huang and Li, 2006). The hydrodynamic characteristics of some reservoirs and tributaries have changed significantly. The velocity of the water flow has been markedly slowed, and the flow rate of many tributaries (A river that flows into another river (or other body of water) rather than directly into the sea.) is less than 0.05 $m \cdot s^{-1}$, which is due to the influence of reservoir hydrodynamics and the backwater effect (Deng and Gong, 2007; Li et al., 2007). The decrease in the flow rate causes the vertical flow of the target area to decrease and the residence time of the water to increase significantly, resulting in the sedimentation of suspended matter in the water (Zheng et al., 2008). Under the appropriate temperature, wind speed, light, and biological factors, such as the impact of phytoplankton, the changing conditions will cause the algae to undergo explosive growth into a "bloom" (Kong and Gao, 2005) and thus have a negative impact on the reservoir ecosystem.

Regarding phytoplankton in the Three Gorges Reservoir, there are many reports on microplankton and picoplankton (Pan et al., 2016; Liu et al.,2012; Zhou et al., 2009), but research data for ultraphytoplankton is lacking. The key and prerequisite for studying ultraphytoplankton are to classify them.

The classical phytoplankton taxonomy mainly uses microscopic observation and flow cytometry. The use of electron microscopy and optical microscopy for traditional morphological observation is the basis on which we can also use the cell count plate for sample identification of the count (Wasilowska et al., 2015). This traditional method is indispensable in phytoplankton classification and identification, but it is extremely difficult to classify phytoplankton with minimal particle sizes (e.g., ultraphytoplankton). Although flow cytometry techniques can accurately and efficiently count microscopic phytoplankton that are difficult to observe, it is a challenge to distinguish the phyla of phytoplankton in the sample (Bonato et al., 2016). On the other hand, if there are aggregates and debris in the sample cells, the resulting fluorescence interference will directly affect the test results. Compared with these methods, chemical classification has the advantages of being fast and accurate, with a high-throughput (Li et al., 2013).

Chlorophyll a plays an important role in photosynthesis and is considered a biomarker of phytoplankton in the world (Alvarez-Fernandez and Riegman, 2014). Scientists (Jeffrey, 1974; Hallegraeff, 1981) have recognized the taxonomic significance of different photosynthetic pigments and their composition in phytoplankton. The distribution of different pigments in algae is distinct and exists only in phytoplankton communities (Wright et al., 1991). Therefore, it is feasible and scientific to determine the characteristic photosynthetic pigments of phytoplankton in order to establish phytoplankton groups. Chromatographic techniques, especially reverse-phase high-performance liquid chromatography (RP-HPLC) technology, can be used in analyzing algae pigment content and composition changes, combined with the characteristic photosynthetic pigment and chlorophyll a initial ratio data, through the matrix factorization program CHEMTAX. In addition, the abundance and composition of the phytoplankton population can also be determined using

http://www.aloki.hu ● ISSN 1589 1623 (Print) ● ISSN 1785 0037 (Online)
DOI: http://dx.doi.org/10.15666/aeer/1705_1193511952

CHEMTAX. The chemical classifications based on HPLC-CHEMTAX pigment analysis can accurately analyze the phytoplankton community structure and abundance composition, and it is not limited by the phytoplankton grain size. The study of biomass change, taxa composition, and community structure succession of the ultraphytoplankton are significant in modern science. Although this method has been widely used in the study of marine phytoplankton composition and abundance (Madhu et al., 2014; Agirbas et al., 2015), it has not been frequently used in fresh water. To explore the dynamics of the ultraphytoplankton community structure in the Three Gorges Reservoir, our group applied this technique, which can quickly and accurately describe the community structure of the ultraphytoplankton (Li, 2014; Liu et al., 2017).

This study used HPLC-CHEMTAX technology aimed at specific pigments of the ultraphytoplankton to analyze the succession of the ultraphytoplankton community structure and its response to environmental factors in the Three Gorges Reservoir. Specifically, the main objectives of this study were as follows: (i) to discover the spatial and temporal distribution of the total biomass of the ultraphytoplankton in the Three Gorges Reservoir; (ii) to determine the concentration of photosynthetic pigments using HPLC to discover the algae community composition and to determine the dominant algal populations in different spatiotemporal and spatial conditions; and (iii) to illustrate the relationship between community structure and environmental factors of ultraphytoplankton by redundancy analysis. Therefore, this study provided Three Gorges Reservoir plant biodiversity research and eco-environmental management with baseline and basic data.

Methods

Sampling point setting

The Three Gorges Reservoir is an artificial channel lake formed after the completion of the Three Gorges Hydropower Station, which is located at east longitude 107°20'-111°02', north latitude 30°31'-30°20', through the provinces of Chongqing and Hubei in China. It covers 19 counties and cities in the Chongqing and Hubei Provinces, with a total area of 54,000 km^2. Based on the topographic features of the Three Gorges Reservoir, the degree of eutrophication, the status of the bloom, the level of nutrients, the hydrodynamic characteristics, and related literature research, the sampling points were determined as follows: we had a total of 26 sample sites, including 9 major tributaries of Chongqing, namely, the Tangxihe (TXH), Pengxihe (Xiaojiang, XJ), and Modaoxi (MDX) in Yunyang County, the Zhuxihe (ZXH), Caotanghe (CTH), and Meixihe (MXH) in Fengjie County, the Quma Town of Xiaojiang (QM) and KaiCoungty of Xiaojiang (KX) in Kai County, and Daninghe (DNH) in Wushan County and 6 tributaries in the Hubei reservoir area, including Shennong Creek (SN01-SN03) and Mianzhuxia (MZX) in Badong county, Xiangxihe (XX01-XX08) in Xiangxi County, and Yuanshuihe (YSH), Qingganhe (QGH), and Tong zhuanghe (TZH) in Zigui County, as well as the main stream of the Yangtze River (CJ01, CJ05). See *Figure 1* for details.

http://www.aloki.hu ● ISSN 1589 1623 (Print) ● ISSN 1785 0037 (Online)
DOI: http://dx.doi.org/10.15666/aeer/1705_1193511952

Figure 1. *Distribution of sampling sites in the Three Gorges Reservoir during 2014*

Monitoring frequency and sampling method

We chose two-month sampling, and the sampling time was from February to December of 2014. A total of 154 samples were collected from 26 stations each time (of which the stations XX08 in June and August were in dry season). Sampling on the 15th-17th of each month, and there were three replicates per site. A 1.5-L water sample was collected using a 5-L organic glass water sampler and was placed in a plastic bottle. Black plastic bags were then used to wrap the plastic bottles, and the samples were returned to the experimental station after the start of filtration. The water samples were passed through a 10-μm sieve, a 5-μm Millipore nuclear membrane, and a 0.7-μm GF/F (Whatman), successively. The sample films containing the ultraphytoplankton were prepared, wrapped with tin foil to avoid light exposure, and kept in liquid nitrogen.

Determination of characteristic photosynthetic pigment contents by HPLC

The sample processing method was as follows: the sample film was cut into 5 mm × 1 cm of debris and placed in a 2-mL Eppendorf tube. After adding 1 mL N,N-dimethylformamide (DMF) for pigment extraction and mixing, the extract was placed in the refrigerator at -20 °C for 40 min. The sample was then centrifuged for 5 min at a rotational speed of 4000 r/min, filtered with a 0.22-M filter membrane, and mixed with 1 M ammonium acetate solution with a volume of 1:1 for Infinity 1260 Series HPLC (Agilent, USA) analysis. The chromatographic separation was carried out on a C8 column (Zorbax Eclipse xdb-C8 4.6 × 150 m, 3.5 um, Agilent, USA) and a 36-min elution procedure.

According to a method in the literature (Li et al., 2015), the external standard method was used to carry out the quantitative analysis, the gradient elution program and the quantitative calculation formula reference (Hu et al., 2011). The identified photosynthetic pigments are as follows: alloxanthin (Allo), chlorophyll *b* (Chl-*b*), chlorophyll *a* (Chl-*a*), fucoxanthin (Fuco), lutein (Lute), neoxanthin (Neox), peridinin (Peri), violaxanthin (Viol), and zeaxanthin (Zeax). Combined with the single factor analysis of variance function in the statistical analysis software SPSS 17.0, the significance was analyzed.

http://www.aloki.hu ● ISSN 1589 1623 (Print) ● ISSN 1785 0037 (Online)
DOI: http://dx.doi.org/10.15666/aeer/1705_1193511952

The community structure of the ultraphytoplankton

The data obtained in the field on the initial ratios of photosynthetic pigments and their concentrations were entered in the matrix of the CHEMTAX software to calculate the characteristics of the ultraphytoplankton community structure in the Three Gorges Reservoir. ANOVA was performed using SPSS 17.0 (Statistical Product and Service Solutions) software, and the significance of functional analysis was analyzed.

Analysis of environmental factors

The environmental and physical indicators of the study included 10 physical and chemical indicators for outdoor measurement, consisting of pH, water temperature (WT), air temperature (AT), transparency (SD), conductivity (SPC), Illumination-water (Illum-W), Illumination-air (Illum-A), Turbidity (Turbidity), and dissolved oxygen (DO), and 7 indoor measurements of water chemistry, consisting of total phosphorus (TP), total nitrogen (TN), ammonium salt ($N\text{-}NH_4^+$), phosphate ($P\text{-}PO_4^{3-}$), nitrate ($N\text{-}NO_3^-$), and chemical oxygen demand (COD). The physical and chemical indicators for outdoor measurement were mainly measured by YSI (dissolved oxygen meter), transparency disk, and photometer. The analysis and test methods of the indoor measurements of water chemistry mainly adhered to the "Surface Water Environmental Quality Standard - GB3838-2002".

Redundancy analysis of the relationship between environmental factors and community structure

If the results of the Monte Carlo test and environmental variables screened showed significant difference ($P < 0.05$), the relationship between environmental factors and the community structure of the ultraphytoplankton could be explained by the RDA analysis module. Ordination plots were made by CANOCO for Windows 4.5 software.

Results

Total biomass of the ultraphytoplankton

It is universally acknowledged that chlorophyll a content indicates the total biomass of the ultraphytoplankton. Therefore, the temporal and spatial distribution of the total biomass of the ultraphytoplankton was identified by analyzing the changes in the content of Chl-*a* at 26 sampling sites (*Fig. 2*).

The concentration range of Chl-a in the Three Gorges Reservoir area was 6.39-18,781.96 μg/m^3, In April, June, and August, the total biomass of the ultraphytoplankton was higher, with the highest value being 18,781.96 μg/m^3 (August; ZXH). In October and December, the total biomass was lower, and the lowest value appeared at the ZXH station in October. The Chl-a concentration of the ultraphytoplankton ranged from 6.39 to 12,704.99 μg/m^3 in the Hubei reservoir area. In April and June, the concentration of Chl-a was the highest, with the highest value at the XX07 station in April. The concentration of Chl-a was lower in October and December, with the lowest value at the ZXH station in October. The concentration range of Chl-a in the Chongqing reservoir area was 28.97-18,781.96 μg/m^3. The Chl-a concentration was higher in August, indicating that the total biomass was the largest, with the highest value at the ZXH site. Lower values were found in December, with the lowest value at the MXH site. Overall, the total biomass of the

http://www.aloki.hu ● ISSN 1589 1623 (Print) ● ISSN 1785 0037 (Online)
DOI: http://dx.doi.org/10.15666/aeer/1705_1193511952

ultraphytoplankton in the Hubei reservoir area was slightly higher than that in Chongqing reservoir area.

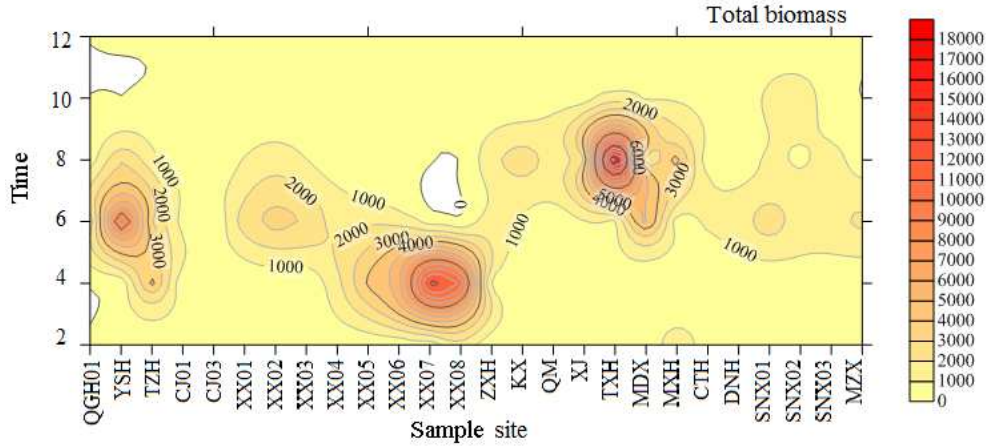

Figure 2. *Temporal and spatial changes of the total biomass*

By using the method of one-way ANOVA, the spatial and temporal differences are analyzed. The results showed that there was significant difference between June and December ($P < 0.05$), and there was no significant difference between the other months ($P > 0.05$). There was also no significant difference in total biomass with space ($P > 0.05$). Therefore, the total biomass is greatly influenced by time of year.

Types of photosynthetic pigments of the ultraphytoplankton

Based on HPLC technology, the photosynthetic pigment composition and content of the ultraphytoplankton in 26 stations in the main stream and tributaries of the Three Gorges reservoir area in 2014 were monitored, and their temporal, spatial, and distribution patterns were analyzed. The results showed that 8 special pigments of the ultraphytoplankton were detected in the Three Gorges Reservoir, including Fuco, Viol, Allo, Lute, Neox, Zeax, Chl-b and Chl-a. Among the target characteristic photosynthetic pigments, Allo, Zeax, Fuco, and Chl-b were the main photosynthetic pigments found in the ultraphytoplankton in the waters of the reservoir area. The total biomass of the ultraphytoplankton, indicated by the content of the Chl-a, has been discussed in the total biomass. The temporal and spatial distribution of the other seven photosynthetic pigments is as follows.

The temporal and spatial distribution of fucoxanthin is shown in *Figure 3A*. In April, the concentration of Fuco was higher, with an average of 534.07 μg/m^3. The highest concentration was 3,621.85 μg/m^3 at the XX08 site. In October and December, the concentration of Fuco was lower, with an average concentration of 13.69 μg/m^3, and the lowest concentration was 3.39 μg/m^3 at the QGH site. The Fuco concentration in the Hubei reservoir area was higher than that in the Chongqing reservoir area.

The temporal and spatial distribution of neoxanthin is shown in *Figure 3B*. In June, the concentration of Neox was higher, with an average of 25.38 μg/m^3 and a maximum of 158.63 μg/m^3 at ZXH. In December, the concentration of Neox was lower, with an average of 0.25 μg/m^3 and a minimum of 0.12 mg/m^3 at CJ03, while the Neox concentration in the Chongqing reservoir area was slightly higher than that of the Hubei reservoir area.

http://www.aloki.hu ● ISSN 1589 1623 (Print) ● ISSN 1785 0037 (Online)
DOI: http://dx.doi.org/10.15666/aeer/1705_1193511952

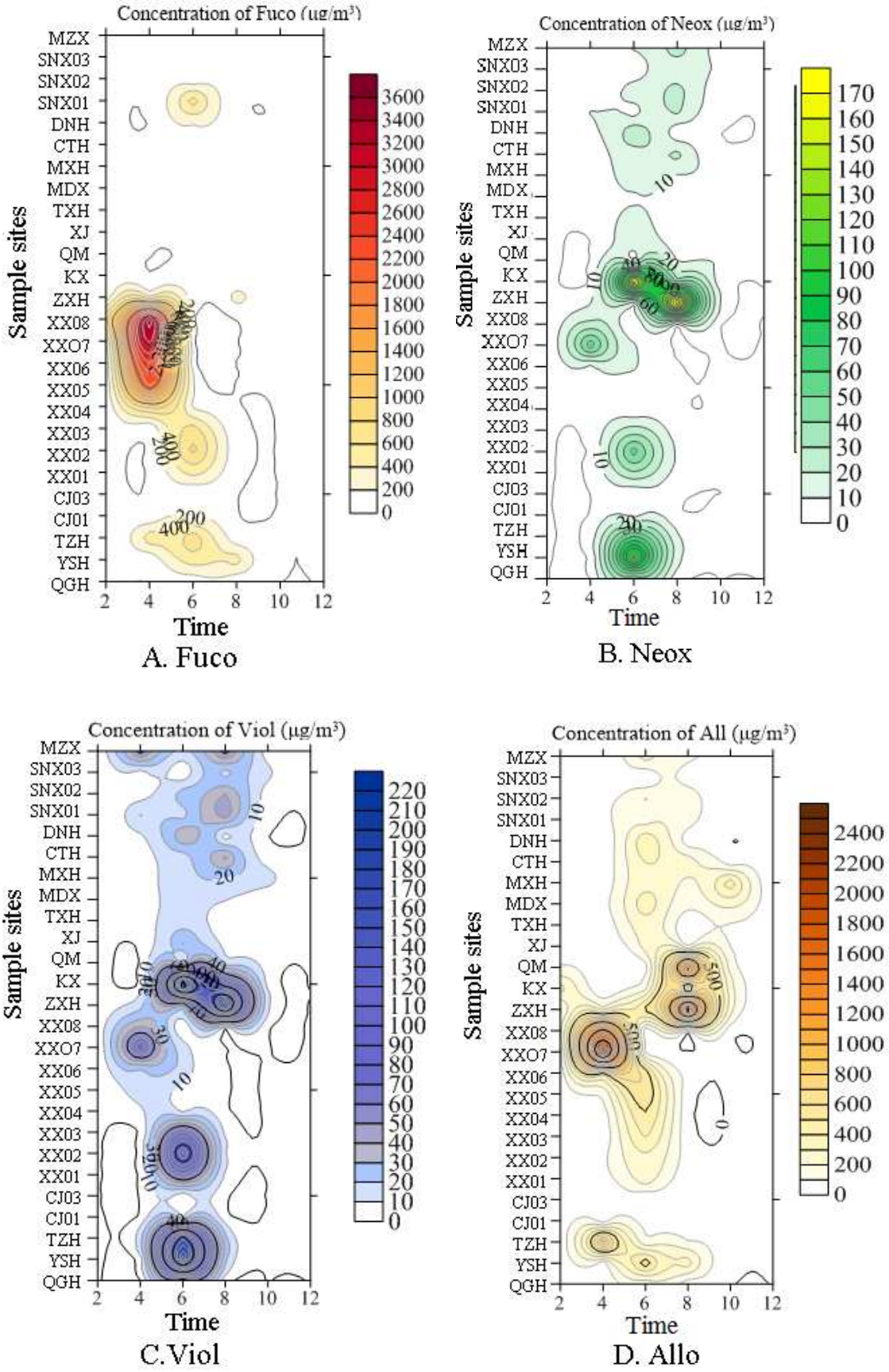

http://www.aloki.hu ● ISSN 1589 1623 (Print) ● ISSN 1785 0037 (Online)
DOI: http://dx.doi.org/10.15666/aeer/1705_1193511952

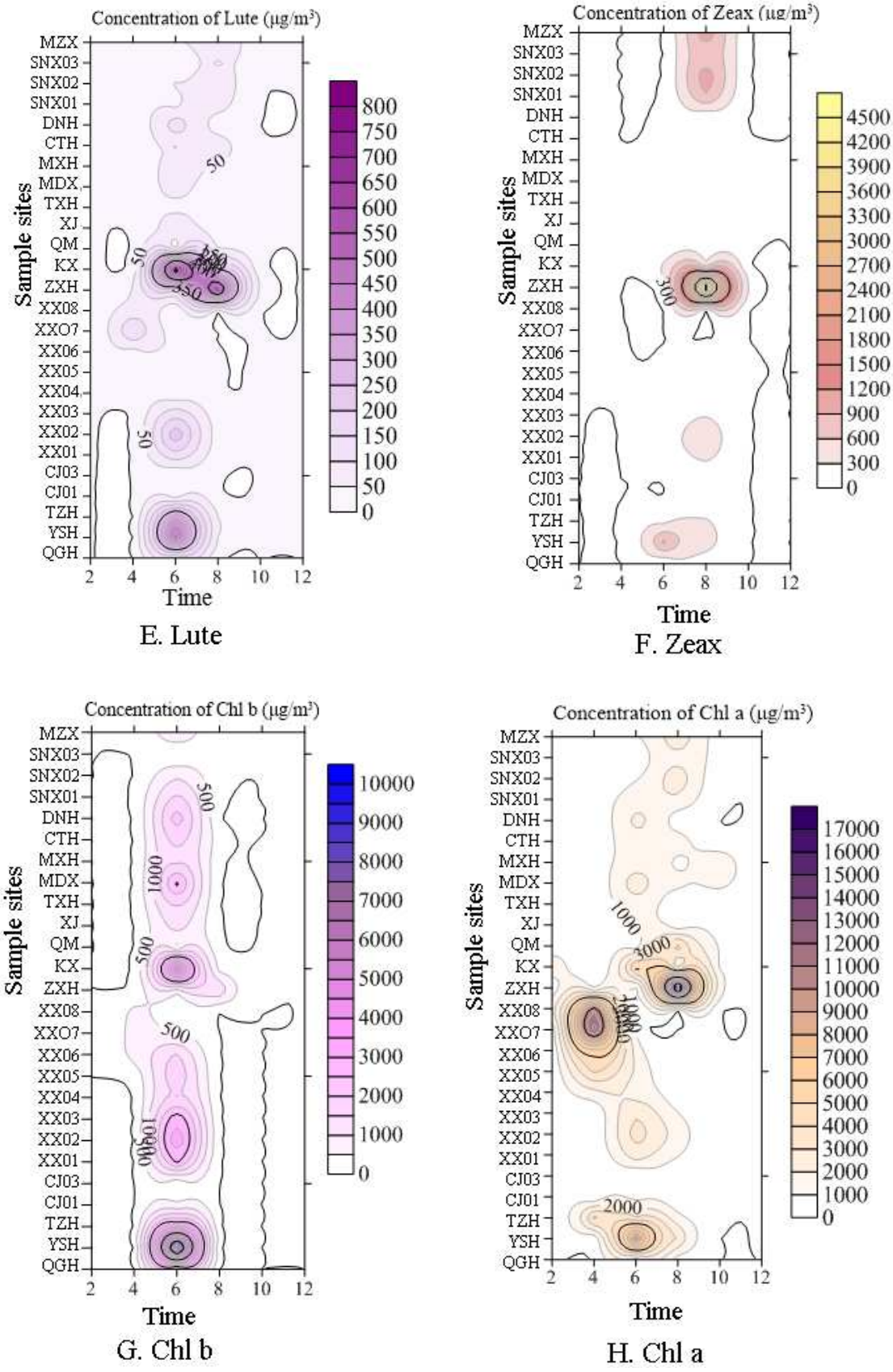

Figure 3. *Biomark photosynthetic pigments temporal and spatial distribution*

http://www.aloki.hu ● ISSN 1589 1623 (Print) ● ISSN 1785 0037 (Online)
DOI: http://dx.doi.org/10.15666/aeer/1705_1193511952

The spatial and temporal distribution of violaxanthin is shown in *Figure 3C*. In June, the concentration of Viol was higher, with an average of 45.8 μg/m^3, and the highest concentration was 198.32 μg/m^3 at YSH. The concentration of Viol in December was lower, with an average of 0.41 μg/m^3, and the lowest value was 0.13 μg/m^3 at CJ01. Its distribution in space showed an obvious difference, while the Viol concentration in the Hubei reservoir area was higher overall than that of the Chongqing reservoir area.

The temporal and spatial distribution of alloxanthin is shown in *Figure 3D*. In April (average: 254.79 μg/m^3) and June (average: 259.64 μg/m^3), the Allo concentration was higher, with a maximum of 2,295.64 μg/m^3 (April; XX07). In December, the Allo concentration was lower, with an average of 10.44 μg/m^3 and a minimum of 0.75 μg/m^3 at the CJ03 site. The concentration of the Chongqing reservoir area was higher than that of the Hubei reservoir area.

The temporal and spatial distribution of lutein is shown in *Figure 3E*. In June, the Lute concentration was higher, with an average of 122.86 μg/m^3, and the highest value appeared at the KX site (851.37 μg/m^3). In December, the concentration of Lute was lower; its average was 1.34 μg/m^3, and the minimum value was 0.46 μg/m^3 at the CJ03 site. The concentration of Lute in the Chongqing reservoir area was higher than that in the Hubei reservoir area.

The temporal and spatial distribution of zeaxanthin is shown in *Figure 3F*. In August, the Zeax concentration was higher, with an average of 482.80 μg/m^3, and the highest value appeared at the ZXH site (5,214.18 μg/m^3). In December, the concentration of Zeax was lower; its average value was 1.98 μg/m^3, and the minimum value of 0.42 μg/m^3 was at the CJ03 site. The concentration of Zeax in the Chongqing reservoir area was significantly higher than that in the Hubei reservoir area.

The temporal and spatial distribution of chlorophyll b was shown in *Figure 3G.* In June, the Chl-*b* had the highest concentration, and its average was 1,927.22 μg/m^3. In December, the Chl-b had the lowest concentration, with an average of 2.05 μg/m^3. In February, the concentration of the Chl-b at sites XX08 and KX was 0 μg/m^3, and the concentration of the Chl-b in the Hubei reservoir area was higher than that in the Chongqing reservoir area.

Except for the Chl-*a*, the other seven characteristic photosynthetic pigments were analysed by a variance homogeneity test and single factor analysis of variance. The results showed that the contents of the photosynthetic pigments including Fuco, Neox, Viol, Allo, Zeax, Lute and Chl-b were significantly different ($P < 0.05$) with time, but there was no significant difference ($P > 0.05$) in the spatial variation.

The community structure rules of the ultraphytoplankton

The community structure rules of the ultraphytoplankton were shown in *Figure 4*, and the significant taxa of the ultraphytoplankton were *Diatoms, Euglenophytes*, *Cryptophytes* and *Chrysophytes* in different samples for the whole year. In February (*Fig. 4A*), the dominant populations were *Diatoms, Cryptophytes* and *Euglenophytes*. The sharp increase in the number of the *Diatom* phyla appeared at the XX08, TXH, MXH, and SNX01 sites; the sharp increase in the number of the *Cryptophyta* phyla appeared at the TZH, CJ01, XX05, KX, MDX and DNH sites. The rest of the site group structures showed more uniform changes. In April (*Fig. 4B*), *Cryptophytes* and *Diatoms* were the principal phyla from sites QGH to XX04, and the *Diatoms* were the dominant population at sites XX05 and XX06; the major phyla were replaced by *Cryptophytes* from sites XX07 to MZX. In June (*Fig. 4C*), the primary phyla was *Cyanobacteria,*

http://www.aloki.hu ● ISSN 1589 1623 (Print) ● ISSN 1785 0037 (Online)
DOI: http://dx.doi.org/10.15666/aeer/1705_1193511952

Euglenophytes and *Diatoms*, and the rest samples did not have excessive changes of community structure. In August (*Fig. 4D*), the number of the *Euglenophytes* was higher than *Cryptophytes*. The community structure of each samples' change was obvious, and the major phyla were changed from *Cryptophytes* to *Euglenophytes*. Among them, the proportion of the *Diatoms* at the YSH site increased sharply, and the proportion of the *Cryptophytes* at the QM site increased sharply, while the proportion of the *Diatoms* at the MZX site decreased drastically. In October (*Fig. 4E*), the *Euglenophytes* accounted for 85% of the taxa at all samples except YSH. In December (*Fig. 4F*), *Euglenophytes* was the superior taxa, and the rest of the algae abundance was equal. However, *Cycanobacteria* were the significant taxa at ZXH, and *Chrysophytes* were the dominant taxa at MXH.

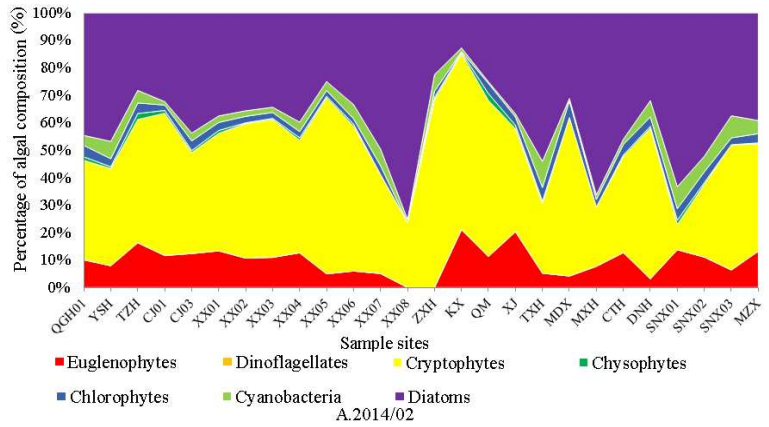

A.2014/02

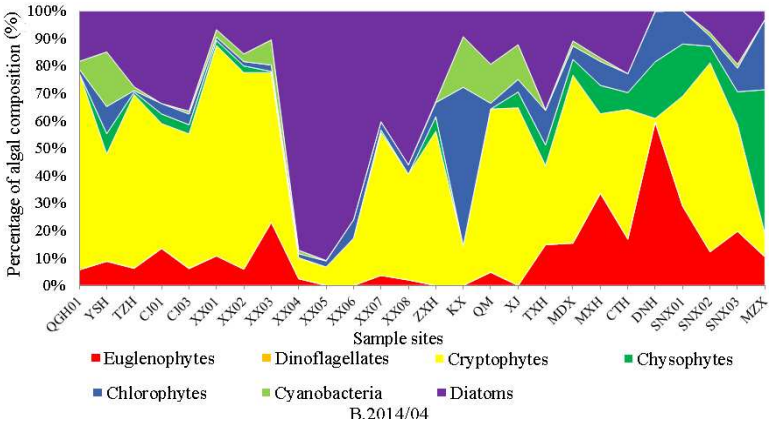

B.2014/04

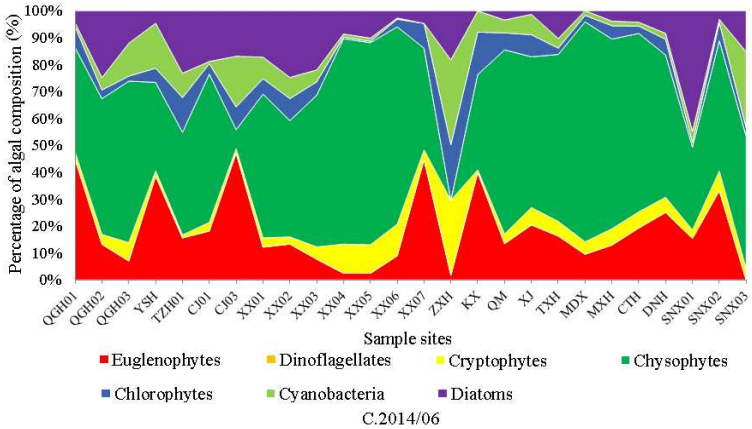

C.2014/06

http://www.aloki.hu ● ISSN 1589 1623 (Print) ● ISSN 1785 0037 (Online)
DOI: http://dx.doi.org/10.15666/aeer/1705_1193511952

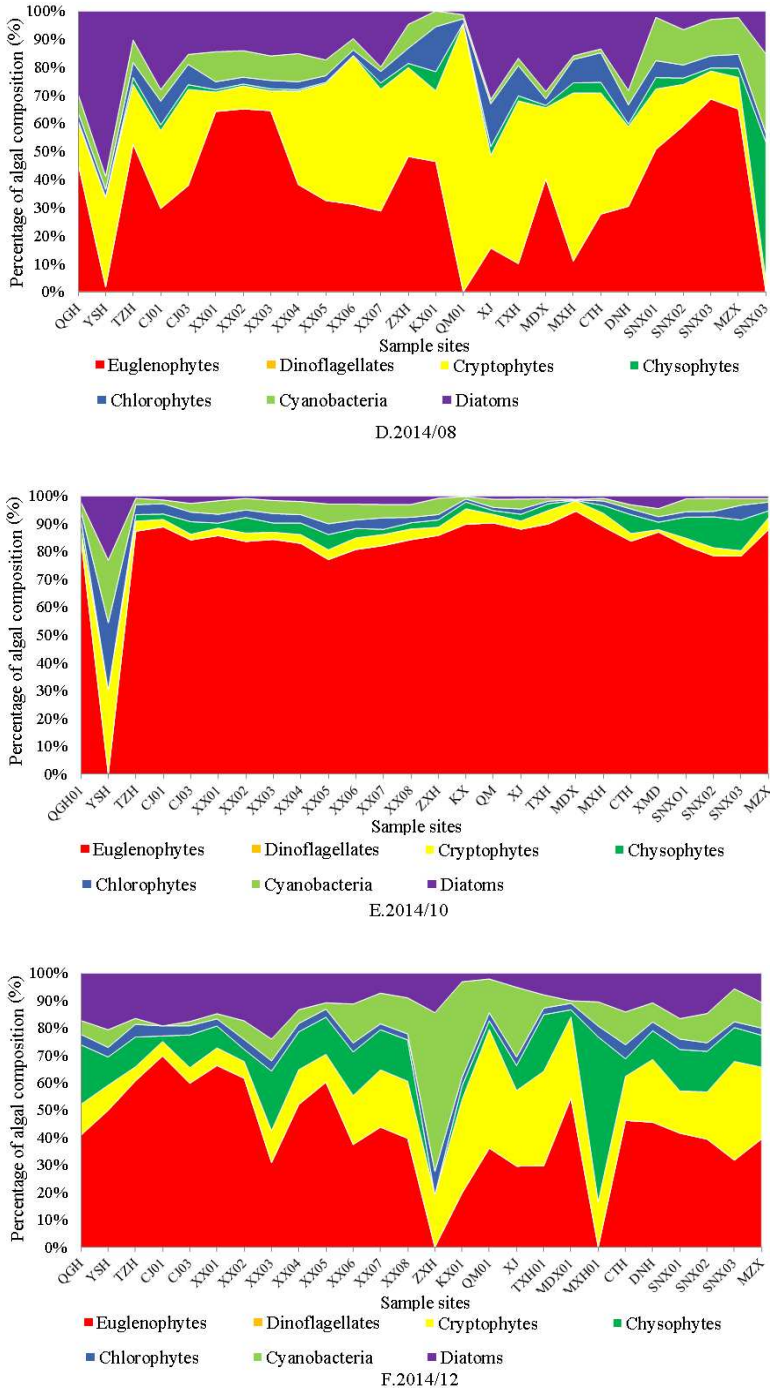

Figure 4. *Temporal and spatial variations of the ultraphytoplankton community structure*

The relationships of time and station were analysed by using the single factor variance of the ultraphytoplankton community structure of the Three Gorges Reservoir. The results showed that the community structure changes over time had significant differences ($P < 0.05$), and there was no significant difference in space ($P > 0.05$). Therefore, community structure was more influenced by the time. The investigation of time change was essential to the change of community structure.

http://www.aloki.hu ● ISSN 1589 1623 (Print) ● ISSN 1785 0037 (Online)
DOI: http://dx.doi.org/10.15666/aeer/1705_1193511952

Environmental responses of ultraphytoplankton

The relationships between the ultraphytoplankton community structure and environmental factors were investigated in the Three Gorges Project. The relevance was significantly different in the ultraphytoplankton community structure and environmental factors in February, April, June, and August ($P < 0.05$) rather than October ($P > 0.05$).

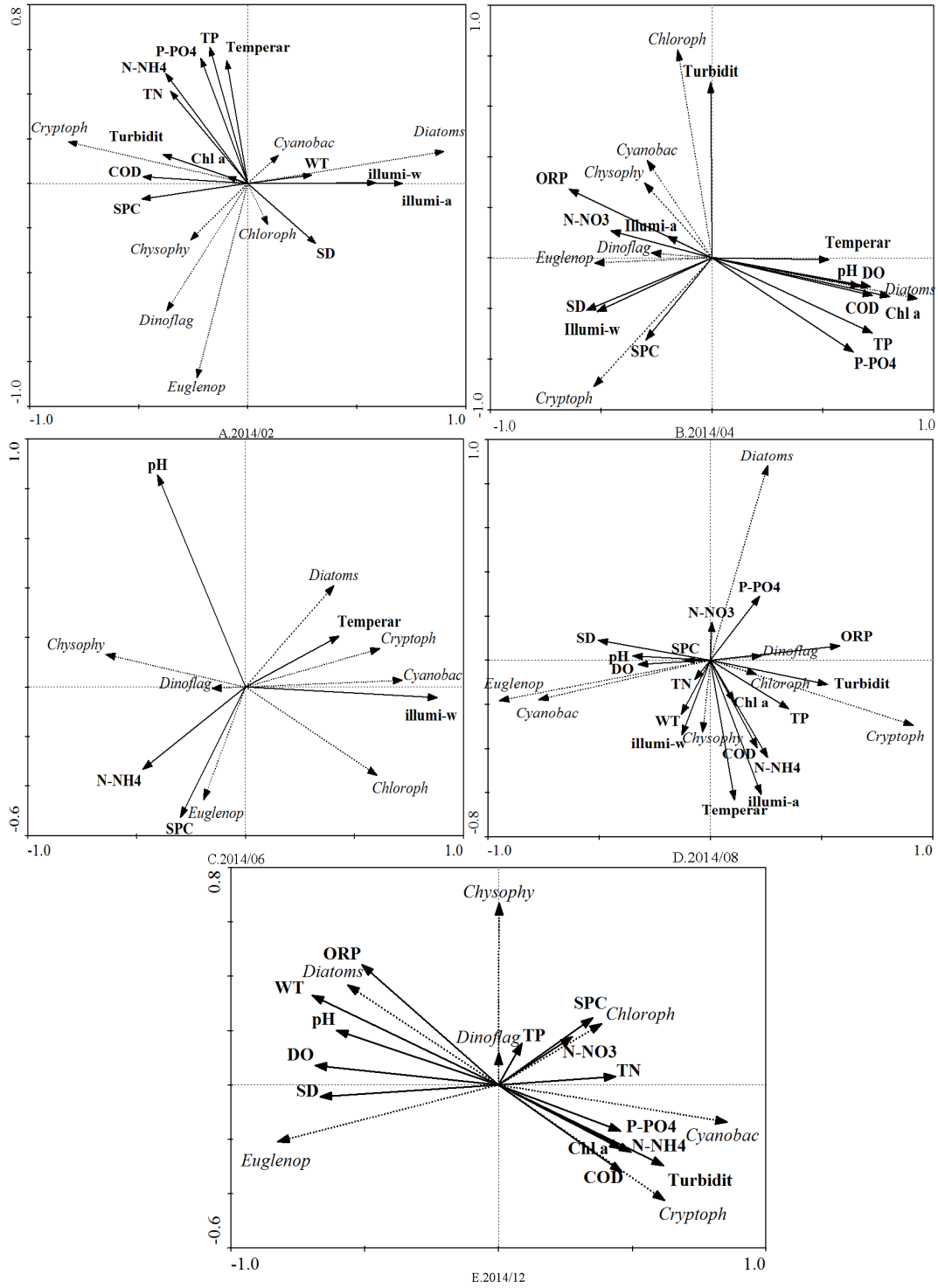

Figure 5. *RDA analysis of the relationship between environmental factors and the ultraphytoplankton phyla assemblages obtained by RDA*

http://www.aloki.hu ● ISSN 1589 1623 (Print) ● ISSN 1785 0037 (Online)
DOI: http://dx.doi.org/10.15666/aeer/1705_1193511952

In February (*Fig. 5A*), the superior taxa of algae were *Diatoms* and *Cryptophytes*. Relevance analysis between the ultraphytoplankton community structure and environmental factors indicated that WT and illumination were the most important limiting environmental factor. The environmental factors had a significant negative correlation with *Cryptophytes*, and algal abundance had a significant positive correlation with *Diatoms*. In April (*Fig. 5B*), the principal phyla of algae were *Diatoms* and *Cryptophytes*. TP was the all-important limiting environmental factor. In June (*Fig. 5C*), the primary phyla of algae were *Cyanobacteria* and *Chysophytes*, and relevance analysis between the ultraphytoplankton community structure and environmental factors indicated that pH and Iillumi-w were the most vital limiting environmental factor. In August (*Fig 5D*), the superior taxa of algae were the *Euglenophytes* and *Cryptophytes*. Relevance analysis between the ultraphytoplankton community structure and environmental factors indicated that DO and SPC were the most essential limiting environmental factor. In October, pre-screening and Monte Carlo tests found that it was unsuited to RDA analysis ($P > 0.5$). In December (*Fig. 5E*), the primary phyla of algae was *Euglenophytes*. RDA analysis showed that SD and DO were the most considerable environmental factor.

Discussion

Studies have shown that there is a positive correlation between the biomass of phytoplankton and the content of the Chl-a (Alvarez-Fernandez and Riegman, 2014). In this study, the Chl-*a* of the ultraphytoplankton was used to represent the biomass, and the Chl-*a* concentration of the ultraphytoplankton (< 5 μm) ranged from 6.39 μg/m^3 to 18,781.96 μg/m^3. It had also been found in earlier research (Silva et al., 2009) that the contribution rate of the ultraphytoplankton of total phytoplankton was 0.2-99.7%. Instead, the contribution rate of the ultraphytoplankton in fresh water was in the low. In keeping with the distribution of the Chl-*a* in the Three Gorges, the biomass of the ultraphytoplankton in April, June, and August were higher than other months, and it reached the maximum in August. Therefore, August probably developed into the outbreak period of the ultraphytoplankton. Liu et al. (2017) have found that the total chlorophyll a content of ultraphytoplankton was higher in the Xiangxi River Basin of the Three Gorges Reservoir in April and August, which is consistent with the results of this study. The research, which was put forth by Xiang Yingchun in 2014, had shown that, during 2011 and 2014 at the ZXH site, every month showed eutrophication. In conclusion, monitoring the change of the ultraphytoplankton biomass could be used to assess environmental status.

Studies (Wright, 1991; Li et al., 2013) have shown that the characteristic pigments only presented in a group of specific phytoplankton, and the distribution in different groups were different, reversed-phase high-performance liquid chromatography was used to analyse the pigment composition of algae, and then a certain mathematical method was used to calculate the ratios of characteristic pigments to the Chl-a, by which the specific phytoplankton contribution to the total biomass could be indicated, and the abundance and composition of a population could be determined. By using high-performance liquid chromatography to detect target waters, eight characteristic photosynthetic pigments were detected, including Fuco, Allo, Viol, Zeax, Neox, Lute, Chl-*b,* and Chl-*a*. After analysis, we found that Fuco, Zeax, Allo, and Chl-*b* were the most important characteristic photosynthetic pigments of the ultraphytoplankton in the Three Gorges Reservoir in 2014,

http://www.aloki.hu ● ISSN 1589 1623 (Print) ● ISSN 1785 0037 (Online)
DOI: http://dx.doi.org/10.15666/aeer/1705_1193511952

it had also been found in earlier research (Chen et al., 2003) that the most important characteristic photosynthetic pigments of the ultraphytoplankton in marine were Fuco, Allo and Chl-b, however, Zeax and Lute were hardly found. The temporal and spatial differences in photosynthetic pigments indicated that the temporal and spatial distribution of the ultraphytoplankton populations (Li, 2014), which said that it was more important to correspond to the community of *Cryptophytes*, *Diatoms*, *Euglenophytes*, *Chrysophytes* and other algae populations in the Three Gorges the ultraphytoplankton during 2014. However, the ultraphytoplankton in the marine are mostly *Chlorophytes*, *Synechococcus*, and *Cyanobacteria* (Li, 1995; Chen et al., 2003).

By using HPLC-CHEMTAX technical analysis, we showed that the changes of the ultraphytoplankton community structure in time and space were different. The dominant populations throughout the whole year were *Euglenophytes*, *Diatoms*, *Cryptophytes*, and *Chrysophytes*. *Chlorophytes*, *Cyanophytes*, and *Dinoflagellates* appeared in lower proportions. This is consistent with the results of Li (2014) and Liu et al. (2017). It shows that Euglenophytes, Diatoms, Cryptophytes and Chrysophytes are the dominant species of Ultraphytoplankton in the Three Gorges Reservoir. Special attention should be paid to February, April and June, as in these three months, dominant populations accounted for a large proportion, more than 50%, easily leading to the outbreak of the ultraphytoplankton blooms. Therefore, a deeper observation and positioning investigation of these months could provide powerful data support for the Three Gorges Reservoir water environment improvement to change the ecological environment in the future. Previous reports (Huang and Huang, 2002) showed that *Cryptophytes* were the dominant phyla in water with high organic matter content and nutrient abundance. Similar phenomena were observed in the Three Gorges Reservoir area throughout the study period, and *Cryptophytes* were widely distributed in February, April, and August. Generally speaking, *Diatoms* prefer to live in an environment with high concentration of nitrates (Liu et al., 2012). According to the annual nutrient level, there was no significant difference in time, except for October, which may be the main reason for the lowest proportion of *Diatoms* in October. In 2014, the *Euglenophytes* occupied a dominant position, especially in the fall, present as high as 80%. Most of them live in a fresh water rich in organic matter, which was an indicator of water pollution. The results showed that it is highly likely that ultraphytoplankton *Euglenophytes* blooms will occur in October.

The succession of phytoplankton is influenced by environmental factors. Based on earlier research about lakes and reservoirs, it was reported that in a poor nutrition system, TP < 0.01 mg/L and TN < 0.2 mg/L, and in a rich nutrition system, TN > 0.5 mg/L and TP > 0.02 mg/L (Peng et al., 2013). The minimum contents of TN and TP were 1.58 and 0.02 mg/L, respectively, in 2014, which showed that the Three Gorges Reservoir area water environments all were of a rich nutrition system. The study of the typical tributaries upstream of the Three Gorges Reservoir area and streamwise nutritional status analysis made by Zhang et al.(2010), showed that the content of TN ranged from 0.58 to 1.67 mg/L, while the content of TP ranged from 0.005 to 0.133 mg/L, the rich nutrition system was not changed. In contrast, the content of TN and TP in the Three Gorges branches and mainstream were significantly higher.

In this research, the relationship between the ultraphytoplankton community structure and environmental factors was not significant ($P > 0.05$) in October, showing that the ultraphytoplankton community structure was weak and affected by environmental factors in this month. The relationships between the ultraphytoplankton community structure and environmental factors were significant ($P < 0.05$) in the other

http://www.aloki.hu ● ISSN 1589 1623 (Print) ● ISSN 1785 0037 (Online)
DOI: http://dx.doi.org/10.15666/aeer/1705_1193511952

five months. The analysis of RDA showed that the most important environmental factors impacting the ultraphytoplankton community structure included illumination (including illumination in air and underwater illumination), TP, and temperature (including air-temperature and water-temperature). These results were the same as another survey (Gonçalvesaraujo et al., 2012), which studied environmental factors influencing algae. Research (Alam et al., 2016) reported that the main limiting factors of phytoplankton growth were nutrients in the water. In these nutrients, TP was the most effective limiting factor to affect the growth of phytoplankton in fresh water, and because of its shape and concentration, can affect the metabolism process of phytoplankton cells. Studies (Sunda and Huntsma, 1997; Siegel et al., 2002) have shown that the correlation between the content of the Chl-*a*, algal cell density, and illumination, and the correlation between illumination and photosynthesis; the results confirmed that illumination was one of the controlling factors of algae growth. The reason was that sufficient illumination was the first condition of phytoplankton growth. The population structure, growth of phytoplankton, and succession of phytoplankton were directly determined by competition, adaptation, light resistance and light of the water environment. The study found that temperature was the most basic condition to control phytoplankton growth and those different groups of phytoplankton have different requirements of temperature (Zhang et al., 2010). In short, this paper discussed the relationships between the ultraphytoplankton distribution and environmental factors in the Three Gorges Reservoir and we should pay more attention to the effects of illumination, temperature and total phosphorus.

Conclusions

By using HPLC-CHEMTAX technical analysis, 8 types of characteristic photosynthetic pigments and 7 divisions of algae phyla of the Three Gorges Reservoir were quickly detected in 2014. The main types of the ultraphytoplankton in the reservoir were *Euglenophytes*, *Chrysophytes*, *Cryptophytes*, and *Cyanophytes*. During the study period, the Three Gorges Reservoir is a eutrophic water body, and the biomass of the ultraphytoplankton in the Hubei reservoir area was higher than that in the Chongqing Reservoir area. The characteristics of the structure and succession of the ultraphytoplankton community were mainly influenced by illumination, total phosphorus, and temperature. The results provided the basic data for the study of phytoplankton biodiversity and ecological environmental monitoring of the Three Gorges Reservoir.

Acknowledgements. We sincerely thank Dr. Yonghong Bi and the Three Gorges Reservoir Ecological Field Station for sampling. We thank the editors and anonymous referees for their professional help and comments on this manuscript.

Funding. This work was funded by the National Natural Science Foundation of China [No. 41171045]; funded the University Science and Technology Innovation Team Research Fund [No. T201504]; and was funded by the Research Fund of Hubei Normal University [No. 2014F014].

http://www.aloki.hu ● ISSN 1589 1623 (Print) ● ISSN 1785 0037 (Online)
DOI: http://dx.doi.org/10.15666/aeer/1705_1193511952

REFERENCES

[1] Agirbas, E., Feyzioglu, A. M., Kopuz, U., Llewellyn, C. A. (2015): Phytoplankton community composition in the south-eastern Black Sea determined with pigments measured by HPLC-CHEMTAX analyses and microscopy cell counts. – Journal of the Marine Biological Association of the United Kingdom 95(1): 35-52.

[2] Alam, R. Q., Benson, B. C., Visser, J. M., Gang, D. D. (2016): Response of estuarine phytoplankton to nutrient and spatio-temporal pattern of physico-chemical water quality parameters in Little Vermilion Bay, Louisiana. – Ecological Informatics 32: 79-90.

[3] Alvarez-Fernandez, S., Riegman, R. (2014): Chlorphyll in North Sea coastal and offshore waters does not reflect long term trends of phytoplankton biomass. – Journal of Sea Research 91(8): 35-44.

[4] Bonato, S., Breton, E., Didry, M., Lizon, F., Cornille, V., Lécuyer, E., Christaki, U., Artigas, L. F. (2016): Spatio-temporal patterns in phytoplankton assemblages in inshore–offshore gradients using flow cytometry: a case study in the eastern English Channel. – Journal of Marine Systems 156: 76-85.

[5] Chen, B. Z., Wang, L., Song, S. Q., Huang, B., Sun, J., Liu, H. (2011): Comparisons of picophytoplankton abundance, size, and fluorescence between summer and winter in northern South China Sea. – Continental Shelf Research 31(14): 1527-1540.

[6] Chen, J. X., Huang, B. Q., Jia, X. W., Hong, H. S., Xie, Y. H. (2003): Study on the structure of ultraphytoplankton community in Xiamen Sea by using photosynthetic pigment. – Marine Environment Science 22(3): 16-21 (in Chinese).

[7] Coclet, C., Garnier, C., Delpy, F., Jamet, D., Durrieu, G., Poupon, C. L., Mayer, M., Misson, B. (2017): Trace metal contamination as a toxic and structuring factor impacting ultraphytoplankton communities in a multicontaminated mediterranean coastal area. – Progress in Oceanography 163: 196-213.

[8] Deng, C. G., Gong, L. (2007): A study on the development trend of eutrophication in the reservoir area of the Xia reservoir. – Chinese Journal of Agricultural Environmental Science 26: 279-282 (In Chinese).

[9] Glover, H. E., Prezelin. B. B., Campbell. L. (1988): Pico- and ultraplankton Sargasso Sea Communities: variability and comparative distributions of Synechococcus spp. and algae. – Marine Ecology Progress 49(1-2): 127-139.

[10] Gonçalvesaraujo, R., De Souza, M. S., Mendes, C. R. B., Tavano, V. M., Pollery, R. C., Garcia, C. A. E. (2012): Brazil-Malvinas confluence: effects of environmental variability on phytoplankton community structure. – Journal of Plankton Research 34(5): 399-415.

[11] Hallegraeff, G. F. (1981): Seasonal study of phytoplankton pigments and species at a coastal station off Sydney: importance of diatoms and nanoplankton. – Marine Biology 61: 107-118.

[12] Hu, J., Liu, X., Wang, L., Huang, B. Q. (2011): Qualitative and quantitative analysis of phytoplankton photosynthetic pigments marine science by reversed phase high performance liquid chromatography. – Marine Science 35(11): 19-28 (in Chinese).

[13] Huang, X. P., Huang, L. M. (2002): Spatial and temporal changes of inorganic nitrogen and activated phosphate content in the waters of the Pearl River estuary. – Journal of Applied Oceanography 21(4): 416-421 (in Chinese).

[14] Huang, Z. L., Li, Y. L. (2006): Water quality prediction and environmental capacity calculation of the Three Gorges Reservoir. – China Water Power Press, Beijing, pp. 14-16 (in Chinese).

[15] Jeffrey, S. W. (1974): Profiles of photosynthetic pigments in the ocean using thin-layer chromatography. – Marine Biology 26: 101-110.

[16] Kong, F. X., Gao, G. (2005): Physiological mechanism of cyanobacteria bloom in large shallow eutrophic lakes. – Acta Ecologica Sinica 25(3): 589-595 (in Chinese).

http://www.aloki.hu ● ISSN 1589 1623 (Print) ● ISSN 1785 0037 (Online)
DOI: http://dx.doi.org/10.15666/aeer/1705_1193511952

[17] Li, C. M., Huang, Z. L., Zhang, S., Chang, J. B. (2007): Algal bloom in the Three Gorges reservoir prediction. – Resources and Environment in the Yangtze River Basin 16(1): 1-6 (in Chinese).
[18] Li, J. Y. (2014): HPLC based on the analysis of photosynthetic pigments in the Three Gorges Reservoir super micro phytoplankton biodiversity research. – Hubei Normal University Master's Thesis, pp. 46-51 (in Chinese).
[19] Li, J. Y., Hou, J. J., Hu, J., Shi, X. Y. (2013): Application of chemical classification method in the study on the diversity of phytoplankton in fresh water. – Journal of Hubei Normal University 33(3): 46-50 (in Chinese).
[20] Li, J. Y., Hu, J., Hou, J. J., Zhou, T., Zheng, H. L, Liu, X. X., Bi, Y. H. (2015): A new method for the preparation of phytoplankton photosynthetic pigments by using pure culture algae. – Journal of Wuhan Textile University 28(6): 79-83 (in Chinese).
[21] Li, W. (1995): Composition of ultraphytoplankton in the Central North Atlantic. – Marine Ecology Progress Series 122(1-3): 1-8.
[22] Liu, X., Lu, X. H., Chen, Y. W. (2012): Temporal and spatial dynamics of the biomass of the algae in the northern part of Taihu Lake. – Journal of Lake Science 24(1): 142-148 (in Chinese).
[23] Liu, X. X., Li, J. Y., Bi, Y. H., Hou, J. J., Li, Y. T., He, Y. Y. (2017): Characterization of ultraphytoplankton pigments and functional community structure in Xiangxi Bay, China, using HPLC-CHEMTAX. – Journal of Freshwater Ecology 32(1): 1-16.
[24] Madhu, N. V., Ullas, N., Ashwini, R., Meenu, P., Rehitha, T. V., Lallu, K. R. (2014): Characterization of phytoplankton pigments and functional community structure in the Gulf of Mannar and the Palk Bay using HPLC-CHEMTAX analysis. – Continental Shelf Research 80(727): 79-90.
[25] Ning, X. R. (1997): Micro and ultra micro organisms in the ocean. – Journal of Marine Sciences 15(3): 60-64 (in Chinese).
[26] Pan, X. J., Liu, C., Zhu, M. L., Zheng, Z. W. Zou, X., Wan, C. Y. (2016): Impact of Three Gorges Reservoir impoundment and discharge on the phytoplankton community structure of Xiaojiang River. – Journal of Hydroecology 37(03); 42-48.
[27] Peng, R. C., Zhang, L., Zheng, Y. Z., Li, D. H. (2013): Seasonal succession of phytoplankton in response to the variation of environmental factors in the Gaolan River, Three Gorges Reservoir, China. – Chinese Journal of Oceanology and Limnology 31(4): 737-749.
[28] Sieburth. J. M. (1978): Pelagic ecosystem structure: Heterotrophic compartments of the plankton and their relationship to plankton size fractions. – Limnology & Oceanography 23(6): 1256-1263.
[29] Siegel, D. A., Doney, S. C., Yoder, J. A. (2002): The North Atlantic spring phytoplankton bloom and Sverdrup's critical depth hypothesis. – Science 296(5568): 730－733.
[30] Silva, R., Negri, R., Lutz, V. (2009): Summer succession of ultraphytoplankton at the EPEA coastal station (Northern Argentina). – Journal of Plankton Research 31(4): 447-458.
[31] Sunda, W. G., Huntsma, S. A. (1997): Interrelated influence of iron, light and cell size on marine phytoplankton growth. – Nature 390(6658): 389-392.
[32] Wasilowska, A., Kopczynska, E. E., Rzepecki, M. (2015): Temporal and spatial variation of phytoplankton in Admiralty Bay, South Shetlands: the dynamics of summer blooms shown by pigment and light microscopy analysis. – Polar Biology 38(8): 1249-1265.
[33] Wright, S. W. (1991): Improved HPLC method for the analysis of chlorophylls and carotenoids from marine phytoplankton. – Marine Ecology Progress Series 77: 183-196.
[34] Xiang, Y. C., Zhang, L. Y., Liu, G. Q., Zhou, N., Ren, J. (2014): Spatial temporal distribution of nutrients in the tributary backwater area of the Wanzhou section of the Three Gorges Reservoir. – Journal of Chongqing Three Gorges University 30(3): 4-9 (in Chinese).

http://www.aloki.hu ● ISSN 1589 1623 (Print) ● ISSN 1785 0037 (Online)
DOI: http://dx.doi.org/10.15666/aeer/1705_1193511952

[35] Zhang, S., Liu, J. H., Li, L. L., Li, S., Xu, J., Gao, J. X. (2006): Distribution features of nutrient and phytoplankton in incipient Three Gorges Reservoir. – Environmental Science 27(6): 1056-1061.
[36] Zhang, S., Song, D., Zhang, K., Zeng, F. H., Li, D. G. (2010): Analysis of nutritional status in the upstream and backwater areas of the typical tributaries of the three gorges reservoir. – Journal of Lake Science 22(2): 201-207 (in Chinese).
[37] Zheng, B. H., Cao, C. J., Qin, Y. W., Huang, M. S. (2008): Characteristics and sources of nitrogen nutrients in the main reservoir of the Three Gorges Reservoir. – Environmental Science 29(1): 1-6 (in Chinese).
[38] Zhou, S., Tang, T., Wu, N., Fu, X., Jiang, W., Li, F., Cai, Q. H. (2009): Impacts of cascaded small hydropower plants on microzooplankton in Xiangxi River, China. – Acta Ecologica Sinica 29(1): 62-68.

http://www.aloki.hu ● ISSN 1589 1623 (Print) ● ISSN 1785 0037 (Online)
DOI: http://dx.doi.org/10.15666/aeer/1705_1193511952

A NEW SCAR MARKER OF HIGH SUGAR GENE IN SWEET SORGHUM [*SORGHUM BICOLOR* (L.) MOENCH]

CHEN, Y. – PANG, H. B. – LI, X. M. – MA, L. J. – WANG, L. L. – ZHANG, Y. – LI, Y. Y.*

College of Life Science, Shenyang Normal University
No. 253 Huanghe North Street, Shenyang, Liaoning 110034, China

**Corresponding author*
e-mail: yueyinglicn@163.com

(Received 25th Apr 2019; accepted 16th Jul 2019)

Abstract. This experiment used molecular marker technology to analyse high sugar genes, clone the target bands and the Random amplified polymorphic DNA (RAPD) molecular markers were converted into Sequence characterized amplified regions (SCAR) molecular markers, and additionally 120 RAPD primers were used to analyse female 3228B (sweet sorghum), paternal 3201B (ordinary sorghum) and their hybrids F_5. The results showed that 95 of 120 pairs amplified products, 25 of them did not amplify products, so the amplification rate reached 79%. The recombination rate of S512 and high sugar genes was 7% in F5 populations. S512 amplified polymorphic bands were recovered, cloned and sequenced, its band length was 441bp. According to the sequence, we transferred the RAPD to SCAR molecular markers and designed SCAR primer. We got the same amplification results with the RAPD in specific amplification progress of sweet sorghum F5 populations, thus the RAPD transfered to SCAR successfully, we called this $SCAR_{S512-441}$.
Keywords: *Random amplified polymorphic DNA (RAPD), Sequence characterized amplified regions (SCAR), amplification, molecular marker, coseparation analysis*

Introduction

Sweet sorghum (*Sorghum bicolour* (L.) Moench) is a variation of common sorghum (Vermerris, 2011), it has a strong resistance, high sugar content, high photosynthesis rates, high productivity, is one of the most important energy plants in the world (Wang et al., 2013; Lu et al., 2013). Sweet sorghum can applied in animal feed and brew as an energy plant, and produce syrup, making sugar. Research shows that the brix of sweet sorghum stems have high heritability, showing great effects on breeding variety (Zhang et al., 2011). We take Liao Tian 6 as a benchmark, the sugar brix of Liao Tian 6 is 18, the sugar brix higher than 18 are regarded as high sugar content. Studies show sugar brix traits of culms of sweet sorghum, is controlled by two major gnes add polygenes (Lu et al., 2012). And sugar contents characters were not a single gene, but have unbalanced multigenes besides a major gene (Wang et al., 2010). As biological research gradually entered the molecular level, molecular marker are more widely used, including germplasm resource research and breeding (Yang et al., 2016). Base on the application of DNA sequence polymorphism, Molecular Marker can mainly divided into three categories: (1) Includes restriction fragment length polymorphism marker and chromosome in situ hybridization marker with molecular hybridization at core. (2) Includes amplified fragment length polymorphism marker and sequence point marker with PCR reaction at core. (3) New molecular marking technique, includes single nucleotide polymorphism marker and expressed sequence tag. It has more advantages which sequence characterization amplified region marker based on RAPD of new molecular technology (Wu et al., 2016). It can overcome the shortcomings of high false

http://www.aloki.hu ● ISSN 1589 1623 (Print) ● ISSN 1785 0037 (Online)
DOI: http://dx.doi.org/10.15666/aeer/1705_1195311962

negative and lacks of repetition that translate the specificity band generated by RAPD marker into SCAR marker (Luo et al., 2013; Wang et al., 2016).

At present, SCAR is used a lot in breeding. In resistance gene marker research, anoectochilus roxburghii polymorphic RAPD marker have been developed based on 20 anoectochilus roxburghii germplasm resource, and transforming specific band into SCAR marker, identify its specificity. Use SCAR marker gene to identify the resistance effect of Soybean anthracnose resistance gene (Gu et al., 2011). Transfer RAPD marker which closely-linked with aphid resistance gene to SCAR marker, and make SCAR determinations to F_3 and some resistant varieties (Li et al., 2003), specific bands of F_3 resistant individual obtained. This experiment aimed to make a RAPD molecular marker analysis to experimental populations, find a RAPD primer related to sweet sorghum's high sugar gene, and give target band cloning and sequencing, then translated into stable SCAR marker, reduce the complexity of field farming, establish the theoretical foundation for choosing fine sweet sorghum variety (Tan et al., 2013; Li et al., 2016).

Materials and Methods

Plant material

Sweet sorghum 3228B (as the female parent in this study) and common grain sorghum 3201B (as the male parent) were supplied by Liaoning Academy of Agricultural Sciences. We created F_5 plants from the cross of 3228B ×3201B, and get total of 100 lines. We get the first leave under the fag leaf of the F_5 plants as plant materials. These sorghums have the same genetic background, and the marker which identify the sugar content.

Experiment methods

DNA extraction of seedling stage

Methods apply modified cetyltrimethylammonium bromide (CTAB) (Li et al., 2009; Lan et al., 2015) to extract DNA of male parent, female parent and F_5 plants.

DNA determination

① Concentration measurement: absorbance of the diluted DNA were measured in different detecting waves which are 230nm, 260nm and 280nm.

② Electrophoresis detection: 0.7% Agarose gel's preparation in ready: point sample, electrophoresis.

Build near isogenic pool

We use Bulked Segregation Analysis (BSA) (Yao et al., 2010) to analyze high sugar population and low sugar population. High sugar bulk: Take 1 μl of DNA of 62 varieties of high sugar content sorghum. Low sugar bulk: Take 1 μl of DNA of 38 varieties of low sugar content sorghum.

Build RAPD-PCR reaction system and condition

25 μl reaction system: which established by 25 mmol/L MgCl2 2.0 μl, 10 × Buffer 2.0 μl, 10 mmol/L dNTPs 1.5 μl, 10 μmol/μl primer 1.0 μl, 5 U/μl Taq enzyme 2.5 μl,

http://www.aloki.hu ● ISSN 1589 1623 (Print) ● ISSN 1785 0037 (Online)
DOI: http://dx.doi.org/10.15666/aeer/1705_1195311962

DNA template (100 ng) 2 μl, and add ddwater to 25 μl. Reaction conditions: 94ºC Initial denaturation 5 min → (94ºC denature 20 s → 50ºC Primer annealing 30 s → 72ºC Primer extension 70 s) 35 cycles → 72ºC extension 10 min → 4ºC storage.

Build SCAR-PCR reaction system

Reaction system: which established by 10 × Buffer 2.5 μ, 10 mmol/L dNTPs 1.0 μl, 25 mmol/L MgCl2 2.5 μL, 5 U/μl Taq enzyme 0.25 μL, 10 μmol/μL S512F 0.5 μl, 10 μmol/μL S512R 0.5 μl, DNA template 1.0 μl (100 ng), and add ddwater to 25 μl. Reaction conditions: 96ºC Initial denaturation 5min → (94ºC denature 1 min → 50ºC Primer annealing 50 s → 72ºC Primer extension 1 min) 35 cycles → 72ºC extension 10 min → 4ºC storage.

Detection of PCR reaction products

① 1.4%Agarose gel's preparation.
② Electrophoresis of PCR product.

Recovery of target band

We sterilize the needle and cut a few times at the polymorphism bands, then put the needle into RAPD-PCR reaction system, repeat this procedure several times and recovery the amplified different bands.

Co-segregated Analysis

Recombination rate (r) = Commutative number/ (High sugar population number + Low sugar population number) ×100% (Wang, 2004).

Genetic distances (cM) = [1/4*ln(1+2r)/(1-2r)]*100.

Marker map (Figure 1)

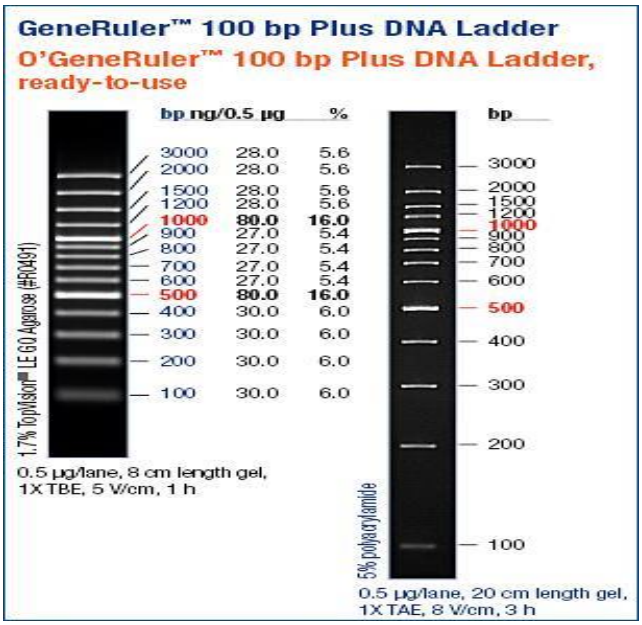

Figure 1. *100bp ladder marker*

http://www.aloki.hu ● ISSN 1589 1623 (Print) ● ISSN 1785 0037 (Online)
DOI: http://dx.doi.org/10.15666/aeer/1705_1195311962

Results and Analysis

Purity analysis of DNA

The electrophoretic pattern as shown in *Fig. 2* is total DNA extracted by improved CTAB method. As seen in *Fig. 2*, these bands are clear and without degrade. Purity and concentration of the DNA which was measured with ultraviolet spectrophotometer show that $OD_{260}/OD_{230} \geq 2.0$, $OD_{260}/OD_{280} \geq 1.7$-1.8, further explain, extracted DNA under these conditions can be used in subsequent RAPD- PCR experiment analysis.

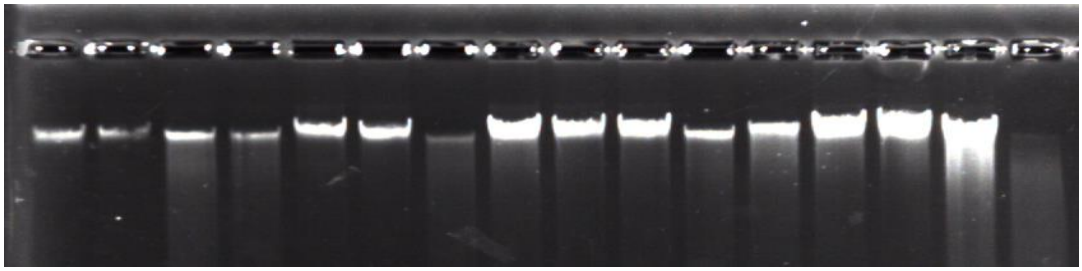

Figure 2. *DNA electrophoresis gel results. Female parent (1) Male parent (2) High sugar individual (3-9) Low sugar individual (10-16)*

RAPD-PCR analysis of sweet sorghum high sugar gene

In this study, with a random selected 120 RAPD primer, the RAPD molecular markers were used to analyze the Sweet sorghum (as the female parent in this study), common grain sorghum (as the male parent), high sugar gene bulk and low sugar gene bulk. The results show that the amplification rate is 79%, 95 primers were amplified bands and 25 primers can not ampliy bands. Most of the primers can amplify more than 6 bands, primer S504 amplify the largest bands, but with low quality images. There was no obvious difference among high sugar gene bulk, low sugar gene bulk and the parents. Primer S506 ampliy 7 bands which are the clearest, and there are also with no obvious difference among high sugar gene bulk, low sugar gene bulk and the parents. Primers S507 have differences between parents and high sugar gene bulk or low sugar gene bulk. Primer S509 amplify the least bands and the bands haven't differences. The amplification results see in *Fig. 3*.

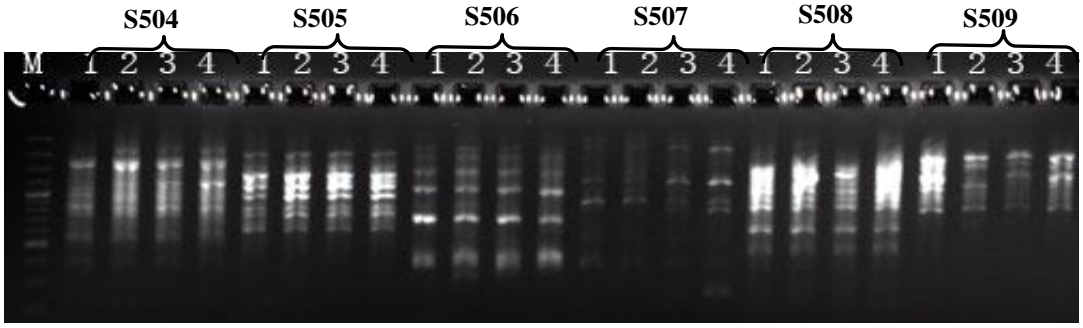

Figure 3. *The PCR-RAPD amplification results of primer S504, S505, S506, S507, S508, S509. Female parent (1) Male parent (2) High sugar gene pool (3) Low sugar gene pool (4) Marker (M)*

http://www.aloki.hu ● ISSN 1589 1623 (Print) ● ISSN 1785 0037 (Online)
DOI: http://dx.doi.org/10.15666/aeer/1705_1195311962

Amplification result of primer S510-S513 showed that bands are amplified by 4 primers. The bands amplified by primer S510 showed high polymorphisms between female parent (1) and male parent (2) and have high definition, but there is no polymorphism between high sugar gene bulk (3) and low sugar gene bulk (4) Only one band amplified by primer S511 and unclear. The bands amplified by primer S513 are clear but there are no polymorphism different bands among parents, high sugar gene bulk and low sugar gene bulk. The bands amplified by primer S512 is clearest, and have different bands between the female parent (sweet sorghum) and high sugar gene bulk, but there are haven't different bands between the male parent (common grain sorghum) and low sugar gene bulk, this different bands located at 450bp (*Fig. 4*), Therefore, our study will continue PCR detection and cosegregation analysis of the primer S512 which is the clearest.

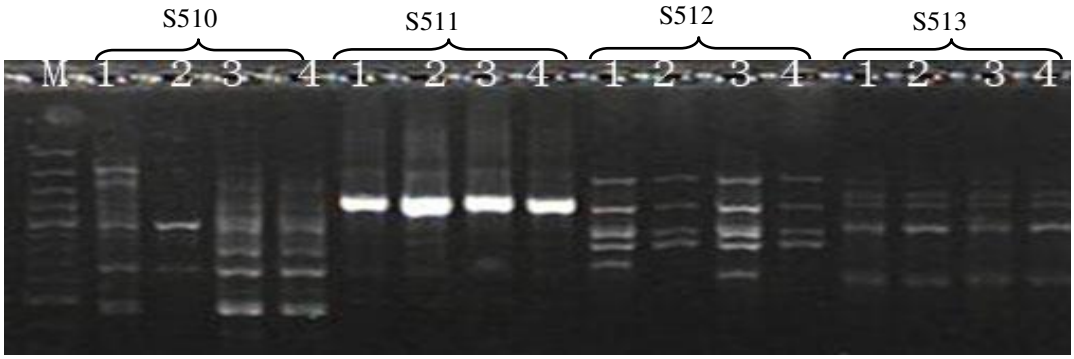

Figure 4. *Amplification results of primer S510, S511, S512, S513. Female parent (1) Male parent (2) High sugar gene pool (3) Low sugar gene pool (4) Marker (M)*

RAPD polymorphism's cosegregation analysis of high sugar gene of sweet sorghum

RAPD-PCR amplification results of the primer S512 in individual

By comparing the individual plant amplification results of parents, high sugar group and low sugar group, we reach that the bands amplified between female parent (sweet sorghum) and high sugar individual by primer S512 are more than the bands between male (common grain sorghum) and low sugar individual (*Fig. 5*).

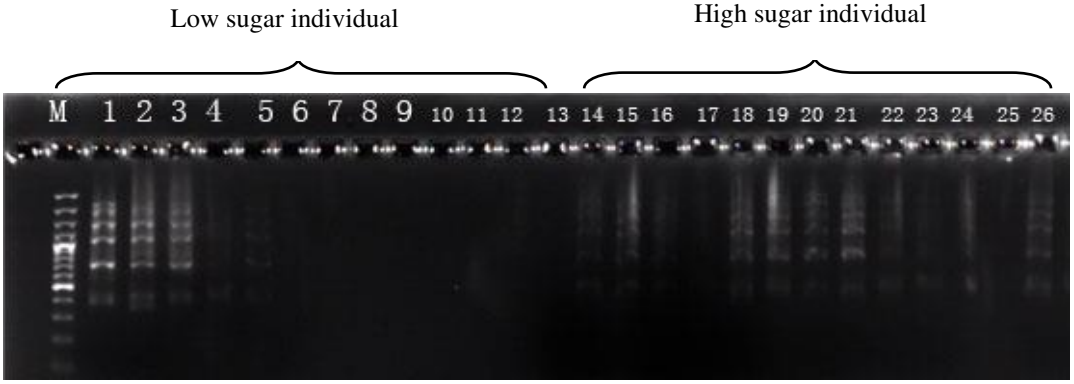

Figure 5. *The single plant amplification results of primer S512. Low sugar individual (1-13), High sugar individual (14-26), Marker (M)*

http://www.aloki.hu ● ISSN 1589 1623 (Print) ● ISSN 1785 0037 (Online)
DOI: http://dx.doi.org/10.15666/aeer/1705_1195311962

Recombination rates analysis

To observe the amplification results of high sugar individual and low sugar individual by primer S512, we get 58 individuals were amplified polymorphism bands and 4 individuals not be amplified in high sugar bulk, and 3 individuals amplified polymorphism, 35 individuals not be amplified, the recombination rate is 7% (*Table 1*). Recover the amplified fragment in the end.

Table 1. *Co-segregation of the S512-441 amplified polymorphic fragment in F_5*

F_5	**Total plants tested**	**Polymorphic fragment**		**Percentage of recombination %**
		Present	Absent	
High sugar	62	58	4	7%
Low sugar	38	3	35	

Recover and clone sequencing of polymmorphism marker

Recover target bands

Recover the difference bands amplified by primer S512, the results of recovery showed that the bands is the same as the target band, both are 450bp (*Figure 6*).

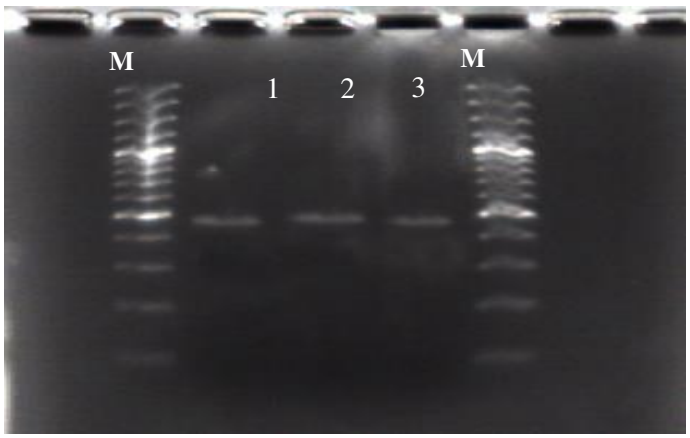

Figure 6. *Recovered fragment of primer S512 (1-3)*

Cloning and sequencing

Cloning and sequencing were given to the recovery difference bands, and results showed the fragment is 441bp.

Transform RAPD molecular marker to SCAR marker

RAPD primer design

Basic sequence and primer design principles of specific primer S512, adding G+C base pairs and designed as follows specific primers sequence ends while avoiding hairpin.

S512F: 5'-ACAGGTGCGTACATCGAATG-3'
S512R: 5'-TTACAGGTGCGTTAATTGCC-3'

http://www.aloki.hu ● ISSN 1589 1623 (Print) ● ISSN 1785 0037 (Online)
DOI: http://dx.doi.org/10.15666/aeer/1705_1195311962

SCAR-PCR response analysis

Above designed specific primer S512 were used to amplify the parents and two sets of individuals in SCAR-PCR. Results show that SCAR marker the same as RAPD marker of high sugar gene's chain reaction of sweet sorghum F_5. Both female parent (sweet sorghum) and high sugar individuals are amplify a specific band at 450bp (*Fig. 8*), but male parent (common grain sorghum) and low sugar individuals haven't this specific band. It shows that SCAR marker is easy to distinguish and has strong specificity, so we can transform RAPD marker to stable SCAR marker successfully, named this marker $SCAR_{S512\text{-}441}$ depending on the sequence results.

1	GACTTAGGTT	TAAGTAAATA	TGGTCCATAT	GGTGTTGGGT	TATCCTATTT
51	CTTAATAGAA	ATTCAGCATA	GTGCAGAGTG	TCATTTCACT	ATATTTTGTT
101	ACA**ACAGGTG**	**CGT**AGTATTC	AAGAGTAGCA	TTCAACTTAT	TCTACCCTAT
151	TTAAGTCAAA	TTAGACATGG	TGTCTAGGTT	GATTTTTGAG	CCAATAGTAT
201	AAACAACCAC	TCCATGGAAG	AGGGTGAACA	AATCACCACC	AGGCCCCTTC
251	TTAGAAAGCT	TTTCTCGATC	TTGGTATGCA	CATAAATGAA	GAACCAAACA
301	CAGAAGTCAC	AAACTGGGAA	GTCCTGAGAT	GAACTCAGAT	GGAGAAAGAA
351	GAGATACATG	AACTTCAACA	ACCTCGCATA	AGGAGAACAT	AGCTTATGGA
401	GAGCCCATGC	AGTTGATCTT	TGCCTTGTCT	TTATGAGCAG	GACACACTTT
451	ATCCAGCAGC	TAGGGATAGC	AGGAGAGGCC	ATGCTGACTG	GTGGATGCCA
501	GATCCGCTGC	TCCGCAGTTG	GGCTCGCTGG	ATCCAGCC**TG**	**TCCACGCA**GT
551	CCGGTAGGAG	CACGGATCCA	CTGCTCTCCA	GATCTACTGC	GACTAGTGCG
601	TGGGCTGGGG	CTCACCAGAT	CTGCTGCTGC	CAGTTGTCTA	CTTGTGATGG
651	GAAGC				

Figure 7. *The recovered fragment sequencing results of S512*

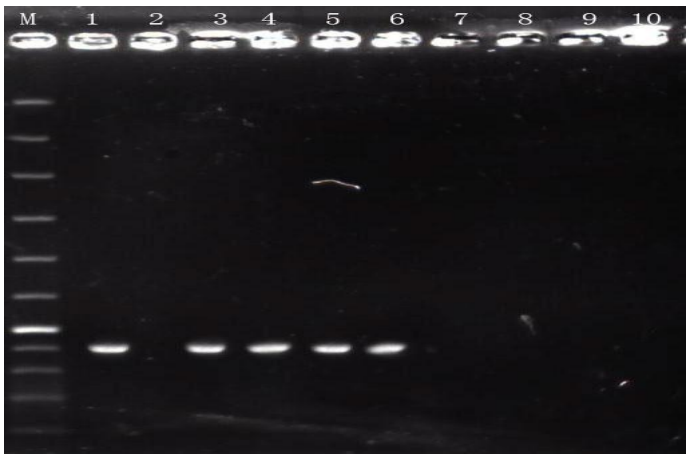

Figure 8. *Part of individuals test results of primer S512's SCAR marker. Female parent (1) Male parent (2) High sugar individual (3-6) Low sugar individual (7-11) Marker (M)*

Conclusion

In this experiment, 120 RAPD primers selected at random, the RAPD techniques were used for molecular marker of experimental population to find the RAPD primer related to high sugar gene of sweet sorghum. In recent years, there are great achievements in fruit varieties identification, hybrid identification and mutant detection, construction of molecular genetic maps, gene map, gene diversity and pedigree analysis

http://www.aloki.hu ● ISSN 1589 1623 (Print) ● ISSN 1785 0037 (Online)
DOI: http://dx.doi.org/10.15666/aeer/1705_1195311962

through RAPD technology (Li et al., 2018). Because of RAPD marker's poor stability and repeatability, it's difficult to use in crop genetic breeding and assistant selection. We clone and sequence target band, to get good stability and high reproduction SCAR marker. The primer used by SCAR marker is longer than RAPD marker and the primer sequence completely complement with template DNA. To get good stability and high reproduction results, we should better amplify in rigorous conditions (Xiong et al., 2010).

Random selecting 120 RAPD primers, analyzing sweet sorghum (female parent), common grain sorghum (male parent), high sugar gene bulk and low sugar gene bulk by the RAPD marker. The result showed that 95 primers could produce bands, 25 primers could not produce bands, amplification rate is 79%. Because of the bands amplified by primer S512 is the clearest, we observe the results of high sugar individual and low sugar individual amplified by primer S512. In high sugar population, 58 plants amplified polymorphic bands, 4 plants haven't amplified, but in low sugar population, 3 plants amplified polymorphic bands, 35 plants haven't amplified, amplification rate is 7%, genetic distances is 7.5CM. Recovering polymorphic bands of PCR production amplified by specific primer S512 and cloning and sequencing. SCAR specific primers were designed.

S512F: 5'-ACAGGTGCGTACATCGAATG-3'.

S512R: 5'-TTACAGGTGCGTTAATTGCC-3'.

Transfer RAPD marker to SCAR marker, named $SCAR_{S512\text{-}441}$. Be compared with $SCAR_{S336\text{-}1119}$, it is a new SCAR marker which fragment length is shorter, and optimize the SCAR marker's reaction system.

Discussion

We can see that it is low efficiency that transfer RAPD marker to SCAR marker. The cause may be: (1) When designing primers, often contain corresponding 10 base RAPD primer. Because of the original polymorphism can be detected. Even as the increases of amplification's stability and success rate, the transformation of RAPD primers was still affected. (2) Transform specific fragment of RAPD to SCAR attention must be paid to primer design length and PCR reaction condition (for instance, when the anneal temperature is constant, the anneal time and extend time should not be too long). (3) Take many factors into consideration, for instance, base sequencing of sequence's head and tail is instability, annealing temperature of specific transform RAPD to SCAR marker primer, the design of primer in SCAR transformation is closer to the medium of sequence, instead of start at both ends of sequence. However, in practical operations, because of these factors, in alone or in combination, the transformation efficiency of transform RAPD marker to SCAR is reduced. These errors should be minimized (Kula, 2012; Li et al., 2014; Liu et al., 2016).

Using identified high sugar population and low sugar population to test SCAR marker closely linked sweet sorghum's high sugar gene. It has great significance to apply it in practice, and use this marker in high sugar gene variety test.

This experiment optimized optimal reaction system and reaction conditions of RAPD molecular markers and optimal reaction system of SCAR marker, recovery polymorphic bands of PCR product amplified by specific primer S512, and cloning and sequencing. Polymorphic bands linked to sorghum F_5 high sugar gene length of 441bp. The RAPD

http://www.aloki.hu ● ISSN 1589 1623 (Print) ● ISSN 1785 0037 (Online)
DOI: http://dx.doi.org/10.15666/aeer/1705_1195311962

marker were converted into SCAR marker, which named $SCAR_{S512\text{-}441}$. Hope to find out more SCAR marker to identify sorghum with high sugar content in the future.

Acknowledgements. The research was partly supported by key project of Liaoning Province Department of Education (2019) and Major incubating project of Shenyang Normal University.

REFERENCES

[1] Gu, Y., Han, Q. H., Wang, W. T., Li, S. W., Sun, D. L., Wu, F. (2011): Application of common bean anthracnose resistance gene SCAR markers in snap bean disease resistance identification. – Acta Horticulturae Sinica 38(5): 911-920.
[2] Lan, B. X., Wang, L., Wu, Z. K. (2015): Rapid miniprep extraction of genomic DNA from micro-endosperm maize with modified CTAB method. – Genomics and Applied Biology 34(1): 190-194.
[3] Li, Y. Y., Zhao, S. H., Yang, L. G. (2003): Study on the molecular markers linked to aphid resistance gene of sorghum. – Acta Agronomica Sinica 29(4): 534-540.
[4] Li, N. Z., Tao, S. Y., Li, Y. Y. (2008): RAPD primers screening and polymorphism analysis of genome on sorghum. – Biotechnology 18(4): 7-10.
[5] Li, R. H., Xia, Y. S., Liu, S. Z. (2009): CTAB – improved method of DNA extraction in plant. – Research and Explorationn in Laboratory.
[6] Li, Q., Liu, Z. Z., Zeng, Z. (2014): Two new RAPD — SCAR markers among wild populations of trachidermus fasciatus. – Freshwater Fisheries 44(3): 17-23.
[7] Liu, S. L., Wang, X. H., Jiang, C. X., Yuan, W., Zhang, J. H. (2016): RAPD-PCR analysis on different germplasm resources of Curcumae Rhizoma. – China Medicine 47(17): 3098-3102.
[8] Li, Y. Y., Li, C. Y., Xing, H. Q. (2016): Research on establishment of head smut of sorghum by using SCAR marker. – Journal of Shenyang Normal University Social Science Edmon (Natural Science Edition) 34(4): 468-472.
[9] Lu, F., Zou, J. Q., Duan, Y. H. (2012): Genetic analysis of stalk sugar content related traits in sweet sorghum (Sorghum bicolor). – Journal Of China Agricultural University 17(06): 111-116.
[10] Lu, F., Zou, J. Q., Duan, Y. H. (2013): Correlation study of stalk sugar content and main agronomic traits. – Liaoning Agricultural Sciences 6: 1-4.
[11] Luo, F. X., Mao, P., Yao, Y. S. (2013): SCAR molecular marker technology and its application in aquatic animal research. – Journal of Jilin Agricultural Sciences 4: 251-252.
[12] Tan, Y., Li, Z. H., Li, J. L. (2013): Application of RAPD Molecular Marker Technology in Plant Research. – Journal of Anhul Agricultural Sciences 41(25): 10236-10238.
[13] Vermerris, W. (2011): Survey of genomics approaches to improve bioenergy traits in maize, sorghum and sugarcanefree access. – Journal of integrative plant biology 53(2): 105-119.
[14] Wang, L. M., Huang, R. D., Jiao, S. J. (2010): Gene effect analysis of sugar content of sweet sorghum. – Crops 4: 62-64.
[15] Wang, H. F., Xin, N., Wu, X. H., Pei, Z. Y. (2013): Current status, problems and countermeasures of sweet sorghum breeding. – Crops 2: 23-26.
[16] Wang, J. K., Li, M. J., Wang, J. M., Wei, K. H., Gu, L., Lin, W. M., Zhang, J. Y., Zhang, Z. Y. (2016): Development of RAPD-SCAR marker for Anoectochilus roxburghii and their utilization to assess genetic diversity of germplasm. – China Medicine 47(1): 122-129.
[17] Wu, Y., Zhou, K. H., Fang, R. (2016): Review of the core collection for horticultural plants based on molecular markers. – Journal of China Capsicum 3: 31-39.

http://www.aloki.hu ● ISSN 1589 1623 (Print) ● ISSN 1785 0037 (Online)
DOI: http://dx.doi.org/10.15666/aeer/1705_1195311962

[18] Xiong, F., Zheng, M. J., Xie, B. G. (2010): Development of SCAR markers based on RAPD and SRAP for rapid identification of pleurotus sajor – caju strain. – Acta Agricultural Turae Universitatis Jiangxiensis 32(3): 601-607.
[19] Yang, H. X., Wu, X. H., Nong, Q. L. (2016): Research progress of sugarcane brown rust resistance gene and its molecule markers. – Sugar Crops of China 38(6): 57-61.
[20] Yao, G. X., Li, J. J., Zhang, Q., Hu, G. L., Chen, C., Tang, B., Zhang, H. L., Li, Z. C. (2010): Mapping QTLs for grain weight and shape using four sister near isogenic lines in rice (Oryza sativa L.). – Acta Agronomica Sinica 36(8): 1310-1317.
[21] Zhang, X. Y., Zhao, W. J. (2011): Study advance in brix in sweet sorghum. – Shanxi Agricultural Science 39(6): 616-618.
[22] Zou, J. Q., Zhu, K., Wang, Y. Q., Li, Y. Y. (2010): Study on inheritance and molecular makers of sorghum resistance to head smut physiological race 3. – Scientia Agricultura Sinica 43(4): 713-720.

http://www.aloki.hu ● ISSN 1589 1623 (Print) ● ISSN 1785 0037 (Online)
DOI: http://dx.doi.org/10.15666/aeer/1705_1195311962

THE EFFECT OF RURAL SETTLEMENT LANDSCAPE PATTERN ON WATER CONSERVATION IN XINBIN COUNTY, CHINA

QI, L.[1,2,3] – LI, N.[4*] – HAN, J. C.[1,2,3] – WANG, H. Y.[1,2,3]

[1]*Shaanxi Provincial Land Engineering Construction Group Co., Ltd.， Shaanxi Key Laboratory of Land Consolidation, Xi'an 710075, China*

[2]*Institute of Land Engineering and Technology, Shaanxi Provincial Land Engineering Construction Group Co., Ltd., Xi'an 710075, China*

[3]*Shaanxi Provincial Land Consolidation Engineering Technology Research Center, Xi'an 710075, China*

[4]*Beijing Huayuan Thick Soil Land Planning and Design , Beijing 100193, China*

**Corresponding author*
e-mail: wdlndudu@163.com

(Received 25th Apr 2019; accepted 11th Jul 2019)

Abstract. Rural settlements are not only the main form of Chinese farmer residence, but also a space for rural production, living as well as other comprehensive functions, being an important part of rural land use. The impact of rural settlement changes on soil and water conservation is studied as it is of great significance for soil and water conservation. Based on the satellites of Xinbin County in 1992, 2001 and 2010, this study analyzes the distribution characteristics of rural settlements by using ArcGIS software spatial analysis function and landscape index method. At the same time, SPSS software is used to analyze the correlation between soil erosion and the size of rural settlements. The results show that soil erosion is positively correlated with rural settlement size and population density. The rural residential areas in Xinbin County are severely fragmented with scattered layout. Soil erosion shows a decreasing trend while increasing in distance from settlements. The bigger the scale, the more serious the erosion.
Keywords: *soil erosion, landscape index, rural habitat, ecological protection, China*

Introduction

Rural settlements are the most significant form of human settlement (Zhou et al., 2013). It has a footprint that interacts with the surrounding social economy, the natural environment and the people. Its layout, form and scale have undergone several major changes (Xi et al., 2018; Yang et al., 2016; Yang, 2015). Although Chinese urbanization level has been greatly improved (Chaolin et al., 2017), the agricultural population quantity is still large. In the future, rural settlement lands will still be an important part of Chinese rural-urban construction land use. Meanwhile, it is still the main form of living for rural populations. There is no overall planning for the layout of rural settlements in most parts of China. Besides, the lack of effective supervision and management of the land result in the spatial layout dispersal (Chen, 2017; Guo et al., 2012). The rural residents have always chosen their settlements spontaneously. Due to the limitations of traditional culture and the natural environment and in order to facilitate the production of farming, the distribution of rural settlements is very fragmented in the mountain areas. This form of layout not only makes it more difficult for farmers to travel, but also negatively affects the natural ecological environment of the mountainous areas, especially the water conservation function in there. The Liaodong mountainous area refers to the mountainous and hilly areas

http://www.aloki.hu ● ISSN 1589 1623 (Print) ● ISSN 1785 0037 (Online)
DOI: http://dx.doi.org/10.15666/aeer/1705_1196311977

of 32 counties in the eastern part of Liaoning province, China, including the counties of Benxi, Fushun, Anshan, Tieling and Dandong. As the main water source conservation area and green barrier area in the Liaohe Plain, the Liaodong mountainous area provides 83% of the province's water supply. The mountainous areas of eastern Liaoning should not only meet the current needs of people for production and life, but also offer ecological security and water resources for the future economic development of Liaoning Province. The third remote sensing survey of soil erosion in Liaoning Province shows that the soil erosion area in the mountainous areas of eastern Liaoning was 1626.27 km^2, accounting for 25.2% of the total area, 35% of the total area of soil erosion in the province. This indicates that there are still potential threats to the water conservation function in the mountainous areas of eastern Liaoning. As one of the important water conservation areas, the areas of eastern Liaoning, Xinbin County where its residents are active is the source of the Hunhe River and belongs to the mountainous area (Ma et al., 2014; Ying, 2017). Therefore, both the protection of water conservation functions by increasing natural vegetation and the adverse effects of human activities on water conservation caused by the layout of rural settlements should be considered. This paper analyzes the distribution features, landscape pattern and soil erosion characteristics of rural settlements in Xinbin County (Christensen et al., 2016; Remmel et al., 2017). From a unique perspective, the influence of the evolution of rural settlement landscape pattern on water conservation function is explored. Based on the discussion of the soil erosion status and the spatial characteristics of residential distribution in the three time periods of Xinbin County, this paper researches the distribution features of residential areas affecting soil erosion, and discusses the coupling relationship between rural residential area distribution and water and soil erosion. Through this study, it provides a scientific basis for optimizing the layout of rural residential areas in ecological protection areas and promoting regional water resources protection.

Methodology and data

Research method

Using four methods – the fusion classification, supervised classification, partition classification and visual interpretation, the SPOT and Landsat data are extracted by ENVI4.5 and ArcGIS software (Maguire, 2015; Ju et al., 2016; Ke, 2016).

Based on the land use data of Xinbin County, the superposition analysis is carried out with the support of ArcGIS software. The landscape index are selected at the plaque level (Rodríguez-Loinaz et al., 2015; Chen et al., 2018), including number of plaques (NP), total plaque area (TA), area-weighted average plaque fractal dimension (AWMPFD), plaque density (PD), average plaque area (MPS) and dispersion (RC). Then, Fragstats 3.3 software is used to calculate the landscape index. Finally, SPSS software is used to analyze the correlation between soil erosion and rural settlement size, the structure of the rural settlements and population density (Green et al., 2016; Cronk, 2017).

Data source and processing

Data source

The research data is derived from the data of Landsat5TM in 1992, 2001 and 2010 of Xinbin County with a resolution of 30 m × 30 m, socio-economic data, the map of the status quo of 110,000 land use and the 1:10,000 topographic map. Among them, remote sensing data mainly uses 3 and 4 bands of data (Ying, 2017).

http://www.aloki.hu ● ISSN 1589 1623 (Print) ● ISSN 1785 0037 (Online)
DOI: http://dx.doi.org/10.15666/aeer/1705_1196311977

Data processing

First, the 3-band and 4-band images are imported into ENVI4.5 software. Second, the Vectors option in the Overlay menu is selected to overlay the boundaries of the study area onto the image. Finally, the ROI Tool in the Region of Interest in the Tools menu and the Subset Data are selected via ROIs option in File in its dialog box, and the Background Value is set to 0, then is saved in a new folder. The other two data are processed in the same way. Next, normalized difference vegetation index (NDVI) and vegetation coverage (VFC) are calculated.

Before calculating NDVI (Gandhi et al., 2015), images of band 3 and band 4 need to be compressed into a layer. The specific operation process is open the 3 and 4 band image in ENVI 4.5 software and Layer Stacking is selected in Basic Tools. Then the dialog box of Layer Stacking Parameters appears. The Import Files button is clicked to output the 3 and 4 band image images, and then they are named. When the results are output, they should be saved in a fixed folder.

Next NDVI is calculated. The specific process is: import the image map of the compressed surface reflectivity into ENVI4.5 software, select band math in the Basic Tools drop-down menu. Input formula (*Eq. 1*), assign 4 channels of surface reflectivity to NIR, assign 3 channels of surface reflectivity to R, then name the output and save the result.

Using NDVI values, vegetation coverage is calculated by *Equation 2*.

$$NDVI = \frac{NIR - R}{NIR + R} \quad \text{(Eq.1)}$$

$$VFC = (NDVI - NDVI_{\min}) / (NDVI_{\max} - NDVI_{\min}) \quad \text{(Eq.2)}$$

Making slope maps and soil erosion maps

The DEM data is obtained from the spatial analysis tool of ArcGIS software to obtain the slope map (Allen, 2016).

According to the soil erosion index *Table 1*, the soil erosion map is obtained using the decision tree in ENVI software (Segatori, 2017). The map is shown in *Figures 1, 2* and *3*.

Table 1. *Ministry of Water Resources soil erosion indicators*

Vegetation coverage (%)	Slope					
	< 5°	5°~8°	8°~15°	15°~25°	25°~35°	> 35°
> 75	Microdegree	Microdegree	Microdegree	Microdegree	Microdegree	Microdegree
60-75	Microdegree	Light erosion	Light erosion	Light erosion	Middle degree	Middle degree
45-60	Microdegree	Light erosion	Light erosion	Middle degree	Middle degree	Serious erosion
30-45	Microdegree	Light erosion	Middle degree	Middle degree	Serious erosion	Very intensive
< 30	Microdegree	Middle degree	Middle degree	Serious erosion	Very intensive	Severe erosion

http://www.aloki.hu ● ISSN 1589 1623 (Print) ● ISSN 1785 0037 (Online)
DOI: http://dx.doi.org/10.15666/aeer/1705_1196311977

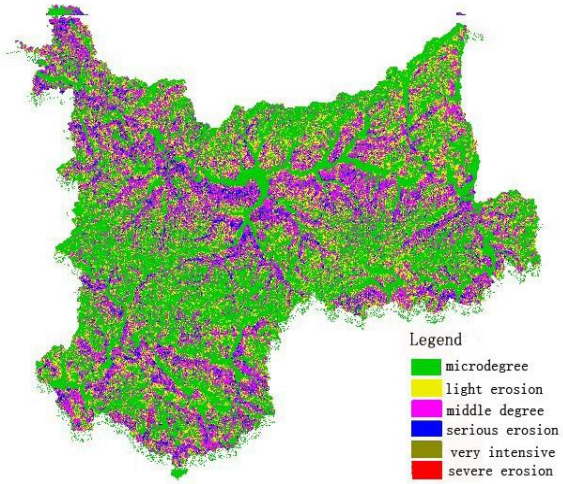

Figure 1. *Soil erosion in 1992*

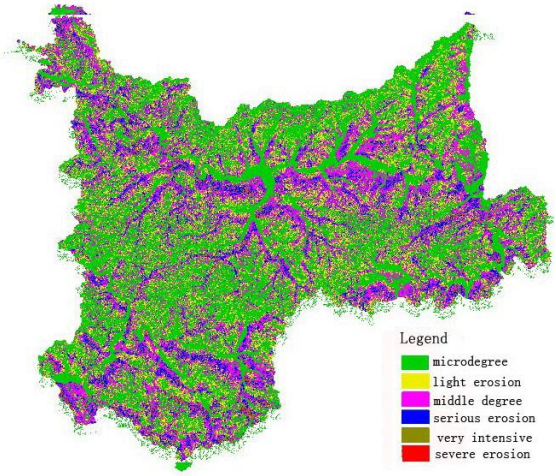

Figure 2. *Soil erosion in 2001*

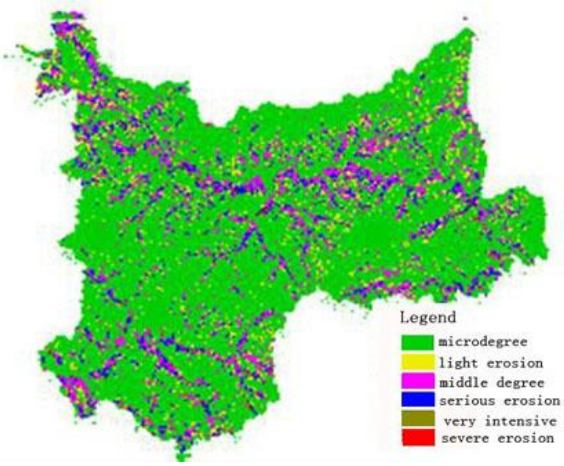

Figure 3. *Soil erosion in 2010*

http://www.aloki.hu ● ISSN 1589 1623 (Print) ● ISSN 1785 0037 (Online)
DOI: http://dx.doi.org/10.15666/aeer/1705_1196311977

Rural settlement data processing

Combined with the overlay module in ArcGIS software, the rural settlement attribute data is superimposed with the elevation and slope related attribute data to calculate the spatial distribution characteristics of the rural settlement (Murasingh et al., 2018; Conrad et al., 2015). The number of rural settlements is measured using statistical data, combined with field surveys. The field research is mainly carried out on-site verification of the population data in the form of a symposium in 2013 to correct the statistical data. According to the density of rural settlements, the distance and mutual influence between rural settlements are considered. Then, the analysis of rural settlements is buffered. A buffer at a distance of 1000 m is created. The rural settlements in each buffer form a composite map that is considered to be the same rural settlement unit.

The composite rural settlement unit is spatially superimposed with four different distances of soil erosion. The four ranges are less than 1000 m, 1000 to 2000 m, 2000 to 3000 m, and 3000 m or more. The erosion of the four distance segments will be obtained. The soil erosion map of three years and four distances is shown in *Figures 4*, *5* and *6*.

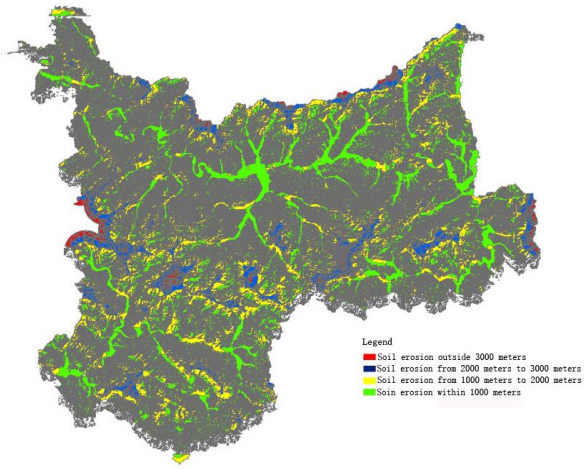

Figure 4. *Soil in various buffer zones in 1992*

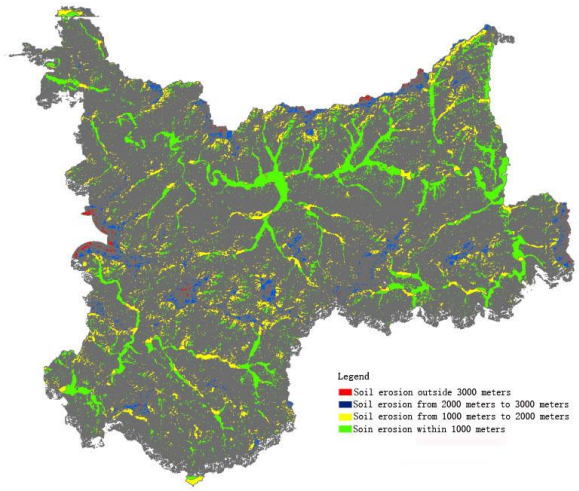

Figure 5. *Soil erosion in various buffer zones in 2001*

http://www.aloki.hu ● ISSN 1589 1623 (Print) ● ISSN 1785 0037 (Online)
DOI: http://dx.doi.org/10.15666/aeer/1705_1196311977

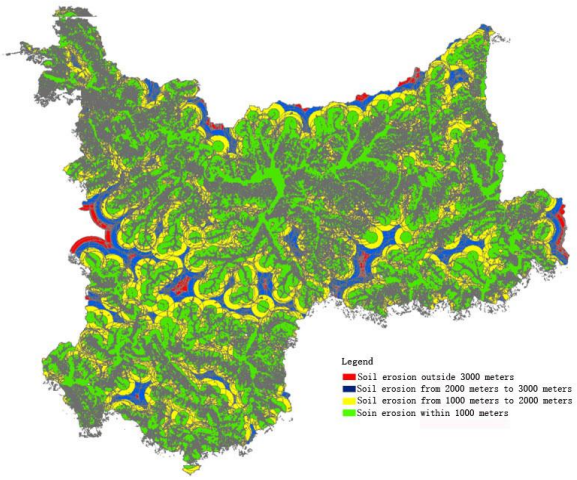

Figure 6. *Soil erosion in various buffer zones in 2010*

Results and analysis

Analysis on the quantity structure of rural settlements in Xinbin County

According to the analysis, at the end of 2010, Xinbin County had a total rural population of 219,805, with a total rural settlement of 6705.7 hm^2 and a per construction land area of 305 m^2/person, exceeding the 150 m^2/person specified in China's "Village and Town Planning Standards" (GB50188-93). In other words, the intensive land consolidation in Xinbin County is not enough, which means there is great potential for consolidation. The largest rural settlement area is Yongling town with 939.88 hm^2, followed by Xinbin town of 732.88 hm^2. While the smallest is Xiangshuihezi Township, which is 207.32 hm^2. The township with the largest per capita area is Muqi town with 431.3 m^2/person. The smallest is Wangqingmen Town with only 227.32 m^2/person. The largest population is Yongling Town, with 27,854 people. The least one is Hongsheng Town, with 7464 people. The rural settlement appears as a single entity on the map, not contiguous. The map is severely fragmented, and it is in a dilapidated state with a scattered layout.

Analysis of spatial distribution landscape index of rural settlement

According to *Table 2*, it can be seen that the number of plaques in Yongling Town is the highest, that is, 473, indicating a high degree of fragmentation. The least is Xiangshuihezi Township, which is 97, showing that its rural settlement is relatively complete. The total area of plaque in Yongling Town is 940 hm^2 while the smallest is Xiangshuihezi Township, which is 207 hm^2. The average plaque area in Nanzamu Town is the largest, which is 3.07 hm^2/per, representing that the average land use size of rural settlements is large. The average plaque area of Muqi Town is the smallest, 1.97 hm^2/per, indicating that the average land use size is small. In terms of plaque density, Muqi Town is the largest one, with 0.51 number/hm^2, which indicates that the degree of fragmentation in Muqi Town is higher. The density of plaques in Nanzamu Town and Xiajiahe Town is the smallest, 0.33 number/hm^2, showing that Nanzamu Town and Xiajiahe Town are relatively complete. Beisiping Township has the largest dispersion, which is 3.98. That implies that the distribution of rural settlements in there is scattered. Yongling Town has the smallest dispersion, suggesting that the rural

http://www.aloki.hu ● ISSN 1589 1623 (Print) ● ISSN 1785 0037 (Online)
DOI: http://dx.doi.org/10.15666/aeer/1705_1196311977

settlements in there are densely distributed. The main reason is affected by the self-sufficient economy in rural areas. In order to obtain the food needed for subsistence, farmers must have a certain amount of cultivated land. Especially in the mountainous areas of eastern Liaoning, the cultivated land resources are scarce. For the facility of farming, the scattered distribution of rural residential areas is an inevitable form. Townships with small rural settlements include Yongling Town, Xinbin Town and Nanzamu Town, which are located at the bottom of the main river and its tributaries. These places are low-lying and flat places. To a certain extent, the dispersion of rural settlements is a reflection of the impact of human activity intensity on landscape structure. Usually, if the average plaque area of the artificial landscape is small, the number of plaques will be less. Therefore, the greater the degree of separation is done, the plaque is dispersed. The separation between the natural landscape and the semi-natural landscape is small, mainly because the distance between the same plaques is short or concentrated.

Table 2. *Landscape index table of rural settlements land in towns and villages of Xinbin County*

Administrative unit	Coordinate	NP (number)	TA (hm^2)	MPS (hm^2/per)	PD (number/hm^2)	RC	AWMPFD
Beisiping town	125°10′E, 41°47′N	109	236	2.17	0.46	3.98	1.1369
Dasiping town	124°43′E, 41°19′N	172	487	2.83	0.35	2.34	1.1282
Hongmiaoz town	125°08′E, 41°31′N	135	387	2.87	0.35	3.78	1.1419
Hongsheng town	125°7′E, 42°12′N	105	211	2.01	0.50	3.56	1.1378
Muqi town	124°38′E, 41°47′N	349	689	1.97	0.51	2.69	1.1198
Nanzamu town	124°25′E, 41°58′N	147	451	3.07	0.33	1.98	1.1168
Pingdingshan town	124°46′E, 41°25′N	170	497	2.92	0.34	2.54	1.1368
Shangjiahe town	124°30′E, 41°56′N	180	411	2.28	0.44	2.78	1.1408
Wangqingmen town	125°18′E, 41°41′N	148	332	2.24	0.45	2.02	1.1265
Weiziyu town	124°31′E, 41°26′N	139	380	2.73	0.37	2.43	1.1247
Xiajiahe town	124°26′E, 41°23′N	115	346	3.01	0.33	3.06	1.1296
Xiangshuihezi town	125°22′E, 41°37′N	97	207	2.13	0.47	3.23.	1.1309
Xinbin town	125°26′E, 41°45′N	309	733	2.37	0.42	1.73	1.0895
Yongling town	124°50′E, 41°43′N	473	940	1.99	0.50	1.56	1.1034
Yushu town	124°50′E, 41°39′N	155	397	2.56	0.39	4.12	1.1383
Xinbin county	125°02′E, 41°44′N	2803	6706	2.39	0.42	2.42	1.1327

Related studies have shown that the rural settlements as artificial plaques have greater stability and small fractal dimension, and the formed plaques are not prone to change. This leads to an increase in the heterogeneity of the natural plaque landscape around it. The fractal dimension is larger than the artificial plaque, and the landscape tends to be unstable. The area-weighted average patch fractal dimension represents the complexity of the margin of land-use plaque at a certain research scale, generally between 1 and 2. The closer the value is to 1, the stronger the self-similarity of the plaque. The smaller the ratio of the length to the axis, the more regular the shape of the plaque, and the shape of the plaque is close to a circle or a square. This shows that the greater the degree of human interference. Because plaques formed by human interference are generally more regular in shape, similar plaque shapes are prone to occur. The larger the value of the area-weighted average patch fractal dimension, the

http://www.aloki.hu ● ISSN 1589 1623 (Print) ● ISSN 1785 0037 (Online)
DOI: http://dx.doi.org/10.15666/aeer/1705_1196311977

larger the ratio of the length to the short axis. At the same time, the more complex the shape of the plaque, the narrower the geometry of the plaque and the less interference it receives (Cheng, 2016; Yang et al., 2018). The weighted average patch fractal dimension of rural settlement areas in Xinbin County is below 1.16, which is close to 1. This is because the rural settlement plaque belongs to the artificial landscape plaque, the plaque shape is relatively regular, close to the square, and the stability is strong. Xinbin Town has the smallest area-weighted average patch fractal dimension of 1.1034. The largest in Hongmiaozi Township is 1.1419. The values of rural towns and villages are all below 1.5, indicating that these rural township settlements are not in a random state similar to Brownian motion but in a steady state.

Analysis of spatial distribution landscape index of rural settlement

This paper selects soil erosion to reflect the water conservation status of the study area.

Analysis of current situation of soil erosion in Xinbin County

It can be seen from *Table 3* that at present, the farmland erosion is the most serious with the total erosion area of 37,768.73 hm^2. The severe erosion is 472.75 hm^2, accounting for 1.25% of the farmland. The proportion of middle degree erosion in farmland is 49.33%. The least eroded is the unutilized land. This means that measures must be taken to control soil erosion. If the treatment effect on soil erosion is good, such a large proportion of eroded land will decrease. It will convert into light erosion land. From the perspective of the total erosion area, the woodland is second behind the farmland, with an area of 3457.33 hm^2. This is because Xinbin county has a relatively large coverage of forest land. The excessive base and the artificial interference in the woodland have caused the erosion area. Being located in the mountainous area, protecting the water and soil means protecting the forest land in Xinbin county.

Table 3. *Soil erosion status statistics within 1000 m in rural settlements in 2010*

	Farmland (hm^2)	**Woodland (hm^2)**	**Grassland (hm^2)**	**Garden land (hm^2)**	**Unutilized land (hm^2)**
Light erosion	3148	15152	340.42	213.11	10.64
Middle degree	18634.05	13129	786.51	262.49	15.12
Serious erosion	12232.64	4853.6	415.2	96.84	8.35
Very intensive	3281.29	1263.4	100.75	25.67	1.76
Severe erosion	472.75	175.33	17	4.73	0

Relationship between soil erosion and rural settlement distance

From *Table 4*, soil erosion was the most severe in 2001 during the three periods, with an erosion rate of 57%. The soil erosion in 2010 was the lightest with an erosion rate of 39.87%. Ranking in the middle place, the soil erosion rate in 1992 is 55.34%. From the point of view of the buffer zone of 1000 m, it was also the most severe erosion in 2001, with an erosion of 39.06%. The rate in 1992 was similar to that in 2001. Compared with 2010, the soil erosion in these two periods was more serious. Because the rural settlement in these two periods had a low degree of concentration and a more dispersed distribution. At the same time, the degree of land use was also low, making erosion

http://www.aloki.hu ● ISSN 1589 1623 (Print) ● ISSN 1785 0037 (Online)
DOI: http://dx.doi.org/10.15666/aeer/1705_1196311977

more serious. Afterwards, with the improvement of living conditions and the guidance of policies such as the revitalization of the Chinese government, the concentration of rural settlement increased, the average plaque area grew, and the intensity of human activities rose, but the density of plaques became larger. The degree of utilization has been improved, and soil erosion has been alleviated to some extent, therefore, the soil erosion rate is lower in 2010 than that of the other two years.

Table 4. *Statistical table of soil erosion at different distances in three time periods*

Years	Distance/m			
	< 1000	**1000-2000**	**2000-3000**	**> 3000**
Erosion rate in 1992	38.49%	12.44%	2.20%	2.21%
Erosion rate in 2001	39.06%	12.81%	2.39%	2.74%
Erosion rate in 2010	21.26%	16.59%	1.79%	0.23%

The soil erosion in the three time periods is gradually decreasing as the distance from the rural settlement increases. This shows that the distribution of rural settlements has a certain impact on soil erosion. Taking 2010 as an example, the erosion rate is 21.26% within 1000 m, and the erosion rate is 16.59% from 1000 to 2 000 m. Because human activities are dependent on land. The closer the rural settlement is, the greater the intensity of human activity, thereby, the erosion is more serious.

Relationship between erosion intensity and rural settlements structure

Table 5 shows the landscape index under different erosion intensities, that is, the different structure of rural settlements under different erosion intensities. Based on the data in *Table 5*, the grey correlation analysis of erosion intensity and the rural settlement structure was carried out by using spss16.0 software, and *Table 6* was obtained. It can be seen from *Table 6* that there is a correlation between soil erosion intensity and the rural settlement structure. The degree of correlation is AWMPFD > PD > NP > RC. From the positive effects of correlation degree, the correlation between AWMPFD, MPS, NP, RC and the soil erosion intensity are positive. In other words, the larger the above indicators, the greater the soil erosion intensity. The larger the value of NP and RC means that the activity range of farmers in the area is large, so the intensity of soil erosion will be severe. The more extensive the farmers use the land, the stronger the interference, and the more regular the shape of the rural settlements, the greater the erosion intensity. From the negative effects of correlation degree, the PD has a negative correlation with soil erosion intensity. The larger it is, the smaller the soil erosion intensity. As the PD value increases, the number of settlements per unit area increases, and the intensive use of land means that the soil erosion intensity may be lower.

Relationship between soil erosion and population density

Arcgis9.3 is applied to compound the map spots of Xinbin county into 33 composite map spots. Through this operation, *Table 7* is obtained. Three of these different patches are eliminated. Correlation and regression analysis use spss16.0. Through this operation, *Table 8* is obtained. *Table 8* shows when the confidence (unilateral) is 0.01, the correlation between population density and erosion area is significant and positively correlated. Because human activities, such as farming and cutting, have aggravated the

http://www.aloki.hu ● ISSN 1589 1623 (Print) ● ISSN 1785 0037 (Online)
DOI: http://dx.doi.org/10.15666/aeer/1705_1196311977

loss of water and soil, making the erosion area larger. In the protection of water and soil, human influence must be considered.

It can be seen from *Table 9* that there is no relationship between soil erosion intensity and population density. And among the 30 plots, almost every plot has the largest area of middle degree erosion intensity.

Table 5. *Soil erosion intensity and rural settlement structure data in 2010*

Erosion intensity	Erosion area (hm^2)	NP (number)	PD (number/hm^2)	RC	AWMPFD
Microdegree	149122.51	1227	317.65	354.76	1.07
Light erosion	25164.45	1295	530.76	677.69	1.05
Middle degree	43437.96	3293	120.24	324.13	1.14
Serious erosion	23154.39	2580	139.44	530.72	1.13
Very intensive	6113.52	1210	271.33	434.03	1.08
Severe erosion	874.98	208	331.58	105.68	1.06

Table 6. *Correlation between erosion intensity and rural settlement structure in 2010*

	Grey correlation
NP (number)	0.51
PD (number/hm^2)	-0.58
RC	0.40
AWMPFD	0.62

Table 7. *Soil erosion in different blocks of Xinbin County*

Plot	1	2	3	4	5	6	7	8	9	10
Erosion area (m^2)	45587.56	20420.79	135.06	309.13	76.74	1216.6	466.18	105.28	147	83.55
Population density (person/km^2)	1193900	921800	85300	475100	576900	647900	397500	669800	412900	503500
Plot	**11**	**12**	**13**	**14**	**15**	**16**	**17**	**18**	**19**	**20**
Erosion area (m^2)	164.56	779.41	15372.25	237.97	156.59	292.57	112.88	88.73	222.21	47.67
Population density (person/km^2)	597800	616200	559000	93200	793500	574200	144300	283600	555100	26400
Plot	**21**	**22**	**23**	**24**	**25**	**26**	**27**	**28**	**29**	**30**
Erosion area (m^2)	25.04	7.3	14.38	6.08	5.45	8.85	0.56	46.42	19.44	47.38
Population density (person/km^2)	866500	9300	9200	9300	9100	8600	8900	9000	9000	18100

Table 8. *Nonparametric correlation coefficient analysis*

		Population density	Erosion area
Population density	Correlation coefficient	1.000	.734**
	Sig. (unilateral)	.	.000
	N	30	30
Erosion area	Correlation coefficient	.734**	1.000
	Sig. (unilateral)	.000	.
	N	30	30

http://www.aloki.hu ● ISSN 1589 1623 (Print) ● ISSN 1785 0037 (Online)
DOI: http://dx.doi.org/10.15666/aeer/1705_1196311977

Table 9. *Statistical data of soil erosion intensity of 30 typical plots*

Plot	Light erosion (m^2)	Middle degree (m^2)	Serious erosion (m^2)	Very intensive (m^2)	Severe erosion (m^2)	Population density (person/km^2)
26	6.33	2.25	0.18	0.09	0	8600
27	0.56	0	0	0	0	8900
28	19.41	17.98	7.35	1.41	0.27	9000
29	13.62	5.82	0	0	0	9000
25	3.1	2.35	0	0	0	9100
23	10.18	3.84	0.27	0.09	0	9200
22	4.76	2.27	0.27	0	0	9300
24	5.09	0.81	0.18	0	0	9300
30	18.67	24.03	4.14	0.54	0	18100
20	15.48	19.8	9.6	2.61	0.18	26400
3	30.62	54.73	42.32	7.39	0	85300
14	125.62	82.4	23.11	6.21	0.63	93200
17	29.89	40.56	36.94	5.49	0	144300
18	31.52	31.74	15.21	6.75	3.51	283600
7	98.71	187.42	129.9	44.43	5.72	397500
9	26.36	54.36	41	23.48	1.8	412900
4	79.01	159.32	47.65	17.25	5.9	475100
10	14.35	31.27	27.94	9.45	0.54	503500
19	57.72	131.4	29.94	3.15	0	555100
13	3675.23	7217.92	3453.17	905.93	120	559000
16	82.22	114.55	71.41	22.59	1.8	574200
5	25.03	30.81	15.75	4.88	0.27	576900
11	40.38	63.07	35.55	21.78	3.78	597800
12	361.06	378.65	35.34	4	0.36	616200
6	202.89	525.71	376.05	98.62	13.33	647900
8	24.13	44.4	28.62	7.68	0.45	669800
15	85.76	101.94	56.89	13.13	0.81	793500
21	12.8	7.74	3.33	0.99	0.18	866500
2	3917.5	8771.43	5590.28	1805.09	336.49	921800
1	10467.94	20607.06	11501.62	2685.41	325.53	1193900

Relationship between soil erosion and the size of rural settlements

In the same way, the spss16.0 software is used to analyze the correlation between soil erosion and the size of rural settlements. The results show that soil erosion is highly correlated with the size of rural settlements and is positively correlated. This means that the greater the size of the rural settlement, the more serious the erosion. Therefore, rural settlements should be determined to a reasonable scale to prevent soil erosion. Spss16.0 is applied to analyze the correlation between rural settlement size and erosion grade (severe erosion as a percentage of erosion area). The results show that the erosion intensity is not related to the size of the settlement. This suggests that the larger the rural settlement, the more serious the erosion, but the erosion intensity is not necessarily severe.

http://www.aloki.hu ● ISSN 1589 1623 (Print) ● ISSN 1785 0037 (Online)
DOI: http://dx.doi.org/10.15666/aeer/1705_1196311977

Discussion

In terms of the features of the rural settlement itself, the rural settlement area gradually decreases with the elevated altitude. Among them, the rural settlement with the elevation of 121-345 m is the largest, accounting for 50.33% of the total area of rural settlements. There are no rural settlements above 734 m. The land use and spatial distribution of rural settlements are influenced by both natural and human factors. Generally, mountainous and hilly areas are significantly affected by natural geographical factors (altitude, slope, aspect, etc.) (Li-Bang et al., 2018; Guo et al., 2012). From the statistics of the rural settlement area at different altitudes within the entire rural settlement, it can be seen that with the rise of altitude, the scale of rural settlements is getting smaller and smaller. The population density is small, and the spatial distribution of rural settlements is random (Yang et al., 2016). According to the results of the slope analysis, the rural settlements in Xinbin county are mainly distributed on the flat land of 0°-5° and hilly-sloppy lands of 8°-15°. Its rural settlement area accounts for 21.25% and 28.55% of the total rural settlement area of the county. Ren (2017) also pointed out in one of his articles. The spatial distribution of rural settlements showed some spatial orientation to low altitude and to low slope, and were significantly close to rivers and towns; thus formed a special pattern of “dense on the plains, and sparse in the mountainous region” (Ren, 2017). However, in the Xinbin county, there are still a large number of peasants living in areas with slopes greater than 15°, which increases the difficulty of ecological management. For such rural settlements, ecological migration should be considered.

From the perspective of landscape pattern analysis (Wenzhi, 2016), Xinbin county, located in the mountainous area of Liaodong, is affected by various natural and social factors, especially the long-term self-sufficient lifestyle and topographical factors that result in insufficient per capita arable land (Zhou et al., 2013). The situation of rural residential areas in the county include the following aspects: the average plaque area of the landscape features is small; the number of plaques is large; the per capita land area exceeds the standard; the average phenotypic fractal dimension is small, and most townships are small in scale. This reveals that the plaque has a certain stability and dispersion. It is the scattered landscape pattern of rural settlements and the stability of the county as artificial landscape patches, which makes the area of human disturbance to the surrounding natural ecological environment expand continuously, and the fragmentation of natural landscape patches is bound to intensify. This leads to an increase in soil erosion and destruction of the ecological environment in a small area.

In addition, when the confidence level is 0.01, the soil erosion in the study area is significantly correlated with the size and population density of the rural, and it is a positive correlation. The erosion intensity is not related to the size of the settlement. This shows that the larger the rural settlement, the more serious the erosion, but the erosion intensity is not necessarily severe, and human activities will increase the erosion area. Therefore, the distribution of rural settlements must reach a reasonable scale to maximize economic and ecological benefits. At the same time, the study found that soil erosion showed a decreasing trend with increasing distance (Gan et al., 2014), because human activities need to rely on the land. In the place closer to the rural settlement, the greater the intensity of human activity, the more serious the erosion. From the perspective of rural settlement structure, erosion intensity is positively correlated with NP, RC and AWMPFD. This shows that the more dispersed the rural settlements, the more extensive the use, the more human disturbance, the stronger the erosion intensity.

http://www.aloki.hu ● ISSN 1589 1623 (Print) ● ISSN 1785 0037 (Online)
DOI: http://dx.doi.org/10.15666/aeer/1705_1196311977

On the contrary, PD is negatively correlated with soil erosion intensity, which indicates that the more the rural settlements gather, the higher the utilization degree, the lower the erosion intensity. Therefore, it is necessary to consider improving and strengthening the spatial agglomeration of rural settlements, thereby reducing the intensity of soil erosion.

The spatial distribution characteristics of rural settlements reflect the relationship between human production, life and its surrounding environment under different productivity levels. The landscape pattern of rural settlements and its dynamic changes affect many environmental factors, such as water and soil conservation, topography and so on. How to change the landscape pattern and spatial distribution of the current rural settlements in Xinbin county and even the entire Liaodong mountainous area, so that its ecological environment protection is in the most reasonable state? One of the most effective ways is to study the landscape pattern of rural settlements and its distribution characteristics, namely ecological migration.

Conclusion

Rural settlements are places where people live and move in mountainous areas. The denser the distribution of settlements, the greater the intensity of people's activities. The rational distribution of rural settlements will contribute to soil and water conservation in the region. Otherwise, it will aggravate soil erosion. At present, the layout of rural settlements in China is relatively poor. The analysis of the rational distribution of rural settlements does not consider the impact of the distribution of rural settlements on soil erosion. This paper takes Xinbin county, Liaoning province, China as an example, using remote sensing technology, ArcGIS and Fragstats 3.3 softwares. Based on the remote sensing satellite and land use status map, the landscape pattern of residential area distribution and soil erosion status in three time periods are analyzed. Via the correlation analysis method, the relationship between the distribution characteristics of rural settlements and soil erosion is quantitatively analyzed. The following is the main conclusion.

(1) In general, the proportion of rural settlement land use in Xinbin county is relatively small. The MPS of rural residential patches is small, the degree of land use is not high, the degree of separation is high, and the distribution of settlements is scattered and chaotic, mostly distributed along rivers and traffic roads.

(2) In three periods, soil erosion was the most serious in 2001, with an erosion rate of 57%; in 2010, soil erosion was the least, with an erosion rate of 39.87%. The intermediate soil erosion rate in 1992 was 55.34%.

(3) Soil erosion is positively correlated with population density and the size of rural settlements. However, the intensity of erosion is not related to the size of the settlement. Soil erosion shows a decreasing trend with increasing distance. From the perspective of rural settlement structure, erosion intensity is positively correlated with NP, RC and AWMPFD. On the contrary, PD is negatively correlated with soil erosion intensity.

Acknowledgments. The study is supported by the Fund Project of Shaanxi Key Laboratory of Land Consolidation (2019-ZD05).

http://www.aloki.hu ● ISSN 1589 1623 (Print) ● ISSN 1785 0037 (Online)
DOI: http://dx.doi.org/10.15666/aeer/1705_1196311977

REFERENCES

[1] Allen, D. W. (2016): GIS Tutorial 2: Spatial Analysis Workbook. – Esri Press, Redlands, CA.
[2] Chaolin, G. U., Weihua, G., Helin, L. (2017): Chinese urbanization 2050: SD modeling and process simulation. – Science China (Earth Sciences) 06: 57-72.
[3] Chen, L., Sun, R., Lv, Y. (2018): A Landscape Index to link landscape pattern with nutrient loss at watershed scale. – AGU Fall Meeting Abstracts. American Geophysical Union, Washington, DC.
[4] Chen, Y., Ge, Y. (2015): Spatial point pattern analysis on the villages in China's poverty-stricken areas. – Procedia Environmental Sciences 27: 98-105.
[5] Cheng, X. (2016): Analysis on the relationship between degree of fragmentation and production profits of arable landscapes upon varying landforms - a case study of Xinjian County, Jiangxi Province. – Agricultural Science & Technology 17(8).
[6] Christensen, A. A., Brandt, J., Svenningsen, S. R. (2016): Landscape Ecology. – In: Richardson, D. et al. (eds.) International Encyclopedia of Geography: People, the Earth, Environment and Technology. Wiley, Hoboken, NJ, pp. 1-10.
[7] Conrad, C., Rudloff, M., Abdullaev, I., Thiel, M., Löw, F., Lamers, J. P. A. (2015): Measuring rural settlement expansion in Uzbekistan using remote sensing to support spatial planning. – Applied Geography 62: 29-43.
[8] Cronk, B. C. (2017): How to Use SPSS®: A Step-by-Step Guide to Analysis and Interpretation. – Routledge, New York.
[9] Gan, C., Li, Y., Wang, Y., Shao, J. (2014): Analysis of the spatial distribution character and its soil erosion of rural settlement in the center region of the Three Gorges Reservoir Area-a case study of 27 towns of Fengjie County. – Journal of Chongqing Normal University 31(4): 52-58.
[10] Gandhi, G. M., Parthiban, S., Thummalu, N., Christy, A. (2015): NDVI: vegetation change detection using remote sensing and GIS - a case study of Vellore District. – Procedia Computer Science 57: 1199-1210.
[11] Green, S. B., Salkind, N. J. (2016): Using SPSS for Windows and Macintosh, Books a la Carte. – Pearson, London.
[12] Guo, X. D., Zhang, Q. Y., Ma, L. B. (2012): Analysis of the spatial distribution character and its influence factors of rural settlement in transition-region between mountain and hilly. – Econ. Geogr 32(10).
[13] Ju, J., Masek, J. G. (2016): The vegetation greenness trend in Canada and US Alaska from 1984-2012 Landsat data. – Remote Sensing of Environment 176: 1-16.
[14] Ke, Y. (2016): Based on ENVI optimization of automatic interpretation of remote sensing image classification results. – World Nonferrous Metals 2016: 59.
[15] Li-Bang, M. A., Ya-Ya, T., Xiao-Dong, G., Mei-Mei, C., Yong-Li, W. (2018): Spatial-temporal change of rural settlements and its spatial coupling relationship with water and soil resources based on grid in the Hexi oasis. – Journal of Natural Resources 33(5): 775-787.
[16] Ma, Y. Q., Shi, Y., Qin, Y. W., Zheng, B. H., Zhao, Y. M., Zhang, L. (2014): Temporal-spatial distribution and pollution assessment of heavy metals in the upper reaches of Hunhe River (Qingyuan section), Northeast China. – Huan Jing Ke Xue 35(1): 108-116.
[17] Maguire, D. J. (2015): ArcGIS: General-Purpose GIS Software. – In: Shekhar, S. et al. (eds.) Encyclopedia of GIS. Springer, Basel, pp. 1-8.
[18] Murasingh, S., Jha, R., Adamala, S. (2018): Geospatial technique for delineation of groundwater potential zones in mine and dense forest area using weighted index overlay technique. – Groundwater for Sustainable Development 7: 387-399.
[19] Remmel, T. K., Fortin, M. J. (2017): What Constitutes a Significant Difference in Landscape Pattern? – In: Gergel, S. E. Turner, M. G. (eds.) Learning Landscape Ecology. – Springer, New York, pp. 105-125.

http://www.aloki.hu ● ISSN 1589 1623 (Print) ● ISSN 1785 0037 (Online)
DOI: http://dx.doi.org/10.15666/aeer/1705_1196311977

[20] Ren, Y. (2017): An analysis of rural settlement patterns and their effect mechanisms based on road traffic accessibility of Guangdong. – Acta Geographica Sinica 72(10): 1859-1871.
[21] Rodríguez-Loinaz, G., Alday, J. G., Onaindia, M. (2015): Multiple ecosystem services landscape index: a tool for multifunctional landscapes conservation. – Journal of Environmental Management 147: 152-163.
[22] Segatori, A., Marcelloni, F., Pedrycz, W. (2017): On distributed fuzzy decision trees for big data. – IEEE Transactions on Fuzzy Systems 26(1): 174-192.
[23] Wenzhi, T. (2016): Rural landscape planning and design based on the perspective of beautiful rural construction. – Chinese Journal of Agricultural Resources & Regional Planning 37(09):229-232.
[24] Xi, H., Xiao, L., Liu, R. Q., Yu, M. M. (2018): Evolution characteristics and driving mechanism of rural settlement in the fringe belt of famous historical and cultural city: taking Hancheng Miaohou village of Shaanxi province for example. – Areal Research & Development 37(2): 158-162.
[25] Yang, R., Liu, Y., Long, H., Qiao, L. (2015): Spatio-temporal characteristics of rural settlements and land use in the Bohai Rim of China. – Journal of Geographical Sciences 25(5): 559-572.
[26] Yang, R., Xu, Q., Long, H. (2016): Spatial distribution `characteristics and optimized reconstruction analysis of China's rural settlements during the process of rapid urbanization. – Journal of Rural Studies 47(47): 413-424.
[27] Yang, Y., Liu, Y., Li, Y., Du, G. (2018): Quantifying spatio-temporal patterns of urban expansion in Beijing during 1985–2013 with rural-urban development transformation. – Land Use Policy 74: 220-230.
[28] Ying, T. (2017): Evaluation of water ecological health of Hunhe River by using diatom index. – Water Resources & Hydropower of Northeast China 5: 19.
[29] Ying, X., Jian-Rong, F., Lei-Lei, L. I., Xuan, L. I. (2017): Comparisons on sparse alpine grassland based on vegetation coverage inversion models of remote sensing. – Journal of Sichuan Agricultural University 35(01): 37-59.
[30] Zhou, G., He, Y., Tang, C., Yu, T., Xiao, G., Zhong, T. (2013): Dynamic mechanism and present situation of rural settlement evolution in China. – Journal of Geographical Sciences 23(3): 513-524.

http://www.aloki.hu ● ISSN 1589 1623 (Print) ● ISSN 1785 0037 (Online)
DOI: http://dx.doi.org/10.15666/aeer/1705_1196311977

COMPARISON OF PRECIPITATION STABLE ISOTOPES DURING WET AND DRY SEASONS IN A SUBTROPICAL MONSOON CLIMATE REGION OF CHINA

XIA, C. C.[1,2] – CHEN, K.[1,2] – ZHOU, J.[1,2] – MEI, J.[1,2] – LIU, Y. P.[1,2] – LIU, G. D.[1,2*]

[1]*State Key Laboratory of Hydraulics and Mountain River Engineering, Sichuan University Chengdu 610065, China*

[2]*College of Water Resources and Hydropower, Sichuan University, Chengdu 610065, China*

[*]*Corresponding author*
e-mail: liugd988@163.com

(Received 25th Apr 2019; accepted 11th Jul 2019)

Abstract. Hydrogen and oxygen stable isotopes are natural tracers and have played an important role in the investigation of hydrological processes. In this paper, year-round precipitation samples were collected and measured in Chengdu, a subtropical monsoon climate region, to compare the stable isotope characteristics in precipitation and their influencing factors between dry and wet seasons. The results showed that the seasonal variation of δD and $\delta^{18}O$ in precipitation was significant, and the isotopic values in precipitation in dry season were more enriched than those in wet season. The slope and intercept of local meteoric water line (LMWL) in Chengdu were lower than those in the southeast monsoon region of China but higher than those in north China, indicating the combined influence of ocean-source and inland water vapor. The slope of LMWL in dry season was obviously lower than that in wet season, revealing more intense sub-cloud secondary evaporation. The effect of temperature and precipitation was not significant in both seasons. Meteorological variables had greater influence on precipitation isotopes in wet season. D-excess had greater fluctuation during the dry season, reflecting more complex water vapor sources, which resulted in the influence of meteorological factors being masked.
Keywords: *water circulation, monsoon activities, moisture source, meteorological parameters, sub-cloud secondary evaporation*

Introduction

As an important part of natural material circulation, water circulation is the link connecting biosphere, atmosphere and hydrosphere. In the study of modern water cycle, hydrogen and oxygen stable isotopes in water bodies can provide a lot of information which is difficult to obtain by traditional hydrological methods due to its sensitive response to climate and environmental changes (Goller et al., 2005; Xie et al., 2011; Wang et al., 2017; Cai et al., 2017; Badaluta et al., 2019). Atmospheric precipitation is an important process of water circulation and a recharge source for rivers, lakes and groundwater. The stable isotopes in precipitation are affected by meteorological conditions, regional geographical position and weather patterns, and usually have a certain spatio-temporal variation law. Therefore, understanding the characteristics of stable isotopes in precipitation can help to understand the processes of water cycle and their feedback mechanism (Celle-Jeanton et al., 2004; Zhang et al., 2005; He et al., 2006). In 1961, the International Atomic Energy Agency (IAEA) and the World Meteorological Organization (WMO) collaborated to establish the Global Network of Isotopes in Precipitation (GNIP) to measure stable isotope data in global precipitation, and more than 800 monitoring sites have been established around the world. Since the 1960s, a large number of studies have been carried out around the world to reveal the

http://www.aloki.hu ● ISSN 1589 1623 (Print) ● ISSN 1785 0037 (Online)
DOI: http://dx.doi.org/10.15666/aeer/1705_1197911993

variation characteristics of stable isotopes in precipitation of different climate types. For example, Guan et al. (2013) sampled and tested the event and intra-event samples of precipitation, and revealed the influence of synoptic weather system and water vapor source on precipitation isotopes in Flinders, an Australian Mediterranean climate region; Balagizi et al. (2018) reported the isotope values in Virunga, an African tropical climate region with strong evaporation, and suggested that the vapor from soil-plant evapotranspiration and that from lake surface evaporation are main causes of the depleted and enriched isotope compositions during wet and dry periods, respectively; a systematic study of stable isotopes was carried out on Crimean Peninsula, a region with different climate types, and temperature were proved to be the major factor correlated with the isotope values (Dublyansky et al., 2018).

Monsoon climate is widely distributed in the world. In the monsoon climate zone, monsoon is an important carrier of water vapor transport, and controls the spatial distribution and seasonal variation of precipitation. The change of the monsoon's onset time and intensity makes the amount and temporal distribution of precipitation in the monsoon region very uncertain, leading to the frequent occurrence of droughts and floods, which has a great impact on human production and life. Therefore, understanding the law of monsoon activities is of great significance to social and economic development. In recent years, many researchers have revealed the influence of monsoon on local meteorological conditions and water vapor source of precipitation by analyzing the stable isotope composition in precipitation in different monsoon regions around the world. For example, Pang et al. (2006) found that Lijiang is mainly controlled by large-scale India Depression System on the weather scale in summer by analysing the $\delta^{18}O$ data in summer daily precipitation. Srivastava et al. (2015) implemented the early detection of the onset of monsoon by measuring the hydrogen and oxygen isotope compositions in atmospheric water vapor and precipitation in Ahmedabad, India. Peng et al. (2016) found that seasonal wind flow is the main factor affecting Yilan area in northeast Taiwan by analyzing the stable isotope compositions of precipitation and river water, and semi-quantitatively estimated the contribution ratio of air masses from different sources to river water volume. Xia et al. (2019) analyzed the monthly accuracy data of 15 stations provided by GNIP, and obtained the relationship between monsoon flow in Asian tropical monsoon region and isotopic composition in precipitation in different seasons. Qu et al. (2018) compared the isotopic characteristics and meteoric water lines of plum and typhoon rain, two typical precipitation types in monsoon region, and determined the relationship between isotopic composition and transport path and water vapor source.

Chengdu is located in southwest China and belongs to subtropical monsoon climate zone. During the wet season, the East Asian monsoon and the Indian monsoon meet here, bringing water vapor from the western Pacific and Indian Ocean; during the dry season, this area is controlled by the northwest monsoon from the high latitude inland. Due to the influence of the complex monsoon system, the stable isotope ratios in precipitation are significantly different between dry and wet seasons. Wu (2009) obtained the LMWL of Chengdu by analyzing precipitation isotope data of monthly accuracy from 1986 to 1998 provided by GNIP, and preliminarily analyzed the influence of precipitation, temperature and water vapor pressure on isotope compositions. However, the isotope data from GNIP is extremely limited, and those of monthly accuracy cannot reflect the variation characteristics of stable isotopes in precipitation at the weather scale. There is a lack of research on stable isotope in

http://www.aloki.hu ● ISSN 1589 1623 (Print) ● ISSN 1785 0037 (Online)
DOI: http://dx.doi.org/10.15666/aeer/1705_1197911993

precipitation in this region. In this study, we collected and measured the stable isotope samples in precipitation during the dry and wet seasons in Chengdu in 2018, recorded local meteorological parameters, and discussed the effects of environmental factors and water vapor sources on the precipitation isotopes during the two seasons. The results of this paper will help to understand the atmospheric circulation and transport processes of water vapor in the southwest subtropical monsoon region of China, and provide isotopic evidence for studying the hydrological cycle mechanism in this region.

Material and methods

Study area

Chengdu, one of the largest cities in southwest China, located in the west of Sichuan Basin and the middle reaches of Minjiang River, is bounded by Longquan Mountain in the east and Qionglai Mountains in the west. Its altitude range is 398~4906 m. Chengdu has a subtropical humid monsoon climate with mild climate, distinct seasons and abundant rain. The long-term distribution characteristics of average monthly precipitation and temperature from Chengdu City Data Site of China Weather Network (www.weather.com.cn) are shown in *Fig. 1(a)*.

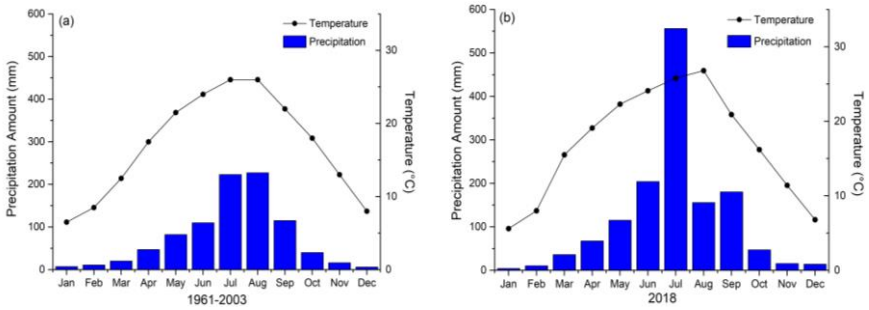

Figure 1. *Monthly precipitation and average temperature in Chengdu in 2018*

The highest and lowest monthly average temperature occurred in August and January, and the largest and smallest monthly precipitation occurred in July and January, respectively. According to the monitoring data provided by Chengdu Public Meteorological Service Website (http://pcc.scqx.gov.cn/sc_cd/fwcp/qhpj/), the average monthly temperature and precipitation in Chengdu in 2018 are shown in *Fig. 1(b)*. In 2018, although the variation trends of temperature and precipitation amount correspond to the multi-year average in Chengdu, the total annual precipitation shows a distinct high value of 1407 mm, which can be attributed to the extremely large precipitation amount in July. The cumulative precipitation from June to September was 1096.9 mm, accounting for 77.96% of the total, and that in other months was 310.1 mm, accounting for 22.04% of the total. According to the temporal distribution of precipitation, June to September was divided into wet season and other months into dry season in Chengdu.

Sample collection and analysis

The sampling point for precipitation was located at the platform test site of the College of Water Resources and Hydropower, Sichuan University (104.08 °E, 30.63 °N, 553 m). This point is far away from local pollution sources and there are no tall

http://www.aloki.hu ● ISSN 1589 1623 (Print) ● ISSN 1785 0037 (Online)
DOI: http://dx.doi.org/10.15666/aeer/1705_1197911993

buildings or trees blocking around. The geographical location of the sampling points is shown in *Fig. 2*. According to the IAEA/GNIP precipitation sampling guide, a simple water collecting device was set up: a plastic cylinder with a diameter of 50 mm and a height of 75 mm was fixed on the ground, with a PE plastic film covered above for collecting water; a 500 mm rain collecting bottle was placed in the cylinder, which connected with a funnel with a diameter of 15 mm and a table tennis ball was placed in the funnel to prevent evaporation. After a precipitation event, the rainwater was collected into a 20 mL plastic bottle, and then placed in a refrigerator for cold storage. The meteorological data (i.e. temperature, precipitation amount and relative humidity) during the precipitation were recorded according to the real-time measurements from Tiaosanta weather station, which is about 1 km away from the sampling site. The samples were collected and analyzed in an event precision, and multiple rainfalls occurring in one day were recorded as independent events respectively. The starting and ending times of an individual event are determined based on whether the rainfall intensity is greater than 0.1 mm/h. A total of 113 precipitation samples were collected in 2018, including 59 for wet season precipitation and 54 for dry season precipitation.

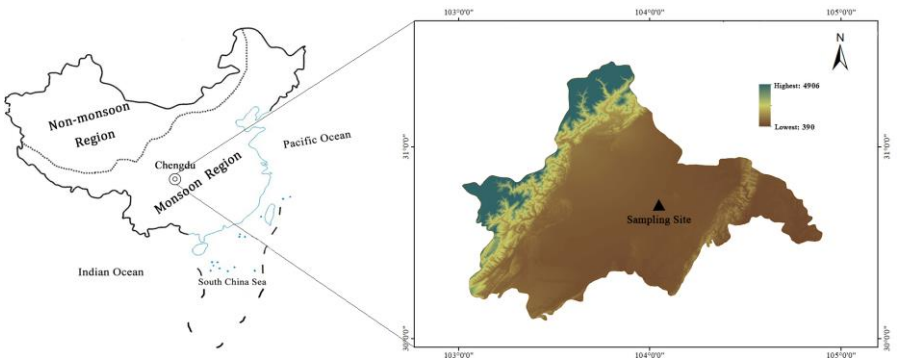

Figure 2. *Location of the study area and sampling site*

The samples were analyzed in College of Water Resources and Hydropower, Sichuan University, using the Triple-Liquid Water Isotope Analyzer produced by Los Gatos Research (LGR). The LGR analyzer uses spectrometry to measure stable isotope content in water and the measurement principle is OFF-AXIS Integrated Cavity Output Spectroscope (OA-ICOS). With the cooperation of a full-automatic sampler, the analyzer measures the samples automatically and continuously according to a computer program. Precipitation samples were filtered using 0.45 μm filter membranes before measurement. Each sample was measured for six times and the first two measurements were rejected for their larger deviation from the actual value. Reference standard samples based on VSOMW-2 and SLAP-2 were measured at an interval of three precipitation samples to diagnose whether abnormalities occur during the measurement. The measurement results are expressed as per mil (‰) deviation from Vienna Standard Mean Ocean Water (VSMOW). The formula is shown in *Eq. 1*:

$$\delta^{18}O(\delta D) = \frac{R_{sample} - R_{standard}}{R_{standard}} \times 1000 \qquad \text{(Eq.1)}$$

For δD and $\delta^{18}O$, the instrumental errors are: δD < 0.3‰, $\delta^{18}O$ < 0.08‰.

http://www.aloki.hu ● ISSN 1589 1623 (Print) ● ISSN 1785 0037 (Online)
DOI: http://dx.doi.org/10.15666/aeer/1705_1197911993

Statistical approaches

Linear equations were established to evaluate the relationships between δD and $\delta^{18}O$ and between meteorological parameters and isotope composition by the method of least square regression. The correlation coefficients and test of significance were analyzed by Pearson's method and two-tailed t tests, respectively. A sinusoidal periodic function was employed to fit the seasonal variation of isotopes. The statistical analysis in this study was conducted by Origin 9.0 and IBM SPSS Statistics 24.

Results and discussion

Characteristics and seasonal variations of δD and $\delta^{18}O$ in precipitation

δD and $\delta^{18}O$ showed obvious seasonal changes in precipitation events in Chengdu. In order to describe these changes, a trigonometric function fitting was employed in *Fig. 3*. The value of δD changed from -119.38 to 22.10, with an arithmetic average of -43.65 and a precipitation weighted average of -50.52. The value of $\delta^{18}O$ changed from -15.84 to 2.68, with an arithmetic average of -6.60 and a precipitation weighted average of -9.01. Wu (2009) reported the average of multi-year isotope values in Chengdu, which is -5.6‰ in $\delta^{18}O$ and -40.7‰ in δD, respectively.

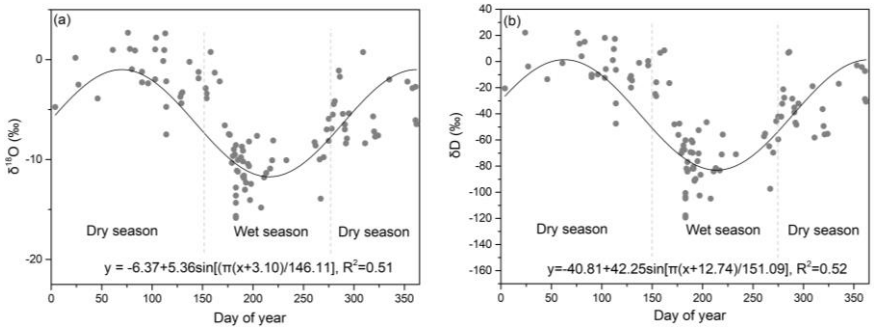

Figure 3. *Seasonal variation of $\delta^{18}O$ and δD in precipitation in 2018*

The average values of both isotopes during our study period are lower than those given by Wu (2009), which may be due to the depletion of heavy isotopes in air masses caused by the heavy summer precipitation in both Chengdu and other areas along the transport path. The maximum and minimum values of δD occurred in January and July, respectively, and those of $\delta^{18}O$ occurred in March and July, respectively. δD and $\delta^{18}O$ showed similar trends and periods of change, while δD showed greater amplitude, indicating that both isotopes in precipitation were affected by the same factors, but δD responded more strongly to environmental changes. Isotopes are enriched in the dry season and depleted in the wet season, which is similar to those in other areas of East Asia affected by subtropical monsoon climate, such as Wuhan, Bangkok and Guangzhou (He et al., 2006; Xie et al., 2011; Deng et al., 2016), but contrast to those in inland areas in the mid-high latitudes (Chen et al., 2017), indicating that the isotopic composition of precipitation in this area is closely related to the characteristics of atmospheric circulation and water vapor sources. Chengdu is located in southwest China, far away from the coastline and its distance from the Indian Ocean is similar to that from the Pacific Ocean. Influenced by different atmospheric circulation systems

http://www.aloki.hu ● ISSN 1589 1623 (Print) ● ISSN 1785 0037 (Online)
DOI: http://dx.doi.org/10.15666/aeer/1705_1197911993

and multiple monsoons, the water vapor sources in this region are complex. During the wet season, Chengdu is jointly affected by Pacific High Pressure and Indian Ocean Low Pressure, and air masses with high humidity in this region came from the surface of the Pacific Ocean and Indian Ocean controlled by southeast and southwest monsoon. Due to frequent precipitation and evaporation caused by high temperature during long-distance transportation, isotopes in water vapor were strongly fractionated and D and ^{18}O in precipitation were depleted. During the dry season, Chengdu is affected by Mongolia High Pressure and Aleutian Low Pressure, and the northerly winds control the area. Air masses with low humidity and temperature originated from inland areas in the middle and high latitudes. During the transportation process, the temperature was lower, the precipitation along the transport path was less, and the "rainout effect" experienced by air masses was weaker, making D and ^{18}O in precipitation more enriched. $\delta^{18}O$ and δD of more events deviated from the fitting line to a large extent in wet season, which may be due to the greater variations of temperature and precipitation, which have a greater impact on isotope fractionation during the rainfall processes.

Local meteoric water line (LMWL) during wet and dry seasons

The linear relationship between δD and $\delta^{18}O$ in precipitation is named as meteoric water line. Craig (1961) first proposed the equation of global meteoric water line (GMWL) by investigating and analyzing the stable isotope compositions of different water bodies around the world: $\delta D = 8\delta^{18}O + 10$; Zheng et al. (1983) reported the Chinese meteoric water line (CMWL) based on stable isotope measurements of precipitation in different regions of China: $\delta D = 7.9\delta^{18}O + 8.2$. The linear relationship between δD and $\delta^{18}O$ in precipitation in Chengdu was obtained by least squares method (*Fig. 4a*). The regression equation is given with *Eq. 2*:

$$\delta D = 7.61\delta^{18}O + 6.58 (R^2 = 0.98) \quad \text{(Eq.2)}$$

The slope and intercept of meteoric water lines are affected by the water vapor sources, transport patterns, condensing temperature and the sub-cloud processes, and can be used to reflect the information of regional geography, meteorological conditions and water vapor source. Compared with GMWL and CMWL, the slope and intercept of the LMWL in Chengdu were small, indicating that the precipitation in Chengdu was affected by both the ocean-source and continental air masses on annual scale. Compared with other areas in China, the slope and intercept of LMWL in Chengdu were lower than those in the southeast coastal areas, such as Guangzhou, Changsha and Fuzhou (Xie et al., 2011; Yao et al., 2018; Xu et al., 2019), but higher than those in northern temperate climate regions, such as Lanzhou, Fengxiang, Ningwu and Beijing (Zhai et al., 2013; Chen et al., 2015; Zhao et al., 2018), indicating that the contribution of marine water vapor in the annual precipitation in Chengdu is lower than that in the southeast coast but higher than that in the northern region.

The LMWLs based on precipitation events during the wet and dry seasons is shown in *Fig. 4b*. It can be observed that the LMWLs in wet and the dry seasons differed greatly, which reflected the differences in characteristics of isotope fractionation in the two seasons, which is mainly caused by atmospheric circulation patterns, water vapor sources and evaporation. In previous studies, the seasonal changes of LMWLs of different monsoon regions have been proved variable. The LMWLs of islands and coastal regions which are dominated by the oceanic water vapor all year round show

http://www.aloki.hu ● ISSN 1589 1623 (Print) ● ISSN 1785 0037 (Online)
DOI: http://dx.doi.org/10.15666/aeer/1705_1197911993

slight variation between wet and dry seasons and plot closely to GMWL (Xia et al., 2019). The slope and intercept of LMWLs in monsoon marginal regions vary greatly seasonally, with high values in wet season and low values in dry (Zhao et al., 2018). In our study area, the slope and intercept of LMWL in wet season were close to those of GMWL and LMWL of low-latitude islands and coastal areas, indicating the dominance of oceanic air masses during this period, and precipitation was less affected by non-equilibrium fractionation. The slope and intercept of LMWL in dry season were significantly lower than those in wet season, but was close to those in mid-high latitudes, for example, Fengxiang in North China (Zhao et al., 2018), indicating that the region was controlled by inland dry air masses and significantly affected by sub-cloud secondary evaporation. Under dry conditions, non-equilibrium fractionation happens when raindrops fall in unsaturated atmosphere, leading to preferential fractionation of D into atmosphere, relative enrichment of ^{18}O, and fractionation ratio of D to ^{18}O to be lower than 8:1, which explains the lower slope and intercept of regression line.

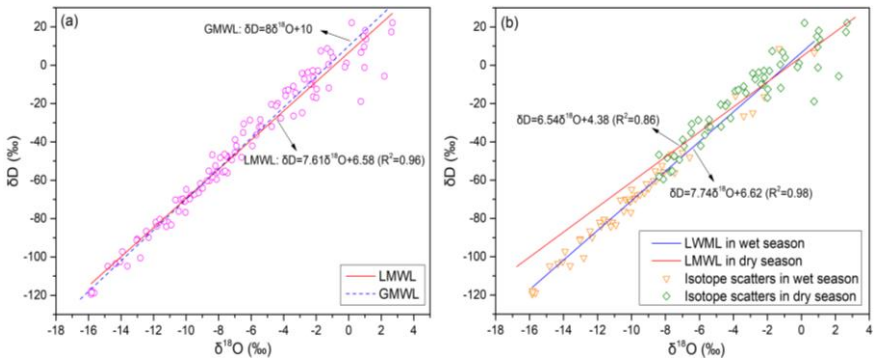

Figure 4. *Year-round and seasonal correlation between $\delta^{18}O$ and δD in precipitation*

Relationship between isotope compositions in precipitation and climatic factors

Precipitation effect

Precipitation effect is an inverse correlation between precipitation stable isotopes and precipitation amount, which is generally significant in tropical and subtropical regions (Dansgaard, 1964). Regression analysis on the $\delta^{18}O$–precipitation amount (P) relationship was performed in dry and wet seasons and the whole year in Chengdu using the least square method. Person's Method and two-tailed tests were used to reflect the degree of correlation and to perform significance test, respectively. The results are shown in *Fig. 5.* On the annual scale, $\delta^{18}O$–P showed a significant negative correlation with a correlation coefficient (r) of -0.42 and passed the significance test of 0.01 confidence level. Compared with other regions in China's monsoon zone, the absolute value of r of Chengdu is lower than that of tropical regions, such as Hong Kong (-0.70, 2015-2016), similar to that of subtropical regions, such as Guangzhou (-0.36, 2007-2009) and Chongqing (-0.40, 2010-2015), and higher than that of temperate regions, such as Fengxiang (0.024, 2016-2017) and Ningwu (-0.05, 2016-2017) (Xie et al., 2011; Zhao et al., 2018; Zhou and Li, 2018; Xia et al., 2019). The geographical difference of r, which is strong in low latitudes and weak in middle and high latitudes, is the same as the results of Araguas-Araguas et al. (1998) in Southeast Asia. This suggested that the influence of precipitation amount on isotopic composition of

http://www.aloki.hu ● ISSN 1589 1623 (Print) ● ISSN 1785 0037 (Online)
DOI: http://dx.doi.org/10.15666/aeer/1705_1197911993

precipitation decreases with the increase of latitude. On the seasonal scale, the $\delta^{18}O$–P correlations of the precipitation in both seasons failed the significance test of 0.05 confidence level and the r values for dry and wet season were -0.11 and -0.26. It is probably due to the complicated formation mechanism of stable isotopes in monsoon precipitation. The meteorological conditions at the source areas of water vapor determine the initial composition of the isotope, the "rainout effect" that isotopes in water vapor experience along the transport path and the recycled water vapor lead to changes in the isotopic composition. In monsoon climate regions, the sources and transport processes of water vapor are unstable and changeable due to the interaction of different monsoon systems, resulting in differences in stable isotopes in cloud when precipitation happens. Compared with the seasonal r values (-0.44 and -0.22 for dry and wet seasons, respectively) of Changsha at the same latitude, the absolute value of r of $\delta^{18}O$-P relationship in wet season is relatively close between the two regions, while that of Chengdu is significantly lower in dry season (Wu et al., 2015). This may be due to the different division of dry and wet season between the two studies. In the study of Wu et al. (2015), the months of May and October, which is the transition periods between summer and winter monsoon with the most complicated water vapor sources, was not included either in dry or wet season. However, the two months were included in dry season in our study. The alternation and transformation of multiple monsoons resulted in the difference of isotope composition in clouds and subsequently in raindrops, which covered up the influence of precipitation amount.

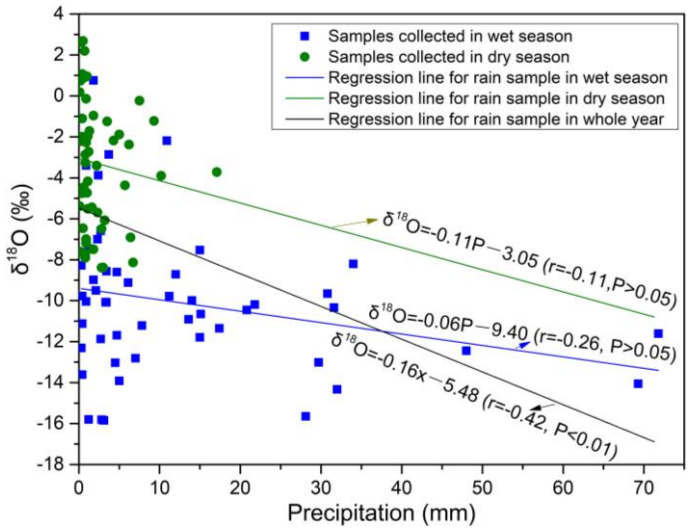

Figure 5. *Linear relationship between $\delta^{18}O$ and precipitation amount in both seasons and the whole year*

According to *Fig. 5*, precipitation intensity is closely related to the variation range of isotopes. The isotopic composition of small-scale precipitation with an amount less than 10 in both seasons had a large variation range, but events with precipitation amount greater than 10 mm all showed low isotopic composition, especially for those occurred in wet season. To determine the influence degree of precipitation intensity on isotope composition, the precipitation data set in this study was divided into two groups (from 0 to 10 mm and from 11 to 70 mm) to examine the $\delta^{18}O$–P correlation separately. The results are shown in *Table 1*. Most precipitation events (88/113) during the study period

http://www.aloki.hu ● ISSN 1589 1623 (Print) ● ISSN 1785 0037 (Online)
DOI: http://dx.doi.org/10.15666/aeer/1705_1197911993

happened with an intensity of less than 10 mm and those with a relatively strong intensity of 10-70 mm were monitored mainly in wet season. The correlation between $\delta^{18}O$ and P (10-70 mm) in the dry season is not obtained because of the scarce sample data. When the precipitation events with strong intensity are taken into consideration individually, the absolute values of r of regression equations increase for both wet season (0.45 vs. 0.26) and whole year (0.49 vs. 0.42). While the absolute values of r of the correlation between $\delta^{18}O$ and P (0-10 mm) are lower in seasonal and annual scale. This could be attributed to the influence of atmospheric circulation and external environment. For the one hand, most precipitation events with strong intensity happened in June and July, when the water vapor sourced from ocean area and travelled along a relative fixed path. The isotopes in the cloud layer were relatively stable when the rainfall happened. Reversely, the isotopes in the cloud layer were variable in dry season for the mixing of water vapor from different sources and transportation paths. For the other hand, the influence of isotope fractionation caused by sub-cloud evaporation, is more significant for small-scale precipitation than large one, which enhanced the variability in isotope composition.

Table 1. *Relationship between $\delta^{18}O$ and precipitation events with different intensity (from 0 to 10 mm and from 11 to 70 mm)*

Period	Precipitation intensity	Number of samples	$\delta^{18}O$–P regression equation
Whole year	<10 mm	88	$\delta^{18}O = -0.49P - 4.57$ ($r = -0.23$, $P > 0.05$)
	10-70 mm	25	$\delta^{18}O = -0.09P - 7.67$ ($r = -0.49$, $P < 0.01$)
Dry season	<10 mm	52	$\delta^{18}O = -0.19P - 2.91$ ($r = -0.13$, $P > 0.05$)
	10-70 mm	2	/
Wet season	<10 mm	36	$\delta^{18}O = -0.30P - 8.89$ ($r = -0.15$, $P > 0.05$)
	10-70 mm	23	$\delta^{18}O = -0.07P - 8.67$ ($r = -0.45$, $P < 0.01$)

Temperature effect

According to the Rayleigh fractionation model, the condensation temperature of water vapor is related to the fractionation coefficient of the isotopes. Dansgaard (1964) defined the positive correlation between precipitation isotopes and temperature as temperature effect. The correlation between $\delta^{18}O$–Temperature (T) in Chengdu was shown in *Fig. 6*. On the annual scale, there was a significant negative correlation between $\delta^{18}O$ in precipitation and temperature in Chengdu, showing a "reverse temperature effect", which is inconsistent with the effect of temperature on isotope fractionation in physics. On the seasonal scale, there was no significant correlation between $\delta^{18}O$ and temperature in either dry season or wet season. In previous studies, monthly accuracy data provided by GNIP presented that most (33/38) stations in Southeast Asia controlled by Pacific and Indian Ocean monsoon showed negative correlation or weak positive correlation ($r^2 \leq 0.24$) between $\delta^{18}O$ and temperature (Araguas-Araguas et al., 1998); the negative correlation between $\delta^{18}O$ and temperature has also been widely observed in studies carried out in the monsoon regions of southern China, for example, in Chongqing ($r = -0.52$) and Changsha ($r = -0.38$), which is consistent with the results of this study (Wu et al., 2015; Zhou and Li, 2018). Recent studies in different regions of China show that the correlation between temperature and

http://www.aloki.hu ● ISSN 1589 1623 (Print) ● ISSN 1785 0037 (Online)
DOI: http://dx.doi.org/10.15666/aeer/1705_1197911993

$\delta^{18}O$ gradually strengthens from monsoon marginal area to inland area (with r value increasing from 0.16 to 0.83), indicating that the influence of temperature on isotope values enhances with the increase of latitude and decrease of monsoon intensity (Wang et al., 2019). These results indicate that the effect of temperature on the isotopic composition is closely related with monsoon activities and was masked by other effects.

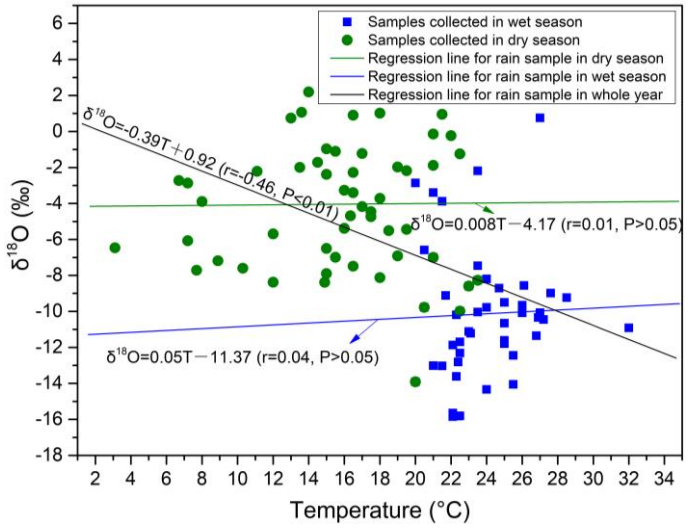

Figure 6. *Linear relationship between $\delta^{18}O$ and temperature in both seasons and the whole year*

Effect of local surface relative humidity

Previous studies have shown that local surface relative humidity (RH) determines the intensity of non-equilibrium isotope fractionation as it is related to evaporation conditions during the falling processes of raindrops, and is considered to be an important factor affecting the isotopic composition of precipitation (Zhang et al., 2007; Crawford et al., 2017). Correlation analysis was performed to determine the relationship between RH and precipitation $\delta^{18}O$ on annual and seasonal scales (*Fig. 7*).

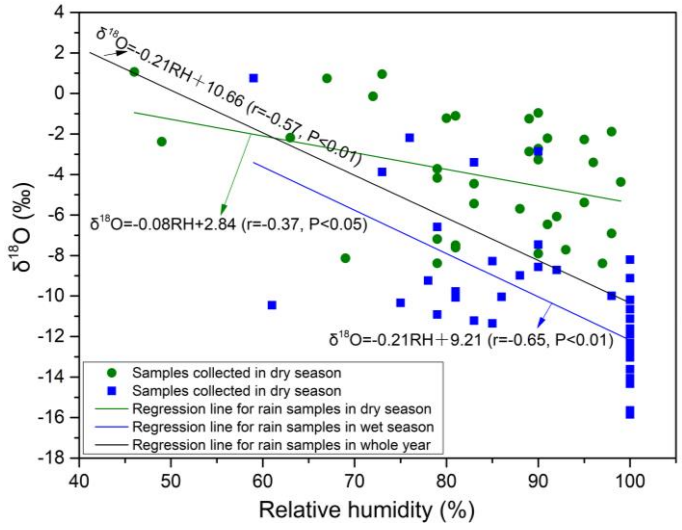

Figure 7. *Correlation between $\delta^{18}O$ and local surface relative humidity before rainfall in both seasons and the whole year*

http://www.aloki.hu ● ISSN 1589 1623 (Print) ● ISSN 1785 0037 (Online)
DOI: http://dx.doi.org/10.15666/aeer/1705_1197911993

Considering the effect of continuous precipitation on atmospheric saturation, the relative humidity in the atmosphere at the beginning of precipitation was selected. A significant negative correlation between $\delta^{18}O$ and RH was observed on both annual and seasonal scales, indicating that evaporation conditions played an important role in the stable isotope composition in precipitation. Under unsaturated atmospheric conditions, the secondary evaporation of raindrops enriches heavy isotopes in the remaining water droplets during the process of falling from cloud to the ground due to the different kinetic energy of molecules in phase transformation. The enrichment degree of heavy isotopes is related to the unsaturated degree of the atmosphere. In the season when precipitation is scarce, the low relative humidity and strong sub-cloud evaporation increase the effect of non-equilibrium fractionation, resulting in an increase in $\delta^{18}O$ value. When heavy or continuous precipitation occurs, the atmosphere approaches saturation and the effect of sub-cloud evaporation is weakened, leading to relatively depleted value of $\delta^{18}O$. The absolute values of slope and correlation coefficient of $\delta^{18}O$–RH regression in wet season were significantly higher than those in dry season, which may be due to the higher temperature in wet season accelerating the evaporation of raindrops during the sub-cloud processes, thus causing stronger non-equilibrium isotopic fractionation.

Comprehensive effects of local climatic variables

Understanding the relationship between meteorological factors and isotopes is the key to reflect climate change using the isotope method. When only the effect of a single factor on $\delta^{18}O$ was considered, there is no expected significant correlation, which is not enough to explain the isotope changes in precipitation. Compared with unary linear regression, multiple linear regression can better reflect the common influence of multiple meteorological factors on stable isotopes in precipitation, which can be used to explore more complex relationships. Therefore, a multiple linear regression model containing temperature (T), precipitation (P), and relative humidity (RH) was established. Regression equations for the whole year, dry season and rainy season are shown in *Eq. 3*, *Eq. 4* and *Eq. 5*, respectively.

$$\delta^{18}O = 0.26T - 0.05P - 0.18RH + 14.16 (R^2 = 0.477, P < 0.001) \quad \text{(Eq.3)}$$

$$\delta^{18}O = 0.43T - 0.01P - 0.23RH + 21.01 (R^2 = 0.506, P < 0.001) \quad \text{(Eq.4)}$$

$$\delta^{18}O = 0.21T - 0.14P - 0.08RH + 0.51 (R^2 = 0.164, P < 0.05) \quad \text{(Eq.5)}$$

Compared with the correlation equation of $\delta^{18}O$–T, $\delta^{18}O$–P and $\delta^{18}O$–RH, the correlation equation considering multiple variables showed higher R^2 values on both annual and seasonal scales, indicating that different meteorological parameters have mutual influences due to their different relationships with precipitation isotopes. During the wet season, about 50.6% of the $\delta^{18}O$ changes can be explained by local meteorological factors, while in the dry season, the proportion dropped to 16.4%, indicating that the influence of local meteorological factors on isotopes was more masked by other variables in dry season than in rainy season.

http://www.aloki.hu ● ISSN 1589 1623 (Print) ● ISSN 1785 0037 (Online)
DOI: http://dx.doi.org/10.15666/aeer/1705_1197911993

Influence of moisture sources on stable isotopes in precipitation

In order to describe the difference in imbalance degree of D and ^{18}O fractionation during two-phase conversion process, Dansgaard (1964) proposed the concept of d-excess: $d = \delta D - 8\delta^{18}O$. In the regional water cycle, d-excess mainly depends on the meteorological conditions of the water vapor source, which is negatively correlated with surface humidity, and positively correlated with temperature. Therefore, d-excess can be used to indicate changes in the source of water vapor. The statistical information and temporal distribution of d-excess in Chengdu's precipitation in 2018 were shown in *Table 2* and *Fig. 8*, respectively.

Table 2. *Comparison of d-excess in precipitation events during dry and wet seasons*

Season	Maximum/‰	Minimum/‰	Range/‰	Average/‰	Standard deviation/‰
Dry	21.13	-24.85	45.97	9.16	9.48
Wet	19.09	-1.95	21.04	9.17	4.34

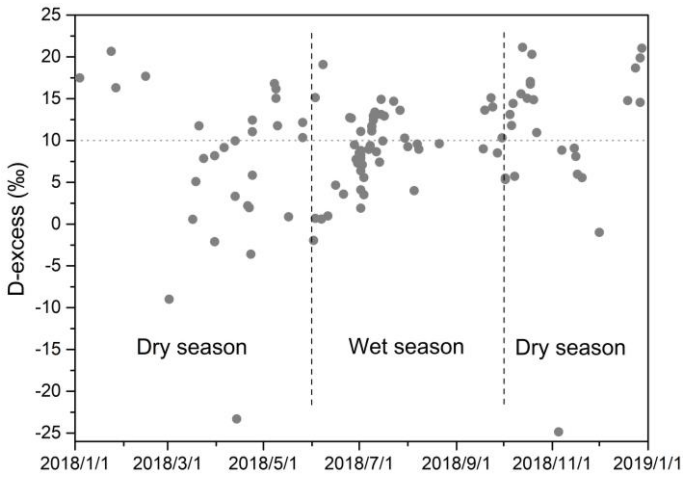

Figure 8. *Temporal variation of d-excess in precipitation in 2018*

Although the d-excess has similar average values in precipitation in dry and wet seasons, it shows a larger variation range and standard deviation in dry season. During the rainy season, the d-excess scatters fluctuate around the global average of 10, indicating that the meteorological conditions of the water vapor source are relatively stable. During the dry season, the scatters of d-excess fluctuate greatly with time, indicating that the source of water vapor in the precipitation is variable. Changes in d-excess can be explained by monsoon activities. During the wet season, the southwest monsoon from the Indian Ocean and the Bay of Bengal, and the southeast monsoon from the South China Sea and the western Pacific controlled the region alternately. Water vapor of precipitation originated from tropical and subtropical oceans, and the weather conditions of the source were relatively close to the transportation path of air masses, so that the temporal variation of d-excess was slight. During the dry season, there were significant temporal differences in monsoon activities. From January to May, the monsoon controlling Chengdu had gradually transitioned from mid-high latitude inland monsoon to mid-low latitude ocean monsoon; from October to December, the

http://www.aloki.hu ● ISSN 1589 1623 (Print) ● ISSN 1785 0037 (Online)
DOI: http://dx.doi.org/10.15666/aeer/1705_1197911993

inland monsoon controlled this area once again as oceanic monsoon subsided gradually. The complicated atmospheric circulation pattern and the contribution of recycled water vapor along the transport path, which is non-negligible under dry conditions, made the water vapor source in the dry season vary greatly in time, explaining the large fluctuation of the d value.

The complexity differences in the source of water vapor (which is related to the initial isotope content in water vapor) and the transport path (which is related to the cumulative precipitation of air masses before reaching the site) can also explain the significant differences in the correlation between $\delta^{18}O$ and meteorological factors in dry and wet season. During the wet season, the temporal variation of the initial isotopic composition in ocean-source water vapor was small, and the uncertainty of transport distance and path was small, which caused smaller difference of isotopic composition in water vapor when the air masses reached Chengdu. During the dry season, Water vapor from different sources and variable transportation paths made the isotopic composition of water vapor over Chengdu significantly different, thus masking the influence of local meteorological conditions on the isotopic composition.

Conclusion

In this paper, a comparison of the stable isotope characteristics during dry and wet seasons in a subtropical monsoon climate region was carried out based on the year-round measured data. The results showed that the stable isotopes in precipitation presented obvious seasonal changes, more negative in wet season and less negative (or positive) in dry season. The LMWL of Chengdu lied between the southeast coast and the northern inland region of China, indicating that Chengdu is affected by both ocean and inland water vapor. The slope of LMWL in dry season was lower than that in rainy season, which indicated that the precipitation in dry season was affected by more intense sub-cloud secondary evaporation. The influence of local meteorological factors on isotopes was analyzed by simple and multiple regressions. The temperature effect and precipitation effect were not significant in both seasons, reflecting the masking effect of other factors. The relative humidity showed a negative correlation with the isotopes during dry and wet seasons, and the correlation difference reflected the strength of sub-cloud secondary evaporation. In a multiple regression that considered the combined influence of multi-factors, the correlation coefficient showed an improvement. The changes in water vapor source under the influence of monsoon reflected by d-excess explained the correlation between meteorological factors and isotopic composition in dry and wet seasons. Compared with the rainy season, more complicated water vapor sources and transport paths in the dry season made the impact of local meteorological variables on isotopes be masked to a greater extent.

REFERENCES

[1] Araguas-Araguas, L., Froehlich, K., Rozanski, K. (1998): Stable isotope composition of precipitation over southeast Asia. – Journal of Geophysical Research-Atmospheres 103: 28721-28742.

[2] Badaluta, C. A., Persoiu, A., Ionita, M., Nagavciuc, V., Bistricean, P. I. (2019): Stable H and O isotope-based investigation of moisture sources and their role in river and

http://www.aloki.hu ● ISSN 1589 1623 (Print) ● ISSN 1785 0037 (Online)
DOI: http://dx.doi.org/10.15666/aeer/1705_1197911993

groundwater recharge in the NE Carpathian Mountains, East-Central Europe. – Isotopes in Environmental and Health Studies 55.

[3] Balagizi, C. M., Kasereka, M. M., Cuoco, E., Liotta, M. (2018): Influence of moisture source dynamics and weather patterns on stable isotopes ratios of precipitation in Central-Eastern Africa. – Science of the Total Environment 628-629: 1058-1078.

[4] Cai, Z. Y., Tian, L. D., Bowen, G. J. (2017): ENSO variability reflected in precipitation oxygen isotopes across the Asian Summer Monsoon region. – Earth and Planetary Science Letters 475: 25-33.

[5] Celle-Jeanton, H., Gonfiantini, R., Travi, Y., Sol, B. (2004): Oxygen-18 variations of rainwater during precipitation: application of the Rayleigh model to selected rainfalls in Southern France. – Journal of Hydrology 289: 165-177.

[6] Chen, F. L., Zhang, M. J., Ma, Q., Wang, S. J., Li, X. F., Zhu, X. F. (2015): Stable isotopic characteristics of precipitation in Lanzhou City and its surrounding areas, Northwest China. – Environmental Earth Sciences 73: 4671-4680.

[7] Chen, F. L., Zhang, M. J., Wang, S. J., Qiu, X., Du, M. X. (2017): Environmental controls on stable isotopes of precipitation in Lanzhou, China: An enhanced network at city scale. – Science of the Total Environment 609: 1013-1022.

[8] Craig, H. (1961): Isotopic Variations In Meteoric Waters. – Science 133: 1702-1703.

[9] Crawford, J., Hollins, S. E., Meredith, K. T., Hughes, C. E. (2017): Precipitation stable isotope variability and subcloud evaporation processes in a semi-arid region. – Hydrological Processes 31: 20-34.

[10] Dansgaard, W. (1964): Stable Isotopes In Precipitation. – Tellus 16: 436-468.

[11] Deng, Z. M., Zhang, X., Pan, G. Y. (2016): Variations of Hydrogen and Oxygen Isotopes in Meteoric Precipitation in Wuhan, China. – Journal of Yangtze River Scientific Research Institute 33: 12-17.

[12] Dublyansky, Y. V., Klimchouk, A. B., Tokarev, S. V., Amelichev, G. N., Langhamer, L., Spotl, C. (2018): Stable isotopic composition of atmospheric precipitation on the Crimean Peninsula and its controlling factors. – Journal of Hydrology 565: 61-73.

[13] Goller, R., Wilcke, W., Leng, M. J., Tobschall, H. J., Wagner, K., Valarezo, C., Zech, W. (2005): Tracing water paths through small catchments under a tropical montane rain forest in south Ecuador by an oxygen isotope approach. – Journal of Hydrology 308: 67-80.

[14] Guan, H. D., Zhang, X. P., Skrzypek, G., Sun, Z., Xu, X. (2013): Deuterium excess variations of rainfall events in a coastal area of South Australia and its relationship with synoptic weather systems and atmospheric moisture sources. – Journal of Geophysical Research-Atmospheres 118: 1123-1138.

[15] He, Y. Q., Pang, H. X., Theakstone, W. H., Zhang, Z. L., Lu, A. G., Gu, J. (2006): Isotopic variations in precipitation at Bangkok and their climatological significance. – Hydrological Processes 20: 2873-2884.

[16] Pang, H. X., He, Y. Q., Lu, A. G., Zhao, J. D., Ning, B. Y., Yuan, L. L., Song, B. (2006): Synoptic-scale variation of $\delta^{18}O$ in summer monsoon rainfall at Lijiang, China. – Chinese Science Bulletin 51: 2897-2904.

[17] Peng, T. R., Huang, C. C., Chen, C. T., Chen, J. E., Liang, W. J. (2016): Using stable hydrogen and oxygen isotopes to reveal monsoonal and related hydrological effects on meteoric water in the Western Pacific monsoon region: A case study of the Ilan region, northeastern Taiwan. – Journal of Asian Earth Sciences 128: 105-115.

[18] Qu, S. M., Chen, X. Q., Wang, Y. F., Shi, P., Shan, S., Gou, J. F., Jiang, P. (2018): Isotopic Characteristics of Precipitation and Origin of Moisture Sources in Hemuqiao Catchment, a Small Watershed in the Lower Reach of Yangtze River. – Water 10.

[19] Srivastava, R., Ramesh, R., Gandhi, N., Jani, R. A., Singh, A. K. (2015): Monsoon onset signal in the stable oxygen and hydrogen isotope ratios of monsoon vapor. – Atmospheric Environment 108: 117-124.

http://www.aloki.hu ● ISSN 1589 1623 (Print) ● ISSN 1785 0037 (Online)
DOI: http://dx.doi.org/10.15666/aeer/1705_1197911993

[20] Wang, T., Chen, J. S., Ge, J., Zhan, L. C. (2017): Isotopic evidence of allogenic groundwater recharge in the Northern Ordos Basin. – Journal of Radioanalytical and Nuclear Chemistry 314: 1595-1606.
[21] Wang, L., Dong, Y., Han, D., Xu, Z. (2019): Stable isotopic compositions in precipitation over wet island in Central Asia. – Journal of Hydrology 573: 581-591.
[22] Wu, X. D. (2009): Stable isotope compositions for meteoric water from Chengdu and their implication of climate. – Acta Geologica Sinica 29: 52-58.
[23] Wu, H., Zhang, X., Xiaoyan, L., Li, G., Huang, Y. (2015): Seasonal variations of deuterium and oxygen-18 isotopes and their response to moisture source for precipitation events in the subtropical monsoon region. – Hydrological Processes 29: 90-102.
[24] Xia, C. C., Liu, G. D., Mei, J., Meng, Y. C., Liu, W., Hu, Y. (2019): Characteristics of hydrogen and oxygen stable isotopes in precipitation and the environmental controls in tropical monsoon climatic zone. – International Journal of Hydrogen Energy 44: 5417-5427.
[25] Xie, L., Wei, G., Deng, W., Zhao, X. (2011): Daily δ18O and δD of precipitations from 2007 to 2009 in Guangzhou, South China: Implications for changes of moisture sources. – Journal of Hydrology 400: 477-489.
[26] Xu, T., Sun, X. S., Hong, H., Wang, X. Y., Cui, M. Y., Lei, G. L., Gao, L., Liu, J., Lone, M. A., Jiang, X. Y. (2019): Stable isotope ratios of typhoon rains in Fuzhou, Southeast China, during 2013-2017. – Journal of Hydrology 570: 445-453.
[27] Yao, T. C., Zhang, X. P., Guan, H. D., Zhou, H., Hua, M. Q., Wang, X. J. (2018): Climatic and environmental controls on stable isotopes in atmospheric water vapor near the surface observed in Changsha, China. – Atmospheric Environment 189: 252-263.
[28] Zhai, Y. Z., Wang, J. S., Zhang, Y., Teng, Y. G., Zuo, R., Huan, H. (2013): Hydrochemical and isotopic investigation of atmospheric precipitation in Beijing, China. – Science of the Total Environment 456: 202-211.
[29] Zhang, X. P., Sun, W. Z., Liu, J. M. (2005): Stable isotopes in precipitation in the vapor transport path in Kunming of Southwest China. – Resources and Environment in the Yangtze Basin 14: 665-669.
[30] Zhang, X. P., Liu, J. M., Sun, W. Z., Huang, Y. M., Zhang, J. M. (2007): Relations between oxygen stable isotopic ratios in precipitation and relevant meteorological factors in southwest China. – Science in China Series D-Earth Sciences 50: 571-581.
[31] Zhao, P., Tan, L., Zhang, P., Wang, S., Cui, B., Li, D., Xue, G., Cheng, X. (2018): Stable Isotopic Characteristics and Influencing Factors in Precipitation in the Monsoon Marginal Region of Northern China. – Atmosphere 9: 97.
[32] Zheng, S. H., Hou, G. F., Ni, B. L. (1983): The studies of hydrogen and oxygen stable isotopes in atmospheric precipitation in China. – Chinese Science Bulletin 13: 801-806.
[33] Zhou, J. L., Li, T. Y. (2018): A tentative study of the relationship between annual delta O-18 & delta D variations of precipitation and atmospheric circulations-A case from Southwest China. – Quaternary International 479: 117-127.

http://www.aloki.hu ● ISSN 1589 1623 (Print) ● ISSN 1785 0037 (Online)
DOI: http://dx.doi.org/10.15666/aeer/1705_1197911993

REASONS FOR THE OCCURENCE OF SMALL FOREST PATCHES WITHIN POST-GLACIAL AREAS USED FOR AGRICULTURE IN NORTHERN POLAND

PIEŃKOWSKI, P.[1*] – PODLASIŃSKI, M.[2] – SZPIGIEL, M.[1]

[1]*Department of Ecology, Environmental Protection and Management, West Pomeranian University of Technology in Szczecin, al. Piastów 17, 70-310 Szczecin, Poland*

[2]*Department of Soil Science, Grasslands and Environmental Chemistry, West Pomeranian University of Technology in Szczecin, al. Piastów 17, 70-310 Szczecin, Poland*

**Corresponding author*
e-mail: pawel.pienkowski@zut.edu.pl; phone: +48-91-449-6347

(Received 25th Apr 2019; accepted 16th Jul 2019)

Abstract. Small forest patches (SFPs) are considered as one of the most important landscape elements, enriching the monotonous agricultural areas. Various studies focus on the ecological role of SFPs, however none provides a comprehensive characteristics of the reasons for their occurrence in post-glacial areas. The location of SFPs within field areas is not incidental, and the occurrence is mainly determined by physiographic factors which prevent or hinder the use of such areas for agriculture. To a large extent, the distribution of SFPs is determined by the origin of the given area which, in the case of Europe and North America, is related to ice sheets and their effects over millennia. Therefore, the aim of the present paper was the assessment of the reasons for the occurrence of SFPs within intensely cultivated agricultural post-glacial areas in Western Pomerania of Poland. It was found that the occurrence of SFPs is related to natural abiotic factors, the most important being gradient of a slope, presence of sandy soils and wetlands. Additionally, the significance of these factors, size of SFPs and their spatial characteristics to a large degree are determined by geomorphological variability of the area.
Keywords: *agricultural landscapes, small remnant habitats, landscape management, forest fragmentations, post-glacial areas*

Introduction

Small-scale landscape elements, such as small forest patches (SFPs), copses, avenues and scattered trees, constitute significant elements enriching the agricultural areas (Gibbons et al., 2008; van Zanten et al., 2016; Solon et al., 2017). Given the increasing intensification of agricultural activity leading to, among others, depletion of the natural environment heterogeneity, the importance of such elements is increasing (Myga-Piatek, 2010). Small forest patches provide, among other things, habitats for various plant and animal species displaced from anthropogenically transformed habitats (Graae, 2000; Lindgren, 2017; Michel et al., 2007; Yahner, 1986; Wuczyński, 2016; Gamrat and Gałczyńska, 2014; Farah et al., 2017; Stanton et al., 2018). Due to their location between larger forest complexes, SFPs act as stepping stone habitats which, similarly to ecological corridors, facilitate connection between landscapes (Jongman, 2002; Burger and Burger, 2005; Estreguil et al., 2013). Small forest patches and mid-field tree stands are considered to be not only an important element of agricultural landscape protection, but also to have a positive effect on biological as well as microclimatic conditions of the surrounding cultivated fields (Zajączkowski, 2005). They also play an important role in both the sequestration and storage of carbon (Brown and Fisher, 2009).

It is believed that intensively used agricultural landscape has a relatively low landscape aesthetic quality (Hermes et al., 2018), that is why numerous authors stress

http://www.aloki.hu ● ISSN 1589 1623 (Print) ● ISSN 1785 0037 (Online)
DOI: http://dx.doi.org/10.15666/aeer/1705_1199512011

the aesthetic and recreation value of SFPs (Arriaza et al., 2004; De Groot, 2006; Van Berkel and Verburg, 2014). In addition, SFPs often provide inspiration and complement cultural heritage (Power, 2010; Schaich et al., 2010; Myga-Piątek, 2012).

The ecological aspect of SFPs was analysed in numerous areas (Baudry et al., 2000; Ryszkowski et al., 2003; Decocq et al., 2016; Varela et al., 2018), however the reasons behind their occurrence within the prevalent agricultural landscape have not yet been fully established. Unarguably, their mid-field location is not incidental and is determined by physiographic factors which prevent or hinder the use of such areas for agriculture. To a large extent, distribution of SFPs is determined by the origin of the given area which, in the case of Europe and North America, is related to ice sheet and its effect over millennia (*Fig. 1*). Additionally, it is conditioned by anthropogenic impact, including economic considerations (Benoit et al., 2012), form of ownership (Crow et al., 1999), development of technology (Vejre and Brandt, 2004; Romanova, 2015), as well as political reasons (Bell et al., 2009).

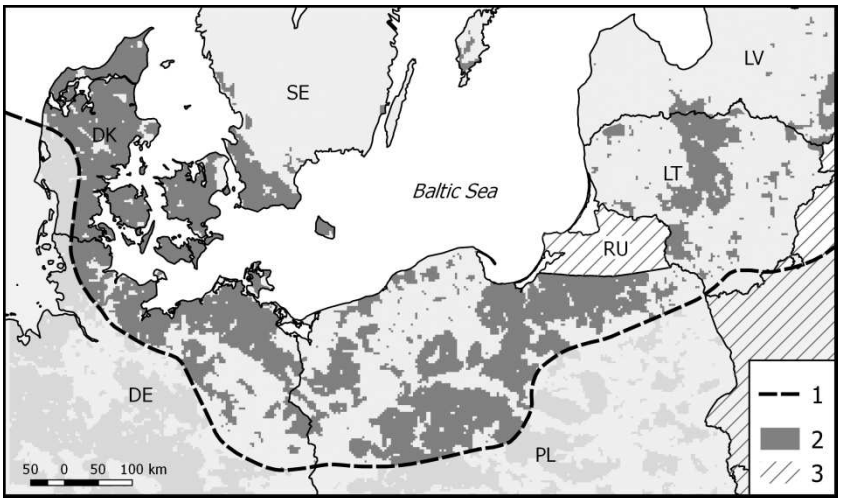

Figure 1. *Predominant agricultural landscape in the area of the last glacial period (based on Corine Land Cover 2000). 1 – limit of Weichselian glaciations, 2 – agricultural landscape, 3 – outside data coverage*

Within the area of intensively used agricultural landscape, the morphological features resulting from glacier retreat (terminal moraines, kames, eskers, dead-ice depression, tunnel valleys) determine the occurrence of small landscape elements including patches of sandy soils, non-runoff depressions (Pieńkowski, 2008) and steep slopes (Najwer et al., 2016). Post-glacial agricultural landscape is additionally diversified by the presence of linear forms, usually not related to physiography, e.g. roadside alleys and hedges (Lenschow, 2005). Given the increasing intensification of agricultural actions, all these forms are in danger of disappearing (Agger and Brandt, 1988; Pieńkowski et al., 2010; Kühne, 2018). It is estimated that in the 2009-2015 period alone, there was a decline in farmland area important to biodiversity in Germany of nearly 13% which, consequently, brought a reduction in the number of trees, hedges, copses and ditches (Agriculture Report, 2017).

Paradoxically, a continuous increase in tree stands has been observed in Europe since the 1960s (European Environment Agency, 2017). An increase in the forest area is also observed in post-glacial areas in Poland (Zając et al., 2014; Pieńkowski, 2015), and the

http://www.aloki.hu ● ISSN 1589 1623 (Print) ● ISSN 1785 0037 (Online)
DOI: http://dx.doi.org/10.15666/aeer/1705_1199512011

increase rate depends on the region (Żarska et al., 2016; Ciesielska and Ciesielski, 2017). However, global increase in forested area is mainly connected with expansion and consolidation of larger patches in the areas of soils of poor quality and does not apply to intensively cultivated areas, where the number of small and isolated forest patches is decreasing (Brown and Fisher, 2009).

The observed landscape simplification leads to reduction in ecosystem services on which agriculture depends. It is assumed that designing agricultural landscapes requires determination of the desired ecosystem services, evaluation of current landscape structure and implementation of targeted modifications (Landis, 2017). It seems reasonable to argue that determination of physiographical diversity of agricultural landscapes and identifying spatial elements determining the presence and distribution of potential biotopes characteristic for SFPs would be beneficial.

For all the reasons outlined above, the aim of the present paper was an attempt to distinguish these elements with respect to small forest patches. The authors believe that such identification and determination of spatial distribution can provide a significant criterion to be adopted in agricultural landscape planning.

Characteristics of the study area

The studied area of Western Pomerania is situated at 52° 51'N and 54° 06'N to 14° 31'E and 16° 17'E and covers the fragments of three macro-regions in Poland: South Pomeranian Lakeland, West Pomeranian Lakeland and the Szczecin Coastal Region. Land relief of these areas is the result of Scandinavian ice sheet in the Pleistocene glaciation. Therefore, predominant are sedimentary rocks of glacial (loam, sandy loam) and fluvial origin (sand). The effect of marine environment on the climate of this area is significant, as the mean air temperature in winter drops to just below 0 °C, whereas the mean annual air temperature amounts to 8.5 °C and is only slightly higher than the average for Poland. Mean annual precipitation sum amounts to 600-650 mm and precipitation occurring in the summer months is prevalent.

The current landscape was formed primarily in the last 16 thousand years, when in the vicinity of retreating glacier, a complex of post-glacial forms began to form as a result of ice sheet and meltwaters activity. Following the climatic change, the developing natural vegetation was preserved only partially, and the existing forest complexes in Western Pomerania are not of primary forest nature. Nevertheless, forest vegetation was found in great majority of areas of Pomerania. Only wetlands, inundated by floods and coastal quicksand were not covered by forest vegetation. With agricultural development and expansion of settlements, the area of cultivated lands increased, which was coupled with a decrease and fragmentation of the forest area. Changes with respect to intensity of land use were mainly determined by the type of soil. The largest forest complexes remained on sandy terrace plains, outwash plains and terminal moraines, whereas in morainic uplands agricultural use was, and still is, predominant (Pieńkowski and Podlasiński, 2002). At present, forest coverage of this area is 36.5% with pine tree being dominant in forests and Pomeranian beech forests in more fertile habitats. Agricultural use of land reaches 36.7% with cereals (mainly wheat) as the prevent crop followed by rapeseed, corn and sugar beet.

The six study sites (*Fig. 2*) were characterised by predominance of agricultural landscape and the largest number of SFPs areas, as compared with other locations. Selected characteristics of testing sites are presented in *Table 1*. Morainic upland is the

http://www.aloki.hu ● ISSN 1589 1623 (Print) ● ISSN 1785 0037 (Online)
DOI: http://dx.doi.org/10.15666/aeer/1705_1199512011

prevalent area, similarly to the whole region of Pomerania, particularly in the area of post-glacial agricultural landscape, where soils developed from loamy sands and clays.

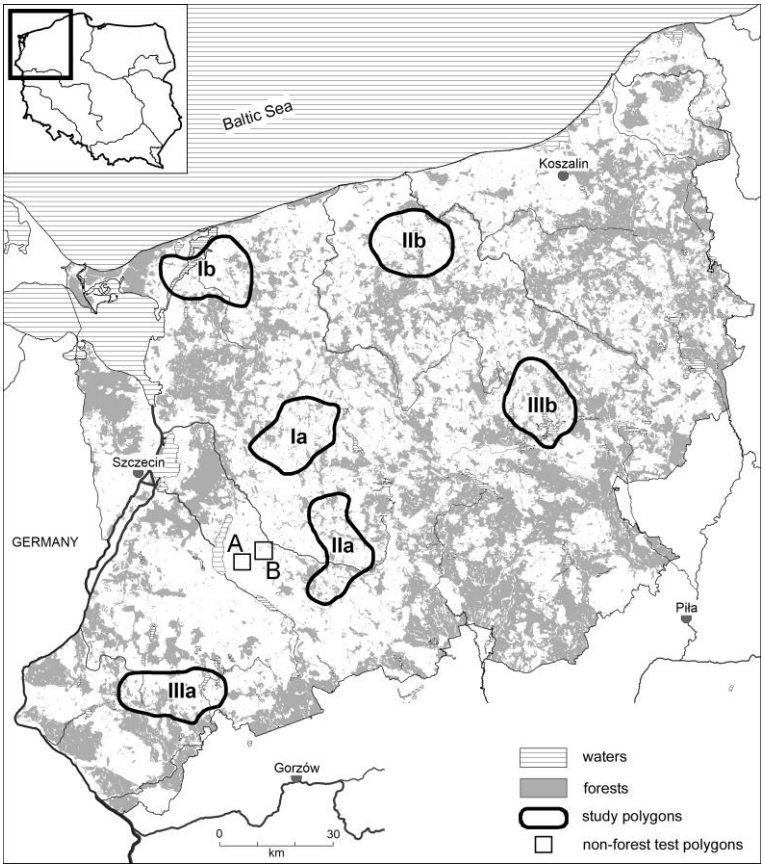

Figure 2. *Study sites in the selected area of Western Pomerania*

Table 1. *Selected properties of study polygons*

Number of polygons	Area [km^2]	Coordinates of polygon centroids		Range of height [m]	Woodiness [%]
Ia	301.1	15° 12’ 15”E	53° 35’45”N	44.0–116.7	16.7
Ib	301.1	14° 46’10”E	53° 56’ 02”N	0.0–31.8	15.0
IIa	301.2	15° 22’ 45”E	53° 18’ 00”N	27.0–103.0	23.1
IIb	301.1	15° 35’ 45”E	54° 01’ 40”N	3.1–85.0	18.2
IIIa	301.0	14° 46’10”E	52° 55’ 50”N	51.0–111.5	21.8
IIIb	301.0	16° 08’ 30”E	53° 39’ 10”N	8.0–221.6	25.4
A	9.0	15° 01’30”E	53° 15’ 20”N	26.7–38.0	0.0
B	9.0	15° 04’ 50”E	53° 16’ 05”N	21.0–42.9	1.1

The distinct nature of relief of the six selected study sites is to a large extent connected with diverse hypsometry. In the regions with high share of terminal moraines, there is a higher ratio of areas with surface inclination of more than 5%. The regions dominated by bottom moraines are characterised by areas of smaller inclination (*Table 2*). Among the analysed study sites, the greatest variability in terms of relief was

http://www.aloki.hu ● ISSN 1589 1623 (Print) ● ISSN 1785 0037 (Online)
DOI: http://dx.doi.org/10.15666/aeer/1705_1199512011

identified in site IIIb where areas of inclination of 5-10% covered 27.9% of the whole area. This was due to the presence of numerous terminal moraine hills in this region. The smallest terrain variability was identified in sites Ia and Ib where flat upland moraine is predominant. It is worth mentioning that all selected study sites were located outside large outwash plain patches which, due to poor quality of soil, are generally covered by forest vegetation.

Additionally, two study sites of an area of 900 ha and characterised by a total lack of forest vegetation were identified. In these areas, the method of identification developed in the present paper with the aim of facilitating determination of the potential of a given area for establishing SFPs was used. The area marked in *Figure 2* as A covers marginal plain, whereas site B flat upland area.

Table 2. *Percentage of average slope in research areas*

Dominated landform	Study area	Slope steepness [%]				
		0–5	5–10	10–18	18–27	> 27
I flat upland moraine	Ia	98.1	1.8	0.1	0	0
	Ib	95.3	4.3	0.4	0	0
II undulating upland moraine	IIa	86.7	11.3	1.9	0.1	0
	IIb	84.5	12.3	2.9	0.3	0
III hummocky upland moraine	IIIa	83.7	14.5	1.7	0.1	0
	IIIb	62.3	27.9	8.1	1.3	0.4
Total		85.10	12.02	2.52	0.30	0.07

Materials and methods

Areas with the largest number of SFPs within the landscape dominated by agricultural lands were defined by VMapL2 using the analysis assessing the distribution of patches centroids. Hot Spot Analysis module of CrimeStat software was used for this purpose (Smith and Bruce, 2008).

To identify the reasons for occurrence of SFPs, layers of VMapL2 were used in MapInfo software, showing the forest cover from the period 2002-2010, orthophotomaps (from 2010) and digital elevation model (DEM). For the purpose of soil conditions analysis, soil-agricultural maps in the scale 1:5000 were used.

For the assessment of the factor determining the presence of SFPs in a given area, a database was compiled. Single database record included an identifier of a given patch and fields proving characteristics: area [ha], centroid coordinates and the dominant factor determining the existence of a patch (W – land wetness, S – soil, H – hypsometry, O – other) identified by cartographic materials and field observations.

The selected landscape metrics were identified using *Fragstats 4.2* software (McGarigal et al., 2012) and the following was calculated:

- AREA_MN – mean area of patches [ha]
- CIRCLE_MN – metrics of the shape of patches showing their complexity; irrespective of the size of patches
- NNS – nearest neighbour distance – mean distance to the closest neighbouring patch [m]
- NNI – nearest neighbour index showing cluster distribution of centroids.

http://www.aloki.hu ● ISSN 1589 1623 (Print) ● ISSN 1785 0037 (Online)
DOI: http://dx.doi.org/10.15666/aeer/1705_1199512011

Results and discussion

Variable factors determining the existence of small forest patches

In many places in Europe, forest landscapes consist of patches of different quality, age, size and isolation, embedded in agricultural matrix (Decocq et al., 2016). Numerous authors called attention to the close link between the geomorphological conditions and agricultural or forest use of land (Iverson, 1988; Hietel et al., 2004; Wulf et al., 2010). However, the studies conducted so far concerned relatively large areas and did not include the reasons behind the occurrence of small forest patches. As opposed to large forest complexes, the presence of small forest patches is determined by abiotic components of relatively small sizes and, consequently, is more prone to transformation due to natural and anthropogenic factors. Particularly in northern Europe, numerous units established by ice sheets are characterised by small size. These are, among others, wet depressions, sandy soil enclaves and slopes of small size – the number, size and distribution of which are frequently connected with land relief. As opposed to flat outwash areas where large forest areas are predominant, morainic areas are dominated by agricultural matrix where the effect of abiotic factors on landscape structure, including distribution of SPFs and spatial patterns of fragmentation, is most evident.

The present paper presents the quantitative and qualitative analysis of these factors on a representative sample of 1237 small forest patches. The analysis of topographic and soil-agricultural maps, aerial photography, digital elevation model and field observations allowed to identify factors determining the existence of SFPs within agricultural land. It was found that the occurrence of SFPs was related to the presence of a series of mutually-interacting natural conditions which were grouped in categories (*Fig. 3*) including factors resulting from:

- Existence of poor soils (S) – of little use for agriculture,
- Area hypsometry (H) – large inclination limiting the agricultural use,
- Excessive land wetness (W) – unfavourable conditions for agricultural use of land.

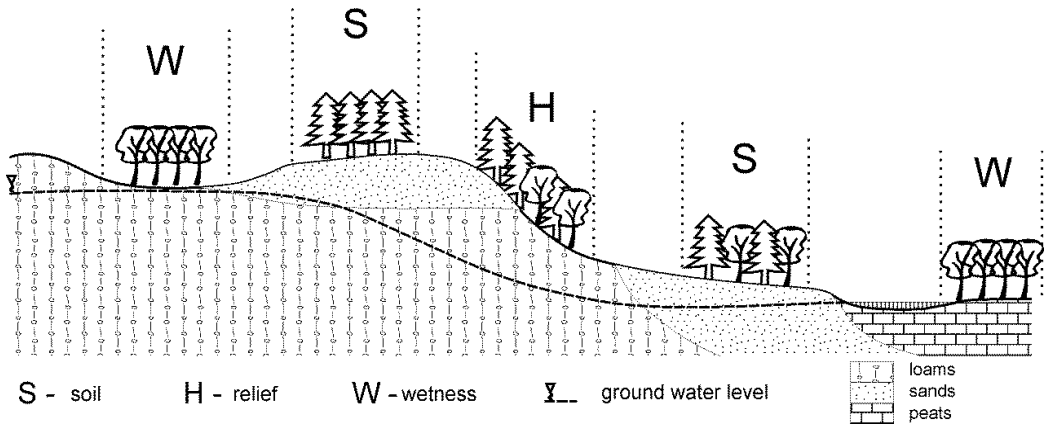

Figure 3. *Diagram illustrating the main abiotic factors determining the existence of SFPs*

In this paper, the category of "other" (O) was distinguished to group mainly the anthropogenic objects including: manor parks, recreational areas, reclaimed areas or discontinued excavation sites. There were no objects not related to the aforementioned factors, which clearly indicates the fact that, apart from the objects classified as "other",

http://www.aloki.hu ● ISSN 1589 1623 (Print) ● ISSN 1785 0037 (Online)
DOI: http://dx.doi.org/10.15666/aeer/1705_1199512011

the occurrence of SFPs in agricultural landscape is closely related to physiographic conditions preventing the agricultural use of a given area. Due to the fact that the patches were isolated from larger forest complexes and located on arable land, there were no other reasons for their existence – as defined by other authors (Erickson et al., 2002; Najwer et al., 2016) such as: area near existing woods, rocky ground and seasonally flooded area.

The selection of soil factor (S) referred to patches located in areas of undifferentiated hypsometry with soils unfit for agricultural use located on a flat area. However, in the case of forest patches located on the area with clear inclination and, at the same time, poor soil conditions, the determining factor was found to be hypsometry (H). Small forest patches located in wetland areas (most often hydrogenic soils) were classified as belonging to a group of objects related to land wetness factor (W). In only few cases (mainly larger objects), where the individual fragments of patches were determined by different conditions, the factor which affected the existence of the predominant area of a given patch was considered to be the dominant factor. Examples of SFPs with the analysis of reasons for their occurrence is presented in *Figure 4*.

Figure 4. *Forest patches in the predominantly agricultural landscape. The reasons for their occurrence: H – relief, W – wetness, S – soil, O – other*

http://www.aloki.hu ● ISSN 1589 1623 (Print) ● ISSN 1785 0037 (Online)
DOI: http://dx.doi.org/10.15666/aeer/1705_1199512011

Variability of the involvement of particular factors affecting the occurrence of SFPs most of all resulted from geomorphological conditions dominating the given area (*Figs. 5* and *6*). In undulating upland area (III), the patches occurring due to high land inclination were predominant. There were, among others, terminal moraine and kame hills of large inclination – more than 25% in both study sites. In the undulating upland area, the presence of SFPs was also attributed to the occurrence of numerous lakes of steep slopes. In the area IIIb, the patches related to a large altitude gradient constituted more than 50% of all recorded objects. However, in flat upland (I) and undulating upland (II) areas, the most common cause of SFPs occurrence was land wetness, often connected with the existence of bog. In the study site Ia, numerous bogs were located in Pomeranian marginal-stream valley, and in the study site Ib – the region of waterlogged subglacial valleys. Within the area of study site IIa, the patches were grouped in the area of the Ina River wide valley, whereas in study site IIb a large share of patches related to land wetness also resulted from the presence of two large bogged subglacial valleys nowadays used as riverbeds. On the slopes of valleys, a relatively large number of patches conditioned by land relief was also identified.

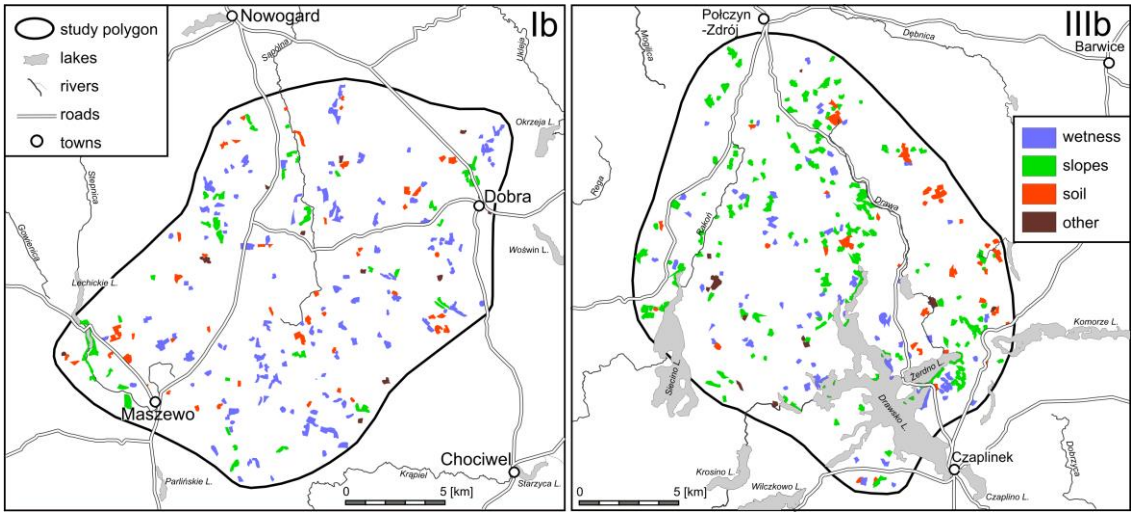

Figure 5. *Variability of the factors determining the occurrence of SFPs in the young glacial area of flat (Ib) and hummocky (IIIb) upland*

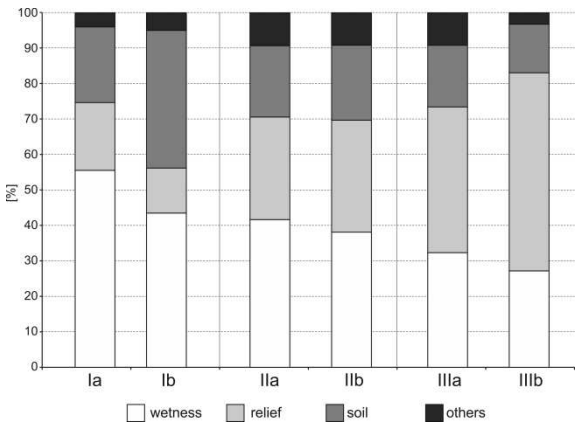

Figure 6. *Share of particular elements determining the occurrence of SFPs in the area of study sites*

http://www.aloki.hu ● ISSN 1589 1623 (Print) ● ISSN 1785 0037 (Online)
DOI: http://dx.doi.org/10.15666/aeer/1705_11995120111

Relatively high share of SFPs, occurrence of which was related to patches of soils of poor quality (38%), was found in study site Ia which, in turn, is attributed to the presence of high soil cover mosaicity manifested, among others, by the existence of small compartments of sandy soils.

The selection of the aforementioned factors allowed determination of the areas in terms of potential occurrence of SFPs in agricultural landscape. For this purpose, cartographic materials listed in the Materials and Methods section were used. In identification of the areas three factors were taken into consideration: altitude gradient of more than 15% which hinders agricultural use of the land (Prus and Budz, 2015), soils of sand granulation and wetlands.

Two study sites were identified in the intensively used agricultural area, characterised by a total lack of forests and SFPs (A and B in *Figs. 2* and *7*). These study sites are located in Pyrzyckie ice-dammed basin area which was used for agriculture as early as in the Neolithic period (Pospieszny, 2014). This ice-dammed basin constitutes the largest area of open landscape (Plit and Myga-Piątek, 2014). Both study sites are of different origin – study site A includes ice-dam level IV, study site B covers a fragment of flat morainic upland.

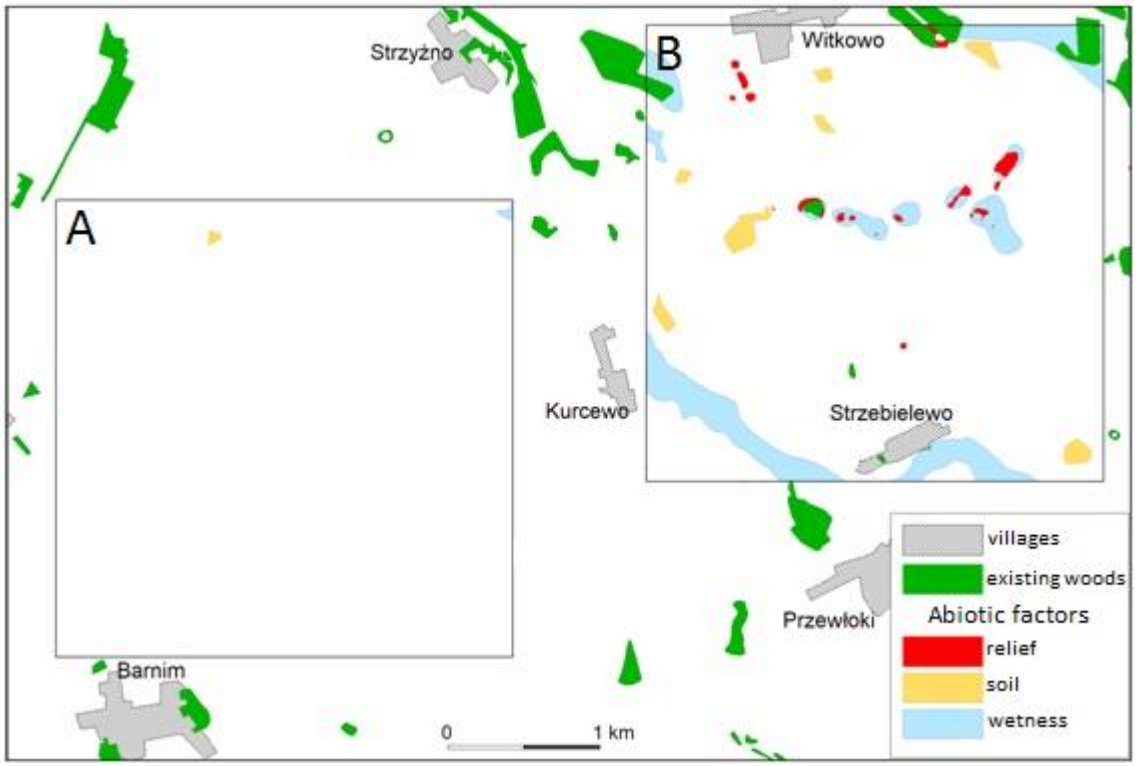

Figure 7. *Variability of the potential of two selected areas of Pyrzyckie ice-dammed basin for constituting possible location of SFPs*

From the perspective of factors conditioning the presence of SFPs, as adopted in this paper, the potential of both study sites for introducing SFPs to landscape is divergent. The analysis of cartographic materials clearly indicates that the first identified study site (A), with the exception of a small compartment of soils of poor quality, does not provide the conditions for the development of tree cover even in the smallest fragments.

http://www.aloki.hu ● ISSN 1589 1623 (Print) ● ISSN 1785 0037 (Online)
DOI: http://dx.doi.org/10.15666/aeer/1705_1199512011

This is due to homogenous flat area of soils of high quality and optimal moisture conditions. In turn, the other study site (B) is located on flat moraine upland with natural conditions of soil moisture, poor quality of soils and hypsometry which may be taken into consideration in possible establishing of SFPs for the purpose of enriching the agricultural landscape.

Selected spatial characteristics of SFPs

The ecological processes and species richness of agricultural landscape is affected by, among others, the size of SFPs, their shape and distribution against one another (Magura et al., 2001; Moser et al., 2002; Decocq et al., 2016). In the case of the smallest patches, the effect of the shape was found to be slight, however, in the case of larger objects, the complexity of the shape shows a significant effect on biodiversity (Heegaard et al., 2007).

The selected spatial characteristics of patches are presented in *Table 3*. It is difficult to attribute the variability between the study sites to a single dominant landform. However, the analysis of size distribution of patches on individual study sites shows a certain relationships. In all analysed study sites, similarly to post-glacial areas in North America (Host and White, 2003), there was a strong representation of lower size classes. Regardless of the origin, in all study sites there was a dominance of small patches of an area below 5 ha. The smallest (< 2.5 ha) occurred most often on hummocky uplands (*Fig. 8*), which can be attributed to frequent occurrence of small enclaves with different habitat conditions such as waterlogged land depressions, steep slopes and small patches of soils of poor quality. In undulating moraine area, and particularly in the area of flat moraine, larger patches (2.5–5.0) connected with relatively larger zones of depression and steep slopes were predominant.

In the study sites located on flat and undulating uplands, the highest mean size of the patches was found for the objects the origin of which was connected with the hypsometric factor (*Table 4*). These patches were characterised by the highest value of development index (Circle MN). This was mainly due to the presence of larger forest patches located in the area of longitudinal slopes surrounding the lakes and river valleys. In this group of patches, the highest mean values of Circle_MN index was found for SFPs in the study site Ia (0.67). In the hummocky upland area, the patches occurrence of which was related to hypsometry, showed relatively smaller size despite the most frequent occurrence. This can be connected with a small degree of radial relief of these areas and, consequently, relatively small and compact slope area of significant inclination.

Table 3. *Selected metrics of SFPs within the study sites area*

Dominated landform	Study area	Amount	Average area [ha]	NNS* [km]	NNI**
I flat upland moraine	Ia	224	3.7	523.7	0.86
	Ib	231	5.8	544.8	0.74
II undulating upland moraine	IIa	168	5.1	618.3	0.80
	IIb	181	3.7	594.6	0.78
III hummocky upland moraine	IIIa	163	4.8	656.0	0.87
	IIIb	270	3.3	468.8	0.77

*Nearest neighbour distance; **nearest neighbour index

http://www.aloki.hu ● ISSN 1589 1623 (Print) ● ISSN 1785 0037 (Online)
DOI: http://dx.doi.org/10.15666/aeer/1705_1199512011

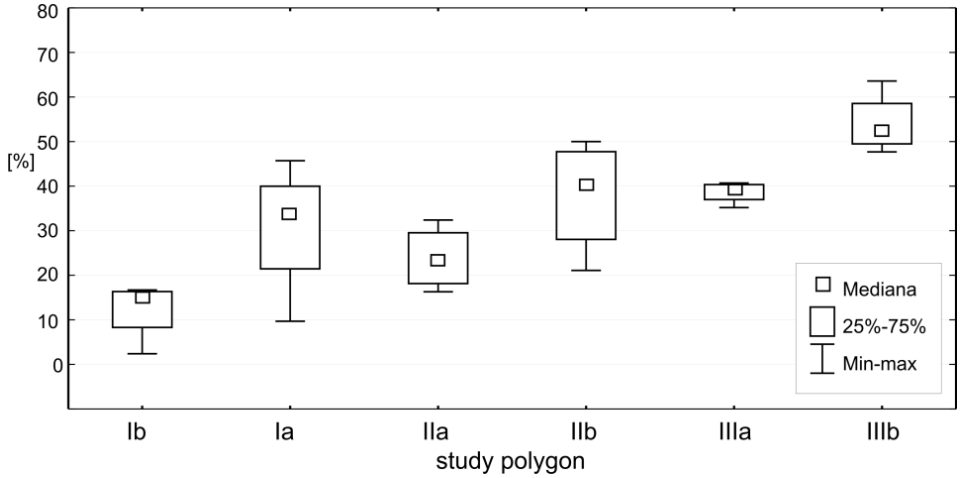

Figure 8. *Share of small patches (0.2-2 ha) within the study sites area*

Table 4. *Landscape metrics of forest patches with different genesis (explanations see Table 2)*

Factor	Study polygon	Amount	Mean area of patches AREA_MN [ha]	Metrics of the shape of patches CIRCLE_ MN	Nearest neighbour distance NNS [m]	Nearest neighbour index NNI
Wetness (W)	Ia	127	5.6	0.55	688.8	0.79
	Ib	96	3.1	0.58	738.5	0.76
	IIa	70	4.8	0.55	1023.2	0.85
	IIb	68	3.5	0.53	927.9	0.86
	IIIa	54	4.6	0.53	1029.4	0.81
	IIb	71	3.6	0.56	786.7	0.74
Relief (H)	Ia	42	7.4	0.67	1090.3	0.75
	Ib	31	6.4	0.62	1601.8	0.99
	IIa	49	5.9	0.61	1353.2	0.90
	IIb	57	6.2	0.61	870.7	0.79
	IIIa	67	4.4	0.53	1052.4	0.98
	IIIb	149	4.0	0.58	624.7	0.77
Soil (S)	Ia	50	4.7	0.50	1013.7	0.83
	Ib	83	3.6	0.56	846.6	0.79
	IIa	34	5.3	0.56	1243.3	0.72
	IIb	40	3.8	0.53	1301.5	1.03
	IIIa	27	5.6	0.55	1621.9	0.91
	IIIb	39	3.6	0.56	1491.8	0.88
Other (O)	Ia	12	3.3	0.46	4359.4	1.57
	Ib	14	2.8	0.54	2086.3	0.96
	IIa	15	4.3	0.48	3991.2	1.12
	IIb	16	2.4	0.49	3326.7	0.95
	IIIa	15	3.7	0.51	2256.2	1.17
	IIIb	11	1.8	0.46	3924.5	1.08

http://www.aloki.hu ● ISSN 1589 1623 (Print) ● ISSN 1785 0037 (Online)
DOI: http://dx.doi.org/10.15666/aeer/1705_1199512011

In all of the six analysed study sites, the patches categorised as "other" were characterised by the most compact size (circle-like). The values of Circle_MN index determined for the study sites Ia and IIb was only 0.46.

The mean distance to the nearest neighbour (NNS) was predominantly dependent on the number of patches in a given group. Accordingly, the smallest distance between the patches was found for the group of the most frequently occurring objects related to hypsometry in the study site IIIb (624.7 m). The greatest distance was found with respect to anthropogenic objects in the same study site (3924.5 m).

The values of the NNI index showing cluster nature of the analysed patches, ranged from 0.72 (IIa; factor S) to 1.57 (Ia, factor: O). Grouping of patches was found mainly for the patches occurrence of which was due to land wetness. The greatest dispersion of patches was found for the category of "other". This can be explained by their anthropogenic origin, not related to physiographical variability of the given area.

Conclusion

Until recently, agricultural landscape management constituted a compromise between "environment" and "development". However, recently more attention is paid to ecological and social benefits of actions undertaken as a part of landscape management (de Groot et al., 2010). Many currently developed agri-environmental programmes entail an increase in the amount and quality of forests within such areas. Still, information enabling the development of practical guidelines regarding the optimum spatial design is relatively scarce (Fuentes-Montemayor et al., 2012). Developing appropriate guidelines and implementing informed landscape policy is hindered by the fact that agricultural landscape in Europe alone is characterised by great variability due to, among others, climate, habitat as well as agricultural management (Van Zanten et al., 2014). Particularly the post-glacial areas are characterised by major differences concerning the forms determining the current fragmentation of forest area (Najwer et al., 2016). Therefore, all actions related to achieving optimum visual and spatial structure of landscapes should be implemented individually for such areas and take into consideration their physiographical features. This also concerns the practice of enriching the monotonous agricultural areas with small landscape elements, including small forest patches. Knowledge on abiotic elements which constitute, or may constitute, potential habitats for small forest patches is limited. There is a lack of information concerning the spatial patterns of fragmentation (patch isolation, size and edge), and on practical use of such patterns in implementation of agri-environmental programmes as well as price estimation of ecosystem services (Valdés et al., 2015). Good knowledge of spatial characteristics of particular abiotic elements, which could potentially form habitats for SFPs on diverse geomorphological units, may also be beneficial in the analysis of landscape transformation trends due to climate change, transformation of economic conditions and technological progress.

Within the analysed post-glacial area, the abiotic elements determining the presence of SFPs are mainly: gradient of slopes, occurrence of patches of sandy soils and land wetness. However, the share of these elements in particular land forms is different. On flat and rolling morainic uplands, the most frequent reason behind the occurrence of SFPs is land wetness, whereas on undulating morainic uplands the patches related to land slopes are predominant. It could be assumed that on flat upland moraine in particular, the forecasted climatic change (Erwin, 2009; Samaniego et al., 2018) could

http://www.aloki.hu ● ISSN 1589 1623 (Print) ● ISSN 1785 0037 (Online)
DOI: http://dx.doi.org/10.15666/aeer/1705_1199512011

be a decisive factor in excessive drying of small non-runoff depressions and facilitate transformation of these previously forested areas for agricultural use. The fact that the size of the SFPs occurring on that area is relatively small can only expedite this process. In turn, global warming and the resulting lowering of groundwater level (Taylor et al., 2013) most likely will not have a significant effect on the number of SFPs on hummocky upland, as on these areas the presence of SFPs is mostly connected with land relief. Regardless of geomorphological unit, excessive drying of patches of poor soil may lead to their exclusion from agricultural use and, as a result, spontaneous forestation and occurrence of shrubs – the fact already reported in some areas in Poland (Śmigielski et al., 2017).

Meeting the increasing demand for agricultural lands without disturbing the biological diversity is indeed a challenge for the 21st century in lowland agricultural landscapes (Decocq et al., 2016). Therefore, knowledge on the elements determining the occurrence of SFPs may also prove useful in identifying the optimum locations for the establishing of new forest patches in a view of minimisation of resulting economic costs. Increasing availability of a given area's resources resulting from, among others, the INSPIRE Directive, allows faster selecting of such habitats especially, as was identified in the present paper, due to the fact that that the post-glacial landscape of Western Pomerania offers a big potential for creation of such habitats. The authors believe that the obtained results may be useful in planning the design of agricultural landscapes for sustainable and resilient biodiversity. Information on the post-glacial areas potential for establishing small landscape elements and the analysis of spatial conditions should be considered as one of the key criteria in decision making process regarding enriching the monotonous agricultural landscape.

REFERENCES

[1] Agger, P., Brandt, J. (1988): Dynamics of small biotopes in Danish agricultural landscapes. – Landscape Ecology 1(4): 227-240.
[2] Agriculture Report (2017): Bioligical Diversity and Agriculture Landscapes. – Federal Ministry for the Environment, Nature Conservation, Building and Nuclear Safety (BMUB), Bonn.
[3] Arriaza, M., Cañas-Ortega, J. F., Cañas-Madueño, J. A., Ruiz-Aviles, P. (2004): Assessing the visual quality of rural landscapes. – Landscape and Urban Planning 69(1): 115-125.
[4] Baudry, J., Bunce, R. G. H., Burel, F. (2000): Hedgerows: An international perspective on their origin, function and management. – Journal of Environmental Management 60(1): 7-22.
[5] Bell, S., Nikodemus, O., Peneze, Z., Kruze, I. (2009): Management of cultural landscapes: what does this mean in the former Soviet Union? A case study from Latvia. – Landscape Research 34(4): 425-455.
[6] Benoit, M., Rizzo, E., Marraccini, A., Camilla, M., Enrico, B. (2012): Landscape agronomy: a new field for addressing agricultural landscape dynamics. – Landscape Ecology 27: 1385-1394.
[7] Brown, N., Fisher, R. (2009): Trees Outside Woods. – A Woodland Trust Publication, Grantham, UK.
[8] Burger, W., Burger, L. (2005): Conservation buffers. – Wildlife Trends 5(2): 2-8.
[9] Ciesielska, K., Ciesielski, M. (2017): Forest cover in different territorial profiles. – Wiadomości Statystyczne 5(672): 62-78.

http://www.aloki.hu ● ISSN 1589 1623 (Print) ● ISSN 1785 0037 (Online)
DOI: http://dx.doi.org/10.15666/aeer/1705_1199512011

[10] Crow, T. R., Host, G. E., Mladenoff, D. J. (1999): Ownership and ecosystem as sources of spatial heterogeneity in a forested landscape, Wisconsin, USA. – Landscape Ecology 14(5): 449-463.
[11] Decocq, G., Andrieu, E., Brunet, J., Chabrerie, O., De Frenne, P., De Smedt, P., Deconchat, M., Diekmann, M., Ehrmann, S., Giffard, B., Mifsud, E. G., Hansen, K., Hermy, M., Kolb, A., Lenoir, J., Liira, J., Moldan, F., Prokofieva, I., Rosenqvist, L., Varela, E., Valdés, A., Verheyen, K., Wulf, M. (2016): Ecosystem Services from Small Forest Patches in Agricultural Landscapes. – Current Forestry Reports 2(1): 30-44.
[12] De Groot, R. (2006): Function-analysis and valuation as a tool to assess land use conflicts in planning for sustainable, multi-functional landscapes. – Landscape and Urban Planning 75(3-4): 175-186.
[13] De Groot, R. S., Alkemade, R., Braat, L., Hein, L., Willemen, L. (2010): Challenges in integrating the concept of ecosystem services and values in landscape planning, management and decision making. – Ecological Complexity 7(3): 260-272.
[14] Erickson, D. L., Ryan, R. L., De Young, R. (2002): Woodlots in the rural landscape: Landowner motivations and management attitudes in a Michigan (USA) case study. – Landscape and Urban Planning 58(2-4): 101-112.
[15] Erwin, K. L. (2009): Wetlands and global climate change: The role of wetland restoration in a changing world. – Wetlands Ecology and Management 17(1): 71-84.
[16] Estreguil, C., Caudullo, G., de Rigo, D., San-Miguel-Ayanz, J. (2013): Forest landscape in Europe: pattern, fragmentation and connectivity. – EUR Scientific and Technical Research 25717: 1-18.
[17] European Environment Agency (2017): Unsustainable land use threatens European landscapes, Copenhagen. – www.eea.europa.eu/highlights/ unsustainable-land-use-threatens-european-landscapes.
[18] Farah, F. T., Muylaert, R. de L., Ribeiro, M. C., Ribeiro, J. W., Mangueira, J. R. de S. A., Souza, V. C., Rodrigues, R. R. (2017): Integrating plant richness in forest patches can rescue overall biodiversity in human-modified landscapes. – Forest Ecology and Management 397: 78-88.
[19] Fuentes-Montemayor, E., Goulson, D., Cavin, L., Wallace, J. M., Park, K. J. (2012): Factors influencing moth assemblages in woodland fragments on farmland: Implications for woodland management and creation schemes. – Biological Conservation 153: 265-275.
[20] Gamrat, R., Gałczyńska, M. (2014): Influence of the forest ecotone structure on the phytodiversity. – Sylwan 158(1): 34-40 (in Polish).
[21] Gibbons, P., Lindenmayer, D. B., Fischer, J., Manning, A. D., Weinberg, A., Seddon, J., Ryan, P., Barrett, G. (2008): The future of scattered trees in agricultural landscapes. – Conservation Biology 22(5): 1309-1319.
[22] Graae, B. J. (2000): The effect of landscape fragmentation and forest continuity on forest floor species in two regions of Denmark. – Journal of Vegetation Science 11(6): 881-892.
[23] Heegaard, E., Økland, R. H., Bratli, H., Dramstad, W. E., Engan, G., Pedersen, O., Solstad, H. (2007): Regularity of species richness relationships to patch size and shape. – Ecography 30(4): 589-597.
[24] Hermes, J., Albert, C., von Haaren, C. (2018): Assessing the aesthetic quality of landscapes in Germany. – Ecosystem Services 31: 296-307.
[25] Hietel, E., Waldhardt, R., Otte, A. (2004): Analysing land-cover changes in relation to environmental variables in Hesse, Germany. – Landscape Ecology 19(5): 473-489.
[26] Host, G. E., White, M. A. (2003): Contemporary forest composition and spatial patterns of north central and northeastern Minnesota: an assessment using 1990s Landsat data. – Minnesota Forest Resources Council Report LT-1203b, Duluth.
[27] Iverson, L. R. (1988): Land-use changes in Illinois, ASA: The influence of landscape attributes on current and historic land use. – Landscape Ecology 2(1): 45-61.

http://www.aloki.hu ● ISSN 1589 1623 (Print) ● ISSN 1785 0037 (Online)
DOI: http://dx.doi.org/10.15666/aeer/1705_1199512011

[28] Jongman, R. H. G. (2002): Homogenisation and fragmentation of the European landscape: Ecological consequences and solutions. – Landscape and Urban Planning 58(2-4): 211-221.
[29] Kühne, S. et al. (2018): Hecken und Raine in der Agrarlandschaft - Bedeutung, Neuanlage, Pflege. – Bundesanstalt für Landwirtschaft und Ernährung, Bonn.
[30] Landis, D. A. (2017): Designing agricultural landscapes for biodiversity-based ecosystem services. – Basic and Applied Ecology 18: 1-12.
[31] Lenschow, U. (2005): Landschaftsökologische Grundlagen zum Schutz, zur Pflege und zur Neuanlage von Feldhecken in Mecklenburg-Vorpommern. – Landesamt für Umwelt, Naturschutz und Geologie, Güstrow.
[32] Lindgren, J. (2017): Small remnant habitas. Important structures in fragmented landscapes. – Stockholm University. http://www.diva-portal.org/smash/record.jsf?pid=diva2%3A1154654&dswid=-814.
[33] Magura, T., Ködöböcz, V., Tóthmérész, B. (2001): Effects of habitat fragmentation on carabids in forest patches. – Journal of Biogeography 25: 129-138.
[34] Michel, N., Burel, F., Legendre, P., Butet, A. (2007): Role of habitat and landscape in structuring small mammal assemblages in hedgerow networks of contrasted farming landscapes in Brittany, France. – Landscape Ecology 22(8): 1241-1253.
[35] Moser, D., Zechmeister, H. G., Plutzar, C., Sauberer, N., Wrbka, T., Grabherr, G. (2002): Landscape patch shape complexity as an effective measure for plant species richness in rural landscapes. – Landscape Ecology 17(7): 657-669.
[36] Myga-Piątek, U. (2010): Transformation of cultural landscapes in the light of the idea of sustainable development. – Problems of Sustainable Development 5(1): 95-108.
[37] Myga-Piątek, U. (2012): Cultural Landscapes. Evolutionary and Typological Aspects. – University of Silesia, Katowice (in Polish).
[38] Najwer, A., Borysiak, J., Gudowicz, J., Mazurek, M., Zwoliński, Z. (2016): Geodiversity and biodiversity of the postglacial landscape (Dębnica River Catchment, Poland). – Quaestiones Geographicae 35(1): 5-28.
[39] Pieńkowski, P. (2008): Distribution of small, water-filled depressions as a component of the analysis of icesheet retreat dynamics in young glacial areas. – Landform Analysis 6: 41-46.
[40] Pieńkowski, P. (2015): Evaluation of the forest cover fragmentation in Western Pomerania. – Sylwan 159(7): 610-616 (in Polish).
[41] Pieńkowski, P., Podlasiński, M. (2002): Changes in forest cover of Szczecin Lowland from the 16th to the end of 20th century, in relation to soil cover. – Electronic Journal of Polish Agricultural Universities 5(2).
[42] Pieńkowski, P., Kupiec, M., Smoter, P. (2010): Changes of selected landscape components in neighbouring areas of Ina and Mała Ina catchments in 20th C. – Prace Komisji Krajobrazu Kulturowego 13: 54-62 (in Polish).
[43] Plit, J., Myga-Piątek, U. (2014): The degree of landscape openness as a manifestation of cultural metamorphose. – Quaestiones Geographicae 33(3): 145-154.
[44] Pospieszny, L. (2014): The Neolithic Landscapes of the Polish Lowlands. Earthen Long-Barrows and Their Histories. – In: Asa, L. P.-D., Larsson, M. (eds.) Uniting Sea II Stone Age Societies in the Baltic Sea Region. Opia 51. Uppsala University, Uppsala, pp. 147-170.
[45] Power, A. G. (2010): Ecosystem services and agriculture: tradeoffs and synergies. – Philosophical Transactions of the Royal Society B: Biological Sciences 365(1554): 2959-2971.
[46] Prus, B., Budz, Ł. (2015): Analysis of relief impact on land structure on an example of Nowy Targ District. – Infrastructure and Ecology of Rural Areas 2(II): 438-497.
[47] Romanova, E. A. (2015): Land use, settlement, and modern landscapes. – International Journal of Economics and Financial Issues 5(5): 25-29.

http://www.aloki.hu ● ISSN 1589 1623 (Print) ● ISSN 1785 0037 (Online)
DOI: http://dx.doi.org/10.15666/aeer/1705_1199512011

[48] Ryszkowski, L., Karg, J., Bernacki, Z. (2003): Biocenotic function of the midfield woodlots in west Poland: Study area and research assumptions. – Polish Journal of Ecology 51(3): 269-281.
[49] Samaniego, L., Thober, S., Kumar, R., Wanders, N., Rakovec, O., Pan, M., Zink, M., Sheffield, J., Wood, E. F., Marx, A. (2018): Anthropogenic warming exacerbates European soil moisture droughts. – Nature Climate Change 8(5): 421-426.
[50] Schaich, H., Bieling, C., Plieninger, T. (2010): Linking ecosystem services with cultural landscape research. – GAIA - Ecological Perspectives for Science and Society 19(4): 269-277.
[51] Śmigielski, M., Pijanowski, J. M., Gniadek, J. (2017): Forest succession and afforestation of agricultural land as a current challenge agricultural works. – Acta Sci. Pol. Formatio Circumiectus 16(4): 51-63.
[52] Smith, S., Bruce, C. (2008): CrimeStat III. Workbook. – The National Institute of Justice, Washington.
[53] Solon, J., Roo-Zielińska, E., Affek, A., Kowalska, A., Kruczkowska, B., Wolski, J., Degórski, M., Grabińska, B., Kołaczkowska, E., Regulska, E., Zawiska, I. (2017): Ecosystem Services in a Postglacial Landscape – Assessment of Potential and Utilisation. Institute of Geography and Spatial Organization, PAS, Warsaw.
[54] Stanton, R. L., Morrissey, C. A., Clark, R. G. (2018): Analysis of trends and agricultural drivers of farmland bird declines in North America: a review. – Agriculture, Ecosystems and Environment 254: 244-254.
[55] Taylor, R. G., Scanlon, B., Döll, P., Rodell, M., Van Beek, R., Wada, Y., Longuevergne, L., Leblanc, M., Famiglietti, J. S., Edmunds, M., Konikow, L., Green, T. R., Chen, J., Taniguchi, M., Bierkens, M. F. P., Macdonald, A., Fan, Y., Maxwell, R. M., Yechieli, Y., Gurdak, J. J., Allen, D. M., Shamsudduha, M., Hiscock, K., Yeh, P. J. F., Holman, I., Treidel, H. (2013): Ground water and climate change. – Nature Climate Change 3(4): 322-329.
[56] Valdés, A., Lenoir, J., Gallet-Moron, E., Andrieu, E., Brunet, J., Chabrerie, O., Closset-Kopp, D., Cousins, S. A. O., Deconchat, M., De Frenne, P., De Smedt, P., Diekmann, M., Hansen, K., Hermy, M., Kolb, A., Liira, J., Lindgren, J., Naaf, T., Paal, T., Prokofieva, I., Scherer-Lorenzen, M., Wulf, M., Verheyen, K., Decocq, G. (2015): The contribution of patch-scale conditions is greater than that of macroclimate in explaining local plant diversity in fragmented forests across Europe. – Global Ecology and Biogeography 24(9): 1094-1105.
[57] Van Berkel, D. B., Verburg, P. H. (2014): Spatial quantification and valuation of cultural ecosystem services in an agricultural landscape. – Ecological Indicators 37(A): 163-174.
[58] Van Zanten, B. T., Verburg, P. H., Espinosa, M., Gomez-Y-Paloma, S., Galimberti, G., Kantelhardt, J., Kapfer, M., Lefebvre, M., Manrique, R., Piorr, A., Raggi, M., Schaller, L., Targetti, S., Zasada, I., Viaggi, D. (2014): European agricultural landscapes, common agricultural policy and ecosystem services: a review. – Agronomy for Sustainable Development 34(2): 309-325.
[59] Van Zanten, B. T., Zasada, I., Koetse, M. J., Ungaro, F., Häfner, K., Verburg, P. H. (2016): A comparative approach to assess the contribution of landscape features to aesthetic and recreational values in agricultural landscapes. – Ecosystem Services 17: 87-98.
[60] Varela, E., Verheyen, K., Valdés, A., Soliño, M., Jacobsen, J. B., De Smedt, P., Ehrmann, S., Gärtner, S., Górriz, E., Decocq, G. (2018): Promoting biodiversity values of small forest patches in agricultural landscapes: Ecological drivers and social demand. – Science of the Total Environment 619-620: 1319-1329.
[61] Vejre, H., Brandt, J. (2004): Contemporary Danish landscape research. – Belgeo (23): 223-230.
[62] Wuczyński, A. (2016): Farmland bird diversity in contrasting agricultural landscapes of southwestern Poland. – Landscape and Urban Planning 148: 108-119 (in Polish).

http://www.aloki.hu ● ISSN 1589 1623 (Print) ● ISSN 1785 0037 (Online)
DOI: http://dx.doi.org/10.15666/aeer/1705_1199512011

[63] Wulf, M., Sommer, M., Schmidt, R. (2010): Forest cover changes in the Prignitz region (NE Germany) between 1790 and 1960 in relation to soils and other driving forces. – Landscape Ecology 25(2): 299-313.
[64] Yahner, R. H. (1986): Structure, seasonal dynamics, and habitat relationships of avian communities in small even-aged forest stands. – Wilson Bulletin 98(1): 61-82.
[65] Zając, S., Kaliszewski, A., Młynarski, W. (2014): Forests and forestry in Poland and other EU countries. – Folia Forestalia Polonica, Series A 56(4): 185-193.
[66] Zajączkowski, K. (2005): Regionalization of Agricultural Landscape Needs or Shelterbelts and Woodlots in Poland. – Forest Research Institute, Warsaw (in Polish).
[67] Żarska, B., Fornal-Pieniak, B., Zaraś-Januszkiewicz, E. (2016): Areas designated for afforestation and areas excluded from afforestation – selected aspects related to the protection of the landscape in view of Poland experience. – Ecological Questions 22: 17-22.

http://www.aloki.hu ● ISSN 1589 1623 (Print) ● ISSN 1785 0037 (Online)
DOI: http://dx.doi.org/10.15666/aeer/1705_1199512011

EFFECTS OF TREATMENT WITH *TRICHODERMA HARZIANUM* AND SOME PLANT ACTIVATORS ON POST-HARVEST DECAY OF APPLE BLUE MOLD *(PENICILLIUM EXPANSUM* LINK.) AND BROWN ROT (*MONILINIA FRUCTIGENA* HONEY EX WHETZEL)

YILDIZ, C.[1] – COSKUNTUNA, A.[2*]

[1]*Istanbul Directorate of Provinical Agriculture and Forestry, Ministry of Agriculture and Forestry, Rebuplic of Turkey, 34728 Kadikoy, Istanbul, Turkey*
(e-mail: cihan.yildiz@tarimorman.gov.tr; phone: +90-216-468-2100)

[2]*Department of Plant Protection, Agriculture Faculty, Tekirdag Namik Kemal University, 59030 Tekirdag, Turkey*

**Corresponding author*
e-mail: acoskuntuna@nku.edu.tr phone: +90-282-250-2083

(Received 25th Apr 2019; accepted 2nd Jul 2019)

Abstract. The post-harvest application of *Trichoderma harzianum* proved to be effective in the control of blue mold and brown rot on apple. The possibilities of separately application of harpin protein (hp) and *Lactobacillus acidophilus*'s fermentation product (Lafp) and boscalid+pyraclostrobin fungicide were evaluated to the shelf-life of apples. TRIC8 and the plant activators applied to the fruits one hour before pathogens inoculations. The apples were inoculated with a micropipette via the artificially created wounds with the pathogens *P. expansum* and *M. fructigena* with suspensions of 1×10^6 conidia/mL^{-1}. After one hour the pathogens inoculations, the fungicide was sprayed onto the fruits at recommended dosage. The apples were stored at (22±2°C) for ten days. TRIC8 was reduced lesion diameter of *P. expansum* and *M. fructigena* by 69.73% and 97.13% respectively. Significant results on brown rot was provided by the application of Lafp (100%) but not had same success on blue mold (29.59%). Hp was provided to reduction of lesion diameter on blue mold and brown rot at 29.76% and 41.65%, respectively. The fungicide demonstrated 37.22% and 100% control of blue mold and brown rot on the apples in the shelf-life study, respectively.
Keywords: *apple, biological control, blue mold, brown rot, harpin protein, Lactobacillus acidophilus, post-harvest*

Introduction

Apple (*Malus domestica*) is an economically important crop in Turkey. According to 2017 data, there were produced 3.032164 tons of apple in the field of 175.357 ha in Turkey (FAOSTAT, 2017). The rate of loss of fresh fruits and vegetables after harvest is 25% in developed countries; however, it can increase to 50% in developing countries (Salunkhe and Kadam, 1998). Fruits and vegetable continue to physiological events such as respiration, sweating, and ethylene production after the harvest. In storage as well, fruits that continue physiological activities like respiration, transpiration, and so on, are exposed to activities of fungal pathogens present in the environment, as well as to biochemical and physical changes. Pathogen fungi cause postharvest disease are usually passive pathogens that can only entrance into wounds on fruit. The fruit are susceptible to the decay caused by several pathogenic fungi including *Penicillium* sp., *Geotrichum* sp., *Rhizopus* sp., *Phytophthora* sp., *Monilinia sp.* and *Botrytis* sp. (Barad, 2016; Benli, 2003; Errampalli et al.,2004; 2005; Fiori et al., 2008; Chávez et al., 2014).

http://www.aloki.hu ● ISSN 1589 1623 (Print) ● ISSN 1785 0037 (Online)
DOI: http://dx.doi.org/10.15666/aeer/1705_1201312022

More than 90 fungal pathogen species have been reported as causal agents in apple decay during storage (Jones and Aldwinckle, 1990).

To control blue mold disease caused by *P. expansum*, is the most common wound pathogen during harvest, transport and storage. So, store should be cleaned, ventilated, disinfected before the fruits are stored, and excessive humidity should be avoided (Ozgonen and Kilic, 2013). Little is known about to mechanism used to decay of caused by *P. expansum* on apple. The secretion of pectolytic enzymes have an important role on pathogenicity. On the other hand patulin known as secondary toxic metabolite that produce by blue mold (Morales et al., 2010; Barad et al., 2016; Snini et al., 2016). *M. fructigena* is a common species of *Monilinia* found on apples and pears in Europe, and is commonly referred to as "apple brown rot" (Jones and Aldwinckle, 1990; Leeuwen et al., 2002). Of pome fruits, apple and pear are sensitive to brown rot disease caused by *M. fructigena,* and of stone fruits, plum is sensitive to brown rot disease (Byrde and Willets, 1977). *M. fructigena* has been reported to infect in more than 40 hosts. These include apples, pears, quince, apricots, peaches, plums and cherries (Sagasta, 1977). Post-harvest disease control is achieved by the use of synthetic fungicides such as sodium *ortho*-phenylphenate, imazalil or thiabendazole (Penrose et al., 1989; Yildiz et al., 2005). Use of the fungicides provides satisfactory control against mold infection. But fungicidal residues can have harmful effect on people and environment. The global trend appear to reduced use of fungicides on produce and demand for reducing disease loss in the harvested commodities (Sharma et al., 2009). So, development of alternative control possibilities has become very important because of the need to reduce the use of fungicides, their residues, concerns about human health and environmental pollution, and development of fungicide-resistant strains for pathogenic fungi (Capdeville et al., 2002; Calvo et al., 2017). Nowadays the researches on using biocontrol agents and alternative chemicals and hot-water treatments on postharvest diseases have been increasing (Falconi and Mendgen, 1994; Janisiewicz et al., 1994; Hong et al., 1998; Ippolito, 1998; Benli, 2003; Li and Yu, 2000; Karabulut et al., 2002; Capdeville et al., 2002, 2003; Irina et al., 2006; Wang et al., 2008; Fiori et al., 2008; Manso and Nunes, 2011; Amiri and Bompeix, 2011; Haıssam et al., 2011; Mari et al., 2012; Zhao et al., 2012; Li et al., 2015; Yaseen et al., 2015; Zhu et al., 2016; Kabelitz et al., 2018). Some antagonistic yeasts such as *Candida sake* Satio & Ota, *C. oleaphila* Montrocher, *C. saitona* Nakase & Sutuki, were used to controlling decay of apple and pear caused by *B. cinerea* Pers.: Fries and *P. expansum* Link. (Sharma et al., 2009). Bacteria as antagonist biological control agents such as *Bacillus amyloliquefaciens* BUZ-14 and *Aureobasidium pullulans* and *Pseudomonas fluorescens* have been used against blue mold in apples (Vinas et al., 1998; Ippolito et al., 2000; Mari et al., 2012; Calvo et al., 2017; Wang et al., 2018).

The aim of the study the control possibilities of blue mold disease caused by *P. expansum* and brown rot caused by *M. fructigena*, with *T. harzianum* (TRIC8), harpin protein (hp), *Lactobacillus acidophilus*'s fermentation product (Lafp), and with boscalid+pyraclostrobin was evaluated to extend the self life of the apples.

Materials and methods

Fruit

Granny Smith apple cultivars not treated with pesticides were harvested in Tekirdag Viticulture Research Institute orchards, Turkey. Healthy fruits were selected without

http://www.aloki.hu ● ISSN 1589 1623 (Print) ● ISSN 1785 0037 (Online)
DOI: http://dx.doi.org/10.15666/aeer/1705_1201312022

physical injuries. The apples were surface disinfected with 70% ethanol and rinsed in sterile distilled water (SDW), dried at room temperature (24 °C).

Pathogens and antagonist isolates

In the study, *P. expansum* was isolated from decayed apples and other pathogen isolate *M. fructigena* (MON14) and biological control antagonist isolate *T. harizanum* (TRIC8, Accession number: MH351669) were provided by Prof. Dr. Nuray Ozer, Tekirdag Namik Kemal University, Agricultural Faculty, Department of Plant Protection.

Postharvest treatments of apples

P. expansum isolate and *T. harzianum* TRIC8 antagonist isolate were grown on potato dextrose agar (PDA) and incubated at 24 °C for 7 days. Petri dishes containing vegetable juice agar (V8 agar) was inoculated with *M. fructigena* isolate (MON14) and incubated at 24 °C for 10 days. The concentration of the *P. expansum* and *M. fructigena* were adjusted to 1×10^6 conidia/mL^{-1} with the aid of a thoma slide. Artificial wounds were performed using sterile needle to make 2 mm deep and 2 mm wide wounds (two wounds for each the apple) along the fruit equatorial areas. Spore suspension of *T. harzianum* (TRIC8) was counted with a thoma slide and adjusted to concentration 1×10^8 conidia/mL^{-1}. Firstly, each wound on apple was inoculated with 20 µL drop of 1×10^8 conidia/mL^{-1} of TRIC8 and left for incubation at room temperature (22 ± 2 °C) for one hour. After one hour, the apples treated with TRIC8 were inoculated with a micropipette into the wounded points with 20 µL drop of 1×10^6 conidia/mL^{-1} of the pathogens.

1% Harpin protein (Hp) (WDG formulation, Eden Bioscience Co.; Messenger Gold, 12 g/100 l water) (Wang et al., 2008). *Lactobacillus acidophilus'*s fermentation product (Lafp) (Alltech Crop Science; ISR 2000; 100 ml/da) (Boyraz et al., 2006). Hp and Lafp plant activators were dissolved in SDW and then sprayed with commercial dosage to fruits one hour before pathogens inoculations.

However, to compare the results of chemical reactions with *T. harzianum* and plant activators, the test fungicide 25.2% boscalid + 12.8% pyraclostrobin (Basf®, Bellis WG; 50 g/100 l water) was applied with the commercial dose by spraying one hour after the inoculation of the pathogens. To maintain humidity environment, two wet papers were placed in each plastic box was wrapped in an unsealed 0.05 mm polyethylene bag. The development of the diseases were determined by measuring the lesion diameters of decay on apples inoculated with 10^6 spores mL^{-1} pathogens inoculum and incubated for 10 days at 24 °C (22 ± 2 °C). Mean lesion diameter was calculated at the end of the study. Non-inoculated with the pathogens: 20 µl drop Sterile Distilled Water (SDW) was used only for each wound on apple in our study as negative control. Each treatment was independently performed two times with five replicate fruit; in each experiment twenty fruit per treatments were included.

We used to the effectiveness of the applications was calculated using Abbott's formula (Abbott, 1925; *Eq 1*):

$$\% \text{ effectiveness} = [(Ic - It) / Ic] \times 100 \qquad \text{(Eq 1.)}$$

http://www.aloki.hu ● ISSN 1589 1623 (Print) ● ISSN 1785 0037 (Online)
DOI: http://dx.doi.org/10.15666/aeer/1705_1201312022

Where: Ic is the disease diameter of the untreated control (+), It is the disease diameter of the treatment.

Statistical analysis

At the end of the storage period, the severity of the diseases was determined by the mean lesion diameter in millimetre on the rotted apples. Statistical significance was judged at level $P \leq 0.05$. When the analysis was statistically significant, the Duncan multiple comparison test was used for means separation. SPSS (Statistical Package for Social Sciences, Inc., 2001, Model 11.0 Chicago) was used analysis program.

Results

The results of this study demonstrated that post-harvest applications of the TRIC8 significantly controlled blue mold caused by *P. expansum* on apple at the rate of 69.73%. This effect was found to be significant at $P \leq 0.05$ level. While the mean lesion diameter of *P. expansum* growth of untreated apples was 5.90 cm, the apples treated with TRIC8 had 1.79 cm, at 10^{th} day. The mean lesion diameters of the hp and Lafp treated apples were 4.14 cm and 4.16 cm, respectively, with both plant activators being equally effective (□29.00%) in reducing decay. The control of blue mold by boscalid+pyraclostrobin indicates that is not highly effective (37.22%) against the sporulation of *P. expansum* in the self-life condition (*Table 1*; *Fig. 1*).

Table 1. *Effects of treatments on lesion development of P. expansum on apple fruits*

Treatments	Lesion diameter (cm)	Effect (%)
Inoculated control	5.90 a	0.00 c
T. harzianum TRIC8	1.79 c	69.73 a
hp	4.14 b	29.76 b
Lafp	4.16 b	29.59 b
B+p (fungicide)	3.56 b	37.22 b

Means of treatment within the same column followed by different letters are significantly (P≤0.05) different according to Duncan's multiple range test.

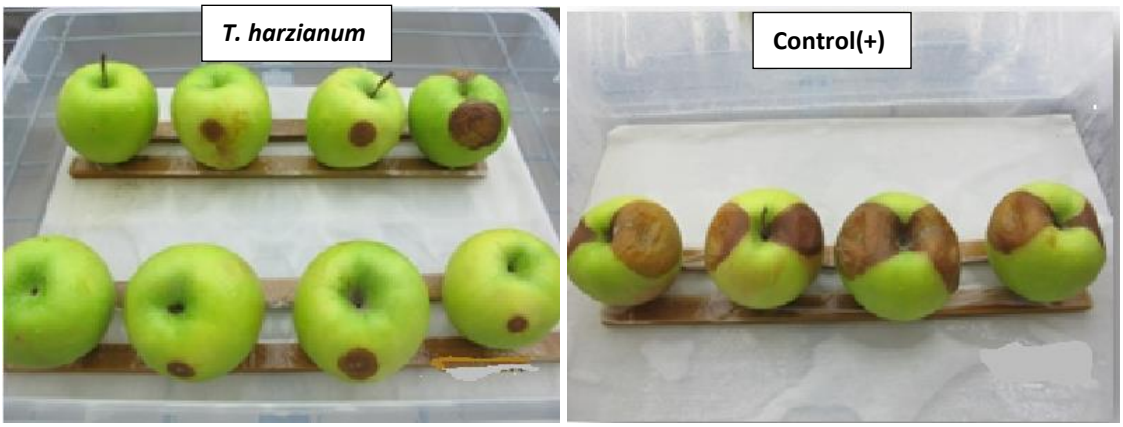

Figure 1. *Biocontrol activity of T. harzianum TRIC8 in inhibiting blue mold caused by P. expansum on apples*

http://www.aloki.hu ● ISSN 1589 1623 (Print) ● ISSN 1785 0037 (Online)
DOI: http://dx.doi.org/10.15666/aeer/1705_1201312022

The results show that TRIC8 is also effective on the mean lesion diameter of *M. fructigena* on apple. While the mean lesion diameter of *M. fructigena* growth of untreated apples was 7.50 cm, the apples treated with TRIC8 had 0.21 cm, at 10th day. The effect of TRIC8 treatment on brown rot was calculated as 97.13%. This value was significantly as statistically (P≤0.05). The mean lesion diameters of the hp and Lafp treated apples were 4.23 cm and 0.00 cm, respectively. Lafp treatment had a significantly greater effect (100%) in reducing decay than hp (41.65%) treatment (*Table 2*) (*Fig. 2*) (*P ≤ 0.05*).

Table 2. *Effects of treatments on lesion development of M. fructigena on apple fruits*

Treatments	Lesion diameter (cm)	Effect (%)
Inoculated control	7.50 a	0.00 c
T. harzianum TRIC8	0.21 b	97.13 a
hp	4.23 b	41.65 b
Lafp	0.00 c	100.00 a
B+p (fungicide)	0.00 c	100.00 a

Means of *M. fructigena* lesions diameter within each column followed by different at (P≤0.05) according to Duncan's multiple range test.

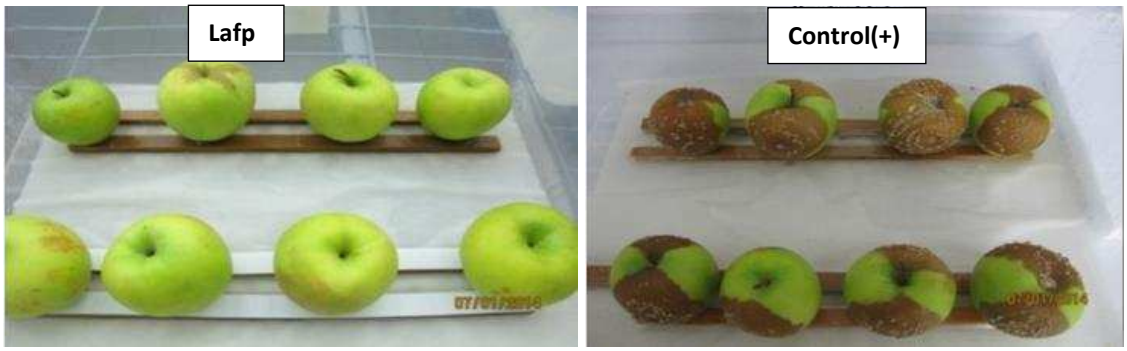

Figure 2. *Plant activator of Lafp in inhibiting brown rot caused by M. fructigena on apples*

Significant differences (P≤0.05) were obtained in *M. fructigena* lesion diameters on wounded the apples when treated with the B+p compared to the treatment with only inoculated *M. fructigena* on the apple (*Table 2*).

Discussion

T. harzianum TRIC8 treatment had a significantly greater effect in reducing decay caused by *M. fructigena* than either decay caused by *P. expansum*. The effectiveness of TRIC8 against both blue mold and brown rot of apple were significantly statistically (P≤0.05). TRIC8 isolate of *T. harzianum* proved its antagonistic potential in controlled reducing blue mold and brown rot on Grany Smith apple cultivars. When the apple treated with TRIC8, demonstrated postharvest pathogens of fruit has the ability to be efficient at 1×10^{8} conidia/mL^{-1} concentration. In apples, Batta (2004) observed low effect (48.8%) of formulated *T. harzianum* against the blue mold on apple is

http://www.aloki.hu ● ISSN 1589 1623 (Print) ● ISSN 1785 0037 (Online)
DOI: http://dx.doi.org/10.15666/aeer/1705_1201312022

significantly attributed to the antagonistic effect of *T. harzianum* but not to because of the formulation ingredients.

Preliminary studies show that different active ingredients with fungicide; such as benomyl, captan, carbendazim, iprodione, mancozeb, myclobutanil, procymidone, thiram, thiophanate methyl, triforin, vinclozolin, and prochloraz etc., were effective to control of *P. expansum* during preharvest and postharvest. Since noticed of thiabendazole resistant blue mold in apple packing houses, study for alternative chemical control strategies have increased greatly (Eckert and Ogawa, 1988; Biyk et al., 1994; Li and Yu, 2000; Moreira and Mio, 2007; Feliziani et al., 2012).

Boscalid + pyraclostrobin active ingredients with fungicide against *M. fructigena* on apples that is only applied postharvest. Also, brown rot was reduced by 100% in apple fruit postharvest with this fungicide in this study. The same fungicide was able to mycelial growth of *P. expansum* on apple. But, this fungicide was effective when applied 7 or 14 days before harvest and reduced blue mold incidence by 41 to 70% (Xiao and Boal, 2009).

Harpin protein and *L. acidophilus* fermentation product elicitors of systemic acquired resistance in the host tissue that could indirectly help to protect apples from pathogens. The effect of application of harpin protein on the apples was less effective against blue mold and brown rot in this study. Capdeville et al. used to Hp in pre and postharvest treatments of apples induced resistance to *P. expansum* on apple. When they inoculated with the concentration 1×10^4 conidia/mL^{-1} *P. expansum* on apple in hp treatment a few days (4-8 days) before harvest was even more effective than the presented study (Capdeville et al., 2002, 2003).

Lafp had successfully controlled the brown rot caused by *M. fructigena* on apple in the present study. Similarly, the control of blue mold and grey mold on apple with Acibenzolar-S- methyl was reported before (Spadaro et al., 2004). β -aminobutyric-acid (BABA) on the activation of resistance responses in apple was investigated by Quaglia et al. (2017). Conversely, BABA resistance was not effective in the control of blue mold on apple such as Lafp.

Successful results similar to our study were obtained concerning the prevention of disease with *Trichoderma* spp. against *M. fructicola* on peaches and plums in the study of Hong et al. (1998) and with *Trichoderma polysporum* against *M. fructigena* on apples. The antagonist fungus *T. polysporum*, which was isolated from the apple leaves, was found to inhibit *B. cinerea* at 93%, *M. fructigena* at 80%, and *P. expansum* at 87% in postharvest apples (Falconi and Mendgen, 1994).

Aureobasidium pullulans, *Candida infirmominiatus*, *C. laurentii*, *Rhodotourula spp*, *M. pulcherrima*, and *Pichia angust*, from the yeasts isolated from the surface of the fruit, leaves and flowers, were found to be successful to prevent the disease, preharvest and postharvest in addition to *T. harzanium* that we applied in the biological control of post-harvest brown rot (Falconi and Mendgen, 1994; Chand and Spots, 1995; Hong et al., 1998; Irina et al., 2006; Fiori et al., 2008). As for our study, a similar effect was achieved (~70%) as the biological control agent *T. harzianum* successfully controlled *P. expansum* (Falconi and Mendgen, 1994). When the lesions were measured for the different postharvest fruits (pear, grape and kiwi) that were treated with the *T. harzianum* emulsion was found to support our research results (Batta, 2006).

In the biological control of *P. expansum* in the postharvest apples, different *Trichoderma* spp. (*T. atrovide*), apart from *T. harzianum*, also were found to have successful decay inhibition ranged of 35-50% while *Pseudomonas syringae* isolates and

http://www.aloki.hu ● ISSN 1589 1623 (Print) ● ISSN 1785 0037 (Online)
DOI: http://dx.doi.org/10.15666/aeer/1705_1201312022

P. agglomorates were found to be 100% and 81% effective, respectively. This may be attributed to the different action mechanisms of antagonist bacteria (Nunes et al., 2002; Quaglia et al., 2010).

Yeast-based and bacteria antagonist isolates isolated from the fruit surface of apples, leaves, flowers and soils such as *Sporobolomyces roseus, Aureobasidium pullulans*, *Metschnikowia andauensis*, *Candida sake*, *Cryptococcus in firomo-miniatus*, *C. laurentii*, *Hanseniaspora uvarum*, *Rhodotourula spp.* and *Bacillus amyloliquefaciens* BUZ-14 have also been successfully applied to the postharvest biologic control of *P. expansum* (Janisiewicz et al., 1994; Leibinger et al., 1997; Ippolito et al., 2000; Nunes et al., 2002; Karabulut et al., 2002; Turkekul, 2003; Spadaro et al., 2004; Manso and Nunes, 2011; Calvo et al., 2017).

There was no study to treatment of the apples with Lafp against *P. expansum* postharvest. However, 14 days and 21 days before the harvest, Lafp plant activator was applied to oranges, followed by the inoculation of *P. digitatum* (1×10^6 conidia/mL^{-1}). The reported 50% success rate as a result of the application of plant activator to the fruit 21 days before pathogen application was more effective than our work. In this study as well, in stimulating durability against disease, it is inferred that the time period after the application of the plant activator should be long (Bower, 2007).

The effective results obtained in this research will contribute to the expansion of the usage areas of plant activators that do not harm human health and the environment. It is thought that promising results can be obtained for different pathogens with different combinations of applications of Lafp and *T. harzianum*, which have been successfully used individually.

Conclusion

Biological control with antagonist fungi have been a promising alternative, with lower environmental effect, either alone or as part of integrated pest management to reduce synthetic fungicide usage in postharvest diseases of fruit and vegetables for many years. The present results indicate that *T. harzianum* (TRIC8) has potential as a biocontrol agent for the control of postharvest decay of apple caused by *P. expansum* and *M. fructigena*. TRIC8 treatment was used to control of *M. fructigena* more effective than *P. expansum* on apple and could become an alternative to fungicide in postharvest decay control of brown rot on apple, but registration and development investigations to acquire a commercial product are needed.

Acknowledgements. This study was supported with financial by Namik Kemal University (NKU_BAP.00.24.YL.13.04), Scientific Research Project Community.

REFERENCES

[1] Abbott, W. S. (1925): A method of computing the effectiveness of an insecticide. – J. Econ. Entomol. 18: 265-267.

[2] Amiri, A., Bompeix, G. (2011): Control of *Penicillium expansum* with potassium phosphite and heat treatment. – Crop Protection 30: 222-227.

[3] Barad, S., Espeso, E. A., Sherman, A., Prusky, D. (2016): Ammonia activates *pacC* and patulin accumulation in an acidic environment during apple colonization by *Penicillium expansum.* – Molecular Plant Pathology 17(5): 727-740. DOI: 10.1111/mpp.12327.

http://www.aloki.hu ● ISSN 1589 1623 (Print) ● ISSN 1785 0037 (Online)
DOI: http://dx.doi.org/10.15666/aeer/1705_1201312022

[4] Batta, Y. A. (2004): Effect of treatment with *Trichoderma harzianum* Rifai formulated in invert emulsion on postharvest decay of apple blue mold. – International Journal of Food Microbiology 96: 281-288.
[5] Batta, Y. A. (2006): Control of postharvest diseases of fruit with an invert emulsion formulation of *Trichoderma harzianum* Rifai. – Postharvest Biology and Technology 43: 143-150.
[6] Benli, M. (2003): Hyperparasitic effect of epiphytic yeasts on *Penicillium expansum* and *Botrytis cinerea* hyphae. – Orlab On-Line Microbiology Journal 1(5): 1-9.
[7] Biyk, H., Wojtas-Koziel, B., Lewandowska, M., Rejnus, M. (1994): Fungi causing apple diseases in storage and their control with several fungicides. – Review of Plant Pathology 73(7): 4522.
[8] Bower, J. P. (2007): The use of isr 2000 as an aid bio control of postharvest decay in citrus. – https://en.engormix.com/agriculture/articles/isr-2000-aid-biocontrol-t33873.htm (accessed on 24.04.2019).
[9] Boyraz, N., Kaymak, S., Baştaş, K. K. (2006)**:** Effects of some plant activators and their combinations with fungicides against apple scab disease (*Venturia inaequalis* (CKE) WINT.) – Journal of Selcuk Agriculture Faculty 20(39): 1-6.
[10] Byrde, R. J. W., Willets, H. J. (1977): The Brown Rot Fungi of Fruit Their Biology and Control. – Pergamon Press, Oxford, UK.
[11] Calvo, H., Marco, P., Blanco, D., Oria, R., Venturini, M. E. (2017): Potential of a new strain of *Bacillus amyloliquefaciens* BUZ-14 as a biocontrol agent of postharvest fruit diseases. – Food Microbiology 63: 101-110.
[12] Capdeville, G., Beer, G., Watkins, V., Wilson, C. B., Tedeschi, L. O., Aist, J. R. (2003): Pre and post-harvest harpin treatments of apples induce resistance to blue mold. – Plant Diseases 87: 39-44.
[13] Capdeville, G., Wilson, C. L., Beer, S. V., Aist, J. R. (2002): Alternative disease control agents induce resistance to blue mold in harvested 'red delicious' apple fruit. – Phytopathology 92: 900-908.
[14] Chand, G. T., Spotts, R. A. (1995): Postharvest biological control of blue mold and brown rot on sweet cherry by natural saprophytic yeast alone or in combination with low doses of fungicides. – Biological Control 6: 253-259.
[15] Chávez, R. A. S., Peniche, R. Á. M., Medrano, S. A., Munoz, L. S., Ortíz, M. del S. C., Espasa, N. T., Sanchis, R. T. (2014): Effect of maturity stage, ripening time, harvest year and fruit, characteristics on the susceptibility to *Penicillium expansum* link of apple genotypes from Queretaro, Mexico. – Scientia Horticulturae 180: 86-93.
[16] Eckert, J. W., Ogawa, J. M. (1988): The chemical control of post harvest diseases: deciduous fruits, berries, vegetables and root/tuber crops. – Annual Review of Phytopathology 26: 433-469.
[17] Errampalli, D. (2004): Effect of fludioxonil on germination and growth of *Penicillium expansum* and decay in apple cvs. Empire and Gala. – Crop Protection 23: 811-817.
[18] Errampalli, D., Northover, J., Skog, L., Brubacher, N. R., Collucci, C. A. (2005): Control of blue mold (*Penicillium expansum*) by fludioxonil in apples (cv Empire) under controlled atmosphere and cold storage conditions. – Pest Management Science 61: 591-596 DOI: 10.1002/ps.1010.
[19] Falconi, C. J., Mendgen, K. (1994): Epiphytic fungi on apple leaves and their value for control of the post harvest pathogens *Botrytis cinerea, Monilinia fructigena, Penicillium expansum* first publ in: – Zeitschrift Pflanzenkrankheiten und Pflanzenschutz 101: 38-47.
[20] FAOSTAT (2017): 2017 data. – faostat.fao.org/site/339/default.aspx.
[21] Feliziani, E., Santini, L., Landi, L., Romanazzi, G. (2012): Pre and postharvest treatment with alternatives to synthetic fungicides to control postharvest decay of sweet cherry. – Postharvest and Biotechnology 78: 133-138.

http://www.aloki.hu ● ISSN 1589 1623 (Print) ● ISSN 1785 0037 (Online)
DOI: http://dx.doi.org/10.15666/aeer/1705_1201312022

[22] Fiori, S., Fadda, A., Giobbe, S., Berardi, E., Migheli, Q. (2008): *Pichia angusta* is an effective biocontrol yeast against postharvest decay of apple fruit caused by *Botrytis cinerea* and *Monilia fructicola*. – FEMS Yeast Res 8: 961-963.
[23] Haıssam, J. M. (2011): *Pichia anomala* in biocontrol for apples: 20 years of fundamental research and practical applications. – Antonie van Leeuwenhoek 99: 93-105. DOI: 10.1007/s10482-010-9541-2.
[24] Hong, C., Michailides, J., Holtz, B. A. (1998): Effects of wounding, inoculum density and biological control agents on postharvest brown rot of stone fruits. – Plant Disease 82: 1210-1216.
[25] Ippolito, A., Ghaouth, A. E., Wilson, C. L., Wisniewski, M. (2000): Control of postharvest decay of apple fruit by *Aureobasidium pullulans* and induction of defense responses. – Postharvest Biology and Technology 19: 265-272.
[26] Irina, G., Cornea, C. P., Mateescu, R., Olteanu, V., Voaides, C. (2006): Control of postharvest fruit rot in apricot and peach by *Methschikowia pulcherrima*. – Buletin USAMV-CN 62: 74-79.
[27] Janisiewicz, W. J., Peterson, D. L., Bors, R. (1994): Control of storage decay of apple with *Sporobolomyces roseus*. – Plant Disease 78: 466-470.
[28] Jones, A. L., Aldwinckle, H. S. (1990): Brown Rot Diseases. Compendium of Apple and Pear Diseases. – American Phytopathology Society Press, USA.
[29] Kabelitz, T., Hassenberg, K. (2018): Control of apple surface microflora for fresh-cut produce by post-harvest hot-water treatment. – LWT - Food Science and Technology 98 492-499.
[30] Karabulut, O. A., Coohen, L., Wiess, B., Daus, A., Lurie, S., Droby, S. (2002): Control of brown rot and blue mold of peach and nectarine by short hot water brushing and yeast antagonists. – Postharvest Biology and Technology 24: 103-111.
[31] Leeuwen, G. C. M., Baayen, R. P., Holb, I. J., Jeger, M. J. (2002): Distinction of the Asiatic brown rot fungus *Monilinia polystroma* sp. Novfrom *M. fructigena*. – Mycological Research 100: 444-451.
[32] Leibinger, W., Breuker, B., Hahn, M., Mendgen, K. (1997): Control of postharvest pathogens and colonization of apple surface by antagonistic microorganism in the field. – Phytopathology 97: 1103-1110.
[33] Li, H., Yu, T. (2000): Effects of chitosan on incidence of brown rot, quality and physiological attributes of postharvest peach fruit. – Journal of the Science of Food and Agriculture 81: 269-274.
[34] Li, Q., Wu, L., Hao, J., Luo, L., Cao, Y., Li, J. (2015): Biofumigation on post-harvest diseases of fruits using a new volatile-producing fungus of *Ceratocystis fimbriata*. – PLoS ONE 10(7): e0132009. DOI: 10.1371/journal.pone.0132009.
[35] Manso, T., Nunes, C. (2011): *Metschnikowia andaunensis* as a new biocontrol agent of fruit postharvest diseases. – Postharvest Biology and Technology 61: 64-71.
[36] Mari, M., Martini, C., Spadoni, A., Rouissi, W., Bertolini, P. (2012): Biocontrol of apple postharvest decay by *Aureobasidium pullulans*. – Postharvest Biology and Technology 73: 56-62.
[37] Morales, H., Marín, S., Ramos, A. J., Sanchis, V. (2010): Influence of post-harvest technologies applied during cold storage of apples in *Penicillium expansum* growth and patulin accumulation: a review. – Food Control 21: 953-962.
[38] Moreira, L. M., Mio, de L. L. M. (2007): Control of peach tree brown rot by fungicides and phosphites evaluated during preharvest and postharvest. – Cienc. Agrotec. Lavras 33(2): 405-411.
[39] Nunes, C., Usall, J., Teixido, N., Fons, E., Viñas, I. (2002): Post-harvest biological control by *Pantoea agglomerans* (CPA-2) on golden delicious apples. – Journal of Applied Microbiology 92: 247-255.
[40] Ozgonen, H., Kılıc, C. H. (2013): Apple and Pear Postharvest Diseases. – Hasat Publishing, Istanbul, Turkey, pp. 25-26.

http://www.aloki.hu ● ISSN 1589 1623 (Print) ● ISSN 1785 0037 (Online)
DOI: http://dx.doi.org/10.15666/aeer/1705_1201312022

[41] Penrose, L. J., Koffman, W., Ridings, H. I. (1989): Factors affecting the efficacy of post-harvest fungicide applications for the control of blue mold (*Penicillium expansum*) in stored apples. – Plant Pathology (1989): 421-426.
[42] Quaglia, M., Baglivo, F., Moretti, C. (2017): Postharvest β-aminobutyric-acide-primed resistance is not effective in the control of *Penicillium expansum* Link. on 'Golden delicious' apple fruit. – Crop Protection 102: 43-48.
[43] Quaglia, M., Ederli, L., Pasqualini, S., Zazzerini, A. (2010): Biological control agents and chemical inducers of resistance for postharvest control of *Penicillium expansum* link. on apple fruit. – Postharvest Biology and Technology 59: 307-315.
[44] Sagasta, E. M. (1977): *Monilinia* diseases. – EPPO Bulletin 7: 105-116.
[45] Salunkhe, D. K., Kadam, S. S. (1998): Handbook of Vegetable Science and Technology: Production, Composition, Storage and Processing. Vol. 1. Introduction. – CRC, Boca Raton, FL, pp. 1-10.
[46] Sharma, R. R., Singh, D., Singh, R. (2009): Biological control of postharvest diseases of fruits and vegetables by microbial antagonists: a review. – Biological Control 50: 205-221.
[47] Snini, S. P., Tannous, J., Heuillard, P., Bailly, S., Lippi, Y., Zehraoui, E., Barreau, C., Oswald, I. P., Puel, O. (2016): Patulin is a cultivar-dependent aggressiveness factor favouring the colonization of apples by *Penicillium expansum*. – Molecular Plant Pathology 17(6): 920-930.
[48] Spadaro, D., Garibaldi, A., Gullino, M. L. (2004): Control of *Penicillium expansum* and *Botrytis cinerea* on apple combining a biocontrol agent with hot water dipping and acibenzolar-*S*-methyl, baking soda, or ethanol application. – Postharvest Biology and Technology 33: 141-151.
[49] Turkekul, S. (2003): Research on the biological control of postharvest diseases *Penicillium expansum* and *Botrytis cinerea* on apples. – MSc. Thesis, Aegean University, Agricultural Faculty, Department of Plant Protection, Izmir, Turkey, 60p.
[50] Vinas, I., Usall, J., Teixido, N., Sanchis, V. (1998): Biological control of major postharvest pathogens on apple with *Candida sake.* – International Journal of Food Microbiology 40: 9-16.
[51] Wang, H., Jiang, M., Chen, K., Wang, K., Du, M., Zalan, Z., Hegyi, F., Kan., J. (2018): Biocontrol of *Penicillium digitatum* on postharvest citrus fruits by *Pseudomonas fluorescens*. – Hindawi Journal of Food Quality, Article ID 2910481. https://doi.org/10.1155/2018/2910481.
[52] Wang, Y., Li., X., Bi, Y., Ge, Y., Li, Y., Xie, F. (2008): Postharvest ASM or Harpin treatment induce resistance of muskmelons against *Trichothecium roseum*. – Agricultural Sciences in China 7(2): 217-223.
[53] Xiao, K., Boal, R. J. (2009): A preharvest application of pyraclostrobin and boscalid for control of postharvest grey mold and blue mold in apples. – Plant Diseases 93: 185-189.
[54] Yaseen, T., Ricelli, A., Turan, B., Albanese, P., D'onghia, M. M. (2015): Ozone for post-harvest treatment of apple fruits. – Phytopathologia Mediterranea 54(1): 94-103. DOI: 10.14601/Phytopathol_Mediterr-14478.
[55] Yildiz, F., Kinay, P., Yildiz, M., Sen, F., Karacali, I. (2005): Effects of preharvest applications of $CaCl_2$, 2,4-d and benomyl and postharvest hot water, yeast and fungicide treatments on development of decay satsuma mandarins. – J. Phytopathology 153: 94-98.
[56] Zhao, Li., Zhang, H., Lin, H., Zhang, X., Ren, X. (2012): Effect of trehalose on the biocontrol efficacy of *Pichia caribbica* against post-harvest grey mould and blue mould decay of apples. – Pest Management Science 69: 983-989.
[57] Zhu, Y. Yu, J., Brecht, J. K., Jiang, T., Zheng, X. (2016): Pre-harvest application of oxalic acid increases quality and resistance to *Penicillium expansum* in kiwifruit during postharvest storage. – Food Chemistry 190: 537-543.

http://www.aloki.hu ● ISSN 1589 1623 (Print) ● ISSN 1785 0037 (Online)
DOI: http://dx.doi.org/10.15666/aeer/1705_1201312022

TRADITIONAL KNOWLEDGE BASED INVENTORY OF WILD PLANTS OF WATALA NATIONAL PARK AND ALLIED VILLAGES FROM BHIMBER DISTRICT, AZAD JAMMU AND KASHMIR, PAKISTAN

MEHWISH, M.[1*] – AJAIB, M.[1] – KHIZAR HAYAT, B.[3] – ISHTIAQ, M.[1*] – HUMAIRA, K[1]. – TANVEER, H.[1] – GHANI, A.[2] – WAHEEDA, M.[1]

[1]*Department of Botany, Mirpur University of Science & Technology (MUST), Mirpur 10250 (AJK), Pakistan*

[2]*Department of Botany, University of Sargodha, Sargodha, Pakistan*

[3]*Department of Botany, University of Gujrat, Gujrat, Pakistan*

**Corresponding authors*
e-mail: mehwishmaqbool11@gmail.com

(Received 26th Apr 2019; accepted 11th Jul 2019)

Abstract. An ethnobotanical (EB) research was conducted on the wild plants of Watala National Park (WNP) and allied villages of Barnala, District Bhimber, Azad Jammu and Kashmir (AJK), Pakistan. EB data have been collected by questionnaire method employing structured and semi-structured interviews. A total of 79 interviewees (47 male, 32 female) having age 25-65 years were included in the EB study. 92 plant species of 37 families were studied and the obtained data were compiled in an inventory form consisting of ethnomedicinal (EM) use, parts used, mode of application and EB use. For validation of EM data of plants different microstatistical tools like frequency of citation (FC), relative frequencies of citation (RFC), use value (UV), fidelity level (FL) and informant consensus factor (ICF) were used. Direct matrix ranking (DMR) and priority ranking (PR) were applied on EB data for quantitative analysis to find multiple use forms of plant(s) and calculate biotic threats for the plants. Study results depicted that FC ranged 59 to 11, RFC was 0.75 to 0.14 and UV was between 0.82 and 0.15. Leaves were the most frequently used (31%) part of plants and powder form (25%) was the most commonly used form. The highest FL was found for *Senegalia modesta* species (100%) and diseases such as fever, flu, headache, bronchitis and cough ranked first (0.94) in ICF analysis. DMR results showed that *Senegalia modesta* was the first regarding multifarious use. Fuel wood cutting and fire burning were top two threats for the flora of the area. Due to anthropogenic pressure and climatic dynamics plants of the area are under severe threats and there is urgent need to conserve the flora of WNP, District Bhimber for future generations and to introduce sustainable applications.

Keywords: *traditional ethnobotanical knowledge, informant consensus factor, relative frequency, folklore therapeutics, green drugs, conservation status*

Introduction

Plants have been used by man for his sustenance on the planet. Wild plants had been part and parcel of daily needs of people inhabiting different rural parts of the world. Plants provide fundamental necessities of daily life because rural communities are primarily dependent on wild plant resources for fulfilling the needs of their life (Ishtiaq and Khan, 2008).

Ethnobotany (EB) is discipline of botany in which we study the native people's relationship with indigenous flora of the area and it encompasses the biocultural diversity of plants and human sociological paradigms (Harshberger, 1895; Ishtiaq et al., 2016). It was demonstrated that ethnobotany and ecology are interlinked with each other and this

http://www.aloki.hu ● ISSN 1589 1623 (Print) ● ISSN 1785 0037 (Online)
DOI: http://dx.doi.org/10.15666/aeer/1705_1202312055

intermingling of two or more disciplines give ecoethnobotany (EEB) discipline which give significant importance of plants in the life of indigenous communities and ecosystem sustainability (Jones, 1941; Ford, 1978; Ajaib et al., 2014a). EB is the study of direct interaction between human beings and the flora through their coinciding biodiversity and civilization/cultural diversity in the form of index of biocultural diversity (IBCD) which describes this interdependence (Pie, 1995; Ahmad et al., 2008; Ishtiaq et al., 2013a). Plants perform variety of keystone roles in our daily life such as plants provide food, fodder, medicines, shelter, cosmetics, shadow, hedging and fencing, dyes, fuel and aesthetics in the form of ornamental taxa. They have a great role in environmental functions such as stabilizing soil, recycling of nutrients, photosynthesis, protecting water drainage areas and help to restraint rainfall through the process of transpiration (Mehmood et al., 2012; Naseem et al., 2018). Plants are also involved in the manufacturing of different phytochemicals also called secondary metabolites which are potential sources of disease treatment through drug discovery and development process (Ajaib et al., 2014b).

Pakistan has rich and abundant plant resources and nearly more than 6000 plants have been reported, particularly more than 2000 species are known as medicinal plants (MPs) being used in the cure of many diseases by local communities of the country (Ali et al., 2001; Umair et al., 2017; Sher et al., 2016). The plants have been playing pivotal role in coping the basic needs of rural communities in various parts of Pakistan and AJK (Ishtiaq et al., 2013b). The indigenous people of mountainous and remote areas of AJK had been dependent primarily on local plants for obtaining needs of life such as food, fodder, shelter and ethnomedicines. The information about plants regarding their role as EMs and other EB necessities is very helpful to ecologists, pharmacologists, taxonomists, watershed and wild life managers. These are documented to conserve the civilization norms and folklore traditions of various ethnic groups and areas and describe how plants are inevitable in the prosperity of indigenous communities of the area (Ishtiaq et al., 2012, 2013a; Ajaib et al., 2014b; Chassagne et al., 2016).

Azad Jammu and Kashmir (AJK) is a territory that connects Pakistan with China and India. Kashmir has a historical background and it was an independent empire in the 18th century but later on during 1940s decade when India and Pakistan emerged on the map of world, this state was tetra-furcated into four sections; one of those is called as AJK (Ishtiaq et al., 2013b). Azad Jammu and Kashmir state has ten districts and Bhimber is one of these and it is located at the southern side connecting District Gujrat of Pakistan and Districts Rajori and Jammu of the Indian part of Kashmir. The study area of Watala National Park (WNP) and allied villages is located in Tehsil Barnala of District Bhimber, AJK. Collectively Districts Mirpur and Bhimber make one division of AJK and it consists of 2526 km^2 area (*Fig. 1*). District Bhimber has plain area with some high mountains in Tehsil Samahni only and its area is 1516 km^2. The population of District Bhimber is 0.343 million with a growth rate of 2.6% and house hold size of 6.7 (Ishtiaq et al., 2016).

The climate of the study area is warm and temperate with an average annual temperature of 23.5 °C. The average rainfall is 752 mm in a year. June is the warmest month of the year, temperature fluctuates with range 40-48.2 °C. January is the coldest month of the year, with an average temperature of 12.1 °C. November is the driest month, with 5 mm of rainfall. In July, the precipitation reaches its peak, with an average of 222 mm (Mehmood et al., 2012; Ishtiaq et al., 2016). Study area (Watala) is located in the North-East of Azad Jammu and Kashmir along 32° 54 (32.9023°) N and 74° 17 (74.2962°) E at an average elevation of 444 m above sea level (GPS Garmin Nuvi) (Nadeem et al., 2014; Ishtiaq et al., 2016).

http://www.aloki.hu ● ISSN 1589 1623 (Print) ● ISSN 1785 0037 (Online)
DOI: http://dx.doi.org/10.15666/aeer/1705_1202312055

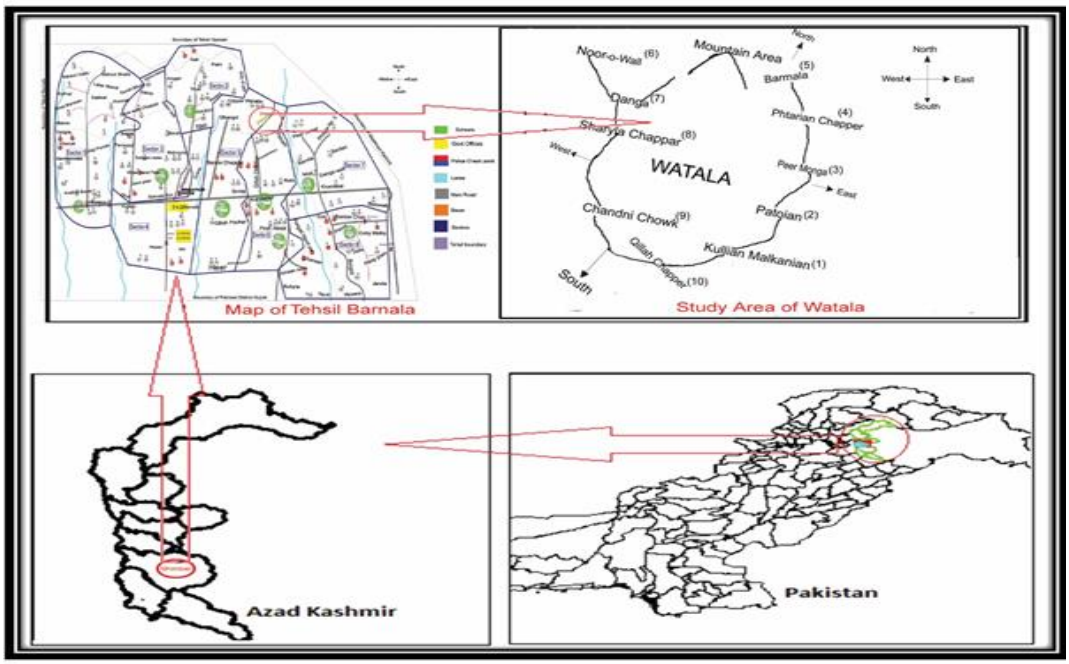

Figure 1. *Map showing location of study area, Watala, District Bhimber within Tehsil Barnala, Azad Kashmir and Pakistan*

WNP area has different ethnic groups residing such as Gojars, Jat, Rajpoot, Jaraal, Syed, Mirza, Kashmiri, Chibs and Awans (Ishtiaq et al., 2007a). In the area key languages spoken are Punjabi, Kashmiri, Saariki, Gojari, and Parhayee and each has different linguistic dialects that fluctuates from one village to other due to mixing of various cultures by bonds of marriages or by migration of people due to Indian firing, long drought spell, or any other cause (Ishtiaq et al., 2013b, 2016).

On many parts of Pakistan commendable work have been reported on EB studies by different workers describing that EB research is very important in drug discovery and development (Shinwari and Khan, 2000; Ishtiaq et al., 2007b). Albeit many sporadic research works are reported on EB studies of different areas of AJK (Qamar, 1996; Amjad et al., 2017; Dar et al., 2018; Ajaib et al., 2015; Ishtiaq et al., 2012, 2013b) but hitherto nothing is published on Watala National Park (WNP) and allied villages of District Bhimber, AJK. This is a first time an attempt to describe the ethnobotanical research on WNP using quantitative analysis by applying various microstatistical indices such as CF, RCF, FL, ICF and UVs. The IBCD, DMR and PR tools were used for determining biotic threat levels on the various plant species of WNP and then recommendations were made for the conservation of these taxa for their sustainable ecosystem services. The pivotal objectives of the research study were to: (i) study the plant biodiversity of the Watala National Park (WNP) and its allied area by preparing check list of plant flora; (ii) investigate and explore ethnobotanical potential of plants of the WNP in the life of rural communities by documenting multiple purpose uses; (iii) traditional folklore therapeutic recipes of medicinal plants (MPs) that may serve drug discovery research in the future; (iv) to document the cultural heritage of the indigenous communities of the WNP area and to calculate the conservation of various plants with recommendations for their protection and conservation for the future.

http://www.aloki.hu ● ISSN 1589 1623 (Print) ● ISSN 1785 0037 (Online)
DOI: http://dx.doi.org/10.15666/aeer/1705_1202312055

Materials and methods

An ethnobotanical (EB) study was conducted during years 2015 and 2016 in Watala National Park (WNP) and allied villages of District Bhimber to collect the plant specimens for experimental analysis. During four seasons of the year, several planned and random field trips were conducted in the study area to collect EB information and data were recorded in triplicate manner for each parameter. The EB data were collected through use of Visual appraisal assessment (VAA) and rapid rural appraisal (RRA) methods (Okuthe et al., 2003; Ishtiaq et al., 2007b). In VAT, observations were made in wild areas and in the community houses and market visits and all of important information were instantly documented in a notebook. In RAA method, questionnaire method following Ishtiaq et al. (2013a, 2016) was used. In the process, structured and semi-structured interview patterns were used and data were collected from field visits and from local market surveys including botanic drug sellers (dealers), timber dealers, fuel wood sellers, local hakims and farmers in the research. The data collected from the local people included: botanical name, vernacular name, local name, folklore uses, therapeutic recipes, plants' part used, occurrence in area, characters involved in the collection, trade marketing, mode of usage and other related information like: disease name cured. According to economic values and drug potential, plants of WNP were further categorized into medicinal plants (MPs), food, fruits, fodder, vegetable, thatching, hedging, shelter, ornamental and fuel wood etc. based on the gathered data through interviewing questionnaire from botanic drug sellers, timber dealers, fuel wood sellers, local hakims and farmers. In this research analysis, preference was given to local elder people and hakims, who were the actual consumers and had a lot of indigenous traditional and cultural information about the plants and local ethnic groups with ritual paradigms (Ishtiaq et al., 2016). The collected data compiled in documentary form and it was compared with published and online papers for authenticity and verification.

Data collection and identification of plants

The plant specimens were collected from the area (WNP) for identification and extraction of EB data from villagers by showing them the plant specimens and asking them to answer the questions asked through different interview formats. The collected plants were dried, pressed, mounted properly on herbarium sheets and voucher numbers were assigned to each taxon according to protocol of Alexiades (1996), Cook (1995) and Ishtiaq et al. (2013b). All of these plant taxa were submitted for further reference in the Herbarium (MUH-), Department of Botany, Mirpur University of Science and Technology (MUST), Bhimber Campus. The plants were identified mainly with the help of Flora of Pakistan (www.eflora.com) following printed Flora book (Nasir and Ali, 1970-1989; Ali and Qaiser, 1993-2015), whereas the International Plant Name Index (IPNI) (www.ipni.org) was also used to obtain authentic botanical names.

Quantitative ethnobotanical data analysis

For the corroboration and to analyze the homogeneity of the collected ethnobotanical data, various quantitative indices were used. The collected EB data were formulated in form of a matrix (MS excel worksheet) and summarized as per protocol of Cook (1995) and Ishtiaq et al. (2013b). The obtained data were compared with previous research work published on the same area or on different areas of AJK but with same topic by

http://www.aloki.hu ● ISSN 1589 1623 (Print) ● ISSN 1785 0037 (Online)
DOI: http://dx.doi.org/10.15666/aeer/1705_1202312055

using online searching for authentication and reliability. Due to stringent peer review procedure only authentic information were kept for the meta-analysis of the study. The applicability, reliability and authenticity of ethnobotanical research work was rechecked and supported by calculating frequency of citation (FC), use value (UV), relative frequency of citation (RFC), fidelity level (FL), informant consensus factor (ICF), data matrix ranking (DMR) and priority ranking (PR) microstatistical tools following protocols of Ishtiaq et al. (2007b) and Fisseha et al. (2009).

Relative frequency of citation (RFC)

The index of relative frequency of citation (RFC) was determined by using the following formula (Vijayakumar et al., 2015).

$$RFC = FC / N \quad \text{(Eq.1)}$$

where FC is the number of informants reporting use of a particular species and N is the total number of informants.

Use value index (UV)

The use value was calculated by using the following formula (Vijayakumar et al., 2015).

$$UV = \sum Ui / N \quad \text{(Eq.2)}$$

where Ui is the number of uses mentioned by each informant for a given species and N is the total number of informants.

Fidelity level (FL)

The fidelity level (FL), the percentage of informants claiming the use of a certain plant for the same major purpose was calculated for the most frequently reported usages or ailments as:

$$FL(\%) = \frac{Np}{N} \times 100 \quad \text{(Eq.3)}$$

where Np is the number of informants that claim a use of a plant species used for a particular purpose/disease and N is the number of informants that use the plants as a botanic/medicine to fill/treat any given demand/disease (Alexiades, 1996).

Informant consensus factor (ICF)

Informant consensus factor (ICF) was calculated for each category of aliments to identify the agreements of the informants on the reported medicures for the group of ICF was calculated as follows: number of use citations in each category (nur) minus the number of species used (nt), divided by the number of use citations in each category minus one (Heinrich et al., 1998).

http://www.aloki.hu ● ISSN 1589 1623 (Print) ● ISSN 1785 0037 (Online)
DOI: http://dx.doi.org/10.15666/aeer/1705_1202312055

$$ICF = \frac{nur - nt}{nur - 1} \quad \text{(Eq.4)}$$

Data matrix ranking (DMR)

Data matrix ranking (DMR) describes the multiple usages of one plant for various purposes by the indigenous community and the data is presented in tabular form with % age index of each use-form aliments (Fisseha et al., 2009; Ishtiaq et al., 2013a).

Priority ranking (PR)

Priority ranking (PR) method was used for indicating the preference of the local people about the potential use of each plant in certain use and it describes the biotic pressure on the plants of the area and it assist to calculate the conservation status of various species in the study area (Ishtiaq et al., 2007a, 2013b).

Results

The Ethnobotanical research work is very important because it provides basic information on plant biodiversity, cultural diversity and traditional ethnomedicinal knowledge (TEK) of an area. The current research work was conducted in the rural area of Tehsil Barnala mainly focused on Watala National Park (WNP) and its allied village areas of Tehsil Barnala, District Bhimber Azad Jammu and Kashmir, Pakistan.

The area of WNP is very rich for biocultural diversity as it has a historic background. King of Dogra empire "Mahraja Hari Singh's" maternal grandparents belonged to this territory of WNP. The princess visited this region during his regime. There is a garden of mangoes in this region that is named as "Princess' Garden" locally called "Raani ka Baagh" which was established by the King in desire of the Princess (Baheem, 1890).

In this research work various parameters were studied which included the following steps: (i) social and geographical characteristics of the sample and study sites, shown in *Table 1*, (ii) Family-wise contribution and ethnomedicinal flora, (iii) plant collection, identification and preservation and (iv) documentation of floristic composition of the plants of the area.

Inhabitants of WNP and allied area (10 villages) were interviewed with the above said methodology for documentation of folklore therapeutics and ethnobotanical knowledge of the plants of the area (*Fig. 1*). The interviewees were of both gender with age range of 25-to-65 years and if age groups were made on the basis of 10 years age differences, then it was found that age group "56-65 years" was more knowledgeable due to their keen interest in local plants uses and their personal experience of life (*Table 1*). Less ethnobotanical knowledge was exhibited by age group "16-25 years" due to their preference for use of western medicines. However, the 56-65 years and 60 < years age group showed high level of traditional knowledge which is a good sign of traditional knowledge consistency in the area. The graphical age difference of respondents is shown in (*Fig. 2*).

http://www.aloki.hu ● ISSN 1589 1623 (Print) ● ISSN 1785 0037 (Online)
DOI: http://dx.doi.org/10.15666/aeer/1705_1202312055

Table 1. *Social characteristics of study sites of Watala National Park, District Bhimber AJK, Pakistan*

Village names of WNP and allied area	Barmala	Saryala-Chapper	Danga	Pataria-Chapper	Noor-o-Wall	Chandni-Choke	Peer-Monga	Patoian	Kulian-Malkanian	Qilla-Chapper
Village size (number of families)	23	52	38	25	26	61	16	42	36	40
Sample size (number of informants)	9	6	10	7	9	11	5	7	9	6
Dependency on livestock as a source of income	82%	50%	87%	65%	55%	40%	51%	55%	62%	59%
Informants average age	56-21	72-18	69-16	46-14	50-12	61-15	67-20	59-25	67-28	62-25
Average number of family members	14-5	12-3	18-3	11-5	10-2	11-4	16-2	12-4	10-2	16-4
Migration ratio	10%	2%	1%	0%	1%	0%	0%	0%	0%	0%
Bilingualism	9%	40%	35%	20%	30%	45%	25%	35%	42%	30%
Elevation (m.a.s.l.)	396	410	465	438	398	472	458	442	394	447

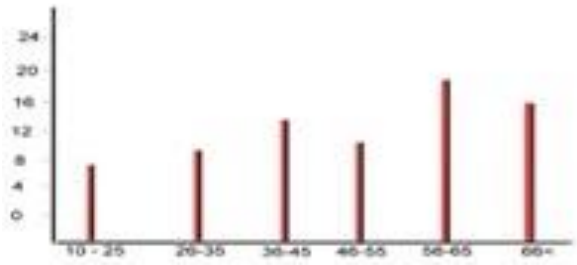

Figure 2. *Graphical age difference of respondents of ethnobotanical study of Watala National Park of AJK, Pakistan*

Family-wise contribution and ethnobotanical flora of Watala National Park and allied areas

For the documentation of ethnobotanical knowledge of the plants of Watala National Park (WNP) different plants were collected from the selected villages and WNP area according to protocol of Ishtiaq et al. (2007b). The collected plants were pressed, dried and mounted on herbarium sheets for preservation in the herbarium of the Department of Botany, Mirpur University of Science and Technology Bhimber AJK. Each collected plant specimen was assigned a herbarium voucher number with prefix: MUH-. The collected plants were herbaria numbers initiating from MUH-3031 to MUH-3122 (*Table 3*). The collected plants were verified and identified mainly with the help of Flora of Pakistan library booklets and online data (www.eflora.com) following Nasir and Ali (1970-1989) and Ali and Qaiser (1993-2015) whereas the International Plant Name Index (IPNI) (www.ipni.org) was also used to obtain correct botanical names, if not found in the herbarium or eflora website. Distribution of medicinal plant (MPs) species according to their family is presented in tabular form and it was

http://www.aloki.hu ● ISSN 1589 1623 (Print) ● ISSN 1785 0037 (Online)
DOI: http://dx.doi.org/10.15666/aeer/1705_1202312055

found that Poaceae was the first having 15 species (16.31%), followed by Amaranthaceae with 08 species (8.69%) and Malvaceae ranked at third with 6 taxa (6.52%) as described in *Table 2* and in *Figure 3* in graphical format.

Table 2. *Percentage distribution of medicinal plants according to their family from Watala National Park of AJK*

Sr. no.	Family name	No. of spp.	Percentage contribution	Sr. no.	Family name	No. of spp.	Percentage contribution
1-	Acanthaceae	3	3.26%	20-	Flacourtiaceae	2	2.17%
2-	Amaranthaceae	8	8.69%	21-	Lamiaceae	3	3.26%
3-	Anacardiaceae	1	1.08%	22-	Malvaceae	6	6.52%
4-	Apocynaceae	2	2.17%	23-	Martyniaceae	1	1.08%
5-	Asclepiadaceae	1	1.08%	24-	Meliaceae	1	1.08%
6-	Asparagaceae	1	1.08%	25-	Mimosaceae	4	4.35%
7-	Asteraceae	4	4.35%	26-	Moraceae	3	3.26%
8-	Boraginaceae	1	1.08%	27-	Nyctaginaceae	1	1.08%
9-	Brassicaceae	1	1.08%	28-	Oxalidaceae	1	1.08%
10-	Cactaceae	1	1.08%	29-	Papilionaceae	4	4.35%
11-	Cannabaceae	1	1.08%	30-	Poaceae	15	16.31%
12-	Capparidaceae	3	3.26%	31-	Potamogetanaceae	1	1.08%
13-	Celastraceae	1	1.08%	32-	Primulaceae	1	1.08%
14-	Combretaceae	1	1.08%	33-	Rhamnaceae	2	2.17%
15-	Commenlinaceae	1	1.08%	34-	Sapindaceae	1	1.08%
16-	Convalvulaceae	4	4.35%	35-	Solanaceae	3	3.26%
17-	Cucurbitaceae	2	2.17%	36-	Tiliaceae	2	2.26%
18-	Cyperaceae	1	1.08%	37-	Verbenaceae	1	1.08%
19-	Euphorbiaceae	3	3.26%				

Documentation of wild plant species

Ethnobotanical data of the wild plants of the WNP of AJK were documented containing voucher numbers, botanical names, vernacular name, family name, plant part used, field collection period, exact gathering sites, traditional medicinal uses and other use forms (*Table 3*). In the investigated area, 92 plant species belonging to 83 genera and 37 families were recorded. Among them, Poaceae ranked first having 15 species (16.31%), Amaranthaceae was second having 8 species (8.69%) whereas Malvaceae showed the third highest number having 6 species (6.52%), respectively. Asteraceae, Convalvulaceae, Mimoaceae and Papilionaceae each having 4 species (4.35%) while Acanthaceae, Capparidaceae, Euphorbiaceae, Lamiaceae, Moraceae and Solanaceae each has 3 species (3.26%). Apocynaceae, Cucurbitaceae, Flacourtiaceae, Tiliaceae and Rhamnaceae each has 2 species (2.17%). Anacardiaceae, Asparagaceae, Boraginaceae, Brassicaceae, Cactaceae, Cannabaceae, Celastraceae Cleomaceae, Combretaceae, Commenlinaceae, Cyperaceae, Martyniaceae, Meliaceae, Nyctaginaceae, Oxalidaceae, Potamogetanaceae, Primulaceae, Sapindaceae and Verbenaceae each has 1 species only (1.08%). A pie-chart of medicinal plant species according to their contribution to each family is shown in (*Fig. 3*). Most of the plant species in the area identified as having an ethnomedicinal value were herbaceous (55%), followed by trees (20%), grasses (12%),

http://www.aloki.hu ● ISSN 1589 1623 (Print) ● ISSN 1785 0037 (Online)
DOI: http://dx.doi.org/10.15666/aeer/1705_1202312055

shrubs (10%) and climbers (3%) (*Fig. 4*). These results reflect the high altitude of the study area where the herbaceous flora is dominant with fewer grasses and trees.

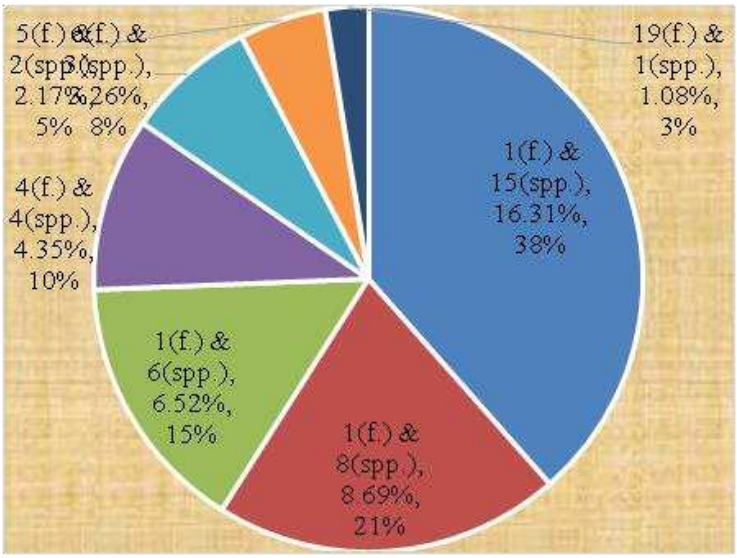

Figure 3. *A pie-chart of medicinal plant species according to their contribution to their family (f: no. of families & spp.: no. of species)*

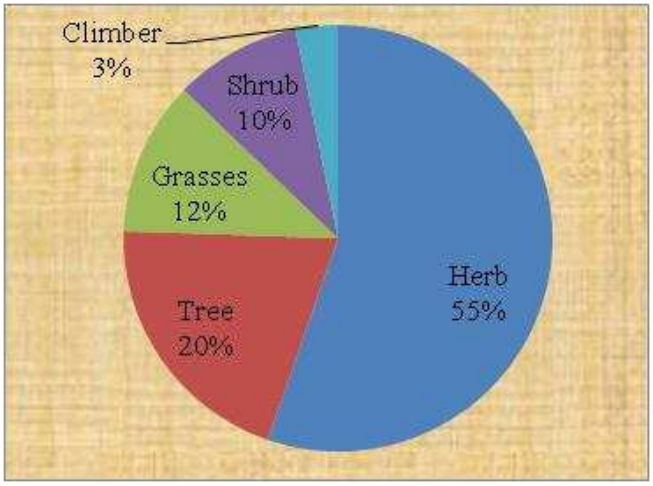

Figure 4. *Life form of plants used in ethnobotanical study of Watala National Park of AJK, Pakistan*

Plant part(s) used

Different plant parts are used in different ways in herbal medicines depending upon the knowledge of indigenous communities and accessibility of those plants to local inhabitants. In the present study, leaves (L = 31%) were the most commonly used plant part in the herbal therapeutic preparations followed by whole plant (WP = 21%), root (R = 10%), fruit & seed (FS = 8.8%), wood (W = 7%), bark (B = 6%), stem (S = 5%), flowers (F = 3%) and legume (Lg = 1%) as shown in *Figure 5*. Ethnobotanical and medicinal uses of plants were also recorded and presented in *Table 3*.

http://www.aloki.hu ● ISSN 1589 1623 (Print) ● ISSN 1785 0037 (Online)
DOI: http://dx.doi.org/10.15666/aeer/1705_1202312055

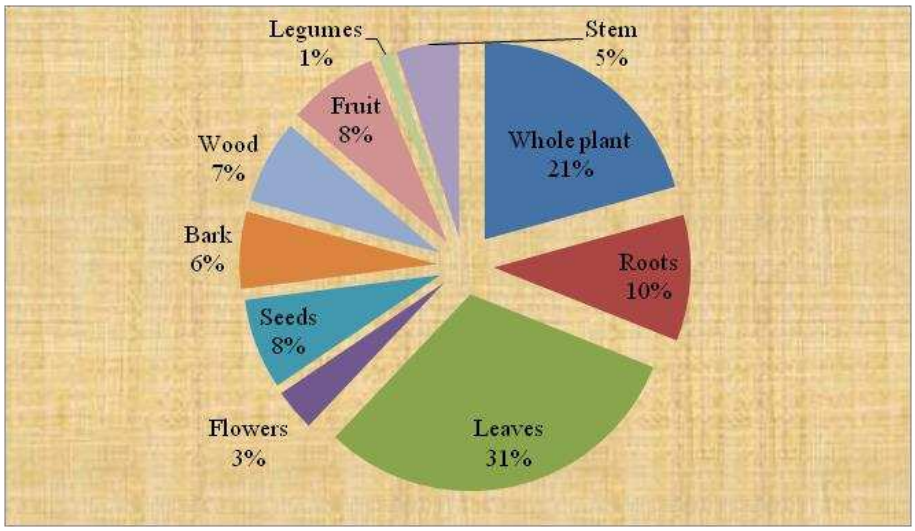

Figure 5. *Plant parts used in herbal recipes in terms of% age from Watala National Park of District Bhimber, AJK*

Method of preparation of folklore therapeutics and mode of administration

Plants are very important source of food and medicines because plants contain many primary and secondary metabolites and the latter ones make them potential sources of medicinal use. Different parts of plants of various types and variable quantity of phytochemicals are used. The different plant parts were mostly used in herbal preparations in various modes such as decoction (22 spp.), extract (18 spp.), wet paste (17 spp.), dry & powder (17 spp.), fuel (16 spp.), juice (11 spp.), palatable (9 spp.), vegetable (8 spp.), poultice (5 spp.) and gum (4 spp.). During the research various methods of folklore tonics' preparation were documented by interviewing the indigenous inhabitants of WNP and allied villages. Common form and mode of herbal therapeutics formation and its administration form were as: food/fodder (direct WP used) with the highest value (25%), and decoction, paste, juice, powder, extract, tea and gum as the least used form (6%) (*Fig. 6*).

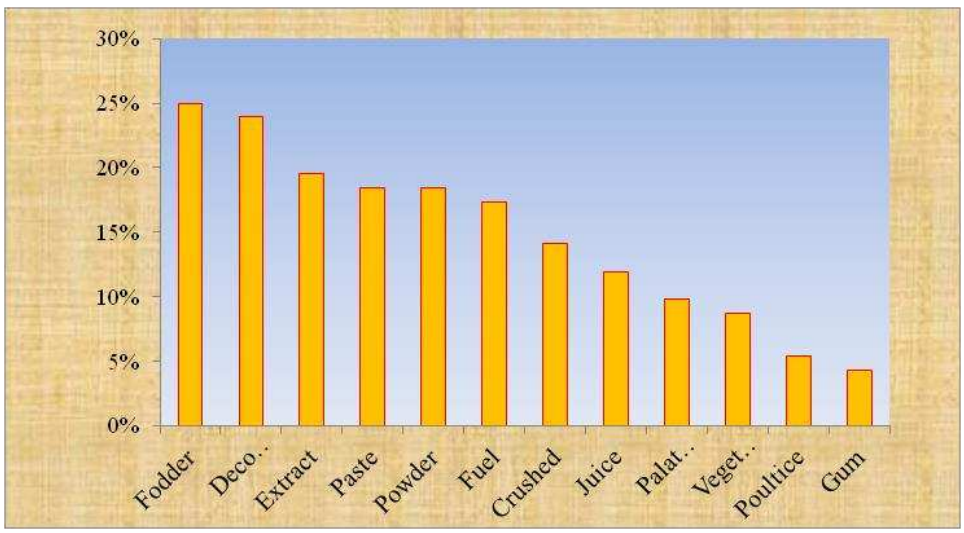

Figure 6. *Common methods of preparation of folklore therapeutics and their mode of administration*

http://www.aloki.hu ● ISSN 1589 1623 (Print) ● ISSN 1785 0037 (Online)
DOI: http://dx.doi.org/10.15666/aeer/1705_1202312055

Table 3. *Traditional ethnomedicinal and ethnobotanical uses of wild plants recorded from study area Watala National Park of District Bhimber of AJK*

Sr#	Family, botanical name & voucher no.	Habit	Common name	Used parts	Gathering period	Gathering area(s)	Traditional medicinal uses	Ethnobotanical uses	FC	RFC	UV
(1) Acanthaceae											
1-	*Dicliptera bupleuroides* Nees MUH-3031	Herb	Kalu	Whole plant	Spring	Waste-land	The poultice is used for scabies. The host insect from this plant is collected to make powder, which is very effective to cure pneumonia and hypertension	It is used as fuel in dried form.	48	0.61	0.63
2-	*Justicia adhatoda* L. MUH-3032	Herb	Bhaker	Leaves and almost whole plant	Spring	Waste-land	Half kg of fresh leaves is extracted with 500ml water, used against diabetes and in blood purification. Leaves and flowers are taken, dried under shade, crushed to acquire powder, 50gm of this powder is mixed in 15ml of honey and used to treatment of chest infection. Decoction of leaves is used for skin infection. The stem and leaves are useful for fever and hypertension	It is used for thatching, fuel ,hedging, shadow for other micro-plants, and used as fodder	No	0.66	0.68
3-	*Peristrophe paniculata* (Forssk.) Brummitt MUH-3033	Herb	Kaluu / Kali-Buti	Whole plant	Spring	Bushy-vegetation	The host insect from this plant is collected to make powder, which is very effective to cure pneumonia and hypertension	It is used as fodder, fuel.	19	0.24	0.31
(2) Amaranthaceae											
4-	*Achyranthes aspera* L. MUH-3034	Herb	Puth-Kanda	Whole plant	Spring	Bushy-vegetation	The paste acquired from the root has been used to cure snake bite. Decoction is diuretic. Seeds and leaves are given in prolepses in cattle. Seed powder is also used in treatment of strong abdominal pain. Shade dried whole plant powder is mixed with honey is effective for pneumonia	It is eaten as fodder, also used as fuel in dried form.	46	0.58	0.52
5-	*Aerva sanguinolenta* (L.) Blume MUH-3035	Herb	Booti	Branches	Spring	Bushy-vegetation	A decoction of immature branches is used to cure haematuria and irregular or painful menstruation	It is used as fodder and bioremediator	11	0.14	0.22
6-	*Alternanthera pungens* Kunth MUH-3036	Herb	Kanda-Buti	Leaves and Roots	Spring	Beside pedestrian passes	Roots and leaves paste is beneficial for liver disorder. Roots are used for eye tumor as well as its decoction for cough and pulmonary disorder. Leaves and roots are diuretic and used in blood purification	It is used for fuel in dried form.	18	0.23	0.16

http://www.aloki.hu ● ISSN 1589 1623 (Print) ● ISSN 1785 0037 (Online)
DOI: http://dx.doi.org/10.15666/aeer/1705_1202312055

7-	*Amaranthus graecizans* L. MUH-3037	Herb	Hardar-Chalei	Whole plant	Spring	Bushy-vegetation	The whole climber plant shade dried and ground to form powder is used for cardiac diseases, diabetes and aphrodisiac. Leaves are crushed with sugar and occupied along with black tea for treating constipation and gastrointestinal problems. Poultice of leaf is prepared along with mustard oil for the cure of abscesses	It is used as vegetable and source of fodder.	12	0.15	0.51
8-	*Amaranthus viridis* L. MUH-3038	Herb	Ganar	Whole plant	Spring	Bushy-vegetation	The leaves are used on snake bite and scorpion sting. Root is used to restraint menstruation. It is also used as vegetable (saag)	It is used as vegetable and fodder	43	0.54	0.24
9-	*Celosia argentea* L. MUH-3039	Herb	Gutta-Buti	Whole plant	Spring	Fertile-valley	About 20ml of root extract is used to check undue menstruation. It is used as fodder for cattle	It is used as fodder for cattle	12	0.15	0.23
10-	*Digera muricata* (L.) Mart. MUH-3040	Herb	Tandola / Dawurra	Whole plant	Spring	Waste-land	Extract of the whole plant juice is used as laxative. Leaves are used as vegetable. The tender tips extract is also used for kidney stones	It is used as bioremediator and fodder and vegetable	29	0.36	0.15
11-	*Pupalia lappacea* (L.) Juss. MUH-3041	Herb	Jojera	Whole plant	Spring	Bushy-vegetation	10-12gm of fresh leaf paste mixed with 50-60ml of *Sesamum indicum* oil, mixture is used for bone fracture	It is used as vegetable and chick feed	57	0.72	0.54
(3) Anacardiaceae											
12-	*Lannea coromandelica* (Houtt.) Merr. MUH-3042	Tree	Gandela	Whole plant	Summer	Forest	The gum acquired from the stem is used in confectionery. The bark powder is used as a flavoring. The plant is grown as a hedge as well as a fence	It is used as Fuel wood, shelter and fodder	32	0.41	0.51
(4) Apocynaceae											
13-	*Carissa opaca* Stapf ex Haines. MUH-3043	Tree	Grunda	Whole plant	Spring	Mountain-forest	1kg decoction of fresh roots is used for asthma, jaundice and kidney pain. 30g dried root is crushed to form powder and used in the cure of animal wounds. Milky juice extracted from ripen fruit is effectively used to cure iron deficiency, liver disorders and blood deficiencies. Leaves are used as fodder for goats and sheep. Stem and root are used as fuel especially in local ovens	It is used as fodder, fuel wood, hedging and fencing, fruit	44	0.55	0.36
14-	*Telosma cordata* (Burm. f.) Merr. MUH-3044	Herb	Pakalana	Roots and flowers	Spring	Waste-land	The plump roots are used to make a sweetmeat. The flowers are used in the treatment of conjunctivitis	It is used as fodder and dry fuel	51	0.65	0.72
(5) Asclepiadaceae											

http://www.aloki.hu ● ISSN 1589 1623 (Print) ● ISSN 1785 0037 (Online)
DOI: http://dx.doi.org/10.15666/aeer/1705_1202312055

15-	*Calotropis procera* (Aiton) Dryand. MUH-3045	Shrub	Desi-aak	Whole plant	Summer	Barren-land	Whole plant extract is used for dog bite. Commonly latex is used for ring worm and skin diseases. The milky juice is toxic	Its toxic material, kills goats if eaten too much	41	0.52	0.23
(6) Asparagaceae											
16-	*Asparagus gracilis* Browicz MUH-3046	Herb	-	Whole plant	Spring	Bushy-vegetation	The plant is used for its anti-oxidant and anti-urease activity	Fodder for animals	23	0.29	0.41
(7) Asteraceae											
17-	*Artemisia scoparia* Waldst. & Kitam. MUH-3047	Herb	Chahuu	Leaves	Spring	Waste-land	Leaves are used as tonic and anthelmintic	It is used as fodder for goats, dry fuel	41	0.52	0.72
18-	*Bidens biternata* (Lour.) Merr. & Sherff MUH-3048	Herb	-	Leaves and seeds	Summer	Waste- land	Leaf juice is used to treat eye and ear infections. The scoured leaves are applied to skin infections as haemostatic on wounds, and enfolded around the umbilical cord of babies. The seeds are used as an anthelmintic in animals	It is used as fodder and bioremediator	12	0.15	0.55
19-	*Tridax procumbens* (L.) L MUH-3049	Herb	Coat button	Whole plant	Spring	Waste-land	The leaves are used in the treatment of bronchial catarrh, dysentery and diarrhea. The leaves paste is applied to reduce swelling of haemorrhoids and to stop bleeding. Smoke produced by burning of the plant is used to repel mosquitoes	It is used as dry fuel, and fodder.	35	0.44	0.65
20-	*Xanthium strumarium* L. MUH-3050	Herb	Motta-Jojera	Whole plant	Spring	Bushy-vegetation	120ml decoction is prepared from 60mg of dried root of this plant and used in diabetes. Leaves decoction is used for long malarial fever	It is used as fuel	59	0.75	0.52
(8) Boraginaceae											
21-	*Ehretia laevis* Roxb. MUH-3051	Tree	Cham-road	Stem and bark	Summer	Forest	Stem bark powder is used internally to check blood dysentery for three days	Fire wood, shelter, fodder	56	0.71	0.29
(9) Brassicaceae											
22-	*Coronopus didymus* (L.) Sm. MUH-3052	Herb	Thandi-Buti	Whole plant	Spring	Fertile-valley	The plant is used as fumigant to repulse the insects. The plant brings feelings of coolness in the body	It is used as bioindicator	24	0.31	0.52
(10) Cactaceae											
23-	*Opuntia monacantha* (Wild.) Haw. MUH-3053	Shrub	Tarapar-thor	Whole plant	Summer	Barren-land	It is used as hedge plant for fencing the fields	It is used as raticide	23	0.29	0.15
(11) Cannabaceae											

http://www.aloki.hu ● ISSN 1589 1623 (Print) ● ISSN 1785 0037 (Online)
DOI: http://dx.doi.org/10.15666/aeer/1705_1202312055

24-	*Cannabis sativa* L. MUH-3054	Herb	Bhaang	Whole plant	Summer	Beside pedestrain passes	The fruit and leaves are used as soporiferous commonly called "Charas". Decoction of seeds is given to cattle for increasing milk. Leaves are also used for constipation, stomach diseases, aphrodisiac and muscle contraction. It is also used for stopping menses and whooping cough. Seeds are used to stop releasing sperms	It is used for fuel, thatching material used in mud-houses	31	0.39	0.44
(12) Capparidaceae											
25-	*Capparis sepiaria* L. MUH-3055	Shrub	Daddur	Whole plant	Spring	Forest	The fruit is used to make powder and effectively used to cure anemia, liver disorder and aphrodisiac. The leaves are used as fodder for goats. Wood is useful as fuel wood	It is used as fuel plant, fodder as well	23	0.29	0.71
26-	*Cleome gynandra* L. MUH-3056	Herb	Talwar-Buti	Leaves	Spring	Hedgerows	Leaf juice is used as an ear-ache drop by drop. Half tea-spoon of leaf juice is used daily for cold. 10g of leaves crushed with the same amount of pepper and garlic extract is used daily for fertility to women after completion of menstrual period	It is used as fodder plant	15	0.18	0.31
27-	*Crateva adansonii* DC. MUH-3057	Tree	Barna	Whole plant	Summer	Barren-land	It is suitable in disorders of urinary organs, urinary tract infections, pain and burning micturition, renal and vesicle calculi.	Fuel wood, shelter and cattle shades	25	0.32	0.29
(13) Celastraceae											
28-	*Maytenus royleana* (Wall. ex M.A. Lawson.) Cufd. MUH-3058	Shrub	Pataki	Whole plant	Summer	Forest	Root extract is abortificent. Leaves are palatable. Whole dry plant is used as fuel wood especially in local ovens	It is used as fodder, hedging plant	31	0.39	0.39
(14) Combretaceae											
29-	*Anogeissus latifolia* (Roxb. ex DC.) Wall.ex Bedd. MUH-3059	Tree	Qaam	Stem bark	Summer	Mountain-forest	Stem bark is crushed and soaked in water over night, 2 spoons of the filtered extract is given twice a day to cure whooping cough	It is used as fuel tree, shelter and fodder	19	0.24	0.18
(15) Commenlinaceae											
30-	*Commelina benghalensis* L. MUH-3060	Herb	Churra	Whole plant	Spring	Shady-land	Leaves are used as vegetable (saag). Plant is used as fodder for cattle. Leaves are laxative	It is used as fodder and vegetable	15	0.18	0.29
(16) Convalvulaceae											

http://www.aloki.hu ● ISSN 1589 1623 (Print) ● ISSN 1785 0037 (Online)
DOI: http://dx.doi.org/10.15666/aeer/1705_1202312055

31-	*Cuscuta reflexa* Roxb. MUH-3061	Climber	Neela-Dhari	Whole plant	Summer	Fertile-valley	Stem juice is useful for epilepsy and other mental disorder. Paste of the plant powder is prepared in butter and visibly useful for wounds. The whole plant is crushed and boiled in 8liter of water for an hour. It is filtered and advised the patient to take a bath with this decoction without using soap for scabies	It is used for roping and knitting of wooden goods	41	0.52	0.32
32-	*Evolvulus alsinoides* (L.) L. MUH-3062	Herb	Vishnuki ranthai	Whole plant	Spring	Fertile-land	Whole plant extract is considered as strong anti-dote for snake bite	It is used as fodder	36	0.45	0.39
33-	*Ipomoea carnea* Jacq. MUH-3063	Shrub	Valeiti-Aak / Jangli	Whole plant	Summer	Waste-land	It is used as a medicinal and hedge plant. It is used to stop the soil erosion in naked land. It is also used as fuel wood	It is used as fuel plant, hedging one	13	0.16	0.24
34-	*Ipomoea pes-tigridis* L. MUH-3064	Climber	Alra-Kalyari / Kangi-poncha	Whole plant	Spring	Bushy-vegetation	It is used for poultice sores, pimples, boils, carbuncles etc. Entire creeper is crushed and the juice is given orally for treatment of rabies, if one is bitten by rabid dog. It is also used for wound healing as well as various painful conditions like head-ache, swelling, poisonous sting, snake bites etc.	It is used as fodder and vegetable	29	0.36	0.82
(17) Cucurbitaceae											
35-	*Coccinia grandis* (L.) Voigt MUH-3065	Herb	Chiwra/ Kandyari	Leaves, root and fruit	Spring	Waste-land	Softened roots are used for diabetes. Softened leaves are applied on swellings. Also its fruit, leaves and stem mixed with neem is used to cure diarrhea, blood purifier, loss of appetite and indigestion	It is used as fodder and dry herb as fuel.	33	0.42	0.69
36-	*Diplocyclos palmatus* (L.) C. MUH-3066	Herb	Cucumber / Sivadond	Leaves	Summer	Waste-land	Slightly warmed leaf juice is used as rheumatic swellings in cattle	It is used as fodder and bioindicator	49	0.62	0.45
(18) Cyperaceae											
37-	*Cyperus iria* L. MUH-3067	Herb	Deela-Kaa / Muthri	Tubers, leaves	Spring	Fertile-land	Decoction of crushed tubers is used for fevers. The plant is considered good tonic, stimulant, stomachic and astringent. It is used as fodder for cattle	It is used as fodder and tonic herb	42	0.53	0.16
(19) Euphorbiaceae											
38-	*Euphorbia hirta* L. MUH-3068	Herb	Duudeil	Whole plant	Spring	House-garden	Whole plant is very effective for liver disorder and ring worms. Leaves juice is taken in diabetes. It is effectively suitable for stomach pain	It is used as fodder herb	21	0.26	0.36

http://www.aloki.hu ● ISSN 1589 1623 (Print) ● ISSN 1785 0037 (Online)
DOI: http://dx.doi.org/10.15666/aeer/1705_1202312055

39-	*Euphorbia prostrata* Aiton MUH-3069	Herb	Hazar-Dani	Whole plant	Spring	Beside pedestrian passes	Dried plant is crushed to make powder and used as anti-renal fall. Plant powder mixed with sugar is effective for liver disorder. The paste is also suitable in skin diseases. Plant decoction is used as dermatocides, especially for ring worm. Dried plant powder is used in diarrhea	It is used as protector	54	0.68	0.82
40-	*Ricinus communis* L. MUH-3070	Shrub	Hernoli	Leaves, seeds and oil	Summer	Waste-land	Leaves are emetics, poisonous and strongly laxative. Poultice is applied to swelling. Castor oil is laxative, oil is given in constipation before and after child birth to mothers. Seeds are sedative	It is use as fuel wood and hedge plants	39	0.49	0.42
(20) Flacourtiaceae											
41-	*Casearia tomentosa* Roxb. MUH-3071	Tree	Cheela / Jeela	Leaves and fruit	Summer	Waste-land	The tender leaves are placed on abdomen of babies to cure abdominal pain. The fruit is used for fish poisoning.	It is used as fuel wood and fodder	44	0.55	0.62
42-	*Flacourtia indica* (Burm. f.) Merr. MUH-3072	Tree	Ko-ko	Fruit and wood	Summer	Forest	Fruit is palatable and also suitable for liver disorder and stomach disorder. Wood is used as fuel wood	It is used as wild fruit tree, fuel wood	47	0.59	0.53
(21) Lamiaceae											
43-	*Anisomeles indica* (L.) Kuntze. MUH-3073	Herb	Boo-Buti / Sankhia	Whole plant	Spring	Fertile-valley	Leaf paste is used to treat snake bite. Whole plant extract is an excellent blood purifier. It is effectively used against cancer, jaundice and hepatitis	It is used as fodder plant	42	0.53	0.26
44-	*Leucas cephalotes* (Roth) Spreng. MUH-3074	Tree	Kareen	Whole plant	Summer	Near human settlement	The seeds are used to control stomach-ache, as contraception and abortifacient. The seed gum is used as a binder. The plant is supposed to be a worm repellent and also used in treating fevers, flu, colds and reduce back pain and menstrual cramps. The immature pods are palatable as well as vegetable. The legumes act as a great source of fodder for cattle	It is used as fuel wood and shadow tree. Leaves as fodder and thatching	49	0.62	0.68
45-	*Ocimum americanum* L. MUH-3075	Herb	Naizboo	Leaves and seeds	Spring	Near shady-land	The seeds are effectively used as aphrodisiac, gas trouble, dyspepsia and indigestion. The leaves paste is used for the treatment of skin diseases. It is also applied to wounds and burns that are not healing well	It is used as fodder	50	0.63	0.55
(22) Malvaceae											

http://www.aloki.hu ● ISSN 1589 1623 (Print) ● ISSN 1785 0037 (Online)
DOI: http://dx.doi.org/10.15666/aeer/1705_1202312055

46-	*Abutilon bidentatum* Hochst. Ex A. Rich MUH-3076	Herb	Kanghi Buti	Whole plant	Spring	Waste-land	The plant is used to comfort childbirth and expel the placenta. The plant is used as bandage to comfort kidney pain and is mixed with sticky rice and it is useful to ulcers. The roots are also used to cure cough and tooth-ache. The leaves are flowers are suitable to abscesses	It is used as bioindicator and fodder	48	0.61	0.59
47-	*Abutilon indicum* (L.) Sweet MUH-3077	Herb	Kanghi Buti	Whole plant	Spring	Waste-land	Leaves decoction is beneficial to cure gout, tuberculosis, ulcers and leucorrhea. The juice of leaves supports to discharge toothache. The whole plant can be stewed down into a decoction to discharge the symptoms of lung ailments, tuberculosis and bronchitis. It is also used in the treatment of colds and fever	It is used as fodder plant	34	0.43	0.53
48-	*Malvastrum coromandelianum* (L.) Garcke MUH-3078	Herb	Hatmii-Khubazii	Leaves and flowers	Spring	Fertile-land	Leaves and flowers are used as aphrodisiac	It is used as bioremediator	52	0.66	0.62
49-	*Sida cordata* (Burm. f.) Borss. Waalk. MUH-3079	Herb	Paavani	Leaves	Spring	Shady-land	Crushed leaves paste is applied externally for body tumors, boils, cuts	It is used as fodder species	38	0.48	0.43
50-	*Sida cordifolia* L. MUH-3080	Herb	Berela	Leaves and root	Spring	Shady-land	Leaf extract is useful in dysentery as well as blood fluctuation. Root extract is used in urinary troubles and haematuria. The plant is used for tonic, in fever, nervous disorders, colic, general debility and heart irregularity	It is used as fodder plant	59	0.75	0.29
51-	*Urena lobata* L. MUH-3081	Herb	Kangi / Burr-Mallow	Whole plant	Spring	Shady-land	The immature leaves are used as vegetable. The leaves are used as poultice on wounds and skin diseases. A decoction of root is used to treat colds, dysentery, goiter, ingestion, malaria etc. The bark is used to heal cuts. A decoction of flowers is used for dry cough. A fiber is acquired from stem which is used to make ropes, papers etc.	It is used as fodder and bioindicator species	54	0.68	0.23
(23) Martyniaceae											
52-	*Martynia annua* L. MUH-3082	Herb	Bichhu / Kutta-buti	Leaves and fruit	Spring	Bushy-land	Leaves and fruit are used in scorpion and snake bite	It is used as fodder plant	18	0.23	0.66
(24) Meliaceae											

http://www.aloki.hu ● ISSN 1589 1623 (Print) ● ISSN 1785 0037 (Online)
DOI: http://dx.doi.org/10.15666/aeer/1705_1202312055

53-	*Azadirachta indica* A. Juss. MUH-3083	Tree	Neem	Leaves, seeds, bark ,wood and stem	Summer	Barren-land	Tender leaves of the plant are given daily to the person suffering from diabetes. 15ml of leaves extract is taken in hollow stomach continuously one month for treatment of diabetes as well as blood purification. Paste of 6 seeds with 50ml rice and 5ml of ghee should be given after meal in case of long standing diabetes. A shade dried powered leaves are useful for blood purification and liver diseases	It is used as fuel wood, kitchen utnesils, mosquito repellent and shelter tree	59	0.75	0.48
(25) Mimosaceae											
54-	*Albizia lebbeck* (L.) Benth. MUH-3084	Tree	Sreeia / shreen	Leaves, Wood and Seeds	Summer	Near human settlement	The flowers decoction is used for heart blockage. Dried leaves and seeds are equal in weight mixed with water then desiccated and honey is added. The mixture is very effective for kidney disorder. Bark decoction is used to treat diarrhea. Seeds are used for treating severe kidney infection. Leaves provide shade which is used as hallowed for the treatment of various diseases. Wood is used as fuel wood and for making agitator. Leaves are also delicious and weight increasing in cattle	It is used as fodder and shelter tree. It is used fuel wood tree	32	0.41	0.68
55-	*Leucaena leucocephala* (Lam.) de Wit. MUH-3085	Herb	Trakhrad -Medana	Whole plant	Spring	Fertile-land	The leaves are used as vegetable. Whole plant is used as fodder for cattle	It is used as fodder tree	28	0.35	0.23
56-	*Senegalia modesta* (Wall.) P. J. Hurter. MUH-3086	Tree	Plai / Pharli	Gum,Leaves and Wood	Summer	Mountain-forest	Gum and powder is prepared fresh leaves of this plant, are mixed with wheat flour and desi ghee and make Halwa that is used for back-ache. Gum extracted from fruits is used as tonic and stimulant. Leaves are used as fodder for goats. Wood is used as fuel. Leaves powder mixed with milk and butter is effectively treat kidney and urinary disorder	It is used as fodder, hedge plant and gum tree, it is used as fuel wood	52	0.66	0.75

http://www.aloki.hu ● ISSN 1589 1623 (Print) ● ISSN 1785 0037 (Online)
DOI: http://dx.doi.org/10.15666/aeer/1705_1202312055

57-	*Vachellia nilotica* (L.) P. J. Hurter & Mabb. MUH-3087	Tree	Kikar	Leaves, Wood, Flowers and Legumes	Summer	Barren-land	Flowers are mixed with mustard oil, which is used in the treatment of skin inflammation. Leaves powder is used as toothpaste and gum is acquired from stem is aphrodisiac. Extraction of fresh roots, leaves and seeds are applied as alcohol (sharab) and also narcotic. Four grams of gum is applied as paste with water that is an effective aphrodisiac. Legume is used as tonic, and for ailment of dysentery and diabetes. Leaves and legumes are used as fodder for goats. Wood is hard and is used for construction, fuel and agricultural tools	It is used as fodder, fuel wood tree, it is shelter tree and used for hedging and thatching	33	0.42	0.41
(26) Moraceae											
58-	*Ficus benghalensis* L. MUH-3088	Tree	Bohar	Whole plant	Summer	Barren-land	The latex acquired from aerial parts of the plants (leaves and immature branches) and mixed with honey is used orally to control high blood glucose level as well as diabetics. Latex from aerial root is energetic and used to fill cracking of feet. Latex is aphrodisiac and effective in dysentery. Wood is used as a fuel wood	It is used as fuel wood, fodder and thatching tree	39	0.49	0.35
59-	*Ficus palmata* Forssk. MUH-3089	Tree	Phugwara	Whole plant	Summer	Waste-land	Fruit is palatable and laxative. It comforts the bee sting by simple rubbing on the skin. Wood is hard and used for making household tools. It is also used as fuel wood	Fruit, fuel wood, and fodder tree	18	0.23	0.42
60-	*Ficus religiosa* L. MUH-3090	Tree	Pipal	Wood, bark and fruit	Summer	Waste-land	Decoction of bark is used in vomiting, gonorrhea and scabies. Burn the bark and make powder from it and take 5g of it orally with water for diarrhea. Fruit is palatable and laxative. Wood is used as fuel wood	It is used as fodder and shelter and fuel	55	0.69	0.49
(27) Nyctaginaceae											
61-	*Boerhavia procumbens* Banks ex Roxb. MUH-3091	Herb	Eeit- seit	Roots and leaves	Spring	Near human settlement	Roots and leaves paste is useful for liver disorder. Root decoction is useful for cough and pulmonary disorder. Leaf paste is lapped on wasp sting as anti-dote	Yes	Yes	58	0.73	0.82
(28) Oxalidaceae											

http://www.aloki.hu ● ISSN 1589 1623 (Print) ● ISSN 1785 0037 (Online)
DOI: http://dx.doi.org/10.15666/aeer/1705_1202312055

62-	*Oxalis corniculata* L. MUH-3092	Herb	Khati / Luuni-Buti	Whole plant	Spring	Beside pedestrian passes	Leaves powder is mixed with silver water, heated and cooled and effectively used for blood purification. Silver water mixed with honey is used effectively for Alzheimer, fever and kidney diseases. Leaves decoction is used in fever and dysentery. Fresh leaves are used as vegetable. It is also used as fodder and forage for cattle	It is used as fodder	39	0.49	0.23
(29) Papilionaceae											
63-	*Butea monosperma* (Lam.) Taub MUH-3093	Tree	Cheechra	Leaves, flowers, gum and wood	Summer	Forest	10ml of leaves extract is applied once a day for 5-10 days on hollow stomach to reduces blood sugar and also useful in glycosuria. Gum is mixed with sugar and milk used as tonic and also given for back-ache after birth in woman. Wood is used as fuel wood	It is used as fuel and fodder tree, thatching plant	38	0.48	0.69
64-	*Dalbergia sissoo* DC. MUH-3094	Tree	Sheesham / Tali	Whole plant	Summer	Mountain-forest	70g of immature leaves of buds are crushed and one glass of water is added to it and strained. The strained decoction is used daily for treatment of piles and jaundice. Wood boiled with water to make syrup is used as blood purifier, irritation, tumors and pimples. Ground leaves is bandaged on mammary glands to reduce pain. Branches are used as Muswak and kills worms in the teeth. Black wood of old tree is used for making furniture as well as fuel wood	It is used timber tree, fodder, shelter making, fuel wood, and hedging and fencing	53	0.67	0.73
65-	*Desmodium gangetium* (L.) DC MUH-3095	Herb	Jojrii / Salpani	Whole plant	Spring	Forest	A decoction of leaves is used against gall bladder and kidneys stones infections while a decoction of root is used to treat kidney problems, swelling, chronic fever, cough, diarrhea and dysentery. The leaves are used for the treatment of head-ache while the root is used for the treatment of tooth-ache. The whole plant is used to be anthelmintic	It is used as fodder plant	50	0.63	0.49
66-	*Tephrosia purpurea* (L.) Pers. MUH-3096	Herb	Sarmak	Whole plant	Summer	Fertile-land	The plant is used for curing many diseases like leprosy, ulcers, asthma, tumors, liver, spleen, heart and blood related diseases. The leaves and seeds is used as fish poison. A decoction of the root is used in treating depression, diarrhea, rheumatism and urinary disorders. The root powder is used for cleaning the teeth and reduces dental pains	It is used for fodder plant	52	0.66	0.67
(30) Poaceae											

http://www.aloki.hu ● ISSN 1589 1623 (Print) ● ISSN 1785 0037 (Online)
DOI: http://dx.doi.org/10.15666/aeer/1705_1202312055

67-	*Apluda mutica* L. MUH-3097	Grasses	Santali / Chofki	Whole plant	Spring	Hedgerows	Root is crushed and mixed with little mustard oil, the paste is applied on the mouth sore of cattle. It is used as a thatching material by Santal clans	It is used as fodder	24	0.31	0.63
68-	*Chrysopogon fulvus* (Spreng.) Chiov MUH-3098	Grasses	Lamb-Kaa / Khandol	Whole plant	Spring	Mountain	Peels of Culm and bark is used for cough and chest pain. It is also used as fodder for cattle	It is used as bioremediator	46	0.58	0.66
69-	*Cynodon dactylon* (L.) Pers. MUH-3099	Grasses	Khabal	Whole plant	Spring	Beside pedestrian passes	Paste of fresh leaves is applied to cut, wound bleeding and piles. Juice of the plant is used for diarrhea as well as diabetes. The whole plant and flowers crushed and mixed with milk and butter is useful on diabetic ulcers. Plant extract mixed with salt is bandaged on bone fracture. It is used as fodder for cattle	It is used as fodder and carpeting for ground. It is used as fuel if dried	22	0.28	0.31
70-	*Dactyloctenium aegyptium* (L.) Willd. MUH-3100	Grasses	Palwan-kaa	Whole plant	Spring	Fertile-land	Decoction of the whole plant is used for the treatment of lumbago (back-ache). Extraction of the leaves mixed with the seeds is used to accelerate childbirth. A decoction of the leaves is used as a cure for dysentery. It is also used as fodder for cattle	It is used fodder and fuel source if dried	16	0.21	0.29
71-	*Dichanthium annulantum* (Forssk.) Stapf MUH-3101	Grasses	Phuul-Kaa / Marvel	Whole plant	Spring	Beside pedestrian passes	The whole plant is used as a favorite fodder grass for animals, and also suitable for silage and hay if cut earlier then flowering	It is fodder and bioindicator	18	0.23	0.58
72-	*Echinochloa colona* (L.) Link MUH-3102	Grasses	Sard-Kaa / Jangli-rice	Leaves	Spring	Fertile-land	The whole plant is used as fodder for animals	It is used as fodder plant	12	0.15	0.28
73-	*Heteropogon contortus* (L.) P. Beauv. Ex Roem. & Schult. MUH-3103	Grasses	Sryalla-Kaa	Whole plant	Spring	Barren-land	The culms of the grass are used for thatching. They are also used in mates. The root is stimulative, diuretic and used in rheumatism. It is also used as fodder for cattle	It is used as fodder and fuel plant in dried form	32	0.41	0.21

http://www.aloki.hu ● ISSN 1589 1623 (Print) ● ISSN 1785 0037 (Online)
DOI: http://dx.doi.org/10.15666/aeer/1705_1202312055

74-	*Lolium temulentum* L. MUH-3104	Herb	Cheeri-Bajra	Whole plant	Spring	Waste-land	The seeds are useful for fever by placing it in sleep bed as well as decoction. Occasionally used to treat head-ache, rheumatism and sciatica. It is used to treat dizziness, insomnia, blood congestion and stomach problems. It may also be used for skin problems like herpes, scurf and sores. The plant is poisonous and can cause death	It is used as fodder and phyto-remediator	57	0.72	0.58
75-	*Panicum antidotale* Retz. MUH-3105	Herb	Gyrum	Whole plant	Spring	Shady-land	The whole plant is used as fodder for grazing animals	It is used as fodder species	19	0.24	0.23
76-	*Paspalidium flavidum* (Retz.) A. Camus MUH-3106	Grasses	Ghass / Arisi pullu	Grains and seeds	Spring	Waste-land	Grains are palatable. Seeds are boiled and eaten as a substitute for rice by kattunaicka and paniya clans	It is used as fodder plant	32	0.41	0.15
77-	*Saccharum spontaneum* L. MUH-3107	Herb	Saroot	Whole plant	Summer	Waste-land	The honey acquired during July from this plant is very effective for diabetes. Its pulped stem is also effective for diabetic condition.	It is used as hedging and thatching plant, fodder	41	0.52	0.41
78-	*Saccharum bengalense* Retz. MUH-3108	Herb	Kaei	Whole plant	Summer	Waste-land	Whole plant juice is mixed with milk for the treatment of cough. Dry plant is used as fodder for cattle. It is also used for making ropes and for roof thatching	It is used as fodder and hedging plant	35	0.44	0.72
79-	*Sporobolus coromandelianus* (Retz.) Kunth MUH-3109	Grasses	Cheeri-Kaa	Whole plant	Spring	Waste-land	The plant is used to augment the blood, reduce swellings and correct gonorrhea. A fiber is acquired from the leaves	It is used as fodder species	23	0.29	0.23
80-	*Themeda anathera* (Nees ex Steud.) Hack. MUH-3110	Grasses	Bhari-Kaaa	Whole plant	Spring	Mountain-forest	It is used as fodder for cattle	It is used as fodder and fuel species	16	0.21	0.24
81-	*Urochloa panicoides* P. Beauv. MUH-3111	Grasses	Harat / Jhun-Kaa	Whole plant	Spring	Waste-land	The whole plant is excellent fodder for cattle and horses	It is used as fodder plant	13	0.16	0.41
(31) Potamogetanaceaet											
82-	*Potamogeton nodosus* Poir. MUH-3112	Climber	Jujuli	Whole plant	Spring	Forest	Leaf extract is applied on irritating skin. Leaves also used for constipation. Whole plant form is excellent bio-fertilizer and used in crops	It is fodder and thatching plant	35	0.44	0.52
(32) Primulaceae											

http://www.aloki.hu ● ISSN 1589 1623 (Print) ● ISSN 1785 0037 (Online)
DOI: http://dx.doi.org/10.15666/aeer/1705_1202312055

83-	*Anagallis arvensis* L. MUH-3113	Herb	Neeli-Buti	Whole plant	Summer	Mountain-forest	Dried whole plant is crushed into powder. 2g of the powder with 5g of wheat flour is mixed for cure of rheumatism. It is also used as fodder for cattle	It is used as fodder plant	43	0.54	0.44
(33) Rhamnaceae											
84-	*Ziziphus jujuba* Mill. MUH-3114	Tree	Jannd	Fruit as well as whole plant	Summer	Forest	Bake the fruit and eat for the treatment of stomach problems. 5 g of root powder and 7 pieces of black pepper, grind mixed and is used to cure diarrhea and abdominal pain. Bark is mixed with honey to use in diarrhea and dysentery. Fruit is palatable, blood purifier and used in indigestion. The leaves are used as fodder for goats. Wood is used as a fuel wood	It is used as fruit tree, fodder and fuel wood species, hedging and fencing	59	0.75	0.29
85-	*Ziziphus mauritiana* Lam. MUH-3115	Shrub	Jangli-Barii	Whole plant	Summer	House-garden	Decoction of fruit and bark is mixed with a cup of milk to treat constipation and dysentery. Fresh leaves are chewed daily to lower blood glucose level. Ripen fruits are palatable. Leaves are used as fodder for goats	It is used as fruit, fuel wood, fodder and hedge plant	53	0.67	0.21
(34) Sapindaceae											
86-	*Dodonaea viscosa* (L.) Jacq MUH-3116	Shrub	Sanatha	Whole plant	Summer	Hilly-forest	Shoots are collected to form besoms for sweeping lawns. Bark is anthelmintic. Oil is extracted from wood by keeping it on pain and used for tooth-ache. Oil is used in cure of paralysis the patient. It is also used as blood purifier. This plant is used for fencing and wood is used as fuel wood. The leaves are warmed and kept on joints to releive pains. (rheumatism)	It is used as fodder, hedging plant and shelter, fuel wood in dried form	41	0.52	0.16
(35) Solanaceae											
87-	*Datura inoxia* Mill. MUH-3117	Herb	Datura	Fruit, leaves and seeds	Spring	Bushy-vegetation	Leaves are used as repellant and vermicide. Fruit is used to heat up the buffalos. Two and half fruit of Datura is used to heat up the cattle. Seeds are antipyretic and soporiferous	It is used as fodder, poisonous plant and pesticide	39	0.49	0.75
88-	*Solanum nigrum* L. MUH-3118	Herb	Canch-manch	Shoots, leaves and fruit	Spring	Fertile-land	Fresh aerial parts of the plant are used as vegetable and to control diabetes. The leaves are crushed to form a paste is used for inflammation, of body such as legs and arms etc. It is also useful for liver disorder. Whole plant juice is abortifacient and the fetus is discharged in a short time. The leaf juice is useful in kidney diseases. Leaf extract is also used to heal up the wounds and tumors	It is used as vegetable, fruit herb, fuel of dried form	26	0.33	0.67

http://www.aloki.hu ● ISSN 1589 1623 (Print) ● ISSN 1785 0037 (Online)
DOI: http://dx.doi.org/10.15666/aeer/1705_1202312055

89-	*Solanum surattense* Burm. f. MUH-3119	Herb	Jangli-Betaun / Mokri	Whole plant	Spring	Barren-land	Fruit is dried, crushed and powder is used for the treatment of abdomen pain, gas trouble, cough, fever and pain in chest. It is expectorant, diuretic and anti-gonorrhea	It is used as fodder, fruit , vegetable herb	31	0.39	0.52
(36) Tiliaceae											
90-	*Grewia optiva* J.R. Drumm. Ex Burret MUH-3120	Tree	Dhaman	Leaves, fruit and wood	Summer	Forest	Fresh leaves are boiled in water to prepare concentrated paste at low temperature. The concentrated paste is used for joint pain. The outer bark and fruit are soaked in water, the yield is a gelatinous material which after drying, is used to make tablets that are used as aphrodisiac. Leaves are palatable for goats. Wood is used as fuel wood	It is used as fodder, fuel wood, hedging and thatching one	23	0.29	0.49
91-	*Triumfetta pentandra* A Rich. MUH-3121	Herb	Permothi i	Whole plant	Spring	Bushy-vegetation	The bark of green shoots of a mucilage used for making sticky soups and sauces. The mucilage is often used as baby food and for young children not so far able to eat common starchy foods. Because of its high energy value, the soup is given to women who have delivered a child. It is also used as appetizer. Fresh roots are used as a poultice on sores and small wounds. The crushed leaf is applied in plaster for treatment of goiter and deformities	It is used as fodder species	34	0.43	0.33
(37) Verbenaceae											
92-	*Vitex negundo* L. MUH-3122	Shrub	Banna	Leaves, root, stem and seeds	Summer	Barren-land	The decoction of leaves is used for jaundice. 60g dried seeds, 30mg prior weed and 2-3 tea-spoon of common salt are crushed to form powder that is used for anti-pyretic, jaundice and gastrointestinal problems. The seeds are crushed to acquire powder and are taken with water for kidney stone. The paste of leaf is used externally to treat snake bite.	It is used as shelter plant, fuel, hedging and fencing plant	37	0.47	0.62

http://www.aloki.hu ● ISSN 1589 1623 (Print) ● ISSN 1785 0037 (Online)
DOI: http://dx.doi.org/10.15666/aeer/1705_1202312055

Relative frequency of citation and use values

The RFC shows the local importance of every species with reference to the informants who cited uses of these plant species (Vitalini et al., 2012). In our work, RFC ranges from 0.75 to 0.14 (*Table 3*). *Senegalia modesta, Grewia optiva, Pupalia lappacea, Xanthium strumarium, Ehretia laevis, Sida cordifolia, Azadirachta indica, Boerhavia procumbens, Ziziphus jujuba* and *Butea monosperma* were the most cited ethnomedicinal plant species. These species are native to the area and have been known to local cultures over a long time period. Thus their specific properties for curing different diseases have become popularized and well-established among the indigenous people.

The use value (UV) is a measure of the types of uses attributed to a particular plant species. In the present study Datura inoxia, Dalbergia sissoo, Tephrosia purpurea, Abutilon bidentatum, Ricinus communis, Cuscuta reflexa, Calotropis procera and Digera muricata had UV values of 0.75, 0.73, 0.67, 0.59, 0.49, 0.32, 0.23 and 0.15, respectively. As the values for the UV and RFC are dynamic and change with location and with the knowledge of the people, so the values of UV and RFC may vary from area to area and even within the area.

Determination of fidelity level (FL)

The plants are used for treatment in different forms by local inhabitants of WNP of District Bhimber, AJK. This fidelity level analysis describes how the people of local area use a particular plant for the cure of specific disease and it also depicts their trust and belief on the specific plant used for cure that ailment. The analysis showed that highest FL values with first rank were *Grewia optiva* and *Senegalia modesta* (100% each) while *Justicia adhatoda* was at number two with 93% FL value and least *Maytenus royleana* with 23% weightage of worthiness in community popularity index (*Table 4*).

Determination of informant consensus factor (ICF) for ethnobotanical study of Watala National Park of AJK

The informant consensus factor (ICF) is a very important tool being used in ethnobotanical analysis and it describes how frequently a herb is used for cure to a particular disease. It indicates that how much community is unanimously agree to use different number of plant species for cure of particular disease or group of specific ailments. In this study, the highest values were obtained for jaundice, spleen and liver disorders (0.93); and kidney and urinary disorder (0.93). The ratio of cardio vascular diseases with reference of ICF was 0.50 (*Table 5*) and it is the least common disease prevailing in the area. These ICF calculations predictive of herbal therapeutics are used in the culture of indigenous communities.

Direct matrix ranking (DMR)

The data matrix ranking is an important microstatistical tool that describes what frequency of utilization is in an invariable form of a particular species for species purpose in daily life of man. This indirectly measures usage pressure on one species that is being exploited for different purposes by human beings. According to the informants' preview and key information *Senegalia modesta* has the highest DMR values and

http://www.aloki.hu ● ISSN 1589 1623 (Print) ● ISSN 1785 0037 (Online)
DOI: http://dx.doi.org/10.15666/aeer/1705_1202312055

ranked at first while two taxa of genus *Ficus* named: *Ficus palmata* and *Ficus religious* were at number two. While plant *Butea monosperma* was third at 6th rank as shown in *Table 6*. This DMR table depicts that there are several severe biotic threats due to anthropogenic interference on plants life.

Table 4. *Fidelity level (FL) values of plants of Watala National Park and allied area, District Bhimber, AJK*

Species and family	Vernacular name	Family	Ethnomedicinal uses	Fidelity level (FL)
Grewia optiva J. R. Drumm. Ex Burret	Dhaman	Tiliaceae	Aphrodisiac, antihypertension	100%
Senegalia modesta (Wall.) P. J. Hurter	Phulai	Mimosaceae	Tonic, anti-inflammatory	100%
Justicia adhatoda L.	Baikar	Acanthaceae	Chest infection, hypertension	93%
Alternanthera pungens Kunth Bot.8	Kand booti	Amaranthaceae	Haematuria and menstrual disorders	82%
Solanum nigrum L.	Makoo	Solanaceae	Spleenic pain, liver disorders	70%
Ziziphus jujuba Mill.	Bairee	Rhamnaceae	Skin disorder, fruit source	69%
Butea monosperma (Lam.) Taub	Cheechra	Rhamnaceae	Hypertension, Hyperlipidemia, glycosuria	66%
Ficus palmata Forssk.	Phakwaree	Solanaceae	Leprosy, Rheumatism	64%
Flacourtia indica (Burm. f.) Merr.	Sheesham	Flacourtiaceae	Jaundice, Stomach disorders	62%
Albizia lebbeck (L.) Benth.	Shereen	Mimosaceae	Kidney, stomach	61%
Dalbergia sissoo DC.	Sheesham	Papilionaceae	Sore throat, cough, dysentery, stomachache	60%
Azadirachta indica A. Juss.	Dhareek	Miliaceae	Syphilis, amenorrheae, edema	58%
Calotropis procera (Aiton) Dryand.	Desi Aak	Asclepiadaceae	Skin disease, dog bite, sting	57%
Casearia tomentosa Roxb.	Cheela	Flacourtiaceae	Anti-ulcer, fish poisoning	43%
Cynodon dactylon (L.) Pers Poaceae	Khabal graas	Poaceae	Antitumor hey fever, flatulation, epilepsy, asthma	40%
Cuscuta reflexa Roxb.	Akaasch Bail	Convolvulaceae	Elipsy, scabies, and wound healer	32%
Maytenus royleana (Wall. ex M. A. Lawson.) Cufd.	Patakee	Celastraceae	Abortifacient agent	23%

Table 5. *Informant consensus factor (ICF) by categories of diseases in the study area (WNP) AJK*

S no	Category/plants used for disease(s)	Species	(%) All species	Use citations	(%) All citations	ICF
1	Diabetics and blood pressure	18	09. 83%	33	08.61%	0.88
2	Fever, flu, headache, bronchitis, cough	37	20.21%	71	18.53%	0.94
3	Epilepsy and mental disorders	14	07.65%	23	06.0%	0.69
4	Stomachic, constipation, haemorrhoids	26	14.20%	48	12.51%	0.88
5	Jaundice, spleen and liver disorders	45	24.59%	86	22.45%	0.93
6	Cardiovascular disorders	13	07.10%	19	04.96%	0.50
7	Rabies and other sting pains	11	06.01%	18	04.69%	0.70
8	Gut, tuberculosis, ulcers and leucorrhea	15	08.19%	27	07.04%	0.85
9	Arthritis and joint disorders	16	08.74%	30	07.83%	0.93
10	Kidney and urinary disorder	15	08.19%	28	07.31%	0.92

http://www.aloki.hu ● ISSN 1589 1623 (Print) ● ISSN 1785 0037 (Online)
DOI: http://dx.doi.org/10.15666/aeer/1705_1202312055

Table 6. *Direct matrix ranking (DMR) of plant species with different uses other than medicinal value (total score of 10 informants) in Watala National Park of District Bhimber AJK*

S. No	Uses	*Senegalia modesta*	*Ficus palmata*	*Butea monosperma*	*Ficus religiosa*	*Carica opaca*	*Ziziphus jujba*
1	Construction	56	26	11	25	11	15
2	Hedge, fencing	22	05	14	21	52	29
3	Fuel wood	40	19	16	37	37	30
4	Shelter, timber	53	38	13	42	12	21
5	Fodder/feed	04	10	33	25	15	16
6	Wild fruit/food	09	04	01	19	30	33
Total		184	102	88	169	157	144
Rank		1st	5th	6th	2nd	3rd	4th

Priority ranking (PR)

The priority ranking (PR) analysis was also determined from the primary data collected from indigenous communities of WNP and allied villages of Barnala AJK. In order to explore the biotic pressure on plants of the study areas PR was calculated in tabular form and destructive threats were categorized in terms of six ranks: 6 < 5 < 4 < 3 < 2 < 1; number 6 represents the most destructive value, as shown in *Table 7*. This determines how respondents of interviewees of the area declare that which parameter is the most dangerous for the flora or specific plant. The PR analysis depicts that fuel wood cutting of plants is a major threat for the flora of the area, followed by fire burnings (that may be accidental or deliberate fires). As village people mostly depend on wood or its products for making shelter or cattle sheds so this is third number key factor of plants degradation or loss from the environment. Among the studied eight threatening factors hedging and fencing cause the least impact on the loss of plant biodiversity of the area.

Table 7. *Priority ranking (PR) of factors perceived as threats to plant biodiversity based on their level of destructive effects in the study area (destructive threat order is: 6 < 5 < 4 < 3 < 2 < 1; 6 is the most destructive value)*

Threat Factors	Respondents (R1-R6)						Total	Percentage	.m
	R1	R2	R3	R4	R5	R6			
Fuel source	6	3	6	4	6	6	31	15.57	1st
Construction of houses	5	3	4	4	2	3	21	11.05	8th
Urbanization mechanism	4	4	6	4	3	4	25	12.56	4th
Agriculture Clearing	5	3	4	4	3	4	23	11.55	6th
Timber Cutting	5	5	4	3	4	5	26	13.06	3rd
Fire Effects	6	4	3	4	6	4	27	13.56	2nd
Fodder and feed	1	4	5	3	6	5	24	12.06	5th
Hedging and Thatching	2	4	5	6	5	2	22	11.07	7th

http://www.aloki.hu ● ISSN 1589 1623 (Print) ● ISSN 1785 0037 (Online)
DOI: http://dx.doi.org/10.15666/aeer/1705_1202312055

Discussion

The plants are very important for the life of all human but their significance is increased many times for rural communities of any area because they depend solely on their natural habitat (plants) while coping their basic needs of life. In this research analysis, plants of the Watala National Park (WNP) and allied villages were surveyed and documented in the form of checklist. The key aim was to explore their traditional ethnomedicinal uses and describe their main ethnobotanical applications in daily life of that area. As indigenous communities of WNP and allied villages are the real owner of flora of that area, so their interviews were conducted using semi-structured and structured format in the form of questionnaires. WNP is an area which is declared as national park by the government and it is located in Tehsil Barnala of District Bhimber AJK, Pakistan. The area under study comprised of WNP area and allied ten villages and out of these "Chandni chowk" and "Danga" villages have high altitude 472 and 465 m.a.s.l., respectively. There is low literacy rate in these remote areas as compared to main stream city of Barnala and Bhimber District. The low education is due to remote areas and low income resources with less approach to good educational institutes (Mehmood et al., 2012). It is also compatible with work past ethnobotanists that modern generations and people living in urban areas have almost no knowledge about medicinal properties of plants (Alcorn, 1984; Altieri et al., 1987). This emphasis that the work conducted on EMs and EB of WNP and allied areas is of paramount significance to conserve the traditional ethnomedicinal knowledge on the plants of the area before it is diminished completely from this area.

In the EB investigation data on medicinal and folklore uses of plants of the Watala National Park (WNP) and allied villages was surveyed and 92 plant species were recorded in ethnomedicinal (EMs) and ethnobotanical (EB) perspectives. The analysis showed that people of age group "56-65 years" had the highest level of EB and EMs knowledge about the local flora of the area (*Fig. 2*). This is in coincidence with previous report of Ishtiaq et al. (2013a) that mostly old people have more EMs knowledge and traditional rituals are preferably followed by them. It was concluded that people of the study area primarily depend on the local vegetation to cope many of their daily needs. Generally inhabitants of the area cut trees/and other plants not only to make shelters and other household items but also sell them as timber and fuel wood for domestic and commercial purposes to earn livelihood and source of revenue; similar findings have been reported in past researchers that rural people of many other countries are also dependent on indigenous plant resources for their needs of life (Mcdichen and Mehl (1990).

Ethnobotany is an important and recent approach to study natural resource management by local people involvement. The EB study gives provision for the protection of traditional and cultural knowledge and rights of native people as intellectual property rights. This research on EB analysis of any area cascades significance on how plants and indigenous people of an area are mutually interconnected and dependent on each other in terms of ecosystem sustainability format. In the past some sporadic work has been conducted on other parts of AJK (Ajaib et al., 2014a) and very little is known on District Bhimber flora, particularly no research project is conducted on EB analysis of WNP and allied villages.

Very little work has been undertaken by legal professionals, environmentalists, NGOs or even human rights groups to secure Intellectual Property Rights for native people, as expressed by Martin (1995) and here WNP and allied villages are very

http://www.aloki.hu ● ISSN 1589 1623 (Print) ● ISSN 1785 0037 (Online)
DOI: http://dx.doi.org/10.15666/aeer/1705_1202312055

neonate and nothing is found in printed or online literature. The present study area WNP and allied villages is an ecologically important area of District Bhimber, AJK but no attention previously had been given for the documentation and conservation of indigenous knowledge of the area.

Most of the native plants now exist only in graveyards and local people had a lot more information about these plants than the introduced plants. Similar results were also recorded by Meza and Vilagram (1991) in Chile on the level of knowledge of native flora, which was always greater for native flora than introduced species. The local inhabitants, having a little knowledge about the species and proper time of collections, from the poorest link in the trade of medicinal plants as reported by Ajaib et al. (2016) during ethnobotanical studies of wild plants of Tehsil Jatlan Azad Jammu and Kashmir. In WNP and allied areas the highest number of plants recorded for EMs and EB studies belonged to families Poaceae, Amaranthaceae and Malvaceae (*Table 2*) and the cause of this might be that taxa of these families have short life spell and can be grown out soon after monsoon rainfall and secondly the tree line is becoming scarce due to cutting and fire burnings (Ishtiaq et al., 2013a). Other taxa of families were also present in the form of herbs (55%), shrubs (10%), climbers and trees (20%) with variable population occurrence in different villages but their community structures have not well established (*Figs. 3* and *4*), which might be underneath cause of sandy stone soil with few rainfall and deep water table in the area (Ishtiaq et al., 2016).

The present study revealed that the local people used some plant species for more than one purpose as tribal totally depended on the vegetation of the area for a variety of their needs. Some of the important multiple-usage plants included *Senegalia modesta* (Wall.) P. J. Hurter, *Albizia lebbeck* (L.) Benth, *Carissa opaca* Stapf ex Haines, *Capparis sepiaria* L, *Dalbergia sissoo* DC, *Dodonaea viscosa* (L.) Jacq, *Flacourtia indica* (Burm. f.) Merr, *Ficus palmata* Forssk, *Ficus religiosa* L, *Heteropogon contortus* (L.) P. Beauv. Ex Roem. & Schult, *Maytenus royleana* (Wall. ex M. A. Lawson.) Cufd., *Oxalis corniculata* L, *Grewia optiva* J. R. Drumm. Ex Burret, *Saccharum spontaneum* L, *Urena lobata* L, *Vachellia nilotica* (L.) P. J. Hurter & Mabb, *Ziziphus jujuba* Mill. Multiple-usage species provided fruits, vegetables, fuel wood, medicines and other requirements to the local population. This is being described in *Table 4* that many plants are being utilized in admixture to cure one or more disease (s) and fidelity level (FL) also proves it (Ishtiaq et al., 2007b). The plant *Senegalia modesta* (Wall.) P. J. Hurter, has the highest FL (100%), followed by *Justicia adhatoda* L. with 93% FL value. *Flacourtia indica* (Burm. f.) Merr. had an FL value of 62%. It is also believed by indigenous rural communities of the area that plants originated drugs “green drugs” are pure and with least or without toxic effects and this coincides with the doctrine of previous researchers (Ishtiaq et al., 2006b, 2007a). The VAA procedure described that ICF analysis of the data culminated that as people of the area living in rural areas and with hard working life style, so they suffer from the least cardiovascular disorders (ICF: 0.50) while common problems in the area were only minor seasonal diseases like fever, flu, headache, bronchitis, cough having the highest ICF (100%), followed by jaundice, spleen and liver disorders (0.93 5) as shown in *Table 5*. Open life pattern and mosquito and high temperature with heat stroke waves may be the cause of this. Other cause of the liver and spleen disorders may be the use of open spring waters or ponds without proper hygienic measures (Erasto et al., 2005; Ishtiaq et al., 2006a, 2007a, 2010b).

One could assess the pressure on the flora of the area by the process of direct matric ranking (DMR) and the results depicted that many plants have been used in multifarious

http://www.aloki.hu ● ISSN 1589 1623 (Print) ● ISSN 1785 0037 (Online)
DOI: http://dx.doi.org/10.15666/aeer/1705_1202312055

forms to cope the needs of life. In this study it was found that *Senegalia modesta* and *Ficus palmata* were being used for different purposes of life by indigenous people and hence in DMR analysis these were at first two positons, respectively (*Table 6*). This describes how the biotic pressure is present on flora of the area and same type of investigations had been recorded that multiple-propose uses creates conservation threats for trees and other plants (Medicken and Mehl, 1990). This all give potential picture of anthropogenic pressure on the local plants of the area and it thrills towards the loss of plants gradually and may be categorized as threatened, endangered or rare taxa, as it was also demonstrated by Ishtiaq et al. (2006b, 2007b) in their previous articles on other areas of AJK.

The research work on WNP and allied areas depicted that as local communities are dwelling in rural area, mostly illiterate with low income resources, so they have to solely depend on wild resources (plants and animals) utilization for livelihood. The priority ranking (PR) statistics is being used as to measure the highly threatening factors for the indigenous plants. The local people use plants for fuel wood, construction, food, fodder, shelter making for livestock, agricultural land preparation by clearing the wild flora of the area. It was found that using plants as fuel is the first threat followed by the fire burning at second (*Table 7*). The hedging and fencing is the least pressure generating factor being at number 7^{th} in analyzed factors. All these factors are keystone threats for the local plants of the area and similar information on threats for plant biodiversity of different areas of AJK and other countries as well (Ahmed and Siraj; 1996; Ishtiaq et al., 2007b). In the analysis it was found that the most threatened species was *Butea monosperma* with highest threatening frequency (29.5%) being used in many needs by local people. Other commonly under threat plants are *Dalbergia sissoo* (19.5%), *Senegalia modesta* (11.25%), *Grewia optiva* (10.25%), *Ziziphus jujuba* (9.25%) as data shown in *Table 8*. These MPs and other taxa are being ruthlessly and unsustainably used by the local communities of the WNP and allied areas for domestic and commercial means that is the main cause of debilitation of plant biodiversity occurrence in the area, ultimately leading towards threatening zone (Mehmood et al., 2012; Ahmed and Siraj, 1996). This all proves that the current scenario should not be ignored and planned biodiversity conservation activities may be introduced and implemented in collaboration with NGOs and Department of Forest with direct participation of the indigenous communities. Main plinth of the problem is unawareness cutting, timber mafia and ignition of fires and it should be tackled by application of incessant methodologies in cooperation with public and private joint venture programs.

Table 8. *Frequency (%) of threatened species in Watala National Park and Allied areas of District Bhimber AJK*

Species name	Frequency (%)
Butea monosperma	29.5
Dalbergia sissoo	19.5
Senegalia modesta	11.25
Grewia optiva	10.25
Ziziphus jujuba	9.25
Azadirachta indica	8.5
Calotropis procera	7.75
Ricinus communis	2.25
Datura inoxia	1.75

http://www.aloki.hu ● ISSN 1589 1623 (Print) ● ISSN 1785 0037 (Online)
DOI: http://dx.doi.org/10.15666/aeer/1705_1202312055

Conclusion and future recommendations

The research work of WNP is of paramount significance as this area is first time explored for ethnomedicinal (EMs) and ethnobotanical (EB) analysis and it has provided the detailed list of all plants of the area in checklist form. It also describes how local people of the area fulfil their daily life needs from indigenous plants and their traditional culture was also recorded in document form. Rural people of the area depend on tree species for shelter, fuel, households, fodder, shadow and food purposes. *Butea monosperma, Grewia optiva, Carica opaca, Dalbergia sissoo, Bauhenia variegata, Senegalia modesta*, *Acacia nilotica* and *Mangifera indica* are key species being used in multiple uses. *Dalbergia sissoo, Butea monosperma* and *Mangifera indica* are under severe threat due to microbial attack and anthropogenic activities. There is dare need to protect and devise *ex-situ* and *in-situ* conservation methods in order to keep the ecosystem of WNP in a sustainable form to cope with the primary needs of village communities, whose whole life depends on the biodiversity of the area. Many plants of the area have good medicinal potential and further ethnopharmacological research should be carried out for novel drug discovery and subsequent drug development and "green drugs" are better than allopathic medicines. It is inevitable to mention that participation and cooperation of indigenous communities is very paramount devoid of that all efforts will be futile and fruitless.

Acknowledgements. This research work is part of the first author's doctoral thesis work who (Ms Mehwish Maqbool) is highly obliged to Chairperson and Lab staff of the Department of Botany, Mirpur University of Science and Technology (MUST) Bhimber Campus Azad Jammu and Kashmir, Pakistan for their kind assistance in the Ph.D. research work conducted in field and lab. The first author is highly indebted to her supervisor Dr Muhammad Ajaib for his all-time coaching and gracious guidance in the completion of this part of her doctoral thesis.

REFERENCES

[1] Ahmad, I., Hussain, M., Ahmad, M. S. A., Hameed, M. (2008): Spatio-temporal effects on association of plant species in some valley of Pakistan. – Pak. J. Bot. 40: 1865-1867.

[2] Ajaib, M., Haider, S. K., Zikrea, A., Siddiqui, M. F. (2014a): Ethnobotanical studies of herbs of Agra Valley Parachinar, Upper Kurram Agency, Pakistan. – Int. J. Biol. Biotech. 11: 71-83.

[3] Ajaib, M., Zabta, K. S., Zikrea, A. (2014b): Ethnobotanical survey of some important herbaceous plants of District Kotli, Azad Jammu & Kashmir. – Biologia (Pakistan) 60: 11-22.

[4] Ajaib, M., Anjum, M., Malik, N. Z., Siddique, M. F. (2015): Ethnobotanical study of some plants of Darguti Tehsil Khuiratta Azad Jammu and Kashmir. – Int. J. Biol. Res. 3(2): 101-107.

[5] Ajaib, M., Islam, A., Siddiqui, M. F. (2016): A contribution to ethnobotanical study of wild plants of Tehsil Jatlan Azad Jammu & Kashmir. – FUUAST J. Biol. 6: 247-256.

[6] Alcorn, J. B. (1984): Development policy forests and peasant farms: reflection on Huastec-managed forests contributions to commercial production and resource conservation. – Econ. Bot. 38(4): 389-406.

[7] Ali, S. I., Qaiser, M. (eds.) (1993-2015): Flora of Pakistan. – Nos, Karachi.

[8] Ali, S. I., Omer, S., Qaiser, M. (2001): Flora of Pakistan. – In: Afzal, M., Mufti, S. A. (eds.) Natural History Research in Pakistan. PASTIC, Islamabad.

http://www.aloki.hu ● ISSN 1589 1623 (Print) ● ISSN 1785 0037 (Online)
DOI: http://dx.doi.org/10.15666/aeer/1705_1202312055

[9] Altieri, M. A., Merick, L. C. (1987): In situ conservation of crop genetic resources through maintenance of traditional farming system. – Econ. Bot. 4(1): 86-96.
[10] Amjad, M. S., Qaeem. M. F., Ahmad, I., Khan, S., Chaudhari, S. K., Malik, N. Z., Shaheen, H., Khan, A. M. (2017): Description study of plant resources in the context of the ethnomedicinal relevance of indigenous flora: a case study from Toli Peer National Park, Azad Jammu and Kashmir, Pakistan. – J Plos One 12(2): 1-31.
[11] Alexiades, M. N. (1996): Selected Guidelines for Ethnobotanical Research: A Field Manual. – In: Advances in Economic Botany Vol. 10. The New York Botanical Garden, Bronx.
[12] Baheem, S. (1890): Tradition and History of Kashmir, Watala Area of District Bhimber Azad Kashmir. – Verinaag Publishers, Srinagar, Kashmir, pp. 110-145.
[13] Chassagne, F., Hul, S., Deharo, E., Bourdy, G. (2015): Natural remedies used by Bunong people in Mondulkiri province (Northeast Cambodia) with special reference to the treatment of 11 most common ailments. – J Ethnopharmacol. 191: 41-70. DOI: 10.1016/j.jep.2016.06.003.
[14] Cook, F. M. (1995): Economic Botany Data Collection Standard. – R. B. G., Kew.
[15] Dar, M. E. U. I., Gillani, N., Shaheen, H., Firdous, S. S., Ahmad, S., Khan, M. Q., Hussain, M. A., Habib, T. M. N. Z., Ullah, T. S., Rafique, S., Aziz, S., Khan, W. A., Hussain, K. (2018): Comparative analysis of vegetation from eroded and non-eroded areas, a case study from Kashmir Himalayas, Pakistan. – Applied Ecology and Environmental Research 16(2) 1725-1737.
[16] Erasto, P., Adebola, P. O., Grierson, D. S., Afolayan, A. J. (2005): An ethnobotanical study of plants used for the treatment of diabetes in the Eastern Cape Province, South Africa. – African Journal of Biotechnology 4(12): 1458-1460.
[17] Ford, R. I. (1978): Ethnobotany: Historical Diversity and Synthesis. – University of Michigan, Museum of Anthropology, Ann Arbor.
[18] Harshberger, J. W. (1896): The purpose of ethnobotany. – Bot. Gaz. 21: 146-158.
[19] Ishtiaq, M., Khan, M. A. (2008): An ethnopharmacological inventory of plants used in midwifery in Tehsil Samahni, District Bhimber Azad Kashmir, Pakistan. – Indian Journal of Traditional Knowledge 7(2) 277-283.
[20] Ishtiaq, M., Mir, A. K., Wajahat, H. (2006a): Ethnoveterinary medicinal uses of plants of from Samahni Valley District Bhimber, (Azad Kashmir) Pakistan. – Asian J. Pl. Sci. 5(2): 390-396.
[21] Ishtiaq, M., He, Q., Cheng, Y. Y., Xiao, P. G. (2006b): Ethnobotany of medicinal plants from Tian Mu Shan Biosphere Reserve, Zhejiang Province, China. – Asian J. of Pl. Sci 5(4): 646-653.
[22] Ishtiaq, M., Wajahat, H., Mir, A. K, Muhammad, A., Ansar, M. B. (2007a): An ethnomedicinal survey and documentation of important medicinal folklore food phytonyms of flora of Samahni Valley, (Azad Kashmir) Pakistan. – Pak. J. Biol. Sci. 10(13): 2241-2256.
[23] Ishtiaq, M., Qing, H., Xiao, P. G. Cheng, Y. Y. (2007b): *Clematis huchouensis* Tamura: a traditional Chinese Herbal medicine and its quality control using a high performance liquid chromatography technique. – Biol. Pharm. Bull. 30(1): 165-168.
[24] Ishtiaq, M., Mehwish, M., Tanveer, H. (2012): Interrelationship of cultural diversity and biodiversity and its impact on conservation. – Pak. J Bot. 44: 245-256.
[25] Ishtiaq, M., Mehwish, M., Tanveer, H., Amin, S. (2013a): Role of indigenous knowledge in biodiversity conservation of an area: a case study on tree ethnobotany of Soona valley, district Bhimber Azad Kashmir, Pakistan. – Pak J Bot 45(SI): 389-399.
[26] Ishtiaq, M., Pazeer, I., Tanveer, H. (2013b): Ethnomedicinal and economic uses of gymnosperms of Neelum Valley District Muzaffarabad Azad Kashmir Pakistan. – Ind J. of Trad Knowl. 12(3): 404-410.

http://www.aloki.hu ● ISSN 1589 1623 (Print) ● ISSN 1785 0037 (Online)
DOI: http://dx.doi.org/10.15666/aeer/1705_1202312055

[27] Ishtiaq, M., Mehwish, M., Tanvir, H., Shehzad, A. (2016): Ethnomedico profile of indigenous flora of Tehsil Barnala District Bhimber Azad Jammu and Kashmir. – J. of Med. Pl. Stud. 3(2): 97-104.
[28] Jones, V. H. (1941): The nature and scope of ethnobotany. – Chronica Botanica 6: 219-22.
[29] Martin, J. (1995): Ethnobotany: A Method Manual, People and Plants Conservation Manual. – Champman and Hall, London.
[30] Mahmood, A., Mahmood, A., Malik, R. N. (2012): Indigenous knowledge of medicinal plants from Leepa valley, Azad Jammu and Kashmir, Pakistan. – J Ethnopharmacol. 143(1): 338-46.
[31] Mcdichen, K. G., Mehl, C. B. (1990): Farmer Prospective of Improvement Objective of MPTS. – In: Glover, N., Adams, N. (eds.) Improvement of Multiple-Purpose Species. Tech-Services Vol. 2. Winrock Instt. for Inter Development and USAID, Little Rock, AR, pp. 50-56.
[32] Meza, P. L., Villagran, C. (1991): Ethnobotany of Alao Island, Chile. – Mus Nac His Nat Bol. (Santiago) 42: 39-78.
[33] Nadeem, A., A. Mehmood, S. Adeel, S. Tahir, B. Asghari, Rifat, N. M. Seema, H., Ishtiaq, M. (2014): Relative importance of indigenous medicinal plants from Layyah district, Punjab Province, Pakistan. – J Ethnopharm 155(1): 509-523.
[34] Naseem, H., Ahsan, M., Shahid, M. A., Khan, N. (2018): Exopolysaccharides producing rhizobacteria and their role in plant growth and drought tolerance. – Basic Microbiol. 58(12): 1009-1022.
[35] Nasir, E., Ali, S. I. (eds.) (1970-1989): Flora of Pakistan. – Islamabad, Karachi.
[36] Okuthe, O. S., McLeod, A., Otte, J. M., Buyu, G. E. (2003): Use of rapid rural appraisal and cross-sectional studies in the assessment of constraints in smallholder cattle production systems in the western Kenya highlands. – Onderstepoort J Vet Res. 70(3):237-42.
[37] Pei, S. (1995): Ethnobotany and sustainable use of plant resource in the HKH mountain region. Proceedings of the Planning Workshop on Ethnobotany and Its Application to Conservation and Community Development in the Hindu Kush Himalayan (HKH) Region. – Biol. Conser. 63(3): 205-210.
[38] Qamar, Q. Z. (1996): Status of major wildlife species and their management in Ghamot game reserve Neelum Valley, District Muzaffarabad. – M.Sc. Thesis submitted to the University of AJK, Muzaffarabad.
[39] Sher, H., Bussmann, R. W., Hart, R., de Boer, H. J. (2016): Traditional use of medicinal plants among Kalasha, Ismaeli and Sunni groups in Chitral District, Khyber Pakhtunkhwa province, Pakistan. – J Ethnopharmacol.188: 57-69. DOI: 10.1016/j.jep.2016.04.059.
[40] Shinwari, M. I., Khan, M. A. (2000): Folk use of medicinal herbs at Margalla Hills National Park, Islamabad. – Journal of Ethnopharmacology 69: 45-65.
[41] Umair, M., Altaf, M., Abbasi, A. M. (2017): An ethnobotanical survey of indigenous medicinal plants in Hafizabad District, Punjab, Pakistan. – PLoS One 12(6): e0177912. DOI: 10.1371/journal.pone.0177912.
[42] Vijayakumar, S., Yabesh, J. M., Prabhu, S., Manikandan, R., Muralidharan, B. (2015): Quantitative ethnomedicinal study of plants used in the Nelliyampathy hills of Kerala, India. – J. Ethnopharma. 161: 238-254.
[43] Vitalini, S., Iriti, M., Puricelli, C., Ciuchi, D., Segale, A., Fico, G. (2012): Traditional knowledge on medicinal and food plants used in ValSan Giacomo (Sondrio, Italy) an alpine ethnobotanical study. – J. Ethnopharma. 145: 517-529.

http://www.aloki.hu ● ISSN 1589 1623 (Print) ● ISSN 1785 0037 (Online)
DOI: http://dx.doi.org/10.15666/aeer/1705_1202312055

THE IMPACT OF SALT (NaCl) STRESS ON GERMINATION CHARACTERISTICS OF GIBBERELLIC ACID PRETREATED WHEAT (*TRITICUM DURUM* DESF) SEEDS

ORAL, E.[1*] – ALTUNER, F.[2] – TUNÇTÜRK, R.[1] – TUNÇTÜRK, M.[1]

[1]*Department of Field Crops, Faculty of Agriculture, Yüzüncü Yıl University, 65080 Van, Turkey*

[2]*Department of Plant and Animal Production, Gevaş Vocational School of Higher Education, Yüzüncü Yıl University, Gevaş, Van, Turkey*

**Corresponding author*
e-mail: eroloral65@gmail.com; phone: +90-546-746-6266

(Received 26th Apr 2019; accepted 16th Jul 2019)

Abstract. This research was conducted to examine the effects of gibberellic acid (GA3), which was treated to wheat (*Triticum durum* Desf) seeds before germination, on their germination and the seedling growth under saline conditions. Durum wheat Güney Yıldızı variety, four different GA3 (0 (control), 100, 200 and 300 ppm), and four different salt (0 (control), 50 mM, 100 mM and 200 mM NaCl) concentrations were used in the research. Germination power, germination ratio (%), germination index, mean germination time, sensitivity index (%), radicula length (cm), plumula length (cm), radicula fresh weight (mg), radicula dry weight (mg), plumula fresh weight (mg), and plumula dry weight (mg) were examined. The results indicated that the increasing doses of salt prevented germination and growth parameters of wheat (*Triticum durum Desf*) seeds. It was observed that the doses of GA3 (Gibberellic acid), which were increased gradually before the doses of salt (NaCl), affected germination and growth positively and significantly. The best results of germination characteristics of wheat seed were obtained from the combination of 300 ppm Gibberellic acid + 0 mM (control) salt.
Keywords: *wheat, gibberellic acid (GA3), germination, salt stress, salt doses*

Introduction

There are many important factors that restrict the efficiency of agricultural production in the world and in Turkey. The first step to eliminate these factors is planting and germinating the seed under suitable conditions (Yıldız et al., 2007). Many vegetative and environmental factors such as seed coat, age, dormancy, temperature, humidity, and light play a role in providing these conditions (Hartmann et al., 1990; De Villiers et al., 1994; Khan and Ungar, 1997). Plants are the most sensitive to environmental factors during germination, emergence, and early seedling periods. All of these environmental factors are called stress factors. The effects of these factors on plants often emerge either one by one or together. Because of that, they are examined as either abiotic or biotic factors based on their sources (Anonymous, 2015). One of the abiotic stress factors that were discussed in this study is salinity (Yılmaz et al., 2011). Salinity is observed in a great portion of the lands on which irrigated farming is practiced especially thanks to the development of irrigation practices. Approximately one third (950 million ha) of the agricultural lands in the world are estimated to suffer from high salinity (Hasegawa et al., 1986; Özkaldı et al., 2004; Taghipour and Salehi, 2008). In Turkey, the salinity problem exists in about 1.5-2 million hectares of the agricultural lands. Wheat is the most grown product in the regions where irrigated agriculture has been started with the GAP project. Especially the majority of durum wheat production is met from this region. Therefore, increasing salinity and alkalinity

http://www.aloki.hu ● ISSN 1589 1623 (Print) ● ISSN 1785 0037 (Online)
DOI: http://dx.doi.org/10.15666/aeer/1705_1205712071

problems in wheat agriculture must be solved. Seen particularly in the regions where wheat is cultivated, the use of poor drainage and faulty irrigation systems is the most important reason. Alkalinity and salinity problems have emerged in our soils as a result of this faulty practice. Salinity that occurs in soil affects transpiration, respiration, and water intake negatively, and also causes root and stem growth to retard. In consequence, hormonal imbalance, transpiration disorder, and inadequate water and nitrate intake occur (Leopold and Willing, 1984; Dölarslan and Gül, 2012). Another problem is that the toxic effects that occur because of Na and Cl ions existing in saline soils cause the loss of ionic equilibrium (Siegel et al., 1980; Flowers and Yeo, 1981; İnal et al., 1995).

For this purpose, these harmful effects on the plants should be detected by conducting research on various plants (Gupta and Srivastava, 1989; Pessarkli et al., 1991; Van Hoorn, 1991). In determining salt resistance, the seeds of the varieties are kept in saline conditions and the effects of these conditions on germination criteria are taken into consideration (Begum et al., 1992). In similar studies, it was stated that plants were the most sensitive during their early germination and seedling periods in terms of salt resistance (Shannon, 1984). Also, the threshold of tolerance to salt in each plant varies by periods (Shannon, 1985). Suitable varieties and practices that will minimize yield losses arising from salinity problem, which restricts productivity in plant cultivation, are needed (Şenay et al., 2005). Salt resistance varies much among the plant species. The most sensitive periods in detecting the salt resistance of species are the germination and the early seedling periods (Van Hoorn et al., 2001). Various research studies that will enable a homogeneous emergence by expediting germination under soil conditions are conducted (Duman and Eşiyok, 1998). For this purpose, different methods such as stratification, hydropriming, acid etching, and hormopriming with growth and development regulators and hormones are applied and these methods are called priming treatments (Ercişli et al., 1999; Yıldız et al., 2017). Among these, hormones and especially GA3 (Gibberellic acid) have been used extensively. Salinity is considered to be one of the environmental stresses that reduce the growth and efficiency of most glycophytic plants worldwide. Induces both osmotic and ionic stresses leading to deterioration of many physiological and biochemical processes including salinity, water relations, ionic homeostasis, gas exchange and mineral nutrition (Parida and Das, 2005) Gibberellins are involved in the stimulation of enzymes involved in seed germination. Gibberellic acid (GA3) is one of the hormones proposed to control primary dormancy by inducing germination. Cavusoglu et al. (2007) reported that GA3 was the most effective salt stress reducing agent among plant growth regulators used in the research.

The aim of this study was to reduce the negative effects of salt in saline soils by treating GA3 (Gibberellic acid) on durum wheat seeds (Zheng et al., 2009; Kayış, 2014).

Materials and methods

In order to evaluate the effect of seed priming on the germination and seedlings' growth traits of Triticum durum Desf. under different salinity stress levels, a factorial experiment was conducted in completely randomized design (CRD) with four replications, at the laboratory of Seed Science and Techonology in the Department of Field Crops, Faculty of Agriculture, Van Yuzuncu Yil University, Turkey in 2019. In the research, Güney Yıldızı variety of durum wheat (*Triticum durum* Desf.) was

http://www.aloki.hu ● ISSN 1589 1623 (Print) ● ISSN 1785 0037 (Online)
DOI: http://dx.doi.org/10.15666/aeer/1705_1205712071

provided from GAP Agricultural Research Institute. Wheat is the most grown product in the regions where irrigated agriculture has been started with the GAP project. Especially the majority of durum wheat production is met from this region. Therefore, increasing salinity and alkalinity problems in wheat agriculture must be solved. The Güney Yıldızı durum wheat cultivar developed by the Diyarbakır Agricultural Research Institute is a high yield genotype grown in large quantities in the region. The yield of other varieties in saline soils is low compared to this variety. For this reason, Güney Yıldızı variety was preferred in the study.

Four different GA3 (0, 100, 200, and 300 ppm) and four different salt concentrations (0, 50, 100, and 200 mM NaCl) were used in the research. Wheat seeds were surface-sterilized for 5 min using 2.5% (v/v) sodium hypochlorite, were washed with pure water 7 times, and were left for drying in a sterile container (Azizi et al., 2011). In the experiment, durum wheat seeds were kept under dark conditions at 20 ± 1 °C in three different doses of GA3 (100, 200, and 300 ppm) and distilled water (H_2O) for 24 h until the humidity of the seeds became 12-13%. After the waiting period, the seeds were drained; two folds of blotting papers were placed; and the seeds were placed into 9-cm-diameter sterile petris, putting 20 seeds in each petri. Then, 5 ml from the prepared NaCl solutions at different doses (50, 100, 200, and 300 mM) and pure water were applied to meet the water demand of the seeds in the petri that was used for control. After these applications, the seeds in the petris were placed into incubators under 20 ± 1 °C temperature for germination and emergence test. The initial tests of the seeds were identified according to ISTA (1996) rules. For the tests applied during germination, the seeds were placed between the two-fold blotting papers, 4 × 20 seeds (*Photo 1*) were used for the tests and the tests lasted for 14 days (ISTA, 1996).

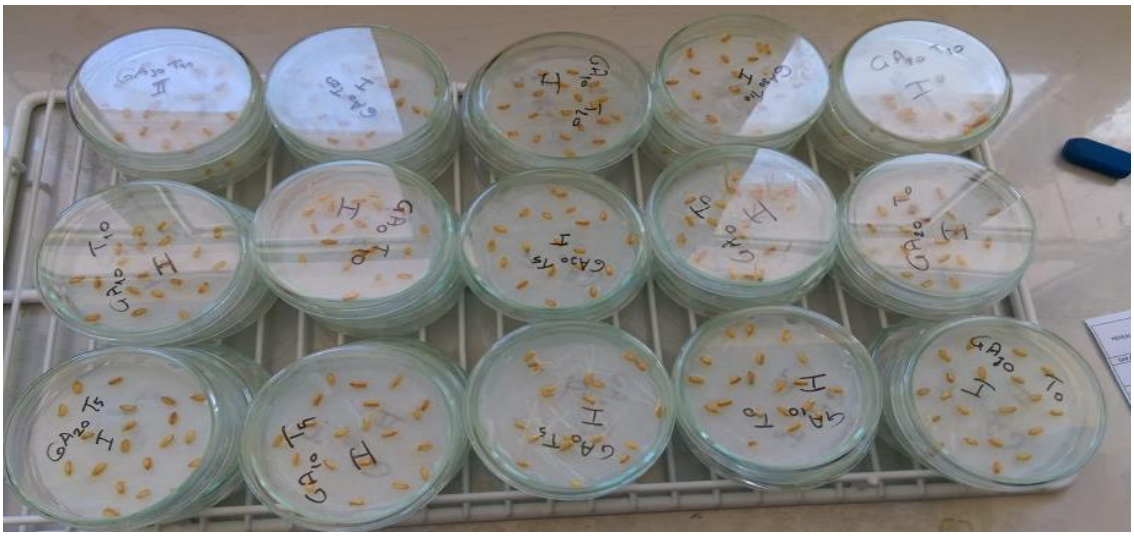

Photo 1. *Seeds in petri dishes*

In this study: germination power, germination ratio (%), germination index, mean germination time, sensitivity index (%), radicula length (cm), plumula length (cm), radicula fresh weight (mg), radicula dry weight (mg), plumula fresh weight (mg), and plumula dry weight (mg) were examined.

Accordingly: root and shoot dry masses were weighed germination rate, germination power, germination index, mean germination time and sensitivity index were calculated

http://www.aloki.hu ● ISSN 1589 1623 (Print) ● ISSN 1785 0037 (Online)
DOI: http://dx.doi.org/10.15666/aeer/1705_1205712071

with the following formulas. It was considered that number of germinated seeds on 7th day as "germination rate" and number of germinated seeds on 14th day as "germination power".

Germination rate (GR) was calculated using *Equation 1* (Akıncı and Calıskan, 2010).

$$GR = \text{Total seeds germinated after day 14} / \text{Total number of planted seeds} \quad \text{(Eq.1)}$$

Germination index (GI) was calculated using *Equation 2* (Wang et al., 2004).

$$GI = \Sigma(Gi / Tt) \quad \text{(Eq.2)}$$

GI: Germination index; Gi: i days germinated seed rate; Tt: count day.

Mean germination time (MGT) was calculated using *Equation 3* (Ellis and Roberts, 1980).

$$MGT = \Sigma(fx) / \Sigma f \quad \text{(Eq.3)}$$

f: Number of seeds germinated x: germination day.

Sensitivity index (SI) was calculated using *Equation 4* (Foolad and Lin, 1997).

$$SI = \text{MGT in the salt application} / \text{MGT in the control application} \quad \text{(Eq.4)}$$

Statistical analyses of the obtained data were done using COSTAT (version 6.3) software, and multiple comparison tests of the data were performed according to the Duncan test (Duzgunes et al., 1987).

Results

According to the results obtained from the research, the effect of salt (NaCl) stress on germination characteristics of GA3 pretreated wheat (Triticum durum Desf) seed was found to be statistically significant. In addition, salt doses × GA3 interactions were found to be significant in all parameters ($P < 0.01$) (*Tables 1* and *2*).

According to the results, the highest germination power and ratio (93.89% and 39.33%, respectively) were obtained from 0 mM and NaCl application; and the lowest values (61.65% and 11.78, respectively) were obtained from the 200 mM salt (NaCl) concentration (*Table 1; Figs. 1* and *2*). The effects of gibberellic acid on germination power and ratio were also found to be significant; and the highest germination power and ratio were obtained from the 200 ppm GA3 application with 81.39% and 32.59%. But it is determined that not found significant differences as statistically between 200 and 300 ppm GA3 applications. The lowest values observed as (75.05% and 14.01%) from 0 ppm (control) applications. But it is in the same Duncan groups with 300 ppm GA3 dose application. The salt × GA3 interactions over the wheat seeds were also found to be significant, and the highest germination power and ratio were obtained from the 300 ppm GA3 concentration (98.00%, 58.33%) of the control application (0 mM). But, there are not different statistically among all GA3 applications for germination power whereas the lowest germination power (56.33%) was detected in the 100 ppm GA3 application of the 200 mM salt concentration.

http://www.aloki.hu ● ISSN 1589 1623 (Print) ● ISSN 1785 0037 (Online)
DOI: http://dx.doi.org/10.15666/aeer/1705_1205712071

Table 1. *The effect of salt stress on the germination characteristics in the Gibberellic acid treated wheat (T. durum Desf) seeds*

Stress applications		Germination power (%)	Germination ratio (%)	Mean germination time (day)	Germination index (%)	Sensitivity index (%)
Salt doses	**GA3**					
Control (T0)	GA0	90.00 a	25.30 c	3.67 c	13.41 a	-
	GA100	92.36 a	33.25 bc	3.83 bc	12.56 a	0.28 e
	GA200	93.22 a	40.25 b	2.68 d	11.25 ab	0.72 bc
	GA300	98.00 a	58.33 a	0.92 f	10.65 c	1.04 ab
T0 mean		93.39 A	39.33 A	2.70 D	11.96 A	0.68 B
50 mM (T50)	GA0	85.32 b	15.50 e	3.90 a	12.27 a	0.38 d
	GA100	85.36 b	20.30 d	4.10 b	13.34 a	0.72 bc
	GA200	85.67 b	40.33 b	3.32 cd	10.95 bc	1.06 ab
	GA300	88.36 ab	49.25 ab	2.30 de	11.05 b	1.12 ab
T50 mean		86.17 B	32.10 B	3.40 B	11.90 B	0.74 B
100 mM (T100)	GA0	66.70 c	9.46 g	4.15 ab	10.36 c	0.55 c
	GA100	75.00 bc	27.70 cd	2.92 d	9.57 cd	0.57 c
	GA200	76.67 bc	35.45 bc	2.67 d	8.78 d	0.89 b
	GA300	71.70 c	11.70 de	2.20 e	7.95 de	1.46 a
T100 mean		72.51 C	21.07 C	2.98 C	9.16 C	0.86 A
200 mM (T200)	GA0	60.00 d	5.75 g	6.33 a	5.61 e	0.34 d
	GA100	56.33 de	10.68 de	3.42 c	4.69 ef	0.45 cd
	GA200	70.00 c	14.36 ef	4.12 ab	4.35 f	1.24 b
	GA300	60.30 d	16.45 e	5.25 a	3.97 g	1.33 a
T200 mean		61.65 D	11.78 D	4.78 A	4.65 D	0.84 A
Mean GA_3 doses	GA0	75.05 C	14.01 C	4.51 A	8.04 D	0.31 D
	GA100	77.26 B	22.98 B	3.56 B	10.04 B	0.50 C
	GA200	81.39 A	32.59 A	2.26 C	8.83 C	0.97 B
	GA300	80.14 A	31.93 A	2.66 C	10.41 A	1.23 A
CV (%)		8.6	17.5	13.3	10.8	11.2

GA0: control doses, GA100: 100 ppmdoses, GA200: 200 ppm doses, GA300: 300 ppm doses, T0: control doses, T50: 50 mM salt doses, T100: 100 mM salt doses, T200: 200 mM salt doses
*The difference between the means was evaluated at $P < 0.05$ and $P < 0.01$ level with the Duncan multiple comparison method

The results showed that the difference between salt, GA3, and their interaction regarding the mean germination time was significant ($P < 0.01$) (*Table 1*). The lowest mean germination time (2.70 days) was obtained from the control application (0 mM) of the salt concentration and the longest time (4.78 days) was obtained from the 200 mM application (*Fig. 3*). Also, the effect of gibberellic acid on the mean germination time was significant, and the shortest time was obtained from the 300 ppm application (2.66 days), and the longest time (4.51 days) was obtained from the control application at 0 ppm dose. In terms of salt × GA3 interactions, the shortest time (0.92 days) was obtained from the control application (0 ppm, 0 mM), and the longest time was obtained from the 200 mM salt concentration with the 0 ppm GA3 dose (6.33 days).

http://www.aloki.hu ● ISSN 1589 1623 (Print) ● ISSN 1785 0037 (Online)
DOI: http://dx.doi.org/10.15666/aeer/1705_1205712071

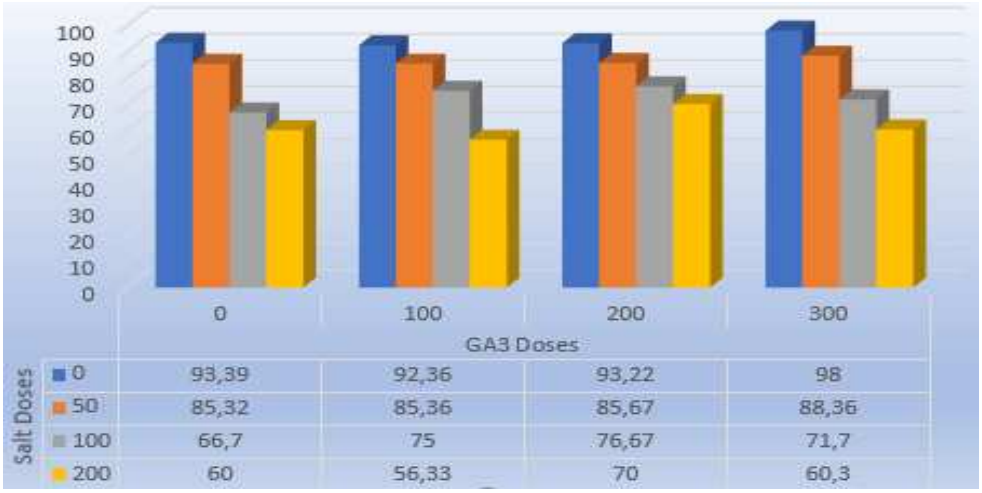

Figure 1. *The impact of salt × GA3 interactions on the germination power (%)*

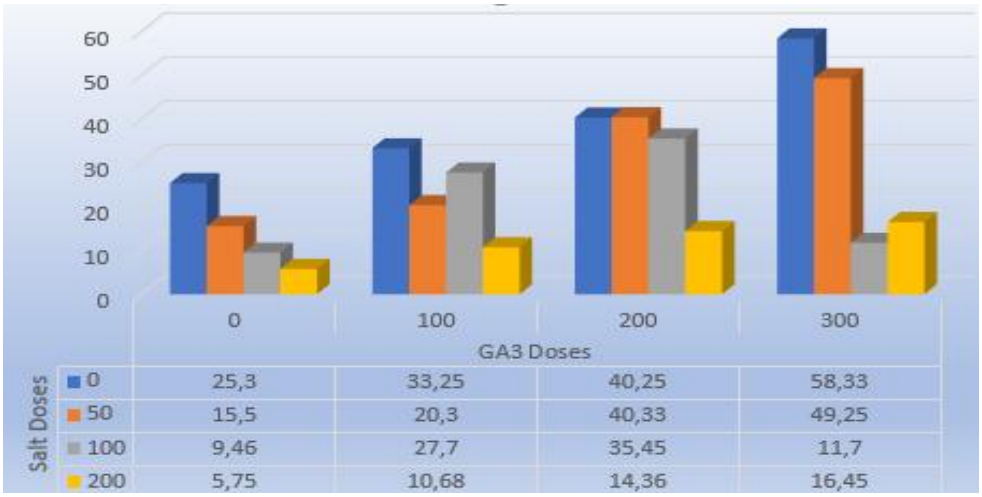

Figure 2. *The impact of salt × GA3 interactions on the germination ratio (%)*

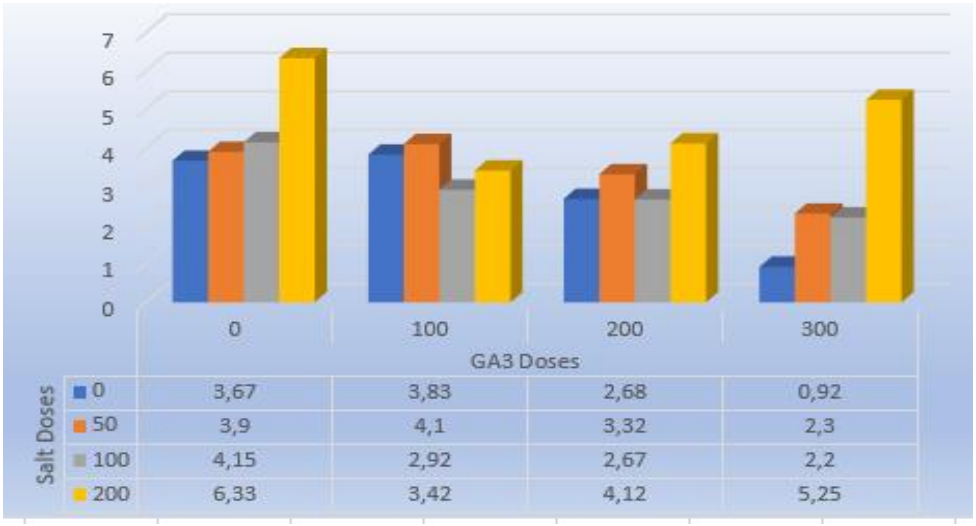

Figure 3. *The impact of salt × GA3 interactions on the mean germination time (days)*

http://www.aloki.hu ● ISSN 1589 1623 (Print) ● ISSN 1785 0037 (Online)
DOI: http://dx.doi.org/10.15666/aeer/1705_1205712071

When the germination index (%) values of the wheat seeds were examined, it was observed that the difference between salt, GA3, and their interactions was significant (*Table 1; Fig. 4*). The highest germination index between the salt doses was obtained from the 0 mM control with 11.96%, and the lowest index value was obtained from the 200 mM concentration (4.65%). Regarding the germination index values of the gibberellic acid doses, the highest index value was obtained from the 300 ppm dose (10.41%), and the lowest value was obtained from the control. The highest value of the germination index of the wheat seeds obtained from the salt × GA3 interaction was in 0 mM and 0 ppm GA3 with 13.41%. There is not difference statistically among 100 and 200 ppm GA3 in the 0 and 50 mM of salt applications. The lowest value (3.97%) was obtained from the 200 mM salt and 300 ppm GA3 applications.

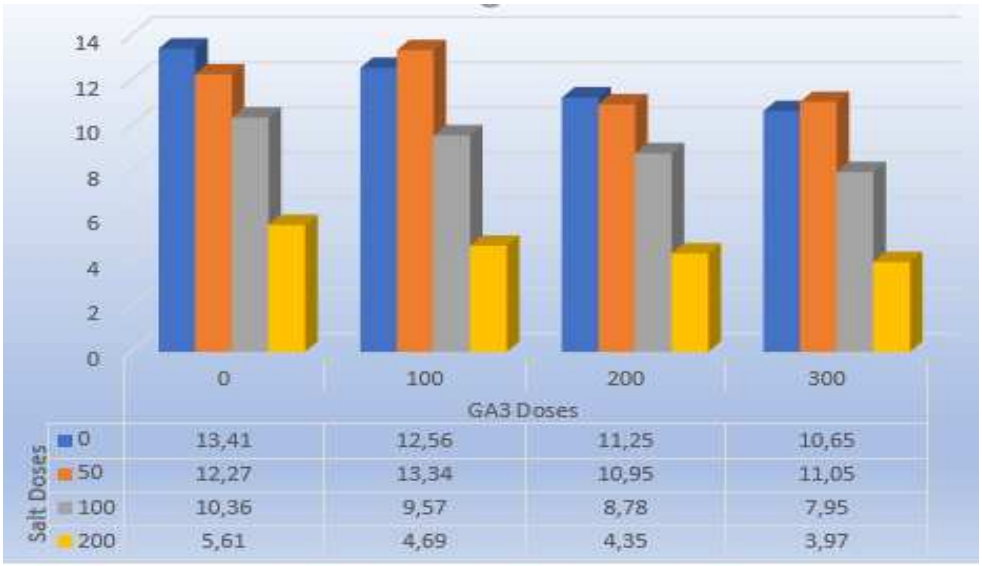

Figure 4. *The impact of salt × GA3 interactions on the germination index (%)*

According to the obtained results, the applications and their interactions were found to be significant regarding the sensitivity index values of the wheat seeds (*Table 1, Fig. 5*). It was observed that increasing salt concentrations decreased the sensitivity index values. The highest sensitivity index value was observed in the 100 nm application (0.84%). But, it is in the same Duncan group with 200 mM salt application. The lowest sensitivity index value was obtained from the control application (0.46%) it is in the same Duncan group with 50 mM salt application. The highest sensitivity index values of the wheat seeds to the gibberellic acid doses were obtained from the 200 ppm concentration (1.23%), and the lowest value was obtained from the 0 ppm concentration (0.31%). The highest sensitivity index in the salt × GA3 interaction was found to be 1.46% (100 mM salt × 300 ppm GA3), and the lowest was found to be 0.28% (0 Mm NaCl × 100 ppm GA3).

Radicula length values were found to be significant in the wheat seeds in terms of the applications and their interactions (*Table 2; Fig. 6*). The lowest radicula length was found to be 1.50 cm in the 200 mM salt concentration, and the highest radicula length (4.5 cm) was obtained from the 50 mM NaCl application In the gibberellic acid applications, the longest root was obtained from the 300 ppm dose (5.54 cm), and the lowest value (1.21 cm) was obtained from the 100 ppm dose. In the salt × GA3

http://www.aloki.hu ● ISSN 1589 1623 (Print) ● ISSN 1785 0037 (Online)
DOI: http://dx.doi.org/10.15666/aeer/1705_1205712071

interaction, the highest radicula length was 5.64 cm (0 mM × 300 ppm GA3). It is in same Duncan with 0 mM NaCl and 300 ppm GA3. The lowest radicula length was found to be 0.19 cm (50 mM ×100 ppm).

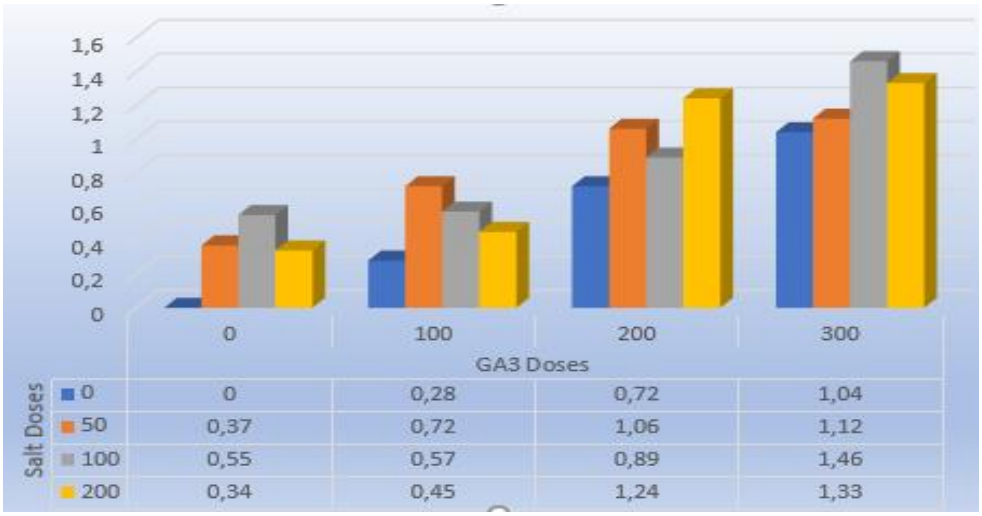

Figure 5. *The impact of salt × GA3 interactions on the sensitivity index (%)*

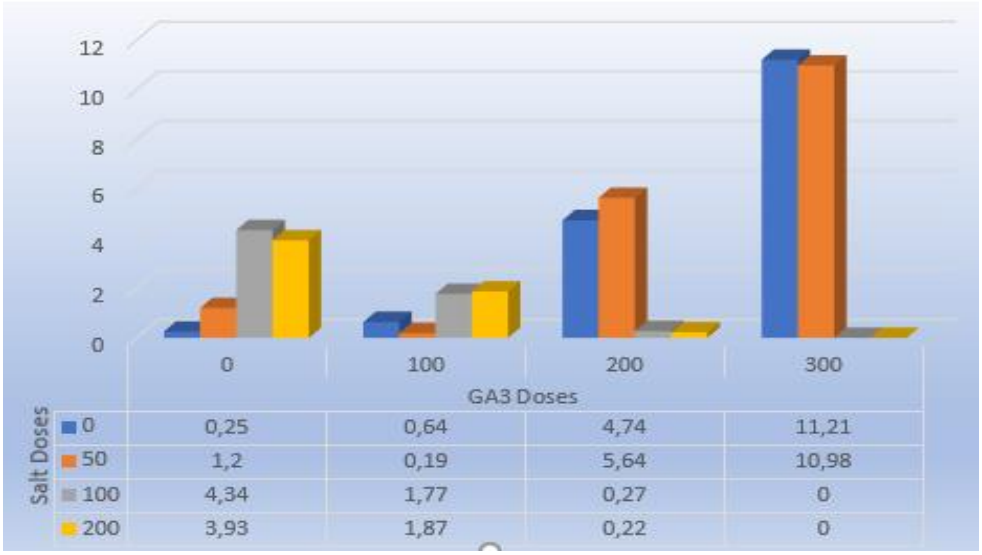

Figure 6. *The impact of salt × GA3 interactions on the radicula lenght (cm)*

According to the results, the effects of the applications on plumula length were found to be significant (*Table 2; Fig. 7*). Depending on the salt concentrations, the highest plumula length (7.29 cm) was observed in the 50 Mm NaCL dose. It is in the same with control. The shortest stem length was observed to be 2.91 cm (T_{200}). Despite this suppressive characteristic of salt, it was observed that the gibberellic acid doses increased the plumula length. The highest stem length (6.20 cm) was obtained from the GA100 dose, and the lowest was 4.86 cm (GA_0). In the salt × GA3 interaction, the highest plumula length (11.50 cm) was obtained from the $T_{50} \times GA_{100}$ application, and the lowest value was observed to be 1.50 cm ($T_{100} \times GA_{300}$).

http://www.aloki.hu ● ISSN 1589 1623 (Print) ● ISSN 1785 0037 (Online)
DOI: http://dx.doi.org/10.15666/aeer/1705_1205712071

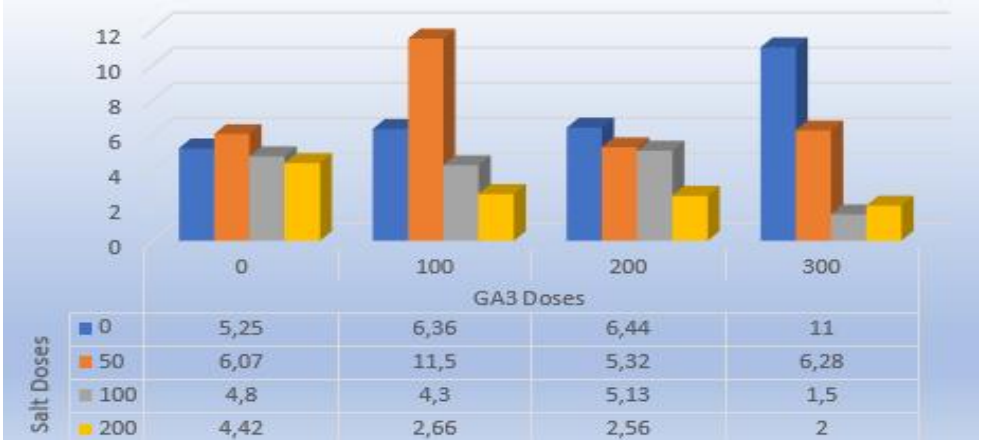

Figure 7. *The impact of salt × GA3 interactions on the plumula length (cm)*

Table 2. *The effect of salt stress on germination characteristics in the Gibberellic acid treated wheat (Triticum durum Desf.) seeds*

Stress applications		Radicula length (cm)	Plumula length (cm)	Radicula fresh weight (mg)	Plumula fresh weight (mg)	Radicula dry weight (mg)	Plumula dry weight (mg)
Salt doses	**GA3**						
Control (T0)	GA0	0.25 e	5.25 cd	32.5 bc	184.2 c	3.17 c	17.7 bc
	GA100	0.64 de	6.36 bc	35.6 b	205.6 bc	3.25bc	19.3 b
	GA200	4.74 b	6.44 bc	34.8 b	220.8 b	3.22bc	19.5 b
	GA300	11.21 a	11.00 b	42.5 a	240.5 a	4.13 a	25.6 a
T0 means		4.21 B	7.26 A	36.3 A	213.5 A	3.44 A	20.5 A
50 mM (T50)	GA0	1.20 de	6.07 c	31.2 c	186.4 d	3.08 c	16.4 cd
	GA100	0.19 ef	11.50 a	32.5 bc	189.3cd	3.07 c	17.2 c
	GA200	5.64 b	5.32 cd	29.8 c	195.4 c	2.75cd	20.2 b
	GA300	10.98 a	6.28 h	24.5 cd	196.4 c	3.55 b	22.4 ab
T50 means		4.50 A	7.29 A	29.5 B	191.8 B	3.11 B	19.1 B
100 mM (T100)	GA0	4.34 b	4.80 d	21.5 d	132.5 e	2.03 d	12.2 d
	GA100	1.77 d	4.30 de	19.8 de	120.5 ef	1.86de	11.9 de
	GA200	0.27 e	5.13 d	13.5 e	95.7 f	1.23 e	10.6 e
	GA300	0.00 f	1.50 h	14.8 ef	88.6 g	1.20 ef	9.3 ef
T100 means		1.59 C	3.93 C	15.4 C	109.3 C	1.63 C	11.0 C
200 mM (T200)	GA0	3.93 c	4.42 de	9.8 f	85.2 g	1.15 ef	9.3 ef
	GA100	1.87 d	2.66 f	10.8 ef	65.4 h	1.62 e	6.7 f
	GA200	0.22 e	2.56 f	12.5 e	65.4 h	1.85de	6.4 f
	GA300	0.00 f	2.00 ı	10.5 fg	71.7 ı	0.98 f	6.0 fg
T200 means		1.50 D	2.91 D	10.9 D	71.9 D	1.40 D	7.1 D
Mean GA3 doses	GA0	2.43 B	4.86 C	24.4 B	146.3 A	2.35 B	13.9 C
	GA100	1.11 C	6.20 A	33.3 A	145.2 C	2.45 A	13.8 C
	GA200	2.71 B	5.13 B	21.9 D	144.3 D	2.31 C	14.2 B
	GA300	5.54 A	5.19 B	25.1 C	149.8 B	2.46 A	15.8 A
CV (%)		8.9	13.3	12.5	15.5	13.5	11.1

GA0: Control doses, GA100: 100 ppmdoses, GA200: 200 ppm doses, GA300: 300 ppm doses. T0: Control doses, T50: 50 mM salt doses, T100: 100 mM salt doses, T200: 200 mM salt doses
*Difference between the means was evaluated at $P < 0.05$ and $P < 0.01$ level with the Duncan multiple comparison method

http://www.aloki.hu ● ISSN 1589 1623 (Print) ● ISSN 1785 0037 (Online)
DOI: http://dx.doi.org/10.15666/aeer/1705_1205712071

The results obtained from the applications on radicula fresh and dry weights were found to be statistically significant (*Table 2; Figs. 8* and *9*). The highest radicula fresh and dry weights were observed in the 0 mM (NaCl) application with 36.3 and 3.44 mg, respectively. The lowest values (10.9, 1.40 mg) were obtained from the 200 mM salt (NaCl) concentration. The effects of Gibberellic acid on the radicula fresh and dry weights were significant, and the highest radicula fresh and dry weights were obtained from the 300 ppm application (25.1 and 2.46 mg). The lowest values (21.9 and 2.31) were detected in the 0 ppm dose. The salt × GA3 interactions on the wheat seeds were found to be statistically significant. The highest radicula fresh and dry weights were obtained from the T_0 (0 mM) and 300 ppm GA3 concentration (42.5 and 4.13 mg), and the lowest radicula fresh weights (9.8 mg) was obtained from 200 mM NaCl and 0 ppm GA3 doses. The lowest radicula dry weights (0.98 mg) were detected in the 300 ppm GA3 application of the 200 mM salt concentration.

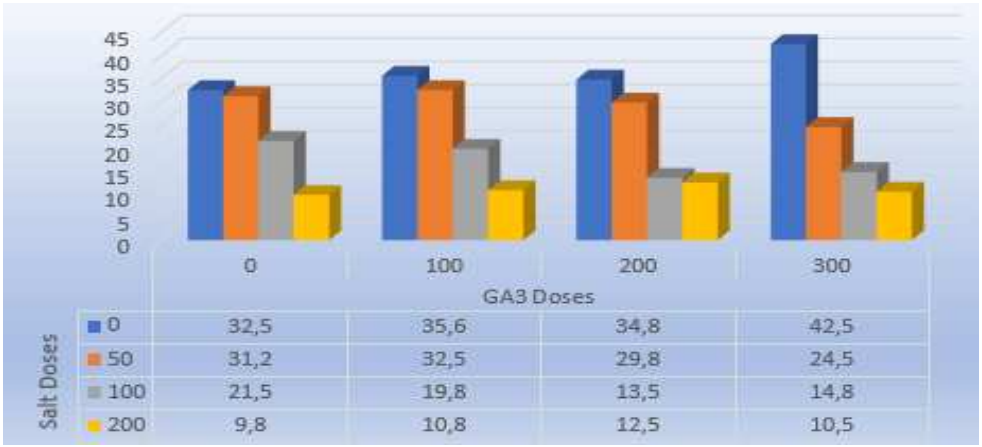

Figure 8. *The impact of salt × GA3 interactions on the radicula fresh weights (mg)*

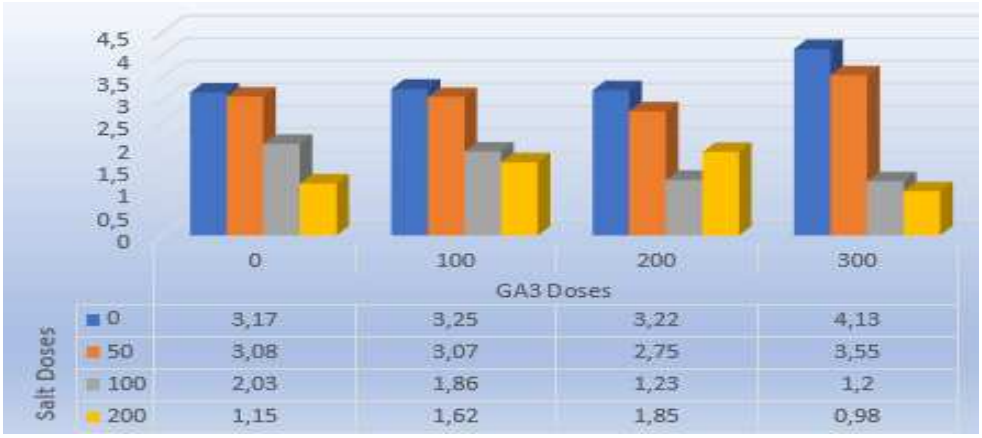

Figure 9. *The impact of salt × GA3 interactions on the radicula dry weights (mg)*

The difference between the plumula fresh and dry weights in the applications was found to be statistically significant according to the results (*Table 2; Figs. 10* and *11*). Considering the results, the results between the plumula fresh and dry weights had parallels regarding the applications. The highest plumula fresh and dry weights were

http://www.aloki.hu ● ISSN 1589 1623 (Print) ● ISSN 1785 0037 (Online)
DOI: http://dx.doi.org/10.15666/aeer/1705_1205712071

found to be 213.5 and 20.5 mg, respectively, in the 0 mM (NaCl) application, and the lowest values (71.9 and 7.1 mg) were obtained from the 200 mM salt (NaCl) concentration. The effects of Gibberellic acid on the plumula fresh and dry weights are significant, and the highest fresh and dry weights (149.8 and 15.8 mg) were obtained from the 300 ppm application. The lowest values (144.3) were detected in the 200 ppm GA3 doses. The lowest plumula dry weight (13.8 mg) was recorded in the 100 ppm GA3. The salt × GA3 interactions on the wheat seeds were also found to be statistically significant. The highest plumula fresh and dry weights (240.5 and 25.6 mg) were obtained from the T_0 (0 mM) and 300 ppm GA3 concentration, and the lowest plumula fresh weight values (65.4) was detected in the 200 ppm GA3 concentration of the 200 mM salt concentration. The lowest plumula dry weight (6.0 mg) was detected in the 300 ppm GA3 concentration of the 200 mM salt concentration

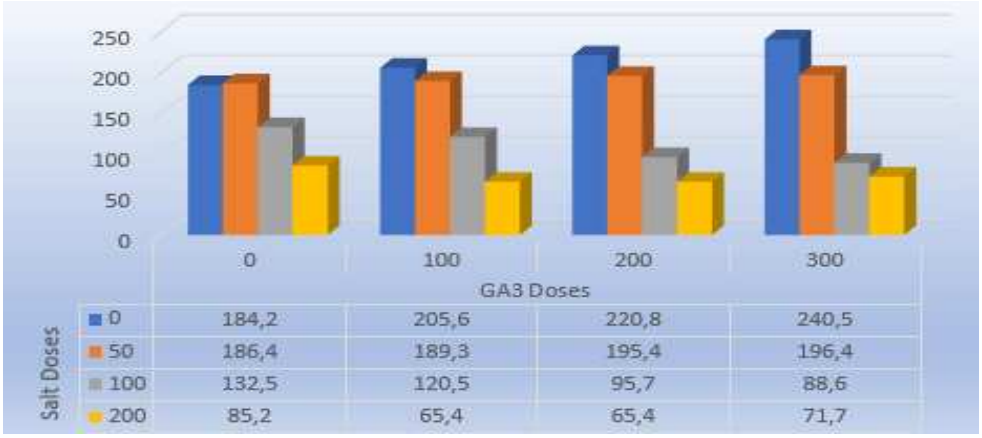

Figure 10. *The impact of salt × GA3 interactions on the plumula fresh weights (mg)*

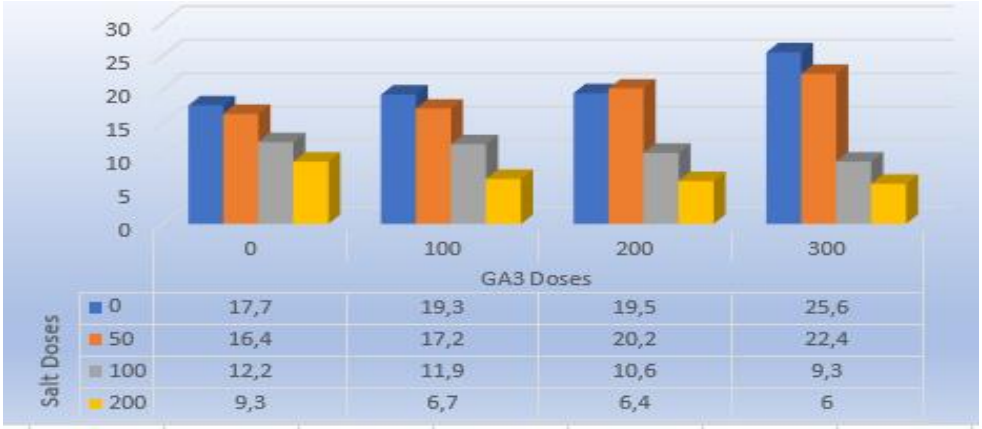

Figure 11. *The impact of salt × GA3 interactions on the radicula dry weights (mg)*

Discussion

The results indicated that the GA3 applications caused the germination power and the germination ratio to increase. However, in the similar studies, it was stated that the increasing salt concentrations had negative and important effects on these ratios (Sharma et al., 2004; Khan et al., 2005; Kızılgeci et al., 2010).

http://www.aloki.hu ● ISSN 1589 1623 (Print) ● ISSN 1785 0037 (Online)
DOI: http://dx.doi.org/10.15666/aeer/1705_1205712071

According to the results, growth and development of the wheat seeds were prevented due to the salinity concentration, which increased gradually. Many researchers had revealed this effect before (Öztürk et al., 1994; Gulzar and Khan, 2002; Yıldız et al., 2017).

When the GA3 pretreatments on the wheat seeds are examined, mean germination days decreased in parallel with the increasing doses, and it was observed in similar studies that this time lengthened together with the increasing doses in salt concentrations (Öztürk et al., 1994; Ghoulam and Fores, 2001; Gulzar and Khan, 2002; Çavuşoğlu et al., 2007).

In their studies, Yuonesi and Moradi (2015) stated that the gibberellic acid applications had positive and significant effects on germination index despite the increasing salt doses.

It was observed that the gibberellic acid pretreatments were useful regarding the sensitivity index values as in the other parameters (Yuonesi and Moradi, 2015).

As significant decreases in the water intake capabilities occur in the plants that are under salt stress, root and shoot lengths decrease (Kızılgeçi and Yıldırım, 2014). While radicula length is important from this point of view, it should be considered as a selection criterion in salt resistance improvement. According to the results, radicula length decreased depending on the increasing salt concentration (Atak et al., 2006; Saboora and Kriarostami, 2006).

The highest stem length (6.20 cm) was obtained from the GA100 dose, and the lowest was 4.86 cm (GA_0). In the salt × GA3 interaction, the highest plumula length (11.50 cm) was obtained from the $T_{50} \times GA_{100}$ application, and the lowest value was observed to be 1.50 cm ($T_{100} \times GA_{300}$). Sadat Noori and McNeilly (2011) found similar results.

It was observed that increasing salt concentrations reduced the radicula fresh and dry weights (Kızılgeçi and Yıldırım, 2014).

According to the results obtained in our research, it was observed that the GA3 applications increased radicula fresh and dry weights relatively. In a study they conducted with local bread wheat varieties, Shahzad et al. (2012) detected that radicula fresh and dry weights decreased. It was stated that this parameter could be used in improvement works.

It was observed that increasing salt concentrations reduced the plumula fresh and dry weights (Kızılgeçi and Yıldırım, 2014).

In similar studies, it was stated that increasing salt concentrations reduced plumula fresh and dry weights in plants (Muhammad and Hussain, 2012; Akbari et al., 2007).

Conclusion

According to the results, germination and growth of wheat seeds were prevented depending on the gradually increasing salinity concentration. Many researchers had revealed this effect before. It prevents water intake especially in high salt concentrations, and based on this, it causes the enzymes to not to be able to activate and in consequence leads to retardation in germination and growth. In this study, this negative and important effect of salt on the germination parameters was reduced as a result of GA3 applications and successful results were obtained. When the results were evaluated in terms of all the parameters, the best results were obtained from the 300 ppm GA3 applications in 0 mM salt concentration. In conclusion, it was observed that

http://www.aloki.hu ● ISSN 1589 1623 (Print) ● ISSN 1785 0037 (Online)
DOI: http://dx.doi.org/10.15666/aeer/1705_1205712071

GA3 (Gibberellic acid) pretreatments lessened the effect of salt (NaCl) stress on germination in wheat seeds. In the world and in our country, as well as fallow fields, soil salinity and alkalics are an important problem. It will be possible to bring these areas to agriculture and increase agricultural production only through these and similar studies.

REFERENCES

[1] Anonymous (2015): www.agri.ankara.edu.tr/fcrops/1289_Bıtkılerde_Stres.pdf. – Access date: 15.05.2015 (in Turkish).
[2] Akbari, G., Sanavy, S., Yousafzadeh, S. (2007): Effect of auxin and salt stress (NaCl) on seed germination of wheat cultivars (*Triticum aestivum* L). – Pak. J. Biol. Sci. 10(15): 2557-2561.
[3] Akıncı, I. E., Calıskan, U. (2010): Effect of lead on seed germination and tolerance levels in some summer vegetables. – Ekoloji Dergisi 19: 164-172 (in Turkish).
[4] Atak, M., Kaya, M. D., Kaya, G., Kıllı, Y., Ciftci, C. Y. (2006): Effects of NaCl on the germination, seedling growth and water uptake of Triticale. – Turkish J. Agric. Forestry 30: 39-47.
[5] Azizi, M., Chehrazi, M., Zahedi, S. M. (2011): Effects of salinity stress on germination and early growth of sweet william (*Dianthus barbatus* L.). – Asian Journal of Agricultural Sciences 3(6): 453-458.
[6] Begum, F., Karmoker, J. L., Fattah, Q. A., Maniruzzaman, A. F. M. (1992): The effect of salinity and Its correlation with K+, Na+, Cl accumulation in germinating seeds of Triticum aestivum L. cv. – Akbar. Plant Cell Phsysiol 33(7): 1009-1114.
[7] Çavuşoğlu, K., Kılıç, S., Kabar, K. (2007): Some morphological and anatomical observations in alleviating salt stress with gibberellic acid, kinetin and ethylene during germination of barley seeds. – Sdü Fen Edebiyat Fakültesi Fen Dergisi (E-Journal) 2(1): 27-40 (in Turkish).
[8] De Villiers, A. J., Van Rooyen, M. W., Theron, G. K., Van De Venter, H. A. (1994): Germination of three Namaqualand pioneer species, as influenced by salinity, temperature and light. – Seed Sci. Technol. 22: 427-433.
[9] Dölarslan, M., Gül, E. (2012): Soil salinity in terms of plant relations. – Türk Bilimsel Derlemeler Dergisi 5(2): 56-59 (in Turkish).
[10] Duman, İ., Eşiyok, D. (1998): Effects of PEG and KH2PO4 applications before germination on germination rate and yield of carrot seeds. – Tr. J. of Agriculture and Forestry 22: 445-449 (in Turkish).
[11] Duzgunes, O., Kesici, T., Kavuncu, O., Gurbuz, F. (1987): Research and experimental methods. Statistical methods-II. – Ankara University, Agr Fac Press 1021: 295 (in Turkish).
[12] Ellis, R. H., Roberts, E. H. (1980): Towards a Rational Basis for Testing Seed Quality. – In: Hebblethwaite, P. D. (ed.) Seed Production. Butterworths, London, pp. 605-63.
[13] Ercişli, S., Eşitken, A., Güleryüz, M. (1999): The effect of vitamines on the seed germination of apricots. – Acta Hort. 488: 437-440.
[14] Flowers, T. J., Yeo, A. R. (1981): Variability in the resistance of sodium chloride salinity within rice (*Oryza sativa* L.) varieties. – New Phytology 88: 363-373.
[15] Foolad, M. R., Lin, G. Y. (1997): Genetic potential for salt tolerance during germination in *Lycopersicon* species. – HortScience 32: 296-300.
[16] Gupta, S. C., Srivastava, J. P. (1989): Effect of salt stress on morpho-physiological parameters in wheat. – Indian J. Plant Physiol. 32(2): 169-171.
[17] Ghoulam, C., Fores, K. (2001): Effect of salinity on seed germination and early seedling growth of sugar beet (*Beta vulgaris* L.). – Seed Science Technology 29: 357-364.

http://www.aloki.hu ● ISSN 1589 1623 (Print) ● ISSN 1785 0037 (Online)
DOI: http://dx.doi.org/10.15666/aeer/1705_1205712071

[18] Gulzar, S., Khan, M. (2002): Alleviation of salinity-induced dormancy in perennial grasses. – Biologia Plantarum 45(4): 617-619.
[19] Hartmann, H. T., Kester, D. E., Davies, F. T. (1990): Plant Propagation. Principles of Propagation by Seed. – Prentice Hall, Upper Saddle River, NJ.
[20] Hasegawa, P. M., Bressan, R. A., Handa, A. V.(1986): Cellular mechanism of salinity tolerance. – Horticultural Science 21(6): 1317-1324.
[21] İnal, A., Güneş, A., Aktaş, M. (1995): Effects of chloride and partial substitution of reduced forms of nitrogen for nitrate in nutrient solution of the nitrate, total nitrogen and chlorine contents of onion. – Journal of Plant Nutrition 18: 2219-2227.
[22] ISTA (1996): International Rules for Seed Testing. Edition 1996/6. – International Seed Testing Association, Zurich.
[23] Khan B. A., Khan, A. N., Khan, T. H. (2005): Effect of salinity on the germination of fourteen wheat cultivars. – Gomal University Journal of Research 21: 31-33.
[24] Khan, M. A., Ungar, I. A. (1997): Effects of light, salinity and thermoperiod on the seed germination of halophytes. – Can. J. Bot. 75: 835-541.
[25] Kızılgeçi, F., Yıldırım, M., Akinci, C. (2010): Determination of salinity responses of some bread wheat genotypes. – 1. Uluslararası Katılımlı Kamu-Üniversite-Sanayi işbirliği Sempozyumu ve ermercilik şurası, 24-26 May 2010, Diyarbakır, Turkey, pp. 301-307 (in Turkish).
[26] Leopold, A. C., Willing, R. P. (1984): Evidence of Toxicity Effects of Salt on Membranes. – In: Staples, R. C., Toenniessen, G. H. (eds.) Salinity Tolerance in Plants. Wiley, New York, pp. 67-76.
[27] Muhammad, Z., Hussain, F. (2012): Effect of NaCl salinity on the germination and seedling growth of seven wheat genotypes. – Pak. J. Bot. 44(6): 1845-1850.
[28] Özkaldı, A., Boz, B., Yazıcı, V. (2004): Drainage problems and solutions in GAP. – Sulanan Alanlarda Tuzluluk Yönetimi Sempozyumu, 20-21 May, Ankara, pp: 97-105.
[29] Öztürk, M., Gemici, M., Özdemir, F., Keyikçi, N. (1994): The role of plant hormones and germination simulator in reducing salt stress in seed germination. – XII. Ulusal Biyoloji Kongresi, Edirne, pp. 44-48.
[30] Parida, A. K., Das, A. B. (2005): Salt tolerance and salinity effects on plants: a review. – Ecotoxicol. Environ. Saf. 60: 324-349.
[31] Pessarakli, M., Tucker, T. C., Nakabayashi, K. (1991): Growth response of barley and wheat to salt stress. – Journal of Plant Nutrition 14(4): 331-340.
[32] Saboora, A., Kriarostami, K. (2006): Salinity (NaCl) tolerance of wheat genotypes at germination and early seedling growth. – Pakistan J. of Bio. Sci. 9(11): 2009-2021.
[33] Sadat Noori, S. A., McNeilly, T. (2000): Assessment of variability in salt tolerance based on seedling growth Triticum durum Desf. – Genetic Resources and Crop Evolution 47: 285-291.
[34] Sariye, U. K. (2014): Tolerance of salt of some lentil (*Lens culinaris* Medic.) Varieties during germination and seedling period. – Diss. Selçuk Üniversitesi Fen Bilimleri Enst., Konya (in Turkish).
[35] Shahzad, A., Ahmad, M., Iqbal, M., Ahmed, I., Ali, G. M. (2012): Evaluation of wheat landrace genotypes for salinity tolerance at vegetative stage by using morphological and molecular markers. – Genet. Mol. Res. 11(1): 679-692.
[36] Shannon, M. C. (1984): Breeding Selection and the Genetics of Salt Tolerance. Salinity Tolerance in Plant Strategies for Crop Improvement. – Wiley-Interscience, New York, 231-254.
[37] Shannon, M. C. (1985): Principles and strategies in breeding for higher salt tolerance. – Plant and Soil 89: 227-241.
[38] Sharma, A. D., Thakur, M., Rana, M., Singh, K. (2004): Effect of plant growth hormones and abiotic stresses on germination, growth and phosphoaphatse activities in *Sorghum bicolour* (L.) moench seeds. – Afr. J. Biotechnol. 3: 308-312.

http://www.aloki.hu ● ISSN 1589 1623 (Print) ● ISSN 1785 0037 (Online)
DOI: http://dx.doi.org/10.15666/aeer/1705_1205712071

[39] Şenay, A., Kaya, M. D., Atak, M., Çiftçi, C. Y. (2005): Effects of different salt concentrations on germination and seedling growth of some bread wheat varieties. – Tarla Bitkileri Merkez Araştırma Enstitüsü Dergisi 14(1-2): 50-55.
[40] Siegel, S. M., Siegel, B. Z., Massey, J., Lahne, P., Chen, J. (1980): Growth of corn in saline water. – Physiology Plant 50: 71-73.
[41] Taghipour, F., Salehi, M. (2008): The study of salt tolerance of Iranian barley (*Hordeum vulgare* L.) genotypes in seedling growth stages. – American-Eurasian J Agric. & Environ. Sci. 4(5): 525-529.
[42] Van Hoorn, J. W. (1991): Development of soil salinity during germination and early seedling growth and its effect on several crops. – Agricultural Water Management 20: 17-28.
[43] Van Hoorn, J. W., Katerji, N., Hamdy, A., Mastrorilli, M. (2001): Effect of salinity on yield and nitrogen uptake of four grain legumes and on biological nitrogen contribution from the soil. – Agricultural Water Management 51: 87-98.
[44] Wang, Y. R., Yu, L., Nan, Z. B., Liu, Y. L. (2004): Vigor tests used to rank seed lot quality and predict field emergence in four forage species. – Crop Sci. 44(2): 535-541.
[45] Younesi, O., Moradi, A. (2015): Effect of different priming methods on germination and seedling establishment of two medicinal plants under salt stress conditions. – Cercetari Agronomice în Moldova 48(3): 43-51.
[46] Yıldız, M., Kasap, E., Konuk, M. (2007): Salinity, temperature and effects of light on seed germination. – Afyon Kocatepe Üni. Fen Bilimleri Dergisi 7(1): 225-243 (in Turkish).
[47] Yıldız, S., Karagöz, F. P., Dursun, A. (2017): Germination of Hüsnüyusuf (*Dianthus barbatus* L.) seeds subjected to gibberellic acid pretreatment in salt stress. – Atatürk Üniv. Ziraat Fak. Derg. 48(1): 1-7 (in Turkish).
[48] Yılmaz, E., Tuna, M., Bürün, B. (2011): Tolerance strategies developed by plants against salt stress effects. – C. B. Ü. Fen Bilimleri Dergisi 7(1): 47-66 (in Turkish).
[49] Zheng, C., Jiang, D., Liu, F., Dai, T., Liu, W., Jing, Q., Cao, W. (2009): Exogenous nitric oxide improves seed germination in wheat against mitochondrial oxidative damage induced by high salinity. – Environ. Exp. Bot. 67: 222-227.

http://www.aloki.hu ● ISSN 1589 1623 (Print) ● ISSN 1785 0037 (Online)
DOI: http://dx.doi.org/10.15666/aeer/1705_1205712071

LOW HOST SPECIFICITY OF ARBUSCULAR MYCORRHIZAL FUNGI ASSOCIATED WITH DOMINANT STEPPE PLANTS IN INNER MONGOLIA

MUNEER, M. A.[1#] – WANG, M.[2#] – JING, Z.[1] – ZHOU, X.[1] – WANG, P.[1] – LI, L.[3] – JI, B.[1*]

[1]*College of Grassland Science, Beijing Forestry University, Beijing 100083, China*

[2]*Key Laboratory for Biodiversity Science and Ecological Engineering, Ministry of Education, Fudan University, Shanghai, China*

[3]*College of Biological Sciences and Technology, Beijing Forestry University, Beijing 100083, China*

[#]*These authors have contributed equally to this work.*

**Corresponding author*
e-mail: baomingji@bjfu.edu.cn

(Received 27th Apr 2019; accepted 2nd Jul 2019)

Abstract. Arbuscular mycorrhizal fungi (AMF) play potentially essential roles in maintaining the diversity and functioning of plant communities in Eurasian steppe representing one of the most important terrestrial ecosystems. However, it remains unclear about the symbiotic relationship between AM fungal communities and the dominant grass species in the steppe ecosystem. We thus examined the species diversity and community composition of AM fungi colonizing three dominant plant species (*Leymus chinensis*, *Stipa grandis* and *Cleistogenes squarrosa*), using field sampling and molecular analyses, in Xilinguole steppe, Inner Mongolia. Our results showed all three plants were well colonized by AM fungi, and 51 operational taxonomic units (OTUs) belonging to six genera with members of *Glomus* dominating in the roots of all the three plants species. By comparison, we found that *L. chinensis* had the most diverse AM fungi within the roots. OTU richness of AM fungi was higher in the roots of *S. grandis* than in the roots of *C. squarrosa* and *L. chinensis*. However, the community composition of AM fungi in three host plant species showed no significant difference. Based on these findings, we concluded that the dominant plant species held diverse AM fungal taxa in their roots, while the host preference did not significantly drive the differences in AM fungal community composition within their roots and resulted in low host specificity. Findings of this study would broaden the concept of host specificity and its implications on plant succession in the largest grassland ecosystem of China.

Keywords: *arbuscular mycorrhizal fungi, diversity, community composition, host specificity, symbiosis*

Introduction

Arbuscular mycorrhizal (AM) symbiosis formed between higher plant roots and the fungi belonging to the phylum *Glomeromycota* is one of the most common mutualistic associations in terrestrial ecosystems (Desai et al., 2016; Stürmer, 2012). In grasslands, the vast majority of plant species are AMF hosts (Bonfante and Genre, 2010; Eom et al., 2000; Harrier, 2001). In these symbiotic associations, plants provide carbon to the fungi to complete their life cycle (Zhang et al., 2016b). In return, AMF benefits their hosts in various ways including enhanced nutrient acquisition and improved protection against biotic and abiotic stresses (Latef et al., 2016; Huang et al., 2017; Chen et al., 2017). Therefore, AM symbionts could play potentially

http://www.aloki.hu ● ISSN 1589 1623 (Print) ● ISSN 1785 0037 (Online)
DOI: http://dx.doi.org/10.15666/aeer/1705_1207312089

important roles in plant growth, community diversity and ecosystem stability (Torrecillas et al., 2012).

The host plant strongly influences the AMF diversity and community composition inside the roots (Pivato et al., 2007; López-García et al., 2014; Zheng et al., 2016). However, owing to the wide range of preference for host plants (Krüger et al., 2012), the AMF normally show low host specificity (Lee et al., 2013), and most of the previous studies found that AMF had no host specificity (Clapp et al., 1995; Santos et al., 2006; Smith and Read, 2008). For example, Su et al. (2011) studied the AMF community composition in five plant species of Inner Mongolia and found 18 AMF species belonging to five genera and concluded that most of the AMF had no host specificity, but few species showed a certain degree of the host preference. However, some findings showed that AMF community composition is host-dependent (Lugo and Cabello, 2002; del Mar Alguacil et al., 2018). Bentivenga and Hetric (1992) found host plant had a significant effect on AM fungal sporulation in tallgrass prairie grasses. Li et al. (2010) explored three plant species of hot and arid ecosystem of southwest China and found different AM fungal community composition. Several studies have documented that selectivity between AMF and host plants may be the cause of presence or absence of host specificity (Bever, 2002; Helgason et al., 2002; Zhang et al., 2010). Moreover, Yang et al. (2012) hypothesized that discerning pressure from host plant at different levels (functional groups and taxonomic order) may be a driver for the distribution of AMF. However, the detailed explanation still needs several studies. The previous suppositions are mainly based on morphological investigations and a little molecular work is involved. Therefore, considering the contrasting opinions regarding AMF host specificity and insufficient investigations, further studies are needed to deepen the understanding about the role of AMF in typical steppe. This would broaden the concept of host specificity and its implications on plant succession in the largest grassland ecosystem of China because the low host specificity favours underground communication and nutrient transfer pathways via mycorrhizal networks.

The typical steppe in Inner Mongolia covers more than 20% of total grassland area in China (Xu et al., 2014), and AMF holds a significant value in the success of plant species in the steppe. In this study, we analyzed and compared the diversity and community composition of AMF colonizing the roots of three dominant perennial plant species; *Leymus chinensis* (*L. chinensis*), *Stipa grandis* (*S. grandis*), and *Cleistogenes squarrosa* (*C. squarrosa*). These three plant species are considered long-lived dominant grass species of the typical steppe, Xilinguole (Vandenkoornhuyse et al., 2003). The sheepgrass (*L. chinensis*) is a perennial forage plant and of great significance for grassland productivity and ecosystem (He et al., 2017). While, *S. grandis* is known as needlegrass also has significant nutritional value for the cattle and sheep in this region of Inner Mongolia (Su et al., 2010). The *Cleistogene squarrosa* is the most abundant C_4 perennial bunchgrass species of this region and the importance of *Cleistogene* has been recognized for the development of sustainable grassland system (Liang et al., 2002). Concerning the ecological and economic importance of these three plant species, our goal was to identify the differences in diversity and community composition of AMF in three plant species belonging to the same family (Poaceae) to determine the host specificity. These findings can do a great deal towards a comprehensive understanding of AM fungi associations with roots of perennial plant species and host specificity.

http://www.aloki.hu ● ISSN 1589 1623 (Print) ● ISSN 1785 0037 (Online)
DOI: http://dx.doi.org/10.15666/aeer/1705_1207312089

Materials and methods

Study site

The study was carried out in the Inner Mongolia Grassland Ecosystem Research Station (43°38′55.9″N, 116°09′06.3″E), Inner Mongolia Autonomous of China (*Fig. 1*). This grassland system has semiarid climatic conditions with a short plant growing period ranging from May to September. The average annual precipitation is 343 mm, and the mean annual temperature is 0.3 °C with average monthly temperature ranging from -21.6 °C (January) to 19.0 °C (July). The main soil type in this site is chestnut soil with relatively homogenous physical and chemical properties (Li et al., 2015; Ren et al., 2016).

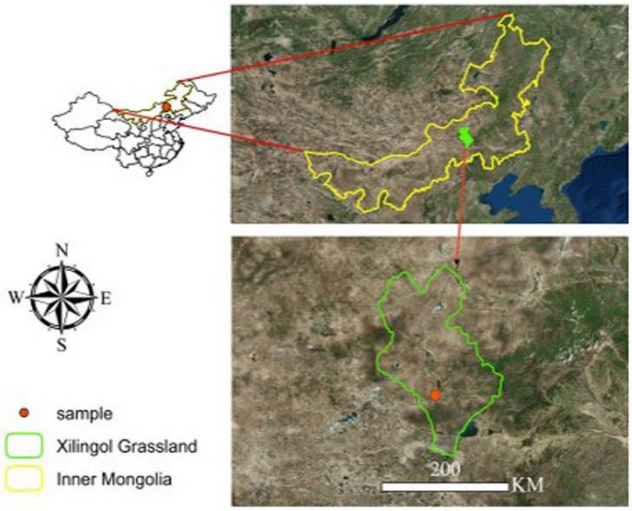

Figure 1. *The geographic location of the sampling site. The green line is the boundary of grassland and red dot is the location of sample plot. The map was created with ArcGIS 10.2*

Field sampling

The sampling was performed on June 24, 2014, and we randomly selected seven sampling points with a distance of 100 m from each other in a 1 × 1 km area as replicates. So, we collected 21 total plant samples and seven samples per species. To diminish the influence of soil type and geographic factors for each point, we selected closely adjacent *L. chinensis, S. grandis, and C. squarrosa* species for each sampling point. Corresponding, we obtained the roots and the rhizosphere soil of each plant using the soil drill. All the samples were preserved in zip lock bags and stored at 4 °C.

AMF structure and colonization

AMF colonization or root length colonization is an indicator of fungal growth within plant roots. In this study, the roots of the collected plants were washed carefully with tap water and cut into segments of 1 cm length. For each sample, approximately 100 root segments were randomly chosen and cleared in 10% KOH at 90 °C and stained with 0.05% Trypan blue, and then examined the percentage of AMF colonization using the magnified intersection method at 200× magnification (Nikon-E100) (Mcgonigle et al., 1990).

http://www.aloki.hu ● ISSN 1589 1623 (Print) ● ISSN 1785 0037 (Online)
DOI: http://dx.doi.org/10.15666/aeer/1705_1207312089

DNA extraction and sequencing

In our study, the AM fungi within the roots of *L. chinensis, S. grandis,* and *C. squarrosa* was identified through PCR amplified 18S-rRNA gene fragments with AMF-specific primers, as partial sequences of small subunit (SSU) genes appeared to be more informative than ITS genes for AM fungi (Redecker et al., 2006). For each sample, the total DNA was extracted from 80 randomly obtained fine roots using MoBio Power Soil®DNA Isolation kits (QIAGEN, Valencia, CA, USA). 18S rRNA gene was amplified using a nested PCR protocol. Based on the previous study (Krüger et al., 2009), the chosen primers were AML1/AML2 because they have better coverage and specificity than NS31/AM1, which have been extensively used in recent years (Helgason et al., 1999; Simon et al., 1992). A 10-fold dilution of the DNA was first amplified using the general eukaryotic primers NS1/NS4 (White et al., 1990). In the second phase of nested PCR, the product was amplified using AML1/AML2, and the PCR product was visualized on 1% agarose gel. The expected 800 bp bands were cut out and purified using an AxyPrep DNA Gel Extraction Kit (Axygen, Union City, CA, USA). The purified product was sequenced using the Sanger platform to confirm the presence of AM fungi before proceeding further. Purified DNA was cloned into the pGEM-T Easy vector (Promega, Madison, WI, USA) and then transformed into *E. coli* DH-5α (Tiangen, Beijing, China). The resulting DNA sequences were aggregated using BioEdit to perform the subsequent analysis.

Sequence analysis

We compared our clone DNA sequences with the GenBank database on the NCBI website (http://www.ncbi.nlm.nih.gov/). The closest match was selected to identify the sequences, and only those recognized as *Glomeromycota* were included for further taxonomic analysis.

All the selected AM fungal sequences were gathered from the previous steps, then we conducted standard operational taxonomic units (OTUs) analysis using the Mothur software (Schloss et al., 2009). The sequences with not less than 97% matched, were grouped into OTU (Helgason et al., 1998). After finishing clustering, we selected one sequence in each OTU as the representative sequence and aligned them together with their closest matched identified AM fungal sequences from the NCBI database; then Mega 6.06 program (Kumar et al., 2007) was utilized to align the sequences. Furthermore, in Mega, Kimura2-parameter model was computed to perform neighbor-joining phylogenetic analysis with 1000 bootstrap replicates to calculate the support value of the tree with *Mortierella polycephala* (ID: X89436) and *Endogone pisiformis* (ID: X58724) as outgroups to root the tree (Tamura et al., 2007; Öpik et al., 2003). To further quantify and compare the fungal community diversity, the Shannon-Wiener index was computed with vegan package (Oksanen et al., 2007) in R (Team, 2013) based on the identified OTUs. The Shannon diversity index was calculated according to the following equation:

$$D = \sum_{i=1}^{s} p_i \times \ln p_i$$

where S is the total number of species in the sample and p_i is the relative abundance of certain AM fungus species of the sample (Shannon and Weaver, 1949).

http://www.aloki.hu ● ISSN 1589 1623 (Print) ● ISSN 1785 0037 (Online)
DOI: http://dx.doi.org/10.15666/aeer/1705_1207312089

Nucleotide sequence accession numbers

A total of 51 representative sequences of the clones detected were submitted to NCBI (National Center for Biotechnology Information) GenBank (http://www.ncbi.nlm.nih.gov) with the accession number LS997508-LS997558.

Statistical analysis

The SPSS statistical software was used to compare the AMF colonization rate, species richness, and Shannon diversity indexes among the three species. The data were analyzed using one-way Analysis of Variance method (ANOVA) and significant differences between the different plant species in ANOVA were compared based on Tukey's HSD post-hoc test at $P \leq 0.05$. To gain further insight into the potential relationship between AM fungal communities and their host plant species, NMDS (nonmetric multidimensional scaling) was conducted using PAST (Paleontological Statistics) version 3.21.

Results

AMF colonization

The results showed that all the plant species were well colonized by AMF. *S. grandis* showed an average of 92% colonization, whereas *C. squarrosa* and *L. chinensis* showed average colonization rates of 87% and 90%, respectively (*Fig. 2*). One-way analysis of variance (ANOVA) indicated that there were no significant differences as shown by Tukey's HSD test ($F = (2,18) = 0.054$) in the AMF colonization among the three dominant species.

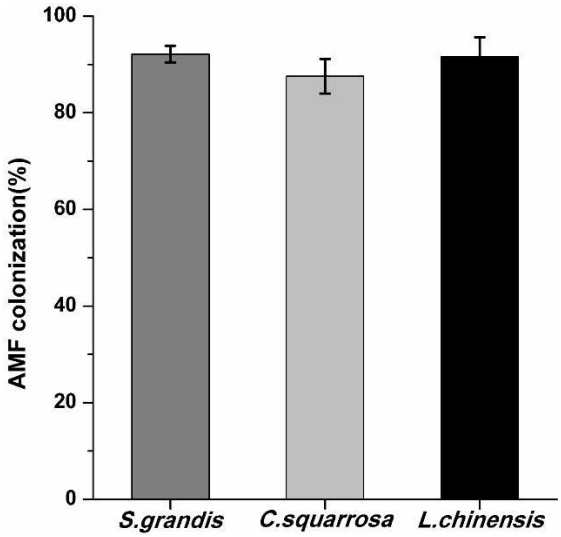

Figure 2. *AMF colonization. AM fungal colonization (%) observed in three plant species. Data are means ± SE*

Identification and phylogenetic analysis of AM fungi

A total of 750 clones were sequenced, and among them, 587 non-chimeric sequences were identified as AMF and clustered into 51 OTUs at 97% sequence similarity. These

http://www.aloki.hu ● ISSN 1589 1623 (Print) ● ISSN 1785 0037 (Online)
DOI: http://dx.doi.org/10.15666/aeer/1705_1207312089

phylotypes or sequences types classified into six genera including *Rhizophagus*, *Glomus*, *Diversispora*, *Claroideoglomus*, *Paraglomus,* and *Ambispora* (*Fig. 3*). Of all these AM fungal phylotypes, 19 belonged to *Rhizophagus* (*Rhizophagus* 01-19), 24 to *Glomus* (*Glomus* 01-24), one from each *Diversispora* (*Diversispora* 01) and *Claroideoglomus* (*Claroideoglomus* 01), four from *Paraglomus* (*Paraglomus* 01-04), and *Ambispora* (*Ambispora* 01-02) group contains two phylotypes.

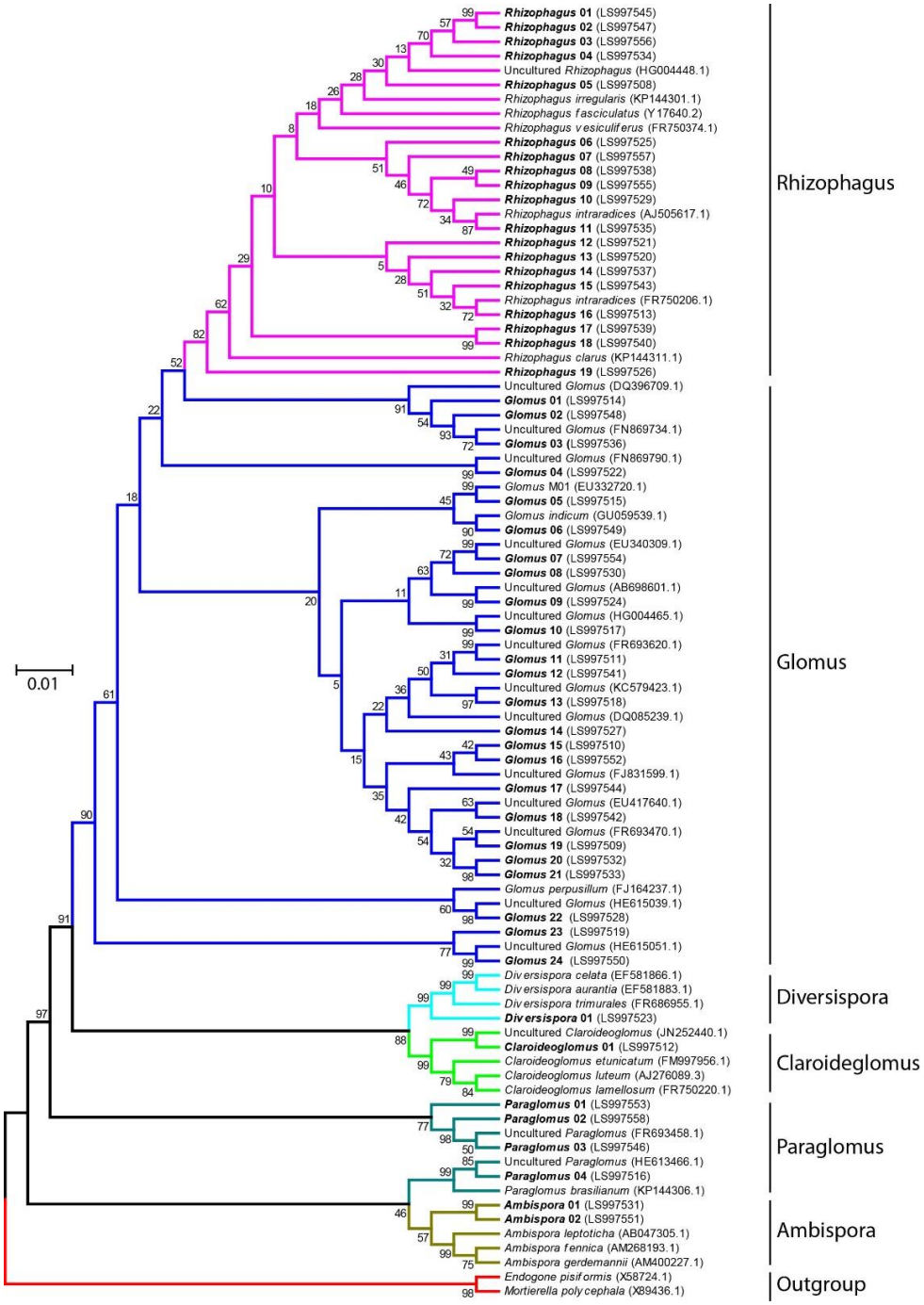

Figure 3. *Phylogenetic tree. The neighbor-joining phylogenetic tree was constructed based on 18S rDNA sequences of the 51 OTUs (bold), and the reference sequences were downloaded from NCBI (their corresponding numbers are shown in the parentheses). The bootstrap values by 1000 replications were calculated. The scale bar represents the sequence divergence at 1%*

http://www.aloki.hu ● ISSN 1589 1623 (Print) ● ISSN 1785 0037 (Online)
DOI: http://dx.doi.org/10.15666/aeer/1705_1207312089

In terms of OTUs, *Rhizophagus*-05 and *Glomus*-15 were the most abundant in all three species, with a relative abundance of 27% and 11% respectively, whereas *Glomus*-19 was found only in *S. grandis* and *C. squarrosa* and had a relative abundance of 13% (*Table 1*).

Table 1. *Number of clones detected for each AM fungi phylotype and relative richness. The most closely related sequences with their accession number from the http://www.ncbi.nlm.nih.gov are given*

OTUs identified	*SG*	*CS*	*LC*	Accession	Identity (%)
***Rhizophagus* 01** (LS997545)	0	0	1	HG004448.1	0.99
***Rhizophagus* 02** (LS997547)	0	0	1	FR693470.1	0.99
***Rhizophagus* 03** (LS997556)	0	1	0	FJ831599.1	0.99
***Rhizophagus* 04** (LS997534)	1	0	1	FR693620.1	0.99
***Rhizophagus* 05** (LS997508)	40	54	62	JN252440.1	0.99
***Rhizophagus* 06** (LS997525)	5	0	0	FR750206.1	0.99
***Rhizophagus* 07** (LS997557)	1	0	0	DQ396709.1	0.99
***Rhizophagus* 08** (LS997538)	2	0	0	EU332720.1	0.99
***Rhizophagus* 09** (LS997555)	0	0	1	HE613466.1	0.99
***Rhizophagus* 10** (LS997529)	0	2	1	HG004465.1	0.99
***Rhizophagus* 11** (LS997535)	0	2	0	KC579423.1	0.99
***Rhizophagus* 12** (LS997521)	4	0	7	EU340309.1	0.96
***Rhizophagus* 13** (LS997520)	10	0	3	FR750206.1	0.99
***Rhizophagus* 14** (LS997537)	1	1	0	FR750206.1	0.99
***Rhizophagus* 15** (LS997543)	0	1	0	FN869790.1	0.99
***Rhizophagus* 16** (LS997513)	5	15	1	FR686955.1	0.95
***Rhizophagus* 17** (LS997539)	0	1	0	AB698601.1	0.99
***Rhizophagus* 18** (LS997540)	1	0	0	FR750374.1	0.98
***Rhizophagus* 19** (LS997526)	2	1	1	Y17640.2	0.98
***Glomus* 01** (LS997514)	2	17	0	DQ085239.1	0.98
***Glomus* 02** (LS997548)	1	0	0	HE615039.1	0.98
***Glomus* 03** (LS997536)	2	0	0	Y17640.2	0.97
***Glomus* 04** (LS997522)	1	0	10	EU340309.1	0.99
***Glomus* 05** (LS997515)	12	6	0	AM268193.1	0.88
***Glomus* 06** (LS997549)	1	0	0	FR693470.1	0.96
***Glomus* 07** (LS997554)	0	0	1	FR693470.1	0.98
***Glomus* 08** (LS997530)	3	0	0	HG004448.1	0.98
***Glomus* 09** (LS997524)	1	0	6	AJ505617.1	0.97
***Glomus* 10** (LS997517)	3	0	14	FN869790.1	0.98
***Glomus* 11** (LS997511)	3	23	5	FR750206.1	0.96
***Glomus* 12** (LS997541)	0	1	0	Y17640.2	0.97
***Glomus* 13** (LS997518)	7	3	6	Y17640.2	0.97
***Glomus* 14** (LS997527)	2	0	1	Y17640.2	0.87
***Glomus* 15** (LS997510)	20	23	22	FR693620.1	0.97
***Glomus* 16** (LS997552)	0	1	0	EU417640.1	0.98
***Glomus* 17** (LS997544)	1	0	0	FR750206.1	0.96
***Glomus* 18** (LS997542)	0	1	0	FR693470.1	0.97
***Glomus* 19** (LS997509)	27	48	0	HG004448.1	0.97

http://www.aloki.hu ● ISSN 1589 1623 (Print) ● ISSN 1785 0037 (Online)
DOI: http://dx.doi.org/10.15666/aeer/1705_1207312089

***Glomus* 20** (LS997532)	0	2	0	FR693458.1	0.97
***Glomus* 21** (LS997533)	2	0	0	HG004448.1	0.96
***Glomus* 22** (LS997528)	3	0	0	DQ396709.1	0.95
***Glomus* 23**(LS997519)	1	0	13	GU059539.1	0.97
***Glomus* 24**(LS997550)	0	0	1	HE615051.1	0.97
Diversispora 01 (LS997523)	0	0	8	AM268193.1	0.87
***Claroideoglomus* 01** (LS997512)	0	0	30	FJ831599.1	0.98
***Paraglomus* 01** (LS997553)	1	0	0	FR693458.1	0.96
***Paraglomus* 02** (LS997558)	0	0	1	EU340309.1	0.98
***Paraglomus* 03** (LS997546)	1	0	0	Y17640.2	0.97
***Paraglomus* 04** (LS997516)	0	17	0	HG004448.1	0.96
***Ambispora* 01** (LS997531)	1	0	2	AJ505617.1	0.97
***Ambispora* 02** (LS997551)	0	0	1	FR693458.1	0.96
Total clones	**167**	**220**	**200**		
Total richness	**32**	**20**	**25**		

AMF diversity inside roots

The most dominant genera were *Glomus* and *Rhizophagus*, accounting for 50% and 39% of the total clones, respectively, whereas, the *Ambispora* and *Diversispora* were the least frequent genera, making up only 0.6% and 1% of the total clones, respectively (*Fig. 4*). At the genus level, all six AM fungal genera were found *in L. chinensis* whereas only four and three genera were found in *S. grandis* and *C. squarrosa*, respectively (*Fig. 4*).

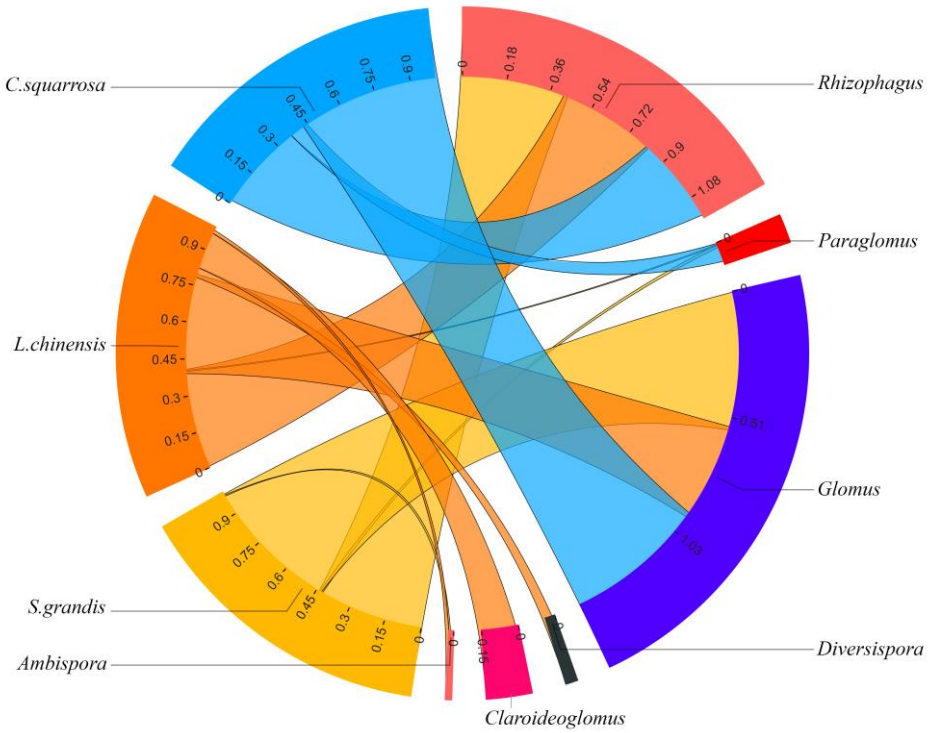

Figure 4. *Chord diagram showing the relative abundance of AMF. The relative abundance of AMF genera detected in the roots of the three plant species*

http://www.aloki.hu ● ISSN 1589 1623 (Print) ● ISSN 1785 0037 (Online)
DOI: http://dx.doi.org/10.15666/aeer/1705_1207312089

Likewise, the detected OTUs (identified genus) were not evenly distributed among the three plant species. Among the 587 sequence types classified as AM fungi, 167 were from *S. grandis*, 220 were from *C. squarrosa*, and 200 were from *L. chinensis;* however, regarding the OTUs identified data (*Table 1*), *S. grandis* appeared to possess the most AMF phylotypes, i.e., 32, whereas, *C. squarrosa* and *L. chinensis* possessed 20 and 25 AMF phylotypes, respectively.

Concerning species richness, *S. grandis* also showed the higher richness of the AMF OTUs, followed by *C. squarrosa* and *L. chinensis* (*Fig. 5*). Analysis of variance showed that there were statistically significant differences found in species richness ($p < 0.05$). Therefore, we concluded that *S. grandis* had significantly more diversified AM fungal phylotypes than *L. Chinensis* and *C. squarrosa*. Notably, some OTUs were observed for limited hosts. *Rhizophagus* 06, 07, 08, and 18, *Glomus* 02, 03, 06, 08, 17, 21, and 22, *Paraglomus* 01 and 03 were found in *S. grandis*, *Rhizophagus* 03, 11, 15, and 17, *Glomus* 12, 16, 18, 20, and *Paraglomus* 04 were observed in *C. squarrosa,* and in *L. chinensis*, *Rhizophagus* 01, 02, 09, *Glomus* 07, 24, *Diversispora* 01, *Claroideoglomus* 01, *Paraglomus* 02, and *Ambispora* 02 were found (*Table 1*).

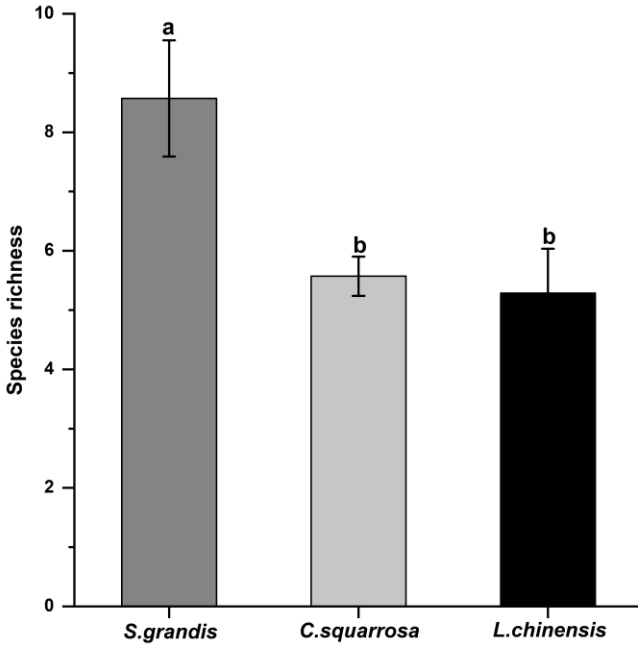

Figure 5. *AMF richness. AMF richness in three different plant species. The analysis of variance revealed that S. grandis deviated significantly from the other two plant species and showed more species richness. Data are means ± SE. Identical letters denote non-significant differences, whereas different letters indicate significant differences, as shown by Tukey's HSD test at P < 0.05*

Furthermore, the Shannon-Wiener index used to indicate species diversity in a community. As our results showed, *S. grandis*, *C. squarrosa* and *L. chinensis* exhibited an average value of Shannon diversity index 1.62, 1.30, and 1.08 respectively, and non-significant differences were found ($p = 0.17$) (*Fig. 6*).

The number of OTUs specific to their host plant was 13 for *S. grandis* and 9 for both *C. squarrosa* and *L. chinensis* (*Fig. 7*). The OTUs data set thus demonstrated the

http://www.aloki.hu ● ISSN 1589 1623 (Print) ● ISSN 1785 0037 (Online)
DOI: http://dx.doi.org/10.15666/aeer/1705_1207312089

uniqueness of AMF-plant combinations of dominant plant species found in Xilinguole steppe regions.

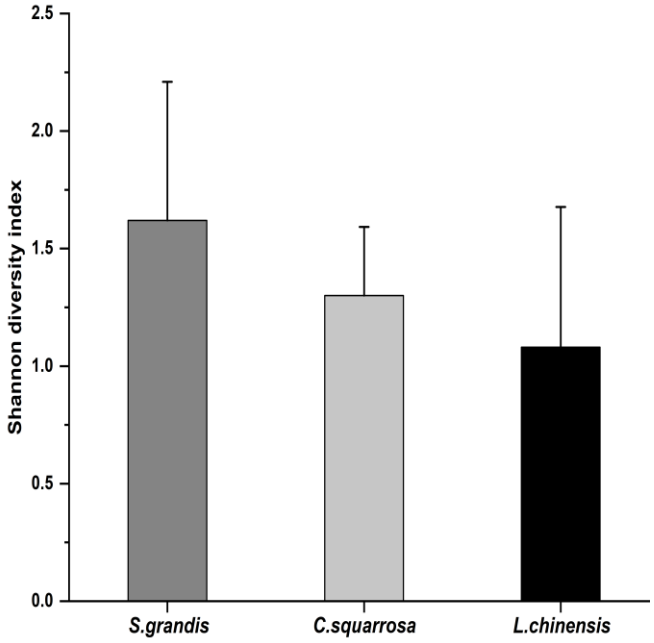

Figure 6. *Shannon-Wiener index. The Shannon's diversity index (mean ± SE), and the analysis of variance revealed a non-significant difference in S. grandis, C. squarrosa, and L. chinensis*

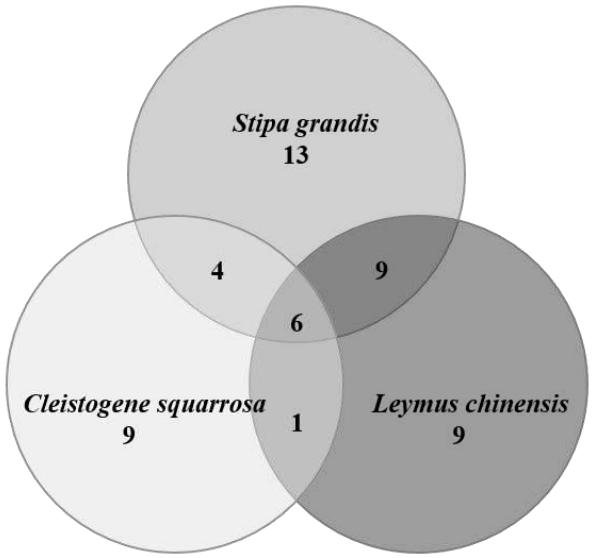

Figure 7. *Venn diagram showing the number of shared and unique OTUs among the host plants*

Moreover, the NMDS analysis indicated that the AMF community components living with one plant species did not tightly group according to their host plant species (*Fig. 8*). It implies that at both the genus and OTU levels, AMF showed a host preference character to a certain extent; however, the host plant species may not be solely the determinant for shaping the overall AM fungal community within roots.

http://www.aloki.hu ● ISSN 1589 1623 (Print) ● ISSN 1785 0037 (Online)
DOI: http://dx.doi.org/10.15666/aeer/1705_1207312089

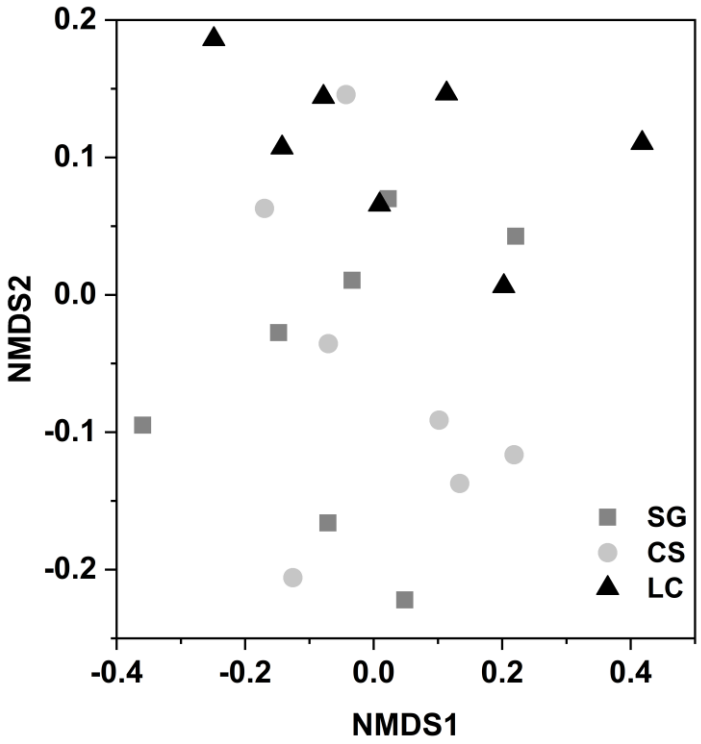

Figure 8. *NMDS analysis. Non-metric multidimensional scaling (NMDS) of the community composition of arbuscular mycorrhizal fungi in the three plant species from seven different sites (stress = 0.189). Gray square boxes correspond to SG (S. grandis), light gray circles to CS (C. squarrosa), and black triangles to LC (L. chinensis)*

Discussion

AMF colonization

In this study, AM fungal colonization in different plant species was high (85%) at the beginning of the growing season, which is in line with the distinct colonization rates studied previously among different co-occurring plants (Li et al., 2010; Lugo et al., 2003; Su et al., 2011). However, the rate of colonization was non-significant among the threes species, which is consistent with Su et al. (2011). Studies on AM fungal colonization in Inner Mongolia, tallgrass prairie grasses and six locations on the European coast showed similar results in early growth seasons, and AMF colonization was the highest in this period (Bentivenga and Hetrick, 1992; Rodríguez-Echeverría et al., 2008; Su et al., 2011). This is because during the early growing season, the plants grow fast with high metabolic activity and high level of nutrient exchange between host plants and fungi, leading to a higher percentage of AM colonization (Baslam et al., 2011; Bentivenga and Hetrick, 1992; Muthukumar and Udaiyan, 2002; Wang et al., 2015; Su et al., 2011). The structures of AMF, including vesicles and arbuscules are essential sites for nutrient storage and their exchange between the host plants and fungi (Müller et al., 2017; Berruti et al., 2016). Moreover, genus *Glomus* was found to be the most abundant, suggesting that the AMF species belonging to this genus can produce more hyphal segments and spores that can colonize onto plant roots extensively (Zhao et al., 2017). Consistent with this, all three plant species, in our study, were dominated by *Glomus* showing the highest percentage of AMF colonization.

http://www.aloki.hu ● ISSN 1589 1623 (Print) ● ISSN 1785 0037 (Online)
DOI: http://dx.doi.org/10.15666/aeer/1705_1207312089

AM fungal diversity and community composition

We found that the number of sequence types/OTUs detected were 51, inferring the rich AMF diversity in this typical steppe. The species richness of AMF in the roots of *S. grandis*, *C. squarrosa,* and *L. chinensis* was 32, 20, and 25, respectively. Moreover, the diversity indexes also indicated the high diversity in all three plant species, especially in *S. grandis*. These findings are supported by the previous studies showing that the plant species in the field conditions held higher AMF diversity in their roots (Öpik et al., 2006; Torrecillas et al., 2012), and perennial plant species of semiarid region hosted the higher AM fungal diversity in their roots (Alguacil et al., 2012). Moreover, the AM fungal community in the current research exhibited that 50% of the total OTUs were contributed from the genus *Glomus*, suggesting it as the most abundant and wide spread genus among the three plant species. These results supported the previous reports that widely distributed AMF had higher abundance in the local environment but with low host specificity (Husband et al., 2002; Öpik et al., 2006; Wirsel, 2004). Moreover, it is also documented that AMF diversity increases with the increase in plant diversity (Alguacil et al., 2011; Torrecillas et al., 2012) because different plant species dominate the typical steppe of Inner Mongolia during the growing season (Su et al., 2011). This explanation is in agreement with our results that *S. grandis* showed a greater extent of AM fungal diversity when compared to *L. chinensis* and *C. squarrosa*, as *S. grandis* also held the highest AMF colonization, which may be attributed to the colonization of more diversified AMF taxa. Alguacil et al. (2011) also concluded that the non-metric multidimensional scaling plot revealed that AM fungal communities of all three plants overlapped, suggesting low host specificity of AMF for these species. This might be because all the species belong to the same family *poaceae*. This is also in line with previous finding stating the absence of host specificity in *poaceae* (Torrecillas et al., 2012). Another explanation could be that the composition of host plant does not effectively influence AM fungal communities. There are also some environmental factors that have substantial effects on the community composition of AMF such as soil properties including structure (Lekberg et al., 2007), fertility (Egerton-Warburton et al., 2007; del Mar Alguacil et al., 2010), moisture content (Wolfe et al., 2007), disturbance (Rodríguez-Echeverría and Freitas, 2006), and climatic factors including temperature and precipitation (Treseder, 2013). Widespread study in Tibetan alpine steppe stated that different plants at the same site had no significant difference in AMF community composition in their rhizosphere soil (Zhang et al., 2016a). In most cases, the AMF community associated with the respective host is not so unique, and there is the probability that a subset of that AMF community is also connected with many other host plants, and it has been reported that a limited number of fungal species associated with globally 90% of plant families, resulting in lower host specificity of AMF (Natasha Teutsch and Hawkes, 2010). In contrast, there are also mounting evidences indicating that co-occurring plant species held apparently distinct AM fungal communities within their roots, including plants in tropical forests (Husband et al., 2002), permanent grasslands (Vandenkoornhuyse et al., 2003), oak-woodlands (Douhan et al., 2005), semiarid coastal dunes (Martínez-García and Pugnaire, 2011), high mountainous meadows (Sýkorová et al., 2007), and farmland (Paul et al., 2013).

Despite the overall community composition similarity, in terms of genus and OTUs, some AMF were still found to be specific to their host plants in our study (*Table 1*). Likely, Lugo and Cabello (2012) found that some AMF species were limited to *B. subarista* and *P. stuckertii*, whereas the *Glomus* species was only associated with *P.*

http://www.aloki.hu ● ISSN 1589 1623 (Print) ● ISSN 1785 0037 (Online)
DOI: http://dx.doi.org/10.15666/aeer/1705_1207312089

stuckertii. Thus, the effects of host plant on AM fungal community composition are still controversial and needs further research to disentangle the reality.

Conclusion

In summary, the overall higher rate of mycorrhizal colonization in the roots of three dominant species of Xilinguole typical grassland reflects the strong association and mutual relationship of plant-AMF. Moreover, there were significant differences in species richness of AMF among the three perennial plant species. However, there were no significant differences in community composition of AMF; some genera exposed a little host preference, wherein *Glomus* was the most dominant in reflecting the actual community composition. These findings can be of vital importance in studying the success of plant species in their ecosystems based on the integrity of their symbiotic relationships with AMF.

Acknowledgements. The authors would like to appreciate Lin Zhang, Xin Lin, M. Zeeshan Munir, Zaib-Un-Nisa, Sagheer Ahmad, M. Imran, Arshad Iqbal, M. Amir, and Xinling Dai for their valuable suggestions in improving the manuscript and their help in different bioinformatics tools. We would like to thank Qiang Dong, Xin Guo, Yaoyao Lu for the assistance with field sampling, and Chengdu Institute of Biology of the Chinese Academy of Sciences for the support on DNA sequencing and bioinformatics analysis. This work was funded by the Special Fund for Forest Scientific Research in the Public Welfare (201404204-05A), the National Key Research and Development Program of China (2016YFC0501802), and the National Natural Science Foundation of China (31770542, 31761123001-1).

REFERENCES

[1] Alguacil, M., Torres, M., Torrecillas, E., et al. (2011): Plant type differently promote the arbuscular mycorrhizal fungi biodiversity in the rhizosphere after revegetation of a degraded, semiarid land. – Soil Biology and Biochemistry 43: 167-173.
[2] Alguacil, M., Torrecillas, E., Roldán, A., et al. (2012): Perennial plant species from semiarid gypsum soils support higher AMF diversity in roots than the annual Bromus rubens. – Soil Biology and Biochemistry 49: 132-138.
[3] Baslam, M., Garmendia, I., Goicoechea, N. (2011): Arbuscular mycorrhizal fungi (AMF) improved growth and nutritional quality of greenhouse-grown lettuce. – Journal of Agricultural and Food Chemistry 59: 5504-5515.
[4] Bentivenga, S., Hetrick, B. (1992): Seasonal and temperature effects on mycorrhizal activity and dependence of cool-and warm-season tallgrass prairie grasses. – Canadian Journal of Botany 70: 1596-1602.
[5] Berruti, A., Lumini, E., Balestrini, R., et al. (2016): Arbuscular mycorrhizal fungi as natural biofertilizers: let's benefit from past successes. – Frontiers in Microbiology 6: 1559.
[6] Bever, J. D. (2002): Host-specificity of AM fungal population growth rates can generate feedback on plant growth. – Plant and Soil 244: 281-290.
[7] Bonfante, P., Genre, A. (2010): Mechanisms underlying beneficial plant–fungus interactions in mycorrhizal symbiosis. – Nature Communications 1: 48.
[8] Chen, M., Yang, G., Sheng, Y., et al. (2017): Glomus mosseae inoculation improves the root system architecture, photosynthetic efficiency and flavonoids accumulation of Liquorice under nutrient stress. – Frontiers in Plant Science 8: 931.
[9] Clapp, J., Young, J., Merryweather, J., et al. (1995): Diversity of fungal symbionts in arbuscular mycorrhizas from a natural community. – New Phytologist 130: 259-265.

http://www.aloki.hu ● ISSN 1589 1623 (Print) ● ISSN 1785 0037 (Online)
DOI: http://dx.doi.org/10.15666/aeer/1705_1207312089

[10] del Mar Alguacil, M., Lozano, Z., Campoy, M. J., et al. (2010): Phosphorus fertilisation management modifies the biodiversity of AM fungi in a tropical savanna forage system. – Soil Biology and Biochemistry 42: 1114-1122.
[11] del Mar Alguacil, M., Díaz, G., Torres, M. P., et al. (2018): Host identity and functional traits determine the community composition of the arbuscular mycorrhizal fungi in facultative epiphytic plant species. – bioRxiv 307991.
[12] Desai, S., Kumar, G. P., Amalraj, L. D., et al. (2016): Exploiting PGPR and AMF Biodiversity for Plant Health Management. – In: Singh, D. P. et al. (eds.) Microbial Inoculants in Sustainable Agricultural Productivity. Springer, India, pp. 145-160.
[13] Douhan, G. W., Petersen, C., Bledsoe, C. S., et al. (2005): Contrasting root associated fungi of three common oak-woodland plant species based on molecular identification: host specificity or non-specific amplification? – Mycorrhiza 15: 365-372.
[14] Egerton-Warburton, L. M., Johnson, N. C., Allen, E. B. (2007): Mycorrhizal community dynamics following nitrogen fertilization: a cross-site test in five grasslands. – Ecological Monographs 77: 527-544.
[15] Eom, A.-H., Hartnett, D. C., Wilson, G. W. (2000): Host plant species effects on arbuscular mycorrhizal fungal communities in tallgrass prairie. – Oecologia 122: 435-444.
[16] Harrier, L. (2001): The arbuscular mycorrhizal symbiosis: a molecular review of the fungal dimension. – Journal of Experimental Botany 52: 469-478.
[17] He, F., Wang, K., Hannaway, D. B., et al. (2017): Effects of precipitation and clipping intensity on net primary productivity and composition of a Leymus chinensis temperate grassland steppe. – PloS One 12: e0190450.
[18] Helgason, T., Daniell, T. J., Husband, R., et al. (1998): Ploughing up the wood-wide web? – Nature 394: 431.
[19] Helgason, T., Fitter, A. H., Young, J. P. W. (1999): Molecular diversity of arbuscular mycorrhizal fungi colonising Hyacinthoides non-scripta (bluebell) in a seminatural woodland. – Mol Ecol 8(4): 659-666.
[20] Helgason, T., Merryweather, J., Denison, J., et al. (2002): Selectivity and functional diversity in arbuscular mycorrhizas of co-occurring fungi and plants from a temperate deciduous woodland. – Journal of Ecology 90: 371-384.
[21] Huang, Y.-M., Zou Y-N and Wu Q-S. (2017): Alleviation of drought stress by mycorrhizas is related to increased root H 2 O 2 efflux in trifoliate orange. – Scientific Reports 7: 42335.
[22] Husband, R., Herre, E. A., Turner, S., et al. (2002): Molecular diversity of arbuscular mycorrhizal fungi and patterns of host association over time and space in a tropical forest. – Molecular Ecology 11: 2669-2678.
[23] Krüger, M., Stockinger, H., Krüger, C., et al. (2009): DNA-based species level detection of Glomeromycota: one PCR primer set for all arbuscular mycorrhizal fungi. – New Phytologist 183: 212-223.
[24] Krüger, M., Krüger, C., Walker, C., et al. (2012): Phylogenetic reference data for systematics and phylotaxonomy of arbuscular mycorrhizal fungi from phylum to species level. – New Phytologist 193: 970-984.
[25] Kumar, S., Tamura, K., Jakobsen, I. B., et al. (2007): MEGA4: Molecular Evolutionary Genetics Analysis (MEGA) software version 4.0. – Molecular Biology & Evolution 24: 1596.
[26] Latef, A. A. H. A., Hashem, A., Rasool, S., et al. (2016): Arbuscular mycorrhizal symbiosis and abiotic stress in plants: A review. – Journal of plant biology 59: 407-426.
[27] Lee, E.-H., Eo, J.-K., Ka, K.-H., et al. (2013): Diversity of arbuscular mycorrhizal fungi and their roles in ecosystems. – Mycobiology 41: 121-125.
[28] Lekberg, Y., Koide, R. T., Rohr, J. R., et al. (2007): Role of niche restrictions and dispersal in the composition of arbuscular mycorrhizal fungal communities. – Journal of Ecology 95: 95-105.

http://www.aloki.hu ● ISSN 1589 1623 (Print) ● ISSN 1785 0037 (Online)
DOI: http://dx.doi.org/10.15666/aeer/1705_1207312089

[29] Li, L.-F., Li, T., Zhang, Y., et al. (2010): Molecular diversity of arbuscular mycorrhizal fungi and their distribution patterns related to host-plants and habitats in a hot and arid ecosystem, southwest China. – FEMS Microbiology Ecology 71: 418-427.
[30] Li, X., Zhu, T., Peng, F., et al. (2015): Inner Mongolian steppe arbuscular mycorrhizal fungal communities respond more strongly to water availability than to nitrogen fertilization. – Environmental Microbiology 17: 3051-3068.
[31] Liang, C., Michalk, D., Millar, G. (2002): The ecology and growth patterns of Cleistogenes species in degraded grasslands of eastern Inner Mongolia, China. – Journal of Applied Ecology 39: 584-594.
[32] López-García, Á., Palenzuela, J., Barea, J. M., et al. (2014): Life-history strategies of arbuscular mycorrhizal fungi determine succession into roots of Rosmarinus officinalis L., a characteristic woody perennial plant species from Mediterranean ecosystems. – Plant and Soil 379: 247-260.
[33] Lugo, M. A., Cabello, M. N. (2002): Native arbuscular mycorrhizal fungi (AMF) from mountain grassland (Córdoba, Argentina) I. Seasonal variation of fungal spore diversity. – Mycologia 94: 579-586.
[34] Lugo, M. A., González Maza, M. E., Cabello, M. N. (2003): Arbuscular mycorrhizal fungi in a mountain grassland II: Seasonal variation of colonization studied, along with its relation to grazing and metabolic host type. – Mycologia 95: 407-415.
[35] Martínez-García, L. B., Pugnaire, F. I. (2011): Arbuscular mycorrhizal fungi host preference and site effects in two plant species in a semiarid environment. – Applied Soil Ecology 48: 313-317.
[36] Mcgonigle, T. P., Miller, M. H., Evans, D. G., et al. (1990): A new method which gives an objective measure of colonization of roots by vesicular—arbuscular mycorrhizal fungi. – New Phytologist 115: 495-501.
[37] Müller, A., Ngwene, B., Peiter, E., et al. (2017): Quantity and distribution of arbuscular mycorrhizal fungal storage organs within dead roots. – Mycorrhiza 27: 201-210.
[38] Muthukumar, T., Udaiyan, K. (2002): Seasonality of vesicular-arbuscular mycorrhizae in sedges in a semi-arid tropical grassland. – Acta Oecologica 23: 337-347.
[39] Natasha Teutsch, H., Hawkes, C. V. (2010): Plant neighborhood control of arbuscular mycorrhizal community composition. – New Phytologist 183: 1188-1200.
[40] Oksanen, J., Kindt, R., Legendre, P., et al. (2007): The vegan package. – Community Ecology Package 10: 631-637.
[41] Öpik, M., Moora, M., Liira, J., et al. (2003): Divergent arbuscular mycorrhizal fungal communities colonize roots of Pulsatilla spp. in boreal Scots pine forest and grassland soils. – New Phytologist 160: 581-593.
[42] Öpik, M., Moora, M., Liira, J., et al. (2006): Composition of root-colonizing arbuscular mycorrhizal fungal communities in different ecosystems around the globe. – Journal of Ecology 94: 778-790.
[43] Paul, G., Andrew, M., Maude, P., et al. (2013): Contrasting arbuscular mycorrhizal communities colonizing different host plants show a similar response to a soil phosphorus concentration gradient. – New Phytologist 198: 546-556.
[44] Pivato, B., Mazurier, S., Lemanceau, P., et al. (2007): Medicago species affect the community composition of arbuscular mycorrhizal fungi associated with roots. – New Phytologist 176: 197-210.
[45] Redecker, D., Cooper, J. E., Rao, J. R. (2006): Molecular Ecology of Arbuscular Mycorrhizal Fungi: A Review of PCR-Based Techniques. – In: Rao, J. R., Cooper, J. E. (eds.) Molecular Approaches to Soil Rhizosphere & Plant Microorganism Analysis. CABI, Wallingford, UK.
[46] Ren, H., Han, G., Lan, Z., et al. (2016): Grazing effects on herbage nutritive values depend on precipitation and growing season in Inner Mongolian grassland. – Journal of Plant Ecology 9: 712-723.

http://www.aloki.hu ● ISSN 1589 1623 (Print) ● ISSN 1785 0037 (Online)
DOI: http://dx.doi.org/10.15666/aeer/1705_1207312089

[47] Rodríguez-Echeverría, S., Freitas, H. (2006): Diversity of AMF associated with Ammophila arenaria ssp. arundinacea in Portuguese sand dunes. – Mycorrhiza 16: 543-552.
[48] Rodríguez-Echeverría, S., Hol, W. G., Freitas, H., et al. (2008): Arbuscular mycorrhizal fungi of Ammophila arenaria (L.) Link: spore abundance and root colonisation in six locations of the European coast. – European Journal of Soil Biology 44: 30-36.
[49] Santos, J. C., Finlay, R. D., Tehler, A. (2006): Molecular analysis of arbuscular mycorrhizal fungi colonising a semi-natural grassland along a fertilisation gradient. – New Phytologist 172: 159-168.
[50] Schloss, P. D., Westcott, S. L., Ryabin, T., et al. (2009): Introducing mothur: open-source, platform-independent, community-supported software for describing and comparing microbial communities. – Applied & Environmental Microbiology 75: 7537-7541.
[51] Shannon, C. E., Weaver, W. (1949): The Mathematical Theory of Communication. – University of Illinois Press, Urbana, pp. 24-30.
[52] Simon, L., Lalonde, M., Bruns, T. D. (1992): Specific amplification of 18S fungal ribosomal genes from vesicular-arbuscular endomycorrhizal fungi colonizing roots. – Applied & Environmental Microbiology 58: 291-295.
[53] Smith, S., Read, D. (2008): Mycorrhizal Symbiosis. 3rd Ed. – Academic-Elsevier, London.
[54] Stürmer, S. L. (2012): A history of the taxonomy and systematics of arbuscular mycorrhizal fungi belonging to the phylum Glomeromycota. – Mycorrhiza 22: 247-258.
[55] Su, Y.-Y., Guo L.-D., Hyde, K. D. (2010): Response of endophytic fungi of Stipa grandis to experimental plant function group removal in Inner Mongolia steppe, China. – Fungal Diversity 43: 93-101.
[56] Su, Y.-Y., Sun, X., Guo L-D. (2011): Seasonality and host preference of arbuscular mycorrhizal fungi of five plant species in the Inner Mongolia steppe, China. – Brazilian Journal of Microbiology 42: 57-65.
[57] Sýkorová, Z., Wiemken, A., Redecker, D. (2007): Cooccurring Gentiana verna and Gentiana acaulis and their neighboring plants in two Swiss upper montane meadows harbor distinct arbuscular mycorrhizal fungal communities. – Applied and Environmental Microbiology 73: 5426-5434.
[58] Tamura, K., Dudley, J., Nei, M., et al. (2007): MEGA4: Molecular Evolutionary Genetics Analysis (MEGA) software version 4.0. – Molecular Biology & Evolution 24: 1596-1599.
[59] Team R Core (2013): R: A Language and Environment for Statistical Computing. – R Core Team, Vienna.
[60] Torrecillas, E., Alguacil, M., Roldán, A. (2012): Host preferences of AM fungi colonizing annual herbaceous plant species in semiarid Mediterranean prairies. – Applied and Environmental Microbiology AEM. 01287-01212.
[61] Treseder, K. K. (2013): The extent of mycorrhizal colonization of roots and its influence on plant growth and phosphorus content. – Plant and Soil 371: 1-13.
[62] Vandenkoornhuyse Á., Ridgway, K., Watson, I., et al. (2003): Co-existing grass species have distinctive arbuscular mycorrhizal communities. – Molecular Ecology 12: 3085-3095.
[63] Wang, Y., Li, T., Li, Y., et al. (2015): Community dynamics of arbuscular mycorrhizal fungi in high-input and intensively irrigated rice cultivation systems. – Applied and Environmental Microbiology AEM. 03769-03714.
[64] White, T. J., Bruns, T., Lee, S., et al. (1990): Amplification and Direct Sequencing of Fungal Ribosomal RNA Genes for Phylogenetics. – In: Innis, M. A. et al. (eds.) PCR Protocols. A Guide to Methods and Applications. Academic Press, New York, pp. 315-322

http://www.aloki.hu ● ISSN 1589 1623 (Print) ● ISSN 1785 0037 (Online)
DOI: http://dx.doi.org/10.15666/aeer/1705_1207312089

[65] Wirsel, S. G. (2004): Homogenous stands of a wetland grass harbour diverse consortia of arbuscular mycorrhizal fungi. – FEMS Microbiology Ecology 48: 129-138.
[66] Wolfe, B. E., Mummey, D. L., Rillig, M. C., et al. (2007): Small-scale spatial heterogeneity of arbuscular mycorrhizal fungal abundance and community composition in a wetland plant community. – Mycorrhiza 17: 175-183.
[67] Xu, H., Su, H., Su, B., et al. (2014): Restoring the degraded grassland and improving sustainability of grassland ecosystem through chicken farming: a case study in northern China. – Agriculture, Ecosystems & Environment 186: 115-123.
[68] Zhang, J., Wang, F., Che, R., et al. (2016a): Precipitation shapes communities of arbuscular mycorrhizal fungi in Tibetan alpine steppe. – Scientific Reports 6: 23488.
[69] Zhang, L., Xu, M., Liu, Y., et al. (2016b): Carbon and phosphorus exchange may enable cooperation between an arbuscular mycorrhizal fungus and a phosphate-solubilizing bacterium. – New Phytologist 210: 1022-1032.
[70] Zhang, Q., Yang, R., Tang, J., et al. (2010): Positive feedback between mycorrhizal fungi and plants influences plant invasion success and resistance to invasion. – PloS One 5: e12380.
[71] Zhao, H., Li, X., Zhang, Z., et al. (2017): Species diversity and drivers of arbuscular mycorrhizal fungal communities in a semi-arid mountain in China. – Peerj 5: e4155.
[72] Zheng, Y., Chen, L., Luo, C.-Y., et al. (2016): Plant identity exerts stronger effect than fertilization on soil arbuscular mycorrhizal fungi in a sown pasture. – Microbial Ecology 72: 647-658.

http://www.aloki.hu ● ISSN 1589 1623 (Print) ● ISSN 1785 0037 (Online)
DOI: http://dx.doi.org/10.15666/aeer/1705_1207312089

A REVIEW: MOLECULAR REGULATION OF STOMATAL DEVELOPMENT RELATED TO ENVIRONMENTAL FACTORS AND HORMONES IN PLANTS

GUO, Z. F.[1] – ZHAN, L.[1] – ZHANG, Y.[1] – LI, J. J.[1] – ZHAO, M. H.[2] – XU, Z. J.[2*] – LI, M. M.[3*]

[1]*Key Laboratory of Agricultural Biotechnology of Liaoning Province, College of Biosciences and Biotechnology, Shenyang Agricultural University, Shenyang 110866, China*

[2]*Rice Research Institute, College of Agronomy, Shenyang Agricultural University, Shenyang 110866, China*

[3]*Rice Research Institute, Jiangxi Academy of Agricultural Sciences, Nanchang 330200, China*

**Corresponding authors*
e-mail/phone/fax: xuzhengjin@126.com, +86-24-8848-7183; lmm3056@163.com, +86-791-8709-0751

(Received 27th Apr 2019; accepted 11th Jul 2019)

Abstract. Plants regulate leaf transpiration rate and water potential by changing the number of stomata and their rate of opening and closing. Stomata act as turgor-operated valves for gas exchange and water evaporation based on environmental needs. During stomatal development, various transcription factors and related genes are involved in the reception or transduction of environmental factors and hormones. Recent studies have led to significant advances in our understanding of intercellular signaling, the underlying pathways, and the polarity of the asymmetric division that controls stomatal development. The endogenous and exogenous factors that regulate these elements have also been identified. However, the mechanism of stomatal formation and development is highly complex and several morphogenesis-related questions are still unresolved. In this review, the molecular basis of stomatal development, including transcription factors, functional genes, and regulatory pathways, is described in detail. The connection between stomatal development and environmental factors such as CO_2, light, temperature and air humidity is discussed. In addition, the influences of plant hormones on stomatal development are sketched out in the review. We also highlight critical questions requiring future research and form a detailed list involving in gene functions and trait changes in mutants.
Keywords: *stomata, molecular mechanism, epidermal patterning factors, bHLH transcription factors, leucine-rich repeat receptor-like proteins*

Introduction

Stomata are apertures typically observed on plant outer leaf layers; they maintain the optimal balance between CO_2 uptake and water loss as a way to adapt environmental conditions in plants (Ni, 2012). In primary leaves of Arabidopsis, stomatal formation involves three types of cells: meristemoid mother cells (MMCs), guard mother cells (GMCs), and meristemoids (Behzadi et al., 2014). A protodermal cell develops into a stoma via three rounds of unequal cell divisions. First, the epidermal cell differentiates into a MMC through a series of unknown steps. The MMC then undergoes an asymmetric division to produce a small meristemoid cell and a stomatal-lineage ground cell (SLGC). The GMC develops into two GCs that flank a central pore to constitute a stoma (Bergmann and Sack, 2007). In addition, a SLGC can form satellite meristemoids (SMs) by spacing asymmetric division, with the SMs gradually differentiating into stomata. Most stomata are formed from SMs in this fashion. In addition to their balancing function, stomata play a significant role in water, carbon, and nutrient cycles.

http://www.aloki.hu ● ISSN 1589 1623 (Print) ● ISSN 1785 0037 (Online)
DOI: http://dx.doi.org/10.15666/aeer/1705_1209112109

Thorough investigation of stomatal regulation is therefore essential for understanding plant physiological responses to the environment and their physical functions (Von et al., 2002).

The traditional model explains stomatal development and distribution in terms of cell developmental lineages, cell–cell interactions, and long-distance signaling. In monocotyledons, stomata are arranged in chains parallel to leaf veins (Geisler et al., 2000). In Arabidopsis and other dicotyledons, however, stomatal distribution on the leaf surface is irregular and individual stomata are spaced from one another (Serna and Fenoll, 2000). Although in-depth examinations would be beneficial to understand gas exchange and to reduce moisture loss, such investigations can be very difficult because of this stomatal variation and the complex relationship between stomatal development and the environment.

Many studies have recently shown that stomatal development is a tightly controlled process. The various transcription factors, secreted protein, protease and some regulatory pathways have been shown to play an important role. While several environmental and hormonal factors are known to affect stomatal development, very little is known about the molecular mechanism for these changes. In this review, we describe stomatal distribution patterns and formation, signaling pathways, and genes related to stomatal development accordingly, and discuss directions for future research. We also form a detailed list involved in genes function and trait changes in mutants (*Table 1*).

Table 1. *Genes with mutations known to affect stomatal development in plant*

Locus	Symbol	Mutant phenotype (or overexpression phenotype)	Identity	References
EPIDERMAL PATTERNING FACTOR 1	EPF1	Increase stomatal densities	Cysteine-rich secreted peptide	Hara et al., 2009
EPIDERMAL PATTERNING FACTOR 2	EPF2	Increase the number of MMCs	Cysteine-rich secreted peptide	Hara et al., 2009
STOMAGEN	STOMAGEN	Reduce stomatal density	Cysteine-rich secreted peptide	Sugano et al., 2010
CHAL-LAH/EPFL6	CHAL	Increase stomatal density	Cysteine-rich secreted peptide	Abrash and Bergmann, 2010
Too Many Mouths	TMM	Stomatal clusters in leaves and no stomata in stems	Leucine-rich repeat receptor	Geisler et al., 2000
STOMATAL DENSITY AND DISTRIBUTION	SDD1	Higher stomatal density and some clusters	Subtilisin processing protease	Von et al., 2002
SPEECHLESS	SPCH	Fails to form stomata	bHLH transcription factor	MacAlister et al., 2007
MUTE	MUTE	Fails to form stomata	bHLH transcription factor	Pillitteri et al., 2007
FAMA	FAMA	Fail to progress into GCs and instead continue dividing	bHLH transcription factor	Ohashi-Ito and Bergmann, 2006
SCREAM/ICE1	SCRM	Fails to form stomata	bHLH transcription factor	Kanaoka et al., 2008
SCREAM2	SCRM2	Fails to form stomata	bHLH transcription factor	Kanaoka et al., 2008
PHYTOCHROME-INTERACTING FACTOR 4	PIF4	Fail to produce more stomata	bHLH transcription factor	Casson et al., 2009
FOUR LIPs	FLP	Induce the formation of clusters of four or more GCs	R2R3 MYB transcription factors	Lee et al., 2014
CO2 RESPONSE SECRETED PROTEASE	CRSP	More stomata at the elevated CO2 concentration	Extracellular protease	Engineer et al., 2014
High carbon dioxide	HIC	Increase stomatal density	3-keto acyl coenzyme A synthase	Gray et al., 2000
Carbonic anhydrase 1, 4	CA1, CA4	Increase stomatal density	Carbonic anhydrase	Hu et al., 2010; Engineer et al., 2014

http://www.aloki.hu ● ISSN 1589 1623 (Print) ● ISSN 1785 0037 (Online)
DOI: http://dx.doi.org/10.15666/aeer/1705_1209112109

Locus	Symbol	Mutant phenotype (or overexpression phenotype)	Identity	References
RETINOBLASTOMA-RELATED	RBR	Promoting initial GC identity, but unable to maintain commitment	Similar to a human protein called Retinoblastoma	Matos et al., 2014
CONSTITUTIVE PHOTOMORPHOGENIC 1	COP1	Producing stomatal clusters	Ubiquitin Ligase	Liu et al., 2008
CONSTITUTIVE PHOTOMORPHOGENIC 10	COP10	Producing stomatal clusters	Ubiquitin Ligase	Delgado et al., 2012
Phytochrome B	phyB	Fail to produce more stomata	Red light photoreceptor	Casson et al., 2009
YODA MAPK(kk)	YDA	Fails to form stomata	Mitogen activated protein kinase	Lampard et al., 2009
BRI SUPPRESSOR1	BSU1	Massive stomata formation	Phosphatase	Kim et al., 2012
Cytochrome	CYP707A1	Prevent stomatal closure at high RH (Overexpression phenotype)	ABA catabolism protein	Arve et al., 2015; Jalakas et al., 2018
BRI1-ASSOCIATED RECEPTOR KINASE 1	BAK1	ABA insensitivity in stomatal closure	BRASSINOSTEROID-INSENSITIVE 1 ASSOCIATED RECEPTOR KINASE	Shang et al., 2016
ANGUSTIFOLIA3	AN3	Decreased stomatal index (loss-of-function) clusters of stomata (overexpression phenotype)	Homolog of the human transcription co-activator	Meng et al., 2018
CONVERGENCE OF BL AND CO2 1/2	CBC1/2	Stomata in leaves closed tighter	Mitogen-activated protein kinase kinase kinase	Hiyama et al., 2017
BLUE LIGHT-DEPENDENT H+-ATPASE PHOSPHORYLATION	BHP	Impairments of stomatal opening and H+-ATPase phosphorylation in response to blue light	Raf-like protein kinase	Hayashi et al., 2017
ABA-INSENSITIVE PROTEIN KINASE1	AIK1	Stomatal closing is less sensitive to ABA; slightly greater stomatal density and significantly increased stomatal index	MAPKKK20	Li et al., 2017
MPK12	MPK12	Stomatal CO_2-insensitivity phenotypes of a mutant *cis* (CO_2-insensitive) and the higher degree of stomatal opening	MAP kinase	Jakobson et al., 2016
SLOW ANION CHANNEL-ASSOCIATED 1	SLAC1	Dramatically impair stomatal closure induced by CO_2	S-type anion channel protein	Vahisalu et al., 2008
H^+-ATPase translocation control 1	PATROL1	Impair stomatal opening in response to low CO_2 concentration and light	Protein with a MUN domain	Hashimoto-Sugimoto et al., 2013; Engineer et al., 2016
HIGH LEAF TEMPERATURE 1	HT1	Constitutively open stomata and impaired stomatal CO_2 responses	Protein kinase	Jakobson et al., 2016
Open Stomata 1	OST1	Insensitivity to ABA promotion of stomatal closure and ABA inhibition of stomatal opening	Protein kinase	Mustilli et al., 2002
ABA INSENSITIVE 1/2	ABI1 and ABI2	ABA-induced stomatal closing is abolished	Protein phosphatase 2C	Hirayama et al., 2007
BIG/CIS1	BIG/CIS1	Fail to show reductions in stomatal density and index, but display inhibition of stomatal opening with eCO_2 concentration	Calossin-like protein	He et al., 2018
BLUE LIGHT-DEPENDENT H+-ATPASE PHOSPHORYLATION	BHP	Impairments of stomatal opening	Raf-like kinase subfamily in the MAPKKK family	Hayashi et al., 2017
Phot1 and phot2	Phot1 and phot2	Blue light-dependent stomatal opening and the H^+-ATPase activation were absent	Light-activated receptor kinases	Doi et al., 2004

http://www.aloki.hu ● ISSN 1589 1623 (Print) ● ISSN 1785 0037 (Online)
DOI: http://dx.doi.org/10.15666/aeer/1705_1209112109

Locus	Symbol	Mutant phenotype (or overexpression phenotype)	Identity	References
Rac-interactive binding motif-containing protein 7	RIC7	Promoted light-induced stomatal opening	Rac-interactive binding motif-containing protein	Hong et al., 2016
ENHANCED RESPONSE TO ABA 1	ERA1	More closed stomata phenotype; stomatal opening induced by blue light was impaired	Farnesyl transferase beta subunit	Jalakas et al., 2017
Photosystem II Subunit S	PsbS	Less stomatal opening in response to light (over-expression)	Integral membrane protein	Głowacka et al., 2018
RESPIRATORY BURST OXIDASE 1	RBOH1	Impaired eCO_2-induced stomatal closure and the compromised eCO_2-enhanced water use efficiency as well as the heat tolerance	RESPIRATORY BURST OXIDASE	Zhang et al., 2018
JASMONATE ZIM DOMAIN 2	JAZ 2	Impaired pathogen-induced stomatal closing	JASMONATE ZIM DOMAIN (JAZ) proteins	Gimenez-Ibanez et al., 2017
MORE AXILLARY GROWTH 2	MAX2	More widely opening stomata or increased stomatal conductance	MORE AXILLARY GROWTH protein	Piisilä et al., 2015

Basic signal transduction and molecular regulation

Various transcription factors and other proteins involved in stomatal development have been studied along with their related genes. The encoded proteins include a family of epidermal patterning factors (EPFs), subtilisin-type proteinases (stomatal distribution and density 1 [SDD1]), leucine-rich repeat receptor-like proteins (TOO MANY MOUTHS [TMM]), basic helix-loop-helix (bHLH) transcription factors, and MAPK phosphatases (Geisler et al., 2000; Von et al., 2002; Hara et al., 2009; Jakobson et al., 2016). These studies, to some extent, have expounded the mechanisms of stomatal formation and development.

Role of EPF

EPF genes encode a protein family of cysteine-rich peptides that include 11 member ligands in Arabidopsis. The EPF family peptides are classified into four subgroups based on their amino acid sequences. Some proteins have been identified as involved in stomatal development, such as epidermal patterning factor 1 (EPF1), epidermal patterning factor 2 (EPF2), STOMAGEN/EPFL9, and CHAL etc. (Hara et al., 2009; Abrash and Bergmann, 2010; Sugano et al., 2010).

EPF1 and EPF2

EPF1 and EPF2 affect the formation of stomatal precursors through distinct yet overlapping functions. Asymmetric cell division and the formation of stomatal clusters or pairs is controlled by EPF1, which is produced in meristemoids, GMCs, and GCs. Mature leaves lacking *EPF1* consequently show an increase in the number of stomata and frequent stomatal pairing. EPF2 inhibits meristemoid formation and promotes the formation of pavement cells. The *epf2* mutant increases stomatal densities and leads to the formation of small, arrested stomatal lineage cells. In contrast, ectopic expression of *EPF2* suppresses entry divisions, which leads to an epidermis composed only of pavement cells. The double mutant *epf1*/*epf2* displays additive effects, causing greatly increased stomatal densities, stomatal pairing, and arrested cells (Hara et al., 2009; Hunt

http://www.aloki.hu ● ISSN 1589 1623 (Print) ● ISSN 1785 0037 (Online)
DOI: http://dx.doi.org/10.15666/aeer/1705_1209112109

and Gray, 2009). Over-expression of either *EPF1* or *EPF2* has been found to suppress stomatal formation, but has revealed that they act on different developmental processes. EPF1 enforces the one-cell spacing rule, whereas EPF2 inhibits the population of cells from acquiring the stomatal lineage fate. *EPF2* can partly substitute for *EPF1* in function, but *EPF2* cannot be replaced by *EPF1*. In addition, *EPF2* expression requires the bHLH transcription factor SPEECHLESS (*SPCH*) and a MAPK (YODA [*YDA*]), suggesting that EPF2 is mediated by the MAPK cascade (Hara et al., 2009). EPF1 and its primary receptor ERECTA-LIKE1 (ERL1) target MUTE as a bHLH protein that controls the transition from meristemoids to GMCs and specifies the proliferation-to-differentiation switch within the stomatal cell lineages, while MUTE directly induces ERL1 (Du et al., 2018).

Although the function of *EPF1* and *EPF2* has been studied deeply in many aspects. Compared with EPF1, however, the function of EPF2 still remains some unknown domains that need to study further in the future. For example, how do the EPF2 peptide and ERECTA receptor affect the downstream signaling components? What proteases activate EPF2?

STOMAGEN/EPFL9

STOMAGEN/EPFL9 is an EPF known to positively influence stomatal development (Von et al., 2002). Over-expression of *EPFL9* shows increased stomatal density and clustering, while loss of *EPFL9* function leads to reduced stomatal density with no clustering. *EPFL9* acts independently of *EPF* to regulate stomatal density and control stomatal clustering, while acts independently of *SDD* to control both stomatal density and clustering (Hunt et al., 2010). In another study, it was showed that STOMAGEN controls stomatal development by binding with the TMM receptor protein to compete with EPF1 and EPF2. Genetic analysis has revealed that TMM is epistatic to STOMAGEN, which suggests that stomatal development is mediated by competitive binding of positive and negative regulators to the same receptor. Loss of *STOMAGEN* function results in fewer stomata. Conversely, *STOMAGEN* over-expression increases stomatal cluster formation and stomatal density (Hunt and Gray, 2009).

Even though the placement of stomata relative to one another has been demonstrated to be controlled by intercellular signaling via several EPFs, the extracellular proteases that function in EPFs pathways still remain unknown (Lee et al., 2015). Environmental signals that regulate the stomatal development via the extracellular propeptides EPFs or the protease SDD1 have still not been certified. Fortunately, the mechanism underlying the interaction of β-carbonic anhydrase and CO_2 RESPONSE SECRETED PROTEASE (CRSP) that influences the action of EPF2 in the CO_2 signaling pathway for stomatal development has been recently uncovered (Engineer et al., 2014). The elucidation of the detailed functions of EPFs other than EPF2 and their impacts on extracellular proteases and environmental signaling during stomatal development obviously requires further investigation.

CHAL

Similar to EPF1 and EPF2, CHAL inhibits stomatal formation. *CHAL* was studied during a screening designed to detect suppressors of *tmm* mutant, and only presented a phenotype in the presence of the *tmm* mutation. Although excess stomata were observed on leaf surfaces of *tmm* mutants, stomata were completely absent from stems.

http://www.aloki.hu ● ISSN 1589 1623 (Print) ● ISSN 1785 0037 (Online)
DOI: http://dx.doi.org/10.15666/aeer/1705_1209112109

Interestingly, stomata reappeared on stems when *CHAL* was knocked out in the *tmm* mutant. Over-expression of *CHAL* requires ERECTA family (ERf) to suppress stomatal development. These differing results indicate that TMM may play a buffering role in the ERf receptor system, preventing EPF1 and EPF2 from disturbing the formation of normal epidermal patterns by absorbing excess CHAL (Abrash and Bergmann, 2010).

Role of TMM

TMM, a LRR-RLP receptor protein, negatively regulates stomatal density and placement. STOMAGEN positively regulates stomatal development, while EPF1 and EPF2 negatively regulate stomatal development by interacting with TMM as ligands. Loss of *TMM* function fails to orient and suppress asymmetric divisions of cells adjacent stomata or their precursors; in addition, loss-of-function mutants undergo a reduced number of divisions, resulting in the premature conversion of meristemoids into GMCs (Geisler et al., 2000). TMM plays an important role in cell-cell communication and perceives information regarding transient contiguous cell confirmation and location (Bergmann and Sack, 2007). The secretory peptides encoded by EPFs are expressed in meristemoids, with their activity dependent on the function of TMM and ERf members. ERfs and TMM work cooperatively to inhibit stomatal production. EPFs require TMM or ERfs to certify their over-expression phenotypes, which indicates the importance of these three proteins in EPf perception (Horst et al., 2015; de Marcos et al., 2016).

Role of SDD

SDD1 is a negative regulator of stomatal development, which encodes a subtilisin-like serine protease. SDD1 affects both protoderm and neighboring cell fates. During the development of neighboring cells, the shift from pavement cells to SM precursors may be controlled by a SDD1-dependent reaction signal in meristemoids/GMCs. Whether the meristemoid/GMC response causes the neighboring cell shift or instead triggers or extends *SDD1* expression is unclear (Von et al., 2002). Loss of SDD1 function leads to properly spaced but denser stomata. In one investigation, a 1.5-fold increase in stomatal density and index were reported in two *sdd1-1* mutants of Arabidopsis (Bergmann and Sack, 2007). *SDD1* overexpression causes a two- to four-fold decrease in stomatal density but does not considerably alter leaf and epidermal cell sizes (Von et al., 2002).

Role of bHLH transcription factors

In plants, bHLH transcription factors constitute an evolutionarily ancient group known to specify cellular identity. Some homologous bHLH proteins play important roles in the determination of the fate of successive stomatal precursor cells. For example, SPCH, MUTE, and FAMA act to activate cellular transition about stomatal development, share 88% structural homology and 39% sequence homology. Despite their similarities, they can not functionally replace each other during stomatal development because of the specific features of each protein (Ohashi-Ito and Bergmann, 2006).

SPCH

The *SPCH* gene is the key factor in the process of protodermal cell division into MMCs. *SPCH* involves in a basic pathway that initiates asymmetric division in the stomatal lineage (MacAlister et al., 2007; Vatén et al., 2018). The *spch* mutant fails to

http://www.aloki.hu ● ISSN 1589 1623 (Print) ● ISSN 1785 0037 (Online)
DOI: http://dx.doi.org/10.15666/aeer/1705_1209112109

produce interlocking pavement cells and promote stomatal lineages, while over-expression of *SPCH* raises the number of cells in the stomatal pathway. In addition, SPCH can prolong meristemoid identity, as loss of SPCH function leads to that meristemoids divide significantly fewer times. SPCH is also a target of brassinosteroid (Br) and MAPK signaling, and is an integration point for environmental information that allows for appropriate patterning and optimization of stomatal density under changing conditions (Ohashi-Ito and Bergmann, 2006).

MUTE

MUTE is a bHLH protein that controls the transition from meristemoids to GMCs, which promotes the differentiation of meristemoids into stomata (Pillitteri et al., 2007; Mahoney et al., 2016). The *mute* mutant fails to form stomata, but has no effect on meristemoid formation. Over-expression of *MUTE* has been shown to shift all epidermal cells toward stomata. The promoter of *MUTE* is not active in meristemoids, but is specifically activated in late-stage meristemoids. It was suggested that *MUTE* promoters binding with one finger regulatory elements is important for regulation (Mahoney et al., 2016). Because it is difficult to predicate the number of meristemoid divisions, how meristemoids regulate the timing of *MUTE* expression and the end of meristemoid division is unclear.

FAMA

FAMA, which controls GC fate, is expressed during the symmetric division that produces the two young GCs, but not in mature stomata (Ohashi-Ito and Bergmann, 2006). This protein likely acts as a transcriptional activator to regulate the transition from GMCs to GCs during symmetric division. Loss of FAMA function results in lack of mature stomata, while it develops clusters of GMCs or incipient GCs. Over-expression of *FAMA* converts non-stomatal cells to GCs in *fama* mutant plants (Ohashi-Ito and Bergmann, 2006). Matos et al. (2014) found that FAMA must bind to another protein, RETINOBLASTOMA-RELATED (RBR), to control the GMC to GC transition. These two proteins cause a permanent transition from stem cells to GCs. When the partnership between FAMA and RBR is broken, reversion of the GCs into stem cells can be observed.

SCRM and SCRM2

SCRM and SCRM2 are two additional bHLH proteins, which promote cellular transitions during stomatal development. Both of these proteins share high sequence homology and encode bHLH-type leucine zipper nucleoproteins. SCRM and SCRM2, which exist in cells of all stages, are similar in expression and function (Kanaoka et al., 2008). A *scrm* single mutant displays phenotypes similar to the *fama* mutant, while the *scrm-scrm2* double mutant produces occasional *spch*-like columns. It was showed that SCRM and SCRM2 interact with SPCH, MUTE, and FAMA. Map-based cloning has shown that SCRM is one of the key regulatory factors during cold stress, indicating that the ability of plants to adapt to environmental conditions may be related to developmental factors (Serna and Fenoll, 2000). Both environmental and developmental factors regulate stomatal development, which implicates SCRM as a participant in the integration of environmental signals directly into the stomatal differentiation pathway (Lee et al., 2017).

http://www.aloki.hu ● ISSN 1589 1623 (Print) ● ISSN 1785 0037 (Online)
DOI: http://dx.doi.org/10.15666/aeer/1705_1209112109

Taken together, these three bHLH family members-SPCH, MUTE, and FAMA-control formation, amplification, division, and final differentiation in stomatal development (*Fig. 1*). Remarkably, the SPCH protein can be phosphorylated by MPK3 and MPK6, whereas no such phosphorylation has been reported for MUTE and FAMA. SPCH generates stem cells and triggers their asymmetric division, while MUTE controls the meristemoid-to-GMC transition. SPCH, MUTE, and FAMA form obligate heterodimers with ICE1/SCRM and SCRM2, but not among themselves. These genes non-redundantly and positively regulate the stomatal development. However, interaction with RBR is inadequate to define the feature of FAMA and indicate a version of FAMA that behaves like MUTE or SPCH (Davies and Bergmann, 2014). It is necessary to study the larger interacted complexes that contribute to stomatal lineage by further work on protein interactions. It is also needed to identify what kind motifs are involved in these protein interactions.

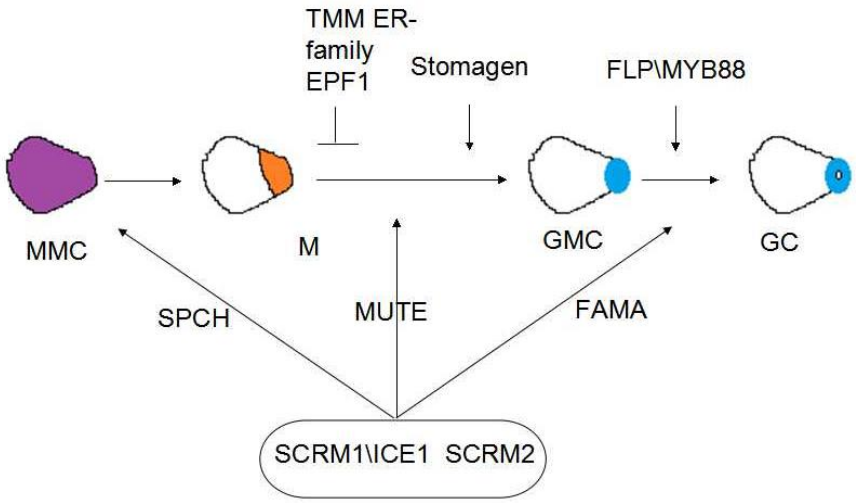

Figure 1. *Model of the differentiation steps regulated by sequential actions of bHLH transcription factors and related genes. MMC: meristeoid mother cell (purple), M: meristemoid (orange), GMC: guard mother cell (blue), GC: guard cell (blue with circle)*

Role of MAPK cascades

The MAPK signaling pathway controls cell fate and division during stomatal development. MAPK cascades are organized into a core module comprising three protein kinases: a MAPK, a MITOGEN-ACTIVATED PROTEIN (MAP) kinase kinase (MKK), and a MAP kinase kinase kinase (MAPKKK). YDA, a MAPKKK in the MAPK cascade, negatively regulates stomatal development. The associated signaling pathway consists of YDA, MKK4/5/7/9, and MPK3/6/9. The YDA-MKK4/5-MPK3/6 complex negatively regulates processes involved in the formation of GMCs from MMCs and of GCs from GMCs. YDA-MKK7/9, in contrast, positively controls these processes (Lampard et al., 2009). Loss of *AtYDA* function generates a clear increase in the production of leaf stomata in Arabidopsis, whereas expression of constitutively active mutants of *AtYDA* causes repressed stomatal formation in leaf epidermis. Furthermore, epidermal cells of *yda* mutant cotyledons display excessive entry divisions, thereby failing to prevent division of neighboring cells that connect two stomatal lineage cells. Asymmetry of cell fates is also compromised in *yda* mutants.

http://www.aloki.hu ● ISSN 1589 1623 (Print) ● ISSN 1785 0037 (Online)
DOI: http://dx.doi.org/10.15666/aeer/1705_1209112109

Over-expression of *YDA* leads to a significant decrease in stomatal density and the rate of water loss (Bergmann and Sack, 2007). *ABA-INSENSITIVE PROTEIN KINASE1 (AIK1)* gene encodes MAPKKK20 and positively regulates ABA-induced stomatal closure. The stomatal closing in *aik1* mutants was less sensitive to ABA than that in wild-type plants. In addition, the *aik1* mutants exhibit slightly greater stomatal density and significantly increased stomatal index. It was revealed that MKK4 and MKK5 could interact with AIK1 in vivo (Li et al., 2017). As another MAPK cascade**,** MPK12 regulates the stomatal aperture. Loss of MPK12 function results in the stomatal CO_2-insensitivity phenotypes and the higher degree of stomatal opening. It was showed that MPK12 interact with the protein kinase HIGH LEAF TEMPERATURE 1 (HT1) to inhibit the activity of HT1. Because of the higher degree of stomatal opening, the instantaneous water use efficiency is lower in *mpk12* mutants, suggesting that MPK12 is a important regulator of stomatal conductance (Jakobson et al., 2016).

The influence of environmental factors

Role of CO_2 concentration

In the plant epidermis, the adjustable stomatal pores formed by GCs allow CO_2 to enter for photosynthesis and water from transpiration to escape to the atmosphere. Plants accommodate to a continuous rise in atmospheric CO_2 concentration by adjusting stomatal density and closing stomata (Hu et al., 2015; Engineer et al., 2016). Gray et al. (2000) have identified a gene, designated as *HIC* (for high carbon dioxide), that is related to the signal transduction pathway responsible for regulating stomatal numbers at elevated CO_2 (eCO_2). *HIC* encodes a protein similar to 3-ketoacyl coenzyme A synthase, which is expressed specifically in GCs. Loss of *HIC* function results in an increase in stomatal density for reacting to a doubling of CO_2. *HIC* is the first gene to be identified that affects plant developmental responses to global changes in atmospheric composition. β-carbonic anhydrase (βCA) is a CO_2-binding protein that functions early in the CO_2 signaling pathway for stomatal development. Two βCAs, CA1 and CA4, were identified that function in the CO_2 response. Double mutants (*ca1 ca4*) result in an inversion in response to eCO_2 by increasing stomatal development (Hu et al., 2010). Over-expression of *CA4* and *CA1* could refresh CO_2-induced stomatal responses in double mutants. The *ca4* mutant shows a slightly altered sensitivity to the CO_2 stimulus (Hu et al., 2015; Engineer et al., 2016).

A novel CO_2-induced extracellular protease, CRSP, has been identified as a mediator of CO_2 regulation of stomatal development during atmospheric CO_2 elevation. Interaction of CA1, CA4, and CRSP degrades the pro-peptide EPF2, repressing stomatal development. However, EPF2 is vital to CO_2 regulation of stomatal development (Engineer et al., 2014). Future research should focus on if feedback modulation results in CO_2 regulation of EPF2 and CRSP transcripts and what are the transcriptional regulators regulating the eCO_2 response. SLOW ANION CHANNEL-ASSOCIATED 1 (SLAC1) is an S-type anion channel protein, which plays a important role in stomatal closure in response to eCO_2. Loss of *AtSLAC1* function dramatically represses stomatal closure induced by CO_2 (Vahisalu et al., 2008; Hedrich and Geiger, 2017).

Stomatal opening is promoted by the activation of H^+-ATPases (AHA1) in the guard cell plasma membrane, and eCO_2 concentration inhibits proton efflux by plasma membrane AHA1 (Hashimoto-Sugimoto et al., 2013). The *PATROL1* gene encodes a

http://www.aloki.hu ● ISSN 1589 1623 (Print) ● ISSN 1785 0037 (Online)
DOI: http://dx.doi.org/10.15666/aeer/1705_1209112109

protein with a MUN domain, which is involved in the membrane trafficking of neurotransmitter release. Loss of *PATROL1* function results in the impaired stomatal opening in response to low CO_2 concentration, disturbing the normal plasma membrane targeting of H^+-ATPases (Engineer et al., 2016).

HT1 is a protein kinase and an essential regulator of stomatal CO_2 responses. Loss of HT1 function results in constitutively stomata opening and repressed stomatal CO_2 responses (Jakobson et al., 2016). The open stomata 1 (OST1) protein kinase is involved in CO_2- and ABA-induced stomatal closing (details in ABA section). It was suggested that HT1 phosphorylates the OST1 protein kinase, which inactivates OST1 (Mustilli et al., 2002; Tian et al., 2015). BIG/CIS1 is a calossin-like protein, which regulates CO_2-induced stomatal closure (He et al., 2018). Loss of BIG/CIS1 function fails to show reductions in stomatal density and index, but displays inhibition of stomatal opening with eCO_2 concentration. It was showed that BIG/CIS1 is only demanded in eCO_2-induced stomatal closure, suggesting the signaling pathways of CO_2-mediated promotion of stomatal closure are distinguishable with inhibition of opening (He et al., 2018). Because BIG/CIS1 is associated with auxin transport, further research should focus on if disruptions to auxin signaling underlie the BIG/CIS1 stomatal mutant phenotype. These studies could help researchers to choose plant germplasm for adapting to CO_2 levels.

Role of light

Light intensity affects stomatal density and the stomatal index, which play an important role in cell fate decisions in the epidermis (Casson et al., 2009). CONSTITUTIVE PHOTOMORPHOGENIC 1 (COP1), a E3 ubiquitin-protein ligase, is a repressor of light-controlled stomatal development (Liu et al., 2008). A current study showed that COP1 degrades ICE through ubiquitination pathways in leaf abaxial epidermal cells. Loss of *COP1* function results in the ICE proteins accumulate in the nuclei of leaf abaxial epidermal cells. Interestingly, light impairs the COP1-mediated degradation of the ICE to induce stomatal development, which upregulates EPF2 activity at the transcriptional level, thereby conferring proper stomatal spacing and distribution. Thus, it is likely that the COP1-ICE-EPF2 signaling module integrates light signals into developmental programs that regulate stomatal development (Lee and Park, 2017). ANGUSTIFOLIA3 (AN3) is a positive regulator of stomatal development, which interacts with the *COP1* promoter to regulate light-induced stomatal development. Loss of *AN3* function results in decreased stomatal index, whereas overexpression of *AN3* leads to clusters of stomata (Meng et al., 2018). These suggest that the AN3–COP1–E3 pathway regulates stomatal development with the integration of light signaling. COP10 is another dominant component of stomatal-lineage divisions, which represses stomatal fate and adjusts the initiation frequency and extension of stomatal lineages. Loss of *COP10* function results in the production of stomatal clusters. COP10 regulates genetically in parallel with SDD1 and does not affect epidermal cell differentiation (Delgado et al., 2012). Phytochrome B (phyB) plays an important role in red light-induced stomatal development. Loss of *phyB* function prevents this increased production of stomata under high intensity red light. phyB can also promote the expression of *FAMA* and *TMM* genes in young leaves (Casson et al., 2009). Consequently, phyB has a significant role in the mediation of epidermal cell division and stomatal development. PHYTOCHROME-INTERACTING FACTOR 4 (PIF4), a bHLH transcription factor, can be transported to the nucleus upon binding to

http://www.aloki.hu ● ISSN 1589 1623 (Print) ● ISSN 1785 0037 (Online)
DOI: http://dx.doi.org/10.15666/aeer/1705_1209112109

phyB. PIF4 may also regulate stomatal development with SPCH, MUTE, and FAMA. Mutations of *PIF4* display a similar defect as in the absence of *phyB* (Casson et al., 2009).

Plasma membrane H^+-ATPase regulates blue light-induced stomatal opening. It is activated via a signaling mediator BLUE LIGHT SIGNALING1 (BLUS1) and blue light-receptor phototropins (phot1 and phot2). BLUS1 and phosphatase act as positive mediators between the H+-ATPase and the phots during stomatal opening. BLUE LIGHT-DEPENDENT H^+-ATPASE PHOSPHORYLATION (BHP) is a novel signaling regulator in blue light-induced stomatal opening interacting with BLUS1, which is owned by the MAPKKK family. Loss of *BHP* function results in impaired stomatal opening in response to blue light (Hayashi et al., 2017). The phots are light-induced receptor kinases, which mediate stomatal opening and phototropism. the *phot1 phot2* double mutant fails to show the blue light-induced stomatal opening and the H^+-ATPase activation, but *phot1* and *phot2* single mutants retain these responses (Doi et al., 2004). A recent study displayed that BLUS1 kinase is phosphorylated by phot1 and phot2, which acts as a common substrate in stomatal opening through the activation of the plasma membrane H^+-ATPase via phosphatase (Takemiya and Shimazaki, 2016).

The light-induced stomatal opening is also inhibited by Rho-type (ROP) GTPase 2 (ROP2). ROP-interactive Cdc42- and Rac-interactive binding motif-containing protein 7 (RIC7) interacts ROP2 and mediates downstream processes. Loss of *RIC7* function activates light-induced stomatal opening, while overexpression of *RIC7* represses light-induced stomatal opening. RIC7 interacts also with Exocyst subunit Exo70 family protein B1 (Exo70B1), a positive regulator of stomatal opening, to optimize the extent of stomatal opening by inhibiting the function of Exo70B1. The mutant *exo70b1* and double mutant *ric7/exo70b1* both display inhibited light-induced stomatal opening (Hong et al., 2016). ENHANCED RESPONSE TO ABA 1 (ERA1) encodes the farnesyl transferase β subunit, which dominates stomatal closure in plants. Loss of *ERA1* function results in more closed stomata phenotype. Further studies indicated that *era1* mutants shows impaired blue light-induced stomatal opening, which suggested a potential function for ERA1 farnesylation in blue light-induced stomatal opening (Jalakas et al., 2017). In addition, Photosystem II Subunit S (PsbS), a integral membrane protein, affects a chloroplastderived signal for light-induced stomatal opening. Over-expression of *PsbS* results in impaired light-induced stomatal opening and a 25% reduction in water loss per CO_2 assimilated under field conditions (Głowacka et al., 2018).

Synergy effects of light and CO_2

The stomatal opening is mediated by light and low concentrations of CO_2 with synergy effects. CONVERGENCE OF BLUE LIGHT AND CO2 1/2 (CBC1/CBC2) are protein kinases related to blue light, which redundantly promote stomatal opening in response to both blue light and low concentrations of CO_2. It was suggested that CBCs positively mediate stomatal aperture by integrating signals from blue light and low CO_2 (Hiyama et al., 2017). In contrast to blue light-induced stomatal opening, the viewpoints about red light-induced stomatal opening are controversial. Some studies showed that red light-induced stomatal opening may be resulted in a low intercellular concentration of CO_2 brought about by mesophyll photosynthesis (Horrer et al., 2016) However, other investigators suggested that such a reduction in the intercellular concentration of CO_2 of leaves was insufficient to lead to stomatal opening. Hiyama et al. (2017) speculated that

http://www.aloki.hu ● ISSN 1589 1623 (Print) ● ISSN 1785 0037 (Online)
DOI: http://dx.doi.org/10.15666/aeer/1705_1209112109

the reduced intercellular concentration of CO_2 might result in stomatal opening by inhibiting the S-type channels through CBCs, but such a response did not display in the *cbc* mutants. Further study is needed to elucidate the role of CBCs in red light-induced stomatal opening.

Temperature and air humidity

Temperature affects stomatal development in a complex manner. Temperature increases often leads to somatal opening, whereas heat stress often promptly mediates stomatal closure to decrease transpirational water loss in some plant species (Lahr et al., 2015). Increased temperature restrains the expression of SPCH that acts as the major mediator of stomatal lineage initiation (Vatén et al., 2018). PIF4 is also a core component of high-temperature signaling, which accumulates in the stomatal precursors and combines with the promoter of SPCH in increased temperature. In addition, PIF4 represses also SPCH activation and stomatal production. This study proposed a model where warm-temperature-activated PIF4 binds and represses SPCH expression to restrict stomatal production at increased temperatures (Lau et al., 2018). The CO_2-induced variations of stomatal closure associates with heat stress tolerance. The eCO_2 moderates the negative effects of heat stress, which is accompanied by greater amounts of *RESPIRATORY BURST OXIDASE 1* (*RBOH1*) transcripts and decreased stomatal aperture. Loss of *RBOH1* function results in the impaired eCO_2-induced stomatal closure and the compromised eCO_2-enhanced water use efficiency as well as the heat tolerance (Zhang et al., 2018).

Stomatal movement is influenced by relative air humidity (RH) with ABA content. High elevated air movement (MOV) reduced length and aperture of stomata in plants developed at high RH and increased stomatal sensitivity to ABA (Carvalho et al., 2015). In this process, *CYP707A1,* a ABA catabolism gene, plays a prominent role for influencing stomata development and ABA content. Over-expression of *CYP707A1* during dark in high RH reduced the ABA content in the guard cells and prevented stomatal closure, whereas loss of CYP707A1 gene function resulted in reduced stomatal aperture (Arve et al., 2015; Jalakas et al., 2018). Compared with the influence of CO_2 and light on stomatal development, the molecular mechanisms underlying the action of temperature and air humidity on stomatal development should be further and deeper to study.

The influence of plant hormones

Some hormones, such as Abscisic acid (ABA), jasmonate (MeJA), Brassinosteroids (BRs), Strigolactones (SLs), Salicylic acid (SA) etc. have a strong correlation with stomatal development. With the mechanism of stomatal development being studied in the past decade, many researches have opened the door to understand the function of plant hormone in stomatal development.

Role of ABA

ABA is well known to mediate the opening and closing of stomata in response to changes in water balance. ABA levels are low in the Arabidopsis *aba2* mutant, with the mutant displaying high stomatal density. ABA INSENSITIVE 1 and ABA INSENSITIVE 2 (ABI1 and ABI2) are protein phosphatase 2C proteins, which regulate

http://www.aloki.hu ● ISSN 1589 1623 (Print) ● ISSN 1785 0037 (Online)
DOI: http://dx.doi.org/10.15666/aeer/1705_1209112109

ABA-mediated stomatal closure interacting with protein kinases OST1 (Tanaka et al., 2013). The pathway for ABA-mediated stomatal closure is related to perception of ABA that results in the activation of guard cell anion channels by OST1. Loss of *OST1* function results in insensitivity to ABA-mediated stomatal closure and opening, which indicates that OST1 is a positive regulator in ABA signaling (Mustilli et al., 2002; Acharya et al., 2013). OST1 needs normal ABI1 function for its ABA-dependent activation and interacts directly with ABI1 protein (Park et al., 2009). In addition, ABA-induced stomatal closing are abolished in *abi1* and *abi2* mutants (Pei et al., 1997). Although ABA interacts with different functional proteins, transcription factors, kinases, and various environmental factors, the molecular mechanisms about these interaction are massively complex and are not entirely clear.

Role of MeJA

The exogenous MeJA can reduce the stomatal index and stomata density on the cotyledons of Arabidopsis. Coronatine (COR) is perceived via a receptor complex formed by CORONATINEINSENSITIVE 1 (COI1) and JASMONATE ZIM DOMAIN (JAZ) proteins, which promotes entry of bacteria into the plant apoplast by facilitating stomata opening (Yan et al., 2009). COR and jasmonate isoleucine (JA-Ile) co-receptor JAZ2 modulates stomatal aperture by the signaling module COI1-JAZ2-MYC2,3,4-ANAC19,55,72 during bacterial invasion. The jaz2 mutant shows partially repressed pathogen-induced stomatal closing, which is more sensitive to Pseudomonas. The JAZ2 binds to the MYC transcription factors directly mediate the expression of ANAC19,55,72 to control stomata aperture (Gimenez-Ibanez et al., 2017). In addition, the MYC transcription factors negatively modulate jasmonate-inhibited stomatal development and act upstream of the SPCH and FAMA to regulate stomatal development. The stomatal development of the *myc2 myc3 myc4* triple mutant is insensitive to MeJA treatment (Han et al., 2018).

Role of BRs

BRs are steroid hormone that promotes stomatal closure in an ABA-independent manner (Kim et al., 2012). BRASSINOSTEROID INSENSITIVE2(BIN2), a important regulator in BR signaling, encode a glycogen synthase kinase 3 (GSK3)-like kinase (He et al., 2002). BRs negatively modulate stomatal development by repressing BIN2 kinase-induced inhibition of YDA. BIN2 phosphorylates and inactivates the YDA, which inhibits stomata formation. Overexpression of *BIN2* displays a similar stomatal overproduction phenotype as *bsu* mutants. Besides, BRs have been directly involved in stimulating stomatal development in hypocotyls through BIN2 phosphorylation and inactivation of SPCH, which acts downstream of the MAPKs and stimulates cell division and stomatal development. BRASSINOSTEROID-INSENSITIVE 1 (BRI1) kinase binding with BR recruits BRI1-ASSOCIATED RECEPTOR KINASE 1 (BAK1) to produce a receptor complex on plasma membranes (Shang et al., 2016). Transphosphorylation between BRI1 and BAK1 further enlarges BRI1 and BAK1 kinase activities, which results in inactivation of BIN2 by the upstream phosphatase BRI SUPPRESSOR1(BSU1) under high BR levels (Zhu et al., 2013). Loss of *BSU1* function results in massive stomata formation, which needs BIN2 activity (Kim et al., 2012). Loss of *BAK1* function results in insensitivity of ABA-mediated stomatal closure and inhibition of OST1 expression and ROS production. It was further indicated that

http://www.aloki.hu ● ISSN 1589 1623 (Print) ● ISSN 1785 0037 (Online)
DOI: http://dx.doi.org/10.15666/aeer/1705_1209112109

BAK1 interacts with OST1 near the plasma membrane, which increases sensitivity in response to ABA. In addition, ABI1 interacts with BAK1 and impairs the interaction of BAK1 and OST1 (Shang et al., 2016).

Role of SLs

SLs play a vital role in regulating stomatal closure in an ABA-independent mechanism. SLs promotes a significant increase in H_2O_2 and NO contents, which is needed for stomatal closure. Disruption of MORE AXILLARY GROWTH 2 (MAX2), DWARF14 (D14), and SLAC1 represses SL-induced stomatal closure. Loss of MAX2 function leads to increased stomatal conductance and more widely opening stomata (Piisilä et al., 2015). The *slac1* mutant shows compromised SL-mediated stomatal closure, showing that SLAC1 is necessary for SL-mediated stomatal closure. Although SL-induced stomatal closure requires H_2O_2, NO, and SLAC1, the detailed molecular mechanism by if SLs regulate the stomatal response remains unknown. It will be required to study whether H_2O_2-activated Ca^{2+} channels are also needed for SL-induced stomatal closure (Lv et al., 2018).

Role of SA

SA regulates ROS production in guard cells through peroxidase-catalyzed reaction, leading to stomatal closure. AtSIZ1 is a small ubiquitin-like modifier (SUMO) E3 ligase, which negatively mediates stomatal apertures via the SA-triggered ROS accumulation. Loss of AtSIZ1 function leads to the accumulation of endogenous SA, which enhances the production of ROS mediated by salicylhydroxamic acid (SHAM)-sensitive peroxidases and impairs stomatal aperture (Miura et al., 2013). In addition, plants growing in the ethylene precursor 1-aminocyclopropane-1-carboxylic acid display increased stomatal density. Stomatal division and development is enhanced in cucumber hypocotyls after brief treatment with ethylene. Furthermore, auxin and gibberellin modulate stomatal aperture opening and closing (Saibo et al., 2003). Compared with other molecular regulatory pathways, the molecular mechanisms underlying the action of ABA and other hormones on stomatal development have not been clearly established.

Future directions

Stomata enable plants to regulate the entry of CO_2 assimilated in photosynthesis and adjust evaporation of water. Although some underlying mechanisms and genes related to stomatal development have been studied, many complex questions related to stomatal morphogenesis and division are still largely unanswered. Future research should involve bioinformatics mining of published gene data, information analysis of transcriptomic and proteomic for deeply studying stomatal development and guard cell responses to environmental factors. In addition, very little is known about the underlying molecular basis for the changes of hormonal factors such as ABA, ethylene, auxin, and gibberellin. The mechanism and regulatory pathway controlling variation in stomatal development in response to environmental signals such as photoreceptors, temperature, and humidity is uncertain. Other problems include determining the genes and pathways involved in stomatal development, ascertaining whether the molecular mechanism of stomatal development differs between monocotyledons and dicotyledons, and understanding how

http://www.aloki.hu ● ISSN 1589 1623 (Print) ● ISSN 1785 0037 (Online)
DOI: http://dx.doi.org/10.15666/aeer/1705_1209112109

intercellular signaling is superimposed and orients the intrinsic polarity. Finally, how environmental signals modulate stomatal development needs to be elucidated. Many questions thus remain to be addressed. In a word, the genetic network for the regulation of stomatal development is too complex and tightly impacted by both intrinsic and external signals. The exact molecular mechanisms underlying the interactions among the various impact factors and environmental signals during stomatal development deserve further investigation.

Acknowledgments. We express our gratitude to the anonymous reviewers for helpful comments to improve the manuscript. This work was supported by the National Key R&D Program of China (Grant No. 2018YFD0300305-01) and the Open Projects Program of the Key Laboratory of Ministry of Agriculture and Ministry of Education of the People's Republic of China.

REFERENCES

[1] Abrash, E. B., Bergmann, D. C. (2010): Regional specification of stomatal production by the putative ligand CHALLAH. – Development 13: 447-455.
[2] Acharya, B. R., Jeon, B. W., Zhang, W., Assmann, S. M. (2013): Open Stomata 1 (OST1) is limiting in abscisic acid responses of Arabidopsis guard cells. – New Phytol. 200: 1049-1063.
[3] Arve, L. E., Kruse, O. M. O., Tanino, K. K., Olsen, J. E., Futsæther, C., Torre, S. (2015): ABA regulation and stomatal malfunctioning in *Arabidopsis thaliana* developed in continuous high air humidity. – Environ. Exp. Bot. 115: 11-19.
[4] Bergmann, D. C., Sack, F. D. (2007): Stomatal development. – Annu. Rev. Plant Biol. 58: 163-181.
[5] Caine, R. S., Chater, C. C., Kamisugi, Y., Cuming, A. C., Beerling, D. J., Gray, J. E., Fleming, A. J. (2016): An ancestral stomatal patterning module revealed in the non-vascular land plant Physcomitrella patens. – Development 143: 3306-3314.
[6] Carvalho, D. R. A., Torre, S., Kraniotis, D., Almeida, D. P. F., Heuvelink, E., Carvalho, S. M. P. (2015): Elevated air movement enhances stomatal sensitivity to abscisic acid in leaves developed at high relative air humidity. – Front. Plant Sci. 6: 11.
[7] Casson, S. A., Hetherington, A. M. (2010): Environmental regulation of stomatal development. – Curr. Op. in Plant Biol. l3: 90-95.
[8] Casson, S. A., Franklin, K. A., Gray, J. E., Grierson, C. S., Whitelam, G. C., Hetherington, A. M. (2009): Phytochrome B and PIF4 regulate stomatal development in response to light quantity. – Curr. Biol. 19: 229-234.
[9] Davies, K. A., Bergmann, D. C. (2014): Functional specialization of stomatal bHLHs through modification of DNA-binding and phospho regulation potential. – Proc. Natl. Acad. Sci. USA.111(43): 15585-15590.
[10] de Marcos, A., Triviño, M., Fenoll, C., Mena, M. (2016): Too many faces for TOO MANY MOUTHS? – New Phytol. 210(3): 779-785.
[11] Delgado, D., Ballesteros, I., Torres-Contreras, J., Mena, M., Fenoll, C. (2012): Dynamic analysis of epidermal cell divisions identifies specific roles for COP10 in Arabidopsis stomatal lineage development. – Planta 236: 447-461.
[12] Doi, M., Shigenaga, A., Emi, T., Kinoshita, T., Shimazaki, K. (2004): A transgene encoding a blue-light receptor, phot1, restores bluelight responses in the *Arabidopsis phot1 phot2* double mutant. – J. Exp. Bot. 55: 517-523.
[13] Du, J., Jiang, H., Sun, X., et al. (2018): Auxin and gibberellins are required for the receptor-like kinase ERECTA regulated hypocotyl elongation in shade avoidance in arabidopsis. – Frontiers in Plant Science 9: 124.

http://www.aloki.hu ● ISSN 1589 1623 (Print) ● ISSN 1785 0037 (Online)
DOI: http://dx.doi.org/10.15666/aeer/1705_1209112109

[14] Engineer, C. B., Ghassemian, M., Anderson, J. C., Engineer, C. B., Ghassemian, M., Anderson, J. C. (2014): Carbonic anhydrases, EPF2 and a novel protease mediate CO_2 control of stomatal development. – Nature 513: 246-250.
[15] Engineer, C. B., Hashimoto-Sugimoto, M., Negi, J., Israelsson-Nordström, M., Azoulay-Shemer, T., Rappel, W. J., Iba, K., Schroeder, J. I. (2016): CO_2 sensing and CO_2 regulation of stomatal conductance: advances and open questions. – Trends in Plant Science 21(1): 16-30.
[16] Geisler, M., Nadeau, J., Sack, F. D. (2000): Oriented asymmetric divisions that generate the stomatal spacing pattern in *Arabidopsis* are disrupted by the too many mouths mutation. – Plant Cell 12: 2075-2086.
[17] Gimenez-Ibanez, S., Boter, M., Ortigosa, A., García-Casado, G., Chini, A., Lewsey, M. G., Ecker, J. R., Ntoukakis, V., Solano, R. (2017): JAZ2 controls stomata dynamics during bacterial invasion. – New Phytol. 213: 1378-1392.
[18] Głowacka, K., Kromdijk, J., Kucera, K., Xie, J. Y., Cavanagh, A. P., Leonelli, L., Leakey, ADB., Ort, D. R., Niyogi, K. K., Long, S. P. (2018): Photosystem II Subunit S overexpression increases the efficiency of water use in a field-grown crop. – Nature Communication 9: 868.
[19] Gray, J. E., Holroyd, G. H., Lee, F. M., Bahrami, A. R., Sijmons, P. C., Woodward, F. I., Schuch, W., Hetherington, A. M. (2000): The HIC signalling pathway links CO_2 perception to stomatal development. – Nature 408: 713-716.
[20] Han, X., Hu, Y., Zhang, G., Jiang, Y., Chen, X., Yu, D. (2018): Jasmonate negatively regulates stomatal development in Arabidopsis cotyledons. – Plant Physiology 176(4): 2871-2885.
[21] Hara, K., Yokoo, T., Kajita, R., Onishi, T., Yahata, S., Peterson, K. M., Torii, K. U., Kakimoto, T. (2009): Epidermal cell density is auto-regulated via a secretory peptide, EPIDERMAL PATTERNING FACTOR 2 in Arabidopsis leaves. – Plant Cell Physiol. 50: 1019-l031.
[22] Hashimoto-Sugimoto, M., Higaki, T., Yaeno, T., Nagami, A., Irie, M., Fujimi, M., Miyamoto, M., Akita, K., Negi, J., Shirasu, K., Hasezawa, S., Iba, K. (2013): A Munc13-like protein in Arabidopsis mediates H+-ATPase translocation that is essential for stomatal responses. – Nat. Commun. 4: 2215.
[23] Hayashi, M., Inoue, S. I., Ueno, Y., Kinoshita, T. (2017): A Raf-like protein kinase BHP mediates blue light-dependent stomatal opening. – Sci. Rep. 7: 45586.
[24] He, J., Zhang, R., Peng, K., Tagliavia, C., Li, S., Xue, S., Hetherington, A. M. (2018): The BIG protein distinguishes the process of CO_2-induced stomatal closure from the inhibition of stomatal opening by CO_2. – New Phytologist 218(1): 232-241.
[25] He, J. X., Gendron, J. M., Yang, Y., Li, J., Wang, Z. Y. (2002): The GSK3-like kinase BIN2 phosphorylates and destabilizes BZR1, a positive regulator of the brassinosteroid signaling pathway in Arabidopsis. – Proc. Natl. Acad. Sci. USA 99: 10185-10190.
[26] Hedrich, R., Geiger, D. (2017): Biology of SLAC1-type anion channels from nutrient uptake to stomatal closure. – New Phytol. 216: 46-61.
[27] Hirayama, T., Shinozaki, K. (2007): Perception and transduction of abscisic acid signals: Keys to the function of the versatile plant hormone ABA. – Trends Plants Sci. 12: 343-351.
[28] Hiyama, A., Takemiya, A., Munemasa, S., et al. (2017): Blue light and CO_2 signals converge to regulate light-induced stomatal opening. – Nature Communications 8: 1284.
[29] Hong, D., Jeon, B. W., Kim, S. Y., Hwang, J., Lee, Y. (2016): The ROP2-RIC7 pathway negatively regulates light-induced stomatal opening by inhibiting exocyst subunit Exo70B1 in Arabidopsis. – New Phytol. 209: 624-635.
[30] Horrer, D., Flütsch, S., Pazmino, D., Matthews, J. S., Thalmann, M., Nigro, A., Leonhardt, N., Lawson, T., Santelia, D. (2016): Blue light induces a distinct starch degradation pathway in guard cells for stomatal opening. – Curr. Biol. 26: 1-9.

http://www.aloki.hu ● ISSN 1589 1623 (Print) ● ISSN 1785 0037 (Online)
DOI: http://dx.doi.org/10.15666/aeer/1705_1209112109

[31] Horst, R. J., Fujita, H., Lee, J. S., Rychel, A. L., Garrick, J. M., Kawaguchi, M., Peterson, K. M., Torii, K. U. (2015): Molecular framework of a regulatory circuit initiating two-dimensional spatial patterning of stomatal lineage. – PLOS Genetics 11: e1005374.
[32] Hu, H., Boisson-Dernier, A., Israelsson-Nordström, M., Böhmer, M., Xue, S., Ries, A., Godoski, J., Kuhn, J. M., Schroeder, J. I. (2010): Carbonic anhydrases are upstream regulators of CO_2-controlled stomatal movements in guard cells. – Nature Cell Biol. 12: 87-93.
[33] Hu, H., Rappel, W. J., Occhipinti, R., Ries, A., Böhmer, M., You, L., Xiao, C. L., Engineer, C. B., Boron, W. F., Schroeder, J. I. (2015): Distinct cellular locations of carbonic anhy-drases mediate CO_2 control of stomatal movements. – Plant Physiology 169: 1168-1178.
[34] Hunt, L., Gray, J. E. (2009): The signaling peptide EPF2 controls asymmetric cell divisions during stomatal development. – Curr. Biol. 19: 864-869.
[35] Hunt, L., Bailey, K. J., Gray, J. E. (2010): The signaling peptide EPFL9 is a positive regulator of stomatal development. – New Phytol. 186: 609-614.
[36] Jakobson, L., Vaahtera, L., Tõldsepp, K., Nuhkat, M., Wang, C., Wang, Y. S., et al. (2016): Natural variation in *Arabidopsis* Cvi-0 accession reveals an important role of MPK12 in guard cell CO_2 signaling. – PLoS Biol 14(12): e2000322.
[37] Jalakas, P., Huang, Y., Yeh, Y., Zimmerli, L., Merilo, E., Kollist, H., Brosché, M. (2017): The role of ENHANCED RESPONSES TO ABA1 (ERA1) in Arabidopsis stomatal responses is beyond ABA signaling. – Plant Physiology 174(2): 665-671.
[38] Jalakas, P., Merilo, E., Kollist, H., Brosché, M. (2018): ABA-mediated regulation of stomatal density is OST1-independent. – Plant Direct. 2: 1-7.
[39] Kanaoka, M. M., Pillitteri, L. J., Fujii, H., Yoshida, Y., Bogenschutz, N. L., Takabayashi, J., Zhu, J. K., Torii, K. U. (2008): SCREAM/ICE1 and SCREAM2 specify three cell-state transitional steps leading to Arabidopsis stomatal differentiation. – Plant Cell 20: 1775-1785.
[40] Kim, T. W., Michniewicz, M., Bergmann, D. C., Wang, Z. Y. (2012): Brassinosteroid regulates stomatal development by GSK3-mediated inhibition of a MAPK pathway. – Nature 482: 419-422.
[41] Lahr, E. C., Schade, G. W., Crossett, C. C., Watson, M. R. (2015): Photosynthesis and isoprene emission from trees along an urban-rural gradient in Texas. – Glob Chang Biol. 21: 4221-4236.
[42] Lampard, G. R., Lukowitz, W., Ellis, B. E., Bergmann, D. C. (2009): Novel and expanded roles for MAPK signaling in Arabidopsis stomatal cell fate revealed by cell type-specific manipulations. – Plant Cell 21: 3506-3517.
[43] Lau, O. S., Song, Z. J., Zhou, Z. M., Davies, K. A., Chang, J., Yang, X., Wang, S. Q., Lucyshyn, D., Tay, I. H. Z., Wigge, P. A., Bergmann, D. C. (2018): Direct control of SPEECHLESS by PIF4 in the high-temperature response of stomatal development. – Current Biology 28(8): 1273-1280.
[44] Lee, E., Lucas, J. R., Goodrich, J., Sack, F. D. (2014): Arabidopsis guard cell integrity involves the epigenetic stabilization of the FLP and fama transcription factor genes. – The Plant Journal 78: 566-577.
[45] Lee, J. H., Park, C. M. (2017): Light inhibits COP1-mediated degradation of ICE transcription factors to induce stomatal development in Arabidopsis. – Plant Cell 29: 2817-2830.
[46] Lee, J. S., Hnilova, M., Maes, M., Lin, Y. C. L., Putarjunan, A., Han, S. K., Avila, J., Torii, K. U. (2015): Competitive binding of antagonistic peptides fine-tunes stomatal patterning. – Nature 522: 439-443.
[47] Li, K., Yang, F. B., Zhang, G. Z., Song, S. F., Li, Y., Ren, D. T., Miao, Y. C., Song, C. P. (2017): AIK1, a mitogen-activated protein kinase, modulates abscisic acid responses through the MKK5-MPK6 kinase cascade. – Plant Physiology 173: 1391-1408.

http://www.aloki.hu ● ISSN 1589 1623 (Print) ● ISSN 1785 0037 (Online)
DOI: http://dx.doi.org/10.15666/aeer/1705_1209112109

[48] Liu, L. J., Zhang, Y. C., Li, Q. H., Sang, Y., Mao, J., Lian, H. L., Wang, L., Yang, H. Q. (2008): COP1-mediated ubiquitination of CONSTANS is implicated in cryptochrome regulation of flowering in Arabidopsis. – Plant Cell 20: 292-306.
[49] Lv, S., Zhang, Y., Li, C., Liu, Z., Yang, N., Pan, L., Wu, J., Wang, J., Yang, J., Lv, Y., Zhang, Y., Jiang, W., She, X., Wang, G. (2018): Strigolactone-triggered stomatal closure requires hydrogen peroxide synthesis and nitric oxide production in an abscisic acid-independent manner. – New Phytol. 217: 290-304.
[50] MacAlister, C. A., Ohashi-Ito, K., Bergmann, D. C. (2007): Transcription factor control of asymmetric cell divisions that establish the stomatal lineage. – Nature 445: 537-540.
[51] Mahoney, A. K., Anderson, E. M., Bakker, R. A., Williams, A. F., Flood, J. J., Sullivan, K. C., Pillitteri, L. J. (2016): Functional analysis of the Arabidopsis thaliana MUTE promoter reveals a regulatory region sufficient for stomatal-lineage expression. – Planta 243(4): 987-998.
[52] Matos, J. L., Lau, O. S., Hachez, C., Cruz-Ramírez, A., Scheres, B., Bergmann, D. C. (2014): Irreversible fate commitment in Arabidopsis stomatal lineage requires a FAMA and RETINOBLASTOMA-RELATED module. – elife 3: e03271.
[53] Meng, L. S., Li, C., Xu, M. K., Sun, X. D., Wan, W., Gao, X. Y., Zhang, J. L., Chen, K. M. (2018): Arabidopsis ANGUSTIFOLIA3 (AN3) is associated with the promoter of *CONSTITUTIVE PHOTOMORPHOGENIC1* (*COP1*) to regulate light-mediated stomatal development. – Plant Cell Environ. https://doi.org/10.1111/pce.13212.
[54] Miura, K., Okamoto, H., Okuma, E., Shiba, H., Kamada, H., Hasegawa, P. M., Murata, Y. (2013): *SIZ1* deficiency causes reduced stomatal aperture and enhanced drought tolerance via controlling salicylic acid-induced accumulation of reactive oxygen species in Arabidopsis. – Plant J. 73: 91-104.
[55] Mustilli, A. C., Merlot, S., Vavasseur, A., Fenzi, F., Giraudat, J. (2002): Arabidopsis OST1 protein kinase mediates the regulation of stomatal aperture by abscisic acid and acts upstream of reactive oxygen species production. – Plant Cell 14: 3089-3099.
[56] Ni, D. A. (2012): Role of vacuolar invertase in regulating Arabidopsis stomatal opening. – Acta Physiologiae Plantarum 34(6): 2449-2452.
[57] Ohashi-Ito, K., Bergmann, D. C. (2006): Arabidopsis FAMA controls the final proliferation/differentiation switch during stomatal development. – Plant Cell 18: 2493-2505.
[58] Park, S. Y., Fung, P., Nishimura, N., Jensen, D. R., Fujii, H., Zhao, Y., Lumba, S., Santiago, J., Rodrigues, A., Chow, T. F., et al. (2009): Abscisic acid inhibits type 2C protein phosphatases via the PYR/PYL family of START proteins. – Science 324: 1068-1071.
[59] Pei, Z. M., Kuchitsu, K., Ward, J. M., Schwarz, M., Schroeder, J. I. (1997): Differential abscisic acid regulation of guard cell slow anion channels in Arabidopsis wild-type and *abi1* and *abi2* mutants. – Plant Cell 9(3): 409-423.
[60] Piisilä, M., Keceli, M. A., Brader, G., Jakobson, L., Joesaar, I., Sipari, N., Kollist, H., Palva, E. T., Kariola, T. (2015): The F-box protein MAX2 contributes to resistance to bacterial phytopathogens in Arabidopsis thaliana. – BMC Plant Biology 15: 53.
[61] Pillitteri, L. J., Sloan, D. B., Bogenschutz, N. L., Torii, K. U. (2007): Termination of asymmetric cell division and differentiation of stomata. – Nature 445: 501-505.
[62] Saibo, N. J., Vriezen, W. H., Beemster, G. T., Van, D. Straeten, D. (2003): Growth and stomata development of Arabidopsis hypocotyls are controlled by gibberellins and modulated by ethylene and auxins. – The Plant Journal 33: 989-1000.
[63] Serna, L., Fenoll, C. (2000): Stomatal development in Arabidopsis: how to make a functional pattern. – Trends in Plant Science 5: 458-460.
[64] Shang, Y., Dai, C., Lee, M. M., Kwak, J. M., Nam, K. H. (2016): BRI1-associated receptor Kinase 1 regulates guard cell ABA signaling mediated by open stomata 1 in Arabidopsis. – Mol. Plant. 9: 447-460.

http://www.aloki.hu ● ISSN 1589 1623 (Print) ● ISSN 1785 0037 (Online)
DOI: http://dx.doi.org/10.15666/aeer/1705_1209112109

[65] Sugano, S. S., Shimada, T., Imai, Y., Okawa, K., Tamai, A., Mori, M., Hara-Nishimura, I. (2010): Stomagen positively regulates stomatal density in Arabidopsis. – Nature 463: 241-244.
[66] Takemiya, A., Shimazaki, K. (2016): Arabidopsis phot1 and phot2 phosphorylate BLUS1 kinase with different efficiencies in stomatal opening. – J. Plant Res. 129(2): 167-174.
[67] Tanaka, Y., Nose, T., Jikumaru, Y., Kamiya, Y. (2013): ABA inhibits entry into stomatal lineage development in Arabidopsis leaves. – Plant J. 74(3): 448-457.
[68] Tian, W., Hou, C. C., Ren, Z. J., Pan, Y. J., Jia, J. J., Zhang, H. W., Bai, F. L., Zhang, P., Zhu, H. F., He, Y. K., Luo, S. L., Li, L. G., Luan, S. (2015): A molecular pathway for CO_2 response in Arabidopsis guard cells. – Nat. Commun. 6: 6057.
[69] Vahisalu, T., Kollist, H., Wang, Y. F., Nishimura, N., Chan, W. Y., Valerio, G., Lamminmäki, A., Brosché, M., Moldau, H., Desikan, R., Schroeder, J. I., Kangasjärvi, J. (2008): SLAC1 is required for plant guard cell S-type anion channel function in stomatal signalling. – Nature 52(7186): 487-491.
[70] Vatén, A., Soyars, C. L., Tarr, P. T., Nimchuk, Z. L., Bergmann, D. C. (2018): Modulation of asymmetric division diversity through Cytokinin and SPEECHLESS regulatory interactions in the Arabidopsis stomatal lineage. – Developmental Cell 47: 1-14.
[71] Von, G. U., Berger, D., Altmann, T. (2002): The subtilisin-like serine protease SDD1 mediates cell-to-cell signaling during Arabidopsis stomatal development. – The Plant Cell 14: 1527-1539.
[72] Yan, J., Zhang, C., Gu, M., Bai, Z., Zhang, W., Qi, T., Cheng, Z., Peng, W., Luo, H., Nan, F., et al. (2009): The *Arabidopsis* CORONATINE INSENSITIVE1 protein is a jasmonate receptor. – Plant Cell 21: 2220-2236.
[73] Zhang, H., Pan, C., Gu, S., Ma, Q., Zhang, Y., Li, X., Shi, K. (2018): Stomatal movements are involved in elevated CO_2-mitigated high temperature stress in tomato. – Physiol Plantarum. DOI: 10.1111/ppl.12752.
[74] Zhu, J. Y., Sae-Seaw, J., Wang, Z. Y. (2013): Brassinosteroid signalling. – Development 140: 1615-1620.

http://www.aloki.hu ● ISSN 1589 1623 (Print) ● ISSN 1785 0037 (Online)
DOI: http://dx.doi.org/10.15666/aeer/1705_1209112109

GREENHOUSE GAS EMISSIONS DUE TO THE CONSTRUCTION OF RESIDENTIAL BUILDINGS IN MORADABAD, INDIA

TIRTH, V.[1*] – ALGARNI, S.[1] – AGARWAL, N.[2] – SAXENA, A.[2]

[1]Mechanical Engineering Department, College of Engineering, King Khalid University, Guraiger, Abha-61411, Asir, Kingdom of Saudi Arabia (phone: +966-59-211-8330; fax: +966-17-241-8152)

[2]Mechanical Engineering Department, Moradabad Institute of Technology, Moradabad 244001, India

**Corresponding author*
e-mail: v.tirth@gmail.com, vtirth@kku.edu.sa

(Received 27th Apr 2019; accepted 12th Jul 2019)

Abstract. In this study, greenhouse gas emitted during the construction stages of three residential buildings with land areas of 204 m^2, 150 m^2 and 120 m^2 in Moradabad city (8.866790 °N, 78.755921 °E) in northern India have been estimated and analyzed. Post design, the construction of a residential building involves five stages viz. design, production of building materials, mobilization of materials, building construction, and disposal of construction waste. Mathematical equations have been developed to calculate the greenhouse gas emissions in all the five stages as well as to estimate the aggregate emissions. Emissions from human-related activities like on-site cooking and water consumption have been included. The results indicate that the production of building materials is responsible for 74% of the total emissions. Steel, concrete, bricks, and cement are consumed in a large volume during the construction and have an environmental impact. Average Greenhouse Gas emissions of the three residential buildings were estimated to be about 0.784 tCO_2e/m^2. Selecting the alternative building materials with low greenhouse gas emissions and incorporating a major renewable energy source are foremost priorities for future construction projects.
Keywords: *construction stages, building materials, human activities, environment, global warming potential, carbon footprint*

Abbreviations: Greenhouse Gas: GHG, Gross Domestic Product: GDP, Global Warming Potential: GWP, Carbon Foot Print: CFP, Liquefied Petroleum Gas: LPG

Introduction

Energy systems are essential for human activities and play a crucial part in the economic growth of the nation. On the other hand, they have ecological implications, including the release of greenhouse gases (GHG) into the atmosphere resulting in the degradation of the environment. The growth of energy systems is difficult to forecast as they are governed by several dynamic factors like population growth, technological development, and socio-economic factors. In the year 2012, the worldwide CO_2 emissions due to energy use touched a remarkable high level of 31.6 Gt (Hong et al., 2015), stagnated in 2014 (32.2 Gt), in spite of about 3% economic growth of the world. It was the first of such observations in the last four decades in which stagnation in emissions was not related to the economic slowdown (International Energy Agency, 2015).

The economic development of the countries is mainly related to the development of infrastructure for which construction activities are key consumers of resources and energy. Therefore, for a sustainable society, it becomes important to engross the construction industries (Asif et al., 2007). The building construction has an effect on numerous secondary commercial activities due to the consumption of a wide range of

http://www.aloki.hu ● ISSN 1589 1623 (Print) ● ISSN 1785 0037 (Online)
DOI: http://dx.doi.org/10.15666/aeer/1705_1211112126

materials, manufactured in diversified small and big industries (Suzuki et al., 1995). Typical building construction requires about 40% of the gravel-stone-sand, 25% wood and, 16% water per annum globally (Arena et al., 2003). The Statics times (2015), reported that the construction industry occupied 8.09% of Gross Domestic Product (GDP) in 2014 with its production amounting to 928,418 crore Indian rupees. According to Nation Master Statistic (2013), more than 33% of the global emissions and the energy consumption were due to the building construction industry in developing as well as the developed nations. This resulted in the diminution of non-renewable energy assets, obliteration of landscapes, leading to the generation of environmental issues, linked indirectly or directly to the community working in this sector. The total embodied energy involved in building construction is proportionate to the quantity of the building material consumed during the different stages of construction and to the embodied energy of materials (Dimoudi et al., 2008). Therefore, it is imperative to consider the impact on the environment and aim to mitigate the effects of building construction on it.

Reducing GHG emissions from construction industries may fetch numerous advantages to society as well as the economy. The construction, maintenance, and renovation activities contribute between 10–40% of the GDP of countries', and about 10% of employment (UNEP, 2009). The meticulous design of the buildings and proper planning of the construction activities may help in the mitigation of GHG and, at the same time, can rouse the new job opportunities in India and other developing countries. It can also help in social development by providing improved accommodations, clean water and, energy to the community. Top management and policymakers should grab the business prospects due to the environmental crisis, to take a lead in sustainable development. To adopt any mitigation policy, it is, therefore significant to estimate the GHG emissions caused due to different construction stages in developing countries such as India.

GHG emissions

The GHG such as carbon dioxide, ozone, methane, water vapor, and nitrous oxide have a tendency to captivate and release radiations in the thermal infrared range, causing the greenhouse effect, which is a primary reason for global warming.

Due to human activities, the CO_2 level in the atmosphere has increased to 400 ppm compared to 280 ppm in 1750, a rise of 40% (Blasing et al., 2014). The main reasons for the increase in anthropogenic carbon emissions are due to the use of fuels namely; oil, gas, coal, wood, etc. and rapid deforestation.

It is projected that with the current rate of increase in carbon emissions, the atmospheric temperature can rise more than historic limits within 30 years. The rise in the temperature of the earth's atmosphere will not only result in rising sea level, but it will cause severe threats to the ecological balance and survival of biodiversity across the globe (Mora et al., 2013).

Indirect and direct emissions

The present work includes both indirect and direct GHG emissions, as well as the emissions during building construction. The construction activities may not directly consume large quantum of energy but their indirect energy footprint is huge due to the consumption of materials processed through high energy-intensive processing. A few examples of high-energy intensive materials used in the construction industry are steel, bricks, aluminum, cement, glass, etc. In this study, the direct emissions during

http://www.aloki.hu ● ISSN 1589 1623 (Print) ● ISSN 1785 0037 (Online)
DOI: http://dx.doi.org/10.15666/aeer/1705_1211112126

construction stages refer to those due to the direct energy use at the site and the indirect emissions are due to the energy footprint and hence add to the carbon emissions of the materials used in building construction. It is expected that this study shall give a comprehensive understanding of emissions from building construction stages in northern India and help in determining the solution for the mitigation of carbon emissions in a phased manner.

Review of literature

In recent decades, varieties of studies have been carried out to analyze the carbon and energy footprints of building and construction activities. The studies carried out are different in scope and methodology. The building life cycle activities were also analyzed. Some related research findings are discussed in this section.

Onat et al. (2014) addressed the rapidly growing emission tendency in the residential buildings in the United States in an attempt to minimize the emissions. The authors concluded that promoting the construction of green buildings is insufficient to curb the emissions unless the existing buildings are retrofitted. Therefore, it becomes necessary to implement a strict green building policy, which should include the new as well as old buildings. Chou and Yeh (2015) proposed a method to augment the CO_2 emissions and their implications on the environment while assessing the life cycle of the buildings. This methodology may be useful in the valuation of major environmental risks for the life cycle of buildings and the selection of a suitable method for construction. Lin et al. (2015) studied the emissions in residential and commercial buildings in China and evaluated the energy-related economic factors. The results indicate that emissions related to energy during building construction are growing briskly and are expected to shoot further in China's eastern regions, particularly in South Asia due to significant migration of people to the urban areas from rural regions.

Akten and Akyol (2018), in their study on Izmir province in Turkey, suggested that the ecological footprint of many countries has exceeded their biocapacity. The human activities and their consumption habits have resulted in an ecological deficit, and the problem is increasing with every passing day.

Doğan (2018) in his detailed study on Eurasian regions and Turkey over a period of 13 years emphasized the connection between global warming and CO_2 concentration. He found that awareness among the population plays a major role in the success of the mitigation policies.

Yang et al. (2018) observed CO_2 concentration around China and raised questions on assumptions of uniform CO_2 level in the atmospheres.

Zheng et al. (2018) in a study on urbanization in China, recommended different policies for reducing carbon emissions for different levels of urbanization.

Marsono et al. (2015) proposed a methodology to reduce the effect of CO_2 emission for buildings as well as to improve their structural stability by encouraging the Malaysian construction industry to increase the use of wood in their building schemes. This methodology can help decision-makers to select the most flexible scheme for Malaysian housing. Lai (2015) conducted a study to explore the carbon footprints (CFP) of three typical hotels in Hong-Kong and found that electricity consumption was the main source of carbon emission. Sharma et al. (2012) assessed a three-story building in the northern region of India. They concluded that the reinforced cement concrete (RCC) framework and steel are the biggest contributors in GHG emissions. Devi and

http://www.aloki.hu ● ISSN 1589 1623 (Print) ● ISSN 1785 0037 (Online)
DOI: http://dx.doi.org/10.15666/aeer/1705_1211112126

Palaniappan (2014) presented a life cycle analysis of energy in a residential apartment located in the southern region of India. The effect of the service life of the building and monthly electricity consumption on the energy used in construction was predicted using sensitivity analysis. Wang et al. (2015) calculated the carbon emissions from the highway construction activities namely road construction, bridge construction and making the tunnels as 5229, 35547, and 42302 $kgCO_{2e}$/m respectively. They suggested a simple mathematical model to assess the CO_2 emissions from road construction activities. A similar model to assess the emissions from the building construction will be very useful.

Li et al. (2019) assessed the GHG emission in China in different phases of building construction. Their work was focused on the CO_{2e} of building materials procured from urban, national, and global markets. Ceramics and basic construction material were obtained from the urban market, paints and chemicals were obtained from the national market, and metals and petroleum were the materials, which were derived from global sales. The contribution of urban, national, and global materials was estimated to be 68.78%, 24.41%, and 6.8% respectively.

In a study on a Norwegian office building, Moschetti et al. (2019) explored the pathways towards zero-emission buildings. To achieve their objective, they emphasized on alternative design solutions and use of solar energy and building materials with low global warming potential (GWP). The use of solar energy reduced emissions by 30%.

Buildings and construction activities are responsible for the diminution of natural resources and impact the environment and so, this sector has attracted the environmentalists for assessment of emissions and attempts to suggest methods for controlling the impact on environment and depletion of natural resources. Hossain and Thomas (2019) studied the adopted resource recovery principle to reduce waste, increase the efficiency of waste disposal and resource-efficient constructions. They suggested a few sustainable strategies for waste treatments. Some of these strategies included recycling and recovery of secondary materials like timber waste, mortar, etc.

In a study on the building life-cycle carbon emissions in China (Can et al., 2019) reported that the production of building material is a major contributor to the emissions, followed by the construction activities. The study also suggested that the variables such as GDP, income, urbanization, price and overall economy directly affect the emissions by influencing the surge in the construction industry. The effective methods to curb the emissions from building and construction activities may be focused on implementing cleaner technology during the production stages of construction materials and the building design.

Wong et al. (2019) in a study in Australia suggested that the estimation of the embodied emission due to stages of building construction shall be made a mandatory practice. The construction industry has misnomer about carbon accounting and sees it as a threat to increase its cost and efficiency. The regulations of the government to promote designs of low CFP buildings and construction activities may have an immediate positive impact on carbon emissions.

From the literature review it may be extracted that though the effect of building construction materials on the environment and CO_2 emissions have been investigated and analyzed in different regions for different sizes and utilities of the buildings, it is apparent that construction-related human activities like on-site cooking, water consumption has been ignored in the published research. Without the incorporation of human activities, the assessment and GHG emissions from the construction activities

http://www.aloki.hu ● ISSN 1589 1623 (Print) ● ISSN 1785 0037 (Online)
DOI: http://dx.doi.org/10.15666/aeer/1705_1211112126

and their analysis is incomplete. Human activities should be given special consideration by the researchers as they affect the GHG emission during the construction phase. Apart from the earlier research work, the present work includes the carbon emissions due to various human actions based on comprehensive process data and the case studies selected in India. The previous research has given limited attention to the buildings of the size and classification identified for the present analysis. The size and carpet areas of the buildings identified for the study are those, which are expected to develop the most in near future and so, with about one-sixth of the world population and being a fast developing country, the study made in the present manuscript is a relevant one.

Materials and methods

Methodologies

Scope of study

The study encompasses the GHG emissions during the stages of construction including several construction activities in the residential buildings, identified and closely studied from the start of construction to its completion. The inherited associated emissions from the materials, GHG emissions from the fuel burned to transport the building materials to the construction site and to transport the construction waste, emissions due to human activities, direct emissions due to electric power consumption at the site and, emissions due to the processing of water and sewage are included in the study.

System boundaries

System boundaries demonstrate the activities included in the analysis. Several aspects influence the GHG emissions of residential buildings during the construction stages. It is relevant to analyze the system boundaries to make certain that the contribution of all significant factors to the CFP is incorporated. A schematic representation of the system boundaries adopted in the present study is given in *Figure 1*.

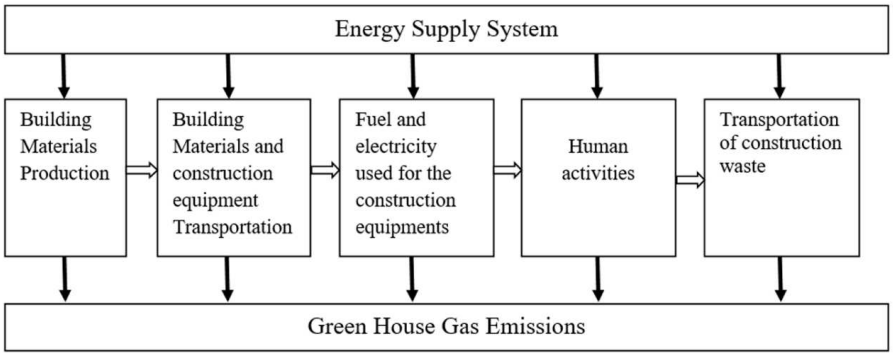

Figure 1. *The system boundary of GHG emissions in the construction of residential houses*

http://www.aloki.hu ● ISSN 1589 1623 (Print) ● ISSN 1785 0037 (Online)
DOI: http://dx.doi.org/10.15666/aeer/1705_1211112126

Quantification of GHG emissions

Greenhouse gases emissions from the production of building materials

The GHG emissions due to the consumption of the building materials can be estimated by *Equation 1*. The units of GHG emissions are tons of Carbon dioxide equivalent (tCO_{2e}).

$$GHG_1=\sum_{i=1}^{m} M_{1i} \times F_{1i} /1000 \quad \text{(Eq.1)}$$

where GHG_1 is the total GHG emissions due to the consumption of all building materials; m is the number of materials considered; M_{1i} is the quantity (tones) of the i^{th} material, and F_{1i} is emission factor of the i^{th} material in tCO_{2e}/kg.

The GHG emission factor of building materials considered in the present analysis is given in *Table 1*.

Table 1. *Building materials used in the construction of residential houses. (Data source: Kilbert, 2007; Shams et al., 2011)*

S.N.	Material	Unit	Emission factor ($kgCO_2e$/unit)	Consumption		
				Case A (204 m^2)	Case B (150 m^2)	Case C (120 m^2)
1.	Cement	kg	0.967	31884	23913	19130.4
2.	Concrete mixture	kg	0.159	578271	433703.2	346962.6
3.	Stainless Steel bars	kg	5.457	25220	18915	15132
4.	Granite	kg	0.04	74	55.5	44.4
5.	Marble	kg	0.436	422.5	318.8	255
6.	Bricks	kg	0.327	216075	162056	129645
7.	Glass	kg	1.735	1286	964.5	771.6
8.	LPG (on site)	kg	3.27	65	48.75	39
9.	PVC pipes	kg	3.23	148	111	88.8
10.	Aluminum	kg	0.622		134	
11.	Diesel	kg	3.17	1145	855	683
12.	Electricity	kWh	0.7898	995	647	591
13.	Cooking oil (on site use)	kg	3.07	72	54	43
14.	Copper pipes	Kg	3.02	38	28.5	22.8
15.	Plastic pipes	m	0.40	140	105	84
16.	Electric wires	kg	2.84	212	159	127.2
17.	Lighting fixtures	Set	35.65	32	24	19.2
18.	Tiles (floor and wall)	m^2	18.33	535	401	321
19.	Plywood	kg	0.61	210	157.5	126
20.	Plaster board	Sheet	11.35	28	21	16
21.	Ceramic (wall care putty)	kg	0.78	2500	1875	1500
22.	Welding rod	kg	20.5	23	17	14
23.	Timber plates	m^3	583	52	39	31.2
24.	Mosaic	kg	0.238	708	531	424.8
25.	Polyurethane	kg	4.31	61	46	36.8
26.	Perlite	kg	0.995	174	131	104.8
27.	Gravel	kg	0.00241	26485	19864	15891.2
28.	Alcohol	kg	0.828	48	36.5	29.2
29.	Fugitive discharge	kgBOD	0.03	112	84	67.2
30.	Water	Liter	0.42	21768	16295	12905

http://www.aloki.hu ● ISSN 1589 1623 (Print) ● ISSN 1785 0037 (Online)
DOI: http://dx.doi.org/10.15666/aeer/1705_1211112126

Emissions from the transportation of construction equipment and materials

GHG emissions from fuel combustion during the transportation of construction equipment and materials and (in tCO_{2e}) are calculated by *Equation 2*.

$$GHG_2 = \sum_{i=1}^{n} M_{2i} * (D_{il} * f_2 + D_{is} * f_3)/1000 \quad \text{(Eq.2)}$$

Where n represents the number of building materials and construction equipment transported to the construction site. M_{2i} is the amount of the i^{th} building material or weight of construction equipment in tones. D_{il} is the transportation distance of the i^{th} material or equipment by land (km). D_{is} is the transportation distance of i^{th} material or equipment by sea (km). f_1 and f_2 are emission factors for land and sea transportation, respectively (Yan et al., 2010). The transportation distances of different materials and equipment are obtained from Google maps.

Emissions from the construction equipment due to the consumption of fuel and electricity

Scientific research has discovered that the fuel consumed by the construction equipment viz. dozer, concrete mixture, channel, and angle type tower hoist, etc. results in the emission of different quantities of N_2O and CH_4, categorized as off-road construction (Eggleston et al., 2006). GHG emission from fuels consumptions of the construction equipment can be calculated (in tCO_{2e}) by *Equation 3*.

$$(GHG)_3 = \sum_{k=1}^{n_3} FC_k \times f_{3k} / 1000 \quad \text{(Eq.3)}$$

Where GHG_3 is the total GHG emission from fuel consumptions by different construction equipment; n_3 is the types of fuels (number) used by different construction equipment viz. diesel, LPG, gasoline, etc., FC_k is the quantity (liters) of the k^{th} fuel used by the construction equipment; F_{3k} is the emission factor of the k^{th} fuel ($kgCO_2$ e/L).

The emission factor of the k^{th} fuel is calculated by *Equation 4*.

$$F_{3k} = F_{CO2} + F_{CH4} \text{ x } GWP_{CH4} + F_{N2O} \text{ x } GWP_{N2O} \quad \text{(Eq.4)}$$

Where F_{CO2}, F_{CH4}, and F_{N2O} is the emission factor of CO_2, CH_4, and N_2O, respectively for fuel 'k'. GWP_{CH4} and GWP_{N2O} are the global warming potentials of CH_4 and N_2O, respectively. In India, the on-site construction equipment is either run on diesel or by electricity, so the emission factor and GWP of diesel are given in *Table 2* (Yan et al., 2010).

Table 2. *Emission factor and GWP of diesel fuel*

Gases	Emission factor ($kgCO_2e/kg$)	GWP
CO_2	2.6140	1
CH_4	0.0239	21
N_2O	0.0074	310

http://www.aloki.hu ● ISSN 1589 1623 (Print) ● ISSN 1785 0037 (Online)
DOI: http://dx.doi.org/10.15666/aeer/1705_1211112126

GHG Emissions from electrical energy use for construction equipment like; vibratory plate compactor, sand screening machine, etc., can be calculated by *Equation 5*.

$$GHG_4 = E * f_5 / 1000 \quad \text{(Eq.5)}$$

Where GHG_4 is the total emission of GHG (tCO_{2e}) due to the electricity consumed by the construction equipment, E is the amount of electric power consumed by the construction equipment during the construction period in kWh. The electricity was supplied by the state electricity board. f_5 is the emission factor for electricity in India. Its default value is 0.93 kg/kWh. *Table 3* shows the emission factor of electricity in India from 2008 to 2012 (tCO_{2e}/MWh) (User Guide Version 8.0, 2013).

Table 3. *The emission factor of electricity in India from 2008 to 2012*

Grid	2012	2011	2010	2009	2008
Southern grid	0.91	0.84	0.85	0.9	0.85
North Eastern grid	0.94	0.91	0.9	0.84	0.8
Pan India	0.93	0.9	0.88	0.85	0.81

GHG emissions from human activities

GHG emissions from human activities include electricity use for processing fresh water and sewage and, consumption of liquefied petroleum gas (LPG) for on-site cooking. Following equations are used to calculate the GHG emissions by these two human activities.

$$GHG_6 = W_W * f_6 / 1000 \quad \text{(Eq.6)}$$

$$GHG_7 = W_G * f_7 / 1000 \quad \text{(Eq.7)}$$

Where GHG_6 represent the emissions (tCO_{2e}) due to the consumption of electric power for processing the fresh and sewage water. W_W is the quantity of the water used (m^3), f_6 is the emission factor of electricity used in handing out fresh and sewage water ($kgCO_{2e}/m^3$). GHG_7 is the GHG emission due to LPG used for on-site cooking (tCO_{2e}), W_G is the quantity of LPG used (m^3) and, f_7 is the emission factor for LPG ($kgCO_{2e}/m^3$).

Emissions from the transportation of construction waste

The emissions from combustion of fuel consumed by vehicles used for disposal of construction waste can be estimated by *Equation 8*.

$$GHG_8 = W_S * D*f_8 / 1000 \quad \text{(Eq.8)}$$

Where W_S is the amount of construction waste (tones), D is the distance traveled by disposal vehicles for transporting the waste to dumpsite (km), and f_8 is the emission factor of the fuel (diesel) used in transportation vehicles ($kgCO_{2e}$/ton-km). The emission factor for diesel is 3.17 $kgCO_{2e}$/kg (Hong et al., 2015).

http://www.aloki.hu ● ISSN 1589 1623 (Print) ● ISSN 1785 0037 (Online)
DOI: http://dx.doi.org/10.15666/aeer/1705_1211112126

Estimation of total emissions

The aggregate emissions during different construction phases of the residential buildings can be calculated by *Equation 9*.

$$GHG_{Total} = \sum_{k=1}^{8} CHG\,\kappa \quad \text{(Eq.9)}$$

Case studies of residential buildings

The present research work has been carried out on real construction projects: three residential houses located in Moradabad district of Uttar Pradesh, India. The land areas are 120 m^2, 150 $m^{2,}$ and 204 m^2. *Figure 2* represents the layout and floor plan of the residential houses. The residential buildings under study represent typical middle-class society with independent houses or floors, common in non-metropolitan cities in India like Moradabad.

The description of three residential houses is presented in *Table 4* and the materials used for construction are presented in *Table 1*. The materials include those used in foundation, civil structure, finishing, landscape architecture, and engineering materials.

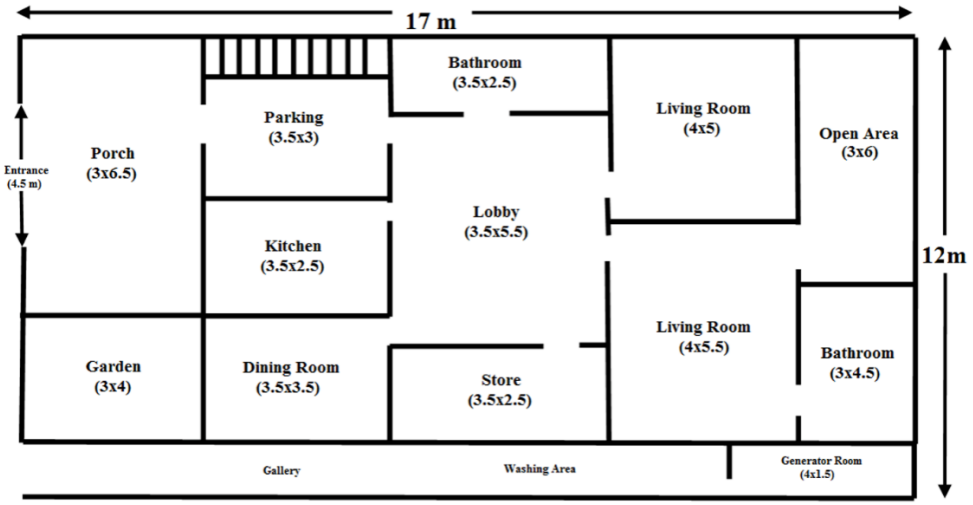

(a)

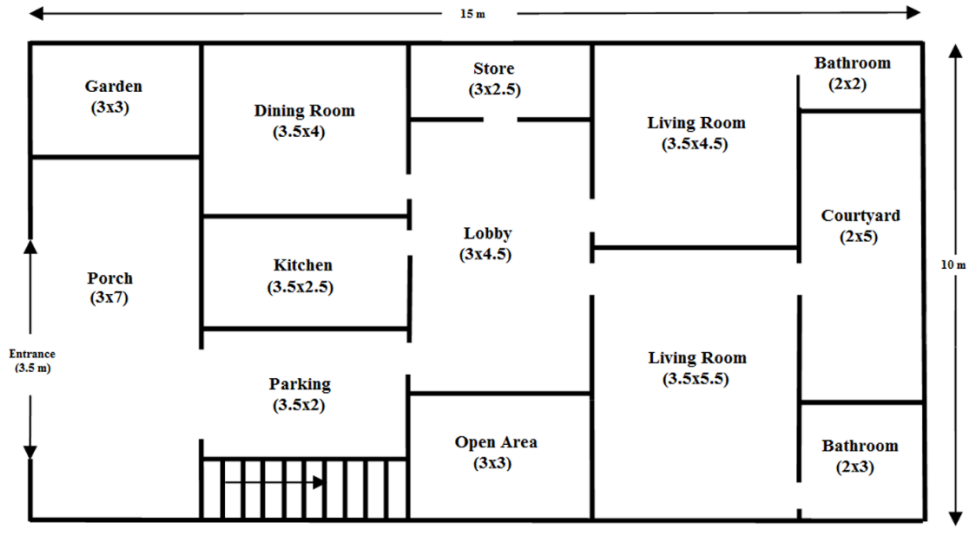

(b)

http://www.aloki.hu ● ISSN 1589 1623 (Print) ● ISSN 1785 0037 (Online)
DOI: http://dx.doi.org/10.15666/aeer/1705_1211112126

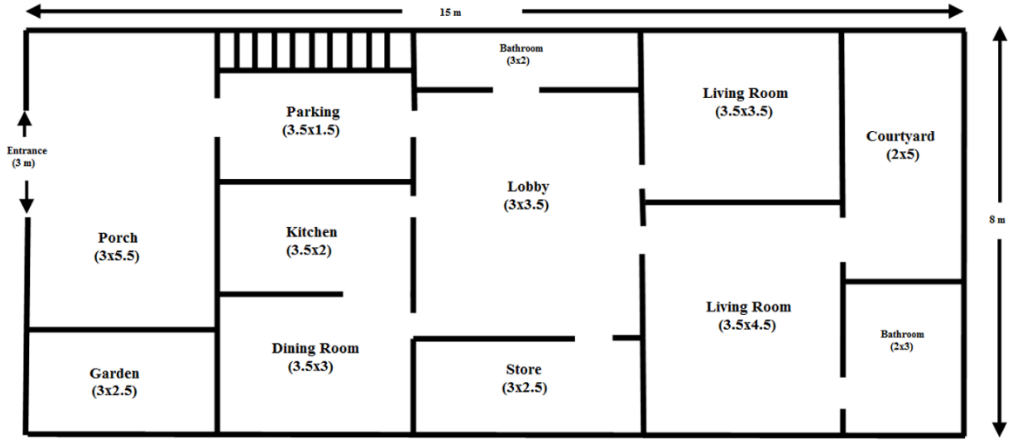

(c)

Figure 2. *Floor plan of the three residential buildings with area and GPS coordinates (given in brackets); (a) 204 m^2 (28.865838°N, 78.753071°E); (b) 150 m^2 (28.866891°N, 78.750128°E) and; (c) 120 m^2 (28.869725°N, 78.752629°E)*

Table 4. *Description of three residential houses under study*

Building	Land area m^2	Number of floors	Covered area (ground floor)	Covered area (first floor)	Construction period	Height of ceiling	Structure	Concrete strength
Case A	204	02	144.5	110.5	25 months and 12 days	3.35 m	Reinforced concrete	22 MPa
Case B	150	02	108.2	82.8	22 months and 15 days	3.35 m	Reinforced concrete	22 MPa
Case C	120	02	86.4	66.4	21 months and 22 days	3.35 m	Reinforced concrete	22 MPa

Results and discussion

The GHG emissions during the construction of each house have been calculated using *Equations 1–8* by substituting the value of appropriate emission factor and the average emission percent due to the factors included in the study is represented in *Figure 3*.

From *Figure 3* we can see that the production of building materials account for 74% of the aggregate GHG emissions, 12% of the aggregate emissions are from transportation of building material and construction equipment, 10% from fuel and electricity used for construction equipment, 2% from human activities, and 2% are from transportation of construction waste. It is observed that besides the massive emission contribution of the productions of building material and their transportation, human activities also contribute 2% of overall emissions during the construction of the residential building. This requires adequate attention of the researchers. The average GHG emission of the three residential buildings was estimated to be around 0.784 tCO_{2e}/m^2.

Figure 4 indicates GHG emissions from primary building materials. It can be seen that GHG emissions from steel, cement, bricks, and concrete mixture were 0.54 tCO_{2e}/m^2 for residential buildings and account for about 68.87% of the total emissions.

http://www.aloki.hu ● ISSN 1589 1623 (Print) ● ISSN 1785 0037 (Online)
DOI: http://dx.doi.org/10.15666/aeer/1705_1211112126

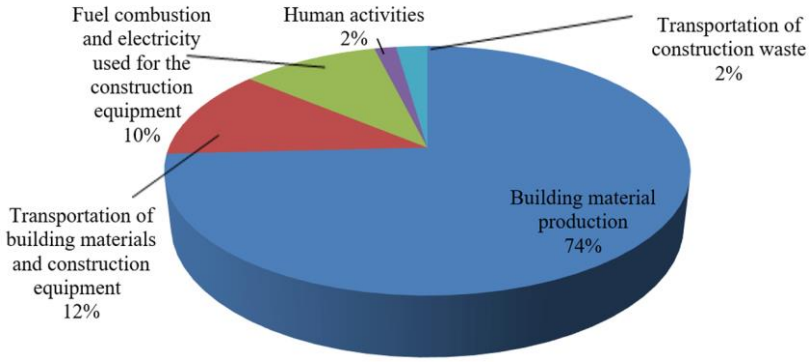

Figure 3. *Distribution of average of the aggregate GHG emissions, in three houses*

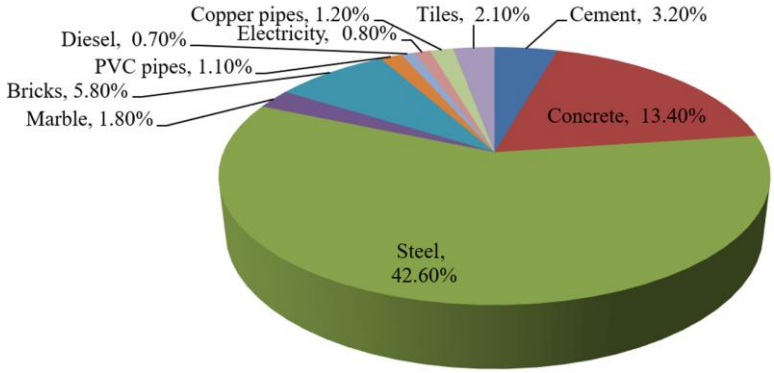

Figure 4. *GHG emissions of primary building materials*

The GHG emissions from steel and cement, the most important construction materials, was approximately 0.349 tCO_{2e}/m^2 and 0.025 tCO_{2e}/m^2 respectively. Other materials like PVC pipes, copper pipes, tiles, marble, diesel, aluminum, plywood, mosaic, etc. have a relatively small contribution.

The consumption of electricity, water and fuel (diesel) in the three residential building are given in *Table 5* month wise. The blank column indicates no consumption due to the completion of construction of the building. The GHG emissions due to the consumption of electricity, water and fuel during the construction stages were estimated from this data.

In the Moradabad district of northern India, nearly 3000 residential houses were constructed in the year 2012-13, with a covered area of approximately 390,000 m^2 (discussion with the town planner, 2013), at this pace of construction of new residential buildings, it is estimated that total GHG emissions may be about 305,760 tCO_{2e} annually.

In order to reduce the emissions due to the construction activities, the recycled building materials along with the environmentally friendly construction practices are recommended to minimize the harm to the environment. Prefabricated building materials and components should be preferred to recover the environmental losses due to GHG emissions. Published research shows that adoption of prefabrication technology during the construction stage add appreciably in the sustainable development of the construction sector (Hong et al., 2015; Aye et al., 2012; Mao et al., 2013; Pons et al.,

http://www.aloki.hu ● ISSN 1589 1623 (Print) ● ISSN 1785 0037 (Online)
DOI: http://dx.doi.org/10.15666/aeer/1705_1211112126

2011). The comparative values of GHG emissions estimated using *Equations 1–9* are given in *Table 6*. Based on the analysis of results, the major contributors to GHG emissions have been selected. The consumption of materials is directly related to the emissions and the covered area.

Table 5. *Diesel, electricity, and water used in the construction of residential houses*

Month	Case A (204 m^2)			Case B (150 m^2)			Case C (120 m^2)		
	Diesel (kg)	**Electricity (kWh)**	**Water (Liter)**	**Diesel (kg)**	**Electricity (kWh)**	**Water (Liter)**	**Diesel (kg)**	**Electricity (kWh)**	**Water (Liter)**
01	29	32	485	22	24	364	17	19	291
02	27	18	1003	20	13	752	16	11	602
03	29	1	728	22	1	546	17	1	437
04	30	8	874	23	6	655	18	5	524
05	30	4	644	23	3	483	18	2	386
06	46	37	694	35	28	520	28	22	416
07	49	17	759	37	13	569	29	10	455
08	66	28	1014	49	21	760	39	17	608
09	73	29	1135	54	22	851	44	18	681
10	105	38	1285	79	29	964	63	23	771
11	139	37	2468	104	27	1851	84	22	1481
12	119	58	2191	89	43	1643	71	35	1315
13	101	21	2640	76	16	1980	61	13	1584
15	213	46	1879	160	35	1409	128	28	1127
16	78	26	1638	58	20	1228	47	16	983
17	6	102	1571	4	76	1178	3	61	943
18	5	97	602	--	73	408	--	58	301
19	--	84	102	--	63	96	--	51	--
20	--	97	56	--	73	38	--	58	--
21	--	101	--	--	61	--	--	121	--
22	--	87	--	--	--	--	--	--	--
23	--	27	--	**--**	**--**	**--**	--	--	--

Table 6. *Comparative GHG emissions from major building materials in three houses*

Case	**A**	**B**	**C**
Plot area [m^2]	204	150	120
Covered area [m^2]	144.5	108.2	86.4
CO_2 emissions [tCO_{2e}] due to major construction materials			
Cement	3.6125	2.705	2.16
Steel	50.4305	37.7618	30.1536
Bricks	6.5025	4.869	3.888
Concrete	15.1725	11.361	9.072
Tiles	2.312	1.7312	1.3824
Marble	2.023	1.5148	1.2096
PVC	1.2427	0.93052	0.74304
Copper pipes	1.3583	1.01708	0.81216
Electricity	0.8959	0.67084	0.53568
Diesel	0.7803	0.58428	0.46656

http://www.aloki.hu ● ISSN 1589 1623 (Print) ● ISSN 1785 0037 (Online)
DOI: http://dx.doi.org/10.15666/aeer/1705_1211112126

Comparative and critical discussion

Based on the study and in correlation with the published research on GHG emissions in different parts of the world, it is deduced that the building construction activities need restructuring to consider the impact of the construction activities and building materials on the environment. It is recommended that the management, contractors, labor and, other stakeholders ought to refer the following guidelines to lower the GHG emissions during the construction stage of buildings.

1. Choose construction sites having low ecological and agricultural significance without any interference with biodiversity.
2. Every construction project should set goals to minimize GHG emissions and watch the performance. GHG emissions should be an important consideration in the design process.
3. Include materials that are more competent and less harmful to the environment.
4. Incorporate features like green roofs and walls and use local species in plantation and landscaping.
5. Saving energy at every stage of the construction process should be a top priority.
6. Poor management and tardy design modifications are the main contributors to waste. Therefore, avoid late modifications to design and intend all work from the commencement of the construction process in order to minimize waste.
7. Strike down over-ordering and facilitate the recycling of waste. Prefer way outs that produce a lesser amount of waste and design material goods that can be dismantled and reused.
8. Make use of materials that can be recycled. Use minimum packing to shield the product. Prefer reuses and avoid landfill.
9. Put the target to minimize water consumption and evaluate progress throughout the construction phase. Use machines and equipment that save water, inspire everyone to detect and report water leaks, and fix them at the earliest possible.
10. Proper project management with time-activity scheduling, deriving benefits from weather and climate, minimize curing and encourage use to solar energy and daylight.

Conclusions

Three residential buildings were identified in Moradabad region of northern India and their construction stages were carefully monitored over a period of two years from 2010-11 to 2012-13 until the buildings were completed. The authors 1, 3 and 4, owned the three buildings, identified as the research subject and so the research and results are 100% authentic and established. The consumption of the construction material, fuel and, electric power was maintained on a day-to-day basis. The equations used to estimate the GHG emissions at a different stage of construction and the aggregate emissions under the framework of the study were developed by the authors. The main deductions from the study highlight that the emissions from building material production account for 74% of the aggregate emissions. Among the construction materials steel, bricks, cement and, concrete together account for about 66% of the aggregate emissions. On-site human activities during the construction phases, which is yet to be published in the research domain, also contribute to the GHG emissions. The deductions of this study are beneficial for the sustainable design and construction management of the residential

http://www.aloki.hu ● ISSN 1589 1623 (Print) ● ISSN 1785 0037 (Online)
DOI: http://dx.doi.org/10.15666/aeer/1705_1211112126

buildings in India and may be used as a reference for developing the strategy and policy to minimize GHG emissions in the building construction industry in any part of the world. The authors are presently working on the life cycle assessment of GHG emissions of the residential buildings taken as research subjects in this study. A life cycle approach is aimed to be developed to investigate the GHG consequences of orthodox as well as low energy forms of residential building construction in India. The authors also aim at extending their work in estimating the life cycle carbon emissions of the residential buildings and further extending the scope of the study to the Kingdom of Saudi Arabia.

Acknowledgments. Authors thankfully acknowledge the funding and support provided by Scientific Research Deanship, King Khalid University, Abha-Asir, Kingdom of Saudi Arabia, with project grant number G.R.P-260-39 to complete the research work.

REFERENCES

[1] Akten, M., Akyol, A. (2018): Determination of environmental perceptions and awareness towards reducing carbon footprint. – Applied Ecology and Environmental Research 16(4): 5249-5267. DOI: http://dx.doi.org/10.15666/aeer/1604_52495267.

[2] Arena, A. P., Rosa, C. de (2003): Life cycle assessment of energy and environmental implications of the implementation of conservation technologies in school buildings in Mendoza - Argentina. – Building and Environment 38:359-368. DOI: https://doi.org/10.1016/S0360-1323(02)00056-2.

[3] Asif, M. A, Muneer, T, Kelley, R. (2007): Life cycle assessment : A case study of a dwelling home in Scotland. – Building and Environment 42:1391-1394. DOI: 10.1016/j.buildenv.2005.11.023.

[4] Aye, L., Ngo, T., Crawford, R. H., Gammampila, R., Mendis, P. (2012): Life cycle greenhouse gas emissions and energy analysis of prefabricated reusable building modules. – Energy and Buildings 47:159-168. DOI: 10.1016/j.enbuild.2011.11.049.

[5] Blasing, T. J. (2014): Recent Greenhouse Gas Concentrations. – Carbon Dioxide Information Analysis Center. DOI:10.3334/CDIAC/atg.032.

[6] Cui, C., Wang, Z., Bin, G. (2019): Life-cycle CO_2 emissions and their driving factors in construction sector in China. – Chinese Geographical Science 29: 293-305. DOI.org/10.1007/s11769-019-1029-z.

[7] Chou, J., Yeh, K. (2015): Life cycle carbon dioxide emissions simulation and environmental cost analysis for building construction. – Journal of Cleaner Production 101:137-147. DOI: 10.1016/j.jclepro.2015.04.001.

[8] Devi, P., Palaniappan, S. (2014): A case study on life cycle energy use of residential building in Southern India. – Energy and Buildings 80: 247-259. DOI: http://dx.doi.org/10.1016/j.enbuild.2014.05.034.

[9] Dimoudi, A., Tompa, C. (2008): Energy and environmental indicators related to construction of office buildings. – Resources, Conservation and Recycling 53: 86-95. DOI: 10.1016/j.resconrec.2008.09.008.

[10] Discussion with the Town Planner (2013): Moradabad Development Authority. – Govt. of Uttar Pradesh, India on 09.12.2013.

[11] Doğan, H. G. (2018): Nexus of agriculture, GDP, population and climate change : case of some Eurasian countries and Turkey. – Applied Ecology and Environmental Research 16(5): 6963-6976. DOI: http://dx.doi.org/10.15666/aeer/1605_69636976.

http://www.aloki.hu ● ISSN 1589 1623 (Print) ● ISSN 1785 0037 (Online)
DOI: http://dx.doi.org/10.15666/aeer/1705_1211112126

[12] Eggleston, H. S., Buendia, L., Miwa, K., Ngara, T., Tanabe, K. (2006): IPCC Guidelines for National Greenhouse Gas Inventories, Prepared by the National Greenhouse Gas Inventories Programme. – IGES, Japan.
[13] Hong, J., Qiping, G., Feng, Y., Lau, W. S., Mao, C. (2015): Greenhouse gas emissions during the construction phase of a building : a case study in China. – Journal of Cleaner production 103:249-259. DOI: 10.1016/j.jclepro.2014.11.023.
[14] Hossain, U., Ng, S. T. (2019): Influence of waste materials on buildings' life cycle environmental impacts: adopting resource recovery principle. – Resources, Conservation & Recycling 142: 10-23. DOI: 10.1016/j.resconrec.2018.11.010.
[15] International Energy Agency (IEA) (2015): World Energy Outlook Special Report: Energy and Climate Change. – IEA, Paris.
[16] Kilbert, C. J. (2007): Sustainable Construction: Green Building Design and Delivery. – Wiley, Hoboken, NJ.
[17] Lai, J. H. K. (2015): Carbon footprints of hotels: analysis of three archetypes in Hong Kong. – Sustainable Cities and Society 14: 334-341. DOI: 10.1016/j.scs.2013.09.005.
[18] Li, Y. L., Han, M. Y., Liu, S. Y., Chen, G. Q. (2019): Energy consumption and greenhouse gas emissions by buildings : A multi- scale perspective. – Building and Environment 151:240-250. DOI: 10.1016/j.buildenv.2018.11.003.
[19] Lin, B., Liu, H. (2015): CO_2 emissions of China's commercial and residential buildings: Evidence and reduction policy. – Building and Environment 92: 418-431. DOI: 10.1016/j.buildenv.2015.05.020.
[20] Mao, C., Shen, Q., Shen, L., Tang, L. (2013): Comparative study of greenhouse gas emissions between off-site prefabrication and conventional construction methods : Two case studies of residential projects. – Energy and Buildings 66:165-176. DOI: 10.1016/j.enbuild.2013.07.033.
[21] Marsono, A. K. B., Balasbaneh, A. T. (2015): Combinations of building construction material for residential building for the global warming mitigation for Malaysia. – Construction and Building Materials 85: 100-108. DOI: http://dx.doi.org/10.1016/j.conbuildmat.2015.03.083.
[22] Mora, C., Frazier, A. G., Longman, R. J., Dacks, R. S., Walton, M. M., Tong, E. J., Sanchez, J. J., Kaiser, L. R., Stender, Y. O., Anderson, J. M., Ambrosino, C. M., Fernandez-silva, I., Giuseffi, L. M., Giambelluca, T. W. (2013): The projected timing of climate departure from recent variability. – Nature 502:183-187. DOI: 10.1038/nature12540.
[23] Moschetti, R., Brattebø, H., Sparrevik, M. (2019): Energy & Buildings Exploring the pathway from zero-energy to zero-emission building solutions : a case study of a Norwegian office building. – Energy and Buildings 188-189:84-97. DOI: 10.1016/j.enbuild.2019.01.047.
[24] Nation Master Statistic (2013): CO_2 Emission by Country. – www.nationmaster.com.
[25] Onat, N. C., Egilmez, G., Tataria, O. (2014): Towards greening the U.S. residential building stock: a system dynamics approach. – Building and Environment 78: 68-80. DOI: http://dx.doi.org/10.1016/j.buildenv.2014.03.030.
[26] Pons, O., Wadel, G. (2011): Environmental impacts of prefabricated school buildings in Catalonia. – Habitat International 35:553-563. DOI: 10.1016/j.habitatint.2011.03.005.
[27] Shams, S., Mahmud, K., Al-Amin, M. (2011): A comparative analysis of building materials for sustainable construction with emphasis on CO_2 reduction. – Int. J. Environment and Sustainable Development 10: 364-374. DOI: 10.1504/IJESD.2011.047767.
[28] Sharma, A., Shree, V., Nautiyal, H. (2012): Life cycle environmental assessment of an educational building in Northern India: a case study. – Sustainable Cities and Society 4:22-28. DOI: 10.1016/j.scs.2012.03.002.
[29] Statics Times (2015): Sector-wise contribution of GDP of India. – http://statisticstimes.com/economy/sectorwise-gdp-contribution-of-india.php.

http://www.aloki.hu ● ISSN 1589 1623 (Print) ● ISSN 1785 0037 (Online)
DOI: http://dx.doi.org/10.15666/aeer/1705_1211112126

[30] Suzuki, M., Oka, T., Okada, K. (1995): The estimation of energy consumption and CO_2 emission due to housing construction in Japan. – Energy and Buildings 22: 165-169. DOI: https://doi.org/10.1016/0378-7788(95)00914-J.
[31] UNEP (2009): Buildings and Climate Change Summary for Decision-Makers. – http://www.unep.org/sbci/pdfs/SBCI-BCCSummary.pdf.
[32] User Guide, Version 8.0 (2013): CO_2 Baseline Database for the Indian Power Sector. – Government of India, Ministry of Power, Central Electricity Authority, New Delhi.
[33] Wang, X., Duan, Z., Wu, L., Yang, D. (2015): Estimation of carbon dioxide emission in highway construction : a case study in southwest region of China. – Journal of Cleaner Production 103:705-714. DOI: 10.1016/j.jclepro.2014.10.030.
[34] Wong, P. S. P., Holdsworth, S., Crameri, L., Lindsay, A. (2019): Does carbon accounting have an impact on decision-making in building design? – International Journal of Construction Management 19(2): 149-161. DOI: 10.1080/15623599.2017.1401290.
[35] Yan, H., Shen, Q., Fan, L. C. H., Wang, Y., Zhang, L. (2010): Greenhouse gas emissions in building construction: a case study of One Peking in Hong Kong. – Building and Environment 45:949-955. DOI: 10.1016/j.buildenv.2009.09.014.
[36] Yang, C. Y., Wang, H. J., Zhao, S. X., Cui, X. Y., Deng, B., Liu, X. P. (2018): Exaggerated climate warming on the assumption of uniform atmospheric CO_2 concentration. – Applied Ecology and Environmental Research 16(4): 3711-3728. DOI: http://dx.doi.org/10.15666/aeer/1604_37113728.
[37] Zheng, D. C., Liu, W. X., Li, X. X., Lin, Z. Y., Jiang, H. (2018): Research on carbon emission diversity from the perspective of urbanization. – Applied Ecology and Environmental Research 16(5): 6643-6654. DOI: http://dx.doi.org/10.15666/aeer/1605_66436654.

http://www.aloki.hu ● ISSN 1589 1623 (Print) ● ISSN 1785 0037 (Online)
DOI: http://dx.doi.org/10.15666/aeer/1705_1211112126

EFFECTS OF LEAD WATER IRRIGATION UNDER ZEOLITE STRESS ON RICE GROWTH

ZHANG, L. – BAI, Y. K.* – LI, Y. Q. – JIANG, G. H.

Shenyang Agricultural University, No. 120 Dongling Road, Shenyang, Liaoning, China (phone: +86-24-8848-7134; fax: +86-24-8848-7134)

**Corresponding author*
e-mail: baiyikui@163.com; phone: +86-133-8683-4288

(Received 28th Apr 2019; accepted 12th Jul 2019)

Abstract. This paper aims to study the effects of lead concentration in irrigation water on the yield and growth traits of rice under soil zeolite stress, with the addition of lead accumulation in rice plants, which were tested in a micro zone at the Experimental Base of Water Conservancy in Shenyang Agricultural University of Liaoning Province, China, through the application of different amounts of zeolite (0, 2500, 5000kg·ha^{-1}) and different lead concentrations (0, 0.25, 0.2, 0.15 mg·L^{-1}) in irrigation water. It was concluded that the lead contents in paddy root, stem, leaf and rice significantly varied with different exogenous lead concentrations. With the increase of the concentration, the lead contents in each part were significantly increased. More importantly, the effect on aboveground material weight was greater than that on underground material weight. The water contents of rice were increased with the decrease in the protein content, and starch content was decreased under zeolite stress. When the concentration of lead increased, the effect was more pronounced. Comprehensive test with various factors indicated that the incorporation of zeolite in soil for rice cultivation with lead-contaminated water irrigation or lead contaminated soil could restrain the movement of lead ions into the rice.
Keywords: *zeolite, lead, quality of rice, enrichment ability, interaction*

Introduction

In recent years, the use of one of China's shortage resources-agricultural irrigation water-has seen an increasing trend concerning industries and urban environments due to the acceleration of industrialization and urbanization, and the rapid development of technology, economy, civilization and people's quality of life. Therefore, the condition of agricultural water is getting worse. To make matters worse, irrigation with contaminated water is becoming one of the major methods to deal with the deficiency of water. In such cases, researches about the effects of recycling water irrigation on the yield and quality of agricultural products attract more attention recently (Galvis et al., 2018; Becerra, 2015). Lead is one of the most toxic elements among all known metal contaminations causing fertility deterioration, reproductive organ tumors, decreased immunity as well as physical anomalies (Zhao et al., 2015) of various organisms including humans. The increased lead level in children's body would damage the brain and nervous system, destroying cerebral cortical cells, which results in mental decline and impaired attention (Zhang et al., 2014). The Pb^{2+} in contaminated water will enter soil, get absorbed by root system and accumulate in plants. Once the concentration of Pb^{2+} exceeds a certain level, plants will be poisoned, and eventually Pb^{2+} will enter human bodies through the food chain to damage our health (Chen et al., 2018; Abrahams, 2002; Luo, 2012). It was revealed that lead would accumulate in rice plants to inhibit their growth, and to degrade their yield and quality (Ashraf et al., 2015; Chen et al., 2010). In China, paddy rice is one of the staple food crops for food supply (Khush, 2013; Huang, 2011). Therefore, it is of key

http://www.aloki.hu ● ISSN 1589 1623 (Print) ● ISSN 1785 0037 (Online)
DOI: http://dx.doi.org/10.15666/aeer/1705_1212712137

importance to study how to reduce the absorption and accumulation of lead in paddy rice.

In recent years, many scholars have been focusing on heavy metal contaminated soil treatment with soil conditioner, such as commonly used lime, phosphate, compost, blast furnace slag, molysite, silicate, and zeolite (Gray, 2006; Theodoratos, 2002; Qian, 2009). As a common adsorbent, zeolite can not only improve soil condition, but also purify waste water by removing of heavy metal (Merrikhpour et al., 2013; Shi et al., 2009). Zeolite has porous aluminosilicate mineral, its unique three-dimensional space frame structure makes it have a huge specific surface area, ion has a great adsorption capacity and adsorption exchange capacity, is considered as an economic and efficient heavy metal pollution remediation material, the lead in wastewater has adsorption effect. In addition, some scholars believe that the passivation of zeolite is due to the strong adsorption of heavy metal through its silicon oxygen and aluminum oxygen tetrahedron structure. Zeolite has a certain passivation effect on heavy metal lead in soil, which can effectively inhibit the migration and ecological effectiveness of soil lead (Zhou et al., 2014a). Natural zeolite, as an inorganic soil conditioner, has been widely used to improve the growth and yield of upland crops due to its high cation exchange capacity and intensive affinity for nutrients and water (Malekian et al., 2011; Aghaalikhani et al., 2012; Hazrati, 2017). On top of that, zeolite can also passivate lead in soil to inhibit lead migration and ecological availability in soil (Altaf et al., 2019). Several studies have been conducted for joint use of various soil conditioners (Zhou et al., 2014b, 2017; Wu al., 2016; Yang et al., 2016) for lead-contaminated soil. However, most of these studies are performed in pot experiments with only a few in regional experiments. At the same time, most studies focused on the influence of composite conditioners on soil contamination or improvement of wastewater through zeolite, while researches on rice yield, lead concentration and growth traits of paddy plant affected by zeolite and lead-containing water were rare. Therefore, this paper aims to analyze effects of exogenous lead on the yield of rice under soil zeolite stress, lead accumulation in rice plant, and growth traits through paddy rice planting in small regions to provide a reference for finding ways to reduce lead contamination in paddy rice.

Materials and methods

Material for experiment

This study used a local, mid-late season rice (Oryza sativa L.) cultivar, Shennong 9816, bred by the Rice Research Institute of Shenyang Agricultural University and characterized by high yield, good quality, and strong disease resistance, with brown earth soil for the base. All physicochemical indices are as follows: pH value 7.41; organic substance contents 20.48 $g \cdot kg^{-1}$; total nitrogen contents 1.3 $g \cdot kg^{-1}$, rapidly available phosphorus 20.69 $mg \cdot kg^{-1}$; rapidly available potassium 50.11 $mg \cdot kg^{-1}$. Applied regular fertilizers are as follows: potassium sulfate 100 $kg \cdot ha^{-1}$; carbamide 300 $kg \cdot ha^{-1}$; monocalcium phosphate 200 $kg \cdot ha^{-1}$. The irrigation water is from the comprehensive experiment base of College of Water Resource. As verified through inspection, the irrigation water met potable water standards, with lead concentrations $< 0.06\ \mu g \cdot L^{-1}$.

Methods

http://www.aloki.hu ● ISSN 1589 1623 (Print) ● ISSN 1785 0037 (Online)
DOI: http://dx.doi.org/10.15666/aeer/1705_1212712137

The experiment was carried out in non-weighing lysimeters at the College of Water Resource of Shenyang Agricultural University of Liaoning Province, China (42°08′57″ N, 120°30′45″ E, 47 m altitude), during one rice-growing seasons (May to October in 2018). The study area has a temperate continental monsoon climate with 7.5 °C average annual air temperature. Average annual rainfall is 672.9 mm, with the main rainy season from June to September. The regional area for experiment (3.5 m long × 1.2m wide × 0.3m deep) were constructed from concrete blocks and sealed with waterproof paint to prevent seepage between plots. In order to prevent irrigation water in the micro zone from being diluted by rain and thus affecting the test results, transparent awnings were set up, covered by rainy days, and all opened on sunny days, and the planting rate between rice plants was 20 × 25 cm. The experiment has two factors (lead and zeolite) with four levels of lead concentration and three zeolite application rates. There were nine treatment methods as shown in *Table 1*. Each treatment was repeated 3 times. Zeolite was applied all at once during soil harrowing before fertilization and transplantation of paddy plant. During the growth delaying period, all of the nine treatment the areas were irrigated with water from the experiment base, and since seedling establishment period, the areas were irrigated with water of different lead concentrations. The CK area was irrigated with clean water.

Table 1. *Factors and levels of the experiment*

Treatment	**CK**	**I**	**III**	**IV**	**V**
W_0/kg·ha^{-1}	0	2 500	2 500	2 500	2 500
Pb/mg·L^{-1}	0	0	0.15	0.2	0.25
Treatment	**CK**	**II**	**VI**	**VII**	**VIII**
W_0/kg·ha^{-1}	0	5 000	5 000	5 000	5 000
Pb/mg·L^{-1}	0	0	0.15	0.2	0.25

The sampling procedure consisted of randomly taking 5 plants for each treatment during the maturity period of the paddy rice. A soil auger was used to obtain 0.5-1 kg of soil at a depth of 0-20 cm. The roots were carefully rinsed from the soil with a hydropneumatic device and detached from their nodal bases. For the growth traits measurements, the height of the sample plants, the tiller number and the biomass of the substances above ground and below ground were all taken. The samples were then treated as follows. The soil samples were dried naturally in the shade, ground and screened with a 100 mesh screen. The plants were oven-dried, crushed with a plant pulverizer, ground into powder via a mortar, and screened with a 100 mesh screen.

Using a GB5009.12-2017 A pressure dissolution vessel was used to treat samples via the digestion method, and an atomic absorption spectrophotometer (HITACHI Z-2000) (*Fig. 1*) was used to determine the lead content via the flame method. The FOSS (*Fig. 2*) was utilized to determine rice qualities, such as water content, protein, and amylase.

Data processing

The analysis software SPSS19.0 was used for one-way ANOVA. Notable comparison of data was made by using Duncan inspecting method ($P < 0.05$). Software Design-Expert 8.0 was used to calculate the optimum point.

http://www.aloki.hu ● ISSN 1589 1623 (Print) ● ISSN 1785 0037 (Online)
DOI: http://dx.doi.org/10.15666/aeer/1705_1212712137

Figure 1. *Photo of HITACHI Z-2000*

Figure 2. *Photo of FOSS*

Results and analysis

Lead accumulation in soil and paddy plant under soil zeolite stress

Table 2 shows the lead contents of the root, stem, leaf and rice unit masses at treatment I was 1.27, 0.87, 0.96 and 0.91 times that of the CK group respectively. The Pb content per unit mass of soil increases from treatment III to treatment V, however, no obvious difference was observed. The maximum value of Pb content in soil at treatment V was 2.06 times that of treatment I ($P < 0.05$). The Pb content per unit mass of root first rose and then dropped, and difference among various treatment methods was obvious. The maximum value of Pb content in roots at treatment IV was 2.13 times that of treatment I ($P < 0.05$). The values of Pb content per unit mass of stems, leaves and rice increases, and values of treatment V were 146%, 159% and 146% ($P < 0.05$) that of treatment I, respectively. The Pb content per unit mass of roots, stems, leaves and rice under treatment II were 1.48, 0.84, 0.81 and 0.81 times that of CK group. The Pb content per unit mass of soil increased from treatment VI to treatment VIII, but the difference seemed to be non-significant. The maximum value of Pb content in soil at treatment VIII was 1.83 times that of treatment II ($P < 0.05$). The Pb content per unit mass of roots first rose and then dropped, and the difference among various treatment was significant. The maximum value of Pb content in roots at treatment VII was 1.93 times that of treatment II ($P < 0.05$). The values of Pb content per unit mass of stem, leaf and rice increased and the values of treatment VIII were 142%, 169% and 139%

http://www.aloki.hu ● ISSN 1589 1623 (Print) ● ISSN 1785 0037 (Online)
DOI: http://dx.doi.org/10.15666/aeer/1705_1212712137

that of treatment II ($P < 0.05$). With 0.15 $mg \cdot L^{-1}$ extraneous lead concentration, the Pb content per unit mass of roots under 5000 $kg \cdot ha^{-1}$ zeolite application is 18.39% higher than that of 2500 $kg \cdot ha^{-1}$ zeolite application, while the Pb content per unit mass of stem, leaf and rice was lower by 18.10%, 24% and 10.84% respectively. Treated with 0.20 $mg \cdot L^{-1}$ extraneous lead concentration, the Pb content per unit mass of roots increased by 5.01%, while the Pb content per unit mass of stem, leaf and rice declined by 14.63%, 13.27% and 11.70% respectively. Treated with 0.25 $mg \cdot L^{-1}$ extraneous lead concentration, the Pb content per unit mass of roots rose by 2.38%, while the Pb content per unit mass of stem, leaf and rice declined by 5.29%, 9.77% and 15.87%, respectively.

Table 2. *Effects of exogenous Pb on Pb contents of rice seedlings under zeolite stress ($mg \cdot kg^{-1}$)*

Treatment	Soil	Root	Stem	Leaf	Rice
CK	32.89 + 0.00c	20.42 + 0.00e	3.44 + 0.00cd	2.87 + 0.00b	0.94 + 0.00c
I	32.89 + 0.00c	26.04 + 0.00d	3.00 + 0.00e	2.76 + 0.00b	0.86 + 0.00cd
II	33.91 + 0.00c	30.30 + 0.00d	2.89 + 0.00e	2.35 + 0.00bc	0.76 + 0.00d
III	64.49 + 3.58ab	41.60 + 6.14c	2.21 + 0.03f	2.00 + 0.57cd	0.83 + 0.01cd
IV	65.47 + 0.61ab	55.71 + 0.54a	3.76 + 0.14bc	2.94 + 0.63b	0.94 + 0.00c
V	67.84 + 1.94a	46.16 + 1.18b	4.34 + 0.05a	4.40 + 0.05a	1.26 + 0.15a
VI	61.05 + 4.86b	49.25 + 4.24b	1.81 + 0.72f	1.52 + 0.05d	0.74 + 0.01d
VII	61.59 + 4.78b	58.50 + 0.67a	3.21 + 0.11de	2.55 + 0.03bc	0.83 + 0.01cd
VIII	62.11 + 4.11b	47.26 + 1.41b	4.11 + 0.14ab	3.97 + 0.54a	1.06 + 0.13b

Different lowercase indicates significant differences ($P < 0.05$) among treatments

Effects of exogenous Pb on biomass of rice seedlings

The biomass of rice at maturation period is given in *Table 3*. *Table 3* shows the biomass of root, shoot and whole plant in treatment I was higher than that of the CK group by 45.08%, 8.58% and 11.48% respectively. The biomass of root, shoot and whole plant in treatment III was 0.71, 1.16 and 1.10 times that of treatment I. According to the coefficients, the biomass of each part of the plants first rose and then dropped with the increase of exogenous Pb concentration. The biomass of root in treatment IV was 8.65% less than that of treatment I, while the biomass of shoot and whole plant in treatment IV was more than that of treatment I by 4.22% and 4.08%, but all values were still higher than CK group. The difference between treatment IV and treatment V was significant. In addition, the height of rice was positively correlated with the dry weight of the whole plant with a correlation coefficient of 0.359 ($P < 0.05$).

The biomass of root, shoot and whole plant in treatment II was higher than that of the CK group by 63.04%, 2.47% and 14.01% respectively. The biomass of root, shoot and whole plant in treatment VI was 0.93, 1.27 and 1.17 times that of treatment II. According to the coefficients, the biomass of each parts of the plant first rose and then dropped with the increase of exogenous Pb concentration. The biomass of root and whole plant in treatment VII was less than that of treatment II by 34.85% and 5.34% respectively, while the biomass of shoot in under treatment VII was 5.59% more than that of treatment II, but the values were still higher than that of the CK group. There was an obvious difference between treatment VII and VIII. There was positive correlation between the tiller number and dry weight of whole plant with the correlation coefficient at 0.491 ($P < 0.05$). At an extraneous lead concentration of 0.15 $kg \cdot L^{-1}$, the

http://www.aloki.hu ● ISSN 1589 1623 (Print) ● ISSN 1785 0037 (Online)
DOI: http://dx.doi.org/10.15666/aeer/1705_1212712137

dry weight of whole plant applied by 5000 kg·ha^{-1} zeolite was higher than that of 2500 kg·ha^{-1} zeolite by 9.07%, 0.20 mg·L^{-1} by 1.83%, 0.25 mg·L^{-1} by 1.92%.

Table 3. *Effects of the exogenous Pb on the growth of rice under zeolite stress*

Treatment	Biomass (dry weight)/g·treatment^{-1}			Plant height/cm	Tiller number	Coefficient
	Root	Shoot	Whole plant			
CK	24.69 ± 5.06cd	141.24 ± 16.72c	165.93 ± 16.36c	101.00 ± 2.65ab	15.33 ± 4.51ab	—
I	35.82 ± 13.73abc	153.36 ± 7.69abc	184.98 ± 3.57abc	93.33 ± 4.16c	11.00 ± 0.00b	1.11
II	40.25 ± 7.65d	144.73 ± 6.56bc	189.18 ± 16.68abc	101.00 ± 3.00ab	18.67 ± 5.77a	1.14
III	25.30 ± 0.71bcd	177.41 ± 6.69ab	202.7 ± 6.03abc	105.000 ± 1.73a	11.00 ± 3.61b	1.22
IV	32.72 ± 2.54abc	159.84 ± 10.27abc	192.53 ± 8.19abc	105.00 ± 4.36a	14.00 ± 1.73ab	1.16
V	29.04 ± 8.43d	151.89 ± 9.37d	180.93 ± 16.50e	93.33 ± 1.53c	12.00 ± 0.00b	1.09
VI	37.63 ± 4.97cd	183.45 ± 8.50a	221.08 ± 13.21a	102.33 ± 3.79a	13.00 ± 1.00ab	1.33
VII	36.22 ± 5.26d	159.82 ± 7.67abc	196.05 ± 11.25bc	104.33 ± 3.79a	14.00 ± 2.00ab	1.18
VIII	29.13 ± 8.03abcd	155.27 ± 9.93d	184.40 ± 4.87d	96.67 ± 2.31bc	13.67 ± 0.58ab	1.11

The coefficient = total biological yield in all treatments/total biological yield in CK group

Zeolite was applied to paddy soil irrigated with lead wastewater. The effects of different zeolite application rates on rice yield are shown in *Table 4*. *Table 4* shows when the application amount of zeolite was 2500 kg·ha^{-1}, the 0 kg·ha^{-1} group without zeolite was used as the control group. The irrigation with different concentrations of lead water increased the yield of clean water by 5.9%, while the other treatments decreased by 3.77%, 8.7% and 17.6%, respectively. When the amount of zeolite was 5000 kg·ha^{-1}, the rice yield showed an upward trend compared with that of 0 kg·ha^{-1}. The rice yield was 8.84%, 11.20%, 16.84% and 8.50% higher than that of the control group under different concentrations of lead-containing water irrigation, and the difference reached a significant level ($p < 0.05$).

Table 4. *Effects of different lead concentrations of irrigation water and different amount of zeolite application on rice yield (g·area^{-1})*

Concentration of irrigation water/mg·L^{-1}	Application amount of zeolite/kg·ha^{-1}		
	0	2500	5000
CK	2058.84 + 105.09ab	2180.88 + 50.64a	2240.88 + 50.64d
0.25	2010.48 + 121.08ab	1655.08 + 44.62a	2235.56 + 50.99b
0.2	2396.04 + 339.83a	2187.84 + 24.9a	2799.68 + 59.51a
0.15	2273.48 + 12.143b	2113.16 + 53.15b	2467.92 + 48.52c

The coefficient = total biological yield in all treatments/total biological yield in CK group

When the concentration of lead water was 0.15, the production of 0 kg·ha^{-1} increased by 10.43%, that of 2500 kg·ha^{-1} increased by 0.1%, and that of 5000 kg·ha^{-1} increased by 10.13% with the addition of different zeolite. When the lead concentration was 0.2 mg·L^{-1}, the 0 kg·ha^{-1} yield increased by 16.38% with different zeolite addition. The yield of 5000 kg·ha^{-1} increased by 24.94% and 14.08% respectively. When the concentration of lead water is 0.25 mg·L^{-1}, the 0 kg·ha^{-1} yield decreases by 2.35% with different zeolite addition. The yield of 5000 kg·ha^{-1} decreased by 0.24% and 24.11% respectively.

http://www.aloki.hu ● ISSN 1589 1623 (Print) ● ISSN 1785 0037 (Online)
DOI: http://dx.doi.org/10.15666/aeer/1705_1212712137

The results showed that when the amount of zeolite in soil was 2500 $kg \cdot ha^{-1}$, it had an inhibitory effect on rice yield, while when the amount of zeolite was increased to 5000 $kg \cdot ha^{-1}$, it had an promoting effect on rice yield, and in irrigation water with different lead concentrations, the effect of zeolite on rice yield was different, and it played an promoting role in CK.

Effects of different treatment on nutritional quality of rice

The water content in rice irrigated by lead water fluctuated under soil zeolite stress. *Table 5* shows the water contents of rice at treatment I were higher than that of the CK group. The water contents of rice from treatment III to treatment V were obviously higher than that of treatment I, which indicated that the effect of exogenous Pb on water content were not significant under soil zeolite stress. In this experiment, the protein content in rice irrigated by lead water fluctuated under soil zeolite stress. When irrigated with water of the same lead concentration, the protein content of rice treated with treatment VI-VIII was lower than that of treatment III-V, but higher than the CK group irrigated by clean water. It indicated that exogenous Pb under soil zeolite stress had negative effects on the protein content in rice at different extents. The amylase content in rice fluctuated in a non-significant range. The rice under treatment VIII had the lowest amylon content at 15.6%, which was lower than the CK group by 6.02%. Therefore, the effect seemed significant ($P < 0.05$). The water and amylase contents of rice in different treatment satisfied the green rice standard (water content $\leq$ 15.5%, amylase content = 13.0% $\sim$ 20.0%).

Table 6 shows the regression equation is based on effect of interaction of zeolite and lead on protein content in rice. It is shown that the effect of interaction of zeolite and lead on protein content in rice is significant, especially the effect of A^2B and AB^2 on the results is quite influential based on the F values, which represents the concentration of zeolite and lead. The effect of lead concentration on protein content is stronger than zeolite amount.

The taste of rice mainly depends on amylase, protein water contents as well as fatty acid value. The taste is in inversely proportional to the amylase and protein contents but proportional to water content. Calculated using software Design-Expert 8.0, the optimum combination is as follows: zeolite 5000 $kg \cdot ha^{-1}$, lead concentration in water 0.19 $mg \cdot L^{-1}$. Under such optimum condition, the predicted protein content is 6.96%, water content is 11.07% and amylase content is 16.29%, which all meet the green rice standard.

Table 5. *The notability analysis after different treatments*

Treatment	Water content	Protein content	Amylase content
CK	10.43b	7.33b	16.56b
I	10.47b	8.23a	16.67b
II	11.07a	7.33b	16.63b
III	11.07ab	6.97bc	16.73b
IV	10.26b	6.23d	16.4b
V	10.6b	7.1bc	15.9a
VI	11.07a	7.2bc	16.57b
VII	11.07ab	6.77c	16.67b
VIII	10.8ab	6.1bc	15.6a

http://www.aloki.hu ● ISSN 1589 1623 (Print) ● ISSN 1785 0037 (Online)
DOI: http://dx.doi.org/10.15666/aeer/1705_1212712137

Table 6. *Significance test with coefficient of regression equation*

Source	Quadratic sum	Degree of freedom	Mean square	F value	P value
Model	6.64	8.00	0.83	19.48	0.0165
A-zeolite	0.00	1.00	0.00	0.06	0.8224
B-lead concentration	0.01	1.00	0.01	0.24	0.6549
AB	0.73	1.00	0.73	17.06	0.0258
A^2	0.00	1.00	0.00	0.02	0.9060
B^2	0.02	1.00	0.02	0.47	0.5435
A^2B	1.15	1.00	1.15	27.05	0.0138
AB^2	0.89	1.00	0.89	20.90	0.0196
A^3	0.00	0.00			
B^3	0.06	1.00	0.06	1.48	0.3101

Discussion

Over the recent years, several heavy metal pollution accidents have occurred, threatening lives and health. Much research on heavy metal pollution has been carried out, with some progress achieved. It has been discovered that biochar itself has a high pH value, thus the addition of 5% biochar in soil can enhance its pH value. With the addition of biochar, the effectiveness of Pb and Cd can be reduced, and the state conversion of Pb and Cd can thus be stabilized. The addition of biochar can also improve the physical and chemical properties of soil affected by combined pollution. Moreover, it can effectively adsorb heavy metal ions, therefore promoting the adsorption of Pb and Cd in soil and reducing the biological effectiveness of Pb and Cd (Gao et al., 2016). Under certain conditions, heavy metals in the adsorption and precipitation states were able to be exchanged between soil solutions, thus reducing the pH value and promoting the release of heavy metals in the adsorption state into the soil. In such cases, the absorption of heavy metals by plants will increase. In the current study, the application of zeolite in paddy plant soil irrigated with water of different lead concentrations was demonstrated to inhibit the migration of Pb to paddy plants, thus improving the quality of paddy plants. The effect of the zeolite application in soil on pH values is worth further research.

Several studies have reported that zeolite mixed with urea increased rice grain yields in flooded paddy fields (Kavoosi, 2007; Gevrek et al., 2009; Sepaskhah and Barzegar, 2010), the results are consistent with the experimental results. However, Research on the effect of lead on the growth of toona ciliata indicated that the total biomass of the whole toona ciliata plant decreases significantly with the increase of the Pb stress gradient, while the biomass of the plant organs (withered leaves, leafstalk) increased with the increase of the Pb stress gradient. This differs from the results of the effects on paddy rice biomass in this study. The soil condition was also an important factor found to affect the growth of toona ciliata and Pb absorption and accumulation. With the same Pb stress gradient, alkaline purple calcium soil had an impact on the Pb effectiveness, and was able to reduce the toxic effect of Pb on toona ciliate (Hu et al., 2012). The study demonstrated that when exogenous Pb entered the soil, the original forms of Pb in the soil clearly changed, revealing that exogenous Pb is maintained in a dynamic conversion process. The application of soil conditioner reduced the content of Pb in an effective state and inhibited the migration of Pb in the soil-plant system. It benefited safe production of plants (Chen et al., 2008). The study of Zhao et al. (2012) suggested that a single treatment with low concentrations of Cd and Pb can promote the growth of

http://www.aloki.hu ● ISSN 1589 1623 (Print) ● ISSN 1785 0037 (Online)
DOI: http://dx.doi.org/10.15666/aeer/1705_1212712137

pilea cadierei, but inhibit its growth when the concentration exceeds a certain level. Under a combined treatment with various concentrations, the inhibiting effect on the growth of pilea cadierei was strengthened with the increase of metal concentrations. The Cd and Pb absorbing capacities of the leaf, stalk and root of pilea cadierei demonstrated strong significant positive correlations, with the accumulation in the root being the most influential. Under a combined treatment, the heavy metal accumulation in each part of the plant rose. Total migration of Cd and Pb in the above ground part of pilea cadierei was large. In particular, under Cd-Pb combined treatment, the total migration of Pb in the above ground part was much more than that under a single treatment with the same concentration of Pb. Therefore when the soil is polluted by heavy metals, ornamental plants can be planted to absorb the heavy metal, thus promoting ecological restoration.

Conclusions

(1) *Table 2* shows that most of the lead remains in soil and rice roots, and only a small amount migrates to aboveground plants. The unit content of lead in each part of the paddy plant was affected on different levels. The application of zeolite can reduce above ground plant absorption of Pb, inhibit the migration of Pb into rice and optimize the quality of rice. The effect of zeolite application in soil on pH value is worth further studying.

(2) *Tables 3* and *4* show that shows that for lead water irrigation under soil zeolite stress, the paddy rice plant height, and the above, below ground dry weight and yield all increased significantly. The effect of zeolite was influenced by Pb concentration in the irrigation water. Higher Pb concentrations resulted in a higher inhibition effect.

(3) *Table 5* shows that the water content in rice increased and the protein content decreased with the increase of zeolite addition. Thus, the application of zeolite has a negative effect on protein content. The starch content decreased with the increase of zeolite addition. Under different treatments, both water content and amylose content in the rice satisfy the green rice standard (water content $\leq$ 15.5%; amylose content 13.0-20.0%).

REFERENCES

[1] Abrahams, P. W. (2002): Soils: their implications to human health. – Science of the Total Environment 29(1/2/3): 1-32.

[2] Aghaalikhani, M., Gholamhoseini, M., Dolatabadian, A., Khodaei-Joghan, A., Sadat Asilan, K. (2012): Zeolite influences on nitrate leaching, nitrogen-use efficiency, yield and yield components of canola in sandy soil. – Arch. Archives of Agronomy and Soil Science 58: 1149-1169.

[3] Altaf, H. L., Zhang, Z., Sabry, M., Shaheen, J. R., Guo, Z., Li, R., Amanullah, M., Wang, Z., Ren, C., Mi, S., Liu, T., Jing, R. (2019): Mono-and co-applications of Ca-bentonite with zeolite, Ca-hydroxide, and tobacco biochar affect phytoavailability and uptake of copper and lead in a gold mine-polluted soil. – Journal of Hazardous Materials 374.

[4] Ashraf, U., Kanu, A. S., Mo, Z. W., Hussain, S., Anjum, S. A., Khan, I., Abbas, R. N., Tang, X. (2015): Lead toxicity in rice; effects, mechanisms and mitigation strategies-a mini review. – Environmental Science and Pollution Research 22: 18318-18332.

[5] Becerra, C., Lopes, A., Vaz, I., Silva, E., Manaia, C., Nunes, O. (2015): Wastewater reuse in irrigation: a microbiological perspective on implications in soil fertility and human and environmental health. – Environment International 75: 117-135.

http://www.aloki.hu ● ISSN 1589 1623 (Print) ● ISSN 1785 0037 (Online)
DOI: http://dx.doi.org/10.15666/aeer/1705_1212712137

[6] Chen, D., Zhou, Y., Zhang, J., et al. (2018): Human health risk assessment owing to Pb and Zn of farmland soils in Shifang City, Southwest China. – Journal of Agro-Environment Science 37(12): 2687-2693.
[7] Chen, H., Zheng, W., Tang, W. (2008): The effectiveness of amendment on Pb form and bioavailability in Pb contaminated soil. – Journal of Agro. Environment Science 27(1): 0170-0173.
[8] Chen, X., Niu, J., Cui, Y. (2010): Bioaccessibility of lead in urban topsoil and its health risk assessment: a case study of a small area near Shougang group. – Environmental Science 3(12): 3028-3035.
[9] Galvis, A., Jaramillo, M. F., van der Steen, P., Gijzen, H. J. (2018): Financial aspects of reclaimed wastewater irrigation in three sugarcane production areas in the Upper Cauca river Basin, Colombia. – Agricultural Water Management 209: 102-110.
[10] Gao, R., Zhu, J., Tang, F., Hu, H., Fu, Q., Wan, T. (2016): Fractions transformation of Cd, Pb in contaminated soil after short-term application of rice straw biochar. – Acta Scientiae Circumstantiae 01: 251-256.
[11] Gevrek, M. N., Tatar, Ö., Yagmur, B., Özaydin, S. (2009): The effects of clinoptilolite application on growth and nutrient ions content in rice grain. – Turkish Journal of Field Crops 14: 79-88.
[12] Gray, C. W., Dunham, S. J., Dennis, P. G., et al. (2006): Field evaluation of in situ remediation of a heavy metal contaminated soil using lime and red-mud. – Environmental Pollution 142(3): 530-539.
[13] Hazrati, S., Tahmasebi-Sarvestani, Z., Mokhtassi-Bidgoli, A., Modarres-Sanavy, S. A. M., Mohammadi, H., Nicola, S. (2017): Effects of zeolite and water stress on growth, yield and chemical compositions of Aloe vera L. – Agric-Water Manage 181: 66-72.
[14] Hu, F., Zhang, J., Yang, W., Wu, F., Liu, Y., Liu, Yan, B., Huang, X. (2012): Effects of Pb stress on the growth, development and Pb enrichment properties of Toona ciliata Roem saplings. – Journal of Agro-Environment Science 02: 284-291.
[15] Huang, J., Hsu, S., Wang, S. (2011): Effects of rice straw ash amendment on Cu solubility and distribution in flooded rice paddy soil. – Journal of Hazardous Materials 186: 1801-1807.
[16] Kavoosi, M. (2007): Effects of zeolite application on rice yield, nitrogen recovery, and nitrogen use efficiency. – Communications in Soil Science and Plant Analysis 38: 69-76.
[17] Khush, G. S. (2013): Strategies for increasing the yield potential of cereals: case of rice as an example. – Plant Breed 132: 433-436.
[18] Luo, X., Yu, S., Li, X. (2012): The mobility, bioavailability and human bioaccessibility of trace metals in urban soils of Hong Kong. – Applied Geochemistry 27(5): 995-1004.
[19] Malekian, R., Abedi-Koupai, J., Eslamian, S. (2011): Influences of clinoptilolite and surfactant-modified clinoptilolite zeolite on nitrate leaching and plant growth. – Journal of Hazardous Materials 185: 970-976.
[20] Merrikhpour, H., Jalali, M. (2013): Comparative and competitive adsorption of cadmium, copper, nickel, and lead ions by Iranian natural zeolite. – Clean Technologies and Environmental Policy 15(2): 303-316.
[21] Qian, G., Chen, W., Lim, T., et al. (2009): In-situ stabilization of Pb, Zn, Cu, Cd and Ni in the multi-contaminated sediments with ferrihyrite and apatite composite additives. – Journal of Hazardous Materials 170(2/3): 1093-1100.
[22] Sepaskhah, A. R., Barzegar, M. (2010): Yield, water and nitrogen-use response of rice to zeolite and nitrogen fertilization in a semi-arid environment. – Agricultural Water Management 98: 38-44.
[23] Shi, W., Shao, H., Li, H., Shao, M., Du, S., et al. (2009): Progress in the remediation of hazardous heavy metal-polluted soils by natural zeolite. – Journal of Hazardous Materials 170(1): 1-6.

http://www.aloki.hu ● ISSN 1589 1623 (Print) ● ISSN 1785 0037 (Online)
DOI: http://dx.doi.org/10.15666/aeer/1705_1212712137

[24] Theodoratos, P., Papassiopi, N., Xenidis, A. (2002): Evaluation of monobasic culcium phosphate for the immobilization of heavy metals in contaminated soils from Lavrion. – Journal of Hazardous Materials 94(2): 135-146.
[25] Wu, Y., Zhou, H., Yang, W., Zou, Z., Zhu, W., Gu, J., Peng, P., Zhang, P., Zeng, M., Liao, B. (2016): Comparison of the persistence of a combined amendment stabilizing Pb, Cd, Cu and Zn in polluted paddy soil. – Environmental Science 37(7).
[26] Yang, W., Zhou, H., Deng, G., et al. (2016): Effects of combined amendment on bioavailability of Pb, Cd, and As in polluted paddy soil. – Acta Scientiae Circumstantiae 36(1): 257-263.
[27] Zhang, L., Mo, Z., Qin, J., et al. (2014): Contamination of heavy metals in soils and health risk assessment in children in a downstream village of Dachang mining area in Guangxi. – Journal of Environmental and Health 31(6): 512-516.
[28] Zhao, F., Ma, Y., Zhu, Y., Tang, Z., McGrath, S. P. (2015): Soil contamination in China: current status and mitigation strategies. – Environmental Science & Technology 49: 750-759.
[29] Zhao, Y., Pan, Y., Liu, B., Yang, H., Hou, Y., Zhang, J., Cai, L. (2012): Pilea cadierei Gagnep. et Guill's growth and accumulation under single and combined pollution of Cd and Pb. – Journal of Agro-Environment Science 31(1): 48-53.
[30] Zhou, H., Zhou, X., Zeng, M., Liao, B., Liu, B., Yang, W., Wu, Y., Qiu, Q., Wang, Y. (2014a): Effects of combined amendments on heavy metal accumulation in rice (Oryza sativa L.) planted on contaminated paddy soil. – Ecotoxicology and Environmental Safety 101: 226-232.
[31] Zhou, H., Zhou, X., Zeng, M., Liu, L., Yang, W., Wang, Y., Liao, B. (2014b): Effects of two combined amendments on heavy metal bioaccumulation in paddy soil. – China Environmental Science 34(2): 437444.
[32] Zhou, R., Liu, X., Luo, L., Zhou, Y., Wei, J., Chen, A., Tang, L., Wu, H., Deng, Y., Zhang, F., Wang, Y. (2017): Remediation of Cu, Pb, Zn and Cd-contaminated agricultural soil using a combined red mud and compost amendment. – International Biodeterioration & Biodegradation 118: 73-81.

http://www.aloki.hu ● ISSN 1589 1623 (Print) ● ISSN 1785 0037 (Online)
DOI: http://dx.doi.org/10.15666/aeer/1705_1212712137

NITROGEN-DOPED CARBON QUANTUM DOTS WITH *PINELLIA TERNATA* AS CARBON SOURCE FOR HIGH SENSITIVE DETERMINATION OF CHROMIUM (VI)

DAI, J.[1] – WANG, Y. J[2*]

[1]*College of Biological and Pharmaceutical Engineering, West Anhui University, Luan 237012, Anhui, China*

[2]*College of Materials and Chemical Engineering, West Anhui University, Luan 237012, Anhui, China*

**Corresponding author*
e-mail: 3070714927@qq.com

(Received 29th Apr 2019; accepted 16th Jul 2019)

Abstract. A novel nitrogen-doped fluorescent carbon dots was successfully prepared via a simple one-step hydrothermal method using the medicinal plant *Pinellia ternata* as an environment-friendly carbon-containing precursor for the first time and ethylenediamine as nitrogen source. The diameter, morphology, ultimate composition and optical performance of the prepared *Pinellia ternata* nitrogen-doped carbon quantum dots (N-CQDs) were characterized by a series of analytical characterization techniques. The photostability was also investigated through the conditions of ionic strength, pH, and storage time. The obtained results showed that the particle size distribution of *Pinellia ternata*-based N-CQDs was uniform with the fluorescence quantum yield as high as 21.3%, and it also exhibited good excitation dependence and excellent light stability. Based on the fluorescence quenching mechanism of fluorescent inner filter effect, it has high sensitivity, selectivity and anti-interference ability for chromium (VI). Under optimal working conditions, the nanoprobe showed a good and sensitive linear response (R^2 = 0.9955) toward chromium (VI) within the concentration range of 0~200 μM with a low detection limit of 15 nM. This method has been successfully applied to the detection of chromium (VI) in environmental water samples, providing a new idea for the development of green natural compound carbon materials.

Keywords: *N-CQDs, fluorescence quecnching mechanism, fluorescent nanoprobe, Cr(VI), environmental samples*

Introduction

Chromium is a steel-gray metal. There is no free state chromium in nature. Chromium (II) is a strong reductant, which is extremely unstable and can be rapidly oxidized to chromium (III) (Abdolmohammad-Zadeh and Sadeghi, 2012; Barrera-Díaz et al., 2012). Therefore, it mainly exists in two forms: chromium (III) and chromium (VI). In addition, as one of the most important micronutrient elements in human body, chromium is an important blood sugar regulator and also one of the components of proteolytic enzymes (Bauer et al., 2013; Broadhurst et al., 2006; Sedman et al., 2006). It plays an important role in the metabolism of glucose and lipid and protein synthesis. The toxicity of chromium was related to its valence (Cosata and Klein, 2006; Gagneten and Imhof, 2009). As a component of glucose tolerance factor, activator of some metabolic enzymes and stabilizer of nucleic acid (Ahmad et al., 2011; Costa, 1997; Kim et al., 2015), chromium (III) could promote insulin to play a role, maintain normal glucose metabolism, promote the production of cholesterol and fatty acids and promote hematopoietic function (Vallejos et al., 2012). Chromium (III) deficiency in human

http://www.aloki.hu ● ISSN 1589 1623 (Print) ● ISSN 1785 0037 (Online)
DOI: http://dx.doi.org/10.15666/aeer/1705_1213912153

body could cause diabetes, coronary atherosclerosis and cardiovascular diseases. The toxicity of chromium (VI) was about 100 times higher than that of chromium (III) (Wang et al., 2017). It was also one of the most susceptible metals to allergy. It was second only to nickel, and more easily absorbed and accumulated by human body, causing a series of pathological changes, such as chromium rhinopathy, and even inducing cancer (Ma et al., 2018; Kong et al., 2017; Yuhua et al., 2018). The International Agency for Research on Cancer (IARC) had rated chromium (VI) as a class I carcinogen (Ohira et al., 2015). Therefore, the monitoring of chromium (VI) had attracted the attention of environmental health workers.

Fluorescent carbon quantum dots (CQDs) had been widely used in various research fields due to their advantages of simple preparation, good chemical stability, easy functionalization, good biocompatibility, low toxicity and special optical properties (Wang and Zhou, 2014; Zhang et al., 2014; Zheng et al., 2015; Carrasco et al., 2016). In recent years, many carbon materials had been used to prepare fluorescent carbon quantum dots (Baker and Baker, 2010; Li et al., 2018; Huang et al., 2015). The synthesis of nitrogen-doped carbon quantum dots with excellent optical properties using green natural carbohydrates as precursors had become one of the most popular research topics (Gong et al., 2017; Wang et al., 2018; Gao et al, 2018).

Pinellia ternata is a kind of nourishing medicinal plant. Its raw materials were cheap and easy to obtain. It could be produced on a large scale. Its main bioactive substances included coumarin, alkaloids, amino acids and polysaccharides. *Pinellia ternata* was rich in carbon, nitrogen and oxygen elements. It was one of the ideal carbon materials for preparing carbon quantum dots (Teixeira da Silva et al., 2017; Ng et al., 2012; Zheng et al., 2015).

In this paper, *Pinellia ternata*-based nitrogen-doped fluorescent carbon quantum dots (*Pinellia ternata* N-CQDs) with blue fluorescence were prepared by a simple hydrothermal method using *Pinellia ternata* as precursor and ethylenediamine. The fluorescence quantum yield of *Pinellia ternata*-based N-CQDs was about 21.3%, which had excellent excitation wavelength dependence and optical stability. Based on the fluorescence quenching mechanism (Gunnlaugsson et al., 2005; Alizadeh et al., 2016; Algar and Krull, 2008; Zhang et al., 2017; Wang et al., 2010), a novel fluorescent probe had been developed for the sensitivity and selectivity detection of chromium (VI). This method could be successfully applied to the rapid detection of environmental water and soil samples, as well as subsequent research.

Experiment

Materials and apparatus

Pinellia ternata was purchased from local flower market (Anhui, China); ethylenediamine (EDA) was purchased from Shanghai Aladdin Biochemical Technology Co., Ltd. (Shanghai, China); citric acid, sodium hydrogen phosphate (Na_2HPO_4) and sodium hydroxide (NaOH) were purchased from Tianjin Zhiyuan Chemical Reagent Co., Ltd. (Tianjin, China). Metal salts mainly include $AlCl_3$, $K_2Cr_2O_7$, $MgCl_2$, $ZnCl_2$, $CuCl_2$, $CdCl_2$, $PbCl_2$, $CrCl_3$, $CoCl_2$, $SnCl_2$, $FeCl_3$ and $FeCl_2$. All solutions were prepared from ultrapure water (18.2 MΩ.cm, 25 °C) of Milli-Q system.

G9800A fluorescence spectrophotometer (Agilent Technologies, USA) was used to determine fluorescence spectrum and its intensity; UV-2600 UV-Visible

http://www.aloki.hu ● ISSN 1589 1623 (Print) ● ISSN 1785 0037 (Online)
DOI: http://dx.doi.org/10.15666/aeer/1705_1213912153

spectrophotometer (Shimadzu, Japan) was used to determine the UV-Visible spectrum; Tecnai G2 F30s-Twin high resolution field emission transmission electron microscopy (FEI, Netherlands) was used to detect particle size and morphology characteristics of nitrogen doped fluorescent quantum dots; TENSOR 27 Fourier transform infrared spectrometer (FT-IR, Bruker, Germany) was used to determine the infrared spectrum and the structure of materials; D8-advance X-ray powder diffractometer (XRD, Bruker, Germany) was used to determine the crystal morphology; Thermo Scientific k-alpha X-ray photoelectron spectrometer (Thermo Fisher Scientific Inc. U.S.A.) was used to analyze the proportion of its elements and chemical oxidation state; Z-2000 atomic absorption spectrometer (Hitachi, Japan) was used for the determination of metal ionization; XH-B vortex instrument (Shanghai Hannuo Instrument Co., Ltd., China) was used for vortex blending; 80-2 high-speed centrifuge (Shanghai Surgical Instrument Factory, China) was used for centrifugal filtration; TOP wave microwave digestion device was equipped with PM 60 microwave digestion tank (Jena, Germany) for soil sample digestion; and BPZ-6003 vacuum drying chamber (Shanghai Yiheng Scientific Instrument Co., Ltd., China) was used for vacuum drying.

Preparation of Pinellia ternata-based N-CQDs

Pinellia ternata-based N-CQDs were prepared by hydrothermal method according to the reported method. The stems of *Pinellia ternata* were dried naturally at room temperature and ground into fine powder. The powder prepared by weighing 2.0 g was evenly dispersed in 90 mL of hot water at 60 °C. Ethanol (10 mL) and EDA (1 mL) were added to mixture evenly at constant temperature. The powder was transferred to a PTFE lined autoclave (200 mL) and heated at 180 °C for 9 h. After cooling down to room temperature naturally, the bright yellow aqueous solution was centrifuged at 10000 rpm for 15 min to remove large particles of sediment. The sediment was purified by 0.22 μm membrane filtration. The N-CQDs was stored in a refrigerator at 4 °C and diluted with deionized water to the required concentration. The synthetic reaction diagram of *Pinellia ternata* N-CQDs is shown in *Figure 1*.

Figure 1. *The reaction scheme of the synthesis of the Pinellia ternata-based N-CQDs*

Fluorescence quenching test of chromium (VI)

In 10.0 mL glass centrifuge tube, 30 mL water-soluble *Pinellia ternata*-based N-CQDs solution, 2 mL pH 7.0 citric acid-disodium hydrogen phosphate buffer solution and different concentration of Cr^{6+} were added in turn, and then diluted to 4.0 mL with deionized water. At room temperature, the full eddy mixing reaction lasts for 10 min. The slit width of excitation and emission on the fluorophotometer is 5 nm, the excitation wavelength is lambda ex = 356 nm, and the emission wavelength is lambda em = 444 nm. In order to evaluate the influence of coexisting ions on the fluorescence

http://www.aloki.hu ● ISSN 1589 1623 (Print) ● ISSN 1785 0037 (Online)
DOI: http://dx.doi.org/10.15666/aeer/1705_1213912153

intensity of N-CQDs and to evaluate the selectivity of Cr^{6+}, other metal ions (including Zn^{2+}, Cu^{2+}, Al^{3+}, Mg^{2+}, Cd^{2+}, Pb^{2+}, Cr^{3+}, Sn^{2+}, Co^{2+}, Hg^{2+}, Fe^{3+} and Fe^{2+}) were detected under the same procedure.

Pretreatment of environmental water and soil samples

In this study, three different water samples (tap water, lake water and waste water) were selected for analysis and detection. All water samples were filtered by simple centrifugal filtration to remove solid particles and suspended solids, then filtered by 0.22 μm membrane, and stored in a 4 °C refrigerator for storage. In this study, three different soil samples (parking lot, highway) were selected for analysis and detection. Soil samples of 1.0 g were weighed and added with 1 mL nitric acid and 3 mL hydrochloric acid. They were placed in a microwave digestion tank of polytetrafluoroethylene (PTFE). Microwave digestion was carried out at 140 °C for 15 min, then cooled to room temperature. The digestion was diluted to 50 mL and stored in a refrigerator at 4 °C.

Results and discussion

Characterization of Pinellia ternata-based N-CQDs

In order to further study the nanostructure characteristics of *Pinellia ternata*-based N-CQDs, the morphology and particle size of *Pinellia ternata*-based N-CQDs were characterized by transmission electron microscopy (TEM). As shown in *Figure 2,* the *Pinellia ternata*-based N-CQDs were uniformly dispersed without agglomeration and were spherical carbon nanoparticles. In addition, the particle size distribution of biomass-based N-CQDs is narrow, mainly between 5 and 6 nm, and the average particle size is about 5.2 nm.

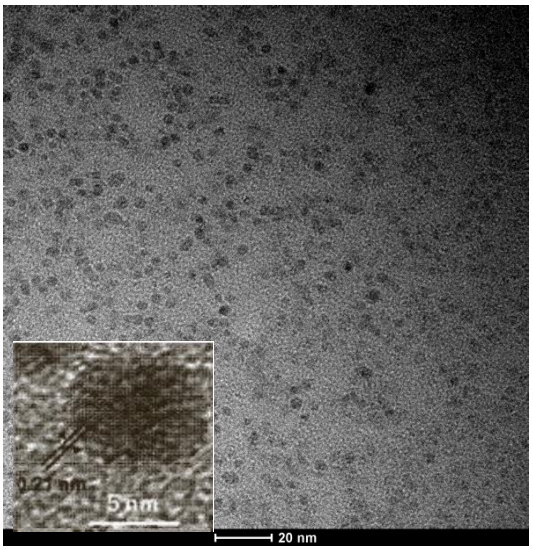

Figure 2. *The TEM image of the synthesized N-CQDs*

The composition and surface chemical structure of *Pinellia ternata*-based N-CQDs were determined by Fourier transform infrared spectroscopy (FT-IR) and X-ray electron

http://www.aloki.hu ● ISSN 1589 1623 (Print) ● ISSN 1785 0037 (Online)
DOI: http://dx.doi.org/10.15666/aeer/1705_1213912153

spectroscopy (XPS). *Figure 3* is the infrared spectra of N-CQDs. The broad and strong absorption peaks at 3442 cm^{-1} are attributed to the stretching vibration absorption peaks of O-H and N-H; the peak at 1637 cm^{-1} is attributed to the stretching vibration absorption peak of O = C-NH; the absorption peaks at 1467 cm^{-1} are attributed to the stretching vibration peak of COOH; and the absorption peaks at 1119 cm^{-1} and 1078 cm^{-1} are attributed to the C-N bend. Bending vibration peak and C-O stretching vibration peak. The results show that the *Pinellia ternata* N-CQDs have abundant hydrophilic functional groups, such as hydroxyl, carboxyl and carbonyl groups, which have good water solubility and broad application prospects.

The elements of *Pinellia ternata*-based N-CQDs were characterized by XPS, as shown in *Figure 4*. XPS elemental analysis is consistent with FT-IR results, which proves that the functional groups containing oxygen and nitrogen, such as hydroxyl, carboxyl, amino groups, etc.

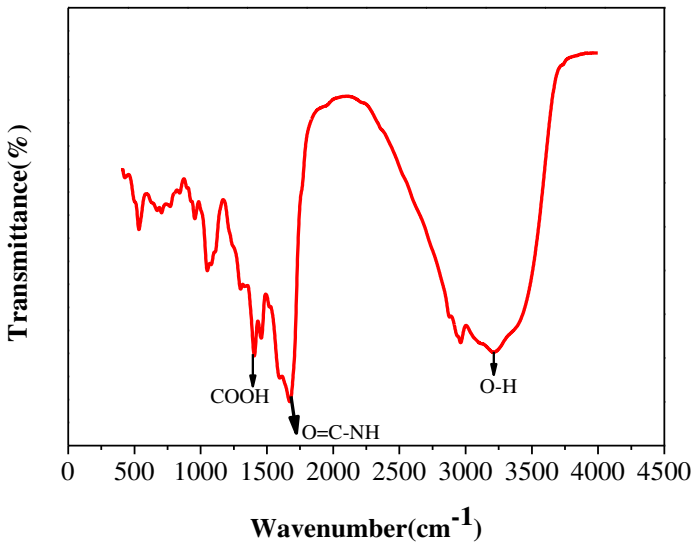

Figure 3. *The FT-IR spectrum of the Pinellia ternata-based N-CQDs*

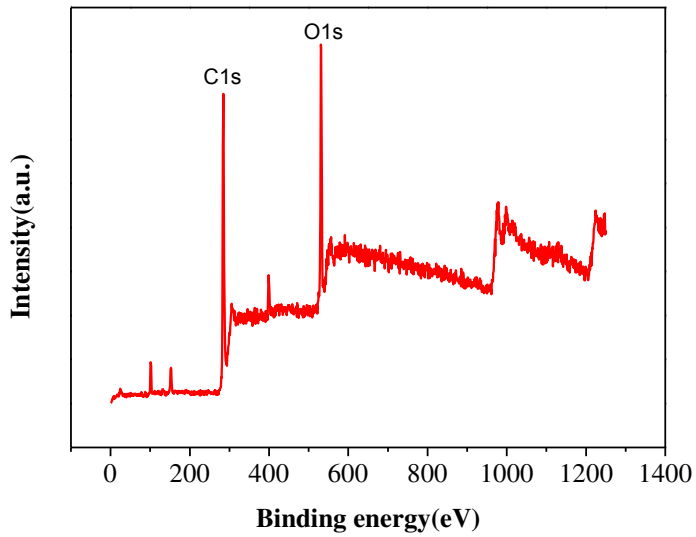

Figure 4. *The XPS spectra of the synthesized N-CQDs*

http://www.aloki.hu ● ISSN 1589 1623 (Print) ● ISSN 1785 0037 (Online)
DOI: http://dx.doi.org/10.15666/aeer/1705_1213912153

Optical properties of Pinellia ternata-based N-CQDs

The optical properties of *Pinellia ternata*-based N-CQDs were characterized by UV-Vis absorption spectra and fluorescence emission spectra. In addition, the illustrations in *Figure 5A* show that *Pinellia ternata*-based N-CQDs are golden in natural light (left) and bright blue fluorescence in 365 nm ultraviolet light (right). Benefiting from its narrow size distribution, *Pinellia ternata*-based N-CQDs exhibit relatively symmetrical fluorescence spectra, as shown in *Figure 5B*. Under 356 nm excitation light, the maximum emission wavelength is 444 nm. The principle of fluorescence depends mainly on the bandgap transition formed by conjugated pion electrons and the surface defects of fluorescent carbon quantum dots. *Figure 5C* is the fluorescence emission spectra of *Pinellia ternata*-based N-CQDs at different excitation wavelengths, showing good excitation wavelength-dependent fluorescence behavior. The results shown that nitrogen doping can adjust the intrinsic electronic and surface properties of CQDs, enhance their effective surface defects and internal carbon core structure, and thus significantly improve their optical properties.

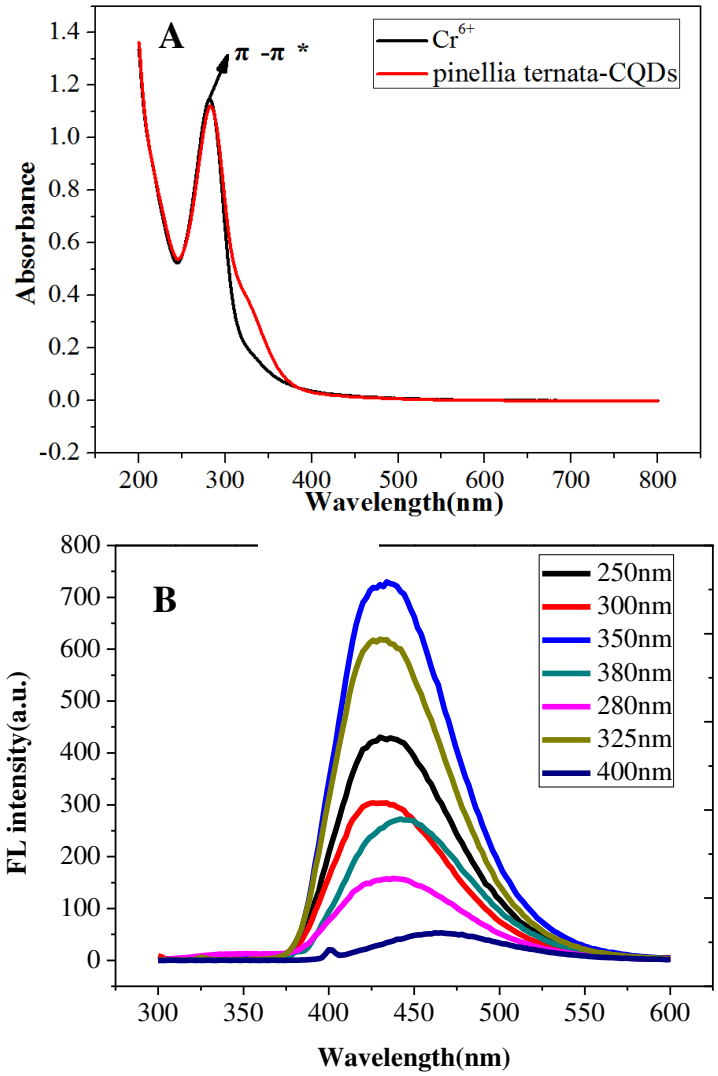

Figure 5. *UV absorption spectra of the Pinellia ternata-based N-CQDs and Cr^{6+}(A); fluorescence excitation and emission spectra of the Pinellia ternata-based N-CQDs (B)*

http://www.aloki.hu ● ISSN 1589 1623 (Print) ● ISSN 1785 0037 (Online)
DOI: http://dx.doi.org/10.15666/aeer/1705_1213912153

Photostability of Pinellia ternata-based N-CQDs

In order to explore the anti-interference ability of *Pinellia ternata*-based N-CQDs to the external environment, the light stability test was carried out, and the conditions of ion strength, pH and storage time were investigated. As shown in *Figure 6A*, when the pH value of citric acid-disodium hydrogen phosphate buffer changes from 2.2 to 8.0, its fluorescence intensity does not change obviously under acidic and neutral conditions of pH 2.2-7.0, but decreases sharply under alkaline conditions of pH 8.0, which indicates that the probe can be used as a fluorescent nanoprobe in acidic medium. *Figure 6B* investigated the effect of ion strength on the fluorescence intensity of *Pinellia ternata*-based N-CQDs. As can be seen from the figure, the fluorescence intensity only fluctuates slightly with the increasing concentration of NaCl solution, and there is no obvious change. Therefore, *Pinellia ternata*-based N-CQDs still have strong stability in high ionic strength environment. As shown in *Figure 6C* and D, *Pinellia ternata*-based N-CQDs with the same concentration were stored in refrigerator at room temperature for 3 h or even 4 °C for 3 months under the same experimental conditions. The fluorescence intensity of *Pinellia ternata*-based N-CQDs remained basically unchanged and stable, and no floating or sediment could be seen in its aqueous solution by naked eyes. The above experimental results show that the *Pinellia ternata*-based N-CQDs have excellent optical stability.

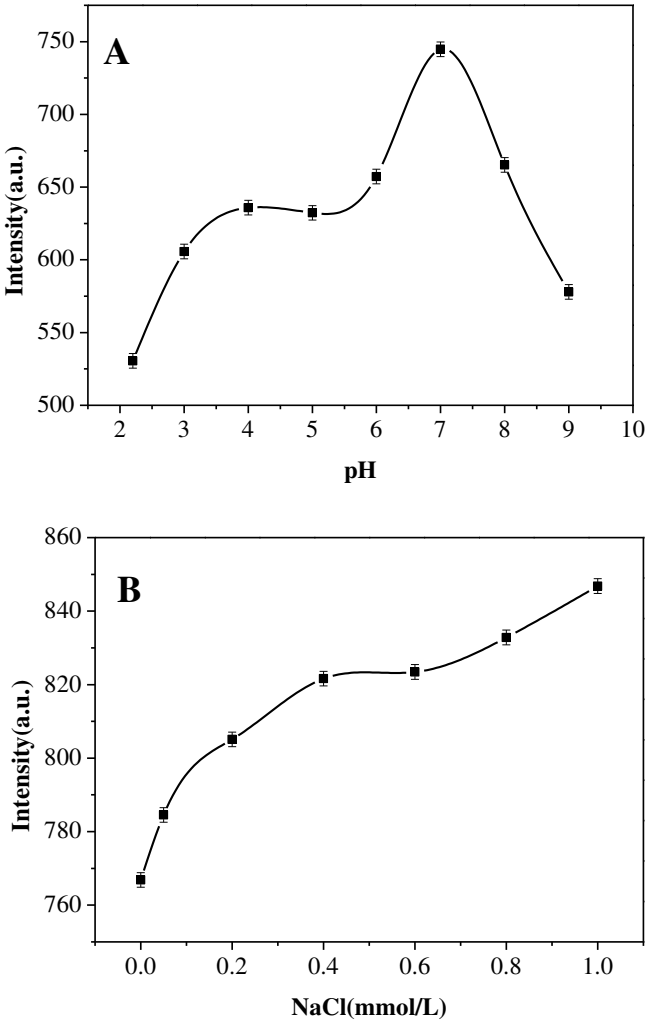

http://www.aloki.hu ● ISSN 1589 1623 (Print) ● ISSN 1785 0037 (Online)
DOI: http://dx.doi.org/10.15666/aeer/1705_1213912153

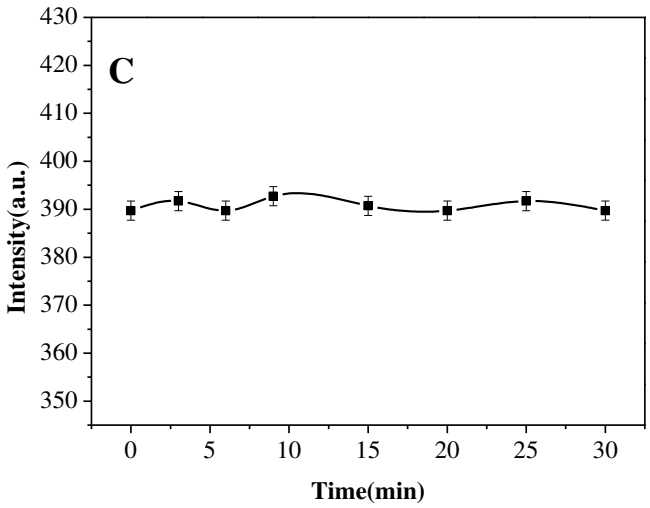

Figure 6. *Effects of various conditions on the fluorescence intensity of the Pinellia ternata-based N-CQDs: (A) pH; (B) NaCl concentrations; (C) storage time*

Selective investigation test

In order to investigate the selectivity of *Pinellia ternata*-based N-CQD fluorescence intensity to different metal ions, 12 metal ions with the same concentration of Al^{3+}, Mg^{2+}, Zn^{2+}, Cu^{2+}, Cr^{6+}, Cr^{3+}, Cd^{2+}, Co^{2+}, Sn^{2+}, Ag^{+}, Pb^{2+}, Fe^{3+}, Fe^{2+}, were investigated. As shown in *Figure 7*, only Cr^{6+} can effectively quench the fluorescence intensity of *Pinellia ternata*-based N-CQDs, while the introduction of other metal ions does not cause significant changes in the fluorescence intensity of *Pinellia ternata*-based N-CQDs. This indicates that *Pinellia ternata*-based N-CQDs have high selectivity to Cr (VI) and can be used as nanoprobe for fluorescence quenching detection of Cr (VI). In addition to Cr^{6+}, other metal ions will coexist with the actual samples. Therefore, this study further investigated the ion interference problem in the detection of Cr^{6+} through competitive experiments, that is, in the presence of other metal ions, the detection of Cr^{6+} was carried out. As shown in *Figure 7*, the experimental results show that the presence of interfering ions has little effect on the detection of Cr^{6+}. In particular, the potential interference ion Cr^{3+}, although causing a slight reduction in the fluorescence intensity of the detection of Cr^{6+}, has a negligible effect, and can be used to distinguish between Cr^{3+} and Cr^{6+}, which is a characteristic that some fluorescent nanoprobes for the detection of Cr^{6+} do not possess. In conclusion, *Pinellia ternata*-based N-CQDs have good selectivity and anti-interference ability as a fluorescent nanoprobe for detection of Cr(VI).

Optimization of experimental conditions

The fluorescence quenching mechanism can be used for rapid detection of Cr (VI). In order to obtain the best fluorescence response signal, some key experimental factors such as solution pH and reaction time were further investigated and optimized. Firstly, the fluorescence intensity of *Pinellia ternata*-based N-CQDs was studied in different pH ranges (2.0-12.0). It can be seen from *Figure 8A* that the fluorescence quenching efficiency is the highest when the pH value is 7.0. The influence of pH value on the quenching process may be related to the form and distribution of acid-base equilibrium

http://www.aloki.hu ● ISSN 1589 1623 (Print) ● ISSN 1785 0037 (Online)
DOI: http://dx.doi.org/10.15666/aeer/1705_1213912153

groups on *Pinellia ternata* N-CQDs surface and Cr (VI) in solution (Vaz et al., 2017). Cr(VI) exhibits a pH-dependent dynamic equilibrium in aqueous solution: $2CrO_4^{2-} + 2H^+ \rightleftharpoons Cr_2O_7^{2-} + 2H_2O$. Cr(VI) mainly exists in the form of chromium (CrO_4^{2-}) and dichromate ($Cr_2O_7^{2-}$). Although it has the same charge number, it has higher molar volume, so it has lower electron density and lower effective interaction with *Pinellia ternata*-based N-CQDs. Its fluorescence quenching efficiency is lower than that of chromite (CrO_4^{2-}). In acidic medium, Cr (VI) mainly exists in the form of dichromate ($Cr_2O_7^{2-}$), so its fluorescence quenching efficiency is low, and gradually increases with the increase of pH.

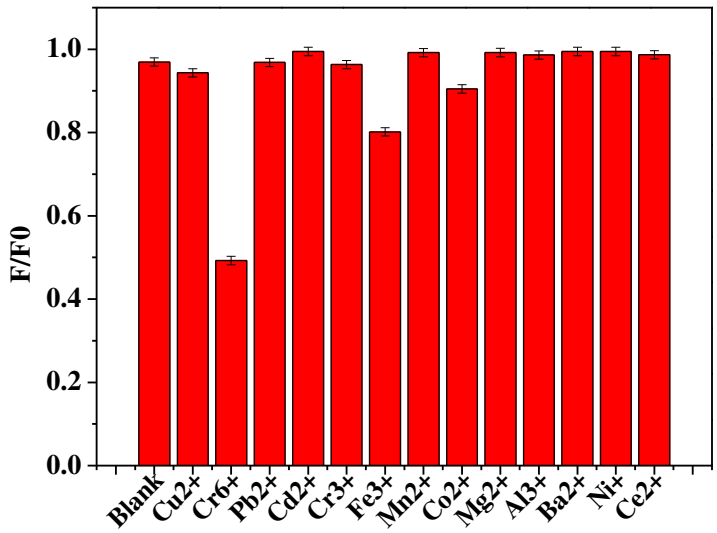

Figure 7. *Evaluation of method selectivity against possible interferents*

In addition, in alkaline medium, the oxygen-containing functional groups on *Pinellia ternata*-based N-CQDs are mainly in the form of chromate (CrO_4^{2-}), which is easy to dephosphorize and increase the negative charge on the surface. The interaction between Cr (VI) and negatively charged chromite (CrO_4^{2-}) is weakened due to electrostatic repulsion, which shows that the fluorescence quenching efficiency begins to decrease gradually. Therefore, pH 7.0 is defined as the optimum determination condition.

In order to determine the quenching response time of Cr^{6+} to *Pinellia ternata* N-CQDs, the reaction time was also discussed in this study. *Figure 8B* shows the fluorescence intensity of *Pinellia ternata* N-CQDs with time after adding Cr^{6+}. The fluorescence intensity of *Pinellia ternata*-based N-CQDs decreases sharply in 0-2 min, and reaches the lowest fluorescence intensity in 2 min. Later, the fluorescence intensity of *Pinellia ternata*-based N-CQDs decreases slightly but tends to stabilize gradually with the extension of time. Therefore, the optimal fluorescence quenching response time is 2 min.

Study on methodological performance

Under the optimum experimental conditions, the relationship between the fluorescence quenching intensity of *Pinellia ternata* N-CQDs and the concentration of Cr^{6+} was studied, and a quantitative analysis method for the fluorescence quenching of Cr^{6+} was established. As shown in *Figure 9A,* the fluorescence intensity of N-CQDs

http://www.aloki.hu ● ISSN 1589 1623 (Print) ● ISSN 1785 0037 (Online)
DOI: http://dx.doi.org/10.15666/aeer/1705_1213912153

decreases gradually with the increase of the concentration of Cr^{6+} and changes regularly, which further proves the feasibility and application prospects of N-CQDs as a fluorescent probe for the detection of Cr^{6+}. As shown in *Figure 9B,* the fluorescence quenching efficiency (F0/F) has a good linear relationship with the concentration of Cr^{6+} in the range of 0-200 μM. The linear equation is F0/F = 1.0218 + 0.1156 C (Cr^{6+}), R^2 = 0.9955, and the detection limit is 15 nM (S/N = 3).

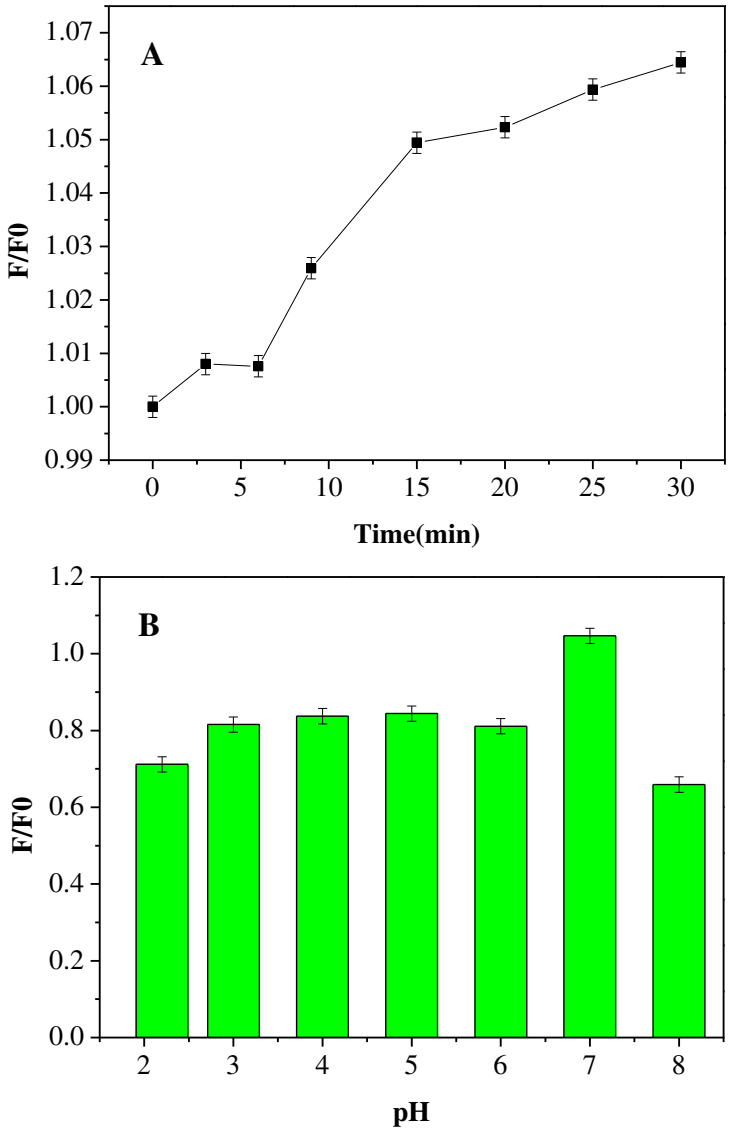

Figure 8. *Effect of reaction time (A) and pH (B) on the fluorescence intensity of the Pinellia ternata-based N-CQDs*

Analysis of fluorescence quenching mechanism

The fluorescence quenching mechanism of *Pinellia ternata*-based N-CQDs for detecting chromium (VI) is similar to that of polyacrylamide-based N-CQDs for detecting Hg^{2+}. It is caused by the synergistic effect of fluorescent inner filter effect (IFE) and electron transfer. As shown in *Figure 10,* at pH 7.0, the ultraviolet-visible absorption spectra of Cr (VI) show two absorption peaks at 272 and 371 nm,

http://www.aloki.hu ● ISSN 1589 1623 (Print) ● ISSN 1785 0037 (Online)
DOI: http://dx.doi.org/10.15666/aeer/1705_1213912153

respectively, while *Pinellia ternata*-based N-CQDs have ultraviolet absorption peaks at 337 nm, and the maximum excitation and emission wavelengths are 356 and 444 nm, respectively. It is obvious that the absorption spectra of Cr (VI) overlap with the excitation and absorption spectra of *Pinellia ternata*-based N-CQDs. Therefore, Cr (VI) partially shields the excitation spectra of *Pinellia ternata*-based N-CQDs and partially absorbs the light emitted by *Pinellia ternata*-based N-CQDs, resulting in the fluorescence endofiltration effect between *Pinellia ternata*-based N-CQDs and Cr^{6+}, resulting in the quenching of the fluorescence of *Pinellia ternata*-based N-CQDs. In addition, Cr^{6+} has strong electron acceptance and affinity, and it is easy to capture electrons. When the excited state molecule of *Pinellia ternata*-based N-CQDs collides with Cr^{6+}, the nitrogen and oxygen functional groups on its surface can combine with Cr^{6+} to form complexes, which lead to electron transfer and non-radiative transition, leading to fluorescence quenching.

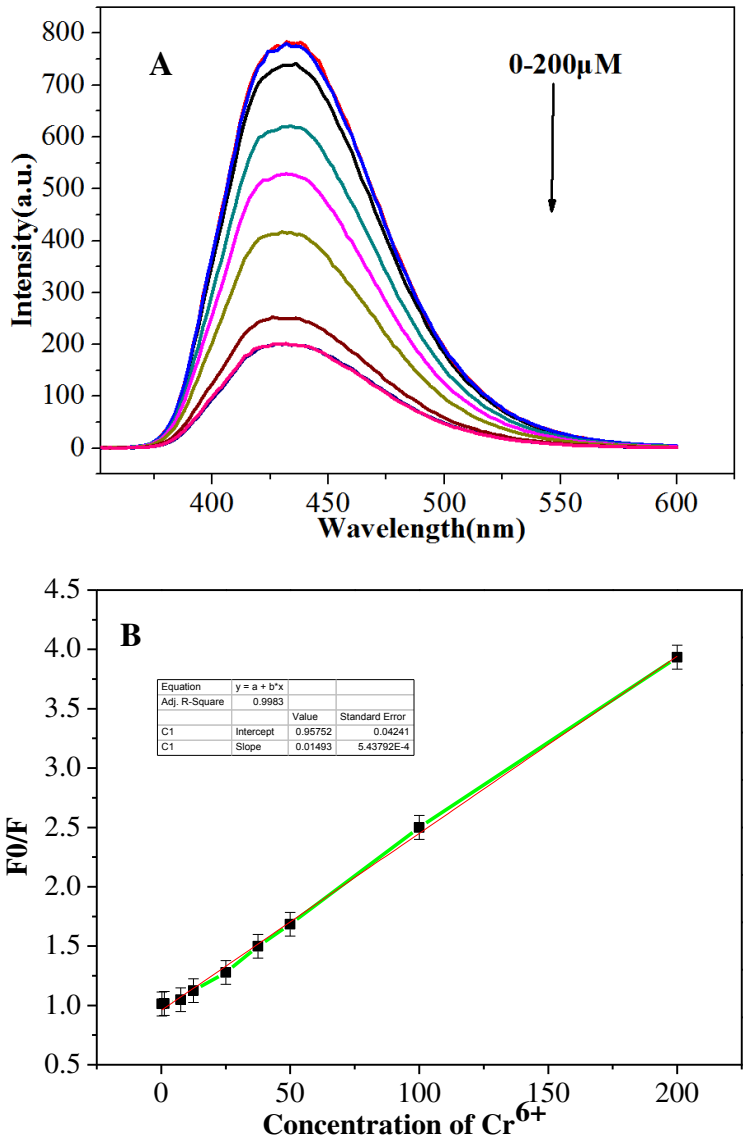

Figure 9. *The fluorescence response of the Pinellia ternata-based N-CQDs upon the addition of different concentrations of Cr^{6+}(A) and a linear correlation of F0/F values versus the concentration of Cr^{6+} over the range from 0 to 200 μM (B)*

http://www.aloki.hu ● ISSN 1589 1623 (Print) ● ISSN 1785 0037 (Online)
DOI: http://dx.doi.org/10.15666/aeer/1705_1213912153

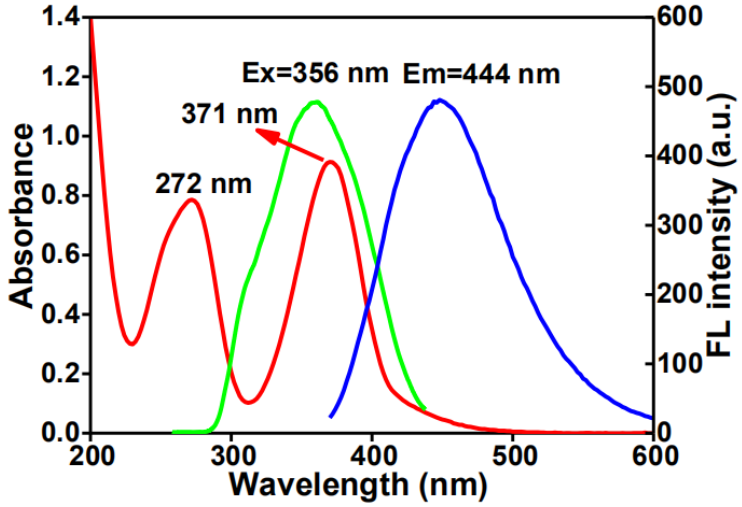

Figure 10. *UV-Vis absorption spectra of Cr (VI) and fluorescence excitation/emission spectra of the Pinellia ternata-based N-CQDs*

Detection of actual samples

In order to verify the practicability of this method, the content of Cr^{6+} in different water samples was investigated. As shown in *Table 1,* the recoveries of water samples were 94.2-102.5% and RSD was less than 5.8%. In order to evaluate the accuracy of this method, FAAS method was used to detect the content of Cr in water samples with the same concentration. The results show that in *Table 1,* the results of the two methods are very close, so, this method can be used for the rapid analysis and detection of Cr^{6+} in environmental water samples, and can be effectively applied to further research.

Table 1. *Analytical results of Cr (VI) in the water samples (n = 3)*

Samples	Spiked (μM)	Found (μM)	Recovery (%)	RSD (%, n = 3)	FAAS Found (μM)
Tap water	0	-	-	-	-
	5	4.71	94.2	4.3	4.82
	20	19.3	96.5	3.6	19.3
Lake water	0	-	-	-	-
	5	4.92	98.4	5.8	4.98
	20	20.5	102.5	2.5	20.1
Waste water	0	-	-	-	-
	5	5.10	102.0	5.3	5.04
	20	20.05	100.3	4.7	19.75

"-" not detected

Conclusion

In this study, for the first time, *Pinellia ternata* was used as a carbon precursor and ethylenediamine as a nitrogen source. Nitrogen-doped fluorescent carbon quantum dots with excellent optical properties and fluorescent quantum yield of 21.3% were prepared

http://www.aloki.hu ● ISSN 1589 1623 (Print) ● ISSN 1785 0037 (Online)
DOI: http://dx.doi.org/10.15666/aeer/1705_1213912153

by a simple one-step hydrothermal method. The morphology, particle size, crystalline form, chemical element composition and optical properties were characterized by TEM, FT-IR, XPS, UV-Vis and FS. The results show that *Pinellia ternata* N-CQDs have uniform size distribution, rich oxygen and nitrogen functional groups on their surface, and show good excitation wavelength dependence and tunability. Based on the quenching mechanism of fluorescence internal filter effect, Cr^{6+} has high sensitivity, selectivity and anti-interference ability. It can be used as a fluorescent nanoprobe for the analysis and detection of Cr^{6+} in complex environmental samples. The method has good linear relationship, fast reaction, simple operation, high sensitivity, high selectivity and low detection limit. It provides a new idea for developing carbon quantum dot fluorescent nanoprobe for detecting Cr^{6+} and has broad application prospects.

Acknowledgements. The subject is supported by the Fund of Nature Science Research Project of Anhui Province (1808085QB33).

REFERENCES

[1] Abdolmohammad-Zadeh, H., Sadeghi, G. H. (2012): A nano-structured material for reliable speciation of chromium and manganese in drinking waters, surface waters and industrial wastewater effluents. – Talanta 94: 201-208.
[2] Ahmad, M. K., Syma, S., Mahmood, R. (2011): Cr (VI) induces lipid peroxidation, protein oxidation and alters the activities of antioxidant enzymes in human erythrocytes. – Biological trace Element Research 144: 426-435.
[3] Algar, W. R., Krull, U. J. (2008): Quantum dots as donors in fluorescence resonance energy transfer for the bioanalysis of nucleic acids, proteins, and other biological molecules. – Analytical & Bioanalytical Chemistry 391(5): 1609-1618.
[4] Alizadeh, A., Ghouzivand, S., Khodaei, M. M., et al. (2016): An interesting spectroscopic method for chromofluorogenic detection of cyanide ion in aqueous solution: Disruption of intramolecular charge transfer (ICT). – Journal of Chemical Sciences 128(4): 537-543.
[5] Baker, S. N., Baker, G. A. (2010): Luminescent carbon nanodots: emergent nanolights. – Angew. Chem. Int. Ed. 49: 6726-6744.
[6] Barrera-Díaz, C. E., Lugo-Lugo, V., Bilyeu, B. (2012): A review of chemical, electrochemical and biological methods for aqueous Cr(VI) reduction. – J. Hazard. Mater. 1(12): 223-224.
[7] Bauer, G., Neouze, M.-A., Limbeck, A. (2013): Dispersed particle extraction. A new procedure for trace element enrichment from natural aqueous samples with subsequent ICP-OES analysis. – Talanta 103: 145-152.
[8] Broadhurst, C. L., Domenico, P. (2006): Clinical studies on chromium picolinate supplementation in diabetes mellitus. A review. – Diabetes Technol Ther 8: 677-87.
[9] Carrasco, P. M., Garcia, I., Yate, L., Zaera, R. T., Cabanero, G., Grande, H. J., Ruiz, V. (2016): Graphene quantum dot membranes as fluorescent sensing platforms for Cr(VI) detection. – Carbon 109: 658-665.
[10] Costa, M. (1997): Toxicity and carcinogenicity of Cr(VI) in animal models and humans. – Critical Reviews in Toxicology 27: 431-442.
[11] Costa, M., Klein, C. B. (2006): Toxicity and carcinogenicity of chromium compounds in humans. – Critical Reviews in Toxicology 36: 155-163.
[12] Gagneten, A. M., Imhof, A. (2009): Chromium (Cr) accumulation in the freshwater crab, Zilchiopsis collastinensis. – Journal of Environmental Biology 30: 345-348.
[13] Gao, Y., Jiao, Y., Lu, W., Liu, Y., Han, H., Gong, X., Xian, M., Shuang, S. and Dong, C. (2018): Carbon dots with red emission as a fluorescent and colorimeteric dual-readout

http://www.aloki.hu ● ISSN 1589 1623 (Print) ● ISSN 1785 0037 (Online)
DOI: http://dx.doi.org/10.15666/aeer/1705_1213912153

probe for the detection of chromium(VI) and cysteine and its logic gate operation. – Mater. Chem. B 38: 1-10.

[14] Gong, X. J., Liu, Y., Yang, Z. H., Shuang, S. M., Zhang, Z. Y., Dong, C. (2017): An "on-of-on" fluorescent nanoprobe for recognition of chromium(VI) and ascorbic acid based on phosphorus/nitrogen dual-doped carbon quantum dot. – Anal. Chim. Acta 968: 5-96.

[15] Gunnlaugsson, T., Ali, H. D. P., Glynn, M., et al. (2005): Fluorescent photoinduced electron transfer (PET) sensors for anions. From design to potential application. – Journal of Fluorescence 15(3): 287-299.

[16] Huang, S., Qiu, H. N., Zhu, F. W., Lu, S. Y., Xiao, Q. (2015): Graphene quantum dots as on-of-on fluorescent probes for chromium(VI) and ascorbic acid. – Microchim. Acta 182: 1723-1731.

[17] Kim, H., Lee, B.-I., Byeon, S.-H. (2015): The inner filter effect of Cr(VI) on Tb-doped layered rare earth hydroxychlorides: new fluorescent adsorbents for the simple detection of Cr(VI). – Chem. Commun. 51: 725-728.

[18] Kong, W., Wu, D., Li, G., Chen, X., Gong, P., Sun, Z., Chen, G., Xia, L., You, J., Wu, Y. (2017): A facile carbon dots based fluorescent probe for ultrasensitive detection of ascorbic acid in biological fluids via non-oxidation reduction strategy. – Talanta 165: 677-684.

[19] Li, Y. K., Yang, T., Chen, M. L., Wang, J. H. (2018): Supported carbon dots serve as high-performance adsorbent for the retention of trace cadmium. – Talanta 180: 18-24.

[20] Ma, X. Y., Chena, Y., Liua, J., Hana, Y., Ma, S., Chen, X. (2018): Ratiometric fluorescent detection of chromium(VI) in real samples based on dual emissive carbon dots. – Talanta. 185(1): 249-257.

[21] Ng, T. B., Liu, J., Wong, J. H., Ye, X., Wing, S. C., Tong, Y., Zhang, K. Y. (2012): Review of research on dendrobium candidum, a prized folk medicine. – Appl. Microbiol. Biotechnol. 93(5) 1795-1803.

[22] Ohira, S. I., Nakamura, K., Shelor, C. P., Dasgupta, P. K., Toda, K. (2015): Simultaneous electrodialytic preconcentration and speciation of chromium(III) and chromium(VI). – Anal. Chem. 87: 11575-11580.

[23] Sedman, R. M., Beaumont, J. A. Y., McDonald, T. A., Reynolds, S., Krowech, G., Howd, R. (2006): Review of the evidence regarding the carcinogenicity of hexavalent chromium in drinking water. – J. Environ. Sci. Heal. C 24: 155-182.

[24] Teixeira da Silva, J. A., Ng, T. B. (2017): The medicinal and pharmaceutical importance of Dendrobium candidum species. – Appl. Microbiol. Biotechnol. 101(6) 2227-2239.

[25] Vallejos, S., Munoz, A., Garcia, F. C., Serna, F., Ibeas, S., Garcia, J. M. (2012): Methacrylate copolymers with pendant piperazinedione-sensing motifs as fluorescent chemosensory materials for the detection of Cr(VI) in aqueous media. – J. Hazard. Mater. 227-228: 480-483.

[26] Vaz, R., Bettini, J., Júnior, J. G. F., et al. (2017): High luminescent carbon dots as an eco-friendly fluorescence sensor for Cr(VI) determination in water and soil samples. – Journal of Photochemistry & Photobiology A Chemistry 346: 502-511.

[27] Wang, H. S., Xie, Y., Bi, J., Li, Y., Song, Y., Cheng, S., Li, D., Tan, M. (2018): Facile one-step synthesis of highly luminescent N-doped carbon dots as efficient fluorescence probe for chromium (VI) detection based on inner filter effect. – New, J. Chem. 5: 1-8.

[28] Wang, L., Zhou, H. S. (2014): Green synthesis of luminescent nitrogen-doped carbon dots from milk and its imaging application. – Anal. Chem. 86: 8902-8905.

[29] Wang, M., Zhang, G., Zhang, D., et al. (2010): Fluorescent bio/chemosensors based on silole and tetraphenylethene luminogens with aggregation-induced emission feature. – Journal of Materials Chemistry 20(10): 1858-1867.

[30] Wang, W., Bai, H., Li, H., Lv, Q., Wang, Z., Zhang, Q. (2017): Disposable plastic electrode for electrochemical determination of total chromium and hexavalent chromium. – J. Electroanal. Chem. 794: 148-155.

http://www.aloki.hu ● ISSN 1589 1623 (Print) ● ISSN 1785 0037 (Online)
DOI: http://dx.doi.org/10.15666/aeer/1705_1213912153

[31] Yuhua, Z., Xian, F., Hong, Z., Li, Z. (2018): A highly sensitive and selective detection of Cr(VI) and ascorbic acid based on nitrogen-doped carbon dots. – Talanta 181: 318-325.
[32] Zhang, H. J., Chen, Y. L., Liang, M. J., Xu, L. F., Qi, S. D., Chen, H. L., Chen, X. G. (2014): Solid phase synthesis of highly fluorescent nitrogen-doped carbon dots for sensitive and selective probing ferric ions in living cells. – Anal. Chem. 86: 9846-9852.
[33] Zhang, H. Y., Wang, Y., Xiao, S., et al. (2017): Rapid detection of Cr(VI) ions based on cobalt(II)-doped carbon dots. – Biosensors & Bioelectronics 87: 46-52.
[34] Zheng, Q., Qiu, D., Liu, X., Zhang, L., Cai, S., Zhang, X. (2015): Antiproliferative effect of Dendrobium candidum catenatum Lindley polypeptides against human liver, gastric and breast cancer cell lines. – Food Funct. 6(5) 1489-1495.
[35] Zheng, X. T., Ananthanarayanan, A., Luo, K. Q., Chen, P. (2015): Glowing graphene quantum dots and carbon dots: properties, syntheses, and biological applications. – Small 11: 1620-1636.

http://www.aloki.hu ● ISSN 1589 1623 (Print) ● ISSN 1785 0037 (Online)
DOI: http://dx.doi.org/10.15666/aeer/1705_1213912153

GENETIC DIVERSITY AMONG ENDANGERED FRESHWATER MUSSELS BASED ON SHELL DNA SEQUENCES

DOĞANKAYA, L.* – COŞKUN, T. – GÜLTEKIN, T.

Ankara University, Faculty of Agriculture, Department of Fisheries and Aquaculture Engineering, 06110 Dışkapı, Ankara, Turkey
(phone: +90-312-596-1438; fax: +90-312-318-5298)

**Corresponding author*
e-mail: dogankaya@ankara.edu.tr; phone: +90-312-596-1439; fax: +90-312-318-5298

(Received 30th Apr 2019; accepted 11th Jul 2019)

Abstract. Molecular genetic information on mollusk species is being increasingly considered for identification and taxonomic status. In this study, we examined the potential of shell material of freshwater mussels from four different locations in Turkey for DNA sequence analysis. A total number of 212 specimens including empty shells were sampled from a river and three lakes. Mitochondrial DNA was extracted from ground shell material with isolation kits and tissue material was also used for reference. Even though the majority of empty shells did not produce high-quality material, DNA extraction from fresh shells had similar results with tissue material. Mitochondrial 28S rDNA partial sequences were analyzed using the neighbour-joining method for genetic divergence. Phylogenetic analysis revealed two well-differentiated clades of *Anodonta cygnea* and *Unio crassus*. The results clearly indicated that 28S rRNA sequences obtained from shell material are informative enough to reveal major clades, haplotypes and phylogenetic relationship between four populations. These findings support that quite fresh shell material from freshwater mussels can be a convenient DNA source for molecular studies.
Keywords: *Unionidae, phylogeny, shell DNA, bivalve diversity, 28S rDNA*

Introduction

Freshwater mussels as prehistoric bivalve inhabitants of inland waters are represented on all continents except Antarctica. They are classified into six families, about 180 genera and 800 species (Bogan, 2008). Bivalves are remarkable aquatic organisms with heavy impact on ecosystems through filtration, bio-accumulation, energy transfer, being host for other organisms and their role in food web. Such factors as pollution, loss of host fishes and the introduction of non-native species are causing changes in diversity and population structure (Lopez-Lima et al., 2017). Freshwater mussels are globally in decline and are among the most endangered aquatic species (Strayer, 2008). Lopez-Lima et al. (2017) recorded 224 (44%) of the 511 freshwater mussel species as Near Threatened or Threatened in the 2015 *IUCN Red List of Threatened Species*. Despite having highly important ecosystem roles, gaps exist on biology and population structure of freshwater bivalves still standing as the primary obstacle to management and conservation.

Recently, European freshwater mussels have also been gaining increasing attention and 16 species have been recognized in Unionida Margaritiferidae: 2 and Unionidae: 14 (Lopez-Lima et al., 2017). The current taxonomy of freshwater mussels is based on morphological characteristics and studies on genetic diversity are very scarce. Due to variable characteristics as size and shell shape which are affected by the current velocity, substratum and environment, freshwater mussels exhibit high phenotypic plasticity (Baker et al., 2004).

http://www.aloki.hu ● ISSN 1589 1623 (Print) ● ISSN 1785 0037 (Online)
DOI: http://dx.doi.org/10.15666/aeer/1705_1215512163

Population size, distribution and species data are primary requirements for successful conservation management so the taxonomic status of the order Unionida is to be resolved and DNA sequence would serve valuable data for systematic updates.

Mantle clipping is the widespread method for tissue sampling from mollusks in genetic studies but non-invasive sampling methods are needed for endangered species and in case of lacking live specimens. Henley et al. (2006) described integumental swabbing as a noninvasive method for cell collection from freshwater mussels. A more recent study presented a method for DNA extraction from empty apple snail shells (Andree and Lopez, 2013).

To avoid the phenomenon phenotypic plasticity and facilitate genetic analysis through small shell fragments from live or empty shells, we examined genetic diversity in four populations of freshwater mussels using 28S rDNA sequences. Here we present a successful method and first genetic data on Turkish populations of freshwater mussels.

Materials and Methods

Live specimens and empty freshwater mussel shells

Freshwater mussels and empty shells were collected from Gölmarmara/Manisa (lake), Manavgat/Antalya (dam lake downstream), Küçük Akgöl/Adapazarı (lake), Karasu/Sinop (river) in Turkey (*Table 1*) with the permission of the Ministry of Agriculture and Forestry (*Figure 1a*). While empty shells were placed in plastic bags, tissue samples were taken from live specimens into ethanol 70% and transferred to the laboratory in cooler boxes. Samples were stored at -20°C until analysis.

Table 1. *Sampling locations*

Location	Waterbody	Coordinates	Number of specimens
Karasu	Stream	41.56162"N – 35.04827"E	150
Küçük Akgöl	Lake	40.52365"N – 30.25582"E	40
Gölmarmara	Lake	38.35449"N – 27.59487"E	4
Manavgat	Dam Lake	36.52434"N – 31.31211"E	11

DNA preparation, PCR and sequencing

Total DNA was extracted using EurX GeneMATRIX Tissue & Bacterial DNA Purification Kit (Poland) according to the manufacturer protocol with minor modifications. Samples from each shell were removed with an 8 mmØ ceramic cutting hand drill and crushed into fine powder in a mortar. To avoid contamination, cutting edges were changed with new between samples. Sample material was placed into the 2 ml tube and 350 µl Lyse T buffer added and the precipitate was suspended. Tissue samples were cut into small pieces and buffered. 2 µl RNaseA and 20 µl Proteinase K were added and vortexed. Samples were incubated at 56°C during 3 h after adding 350 µl buffer, the samples were incubated for 10 min at 70°C. Pure ethanol of 350 µl was added and the tubes were centrifuged for 1 min at 12 000g. The supernatant was transferred into DNA binding spin-column and centrifuged repeatedly. After placing the column in the collection tube 500 µl washing buffers were added and centrifuged. Elution buffer was added in new tubes and incubated at room temperature. DNA products were stored at 4°C. The recovered DNA was checked with Thermo Scientific Nanodrop 2000 (USA) for integrity.

http://www.aloki.hu ● ISSN 1589 1623 (Print) ● ISSN 1785 0037 (Online)
DOI: http://dx.doi.org/10.15666/aeer/1705_1215512163

Figure 1a. *Map showing the sampling locations*

Figure 1b. *Shells from collection sites. (a)Karasu, (b)Akgöl, (c) Gölmarmara and (d) Manavgat*

A universal primer set (Justine et al., 2002) was employed for mitochondrial 28S rDNA gene amplification (*Table 2*).

Table 2. *Primer set used for 28S rDNA amplification*

Primer	Direction	Primer Sequence	Reference
C1	Forward	5′-ACCCGCTGAATTTAAGCAT-3′	Justin et al., 2002
C2	Reverse	5′-CTCTCTYTYCAAAGTTCTTTTC-3′	

Each PCR reaction mixture contained 1.5 µl DNA template (880 ng/µl), 1 µl DNA FIREPol® DNA Polymerase (5 U/µl), 10 µl 10X Buffer, 1 µl dNTP (20 mM), 6 µl 25 mM $MgCl_2$ (1.5 nM) and 10 pmol/µl of each primer (0.15 µM), completed with ddH_2O to a total volume of 100 µl. The thermal cycler profile was as one cycle initial denaturation step at 95°C for 5 min, 35 cycles of denaturation at 95°C for 45 sec, annealing at 57°C for 45 sec, elongation at 72°C for 1 min and a final extension step at 72°C for 5 min. The amplified DNA fragments were controlled with agarose gel electrophoresis and purified using ExoSAP-IT™ PCR Product Cleanup Reagent"

http://www.aloki.hu ● ISSN 1589 1623 (Print) ● ISSN 1785 0037 (Online)
DOI: http://dx.doi.org/10.15666/aeer/1705_1215512163

(ThermoFisher Scientific, USA). PCR amplified DNA fragments were sequenced with automated 3500xL Genetic Analyzer (Applied Biosystems).

The sequences were aligned with Sequencer v5.4.6 and consensus alignments for each sampling location were deposited to GenBank under accession numbers MK530498, MK530499, MK530500, MK530501.

The number of polymorphic sites, DNA polymorphism, conserved regions, haplotype number, haplotype diversity and Tajima's D statistics were performed with DnaSP v.5.0 (Librado and Rozas, 2009).

Phylogenetic analysis for the 28S rDNA sequence set was performed using the software MEGA X (Kumar et al., 2018). The tree was produced with the Neighbor-Joining (NJ) method using the Kimura 2-parameter model for genetic distance estimation (Kimura, 1980). Percentage of replicate trees in the bootstrap test (1000 replicates) indicated alongside the branch nodes (Felsenstein, 1985).

Results

DNA extraction from all three types of material was affordable. *Figure 2* demonstrates the gel electrophoresis screenshot for mitochondrial DNA from mantle clipping, fresh shell and old empty shell material. Even though mitochondrial DNA can be isolated from all samples, sequencing performance was not the same. While 97% of tissue and 70% of fresh shell samples were sequenced succesfully, only 10% of the PCR products from old empty shells served quality sequences (*Table 3*).

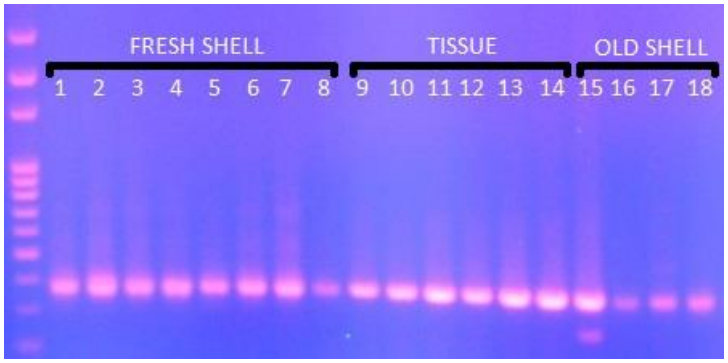

Figure 2. *Gel electrophoresis of mantle tissue, fresh shell and old shell samples*

Table 3. *Number of successfully sequenced specimens from different DNA sources*

Location	Tissue		Fresh Shell Material		Old Empty Shell Material	
	Template DNA (n)	Sequenced (n)	Template DNA (n)	Sequenced (n)	Template DNA (n)	Sequenced (n)
Karasu	10	10	10	10	10	2
Küçük Akgöl	10	10	10	7	10	-
Gölmarmara	6	5	6	4	10	1
Manavgat	10	10	10	4	10	1

Twenty-five 28S rDNA sequences have an average length of 339 bp. Mean G+C ratio found 54.1% ranging between a high scale of min 52.9% and max 54.8%. (*Table 4*). Specimens from each sampling location were given in consensus sequences

http://www.aloki.hu ● ISSN 1589 1623 (Print) ● ISSN 1785 0037 (Online)
DOI: http://dx.doi.org/10.15666/aeer/1705_1215512163

in NJ tree construction. Nucleotide compositions of consensus sequences are given in *Table 4*.

For all data set, 136 variable sites exist in 339 bg sequence (5.04%). *Table 5* shows conserved, variable and parsimony informative sites, identical, transitional and transversional pair frequencies and transition/transversion ratio (R). The data set has 82 polymorphic and 52 parsimony informative sites and transitional/transversional pair ratio of 0.8 (R).

Table 4. *Nucleotide composition*

Location	T (U)	C	A	G	G+C	A+T
Karasu	20.4	24.3	26.7	28.5	52.9	47.1
Küçük Akgöl	20.1	24.7	25.6	29.6	54.3	45.7
Gölmarmara	19.6	25.2	25.8	29.5	54.7	45.3
Manavgat	20.4	24.5	24.8	30.3	54.8	45.2
Avg.	20.1	24.7	25.7	29.5	54.1	45.9

Table 5. *Nucleotide pair frequency*

Conserved sites	199/339
Variable sites	136/339
Parsimony informative sites	52/339
Singleton sites	83/339
Identical pairs ii	259
Transitional pairs si	10
Transversional pairs sv	13
R si/sv	0.8

The sequence data set represented 16 haplotypes. While haplotype H9 existed in six samples (2 from Golmarmara and 4 from Akgol), haplotype H10 was found in three samples (1 from Golmarmara, 1 from Akgol and 1 from Manavgat). Other 14 haplotypes were found for each sample from all locations. Mean haplotype diversity (Hd), nucleotide diversity (π), Tajima's D test results are given in *Table 6*. Haplotype diversity changed between 0.714 and 1.000 min/max from Akgöl and Manavgat. Average Hd and π were calculated as 0.0881 and 0.062 respectively. Test of neutrality on allele frequency distribution with Tajima's D indices resulted negative for all four populations and was not statistically significant ($p>0.05$).

Table 6. *Genetic diversity and neutrality results (Hd: Haplotype diversity, π: nucleotide diversity)*

Location	n	h	Hd	π	Tajima's D
Karasu	10	9	0.977	0.065	-0.419
Küçük Akgöl	7	4	0.714	0.117	-1.543
Gölmarmara	4	3	0.833	0.006	-0.780
Manavgat	4	4	1.000	0.059	-0.635

Nucleotide substitution rates were calculated with maximum likelihood method using Tamura 3-parameter model (*Table 7*). The nucleotide frequencies are A=23.13%, T/U=23.13%, C=26.87%, and G=26.87%.

http://www.aloki.hu ● ISSN 1589 1623 (Print) ● ISSN 1785 0037 (Online)
DOI: http://dx.doi.org/10.15666/aeer/1705_1215512163

The divergence between four populations ranged between 0.019 and 0.045 with an average value of 0.031 (3.1%) indicating a correlation between divergence and location. While the highest diversity was found between Karasu and Manavgat populations (4.5%), the populations from Gölmarmara and Akgöl were the genetically closest ones (1.9%) (*Table 8*). The high distance value of Karasu samples is due to the species difference. The Karasu population is clearly located on a separate branch in the phylogenetic tree given in *Figure 3*.

Table 7. *Nucleotide substitution matrix*

	A	T	C	G
A	-	6.77	7.86	**11.15**
T	6.77	-	**11.15**	7.86
C	6.77	**9.60**	-	7.86
G	**9.60**	6.77	7.86	-

Each entry is the probability of substitution (*r*) from one base (row) to another base (column). Rates of different transitional substitutions are shown in **bold** and those of transversional substitutions are shown in *italics*

Table 8. *Average p distances for 28S rDNA between different geographic populations*

n		1	2	3	4
4	Manavgat	-			
7	Akgol	0.028	-		
4	Golmarmara	0.019	0.003	-	
10	Karasu	0.045	0.044	0.045	-

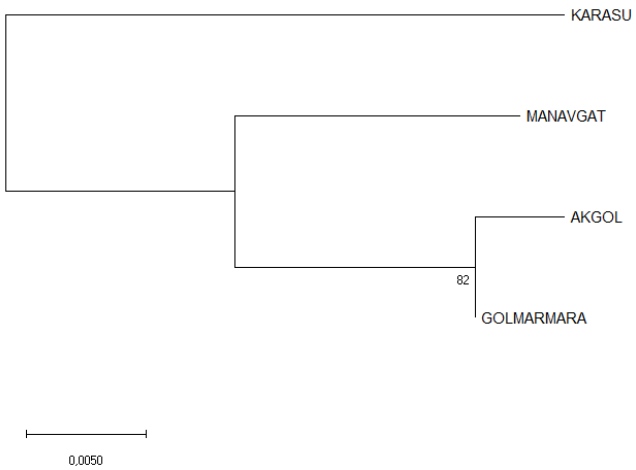

Figure 3. *Phylogenetic relationships among four taxa inferred from 28S rDNA sequences. The evolutionary history was inferred using the Neighbor-Joining method (Saitou and Nei, 1987). The percentage of replicate trees in which the associated taxa clustered together in the bootstrap test (1000 replicates) are shown next to the branches (Felsenstein, 1985). The evolutionary distances were computed using the Kimura 2-parameter method (Kimura, 1980). Evolutionary analyses were conducted in MEGA X (Kumar et al., 2018)*

Figure 3 shows the evolutionary relationship between the four populations. The tree was obtained by Neighbor-Joining method (Saitou and Nei, 1987) in MEGA X (Kumar

http://www.aloki.hu ● ISSN 1589 1623 (Print) ● ISSN 1785 0037 (Online)
DOI: http://dx.doi.org/10.15666/aeer/1705_1215512163

et al., 2018). The optimal tree with the sum of branch length was 0,058775. Genetic distances between four populations were estimated by Kimura 2-parameter method (Kimura, 1980). The percentage of replicate trees in which the associated taxa clustered together in the bootstrap test (1000 replicates) are shown next to the branches (Felsenstein, 1985). The analysis involved 4 nucleotide sequences. All ambiguous positions were removed for each sequence pair. There were a total of 339 positions in the final dataset.

Discussion

This is the first study investigating the genetic diversity of freshwater bivalvia through shell DNA analysis. The results clearly indicated that 28S rRNA sequences obtained from shell material are informative to reveal major clades, haplotypes and phylogenetic relationship between four populations. These findings support that quite fresh shell material from freshwater mussels is to be a convenient DNA source for molecular-based studies. Degradation of shells due to the exposure time to environmental components, basically the water, is the primary limiting factor for shell DNA.

G+C ratio (average 54.1%) represented in *Table 4* indicates heterogeneity between four populations. The high number of variable sites supports that the 339 bp 28S rRNA sequence from the shell is a successful molecular marker for freshwater mussels. Transitional/Transversional pair rate R (si/sv) found 0.8 while substitution rate R which is calculated using Kimura-2 parameter was 0.7. These close rates also support the reliability of data analysis.

Consensus sequence analyses supported two well-differentiated clades of unionid species swan mussel *Anodonta cygnea* from Manavgat, Akgol and Golmarmara Lakes and thick shelled river mussel *Unio crassus* from Karasu River. Genetic distance between populations found between 0.003 and 0.045 (*Table 8*) with an average of 0.030. Akgol and Golmarmara populations have exhibited the lowest genetic distance while Karasu River samples have a constant high distance value which is compatable with species difference.

According to Gürlek et al. (2014) Modell has defined four main groups of freshwater mussels of Anatolia according to geographic distribution containing Unio, Anodonta, Potomida, Leguminaia, Gabillotia, Pseudodontopsis, Sinanodonta species. There are only a few more studies on freshwater mollusks of Turkey which all used the morphological description of species. This study is being the first as using shell DNA for genetic classification of freshwater bivalvia from Turkey. Due to the difference between sampling locations, there is a lack of chance to conclude data from the literature. Only Şahin (2013) defined bivalvia specimens from Karasu as *Unio pictorum* through morphological identification methods but our findings indicated a different taxonomy of specimens from the same locality as *Unio crassus* according mtDNA sequence.

The phylogenetic tree of 28S rRNA sequences clearly revealed the genetic difference between four populations (*Figure 3*). Karasu samples were located on a separate branch. Akgol and Golmarmara populations stand close with a result of the hypotheses of geographic isolation.

Ricciardi and Rasmussen (1999) have reported the rapid extinction of freswater species in Nort America and made an extinction rate estimation for freshwater mussels

http://www.aloki.hu ● ISSN 1589 1623 (Print) ● ISSN 1785 0037 (Online)
DOI: http://dx.doi.org/10.15666/aeer/1705_1215512163

about two fold than the avarage of freshwater species. Lopes-Lima et al. (2017) have underlined the lack of data on freshwater mussels especially in south-eastern European countries and the importance of more studies for effective management measures.

While thick shelled river mussel *Unio crassus* is classified as "globally endangered" on IUCN Red List (Lopes-Lima et al., 2014), the swan mussel *Anodonta cygnea* is referred as "near threatened" by Killeen and Aldridge (2011). Also, it is noted that the population trend of *Unio crassus* is unknown for the Mediterranean basis so referred to DD (Data Deficient) by Vavrova (2011). Since the taxonomy of freshwater bivalve is still ambiguous and species distribution and population sizes are unclear, molecular studies can serve valuable information for conservation management plans.

Conclusion

The need for effective conservation and management strategies for freshwater ecosystems which are under intense pressure, especially human activities, requires wider monitoring using standardized protocols and methods. But there are gaps on population structures, distribution and taxonomic data for many species as well as freshwater mussels. On country basis, large scale taxonomic studies which are supported with molecular data will help filling these gaps. International cooperation is strongly suggested for database and management projects.

Overall this study suggests shell DNA as a reliable source of divergence data on freshwater bivalve species against the problematic systematic relationships and phenotypic plasticity. Partial sequences of 28S rDNA derived from four populations provide the first genetic data in Turkey with this study.

Future researches are needed for large scale data collection on freshwater bivalves by using non-invasive standardized methods.

Acknowledgments. This research has been supported by Ankara University Scientific Research Projects Coordination Unit. Project Number: 16B0759001, 2018.

REFERENCES

[1] Andree, K. B., López, M. A. (2013): Species identification from archived snail shells via genetic analysis: a method for DNA extraction from empty shells. – Molluscan Research 33(1): 1-5.

[2] Baker, A. M., Sheldon, F., Somerville, J., Walker, K. F., Hughes, J. M. (2004): Mitochondrial DNA phylogenetic structuring suggests similarity between two morphologically plastic genera of Australian freshwater mussels (Unionoida: Hyriidae). – Molecular Phylogenetics and Evolution 32(3): 902-912.

[3] Bogan, A. E. (2008): Global diversity of freshwater mussels (Mollusca, Bivalvia) in freshwater. – Hydrobiologia 595: 139-147.

[4] Felsenstein, J. (1985): Confidence limits on phylogenies: An approach using the bootstrap. – Evolution 39: 783-791.

[5] Gürlek, M., Kara, C., Kebapçı, Ü. (2014): Adıyaman Azaplı Gölü'nde yaşayan *Unio terminalis* (Bourguignat, 1852)'in bazı konkolojik özellikleri. – Aquaculture Studies 2014(3): 23-28.

[6] Henley, W. F., Grobler, P. J., Neves, R. J. (2006): Non-invasive method to obtain DNA from freshwater mussels (Bivalvia: Unionidae). – Journal of Shellfish Research 25(3): 975-978.

http://www.aloki.hu ● ISSN 1589 1623 (Print) ● ISSN 1785 0037 (Online)
DOI: http://dx.doi.org/10.15666/aeer/1705_1215512163

[7] Justine, J. L., Jovelin, R., Neifar, L., Mollaret, I., Lim, L. H. S., Hendrix, S. S., Euzet, L. (2002): Phylogenetic positions of the Bothitrematidae and Neocalceostomatidae (monopisthocotylean monogeneans) inferred from 28S rDNA sequences. – Comparative Parasitology 69(1): 20-25.
[8] Killeen, I., Aldridge, D. (2011): Anodonta cygnea. – The IUCN Red List of Threatened Species 2011: e.T156066A4907255. Downloaded on 25 April 2019.
[9] Kimura, M. (1980): A simple method for estimating evolutionary rate of base substitutions through comparative studies of nucleotide sequences. – Journal of Molecular Evolution 16: 111-120.
[10] Kumar, S., Stecher, G., Li, M., Knyaz, C., Tamura, K. (2018): MEGA X: Molecular Evolutionary Genetics Analysis across computing platforms. – Molecular Biology and Evolution 35: 1547-1549.
[11] Librado, P., Rozas, J. (2009): DnaSP v5: A software for comprehensive analysis of DNA polymorphism data. – Bioinformatics 25: 1451-1452.
[12] Lopes-Lima, M., Kebapçı, U., Van Damme, D. (2014): Unio crassus. – The IUCN Red List of Threatened Species 2014: e.T22736A42465628. http://dx.doi.org/10.2305/IUCN.UK.2014-1.RLTS.T22736A42465628.en. Downloaded on 25 April 2019.
[13] Lopes-Lima, M., Sousa, R., Geist, J., Aldridge, D. C., Araujo, R., Bergengren, J., Douda, K. (2017): Conservation status of freshwater mussels in Europe: state of the art and future challenges. – Biological Reviews 92(1): 572-607.
[14] Ricciardi, A., Rasmussen, J. B. (1999): Extinction rates of North American freshwater fauna. – Conservation Biology 13: 1220-1222.
[15] Saitou, N., Nei, M. (1987): The neighbor-joining method: A new method for reconstructing phylogenetic trees. – Molecular Biology and Evolution 4: 406-425.
[16] Strayer, D. L. (2008): Freshwater Mussel Ecology: A multifactor approach to distribution and abundance. – University of California Press, Berkeley, CA.
[17] Şahin, S. K. (2013): Mollusca species of Down Sakarya River (Karasu) and some physico-chemical variables effecting their abundance. – Aquaculture Studies 13: 011-019.
[18] Vavrova, L. (2011): Unio crassus. – The IUCN Red List of Threatened Species 2011: e.T22736A9382322. Downloaded on 25 April 2019.

http://www.aloki.hu ● ISSN 1589 1623 (Print) ● ISSN 1785 0037 (Online)
DOI: http://dx.doi.org/10.15666/aeer/1705_1215512163

ORGANIC CARBON CYCLE IN THE ULLEUNG BASIN SEDIMENT, EAST/JAPAN SEA

LEE, T.[1] – JUNG, S. K.[2] – KIM, K. H.[3] – LEE, S. H.[4] – SON, Y. B.[1*]

[1]Jeju Environmental Research Center, Korea Institute of Ocean Science & Technology
Iljudong-ro 2670, Gujwa, Jeju 63349, Republic of Korea
(e-mail: thlee@kiost.ac.kr; phone: +82-64-798-6072; fax: +82-64-798-6085)

[2]Marine Security and Safety Research Center, Korea Institute of Ocean Science & Technology
49111 Busan, Republic of Korea

[3]Deep-sea Mineral Resource Research Center, Korea Institute of Ocean Science & Technology
49111 Busan, Republic of Korea

[4]Department of Oceanography, Pusan National University, 46241 Busan, Republic of Korea

[*]Corresponding author
e-mail: sonyb@kiost.ac.kr; phone:+82-64-798-6071; fax:+82-64-798-6085

(Received 30th Apr 2019; accepted 4th Jul 2019)

Abstract. Organic carbon (OC) fluxes in the Ulleung Basin (UB) sediments, East/Japan Sea (E/JS) were investigated through geochemical analyses and sediment chamber experiment. The UB sediment has high organic carbon contents of over 2% and the mean C/N molar ratio is 7.09, therefore suggesting that the organic matter deposited in the UB is predominantly of marine origin. Apparent sedimentation rates (ASR) calculated from excess ^{210}Pb activity distribution, ranged between 0.036-0.047 cm year^{-1}. The mass accumulation rates (MAR) calculated from porosity, grain density (GD) and ASR, ranged between 131-184 g m^{-2} year^{-1}. Input fluxes of OC (IF) and burial fluxes of OC (BF) varied between 7.89-11.08 and 2.02-3.10 gC m^{-2} year^{-1}, respectively. Regenerated fluxes of OC (RF) estimated with oxygen consumption rate, varied between 6.22-6.59 gC m^{-2} year^{-1}. However, the RF calculated by subtracting BF from IF, varied between 5.87-7.98 gC m^{-2} year^{-1}. The proportions of the IF, RF, and BF to the primary production (177.1 gC m^{-2} year^{-1}) in the UB were about 5.4%, 3.9%, and 1.5%, respectively. These proportions were over 5 times higher than the average of world open ocean. Based on these results, the UB appears to play an important role in the deposition and removal of organic carbon in the E/JS.
Keywords: *particulate organic carbon (POC), input flux of organic carbon (IF), regenerated flux of organic carbon (RF), burial flux of organic carbon (BF), Ulleung Basin (UB)*

Introduction

The amount of organic matter in marine sediments reflect the supply and preservation of organic materials from marine and terrestrial sources (Tissot et al., 1980; Summerhayes, 1981). The export and preservation of organic matter from the surface waters, where they are produced, down to the basin floor determines the role of basins as a potential carbon sink. The export fluxes of particulate organic carbon (POC) play an important role in the transfer of carbon between the atmosphere and the ocean (Savoye et al., 2006; Waples et al., 2006). In the open ocean, the main source of particles is biological production. Organic particles are produced from carbon fixation through photosynthesis and uptake of nutrients. Most of the POC is recycled in the surface water by decomposition into dissolved organic carbon and remineralization into inorganic carbon. Only a small fraction of POC is exported from the euphotic layer and subsequently either recycled in the deep waters or reaching the sediments. The POC

http://www.aloki.hu ● ISSN 1589 1623 (Print) ● ISSN 1785 0037 (Online)
DOI: http://dx.doi.org/10.15666/aeer/1705_1216512179

export out of the surface layer is the most important process for the transport of atmospheric CO_2 to the deep ocean (Trull et al., 2011).

Export of organic material from the euphotic zones into deeper oceanic zones occurs in different ways. Particulate materials as biogenic materials, detrital materials and fecal pellets are transported by gravitational settling and lateral transport. Whereas the dissolved organic matter export largely depends on the extent of downward diffusion and mixing. Generally, most of this particle flux is affected by early diagenesis during settling: concentration decreases significantly with increasing water depth preferentially due to biogenically mediated organic matter degradation and dissolution processes (Suess, 1980). So, only a small fraction, which is not reintroduced back into the oceanic water column and the euphotic zone, reaches marine sediments.

Marine sediments acting as important sinks for organic matter are known from, for example, upwelling areas, shelf mud depocentres and marginal sea basins (Leipe et al., 2011). Organic carbon (OC) in marine sediments represents a major component of the global carbon cycle (Seiter et al., 2004). OC cycles in deep basin sediments are of interest for assessment of the long-term removal of CO_2 from surface waters and the regeneration of nutrients from the sediments (Eimeis et al., 2000). A key step in this cycle is represented by the reminelalization of organic matter at the sediment-water interface, via a number of oxidative processes.

The E/JS is a semi-enclosed marginal sea between continental Asia and the Japanese archipelago, connected to open ocean through straits 12–140 m in depth (Chough et al., 2000). The E/JS is considered as a miniature ocean, since it has typical characteristics of open oceans, such as a deep ventilation system, subpolar and subtropical gyres, and a western boundary current (Masuda, 2000). The E/JS has three deep basins (Ulleung Basin, Yamato Basin, and Japan Basin). The UB, located in the southwestern part of the E/JS, is surrounded by continental slopes of the Korean Peninsula, the southwestern part of Japan's main island of Honshu, and Ulleung and Dok island (*Fig. 1*). The northern and western margins of the basin are steep (> 10°), whereas the southern and eastern margins have smooth slopes (1~2°) and a broad continental shelf (Park et al., 2005). The basin floor lies at depths of 2000~2300 m, with the boundary between the continental slope and the UB approximately 2000 m in depth. Recent sediments appear to be primarily hemipelagic (Chough and Brag, 1987), no major rivers drain into the basin along the coast of the Korean Peninsula (Ikehara et al., 1994; Hong et al., 2008).

This study focused on OC cycle at the sediment-water interface and ultimately removal of OC in the UB sediments. The E/JS is a small local sea, but it is similar to the characteristics of the ocean. It is therefore the most suitable model for studying the carbon sinking to the deep ocean floor. The main purpose of this paper is to present a carbon storage and removal mechanisms of deep UB sediments, and to understand role of deep basin sediment for the removal of CO_2 from the E/JS surface water. This result is crucial for future carbon cycle and deep ocean ecosystem modelling.

Materials and methods

Sediment sampling and analyses

Sediment samples were collected using a box corer at sites on the deep basin (D2, D3, and D4) in April 2006 and August 2007. Sediment samples for geochemical analysis were collected from the box core using acrylic core samplers (8 cm i.d.) that were then immediately sealed with polyethylene stoppers (*Fig. 2*). The core samples

http://www.aloki.hu ● ISSN 1589 1623 (Print) ● ISSN 1785 0037 (Online)
DOI: http://dx.doi.org/10.15666/aeer/1705_1216512179

were transferred to the laboratory onboard the research vessel, where the sediment was sectioned at intervals of 1 or 2 cm and transferred to acid-cleaned polyethylene bottles that were sealed with caps. The sediment samples for measuring organic carbon content, total nitrogen content, $CaCO_3$ content, opal content, sediment density, water content, and ^{210}Pb activity were stored at 4°C.

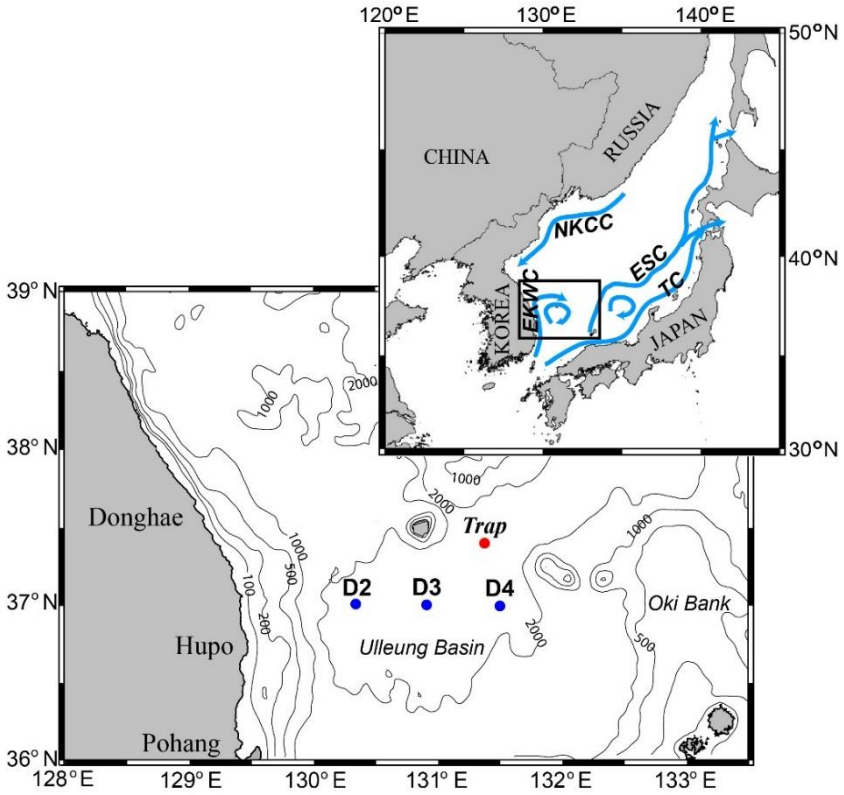

Figure 1. *Study area and sampling sites in the Ulleung Basin, East/Japan Sea. Trap is sediment trap mooring site (KORDI, 2003)*

The organic carbon content was determined by comparing the total carbon measured by a Carlo Erba NA 1500 nitrogen–carbon–sulfur (NCS) analyzer to the inorganic carbon content measured by a Coulometrics inorganic carbon analyzer. Dried samples were combusted at 900ºC in an oxygen atmosphere in the NCS analyzer. The resulting products were chromatographically separated and quantified to obtain the total carbon and total nitrogen contents.

Calculation of the sedimentation rate and sediment mass accumulation rate (MAR)

Dried sediment samples taken from various depths were used to determine the sediment density and porosity. Density was measured by a Micromeritics AccuPyc 1330 density analyzer, and porosity was calculated from water content. A portion of the dried samples were ground and spiked with a known quantity of ^{208}Po to determine the accuracy of the analyses. These samples were leached and brought to dryness three times in the presence of concentrated HNO_3 and 6N HCl. Dilute HCl was then added to the sample, and the solution was separated from the residual solids by centrifugation. For each sample, the dissolved polonium isotopes were plated onto a silver planchet.

http://www.aloki.hu ● ISSN 1589 1623 (Print) ● ISSN 1785 0037 (Online)
DOI: http://dx.doi.org/10.15666/aeer/1705_1216512179

The ^{210}Pb activity was determined by measuring the alpha activity of its granddaughter, ^{210}Po, using a silicon-surface-barrier detector coupled to a multi-channel analyzer. All measurements were conducted at the Korea Basic Science Institute.

Aparent sedimentation rates (ASR) were estimated based on the ^{210}Pb profiles. The exact relation is *Equation 1*.

$$S = -\lambda/b \qquad \text{(Eq.1)}$$

where ***S*** is the sedimentation rate (cm year^{-1}), λ is the decay constant of ^{210}Pb (0.0311 year^{-1}), and b is the slope of the curve. The calculation of sedimentation rates assumes that the excess ^{210}Pb flux and sedimentation are constant over time. Sedimentation rates calculated from profiles of excess ^{210}Pb activity often overestimate actual accumulation rates because the gradual decrease in mixing efficiency with increasing depth results in a depth profile indicating exponential decay (Niggemann et al., 2007), which can be falsely interpreted as undisturbed sediment accumulation.

The sediment mass accumulation rate (MAR) was calculated by following *Equation 2*.

$$\text{MAR (g m}^{-2}\text{ year}^{-1}\text{)} = (1-\varphi) \times \text{GD (g cm}^{-3}\text{)} \times \text{ASR (cm year}^{-1}\text{)} \times 10^4 \qquad \text{(Eq.2)}$$

where φ is porosity, and GD is sediment grain density. The porosity was calculated from the water content. At all stations, water contents decreased rapidly within the top 10-15 cm and were relatively constant below it. We used an average of porosities below 15 cm at each station for the MAR calculation. An average of GD below 15 cm was also used for the MAR calculation.

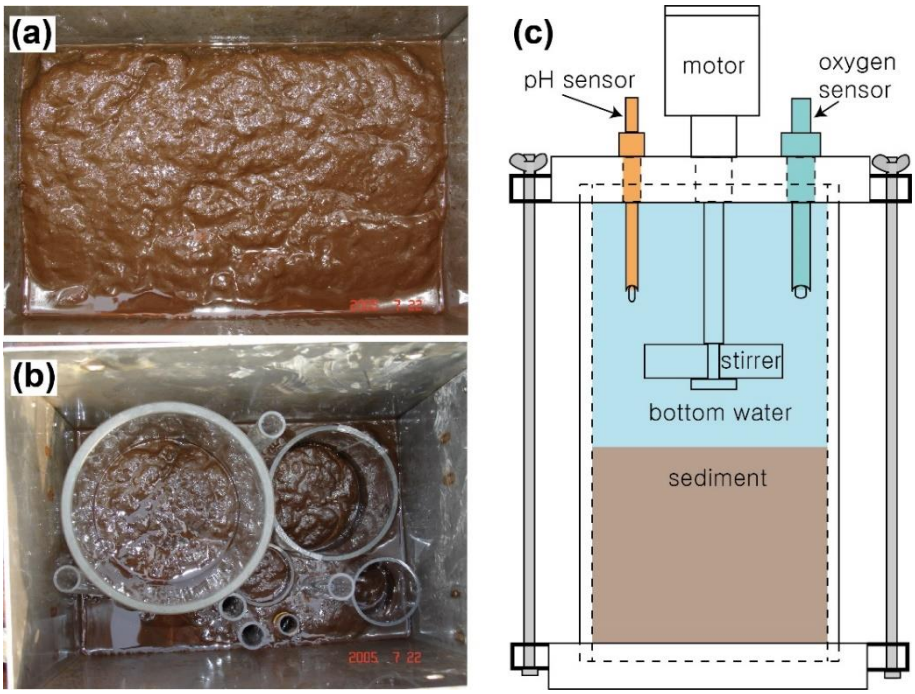

Figure 2. *Photographs of (a) sediment sampling using a box corer and (b) subsampling for geochemical analyses and sediment incubation chamber experiment. A schematic diagram of (c) sediment incubation chamber (Lee et al., 2019)*

http://www.aloki.hu ● ISSN 1589 1623 (Print) ● ISSN 1785 0037 (Online)
DOI: http://dx.doi.org/10.15666/aeer/1705_1216512179

Sediment incubation for calculation of oxygen consumption rate (OCR)

Bottom water taken from the Rosette-sampler was carefully added on top of the sediment at each stations where sediment sampling was performed using the box corer (*Fig. 2*). The water column height overlying the 30 cm sediment core was 18 cm, corresponding to a water volume of approximately 2 L. Immediately after adding bottom water, acryl cover was put on acryl core liner without trapping any air. The core was incubated together with the overlying water at approximately *in-situ* temperature (0.4°C) in a darkened, refrigerator for benthic exchange measurement of oxygen. A stirring speed in the overlying water of approximately 9 rpm was obtained by using a Poly Ethylene stirring bar attached to a Poly Ethylene rod 10 cm above the sediment surface during incubation time of 1-2 days (*Fig. 2*). The sediment incubation was performed until the oxygen was completely depleted or the reduction in oxygen became steady. At the beginning and end of the incubation, overlying water was collected, and the DO concentration was adjusted via Winkler titration. The oxygen consumption rate (OCR) was estimated by reference to the changes in the concentrations measured by the respective sensors in the chamber (Lee et al., 2019), and calculated using the *Equation 3*.

$$F = dC/dt \times V/A \quad \text{(Eq.3)}$$

where F is the net flux of substance via the water-sediment boundary layer (mmol m^{-2} day^{-1}), dC/dt is the slope of the changes in the concentration of oxygen over time (mmol L^{-1} d^{-1}), V is the chamber volume (L), and A is the area of the chamber's horizontal plane (m^2).

Surface chlorophyll-a concentration

The monthly surface chlorophyll-a concentration (mg/m^3) were used MODerate resolution Imaging Spectroradiometer (MODIS)-aqua level 3 data (4x4 km spatial resolution and Standard Mapped Image (SMI) projection) and obtained from NASA Ocean Biologoy Processing Group (http://oceancolor.gsfc.nasa.gov/). The chlorophyll-a concentration data on August, 2007 covered the study area was resampled from the level 3 data.

Results

Surface sediment characteristics

Figure 3 shows contents of the total organic carbon (TOC), total nitrogen (TN), calcium carbonate ($CaCO_3$) and biogenic opal (Si) in the UB sediment. TOC contents in the surface sediments were over 2.6% except station D3. TOC contents profiles showed dramatically decreasing from 2.6 to 1.7% in the uppermost 5 cm, and slightly decline below it. TN content profiles displayed same profiles of organic carbon contents at all stations. At surface sediments, TN contents varied from 0.25% to 0.4%. At all stations, calcium carbonate contents were under 1% at whole depth. The Si contents ranged from 10% to 16% at stations D2 and D4 (*Fig. 3*).

TOC contents are positively correlated with TN values at the UB sediments, with mean TOC/TN (C/N) molar ratio of 7.09, which is almost same as the Redfield ratio (6.63), indicating that the organic matter deposited in the UB is predominantly of

http://www.aloki.hu ● ISSN 1589 1623 (Print) ● ISSN 1785 0037 (Online)
DOI: http://dx.doi.org/10.15666/aeer/1705_1216512179

marine origin. Biogenic opal/TOC (Si/C) ratio ranged from 4.8 to 9.9, with a mean Si/C ratio is 7.2 (*Fig. 4*). The mean Si/C ratio of station D2 is 7.6, and station D4 is 6.7.

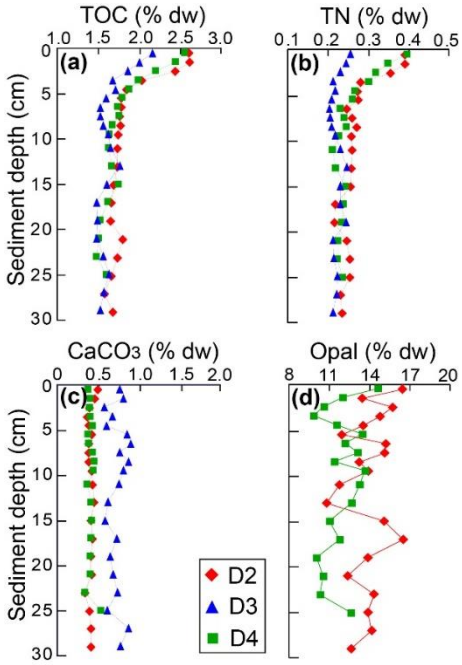

Figure 3. *Depth profiles of (a) total organic carbon (TOC), (b) total nitrogen (TN), (c) calcium carbonate ($CaCO_3$) and (d) biogenic opal in the Ulleung Basin sediment. In site D3, the biogenic opal content could not be analyzed*

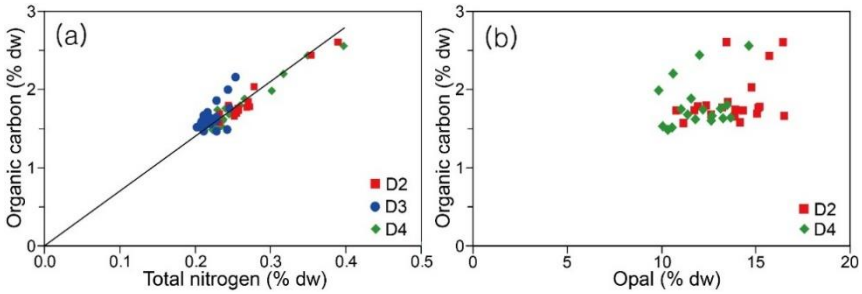

Figure 4. *Organic carbon versus (a) total nitrogen contents and (b) biogenic opal contents at the Ulleung Basin sediment. The C/N ratio was calculated from the slope of the best-fit regression line*

Sedimentation rate

Sedimentation rates were calculated primarily from excess ^{210}Pb distribution, with the common assumption that fluxes of sediment and the associated excess ^{210}Pb activity are reasonably constant on decadal to centennial timescales in the UB. The apparent sedimentation rates (ASR) varied between 0.036-0.047 cm year^{-1} (*Fig. 5*). The sediment mass accumulation rate (MAR) was calculated by porosity, sediment grain density (GD), and ASR in UB sediments. The porosity varied from 0.85 to 0.86, and the GD varied from 2.61 to 2.63 g cm^{-3} (*Table 1*). The calculated MARs ranging from 131 to 184 g m^{-2} year^{-1}, was relatively higher at the station D3 than at the station D4.

http://www.aloki.hu ● ISSN 1589 1623 (Print) ● ISSN 1785 0037 (Online)
DOI: http://dx.doi.org/10.15666/aeer/1705_1216512179

Organic carbon fluxes in the sediment

Time-series sediment trap was deployed at 2,100 m water depth in the UB from December 1998 to January 2000 (KORDI, 2003), which reported that OC content was approximately 6%. Input flux of organic carbon (IF) was calculated from the MAR and OC content at 2,100 m water depth. The calculated IFs varied from 7.89 to 11.08 gC m^{-2} $year^{-1}$. Burial flux of organic carbon (BF) was calculated from the MAR and the averaged OC content below the sediment depth 15 cm where it was not changed considerably (*Fig. 3*). The calculated BFs varied between 2.02-3.10 gC m^{-2} $year^{-1}$ (*Table 1*).

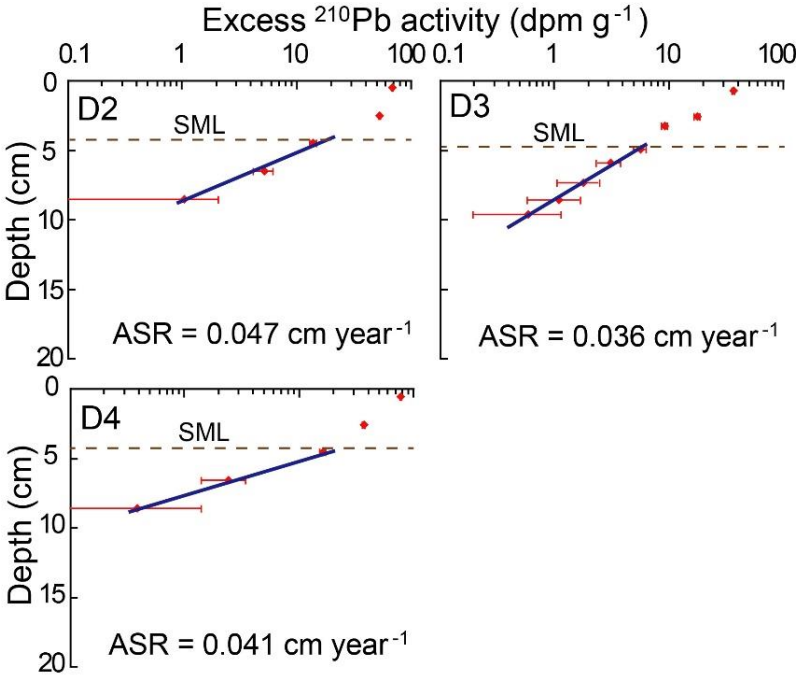

Figure 5. *Depth profiles of excess ^{210}Pb activities (error bars denote standard deviations) at site D2, D3 and D4 in Ulleung Basin sediment. The dotted lines indicate the surface mixed layer (SML)*

Table 1. *Water depth (m), Porosity(φ), grain density (GD), apparent sedimentation rate (ASR), mass accumulation rate (MAR), Input flux of organic carbon (IF), regenerated flux of organic carbon (RF), and burial flux of organic carbon (BF) in the Ulleung Basin sediment*

Site	Water Depth (m)	φ	GD (g cm^{-3})	ASR (cm $year^{-1}$)	MAR (g m^{-2} $year^{-1}$)	IF	RF	BF
						(gC m^{-2} $year^{-1}$)		
D2	2,208	0.85	2.62	0.047	184	11.08	6.59 (7.98)[a]	3.10
D3	2,190	0.86	2.61	0.036	131	7.89	6.22 (5.87)[a]	2.02
D4	2,143	0.85	2.63	0.041	161	9.70	6.22 (7.15)[a]	2.55

[a] Regenerated flux of organic carbon calculated by subtracting burial flux from input flux

In sediments underlying well-oxygenated bottom waters, oxygen is the most important electron accepter for organic matter decomposition. The sedimentary oxygen consumption rate (OCR) is a good first-order indicator of organic matter oxidation rates in many locations. Concentrations of oxygen in the overlying water decreased linearly

http://www.aloki.hu ● ISSN 1589 1623 (Print) ● ISSN 1785 0037 (Online)
DOI: http://dx.doi.org/10.15666/aeer/1705_1216512179

with time over the entire period of the sediment incubations in this study (*Fig. 6*). A linear decrease was to be expected since oxygen concentration did not decrease by more than 5-10% of the almost initial bottom water values. At the stations D2 and D3 in April 2006, sedimentary OCRs were 1.85 and 2.05 mmol m^{-2} day^{-1}, respectively. At the stations D2 and D4 in August 2007, the measured sediment OCRs were 1.87 and 1.85 mmol m^{-2} day^{-1}, respectively (*Fig. 6*).

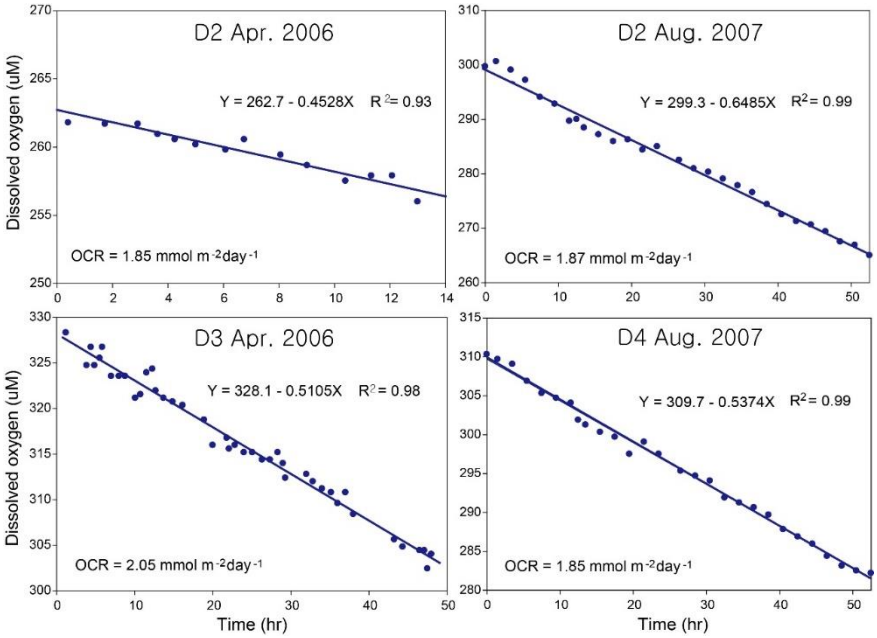

Figure 6. *Time-series of dissolved oxygen concentration in overlying water of chamber experiment at sites D2 and D3 in basin sediment in April 2006, at sites D2 and D4 in August 2007. The solid lines indicate the result of linear regression at considerable oxygen reduced section*

Regenerated flux of organic carbon (RF) was calculated from the sedimentary OCR, since oxygen most likely is the predominant electron acceptors in the mineralization process of sediment, and the oxygen is used in the reduction of the reduced species. In deep sediment, 90% of oxygen is consumed in the mineralization of organic matter and the rest is consumed in the reduction of the reduced species. So, the oxygen consumption and mineralization of organic matter coincides with nearly. In general, 138 moles of oxygen needed to oxidize 106 moles of organic carbon undergoing mineralization. At the stations D2 and D3 in April 2006, the RFs calculated with the OCR were 6.22-6.90 gC m^{-2} $year^{-1}$, respectively. At the stations D2 and D4, the RFs were 6.29-6.22 gC m^{-2} $year^{-1}$ in August 2007, respectively (*Table 1*).

Discussion

Sedimentary organic carbon

At the UB, the high organic contents (> 2.5%) are rarely found in the deep sea sediments, except for the Black Sea with a large river discharge (Cociasu et al., 1996; Reschke et al., 2002) and the Chilean upwelling areas with high primary productivity

http://www.aloki.hu ● ISSN 1589 1623 (Print) ● ISSN 1785 0037 (Online)
DOI: http://dx.doi.org/10.15666/aeer/1705_1216512179

(Schubert et al., 2000; Böning et al., 2005). The UB sediments are less influenced by river discharge since no major rivers drain into the sea along the east coast of Korea (Ikehara et al., 1994).

In the UB, OC flux estimated by the Honjo-type time-series sediment trap was 8.8 gC m^{-2} $year^{-1}$ at the 1020 m water depth from December 1998 to January 2001 (KORDI, 2003), which is about 3 times higher than that in the Bering Sea (Takahashi et al., 2000) and comparable with that in the Chilean upwelling area (Hebbeln et al., 2000). Therefore, the high OC contents in the UB appear to be resulted from the high export production in this area. Besides the high export production, the high OC contents in the UB may be due to the less dilution effect by calcium carbonate (Lee et al., 2008). Chen et al. (1995) suggested that carbonate saturation depths for aragonite and calcite in the E/JS were 300 and 1300 m, respectively. Thus, calcium carbonate contents in the UB sediments were less than 1% (*Fig. 3*), which caused the high OC contents in the UB.

The OC and TN values were used to calculate the C/N molar ratios, which were used to identify whether sedimentary organic matter had originated from algal or land–plant sources. The average C/N molar ratio is 7.09 (*Fig. 4*). Algae have C/N molar ratios between 4 and 10, whereas vascular land plants have ratios of 20 or greater (Jasper and Gagosian, 1990; Meyers, 1994; Prahl et al., 1994). The average Si/C ratios are 7.6 and 6.7 in sites D2 and D4, respectively (*Fig. 4*). The typical stoichiometric proportion of OC to biogenic opal in diatoms with adequate light and nutrients is approximate 7 (Haskell et al., 2013), this suggests that the deposited organic matter in the UB sediment was predominantly of diatoms.

In the UB sediment, more than 80% of deposited organic matter is composed of marine origin biogenic matter, which are dominated by silicate diatoms (Niggemann et al., 2007). In the surface ocean, they sink with POC and ballast minerals, such as siliceous opal and $CaCO_3$ at the same time (Amstrong et al., 2001; Honda and Watanabe, 2010). A $CaCO_3$ is mostly dissolved at a 1,300 m or shallower water depth, but POC and opal settle down on the deeper sea bed. Therefore, at over 2,100 m water depth, the $CaCO_3$ was slightly dissolved and did not significantly affect POC flux. However, the POC sink with high content of biogenic opal, leading to higher POC flux, which may have increased the OC content in the UB sediment.

Fluxes of organic carbon in the sediment

The ASR tends to decrease with increasing water depth, which is consistent with the previous result found by Hong et al. (1997) in the UB. In addition, the sedimentation rates of this study are very similar to those measured by Hong et al. (1997), 0.04-0.17 cm $year^{-1}$, in the same study area. Miralles et al. (2005) proposed an inverse linear relationship between the ASR and water depth in the northwestern Mediterranean margin sediments; ASR (cm $year^{-1}$) = $0.155 - 4.978 \times 10^{-5} \times$ water depth (m). This relation holds strongly in this study area, with only 10 % deviation between the measured values and the expected values from the above relationship.

The high BF values (over 2 gC m^{-2} $year^{-1}$) have rarely been found in the deep sea sediments (deeper than 2000 m), except for the Black Sea deep basin and intense upwelling areas. The BFs obtained from the deep basin of the Black Sea are similar to, or 2–3 times higher than those in the UB (Hay, 1998). In the Peruvian and Namibian upwelling areas, the IF is about an order of magnitude higher than in the UB (Calvert and Price, 1983; Böning et al., 2004). Although MAR estimated in the northern Gulf of

http://www.aloki.hu ● ISSN 1589 1623 (Print) ● ISSN 1785 0037 (Online)
DOI: http://dx.doi.org/10.15666/aeer/1705_1216512179

Mexico is similar to that in the UB, the IF is much lower due to low organic carbon contents (Yeager et al., 2004).

Since oxygen respiration is the principal mineralization process in the sediment of the UB (Lee et al., 2008), a respiratory quotient of 0.77, which is consistent with the Redfiled stoichiometry for the oxidation of organic matter. But Accornero et al. (2003) presented that a respiratory quotient of 0.85 was assumed to convert sediment oxygen consumption into organic carbon remineralization in the sediment of the Gulf of Lions. In the conversion of oxygen consumption into mineralization rates, we assumed that oxygen was consumed by re-oxidation of reduced components within the sediment chamber. This process was found to significantly affect OC oxidation in other continental margin sediments (Canfiel et al., 1993). Previous studies have demonstrated that in sediments of the UB, oxygen and other processes such as Mn-oxide and Fe-oxide reduction, sulfate reduction does play a considerable role in the OC oxidation (Lee et al., 2008; Choi et al., 2009). In the UB, near the sediment-water interface is anoxic condition due to oxygen penetration depth is a few millimeters, and stimulate the heterotrophic activity. Consequently, converted RF by OCR is lower than calculated RF by subtracting BF from IF (*Table 1*).

Organic carbon cycle in the Ulleung Basin

In the UB, Hahm and Kim (2001) estimated the export flux of OC (EF, 64 gC m^{-2} $year^{-1}$) using tritium and helium isotopes and Kim et al. (2011) determined an annual average EF (59 ± 3 gC m^{-2} $year^{-1}$) using $^{238}U/^{234}Th$ disequilibrium. Based on Kim et al. (2011) seasonal average EFs were 216.0, 102.2, 55.2 and 84.2 mgC m^{-2} day^{-1} in spring, summer, autumn and winter, respectively. In spring, the EF was higher than other seasons. This value was attributed to the highest value of the phytoplankton biomass, and the primary production was higher than in summer and autumn. In summer, the EF was moderate value. In autumn, the value was about four times lower than spring. This lower EF value was attributed to the lower primary production in autumn. In winter, however, despite of high primary production, the EF was relatively very low.

Berger et al. (1989) suggested the proportions of OC export flux to primary production in the world open ocean and coastal ocean. The world open ocean and coastal ocean EF/PP ratios are 0.10 and 0.25, respectively. The annual average primary production in the UB was about 177.1 gC m^{-2} $year^{-1}$ (Kim et al., 2011), the EF/PP ratios are 0.36, 0.07 and 0.29 at station D2, D3 and D4, respectively (*Table 2*), average EF/PP ratio is 0.299 (Kim et al., 2011). Satellite-derived primary production ranged between 161-222 gC m^{-2} $year^{-1}$ in the E/JS and the UB is much higher than the Japan basin (Yamada et al., 2005). The EF in the UB was 2 times higher than the world open oceans.

The exported POC from the UB surface ocean is one of the largest sinks of atmospheric carbon dioxide. For example, *Figure 7* showed the satellite-derived chlorophyll-a concentration image in August, 2007. Increasing chlorophyll-a concentration was covered in the study area compared to around area. Hyun et al. (2009) proposed that phytoplankton and bacterioplankton production is enhanced by coastal upwelling and anticyclonic eddy (i.e. Ulleung warm eddy) in the UB. Omand et al. (2015) proposed that a submesoscale eddy-driven flux of POC is unresolved in global carbon cycle models but can contribute as much as half of the total springtime export of POC from the highly productive oceans. Yoo and Park (2009) suggested that the southwest region in the E/JS is highly productive due to southerly wind-driven

http://www.aloki.hu ● ISSN 1589 1623 (Print) ● ISSN 1785 0037 (Online)
DOI: http://dx.doi.org/10.15666/aeer/1705_1216512179

coastal upwelling from spring to fall. Various studies noted that East Korea Warm Current (EKWC) is important factor, which the production in the coastal region transported into the UB by anticyclonic Ulleung Warm Eddy (Isoda and Saitoh, 1993; Michell et al., 2005; Hyun et al., 2009). Time-series sediment trap was deployed at 2100 m water depth in the UB from December 1998 to January 2000 in order to estimate an annual flux of particulate matter (KORDI, 2003), which was 122 g m^{-2} $year^{-1}$, less than the MAR (161 g m^{-2} $year^{-1}$) estimated at site D4. The location of sediment trap deployment was apart about 50 km from site D4 (*Fig. 1*). The site D4 located in eddy region, so export production at D4 is higher than that of sediment trap mooring site.

Table 2. *POC Export flux (EF), Input flux (IF), regenerated flux (RF), and burial flux (BF) of organic carbon/primary production (PP) ratios in the Ulleung Basin. The average primary production in the Ulleung Basin was about 177.1 gC m^{-2} $year^{-1}$ (Kim et al., 2011). Open ocean and Coastal ocean are the average proportions of organic carbon flux to primary production in the world open ocean and coastal ocean (Berger et al., 1989)*

Site	EF / PP ratio	IF / PP ratio	RF / PP ratio	BF / PP ratio
D2	0.328	0.062	0.045	0.017
D3	0.062	0.044	0.033	0.012
D4	0.254	0.055	0.040	0.015
Ave. UB	0.211	0.054	0.039	0.015
Open ocean	0.100	0.010	0.009	0.001
Coastal ocean	0.250	0.066	0.058	0.008

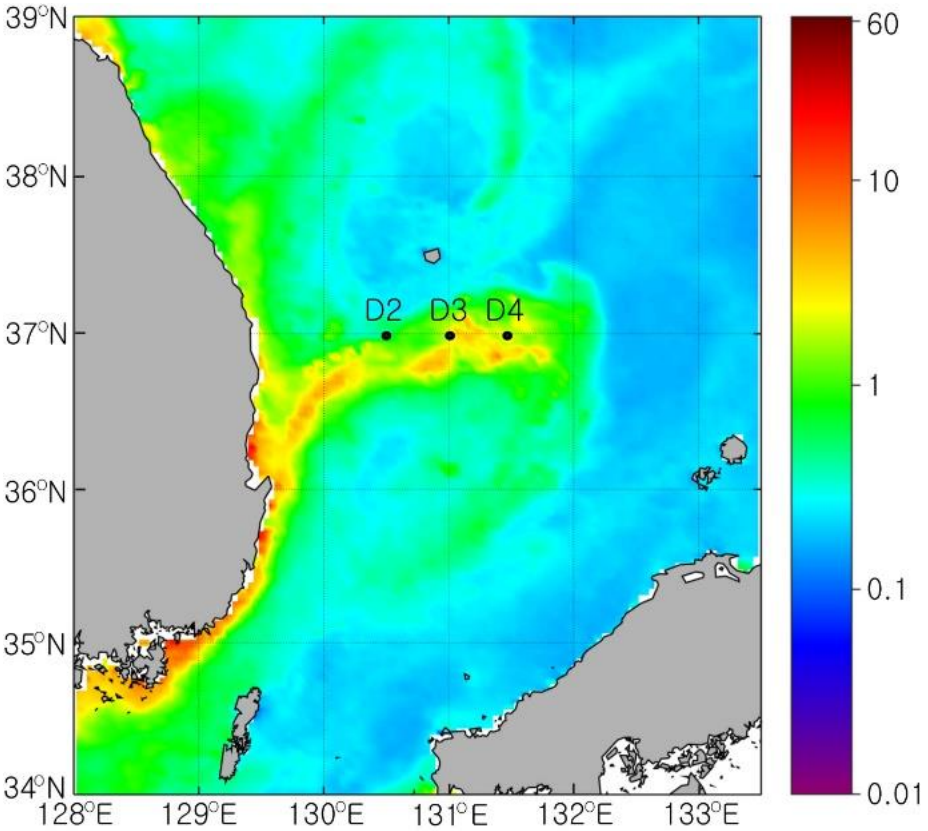

Figure 7. *Monthly mean of surface chlorophyll-a concentration derived from MODIS-aqua in the Ulleung Basin in August, 2007*

http://www.aloki.hu ● ISSN 1589 1623 (Print) ● ISSN 1785 0037 (Online)
DOI: http://dx.doi.org/10.15666/aeer/1705_1216512179

Berger et al. (1989) suggested the proportions of IF, RF, and BF to primary production in the world open ocean and coastal ocean. In the world open ocean and coastal ocean benthic boundary layer, IF/PP ratios are about 0.010 and 0.066, respectively. In the UB deep benthic boundary layer, IF/PP ratio is 0.054 (*Table 2*). In the UB, the POC input to the benthic boundary layer is 5 times higher than in the world open ocean. In the world open ocean, coastal ocean, and UB sediments, RF/PP ratios are about 0.009, 0.058, and 0.039, respectively. The BF/PP ratios are 0.001, 0.008, and 0.015 in the open ocean, coastal ocean and UB, respectively (*Table 2*). Over 1% of primary production is buried on the UB sediment. It is a very rare case in the world coastal ocean and open ocean. Although a large value of IF in the coastal ocean sediment does not contribute significantly to carbon removal. In the coastal area, about 90% of OC deposited in sediments is remineralized, and returned to the water mass with CO_2. In the UB sediment, however, only approximately 80% of the deposited OC is remineralized and approximately 20% is buried. It is important that the UB play a significant role in deep ocean carbon storage.

Conclusion

The UB sediment of E/JS are characterized by high OC contents and high IF of OC. High OC contents (over 2.5%) and high IFs in the deep basin sediments have rarely been found, except for the Black Sea deep basin and intense upwelling areas. The high OC content appeared to result from high export production at surface water in UB. A mean organic matter C/N molar ratio is 7.09, indicating that the organic matter is predominantly of marine origin. The ASRs calculated by activities of excess ^{210}Pb were ranged between 0.036-0.047 cm year^{-1}. The MARs calculated from the ASR and GD, ranged between 131-184 g m^{-2} year^{-1} and agree well with mass flux determined by the previous time-series sediment trap result (122 g m^{-2} year^{-1}). The IF and BF estimated by the MAR were ranged between 7.89-11.08 gC m^{-2} year^{-1}, 2.02-3.10 gC m^{-2} year^{-1}, respectively. The RF estimated by OCR were ranged 6.22-6.59 gC m^{-2} year^{-1}, but RF calculated by subtracting BF from IF were ranged between 5.87-7.98 gC m^{-2} year^{-1}. The average IF/PP, RF/PP and BF/PP ratios of UB sediments were 0.054, 0.039, and 0.015, respectively.

In the UB, high proportion exported to the deep ocean with organic carbon produced by the primary production, high efficiency deposited to the deep boundary layer, high efficiency buried in the sediment. The UB might play an integral role in the deposition and removal of organic carbon. The area of E/JS is only 0.3% of the world ocean, however, may play a fundamental role in the global carbon cycle. These results show promise in terms of carbon cycle in the regions with high production input. The combined data on the in-situ and remote-sensing data clearly reproduce the understanding of the spatial and temporal pattern than is possible by using hydrographic cruise data. This approach is particularly important for interpreting deep waters in the regional and/or global scales.

Acknowledgements. The authors thank the captain, officers and crew of the *R/V Eardo* who were most helpful in all our shipboard operations. We also thank to Dr. Jeong Hee Han of Korea Basic Science Institute, Republic of Korea for ^{210}Pb measurements. This research was funded by KIOST, grant number PE99712 and titled “Biogeochemical cycling and marine environmental changes studies”.

http://www.aloki.hu ● ISSN 1589 1623 (Print) ● ISSN 1785 0037 (Online)
DOI: http://dx.doi.org/10.15666/aeer/1705_1216512179

REFERENCES

[1] Accornero, A., Picon, P., de Bovée, F., Charrière, B., Buscail, R. (2003): Organic carbon budget at the sediment-water interface on the Gulf of Lions continental margin. – Continental Shelf Research 23: 79-92.

[2] Armstrong, R. A., Lee, C., Hedges, J. L., Honjo, S., Wakeham, S. G. (2001): A new, mechanistic model for organic carbon fluxes in the ocean based on the quantitative association of POC with ballast minerals. – Deep-Sea Research II 49: 219-236.

[3] Berger, W. H., Smetacek, V. S., Wefer, G. (1989): Ocean productivity and paleoproductivity - an overview, productivity of the oceans present and past. – In: Report of the Dahlem workshop on productivity of the ocean; Berlin, Life science research report 44, Wiley & Sons, Chicherster, pp. 1-34.

[4] Böning, P., Brymsack, H. J., Böttcher, M. E., Schnetger, B., Kriete, C., Kallmeyer, J., Borchers, S. L. (2004): Geochemistry of Peruviam near-surface sediments. – Geochimica et Cosmochimica Acta 68: 4429-4451.

[5] Böning, P., Cuypers, S., Grunwald, M., Schnetger, B., Brumsack, H. J. (2005): Geochemical characteristics of Chilean upwelling sediments at ~36°S. – Marine Geology 220: 1-21.

[6] Calvert, S. E., Price, N. B. (1983): Geochemistry of Namibian sediments: Coastal upwelling, part A. – Response of the sedimentary regime to present coastal upwelling. Plenum, New York, USA, pp. 333-375.

[7] Canfiel, D. E., Jorgensen, B. B., Fossing, H., Glud, R., Gundersen, J., Ramsing, N. B., Thamdrup, B., Hansen, J. W., Nielsen, L. P., Hall, P. O. J. (1993): Pathways of organic carbon oxidation in the continental margin sediments. – Marine Geology 113: 27-40.

[8] Chen, C. T. A., Wang, S. L., Bychkov, A. S. (1995): Carbonate chemistry of the Sea of Japan. – Journal of Geophysical Research 100: 13737-13745.

[9] Choi, Y. J., Kim, D., Lee, T., Lee, C. B. (2009): Estimate of manganese and iron oxide reduction rates in slope and basin sediments of Ulleung Basin, East Sea. – Journal of Korean Society Oceanography 14: 127-133. (in Korean).

[10] Chough, S. K., Brag, E. (1987): Tectonic history of Ulleung basin margin, East Sea (Sea of Japan). – Geology 15(1): 45-48.

[11] Chough, S. K., Lee, H. J., Yoon, S. H. (2000): Marine Geology of Korean Seas. – 2nd Ed, Elsevier, Amsterdam, 313p.

[12] Cociasu, A., Dorogan, L., Humborg, C., Popa, L. (1996): Long-term ecological changes in the Romanian coastal waters of the Black Sea. – Marine Pollution Bulletin 32: 32-38.

[13] Emeis, K. C., Struck, U., Leipe, T., Pollehne, F., Kunzendorf, H., Christiansen, C. (2000): Changes in the C, N, P burial rates in some Baltic Sea sediments over the last 150 years-relevance to P regeneration rates and the phosphorus cycle. – Marine Geology 167: 43-59.

[14] Hahm, D., Kim, K. R. (2001): An estimation of the new production in the southern East Sea using helium isotopes. – Journal of Korean Society Oceanography 36: 19-26. (in Korean).

[15] Haskell, W. Z., Berelson, W. M., Hammond, D. E., Capone, D. G. (2013): Particle sinking dynamics and POC fluxes in the Eastern Tropical South Pacific based on ^{234Th} budgets and sediment trap deployments. – Deep-Sea Research I 81: 1-13.

[16] Hay, B. J. (1998): Sediment accumulation in the central western Black Sea over the past 5100 years. – Paleoceanography 3: 491-508.

[17] Hebbeln, D., Marchant, M., Wefer, G. (2000): Seasonal variations of the particle flux in the Peru-Chile current at 30°S under 'normal' and El Nino conditions. – Deep-Sea Research II 47: 2101-2128.

http://www.aloki.hu ● ISSN 1589 1623 (Print) ● ISSN 1785 0037 (Online)
DOI: http://dx.doi.org/10.15666/aeer/1705_1216512179

[18] Honda, M. C., Watanabe, S. (2010): Importance of biogenic opal as ballast of particulate organic carbon (POC) transport and existence of mineral ballast-associated and residual POC in the Western Pacific Subarctic Gyre. – Geophysical Research Letters 37: L02605, doi:10.1029/2009GL041521.

[19] Hong, G. H., Kim, S. H., Chung, C. S., Kang, D. J., Shin, D. H., Lee, H. J., Han, S. J. (1997): ^{210}Pb-drived sediment accumulation rates in the southwestern East Sea (Sea of Japan). – Geo-Marine Letters 17: 126-132.

[20] Hong, G. H., Kim, Y. I., Baskaran, M., Kim, S. K., Chung, C. S. (2008): Distribution of ^{210}Po and export of organic carbon from euphotic zone in the Southwestern East Sea (Sea of Japan). – Journal of Oceanography 64: 277-292.

[21] Hyun, J. H., Kim, D., Shin, C. W., Noh, J. H., Yang, E. J., Mok, J. S., Kim, S. H., Kim, H. C., Yoo, S. (2009): Enhanced phytoplankton and bacterioplankton production coupled to coastal upwelling and an anticyclonic eddy in the Ulleung basin, East Sea. – Aquatic Microbial Ecology 54: 45-54.

[22] Ikehara, K., Kikkawa, K., Oshima, H. (1994): Late Quaternary paleoenvironments of the Japan Sea as revealed by tephrochronology, AMS-14 dating and palynological data. – In: Proceedings of 1994 Sapporo Symposium global fluxes of carbon and its related substances in the coastal Sea-Ocean-Atmosphere system. pp. 505-510.

[23] Isoda, Y., Saitoh, S. (1993): The northward intruding eddy along the east coast of Korea. – Journal of Oceanography 49: 443-458.

[24] Jasper, J. P., Gagosian, R. B. (1990): The source and deposition of organic matter in the Late Quaternary Pygmy Basin, Gulf of Mexico. – Geochimica et Cosmochimica Acta 54: 117-132.

[25] Kim, D., Choi, M. S., Oh, H. Y., Song, Y. H., Noh, J. H., Kim, K. H. (2011): Seasonal export fluxes of particulate organic carbon from ^{234}Th/^{238}U disequilibrium measurements in the Ulleung Basin (Tsushima Basin) of the East Sea (Sea of Japan). – Journal of Oceanography 67: 577-588.

[26] KORDI. (2003): Marine ecosystem responses to climate variability in the East Sea. – KORDI Tech. Rep. BSPE 825-00-1495-3 498p. (in Korean).

[27] Lee, T., Hyun, J. H., Mok, J. S., Kim, D. (2008): Organic carbon accumulation and sulfate reduction rates in slope and basin sediments of Ulleung Basin, East/Japan Sea. – Geo-Marine Letters 28: 153-159.

[28] Lee, T., Kim, H. C., Son, Y. B. (2019): Sediment oxygen consumption and hydrogen sulfide release in hypoxic areas of Gamak Bay, Korea. – Applied Ecology and Environmental Research 17: 3199-3214.

[29] Leipe, T., Tauber, F., Vallius, H., Virtasalo, J., Uścinowicz, S., Kowalski, N., Hille, S., Lindgren, S., Myllyvirta, T. (2011): Particulate organic carbon (POC) in surface sediments of the Baltic Sea. – Geo-Marine Letters 31: 175-188.

[30] Masuda, A. (2000): Toward the clarification of variabilities in atmospheric and oceanic conditions in the Japan Sea. – In: Proceedings of 49th conference of applied mechanics. pp. 285-288.

[31] Meyers, P. A. (1994): Preservation of elemental and isotopic source identification of sedimentary organic matter. – Chemical Geology 144: 289-302.

[32] Michell, D. A., Watts, D. R., Wimbush, M., Teague, W. J., Tracey, K. I., Book, J. W., Chang, K. I., Suk, M. S., Yoon, J. H. (2005): Upper circulation patterns in the Ulleung Basin. – Deep-Sea Research II 52: 1617-1638.

[33] Miralles, J., Radakovitch, O., Aloisi, J. C. (2005): ^{210}Pb sedimentation rates from the Northwestern Mediterranean margin. – Marine Geology 216: 155-167.

[34] Niggemann, J., Ferdelman, T. G., Lomstein, B. A., Kallmeyer, J., Schubert, C. J. (2007): How depositional conditions control input, composition, and degradation of organic matter in sediments from the Chilean coastal upwelling region. – Geochimica et Cosmochimica Acta 71: 1513-1527.

http://www.aloki.hu ● ISSN 1589 1623 (Print) ● ISSN 1785 0037 (Online)
DOI: http://dx.doi.org/10.15666/aeer/1705_1216512179

[35] Omand, M. M., D'Asaro, E. A., Lee, C. M., Perry, M. J., Briggs, N., Cetinic, I., Mahadevan, A. (2015): Eddy-driven subduction expores particulate organic carbon from the spring bloom. – Science 348: 222-225.
[36] Park, M. H., Kim, J. H., Kim, I. S., Ryu, B. J., Yu, K. M. (2005): Tehprostratigraphy and paleo-environmental implications of Late Quaternary sediments and interstitial water in the western Ulleung Basin, East/Japan Sea. – Geo-Marine Letters 25: 54-62.
[37] Prahl, F. G., Ertel, J. R., Goni, M. A., Sparrow, M. A., Eversmeyer, B. (1994): Terrestrial organic carbon contributions to sediments on the Washington margin. – Geochimica et Cosmochimica Acta 58: 3055-3048.
[38] Reschke, S., Ittekkot, V., Panin, N. (2002): The nature of organic matter in the Danube river particles and north-western Black Sea sediments. – Esturine, Coastal and Shelf Science 54: 563-574.
[39] Savoye, N., Benitez-Nelson, C., Burd, A. B., Cochran, J. K., Charette, M., Buesseler, K. O., Jackson, G. A., Roy-Barman, M., Schmidt, S., Elskens, M. (2006): ^{234}Th sorption and export models in the water column: a review. – Marine Chemistry 100: 234-249.
[40] Schubert, C. J., Ferdelman, T. G., Strotmann, B. (2000): Organic matter composition and sulfate reduction rates in sediment of Chile. – Organic Geochemistry 31: 351-361.
[41] Seiter, K., Hensen, C., Schröter, J., Zabel, M. (2004): Organic carbon content in surface sediments-defining regional provinces. – Deep-Sea Research I 51: 2001-2026.
[42] Suess, E. (1980): Particulate organic carbon flux in the ocean-surface productivity and oxygen utilization. – Nature 288: 260-263.
[43] Summerhayes, C. P. (1981): Organic facies of middle Cretaceous black shales in deep north Atlantic. – AAPG Bulletin 65: 2364-2380.
[44] Takahashi, K., Fujitani, N., Yanada, M., Maita, Y. (2000): Long-term biogenic particle fluxes in the Bering Sea and central subarctic Pacific Ocean, 1990-1995. – Deep-Sea Research I 47: 1723-1759.
[45] Tissot, B. P., Demaison, G., Masson, P., Delteil, J. R., Combaz, A. (1980): Paleoenvironment and petroleum potential of middle Cretaceous black shales in Atlantic basins. – AAPG Bulletin 64: 2051-2063.
[46] Trull, T., Bray, S., Manganini, S., Honjo, S., Francois, R. (2011): Moored sediment trap measurement of carbon export in the Sub-antarctic and Polar Frontal Zones of the Southern Ocean, south of Australia. – Journal of Geophysical Research 106: 31489-31509.
[47] Waples, J. T., Benitez-Nelson, C. R., Savoye, N., Rutgers van der Loeff, M., Baskaran, M., Gustafsson, O. (2006): An introduction to the application and future use of ^{234}Th in aquatic systems. – Marine Chemistry 100: 166-189.
[48] Yamda, K., Ishizaka, J., Nagata, H. (2005): Spatial and temporal variability of satellite estimated primary production in the Japan Sea from 1998 to 2002. – Journal of Oceanography 61: 857-869.
[49] Yeager, K. M., Santschi, P. H., Rowe, G. T. (2004): Sediment accumulation and radionuclide inventories (^{239,240}Pu, ^{210}Pb and ^{234}Th) in the northern Gulf of Mexico, as influenced by organic matter and macrofaunal density. – Marine Chemistry 91: 1-14.
[50] Yoo, S., Park, J. (2009): Why is the southwest the most productive region of the East Sea/Sea of Japan? – Journal of Marine Systems 78: 301-315.

http://www.aloki.hu ● ISSN 1589 1623 (Print) ● ISSN 1785 0037 (Online)
DOI: http://dx.doi.org/10.15666/aeer/1705_1216512179

CELLULAR BIOLOGICAL AND EUMELANIN-RELATED GENE EXPRESSIONAL BASES OF PIGMENT DEVIATION OF *LEPTOBOTIA TAENIOPS*

JIANG, H.[1,2,3] – LIU, S.[1,2,3] – XIAO, T. Y.[1,2,3*] – CAO, Y. K.[4] – XIE, M.[5] – YIN, Z. F.[1,2,3]

[1]*College of Animal Science and Technology, Hunan Agricultural University, Changsha 410128, China*

[2]*Hunan Engineering Technology Research Center of Featured Aquatic Resources Utilization, Hunan Agricultural University, Changsha 410128, China*

[3]*Collaborative Innovation Center for Efficient and Health Production of Fisheries in Hunan Province, Changde 415000, China*

[4]*R&D Center, Guangdong Meilikang Bio-Science Ltd., Dongguan 523808, China*

[5]*Hunan Fisheries Science Institute, Chiangsha 410153, China*

**Corresponding author*
e-mail: tyxiao1128@163.com; phone: +86-731-8461-8176

(Received 1st May 2019; accepted 11th Jul 2019)

Abstract. Pigmentation is closely associated with various behaviors, and it is also an important feature that influences the popularity and price of ornamental fish. However, the molecular mechanism that regulates the pigmentation of fish is barely understood. There are two clearly different pigmentation phenotypes, i.e. light and dark phenotypes, in the same natural population of *Leptobotia taeniops*. Type and distribution of chromatophores is the cellular basis of the pigmentation. To analyze the composition of chromatophores in the light and dark phenotypes of *L. taeniops* and the correlation of the pigmentation to the expressions of pigment synthesis genes, we studied the pigment cell types and distribution in the skin of *L. taeniops* by microscope, and analyzed the expressions of genes that regulate melanin production using real-time qRT-PCR. Our results showed that the amount of melanophores in the skin was the major factor that caused the pigment deviation of *L. taeniops* living in the same habitat. The expressions of *TYR*, *Tyrp1*, and *Dct* genes were significantly higher in the skin of the dark phenotype than those in the light phenotype. This result implied that the amount of melanophores was influenced by the expression of these genes in the skin of *L. taeniops*.
Keywords: *chromatophores, ecological adaptation, fish skin, melanin-related gene, pigment cell, real-time fluorescent quantitative PCR*

Introduction

Pigmentation of fish is associated with various behaviors, such as warning, courtship, and hiding (Blakeslee et al., 2009; Culumber, 2013; Jiang et al., 2019). Additionally, in some species of fish, such as *Poecilia reticulate*, bright flashy colors may show a parasite infection (Houde and Torio, 1992) and the pigmentation has also been associated with immunocompetence in *Betta splendens* (Clotfelter et al., 2007). In ornamental fish market, pigmentation is an important feature that influences the popularity and price of ornamental fish. However, although cellular basis and development pattern of pigmentation of some fish species, such as *Betta splendens*, has been studied (Khoo et al., 2014; Carey et al., 2015), the molecular mechanism that regulates the pigmentation of fish is still rarely studied.

http://www.aloki.hu ● ISSN 1589 1623 (Print) ● ISSN 1785 0037 (Online)
DOI: http://dx.doi.org/10.15666/aeer/1705_1218112189

Leptobotia taeniops is a small freshwater fish living in Yangtze River basin (Hunan Fisheries Science Institute, 1980; Ding, 1994; Ni and Wu, 2006; Fang et al., 2011). There are two obviously different pigment phenotypes, i.e. light and dark phenotypes, in the same natural population of *L. taeniops* (Jiang et al., 2019), and the difference is not influenced by heredity (Meng, 2011).

Type and distribution of chromatophores is cellular basis of the pigmentation (Khoo et al., 2014). It has been well documented that teleost fish have various chromatophore types, such as melanophores, xanthophores, erythrophores, iridophores, cyanophores, and leucophores (Jeon et al., 1993). Since the light phenotype of *L. taeniops* is of a near golden color and the dark one is yellowish-brown, and there are black stripes and splashes on their body (Jiang et al., 2019), melanophores and xanthophores were maybe the major chromatophores that influence the pigmentation of *L. taeniops*. In addition, melanin is the chromogenic substance in melanophores and tyrosinase plays an important role in synthesis of melanin (Lamoreux et al., 2001), and in our previous study, we have proved that the expression of tyrosinase gene in skin significantly higher in the light phenotype of *L. taeniops* than those in the dark phenotypes (Jiang et al., 2019). However, although it is important to elucidate the molecular mechanism that regulates the pigmentation of *L. taeniops* to adapt their external environment and protect wild *L. taeniops*, how the expression of tyrosinase gene in skin influences the pigmentation of *L. taeniops* and whether it associates with other genes is still unknown.

To analyze the composition of chromatophores in the light and dark phenotypes of *L. taeniops* and the correlation of the pigmentation to the expressions of pigment synthesis genes, we studied the pigment cell types and distribution by microscope, and analyzed the expressions of genes that regulate melanin production using real-time quantitative reverse transcription PCR (qRT-PCR). The results would provide important reference to elucidate the molecular mechanism that regulates the pigmentation of *L. taeniops* to adapt their external environment.

Materials and methods

Sample collection

The fish samples were collected from Yueyang Section (113.2051 N, 29.5140 E) of the Yangtze River during July to September, 2017, and transported to the Aquaculture Laboratory of Hunan Agricultural University to temporary culture in a circulating water system at 25 ± 1 °C. Healthy light and dark phenotype samples (6 specimens of each phenotype) were anaesthetized using MS-222, photographed, and measured body lengths and body weights. Subsequently, they were dissected and their sex was identified through sex gland. The skins at both sides of the dorsal fin base were collected using anatomical tools for microscopic examination of chromatophores and total RNA extraction.

Microscopic examination of chromatophores in skin of L. taeniops

The skins for microscopic examination of chromatophores were washed using phosphate buffer and made temporary slides. The temporary slides were examined and photographed using an Olympus BX53 microscope (Olympus, Japan). Amount of chromatophores in randomly selected 100 × 100 μm square regions of the photographs was counted and each phenotype was examined 10 times.

http://www.aloki.hu ● ISSN 1589 1623 (Print) ● ISSN 1785 0037 (Online)
DOI: http://dx.doi.org/10.15666/aeer/1705_1218112189

Another 1 × 1 cm of skins were fixed 24 h using 4% paraformaldehyde tissue stationary fluid and paraffin sections of the skins were prepared and hematoxylin and eosin (HE) staining was conducted according to previous reports (Huang et al., 2018; Li et al., 2019). Then the skin tissue slices were examined and photographed using an Olympus BX53 microscope (Olympus, Japan).

Total RNA extraction and qRT-PCR

Total RNA was extracted from 50–80 mg of each skin sample using E.Z.N.A total RNA kit I (OMEGA, China) according to the manufacturer's introduction. The first stand of cDNA was synthetized using a RevertAid first strand cDNA synthesis kit (Fermentas, USA) with Oligo(dT)$_{18}$ primer according to the manufacturer's introduction (Jiang et al., 2019). Fluorescent quantitative PCR primers were designed using primer 6.0 software according to tyrosinase (*TYR*), tyrosinase-related protein 1 (*Tyrp1*), dopachrome tautomerase (*Dct*), Microphthalmia-associated transcription factor (*Mitfa*), Sox10 and melanocortin 1 receptor (*MC1R*) gene sequences of Cyprinidae fish in GenBank database (*Table 1*). β-Actin gene was used as endogenous reference (Jiang et al., 2019).

Table 1. *Real-time fluorescent quantitative PCR primers of melanin-related genes*

Gene name	Primer name	Primer sequence (5'-3')	Description	Reference
TYR	qRT-TYR-F	ATGCCTATTTGCTGGACCCC	qRT-PCR primer	Present study
TRY	qRT-TYR-R	TATGCCGACATCTTCCTGCG	qRT-PCR primer	Present study
Tyrp1	qRT-Tyrp1-F	ACCACCATATTACTCAACGTCCTCT	qRT-PCR primer	Present study
Tyrp1	qRT-Tyrp1-R	AGTCTGTCCACCTGTGCCATTAAG	qRT-PCR primer	Present study
Dct	qRT-Dct-F	GCAGAGGCATCACCGACAGAAC	qRT-PCR primer	Present study
Dct	qRT-Dct-R	CCTGAAGCTGAAGGTTGAGTTGGT	qRT-PCR primer	Present study
MITFa	qRT-Mitfa-F	TGCTCACGGACTTGCTGTAG	qRT-PCR primer	Present study
MITFa	qRT-Mitfa-R	AGAGATCGGAGGAGCAGTCT	qRT-PCR primer	Present study
Sox10	qRT-Sox10-F	CGATCAGTACCCGCACCTG	qRT-PCR primer	Present study
Sox10	qRT-Sox10-R	CTGTTTCCGCAAACGCTCG	qRT-PCR primer	Present study
MC1R	qRT-MC1R-F	CCATCTTTTACGCGCTTCGG	qRT-PCR primer	Present study
MC1R	qRT-MC1R-R	AACGTGACAAGACAGGCGAT	qRT-PCR primer	Present study
β-Actin	β-Actin-F	CTGGACTTGGCTGGTCGTG	Internal control primer	Jiang et al., 2019
β-Actin	β-Actin-R	CTCGAAGTCAAGGGCAACAT	Internal control primer	Jiang et al., 2019

To calculate the amplification efficiencies (*E%*) and the correlation coefficients (R^2) of the primers, the cDNA was gradiently diluted to 5, 25, 125, and 625 times and the E% and R^2 of the primers were calculated by qRT-PCR. The qRT-PCR was conducted as our previous description (Ni et al., 2018; Jiang et al., 2019). Three technical repetitions of each sample were set to exclude technical error. The results were collected and analyzed using CFX manager software 3.1. Relative expressions of the genes were calculated by the comparative Ct ($2^{-\Delta\Delta Ct}$) method (Spivak et al., 2012).

Data analysis

Each parameter result is presented as means ± standard deviation (SD). Independent *t*-test was used to compare the significance of difference between the light and dark

http://www.aloki.hu ● ISSN 1589 1623 (Print) ● ISSN 1785 0037 (Online)
DOI: http://dx.doi.org/10.15666/aeer/1705_1218112189

phenotypes. p-values < 0.05 were considered statistically significant. The statistical analyses and plotting were conducted using R 3.5.1 (R Core Team, 2017).

Results and discussion

Amount of melanophores caused pigment deviation of L. taeniops

Type and distribution of chromatophores is cellular basis of the pigmentation. Specific combinations of chromatophores in skin of *Betta splendens* formed the pigmentation patterns of the dark blue, ultra-maine, turquoise-bronze, and golden strains (Khoo et al., 2014). There were two major chromatophores, i.e. melanophores and xanthophores in the skin of *L. taeniops* (*Fig. 1*). There was no significant difference of the xanthophore amounts in the skin between light and dark phenotypes (Independent *t*-test, $t = 0.893$, $p = 0.384$). However, the melanophore amounts were significantly increased in dark phenotype skin than those in light phenotype skin (Independent *t*-test, $t = 10.622$, $p < 0.001$; *Fig. 1*). The result showed that the pigment deviation between light and dark phenotypes of *L. taeniops* mainly caused by the difference of melanophore amount.

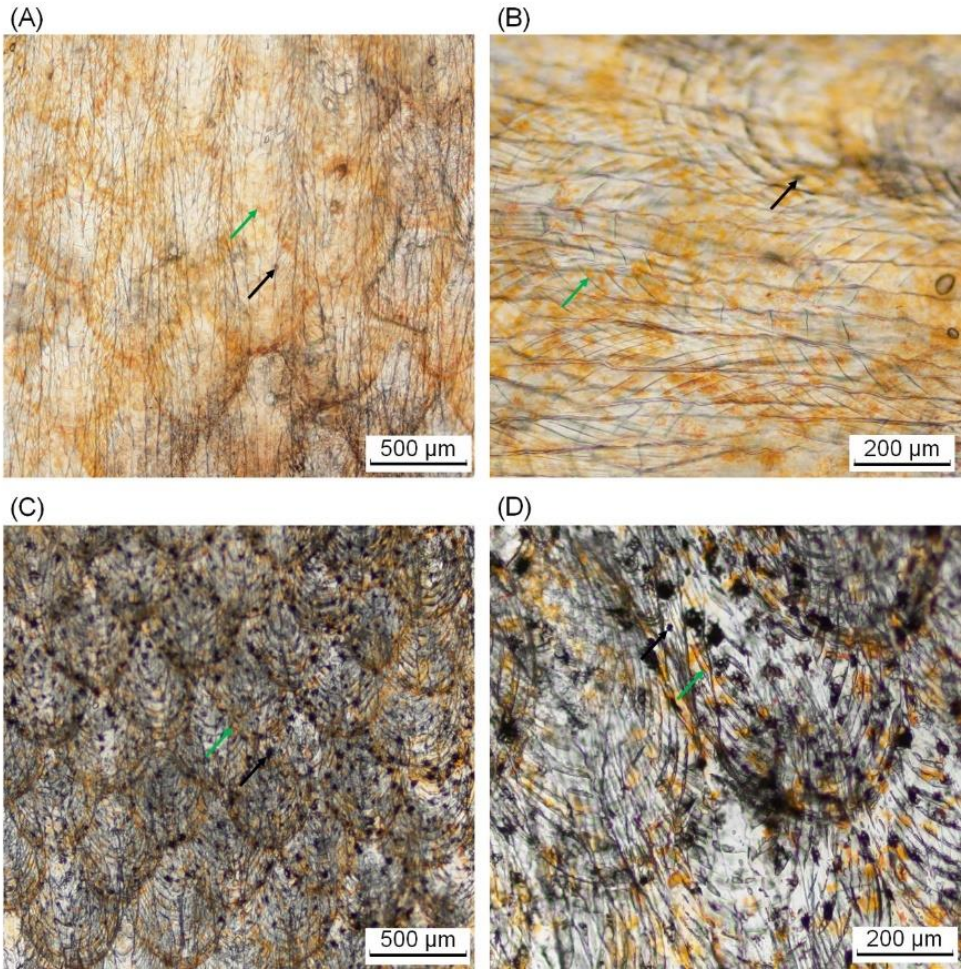

Figure 1. *Microscopic profiles of skin temporary slides showed pigment cells of Leptobotia taeniops. A and B: light phenotype of L. taeniops; C and D: dark phenotype of L. taeniops. The black arrows indicate the melanophores, and the green arrows indicate the xanthophores*

http://www.aloki.hu ● ISSN 1589 1623 (Print) ● ISSN 1785 0037 (Online)
DOI: http://dx.doi.org/10.15666/aeer/1705_1218112189

The tissue structure of *L. taeniops* skin was analogous to other fish, including epidermis (EP; Approximately 50-100 μm), dermis (D; Approximately 130-200 μm), and subcutaneous layer (SL). The epidermis did not keratinization and covered by multilayer epithelial cells. The epithelial cells were flat and arranged closely. Under the epithelial cells, glandular layer occupied the majority of the epidermis. It was composed by goblet-cell (GC), club cell (CC), and epithelial cell (EC). The malpighian layer was close to the basement membrane. The dermis was constituted by dense connective tissue and was rich in fiber. The dermis was divided into the loose layer (SS) and the compact layer (SC) according to the fiber arrangement. The loose layer occupied a large part of the dermis, and the fibers in the loose layer arranged loosely. The fibers in the compact layer arranged closely. The subcutaneous layer located below the dermis, and contained a large number of fat cells, vessels and nerves (*Fig. 2*). The pigment cells of *L. taeniops* mainly distributed in the dermis, and a small amount of the pigment cells distributed in the epidermis. The pigment cells were stained into deep color by HE staining as the cells contain pigment granule. Shapes of the pigment cells were diversiform, and were mainly long strip and asteroid. A large number of pigment cells distributed in the loose layer and their distribution was not continuously and evenly (*Fig. 2*). This result implied that the pigment cells were not even-distributed in the skin of *L. taeniops*, in accordance with the results of the skin temporary slides.

The dermis of light *L. taeniops* was thicker than those of dark phylotype, while the epidermis and subcutaneous layer of light *L. taeniops* was thinner. The epithelial cells in the skin of light *L. taeniops* were more than those of dark phylotype (*Fig. 2*). These results implied that although the amount of melanophores caused the pigment deviation of *L. taeniops*, there was a deeply histological basis that influenced the amount of melanophores. This may be influenced by expression of the pigment genes.

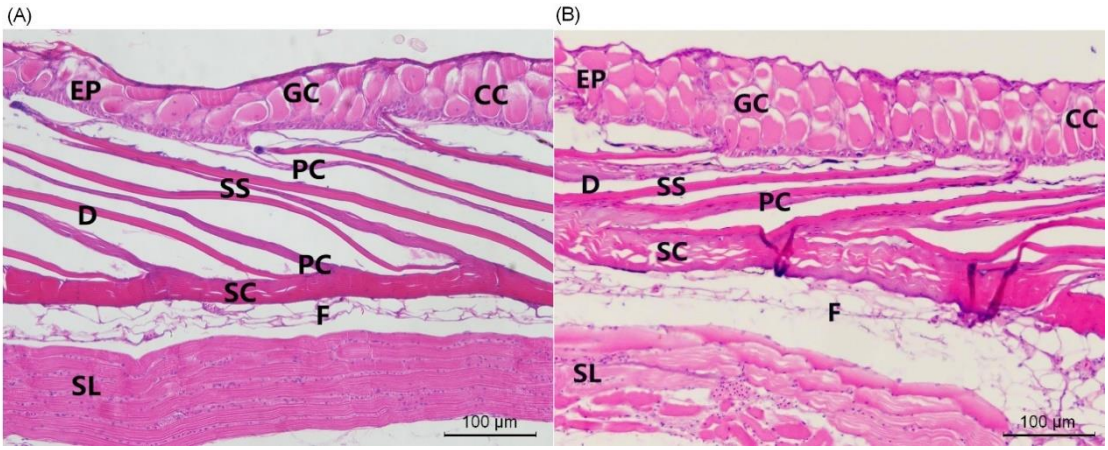

Figure 2. *Microscopic profiles of the skin paraffin sections with H-E dyeing of Leptobotia taeniops. A: Light phenotype; B: dark phenotype. EP, epidermis; D, dermis; SL, subcutaneous layer; SS, loose layer; SC, compact layer; GC, goblet cells; CC, club cell, EP, epithelial cells; PC, pigment cells; F, fat cells*

TYR, Tyrp1, and Dct genes were higher expressed in light than in dark L. taeniops

The first step of melanin production involves *TYR* which catalyzes the transformation of tyrosine to dopaquinone and then dopachrome in the eumelanin pathway. Then, *Dct*

http://www.aloki.hu ● ISSN 1589 1623 (Print) ● ISSN 1785 0037 (Online)
DOI: http://dx.doi.org/10.15666/aeer/1705_1218112189

catalyzes the transformation of dopachrome to dihydroxyindole carboxylic acid (DHICA) and *Tyrp1* catalyzes the oxidation of DHICA and finally biosynthesis of eumelanin (*Fig. 3*; Murisier and Beermann, 2006). In addition, *MC1R* protein shows high affinity for α-melanocyte-stimulating hormone (α-MSH) and bingding of α-MSH to *MC1R* activated adenylate cyclase and increased cyclic adenosine monophosphate production, thus activating a variety of intracellular pathways which promote a switch in melanin synthesis from pheomelanin to eumelanin (Sturm et al., 1998). *Mitf* is critically involved in melanin synthesis, which enhances transcription of the genes encoding major enzymes in the melanin synthesis pathway, including *TYR*, *Tyrp1*, *Tyrp2*, and *Dct* (Yasumoto et al., 1994, 1997; Udono et al., 2000; Saito et al., 2003). Sox10 regulates the development of neural crest-derived melanocytes and the early development of the prospective neural crest (Aoki et al., 2003; Honoré et al., 2003). Therefore, we analyzed the expression of these genes in the skin of the light and dark *L. taeniaps*. The *E%* of TYR, Tyrp1, Dct, Mitfa, Sox10, and MC1R primers were 104.8%, 101.8%, 102.6%, 103.8%, 101.4%, and 95.5%, respectively; and the R^2 were 0.991, 0.998, 0.997, 0.997, 0.994, and 0.987, respectively. All of them were achieved the technical requirements of qRT-PCR that 90% < *E%* < 105% and $R^2 > 0.98$. The results showed that these primers could be used to quantify the expressions of these genes in the skins of *L. taeniops* with different pigmentation.

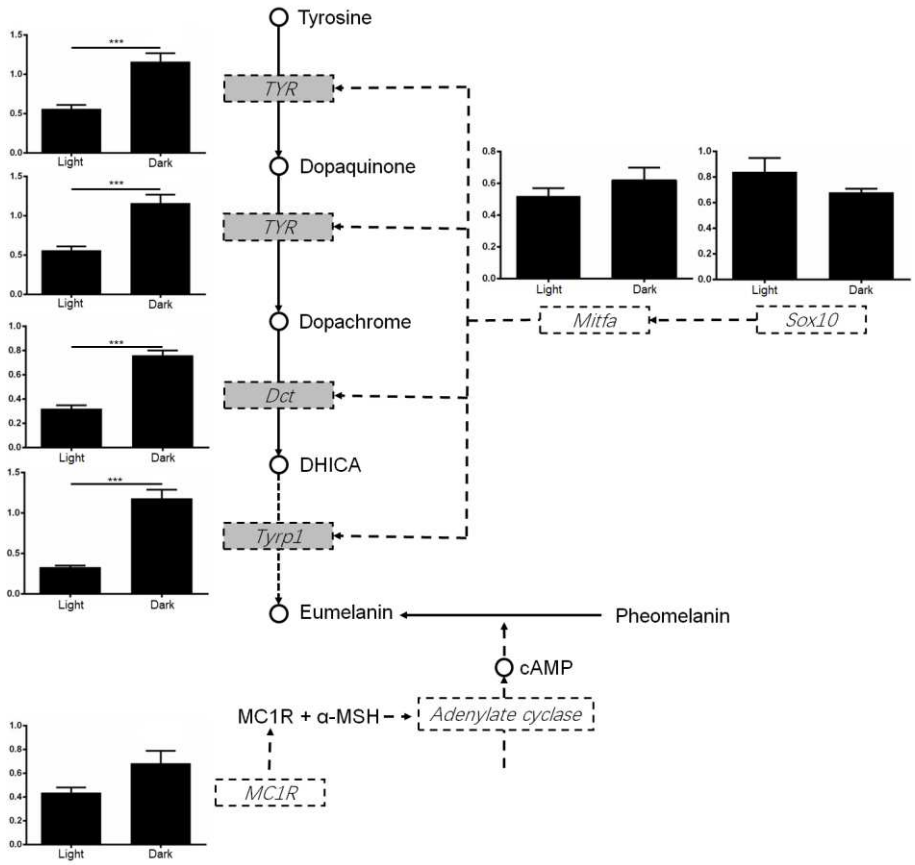

Figure 3. *Regulatory pathway of eumelanin biosynthesis in the skin tissue of Leptobotia taeniaps. TYR, tyrosinase; Tyrp1, tyrosinase-related protein 1; Dct, dopachrome tautomerase; MC1R, melanocortin 1 receptor; α-MSH, α-melanocyte-stimulating hormone; cAMP, cyclic adenosine monophosphate; Mitfa, microphthalmia-associated transcription factor. *p < 0.05; **p < 0.01; **p < 0.001*

http://www.aloki.hu ● ISSN 1589 1623 (Print) ● ISSN 1785 0037 (Online)
DOI: http://dx.doi.org/10.15666/aeer/1705_1218112189

Although only six specimens of each phenotype were analyzed through qRT-PCR, qRT-PCR experiments with small sample size had been reported in previous reports, and their results were also considered reliable (Varkonyi-Gasic et al., 2007; Vieth et al., 2007). In the present study, the expressions of *TYR* (Independent *t*-test, $t = 4.966$, $p < 0.001$), *Tyrp1* (Independent *t*-test, $t = 7.603$, $p < 0.001$), and *Dct* (Independent *t*-test, $t = 8.800$, $p < 0.001$) genes in the skin of the dark phenotype were significantly higher than those in the light phenotype, while the expressions of Mitfa (Independent *t*-test, $t = 1.060$, $p = 0.314$), Sox10 (Independent *t*-test, $t = 1.403$, $p = 0.191$), and *MC1R* (Independent *t*-test, $t = 1.986$, $p = 0.075$) were not detected significant difference (*Fig. 3*). These results showed that the eumelanin biosynthesis was the major reason that caused the pigment deviation of *L. taeniops*. However, the expressions of the upstream regulation factors, i.e. *Mitfa*, *Sox10*, and *MC1R*, were not significantly different. This result implied that there was probably another undiscovered way to regulate the expression of *TYR*, *Dct*, and *Tyrp1* genes and the eumelanin biosynthesis.

Sox10 is a major regulator of neural crest formation (Honoré et al., 2003) and it is reported that regulates the development of neural crest-derived melanocytes in *Xenopus* (Aoki et al., 2003). In addition, MITF expression is maintained in about 90% of melanomas and a genomic amplification of MITF has been frequently observed in metastatic melanomas (Beuret et al., 2011). However, our results showed that both *Sox10* and *Mitfa* genes were not significantly upregulated in the skin of *L. taeniops*. These results implied that the developments of neural crest melanocytes and skin melanocytes were through different pathways, and pigmentation was probably not a direct factor that causes melanomas. In addition, our results also implied that through regulating *TYR* pathway, but not *Sox10* pathway, probably changed the production of melanophores and produced novel ornamental fish species.

Conclusion

In summary, amount of melanophores in the skin was the major factor that caused the pigment deviation of *L. taeniops* living in the same habitat. The amount of melanophores was influenced by the expression of *TYR*, *Tyrp1*, and *Dct* genes in the skin of *L. taeniops*. The expressions of these genes were significantly higher in the skin of the dark phenotype than those in the light phenotype. However, what and how external factors regulate the expression of these genes still need to be further studied in future.

Acknowledgements. This work was funded by the Earmarked Funds for China Agriculture Research System (CARS-45-48). The authors thank anonymous technicians at Guangdong Meilikang Bio-Science Ltd., China for assistance with data re-analysis and figure preparation.

REFERENCES

[1] Aoki, Y., Saint-Germain, N., Gyda, M., Magner-Fink, E., Lee, Y., Credidio, C., Saint-Jeannet, J. (2003): *Sox10* regulates the development of neural crest-derived melanocytes in *Xenopus*. – Developmental Biology 259: 19-33.

[2] Beuret, L., Ohanna, M., Strub, T., Allegra, M., Davidson, I., Bertolotto, C., Ballotti, R. (2011): BRCA1 is a new MITF target gene. – Pigment Cell & Melanoma Research 24: 725-727.

http://www.aloki.hu ● ISSN 1589 1623 (Print) ● ISSN 1785 0037 (Online)
DOI: http://dx.doi.org/10.15666/aeer/1705_1218112189

[3] Blakeslee, C., McRobert, S. P., Brown, A. C., Clotfelter, E. D. (2009): The effect of body coloration and group size on social partner preferences in female fighting fish (Betta splendens). – Behavioural Processes 80: 157-161.
[4] Carey, A. N., Lyvers, B. H., Ferrill, R. N., Johnson, R. L., Dumaine, A. M., Sly, B. J. (2015): Development of Betta splendens embryos and larvae reveals variation in pigmentation patterns. – Zygote 24: 396-400.
[5] Clotfelter, E. D., Ardia, D. R., McGraw, K. J. (2007): Red fish, blue fish: trade-offs between pigmentation and immunity in Betta splendens. – Behavioral Ecology 18: 1139-1145.
[6] Culumber, Z. W. (2013): Pigmentation in Xiphophorus: an emerging system in ecological and evolutionary genetics. – Zebrafish 11(1): 57-70.
[7] Ding, R. (1994): Fish Fauna of Sichuang. – Sichuan Science and Technology Press, Chengdu.
[8] Fang, C., Meng, Y., Zu, G., Tang, Y., Xu, D., Hong, B. (2011): Individual biology and resource conservation of Leptobotia taeniops in Tongling Section of the Yangtze River. – Journal of Hydroecology 32(2): 100-104.
[9] Honoré, S. M., Aybar, M. J., Mayor, R. (2003): Sox10 is required for the early development of the prospective neural crest in Xenopus embryos. – Developmental Biology 260: 79-96.
[10] Houde, A. E., Torio, A. J. (1992): Effect of parasitic infection on male color pattern and female choice in guppies. – Behavioral Ecology 3(4): 346-351.
[11] Huang, R., Li, T., Ni, J., Bai, X., Gao, Y., Li, Y., Zhang, P., Gong, Y. (2018): Different sex-based responses of gut microbiota during the development of hepatocellular carcinoma in liver-specific *Tsc1*-knockout mice. – Frontiers in Microbiology 9: 1008.
[12] Hunan Fisheries Science Institute (1980): Fish Fauna of Hunan. – Hunan Science and Technology Press, Changsha.
[13] Jeon, K., Friedlander, J., Jarvik, J., Fujii, R. (1993): Cytophysiology of fish chromatophores. – International Review of Cytology 143: 191-255.
[14] Jiang, H., Liu, S., Xiao, T. Y., Xie, M. (2019): Body color regulation of *Leptobotia taeniops* through tyrosinase gene expression. – Applied Ecology and Environmental Research 19(3): 5525-5537.
[15] Khoo, G., Lim, T. M., Phang, V. P. E. (2014): Cellular basis of metallic iridescence in the Siamese fighting fish, *Betta splendens*. – Israeli Journal of Aquaculture 66: 988.
[16] Lamoreux, M. L., Wakamatsu, K., Ito, S. (2001): Interaction of major coat color gene functions in mice as studied by chemical analysis of eumelanin and pheomelanin. – Pigment Cell & Melanoma Research 14(1): 23-31.
[17] Li, Z. F., Wang, G., Zhang, K., Gong, W., Yu, E., Tian, J., Xie, J., Yu, D. (2019): Epizootic ulcerative syndrome causes cutaneous dysbacteriosis in hybrid snakehead (Channa maculate ♀ × Channa argus ♂). – Peer J 7: e6674.
[18] Meng, Y. (2011): Research on Karyotype and Genetic Diversity of Leptobotia Taeniops. – Anhui Agricultural University, Hefei.
[19] Murisier, F., Beermann, F. (2006): Genetics of pigment cells: lessons from the tyrosinase gene family. – Histology & Histopathology 21(5): 567-578.
[20] Ni, J., Li, X., Chen, F., Wu, H., Xu, M. (2018): Community structure and potential nitrogen metabolisms of subtropical aquaculture pond microbiota. – Applied Ecology and Environmental Research 16(6): 7687-7697.
[21] Ni, Y., Wu, H. (2006): Fish Fauna of Jiangsu. – China Agriculture Press, Beijing.
[22] R Core Team (2017): R-A Language and Environment for Statistical Computing. – R Foundation for statistical computing. R version 3.4.3, Vienna.
[23] Saito, H., Yasumoto, K., Takeda, K., Takahashi, K., Yamamoto, H., Shibahara, S. (2003): Microphthalmia-associated transcription factor in the Wnt signaling pathway. – Pigment Cell Research 16(3): 261-265.

http://www.aloki.hu ● ISSN 1589 1623 (Print) ● ISSN 1785 0037 (Online)
DOI: http://dx.doi.org/10.15666/aeer/1705_1218112189

[24] Spivak, C. E., Kim, W., Liu, Q., Lupica, C. R., Doyle, M. E. (2012): Blockade of β-cell KATP channels by the endocannabinoid, 2-arachidonoylaglycerol. – Biochemical and Biophysical Research Communications 423(1): 13-18.
[25] Sturm, R. A., Box, N. F., Ramsay, M. (1998): Human pigmentation genetics: the difference is only skin deep. – Bioessays 20: 712-721.
[26] Udono, T., Yasumoto, K., Takeda, K., Amae, S., Watanabe, K., Saito, H., Fuse, N., Tachibana, M., Takahashi, K., Tamai, M., Shibahara, S. (2000): Structural organization of the human microphthalmia-associated transcription factor gene containing four alternative promoters. – Biochimica et Biophysica Acta (BBA) - Gene Structure and Expression 1491(1-3): 205-219.
[27] Varkonyi-Gasic, E., Wu, R., Wood, M., Walton, E. F., Hellens, R. P. (2007): Protocol: a highly sensitive RT-PCR method for detection and quantification of microRNAs. – Plant Methods 3: 12.
[28] Vieth, S., Drosten, C., Lenz, O., Vincent, M., Omilabu, S., Hass, M., Becker-Ziaja, B., ter Meulen, J., Nichol, S. T., Schmitz, H., Günther, S. (2007): RT-PCR assay for detection of Lassa virus and related Old World arenaviruses targeting the L gene. – Transactions of the Royal Society of Tropical Medicine and Hygiene 101: 1253-1264.
[29] Yasumoto, K., Yokoyama, K., Shibaba, K., Tomita, Y., Shibahara, S. (1994): Microphthalmia-associated transcription factor as a regulator for melanocyte-specific transcription of the human tyrosinase gene. – Molecular and Cellular Biology 14(12): 8085-8070.
[30] Yasumoto, K., Yokoyama, K., Takahashi, K., Tomita, Y., Shibahara, S. (1997): Functional analysis of microphthalmia-associated transcription factor in pigment cell-specific transcription of the human tyrosinase family genes. – Journal of Biological Chemistry 272(1): 503-509.

http://www.aloki.hu ● ISSN 1589 1623 (Print) ● ISSN 1785 0037 (Online)
DOI: http://dx.doi.org/10.15666/aeer/1705_1218112189

INFLUENCE OF TRANSIENT CHANGE OF WATER TEMPERATURE ON PILOT-SCALE ANAEROBIC-ANOXIC-OXIC PROCESS UNDER PLATEAU ENVIRONMENTAL FACTORS

ZONG, Y.[1,2] – LI, Y.[2] – HAO, K.[2] – LU, G.[1,2*] – HUANG, D.[2]

[1]*Res. Institute of Tibet Plateau Ecology, Tibet Agriculture & Animal Husbandry University, Linzhi 860000, China*

[2]*Water Conservancy Project & Civil Engineering College, Tibet Agriculture & Animal Husbandry University, Linzhi 860000, China*

**Corresponding author*
e-mail:ghlu@hhu.edu.cn

(Received 1st May 2019; accepted 11th Jul 2019)

Abstract. The objective of this study was to explore the effect of transient changes of Pilot-Scale Anaerobic-Anoxic-Oxic Process (A2O). The effects of transient changes in Tibet, China of water temperature on water quality indicators such as chemical oxygen demand (COD), the total phosphorous (TP), total nitrogen (TN) and ammoniacal nitrogen (NH_4^+-N), as well as microorganism and mixed liquor suspended solids were analyzed. The A2O system had a hydraulic retention time of 21 h, a mixture of the reflux ratio of the mixed liquor of 200%, a reflux ratio of the sludge of 100%, a temperature fluctuation range of 8-25 °C, and a water sampling interval of 3 h. The results showed that the optimal removal rates of different water quality indicators were different. The removal of COD, TN and NH_4^+-N mainly occurred in anaerobic tank and TP mainly in anaerobic tank and oxic tank. There was no obvious relationship between microorganism density and indicator organisms in anoxic tank, oxic tank and anaerobic tank. The concentrations of COD, TP, TN and NH_4^+-N in the effluents did not meet the first grade A standards, and the mixed liquid suspended solids did not show a significant growth trend with increasing temperature.
Keywords: *nitrogen and phosphorus removal, dissolved oxygen, microorganism, A2O, Tibet*

Introduction

Currently, the Anaerobic-Anoxic-Oxic (A2O) process, improved from the traditional activated-sludge process, has become the most popular sewage treatment method in Tibet, China (Chen et al., 2018). The sewage temperature in Tibet has obvious inter-annual and diurnal changes, the daily temperature difference can reach about 10 ℃, and the inter-annual temperature difference can reach about 15 ℃, which is mainly caused by drastic change of environmental temperature and centralized of water consumption time. Frequent change of water temperature could influence microbial growth and community structure, and adsorption performance and sedimentation performance of activated sludge, which ultimately leads to large fluctuations in wastewater treatment efficiency.

It is widely agreed that the effect of A2O is influenced by the unique environment factors of the plateau, namely, water temperature and atmospheric pressure. At present, according to the on-site measurement, the lowest temperature of sewage in Linzhi City is -1 ℃, the highest is 14 °C (Zong et al., 2018). According to the comprehensive analysis of the survey, the reason for the sewage temperature of -1 °C in Linzhi City is mainly due to the following two reasons: firstly, the sewage pipeline in Linzhi City is too long, and the sewage flow is too small, resulting to a large heat loss in the sewage flow; secondly, the

http://www.aloki.hu ● ISSN 1589 1623 (Print) ● ISSN 1785 0037 (Online)
DOI: http://dx.doi.org/10.15666/aeer/1705_1219112202

groundwater level is too high, and some groundwater seeps into the sewage pipeline, causing its average temperature to be too low (Zong, 2017).

Our previous study has shown that the traditional activated-sludge process cannot satisfactorily remove nitrogen and phosphorus from domestic sewage in Tibet (Zong, 2017). Temperature is a main influencing factor of sewage treatment efficiency (Ai et al., 2018). In the process of the phosphorus removal of sludge denitrification, the release and absorption rates of phosphorus are changed under excessively high or low temperatures, and the proportion of denitrifying phosphorus accumulating organisms in the activated sludge is greatly affected by temperature variation (Zhang et al., 2016). In addition, the nitrification capacity of the sewage treatment system is obviously weakened when the water temperature falls below 15 °C, and even lost totally when the temperature drops below 4 °C (He et al., 2010; Li et al., 2013). Thus, the nitrogen removal is severely inhibited under a low temperature (Li et al., 2014).

As for the A2O process, the nitrification/denitrification is weakened at a low temperature and a high sludge load. In this case, nitrite nitrogen will accumulate in the system, and denitrifying phosphorus removal will happen in the anoxic tank. The phosphorus removal efficiency of the system could decline due to the sludge bulking induced by non-filamentous bacteria (Li et al., 2014), and the lack of small molecular carbons required for phosphorus release by phosphorus-concentrating bacteria (as the hydrolysis of macromolecular organic matter is suppressed under a low temperature) (Shen et al., 2017).

The atmospheric pressure has a direct bearing on the oxygen partial pressure, and the oxygen partial pressure controls the dissolved oxygen (DO) in water. When partial oxygen pressures was below 40 kPa, the removal efficiencies of chemical oxygen demand (COD), and ammoniacal nitrogen (NH_4^+-N) increased with the increase of DO, meanwhile, nitrification was the main control process in simultaneous nitrification and denitrification (SND). However, partial oxygen pressures above 40 kPa did not affect their removal efficiencies, and denitrification became the main control process in SND (Xing et al., 2013). The nitrification can be enhanced by extending the aeration time, while the denitrification can be stimulated by prolonged exposure to anaerobic conditions (Yoo and Lee, 2015). Under low aeration, the nitrogen and phosphorus removal were greatly hindered in the A2O system (Li et al., 2013). The DO could affect the conversion of polyhydroxy alkyl ester and glycogen (Chen et al., 2014), as well as the activity of desulfurase and polyphosphatase, and affect phosphorus removal subsequently. The total number and activity of ammonia oxidizing bacteria are respectively determined by the hydraulic retention time (HRT) of solids and the DO concentration (Limpiyakorn et al., 2005).

Transient and non-steady state of domestic sewage is relatively common, and the temperature of sewage varies significantly during a day in Tibet. The present study used A2O system as a typical sewage treatment process to investigate the removal rates of nitrogen and phosphorus in daily responding to water temperature change, analyze the characteristics of the microbes in anaerobic tank, anoxic tank and oxic tank, and explore the mechanisms of nitrogen and phosphorus removal and microbial transient response under plateau environmental factors.

Materials and methods

Description of the anaerobic-anoxic-oxic process system and wastewater

A pilot-scale A2O sewage treatment device was designed and fabricated with plexiglass in Tibet, China. With an effective volume of 210 L, the device consists of 8 segments: the

http://www.aloki.hu ● ISSN 1589 1623 (Print) ● ISSN 1785 0037 (Online)
DOI: http://dx.doi.org/10.15666/aeer/1705_1219112202

first 2 are anaerobic tanks with an effective volume of 35 L, the middle 2 are anoxic tanks with an effective volume of 58 L, and the last 4 are oxic tanks with an effective volume of 117 L. Besides, the effective volume of the sedimentation tank is 210 L. In both anaerobic and anoxic sections, each tank has a 50 rpm stirring device at the bottom; in each oxic tank, there is an aerator for oxygen supply. Inflow, return sludge and nitrifying liquid are controlled by a peristaltic pump. To maintain a constant temperature, the water temperature was regulated by a constant temperature circulator. In each tank, a sampling hole was opened on the tank wall. Before the experiment, the activated sludge was cured for 32 d. The temperature, MLSS, and volume percent of MLSS after settling for 30 min (SV30) were set to 22.5 °C, 4,787 mg/L and 35%, respectively.

The urban domestic sewage in Linzhi was directly adopted for our experiments. The main water quality indices of the sewage are given in *Table 1*.

Table 1. *Quality indicators of sewage*

Potential of hydrogen	Dissolved oxygen (mg/L)	Temperature (°C)	Chemical oxygen demand (mg/L)	Total nitrogen (mg/L)	Total phosphorous (mg/L)	Ammoniacal nitrogen (mg/L)
6.20~8.70	1.87~4.68	8.05~23.10	217.17~526.36	23.12~112.51	2.59~7.28	12.09~45.15

Operation of the anaerobic-anoxic-oxic process

The operation of the A2O device was studied under transient change of water temperature, in order to disclose the law of removal rates under different water temperatures. The control plans for the three parameters are specified below. On water temperature control, the inlet water flow was designed as 10.0 ± 0.1 L/s, HRT as 21.0 ± 0.2 h (the HRT ratio between anaerobic tank, anoxic tank and oxic tank = 35:58:117), DO as 3.0~4.0 mg/L, the reflux ratio of the mixed liquor $R_i = 200\%$, and the reflux ratio of the sludge R = 100%. Both the mixed liquor and the sludge were continuously refluxed. Temperature fluctuation range is set to 8~25 °C. The temperature was controlled with an error of or less than 0.1 °C. The experiment was replicated three times. Water quality sampling interval was 3 h (*Fig. 1*).

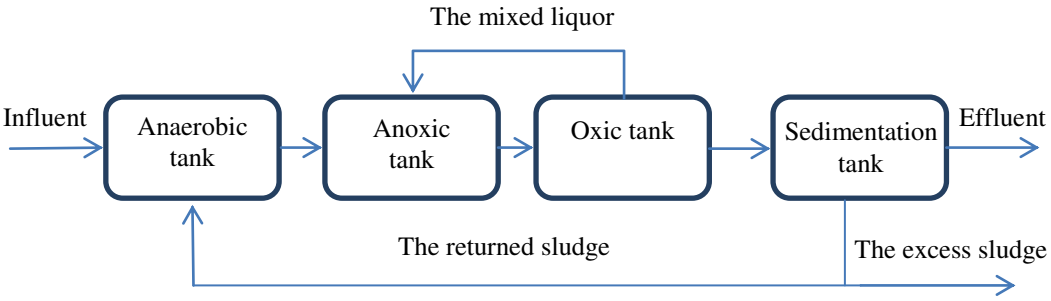

Figure 1. *Schematic of anaerobic-anoxic-oxic process*

Analytical methods

The measurement methods of the test indicators are selected according to the existing standards (State Environmental Protection Administration of China, 2002).

http://www.aloki.hu ● ISSN 1589 1623 (Print) ● ISSN 1785 0037 (Online)
DOI: http://dx.doi.org/10.15666/aeer/1705_1219112202

Statistical analysis

All data were initially verified for normality using the Shapiro-Wilk method. The differences between different treatments were evaluated by one-way analysis of variance in SPSS, followed by Tukey's test. All differences were considered significant at $p < 0.05$. All these statistical analyses were performed using the SPSS statistical package (ver. 22.0, SPSS Company, Chicago, IL, USA).

Results

Removal rate at temperature transients

Figures 2–5 provide the removal rates of COD, TP, TN and NH_4^+-N in anaerobic, anoxic and Oxic tanks at different temperatures.

As shown in *Figure 2,* the COD removal effect in the anaerobic tank maintains a good removal efficiency under the temperature from 8 °C to 25 °C. The removal efficiency of individual temperatures is low, and the average removal rate is 67.18%, which is lower than 75.69% (Huang et al., 2017); COD is mainly removed in the anaerobic tank with a maximum removal rate of 89.09% and a minimum removal rate of 34.11% corresponding to the temperature of 18.2 °C and 22.3 °C, respectively. The COD removal effect in the anoxic tank is generally acceptable, and the COD removal rate in the anoxic tank is only increased by 4.44%, which is lower than 12.72% (Huang et al., 2017), which increases the maximum value by 15.91% and the minimum value of -8.13% corresponding temperature are 22.3 °C and 15.1 °C, respectively; the maximum removal rate of 87.48% and the minimum value of 50.02% corresponding temperatures are 18.2 °C and 22.3 °C. The COD in the oxic tank can be removed as a whole due to the removal of the anaerobic tank and anoxic tank, but the average value of the relative anoxic removal rate is 10.07%, which is larger than 5.98% (Huang et al., 2017), the removal rate increases by a maximum of 27.69% and the minimum value of -0.90%, the corresponding temperatures are 8.98 °C and 18.2 °C; the average COD removal rate is 81.69%, and the maximum value of 91.15% and the minimum value of 70.06% corresponding temperature are 8.45 °C and 17.50 °C. The above trend is also consistent with the low temperature and room temperature COD treatment effects, but the effect is poor (Li et al., 2012); according to the COD removal rate effect, the test temperature is 18.2 °C, the removal rate can reach 92.19%, the measured COD effluent can reach the first grade A standards (GB18918-2002), but other temperatures are difficult to reach this standard.

As shown in *Figure 3,* the TP removal effect in the anaerobic tank changes obviously between 3.54% and 83.41% at the temperature of 8~25 °C. The removal efficiency of individual temperatures is low, and the average removal rate is 30.15%, which is lower than 69% (Bao et al., 2012). The highest TP removal rate of 63.58% and the lowest value of 5.56% corresponding temperatures are 12.00 °C and 22.40 °C, respectively. The anoxic tank contributes very little to the TP removal rate which is only increased by only 2.50%, which was lower than 56.00% (Zhou et al., 2013), which increased the maximum value by 20.19% and the minimum value by -13.86% corresponding to temperatures of 14.70 °C and 8.05 °C, respectively; the maximum removal rate of 71.95% and the minimum value of 6.06% corresponding temperatures are12.00 °C and 22.4 °C. The TP in the oxic tank is not obvious due to the poor removal rate of the anaerobic tank and anoxic tank, but the average value of the relative anoxic removal

http://www.aloki.hu ● ISSN 1589 1623 (Print) ● ISSN 1785 0037 (Online)
DOI: http://dx.doi.org/10.15666/aeer/1705_1219112202

rate is 11.90%. Considering the dilution of the anaerobic section, the effect of removing TP is more significant, but the overall TP removal rate is still low (Zhou et al., 2013), the removal rate increases by 46.93% and the minimum value by -3.50%, and the corresponding temperatures are 8.49 °C and 22.3 °C, respectively; The average removal rate was 44.55%, and the maximum values of 83.41% and the minimum value of 3.54% corresponding to the temperature of 12.00 °C and 22.40 °C, respectively. When the test temperature is 12.00 °C, the removal rate of TP can reach 83.41%, and the sedimentation tank effluent regarding the TP can reach the grade 1 B standard (GB18918-2002), but TP removal rate can not reach this standard at the other temperatures. Overall, the removal rate of TP has two critical points of 9.54 °C and 14.70 °C.

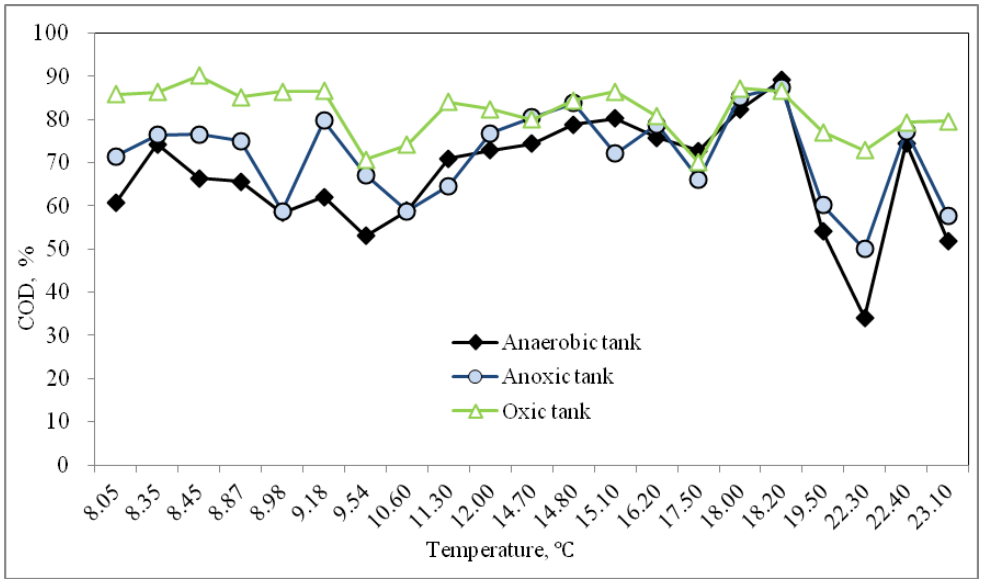

Figure 2. *Removal rate of chemical oxygen demand at different temperatures*

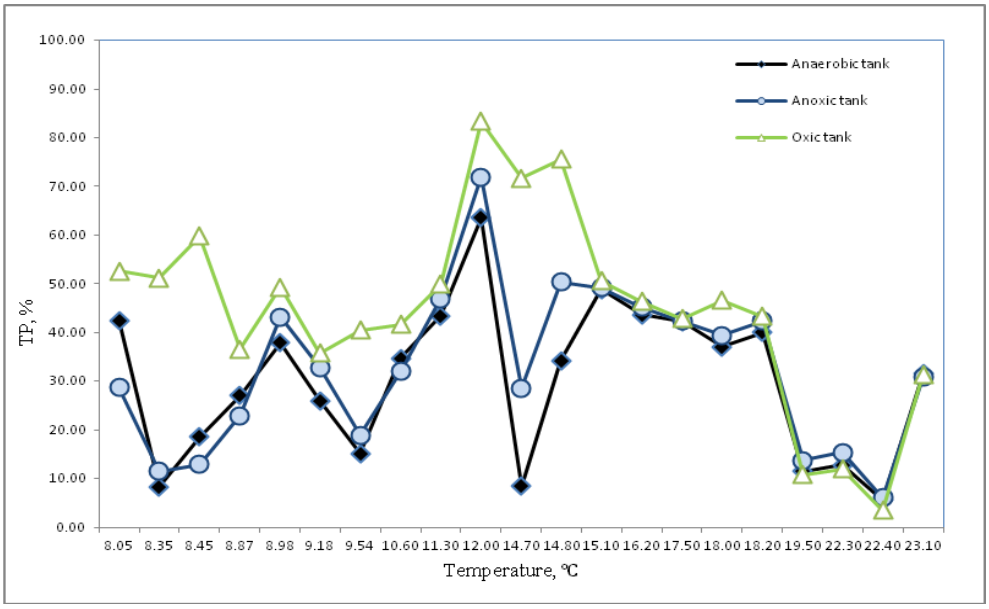

Figure 3. *Removal rates of total phosphorous at different temperatures*

http://www.aloki.hu ● ISSN 1589 1623 (Print) ● ISSN 1785 0037 (Online)
DOI: http://dx.doi.org/10.15666/aeer/1705_1219112202

As shown in *Figure 4,* the TN removal rates in the anaerobic tank changes obviously between 1.34% and 95.37% when the temperature changed from 8 °C to 25 °C. The removal rate of TN is higher than other studies (Zhou et al., 2013). The average removal rate is 51.56%, which is higher than the result obtained by Zhou et al. (2013). The anoxic tank contributes very little to the TN removal rate which is only increased by 5.53%. The values corresponding to the value of 93.20% and the minimum of 20.23% corresponding to the temperatures were 9.18 °C and 8.35 °C. The TN in the oxic tank is not obvious due to the poor removal rate of the anaerobic tank and anoxic tank, but the average value of the relative anoxic removal rate is 4.53%, and the removal rate increases by 48.22% and -27.22%. The corresponding temperatures are 22.40 °C and 19.50 °C respectively; the average TN removal rate is 61.62%, and the maximum values of 95.37% and the minimum values of 23.16% correspond temperatures are 9.54 °C and 16.2 °C, respectively. According to the TN removal rate, the better temperature is 9.54 °C, and the removal rate can reach 95.37%, which is better than 80% (Wang et al., 2011). However, the dissolved oxygen value is as high as 3.70 mg/L, which is much higher than 1.20 ± 0.2 mg/L (Liu et al., 2011). Other temperatures are difficult to reach the Grade 1 B standard (GB18918-2002). Overall, the removal rate of TN has two critical points of 10.60 °C and 16.20 °C, and it is possible that 10.60 °C and 16.20 °C are the extreme temperatures of certain low temperature denitrifying microorganisms and these require additional attention in future research.

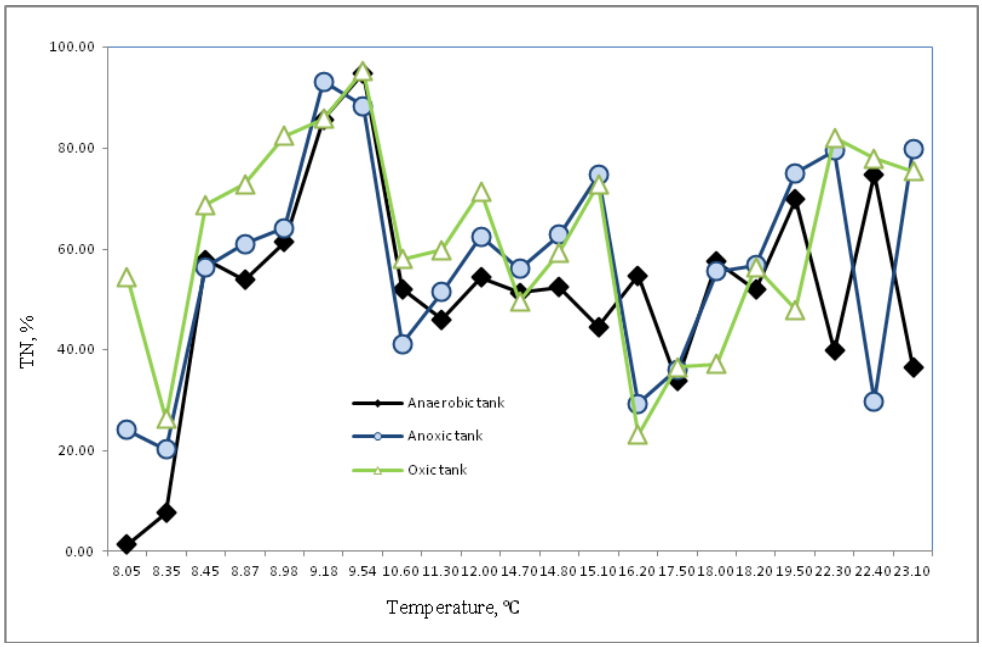

Figure 4. *Removal rates of total nitrogen at different temperatures*

As shown in *Figure 5,* the removal rate of NH_4^+-N in the anaerobic tank changes obviously between 9.36% and 97.23% under the fluctuation of temperature between 8 °C and 25 °C, the removal rate of NH_4^+-N changes obviously. The average removal rate is 61.46%, which is lower than 67.0% (Sohsalam and Sirianuntapiboon, 2008); the highest NH_4^+-N removal rate of 95.87% and the lowest value of 6.16% correspond temperatures are 22.30 °C and 8.35 °C, respectively. The anoxic tank contributes very little to the NH_4^+-N removal rate which is only increased by 4.04%, which is lower than

http://www.aloki.hu ● ISSN 1589 1623 (Print) ● ISSN 1785 0037 (Online)
DOI: http://dx.doi.org/10.15666/aeer/1705_1219112202

16.12% (Sahariah et al., 2015), which increases the maximum value by 85.65% and the minimum value of -1.38% corresponding to the temperatures of 9.18 °C and 8.05 °C, respectively; the maximum removal rate of 95.08% and the minimum value of 9.36% corresponding temperatures are 95.02 °C and 8.05 °C. The NH_4^+-N in the oxic tank is not obvious due to the poor removal rate of anaerobic tank and anoxic tank, but the average value of the relative anoxic removal rate is 11.29%, which is larger than 11% (Peng et al., 2005), the removal rate increases the maximum value 57.14% and the minimum value of -2.50%, the corresponding temperatures were 8.05 °C and 17.50 °C, respectively; the average removal rate of NH_4^+-N was 77.42%, and the maximum value of 98.12% and the minimum value of 34.83% corresponding temperatures are 22.30 °C and 8.35 °C, respectively. According to the removal rate of NH_4^+-N, the better temperature is 22.30 °C, the removal rate can reach 98.12%, and the measured NH_4^+-N effluent in the sedimentation tank can reach the first grade A standards (GB18918-2002), and the initial concentration is low so other temperatures can also reach this standard. In general, the two critical temperatures of 10.60 °C and 17.50 °C divide the curve into three parts. 8.05~9.54 °C is the first part, which is a significant increase in the NH_4^+-N removal rate. 10.60~17.50 °C is the second part, which is not obvious for the NH_4^+-N removal rate. 17.50~23.10 °C is the third part, which is a significant change in the TP removal rate. And it is possible that 10.60 °C and 17.50 °C are the extreme temperatures of certain low temperature denitrifying microorganisms.

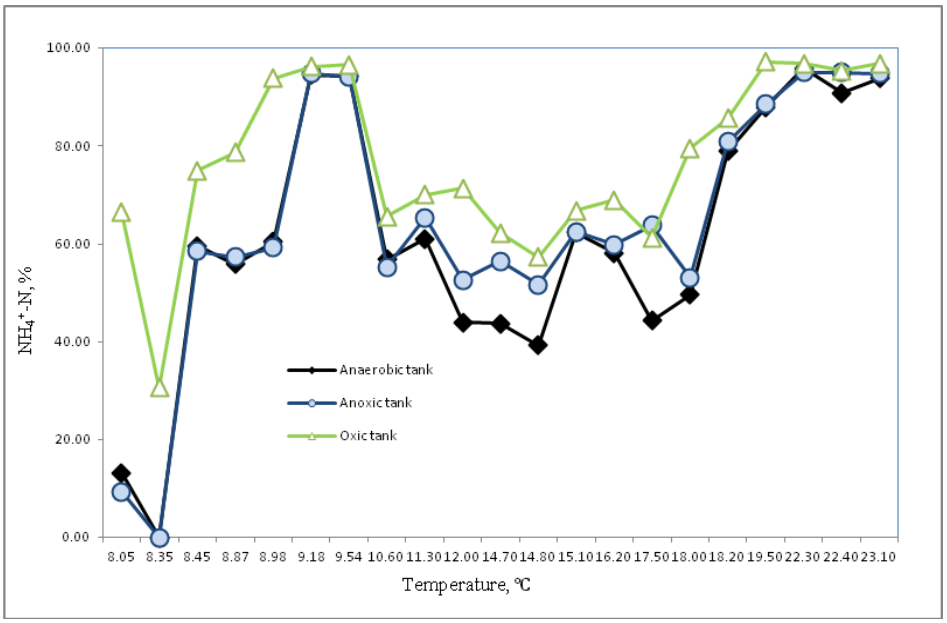

Figure 5. *Removal rates of ammoniacal nitrogen at different temperatures*

Microorganisms

The response of microorganisms in anaerobic tank, anoxic tank and oxic tank under temperature fluctuation of 8–25 °C is shown in *Figure 6.*

It can be seen from *Figure 6a* that the microbial density of anaerobic tanks generally shows a process of gradually decreasing from the high level and then increasing. The microbial density of the anoxic tank and oxic tank is flatter. The experiment showed that the microbial density in each tank was from 8 °C to 12 °C and 12 °C to 23.1 °C.

http://www.aloki.hu ● ISSN 1589 1623 (Print) ● ISSN 1785 0037 (Online)
DOI: http://dx.doi.org/10.15666/aeer/1705_1219112202

The microbial density of 8~12 °C showed a downward trend, which may be related to the higher temperature of sludge culture and domestication. The trend appeared in density; the microbial density of each tank showed a oscillating upward trend at 12 °C to 23.1 °C. Overall, the microbial density of anaerobic tanks was higher than that of anoxic tank and oxic tank. There was no significant difference in microbial density between anoxic tank and oxic tank, but the experimental microbial density was lower than 10^8 CFU/L (Yang, 2017).

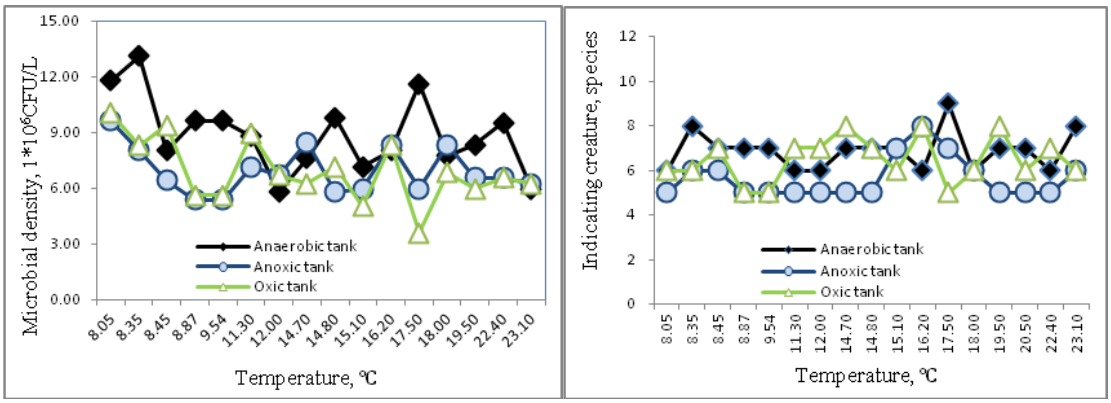

a **b**

Figure 6. *Microbial response at different temperatures*

It can be seen from *Figure 6b* that the relative changes of indicating creature are not significant in the three reaction cells, and the anaerbic tank and oxic tank indicate that the indicating creature are significantly better than the anoxic tank. Microscopic observations showed that the indicated microorganisms in each tank were pointed caterpillars, bell worms and trichinella, and the number of pointed caterpillars and bell worms decreased gradually while the trichinella showed an increasing trend. It has also been observed that Surticae has an increasing trend, which may be related to DO, and DO is greater than the minimum limit of 2.5 mg/L (Bernot and Wilson, 2012).

Mixed liquid suspended solids and volume percent after settling for 30 min

It can be seen from *Figure 7* that MLSS shows a certain increasing trend with increasing temperature in the range of 8.05 °C to 11.3 °C. In the range of 11.3 °C to 23.1 °C, MLSS shows a certain downward trend with increasing temperature; MLSS is less than 3,000 mg/L (Whang and Lim, 2008). SV30 shows a slow downward trend with increasing temperature.

Discussion

The removal contributions of anaerobic tank, anoxic tank, oxic tank and secondary sedimentation tank at the average removal rate of COD, TN, NH_4^+-N and TP are shown in *Figure 8*.

In addition to TP, the removal of COD, TN, and NH_4^+-N mainly occurs in anaerobic tank, while TP mainly occurs in anaerobic tank and oxic tank. The COD removal effect in each tank is consistent with the microbial density in the corresponding tank; the TP removal effect in each tank is consistent with the change trend of MLSS, and the two

http://www.aloki.hu ● ISSN 1589 1623 (Print) ● ISSN 1785 0037 (Online)
DOI: http://dx.doi.org/10.15666/aeer/1705_1219112202

also exhibit a certain positive correlation, which is related to MLSS was key factors, which had a significant impact on Anaerobic phosphorus release and anoxic phosphorus uptake in the biological phosphorous removal process. Wang et al. (2007) are more consistent; TN and NH_4^+-N removal effects have a more consistent trend.

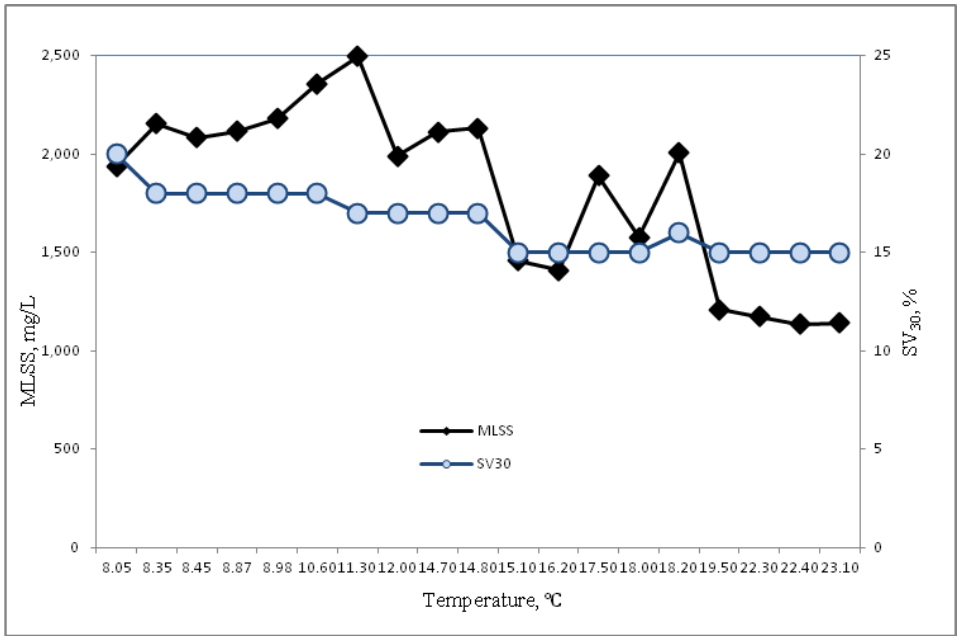

Figure 7. *Mixed liquor suspended solids and volume percent after settling for 30 min at different hydraulic retention times*

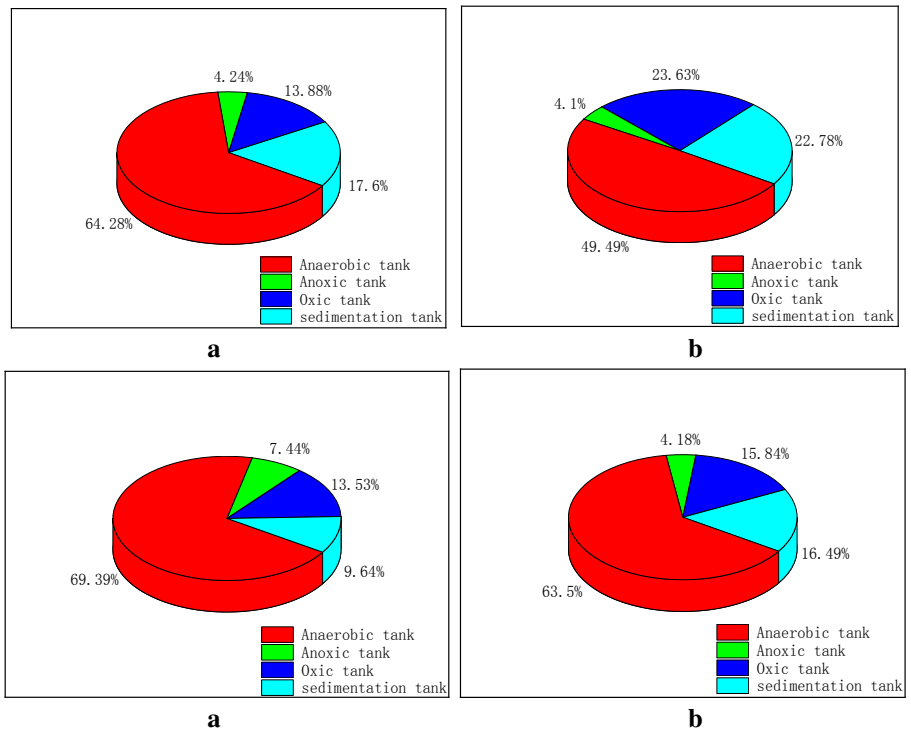

Figure 8. *Removal contribution ratios of **a** chemical oxygen demand, **b** total phosphorous, **c** total nitrogen and **d** ammoniacal nitrogen of each tank*

http://www.aloki.hu ● ISSN 1589 1623 (Print) ● ISSN 1785 0037 (Online)
DOI: http://dx.doi.org/10.15666/aeer/1705_1219112202

Conclusion

Under the unique plateau environmental factors, the effects of temperature transients on COD, TP, TN, NH_4^+-N removal rate and microbial response were studied using a pilot-scale A2O process. The transient temperature changes show that the optimal removal rate of each water quality index is different. The COD removal rate maintains a good removal efficiency and the removal rate of TN, TP and NH_4^+-N in the anaerobic tank changes obviously under the temperature from 8 °C to 25 °C. The removal of COD, TN and NH_4^+-N mainly occurs in anaerobic tanks while TP mainly occurs in anaerobic and oxic tanks, anaerobic There is no obvious response relationship between microorganisms and indicator organisms in the tank, anoxic tank and oxic tank. The COD, TP, TN, NH_4^+-N in the effluent do not meet the Grade A standard, and the MLSS follows the increased temperature. The increase has not shown a significant growth trend. There are two distinct critical temperatures of 10.60 °C and 16.20 °C to the NH_4^+-N removal rate, of 10.60 °C and 17.50 °C to the TN removal rate and of 9.54 °C and 14.70 °C to the TP removal rate, and it is possible that two distinct critical temperatures are the extreme temperatures of certain low temperature denitrifying microorganisms. The above problems may be related to the long-term response time of temperature transient changes under high altitude environmental factors, and the corresponding mechanism needs to be studied later.

Acknowledgements. This work was supported by the National Natural Science Foundation of China (NO.51868069, 51769034）, Natural Science Foundation of Tibet (NO.XZ 2018 ZR G-20), the Program for Scientific Research Innovation Team in Colleges and Universities of Tibet Autonomous Region, Snowy Plateaus of Tibet Agriculture and Animal Husbandry College (Study on the operation status of typical sewage treatment plants in Tibet in China).

REFERENCES

[1] Ai, S. S., Zhang, X. H., Xiao, Y. B. (2014): Study on characteristics of activated sludge at low temperature. – Applied Mechanics & Materials 675-677: 574-577.

[2] An, J., Xue, M., Xiang, C., et al. (2002): Isolation of psychrotrophs and their application to treatment of sewage in cold area. – Journal of Harbin Institute of Technology 34(4): 563-565 + 569.

[3] Bao, K., Q., Gao, J. Q., Wang, Z. B. (2012): Enhanced removal of chemical oxygen demand, nitrogen and phosphorus using the ameliorative anoxic/anaerobic/oxic process and micro-electrolysis. – Water Science & Technology 66(4): 850-857.

[4] Bernot, M. J., Wilson, K. P. (2012): Spatial and temporal variation of dissolved oxygen and ecosystem energetics in Devils Hole, Nevada. – Western North American Naturalist 72(3): 265-275.

[5] Chen, H., Wang, D., Li, X. (2014): Effect of dissolved oxygen on biological phosphorus removal induced by aerobic/extended-idle regime. – Biochemical Engineering Journal 90(9): 27-35.

[6] Chen, X. Y., Hao, K. Y., Su, D. (2018): Characteristic study on wastewater treatment in high altitude area by A2/O process. – Technology of water treatment 38(6): 93-96.

[7] He, J. G., Ke, L., Han, B. P. (2010): Study on the operational characteristics of hybrid A2/O process at low temperature. – Applied Mechanics & Materials 39: 326-331.

[8] Huang, X., Dong, W., Wang, H. (2017): Biological nutrient removal and molecular biological characteristics in an anaerobic- multistage anaerobic/oxic (A-MAO) process to treat municipal wastewater. – Bioresource Technology 24: 969-978.

http://www.aloki.hu ● ISSN 1589 1623 (Print) ● ISSN 1785 0037 (Online)
DOI: http://dx.doi.org/10.15666/aeer/1705_1219112202

[9] Li, S. M., Du, G. S., Tang, F. B. (2013): Nitrogen and phosphorus removal of modified A2/O process on low-carbon domestic sewage under low temperature. – Advanced Materials Research 777: 187-191.
[10] Li, S. M., Tong, H., Wang, R. B. (2014): Operation of modified A2/O process at low temperature and different sludge loadings. – China Water & Wastewater 13: 64-68.
[11] Li, T., Bo, L., Yang, F. (2012): Comparison of the removal of COD by a hybrid bioreactor at low and room temperature and the associated microbial characteristics. – Bioresource Technology 108(3): 28-34.
[12] Li, Y. F., Yang, J. Y., Zhang, G. C. (2013): Effects of aeration on nitrogen and phosphate removal with A2O process. – Advanced Materials Research 622-623: 1738-1741.
[13] Limpiyakorn, T., Shinohara, Y., Kurisu, F. (2005): Communities of ammonia-oxidizing bacteria in activated sludge of various sewage treatment plants in Tokyo. – Fems Microbiology Ecology 54(2): 205-217.
[14] Liu, G., Xu, X., Zhu, L. (2011): Biological nutrient removal in a continuous anaerobic–aerobic–anoxic process treating synthetic domestic wastewater. – Chemical Engineering Journal 225: 223-229.
[15] Peng, Y. Z., Wang, X. L., Li, B. K. (2005): Anoxic biological phosphorus uptake and the effect of excessive aeration on biological phosphorus removal in the A2O process. – Desalination 189(1): 155-164.
[16] Ruiz-Urbieta, M., Sparrow, E. M., Parikh, P. D. (1975): Two-film reflection polarizers: theory and application. – Applied Optics 14(2): 486-492.
[17] Sahariah, B. P., Anandkumar, J., Chakraborty, S. (2015): Treatment of coke oven wastewater in an anaerobic–anoxic–aerobic moving bed bioreactor system. – Desalination & Water Treatment 57(31): 1-7.
[18] Shen, N., Chen, Y., Zhou, Y. (2017): Multi-cycle operation of enhanced biological phosphorus removal (EBPR) with different carbon sources under high temperature. – Water Research 114: 308-315.
[19] Sohsalam, P., Sirianuntapiboon, S. (2008): Feasibility of using constructed wetland treatment for molasses wastewater treatment. – Bioresource Technology 99(13): 5610-5616.
[20] Wang, Y. Y., Pan, M. L., Yan, M. (2007): Characteristics of anoxic phosphors removal in sequence batch reactor. – Journal of Environmental Sciences 19(7): 776-782.
[21] Wang, Y. Y., Geng, J. J., Guo, G. (2011): N2O production in anaerobic/anoxic denitrifying phosphorus removal process: the effects of carbon sources shock. – Chemical Engineering Journal 172(2-3): 9 99-1007.
[22] Whang, G. D., Lim, D. M. (2008): A study on the treatment efficiency of A2O process coupled with mesh screening reactor. – Journal of Korean Society of Water and Wastewater 22(6): 705-714.
[23] Xing, J., Yu, C., Wang, W. (2013): Effect of partial oxygen pressures on pollutant removal with membrane-aerated bioreactor. – Advanced Materials Research 773: 347-352.
[24] Yang, T. (2017): Study on Degradation Regularity of Three Characteristic Pollutants of Pharmaceutical Park Tail Water in A2O Treatment Process. – Liaoning University, Shenyang.
[25] Yoo, H. S., Lee, B. (2015): A study on adjustment of operational factor in A2O process. – Korea Organic Resource Recycling Association 23(3): 33-41.
[26] Zhang, L. H., Zhuang, Y. P., Wang, X. M. (2016): Effect of temperature on denitrifying phosphorus removal efficiency using modified A2/O process. – Transactions of the Chinese Society of Agricultural Engineering 32(10): 213-219.
[27] Zhou, J., Gao, J., Liu, Y. (2013): Contaminant removal performances on domestic sewage using modified anoxic/anaerobic/oxic process and micro-electrolysis. – Environmental Technology 34(19): 2773-2779.

http://www.aloki.hu ● ISSN 1589 1623 (Print) ● ISSN 1785 0037 (Online)
DOI: http://dx.doi.org/10.15666/aeer/1705_1219112202

[28] Zong, Y. C. (2017): Preliminary influence study of Tibet natural environment on sewage treatment effect. – Municipal Technology 35(3): 132-136.
[29] Zong, Y. C., Zhang, Y. H., Lu, G. H. (2018): Study on process characteristics of high altitude A2/O process based on principal component analysis. – Technology of Water Treatment 38(9): 116-119.

http://www.aloki.hu ● ISSN 1589 1623 (Print) ● ISSN 1785 0037 (Online)
DOI: http://dx.doi.org/10.15666/aeer/1705_1219112202

THE DETECTION AND MIDGUT INTRACELLULAR LOCATION OF *RICKETTSIA* SYMBIONT IN THE CAMELLIA APHID (*APHIS AURANTII*)

DENG, J. – LIU, Q. – YU, Y. H. – LI, J. J. – HUANG, X. L.*

State Key Laboratory of Ecological Pest Control for Fujian and Taiwan Crops, College of Plant Protection, Fujian Agriculture and Forestry University, Fuzhou 350002, China

**Corresponding author*
e-mail: huangxl@fafu.edu.cn

(Received 2nd May 2019; accepted 16th Jul 2019)

Abstract. The *Rickettsia*, secondary symbiotic bacteria prevalent in arthropods, has been gradually recognized to play a significant role in the biology of their hosts in the past 20 years. A few previous studies have reported the occurrence of *Rickettsia* in several aphid species, located in the secondary bacteriocyte, sheath cell, or aphid hemolymph extracellularly. In this study, we found that *Rickettsia* symbiont infected camellia aphid, *Aphis aurantii*, with a relatively high infection rate (22%). Moreover, based on the next-generation sequencing of 16S rRNA genes, the relative abundance of *Rickettsia* from an *A. aurantii* sample could even reach 59.1%, which exceeded that of *Buchnera*, the primary endosymbiont of aphids. By using transmission electron microscopy, we also observed dense populations of rod-shaped *Rickettsia* symbionts in midgut epithelial cells of *A. aurantii*. Our study is the first to confirm that the *Rickettsia* can invade into midgut epithelial cells of *A. aurantii*, offering new insights into the location and possible infection route of *Rickettsia* in aphids.
Keywords: *bacteria, arthropods, Next Generation Sequencing, electron microscopy, endosymbiont*

Introduction

Aphids (Hemiptera, Aphididea) are considered notorious agricultural pests that cause severely damage to host plants via sucking on the phloem sap and transmitting phytopathogenic viruses (Eastop, 1977; Huang and Qiao, 2014; Skaljac, 2016). Due to the lack of various essential amino acid in the plant phloem sap, primary/obligate symbionts play an important role in providing essential nutrition to complete the diet of sap-feeding insects (Brumin et al., 2012; Hansen and Moran, 2013). For aphids, *Buchnera aphidicola* supplying nutrients as a primary endosymbiont has been reported in numerous studies (Baumann et al., 1995; Shigenobu et al., 2000; Wilson et al., 2010). Besides primary symbionts, insect secondary/facultative symbionts have generally been considered not necessary for host development and reproduction in the past. However, increasing evidence shows that multiple facultative symbionts might have significant influence on aphid fitness (Oliver et al., 2010), including *Hamiltonella defensa* for protection against parasitoids and predators (Schmid et al., 2012; Costopoulos et al., 2014), *Regiella insecticola* for protection against entomopathogen (ŁUkasik et al., 2013), *Wolbachia* for possible nutritional function (Augustinos et al., 2011). Furthermore, the endosymbiont *Serratia* symbiotica seems to undergo an evolutionary scenario from facultative stage to obligate stage, and establish a co-obligate endosymbiotic consortium with *B. aphidicola* in *Cinara cedri* (Lamelas et al., 2011) and *Cinara tujafilina* (Manzano-Marín and Latorre, 2014).

The *Rickettsia* are intracellular symbionts of eukaryotes and ubiquitous in arthropods (Weinert et al., 2009; Merhej and Raoult, 2011), some of which are best known as

http://www.aloki.hu ● ISSN 1589 1623 (Print) ● ISSN 1785 0037 (Online)
DOI: http://dx.doi.org/10.15666/aeer/1705_1220312212

human and animal pathogens vectored by blood-sucking arthropods, being responsible for epidemic typhus, murine typhus or spotted fever (Raoult and Roux, 1997; Sakurai et al., 2005). *Rickettsia* bacteria are thought to be maternally (Weinert et al., 2009) and also plant-mediated horizontally transmitted (Caspi-Fluger et al., 2011). In general, *Rickettsia* bacteria are facultative symbionts in most arthropods, with influences on host fitness such as fitness benefits, female bias and sensitivity to insecticides in whitefly (Kontsedalov et al., 2008; Himler et al., 2011), male killing in ladybird beetle (Von Der Schulenburg et al., 2001), and thelytokous parthenogenesis induction in a parasitoid wasp (Hagimori et al., 2006). However, considering such wide occurrence in arthropods, more distinct and specific functions of *Rickettsia* symbionts await to be discovered in the vast majority of hosts.

For aphids, some studies have shown that *Rickettsia* can live in secondary bacteriocytes, sheath cells (Fukatsu et al., 2000; Skaljac, 2016), as well as in the hemolymph of hosts with extracellular stage (Tsuchida et al., 2005). A recent study using 454 pyrosequencing of 16S rRNA genes indicated the presence of *Rickettsia* in insect guts of 19 taxonomic orders (Yun et al., 2014). It seems to indicate that *Rickettsia* might be distributed more widely across the digestive system of insect taxa than previously thought. However, further studies are needed to investigate the real location of *Rickettsia* in insect digestive system, for example, free living in the gut or within the midgut epithelial cells. The camellia aphid *Aphis Aurantii* is a common pest species in the subtropical and tropical regions. In our study, we found that *Rickettsia* existed in wild *A. Aurantii* populations feeding on the plant *Loropetalum chinense*. We further investigate three questions: 1) whether the *Rickettsia* is common in *A. aurantii* populations; 2) how much can the relative abundance of *Rickettsia* in the symbiotic microbiome of *A. aurantii*; 3) whether the gut cells of *A. aurantii* contain *Rickettsia* symbiont.

Materials and Methods

The samples of *A. aurantii* were collected from seven different localities distributed in Yunnan, Guangxi, Fujian and Zhejiang provinces of southern China (*Fig. 1*). All samples were collected from different locations and plant individuals, making sure these samples were from different clones. All samples were directly preserved in 95%-ethanol in the wild and frozen at −80°C for further experiment in laboratory. For eliminating possible surface contaminants, all 27 individuals from 19 different clones were washed thrice in 70% ethanol, and then rinsed in sterile deionized water. DNA was isolated with DNeasy Blood & Tissue Kit (QIAGEN) as following the manufacturer manual. The specific primer pair (Ric16SF1: 5'-TGGCTGTCGTCAGCTCGT-3' and 5'-Ric16SR1: TCCACGTCACCGTCTTGC-3') (Sakurai et al., 2005) was used to detect and classify the *Rickettsia* infection. All PCRs were carried out in a 50 μl volume with 4 μl DNA template (2-20 ng/μl), 5 μl 10×Buffer, 2.5 mM dNTP mixture, 10 pmol of each primer and 1 unit of ExTaq DNA polymerase (TaKaRa Bio Inc., Otsu, Japan). The PCR conditions were an initial step of 3 min at 95°C followed by 30 cycles of 30 s at 94°C, 30 s at 52°C and 1 min at 72°C followed in turn by final extension of 10 min at 72°C. PCR products were visualized on 1% agarose. To assure the accuracy of results, sterile deionized water was used as a negative control and some positive products (Individual ID: 17, 22 and 23) were sequenced (*Table 1*).

http://www.aloki.hu ● ISSN 1589 1623 (Print) ● ISSN 1785 0037 (Online)
DOI: http://dx.doi.org/10.15666/aeer/1705_1220312212

To investigate relative abundance of *Rickettsia* in the symbiotic microbiome of *A. aurantii*, three aphid clones (HCX25 from *Mangifera indica*, HCX30 and HCX31 from *L. chinense*) were selected for NGS of bacterial 16S rRNA genes. Ten individuals of each clone followed the above steps of DNA extraction. The primer set (338F: 5'-ACTCCTACGGGAGGCAGCA-3' and 806R: 5'-GGACTACHVGGGTWT CTAAT-3') (Srinivasan et al., 2012) was used to amplify the V3 and V4 region of the bacterial 16S rRNA genes with 95°C for 5 min (1 cycle), 95°C for 30 s, 50°C for 30 s, 72°C for 40 s (25 cycles), followed by 72°C for 7 min. The PCR products was purified using a GeneJET Gel Extraction Kit (Thermo Fisher Scientific, Waltham, MA, United States). Finally, paired-end sequencing of the 16S rRNA was conducted on Illumina HiSeq 2500 with 2×250bp reads (Illumina, Inc., SanDiego, CA, United States) at Biomarker Bioinformatics Technology, Co., Ltd. (Beijing, China).

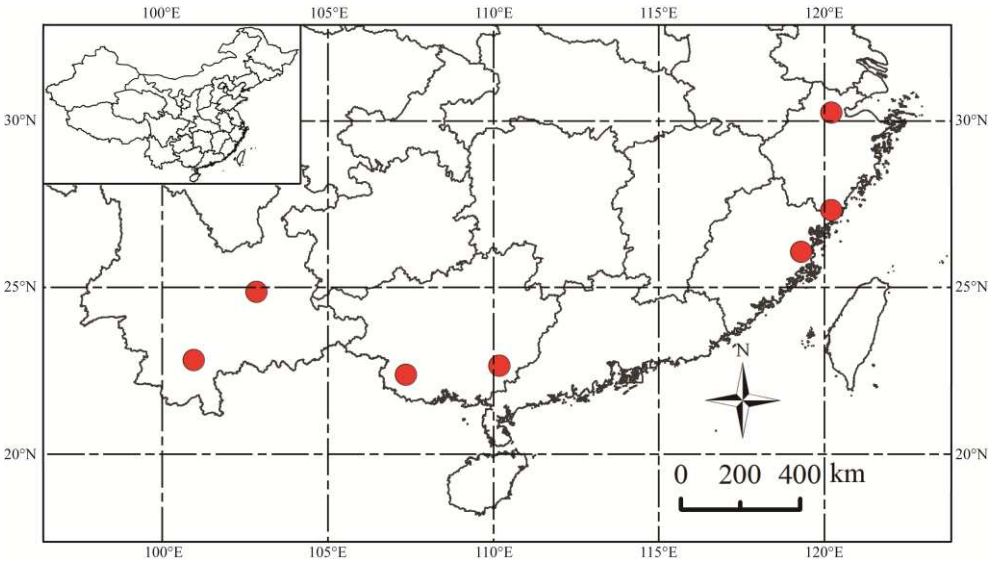

Figure 1. *Overview of geographic distribution of Aphis Aurantii clones collected in this study. Collection sites are labeled with red circle*

The paired-end reads were merged using FLASH v1.2.11 (Magoč and Salzberg, 2011), sequences were further quality trimmed using Trimmomatic v0.33 (Bolger et al., 2014), ensuring >20 quality scores on a sliding window of 50 bp. The chimera sequences were identified and removed using the UCHIME algorithm (Edgar et al., 2011). Sequences with ≥ 97% similarity were clustered into the same operational taxonomic units (OTUs) using UCLUST v10.0 (Edgar, 2010). All OTUs were identified with the RDP classifier (Version 2.2) (Wang et al., 2007) to obtain taxonomic information. The raw sequences have been submitted to the NCBI Sequence Read Archive (accession number SRR8668504, SRR8668505 and SRR8668506).

The 16S sequence of *Rickettsia* from HCX31 was extracted from the NGS sequences of bacterial 16S rRNA genes. The 16S sequences of other *Rickettsia* species was selected and download from GenBank. The data was aligned using MAFFT v 7.409 (Katoh and Standley, 2013), and some sequences not in the same regions were removed using BioEdit 7.0.5 (Hall, 1999). *Orientia tsutsugamushi* (AF062074.1) was chosen as outgroup. Finally, maximum likelihood (ML) tree was conducted using IQTree v1.5.4 and the HKY+F+I model with 1000 ultrafast bootstraps (Nguyen et al., 2014).

http://www.aloki.hu ● ISSN 1589 1623 (Print) ● ISSN 1785 0037 (Online)
DOI: http://dx.doi.org/10.15666/aeer/1705_1220312212

The aphid guts of HCX31 individuals were dissected in 1×PBS using fine forceps. The dissected guts were prefixed in 2.5% glutaraldehyde at room temperature for 2h, and postfixed in 1% osmium tetroxide at room temperature for 60 min. After dehydration through an ethanol series and acetone, the guts were embedded through an SPURR embedding medium series. Ultrathin sections were made on an ultramicrotome (EM UC7; Leica), stained with uranyl acetate and lead citrate, and observed under an H-7650 Hitachi transmission electron microscopy at 80KV.

Table 1. *The detail information of samples from our study*

Clone	SD	NGS	Individual ID	Data	Location collected	Accession number
C1	+		1	04/03/2017	Fuding, Fujian	
C2	+		2	08/06/2017	Kunming, Yunnan	
C3	+		3	04/15/2017	Fuzhou, Fujian	
C4	+		4	10/16/2016	Fuzhou, Fujian	
C5	+		5	09/07/2015	Fuzhou, Fujian	
C6	+		6	10/23/2015	Fuzhou, Fujian	
C7(HCX30)	+	+	7	05/29/2017	Fuzhou, Fujian	SRR8668504
C8(HCX31)	+R	+	8	09/22/2017	Fuzhou, Fujian	SRR8668506
C9	+		9	11/04/2017	Fuzhou, Fujian	
C10	+		10	04/01/2018	Fuzhou, Fujian	
C11	+		11	09/24/2018	Fuzhou, Fujian	
C12	+		12	10/17/2018	Fuzhou, Fujian	
C13	+		13	11/18/2017	Pu'er, Yunnan	
C14	+		14	11/17/2017	Pu'er, Yunnan	
C14	+R		15	11/17/2017	Pu'er, Yunnan	
C15	+		16	11/01/2017	Chongzuo, Guangxi	
C16	+R		17	10/31/2017	Chongzuo, Guangxi	MK577785
C16	+R		18	10/31/2017	Chongzuo, Guangxi	
C2	+		19	08/06/2017	Kunming, Yunnan	
C2	+		20	08/06/2017	Kunming, Yunnan	
C2	+		21	08/06/2017	Kunming, Yunnan	
C17	+		22	10/29/2017	Yulin, Guangxi	MK577784
C18	+R		23	10/27/2017	Yulin, Guangxi	MK577783
C18	+R		24	10/27/2017	Yulin, Guangxi	
C19	+		25	06/17/2018	Hangzhou, Zhejiang	
C19	+		26	06/17/2018	Hangzhou, Zhejiang	
C19	+		27	06/17/2018	Hangzhou, Zhejiang	
C20(HCX25)		+		04/25/2016	Fuzhou, Fujian	SRR8668505

All Clones were collected from *Loropetalum chinense* except for C20 (HCX25) from *Mangifera indica*. NGS=NGS of bacterial 16S rRNA genes; SD=Specific detection using specific primers for *Rickettsia*. + represents using this method. +R represents a fragment of 300 bp obtained from specific primers, indicating the present of *Rickettsia* species

Results

The *Fig. 2* showed the rapid identification result of *Rickettsia* symbiont using the specific primers. A fragment of 300 bp was observed in 6 of 27 individuals. The result suggested a *Rickettsia* occurrence rate of 22.2% in our study. A total of 19 *Rickettsia* species with 403 bp length were selected to construct a ML phylogenetic tree. In the phylogenetic tree (*Fig. 3*), *Rickettsia* were classified into three major clades with high support values: one including *Rickettsia* from leeches, arthropods and our sample; a second clade including *Rickettsia* endosymbiont from *Bemisia tabaci* and some vertebrate pathogen *Rickettsia* such as *R. typhi* and *R. japonica*; a third clade containing sequences obtained from environmental samples.

http://www.aloki.hu ● ISSN 1589 1623 (Print) ● ISSN 1785 0037 (Online)
DOI: http://dx.doi.org/10.15666/aeer/1705_1220312212

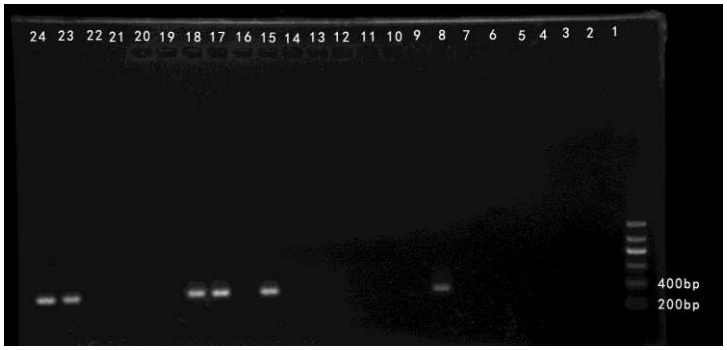

Figure 2. *Specific detection of Rickettsia sp. with primers Ric16SF1 and Ric16SR1 in 19 clones and 27 individuals of A. aurantii. Lanes 1-24: 1-24 individuals, Marker: marker F (200bp 400bp 700bp 1000bp 1500bp 2000bp). The remaining three are not shown due to observation in a small gel, and negative control does not show a fragment of 300 bp. The products in lanes 15, 17 and 23 have been sequenced and submitted to GenBank (Table 1)*

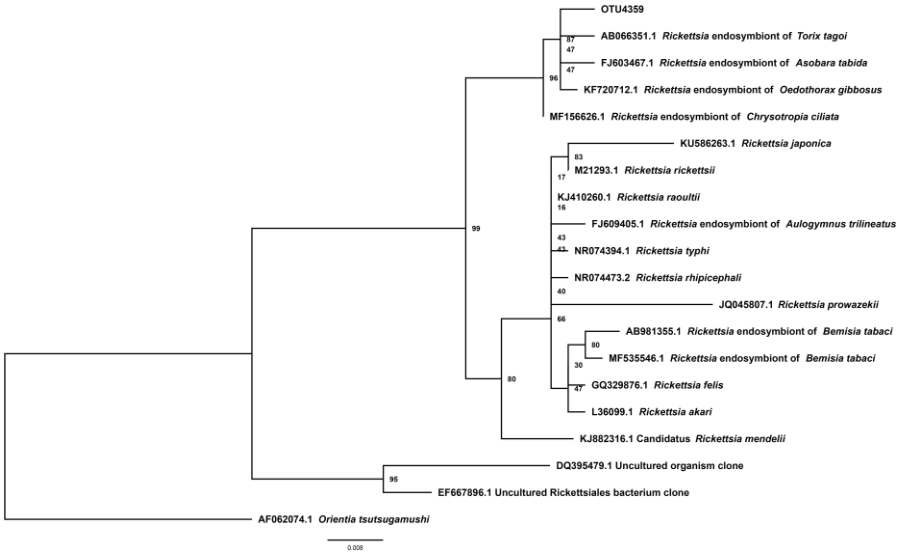

Figure 3. *ML phylogenic tree of Rickettsia based on 16S rDNA sequences. OUT4359 is the sequence from our sample HCX 31. The node values represent the bootstrap values*

The NGS of bacterial 16S rRNA gene yielded 47,579, 54,211 and 54,337 effective tags from HCX25, HCX30 and HCX31, respectively. The average length of effective tags was about 420bp. The OTUs number of the rarefaction curves had very slow growth with the increase of sequencing depth, indicating that the majority of bacterial OTUs had been observed (*Fig. 4A*). A total of 42 OTUs were obtained at 97% sequence-similarity level (31 OTUs for HCX25; 34 OTUs for HCX30 and 34 OUTs for HCX31) (*Fig. 4B*). The top 10 genera based on relative abundance in three samples were illustrated in *Fig. 4C*. For HCX25 and HCX30, the genus of dominant bacteria was *Buchnera*, the primary endosymbiont of aphids, accounting for 98.3% and 98.8%, respectively. For HCX31, the dominant bacteria were *Rickettsia* with 59.1% relative abundance, followed by *Buchnera* with 39.2%. Electron microscopic observation of the gut of HCX31 with dense populations of rod-shaped bacteria in the gut cells (*Fig. 5*). The *Rickettsia* cells ranged from 0.35-0.5 μm in width to 0.5-1 μm in length.

http://www.aloki.hu ● ISSN 1589 1623 (Print) ● ISSN 1785 0037 (Online)
DOI: http://dx.doi.org/10.15666/aeer/1705_1220312212

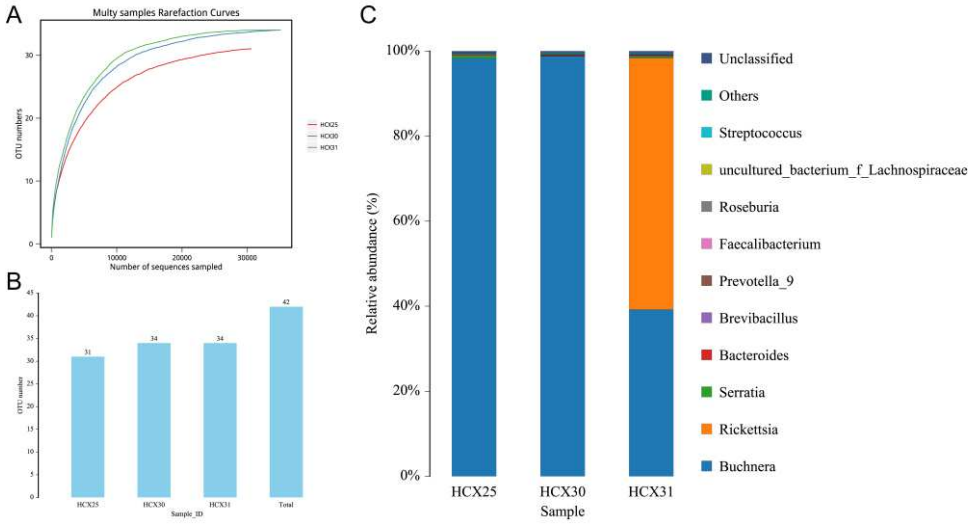

Figure 4. *The NGS analysis results of bacterial 16S rRNA genes. (A) The rarefaction curves. (B) The histogram of the OTUs numbers. (C) Taxonomic composition of bacteria for three A. aurantii samples*

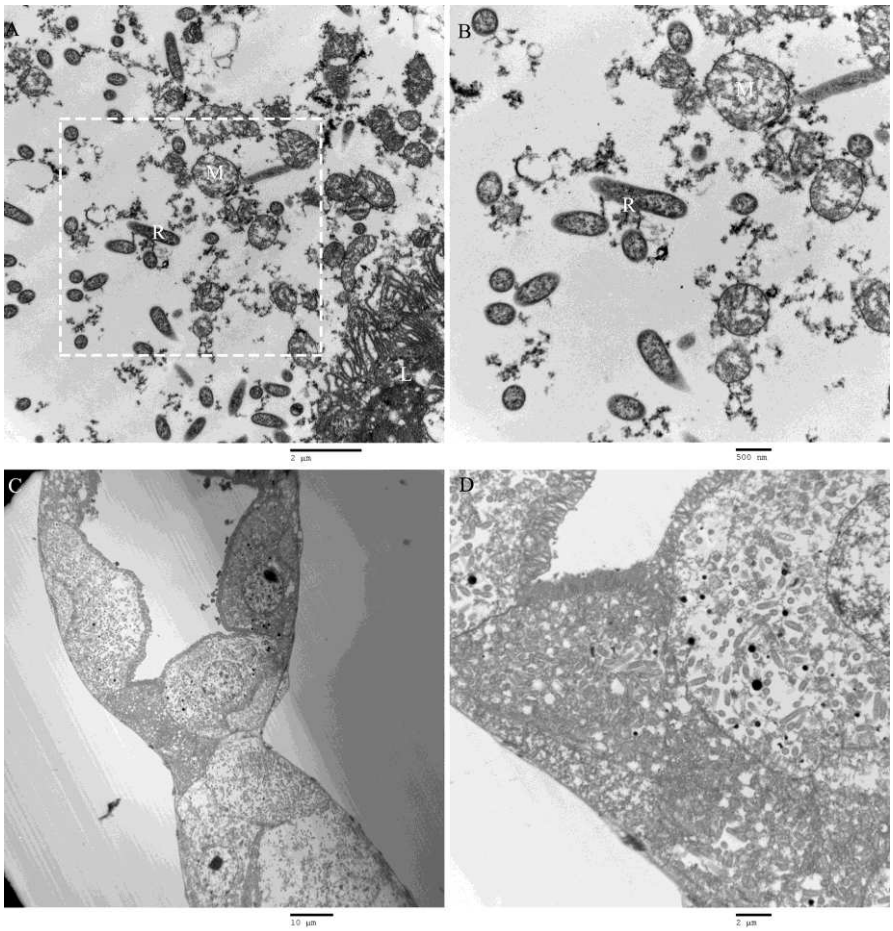

Figure 5. *(A) Electron microscopic observation of the midgut epithelial cells of A. aurantii. (B) Details of the box in A. L, lumen; M, mitochondria; R, Rickettsia. (C) and (D) High density Rickettsia symbionts with rod-shape in the gut cells*

http://www.aloki.hu ● ISSN 1589 1623 (Print) ● ISSN 1785 0037 (Online)
DOI: http://dx.doi.org/10.15666/aeer/1705_1220312212

Discussion

Although all 27 individuals in our study were collected from *L. chinense*, the *Rickettsia* occurrence rate was similar with 17% of Guidolin and Cônsoli (2018) in *Aphis aurantii*. Cautiously, some bacteria occur at low proportion within a host, making limits of detection of specific primers due to low bacterial DNA concentration. The *Rickettsia* occurrence rate of 22.2% might be underestimated. Like other pathogens, some evidence have shown that the plant can be a media and provide a place for horizontal transmission of *Rickettsia* (Perlman et al., 2006; Caspi-Fluger et al., 2011). This may explain the phylogenetically similar symbionts occur in unrelated phytophagous insect species (Caspi-Fluger et al., 2011). The *Rickettsia* sequence from our sample is clustered together with *Rickettsia* from other arthropods in ML tree. *Rickettsia* are popular in many arthropod groups also including some other sap-feeders, but it is rare in aphids (Oliver et al., 2010). All records only include *Acyrthosiphon pisum* (Chen et al., 1996; Sakurai et al., 2005; Sepúlveda et al., 2017), *Amphorophora rubi* (Haynes et al., 2003), *Aphis citricidus* (Guidolin and Cônsoli, 2017, 2018). Haynes et al. (2003) also reported that the *Rickettsia* was very rarely detected in just 1% and 2% occurrence rates in natural populations of *Am. rubi* and *Ac. pisum*, respectively. A relatively high infection rate (22%) of *A. aurantii* was reported in our study, showing a significant difference compared to *Am. rubi* and *Ac. pisum*. Interestingly, the range of host plants of *A. aurantii* is also wider with 104 plant families compared to three families of *Am. rubi* and 23 families of *Ac. Pisum* (host plant information from http://www.aphidsonwor ldsplants.info), which is concordant with the comparative result of *Rickettsia* infection rates among the three aphid species. Guidolin and Cônsoli (2018) also consider that the polyphagous species may tend to more frequently infected with secondary symbionts than the oligophagous one.

Little is known about the influences of *Rickettsia* on their aphid hosts. A few studies show that *Rickettsia* symbionts can enhance aphid host's resistance to natural enemies (ŁUkasik et al., 2013) and cause reductions in body weight and fecundity in the pea aphid (Chen et al., 2000). The invasive order of the most *Rickettsia* is considered from the gut to the haemocoel and then to the salivary glands (Perlman et al., 2006). Brumin et al. (2012) investigated the subcellular localization of *Rickettsia* endosymbiont in the whitefly, showing that *Rickettsia* infected the digestive salivary and had the possible digestive purposes. For aphids, several previous works of *Rickettsia* location only have shown the distribution of *Rickettsia* endosymbiont in secondary bacteriocytes, sheath cells and hemolymph (Fukatsu et al., 2000; Tsuchida et al., 2005; Skaljac, 2016) with the exception of the gut.

Conclusion

Our research confirms the *Rickettsia* location in gut cells, providing a necessary supplement to reveal a complete and clear *Rickettsia* localization in aphids, contributing to understanding its evolution and function in the future research. To understand *Rickettsia* evolution and pathogenesis, more works such as a comprehensive analysis of the entire genome need be done. Meanwhile, it will be interesting to test whether wider host plant range increases the infection possibility of *Rickettsia* in other aphids in the future.

http://www.aloki.hu ● ISSN 1589 1623 (Print) ● ISSN 1785 0037 (Online)
DOI: http://dx.doi.org/10.15666/aeer/1705_1220312212

Acknowledgements. The work was supported by grants from the National Natural Science Foundation of China (Grant Numbers: 31772504, 31601860), National Key R&D Program of China (2016YFE0203100), and Fujian Provincial Department of Science & Technology (2015J06005). We thank Qianzhuo Mao and Haitao Wang's help for the electron microscopic observation.

REFERENCES

[1] Augustinos, A. A., Santos-Garcia, D., Dionyssopoulou, E., Moreira, M., Papapanagiotou, A., Scarvelakis, M., Doudoumis, V., Ramos, S., Aguiar, A. F., Borges, P. A. V., Manhaz, K., Latorre, A., Tsiamis, G., Bourtzis, K. (2011): Detection and characterization of *Wolbachia* infections in natural populations of aphids: is the hidden diversity fully unraveled? – PLoS One 6: e28695.

[2] Baumann, P., Baumann, L., Lai, C. Y., Rouhbakhsh, D., Moran, N. A., Clark, M. A. (1995): Genetics, physiology, and evolutionary relationships of the genus *Buchnera*: intracellular symbionts of aphids. – Review of Microbiology 49: 55-94.

[3] Bolger, A. M., Lohse, M., Usadel, B. (2014): Trimmomatic: a flexible trimmer for Illumina sequence data. – Bioinformatics 30: 2114-2120.

[4] Brumin, M., Levy, M., Ghanim, M. (2012): Transovarial transmission of *Rickettsia spp*. and organ-specific infection of the whitefly *Bemisia tabaci*. – Applied and Environmental Microbiology 78: 5565-5574.

[5] Caspi-Fluger, A., Inbar, M., Mozes-Daube, N., Katzir, N., Portnoy, V., Belausov, E., Hunter, M. S., Zchori-Fein, E. (2011): Horizontal transmission of the insect symbiont *Rickettsia* is plant-mediated. – Proceedings of the Royal Society B: Biological Sciences 279: 1791-1796.

[6] Chen, D. Q., Campbell, B. C., Purcell, A. H. (1996): A new Rickettsia from a herbivorous insect, the pea aphid *Acyrthosiphon pisum* (Harris). – Current Microbiology 33: 123-128.

[7] Chen, D. Q., Montllor, C. B., Purcell, A. H. (2000): Fitness effects of two facultative endosymbiotic bacteria on the pea aphid, *Acyrthosiphon pisum*, and the blue alfalfa aphid, *A. kondoi*. – Entomologia Experimentalis et Applicata 95: 315-323.

[8] Costopoulos, K., Kovacs, J. L., Kamins, A., Gerardo, N. M. (2014): Aphid facultative symbionts reduce survival of the predatory lady beetle *Hippodamia convergens*. – Bmc Ecology 14: 1-7.

[9] Eastop, V. F. (1977): Worldwide importance of aphids as virus vectors. – In Aphids As Virus Vectors Academic Press, UK.

[10] Edgar, R. C. (2010): Search and clustering orders of magnitude faster than BLAST. – Bioinformatics 26: 2460-2461.

[11] Edgar, R. C., Haas, B. J., Clemente, J. C., Quince, C., Knight, R. (2011): UCHIME improves sensitivity and speed of chimera detection. – Bioinformatics 27: 2194-2200.

[12] Fukatsu, T., Nikoh, N., Kawai, R., Koga, R. (2000): The secondary endosymbiotic bacterium of the pea aphid *Acyrthosiphon pisum* (Insecta: Homoptera). – Applied and Environmental Microbiology 66: 2748-2758.

[13] Guidolin, A. S., Cônsoli, F. L. (2017): Symbiont diversity of Aphis (Toxoptera) citricidus (Hemiptera: Aphididae) as Influenced by host plants. – Microbial Ecology 73: 201-210.

[14] Guidolin, A. S., Cônsoli, F. L. (2018): Diversity of the most commonly reported facultative symbionts in two closely-related aphids with different host ranges. – Neotropical entomology 47: 440-446.

[15] Hagimori, T., Abe, Y., Date, S., Miura, K. (2006): The first finding of a *Rickettsia* bacterium associated with parthenogenesis induction among insects. – Current Microbiology 52: 97-101.

[16] Hall, T. A. (1999): BioEdit: a user-friendly biological sequence alignment editor and analysis program for Windows 95/98/NT. – In Nucleic acids symposium series, Information Retrieval Ltd, London.

http://www.aloki.hu ● ISSN 1589 1623 (Print) ● ISSN 1785 0037 (Online)
DOI: http://dx.doi.org/10.15666/aeer/1705_1220312212

[17] Hansen, A. K., Moran, N. A. (2013): The impact of microbial symbionts on host plant utilization by herbivorous insects. – Molecular Ecology 23: 1473-1496.
[18] Haynes, S., Darby, A. C., Daniell, T. J., Webster, G., Van Veen, F. J. F., Godfray, H. C. J., Prosser, J. I., Douglas, A. E. (2003): Diversity of bacteria associated with natural aphid populations. – Applied and Environmental Microbiology 69: 7216-7223.
[19] Himler, A. G., Adachi-Hagimori, T., Bergen, J. E., Kozuch, A., Kelly, S. E., Tabashnik, B. E., Chiel, E., Duckworth, V. E., Dennehy, T. J., Zchori-Fein, E. (2011): Rapid spread of a bacterial symbiont in an invasive whitefly is driven by fitness benefits and female bias. – Science 332: 254-256.
[20] Huang, X. L., Qiao, G. X. (2014): Aphids as models for ecological and evolutionary studies. – Insect Science 21: 247-250.
[21] Katoh, K., Standley, D. M. (2013): MAFFT multiple sequence alignment software version 7: improvements in performance and usability. – Molecular Biology and Evolution 30: 772-780.
[22] Kontsedalov, S., Zchori-Fein, E., Chiel, E., Gottlieb, Y., Inbar, M., Ghanim, M. (2008): The presence of *Rickettsia* is associated with increased susceptibility of *Bemisia tabaci*(Homoptera: Aleyrodidae) to insecticides. – Pest Manag Sci 64: 789-792.
[23] Lamelas, A., Gosalbes, M. J., Manzano-Marin, A., Pereto, J., Moya, A., Latorre, A. (2011): Serratia symbiotica from the aphid *Cinara cedri*: a missing link from facultative to obligate insect endosymbiont. – PLoS Genet 7: e1002357.
[24] ŁUkasik, P., Asch, M. V., Guo, H., Ferrari, J. J., Godfray, H. C. (2013): Unrelated facultative endosymbionts protect aphids against a fungal pathogen. – Ecology Letters 16: 214-218.
[25] Magoč, T., Salzberg, S. L. (2011): FLASH: fast length adjustment of short reads to improve genome assemblies. – Bioinformatics 27: 2957-2963.
[26] Manzano-Marín, A., Latorre, A. (2014): Settling down: the genome of *Serratia symbiotica* from the *Aphid Cinara* tujafilina zooms in on the process of accommodation to a cooperative intracellular life. – Genome Biology and Evolution 6: 1683-1698.
[27] Merhej, V., Raoult, D. (2011): Rickettsial evolution in the light of comparative genomics. – Biological Reviews 86: 379-405.
[28] Nguyen, L. T., Schmidt, H. A., von Haeseler, A., Minh, B. Q. (2014): IQ-TREE: a fast and effective stochastic algorithm for estimating maximum-likelihood phylogenies. – Molecular Biology and Evolution 32: 268-274.
[29] Oliver, K. M., Degnan, P. H., Burke, G. R., Moran, N. A. (2010): Facultative symbionts in aphids and the horizontal transfer of ecologically important traits. – Annual Review of Entomology 55: 247-266.
[30] Perlman, S. J., Hunter, M. S., Zchori-Fein, E. (2006): The emerging diversity of *Rickettsia*. – Proceedings of the Royal Society B: Biological Sciences 273: 2097-2106.
[31] Raoult, D., Roux, V. (1997): Rickettsioses as paradigms of new or emerging infectious diseases. – Clinical Microbiology Reviews 10: 694-719.
[32] Sakurai, M., Koga, R., Tsuchida, T., Meng, X. Y., Fukatsu, T. (2005): *Rickettsia* symbiont in the pea aphid *Acyrthosiphon pisum*: novel cellular tropism, effect on host fitness, and interaction with the essential symbiont *Buchnera*. – Applied and Environmental Microbiology 71: 4069-4075.
[33] Schmid, M., Sieber, R., Zimmermann, Y. S., Vorburger, C. (2012): Development, specificity and sublethal effects of symbiont-conferred resistance to parasitoids in aphids. – Functional Ecology 26: 207-215.
[34] Sepúlveda, D. A., Zepeda-Paulo, F., Ramírez, C. C., Lavandero, B., Figueroa, C. C. (2017): Diversity, frequency, and geographic distribution of facultative bacterial endosymbionts in introduced aphid pests. – Insect Science 24: 511-521.
[35] Shigenobu, S., Watanabe, H., Hattori, M., Sakaki, Y., Ishikawa, H. (2000): Genome sequence of the endocellular bacterial symbiont of aphids *Buchnera sp*. APS. – Nature 407: 81-86.

http://www.aloki.hu ● ISSN 1589 1623 (Print) ● ISSN 1785 0037 (Online)
DOI: http://dx.doi.org/10.15666/aeer/1705_1220312212

[36] Skaljac, M. (2016): Bacterial symbionts of aphids (Hemiptera: Aphididae). – In: Biology and Ecology of Aphids. CRC Press: Boca Raton, FL, USA.
[37] Srinivasan, S., Hoffman, N. G., Morgan, M. T., Matsen, F. A., Fiedler, T. L., Hall, R. W., Ross, F. J., McCoy, C. O., Bumgarner, R., Marrazzo, J. M. (2012): Bacterial communities in women with bacterial vaginosis: high resolution phylogenetic analyses reveal relationships of microbiota to clinical criteria. – PLoS One 7: e37818.
[38] Tsuchida, T., Koga, R., Meng, X. Y., Matsumoto, T., Fukatsu, T. (2005): Characterization of a facultative endosymbiotic bacterium of the pea aphid *Acyrthosiphon pisum*. – Microbial Ecology 49: 126-133.
[39] Von Der Schulenburg, J. H., Habig, M., Sloggett, J. J., Webberley, K. M., Bertrand, D., Hurst, G. D. D., Majerus, M. E. N. (2001): Incidence of male-killing *Rickettsia spp*. (alpha-proteobacteria) in the ten-spot ladybird beetle *Adalia decempunctata* L. (Coleoptera: Coccinellidae). – Applied and Environmental Microbiology 67: 270-277.
[40] Wang, Q., Garrity, G. M., Tiedje, J. M., Cole, J. R. (2007): Naive Bayesian classifier for rapid assignment of rRNA sequences into the new bacterial taxonomy. – Applied and Environmental Microbiology 73: 5261-5267.
[41] Weinert, L. A., Werren, J. H., Aebi, A., Stone, G. N., Jiggins, F. M. (2009): Evolution and diversity of *Rickettsia* bacteria. – BMC BIOLOGY 7: 6.
[42] Wilson, A. C. C., Ashton, P. D., Calevro, F., Charles, H., Colella, S., Febvay, G., Jander, G., Kushlan, P. F., Macdonald, S. J., Schwartz, J. F. (2010): Genomic insight into the amino acid relations of the pea aphid, *Acyrthosiphon pisum*, with its symbiotic bacterium *Buchnera aphidicola*. – Insect Molecular Biology 19: 249-258.
[43] Yun, J. H., Roh, S. W., Whon, T. W., Jung, M. J., Kim, M. S., Park, D. S., Yoon, C., Nam, Y. D., Kim, Y. J., Choi, J. H. (2014): Insect gut bacterial diversity determined by environmental habitat, diet, developmental stage, and phylogeny of host. – Applied and Environmental Microbiology 80: 5254-5264.

http://www.aloki.hu ● ISSN 1589 1623 (Print) ● ISSN 1785 0037 (Online)
DOI: http://dx.doi.org/10.15666/aeer/1705_1220312212

NITROGEN AND PHOSPHOROUS REMOVAL OF PILOT-SCALE ANAEROBIC-ANOXIC-AEROBIC PROCESS UNDER PLATEAU ENVIRONMENTAL FACTORS

ZONG, Y. C.[1,2,3,4,5,6] – HAO, K. Y.[6] – LI, Y. W.[6] – LU, G. H.[1,2,3,4,5,6*] – HUANG, D. C.[6]

[1]Res. Institute of Tibet Plateau Ecology, Tibet Agriculture & Animal Husbandry University Linzhi 860000, China

[2]Tibet Key Laboratory of Forest Ecology in Plateau Area, Ministry of Education Linzhi 860000, China

[3]National Key Station of Field Scientific Observation & Experiment, Linzhi 860000, China

[4]Key Laboratory of Forest Ecology in Plateau Area, Tibet Autonomous Region Linzhi 860000, China

[5]United Key Laboratories of Ecological Security, Tibet Autonomous Region Linzhi 860000, China

[6]Water Conservancy Project & Civil Engineering College, Tibet Agriculture & Animal Husbandry University, Linzhi 860000, China (phone: +86-13062577435)

[*]Corresponding author e-mail: ghlu@hhu.edu.cn; phone: +86-13062577435

(Received 3rd May 2019; accepted 11th Jul 2019)

Abstract. Considering the two unique factors of the plateau environment (i.e. water temperature and oxygen partial pressure), this paper explores the nitrogen and phosphorous removal of pilot-scale anaerobic-anoxic-aerobic (A2O) process. The experimental results show that none of the total phosphorous (TP), total nitrogen (TN) or NH_4^+-N of the outlet water satisfied the Chinese national standard GB18918-2002, while COD only fulfilled the standard requirements under a few working parameters. The optimal values of the four working parameters were determined as: the optimal HRT=26.25 h, the optimal DO=3.0 mg/L, the optimal temperature=15°C. All these optimal values deviated greatly from the existing studies. The microbial densities corresponded poorly to the three working parameters, and were smaller than those under non-plateau environment; the number of indicator microorganisms had good correspondence with the optimal values of our experimental parameters.
Keywords: *anaerobic-anoxic-aerobic (A2O) process, water temperature, hydraulic retention time (HRT), dissolved oxygen (DO), nitrogen and phosphorous removal*

Introduction

The anaerobic-anoxic-aerobic (A2O) process, improved from the traditional activated-sludge process, has become the most popular sewage treatment method in Tibet (Chen et al., 2018), China. It is widely agreed that the effect of A2O is influenced by the unique environment factors of the plateau, namely, water temperature and pressure.

With a mean elevation of more than 4,000 m, Tibet can be categorized as a typical plateau region with low temperature. Taking Linzhi for instance, the domestic sewage falls in the range of 4°C and 14°C (Zong et al., 2018), which is a typical low-

http://www.aloki.hu ● ISSN 1589 1623 (Print) ● ISSN 1785 0037 (Online)
DOI: http://dx.doi.org/10.15666/aeer/1705_1221312226

temperature sewage. The water temperature in other parts of Tibet is theoretically below this range, because Linzhi is a city with below-average elevation in Tibet.

According to Lewis-Whitman's two-film theory (Ruiz-Urbieta et al., 1975), the maximal concentration of oxygen that can be dissolved in liquid medium decreases with the pressure. The atmospheric pressure is only 67.24 kPa in Linzhi. The elevation and atmospheric pressure of other cities in Tibet are listed in *Table 1* below.

Table 1. *Elevation, pressure of Tibet in China*

	Lhasa	**Changdu**	**Shigatse**	**Linzhi**	**Shannan**	**Naqu**	**Ali**
Elevation (m)	3658.0	3306.0	3836.0	3000.0	3551.7	4507.0	4278.0
The local pressure (kPa)	59.87	63.81	57.88	67.24	61.06	50.36	52.93
Oxygen partial pressure (kPa)	12.54	13.37	12.13	14.09	12.79	10.55	11.09
Oxygen levels (%)	59.87	63.81	57.88	67.24	61.06	50.36	52.93

Note: Standard Oxygen levels are 100%

Temperature is a main influencing factor of sewage treatment (Ai et al., 2014; Abourabia and Abdel Moneim, 2019). Its influence mainly exists in the following aspects: On the phosphorus removal of sludge denitrification, the release and absorption rates of phosphorus are changed under excessively high or low temperatures, and the proportion of denitrifying phosphorus accumulating organisms (DPAOs) in the activated sludge is greatly affected by temperature variation (Zhang et al., 2016; Wu, 2017); the nitrification capacity of the sewage treatment system is obviously weakened when the water temperature falls below 15°C, and basically disappears when the temperature drops below 4°C (He et al., 2010; Li et al., 2013). Thus, the nitrogen removal is severely inhibited under a low temperature (Li et al., 2014).

In view of the above, this paper explores the mechanism of nitrogen and phosphorus removal of A2O system, as a typical sewage treatment process. Starting from the microbial variation law, the author discussed the influence of water temperature, dissolved oxygen concentration, hydraulic retention time (HRT) and other factors on nitrogen and phosphorus removal, analyzed the operation features of A2O system at high elevations, and investigated the microbial features in the anaerobic section, anoxic section and aerobic section. The research discloses the mechanism of nitrogen and phosphorus removal in the reactor, shedding light on how plateau environmental factors affect the mechanism of nitrogen and phosphorus removal. Moreover, our research results lay a theoretical basis for the biological sewage treatment system in the plateau environment.

Materials and methods

Description of the A2O system and wastewater

As mentioned above, our experiment aims to disclose the law of removal rates under different water temperatures, HRTs and dissolved oxygens (DOs). For this purpose, the process flow of our experiment was designed as the following chart.

A pilot-scale A2O sewage treatment device was designed and fabricated with plexiglass. With an effective volume of 210 L, the device consists of 8 segments: the first 2 are anaerobic tanks, the middle 2 are anoxic tanks, and the last 4 are aerobic tanks.

http://www.aloki.hu ● ISSN 1589 1623 (Print) ● ISSN 1785 0037 (Online)
DOI: http://dx.doi.org/10.15666/aeer/1705_1221312226

The volume ratio of the anaerobic, anoxic and aerobic sections is 1:1:2. Besides, the effective volume of the sedimentation tank is 26.25 L. In both anaerobic and anoxic sections, each tank has a 50 rpm stirring device at the bottom; in each aerobic tank, there is an aerator for oxygen supply. Inflow, return sludge and nitrifying liquid are controlled by a peristaltic pump. To maintain a constant temperature, the water temperature was regulated by a constant temperature circulator. In each tank, a sampling hole was opened on the tank wall. Before the experiment, the activated sludge was cured for 32 d. The temperature, mixed liquor suspended solids (MLSS), and volume percent of MLSS after settling for 30 min (SV_{30}) were set to 22.5ºC, 4,787 mg/L and 35%, respectively. The number of parallel samples per point is three, and the average of three samples is taken when the accuracy requirement is met, otherwise resampling is considered (*Figure 1*).

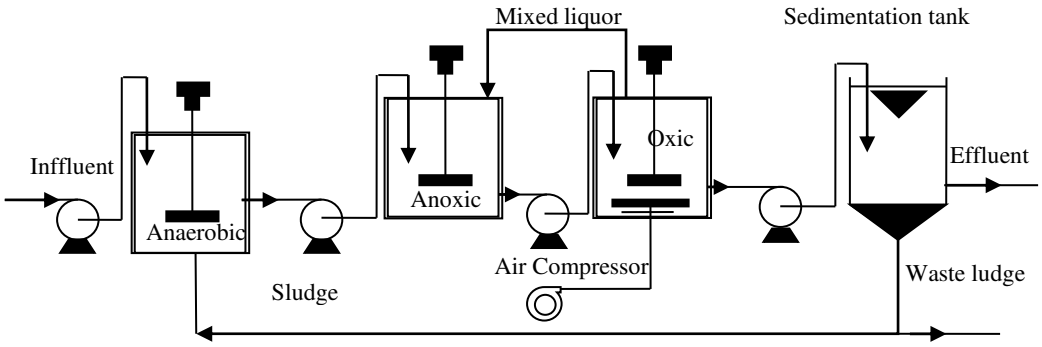

Figure 1. *Schematic of anaerobic-anoxic-aerobic (A2O) process*

The urban domestic sewage in Linzhi was directly adopted for our experiments. The main water quality indices of the sewage are given in the table below (*Table 2*).

Table 2. *Quality indicators of sewage*

pH	DO (mg/L)	Temperature (°C)	COD (mg/L)	TN (mg/L)	TP (mg/L)	NH_4^+-N (mg/L)
6.99~8.41	1.12~5.08	8.98~29.10	149.48~526.36	36.51~147.08	3.96~11.56	30.81～54.16

Operation of the A2O device

The operation of the A2O device was studied under three working parameters, i.e. water temperature, hydraulic retention time (HRT) and DO, in order to disclose the law of removal rates under different water temperatures, HRTs and DOs. The control plans for the three parameters are specified below.

On water temperature control, the inlet water flow was designed as 10.0±0.1 L/s, HRT as 21.0±0.2 h (the HRT ratio between anaerobic tank, anoxic tank and aerobic tank=1: 1: 2), DO as 2.0±0.1 mg/L, the reflux ratio of the mixed liquor Ri=200%, and the reflux ratio of the sludge R=100%. Both the mixed liquor and the sludge were continuously refluxed. The temperature was changed by an electric heater between five levels: 10, 15, 20, 25 and 30°C. The water samples were collected 72 h after the temperature reached the design temperature. The temperature was controlled with an error of or less than 0.1°C.

http://www.aloki.hu ● ISSN 1589 1623 (Print) ● ISSN 1785 0037 (Online)
DOI: http://dx.doi.org/10.15666/aeer/1705_1221312226

On HRT control, the inlet water temperature was designed as 20±0.1°C, the HRT ratio between anaerobic tank, anoxic tank and aerobic tank as 1: 1: 2, DO as 2.0±0.1 mg/L, the reflux ratio of the mixed liquor Ri=200%, and the reflux ratio of the sludge R=100%. Both the mixed liquor and the sludge were continuously refluxed. HRT was adjusted by changing the inlet water flow between five levels: 4, 8, 12, 16 and 20 L/s. HRTs corresponding to the five levels were respectively 52.5, 26.26, 17.5, 13.125 and 10.5 h. The water samples were collected 72 h after the change of the inlet water flow. The flow was controlled with an error of or less than ±0.1 L/s.

On DO control, the inlet water temperature was designed as 20±0.1°C, the inlet water flow as 10.0±0.1 L/s, HRT as 21.0±0.2 h (HRT ratio between anaerobic tank, anoxic tank and aerobic tank=1:1:2), the reflux ratio of the mixed liquor Ri=200%, and the reflux ratio of the sludge R=100%. Both the mixed liquor and the sludge were continuously refluxed. DO was altered between 10 levels (1, 2, 2.5, 2.8, 3, 3.2, 3.5, 4, 4.5 and 5 mg/L) by changing the amount of blast aeration. The water samples were collected 72 h after DO reached the design level. DO was controlled with an error of or less than ±0.1 mg/L.

Analytical methods

According to the working standards, the experimental indices were respectively measured by the following methods: COD was determined by the potassium dichromate method, the TN by the ion chromatography, TP by potassium persulfate oxidation, MLSS by the gravimetric method, the SV30 by the standard method, DO by membrane electrode method, pH by the portable pH meter, NH_4^+-N by the Nessler's reagent photometry, the water temperature by water thermometer, the inlet water flow by float flowmeter, and the microorganisms by biochemical microscope counting.

Results

Sewage treatment at different HRTs

Table 3 displays the operation parameters like DO, MLSS, pH and temperature at different HRTs.

Table 3. *Process Parameter at different hydraulic retention times (HRTs)*

Designed Flow (L/h)	4	8	12	16	20
HRTs (h)	52.50	26.25	17.50	13.13	10.50
DO (mg/L)	3.16	2.30	1.64	1.98	2.04
pH	8.10	8.00	8.27	8.40	8.41
MLSS (mg/L)	964	996	1084	930	920
SV_{30} (%)	10	10	10	10	10
Temperature (°C)	21.4	20.0	19.5	20.7	20.6

Effect on removal rates

Figure 2 provides the removal rates of COD, TP, TN and NH_4^+-N in anaerobic, anoxic and aerobic tanks at different HRTs.

http://www.aloki.hu ● ISSN 1589 1623 (Print) ● ISSN 1785 0037 (Online)
DOI: http://dx.doi.org/10.15666/aeer/1705_1221312226

As shown in *Figure 2(a)*, the COD removal rate ranged between 69.65% and 93.98% under the five HRTs; in descending order of the COD removal rate, the inlet water flows were ranked as 8, 12, 16, 4 and 20 L/h, and HRTs as 26.25, 17.50, 13.13, 52.50 and 10.50 h; the optimal HRT was much greater than 7~14 h; the highest COD removal rate was observed at the design inlet water flow of 8 L/h; the removal effect was obvious in anaerobic and aerobic sections, but the removal rate was not significantly enhanced in the anoxic section.

As shown in *Figure 2(b)*, the TP removal rates fell in the range of 4.53%~64.56% under the five HRTs; in descending order of TP removal rate, the inlet water flows were ranked as 8, 12, 20, 16 and 4 L/h, and HRTs as 26.25, 17.50, 10.50, 13.13 and 52.50 h; the optimal HRT was much greater than 7~14 h; the highest TP removal rate was observed at the design inlet water flow of 8 L/h; the removal effect was obvious in anaerobic and aerobic sections, but the removal rate was not significantly enhanced in the anoxic section.

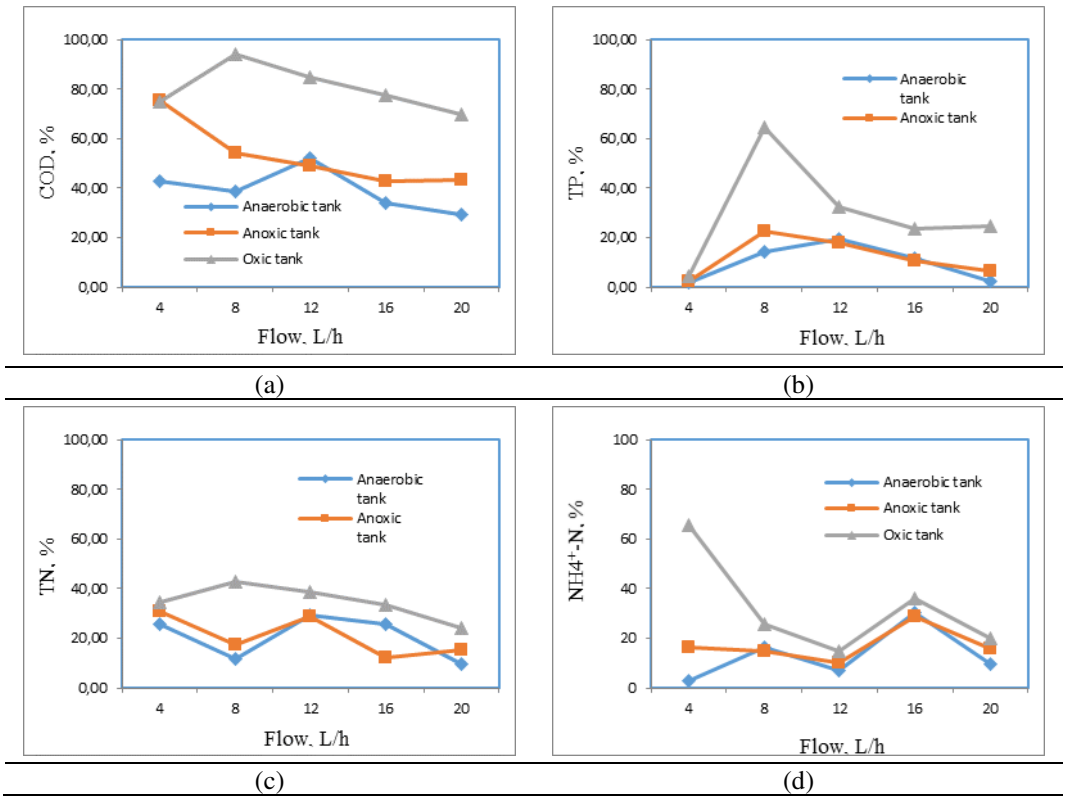

Figure 2. *Removal rate at different hydraulic retention times (HRTs)*

As shown in *Figure 2(c)*, the TN removal rates shifted from 23.92% to 42.85% under the five HRTs; in descending order of the TN removal rate, the inlet water flows were ranked as 8, 12, 4, 16 and 20 L/h, and HRTs as 26.25, 17.50, 52.50, 13.13 and 10.50 h; the optimal HRT was much greater than 7~14 h; the highest TN removal rate was observed at the design inlet water flow of 8 L/h; the removal effect was obvious in anaerobic and aerobic sections, but the removal rate was not significantly enhanced in the anoxic section.

http://www.aloki.hu ● ISSN 1589 1623 (Print) ● ISSN 1785 0037 (Online)
DOI: http://dx.doi.org/10.15666/aeer/1705_1221312226

As shown in *Figure 2(d)*, the NH_4^+-N removal rates changed within 14.92% and 65.47%; in descending order of the NH_4^+-N removal rate, the inlet water flows were ranked as 4, 16, 8, 20, 12 L/h, and the HRTs as 52.50, 13.13, 26.25, 10.50 and 17.50 h; the optimal HRT was much greater than 7-14 h; the highest NH_4^+-N removal rate was observed at the design inlet water flow of 4 L/h; the removal effect was obvious in the aerobic sections, but the removal rate was not significantly enhanced in the anaerobic or anoxic section.

To sum up, the optimal HRT was 26.25 h among the five designed HRTs; HRT increased more significantly in the plateau environment than other regions.

Microbial response

The microbial density and indicator microorganisms under the above five HRTs are shown in *Figure 3*.

It can be seen from *Figure 3(a)* that, under the five HRTs, the different levels of inlet water flows could be ranked as 20, 16, 8, 4 and 12 L/h in descending order of the number of microorganisms in the anaerobic section, 4, 16, 12, 20 and 8 L/h in the anoxic section, and 20, 4, 12, 16 and 8 L/h in the aerobic section. Since the microbial effect is correlated with microbial density, microbial residence time, and inlet/outlet water quality, it is not reasonable to evaluate the microbial response with the bulk density of the microorganisms.

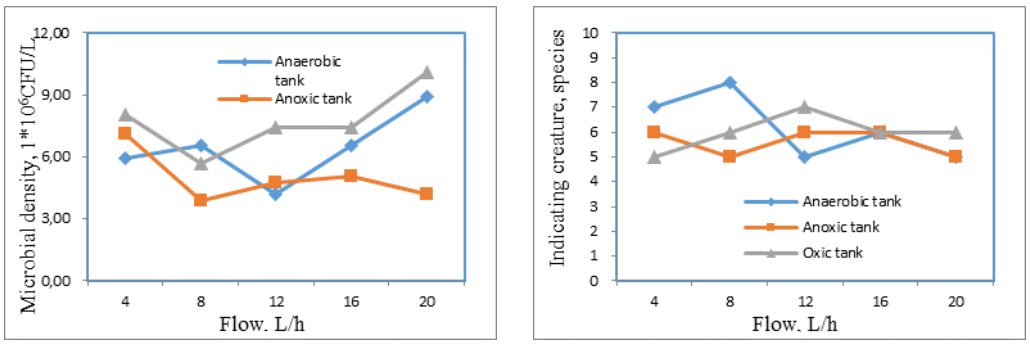

(a) (b)

Figure 3. *Microbial response at different hydraulic retention times (HRTs)*

It can be seen from *Figure 3(b)* that, under the five HRTs, the different levels of inlet water flows could be ranked as 8, 4, 16, 12 and 20 L/h in descending order of the diversity of indicator microorganisms in the anaerobic section, 16, 4, 12, 8 and 20 L/h in the anoxic section, and 12, 8, 16, 20 and 4 L/h in the aerobic section. The indicator microorganisms reached the peak diversity at 8 L/h. The most populous microorganisms include vorticella, trochilia, rotifera and oxytricha.

The microbial analysis show that the microbial density is not directly correlated with the optimal HRT, because the treatment effect depends on retention time and inlet/outlet water quality, in addition to microbial density; moreover, the indictor microorganism analysis confirmed that the indicator microorganisms reached the peak diversity at 8 L/h and the most populous microorganisms were vorticella, trochilia, rotifera and oxytricha.

http://www.aloki.hu ● ISSN 1589 1623 (Print) ● ISSN 1785 0037 (Online)
DOI: http://dx.doi.org/10.15666/aeer/1705_1221312226

Sewage treatment at different DOs

Table 4 lists the operation parameters like DO, MLSS, pH and temperature at different DOs.

Table 4. *Process parameter at different dissolved oxygens (DOs)*

Designed DO (mg/L)	**1.0**	**2.0**	**2.5**	**2.8**	**3.0**	**3.2**	**3.5**	**4.0**	**4.5**	**5.0**
HRT (h)	26.25	26.25	26.25	26.25	26.25	26.25	26.25	26.25	26.25	26.25
DO (mg/L)	1.12	2.01	2.42	2.82	2.92	3.20	3.54	3.90	4.50	5.08
pH	7.43	7.21	7.55	8.18	7.61	7.91	8.03	7.46	7.43	7.34
MLSS (mg/L)	247	568	714	928	1089	1043	1015	957	724	616
SV_{30} (%)	8	9	10	10	10	10	10	10	9	8
Temperature (°C)	20.10	21.00	18.80	20.00	18.70	20.00	20.40	19.70	19.80	20.80

Effect on removal rates

Figure 4 gives the removal rates of COD, TP, TN and NH_4^+-N in anaerobic, anoxic and aerobic tanks at different DOs.

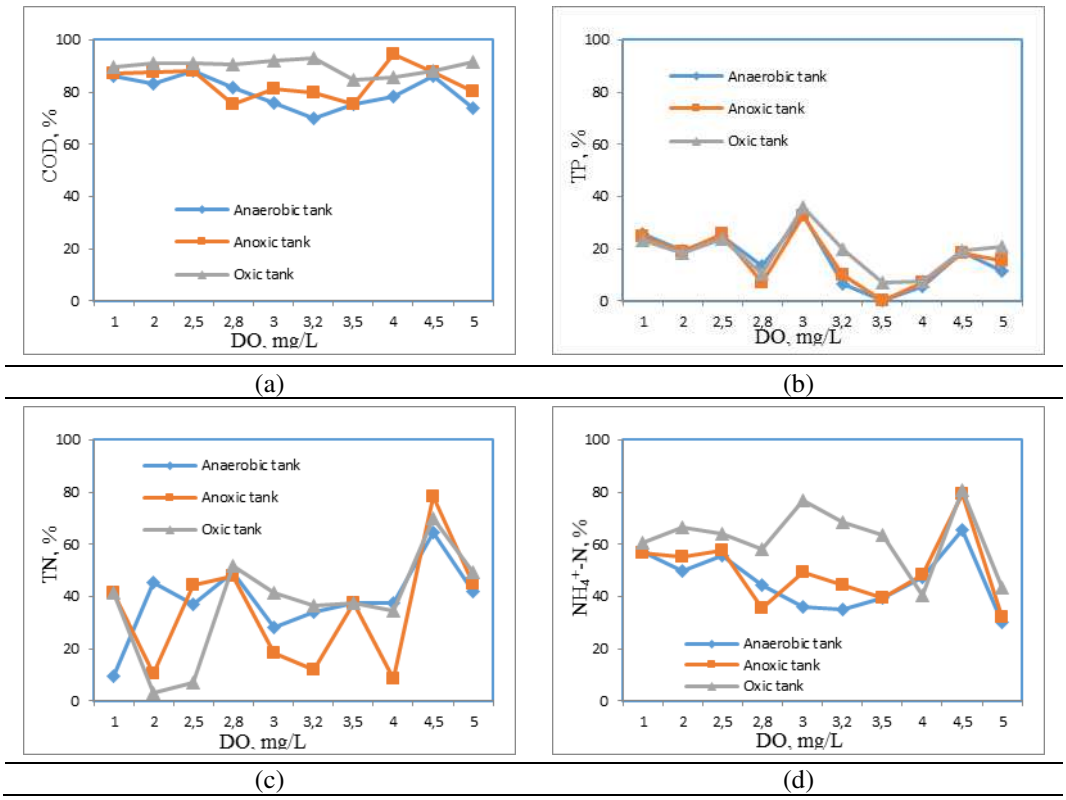

Figure 4. *Removal rate at different dissolved oxygens (DOs)*

As shown in *Figure 4(a)*, the COD removal rate ranged between 84.59% and 92.84% under the ten DOs; in descending order of the COD removal rate, the DOs were ranked as 3.2, 3.0, 5.0, 2.5, 2.0, 2.8, 1.0, 4.5, 4.0 and 3.5 mg/L; the optimal DO was far higher

http://www.aloki.hu ● ISSN 1589 1623 (Print) ● ISSN 1785 0037 (Online)
DOI: http://dx.doi.org/10.15666/aeer/1705_1221312226

than 2.0 mg/L, but the COD differed slightly between the working parameters; the COD removal rate peaked at the design DO of 3.2 mg/L; the removal effect was obvious in anaerobic section, but the removal rate was not significantly enhanced in the anoxic or aerobic section.

As shown in *Figure 4(b)*, the TP removal rate fluctuated between 7.27% and 35.84% under the ten DOs; in descending order of the TP removal rate, the DOs were ranked as 3, 2, 1, 5, 3.2, 4.5, 2, 2.8, 4 and 3.5 mg/L; the optimal DO was far higher than 2.0 mg/L; the highest TP removal rate appeared at the design DO of 3 mg/L; the removal effect was obvious in anaerobic section, but the removal rate was not increased in the anoxic or aerobic section.

As shown in *Figure 4(c)*, the TN removal rate fell between 7.27% and 35.84% under the ten DOs; in descending order of the TN removal rate, the DOs were ranked as 3, 2, 1, 5, 3.2, 4.5, 2, 2.8, 4 and 3.5 mg/L; the optimal DO was much higher than 2.0 mg/L; the highest TN removal rate appeared at the design DO of 3 mg/L; the removal effect was obvious in aerobic section, but the removal rate was not increased significantly in the anoxic or anaerobic section.

As shown in *Figure 4(d)*, the NH_4^+-N removal rate changed between 80.76% and 40.35% under the ten DOs; in descending order of the NH_4^+-N removal rate, the DOs were ranked as 4.5, 3.0, 3.2, 2.0, 2.5, 3.5, 1.0, 2.8, 5.0 and 4.0 mg/L; the optimal DO was much higher than 2.0 mg/L; the NH_4^+-N removal rate reached the maximum at the design DO of 4.5 mg/L; the removal effect was obvious in aerobic section, but the removal rate was not increased significantly in the anoxic or anaerobic section.

In summary, the optimal DO was 3 mg/L among the ten designed DOs; the DO in the plateau environment was much greater than that in the other regions; however, the removal rates of TP, TN and NH_4^+-N were not high under plateau environmental factors; in particular, only about 35% of TP were removed.

Microbial response

The microbial density and indicator microorganisms under the above seven DOs are displayed in *Figure 5*.

It can be seen from *Figure 5(a)* that the seven DOs could be ranked as 2.8, 4.5, 2.5, 5, 2, 3.2 and 1 mg/L in descending order of the number of microorganisms in the anaerobic section, 2.5, 5.0, 2.8, 3.2, 2, 4.5 and 1 mg/L in the anoxic section, and 2.5, 2.8, 5.0, 3.2, 4.5, 2 and 1 mg/L in the aerobic section. Since the microbial effect is correlated with microbial density, microbial residence time, and inlet/outlet water quality, it is not reasonable to evaluate the microbial response with the bulk density of the microorganisms.

It can be seen from *Figure 5(b)* that the seven DOs could be ranked as 2.8, 4.5, 1, 2, 2.5, 5 and 3.2 mg/L in descending order of the diversity of indicator microorganisms in the anaerobic section, 1, 5, 2.5, 3.2, 4.5, 2.8 and 2 mg/L in the anoxic section, and 5, 2, 2.5, 3.2, 1, 2.8 and 4.5 mg/L in the aerobic section. The indicator microorganisms reached the peak diversity at 5 mg/L, when the most populous microorganisms were vorticella and rotifera. Meanwhile, the most populous microorganisms became vorticella, rotifera and trochilia at the DO of 3 mg/L.

The microbial analysis show that the microbial density is not directly correlated with the optimal DO, because the treatment effect depends on retention time and inlet/outlet water quality, in addition to microbial density; moreover, the indictor microorganism

http://www.aloki.hu ● ISSN 1589 1623 (Print) ● ISSN 1785 0037 (Online)
DOI: http://dx.doi.org/10.15666/aeer/1705_1221312226

analysis confirmed that the indicator microorganisms reached the peak diversity at 5mg/L, when the most populous microorganisms were vorticella and rotifera.

Sewage treatment at different water temperatures

Table 5 lists the operation parameters like DO, MLSS, pH and HRT at different water temperatures.

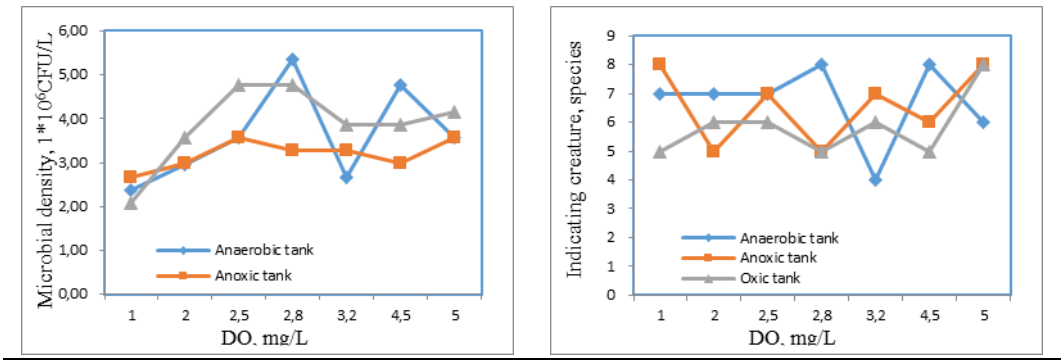

(a) (b)

Figure 5. *Microbial response at different dissolved oxygens (DOs)*

Table 5. *Process parameter at different temperatures*

Designed Temperature(°C)	10	15	20	25	30
HRT(h)	26.25	26.25	26.25	26.25	26.25
DO(mg/L)	1.80	1.87	1.76	1.80	1.63
pH	7.52	7.69	7.58	7.52	8.18
MLSS(mg/L)	1137	2132	1889	1137	983
SV30(%)	15	17	15	15	13
Temperature(°C)	8.98	14.8	17.5	22.4	29.1

Effect on removal rates

Figure 6 shows the removal rates of COD, TP, TN and NH_4^+-N in anaerobic, anoxic and aerobic tanks at different water temperatures.

As shown in *Figure 6(a)*, the COD removal rate ranged between 70.06% and 84.33% under the five water temperatures; in descending order of the COD removal rate, the water temperatures were ranked as 15, 30, 25, 10 and 20°C; the optimal water temperature was obviously 15°C, as the COD removal rate reached the peak value under this temperature; the removal effect was obvious in anaerobic section, but the removal rate was not significantly enhanced in the anoxic or aerobic section.

As shown in *Figure 6(b)*, the TP removal rate fluctuated between 3.54% and 75.55% under the five water temperatures; in descending order of the TP removal rate, the water temperatures were ranked as 15, 20, 30, 10 and 25°C; the optimal water temperature was obviously 15°C, as the TP removal rate was the highest under this temperature; the removal effects were obvious in anaerobic and aerobic sections, but the removal rate was not significantly enhanced in the anoxic section.

http://www.aloki.hu ● ISSN 1589 1623 (Print) ● ISSN 1785 0037 (Online)
DOI: http://dx.doi.org/10.15666/aeer/1705_1221312226

As shown in *Figure 6(c)*, the TN removal rate fell between 36.60% and 77.98% under the ten DOs; in descending order of the TN removal rate, the water temperatures were ranked as 10, 25, 15, 30 and 20°C; the optimal water temperatures were 10 and 25°C, as the peak TN removal rate was measured under the two temperatures; the removal effects were obvious in anaerobic and aerobic sections, but the removal rate was not significantly enhanced in the anoxic section.

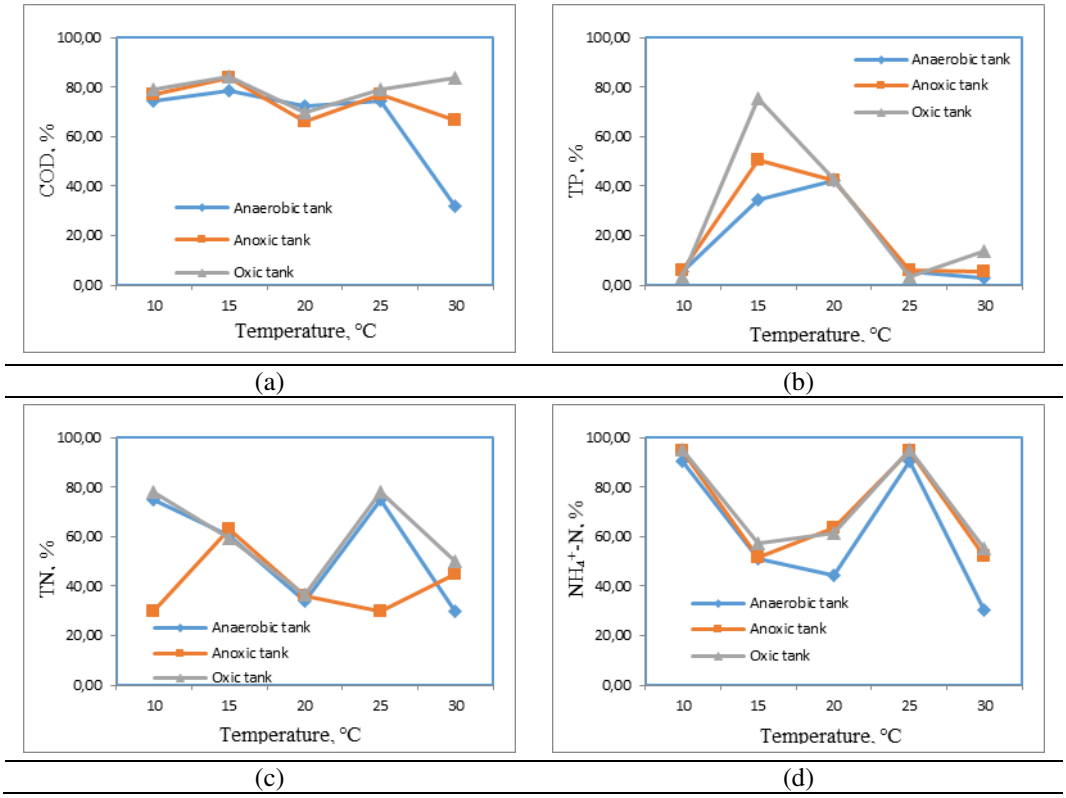

Figure 6. *Removal rate at different temperatures*

As shown in *Figure 6(d)*, the NH_4^+-N removal rate changed between 55.44% and 95.44% under the five water temperatures; in descending order of the NH_4^+-N removal rate, the water temperatures were ranked as 10, 25, 20, 15 and 30°C; the optimal temperatures were 10 and 25°C, as the peak NH_4^+-N removal rate was obtained under these two temperatures; the removal effect was obvious in anaerobic section, but the removal rate was not significantly enhanced in the anoxic or aerobic section.

Overall, the optimal water temperature was 15°C among the five designed water temperatures; the optimal temperature in the plateau environment was lower than that in the other regions.

Microbial response

The microbial density and indicator microorganisms under the above five water temperatures are displayed in *Figure 7*.

It can be seen from *Figure 7(a)* that the five water temperatures could be ranked as 20, 15, 10, 25 and 30°C in descending order of the number of microorganisms in the anaerobic section, 30, 25, 10, 20 and 15°C in the anoxic section, and 15, 30, 25, 10 and

http://www.aloki.hu ● ISSN 1589 1623 (Print) ● ISSN 1785 0037 (Online)
DOI: http://dx.doi.org/10.15666/aeer/1705_1221312226

20°C in the aerobic section. Since the microbial effect is correlated with microbial density, microbial residence time, and inlet/outlet water quality, it is not reasonable to evaluate the microbial response with the bulk density of the microorganisms.

It can be seen from *Figure 7(b)* that the five water temperatures could be ranked as 20, 10, 25, 15 and 30°C in descending order of the diversity of indicator microorganisms in the anaerobic section, 20, 10, 25, 15 and 30°C in the anoxic section, and 15, 30, 10, 25 and 20°C in the aerobic section. The indicator microorganisms reached the peak diversity at the water temperature of 20°C, when the most populous microorganisms were vorticella, trochilia and oxytricha. Meanwhile, the most populous microorganisms were also vorticella, trotifera and trochilia at the water temperature of 15°C.

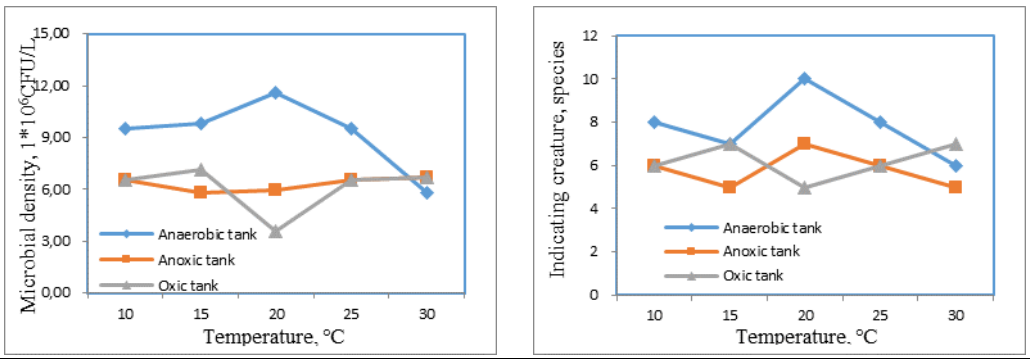

(a) (b)

Figure 7. *Microbial response at different temperatures*

The microbial analysis show that the microbial density is not directly correlated with the optimal water temperature, because the treatment effect depends on retention time and inlet/outlet water quality, in addition to microbial density; moreover, the indictor microorganism analysis found that the indicator microorganisms reached the peak diversity at 15°C, when the most populous microorganisms were vorticella, rotifera and oxytricha; furthermore, it should be noted that the diversity did not increase with the water temperature (Tian et al., 2013).

Discussion

Discussion of HRTs

Some of the recent studies on the optimal HRT are as follows. Wang et al. (2014) suggested that the optimal HRT was 8~12 h for the processing of high-load sewage by A2O and electro-coagulation. Ye et al. (2018) put the optimal HRT to 6 h for the removal of organic matters and nutrients from urban sewage with dual-A2O (D-A2O).

In our experiment, the optimal HRT is determined as 26.25 h based on the removal rates and microorganism response. This conclusion differs greatly from the results of the previous studies. The difference may be attributed to the environmental factor of low water temperature. The microbial density in low-temperature water body treated by the A2O is generally considered as 10^8CFU/L (Yang, 2017). In our experiment, however, the microbial density was merely 10^6CFU/L under the plateau environmental factors.

http://www.aloki.hu ● ISSN 1589 1623 (Print) ● ISSN 1785 0037 (Online)
DOI: http://dx.doi.org/10.15666/aeer/1705_1221312226

Discussion of DO

Large numbers of DOs come to the anoxic unit through International recirculation flow and destroyed the hypoxic environment, affecting the nitrogen removal (Li et al., 2012). With respect to total nitrogen removal, nitritation–denitritation at low DO levels of 0.3–0.5 mg/L was essentially equal to the complete nitrification– denitrification at DO levels of 1.5-2.5 mg/L with the addition of external carbon sources (Zeng et al., 2010). Under the conditions of 11 h HRT, 1.0-2.0 mg/L DO concentration, 200% mixture reflux proportion, 80% sludge reflux proportion and 20d sludge age, the effluent concentration can achieve the first order A standard of Discharge Standard of Pollutants for Municipal Wastewater Treatment Plant (Zhang et al., 2011). Controlling to DO at 0.8-1.5 mg/L, the treatment efficiency of full-scale Biolak/A^2O process was near optimal with the total nitrogen efficiency of 69.45% (Ju et al., 2013). DO levels in the range of 0.5 to 3.5 mg/L in the aeration basin did not have significant impact on effluent ortho-P concentration in a completely mixed basin within the EBPR process (Gu et al., 2006). In our experiment, the optimal DO is determined as 3.0 mg/L based on the removal rates and microorganism response. This conclusion deviates greatly from the results of the previous studies. A possible cause for the deviation lies in the unique environmental factors of the plateau.

Discussion of temperature

The temperature and functions of A2O process were closely related (Zhao et al., 2010). Under the condition of average temperature of 14.2°C and carbon-to-nitrogen radio of 4.81, enhanced nitrogen and phosphorus removal was achieved (Wang, 2010). The changes of temperature could affect the community structure and the Shannon diversity index of nitrifying bacteria (Tao et al., 2009). In our experiment, the optimal water temperature was determined as 15°C based on the removal rates and microorganism response. This conclusion was very inconsistent with the results of the previous studies, which may be ascribed to the unique properties of microorganisms at low temperatures on the plateau. Because Nitrification rates at high altitude aquatic ecosystems are scarce (Hayden and Beman, 2014; Molina et al., 2018).

Conclusions

Under the unique environmental factors of plateau, this paper designs a pilot-scale A2O device to explore the effects of DO, HRT and water temperature on the removal rates of COD, TP, TN and NH_4^+-N, and the law of microbial response to these working parameters. The results show that none of the TP, TN or NH_4^+-N of the outlet water satisfied the Chinese national standard GB18918-2002, while the COD only fulfilled the standard requirements under a few working parameters. The optimal values of the four working parameters were determined as: the optimal HRT=26.25 h, the optimal DO=3.0 mg/L, the optimal temperature=15°C. All these optimal values deviated greatly from the existing studies. The microbial densities corresponded poorly to the three working parameters, and differed significantly from those under normal conditions; the number of indicator microorganisms was basically consistent with the optimal values of our experimental parameters. In addition, the SV30 (Xu et al., 2013) and NLSS (Zhang et al., 2018) were both low in our experiment.

http://www.aloki.hu ● ISSN 1589 1623 (Print) ● ISSN 1785 0037 (Online)
DOI: http://dx.doi.org/10.15666/aeer/1705_1221312226

Acknowledgements. This work was supported by the National Natural Science Foundation of China (NO.51868069, 51769034), Natural Science Foundation of Tibet (NO. XZ 2018 ZR G-20), the Program for Scientific Research Innovation Team in Colleges and Universities of Tibet Autonomous Region, Snowy Plateaus of Tibet Agriculture and Animal Husbandry College (Study on the operation status of typical sewage treatment plants in Tibet in China).

REFERENCES

[1] Abourabia, A. M., Abdel Moneim, S. A. (2019): Analytical solution of sea water steady magneto-hydrodynamic equations subjected to stretching sheet under induced magnetic field and heat transfer. – Mathematical Modelling of Engineering Problems 6(1): 141-151.
[2] Ai, S. S., Zhang, X. H., Xiao, Y. B. (2014): Study on characteristics of activated sludge at low temperature. – Applied Mechanics & Materials 675-677: 574-577.
[3] Chen, X. Y., Hao, Ka. Y., Su, D. (2018): Characteristic study on wastewater treatment in high altitude area by A2/O process. – Technology of Water Treatment 38(6): 93-96.
[4] Gu, A. Z., Hughes, T., Fisher, D. (2006): The devil is in the details: full-scale optimization of the EBPR process at the city of las vegas WPCF. – Proceedings of the Water Environment Federation 2006(7): 5110-5130.
[5] Hayden, C. J., Beman, M. (2014): High abundances of potentially active ammonia-oxidizing bacteria and archaea in oligotrophic, high-altitude lakes of the sierra nevada, California, USA. – Plos One 9(11): e111560.
[6] He, J. G., Ke, L., Han, B. P. (2010): Study on the operational characteristics of hybrid A2/O process at low temperature. – Applied Mechanics & Materials 39: 326-331.
[7] Ju, Y. K., Wang, H. L., Zhang, Q. (2013): Effect of dissolved oxygen on nitrogen and phosphorus removal rate in biolak process. – Advanced Materials Research 779-780: 1629-1633.
[8] Li, Y. F., Yang, J. Y., Zhang, G. C. (2012): Effects of Aeration on Nitrogen and Phosphate Removal with A2O Process. – Advanced Materials Research 622-623: 1738-1741.
[9] Li, Y. F., Yang, J. Y., Zhang, G. C. (2013): Effects of aeration on nitrogen and phosphate removal with A2O process. – Advanced Materials Research 622-623: 1738-1741.
[10] Li, S. M., Du, G. S., Tang, F. B. (2013): Nitrogen and phosphorus removal of modified A2/O process on low-carbon domestic sewage under low temperature. – Advanced Materials Research 777: 187-191.
[11] Li, S. M., Hao, T., Wang, R. B. (2014): Operation of modified A~2/O process at low temperature and different sludge loadings. – China Water & Wastewater 2014(13): 64-68.
[12] Molina, V., Dorador, C., Fernández, C. (2018): The activity of nitrifying microorganisms in a high altitude Andean wetland. – FEMS Microbiology Ecology 94(6).
[13] Ruiz-Urbieta, M., Sparrow, E. M., Parikh, P. D. (1975): Two-film reflection polarizers: theory and application. – Applied Optics 14(2): 486-492.
[14] Tao, F., Huang, Y., Gao, S., Huang, M. S., Chen, C. (2009): Application of PCR-DGGE to analyze the effect of temperatureon structure of nitrifying bacteria in A/O system (Chinese). – Journal of East China Normal University.
[15] Tian, X., Ai, S. S., Zuo, Y. (2013): Study on activated sludge microorganisms of northern winter sewage treatment plant. – Applied Mechanics and Materials 361-363: 1032-1035.
[16] Wang, J. H. (2010): Biological nutrients removal from domestic wastewater with low carbon-to-nitrogen ratio in A~2O-BAF system at low temperature. – China Environmental Science 30(9): 1195-1200.
[17] Wang, W., Chen, S., Bao, K. (2014): Enhanced removal of contaminant using the biological film, anoxic-anaerobic-aerobic and electro-coagulation process applied to high-load sewage treatment. – Environmental Technology 35(7): 833-840.

http://www.aloki.hu ● ISSN 1589 1623 (Print) ● ISSN 1785 0037 (Online)
DOI: http://dx.doi.org/10.15666/aeer/1705_1221312226

[18] Wu, C., Guo, L. (2017): Influence of temperature and dissolved oxygen on nitrogen and phosphorus removal of integrated bioreactor. – International Journal Bioautomation 21(1): 207-216.
[19] Xu, X. P., Tao, X. W., Du, J., Wu, F. S. (2013): Effect of SRT on nitrogen and phosphorus removal in A2/O process. – China Water & Wastewater 29(21): 69-71.
[20] Yang, T. (2017): Study on degradation Regularity of three characteristic pollutants of pharmaceutical park tail water in a2o treatment process. – Liaoning University.
[21] Ye, C., Zhou, Z., Li, M. (2018): Evaluation of simultaneous organic matters and nutrients removal from municipal wastewater using a novel bioreactor (D-A2O) system. – Journal of Environmental Management 218: 509-515.
[22] Zeng, W., Li, L., Yang, Y. (2010): Nitritation and denitritation of domestic wastewater using a continuous anaerobic–anoxic–aerobic (A2O) process at ambient temperatures. – Bioresource Technology 101(21): 8074-8082.
[23] Zhang, S. R., Zhang, T. J., Liu, J. L. (2011): Study on A2O Method for co-treatment of landfill leachate and municipal sewage. – Advanced Materials Research 356-360: 2908-2913.
[24] Zhang, L., Zhuang, Y., Wang, X., Zhang, H. (2016): Effect of temperature on denitrifying phosphorus removal efficiency using modified A2/O process. – Transactions of the Chinese Society of Agricultural Engineering.
[25] Zhang, J. X., Sun, W. G., Niu, F. S., Wang, L., Zhao, Y. W., Han, M. M. (2018): Atmospheric sulfuric acid leaching thermodynamics from metallurgical zinc-bearing dust sludge. – International Journal of Heat and Technology 36(1): 229-236.
[26] Zhao, F., Dai, X. C., Huang, M. S. (2010): Influence of temperature on nitrogen removal in A2/O process. – Environmental Science & Technology 33(3): 49-53.
[27] Zong, Y. C., Zhang, Y. H., Lu, G. H. (2018): Study on Process Characteristics of High Altitude A2/O Process Based on Principal Component Analysis. – Technology of water treatment 38(9): 116-119.

http://www.aloki.hu ● ISSN 1589 1623 (Print) ● ISSN 1785 0037 (Online)
DOI: http://dx.doi.org/10.15666/aeer/1705_1221312226

SPATIAL AND TEMPORAL EVOLUTION CHARACTERISTICS OF DROUGHT-FLOOD ABRUPT ALTERNATION IN GUIZHOU PROVINCE IN RECENT 50 YEARS BASED ON DWAAI INDEX

FAN, H.[1] – ZHANG, Z. Z.[1] – WU, F.[1*] – XU, J. X.[1] – SHEN, D. F.[2] – YUAN, Y. J.[1]

[1]*School of Water Conservancy, North China University of Water Resources and Electric Power Zhengzhou 450011, China*

[2]*Guizhou Water Conservation Science and Research Institute, Guiyang 550002, China*

[*]*Corresponding author*
e-mail: 36560797@qq.com

(Received 3rd May 2019; accepted 11th Jul 2019)

Abstract. Based on the daily rainfall data of 19 meteorological stations in Guizhou Province from 1968 to 2017 and combining the characteristic of hydrogeology in Guizhou Province, this study revised the Dry-Wet Abrupt Alternation Index (DWAAI) and analyzed the spatial and temporal evolution characteristics of drought-flood abrupt alternation in Guizhou Province in recent 50 years. The results show that: 1. the revised DWAAI index has good applicability in Guizhou Province; 2) The time of drought-flood abrupt alternation is mainly distributed from April to October. In terms of the interannual variation, the station proportion and intensity show an increasing trend, and the increasing trend was significant in station proportion. The intensity of drought-flood abrupt alternation in autumn shows a decreasing trend, and the station proportion and intensity increase in other seasons, in which the intensity of the drought-flood abrupt alternation in spring and summer and the station proportion of the drought-flood abrupt alternation in summer increase significantly. (3) The frequency of the drought-flood abrupt alternation in Guizhou Province decreased from east to west as a whole. It is easy to occur in spring in the south, in summer in the middle and the north with the largest area, and in autumn in the east. With the increase of the years, the scope of prone areas has been expanding. The results are of great significance for disaster prediction and early warning and drought and flood control in this area.
Keywords: *drought and flood, revised index, trend analysis, spatial analysis*

Introduction

Guizhou is a province with frequent natural disasters, mainly including flood and drought disasters, low-temperature freezing, wind and hail, landslide and debris flow, among which the occurrence frequency of flood and drought disasters is higher, with the larger disaster area, which mostly appear as flower arrangement, so it is easy to form drought-flood abrupt alternation events and pose a serious threat to the local social and economic development. The drought-flood abrupt alternation refers to the meteorological and hydrological events such as floods when there is no precipitation or little precipitation in the early stage and the drought has occurred, and then high-intensity precipitation occurs in a short period of time (Huang, 2015). The drought-flood abrupt alternation usually coincides with the growth period of autumn harvest and summer harvest crops, encounters the abrupt alteration of drought and flood disasters in a short period, the influence and loss of the region is multiplied, and climate change leads to the increase of extreme hydrological events, which increases the risk of drought-flood abrupt alternation to a large extent. Many scholars in China and abroad studied flood and drought disasters from the aspects of forming factors (Djebou et al., 2014), physical processes (Langousis and Kaleris, 2014; Goswami et al., 2018) and

http://www.aloki.hu ● ISSN 1589 1623 (Print) ● ISSN 1785 0037 (Online)
DOI: http://dx.doi.org/10.15666/aeer/1705_1222712244

evolution rules (Grinsted et al., 2014; Andrea et al., 2018), but most of them focused on relatively independent elements such as "flood" and "drought" (Zhou et al., 2013; Han et al., 2014; Liu et al., 2014; Rajsekhar et al., 2015) or uses drought-flood abrupt alternation as a fixed element. With the intensification of climate change, especially the frequent and wide occurrence of drought and flood events in China, the study of "flood" and "drought" coupling has entered into a development period in China. Many scholars used conventional meteorological dry and wet indicators such as continuous rain-free days (Cheng et al., 2012), precipitation anomaly (Shen et al., 2012) and SPI (Wu et al., 2006a,b) to study the drought-flood abrupt alternation, with good results in macroscopic law recognition and characteristic analysis, but failing to completely describe the process and intensity of the drought-flood abrupt alternation. For better quantify, Wu et al. (2006b) compared the differences in precipitation between May-June and July-August, and defined a Long-cycle Drought-Flood Abrupt Alternation Index (LDFAI); Zhang et al. (2012) referred to LDFAI, and defined the Runoff Drought-Flood Abrupt Alternation Index (RDFAI); Shan et al. (2018) improved the problem of large time scale of LDFAI index and constructed the Dry-Wet Abrupt Alteration Index (DWAAI), which not only reflects the difference of drought and flood in the former and later stages, but also reflects the degree of urgency from drought to flood, that's, it can comprehensively reflect the "abrupt" and "alternation" of the drought-to-flood.

Based on DWAAI and combining with the characteristics of hydrology, meteorology, soil and geology in Guizhou Province, this study revised the degree of drought and flood in the former and later stages of the index. Based on the calculated results, the temporal and spatial evolution characteristics and regularities of drought-flood abrupt alternation events in Guizhou Province are analyzed by using climatic tendency rate, Mann-Kendall method and Inverse Distance Weighting (IDW). The purpose of the study is to monitor and warn drought-flood abrupt alternation disasters, formulate comprehensive response plans for the sudden disasters of drought-flood abrupt alternation, reduce disaster losses, and provide scientific support for agricultural production safety in this region.

Materials and methods

Overview of the research area

Guizhou Province belongs to the Yangtze River Basin and the Pearl River Basin, and its geographical position is between 103°36′E-109°35′E and 24°37′N-29°13′N. The territory is high in the west and low in the east, sloping northward, eastward and southward from the middle, with an average elevation of about 1,000 m above sea level and over 1,600-2,800 m above sea level in the west. The river network of the whole province is dense, the river slope is steep, the landform is complex and diverse, mainly with mountainous and hilly areas, and the karst landform is widely distributed, accounting for about 73% of the total area of the province. Guizhou Province belongs to the sub-tropical temperate and humid monsoon climate region. The basic meteorological data of 19 meteorological stations in the province over the past 50 years have been collated and counted,and the annual average temperature is about 15 ℃ and rain and heat are in the same season, with the annual rainfall of 1,179 mm but the uneven spatial and temporal distribution, descending from southeast to northwest. The annual rainfall from May to October accounts for 75% of the total.

http://www.aloki.hu ● ISSN 1589 1623 (Print) ● ISSN 1785 0037 (Online)
DOI: http://dx.doi.org/10.15666/aeer/1705_1222712244

Data sources

The data of this study are obtained from the National Meteorological Information Center of China Meteorological Administration (http://data.cma.cn), using daily rainfall data of 19 basic meteorological stations in Guizhou Province from 1968 to 2017 to sort and make up the difference in the quality of the original data. See *Figure 1* for spatial distribution of meteorological stations.

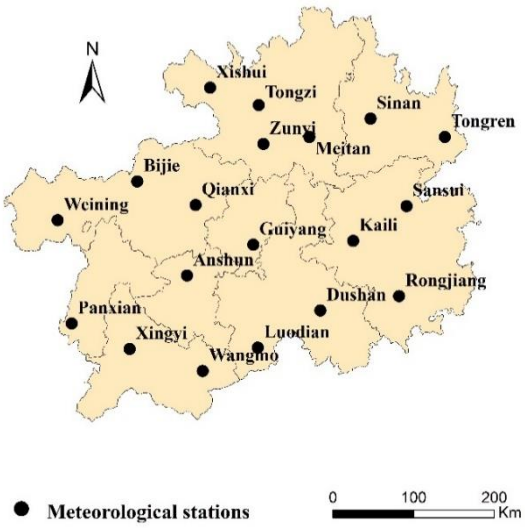

Figure 1. *Distribution of meteorological stations in Guizhou province*

Indicators and methods

Revised DWAAI index

(1) DWAAI index

The DWAAI index calculation model is derived from the LDFAI defined by Wu et al (2006b). The LDFAI index was improved by Shan et al. (2018) to construct the DWAAI index, with equation as follows:

$$DWAAI_i = \left[K + \left(SPA_{la\,i} - SPA_{ea\,i}\right) \times \left(\left|SPA_{ea\,i}\right| + \left|SPA_{la\,i}\right|\right)\right] \times a^{-\left|SPA_{ea\,i} + SPA_{la\,i}\right|} \quad \text{(Eq.1)}$$

$$K = \sum_{i=1}^{n} \left(\frac{SAPI_i - SAPI_0}{i} \right) \quad \text{(Eq.2)}$$

In *Equation (1)*, $SPA_{ea\,i}$ and $SPA_{la\,i}$ represent the anomalies of normalized precipitation in the early and late periods (Maheras et al., 1999); in *Equation (2)*, $SAPI_i$ and $SAPI_0$ represent the value of the Standard Antecedent Precipitation Index (SAPI) in the *i*-th day and the antecedent last day of the flood period, which is calculated with the standardization of Antecedent Precipitation Index (API); n represents days in flood period; *a* represents weight coefficient, with the value range of $1<a\leq1.4$ as recommended by Literature (Shan et al., 2018), and $a=1.1$ according to the actual situation of Guizhou and the comparison and rationality analysis of various calculation results.

http://www.aloki.hu ● ISSN 1589 1623 (Print) ● ISSN 1785 0037 (Online)
DOI: http://dx.doi.org/10.15666/aeer/1705_1222712244

(2) DWAAI index revision

In the drought-flood abrupt alternation events, the formation of drought in the early stage and drought-flood abrupt alternation in the late stage are two different stages, with different mechanisms. The formation of drought is the result of drought accumulation in the early stage, and the influence of daily precipitation on drought in the early stage decreases exponentially with the increase of drought date (Lu, 2009); floods caused by late heavy rainfall have short-term characteristics, and there is no attenuation and accumulation process. Therefore, this study revise $SPA_{ea\,i}$ and $SPA_{la\,i}$ as follows:

$$SPA_{ea\,i} = \sum_{j=0}^{m} k^j SPA_{i-j} \quad (i \geq 45 and\, i, j \in N) \tag{Eq.3}$$

$$SPA_{la\,i} = \frac{1}{n} \sum_{j=1}^{n} SPA_{i+j} \quad (i \geq 1 and\, i, j \in N) \tag{Eq.4}$$

In *Equation (3)*, m represents the number of drought days, and the influence of the 44th day in the early stage on the drought is less than 1‰, so m takes 44 herein; k represents the attenuation index; Lu (2009) recommends k as 0.9 in the study of the Mississippi Valley. But Guizhou Province is of mainly karst landform, mountainous and hilly, the soil thickness is thin and the groundwater layer is deep, so the attenuation degree is larger. Combined with the actual parameter optimization, k=0. 87 is selected in this study. In *Equation (4)*, n represents the days of flood period, because of the short-term nature of flood and flood, the excessively large value of n will cause "drought and flood neutralization". Combined with the meteorological characteristics of Guizhou Province and the actual calculation results, n=5 in this study. According to the calculation results and the actual situation of Guizhou, the classification of drought-flood abrupt alternation grade based on DWAAI index is shown in *Table 1*.

Table 1. *Grade division of drought-flood abrupt alternation*

Grade	None	Light	Moderate	Heavy
Value range of DWAAI	(0,12.0)	[12.0,18.0)	[18.0,25.0)	[25.0,∞)

Research methods

Referring to the regional drought assessment index constructed by Huang et al. (2010), this study uses frequency, station proportion and intensity of drought-flood abrupt alternation to reflect the spatial and temporal characteristics of drought-flood abrupt alternation events in Guizhou Province, among which station proportion reflects the range of drought-flood abrupt alternation events with equation as follows:

$$P = \frac{m}{M} \times 100\% \tag{Eq.5}$$

In *Equation (5)*, P represents station proportion; m represents the number of the meteorological stations which occurred drought-flood abrupt alternation event in study

http://www.aloki.hu ● ISSN 1589 1623 (Print) ● ISSN 1785 0037 (Online)
DOI: http://dx.doi.org/10.15666/aeer/1705_1222712244

area; M represents the number of all the meteorological stations in study area. It indicates the scope of drought-flood abrupt alternation in a certain region.

The climate tendency rate and Mann-Kendall method are used to analyze the trend. The climate tendency rate is linear tendency rate. The least square method is used to fit the unitary regression equation of the long-time element sequence, which is expressed as 10 times of the regression coefficient. Mann-Kendall method is used to test the significance of the trend. ArcGIS Inverse Distance Weighting (IDW) method is used to analyze spatial evolution characteristics.

Results

Verification of indicator applicability

At present, the research on the drought-flood abrupt alternation in China is mainly concentrated in the middle and lower reaches of the Yangtze River and the Huaihe River Basin while the characteristics and types of rainfall, drought and flood in Guizhou Province are different from those in the above areas. Therefore, this study takes the typical drought and flood abrupt alternation events in 2011 and 2012 as examples to verify the applicability of the revised DWAAI index in Guizhou Province. According to the calculation results, the spatial distribution of drought-flood abrupt alternation events in Guizhou Province in 2011 and 2012 is shown in *Figure 2*.

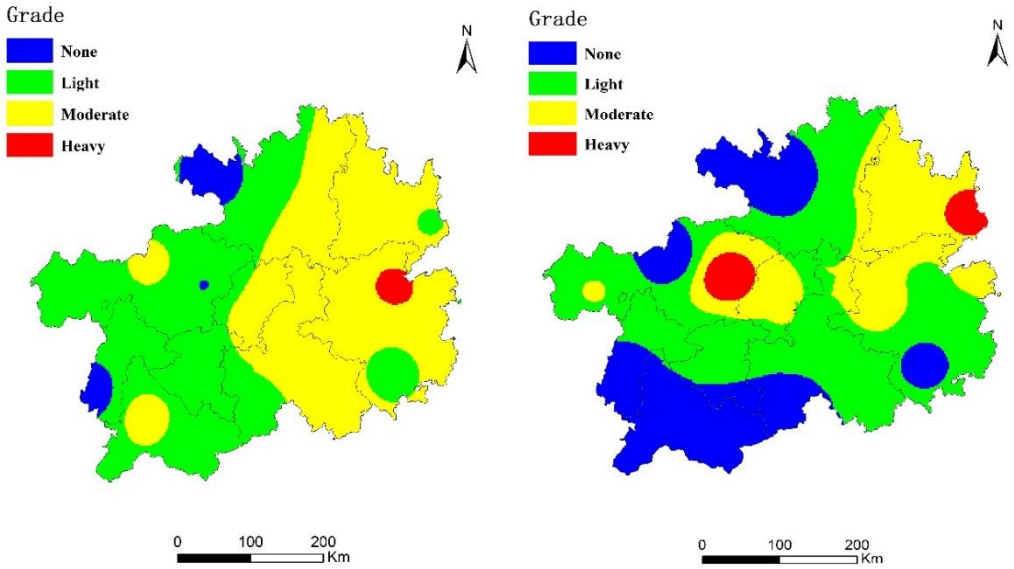

(a) 2011 (b) 2012

Figure 2. *Spatial distribution of drought-flood abrupt alternation events in 2011 and 2012 in Guizhou province*

According to the actual situation, in the middle and upper part of June 2011, there was a strong precipitation process in the northern-central Jiangxi, the central Hunan and the eastern Guizhou. Although the drought was alleviated, the drought-flood abrupt alternation occurred in some areas of the three provinces. In late May 2012, due to uneven distribution of rainfall, serious drought-flood abrupt alternation occurred in

http://www.aloki.hu ● ISSN 1589 1623 (Print) ● ISSN 1785 0037 (Online)
DOI: http://dx.doi.org/10.15666/aeer/1705_1222712244

Yanhe County and Dejiang County of Tongren City and Qianxi County of Bijie City. As can be seen from *Figure 2a*, in 2011, except for a few areas such as the west of Zunyi City and the southwest of Liupanshui City, most regions of Guizhou Province experienced drought-flood abrupt alternation in different degrees, with the most serious in the east. As can be seen from *Figure 2b*, in 2012, except for the southern and northwest regions of Guizhou Province, the drought-flood abrupt alternation occurred in different degrees in other regions, and the high-intensity regions are consistent with the historical reality.

Combining with the actual situation of the drought-flood abrupt alternation in Guizhou Province from 2011 to 2012, this paper selected data of the rainfall process and the corresponding DWAAI indices before and after the occurrence of drought-flood abrupt alternation happened in Rongjiang County in 2011, and in Qianxi County and Tongren City in 2012, as shown in *Figure 3*.

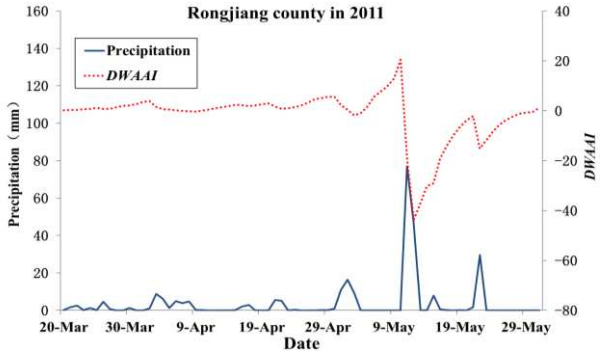

(a) Rongjiang county in 2011

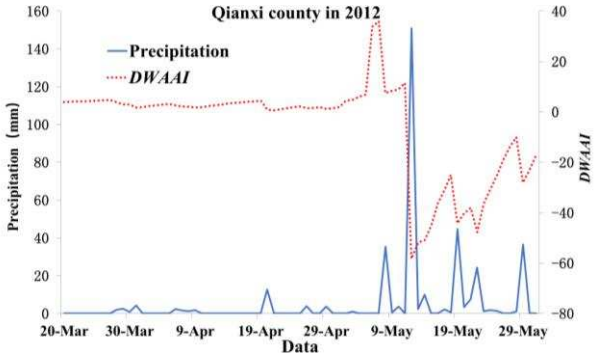

(b) Qianxi county in 2012

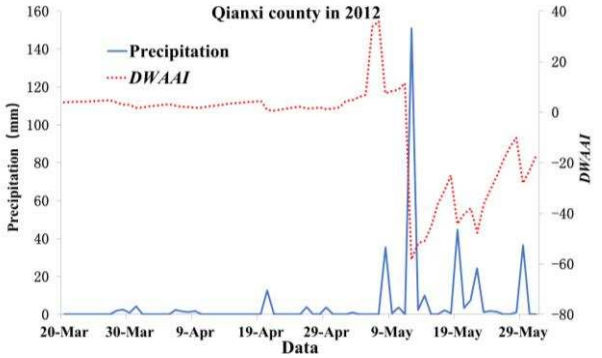

(c) Tongren city in 2012

Figure 3. *The process of typical drought-flood abrupt alternation events in 2011 and 2012 in Guizhou province*

http://www.aloki.hu ● ISSN 1589 1623 (Print) ● ISSN 1785 0037 (Online)
DOI: http://dx.doi.org/10.15666/aeer/1705_1222712244

From *Figure 3a* we can see that, in the Rongjiang County, the accumulated precipitation in 45 days before May 10th 2011 was 87.5mm, and the accumulated precipitation in 5 days after May 10th was 132.2 mm, wherein the single-day precipitation on May 11th was 77 mm, and the DWAAI of May 10th was 20.5, which had reached an extremum, so the May 10th had been determined as the date of the drought-flood abrupt alternation occurrence, with a degree of moderate; moreover, from *Figure 3b* we can see that, in the Qianxi County, the accumulated precipitation in 45 days before May 7th 2011 was 35.3 mm, and the accumulated precipitation in 5 days after May 7th was 190.5 mm, although the single-day precipitation reached 150.9 mm on May 12th, the DWAAI extreme value 35.9 appeared on May 7th with a degree of severe, this is because the single-day precipitation on May 8th was 35.4 mm, which can better reflect the "abrupt" degree of the change of drought and flood since that day, therefore, the May 7th had been determined as the date of the drought-flood abrupt alternation occurrence, and after a certain period of flood season, the drought-flood abrupt alternation had produce serious impact in mid- and late-May; similarly, as can be seen from *Figure 3c*, Tongren City had determined the May 8th as the date of the drought and flood abrupt alternation occurrence, but its DWAAI was 15.4, indicating it was a slight degree drought-flood abrupt alternation. This is because the accumulated precipitation in the previous period reached 204.9mm, indicating from the perspective of the "alternation" of the drought-flood that the degree of drought-flood abrupt alternation is not as severe as the Qianxi County, which further proves the applicability and rationality of the indices. Therefore, the applicability of the revised DWAAI in Guizhou Province has been verified.

Characteristics of temporal evolution

Distribution characteristics within a year

As can be seen from *Figure 4*, the time of drought-flood abrupt alternation in Guizhou Province is mainly distributed from April to October, and the cumulative drought-flood abrupt alternations account for 93.51% of the total; from July to September, it's relatively concentrated with 75 times, 59 times and 67 times respectively, accounting for 19.48%, 15.32% and 17.40% of the total number of events, respectively.

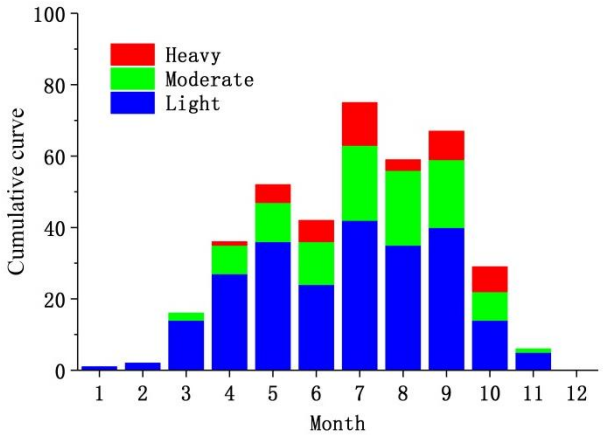

Figure 4. *Annual distribution of drought-flood abrupt alternation events over 1968-2017 in Guizhou province*

http://www.aloki.hu ● ISSN 1589 1623 (Print) ● ISSN 1785 0037 (Online)
DOI: http://dx.doi.org/10.15666/aeer/1705_1222712244

From December to February of the following year, the drought-flood abrupt alternation rarely occurred; from the point of view of the cases of moderate and above drought-flood abrupt alternation, it mainly occurs from July to September, 33 times, 24 times and 27 times, accounting for 8.57%, 6.23% and 7.01% of the total times respectively, which is basically consistent with the research results by Chen et al. (2015) and Lu (2010) on the characteristics of drought, rainstorm and flood in Guizhou Province, respectively. The drought-prone type is summer drought and spring drought in Guizhou Province, and the rainfall is concentrated in May-October in the whole province, so the period from the end of spring to early autumn is the period of drought-flood abrupt alternation, which is consistent with the *Figure 4*, further proving the applicability of the DWAAI index in Guizhou Province.

Interannual variation

(1) Station proportion. As can be seen from *Figure 5* ,the station proportion of drought-flood abrupt alternation in Guizhou province fluctuates from 10.53% to 78.95% in recent 50 years with greater interannual difference. In 2015 and 1986, there were partially regional drought-flood abrupt alternations for 5 years; in 2013 and 2007, there were partially regional drought-flood abrupt alternations for 14 years; in 2016-2017 and 2014, there were regional drought-flood abrupt alternations for 21 years; in 2011-2012 and 2002, there were regional drought-flood abrupt alternations for 10 years; before 2000, there were mainly partially regional and regional drought-flood abrupt alternation; after 2000, the regional drought-flood abrupt alternation occurred frequently, and the years with the highest station proportion were all after 2000, i.e., 2002 and 2011, respectively (78.95% of station proportion), which shows that the occurrence range of drought-flood abrupt alternation in recent 20 years is expanding.

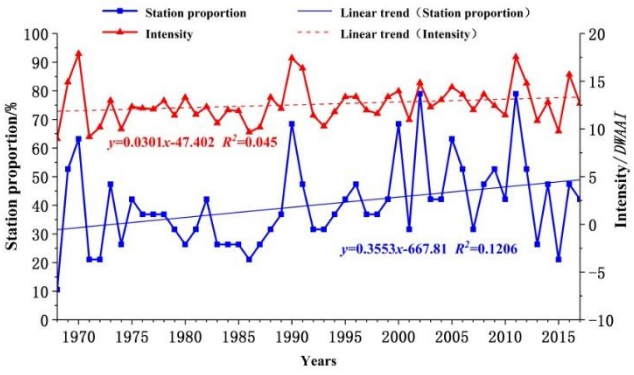

Figure 5. *Variation characteristics of station proportion and intensity of drought-flood abrupt alternation over 1968-2017 in Guizhou province*

(2) Intensity. As can be seen from *Figure 5*, the intensity of drought-flood abrupt alternation in Guizhou Province in recent 50 years fluctuated from 8.96 to 17.88, and the average intensity of drought-flood abrupt alternation is 12.59, which shows that the drought-flood abrupt alternation in Guizhou Province is mainly mild, and the intensity of drought-flood abrupt alternation is higher than 12.00 for 29 years, during which in 1970, 2011 and 1990, the intensity is higher than 17.00, that's, 17.88, 17.55 and 17.43, respectively. They are the three years with the highest intensity of drought-flood abrupt alternation over the past 50 years.

http://www.aloki.hu ● ISSN 1589 1623 (Print) ● ISSN 1785 0037 (Online)
DOI: http://dx.doi.org/10.15666/aeer/1705_1222712244

From the change trend of station proportion and intensity (*Table 2*), the climate tendency rate is consistent with the result of Mann-Kendall method. The station proportion and intensity have increased in Guizhou Province in recent 50 years, and the increasing trend of station proportion is significant, which shows that with the increase of time, the intensity and range of drought-flood abrupt alternation in Guizhou Province increased.

Table 2. *Trend detection results of station proportion and intensity of drought-flood abrupt alternation over 1968-2017 in Guizhou province*

	Linear tendency rate/10a-1	**Mann-Kendall test**	
		Z	**β**
Station proportion/%	3.55*	2.06*	0.39
Intensity	0.3	1.4	0.04

Note: Z is Statistics of Mann-Kendall test; β is Sen's slope, means trend of annual average; * means significant trend when α=0.05; the same below

Characteristics of seasonal drought-flood abrupt alternation over the years

(1) Spring (March-May). As can be seen from *Figure 6a*, the station proportion of drought-flood abrupt alternation in spring in Guizhou Province in the past 50 years ranged from 0.00% to 42.11%, averaging 10.84%; only in 1973 occurred the regional drought-flood abrupt alternation, with the station proportion of 42.11%. In 1969, 1977, 1999 and 2006, there were partially regional drought-flood abrupt alternations or non-obvious drought-flood abrupt alternation for 4 years, while there were regional drought-flood abrupt alternations for the other 45 years, and large-scale drought-flood abrupt alternation occurred frequently from 1994 to 2007 in spring. The interannual intensity of drought-flood abrupt alternation in spring varies from 0.00 to 16.80, averaging 10.91; the intensity of drought-flood abrupt alternation in spring exceeded 12.00 for 15 years, of which it occurred after 2000 for 7 years and occurred for 4 years in recent 10 years, that's, 2009, 2011-2012 and 2016, respectively.

(2) Summer (June-August). As can be seen from *Figure 6b*, the station proportion of drought-flood abrupt alternation in summer in Guizhou Province over the past 50 years is between 0.00% ~ 57.89% (average 18.74%), which is generally higher, indicating that the occurrence range of drought-flood abrupt alternation in summer is large in Guizhou Province. The years with the highest station proportion in summer is 2002, and the station proportion is 57.89%, which is regional drought-flood abrupt alternation. In 1982, 1991, 2009 and 2012, there were regional drought-flood abrupt alternation for 4 years. In 2011 and 2005, there were partially regional drought-flood abrupt alternation for 10 years, and in 2016 and 2014, there were regional drought-flood abrupt alternation for 23 years. The interannual intensity of drought-flood abrupt alternation in spring varies from 0.00 to 27.02, averaging 13.74; the intensity of drought-flood abrupt alternation exceeded 12.00 for 37 years, of which it reached 27.02 in 2004, which is generally at a severe level, and it is the year with the strongest intensity of drought-flood abrupt alternation.

(3) Autumn (September-November). As can be seen from *Figure 6c*, the station proportion of drought-flood abrupt alternation in autumn for 50 years is between 0.00% and 47.37%, averaging 10.63%; in 1990 and 2011, there were regional drought-flood abrupt alternation in autumn for 2 years; in 1970, 1978 and 1996, there were partially

http://www.aloki.hu ● ISSN 1589 1623 (Print) ● ISSN 1785 0037 (Online)
DOI: http://dx.doi.org/10.15666/aeer/1705_1222712244

regional drought-flood abrupt alternation in autumn for 3 years; in 1969 and 1975-1976, there were regional drought-flood abrupt alternation in autumn for 21 years, among which it occurred after 2000 for 9 years and after 2010 for 4 years.

The interannual intensity of drought-flood abrupt alternation in autumn varies from 0.00 to 19.36, averaging 11.15; the intensity of drought-flood abrupt alternation in autumn exceeded 12.00 for 22 years, of which it reached 19.36 in 2011, which is generally at a moderate level, and it is the year with the strongest intensity of drought-flood abrupt alternation in autumn.

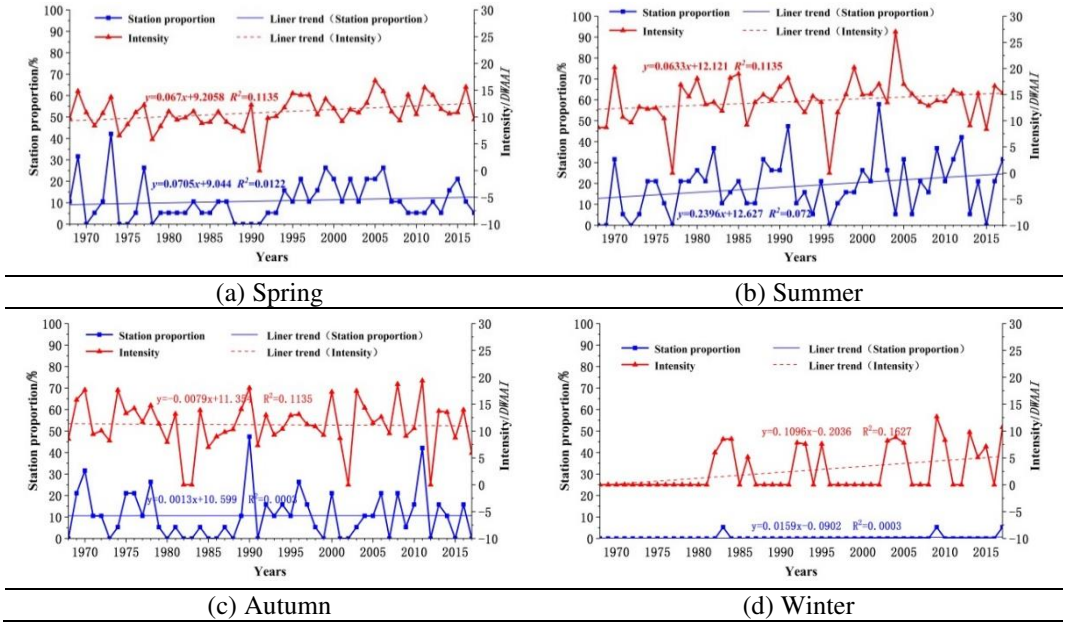

(a) Spring (b) Summer

(c) Autumn (d) Winter

Figure 6. *The seasonal variation characteristics of station proportion and intensity of drought-flood abrupt alternation over 1968-2017 in Guizhou province*

(4) Winter ((December-February). According to the calculation results, there were only three drought-flood abrupt alternation in winter in Guizhou Province in the past 50 years, which were in 1983, 2009 and 2017, and all of them were mild events. From Figure 6d, we cannot find the change rules from the station proportion. The interannual intensity of drought-flood abrupt alternation in winter ranges from 0.00 to 12.66, averaging 2.59. Therefore, there is no obvious drought-flood abrupt alternation in winter in Guizhou Province.

According to the station proportion and intensity variation trend of drought-flood abrupt alternation in different seasons (*Table 3*), the climatic tendency rate is basically consistent with the result of Mann-Kendall method. In spring, the station proportion of drought-flood abrupt alternation in spring tends to increase slightly, and the intensity tends to increase significantly. The station proportion and intensity of drought-flood abrupt alternation increase significantly in summer. The intensity of drought-flood abrupt alternation in autumn tends to slightly decrease. The station proportion linear tendency rate isn't consistent with the result of the Mann-Kendall test statistic Z, but the absolute values of them are both lower, so there is no obvious change trend in station proportion in autumn; the station proportion and intensity of drought-flood abrupt alternation in winter increased, but not significantly.

http://www.aloki.hu ● ISSN 1589 1623 (Print) ● ISSN 1785 0037 (Online)
DOI: http://dx.doi.org/10.15666/aeer/1705_1222712244

Characteristics of spatial evolution

Spatial distribution characteristics of occurrence frequency

As can be seen from *Figure 7*, the frequency of drought-flood abrupt alternation in Guizhou Province from 1968 to 2017 is obviously different, decreasing from east to west as a whole. The prone areas of drought-flood abrupt alternation are mainly concentrated in central and southern Tongren and southeastern, central and eastern Guizhou, with a frequency of 50.85% ~ 68.00%, once every 1-2 year; the frequency in the western part of Bijie is low, ranging from 24.01% to 33.90%.

Table 3. *Trend detection results of station proportion and intensity of drought-flood abrupt alternation on different seasons over 1968-2017 in Guizhou province*

Season		Linear tendency rate/10a-1	Mann-Kendall test	
			Z	β
Spring	Station proportion/%	0.71	1.35	0
	Intensity	0.67*	2.11*	0.06
Summer	Station proportion/%	2.4*	2.87*	0.25
	Intensity	0.63*	1.97*	0.07
Autumn	Station proportion/%	0.01	-0.02	0
	Intensity	-0.08	-0.09	-0.01
Winter	Station proportion/%	0.16	0.4	0
	Intensity	1.1	1.74	0

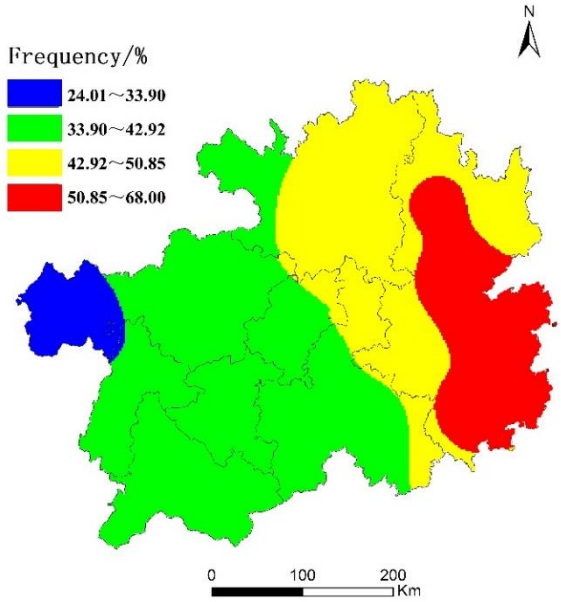

Figure 7. *Spatial distribution of drought-flood abrupt alternation frequency over 1968-2017 in Guizhou province*

Characteristics of seasonal spatial variation

In accordance with the calculation result, the frequency of drought-flood abrupt alternation in different seasons is calculated by four zones including once every more than 10 years (0 ~ 10%), once every 7 ~ 10 years (10% ~ 15%), once every 5 ~ 7 years

http://www.aloki.hu ● ISSN 1589 1623 (Print) ● ISSN 1785 0037 (Online)
DOI: http://dx.doi.org/10.15666/aeer/1705_1222712244

(15% ~ 20%) and once every less than 5 years (> 20%), with the spatial distribution shown in Figure 7 and the area proportion of different zones shown in *Table 4*. The area proportion of each frequency and the product of the frequency are used to express the severity index of the zone with drought-flood abrupt alternation.

Table 4. *The area proportion of each frequency on different seasons over 1968-2017 in Guizhou province (%)*

Frequency / Season	0~10%	10%~15%	15%~20%	>20%	Severity index
Spring	48.43	31.97	17.47	2.13	9.90
Summer	3.53	21.25	21.44	53.78	17.34
Autumn	38.79	41.65	19.56	0.00	10.57
Winter	100.00	0.00	0.00	0.00	5.00

As can be seen from *Figure 8*, the spatial distribution of the frequency of drought-flood abrupt alternation varies greatly in different seasons.

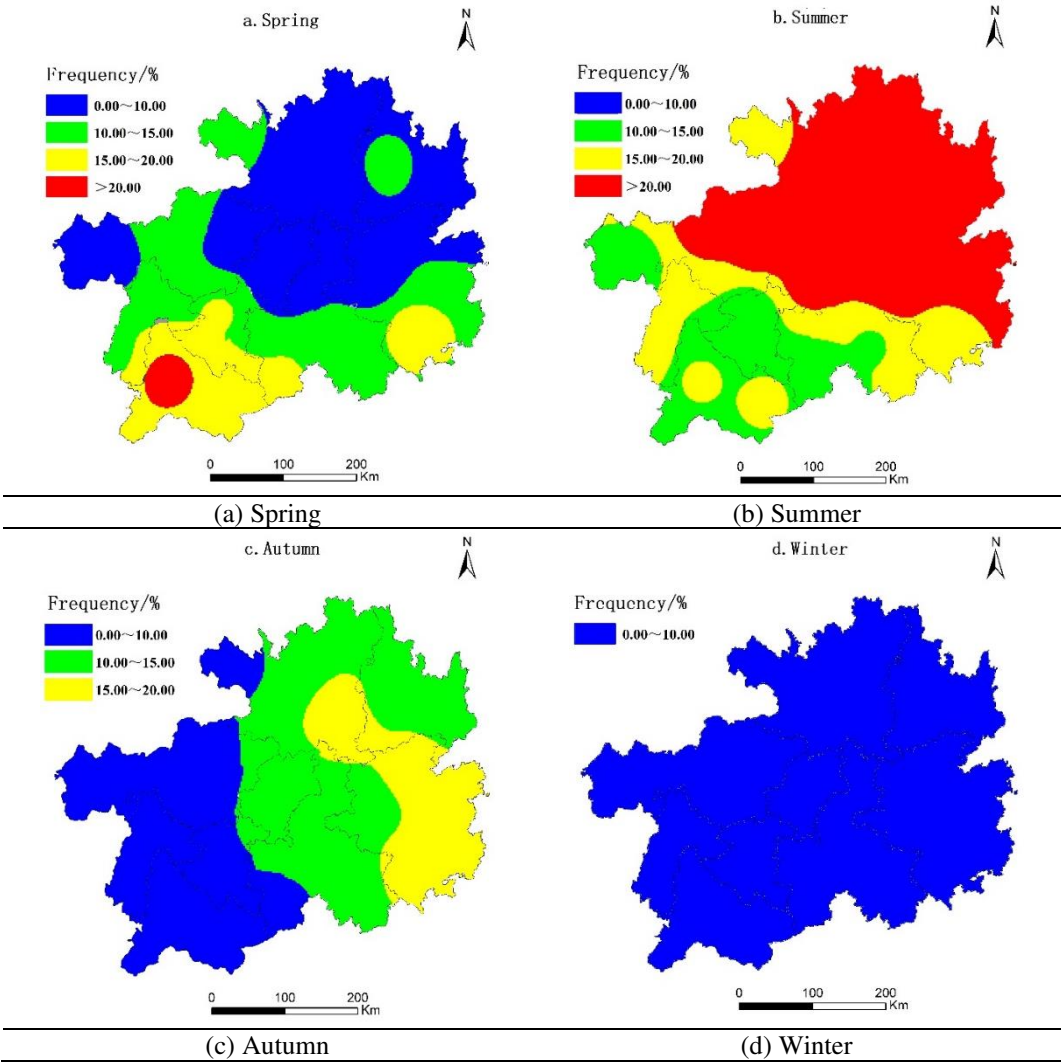

(a) Spring (b) Summer

(c) Autumn (d) Winter

Figure 8. *Spatial distribution of drought-flood abrupt alternation frequency on different seasons over 1968-2017 in Guizhou province*

http://www.aloki.hu ● ISSN 1589 1623 (Print) ● ISSN 1785 0037 (Online)
DOI: http://dx.doi.org/10.15666/aeer/1705_1222712244

The frequency of drought-flood abrupt alternation in spring is higher in the south than in the north, and the prone area is mainly in the southwest of Guizhou, of which the frequency in Xingyi City is more than 20%, that's, once every less than 5 years; the frequency in most of the central and northern regions and the western part of Bijie is less than 10% (*Figure 8a*). Summer is the opposite to spring, with the overall decline from north to south, the prone areas with the frequency of more than 20% run throughout most of the north-central region, and only in the southwest of Guizhou, the frequency is less than 10% (*Figure 8b*). In autumn, the frequency of drought-flood abrupt alternation decreases from east to west, and the southeast of Guizhou, the southwest of Tongren and the southeast of Zunyi are relatively vulnerable to drought-flood abrupt alternation, with the frequency of 15% ~ 20%, that's, the frequency in most areas of northwest and southwest Guizhou is less than 10% (*Figure 8c*). Fewer drought-flood abrupt alternation occurs in winter, without obvious characteristics of the spatial distribution, and the frequency is below 10% in the whole province (*Figure 8d*).

From *Table 4*, it can be seen that the frequency of drought-flood abrupt alternation in more than 80% areas of the province in spring and autumn is less than 15%; the frequency of drought-flood abrupt alternation in summer is over 50% in more than 50% of the whole province, and only 3.53% of the area have the frequency of lower than 10%. In winter, there are less drought-flood abrupt alternation events. In terms of severity, drought-flood abrupt alternation is the severest in summer, with the order from high to low as summer, autumn, spring and winter.

Characteristics of interdecadal spatial change

In order to describe the characteristics of interdecadal change conveniently, every 10 years has been counted as one decade since 1968. In accordance with the calculation result, the frequency of drought-flood abrupt alternation in different decades is calculated by four zones including once every 5 years (0 ~ 20%), once every 3 ~ 5 years (20% ~ 33.33%), once every 2 ~ 3 years (33.33% ~ 50%) and once every 1~2 years (> 50%), with the spatial distribution shown in *Figure 8*, and the area ratios of different zones shown in *Table 5*.

Table 5. *The area proportion of each frequency in different decades in Guizhou province(%)*

Frequency / Decade	0~20%	20%~33.33%	33.33%~50%	>50%	Severity index
1968-1977	2.39	33.78	60.37	3.46	36.13
1978-1987	13.79	35.48	47.79	2.94	32.22
1988-1997	4.31	8.16	49.05	38.48	42.29
1998-2007	0.00	0.45	48.62	50.94	45.84
2008-2017	1.38	5.14	58.45	35.02	43.38

As can be seen from *Figure 9*, except for 1998-2007, the spatial distribution of drought-flood abrupt alternation in each decade basically declines from east to west. With the increase of the decades, the scope of prone areas has been expanding. From 1968 to 1987, the frequency is higher than 50%, i.e. once every 1-2 years, the drought-flood abrupt alternation is sporadically distributed in southeast Quizhou, Bijie, Zunyi and Tongren (*Figures 9a,b*). From 1988 to 1997, the scope of prone areas has been extended to Guiyang, Zunyi, Tongren and southeast Quizhou (*Figure 9c*). From 1998 to 2007, except for some areas in Anshun, the drought-flood abrupt alternation occurred

http://www.aloki.hu ● ISSN 1589 1623 (Print) ● ISSN 1785 0037 (Online)
DOI: http://dx.doi.org/10.15666/aeer/1705_1222712244

once every 1 ~ 3 years in the whole province, among which, the scope of the prone areas once every 1 ~ 2 years was further expanded to the northwest, southwest and southeast Guizhou (*Figure 9d*). From 2008 to 2017, except for some areas in Zunyi and southwest Guizhou, the drought-flood abrupt alternation occurred once every 1-3 years in the whole province, and the range of prone areas was slightly reduced compared with that in 1998-2007. However, the overall distribution range is still relatively large (*Figure 9e*).

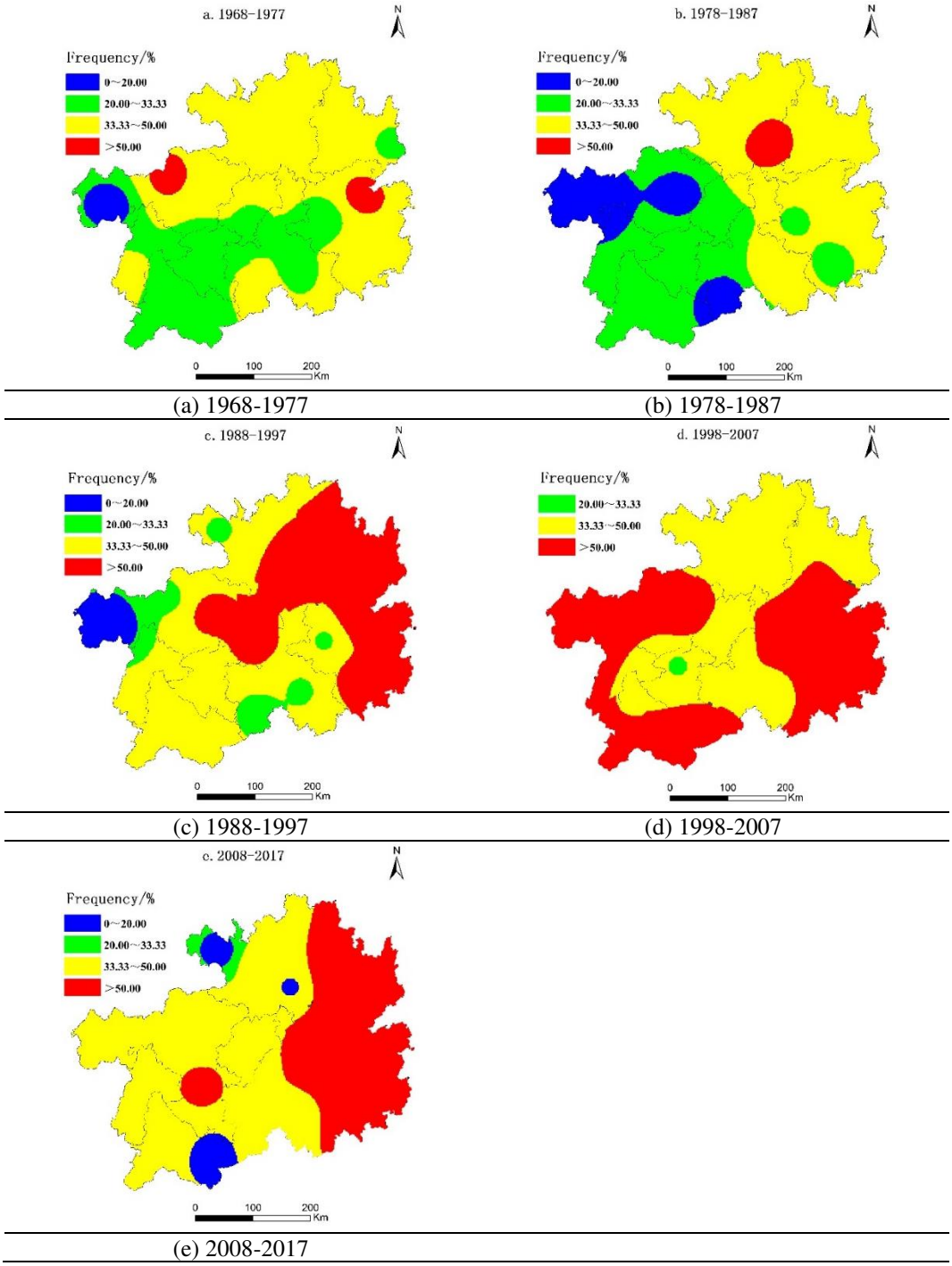

(a) 1968-1977 (b) 1978-1987

(c) 1988-1997 (d) 1998-2007

(e) 2008-2017

Figure 9. *Spatial distribution of drought-flood abrupt alternation frequency in different decades in Guizhou province*

http://www.aloki.hu ● ISSN 1589 1623 (Print) ● ISSN 1785 0037 (Online)
DOI: http://dx.doi.org/10.15666/aeer/1705_1222712244

As can be seen from *Table 5*, from 1988 to 1997, the area of the prone areas with drought-flood abrupt alternation once every 1-2 years increases sharply. In 1998-2007, more than 50% of the area of the province suffered from drought-flood abrupt alternation once every 1-2 years. In recent 10 years, the area of prone areas has decreased, and the frequency is 33% ~ 50%, that's, the area with drought-flood abrupt alternation once every 2 ~ 3 years is relatively stable. The frequency of drought-flood abrupt alternation is 20% ~ 33.33%, that's, the area with drought-flood abrupt alternation once every 3 ~ 5 years decreased significantly. In terms of severity, from 1998 to 2007, the drought-flood abrupt alternation is the severest, followed by it from 2008 to 2017 and it is the lowest from 1978 to 1987.

Discussion

Chen et al. (2015) studied the temporal and spatial variation characteristics of drought in Guizhou Province. Lu (2010) carried out research in the climate characteristics of rainstorms and floods in Guizhou Province, and concluded that spring and summer are the high incidence periods of drought in Guizhou Province, the spring drought tends to occur in the western region of Guizhou, and the summer drought tends to occur in the northeastern region of Guizhou, from late-December to early-February, there is no rainstorm in the whole province, from mid-November to mid-March, there is no heavy rainstorm, and the extraordinary rainstorm concentrates from late-May to mid-September, which is consistent with the spatial and temporal characteristics of drought-flood abrupt alternation in the search results of this paper. Compared with 1998-2007, although the range in the recent 10 years is slightly reduced, high-intensity drought and flood abrupt alternation occurs more frequently, such as in 2011~2012, 2014 and 2016, and the resulted social and economic losses are much higher than in the past, which indicates that the drought -flood abrupt alternation has a tendency of becoming more intense. Therefore, it's of important practical significance to study the evolution law of drought and flood abrupt alternation, monitor it and alarm early warnings.

The drought in earlier period is the premise of the formation of drought-flood abrupt alternation, and the extreme precipitation event is a necessary condition for drought and flood abrupt alternation. Raksekhar et al. (2015), Liu et al. (2014) assessed or analyzed the drought characteristics of the study area by establishing or improving drought indicators. Goswami et al. (2018), Andrea et al. (2018) studied the formation factors of extreme precipitation. Compared with the above research results, the DWAAI can couple "droughts" and "floods", and describe the entire process of drought-flood abrupt alternation events completely, which has laid a foundation for exploring the formation mechanism of drought-flood abrupt alternation events.

The food crops and economic crops in Guizhou are mainly harvested in the autumn, and the crucial growth period of most crops coincides with the period of the occurrence of drought-flood abrupt alternation, therefore, the drought-flood abrupt alternation has a great impact on agricultural production. And the influencing mechanism of drought-flood abrupt alternation on crops is quite complicated, generally speaking, both droughts and floods would affect the growth and development of crops and thus leading to production reduction. In addition, if drought-d flood abrupt alternation occurs, it would produce superposed losses; but for some dryland crops, a certain-degree drought during the rooting period can effectively increase the root length and thus enhancing the drought tolerance; if the drought is relieved or there is a slight flood, there may be a

http://www.aloki.hu ● ISSN 1589 1623 (Print) ● ISSN 1785 0037 (Online)
DOI: http://dx.doi.org/10.15666/aeer/1705_1222712244

certain "compensation" effect (Gao et al., 2017). Therefore, it is necessary to combine specific physiological indicators of crops and the soil moisture conditions to carry out more in-depth experimental research on the crops' response mechanism to the abrupt alternation of droughts and floods.

Conclusions

(1) The revised DWAAI index has the advantages of high accuracy, comprehensive reflection, reasonable calculation results and good agreement with the real situation, so it has a good applicability in Guizhou Province.

(2) Temporally, the drought-flood abrupt alternation mainly occurs from April to October in Guizhou Province. In terms of interannual variation, the station proportion and intensity have the trend of increasing year by year, and the increasing trend of station proportion is significant. In terms of seasonal characteristic, except autumn, the station proportion and intensity all have an increasing trend, among which the intensity of drought-flood abrupt alternation in spring and summer and the station proportion of drought-flood abrupt alternation in summer increase obviously, the intensity of drought-flood abrupt alternation in autumn has a decreasing trend and the trend of station proportion is not obvious.

(3) Spatially, the frequency of drought-flood abrupt alternation in Guizhou Province is decreasing from east to west, varying greatly in different seasons, i.e., in the southern region in spring, in the middle and north in summer with the largest area of the prone areas, and in the eastern region in autumn. Along with the increase of the decades, the scope of the areas where drought and waterlogging change rapidly is expanding, among which the drought-flood abrupt alternation is the severest from 1998 to 2007.

(4) The spatial and temporal characteristics of drought-flood abrupt alternation events could be discussed by improving the index. In the future research, on the one hand, we can try to combine atmospheric circulation and other factors to study the formation mechanism of the drought-flood abrupt alternation events, so as to better predict and give warning; on the other hand, we can use modeling, experimentation and other approaches to study the influencing mechanism of drought-flood abrupt alternation on certain crops, such as rice, corn or wheat, so as to develop scientific countermeasures for disaster prevention and alleviation.

Acknowledgements. This paper is supported by General Project of National Natural Science Foundation of China (51779093); Science and Technology Project of Water Resources Department of Guizhou Province (KT201705); Scientific Research Project of Public Welfare Industry of Ministry of Water Resources (201301039); Innovation fund for doctoral students of North China University of Water Resources and Electric Power.

REFERENCES

[1] Chen, X. K., Xu, J. X., Lei, H. J., Hu, J. P., Zhang, Z. Z., Huang, X., Shang, C, J., Yang, J. (2015): Spatial and temporal distribution characteristics of drought and its regional response to climate change in Guizhou Province. – Journal of Irrigation and Drainage 34(8): 74-81.

http://www.aloki.hu ● ISSN 1589 1623 (Print) ● ISSN 1785 0037 (Online)
DOI: http://dx.doi.org/10.15666/aeer/1705_1222712244

[2] Cheng, Z., Xu, M., Luo, L. S., Ding, X. J. (2012): Climate Characteristics of Drought-flood Abrupt Change Events in Huaihe River Basin. – Journal of China Hydrology 32(1): 73-79.
[3] Dittus, A. J., Karoly, D. J., Donat, M. G. (2018): Alexander. Understanding the role of sea surface temperature-forcing for variability in global temperature and precipitation extremes. – Weather and Climate Extremes 21(9): 1-9.
[4] Djebou, D. C. S., Singh, V. P., Frauenfeld, O. W. (2014): Analysis of watershed topography effects on summer precipitation variability in the southwestern United States. – Journal of Hydrology 511: 838-849.
[5] Gao, Y., Hu, T. S., Yuan, H. W., Yang, J. W. (2017): Analysis on yield reduced law of rice in Huaibei plain underdrought-flood abrupt alternation. – Transactions of the Chinese Society of Agricultural Engineering 33(21): 128-136.
[6] Goswami, P. U., Hazra, B., Goyal, K. M. (2018): Copula-based probabilistic characterization of precipitation extremes over north sikkim himalaya. – Atmospheric Research 212: 273-284.
[7] Grinsted, A., Moore, J. C., Jevrejeva, S. (2014): Application of the cross wavelet transform and wavelet coherenceto geophysical time series. – Nonlinear Processes in Geophysics 11(5/6): 561-566.
[8] Han, D. M., Yang, G. Y., Yan, D. H. (2014): Spatial-temporal Feature Analysis of Drought and Flood in Northeast China in Recent 50 Years. – Water Resources and Power 32(6): 5-8.
[9] Huang, W. H., Yang, X. G., Li, M. S., Zhang, X. Y., Wang, M. T., Dai, Z. W., Ma, J. H. (2010): Evolution characteristics of seasonal drought in the south of China during the past 58 years based on standardized precipitation index. – Transactions of the Chinese Society of Agricultural Engineering 26(7): 50-59.
[10] Huang, R. (2015): Research on evolution and Countermeasures of drought-floods abrupt alternation events in Huaihe River basin. – China Institute of Water Resources & Hydropower Research.
[11] Langousis, A., Kaleris, V. (2014): Statistical framework to simulate daily rainfall series conditional on upper- air predictor variables. – Water Resources Research 50(5): 3907-3932.
[12] Liu, Z. Y., Zhang, J. P., Luo, H. X., He, Y. K. (2014): Temporal and spatial distribution of maize drought in Southwest of China based on agricultural reference index for drought. – Transactions of the Chinese Society of Agricultural Engineering 30(2): 105-115.
[13] Lu, E. (2009): Determining the start, duration, and strength of flood and drought with daily precipitation: Rationale. – Geophysical Research Letters 36: L12707.
[14] Lu, R. J. (2010): Analysis of Climate Characteristic of Rainstorm in Guizhou Province. – Lanzhou University.
[15] Maheras, P., Xoplaki, E., Kutiel, H. (1999): Wet and Dry Monthly Anomalies Across the Mediterranean Basin and Their Relationship with Circulation, 1860-1990. – Theoretical Applied Climatology 64: 189-199.
[16] Raksekhar, D., Singh, V. P., Mishra, A. K. (2015): Multivariate drought index: An information theory based approach for integrated drought assessment. – Journal of Hydrology 526(11/12): 164-182.
[17] Shan, L. J., Zhang, L. P., Zhang, Y. J., She, D. X., Xia, J. (2018): Characteristics of dry-wet abrupt alternation events in the middle and lower reaches of the Yangtze River Basin and their relationship with ENSO. – Acta Geographica Sinica 37(1): 25-40.
[18] Shen, B. Z., Zhang, S. X., Yang, H. W., Wang, K., Feng, G. L. (2012): Analysis of characteristics of a sharp turn from drought to flood in the middle and lower reaches of the Yangtze River in spring and summer in 2011. – Acta Physica Sinica 61(10): 530-540.
[19] Wu, Z. W., Li, J. P., He, J. H., Wang, Z. H. (2006a): Large-scale Atmospheric Circulation Anomaly and Long Period of Drought and Flood Abrupt Alternation in the Middle and

http://www.aloki.hu ● ISSN 1589 1623 (Print) ● ISSN 1785 0037 (Online)
DOI: http://dx.doi.org/10.15666/aeer/1705_1222712244

Lower Reaches of the Yangtze River in Summer. – Chinese Science Bulletin 51(14): 1717-1724.

[20] Wu, Z., Li, J., He, J. (2006b): Occurrence of droughts and floods during the normal summer monsoons in the mid and lower reaches of the Yangtze River. – Geophysical Research Letters 33(5): 813-816.

[21] Zhang, S. F., Zhang, J. C., Min, J. J., Zhang, Z. X., Zhuang, J. Y., Lin, J. (2012): Drought-flood abrupt alternation based on runoff in the Huaihe River Basin during rainy season. – Journal of Lake Sciences 24(5): 679-686.

[22] Zhou, Y., Li, N., Ji, Z. H., Gu, X. T., Fan, B. H. (2013): Temporal and Spatial Patterns of Droughts Based on Standard Precipitation Index (SPI) in Inner Mongolia during 1981-2010. – Journal of Natural Resources 28(10): 1694-1706.

http://www.aloki.hu ● ISSN 1589 1623 (Print) ● ISSN 1785 0037 (Online)
DOI: http://dx.doi.org/10.15666/aeer/1705_1222712244

DEVELOPMENT STATUS AND ENVIRONMENTAL IMPACT EVALUATION OF CHINA'S GREEN FINANCE

WANG, L.[1*] – QIU, X. M.[1] – ZHANG, X. X.[2] – MA, R. H.[1] – JIANG, Y. H.[1]

[1]*College of Economic and Trade, University of Electronic Science and Technology of China, Zhongshan Institute, Zhongshan 528499, China*

[2]*Management College, University of Electronic Science and Technology of China, Zhongshan Institute, Zhongshan 528499, China*
(phone: +86-159-1729-3187)

[*]*Corresponding author*
e-mail: 838241358@qq.com

(Received 3rd May 2019; accepted 11th Jul 2019)

Abstract. Green finance is a financial activity for supporting environmental improvement, for tackling climate change and for conserving and efficiently utilizing resources, which is also a requirement for sustainable economic development. Existing researches on the green finance policies and policy systems are still in their infancy, which are predominantly qualitative analyses, while empirical studies concerning the green finance policies are scarce. This paper combs the development course of China's green finance, and then evaluates the effectiveness of carbon emissions trading pilot programs through robust regression. The results reveal that China's total carbon emissions are still on the rise, though the emission intensity is declining by years. The carbon emission intensity is lower in the pilot areas with relatively developed economy, where the carbon emissions trading pilot programs are obviously effective in reducing the carbon emissions. Referring to the control variables, the increase of foreign direct investment (FDI) and technology progress (TE) both reduce the intensity of carbon emissions, while the increase of per capita GDP will lead to the deterioration of the environment; Environmental support effort (ENVI) has not yet played a role in slowing down environmental pollution. Thus, China's current green finance policy system should strengthen the reform of policy guarantee and market operation, which has certain reference value for further improving the policy system and promoting the development of green finance.
Keywords: *green finance, robust regression, CO_2 emission intensity, dynamic panel regression, environmental support effort*

Introduction

Green finance, as the product of a combination of financial theory with economic practice, redefines the management policies and business processes of financial industry from the perspectives of environmental protection and sustainable development. While assisting in the economic transition, it can also realize the sustainable development of finance itself. Therefore, green finance is also known as "environmental financing", "sustainable finance", "ecological finance" or "carbon finance". Although the theoretical community has differing descriptions of its meaning, the basic connotation is always how the financial institutions carry out financial activities around improving environment and tackling climate change.

With the rapid and extensive growth of China's economy since the reform and opening up, ecological environment is increasingly deteriorating, which has become a major bottleneck restricting sustainable economic development. Finance, as the core of modern economy, plays an important role in resource allocation. Green finance can shift investment from the energy-intensive and high-polluting industries to the green and environmental, which is a powerful guarantee for promoting sustainable economic

http://www.aloki.hu ● ISSN 1589 1623 (Print) ● ISSN 1785 0037 (Online)
DOI: http://dx.doi.org/10.15666/aeer/1705_1224512258

development and industrial restructuring. However, green finance is an emerging financial industry. Although it is featured with positive externalities, it is difficult to clarify property rights and bring benefits to it, which hinders the development of green finance. Therefore, studying the healthy development of green finance is not only an urgent task, but also a requirement for the sustainable development of China's economy.

Literature review

In recent years, green finance has been studied by many scholars at home and abroad mainly from the following two aspects: One is the connotation of green finance; and the other is the empirical analysis on green finance evaluation. Regarding research on the connotation of green finance, Salazar (1998) argued that green finance is a financial innovation that seeks economic development along the path of environmental protection, with purposes of seeking economic development alongside environmental protection and achieving a balance between economy and environment. In Cowan's (1999) opinion, green finance is a discipline that studies the relationship between environment and financing. According to Labatt and White (2002), green finance is a market-based financial instrument that aims to improve environmental quality and transfer environmental risks. Scholtens (2006) focused on analyzing the transmission mechanism between finance and sustainable development, who pinpointed that the green finance can address resource and environmental issues via the optimal combination of financial instruments. There are also a number of scholars who have done similar researches (Vyas, 2015; Wang and Zhi, 2016; Raberto et al., 2018; Volz, 2018).

Meanwhile, the empirical analyses on green finance evaluation concentrate mainly on three aspects. Firstly is the impact of green finance on financial institutions. Many scholars believe that the financial institutions should implement green financial strategies because by doing so, they can better attain the corporate risk management objectives and make strategic decisions that are conducive to the long-term corporate development, which is an objective requirement for the sustainable development of financial industry (Chami, 2002). There is also an argument that the financial institutions' implementation of green finance policies does not pose significant influence on their profits or risks (Gelema et al., 2011). Thus, clearly, the theoretical community has failed to reach a consensus as to the impact of green finance on the financial institutions. Secondly is the empirical analysis concerning green finance and green financial products. Brennan and Schwartz (1985) initiated the inclusion of environmental factors in the financial instrument pricing, who took into account the natural consumption cost in the corporate options pricing method. On this basis, Cortazar et al. (1998) extended the calculation method of the above model to propose a real options model for optimal timing of corporate investment in environmental technologies based on the corporate operating costs and environmental protection policies. Climent and Soriano (2011) have also done relevant research. Thirdly is the evaluation of green finance and environmental risks. By establishing index systems measuring the relationship between bank channels and green performance, Street and Monaghan (2001) and Cleene and Wood (2004) evaluated the green performance level of banks during operation. There are also a number of scholars who have done similar researches (Hoti and Mcaleer, 2004; Thomas, 2010; Zeng, 2014; Liu et al., 2018).

The above literatures offer substantial implications. In this study, green finance is defined as financial activities that support environmental improvement, tackle climate

http://www.aloki.hu ● ISSN 1589 1623 (Print) ● ISSN 1785 0037 (Online)
DOI: http://dx.doi.org/10.15666/aeer/1705_1224512258

change, and conserve and efficiently utilize resources. It channels funds into projects like environmental protection, energy conservation, clean energy, green transportation and green buildings through tools and policies such as credits, bonds, funds, insurance and carbon finance. Despite respective emphases of the above literatures, the research on the effect of China's green finance policies is still in its infancy, which needs to be deepened urgently.

Development history of China's green finance

The development course of China's green finance can be divided roughly into three stages:

(1) Years 2005-2008: The emerging stage of green finance

At the national policy level, energy conservation, emission reduction and environmental protection received increasing attention during this period. The *Eleventh Five-Year Plan* (2006-2010) put forward clear quantitative targets for the energy conservation and emission reduction. In this stage, green credit policies began to be formulated and issued in succession, such as the *Opinions on Implementing Environmental Protection Policies and Regulations for Preventing Credit Risks* (2007) and the *Green Credit Guidelines* (2008), which mark the sprouting of green finance in China.

(2) Years 2009-2014: The initial developing stage of green finance

During this period, the national green policies kept stepping up. Firstly, the Chinese government made international commitments on greenhouse gas emission control target. Secondly, the energy-saving and emission-reducing policies were launched continuously. Thirdly, ecological civilization was emphasized and the "strictest ever environmental law", i.e. the *Environmental Protection Law* (2014), was introduced.

In this stage, the green credit policy system began to be established, developed and improved gradually. Policies like the *International Experiences in Promoting Green Credit: Equator Principles and IFC's Performance Standards and Guidelines* (2010), the *China Green Credit Development Report 2010* (2011), the *Green Credit Guidelines* (2012), the *Opinions on Green Credit Practice* (2013), the *Green Credit Statistics System* (2013) and the *Key Evaluation Indices for the Implementation of Green Credit* (2014) were introduced. As a result, China formed a rather complete green credit policy system that centered on the *Green Credit Guidelines* with the green credit statistics system and evaluation mechanism as the two major cornerstones.

(3) Year 2015–present: The scale development stage of green finance

The main features of this stage are as follows: Firstly, the green development and ecological civilization policies have been introduced intensively. In 2015, the top-level design scheme for ecological civilization, i.e. *The Overall Plan for the Reform of Ecological Civilization System*, was launched. Subsequently, numerous environmental related policies, regulations, regimens and plans were introduced in succession, including the *Action Plan for Water Pollution Prevention and Control*, the *Action Plan for Air Pollution Prevention and Control*, the *Atmospheric Pollution Prevention and Control Law of The People's Republic of China*, and the *Action Plan for Soil Pollution Prevention and Control*. Secondly, the green finance system has begun to be established.

http://www.aloki.hu ● ISSN 1589 1623 (Print) ● ISSN 1785 0037 (Online)
DOI: http://dx.doi.org/10.15666/aeer/1705_1224512258

In 2015, the People's Bank of China issued the *Energy Efficiency Credit Guidelines*, the *Green Financial Bonds Announcement* and the *Green Bond Support Project Catalogue*, which mark the opening of China's green bond market. The *Guiding Opinions on Building a Green Finance System* released in 2016 marks the establishment of China's top-level green finance framework system, thus making China the first nation in the world to set up a rather complete green finance policy system.

After more than a decade's accumulation, China's achievements in the green finance field have drawn worldwide attention. Countries around the world are increasingly understanding China's concept, listening to China's wisdom, appreciating China's programs, and taking China's development opportunities as their own. The development of China's green finance is characterized by giving equal consideration to the domestic and international green development, and actively leading green development at the international level while continuously progressing the reform of domestic green development towards the deep water zones.

This paper uses empirical method to analyze the impact of China's green finance policies on environmental pollution. The significance could be explained by two points. First of all, it analyzes the formation process of the green finance policy system in China so as to deepen understanding about green finance policy system and combine with green finance industry development course to observe limitations of the policy. Secondly, based on the analysis on green finance policy and literature, the paper begins with "carbon emission permit trading policy" and adopts robust regression method to test policy implementation effects, therefore objectively assessing the advantages and disadvantages of the policy and exploring the validity of this policy in explaining green finance policy. Finally, by reference to empirical analysis, the paper proposes two pertinent countermeasures so as to provide new thought for the further research on green finance and economic sustainable development in China.

Materials and methods

Emerged in China, the green finance originated from the *Notice on the Use of Credit Policies for Promoting Environmental Efforts* promulgated by the China Environmental Protection Administration and the *Notice on Issues Concerning the Implementation of Credit Policies and Strengthening of Environmental Efforts* issued by The People's Bank of China in 1995. Restricted by the economic development level and public ideology at the time, the green finance did not receive enough attention when it was initially introduced. It was not until China's official launch of green credit-related policy in 2007 that the green finance gained further development.

Materials

China's overall ecological environment has been improved positively as its green finance policy matures and functions. During the 13th Five-Year Plan period, China is expected to totally reverse the deterioration of ecological environment. From a macro perspective, the allocation of financial resources is optimized by establishing a green finance system, whose influence is then propagated to the real economy, thus transforming the extensive growth towards a green, comprehensive and intensive direction. From 2007 to 2017, the funds for pollutants discharge reduction increased by years in the national public fiscal expenditure (including central and local governments)

http://www.aloki.hu ● ISSN 1589 1623 (Print) ● ISSN 1785 0037 (Online)
DOI: http://dx.doi.org/10.15666/aeer/1705_1224512258

(see *Figure 1*), which reached 561.733 billion yuan in 2017, suggesting the Chinese government's determination to govern environment.

From a micro perspective, policies on green credit, green bonds and environmental insurance were introduced intensively from 2015 to 2018. The increasingly perfect policy system has promoted the rapid development of related industries effectively while laying a solid foundation for the establishment of a sound green finance system. The green credit supply and green bond issuance in China are increasing by years. *Table 1* presents the status of China's green bond issuance from October 2016 to October 2018. As can be seen, the issuing scale of green bonds has been maintained at higher levels since 2016.

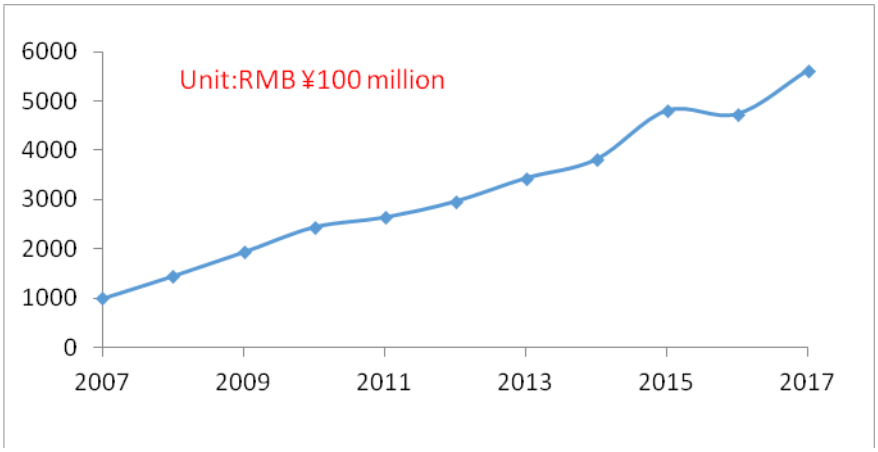

Figure 1. *General public budget fiscal expenditure for pollutants discharge reduction. Data Source: China Statistical Yearbook 2008-2018*

Table 1. *Issuance of green bonds (excluding asset-backed securities) from 2016 to October 2018*

	2016	**2017**	**January-October 2018**
issue number	29	68	65
issuing scale (billion)	1985.3	1908.75	1252.89

In *Figure 2*, the amount of green debt financing instruments managed by Shanghai Clearing House is displayed, which was up to 34.48 billion yuan in December 2018. From the figure, it is also clear that the amount of China's green debt financing has been increasing continuously.

Concerning insurance, China's environmental insurance is primarily the environmental pollution liability insurance, which is also known as the green insurance. In 2014, about 5,000 companies signed for the environmental pollution liability insurance. In 2015, the number of insurance sign-ups was 14,000, with a signing premium of 280 million yuan, offering risk protection of 24.421 billion yuan. In 2016, the premium income from the environmental pollution liability insurance was nearly 300 million yuan, offering risk protection of over 26 billion yuan. In 2017, the environmental pollution liability insurance provided risk protection of 30.6 billion yuan to more than 16,000 companies.

http://www.aloki.hu ● ISSN 1589 1623 (Print) ● ISSN 1785 0037 (Online)
DOI: http://dx.doi.org/10.15666/aeer/1705_1224512258

Methods

The *Notice on Launching Pilot Programs of Carbon Emissions Trading* issued in 2011 has initiated the exploration of issues pursuant to carbon emissions trading in China. As an important supplement to China's green finance system, the *Notice* will have a profound impact on the future of China's green finance industry. In 2013, carbon markets were launched and started trading in seven pilot provinces and municipalities (Beijing, Tianjin, Chongqing, Shanghai, Hubei, Guangdong and Shenzhen). As of now, the trading volume has reached 270 million tons of carbon dioxide, and the transaction amount exceeded 800 million euros, hence making China the world's largest carbon emissions trading market. This paper employs the robust regression technique to empirically analyze the effectiveness of implementing the carbon emissions permit policies.

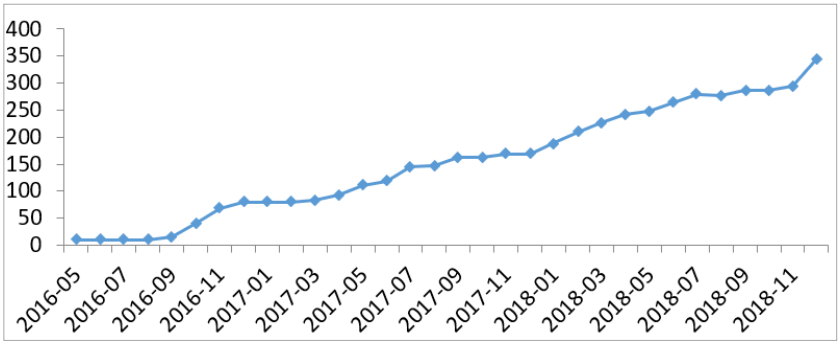

Figure 2. *The amount of green debt financing instruments managed by Shanghai Clearing House. Data Source: http://www.shclearing.com/sjtj/tjyb/*

Econometric model

(1) Traditional Econometric Model

The following dynamic panel regression model is finalized based on the research of green finance in the classic literatures combined with the theoretical analysis of green finance policies herein:

$$CO_{2_{it}} = \beta_1 + \beta_1 D_{it} + \sum \alpha X_{it} + \varepsilon_{it} \quad \text{(Eq.1)}$$

where, CO_2 denotes the intensity of carbon dioxide emissions; D is the dummy variable (D= 0 indicates that the green finance policy is not implemented in the non-pilot or pilot areas, while D= 1 indicates that the green financial policy is implemented in the pilot areas); X is the control variable (including foreign direct investment, technological progress, economic development level and environmental support effort); and i, t represent the region and year, respectively.

Most regressions are based on the ordinary least square (OLS) method at present. However, when many outliers are present in the data, the traditional least squares-based regression is no longer applicable. Robust regression, on the other hand, is a method in statistical robust estimation, whose main idea is to modify the objective function in the classical least squares regression that is highly sensitive to outlier values. Since the data

http://www.aloki.hu ● ISSN 1589 1623 (Print) ● ISSN 1785 0037 (Online)
DOI: http://dx.doi.org/10.15666/aeer/1705_1224512258

in this paper involves 30 provinces of China, there are huge interprovincial differences, so it seems more reasonable to estimate the above model via robust regression.

Common robust regression methods include least median square (LMS) method, M estimation method, etc. This paper adopts M estimation method.

(2) Robust regression algorithm based on M estimation

In case of any abnormal value in sample data, the residual estimated by OLS is often not in normal distribution, but biased tail instead. Considering residual quadratic sum, the role of abnormal value significantly increases, which leads to poorer estimation accuracy. Robust regression method mainly aims to improve the drawback of OLS in its great susceptibility to abnormal value. The basic thought is to minimize residual function $\rho(e_i)$, and derive each regression coefficient. The chosen residual function $\rho(e_i)$ does not endow all sample data with similar impact factor like how OLS chooses residual quadratic sum. On the contrary, it givens different weights according to the size of residual and therefore weakens the impact of abnormal value on regression result.

Common robust regression method is the M estimation method proposed by Huber in 1964. *Eq.2* presents its fundamental principle

$$Y_i = \beta_0 + \beta_1 X_{i1} + \cdots + \beta_p X_{ip} + e_i = X_i'\beta + e_i \ \ (\mathrm{i} = 1,2,\ldots,\mathrm{n}) \tag{Eq.2}$$

where, in β_0, β_1, ..., β_p are regression coefficients and e_1, e_2, ..., e_n are independent identically distributed with $\mathrm{E}[e_i] = 0$.

The M estimation method is exactly to seek β so as to reach the minimum of *Eq.3*.

$$\sum_{i=1}^{n} \rho(e_i) = \sum_{i=1}^{n} \rho(Y_i - X_i'\beta) \tag{Eq.3}$$

For reducing the role of abnormal value in Y_1, Y_2, ..., Y_n, it is necessary to take a function of growth rate of $\rho(x)$ slower than that of x^2, and meet the following conditions.

- $\rho(x)$continuity, $-\infty < x < +\infty$;
- $\rho(0)$=0, $\rho(x) = \rho(-x)$, and $\rho(x) \geq \rho(y)$ under the condition of $|x| \geq |y|$;
- $\lim_{x\to+\infty} \rho(x)x^{-2} = 0$.

Obviously, when $\rho(e_i) = e_i^2$, M estimation is OLS. Consequently, M estimation can be considered as the extension of OLS estimation as shown in *Eq.4*.

$$\rho'(x) = \psi(x) \tag{Eq.4}$$

If the target function solves the partial derivative of parameter β and set its value as 0, then *Eq.5* about parameter k+1 formula will be obtained.

$$\sum_{i=1}^{n} \psi(Y_i - X_i'\beta)X_i' = 0 \tag{Eq.5}$$

For ensuring the validity of above formula, $\rho(x)$meets the conditions as below: p(x) is defined as the non-negative convex function on （-∞，+∞）. $\rho'(x) = \psi(x)$ is valid under all conditions, in which $\lim_{|x|\to\infty} \rho(x) = \infty$.

http://www.aloki.hu ● ISSN 1589 1623 (Print) ● ISSN 1785 0037 (Online)
DOI: http://dx.doi.org/10.15666/aeer/1705_1224512258

Therefore, M estimation property is greatly related to chosen function $\rho(x)$. In measuring β, the choice of initial value is very important. Throughout scale quivariance, *Eq.6* may be simplified as *Eq.6*.

$$\sum_{i=1}^{n} W_i X_i' e_i = 0 \quad \text{(Eq.6)}$$

Eq.6 is a weighted least square (WLS) problem, of which the weight depends on the size of residual e_i, the residual reversely depends on regression coefficient β, and regression coefficient reversely depends on estimated weight W_i. In this case, it is necessary to adopt the iteration method to solve the formula. Moreover, in this process, the key is to choose proper objective function $\rho(x)$ and weight function $W(x)$ so as to decrease residual abnormal value weight, increase the weight of sample data with minor residua, weaken the influence of abnormal value on regression analysis and reinforce regression formula robustness.

(3) Variable setting

According to *Eq.1* and economic principle, the paper chooses the following variables.

Carbon intensity (CO_2): Carbon dioxide emissions are calculated based on the carbon emission coefficient of energies. Considering the GDP variance among provinces, the variable is measured by CO_2 emissions/GDP.

Foreign direct investment (FDI): Measured by RMB-denominated FDI/GDP, FDI brings promotion of the green and energy-saving technologies, which thus may contribute to reducing the carbon intensity.

Technological progress (TE): Technological progress can improve the energy efficiency of industrial enterprises to lower the carbon intensity. The variable is herein measured by the volume of invention patent applications that best reflects the technological level.

Economic development level (Pgdp): It is measured by the natural logarithm of GDP per capita. The higher the level of economic development, the more it contributes to the increase in environmental investments, thus lowering the intensity of industrial pollution.

Environmental support effort (ENVI): It is measured by the regional investment in governing industrial pollution/GDP. The government's efforts to strengthen the environmental protection promote the use of environmental technologies by companies, and prompt the shift of highly polluting companies to areas with weak environmental regulations.

Results

Descriptive statistics for every variable

Considering the availability and consistency of data, this paper selects the panel data of 30 provincial-level regions (excluding Tibet) from 2000 to 2016. The raw data comes from *China Statistical Yearbook*, *China Environmental Statistics Yearbook*, *China Science and Technology Statistical Yearbook*, as well as the statistical yearbooks of various provinces. *Table 2* lists the descriptive statistics for each variable.

Three carbon emissions trading pilots and three non-pilot provinces are selected to explore the variation trends of CO_2 emissions and CO_2 intensity since 2000. In *Table 3*,

http://www.aloki.hu ● ISSN 1589 1623 (Print) ● ISSN 1785 0037 (Online)
DOI: http://dx.doi.org/10.15666/aeer/1705_1224512258

relevant minimums and minimums are listed. The numbers in brackets indicate the years in which the values appear.

It can be seen from the above table that the minimum CO_2 emissions occur in 2000 for all provinces, while the maximums all appear in 2013 and beyond, showing an upward trend of emissions. Regarding the CO_2 intensity, all minimums appear in 2016, while all maximums occur in 2000, so the emission intensity is declining by years.

Table 2. *Descriptive statistics for every variable*

	Mean	**Min**	**Max.**	**s.d.**
CO_2 (Kg/10000 yuan)	3.580	0.752	14.27	2.212
FDI (10000 yuan)	3752484	9930	22573222	4388323
TE	36146	124	512429	71974
Pgdp (Yuan / person)	29432	2759	118198	22861
ENVI (Yuan/10000 yuan GDP)	17.476	0.684	99.185	14.08

Table 3. *Trends of CO_2 emissions and CO_2 emission intensity in some provinces*

	Beijin		Shanghai		Guangdong	
	emissions	intensity	emissions	intensity	emissions	intensity
Min	11489 (2000)	0.752 (2016)	15247 (2000)	1.152 (2016)	26194 (2000)	1.071 (2016)
Max.	19900 (2012)	3.634 (2000)	32473 (2016)	3.196 (2000)	86615 (2016)	2.439 (2000)
	Jiangsu		Sanxi		Heibei	
	emissions	intensity	emissions	intensity	emissions	intensity
Min	23878 (2000)	1.113 (2016)	18673 (2000)	4.122 (2016)	31040 (2000)	2.576 (2016)
Max.	86097 (2016)	2.792 (2000)	55070 (2014)	11.139 (2000)	86420 (2013)	6.175 (2000)

Note: Parentheses are the year.The unit of emission is ton, and intensity is ton/billion yuan

Analysis of empirical results

In this paper, robust regression is performed using *formula (1)* with the control variables FDI, TE, Pgdp and ENVI. The results are shown in *Table 4*.

Table 4. *Regression models results*

Variable	**Coefficient**	**Z-Statistic**	**Prob.**
D	-0.750841	-2.299761	0.0215
Pgdp	1.05811	17.63547	0.0000
FDI	-0.001119	-3.888342	0.0001
TE	-0.851207	-14.1518	0.0000
ENVI	0.066388	13.32519	0.0000

After analyzing the significance (Prob.) and coefficient of the control variables in the empirical model, we find that:

The p values of explanatory variables are all less than 0.05, indicating their significance in the present experiment.

The coefficient of green finance policy(dummy variable D) is negative, suggesting that the green finance policies are helpful for lowering the carbon intensity. This implies that there should be a transmission mechanism whereby the green finance policies promote the development of green finance and the green finance development reduces the carbon intensity.

http://www.aloki.hu ● ISSN 1589 1623 (Print) ● ISSN 1785 0037 (Online)
DOI: http://dx.doi.org/10.15666/aeer/1705_1224512258

Concerning control variables, the coefficients of FDI and TE are negative, suggesting that the promotion of green and energy-saving technologies brought by FDI and the technological advancement in China have led to an improved energy efficiency of industrial enterprises, both of which have lowered carbon intensity. The coefficient of per capita GDP (Pgdp) is positive, indicating that the environmental pollution in China has become increasingly serious with the growth of per capita income. So far, there has been no inflection point on the environmental Kuznets curve in China. The coefficient of environmental support effort (ENVI) is also positive, but very small, which is 0.066, indicating that China's investment in environmental governance has not yet abated the environmental pollution.

Discussion

Foreign green finance practice and experience

Comparing with western developed countries, China has obtained great progress in green finance. But the large gap should not be overlooked. Firstly, foreign green finance starts early. German government had already established the world's first environment policy bank as early as 1974. Later on, large foreign banks represented by Citibank took the lead to formulate and implement a full set of environment assessment standards and mechanisms in 2002, namely the "equator principle". Secondly, green finance products in foreign developed countries are in wide variety and scope, including both fundamental products like green credit and green bond but also derivatives like carbon fund. However, the green finance system in China is rather unsound, and related laws and regulations are imperfect. This may be evidenced by inadequate incentive mechanism, untimely environmental protection information disclosure, insufficient internal impetus of companies, poor innovation of green finance products, and many other internal problems. In consequence, the practice and development experience of foreign green finance provide great reference for the construction and development of green finance in China.

As to the green finance policy practice of foreign developed countries, it should be noted that these countries do not have identical policy and system, but they all combine a series of international standards of international banks like the "equator principle" with domestic reality, and formulate proper green finance implementation tenets and policies. *Table 5* shows the comparison of foreign green finance policy in developed countries.

As shown in *Table 5*, America primarily implements green finance policies by large banks, while Germany and Japan rely on large banks and policy banks. From the perspective of policy, these policies are all based on the equator principle. From the perspective of core system, Germany implement green finance policy by interest subsidy policy. From the perspective of advantages, German government take part in the implementation of green finance policy and offer pertinent guarantee.

Countermeasures to green finance development in China

Based on the above analysis, the following suggestions are put forward for the sustainable development of China's green finance:

http://www.aloki.hu ● ISSN 1589 1623 (Print) ● ISSN 1785 0037 (Online)
DOI: http://dx.doi.org/10.15666/aeer/1705_1224512258

(1) Establishment of a green finance policy guarantee mechanism

The policy guarantee mechanism refers mainly to the institutional construction and policy design by relevant governmental departments. Firstly, the green finance system must be improved by establishing a systematic finance system from the aspects of basic legal system, business standard system, business implementation system and supervision system of green finance. Secondly, the fiscal and taxation support system needs to be improved. According to estimations, the funds required for green development in China account for more than 15% of China's fiscal revenue. Apparently, fiscal funds cannot afford all the demands for green development. In such a context, innovations should be made by "transforming subsides into equity investment, into financing guarantee, into risk compensation, into special incentives and by relieving taxes". By doing so, the fiscal funds are used for stimulating the supply of market-oriented green finance instead of being directly used for green finance supply, thereby ensuring the efficiency and fairness of fiscal fund utilization by market means. Thirdly, the information communication mechanism should be set up. Green finance is not only an issue of eco-environmental protection, but also a financial reform issue involving multiple governmental and market sectors such as the environmental protection departments, the fiscal and taxation departments, the financial regulatory departments, financial institutions and intermediary service agencies. To promote the information communication between various departments, a sound cross-functional coordination mechanism must be established, and a bridge should be built between the government and the market.

(2) Improvement of the market operation mechanism

To play the role of green finance in supporting green industries, we must start from two aspects. On the one hand, the green finance organizational system needs to be improved. First of all, it is necessary to expand the participants of green finance market, and encourage the further greening of existing banks to adjust business operations in accordance with the *Equator Principles*. Meanwhile, the enthusiasm of non-bank financial institutions such as securities, insurance and fund companies should be fully mobilized for participating in the green finance business. Secondly, it is necessary to set up professional green development banks by the national, provincial and municipal governments after learning from international experience. Finally, it is necessary to foster green finance intermediary service agencies, encourage the existing intermediary services to actively participate in green financial operations, and accelerate the cultivation and development of professional intermediaries like the green credit rating agencies, green financial product certification institutions, green asset assessment firms, green financial information consulting services and environmental risk assessment agencies, so as to provide technical support for financing of green projects.

On the other hand, green financial products and instruments need to be innovated. First of all, it is necessary to promote the green credit innovation, such as innovating the mode of mortgage guarantee, tapping the intrinsic values of emission permits, energy efficiency improvement and other intangible assets, and developing innovative tools like emission permit mortgage loans, patent pledge loans and contract energy management financing. Secondly, it is necessary to promote the green insurance business, and comprehensively popularize the compulsory liability insurance system for environmental pollution. Meanwhile, developing other innovative types of green

http://www.aloki.hu ● ISSN 1589 1623 (Print) ● ISSN 1785 0037 (Online)
DOI: http://dx.doi.org/10.15666/aeer/1705_1224512258

insurance is also necessary, such as green auto insurance and green construction insurance, so as to reflect the support for green industries through insurance mechanism. Thirdly, it is necessary to develop a green capital market dominated by green stocks, bonds and funds to form a green financial market structure with diversified participants and financial products. Finally, carbon finance should be developed vigorously. At the end of 2017, the construction of national carbon emissions trading market formally began. Expected to be formally completed in 2020, the market will effectively slow down the growth of China's carbon emissions and bring a new impetus to the sustainable development of China's economy.

Table 5. *Comparison of foreign green finance policy*

America	
Main banks involved	Export-Import Bank of Washington HSBC Citibank
Policy	OECD public method Pollution Prevention and Control measures Environment Credit and Ethical Investment Guiding Principle Equator Principle *IFC Environment and Social Risk Standards*
Core system	Environment assessment procedures and guidelines Environment credit and ethical investment Environment and social risk management mechanism
Advantages	*Guidelines* consistent with *Common Method* Environmental protection should begin with ourselves Expand the concept of environmental protection and affect the market and client International organization authentication Forest protection EPS initiator, core, and leadership role
Germany	
Main banks involved	Dresdner Bank HVB KFW
Policy	Equator Principle Environment, Health and Security Guide Circular Economy and Waste Management Act
Core system	Discount allowance Interest subsidy loan
Advantages	Government participation in the development and design of green credit products Low-interest rate loan accessible to small and medium-sized companies Approval of environmental protection sectors Add new tax categories
Japan	
Main banks involved	JBIC DJB Mizuho Bank
Policy	International finance business instructions Overseas economic cooperation business instructions EEG Equator Principle
Core system	New environment social guiding principle Environmental protection grading loan project
Advantages	Seven basic principles in environment and society Equal attention to reward and punishment Full-process comprehensive governance Guide business banks, and financial institutions to develop green credit business

http://www.aloki.hu ● ISSN 1589 1623 (Print) ● ISSN 1785 0037 (Online)
DOI: http://dx.doi.org/10.15666/aeer/1705_1224512258

Conclusions

In this paper, the history and status quo of China's green finance development are combed first. On this basis, robust regression is employed to evaluate the effectiveness of the "carbon emissions trading pilot policies". The following conclusions are drawn:

China's green finance has undergone three stages of development. With the establishment of the top-level green finance framework system in 2016, China has become the first nation in the world to set up a relatively complete green finance policy system. At the macro level, China's support for environmental protection has been strengthened, and the funds used for emission reduction are growing by years in the public fiscal expenditure. At the micro level, the green credit, green bonds and environmental insurance have shown year-over-year growth.

According to the results of empirical analysis, the CO_2 emissions in various regions of China are on the rise, but the emission intensity is declining, suggesting China's certain achievements in the environmental governance. All the pilot provinces and cities that have adopted the carbon emissions permit policy are economically developed regions of China. They exhibit lower carbon intensity on average as compared to the non-pilot areas, and the green finance pilot policy is effective in significantly reducing carbon emissions. Similarly, the increases in foreign direct investment and technological progress have both contributed to lowering the carbon intensity, while the elevated level of economic development has aggravated the environmental pollution. These conclusions have an explanatory role in answering the issues faced by China's green finance policies. On this basis, we put forward two suggestions: establishing a green finance policy guarantee mechanism and improving the market operation mechanism.

Based on robust regression model, the paper analyzes and assesses the validity of "carbon emission permit trading experimental unit policy". Though some periodical results have been reached, some problems still deserve further research. The first one is data accessibility. As the paper does not collect any data about the application of green credit in specific projects, it does not show the preference of green finance policy to specific industries in China. The second one is about the choice of independent variable in regression analysis model. Because of data accessibility, the paper expresses it with some alternative variables. This lowers the persuasiveness of conclusion. Targeted at these problems, future studies should compare the green finance practice in other countries and make long-term tracking of related statistics in Chinese green finance business to raise useful policy suggestions in favor of the development of green finance in China.

Acknowledgements. The authors are grateful for the financial support provided by Zhongshan science and Technology Bureau (2016B2154), University of Electronic Science and Technology of China, Zhongshan Institute Scientific Research Starting Foundation for PHD (26-415YKQ12) and Educational Reform Project (23-JY201616).

REFERENCES

[1] Brennan, M. J., Schwartz, E. S. (1985): Evaluating natural resource investments. – Journal of Business 58(2): 135-157.

[2] Chami, R., Cosimano, T. F., Fullenkamp, C. (2002): Managing ethical risk: How investing in ethics adds value. – Journal of Banking & Finance 26(9): 1697-1718.

http://www.aloki.hu ● ISSN 1589 1623 (Print) ● ISSN 1785 0037 (Online)
DOI: http://dx.doi.org/10.15666/aeer/1705_1224512258

[3] Cleene, S., Wood, C. (2004): Sustainability banking in Africa. – African Institute of Corporate Citizenship: 18-20.
[4] Climent, F., Soriano, P. (2011): Green and good? The investment performance of US environmental mutual funds. – Journal of Business Ethics 103(2): 275-287.
[5] Cortazar, G., Schwartz, E. S., Salinas, M. (1998): Evaluating environmental investments: A Real Options Approach. – Management Science 44(44): 1059-1070.
[6] Cowan, E. (1999): Topical Issues In Environmental Finance. – Research Paper Was Commissioned by the Asia Branch of the Canadian International Development Agency(CIDA) 1: 1-20
[7] Gelema, R., Lensink, R., Spierdijk, L. (2011): International diversification and Microfinance. – Journal of International Money & Finance 30(3): 507-515.
[8] Hoti, S., Mcaleer, M. (2004): An empirical assessment of country risk ratings and associated models. – Journal of Economic Surveys 18(4): 50.
[9] Labatt, S., White, R. R. (2002): Environmental Finance: A Guide to Environmental Risk Assessment and Financial Products. – Transplantation 66(8): 405-409.
[10] Liu, R., Wang, D., Zhang, L. (2018): Can green financial development promote regional ecological efficiency? A case study of China. – Natural Hazards: 1-17.
[11] Raberto, M., Ozel, B., Ponta, L. (2018): From financial instability to green finance: the role of banking and credit market regulation in the Eurace model. – Journal of Evolutionary Economics 1.
[12] Salazar, J. (1998): Environmental finance: linking two world. – A Workshop on Financial Innovations for Biodiversity Bratislava 1: 2-18.
[13] Scholtens, B. (2006): Finance as a Driver of Corporate Social Responsibility. – Journal of Business Ethics 68(1): 19-33.
[14] Street, P., Monaghan, P. (2001): Assessing the sustainability of bank service channels: The case of the Co-operative Bank. – Sustainable Banking: The Greening of Finance: 72-87.
[15] Thomas, S., Repetto, R., Dias, D. (2010): Integrated environmental and financial performance metrics for investment analysis and portfolio management. – Corporate Governance An International Review 15(3): 421-426.
[16] Volz, U. (2018): Fostering Green Finance for Sustainable Development in Asia. – Adbi Working Papers.
[17] Vyas, M. (2015): Green Finance and Sustainable Development. – Finance Forum.
[18] Wang, Y., Zhi, Q. (2016): The Role of Green Finance in Environmental Protection: Two Aspects of Market Mechanism and Policies. – Energy Procedia 104: 311-316.

http://www.aloki.hu ● ISSN 1589 1623 (Print) ● ISSN 1785 0037 (Online)
DOI: http://dx.doi.org/10.15666/aeer/1705_1224512258

IDENTIFICATION OF DROUGHT-FLOOD ABRUPT ALTERNATION IN TOBACCO GROWTH PERIOD IN XINGREN COUNTY UNDER CLIMATE CHANGE IN CHINA

ZHANG, Z. Z.[1] – YUAN, Y. J.[1*] – SHEN, D. F.[2] – FAN, H.[1]

[1]*School of water conservancy engineering, North China University of Water Resources and Electric Power, Zhengzhou 450046, China*

[2]*Guizhou Water Conservancy Research Institute, Guiyang 550002, China*

[*]*Corresponding author*
e-mail: 534012813@qq.com

(Received 3rd May 2019; accepted 11th Jul 2019)

Abstract. Climate change causes drought and rainstorm, two extreme hydrological events, to occur interlock, and in a short period of time the rapid transformation of drought and flood disasters, resulting in more difficult rescue and relief, agricultural losses more serious. In order to study the characteristics of drought and flood in tobacco growing period in Xingren County. By defining the Long-cycle Drought-Flood Abrupt Alternation Index (LDFAI) and Short-cycle Drought-Flood Abrupt Alternation Index (SDFAI), the moving average method and precipitation anomaly are used. For the daily precipitation data during the tobacco growth period (5~8 months) from 1961 to 2012 in Xingren County, A comprehensive analysis of the (LDFAI SDFAI) change trends and monthly precipitation changes during the growth period of tobacco. The characteristics of rapid change of drought and flood in tobacco growing period were identified. The results showed that: the LDFAI in the tobacco growth period are mainly from drought to flood. In the future, there will be an increasing trend from flood to drought, and the strength is reduced; The trend of SDFAI is: increase-decrease-decrease; there is an increasing trend from drought to flood events in May-June; June-July is a period of drought-flood abrupt alternation, and the intensity is higher. In July-August, the flood to drought event has a decreasing trend and the intensity is reduced. During the tobacco maturity period, Monthly average precipitation is higher, the precipitation fluctuates greatly, Extremely prone to Drought-Flood Abrupt Alternation. The research results can provide theoretical basis for the formulation of countermeasures for disaster prevention and mitigation in Xingren County in China.

Keywords: *climate change, drought-flood abrupt alternation, moving average method, precipitation anomaly method, tobacco growth period, Xingren County*

Introduction

The Fifth Assessment Report of the Intergovernmental Panel on Climate Change (IPCC, 2013) points out that global warming has become an indisputable fact. Affected by climate change, extreme hydrological events present with the special complex phenomenon of flood and drought. Xingren County experienced the worst drought in 100 years in 2010. It lasted from August of the previous year to April. It lasted for 9 months and the soil moisture was extremely poor, which seriously affected tobacco seedlings and transplanting. The drought-flood abrupt alternation is a meteorological and hydrological event in which there is no rainfall or less rainfall in the early period, followed by high intensity rainfall and flood disaster in the short term, with the superimposed losses of drought and flood disasters in the region (Huang, 2015). Climate change causes two extreme hydrological events, drought and floods, which occur alternately and change rapidly in a short period of time to form a drought-flood disaster, which makes it more difficult to rescue and causes more serious losses on

http://www.aloki.hu ● ISSN 1589 1623 (Print) ● ISSN 1785 0037 (Online)
DOI: http://dx.doi.org/10.15666/aeer/1705_1225912269

social economy and the people's production and life. It has a significant and far-reaching impact on agricultural production and food security, water resources security, and ecological environment security (Niu et al., 2013). In 2010, drought and drought caused a loss of 50,000 tons of Xingren Tobacco and an economic loss of 60 million yuanRMB.

At present, foreign scholars mainly focus on the extreme hydrological events. Vogel (1978) studied the climate causes of abnormal precipitation in St. Louis; Ting et al. (1997) studied the variation of summer precipitation in the United States and its relationship with the Pacific SST. Domestic studies mainly focus on the causes for the change between drought and flood (Li et al., 2014), the analysis of the law on the drought-flood abrupt alternation (Shen et al., 2012; Sun et al., 2012) and the impact of the drought-flood abrupt alternation on rice and peanut yield in the Yangtze River Basin (Yuan et al., 2008; Zhou et al., 2012). However, there are few reports on the drought-flood abrupt alternation in a short time scale and the disaster caused by the drought-flood abrupt alternation in tobacco growth period. Drought seriously affects the growth and development of flue-cured tobacco and the accumulation of dry matter. Excessive soil moisture is not conducive to tobacco growth and reduces the biomass of tobacco plants. In fact, Xingren County is one of the main tobacco growth areas in China, and also one of the prone areas to drought and flood disasters. Drought and flood disasters mainly occur in May to August, which has a greater impact on tobacco planting.

In view of this, according to the daily precipitation data from May to August at the meteorological station in Xingren County from 1961 to 2012, this study uses the precipitation anomaly percentage, the long-period drought-flood abrupt alternation index and the short-period drought-flood abrupt alternation index to systematically analyze the evolution characteristics of drought-flood abrupt alternation time in the tobacco growth period in this area, so as to provide reference for tobacco cultivation, flood control and drought relief.

Xingren County is located in QianXiNa buyi and miao minority autonomous prefecture is located in east longitude 104°54' - 105°34', north latitude 25°16' to 25°47' in Guizhou, China, *Figure 1*.

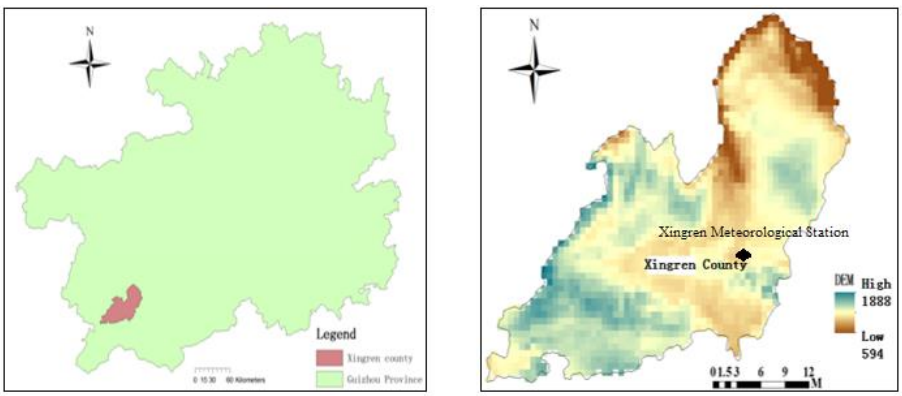

Figure 1. *Overview of the research area*

It is a low-latitude plateau temperate and humid monsoon climate region in mid-subtropical zone. There is no severe cold in winter and no intense heat in summer. The frost-free period is longer, the rain and heat is in the same season, the annual average

http://www.aloki.hu ● ISSN 1589 1623 (Print) ● ISSN 1785 0037 (Online)
DOI: http://dx.doi.org/10.15666/aeer/1705_1225912269

temperature is 15.2ºC, the annual rainfall is 1,315.3 mm, and the annual accumulated temperature of 10.0 ℃ is 4,588.0 ℃. Superior light, heat, water and other climatic conditions make the county a suitable flue-cured tobacco growth areas. However, drought, hail, flood and other disasters seriously affect the yield and quality of flue-cured tobacco (Xiao and Cui, 2014).

Materials and methods

Data source

The data used in the analysis of drought-flood abrupt alternation events are the daily precipitation data of Xingren National Reference Meteorological Station from 1961 to 2012, which are provided by the National Meteorological Information Center in China. Xingren National Reference Meteorological Station is located in east longitude 105°11', north latitude 25°26'.

Research method

Precipitation anomaly percentage (Pa)

The precipitation anomaly percentage reflects the deviation degree of precipitation from the average state at a certain period of time, and its calculation formula is as follows (Guizhou Provincial Bureau of quality and Technology Supervision, 2015).

$$Pa = \frac{P - \overline{P}}{\overline{P}} \times 100\% \quad \text{(Eq.1)}$$

where, P precipitation for a certain period of time, *mm*; $\overline{P}$ annual mean precipitation at a certain period of time, *mm*.

For the classification of drought and flood grades, refer to the monthly scale classification standard in DB52/T1030-2015 *Drought Standard of Guizhou Province*, as shown in *Table 1*.

Table 1. *Classification of drought and flood grades by precipitation anomaly percentage (unit: %)*

Type of drought	Pa	Type of flood	Pa
Extraordinary	Pa≤-95	Light	40≤Pa<60
Severe	-95<Pa≤-80	Moderate	60≤Pa<80
Moderate	-80<Pa≤-60	Severe	80≤Pa<95
Light	-60<Pa≤-40	Extraordinary	95≤Pa
Normal	-40<Pa<40		

Long-period drought-flood abrupt alternation index in tobacco growth period

The time scale of drought-flood change is defined as two months, that's, drought in May-June and flood in July-August, which is called drought-flood, and vice versa. There is no standard definition for the drought-flood abrupt alternation index. This paper refers to the definition of the drought-flood abrupt alternation index proposed by Wu et al. (2006) on the Yangtze River Basin, and adjusts the weight coefficient.

http://www.aloki.hu ● ISSN 1589 1623 (Print) ● ISSN 1785 0037 (Online)
DOI: http://dx.doi.org/10.15666/aeer/1705_1225912269

a) Standardization of precipitation

$$R = \frac{P_i - \overline{P}}{\sqrt{\frac{1}{N}\sum_{i=1}^{N}(P_i - \overline{P})^2}} \quad \text{(Eq.2)}$$

where R- standardized precipitation; P_i- original value of precipitation, *mm; i=1, 2, 3, ..., N*; $\overline{P}$- Average precipitation, *mm; N*- The total number of samples.

b) *LDFAI*

$$LDFAI = (R_{78} - R_{56}) \times (|R_{56}| + |R_{78}|) \times 2^{-|R_{56}+R_{78}|} \quad \text{(Eq.3)}$$

where, R_{78}- Standardized precipitation from July to August; R_{56}- Standardized precipitation from May to June; R_{78}-R_{56}- The intensity of drought-flood abrupt alternation; $|R_j|+|R_i|$- Intensity term of drought-flood abrupt alternation; $2^{-|R_{56}+R_{78}|}$ is weight coefficient, which functions to increase the weight of drought-flood abrupt alternation events and reduce the weight of all-drought or total-flood event. The criteria for judging the drought-flood abrupt alternation are as follows: if *LDFAI* is great than 1, it's drought-flood event; if *LDFAI* is less than 1, it's the flood-drought event; if *LDFAI* is in the middle, it's normal; the absolute value of *LDFAI* reflects the intensity of the drought-flood abrupt alternation, the greater the absolute value is, the more serious the drought and flood rapid change event is (Shan et al., 2015).

Short-term drought-flood abrupt alternation index during the tobacco growth period

The calculation method of SDFAI is basically the same as that of LDFAI, with the formula is (Wu et al., 2006)

$$SDFAI = (R_j - R_i) \times (|R_i| + |R_j|) \times 3.2^{-|R_i+R_j|} \quad \text{(Eq.4)}$$

where R_j- Standardized precipitation in the *j*-th month; R_i- Standardized precipitation in the *i*-th month; R_j-R_i- The intensity of drought-flood abrupt alternation; $|R_j|+|R_i|$- The intensity item of drought-flood abrupt alternation; $3.2^{-|R_i+R_j|}$- Weight coefficient; j=i+1(i=5, 6, 7).

Non-uniformity of precipitation distribution

The non-uniformity of precipitation distribution is studied and analyzed by using the non-uniformity and coefficient of rainfall distribution. The formula is as follows:

$$C_V = \frac{\sigma}{\overline{P}} \quad \text{(Eq.5)}$$

$$\sigma = \sqrt{\frac{1}{N}\sum_{i=1}^{N}(P_i - \overline{P})^2} \quad \text{(Eq.6)}$$

http://www.aloki.hu ● ISSN 1589 1623 (Print) ● ISSN 1785 0037 (Online)
DOI: http://dx.doi.org/10.15666/aeer/1705_1225912269

where σ- Mean square error; $\overline{P}$- Average precipitation over the same period of years, *mm*; P_i- Rainfall in the *i*-th year, *mm*.

Results and analysis

Trend of long-term drought-flood abrupt alternation

Characteristics of typical long-term drought-flood abrupt alternation

According to the precipitation sequence during the tobacco growth period in Xingren County, the Pa value and LDFAI value from May to June and from July to August from 1961 to 2012 are calculated by the *Eq.1* to *Eq.3*. *Table 2* lists the years with the highest (lowest) LDFAI values from 1961 to 2012 and its Pa value from May to June and from July to August by the *Eq.1* to *Eq.3*.

Table 2. *Six highest (lowest) LDFAI values and its Pa value from 1961 to 2012*

Year	Highest (LDFAI)			Year	Lower (LDFAI)		
	LDFAI	May-June Pa/%	July-August Pa/%		LDFAI	May-June Pa/%	July-August Pa/%
1999	9.73	-40.84	67.40	1978	-3.14	43.92	-26.46
1986	8.12	-37.24	68.54	1972	-3.04	18.96	-59.52
1988	3.33	-46.93	27.60	1966	-1.94	21.76	-22.59
1970	3.00	-39.41	25.99	1974	-1.80	24.40	-20.17
2004	2.92	-39.07	25.51	1962	-1.54	16.05	-21.63
1961	1.96	-42.05	16.25	1994	-1.39	15.33	-20.52

It can be seen that in the years with higher *LDFAI*, the precipitation in from May to June is less (35%), and drought event occurs, and the precipitation from July to August is more (15%), and flood event occurs, so the drought-to-flood event is formed. From May to June in 1999, the precipitation generally decreased by 40.84%, belonging to light drought event, but from July to August in 1999, the precipitation generally increased by 67.40%, and moderate flood occurs, with *LDFAI* as high as 9.73, belonging to typical drought-flood event. In the years with lower *LDFAI*, the precipitation from May to June is more (15%), which belongs to flood event, and from July to August, the precipitation is less (20%), which leads to the drought event, so the flood-to-drought event occurs. The precipitation from May to June in 1978 is more (43.92%) and the light flood occurs; the precipitation from July to August is less (26.46%) and the drought occurs, with the *LDFAI* of -3.14, belonging to typical flood-to-drought event. Therefore, *LDFAI* can reflect the phenomenon of drought-flood abrupt alternation to a certain extent.

Interannual trend of long-term drought-flood abrupt alternation

Figure 2 depicts that interannual change of LDFAI from 1961 to 2012. It can be seen from the figure that most of LDFAIs are positive, indicating that the long-term drought-flood abrupt alternation in Xingren County is mainly drought-to-flood. LDFAI fluctuated more frequently from the end of 1960s to the end of 1970s, which indicates that there are more drought-flood abrupt alternations from the end of 1960s to the end of 1970s. LDFAI appeared two anomalously large in the early 1980s and the end of 1990s,

http://www.aloki.hu ● ISSN 1589 1623 (Print) ● ISSN 1785 0037 (Online)
DOI: http://dx.doi.org/10.15666/aeer/1705_1225912269

mainly due to two high intensity drought-to-flood events. According to the 3a moving average curve and 5a moving average curve, the occurrence frequency and intensity of the long-term drought-flood abrupt alternation events are decreasing.

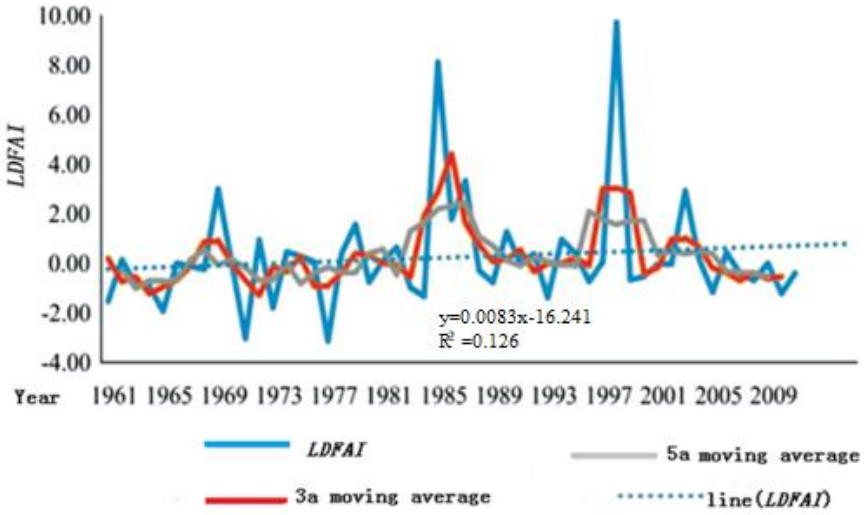

Figure 2. *Trend of the long-term drought-flood abrupt alternation in the tobacco growth period in Xingren County*

Trend of the short-term drought-flood abrupt alternation

Characteristics of typical short-term drought-flood abrupt alternation

According to the precipitation sequence during the tobacco growth period in Xingren County, the short-period drought-flood abrupt alternation index in the tobacco growth period from 1961 to 2012 is calculated by the *Eq.4* to *Eq.6*. *Tables 3, 4 and 5* show *SDFAI* and its *Pa* values of the typical drought-flood abrupt alternation years from 1961 to 2012.

Table 3. *SDFAI and characteristics of drought-flood from May to June in Xingren County*

Year	May Pa/%	June Pa/%	SDFAI	Type
1979	-42.51	55.95	3.66	Light drought to light flood
1980	43.12	-46.29	-4.10	Light flood to light drought
1991	-74.88	41.74	3.86	Moderate drought to light flood
2007	-51.48	60.33	5.26	Light drought to light flood
2008	132.14	-45.31	-1.96	Extraordinary flood to light drought
2011	-73.16	49.36	5.72	Moderate drought to light flood

Table 4. *SDFAI and characteristics of drought-flood from June to July in Xingren County*

Year	June Pa/%	July Pa/%	SDFAI	Type
1965	58.94	-39.84	-4.75	Light flood to light drought
1970	-51.57	74.17	6.40	Light drought to moderate flood
1980	-46.29	44.61	1.80	Light drought to light flood
1999	-68.08	86.77	8.44	Moderate drought to serious flood
2004	-43.70	51.29	2.49	Light drought to light flood
2011	49.36	-63.01	-5.97	Light flood to moderate drought

http://www.aloki.hu ● ISSN 1589 1623 (Print) ● ISSN 1785 0037 (Online)
DOI: http://dx.doi.org/10.15666/aeer/1705_1225912269

Table 5. *SDFAI and characteristics of drought-flood from July to August in Xingren County*

Year	July Pa/%	August Pa/%	SDFAI	Type
1965	-39.84	50.18	2.92	Light drought to light flood
1977	80.18	-48.13	-3.54	Serious flood to light drought
1988	-40.97	110.08	1.84	Light drought to extraordinary flood
1997	69.66	-46.07	-3.57	Moderate flood to light drought
2002	-54.83	65.70	5.12	Light drought to moderate flood

The comparison shows that SDFAI is mainly positive from May to June, mainly from light and moderate drought to light flood, with the only event from extraordinary flood to light drought in 2008. SDFAI is higher from May to June, which indicates that the intensity of drought-flood abrupt alternation events is higher in this period and the period when drought-flood abrupt alternation events are prone to occur. From July to August, SDFAI is low, which indicates that the intensity of drought-flood abrupt alternation events is decreased and the number of drought-flood abrupt alternation events is decreased. From May to June of 1980, the light flood to light drought occurred, but from June to July of 1980, the light drought to light flood occurred again, the drought and flood occurred frequently in a year, and it is the tobacco flourishing period (Qiu et al., 2013), so we should guard against the adverse effects brought by the drought-flood abrupt alternation.

Interannual trend of short-term drought-flood abrupt alternation

Figure 3 depicts the interannual change of SDFAI from 1961 to 2012. Through the analysis, we can conclude that the short-term drought-flood abrupt alternation has the following characteristics in the tobacco growth period.

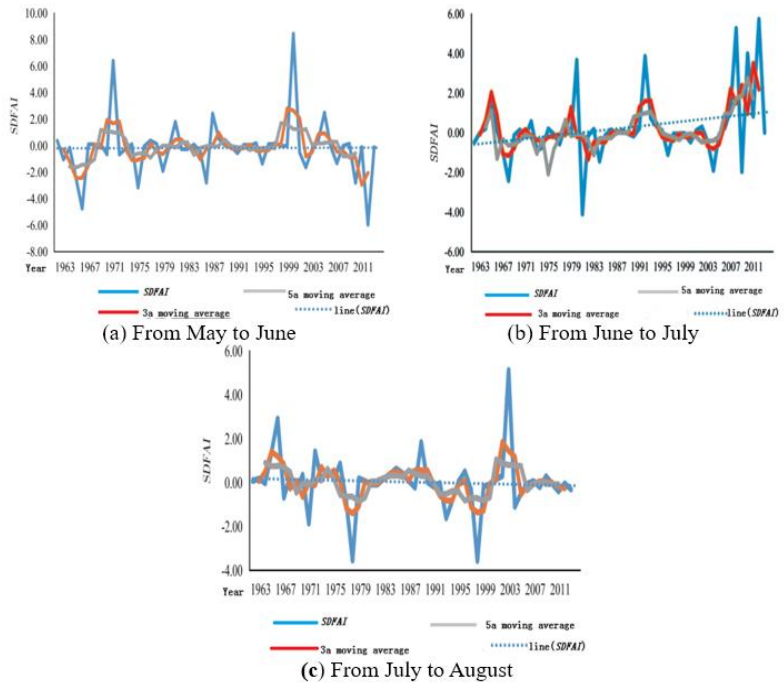

(a) From May to June (b) From June to July

(c) From July to August

Figure 3. *Trend of the short-term drought-flood abrupt alternation in the tobacco growth period in Xingren County*

http://www.aloki.hu ● ISSN 1589 1623 (Print) ● ISSN 1785 0037 (Online)
DOI: http://dx.doi.org/10.15666/aeer/1705_1225912269

a) From May to June mainly occurs the drought-to-flood; SDFAI oscillated frequently and violently after the 21st century. The drought-to-flood events with higher intensity mainly occurred after the 21st century, the flood-to-drought events with higher intensity mainly occurred before 1980s, and only two drought-to-flood events with higher intensity occurred after 1980s. From 3a moving average curve, 5a moving average curve and SDFAI trend curve, it can be seen that the drought-to-flood events have an increasing trend, which is obvious.

b) From June to July mainly occurs the flood-to-drought; SDFAI oscillated frequently from the beginning of 1960s to the beginning of 1980s. The drought-to-flood events with higher intensity mainly occurred after 1990s, and only one drought-to-flood event with higher intensity occurred in 1960s. From 3a moving average curve, 5a moving average curve and SDFAI trend curve, it can be seen that the flood-to-drought events have a slight increasing trend.

c) From July to August mainly occurs the flood-to-drought; SDFAI oscillated frequently from the beginning of 1960s to the beginning of 1980s. The drought-to-flood events with higher intensity mainly occurred after 1990s and only one drought-to-flood event with higher intensity occurred in 2002 after entering the 21st century, without any drought-to-flood event event afterwards. From 3a moving average curve, 5a moving average curve and SDFAI trend curve, it can be seen that the flood-to-drought events have a slight increasing trend.

Changes of monthly precipitation during tobacco growth period

The maximum, minimum, average and non-uniform coefficient of monthly precipitation distribution during the tobacco growth period from 1961 to 2012 in Xingren County are analyzed. The calculation results are shown in *Table 6*.

Table 6. *Statistics on monthly precipitation characteristic amount of 52a tobacco growth period in Xingren County*

Month	Maximum precipitation		Minimum precipitation		Monthly average precipitation in tobacco growth period	$C_{V,M}$	Annual extreme ratio of monthly rainfall
	Year	Precipitation (mm)	Year	Precipitation (mm)			
5	2008	390.9	2011	45.2	168.39	0.42	8.65
6	2006	480.4	1961	81.4	274.44	0.37	5.90
7	1987	474.3	1972	57.1	239.54	0.46	8.31
8	1988	418.4	2011	26.2	199.16	0.46	15.97

As can be seen from *Table 6*, the precipitation in Xingren County increased firstly and then decreased during tobacco growth period, among which the maximum precipitation, the minimum precipitation and the maximum of monthly average precipitation are all in June, indicating that the precipitation in June is more and June is prone to flood disasters; the annual extreme value ratio of monthly precipitation is also smaller in June, and the value of $C_{V,M}$ is also smaller in June,, indicating that the monthly precipitation fluctuation is small. The value of $C_{V,M}$ is larger in August and the annual extreme value ratio of monthly precipitation is the largest in August, which indicates that precipitation fluctuates greatly in this period and drought-flood abrupt alternation events are easy to occur.

http://www.aloki.hu ● ISSN 1589 1623 (Print) ● ISSN 1785 0037 (Online)
DOI: http://dx.doi.org/10.15666/aeer/1705_1225912269

Discussion

The growth period of spring tobacco in the field is from May to August, including root elongation period (30-35 d), flourishing period (30 d) and mature period (60-65 d) (Tang, 2011). In the growth period of spring tobacco in the field, the precipitation is suitable in the range of 400 ~ 520 mm, the monthly average water requirement is about 100 mm at the elongation period, about 200 mm at the flourishing period is and about 100 mm at maturity period (Ran et al., 2010). In May, which is the elongation period, the monthly rainfall could meet the needs of tobacco growth, moderate water shortage could promote root development, and excessive water would lead to root necrosis. Due to the increasing trend of short-term drought-to-flood events, irrigation and drainage work should be done well to ensure the survival rate of tobacco seedlings. In June, when tobacco is flourishing, the monthly average rainfall can meet the demand of tobacco growth, and with small fluctuation of rainfall, drought and flood events are not easy to occur, but the drought-flood abrupt alternation events with high intensity are easy to occur in this stage, so the precautions are required. July to August is the maturity period of tobacco, the precipitation fluctuates greatly, and the monthly average rainfall is relatively large. The excessive rainfall may cause the tobacco leaves to be too thin to modulate, low nicotine content and the insipid aroma. The mature tobacco leaves should be picked in time according to the forecast situation of the meteorological department, with the efforts made in the drainage of tobacco fields to ensure the quality of tobacco leaves.

Mechanism of the drought-flood abrupt alternation

Xingren County belongs to the typical monsoon climate fragile area, and the monsoon change causes the uneven annual precipitation distribution. What's more, the local is of the karst landform, and with strong water permeability and poor water retention, so it's extremely easy to suffer from the drought. In addition, the abnormal atmospheric circulation over the Qinghai-Xizang Plateau results in the formation of cold and high-pressure air masses in the plateau, which block the warm and humid air flow from the Indian Ocean and the Bay of Bengal. However, it's not easy for the cold air from the north to reach the area and it's difficult for the cold and warm air flows to intersect to form precipitation. The water vapor producing strong precipitation mainly comes from the South China Sea and the Bay of Bengal in the northern Indian Ocean (Sun et al., 2017). In summer, the southwest monsoon intensifies, and the transported water vapor increases. When cold air intrudes, the cold and warm air flows converge, resulting in relatively strong precipitation, resulting in drought-flood abrupt alternation. Another factor that produces strong precipitation in a short period of time is that the topographic relief within the territory is large, and the topography is high in the west and low in the east; blocked by the topography, during the day, the foot of the mountain, receives less solar radiation, air heating is not as fast as the top of the mountain, leading to heat air on the mountain top, floating in the sky; the air at the foot of the mountain, is cold and the atmosphere is relatively stable. At night, the temperature at the top of the mountain drops faster than that at the foot of the mountain, and the air sinks after cooling, raising the warm and humid air at the foot of the mountain. As the air rises, the water vapor cools down continuously, resulting in heavy rainfall and a sharp drought-to-flood.

http://www.aloki.hu ● ISSN 1589 1623 (Print) ● ISSN 1785 0037 (Online)
DOI: http://dx.doi.org/10.15666/aeer/1705_1225912269

Conclusions

The main conclusions are as follows:

(a) During the tobacco growth period in Xingren County, the long-term drought-flood abrupt alternation is dominant, and the frequency of the l long-term drought-flood abrupt alternation events generally decreases. In the 21st century, the trend of flood-to-drought events increases and the intensity decreases.

(b) The evolution trend of short-term drought-to-flood events during the tobacco growth period in Xingren County is as follows: increase-decrease-decrease; and the increasing trend is obvious, which is identical with the change trend of short-term drought-to-flood events. From May to June, the drought-to-flood increases; from June to July, it's easy to suffer from the drought-to-flood rapid change, with the relatively high intensity, and then at the transition period of tobacco from flourishing to maturing period, excessive or insufficient water should be prevented from to avoid the decline in tobacco yield and quality; from July to August, the flood-to-drought has a increasing trend, with the increasing intensity, and it's the tobacco maturity period, it's necessary to prevent tobacco quality from deteriorating due to the drought-flood abrupt alternation.

(c) In the tobacco flourishing period, the monthly average precipitation is the most and the fluctuation of precipitation is the least, so the flood disaster is very easy to happen. In the tobacco maturity period, the monthly average precipitation is more and precipitation fluctuation is greater, so it's extremely prone to drought-flood abrupt alternation and we should take precautions.

Acknowledgements. This paper is funded by the Water Conservancy Research Project of Guizhou Provincial Water Resources Department (Grant No.: KT201705) and National Natural Science Foundation (Grant No.: 51779093).

REFERENCES

[1] Guizhou Provincial Bureau of quality and Technology Supervision (2015): Guizhou drought standard DB52/T1030-2015.

[2] Huang, R. (2015): Research on evolution and Countermeasures of drought-floods abrupt alternation events in Huaihe River basin. – China Institute of Water Resources & Hydropower Research, Beijing.

[3] IPCC. Climate Change (2013): The Physical Science Basis, Contribution of Working Group I to the Fifth Assessment Report of the Inter-governmental Panel on Climate Change. – Cambridge, United Kingdom and New York, NY, USA: Cambridge University Press, 2013.

[4] Li, X., Yuan, D. M., Yin, Z. C. Li, W. J., Xie, Z. (2014): Preliminary Analysis of Sudden Turn of Drought and Flood in the Middle and Lower Reaches of the Yang. – Climatic and Environmental Research 19(1): 41-50.

[5] Niu, J. L., He, Z. Y., Zhang, T. Y., Chen, X. Y. (2013): Impacts of Sudden Drought to Flood Change on Manufacture Livelihood and Ecology. – Resources and environment in the Yangtze River Basin 22(Z1): 108-115.

[6] Qiu, X. B., Yin, P. D., Chen, W., Ding, F. Z., Liang, G. L., Li, J. W., Pan, W. J. (2013): Effect of Climate Change on Transplanting Time of Flue-cured Tobacco in Zunyi County during 51 Years. – Chinese Tobacco Science 34(4): 36-41.

[7] Ran, F. F., Wang, H. T., Xun, Z. C., Wang, M., Hu, H. Y. (2010): Changes of climate and comprehensive evaluation of climate feasibility Under different transplanting dates in

http://www.aloki.hu ● ISSN 1589 1623 (Print) ● ISSN 1785 0037 (Online)
DOI: http://dx.doi.org/10.15666/aeer/1705_1225912269

Xuchang tobacco-growing areas. – Journal of Henan Agricultural University 44(2): 217-223.

[8] Shan, L. J., Zhang, L. P., Chen, X. C., Yang, W. (2015): Spatio-temporal Evolution characteristics of Drought-Flood abrupt alternation in the Middle and Lower reaches of the Yangtze River Basin. – Resources and Environment tin the Yangtze Basin 24(12): 2100-2107.

[9] Shen, B. Z., Zhang, S. X., Yang, H. W., Wang, K., Feng, G. L. (2012): Analysis of characteristics of a sharp turn from drought to flood in the middle and lower reaches of the Yangtze River in spring and summer in 2011. – Acta Physica Sinica 61(10): 530-540.

[10] Sun, P., Liu, C. L., Zhang, Q. (2012): Spatio-temporal variations of drought -flood abrupt alternation during main flood season in East River Basin. – Pearl River 33(5): 29-34.

[11] Sun, X. T., Li, Q. Q.,Wang, L. J. (2017): Characteristics of Long-Cycle Abrupt Drought-Flood Alternations in Southwest China and Anomalies of Atmospheric Circulation in Summer. – Chinese Journal of Atmospheric Sciences 41(6): 1332-1342.

[12] Tang, S. K. (2011): The environment of tobacco growth. – Yun Yunnan Science and Technology Publishing Press.

[13] Ting, M. F., Wang, H., Summertime, U. S. (1997): Precipitation variability and its relation to Pacific sea surface temperature. – Journal of Climate 10: 1853-1873.

[14] Vogel, J. L., Huff, F. A. (1978): Relation between St-Louis Urban Precipitation Anomaly and Synoptic Weather Factors. – Journal Of Applied Meteorology 17(8): 1141-1152.

[15] Wu, Z. W., Li, J. P., He, J. H., Jiang, Z. H. (2006): Large-Scale Atmospheric Circulation anomaly and long period drought and Flood in the Middle and Lower reaches of the Yangtze River in Summer. – Chinese Science Bulletin (14): 1717-1724.

[16] Xiao, W., Cui, T. (2014): Study on the Climate conditions of developing Flue-cured Tobacco planting in Xingren County, Guizhou Province. – Beijing Agriculture 198-200.

[17] Yuan, J., Jiang, X. H., Huang, J. Z., Zhang, E. Z. (2008): Effects of Fast Conversion from Drought to Waterlogging Stress on Physiological Characteristics of Rice in Jointing-booting Stage. – Water Conservancy Science and Technology and Economy 2008(4): 259-262.

[18] Zhou, X., Li, L., Shan, S. H. (2012): Effect of abrupt droughts-floods on physiology and biochemistry of different peanut varieties. – Chinese Journal of Oil Crop Sciences 34(1): 56-61.

http://www.aloki.hu ● ISSN 1589 1623 (Print) ● ISSN 1785 0037 (Online)
DOI: http://dx.doi.org/10.15666/aeer/1705_1225912269

ANALYSIS OF DROUGHT-FLOOD ABRUPT ALTERNATION OF TOBACCO BASED ON PRECIPITATION AND SOIL PONDING IN SIUWEN CHINA

ZHANG, Z. Z.[1] – YUAN, Y. J.[1*] – SHEN, D. F.[2] – FAN, H.[1]

[1]*School of water conservancy engineering, North China University of Water Resources and Electric Power, Zhengzhou 450046, China*

[2]*Guizhou Water Conservancy Research Institute, Guiyang 550002, China*

[*]*Corresponding author*
e-mail: 534012813@qq.com

(Received 3rd May 2019; accepted 11th Jul 2019)

Abstract. Drought-flood abrupt alternation disaster caused by climate change results in greater difficulty in disaster relief and more serious agricultural losses. In order to identify the characteristics of drought-flood abrupt alternation in the tobacco growth period and effectively prevent and reduce the drought-flood abrupt alternation disaster, the daily precipitation data in the tobacco growth period from 1951 to 2017 in Guiyang City are used and the data of soil moisture content in the Xiuwen country Irrigation Test Base of Guizhou Irrigation Test Center are adopted. By defining continuous days without available precipitation and the cumulative available precipitation during the flood period, the characteristics of drought-flood abrupt alternation in Guiyang are comprehensively analyzed. The results are as follows: (1) it can be verified by soil moisture content data that the law of drought-flood abrupt alternation in tobacco growth period can be accurately described based on continuous days without available precipitation and the cumulative available precipitation during the flood period. (2) In the tobacco growth period, there are two or more times of drought-flood abrupt alternation with low intensity. (3) In tobacco root extension period, there is no drought-flood abrupt alternation; during the flourishing growing period of tobacco, drought-flood abrupt alternation with low intensity prevails, and the intensity and frequency of drought-flood abrupt alternation increase; in tobacco mature period, the intensity of drought-flood abrupt alternation fluctuates greatly, and the intensity and frequency of drought-flood abrupt alternation increase. The research results can provide theoretical basis for the formulation of tobacco disaster prevention and mitigation countermeasures in Guiyang China.
Keywords: *climate change, drought-flood abrupt alternation disaster, continuous days without available precipitation, accumulative available precipitation during flood period, tobacco, Guiyang City*

Introduction

The IPCC's fifth assessment report points out that the global warming has been no longer in question (IPCC, 2013). Extreme climate events such as torrential rain, flood, high temperature and drought caused by climate change frequently occur in the world, which has attracted wide attention of scholars both at home and abroad (Mesmoudi et al., 2017; Nocera et al., 2017; Scafetta et al., 2017; Bello and Mamman, 2018; Kong, 2018; Magrini et al., 2018; Zhao et al., 2018; Uttam et al., 2018; Dittus et al., 2018).

Tobacco is an important economic crop in Guiyang. Guiyang has a long history of flue-cured tobacco planting, and the quality of tobacco leaves is better. In 2017, the city planted 13,700 hectares of flue-cured tobacco, and acquired 16,700 tons of flue-cured tobacco, with 36. 72% of fine tobacco and 96. 70% of medium tobacco. Tobacco industry is the dominant traditional industry in Guiyang and plays an important role in local economic construction. However, due to the influence of special karst landform and the continuous occurrence of Nino phenomenon (ElNino) in recent years, the spatial

http://www.aloki.hu ● ISSN 1589 1623 (Print) ● ISSN 1785 0037 (Online)
DOI: http://dx.doi.org/10.15666/aeer/1705_1227112286

and temporal distribution of precipitation in Guiyang tobacco area is uneven, drought and flood disasters occur frequently, which seriously threatens the output and quality of tobacco in Guiyang. Therefore, it is necessary to study the characteristics of drought-flood abrupt alternation in Guiyang tobacco area so as to provide scientific basis for disaster prevention and reduction.

Drought-flood abrupt alternation refers to the meteorological and hydrological events in which there is no precipitation or little precipitation in the early period and the drought has occurred, and then high-intensity precipitation and flood occurs in a short period (Huang, 2015). Many scholars in China have made in-depth study on drought-flood abrupt alternation from different points of view. Wu et al. (2006) first define a summer long-cycle drought-flood abrupt alteration index (LDFAI). On the basis of this, most of the scholars study the space-time evolvement law of drought-flood abrupt alternation in different areas (Shan et al., 2015; He et al., 2016; Liu et al., 2017; Peng et al., 2018). If LDFAI is used to study the law of drought-flood abrupt alternation in tobacco growth period, this only considers the difference of drought and flood in the early and late period and the time scale is too large. The drought-flood abrupt alternation degree can be evaluated only after the end of the whole growing period of tobacco, which is unable to meet the needs of real-time monitoring and early warning assessment. Based on LDFAI, the dry-wet abrupt alteration index (DWAAI) is constructed, which can well reflect the abrupt alternation degree. According to the theory, there is only one time of drought-flood abrupt alteration in a year, and the date of abrupt alteration is the day when the value of DWAAI is the highest. In fact, the tobacco growth period is also the season of frequent occurrence of drought and flood in Guiyang. Thus, DWAAI can't be used to study the evolvement law of drought-flood abrupt alternation in tobacco growth period because there may be two or more times of drought-flood abrupt alteration.

The analysis of drought in continuous days without precipitation from the point of view of daily precipitation can make drought monitoring and assessment more precise on time scale (Jiang et al., 2009; Wang et al., 2014; Gu, 2014; Shan et al., 2015), the application is more mature, and is determined as local standard in Gansu and Guizhou (Gansu provincial bureau of quality and technical supervision, 2011; Guizhou provincial bureau of quality and technology supervision, 2015). However, the index of continuous days without available precipitation is considered only in the sense of meteorology. In fact, precipitation can be used by crops only if it reaches a certain level, so the effectiveness of precipitation should be considered. Huang et al. (2014) improve continuous days without available precipitation, considering that the continuous days without available precipitation can integrate both precipitation and precipitation days, and indirectly reflect the income and expenditure of farmland precipitation and profit and loss of soil moisture. Flood disaster of crops is not only directly affected by excessive and concentrated precipitation, but also closely related to soil texture, light conditions, crop species and their developmental stages (Huo and Wang, 2009). Yang et al. (2017) put forward the concept of "equivalent precipitation" that represents the cumulative effect of precipitation in the early period and current process on flood. Based on this, the grade index of spring corn flood is constructed. In consideration of the cumulative effect of precipitation on flood process, Fan (2018) constructs the catastrophic index of oilseed rape flood process by taking the effective cumulative precipitation and the number of rainy days as the cause of flood disaster.

http://www.aloki.hu ● ISSN 1589 1623 (Print) ● ISSN 1785 0037 (Online)
DOI: http://dx.doi.org/10.15666/aeer/1705_1227112286

During the study of drought period of drought-flood abrupt alteration, continuous days without available precipitation are used as the drought index of tobacco in order to analyze the drought characteristics of tobacco in different growing periods from the daily dynamic perspective. The formation process of tobacco flood can be objectively and quantitatively characterized by the classification of flood grades by accumulative available precipitation in flood period. Based on this, this study explores the evolvement law of drought-flood abrupt alteration in tobacco growth period, which can provide scientific and technical support for timely and accurate evaluation of the impact of drought-flood abrupt alteration on tobacco growth and realize flood control, drought resistance, high and stable yield and evaluation of disaster reduction benefits of water conservancy projects.

Materials and methods

Data sources

The data are the daily precipitation data of Guiyang National Standard Meteorological Station from 1951 to 2017 provided by the National Meteorological Information Center, and soil moisture content data the No. 2 test pit of Xiuwen country Irrigation Test Base of Guizhou Irrigation Test Center in 2015 and 2016 in China.

Overview of the study area

Guiyang City, located in the east of Yunnan-Guizhou Plateau and the central part of Guizhou Province, is an important central city in southwest China in *Figure 1*.

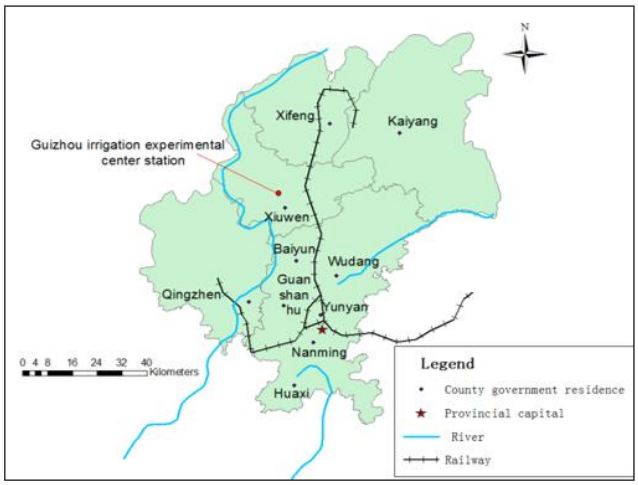

Figure 1. *Overview of the study area*

Guiyang city has a total area of 8,034 square kilometers and an area for tobacco cultivation, planted 13,700 hectares of flue-cured tobacco. With the altitude of around 1,100 m, it is located in the Federl circulation cell and is controlled by the westerlies all the year round. It belongs to the subtropical humid and mild climate with the annual average total precipitation of about 1,130 mm. The precipitation distribution is uneven. Rainwater is abundant in summer, accounting for about 70% of the annual precipitation, so that it is easy for drought-flood abrupt alteration to occur.

http://www.aloki.hu ● ISSN 1589 1623 (Print) ● ISSN 1785 0037 (Online)
DOI: http://dx.doi.org/10.15666/aeer/1705_1227112286

Calculation of accumulative available precipitation

Available precipitation refers to the part of total precipitation that can be preserved in the root layer of crops to meet the needs of crop evapotranspiration, excluding surface runoff and the part that leaks below the water-absorbing layer of crop roots. The main factors affecting available precipitation are precipitation intensity, soil texture and structure, topography and flatness, soil water content before precipitation, crop species and growing period (Guo et al., 2012). Available precipitation calculation formula for a certain precipitation (Xu, 2009) is:

$$P_{e\mathrm{i}} = \alpha_i P_i \quad \text{(Eq.1)}$$

where, P_i is total precipitation of i^{th} time of precipitation, *mm*; a_i is the available utilization coefficient. Considering the factors such as large terrain slope, barren land and unique karst landform in Guiyang, the values of a_i are as follows, by combination of the available utilization coefficient of precipitation studied by the scholars (Dastane, 1974; Liu et al., 2009): when $P_i \leq 5$ mm, $a_i=0$; when 5 mm$\leq P_i \leq$50 mm, $a_i=0.85$; when $P_i>50$ mm, $a_i=0.85$.

The accumulative available precipitation during the flood period P_E is equal to the sum of the multiple time of available precipitation during the flood period, and the calculation formula is as follows:

$$P_E = \sum_{i=1}^{n} P_{ei} \quad \text{(Eq.2)}$$

In general, tobacco has certain flood tolerance. Considering the different flood tolerance of tobacco in different growing periods and the different critical values of precipitation in effective process of different growing periods, this study classifies the flood standards of tobacco in different growing periods (Tang, 2011), in *Table 1*.

Table 1. *Classification of tobacco flood grade based on accumulative available precipitation*

Tobacco growth period	**Process effective precipitation critical value P_k (mm)**	**Grading**			
		Light flood	**Moderate flood**	**Severe flood**	**Extreme flood**
Root extension stage	25	≤40	40~55	55~70	>85
Grow prosperous stage	35	≤50	50~75	75~100	>125
pre-mature stage	25	≤45	40~65	65~85	>105
mature late stage	20	≤40	40~55	55~70	>85

Continuous days without available precipitation

Continuous days without available precipitation refer to the duration days when the precipitation is less than the available precipitation critical value in the crop growing season. This index combines the precipitation and the precipitation days, but the daily water requirement of the crops is basically close under the non-precipitation

http://www.aloki.hu ● ISSN 1589 1623 (Print) ● ISSN 1785 0037 (Online)
DOI: http://dx.doi.org/10.15666/aeer/1705_1227112286

meteorological conditions. Therefore, the index can indirectly reflect the income and expenditure of farmland precipitation and profit and loss of soil moisture. Combined with the law and actual situation of tobacco water demand in Guiyang (Cai et al., 2005; Cheng, 2006; Gao, 2006), the formula for calculating continuous days without available precipitation is as follows (Huang et al., 2014):

$$Dnp = \sum_{j=1}^{m} a \cdot Dnp_j \quad \text{(Eq.3)}$$

where, *Dnp* is number of continuous days without available precipitation, *d*; *a* is the adjustment coefficient of tobacco in different growing periods and the specific value is shown in *Table 2*. The calculation formula of Dnp_j is as follows:

$$Dnp_j = \begin{cases} 1 & P_{ei} \le P_0 \\ 0 & P_{ei} > P_0 \text{ and } P_n \le P_k \text{ or } P_{ei} > P_k \end{cases} \quad \text{(Eq.4)}$$

where, P_{ei} is the daily available precipitation, mm; P_0 is the critical value of daily available precipitation, mm; P_0 is 5 mm during the critical water demand period (flourishing growing period) of tobacco, and is 3 mm in the rest periods. P_n and P_k is the process accumulative precipitation, of which P_n refers to the accumulation of available precipitation process that can alleviate drought and reach the root layer of crops to be used by crops, mm; P_k is the critical value of available precipitation, mm. The meaning of *Eq. 4* is:

1) When $P_{ei} \le P_0$, that is, the daily precipitation is below the critical value of daily available precipitation, drought occurs or continues, and days without available precipitation are calculated, that is $Dnp_j=1$;

2) When $P_{ei} > P_0$ and $P_n < P_k$, that is, the daily precipitation forms available precipitation, but the process available precipitation is still insufficient to end the drought, the drought is interrupted but not alleviated and the drought continues after the precipitation process ends, and the drought days don't accumulate, $Dnp_j=0$;

3) When $P_{ei} \ge P_0$, that is, the accumulative precipitation of one effective precipitation process is greater than the critical value of the effective process precipitation, excessive precipitation will be lost in the form of surface runoff, and the drought will continue after the precipitation process ends, and the drought days don't accumulate, $Dnp_j=0$;

Application of Dnp to evaluate multiple drought processes in tobacco growth period

The tobacco growth period is in the season of frequent drought in Guiyang City, and sometimes there are two or more times of drought, so it is necessary to evaluate the accumulative process of drought in the whole growing period of tobacco. Perfect the *Eq. 3* (Huang et al., 2014):

$$Dnp = \sum_{i=1}^{n} a \times (\sum_{j=1}^{m} Dnp_{ji} - D_{pj}) \quad \text{(Eq.5)}$$

where, *Dnp* is the accumulative continuous days without available precipitation during *n* times of drought processes in the whole growing period of tobacco; Dnp_j is

http://www.aloki.hu ● ISSN 1589 1623 (Print) ● ISSN 1785 0037 (Online)
DOI: http://dx.doi.org/10.15666/aeer/1705_1227112286

continuous days without available precipitation in a single drought process, and the meaning is the same as *Eq. 4*; *n* is the time of drought in the whole growing period of tobacco; *m* is the number of day of j^{th} drought. The meaning and value of *a* are the same as *Eq. 3*; *Dpj* is the equivalent days of available precipitation in the process of relieving drought to reduce the drought in the later period of j^{th} drought in tobacco growth period; *j* is the time of drought. The calculation formula of *Dpj* is as follows:

$$Dpj = P_{nj} / 2P_0 \quad \text{(Eq.6)}$$

where, P_{nj} is accumulative available precipitation in the course of a drought mitigation when $P_n \geq P_k$, mm, the calculation process of P_{nj} is the same as *Eq. 2*. The result of the calculation of *Dpj* is taken as an integer. The meaning of P_0 is the same as *Eq. 4*. According to the previous calculation result of crop water demand (Tang, 2011), the daily water demand of tobacco ET_c is close to the critical value P_0 of available precipitation and can be approximately equal. Therefore, the meaning of the *Equations (5)-(6)* is that the drought can compensate for the drought in the later period of available precipitation. In the process of interrupting the drought, if the precipitation is excessive in a single day, the excessive precipitation will be lost in the form of surface runoff, and the drought can't be relieved.

According to previous research result of available precipitation and the characteristics of tobacco water demand in Guizhou (Tang, 2011), the specific P_k vales be included in the *Table 1*. The values of P_0, P_k and *a* are subdivided and adjust according to the tobacco growth period. P_0 is 4 mm in the root extension period and the pre-mature period, 5 mm in the flourishing growing period, and 3 mm in the pre-mature period. Please refer to the table for the specific values of P_k. *a* is 1.1 in the root extension stage and the post-mature period, 1.3 and 1.2 in the flourishing growing period and the pre-mature period respectively. The days without available precipitation in a single drought process is calculated according to *Eq. 3* and *Eq. 4*. When the continuous days without available precipitation reaches above 10*d*, it is determined as a drought process, and the specific classification is shown in *Table 2*.

Table 2. *Criteria for tobacco drought grades based on continuous days without available precipitation*

Drought grade	Normal	Light drought	Moderate drought	Severe drought	Extreme drought
continuous days without available precipitation	≤10	10~20	20~30	30~45	>45

According to the local agricultural production experience in Guizhou, the tobacco transplanting period is in the first ten-day period of May. Assuming that the transplanting is completed on May 10 and the soil moisture is sufficient, and the drought start date is counted from May 11; if the start day is rainy, the first rain-free day after the end of the precipitation process is taken as the drought start date; if the start day is a rain-free day, this day is the start day of the drought.

http://www.aloki.hu ● ISSN 1589 1623 (Print) ● ISSN 1785 0037 (Online)
DOI: http://dx.doi.org/10.15666/aeer/1705_1227112286

Results and analysis

Analysis on the evolvement law of drought-flood abrupt alternation during the tobacco growth period

In accordance with the daily precipitation data in Guiyang from May to August of 1951, the daily available precipitation P_{ei} is calculated by the *Eq. 1*, and the accumulative available precipitation in different periods is calculated by the *Eq. 2*. *Eqs. 3-6* are used to calculate continuous days without available precipitation to study evolvement process of drought-flood abrupt alternation during the tobacco growth period.

Figure 2 describes the evolvement law of drought-flood abrupt alternation during the tobacco growth period. In a short period of two weeks after tobacco transplanting, the accumulative available precipitation reaches more than 90 mm. At this time, it is tobacco root extension period when the daily average water demand is 3 mm, so serious flood disaster occurs at this period.

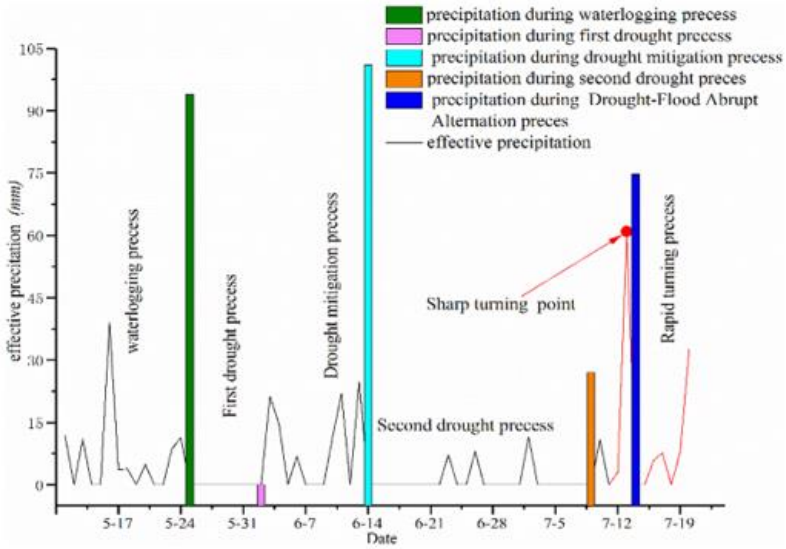

Figure 2. *Evolvement process of drought-flood abrupt alternation during the tobacco growth period*

During the next week, there is no available precipitation and belongs to light drought. In the following two weeks, the total available precipitation is as high as 100 mm. Because there is a light drought process in the early period, this precipitation can alleviate the drought in the early period. At this time, the tobacco is in the flourishing growing period and the daily average water demand is large, so there is no flood disaster. From June 14 to July 10, the accumulative available precipitation is less than 30 mm while it is the critical period of tobacco water demand and the daily average water demand is more than 5 mm. The water shortage will seriously affect the output and quality of tobacco. The *Dnp* value is calculated to be 28 days, belonging to moderate drought. From July 10 to July 13, in a short period of 3 days, the accumulative available precipitation is more than 70 mm, and drought-flood abrupt alternation occurs. The intensity turns from moderate drought to moderate flood, and the point of drought-flood abrupt alternation is on July 13.

http://www.aloki.hu ● ISSN 1589 1623 (Print) ● ISSN 1785 0037 (Online)
DOI: http://dx.doi.org/10.15666/aeer/1705_1227112286

In order to verify the feasibility of the research method, the soil moisture content and precipitation data of No. 2 test pit of Xiuwen Irrigation Test Base of Guizhou Irrigation Test Center from May 1 to August 31, 2016 are selected in this study. The variation law between precipitation and soil moisture content is studied and described in detail in *Figure 3*.

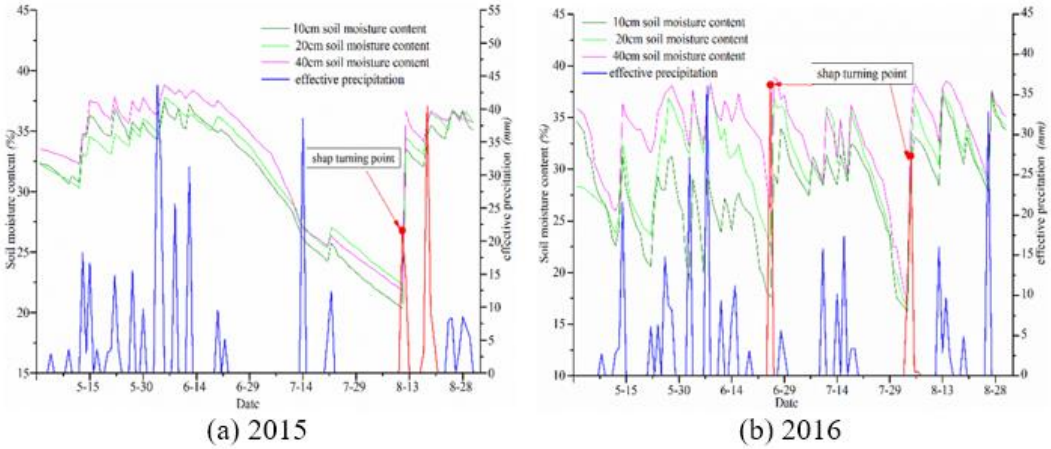

Figure 3. *Variation Law between Precipitation and Soil Moisture in the Irrigation Experimental Station of Xiuwen County in 2015 and 2016*

Li et al. (2007) hold that during the whole growing period of flue-cured tobacco, the soil moisture should be maintained at 60%-68%, 78.5%-81%, 76%-78% of the field water holding capacity during the root extension period, flourishing growth period and mature period, respectively, which is most beneficial to the growth and development of flue-cured tobacco. It can be seen from *Figure 3a* that during the root extension period of tobacco in 2015, 5 times of available precipitation are more than 10 mm and soil moisture content is more than 80% of the field water holding capacity. Han et al. (1992) hold that too high soil moisture is unfavorable for root development during the root extension period of tobacco and that total absorption area and active absorption area of root all decrease, so tobacco is subjected to flood stress at this period. In the flourishing growth period of tobacco, 3 times of available precipitation exceed 20 mm and the soil moisture content is more than 80% of the field water holding capacity. The soil moisture content at this time is beneficial to the growth and development of tobacco and the formation of output and quality because the flourishing growth period is critical for tobacco water demand. In the pre-mature period, there is a precipitation of more than 35 mm. Guiyang City belongs to typical karst landform, the surface water leakage is serious, and the temperature is high, the evaporation is vigorous, so the drought has not been alleviated. In a short week from August 13 to August 17, the total available precipitation is nearly 70 mm and the soil moisture content increases from 50% to 80% of the field water holding capacity. Drought-flood abrupt alternation occurs, and the point of drought-flood abrupt alternation occurs on August 13. According to the calculation, in the drought period of this year, continuous days without available precipitation are as long as 52 days, which belongs to Extraordinary drought. The accumulative available precipitation in the drought period is only 48 mm, which belongs to the transition from Extraordinary drought to moderate flood. Therefore, it is feasible to identify the drought-flood abrupt alternation in tobacco growth period based

http://www.aloki.hu ● ISSN 1589 1623 (Print) ● ISSN 1785 0037 (Online)
DOI: http://dx.doi.org/10.15666/aeer/1705_1227112286

on continuous days without available precipitation and accumulative available precipitation during flood period.

In the tobacco growth period, Guizhou is prone to have droughts and floods, therefore, there may be more than two drought-flood abrupt alternations. According to *Figure 3b*, it can be found that two drought-flood abrupt alternations occurred in 2016, and the abrupt turning point of drought and flood occurred on June 26 and August 2, respectively. The first drought-flood abrupt alternation occurred in the flourishing growing period of tobacco, the number oconsecutive non-effective precipitation days reached 32 days, belonging to heavy drought, the accumulative effective precipitation reached 45 mm in flood period, belonging to middle flood, with the intensity of abrupt alternation from heavy drought to moderate flood. However, it can be seen from the figure that before and after June 26, the soil moisture content rises from 40% to 90% of the field water holding capacity, which is a severe drought-flood abrupt alternation. There is some error in the intensity discrimination, but it can accurately judge the occurrence time of the drought-flood abrupt alternation. The second drought-flood abrupt alternation occurred in the late stage of tobacco maturity, with 35 consecutive days of non-effective precipitation during the drought period, belonging to heavy drought, and the accumulative effective precipitation in the flood period reached 35 mm, belonging to light flood, with the intensity of abrupt alteration from heavy drought to light flood. Before and after August 2, the soil moisture content increased from 40% to 90% of field capacity, belonging to the severe drought-flood abrupt alternation. In the drought period, the number of the continuous non-effective precipitation days in the first drought-flood abrupt alternation is almost the same as the cumulative effective precipitation in the flood period. Therefore, in the whole tobacco growth period, it is possible to have many drought-flood abrupt alternations, but the intensity of drought-flood abrupt alternation will not be too high.

Characteristics of drought-flood abrupt alternation in typical years

The number of days of non-effective precipitation and the accumulative effective precipitation in the flood period during the whole growing period of tobacco in Guiyang from 1951 to 2017 are counted and screened year by year, with the specific screening results shown in *Table 3*.

Table 3. *characteristics of Drought-Flood Abrupt Alternation in typical years of tobacco growth in Guiyang*

Year	Continuous days without available precipitation (d)	Cumulative effective precipitation during waterlogging (mm)	Sharp turning degree	Sharp turning point
1957	18	93	Light drought turn Severe flood	June 14th
	16	158	Light drought turn Extreme flood	July 28th
	40	50.49	Severe drought turn Light flood	July 6th
1958	18	43.03	Light drought turn Light flood	August 3rd
	14	82.62	Light drought turn Moderate flood	August 23th
1970	47	228.75	Extreme drought turn Extreme flood	July 11th
1975	72	100.98	Extreme drought turn Severe flood	August 9th
1988	48	171.02	Extreme drought turn Extreme flood	August 22th
1991	51	363.72	Extreme drought turn Extreme flood	July 9th
2010	52	76.58	Extreme drought turn Moderate flood	August 24th
2016	42	54.91	Severe drought turn Light flood	August 4th

http://www.aloki.hu ● ISSN 1589 1623 (Print) ● ISSN 1785 0037 (Online)
DOI: http://dx.doi.org/10.15666/aeer/1705_1227112286

It can be seen from *Table 3* that in the years with severe drought, the number of consecutive non-effective precipitation days is more than 45 days, and the number of consecutive non-effective precipitation days in 1972 is as high as 72 days, from May 28 to August 9, when is flourishing growing period and pre-mature period of tobacco, with the accumulative effective precipitation less than 100 mm, which results in extraordinary drought events, and then within the following 3 days, the accumulative effective precipitation is as high as 100 mm, resulting in heavy flood disaster. In 1957, two drought-flood abrupt alternation occurred, and the abrupt alternation was relatively low. Because of the low intensity of drought in the early period and the high level of flood in the later period, we should focus on preventing the adverse effects of flood in the later period. In the 1970s, two high-intensity drought-flood abrupt alternation occurred, and due to the severe drought in the early period, we did not forget the late flood prevention work while doing the early drought relief work. In the 21st century, the drought degree in the drought period is still serious, and the cumulative effective precipitation in the flood period has been reduced, so we should focus on addressing drought in the early period, especially in the flourishing growing period, when there may be summer drought.

The trend of drought-flood abrupt alternation in different growing periods of tobacco

Figure 4 shows the trend of drought-flood abrupt alternation in different growing periods of tobacco. (Since the root extension period of tobacco is dominated by waterlogging, and only 4 times of drought-flood abrupt alternation occur, it will not be described here).

Nearly 20 drought-flood abrupt alternations in different degrees occur during the flourishing growing period of tobacco. The duration of drought varies from 20 to 30 days, which is due to excessive cumulative effective precipitation in the root extension period of tobacco, which compensates for the later drought. The cumulative effective precipitation during the flood period is mostly concentrated in 50~100 mm, and the intensity of abrupt alternation is mostly from moderate drought to moderate flood. As can be seen from the change trend curve, during this growing period, the duration of drought increases significantly, and the cumulative effective precipitation in the flood period shows a significant decreasing trend, indicating that the intensity of abrupt alternation is lightening and the drought is increased in the future, when is the critical period of tobacco water demand. Severe drought would make leaves lose water seriously, and the water in the lower leaves is transferred to the upper leaves excessively, causing the lower leaves to wither and form "dry drying". Therefore, the adverse effects of summer drought on tobacco growing should be prevented emphatically.

There are about 25 drought-flood abrupt alternations with varying degree in the pre-mature period of tobacco. The duration of drought fluctuates greatly, because if the accumulative effective precipitation is too much in the flourishing growing period of tobacco, it can compensate for relieving the drought in the later period, and if the tobacco suffers from summer drought in the flourishing growing period, which may aggravate the drought in the later period. The cumulative effective precipitation in flood period is mostly concentrated in the range of 50~150 mm, and the intensity of abrupt alternation is mostly from heavy drought to heavy flood.

It can be seen from the trend curve that during the growing period of tobacco, the duration of drought has a significant increasing trend, and the cumulative effective precipitation during the flood period has an increasing trend, which indicates an

http://www.aloki.hu ● ISSN 1589 1623 (Print) ● ISSN 1785 0037 (Online)
DOI: http://dx.doi.org/10.15666/aeer/1705_1227112286

increasing trend in the intensity of abrupt alternation in the future. If the tobacco field waterlogging time is too long, resulting in the root oxygen deficiency, it's easy to form "water drying". Therefore, while doing a good job in drought relief, we should pay attention to preventing the adverse effects caused by the drought-flood abrupt alternation.

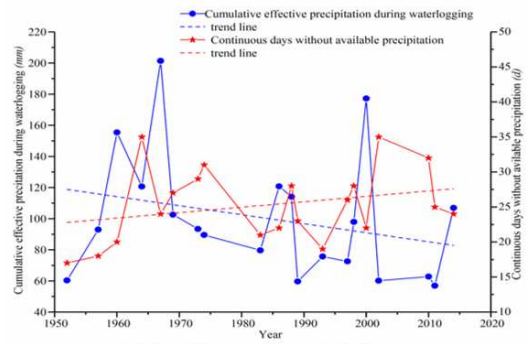

(a) Flourishing growing period of tobacco

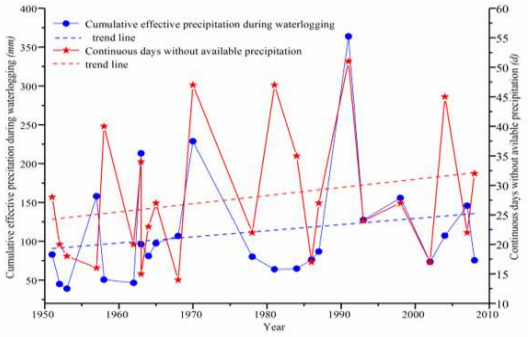

(b) Pre-mature period of tobacco

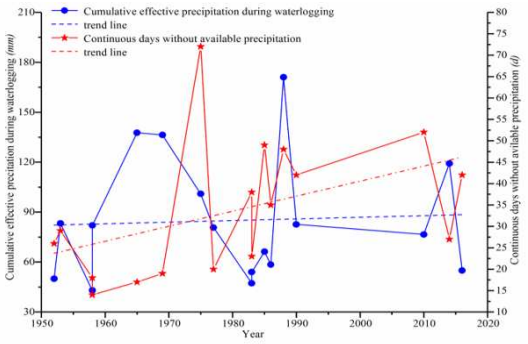

(c) Post-mature period of tobacco

Figure 4. *Trend of drought-flood abrupt alternation in different growing periods of tobacco*

In the post-mature period of tobacco, there are 15 drought-flood abrupt alternations in different degrees. Before 1970s, the drought lasted about 20 days in the drought period, and after 1980s, the drought lasted about 40 days in the drought period. The cumulative effective precipitation during the flood period is mostly concentrated in 50~100 mm, and the intensity of abrupt alternation is mostly from heavy drought to moderate flood. According to the changing trend curve, during the growing period, the duration of drought is obviously rising, and the accumulative effective precipitation in flood period is increasing, which indicates that there is an increasing trend in the

http://www.aloki.hu ● ISSN 1589 1623 (Print) ● ISSN 1785 0037 (Online)
DOI: http://dx.doi.org/10.15666/aeer/1705_1227112286

intensity of drought-flood abrupt alternation in the future, and then there is less water demand for tobacco. If the precipitation is too much, the temperature will decrease, the sunshine will weaken, the accumulation of organic matter in the tobacco leaves will decrease, the air humidity will increase, and diseases and pests will easily occur under high temperature. It is important to prevent the adverse effects of flood on tobacco yield and quality.

Discussion

Guiyang is a typical monsoon climate fragile area, and is extremely prone to drought-flood abrupt alternation because of the monsoon changes, atmospheric circulation anomalies and local unique geographical factors such as geomorphology. The water vapor of heavy rainfall mainly comes from the South China Sea and the Bay of Bengal in the northern Indian Ocean. In the early March-April of the years with drought-flood abrupt alternation, the intensity of the Bay of Bengal monsoon, the East Asian monsoon, the Indian Ocean monsoon and the South China Sea monsoon is all remarkably weak, and the water vapor transport is insufficient, so it is easy to form drought. In summer, the southwest monsoon strengthens and the water vapor transported increases. When the cold air invades, the cold and warm air flow intersects, which is easy to form strong precipitation and cause the drought-flood abrupt alternation. Sun et al. (2017) analyzed the characteristics of atmospheric circulation anomalies, and found that in the early period of the years with drought-flood abrupt alternation, the western Pacific subtropical high is westward strong, the zonal motion of mid-latitude and high-latitude circulation is strong, the upper weaterlies are strong, and the cold air cannot move southward, which is not conducive to precipitation. In the later period, the meridional motion of the mid-latitude and high-latitude circulation is enhanced, the trough beyond the east of Ural Mountains is deepened, the East Asian coastal ridge is strengthened, and the water vapor from southeast and southwest directions is transported to southwest China, resulting in more precipitation in southwest China and the drought-flood abrupt alternation. The terrain in the territory is undulating and blocked by the terrain, the mountain is less exposed to solar radiation in the days, and the air is not as hot as the top of the mountain, causing the air on the top of the mountain to be hot and floating in the sky. The air at the foot of the mountain is cold, and the atmosphere below is relatively stable. In the evening, the temperature at the top of the mountain drops faster than that at the foot of the mountain. The air becomes cooler and then sinks, raising the warm and humid air at the foot of the mountain. The water vapor cools down continuously in the process of air rising, producing heavy rainfall and prone to drought-flood abrupt alternation.

Peng et al. (2018) uses the long and short period drought-flood abrupt alternation index to analyze the characteristics of drought-flood abrupt alternation in Zhengzhou in summer. If this method is used to study the law of drought-flood abrupt alternation in the growing period of tobacco, only the difference of drought and flood in the early and late periods is considered, and the time scale is too large. Only when the whole growing period of tobacco is over, can the degree of drought-flood abrupt alternation be evaluated, which cannot meet the needs of real-time monitoring and early warning evaluation. Chen et al. (2018) used hydrus-1d model to simulate soil moisture movement and study drought-flood abrupt alternation in the growing period of rice. The author thinks that this method not only considers meteorological factors, but also

http://www.aloki.hu ● ISSN 1589 1623 (Print) ● ISSN 1785 0037 (Online)
DOI: http://dx.doi.org/10.15666/aeer/1705_1227112286

considers soil moisture condition and water requirement during the crop growing period, with the certain feasibility. However, the continuous non-effective precipitation days and the accumulative effective precipitation during the flood period can indirectly reflect the income and expense of farmland precipitation and loss of soil moisture, and can accurately describe the law of drought-flood abrupt alternation in the growing period of tobacco. The method does not involve complex operations, and does not require a large number of data to simulate, so it can quickly achieve the monitoring and early warning evaluation of drought-flood abrupt alternation during the growing period of tobacco.

Conclusions

(1) In this study, the drought index of tobacco growth period constructed by continuous non-effective precipitation days is used to take into account the dual factors of precipitation and precipitation days, which can indirectly reflect the income and expenditure of farmland precipitation and soil moisture profit and loss. The flood index of different growing periods is constructed by using cumulative effective precipitation in the flood period, and the effects of water requirement, flood tolerance and precipitation process on tobacco growth were comprehensively considered. The precipitation and soil moisture data of Xiuwen County Irrigation Experimental Base in 2015 and 2016 are used to verify that the continuous non-effective precipitation days and cumulative effective precipitation in flood period could accurately describe the evolution of drought-flood abrupt alternation in tobacco growth period. It can realize the real-time monitoring and early warning evaluation of the drought-flood abrupt alternation during the growing period of tobacco in this area, and provide scientific basis for timely and accurate disaster prevention and reduction.

(2) In the tobacco root extension period, waterlogging is the main cause. It is easy to suffer from drought-flood abrupt alternation in flourishing period. Guiyang is located in the Yunnan-Guizhou plateau, where there is a severe drought-flood abrupt alternation in the tobacco growing period. In the later stage of maturation drought, the duration of drought increased obviously, and the intensity of drought-flood abrupt alternation increased rapidly, so the adverse effects of flood stress on the yield and quality of tobacco should be prevented.

(3) In the next step, artificial precipitation simulation test of drought and waterlogging is carried out to further improve the accuracy of the coupling method in this paper.

Acknowledgements. This paper is funded by the Water Conservancy Research Project of Guizhou Provincial Water Resources Department (Grant No.: KT201705) and National Natural Science Foundation (Grant No.: 51779093).

REFERENCES

[1] Bello, A. A., Mamman, M. B. (2018): Monthly rainfall prediction using artificial neural network: A case study of Kano, Nigeria. – Environmental and Earth Sciences Research Journal 5(2): 37-41.

http://www.aloki.hu ● ISSN 1589 1623 (Print) ● ISSN 1785 0037 (Online)
DOI: http://dx.doi.org/10.15666/aeer/1705_1227112286

[2] Cai, H. Y., Wang, Y. W., Li, J. P., Chen, Z. G. (2005): Effect of Soil Water on Configuration and Character of Water Consumption inFlue-cured Tobacco. – Journal of Irrigation and Drainage (3): 38-41.
[3] Chen, C., Hu, T. S., Gao, Y. (2018): Research on the Definition of Drought and Flood Alternation in Rice Irrigation. – China Rural Water and Hydropower (7): 56-61.
[4] Cheng, J. B. (2006): A preliminary Study on Water Requirement character of flued-cured tobacco of high-quality in karst mountain area. – Guizhou University, Guizhou Province.
[5] Dastane, N. G. (1974): Effective rainfall in irrigated agriculture. – Irrigation and Drainage Paper No. 25. New York: Food and Agriculture Organization, United Nations.
[6] Dittus, A. J., Karoly, D. J., Donat, M. G., Lewis, S. C., Alexander, L. V. (2018): Understanding the role of sea surface temperature-forcing for variability in global temperature and precipitation extremes. – Weather and Climate Extremes 21(9): 1-9.
[7] Fan, Y. X. (2018): Catastrophe distinction index of oilseed rape vernal waterlogging and waterlogging impact analysis in Huna. – China Academy of Meteorological Sciences, Beijing.
[8] Gansu Provincial Bureau of Quality and Technical Supervision (2011): Gansu drought Standard DB62/T2034/2011.
[9] Gao, H. J. (2006): Study on Water-saving Irrigation Schedule and Optimum Irrigation Index of Flue-cured Tobacco. – Henan Agricultural University, Henan Province.
[10] Gao, X. R., Wang, C. Y., Zhang, J. Q., Xue, X. Z. (2012): Crop water requirement and temporal-spatial variation of drought and flood disaster during growth stages for maize in Northeast during past 50 years. – Transacti ons of the Chinese Society of Agricultural Engineering 28(12): 101-109.
[11] Gu, X. (2014): Analysis of suitability and climatic characteristics of meteorological drought index in summer in southeastern Guizhou. – 31st Annual meeting of Chinese Meteorological Society, Beijing.
[12] Guizhou Provincial Bureau of quality and Technology Supervision (2015): Guizhou drought standard DB52/T1030-2015.
[13] Han, J. F., Wang, Y. F., Zhang, X. T. (1992): Effects of soil moisture on root development and root activity of flue-cured tobacco. – China Tobacco (3): 14-17.
[14] He, H., Liao, X. P., Lu, H., Chen, S. R. (2016): Features of long-cycle drought-flood abrupt alternation in South China during summer in1961-2014. – Acta Geographica-Sinica 71(1): 130-141.
[15] Huang, R. (2015): Research on evolution and Countermeasures of drought-floods abrupt alternation events in Huaihe River basin. – China Institute of Water Resources & Hydropower Research, Beijing.
[16] Huang, W. H., Sui, Y., Yang, X. G., Dai, S. W., Qu, H. H., Li, M. S. (2014): Spatio-temporal characteristics of crop drought in southern China based on drought index of continuous days without available precipitation. – Transactions of the Chinese Society of Agricultural Engineering 30(4): 125-135.
[17] Huo, Z. G., Wang, S. L. (2009): Agricultural and bio-meteorological disasters. – Meteorological Press, Beijing.
[18] IPCC (2013): Climate Change 2013: the Physical Science Basis, Contribution of Working Group I to the Fifth Assessment Report of the Inter-governmental Panel on Climate Change. – Cambridge, United Kingdom and New York, NY, USA: Cambridge University Press, 2013.
[19] Jiang, X. N., Feng, J., Jian, M. Q. (2009): Comparative Analysis of Seasonal Drought Events in Guangzhou With Precipitation and Day without Rain. – Guangdong Meteorology 31(5): 4-5.
[20] Kong, F. (2018): Diagnosis of spatio-temporal pattern changes of global multi-scale rainstorm. – 35th Annual meeting of China Meteorological Society, Anhui Province.

http://www.aloki.hu ● ISSN 1589 1623 (Print) ● ISSN 1785 0037 (Online)
DOI: http://dx.doi.org/10.15666/aeer/1705_1227112286

[21] Li, J. P., Chen, Z. G., Yang, Y. H., Cai, H. Y. (2007): Study on the Adequate Soil Moisture Indexes of Flue-cured Tobacco Irrigation Based on Some Physiological Indexes. – Journal of Irrigation and Drainage 1: 93-96.
[22] Liu, Z. D., Duan, A. W., Xiao, J. F., Gao, Y., Liu, H. (2009): Calculation Model of Effective Precipitation at Growth Stages for Winter Wheat. – Journal of Irrigation and Drainage 28(2): 21-25.
[23] Liu, Y. F., Yuan, Z. H, Guo, L. X., Kong, W., Zhang, L.,Wu, L. (2017): Characteristics of Spatio-Temporal Variation of Abrupt Alternation of Drought and Flood in Shanxi Province During Summers in 1961-2013. – Journal of Ecology and Rural Environment 33(4): 332-340.
[24] Magrini, A., Lazzari, S., Marenco, L., Guazzi, G. (2018): Cost optimal analysis of energy refurbishment actions depending on the local climate and its variations. – Mathematical Modelling of Engineering Problems 5(3): 268-274.
[25] Mesmoudi, K., Meguellati, K., Bournet, P. E. (2017): Thermal analysis of greenhouses installed under semi arid climate. – International Journal of Heat and Technology 35(1): 474-486.
[26] Nocera, F., Gagliano, A., Evola, G., Marletta, L., Faraci, A. (2017): The Kyoto Rotation Fund as a policy tool for climate change mitigation: The case study of an Italian school. – International Journal of Heat and Technology 35(S1): S159-S165.
[27] Peng, G. H., Qin, L. L., Ma, J. Q., Huang, M. Y. (2018): Analysis of drought-flood abrupt alternation in Zhengzhou during summer in 1955-2015. – South-to-North Water Transfers and Water Science & Technology 16(6): 27-32.
[28] Scafetta, N., Mirandola, A., Bianchini, A. (2017): Natural climate variability, part 1: Observations versus the modeled predictions. – International Journal of Heat and Technology 35(S1): S9-S17.
[29] Scafetta, N., Mirandola, A., Bianchini, A. (2017): Natural climate variability, part 2: Interpretation of the post 2000 temperature standstill. – International Journal of Heat and Technology 35(S1): S18-S26.
[30] Shan, L. J., Zhang, L. P., Chen, X. C., Yang, W. (2015): Spatio-temporal Evolution characteristics of Drought-Flood abrupt alternation in the Middle and Lower reaches of the Yangtze River Basin. – Resources and Environment tin the Yangtze Basin 24(12): 2100-2107.
[31] Shan, L. J., Zhang, L. P., Zhang, Y. J., She, D. X. (2018): Characteristics of dry-wet abrupt alternation events in the middle and lowerreaches of the Yangtze River Basin and their relationship with ENSO. – Acta Geographica Sinica 37(1): 25-40.
[32] Sun, X. T., Li, Q. Q., Wang, L. J. (2017): Characteristics of Long-Cycle Abrupt Drought-Flood Alternations in Southwest China and Anomalies of Atmospheric Circulation in Summer. – Chinese Journal of Atmospheric Sciences 41(6): 1332-1342.
[33] Tang, S. K. (2011): The environment of tobacco growth. – Yun Yunnan Science and Technology Publishing Press, Yunnan Province.
[34] Uttam, P., Goswami, B., Hazra, M. K. (2018): Copula-based probabilistic characterization of precipitation extremesover North Sikkim Himalaya. – Atmospheric Research 212(11): 273-284.
[35] Wang, N., Wang, Q., Fang, F., Cai, X. L., Xiao, K. L., Fang, J. G. (2014): Characteristics of spatial and temporal variation of extreme no rain days in each season in Shaanxi province. – Agricultural Research in the Arid Areas 32(6): 221-228, 267.
[36] Wu, Z. W., Li, J. P., He, J. H., Jiang, Z. H. (2006): Occurrence of droughts and floods during the normal summer monsoons in the mid and lower reaches of the Yangtze River. – Geophysical Research Letters 33(5): 813.
[37] Xu, F. Q. (2009): Concise analysis of effective precipitation. – Meteorological, Hydrological and Marine Instruments 26(1): 96-100.

http://www.aloki.hu ● ISSN 1589 1623 (Print) ● ISSN 1785 0037 (Online)
DOI: http://dx.doi.org/10.15666/aeer/1705_1227112286

[38] Yang, H. Y., Huo, Z. G., Yang, J. Y., Zhang, G. X., Wu, L., Fan, Y. X. (2017): Indicators and Risk o f Spring Corn Waterlogging Disaster in Jianghan and West Region of Jiangnan. – Journal of Applied Meteorological Science 28(2): 237-246.
[39] Zhao, G. Y., Han, Y., Liu, M. H., Hou, J. L., Shi, H. P., Liu, W. Z., Guo, Y. L., Qiao, Q. (2018): Spatial-temporal Variation of Extreme Precipitation Events in Henan Province from 1961 to 2013. – Research of Soil and Water Conservation 25(6): 115-120.

http://www.aloki.hu ● ISSN 1589 1623 (Print) ● ISSN 1785 0037 (Online)
DOI: http://dx.doi.org/10.15666/aeer/1705_1227112286

EFFECTS OF Pb AND Cd STRESS ON THE PHOTOSYNTHETIC PHYSIOLOGICAL CHARACTERS OF POTATO IN HEAVY METAL POLLUTION OF SOIL

LI, P. H. – LIN, Q.* – XU, G. Z.

Institution Xichang University, Sichuan potato key laboratory
Xichang 61500, China

**Corresponding author*
e-mail: 13778672269@qq.com; phone: +86-137-7867-2269

(Received 3rd May 2019; accepted 11th Jul 2019)

Abstract. Study on the effects of Pb and Cd stress on the photosynthetic physiological characters of potato. The single-factor randomized block experiments with the potato variety Xishu 1 as the test material. The photosynthetic rate (Pn), stomatal conductance (Gs), transpiration rate (Tr), intercellular CO_2 concentration (Ci) and SPAD value of the potato decreased with the increased concentrations and prolonged treatment. As the concentrations of Pb and Cd continued to increase, most of the photosynthetic physiological indices tended to be stable. But in the treatment with high concentration of Cd, the SPAD value decreases sharply. The potato photosynthetic system has certain tolerance to Pb and Cd, and the effect of Cd on the photosynthesis of potato is greater than that of Pb.
Keywords: *Pb and Cd, potato, photosynthetic, physiological characters, stress*

Introduction

With the progress of the human society and the accelerated industrialization process, environmental pollution has become one of the most prominent ecological problems in the world, including the heavy metal pollution of soil (Wan et al., 2008). Heavy metal pollution has been one of the hotspots in ecological and environmental biology research. So far, there have been a lot of studies on the effects of heavy metals on the biological morphology, their physiological and biochemical effects and the resistance mechanism of plants against heavy metal pollution (Kong et al., 2007; Zhou et al., 2007; Li et al., 2008). The current research mainly focuses on the toxic effects of heavy metals on plants, toxic mechanisms and the resistance mechanisms of plants, but little research involves the photosynthetic physiological characters of plants under heavy metal stress.

At present, 20 million hm^2 of soil has been polluted by heavy metals such as Pb and Cd in China, accounting for about one-fifth of the total cultivated land area (Lee, 2016). Every year, the economic loss caused by heavy metal pollution can be as high as 20 billion RMB (Gu et al., 2003). According to statistics, the land area suffering from heavy metal pollution accounts for 64.8% of the total wastewater irrigation area, including 46.7% mild pollution, 9.7% moderate pollution and 8.4% serious pollution (Chen et al., 2002). At present, the soil in the suburbs of most cities in China has been polluted to varying degrees. In many places, the contents of heavy metals such as Pb and Cd in grains, vegetables, fruits and other foods already exceed the standards and are close to the critical values. According to the survey conducted by the Ministry of Agriculture, among the 320 key polluted areas including suburbs, wastewater irrigation areas and industrial mines in 24 provinces (cities), 606,000 hm^2 of field crops suffer from excessive pollution, accounting for 20% of the total area monitored. In particular, the output and area of agricultural products with excessive heavy metal content account for about 80% of

http://www.aloki.hu ● ISSN 1589 1623 (Print) ● ISSN 1785 0037 (Online)
DOI: http://dx.doi.org/10.15666/aeer/1705_1228712295

the total output and area of the agricultural products with excessive amount of pollutants. The pollution of Pb, Cd, Hg, Cu and their combinations is the most serious (Hou et al., 2017). Pb and Cd are the elements toxic to the plant growth. A large number of studies have confirmed that Pb can affect the antioxidant enzyme systems of plants (Sun et al., 2009; Cai et al., 2012); that the root tips of Cd-polluted broad bean seedlings turn dark brown and suffer from necrosis (Mo and Li, 1992); and that Cd can inhibit the growth of corn, wheat (Parlak, 2016), cucumber (Chen, 1990) and tomato (Moral et al., 1994), etc., and result in symptoms like leaf chlorosis and yellowing, which all affect the crop yield. In recent years, through research, Wang et al. (2009) found that the chlorophyll content, photosynthetic rate, transpiration rate and other indicators of radish leaves significantly dropped with the increase in the concentration of the Pb and Cd mixed solution (Wang and Shi, 2008); Wang et al. (2009) found that low-concentration Pb and Cd mixed solution has certain promoting effects on various physiological indicators of wheat, and that with the increase of concentration, the synthesis of chlorophyll will be blocked (Wang and Zheng, 2009). This reveals that Pb and Cd have certain impacts on the photosynthesis of plants; however, no research has been reported on the effects of Pb and Cd on the photosynthetic physiological characters of potato.

Potato (*Solanum tuberosum* L.), an annual herb of the Solanaceae family, is an important type of staple food and vegetable (Furrer et al., 2018). Potato is rich in nutrients and has high edible value. The starch in the dry matters' accounts for 75%-80%, which can be easily absorbed by the human body; the protein availability is 71%, which is 21% higher than that of grain, and what is more, it is rich in vitamin C (Li, 2013). In China, potato is an important kind of export goods; and in agricultural production, it is an excellent fore crop for cereal crops, and also an excellent crop for intercropping and replanting. Therefore, developing potato production is of great significance to improving the living standards of the people and promoting the development of light industry, food industry and grain production. With the development of industrialization and urbanization, large amount of Pb and Cd are continuously entering the soil, resulting in more and more serious pollution, which brings great harm to humans, environment and agriculture. So far, heavy metal elements have been accumulated to varying degrees in the soil (Bat, 1997; Fang, 2015; Jing et al., 2018; Pozza and Bishop, 2019), especially in suburban soil. The contents of Pb and Cd in soil have already greatly exceeded the world soil background values. For plant growth, Pb and Cd are non-essential elements, and both of them can adversely affect the chlorophyll synthesis and antioxidant enzymes of plants. When the dose exceeds a certain level, they may seriously affect the physiological metabolism of plants, hinder their growth and even lead to plant deaths (Bai et al., 2012). However, no research has been reported on the effects of Pb and Cd stress on the photosynthetic physiological characters of potato. This experiment explored the relationship between the photosynthetic physiological characters of potato and the heavy metal pollution of soil, so as to reveal the response of the potato photosynthetic system to heavy metal stress, and provide theoretical guidance for potato production.

Materials and Methods

Test materials

The potato variety tested was Xishu No. 1, supplied by Plateau and Subtropical Crop Laboratory, Xichang University.

The height, diameter, volume of pots is 150 g, 35 cm, 1750 cm^3.

http://www.aloki.hu ● ISSN 1589 1623 (Print) ● ISSN 1785 0037 (Online)
DOI: http://dx.doi.org/10.15666/aeer/1705_1228712295

Experimental design

The experiment was carried out in the phytotron at Xichang University. We arrange the condition of enviroment on normal status which potato can grow healthy. During the experiment, the indoor CO_2 concentration was (450±50) $\mu mol \cdot mol^{-1}$, the light intensity (420±50) $\mu mol \cdot m^{-2} \cdot s^{-1}$, the relative humidity (55±8)%, the daytime temperature (25±2)ºC, the nighttime temperature (15±2)ºC and the illumination 12 h per day. The test soil was collected from the surface soil in the experiment field at Xichang College. The physical and chemical properties were as follows: the pH value was 6.30 (water)/7.71 ($CaCl_2$), the total P content was 441 $mg \cdot kg^{-1}$, the total N content 853 $mg \cdot kg^{-1}$, the total K content 2313 $mg \cdot kg^{-1}$, CEC 11.23 meq/100g, the organic matter content 25.1 $mg \cdot kg^{-1}$, and the contents of the heavy metals Pb and Cd 20 and 0.2 $mg \cdot kg^{-1}$, respectively. The Pb stress treatment levels were respectively 0(CK), 200, 500 and 1000 $mg \cdot kg^{-1}$, and Pb was added in the form of $Pb(CH_3COO)_2$; the Cd stress treatment levels were 0(CK), 20, 50, 100 $mg \cdot kg^{-1}$, and Cd was added in the form of $CdCl_2 \cdot 2.5H_2O$. After being treated, the soil was mixed well and stabilized for two weeks, and then potato seedlings were transplanted. The plants with roughly the same weight and height (about 8-10 cm) were selected and randomly allocated to the soil with different concentrations. For each treatment level, 16 pots were planted, and each pot had one plant. After transplantation, the water was added by the weighing method to maintain the soil moisture at about 60% of the field moisture capacity. After 30 days of heavy metal stress treatment, the photosynthetic physiological indices were determined.

Determination of the photosynthetic physiological indices

The potato leaves (the 3rd and 4th pairs of leaves of the main stem from top down) were measured during the period from 10:00 to 11:30 using the CI-340 portable photosynthetic measure system (CID (Beijing) Ecological Scientific Instrument Co., Ltd.). The indices determined included net photosynthetic rate (Pn), transpiration rate (Tr), stomatal conductance (Gs) and intercellular CO_2 concentration (Ci). At the same time, the SPAD value of the leaves was measured by SPAD-502 (Minota, Japan) chlorophyll meter. For each leaf, the indicators were determined for three times.

Data analysis

The above experiment was repeated 3 times, and the average values were taken as the results. And then statistical analysis and plotting were performed using the software SAS 8.2 and Excel.

Results

Effects of Pb and Cd on the photosynthetic physiological characters of potato

Effects of Pb on the photosynthetic physiological characters of potato

It can be seen from *Fig. 1* that under different concentrations of Pb, the photosynthetic physiological characters of potato showed different variation patterns. Under the action of Pb, the photosynthesis rate of potato decreased with the increase of the Pb concentration, and the treatment groups were significantly different from the control group. When the concentration of Pb was 200 $mg \cdot kg^{-1}$, the net photosynthetic rate decreased the most – by 22.97%, and then the decline gradually slowed down.

http://www.aloki.hu ● ISSN 1589 1623 (Print) ● ISSN 1785 0037 (Online)
DOI: http://dx.doi.org/10.15666/aeer/1705_1228712295

When the concentration of Pb was 1000 mg·kg^{-1}, the net photosynthetic rate was 52.55% of that in the control group. After Pb treatment, Tr of the potato leaves decreased with the increase of the Pb concentration, and the results of the treatment groups were significantly different from those of the control group. When the concentration of Pb exceeded 200 mg·kg^{-1}, the decrease of Tr became slower; and when the concentration of Pb was 1000 mg·kg^{-1}, Tr was 74.66% of that in the control group. When the concentration of Pb was 200 mg·kg^{-1}, Gs was not significantly different from that in the control group. With the increase of the Pb concentration, the decrease of Gs became faster. When the concentration of Pb was 1000 mg·kg^{-1}, Gs was 74.67% of that in the control group. With the increase of the Pb concentration, the decrease of Ci gradually slowed down and the content tended to be stable. At the Pb concentration of 500 and 1000 mg·kg^{-1}, Ci was 84.21% and 83.32% of that in the control group, respectively.

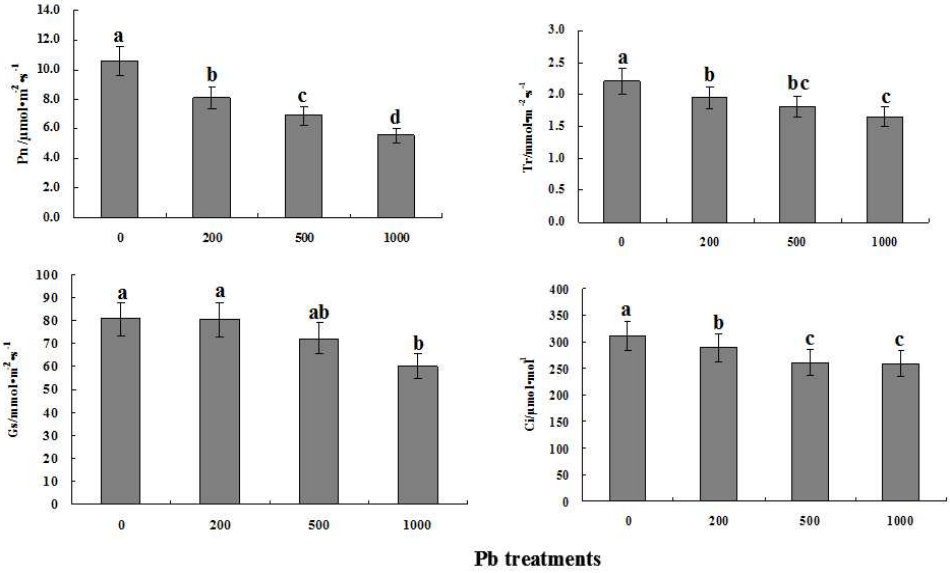

Figure 1. *Effects of Pb on the photosynthetic physiological indices of potato. The data are displayed as mean±SD, n=3. Different letters indicate the significant differences between treatments, P<0.05*

Effects of Cd on the photosynthetic physiological characters of potato

It can be seen from *Fig. 2* that under different concentrations of Cd, the photosynthetic physiological characters of potato showed different variation patterns. Under the action of Cd, the photosynthesis rate of potato decreased with the increase of the Cd concentration. When the concentration of Cd was 20 mg·kg^{-1}, the photosynthetic rate of potato did not differ much from that in the control group; but when the concentration was 50 mg·kg^{-1}, the net photosynthetic rate decreased the most – by 26.75%, and after that, the decline gradually slowed down. When the concentration of Cd was 100 mg·kg^{-1}, the net photosynthetic rate was 50.28% of that in the control group. After Cd treatment, Gs showed a different decline trend from that in the Pb treatment – it decreased more slowly with the increase of the Cd concentration. When the concentration of Cd exceeded 50 mg·kg^{-1}, Gs tended to be stable; and when the concentration of Cd was 1000 mg·kg^{-1}, Gs was 68.04% of that in the control group.

http://www.aloki.hu ● ISSN 1589 1623 (Print) ● ISSN 1785 0037 (Online)
DOI: http://dx.doi.org/10.15666/aeer/1705_1228712295

With the increase of the Cd concentration, Ci first declined and then increased. When the Cd concentration was 50 mg·kg^{-1}, Ci declined the most and was 89.39% of that in the control group. When the Cd concentration was 50 mg·kg^{-1}, Ci started to increase. At the Cd concentration of 100 mg·kg^{-1}, Ci increased to 98.47% of that in the control group.

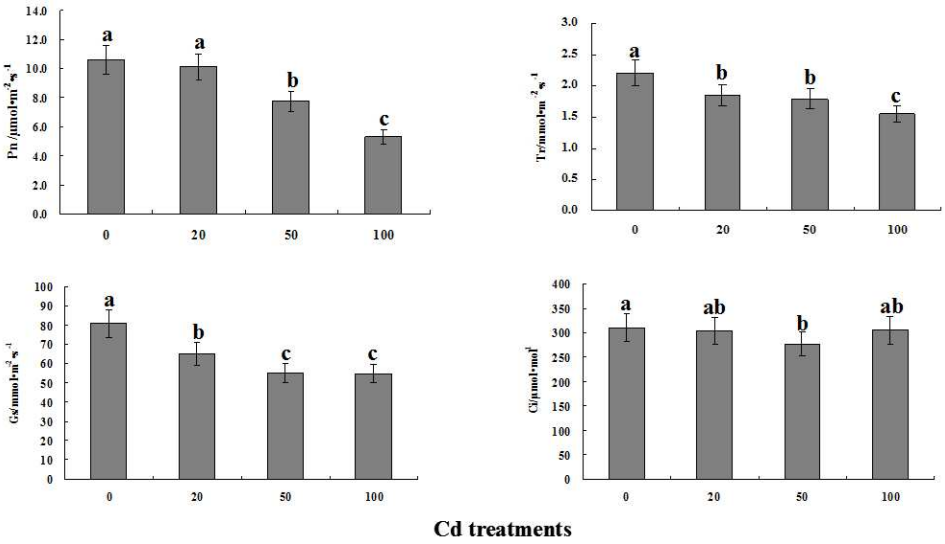

Figure 2. *Effects of Cd on the photosynthetic physiological indices of potato. The data are displayed as mean±SD, n=3. Different letters indicate the significant differences between treatments, P<0.05*

Effects of Pb and Cd on the chlorophyll content of potato

It can be seen from *Fig. 3* that the SPAD value of potato decreased with the increase of Pb and Cd concentrations, and the variation patterns were different. Under the Pb stress, the SPAD value showed a downward trend with the increase of the Pb concentration, and the decrease rate became smaller. When the Pb concentration exceeded 500 mg·kg^{-1}, the SPAD value tended to be stable. Under the Cd stress, the SPAD value decreased with the increase of the Cd concentration, and when the concentration of Cd exceeded 50 mg·kg^{-1}, the decrease of SPAD value became much faster.

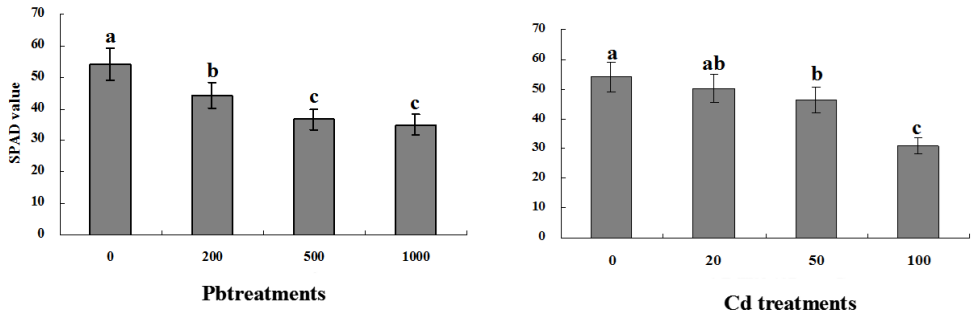

Figure 3. *Effects of Pb and Cd on the photosynthetic physiological indices of potato. The data are displayed as mean±SD, n=3. Different letters indicate the significant differences between treatments, P<0.05*

http://www.aloki.hu ● ISSN 1589 1623 (Print) ● ISSN 1785 0037 (Online)
DOI: http://dx.doi.org/10.15666/aeer/1705_1228712295

Discussion

The photosynthesis of plants mainly depends on three physiological processes, namely, the conduction, light and dark reaction of the photosynthetic substrate CO_2. The leaves have strong CO_2 conductivity, and high light and dark reactions are the important foundations for plant leaves to achieve a higher photosynthetic rate (Liu et al., 2007; Yang, 2012). Environmental stress has multiple impacts on the photosynthesis of plants. It not only directly causes damages to the photosynthetic structure, but also affects the photosynthetic electron transport, the photosynthetic phosphorylation and the dark-reaction-related enzyme systems. It is generally believed that the factors causing a decrease of the photosynthetic rate include stomatal limitation and non-stomatal limitation (Jing et al., 2018). The net photosynthetic rate (Pn) of plant leaves is an important indicator to measure the photosynthesis of plants, and its changes can also directly reflect the degree and variations of photosynthesis. Factors affecting Pn mainly include Ci, Gs and Tr. They work synergistically during the plant photosynthesis to promote the photosynthetic reactions. Tr can measure the transpiration intensity and stomatal opening of plant leaves, of which the latter can directly affect the velocity of CO_2 entering the leaves and the intercellular CO_2 concentration, and thus affecting the carbon assimilation (Shabbir et al., 2016).

In recent years, the inhibition of plant photosynthesis by heavy metal has been confirmed by many studies. It is generally believed that the inhibition mechanisms include (Quartacci et al., 2000; Mukhopadhyay et al., 2015): heavy metals can destroy the photosynthetic enzymes in leaves and cause photosynthetic pigments to decrease; heavy metals reduce the chlorophyll content and cause the structural damages of the chloroplast and destruction of the chloroplast membrane. Chlorophyll is the initiator of photosynthesis. Within a certain range, the higher the chlorophyll content, the higher the net photosynthetic rate. After the Pb treatment, the photosynthetic pigments of plants were damaged, especially chlorophyll a. Its content decreased rapidly after the concentration of Pb increased, and the inhibitory effect was even more obvious under high-concentration Pb stress (Wang et al., 2009). The reduction of the chlorophyll content is related to the damage of the enzymes for the synthesis of chlorophyll. Some research proposes that, after being absorbed by plants, heavy metal ions act on the SH part of the peptide chain of the chlorophyll synthase and change its normal configuration to inhibit the activity of the synthase and block the synthesis of chlorophyll (Qiu et al., 2006). In addition, according to some studies, heavy metal ions can make the chloroplast envelope disappear, resulting in irreversible damages of chloroplast (Kutschera, 2015; Soares et al., 2016); under the Pb stress, the chloroplast structure will change significantly (Bashmakov et al., 2017); and under the high-concentration Pb stress, the chloroplast membrane system will collapse and the chloroplast will shrink, resulting in numerous large lipid globules (Zhou et al., 2005). It shows that heavy metal can cause great damages to the function of chloroplast and significantly reduce the chlorophyll content of plant leaves.

Heavy metals inhibit plant photosynthesis by affecting the stomatal opening of leaves, especially cadmium and lead. In this experiment, under the treatment of high-concentration Pb and Cd, the decrease of Pn became significantly faster, Gs significantly decreased, and at the same time Ci increased. According to the study of Farquhar and Sharkey (1982) on the determination of stomatal limitation and non-stomatal limitation, the inhibition of potato photosynthesis by Pb and Cd in this experiment was caused by non-stomatal factors. It was not because the decrease of

http://www.aloki.hu ● ISSN 1589 1623 (Print) ● ISSN 1785 0037 (Online)
DOI: http://dx.doi.org/10.15666/aeer/1705_1228712295

stomatal conductance resulted in insufficient CO_2 supply, but because the photosynthetic structure was destroyed, which inhibited the activity of the dark reaction enzyme and thus reduced the photosynthetic rate of the plant (Mobin and Khan, 2007; Huang et al., 2018).

Conclusions

This experiment studied the effects of Pb and Cd on the photosynthesis of potato. After the treatment of Pb and Cd within a certain range of concentration, the photosynthetic rate (Pn), stomalal conductance (Gs), transpiration rate (Tr), intercellular CO_2 concentration (Ci) and chlorophyll content (SPAD) of potato were on a downward trend. As the concentrations of Pb and Cd continued to increase, most of the photosynthetic physiological indices tended to be stable, indicating that the potato photosynthetic system has certain resistance to Pb and Cd. Under the high-concentration Cd treatment, the SPAD value decreased sharply, which indicates that the effect of Cd on potato photosynthesis is greater than that of Pb.

Acknowledgements. Breeding and Promotion of New Specialized Potato Varieties for Staple Food in Panxi Area (Project No. 2016NYZ0032-4), Sichuan Potato Innovation Team Project. "Study on Agricultural Meteorological Indicators of Main Grain Crops in Sichuan Province" (Province key Laboratory 2018-Key -05-01)

REFERENCES

[1] Bai, R., Meng, H., Zhou, S. (2012): Effect of Cadmium on Growth and Development of Two Potato Varieties. – Acta Agriculturae boreali-simica 27(1): 168-172.
[2] Bashmakov, D. I., Kluchagina, A. N., Malec, P. (2017): Lead accumulation and distribution in maize seedlings: relevance to biomass production and metal phytoextraction. – International journal of phytoremediation 19(11): 1059-1064.
[3] Bot, L. (1997): Natural enrichment of topsoils with chromium and other heavy metal. Port Macquaria New south wales, Austrilia. – Australian Journal of soil Researeh 35: 1165-1176.
[4] Cai, Z., Lu, D., Liang, X., Mo, C., Du, L., Mo, L., Huang, F. (2012): Study on effects of lead on the antioxidant activities of Aloe vera. – Journal of Guangxi University (Natural Science Edition) 37(3): 515-520.
[5] Chen, G. (1990): Studies on the Effects of Heavy Metal on Growth of Cucumis Sativus Seedling. – Chinese Bulletin of Botany 7(1): 34-39.
[6] Chen, Z., Qiu, R., Zhang, J., Wan, Y. (2002): Removed Technology of Heavy Metal Pollution in Soil. – Environmental Protection (6): 21-23.
[7] Fang, S., Qiao, Y., Yin, C. (2015): Characterizing the physical and demographic variables associated with heavy metal distribution along urban-rural gradient. – Environmental monitoring and assessment 187(9): 570.
[8] Farquar, G. D., Sharkey, T. D. (1982): Stomatal conductance and photosynthesis. – Annual. Review of Plant Physiol 33: 317-345.
[9] Furrer, A. N., Chegeni, M., Ferruzzi, M. G. (2018): Impact of potato processing on nutrients, phytochemicals, and human health. – Critical reviews in food science and nutrition 58(1): 146-168.
[10] Gu, J., Zhou, Q., Wang, X. (2003): Reused Path of Heavy Metal Pollutionin Soils and its Research Advance. – Journal of Basic Science and Engineering 11(2): 143-151.

http://www.aloki.hu ● ISSN 1589 1623 (Print) ● ISSN 1785 0037 (Online)
DOI: http://dx.doi.org/10.15666/aeer/1705_1228712295

[11] Hou, D., O'Connor, D., Nathanail, P. (2017): Integrated GIS and multivariate statistical analysis for regional scale assessment of heavy metal soil contamination: A critical review. – Environmental Pollution 231: 1188-1200.
[12] Huang, H. Y., Li, J. L., Liu, H. (2018): Thermal analysis kinetics of Tartary buckwheat flour. – International Journal of Heat and Technology 36(4): 1414-1422.
[13] Jing, T., Xie, H. C., Chen, M. (2018): The Response of Antioxidant Enzymes and Photosynthesis Dynamics of Sunflower Exposed to Aniline Wastewater. – International Journal of Biochemistry Research & Review 2018: 1-9.
[14] Kong, X., Qu, D., Zhou, L. (2007): Effects of Sulfur Nutrition on Root Hydraulic Conductivity of Maize and Wheat under Heavy Metals Stress. – Acta Botanica Boreali-Occidentalia Sinica 27(11): 2257-2262.
[15] Kutschera, U. (2015): 150 years of an integrative plant physiology. – Nature plants 1: 15131-15131.
[16] Lee, K. M., Lai, C. W., Ngai, K. S. (2016): Recent developments of zinc oxide based photocatalyst in water treatment technology: a review. – Water research 88: 428-448.
[17] Li, Q., Yang, F., Zhang, B., Zhang, X., Zhou, G. (2008): Biogeochemistry Responses and Spectral Character istics of Rhus Chinensis Mill Under Heavy Meta Contam ination Stress. – Journal of Remote Sensing (2): 284-290.
[18] Li, P. (2013): Panxi district High yield cultivation of potato. – Chengdu: Sichuan university press 12: 2-8.
[19] Liu, H., Zhu, Z., Shi, Q. (2007): Effect of Low Temperature Stress on Characteristics of Photosynthesis in Leaves of Own-rooted and Grafted Watermelon Seedling. – Journal of Shihezi University (Natural Science) 25(2): 163-167.
[20] Mo, W., Li, M. (1992): Effect of Cdcl2 on the Growth and Mitosis of Root Tip Cells in Vicia Faba. – Chinese Bullctiu of Botuny 9(3): 30-34.
[21] Mobin, M., Khan, N. A. (2007): Photosynthetic activity, pigment composition and antioxidatvie response of two mustard (Brassica juncea) cultivars differing in photosynthetic capacity subjected to cadmium stress. – Plant Physiol 164: 601-610.
[22] Moral, R., Gomez, I., Navarro, P. J. (1994): Effects of cadmium on nutrient distribution, yield, and growth of tomato grown in soilless culture. – Journal of plant nutrition 17(6): 953-962.
[23] Mukhopadhyay, M., Mondal, T. K. (2015): Effect of zinc and boron on growth and water relations of Camellia sinensis (L.) O. Kuntze cv. T-78. – National Academy Science Letters 38(3): 283-286.
[24] National Environmental Protection Agency. (1990): Chinese soil background. – Beijing: China Environmental Science Press.
[25] Parlak, K. U. (2016): Effect of nickel on growth and biochemical characteristics of wheat (Triticum aestivum L.) seedlings. – NJAS-Wageningen Journal of Life Sciences 76: 1-5.
[26] Pozza, L. E., Bishop, T. F. A. (2019): A meta-analysis of published semivariograms to determine sample size requirements for assessment of heavy metal concentrations at contaminated sites. – Soil Research.
[27] Qiu, Y., Cai, N., Wu, Q. (2006): Effect of Pb on root growth and plant photosynthesis of sweetpotato. – Acta Agriculturae Zhejiangensis 18(6): 429-432.
[28] Quartacci, M. F., Pinzino, C., Cristina, L. M. (2000): Growth in excess copper induces changes in the lipid composition and fluidity pf PS Ⅱ-enriched membranes in wheat. – Physiologia Plantarum 108: 87-93.
[29] Shabbir, R. N., Waraich, E. A., Ali, H. (2016): Supplemental exogenous NPK application alters biochemical processes to improve yield and drought tolerance in wheat (Triticum aestivum L.). – Environmental Science and Pollution Research 23(3): 2651-2662.
[30] Soares, C., de Sousa, A., Pinto, A. (2016): Effect of 24-epibrassinolide on ROS content, antioxidant system, lipid peroxidation and Ni uptake in Solanum nigrum L. under Ni stress. – Environmental and experimental botany 122: 115-125.

http://www.aloki.hu ● ISSN 1589 1623 (Print) ● ISSN 1785 0037 (Online)
DOI: http://dx.doi.org/10.15666/aeer/1705_1228712295

[31] Sun, S., He, M., Cao, T., Cheng, S., Song, H. (2009): Effects of Pb and Ni stress on antioxidant enzyme system of Thuidium cymbifolium. – Chinese Journal of Applied Ecology 20(4): 937-942.
[32] Wan, Y. J., Zheng, W. J., Fang, Y., Wang, Z. M., Qiu, J. (2008): Effects of Cr (Ⅲ) Stress on Activities and Isozymes of SOD and POD of Kandelia candel Mangrove Seedlings. – Journal of Xiamen University (Natural Science) 47(4): 571-574.
[33] Wang, L., Shi, Y. (2008): Effects of cadmium, lead and their compound pollution on physiological and biochem ical character istics of radish. – Chinese Journal of Eco-Agriculture 16(2): 411-414.
[34] Wang, L., Zheng, S. (2009): Effect of Cadmium,Lead and Their Combined Pollution on Seed Germination of Wheat. – Journal of Triticeae Crops 29(1): 146-148.
[35] Wang, L., Xu, X., Li, Y., Chen, S., Wang, S., Huang, D. (2009): Effects of Pb stress on the physiological and biochemical characterristics of leaf in six greening trees. – Journal of Agricultural University of Heibei 32(2): 29-33.
[36] Yang, W. (2012): Study on Rapid Determination of Chlorophyll Content of Leaves. – Acta Agriculturae boreali-simica 27(1): 168-172.
[37] Zhou, B., Hu, T., Xu, X. (2005): Effect of Lead Stress on Chlorophyll Content and Photosynthetic Characters in Leaf of Melilotus suavena. – Journal of Sichuan Agricultural University 23(4): 432-435.
[38] Zhou, S., Wang, C., Yang, H., Bi, D., Li, J., Wang, Y. (2007): Stress responses and bioaccumulation of heavy metals by Zizan ia la tifo lia and Acorus calamus. – Acta Ecologica Sinica 27(1): 281-287.

http://www.aloki.hu ● ISSN 1589 1623 (Print) ● ISSN 1785 0037 (Online)
DOI: http://dx.doi.org/10.15666/aeer/1705_1228712295

U-PB CHRONOLOGICAL CHARACTERISTICS OF MESOPROTEROZOIC LA-ICP-MS DETRITAL ZIRCONS IN THE XIONG'ER RIFTING TROUGH AND ITS PALEOENVIRONMENT ANALYSIS

DAI, R.[1] – ZHANG, Y.[2*] – LUO, S. S.[1,3] – WANG, Z. C.[4] – WANG, T. S.[4] – LYU, Q. Q.[2] – GUAN, Y. L.[2]

[1]*Laboratory of Exploration Technologies for Oil and Gas Resources of Ministry of Education Yangtze University, Wuhan 430100, China*

[2]*School of Geosciences, Yangtze University, Wuhan 430100, China*

[3]*Hubei Cooperative Innovation Center of Unconventional Oil and Gas, Wuhan 430100, China*

[4]*Research Institute of Petroleum Exploration & Development, Beijing 100083, China*

[*]*Corresponding author*
e-mail: 201671301@yangtzeu.edu.cn

(Received 3rd May 2019; accepted 11th Jul 2019)

Abstract. In order to understand the sedimentary age and geotectonic environment characteristics of the Ruyang Group in geological history, this study, with the LA-ICP-MS method, focuses on the study of U-Pb isotope geochronology and geotectonic environment analysis of detrital zircons in the bottom of Xiaogoubei Formation of Ruyang Group in Daimeishan of Henan. Results show that the ages of detrital zircons of Xiaogoubei Formation range from 1720 Ma to 2727 Ma, the youngest detrital zircon age near the harmonic line is 1720 ±65 Ma, the main peak age is 2547 Ma, and the second peak ages include 2178 Ma and 1832 Ma. Therefore, we consider that the lower age limit of Xiaogoubei Formation is ~1720 Ma; the sediment sources of Xiaogoubei Formation mainly come from the geological bodies of the interior of the North China craton in the late Neoarchean, early Paleoproterozoic, middle Paleoproterozoic, late Paleoproterozoic and early Neoproterozoic. At the same time, the detrital zircon age of samples has a good response relationship with the Precambrian geological events in North China Craton, which reveals the then construction environment.
Keywords: *zircon LA-ICP-MS U-Pb dating, xiaogoubei formation, changchengian system, xiong'er rift trough, North China Craton*

Introduction

There are many opinions on the division of the stratigraphic ages of Xiong'er rift trough: Guan et al. (1980) and Xing et al. (1996) advocated that the Ruyang Group composed of Bingmagou Formation and Beidajian Formation should be classified into the Mesoproterozoic Jixian System and the Luoyu Group composed of the Cuizhuang Formation and the Luoyukou Formation into the New Proterozoic Qingbaikou System. Chen et al. (1999) called the Bingmagou Formation - Luoyukou Formation collectively the "Ruyang Group", unifying into the Mesoproterozoic Jixian System. In order to limit the stratigraphic age, Guan et al. (1980) first obtained glauconite K-Ar dating data in the Sanjiaotang Formation and Cuizhuang Formation, i.e., 1071 Ma-1089 Ma and 1138 Ma-1159 Ma, respectively, which is the basis to classify Luoyu Group into Qingbaikou System; Qiao et al. (1997) obtained the Pb-Pb age of carbonate rocks in Luoyukou Formation as 855 ± 54 Ma; Liu et al. (1999) obtained the Rb-Sr age of clay

http://www.aloki.hu ● ISSN 1589 1623 (Print) ● ISSN 1785 0037 (Online)
DOI: http://dx.doi.org/10.15666/aeer/1705_1229712304

minerals as 1125 ± 3 Ma in the Cuizhuang Formation and the Ar-Ar age as 918.8 Ma in the flints of Dongjia Formation. In recent year, Su et al. (2012) has made important progress in this area, studied the zircon U-Pb dating of the "sedimentary tuff" interbedded in the middle part of the Luoyukou Formation near Yangpo Village in Ruzhou, Henan Province, and obtained the high-precision dating date of 1611 ± 8 Ma, which provides accurate age data for Luoyukou Formation and its underlying strata such as Luoyu Group and Ruyang Group in this area. In the same year, Hu et al. (2012) carried out U-Pb dating of LA-ICP-MS zircon in the Maanshan Formation at the bottom of the Wufoshan Group in Songshan area, found the youngest zircon age of two samples is 1732 ± 11 Ma and 1655 ± 22 Ma, respectively and defined the sedimentary age of the Songshan-Jishan Formation area, believing that the sedimentary age of the Foshan Group is later than 1655 Ma; Hu et al. (2014) obtained the youngest detrital zircon age of 1744 ± 22 Ma at the bottom of Yunmeng Mountain, defined the detrital sedimentary age of the rift trough after the volcanic rocks of the Xiong'er Group. All of the researches are of great significance for the stratigraphic comparison and the establishment of chronostratigraphic framework in this area.

In addition, Daimeishan area is a national geological park and AAAAA scenic spot. Its unique natural environment can not be separated from the joint action of tectonic activities, rock types and climate. Among them, tectonic activities are of great significance to its later genesis. Therefore, the analysis of tectonic environment in its geological and historical period is conducive to strengthening the understanding of its modern geographical environment. We can also understand the tectonic background and the characteristics of the surrounding environment and the large paleogeographic pattern in the western part of Henan Province of the North China Craton at that time.

This study involves the U-Pb dating of the LA-ICP-MS detrital zircon of Xiaogoubei Formation of Ruyang Group in Daimei Mountain, Henan Province. Combining the results of previous researches, this study compares the zircon ages of different regions in the southern margin of the North China Craton, and reveals the characteristics of the formation and evolution of the crystalline basement and the Xiong'er rift trough in the southern margin of the North China Craton. It is of great significance to understand the tectonic environment of the study area and restore the characteristics of paleoenvironment.

Materials and methods

Regional geological background

Xiong'er rift trough is mainly distributed in the junction of Henan, Shanxi and Shaanxi provinces in China (*Figure 1a*), particularly in the west of Henan, and the Neoproterozoic strata are mainly composed of neutral+acidic volcanic basement with an extremely thick (7000 m) of Xiong'er Group, upper detrital rock and carbonate sedimentary caprocks. The Neoproterozoic strata are divided into the Xiaoqinling-Luanchuan stratigraphic block (I), the Mianchi-Qushan stratigraphic block (II), and the Songshan-Jishan stratigraphic block (III) according to the lithological combination and sedimentary characteristics of the area *(Figure 1b*).

http://www.aloki.hu ● ISSN 1589 1623 (Print) ● ISSN 1785 0037 (Online)
DOI: http://dx.doi.org/10.15666/aeer/1705_1229712304

Profile and sampling location

The section of this study is located in the area of Daimei Mountain (35°2'1.72"N, 111°57'44.26"E), Xin'an County, Luoyang City, Henan Province (*Figure 1b*). The Xiaogoubei Formation and Yunmenshan Formation are observed and measured in detail in the early stage. Xiaogoubei Formation (73.0 m thick) is not integrated on the metamorphic rocks of Majiahe Formation of Xiong'er Group, mainly composed of gray-grayish white medium-thick layers containing gravel sandstone and purplish red medium-fine feldspar quartz sandstone, with large-scale cross-bedding and lenticular bedding, and parallel bedding, and is of fan-delta deposit. Samples used for zircon dating are taken from the first layer of brown-yellow thick-bedded quartzite-fine medium-grained feldspar quartz sandstone (palimpsest structure can be seen) (*Figure 2*).

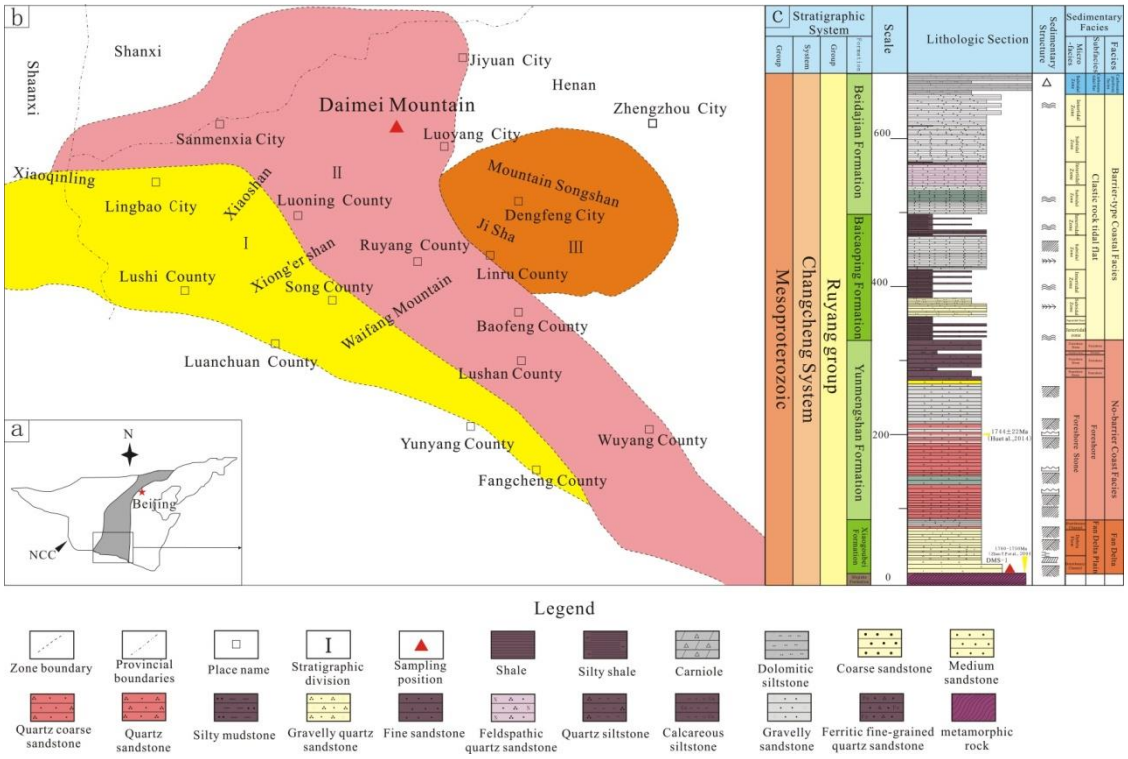

Figure 1. *Geotectonic setting (a), stratigraphic zoning map (b) and sampling location map (c) of the Xiong'er rift trough (as modified by Su et al. (2012))*

Methods of analysis and data processing

Sample crushing and zircon selection are completed by Langfang Keda Rock and Mineral Separation Technology Co., Ltd. By means of flotation and electromagnetic separation, single-grain zircons with different crystal shapes and sizes are selected under binocular lens to ensure their representativeness.

In general, the $^{206}Pb/^{238}U$ age is generally used for younger zircons of less than 1000 Ma, whereas the $^{207}Pb/^{206}Pb$ age, which is more reliable, is generally used for older zircons of greater than 1000 Ma due to lead loss (Black et al., 2003). After the experiment, ICPMSDataCal software (Liu et al., 2009) and Isoplot program (Ludwig, 2003) (Version 3.0) are used to analyze and process the data with the weighted average age calculated and a harmonic graph plotted.

http://www.aloki.hu ● ISSN 1589 1623 (Print) ● ISSN 1785 0037 (Online)
DOI: http://dx.doi.org/10.15666/aeer/1705_1229712304

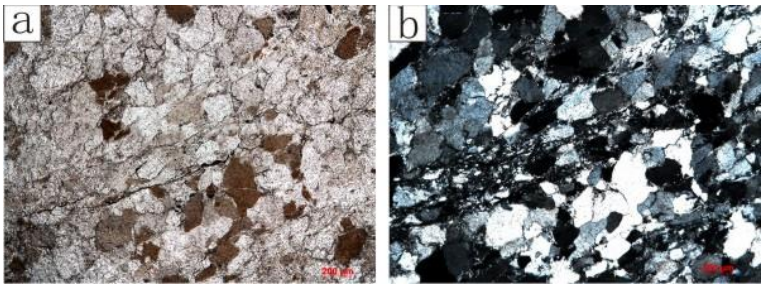

Figure 2. *Photos of Xiaogoubei Formation (DMS-1) in Daimei Mountain Area, Henan Province.*
Note: Fine medium-grained feldspar quartz sandstone can be seen as secondary enlargement with obvious cataclasite phenomenon. It seems to have carbon-filled micro-fissure and argillaceous complex-base filling. Photos under the thin slice of Xiaogoubei Formation (DMS(Daimeishan)-1), single polarization (a), and orthogonal polarized light (b)

Results

Morphology and Th/U ratio of zircons

Among samples, the size of zircon particles is different and mainly in the shape of equiaxial shape, followed by long column and spindle shape, with the particle diameter between 50-150 μm. The grinding circle is mainly sub-circular and sub-angular with occasional round grains, so it can be seen that the zircons in the samples may come from a distant source region and have been subject to long-time handling and strong abrasion.

The cathodoluminescence image analysis shows that there are obvious differences in the internal characteristics of zircons in the samples, most of the zircons have obvious magmatic growth oscillation zonal structure, and most of the crystal zoning is narrow, indicating that the magmatic rocks are more acidic (*Figure 3*). The core-mantle structure can be seen in individual zircons.

U-Pb age

A total of 86 valid data points are obtained from the Xiaogoubei Formation (sample DMS-1), and the harmonic degree of its surface age is greater than 90 on average. A harmonic graph and a histogram of age distribution are made for the valid data of the samples, and most of the data points are distributed along and near the harmonic line (*Figure 4*). As the average age of zircons measured is more than 1000 Ma, $^{207}Pb/^{206}Pb$ is selected as the age of zircon formation. The zircon age of Xiaogoubei Formation (sample DMS-1) is 1720~2727 Ma, and the youngest detrital zircons near the harmonic line is 1720 ± 60 Ma (measuring point DMS-1-03). The main peak age is 2547 Ma, and the second peak ages are 2178 Ma and 1832 Ma (*Figure 4*).

Discussion

Restriction of harmonic age of the youngest detrital zircons on the age of Xiaogoubei Formation

The youngest age data obtained for the detrital zircons in the sedimentary rocks will provide the largest age for the sediments, provided the samples are not contaminated

http://www.aloki.hu ● ISSN 1589 1623 (Print) ● ISSN 1785 0037 (Online)
DOI: http://dx.doi.org/10.15666/aeer/1705_1229712304

and the test system is stable. The minimum harmonic age of detrital zircons from Xiaogoubei Formation studied in this paper is 1720 ± 60 Ma (measuring point DMS-1-03), which represents the largest sedimentary age of Xiaogoubei Formation. The top-boundary age of Ruyang Group-Luoyu Group is limited to 1.6 Ga, and the bottom-boundary age is limited to 1.75 Ga. In combination with the result of dating, it is shown that between 1750 Ma and 1720 Ma, or showing a deposition discontinuity. However, due to the lack of more accurate tuff age data, this conjecture needs to be further verified.

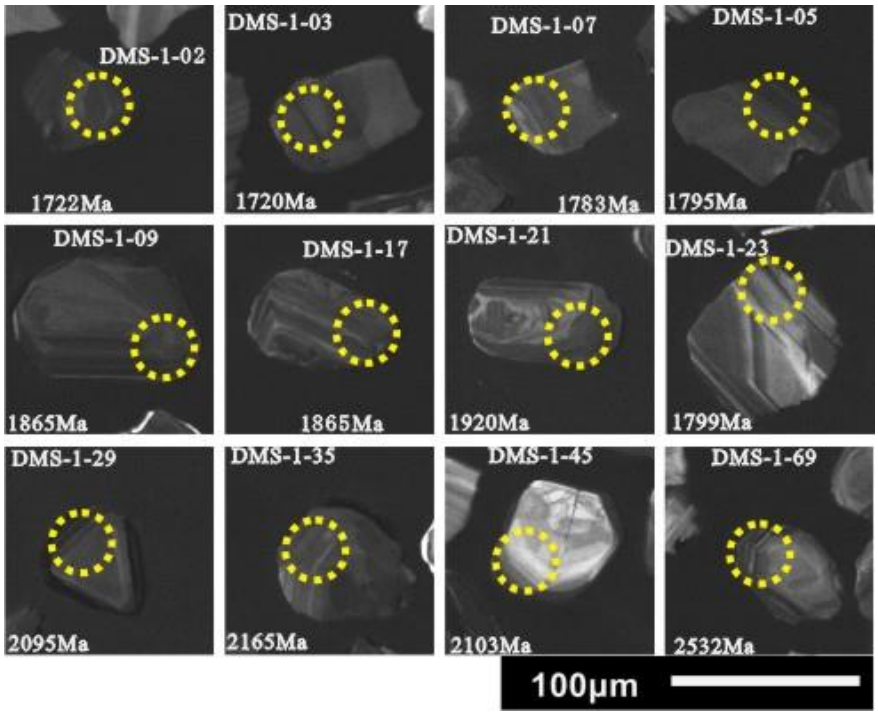

Figure 3. *Xiaogoubei Formation (DMS-1) in Daimei Mountain Area, Henan Province, representative zircon cathodoluminescence (CL) image (beam spot diameter of 24 μm)*

Source analysis of detrital zircons

According to the analysis of zircon age distribution histogram, the age distribution of Xiaogoubei Formation is divided into three groups: 2.75~2.4 Ga (peak value is 2547 Ma), 2.4~2.0 Ga (peak value is 2178 Ma), and 2.0~1.7 Ga (peak value is 1832 Ma), which accounts for 34%, 37% and 29% of the entire zircon age distribution respectively (*Figure 4*). It is considered that the source of Xiaogoubei Formation comes from the geological bodies in late Neoproterozoic, early Palaeoproterozoic, middle Palaeoproterozoic, late Paleoproterozoic and early Neoproterozoic (Wan et al., 2009; Hu et al., 2010; Zhou et al., 2011).

Response of detrital zircons to the precambrian geological events in the North China Craton

Crust growth and caratization events

The peak age of ~2.5 Ga and the age distribution of few ~2.7 Ga are recorded in the detrital zircons of the Xiaogoubei Formation. For a long time, 2.9~2.7 Ga is considered

http://www.aloki.hu ● ISSN 1589 1623 (Print) ● ISSN 1785 0037 (Online)
DOI: http://dx.doi.org/10.15666/aeer/1705_1229712304

as a period of large-scale continental crust growth in the North China Craton. The main evidences from the rocks are greenstone belts and TTG gneiss in the western Shandong region and the TTG gneiss from Jiaodong, Hengshan, Fuping, Jidong, Zhongtiao Mountains, Henan and Inner Mongolia. In addition, the peak age of ~2.7 Ga in the Proterozoic sedimentary basins of North China can also be observed, which indicates that the rocks of 2.9~2.7 Ga are common, together with the age records of ~2.7 Ga zircons from the Xiaogoubei Formation and Yunmengshan Formation of Xiong'er rift trough. In the meantime, the gneiss, TTG and granitic gneiss in the craton have the Hf and Nd model age of 2.9~2.7 Ga, and the age of their formation or upwelling from the mantle is considered to be 2.9 to 2.7 Ga, which indicates that the North China Craton has a large-scale continental crust formation during this period (Jahn et al., 2008).

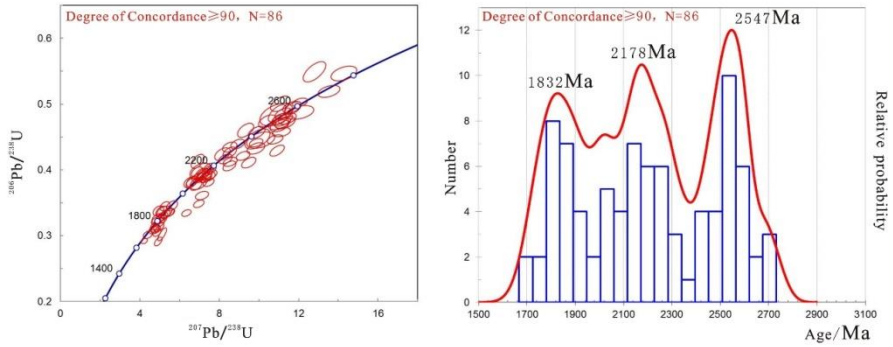

Figure 4. *U-Pb harmonic curve and age distribution histogram of detrital zircons in middle Paleoproterozoic Xiaogoubei Formation (Sample DMS-1) in Daimei Mountain Area, Henan Province*

Paleoproterozoic rift events

The U-Pb age distribution of detrital zircons from Xiaogoubei Formation shows a large amount of age distribution of 2.4~1.95 Ga, with a peak value of ~2.1 Ga. It is reported that during the period of 2.3~2.0 Ga, the North China Craton may have experienced a fracture-tension event of the basement continental block, and three rift belts of Fengzhen, Jiaoliao and Jinyu formed in the northern margin, eastern margin and central regions of North China, thus forming three internal sag basins (or rift belts) in Fengzhen, Jiaoliao and Jin-Henan cratons, which, along with the basic dykes, rift volcanic rocks and A-type granites found at the same time, have extensional properties, which can be proved effectively.

Paleoproterozoic orogenic belt and Mesoproterozoic rift events

In addition, the U-Pb ages of the detrital zircons in the Xiaogoubei Formation are mostly in the range of 1.95 ~ 1.7 Ga, with the peak age of ~1.8 Ga. It is reported that the large-scale metamorphism of the North China Craton at 1.95~1.82 Ga and the intrusion of granite and pegmatite veins related to metamorphism may be related to 1.9~1.8 Ga orogenic activities of three lift belts in Fengzhen, Jiaoliao and Jinyu. The zircons with the age distribution from 1.8 to 1.75 Ga correspond to the development of the Xiong'er rift trough, accompanied by the intrusion of 1.78 Ga basic dykes (Cui et al., 2011). This event also foreshadowed the beginning of the Mesoproterozoic rift and sedimentary events throughout the North China Craton.

http://www.aloki.hu ● ISSN 1589 1623 (Print) ● ISSN 1785 0037 (Online)
DOI: http://dx.doi.org/10.15666/aeer/1705_1229712304

Conclusions

(1) The lower age limit of Xiaogoubei Formation is 1.72 Ga and the Mesoproterozoic Ruyang Group is dominated by delta-clastic littoral sedimentary environment, which is obviously different from the underlying Xiong'er Group.

(2) Xiaogoubei Formation comes from the geological bodies in late Neoproterozoic, early Palaeoproterozoic, middle Palaeoproterozoic, late Paleoproterozoic and early Neoproterozoic.

(3) The detrital zircon peak age of Xiaogoubei Formation has a good response relationship with the Precambrian geological events in North China Craton: the detrital zircon age of ~2.7 Ga mainly reflects the crustal growth of the craton, the peak age of ~2.5 Ga reflects the evolution of the North China cratonization, the detrital zircon age of 2.4~1.9 Ga mainly reflects the Paleoproterozoic rift event, the detrital zircon age of 1.95~1.8 Ga is mainly related to the orogenic activities of the three rift belts including Fengzhen, Jiaoliao and Shanxi-Henan and the detrital zircon age of 1.8~1.75 Ga mainly reflects the development period of the Xiong'er rift trough, foreshadows the beginning of the Mesoproterozoic rift event in the North China Craton.

Acknowledgements. This paper is supported by National Major Special Project of Science and Technology (2016ZX05004-001); Advanced Basic Research Project of Research Institute of Petroleum Exploration & Development (2015yj-09).

REFERENCES

[1] Black, L. P., Kamo, S. L., Allen, C. M., Aleinikoff, J. N., Davis, D. W., Korsch, R. J., Foudoulis, C. (2003): TEMORA 1: A new zircon standard for Phanerozoic U-Pb geochronology. – Chemical Geology 200: 155-170.

[2] Chen, J. B., Gao, Z. J., Zhang. P. Y. (1999): Stratigraphic Code of Chian-Mesoproterozoic. – Geological Publishing House: 1-89.

[3] Cui, M. L., Zhang, B. L., Zhang, L. C. (2011): U-Pb dating of baddeleyite and zircon from the Shizhaigou diorite in the southern margin of North China craton: Constrains on the timing and tectonic setting of the Paleoproterozoic Xiong'er Group. – Gondwana Research 20(1): 184-193.

[4] Guan, B. D., Pan, Z. C., Geng, W. C. (1980): Sinian Suberathem on the North Slope of East Qinling Mountains. Sinian Suberathem In China. – Tianjin Science and Technology Press: 288-313.

[5] Hu, G. H., Hu, J. L., Chen, W., Zhao, T. P. (2010): Geochemistry and tectonic setting of the 1.78 Ga mafic dyke swarms in the Mt.Zhongtiao and Mt.Song areas, the southern margin of the North China Craton. – Acta Petrologica Sinica 26(5): 1563-1576.

[6] Hu, G. H., Zhao, T. P., Zhou, Y. Y., Yang, Y. (2012): Depositional age and provenance of the Wufoshan Group in the southern margin of the North China Craton:Evidence from detrital zircon U-Pb ages and Hf isotopic compositions. – Geochimica 41(4): 326-342.

[7] Hu, G. H., Zhao, T. P., Zhou, Y. Y. (2014): Depositional age, provenance and teconic setting of the Proterozoic Ruyang Group, southern margin of the NorthChina Craton. – Precambrian Research 246: 296-318.

[8] Jahn, B. M., Liu, D. Y., Wan, Y. S., Song, B., Wu, J. (2008): Archean crustal evolution of the Jiaodong Peninsula, China, as revealed by zircon SHRIMP geochronology, elemental and Nd-isotope geochemistry American. – Journal of Science 308(3): 232-269.

[9] Liu, H. Y., Hao, J., Li, Y. J. (1999): Late Precambrian Stratigraphic and Geological Evolution in Central-Eastern China. – Science Press: 1-200.

http://www.aloki.hu ● ISSN 1589 1623 (Print) ● ISSN 1785 0037 (Online)
DOI: http://dx.doi.org/10.15666/aeer/1705_1229712304

[10] Liu, Y. S., Gao, S., Hu, Z. C., Gao, C. G., Zong, K. Q., Wang, D. B. (2009): Continental and oceanic crust recycling-induced melt-peridotite interactions in the Trans-North China Orogen: U-Pb dating, Hf isotopes and trace elements in zircons from mantle xenoliths. – Journal of Petrology 51(1-2): 537-571.
[11] Ludwig, K. R. (2003): User's manual for Isoplot/Ex, version3.00. A geochronological toolkit for Microsoft Excel. – Geochronology Center Special Publication 4: 1-70.
[12] Qiao, X. F., Gao, L. (1997): Carbonate Pb-Pb Isotopic Dating of Qingbaikouan System in Northern China and its Significance. – Journal of Earth Science 22(1): 1-7.
[13] Su, W. B., Li, H. K., Xu, L., Jia, S. H., Geng, J. Z., Zhou, Y. H., Wang, Z. H., Pu, H. Y. (2012): Luoyu and Ruyang Group at the South Margin of the North China Craton (NCC) Should Belong in the Mesoproterozoic Changchengian System: Direct Constraints from the LA-MC-ICPMS U-Pb Age of the Tuffite in the Luoyukou Formation, Ruzhou, Henan, China. – Geological Survey and Research 35(2): 96-108.
[14] Wan, Y. S., Liu, D. Y., Wang, S. Y., Zhao, X., Dong, C. Y., Zhou, H. Y., Yin, X. Y., Yang, C. X., Gao, L. Z. (2009): Early Precambrian Crustal Evolution in the Dengfeng Area, Henan Province (eastern China) Constraints from Geochemistry and SHRIMP U-Pb Zircon Dating. – Acta Geologica Sinica 83(7): 982-999.
[15] Xing, Y. S., Gao, Z. J., Wang, Z. Q. (1996): Stratigraphic Code of Chian- Neoproterozoic. – Geological Publishing House: 1-117.
[16] Zhou, Y. Y., Zhao, T. P., Wang, C. Y., Hu, G. H. (2011): Geochronology and geochemistry of 2.5 to 2.4 Ga granitic plutons in the southern margin of the North China Craton: Implications for a tectonic transition from arc to post- collisional setting. – Gondw Res 20(1): 171-183.

http://www.aloki.hu ● ISSN 1589 1623 (Print) ● ISSN 1785 0037 (Online)
DOI: http://dx.doi.org/10.15666/aeer/1705_1229712304

EFFECTS OF VEGETATION COVER/LAND USE AND SLOPE ASPECT ON SURFACE SOIL PROPERTIES NEAR THE COPPER SMELTER FACTORY IN MURGUL, TURKEY

KUCUK, M.[1] – YENER, I.[1*] – DUMAN, A.[2]

[1]*Faculty of Forestry, Artvin Coruh University, Artvin, Turkey*

[2]*Artvin Vocational School, Artvin Coruh University, Artvin, Turkey*

**Corresponding author*
e-mail: ismetyener@hotmail.com; phone: +90-505-351-0085; fax: +90-466-215-1034

(Received 4th May 2019; accepted 16th Jul 2019)

Abstract. The mining activities, one of the most drastic examples of human intervention to nature, have considerably deteriorated the environment. Although being one of the smallest and least populated cities of Turkey, Artvin is notably affected by mining in many ways such as acid rains, water contamination and medical problems. The activities also affect soil properties. The present study aimed to assess the effects of restoration and reclamation of the former smelter factory and determine the changes in some soil properties according to land use/land cover (LULC) and slope aspect. With this purpose, Pearson correlation and two-way ANOVA methods were used. Results showed that while LULC significantly affected ($p < 0.05$) all soil properties except silt content, bulk density, $CaCO_3$ content, C:N ratio, Cd and Zn; slope aspect significantly affected less soil properties such as sand, silt, pH, EC, $CaCO_3$ and Pb. The interaction between factors also significantly affected ($p < 0.05$) soil properties like LULC. According to partial eta squared ($\eta 2$) values, while the most significantly affected soil properties by LULC, slope aspect and their interaction were found to be Cr (0.93), Clay (0.59) and Cr (0.94), respectively; the ones least affected were found to be total nitrogen (0.12), $CaCO_3$ (0.14) and total nitrogen for 63-day (0.18), respectively. Despite the black alder's and black locust's lack of phytoremediation abilities concerning soil heavy metal content except Pb, *Alnus glutinosa* and *Robinia pseudoacacia* may be suggested for the restoration and reclamation of mining soils in terms of phytoremediation beside their advantages such as improving nitrogen mineralization.
Keywords: *copper mining, two-way ANOVA, black alder, black locust, partial eta squared*

Introduction

The human being has been forced to find new resources for energy and row material and to change land use because of increasing population since ancient times. Pollution, deforestation, erosion, drought-desertification and global climate change are only a few negative results of human activities causing the land use and land cover changes (LUCC) (Deng et al., 2013; Mahmood et al., 2010). The mining, one of the human activities, also has some negative impacts on the environment such as hydrologic, biologic, societal, blasting, subsidence, air quality and land surface effects (Allgaier, 1997).

Artvin has recently come into question with LUCC due to the construction of hydropower plants and mining activities. In this scope, there are 72 mineral deposit reserves determined in Artvin province consisting of 44-Cu-Pb-Zn, 1-Fe, 17-Mn, 5-Cu-Mo and 5-Au (TUİK, 2013). Total copper reserve including Artvin province and Murgul is 329.681 tones (DPT, 2001). Murgul mining entity, dated back to Genoese era, operated in between 1907-1914 by Russians, reactivated in 1951 with the copper smelter by General Directorate of Mineral Research and Exploration (MTA). The

http://www.aloki.hu ● ISSN 1589 1623 (Print) ● ISSN 1785 0037 (Online)
DOI: http://dx.doi.org/10.15666/aeer/1705_1230512321

sulphuric acid factory, operated in between 1963-1975 and 1986-199 was also added to the entity to prevent SO2 emission. The SO2 production, emitted from the factory in between 1951-197 was estimated as 795431 tons (Erdin, 1983; Oruc, 2013). Damages to the ecosystems such as soil loss, lesions and color changes especially on the leaves of fruit trees, lower pH and organic matter content in soil and sulphur accumulation in needles around smelter due to SO2 and other emissions from the factory, were reported by some researchers (Erdin, 1983; Hutchinson and Whitby, 1977; Oruc, 2013). The current physical and chemical properties of soils which influence some vital processes such as carbon storage and nitrogen retention are determined by the duration and the type of land use. On the other hand, heavy metal contamination of soil is another environmental problem, which threatens human health beside the environment by affecting the food chain (Liu et al., 2017; Yesilonis et al., 2016). The area around the factory was planted by Artvin Forest Directorate in 1996 with *Robinia pseudoacacia* and *Alnus glutinosa* sp. to remediate the area. In remediation, beside above mentioned species pine, oak, lime, larch, poplar and birch also have been used in the world. The afforestation of these sites after soil amelioration results in good results (Fischer and Fischer, 2006).

Mining activities cause extreme influences on ecosystem and soil properties and it requires more time to restore soil quality. Therefore, assessing the changes in soil properties is important to see the effects of reclamation of mining areas (Shrestha and Lal, 2011). One of the most important factors affecting restoration and quality of soil is LUCC resulted from human-being, which have an effect on the changes in biological properties. Biomass and forest floor affect many features such as microbial biomass, soil nutrients and soil organic matter (Qi et al., 2018) which have a vital role in carbon balance. The amount of carbon sequestrated in soil in global scale has been estimated 3.3 and 4.5 times more than that in atmosphere and biosphere, respectively (Lal, 2004). The soil properties are expected to change by also slope aspect which is one of the topographic features and closely related to local climate (e.g. precipitation, evaporation and solar incident radiation) (Xu et al., 2008) beside LUCC. Therefore, the slope aspect was taken as the main second factor expected to change selected soil properties.

The aim of the present study was to test our hypothesis that assumes afforestation with black alder and black locust compared to grasslands would improve the soil properties, affecting soil quality after the mining (smelter factory).

Materials and methods

Site description

The study area is located between 41°15’53” - 41°16’21” N latitudes and 41°33’21” - 41°34’04” E longitudes (*Fig. 1*). It is found in Murgul district which is composing of two deep valley surrounded by high mountains with steep slopes (Acatay, 1968). The average elevation of the study site is 600 m above sea level. This region is characterized by mountainous topography with steep slopes. The average slope ranges between 40 and 60%. Soil parent material varies widely from sedimentary marl to igneous dacite, rhyodacite, rhyolite (Anonymous, 2002). The soil texture ranges from clay loam, silty clay loam to sandy loam, loam and loamy clay. Humus form includes both moder and mulls. The soil in the district is generally acidic due to high precipitation causing leaching of base cations (Yener, 2013).

http://www.aloki.hu ● ISSN 1589 1623 (Print) ● ISSN 1785 0037 (Online)
DOI: http://dx.doi.org/10.15666/aeer/1705_1230512321

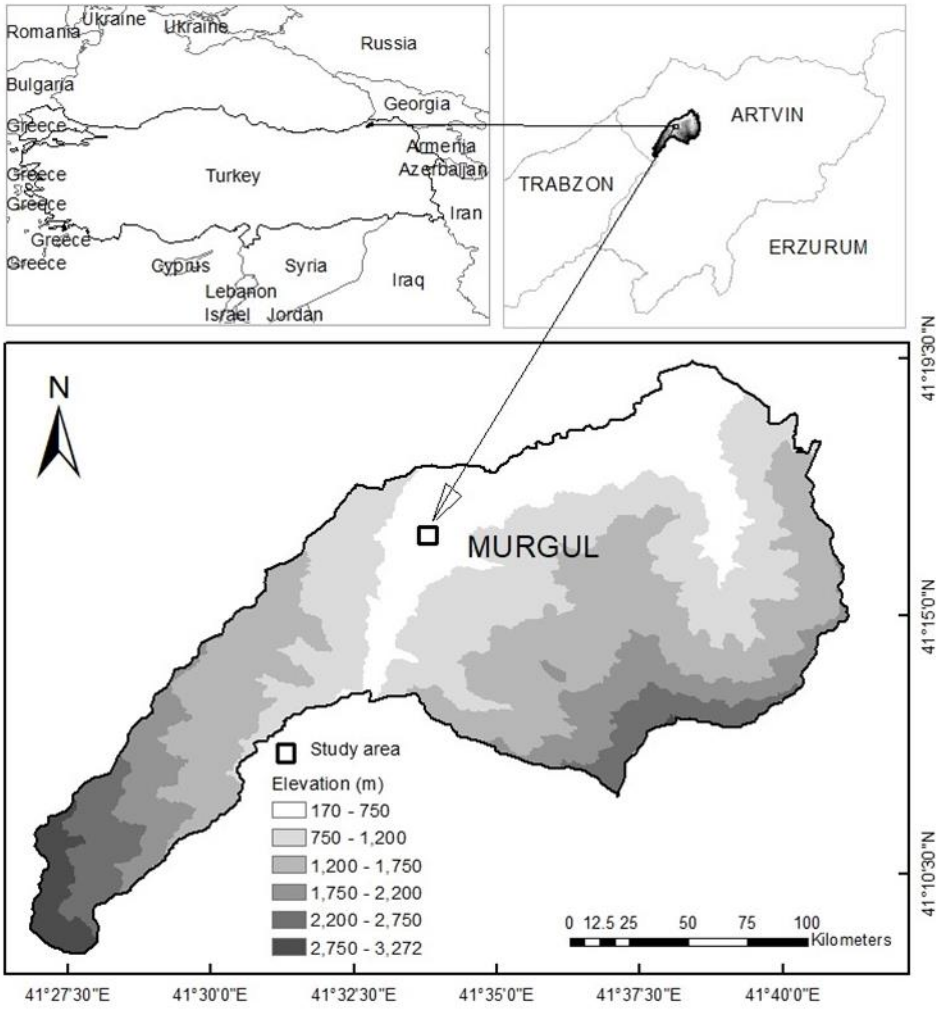

Figure 1. *Location of the study area in Murgul province, northeast Turkey*

The study area shows Eastern Black Sea climate under Black Sea macroclimate type, temperate in winter, warmer in summer and quite rainy in all seasons. According to the extrapolated climate data from the meteorological station closest to the study area, the annual mean temperature and the annual mean precipitation are 11.2 °C and 1213 mm, respectively. Mean annual minimum and maximum temperature are 7.1 °C and 16.6 °C, respectively (DMI, 2005). The growing season in the region is about six months (from May to October). The climate type is AB'1rb'3 (perhumid, mesothermal with no season of water deficiency, close to oceanic climate) according to Thornthwaite (1948).

In the district, along with oriental spruce, beech (*Fagus orientalis*), fir (*Abies nordmanniana)*, Scotch pine (*Pinus sylvestris)* and alder (*Alnus glutinosa)* species are found. Regarding understory vegetation, European mountain ash (*Sorbus aucuparia),* Caucasina laurel *(Prunus officinalis),* black sea holly *(Ilex colchica), common elder (Sambucus nigra),* European blueberry *(Vaccinium myrtillus),* Caucasian honeysuckle *(Lonicera caucasica),* fly honeysuckle *(Lonicera xylosteum),* rock red currant *(Ribes biebersteinii), oriental currant (Ribes orientale),* pontic azalea *(Rhododendron ponticum),* and yellow azalea *(Rhododendron luteum)* species are widely spread on the forest floor (Ansin, 1980).

http://www.aloki.hu ● ISSN 1589 1623 (Print) ● ISSN 1785 0037 (Online)
DOI: http://dx.doi.org/10.15666/aeer/1705_1230512321

Soil sampling and analyses

The sampling was done during the summer season of 2017. 54 sample plots were determined and equally distributed in 2-slope aspects such as north facing slopes (NFS) and south facing slopes (SFS), and 3 land use/land cover (LULC) types including 18-black alder, 18-black locust and 18-grassland with 9-replicate (2 slope aspects × 3 LULC × 9-replicate = 54). Top soil is the most common used part in related to LUCC-soil quality studies because of its susceptibility to LUCC (Gol, 2017). Therefore, 54-top soil (disturbed) and 54-soil-core (undisturbed) samples were collected at 0-20 cm soil depth to determine some soil properties. All soil samples were air-dried and sieved through 2-mm mesh before analyses. All measurements were done with two repetitions. Bulk density (BD) was determined by steel core sampler after soil samples were oven-dried at 105 °C (Blake and Hartge, 1986). Soil skeleton (Stoniness) was determined using undisturbed soil core samples. Soil texture analysis was done using Bouyoucos hydrometer method (Bouyoucos, 1962). Soil acidity (pH) and electrical conductivity (EC) were determined in 1:2.5 and 1:5 soil: distilled water ratio, respectively with glass electrode, and organic carbon (SOC) was determined using Walkley & Black wet digestion method and soil organic matter was calculated by multiplying percent of organic carbon with a factor of 1.724 2001 (Kalra and Maynard 1991). Soil lime content ($CaCO_3$) was determined with Schreiber's Calcimeter (Nelson, 1982). Total nitrogen (TN) was determined following Kjelhdal digestion, distillation, and titration method (Pansu and Gautheyrou, 2007). Carbon-nitrogen ratio (C:N) was determined as the ratio of total carbon to total nitrogen. Potentially mineralisable-N (NO_3^--N plus NH_4^+-N) was determined by microdestillation method following Bremner and Keeney (1965) in the beginning and at the 63rd days of incubation, and the net mineral nitrogen was calculated for 63 days (Ammonium for 63 days: Ammon63; Nitrate for 63 days: Nitrate63; Total N for 63 days: T63) using the difference between beginning and 63rd day (Guleryuz et al., 2007). Heavy metals in soil such as Cadmium (Cd), Chromium (Cr), Cupper (Cu), Lead (Pb) and Zinc (Zn) were determined with ICP-OES following EPA (1996) 3051 procedure.

Data analyses

Pearson correlation analysis was performed to determine the significant ($p < 0.005$) relationships among variables. Then, two-way analysis of variance (ANOVA) was used following the general linear model procedure to determine the effects of factors (vegetation cover, slope aspect) and their interaction (vegetation cover*slope aspect) on dependent variables. Tukey HSD test were used to determine differences between vegetation cover groups. To interpret the interaction, six new variables were computed with original cells as a level. Then, one-way ANOVA was run and simple main effects from one-way ANOVA was examined using the contrast results 2005). An anthropogenic index (AI) which indicates antropogenic impacts on selected soil properties with a specific number, using partial eta-squared values from two-way ANOVA, developed by Zhang et al. (2012) was used using the formula below:

$$AI = \frac{1}{n} + \sum_{i=1}^{n} \left(\frac{\eta 2ai}{\eta 2ni + \eta 2ai} \right) \times 100 \qquad \text{(Eq.1)}$$

http://www.aloki.hu ● ISSN 1589 1623 (Print) ● ISSN 1785 0037 (Online)
DOI: http://dx.doi.org/10.15666/aeer/1705_1230512321

where $\eta 2_{ai}$ and $\eta 2_{ni}$ refer to partial eta-squared values of land use and soil series for a certain soil property, respectively, and n is the number of soil properties. In this study, $n = 19$. Anthropogenic index ranges from 0 to 1: the larger the AI value, the higher the anthropogenic impact. All statistical analyses were performed using SPSS v20.0 (IBM.Corp, 2011).

Results and discussion

Changes in physical soil properties

Soil texture among the land uses ranged from sandy loam to loamy clay. The texture classes were determined as loamy clay (44%), clayey loam (44%) and the remaining (12%) for black locust; loamy clay (50%), clayey loam (28%) and the remaining (22%) for black alder; and sandy loam (39%), loam (33%) and the remaining (28%) for grasslands. Sand content of soil differed significantly ($p < 0.001$) both for vegetation cover and slope aspect (*Fig. 2b; Table 1*). Sand content of soil on NFS (60.3%) was found significantly ($p < 0.001$) higher than that on SFS (52.1%). Sand content of grassland soils (64.9%) was significantly ($p < 0.001$) higher than that of black alder (52.8%) and black locust (51.4%). Mean sand content did not differ significantly ($p = 0.33$) for their interaction (*Table 1*).

Clay content of soils also differed significantly ($p < 0.01$) with vegetation cover, slope aspect and their interaction (*Fig. 2a; Table 1*). Clay content of NF slope soils (17.3%) was found significantly lower than that of SF slope soils (27.1%). Clay content of grassland soils (14.3%) was significantly ($p < 0.001$) lower than that of black alder (26.1%) and black locust (26.3%). Clay content of NF black alder soils (19.1%) was found significantly ($p < 0.001$) lower than that of SF ones (33.5%) and mean clay content of NF black alder soils (19.1%) was found significantly ($p = 0.015$) higher than that of NF grassland soils (12.0%) (*Table 1*). The lower clay and higher sand contents in grasslands, having little or no protective vegetation cover, may be due to the removal of clay by erosion (Miheretu and Yimer, 2018; Tsehaye and Mohammed, 2013; Bewket and Stroosnijder, 2003). Hung et al. (2017) stated that the higher clay content in tree systems (e.g. forests) compared to other land uses may attribute to the protective cover by tree crowns, roots and litter reducing soil erosion. BD in the present study ranged from 1.38 gr/cm3 to 1.84 gr/cm3 and was not significantly affected by any of the factors according to two-way ANOVA ($p > 0.05$) (*Table 1*). BD in forests was found lower than that in other land uses (e.g. grassland) by some other researchers (Assefa et al., 2017; Gol, 2017; Tesfaye et al., 2016; Toohey et al., 2018; Yesilonis et al., 2016). The lower BD in forests as compared to the other land uses can be attributed to higher clay content and loosening of the surface soil with plant root growth (Qi et al., 2018). Vegetation cover, slope aspect and their interaction significantly affected soil stoniness ($p < 0.001$). The stoniness of soil was not differed significantly between NFS and SFS ($p = 0.91$). The stoniness of grassland soil (46.9%) was higher than that of black alder (38.9%) and black locust (35.6%) soils ($p < 0.005$). The interaction between vegetation cover and slope aspect also significantly affected soil stoniness (*Fig. 2c; Table 1*). Soil stoniness of SF grassland (53.8%) was significantly higher than that of black alder (32.2%) and black locust (32.0%) ($p < 0.001$). The slope aspect significantly affected only grassland soil ($p = 0.005$). The soil stoniness of NF grassland (35.8%) was found lower than that of SF grassland (53.8%).

http://www.aloki.hu ● ISSN 1589 1623 (Print) ● ISSN 1785 0037 (Online)
DOI: http://dx.doi.org/10.15666/aeer/1705_1230512321

Table 1. *Physical properties (mean ± standard error) of surface soils according to LULC and slope aspect*

LULC	SASP	Sand (%)	Clay (%)	Silt (%)	BD (gr/cm^3)	Stoniness (%)
Black locust	NFS	55.9±0.9_a_A	19.1±0.8_a_A	25.0±0.7_a_A	1.6±0.0_a_A	39.2±1.5_a_A
	SFS	46.9±1.9_a_A	33.5±1.1_b_A	19.6±1.4_a_A	1.6±0.0_a_A	32.0±1.6_a_A
Black alder	NFS	58.4±3.2_a_AB	20.7±2.1_a_A	20.9±1.4_a_A	1.7±0.0_a_A	41.9±1.9_a_A
	SFS	47.2±2.5_b_A	31.4±2.0_b_A	21.4±0.9_a_A	1.5±0.0_a_A	35.8±3.8_a_A
Grassland	NFS	66.6±2.4_a_B	12.0±1.3_a_B	21.4±2.6_a_A	1.6±0.0_a_A	39.9±3.4_a_A
	SFS	62.0±1.8_a_B	16.6±1.0_a_B	21.4±1.7_a_A	1.6±0.0_a_A	53.8±2.2_b_B
Two-way ANOVA	LULC	F=20.1 p<0.001	F=43.8 p<0.001	F=0.0 p>0.05	F=0.0 p>0.05	F=10.1 p<0.001
	SASP	F=20.3 p<0.001	F=68.5 p<0.001	F=1.7 p>0.05	F=0.0 p>0.05	F=0.0 p<0.001
	Interaction	F=1.1 p>0.05	F=5.7 p<0.01	F=2.2 p>0.05	F=3.1 p>0.05	F=10.6 p<0.001

LULC: land-use/land cover, SASP: slope aspect, NFS: north facing slopes, SFS: south facing slopes, BD: bulk density. By slope aspect, values of same LULC follow the various lower-case letters indicate significant difference. By LULC, values of same slope aspect follow the various upper-case letters differ significantly

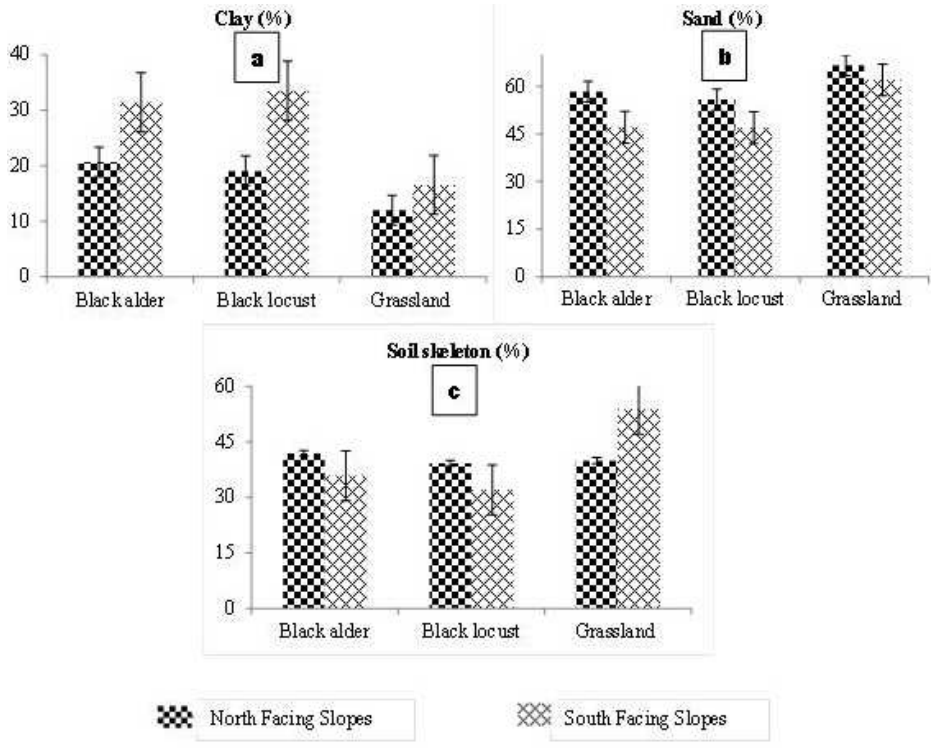

Figure 2. *Physical soil properties significantly affected by LULC and slope aspect*

Changes in chemical soil properties

The pH in the study area ranged from 3.93 (very strongly acidic) to 7.79 (weakly alkaline) according to Hazelton and Murphy (2016). This range is consistent with other

http://www.aloki.hu ● ISSN 1589 1623 (Print) ● ISSN 1785 0037 (Online)
DOI: http://dx.doi.org/10.15666/aeer/1705_1230512321

studies (Kuo et al., 1983). pH was significantly affected by vegetation cover ($p < 0.001$), slope aspect ($p = 0.005$) and their interaction ($p < 0.001$) (*Fig. 3a; Table 3*). pH of grassland soils (5.29) was found significantly lower than that of black locust (6.03) and black alder (6.72) soils ($p < 0.001$). As the slope aspect changes from north to south for all vegetation covers, soil pH significantly increased from 5.82 to 6.21 (*Table 3*). The interaction also affected soil pH ($p < 0.001$). While, black locust soil pH was significantly found lower than that of other vegetation cover soils in NFS, grassland soil pH was significantly lower than that of other vegetation cover soils in SFS. The change of land use from forests to grasslands resulted in a decrease in soil pH may be attributed to either removal of basic cations by harvesting/grazing or leaching of them because of sparse vegetation cover 2018). Shrestha and Lal (2011) also reported a significant increase in soil pH after reclamation of soil. Some researchers (Kucuk, 2013; Tufekcioglu and Kucuk, 2004) reported the results unlike ours. Kucuk (2013) for example, reported that soil pH in forests (5.35) was lower than that in grasslands (6.87).

Soil EC in the study area changed between 19.5 and 421 µS/cm which is in the class of non-saline soils meaning salinity effects are mostly negligible according to Hazelton and Murphy (2016). All factors including also interaction significantly affected soil EC ($p < 0.001$) (*Fig.3b; Table 3*). EC significantly decreased in the order of black alder > black locust > grasslands. As the aspect changed from north to south, EC increased from 97.5 to 179.1 µS/cm. According to interaction between two-factors, while the lowest soil EC in north and south aspects was determined in black locust and grasslands respectively as 40.1 and 29.9 µS/cm (*Table 3*). This change may be attributed to the leaching of soil bases and subsequent reduction in soil carbonate (Biro et al., 2013). The correlation between EC and $CaCO_3$ in the study area was significant ($r = 0.71$ and $p < 0.01$) (*Table 2*).

Table 2. *Pearson correlation coefficient (r) between selected soil properties*

		(1)	(2)	(3)	(4)	(5)	(6)	(7)	(8)	(9)	(10)	(11)	(12)	(13)	(14)	(15)	(16)	(17)	(18)	(19)
(1)	Sand	1																		
(2)	Clay	-.87**	1																	
(3)	Silt	-.41**	-.09	1																
(4)	pH	-.35**	.53**	-.28*	1															
(5)	OM	.48**	-.48**	-.08	-.38**	1														
(6)	CaCO3	-.38**	.47**	-.10	.53**	-.20	1													
(7)	EC	-.50**	.69**	-.27*	.85**	-.28*	.71**	1												
(8)	TN	-.03	-.02	.10	-.07	.35**	-.13	-.01	1											
(9)	CN	.33*	-.33*	-.06	-.16	.27*	-.12	-.21	-.49**	1										
(10)	BD	.01	-.04	.04	.03	-.12	-.10	-.08	.06	-.13	1									
(11)	Stoniness	.36**	-.38**	-.03	-.41**	.51**	-.07	-.34*	.36**	-.04	.12	1								
(12)	Ammon63	.45**	-.51**	.03	-.51**	.36**	-.09	-.41**	-.12	.13	.12	.55**	1							
(13)	Nitrat63	-.04	.17	-.24	.43**	-.08	-.05	.28*	.24	-.09	.05	-.17	-.42**	1						
(14)	T63	.22	-.12	-.24	.16	.13	-.11	.06	.19	-.02	.12	.14	.14	.84**	1					
(15)	Cd	.11	-.08	-.07	.02	.07	-.04	.18	.01	-.06	-.17	-.10	.02	.28	.30	1				
(16)	Cr	-.49**	.57**	-.04	.69**	-.51**	.42*	.66**	-.30	-.04	-.14	-.71**	-.49**	.17	-.12	-.07	1			
(17)	Cu	-.02	-.15	.32	-.26	-.05	-.13	-.16	.05	-.09	-.35*	-.18	.00	-.12	-.13	.38*	.13	1		
(18)	Pb	.24	-.27	.00	-.59**	.28	-.27	-.37*	.11	-.03	-.12	.41*	.53**	-.16	.17	.45**	-.67**	.27	1	
(19)	Zn	.24	-.26	-.02	-.25	.21	-.22	-.13	.05	.11	-.20	.00	.14	.23	.33	.81**	-.41*	.29	.66**	1

**Correlation is significant at the 0.01 level. *Correlation is significant at the 0.05 level. pH: soil acidity, EC: electrical conductivity, TN: total nitrogen, CN: carbon: nitrogen ratio, BD: bulk density, stoniness: soil skeleton, Ammon6 Nitrat63 and T 63: ammonium, nitrate and total nitrogen mineralization for 63-day, Cd: cadmium, Cr: chromium, Cu: copper, Pb: lead, Zn: zirconium

http://www.aloki.hu ● ISSN 1589 1623 (Print) ● ISSN 1785 0037 (Online)
DOI: http://dx.doi.org/10.15666/aeer/1705_1230512321

Table 3. *Chemical properties (mean ± standard error) of surface soils according to LULC and slope aspect*

LULC	SASP	pH	OM (%)	CaCO3 (%)	EC (µS/cm)	TN (%)
Black locust	NFS	4.7±0.0_a_A	1.9±0.2_a_A	1.2±0.1_a_A	40.1±2.8_a_A	0.094±0.003_a_AB
	SFS	7.4±0.2_b_A	1.5±0.2_a_A	3.0±0.7_a_A	248.5±30.1_b_A	0.080±0.004_a_A
Black alder	NFS	6.4±0.1_a_B	2.7±0.3_a_A	1.6±0.3_a_A	162.6±26.5_a_B	0.117±0.008_a_A
	SFS	7.0±0.3_a_A	1.5±0.2_b_A	2.8±0.7_a_A	258.8±30.8_b_A	0.085±0.004_b_A
Grassland	NFS	6.3±0.2_a_B	2.0±0.1_a_A	1.2±0.2_a_A	90.0±11.7_a_A	0.078±0.009_a_B
	SFS	4.3±0.1_b_B	3.1±0.4_b_B	1.2±0.1_a_A	29.9±2.9_a_B	0.096±0.007_a_A
Two-way ANOVA	LULC	F=38.5 p<0.001	F=6.5 p<0.01	F=3.2 p>0.05	F=25.3 p<0.001	F=3.3 p<0.01
	SASP	F=8.5 p<0.01	F=0.0 p>0.05	F=7.7 p<0.01	F=22.0 p<0.001	F=3.3 p<0.01
	Interaction	F=103.0 p<0.001	F=10.6 p<0.001	F=1.9 p>0.05	F=20.1 p<0.001	F=7.6 p<0.01
LULC	**SASP**	**CN**	**Ammon63 (kg/ha)**	**Nitrat63 (kg/ha)**	**T63 (kg/ha)**	
Black locust	NFS	11.6±1.1_a_A	28.5±1.3_a_AB	32.0±2.9_a_A	60.5±2.3_a_A	
	SFS	11.1±1.4_a_A	23.8±3.6_a_A	42.5±2.8_a_AB	66.3±4.4_a_A	
Black alder	NFS	13.2±1.2_a_A	22.3±1.9_a_A	66.4±5.9_a_B	88.7±5.8_a_B	
	SFS	10.0±1.4_a_A	21.2±1.9_a_A	51.4±4.7_a_B	72.6±5.4_a_A	
Grassland	NFS	25.7±11.9_a_A	31.2±2.2_a_B	39.7±5.0_a_A	70.9±5.5_a_A	
	SFS	20.0±2.9_a_B	40.6±2.1_a_B	30.5±2.7_a_A	71.2±3.2_a_A	
Two-way ANOVA	LULC	F=3.3 p>0.05	F=20.3 p<0.001	F=19.7 p<0.001	F=19.7 p<0.001	
	SASP	F=0.0 p>0.05	F=0.0 p>0.05	F=1.8 p>0.05	F=1.8 p>0.05	
	Interaction	F=0.0 p>0.05	F=5.2 p<0.01	F=5.1 p<0.01	F=5.1 p<0.01	

LULC: land-use/land cover, SASP: slope aspect, NFS: north facing slopes, SFS: south facing slopes, OM: organic matter, EC: electrical conductivity, TN: total nitrogen, CN: carbon: nitrogen ratio, Ammon6 Nitrat63 and T63: ammonium, nitrate and total nitrogen mineralization for 63-day. By slope aspect, values of same LULC follow the various lower-case letters indicate significant difference. By LULC, values of same slope aspect follow the various upper-case letters differ significantly

Organic matter classes of soils in the study area ranged from weak (1.69%) in black locust to moderate (2.59%) in grasslands according to 2016). Organic matter content of black alder soils (1.70%) were significantly found lower than that of grassland soils (2.59%)($p = 0.002$) (*Fig. 3c; Table 3*). Similar results were found by some other researchers (Pu et al., 2018; Wei et al., 2011; Yesilonis et al., 2016). The slope aspect alone did not affect soil organic matter ($p = 0.46$). In SFS, soil organic matter content of grasslands (3.13%) was higher than that of black locust (1.51%) and black alder (1.49%) (*Fig. 3c; Table 3*). While soil organic matter content of black alder increased from south (1.49%) to north (2.66%) facing slopes ($p = 0.02$), that of grasslands decreased ($p = 0.037$). The positive effect of north aspect on organic matter content by also found by Qin et al. (2017). Increasing organic matter content in north aspect can be attributed to more organic carbon and more total nitrogen accumulation in the soil because of higher soil water content and less evaporation (Johnson et al., 2011).

http://www.aloki.hu ● ISSN 1589 1623 (Print) ● ISSN 1785 0037 (Online)
DOI: http://dx.doi.org/10.15666/aeer/1705_1230512321

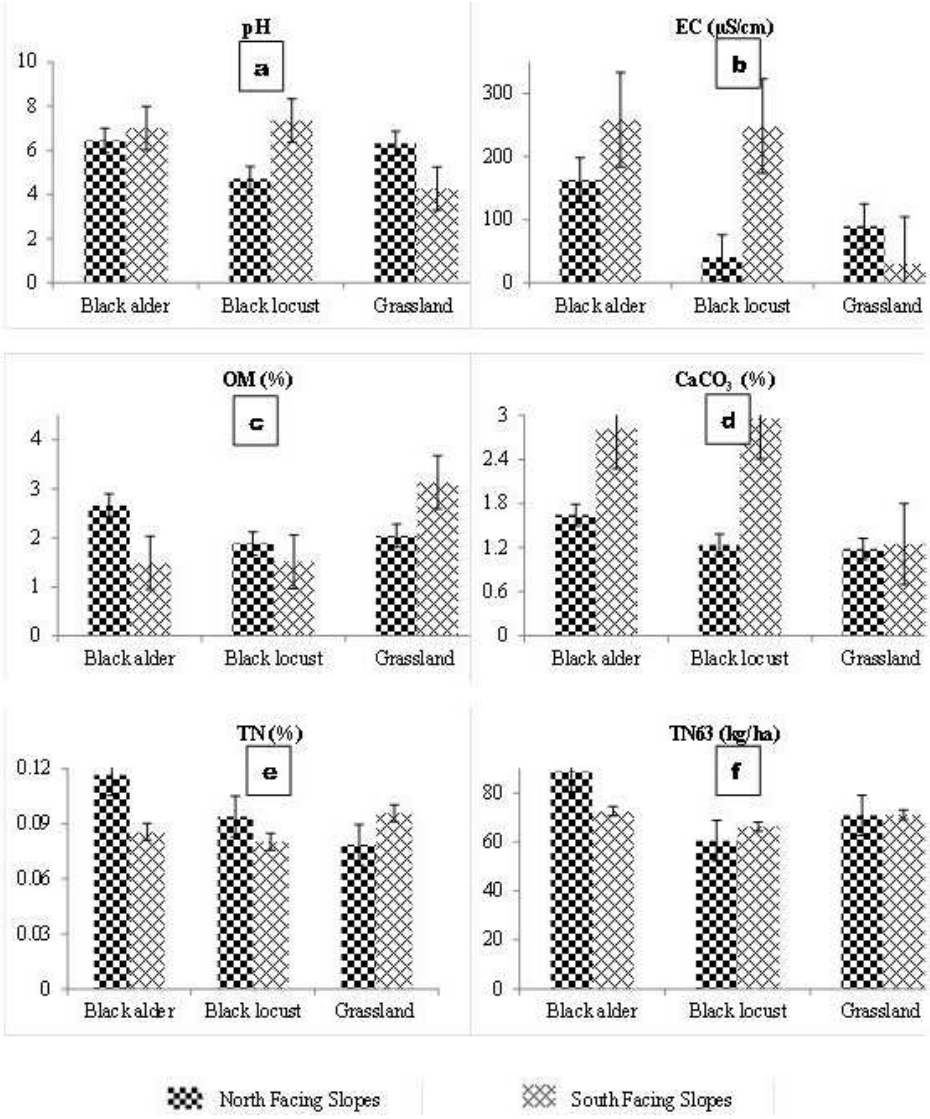

Figure 3. *Chemical soil properties significantly affected by LULC and slope aspect*

On the one hand, $CaCO_3$ content of soils was not significantly affected by vegetation cover ($p = 0.05$) and vegetation cover*slope aspect interaction ($p = 0.164$), on the other hand, the content decreased from south (2.34%) to north (1.35%) without considering vegetation cover effect ($p = 0.008$) (*Fig. 3d; Table 3*).

When not considered the effects of vegetation cover, soil EC in SFS (179.1 µS/cm) was also significantly greater than that in NFS (97.5 µS/cm)($p < 0.001$). Soil EC in grasslands (59.9 µS/cm) was found significantly lower than that in black locust (144.3 µS/cm, $p = 0.01$) and black alder (210.7 µS/cm, $p < 0.001$) without considering slope aspect effect. In SFS, soil EC of grassland (29.9 µS/cm) was found significantly less than that of other vegetation covers ($p < 0.001$). Soil EC of vegetation covers except grasslands increased from NFS to SFS (*Table 3*).

TN of soils was not affected by vegetation covers ($p = 0.05$) and slope aspect ($p = 0.07$) but significantly affected by their interaction. It significantly increased from south (0.085%) to north (0.117%) for only black alder ($p = 0.012$) (*Fig. 3e; Table 3*). That increase may be attributed to improving ecological condition depending on more

http://www.aloki.hu ● ISSN 1589 1623 (Print) ● ISSN 1785 0037 (Online)
DOI: http://dx.doi.org/10.15666/aeer/1705_1230512321

moisture in north. Similar results were found by some other researchers (Bangroo et al., 2017; Gol, 2017; Rezaei et al., 2006). Soil TN of north –facing black alder (0.117%) was found significantly greater than that of NF grasslands (0.078%) ($p = 0.001$). This can be attributed to removal of organic matter with grazing and higher level of N-fixation in black alder (Ripley et al., 2010; Wilson et al., 2011). Similar results were reported by some other researchers (Beheshti et al., 2012; Miheretu and Yimer, 2018; Tesfaye et al., 2016; Wilson et al., 2011). Soil C:N ratio was not significantly affected by vegetation cover ($p = 0.05$), slope aspect ($p = 0.46$) and their interaction ($p = 0.87$) (*Table 3*). While Miheretu and Yimer (2018) and Chacon et al. (2009) also found similar results like in the present study. Significant effects of land use on soil C:N ratio also found in some other studies (Assefa et al., 2017; Kucuk, 2013).

Looked at variables regarding 63-day nitrogen mineralization (ammonium, nitrate and total); slope aspect alone had no significant effect on 63-day nitrogen mineralization. Vegetation cover alone had significant effect on 63-day ammonium, nitrate and total nitrogen mineralization. 63-day ammonium mineralization of grassland soils (35.9 kg/ha) was found significantly higher than that of black locust (26.1 kg/ha) and black alder (21.8 kg/ha) ($p < 0.001$). Higher ammonium mineralization in grassland soils can be attributed to lower pH (Xue et al., 2013). The correlation between NH4-N and pH was negative ($p < 0.0$ $r = -0.59$) (*Table 2*). Similar results were found by Wei et al. (2011) in loess plateau of China who reported higher nitrogen mineralization in grassland soils compared to others due to lower bulk density. Nitrate and total nitrogen mineralization in 63-day period of black alder soils (58.8 kg/ha and 80.6 kg/ha) were found significantly higher than that of the other vegetation covers (*Fig. 3f; Table 3*). Higher nitrate mineralization in forest (alder) soils compared to the other land uses can be attributed to that on the one hand, black alder, being one of the N-fixing trees provides resources both easily accessible and abundant for soil microbes and facilitates N mineralization, on the other hand, it contributes to the supply of organic substrates which are easily decomposed and decrease C:N ratio (Cui et al., 2018). The higher nitrate mineralization can also be attributed to positive correlation with pH ($r = 0.4$ $p < 0.01$) (*Table 2*). Similar results were found also by some other researchers (Hart et al., 1997; Tecimen et al., 2013; Uri et al., 2008). Uri et al. (2008), for example, reported higher annual net nitrogen mineralization (99 kg/ha) in the birch stand than that (51 kg/ha) of in grasslands in Estonia. Tecimen et al. (2013) explained the difference with the effect of increasing organic carbon. The 63-day ammonium mineralization of SF grassland soils (40.6 kg/ha) was found significantly higher than that of SF black locust (23.7 kg/ha) and black alder (21.2 kg/ha) soils ($p < 0.001$). Both in NFS and SFS, 63-day nitrate mineralization of black alder soils (66.4 kg/ha and 51.4 kg/ha respectively) was significantly higher than that of grassland soils (39.7 kg/ha and 30.5 kg/ha respectively). 63-day total nitrogen mineralization of NF black locust soils (60.5 kg/ha) was lower than that of black alder soils in the same aspect (88.7 kg/ha).

Changes in heavy metal concentrations

Average Cd and Zn contents of soils in the study area were 0.7 ppm (0 to 6.3 ppm) and 148.5 ppm (72 to 312 ppm), respectively. These values are slightly higher than the average concentrations (0.5 ppm for Cd and 64 ppm for Zn) reported by Kabata-Pendias and Mukherjee (2007). This can be due to the copper mine near the study area. Cd and Zn concentrations among heavy metals did not significantly differed according to vegetation cover, slope aspect and their interaction ($p > 0.05$) (*Table 4*).

http://www.aloki.hu ● ISSN 1589 1623 (Print) ● ISSN 1785 0037 (Online)
DOI: http://dx.doi.org/10.15666/aeer/1705_1230512321

Cr concentration in soil ranged from 5.2 to 29.5 ppm with the average value of 20.2 ppm. This value is consistent with the range of world mean (54 ppm) reported by Kabata-Pendias and Mukherjee (2007). Soil Cr concentration of grasslands (13.8 ppm) was found significantly lower than that of black alder (23.3 ppm) and black locust (24.4 ppm)($p < 0.001$). The soil Cr content of black alder and black locust significantly increased from NFS to SFS unlike grasslands ($p < 0.05$). The soil Cr content of SF grassland (6.7 ppm) was significantly lower than that of black alder (28 ppm) and black locust (26.8 ppm) in the same aspect (*Fig. 4a; Table 4*). Higher Cr contents of forest soil may be related to higher pH ($r = 0.6$ $p < 0.01$) (*Table 2*) (Kabata-Pendias and Mukherjee, 2007).

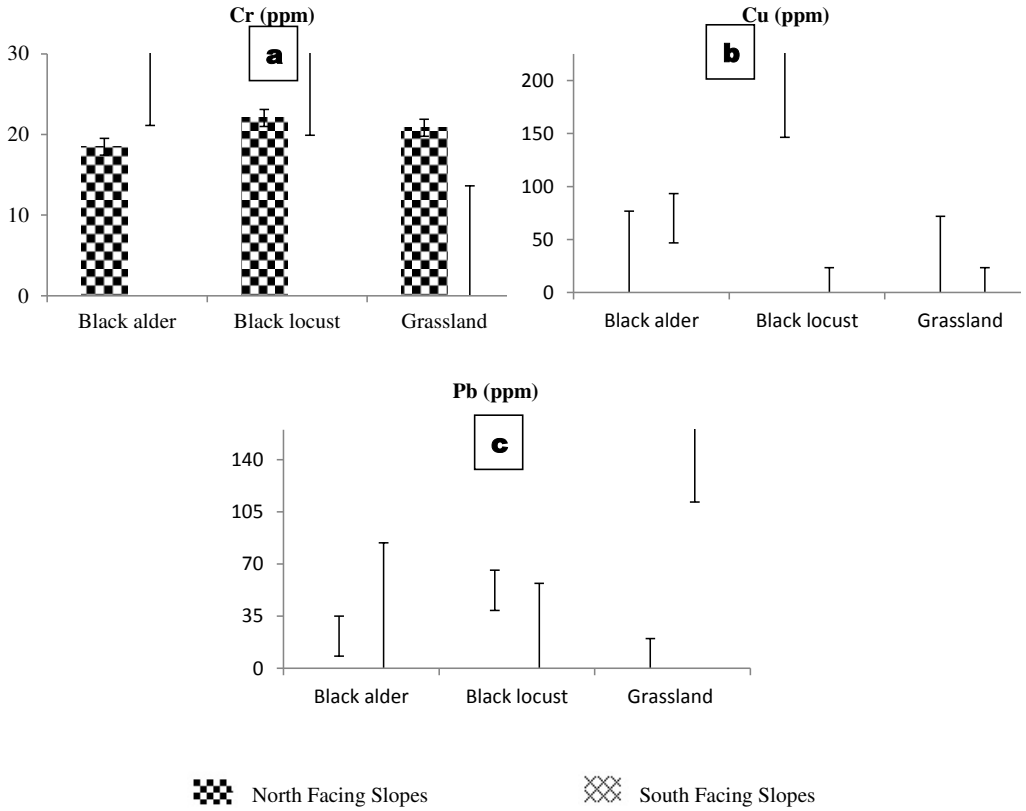

Figure 4. *Heavy metal contents of soils significantly affected by LULC and slope aspect*

Cu content of soils in the study area ranged from 0 to 380 ppm with the average value of 49 ppm. This range is consistent with the range in the world (2 to 250 ppm) reported by Kabata-Pendias and Mukherjee (2007). Soil Cu concentration of black locust (109.1 ppm) was significantly higher than that of grassland (0.001 ppm) ($p = 0.007$). While in north aspects, the lowest and the highest soil Cu concentrations belonged to grasslands (0.001 ppm) and black locust (218.3 ppm), respectively, in south aspects, the lowest and highest soil Cu concentrations belonged to grassland (0.001 ppm) and black alder respectively (70.0 ppm) (*Fig. 4b; Table 4*). Higher Cu contents in forest soils might be related to higher clay contents than that in grassland soils ($r = 0.7$ $p < 0.001$) (*Table 2*). Zheng et al. (2016) also reported positive correlation between Cu and clay contents of soil for coastal soils in China.

http://www.aloki.hu ● ISSN 1589 1623 (Print) ● ISSN 1785 0037 (Online)
DOI: http://dx.doi.org/10.15666/aeer/1705_1230512321

Pb content of soils in the study area ranged from 0 to 254.2 ppm with the average value of 48 ppm. This value is higher than that in the world (up to 90 ppm) Kabata-Pendias and Mukherjee (2007). Pb concentration was found significantly highest in grassland soils (80.5 ppm) compared to black locust (33.2 ppm) and black alder (31.3 ppm) soils. The Pb concentration significantly increased from north (26.8 ppm) to south (69.9 ppm) ($p = 0.002$). In SFS, grassland soils had significantly higher Pb concentration than others ($p < 0.001$). Grassland soil Pb concentration increased from north (6.5 ppm) to SFS (154.5 ppm) (*Fig. 4c; Table 4*). The lower Pb content in forest soils may be related to higher pH ($r = -0.5$ $p < 0.01$) and higher clay content ($r = 0.7$ $p < 0.001$) (*Table 2*). The lower Pb content in black alder and black locust may be related to phytoremediation (Escobar and Dussan, 2016; Babu et al., 2013; Escobar and Dussan, 2016; Lee et al., 2009). *Alnus acuminata* subsp. acuminata for example, took Pb and Cr up as 135 mg/kg and 71 mg/kg, respectively (Escobar and Dussan, 2016).

Many studies have been performed to determine the effects of copper smelter on heavy metal concentration (Adamo et al., 2002; Dudka et al., 1996; Hutchinson and Whitby, 1977; Kuo et al., 1983). For example, Adamo et al. (2002) found the related heavy metal concentrations of soil near the smelter in Ontario, Canada as 43 3 5 2.7 and 63 ppm for Cu, Pb, Zn, Cd and Cr, respectively. Hutchinson and Whitby (1977) reported heavy metal concentrations in soils for Cu, Pb and Zn near the Sudbury smelting region of Canada as 134 51 and 62 ppm, respectively. Cai et al. (2015) reported the average heavy metal concentrations in soil near Tonglushan copper mine in Hubei, China for Cu, Pb and Cd as 38 120 and 2.59 ppm, respectively. While Cu, Pb, Cd and Cr concentrations in soils determined in the present study was consistent with those in the other studies (Adamo et al., 2002; Dudka et al., 1996; Hutchinson and Whitby, 1977; Kuo et al., 1983), Zn was found higher than the others.

Comparison of main factors' effects with partial eta squared (η2)

The anthropogenic index was computed using *Equation 1*. This index indicates which main factor was more effective on selected soil properties, natural (slope aspect) or anthropogenic (land use/land cover). This index was computed as 0.75 closer to indicates adverse human impact on soil properties.

The partial eta-squared values (η2) were also used to compare the effect size (explained proportion of variance by any factor) of main factors and their interaction on selected soil properties. The related values (η2) were presented in *Tables 4* and *Figure 5*. Regarding soil texture, clay was the most affected texture component by land use, slope aspect and their interaction with η2 values of 0.6 0.59 and 0.1 respectively (*Fig. 5*). pH, EC and OM were the most significantly affected soil chemical properties after Cr by land use, slope aspect and their interaction respectively, were pH with values of 0.6 0.1 0.81; EC with values of 0.5 0.3 0.46 and OM with values of 0.2 0.0 0.31 (*Fig. 5*).

The most significantly affected soil properties by land use and interaction was found Cr with values of 0.93 and 0.94 (*Fig. 5*). The significant interaction effect on soil properties such as pH, OM, TN, Stoniness and heavy metals except Cd was found higher than that of main factors. That means the interaction between main factors strengthen the effect. For example, while effect size of land use and slope aspect on Pb content were 0.29 and 0.27 respectively, the interaction effect was found 0.54 which was about two times higher than that of the other factors (*Table 4*).

http://www.aloki.hu ● ISSN 1589 1623 (Print) ● ISSN 1785 0037 (Online)
DOI: http://dx.doi.org/10.15666/aeer/1705_1230512321

Table 4. *Heavy metal contents (mean ± standard error) of surface soils according to LULC and slope aspect*

LULC	SASP	Cd (ppm)	Cr (ppm)	Cu (ppm)	Pb (ppm)	Zn (ppm)
Black locust	NFS	0.3±0.2_a_A	22.0±0.6_a_A	218.3±66.0_a_A	52.3±17.6_a_A	140.6±8.0_a_AB
	SFS	0.0±0.0_a_A	26.8±0.9_b_A	0.0±0.0_b_A	14.0±5.2_a_A	113.3±12.9_a_A
Black alder	NFS	0.7±0.3_a_A	18.5±0.5_a_B	4.9±3.1_a_B	21.6±5.6_a_AB	164.5±15.1_a_B
	SFS	2.1±1.3_a_A	28.1±0.5_b_A	70.0±45.9_a_A	41.1±22.7_a_A	167.2±40.5_a_A
Grassland	NFS	0.0±0.0_a_A	20.8±0.4_a_A	0.0±0.0_a_B	6.5±1.7_a_B	119.5±11.8_a_A
	SFS	1.0±0.3_a_A	6.7±0.5_b_B	0.0±0.0_a__A	154.5±25.1_b_B	186.0±12.1_a_A
Two-way ANOVA	LULC	F=2.4	F=196.1	F=5.7	F=6.1	F=2.0
		p>0.05	p<0.001	p<0.01	p<0.01	p>0.05
	SASP	F=2.2	F=0.0	F=3.6	F=11.0	F=0.0
		p>0.05	p>0.05	p>0.05	p<0.01	p>0.05
	Interaction	F=1.2	F=221.3	F=10.2	F=18.0	F=2.9
		p>0.05	p<0.001	p<0.001	p<0.001	p>0.05

LULC: land-use/land cover, SASP: slope aspect. NFS: north facing slopes, SFS: south facing slopes. By slope aspect, values of same LULC follow the various lower-case letters indicate significant difference. By LULC, values of same slope aspect follow the various upper-case letters differ significantly

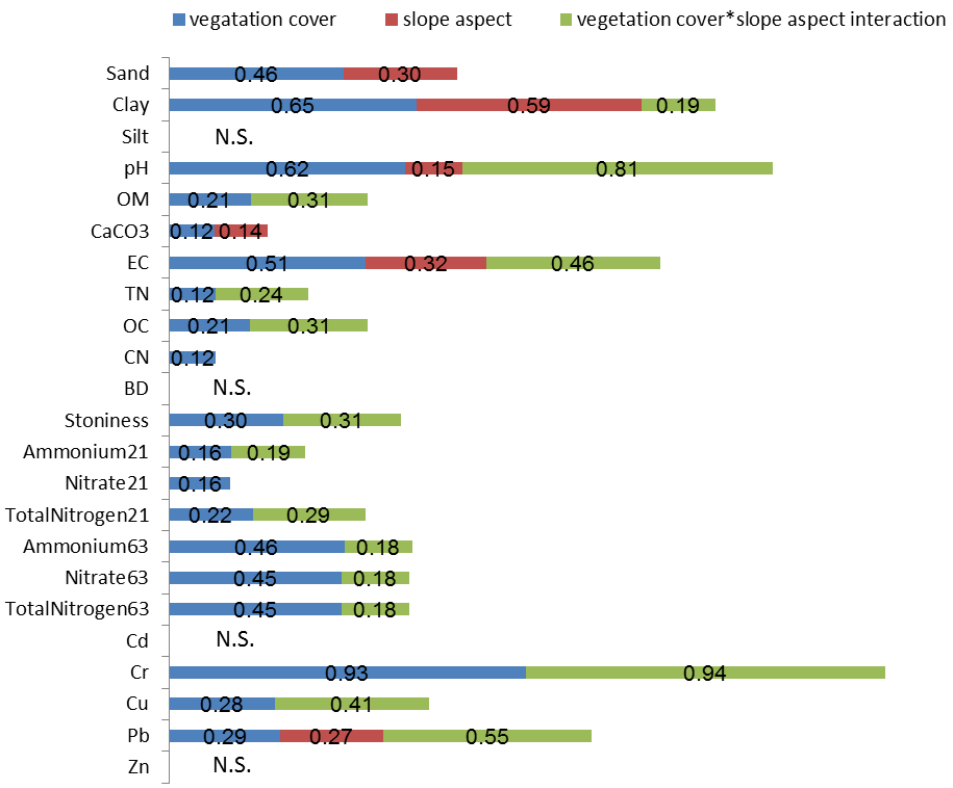

Figure 5. *Effect size (η2) of independent variables on selected soil properties*

Conclusion

The results from the present study showed significant interaction effect beside LULC and slope aspect on selected soil properties. In general, main factors and their interaction improved selected soil properties affecting soil quality. The most affected

http://www.aloki.hu ● ISSN 1589 1623 (Print) ● ISSN 1785 0037 (Online)
DOI: http://dx.doi.org/10.15666/aeer/1705_1230512321

soil properties by LULC and slope aspect were Cr content and clay content, respectively. The improving effects of afforestation compared to grasslands was revealed on only clay contents and soil skeleton among physical properties; pH, nitrate and total nitrogen mineralization for 63-day among chemical properties. Our study showed that changes in LULC from grasslands to forest (especially to black alder) promoted soil quality in terms of total nitrogen and NO_3-N, playing a fundamental role in ecological restoration, beside other soil properties. Although decreasing effect (phytoremediation) of black alder and black locust on heavy metals except Pb in soil was not found In the present study, *Alnus glutinosa* and *Robinia pseudoacacia* may be suggested for the restoration/reclamation of mining soils in terms of phytoremediation beside their advantages such as improving nitrogen mineralization. However, further periodical studies are needed to determine the improving effects of afforestation on soil properties after mining. Results from the present study may be generalized to larger areas which are similar to the study area in terms of land-use and vegetation cover

Acknowledgements. This research was supported by Artvin Coruh University Scientific Research Project Unit, Turkey (Ref. No. 2016.F10.02.13). We thank Dr. Aydin Tufekcioglu and Dr. Funda OGUT from Artvin Coruh University for their valuable proofreading.

REFERENCES

[1] Acatay, A. (1968): Smoke damages from copper smelter factory in Murgul. – Journal of the Faculty of Forestry Istanbul University, Series A, 18(1): 1-17 (in Turkish).

[2] Adamo, P., Dudka, S., Wilson, M. J., McHardy, W. J. (2002): Distribution of trace elements in soils from the Sudbury smelting area (Ontario, Canada). – Water Air Soil Poll 137: 95-116.

[3] Allgaier, F. (1997): Environmental Effects of Mining. – In: Marcus, J. J. (ed.) Mining Environmental Handbook: Effects of Mining on the Environment and American Environmental Controls on Mining. World Scientific, River Edge, NJ, pp 132-189.

[4] Anonymous (2002): 1/500.000 Scaled Trabzon and Samsun Plates. – General Directorate of Mineral Research and Exploration, Ankara.

[5] Ansin, R. (1980): Flora of Eastern Black Sea Region and floristic content of primary vegetation types. – Associate Professorship Thesis, Karadeniz Technical University.

[6] Assefa, D., Rewald, B., Sanden, H., Rosinger, C., Abiyu, A., Yitaferu, B., Godbold, D. L. (2017): Deforestation and land use strongly effect soil organic carbon and nitrogen stock in Northwest Ethiopia. – Catena 153: 89-99. DOI: 10.1016/j.catena2017.02.003.

[7] Babu, A. G., Kim, J. D., Oh, B. T. (2013): Enhancement of heavy metal phytoremediation by *Alnus firma* with endophytic *Bacillus thuringiensis* GDB-1. – J Hazard Mater 250: 477-483.

[8] Bangroo, S., Najar, G., Rasool, A. (2017): Effect of altitude and aspect on soil organic carbon and nitrogen stocks in the Himalayan Mawer Forest Range. – Catena 158: 63-68.

[9] Beheshti, A., Raiesi, F., Golchin, A. (2012): Soil properties, C fractions and their dynamics in land use conversion from native forests to croplands in northern Iran. – Agr Ecosyst Environ 148: 121-133. DOI: 10.1016/j.agee.2011.12.001.

[10] Biro, K., Pradhan, B., Buchroithner, M., Makeschin, F. (2013): Land use/land cover change analysis and its impact on soil properties in the Northern Part of Gadarif region, Sudan. – Land Degrad Dev 24: 90-102. DOI: 10.1002/ldr.1116.

[11] Blake, G. R., Hartge, K. (1986): Bulk Density 1. – In: Klute, A. (ed.) Methods of Soil Analysis. Part 1: Physical and Mineralogical Methods. SSSA, ASA, Madison, WI, pp. 363-375.

http://www.aloki.hu ● ISSN 1589 1623 (Print) ● ISSN 1785 0037 (Online)
DOI: http://dx.doi.org/10.15666/aeer/1705_1230512321

[12] Bouyoucos, G. J. (1962): Hydrometer method improved for making particle size analyses of soils. – Agronomy Journal 54: 464-465.
[13] Bremner, J., Keeney, D. R. (1965): Steam distillation methods for determination of ammonium, nitrate and nitrite. – Analytica Chimica Acta 32: 485-495.
[14] Cai, L. M., Xu, Z. C., Qi, J. Y., Feng, Z. Z., Xiang, T. S. (2015): Assessment of exposure to heavy metals and health risks among residents near Tonglushan mine in Hubei, China. – Chemosphere 127: 127-135.
[15] Chacon, G., Gagnon, D., Pare, D. (2009): Comparison of soil properties of native forests, *Pinus patula* plantations and adjacent pastures in the Andean highlands of southern Ecuador: land use history or recent vegetation effects? – Soil Use Manage 25: 427-433. DOI: 10.1111/j.1475-2743.2009.00233.x.
[16] Cui, J., Hirota, M., Kamijo, T., Yoshitake, S., Katoh, K. (2018): Soil net nitrogen mineralization at different ecosystem development stages after the year 2000 eruption on Miyakejima Island. – Journal of Ecosystem & Ecography 8: 1-9. DOI: 10.4172/2157-7625.250.
[17] Deng, X. Z., Zhao, C. H., Yan, H. M. (2013): Systematic modeling of impacts of land use and land cover changes on regional climate: a review. – Adv Meteorol. DOI: 10.1155/2013/317678.
[18] DMI (2005): Meteorological Bulletin. – Turkish State Meteorological Service, Ankara.
[19] DPT (2001): Mining Special Commission Report. – DPT, Ankara.
[20] Dudka, S., PonceHernandez, R., Tate, G., Hutchinson, T. C. (1996): Forms of Cu, Ni, and Zn in soils of Sudbury, Ontario and the metal concentrations in plants. – Water Air Soil Poll 90: 531-542.
[21] EPA (1996): Microwave Assisted Acid Digestion of Sediments, Sludges, Soils, and Oils. OHW, Method 3051. – EPA, Washington.
[22] Erdin, K. (1983): Remote sensing in forestry and determination of smoke damages by infrared colour films (in Turkish). –
[23] Escobar, M. P., Dussan, J. (2016): Phytoremediation potential of chromium and lead by *Alnus acuminata* subsp *acuminata*. – Environ Prog Sustain 35: 942-948.
[24] Fischer, A., Fischer, H. (2006): Restoration of forests. In: van Andel, J., Aronson, J. (eds.). Restoration ecology. Blackwell Publishing, Malden, Massachusetts, U.S.A. p. 124–140.
[25] Gol, C. (2017): Effects of aspect and changes in land use on organic carbon and soil properties in Uludere catchment, semi-arid region: Turkey. – Rend Lincei-Sci Fis Nat 28: 463-469. DOI: 10.1007/s12210-017-0619-x.
[26] Guleryuz, G., Kirmizi, S., Arslan, H. (2007): Nitrogen mineralisation in the soils of alpine mat communities: an incubation experiment under laboratory conditions. – Turkish Journal of Botany 31: 277-286.
[27] Hart, S. C., Binkley, D., Perry, D. A. (1997): Influence of red alder on soil nitrogen transformations in two conifer forests of contrasting productivity. – Soil Biol Biochem 29: 1111-1123.
[28] Hazelton, P., Murphy, B. (2016): Interpreting Soil Test Results: What Do all the Numbers Mean? – CSIRO Publishing, Clayton.
[29] Hung, T. T., Doyle, R., Eyles, A., Mohammed, C. (2017): Comparison of soil properties under tropical *Acacia* hybrid plantation and shifting cultivation land use in northern Vietnam. – Southern Forests: A Journal of Forest Science 79(1): 9-18.
[30] Hutchinson, T., Whitby, L. (1977): The effects of acid rainfall and heavy metal particulates on a boreal forest ecosystem near the Sudbury smelting region of Canada. – Water, Air, and Soil Pollution 7: 421-438.
[31] IBM.Corp (2011): IBM SPSS Statistics for Windows, Version 20.0. – IBM Corp, Armonk, NY.
[32] Johnson, K. D. et al. (2011): Soil carbon distribution in Alaska in relation to soil-forming factors. – Geoderma 167-68: 71-84. DOI: 10.1016/j.geoderma.2011.10.006.

http://www.aloki.hu ● ISSN 1589 1623 (Print) ● ISSN 1785 0037 (Online)
DOI: http://dx.doi.org/10.15666/aeer/1705_1230512321

[33] Kabata-Pendias, A., Mukherjee, A. B. (2007): Trace Elements from Soil to Human. – Springer Science & Business Media, Berlin.
[34] Kalra, Y. P., Maynard, D. G. (1991): Methods Manual for Forest Soil and Plant Analysis (Vol. 319). – Forestry Canada, Northwest Region, Northern Forestry Centre, Edmonton, Alberta.
[35] Kucuk, M. (2013): Determination of nitrogen mineralization and soil respiration in different slope and aspect groups of oak stands and pasture. – Ph. D. Thesis, Karadeniz Technical University.
[36] Kuo, S., Heilman, P. E., Baker, A. S. (1983): Distribution and forms of copper, zinc, cadmium, iron, and manganese in soils near a copper smelter. – Soil Science 135: 101-109.
[37] Lal, R. (2004): Soil carbon sequestration to mitigate climate change. – Geoderma 123:1-22.
[38] Lee, D.-B., Nam, W., Kwak, Y.-S., Cho, N.-H., Lee, S.-S. (2009): Phytoremediation of heavy-metal-contaminated soil in a reclaimed dredging area using *Alnus* species. – Journal of Ecology and Environment 32: 267-275.
[39] Leech, N., Barrett, K., Morgan, G. A. (2013): SPSS for Intermediate Statistics: Use and Interpretation. – Routledge, New York.
[40] Liu, X. Y., Bai, Z. K., Zhou, W., Cao, Y. G., Zhang, G. J. (2017): Changes in soil properties in the soil profile after mining and reclamation in an opencast coal mine on the Loess Plateau, China. – Ecological Engineering 98: 228-239. DOI: 10.1016/j.ecoleng.2016.10.078.
[41] Mahmood, R. et al. (2010): Impacts of land use/land cover change on climate and future research priorities. – Bulletin of the American Meteorological Society 91: 37-46.
[42] Miheretu, B. A., Yimer, A. A. (2018): Spatial variability of selected soil properties in relation to land use and slope position in Gelana sub-watershed, Northern highlands of Ethiopia. – Phys Geogr 39: 230-245. DOI: 10.1080/02723646.2017.1380972.
[43] Negasa, T., Ketema, H., Legesse, A., Sisay, M., Temesgen, H. (2017): Variation in soil properties under different land use types managed by smallholder farmers along the toposequence in southern Ethiopia. – Geoderma 29: 40-50.
[44] Nelson, R. (1982): Carbonate and Gypsum. – In: Page, A. L. (ed.) Methods of Soil Analysis. Part 2: Chemical and Microbiological Properties. SSSA, ASA, Madison, WI, pp. 181-197.
[45] Oruc, N. (2013): Environmental effects of Murgul Copper Factory: a review. – International Caucasia Forestry Symposium, Artvin Coruh University, October 24-26.
[46] Pansu, M., Gautheyrou, J. (2007): Handbook of soil Analysis: Mineralogical, Organic and Inorganic Methods. – Springer, Berlin Heidelberg.
[47] Pu, X., Cheng, H. G., Tysklind, M., Xie, J., Lu, L., Yang, S. T. (2018): Indications of soil properties on dissolved organic carbon variability following a successive land use conversion. – Ecological Engineering 117: 115-119. DOI: 10.1016/j.ecoleng.2018.03.018.
[48] Qi, Y., Chen, T., Pu, J., Yang, F., Shukla, M. K., Chang, Q. (2018): Response of soil physical, chemical and microbial biomass properties to land use changes in fixed desertified land. – Catena 160: 339-344.
[49] Qin, Y.Y., Holden, N., Feng, Q., Zhu, M. (2017): Influence of Slope Aspect on Plant Community Composition and its Implications for Restoration of a Chinese Mountain Range. – Pol J Environ Stud 26: 375-383 doi:10.15244/pjoes/64458.
[50] Rezaei, S. A., Arzani, H., Tongway, D. (2006): Assessing rangeland capability in Iran using landscape function indices based on soil surface attributes. – Journal of Arid Environments 65: 460-473.
[51] Ripley, S.W., Krzic, M., Bradfield, G.E., Bomke, A.A. (2010): Land-use impacts on selected soil properties of the Yungas/Chaco transition forest of Jujuy province,

http://www.aloki.hu ● ISSN 1589 1623 (Print) ● ISSN 1785 0037 (Online)
DOI: http://dx.doi.org/10.15666/aeer/1705_1230512321

northwestern Argentina: a preliminary study. – Canadian Journal of Soil Science 90: 679-683 doi:10.4141/cjss09101.

[52] Shrestha, R. K., Lal, R. (2011): Changes in physical and chemical properties of soil after surface mining and reclamation. – Geoderma 161: 168-176.

[53] Tecimen, H. B., Sevgi, O., Yurtseven, H., Sevgi, E., Ozturk, M. (2013): Net nitrogen mineralization and nitrification rates in different land uses: an in situ incubation. – Fresen Environ Bull 22: 1173-1178.

[54] Tesfaye, M. A., Bravo, F., Ruiz-Peinado, R., Pando, V., Bravo-Oviedo, A. (2016): Impact of changes in land use, species and elevation on soil organic carbon and total nitrogen in Ethiopian Central Highlands. – Geoderma 261: 70-79. DOI: 10.1016/j.geoderma.2015.06.022.

[55] Thornthwaite, C. W. (1948): An approach toward a rational classification of climate. – Geographical Review 38: 55-94.

[56] Toohey, R. C., Boll, J., Brooks, E. S., Jones, J. R. (2018): Effects of land use on soil properties and hydrological processes at the point, plot, and catchment scale in volcanic soils near Turrialba, Costa Rica. – Geoderma 315: 138-148. DOI: 10.1016/j.geoderma.2017.11.044.

[57] Tsehaye, G., Mohammed, A. A. (2013): Effects of land-use/cover changes on soil properties in a dryland watershed of Hirmi and its adjacent agro ecosystem: northern Ethiopia. – International Journal of Geosciences Research 1(1): 45-57.

[58] Tufekcioglu, A., Kucuk, M. (2004): Soil respiration in young and old oriental spruce stands and in adjacent grasslands in Artvin, Turkey. – Turkish Journal of Agriculture and Forestry 28: 429-434.

[59] TUİK (2013): Artvin with Selected Indicators. – Turkish Statistical Institute, Ankara.

[60] Uri, V., Lohmus, K., Kund, M., Tullus, H. (2008): The effect of land use type on net nitrogen mineralization on abandoned agricultural land: Silver birch stand versus grassland. – Forest Ecology and Management 255: 226-233.

[61] Wei, X. R., Shao, M. A., Fu, X. L., Agren, G. I., Yin, X. Q. (2011): The effects of land use on soil N mineralization during the growing season on the northern Loess Plateau of China. – Geoderma 160: 590-598.

[62] Wilson, B. R., Koen, T. B., Barnes, P., Ghosh, S., King, D. (2011): Soil carbon and related soil properties along a soil type and land-use intensity gradient, New South Wales, Australia. – Soil Use Manage 27: 437-447. DOI: 10.1111/j.1475-2743.2011.00357.x.

[63] Xu, X. L., Ma, K. M., Fu, B. J., Song, C. J., Liu, W. (2008): Relationships between vegetation and soil and topography in a dry warm river valley, SW China. – Catena 75: 138-145.

[64] Xue, Z.J., Cheng, M., An, S.S. (2013): Soil nitrogen distributions for different land uses and landscape positions in a small watershed on Loess Plateau. – China Ecological Engineering 60: 204-213.

[65] Yener, I. (2013): Investigation of relationships between some ecological factors and the growth of pure oriental spruce (*Picea orientalis* (L.) link) forests at different sites. – Ph. D. Thesis, Karadeniz Technical University.

[66] Yesilonis, I., Szlavecz, K., Pouyat, R., Whigham, D., Xia, L. (2016): Historical land use and stand age effects on forest soil properties in the Mid-Atlantic US. – Forest Ecology and Management 370: 83-92. DOI: 10.1016/j.foreco.2016.03.046.

[67] Zhang, W. T., Weindorf, D. C., Zhu, Y. D., Haggard, B. J., Bakr, N. (2012): Soil series and land use impacts on major soil properties: a quantitative comparison. – Soil Res 50: 390-396. DOI: 10.1071/sr11247.

[68] Zheng, R., Zhao, J. L., Zhou, X., Ma, C., Wang, L., Gao, X. J. (2016): Land use effects on the distribution and speciation of heavy metals and arsenic in coastal soils on Chongming Island in the Yangtze River Estuary, China. – Pedosphere 26: 74-84. DOI: 10.1016/s1002-0160(15)60024-8.

http://www.aloki.hu ● ISSN 1589 1623 (Print) ● ISSN 1785 0037 (Online)
DOI: http://dx.doi.org/10.15666/aeer/1705_1230512321

PREPARATION AND APPLICATION OF MONOCLONAL ANTIBODY TO SUGARCANE (*SACCHARUM* L. SPP. HYBRIDS) SOP5CS PROTEIN

LI, J.[1] – WANG, L. R.[1] – HUANG, X.[2] – XING, Y. X.[1] – YANG, L. T.[1*] – LI, Y. R.[2*]

[1]*College of Agriculture, Guangxi University, Nanning 530005, China*

[2]*Key Laboratory of Sugarcane Biotechnology and Genetic Improvement (Guangxi), Ministry of Agriculture and Rural Area; Guangxi Key Laboratory of Sugarcane Genetic Improvement; Sugarcane Research Center, Chinese Academy of Agricultural Sciences-Guangxi Academy of Agricultural Sciences, Nanning 530007, China*

**Corresponding authors*
e-mail: litao61@hotmail.com (L. T. Yang), liyr@gxaas.net (Y. R. Li)

(Received 5th May 2019; accepted 16th Jul 2019)

Abstract. Δ[1]-pyrroline-5-carboxylate synthase (P5CS) is a key enzyme in proline biosynthesis. In this study, the nucleotide sequence of sugarcane *P5CS* (*SoP5CS*) gene was obtained from sugarcane. Then the ORF of *SoP5CS* linked with pET-30a vector and the SoP5CS protein was expressed successfully in *E. coli* by the induction of 1.0 mM IPTG at 28 °C for 6 h. The prokaryotic expression protein was expressed as inclusion bodies (IBs). It was purified by Ni- NTA Resin firstly and then refolded, dialyzed and further purified by gel filtration. The monoclonal antibody of SoP5CS was prepared using mice. The expression of *SoP5CS* gene and the corresponding protein and physiological parameters associated with drought resistance were detected in sugarcane leaves under different drought stresses, they worked together to regulate the drought resistance process of sugarcane. This is the first report on the preparation of P5CS monoclonal antibody and the expression of the antibody in sugarcane, which would provide new methods to study the function of SoP5CS response to various abiotic stresses and other aspects.
Keywords: *sugarcane, P5CS gene; proline, monoclonal antibody, physiological index*

Abbreviations: ABA: Abscisic acid; CAT: Catalase; cDNA: Complementary DNA; DTT: Dithiothreitol; ELISA: Enzyme-linked immunosorbent assay; IBs: Inclusion bodies; IPTG: Isopropyl-β-D-thiogalactopyranoside; LB: Luria-Bertani; MDA: Maleic dialdehyde; ORF: Open reading frame; P5CS: Δ[1]-pyrroline-5-carboxylate synthase; PBS: Phosphate buffer saline; PCR: Polymerase chain reaction; POD: Peroxidase; ROS: Reactive oxygen species; RWC: Relative water content; SDS-PAGE: Sodium dodecyl sulfate polyacrylamide gel electrophoresis; So: *Saccharum officinarum;* SOD: Superoxide dismutase

Introduction

Proline plays an important role in plant osmotic adjustment processes, and it is a penetration protective agent, protein stabilizer and free-radical scavenger (Kishor et al., 2005). Studies have shown that the accumulation of proline showed a positive correlation with stress adaptation of drought and salt in plants (Kishor et al., 1995). In normal conditions, proline is synthesized mainly by ornithine pathway, whereas it is made directly through the glutamate pathway under stress conditions (Delauney et al., 1993). P5CS is a bifunctional enzyme and catalyzes the first two steps of glutamate pathway (Kishor et al., 1995).

In plants, the activity of P5CS was assayed in duckweed under gradually increasing cadmium stress (Qiao et al., 2015), and in *Arabidopsis thaliana* under salt tolerance (Saibi et al., 2015). More researches concentrated on the *P5CS* gene, which has been

http://www.aloki.hu ● ISSN 1589 1623 (Print) ● ISSN 1785 0037 (Online)
DOI: http://dx.doi.org/10.15666/aeer/1705_1232312335

isolated from many plants, such as cowpea (Hu et al., 1992), alfalfa (Ginzberg et al., 1998, barley (Romman et al., 2011), sorghum (Su et al., 2011), Chinese wolfberry (Guan et al., 2014); Nitraria tangutorum (Zheng et al., 2014), mulberry (Zhou et al., 2016), and others. The expression of *P5CS* gene was analyzed by RT-PCR under salt stress (Ortega et al., 2008), Northern blotting under drought (Porcel et al., 2004), salt (Do et al., 2003) stress and qRT-PCR (Jain et al., 2015) under drought stress. And previous research showed that drought stress could induce the changes in gene and protein expression and physiological parameters associated with drought resistance (Kuzuoglu-Ozturk et al., 2012; Dey et al., 2016; Wang et al., 2016; Cao et al., 2017).

Monoclonal antibody is widely employed in the detection and identification of protein in plants by Western blotting and enzyme-linked immunosorbent assay (ELISA). The former is widely used in studying the expression of a protein in different plant tissues (Pereira et al., 2005), under various stresses (Pruvot et al., 1996; Ozturk et al., 2012). Most reports have been focusing on transgenic plants accumulation of a foreign protein resistant to virus (Yu et al., 2011), disease (Maruthasalam et al., 2007), pest (McManus et al., 1999), abiotic stress (Subramanyam et al., 2012) and so on.

To our knowledge, there have not been any reports about P5CS monoclonal antibody in plants. Sugarcane (*Saccharum* L. spp. hybrids) is the most important sugar crop and one of the main agricultural commodities in the world. Guangxi is the largest sugarcane producing areas in China, however, about 80% of the sugarcane is planted in upland areas with shallow tillage layer and no irrigation system, so drought is a main constraint factor for sugarcane production (Li and Yang, 2015). The purpose of this study was to prepare monoclonal antibody of sugarcane P5CS gene to provide a reference for further study on the mechnism of sugarcane resistance to drought stress.

Materials and methods

Sugarcane material and treatments

The sugarcane variety GT 21 was used as plant material, and the single bud cane setts were planted in sand. After the seedlings grew to 3-4 leaves, they were transplanted to plastic pots containing sand and soil with the ratio of 1:2 for culturing. When the seedlings grew to 7-8 leaves, the consistent plants were selected for drought treatment, that is, the plants were subjected to withholding water and the control plants were well-watered. The leaf samples were collected from leaf + 1 (top visible dewlap leaf) at 0, 1, 3, 5 and 7 d, respectively, after drought treatment. There were three replications for each treatment and all the samples were wrapped in aluminum foil, placed in liquid nitrogen and stored at -80 °C.

Experiment reagents

The Trizol reagent and anti β-Actin mouse monoclonal antibody were bought from Beijing ComWin Biotech Co., Ltd. (Beijing, China); *Eco*R I and *Xho* I restriction enzymes and RevertAid First Strand cDNA Synthesis Kit were bought from Thermo Fisher Scientific (Shanghai, China); PMD18-T vector and DNA Ligation Kit were got from TaKaRa Company (Dalian, China). Escherichia coli DH5α and BL21 (DE3) were bought from TransGen Biotech (Beijing, China). Protein A Sefinose™ Kit, Ni-NTA-Sefinose Column, Sefinose™ CL-6B and Non-Interference Protein Assay Kit were products of Sangon Biotech Company (Shanghai, China). pET-30a was kept by the

http://www.aloki.hu ● ISSN 1589 1623 (Print) ● ISSN 1785 0037 (Online)
DOI: http://dx.doi.org/10.15666/aeer/1705_1232312335

laboratory. All other chemicals were obtained from commercial sources and analytical grade.

Isolation of SoP5CS

Total RNA of sugarcane leaves was extracted and tested the concentration and integrity by Implen P 300 NanoPhotometer and 1% agarose gel electrophoresis. The cDNA for gene cloning was synthesized using RevertAid First Strand cDNA Synthesis Kit. Based on the sugarcane *P5CS* gene sequences in GenBank (Accession No. Eu005373), the primers of upstream and downstream for both sides of its largest open reading frame (2148 bp) designed with Primer Premier 5.0 software are 5'-TCAGAATTCATGGCCACCGTGGACCGGACC-3', and 5'-TGTCTCGAGTTG-CAAAGGAAGGTTCTTATG-3', respectively, that *Eco*R I and *Xho* I restrict enzyme sites are underlined. The PCR products were purified and cloned into PMD18-T vector and sequenced on both strands in Beijing Genomics Institute (Shenzhen, China).

Prokaryotic expression, extraction and purification of SoP5CS protein

The pET-30a was used as the prokaryotic expression vector. The plasmids of recombinant strain PMD-SoP5CS and pET-30a were extracted and double digested with *Eco*R I and *Xho* I. Then *SoP5CS* and the vector fragments were ligated and transformed into the *E. coli* BL 21 (DE 3) cells. The recombinant plasmid was detected by PCR and sequenced (The Beijing Genomics Institute, Shenzhen), and verified by double enzymes digestion. The recombinant strain was incubated in liquid LB medium (contained 100 mg/L kanamycin) until the value of OD_{600} reached 0.4–0.6, and the target protein was induced with 1.0 mM IPTG for an additional 6 h. The cell pellets were collected by centrifugation and resuspended in lysis buffer (500 mM NaCl, 50 mM NaH_2PO_4, and 10 mM imidazole, pH 8.0), then lysed by sonication (pulse 5 s, pause 5 s, 20 min) using an ultrasonic processor VCX 750 (Sonics & Materials, Inc.). Then the cell lysate was centrifuged to precipitate the cellular debris and the supernatant was transferred to fresh microcentrifuge tubes for further purification using a Ni-NTA-Sefinose Column. Then the wash fractions were collected and analyzed by SDS-PAGE.

Refolding, dialysis and concentration of SoP5CS protein

The over expressed SoP5CS proteins were refolded under the buffer (PBS, 2 mM DTT, 0.05% SKL, pH 7.4) and centrifuged, then the supernatant was collected and dialyzed for overnight at 4 °C with dialysis tubing cellulose membrane (MW 10,000 Da, Sigma). The proteins were further dialyzed twice with fresh dialysis buffer each time for 3 h. The dialyzed proteins were analyzed by SDS–PAGE to confirm it remained intact and then purified by gel filtration using Sefinose™ CL-6B. Then the protein was concentrated by PEG 20000 and determined using the Non-Interference Protein Assay Kit.

Preparation of monoclonal antibody

Female BALB/c mice were immunized subcutaneously using conventional methods. The immunization was given 3 times with 2 week intervals after the first immunization. And the mice would have an ictus immunisatorius before the cell fusion. The antiserum was collected in 10 days after the last immunization and the SoP5CS antibody titer was

http://www.aloki.hu ● ISSN 1589 1623 (Print) ● ISSN 1785 0037 (Online)
DOI: http://dx.doi.org/10.15666/aeer/1705_1232312335

determined by indirect ELISA. The mouse whose antiserum exhibited the highest value of the antibody titer was selected for the subsequent fusion. Splenocytes of selected mice were fused with Sp2/0 cells, then the fused cells were suspended and placed into a total of 96 wells cell culture plates under 5% CO_2, 37 °C. Two weeks later, positive hybridomas were selected and subcloned. Supernatants from the positive wells were detected by indirect ELISA and the clones showed high titer and good condition were selected to generate ascites. Antiserum of selected mouse was reacted with different amounts of the purified SoP5CS protein to analyze the quality. For Western blotting, the dilution rate of SoP5CS antibody and goat anti-mouse antibody (Beijing ComWin Biotech Co., Ltd.) was 1:2000. The membrane was placed in FluorChem and HD2 (ProteinSimple) was exposed for 1-10 min for images captured by using electrochemiluminescence (ECL) substrate (PIERCE). Then the monoclonal antibodies were purified by using the protein A column and stored at -80 °C.

Application of monoclonal antibody

After drought treatment, the leaves were sampled to detect the expression of *SoP5CS* gene and its encoded protein. Besides, the physiological parameters, including proline, maleic dialdehyde (MDA) and abscisic acid (ABA) contents, superoxide dismutase (SOD), catalase (CAT) and P5CS activities, relative water content (RWC) and Chlorophyll content (SPAD value) were also measured. Total proteins in sugarcane leaves were extracted with the method of Parrott et al. (2005) and qRT-PCR was used the method described by Niu et al. (2015). RWC of the leaves were calculated with the method of Kautz et al. (2015). SPAD value was measured as the method of Phan et al. (2016). Other physiological parameters (contents of proline, MDA and ABA, and activities of SOD, CAT and P5CS) were measured using ELISA Kit (ColorfulGene Biological Technology Co., Ltd., Wuhan, China).

Statistical analysis

The data were analyzed using the IBM SPSS Statistics 20 software and Excel 2013 (Microsoft). There were three replicates for each experiment, and statistical differences were compared based on the Duncan's test with P values set at 0.05 and 0.01 levels.

Statement on ethical approval

All experimental procedures were conducted in conformity with institutional guidelines for the care and use of laboratory animals in The Animal Experimental Center of Shanghai General Hospital, Shanghai, China, and conformed to the National Institutes of Health Guide for Care and Use of Laboratory Animals.

Results

Construction of prokaryotic expression vector

Bands of about 2150 bp were obtained by RT-PCR (*Fig. 1A*) and they were recovered together and inserted into pMD-18T to get the recombinant plasmid pMD-SoP5CS which showed a fragment of 2148 bp by sequencing. ORF of *SoP5CS* was ligated with pET-30a and the recombinant plasmid pET-SoP5CS was expressed in *E. coli* BL 21 (DE 3) and confirmed by double digested with *Eco*R I and *Xho* I. The result

http://www.aloki.hu ● ISSN 1589 1623 (Print) ● ISSN 1785 0037 (Online)
DOI: http://dx.doi.org/10.15666/aeer/1705_1232312335

showed that the prokaryotic expression vector with *SoP5CS* gene pET-SoP5CS had been built successfully (*Fig. 1B*).

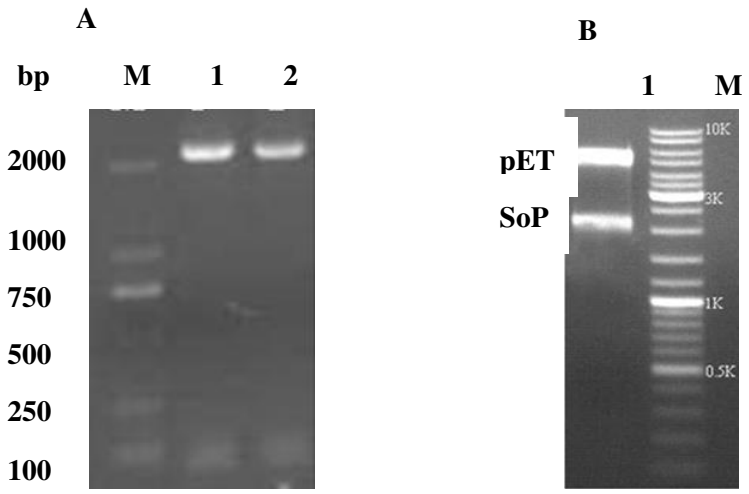

Figure 1. *Amplification of SoP5CS and verification of recombinant plasmid.* ***A*** *Products of RT-PCR from cDNA of sugarcane leave by. Lane 1-2, products of RT-PCR; Lane M, DNA marker.* ***B*** *Restriction enzymes digestion analysis of pET-SoP5CS plasmid. Lane 1, Products of double enzymes digestion. Lane M, DNA marker*

Expression, purification, AND concentration of SoP5CS protein

The molecular weight of the fusion SoP5CS protein is ~84 kDa according to the sequences of pET-30a and ORF of *SoP5CS*. SDS-PAGE analysis revealed that the target protein was expressed only in the insoluble inclusion bodies (IBs) (*Fig. 2A*). Then the SoP5CS protein was purified using Ni–NTA Resin (*Fig. 2B*), the final product was refolded and dialyzed. After gel filtration, the pure SoP5CS protein was obtained (*Fig. 2C*). Then the protein was concentrated using PEG 20000 and a expected single band of ~84 kDa protein was observed (*Fig. 2D*). About 15 mg of SoP5CS at the concentration of 1.37 mg/ml was obtained by the protein quantitative kit, and the purity was more than 90%, which meet the requirement of preparing the monoclonal antibody.

Titer and specificity analysis of SoP5CS antibody

After fusion of immunized BALB/c mouse splenocytes and Sp2/0 mouse myeloma cells, cell supernatant was measured by indirect ELISA (OD_{450}). The cell lines with the highest positive value were selected and subcloned. Nine hybridoma cell lines that stably secreted SoP5CS McAb were obtained and they were 1E1, 3D10, 3H10, 5F8, 5E12, 4D6, 4F10, 5C10 and 2F11. The titer of 9 hybridoma cell lines was determined by indirect ELISA method (*Table 1*). Based on the growth state, the cell line of 4F10 was finally selected to collect the supernatant which was purified by Protein A Sefinose™ Kit. The pure supernatant was reacted with different amounts of SoP5CS protein by Western blotting. The expected 84 kDa in different brightness bands were detected with different amount of antigen (*Fig. 3*).

According to the growth state, the cells of 4F10 and 4F10E8 were selected to inject the mice, and the ascites was purified by Protein A Sefinose™ Kit. The concentration of monoclonal antibody was 2.15 mg/ml measured with UV spectrophotometer. The titer

http://www.aloki.hu ● ISSN 1589 1623 (Print) ● ISSN 1785 0037 (Online)
DOI: http://dx.doi.org/10.15666/aeer/1705_1232312335

of the purified antibody was more than 64 k analyzed by indirect ELISA method (*Table 2*), which met the requirement of Western blotting detection. Thus, the preparation of SoP5CS monoclonal antibody was successful and it is ready for further research.

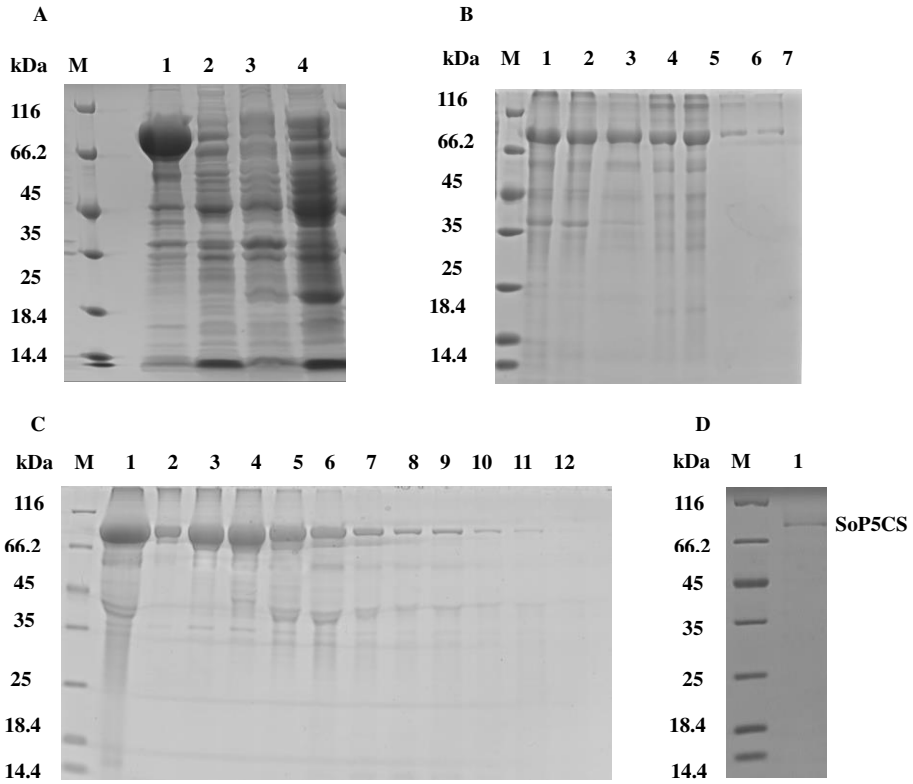

Figure 2. *Analysis of SoP5CS protein expression, purification and concentration by SDS-PAGE from pET-SoP5CS.* ***A*** *SoP5CS protein induced by 1.0 mM IPTG. Lane 1, induced 6 h, 28 °C (Precipitant); Lane 2, induced 6 h, 28 °C (Supernatant); Lane 3, no IPTG (Precipitant); Lane 4, no IPTG (Supernatant); Lane M, protein Marker.* ***B*** *The protein purification by Ni^{2+} affinity chromatography. Lane 1, before loading; Lane 2, flow through; Lane 3, wash with 20 mM imidazole; Lane 4-7, wash with 500 mM imidazole; Lane M, protein marker.* ***C*** *The protein purified with gel filtration (Lane 1-12).* ***D****, SoP5CS protein concentrated (Lane 1)*

Table 1. *Titer determination of supernatant of selected hybridoma cell lines by ELISA*

Sample	+	-	Blank	Dilution rate							
				1:1	1:100	1:200	1:400	1:800	1:1600	1:3200	1:6400
1E1	1.176	0.035	0.062	0.643	0.438	0.287	0.172	0.096	0.081	0.052	0.049
3D10	1.393	0.058	0.061	0.733	0.489	0.324	0.209	0.120	0.079	0.044	0.041
3H10	1.385	0.048	0.056	0.630	0.421	0.279	0.158	0.095	0.077	0.064	0.034
5F8	1.167	0.054	0.057	0.464	0.248	0.134	0.097	0.067	0.069	0.039	0.026
5E12	0.958	0.137	0.053	0.343	0.222	0.125	0.081	0.049	0.051	0.050	0.049
4D6	1.007	0.065	0.075	0.628	0.382	0.269	0.159	0.081	0.049	0.068	0.036
4F10	1.769	0.046	0.057	0.517	0.342	0.207	0.124	0.066	0.049	0.037	0.030
5C10	1.380	0.065	0.058	0.260	0.182	0.146	0.074	0.080	0.064	0.062	0.064
2F11	1.129	0.064	0.075	0.454	0.312	0.215	0.156	0.114	0.095	0.065	0.068

+: Positive control (the mouse serum before fusion). -: Negative control (the mouse serum before immunization). Blank: Antibody dilution buffer. The data are optical density values at 450 nm

http://www.aloki.hu ● ISSN 1589 1623 (Print) ● ISSN 1785 0037 (Online)
DOI: http://dx.doi.org/10.15666/aeer/1705_1232312335

Table 2. *Titer determination of monoclonal antibody by ELISA*

	+	-	Blank	Dilution rate						
				1:1000	1:2000	1:4000	1:8000	1:16000	1:32000	1:64000
OD_{450}	2.128	0.065	0.069	1.253	0.894	0.498	0.337	0.263	0.218	0.192

+: Positive control (the mouse serum before fusion). -: Negative control (the mouse serum before immunization). Blank: Antibody dilution buffer

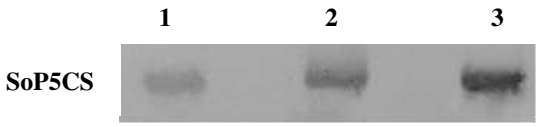

Figure 3. *Specificity analysis of SoP5CS antibody by Western blotting assay. The supernatant of selected hybridoma cell reacted with different amounts of the SoP5CS protein. Lane 1-3, loaded 1, 2 and 4 μg protein, respectively*

Expression of SoP5CS gene and its encoded protein in sugarcane under drought stress

Under drought stress, the expression level of *SoP5CS* increased rapidly, reached the peak at 5 d, which was 11.22-fold higher than that at 0 d, and also maintained at high levels (~5-fold) at 3 and 7 d (*Fig. 4A*). Endogenous SoP5CS proteins from sugarcane leaves under drought stress were detected by Western blotting and β-actin was used as the reference gene. A total of 25 μg protein was loaded in each lane and the results (*Fig. 4B, C*) indicated that the relative expression levels of SoP5CS under drought stress were all higher than that in normal condition (0 d). But the expression level of SoP5CS protein increased slightly that were all below 2-fold while compared to 0 d, and the highest expression was at 7 d (1.99-fold).

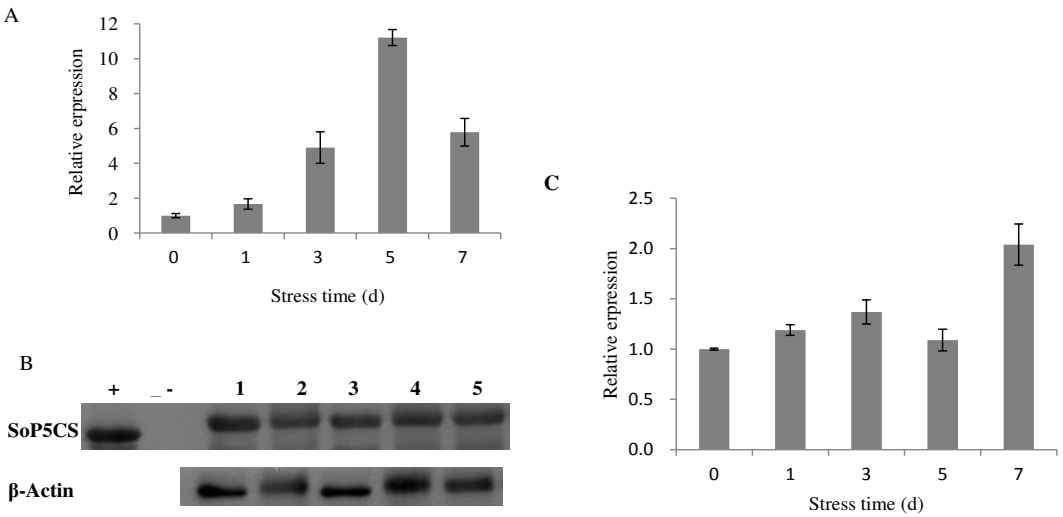

Figure 4. *Relative expression of SoP5CS gene (A) and its encoded protein (B, C) in sugarcane leaves under drought stress. For Western blotting, the anti-SoP5CS antibody reacted with endogenous SoP5CS protein from sugarcane leaves under different drought stresses. Lane 1-6, 0, 1, 3, 5 and 7 d under drought stress, respectively; Lane +, purified SoP5CS protein; Lane -, sterile water. Whiskers indicate the standard deviation of three replicates*

http://www.aloki.hu ● ISSN 1589 1623 (Print) ● ISSN 1785 0037 (Online)
DOI: http://dx.doi.org/10.15666/aeer/1705_1232312335

Physiological changes in sugarcane leaves under drought stress

Under drought stress, contents of proline and MDA increased rapidly and reached the peak at 7 d, and those at 1, 3 and 5 d were also significantly higher than those of 0 day (*Fig. 5A, C*). ABA content increased slightly and also reached the peak at 7 d (*Fig. 5B*).

As shown in *Figure 6A,* there was no significant difference in SOD activity between normal condition (0 d) and 1 d, while it was significantly higher at 3, 5 and 7 d. Drought stress treatments showed significantly higher CAT activity than that at 0 d (*Fig. 6B*). P5CS activity showed the trend of increase firstly and then decrease, which reached the peak at 3 d (*Fig. 6C*). Chlorophyll content and RWC decreased slightly firstly and then reduced markedly as the drought stresses were intensified (*Fig. 7*).

Discussion

There have been no literature reports on overexpression and purification of plant P5CS in *E. coli* yet, however, the prokaryotic expression vector of pET-30a has been used in different proteins from other plants (Wan et al., 2010; Zhu et al., 2012; Wang et al., 2015). In this research, the recombinant protein was expressed in *E. coli* as an inclusion body, but it takes long and intricate steps to form soluble proteins and it is difficult for purification (Nahálka et al., 2009). The formation of bacterial IBs is common due to an imbalance between protein deposition and removal (Carrio et al., 1999; Carrio and Villaverde, 2001). The concentration of IPTG, growth temperature and time may influence the expression pattern of recombinant protein (Sorensen and Mortensen, 2005; Montalbán et al., 2006). But in many cases, screening and optimization of these conditions still could not eliminate the formation of IBs (Sahdev et al., 2008; Xue et al., 2011). Although we made efforts to optimize the expression conditions, the recombinant protein still accumulated as IBs. The IBs of SoP5CS were firstly purified by Ni-NTA Resin and about 15 mg purified SoP5CS was obtained from 1 liter of culture broth after refolding, dialysis, gel filtration and concentration. The yield of SoP5CS was not very high compared with other proteins purified from inclusion body (Ruan et al., 2016), but it was enough for further use.

Under drought stress, drought resistance genes could be induced. And previous research showed that the expression of *P5CS* gene was up-regulated under drought stress (Jain et al., 2015; Zhou et al., 2016; Wei et al., 2016), which was consistent with the results of our study. The expression of SoP5CS protein in different drought stresses was also up-regulated but showed lower expression quantity compared to the corresponding gene. In this study, distinct changes in physiological parameters associated with drought resistance were also detected. The increased activities of both SOD and CAT could protect sugarcane cells against reactive oxygen species (ROS). The free proline acts as a multifunctional osmolyte in plants and plays important roles in enhancing osmotic stress tolerance (Krasensky and Jonak, 2012). Higher activity of P5CS could help synthesize more proline that act as an osmoprotectant thus help tolerate drought stress. Endogenous ABA was also increased with the up-regulated of *SoP5CS*, thus *SoP5CS* may be involved in an ABA-dependent stress signaling pathway. Previous studies showed that accumulation of ABA was important for the regulation of *P5CS* expression and proline accumulation level in *Lycium chinense* (Guan et al., 2014). The up-regulated expression of *SoP5CS* gene and the corresponding protein and physiological changes in sugarcane leaves might work together to regulate the drought resistance process of sugarcane.

http://www.aloki.hu ● ISSN 1589 1623 (Print) ● ISSN 1785 0037 (Online)
DOI: http://dx.doi.org/10.15666/aeer/1705_1232312335

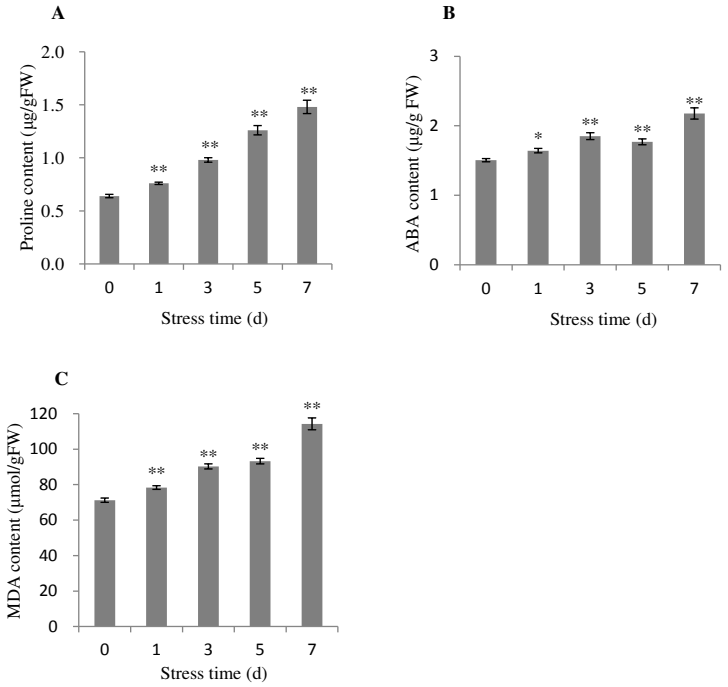

Figure 5. *Contents of proline (A), ABA (B) and MDA (C) in sugarcane leaves under drought stress. All data are means ± SD calculated from three replicates. Symbols * and ** indicate significant difference between different drought stresses and normal condition (0 d) at 0.05 and 0.01 levels, respectively*

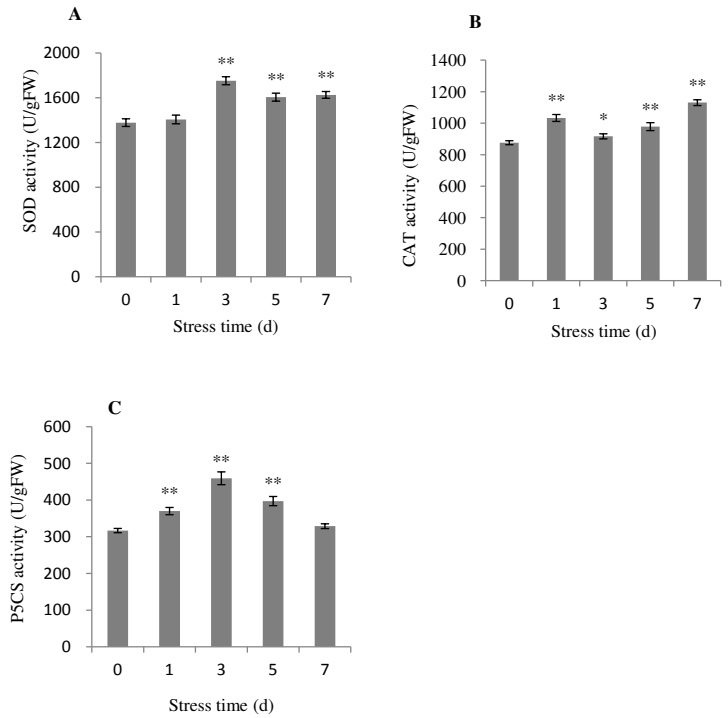

Figure 6. *Activities of SOD (A), CAT (B) and P5CS (C) in sugarcane leaves under drought stress. All data are means ± SD calculated from three replicates. Symbols * and ** indicate significant difference between different drought stresses and normal condition (0 d) at 0.05 and 0.01 levels, respectively*

http://www.aloki.hu ● ISSN 1589 1623 (Print) ● ISSN 1785 0037 (Online)
DOI: http://dx.doi.org/10.15666/aeer/1705_1232312335

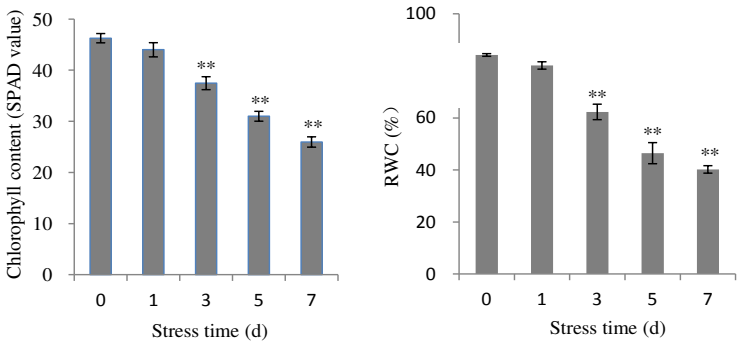

Figure 7. *Chlorophyll content (A) and RWC (B) in sugarcane leaves under drought stress. All data are means ± SD calculated from three replicates. Symbols * and ** indicate significant difference between different drought stresses and normal condition (0 d) at 0.05 and 0.01 levels, respectively*

Conclusion

In this study, SoP5CS monoclonal antibody was prepared and the expression of SoP5CS protein and the corresponding gene and physiological parameters associated with drought resistance were detected in sugarcane leaves under drought stress. The SoP5CS monoclonal antibody obtained in the present study will be useful for further research on plant stress response, defense signaling pathways, and other aspects in plants. In future research, the function of SoP5CS could be identified by over-expression of SoP5CS protein not only in sugarcane but also in other plants. The preparation of SoP5CS monoclonal antibody could provide a new approach in research of the P5CS protein in plants.

Acknowledgments. This work was supported by the grants from International Cooperation Program Project of China (2013DFA3160), Guangxi Funds for Bagui Scholars and Distinguished Experts (2013), Guangxi Special Fund for Scientific Base and Talent (GKAD17195100), Guangxi Key Laboratory Fund (12-K-05-01) and Fund for Guangxi Innovation Teams of Modern Agriculture Technology (gjnytxgxcxtd-03).

Conflict of interests. The authors declare that they have no conflict of interest.

Author contribution. L. T. Y. and Y. R. L. designed the study. J. L. and L. R. W. conducted the experiments. J. L., L. R. W. and Y. X. X. analyzed data. J. L. L. T. Y. and Y. R. L. wrote the manuscript. L. T. Y. and Y. R. L. revised and finalized the manuscript.

REFERENCES

[1] Cao, Y., Luo, Q. X., Tian, Y., Meng, F. J. (2017): Physiological and proteomic analyses of the drought stress response in *Amygdalus mira* (koehne) yü et luroots. – BMC Plant Biology 17: 53.

[2] Carrio, M. M., Villaverde, A. (2001): Protein aggregation as bacterial inclusion bodies is reversible. – FEBS Letters 489: 29-33.

[3] Carrio, M. M., Corchero, J. L., Villaverde, A. (1999): Proteolytic digestion of bacterial inclusion body proteins during dynamic transition between soluble and insoluble forms. – Biochim Biophys Acta 1434: 170-176.

[4] Delauney, A. J., Hu, C. A. A., Kishor, P. B. K., Verma, D. P. S. (1993): Cloning of ornithine delta-amino- transferase cDNA from *Vigna aconitifolia* by

http://www.aloki.hu ● ISSN 1589 1623 (Print) ● ISSN 1785 0037 (Online)
DOI: http://dx.doi.org/10.15666/aeer/1705_1232312335

transcomplementation in *Escherichia coli* and regulation of proline biosynthesis. – Journal of Biological Chemistry 268: 18673-18678.

[5] Dey, A., Samanta, M. K., Gayen, S., Maiti, M. K. (2016): The sucrose non-fermenting 1-related kinase 2 genesapk9improves drought tolerance and grain yield in rice by modulating cellular osmotic potential, stomatal closure and stress-responsive gene expression. – BMC Plant Biology 16: 158.

[6] Do, T. H., Jacobs, M., Angenon, G., Hermans, C., Tran, T. T., Son, L. V., Roosens, N. H. (2003): Proline accumulation and Δ^1-pyrroline-5-carboxylate synthetase gene properties in three rice cultivars differing in salinity and drought tolerance. – Plant Science 165: 1059-1068.

[7] Ginzberg, I., Stein, H., Kapulnik, Y., Szabados, L., Strizhov, N., Schell, J., Koncz, C., Zilberstein, A. (1998): Isolation and characterization of two different cDNAs of Δ^1-pyrroline-5-carboxylate synthase in *alfalfa*, transcriptionally induced upon salt stress. – Plant Molecular Biology 38: 755-764.

[8] Guan, C. F., Ji, J., Guan, W. Z., Feng, Y. H., Li, X. Z., Jin, C., Li, J., Wang, Y. R., Wang, G. (2014): A Lycium chinense-derived P5CS-like gene is regulated by water deficit-induced endogenous abscisic acid and overexpression of this gene enhances tolerance to water deficit stress in *Arabidopsis*. – Molecular Breeding 34: 1109-1124.

[9] Hu, C. A. A., Delauney, A. J., Verma, D. P. S. (1992): A bifunctional enzyme (Δ^1-pyrroline-5- carboxylate synthetase) catalyzes the first two steps in proline biosynthesis in plants. – Proceedings of National Academy of Science of the United States of America 89: 9354-9358.

[10] Jain, R., Chandra, A., Venugopalan, V. K., Solomon, S. (2015): Physiological changes and expression of *SOD* and *P5CS* genes in response to water deficit in sugarcane. – Sugar Tech 17: 276-282.

[11] Kautz, B., Noga, G., Hunsche, M. (2015): PEG and drought cause distinct changes in biochemical, physiological and morphological parameters of apple seedlings. – Acta Physiologiae Plantarum 37: 1-6.

[12] Kishor, P. B. K., Hong, Z., Miao, G. H., Hu, C. A. A., Verma, D. P. S. (1995): Over expression of Δ^1-pyrroline-5- carboxylate synthetase increase proline production and confers osmotolerance in transgenic plants. – Plant Physiology 108: 1387-1394.

[13] Kishor, P. B. K., Sangam, S., Amrutha, R. N., Laxmi, P. S., Naidu, K. R., Rao, K. R. S. S., Rao, S., Reddy, K. J., Theriappan, P., Sreenivasulu, N. (2005): Regulation of proline biosynthesis, degradation, uptake and transport in higher plants: its implications in plant growth and abiotic stress tolerance. – Current Science 88: 424-438.

[14] Krasensky, J., Jonak, C. (2012): Drought, salt, and temperature stress-induced metabolic rearrangements and regulatory networks. – Journal of Experimental Botany 63: 1593-1608.

[15] Kuzuoglu-Ozturk, D., Cebeci, Y. O., Akpinar, B. A., Mitou, G., Korkmaz, G., Gozuacik, D., Budak, H. (2012): Autophagy-related gene, *TdAtg8*, in wild emmer wheat plays a role in drought and osmotic stress response. – Planta 236: 1081-1092.

[16] Li, Y. R., Yang, L. T. (2015): Sugarcane agriculture and sugar industry in China. – Sugar Tech 17: 1-8.

[17] Maruthasalam, S., Kalpana, K., Kumar, K. K., Loganathan, M., Poovannan, K., Raja, J. A. J., Kokiladevi, E., Samiyappan, R., Sudhakar, D., Balasubramanian, P. (2007): Pyramiding transgenic resistance in elite indica rice cultivars against the sheath blight and bacterial blight. – Plant Cell Reports 26: 791-804.

[18] McManus, M. T., Burgess, E. P. J., Philip, B., Watson, L. M., Laing, W. A., Voisey, C. R., White, D. W. R. (1999): Expression of the soybean (Kunitz) trypsin inhibitor in transgenic tobacco: Effects on larval development of *Spodoptera litura*. – Transgenic Research 8: 383-395.

http://www.aloki.hu ● ISSN 1589 1623 (Print) ● ISSN 1785 0037 (Online)
DOI: http://dx.doi.org/10.15666/aeer/1705_1232312335

[19] Montalbán, N. G., Fruitós, E. G., Ventura, S., Arís, A., Villaverde, A. (2006): The chaperone DnaK controls the fractioning of functional protein between soluble and insoluble cell fractions in inclusion body-forming cells. – Microbial Cell Factories 5: 26.
[20] Nahálka, J., Mislovičová, D., Kavcová, H. (2009): Targeting lectin activity into inclusion bodies for the characterisation of glyco-proteins. – Molecular BioSystems 5: 819-821.
[21] Niu, J. Q., Wang, A. Q., Huang, J. L., Yang, L. T., Li, Y. R. (2015): Isolation, characterization and promoter analysis of cell wall invertase gene socin1, from sugarcane (*Saccharum* spp.). – Sugar Tech 17: 65-76.
[22] Ortega, C. O. S., Alfaro, A. E. O., Agüero, J. A. R., Santacruz, G. A. A., Bremont, J. F. J. (2008): Salt stress increases the expression of *P5CS* gene and induces proline accumulation in cactus pear. – Plant Physiology and Biochemistry 46: 82-92.
[23] Ozturk, D. K., Yalcinkaya, O. C., Akpinar, B. A., Mitou, G., Korkmaz, G., Gozuacik, D., Budak, H. (2012): Autophagy-related gene, *TdAtg8*, in wild emmer wheat plays a role in drought and osmotic stress response. – Planta 236: 1081-1092.
[24] Parrott, D., Yang, L., Shama, L., Fischer, A. M. (2005): Senescence is accelerated, and several proteases are induced by carbon "feast" conditions in barley (*Hordeum vulgare* L.) leaves. – Planta 222: 989-1000.
[25] Pereira, C. S., Costa, D. S. D., Teixeira, J., Pereira, S. (2005): Organ-specific distribution and subcellular localisation of ascorbate peroxidase isoenzymes in potato (*Solanum tuberosum* L.) plants. – Protoplasma 226: 223-230.
[26] Phan, T. T., Sun, B., Niu, J. Q., Tan, Q. L., Li, J., Yang, L. T., Li, Y. R. (2016): Overexpression of sugarcane gene *SoSnRK2.1* confers drought tolerance in transgenic tobacco. – Plant Cell Reports 35: 1891-1905.
[27] Porcel, R., Azcón, R., Lozano, J. M. R. (2004): Evaluation of the role of genes encoding for Δ^1-pyrroline-5-carboxylate synthetase (P5CS) during drought stress in arbuscular mycorrhizal *Glycine max* and *Lactuca sativa* plants. – Physiological and Molecular Plant Pathology 65: 211-221.
[28] Pruvot, G., Cuing, S., Peltier, G., Rey, P. (1996): Characterization of a novel drought-induced 34-kDa protein located in the thylakoids of *Solanum tuberosum* L. plants. – Planta 198: 471-479.
[29] Qiao, X. Q., Wang, P. H., Shi, G. X., Yang, H. Y. (2015): Zinc conferred cadmium tolerance in *Lemna minor* L. via modulating polyamines and proline metabolism. – Plant Growth Regulation 77: 1-9.
[30] Romman, S. M. A., Ammari, T. G., Irshaid, L. A., Salameh, N. M., Hasan, M. K., Hasan, H. S. (2011): Cloning and expression patterns of the *HvP5CS* gene from barley (*Hordeum vulgare*). – Journal of Food, Agriculture & Environment 9: 279-284.
[31] Ruan, L. T., Zheng, R. C., Zheng, Y. G. (2016): A novel amidase from *Brevibacterium epidermidis* ZJB–07021: gene cloning, refolding and application in butyrylhydroxamic acid synthesis. – Journal of Indian Microbiology and Biotechnology 43: 1071-1083.
[32] Sahdev, S., Khattar, S. K., Saini, K. S. (2008): Production of active eukaryotic proteins through bacterial expression systems: a review of the existing biotechnology strategies. – Molecular and Cell Biochemistry 307: 249-264.
[33] Saibi, W., Feki, K., Yacoubi, I., Brini, F. (2015): Bridging between proline structure, functions, metabolism, and involvement in organism physiology. – Applied Biochemistry and Biotechnology 176: 2107-2119.
[34] Sorensen, H. P., Mortensen, K. K. (2005): Soluble expression of recombinant proteins in the cytoplasm of *Escherichia coli*. – Microbial Cell Factories 4: 1-8.
[35] Su, M., Li, X. F., Ma, X. Y., Peng, X. J., Zhao, A. G., Cheng, L. Q., Chen, S. Y., Liu, G. S. (2011): Cloning two *P5CS* genes from bioenergy sorghum and their expression profiles under abiotic stresses and MeJA treatment. – Plant Science 181: 652-659.
[36] Subramanyam, K., Arun, M., Mariashibu, T. S., Theboral, J., Rajesh, M., Singh, N. K., Manickavasagam, M., Ganapathi, A. (2012): Overexpression of tobacco osmotin (Tbosm)

http://www.aloki.hu ● ISSN 1589 1623 (Print) ● ISSN 1785 0037 (Online)
DOI: http://dx.doi.org/10.15666/aeer/1705_1232312335

in soybean conferred resistance to salinity stress and fungal infections. – Planta 236: 1909-1925.

[37] Wan, S. B., Wang, W., Luo, M., Huang, W. D., Yin, J. Y., Zhan, J. C. (2010): cDNA Cloning, prokaryotic expression, polyclonal antibody preparation of the *Auxin-Binding Protein 1* gene from grape berry. – Plant Molecular Biology Reporter 28: 373-380.

[38] Wang, F., Tong, W., Zhu, H., Kong, W., Peng, R., Liu, Q., Yao, Q. (2016): A novel Cys_2/His_2 zinc finger protein gene from sweet potato, *ibZFP1*, is involved in salt and drought tolerance in transgenic *Arabidopsis*. – Planta 243: 783-797.

[39] Wang, S., Zhang, K. K., Huang, X., Fan, Y. J., Yang, L. T., Li, Y. R. (2015): Cloning and functional analysis of thylakoidal ascorbate peroxidase (TAPX) gene in sugarcane. – Sugar Tech 17: 356-366.

[40] Wei, C., Cui, Q., Zhang, X. Q., Zhao, Y. Q., Jia, G. X. (2016): Three *P5CS* genes including a novel one from *Lilium regale* play distinct roles in osmotic, drought and salt stress tolerance. – Journal of Plant Biology 59: 456-466.

[41] Xue, Z., Chao, Y., Wang, D., Wang, M., Qian, S. (2011): Overexpression of a recombinant amidase in a complex auto-inducing culture: purification, biochemical characterization, and regio-and stereoselectivity. – Journal of Indian Microbiology and Biotechnology 38: 1931-1938.

[42] Yu, T. A., Chiang, C. H., Wu, H. W., Li, C. M., Yang, C. F., Chen, J. H., Chen, Y. W., Yeh, S. D. (2011): Generation of transgenic watermelon resistant to Zucchini yellow mosaic virus and Papaya ringspot virus type W. – Plant Cell Reports 30: 359-371.

[43] Zheng, L. L., Dang, Z. H., Li, H. Y., Zhang, H. R., Wu, S. B., Wang, Y. C. (2014): Isolation and characterization of a Δ^1-*pyrroline-5-carboxylate synthetase* (*NtP5CS*) from *Nitraria tangutorum* Bobr. and functional comparison with its Arabidopsis homologue. – Molecular Biology Reports 41: 563-572.

[44] Zhou, H., Qian, J., Zhao, M. D., Li, F., Tong, W., Li, L., Fang, R. J., Zhao, W. G., Kim, H. J. (2016): Cloning and sequence analysis of the Δ^1-*pyrroline-5-carboxylate synthase* gene (*MP5CS*) from mulberry (*Morus alba*) and patterns of *MP5CS* gene expression under abiotic stress conditions. – The Journal of Horticultural Science and Biotechnology 91: 100-108.

[45] Zhu, F., Xu, M. Y., Wang, S. D., Jia, S. D., Zhang, P., Lin, H. H., Xi, D. H. (2012): Prokaryotic expression of pathogenesis related protein 1 gene from *Nicotiana benthamiana*: antifungal activity and preparation of its polyclonal antibody. – Biotechnol Letters 34: 919-924.

http://www.aloki.hu ● ISSN 1589 1623 (Print) ● ISSN 1785 0037 (Online)
DOI: http://dx.doi.org/10.15666/aeer/1705_1232312335

EFFECT OF DIETARY CARROT MEAL SUPPLEMENTATION ON PRODUCTIVITY AND CARCASS CHARACTERISTICS OF ARBOR ACRE BROILER CHICKENS AGED 22 TO 42 DAYS

NG'AMBI, J. W. – MOKGOPE, P. K. – BROWN, D. – MANYELO, T. G.*

Department of Agricultural Economics and Animal Production, University of Limpopo, P/Bag X1106, Sovenga 0727, South Africa

**Corresponding author*
e-mail: manyelo.t.g@gmail.com

(Received 6th May 2019; accepted 16th Jul 2019)

Abstract. This study determined the effect of carrot meal supplementation on productivity and carcass characteristics of Arbor acre broiler chickens aged 22 to 42 days in Limpopo province, South Africa. A total of 200 female Arbor acre broiler chickens were randomly allocated to five treatments with five replicates, each having 8 birds, in a completely randomized design. The supplementation levels were 0 (FA0), 20 (FA20), 50 (FA50), 75 (FA75) or 100 (FA100) g of carrot meal per kg DM feed. The results showed that dietary carrot meal supplementation had no ($P > 0.05$) effect on growth rate, live weight and carcass characteristics of female Arbor acre broiler chickens aged 22 to 42 days. Carrot meal supplementation improved feed intake, feed conversion ratio, metabolisable energy intake and nitrogen retention of Arbor acre broiler chickens aged 22 to 42 days. Dietary feed intake, feed conversion ratio, live weight, metabolisable energy intake and nitrogen retention were optimized at different dietary carrot meal supplementation levels of 52.8, 63.8, 38.0, 42.0 and 44.3 g/kg DM feed, respectively. It is concluded that carrot meal supplementation improved intake, feed conversion ratio, metabolisable energy and nitrogen retention of female Arbor acre broiler chickens aged 22 to 42 days.
Keywords: *metabolisable energy, meat sensory attributes, vitamin C, diets, performance*

Introduction

Poultry production is nutritionally, economically and socially important in Limpopo province and the world as a whole. Chicken production is an important source of income and employment, and it contributes substantially to food security among rural people in Africa (Ng'ambi et al., 2012). Much of the poultry meat comes from broiler chickens. Not only are broiler chickens heavier at an early age but they also have better feed conversion ratio (Havenstein, 2004). High mortality in broiler chickens leads to poor productivity and low income for rural people. Carcasses from broiler chickens have high fat content and, thus, reduced carcass quality and feed efficiency. High fat content meat is also not liked by consumers (Steenfeldt et al., 2007). Excessive fat is one of the main problems faced by the broiler chicken industry, since it does not just reduce carcass quality and feed efficiency but also causes consumer rejection and difficulties in meat processing (Macajova et al., 2003).

There is some evidence that carrot meal supplementation reduces chick mortality and improves carcass characteristics (Steenfeldt et al., 2007). Carrot (*Daucus carota)* is a commonly consumed vegetable species belonging to the family Apiacea, which grows in temperate regions of Europe, Asia and Africa (Hammam, 2014). It contains a lot of active ingredients such as steroids, tannins, flavonoids, and carotene (Jasicka-Misiak et al., 2005; Vasudevan et al., 2006). Aromatic plants such as carrots can increase feed intake, feed conversion ratio, weight gain and can improve the oxidative stability of tissues (Ürüşan and Bölükbaşı, 2017). Carrot meal has been tested for its potential as food in livestock industry

http://www.aloki.hu ● ISSN 1589 1623 (Print) ● ISSN 1785 0037 (Online)
DOI: http://dx.doi.org/10.15666/aeer/1705_1233712346

(Rust and Buskirk, 2008; Steenfeldt et al., 2007); however, its prospect in Arbor acre broiler-based diets has not yet been fully exploited. Information generated in this study will help in formulating strategies aimed at improving productivity and carcass characteristics of Arbor acre broiler chickens. Improvement of productivity of broiler chickens may enhance the economic, nutritional and social status of broiler chicken farmers. Therefore, the aim of this study was to determine the effects of supplementing diets with carrot meal on feed intake, digestibility, live weight, growth, feed conversion ratio, mortality and carcass characteristics of Arbor acre broiler chickens.

Materials and methods

Study site and experimental design

This study was conducted as part of the Pahlomoje Poultry Project, Shikwane village in Maruleng Municipality, South Africa. The project site is 64 km north-west of Tzaneen. The chickens were raised on commercial starter mash up to 21 days old before the experiment commenced. Prior to the start of the experiment the chickens were fed a 22% crude protein (CP) diet that would satisfy their nutritional requirements according to NRC (1994). A total of 200 female Arbor acre broiler chickens (Females were used because there were not enough males), weighing 650 ± 4 g per chicken were randomly assigned to five treatments with five replicates, each replicate having 8 Arbor acre female chickens in a completely randomized design. Thus, chickens were raised on 25 floor pens in an environmentally controlled house and temperature maintained at 30 to 33 °C and 23 to 25 °C during the starter and grower phase, respectively. Lighting was provided continuously (*Fig. 1*). The chicks were vaccinated against Newcastle virus disease and infectious bronchitis. A grower diet was offered from day 22-42 days with different carrot supplementation levels (*Table 1*). The nutrient composition of the treatments is presented in *Table 2*. The diets contained similar nutrients but different carrot meal levels ranging from zero to 100 g per kg DM. The carrot meal contained 12% crude protein, 17.1 MJ of gross energy/kg DM, 18% ash, 13.3% neutral detergent fibre (NDF), 8.8% acid detergent fibre (ADF) and 300-700 mg/kg dry matter (DM) of vitamin C. The grower diet was formulated and produced by a commercial feed company, Meadow Feeds, South Africa. Feed and water were offered ad libitum throughout the experiment.

Figure 1. *Ross 308 broiler chickens feeding on treatment diet*

http://www.aloki.hu ● ISSN 1589 1623 (Print) ● ISSN 1785 0037 (Online)
DOI: http://dx.doi.org/10.15666/aeer/1705_1233712346

Table 1. *Diet composition of grower feed for Arbor acre chickens*

Ingredient	Quantity (%)
Yellow maize	567
Sunflower meat	100
Full fat soya meal	290
Fish meal	10
Monocalcium phosphate	13.6
Limestone	13.6
Iodised salt	0.5
DL Methionine	0.3
L Threonine	0.0
Vitamin/mineral premix	5.0
Total	1000
CP (%)	20
Energy (MJ/kg DM)	16.9

Table 2. *Nutrient composition of the diets for Arbor acre broiler chickens (units are in g/kg DM except energy as MJ/kg DM feed and dry matter as g/kg feed)*

Diet code	Nutrient			
	Dry matter	Energy	Protein	Carrot meal supplement
UA_0	930	16.9	200	0
UA_{20}	930	16.9	200	20
UA_{50}	930	16.9	200	50
UA_{75}	930	16.9	200	75
UA_{100}	930	16.9	200	100

Data collection

The initial live weights of the chickens were taken at the beginning of the experiment and weekly weights were taken thereafter using the electronic weighing scale (RADWAG AS 220/C/2). Weekly feed intakes were determined. Daily mean growth rates and feed conversion ratios were calculated. Digestibility was done when the chickens were between 35 and 42 days. Digestibility was conducted in specially designed metabolic cages with separate watering and feeding troughs. Four birds were randomly selected from each replicate and transferred to metabolic cages to measure apparent digestibility. A three-day acclimatization period was allowed prior to a three-day collection period. Droppings voided by each bird were collected daily at 09h00. Care was taken to avoid contamination from feathers, scales, debris and feeds. Dry matter and nitrogen contents of the diets, refusals and faeces were determined. At 42 d of age, 3 chickens per pen were slaughtered according to the rules and regulations of University of Limpopo Animal Research Ethics Committee. After slaughtering, carcass weight of each chicken was measured. Dressing percentage was determined by dividing carcass weight by live weight and then multiplying by 100. Breast, fat pad, thigh, wing, drumstick, gizzard and liver weights were measured using an electronic scale. Breast

http://www.aloki.hu ● ISSN 1589 1623 (Print) ● ISSN 1785 0037 (Online)
DOI: http://dx.doi.org/10.15666/aeer/1705_1233712346

meat samples were further analysed for meat sensory attributes. Breast meat was prepared and the skin was left on the meat samples. Nothing was added to the meat samples to add taste. An oven set at 105 °C was allowed to preheat prior to cooking. The meat samples were put in trays and they were covered with aluminium foil to prevent water loss. Thereafter, the trays with meat were put in an oven for approximately 60 min and the meat samples were turned after every 10 min. Samples were cut into small 5 cm cubic pieces and served immediately after cooking to a total of 30 panel composed of students and staff members of the University of Limpopo that were from the Sepedi, Setswana, Tshivenda and Tsitsonga tribes. The panel was shown how to infer and record scores for each parameter. The waiting period between meats samples tastings was 10 min. Distilled water with lemon was given to panel to clean their palate between sub-sample measurements to avoid crossover effects. Breast meat was evaluated for tenderness, juiciness and flavour using a 5-point ranking scale (AMSA, 1995) (*Table 3*).

Table 3. *Evaluation scores used by the sensory panel*

Score	Sensory attributes		
	Tenderness	**Juiciness**	**Flavour**
1	Too tough	Much too dry	Very bad flavor
2	Tough	Dry	Poor flavor
3	Neither tough nor tender	Neither dry nor juicy	Neither bad nor good flavor
4	Tender	Juicy	Good flavor
5	Too tender	Too juicy	Very good flavor

Chemical analysis

Dry matter and nitrogen contents of the diets, refusals, faeces and meat samples were determined as described by AOAC (2008). Neutral and acid detergent fibre contents were analysed by AOAC (2008) methods. The energy of the diets, excreta samples and meat were determined using an adiabatic bomb calorimeter IKA® C5003 Control.

Statistical analysis

Data on feed intake, feed conversion ratio, growth rate, live weight and carcass characteristics of Arbor acre broiler chickens were analyzed using the general linear model procedures of the statistical analysis of variance (SAS, 2008). Where there was a significant difference, the Duncan test for multiple comparisons was used to test the significance of differences between treatment means (SAS, 2008). The dose - responses in feed intake, live weight, growth rate, feed conversion ratio, metabolisable energy, nitrogen retention and carcass characteristics of the chickens were models using the following quadratic equation:

$$Y = a + b_1x + b_2x^2 \quad \text{(Eq.1)}$$

where y = feed intake, digestibility, live weight, growth rate, feed conversion ratio, metabolisable energy, nitrogen retention and carcass characteristics; a = intercept; b_1 and b_2 = coefficients of the quadratic equation; x = dietary carrot meal supplementation level and $-b_1/2b_2 = x$ value for optimum response. The quadratic model was fitted to

http://www.aloki.hu ● ISSN 1589 1623 (Print) ● ISSN 1785 0037 (Online)
DOI: http://dx.doi.org/10.15666/aeer/1705_1233712346

experimental data by means of the NLIN procedure of SAS (SAS, 2008). The quadratic model was used because it gave the best fit.

The relationships between carrot meal supplementation and optimal responses in meat tenderness, flavour and juiciness were models using a linear regression equation (SAS, 2008) of the form:

$$Y = a + bx \quad \text{(Eq.2)}$$

where Y = optimal tenderness, juiciness and flavour; a = intercept; b = coefficient of the linear equation and x = dietary carrot meal supplementation level.

Results

Results of the effect of carrot meal supplementation on feed intake, growth rate, feed conversion ratio, live weight, metabolisable energy intake and nitrogen retention of female Arbor acre broiler chickens aged 22 to 42 days are presented in *Table 4*. Carrot meal supplementation had no effect ($P > 0.05$) on growth rate of female Arbor acre broiler chickens aged 22 to 42 days. Broiler chickens on a diet supplemented with 50 g of carrot meal per kg DM had higher ($P < 0.05$) feed intakes than those on a diet not supplemented with carrot meal, and those on diets supplemented with 20 or 100 g of carrot meal per kg DM feed. Feed intakes of female Arbor acre broiler chickens aged 22 to 42 days were optimized at dietary carrot meal levels of 52.8 ($r^2 = 0.888$) (*Table 5*).

Carrot meal supplementation improved dietary intake of female Arbor acre broiler chickens aged 22 to 42 days. However, these improvements did not have any impact on growth rates of the chickens. Similarly, improvements in dietary intake, feed conversion ratio, metabolisable energy intake and nitrogen retention did not result in any improvement of live weights of the chickens. Female broiler chickens on a diet supplemented with 50 g of carrot meal per kg DM had higher ($P < 0.05$) live weights than those on diets supplemented with 20 or 100 g of carrot meal per kg DM feed. Broiler chickens on a diet supplemented with 20 g of carrot meal per kg DM feed had higher ($P < 0.05$) live weights than those on a diet supplemented with 100 g of carrot meal per kg DM. Live weights of female Arbor acre broiler chickens aged 22 to 42 days were optimized at dietary carrot meal levels of 63.8 ($r^2 = 0.780$) (*Table 5*). Supplementation with 50 g of carrot meal per kg DM feed improved ($P < 0.05$) feed conversion ratio. Feed conversion ratios of female Arbor acre broiler chickens aged 22 to 42 days were optimized at dietary carrot meal levels of 38.0 ($r^2 = 0.673$) (*Table 5*).

In the present study, dietary intake and feed conversion ratio and live weight of female Arbor acre broiler chickens aged 22 to 42 days were optimized at different dietary carrot meal supplementation levels of 52.8 and 63.8 g/kg DM feed, respectively. Female broiler chickens on a diet supplemented with 20 g of carrot meal per kg DM had higher ($P < 0.05$) metabolisable energy intakes than those on a diet not supplemented with carrot meal and those on diets supplemented with 50, 75 or 100 g of carrot meal per kg DM. Broiler chickens on diets supplemented with 50 or 75 g of carrot meal per kg DM had higher ($P < 0.05$) metabolisable energy intakes than those on a diet not supplemented with carrot meal. Metabolisable energy intakes of female Arbor acre broiler chickens aged 22 to 42 days were optimized at dietary carrot meal levels of 42.0 ($r^2 = 0.385$) g/kg DM (*Table 5*). Female broiler chickens on diets supplemented with 20 or 50 g of carrot meal per kg DM had higher ($P < 0.05$) nitrogen retention values than

http://www.aloki.hu ● ISSN 1589 1623 (Print) ● ISSN 1785 0037 (Online)
DOI: http://dx.doi.org/10.15666/aeer/1705_1233712346

those on a diet not supplemented with carrot meal and those on diets supplemented with 75 or 100 g of carrot meal per kg DM. Nitrogen retention of female Arbor acre broiler chickens aged 22 to 42 days were optimized at dietary carrot meal levels of 44.3 ($r^2 = 0.603$) g/kg DM (*Table 5*). Carrot meal supplementation improved dietary metabolisable energy intakes of female Arbor acre broiler chickens aged 22 to 42 days. In the present study, metabolisable energy intake and nitrogen retention of female Arbor acre broiler chickens were optimized at different carrot meal supplementation levels of 42.0 and 44.3 g/kg DM feed, respectively. This means carrot meal levels for optimal metabolisable intake and nitrogen retention intake will depend on the variable of interest.

Table 4. *Effect of carrot meal supplementation on feed intake (g DM/bird/day), growth rate (g/bird/day), feed conversion ratio (FCR) (g DM feed/g live weight gain), live weight (g/bird aged 42 days), metabolisable energy (MJ/kg DM) and nitrogen retention (g/bird/day) of female Arbor acre broiler chickens aged 22 to 42 days*

Variables	Treatment					SE
	FA_0	FA_{20}	FA_{50}	FA_{75}	FA_{100}	
DM intake	140.0^{b}	150.5^{b}	172.0^{a}	160.3^{ab}	147.5^{b}	3.80
Growth rate	33.3	29.5	27.8	31.8	28.0	1.13
FCR	5.3^{a}	4.5^{ab}	3.3^{b}	4.2^{ab}	4.0^{ab}	0.22
Live weight	1834^{ab}	1755^{b}	1891^{a}	1835^{ab}	1609^{c}	36.84
ME intake	9.4^{c}	13.8^{a}	11.4^{b}	11.4^{b}	10.4^{bc}	0.388
N retention	2.0^{b}	2.8^{a}	3.0^{a}	2.0^{b}	2.0^{b}	0.115

^{a,b,c}Means in the same row not sharing a common superscript are significantly different ($P < 0.05$)
SE: Standard error

Table 5. *Carrot meal supplementation levels for optimal feed intake (g/bird/day), feed conversion ratio (g DM feed/g live weight gain), live weight (g/bird aged 42 days), metabolisable energy (ME) (MJ/kg DM) and nitrogen retention (g/bird/day) of female Arbor acre broiler chickens aged 22 to 42 days*

Trait	Formula	r^2	Carrot meal	Optimal Y-value
Feed intake	$Y = 137.884 + 1.0559x + -0.0094x^2$	0.888	52.8	166.8
FCR	$Y = 5.2775 + -0.0510x + 0.0004x^2$	0.780	63.8	3.65
Live weight	$Y = 1781.939 + 4.7089x + -0.0615x^2$	0.673	38.0	1872
Apparent ME	$Y = 10.427 + 0.0841x + -0.0008x^2$	0.385	42.0	12.4
N retention	$Y = 2.15894 + 0.2811x + -0.0003x^2$	0.603	44.3	2.78

r^2: regression coefficient. Carrot meal: carrot meal supplementation level for optimal variable

Results of the effect of carrot meal supplementation on carcass characteristics of female Arbor acre broiler chickens aged 42 days are presented in *Table 6*. Carrot meal supplementation had no effect ($P > 0.05$) on carcass, breast, drumstick, thigh, liver, gizzard and fat pad weights of female Arbor acre broiler chickens aged 42 days. Results of the effect of carrot meal supplementation on tenderness, juiciness and flavour of meat of female Arbor acre broiler chickens aged 42 days are presented in *Table 7*. Carrot

http://www.aloki.hu ● ISSN 1589 1623 (Print) ● ISSN 1785 0037 (Online)
DOI: http://dx.doi.org/10.15666/aeer/1705_1233712346

meal supplementation did not improve ($P > 0.05$) meat tenderness and flavour of female Arbor acre broiler chickens aged 42 days. Female broiler chickens supplemented with 20, 50 or 100 g of carrot meal per kg DM feed produced meat with higher ($P < 0.05$) juiciness than those of meat from a diet not supplemented with carrot meal and those on a diet supplemented with 75 g of carrot meal per kg DM. A positive relationship was observed between carrot meal supplementation to the diets of female Arbor acre broiler chickens and meat juiciness ($r^2 = 0.085$). Carrot meal supplementation did not affect tenderness and flavour of female Arbor acre broiler chicken meat. However, carrot meal supplementation improved the juiciness of female Arbor acre broiler chicken meat. Thus, there was a weak but positive relationship between carrot meal supplementation and juiciness of female Arbor acre broiler chicken meat.

Table 6. *Effect of carrot meal supplementation on carcass characteristics (g) of female Arbor acre broiler chickens aged 42 days*

Variable	Treatment					SE
	FA_0	FA_{20}	FA_{50}	FA_{75}	FA_{100}	
Carcass	1569	1434	1534	1461	1526	26.03
Breast	205	221	207	214	202	8.42
D/stick	102	99	88	89	96	2.15
Thigh	108	112	104	76	107	5.75
Liver	68	62	62	55	54	3.01
Gizzard	41	34	32	37	33	1.65
Fat pad	39	43	44	31	42	2.62

SE: standard error

Table 7. *Effect of carrot meal supplementation level on tenderness, juiciness and flavour of meat of female Arbor acre broiler chickens aged 42 days*

Sensory attributes	Treatment					SE
	FA_0	FA_{20}	FA_{50}	FA_{75}	FA_{100}	
Juiciness	2.50^b	3.50^a	3.70^a	2.50^b	3.60^a	0.153
Tenderness	3.30	3.30	3.00	3.00	3.30	0.131
Flavour	3.00	3.10	3.00	3.00	3.20	0.131

^{a,b}Means in the same row not sharing a common superscript are significantly different ($P < 0.05$)
SE: standard error

Discussion

In the present study, carrot meal supplementation had no effect on growth rate of female Arbor acre broiler chickens aged 22 to 42 days. Carrot meal supplementation improved dietary intake of female Arbor acre broiler chickens aged 22 to 42 days. However, these improvements did not have any impact on growth rates of the chickens. Similarly, improvements in dietary intake, feed conversion ratio, metabolisable energy intake and nitrogen retention did not result in any improvement of live weights of the chickens. These results are similar to those of Erhan and Bölükbaşı (2017) who found out that supporting the diet with citrus peel oil did not change the weight of the broilers. According to Yu et al. (2005), the obtained results in this study may be attributed to

http://www.aloki.hu ● ISSN 1589 1623 (Print) ● ISSN 1785 0037 (Online)
DOI: http://dx.doi.org/10.15666/aeer/1705_1233712346

antioxidant and antimicrobial properties of carrot meal. However, the present results are contrary to those of Ürüşanet al. (2018) who observed improvements in live weights of chickens supplemented with carrot meal. Similarly, Abdu et al. (2012) reported improvements in live weights of rabbits with carrot meal supplementation. This might also be because large amounts of easily-fermented components as sugars and soluble non-starch polysaccharides contribute some energy to the chickens Steenfeldts et al. (2007).

Supplementation with 50 g of carrot meal per kg DM feed improved feed conversion ratio. Rizal et al. (2010) reported an improvement in feed conversion ratio of broiler chickens supplemented with carrot meal. Improvements in dietary feed conversion ratio observed in the present study are similar to those observed by Hammershøj et al. (2005) and Hammershøj et al. (2010) reported improvements in feed conversion ratio of laying hens when they were supplemented with carrot meals. However, Khan (2019) reported no improvements in feed conversion ratio of broiler chickens fed carrot pulp. In the present study, dietary intake and feed conversion ratio and live weight of female Arbor acre broiler chickens aged 22 to 42 days were optimized at different dietary carrot meal supplementation levels of 52.8 and 63.8 g/kg DM feed, respectively. This means that carrot meal levels for optimal productivity will depend on the particular variable of interest. This has implications on ration formulation where carrot meal is included.

Carrot meal supplementation improved dietary metabolisable energy intakes of female Arbor acre broiler chickens aged 22 to 42 days. These results are similar to those of Magouze et al. (1998) who observed that carrot meal supplementation in growing rabbits improved their metabolisable energy intakes. However, El-Kerdawy et al. (1992) found that carrot meal supplementation to the diets of growing rabbits decreased their metabolisable energy intakes. Similarly, Steenfeldts et al. (2007) observed a decrease in metabolisable energy intakes of laying hens supplemented with carrot meal. The results of the present study indicate that carrot meal supplementation increased nitrogen retention in female Arbor acre broiler chickens aged 22 to 42 days. Their findings may imply that an alteration of tissues takes place, particularly muscle and fat deposits, which may differ in nutrient digestion (Moran and Bilgili, 1990). However, these results contradict with those of El-Kerdawy et al. (1992), which indicated that carrot meal supplementation to the diets of growing rabbits decreased nitrogen retention. Similarly, Steenfeldts et al. (2007) found that nitrogen retention in laying hens supplemented with carrot meal was increasing. In the present study, metabolisable energy intake and nitrogen retention of female Arbor acre broiler chickens were optimized at different carrot meal supplementation levels of 42.0 and 44.3 g/kg DM feed, respectively. This means carrot meal levels for optimal metabolisable intake and nitrogen retention intake will depend on the variable of interest.

Carrot meal supplementation had no effect on carcass, breast, drumstick, thigh, liver, gizzard and fat pad weights of female Arbor acre broiler chickens aged 42 days. Ürüşanet al. (2018) reported increase in hot carcass weight and carcass yield of broiler chickens feed carrot seed oil authors indicated that increase carcass weights which were observed in many studies, occurred because of the appetizer properties of plant extracts by increasing the gastric digestion liquor. Carrot meal supplementation did not affect tenderness and flavour of female Arbor acre broiler chicken meat. Meat sensory attribute values of tenderness and flavour were similar across the dietary treatments. It is not clear how carrot meal supplementation affect the sensory attributes of broiler chickens and this may require further studies. However, carrot meal supplementation

http://www.aloki.hu ● ISSN 1589 1623 (Print) ● ISSN 1785 0037 (Online)
DOI: http://dx.doi.org/10.15666/aeer/1705_1233712346

improved the juiciness of female Arbor acre broiler chicken meat. Thus, there was positive relationship between carrot meal supplementation and juiciness of female Arbor acre broiler chicken meat. No such information was found for either indigenous or broiler chicken breeds. Further research is needed to deepen the knowledge in this area.

Conclusion

Carrot meal supplementation did not have any effect on growth rate, live weight, carcass weight, meat tenderness and flavour of Arbor acre broiler chickens aged 22 to 42 days. However, carrot meal supplementation improved intake, feed conversion ratio, metabolisable energy intake, nitrogen retention and meat juiciness of female Arbor acre broiler chickens aged 22 to 42 days. As a result, carrot meal can be added in the diet of broilers as a beneficial dietary supplement which contains natural antioxidants. Optimal improvements of feed intake, FCR, live weight, metabolisable energy intake and nitrogen retention were achieved at different carrot meal supplementation levels. Thus, carrot meal levels for optimal productivity will depend on the parameter in question. This has a lot of implications in diet formulations where carrot meal is included. Further studies are recommended to repeat and confirm results of this study.

Acknowledgements. The authors wish to acknowledge Agri-SETA and Meadow feeds for financial support.

REFERENCES

[1] Abdu, S. B., Jokthan, G. E., Hassan, M. R., Adamu, H. Y., Yashim, S. M., Ikani, E. (2012): Effects of inclusion levels of carrot leaf meal on performance of growing rabbits. – World Journal of Life Science and Medical Research 2(2): 65-70.

[2] AMSA (1995): Research Guidelines for Cookery, Sensory Evaluation and Instrumental Measurements of Fresh Meat. – American Meat Science Association, Chicago, IL.

[3] AOAC (2008): Association of Analytical Chemists, Official Methods of Analysis. 17th Ed. AOAC, Washington, DC.

[4] El-kerdawy, D. M. A., Rashwan, A. A., Ibrahim, H., El-gendy, K. M. (1992): Digestibility, growth rate, carcass traits and some physiological aspects of growing New Zealand white rabbits as affected by partial substitution of concentrates with carrot–tops hay and feeding time. – Egyptian Journal of Rabbit Science 2(1): 61-71.

[5] Erhan, M. K., Bölükbaşı, Ş. C. (2017): Citrus peel oils supplementation in broiler diet: effects on performance, jejunum microflora and jejunum dietary inclusion of turmeric (*Curcuma longa*) and cinnamon (*Cinnamomum verum*) powders on performance, organs relative weight and some ımmune system parameters in broiler chickens. – Poultry Science 2: 153-163.

[6] Hammam, F. H. (2014): Protective effect of carrot juice against the toxicity of carbon tetrachloride on liver and kidneys in rabbits. – World Journal of Pharmacy and Pharmaceutical Sciences 3: 1229-1239.

[7] Hammershøj, M., Steenfeldt, S. (2005): Effect of blue lupin (*Lupinus angustifolius*) in organic layer diets and supplementation with foraging material on layer performance and some egg quality parameters. – Poultry Science 84: 723-733.

http://www.aloki.hu ● ISSN 1589 1623 (Print) ● ISSN 1785 0037 (Online)
DOI: http://dx.doi.org/10.15666/aeer/1705_1233712346

[8] Hammershøj, M., Kidmose, U., Steenfeldt, S. (2010): Deposition of carotenoids in egg yolk by short-term supplement of coloured carrot (*Daucus carota*) varieties as forage material for egg-laying hens. – Journal of Science and Food Agriculture 90(7): 1163-71.
[9] Havenstein, G. B., Mahmoud, F. W., Eisen, E. J. (2004): The effect of dietary phosphorus on heat shock protein mRNAs during acute heat stress in male broiler chickens (*Gallus gallus*). – British Journal 137: 11-18.
[10] Jasicka-Misiak, I., Wieczorek, P. P., Kafarski, P. (2005): Crotonic acid as a bioactive factor in carrot seeds (*Daucus carota L.).* – Phytochemistry 66: 1485-1491.
[11] Macajova, M. D., Lamosova, D., Zenman, E. (2003): Physiological effects of leptin insulin and triamcin nolon on adult Japanese quail. – Acta Veterinary Brunes 72: 515-522.
[12] Khan, S. (2019): Utilization carrot pulp as corn replacement in the broiler diet. – Journal of Agriculture and Veterinary Science 12(2): 72-74.
[13] Magouze, F. I., Mahmound, S. A., El-kelawy, H. M., Homouda, I. A., Alla, S. A. Z. G. (1998): Productive and reproductive performance of rabbits fed diets containing different agricultural by-products: productive performance of growing rabbits. – Egyptian Journal of Rabbit Science 8(1): 49-60.
[14] Moran, E., Bilgili, S. (1990): Processing losses, carcass quality, and meat yields of broiler chickens receiving diets marginally deficient to adequate in lysine prior to marketing. – Poultry Science 69: 702-710.
[15] Ng'ambi, J. W., Sebola, N. A., Norris, D. (2012): Effect of *Hoodia gordonii* leaf meal supplementation at finisher stage on productivity, carcass characteristics and meat sensory attributes of male Ross 308 broiler chickens. – African Journal of Biotechnology 11(95): 16205-16209.
[16] NRC (1994): Nutrient Requirements of Poultry. 9th Revised Ed. – National Academy Press, Washington, DC.
[17] Rizal, Y., Mahata, M. E., Andriani, M., Wu, G. (2010): Utilization of juice wastes as corn replacement in the broiler diet. – World Academy of Science, Engineering and Technology 44: 1459-1462.
[18] Rust, S., Buskirk, D. (2008): Feeding carrots or sugar beets to cattle. – Cattle Call 13(4).
[19] SAS (2008): Proprietary Software Release 9.2. – Statistical Analysis Systems Institute, Inc., Cary, NC.
[20] Steenfeldt, S., Kjaer, J. B., Engberg, R. M. (2007): Effect of feeding silages or carrots as supplements to laying hens on production performance, nutrient digestibility, gut structure, gut microflora and feather pecking behaviour. – British Poultry Science 48: 454-468.
[21] Ürüşan, H., Bölükbaşı, Ş. C. (2017): Effects of dietary supplementation levels of turmeric powder (curcuma longa) on performance, carcass characteristics and gut microflora in broiler chickens. – Journal of Animal and Plant Sciences 27(3): 732-736.
[22] Ürüşan, H., Erhan, M. K., Bölükbaşı, S. C. (2018): Effect of cold-press carrot seed oil on the performance, carcass characteristics, and shelf life of broiler chickens. – Journal of Animal and Plant Sciences 28(6): 1662-1668.
[23] Vasudevan, M., Gunnam, K. K. (2006): Parle Antinociceptive and anti-inflammatory properties of *Daucus carota* seeds extract. – Journal of Health Sciences 52: 598-606.
[24] Yu, L. L., Zhou, K. K., Parry, J. (2005): Antioxidant properties of coldpressed black caraway, carrot, cranberry, and hemp seeds oils. – Food Chemistry 91: 723-729.

http://www.aloki.hu ● ISSN 1589 1623 (Print) ● ISSN 1785 0037 (Online)
DOI: http://dx.doi.org/10.15666/aeer/1705_1233712346

FIRST MOLECULAR CHARACTERIZATION OF THE PARTIAL COAT PROTEIN AND 3'UTR GENES RELATED TO *DASHEEN MOSAIC VIRUS* ON FLAMINGO FLOWERS (*ANTHURIUM* SPECIES) IN THE MEDITERRANEAN COAST OF TURKEY

KOÇ, G.

Subtropical Fruits Research and Experimental Center, Çukurova University, Adana, Turkey (e-mail: gkmnkoc@hotmail.com.tr)

(Received 7th May 2019; accepted 16th Jul 2019)

Abstract. Observations were carried out on *Anthurium sp* growing at Mediterranean region (Adana, Mersin and Antalya provinces) of Turkey in 2015-2017. During the studies virus-like symptoms in plants; systemic chlorotic mosaic and irregular uniformity on leaf and petals were recognized. Eleven of 73 samples showed positive response with the Potyvirus group specific antibodies and their results were also confirmed by RT-PCR. The 327 bp products via using the Potyvirus-specific primers, MJ1 and MJ2 were run in 1.5% agarose gel. Further amplifications were made with the 3'UTR and 3'end of the coat protein of the viral genome. RT-PCR analysis using the primer MJ1 and M4T resulted in an amplification of 719 bp amplicon. Direct sequencing of RT-PCR products and BLAST results have showed that there were two clades between 96-99% among the Mediterranean coast DsMV isolates. The data are available in Genebank with accession Number MK758088/Antalya; MK758087/Yenice). DsMV infection on *Anthurium sp*, was determined serologically and molecularly. To our knowledge, this is the first molecular record describing the occurrence, distribution and genome organisation of DsMV isolates that have been infecting Flamingo flowers at the Mediterranean coast of Turkey. Findings may have shown an evidence about uncontrolled distribution from Northern corner to Southern side.
Keywords: *DsMV, potygroup serology, RT-PCR, molecular agroecology, evolution*

Introduction

Flamingo flowers (Anthurium plants) are native to Central and South America. Anthurium belongs to the Alismatales ordo, Araceae family, *Anthurium* genus. It is known to have over 500 species. It is grown both to be sold as a potted plant and cut flower. The most grown species are *Anthurium crystallinum, Anthurium veitchii, Anthurium magnificum, Anthurium scherzerianum* and *Anthurium andreanum.* Among the species of *Anthurium*, *Anthurium scherzerianum* is the most cultivated species. As a result of various hybridization studies of this species, different colors were produced. Mostly *Anthurium andreanum* species are produced as cut flowers. The Anthurium plant in Turkey is cultivated in the Marmara, Aegean and Mediterranean regions. The nice plant has 8-15 cm diameter flesh-like flower tray, reproductive organ and 40-70 cm length flower on stem. Flamingo flower shows tropical plants' characters. Therefore, they require high levels of humidity, temperature and shading. Due to the climate requirements, it has been cultivated under cover in the Mediterranean, Aegean and Marmara regions of Turkey.

Like in the case of other ornamental plants, many diseases have been reported in its cultivation areas. For example; members of the Tospovirus, Nepovirus, Potyvirus and Cucumovirus species are among the most important viral factors causing damage and loss due to their infections on ornamental plants (Sutic et al., 1999; Daughtrey et al., 1997; Loebenstein et al., 1995). Such as *Cucumber mosaic virus* (CMV), *Dasheen mosaic virus* (DsMV) (Rivas et al., 1997; Miura et al., 2013) and Tomato spotted wilt

http://www.aloki.hu ● ISSN 1589 1623 (Print) ● ISSN 1785 0037 (Online)
DOI: http://dx.doi.org/10.15666/aeer/1705_1234712365

virus (TSWV) (Fidan et al., 2016; Norman and Ali, 2012; Chen et al., 2003; Uchida et al., 1999). The species of ornamental plants belongs to family Areceae (Aroid) which are the most important hosts of *Dasheen mosaic virus* (DsMV). DsMV attacks at least 16 genera including Aglaonema, Caladium, Dieffenbachia, Philodendron and Zantedeschia genuses. Colocasia, Xanthosoma, Cyrtosperma species are also prone to infection with the virus (Nelson, 2008).

DsMV, has a narrow range to the plants of Aroid family (Brunt et al., 1996), the DsMV has been transmitted through tainted sap and via non-persistent manner by a couple of aphid species, including *Myzus persicae, Aphis gossypii* and *Aphis craccivora* (Buddenhagen et al., 1970). And also DsMV is not transmitted via seed propagation. The disease fundamentally causes tainted planting material which is the most common symptom. If vegetatively propagated cultivated plants have infection, it results in tainted flowers (Zettler et al., 1970; Van der Meer, 1985).

Investigation on commercial Flamingo flower plants have shown mosaic, chlorotic line indications in the veins of many plant leaves. They hindered the growth of the plant and were found to cause deformities in the nodes with color changes in the blossoms. The pathogen causing the symptoms has characterized as Dasheen mosaic infection (DsMV). The *Philodendron verrucosum* plant is a good lesion host for DsMV (Tooyoma, 1975). The other six Philodendron species tested and have deliberately contaminated with virus infection and showed diverse mosaic effects. Pale colored spots were found in *Anthurium scandens* the leaves of the cv violaceum plant. Further deformation of blossoms as well as the color quality of the knot were observed (Chagas et al., 1993). The DsMV infection results in deterioration of the appearance and nature of the blossoms. The mosaic, deformity and little protuberance indications of *Anthurium sp. cv. river* have been related with the Dasheen mosaic potyvirus and isolated the agent (Chagas et al., 1993).

If physical and molecular properties are focused on The DsMV, it is 750 nm in length and 11-13 nm wide which has flexuous, non-enveloped particles (De Brot and Ordosgoitti, 1974). The viral genome includes a monopartite single-stranded (ss) molecule of positive sense RNA of about 10 kbp, which contains 5ˈ and 3ˈ terminal UTRs flanking an imperative single ORF and the 3ˈ UTR finishing with a poly-A tail (Hull, 1994; Adams et al., 2005; Ha et al., 2008; Cuevas et al., 2012). The ten utilitarian proteins in their solicitation from 5ˈ to 3ˈ are P1 (1st protein), Helper Component-Pro (accomplice fragment protease), P3 (3rd protein), 6K1, CI (barrel molded thought protein), 6K2, VPg (genome-associated), NIa-Pro (genuine protease of minimal nuclear fuse protein - NIa), NIb (broad nuclear consolidation protein) and (CP) coat protein (Colinet et al., 1998; Adams et al., 2005; Cuevas et al., 2012; Hull, 1994).

Essentially, plants that gave signs were subjected to Enzyme Linked Immuno Sorbent Assay (ELISA) testing utilizing DsMV polyclonal antisera and gave a negative outcome. ELISA tests with potyvirus monoclonal antiserum PTY 1, a particular antiserum explicit to the potyviral coat protein region, gave a positive response. ELISA is the most convenient procedure for routine distinguishing proof of DsMV in huge amounts of plant tests with variable contamination titres. Nevertheless, DsMV IgG is in limited facility, and the exceedingly thick concentrate of aroid sap is represented to intrude with ELISA tests (Rodoni and Moran, 1988). Moreover, past examination exhibited that recognizable proof of DsMV by ELISA was clashing obviously due to uneven course of DsMV (Hu et al., 1994). Serological investigation of potyviruses is routinely mismatched, due to immunological cross-reactions among species (Brunt,

http://www.aloki.hu ● ISSN 1589 1623 (Print) ● ISSN 1785 0037 (Online)
DOI: http://dx.doi.org/10.15666/aeer/1705_1234712365

1992) and biological identification is extremely unbalanced. On the other hand, continuous advances in nucleic acid advances have enabled the improvement of stunning acknowledgment and recognizing proof instruments.

The currently accepted criteria for detecting disease species in the Potyviridae family are based on the collection of genomic information. Moreover, differentiation in host range and host reaction, antigenic properties and the morphology of inclusion bodies can be considered as criteria for limiting (King et al., 2012; Babu et al., 2011). In the same study, the 327-bp part of the coat protein gene area from the contaminated *Colocasia esculenta* plant, which has whitepox symptoms, has researched by Reverse Transcriptase Polymerase Chain reaction (RT-PCR) technique utilizing primers specific to the Potyviruses. DNA sequence investigation and BLAST examination demonstrated a close association with DsMV. Similarly, the presence of Dasheen mosaic infection (DsMV-Sc) has been verified on *Spiranthes cernua* plants that show chlorotic spots and mosaic indications (Guaragna et al., 2006).

The conspicuous confirmation was reliant on the Polymerase Chain Reaction, which was used for Potyvirus (Langeveld et al., 1991). Grisoni et al. (2006) has been used Potyvirus group specific primers for recognizable evidence of Potyvirus tainting Vanilla. Same researchers reported primer pair MJ1 and MJ2, which amplify a short fragment (327 bp centered on coat protein gene) of an extensive part of the potyviruses.

In the Mediterranean Region of Turkey, which has an important place in the production of ornamental plants, the studies of viral diseases started on the demands of the producers of Flamingo flower cultivations as interior and cut flowers. The symptoms; systemic chlorotic mosaic and irregular uniformity on leaf and petals) were considered to be related to Dasheen mosaic virus. As the production areas are usually intertwined with undergrowth vegetable production areas, it has been investigated in terms of viral diseases which are problem in both vegetable and ornamental plants.

Therefore, aims of the studies were to clarify the recognition and recognizable proof of the Potyvirus species tainting Flamingo flower (Anthurium sp.), through sequencing of fractional coat protein gene and the 3'UTR area of the viral genome. Then, the nearness of DsMV in Flamingo flower plants will be recognized by DAS-ELISA and RT-PCR systems. Finally, the CP and 3'UTR of some DsMV isolates will be sequenced in molecular genetic for distinguishing proof. The study may be the broadest research on DsMV in recent years at Turkey.

Materials and methods

Experiments have been set in Antalya, Mersin and Adana cities located at the Mediterranean region of Turkey (*Fig. 1*). Seventy-three samples from symptomatic Flamingo flower plants showing common DsMV symptoms (upward leaf curling, mosaic, yellowing, distortion and flower mosaics) and some asymptomatic leaf samples were used in molecular analyses (*Fig. 2*).

Serological tests

Collected samples were labelled and placed into plastic packs, then were conveyed to the Virology Lab via putting them in ice pail and kept at 4 °C. All samples were used within 24 h.

http://www.aloki.hu ● ISSN 1589 1623 (Print) ● ISSN 1785 0037 (Online)
DOI: http://dx.doi.org/10.15666/aeer/1705_1234712365

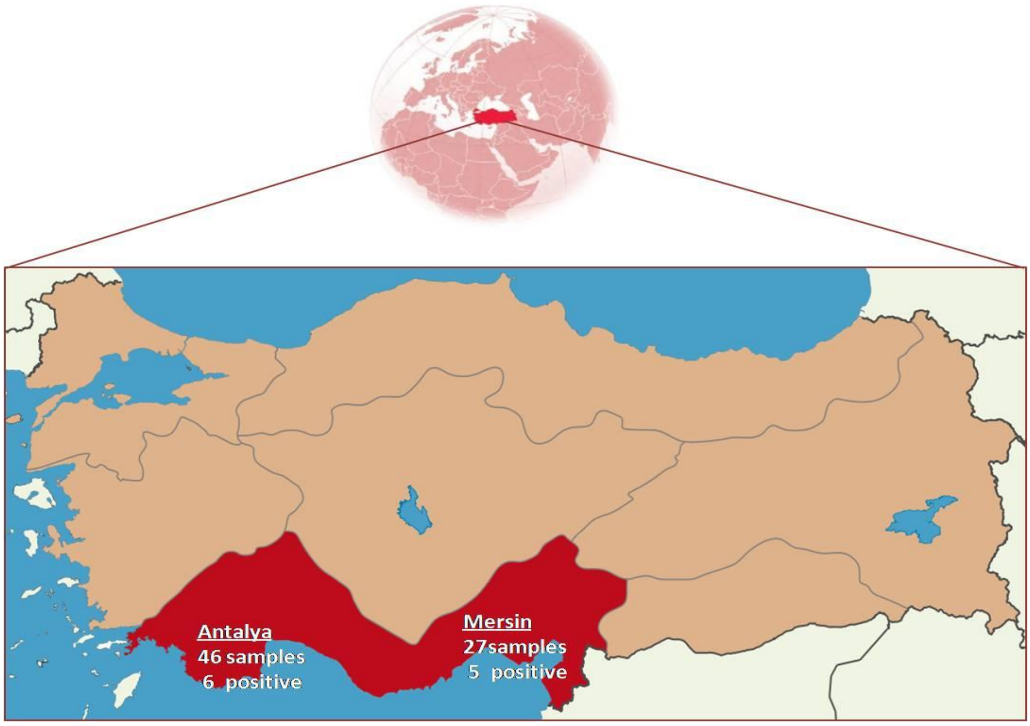

Figure 1. *The map of the Mediterranean region in Turkey with positive locations (https://tr.wikipedia.org/wiki/Akdeniz_Bölgesi)*

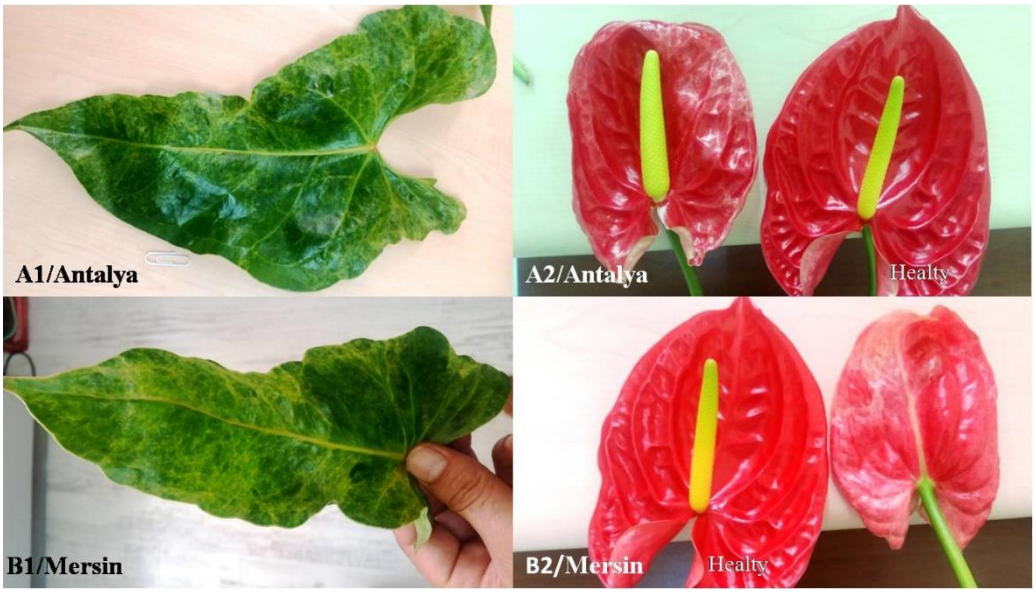

Figure 2. *Athurium plants have showing typical DsMV symptoms (upward leaf curling, mosaic, yellowing, distortion and flower mosaics)*

Enzyme linked immunosorbent assay

For distinguishing evidence infections contaminating Flamingo flower, leaves were attempted through ELISA utilising polyclonal antiserum specific to infections. The ELISA tests contained various virus species which are found in ornamental plants. All

http://www.aloki.hu ● ISSN 1589 1623 (Print) ● ISSN 1785 0037 (Online)
DOI: http://dx.doi.org/10.15666/aeer/1705_1234712365

the tested polyclonal antibodies were given in *Table 1*. ELISA antisera one by one received from Agdia U.S. and Bioreba AG, Switzerland. Tests covered location of infections in tainted fresh leaves and conveyed according to Clark and Adams (1977). To each well of ELISA plates (Nunc F96 Maxisorp) 200 µl of IgG diluted in coating buffer (BIOREBA antisera 1: 1000 ratio or Agdia antisera 1: 200 ratio) was added and they were incubated for 4 h at 30 °C. The ELISA plate was washed with wash buffer and left for 3 min, which was repeated 3 times. Samples prepared with extraction buffer were incubated for 16 h at 4 °C by adding 200 µl of positive and negative controls to each well. The ELISA plate was washed again as described in the second step. IgG diluted 1: 1000 (Bioreba) and 1: 200 (Agdia) in conjugated buffer was incubated at 30 °C for 4 h by adding 200 µl to each well and the ELISA plate was washed again as described in the second step. Subsequently, 200 µl of the substrate solution (1 mg/ml paranitrophenylphosphate) was added to each well and allowed to stand at room temperature in the dark for 1 h.

The results were obtained by observing the formation of yellow color in the ELISA reader and measuring the absorbance values at 405 nm wavelength. Samples that gave at least twice the absorbance value of the healthy control value were considered infected or positive. Values close to positive but not definite were considered suspicious.

Nucleic acid based assays

We focus on DsMV in molecular studies because serologically positive results were obtained by *Potyviru*s genus-specific antibodies (Agdia). Moreover, the most obvious disease in Flamingo flower is DsMV and typical symptoms in the collected samples indicate DsMV.

Total RNA isolation and reverse-transcription polymerase chain reaction (RT-PCR)

Total nucleic acid was extracted from contaminated Flamingo flower plants according to Dellaporta et al. (1983) and their RNAs were used in Reverse-Transcriptase Polymerase Chain Reactions (RT-PCR). In the first place the samples were prepared from different tissues of infected Anthuriums such as Leaf, Petal, stamen + pistil, Peduncle or stem due to covering causal disease agent.

RT-PCR detection of CP region by MJ1 and MJ2

Sense MJ1 (5'-ATGGTHTGGTGYATHGARAAYGG-3' and MJ2 (5'-TGCTGCKGCYTTCATYTG-3') designed by Marie-Jeanne et al. (2000) (*Fig. 3*). Grisoni et al. (2006) published a single letter code H: A/C/T\, Y:C/T, R:A/G, K:G/T that amplify a 327 nt fragment in the CP gene of potyviruses of DsMV isolates. The cDNAs were obtained using Thermo Sci. Verso 1-Step RT-PCR Kit pack according to producer's manual. DsMV PCR mix was replicated by program through a cycle of RT at 49 °C for 45 min (m), 94 °C for 2 min; following 38 cycles of 94 °C for 30 s, 50 °C for 55 s., extension 72 °C for 55 s, and a final step of 72 °C for 10 min in a thermal cycler (Babu et al., 2011).

Amplification of partial coat protein gene and 3'UTR; The universal primer sequence M4T, which trigers to the 3'end of the potyviral gene and the reverse primer in combination with the forward primer MJ1 were used. The RT-PCR was performed in a 20 mL volume. Each primers MJ1 and M4T-5'-GTTTTCCCAGTCACGACTTTTTTTTTT-3' are shown in (*Fig. 3*). The RT-PCR mix

http://www.aloki.hu ● ISSN 1589 1623 (Print) ● ISSN 1785 0037 (Online)
DOI: http://dx.doi.org/10.15666/aeer/1705_1234712365

was subjected to thermal programme: RT at 48 °C for 45 min, denaturation at 94 °C for 2 min; 38 cycles of 94 °C for 30 s, annealing. at 50 °C for 55 s and extension at 72 °C for 55 s, and last step of 72 °C in 10 at thermal cycler (Babu et al., 2011).

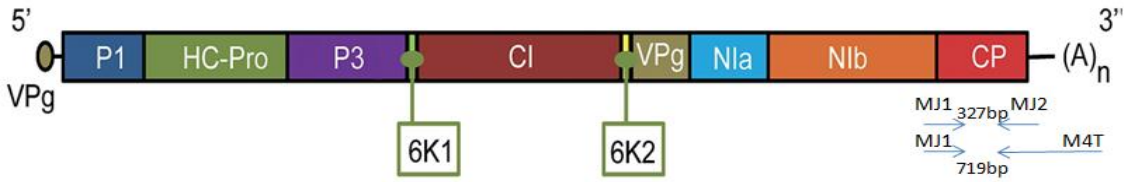

Figure 3. *Schematic representation of Potyvirus genome (Cuevas et al., 2012) and the primers' amplicon ranges for DsMV Mediteranean isolates in this study*

Analysis of RT-PCR products

10 µl of PCR product was utilized within gel loading buffer and dissected on a 1.5% agarose gel containing 0.5 mg/ml of ethidium bromide (Sambrook et al., 2001). 100 bp DNA stepping ladder (thermo) was also used on each gel to compare PCR products' size.

Phylogenetic analysis

The DsMV containing RT PCR products obtained by MJ1 and MT4 primer sequences and dnasp5 program was conducted. Phylogenetic analyses were performed by MEGA 7 software and neighbour joining process, according to conventional analysis. Obtained sequences were compared with strains of DsMV genebank (NCBI, National Center for Biotechnology Information). Sequences from the accessions (accession Number MK758088/Antalya; MK758087/Yenice) were considered. Sequence alignment of the DsM virus isolates and homology between sequences were calculated according to Thompson et al. (1994). A sequence identity matrix of the 3'UTR region and partial CP gene of the DsMV isolates were constructed using the BIOEDIT with worldwide DsMV sequences obtained from the GeneBank.

Results

Type of symptoms on Anthurium sp.

Upward leaves curling, mosaic, yellowing, distortion and mosaic flower associated with Flamingo flower plants were indicating DsMV symptoms (*Fig. 2*). Virus infected leaves in the fields were light yellow and leaf margin areas resembled to distortion (*Fig. 2A1-A2*); There were leaf mosaics reduced in size and shapeless malformated leaves (*Fig. 2A1-A2*). General flower discoloration was observed and petals had mild whitish mosaics on the Flamingo plants (*Fig. 2B1-B2*).

Occurrence of viruses by serology (ELISA)

Immunological assay performed in ELISA serological tests: they were individually repeated at least two times to approve presence of the virus. 11 out of 73 samples have given positive reactions (with 15.06% incidence) with the potyvirus genus group

http://www.aloki.hu ● ISSN 1589 1623 (Print) ● ISSN 1785 0037 (Online)
DOI: http://dx.doi.org/10.15666/aeer/1705_1234712365

specific antiserum. The 11 positive samples of Flamingo flowers were collected from 2 provinces, 6 of them were from Antalya and other 5 were from Yenice, Mersin, Turkey (*Fig. 2*).

Further verification tests have applied RT-PCR with total nucleic acids isolated from the samples following ELISA tests. Due to having positive result to Potyvirus group, any positive reaction for other tested virus species and groups, cellar DsMV symptoms and not in laboratory opportunities of DsMV commercial antiserum. As well DsMV is previously reported on many aroid species (Nelson, 2008).

The RT-PCR amplification

For confirming the serology test results, RT-PCR analyses were conducted. DsMV; 327 bp sections as the objective RNA have been put in CP focal areas and DsMV; 719 bp on 3'UTR and coat protein partial genes, are identical for detection experiments. Selected MJ1–MJ2 were published as degenerate primers by different researchers (Chen et al., 2001; Pappu et al., 1993; Langeveld et al., 1991). For the reason of couple of these primers good at for RT-PCR based detection.

Extracted RNAs (327 nt) were chosen symptomologically from two samples, and they yielded expected products (*Fig. 4*) on agarose gel (1.5%) electrophoresis. The RT-PCR results affirmed DsMV in Flamingo plants.

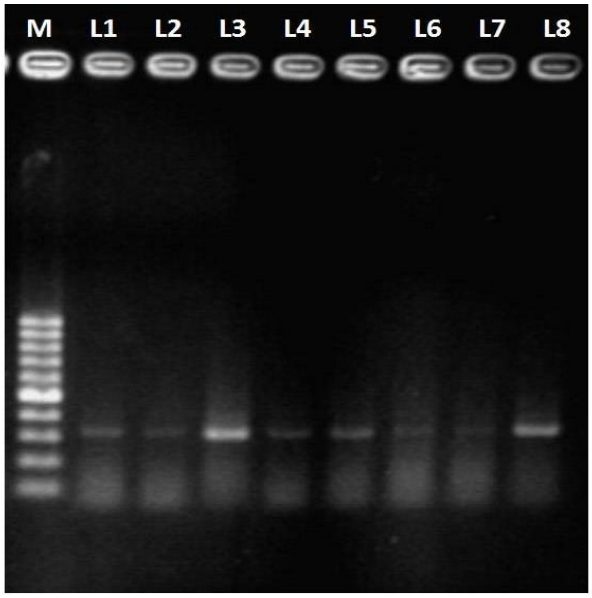

Figure 4. *First lane M DNA ladder; RT-PCR products of 327 bp of DsMV CP on agarose gel (1.5%) (Lane1, A1 Leaf; L2, A2 Petal; L3, A2 stamen + pistil; Lane4, A2 Peduncle or stem; Lane5, B1 Leaf; Lane 6, B2 Petal; Lane 7, B2 stamen + pistil; Lane 8, B2 Peduncle or stem) positive Flamingo flower samples ("A" coded samples from Antalya and "B" coded samples from Yenice/Mersin of Mediterranean Cost in Turkey)*

Additionally, conserved CP central regions resulted bands in RT-PCR analysis using primer pairs combination of MJ1 and M4T. We obtained 719 bp cDNA bands of DsMV located between partial CP and 3'UnTranslated Region verifying discrimination of different isolates in RT-PCR system (*Fig. 5*). The 3'UTR sequences of potyviruses have an opportunity for understanding different isolates (Frenkel et al., 1989; Pappu et al., 1993).

http://www.aloki.hu ● ISSN 1589 1623 (Print) ● ISSN 1785 0037 (Online)
DOI: http://dx.doi.org/10.15666/aeer/1705_1234712365

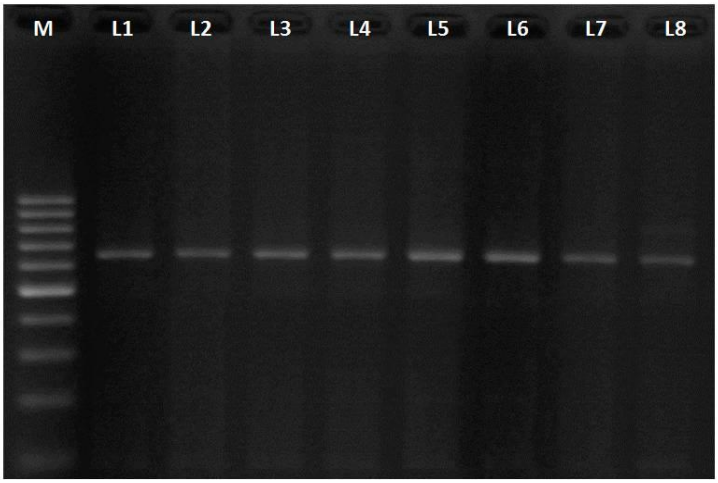

Figure 5. *RT-PCR product of 719 bp of DsMV CP on agarose gel (1.5%); First lane, M DNA ladder; Lane1, A1 Leaf; L2, A2 Petal; L3, A2 stamen + pistil; Lane4, A2 Peduncle or stem; Lane5, B1 Leaf; Lane 6, B2 Petal; Lane 7, B2 stamen + pistil; Lane 8, B2 Peduncle or stem) positive Flamingo flower samples ("A" coded samples from Antalya and "B" coded samples from Yenice/Mersin of Mediterranean Coast in Turkey*

ELISA tests were conducted against 20 viruses where two types of group specific antiserums were used. Positive results were obtained only against Potygroup specific polyclonal antiserums and 327 nt CP core regional primers by RT-PCR (*Fig. 4*) among all viruses infected samples (*Table 1*). In addition to the species specific ELISA tests, *Tospo* group specific antiserums did not give any positive results for all collected samples. RT-PCR resulted 719 nt amplicon that was specific for DsMV. There were additional results found from different plant tissues; leaf; petal; stamen + pistil and peduncle or stem (*Fig. 5*).

Phylogenetic analysis

Phylogenetic analysis was performed by MEGA 7 programming, entire DsMV sequences were distinguished (*Fig. 6*). Two distinct haplotypes which were symptomologically chosen from Anthurium sp plants at Mediterranean region of Turkey were determined from present DsMV isolates by either RT-PCR or sequences. Two different but not so significantly distinct haplotypes have been analyzed in NCBI system and their sequences were submitted to NCBI as new records.

The Flamingo flower samples from Turkey in Genebank have accession numbers MK758088/Antalya and MK758087/Yenice. The accession numbers were first recorded to NCBI system (*Fig. 6*) and they listed with other isolates from worldwide in *Table 2*. The two isolates of DsMV have approximately 99.49% similarity with each other isolate in Turkey. They were replaced in two clades as they were isolated from two Anthurium species. This is may be caused by two production materials imported from different origins. Phylogenetic tree showed that both isolates are related with each other at the Mediterranean region of Turkey. Their sequences were clarified that two Anthurium sp DsMV isolates from the Mediterranean region of Turkey have similar homology with *Xanthosoma* sp Et56 from Ethiopia (Accession Num. MG602233.1) and *Colocosia esculenta* TW from Japan: Utsunomiya (Accession Num. AJ298036.1) isolates.

http://www.aloki.hu ● ISSN 1589 1623 (Print) ● ISSN 1785 0037 (Online)
DOI: http://dx.doi.org/10.15666/aeer/1705_1234712365

The DsMV from Flamingo flower Antalya, Turkey isolates (accessed as new record to NCBI system with accession number: MK758088) (100%-Turkey) have showed approximately 91.40% similarity with Japan: Utsunomiya (Accession Num.AJ298036.1) isolate and 90.54% Nicaragua NiNG1 (Accession Num.AM910398.1); 87.32%. Tanzania *Xanthosoma* sp. Tz24 (Accession Num.MG602242.1) around the world (*Table 2*; *Fig. 6; Table 3*). The other DsMV isolate, Yenice was reported to NCBI system with accession number: MK758087 (99.49%-Turkey). The DsMV Yenice has approximately 89.54% similarity with *Xanthosoma* sp Et56 from Ethiopia (Accession Num. MG602233.1) isolate and 84.55% New Zealand Taro DsMV1 (Accession Num.AY994104.1); 83.50% French Polynesia *Vanilla tahitensis* FP (WP013, Accession Num. AJ616719.1) (*Table 2*; *Fig. 6; Table 3*, respectively).

The developmental history was derived utilizing the Neighbor-Joining technique. The ideal tree with the aggregate of branch length = 24.38716469 is appeared. The level of recreate trees in which the related taxa bunched together in the bootstrap test (1000 repeats) are appeared at the branches. The tree is attracted to scale, with branch lengths in indistinguishable units from those of the evolutionary distances used to deduce the phylogenetic tree (*Fig. 6*).

Table 1. *Serological and molecular studies and results of Flamingo flower plant samples*

Virus species	**Plant species**	**Assays**	**Number of samples *Result**	
			27/Yenice	**46/Antalya**
ArMV (Arabis Mosaic Virus)	Anthurium sp	ELISA	-	-
SLRSV (Strawberry Latent Ringspot Virus)	Anthurium sp	ELISA	-	-
TRSV (Tobacco Ringspot Virus)	Anthurium sp	ELISA	-	-
ToRSV (Tomato Ringspot Virus)	Anthurium sp	ELISA	-	-
TMV (Tobacco Mosaic Virus)	Anthurium sp	ELISA	-	-
TRV (Tobacco Rattle Tobravirus)	Anthurium sp	ELISA	-	-
TNV (Tobacco Necrosis Virus)	Anthurium sp	ELISA	-	-
ToMV (Tomato Mosaic Virus)	Anthurium sp	ELISA	-	-
PepMoV (Pepper Mottle Potyvirus)	Anthurium sp	ELISA	-	-
Tospo (Tospovirus)	Anthurium sp	ELISA	-	-
TSWV (Tomato Spotted Wilt Virus)	Anthurium sp	ELISA	-	-
Poty (Genus group Poty Virus)	**Anthurium sp**	ELISA	**5 +**	**6 +**
PVY (Potato Virus Y)	Anthurium sp	ELISA	-	-
AMV (Alfalfa Mosaic Virus)	Anthurium sp	ELISA	-	-
ZYMV (Zucchini Yellow Mosaic Virus)	Anthurium sp	ELISA	-	-
BCMV (Bean common mosaic potyvirus)	Anthurium sp	ELISA	-	-
LMV (Lettuce mosaic potyvirus)	Anthurium sp	ELISA	-	-
PVX (Potato Virus X)	Anthurium sp	ELISA	-	-
INSV (Impatiens necrotic spot virus)	Anthurium sp	ELISA	-	-
TuMV (Turnip Mosaic Potyvirus)	Anthurium sp	ELISA	-	-
DsMV (Dasheen mosaic virus).	**Anthurium sp**	RT-PCR	**5 +**	**6 +**
CMV (Cucumber Mosaic Virus)	Anthurium sp	ELISA	-	-

*(-) Negative (not infected); (+) Positive (infected)

http://www.aloki.hu ● ISSN 1589 1623 (Print) ● ISSN 1785 0037 (Online)
DOI: http://dx.doi.org/10.15666/aeer/1705_1234712365

Table 2. *The Anthurium sp DsMV isolates in Turkey, which are ranked in phylogenetic tree*

No	Accession num.	Isolate name	Host	Country	Per ident.
1	MK758088	Antalya	*Anthurium* sp.	Turkey	-
2	MK758087	Yenice	*Anthurium* sp.	Turkey	99.49-
3	KJ786965.1	T10	*Amorphophallus paeoniifolius*	India	99.59
4	MG602229.1	Et26	*Colocasia esculenta*	Ethiopia	90.65
5	AJ298036.1	TW	*Colocosia esculenta*	Japan: Utsunomiya	91.40
6	LC114515.1	Ds23	*Amorphophallus konjac*	Japan: Gunma, Shibukawa	90.95
7	DQ925466.1	DsMV-VN/Tt1	*Typhonium trilobatum*	Viet Nam: Hanoi	90.66
8	MG602233.1	Et56	*Xanthosoma* sp	Ethiopia	89.54
9	AM910398.1	NiNG1		Nicaragua	90.54
10	AJ298033.1	M13	*Zantedeschia aethiopica*	China: Zhejiang	89.54
11	MG602235.1	Ug31	*Xanthosoma* sp.	Uganda	87.95
12	KY242359.1		*Colocasia esculenta*	USA: Hawaii Strain (II)	87.91
13	KT372699.1	ZAN	*Zantedeschia* sp.	Taiwan	88.24
14	KP729477.1	66/14	*Zantedeschia* sp.	Bosnia and Herzegovina	90.19
15	AY994104.1	DsMV1	Taro	New Zealand	84.55
16	KY242358.1		*Colocasia esculenta*	USA: Hawaii Strain I	84.38
18	AY994105.2	DsMV2	Taro	New Zealand	84.40
19	MG602242.1	Tz24	*Xanthosoma* sp.	Tanzania	87.32
20	AJ616719.1	FP (WP013)	*Vanilla tahitensis*	French Polynesia	83.50

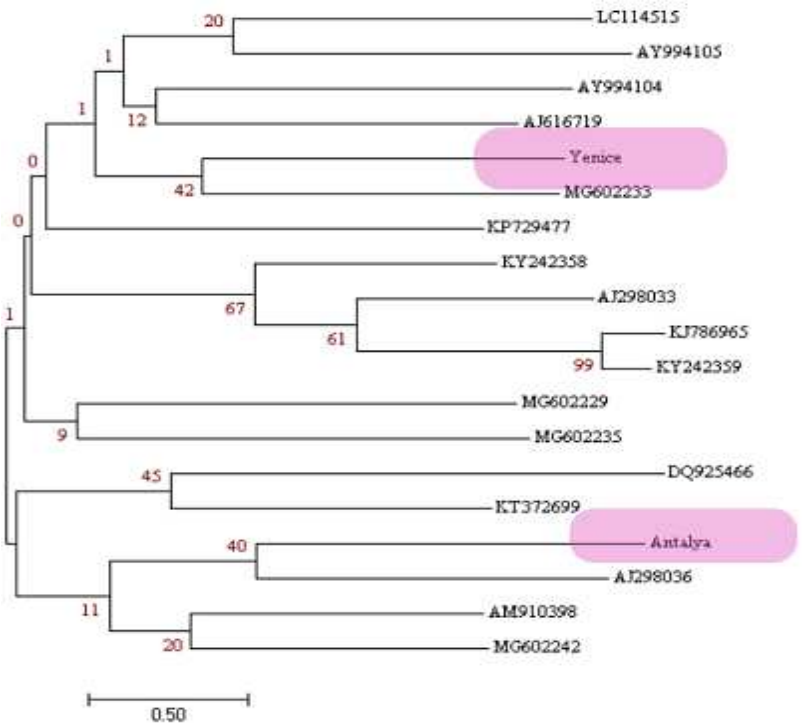

Figure 6. *Phylogenetic tree of two different DsMV isolates from Mediterranean region of Turkey were clustered within the GenBank database (detailed in Table 2)*

http://www.aloki.hu ● ISSN 1589 1623 (Print) ● ISSN 1785 0037 (Online)
DOI: http://dx.doi.org/10.15666/aeer/1705_1234712365

Table 3. *Phylogenetic tree pair wise distance matrix of DsMV haplotypes of different countries and Turkey (Antalya and Yenice)*

Yenice																		
Antalya	4.62																	
KJ786965	3.15	4.95																
MG602229	2.72	3.39	2.80															
AJ298036	4.61	2.32	5.08	3.97														
LC114515	3.12	4.08	3.06	3.00	3.01													
MG602233	2.25	4.33	2.76	4.50	3.44	3.23												
AJ298033	4.52	4.52	1.51	4.21	3.28	3.42	3.00											
DQ925466	4.70	3.34	4.21	3.41	3.87	4.15	2.97	3.33										
AM910398	2.90	2.96	3.10	3.25	1.80	2.63	4.28	2.82	3.37									
MG602235	3.06	2.95	4.39	2.79	3.53	3.22	2.63	2.68	4.66	2.61								
KT372699	2.76	3.36	2.47	2.89	4.33	4.57	2.71	3.31	2.54	2.86	2.79							
KY242359	3.26	4.40	0.35	3.12	4.81	3.12	2.78	1.85	4.15	2.52	4.37	4.33						
KP729477	2.96	3.39	4.48	2.71	3.50	3.08	3.01	3.11	3.29	3.35	3.32	2.93	3.27					
AY994104	2.99	2.99	3.33	3.62	3.47	3.09	2.73	4.35	3.23	4.01	3.15	2.81	3.07	3.17				
KY242358	3.52	3.84	1.86	3.23	3.09	2.97	2.89	1.46	4.44	2.22	2.66	2.92	2.90	2.63	3.36			
AY994105	3.43	2.88	3.47	3.01	3.99	2.37	2.74	3.56	4.44	3.29	3.33	4.92	2.90	3.19	2.84	4.53		
AJ616719	2.43	3.41	4.41	3.11	3.10	3.08	3.07	3.05	4.05	2.71	3.44	3.19	3.43	2.66	2.44	2.75	2.40	
MG602242	2.49	3.90	4.32	3.25	2.52	2.08	3.25	3.45	3.45	1.84	3.52	2.99	4.35	3.26	3.44	2.17	3.44	3.04

Discussion

The sanitary status of Dasheen viruses in Turkey has not been broadly studied. Therefore, in the project, we aimed to determine and identify how to detect the virus and possibly control economically important viruses associated with Flamingo flower.

Typical symptomatic Flamingo flower plants in this study, were tested with ELISA and RT-PCR analyses. 73 samples were collected from Mersin and Antalya provinces in the in Mediterranean region: among which 11 were positive with the potyvirus infection in ELISA and RT-PCR similarly to previous works (Kibar, 2014; Kidanemariam, 2016, 2018)

In our study frame, virus infected leaves in the fields were light yellow and leaf margin areas resembled distortion, leaves having mosaics reduced in size and shapeless, malformated leaves were observed, flowers had discoloration and petal mosaics were also observed on flamingo plants. The same was found in the case of several aroids (Elliott et al., 1997; Lima et al., 2004; Nelson, 2008; Cabrera et al., 2010; Babu and Hegde, 2014). Infrequently, yellow and green patterns occurred over the whole leaf surface, which may have seemed slender with a distorted edge (Kohler et al., 1997).

In a close study, an excessive strain of DsMV caused pale green and yellowish designs on stunted and extremely distorted leaves in French Polynesia (Jackson, 1982). A few of which can be decreased to strap-like structures without flaps. The presence of DsMV in *Anthurium andreanum* (Flamingo blossom) and a few orchid (*Cymbidium spp*.) species was just investigated by means of serological methods. DsMV was verified in two *Anthurium andreanum* leaf samples in Trace location of Turkey (Kibar, 2014). Similarly, Greber and Shaw (1986) diagnosed Dasheen mosaic virus (DsMV) via mechanical inoculation of plant sap and serological tests in wild and cultivated plant species. Also close results, reported by Simone and Zettler (1990) that there are hosts of DsMV in a few different tropical plants besides Araceae family ornamental flora. Viral

http://www.aloki.hu ● ISSN 1589 1623 (Print) ● ISSN 1785 0037 (Online)
DOI: http://dx.doi.org/10.15666/aeer/1705_1234712365

agents belonging to the genera Tospovirus, Nepovirus, Potyvirus and Cucumovirus had been among the main viral agents inflicting loss of ornamental plants which were reported (Daughtrey et al., 1997; Loebenstein et al., 1995; Sutic et al., 1999).

The Flamingo flower samples, in Mersin (Yenice) and Antalya, gave positive reactions (with 15.06% incidence) against the potyvirus genus group specific antiserum but there were not any serological reactions against other tested viruses and groups. Likewise, Lima et al. (2004) reported that their collected samples from 20 symptomatic Anthurium flowers were revealed positive results in ELISA. Our results were consistent with the potyvirus specific antiserum in ELISA but negative response obtained with the antiserum for CMV. Only difference between the above study and ours were antisera which we did not have DsMV antiserum.

Valverde et al. (1997) reported DsMV in Dasheen vegetation, which was produced in in vitro environment. DsMV was determined by means of ELISA check in distinctive forms of *Colocasia esculenta* plant in different researches (Hu et al., 1994; Rodrigues et al., 1984; Zettler et al., 1987; De Brot and Ordosgoitti, 1974). Kibar (2014) reported the DsMV serologically by ELISA on Anthurium and Cymbidium flowers. Shukla et al. (1992) referenced a couple of challenges related to serological identification of some potyviruses, which were direct result of characteristic complexities related with the potyvirus coat proteins (Shukla and Ward, 1989a, b; Ward and Shukla, 1991). Shukla et al. (1994) expressed that the complexities came about because of 3 overwhelming inconveniences. Those are especially in the first place variable cross-reactivity of potyvirus antisera; in second placeamazing and conflicting combined pursuing; and in the third place absence of cross-response between certain strains.

ELISA and molecular assays have been used for the detection of DsMV by different papers (Abo El-Nil et al., 1977; Nelson, 2008; Babu and Hegde, 2014), both techniques are sensitive for the detection of viruses but RT-PCR is more reliable with high selectivity to detect such viruses (Randles et al*.,* 1996).

Among molecular analyses of this study, the RT-PCR have been intensified with degenareted primers MJ1–MJ2 and 327 bp target fragments were obtained for the detection of DsMV. Based on many previous results (Chen et al., 2001; Pappu et al., 1993; Langeveld et al., 1991) MJ1–MJ2 were selected which were reported as degenerate for the DsM virus from different aroid isolates. The 327 bp fragments as the target RNA have been amplified for both potygroup and DsMV due to highly conserved CP core central regions. Similarly, Marie-Jeanne et al. (2000) reported a 327 bp fragment in the Coat Protein genes of potyviruses. Since they amplify a short part and gave superior enhancement signals in preliminary experiments of diverse isolates DsMV isolates Marie Jeanne et al. (2000) also concluded similar results with DsMV. 719 bp on coat protein partial genes and 3'UTR, were resulted for specific detection and discriminations.

Likewise, Babu et al. (2011) clarified the 327 bp CP fragments from the infected *Colocasia esculenta* plants via RT-PCR. The processing of unique primers particular to the Potyviruses and cDNA sequence evaluation confirmed for DsMV.

As well Grisoni et al. (2006) applied Potyvirus group specific primers for recognizable proof of Potyvirus contaminating Vanilla plants. The primer pair MJ1 and MJ2 explicitly amplify a brief piece (327 bp) of the middle district of coat protein gene of a big portion of the potyviruses.

In Addition to 327 bp region amplification; primer pairs combination of MJ1 and M4T were studied for 719 bp cDNA bands of DsMV to compare the isolates with

http://www.aloki.hu ● ISSN 1589 1623 (Print) ● ISSN 1785 0037 (Online)
DOI: http://dx.doi.org/10.15666/aeer/1705_1234712365

worldwide isolates via ncbi database in project scope. RT-PCR sequences of 719 bp affirmed the diseases for DsMV positive plants from East Mediterranean isolates in ELISA. The amplified PCR 719 bp products were applied for sequencing and phylogenetic tree discrimination. No critical differences was observed among the plant tissues when the RT-PCR was applied. That is identical to the result obtained on exceptional tissues in agarose gel electrophoresis in our study. Frenkel et al. (1989) and Pappu et al. (1993) decided that the 3'UTR sequences of potyviruses were useful for differentiation of strains and species of potyviruses

Edited DsMV sequences from East Mediterranean isolates were compared with strains of gen bank (NCBI). Sequences of The Mediterranean region isolates of Turkey were edited as accession Number MK758088/Antalya and MK758087/Yenice for the first time in Turkey (*Fig. 6*).

The main outcome from analysis of sequence revealed that DsMV Yenice (Mersin) and Antalya isolates were most similar to both in itself and all the other compared geographically originated isolates. In the same way, Babu et al. (2011) compared 3'UTR region of different isolates by universal primers MJ1 and M4T and also they identified DsMV was closely related to DeSLK2 isolate. Finally, same papers reported DsMV as the first report of molecular based detection of the DSMV infecting *Amorphophallus paeoniifolius i*n India. Briefly, it was determined that the 3'UTR sequences of potyviruses had an opportunity that benefited for differentiation of isolates (Frenkel et al., 1989; Pappu et al., 1993).

Similarly, Zavareh et al. (2013) determined the DsMV in Anthurium plant by means of PCR method. Furthermore, it is reported that the Areceae family is a few of the most essential hosts of Dasheen mosaic virus (DsMV) in ornamental plant species Nelson (2008).

In another group of studies, presence of DsMV with molecular techniques was detected by Reyes et al. (2009) in a tropical plant Cocoyam (*Xanthosoma spp*.); Babu et al. (2011) in *Colocasia esculenta*, and Chen and Adams (2001) identified the complete genome sequences of an isolate of Dasheen mosaic virus (DsMV) in *Zantedeschia aethiopica*. Likewise, Maino (2003) concluded the variability within the coat protein-CR of DsMV isolates from French Polynesia, Papua New Guinea, Vietnam Solomon Islands, Samoa, and New Caledonia via amplifying, cloning and sequencing. In comparison with the DsMV sequences at the database, the most variability changed into taken as 21.9%, while the center district of the CP become analysed, while the greatest variability dropped to 6%. Additionally, equivalent guide was demonstrated, most variability become present in the N end.

Li et al. (1998) ordinarily cloned and sequenced the 3' - terminal 3158 nts of the Caladium isolate of (DsMV-Ch). The sequences included the 3' end of the Nia, Nib and CP-coding regions and a 246 nt UTR (with the exception of the poly-A tail) in the long run. The comparisons of DsMV-Ch CP with that of DsMV-LA and DsMV-TEN isolates found a closeness of 84-88% on the nucleotide level, and 92-94% at the amino acid level. When all data considered an arrangement of the amino acid sequencing of the 3 isolates discovered N terminal variability and a close similarity among the DsMV-Ch and DsMV-TEN.

http://www.aloki.hu ● ISSN 1589 1623 (Print) ● ISSN 1785 0037 (Online)
DOI: http://dx.doi.org/10.15666/aeer/1705_1234712365

Conclusion

The Mediterranean region of Turkey is a critical agricultural cultivation area for many types of plants grown. Ornamental vegetation has a vital importance inside the production of cultivated crops which contribute substantially to the financial system and have an excessive export capacity.

Decorative plants' leaves and cut flowers are the most common wealth of ornamental plant market in global scale. Productivity and quality losses occur because of adverse outcomes of diseases in decorative flowers that economic importance is increasing day by day. Especially in practice, there is no chemical application to control virus diseases. Consequently, the virus diseases can restrict the production via reducing flower production within the Mediterranean region of Turkey. It should be understood to apply control measures and their epidemiology and molecular origin ought to be known.

Studying the Anthurium sp. as cut flower species in greenhouses (Flamingo plant) becomes important for economical reasons. Viral disease agents have reduced their market value and their aesthetic value for consumers.

Natural distribution and occurrence of Dasheen viruses in the studied area have determined as very limited distribution in Turkey. Our results have already mentioned above sanitary situations in Flamingo flowers growing regions are very vitally important in Turkey. As well as, to prevent the spreading of common plant viruses and DsMV is only possible with the detection of the agent. All of DsMV positive samples in this study have already been eradicated. Therefore, maintaining Turkey's disease free status with the definite destruction of the inoculum sources needs controlled quarantine applications. Probably, DsMV's insect vectors, are actually second main factors, are responsible for the epidemiology by re-infection in the green houses. Insecticide applications are commonly used technique for management strategy against aphids (Knauss et al., 1975; Monge et al., 1987; Valverde et al., 1997). Even it is one of the main threatening elements to the ecology and environment. Resistant cultivars and sanitation should be used for control of the DsMV in practices. Sometimes resistance breaking isolates can be developed in greenhouses (Fidan and Sarı, 2019). Infected plants, presence of vectors and presence of virus have vital effects on the spread of DsMV at infected areas (Çolak Ateş et al., 2018).

Some potyvirus isolates, such as Alfalfa Mosaic Virus (AMV), Zucchini Yellow Mosaic Virus (ZYMV) and Plum Pox Potyvirus (PPV), etc.) are highly infectious and are able to transmit with aphids. They have been studied and molecularly characterised from different hosts both in Turkey and in Cyprus (important for material exchange) (Özer et al., 2012; Fidan et al., 2012; Koç, 2010; Koç and Baloğlu, 2006).

Therefore, molecular epidemiology should be well understood and spread to field or outdoor plants should be prevented. In addition, the presence of broad range vector aphids in the greenhouses and outside, and the lack of biological and more ecologically friendly chemical protection, the risk of infection increases that will allow DsMV to spread more by aphids from cultivated plant crops. It also originates progressively from different weed species and occurs after infection with infected seedlings or inoculum sources if it is not well controlled.

This is the first molecular event report of DsMV in Anthurium sp in the Mediterranean region of Turkey. Our results have shown reliable laboratory molecular methods with immunological ELISA and molecular RT-PCR analyses. Further advanced techniques such as Next Generation Sequencing should be used to confirm our results. Due to the fact that DsMV have been transmitted not only by aphids but also

http://www.aloki.hu ● ISSN 1589 1623 (Print) ● ISSN 1785 0037 (Online)
DOI: http://dx.doi.org/10.15666/aeer/1705_1234712365

by infected material and cuttings, certified plant materials, eradication and vector management are powerful strategies to overcome the DsMV disease. Otherwise, the disease transmitted to the open field rotates with vectors in every season and returns as an epidemiological threat of agroecological origin.

This paper additionally indicates that uncontrolled distribution of infected ornamental plants between countries will allow the spread of plant viruses. In the present paper RT- PCR was a standardized method for reliable detection of DsMV. The results have also revealed that all exported plant materials should be distributed with certain quarantine regulations.

The harvest should be made with sterilized cutting equipments by the practitioners. Otherwise, if eradication or sterilization rules are not followed, infection may spread to more plants and areas. Mechanical harvesting might cause more spread of DsMV than vector transmission in time. Moreover, correct decoding of molecular epidemiology codes may open new doors to the fight against DsMV. Deep impacts on the ecological environment can be prevented provided that virus vector relationships are understood correctly. Therefore, more detailed and multidisciplinary studies should be focused. Moreover, these studies should not only be limited to in vivo, but also projects that can be applied in vitro.

Acknowledgements. Thanks to Assist. Prof. Ozer Çalış, Dr. Hakan Fidan and MSc. Nuray Sarı for the critical review of the publication.

Conflict of interests. The author declares that he has no conflict of interests.

Ethical approval. This article does not contain any studies with human participants or animals performed by any of the authors.

REFERENCES

[1] Abo El-Nil, M. M., Zettler, F. W., Hiebert, E. (1977): Purification, serology and some physical properties of dasheen mosaic vims. – Phytopathology 67: 1445-1450.

[2] Adams, M., Antoniw, J., Fauquet, C. (2005): Molecular criteria for genus and species discrimination within the family Potyviridae. – Arch. Virol. 150: 459-479.

[3] Babu, B., Hegde, V. (2014): Molecular characterization of dasheen mosaic virus isolates infecting edible aroids in India. – Acta Virologica 58: 34-42.

[4] Babu, B., Hegde, V., Makeshkumar, T., Jeeva, M. (2011): Characterisation of the coat protein gene of dasheen mosaic virus infecting elephant foot yam. – J. Plant Pathol. 93: 199-203.

[5] Brunt. A. A. (1992): The general properties of Potyviruses. – Arch Virol.;Supplementum 5: 3-16.

[6] Brunt, A. A., Crabtree, K., Dallwitz, M. J., Gibbs, A. J., Watson, L. (1996): Viruses of Plants. – Wallingford: CAB International; p. 1484.

[7] Buddenhagen, I. W., Milbrath, G. M., Hsieh, S. P. (1970): Virus diseases of Taro and other Aroids. – Proceedings of the Second International Symposium on Tropical Root and Tuber Crops 2: 53-55.

[8] Cabrera, D., González, J. E., Portal, O., Hernández, R. (2010): Influencia Del Virus Del Mosaico De La Malanga Sobre El Contenido De Clorofilas En *Xanthosoma Nigrum* (Vell.) Genotıpo Inivit M 95-1. – Rev. Protección Veg. 25(3): 194-196.

[9] Chagas, C. M., Colariccio, A., Galleti, S. R., Kitajima, E. W. (1993): Natural infection of *Amorphophallus konjac* with Dasheen mosaic virus in Brazil. – Fitopatologia Brasileira 18(4): 551-554.

http://www.aloki.hu ● ISSN 1589 1623 (Print) ● ISSN 1785 0037 (Online)
DOI: http://dx.doi.org/10.15666/aeer/1705_1234712365

[10] Chen, J., Adams, M. J. (2001): Molecular characterisation of an isolate of dasheen mosaic virus from *Zantedeschia aethiopica* and comparisons in the genus potyvirus. – Archives of Virology 146: 1821-1829.
[11] Chen, J., McConnell, D. B., Henny, R. J., Everitt, K. C. (2003): Cultural Guidelines for Commercial Production of Interiorscape *Anthurium.* ENH956. – University of Florida, Gainesville.
[12] Clark, M. R., Adams, A. N. (1977): Characteristics of the microplate method of enzyme-linked immunosorbent assay for the detection of plant viruses. – J. Gen. Virol. 34: 475-483.
[13] Çolak Ateş, A., Fidan, H., Büyüköztürk, D., Torun, H., Dinçer, D., Yüzbaşıoğlu, E. G. (2018): Studies on the determination of diseases, pests and weeds in leafy vegetables in eastern Mediterranean region. – 4th International Agriculture Congress 05-08 July, 2018.
[14] Colinet, D., Nguyen, M., Kummert, J., Lepoivre, P., Xia, F. Z. 1998 Differentiation among Potyviruses infecting sweet potato based on genus- and virus specific reverse transcription polymerase chain reaction. – Plant Dis. 82: 223-9.
[15] Cuevas, J. M., Delaunay, A., Visser, J. C., Bellstedt, D. U., Jacquot, E., Elena, S. F. (2012): Phylogeography and molecular evolution of potato virus Y. – PLoS One 7: e37853.
[16] Daughtrey, M. L., Jones, R. K., Moyer, J. W., Daub, M. E., Baker, J. R. (1997): Tospoviruses Strike the greenhouse industry: INSV has become a major pathogen on flower crops. – Plant Disease. 81(11): 1220-1230.
[17] De Brot, E. A., Ordosgoitti, A. (1974): Dasheen mosaic virus infection of *Colocasia* and *Xanthosoma* in Venezuela. – Plant Disease Reporter 58: 1032-1034.
[18] Dellaporta, S. L., Wood, J., Hicks, J. B. (1983): A plant DNA mini-preparation: version 2. – Plant Mol Biol Rep. 1(4): 19-21.
[19] Elliott, M. S., Zettler, F. W., Brown, L. G. (1997): Dasheen Mosaic Potyvirus of Edible and ornamental Aroids. – Plant Pathol. Circular 384. Dept. Agric. & Consumer Services, Florida.
[20] Fidan, H., Sari, N. (2019): Molecular characterization of resistance breaking tomato spotted wilt virus (TSWV) isolate medium segment in tomato. – Applied Ecology and Environmental Research 17(2): 5321-5339.
[21] Fidan, H., Adak, N. A., Konuksal, A., Akerzurumlu, E., Yılmaz, M. A. (2012): Occurrence of alfalfa mosaic virus (Amv) diseases on potato crops in northern Cyprus. – Acta Hort. (ISHS) 960: 341-346.
[22] Fidan, H., Koç, G., Topçu, T. (2016): Tomato spotted wilt virus (TSWV) infection and molecular characterization in Anthurium sp (Anthurium sp.' de Tomato Spotted Wilt Virus (TSWV) Enfeksiyonu ve Moleküler Karakterizasyonu). – Alatarım 15(2): 28-36.
[23] Frenkel, M. J., Ward, C. W., Shukla, D. D. 1989. The use of 3'noncoding nucleotide sequences in the taxonomy of Potyviruses: application to Water Melon Mosaic Virus 2 and Soybean Mosaic Virus-N. – J Gen Virol. 70: 2775-2783.
[24] Greber, R. S., Shaw, D. E. (1986): Dasheen mosaic virus in Queensland. – Australasian Plant Pathology 15(2): 29-33.
[25] Grisoni, M., Moles, M., Farreyrol, K., Rassaby, L., Davis, R., Pearson, M. (2006): Identification of Potyviruses infecting vanilla by direct sequencing of a short RT-PCR amplicon. – Plant Pathol. 55: 523-9.
[26] Guaragna, M., Ndum, O., Jordan, R. (2006): Detection and characterization of two previously undescribed potyviruses in the terrestrial orchid *Spiranthes cernua.* – Acta Hart. 722. DOI: 10.17660/ActaHortic.2006.722.26.
[27] Ha, C., Revill, P., Harding, R. M., Vu, M., Dale, J. L. (2008): Identification and sequence analysis of potyviruses infecting crops in Vietnam. – Arch. Virol. 153: 45-60.
[28] Hu, J. S., Meleisea, S., Wang, M. (1994): Detection of dasheen mosaic virus from taro plants in the field and in tissue culture. – Plant Disease 78: 754.

http://www.aloki.hu ● ISSN 1589 1623 (Print) ● ISSN 1785 0037 (Online)
DOI: http://dx.doi.org/10.15666/aeer/1705_1234712365

[29] Hull, R. (1994): Resistance to plant viruses: obtaining genes by non-conventional approaches. – Euphytica 75: 902-906.
[30] Jackson, G. V. H. (1982): A Virus disease of Taro in French Polynesia. – Report to the South Pacific Commission, Noumea.
[31] Kibar, H. (2014): Investigations on the determination of tomato spotted wilt virus (TSWV), dasheen mosaic virus (DSMV) and cucumber mosaic virus (CMV) in Yalova Province, Turkey (Yalova İli Kesme Çiçek Üretimi Yapılan Alanlarda *Tomato Spotted Wilt Virus* (TSWV), *Dasheen Mosaic Virus* (DSMV) ve *Cucumber Mosaic Virus* (CMV)'lerinin Saptanmasi Üzerine Araştırmalar). – T. C. Namık Kemal Üniversitesi Fen Bilimleri Enstitüsü Yüksek Lisans Tezi.
[32] Kidanemarıam, D. B. (2018): Viruses of taro and other edible aroids in East Africa. – A thesis for the degree of Doctor of Philosophy, Queensland University of Technology Brisbane, Australia.
[33] Kidanemariam, D. B., Abraham, A. D., Sukal, A. C., Holton, T. A., Dale, J. L., James, A. P., Harding, R. M. (2016): Complete genome sequence of a novel zantedeschia mild mosaic virus isolate: the first report from Australia and from Alocasia sp. – Archives of Virology 161: 1079-1082.
[34] King, A. M., Adams, M. J., Lefkowitz, E. J., Carstens, E. B. (2012): Virus Taxonomy: Classification and Nomenclature of Viruses: Ninth Report of the International Committee on Taxonomy of Viruses. – Elsevier, Amsterdam.
[35] Knauss, J. F., Zettler, F. W., Conover, C. A. (1975): Field evaluation of caladiums derived from tissue culture. – Proc. Am. Phytopathol. Sot. 2: 69.
[36] Koç, G. (2010): Determination and characterization of plum pox potyvirus (PPV, Sharka) 'Situation in Stone fruit in eastern Mediterranean Region (Doğu Akdeniz Bölgesinde Sert Çekirdekli Meyvelerde Plum Pox Potyvirüs (PPV, Sharka)' Ünün Durumunun Belirlenmesi Ve Karakterizasyonu). – Çukurova Üniversitesi Fen Bilimleri Enstitüsü Dr. Tezi.
[37] Koç, G., Baloğlu, S. (2006): First report of sharka in the Çukurova region of Turkey. – Journal of Plant Pathology 88: 65-67.
[38] Kohler, F., Pellegrin, F., Jackson, G., Mckenzie, E. (1997): Diseases of Cultivated crops in Pacific Islands Countries. – South Pacific Commission, Noumea, New Caledonia.
[39] Langeveld, S. A., Dore, J. M., Memelink, J., Derks, A. F. L. M., van der Vlugt, C. I. M., Asjes, C. J., Bol, J. F. (1991): Identification of potyviruses using the polymerase chain reaction with degenerate primers. – J Gen Virol. 72: 1531-41.
[40] Loebenstein G, Lawson, R. H., Brunt, A. A. (1995): Virus and Virus-Like Diseases of Bulb and Flower Crops. Chapter 1. – Wiley, New York, pp. 1-14.
[41] Li, R. H., Zettler. F. W., Purcifull, D. E., Hiebert, E. (1998): The nucleotide sequence of the 3 '-terminal region of dasheen mosaic virus *(Caladium* isolate) and expression of its coat protein in *Escherichia coli* for antiserum production. – Archives ofVirology 143: 2461-2469.
[42] Lima Roberto, C. A., Lima Albersio, J. A., Aguiar Rubens, J. (2004): Serological Identification of *Dasheen mosaic virus* in *Anthurium* sp. in the State of Ceará. – Fitopatol. Bras. 29(1): 105.
[43] Maino, M. K. (2003): The development of a serological-based diagnostic test for *dasheen mosaic potyvirus* (DsMV). – A thesis submitted for the degree of Master of Applied Science, Centre for Molecular Biotechnology, School of Life Sciences, Queensland University of Technology.
[44] Marie-Jeanne, V., Loos, R., Peyre, J., Alliot, B., Signoret, P. (2000): Differentiation of Poaceae potyviruses by reverse transcription polymerase chain reaction and restriction analysis. – J Phytopathol. 148: 141-51.
[45] Miura, N. S.; Beriam, L. O. S., Rivas, E. B. (2013): Detection of *Cucumber mosaic virus* in commercial Anthurium crops and genotypes evaluation. – Horticultura Brasileira 31: 322- 327.

http://www.aloki.hu ● ISSN 1589 1623 (Print) ● ISSN 1785 0037 (Online)
DOI: http://dx.doi.org/10.15666/aeer/1705_1234712365

[46] Monge, M., Arias, O., Ramirez, P. (1987): Obtencion de plantas de tiquisque blanco *(Xanthosoma sugittifolium)* de tiquisque morado (X. *oioluceum) y* de iampi *(Colocucia esculenta)* libres de virus por medio del cultivo in vitro de apices. – Agron. Costarricense 11(1): 71-79.
[47] Nelson, S. C. (2008): Dasheen mosaic of edible and ornamental aroids. – Plant Disease CTAHR. http://www.ctahr.hawaii.edu/oc/freepubs/pdf/PD-44.pdf (accessed: January 23, 2012.
[48] Norman, D. J., Ali, G. (2012): *Anthurium* Diseases: Identification and Control in Commercial Greenhouse Operations. – UF/IFAS Extension, Gainesville. http://edis.ifas.ufl.edu.
[49] Özer, M., Sipahioğlu, H. M., Usta, M., Fidan, H. (2012): Cloning and sequencing of coat protein gene of zucchini yellow mosaic virus isolated from squash and muskmelon in Turkey. – Turk J Biol 36: 423-429. DOI: 10.3906/biy-1110-16.
[50] Pappu, S. S., Brand, R., Pappu, H.R, Rybicki, E. P., Gough, K. H., Frenkel, M. J., Niblett, C. L. (1993): A polymerase chain reaction method adapted for selective amplification and cloning of 3' sequences of potyviral genomes: application to Dasheen Mosaic Virus. – Journal of Virological Methods 41: 9-20.
[51] Randles, J. W., Hodgson, R. A. J., Wefels, E. (1996): The rapid and sensitive detection of plant pathogens by molecular methods. – Australasian Plant Pathology 25: 71-85.
[52] Reyes G, Rönnberg-Wastljung, A. C., Nyman, M. (2009): Comparison of field performance between *Dasheen mosaic virus* free and virus infected in vitro plants of Cocoyam (*Xanthosoma spp*.) in Nicaragua. – Experimental Agriculture 42(3): 301-310.
[53] Rivas, E. B., Duarte, L. M. L., Alexandre, M. A. V., Galleti, S. R. (1997): Dasheen Mosaic Virus in *Anthurium* species. – Virus Reviews & Research 2: 192-193.
[54] Rodoni, B. C., Moran, J. R. (1988): The detection of dasheen mosaic virus using the enzyme-linked immunosorbent assay (ELISA). – Acta Horticulturae 234: 281-285.
[55] Rodrigues, M. G. R., Kitajima, E. W., Lin, M. T. (1984): Mosaic of edible and ornamental Araceae caused by Dasheen Mosaic Virus. – Fitopatologia Brasileira 9: 291-299.
[56] Sambrook, J., Russel, D. W. (2001): Molecular Cloning: A Laboratory Manual. 3rd Ed. – Cold Spring Harbour Laboratory Press, Cold Spring Harbour.
[57] Shukla, D. D., Ward, C. W. (1989a): Structure of potyvirus coat proteins and its application in the taxonomy of potyvirus group. – Advances in Virus Research 36: 273-314.
[58] Shukla, D. D., Ward, C. W. (1989b): Identification and classification of potyviruses on the basis of coat protein sequence data and serology. – Archives of Virology 106: 171-200.
[59] Shukla, D. D., Lauricella, R., Ward, C. W. (1992): Serology of Potyviruses: Current Problems and Some Solutions. – In: Barnett, O. W. (ed.) Potyvirus Taxonomy. Springer, Wien, pp. 57-69.
[60] Shukla, D. D., Ward, C. W., Brunt, A. A. (1994): The Potyviridae. – CAB International, Wellington.
[61] Simone, G.W, Zettler, F.W (1990): Dasheen mosaic disease of araceous foliage plants. – Plant Pathology. https://plantpath.ifas.ufl.edu/misc/media/factsheets/pp0042.pdf.
[62] Sutic, D. D., Ford, R. E., Tošić, M. T. (1999): Handbook of Plant Virus Diseases. – CRC Press, Boca Raton, FL.
[63] Thompson, J. D., Higgine, D. G., Gibson, T. J. (1994): CLUSTAL W: improving the sensitivity of multiple sequence alignment through sequence weighting, position specific gap penalties and weight matrix choice. – Nucleic Acids Res. 22: 4673-80.
[64] Tooyama, A. (1975): Indicator plants for dasheen mosaic virus. – Ann. Phytopathology. Soc. Japan 41: 504-505.

http://www.aloki.hu ● ISSN 1589 1623 (Print) ● ISSN 1785 0037 (Online)
DOI: http://dx.doi.org/10.15666/aeer/1705_1234712365

[65] Uchida, J. Y., Ogata, D., Nagata, N. (1999): Tomato Spotted Wilt Virus on Anthurium. – Plant Disease 17. Cooperative Extension Service, College of Tropical Agriculture and Human Resources, University of Hawaii at Manoa, Honolulu.
[66] Valverde, R., Gomez, L., Saborio, F., Torres, S., Arias, O., Thorpe, T. (1997): Field evaluation of dasheen mosaic virus-free cocoyam plants produced by *in vitro* techniques. – Scientia Horticulturae 68: 37-47.
[67] Van der Meer, F. W. (1985): Occurrence of dasheen mosaic virus in South Africa. – Phytophylactica 17: 95-98.
[68] Ward, C. W., Shukla, D. D. (1991): Taxonomy of potyviruses: current problems and some solutions. – Intervirology 32: 269-296.
[69] Zavareh, N., Maleki, M., Ghotbi, T. (2013): Serological and molecular detection of *Cucumber Mosaic Virus* from two maincommercial Anthurium cultivars in Iran. – Annals of Biological Research 4(4): 120-125.
[70] Zettler, F. W., Hartman, R. D. (1987): Dasheen mosaic virus as a pathogen of cultivated Aroids and control of the virus by tissue culture. – Plant Dis. 71(1I): 958-962.
[71] Zettler, F. W., Foxe, M. J., Hartman, R. D., Edwarson, J. R., Christie, R. G. (1970): Filamentous Viruses infecting dasheen and other araceas plants. – Phytopathology 60: 983-987.

http://www.aloki.hu ● ISSN 1589 1623 (Print) ● ISSN 1785 0037 (Online)
DOI: http://dx.doi.org/10.15666/aeer/1705_1234712365

PLANT GROWTH AND GLUTAMINE SYNTHASE GENE *SCGS1* EXPRESSION IN SUGARCANE (*SACCHARUM* L. SPP. HYBRIDS) UNDER DIFFERENT NITROGEN LEVELS

ZHU, K.[1] – YUAN, D.[1] – XING, Y. X.[1] – NONG, Y. Y.[1] – YANG, L. T.[1*] – LI, Y. R.[2*]

[1]*College of Agriculture, Guangxi University, Nanning 530005, China*

[2]*Key Laboratory of Sugarcane Biotechnology and Genetic Improvement (Guangxi), Ministry of Agriculture and Rural Area; Guangxi Key Laboratory of Sugarcane Genetic Improvement; Sugarcane Research Center, Chinese Academy of Agricultural Sciences-Guangxi Academy of Agricultural Sciences, Nanning 530007, China*

K. Zhu and D. Yuan have contributed equally to this work.

**Corresponding authors*
e-mail: litao61@hotmail.com (L. T. Yang), liyr@gxaas.net (Y. R. Li)

(Received 8th May 2019; accepted 16th Jul 2019)

Abstract. The main aim of this study was to investigate the responses of agronomic traits, photosynthesis and glutamine synthase (GS) expression in different sugarcane (*Saccharum* L. spp. hybrids) varieties under different nitrogen levels. Sugarcane varieties GT11 (nitrogen inefficient) and GXB9 (nitrogen efficient) were planted at three levels of nitrogen supply, e.g. 0 kg/ha (low nitrogen level, L-N), 150 kg/ha (medium nitrogen level, M-N) and 300 kg/ha (high nitrogen level, H-N) of urea application. The agronomic traits, photosynthesis, and GS activity and expression were determined at different growth stages of sugarcane. The results showed that the plant height, stalk diameter, leaf area, chlorophyll content, net photosynthetic rate, GS activity and GS1 protein expression in GT11 increased with the increase of nitrogen application, while the plant height, stalk diameter, chlorophyll content, net photosynthetic rate, GS activity and GS1 protein expression in GXB9 reached the maximum on medium nitrogen level. The leaf area of GXB9 was always higher than that of GT11 on the same nitrogen level. Under the low and medium nitrogen levels, the activities of GS and expression of GS1 protein were higher in GXB9 than GT11. The transcription expression levels of *scGS1.a* and *scGS1.b* were down-regulated while that of *scGS1.c* up-regulated by the increase of nitrogen application level. In conclusion, the nitrogen inefficient sugarcane variety needs more nitrogen application, but excessive nitrogen application is not good for the nitrogen efficient sugarcane variety.

Keywords: *physiological characteristic, photosynthesis, molecular response, chlorophyll, nitrogen utilization*

Abbreviations: GS: Glutamine synthase; H-N: High nitrogen; L-N: Low nitrogen; M-N: Medium nitrogen

Introduction

Sugarcane is the most important sugar crop and a regenerative energy crop grown worldwide in tropical and subtropical areas, which contributes more than 90% of the total sugar in China (Li and Yang, 2015). Nitrogen is the main nutrition element of crops, it is required for protein synthesis, nucleic acid, phospholipid and many organic substances, and also plays an important role in photosynthesis. Previous studies have indicated that application of nitrogenous fertilizer is considered a significant measure to guarantee the productivity in sugarcane. However, excessive application of nitrogen fertilizer is common in sugarcane commercial production in China, and the application rate of urea is usually 500-700 kg/ha or higher, much higher than the world average. In our previous study, the effects of different nitrogen application levels (150, 300, 600 kg/ha urea) on

http://www.aloki.hu ● ISSN 1589 1623 (Print) ● ISSN 1785 0037 (Online)
DOI: http://dx.doi.org/10.15666/aeer/1705_1236712384

key enzymes of nitrogen metabolism and contents of related active substances in different sugarcane varieties were investigated, which indicated that the nitrogen metabolism of sugarcane was significantly enhanced with the increase of nitrogen application amount within a certain range of nitrogen application level (150-300 kg/ha urea) (Zhang et al., 2015). Over application of nitrogen fertilizer not only declines nitrogen use efficiency and increases the cost of sugarcane production, but also results in a series of negative effects such as cane quality degradation and agricultural environmental pollution (Bijay et al., 1995; Li et al., 2016).

Nitrogen assimilation is a vital process controlling plant growth and development. Plants absorb nitrogen in nitrate, ammonium and amino acid forms, and ultimately transform it into ammonium form. Majority of the organic nitrogen in plants is derived from the assimilation of ammonia into the amide position of glutamine by the enzyme GS (Lea and Miflin, 2011). GS is a key enzyme involved in the nitrogen assimilation and metabolism of nitrogen compounds, and is also the first enzyme to transformed inorganic nitrogen into organic nitrogen in plants. GS pathway of ammonia assimilation is of crucial importance for crop growth and productivity. In most plant leaves, GS mainly exists in the form of GS1 and GS2; the expression of GS1 was evidently affected by the concentration and the form of nitrogen, while the expression of GS2 was mainly affected by light (Edwards et al., 1990). For higher plant, GS1 are mainly distributed in the companion cells of leaf vascular tissue phloem. The main functions of GS1 are assimilating ammonia produced by endogenous protein degradation, amino acid catabolism and stored nitrogen source, involving in the transfer of nitrogen source, and reusing finally (Swarbreck et al., 2011). GS1 was generally encoded by 3-5 genes, for Arabidopsis, tobacco and maize, GS1 was encoded by at least five homologous genes (Keegstra and Cline, 1999; Keiki et al., 2004; Li et al., 2006; Lightfoot et al., 1988; Lothier et al., 2011; Tingey et al., 1988), and it was encoded by three genes in rice (May and Soll, 1999). Previous researches indicate that GS1.a mainly participates in nitrogen remobilization during leaf senescence and nitrogen migration under low nitrogen condition, and affects grains' size, number and grouting (Antoine et al., 2006; Bernard et al., 2008; Kusano et al., 2011; Mayumi et al., 2005). GS1.b is mainly responsible for the primary NH_4^+ assimilation in roots, nitrogen remobilization during leaf ageing, assisting in the primary nitrogen assimilation of GS2 (Bernard et al., 2008; Kazuhiro et al., 2013). GS1.c can ease the ammonia poisoning, and also remission nitrogen assimilation in grain growth period (Goodall et al., 2013). Nogueira et al. (2005) have identified and characterized the *GS1* (*scGS1.a*, *scGS1.b* and *scGS1.c*) in sugarcane.

To our knowledge, there is no report about the impact of different nitrogen levels on the *GS1* gene expression in sugarcane. The purpose of this study was to investigate the effects of different nitrogen application rates on plant growth and photosynthesis in different sugarcane varieties, the response of *GS1* in sugarcane to nitrogen levels, and further reveal the role of GS1 in nitrogen metabolism and the related regulation mechanism, to provide a reference for efficient nitrogen utilization and regulation in sugarcane.

Materials and methods

Experimental materials

The experiment was conducted at College of Agriculture, Guangxi University in Nanning, China. The sugarcane variety GT11 (Nitrogen inefficient variety) and GXB9

http://www.aloki.hu ● ISSN 1589 1623 (Print) ● ISSN 1785 0037 (Online)
DOI: http://dx.doi.org/10.15666/aeer/1705_1236712384

(nitrogen efficient variety) were used for the experiment (Zhang et al., 2015). The soil used for experiment was red soil with pH 7.32, organic matter 4.23 g/kg, total nitrogen 0.27 g/kg, total phosphorus 0.33 g/kg, total potassium 7.85 g/kg, alkali-hydrolyzable nitrogen 21.55 g/kg, effective phosphorus 8.4 mg/kg, and available potassium 96 mg/kg. Urea (N 46%) was used as the nitrogenous fertilizer.

Plant culture and nitrogenous fertilizer application

Single-budded seedcane sets of the two sugarcane varieties were planted in sands for germination under warm and wet condition on March 3, 2016. After 45 days, the healthy and consistent plants were selected and transplanted into plastic pots of 36.3 × 30 cm (height × diameter) filled with 20 kg soil, and two plants of the same variety were grown in each pot.

Three levels of nitrogen supply were set and applied after transplanting, that is, 0, 150 and 300 kg/ha, or 0, 1.55 and 3.10 g urea per pot were applied at seedling stage (May 15), referred to as the low nitrogen, medium nitrogen and high nitrogen levels, respectively. There was a low nitrogen content (total nitrogen 0.27 g/kg, alkali-hydrolyzable nitrogen 21.55 g/kg) in the soil used in the experiment, which could not be ignored. Therefore, we used the low nitrogen level to represent the actual nitrogen level in the soil even if we gave no nitrogen in the soil. Therefore, the experiment consisted of six treatments (two varieties and three nitrogen levels), and 9 replicates were arranged in a completely randomized block design, so total had 54 pots (*Fig. 1*).

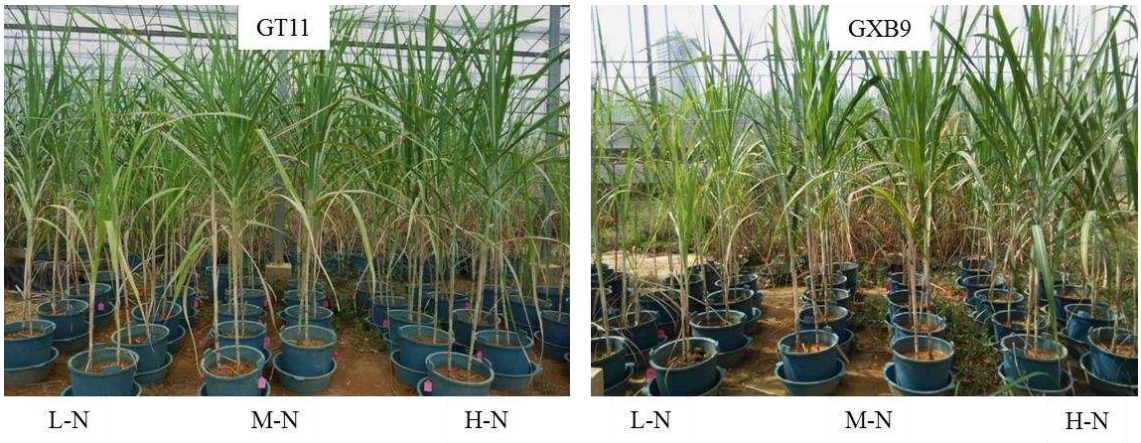

Figure 1. *Growth photos of two sugarcane varieties (GT11 and GXB9) under three nitrogen application levels at sampling day (2016-07-12)*

Sampling and assay

The leaf + 1 (the top visible dewlap leaf) was sampled on June 10, July 12, August 12, and September 15, respectively. Part of the fresh leaf sample was used for determination of GS activity with the method as described by Wei (2005), and the rest was frozen in liquid N_2 and kept at -80°C before use.

Investigation of agronomic traits

Nine plants were chosen randomly for agronomic trait investigation at sampling days after treatment. The plant height and stem diameter were estimated with conventional

http://www.aloki.hu ● ISSN 1589 1623 (Print) ● ISSN 1785 0037 (Online)
DOI: http://dx.doi.org/10.15666/aeer/1705_1236712384

methods. Leaf area of leaf + 1 was estimated using CI-203 Handheld Leaf Area Meter (CID Bio-Science, Inc., Camas, USA) and the leaf chlorophyll was estimated by SPAD readings measured with SPAD-502 chlorophyll meter (Konica Minolta, Inc., Tokyo, Japan).

Assay of photosynthetic rate

Net photosynthetic rate was measured using a LC Pro-SD portable photo system unit (Opti-Sciences Inc., Hudson, USA) at a photon irradiance of 1504 μmol m^{-2} s^{-1}. The measurement was conducted at a gas flow rate 200 μmol s^{-1}. Nine plants in each treatment were randomly selected for measurement from 9:00 to 11:00 am in the morning of September 3 when it was sunny.

Quantification of scGS1 gene expression on transcription level

The relative expression of *scGS1.a* (AY835453), *scGS1.b* (AY835454) and *scGS1.c* (AY835455) was quantified at the sampling days (June 10, July 12, August 12, and September 15, respectively) after treatment. The expression of *scGS1* in sugarcane leaf + 1 was performed in randomly selected 9 plants with a Light Cycler® 480II (Roche Applied Science, Basel, Switzerland) using the SYBR Premix Ex TapTM II (TaKaRa, Dalian, China) in accordance with the product manual. The GAPDH gene of sugarcane (accession number EF189713) was used as an internal control to quantify the relative transcript level. Specific primers for those genes were designed using the Primer Premier 5 software based on their cDNA sequences (*Table A1* in the *Appendix*). The relative level of gene expression was calculated using the $2^{-\Delta\Delta Ct}$ formula (Livak and Schmittgen, 2001).

Western blot analysis of scGS1 protein in sugarcane

Total soluble protein was extracted from sugarcane leaf with 100 mM Tris (pH 7. 8, containing 10 mM $MgCl_2$, 100 mM 2-mercatoetanol, 5% Polyvinylpolypyrrolidone) (Nogueira et al., 2005), and quantified using the method of Bradford (1976). For Western blot, denatured proteins were fractionated by SDS-PAGE [12.5% (w/v) polyacrylamide] according to Laemmli (1970) and transferred to nitrocellulose membrane as described by Towbin et al. (1979). Anti-GS1 primary polyclonal antibody was used to detect GS1 protein. Protein–antibody complexes were located using horse reddish peroxidase, and conjugated goat anti-rabbit immunoglobulin G. Pierce® ECL Western Blotting Substrate (Thermo, U.S.A.) was used for development and then observed under FluorChem HD2 (Alpha, Protein Simple, U.S.A.). The GS1 polyclonal antibody (AS08295, Agrisera, Sweden) and secondary antibody (Goat anti-rabbit lgG, HRP conjugated, CoWin Biosciences, Beijing, China) were purchased in a biological reagent company.

Data analysis

All the data were analyzed using Microsoft Excel 2010 and SPSS 21.0. ANOVA test was used to compare the mean values of each treatment. Significant differences between the means of parameters were determined by using the LSD test ($P < 0.05$).

http://www.aloki.hu ● ISSN 1589 1623 (Print) ● ISSN 1785 0037 (Online)
DOI: http://dx.doi.org/10.15666/aeer/1705_1236712384

Results

Effects of different nitrogen levels on agronomic traits in different sugarcane varieties

The data in *Table 1* show the growth rate of two sugarcane varieties under medium and high nitrogen levels increased with the course of growth, and the highest growth rate occurred between August and September. In general, the plant height and stem diameter in the variety GT11 increased with the level of nitrogen application. For the variety GXB9, the highest plant height and stem diameter were recorded on medium nitrogen level (*Table 1*). The leaf area of two sugarcane varieties significantly increased with the level of nitrogen application (*Table 1*). Under the same nitrogen level, the leaf area is basically characterized by GXB9 > GT11 (*Fig. A1* in the *Appendix*).

Table 1. *Effects of different nitrogen levels on agronomic traits in different sugarcane varieties*

Variety		GT11			GXB9		
Date nitrogen levels		L-N	M-N	H-N	L-N	M-N	H-N
2016-06-10	Plant height (cm)	27.1 ± 3.4^{a}	32.3 ± 3.7^{a}	32.7 ± 4.5^{a}	26.9 ± 3.1^{a}	27.2 ± 3.5^{a}	27.5 ± 3.5^{a}
	Stalk diameter (mm)	10.5 ± 0.7^{c}	11.9 ± 0.8^{b}	12.7 ± 0.7^{a}	7.8 ± 0.8^{c}	9.5 ± 0.7^{a}	8.6 ± 0.7^{b}
	Leaf area (cm^2)	80.1 ± 8.4^{a}	89.21 ± 8.52^{a}	89.2 ± 7^{a}	88 ± 9.6^{a}	87.6 ± 2.5^{a}	87.8 ± 7.7^{a}
	SPAD	36.7 ± 0.9^{a}	38.5 ± 0.8^{a}	40.4 ± 1.4^{a}	39.9 ± 1.8^{b}	45.2 ± 2^{a}	42 ± 1.5^{ab}
2016-07-12	Plant height (cm)	43.8 ± 1.8^{c}	49.2 ± 2.3^{b}	55.5 ± 2.5^{a}	43.6 ± 3^{b}	49.8 ± 2.6^{a}	48.7 ± 3.2^{a}
	Stalk diameter (mm)	15.6 ± 0.6^{c}	16.3 ± 0.9^{b}	17.7 ± 0.6^{a}	13.4 ± 0.6^{c}	15.5 ± 0.6^{a}	14.9 ± 0.7^{b}
	Leaf area (cm^2)	317 ± 17.4^{a}	330 ± 18.5^{a}	343 ± 11.4^{a}	353 ± 15.7^{a}	366 ± 31.4^{a}	386 ± 36.1^{a}
	SPAD	34 ± 1.7^{b}	37.1 ± 1.4^{ab}	39.8 ± 1.5^{a}	35.2 ± 1.8^{b}	47.8 ± 1.9^{a}	48 ± 1.7^{a}
2016-08-12	Plant height (cm)	73.2 ± 4.3^{c}	81.3 ± 5.2^{b}	93.8 ± 5.5^{a}	82.7 ± 4.6^{b}	97.5 ± 4.5^{a}	95.5 ± 3.9^{a}
	Stalk diameter (mm)	13.9 ± 0.7^{b}	15.3 ± 0.8^{a}	15.1 ± 0.7^{a}	14.5 ± 0.8^{b}	16.9 ± 0.7^{a}	17 ± 0.7^{a}
	Leaf area (cm^2)	313 ± 15.2^{c}	393 ± 24.9^{b}	537 ± 22^{a}	356 ± 10^{c}	467 ± 20^{b}	582 ± 27.5^{a}
	SPAD	28 ± 1.8^{b}	39.1 ± 2.^{a}	39 ± 2.3^{a}	29.9 ± 1.2^{b}	51.8 ± 1.8^{a}	49.6 ± 1.7^{a}
2016-09-15	Plant height (cm)	102 ± 5.6^{c}	146 ± 2.4^{b}	154 ± 4.7^{a}	113 ± 4.1^{c}	175 ± 5^{a}	165 ± 4.1^{b}
	Stalk diameter (mm)	14.5 ± 0.6^{c}	15.5 ± 0.9^{b}	16.2 ± 0.6^{a}	14.7 ± 0.6^{c}	17.9 ± 0.6^{a}	17.1 ± 0.7^{b}
	Leaf area (cm^2)	263 ± 16^{c}	388 ± 20^{b}	553 ± 25^{a}	343 ± 30^{c}	476 ± 30^{b}	609 ± 23^{a}
	SPAD	23.2 ± 0.8^{b}	35 ± 0.8^{a}	37 ± 1.4^{a}	30. 9 ± 1.1^{b}	40.6 ± 0.8^{a}	42.2 ± 1^{a}

Data are presented as mean ± SE, and data points with different letters are significantly different ($P < 0.05$) between different nitrogen levels from the same sugarcane variety at the same time. L-N, low nitrogen level; M-N, medium nitrogen level; H-N, high nitrogen level

Effect of different nitrogen levels on chlorophyll content in different sugarcane varieties

Overall, the chlorophyll relative content in the variety GT11 is characterized by high nitrogen > medium nitrogen > low nitrogen levels, increased with the levels of nitrogen application. The chlorophyll relative content in the variety GXB9 showed the order of medium nitrogen > high nitrogen > low nitrogen levels (*Table 1*).

Effect of different nitrogen levels on net photosynthetic rate in different sugarcane varieties

At booming stage of sugarcane (September 3), the net photosynthetic rate in the variety GT11 was significantly higher in the high nitrogen treatment than the low

http://www.aloki.hu ● ISSN 1589 1623 (Print) ● ISSN 1785 0037 (Online)
DOI: http://dx.doi.org/10.15666/aeer/1705_1236712384

nitrogen treatment. For the variety GXB9, the net photosynthetic rate was significantly higher under medium nitrogen level than low and high nitrogen levels. Under low and medium nitrogen levels, the net photosynthetic rate was higher in the variety GXB9 than the variety GT11, but had no significant difference between them under high nitrogen level (*Fig. 2*).

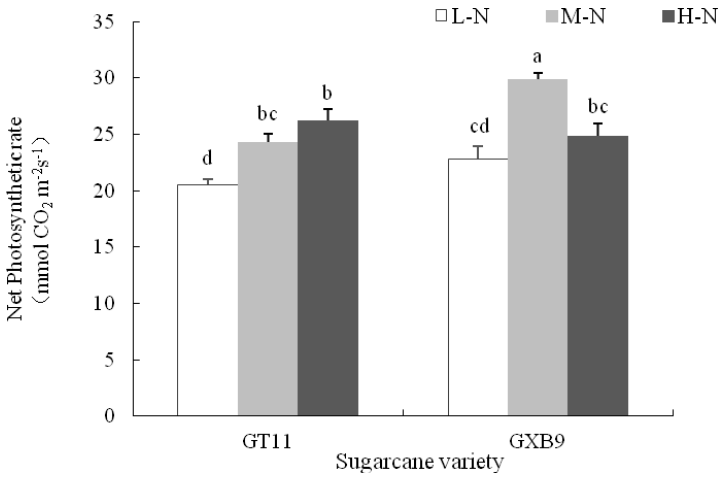

Figure 2. *Photosynthetic rate in leaves of two sugarcane varieties under different nitrogen levels measured on September 15, 2016. Treatments labeled with different small letters represent statistically significant difference at $P < 0.05$. L-N, low nitrogen level; M-N, medium nitrogen level; H-N, high nitrogen level*

Effect of different nitrogen levels on GS activity in different sugarcane varieties

The data in *Figure 3* showed that the GS activity in leaves of the variety GT11 increased with the level of nitrogen application (*Fig. 3A*), and peaked on August 12 in all the treatments except for the high nitrogen treatment in GXB9. The GS activity was significantly higher on high nitrogen level than that on low and medium nitrogen levels. The highest GS activity was recorded in the variety GXB9 under medium nitrogen level on August 12 (*Fig. 3B*). Under low and medium nitrogen levels, the GS activity was always higher in the variety GXB9 than the variety GT11 (*Fig. A2*), and this may be related to the higher biological nitrogen fixation ability and nitrogen efficiency of the variety GXB9.

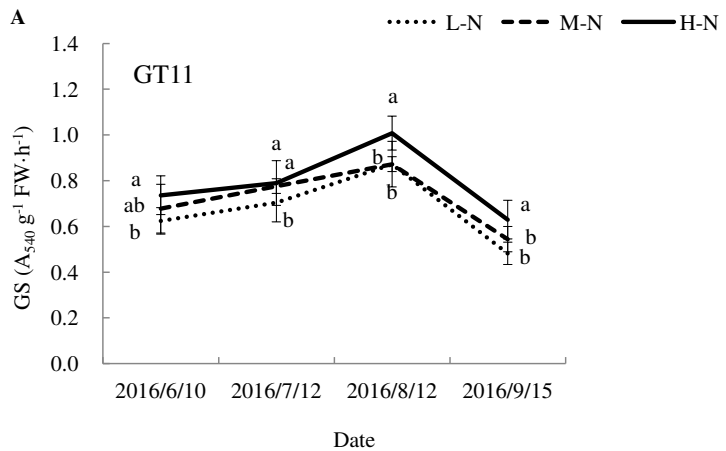

http://www.aloki.hu ● ISSN 1589 1623 (Print) ● ISSN 1785 0037 (Online)
DOI: http://dx.doi.org/10.15666/aeer/1705_1236712384

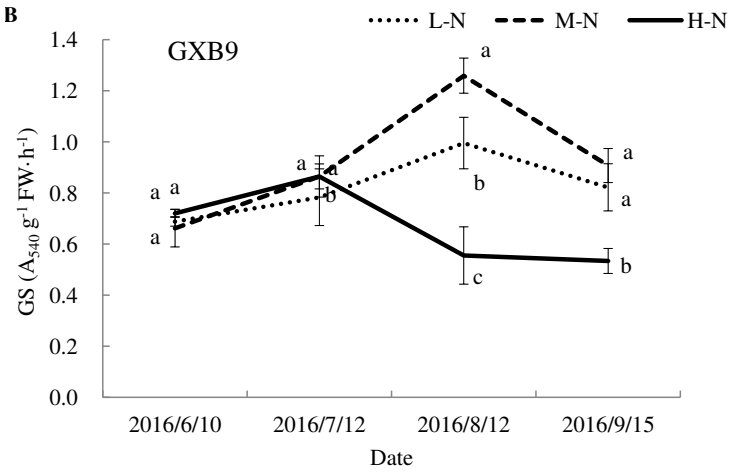

Figure 3. *GS activity in leaves of two sugarcane varieties under different nitrogen levels. Treatments labeled with different small letters represent statistically significant difference at $P < 0.05$ at the same date. L-N, low nitrogen level; M-N, medium nitrogen level; H-N, high nitrogen level*

Effect of different nitrogen levels on scGS1 expression in different sugarcane varieties

From *Figure 4,* we can see that for most treatments, *scGS1.a* expression was higher in August and September than June and July. *scGS1.a* expression tended to decrease with the level of nitrogen application in both sugarcane varieties. Under low nitrogen level, *scGS1.a* expression was higher in GXB9 than GT11 (*Fig. A3A*), while under high nitrogen level, *scGS1.a* expression in GXB9 is lower (*Fig. A3B*).

From *Figure 5,* we can find that in June and July, *scGS1.b* expression tended to decrease with the level of nitrogen application in both two sugarcane varieties except for that in GT11 in August and September when it showed the highest under medium nitrogen level.

The data in *Figure 6* showed that the *scGS1.c* expression tended to increase with the level of nitrogen application from June to September and the growth course from June to August in both sugarcane varieties. For different sugarcane varieties, the *scGS1.c* expression showed the order of GXB9 > GT11 under the same nitrogen level (*Fig. A4*).

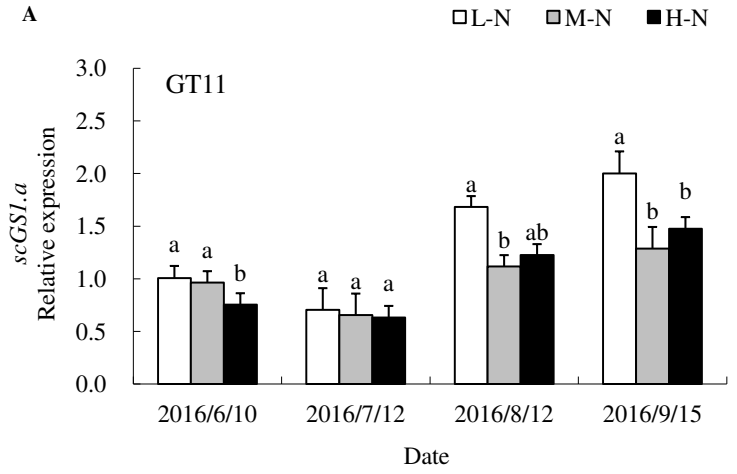

http://www.aloki.hu ● ISSN 1589 1623 (Print) ● ISSN 1785 0037 (Online)
DOI: http://dx.doi.org/10.15666/aeer/1705_1236712384

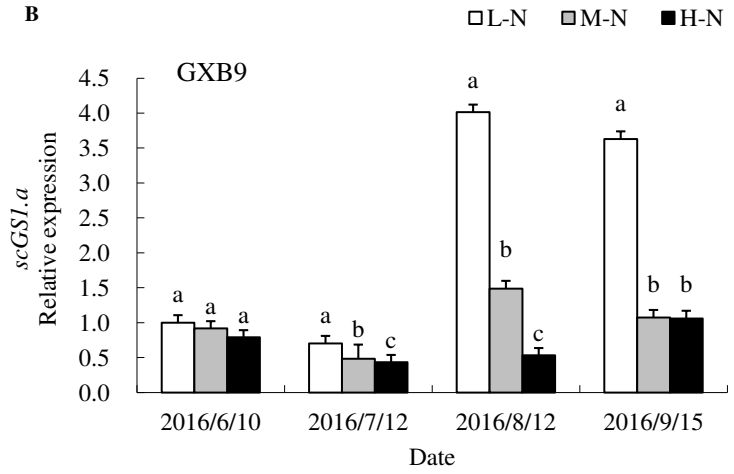

Figure 4. *Expression of scGS1.a mRNA in leaves of two sugarcane varieties under different nitrogen levels. Treatments labeled with different small letters represent statistically significant difference at P < 0.05 at the same date. L-N, low nitrogen level; M-N, medium nitrogen level; H-N, high nitrogen level*

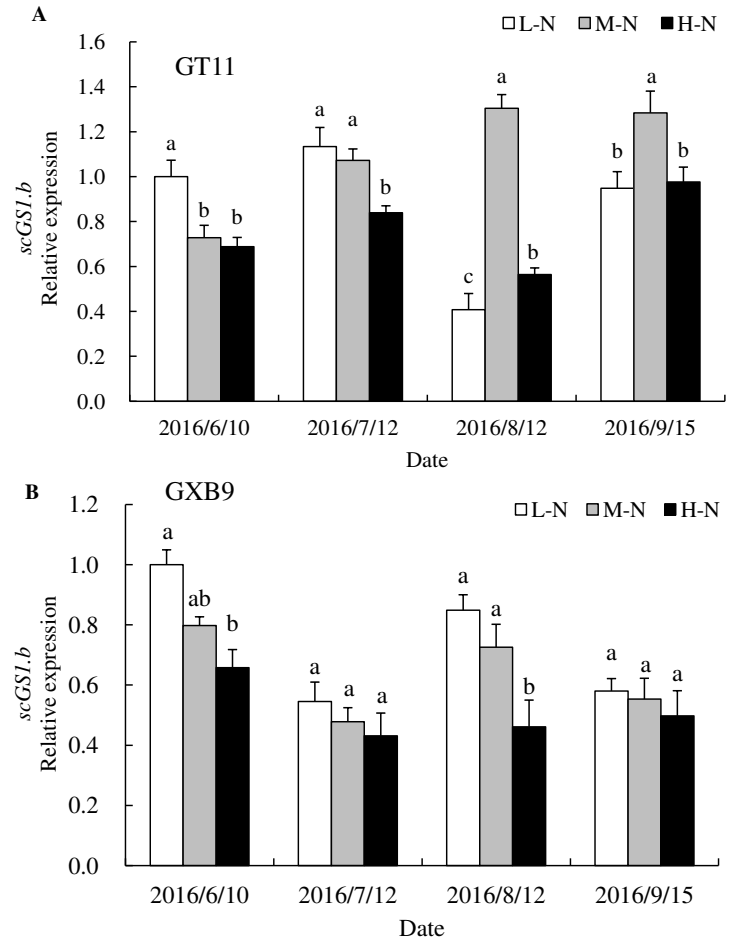

Figure 5. *Expression of scGS1.b mRNA in two sugarcane varieties under different nitrogen levels. Treatments labeled with different small letters represent statistically significant difference at P < 0.05 at the same date. L-N, low nitrogen level; M-N, medium nitrogen level; H-N, high nitrogen level*

http://www.aloki.hu ● ISSN 1589 1623 (Print) ● ISSN 1785 0037 (Online)
DOI: http://dx.doi.org/10.15666/aeer/1705_1236712384

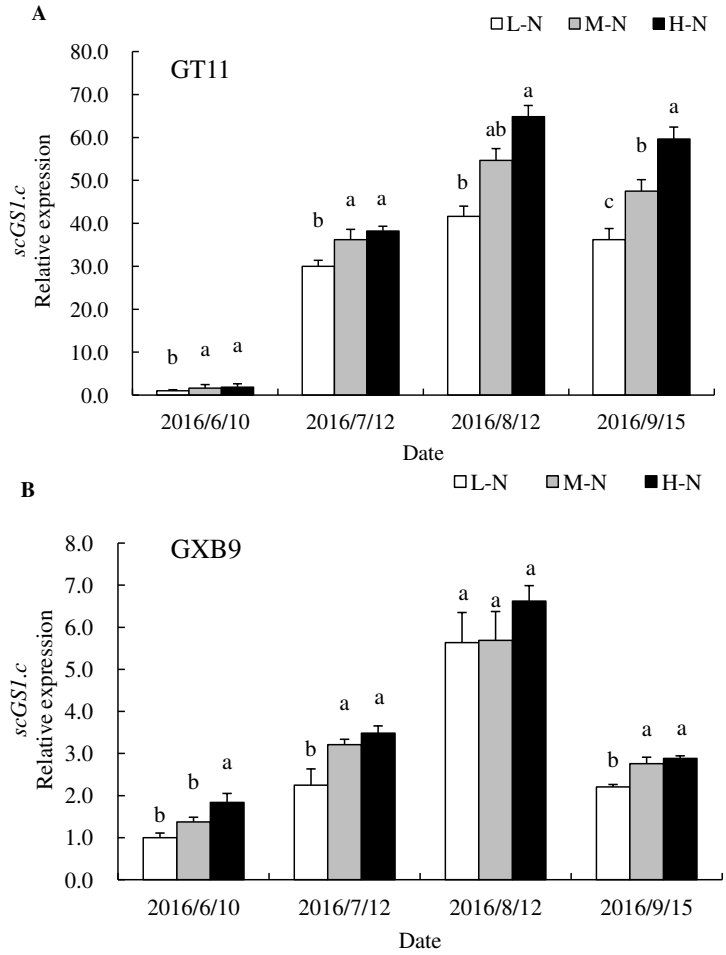

Figure 6. *Expression of scGS1.c mRNA in two sugarcane varieties under different nitrogen levels. Treatments labeled with different small letters represent statistically significant difference at $P < 0.05$ at the same date. L-N, low nitrogen level; M-N, medium nitrogen level; H-N, high nitrogen level*

Influence of different nitrogen levels on GS1 protein expression in different sugarcane varieties

The GS1 protein expression in the variety GT11 increased with the level of nitrogen application, and that in GXB9 reached the maximum under medium nitrogen level (*Figs. 7* and *8*). The GS1 protein expression is higher in GXB9 than GT11 under low and medium nitrogen levels (*Fig. A5*).

Discussion

Nitrogen is the biggest nutrient element for crop growth and development demand. However, excessive nitrogen fertilizer application will reduce plant nitrogen utilization efficiency and cause serious environmental pollution. Zhou et al. (2006) found that different sugarcane varieties responded differently to different nitrogen levels, and the sugarcane variety RB72-454 with high biological nitrogen fixation ability has better growth potential than others under low nitrogen condition. In this study, the plant height, stem diameter increased with the level of nitrogen application in the nitrogen

http://www.aloki.hu ● ISSN 1589 1623 (Print) ● ISSN 1785 0037 (Online)
DOI: http://dx.doi.org/10.15666/aeer/1705_1236712384

inefficient sugarcane variety GT11 while showed the highest at medium nitrogen level in the nitrogen efficient sugarcane variety GXB9 with high biological nitrogen fixation ability, which suggested that the responses of different sugarcane varieties to nitrogen application are varied, and nitrogen efficient sugarcane variety needs less nitrogen fertilizer application.

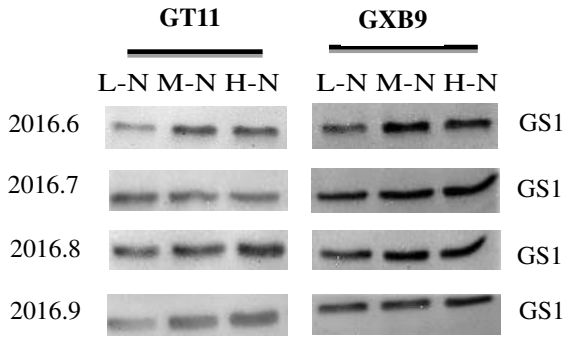

Figure 7. *Western blotting analysis of sugarcane GS1 protein under different nitrogen levels. L-N, low nitrogen level; M-N, medium nitrogen level; H-N, high nitrogen level*

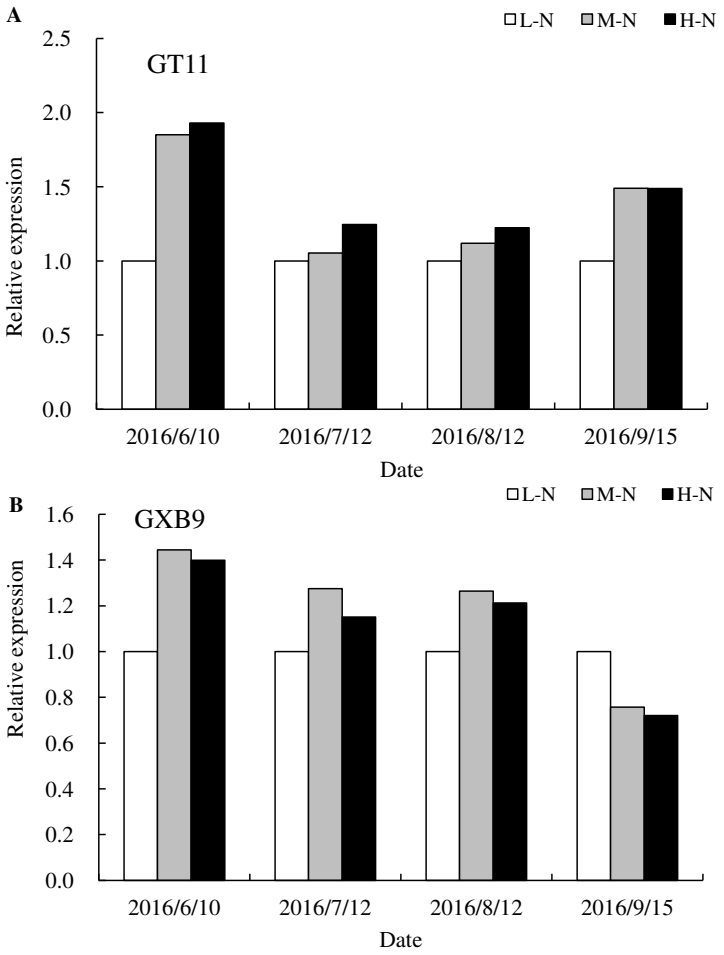

Figure 8. *Effects of different nitrogen levels on the expression of GS1 protein in different sugarcane varieties. L-N, low nitrogen level; M-N, medium nitrogen level; H-N, high nitrogen level*

http://www.aloki.hu ● ISSN 1589 1623 (Print) ● ISSN 1785 0037 (Online)
DOI: http://dx.doi.org/10.15666/aeer/1705_1236712384

Accumulation distribution rate of nitrogen reached 60 to 80% in leaves, and the proportion of nitrogen in leaves increased with the growth course of sugarcane (Jiang, 2016). Sugarcane leaf segments had contrasting amount of chlorophyll, nitrogen and sugars (Mattiello et al., 2015). Nitrogen fertilizer application can obviously increase the chlorophyll content and leaf area in wheat (Li et al., 2007). In this study we found that sugarcane leaf area significantly increased with the increase of nitrogen application levels. We also found that appropriate nitrogen fertilizer application could increase the content of chlorophyll in leaves, which is consistent with the results reported by Shao et al. (2009).

Wu and Zhao (2010) reported that nitrogen has the best level range for promoting photosynthetic rate. Out of this range, photosynthetic rate decreases. Nitrogen efficient wheat genotypes have strong photosynthetic capacity under low nitrogen condition, but inefficient genotypes need sufficient fertilizer to get higher photosynthetic capacity and higher yield (He et al., 1999). N supply and the sugarcane ability to respond to N influenced photosynthesis (Bassi et al., 2018). In this study we proved that the photosynthetic rate increased with the increase of nitrogen level in the nitrogen inefficient variety GT11, while it showed the highest on the medium nitrogen level in the nitrogen efficient variety GXB9, and significantly higher in the latter than the former.

In this study, the GS activity in all the treatments presented a typical single peak during whole detection duration, and most reached peak on August 12. August belongs to the booming stage, and the plant growth needs large amount of nitrogen. Luo (2007) pointed out that nitrogen can significantly improve GS activity in rice leaf, and the GS activity presented a single peak during whole growth period and reached peak at the heading stage. In this study, the GS activity in the variety GT11 increased with the increase of nitrogen level, while that in the variety GXB9 presented medium nitrogen > low nitrogen > high nitrogen from August to September, which is similar to the result reported by Gui (2007). The variety GXB9 also showed high GS activity under low nitrogen condition, and it always showed significantly higher than the variety GT11, but it seems that high nitrogen has inhibitory effect on the GS activity in the variety GXB9. Nitrogen could induce GS gene expression (Higashi et al., 1998; Ortega et al., 2001). The expression of *GS1-1* in wheat was raised when the nitrogen supply decreased, and high NH_4^+ supply specifically induced *GS1-3* gene expression in barley and sorghum (Caputo et al., 2009; Elomari et al., 2010; Goodall et al., 2013). In the present study, the *scGS1.a* expression decreased with the increase of nitrogen application in the variety GXB9, while the highest under low nitrogen in the variety GT11, which is consistent with the results in wheat reported by Caputo et al. (2009). The relative expression of *scGS1.a* in plant showed the highest level under low nitrogen supply could reduce plant damage due to nitrogen deficiency. Robinson et al. (2007) used NH_4^+ labeled ^{15}N as nitrogen source in a sugarcane hydroponic cultural experiment, and found marked nitrogen transport from xylem to leaves accumulated in the form of glutamic acid and glutamine, forming a marked small nitrogen library. In the present study, the expression of *scGS1.a* was significantly higher in the variety GXB9 than the variety GT11 at the booming stage of sugarcane under the medium and low nitrogen condition, reflecting that the variety GXB9 could have stronger ability for transfer of nitrogen from library to source, which could be related with its low nitrogen resistance characteristics. At the early stage of the sugarcane growth, the expression of *scGS1.b* decreased with the increase of nitrogen application rate while the expression of

http://www.aloki.hu ● ISSN 1589 1623 (Print) ● ISSN 1785 0037 (Online)
DOI: http://dx.doi.org/10.15666/aeer/1705_1236712384

scGS1.c increased with the increase of nitrogen application rate for both sugarcane varieties. The enzyme scGS1.c can accelerate the assimilation of NH_4^+ and reduce ammonia poisoning. The expression of *scGS1.c* is 15 times higher in the variety GXB9 than the variety GT11 in June, indicating that the NH_4^+ assimilation ability of the variety GXB9 is significantly higher than the variety GT11.

The results in the present study showed that, application of 150 kg/ha urea can keep or significantly increase the GS1 protein expression in the leaves of sugarcane variety GXB9, but more nitrogen fertilizer application rate was needed for the variety GT11. The GS1 protein expression level was higher in the variety GXB9 than the variety GT11, which indicated that the former has stronger low nitrogen endurance than the latter. GS1 protein in sugarcane was commonly encoded by the genes *scGS1.a*, *scGS1.b* and *scGS1.c*. We found that the relative expression ratio of *scGS1.a* : *scGS1.b* : *scGS1.c* on transcription level is approximately 60 : 26 : 0.6, which indicated that *scGS1.a* is the most highly expressed sugarcane *GS1* gene. We also found that the GS1 protein relative expression increased with the increase of nitrogen application in sugarcane. However, there was big difference between transcription expression and enzyme activity due to the influences of various factors. Ortega et al. (2001) reported that there is no GS enzyme activity increase when the GS1 gene transcription increased in alfalfa. GS enzyme in plants is in a dynamic process of biosynthesis and decomposition, and enzyme synthesis is positively correlated with the substrate concentration (Guan et al., 2007). Under low nitrogen condition, lack of GS substrate will cause primary oxidative modification of GS activity sites His residues, followed by protein conformation change or enzyme split, and the process will only be suspended until the GS peptides is hydrolyzed. It is thus clear that lack of substrate prompts enzyme decomposition under insufficient nitrogen condition, and rich substrate helps GS enzyme synthesis and keeps its stability under rich nitrogen conditions. It is also clarified that GS1 transcription level increased but the GS protein expression quantity decreased under low nitrogen condition in the present study.

Conclusion

The nitrogen inefficient sugarcane variety GT11 had the best performance in plant height, stalk diameter, leaf area, SPAD, net photosynthetic rate, GS activity and GS1 protein under high nitrogen levels, while the nitrogen efficient sugarcane variety GXB9 performed the best under medium nitrogen level. Under the low and medium nitrogen levels, the activities of GS and expression of GS1 protein were higher in GXB9 than GT11. The genes *scGS1.a* and *scGS1.b* had higher expression levels in leaves under low nitrogen level while the gene *scGS1.c* increased the relative expression level with the increase of nitrogen application rate. It is suggested that scGS1.a and scGS1.b be more important for nitrogen metabolism, possibly taking part in the nitrogen assimilation in sugarcane under low nitrogen level.

Acknowledgments. This work was supported financially in part by the grants from the National Natural Science Foundation of China (31471449, 31560352), Guangxi Special Fund for Scientific Base and Talent (GKAD17195100), Guangxi Special Funds for Bagui Scholars and Distinguished Experts (2013-3), Guangxi Sugarcane Innovation Team of National Agricultural Industry Technology System (gjnytxgxcxtd-03-01).

Conflict of interests. The authors declare that they have no conflict of interests.

http://www.aloki.hu ● ISSN 1589 1623 (Print) ● ISSN 1785 0037 (Online)
DOI: http://dx.doi.org/10.15666/aeer/1705_1236712384

Author contribution. L. T. Y. and Y. R. L. designed the study. K. Z. and D. Y. conducted the experiments. K. Z. and D. Y. analyzed data. K. Z., D. Y., L. T. Y. and Y. R. L. wrote the manuscript. L. T. Y. and Y. R. L. revised and finalized the manuscript.

REFERENCES

[1] Antoine, M., Judy. L., Thomas, K., Denise, G., Michel, Z., Christophe, T., Frédéric, D., Thierry, B., Beno, T. V., Marlène, D. (2006): Two cytosolic glutamine synthetase isoforms of maize are specifically involved in the control of grain production. – Plant Cell 18(11): 3252-3274.

[2] Bassi, D., Menossi, M., Mattiello, L. (2018): Nitrogen supply influences photosynthesis establishment along the sugarcane leaf. – Scientific Reports 8(1): 2327.

[3] Bernard, S. M., Møller, A. L. B., Dionisio, G., Kichey, T., Jahn, T. P., Dubois, F., Baudo, M., Lopes, M. S., Tercélaforgue, T., Foyer, C. H. (2008): Gene expression, cellular localisation and function of glutamine synthetase isozymes in wheat (Triticum aestivum L.). – Plant Molecular Biology 67(1-2): 89-105.

[4] Bijay, S., Yadvinder, S., Sekhon, G. S. (1995): Fertilizer-N use efficiency and nitrate pollution of groundwater in developing countries. – Journal of Contaminant Hydrology 20(3): 167-184.

[5] Bradford, M. M. (1976): A rapid method for the quantitation of microgram quantities of protein utilizing the principle of protein-dye binding. – Analytical Biochemistry 72: 248-254.

[6] Caputo, C., Criado, M. V., Roberts, I. N., Gelso, M. A., Barneix, A. J. (2009): Regulation of glutamine synthetase 1 and amino acids transport in the phloem of young wheat plants. – Plant Physiology & Biochemistry 47(5): 335-342.

[7] Edwards, J. W., Walker, E. L., Coruzzi, G. M. (1990): Cell-specific expression in transgenic plants reveals nonoverlapping roles for chloroplast and cytosolic glutamine synthetase. – Proceedings of National Academy of Science of the United States of America 87(9): 3459-3463.

[8] Elomari, R., Ruedalópez, M., Avila, C., Crespillo, R., Nhiri, M., Cánovas, F. M. (2010): Ammonium tolerance and the regulation of two cytosolic glutamine synthetases in the roots of sorghum. – Functional Plant Biology 37(1): 55.

[9] Goodall, A. J., Pankaj, K., Tobin, A. K. (2013): Identification and expression analyses of cytosolic glutamine synthetase genes in barley (Hordeum vulgare L.). – Plant & Cell Physiology 54(4): 492-505.

[10] Guan, S. Q. (2007): Cloning and expression analysis of glutamine synthetase gene from melon. – M. S. Thesis of Shanghai Jiao Tong University, Shanghai.

[11] Gui, Y. Y. (2007): Influence of different levels of nitrogen on nitrogen fixation in sugarcane. – M.S. Thesis of Guangxi University, Nanning.

[12] He, W. S., Guo, R. Y., Kang, J. H. (1999): Studies on physiological mechanism of genotypic differences in NPK-efficiency among spring wheat genotypes. – Journal of Ningxia Agricultural College 21(2): 33-38.

[13] Higashi, K., Shiota, H., Kamada, H. (1998): Patterns of expression of the genes for glutamine synthetase isoforms during somatic and zygotic embryogenesis in carrot. – Plant & Cell Physiology 39(4): 418-24.

[14] Jiang, Y. (2016): Effects of nitrogen fertilization levels on accumulation and utilization of nitrogen and yield and quality in different sugarcane varieties. – M.S. Thesis of Guangxi University, Nanning.

[15] Kazuhiro, F., Soichi, K., Mayumi, T. K., Yuki, S., Yosuke, N., Toshihiko, H., Tomoyuki, Y. (2013): Cytosolic glutamine synthetase1;2 is responsible for the primary assimilation of ammonium in rice roots. – Plant & Cell Physiology 54(6): 934-943.

http://www.aloki.hu ● ISSN 1589 1623 (Print) ● ISSN 1785 0037 (Online)
DOI: http://dx.doi.org/10.15666/aeer/1705_1236712384

[16] Keegstra, K., Cline, K. (1999): Protein import and routing systems of chloroplasts. – The Plant Cell 11(4): 557-570.
[17] Keiki, I., Eri, I., Akiko, W. T., Mitsuhiro, O., Tomoyuki, Y., Hideki, T. (2004): Kinetic properties and ammonium-dependent regulation of cytosolic isoenzymes of glutamine synthetase in Arabidopsis. – Journal of Biological Chemistry 279(16): 16598-605.
[18] Kusano, M., Tabuchi, M., Fukushima, A., Funayama, K., Diaz, C., Kobayashi, M., Hayashi, N., Tsuchiya, Y. N., Takahashi, H., Kamata, A. (2011): Metabolomics data reveal a crucial role of cytosolic glutamine synthetase 1;1 in coordinating metabolic balance in rice. – Plant Journal 66(3): 456-466.
[19] Laemmli, U. K. (1970): Cleavage of structural proteins during the assembly of the head of bacteriophage T4. – Nature 227: 680.
[20] Lea, P. J., Miflin, B. J. (2011): Nitrogen assimilation and its relevance to crop improvement. – Plant Review 42: 1-40.
[21] Li, J. H. (2017): Effects of nitrogen fertilizer on the expression nifH gene in the leaves of different sugarcane varieties. – Thesis of Guangx i University, Nanning.
[22] Li, J. T., Li, W. X., Liu, Y. G., Huang, L. F., Lin, Q. (2007): Effects of long-term located fertilization on the decrepitude characteristics of the flag leaf of winter wheat in the later growing stage. – Journal of Qingdao Agricultural University: Natural Science Edition 24: 279-282.
[23] Li, R. J., Hua, W., Lu, Y. T. (2006): Arabidopsis cytosolic glutamine synthetase AtGLN1;1 is a potential substrate of AtCRK3 involved in leaf senescence. – Biochemical & Biophysical Research Communications 342(1): 119-126.
[24] Li, Y. R., Yang, L. T. (2015): Sugarcane agriculture and sugar industry in China. – Sugar Tech 17(1): 1-8.
[25] Li, Y. R., Song, X. P., Wu, J. M., Li, C. N., Liang, Q., Liu, X. H., Wang, W. Z., Tan, H. W., Yang, L. T. (2016): Sugar industry and improved sugarcane farming technologies in China. – Sugar Tech 18(6): 603-611.
[26] Lightfoot, D. A., Green, N. K., Cullimore, J. V. (1988): The chloroplast-located glutamine synthetase of Phaseolus vulgaris L.: nucleotide sequence, expression in different organs and uptake into isolated chloroplasts. – Plant Molecular Biology 11(2): 191.
[27] Livak, K. J., Schmittgen, T. D. (2001): Analysis of relative gene expression data using real-time quantitative PCR and the $2^{-\Delta\Delta CT}$ method. – Methods 25(4): 402-408.
[28] Lothier, J., Gaufichon, L., Sormani, R., Lemaître, T., Azzopardi, M., Morin, H., Chardon, F., Reisdorf-Cren, M., Avice, J. C., Masclaux-Daubresse, C. (2011): The cytosolic glutamine synthetase GLN1;2 plays a role in the control of plant growth and ammonium homeostasis in Arabidopsis rosettes when nitrate supply is not limiting. – Journal of Experimental Botany 62(4): 297-305.
[29] Luo, L. F., Zheng, S. X., Liao, Y. L., Nie, J., Xie, J., Xiang, Y. W. (2007): Effect of controlled release nitrogen fertilizer on protein quality of brown rice and key enzyme activity involved in nitrogen metabolism in hybrid rice. – Chinese Journal of Rice Science 21(4): 403-410.
[30] Mattiello, L., Riaño-Pachón, D. M., Martins, M. C. M., da Cruz, L. P., Bassi, D., Marchiori, P. E. R., Ribeiro, R. V., Labate, M. T. V., Labate, C. A., Menossi, M. (2015): Physiological and transcriptional analyses of developmental stages along sugarcane leaf. – BMC Plant Biology 15(1): 300.
[31] May, T., Soll, J. (1999): Chloroplast precursor protein translocon. – Febs Letters 452(1-2): 52-56.
[32] Mayumi, T., Kenjiro, S., Keiki, I., Eri, I., Tadashi, S., Hideki, T., Tomoyuki, Y. (2005): Severe reduction in growth rate and grain filling of rice mutants lacking OsGS1;1, a cytosolic glutamine synthetase1;1. – Plant Journal 42(5): 641-651.

http://www.aloki.hu ● ISSN 1589 1623 (Print) ● ISSN 1785 0037 (Online)
DOI: http://dx.doi.org/10.15666/aeer/1705_1236712384

[33] Nogueira, D. M., Eduardo, Olivares, L., Fabio, Japiassu, C., Janaina, VILAR, Claudia, Fabiano. (2005): Characterization of glutamine synthetase genes in sugarcane genotypes with different rates of biological nitrogen fixation. – Plant Science 169(5): 819-832.
[34] Ortega, J. L., Temple, S. J., Sengupta-Gopalan, C. (2001): Constitutive overexpression of cytosolic glutamine synthetase (GS(1)) genein transgenic alfalfa demonstrates that GS(1) may be regulated at the level of RNA stability and protein turnover. – Plant Physiology 126(1): 109-121.
[35] Robinson, N., Fletcher, A., Whan, A., Critchley, C., Wirén, N. V., Lakshmanan, P., Schmidt, S. (2007): Sugarcane genotypes differ in internal nitrogen use efficiency. – Functional Plant Biology 34(12): 1122-1129.
[36] Shao, X. W., Han, M., Han, Z. M. (2009): Relationship between diurnal changes of photosynthesis of Scutellaria baicalensis and environmental factors in different habitats. – Acta Ecologica Sinica 29(3): 1470-1477.
[37] Swarbreck, S. M., Defoin-Platel, M., Hindle, M., Saqi, M., Habash, D. Z. (2011): New perspectives on glutamine synthetase in grasses. – Journal of Experimental Botany 62(4): 1511.
[38] Tingey, S. V., Tsai, F. Y., Edwards, J. W., Walker, E. L., Coruzzi, G. M. (1988): Chloroplast and cytosolic glutamine synthetase are encoded by homologous nuclear genes which are differentially expressed in vivo. – Journal of Biological Chemistry 263(20): 9651-9657.
[39] Towbin. H., Staehelin, T., Gordon, J. (1979): Electrophoretic transfer of proteins from polyacrylamide gels to nitrocellulose sheets: procedure and some applications. – Proceedings of National Academy of Science of the United States of America 76(9): 4350-4.
[40] Wei, L. P. (2005): Effects of different levels of molybdenum on the physiological and biochemical characteristic in relation to nitrogen fixation in sugarcane. – Thesis of Guangxi University, Nanning.
[41] Wu, W., Zhao, J. (2010): Advances on plants' nitrogen assimilation and utilization. – Chinese Agricultural Science Bulletin 26(13): 75-78.
[42] Zhang, Y. M., Yang, L. T., Li, X., Li, Y. R. (2015): Effects of different nitrogen levels on key enzymes of nitrogen metabolism and contents of related active substances for three sugarcane varieties. – Journal of Southern Agriculture 46(5): 766-771.
[43] Zhou, Z. B., Gong, D. Y., Dai-Yong, Y. I., Liu, F. Z., Xie, H. Y. (2006): Fertilizer effects of different amount of nitrogen applied on nitrogen fixation RB72-454 (sugarcane variety). – Guizhou Agricultural Science 34: 52-55.

APPENDIX

Table A1. *The primers of scGS1.a, scGS1.b, scGS1.c and GAPDH used to detect the relative expressions in sugarcane*

Primer	Primer sequence	
GS1.a	-AGACAGAGCAGAACGGCAAG-3'	F1
	-CTTCCAGAGGATGGTGGTGT-3'	R1
GS1.b	-CAAAGCAAGGACGGTGAAA-3'	F1
	-TGAGGGTAGAGGATGACTTCG-3'	R1
GS1.c	-CTGGGATGGATGTGAGGAGC-3'	F1
	-GTCTCTGAAGATGGCCCGAG-3'	R1
GAPDH	-CTCTGCCCCAAGCAAAGATG-3	F1
	-TGTTGTGCAGCTAGCATTG-3'	R1

http://www.aloki.hu ● ISSN 1589 1623 (Print) ● ISSN 1785 0037 (Online)
DOI: http://dx.doi.org/10.15666/aeer/1705_1236712384

Figure A1. *Leaf area of two sugarcane varieties under different nitrogen levels. Treatments labeled with different small letters represent statistically significant difference at $P < 0.05$ at the same date*

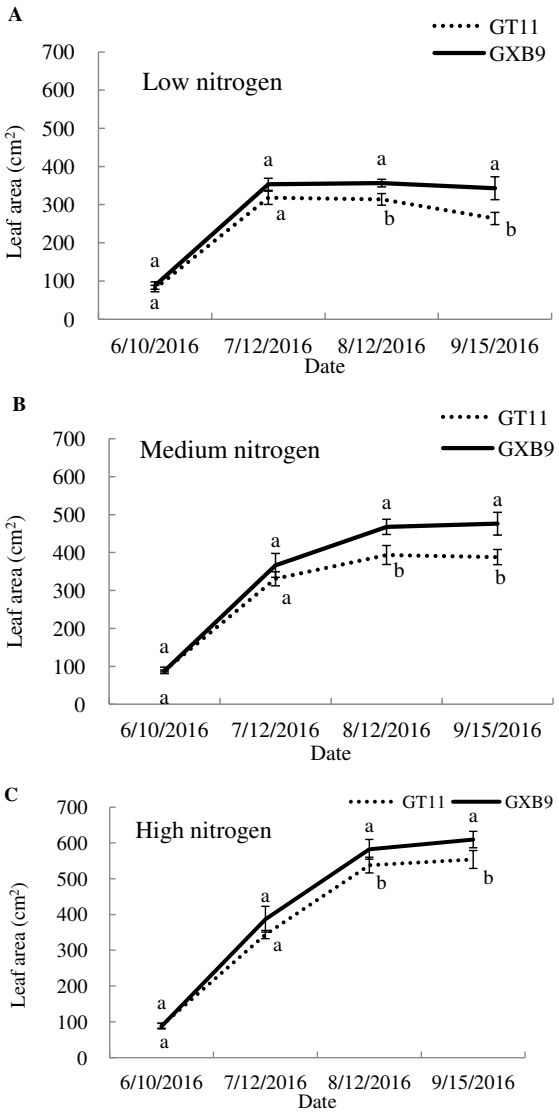

Figure A2. *GS activity in two sugarcane varieties under different nitrogen levels. Treatments labeled with different small letters represent statistically significant difference at $P < 0.05$ at the same date*

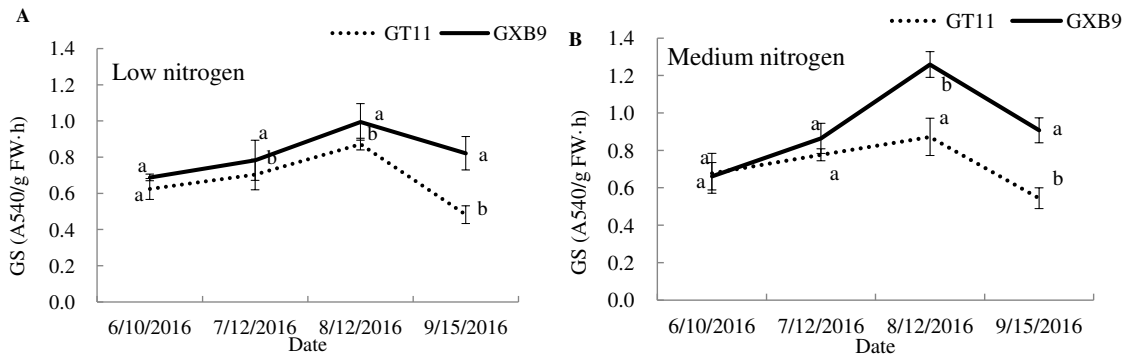

http://www.aloki.hu ● ISSN 1589 1623 (Print) ● ISSN 1785 0037 (Online)
DOI: http://dx.doi.org/10.15666/aeer/1705_1236712384

Figure A3. *Expression of scGS1.a mRNA in two sugarcane varieties under different nitrogen levels. Treatments labeled with different small letters represent statistically significant difference at P < 0.05 at the same date*

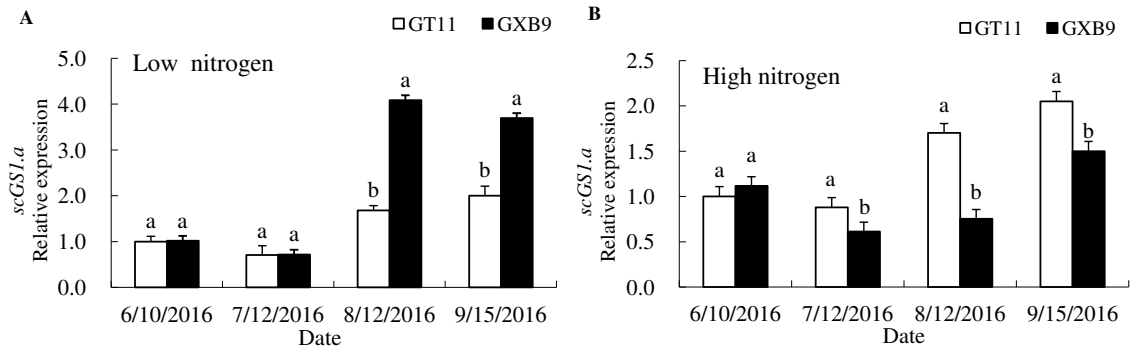

Figure A4. *Expression of scGS1.c mRNA in two sugarcane varieties under different nitrogen levels. Treatments labeled with different small letters represent statistically significant difference at P < 0.05 at the same date*

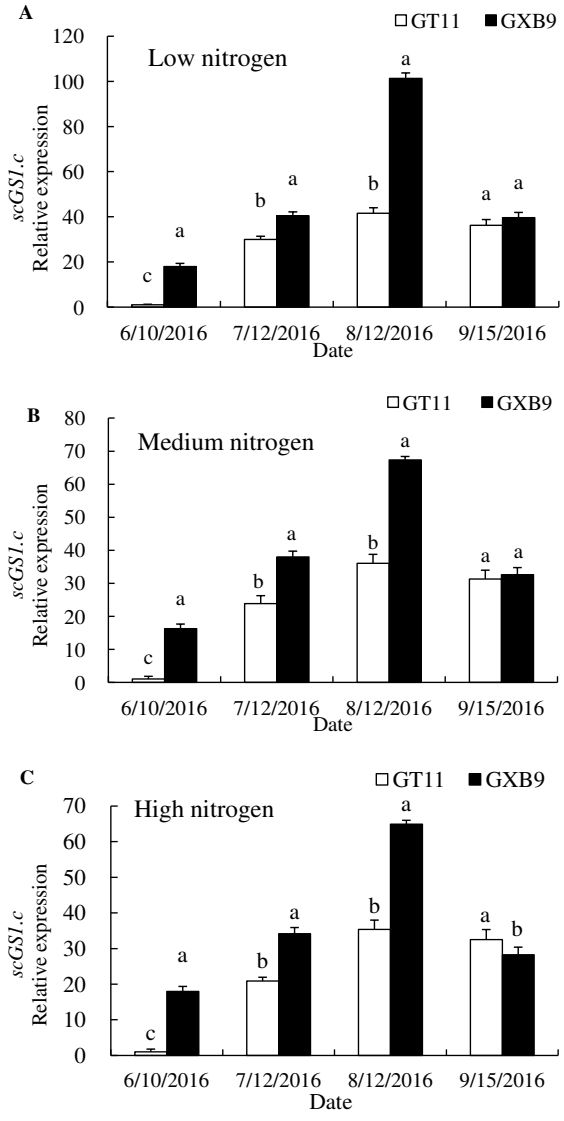

http://www.aloki.hu ● ISSN 1589 1623 (Print) ● ISSN 1785 0037 (Online)
DOI: http://dx.doi.org/10.15666/aeer/1705_1236712384

Figure A5. *Expression of GS1 protein in two sugarcane varieties under different nitrogen levels*

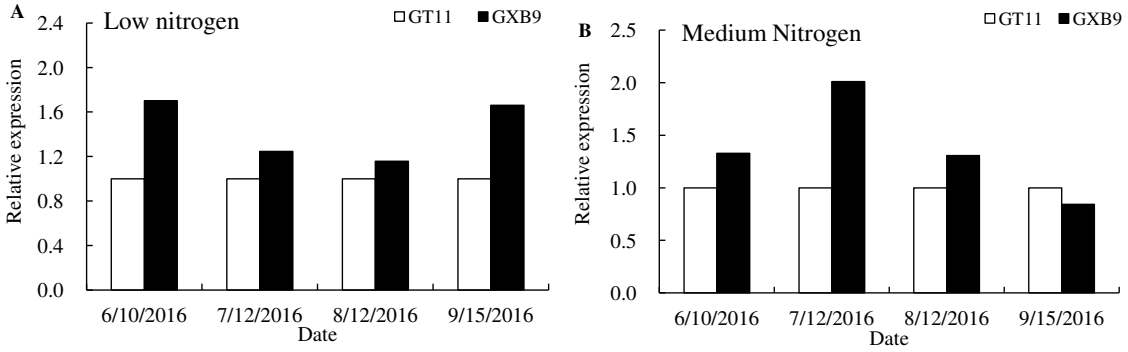

http://www.aloki.hu ● ISSN 1589 1623 (Print) ● ISSN 1785 0037 (Online)
DOI: http://dx.doi.org/10.15666/aeer/1705_1236712384

THE IMPACT OF THE LONG – TERM FERTILISATION WITH MINERAL FERTILISERS ON THE CHEMICAL PROPERTIES OF VERTISOL (CENTRAL SERBIA)

GUDŽIĆ, N.[1] – ŠEKULARAC, G.[2*] – DJIKIĆ, A.[1] – DJEKIĆ, V.[3] – AKSIĆ, M.[1] – GUDŽIĆ, S.[1]

[1]*Faculty of Agriculture, Lešak, University of Priština, Serbia*

[2]*Faculty of Agronomy, Čačak, University of Kragujevac, Serbia*

[3]*Centre of Small Grains, Kragujevac, Serbia*

**Corresponding author*
e-mail: gordasek@kg.ac.rs

(Received 8th May 2019; accepted 16th Jul 2019)

Abstract. The study is based on establishing soil acidity and fertility of Vertisols after the mineral fertilisers had continuously been applied from 1984 to 2016. The two phosphorus (35 and 70 kg P ha^{-1}), the invariable nitrogen (120 kg N ha^{-1}) and potassium (66.4 kg K ha^{-1}) doses were used in Kragujevac location (central Serbia) for over 33 study years. The impact of fertilisation with mineral fertilisers on soil acidity, organic carbon content, the total N, P and K as well as on P, K forms balance and on some microelements (Fe, Mn, Cu and Zn) availability was studied at soil depths of 0-20 and 20-40 cm. After 33 years, the highest changes were noticed in the surface layer (0-20 cm), with an increase in the acidity level and a decrease in organic carbon content and in the total N. Simultaneously, a higher P and K content and a higher Fe and Mn mobility were established in the same soil layer whereas mineral fertilisers had no significant effect on the changes in chemical properties at 20-40 cm deep soils.
Keywords: *plant production, soil properties, nutrient, acidification, farming sustainability*

Introduction

Constantly used mineral fertilisers in conventional plant production were found to affect numerous soil properties. In this regard, continuously used nitrogen, phosphorus and potassium in mineral form were found to somewhat influence soil physical characteristics (Herencia et al., 2011; Suwara et al., 2016), and to a larger extent the soil chemical and biological properties (Belay et al., 2002; Zhong et al., 2010) as well as the soil enzyme activity (Piotrowska and Wilczewski, 2012; Chen et al., 2018). Soil physical and chemical properties and fungi diversity and abundance were also found to be significantly affected by long-term mineral fertilisation, especially in terms of fungi diversity reduction and soil acidification (Yan et al., 2019).

Soil and water contamination most often bring about soil acidification (Herencia et al., 2007; Undurraga et al., 2009). One of the solutions made to the potential harmful effect of the long-term and one-sided use of fertilisers is considered to be fertilisation management system managing the nutrients put into and taken out of the soil within the crop rotation system (Hirzel et al., 2011). Therefore, a reasonable use of the mineral fertilisers over a longer period of time may keep up or even upgrade the soil quality and its production capacities, too (Belay et al., 2002).

One of the best ways to assess how fertilisation affects fertility and other soil properties is through the long-term experiments (Mitchell et al., 1991). Such experiments may provide useful information about farming systems sustainability,

http://www.aloki.hu ● ISSN 1589 1623 (Print) ● ISSN 1785 0037 (Online)
DOI: http://dx.doi.org/10.15666/aeer/1705_1238512396

particularly when fertilisers are invariably used and for quite a long time. That is why the current study was aimed at establishing the changes in soil chemical properties caused by these fertilisers on Vetisols in the central Serbia.

Materials and methods

Experimental location

The investigation was performed in a long-term trial field of the Centre of Small Grains, in Kragujevac (44º02´ N and 20º56´ E, altitude: 185 m asl), central Serbia (*Fig. 1*), on Vertisols (IUSS Working Group WRB, 2014). The study location of Kragujevac is approximately 113 km away from Belgrade.

Figure 1. *Study location map (Kragujevac, central Serbia)*

Climatic conditions of the study location

Based on the climatic data outlined in Walter climate-diagram (Walter et al., 1975) (*Fig. 2*), the annual air temperature of Kragujevac location averaged 12.2ºC and the total annual rainfalls averaged 673 mm over the last twenty years (Republic Hydrometeorological Service of Serbia, 1998-2017). July and August were found to be the hottest (22.9ºC and 22.4ºC, respectively) and January and December the coldest months (1.3ºC and 2.3ºC, respectively). On average, May (74 mm) and June (70 mm) were the rainiest and February (42 mm) and January (45 mm) the driest months.

Walter climate-diagram denotes that, on average, humid periods over the year were present from January to June and from September to December whereas dry periods prevailed in July and in August. According to Köppen classification (1936) and based on the previously outlined data, the climate of Kragujevac location could be determined as moderately warm and humid with hot summers and dry winters.

http://www.aloki.hu ● ISSN 1589 1623 (Print) ● ISSN 1785 0037 (Online)
DOI: http://dx.doi.org/10.15666/aeer/1705_1238512396

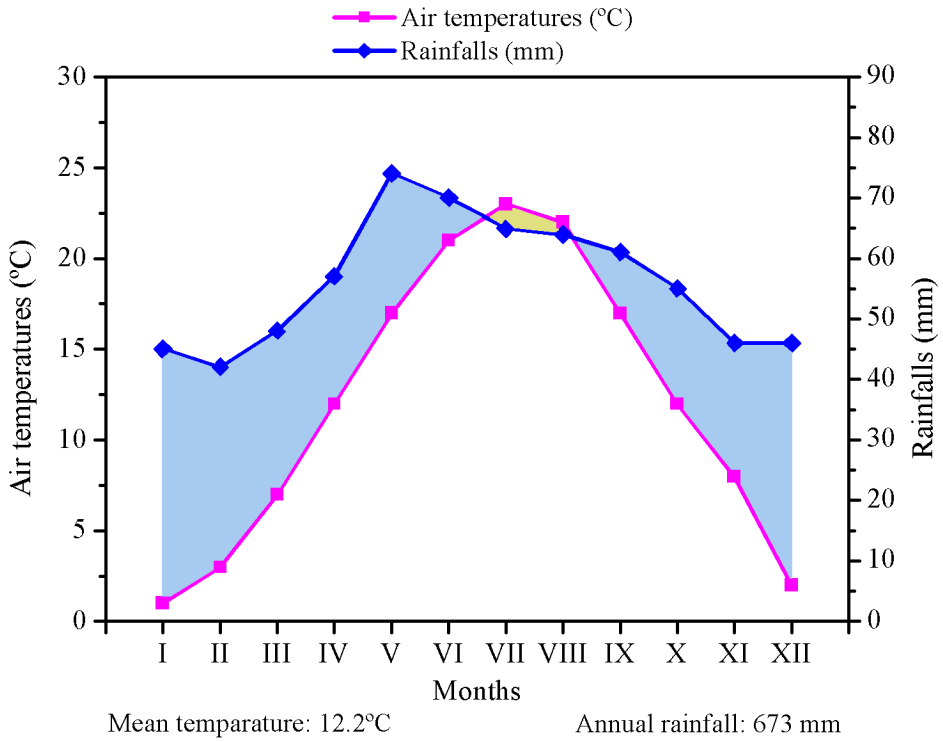

Figure 2. *Walter climate-diagram of research area (1998-2017)*

Agrochemical soil properties

The soil studied is characterised by lessivage process. Prior to the experiment, the soil had an excessive acid reaction, a low phosphorus content, moderate organic carbon (OC) and potassium content (*Table 1*). Soil acidity and the total and available K content were found to increase at 20-40 cm depth whereas OC content, total N and total and available P contents were found to decrease. The available Fe, Mn and Cu contents also decreased whereas Zn one increased.

Table 1. *Agrochemical properties before setting up of the experiment*

Depth cm	pH		Hh cmol kg^{-1}	OC %	Total			Available					
	H_2O	KCl			N	P	K	P	K	Fe	Mn	Cu	Zn
					%	mg kg^{-1}							
0-20	5.90	4.60	13.29	1.56	0.17	977.4	15000	260	186	71	118	2.4	1.7
20-40	5.90	4.47	11.11	0.96	0.11	763.6	15700	190	215	64	110	2.2	2.8

Experimental design

Having started in 1984, the experiment was continuoulsy carried out till 2016 within the two-field crop rotation of the winter wheat (*Triticum aestivum*) and of maize (*Zea mays* L.). Soil cultivation was typical of the existing environmental conditions with standard agronomical measures suiting maize and wheat used and plant remains from the previous vegetation removed.

http://www.aloki.hu ● ISSN 1589 1623 (Print) ● ISSN 1785 0037 (Online)
DOI: http://dx.doi.org/10.15666/aeer/1705_1238512396

In the course of the experiment, the phosphorus doses were continuously used, the lower dose of 35 kg P ha^{-1} (P1) and the higher one of 70 kg P ha^{-1} (P2). The two P doses were combined with the constant N dose (120 kg N ha^{-1}) in the variants NP1 and NP2 with the constant N (120 kg N ha^{-1}) and K (66.4 kg K ha^{-1}) doses in the variants NP1K and NP2K. Nitrogen and potassium were also used in the same rates in the variant – NK. Fertilisation treatments were compared with the control treatment in which no fertilisers were used (0). Super-phosphate – $Ca(H_2PO_4)_2 \cdot CaSO_4$, urea – $CO(NH_2)_2$ and potassium chloride – KCl were used for fertilisation. Fertilisation technology was standard for each vegetation season, in which the total amounts of super-phosphate and pottasium chloride as well as 1/3 of urea were always applied before sowing. The remaining urea amount was used during vegetation depending on the climatic circumstances so that for wheat, it was used in the period from the end of March to the beginning of April and for maize during the second half of May.

The experiment proceeded according to the random system block design (RSBD) with four replications. Each plot was 15 m^2 in size. The average (composite) soil sample was taken for each treatment and formed from the five sub-samples. In every treatment, firstly at the depth 0-20 cm, the probe (Eijkelkamp) was used to take five individual samples (sub-samples) being mixed together and an average or composite sample was singled out from the total mass. The procedure was repeated for each treatment (0-20 cm) as well as for that of 20-40 cm. Composite samples (24 for 0-20 cm and 24 for 20-40 cm) were chemically analysed after the corresponding treatment. Soil samples were collected in the period from the 10^{th} to the12^{th} October, 2016 after the maize harvest.

Soil laboratory analysis

Soil pH was determined on the pH meter (MA 5730 ISKRA) in 1 : 2.5 suspension with water (AA) and l M KCl (SA). Hydrolytic acidity (Hh) was determined following the method of Kappen while the availability of phosphorus (AP) and potassium (AK) was determined following that of Egner-Riehm with ammonium-lactate (pH = 3.7) used as the extraction means. Upon the extraction, potassium was determined through the atomic absorption spectrometry (AAS) and phosphorus through spectrophotometry UV/Vis S2000 (WPA, England) after the colour had been developed with NH_4MoO_4 and $SnCl_2$. The total phosphorus (TP) was determined through spectrophotometry at the wave length of 400-490 nm after digestion with $HClO_4$ and treatment with ammonium paramolybdate-vanadate reagent (Olsen and Sommers, 1982) and the total potassium (TK) AAS after degrading the sample with mixture HF and H_2SO_4. Further, the content of soil microelements available forms (Fe, Mn, Cu and Zn) was determined through atomic absorption spectrophotometry (AAS) using the apparatus AAS N-1 (Carl Zeiss Jena, Germany). The available Fe (AFe) was determined after being extracted in the solution l M CH_3COONH_4 (pH 7). Determining the available Mn (AMn) content was done using the extraction means of 0.l M H_2SO_4 and that of Cu (ACu) and Zn (AZn) using 0.l M HCl.

Statistical analysis

The data obtained from the parameters were subjected to statistical analysis using the WinSTAT program being the statistics Add-In for Microsoft Excel (Copyright © 2018 Robert K. Fitch). The effects of treatment with fertilisers were tested using ANOVA and the differences between the treatments were registered using t-test for the levels of

http://www.aloki.hu ● ISSN 1589 1623 (Print) ● ISSN 1785 0037 (Online)
DOI: http://dx.doi.org/10.15666/aeer/1705_1238512396

95 and 99%, whereas the balance of available microelements dependant on the substantial acidity and available P, was tested using the square regression.

Results and discussion

The experiment conducted for 33 years was characterised by monitoring acidifying of both layers tested. AA and SA were found to have significantly increased in the surface layer whereas Hh was found to have had just a mild increase. Thus, AA of 5.90 fell in the control variant after 33 years amounting to 5.57. In addition, SA pH in KCl decreased from 4.60 to 4.18 whereas Hh mildly increased from 13.29 cmol kg^{-1} to 14.10 cmol kg^{-1} for the same period. The process of somewhat milder acidification also prevailed in the 20-40 cm deep layer.

Table 2. *Characteristics of the acidity after 33 years of fertilisation*

Variants	pH		Hh
	H_2O	KCl	cmol kg^{-1}
	0-20 cm		
0	5.58 ± 0.08	4.18 ± 0.14	14.10 ± 0.41
NK	5.30 ± 0.13	4.02 ± 0.10	17.80 ± 0.23
NP1	5.36 ± 0.15	4.10 ± 0.09	16.98 ± 0.22
NP2	5.40 ± 0.08	4.12 ± 0.07	16.37 ± 0.16
NP1K	5.42 ± 0.07	4.10 ± 0.12	16.43 ± 0.15
NP2K	5.52 ± 0.08	4.13 ± 0.11	16.18 ± 0.30
Lsd 0.05	0.066	0.069	0.174
Lsd 0.01	0.091	0.094	0.238
	20-40 cm		
0	5.60 ± 0.10	4.40 ± 0.11	10.51 ± 1.44
NK	5.63 ± 0.11	4.16 ± 0.11	12.30 ± 0.11
NP1	5.50 ± 0.09	4.30 ± 0.11	10.92 ± 0.10
NP2	5.60 ± 0.09	4.33 ± 0.19	10.53 ± 0.17
NP1K	5.50 ± 0.09	4.23 ± 0.11	11.11 ± 0.11
NP2K	5.90 ± 0.13	4.26 ± 0.13	11.17 ± 0.20
Lsd 0.05	0.0679	0.084	0.408
Lsd 0.01	0.0929	0.116	0.559

In addition to the natural acidification, the long-term and continuous use of mineral fertilisers also favoured additional acidification of the Vertisol in both soil layers (*Table 2*) in that the acidification of the surface layer seemed to be more expressed. This may be accounted for by the fact that it was the zone of fertilisers used and, therefore, of their direct impact on this layer. In the 0-20 cm deep layer, the differences in AA, SA i Hh between the control variant and those with fertilisation appeared to be highly significant ($P \leq 0.01$). However, the highest acidification was established in NK variant, meaning that their long-term use increased acidity more significantly than their combination with phosphorus fertilisers did. Such a trend was expected considering that soil acidification over a long period of nitrogen fertilisation is well-known and already confirmed. However, the long-term and continuous application of the fertilisers, which, beside nitrogen, also contain phosphorus such as MAP, may often result in higher acidification (Belay et al., 2002; Saleque et al., 2004).

http://www.aloki.hu ● ISSN 1589 1623 (Print) ● ISSN 1785 0037 (Online)
DOI: http://dx.doi.org/10.15666/aeer/1705_1238512396

Therefore, at 20-40 cm depth, the differences in AA between the control and fertilisation treatments were lower, denoting at fertilisation to have a lower impact on this type of acidity in deeper soil layers even after 33 years of being applied. On the other hand, the variations in SA and Hh between fertilisation and control treatments seemed to be more pronounced. Identically with the changes in soil acidity in the surface layer, those in the deeper ones also suggested the highest acidity in NK variant.

When comparing the initial (1984) organic carbon (OC) content and the total nitrogen (TN) one in 2016 in the control variant, study period was not found to be profoundly reflected on their balance. However, more significant changes did happen in the experimental stage with fertilisers applied (*Table 3*). Namely, in all the fertilisation variants, the OC content and TN one were significantly reduced in the surface layer compared to the control variant ($P \leq 0.01$). In contrast to the significant impact of the long-term fertilisation with nitrogen on sustaining and improving OC content (Bundy et al., 2011), the total and nitrate nitrogen (Zhang et al., 2012), then that contained in the fertilisers used over the current research had, however, no positive effect. The content of these two components could be expected to drop with the depth (*Table 4*).

Table 3. *The content of OC, TN, TP, TK, AP and AK in the 0-20 cm layer after 33 years*

	OC	TN	TP	TK	AP	AK
Variants	**%**		**mg kg^{-1}**			
0	1.57 ± 0.06	0.157 ± 0.007	924 ± 79	13200 ± 600	18.9 ± 4.5	188.0 ± 4.0
NK	1.25 ± 0.07	0.125 ± 0.007	967 ± 166	16500 ± 1200	20.2 ± 2.9	258.3 ± 4.4
NP1	1.38 ± 0.10	0.138 ± 0.010	1202 ± 86	14100 ± 700	104.4 ± 7.6	168.9 ± 9.5
NP2	1.39 ± 0.10	0.140 ± 0.011	1381 ± 213	14000 ± 600	115.5 ± 10.5	154.8 ± 5.3
NP1K	1.37 ± 0.10	0.137 ± 0.010	1283 ± 96	15000 ± 600	125.5 ± 4.8	288.3 ± 3.8
NP2K	1.44 ± 0.14	0.144 ± 0.020	1605 ± 107	16000 ± 800	168.2 ± 5.8	255.5 ± 7.4
Lsd 0.05	0.078	0.0078	86.56	530.33	4.37	4.08
Lsd 0.01	0.107	0.0107	118.57	726.46	5.99	5.58

OC: organic carbon; TN: total nitrogen; TP: total phosphorus; TK: total potassium; AP: available phosphorus; AK: available potassium

When phosphorus and potassium content in Vertisols are concerned with, the fertilisers containing these two elements were reported to directly influence their concentration in relation to the initial level in 1984. So, after 33 years, in all the variants with P fertilisers, the TP and AP content increased with variations in relation to the control and NK treatment was found to be statistically highly significant ($P \leq 0.01$) proportionally to the applied fertilisers rates. The highest changes were noticed in the surface layer while the long-term use of fertilisers strongly favoured the accumulation of the available forms in the zone of their input (Otto and Kilian, 2001; Cakmak et al., 2010).

Such a balance of phosphorus was influenced by both, phosphorus doses used on a year basis (35 and 70 kg ha^{-1}) and by its being incompletely utilised. Thus, in this layer, the same phosphorus rates were found to favour the accumulation of this element considerably more in NP1K and NP2K than in NP1 and NP2 variants. The long-term use of lower P rates with NP1K treatment favoured the increase in AP highly significantly ($P \leq 0.01$) compared with the higher rate used in NP2 treatment. Similar trend was reported for the fertilisers impact on TK and AK.

http://www.aloki.hu ● ISSN 1589 1623 (Print) ● ISSN 1785 0037 (Online)
DOI: http://dx.doi.org/10.15666/aeer/1705_1238512396

Table 4. *The content of OC, TN, TP, TK, AP and AK in the 20-40 cm layer after 33 years*

	OC	TN	TP	TK	AP	AK
Variants	**%**		**mg kg^{-1}**			
0	0.90 ± 0.11	0.089 ± 0.011	924 ± 79	13400 ± 450	19.3 ± 1.7	204.5 ± 8.8
NK	1.06 ± 0.09	0.105 ± 0.011	704 ± 129	16500 ± 300	18.7 ± 2.7	266.0 ± 7.1
NP1	1.11 ± 0.03	0.111 ± 0.005	984 ± 86	12500 ± 450	52.0 ± 7.2	208.0 ± 8.0
NP2	1.09 ± 0.06	0.109 ± 0.007	1158 ± 93	13100 ± 400	54.0 ± 5.3	181.0 ± 5.8
NP1K	1.15 ± 0.07	0.116 ± 0.007	994 ± 108	14800 ± 600	51.0 ± 4.0	237.4 ± 3.6
NP2K	1.13 ± 0.05	0.112 ± 0.005	1093 ± 155	14800 ± 350	63.3 ± 2.2	237.0 ± 7.4
Lsd 0.05	0.049	0.0053	75.13	284.48	2.85	6.26
Lsd 0.01	0.067	0.0072	102.92	389.68	3.90	8.58

P content in 20-40 cm deep layer unambiguously suggested its barely slight mobility compared to its input zone (*Table 4*) whereas a much better mobility applied to potassium, with its content in the 20-40 cm layer considerably matching that in the surface layer. Therefore, the potassium introduced through fertilisation over 33 years of the experiment was continuously leached and more or less evenly distributed in the 40 cm layer being analysed.

Table 5. *The content of the available microelements in the Vertisol after 33 years*

Variants	**Fe**	**Mn**	**Cu**	**Zn**
	mg kg^{-1}			
	0 - 20 cm			
0	88 ± 20	134 ± 18	2.9 ± 0.7	1.4 ± 0.5
NK	94 ± 15	125 ± 20	2.5 ± 0.5	0.8 ± 0.4
NP1	81 ± 15	105 ± 18	2.6 ± 0.9	1.3 ± 0.3
NP2	88 ± 24	110 ± 25	2.0 ± 0.4	1.2 ± 0.3
NP1K	93 ± 32	121 ± 19	2.8 ± 1.1	1.6 ± 0.2
NP2K	84 ± 19	118 ± 30	2.4 ± 0.5	1.5 ± 0.7
Lsd 0.05	14.77	14.90	0.496	0.300
Lsd 0.01	20.23	20.41	0.678	0.412
	20 - 40 cm			
0	83 ± 26	122 ± 15	2.5 ± 0.6	1.4 ± 0.5
NK	89 ± 24	121 ± 17	2.0 ± 0.7	0.8 ± 0.5
NP1	81 ± 12	103 ± 10	2.2 ± 0.5	1.2 ± 0.6
NP2	86 ± 18	100 ± 11	2.1 ± 0.4	1.4 ± 0.6
NP1K	81 ± 14	118 ± 16	2.4 ± 1.0	1.5 ± 0.7
NP2K	78 ± 14	115 ± 18	2.1 ± 0.4	1.5 ± 1.1
Lsd 0.05	12.48	10.15	0.449	0.460
Lsd 0.01	17.10	13.90	0.616	0.630

Fertilisation lasting thirty-three years exhibited its effect on the available microelements forms content *(Table 5)* in that the highest available Fe content was established with NK and the lowest one with NP1 in 0-20 cm and with NP2K in 20-40 cm, respectively. Neither statistically significant differences between the variants with the highest and lowest Fe content were revealed nor those between the other variants, were. Contrary to Fe content, the lowest Zn content was recorded in both studied layers in NK variant in that in 0-20 cm layer the differences between NK and NP2 variants were statistically significant ($P \leq 0.05$) and those between NK and remaining variants

http://www.aloki.hu ● ISSN 1589 1623 (Print) ● ISSN 1785 0037 (Online)
DOI: http://dx.doi.org/10.15666/aeer/1705_1238512396

highly statistically significant ($P \leq 0.01$). As for 20-40 cm layer, highly significant differences could be recorded only between NK with the lowest Zn content and NP1K and NP2K in which the highest Zn content was established.

Thus, the lowest Mn content was recorded in NP1 and NP2 variants but with no clearly established effect of the phosphorus rate. On the other hand, Cu content decreased with fertiliser rate increased, with Cu lowest content established in the NP2 and NP2K variants.

The decreasing trend of active Mn and Cu forms with NP1 and NP2 variants in relation to the control and Zn with NK, NP1 and NP2 variants, was observed at the 20-40 cm depth, at which the lower content of all the four microelements analysed in relation to the surface layer, was also observed.

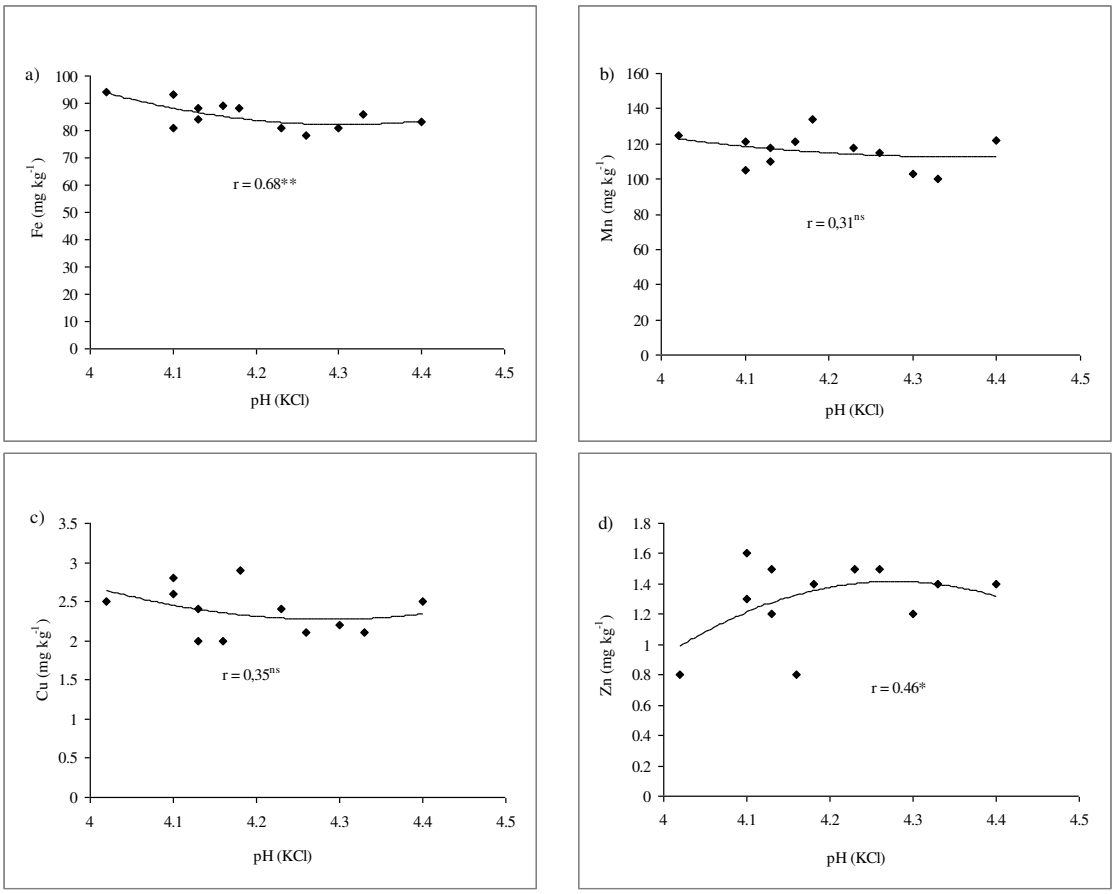

Figure 3. *The ratio between the available microelements forms rates (Fe, Mn, Cu, Zn) and pH (KCl) in the surface layer*

Therefore, the experience about fertilisers impact on the microelements available forms, some of which being Fe, Mn, Cu and Zn content in the soil, seemed to vary but mainly denying that mineral fertilisers had significantly altered their concentration (Rutkowska et al., 2009) and also stressing a more significant long-term use of organic fertilisers compared with the mineral ones (Li et al., 2010; Richards et al., 2011). As supported by Thakur et al. (2011), in addition to the organic, mineral fertilisers, of which particularly the phosphorus ones (Molina et al., 2009), mainly containing heavy metals (As, Cd, Cr) as well as numerous micronutrients, particularly Zn, may also

http://www.aloki.hu ● ISSN 1589 1623 (Print) ● ISSN 1785 0037 (Online)
DOI: http://dx.doi.org/10.15666/aeer/1705_1238512396

influence the microelements content. Thus, the input of P fertilisers may result in a higher Zn content, which was evident in NP1K and NP2K variants in both layers studied.

The availability of microelements in the soil may result from numerous factors, of which OC, soil response in the presence of the phosphorus soluble forms, take an important part (Wei et al., 2006; Asadu et al., 2014). Thus, micronutrients and toxic ions, cations availability, increased with the increase in soil acidity (Khabaz-Saberi and Rengel, 2010). When comparing the dependence between SA and Fe, Mn, Cu and Zn content in the surface layer, highly significant correlation between this trait of the studied soil and available Fe in it, could be found (*Fig. 3*). In addition, the correlation with the available Zn content seemed to be significant whereas no interdependence between Mn, Cu and SA was revealed.

Overall, significant correlation existed between the soluble forms of phosphorus and available Mn and Zn whereas it did not between phosphorus and available Fe and Cu content (*Fig. 4*).

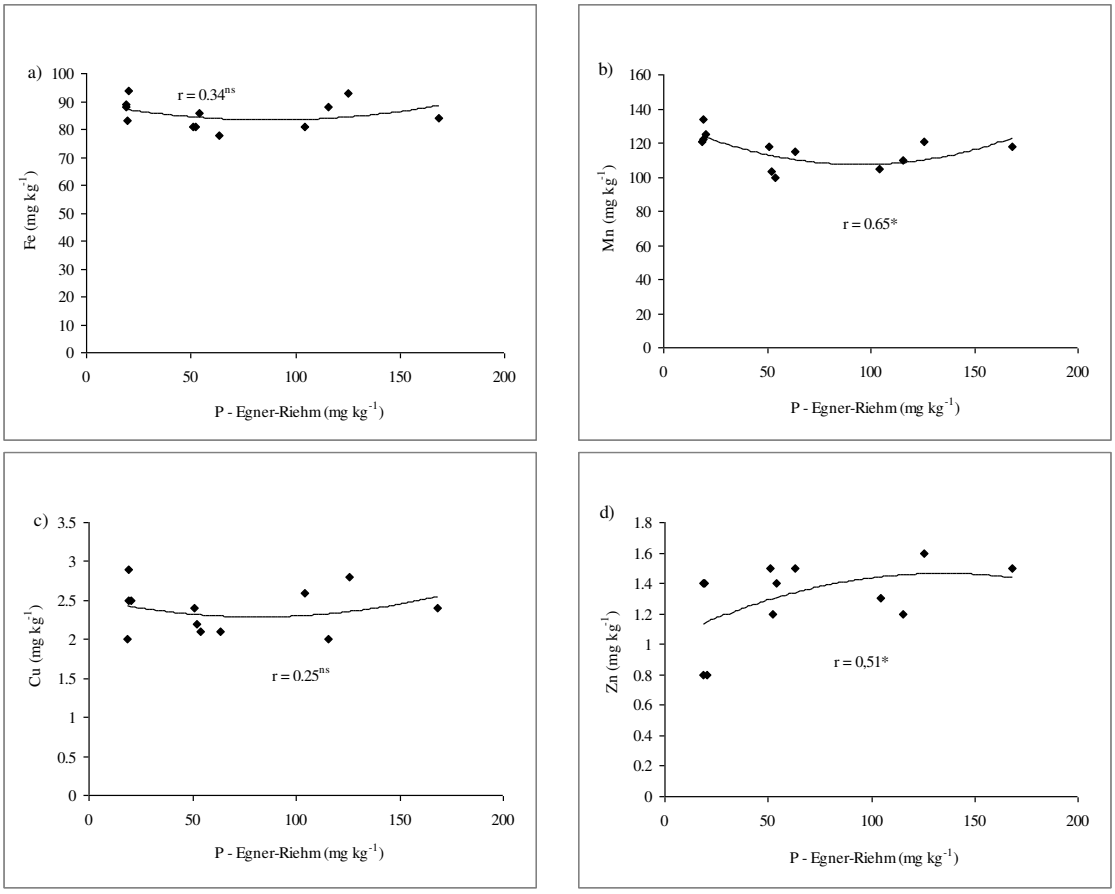

Figure 4. *The ratio between the available microelements forms rates (Fe, Mn, Cu, Zn) and the available P in the surface layer*

http://www.aloki.hu ● ISSN 1589 1623 (Print) ● ISSN 1785 0037 (Online)
DOI: http://dx.doi.org/10.15666/aeer/1705_1238512396

Conclusion

Mineral fertilisers, particularly nitrogen and potassium ones used over thirty-three years, were reported to have caused the acidification of Vertisol, reduced organic carbon content and the total nitrogen one in the surface layer. The changes in the same parameters seemed to be less expressed in the 20-40 cm deep layer. Simultaneously, the total and available phosphorus and potassium content increased in all the cases in which the fertilisers containing these two elements were used, being in proportion with their rates used. Due to low mobility, phosphorus remained in the input zone so that even thirty-three years of its continuous use exhibited a limited effect on its content in deeper horisons. To sum up, Fe, Mn, Cu and Zn available forms content was revealed to depend upon a fertiliser type and phosphorus amount introduced. While NK fertilisers exhibited a significant effect on Zn content, the NP and NPK ones had it on Mn and Cu content. Cu was also found to respond mostly to the amount of phosphorus input in that Cu availability forms decreased with increase in the phosphorus used.

Acknowledgements. Supported by the Ministry of Education, Science and Technological Development of the Republic of Serbia, Projects No. TR 31054 and TR 31092.

REFERENCES

[1] Asadu, C.L.A., Chibuike, G.U., Dixon, A.F.O. (2014): Micronutrients availability in a cleared forestland after seven years of continuous cultivation and eight years of natural fallow in a Alfisol, Eastern Nigeria. – Scientica Agriculturae 4: 86-90.

[2] Belay, A., Claassens, A., Wehner, F. (2002): Effect of direct nitrogen and potassium and residual phosphorus fertilizers on soil chemical properties, microbial components and maize yield under long-term crop rotation. – Biology and Fertility of Soils 35: 420-427.

[3] Bundy, L.G., Andraski, T.W., Ruark, M.D., Peterson, A.E. (2011): Long-Term Continuous Corn and Nitrogen Fertilizer Effects on Productivity and Soil Properties. – Agronomy Journal 103: 1346-1351.

[4] Cakmak, D.B., Saljnikov, E., Mrvic, V.V., Jakovljevic, M.D., Marjanovic, Z.S., Sikiric, B., Maksimovic, S. (2010): Soil Properties and Trace Elements Contents Following 40 Years of Phosphate Fertilization. – Journal of Environmental Quality 39: 541-547.

[5] Chen, Y.I., Liu, J.T., Liu, S.T. (2018): Effect of long-term mineral fertilizer application on soil enzyme activities and bacterial community composition. – Plant, Soil and Environment 64: 571-577.

[6] Herencia, J.F., Ruiz-Porras, J.C., Melero, S., Garcia-Galavis, P.A., Morillo, E., Maqueda, C. (2007): Comparison between Organic and Mineral Fertilization for Soil Fertility Levels, Crop Macronutrient Concentrations, and Yield. – Agronomy Journal 99: 973-983.

[7] Herencia, J.F., Garcia-Galavis, P.A., Maqueda, C. (2011): Long-Term Effect of Organic and Mineral Fertilization on Soil Physical Properties Under Greenhouse and Outdoor Management Practices. – Pedosphere 21: 443-453.

[8] Hirzel, J., Undurraga, P., González, J. (2011): Chemical properties of volcanic soil affected by seven-year rotations. – Chilean Journal of Agricultural Research 71: 304-312.

[9] IUSS Working Group WRB (2014): World Reference Base for Soil Resources 2014. – In: Schad, P., Huyssteen, van C., Michéli, E. (eds.) International soil classification system for naming soils and creating legends for soil maps, World Soil Resources Reports No. 106, FAO, Roma

http://www.aloki.hu ● ISSN 1589 1623 (Print) ● ISSN 1785 0037 (Online)
DOI: http://dx.doi.org/10.15666/aeer/1705_1238512396

[10] Khabaz-Saberi, H., Rengel, Z. (2010): Aluminum, manganese, and iron tolerance improves performance of wheat genotypes in waterlogged acidic soils. – Journal of Plant Nutrition and Soil Science 173: 461-468.
[11] Köppen, W. (1936): Das Geographisca System der Klimate. – In: Köppen, W. and Geiger, G.C. (eds.). Handbuch der Klimatologie, Gebr, Borntraeger
[12] Li, B.Y., Huang, S.M., Wei, M.B., Zhang, H.L., Shen, A.L., Xu, J.M., Ruan, X.L. (2010): Dynamics of Soil and Grain Micronutrients as Affected by Long-Term Fertilization in an Aquic Inceptisol. – Pedosphere 20: 725-735.
[13] Mitchell, C.C., Westerman, R.L., Brown, J.R., Peck, T.R. (1991): Overview of Long-Term Agronomic Research. – Agronomy Journal 83: 24-29.
[14] Molina, M., Aburto, F., Calderon, R., Cazanga, M., Escudey, M. (2009): Trace Element Composition of Selected Fertilizers Used in Chile: Phosphorus Fertilizers as a Source of Long-Term Soil Contamination. – Soil and Sediment Contamination 18: 497-511.
[15] Olsen, S.R., Sommers, L.E. (1982): Phosphorus. – In: Page, A.L., Miller, R.H., Keeney, D.R. (eds.) Methods of Soil Analysis, Part 2, Chemical and Microbiological Properties, American Society of Agronomy, Inc., Madison, pp. 403-427.
[16] Otto, W.M., Kilian, W.H. (2001): Respons of soil phosphorus content, growth and yield of wheat to long-term phosphorus fertilization in a conventional cropping system. – Nutrient Cycling in Agroecosystems 61: 283-292.
[17] Piotrowska, A., Wilczewski, E. (2012): Effects of catch crops cultivated for green manure and mineral nitrogen fertilization on soil enzyme activities and chemical properties. – Geoderma 189-190: 72-80.
[18] Republic Hydrometeorological Service of Serbia (1998-2017): Meteorological Yearbook-Climatological data. – Republic Hydrometeorological Service of Serbia. – http://www.hidmet.gov.rs/ciril/meteorologija/klimatologija_godisnjaci.php (accessed on 20th June 2019).
[19] Richards, J.R., Zhang, H., Schroder, J.L., Hattey, J.A., Raun, W.R., Payton, M.E. (2011): Micronutrient availability as affected by the long-term application of phosphorus fertilizer and organic amendments. – Soil Science Society of America Journal 75: 927-939.
[20] Rutkowska, B., Szulc, W., Labetowicz, J. (2009): Influence of soil fertilization on concentracion of microelements in soil solution of sandy soil. – Journal of Elementology 14: 349-355.
[21] Saleque, M.A., Naher, U.A., Islam, A., Pathan, A.B.M.B.U., Hossain, A.T.M.S., Meisner, C.A. (2004): Inorganic and organic phosphorus fertilizer effects on the phosphorus fractionation in wetland rice soils. – Soil Science Society of America Journal 68: 1635-1644.
[22] Suwara, I., Pawlak-Zareba, K., Gozdowski, D., Perzanowska, A. (2016): Physical properties of soil after 54 years of long-term fertilization and crop rotation. – Plant, Soil and Environment 62: 389-394.
[23] Thakur, R., Kauraw, D.L., Singh, M. (2011): Profile Distribution of Micronutrient Cations in a Vertisol as Influenced by Long-term Application of Manure and Fertilizers. – Indian Society of Soil Science 59: 239-244.
[24] Undurraga, P., Zagal, E., Sepúlveda, G., Valderrama, N. (2009): Dissolved organic carbon and nitrogen in Andisol for six crop rotations with different soil management intensity. – Chilean Journal of Agricultural Research 69: 445-454.
[25] Walter, H., Harnickell, E., Mueller Domboi, D. (1975): Climate-Diagram Maps of the Individual Continents and the Ecological Climatic Regions of the Earth. – Springer-Verlag, Berlin
[26] Wei, X., Hao, M., Shao, M., Gale, W.J. (2006): Changes in soil properties and the availability of soil micronutrients after 18 years of cropping and fertilization. – Soil and Tillage Research 91: 120-130.

http://www.aloki.hu ● ISSN 1589 1623 (Print) ● ISSN 1785 0037 (Online)
DOI: http://dx.doi.org/10.15666/aeer/1705_1238512396

[27] Yan, L., Wang, C., Feng, G., Gao, Q., Zhang, J., Wei, D. (2019): Effect of mineral fertilizers on fungi communities in a Mollisol of Northeast China. – Applied Ecology and Environmental Research 17: 7421-7429.
[28] Zhang, J.B., Zhu, T.B., Cai, Z.C., Qin, S.W., Müller, C. (2012): Effects of long-term repeated mineral and organic fertilizer applications on soil nitrogen transformations. – European Journal of Soil Science 63: 75-85.
[29] Zhong, W., Gu, T., Wang, W., Zhang, B., Lin, X., Huang, Q., Shen, W. (2010): The effects of mineral fertilizer and organic manure on soil microbial community and diversity. – Plant and Soil 326: 511-522.

http://www.aloki.hu ● ISSN 1589 1623 (Print) ● ISSN 1785 0037 (Online)
DOI: http://dx.doi.org/10.15666/aeer/1705_1238512396

EFFECT OF METEOROLOGY AND SOIL FERTILITY ON DIRECT-SEEDED RICE (*ORYZA SATIVA* L.) PERFORMANCE IN CENTRAL CHINA

JIANG, S. C.[1,2] – WANG, J. M.[1,2] – LUO, H. W.[3] – XIE, Y. M.[4] – FENG, D. H.[1] – ZHOU, L.[4] – SHI, L.[1] – CHEN, H.[4] – XU, Y. Y.[1] – WANG, M.[1] – XING, D. Y.[1,2*]

[1]*College of Agriculture, Yangtze University, 434025 Jingzhou, PR China*

[2]*Hubei Cooperative Innovation Center for Major Food Crops, 434025 Jingzhou, PR China*

[3]*Department of Crop Science and Technology, College of Agriculture, South China Agricultural University, Guangzhou 510642, PR China*

[4]*National Quality Supervision and Testing Center for Selenium Products 445000 Enshi, PR China*

[#]*These authors have contributed equally to this work*

[*]*Corresponding author*
e-mail: xingdy_2006@126.com

(Received 9th May 2019; accepted 16th Jul 2019)

Abstract. The aim of this study was to study the effect of meteorology and soil fertility on direct-seeded rice growing period and yield formation. A two year field experiment was conducted with six rice varieties (*Fengliangyou 2 (FYL-2), Fengliangyouxiang-1 (FLYX-1), Liangyou 168 (LY-168), Guofeng-1 (GF-1), Quanyou-801 (QY-801)* and *Japonica Rice-107 (WD-107)*) in Central China during 2017 and 2018. Two soil fertilities (high fertility and low fertility) were texted in present study. The result showed that the difference in temperature and sunshine hours during the growth periods between 2017 and 2018 induced the difference in growing period and grain yield. On the other hand, compared to low soil fertility, high soil fertility significantly increased grain yield of direct seeded rice by promoting panicle number and grain number. The highest yield was recorded in *QY-801* in both years and both soil fertilities, Quanyou-801 might be the most suitable variety for direct-seeded rice planting in Central China.
Keywords: *soil condition, yield, yield component, path analysis, fertilization method*

Introduction

As the main crop in China, rice is the first in terms of planting area and yield, thus, ensuring a stable increase in rice production is the basic condition of Chinese food security (Chen et al., 2016). As far as seedling raising methods are concerned, rice cultivation can be divided into direct seeding cultivation and transplanting cultivation. Compared with traditionally transplanted rice production system, the technology of direct-seed rice has the advantages of labor-saving, rice seedling field-saving, short growth period, high yield and high efficiency, and it is more suitable for large-scale cultivation and plays an important role in the process of agricultural mechanization in China (Pan et al., 2017). Direct-seeded rice is characterized by continuous growth, low tiller node position, rapid growth process, few leaves, rapid population formation and large scale (Hu et al., 2019). Its photosynthetic capacity is high in the early stage, low in the middle and late stages, and its yield formation is characterized by more panicles,

http://www.aloki.hu ● ISSN 1589 1623 (Print) ● ISSN 1785 0037 (Online)
DOI: http://dx.doi.org/10.15666/aeer/1705_1239712406

smaller panicle type, and lower grain filling and setting level (Wang et al., 2018; Du et al., 2019). Normally, the yield of direct-seeded rice is not only affected by its own genetic conditions and acquired crop management, but also influenced by the environment of paddy field.

Meteorology and soil are the main influencing factors for rice growth and development. Some previous studies showed the influence of climate on rice performance. For example, the study of Mo (2017) found that temperature fluctuations at critical growth stages of rice may cause crop yield loss, shifts in crop growth periods as well as in sowing and harvesting times. Kong (2017) demonstrated high temperature during the grain filling stage not only reduced the fragrant rice yield, but also affected grain quality. Rao (1988) even obtained the correlations between weather parameters and the biomass of rice. As far as soil condition is concerned, there are regional differences in soil conditions in China and the spatial variation is small (Sun et al., 2008). Tang (2009) compares the influence of soil fertility on three major food crops and finds the soil contribution rate to rice production and basic yield. Seyfferth (2014) investigated the effect of arsenic concentrations in soil on major rice-growing regions in Cambodia. Furthermore, there is a significant difference in fertilizer contribution rate, basic soil contribution rate and yield when the same rice genotype grows under different soil conditions (Zou et al., 2015). However, there was no much study about environmental effect on direct-seeded rice performance reported.

Thus, present study was conducted in Hubei province (major rice producing province in Central China) in order to study the effect of different soil fertility and meteorology on direct-seeded rice performance in different rice genotypes.

Materials and methods

Experimental design and crop management

Two years experiment was conducted in Taihu Farm, Jingzhou City during 2017 and 2018 (longitude 30°34'57, dimension 112°04'78). Six rice varieties were used in present study: *Fengliangyou 2 (FYL-2), Fengliangyouxiang-1 (FLYX-1), Liangyou 168 (LY-168), Guofeng-1 (GF-1), Quanyou-801 (QY-801) and Japonica Rice-107 (WD-107)*, which are provided by Jingzhou Fulongxing Seed Industry Co., Ltd. The rice seeds were sowed into experiment fields on June 20, 2017 and 2018. Before sowing, the seeds were soaked in water for 24 h, germinated in manual climatic boxes for another 10 h (33°C), then shade-dried. Pre-germinated seeds of six rice genotypes were hill-seeded with direct-seeded machine into two different fertility soils at a space of 25 × 15 cm while each hill was planted with 3–5 seeds. The soil fertilities were shown in *Table 1*.

The treatments were arranged in randomized complete block design (RCBD) in triplicate with net plot size of 12 m^2. The temperature and sunshine hours during the experiment were shown in *Figure 1*.

Nitrogen fertilizer was applied to the field in the form of urea 1 day before sowing, rice 3 leaf stage and rice booting stage according to the ratio of 6:2:2. The total amount was N 134.60 kg hm^{-2}, and the phosphate fertilizer passed the superphosphate one day before sowing. The form is applied to the field at one time, the total dosage is P_2O_5 79 kg hm^{-2}, and the potassium fertilizer is applied to the field in the form of potassium chloride in the ratio of 7:3, 1 day before sowing and rice booting stage, the total dosage is K_2O 97 kg hm^{-2}. Fertilization management for two years is exactly the same. The

http://www.aloki.hu ● ISSN 1589 1623 (Print) ● ISSN 1785 0037 (Online)
DOI: http://dx.doi.org/10.15666/aeer/1705_1239712406

field management refers to the local rice high-yield management requirements, timely drying the fields, and doing pest control and weed control.

Table 1. *The fertility from two soil conditions*

	Total nitrogen (g kg^{-1})	**Total phosphorus** (g kg^{-1})	**Total potassium** (g kg^{-1})	**Available nitrogen** (mg kg^{-1})	**Available phosphorus** (mg kg^{-1})	**Available potassium** (mg kg^{-1})	**Organic matter** (g kg^{-1})	**PH**
Low	1.99	0.99	13.55	87.21	38.43	129.23	17.80	5.56
High	2.78	1.08	14.69	151.63	28.41	209.10	25.86	5.45

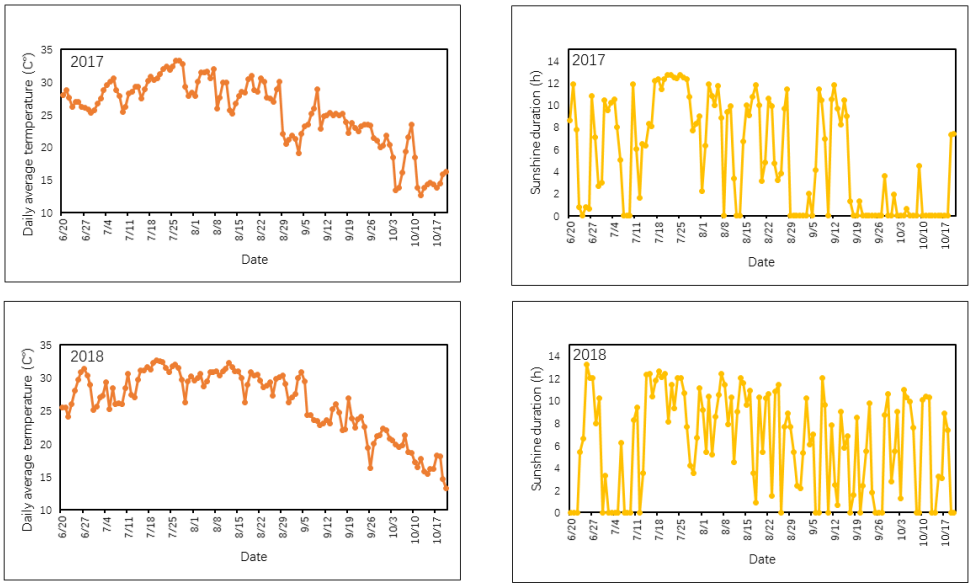

Figure 1. *The air temperature and sunshine duration during the experiment*

Water managements were followed as adopted by local farmers. No standing water was kept in the field from sowing to the three-leaf stage of rice, subsequently, the field was reflooded to about 3 cm water depth until the end of the tillering stage. Then, water was drained for about 7 days to control the production of non-productive tillers. At the following stages, water layer at soil surface was maintenance at 5 cm until grain filling stage. All other agronomic practices i.e., pest and diseases management, and weed control were the same in all treatments by following the guidelines and standards recommended by the province.

Determination of rice yield and growth period

After the direct-seeding, the three-leaf stage, booting stage, heading stage, flowering stage and maturity stage of rice were recorded. At maturity, the rice grains were harvested from ten-unit sampling area (10.00 m^2) in each plot and then threshed by machine. The harvested grains were sundried by a small thresher (150A, Maizhe, Hangzhou, China) and dried (101-0A, Keheng, Shanghai, China), then and weighed to estimate grain yield. Thirty hills of rice from different locations in each plot were sampled for estimating the average effective panicles number per hill. Six hills representative plants were taken for estimation of the yield related traits.

http://www.aloki.hu ● ISSN 1589 1623 (Print) ● ISSN 1785 0037 (Online)
DOI: http://dx.doi.org/10.15666/aeer/1705_1239712406

Statistical analysis

Data were analyzed by using statistical software by ANOVA (SPSS, 21.0) while differences amongst means were separated by using least significant difference (LSD) test at 5% probability level. Graphical representation was conducted via Sigma Plot 14.0 (Systat Software Inc., California, USA).

Results

Growth period

The growth process of rice was shown in *Table 2*. It could be observed the growth period of all varieties is within 130 days, of which the growth period of 2018 is in the range of 113-125 days, and the whole growth period of *FLY-2* and *WD-107* under low soil fertility was 1 day longer than high fertility. However, there was no remarkable difference between two soil fertility conditions in other rice varieties.

Table 2. *Fertility progress of various varieties in 2017 and 2018*

Variety		2017					2018				
		SS-TI	**TI-PI**	**PI-HD**	**HD-MA**	**AA-MA**	**SS-TIa**	**TI-PI**	**PI-HD**	**HD-MA**	**AA-MA**
High	*GF-1*	20	36	20	39	115	20	35	19	39	113
	FLY-2	25	42	22	40	129	25	40	20	39	124
	WD-107	22	40	22	40	124	22	38	21	40	121
	LY-168	20	37	20	39	116	20	36	19	39	114
	FLYX-1	23	37	20	39	119	23	36	19	39	117
	QY-801	24	39	22	40	125	24	38	21	40	123
Low	*GF-1*	20	37	20	39	116	20	35	19	39	113
	FLY-2	25	44	21	40	130	25	41	20	39	125
	WD-107	22	41	22	40	125	22	39	21	40	122
	LY-168	20	37	20	39	116	20	36	19	39	114
	FLYX-1	23	37	20	39	119	23	36	19	39	117
	QY-801	24	39	22	40	125	24	38	21	40	123

Three-leaf stage (SS-TI): time from seeding to trifoliate; booting stage (SS-PI): time from tillering to booting stage; heading period (PI-HD): time from the end of the booting to the heading; maturity: time from the head to maturity; total growth period: the time from the start of sowing to maturity. The same below

The growth period in 2017 ranged between 115-130 days. The entire growth periods of *GF-1, FLY-2, WD-107* under low soil fertility were 1 more day than the high fertility, whilst there was no significant difference observed between different soil fertility among the other varieties. Moreover, the growth period in 2017 is 2 to 5 days older than 2018. The growth period of *FLY-2* in 2017 is 5 days longer than 2018 while other varieties were 2 to 3 days longer.

Grain yield and its related trails

As shown in *Table 3*, the yield of direct-seeded rice varies among years, soil fertilities and genotype. Compared to low soil fertility, high soil fertility remarkably increased the rice yield by 6.52% - 12.22%. The increment could be explained by the improvement in the panicle number. Compared with low soil fertility, the number of

http://www.aloki.hu ● ISSN 1589 1623 (Print) ● ISSN 1785 0037 (Online)
DOI: http://dx.doi.org/10.15666/aeer/1705_1239712406

effective panicles increased by 0.56% - 8.51% due to high soil fertility. Moreover, higher grain number per panicles were recorded in high soil fertility than low soil fertility for *LY-168, FLYX-1, QY-801* in both 2017 and 2018. On the other hand, compared to 2017, lower seed-setting rates were recorded in 2018 for *GF-1, LY-168, FLYX-1*.

Table 3. *Effect of different soil fertility on rice yield and related trails*

Year	Soil fertility	Variety	Panicle number (10^4 ha^{-1})	Grain number per panicle	Seed-setting rate (%)	1000-grain weight (g)	Grain yield (kg ha^{-1})
2017	Low	GF-1	201.5b	182.6a	86.4a	27.7bc	7837.0a
		FLY-2	205.4ab	187.0a	83.1ab	27.3c	7589.4b
		WD-107	217.3a	181.3a	80.0b	28.1bc	7388.6d
		LY-168	207.4ab	173.9a	80.1b	29.6a	7918.2a
		FLYX-1	210.1ab	173.8a	81.90b	27.4c	7496.9c
		QY-801	199.7ab	203.9a	83.0ab	28.4b	7940.4a
		Mean	**207.0**	**183.7**	**82.4**	**28.1**	**7695**
	High	GF-1	214.3b	182.9b	84.4a	28.5ab	8584.0a
		FLY-2	225.6ab	184.9b	82.8ab	28.4ab	8468.3ab
		WD-107	232.8a	187.1b	81.2ab	28.0b	8404.2b
		LY-168	220.5ab	198.2ab	79.9b	28.8a	8472.0ab
		FLYX-1	213.4b	198.8ab	84.9a	27.8b	8413.6ab
		QY-801	207.0b	233.0a	81.7ab	28.9a	8553.4a
		Mean	**219.0**	**197.5**	**82.5**	**28.4**	**8399.2**
2018	Low	GF-1	208.6a	182.4a	80.9bc	27.4c	7567.1b
		FLY-2	202.8a	174.2ab	84.0a	28.5b	7638.5b
		WD-107	222.3a	165.0b	79.9cd	27.6c	7466.6c
		LY-168	215.4a	175.6ab	75.5d	28.3bc	7399.6cd
		FLYX-1	211.7a	173.4ab	78.9cd	28.5b	7363.6d
		QY-801	205.5a	176.8ab	84.0a	30.7a	8011.4a
		Mean	**211**	**174.6**	**80.5**	**28.5**	**7574.5**
	High	GF-1	220.6a	183.9ab	82.8bc	28.2b	8409.9b
		FLY-2	219.7a	173.8b	83.4ab	29.7a	8505.4a
		WD-107	229.9a	166.4c	80.3bc	28.4b	8425.8b
		LY-168	228.5a	182.8b	78.0c	27.8b	8114.5d
		FLYX-1	212.9a	178.7b	79.3c	28.2b	8263.1c
		QY-801	212.6a	199.2a	82.2a	30.8a	8534.2a
		Mean	**224.9**	**180.8**	**81.0**	**28.9**	**8375.5**
Analysis of Variance	Soil fertility (F)		**	*	*	**	**
	Varieties (V)		**	**	**	**	**
	Year (Y)		ns	*	**	*	**
	F × V		**	*	ns	ns	*
	F × Y		ns	ns	ns	ns	ns
	V × Y		ns	ns	ns	ns	ns
	F × V × Y		ns	ns	ns	ns	ns

The same letter indicates that the variety is not significantly different under the LSD (0.05) method at the same place and year, and the same letter is reversed. The total line represents a comparison of differences between different fertility. The same below

Correlation analysis and path analysis

The correlation analysis between yield structure and yield was shown in *Table 4*. For low soil fertility, the effective panicle per had a negative significant correlation with both seed setting rate and grain weight whilst there exited a significant positive correlation between seed setting rate and grain yield. For high soil fertility, there exited a significant negative correlation between grain number and effective panicle whilst the

http://www.aloki.hu ● ISSN 1589 1623 (Print) ● ISSN 1785 0037 (Online)
DOI: http://dx.doi.org/10.15666/aeer/1705_1239712406

grain yield had a significant positive correlation with both seed setting rate and 1000-grain yield.

The path analysis of yield structure and yield was shown in *Table 5*. The order of the effects of the two fertility on yield is 1000-grain weight > seed setting rate > effective panicle per unit area > number per panicle. The effective panicle number per unit area under low fertility had a high negative impact on yield through yield (-0.0676), with a high positive impact on yield through 1000-grain weight (0.0452), and the effective panicle number per unit area under high fertility through seed set rate (-0.0141) and 1000-grain weight (-0.0380) had a high negative impact on yield. The seed setting rate under two fertility conditions had a high positive impact on yield through 1000-grain weight.

Table 4. *Correlation between yield component factors and yield*

	Low					High				
	X_1	X_2	X_3	X_4	Y	X_1	X_2	X_3	X_4	Y
X_1	1					1				
X_2	-0.029	1				-0.610*	1			
X_3	-0.731**	0.3491	1			-0.390	0.123	1		
X_4	-0.209	-0.100	0.043	1		-0.384	0.192	0.259	1	
Y	-0.726**	0.413	0.631*	0.593*	1	-0.416	0.343	0.707**	0.557**	1

X1: effective panicle per unit area (plant/hm2); X2: number of grains per panicle; X3: seed setting rate; X4: 1000-grain weight; Y: grain yield (kg ha^{-1}) the same.
* represents a significant correlation at the 0.05 level, and ** represents a very significant correlation at the 0.01 level

Table 5. *Path analysis of yield components and yield*

		Direct effect	**Indirect effect**				
			Total	→X_1	→X_2	→X_3	→X_4
Low	X_1	0.074	-0.0239		-0.0015	-0.0676	0.0452
	X_2	0.061	-0.0184	-0.0018		-0.0232	0.0066
	X_3	0.227	0.0024	-0.0221	-0.0062		0.0307
	X_4	0.234	0.0171	-0.0143	0.0017	0.0297	
High	X_1	0.052	-0.0517		0.0004	-0.0141	-0.0380
	X_2	-0.009	0.0405	-0.0024		0.0159	0.0270
	X_3	0.113	0.0491	-0.0065	-0.0013		0.0569
	X_4	0.239	0.0176	-0.0083	-0.0010	0.0269	

Discussion

Present study investigated the effect of climate and soil fertility on direct-seeded rice yield and growing period. There are many factors which could affect the rice growing period such as climate, variety and cultivation management. Early study revealed a significant influence of water stress on growing period for rainfed lowland rice (Inthavong et al., 2011). Present study showed that the growth period of direct-seeded rice in 2017 was longer 2 to 5 days than 2018, which may attribute to the lower average daily temperature in 2017. This result agreed with the study of Fulu et al. (2013) who demonstrated that the increase in temperature will lead to the advancement of rice phenology and the shortening of growth period. The difference in growth period between varieties was large and it might be related to the difference in rice genotypes. However, there was no remarkable difference between two soil fertilities in rice

http://www.aloki.hu ● ISSN 1589 1623 (Print) ● ISSN 1785 0037 (Online)
DOI: http://dx.doi.org/10.15666/aeer/1705_1239712406

growing period and thus the growth period of direct-seeded rice might be mainly affected by climate condition and rice genotypes.

As far as yield formation was concerned, both soil fertility and meteorology had influences on direct-seeded rice yield in present study. The grain yield of GF-1, LY-168 and FLYX-1 in 2018 was significantly lower than 2017 and it could be explained by the decrement in seed-setting rate. Further reason might be related to the higher temperature of the flowering stage in 2017. Previous study already evidenced that heat stress could induce rice spikelet degeneration (Zhang et al., 2017). The study of Tang et al. (2018) also revealed that high temperature during the early grain filling stage could reduce rice yield by affecting the photosynthesis and antioxidant capacity. Furthermore, the study of Xuan et al. (2015) showed that average temperature at the flowering stage is higher than 30°C will reduce the rice seed setting rate. Moreover, we observed that the panicle number of *GF-1, LY-168* and *QY-801* in 2018 was higher than 2017. It might relate to the higher sunshine hour in 2018 during the experiment. This result was consistent with the research of Liu et al. (2013) who demonstrated there was a correlation between sunshine hours and rice productivity. On the other hand, present study showed that soil fertility greatly affected the yield formation of direct-seeded rice. Soil fertility is an important indicator of soil fertility. It is a measure of the ability of soil to provide various nutrients needed for crop growth and it is also the comprehensive expression of various basic properties of soil, the most essential characteristic of soil which is different from parent material and other natural bodies, and the material basis of soil as natural resources and agricultural means of production (Rahman and Parkinson, 2007). Compared with low soil fertility, the grain yield of all rice varieties increased due to high soil fertility and the increment was attributed to the enhancement in grain number and panicle number. It indicated that the rice plant could develop more effective tillers under high fertility conditions. Our result was consistent with early study (Fan et al., 2016) which indicated that higher soil fertility could improve rice yield and its related trail. Our result also agreed with the investigation of Yadivinder et al. (2004) who indicated that there was a correlation between rice yield and soil fertility. Early study also evidenced the benefits of improved soil fertility on irrigated rice performance (Haefele et al., 2000). Furthermore, the study of Huang et al. (2010) showed that A. bisporus residues return could induce positive regulation in soil nutrients, soil enzymatic activities, N use efficiency and crop yields as organic manure in a paddy soil.

Combined with correlation analysis and path analysis, it can be found that the 1000-grain weight is a factor which had the greatest impact on grain yield and is different from previous studies (Mirza et al., 1976) which showed that there was no significant correlation between grain yield and grain weight. The source of the difference was mainly caused by different varieties and cultivation management. Present study showed that soil fertility affected direct seeded rice yield by influencing the panicle number and grain number, however, the path analysis in this study divided two soil condition so that the difference in soil fertility was ignored. Therefore, the constituent factor that had the greatest impact on yield was not the panicle number and grain number. The effective panicle number under low fertility had a high negative impact on yield through the seed setting rate whilst the 1000-grain weight had a high positive impact on yield. Under high fertility, the number of effective panicles had a negative effect on the yield through seed setting rate and 1000-grain weight, which was related to the yield potential of rice. The light energy and the absorbed fertility are limited in the limited growth time of rice so the yield potential is limited (Du et al., 2018). Hence, the yield components are

http://www.aloki.hu ● ISSN 1589 1623 (Print) ● ISSN 1785 0037 (Online)
DOI: http://dx.doi.org/10.15666/aeer/1705_1239712406

generally negatively correlated. However, the number of effective panicles per unit area under low fertility didn't reach the highest level in present study, and the yield potential was not fully realized, so the yield could be increased by other yield components. The seed-setting rate had a high positive impact on yield through 1000-grain weight, indicating that the rice has not reached the rice yield potential level in the late growth stage, and rice self-regulation by strengthening individual growth may attribute to insufficient fertility in the later stage (Ren et al., 2017).

Conclusion

Present study showed that the growing period of direct-seed rice was mainly affected by climate and genotypes. The soil fertility, meteorology and genotypes all had impact on yield formation of direct-seeded rice. The soil fertility influenced the grain yield by affecting the panicle number and grain number. was affected by Different soil fertility affected grain yield and related trail significantly. In addition, considered the highest yield was recorded in *QY-801* in both years and both soil fertilities, Quanyou-801 might be the most suitable variety for direct-seeded rice planting in Central China. In order to revealed the mechanism of how meteorology and soil fertility affect the growth and development of rice, more study should be conducted at molecular and physiological level.

Acknowledgements. This study was supported by National Key Research and Development Program of China (2017YFD0301403). The authors declare no conflict of interests.

REFERENCES

[1] Chen, S., Xu, C., Yan, J., Zhang, X., Zhang, X., Wang, D. (2016): The influence of the type of crop residue on soil organic carbon fractions: An 11-year field study of rice-based cropping systems in southeast China. – Agriculture ecosystems & Environment 223: 261-269.

[2] Du, B., Luo, H. W., He, L. X., Zheng, A. X., Chen, Y. L., Zhang, T. T., Wang, Z. M., Hu, L., Tang, X. R. (2018): Deep fertilizer placement improves rice growth and yield in zero tillage. – Applied Ecology and Environmental Research 16: 8045-8054.

[3] Du, B., Luo, H. W., Liu, C., Lei, C. Y., Jiang, S. C., Lou, Y. G., Xu, Y. Y., Wang, M., Shi, L., Xing, D. Y. (2019): Effects of different water management methods on seeding rate, phenological and yielding properties of different rice cultivars (Oryza sativa L.). – Applied Ecology and Environmental Research 17: 4269-4279.

[4] Fan, L. H., Shan-Shan, X. U., Hou, P. F., Xue, L. H., Gang-Hua, L. I., Ding, Y. F., Yang, L. Z. (2016): Effect of Different Ratios of Basal to Tiller Nitrogen on Rice Yield and Nitrogen Utilization Under Different Soil Fertility. – Scientia Agricultura Sinica.

[5] Fulu, T., Zhao, Z., Wenjiao, S., Yujie, L., Dengpan, X., Shuai, Z., Zhu, Z., Meng, W., Fengshan, L. (2013): Single rice growth period was prolonged by cultivars shifts, but yield was damaged by climate change during 1981-2009 in China, and late rice was just opposite. – Glob Chang Biol 19: 3200-3209.

[6] Haefele, S. M., Johnson, D. E., Diallo, S., Wopereis, M. C. S., Janin, I. (2000): Improved soil fertility and weed management is profitable for irrigated rice farmers in Sahelian West Africa. – Field Crops Research 66: 101-113.

[7] Hu, L., Du, P., Luo, H. W., Cheng, S. R., Wu, T. Y., He, J., Liu, Y. F., Meng, S. B., Chen, B. Y., Wang, Z. M., Tang, X. R. (2019): The effect of different cultivation methods

http://www.aloki.hu ● ISSN 1589 1623 (Print) ● ISSN 1785 0037 (Online)
DOI: http://dx.doi.org/10.15666/aeer/1705_1239712406

on rice growth and development. – Applied Ecology and Environmental Research 17: 3867-3875.

[8] Huang, C., Deng, L., Gao, X., Zhang, S., Luo, T., Ren, Q. (2010): Effects of fungal residues return on soil enzymatic activities and fertility dynamics in a paddy soil under a rice-wheat rotation in Chengdu Plain. – Soil & Tillage research 108: 16-23.

[9] Inthavong, T., Tsubo, M., Fukai, S. (2011): A water balance model for characterization of length of growing period and water stress development for rainfed lowland rice. – Field crops research 121: 291-301.

[10] Kong, L., Ashraf, U., Cheng, S., Rao, G., Mo, Z., Tian, H., Pan, S., Tang, X. (2017): Short-term water management at early filling stage improves early-season rice performance under high temperature stress in South China. – European journal of agronomy 90: 117-126.

[11] Liu, L., Zhu, Y., Tang, L., Cao, W., Wang, E. (2013): Impacts of climate changes, soil nutrients, variety types and management practices on rice yield in East China: A case study in the Taihu region. – Field crops research 149: 40-48.

[12] Mirza, M. J., Faiz, F. A., Mazid, A. (1976): Correlation studies and path analysis of plant height, yield and yield components in rice (Oryza sativa L.). – Nature 262: 17.

[13] Mo, Z. W., Pan, S. G., Ashraf, U., Kanu, A. S., Li, W., Wang, Z. M., Duan, M. Y., Tian, H., Kargbo, M. B., Tang, X. R. (2017): Local climate affects growth and grain productivity of precision hill-direct-seeded rice in South China. – Applied Ecology and Environmental Research 15: 113-125.

[14] Pan, S., Wen, X., Wang, Z., Ashraf, U., Tian, H., Duan, M., Mo, Z., Fan, P., Tang, X. (2017): Benefits of mechanized deep placement of nitrogen fertilizer in direct-seeded rice in South China. – Field Crops Research 203: 139-149.

[15] Rahman, S., Parkinson, R. J. (2007): Productivity and soil fertility relationships in rice production systems, Bangladesh. – Agricultural systems 92: 318-333.

[16] Rao, A. S., Alexander, D. (1988): Prediction of evapotranspiration and grain yield of rice (Oryza sativa L. cv Thriveni) in a humid tropical climate. – International Journal of Biometeorology 32: 81-86.

[17] Ren, Y., Ashraf, U., He, L. X., Mo, Z. W., Wang, F., Wan, X. C., Kong, H., Ran, X. L., Tang, X. R. (2017): Irrigation and nitrogen management practices affect grain yield and 2-ACETYL-1-PYRROLINE content in aromatic rice. – Applied Ecology and Environmental Research 15: 1447-1460.

[18] Seyfferth, A. L., McCurdy, S., Schaefer, M. V., Fendorf, S. (2014): Arsenic Concentrations in Paddy Soil and Rice and Health Implications for Major Rice-Growing Regions of Cambodia. – Environmental science & technology 48: 4699-4706.

[19] Sun, B., Pan, X., Wang, D., Han, X., Zhang, Y., Hao, M., Chen, X. (2008): Effect of Nutrient Balance on Spatial and Temporal Change of Soil Fertility in Different Agriculture Area in China. – Advances in Earth Science 23: 1201-1208.

[20] Tang, S., Zhang, H., Li, L., Liu, X., Chen, L., Chen, W., Ding, Y. (2018): Exogenous spermidine enhances the photosynthetic and antioxidant capacity of rice under heat stress during early grain-filling period. – Functional plant biology 45: 911-921.

[21] Wang, Z., Gu, D., Beebout, S. S., Zhang, H., Liu, L., Yang, J., Zhang, J. (2018): Effect of irrigation regime on grain yield, water productivity, and methane emissions in dry direct-seeded rice grown in raised beds with wheat straw incorporation. – Crop journal 6: 495-508.

[22] Xuan, S., Shi, C., Yang, L., Zhao, Y., Zhang, W., Cao, H., Xue, C. (2015): Prediction of the Natural Environmental High Temperature Influences on Mid-Season Rice Seed Setting Rate in the Middle-Lower Yangtze River Valley.

[23] Yadvinder-Singh, Bijay-Singh, Ladha, J. K., Khind, C. S., Gupta, R. K., Meelu, O. P., Pasuquin, E. (2004): Long-term effects, of organic inputs on yield and soil fertility in the rice-wheat rotation. – Soil Science Society of America Journal 68: 845-853.

http://www.aloki.hu ● ISSN 1589 1623 (Print) ● ISSN 1785 0037 (Online)
DOI: http://dx.doi.org/10.15666/aeer/1705_1239712406

[24] Yonghua, T. Y. H. S. (2009): Distribution Characteristics of the Percentage of Soil Fertility Contribution and Its Associated Basic Crop Yield in Mainland China. – Journal of Agro-Environment Science 5: 1070-1078. (In Chinese).
[25] Zhang, C. X., Feng, B. H., Chen, T. T., Zhang, X. F., Tao, L. X., Fu, G. F. (2017): Sugars, antioxidant enzymes and IAA mediate salicylic acid to prevent rice spikelet degeneration caused by heat stress. – Plant growth regulation 83: 313-323.
[26] Zou, Y. B., Xia, B., Peng, J., Xie, X. B., Huang, M. (2015): Discussion on the Theory and Methods for Determining the Target Yield in Rice Production. – Scientia Agricultura Sinica.

APPENDIX

Appendix 1. *Photo of the experiment*

http://www.aloki.hu ● ISSN 1589 1623 (Print) ● ISSN 1785 0037 (Online)
DOI: http://dx.doi.org/10.15666/aeer/1705_1239712406

THE EFFECT OF BIOSTIMULANTS DERIVED FROM VARIOUS MATERIALS ON THE YIELD AND SELECTED ORGANIC COMPONENTS OF ITALIAN RYE GRASS (*LOLIUM MULTIFLORUM* LAM.) AGAINST THE BACKGROUND OF NITROGEN REGIME

CIEPIELA, G. A. – GODLEWSKA, A.*

Institute of Health Sciences, Faculty of Natural Science, Siedlce University of Natural Sciences and Humanities, B. Prusa 12 st., 08-110 Siedlce, Poland
(ORCID number: G. A. Ciepiela - 0000-0002-9235-3000; A. Godlewska - 0000-0003-1553-0867)

**Corresponding author*
e-mail: godlewskaa@uph.edu.pl

(Received 9th May 2019; accepted 16th Jul 2019)

Abstract. The present work is an attempt to assess the effect of biostimulants derived from various materials on the yield and selected organic components in Italian rye grass against the background of nitrogen regime. A field experiment was arranged as a randomized subblock design (split-plot) in Poland in August 2013. The following factors were examined: type of biostimulant: Algex, Tytanit, Asahi SL and a control (no biostimulant addition); and nitrogen application rate: 0 (control); 120 and 180 kg ha^{-1}. The results reported here indicate that biostimulants applied in the study contributed to similar yield performance to plants fertilised with a 60 kg ha^{-1} lower nitrogen rate, the highest increase in yield (42.2%) being recorded for Algex-treated grass. An application of biostimulants beneficially affected Italian rye grass yield quality as it was followed by a significant increase in chlorophyll content in leaves as well as protein compounds and soluble carbohydrates in the dry matter of the test grass. The nitrogen rate of 120 and 180 kg ha^{-1} significantly increased Italian rye grass yields, chlorophyll content in plant leaves and protein compounds, the concentration of soluble carbohydrates being significantly lower in the dry matter of test plants.
Keywords: *grass, fertilisation, chlorophyll, protein compounds, soluble carbohydrates*

Introduction

Agriculture intensification has undoubtedly contributed to an increase in the effectiveness and efficiency of crop and animal production. Simultaneously, such farming relying on an application of high rates of mineral fertiliser and plant protection agents negatively influences soil effectiveness (Reguraman et al., 2019), and the quality of the final products. Moreover, it leads to natural environment degradation. In recent years, there has been an increase in the plant growth and frequency development regulator use frequency in crop production, also called biostimulants, in order to counteract intensive fertilisation, nitrogen application in particular. The products contain biologically active substances which affect metabolism and so make it possible to obtain higher plant efficiency (Kocira et al., 2015). On their own, biostimulants are not nutritional products but they increase nutrient uptake from soil (Brown and Saa, 2015). Growth stimulants are of either mineral or organic origins (Kocira et al., 2016) and are produced from algae and seaweed extracts (Algex), microorganisms, phytohormones as well as macro- and microelements (Tytanit, Asahi). An application of these products is safe for the environment (Tuhy et al., 2013) and may partly complement the influence of crop plant production chemicals, including mineral

http://www.aloki.hu ● ISSN 1589 1623 (Print) ● ISSN 1785 0037 (Online)
DOI: http://dx.doi.org/10.15666/aeer/1705_1240712418

fertilisation (Murawska et al., 2017). Relevant literature on the subject has demonstrated that individual biostimulants may have a different effect on yield quality and quantity, an increase in nutrient availability for plants, water retention ability, antioxidant content and chlorophyll production in plants (Khan et al., 2009; Sharma et al., 2014; Godlewska and Ciepiela, 2016a). Growth stimulants affect synthesis of natural plant hormones and an increase in their activity. According to research reports (Haider et al., 2012; Renuka et al., 2018), biostimulant application can also reduce abiotic and biotic stress of crop plants. Research has confirmed a positive effect of this type of products on crop plants, but it has also demonstrated that their effect is more dependent on crop plant species and cultivar than biostimulant rate (Sultana et al., 2005). Growth regulators are applied worldwide in vegetable and fruit production as well as cereals, oil seed rape and maize. However, there is still a paucity of reports on the efficiency of these products applied to fodder grasses constituting grassland established on ploughed land. Thus, the authors of the present work attempted to assess the effect of biostimulants derived from various materials on the yielding, chlorophyll content, protein content and simple sugars in *Lolium multiflorum* against the background of nitrogen regime.

Materials and methods

A field experiment was arranged as a randomized subblock design (split-plot) with three replicates at the Siedlce Experimental Unit of the University of Natural Sciences and Humanities in Poland (52.169° N, 22.280° E) in the second decade of August 2013. The plot area was 10 m^2. According to the Polish soil classification system (Systematics of Polish Soils, 2011), the soil used in the experiment was the culture soils with the hortisole type, developed from loamy sand. Based on the analysis performed at the Regional Chemical Station in Wesoła (*Table 1*). The following factors were examined:

- Type of biostimulant: Algex, Tytanit, Asahi SL and a control (no biostimulant addition)
- Nitrogen application rate: 0 (control); 120 and 180 kg· ha^{-1}

Table 1. *The chemical composition of soil*

pH in 1 n KCL	Content of soil				
	Humus (%)	Assimilable components (mg kg^{-1} of soil)			N – total (g kg^{-1} d.m. soil)
		$P_2O_4^-$	K^+	Mg^{2+}	
6.8	3.78	170	114	84	1.3

Algex is an extract of the sea alga *Ascophyllum nodosum* which contains vitamins, amino acids, phytohormones (auxins, cytokinins, gibberellins), polysaccharides, betaine as well as macro- and microelements such as N − 8%, P − 3.6%, K − 7%, B − 0.036%, Zn − 0.025%, Cu − 0.009%, Fe − 0.016%, Mn − 0.036% and Mo − 0.0036%. Algex is manufactured by Rosier, Moustier, Belgium.

Tytanit is produced by INTERMAG Ltd., Olkusz, Poland. Tytanit contains 8.5 g Ti per 1 dm^3 (0.8% m/m) in the form of Ti-ascorbate.

Asahi SL is produced by Arysta Life Science Ltd., Warsaw, Poland. The product contains the following phenolic compounds: sodium p-nitrophenolate − 0.3%, sodium o-nitrophenolate − 0.2% and sodium 5-nitroguaiacolate − 0.1%.

http://www.aloki.hu ● ISSN 1589 1623 (Print) ● ISSN 1785 0037 (Online)
DOI: http://dx.doi.org/10.15666/aeer/1705_1240712418

The sowing rate of *Lolium multiflorum* Lam. cv. Dukat was calculated based on the standards drawn up by IMUZ (the Institute for Land Reclamation and Grassland Farming) (Jankowski et al., 2005). Standard cultivation methods were applied in the experiment and, additionally, plants were fertilised with different biostimulants.

The grass sowing rate was 31 kg ha^{-1} (TWG - thousand-grain weight – 2.8 g, 11071429 kernels per hectare). In 2013, when seeds were sown, neither biostimulants nor nitrogen fertiliser was applied. In October 2013 only one cut was performed at the plant height of 6 cm. Over the study period (2014-2015), the cutting regime consisted of three harvests per year. Ammonium nitrate was applied three times per year. The total nitrogen amount was split into three equal rates which were applied before each cutting. P and K fertilisation was applied to all the plots. Phosphorus was applied once as triple superphosphate at the rate of 40 kg ha^{-1} P_2O_5 in the spring. The amount of potassium (160 kg ha^{-1} K_2O) was split into three equal rates and applied prior to each cutting as 60% potash salt. The biostimulants was sprayed as an aqueous solution. The spraying was performed before each cutting: the first application was three weeks before the first cutting, the second one two weeks after the first harvest and the last one three weeks after the second harvest. Biostimulant rates following each cut were applied as recommended by the manufacturer, that is thinned with water to obtain the volume of 400 dm^3: Algex − 6 dm^3 ha^{-1}, Tytanit − 0.4 dm^3 ha^{-1}, Asahi SL − 0.6 dm^3 ha^{-1}.

Leaf chlorophyll was determined using a Minolta Chlorophyll Meter SPAD-502. It measures the light absorption by leaves at the wavelength of 650 and 940 nm. The quotients of light absorption at the two wavelengths are unitless and are called SPAD values. They reflect the leaf greenness index which corresponds to the total chlorophyll content (Blackmer and Schepers, 1994). Measurements were taken in each plot on 10 randomly selected grass leaves (top leaves) the day before harvest.

During harvest of each cut, green matter from each plot (whole area, that is 10 m^2) was weighed to determine the yield, and 0.5 kg green matter samples of grass were taken to determine the drying-up coefficient and to carry out chemical analyses. The samples were left to dry in a ventilated room. Airy dry matter was weighed (to determine dry matter yield per plot) and was then shredded and ground. The obtained material was subjected to chemical analysis to determine dry matter (by determining moisture content), protein compounds, and soluble carbohydrates. The method of determination was near-infrared spectroscopy (NIRS) using a NIRFlex N-500 spectrometer and ready-to-use INGOT calibration applications.

Statistical analysis was conducted using the program STATISTICA StatSoft, Inc. (2011), STATISTICA (data analysis software system), version 10 (www.statsoft.com). Significance of differences between means was checked using the Tukey test at the significance level of $\alpha \leq 0.05$.

Meteorological conditions during the study period were changeable and precipitation was very unevenly distributed (*Table 2*). The mean air temperature in the 2015 growing season was by 2 degrees lower than the mean across 2006-2015. By contract, unusual precipitation shortages occurred in September 2014, April and August 2015.

Results and discussion

The results of the research demonstrated that all the biostimulants affected Italian rye grass yielding. Regardless of the study years and nitrogen rate (*Table 3*), significantly higher grass biomass yields were determined following an application of biostimulants

http://www.aloki.hu ● ISSN 1589 1623 (Print) ● ISSN 1785 0037 (Online)
DOI: http://dx.doi.org/10.15666/aeer/1705_1240712418

compared with control yields of grass dry matter. Algex, Tytanit and Asahi contributed to an increase in biomass yield, respectively by 42.2, 27.3 and 18.8%, on average, compared with control yields. An application of Tytanit and Asahi significantly increased plant dry matter yields compared with control (where no biostimulants had been used). However, in each study year and for all the nitrogen rates biomass yields of plants treated with these biostimulants were significantly lower compared with biomass yields harvested in Algex-treated plots. Many authors have confirmed a positive effect of these biostimulants on yield amount for various crop plants (Nerrisa et al., 2016; Godlewska and Ciepiela, 2016b; Kovacik et al., 2018; Whitted-Haag et al., 2014; Przybysz et al., 2014). However, Lola-Luz et al. (2013) reported different results of their studies. Following an application of *Ascophyllum nodosum* extract, they found no statistical increase in cabbage yield. Thus, it should be noted that the effect of biostimulants may be highly influenced by crop plant species (Michałek et al., 2018) and further investigation of this issue is warranted.

Italian rye grass is a short-lived species as have been demonstrated by results of this research. In the first study year, yields of this grass species were by 49.6% higher compared with the second year, the differences being statistically significant.

Nitrogen regime significantly increased yields of the grass. In both the study years, increasing nitrogen fertiliser rates contributed to a significant increase in Italian rye grass yields compared with control where no nitrogen had been applied. The highest increase in Italian rye grass yield (by 73.9%), compared with control, was recorded in the second study year after the rate of 180 kg N ha^{-1} had been applied.

An increase in nitrogen rate was followed by a significant increase in the dry matter of the grass in the control unit and the biostimulant-treated plots.

Dry matter yields (t ha^{-1}) for individual cuts as affected by nitrogen regime and biostimulant type are shown in *Table 4*. Regardless of the remaining factors, the highest Italian rye grass biomass yields were harvested with the second cut, which may have been associated with meteorological conditions (*Table 2*). The yields differed significantly from those harvested with the first and third cut.

Table 2. *Meteorological condition in years 2014-2015 by meteorological station in Siedlce*

Years	Means monthly air temperatures (°C)						Means in growing season (IV-IX) (°C)
	Month						
	IV	V	VI	VII	VIII	IX	
2014	9.7	13.7	15.1	20.4	17.8	13.7	15.1
2015	8.1	12.3	16.5	14.3	21.1	8.8	13.5
Mean of many years (2006-2015)	9.6	14.0	17.2	19.9	18.4	13.6	15.5
Years	**Monthly precipitation (mm)**						**Sum in season (IV-IX) (mm)**
	Month						
	IV	**V**	**VI**	**VII**	**VIII**	**IX**	
2014	39.5	79.3	50.3	62.5	66.3	26.7	324.6
2015	29.7	100.6	41.1	68.3	12.0	77.5	329.2
Mean of many years (2006-2015)	26.9	68.9	64.6	55.8	65.3	44.3	325.8

http://www.aloki.hu ● ISSN 1589 1623 (Print) ● ISSN 1785 0037 (Online)
DOI: http://dx.doi.org/10.15666/aeer/1705_1240712418

Table 3. *Dry matter yield of Italian rye grass (t ha^{-1}) (sum of three cuts)*

Year	Dose of N kg ha^{-1}	Biostimulant				Mean
		Without biostimulant (control)	Algex	Tytanit	Asahi SL	
2014	0	A 12.6 a	A 17.7 b	A 15.8 c	A 14.5 d	15.2 A
	120	B 17.4 a	B 22.4 b	B 20.2 c	B 18.7 d	19.7 B
	180	C 19.0 a	C 23.3 b	C 22.2 c	C 20.7 d	21.3 C
2015	0	A 5.6 a	A 10.8 b	A 9.7 c	A 9.1 c	8.8 A
	120	B 9.9 a	B 15.8 b	B 14.4 c	B 13.7 c	13.5 B
	180	C 12.4 a	C 18.9 b	C 15.4 c	C 14.6 c	15.3 C
2014	Mean	A 16.3 a	A 21.1 b	A 19.4 c	A 18.0 c	18.7 A
2015		B 9.3 a	B 15.2 b	B 13.2 c	B 12.5 c	12.5 B
Mean	0	A 9.1 a	A 14.3 b	A 12.8 c	A 11.8 c	12.0 A
	120	B 13.7 a	B 19.1 b	B 17.3 c	B 16.2 c	16.6 B
	180	C 15.7 a	C 21.1 b	C 18.8 c	C 17.7 c	18.3 C
Mean		12.8 a	18.2 b	16.3 c	15.2 c	15.6

Different lower-case letters within the same line indicate significant differences. Different uppercase letters indicate that the values in the column for individual factors (Dose N and Year) and their interaction differ significantly

Table 4. *The effect of the biostimulants on dry matter yield of Italian rye grass by cut and nitrogen fertilization (t ha^{-1}) (mean of two years)*

Cut	Dose of N kg ha^{-1}	Biostimulant				Mean
		Without biostimulant (control)	Algex	Tytanit	Asahi SL	
1	0	A 2.6 a	A 3.2 b	A 3.0 ab	A 2.9 ab	2.9 A
	120	B 4.2 a	B 5.4 b	B 5.3 b	B 4.6 ac	4.9 B
	180	B 4.3 a	C 6.7 b	B 5.7 c	C 5.3 c	5.5 C
2	0	A 4.3 a	A 6.6 b	A 5.9 c	A 5.4 d	5.6 A
	120	B 6.3 a	B 8.6 b	B 7.7 c	B 7.4 c	7.5 B
	180	C 7.1 a	B 8.9 b	C 8.3 c	C 8.0 c	8.1 C
3	0	A 2.3 a	A 4.4 b	A 3.9 c	A 3.5 c	3.5 A
	120	B 3.2 a	B 5.0 b	AB 4.4 c	B 4.2 c	4.2 B
	180	C 4.3 a	C 5.6 b	B 4.9 c	B 4.4 a	4.8 C
1	Mean	A 3.7 a	A 5.1 b	A 4.7 bc	A 4.3 c	4.4 A
2		B 5.9 a	B 8.0 b	B 7.3 c	B 6.9 c	7.0 B
3		A 3.3 a	A 5.0 b	A 4.4 c	A 4.0 c	4.2 A
Mean	0	A 3.1 a	A 4.7 b	A 4.3 bc	A 3.9 c	4.0 A
	120	B 4.6 a	B 6.3 b	B 5.8 c	B 5.4 c	5.5 B
	180	C 5.2 a	C 7.1 b	B 6.3 c	B 5.9 c	6.1 C
Mean		4.3 a	6.1 b	5.4 c	5.1 c	5.2

Different lower-case letters within the same line indicate significant differences. Different uppercase letters indicate that the values in the column for individual factors (Dose N and Cut) and their interaction differ significantly

http://www.aloki.hu ● ISSN 1589 1623 (Print) ● ISSN 1785 0037 (Online)
DOI: http://dx.doi.org/10.15666/aeer/1705_1240712418

Regardless of nitrogen regime, biostimulants significantly increased Italian rye grass yields. Moreover, compared with control, higher dry matter yields were recorded for Tytanit-treated plants harvested with the first cut in units without nitrogen fertilisation, and Asahi-sprayed grass harvested in plots without nitrogen fertilisation and fertilised with 120 kg N ha^{-1}, the differences being statistically insignificant. It should be mentioned that, following an application of biostimulants, similar yields were produced at a lower (by 60 kg ha^{-1}) nitrogen rate.

Nitrogen fertilisation at the rate of 120 and 180 kg ha^{-1} resulted in a significant increase in Italian rye grass yields harvested with all the cuts compared with the biomass of the non-fertilised control.

Increased nitrogen rates contributed to an increase in the dry matter yield of Italian ryegrass in all the plots treated with the biostimulants and in the control unit although not all the differences were statistically significant.

Chlorophyll content in Italian rye grass leaves harvested with individual cuts as affected by nitrogen regime and biostimulant application is presented in *Table 5*. Regardless of biostimulant use and nitrogen fertilisation, chlorophyll content in the leaves of the test grass fluctuated significantly during the growing season. Chlorophyll content was the lowest in the leaves of grass harvested with the first cut, it being the highest in the leaves of plants harvested with the third cut. Similar results were reported by Ciepiela and Godlewska (2015).

Table 5. *The effect of the biostimulants on content of chlorophyll in leaves of Italian rye grass (value of SPAD) by cut and nitrogen fertilization (mean of two years)*

Cut	Dose of N kg ha^{-1}	Biostimulant				Mean
		Without biostimulant (control)	Algex	Tytanit	Asahi SL	
1	0	A 35.0 a	A 36.5 ab	A 38.1 b	A 40.9 bc	37.6 A
	120	A 34.9 a	A 36.7 ab	A 38.6 b	A 42.3 c	38.1 A
	180	A 32.6 a	A 35.6 a	B 41.8 b	B 43.8 b	38.5 A
2	0	A 34.2 a	A 35.0 a	A 40.1 b	A 42.9 c	38.1 A
	120	A 33.9 a	B 40.0 b	A 40.1 bc	B 46.1 d	40.0 B
	180	B 41.1 a	C 42.2 ab	B 43.9 b	B 44.7 bc	43.0 C
3	0	A 36.7 a	A 38.4 a	A 40.2 b	A 42.6 c	39.5 A
	120	B 38.5 a	A 39.7 a	B 45.7 b	B 47.6 c	42.9 B
	180	B 38.8 a	B 42.4 b	B 45.2 c	B 46.1 c	43.1 B
Mean	0	A 35.3 a	A 36.6 a	A 39.5 b	A 42.1 c	38.4 A
	120	A 35.8 a	B 38.8 b	B 41.5 c	B 45.3 d	40.3 B
	180	B 37.5 a	B 40.1 b	C 43.6 c	B 45.0 d	41.5 B
1	Mean	A 34.2 a	A 36.3 a	A 39.5 b	A 42.3 c	38.1 A
2		B 36.4 a	B 39.1 b	B 41.4 c	B 44.6 d	40.4 B
3		C 38.0 a	B 40.2 b	C 43.7 c	B 45.4 d	41.8 C
Mean		36.2 a	38.5 b	41.5 c	44.1 d	40.1

Different lower-case letters within the same line indicate significant differences. Different uppercase letters indicate that the values in the column for individual factors (Dose N and Cut) and their interaction differ significantly

http://www.aloki.hu ● ISSN 1589 1623 (Print) ● ISSN 1785 0037 (Online)
DOI: http://dx.doi.org/10.15666/aeer/1705_1240712418

Regardless of the remaining factors, all the biostimulants applied in the experiment contributed to a significant increase in chlorophyll content in Italian rye grass leaves although their effect was not the same. Tytanit and Asahi significantly increased (by 14.6 and 21.8%, respectively) chlorophyll content in plant leaves compared with control grass which had not been treated with the biostimulants. A positive effect of biostimulants on chlorophyll amount in leaves has been confirmed by Kováčik et al. (2018), Radkowski (2013) who applied Tytanit, as well as by Borowski and Blamowski (2009) and Przybysz et al. (2014) who used Atonik (equivalent of Asahi). An application of Algex was also associated with an increase in chlorophyll content in grass leaves but the increase was barely 6.4% compared with control and it was insignificant. El-Miniawy et al. (2014) applied Algreen and observed an increase in chlorophyll content in strawberry leaves whereas Pacheco et al. (2019), who applied *Ascophyllum nodosum* extract, observed lower chlorophyll contents in *Achilleamille folium* L. leaves.

Analysis of the average chlorophyll content in Italian rye grass leaves revealed that the rate of 120 and 180 kg N ha^{-1} resulted in a significant increase in the amount of this pigment in the test grass leaves. Distribution of chlorophyll content in the leaves of plants harvested with individual cuts indicated that nitrogen regime had no significant effect on the characteristic tested for plants harvested with the first cut.

Increasing nitrogen rates significantly affected chlorophyll content in Italian ryegrass harvested in units treated with Tytanit. In the remaining plots, an increase in nitrogen rate contributed to an increase in chlorophyll content in the grass although the majority of the differences were statistically insignificant.

The concentration of protein compounds in the dry matter of Italian rye grass averaged 106.4 g kg^{-1} DM (*Table 6*) and was influenced by all the experimental factors. Regardless of the nitrogen regime and biostimulant application, the lowest amount of protein compounds was determined in grass harvested with the first cut, and the highest in the third cut, the differences being statistically significant.

Biostimulants tend to increase certain contents, for example protein content or sugars, affecting yield quality (Aydin et al., 2012; Kocira et al., 2017). In the study reported here, the average highest increase in the plant content of protein compounds following an application of Tytanit was 27.5% compared with control. Both Tytanit and Asahi significantly increased protein compounds in the dry matter of Italian rye grass harvested with all the cuts at each nitrogen rate. Also Algex had a positive effect on the amount of protein compounds in the test grass but the effect of an application of the biostimulant was frequently dependent on the cut and nitrogen rate. An application of this biostimulant resulted in a significant increase in protein compounds determined in grass harvested with the first and second cut in plots without nitrogen fertilisation, and with the third cut at all the nitrogen rates. There are research papers published worldwide which have confirmed a positive effect of the above-mentioned biostimulants on protein compounds in crop plants (Haroun et al., 2011; Ciepiela and Godlewska, 2015; Murawska et al., 2017; Hidangmayum and Sharma, 2017).

Nitrogen fertilisation significantly increased protein compounds in Italian rye grass dry matter. Their amount in plants harvested with all the cuts increased as increasing nitrogen rates were applied, the differences being statistically significant. Nitrogen applied at the rate of 120 and 180 kg ha^{-1} contributed to an increase in the dry matter content of protein compounds, the respective increases being 22.1 and 43.1%, compared with plants harvested in plots where no nitrogen had been applied.

http://www.aloki.hu ● ISSN 1589 1623 (Print) ● ISSN 1785 0037 (Online)
DOI: http://dx.doi.org/10.15666/aeer/1705_1240712418

Table 6. *The effect of the biostimulants on content of protein compounds in Italian rye grass by cut and nitrogen fertilization (g kg^{-1} DM) (mean of two years)*

Cut	Dose of N kg ha^{-1}	Biostimulant				Mean
		Without biostimulant (control)	Algex	Tytanit	Asahi SL	
1	0	A 59.2 a	A 91.7 b	A 79.2 c	A 76.1 c	76.6 A
	120	B 83.2 a	A 89.7 ac	B 124.0 b	B 94.1 c	97.8 B
	180	C 108.9 a	B 116.6 ab	B 123.4 b	C 127.8 bc	119.2 C
2	0	A 63.6 a	A 112.4 b	A 86.9 c	A 77.3 d	85.1 A
	120	B 90.2 a	B 94.4 a	B 127.6 b	B 103.7 c	104.0 B
	180	C 106.7 a	A 112.1 ab	C 115.4 b	C 141.1 c	118.8 C
3	0	A 66.4 a	A 129.8 b	A 107.1 c	A 98.8 d	100.5 A
	120	B 106.6 a	B 113.3 b	B 136.0 c	B 117.2 bd	118.3 B
	180	C 126.6 a	A 132.6 b	B 135.8 bc	C 154.1 d	137.3 C
Mean	0	A 63.1 a	A 111.3 b	A 91.1 c	A 84.1 c	87.4 A
	120	B 93.3 a	B 99.1 ac	B 129.2 b	B 105.0 c	106.7 B
	180	C 114.1 a	C 120.4 b	B 124.9 b	C 141.0 c	125.1 C
1	Mean	A 83.8 a	A 99.3 b	A 108.9 b	A 99.3 b	97.8 A
2		A 86.8 a	A 106.3 b	A 110.0 b	A 107.4 b	102.6 A
3		B 99.9 a	B 125.2 b	B 126.3 b	B 123.4 b	118.7 B
Mean		90.2 a	110.3 bc	115.0 b	110.0 c	106.4

Different lower-case letters within the same line indicate significant differences. Different uppercase letters indicate that the values in the column for individual factors (Dose N and Cut) and their interaction differ significantly

An increase in nitrogen rate was followed by a significant increase in protein content in Italian ryegrass grown in units which were either without biostimulant or treated with Algex or Asahi SL.

Soluble carbohydrates in Italian rye grass were affected by cuts, an application of biostimulants and nitrogen regime (*Table 7*). Regardless of the experimental factors, the average concentration of these compounds in dry matter was 123.7 g kg^{-1}. The highest concentration of soluble carbohydrates was determined in the grass of the cut harvested in spring, which may have been due to a substantial utilisation of these compounds because of increased plant respiration at high temperatures (the second and third cut) which makes use of sugars. Similar findings were reported in previous works which examined a biostimulant produced from brown algae applied to *Dactylis glomerata* and *Festulolium braunii* (Ciepiela and Godlewska, 2014).

Regardless of the cuts and nitrogen regime, all the biostimulants applied in the experiment significantly increased soluble carbohydrates in Italian rye grass compared with control plants (by 35.2%, on average). A positive effect of extracts obtained from sea algae on the concentration of soluble carbohydrates in plants has been reported by other authors, too (Zodape et al., 2010; Haroun et al., 2011). However, not all studies have confirmed the above tendencies. Cwalina-Ambroziak and Amarowicz (2012) applied Asahi SL and observed a decline in the sugar content of tomato and red pepper fruit.

http://www.aloki.hu ● ISSN 1589 1623 (Print) ● ISSN 1785 0037 (Online)
DOI: http://dx.doi.org/10.15666/aeer/1705_1240712418

Table 7. *The effect of the biostimulants on content of soluble carbohydrates in Italian rye grass by cut and nitrogen fertilization (g kg^{-1} DM) (mean of two years)*

Cut	Dose of N kg ha^{-1}	Biostimulant				Mean
		Without biostimulant (control)	Algex	Tytanit	Asahi SL	
1	0	A 123.4 a	A 160.5 b	A 151.7 b	A 196.7 c	158.1 A
	120	B 105.6 a	A 171.6 b	A 142.1 c	B 183.5 d	150.7 A
	180	B 100.1 a	B 128.8 b	B 112.5 c	C 154.7 d	124.0 B
2	0	A 88.8 a	A 135.6 b	A 140.2 b	A 163.2 c	132.0 A
	120	B 101.9 a	B 111.0 b	A 136.5 c	B 148.6 d	124.5 A
	180	AB 92.6 a	B 114.2 b	B 121.9 bc	C 129.6 c	114.6 B
3	0	A 94.6 a	A 107.3 b	A 121.2 c	A 112.2 b	108.8 A
	120	AB 88.3 a	B 97.4 b	B 113.1 c	A 108.3 c	101.8 B
	180	B 85.3 a	B 90.4 a	B 114.8 b	A 103.9 c	98.6 B
Mean	0	A 102.3 a	A 134.5 b	A 137.7 b	A 157.4 c	133.0 A
	120	A 98.6 a	A 126.7 b	A 130.6 b	A 146.8 c	125.7 A
	180	A 92.7 a	B 111.1 b	B 116.4 b	B 129.4 c	112.4 B
1	Mean	A 109.7 a	A 153.6 b	A 135.4 c	A 178.3 d	144.3 A
2		B 94.4 a	B 120.3 b	A 132.9 c	B 147.1 d	123.7 B
3		C 89.4 a	C 98.4 b	B 116.4 c	C 108.1 d	103.1 C
Mean		97.8 a	124.1 b	128.2 b	144.5 c	123.7

Different lower-case letters within the same line indicate significant differences. Different uppercase letters indicate that the values in the column for individual factors (Dose N and Cut) and their interaction differ significantly

Nitrogen applied at the rate of 120 and 180 kg ha^{-1} significantly reduced soluble carbohydrates in Italian rye grass dry matter (by 21.4%, on average), regardless of the remaining experimental factors, compared with control where no nitrogen had been applied, the finding having been reported in earlier works of the authors of this paper.

Increased nitrogen rates were followed by the decline in solouble carbohytrates in the test grass harvested in units treated with different biostimulants although most of the differences were statistically insignificant.

Conclusions

Regardless of biostimulant application and nitrogen regime, Italian rye grass yield quality and quantity differed significantly for individual cuts and in study years. The highest concentration of chlorophyll in Italian rye grass leaves and protein compounds in dry matter were determined in plants harvested with the third cut. Significantly the highest amount of soluble carbohydrates was determined in the dry matter of Italian rye grass harvested with the first cut. The results reported here indicate that biostimulants applied in the study contributed to similar yield performance of plants fertilised with a nitrogen rate which was by 60 kg ha^{-1} lower, the highest increase in yield (by 42.2%) being recorded for Algex-treated grass. This finding indicates that it is possible to reduce nitrogen rates without compromising the yield, which is beneficial for the

http://www.aloki.hu ● ISSN 1589 1623 (Print) ● ISSN 1785 0037 (Online)
DOI: http://dx.doi.org/10.15666/aeer/1705_1240712418

environment. An application of biostimulants beneficially affected Italian rye grass yield quality as it was followed by a significant increase in chlorophyll content in leaves as well as protein compounds and soluble carbohydrates in the dry matter of the test grass. Of the three biostimulants, the best effects were observed for Asahi-treated plants in terms of the concentration of chlorophyll in leaves and soluble carbohydrates, and for Tytanit-treated plants as far as protein compounds were concerned. The nitrogen rate of 120 and 180 kg ha^{-1} significantly increased Italian rye grass yields, chlorophyll content in plant leaves and protein compounds, the concentration of soluble carbohydrates being significantly lower in the dry matter of test plants. Treatment of Italian ryegrass grown for animal feed with the test biostimulants is reasonable because they contribute to an increase in plant dry matter yield, chlorophyll content, protein compounds and soluble carbohydrates at each nitrogen fertilisation level. It should also be stressed that yields harvested in biostimulant-treated units fertilised with 120 kg N ha^{-1} were higher compared with non-treated plots fertilised with 180 kg N ha^{-1}. Of the test biostimulants, Algex was superior in terms of yield-formation properties. The favourable results of the study reported here as well as the fact that the effect of biostimulants is species- or even cultivar-dependent are a stimulus to continue research into an application of biostimulants to other species of meadow plants.

Acknowledgments. The results of the research carried out under the research theme No. 340/S/13 were financed from the science grant granted by the Ministry of Science and Higher Education

REFERENCES

[1] Aydin, A., Kant, C., Turan, M. (2012): Humic acid application alleviate salinity stress of bean (*Phaseolus vulgaris* L.) plants decreasing membrane leakage. – African Journal of Agricultural Research 7: 1073-1086.

[2] Blackmer, T. M., Schepers, J. S. (1994): Techniques for monitoring crop nitrogen status in corn. – Commun. Soil Science and Plant Analysis 24: 2507-2516.

[3] Borowski, E., Blamowski, Z. K. (2009): The effects of triacontanol 'TRIA' and Asahi SL on the development and metabolic activity of sweet basil (*Ocimum basilicum* L.) plants treated with chilling. – Folia Horticulturae 21(1): 39-48. DOI: 10.2478/fhort-2013-0124.

[4] Brown, P., Saa, S. (2015): Biostimulants in agriculture. – Frontiers in Plant Science. doi.org/10.3389/fpls.2015.00671.

[5] Ciepiela, G. A., Godlewska, A. (2014): Changes in protein compounds and monosaccharides in selected grass species following an application of seaweed extract. – Polish Journal and Environmental Study 23(1): 35-41.

[6] Ciepiela, G. A., Godlewska, A. (2015): The effect of the biostimulant Kelpak SL on *Lolium perenne* L. yield, protein and chlorophyll contents at different nitrogen levels. – Agrochimica 59(2): 124-135.

[7] Cwalina-Ambroziak, B., Amarowicz, R. (2012): Effects of Biological and Fungicidal Environmental protection on chemical composition of tomato and red pepper fruits. – Polish Journal of Environmental Study 21(4): 831-836.

[8] El-Miniawy, S. M., Ragab, M. E., Youssef, S. M., Metwally, A. A. (2014): Influence of foliar spraying of seaweed extract on growth, yield and quality of strawberry plants. – Journal of Applied Sciences Research 10(2): 88-94.

[9] Godlewska, A., Ciepiela, G. A. (2016 a): The effect of the biostimulant Kelpak SL on the content of some microelements in two grass species. – Journal of Elementology 21(2): 373-381. doi.org/10.5601/jelem.2015.20.2.858.

http://www.aloki.hu ● ISSN 1589 1623 (Print) ● ISSN 1785 0037 (Online)
DOI: http://dx.doi.org/10.15666/aeer/1705_1240712418

[10] Godlewska, A., Ciepiela, G. A. (2016b): The effect of growth regulator on dry matter yield and some chemical components in selected grass species and cultivars. – Soil Science and Plant Nutrition 62(3): 297-302. doi.org/10.1080/00380768.2016.1185741.
[11] Haider, M. W., Ayyub, C. H. M., Pervez, M. A., Asad, H. U., Manan, A., Raza, S. A., Ashraf, I. (2012): Impact of foliar application of seaweed extract on growth, yield and quality of potato (*Solanum tuberosum* L.). – Soil and Environment 31(2): 157-162.
[12] Haroun, S. A., Shukry, W. H., Abbas, M. A., Mowafy, A. M. (2011): Growth and physiological responses of Solanum lycopersicum to atonik and benzyl adenine under vernalized conditions. – Journal of Ecology and the Natural Environment 3(9): 319-331.
[13] Hidangmayum, A., Sharma, R. (2017): Effect of different concentrations of commercial seaweed liquid extract of Ascophyllum nodosum as a plant bio stimulant on growth, yield and biochemical constituents of onion (Allium cepa L.). – Journal of Pharmacognosy and Phytochemistry 6(4): 658-663.
[14] Jankowski, K., Ciepiela, G. A., Jodełka, J., Kolczarek, R. (2005): Grassland. – University of Podlasie Press, Siedlce, pp. 119-122 (in Polish).
[15] Khan, W., Rayorath, U. P., Subramanian, S., Jithesh, M. N., Rayorath, P., Hodges, D. M., Critchley, A. T., Craigie, J. S., Norrie, J., Prithiviraj, B. (2009): Seaweed extracts as biostimulants of plant growth and development. – Journal of Plant Growth Regulation 28: 386-399. https://doi.org/10.1007/s00344-009-9103-x.
[16] Kocira, A., Kocira, S., Stryjecka, M. (2015): Effect of Asahi SL application on common bean yield. – Agriculture and Agricultural Science Procedia 7: 103-107.
[17] Kocira, A., Świeca, M., Kocira, S., Złotek, U., Jakubczyk, A. (2016): Enhancement of yield, nutritional and nutraceutical properties of two common bean cultivars following the application of seaweed extract (*Ecklonia maxima*). – Saudi Journal of Biological Sciences 25: 563-571.
[18] Kocira, S., Kocira, A., Kornas, R., Koszel, M., Szmigielski, M., Krajewska, M., Szparaga, A., Krzysiak, Z. (2017): Effect of seaweed extract on yield and protein content of two common bean (*Phaseolus vulgaris* L.) cultivars. – Legume Research 41(4): 589-593. https://doi: 10.18805/LR-383.
[19] Kováčik, P., Wiśniowska-Kielian, B., Smoleń, S. (2018): Effect of application of mg-tytanit stimulator on winter wheat yielding and quantitative parameters of wheat straw and grain. – Journal of Elementology 23(2): 697-708. doi.org/10.5601/jelem.2017.22.2.1461.
[20] Lola-Luz, T., Hennequart, F., Gaffney, M. (2013): Enhancement of phenolic and flavonoids compounds in cabbage (Brassica oleraceae var italica) following application of commercial seaweed extracts of the brown seaweed, Ascophyllum nodosum. – Agricultural and Food Science 22: 288-295.
[21] Michałek, W., Kocira, A., Findura, P., Szparaga, A., Kocira, S. (2018): The Influence of Biostimulant Asahi SL on the Photosynthetic Activity of Selected Cultivars of Phaseolus vulgaris L. – Middle Pomerania Scientific Society of The Environmental Protection 20: 1286-1301.
[22] Murawska, B., Gabrowska, M., Spychaj-Fabisiak, E., Wszelaczyńska, E., Chmielewski, J. (2017): Production and environmental aspects of the application of biostimulators Asahi SL, Kelpak SL and stimulator Tytanit with limited doses of nitrogen. – Environmental Protection and Natural Resources 28(4): 10-15.
[23] Nerissa, A., Farrell, A., Ramsubhag, A., Jayaraman, J. (2016): The effect of *Ascophyllum nodosum* extract on the growth, yield and fruit quality of tomato grown under tropical conditions. – Journal of Applied Phycology 28: 1353-1362. doi.org/10.1007/s10811-015-0608-3.
[24] Pacheco, A. C., Sobral, L. A., Gorni, P. H., Carvalho, M. E. A. (2019): *Ascophyllum nodosum* extract improves phenolic compound content and antioxidant activity medicinal and functional food plant *Achillea millefolium* L. – Australian Journal of Crop Science 13(03): 418-423. DOI:10.21475/ajcs.19.13.03.p1342.

http://www.aloki.hu ● ISSN 1589 1623 (Print) ● ISSN 1785 0037 (Online)
DOI: http://dx.doi.org/10.15666/aeer/1705_1240712418

[25] Przybysz, A., Gawronska, H., Gajc-Wolska, J. (2014): Biological mode of action of a nitrophenolates-based biostimulant: case study. – Frontiers in Plant Science 5: 1-15. DOI: 10.3389/fpls.2014.00713.
[26] Reguraman, V., Abraham, L. S., Inbakandan, D., Thirugnanasambandam, R., Senthilvelan, T., Jabeen, S. K. A., Prakash, P. (2019): Influence of seaweed extracts on growth, phytochemical content and antioxidant capacity of cowpea (*Vigna unguiculata* L. Walp). – Biocatalysis and Agricultural Biotechnology 17: 589-594.
[27] Radkowski, A. (2013): Leaf greenness (SPAD) index in timothy-grass seed plantation at different doses of titanium foliar fertilization. – Ecological Chemistry Engineering A 20(2): 167-174.
[28] Renuka, N., Guldhe, A., Prasanna, R., Singh, P., Bux, F. (2018): Microalgae as multi-functional options in modern agriculture: current trends, prospects and challenges. – Biotechnology Advances 36: 1255-1273. doi.org/10.1016/j.biotechadv.2018.04.004.
[29] Sharma, H. S. S., Fleming, C., Selby, C. H., Rao, J. R., Martin, T. (2014): Plant biostimulants: a review on the processing of macroalgae and use of extracts for crop management to reduce abiotic and biotic stresses. – Journal of Applied Phycology 26: 465-490. http://dx.doi.org/10.1007/s10811-013-0101-9.
[30] Sultana, V., Ehteshamul-Haque, S., Ara, J., Athar, M. (2005): Comparative efficacy of brown, green and red seaweeds in the control of root infesting fungi and okra. – International Journal of Environmental Science and Technology 2(2): 129-132. doi.org/10.1007/BF03325866.
[31] Systematics of Polish Soil (2011): Without title. – Annals of Soil Science 62(3): 1-193.
[32] Tuhy, Ł., Chowańska, J., Chojnacka, K. (2013): Seaweed extracts as biostimulants of plant growth: review. – Chemik 7(67): 636-641.
[33] Whitted-Haag, B., Kopsell, D. E., Kopsell, D. A., Rhykerd, R. L. (2014): Foliar silicon and titanium application influence growth and quality characteristics of annual bedding plants. – Open Horticulture Journal 7: 6-15. doi.org/10.2174/1874840601407010006.
[34] Zodape, S. T., Mukhopadhyay, S., Eswaran, K., Reddy, M. P., Chikara, J. (2010): Enhanced yield and nutritional quality in green gram (*Phaseolus radiata* L.) treated with seaweed (*Kappaphycus alvarezii*) extract. – Journal of Scientific and Industrial Research 69(6): 468-471.

http://www.aloki.hu ● ISSN 1589 1623 (Print) ● ISSN 1785 0037 (Online)
DOI: http://dx.doi.org/10.15666/aeer/1705_1240712418

THE EFFECT OF ENVIRONMENTAL CONDITIONS AND BREEDER AGE ON EGG QUALITY CHARACTERISTICS

HEMIN, N. M.* – KHASRAW, A. A.

Department of Animal Sciences, College of Agricultural Sciences Engineering, University of Sulaimani, Sulaymaniyah, Iraq
(e-mail: xasrao.ali@gmail.com)

**Corresponding author*
e-mail: hemin.mohammed@univsul.edu.iq

(Received 10th May 2019; accepted 16th Jul 2019)

Abstract. The study was carried out to investigate the effect of broiler breeder age (35 and 50 weeks), storage period (2 and 6 days) and storage type (cooling, 30 °C hot room and partially oil covered in a hot room 30 °C) and their interactions on egg quality traits and hatchability of the Ross-308 broiler breeder eggs. The experiment included the measurements of the egg quality characteristics in the research laboratory. The results obtained from this experiment were summarized as the following: Broiler breeder ages had significant ($p \leq 0.05$) effects on some of the improved quality traits of the eggs such as: egg weight, albumin weight, yolk weight, haugh unit, yolk height, yolk index, hatchability and fertile egg hatchability percentage. Storage periods had significant ($p \leq 0.05$) effects on the egg weight, albumin weight, haugh unit, yolk index, hatchability and fertile egg hatchability percentage. Storage types (conditions) had significant ($p \leq 0.05$) effects on the egg weight, albumin weight, yolk weight, haugh unit, albumin and yolk percentage, albumin height, egg specific gravity and yolk height, yolk diameter, yolk index, hatchability and fertile egg hatchability percentage.
Keywords: *egg quality, storage period, storage type, egg storage, hatchability*

Introduction

Breeder age could be considered as one of the major factors affecting variability in egg characteristics, fertility, hatchability and broiler performance (Elibol et al., 2002; Guibert et al., 2012; Peebles et al., 2001). It is known that young breeders tend to have smaller eggs with higher proportion of albumen to yolk, lower albumen pH and higher shell thickness than eggs from old breeders (Peebles et al., 2000). Breeder age could be also a contributing factor to post- hatch performance of broilers, smaller yolk proportions of eggs from a young flock may be associated with low final body weight of their offspring (Ulmer-Franco et al., 2010). Hulet et al. (2007) reported that broilers from old breeders had higher body weight until 35 d compared to broilers from the young breeders. Generally, breeders kept in production till ages of 60-65 weeks. The main factors directly associated with egg deterioration are temperature and relative humidity, besides manipulation and storage period, however, during egg storage, some components of albumen and yolk may alter and tend to deteriorate egg quality (Feddern et al., 2017).

A storage duration beyond 7 d increases incubation duration (Tona et al., 2003) and has a negative effect on hatchability (Fasenko et al., 2001b; Tona et al., 2004; Yassin et al., 2008) and chick quality (Tona et al., 2003, 2004). The negative effects of prolonged egg storage may be caused by changes in egg characteristics, embryo quality or by both (Reijrink et al., 2008). Poor shell quality was associated with a higher percentage of egg moisture loss during incubation (Peebles et al., 2001) and low hatchability (Narushin and Romanov, 2002). It is suggested that prolonged egg storage may cause embryonic

http://www.aloki.hu ● ISSN 1589 1623 (Print) ● ISSN 1785 0037 (Online)
DOI: http://dx.doi.org/10.15666/aeer/1705_1241912439

stress, manifesting in increasing embryonic necrotic and apoptotic cell death, decreased embryonic metabolism, and developmental delays; as a result, irreparable damage to the embryo may occur, thus resulting in increased embryonic mortality and decreased chick performance (Christensen et al., 2001; Fasenko, 2007; Hamidu et al., 2010).

Preincubation of hatching eggs before or during storage was reported to reduce the detrimental effects of periods of storage more than 7 d (Fasenko et al., 2001a; Reijrink et al., 2009). The effect of preincubation on hatchability was found to be influenced by the length of egg storage period and the developmental stage of the embryo before (Reijrink et al., 2009) or after (Fasenko et al., 2001a) the heating. According to Santos (2005), ambient temperature and prolonged egg storage negatively influenced the quality of eggs and significantly reduced the Haugh unit. Factors associated with the management and feeding of hens can play a role in internal egg quality, but egg handling and storage practices also had a significant impact on the quality of eggs reaching consumers (Jin et al., 2011).

The aim of this study was to investigate the effects of broiler breeder ages, egg storage periods and egg storage types on egg quality traits and hatching percentage.

Materials and methods

This study was conducted at the laboratory and poultry farm of College of Agricultural Sciences, University of Sulaimani, in Iraq. A total of (4200 eggs) of broiler breeder (Ross-308) were used in this experiment, at 35 and 50 weeks of breeder's age.

The experiment was divided in to two stages, the first stage included storing the eggs for 2 and 6 days in three types of storage conditions including (cooling, hot room 30 °C and partially oil covered in hot room), followed by the second stage which started to measure the egg quality characteristics in the laboratory.

The experimental studied factors were as the following:
Factor one: included two levels of broiler breeder ages (35 and 50) weeks.
Factor two: included two levels of storage periods (2 and 6 days).
Factor three: included three levels of storage type (storing of the eggs in cooling, hot room at 30 °C and partially covered the eggs (blunt side) with oil in the hot room).

Egg test

Two thousand one hundred (2100) eggs were taken from each different breeder ages and 1050 eggs were stored for each 2 and 6 days in the three types of storage condition where 350 eggs selected for each type (storage types were denoted by cooling = C, hot room 30 °C = H and partially oil covered in hot room = O), after storage periods 50 eggs from each group were taken to measure the quality characteristic of the eggs and remain 300 eggs to for measure hatchability percentage.

Egg weight (g)

The eggs were weighed individually using sensitive electric balance type Mettler toledo (max = 101 g and e = 0.1 mg) and recorded in gram (*Fig. 1*).

Albumin weight (g)

After yolk separation from albumin, albumin was weighed by using sensitive electric balance type Mettler Toledo (max = 101 g and e = 0.1 mg) (*Fig. 2*).

http://www.aloki.hu ● ISSN 1589 1623 (Print) ● ISSN 1785 0037 (Online)
DOI: http://dx.doi.org/10.15666/aeer/1705_1241912439

Figure 1. *Sensitive electric balance type Mettler Toledo used to measure egg weight*

Figure 2. *Sensitive electric balance type Mettler Toledo used to measure albumin weight*

Yolk weight (g)

After yolk separation from albumin, yolk was weighed by the same balance (*Fig. 3*).

Shell weight (g)

Shell weight was calculated by the following equation:

$$\text{Egg shell weight} = \text{Egg weight (g)} - \text{Yolk with albumin weight (g)}$$

http://www.aloki.hu ● ISSN 1589 1623 (Print) ● ISSN 1785 0037 (Online)
DOI: http://dx.doi.org/10.15666/aeer/1705_1241912439

Figure 3. *Sensitive electric balance type Mettler Toledo used to measure yolk weight*

Yolk, albumin and shell percentage

Traits were calculated by the following equations:

$$\text{Yolk } \% = \frac{\text{Yolk weight } (\text{g})}{\text{Egg weight } (\text{g})} \times 100$$

$$\text{Albumin } \% = \frac{\text{Albumin weight } (\text{g})}{\text{Egg weight } (\text{g})} \times 100$$

$$\text{Shell } \% = \frac{\text{Shell weight } (\text{g})}{\text{Egg weight } (\text{g})} \times 100$$

Yolk, albumin ratio

The following equation was used to measure this trait:

$$\text{Yolk, albumin ratio} = \frac{\text{Yolk weight } (\text{g})}{\text{Albumin weight } (\text{g})}$$

Albumin height (mm)

Albumin height was recorded after pouring albumin on the phial-layer by Spherometer (*Fig. 4*).

http://www.aloki.hu ● ISSN 1589 1623 (Print) ● ISSN 1785 0037 (Online)
DOI: http://dx.doi.org/10.15666/aeer/1705_1241912439

Haugh unit (HU)

Haugh unit was calculated depending on the albumin height (mm) and egg weight (g) by the following equation:

$$HU = 100 [\log (H + 7.57 - 1.7 W^{0.37})]$$

H = height of albumin (mm)

W = weight of egg (g)

Figure 4. *Spherometer used for measure albumin height*

Yolk height (mm)

Yolk height was recorded by the Spherometer after pouring yolk in to the Petri-dish (*Fig. 5*).

Yolk diameter (mm)

Yolk diameter was recorded by the same Vernier after pouring yolk in to the Petri-dish (*Fig. 6*).

Yolk index

Yolk index was calculated depending on the yolk height and yolk diameter (mm) by using this equation:

$$\text{Yolk index} = \frac{\text{Yolk height}}{\text{Yolk diameter}}$$

Egg specific gravity

Egg specific gravity was recorded after storing the eggs. Eggs were put-in the 9 of salt solution and egg specific gravity takes the same specific gravity of solution that float it.

http://www.aloki.hu ● ISSN 1589 1623 (Print) ● ISSN 1785 0037 (Online)
DOI: http://dx.doi.org/10.15666/aeer/1705_1241912439

Figure 5. *Spherometer used for measure yolk height*

Figure 6. *Digital Vernier used for measure yolk diameter*

Fertility and hatchability

These traits were calculated by the following equations:

$$\text{Fertility } \% = \frac{\text{No. of fertile egg}}{\text{No. of total settable eggs}} \times 100$$

$$\text{Total egg hatchability } \% = \frac{\text{No. of hatched chicks}}{\text{No. of total egg set}} \times 100$$

http://www.aloki.hu ● ISSN 1589 1623 (Print) ● ISSN 1785 0037 (Online)
DOI: http://dx.doi.org/10.15666/aeer/1705_1241912439

$$\text{Fertile egg hatchability \%} = \frac{\text{No. of hatched chicks}}{\text{No. of fertile eggs}} \times 100$$

Statistical analysis

The present experiment was conducted using Completely Randomized Design (C.R.D) with three factors namely broiler breeder ages, storage periods and storage types to study the effect of these factors on the egg quality and hatchability traits. Statistical analysis was accomplished using (Xlstat-2017 Program for Windows version 19.6). Duncan's multiple range tests were used to determine the significance of differences among treatments means. Level of significance used in all results was ($P \leq 0.05$).

Results

Egg weight (g) and albumin weight (g)

The effects of interactions between broiler breeder ages, storage periods and storage types had significant ($p \leq 0.05$) effect on egg weight (g) (*Table 1*), the highest weight (58.179 g) was recorded by broiler breeder 50 weeks of age with 2 day of storage period and cooling condition of storage type and the lowest weight (46.931 g) was recorded by broiler breeder 35 weeks of age with 6 day of storage period and hot room condition of storage type.

Table 1. *Effect of interactions between breeder ages, storage periods and storage types on egg weight (g) and albumin weight (g) (mean ± SEM)*

Factors			Traits	
			Egg weight (g)	Albumin weight (g)
Breeder ages (week) × Storage periods (day) × Storage types (C, H and O)				
35	2	C	$56.012^{ab} \pm 0.81$	$35.012^{abc} \pm 0.2$
		H	$50.139^{cd} \pm 0.29$	$30.717^{def} \pm 0.25$
		O	$55.836^{ab} \pm 0.72$	$35.079^{abc} \pm 0.15$
	6	C	$54.785^{ab} \pm 0.6$	$34.063^{bcd} \pm 0.37$
		H	$46.931^{d} \pm 0.98$	$27.980^{f} \pm 2.27$
		O	$52.803^{bc} \pm 1.83$	$34.579^{abc} \pm 1.16$
50	2	C	$58.179^{a} \pm 2.12$	$37.921^{a} \pm 0.51$
		H	$51.120^{c} \pm 1.12$	$31.600^{cde} \pm 0.59$
		O	$57.083^{a} \pm 0.65$	$36.103^{ab} \pm 0.86$
	6	C	$56.015^{ab} \pm 0.66$	$36.108^{ab} \pm 0.72$
		H	$50.932^{c} \pm 0.14$	$30.360^{ef} \pm 1.15$
		O	$54.720^{ab} \pm 0.49$	$34.110^{bcd} \pm 1.38$

Mean values in the same column having different superscripts are significantly different at $P \leq 0.05$. Mean values in the same column having the same superscripts are not significantly different at $P \leq 0.05$. C = cooling, H = hot room 30 CO and O = partially oil covered in hot room

The effects of interactions between broiler breeder ages, storage periods and storage types had significantly ($p \leq 0.05$) affected albumin weight (g) (*Table 1*), the highest weight of albumin (37.921 g) was recorded by broiler breeder 50 weeks of age with

http://www.aloki.hu ● ISSN 1589 1623 (Print) ● ISSN 1785 0037 (Online)
DOI: http://dx.doi.org/10.15666/aeer/1705_1241912439

2 day of storage period and cooling condition of storage type and the lowest (27.980 g) was recorded by broiler breeder 35 weeks of age with 6 day of storage period and hot room condition of storage type.

Yolk weight (g) and shell weight (g)

The effects of interactions between broiler breeder ages, storage periods and storage types had significantly ($p \leq 0.05$) affected egg yolk weight (g) (*Table 2*), the highest value of yolk weight (15.780 g) was recorded by broiler breeder 50 weeks of age with 2 day of storage period and oil covered condition of storage type and the lowest (12.360 g) was recorded by broiler breeder 35 weeks of age with 6 day of storage period and oil covered condition of storage type. Also, there were no significant ($p \leq 0.05$) effects of interactions between broiler breeder ages, storage periods and storage types on egg shell weight (g) (*Table 2*).

Table 2. *Effect of interactions between breeder ages, storage periods and storage types on yolk weight (g) and shell weight (g) (mean ± SEM)*

Factors			Traits	
			Yolk weight (g)	Shell weight (g)
Breeder ages (week)× Storage periods (day) × Storage types (C, H and O)				
35	2	C	$15.000^{a} \pm 0.1$	$6.000^{a} \pm 0.12$
		H	$13.668^{bc} \pm 0.28$	$5.754^{a} \pm 0.19$
		O	$14.131^{b} \pm 0.06$	$6.626^{a} \pm 0.2$
	6	C	$14.200^{b} \pm 1.63$	$6.522^{a} \pm 0.73$
		H	$13.000^{c} \pm 0.89$	$5.951^{a} \pm 0.32$
		O	$12.360^{c} \pm 1.02$	$5.864^{a} \pm 1.4$
50	2	C	$15.090^{a} \pm 0.18$	$5.168^{a} \pm 0.26$
		H	$14.800^{ab} \pm 0.71$	$4.720^{a} \pm 0.03$
		O	$15.780^{a} \pm 0.06$	$5.200^{a} \pm 0.31$
	6	C	$15.110^{a} \pm 0.32$	$4.797^{a} \pm 0.3$
		H	$14.920^{ab} \pm 0.24$	$5.652^{a} \pm 0.26$
		O	$15.180^{a} \pm 0.08$	$5.430^{a} \pm 0.76$

Means values in the same column having different superscripts are significantly different at $P \leq 0.05$. Means values in the same column having the same superscripts are not significantly different at $P \leq 0.05$. C = cooling, H = hot room 30 CO and O = partially oil covered in hot room

Albumin and yolk percentage

The effects of interactions between broiler breeder ages, storage periods and storage types had a significant ($p \leq 0.05$) effect on albumin percentage (*Table 3*), the highest value of albumin percentage (65.487%) was recorded by broiler breeder 35 weeks of age with 6 day of storage period and oil covered condition of storage type and the lowest (59.609%) was recorded by broiler breeder 50 weeks of age with 6 day of storage period and hot room condition of storage type.

The effects of interactions between broiler breeder ages, storage periods and storage types had a significant ($p \leq 0.05$) effect on yolk percentage (*Table 3*), the highest value of yolk percentage (29.294%) was recorded by broiler breeder 50 weeks of age with

http://www.aloki.hu ● ISSN 1589 1623 (Print) ● ISSN 1785 0037 (Online)
DOI: http://dx.doi.org/10.15666/aeer/1705_1241912439

6 day of storage period and hot room condition of storage type and the lowest (23.408%) was recorded by broiler breeder 35 weeks of age with 6 day of storage period and oil covered condition of storage type.

Table 3. *Effect of interactions between breeder ages, storage periods and storage types on albumin and yolk percentage (mean ± SEM)*

Factors			Traits	
			Albumin (%)	**Yolk (%)**
Breeder ages (week)× Storage periods (day) × Storage types (C, H and O)				
35	2	C	$62.508^{abc} \pm 0.1$	$26.780^{abc} \pm 0.23$
		H	$61.264^{bc} \pm 0.49$	$27.260^{ab} \pm 0.2$
		O	$62.825^{abc} \pm 0.93$	$25.308^{bc} \pm 0.11$
	6	C	$62.176^{abc} \pm 0.36$	$25.920^{abc} \pm 0.16$
		H	$59.619^{c} \pm 0.42$	$27.700^{ab} \pm 0.29$
		O	$65.487^{a} \pm 0.2$	$23.408^{c} \pm 0.17$
50	2	C	$65.180^{a} \pm 0.51$	$25.937^{abc} \pm 0.4$
		H	$61.815^{abc} \pm 0.25$	$28.951^{ab} \pm 0.18$
		O	$63.247^{abc} \pm 0.45$	$27.644^{ab} \pm 0.21$
	6	C	$64.461^{ab} \pm 0.21$	$26.975^{abc} \pm 0.11$
		H	$59.609^{c} \pm 0.33$	$29.294^{a} \pm 0.24$
		O	$62.336^{abc} \pm 0.36$	$27.741^{ab} \pm 0.22$

Means values in the same column having different superscripts are significantly different at $P \leq 0.05$. Means values in the same column having the same superscripts are not significantly different at $P \leq 0.05$. C = cooling, H = hot room 30 CO and O = partially oil covered in hot room

Shell percentage and yolk albumin ratio

The effects of interactions between broiler breeder ages, storage periods and storage types had a significant ($p \leq 0.05$) effect on shell percentage (*Table 4*), the highest value of shell percentage (12.680%) was recorded by broiler breeder 35 weeks of age with 6 day of storage period and hot room condition of storage type and the lowest (8.564%) was recorded by broiler breeder 50 weeks of age with 6 day of storage period and cooling condition of storage type. Also, there were no significant ($p \leq 0.05$) effects of interactions between broiler breeder ages, storage periods and storage types on yolk albumin ratio (*Table 4*).

Albumin height (mm) and haugh unit

The effects of interactions between broiler breeder ages, storage periods and storage types had a significant ($p \leq 0.05$) effect on Albumin height (mm) (*Table 5*), the highest value of albumin height (7.500 mm) was recorded by broiler breeder 50 weeks of age with 2 day of storage period and cooling condition of storage type and the lowest value (3.400 mm) was recorded by broiler breeder 35 weeks of age with 6 day of storage period and hot room condition of storage type.

The effects of interactions between broiler breeder ages, storage periods and storage types had a significant ($p \leq 0.05$) effect on Haugh unit (*Table 5*), the highest value of Haugh unit (87.066 mm) was recorded by broiler breeder 50 weeks of age with 2 day of

http://www.aloki.hu ● ISSN 1589 1623 (Print) ● ISSN 1785 0037 (Online)
DOI: http://dx.doi.org/10.15666/aeer/1705_1241912439

storage period and cooling condition of storage type and the lowest (59.202 mm) was recorded by broiler breeder 35 weeks of age with 6 day of storage period and hot room condition of storage type.

Table 4. *Effect of interactions between breeder ages, storage periods and storage types on shell percentage and yolk albumin ratio (mean ± SEM)*

Factors			Traits	
			Shell (%)	Yolk albumin ratio
Breeder ages (week)× Storage periods (day) × Storage types (C, H and O)				
35	2	C	$10.712^{ab} \pm 0.12$	$0.428^{a} \pm 0$
		H	$11.476^{ab} \pm 0.24$	$0.445^{a} \pm 0.01$
		O	$11.867^{ab} \pm 0.48$	$0.403^{a} \pm 0.01$
	6	C	$11.905^{ab} \pm 0.25$	$0.417^{a} \pm 0.005$
		H	$12.680^{a} \pm 0.24$	$0.465^{a} \pm 0.008$
		O	$11.105^{ab} \pm 0.14$	$0.357^{a} \pm 0.005$
50	2	C	$8.883^{ab} \pm 0.27$	$0.398^{a} \pm 0.011$
		H	$9.233^{ab} \pm 0.17$	$0.468^{a} \pm 0.005$
		O	$9.110^{ab} \pm 0.14$	$0.437^{a} \pm 0.003$
	6	C	$8.564^{b} \pm 0.15$	$0.418^{a} \pm 0.003$
		H	$11.097^{ab} \pm 0.15$	$0.491^{a} \pm 0.01$
		O	$9.923^{ab} \pm 0.22$	$0.445^{a} \pm 0$

Means values in the same column having different superscripts are significantly different at $P \leq 0.05$. Means values in the same column having the same superscripts are not significantly different at $P \leq 0.05$. C = cooling, H = hot room 30 CO and O = partially oil covered in hot room

Table 5. *Effect of interactions between breeder ages, storage periods and storage types on albumin height (mm) and haugh unit (mean ± SEM)*

Factors			Traits	
			Albumin height (mm)	HU
Breeder ages (week)× Storage periods (day) × Storage types (C, H and O)				
35	2	C	$6.990^{ab} \pm 0.12$	$84.64^{a} \pm 1.2$
		H	$4.100^{ab} \pm 0.12$	$64.677^{d} \pm 1.02$
		O	$6.300^{ab} \pm 0.13$	$80.207^{b} \pm 0.96$
	6	C	$5.030^{ab} \pm 0.09$	$70.949^{c} \pm 0.49$
		H	$3.400^{b} \pm 0.02$	$59.202^{e} \pm 0.35$
		O	$5.010^{ab} \pm 0.03$	$71.632^{c} \pm 0.49$
50	2	C	$7.500^{a} \pm 0.03$	$87.066^{a} \pm 0.67$
		H	$4.600^{ab} \pm 0.04$	$68.857^{c} \pm 0.22$
		O	$7.300^{a} \pm 0.07$	$86.201^{a} \pm 0.6$
	6	C	$7.100^{ab} \pm 0.18$	$85.314^{a} \pm 1.59$
		H	$3.760^{ab} \pm 0.18$	$60.763^{e} \pm 1.03$
		O	$6.010^{ab} \pm 0.11$	$78.574^{b} \pm 0.84$

Means values in the same column having different superscripts are significantly different at $P \leq 0.05$. Means values in the same column having the same superscripts are not significantly different at $P \leq 0.05$. C = cooling, H = hot room 30 CO and O = partially oil covered in hot room

http://www.aloki.hu ● ISSN 1589 1623 (Print) ● ISSN 1785 0037 (Online)
DOI: http://dx.doi.org/10.15666/aeer/1705_1241912439

Egg specific gravity and yolk height

Also, The effects of interactions between broiler breeder ages, storage periods and storage types had significant ($p \leq 0.05$) effect on egg specific gravity (*Table 6*), the highest value (1.090) was recorded by both broiler breeder 35 and 50 weeks of age with 2 day of storage period and cooling condition of storage type and the lowest (1.070) was recorded by broiler breeder 35 weeks of age with 6 day of storage period and hot room condition of storage type, also, the value (1.070) obtained from breeders 50 weeks of age with 2 and 6 day of storage period and hot room condition of storage type.

The interactions between broiler breeder ages, storage periods and storage types had significant ($p \leq 0.05$) effect on yolk height (mm) (*Table 6*), the highest value of yolk height (19.290 mm) was recorded by broiler breeder 50 weeks of age with 2 day of storage period and cooling condition of storage type and the lowest (16.300 mm) was recorded by broiler breeder 35 weeks of age with 6 day of storage period and hot room condition of storage type.

Table 6. *Effect of interactions between breeder ages, storage periods and storage types on egg specific gravity and yolk height (mm) (Mean ± SEM)*

Factors			Traits	
			Egg specific gravity	Yolk height (mm)
Breeder ages (week)× Storage periods (day) × Storage types (C, H and O)				
35	2	C	$1.090^{a} \pm 0.002$	$18.640^{a} \pm 0.12$
		H	$1.075^{b} \pm 0.001$	$16.680^{bc} \pm 0.09$
		O	$1.080^{ab} \pm 0.002$	$18.400^{a} \pm 0.29$
	6	C	$1.080^{ab} \pm 0.002$	$17.480^{ab} \pm 0.24$
		H	$1.070^{b} \pm 0$	$16.300^{c} \pm 0.21$
		O	$1.080^{ab} \pm 0.001$	$17.060^{ab} \pm 0.18$
50	2	C	$1.090^{a} \pm 0$	$19.290^{a} \pm 0.05$
		H	$1.070^{b} \pm 0.001$	$18.120^{a} \pm 0.15$
		O	$1.080^{ab} \pm 0.001$	$19.260^{a} \pm 0.05$
	6	C	$1.080^{ab} \pm 0.001$	$18.590^{a} \pm 0.11$
		H	$1.070^{b} \pm 0.001$	$17.510^{ab} \pm 0.13$
		O	$1.075^{b} \pm 0$	$18.390^{a} \pm 0.23$

Means values in the same column having different superscripts are significantly different at $P \leq 0.05$. Means values in the same column having the same superscripts are not significantly different at $P \leq 0.05$. C = cooling, H = hot room 30 CO and O = partially oil covered in hot room

Yolk diameter (mm) and yolk index

The interactions between broiler breeder ages, storage periods and storage types had a significant ($p \leq 0.05$) effect on yolk diameter (mm) (*Table 7*), the highest value of yolk diameter (40.110 mm) was recorded by broiler breeder 50 weeks of age with 6 day of storage period and hot room condition of storage type and the lowest value (35.280 mm) was recorded by broiler breeder 35 weeks of age with 2 day of storage period and cooling condition of storage type.

http://www.aloki.hu ● ISSN 1589 1623 (Print) ● ISSN 1785 0037 (Online)
DOI: http://dx.doi.org/10.15666/aeer/1705_1241912439

The interactions between broiler breeder ages, storage periods and storage types had significant ($p \leq 0.05$) effects on yolk index (*Table 7*), the highest value of yolk index (0.544) was recorded by broiler breeder 50 weeks of age with 2 day of storage period and cooling condition of storage type and the lowest value (0.408) was recorded by broiler breeder 35 weeks of age with 6 day of storage period and hot room condition of storage type.

Table 7. *Effect of interactions between breeder ages, storage periods and storage types on yolk diameter (mm) and yolk index (mean ± SEM)*

Factors			Traits	
			Yolk diameter (mm)	Yolk index
Breeder ages (week)× Storage periods (day) × Storage types (C, H and O)				
35	2	C	$35.280^{d} \pm 0.16$	$0.528^{a} \pm 0.47$
		H	$38.570^{abcd} \pm 0.41$	$0.432^{ef} \pm 0.51$
		O	$36.140^{cd} \pm 0.24$	$0.509^{ab} \pm 0.44$
	6	C	$35.910^{cd} \pm 0.28$	$0.486^{bc} \pm 0.46$
		H	$39.890^{ab} \pm 0.2$	$0.408^{f} \pm 0.47$
		O	$36.440^{bcd} \pm 0.16$	$0.468^{cd} \pm 0.45$
50	2	C	$35.410^{d} \pm 0.22$	$0.544^{a} \pm 0.44$
		H	$39.450^{abc} \pm 1.28$	$0.459^{cde} \pm 0.57$
		O	$35.830^{cd} \pm 0.16$	$0.537^{a} \pm 0.45$
	6	C	$35.780^{cd} \pm 0.08$	$0.519^{ab} \pm 0.44$
		H	$40.110^{a} \pm 0.31$	$0.436^{def} \pm 0.47$
		O	$36.010^{cd} \pm 0.35$	$0.510^{ab} \pm 0.45$

Means values in the same column having different superscripts are significantly different at $P \leq 0.05$. Means values in the same column having the same superscripts are not significantly different at $P \leq 0.05$. C = cooling, H = hot room 30 CO and O = partially oil covered in hot room

Hatchability and fertility percentage

The interactions between broiler breeder ages, storage periods and storage types had a significant ($p \leq 0.05$) effect on value of hatchability (*Table 8*), the highest value (91.00%) of hatchability was recorded by broiler breeder 50 weeks of age with 2 day of storage period and cooling condition of storage type and the lowest value (32.33%) was recorded by broiler breeder 50 weeks of age with 6 day of storage period and hot room condition of storage type. Also, there were no significant ($p \leq 0.05$) effects of interactions between broiler breeder ages, storage periods and storage types on fertility (*Table 8*).

Fertile egg hatchability

The interactions between broiler breeder ages, storage periods and storage types had significant ($p \leq 0.05$) effect on values of fertile egg hatchability percentage (*Table 9*), the highest value (96.26%) of fertile egg hatchability was recorded by broiler breeder 35 weeks of age with 2 day of storage period and cooling condition of storage type and the lowest value (35.14%) was recorded by broiler breeder 50 weeks of age with 6 day of storage period and hot room condition of storage type.

http://www.aloki.hu ● ISSN 1589 1623 (Print) ● ISSN 1785 0037 (Online)
DOI: http://dx.doi.org/10.15666/aeer/1705_1241912439

Table 8. *Effect of interactions between breeder ages, storage periods and storage types on hatchability and fertility eggs percentage (mean ± SEM)*

Factors			Traits	
			Hatchability (%)	Fertility (%)
Breeder ages (week)× Storage periods (day) × Storage types (C, H and O)				
35	2	C	90.00 ^{a} ± 4.83	93.50 ^{a} ± 4.67
		H	63.33 ^{d} ± 6.71	94.33 ^{a} ± 8.56
		O	77.00 ^{c} ± 11.76	± 7.99
	6	C	85.50 ^{b} ± 4.27	92.50 ^{a} ± 10.03
		H	40.00 ^{f} ± 2.36	91.67 ^{a} ± 7.66
		O	51.00 ^{e} ± 3.79	92.00 ^{a} ± 11.02
50	2	C	91.00 ^{a} ± 4.44	95.00 ^{a} ± 8.01
		H	64.00 ^{d} ± 10	93.00 ^{a} ± 10.41
		O	77.33 ^{c} ± 5.88	92.33 ^{a} ± 8.89
	6	C	83.00 ^{b} ± 7.41	91.50 ^{a} ± 5.56
		H	32.33 ^{g} ± 8.82	± 10
		O	50.00 ^{e} ± 3.41	94.00 ^{a} ± 4.24

Means values in the same column having different superscripts are significantly different at $P \leq 0.05$. Means values in the same column having the same superscripts are not significantly different at $P \leq 0.05$. C = cooling, H = hot room 30 CO and O = partially oil covered in hot room

Table 9. *Effect of interactions between breeder ages, storage periods and storage types on fertile egg hatchability percentage (mean ± SEM)*

Factors			Traits
			Fertile egg hatchability (%)
Breeder ages (week)× Storage periods (day) × Storage types (C, H and O)			
35	2	C	96.26 ^{a} ± 4.52
		H	67.14 ^{d} ± 14.43
		O	82.50 ^{c} ± 14.43
	6	C	92.43 ^{b} ± 19.25
		H	43.64 ^{f} ± 10.99
		O	55.43 ^{e} ± 14.53
50	2	C	95.79 ^{a} ± 10.32
		H	68.82 ^{d} ± 11.25
		O	83.75 ^{c} ± 9.87
	6	C	90.71 ^{b} ± 7.66
		H	35.14 ^{g} ± 16.67
		O	53.19 ^{e} ± 3.82

Means values in the same column having different superscripts are significantly different at $P \leq 0.05$. Means values in the same column having the same superscripts are not significantly different at $P \leq 0.05$. C = cooling, H = hot room 30 CO and O = partially oil covered in hot room

http://www.aloki.hu ● ISSN 1589 1623 (Print) ● ISSN 1785 0037 (Online)
DOI: http://dx.doi.org/10.15666/aeer/1705_1241912439

Discussion

The increase of egg weight with advancing age of broiler breeders (older breeders) may be due to increase the parts of egg components (especially yolk and albumin weight) giving more growth and activation of the reproductive system of broiler breeders compared to younger breeders. This can be explained by the associated increase in egg weight with age. Similar results were reported by several investigators with respect to egg weight increase with advancing age of broiler breeders (Javid et al., 2016; Akyurek and Okur, 2009; Yildirim, 2005; Vieira et al., 2005).

Also, the results of the present study indicated that egg weight of fresh egg decreased and egg weight loss increased with prolonged eggs storage period and storage condition. When the storage period is extended the egg weight declines due to loss of moisture from the egg, and the value of egg weight in oil covered was similar to eggs stored in cooling condition, because of the oil covered condition preventing the loss of more moisture from the eggs compared with un covered eggs in the hot room. These results with respect to the effect of storage period on egg weight loss agreed with those of Reijrink et al. (2010) and Gonzalez (2010).

Gualhanone et al. (2011) also, showed that heavier eggs resulted in heavier chicks, as expected, corroborating several authors that reported a positive correlation between egg weight and chick weight, older breeders with heavier eggs produced heavier chicks, irrespective of incubation temperature, chick weight is an important factor in broiler growth, since it was reported that there is a positive and strong correlation between chick weight at hatch and broiler market weight (42 to 45 days of age). Similar results were reported by several investigators with respect to egg weight increase with advancing age of breeders (Yildirim, 2005; Vieira et al., 2005; Zakaria et al., 2009). This severe effect of older breeders may be considered as a method of improving the percentage of high quality chicks obtained from older breeders.

The increase in the albumin egg weight in older breeders may be due to more growth and activation of the reproductive system of females compared to younger breeders (Javid et al., 2016). And albumin weight was decreased with a longer storage period of egg and storage condition, this is caused by water loss or migration from the albumin. These results were in agreement with the suggestions of Yeasmin et al. (2014) and Jin et al. (2011) whom reported that the albumin weight was greatly influenced by the storage temperature condition and storage period of the eggs.

Generally, the present study showed that the interaction between the main factors showed clearly the decreased the egg weight and albumin weight for old broiler breeders (50 weeks), this was may be due to the storage periods and storage condition that caused the loss of moisture from the egg. The present results are very similar to those reported by Reijrink et al. (2010), Gonzalez-Redondo (2010) and Jin et al. (2011).

Yolk weight increasing by progressing the age may be due to more activation of reproductive system of females and liver activity compared to younger breeders; these results were similar to the finding by Javid et al. (2016) that recorded the increase in egg components by old breeders compared with young breeders. And yolk weight increased with a longer storage period of egg and storage condition this was caused by some of water migration from the albumin to the yolk, these finding of the present study were in agreement with chose by several authors (Khan et al., 2014, 2013; Demirel and Kirikci, 2009) who reported positive correlation between increased yolk weight with increased storage periods and condition. The interaction between the main factors showed clearly the increase of yolk weight for old broiler breeders (50 weeks) was caused by activity of

http://www.aloki.hu ● ISSN 1589 1623 (Print) ● ISSN 1785 0037 (Online)
DOI: http://dx.doi.org/10.15666/aeer/1705_1241912439

reproductive system of females and liver, and for storage periods and conditions, this was may be due to the and migration of moisture from the albumin to the yolk. The results were very similar to the results reported by Javid et al. (2016), Khan et al. (2014, 2013) and Demirel and Kirikci (2009).

According to the present results there were no effects of main factors and their interactions on shell weight, however, numerically shell weight increased with advancing of age in broiler breeders and the other factors (storage periods and storage conditions) had no effect on shell weight. These findings were in line with Yeasmin et al. (2014), Akyurek and Okur (2009) and Silversides and Scott (2001), who reported no effect of storage period and storage temperature on egg shell weight.

Albumin and yolk percentage of eggs were affected significantly by storage conditions and the interaction between broiler breeder ages, storage periods and storage conditions. When decreased albumin ratio already increased yolk ratio, this was because albumin loses more water than yolk, which caused a proportional increase in yolk ratio. The results were similar to the finding of Demirel and Kirikci (2009) and Kırıkçı et al. (2005) whom found the effect of storage period on albumin and yolk percentage.

The cause of affecting of interaction between broiler breeder ages, storage periods and storage type conditions on increasing of shell percentage may be due to decrease of other eggs component ratio during storage period. Shell ratio determined in the present study was similar to the finding of Demirel and Kirikci (2009).

According to the results there were no effects of main factors and their interactions on yolk albumin ratio. However, numerically there was a little difference between the interactions of main factors; this is may be due to the variety and the proportion of the yolk and albumin of eggs during the storage periods and storage conditions. These results were in agreement with those suggested by Suk and Park (2001).

In the present study, there was not effect of broiler breeder ages on albumin height, but there was a significantly effect of interactions between broiler breeder ages with storage temperature condition on albumin height. These results were consistent with the findings of Yeasmin et al. (2014) and Silversides and Scott (2001), who reported the reduction of albumin height was due to the decrease in thick albumen height, because of breakdown of the ovomucin-lysozyme complex during storage periods.

In the present study the storage of eggs clearly reducing of (HU) between young and older breeders. Also, these disparate effects caused by the influence of interaction of age with storage (Tona et al., 2004), these results may be due to increase of egg weight and albumin height of eggs from old broiler breeders compared to young broiler breeders. This result of reduced HU was due to age of broiler breeders or storage periods which were consistent with the reports of Akyurek and Okur (2009), Tona et al. (2004) and Silversides and Scott (2001).

The results showed that Haugh unit values decreased with increased egg storage periods and conditions in the present study, water loss from the egg, or migration of water from the albumen to the yolk or evaporation from the eggs components is the most likely reason of it. These results were consistent with the findings of Monira et al. (2003), who reported that values decreased with storage period. The present results relating to the effect of storage period on Haugh unit were similar with the findings of Grashorn et al. (2016), Alsobayel and Albadry (2011), Nowaczewski et al. (2010), Demirel and Kirikçi (2009) and Tilki and Saatçi (2004), who reported that the Haugh unit significantly decreased with increasing days of storage, due to loss of water from the eggs.

http://www.aloki.hu ● ISSN 1589 1623 (Print) ● ISSN 1785 0037 (Online)
DOI: http://dx.doi.org/10.15666/aeer/1705_1241912439

There was no significant effect of broiler breeder ages on egg specific gravity, these results were in agreement with Gualhanone et al. (2011) and Akyurek and Okur (2009), who reported that no effect of breeder age on (ESG). On the other hand, specific gravity of eggs declined gradually with the advancing storage period as a resulted in maximum decreases at hot room of storage condition in both covered and non-covered with oil, but the specific gravity of eggs kept at room temperature declined more rapidly than that of cooling temperature condition, this might be due to the size of the air cell with increase of storage period and temperature the size of the air cell increased. These results were in agreement with Yeasmin et al. (2014), Alsobayel and Albadry (2011) and Akyurek and Okur (2009), who observed the size of the air cell increased with different storage temperatures.

In the present study the yolk height values were increased by advancing the age of broiler breeders, this was may be due to the size of yolk in heavy egg (this was clearly observed in continued *Table 1* that the highest egg weight (58.179 g) was recorded by broiler breeder 50 weeks of age with 2 day of storage period and cooling condition of storage type) compared to light egg, but yolk height decreased with increase of storage periods and storage temperature, this was may be due to the decrease of the strength of vitelline membrane that caused loss a little of water from the yolk and finally it caused the change in yolk index value. These results were confirmed with Abdel-Azim and Farahat (2009) and Günlü et al. (2007), who found the change of yolk index value under the effect of changing yolk height value.

The increase in yolk diameter observed in the present study could be due to decrease of the strength of vitelline membrane. When eggs are stored under room temperature for long periods, the strength of vitelline membrane breaks which makes the yolk to spread into the albumin. These results were in agreement with Kirunda and McKee (2000), who reported that vitelline membrane strength decreases during storage and makes the yolk more susceptible to breaking, as a result, water slowly enters into the yolk from the albumen, so this creates a mottled appearance in yolk, and the yolk becomes flattened. The yolk diameter values were higher in room temperature, because at a very high temperature, the amount of water migration from the albumen to the yolk is high, which helped to increase yolk diameter (Yeasmin et al., 2014).

The results of *Table 7* also showed that the yolk index (YI) values were significantly decrease with increased storage periods which was most likely due to water loss from the egg. On the other hands, the yolk index values equation depended on the yolk height and yolk diameter, when the yolk diameter increased with increase storage periods and conditions which resulted in an increase the YI values. These results were similar to those found by Abdel-Azim and Farahat (2009), Günlü et al. (2007), Gupta et al. (2007) and Kuzniacka et al. (2005).

The results in the present study showed that hatchability percentage was significantly affected by ages of broiler breeders, storage periods and storage type conditions. These results may be return to the effect of these factors on the egg quality; changes in the quality of eggs can affect the embryonic development during the incubation period and finally the hatchability results. On the basis of the results obtained, it can be concluded that present results in this study were confirmed by Sebastian et al. (2016), who found the lower levels of hatchability parameters were recorded in Ross 308 broiler breeders over 40th weeks of age. Hatchability was significantly lower in the eggs incubated at high ambient temperature (Gualhanone et al., 2011). Some negative changes in egg quality of all poultry species were reported due to prolonged storage period. For

http://www.aloki.hu ● ISSN 1589 1623 (Print) ● ISSN 1785 0037 (Online)
DOI: http://dx.doi.org/10.15666/aeer/1705_1241912439

example, water loss from eggs was related to hatchability (Kozuszek et al., 2009). Also, variations in hatchability may be explained various factors, such as: storage duration, care of hatching eggs, age of breeder, age of broody birds, quality of eggs, seasons, nutrition (Miazi et al., 2012).

The hatchability values recorded by Khan et al. (2013), Mustafa and Al-Sardary (2009), Reijrink et al. (2009), Demirel and Kırıkçı (2009) and Fasenko et al. (2001b) were very close to the results of the present study. Some embryos of eggs stored for a long period could not begin developing instantly after normal incubation temperatures were provided. Khan et al. (2013) found the significant differences in the hatchability of the total of the incubated eggs according to the duration of the storage period before the incubation.

Mustafa and Al-Sardary (2009) finding that the highest hatchability percentage was obtained in the young breeders (33 weeks) compared with old breeders (53 weeks).

Also, Reijrink et al. (2009) noted the detrimental or beneficial effect of pre-storage incubation when storage period was prolonged. Hatchability characteristics were affected by storage period, decreasing with increased storage period, similar results were found by Demirel and Kırıkçı (2009).

According to Fasenko et al. (2001b), the effect of pre-storage incubation on hatchability when storage period is prolonged depends on the developmental stage of the embryo after pre-storage incubation.

According to the present results there were no significant effects of storage periods and storage conditions on the fertility percentage, these results may be due the occurrence of the fertilization of the eggs in the fundamental part of female reproductive system inside the body therefore these factors did not affect on the fertility percentage.

On the other hands, it was shown that the eggs' fertility depends on various factors, such as: age, breed, season, lighting, level of nutrition, time of mating and number of mail with females (Miazi et al., 2012).

Fertility percentage found in the present study was similar to fertility percentage reported in previous studies of Khan et al. (2014) and Demirel and Kırıkçı (2009), who reported that there was no positive or negative effect of storage period on the fertility value.

According to the results of the present study there were significant effects of main factors and their interactions on hatchability of fertile eggs. Hatchability of fertile eggs also may be influenced by same factors that affected total hatchability such as storage duration, care of hatching eggs, age of broody birds, quality of eggs, seasons and nutrition (Miazi et al., 2012). Also, Mustafa and Al-Sardary (2009) found that the highest hatchability of fertile eggs percentage was obtained in the young breeders (33 weeks) compared with old breeders (53 weeks). In embryos less or further advanced damage caused by prolonged storage period might be irreversible and sometimes might cause embryonic mortality. Similarly, Tona et al. (2001) reported the process of embryo development in Cobb hens at different ages (27-60 weeks) also reported a rapid increase in the total embryonic mortality during incubation of eggs laid by older hens (46-64 weeks of age). Significant differences were found in the hatchability of the fertile eggs according to the duration of the storage period before the incubation conducted by Khan et al. (2013).

Reijrink et al. (2009) found that hatchability of fertile eggs in broiler breeder stored for 3, 5 and 8 d were higher than hatchability of fertile eggs stored for 12 d at 16 °C to 18 °C.

http://www.aloki.hu ● ISSN 1589 1623 (Print) ● ISSN 1785 0037 (Online)
DOI: http://dx.doi.org/10.15666/aeer/1705_1241912439

Some embryos could not begin developing immediately after normal incubation temperatures if stored for a long period reported by Tona et al. (2001).

In conclusion, some of the quality traits of the eggs were significantly affected by broiler breeder ages, storage periods and storage types such as: egg weight, albumin weight, yolk weight, haugh unit, yolk height, yolk index, hatchability and fertile egg hatchability percentage.

Conclusions

Some of the quality traits of the eggs were significantly affected by broiler breeder ages, storage periods and storage types such as: egg weight, albumin weight, yolk weight, haugh unit, yolk height, yolk index, hatchability and fertile egg hatchability percentage. According to the results of the present study**,** the following points can be recommended: If the purpose of eggs production was for hatching, we recommend purchasing eggs laid by younger breeders than older breeders that is useful for owners of the hatcheries, but if the purpose of eggs production was for table eggs (consumption) we recommend to purchasing the eggs laid by older layers than younger layers that is useful for the commercial sellers and for consumers. Also, the best storage condition for storage (keeping) the eggs was under the cooling condition, but if this condition is not prepared because of disorder or disable of hatcheries machine, disconnect of electric source or prepare the large number of the eggs we recommended storage the eggs under oil covered condition (partially covered by oil) for short period (1-2 days) to prevent the water loss from the eggs.

REFERENCES

[1] Abdel-Azim, A. M., Farahat, G. S. (2009): Breed differences and phenotypic correlations of antioxidant enzymes activities, some physiological parameters and productive traits of chicken. Phenotypic correlations. – Egypt. P. Sci. J. 29: 645-666.

[2] Akyurek, H., Okur, A. A. (2009): Effect of storage time, temperature and hen age on egg quality in free-range layer hens. – J. of A. and V. A. 8: 1953-1958.

[3] Alsobayel, A. A., Albadry, M. A. (2011): Effect of storage period and strain of layer on internal and external quality characteristics of eggs marketed in Riyadh area. – J. of the Saudi S. of A. Sci. 10: 41-45.

[4] Christensen, V. L., Grimes, J. L., Wineland, M. J. (2001): Effects of breeder hen age, strain, and length of the incubation period on survival of embryos and hatchlings. – J. Appl. Poult. Res. 10: 5-15.

[5] Demirel, Ş., Kırıkçı, K. (2009): Effect of different egg storage times on some egg quality characteristics and hatchability of pheasants (Phasianus colchicus). – Poultry Sci. 88: 440-444.

[6] Elibol, O., Peak, S. D., Brake, J. (2002): Effect of flock age, length of egg storage, and frequency of turning during storage on hatchability of broiler hatching eggs. – Poult. Sci. 81: 945-950.

[7] Fasenko, G. M. (2007): Egg storage and the embryo. – Poult. Sci. 86: 1020-1024.

[8] Fasenko, G. M., Christensen, V. L., Wineland, M. J., Petitte, J. N. (2001a). Examining the effects of pre-storage incubation of turkey breeder eggs on embryonic development and hatchability of eggs stored for four to fourteen days. – Poult. Sci. 80: 132-138.

[9] Fasenko, G. M., Robinson, F. E., Whelan, A. I., Kremeniuk, K. M., Walker, J. A. (2001b): Prestorage incubation of long-term stored broiler breeder eggs effects on hatchability. – Poult. Sci. 80: 1406-1411.

http://www.aloki.hu ● ISSN 1589 1623 (Print) ● ISSN 1785 0037 (Online)
DOI: http://dx.doi.org/10.15666/aeer/1705_1241912439

[10] Feddern, V., Celant De Prá, M., Mores, R., da Silveira Nicoloso, R., Coldebella, A., Giovanni de, A. P. (2017): Egg quality assessment at different storage conditions, seasons and laying hen strains. – Ciência e Agrotecnologia 41(3): 322-333.
[11] Gonzalez, R. (2010): Effect of long-term storage on the hatchability of red-legged partridge (Alectoris rufa) eggs. – Poultry Sci. 89: 379-383.
[12] Gualhanone, A., Furlan, R. L., Fernandez-Alarcon, M. F., Macari, M. (2011): Effect of Breeder Age on Eggshell Thickness, Surface Temperature, Hatchability and Chick Weigh. – Brazilian J. of P. Sci. 14(1): 09-14.
[13] Guibert, F., Richard-Yris, A. M., Lumineau, S., Kotrschal, K., Möstl, E., Houdelier, C. (2012): Yolk testosterone levels and offspring phenotype correlate with parental agein aprecocial bird. – Physiol. Behav. 105: 242-250.
[14] Günlü, A., Kırıkçı, K., Çetin, O., Garip, M. (2007): Effect of hen age on some egg quality characteristics of Pheasants (P. colchicus). Current Problems of Breeding, Health. – Growth and Production of Poultry Congress (February 14-17). Ceske Budejovice, Czech Republic, pp. 211-215.
[15] Gupta, C. S., Kumar, A., Arya, R., Patel, M., Ghosh, A. K., Palod, J. (2007): Evaluation of egg quality of crossbred chickens reared under backyard farming in Tarai areas of Uttaranchal. – Indian J. Anim. Res. 41: 216-219.
[16] Hamidu, J. A., Rieger, A. M., Fasenko, G. M., Barreda, D. R. (2010): Dissociation of chicken blastoderm for examination of apoptosis and necrosis by flow cytometry. – Poult. Sci. 89: 901-909.
[17] Hulet, R., Gladys, G., Hill, D., Meijerhof, R., El-Shiekh, T. (2007): Influence of eggshell embryonic incubation temperature and broiler breeder flock age on posthatch growth performance and carcass characteristics. – Poul. Sci. 86: 408-412.
[18] Javid, I., Sohail, H. K., Nasir, M., Tanveer, A., Riaz, A. P. (2016): Effects of egg size (weight) and age on hatching performance and chick quality of broiler breeder. – Journal of Applied Animal Research 44(1): 54-64. DOI: 10.1080/09712119.2014.987294.
[19] Jin, Y. H., Lee K. T., Lee W. I., Han Y. K. (2011): Effects of Storage Temperature and Time on the Quality of Eggs from Laying Hens at Peak Production. – Asian-Aust. J. Anim. Sci. 24(2): 279-284.
[20] Khan, M. J. A., Khan, S. H., Bukhsh, A., Abbass, M. I., Javed, M. (2013): Effect of Different Storage Period on Egg Weight, Internal Egg Quality and Hatchability Characteristics of Fayumi Eggs. – Italian J. of A. S. 12: 2: e51. DOI: 10.4081/ijas.2013.e51.
[21] Khan, M. J. A., Khan, S. H., Bukhsh, A., Abbass, M. I. (2014): The effect of storage time on egg quality and hatchability characteristics of Rhode Island Red (RIR) hens. – Veterinarski Arhiv 84(3): 291-303.
[22] Kırıkçı , K., Günlü, A., Garip, M. (2005): Some quality characteristics of Pheasant (*P. colchicus*) eggs which different shell colors. – Türk. J. Vet. Anim. Sci. 29: 315-318.
[23] Kirunda, D. F. K., McKee, S. R. (2000): Relating quality characteristics of aged eggs and fresh eggs to vitelline membrane strength as determined by a texture analyzer. – Poultry Science 79(8): 1189-1193.
[24] Kozuszek, R., Kontecka, H., Nowaczewski, S., Rosiñski, A. (2009): Storage time and eggshell colour of pheasant eggs vs. the number of blastodermal cells and hatchability results. – Folia Biologica (Kraków) 57: 121-130.
[25] Kuzniacka, J., Bernacki, Z., Adamski, M. (2005): Effect of the date of egg-laying on the biological value of eggs and reproductive traits in pheasants (*Phasianus colchicuc* L.). – Folia Biol. (Krakow) 53: 73-78.
[26] Miazi, O. F., Miah, G., Miazi, M. M., Uddin, M. M., Hassan, M. M., Faridahsan, M. (2012): Fertility and hatchability of Fayoumi and Sonali chicks. – Scholarly J. Agric. Sci. 2: 83-86.
[27] Grashorn, M., Juergens, A., Bessei, W. (2016): Effects of storage conditions on egg quality. – Lohman Information 50(1).

http://www.aloki.hu ● ISSN 1589 1623 (Print) ● ISSN 1785 0037 (Online)
DOI: http://dx.doi.org/10.15666/aeer/1705_1241912439

[28] Monira, K. N., Salahuddin, M., Miah, G. (2003): Effect of breed and holding period on egg quality characteristics of chicken. – Int. J. Poult. Sci. 2: 261-263.
[29] Mustafa, M. M., Al-Sardary, S. Y. (2009): Effect of broiler breeder age and short egg storage period on hatching trait and broiler performance. – M.Sc. Thesis, University of Duhok.
[30] Narushin, V. G., Romanov, M. N. (2002): Egg physical characteristics and hatchability. – World's Poult. Sci. J. 58: 297-303.
[31] Nowaczewski, S., Witkiewicz, K., Kontecka, H., Krystianiak, S., Rosiński, A. (2010): Eggs weight of Japanese quail vs. eggs quality after storage time and hatchability results. – Archiv. Tierzucht. 53: 720-730.
[32] Peebles, E. D., Gardner, C. W., Brake, J., Benton, C. E., Bruzual, J. J., Gerard, P. D. (2000): Albumen height and yolk and embryo compositions in broiler hatching eggs during incubation. – Poult. Sci. 79: 1373-1377.
[33] Peebles, E. D., Doyle, S. M., Zumwalt, C. D., Gerard, P. D., Latour, M. A., Boyle, C. R., Smith, T. W. (2001): Breeder age influences embryogenesis in broiler hatching eggs. – Poult. Sci. 80: 272-277.
[34] Reijrink, D., Berghmans, R., Kemp Meijerof, B., van den Brand, H. (2010): Influence of egg storage time and preincubation warming profile on embryonic development, hatchability, and chick quality. – Poultry Sci. 89: 1225-1238.
[35] Reijrink, I. A. M., Meijerhof, R., Kemp, B., van den Brand, H. (2008): The chicken embryo and its micro environment during egg storage and early incubation. – World's Poult. Sci. J. 64: 581- 598.
[36] Reijrink, I. A. M., Meijehof, R., Kemp, B., Graat, E. A. M., Van den Brand, H. (2009): Influence of prestorage incubation on embryonic development, hatchability, and chick quality. – Poult. Sci. 88: 2649-2660.
[37] Santos, M. S. V. (2005): Avaliação do desempenho e qualidade dos ovos de poedeiras comerciais, submetidas às dietas suplementadas com diferentes óleos vegetais. – Tese (Doutorado em Zootecnia), Universidade Federal do Ceará, Fortaleza.
[38] Sebastian, N., Mateusz, B., Sebastian, K. (2016): Effect of broiler breeders' age on eggshell temperature, embryo viability and hatchability parameters. – Ann. Anim. Sci. 16(1): 235-243.
[39] Silversides, F. G., Scott, T. A. (2001): Effect of storage and layer age on quality of eggs from two lines of hens. – Poult. Sci. 80: 1240-1245.
[40] Suk, Y. O., Park, C. (2001): Effect of breed and age of hens on the yolk to albumen ratio in two different genetic stocks. – Poultry Science 80: 855-858.
[41] Tilki, M., Saatci, M. (2004): Effects of storage time on external and internal characteristics in partridge (*Alectoris graeca*) eggs. – Revue Méd. Vét. 155: 561-564.
[42] Tona, K., Bamelis, F., Coucke, W., Bruggeman, V., Decuypere, E. (2001): Relationship between broiler breeder's age and egg weight loss and embryonic mortality during incubation in largescale conditions. – J. Appl. Poult. Res. 10: 221-227.
[43] Tona, K., Bamelis, F., De Ketelaere, B., Bruggeman, V., Moraes, V. M. B., Buyse, J., Onagbesan, O., Decuypere, E. (2003): Effects of egg storage time on spread of hatch, chick quality, and chick juvenile growth. – Poult. Sci. 82: 736-741.
[44] Tona, K., Onagbesan, O., Ketelaere, B., De Decuypere, E., Bruggeman, V. (2004): Effects of age of broiler breeders and egg storage on egg quality, hatchability, chick quality, chick weight, and chick post-hatch growth to forty-two days. – J. Appl. Poult. Res. 13: 10-18.
[45] Ulmer, A. M., Fasenko, G. M., Dea, E. E. (2010): Hatching egg characteristics, chick quality, and broiler performance at 2 breeder flock ages and from 3 egg weights. – Poul. Sci. 89: 2735-2742.
[46] Vieira, S. L., Almeida, J. G., Lima, A. R., Conde, O. R. A., Olmos, A. R. (2005): Hatching distribution of eggs varying in weight and breeder age. – Braz. J. Poultry Sci. 7(2): 73-78.

http://www.aloki.hu ● ISSN 1589 1623 (Print) ● ISSN 1785 0037 (Online)
DOI: http://dx.doi.org/10.15666/aeer/1705_1241912439

[47] Yassin, H., Velthuis, A. G. J., Boerjan, M., van Riel, J., Huirne, R. B. M. (2008): Field study on broiler eggs hatchability. – Poult. Sci. 87: 2408-2417.
[48] Yeasmin, A., Azhar, K., Hishamuddin, O., Awis, Q. S. (2014): Effect of storage time and temperature on the quality characteristics of chicken eggs. – Journal of Food, Agriculture & Environment 12(3-4): 87-92.
[49] Yildirim, I. E. (2005): Effects of breeder age and pre-incubation storage of eggs on hatchability, time of hatch and relative organ weight of quail chicks at hatch. – S. Afr. J. Anim. Sci. 35(2): 135-142.
[50] Zakaria, A. H., Plumstead, P. W., Romero-Sanchez, H., Leksrisompong, N., Brake, J. (2009): The effects of oviposition time on egg weight loss during storage and incubation, fertility, and hatchability of broiler hatching eggs. – Poultry Sci. 88: 2712-2717.

http://www.aloki.hu ● ISSN 1589 1623 (Print) ● ISSN 1785 0037 (Online)
DOI: http://dx.doi.org/10.15666/aeer/1705_1241912439

YIELD AND QUALITY OF SULTANI GRAPES (*VITIS VINIFERA* L.) TREATED WITH 28-HOMOBRASSINOLIDE AND GIBBERELLIC ACID

IŞÇI, B.

Department of Horticulture, Faculty of Agriculture, Ege University, Bornova/İzmir, Turkey
(ORCID ID: 0000-0002-6542-0271)
e-mail: burcak.isci@ege.edu.tr

(Received 10th May 2019; accepted 16th Jul 2019)

Abstract. In this study, the effects of gibberellic acid (GA_3) and brassinosteroid (BRs) applications on the yield and berry quality of Sultani grapes were determined during the 2017-2018 period. 28-homobrassinolide (Hbl) solutions with concentrations 4 ppm (Hbl-4) and 8 ppm (Hbl-8) were spray-applied at veraison. Three GA_3 concentrations were implemented by spraying method. The applications times were as follows; Application 1: 10 ppm, clusters 5-10 cm in length at pre-bloom stage (first week of May), Application 2: 15 ppm at 45-50% flowering (mid-June), and Application 3: 20 ppm with 3-5 mm berry diameter stage. GA_3 and BRs on yield components, some quality characteristics relating to clusters and berries (weight, breadth and length, etc.), color of bunches, total phenol content and antioxidant activity were investigated. Results showed that the effects differed, and they were not consistent on all the variables. Effects of the HBl treatments on yield were not as high as GA_3 but there were some positive improvements. Hbl was found to be influential on increasing cluster breadth. Berries were harder with the hormone applications. Quality characteristics were more influenced by the seasons rather than the hormones. Color and total anthocyanin contents were better with the hormones. Fructose content indicated a significant increase with the Hbl-4 application. 28-homobrassinolide might carry some potentially useful effects on improving yield, not to the extent of GA_3, and also on color along with increasing sweetness during the production of 'Sultani' grapes.
Keywords: *Vitis vinifera, Sultani, berry, hormone, gibberellic acid (GA_3), brassinosteroid*

Introduction

In Turkey, only about 50-60 grape cultivars are economically cultivated despite their vast variety (about 1200). Seedless table grape production constitutes about 37% of all production. Sultani (aka 'Thompson Seedless'), originated from the Aegean region of Turkey, since it is the most valuable raisin and table grape variety in the world. Its berries are green-yellow in color, seedless and small, with ellipsoid shaped berries, and the bunches are very large in size with long cylindrical body with wings on both sides (İşçi and Altındişli, 2015).

Applications of growth regulators such as gibberellins, ethylene or auxin in grape growing aim to improve fruit yield and quality. Especially gibberellic acid is the most effective growth regulator in improving bunch compactness, berry characters as well as yield and quality of berries. Gibberellic acid is mostly commercially used in seedless varieties to increase yield of grapes depending on its concentration and the time of application (İşçi and Gökbayrak, 2015; Reynolds et al., 2016; Ghorbani et al., 2017).

Brassinosteroids promote a dual response of cell division and cell elongation resulting in both enhancement and acceleration of the overall growth of the plants (Bartwal et al., 2013; Ali, 2017; Chai, 2012). They show growth regulatory effects in plants similar to those of endogenous plant hormones, auxins and gibberellins. In carrot, application of 24-epibrassinolide resulted in longer plants with increased vegetation weight (Que et al., 2017). Chai et al. (2013) determined that keeping brassinosteroids

http://www.aloki.hu ● ISSN 1589 1623 (Print) ● ISSN 1785 0037 (Online)
DOI: http://dx.doi.org/10.15666/aeer/1705_1244112450

from expression resulted in delayed color development in strawberries. It was shown that the application of brassinosteroid to grape berries evidently enhanced skin coloration and the final sugar level of the flesh, and significantly promoted ripening (Mitchell et al., 1970; Vardhini and Rao, 2002; Symons et al., 2006).

The objective of this study was to determine and compare the effects of gibberellic acid (GA_3) and 28-homobrassinolide applied at different phenological stages on quantity and quality of the 'Sultani' vines.

Materials and methods

Plant material

Vitis vinifera L. 'Sultani', a seedless grape, was grafted on 41B rootstock in 2005. Implementations were carried out at the experimental vineyard located in Bornova, İzmir. The vineyard is on sandy and silt soil 2.0 × 3.0 m spacing. Each vine carried approximately 20 grape clusters. Guyot-trained vines with four canes carrying 11-12 buds were drip irrigated. All viticulture practices were performed according to standard vineyard practices. During winters of 2017 and 2018, Bordeaux mix was applied following pruning, and wettable powder sulphur was used when the summer shoots were 10 cm long. Lateral shoots were accordingly removed in order to facilitate pest management.

Hormone treatments including the control were carried out freshly prepared solutions that contained 0.1% Tween 20 as the surfactant. Control vines were sprayed with distilled water. There were no other manipulations on the clusters. 28-homobrassinolide (Hbl, 0.1%; Repar, MD, USA) solutions with concentrations 4 ppm (Hbl-4) and 8 ppm (Hbl-8) were applied at veraison (last week of July) by spraying with a handgun sprayer at a rate of 10 ml/cluster, and the solution was made sure to cover the entire surface area of the berries in each cluster. Three GA_3 concentrations were implemented by spraying method. The applications times were as following; 1. application: 10 ppm, clusters 5-10 cm in length at pre-bloom stage (first week of May), 2. application: 15 ppm at 45-50% flowering (mid-June), and 3. application: 20 ppm with 3-5 mm berry diameter stage (last week of July).

The weather conditions in the two seasons (2017 and 2018, respectively) were as follows: average monthly temperature in year round was 18.2 °C and 19.2 °C. Mean temperature during the months of vegetation period (April-October) was 24.2 and 24.3 °C. Mean total precipitation was 1.78 mm and 1.65 mm, during which the vegetation period it was recorded as 0.64 and 0.93 mm. Average humidity was 60.6% and 64.3% throughout the seasons. The relative humidity during the vegetation period in 2018 was 4.2% higher compared to that in 2017.

The vines were monitored and harvested when the control vines reached 16°Brix. Yield components (yield per vine and per hectare) were recorded and some quality characteristics relating to clusters and berries (weight, breadth and length, etc.) were determined under lab conditions. Tensile strength of the pedicel (Newton, N) was measured with a penetrometer (Somyftec, France) on 50 berries taken from the clusters. The external berry color was measured at the equatorial area of each side of 50 berries using a colorimeter (CR-300, Minolta Co, Osaka, Japan), average scores were recorded in terms of CIE-L* a* b* values. The colorimeter had an 8 mm diameter viewing area and was calibrated with a white tile (L* = 97.26, a* = + 0.13, b* = + 1.71). From these data, the Color Index of Red Grapes (CIRG) (Carreño et al., 1996) was calculated as:

http://www.aloki.hu ● ISSN 1589 1623 (Print) ● ISSN 1785 0037 (Online)
DOI: http://dx.doi.org/10.15666/aeer/1705_1244112450

CIRG = (180- h^o)/(C* + L*). Based on this index, the berries were classified into five categories: green-yellow (CIRG < 2); pink (2 < CIRG < 4); red (4 < CIRG < 5); dark red (5 < CIRG < 6); and blue-black (CIRG > 6).

The total soluble solids (°Brix) content in the juice was determined with a digital refractometer (PR-1, Atago, Tokyo, Japan) and expressed as percentage. Titratable acidity was measured by titration with 0.1 N NaOH to pH 8.1, and the results were expressed as g tartaric acid·100 mL-1 fruit juice. Sugar composition of grape (fructose and glucose) was determined with HPLC (Thermo Dionex Ultimate 3000) according Camara et al. (1996) only in year 2017. Total phenol content and extraction for antioxidant activity was measured by Thaiponga et al. (2006).

Statistical analysis

The trial was completely randomized with three replicates in each treatment. Each replicate had four vines. A total of 12 vines was used for each application. The mean data collected relating to different parameters of 'Sultani' grapes were statistically analyzed by Minitab® 16.1.1 statistical software. The differences between the significant means were determined with the Tukey's test ($p \leq 0.05$).

Results and discussion

Yield components of the cultivar were not affected by the treatments (*Table 1*). However, the seasonal variations exhibited significant differences and always in the second year that decreases were observed. The weather data indicated that although mean values of temperature, humidity and precipitation all year round were not quite apart, the values during the vegetation period showed that the second period was hotter, more humid and had more rain. This might have caused the yield to be lower. Interestingly, in the first year of hormone applications, GA_3 had always the highest values, followed by mostly the control group. In second year of the experiment, on the other hand, it was the control group that had the highest cluster and vine yield. One stipulation on this observation could be that hormone treated vines might be more prone to the adverse effects of the weather conditions or that they might exert some negative effects on bud fruitfulness. Vergara et al. (2018) also stated that exogenous applications of brassinosteroids at veraison did not improve yield. Senthilkumar et al. (2018) investigated preharvest application of GA_3 and brassinosteroid together and found that they provided best vine yield and highest cluster weight. Champa et al. (2015) showed that 0.5 ppm brassinosteroid at pea stage and veraison significantly increased bunch weight in 'Flame Seedless'. Baneh et al. (2017) reported positive effects of GA_3 on increasing yield of Iranian seeded grape cultivars. In their study involving application of a GA_3 based growth regulator, Nicolaescu et al. (2015) indicated its promoting activity on cluster productivity in 'Beauty Seedless' cultivar. Reynolds et al. (2016) also reported effects of GA_3 on increasing yield as positive and negative dependent on the cultivars. Ghorbani et al. (2017) stated that effects of 24-epibrassinolide on yield of 'Thompson Seedless'vines were mainly dependent on the time of the applications, such that after bloom it tended to provide the highest yield, but it gave the lowest yield when applied at budbreak.

Cluster characteristics, except for the cluster length, did not change with the hormone applications (*Table 2*). The clusters were wider than they were longer, showing that 28-homobrassinolide was as effective as GA_3. Fresh and dry weight of the rachis were

http://www.aloki.hu ● ISSN 1589 1623 (Print) ● ISSN 1785 0037 (Online)
DOI: http://dx.doi.org/10.15666/aeer/1705_1244112450

higher in the first year. Cluster length showed a significant increase in the second year. Although Haubrick and Assmann (2006) stated promoting effect of brassinosteroids on stem elongation, this effect was not observed in this study. This might be due to circumstances of the trial conducted. The increase was seen in all the clusters in the experiment. Champa et al. (2015) stated in their study with double application of brassinosteroid that cluster size significantly increased in 'Flame Seedless'.

The hormone treatments generally caused no significant differences in the characteristics of berries (*Table 3*). Berry breadth, berry weight and tensile strength of the pedicel differed between the seasons, being higher in the first season. Berry firmness was affected by the hormone application. Clear difference was observed between GA_3 and the Hbl-4/control groups. It seems that H8 was also capable of increasing berry firmness as GA_3 did. This might be the result of brassinosteroids, keeping the pectins in the cell walls from solubilization and/or depolymerization which lead to pulp softening (Villareal et al., 2008). Suehiro et al. (2018) reported enlarging effect of GA_3 in 'Shine Muscat' grapes. There are many reports on the effects of GA and CK on berry enlargement throughout the developmental stage (Peppi and Fidelibus, 2008; Zoffoli et al., 2009; Acheampong et al., 2015). In Flame Seedless (Champa et al., 2015) berry weight and berry size showed an increase after brassinosteroid applications at pea stage and veraison. GA_3 treated vines of 'Thompson Seedless' produced heavier berries with greater size compared to the control vines (Koukourikou et al., 2015). 'Skookum Seedless' berries increased their firmness following application of GA_3 (Reynolds et al., 2016).

Quality of the 'Sultani' berries were not affected by the treatment (*Table 4*), but they showed a significant increase in the second season compared to the first season. Soluble solids content between GA_3 and Hbl-4 treatment was comparably high in 2016, and a balance was observed in all the applications in 2017. Total acidity exhibited a slight increase in the second season. Maturity index was under the influence of the hormones. Hbl-4 resulted in the highest index value in both seasons. The others showed a minor decrease in the second season. Our findings were in consistent with those of Vergara et al. (2018) in 'Red Globe' and in contrast with those of Ashgari and Rezaei-Rad (2018) in 'Thompson Seedless". Reynolds et al. (2016) also showed that response of berry quality characteristics was cultivar specific. İşçi and Gökbayrak (2015) indicated no effects of homobrassinolide applied at anthesis on Brix and pH of 'Alphonse Lavallee', but they showed that seasonal effects were clear on total acidity.

Color of the berries were interactively affected by the treatments and the season (*Table 5*). Brightness (L*) was higher and generally the same in the second season. Yellowness (b*) was generally similar between the seasons, except for the Hbl-8 treatment. As was with the brightness, b* was higher in the treated berries compared to the control berries. Redness (a*) stayed at similar levels among the hormone applications, but significantly increased between the seasons. CIRG value (Carreño et al., 1996) of the grapes showed that the 'Sultani' berries fall within the class of green-yellow. It did not change with the applications, but seasonal differences were found significant even though the class they belonged to be the same. In agreement with our findings, Vergara et al. (2018) stated that brassinosteroid analogs applied to Red Globe berries at veraison resulted in better coloration. However, the response here was also dependent on the seasonal effects.

Biochemical aspects of the berries treated with various hormones indicated that hormones resulted with significant contributions to the contents of total anthocyanin and

http://www.aloki.hu ● ISSN 1589 1623 (Print) ● ISSN 1785 0037 (Online)
DOI: http://dx.doi.org/10.15666/aeer/1705_1244112450

total phenolics (*Table 6*). TAC increased with the hormones. TPC on the other hand responded differently to the type of the hormones. GA_3 treated berries had the highest TPC, but 28-homobrassinolid comparably lowered it. Ma et al. (2012), in agreement, showed that 24-epibrassinolide increased phenolic contents in grapes. Since the responses of TAC and TPC were similar to the treatments, it can be assumed that the phenolics contents in the 'Sultani' berries might be mainly related to anthocyanin accumulation as also stated by (Xi et al., 2013). Fructose content of the berries showed a significant increase with Hbl-4 treatment. Glucose accumulated more with the hormones than the control group. In a similar study Asghari and Rezaei-Rad (2018) indicated that three times applied 24-epibrassinolide made a significant contribution to the total anthocyanin contents of 'Thompson Seedless' table grapes. Vergara et al. (2018) also showed that brassinosteroid analogs improved the anthocyanin content of 'Red Globe' grapes. Application of 0.6 ppm at veraison resulted in highest total phenolics and total anthocyanin contents in 'Thompson Seedless' berries (Ghorbani et al., 2017).

Table 1. *Yield components of 'Sultani' vines at harvest for growing seasons of 2017 and 2018 (mean ± SD)*

	Cluster weight (g)		**Yield per vine (kg)**		**Yield per ha (ton)**	
Hormones	2017	2018	2017	2018	2017	2018
GA_3 (10-15-20 ppm)	762.58±181.2	383.93±57.0	15.23±3.62	7.68±1.14	25.41±6.03	12.79±1.90
Hbl 4 ppm	608.72±63.2	326.99±155.6	12.17±1.26	6.54±3.11	20.29±2.11	10.90±5.18
Hbl 8 ppm	548.33±72.1	352.77±124,2	10.97±1.44	7.05±2.48	18.27±2.40	11.75±4.14
Control	601.14±8.7	490.92±46.9	12.02±0.97	9.82±0.94	20.03±3.30	16.35±1.57
Mean	630.19±128A*	388.65±111.5B	12.60±2.56A	7.77±2.23B	21.00±4.26A	12.95±3.72B
p value	0.000		0.000		0.000	

*Uppercase letters in the rows indicate the significant differences between the seasons

Table 2. *Effects of hormone treatments on cluster traits of 'Sultani' grapes (mean ± SD)*

	Cluster breadth (cm)		**Cluster length (cm)**		**Rachis fresh weight (g)**		**Rachis dry weight (g)**	
Hormones	2017	2018	2017	2018	2017	2018	2017	2018
GA_3 (10-15-20 ppm)	26.50±2.18	27.22±3.13	11.67±1.26	14.92±1.81	20.56±2.6	13.43±3.92	8.99±0.46	6.08±0.38
Hbl 4 ppm	28.35±3.43	26.53±3.33	10.33±2.57	11.78±1.36	20.42±1.42	12.67±1.96	8.42±1.37	6.32±0.55
Hbl 8 ppm	25.17±3.01	23.90±2.50	9.50±3.50	12.20±0.00	16.58±5.22	14.90±7.21	7.08±1.87	7.35±1.80
Control	27.50±4.3	26.47±1.70	9.33±1.04	12.25±2.21	22.03±6.43	23.48±9.72	9.16±2.59	9.62±3.16
Mean	26.88±3.11	26.03±2.68	10.26±2.20B	12.78±2.27A	19.90±4.27	16.12±7.12	8.41±1.72	7.34±2.15
p value	>0.05		0.013		>0.05		>0.05	

*Uppercase letters in the rows indicate the significant differences between the seasons

http://www.aloki.hu ● ISSN 1589 1623 (Print) ● ISSN 1785 0037 (Online)
DOI: http://dx.doi.org/10.15666/aeer/1705_1244112450

Table 3. *Effects of hormone treatments on berry traits of 'Sultani' grapes (mean ± SD)*

	Berry breadth (mm)		**Berry length (mm)**		**100 berry weight (g)**		**Berry firmness (N)**			**Tensile strength (N)**	
Hormones	2017	2018	2017	2018	2017	2018	2017	2018	Mean	2017	2018
GA_3 (10-15-20 ppm)	16.2±2.44	12.72±0.08	17.40±0.72	16.12±0.73	243.22±59.2	174.63±11.90	8.51±0.72	7.25±0.73	7.88±0.95 a	293.83±48.66	217.40±25.63
Hbl 4 ppm	14.26±0.77	12.25±0.60	16.51±0.84	15.33±0.40	218.41±29.66	148.63±33.48	6.42±0.84	5.60±0.40	6.01±0.74 b	246.83±9.02	211.00±19.94
Hbl 8 ppm	13.90±1.07	12.57±0.35	16.24±0.96	16.84±0.18	201.17±6.2	186.35±0.95	6.80±0.95	7.43±0.18	7.11±0.70 ab	243.17±22.83	231.10±24.30
Control	13.75±0.16	12.92±0.77	16.45±0.25	18.19±0.86	203.93±11.90	213.80±49.97	6.19±0.25	6.18±0.86	6.19±0.57 b	293.00±63.72	232.00±10.46
Mean	14.53±1.57A*	12.62±0.51B	16.72±1.14	16.63±0.95	216.68±39.15A	180.85±35.80B	6.98±1.14	6.62±0.94		269.21±43.81A	222.88±20.17 B
p value	0.000		>0.05		0.028		0.001			0.003	

*Lowercase letters within a column indicate significant differences among the treatments. Uppercase letters in the rows indicate the significant differences between the seasons

Table 4. *Quality parameters evaluated at harvest after hormone treatments in 'Sultani' grapes (mean ± SD)*

	Soluble solids (Brix)		**Total acidity g (100 g FW)**		**pH**		**Maturity index (SS/TA)**		
Hormones	2017	2018	2017	2018	2017	2018	2017	2018	Mean
GA_3 (10-15-20 ppm)	18.63±0.55	22.32±0.68	6.64±0.28	8.20±0.23	4.02±0.02	3.94±0.02	28.31±1.42	27.26±1.32	27.69±1.31 ab
Hbl 4 ppm	20.20±0.92	21.20±1.30	5.81±,0.47	7.13±0.05	4.11±0.07	3.98±0.01	35.02±4.27	29.71±1.64	32.37±4.10 a
Hbl 8 ppm	18.98±0.21	21.03±1.72	6.88±0.79	7.80±0.27	3.93±0.09	3.97±0.04	27.83±2.94	26.97±2.37	27.40±2.44 ab
Control	17.90±1.72	20.13±0.58	7.07±1.24	8.12±1.34	4.02±0.13	4.02±0.03	26.12±6.52	25.24±4.21	25.68±4.93 b
Mean	18.94±1.22B*	21.18±1.29A	6.60±0.84B	7.82±0.74A	4.02±0.10	3.98±0.04	29.87±5.06	27.30±2.80	
p value	0.000		0.001		>0.05		0.027		

*Lowercase letters within a column indicate significant differences among the treatments. Uppercase letters in the rows indicate the significant differences between the seasons

http://www.aloki.hu ● ISSN 1589 1623 (Print) ● ISSN 1785 0037 (Online)
DOI: http://dx.doi.org/10.15666/aeer/1705_1244112450

Table 5. *Chromatic parameters of the 'Sultani' berries treated with hormones (mean ± SD)*

	L*		***a****		***b****		**CIRG (scale)**	
Hormones	2017	2018	2017	2018	2017	2018	2017	2018
GA_3 (10-15-20 ppm)	42.55±3.88Bab*	48.87±0.49Aa	-7.29±0.33	-8.67±1.12	20.62±1.68Aab	20.91±0.53 Aa	1.10±0.07	0.94±0.04
Hbl 4 ppm	44.03±3.4Ba	48.94±0.61Aa	-7.51±0.52	-9.16±0.73	20.76±1.21Aa	21.48±0.48 Aa	1.06±0.06	0.93±0.03
Hbl 8 ppm	42.08±2.32Bab	50.98±1.92Aa	-7.21±0.69	-8.87±0.36	20.37±1.16Bab	25.12±3.31 Aa	1.11±0.05	0.91±0.04
Control	34.59±7.55Bb	51.12±2.19Aa	-7.22±0.98	-8.26±0.73	16.32±0.76Ab	24.04±2.53 Aa	1.29±0.22	0.93±0.03
Mean	40.81±5.56	49.98±1.71	-7.31±0.59 B	-8.74±0.75 A	19.52±2.21	22.89±2.56	1.14±0.14 A	0.93±0.03 B
p value	0.049		0.000		0.005		0.000	

*Lowercase letters within a column indicate significant differences among the treatments. Uppercase letters in the rows indicate the significant differences between the seasons

Table 6. *Total anthocyanin, total phenolics, fructose and glucose contents of 'Sultani' berries treated with hormones (mean ± SD)*

	TAC (mg/100 g FW)			**Total phenolics (mg GAE/100 g FW)**			**Fructose (%)**	**Glucose (%)**
Hormones	2017	2018	Mean	2017	2018	Mean	2017	2018
GA_3 (10-15-20 ppm)	3.23±0.83	6.08±0.93	4.66±1.74 a*	40.38±4.90	76.51±6.0	58.45±20.39 a*	5.69±2.60 b	5.06±0.13 a
Hbl 4 ppm	2.32±0.37	5.86±0.92	4.09±2.03 ab	34.64±10.11	63.67±3.76	49.16±17.30 b	7.93±0.85 a	5.58±0.39 a
Hbl 8 ppm	2.37±0.22	5.43±1.69	3.90±1.69 ab	38.78±4.03	61.89±1.21	50.34±13.99 b	6.60±0.33 ab	5.01±0.17 a
Control	1.99±0.65	4.46±0.57	3.23±1.43 b	28.23±5.00	63.51±0.21	55.87±19.60 ab	5.38±0.48 b	4.33±0.03 b
Mean	2.48±0.66B	5.46±0.89A		35.51±7.38B	66.40±7.77A		6.40±1.14	4.92±0.51
p value	0.000 (years) 0.010 (treatments)			0.000 (years) 0.015 (treatments)			0.000	0.000

*Lowercase letters within a column indicate significant differences among the treatments. Uppercase letters in the rows indicate the significant differences between the seasons

http://www.aloki.hu ● ISSN 1589 1623 (Print) ● ISSN 1785 0037 (Online)
DOI: http://dx.doi.org/10.15666/aeer/1705_1244112450

Conclusion

No matter the information gathered from this study and from all previous conducted valuable studies indicate that hormones do not greatly influence fruit growth and quality, understanding the role of plant growth regulators in composing grape quality and improving yield still requires some researches. Despite its relatively new-found place among plant hormones, brassinosteroids do have some promising effects on quality and quantity, obviously depending on its type, concentration and the time of application. Due to their degradation and limited transport, it might be useful to apply at the closest time or phenological stage to the intended outcome and therefore, repeated applications may be more effective. Improvement shown by brassinosteroid applications in berry firmness, color development and anthocyanin increases validate these hormones to be the subject of further research.

Acknowledgment. The author thanks Dr. Bhushan Mandava and Prof. Dr. Zeliha Gökbayrak for kindly providing the 28-homobrassinolide.

REFERENCES

[1] Acheampong, A. K., Hu, J., Rotman, A., Zheng, C., Halaly, T., Takebayashi, Y., Jikumaru, Y., Kamiya, Y., Lichter, A., Sun, T. P., Or, E. (2015): Functional characterization and developmental expression profiling of gibberellin signaling components in *Vitis vinifera*. – Journal of Experimental Botany 66: 1463-1476. DOI: 10.1093/jxb/eru504.

[2] Ali, B. (2017): Practical applications of brassinosteroids in horticulture—some field perspectives. – Scientia Horticulturae 225: 15-21. DOI: 10.1016/j.scienta.2017.06.051.

[3] Asghari, M., Rezaei-Rad, R. (2018): 24-Epibrassinolide enhanced the quality parameters and phytochemical contents of table grape. – Journal of Applied Botany and Food Quality 91: 226-231. DOI: 10.5073/JABFQ.2018.091.030.

[4] Baneh, H. D., Jafari, H., Marandi, J., Abdolahi, R. (2017): Effect of pre-bloom gibberellic acid application on aeedlessness and some fruit traits of three Iranian seeded grape cultivars. – Majallah-i Ulum-i Bāghbānī 31(1): 110-121(12). DOI: 10.22067/jhorts4.v0i0.44918.

[5] Bartwal, A., Mall, R., Lohani, P., Guru, S. K., Arora, S. (2013): "Role of secondary metabolites and brassinosteroids in plant defense against environmental stresses". – Journal of Plant Growth Regulation 32: 216-232. DOI: 10.1007/s00344-012-9272-x.

[6] Camara, M., Diez, C., Torija, M. E. (1996): Free sugars determination by HPLC in pineapple products. – Zeitschrift für Lebensmittel-Untersuchung und -Forschung 202: 233-237.

[7] Chai, Y. M., Zhang, Q., Tian, L., Li, C. L., Xing, Y., Qın, L., et al. (2013): Carreño, J., Martinez, A., Almela, L., Fernadezlopez, J. A. (1996): Measuring the color of table grapes. – Color Research & Application 21: 50-54. DOI: 10.1002/(SICI)1520-6378(199602)21:1<50::AID-COL5>3.0.CO;2-4.

[8] Chai, Y. M., Zhang, Q. (2012): Brassinosteroid is involved in strawberry fruit ripening. – Plant Growth Regulator 69: 63-69.

[9] Champa, W., Gill, M., Mahajan, B. V. C., Aror, N. K., Bedi, S. (2015): Brassinosteroids improve quality of table grapes (*Vitis vinifera* L.) cv. Flame Seedless. – Tropical Agricultural Research 26: 368-379. DOI: 10.4038/tar.v26i2.8099.

http://www.aloki.hu ● ISSN 1589 1623 (Print) ● ISSN 1785 0037 (Online)
DOI: http://dx.doi.org/10.15666/aeer/1705_1244112450

[10] Ghorbani, P., Eshghi, S., Haghi, H. (2017): Effects of brassinosteroid (24-epibrassinolide) on yield and quality of grape (*Vitis vinifera* L.) 'Thompson Seedless'. – Vitis 56: 113-117. DOI: 10.5073/vitis.2017.56.113-117.
[11] Haubrick, L. L., Assmann, S. M. (2006): Brassinosteroids and plant function: some clues, more puzzles. – Plant, Cell Environment 29: 446-457. DOI: 10.1111/j.1365-3040.2005.01481.x.
[12] İşçi, B., Altındişli, A. (2015): Drying of *Vitis vinifera* L. cv "Sultanina" in tunnel solar drier. – BIO Web of Conferences 5: 01016. DOI: 10.1051/bioconf/20150501016.
[13] İşçi, B., Gökbayrak, Z. (2015): Influence of brassinosteroids on fruit yield and quality of table grape 'Alphonse Lavallée'. – Vitis 54: 17-19.
[14] Koukourikou, M., Zioziou, E., Pantazaki, A., Nikolaos, Nikolaou, N., Kyriakidis, D. (2015): Effects of gibberellic acid and putrescine on 'Thompson Seedless' grapes. – American International Journal of Biology 3: 19-29. DOI: 10.15640/aijb.v3n2a2.
[15] Ma, L. N., Xi, Z. M., GAO, X., Huo, S. S., Luan, L. Y. (2012): Effects of abscisic acid and 24 epibrassinolide on the endogenous contents of the plant hormone of berries in the process of grape ripening. – North Horticulture 17: 16-19.
[16] Mitchell, J. W., Mandava, N., Worley, J. F., Plimmer, J. R.. (1970): Brassins—a New family of plant hormones from rape pollen. – Nature 225: 1065-1066. DOI: 10.1038/2251065a0.
[17] Nicolaescu, G., Derendovskaia, A., Secrieru, S., Mihov, D., Procopenc, V., Godoroj, M., Lungu, C. (2015): The influence of treatment with growth stimulator (gobbi gib 2lg) on the quantity and quality of seedless grape 'Beauty Seedless'. – Agro Life Scientific Journal 4: 72-79.
[18] Peppi, M. C., Fidelibus, M. W. (2008): Effects of forchlorfenuron and abscisic acid on the quality of 'Flame Seedless' grapes. – HortScience 43: 173-176. DOI: 10.21273/HORTSCI.43.1.173.
[19] Que, F., Wang, G. L., Xu, Z. S., Wang, F., Xiong, A. S. (2017): Transcriptional regulation of brassinosteroid accumulation during carrot development and the potential role of brassinosteroids in petiole elongation. – Front Plant Science 8: 1356. https://doi.org/10.3389/fpls.2017.01356.
[20] Reynolds, A., Robbins, N., Lee, H. S., Kotsaki, E. (2016): Impacts and interactions of abscisic acid and gibberellic acid on sovereign coronation and Skookum Seedless Table Grapes. – American Journal of Enology and Viticulture 67: 327-338. DOI: 10.5344/ajev.2016.15108.
[21] Senthilkumar, S., Vijayakumar, R. M., Soorianathasundaram, K., Devi, D. D. (2018): Impact of pre-harvest sprays with gibberellic acid on yield and economics of grape (*Vitis vinifera* L.) cv. Italia. –Annals of Biology 34: 170-175.
[22] Suehiro, Y., Mochida, K., Tsuma, M., Yasuda, Y., Hiroyuki, Itamura, H., Esumi, T. (2018): Effects of gibberellic acid/cytokinin treatments on berry development and maturation in the yellow-green skinned 'Shine Muscat' grape. – Japanese Society for Horticultural Science 1-12. DOI: 10.2503/hortj.UTD-046.
[23] Symons, G. M., Davies, C., Shavrukov, Y., Dry, I. B., Reid, J. B., Thomas, M. R. (2006): Grapes on steroids: brassinosteroids are involved in grape berry ripening. – Plant Physiol. 140: 150-158. DOI: 10.1104/pp.105.070706.
[24] Thaiponga, K., Boonprakoba, U., Crosbyb, K., Cisneros, Z. L., Hawkins, B. D. (2006): Comparison of ABTS, DPPH, FRAP, and ORAC assays for estimating antioxidant activity from guava fruit extracts. – Journal of Food Composition and Analysis 19: 669-675. DOI: 10.1016/j.jfca.2006.01.003.
[25] Vardhini, B. V., Ram, Rao, S. S. (2002): Acceleration of ripening of tomato pericarp discs by brassinosteroids. – Phytochem 61: 843-847. DOI: 10.1016/50031-9422(02)00223-6.
[26] Vergara, A. E., Díaz, K., Carvajal, R., Espinoza, L., Alcalde, J. A., Pérez-Donoso, A. G. (2018): Exogenous applications of brassinosteroids improve color of red table grape

http://www.aloki.hu ● ISSN 1589 1623 (Print) ● ISSN 1785 0037 (Online)
DOI: http://dx.doi.org/10.15666/aeer/1705_1244112450

(*Vitis vinifera* L. Cv. "Redglobe") berries. – Frontiers in Plant Science 9: 363-374. DOI: 10.3389/fpls.2018.00363.

[27] Villarreal, N. M., Rosli, H. G., Martínez, G. A., Civello, P. M. (2008): Polygalacturonase activity and expression of related genes during ripening of strawberry cultivars with contrasting fruit firmness. – Postharvest Biology and Technology 47: 141-150.

[28] Xi, Z., Zhang, Z., Huo, S., Luan, L., Gao, X. M. L., Fang, Y. (2013): Regulating the secondary metabolism in grape berry using exogenous 24-epibrassinolide for enhanced phenolics content and antioxidant capacity. – Food Chemistry 141: 3056-3065.

[29] Zoffoli, J. P., Latorre, B. A., Naranjo, P. (2009): Preharvest applications of growth regulators and their effect on postharvest quality of table grapes during cold storage. – Postharvest Biology and Technology 51: 183-192. DOI: 10.1016/j.postharvbio.2008.06.013.

http://www.aloki.hu ● ISSN 1589 1623 (Print) ● ISSN 1785 0037 (Online)
DOI: http://dx.doi.org/10.15666/aeer/1705_1244112450

EFFICACY OF *PENICILLIUM CHRYSOGENUM* STRAIN SNEF1216 AGAINST ROOT-KNOT NEMATODES (*MELOIDOGYNE INCOGNITA*) IN CUCUMBER (*CUCUMIS SATIVUS* L.) UNDER GREENHOUSE CONDITIONS

SIKANDAR, A.[1] – ZHANG, M. Y.[1] – ZHU, X. F.[1] – WANG, Y. Y.[2] – AHMED, M.[3] – IQBAL, M. F.[2] – JAVEED, A.[2] – XUAN, Y. H.[1] – FAN, H. Y.[1] – LIU, X. Y.[4] – CHEN, L. J.[1] – DUAN, Y. X.[1*]

[1]*Nematology Institute of Northern China, Shenyang Agricultural University*
120 Dongling road, Shenyang 110866, China

[2]*College of Biosciences and Biotechnology, Shenyang Agricultural University*
120 Dongling road, Shenyang 110866, China

[3]*College of Plant Protection, Shenyang Agricultural University*
120 Dongling road, Shenyang 110866, China

[4]*College of Sciences, Shenyang Agricultural University*
120 Dongling road, Shenyang 110866, China

[*]*Corresponding author*
e-mail: duanyx6407@163.com; phone: +86-13-99825-3910

(Received 12th May 2019; accepted 16th Jul 2019)

Abstract. Root-knot nematode (*Meloidogyne incognita*) has become a serious risk for cucumber globally. Haphazard use of synthetic chemicals poses a serious threat to agricultural crops, eliminating predators and also polluting natural community. Thus these negative effects led towards development of eco-friendly approaches which are safe and effective for *M. incognita* management. The study has been planned to coat seeds with Snef1216 (*Penicillium chrysogenum*) and evaluate its ability to control *M. incognita* in cucumber. It reduced *M. incognita* invasion rate significantly in different inoculums 500J2 (second stage juveniles) 67.09% followed by 1000J2 and 2000J2 plant^{-1} 60.44% and 36.02%, respectively. It inhibited development of nematodes 60.30%, 50.37% and 38.77% at 500, 1000 and 2000J2 plant^{-1} inoculation levels respectively compared to control. Snef1216 reduced significant ($P<0.05$) reproduction rate at 500J2 (69.46%), 1000J2 (62.89%) and 2000J2 (63.62%) of *M. incognita*. It interfered in galls formation and nematodes g^{-1} in root mass. Snef1216 enhanced seed germination (22.09%) with germination index (53.77%) and germination rate (64.49%). Additionally, seed dressing with Snef1216 exhibited additional biomass, reduced invasion of second-stage juveniles and also restrained development of nematode. Our results suggest that Snef1216 can be introduced as a biomass enhancer and potential bio-control agent against *M. incognita* in cucumber.
Keywords: *biological control, seed dressing, invasion, penetration, biological control agents, biomass*

Introduction

Plant parasitic nematodes can easily damage crops not only by direct feeding but also acting as a facilitator for other organisms (Palomares-Rius et al., 2017; Smant et al., 2018). However, damage caused by nematodes is often not easy to differentiate from other agents due to their microscopic size. These are usually soil, roots and leaves inhibiting microorganisms cause an enormous threat to agriculture, manifested in up to 157 billion US$ worth of damage (Youssef et al., 2013).

Root-knot nematodes (RKNs) are common and have an extremely broad host range which includes more than 5500 plant species (Trudgill and Blok, 2001). Among

http://www.aloki.hu ● ISSN 1589 1623 (Print) ● ISSN 1785 0037 (Online)
DOI: http://dx.doi.org/10.15666/aeer/1705_1245112464

different genera, *Meloidogyne* is one of the most destructive plant parasitic nematodes (Xiang et al., 2017; Li and Chen, 2017). However, four main species of this genus, i.e. *Meloidogyne incognita*, *Meloidogyne hapla*, *Meloidogyne arenaria* and *Meloidogyne javanica* have been reported to decrease yields, among them *M. incognita* is one of the most widespread species (Dong et al., 2014).

Cucumber (*Cucumis sativus*) is a commonly cultivated plant belonging to the family Cucurbitaceae, is ranked as an important vegetable globally (Sebastian et al., 2010; Mao et al., 2016). However, China has been ranked as number one and accepted as the world's largest producer of cucumber (FAOSTAT, 2018). This is an important vegetable crop cultivated widely throughout the country, especially in North China (Tian et al., 2011; Huang et al., 2014; Huang et al., 2016). The researcher reported that about 50% of vegetables grown in greenhouse infected by root-knot nematodes with annual loss up to 400 million US dollars (Huang et al., 2014) and it is hard for farmer to diagnose its damage due to similarities with nutritional deficiencies such as chlorosis (Zeng et al., 2018).

The infestation of *M. incognita* adversely affects the growth of the plant, yellowing and stunted leaves growth and ultimately the destruction of whole plants due to absorption of important nutrients (Escobar et al., 2015; Li and Chen, 2017). Infected roots showed bushier and shorter length compared with healthy roots (Miyashita et al., 2014). They directly feed upon plants and caused the lesion in it which helps in development of secondary pathogens such as pathogenic bacteria, fungus and viruses which caused secondary infections (Smant et al., 2018). Unfortunately, it is difficult to control it in soil because of its interaction with other pathogens and plant-parasitic nematodes (PPNs), and developing disease complextion (Back et al., 2002; Divon and Fluhr, 2007; Son et al., 2009; Björsell et al., 2017).

Chemical nematicides have been used to control this pest but their continues and indiscriminate use poses adverse effects on soil and environment (Huang et al., 2014). Due to their hazardous effect on human, availability of such pesticides has become limited in local markets such as methyl bromide, ethylene dibromide (EDB) and dibromochloropropane (Oka et al., 2000; Gotlieb et al., 2003; Dong and Zhang, 2006; Nicol et al., 2011; Onkendi et al., 2014). To overcome this problem, eco-friendly and safe approaches for prevention and management of this nematode are needed urgently because root-knot nematodes have high reproduction rates and short generation times (Trudgill and Blok, 2001; Jang et al., 2016). With increasing demands of organic and chemical free crops, there is a dire need to develop strategies for this destructive pathogen (Huang et al., 2014; Kokalis-Burelle, 2015).

Signs of Progress in recent decades regarding biocontrol agents have led to several products. Biological control is usually safe as compared to chemical control. Meanwhile, Fungi belonging to genera *Fusarium*, *Trichoderma*, *Phyllosticta*, *Acremonium, Chaetomium, Paecilomyces,* and *Penicillium* have been known as antagonistic to plant-parasitic nematodes (Kalele et al., 2007; Govinden-Soulange and Levantard, 2008; Sharon et al., 2009; Siddiqui and Akhtar, 2009). Within an integrated and more sustainable management strategy the use of biocontrol agents, like *P. chrysogenum*, seems to be a promising alternative in the future. However, some studies reported the effectiveness of such fungus against *M. incognita* in different crops. The biocontrol effect against different pathogens in the presence of *P. chrysogenum* is reported in a wide range of plants and pathogens providing evidence for the effect of *P. chrysogenum* on nematode infection. Dry mycelium enhanced plant growth and

http://www.aloki.hu ● ISSN 1589 1623 (Print) ● ISSN 1785 0037 (Online)
DOI: http://dx.doi.org/10.15666/aeer/1705_1245112464

reduced root galls to protect cucumber and tomato plants against *M. javanica* (Gotlieb et al., 2003). *P. chrysogenum* used alone and in the combination of two (*Aspergillus niger*, Plant growth promoting rhizobacteria PGPRS and Arbuscular mycorrhizal fungi) could boost plant growth and reduce reproduction of *M. incognita* in tomato (Siddiqui and Akhtar, 2009). Yao et al. (2014) also reported that *P. chrysogenum* is one of the most important fungi to control *M. incognita* in tomato. Thus, keeping in view the biocontrol potential of Snef1216 (*P. chrysogenum*) against *M. incognita* on different crops, the present study was planned to explore the nematicidal activity of fungus fermentation for control of *M. incognita* by seeds dressing on cucumber seeds and to enhance biomass at Nematology Institute of Northern China, Shenyang Agricultural University, Liaoning, China. The results of the present study should help as a theoretical foundation for the development of marketable and valuable biocontrol agent.

Material and methods

Experimental design

The study has been designed to evaluate the efficacy of Snef1216 (*Penicillium chrysogenum*) against *M. incognita* on cucumber by seed coating with randomized complete block design (RCBD) during 2018. Each treatment have been replicated five time.

Preparation of PDA

200 g of potatoes were boiled in 1 L of distilled water and filtered through cheesecloth on becoming soft. After that, 20 g of glucose and 17 g of agar were added into it and boiled again for 1 minute. Then, 100 ml PDA was poured in 250 ml conical flasks and sealed. PDA containing flask were sterilized into a steam autoclave machine for 30 minutes at 121^{o}C and preserved at room temperature.

Activation of Strain Snef1216 (Penicillium chrysogenum)

P. chrysogenum strain Snef1216 was obtained from the China General Microbiological Culture Collection Center. Jiang et al. (2011) identified it and stored at -80^{o}C at Nematology Institute of Northern China (NINC), Shenyang Agricultural University, China. Before use, a small quantity of strain was added into PDA filled cavities by the help of a sterilized needle and placed into an incubator for 7 days at 25-28^{o}C for the confirmation and purity level and strain activation.

Fermentation preparation

For the preparation of fermentation (nutrition medium) 50 g Sucrose, 8 g $NaNO_3$, 2 g K_2HPO_4, 0.08 g $MgSO_4.7H_2O$, 0.4 g KCl, and 0.003 g $FeSO_4.7H_2O$ were mixed together into 1000 ml distill water and the consequent mixture was boiled for few minutes. Then, 100 ml nutrition medium was poured into 250 ml conical flasks and sterilized into steam autoclave machine for 30 minutes at 121^{o}C. Five fungus cakes were added (1 mm diameter of each) into 100 ml nutrition medium and put on a shaker for 3 days at 28^{o}C and 150 rpm. After that, 100 ml new medium was poured into each flask and were again put on a shaker for 8 days at 28^{o}C and 150 rpm for fermentation development and then stored at 4^{o}C after filtration (Jiang et al., 2011).

http://www.aloki.hu ● ISSN 1589 1623 (Print) ● ISSN 1785 0037 (Online)
DOI: http://dx.doi.org/10.15666/aeer/1705_1245112464

Sterilization of seeds and seeds coating

Seeds were surface sterilized by 1-2 ml 75% ethanol and 0.05% Tween 20. After that 1-2 ml 95% ethanol was added and left for 1 minute then, 1-2 ml absolute ethanol was added and allowed for a few minutes to rinse with sterilized distilled water and air-dried. After that seeds were divided equally into two Petri dishes, half-seeds were coated with Snef1216 (*P. chrysogenum*) and half were taken as a control treatment. Uncoated or control seeds were placed into Petri dish containing double layers of wet filter papers for seed germination. For seeds coating, fermentation of Snef1216 (*P. chrysogenum*) was added and properly mixed for uniform coating on all seeds and left for complete drying, and was placed into Petri dish containing double layers of wet filter papers for seed germination. Germination % (G%), germination index (GI), and germination rate (GR) were calculated by *Eqs.1-3* (Bartlett, 1937; Mukhtar, 2008; Mukhtar et al., 2012).

$$G\% = \frac{N.G.S}{T.N.S} \times 100 \quad \text{(Eq.1)}$$

Whereas, N.G.S. is no. of germinated and T.N.S. is total no. of seeds.

$$GI = \frac{N.G.S.(1)}{D.C.(1)} + \frac{N.G.S.(2)}{D.C.(2)} + \frac{N.G.S.(f)}{D.C.(f)} \quad \text{(Eq.2)}$$

Whereas, N.G.S. (1), N.G.S. (2) and N.G.S. (f) are the numbers of germinated seeds in 1st, 2nd and final counts; D.C. (1), D.C. (2) and D.C. (f) are stand for days to 1st, 2nd and final counts.

$$GR = \frac{a + (a+b) + (a+b+c)(a+b+c+m)}{n(a+b+c+m)} \quad \text{(Eq.3)}$$

Whereas, a, b and c are the number of seedling in the first, second and third counts, m stands for the number of seedling in final count and n is number of counts.

Germinated seedlings were transferred into seedling trays which were filled with sterilized substrate. At four leaves stage plants were transferred into pots (20 cm diameter), those filled with 800-1000 g sterilized sand, soil and substrate (1:1:1).

Nematode Inoculums

The population of root-knot nematode (*M. incognita*) was maintained in tobacco and tomato plants, grown in greenhouse of Nematology Institute of Northern China (NINC), Shenyang Agricultural University, China. Plants were uprooted and roots were washed gently then, cut into 1-2 cm pieces and macerated for 30 seconds in a small amount of water by using the electric blender. Macerate was transferred into the funnel and added 0.05% NaOCl into it. The mixture was manually shaken for 1-2 minutes to separate the eggs from the gelatinous matrix. Then, the suspension was poured through 200 and 500 µm size meshes respectively and washed with tap water to remove NaOCl. Eggs were further purified by centrifugation in 454 g L^{-1} sucrose for 4 minutes at 3000 rpm. The supernatant was poured into 25 µm (500 µm mesh and rinsed several times with

http://www.aloki.hu ● ISSN 1589 1623 (Print) ● ISSN 1785 0037 (Online)
DOI: http://dx.doi.org/10.15666/aeer/1705_1245112464

sterilized water. Eggs inoculums were transferred into a funnel and allowed to hatch into second stage juveniles (J2). These (J2) were then allowed to crawl through eight layers of Kim-wipe tissues into sterilized water by using the Baermann funnels method (Baermann, 1917). The J2 in the resulting suspension adjusted at 500J2, 1000J2 and 2000J2/3 ml used as inoculums. These inoculums were injected 2-4 cm deep into rhizosphere with a plastic rod into 3 holes made around the base of the stem (Selim, 2010). The plants were monitored regularly to examine the different stages of the nematodes in the roots at different intervals viz., 7, 14, 21 and 28 dpi (days post inoculation).

Staining of roots

Plants were uprooted; carefully washed the roots under running tap water to remove soil particles and bleached in 10, 20 and 30 ml for young, mature and older roots respectively. Bleaching process was performed in 5.25% NaOCl into 50 ml distilled water for 4 minutes and washed for 45 seconds under running water and soaked into distilled water for 15 minutes. For stain preparation, 1 ml fuchsin acid was added into 30-50 ml distilled water and heated for 1 minute in the microwave. Then these roots were put into the preheated stain and reheated the stain untill boils. Washing was performed under water for color fading. Then, 2-3 drops of 5 mol/L HCl was added into 20-30 ml glycerol heated and placed the roots into it. Roots were examined after cooling under the microscope and observed different stages of RKN (Hussey, 1985).

Growth Index observation and determination

Growth parameters like plant height (cm) by using scale, stem diameter (mm) by using Vernier calipers, root length (cm), root and shoot weight (g) were calculated. Leaf area (LA) was calculated by using *Eq.4* Quarrie and Jones equation (Aldesuquy et al., 2014; Ahmad et al., 2015). Germinated plants were maintained in greenhouse at ambient light at 26-32°C and were irrigated by showering of tap water with the interval of three days. Five plants were selected randomly from each treatment at 28 dpi (Days post inoculation) for evaluating the variation among growth parameters.

$$LA = (Length \times Width) \times 0.75 \quad \text{(Eq.4)}$$

Following treatments were used (T1) control with (2000 J2) RKN (T2); control with (1000 J2) RKN; (T3) control with (500 J2) RKN; (T4) control without inoculation (T5); Coated or treated with (2000 J2) RKN; (T6) Coated or treated with (1000 J2) RKN; (T7) Coated or treated with (500 J2) RKN; (T8) coated or treated without inoculation.

Statistical Analysis

In order to assess the significant effects of all treatments on cucumber, all recorded data were analyzed by one-way Analysis of Variance (ANOVA). Mean difference between treatments were calculated for the significance test through Duncan's multiple range test (P>0.05). All statistical processes were administered by different statistical packages such as IBM-SPSS statistics 25.0 version software and MS Excel. Graphs were constructed through Sigma Plot 10.0 software.

http://www.aloki.hu ● ISSN 1589 1623 (Print) ● ISSN 1785 0037 (Online)
DOI: http://dx.doi.org/10.15666/aeer/1705_1245112464

Results

Seed Germination

The effect of fermentation on the seed germination is shown in *Fig. 1A, B and C*. Significant difference among treatments was observed. However, significant results (P<0.05) showed that seeds coated with fermentation broth of Snef1216 (*P. chrysogenum*) were found efficient to enhance 22.09% germination (G%) compared to control. Seed germination index (GI) noticeably demonstrated the potential of Snef1216 (*P. chrysogenum*) which increased to 53.77%. While, germination rate was boosted to 64.49% by pretreated seeds with fermentation as compared to control.

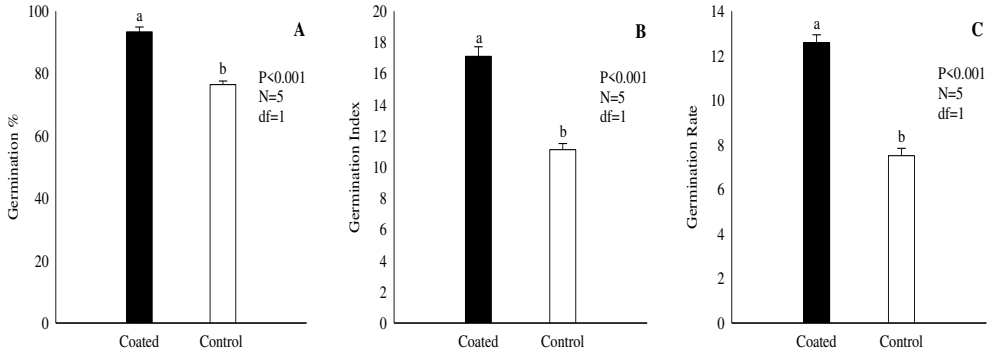

Figure 1. *(A) Germination percentage of cucumber seeds. (B) Germination index of treated and untreated seeds. (C) Effect of coating on germination rate. The error bars illustrated the mean±Standard error. Different letters on bar indicates that values are significantly different according to Duncan's multiple range test at P>0.05*

Growth Parameters

Table 1 and *Fig. 2* demonstrated that all treated seed efficiently promoted plant growth; like maximum plant height, 104.3 cm was observed in T8 followed by T4 and T7 96.8 and 94.9 cm, respectively.

Table 1. *Treatment effect on growth parameters of cucumber plants infected Meloidogyne incognita*

Treatments	Growth Parameters					
	Plant height (cm)	Stem diameter (mm)	Leaf area (cm^2)	Root length (cm)	Shoot weight (g)	Root weight (g)
Ck+2000J_2 (T1)	66.7±2.8^{e}	4.7±.01^{f}	72.5±2^{h}	20.3±0.9^{g}	27.8±2.1^{f}	6.3±.2^{e}
Ck+1000J_2 (T2)	70.2±1.7^{d}	5.1±.03^{e}	77.2±1^{g}	23.8±1.4^{f}	29.1±2.4^{ef}	6.9±.1^{e}
Ck+500J_2 (T3)	75.5±1.5^{c}	5.1±.04^{e}	80.4±1^{f}	24.4±1.5^{f}	30.9±1.1^{e}	7.9±.2^{d}
Ck no J_2 (T4)	76.7±2.8^{c}	5.3±.05^{d}	86.7±.3^{e}	28.8±0.8^{e}	36.4±1.5^{d}	9.6±.1^{c}
Trt.+2000J_2 (T5)	93.7±2.8^{b}	6.2±.03^{c}	103.3±1^{d}	31.3±1.8^{d}	40.8±2.3^{c}	9.4±.1^{c}
Trt.+1000J_2 (T6)	94.9±2.5^{b}	6.2±.02^{bc}	106.4±0^{c}	35.4±1.4^{c}	45.1±2.1^{b}	9.9±.1^{c}
Trt.+500J_2 (T7)	96.8±2.8^{b}	6.4±.01^{b}	109.5±1^{b}	39.2±1.0^{b}	47.7±2.2^{b}	11.9±0^{b}
Trt. no J_2 (T8)	104.3±3^{a}	6.6±.03^{a}	116.2±2^{a}	45.3±2.4^{a}	52.1±2.2^{a}	16.6±2^{a}
ANOVA Test						
Sum of square	699.459	18.182	9755.19	2526.216	2867.608	381.197
Mean Square	998.780	2.597	1393.60	360.888	409.658	54.457
F-value	156.631	101.247	1008.11	166.394	103.964	182.451

Data repesent the Mean±Standard deviation of growth parameters. The different letter within columns are significantly different according to Duncan's multiple range test (P>0.05)

http://www.aloki.hu ● ISSN 1589 1623 (Print) ● ISSN 1785 0037 (Online)
DOI: http://dx.doi.org/10.15666/aeer/1705_1245112464

Significant (P<0.05) stem diameter was recorded in T8 6.6 mm followed by T7 and T6 6.4 and 6.2 mm, respectively. The leaf area was ranged between 72.5-116.2 cm^2 in T1 and T8. Maximum root length observed was 45.30 cm in T8 compared to a minimum in T1 20.3 cm. Similarly, the highest shoot and root weight was recorded in T8 52.1 and 16.6 g compared to T1 27.8 and 6.3 g. The results revealed that pathogenicity of root-knot nematode (RKN) at different levels of inoculums viz., 500, 1000 and 2000 J2 of *M. incognita* per pot resulted into a significant (P<0.05) decrease in plant growth, however, treated plants showed significant biomass over control.

Figure 2. *Efficacy of coating of Snef 1216 (P. chrysogenum) on the growth of cucumber*

Nematode Infection

The Snef1216 *P. chrysogenum* was tested for its potential control toward *M. incognita* on the cucumber plant. The plants were monitored regularly to examine the different stages of the nematodes in roots at different intervals viz., 7, 14, 21 and 28 dpi (days post inoculums). Data presented in *Figs. 3* and *4*. showed that all the seed treated with Snef1216 efficiently reduced the penetration rate of J2 into cucumber roots at different inoculums levels such as 500J2/plant reduced invasion 67.09% followed by 1000 and 2000J2/plant 60.44 and 36.02%, respectively. It also inhibited the development of nematodes (J3 and J4) like 500J2/plant reduced 60.30% followed by 1000 and 2000J2/plant 50.37 and 38.77%, respectively. Similarly, rate of reproduction was 69.46, 62.89 and 63.62% at the same inoculation level (*Figs. 3* and *4*). At 7 dpi and 28 dpi less nematode population were present. Whereas, at all dpi-s control plants had highest population of nematodes while, seed treated with Snef1216 (*P. chrysogenum*) showed significantly fewer nematodes (*Fig. 5*). It was also observed that fewer females and males were developed in treated plants resulting in the development of few egg masses compared to control. It is obvious from results that the Snef1216 (*P. chrysogenum*) exhibited a drastic reduction in galls and no. of nematodes per gram of root weight as compared with control at different inoculum levels viz., 500, 1000 and 2000J2/per plant (*Fig. 6*).

http://www.aloki.hu ● ISSN 1589 1623 (Print) ● ISSN 1785 0037 (Online)
DOI: http://dx.doi.org/10.15666/aeer/1705_1245112464

Discussion

Seed dressing with fungus enhanced germination percentage, germination index, and germination rate. However, seed treatment with non-pathogenic inoculants like fungus showed boosted seed germination rate, seedling vigor and reduced the occurrence of pathogenic infections (Zheng and Shetty, 2000; Bharath et al., 2006; Dubey et al., 2007). Seed treated with *Trichoderma* species enhanced the germination parameters (Oyarbide et al., 2001; Mukhtar, 2008; Asaduzzaman et al., 2010; Mukhtar et al., 2012). Seed treatment with fermentation broth of Snef1216 could be an effective and reasonable way to enhance the germination of cucumber and reduce nematodes invasion in plant roots.

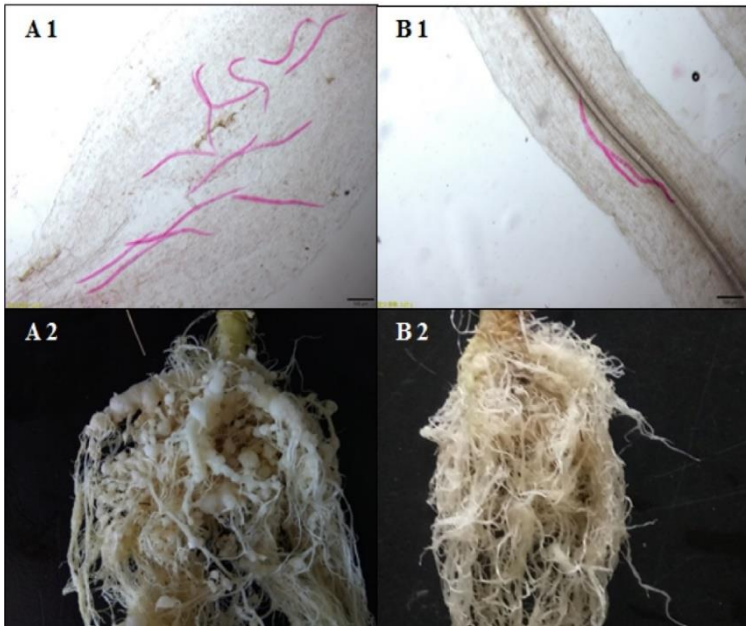

Figure 3. *(A1 and A2) Roots of seeds without coating. (B1 and B2) Roots of seeds coated with Snef 1216 (P. chrysogenum) fermentation*

The results indicated that seed coating resulted in increased biomass with low nematodes attack at different inoculums levels viz., 500, 1000 and 2000 J2/per pot as compared to their controls. Thus, our results are agree with Duggal et al. (2017) who reported that the pathogenic level of root-knot nematode in different inoculums viz., 0, 10, 100, 1000 and 10000 J2/pot resulted into significant reduction in plant growth parameters like plant height, root and shoot weight at or above 1000 J2 inoculums level. It was also reported that plant growth was inversely proportional to inoculums levels, at highest inoculums plant showed less biomass or vice versa. Vos et al. (2012) and Banuelos et al. (2014) supported our findings that *Arbuscular mycorrhizal* fungi improved plant growth and vigor in brinjal, tomato, and ornamental plants. *Syncephalastrum racemosum* efficiently increased plant growth in cucumber (Huang et al., 2014). Siddiqui and Akhtar (2009) described that antagonistic fungi (*P. chrysogenum* and *A. niger*) efficiently enhanced the tomato growth and significantly reduced gall formation. Seed treatment with fungus Snef1216 (*P. chrysogenum*) efficiently promoted the growth parameters compared to control at different levels of inoculums and play a vital role in the promotion of plant growth.

http://www.aloki.hu ● ISSN 1589 1623 (Print) ● ISSN 1785 0037 (Online)
DOI: http://dx.doi.org/10.15666/aeer/1705_1245112464

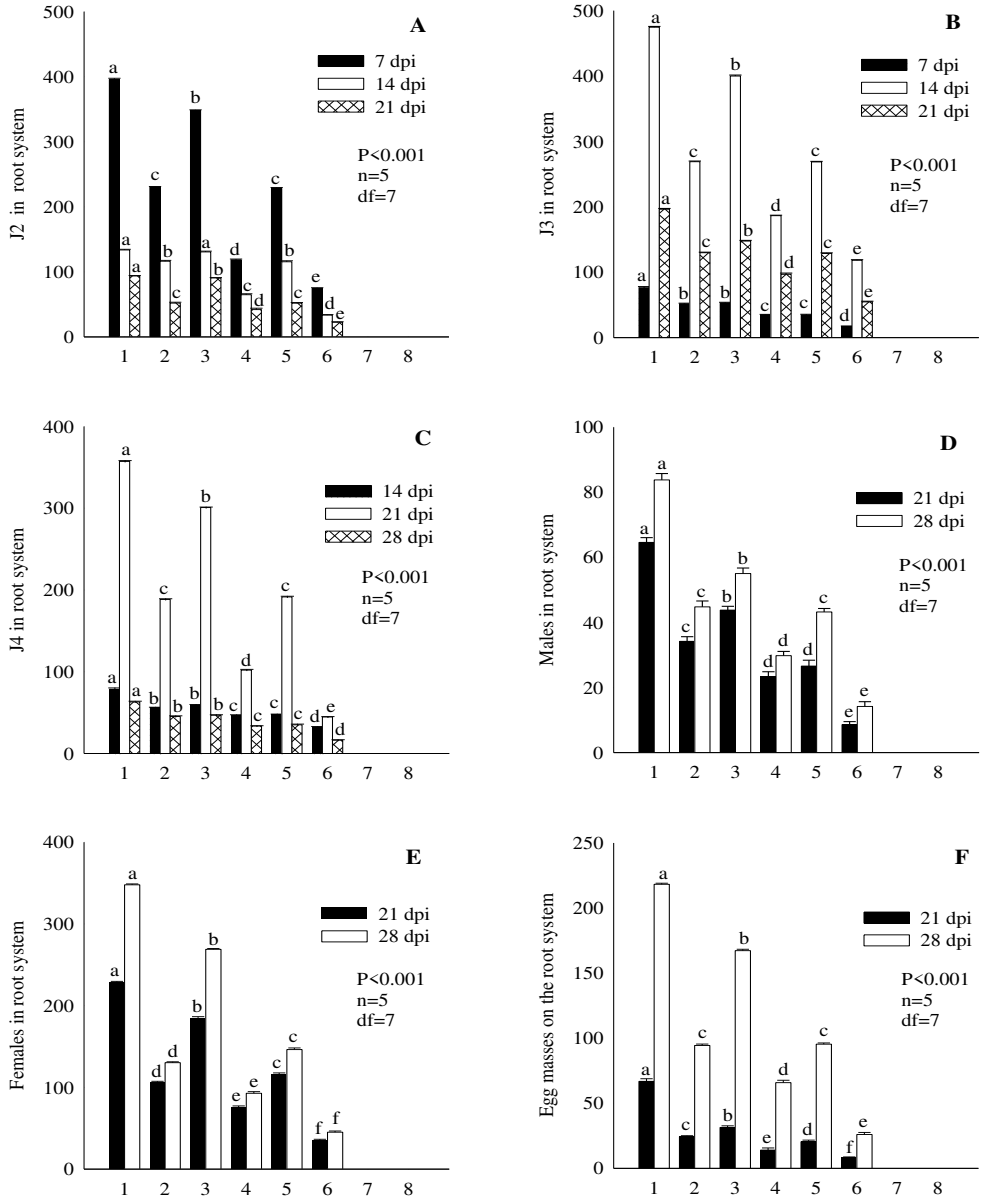

Figure 4. *(A) Number of J2 in the root system. (B) Number of J3 in the root system. (C) Number of J4 in the root system. (D) Number of males in the root system. (E) Number of females in the root system. (F) Number of egg masses on the root. The error bars illustrated the mean±standard error. Different letters on bar indicates that values are significantly different according to Duncan's multiple range test at P>0.05. (1= CK+2000J2; 2= Treated+2000J2; 3=CK+1000J2; 4=Treated+1000J2; 5=CK+500J2; 6=Treated+500J2; 7=CK-without inoculation, 8=Treated-without inoculation)*

Seed treated with endophytic fungi like *Fusarium*, *Trichoderma*, *Chaetomium*, *Acremonium*, *Paecilomyces*, and *Phyllosticta* potentially control *M. incognita* in cucumber (Siddiqui and Akhtar, 2009; Yan et al., 2011). Seed treatment used as a standard way for the application of *P. chrysogenum* that could concurrently confer resistance to root-knot nematodes in agricultural. Mascarin and Junior (2012) reported

http://www.aloki.hu ● ISSN 1589 1623 (Print) ● ISSN 1785 0037 (Online)
DOI: http://dx.doi.org/10.15666/aeer/1705_1245112464

that *T. harzianum* efficiently decrease the population of *M. incognita* in cucumber and enhanced plant growth under greenhouse conditions. *A. niger* had the ability to inhibit the *M. incognita* in tomato (Jang et al., 2016). *Fusarium oxysporum* showed repelling effect towards *M. incognita* in tomato as well as promoted plant growth (Selim, 2010; Terra et al., 2018). Gotlieb et al. (2003) reported that dry mycelium enhanced plant growth and reduced root galls to protect cucumber and tomato against *M. javanica.* Our findings clearly demonstrated that seed treatment with fungus Snef1216 (*P. chrysogenum*) significantly reduced the infection of root-knot nematode and lowered the number of 2nd stage juvenile's invasion in to cucumber roots. The pathogenic level of *M. incognita* in capsicum under greenhouse condition was observed that number of galls, egg masses was increased with increase in levels of inoculum conspicuously at and above 1000 J2 level (Duggal et al., 2017). Our results also revealed that pathogenic level of root-knot nematode was also observed in cucumber that the number of galls and egg masses was increased with increase in inoculums level while, seeds treated with Snef1216 significantly reduced compared to control. It also inhibited the development and rate of reproduction of nematodes in the roots. Cucumber is susceptible and an excellent host for multiplication of *M. incognita* but, seeds treated with Snef1216 significantly reduced the infection of nematodes and galls at a different level of inoculums also enhanced biomass.

Although different biological control approaches have been employed in current agriculture system to control nematodes on crops and vegetables, but seed dressing with strain Snef1216 on cucumber is limited. The outcomes from this study presented that Snef1216 is useful as a seed dressing, in order to decrease nematode infection. These results showed that seed dressing could be an effective alternative and reasonable way to control *M. incognita*.

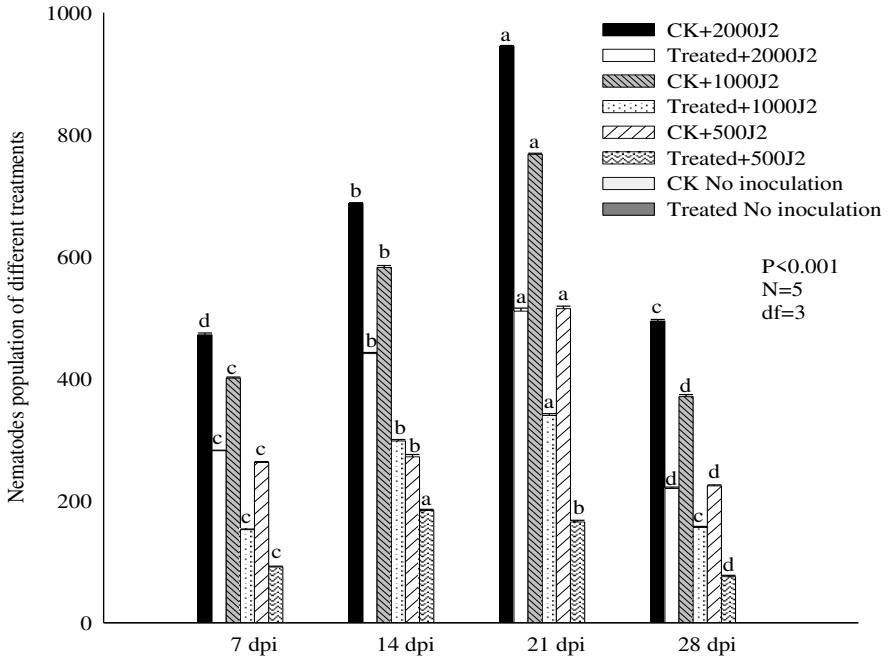

Figure 5. *Population of nematodes in different treatments at different dpi. The error bars illustrated the mean±standard error. Different letters on bar indicates that values are significantly different according to Duncan's multiple range test at P>0.05*

http://www.aloki.hu ● ISSN 1589 1623 (Print) ● ISSN 1785 0037 (Online)
DOI: http://dx.doi.org/10.15666/aeer/1705_1245112464

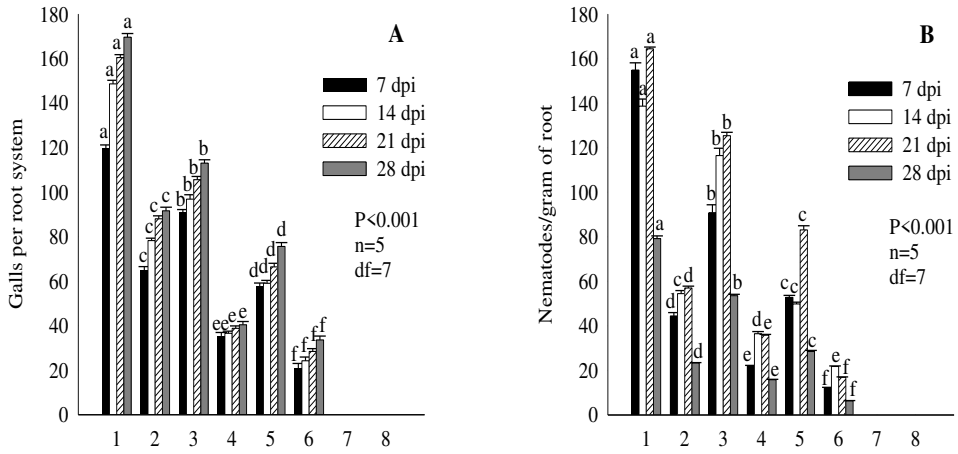

Figure 6. *(A) Number of galls per root system. (B) Number of nematodes present in per gram of root. The error bars illustrated the mean±standard error. Different letters on bar indicates that values are significantly different according to Duncan's multiple range test at P>0.05. (1= CK+2000J2; 2= Treated+2000J2; 3=CK+1000J2; 4=Treated+1000J2; 5=CK+500J2; 6=Treated+500J2; 7=CK-without inoculation, 8=Treated-without inoculation)*

Conclusion

Based on the finding of the present study, it is concluded that Snef1216 (*P. chrysogenum*) showed plant growth-promoting characters as well as have nematicidal activities with potential biocontrol agents against RKNs on cucumber under greenhouse conditions. It can be considered as a commercial biocontrol agent, however, before recommending this Snef1216 as commercial nematicides further study is needed to evaluate its active component screening and mechanisms of action. However, present findings may provide a theoretical foundation as a biocontrol agent for better control of root-knot nematodes (*M. incognita*).

Acknowledgements. The financial support provided by National Natural Science Foundation of China (31471748).

Conflict of interests. The authors have no conflict of interests.

REFERENCES

[1] Ahmad, S., Ali, H., Ur Rehman, A., Khan, R. J. Z., Ahmad, W., Fatima, Z., Abbas, G., Irfan, M., Ali, H., Khan, M. A. (2015): Measuring leaf area of winter cereals by different techniques: A comparison. – Life 13: 117-125.

[2] Aldesuquy, H., Baka, Z., Mickky, B. (2014): Kinetin and spermine mediated induction of salt tolerance in wheat plants: Leaf area, photosynthesis and chloroplast ultrastructure of flag leaf at ear emergence. – Egyptian Journal of Basic and Applied Sciences 1: 77-87.

[3] Asaduzzaman, M., Alam, M., Islam, M. (2010): Effect of *Trichoderma* on seed germination and seedling parameters of chili. – Journal of Science Foundation 8: 141-150.

[4] Back, M., Haydock, P., Jenkinson, P. (2002): Disease complexes involving plant parasitic nematodes and soilborne pathogens. – Plant Pathology 51: 683-697.

http://www.aloki.hu ● ISSN 1589 1623 (Print) ● ISSN 1785 0037 (Online)
DOI: http://dx.doi.org/10.15666/aeer/1705_1245112464

[5] Baermann, G. (1917): Eine einfache methode zur auffindung von Ancylostomum (Nematoden) larven in erdproben. – Geneeskd Tijdschr Ned Indie 57: 131-137.
[6] Banuelos, J., Alarcón, A., Larsen, J., Cruz-Sánchez, S., Trejo, D. (2014): Interactions between arbuscular mycorrhizal fungi and *Meloidogyne incognita* in the ornamental plant Impatiens balsamina. – Journal of Soil Science and Plant Nutrition 14: 63-74.
[7] Bartlett, M. S. (1937): Some examples of statistical methods of research in agriculture and applied biology. – Supplement to the Journal of the Royal Statistical Society 4: 137-183.
[8] Bharath, B., Lokesh, S., Prakash, H., Shetty, H. (2006): Evaluation of different plant protectants against seed mycoflora of watermelon [*Citrullus lanatus* (Thunb.) Matsum and Nakai]. – Research Journal of Botany 1: 1-5.
[9] Björsell, P., Edin, E., Viketoft, M. (2017): Interactions between some plant-parasitic nematodes and *Rhizoctonia solani* in potato fields. – Applied Soil Ecology 113: 151-154.
[10] Divon, H. H., Fluhr, R. (2007): Nutrition acquisition strategies during fungal infection of plants. – FEMS Microbiology Letters 266: 65-74.
[11] Dong, L. Q., Zhang, K. Q. (2006): Microbial control of plant-parasitic nematodes: a five-party interaction. – Plant and Soil 288: 31-45.
[12] Dong, S., Qiao, K., Zhu, Y., Wang, H., Xia, X., Wang, K. (2014): Managing *Meloidogyne incognita* and *Bemisia tabaci* with thiacloprid in cucumber crops in China. – Crop Protection 58: 1-5.
[13] Dubey, S. C., Suresh, M., Singh, B. (2007): Evaluation of *Trichoderma* species against *Fusarium oxysporum* f. sp. ciceris for integrated management of chickpea wilt. – Biological Control 40: 118-127.
[14] Duggal, P., Ram, S., Bhatia, A., Patil, J. (2017): Life Cycle and Pathogenicity of *Meloidogyne incognita* on *Capsicum frutescens* under Poly-House as Compared to Screen-House Conditions. – International Journal of Pure and Applied Bioscience 5: 1017-1024.
[15] Escobar, C., Barcala, M., Cabrera, J., Fenoll, C. (2015): Overview of root-knot nematodes and giant cells. – Advances in Botanical Research, Elsevier.
[16] FAOSTAT (2018): Countries - Select All; Regions - World + (Total); Elements - Production Quantity; Items - Cucumbers and gherkins; Years -2016. – Retrieved 2018-08-25.
[17] Gotlieb, D., Oka, Y., Ben-Daniel, B.-H., Cohen, Y. (2003): Dry mycelium of *Penicillium chrysogenum* protects cucumber and tomato plants against the root-knot nematode *Meloidogyne javanica*. – Phytoparasitica 31: 217-225.
[18] Govinden-Soulange, J., Levantard, M. (2008): Comparative studies of seed priming and pelleting on percentage and meantime to germination of seeds of tomato (*Lycopersicon esculentum* Mill.). – African Journal of Agricultural Research 3: 725-731.
[19] Huang, W.-K., Sun, J.-H., Cui, J.-K., Wang, G.-F., Kong, L.-A., Peng, H., Chen, S.-L., Peng, D.-L. (2014): Efficacy evaluation of fungus *Syncephalastrum racemosum* and nematicide avermectin against the root-knot nematode *Meloidogyne incognita* on cucumber. – PLoS One 9: e89717.
[20] Huang, W.-K., Cui, J.-K., Liu, S.-M., Kong, L.-A., Wu, Q.-S., Peng, H., He, W.-T., Sun, J.-H., Peng, D.-L. (2016): Testing various biocontrol agents against the root-knot nematode (*Meloidogyne incognita*) in cucumber plants identifies a combination of *Syncephalastrum racemosum* and *Paecilomyces lilacinus* as being most effective. – Biological Control 92: 31-37.
[21] Hussey, R. (1985): Staining nematodes in plant tissue - Plant nematology laboratory manual. – Amherst, MA, USA, University of Massachusetts Agricultural Experimental Station 197-199.
[22] Jang, J. Y., Choi, Y. H., Shin, T. S., Kim, T. H., Shin, K.-S., Park, H. W., Kim, Y. H., Kim, H., Choi, G. J., Jang, K. S. (2016): Biological control of *Meloidogyne incognita* by *Aspergillus niger* F22 producing oxalic acid. – PloS One 11: e0156230.

http://www.aloki.hu ● ISSN 1589 1623 (Print) ● ISSN 1785 0037 (Online)
DOI: http://dx.doi.org/10.15666/aeer/1705_1245112464

[23] Jiang, M., Duan, Y., Chen, L., Zhu, X. (2011): Study on the Fermentation of *Penicillium* Snef1216 Inducing the Resistance of Tomato to Root-knot Nematode. – Journal of Henan Agricultural Sciences 4: 032.
[24] Kalele, D. N., Affokpon, A., Coosemans, J. (2007): Efficacy of *Paecilomyces lilacinus* strain 251 against root knot nematodes in tomato under greenhouse conditions. – Communications in Agricultural and Applied Biological Sciences 72: 209-213.
[25] Kokalis-Burelle, N. (2015): *Pasteuria penetrans* for control of *Meloidogyne incognita* on tomato and cucumber, and *M. arenaria* on snapdragon. – Journal of Nematology 47: 207.
[26] Li, X., Chen, S. (2017): Screening and identification of cucumber germplasm and rootstock resistance against the root-knot nematode (*Meloidogyne incognita*). – Genetics and Molecular Research 16.
[27] Mao, L.-g., Wang, Q.-x., Yan, D.-d., Liu, P.-f., Jin, S., Fang, W.-s., Hu, X.-m., Yuan, L., Ouyang, C.-b., Guo, M.-x. (2016): Application of the combination of 1, 3-dichloropropene and dimethyl disulfide by soil injection or chemigation: effects against soilborne pests in cucumber in China. – Journal of Integrative Agriculture 15: 145-152.
[28] Mascarin, G. M., Junior, M. F. B. (2012): *Trichoderma harzianum* reduces population of *Meloidogyne incognita* in cucumber plants under greenhouse conditions. – Journal of Entomology and Nematology 4: 54-57.
[29] Miyashita, N., Yabu, T., Kurihara, T., Koga, H. (2014): The feeding behavior of adult root-knot nematodes (*Meloidogyne incognita*) in rose balsam and tomato. – Journal of Nematology 46: 296-301.
[30] Mukhtar, I. (2008): Influence of *Trichoderma* species on seed germination in okra. – Mycopath 6: 47-50.
[31] Mukhtar, I., Hannan, A., Atiq, M., Nawaz, A. (2012): Impact of *Trichoderma* species on seed germination in soybean. – Pakistan Journal of Phytopathology 24: 159-162.
[32] Nicol, J. M., Turner, S. J., Coyne, D. L., Nijs, L. D., Hockland, S., Maafi, Z. T. (2011): Current Nematode Threats to World Agriculture. – In: Jones, J., Gheysen, G., Fenoll, C. (eds.) Genomics and Molecular Genetics of Plant-Nematode Interactions. Springer Netherlands, Dordrecht.
[33] Oka, Y., Nacar, S., Putievsky, E., Ravid, U., Yaniv, Z., Spiegel, Y. (2000): Nematicidal activity of essential oils and their components against the root-knot nematode. – Phytopathology 90: 710-715.
[34] Onkendi, E. M., Kariuki, G. M., Marais, M., Moleleki, L. N. (2014): The threat of root-knot nematodes (*Meloidogyne* spp.) in Africa: a review. – Plant Pathology 63: 727-737.
[35] Oyarbide, F., Osterrieth, M. L., Cabello, M. (2001): *Trichoderma koningii* as a biomineralizing fungous agent of calcium oxalate crystals in typical Argiudolls of the Los Padres Lake natural reserve (Buenos Aires, Argentina). – Microbiological Research 156: 113-119.
[36] Palomares-Rius, J. E., Escobar, C., Cabrera, J., Vovlas, A., Castillo, P. (2017): Anatomical Alterations in Plant Tissues Induced by Plant-Parasitic Nematodes. – Frontiers in Plant Science 8: 1987.
[37] Sebastian, P., Schaefer, H., Telford, I. R., Renner, S. S. (2010): Cucumber (*Cucumis sativus*) and melon (*C. melo*) have numerous wild relatives in Asia and Australia, and the sister species of melon is from Australia. – Proceedings of the National Academy of Sciences 107: 14269-14273.
[38] Selim, M. E. M. (2010): Biological, chemical and molecular studies on the systemic induced resistance in tomato against *Meloidogyne incognita* caused by the endophytic *Fusarium oxysporum*, Fo162. – PH.D. University of Bonn.
[39] Sharon, E., Chet, I., Spiegel, Y. (2009): Improved attachment and parasitism of *Trichoderma* on *Meloidogyne javanica* in vitro. – European Journal of Plant Pathology 123: 291-299.

http://www.aloki.hu ● ISSN 1589 1623 (Print) ● ISSN 1785 0037 (Online)
DOI: http://dx.doi.org/10.15666/aeer/1705_1245112464

[40] Siddiqui, Z. A., Akhtar, M. S. (2009): Effects of antagonistic fungi, plant growth-promoting rhizobacteria, and arbuscular mycorrhizal fungi alone and in combination on the reproduction of *Meloidogyne incognita* and growth of tomato. – Journal of General Plant Pathology 75: 144.

[41] Smant, G., Helder, J., Goverse, A. (2018): Parallel adaptations and common host cell responses enabling feeding of obligate and facultative plant parasitic nematodes. – The Plant Journal 93: 686-702.

[42] Son, S., Khan, Z., Kim, S., Kim, Y. (2009): Plant growth-promoting rhizobacteria, *Paenibacillus polymyxa* and *Paenibacillus lentimorbus* suppress disease complex caused by root-knot nematode and fusarium wilt fungus. – Journal of Applied Microbiology 107: 524-532.

[43] Terra, W. C., Campos, V. P., Martins, S. J., Costa, L. S. A. S., da Silva, J. C. P., Barros, A. F., Lopez, L. E., Santos, T. C. N., Smant, G., Oliveira, D. F. (2018): Volatile organic molecules from *Fusarium oxysporum* strain 21 with nematicidal activity against *Meloidogyne incognita*. – Crop Protection 106: 125-131.

[44] Tian, Y., Zhang, X., Liu, J., Gao, L. (2011): Effects of summer cover crop and residue management on cucumber growth in intensive Chinese production systems: soil nutrients, microbial properties and nematodes. – Plant and Soil 339: 299-315.

[45] Trudgill, D. L., Blok, V. C. (2001): Apomictic, polyphagous root-knot nematodes: exceptionally successful and damaging biotrophic root pathogens. – Annual Review of Phytopathology 39: 53-77.

[46] Vos, C. M., Tesfahun, A. N., Panis, B., De Waele, D., Elsen, A. (2012): Arbuscular mycorrhizal fungi induce systemic resistance in tomato against the sedentary nematode *Meloidogyne incognita* and the migratory nematode *Pratylenchus penetrans*. – Applied Soil Ecology 61: 1-6.

[47] Xiang, N., Lawrence, K. S., Kloepper, J. W., Donald, P. A., McInroy, J. A., Lawrence, G. W. (2017): Biological control of *Meloidogyne incognita* by spore-forming plant growth-promoting rhizobacteria on cotton. – Plant Disease 101: 774-784.

[48] Yan, X.-n., Sikora, R. A., Zheng, J.-w. (2011): Potential use of cucumber (*Cucumis sativus* L.) endophytic fungi as seed treatment agents against root-knot nematode *Meloidogyne incognita*. – Journal of Zhejiang University Science B 12: 219-225.

[49] Yao, Q., Lu, X., Zhu, X., Wang, Y., Chen, L., Duan, Y. (2014): Resistance against *Meloidogyne incognita* in tomato induced by fermentation liquid of *Penicillium chrysogenum* strain 1216. – Acta Phytopathologica Sinica 44: 693-699.

[50] Youssef, R. M., Kim, K.-H., Haroon, S. A., Matthews, B. F. (2013): Post-transcriptional gene silencing of the gene encoding aldolase from soybean cyst nematode by transformed soybean roots. – Experimental Parasitology 134: 266-274.

[51] Zeng, J., Zhang, Z., Li, M., Wu, X., Zeng, Y., Li, Y. (2018): Distribution and Molecular Identification of *Meloidogyne* spp. Parasitising Flue-cured Tobacco in Yunnan, China. – Plant Protection Science 1-7.

[52] Zheng, Z., Shetty, K. (2000): Enhancement of pea (*Pisum sativum*) seedling vigour and associated phenolic content by extracts of apple pomace fermented with *Trichoderma* spp. – Process Biochemistry 36: 79-84.

http://www.aloki.hu ● ISSN 1589 1623 (Print) ● ISSN 1785 0037 (Online)
DOI: http://dx.doi.org/10.15666/aeer/1705_1245112464

NUMERICAL ANALYSIS OF THE SEEPAGE CHARACTERISTICS OF SLOPES WITH WEAK INTERLAYERS UNDER DIFFERENT RAINFALL LEVELS

YU, S. – ZHANG, J.* – REN, X.

College of Water Conservancy and Hydropower Engineering, Hohai University, Nanjing 210098, China

**Corresponding author*
e-mail: zhangjixun@hhu.edu.cn; phone: +86-159-5050-6212

(Received 13th May 2019; accepted 16th Jul 2019)

Abstract. In order to study the seepage characteristics of slopes with weak interlayers under different rainfall levels, the finite element analysis model was established using the Seep/w module in Geostudio2018. The calculation conditions of big rain, heavy rain and rainstorm were carried out. The variation of pore pressure at different monitoring points and monitoring lines was obtained. The results show that under different rainfall levels, the pore pressure of slope surface increases first and then decreases, reaches saturation in the process of rainfall, and decreases gradually after the rainfall, and the pore pressure presents shapes like a backwards S at the elevation of weak interlayers. The wetting front infiltrates the silty clay layer uniformly and a "sudden change" occurs at the elevation of weak interlayers. The rainfall infiltration degree under low intensity and long duration is greater than that of high intensity and low duration. The research results will provide a reference for the understanding of the rainfall infiltration mechanism of the slope with weak interlayers as well as the slope treatment and prevent the catastrophic disasters occurring in slopes.
Keywords: *numerical studies, unsaturated soils, interlayers, pore water pressure, wetting front, geo-studio*

Introduction

Weak interlayers widely exist in the interior of the slope (Long-Qi and Neng-Pan, 2016; Yang et al., 2018), not only controlling its stability (Kulasingam et al., 2004), but also having a great influence on the seepage characteristics (Thompson, 1984; Ming et al., 2011). Meanwhile, Rainfall is the key factor affecting slope safety (Rahardjo et al., 2005). Rainfall causes the rise of the underground water level (Chaplot et al., 2003) and the reduction of shear strength in rock and soil (Fang et al., 2015), thus leading to catastrophic disasters. According to some relevant studies (Lee et al., 2013), rainfall-induced landslides account for 51% of the total number of landslides. Therefore, it is of great significance to study the effects of rainfall on slopes with weak interlayers.

Rainfall-induced landslides are mainly characterized by shallow instability in the early stage and overall slipperiness in the later period (Zhang and Wang, 2012). The influence of rainfall on slope seepage is mainly reflected in the formation of transient saturation zone at the foot of the slope, and then diffuses to its depth (Philip, 1993). Previous studies have focused on the influence of different rainfall types and different soil or rock mechanical properties on the seepage characteristics and slope safety. For example, soil properties such as the anisotropy ratio (Zhang and Lin, 2016), the saturated hydraulic conductivity (Woolhiser et al., 1996), the matric suction (Lim et al., 1996), the cohesive strength (Schultz et al., 1985) and the internal friction angle (Mitchell et al., 1972) all play important roles, and rainfall types such as different peak

http://www.aloki.hu ● ISSN 1589 1623 (Print) ● ISSN 1785 0037 (Online)
DOI: http://dx.doi.org/10.15666/aeer/1705_1246512478

rainfalls (Sheng, 2000), different rainfall levels (Tian, 2014) and different return periods (Ng et al., 2001) equally have a great impact. Meanwhile, antecedent rainfall should be considered before starting numerical calculations (Rahimi et al., 2011).

As a weak part in the slope, interlayers have the characteristics of high permeability and low shear resistance, and they are sensitive to rainfall. Experimental study on slopes with a thin soft band layer under rainfall has been conducted by Elkamhawy et al. (2018) to study the seepage characteristics and failure modes, but discussions are not sufficient, theoretical methods were proposed such as the shear strength reduction method (Jie-Qun et al., 2013) and the three-dimensional combined rotational-translational mechanism (Huang et al., 2017) but they are applied under the condition without rainfall. In addition, the seepage stability mechanism of weak interlayer under rainfall condition is still lacking, which needs to be further studied.

Previous studies have mostly focused on the impact of rainfall types on the seepage characteristics of homogeneous slopes or its stability with interlayers. However, few studies have involved systematic analysis of seepage characteristics, which can reveal the mechanism of rainfall infiltration and rock and soil deterioration. So in this paper, numerical model of a slope with weak interlayers was established with Geo-studio and seepage characteristics were quantitatively studied under different rainfall levels. The results of the research will provide a reference for the understanding of rainfall infiltration mechanism of the slopes with weak interlayers as well as the its treatment and prevent the catastrophic disasters occurring in slopes.

Methods and theory

Model and boundary conditions

The simulation model was established according to the geometry presented by Yang et al. (2008), as shown in *Figure 1*. However, Yang et al. (2008) did not give a systematic description of the seepage characteristics. In this paper, the monitoring points and monitoring lines are adopted to illustrate the seepage characteristics not only on the slope surface but also along its elevation, which can give a better understanding. The slope height of the first and second grade is 10 m, and the third one is 8 m high. The slope ratios of all the three stages are 1:1. There are two weak interlayers, which are the ribbon structure layer with a thickness of 2 m (8.2°with horizontal direction). For the correct reflection of rainfall infiltration, the depth of the foundation is set to 22 m. The mesh size is refined to 0.2 m in weak interlayers and 0.4 m in other parts. The whole model is divided into 5,481 nodes and 5,375 elements.

In order to study the seepage characteristics of the slope surface at different locations, four monitoring points on the surface of the slope are taken. They are monitoring point 1 located at (30, 50), monitoring point 2 located at (41.5, 42), monitoring point 3 located at (56.5, 34) and monitoring point 4 located at (66, 22). Four monitoring lines are also taken to investigate the seepage law in the slope at different locations; they are monitoring line 1 located at $x = 30$, monitoring line 2 located at $x = 41.5$, monitoring line 3 located at $x = 56.5$ and monitoring line 4 located at $x = 66$.

To study the rainfall infiltration, the initial condition should be defined. In this paper, the initial seepage field is calculated by the initial infiltration line shown in *Figure 1*. CDEF is the rainfall infiltration boundary, BC, FG and AH are the impervious boundary, AB is the fixed head boundary of 26 m and HG is the 15 m fixed head boundary.

http://www.aloki.hu ● ISSN 1589 1623 (Print) ● ISSN 1785 0037 (Online)
DOI: http://dx.doi.org/10.15666/aeer/1705_1246512478

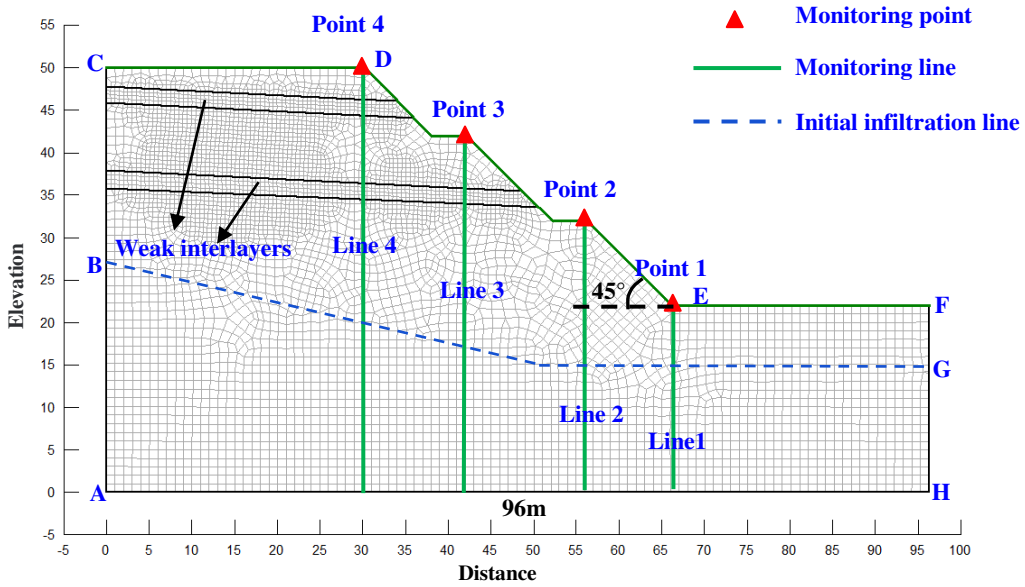

Figure 1. *Slope simulation model*

According to the climate monitoring data of Linchang Highway, three simulation schemes are determined for different rainfall levels: big rain, heavy rain and rainstorm on the basis of the standard of State Meteorological Administration of China. The rainfall intensity is 1.67 mm/h in big rain condition, and the duration is 4 d. The rainfall intensity is 3.33 mm/h in heavy rain condition, and the duration is 2 d, while the rainfall intensity is 6.67 mm/h in rainstorm condition, and the duration is 1 d. The calculation time is set to 5 d in Geo-studio and the specific rainfall conditions are shown in *Table 1*.

Table 1. *Rainfall conditions*

Rainfall level	Rainfall intensity (mm/h)	Rainfall duration time (d)	Rainfall amount (m)
Big rain	1.67	4	0.16
Heavy rain	3.33	2	0.16
Rain storm	6.67	1	0.16

Material properties

The SEEP/W module in Geo-studio is utilized to simulate the rainfall infiltration, and the unsaturated seepage equation can be expressed as (Fredlund and Rahardjo, 1993):

$$\frac{\partial}{\partial x_i}[k_{ij}{}^s k_r(h_c)\frac{\partial h_c}{\partial x_j}+k_{i3}k_r(h_c)]+Q=[C(h_c)+\frac{\theta}{n}S_s]\frac{\partial h_c}{\partial t} \quad \text{(Eq.1)}$$

where x_i, x_j is the position coordinates in i and j direction, $k_{ij}{}^s$ is the saturated permeability tensor, k_r is the relative water permeability, h_c is the pressure head, β is the unsaturated coefficient, S_s is the pondage restored in soil, Q is the input and output of the flux, $C(h_c)$ is the water capacity which is the function of h_c, n is the porosity and t is the time.

http://www.aloki.hu ● ISSN 1589 1623 (Print) ● ISSN 1785 0037 (Online)
DOI: http://dx.doi.org/10.15666/aeer/1705_1246512478

The water characteristic curves (SWCC) characterizing the variation of volumetric moisture content or permeability coefficient with matric suction, which was proposed by Fredlund and Rahardjo (1993) in 1994, can obtain the closed solution of volume water content under the range of negative pore pressure from 0 to -1×10^6 KPa and is adopted in this paper:

$$\theta_w = C_\phi \frac{\theta_s}{\left\{\ln\left[e + \left(\frac{\phi}{a}\right)^n\right]\right\}^m} \quad \text{(Eq.2)}$$

where θ_w is the volumetric moisture content, C_ϕ is the modified function, θ_s is the saturated volumetric moisture content, ϕ is the negative pore water pressure.

According to the volume water content function of Fredlund (Fredlund and Rahardjo, 1993), SEEP/W module in Geo-studio software sets the corresponding governing equation (Fredlund and Rahardjo, 1993), which can be expressed as:

$$k_w = k_s \frac{\sum_{i=j}^{N} \frac{\theta(e^y) - \theta(\psi)}{e_i^y} \theta(e_i^y)}{\sum_{i=1}^{N} \frac{\theta(e^y) - \theta_s}{e_i^y} \theta^0(e_i^y)} \quad \text{(Eq.3)}$$

where k_w is the permeability coefficient calculated by water content or negative pore water pressure, k_s is the saturated permeability coefficient of slope soil, y represents the dummy variable of the negative pore water pressure algorithm, i is the numerical distance between j and N, j is the minimum negative pore water pressure described by the final function, N is the maximum negative pore water pressure described by the final function and Ψ corresponds to the first j of negative pore water pressure. θ_0 is the initial value of the equation.

The slope soil is composed of silty clay. The physical and mechanical properties of silty clay and interlayers are determined according to the experiment and field investigation. The values of parameters are shown in *Table 2,* and the SWCC curves are shown in *Figure 2.*

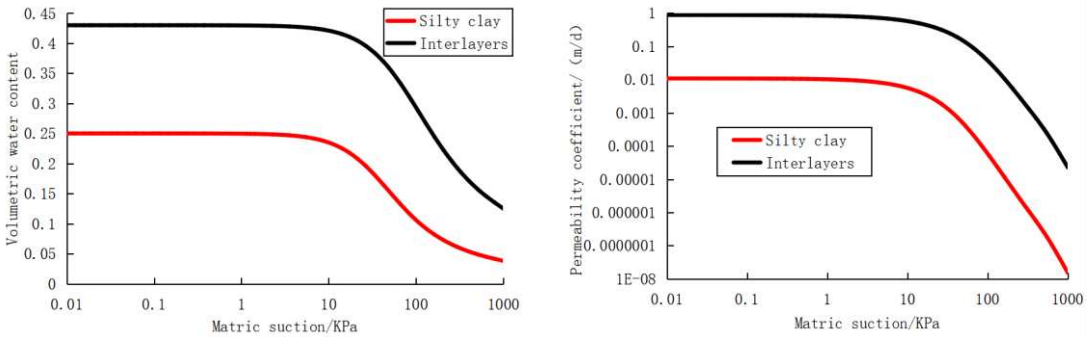

(a) Volume water content function (b) Permeability coefficient function

Figure 2. *Soil-water characteristic curve*

http://www.aloki.hu ● ISSN 1589 1623 (Print) ● ISSN 1785 0037 (Online)
DOI: http://dx.doi.org/10.15666/aeer/1705_1246512478

Table 2. *Physical and mechanical properties of materials*

Materials	Weight (kN/m^3)	Cohesive strength (KPa)	Internal friction angle	Permeability coefficient (m/d)	Saturated water content
Silty clay	25	31	27	0.0108	0.25
Interlayers	12	16	13	0.88128	0.43

Results

Comparison of pore water pressure variation on the slope surface

The variation of pore pressure at different monitoring points (monitoring point 1, monitoring point 2, monitoring point 3 and monitoring point 4) is shown in *Figure 3*. Under the action of rainfall, the slope surfaces at different positions experienced the process from unsaturated to saturated and then to unsaturated, that is, the pore pressure increases to 0 at first and then decreases, except for monitoring point 3, and the variation of pore pressure caused by different rainfall grades is quite different. For monitoring point 1, monitoring point 2 and monitoring point 4, pore pressure goes through a process of rapidly rising to saturation, continuing and then decreasing under different rainfall levels, and the time when the slope surface reaches saturation is positively proportional to the rainfall level. However, it is worth noting that the big rain, which represents the long period of weak rainfall, has the ability to make the duration of slope surface saturation longer (average 0.5 day for rainstorm, 1 day for heavy rain and 2.4 days for big rain). Although the time of the big rain condition when slope surface reaches saturation is later than other rainfall levels (heavy rain and rainstorm). It means that the effect of a short period of heavy rain on the slope seepage characteristics is less than that of a long period of weak rain. This is because prolonged weak rainfall can make slope infiltration more sufficient, and large amounts of rainwater are prevented from draining away from the slope surface, which is closely related to the infiltration rate of the soil (Jun-Ping et al., 2016), if the rain intensity is larger than the infiltration rate of soil, then rainfall infiltration will be determined by infiltration rate rather than rainfall intensity. Therefore, more attention should be paid to slope safety monitoring and drainage in the case of long-term weak rainfall.

For monitoring point 3, the change of pore pressure is different from other monitoring points, although pore pressure increases during rainfall, the slope surface does not reach the saturated state. This is because monitoring point 3 is located at the top of the secondary slope. Under this condition, rainwater not only infiltrates from monitoring point 3, but also drains to the lower part of the slope. This phenomenon is observed in Elkamhawy's works (Elkamhawy et al., 2018) and is discussed in section 4. Therefore, the increase of pore pressure at monitoring point 3 is significantly smaller than that at other monitoring points.

Comparison of pore water pressure variation in the slope

Variation of pore water pressure of different time under a rainstorm

Variation of pore water pressure of different time under rainstorm is shown in *Figure 4*. Pictures on the left side are the pore pressure distribution of the whole monitoring line, while on the right side are the region where local pore pressure changes

http://www.aloki.hu ● ISSN 1589 1623 (Print) ● ISSN 1785 0037 (Online)
DOI: http://dx.doi.org/10.15666/aeer/1705_1246512478

dramatically. The pore pressure distribution on different monitoring lines is also very different, the monitoring line 1 and 2 did not pass through the weak interlayer, while the monitoring line 3 passed through the second weak in

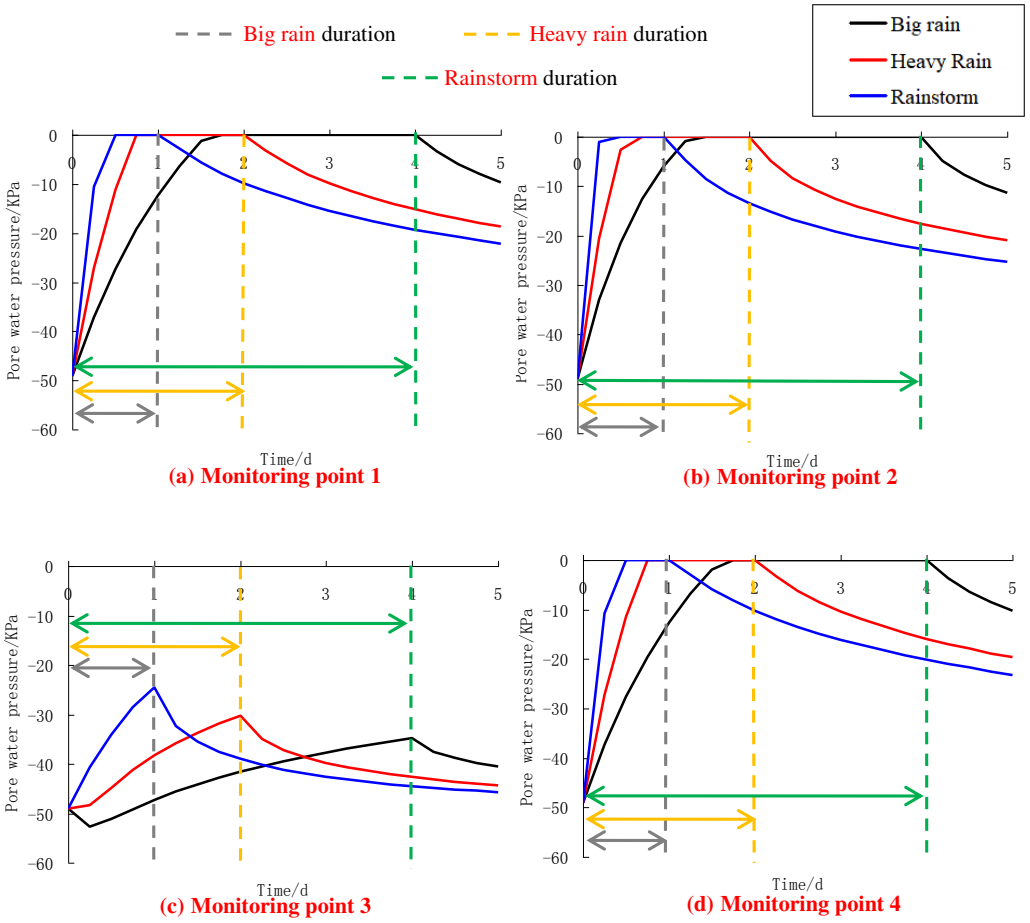

Figure 3. *Pore water pressure of different monitoring points*

terlayer and the monitoring line 4 simultaneously passed through two weak interlayers.

For monitoring line 1, it is not only affected by rainfall infiltration in the process of rainfall, but also by the drainage of upper rainwater because it is located in the lower part of the slope. Therefore, except for the shallow part (elevation 18-22 m), which is greatly affected by rainfall on the surface of the slope, the pore pressure increases linearly with the elevation and remains unchanged during rainfall. Compared with the local enlarged image on the right, the pore pressure on the shallow part rapidly increases to saturation during rainfall, and then gradually develops to the depth. After the rain stops, the pore pressure of the slope surface gradually drops, but the affected area is only limited to the elevation of 18-22 m and has a small impact on the rest.

For monitoring line 2, except the area where the pore pressure in the surface of the slope changes sharply (elevation 28-32 m), the rest of the area first remains unchanged with the elevation (elevation 22-28 m), and then presents a linear increase distribution with the elevation. For the shallow part (figures on the right), the change of pore pressure is similar to that of monitoring line 1.

http://www.aloki.hu ● ISSN 1589 1623 (Print) ● ISSN 1785 0037 (Online)
DOI: http://dx.doi.org/10.15666/aeer/1705_1246512478

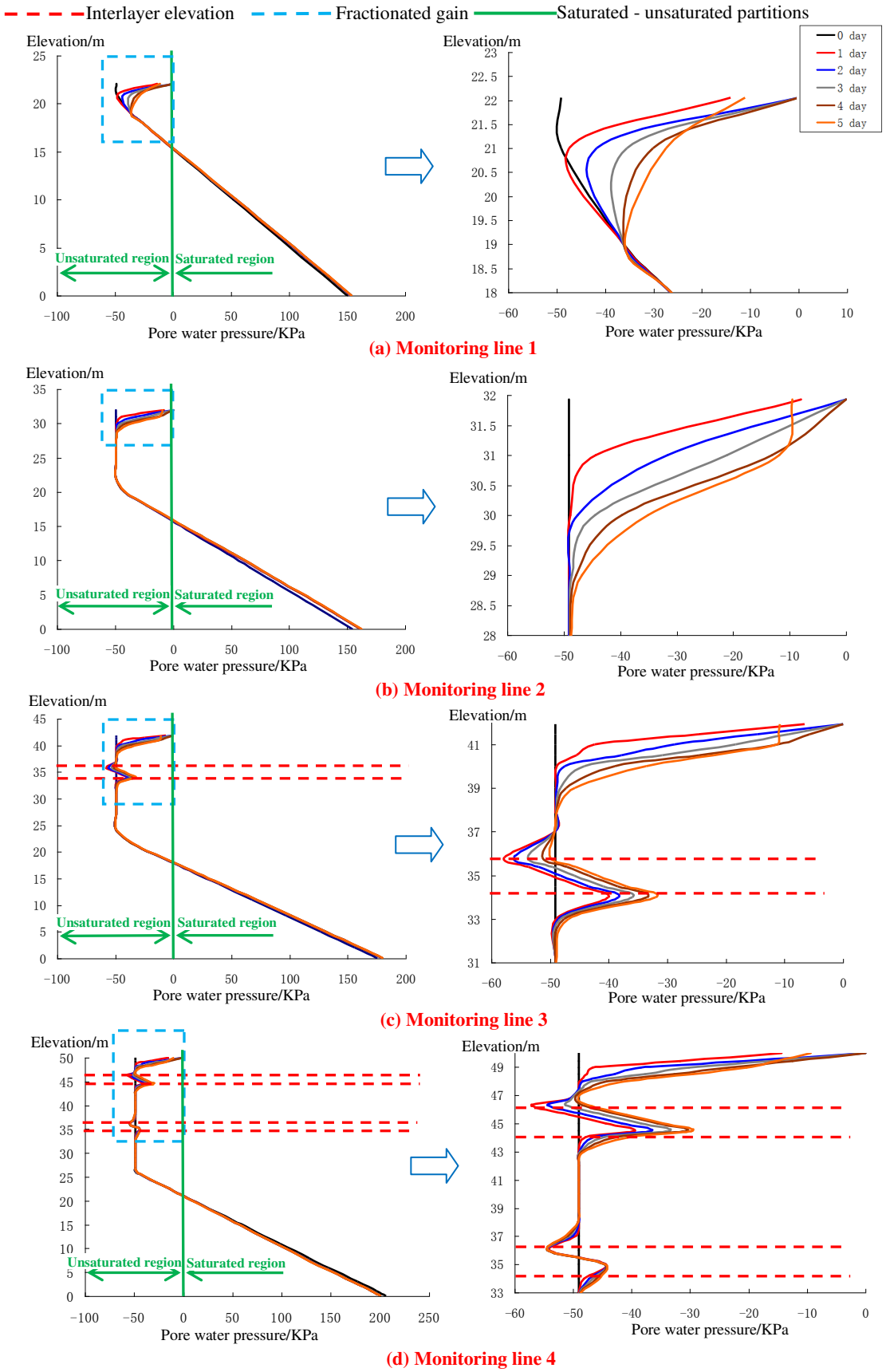

Figure 4. *Variation of pore water pressure of different time under a rainstorm*

http://www.aloki.hu ● ISSN 1589 1623 (Print) ● ISSN 1785 0037 (Online)
DOI: http://dx.doi.org/10.15666/aeer/1705_1246512478

For monitoring line 3, in addition to the dramatical changes of surface pore pressure, there is also an obvious variation at the elevation of the weak interlayer. The pore pressure at the weak interlayer presents obvious shapes like a backwards S along the elevation, that is, the upper and lower surface pressure of the weak interlayer decreases sharply, while the internal pore pressure of the weak interlayer is large, forming a more obvious drainage effect. This is because the permeability coefficient of the weak interlayer is smaller than that of the silty clay, so this kind of shape is formed, and the variation range of pore pressure in the weak interlayer is also large.

For monitoring line 4, it passes through two weak interlayers, so the pore pressure of the monitoring surface presents two shapes like a backwards S. The first one is consistent with the change rule of monitoring point 3, while the second one is slightly different, mainly reflected in that the overall change range of pore pressure is smaller than that of the upper weak interlayer. Meanwhile, the change range of pore pressure in the weak interlayer at different times is also not so obvious, which is mainly due to the deep distance from the second weak interlayer to the slope surface and the impact of rainwater infiltration is small.

Variation of pore water pressure on the 5th day under different rainfall levels

Variation of pore water pressure on the 5^{th} day under different rainfall levels is shown in *Figure 5*. Pictures on the left side are the pore pressure distribution of the whole monitoring line, while on the right side are the region where local pore pressure changes dramatically. As can be seen from the left side, the change of pore pressure with elevation is consistent with that in *Figure 4,* and the shapes like a backwards S also exist in monitoring 3 and 4. However, when the rain stopped, the surface pore pressure would fall back in different order under different levels of rainfall, as shown on the right side of *Figure 5*. Rainstorm falls the fastest in the shallow part of the slope, followed by big rain, followed by a heavy rain. Meanwhile, the pore pressure at the weak interlayer is also different, and the pore pressure of the rainstorm is close to that of the heavy rain, the pore pressure of big rain is relatively backward. This is also easy to understand, because the low rainfall intensity makes the less water needed to be excreted from the weak interlayer, and the pore pressure of heavy rain whose rainfall intensity in the lowest is correspondingly smaller than other rainfall levels.

Variation of the wetting front

Definition of the wetting front

Rainfall infiltration is a typical unsaturated problem, according to Bodman et al. (1944), for the general rainfall process, the water content of the slope can be divided into four parts: saturation zone, transition zone, conduction area and wetting area. The lowest end of the wetting area is the wetting front, as shown in *Figure 6a.*

The soil moisture content is constantly changing with the continuous rainfall process. Fredlund (Fredlund and Rahardjo, 1993) proposed that when rainfall is applied to the slope surface, the soil surface moisture content increases rapidly from initial water content θ_0 to saturated water content θ_s. And as the rainfall continues, the wet front is continuously advanced to the deep side of the slope, and the water content curve gradually becomes smooth. The variation of soil moisture content over time is shown in *Figure 6b.*

http://www.aloki.hu ● ISSN 1589 1623 (Print) ● ISSN 1785 0037 (Online)
DOI: http://dx.doi.org/10.15666/aeer/1705_1246512478

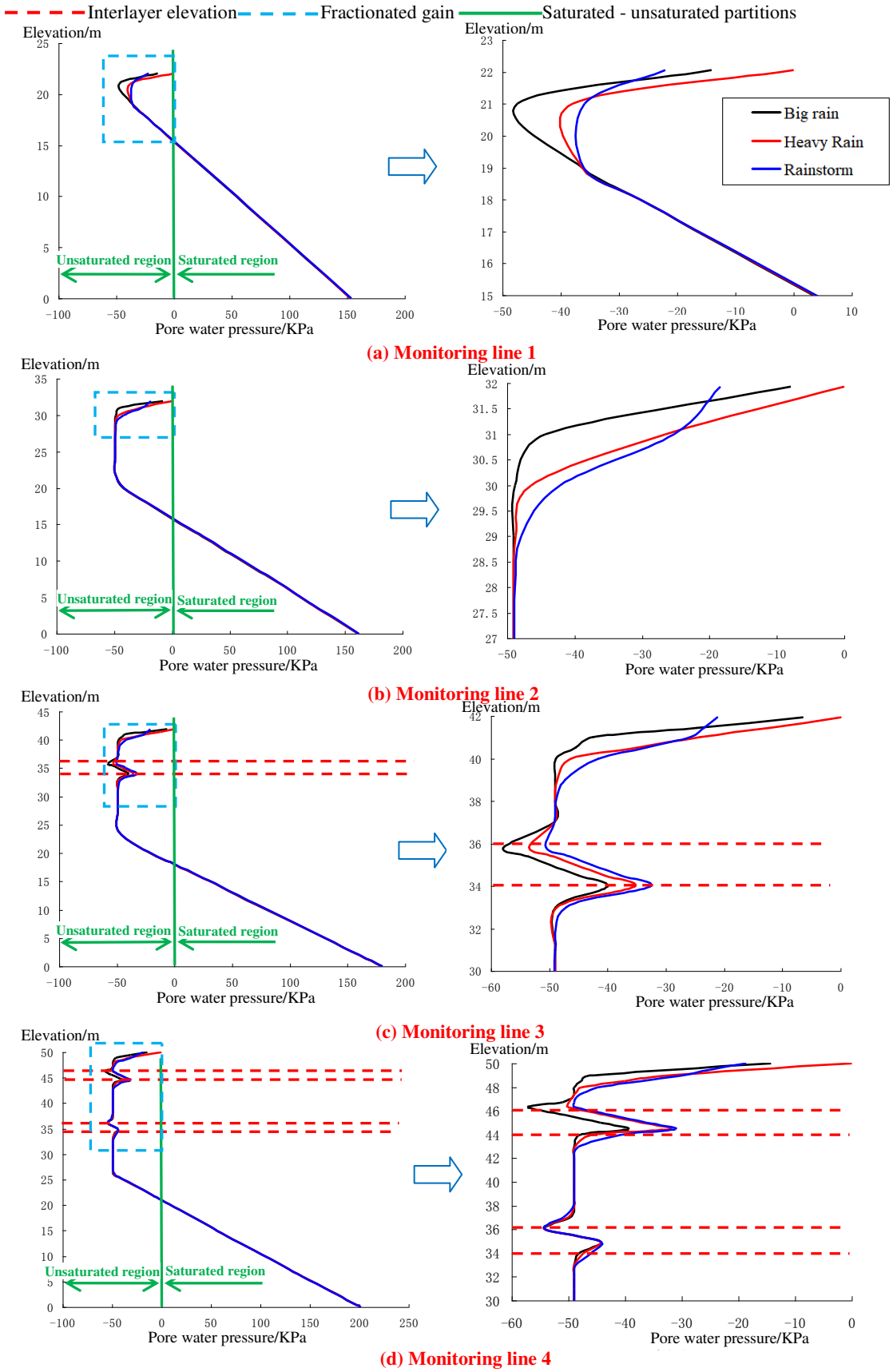

Figure 5. *Variation of pore water pressure in the 5th day under different rainfall levels*

http://www.aloki.hu ● ISSN 1589 1623 (Print) ● ISSN 1785 0037 (Online)
DOI: http://dx.doi.org/10.15666/aeer/1705_1246512478

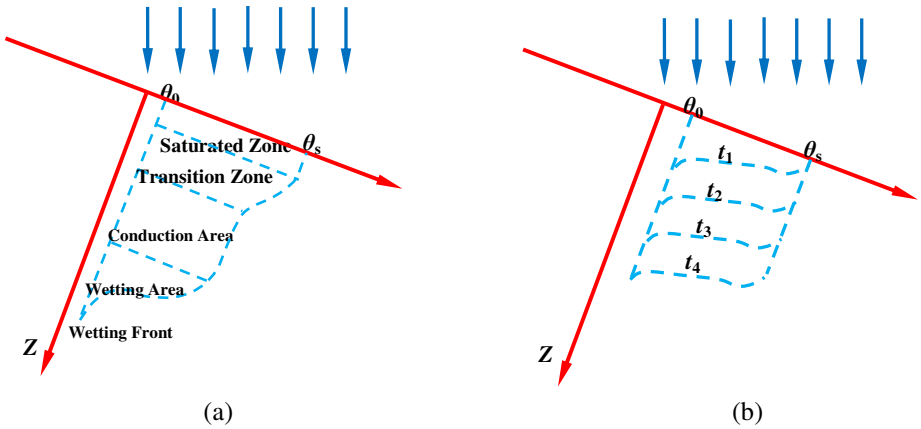

Figure 6. *Wetting front diagram.* ***a*** *and* ***b:*** *Typical water cut profile of water infiltration*

Variation of the wetting front of slope under different rainfall grades

The wetting front changes under different levels of rainfall are shown in *Figure 7*. As can be seen from the graph, the law of the development of wet front under different rainfall grades is almost the same, that is, there is uniform infiltration on the surface of clay slope. However, a sudden change in the weak interlayer occurs because the permeability coefficient in the weak interlayer is larger than that in the silty clay, so that rainfall is easier to infiltrate than other parts of the slope. Under the different rainfall levels, the development of the wetting front of rainstorm is less than that of a heavy rain, and less than that of a big rain, which indicates that rainfall infiltration under the condition of long duration and low rainfall intensity is more abundant than the high rainfall intensity of short duration. This is because, under the same rainfall condition, the high-intensity rainfall cannot completely infiltrate into the slope body, most rainwater is lost on the its surface, while the low-intensity rainfall is just the opposite, and the rainfall can fully infiltrate into the soil mass. Therefore, for the actual slope engineering, it is more likely to lose stability in the case of long duration and low rainfall intensity. At the same time, because of the high permeability of the weak interlayer, the internal pore pressure increases and the soil parameters deteriorate under the condition of rainfall, which makes it easier to form the potential failure surface. Therefore, the reinforcement of weak interlayer is also very important.

Validation and discussion

Elkamhawy et al. (2018) carried out the experimental study on failure mechanism of a slope with weak interlayers triggered by intensive rainfall. Experimental results showed that during the time of rainfall, the infiltrated water flowed out from the slope through the weak interlayer near to the toe causing piping and local failure, then the tensile cracks formed at the top grew and expanded due to sliding of the failed soil blocks along the weak interlayer, which is in accordance with our numerical results. In section 3.1 and 3.2 the pore water pressure in monitoring point 1 and monitoring line 1 have higher values than other parts, which means that rain water is abundant at the foot of the slope. So in order to restrict the growth of positive pore water pressure at the toe, we can apply the method of constructing horizontal and vertical drains to discharge the infiltrated water directly.

http://www.aloki.hu ● ISSN 1589 1623 (Print) ● ISSN 1785 0037 (Online)
DOI: http://dx.doi.org/10.15666/aeer/1705_1246512478

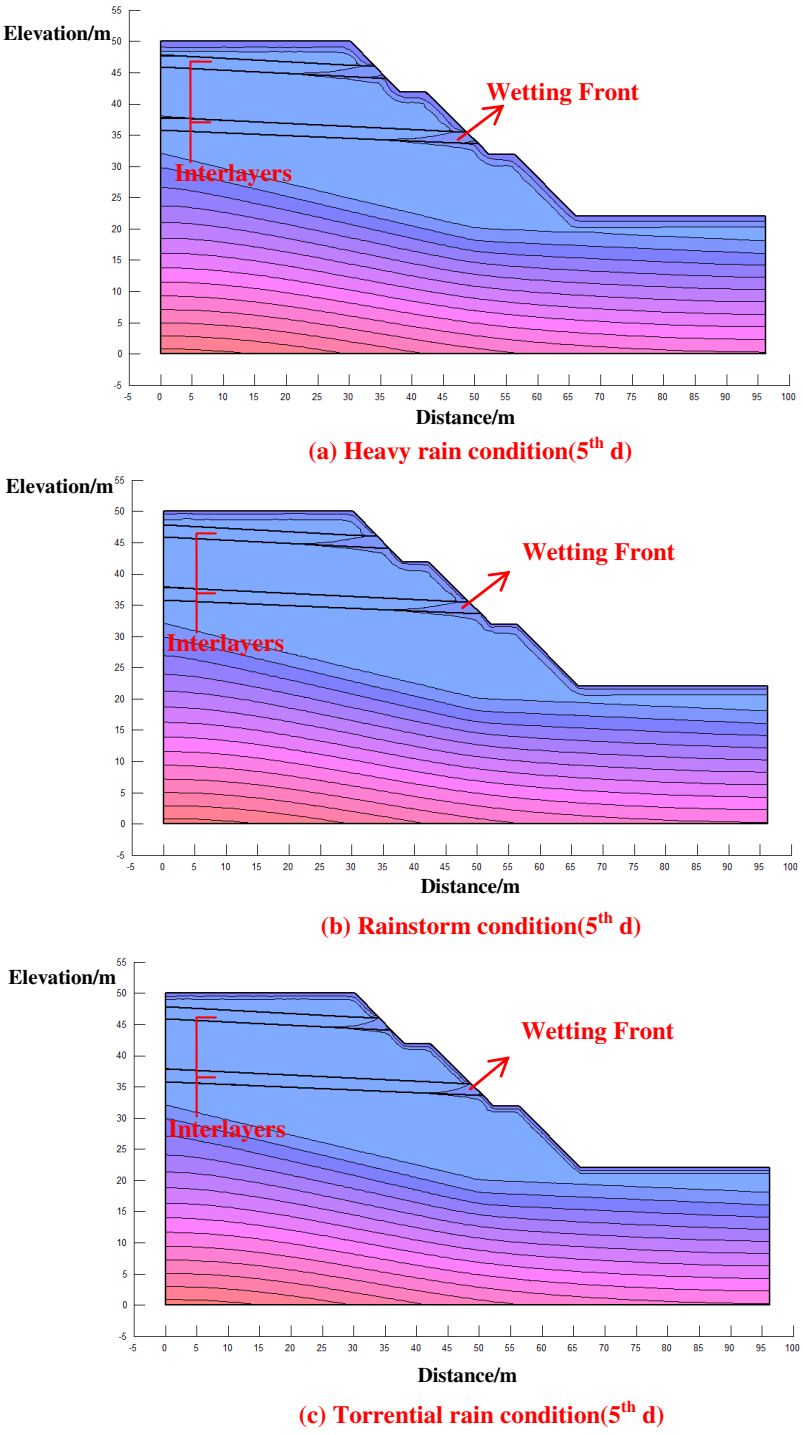

Figure 7. *Variation of the wet front under different rainfall grades*

In addition, the shapes like a backwards S of pore water pressure at the elevation of weak interlayers mean that weak interlayers is a potential leakage passage for rainfall infiltration, and along which the soil block tend to slide, so it is necessary to make proper reinforcement treatments of weak interlayers. For example, we can use soil nailing to link between the wedges prone to slide with the stable soil under the weak interlayers.

http://www.aloki.hu ● ISSN 1589 1623 (Print) ● ISSN 1785 0037 (Online)
DOI: http://dx.doi.org/10.15666/aeer/1705_1246512478

Moreover, in our simulation, we found that the surface pore water pressure undergoes a longer period of saturation in big rain than heavy rain and rainstorm, which means that the the rainfall with low intensity and long duration has a worse effect on slope than the rainfall with high intensity and short duration, so it is very important to pay more attention to the rainfall with low intensity and long duration and prevent the landslides.

Conclusions

In this paper, the seepage characteristics of the slope with weak interlayers under different rainfall levels are numerically simulated, and the following conclusions can be obtained:

(1) Under different rainfall grades, the surface pressure of the slope at different elevations increases rapidly and reaches saturation at the time of rainfall, and decreases rapidly after the rainfall. Under the same rainfall amount, high rainfall grade makes the time when pore pressure reaches saturation earlier, and the long duration of the rainfall makes the longer duration time when the pore pressure reaches saturation.

(2) Rainfall has a great influence on the pore pressure variation in the surface layer and weak interlayer of the slope, but has limited effect on the other parts. The pore pressure distribution in different positions of the slope is also quite different. The pore pressure of the lower part increased linearly with the elevation, and the pore pressure of the middle and lower parts remains unchanged first and then increases linearly with the elevation. The pore pressure of the upper and middle parts shows shapes like a backwards S along with the elevation at the weak interlayer.

(3) Wetting front uniformly infiltrates in silty clay layer, and “sudden change” appears in weak interlayers. Meanwhile, the development of the wetting front of low intensity and long duration rainfall is larger than that of high-intensity short rainfall.

(4) For the actual slope engineering, it is very important to pay more attention to the rainfall with low intensity and long duration and prevent the landslides.

(5) Although systematic analysis of seepage characteristics are discussed in this paper, what occurs in nature is complex, and different conditions such as the variable thickness and angles of weak interlayers, different rainfall types, duration and different slope geometry should be included in future studies.

Acknowledgements. This research was financially supported by The National Natural Science Fund (Grant No. U1765204).

REFERENCES

[1] Bodman, G. B., Colman, E. A. (1944): Moisture and energy conditions during downward entry of water into soils. – Soil Science Society of America Journal 8(8).

[2] Chaplot, V. A. M., Bissonnais, Y. L. (2003): Runoff features for interrill erosion at different rainfall intensities, slope lengths, and gradients in an agricultural loessial hillslope. – Soil Science Society of America Journal 67(3): 844-851.

[3] Elkamhawy, E., Wang, H., Zhou, B. (2018): Failure mechanism of a slope with a thin soft band triggered by intensive rainfall. – Environmental Earth Sciences 77(9): 340.

http://www.aloki.hu ● ISSN 1589 1623 (Print) ● ISSN 1785 0037 (Online)
DOI: http://dx.doi.org/10.15666/aeer/1705_1246512478

[4] Fang, H., Sun, L., Tang, Z. (2015): Effects of rainfall and slope on runoff, soil erosion and rill development: an experimental study using two loess soils. – Hydrological Processes 29(11): 2649-2658.
[5] Fredlund, D. G., Rahardjo, H. (1993): Soil Mechanics for Unsaturated Soils. – Wiley, New York.
[6] Huang, M., Fan, X., Wang, H. (2017): Three-dimensional upper bound stability analysis of slopes with weak interlayer based on rotational-translational mechanisms. – Engineering Geology. DOI: 10.1016/j.enggeo.2017.04.017.
[7] Jie-Qun, L., Lu-Wang, C., Jin-Long, L. (2013): Failure modes and stability of rock mass slope containing multi-weak interlayer. – Journal of Applied Sciences 13(21): 139-141.
[8] Jun-Ping, Y., Yan-Ling, L., Peng, D., Chun-Lei, H. (2016): Influence of anisotropy induced by fissures on rainfall infiltration of slopes. – Chinese Journal of Geotechnical Engineering. DOI: 10.11779/CJGE201601007.
[9] Kulasingam, R., Malvick, E. J., Boulanger, R. W. (2004): Strength loss and localization at silt interlayers in slopes of liquefied sand. – Journal of Geotechnical & Geoenvironmental Engineering 130(11): 1192-1202.
[10] Long-Qi, L. I., Neng-Pan, J. U. (2016): Effect of the inclined weak interlayers on the rainfall response of a bedded rock slope. – Journal of Mountain Science 13(9): 1663-1674.
[11] Lee, D. H., Lai, M. H., Wu, J. H. (2013): Slope management criteria for Alishan Highway based on database of heavy rainfall-induced slope failures. – Engineering Geology 162(14): 97-107.
[12] Lim, T. T., Rahardjo, H., Chang, M. F., Fredlund, D. G. (1996): Effect of rainfall on matric suctions in a residual soil slope. – Canadian Geotechnical Journal 33(4): 618-628.
[13] Ming, L. I., Zhang, G., Zhang, J. M. (2011): Research on failure mode of clay slope containing horizontal sand interlayer under excavation conditions. – Rock & Soil Mechanics 12(8): 197-199.
[14] Mitchell, J. K., Scott, R. F., Houston, W. N., Costes, N. C., Carrier, W. D., Bromwell, L. G. (1972): Mechanical properties of lunar soil: density, cohesion, and angle of internal friction. – Lunar & Planetary Science Conference, January 10-13, 1972, Houston, Texas.
[15] Ng, C. W., Wang, B., Tung, Y. K. (2001): Three-dimensional numerical investigations of groundwater responses in an unsaturated slope subjected to various rainfall patterns. – Canadian Geotechnical Journal 38(5): 1049-1062.
[16] Philip, J. R. (1993): Constant-Rainfall Infiltration on Hillslopes and Slope Crests. – In: Russo, D., Dagan, G. (eds.) Water Flow and Solute Transport in Soils. Springer, Berlin.
[17] Rahardjo, H., Lee, T. T., Leong, E. C. (2005): Response of a residual soil slope to rainfall. – Canadian Geotechnical Journal 42(2): 340-351.
[18] Rahimi, A., Rahardjo, H., Leong, E. C. (2011): Effect of antecedent rainfall patterns on rainfall-induced slope failure. – Journal of Geotechnical and Geoenvironmental Engineering 137(5): 483-491.
[19] Schultz, J. P., Jarrett, A. R., Hoover, J. R. (1985): Detachment and splash of a cohesive soil by rainfall. – Transactions of the ASAE 28(6): 1878-1884.
[20] Sheng, Y. (2000): Joint probability distribution of annual maximum storm peaks and amounts as represented by daily rainfalls. – International Association of Scientific Hydrology Bulletin 45(2): 12.
[21] Thompson, J. N. (1984): Insect diversity and the trophic structure of communities. – Ecological Entomology 9(2): 165-178.
[22] Tian, D. F. (2014): A slope stability analysis method based on unsaturated seepage of slope and its comparison with geo-seep software. – Applied Mechanics & Materials 540: 177-180.
[23] Woolhiser, D. A., Smith, R. E., Giraldez, J. V. (1996): Effects of spatial variability of saturated hydraulic conductivity on hortonian overland flow. – Water Resources Research 32(3): 671-678.

http://www.aloki.hu ● ISSN 1589 1623 (Print) ● ISSN 1785 0037 (Online)
DOI: http://dx.doi.org/10.15666/aeer/1705_1246512478

[24] Yang, Y., He, Z., Wang, B., Ma, Y. (2008): Numerical analysis of seepage characteristics of soil slope with weak interlayer under different rainfall conditions. – Mining and Metallurgical Engineering 38(03): 15-19.
[25] Yang, Y. C., Xing, H. G., Yang, X. G. (2018): Experimental study on the dynamic response and stability of bedding rock slopes with weak interlayers under heavy rainfall. – Environmental Earth Sciences 77(12): 433.
[26] Zhang, G. A., Wang, R., Qian, J. (2012): Effect study of cracks on behavior of soil slope under rainfall conditions. – Soils & Foundations 52(4): 634-643.
[27] Zhang, J., Li, J., Lin, H. (2016): Models and influencing factors of the delay phenomenon for rainfall on slope stability. – European Journal of Environmental & Civil Engineering 22(1): 1-15.

http://www.aloki.hu ● ISSN 1589 1623 (Print) ● ISSN 1785 0037 (Online)
DOI: http://dx.doi.org/10.15666/aeer/1705_1246512478

RESPONSE OF SOME NARBON VETCH VARIETIES TO DIFFERENT DEFOLIATION INTENSITIES CONCERNING FORAGE, SEED YIELD AND GROWTH TRAITS UNDER RAINFED CONDITIONS OF THE SULAIMANI GOVERNORATE, IRAQ

MUHAMMED, S. R. – AHMED, D. A. – SLEMAN, S. M.* – HUSSAEN, R. A.

Department of Biotechnology and Crop Science, College of Agricultural Engineering Sciences, University of Sulaimani, Sulaymaniyah, Iraq
(e-mails: sanarya.muhammed@univsul.edu.iq, dastan.ahmed@univsul.edu.iq, roonak.hussaen@univsul.edu.iq)

**Corresponding author*
e-mail: shokhan.sleman@univsul.edu.iq

(Received 14th May 2019; accepted 20th Aug 2019)

Abstract. To study the response of some narbon vetch varieties to different defoliation intensities on forage, seed yield and their components under rain fed condition. A field experiment was conducted at College of Agricultural Sciences-University of Sulaimani in Iraq country during the winter season of 2017-2018, using split plot design. Three varieties of narbon vetch (ICARDA 2561, ICARDA 2380 and ICARDA 2706) were implemented in the main plots and arranged according to Randomized Complete Block Design and replicated three times, and four defoliation intensities (different height of forage cutting from ground level) Control (not defoliated), Low = 8 cm, Moderate = 6 cm and Severe = 4 cm from ground level) were allotted in subplots. Means comparisons were carried out using the least significant difference test (LSD) at 5% and 1% significant levels. The results of this study indicated that the interaction between ICARDA 2561 and moderate defoliation intensity gave the highest values of fresh forage yield and fresh stem percent, and the interaction between ICARDA 2380 and severe defoliation intensity gave maximum fresh leaf percent, Regarding leaves/stem ratio, maximum ratio showed by interaction between ICARDA 2561 and low defoliation intensity. The interaction between ICARDA 2380 and moderate defoliation intensity awarded the highest values of most traits such as plant height, no. of branches/plant, no. of leaves/plant, leaves weight/plant, leaves dry weight/plant and stem dry weight/plant, Maximum values of these traits biological yield, pods number/m², pod yield, seed number/pod and seed yield reached attained by the interaction between ICARDA 2706 and control treatment, but the interaction between ICARDA 2561 and control treatment gave the highest values of pod length and seeds weight/pod but concerning 100 seeds weight, the highest weight obtained by interaction between ICARDA 2380 and control treatment.

Keywords: *Vicia narbonensis, lines, cutting height, growth, yield, yield components, dry matter percent*

Introduction

The genus Vicia is made up of approximately 190 species worldwide. The genus is primarily found in the Mediterranean and Irano- Turanian regions. However, the genus Vicia is widely distributed in the temperate zone of the northern hemisphere and in extra-tropical South America (Tahereh et al., 2012). Narbon vetch (*Vicia narbonensis* L.*),* which is resistant to cold and drought, is an annual legume species (Açıkgöz, 2001; Fırıncıoğlu et al., 2012). Vetch can be grazed by animals as fresh forage (Haddad, 2006) or can be cut and preserved as hay and silage (Abdullah et al., 2010). Vetches hay can be used as a protein supplement, and their grains serve as energy and protein sources in the rations of ruminants and non-ruminants (Sadeghi et al., 2009).

http://www.aloki.hu ● ISSN 1589 1623 (Print) ● ISSN 1785 0037 (Online)
DOI: http://dx.doi.org/10.15666/aeer/1705_1247912490

The potential of narbon vetch for grain production as livestock feed is greater than other vetch species, and the grain contains tannin and trypsin inhibitors that is directly affecting its efficiency of feed (Berger et al., 2002; Larbi et al., 2010), in general narbon vetch is cultivated for grain production (Buyukburc and Iptas, 2001). The species also has great importance in the system of crop rotation, either as pure stands or in a mixture with cereals for green forage or hay production to provide high-quality of livestock feed (Altınok, 2002; Altınok and Hakyemez, 2002; Iptaş and Karadağ, 2009; Nizam et al., 2011). Furthermore, narbon vetch is used as a valuable green manure plant, because it produce a high amount of green biomass, and its ability to fix large amounts of nitrogen to the soil as a legume (Albayrak et al., 2004a, b; Avcıoğlu et al., 2009; Fırıncıoğlu et al., 2012).

Narbon vetch is a fast-growing crop, with vigorous regrowth ability, and does better under warm temperatures and drier conditions (annual rainfall amount below 350 mm) than faba bean. It is tolerant to cold. When aerial parts damaged by frost may be die, but new shoots regrow when conditions will better in the spring. It can grow in many types of soils from sandy soils to loams provided they are well-drained. The input requirement of narbon vetch has low (fertilizer and pesticides) but does particularly well on alkaline soils and responds positively to P fertilizer (Mebarkia et al., 2013; Sanchez-Vioque et al., 2011). Like many other Vicia species, the culture of *Vicia narbonensis* L. has long been neglected due to the presence of anti-nutritional factors that also cause an undesirable odorand taste in grain and foliage. Once cooked, the anti-nutritional factors removed, and Narbon beans can be eaten and are described as being of high quality (Bryant et al., 2011).

Forage growers cut forages frequently at a height of 3-inches or more. However, recent reports indicate that there may be an advantage to cutting crop closer, leaving an inch or less of stubble height, which was found that annual alfalfa yields were 1.6 tons per acre higher when cutting at 1-inches compared to 5-inches heights (@griculture Online, 1999).

A study from West Virginia reports that alfalfa cut at 1 or 2 inches yielded as much as38% more than alfalfa cut at 4 inches (Belesky and Fedders, 1997). A reduction of a ½ ton of dry matter per inch as cutting height increased from 2 to 6 inches above the ground when combined across three harvests for the year (Wiersma, 2000).

However, there is little information available on the forage yield of narbon vetches grown under climatic conditions of Sulaimani. Therefore, the current study aimed to determine forage and seed yields for three varieties of narbon vetch (*Vicia narbonensis* L.) at different defoliation intensities, and which variety has ability to adapt with our condition and regrowth after defoliation to produce high yield crop.

Materials and methods

A field experiment was conducted at College of Agricultural Engineering Sciences-University of Sulaimani located (Latitude: 35 33’ N, Longitude 45° 27’ E, at altitude of approximately 830 m) during the winter season of 2017-2018, to study the effect of different varieties and defoliation intensities on growth, forage, seed yield and its components of narbon vetch (*Vicia narbonensis* L.) under rainfed condition conducting in split-plot design. Three varieties of narbon vetch (ICARDA 2561, ICARDA 2380 and ICARDA 2706) were implemented in the main plots and arranged according to the randomized complete block design (CRBD) and replicated three times, and four

http://www.aloki.hu ● ISSN 1589 1623 (Print) ● ISSN 1785 0037 (Online)
DOI: http://dx.doi.org/10.15666/aeer/1705_1247912490

defoliation intensities (different height of forage cutting from ground level) (Control (not defoliated), Low = 8 cm, Moderate = 6 cm and Severe = 4 cm from ground level) were allotted in subplots for seed traits, but for forage traits treatments were allotted without control (Low = 8 cm, Moderate = 6 cm and Severe = 4 cm from ground level). Each subplot consists of 3 rows, 2 m long with 0.30 m apart between rows.

Sowing was conducted during 12th December 2017 according to the recommended seed rates 120 kg/ha for three varieties and all plots were fertilized with 120 kg P_2O_5/ha as triple superphosphate, which was broadcasting before sowing, and the germination percentage for each used varieties was higher than % 95. All required agricultural practices were used as needed. Forage cutting conducted for all subplots on 4th January 2018 to determine forage yield traits:

Forage yield traits

- Fresh Forage Yield (ton/ha)
- Dry Forage Yield (ton/ha)
- Fresh Leaf%
- Dry Leaf%
- Fresh Stem%
- Dry Stem%
- Dry Matter%
- Leaves/Stem Ratio

In addition, on the same day of cutting we were taken a sample randomly (5 plants of each subplot) to estimate forage yield component traits were:

Growth traits

- Plant height (cm)
- No. of Branches/plant
- No. of leaves/plant
- Leaves weight/plant (g)
- Dry leaves weight/plant (g)
- Stem weight/plant (g)
- Dry Stem weight/plant (g)
- Root weight (g)
- Dry Root weight (g)

When the plants matured physiologically, harvesting was carried out on 4th June 2018 to record seed yield traits from each plot, but the averages of 10 pods were taken from each plot to estimate yield component traits as follows:

Seed yield and its components

- Seed Yield (ton/ha)**,**
- Biological Yield (ton/ha)**,**
- Pods Number/m^2
- Pod yield (ton/ha)
- Average Pod Length (cm)

http://www.aloki.hu ● ISSN 1589 1623 (Print) ● ISSN 1785 0037 (Online)
DOI: http://dx.doi.org/10.15666/aeer/1705_1247912490

- Average Seeds Number/Pod
- Average Seeds Weight/Pod (g)
- 100 Seeds Weight (g)

The data were statistically analyzed according to the methods of analysis of variance as a general test and combined analysis conducted (AL Mohamad and AL Younis, 2000). Comparison among the means was carried out using the least significant test (L.S.D) at a significant level of 5% and 1% (AL Mohamad and AL Younis, 2000).

Results and discussion

Data in *Table 1* and *Appendix 1* indicated that the effect of varieties on forage yield traits was not significant for most characters but on the other traits such as (fresh forage yield, dry forage yield and fresh leaf percent) were found to be significant, ICARDA 2561 gave maximum value of fresh forage yield (13.356 ton/ha), while ICARDA 2380 recorded minimum value of this trait which was (11.706 ton/ha). But the highest dry forage yield and fresh leaf percent were (1.492 ton/ha and 63.467%) respectively exhibited by V3, in which the lowest values of both traits were (1.302 ton/ha and 60.763%) recorded by ICARDA 2380 and ICARDA 2561 regularly. These differences among varieties may be due to genetic variance and capability of each variety for best production. These results were in agreement with the results of Muhammed (2017).

Table 1. *Effect of varieties on forage yield traits of narbon vetch*

Varieties	Fresh forage yield (ton/ha)	Dry forage yield (ton/ha)	Fresh leaf %	Fresh stem %	Dry leaf %	Dry stem %	Dry matter %	Leaves/stem ratio
ICARDA 2561	13.356	1.393	60.763	39.237	7.450	3.032	10.482	1.337
ICARDA 2380	11.706	1.302	63.358	36.642	7.957	3.167	11.123	1.082
ICARDA 2706	13.130	1.492	63.467	36.867	8.242	3.100	11.342	1.267
LSD ($P \leq 0.05$)	0.923	0.079	2.171	N.S	N.S	N.S	N.S	N.S

N.S: not significant

The results of *Table 2* and *Appendix 1* confirmed that the effect of defoliation intensities on all forage yield traits was significant except these characters' dry forage yield, dry stem percent, and dry matter percent were found to be not significant. Moderate defoliation intensity (6 cm) gave maximum values of fresh forage yield, fresh stem percent and leaves/stem ratio was (13.907 ton/ha, 39.971% and 1.356) respectively, while minimum values of fresh forage yield and fresh stem percent were (12.054 ton/ha and 35.404%) registered by low defoliation intensity (8 cm), but regarding leaves/stem ratio, minimum value was 1.062 obtained by severe defoliation intensity (4 cm).

Concerning both traits (fresh leaf and dry leaf percent), low defoliation intensity (8 cm) gave the best percent (64.929 and 8.283%) respectively, while the lowest percentage of these both traits were (60.029 and 7.606%) recorded by moderate defoliation intensity (6 cm).

In theory, leaving tall stubble and leaves at the base of the plant provides more photosynthetic area and energy for new stem growth following harvest. Prevision results showed that cutting to the soil surface increased forage yield at the first cut by

http://www.aloki.hu ● ISSN 1589 1623 (Print) ● ISSN 1785 0037 (Online)
DOI: http://dx.doi.org/10.15666/aeer/1705_1247912490

increasing the weight of individual shoots harvested. This is simply because defoliation closer to the soil surface removed greater part of individual shoots of plants that had been uniformly managed prior to the first harvest. Plants at the first cut in the second-year growing season had stems arising mainly from the crown. This character- is tic of the plant canopy increased individual shoot weight steeply with decreasing cutting height reported by Shen et al. (2013), this result was in agreement with our results.

Table 2. *Effect of defoliation intensities on forage yield traits of narbon vetch*

Defoliation intensities	Fresh forage yield (ton/ha)	Dry forage yield (ton/ha)	Fresh leaf %	Fresh stem %	Dry leaf %	Dry stem %	Dry matter %	Leaves/stem ratio
Low (8 cm)	12.054	1.371	64.929	35.404	8.283	3.086	11.369	1.268
Moderate (6 cm)	13.907	1.483	60.029	39.971	7.606	3.081	10.687	1.356
Severe (4 cm)	12.231	1.334	62.630	37.370	7.760	3.132	10.892	1.062
LSD ($P \leq 0.05$)	0.656	N.S	1.103	1.216	0.401	N.S	N.S	0.166

N.S: not significant

Data represented in *Table 3* and *Appendix 1* showed that the effect of interactions between varieties and defoliation intensities on forage yield traits was significant on some traits such as fresh forage yield, fresh leaf percent, fresh stem percent, and leaves/stem ratio, but on the others was not significant. The interaction between ICARDA 2561 and moderate defoliation intensity (6 cm) gave the highest values of fresh forage yield and fresh stem percent were 15.587 ton/ha and 42.53% respectively, while the lowest yield of fresh forage was 11.291 ton/ha exhibited by interaction between ICARDA 2380 and low defoliation intensity (8 cm), and the lowest percent of fresh stem was 33.49% obtained by interaction between ICARDA 2380 and severe defoliation intensity (4 cm), also this interaction gave maximum fresh leaf percent 66.51%, in which minimum percent of fresh leaf was 57.47% recorded by ICARDA 2380 when treated with moderate defoliation intensity (6 cm). Regarding leaves/stem ratio, a maximum ratio was 1.432 showed by the interaction between ICARDA 2561 and low defoliation intensity (8 cm), in which the interaction between ICARDA 2380 and severe defoliation intensity (4 cm) recorded minimum leaves/stem ratio 0.532.

Table 4 and *Appendix 1* illustrated Effect of varieties on growth traits of narbon vetch, which was found that the effect was significant on plant height, leaves weight/plant, stem weight/plant and root dry weight, but on the other traits was not significant. The highest values of plant height, leaves weight/plant and stem weight/plant were (44.089 cm, 20.413 g, and 20.013 g) exhibited by ICARDA 2380**,** respectively, but maximum value of root dry weight was 0.922 g showed by variety 3, while the lowest values of these traits plant height, leaves weight/plant, stem weight/plant and root dry weight were (34.386 cm, 16.723 g, 12.490 g and 0.634) g recorded by (ICARDA 2706, ICARDA 2561, ICARDA 2561, and ICARDA 2380) respectively.

The differences between varieties in some growth traits may be positively and strongly related to the differences in genetic map and these adaptations to the climate. These results were in agreement with the results reported by (Muhammed, 2017).

Data in *Table 5* and *Appendix 1* confirmed that most growth traits of narbon vetch such as (no. of branches/plant, no. of leaves/plant, leaves weight/plant, leaves dry weight/plant and stem weight/plant) significantly affected by different defoliation intensities, while the other traits (plant height, stem dry weight/plant, root weight and root dry weight) not affected by this factor. Moderate defoliation intensity (6 cm) gave maximum values of

http://www.aloki.hu ● ISSN 1589 1623 (Print) ● ISSN 1785 0037 (Online)
DOI: http://dx.doi.org/10.15666/aeer/1705_1247912490

(no. of branches/plant, no. of leaves/plant, leaves weight/plant and leaves dry weight/plant) were (2.919, 26.027, 21.941 g and 3.070 g) respectively, on the other hand, maximum stem weight/plant (17.721 g) presented by severe defoliation intensity (4 cm), in which minimum values of these traits (no. of branches/plant, no. of leaves/plant and leaves dry weight/plant) were (2.294, 20.257 and 2.259 g) appeared by severe defoliation intensity (4 cm), but concerning both traits (leaves weight/plant and stem weight/plant), the lowest values showed by low defoliation intensity (8 cm) which was (16.194 and 13.298) g respectively. Previous works confirmed that alfalfa growth in the spring is primarily from crown buds and depends on temperature and available root energy reserves. Shoot growth after the first harvest originates from both crown and auxiliary buds. When the crop is cut very short (1-inch or less) most of the axillary buds are removed and new shoots must come from the crown buds (Wiersma, 2000).

Table 3. *Effect of interactions between varieties and defoliation intensities on growth traits of narbon vetch*

Varieties	Defoliation intensities	Fresh forage yield (ton/ha)	Dry forage yield (ton/ha)	Fresh leaf %	Fresh stem %	Dry leaf %	Dry stem %	Dry matter %	Leaves/ stem ratio
ICARDA 2561	Low (8 cm)	11.918	1.323	65.97	34.03	8.213	2.887	11.100	1.432
	Moderate (6 cm)	15.587	1.537	57.47	42.53	7.010	2.843	9.853	1.316
	Severe (4 cm)	12.564	1.320	58.85	41.15	7.127	3.367	10.493	1.263
ICARD A 2380	Low (8 cm)	11.291	1.310	64.17	35.83	8.163	3.433	11.597	1.307
	Moderate (6 cm)	11.875	1.262	59.39	40.61	7.490	3.150	10.640	1.408
	Severe (4 cm)	11.950	1.334	66.51	33.49	8.217	2.917	11.133	0.532
ICARDA 2706	Low (8 cm)	12.954	1.479	64.65	36.35	8.473	2.937	11.410	1.066
	Moderate (6 cm)	14.257	1.651	63.22	36.78	8.317	3.250	11.567	1.344
	Severe (4 cm)	12.180	1.346	62.53	37.47	7.937	3.113	11.050	1.392
LSD ($P \leq 0.05$)		1.136	N.S	1.911	2.106	N.S	N.S	N.S	0.288

N.S: not significant

Table 4. *Effect of varieties on growth traits of narbon vetch*

Varieties	Plant height (cm)	No. of brunches/ plant	No. of leaves/plant	Leaves weight/plant (g)	Leaves dry weight/plant (g)	Stem weight/plant (g)	Stem dry weight/plant (g)	Root weight (g)	Root dry weight (g)
ICARDA 2561	37.123	2.550	22.101	16.723	2.243	12.490	1.456	2.449	0.729
ICARD A 2380	44.089	2.627	23.804	20.413	2.949	20.013	1.746	2.171	0.634
ICARDA 2706	34.386	2.626	22.923	17.541	2.582	14.572	1.583	2.528	0.922
LSD ($P \leq 0.05$)	1.692	N.S	N.S	2.465	N.S	3.427	N.S	N.S	0.116

N.S: not significant

Table 5. *Effect of defoliation intensities on growth traits of narbon vetch*

Defoliation intensities	Plant height (cm)	No. of brunches/ plant	No. of leaves/ plant	Leaves weight/ plant (g)	Leaves dry weight/ plant (g)	Stem weight/ plant (g)	Stem dry weight/plant (g)	Root weight (g)	Root dry weight (g)
Low (8 cm)	39.631	2.589	22.546	16.194	2.446	13.298	1.482	2.278	0.773
Moderate (6 cm)	38.311	2.919	26.027	21.941	3.070	16.057	1.880	2.410	0.740
Severe (4 cm)	37.656	2.294	20.257	16.542	2.259	17.721	1.422	2.460	0.772
LSD ($P \leq 0.05$)	N.S	0.317	1.726	0.727	0.312	2.010	N.S	N.S	N.S

N.S: not significant

http://www.aloki.hu ● ISSN 1589 1623 (Print) ● ISSN 1785 0037 (Online)
DOI: http://dx.doi.org/10.15666/aeer/1705_1247912490

The results were obtained from *Table 6* and *Appendix 2* indicated that the effect of interactions between varieties and defoliation intensities on all growth traits was significant with the exception of the character root weight which was found to be not significant. The interaction between ICARDA 2380 and moderate defoliation intensity (6 cm) awarded the highest values of (plant height, no. of branches/plant, no. of leaves/plant, leaves weight/plant, leaves dry weight/plant and stem dry weight/plant) were (41.59, 3.553, 34.420, 33.537 g, 4.923 g, and 2.830 g) respectively, but the highest amount of stem weight/plant was 25.163 g offered by ICARDA 2380 when interacted with severe defoliation intensity (4 cm), and maximum root dry weight was (1.073 g) obtained by interaction between ICARDA 2706 and severe defoliation intensity (4 cm). while the lowest height of plant was 30.37 cm exhibited by interaction between ICARDA 2706 and low defoliation intensity (8 cm), but the minimum values of (no. of branches/plant, leaves dry weight/plant and stem weight/plant) were (2.107, 1.953 g and 11.067 g) showed by ICARDA 2380 when interacted with low defoliation intensity (8 cm) respectively. Regarding these traits (no. of leaves/plant, leaves weight/plant, stem dry weight/plant and root dry weight), the interaction between ICARDA 2380 and severe defoliation intensity (4 cm) gave minimum values were 17.997, 13.270 g, 1.087 g and 0.570 g, respectively.

Table 6. *Effect of interactions between varieties and defoliation intensities on growth traits of narbon vetch*

Varieties	Defoliation intensities	Plant height (cm)	No. of brunches/ plant	No. of leaves/ plant	Leaves weight/ plant (g)	Leaves dry weight/ plant (g)	Stem weight/ plant (g)	Stem dry weight/ plant (g)	Root weight (g)	Root dry weight (g)
ICARDA 2561	Low (8 cm)	38.21	3.110	25.533	18.610	2.590	13.000	1.597	2.497	0.780
	Moderate (6 cm)	38.89	2.430	21.773	15.957	2.083	12.123	1.430	2.510	0.733
	Severe (4 cm)	34.27	2.110	18.997	15.603	2.057	12.347	1.340	2.340	0.673
ICARDA 2380	Low (8 cm)	50.32	2.107	18.997	14.433	1.953	11.067	1.320	2.510	0.750
	Moderate (6 cm)	41.59	3.553	34.420	33.537	4.923	23.810	2.830	2.107	0.583
	Severe (4 cm)	40.36	2.220	17.997	13.270	1.970	25.163	1.087	1.897	0.570
ICARDA 2706	Low (8 cm)	30.37	2.550	23.107	15.540	2.793	15.827	1.530	1.827	0.790
	Moderate (6 cm)	34.46	2.773	21.887	16.330	2.203	12.237	1.380	2.613	0.903
	Severe (4 cm)	38.33	2.553	23.777	20.753	2.750	15.653	1.840	3.143	1.073
LSD ($P \leq 0.05$)		2.318	0.550	2.989	1.259	0.540	3.482	0.604	N.S	0.135

N.S: not significant

Data represented in *Table 7* and *Appendix 3* confirmed that the effect of varieties on all seed yield and its components traits was significant with the exception of the characters (pods number/m^2, pods length, and seeds weight/pod) which was found to be not significant. Maximum values of (biological yield, pod yield, average seeds number/pod and seed yield) were (5.082 ton/ha, 2.709 ton/ha, 3.554 and 2.040 ton/ha) respectively recorded by ICARDA 2706, but regarding 100 seeds weight, ICARDA 2380 gave the highest value which was 20.001 g, while ICARDA 2380 gave minimum value of biological yield 3.997 ton/ha, and ICARDA 2561 exhibited the lowest values of (pod yield, seeds number/pod and seed yield) were (2.092 ton/ha, 2.817 and 1.584 ton/ha) respectively, in which minimum weight of 100 seeds was 16.149 g registered by ICARDA 2706. The superiority of ICARDA 2706 in biological, seed yield and some other traits may be due to its adaptation in compare to other variety which

http://www.aloki.hu ● ISSN 1589 1623 (Print) ● ISSN 1785 0037 (Online)
DOI: http://dx.doi.org/10.15666/aeer/1705_1247912490

was well adapted to the Sulaimani region climatic and soil conditions. This result agrees with the results of Baş et al. (2011).

Table 7. *Effect of varieties on seed yield and its components of narbon vetch*

Varieties	Biological yield (ton/ha)	Pods number/m²	Pod yield (ton/ha)	Pods length (cm)	Seeds number/pod	Seeds weight/pod (g)	100 seeds weight (g)	Seed yield (ton/ha)
ICARDA 2561	4.464	215.333	2.092	4.939	2.817	0.624	16.180	1.584
ICARDA 2380	3.997	209.167	2.233	5.311	3.309	0.726	20.001	1.656
ICARDA 2706	5.082	244.250	2.709	4.673	3.554	0.628	16.149	2.040
LSD (P ≤ 0.05)	0.319	N.S	0.271	N.S	0.497	N.S	1.127	0.312

N.S: not significant

All traits of seed yield and its components of narbon vetch were shown in *Table 8* and *Appendix 2* affected significantly by different defoliation intensities. Control (not defoliated) treatment gave the highest values of these traits (biological yield, pods number/m², pods weight/m², pod length, seeds number/pod, seeds weight/pod, 100 seed weight and seed yield) were (15.725 ton/ha, 735.89, 8.0767 ton/ha, 5.936 cm, 4.333, 0.910 g, 22.196 g and 6.201 ton/ha) respectively, in which the lowest values of these previous traits exhibited by severe defoliation intensity (4 cm) were (0.376 ton/ha, 20000, 0.12719 ton/ha, 5.132 cm, 2.323, 0.584 g, 10.378 g and 0.098 ton/ha) respectively. Previously Mitchell et al. (2010), who reported switch grass should not be harvested within below a 10-cm stubble height to ensure carbohydrate translocation to the plant crowns for setting new tiller buds and maintaining stand productivity.

Table 8. *Effect of defoliation intensities on seed yield and its components of narbon vetch*

Defoliation intensities	Biological yield (ton/ha)	Pods number/m²	Pod yield (ton/ha)	Pod length (cm)	Seeds number/pod	Seeds weight/ pod (g)	100 seeds weight (g)	Seed yield (ton/ha)
Control (not defoliated)	15.725	735.89	8.077	5.936	4.333	0.910	22.196	6.201
Low (8 cm)	1.510	101.67	0.850	3.721	2.917	0.633	18.654	0.558
Moderate (6 cm)	0.447	34.111	0.325	5.108	3.333	0.510	18.546	0.184
Severe (4 cm)	0.376	20.000	0.127	5.132	2.323	0.584	10.378	0.098
LSD (P ≤ 0.05)	0.377	47.321	0.253	1.344	0.502	0.201	1.495	0.398

N.S: not significant

Results of *Table 9* and *Appendix 2* confirmed that the effect of interactions between varieties and defoliation intensities on all seed yield and its component traits of narbon vetch were significant. Maximum values of these traits (biological yield, pods number/m^2, pod yield, seeds number/pod and seed yield) were attained by the interaction between ICARDA 2706 and control (not defoliated) treatment were (17.589 ton/ha, 794.33, 9.031 ton/ha, 4.600 and 6.999) ton/ha respectively, but the interaction between ICARDA 2561 and control (not defoliated) treatment gave the highest values of (pod length and seeds weight per pod) were (6.227 cm and 1.013 g) respectively, but concerning 100 seeds weight, the interaction between ICARDA 2380 and control (not defoliated) treatment gave the highest weight which was 24.820 g, while the minimum values of (biological yield and pod yield) were (0.098 and 0.046) ton/ha exhibited by interaction between ICARDA 2380 with severe defoliation intensity (4 cm), but when ICARDA 2561 interacted with severe (4 cm) defoliation intensity

http://www.aloki.hu ● ISSN 1589 1623 (Print) ● ISSN 1785 0037 (Online)
DOI: http://dx.doi.org/10.15666/aeer/1705_1247912490

recorded the lowest values of (pods number/m^2, pod yield, seeds number/pod, 100 seeds weight, and seed yield) were (3.00, 0.008 ton/ha, 1.500, 5.227 g and 0.004 ton/ha) respectively. Regarding the average of pods length, minimum length exhibited by the interaction between ICARDA 2380 and low (8 cm) defoliation intensity which was 3.060 cm, and when ICARDA 2380 interacted with moderate (6 cm) defoliation intensity recorded minimum value of seeds weight/pod was 0.233 g.

Table 9. *Effect of interactions between varieties and defoliation intensities on seed yield and its components of narbon vetch*

Varieties	Defoliation intensities	Biological yield (ton/ha)	Pods number/m^2	Pod yield (ton/ha)	Pods length (cm)	Seeds number/pod	Seeds weight/pod (g)	100 seeds weight (g)	Seed yield (ton/ha)
ICARDA 2561	Control (not defoliated)	15.046	694.33	7.194	6.227	4.467	1.013	22.177	5.500
	Low (8 cm)	2.446	155.67	1.113	5.033	2.367	0.677	19.433	0.820
	Moderate (6 cm)	0.184	8.333	0.053	3.950	2.933	0.233	17.883	0.013
	Severe (4 cm)	0.180	3.000	0.008	4.547	1.500	0.572	5.227	0.004
ICARDA 2380	Control (not defoliated)	14.539	719.00	8.005	6.100	3.933	0.983	24.820	6.102
	Low (8 cm)	1.001	81.000	0.469	3.060	2.733	0.478	19.330	0.328
	Moderate (6 cm)	0.350	29.000	0.410	5.500	3.533	0.802	21.590	0.156
	Severe (4 cm)	0.098	7.667	0.046	6.583	3.037	0.641	14.263	0.036
ICARDA 2706	Control (not defoliated)	17.589	794.33	9.031	5.480	4.600	0.732	19.590	6.999
	Low (8 cm)	1.082	68.333	0.966	3.070	3.650	0.743	17.200	0.526
	Moderate (6 cm)	0.807	65.000	0.512	5.875	3.533	0.494	16.163	0.382
	Severe (4 cm)	0.850	49.333	0.328	4.267	2.433	0.540	11.643	0.253
LSD ($P \leq 0.05$)		0.653	59.826	0.437	59.826	0.870	0.349	2.590	0.690

N.S: not significant

Conclusions

From the results of this study, we concluded that most traits of growth, forage yield, seed yield and its components of narbon vetch were affected significantly by different varieties, defoliation intensities and their interactions as follow:

- The interaction between variety 1 and moderate defoliation intensity (6 cm) gave the highest values of fresh forage yield and fresh stem percent, and maximum fresh leaf percent exhibited by interaction between variety 2 and severe defoliation intensity (4 cm), but maximum leaves/stem ratio, showed by interaction between variety 1 and low defoliation intensity (8 cm).
- The interaction between variety 2 and moderate defoliation intensity (6 cm) awarded the highest values of plant height, no. of branches/plant, no. of leaves/plant, leaves weight/plant, leaves dry weight/plant and stem dry weight/plant, but the highest amount of stem weight/plant was offered by variety 2 when interacted with severe defoliation intensity (4 cm), and maximum root dry weight was obtained by interaction between variety 3 and severe defoliation intensity (4 cm).
- Maximum values of biological yield, pods number/m^2, pod yield, seeds number/pod, and seed yield were attained by the interaction between variety 3 and control (not defoliated) treatment, but the interaction between variety 1 and control treatment gave the highest values of pod length and seeds weight per

http://www.aloki.hu ● ISSN 1589 1623 (Print) ● ISSN 1785 0037 (Online)
DOI: http://dx.doi.org/10.15666/aeer/1705_1247912490

pod, but concerning 100 seeds weight, the highest weight obtained by the interaction between variety 2 and control treatment.

Recommendation

We recommend from this study that there is a forage yield benefit to cutting or defoliation at shorter heights from ground level when the plants are not under stress or low in root carbohydrate levels, medium and high defoliation intensities significantly reduced available forage production. Seed production was adversely affected by defoliation intensity, and further study must be conduct at different locations and conditions to know the performance of these varieties.

REFERENCES

[1] @griculture Online (1999): Cut it close for best performance in alfalfa. – http://www.agriculture.com, April 9, 1999.
[2] Abdullah, Y., Muwalla, M. M., Qudsieh, R. I., Titi, H. H. (2010): Effect of bitter vetch (*Viciaervilia*) seeds as a replacement protein source of soybean meal on performance and carcass characteristics of finishing Awassi lambs. – Trop. Anim. Health Pro. 42: 293-300.
[3] Açıkgöz, E. (2001): Forage Crops. – Uludag Univ. Publ. no: 182, Bursa, Turkey.
[4] AL Mohamad, F., AL Younis, M. A. (2000): Agricultural Experimentation Design and Analysis. – Baghdad Univ. Ministry of Higher Education and Scientific Research, Vol. 374.
[5] Albayrak, S., Güler, M., Tongel, M. O. (2004a): Effects of seed rates on forage production and hay quality of vetch-triticale mixtures. – Asian Journal of Plant Science 3(6): 752-756.
[6] Albayrak, S., Sevimay, C. S., Tongel, M. O. (2004b): The effects of inoculation with Rhizobium on forage yield and yield components of common vetch (*Vicia sativa* L.). – Turkish Journal of Agriculture & Forestry 28: 405-411.
[7] Altınok, S. (2002): The effects of different mixture of hairy vetch (Viciavillosa L.) and Narbonne vetch (*Vicianarbonensis* L.) seeded with barley (*Hordeum vulgare* L.) on silage quality. – TarimBilimleriDergisi-Journal of Agricultural Sciences 8(3): 232-237.
[8] Altınok, S., Hakyemez, H. (2002): The effects on forage yields of different mixture rates of hairy vetch (*Viciavillosa*L.) and Narbonne vetch (*Vicianarbonensis* L.) seeded with barley (Hordeum vulgare L.). – TarimBilimleriDergisi - Journal of Agricultural Sciences 8(1): 45-50.
[9] Avcıoğlu, R., Kavut, Y. T., Okkaoğlu, H. (2009): Narbonne Vetch (*Vicianarbonensis L.*). – In: Avcioglu, R. et al. (eds.) Forages-Legume Forages II. Publication of Turkish Ministry of Agricultural and Rural Affairs, Izmir, pp. 421-425.
[10] Baş, U. et al. (2011): Lathyrus sativus L. – LANDRACES 16(1): 9-14.
[11] Belesky, D. P., Fedders, J. M. (1997): Residue height influences stand dynamics of alfalfa grown on shallow soil. – Agron. J. 89: 975-980.
[12] Berger, J. D., Robertson, L. D., Cocks, P. S. (2002): Genotype × environment interaction for yield and other attributes among undomesticated Mediterranean Vicia species. – Euphytica 126: 421-435.
[13] Brown, E. M., Blaser, R. E., Dunton, H. L. (1966): Leaf-Area Index and Apparent Photosynthesis under Various Microclimates for Different Pasture Species. – In: Hill, A. G. G. (ed.) Proc. 10th Int. Grassl. Congr, Helsinki, Finland. 7-16 July. Finnish Grassland Association, Helsinki, pp. 108-113.

http://www.aloki.hu ● ISSN 1589 1623 (Print) ● ISSN 1785 0037 (Online)
DOI: http://dx.doi.org/10.15666/aeer/1705_1247912490

[14] Bryant, J. A., Hughes, S. G. (2011): Vicia. – In: Kole, C. (ed.) Wild Crop Relatives: Genomic and Breeding Resources. Legume Crops and Forages. Springer, Heidelberg, Chap. 14.
[15] Büyükburç, U., İptaş, S., (2001): The yield and yield components of some narbon vetch (*Vicianarbonensis* L.) lines in Tokat ecological conditions. – Turk J Agric For 25: 79-88.
[16] Fırıncıoğlu, H. K., Unal, S., Pank, Z., Beniwal, S. P. S. (2012): Growth and development of narbon vetch (*Vicianarbonensis L.*) genotypes in the semi-arid central Turkey. – Spanish Journal of Agricultural Research 10(2): 430-442.
[17] Haddad, S. G. (2006): Bitter vetch grains as a substitute for soybean meal for growing lambs. – Livest. Sci. 99: 221-225.
[18] Iptaş, S., Karadağ, Y. (2009): Determination of the yield and yield components of narbon vetch (*Vicianarbonensis L.*) lines grown in spring. – 1st International Symposium on SustainableDevelopment, June 9-10, 2009, Sarajevo, pp. 83-88.
[19] Larbi, A., Abd El-Moneim, A. M., Nakkul, H., Jammal, B., Hassan, S., (2010): Intraspecies variations in yield and quality determinants in Vicia species: 2. Narbon vetch (*Vicianarbonensis* L.). – Anim. Feed Sci. Tech. 162: 20-27.
[20] Mebarkia, A., Abbas, K., Slimani, A. (2013): *Vicianarbonensis* L.: the importance of phosphorus fertilization and seeding rate under rainfall conditions Setif High Plains Algeria. – J. Agronomy 12(2): 93-98.
[21] Mitchell, R. B., Vogel, K. P., Schmer, M. R., Pennington, D. (2010): Switchgrass for biofuel production. – http://www.extension.org/pages/Switchgrass_for_Biofuel_Production. Accessed 30 Nov 2011.
[22] Muhammed, S. R. (2017): Response of two fenugreek *Trigonellafoenum-graecum* varieties to different cutting dates and nitrogen fertilizer for growth and forage yield traits under rainfed condition. – Journal of Tikrit for Agriculture Sciences 17(Special): 134-142.
[23] Nizam, I., Orak, A., Kamburoglu, I., Cubuk, M. G., Moralar, E. (2011): Yield potentials of Narbonne vetch (*Vicianarbonensis L.*) genotypes in different environmental conditions. – Journal of Food Agriculture & Environment 9(1): 314-318.
[24] Sadeghi, G. H., Mohammadi, L., Ibrahim, S. A., Gruber, K. J. (2009): Use of bitter vetch (*Viciaervilia*) as a feed ingredient for poultry. – World Poultry Sci. 65: 51-63.
[25] Sánchez-Vioque, R., Girón-Calle, J., Rodriguez-Conde, M. F., Vioque, J., De-Los-Mozos-Pascual, M., Santana-Méridas, O., Izquierdo-Melero, M. E., Alaiz, M. (2011): Determination of γ-glutamyl-S-ethenyl-cysteine in narbon vetch (*Vicianarbonensis* L.) seeds by high-performance liquid chromatography. – Anim. Feed Sci. Technol. 165(1-2): 125-130.
[26] Sheaffer, C. C., Lacefield, G. D., Marble, V. L. (1988): Cutting Schedules and Stands. – In: Hanson, A. A. et al. (ed.) Alfalfa and Alfalfa Improvement. Agron. Monogr. 29. ASA, CSSA, SSSA, Madison, WI.
[27] Shen, Y., Huixin, J., Guiu, Z., Qingsheng, C. (2013): Effects of cutting height on shoot regrowth and forage yield of alfalfa (Medicago sativa L.) in a short-term cultivation system. – Japanese Society of Grassland Science, Grassland Science 59: 73-79.
[28] Tahereh, R., Arash, A., Ali, M., Karim, K., Farshid, F., Hana, S., Babak, D. (2012): Chemical composition and forage yield of three Vicia varieties (*Vicia spp*.) at the full blooming stage. – Italian Journal of Animal Science 11: 3.
[29] Wiersma, D. W. (2000): Alfalfa cutting height to maximize forage yield and quality. – http://www.uwex.edu/ces/forage/wfc/proceedings2000/wiersma.htm.

http://www.aloki.hu ● ISSN 1589 1623 (Print) ● ISSN 1785 0037 (Online)
DOI: http://dx.doi.org/10.15666/aeer/1705_1247912490

APPENDIX

Appendix 1. *Mean squares of variance analysis for forage yield traits of narbon vetch*

S.O.V	d.f	Fresh forage yield (ton/ha)	Dry forage yield (ton/ha)	Fresh leaf %	Fresh stem %	Dry leaf %	Dry stem %	Dry matter %	Leaves/ stem ratio
Blocks	r-1 = 2	0.018	0.011	0.186	0.573	0.209	0.196	0.765	0.065
A (varieties)	a-1 = 2	7.209*	0.081**	21.077*	18.598$^{n.s}$	1.449$^{n.s}$	0.041$^{n.s}$	1.798$^{n.s}$	0.156$^{n.s}$
Error (a)	(r-1)(a-1) = 4	0.497	0.004	2.751	3.097	0.416	0.074	0.329	0.040
B (defoliation intensities)	b-1 = 2	6.268**	0.036$^{n.s}$	36.061**	31.484**	0.757*	0.005$^{n.s}$	0.735$^{n.s}$	0.136*
AB	(a-1)(b-1) = 4	1.935*	0.022$^{n.s}$	17.090**	18.525**	0.302$^{n.s}$	0.174$^{n.s}$	0.320$^{n.s}$	0.200**
Error (b)	a(b-1)(r-1) = 12	0.408	0.017	1.154	1.402	0.153	0.166	0.360	0.026
Total	abr-1 = 26								

N.S: Not significant; *: Significant; **: Highly significant

Appendix 2. *Mean squares of variance analysis for forage yield component traits of narbon vetch*

S.O.V	d.f	Plant height (cm)	No. of branches/ plant	No. of leaves/ plant	Leaves weight/ plant (g)	Dry leaves weight/ plant (g)	Stem weight/ plant (g)	Dry stem weight/| plant (g)	Root weight (g)	Dry root weight (g)
Blocks	r-1 = 2	2.560	0.015	2.907	2.617	0.390	7.902	0.012	2.697	0.015
A (varieties)	a-1 = 2	225.2**	0.017$^{n.s}$	6.531$^{n.s}$	33.802*	1.121$^{n.s}$	135.8**	0.190$^{n.s}$	0.316$^{n.s}$	0.19**
Error (a)	(r-1)(a-1) = 4	1.672	0.117	4.784	3.548	0.582	6.857	0.390	0.258	0.008
B (defoliation intensities)	b-1 = 2	6.075$^{n.s}$	0.586*	50.65**	62.293**	1.083**	29.95**	0.371$^{n.s}$	0.053$^{n.s}$	0.002$^{n.s}$
AB	(a-1)(b-1) = 4	48.49**	0.632**	71.12**	108.95**	2.581**	49.8**	0.782**	0.518$^{n.s}$	0.03**
Error (b)	a(b-1)(r-1) = 12	1.698	0.096	2.823	0.501	0.092	3.832	0.115	0.409	0.006
Total	abr-1 = 26									

N.S: Not significant; *: Significant; **: Highly significant

Appendix 3. *Mean squares of variance analysis for seed yield and its components of narbon vetch*

S.O.V	d.f	Biological yield (ton/ha)	Pods number/m^2	Pod yield (ton/ha)	Pod length (cm)	Seeds number/pod	Seeds weight/pod (g)	100 seeds weight (g)	Seed yield (ton/ha)
Blocks	r-1 = 2	0.291	220.583	0.019	0.170	0.373	0.046	2.547	0.011
A (varieties)	a-1 = 2	3.554**	4210.083$^{n.s}$	1.257**	1.232 $^{n.s}$	1.693*	0.040$^{n.s}$	58.87**	0.721*
Error (a)	(r-1)(a-1) = 4	0.079	1693.917	0.057	3.122	0.192	0.045	0.988	0.076
B (defoliation intensities)	b-1 = 3	505.1**	1063994**	132.262**	7.612*	6.445**	0.274**	225.6**	79.240**
AB	(a-1)(b-1) = 6	2.420**	5010.82**	0.632**	3.681 $^{n.s}$	0.716*	0.113*	18.11**	0.443*
Error (b)	a(b-1)(r-1) = 18	0.145	1216.324	0.065	1.842	0.257	0.041	2.279	0.162
Total	abr-1 = 35								

N.S: Not significant; *: Significant; **: Highly significant

http://www.aloki.hu ● ISSN 1589 1623 (Print) ● ISSN 1785 0037 (Online)
DOI: http://dx.doi.org/10.15666/aeer/1705_1247912490

CLASSICAL AND MOLECULAR APPROACHES FOR IDENTIFICATION OF *RHIZOBIUM LEGUMINOSARIUM*, *AZOTOBACTER CHROOCOCCUM* AND *BACILLUS MEGATERIUM*

TALABANI, SH. K.[1*] – FATTAH, O. A.[2] – KHIDER, A. K.[1]

[2]*Soil and Water Sciences Department, College of Agricultural Sciences, University of Sulaimani, Sulaimani, Kurdistan Region, Iraq*
e-mail: omar.fattah@univsul.edu.iq; phone: +964-770-153-6011

[1]*Biology Department, College of Education Scientific, University of Salahaddin, Erbil, Kurdistan Region, Iraq*
e-mail: dradelkamal51@yahoo.com phone: +964-750-447-2908

**Corresponding author*
e-mail: shahen.fazil @univsul.edu.iq; phone: +964-770-158-6531

(Received 15th May 2019; accepted 16th Jul 2019)

Abstract. The present study aimed to identify of *Rhizobium leguminosarium* from Broad bean nodules, *Azotobacter chrococcum* and *Bacillus megaterium* from the soil in Sulaimani city/Iraq. Cultural characteristics showed that the colonies of bacteria were circular, smooth convex, and white color in *Rhizobium leguminosarium* and *Bacillus megaterium*, while creamy colored for *Azotobacter chrococcum.* The isolated bacteria were motile, rod, and gram-negative in *Rhizobium leguminosarium* and *Azotobacter chrococcum,* and gram-positive in *Bacillus megaterium*. Biochemical tests found that *Rhizobium leguminosarium* was positive for Catalase and negative for Indole Production, Methyl Red, Vogas Proskauer, Citrate Utilization and Gelatinase, *Azotobacter chrococcum* was positive for Catalase and Citrate Utilization, while *Bacillus megaterium* was positive for Catalase, Citrate Utilization and Gelatinase. *Rhizobium leguminosarium* utilized Starch Glucose, Mannitol, Galactose, Raffinose, Trehalose, Mannose and Xylose, but *Azotobacter chrococcum* did not utilize Galactose and xylose, while *Bacillus megaterium* did not utilize Trehalose**.** The molecular method based on the detection of plasmid DNA*, nod*D2 and *nod*D3 in *Rhizobium leguminosarium*, chromosomal DNA, *nif*H2 and *nif*H3 in *Azotobacter chrococcum*, genomic DNA and two random primers in *Bacillus megaterium* on gel electrophoresis have been successfully applied. We conclude that cultural, morphological and biochemical tests used for identification of these isolates was equivalent to the molecular-based method.
Keywords: *biological nitrogen fixation, nod and nif genes, phosphate solubilization, PCR, gel electrophoresis*

Introduction

Rhizobia are soil bacteria able to form nodules and establish a symbiosis with the roots of leguminous plants. During the symbiotic process, rhizobia reduce atmospheric nitrogen into a form directly assimilated by plants (ammonium) (Berrada and Fikri-Benbrahim, 2014). *Azotobacter* is an aerobic and free-living bacterium that can fix atmospheric nitrogen into the soil. Plants are able to utilize the ammonia as a nutrient (Biomate India, 2008). *Bacillus megaterium* is a gram-positive bacteria; it has a very efficient protein secretion system, grow on several different and cheap carbon sources, lack endotoxins, and are nonpathogenic. Proteins produced from and with it are of great industrial importance (Bunk et al., 2010). *B. megaterium* has the ability to solubilize phosphorus in the soil (Patel et al., 2016).

Nitrogen (N) and Phosphorus (P) are mineral nutrients often limiting plant growth because they are required in large amounts in relation to their availability in the soil

http://www.aloki.hu ● ISSN 1589 1623 (Print) ● ISSN 1785 0037 (Online)
DOI: http://dx.doi.org/10.15666/aeer/1705_1249112506

(Harpole et al., 2011). Biological Nitrogen Fixation (BNF) is known to be a key to sustain agriculture and to reduce soil fertility decline (Kahindi et al., 2009). (BNF) is an efficient source of fixed N2 that plays an important role in land remediation (Mohammadi et al., 2012). Nitrogen fixation in symbionts and free-living microbes is catalyzed by nitrogenase; an enzyme complex encoded *nif*DK and *nif*H genes. Nitrogenase itself consists of a molybdenum-iron protein (MoFe), subunit I and an iron-containing protein (Fe) subunit II. This biological process between *Rhizobium* strains and their legume partners can happen under low levels of available nitrogen with the help of many different genes such as a *nod, nif, fix*, production of polysaccharides, competition, infection process, and host specificity. *Nod*D is appositive transcription regulator from the Lysr family and present in all *rhizobia* (Shamseldin, 2013). The structural *nif* genes from taxonomically diverse microbes are nearly identical and function in a similar manner to encode nitrogenase (Ruvkin et al., 1980). *Azotobacter spp.* studies on the genetics in this genus should take into consideration their *nif* genes which are responsible for fixing nitrogen (Dashti, 2011; Khider, 2011; Abid, 2013; Mohamed, 2017). The *nif*H gene is the biomarker most widely used to study the ecology and evolution of nitrogen-fixing bacteria (Raymond et al., 2004). Phosphate solubilization ability of microorganisms is associated with the release of low molecular weight organic acids (Puenta *et a*l., 2004). The phosphate solubilization ability of microorganisms is regulated by several genes (Young and Lai, 2008), these genes are induced under phosphate starvation and constitute the Pho regulation (Bagyaraj et al., 2000). *Bacillus megaterium var. phosphaticum* was used to create a bio-preparation called Phosphobucterin with the purpose of enhancing mineral phosphorus solubilization (Sylvia et al., 1999).

The present study was carried out to compare two strategies for the isolation and identification of *Rhizobium leguminosarium* from bean nodules, *Azotobacter chroococcum* and *Bacillus megaterium* from soil depending on classical phenotypic approaches and through molecular methods by detection of *nod*D genes in *R. leguminosarium* and *nif*H genes in *A. chroococcum* and cheek the presence of *B. megaterium* that reported in different researches to do significant role in biological nitrogen fixation and phosphorus solubilization up to date. We used the molecular methods addition to the classical taxonomical process to support and to be sure that the bacteria which identified by the classical taxonomical process are same using molecular methods or not, because often the tests or characteristics of the classical taxonomical process of many bacterial species are similar which in some cases make the identification difficult. So, this classification should be confirmed and supported by molecular examination. This study consider the importance report and the first time identified of these bacteria depending on molecular approach in Bakrajow soil in Sulaimani city, Kurdistan region, Iraq.

Materials and methods

Isolation of bacteria

Rhizobium leguminosarium spp.

Nodulated Broad bean was selected from the organic farm of Bakrajow; the plant washed thoroughly with running tap water, then healthy, unbroken, firm and pink nodules were selected for the isolation. Isolation of *Rhizobium* was done on Yeast Extract Mannitol Agar (YEMA) (Handley et al,. 1998; Castro et al., 2003; Kucuk et al., 2006).

http://www.aloki.hu ● ISSN 1589 1623 (Print) ● ISSN 1785 0037 (Online)
DOI: http://dx.doi.org/10.15666/aeer/1705_1249112506

The selected nodules were repeatedly washed in sterile water for 3-4 min, then washed with 70% ethyl alcohol, next rewashed with sterile water, after that crushed with a sterile glass rod. The resulting suspension was streaked on YEMA medium and incubated at 28 °C for 2-3 days. The developed colonies were isolated and purified then identified (Agrawal et al., 2012).

Azotobacter chroococcum spp.

Modified Ashby's Medium (MAM) was used as the specific *A. chroococcum* medium (Astafyeva and Shalabayeva, 2016). Two grams of soil samples were added to 500 ml Erlenmeyer flasks containing 100 ml (MAM), then stirred on rotary shaker 180 rpm for 10 min, streaked out on (MAM) and incubated at 28 ± 2 °C for 2-5 days to be checked for purity (Marwa et al., 2010).

Bacillus megaterium

B. megaterium was isolated through suspending 10 g of soil in 100 ml distilled water in a conical flask. Aerobic spore formers pasteurized a diluted soil sample at 80 °C for 10-15 min and serial dilutions were made from soil suspension, then 100 µl of soil suspension at different dilutions powered onto the surface of Sperber's medium which is a selective medium for isolating *B. megaterium*. Incubated at 28-30 °C for 48 h. Developed colonies of *B. megaterium* appearing on the plates were observed (Shiva et al., 2010).

Purification of bacteria

A single colony of each isolated bacteria (48 h old surface film) was streaked on their selective media; the growth was observed depending on the type of bacteria, *R. leguminosarium* and *B. megaterium* after 24-48 h and *A. chroococcum* after 3-7 days at 28 °C of incubation. The well separated and apparently uncontamination colonies appearing on the plates were streaked on agar medium, plating and picking were repeated at least 4-5 times (Ausubel et al., 1987).

Identification of isolated bacteria by cultural and microscopical characteristics

Cultural characteristics for each isolated were achieved on their media including the shape, color and type of the colonies after 24-48 h for *R. leguminosarium* and *B. megaterium*, and after 3-7 days for *A. chroococcum* at 28 °C of incubation, while microscopical tests for each isolated were carried out for fixed smears using gram stain, shape, and motility followed the method described by Mahon and Manuselis (2000).

Identification of isolated bacteria by biochemical tests

The isolated bacteria were characterized biochemically such as Catalase test and Gelatinase test according to Forbes et al. (2002), methyl red, vogas proskauer and Indole production depending on Atlas et al. (1995) and Citrate utilization according to Mahon and Manuselis (2000).

http://www.aloki.hu ● ISSN 1589 1623 (Print) ● ISSN 1785 0037 (Online)
DOI: http://dx.doi.org/10.15666/aeer/1705_1249112506

Identification of isolated bacteria by carbohydrate fermentation test

Carbohydrate fermentation profiles were conducted in Yeast manitol broth for *R. leguminosarium*, Modified Ashby's broth for *A. chroococcum* and Sperber's broth for B. *megaterium* as carbon sources amended with 0.004% of chlorophenol red and 1% of one of the investigated sugars namely: Starch, Glucose, Mannitol, Galactose, Raffinose, Trehalose, Mannose and Xylose, growth was observed after 5 and even up to 15 days at 28 °C of incubation. Acid and gas production were detected by observing the color change of chlorophenol red from red to yellow (acid) and accumulation of gas in Durham's tube (gas) (Forbes et al., 2002).

Maintenance and storage of bacterial culture

The cultures were maintained for a short time at slant medium, and for a long time without losing their activity in 20% glycerol and stored at - 70 °C (Ausubel et al., 1987).

Identification of bacteria by molecular basis protocol

Extraction of Chromosomal, Genome and Plasmid DNA from bacteria

Plasmid DNA was extracted from pure culture of *R. leguminosarium* using Genet bio, PrmePrep Plasmid DNA isolation kit, and Chromosomal DNA from pure culture of *A. chroococcum* and Genome DNA from pure culture of *B. megaterium* were extracted using the PrestoTM Mini gDNA Bacteria Kit Protocol.

PCR amplification conditions

The conditions of PCR amplification: for *nod*D2 and *nod*D3 were performed according to the modified method of Del Cerro et al. (2015a) at cycling conditions consisted of a single cycle of 95 °C for 10 min, followed by 45 cycles of 95 °C for 2 min, 60 °C for 30 s and 72 °C for 30 s, and a final extension cycle at 72 °C for 6 min., while PCR reactions for *nif*H2 and *nif*H3 were done depending on Setubal et al. (2009), and for random primers 1 and 2 of *B. megaterium* carried out depending on Patil et al. (2013). The forward, reverse and random primers are shown in *Table 1.*

Gel electrophoresis

The PCR products were checked by electrophoresis by dissolve 0.5, 1, 1.5 and 2% (w/v) agarose gel depending on the size of amplified DNA fragments in 100 ml IX TBE buffer by heat in microwave oven for 3 min, then cooled solvent to 45 °C at room temperature, Gels were stained in ethidium bromide and then covered the gel tank by lid and electrophoresis was run at (80 V, 100 V) 10 V/cm. DNA fragments were visualized at 312 nm with a UV-transilluminator Image (Helmut et al., 2004).

Results

Isolation

R. leguminosairum was isolated from Broad bean plant nodules using yeast mannitol agar medium, and colonies observation were done after 2-3 days of incubation at 28 ± 2 °C (*Fig. 1*). The nodules were found positive for the presence of *R. leguminosarium*. *A. chroococcum* was isolated from the soil using Modified Ashby's

http://www.aloki.hu ● ISSN 1589 1623 (Print) ● ISSN 1785 0037 (Online)
DOI: http://dx.doi.org/10.15666/aeer/1705_1249112506

medium, and the growth was observed after 3-7 days of incubation at 28 °C (*Fig. 2*). *B. megaterium* was isolated from soil using Sperber's medium, and the colonies were observed on the plates after 48 h of incubation at 28-30 °C (*Fig. 3*). Then the bacteria were characterized morphologically, biochemically and molecularly.

Table 1. *The forward, reverse and random primers used*

Primer	Sequence (5'-3')	Nucleotide	Reference
*nod*D2- F-	(GTA GGC CAT AAT GTC CAG A)	19	Del Cerro et al., 2015a
*nod*D2- R-	(GCG GCT TTA TAC TCA CCA)	18	
*nod*D3- F-	(GAG CTA CCT CGA CTG CTA)	18	Del Cerro et al., 2015b
*nod*D3- R-	(CTA CCG CCA TGA TCA CCA)	18	
*nif*H2- F-	(CGCCGGCGCAGTGTTTGCGG)	20	Setubal et al., 2009
*nif*H2 -R-	(CACTCGTTGCAGCTGTCGGC)	20	
*nif*H3- F-	(CGATGACTGAAGACTGAACGAG)	22	Setubal et al., 2009
*nif*H3 -R-	(AAGGTGCGGTCAGGAGAGAA)	20	
Random primer1	(GGT GCG GGA A)	10	Patil et al., 2013
Random primer2	(GTA GTC ATA T)	10	

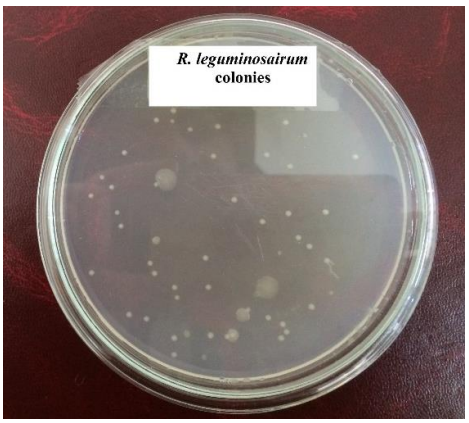

Figure 1. *Single colonies of R. leguminosarium growth on YEMA medium*

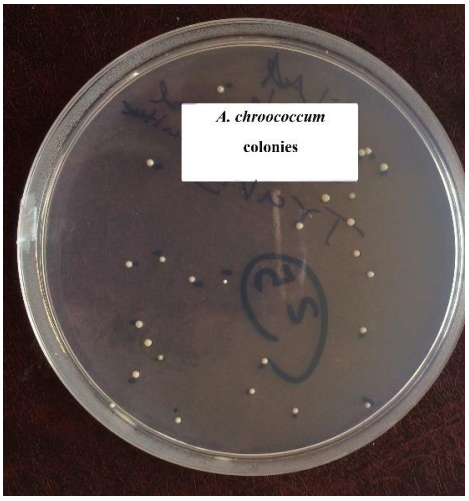

Figure 2. *Single colonies of A. chroococcum growth on modified Ashby's medium*

http://www.aloki.hu ● ISSN 1589 1623 (Print) ● ISSN 1785 0037 (Online)
DOI: http://dx.doi.org/10.15666/aeer/1705_1249112506

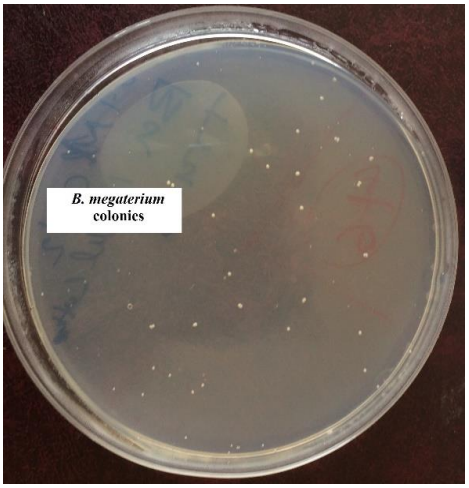

Figure 3. *Single colonies of B. megaterium growth on Sperber's medium*

Identification of isolated bacteria by the morphological and biochemical characteristics

To identify the species, the following were determined: the growth, morphological, biochemical properties, and carbohydrate fermentation tests according to Brenner et al. (2005).

Table 2 represents cultural and microscopical characteristics of *R. leguminosarium, A. chroococcum and B. megaterium*. The colonies of all the bacteria were circular in shape and smooth convex in type, but in color, *R. leguminosarium and B. megaterium* were white while *A. chroococcum* was creamy color. The all bacteria were rod in shape and motile, but in gram stain, *R. leguminosarium* and *A. chroococcum* were negative while *B. megaterium* was positive.

Table 2. *The cultural and microscopical tests of the isolated Rhizobium leguminosarium, Azotobacter chroococcum and Bacillus megaterium*

Test	**Bacteria**		
	Rhizobium leguminosarium	***Azotobacter chroococcum***	***Bacillus megaterium***
Colonies			
Shape	Circular	Circular	Circular
Color	White	Creamy	White
Type	Smooth convex	Smooth convex	Smooth convex
Bacterium			
Gram Stain	-	-	+
Shape	Rod	Rod	Rod
Motile	Flagella	Flagella	Flagella

Table 3 represents the biochemical characterizations of *R. leguminosarium, A. chroococcum* and *B. megaterium*. All the bacteria were found positive for Catalase test, and negative for Indole Production, Methyl Red, Vogas Proskauer tests, but in Citrate Utilization was positive in *A. chroococcum* and *B. megaterium*, and negative for *R.*

http://www.aloki.hu ● ISSN 1589 1623 (Print) ● ISSN 1785 0037 (Online)
DOI: http://dx.doi.org/10.15666/aeer/1705_1249112506

leguminosarium, while Gelatinase test was negative for *R. leguminosarium* and *A. chroococcum* and positive for *B. megaterium*.

Table 3. *The biochemical characteristics of the isolated Rhizobium leguminosarium, Azotobacter chroococcum and Bacillus megaterium*

Characteristics	Bacteria		
	Rhizobium leguminosarium	***Azotobacter chroococcum***	***Bacillus megaterium***
Catalase	+	+	+
Indole Production	-	-	-
Methyl Red	-	-	-
Vogas Proskauer	-	-	-
Citrate Utilization	-	+	+
Gelatinase	-	-	+

R. leguminosarium, A. chroococcum and *B. Megaterium* were also examined for fermentation of the various sugars, *Table 4* shows that the *R. leguminosarium* found positive for assimilation of all sugars, *A. chroococcum* found negative for assimilation of Galactose and xylose while positive for other sugars, and *B. megaterium* found negative assimilation for Trehalose but positive for others.

Table 4. *The Carbohydrate fermentation tests of the isolated Rhizobium leguminosarium, Azotobacter chroococcum and Bacillus megaterium*

Carbon sources	Bacteria		
	Rhizobium leguminosarium	***Azotobacter chroococcum***	***Bacillus megaterium***
Starch	+	+	+
Glucose	+	+	+
Mannitol	+	+	+
Galactose	+	-	+
Raffinose	+	+	+
Trehalose	+	+	-
Mannose	+	+	+
Xylose	+	-	+

Identification of bacteria by the molecular basis

Moreover based on the molecular method, plasmid DNA and *nod*D genes of *R. leguminosarium*, chromosomal DNA and *nif*H genes of *A. chroococcum*, and genome DNA and random primers of *B. megaterium* were detected.

The chromosomal DNA from *A. chroococcum*, genome DNA from *B. megaterium* and plasmid DNA from *R. leguminosarium* were detected on the agarose gel electrophoresis, the result shows in *Figure 4*, lane 2, 4, 6 respectively.

The PCR was carried out for all tested isolates to check the presence of *nod*D2 and *nod*D3 genes in *R. leguminosarium*, *nif*H2 and *nif*H3 genes in *A. chroococcum*, and to know the presence of the *B. megaterium* in the region using two random primers. Their

http://www.aloki.hu ● ISSN 1589 1623 (Print) ● ISSN 1785 0037 (Online)
DOI: http://dx.doi.org/10.15666/aeer/1705_1249112506

banding patterns of DNA on agarose gel electrophoresis were compared with their references' primers. The PCR products for *R. leguminosarium* were: *nod*D2 (100 bp) (*Fig. 5*) and *nod*D3 (150 bp) (*Fig. 6*), for *A. chroococcum* were: *nif*H2 (250 bp) (*Fig. 7*), and *nif*H3 (130 bp) (*Fig. 8*) lanes 2, while these bands did not appear in the negative control (lanes 3) in all figures.

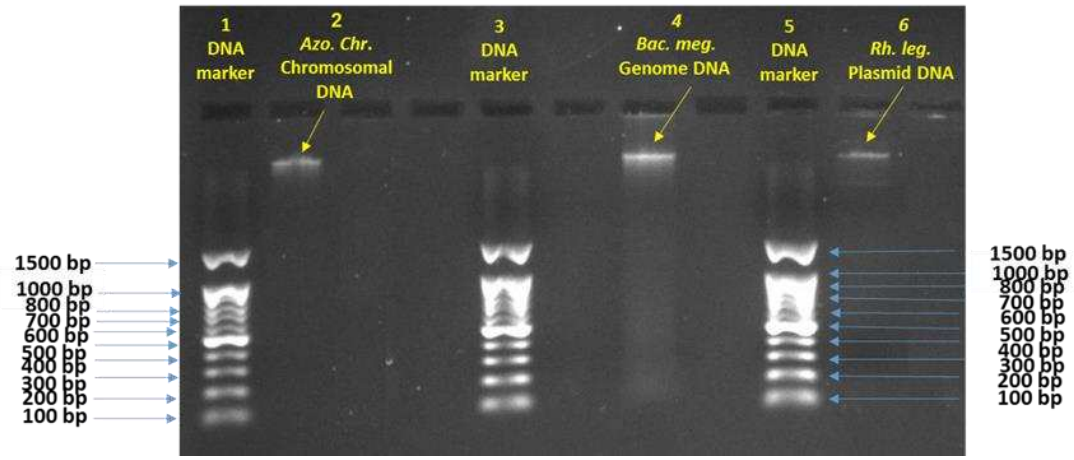

Figure 4. *Agarose gel electrophoresis shows DNA marker lanes (1, 3, and 5), extracted chromosomal DNA from A. chroococcum lane 2, genome DNA from B. megaterium lane 4, and plasmid DNA from R. leguminosarium lane 6*

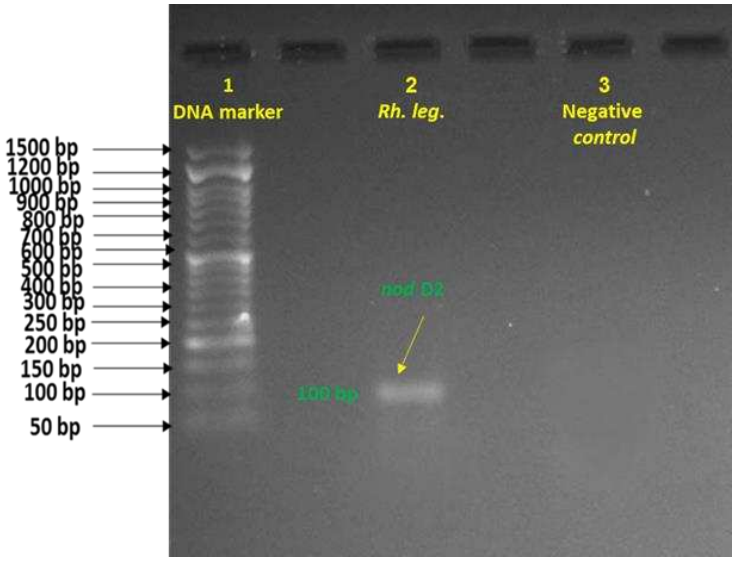

Figure 5. *Agarose gel electrophoresis shows the PCR amplified products of the nodD2 gene (100 bp). Lane 1: DNA marker, lane 2: R. leguminosarium (+ve PCR product), lane 3: negative control (-ve PCR product)*

For *B. megaterium* using random primers (1 and 2) were obtained high amplification rate and reproducible banding pattern which confirmed the existence of *B. megaterium* in the regions (*Fig. 9*) lanes 2 and 3. Therefore, all the bacteria that classified depending on the traditional approach were compared with that of molecular-based methods.

http://www.aloki.hu ● ISSN 1589 1623 (Print) ● ISSN 1785 0037 (Online)
DOI: http://dx.doi.org/10.15666/aeer/1705_1249112506

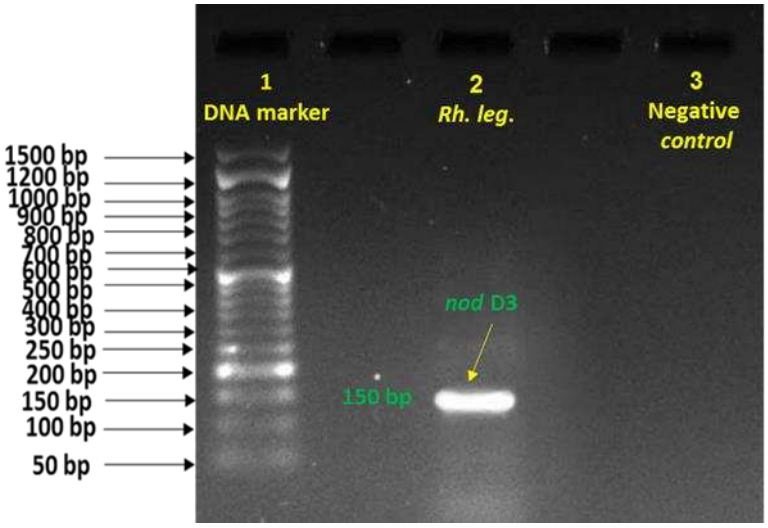

Figure 6. *Agarose gel electrophoresis shows the PCR amplified products of the nodD3 gene (150 bp). Lane 1: DNA marker, lane 2: R. leguminosarium (+ve PCR product), lane 3: negative control (-ve PCR product)*

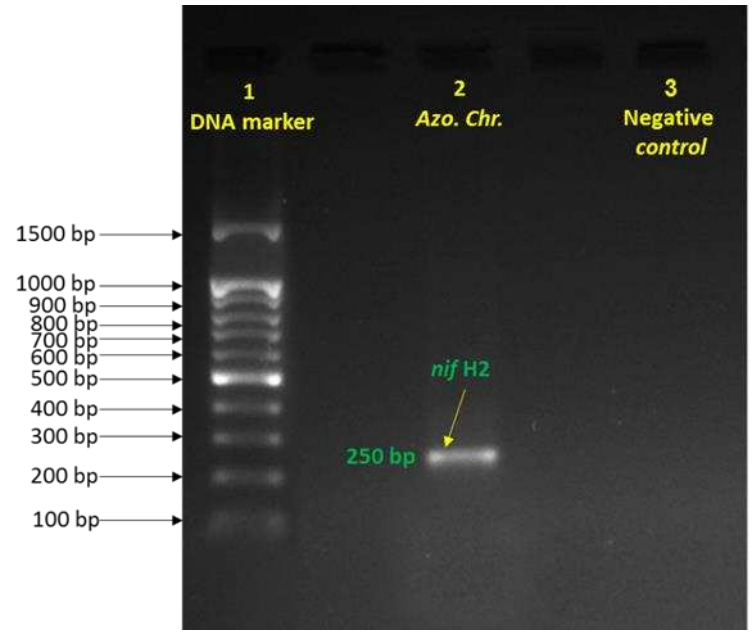

Figure 7. *Agarose gel electrophoresis shows the PCR amplified products of the nifH2 gene (250 bp). Lane 1: DNA marker, lane 2: A. chroococcum (+ve PCR product), lane 3: negative control (-ve PCR product)*

Discussion

This research work aimed to compare two different methods reported in the literature for the isolations of *R. leguminosarium* from Broad bean nodules, *A. chroococcum* and *B. megaterium* bacteria from Bakrajow soil in Sulaimani city, Iraq, in order to prove the presence and identify these bacteria. Different criteria have been presented by several researchers to delimit characteristic which can be used as a key for identification of all studied bacteria, generally included morphological, cultural, biochemical and molecular

http://www.aloki.hu ● ISSN 1589 1623 (Print) ● ISSN 1785 0037 (Online)
DOI: http://dx.doi.org/10.15666/aeer/1705_1249112506

characteristics, highlighting the points which may be used as the diagnostic indications. All bacteria were processed through the characteristics using common procedures for isolation and identification of all isolated bacteria using selective media for each bacteria.

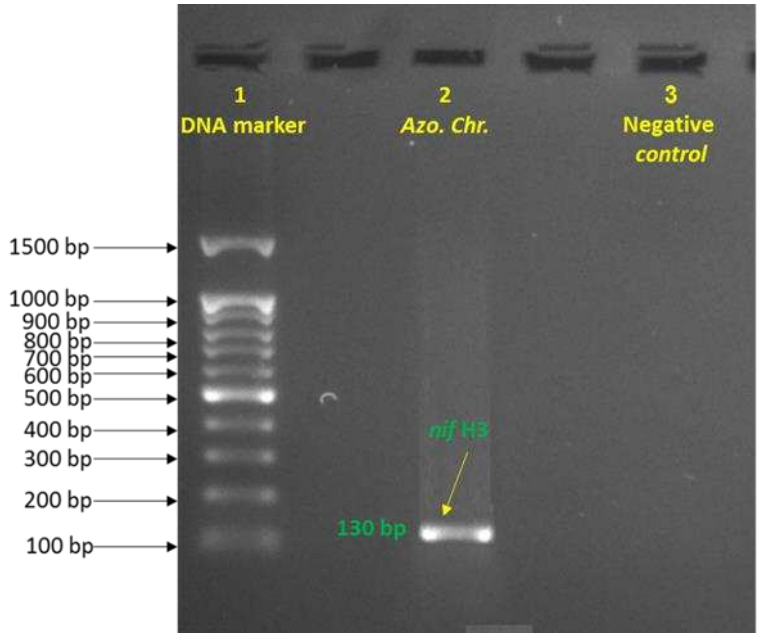

Figure 8. *Agarose gel electrophoresis shows the PCR amplified products of the nifH3 gene (130 bp). Lane 1: DNA marker, lane 2: A. chroococcum (+ve PCR product), lane 3: negative control (-ve PCR product)*

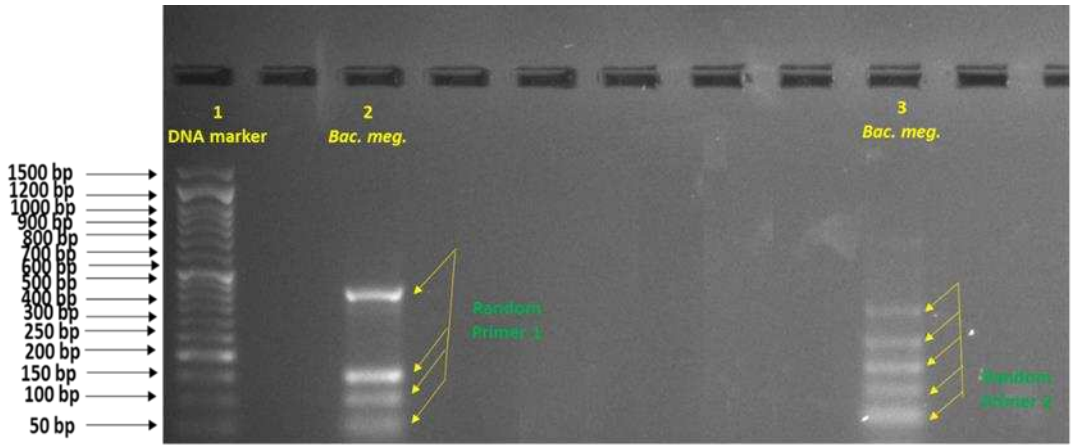

Figure 9. *Agarose gel electrophoresis shows the PCR amplified products of the B. megaterium isolate generated using 10-mer random primers: Lane 1: DNA marker, lanes 2 and 3: random primers 1 and 2 respectively (+ve PCR products)*

The nodules of Broad bean showed presences of *R. leguminosarium* basing on the characteristics, the colony morphology on a selective medium is clearly recognizable (*Fig. 1*), so the isolated bacteria classified as *R. leguminosarium* when the colonies were circular in shape, white color, smooth convex in type, and the bacterium was motile, rod

http://www.aloki.hu ● ISSN 1589 1623 (Print) ● ISSN 1785 0037 (Online)
DOI: http://dx.doi.org/10.15666/aeer/1705_1249112506

and gram-negative. The biochemical characterization found positive for Catalase test, and negative for other biochemical tests, when *R. leguminosarium* utilized starch and all other sugars and produced of gas and acid, considered the important observations to classify the isolated bacteria as *R. leguminosarium*, Depending on these characteristics the isolated *Rhizobium* was classified as *R. leguminosarium* according to Brenner et al. (2005). Same results have also reported by other researchers like Shoukry et al. (2013), Datta et al. (2015) and Tesema (2018).

Obviously molecular characterization of the isolated *Rhizobium* identified based on the extraction and purification of plasmid DNA from pure culture of *R. leguminosarium* to detect of *nod*D genes, because nodulation genes (*nod* genes) are located on the plasmid which is also called mega plasmid (Kumari and Sinha, 2011), which have been successfully applied and the banding pattern of plasmid DNA on agarose gel electrophoresis showed in *Figure 4* lane 6. The PCR was carried out for isolated bacteria by using complementary primers in order to amplify and cheek the presence of *nod*D2 and *nod*D3 for isolated *Rhizobium* which identified as *R. leguminosarium* by the traditional approach. The *nod*D2 and *nod*D3 genes were (100 bp) and (150 bp) in *Figures 5* and *6,* lanes 2, respectively. *Nod*D genes act as the family of regulatory (Kidaj and Wielbo, 2010). In legume nitrogen-fixing symbioses, rhizobial *nod* genes are obligatory for initiating infection thread formation and root nodule development (Fujishige et al., 2007). *Nod*D is the core signaling protein, reacting to plant flavonoids then binding to nod boxes, binding sites upstream of *nod* genes, typically *nod*A and/or *nod*B, triggering the expression of a *nod* gene cascade and thus the construction of the Nod Factor (Jones et al., 2007). The *nod* gene is controlled by *nod*D gene. *Nod*D proteins act as a transcriptional activator of inducible nod gene (Kumari and Sinha, 2011). So the importance of *nod*D in nitrogen fixation process gives importance to our choice of these genes (*nod*D2 and *nod*D3) which are located on the plasmid for this study. The common nodulation genes (*nod*DABC) are found in all bacteria that nodulate legumes (Giraud et al., 2007). Also Black et al. (2012) reported that all fourteen species of *Rhizobium* contained *nod*D, *nod*E, *nod*G, *nod*I, *nod*M, *nod*P, *nod*Q, *nod*V, and *nod*W. As well Rossen et al. (1985), Hu et al. (2000) and Zeze et al. (2001) showed and confirmed presence of *nod*D in *R. leguminosarium.*

The soil sample was processed through the colony characteristics, morphology, and biochemical tests, using common procedures for isolation and identification of *A. chroococcum* and *B. megaterium* species in the soil using selective media for each bacteria. The sample showed presences of the two species depending on their characteristics.

The colony morphology of *A. chroococcum* on Modified Ashby's medium clearly appeared (*Fig. 2*), and the medium that used is to be selective enough, so the isolated classified as *A. chroococcum* when the colonies were circular in shape, creamy color, smooth convex in type and the bacterium was motile, rod and gram-negative, in biochemical characterization found positive for Catalase test and Citrate utilization, but negative for other biochemical tests. The important observations that the isolates classified as *A. chroococcum* when utilized different carbon sources such as starch, glucose, mannitol, raffinose, trehalose and mannose. Marwa et al. (2010), Dashti (2011), Khider (2012), Abid (2013) and Mohamed (2017) obtained same results when they isolated different strains of *Azotobacter* from the soil of different regions in Kurdistan-Iraq. The isolated *Azotobacter* was classified as *A. chroococcum* according to Brenner et al. (2005) in Bergey's Manual of Determinative Bacteriology.

http://www.aloki.hu ● ISSN 1589 1623 (Print) ● ISSN 1785 0037 (Online)
DOI: http://dx.doi.org/10.15666/aeer/1705_1249112506

Indeed molecular characterization of the isolated *Azotobacter* based on the extraction of chromosomal DNA from pure culture of *A. chroococcum* and the banding pattern of the chromosomal DNA on agarose gel electrophoresis showed in *Figure 4* lane 2. Then the *nif*H genes detected on chromosomal DNA of *A. chroococcum*, because *nif* genes in some free-living bacteria are located on the chromosome (Kumari and Sinha, 2011). Using of the complementary primers to well-conserved regions in the bacterial genome, led to amplify the *nif* genes (nitrogenase genes) *nif*H2 and *nif*H3 genes by PCR which identified as *A. chrococcum* by classical approach. The *nif*H2 and *nif*H3 genes were (250 bp) and (130 bp) in *Figures 7* and *8,* lanes 2, respectively. *Nif*H acts as dinitrogenase reductase, obligate electron donor to dinitrogenase during dinitrogenase turnover and is required for FeMo-Co biosynthesis and apodinitrogenase maturation (Shamseldin, 2013). The region of chromosome which contain *nif*K, *nif*D, *nif*M, *nif*A, *nif*N, *nif*B, *nif*Q, *nif*Z, *nif*P, *nif*F, *nif*W, *nif*B, *nif*L, and *nif*Y genes are located between the fragment of chromosome which contains *nif*H2 and *nif*H3 and the fragment contain *nif*V, *nif*S, and *nif*U (Hamilton et al., 2011). Importance of region of *nif*H2 and *nif*H3 genes on chromosome took into consideration to select these genes for this study. Previous studies by Kirshtein et al. (1991), Ueda et al. (1995), Zehr et al. (2003), Aquilantia et al. (2004), Mary Ann and Virginia (2007), Dashti (2011), Hamilton et al. (2011), Khider (2012), Abid (2013) and Mohamed (2017) indicated that N-fixing bacteria were investigated by the diversity of nitrogenase genes in different environments, through amplification of *nif* genes, i.e., *nif*H, *nif*D, *nif*V, *nif*K, *nif*U which encode nitrogenase complex from cultivated organisms.

Sperber's medium was used as a selective medium to identify the *B. megaterium* depending on the colonies (*Fig. 3*) and bacterium morphology, and other characteristics, the isolated classified as *B. megaterium* when the colonies were circular in shape, white color, smooth convex in type and the bacterium was motile, rod and gram-positive. In biochemical characterization found positive for Catalase, Citrate utilization and Gelatinase tests, but negative for Indole Production, Methyl Red and Vogas Proskauer. *B. megaterium* had the ability to utilize all carbon sources except trehalose. Other researchers have also reported same results such as Dunca et al. (2005), Tenzing et al. (2016), Patel et al. (2016) and Environment and Climate Change Canada (2018). So the isolated *Bacillus* was classified and identified as *B. megaterium* according to Brenner et al. (2005) in Bergey's Manual of Systematic Bacteriology.

Molecular characterization of the isolated *B. megaterium* was identified through extraction of the genome DNA from pure culture of *B. megaterium* culture, and the banding pattern of the genome DNA on agarose gel electrophoresis showed in *Figure 4* lane 4. The PCR was carried out for isolated bacteria by using two random primers 1 and 2 to detect and cheek the presence of *B. megaterium* in the region which identified as *B. megaterium* by classical approach. In the results found that the banding patterns were intense, clear and reproducible in *B. megaterium* (*Fig. 9*). Previous studies by Shiva et al. (2010) and Patil et al. (2013) indicated the presence of *B. megaterium* in the different area by these primers.

Conclusion

As the result of the morphological and growth characteristics, physiological and biochemical properties of all isolated bacteria according to Brenner et al. (2005) in Bergey's Manual of Systematic Bacteriology, and based on the molecular methods: the

http://www.aloki.hu ● ISSN 1589 1623 (Print) ● ISSN 1785 0037 (Online)
DOI: http://dx.doi.org/10.15666/aeer/1705_1249112506

isolated *Rhizobium* was taxonomically classified as *Rhizobium leguminosarium*, isolated *Azotobacter* as *Azotobacter chroococcum* and isolated *Bacillus* as *Bacillus megaterium*, so the results of the classical approaches were parallel with molecular methods. Our recommendation is using molecular method with multiplex PCR for one step identification of each bacteria is faster, more accurate and low cost. Detection of other *nod* and *nif* genes required further work.

Acknowledgments. We wish to thank Dr. Zaid Khalaf Khidhir from Faculty of the Agricultural Sciences University of Sulaimani for his cooperation; we also wish to thank Professor Dr. Nawroz Abdul-razzak Tahir from Faculty of the Agricultural Sciences University of Sulaimani for his helpful in the molecular part.

REFERENCES

[1] Abid, S. A. (2013). Microbiological and molecular biology study of *Azotobacter* species from Bakrajow soil in Sulaimani. – M.Sc. Thesis. Faculty of Agricultural Sciences, University of Sulaimani, Kurdistan.

[2] Agrawal, P. K., Agrawal, S., Singh, U., Katiyar, N., Verma, S. K. (2012): Phenotypic characterization of *Rhizobia* from legumes and its application as a bioinoculant. – Journal of Agricultural Technology 8(2): 681-692.

[3] Aquilantia, L., Favillib, F., Clementi, F. (2004): Comparison of different strategies for isolation and preliminary identification of *Azotobacter* from soil samples. – Soil Biol. Biochem. 36: 1475-1483.

[4] Astafyeva, Y., Shalabayeva, K. (2016): Dependence of *Azotobacter chroococcum* culture growth rate on salt concentrations. – Proceedings of Engineering for Rural Development, 25-27 May, 2016, Jelgava, Latvia.

[5] Atlas, R. M., Alfred, A. E., Lawrence, C. P. (1995): Laboratory Manual of Experimental Microbiology. – Mosby-Year Book Inc., USA.

[6] Ausuble, F. M., Kingstonm, R. E., Bernt, R., Moore, D. D., Smith, J. A,. Seidman, J. G., Stuhl, K. (1987): Current Protocols in Molecular Biology. – John Wiley and Sons, Inc., New York.

[7] Bagyaraj, D. J., Krishnaray, P. U., Khanuja, S. P. (2000): Mineral phosphate solubilization Agronomic implications, mechanism and molecular genetics. – Ind. Natu. Sci. Acad. (PINSA) 3: 69-82.

[8] Berrada, H., Fikri-Benbrahim, K. (2014): Taxonomy of the *Rhizobia*: current perspectives. – British Microbiology Research Journal 4(6): 616-639. www.sciencedomain.org.

[9] Biomate India (2008): Project Report for Biofertilizer Laboratory and Production Unit, Inspired by Scientific Technology. An ISO 9001 Certified Company, Near Delhi Technological University (DCE). – Rohini, Delhi. www.biomateindia.com.

[10] Black, M., Moolhuijzen, P., Chapman, B., Barrero, R., Howieson, J., Hungria, M., Bellgard, M. (2012): The genetics of symbiotic nitrogen fixation: comparative genomics of 14 *Rhizobia* strains by resolution of protein clusters. – Genes 3: 138-166. DOI: 10.3390. www.mdpi.com/journal/genes.

[11] Brenner, D. J., Noel, R. K., Staley, J. T. (2005): The Proteobacteria. Part B: The *Gammaproteobacteria*. – In: Garrity, G. M. (ed.) Bergey's Manual of Systematic Bacteriology. Second Ed. Springer Science and Business Media, Inc., New York.

[12] Bunk, B., Jahn, D., Biedendieck, R., Vary, S. P. (2010): *Bacillus Megaterium* and Other Bacilli: Industrial Applications. – In: Flickinger, M. C. (ed.) Encyclopedia of Industrial Biotechnology: Bioprocess, Bioseparation, and Cell Technology. Wiley, Hoboken, NJ.

http://www.aloki.hu ● ISSN 1589 1623 (Print) ● ISSN 1785 0037 (Online)
DOI: http://dx.doi.org/10.15666/aeer/1705_1249112506

[13] Castro, I. V., Ferreira, E. M., McGrat, S. P. (2003): Survival and plasmid stability of *rhizobia* introduced into a contaminated soil. – Soil Biol. Biochem 35: 49-54.
[14] Dashti, A. M. K. (2011): Isolation and characterization of *Azotobacter spp*. in Erbil soils, and study the effect of biofertilzer (*Azotobacter chroococcum* and transconjugant *Lactobacillus plantarum*) on nutrient uptake by wheat. – Ph.D. Thesis. Ministry of High Education and Scientific Research, University of Salahaddin, Erbil, Kurdistan.
[15] Datta, A., Singh, R. K., Tabassum, S. (2015): Isolation, characterization and growth of *Rhizobium* strains under optimum conditions for effective biofertilizer production. – Int. J. Pharm. Sci. Rev. Res. 32(1): 199-208.
[16] Del Cerro, P., Rolla-Santos, A. A. P., Gomes, D. F., Marks, B. B., Pérez-Montaño, et al. (2015a). Regulatory *nod*D1 and *nod*D2 genes of *Rhizobium tropici* strain CIAT 899 and their roles in the early stages of molecular signaling and host-legume nodulation. – BMC Genomics 16(1): 251. DOI: 10.1186/s12864-015-1458-8.
[17] Del Cerro, P., Rolla-Santos, A. A. P., Gomes, D. F., Marks, B. B., Pérez-Montaño, F., et al. (2015b). Opening the "black box" of *nod*D3, *nod*D4 and *nod*D5 genes of *Rhizobium tropici* strain CIAT 899. – BMC Genomics 16: 864. DOI: 10.1186/s12864-015-2033-z.
[18] Dunca, S., Stefan, M., Nimitan, E., Ailesei, O. (2005): Microbiologcal study of a *Bacillus megaterium* strain with soil phosphorus solubilization potential. – Kom. J. Biol. Plant Biol. 49-50: 31-39.
[19] Environment and Climate Change Canada (2018): Final Screening Assessment of *Bacillus megaterium*. – Health Canada, Government of Canada.
[20] Forbes, B. A., Sahm, D. F., Weissfeld, A. S. (2002): Diagnostic Microbiology. 11th Ed. – Mosby, Inc., USA.
[21] Fujishige, N. A., Lum, M. R., De Hoff, P. L., Whitelegge, J. P., Faull, K. F., Hirsch, A. M. (2007): *Rhizobium* common *nod* genes are required for biofilm formation. – Molecular Microbiology 67(3): 504-515.
[22] Giraud, E., Moulin, L., Vallenet, D., Barbe, V., Cytryn, E., Avarre, J. C., Jaubert, M., et al. (2007): Legume symbioses: absence of Nod genes in photosynthetic *bradyrhizobia*. – Science 316: 1307-1312**.**
[23] Hamilton, T. L., Marcus, L., Ray, D., Eric, S. B., Patricia, C., et al. (2011): Transcriptional profiling of nitrogen fixation in *Azotobacter vinelandii*. – J. Bacteriol. 193(17): 4477-4486.
[24] Handley, B. A., Hedges, A. J., Beringer, J. E. (1998): Importance of host plants for detecting the population diversity of *Rhizobium leguminosarum* biovar viciae in soil. – Soil Biology & Biochemistry 3: 241-249.
[25] Harpole, W. S., Ngai, J. T., Cleland, E. E., Seabloom, E. W., Borer, E. T., et al. (2011): Nutrient co-limitation of primary producer communities. – Ecol Lett 14: 852-62.
[26] Helmut, B. F., Widmer, W., Sigler, V., Zeyer, J. (2004): New molecular screening tools for analysis of free-living diazotrophs in soil. – Appl. Environ. Microbial 70: 240-247.
[27] Hu, H., Liu, S., Yang, Y., Chang, W., Honga, G. (2000): In *Rhizobium leguminosarum, NodD* represses its own transcription by competing with RNA polymerase for binding sites. – Nucleic Acids Research 28(14): 2784-2793.
[28] Jones, K. M., Kobayashi, H., Davies, B. W., Taga, M. E., Walker, G. C. (2007): How *rhizobial* symbionts invade plants: the Sinorhizobium–Medicago model. – Nat. Rev. Microbiol. 5: 619-633.
[29] Kahindi, K., Karanja, N., Gueye, M. (2009): Biological Nitrogen Fixation. – In: Doelle, H. W. et al. (eds.) Biotechnology. EOLSS, Oxford, UK.
[30] Khider, A. K. (2011): Chromosomal *nif* genes transfer by conjugation in nitrogen fixing *Azotobacter chrococcum* to *Lactobacillus planetarium*. – Current Research Journal of Biological Sciences 3: 155-164.
[31] Khider, A. K. (2012): Molecular study of *nifH1, nifH2, nifH3, nifU, nifV, VF* genes and classical approach carried out to identification of *Azotobacter chrococcum* from soil. – Curr. Res. J. Biol. Sci. 4(5): 570-577.

http://www.aloki.hu ● ISSN 1589 1623 (Print) ● ISSN 1785 0037 (Online)
DOI: http://dx.doi.org/10.15666/aeer/1705_1249112506

[32] Kidaj, D., Wielbo, J. (2010): Use of rhizobial *Nod* factors as biofertilizers for legumes. – M. Curie-Sklodowska University, Lublin, Poland/Mikkeli, Finland.
[33] Kirshtein, J. D., Paerl, H., Zehr, W. J. (1991): Amplification, cloning and sequencing of a nif H segment from aquatic microorganisms and natural communities. – Appl. Environ. Microbiol. 57: 2645-2650.
[34] Kucuk, C. M., Kivanç, M., Kinaci, E. (2006): Characterization of *Rhizobium Sp*. isolated from bean. – Turk J. Biol. 30: 127-132.
[35] Kumari, S., Sinha, R. P. (2011): Symbiotic and Asymbiotic N2 Fixation. – In: Sinha, R. P. et al. (eds.) Advances in Life Sciences. I.K. International Publishing House Pvt. Ltd., New Delhi, Chap. 5, pp. 133-148.
[36] Mahon, C., Manuselis, G. (2000): Textbook of Diagnostic Microbiology. 2nd Ed. – W. B. Saunders Company, PA.
[37] Marwa, A. S., Elbaz, A. F., Ragab, A. A., Hamza, H. A., El Halafawy, K. A. (2010): Identification and characterization of *Azotobacter chroococcum* isolated from some Egyptian soils. – J. of Agricultural Chemistry and Biotechnology 1(2): 93-104.
[38] Mary Ann, M. E., Virginia, A. R. (2007): Genomes of sea microbes. – Oceanogr 20: 47-55.
[39] Mohamed, A. S. A. (2017): Molecular study on isolated *Azotobacter, Rhizobium* and *Bacillus megaterium var phosphaticum* employment as biofertilizer. – Ph.D. thesis. Salahaddin University, Erbil, Kurdistan.
[40] Mohammadi, K., Sohrabi, Y., Heidari, G., Khalesro, S., Majidi, M. (2012): Effective factors on biological nitrogen fixation. – Afr. J. Agric. Res. 7(12): 1782-1788.
[41] Patel, G., Singh, S., Saxena, S. K., Kaur, K. J. (2016): Isolation, biochemical characterization and production of biofertilizer from *Bacillus megaterium*. – Int. J. Life Sci. Scienti. Res. 2(6): 749-752. DOI: 10.21276/ijlssr.2016.2.6.16.
[42] Patil, H. S. R., Naik, T. V., Avin, B. R. V., Sayeswara, H. A. (2013): Isolation and molecular characterization of *Bacillus megaterium* isolated from various agro climatic zones of Karnataka and its effect on medicinal plant *Ruta gradiolus*. – Curr Res Microbiol Biotechnol. 1(4): 173-182.
[43] Puenta, M. E., Bashan, Y., Li, C. Y., Lebsky, V. K. (2004): Microbial populations and activities in the rhizoplane of rock weather insert plants, root colonization and weathering of igneous rocks. – Plant. Biol. 6: 629-642.
[44] Raymond, J., Siefert, J. L., Staples, C. R., et al. (2004): The natural history of nitrogen fixation. – Mol. Biol. Evol. 21: 541-554.
[45] Rossen, L., Shearman, C. A., Johnston, A. W. B., Downiel, J. A. (1985): The *nodD* gene of *Rhizobium leguminosarum* is autoregulatory and in the presence of plant exudate induces the *nod A, B, C* genes. – The EMBO Journal 4(13A): 3369-3373.
[46] Ruvkin, G. B., Ausubel, F. M. (1980): Interspecies homology of nitrogenase genes. – Proc. Natl. Acad Sci. USA 77: 191-195.
[47] Setubal, J. C., Santos, P. D., Goldman, B. S., Ertesvåg, H., Espin, G., et al. (2009): Genome sequence of *Azotobacter vinelandii*, an obligate aerobe specialized to support diverse anaerobic metabolic processes. – J. Bacteriol. 191: 4534-4545.
[48] Shamseldin, A. (2013): The role of different genes involoved in symbiotic nitrogen fixation - review. – Global Journal of Biotechnology & Biochemistry 8(4): 84-94.
[49] Shiva, R. D. M., Mohan, B. K., Nataraja, S., Krishnappa, M., Abhilash, M. (2010): Isolation and molecular characterization of *Bacillus megaterium* isolated from different agro climatic zones of Karnataka and its effect on seed germination and plant growth of Sesamum indicum. – RJPBCS 1(3): 614.
[50] Shoukry, A. A., Khattab, A. A., Abou-Ellail. M., El-shabrawy, H. (2013): Molecular and biochemical characterization of new *Rhizobium leguminosarum* bio *viciae* strains isolated from different located of Egypt. – Journal of Applied Sciences Research 9(11): 5864-5877.

http://www.aloki.hu ● ISSN 1589 1623 (Print) ● ISSN 1785 0037 (Online)
DOI: http://dx.doi.org/10.15666/aeer/1705_1249112506

[51] Sylvia, D. M., Fuhrmann, J. J., Hartel, P. G., Zuberer, D. A. (1999): Principles and Applications of soil Microbiology. – Prentice Hall Inc., Upper Saddle River, NJ.

[52] Tenzing, B. N., Pandiarajan, G., Makesh, K. B. (2016): Isolation, identification and characterization of phosphate solubilizing bacteria from different crop soils of Srivilliputtur Taluk, Virudhunagar District, Tamil Nadu. – Tropical Ecology 57(3): 465-474.

[53] Tesema, W. M. (2018): Symbiotic and phenotypic characteristics of *Rhizobia* nodulating Faba bean (*Vicia faba L.*) from Bale zone, Oromiya Regional State, Ethiopia. – M.Sc. Thesis. Hawassa University, Hawassa, Ethiopia.

[54] Ueda, T., Suga, Y., Yahiro, N., Matsuguchi, T. (1995): Remarkable N2 fixing bacterial diversity detected in rice roots by molecular evolutionary analysis of *nif*H gene sequences. – J. Bacteriol. 177: 1414-1417.

[55] Young, C., Lai, W. A. (2008): Mechanism of phosphate solubilization and growth promotion by diverse bacteria. – Appl. Soil Ecol. 49: 72-79.

[56] Zehr, J. P., Jenkins, B. D., Shortand, S. M., Steward, G. F. (2003): Nitrogenase gene diversity and microbial community structure: a cross-system comparison. – Environ. Microbiol. 5 :539-554.

[57] Zeze, A., Mutch, L. A., Young, J. P. W. (2001): Direct amplification of *nod*D from community DNA reveals the genetic diversity of *Rhizobium leguminosarum* in soil. – Environmental Microbiology 3(6): 363-370.

http://www.aloki.hu ● ISSN 1589 1623 (Print) ● ISSN 1785 0037 (Online)
DOI: http://dx.doi.org/10.15666/aeer/1705_1249112506

GENETIC DIVERSITY ANALYSIS OF *DENDROCALAMOPSIS BEECHEYANA* VAR. *PUBESCENS* BASED ON ISSR MARKERS

HE, T. Y.[1] – QU, Y. Q.[2] – CHEN, L. Y.[1] – XU, W.[2] – RONG, J. D.[2] – CHEN, L. G.[2] – FAN, L. L.[2] – TARIN, M. W. K.[2] – ZHENG, Y. S.[1,2*]

[1]*College of Art & Landscape Architecture, Fujian Agriculture and Forestry University, Fuzhou 350002, PR China*

[2]*Bamboo Institute, College of Forestry, Fujian Agriculture and Forestry University, Fuzhou 350002, PR China*

**Corresponding author*
e-mail: zsy1960@163.com; phone: + 86-591-8378-6894

(Received 15th May 2019; accepted 16th Jul 2019)

Abstract. *Dendrocalamopsis beecheyana* var. *pubescens* is native to the southern provinces of China. In this study, the genetic diversity of 17 accessions from 6 populations of Fujian and Guangxi provinces were assessed. Genetic diversity was estimated using ISSR (inter-simple sequence repeat) markers. Sixteen selected primers produced 185 ISSR loci, of which 167 (90.27%) were found to be polymorphic. Dendrogram analyses revealed that the 17 accessions formed six major groups, while the six populations were clustered into three major groups. A high genetic diversity was identified at the species level, with the percentage of polymorphic band (*PPB*), Nei's gene diversity (*He*) and Shannon's information index (*I*) was found to be 90.27%, 0.2497, and 0.3949, respectively. In addition, Nei's differentiation coefficient (*Gst*) was relatively high (0.5399) and a low rate of gene flow (*Nm*) of 0.4261 was observed. The results clearly show that there is a high degree of genetic variation at the species level and a low degree of genetic variation at the population level. Moreover, ISSR molecular markers could be effectively utilized for the characterization of *D. beecheyana* var. *pubescens* accessions and identification of the relationships within populations.
Keywords: *D. beecheyana var. pubescens primers, genetic variation, Fujian, species level*

Introduction

Dendrocalamopsis beecheyana var. pubescens is considered to be an important ornamental bamboo with low cold tolerance, which is widely cultivated in the southern region of Guangdong Province, Hongkong, and Taiwan (Editorial Committee of Chinese Flora of Chinese Academy of Sciences, 1996). In China, this bamboo species is used for the manufacture of construction materials, while the bamboo shoots are used in the traditional Chinese cuisine of Fujian and Guangxi Provinces. In addition, it has been used for soil and water conservation and also to improve the environment in the coastal town of Zhangzhou in Fujian Province (Li et al., 2017). Thus, this bamboo has gained its value for ornamental, ecological, economic, and social purposes and is characterized by its wide adaptability, fast breeding, and highly developed root system (Desai et al., 2015).

To date, genetic diversity analysis of bamboo species has been done with molecular marker variations using PCR amplification (Barkley et al., 2005; Tian et al., 2012; Yang et al., 2012). However, studies on *D. beecheyana* var. *pubescens* have been limited to tissue culture, physiological biochemistry, and cultivation techniques with little information reported on genetic diversity. Considering the rich genetic diversity of bamboo species, its genetic diversity analyses can help to determine the genetic

http://www.aloki.hu ● ISSN 1589 1623 (Print) ● ISSN 1785 0037 (Online)
DOI: http://dx.doi.org/10.15666/aeer/1705_1250712519

resources of the species, and also the selection and conservation of improved cultivars.

In recent years, a number of molecular marker technologies have been developed and widely applied in genetic diversity and DNA fingerprinting studies including random amplified polymorphic DNA (RAPD) markers, restriction fragment length polymorphism (RFLP) markers, amplified fragment length polymorphism (AFLP) markers, and inter-simple sequence repeat (ISSR) markers (Grover et al., 2016). RAPD has been regarded as an approach that exhibited high efficiency, sensitivity, and specificity, with rapid and simple method to analyze genomic DNA; however, it is incapable of discriminating between heterozygotes and homozygotes (Williams et al., 1990). The RFLP method offers large numbers of markers, but requires larger quantities of DNA from fresh samples (Yang et al., 1996). Similarly, AFLP markers offer high resolution, stability, and efficiency, but the requirement of high-purity DNA and restriction enzyme makes it expensive to use (Vos et al., 1995). ISSR markers provide a simple, rapid, and highly efficient method that is comparatively economical (Zietkiewicz et al., 1994). Moreover, this technique can detect abundant polymorphic fragments without previous knowledge of the position of the target DNA sequences. Furthermore, ISSR method exhibited high reproducibility since it used long primer lengths and high annealing temperatures (Archak et al., 2003). Due to these advantages, ISSR method was selected to study the analysis of genetic diversity among *D. beecheyana var. pubescens* accessions. In the present study, we applied this approach to estimate the genetic diversity within and among the populations of *D. beecheyana* var. *pubescens* collected from different regions in Fujian and Guangxi Provinces. Moreover, due to limited information based on ISSR marker few related report about the genetic diversity was compared with other species, such as mango (Luo et al., 2011), cucumber and apricot (Li et al., 2014), and *Platycodon grandiflorus* (Nie et al., 2014). These analyses provided insights into the germplasm resources and genetic relationships of natural bamboos populations that can help inbreeding improved varieties and for conservation.

Materials and methods

Plant materials

A total of 17 accessions of *D. beecheyana* var. *pubescens* from 6 natural populations of Fujian and Guangxi Province were used in this study. The geographical location of each population was determined using GPS and are listed in *Table 1*. The samples were cultivated at the Chishan state-owned forest farm, Dongshan, Fujian, China. Fresh young leaves were collected for the analyses (*Fig. 1*).

DNA extraction

Total genomic DNA from each accession was extracted using a Biospin Plant Genomic DNA Extraction kit following the manufacturer's instructions. The qualitative and quantitative analysis of DNA was performed on 1% agarose gels using an ultraviolet spectrophotometer (NANODROP 2000c Thermo Fisher, Beijing, China). The extracted DNA was diluted to 25 ng/μL and stored at -20 °C for future use.

http://www.aloki.hu ● ISSN 1589 1623 (Print) ● ISSN 1785 0037 (Online)
DOI: http://dx.doi.org/10.15666/aeer/1705_1250712519

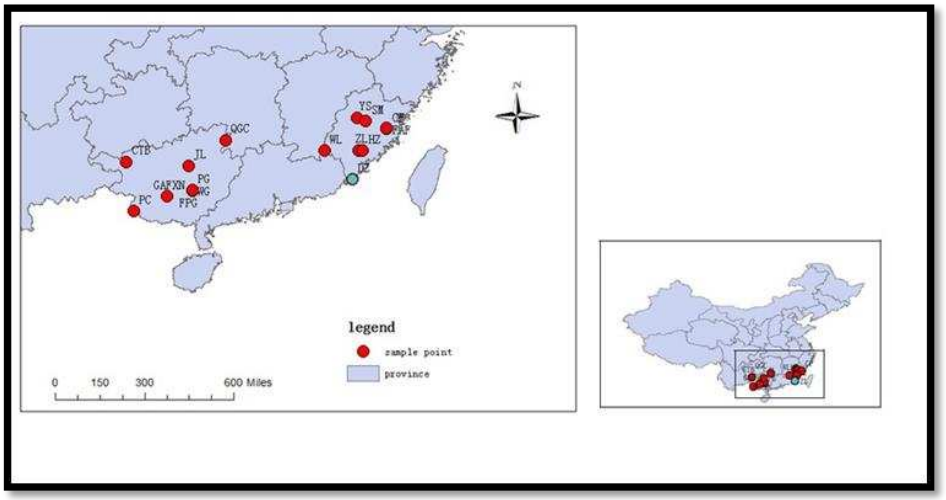

Figure 1. *Map showing the origins of accessions*

Table 1. *Sampling locations of the 17 D. beecheyana var. pubescens accessions*

No.	Accession	Population	Location	Latitude (N)	Longitude (E)
1	YS	Western Fujian Province	Yongan, Sanming	25°98’	117°37’
2	SM	Western Fujian Province	Sanming	26°27’	117°62’
3	WL	Western Fujian Province	Wuping, Longyan	25°01’	116°01’
4	ZL	Western Fujian Province	Zhangping, Longyan	25°03’	117°42’
5	FAF	Central Fujian Province	Fujian Academy of Forestry	26°08’	119°03’
6	CF	Central Fujian Province	Cangshan, Fuzhou	26°05’	119°03’
7	HZ	Southern Fujian Province	Huaan, Zhangzhou	25°02’	117°53’
8	DZ	Southern Fujian Province	Dongshan, Zhangzhou	23°07’	117°43’
9	WG	Eastern Guangxi Province	Watang Town, Guigang	23°04’	109°36’
10	PG	Eastern Guangxi Province	Pingtian Mountain, Guigang	23°06’	109°36’
11	FPG	Eastern Guangxi Province	Forest farm of Pingtian Mountain, Guigang	23°06’	109°36’
12	GAF	Southern Guangxi Province	Guangxi Academy of Forestry	22°49’	108°21’
13	XN	Southern Guangxi Province	Xingning, Nanning	22°48’	108°22’
14	PC	Southern Guangxi Province	Pingxiang, Chongzuo	22°05’	106°45’
15	CTB	Northern Guangxi Province	Cen Wang Laoshan Mountain, Tianlin, Baise	24°29’	106°23’
16	QGG	Northern Guangxi Province	Qianjia Dong, Guanyang, Guilin	25°32’	111°13’
17	JL	Northern Guangxi Province	Jinxiu Mountain, Liuzhou	24°18’	109°25’

http://www.aloki.hu ● ISSN 1589 1623 (Print) ● ISSN 1785 0037 (Online)
DOI: http://dx.doi.org/10.15666/aeer/1705_1250712519

Primer selection and ISSR-PCR amplification

In order to select appropriate primers for *D. beecheyana var. pubescens*, 100 ISSR primer sequences (*Supp. Tab* 1) provided by the University of British, Columbia (UBC) (https://www.ubc.ca/) in Canada were screened using an optimized ISSR-PCR system by the Shanghai Sangon Biological Engineering Technology Service Co. Ltd., China.

ISSR-PCR amplifications were performed in a total reaction volume of 20 μL containing 2.5 mM $MgCl_2$, 0.25 mM dNTPs, 1.25 U of Taq DNA polymerase (TaKaRa Biotechnology, Dalian, China), 0.6 μM primer, 10 ng genomic DNA, and 2 μL 10× buffer. The reactions were performed in a TProfessional Thermocycler (Biometra, Gottingen, Germany) with the following conditions: initial denaturation at 94 °C for 5 min; followed by 40 cycles of 45 s at 94 °C, 30 s at annealing temperature (50-60 °C), 90 s at 72 °C; and final extension at 72 °C for 10 min. The PCR products were stored at 4 °C until further use. These PCR products (0.5 μg/mL in 1× TBE buffer (445 mmol/L Tris, 445 mmol/L borate, 10 mmol/L EDTA)) were subjected to electrophoresis on a 1.5% agarose gel at 120 V for approximately 1 h and the gel was later analyzed using Gel Documentation System (Bio-Rad, Hercules, California, USA).

Data analysis

Polymorphic DNA fragments, obtained with reproducible bands, were scored as present (1) or absent (2). The binary data matrix was analyzed using POPGENE32 (Yeh et al., 2000) to obtain the following genetic diversity parameters within and among populations: percentage of polymorphic bands (*PPB*), number of alleles (*Na*), effective number of alleles (*Ne*), Nei's gene diversity (*He*), Shannon's information index (*I*), total genetic diversity (*Ht*), genetic diversity within populations (*Hs*), coefficient of gene differentiation (*Gst*), and gene flow (*Nm*). A cluster analysis was performed using the DATA processing system (DPS) program and a dendrogram was constructed using an unweighted pair-group method with arithmetic averaging (UPGMA).

Results

ISSR polymorphism

The ISSR primer screening yielded 16 primers exhibiting high polymorphism and stability (*Table* 2). These ISSR primers generated 185 amplified fragments with an average of 11.6 bands per primer and 167 bands (90.27%) were polymorphisms. The fragment sizes ranged from 200 to 2200 bp and the number of bands varied from 9 to 15. The highest proportion (100%) of the polymorphic bands was obtained with the primers UBC818, UBC826, UBC842, UBC888, and UBC889, while the lowest proportion (66.67%) was obtained with the primer UBC850. The results of the amplification using the primer UBC856 for all 17 accessions are illustrated in *Figure 2*. This example showed the high genetic diversity present in the 17 accessions.

Genetic diversity

At the species level, *Na, Ne, He, I* and *PPB* were found to be 1.9027, 1.3873, 0.2497, 0.3949 and 90.27%, respectively that were relatively higher than populations (*Table* 3). The accessions from the Western Fujian population exhibited highest values for the genetic diversity parameters, with *Na* = 1.5676, *Ne* = 1.4243, *He* = 0.2315, *I* = 0.3358,

http://www.aloki.hu ● ISSN 1589 1623 (Print) ● ISSN 1785 0037 (Online)
DOI: http://dx.doi.org/10.15666/aeer/1705_1250712519

and *PPB* = 56.76%. However, genetic diversity in this population was observed to be lower than that at the species level. The lowest level of genetic diversity was found in the Eastern Guangxi population (*Na* = 1.1568, *Ne* = 1.1239, *He* = 0.0673, *I* = 0.0968, *PPB* = 15.68%). At the population level, the values for *Na, Ne, He, I* and *PPB* were found to be in the range of1.1568–1.5676, 1.1239–1.4243, 0.0673–0.2315, 0.0968–0.3358, and 15.68–56.76% respectively. Based on these results, it can be concluded that the highest genetic variations were observed in the Western Fujian population, while the lowest variations were observed in the Eastern Guangxi and Southern Guangxi populations.

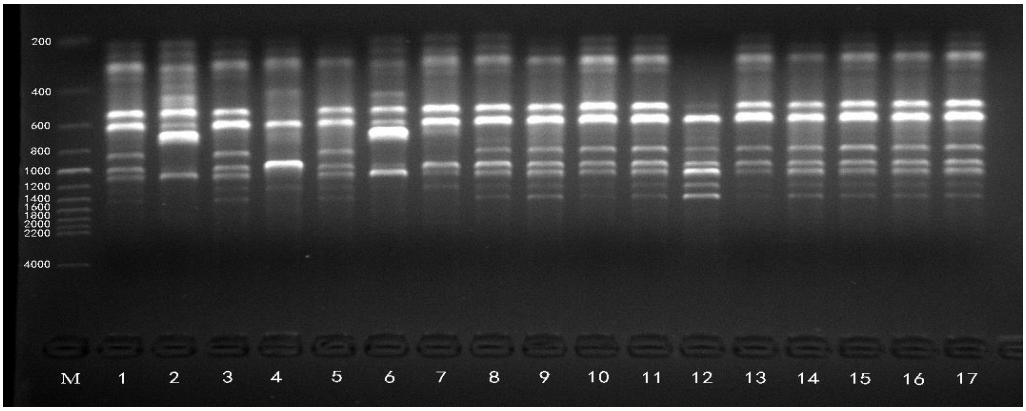

Figure 2. *Amplification products from the 17 D. beecheyana var. pubescens accessions amplified using the primer UBC856*

Table 2. *ISSR primers used to analyze D. beecheyana var. pubescens accessions (R = A, G; Y = C, T)*

Primers	Sequence (5'–3')	Tm (°C)	Number of bands scored	Number of polymorphic bands
UBC811	$(GA)_8C$	52.5	10	9
UBC818	$(CA)_8G$	54.6	11	11
UBC826	$(AC)_8C$	53.2	15	15
UBC827	$(AC)_8G$	54.6	11	10
UBC835	$(AG)_8YC$	56.2	10	9
UBC836	$(AG)_8YA$	53.9	14	11
UBC840	$(GA)_8YT$	51.0	10	9
UBC841	$(GA)_8YC$	53.2	9	8
UBC842	$(GA)_8YG$	53.2	9	9
UBC850	$(GT)_8YC$	56.2	12	8
UBC856	$(AC)_8YA$	53.9	13	12
UBC857	$(AC)_8YG$	56.2	10	9
UBC859	$(TG)_8RC$	56.2	12	10
UBC886	$VDV(CT)_7$	53.0	12	10
UBC888	$BDB(CA)_7$	53.8	12	12
UBC889	DBD(AC)7	55.0	15	15
Total			185	167
Mean			11.6	10.4

http://www.aloki.hu ● ISSN 1589 1623 (Print) ● ISSN 1785 0037 (Online)
DOI: http://dx.doi.org/10.15666/aeer/1705_1250712519

Table 3. *Genetic diversity between populations of D. beecheyana var. pubescens*

Population	Pop ID	*Na*	*Ne*	*He*	*I*	*PPB* (%)
Western Fujian Province	WF	1.5676	1.4243	0.2315	0.3358	56.76
Central Fujian Province	CF	1.4000	1.2828	0.1657	0.2419	40.00
Southern Fujian Province	SF	1.4378	1.3096	0.1814	0.2648	43.78
Eastern Guangxi Province	EG	1.1568	1.1239	0.0673	0.0968	15.68
Southern Guangxi Province	SG	1.1568	1.1267	0.0684	0.0979	15.68
Northern Guangxi Province	NG	1.2000	1.1679	0.0895	0.1274	20.00
Average		1.3198	1.2392	0.1340	0.1941	31.98
Average species level		1.9027	1.3873	0.2497	0.3949	90.27

Na: number of alleles; Ne: effective number of alleles; I: Shannon's information index; He: Nei's gene diversity; PPB: percentage of polymorphic bands

Genetic differentiation and relationships

From Nei's genetic diversity, genetic differentiation (*Gst*) was estimated as 0.5399, indicating that 53.99% of the genetic variation was distributed within populations. The level of the gene flow (*Nm*) was found to be 0.4261 individuals per generation within the six populations, thus, demonstrating that there was minimum gene flow between the populations (*Table* 4).

Table 4. *Nei's analysis of genetic variability of the six populations*

	Ht	*Hs*	*Gst*	*Nm*
Mean	0.2912	0.1340	0.5399	0.4261
SD	0.0253	0.0082		

Ht: total genetic diversity; Hs: genetic diversity within populations; Gst: coefficient of gene differentiation; Nm: gene flow

Genetic diversity was assessed using genetic distances (*D*) and genetic similarity coefficients (*GSC*). It was observed that *D* ranged from 0.0564 (between Western Fujian and Central Fujian populations) to 0.4590 (between Southern Fujian and Eastern Guangxi populations) and *GSC* ranged from 0.6319 (between Southern Fujian and Eastern Guangxi populations) to 0.9451 (Western Fujian and Central Fujian populations) (*Table* 5). This analysis showed similar trends in *D* and *GSC* levels. The highest *GSC* (0.9451) and the lowest *D* (0.0564) were found between the Western Fujian and Central Fujian populations, indicating the closest relationship between them. Moreover, the lowest *GSC* (0.6319) and the highest *D* (0.4590) were found between the Southern Fujian and Eastern Guangxi populations, indicating a distant relationship was between these populations.

The UPGMA tree that was constructed based on genetic distance (*D*) demonstrated that the 17 accessions clustered into six groups (*Fig. 3a*). Group A, C, E and F comprised one accession each, FAF, JL, DZ and HZ respectively. However, Group B consisted of eleven accessions, namely, YS, SM, ZL, CTB, QGG, GAF, PG, FPG, PC, XN, and WG. Group D consisted two accessions, WL and CF. An UPGMA tree constructed from the population data generated three clusters (*Fig. 3b*). Cluster I

http://www.aloki.hu ● ISSN 1589 1623 (Print) ● ISSN 1785 0037 (Online)
DOI: http://dx.doi.org/10.15666/aeer/1705_1250712519

included two populations (WF and CF), cluster II contained three populations (EG, SG and NG), and cluster III consisted one population (SF).

Table 5. *Nei's (1978) genetic similarity coefficient (GSC) (above diagonal) and genetic distance (D) (below diagonal) between populations*

Pop ID*	WF	CF	SF	EG	SG	NG
WF	****	0.9451	0.7410	0.8669	0.8697	0.8728
CF	0.0564	****	0.7911	0.8295	0.8073	0.8004
SF	0.2998	0.2343	****	0.6319	0.6368	0.6717
EG	0.1428	0.1869	0.4590	****	0.9339	0.8912
SG	0.1396	0.2141	0.4513	0.0684	****	0.9071
NG	0.1360	0.2226	0.3979	0.1151	0.0976	****

*The identities of the various populations are explained in *Table 3*

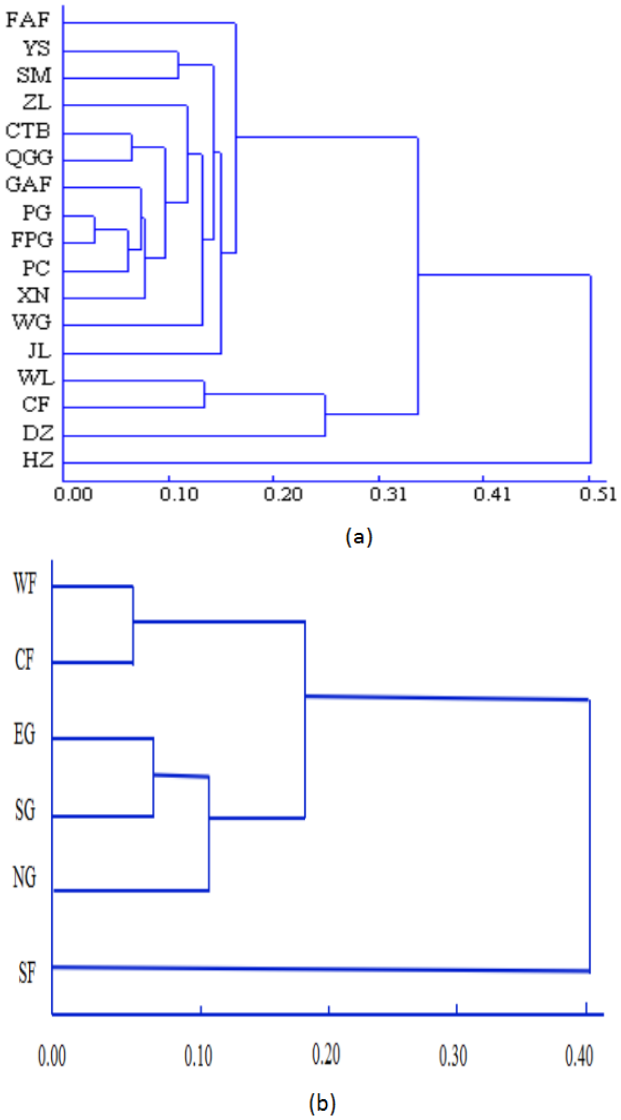

Figure 3. *UPGMA dendrogram of D. beecheyana var. pubescens based on genetic distances indicating the clustering relationships of accessions (a) and populations (b)*

http://www.aloki.hu ● ISSN 1589 1623 (Print) ● ISSN 1785 0037 (Online)
DOI: http://dx.doi.org/10.15666/aeer/1705_1250712519

Discussion

Polymorphism analysis

In this study, after a preliminary screening of 100 ISSR primers, those primers were selected that showed clear, reproducible, and polymorphic bands. The primers that generated fuzzy bands or failed to generate an amplification product were rejected, including those that showed monomorphic bands due to the formation of dimers in the primers. The 16 selected primers were used for the analysis of the 17 *D. beecheyana* var. *pubescens* accessions. The selected primers produced an average of 11.6 bands, which is lower than that observed in other bamboo species (Desai et al., 2015). The present study confirmed that the selection of competent primers is very important when using ISSR markers (Safaei et al., 2016).

Genetic diversity

Genetic diversity data is an essential component of a breeding program. In the present study, 17 accessions of *D. beecheyana* var. *pubescens* showed higher levels of genetic diversity at the species level compared to the population level. However, the accessions demonstrated relatively high levels of diversity within the six populations. These results are consistent with the data reported in *Jatropha* previously (Arolu et al., 2015). It was observed that the genetic diversity of *D. beecheyana* var. *pubescens* (PPB_s = 90.27%, He_s = 0.2497) at the species level was higher than that of the short-lived perennial species *Blysmus sinocompressus* (PPB_s = 74.76%, He_s = 0.1668) (Hu et al., 2016) and mating breeding system species *Platycodon grandiflorum* (PPB_s = 76.29%, He_s = 0.2326) (Nie et al., 2014). At the population level, the average He_p in *D. beecheyana* var. *pubescens* was 0.1340 (*Table* 3) that was almost similar to that of *Taxus fuana* (0.1165) (Shah et al., 2008) but lower than that of apricot (0.1738) (Liu et al., 2016). Low He_p value is attributed to low genetic diversity. Similarly, the low average value of I_p (0.1941) also indicated a low level of genetic diversity (*Table* 3). High value have been reported in *Portulaca oleracea* (I_p = 0.515) (Alam et al., 2015). Further, the average value for PPB_s was found to be 31.98% that was lower than that of *Platycodon longiflorum* (PPB_s = 55.67%) (Nie et al., 2014). Low genetic diversity within populations has been reported in other plant species, such as *Taxus fuana* (Shah et al., 2008) and *Monimopetalum chinense* (Xie et al., 2005).

Our results indicated that *D. beecheyana* var. *pubescens* showed considerable genetic variation between populations and high genetic diversity within populations. A mixed mating system has been recognized as an important factor to determine the level of genetic diversity in a plant species (Godt et al., 2001). However, other factors can also influence the genetic variation including, the geographic factor that can exhibits significant negative effect on genetic diversity and higher temperatures that can boost the seedling growth and increase genetic diversity. However, *D. beecheyana* var. *pubescens* flowers every 10–120 years in an unpredictable mode. The propagation is mainly dependent on selfing by underground rhizomes. Thus, in the present study, the breeding system was not likely to be a contributor towards genetic diversity.

Two possible explanations can be proposed for the high total genetic diversity within populations. Firstly, since *D. beecheyana* var. *pubescens* lives for many years before flowering, it is highly possible that habitat heterogeneity of the long-lived plants could have contributed to the pattern of genetic diversity in this species (Hu et al., 2016). Secondly, the geographical prevalence of this species might have supported high

http://www.aloki.hu ● ISSN 1589 1623 (Print) ● ISSN 1785 0037 (Online)
DOI: http://dx.doi.org/10.15666/aeer/1705_1250712519

genetic diversity compared to a species with restricted distribution (Godt and Hamrick, 1996). The populations of *D. beecheyana* var. *pubescens* examined in this study were narrowly distributed in Fujian and Guangxi Provinces. This restricted distribution might have resulted into low genetic diversity among populations (Ge et al., 2005).

Genetic differentiation and relationships

Various factors such as life history, geographic distribution, and gene flow within populations can influence the genetic structure of plant species (Hilfiker et al., 2004). In this study, we found that the genetic differentiation coefficient among populations of *D. beecheyana* var. *pubescens* (*Gst* = 0.5399) was higher than the average of other long-lived species (*Gst* = 0.19) (Nybom, 2004). This suggested that there was a high level of genetic differentiation in *D. beecheyana* var. *pubescens.* However, genetic variation in *D. beecheyana* var. *pubescens* in the Fujian and Guangxi Provinces was mainly observed at the intra-population level (53.99%) and inter-population level (46.01%). This can be attributed to the geographical location that might have had a significant influence on genetic differentiation leading to the higher genetic diversity at the intra-population level (Yuan et al., 2007). In addition, the complex topography of the region, including remote and isolated mountains, may have hindered the gene flow between populations, thus promoting population differentiation (Wheeler et al., 2011). In the present study, gene flow among *D. beecheyana* var. *pubescens* populations was found to be 0.4261 that indicated limited level of gene flow between populations and thus it could not prevent genetic differentiation at the intra-population level.

Genetic diversity was estimated using genetic distance (*D*) and genetic similarity coefficients (*GSC*), which ranged from 0.0564–0.4590 and 0.6319–0.9451, respectively. This range was consistent with a previous study that reported a range of 0.045455–0.454545 for *D* (Yuan et al., 2014), however, the *GSC* range (0.39–0.95) was lower compared to our study (Noroozisharaf et al., 2015). The *GSC* obtained from our ISSR analysis exhibited a high genetic diversity among *D. beecheyana* var. *pubescens* accessions. Moreover, the 17 accessions were found to form six major groups in the UPGMA dendrogram. The clustering in this dendrogram was not consistent with the geographical distribution, suggesting that there was no obvious correlation between genetic distance and geographic distance of accessions in Fujian and Guangxi Province. However, the 6 populations clustered into three major groups in the UPGMA dendrogram, and in particular, three populations, EG, SG and NG, formed a cluster with high genetic similarities due to the same place of origin. Therefore, based on the findings of this study, it can be concluded that the geographic distribution may have influenced the genetic distance or the genetic relationships of populations and the widespread accessions may have exhibited higher level of genetic diversity than the narrowly distributed ones. The population SF was found to be grouped away from other two groups, thus, supporting the hypothesis that these *D. beecheyana* var. *pubescens* accessions origin from SF were the independent species. Therefore, a high level of genetic variation can be estimated in widespread accessions.

Economical aspects and fiscal policy consideration

D. beecheyana var. *pubescens* as one of the protection forest was introduced to coastal regions of southern and eastern China for soil and water conservation and to improve the environment as well. Since, the southeast coast of China has been suffering

http://www.aloki.hu ● ISSN 1589 1623 (Print) ● ISSN 1785 0037 (Online)
DOI: http://dx.doi.org/10.15666/aeer/1705_1250712519

from typhoons, storm surges and other natural disasters throughout the year, it is crucial to strengthen the coastal shelterbelt system to minimize economic losses. Certainly, some capital investments and fiscal policies would be required to conserve the coastal shelterbelt. In this context, this study provided important genetic information for devising the conservation strategies of *D. beecheyana* var. *pubescens.*

One primary objective of conservation is to protect the genetic diversity. Considering the low genetic diversity among populations and high genetic variation within populations of *D. beecheyana* var. *pubescens* in China, the most effective strategy for maintaining genetic variation is to conserve and cultivate as many populations as possible. Moreover, transplanting individuals from other populations would enhance inter-population gene flow and genetic diversity. Thus, the foremost step for all populations in situ must be the prevention of the anthropogenic disturbance. Subsequently, we should make it a priority to cultivate the high genetic diversity of *D. beecheyana* var. *pubescens* in initial period. Since the WF population exhibited the highest level of genetic diversity, it should be preferred for cultivation. Further, the population with high genetic diversity may have the ability to adapt to the environment as compared to the population with low genetic diversity. For *ex situ* conservation, a germplasm bank is required to be established for this species.

Conclusion

In this study, the ISSR markers were found to be viable for detecting the high level of genetic diversity within populations and considerable genetic differentiation among populations. In addition, the polymorphism generated by ISSR markers was very high. Based on the findings of this study, it was observed that rich genetic diversity existed in *D. beecheyana* var. *pubescens.* Besides, the genetic differentiation and relationships obtained in this study may help in understanding and evaluating the conservation in China. The cluster results of 17 materials related to adaptability, resistance, water and soil conservation and growth period, which need to be further studies. It is necessary to strengthen the collection, identification and excavation of the germplasm resources of D. beecheyana var. Pubescens to enrich the genetic diversity of breeding materials.

Acknowledgements. This work was supported by the Central Fiscal Forestry Science and Technology Extension Project [2013, NO. 7], the Science and Technology Major Projects of Fujian Province [2013NZ0001], the Regional Development Project of Fujian Province [2015 No.3015], Research Development Fund of Fujian Agriculture and Forestry University [KF2015085] and [CXZX2017119], Program for Scientific and Technological Innovation Team for Universities of Fujian Province [2018 No.49].

REFERENCES

[1] Alam, M. A., Juraimi, A. S., Rafii, M. Y., Hamid, A. A., Arolu, I. W., Latif, M. A. (2015): Genetic diversity analysis among collected purslane (Portulaca oleracea, L.) accessions using ISSR markers. – C. R. Biol. 338: 1-11.

[2] Archak, S., Gaikwad, A. B., Gautam, D., Rao, E. V., Swamy, K. R., Karihaloo, J. L. (2003): Comparative assessment of DNA fingerprinting techniques (RAPD, ISSR and AFLP) for genetic analysis of cashew (*Anacardium occidentale* L.) accessions of India. – Genome 46: 362-369.

http://www.aloki.hu ● ISSN 1589 1623 (Print) ● ISSN 1785 0037 (Online)
DOI: http://dx.doi.org/10.15666/aeer/1705_1250712519

[3] Arolu, I. W., Rafii, M. Y., Hanafi, M. M., Mahmud, T. M. M., Askani, S., Abdullah, N. A. (2015): Genetic divergence and evaluation of yield potential of Jatropha curcas accessions collected from peninsular Malaysia. – Pertanika J. Trop. Agric. Sci. 38: 127-142.

[4] Barkley, N. A., Newman, M. L., Wang, M. L., Hotchkiss, M. W., Pederson, G. A. (2005): Assessment of the genetic diversity and phylogenetic relationships of a temperate bamboo collection by using transferred EST-SSR markers. – Genome 48: 731-737.

[5] Desai, P., Gajera, B., Mankad, M., Shah, S., Patel, A., Patil, G., Narayana, S., Kumar, N. (2015): Comparative assessment of genetic diversity among Indian bamboo genotypes using RAPD and ISSR markers. – Mol. Biol. Rep. 42: 1265-73.

[6] Editorial Committee of Chinese Flora of Chinese Academy of Sciences (1996): Flora Reipublicae Popularis Sinicae. – Science Press, Beijing.

[7] Ge, X. J., Zhou, X. L., Li, Z. C., Hsu, T. W., Schaal, B. A., Chiang, T. Y. (2005): Low genetic diversity and significant population structuring in the relict *Amentotaxus argotaenia* complex (Taxaceae) based on ISSR fingerprinting. – J. Plant Res. 118: 415-422.

[8] Godt, M. J. W., Hamrick, J. L. (1996): Genetic diversity and morphological differentiation in *Liatris helleri*, (Asteraceae), a threatened plant species. – Biodivers. Conserv. 5: 461-471.

[9] Godt, M. J. W., Hamrick, J. L., Edwards-Burke, M. A., Williams, J. H. (2001): Comparisons of genetic diversity in white spruce (*Picea glauca*) and jack pine (*Pinus banksiana*) seed orchards with natural populations. – Can. J. Forest Res. 31: 943-949.

[10] Grover, A., Sharma, P. C. (2016): Development and use of molecular markers: past and present. – Critical Reviews in Biotechnology 36: 1-13.

[11] Hilfiker, K., Holderegger, R., Rotach, P., Gugerli, F. (2004): Dynamics of genetic variation in *Taxus baccata*: local versus regional perspectives. – Can. J. Bot. 82: 219-227.

[12] Hu, Y. P., Bao, R., Shi, L., Wang, J. K., Wang, J., Wang, L., Li, Y. (2016): Analysis of population structure of Blysmus sinocompressus, in the Qilian mountains by ISSR markers. – Aquat. Bot. 134: 54-60.

[13] Li, M., Zhao, Z., Miao, X. (2014): Genetic diversity and relationships of apricot cultivars in north China revealed by ISSR and SRAP markers. – Sci. Hort. 173: 20-28.

[14] Li, S. X., Li, M. F., Ping, Y., Fan, Y. M., Shou, J. N., Sun, R. C. (2017): Valorization of bamboo by γ-valerolactone/acid/water to produce digestible cellulose, degraded sugars and lignin. – Biores. Technol. 230: 90-96.

[15] Liu, J., Liao, K., M, Nasir., Peng, X. (2016): Analysis of genetic diversity of the apricot germplasm in the southern region of the Tianshan Mountains in Xinjiang, China using the ISSR technique. – Eur. J. Hort. Sci. 81: 37-43.

[16] Luo, C., He, X. H., Chen, H., Ou, S. J., Gao, M. P., Brown, J. S., et al. (2011): Genetic diversity of mango cultivars estimated using scot and ISSR markers. – Biochem. System. Ecol. 39: 676-684.

[17] Nie, C., Liu, R., Li, S., Li, Y. (2014): Assessment of *Platycodon grandiflorum* germplasm resources from northern Anhui province based on ISSR analysis. – Molecular Biology Reports 41: 8195-8201.

[18] Noroozisharaf, A., Hatamzadeh, A., Lahiji, H. S., Bakhshi, D. (2015): Genetic diversity of endangered primrose (*Primula heterochroma* Stapf.) accessions from Iran revealed by ISSR and IRAP markers. – Sci. Hort. 190: 173-178.

[19] Nybom, H. (2004): Comparison of different nuclear DNA markers for estimating intraspecific genetic diversity in plants. – Mol. Ecol. 13: 1143-1155.

[20] Safaei, M., Sheidai, M., Alijanpoor, B., Noormohammadi, Z. (2016): Species delimitation and genetic diversity analysis in salvia with the use of issr molecular markers. – Acta Botanica Croatica 75: 45-52.

http://www.aloki.hu ● ISSN 1589 1623 (Print) ● ISSN 1785 0037 (Online)
DOI: http://dx.doi.org/10.15666/aeer/1705_1250712519

[21] Shah, A., Li, D. Z., Gao, L. M., Li, H. T., Möller, M. (2008): Genetic diversity within and among populations of the endangered species Taxus fuana, (Taxaceae) from Pakistan and implications for its conservation. – Biochem. System. Ecol. 36: 183-193.
[22] Tian, B., Yang, H. Q., Wong, K. M., Liu, A. Z., Ruan, Z. Y. (2012): ISSR analysis shows low genetic diversity versus high genetic differentiation for giant bamboo, *Dendrocalamus giganteus* (Poaceae: Bambusoideae), in China populations. – Genet. Res. Crop Evol. 59: 901-908.
[23] Vos, P., Hogers, R., Bleeker, M., Reijans, M., Van, d. L. T., Hornes, M., Frijters, A., Pot, J., Peleman, J., Kuiper, M., Zabeau, M. (1995): AFLP: a new technique for DNA fingerprinting. – Nucleic Acids Res. 23: 4407-14.
[24] Wheeler, N. C., Jech, K. S., Masters, S. A., O'Brien, C. J., Stonecypher, R. W., Timmons, D. W., Lupkes, A. (2011): Genetic variation and parameter estimates in *Taxus brevifolia* (Pacific yew). – Can. J. Forest Res. 25: 1913-1927.
[25] Williams, J. G., Kubelik, A. R., Livak, K. J., Rafalski, J. A., Tingey, S. V. (1990): DNA polymorphisms amplified by arbitrary primers are useful as genetic markers. – Nucleic Acids Res. 18: 6531-5.
[26] Xie, G., Wang, D., Yuan, Y., Xuejun, G. E. (2005): Population genetic structure of *Monimopetalum chinense* (Celastraceae), an endangered endemic species of eastern China. – Ann. Bot. 95: 773-777.
[27] Yang, H. Q., An, M. Y., Gu, Z. J., Bo, T. (2012): Genetic diversity and differentiation of *Dendrocalamus membranaceus* (Poaceae: Bambusoideae), a declining bamboo species in Yunnan, China, as based on inter-simple sequence repeat (ISSR) analysis. – Int. J. Mol. Sci. 13: 4446-4457.
[28] Yang, W., Oliveira, A. C. D., Godwin, I., Schertz, K., Bennetzen, J. L. (1996): Comparison of DNA marker technologies in characterizing plant genome diversity: variability in Chinese sorghums. – Crop Sci. 36: 1669-1676.
[29] Yeh, F. C., Yang, R., Boyle, T. J. (2000): POPGENE 32, Microsoft Windows-based Freeware for Population Genetic Analysis, version1.32. Edmonton, Canada. – University of Alberta.
[30] Yuan, C. Y., Zhang, C., Wang, P., Hu, S., Chang, H. P., Xiao, W. J., Lu, X. T., Jiang, S. B., Guo, X. H. (2014): Genetic diversity analysis of okra (*Abelmoschus esculentus* L.) by inter-simple sequence repeat (ISSR) markers. – Genet. Mol. Res. 13: 3165-75.
[31] Yuan, Z., Chen, X., He, T., Feng, J., Feng, T., Zhang, C. (2007): Population genetic structure in apricot (*Prunus armeniaca* L.) cultivars revealed by fluorescent-AFLP markers in southern Xinjiang, China. – J. Genet. Genom. 34: 1037-1047.
[32] Zietkiewicz, E., Rafalski, A., Labuda, D. (1994): Genomic fingerprinting by simple sequence repeat anchored polymerase chain reaction amplification. – Genomics 20: 176-183.

APPENDIX

Table A1. *Selected ISSR primers*

Primer name sequence 5′-3′	Primer name sequence 5′-3′
801 ATA TAT ATA TAT ATA TT	851 GTG TGT GTG TGT GTG TYG
802 ATA TAT ATA TAT ATA TG	852 TCT CTC TCT CTC TCT CRA
803 ATA TAT ATA TAT ATA TC	853 TCT CTC TCT CTC TCT CRT
804 TAT ATA TAT ATA TAT AA	854 TCT CTC TCT CTC TCT CRG
805 TAT ATA TAT ATA TAT AC	855 ACA CAC ACA CAC ACA CYT
806 TAT ATA TAT ATA TAT AG	856 ACA CAC ACA CAC ACA CYA

http://www.aloki.hu ● ISSN 1589 1623 (Print) ● ISSN 1785 0037 (Online)
DOI: http://dx.doi.org/10.15666/aeer/1705_1250712519

807 AGA GAG AGA GAG AGA GT	857 ACA CAC ACA CAC ACA CYG
808 AGA GAG AGA GAG AGA GC	858 TGT GTG TGT GTG TGT GRT
809 AGA GAG AGA GAG AGA GG	859 TGT GTG TGT GTG TGT GRC
810 GAG AGA GAG AGA GAG AT	860 TGT GTG TGT GTG TGT GRA
811 GAG AGA GAG AGA GAG AC	861 ACC ACC ACC ACC ACC ACC
812 GAG AGA GAG AGA GAG AA	862 AGC AGC AGC AGC AGC AGC
813 CTC TCT CTC TCT CTC TT	863 AGT AGT AGT AGT AGT AGT
814 CTC TCT CTC TCT CTC TA	864 ATG ATG ATG ATG ATG ATG
815 CTC TCT CTC TCT CTC TG	865 CCG CCG CCG CCG CCG CCG
816 CAC ACA CAC ACA CAC AT	866 CTC CTC CTC CTC CTC CTC
817 CAC ACA CAC ACA CAC AA	867 GGC GGC GGC GGC GGC GGC
818 CAC ACA CAC ACA CAC AG	868 GAA GAA GAA GAA GAA GAA
819 GTG TGT GTG TGT GTG TA	869 GTT GTT GTT GTT GTT GTT
820 GTG TGT GTG TGT GTG TC	870 TGC TGC TGC TGC TGC TGC
821 GTG TGT GTG TGT GTG TT	871 TAT TAT TAT TAT TAT TAT
822 TCT CTC TCT CTC TCT CA	872 GAT AGA TAG ATA GAT A
823 TCT CTC TCT CTC TCT CC	873 GAC AGA CAG ACA GAC A
824 TCT CTC TCT CTC TCT CG	874 CCC TCC CTC CCT CCC T
825 ACA CAC ACA CAC ACA CT	875 CTA GCT AGC TAG CTA G
826 ACA CAC ACA CAC ACA CC	876 GAT AGA TAG ACA GAC A
827 ACA CAC ACA CAC ACA CG	877 TGC ATG CAT GCA TGC A
828 TGT GTG TGT GTG TGT GA	878 GGA TGG ATG GAT GGA T
829 TGT GTG TGT GTG TGT GC	879 CTT CAC TTC ACT TCA
830 TGT GTG TGT GTG TGT GG	880 GGA GAG GAG AGG AGA
831 ATA TAT ATA TAT ATA TYA	881 GGG TGG GGT GGG GTG
832 ATA TAT ATA TAT ATA TYC	882 VBV ATA TAT ATA TAT AT
833 ATA TAT ATA TAT ATA TYG	883 BVB TAT ATA TAT ATA TA
834 AGA GAG AGA GAG AGA GYT	884 HBH AGA GAG AGA GAG AG
835 AGA GAG AGA GAG AGA GYC	885 BHB GAG AGA GAG AGA GA
836 AGA GAG AGA GAG AGA GYA	886 VDV CTC TCT CTC TCT CT
837 TAT ATA TAT ATA TAT ART	888 BDB CAC ACA CAC ACA CA
838 TAT ATA TAT ATA TAT ARC	889 DBD ACA CAC ACA CAC AC
839 TAT ATA TAT ATA TAT ARG	890 VHV GTG TGT GTG TGT GT
840 GAG AGA GAG AGA GAG AYT	891 HVH TGT GTG TGT GTG TG
841 GAG AGA GAG AGA GAG AYC	892 TAG ATC TGA TAT CTG AAT TCC C
842 GAG AGA GAG AGA GAG AYG	893 NNN NNN NNN NNN NNN
844 CTC TCT CTC TCT CTC TRC	894 TGG TAG CTC TTG ATC ANN NNN
845 CTC TCT CTC TCT CTC TRG	895 AGA GTT GGT AGC TCT TGA TC
846 CAC ACA CAC ACA CAC ART	896 AGG TCG CGG CCG CNN NNN NAT G
847 CAC ACA CAC ACA CAC ARC	897 CCG ACT CGA GNN NNN NAT GTG G
848 CAC ACA CAC ACA CAC ARG	898 GAT CAA GCT TNN NNN NAT GTG G
849 GTG TGT GTG TGT GTG TYA	899 CAT GGT GTT GGT CAT TGT TCC A
850 GTG TGT GTG TGT GTG TYC	900 ACT TCC CCA CAG GTT AAC ACA

http://www.aloki.hu ● ISSN 1589 1623 (Print) ● ISSN 1785 0037 (Online)
DOI: http://dx.doi.org/10.15666/aeer/1705_1250712519

DEVELOPMENT OF CARBON STORAGE MODEL FOR ABOVEGROUND VEGETATION IN CHINA

ZHAO, Z. – FENG, Z.* – LIU, J. – SHEN, Y.

Precision Forestry Key Laboratory of Beijing, Beijing Forestry University, No. 35 East Qinghua Road, Haidian District, Beijing 100083, China

**Corresponding author*
e-mail: zhaozy3358@gmail.com, phone: +86-159-3355-5590; fax: +86-10-6233-7963

(Received 16th May 2019; accepted 16th Jul 2019)

Abstract. Aboveground vegetation is an important component of the terrestrial ecosystem carbon storage, with a significant role in maintaining the global carbon cycle and balance. At present, the estimation method of aboveground vegetation carbon storage was concerned by people. Based on the national data of major trees, forest sample plots and major crops, the carbon storage models of 13 species of tree and 9 types of stands were established through regression analysis, and the carbon storage factors of main crops per unit area was calculated, Moreover, the carbon storage of forest in China was estimated. The results of model fitting showed that the fitting determination coefficients (R^2) were all above 0.9. Evaluation indicators of five regression models were selected to conduct model verification. And the verification results showed that the variation range of total relative error (TRE) of tree regression model is -6.03~4.76%, and that of forest classification regression model is -3.24~7.43%. The China forest carbon storage calculated by regression model is 8.999 Pg, considering that forest inventory is carried out based on a certain degree of canopy density, so the error between the results 8.427 Pg of regression model and forest inventory is within the permit range. Therefore, the aboveground vegetation carbon storage models established in this study can be used to estimate the carbon storage of China's main vegetation types.
Keywords: *forest type, tree, crop, carbon storage, regression model*

Introduction

Global climate change is a scientific problem that mankind has to deal with together, particularly climate warming is widely concerned by the scientific community (Canadell et al., 2000; Zeng et al., 2010). The vegetation ecosystem is an important part of the terrestrial ecosystem, the carbon sinks in vegetation ecosystem plays an important role in the global carbon cycle, it is a key factor in the study of global carbon cycle and carbon balance, it also plays an indispensable role in regulating climate change, absorbing greenhouse gases and mitigating the greenhouse effect (Cao and Woodward, 1998; Li et al., 2011). The quality and dynamics of regional forest cover, including afforestation, deforestation and forest protection, are important factors in mitigating climate change in the context of sustainable development (Koh and Ghazoul, 2010; Aryal et al., 2014; Edenhofer et al., 2014). The aboveground vegetation carbon storage, especially annual carbon increment, is a reliable index to measure the ecological function of vegetation, so how to determine the carbon storage of aboveground vegetation with high efficiency is a hot and important issue in scientific research.

Since the 1960s, many scholars have estimated and predicted the carbon storage of different types of forest (Nunery and Keeton, 2010; Popescu, 2007), many people has been well recognized that forest carbon pools are affected by forest management methods (Berbés-Blázquez, 2012), and they believe that it is a more accurate and feasible method to establish the carbon storage model of individual tree and then make scale transformation (Chave et al., 2005; Navar, 2009). Yangliu using Landsat 8, built a variety

http://www.aloki.hu ● ISSN 1589 1623 (Print) ● ISSN 1785 0037 (Online)
DOI: http://dx.doi.org/10.15666/aeer/1705_1252112535

of forest accumulation prediction models by the method of machine learning information extraction and realized the measurement of coniferous forest, broad-leaved forest and mingled forest (Yang et al., 2017). Kurz, Heath and Holly K had respectively studied the northern forest, temperate forest and tropical forest and update prominent forest biomass carbon databases to create the Abies fabri Craibt complete set of national-level forest carbon stock estimates (Woodbury et al., 2007; Gibbs et al., 2007). Gilabert had conducted a research which is explored the relationships between crop canopy leaf area index, biomass and normalized differential vegetation index (NDVI) used by the method of remote sensing (Martínez and Gilabert, 2009). Chao Zhang were analyzed the forest carbon storage and their spatial distribution in China's small (2,300 km^2) liuxi river basin a, and determined the different contributors of carbon storage (Zhang et al., 2016). Rengtang Chen and Zhongke Feng established regression equations of each organ for Quercus acutidentata and other 7 tree species based on 1259 standard plots and 836 standard trees, measured and studied the biomass of 8 types of forest stands at Xiaolong Mountain (Cheng et al., 2007). Wensheng Cheng established binary volume models and form factor models of the main tree species in China which are based on the single volume tables of each province, and improved efficiency and reduced the workload of large area scale measurement of standing wood volume (Wensheng et al., 2017). The main method to calculate the carbon storage of forest ecosystem at large scale is based on the forest resource inventory data and there are increasing number of studies have been conducted on the application of forest resource inventory data and remote sensing data to the calculation of carbon storage of forest ecosystem (Zolkos et al., 2017; Jenkins et al., 2003). Although it is of high precision to estimate carbon storage of sample plots using forest resource inventory data, there are still some problems when predicting large scale carbon storage of sample plots, such as it is easy to ignore the sparse forest with less than 20% crown density. Moreover, large-scale forest resource inventory takes a lot of manpower and material resources and lasts for a long time, such as China's latest forest inventory took five years which has seriously affected the timeliness of forest carbon storage research. The calculation of regional scale carbon storage based on remote sensing data also has many defects, such as there is great uncertainty in the calculation of various remote sensing vegetation indexes (Moncada Rojas and Botero, 2013; Trishchenko et al., 2002). On the other hand, NDVI and other vegetation indexes always reflect the status of vegetation productivity, and it is quite different from the carbon storage of vegetation.

This study attempts to establish aboveground vegetation carbon storage measurement models to solve the problem of carbon storage estimation in large scale vegetation ecosystem. This paper aims to establish models with high precision and timeliness and partly relies on sample plot inventory data. This study using the national permanent sample plot data and the binary volume table as basic materials, the study was based on the national fixed sample land data and the measured forest sample land data in various regions of the country, using the SPSS software to regression analysis, and establishing 13 types of trees binary carbon storage models, 9 types of forest stands carbon storage models and staple crops carbon storage models.

Materials and methods

Tree data

The data of forest biomass in this study are derived from the eighth national forest inventory data and the measured data of different forest types in different regions of

http://www.aloki.hu ● ISSN 1589 1623 (Print) ● ISSN 1785 0037 (Online)
DOI: http://dx.doi.org/10.15666/aeer/1705_1252112535

China (Department of Forest Resources, 2014). Mainly including place names, longitude and latitude, altitude, annual average temperature, annual average rainfall, forest origin, tree species, composition, age, average DBH, average height, forest density, standing stock volume, arbor biomass (trunk, branch, leaf, ground, etc.) (Wang et al., 2001; Zhao and Zhou, 2004; Fang, 2001). In this study, forest biomass was measured by standard plot method. Standard plot is the miniature of the whole stand. Standard plot is only different from the whole stand in area, but not in quality. The data used in this study include dominant tree species, research area, stand origin, age, stand volume and tree biomass. Some of the data are shown in *Table 1*. Based on the analysis of 160 million sets of forest inventory data in China, the inventory data of dominant tree species in various provinces and cities were selected, and the volume of individual tree was calculated. Then the biomass of sample plot was estimated according to dominant tree species in forest sample plot. National forest data are divided into nine categories, such as: coniferous forest, hardwood broad-leaved forest, soft leaf broad-leaved forest, miscellaneous wood forest, coniferous and broad-leaved mixed forest ecosystem, Coniferous mixed forest, Broad-leaved mixed forest, Chinese fir forest, Mongolica forest, and Tthirteen tree species such as: Pinus tabuliformis, Picea asperata Mast, Cryptomeria fortune, Cunninghamia Lanceolata, Quercus, Abies fabri, Pinus yunnanensis, Pinus massoniana, schima superba, Betula, Pinus elliottii, Larix gmelinii, Liquidambar formosana Hance.

Table 1. *Forest biomass data (part of the data)*

Dominant species	Research area	Stand origin	Stand age (a)	Standing stock (m^3/ha)	Biomass (Mg/ha)
Spruce	Ebian County, Sichuan Province	Planted forest	35	337.8	173.08
Spruce	Heishui County, Sichuan Province	Planted forest	32	125.2	107.82
Larix olgensis Henry	Fengcheng City, Liaoning Province	Planted forest	32	357.63	283.61
Larix principis-rupprechtii Mayr	Quangou Nature Reserve in Shanxi Province	Natural forest	35	287	189.99
Larix gmelinii	Shangzhi City, Heilongjiang Province	Planted forest	24	173.58	168.79
Pinus	Tianshui City, Gansu Province	Planted forest	42	92.94	60.7
Pinus	Zhengning County, Gansu Province	Secondary forest	26	89.41	89.44
Platycladus orientalis	Yongshou County, Shaanxi Province	Planted forest	17	18.53	35.43

Crop data

The crop data in this study mainly include rice, wheat, maize, beans, potato, cotton, oil, sugar, tobacco, vegetables, total of ten species. The yield of sown area of crops originated from the National Statistical Yearbook (2014). Through the method of sample plot investigation and experimental analysis, the sample plot of 1 m × 1 m was randomly selected from the selected experimental observation farmland sample plot before the crop was mature, After the collection of plant samples, the samples were put

http://www.aloki.hu ● ISSN 1589 1623 (Print) ● ISSN 1785 0037 (Online)
DOI: http://dx.doi.org/10.15666/aeer/1705_1252112535

into a constant temperature oven (100 constant temperature) to bake to constant weight according to different organs. After being taken out, the dry matter weight of each organ was weighed, and the biological quantity of crops was calculated by adding, so as to obtain the economic coefficient of crops.

Model selection

Carbon storage model of forest stand

In order to ensure the application value of the model, this paper uses SPSS software to analyze the correlation of the carbon storage between tree species, and generates the scatter plots. According to the data point distribution, it is found that power function is more consistent with data rules, and combined with the results of previous carbon storage models, the model is obtained by nonlinear regression:

Forest stand carbon storage model:

$$C = aV^b \quad \text{(Eq.1)}$$

C is forest stand carbon storage (Mg), V stands for forest stand volume (m^3), a and b are estimated parameters.

Carbon storage model of tree species

Measuring DBH is usually fast, convenient and accurate, but measuring tree height is time-consuming and laborious. In forest survey, only part of dominant tree height is usually measured, and the missing tree height is often predicted by tree height curve model of different tree species (McRoberts et al., 2013). Therefore, the H index coefficient of tree height in tree species biomass model is set to 1, and the expression of tree species carbon storage model is as follows.

$$C = aD^bH \quad \text{(Eq.2)}$$

C is the carbon storage of single tree species (kg/tree), D is diameter at breast height (DBH) (cm), H is the tree height (m), a and b are estimated parameters.

Carbon storage model of crop

The economic yield and economic coefficient of crop production carbon coefficient are selected as independent variables in the crop carbon storage model. Through the model, the crop vegetation carbon storage per unit area can be calculated.

$$C = C_f * D_w = C_f * Y_w/H_t \quad \text{(Eq.3)}$$

C is Crop carbon storage (unit: t/ha), D_w is crop production, Cf is carbon coefficient, Y_w is economic output, H_t is economic coefficient.

Model evaluation standard

The last and most important step of regression analysis is to verify the model. It is not appropriate to evaluate the predictive ability of the sample calculation model only

http://www.aloki.hu ● ISSN 1589 1623 (Print) ● ISSN 1785 0037 (Online)
DOI: http://dx.doi.org/10.15666/aeer/1705_1252112535

by using the fitting or test indicators, the test sample which means that samples not involved in the fitting model also need to be used in fitting or test indicators. Zeng et al. (2011) believed that the applicability test could not reflect the prediction accuracy of the model, and suggested to combine the test sample and modeling sample for modeling in order to make full use of the sample information The statistical indicators of model test and evaluation include the following five items: Coefficients of determination (R2), Standard error of estimated (SEE), Total relative error (TRE), Mean systematic error (MSE) and Mean prediction error (MPE) (Tang et al., 2008), the specific calculation formula was shown in (*Eqs. 4–8*). In the formula: y_i Is the actual observed value; $\hat{y}_i$ is the estimation; $\bar{y}_i$ is the mean of the reference values; n is the number of estimation, and p is number of parameters. R2 and SEE are the most common evaluation indicators which are reflect the goodness of the fit of models. TRE and MSE are the important indexes to reflect the fitting effects which are should be within $\pm 3\%$ or $\pm 5\%$ and it works best when close to zero. MPE is a precision index which reflecting average carbon storage valuation. In addition, the good fitted model should also have the characteristics of parameter stability and residual (symmetric random distribution with 0 as the base).

$$R^2 = 1 - \sum(\hat{y}_i - y_i)^2 / \sum(y_i - \bar{y}_i)^2 \quad \text{(Eq.4)}$$

$$SEE = \sqrt{\sum(y_i - \hat{y}_i)^2 / (n - p)} \quad \text{(Eq.5)}$$

$$TRE = \sum(y_i - \hat{y}_i) / \sum \hat{y}_i \times 100 \quad \text{(Eq.6)}$$

$$MSE = \sum(y_i - \hat{y}_i) / \hat{y}_i / n \times 100 \quad \text{(Eq.7)}$$

$$MPE = t_\alpha (SEE / \bar{y}) / \sqrt{n} \times 100 \quad \text{(Eq.8)}$$

Results

Carbon storage model of stands

Based on the sample data of each forest tree species, Carbon storage model was processed by SPSS 23 software with nonlinear regression analysis method. And the generated carbon storage model of 9 stand types were evaluated by 4 indicators. The results of the indicators evaluation and parameters estimation are shown in *Table 2*.

As shown in *Table 2*, TRE and MPE of carbon storage model in each stand were low, which indicated that the parameters of each model were very accurate. Accurate prediction of model parameters is the basis for the accuracy of model prediction capability. R2 values were over 0.9, which indicated that the fitting precision was perfect. Meanwhile, MSE was also lower, which indicated that the model had a better accuracy in estimating carbon storage. In general, the regression model had an excellent fitting performance on different forest types.

http://www.aloki.hu ● ISSN 1589 1623 (Print) ● ISSN 1785 0037 (Online)
DOI: http://dx.doi.org/10.15666/aeer/1705_1252112535

Table 2. *Results of the regression analyses of carbon storage in 9 types of stand*

No.	Stand type	a	b	R^2	SEE (%)	MPE (%)	TRE (%)	MSE (%)
1	Coniferous forest	2.221	0.647	0.913	43.41	1.27	1.87	5.89
2	Chinese fir forest	3.453	0.635	0.992	32.63	1.86	2.31	6.75
3	Mongolica forest	2.019	0.991	0.993	27.58	1.29	3.37	7.38
4	Hardwood broad-leaved	1.826	0.903	0.982	39.52	2.18	4.96	11.59
5	Soft leaf broad-leaved	5.006	0.603	0.991	41.25	1.65	1.58	6.18
6	Miscellaneous wood	1.329	0.902	0.991	34.66	1.73	1.86	9.46
7	Coniferous and broad-leaved mixed	2.373	0.816	0.987	18.36	1.03	1.28	5.73
8	Broad-leaved mixed forest	1.285	0.875	0.981	10.45	1.41	0.68	5.38
9	Coniferous mixed forest	5.434	0.603	0.973	24.47	1.31	1.23	6.81

Carbon storage model of individual tree

Through process and analysis, the regression model of carbon storage model of 13 types of tree species in China was established, and the sample data were non-linearly fitted, and the fitting results of the model were calculated by evaluation indexes respectively. The parameter estimation and fitting evaluation are shown in *Table 3*.

Table 3. *Results of the regression analyses of carbon storage in 13 types of tree species*

No.	Tree types	a	b	R^2	SEE (%)	MPE (%)	TRE (%)	MSE (%)
1	Pinus tabuliformis	0.00497	2.267	0.924	12.37	2.34	4.93	17.52
2	Picea asperata Mast	0.00408	2.343	0.861	41.17	3.14	1.13	3.07
3	Cryptomeria fortunei	0.00914	2.010	0.925	14.38	2.24	6.41	10.19
4	Cunninghamia Lanceolata	0.00597	2.109	0.926	13.85	2.04	-1.98	-3.91
5	Quercus	0.00507	2.375	0.876	35.36	3.01	4.71	6.65
6	Abies fabri Craib	0.00713	2.130	0.924	25.87	1.73	-3.24	-4.36
7	Pinus yunnanensis	0.00621	2.121	0.928	9.76	1.52	6.15	5.37
8	Pinus massoniana	0.00591	2.201	0.933	13.87	1.68	3.53	9.69
9	Schima superba	0.01012	2.115	0.894	27.85	3.27	-2.24	-6.87
10	Betula	0.01009	2.101	0.948	42.15	2.56	6.42	8.53
11	Pinus elliottii	0.00914	2.104	0.966	12.08	1.98	3.12	7.15
12	Larix gmelinii	0.00897	2.113	0.935	7.75	1.84	5.34	4.58
13	Liquidambar formosana Hance	0.00632	2.292	0.902	34.32	2.58	7.43	8.17

As can be seen from the evaluation results in *Table 3,* the overall fitting degree of the regression model of carbon storage of 9 types of tree species was over 0.9. Among them, only Picea asperata Mast, Quercus, schima superba and Liquidambar formosana Hance trees were slightly less than 0.9. And MPE was an important index in the calculation of carbon storage. It can be seen from the table that the mean square error was controlled within 5%, and the overall influence was small, which was in line with the calculation of carbon storage of major tree species.

http://www.aloki.hu ● ISSN 1589 1623 (Print) ● ISSN 1785 0037 (Online)
DOI: http://dx.doi.org/10.15666/aeer/1705_1252112535

Carbon storage model of crop

We collected and sorted out the crop economic output, economic coefficient, carbon absorption and other related factors in the Statistic Yearbook of China, the biomass per hectare and carbon storage per hectare were obtained by regression model analysis. The parameters were shown in *Table 4*. If the aboveground vegetation density stays the same, the calculated parameters can be used to calculate the carbon storage of crops directly by multiplying the planting area of agricultural crops by the carbon storage per unit area.

Table 4. *Coefficient of crop carbon storage*

No.	Crop	Carbon storage per hectare (t/ha)	Absorptivity of carbon (%)	Carbon sink per hectare (t/ha)
1	Rice	7.60	0.41	6.24
2	Wheat	6.65	0.49	6.52
3	Maize	7.45	0.47	7.01
4	Beans	2.61	0.45	2.34
5	Potato	2.70	0.42	2.27
6	Cotton	7.90	0.45	7.11
7	Oil plants	5.15	0.45	4.63
8	Sugar plant	51.95	0.43	44.68
9	Tobacco	1.95	0.45	1.75
10	Vegetables	2.75	0.41	2.25

Model evaluation and analysis

Model evaluation and analysis of stand carbon storage

We tested the applicability of each aboveground vegetation carbon storage model with data not involved in the model fitting. The evaluation indexes of TRE and MSE were respectively calculated by the regression model of 9 types of forest stand, and the test results were shown in *Table 5*. The range of TRE in the table varied from -4.72% to 2.64%, and MSE variation range was -4.12%~3.25%. The absolute value of the predicted error of all indexes was less than 5%, which meets the requirements of the model method of biomass and the industry standards (Tang et al., 2008). In order to verify the accuracy of the stand carbon storage model, a set of reserved data was used to verify the accuracy of the model. The results of analysis and comparison between the predicted and measured values were shown in *Figure 1*. The above results show that the model can effectively convert forest carbon reserves.

Table 5. *Results of forest carbon storage model test*

Forest stand	TRE (%)	MSE (%)	Forest stand	TRE (%)	MSE (%)
Coniferous forest	-4.72	-3.75	Miscellaneous wood forest	-.346	-2.27
Chinese fir forest	-3.87	-4.12	Coniferous mixed forest	-3.56	-4.08
Mongolica forest	-2.65	-3.42	Broad-leaved mixed forest	2.64	3.25
Hardwood broad-leaved forest	1.96	2.74	Coniferous and broad-leaved mixed forest	1.76	1.87
Soft leaf broad-leaved forest	-2.05	-1.89	-	-	-

http://www.aloki.hu ● ISSN 1589 1623 (Print) ● ISSN 1785 0037 (Online)
DOI: http://dx.doi.org/10.15666/aeer/1705_1252112535

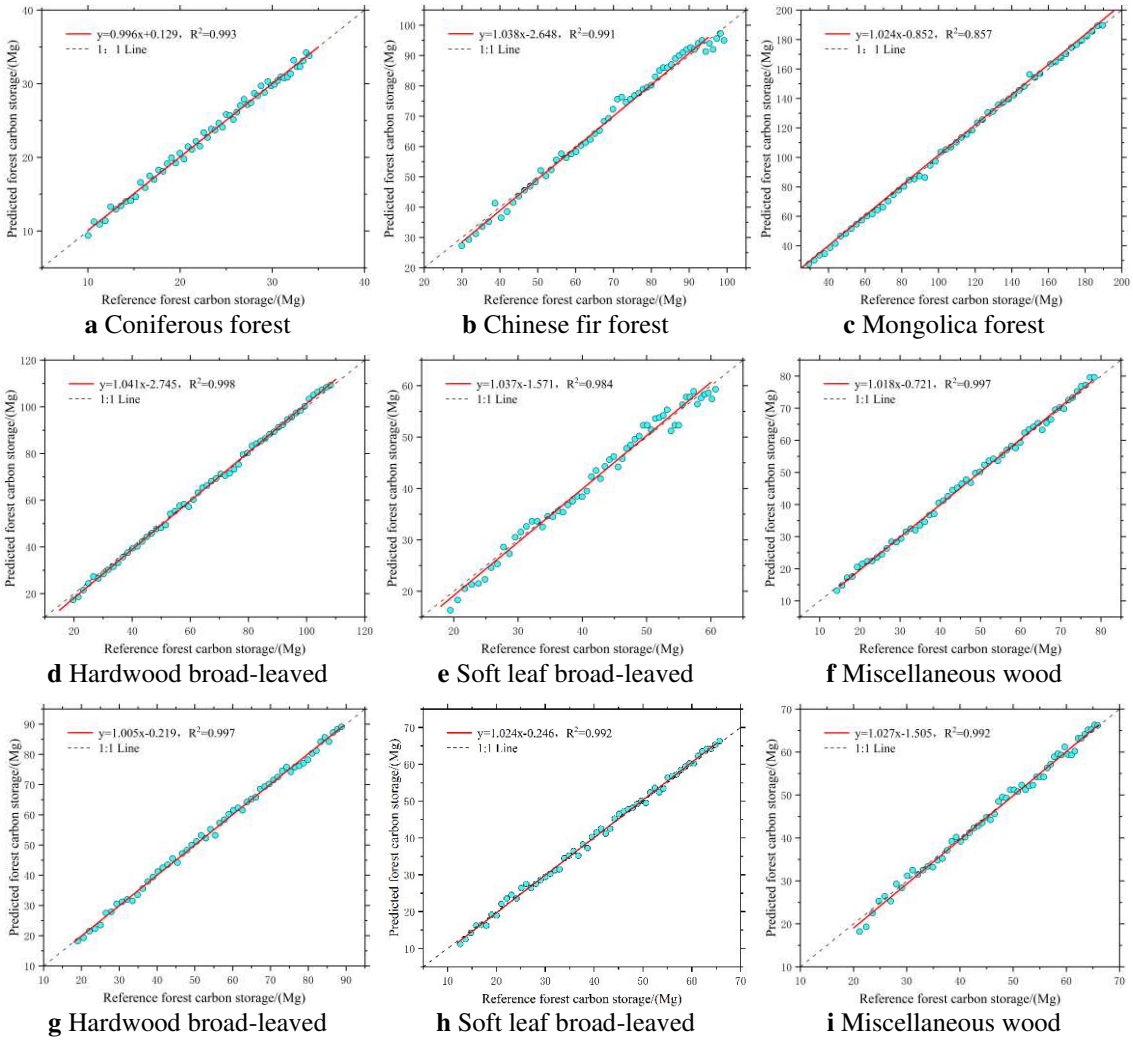

Figure 1. *Reference value and estimation value distribution of forest stand carbon storage*

Model evaluation and analysis of individual tree carbon storage

TRE and MSE were used to test the error of the carbon storage model of 13 species of individual tree. As shown in *Table 6*, experimental investigation showed that the relative TRE of individual tree carbon storage measurements is -6.03%, the relative TRE of hypsometrical measurements is 3.93%, MSE of individual tree carbon storage measurements is -4.72%, and the relative MSE of hypsometrical measurements is 4.37%, all of which are higher than the accuracy required for traditional forestry surveys. In order to verify the accuracy of the tree carbon storage model, a set of reserved data was used to verify the accuracy of the model. The results of analysis and comparison between the predicted and measured values were shown in *Figure 2*. The above results show that the model can effectively convert tree carbon reserves.

Spatial distribution of forest carbon storage in China

In order to quantitatively analyze the spatial distribution characteristics of forest carbon storage in China and verify the accuracy of research model, this paper divides China into six regions (the northeast, the north, the northwest, the southwest, the central

http://www.aloki.hu ● ISSN 1589 1623 (Print) ● ISSN 1785 0037 (Online)
DOI: http://dx.doi.org/10.15666/aeer/1705_1252112535

south and the eastern coasts) and separately estimates the regional carbon storage calculated from forest inventory and the results of carbon storage value obtained in this paper.

It can be seen from *Table 7,* the calculated value based on forest resource inventory is basically match the spatial distribution of carbon reserves value obtained by the simulation in this study. The specific distribution is: the largest is southwest and northeast, followed by central south and north, while northwest and east are relatively small, which is basically consistent with previous studies (Zhao et al., 2014). While there still has some differences between simulation results and results obtained from forest resource inventory, the main reason is the carbon reserve calculated based on forest resource inventory has error. Forest resource inventory is based on 20% crown density standard which means that sparse forests with crown density less than 20% and shrubs were not examined. This error cannot be ignored at the national scale. In addition, there might be some errors also in the process of forest resource inventory and carbon storage calculation. The difference between northeast and southwest is the largest, the reason should be these two areas are the main forest areas in China, and the forest area is large and the terrain is complex. However, the simulation method in this paper can take the calculation of carbon reserves of sparse forests and shrubs into account at the same time, the simulation results match the actual carbon reserves distributions.

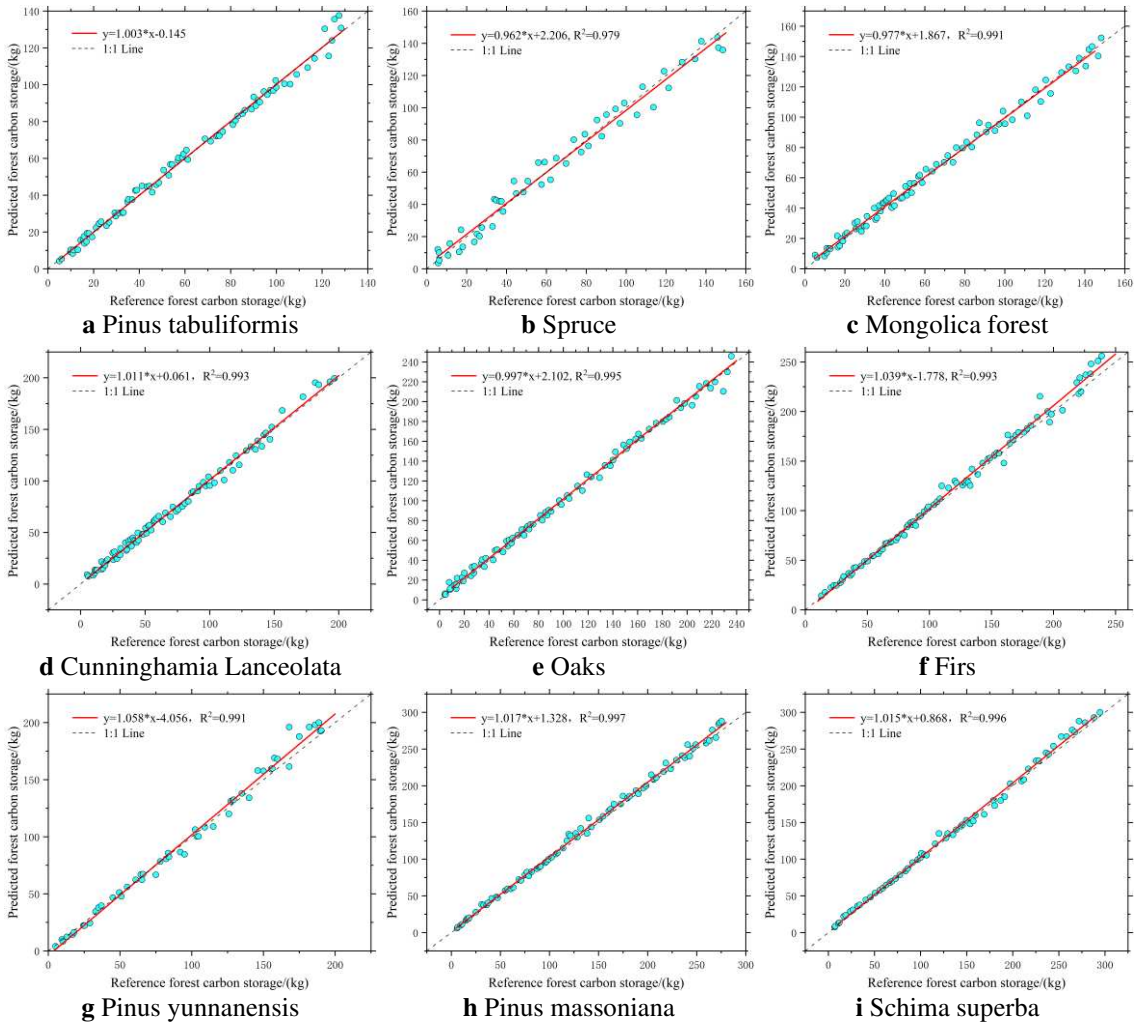

a Pinus tabuliformis **b** Spruce **c** Mongolica forest

d Cunninghamia Lanceolata **e** Oaks **f** Firs

g Pinus yunnanensis **h** Pinus massoniana **i** Schima superba

http://www.aloki.hu ● ISSN 1589 1623 (Print) ● ISSN 1785 0037 (Online)
DOI: http://dx.doi.org/10.15666/aeer/1705_1252112535

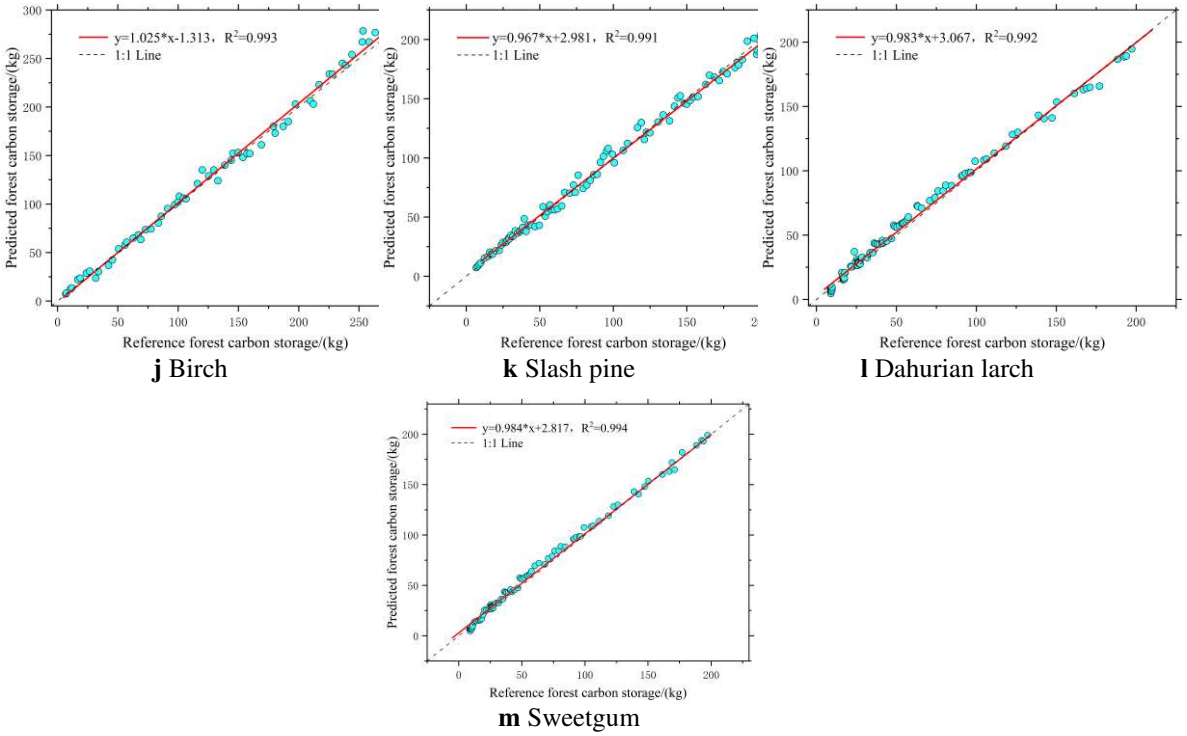

Figure 2. *Reference value and estimation value distribution of tree carbon storage*

Table 6. *Results of tree carbon storage model test*

No.	Tree types	TRE (%)	MSE (%)	No.	tree types	TRE (%)	MSE (%)
1	Pinus tabuliformis	-4.18	-3.87	8	Pinus massoniana	3.87	4.04
2	Picea asperata Mast	-3.58	-3.56	9	Schima superba	2.63	3.28
3	Cryptomeria fortunei	-2.38	-2.28	10	Betula	1.98	2.97
4	Cunninghamia Lanceolata	2.67	2.19	11	Pinus elliottii	2.77	3.26
5	Quercus	-2.39	-2.54	12	Larix gmelinii	-2.76	-3.45
6	Abies fabri Craib	-6.03	-4.72	13	Liquidambar formosana Hance	-2.83	-1.87
7	Pinus yunnanensis	4.76	4.37		-	-	-

Table 7. *Forest carbon storage and density in China at large region level*

Regions	Data of forest resource monitoring (Pg)	Results of model estimates (Pg)	Difference (Pg)	Relative difference (%)
Northeast	1.746	1.923	0.177	10.137
North	0.923	0.867	-0.056	-6.067
Northwest	0.696	0.742	0.046	6.609
Southwest	2.913	3.212	0.299	10.264
Central south	1.145	1.224	-0.079	6.899
Southeast	1.004	1.031	0.027	2.689
total	8.427	8.999	0.572	6.788

http://www.aloki.hu ● ISSN 1589 1623 (Print) ● ISSN 1785 0037 (Online)
DOI: http://dx.doi.org/10.15666/aeer/1705_1252112535

Discussion

The carbon storage conversion model was established by regression model in this study, problem of estimated the carbon storage of single wood level and stand level of each dominant tree species has been solved successfully, It is a less time consuming, lower cost and less laborious approach. Diameter at breast height was the main explanatory tree variable used to estimate the tree carbon storage components for all species. Several authors have noted that inclusion of total height does not usually lead to a substantial increase in the predictive ability of diameter-based biomass regressions, and they also assume that d is sufficient to yield a reliable tree carbon storage prediction (Johansson, 1999; Porté et al., 2002; Jenkins et al., 2003). However, other authors also found that when h was added as a factor, the fitting effect of the model was significantly improved (Reed and Tomé, 1998; Bartelink, 1996), and the accuracy of carbon storage estimation was improved (Menéndez-Miguélez et al., 2013). In this study, D was a good predictor of carbon storage, but the addition of h as the second variable improved the prediction of several species. Tang et al. compared 5 biomass estimation methods based on forest inventory data (Tang, 2016), four carbon storage assessment methods were compared by Gao et al. (2016). Feldpausch et al. (2012) reported that the mean relative error in biomass estimates when h was included was 50% lower than when h was excluded. There are two sets of carbon storage conversion models, one based on DBH and the other based on DBH and tree height, The model of binary was as, D and H are tree DBH and tree height respectively, a, b and c are parameters of the binary model. In the investigation of forest resources, usually only the average tree height of trees was measured, so the coefficient of the tree height parameter H was one in this study.

The combined variable D^2H is usually used in biomass equations (Chave, 2010), and the accuracy of carbon storage estimation has been found to increase significantly (measured as R^2) when h or D^2H was also included, in addition to H. In fact, tree biomass is closely correlated with D^2H, as shown by Parresol (1999) and Carvalho and Parresol (2003). In the models developed by Parresol (1999), height was a good predictor of stem wood but not of stem bark biomass, whereas Carvalho and Parresol (2003) obtained the best estimates for stem, crown and total tree biomass of Pyrenean oak by including the variable D^2H as the sole independent variable in the equation. Bi et al. (2004) reached a similar conclusion, reporting that D^2H performed better for predicting stem and bark components than diameter alone but not for branch and leaf components. In the present study, D、H yielded the best estimates of all biomass components and AGB for P. leiophylla, J. depeanna and Q. crassifolia. The results reported here suggest that the best equations for biomass estimation for most species are based on D and H.

In the total carbon storage of China's forest vegetation, arbor forest accounts for more than 85%, which is the main part. According to the statistics of dominant tree species, the top 10 tree species in terms of area proportion are oak, birch, larch, Pinus massoniana, poplar, yunnan pine, eucalyptus, spruce and cypress, which accounts for 52.54% of the total area in China. In this paper, according to the proportion of dominant tree species in the area, 13 dominant tree species of trees in China were selected. At the same time, according to the composition of dominant tree species, the national arbor forest was divided into 9 categories. such as: coniferous forest, hardwood broad-leaved forest, soft leaf broad-leaved forest, miscellaneous wood forest, coniferous and broad-leaved mixed forest ecosystem, Coniferous mixed forest, Broad-leaved mixed forest, Chinese fir forest, Mongolica forest. Since the bamboo forest in China only accounts for

http://www.aloki.hu ● ISSN 1589 1623 (Print) ● ISSN 1785 0037 (Online)
DOI: http://dx.doi.org/10.15666/aeer/1705_1252112535

1.98% of the national forest area, and the bamboo forest is mainly distributed in several southern provinces of China, the research on bamboo forest is not included in this paper. In future studies, special studies will be conducted on bamboo forest, grassland and shrub.

Conclusions

Based on the general volume table, national forest inventory data and national crop statistic yearbook, this paper proposed a regression modeling method to estimate the carbon storage of large-scale aboveground vegetation in China. The proposed method proved to be capable of reducing field work, evaluating contribution of forests to the global carbon cycle and to support international research on forest carbon and greenhouse gas exchange. According to the results of the modeling, the following conclusions can be drawn.

(1) For Stands and individual trees carbon storage regression model, MSE were within 10% and TRE were within 5%, and it has high fitting precision. Based on the established aboveground vegetation carbon storage model, the regional carbon storage would be directly calculated by using the survey original data. As this method avoids the conversion of tree material volume to biomass, so it has the advantage of high efficiency.

(2) In this study, the carbon storage coefficient of crops can be calculated by directly multiplying the area of crops with the corresponding carbon coefficient, which can be used to estimate carbon storage after UAV detection and the estimation of crop production in a large area.

(3) During the growth and development of aboveground vegetation, the environmental conditions such as water, light, soil characteristics and site conditions have a great influence on the growth and development of trees. Due to the difficulty in collecting and receiving some data, these factors are not considered in this study. Therefore, factors such as rainfall, altitude and site index should be introduced into the model in the future research of carbon storage model.

Acknowledgements. This research was jointly supported by the National Natural Science Foundation of China (No. U1710123).

Author contribution. Ziyu Zhao and Zhongke Feng conceived and designed the experiments; Ziyu Zhao and Jincheng Liu performed the experiments; Ziyu Zhao analyzed the data; Ziyu Zhao and Yajun Shen wrote the main manuscript. All authors contributed in writing and discussing the paper.

Conflict of interests. Ziyu zhao, Zhongke Feng, Jincheng Liu, Yajun Shen declare that they have no conflict of interest or financial conflicts to disclose.

REFERENCES

[1] Aryal, D. R., Jong, B. H. J. D., Ochoa-Gaona, S., et al. (2014): Carbon stocks and changes in tropical secondary forests of southern Mexico. – Agriculture Ecosystems & Environment 195(195): 220-230.

[2] Bartelink, H. H. (1996): Allometric relationships on biomass and needle area of Douglas-fir. – Forest Ecol. Manag 86: 193-203.

http://www.aloki.hu ● ISSN 1589 1623 (Print) ● ISSN 1785 0037 (Online)
DOI: http://dx.doi.org/10.15666/aeer/1705_1252112535

[3] Berbés-Blázquez, M. (2012): A Participatory Assessment of Ecosystem Services and Human Wellbeing in Rural Costa Rica Using Photo-Voice. – Environmental Management 49(4): 862-875.
[4] Bi, H., Turner, J., Lambert, M. (2004): Additive biomass equations for native eucalypt forest trees of temperate Australia. – Trees 18: 467-479.
[5] Canadell, J. G., Mooney, H. A., Baldocchi, D. D., et al. (2000): Carbon metabolism of the terrestrial biosphere: a multitechnique approach for improved understanding. – Ecosystems 3(2): 115-130.
[6] Cao, M., Woodward, I. F. (1998): Net primary and ecosystem production and carbon stocks of terrestrial ecosystems and their responses to climate change. – Global Change Biology 4(2): 283-290.
[7] Carvalho, J. P., Parresol, B. R. (2003): Additivity in tree biomass components of Pyrenean oak (Quercus pyrenaica Willd.). – Forest Ecol. Manag. 179: 269-276.
[8] Chave, J., Andalo, C., Brown, S., et al. (2005): Tree allometry and improved estimation of carbon storage and balance in tropical forests. – Oecologia 145(1): 87-99.
[9] Cheng, T., Ma, Q., Feng, Z. (2007): Research on forest biomass in Xiaolong Mountains Gansu Province. – Journal of Beijing Forestry University 29(1): 31-36 (in Chinese).
[10] Department of Forest Resources Management of State Forestry Administration (2014): Forest Resources Statistics of China – Department of Forest Resources Management of State Forestry Administration, Beijing.
[11] Fang, J., Chen, A., Peng, C., et al. (2001): Changes in forest biomass carbon storage in China between 1949 and 1998. – Science 292(5525): 2320-2322.
[12] Feldpausch, T. R., Lloyd, J., Lewis, S. L., et al. (2012): Tree height integrated into pantropical forest biomass estimates. – Biogeosciences 9: 3381-3403.
[13] Gibbs, H. K., Brown, S., Niles, J. O., et al. (2007): Monitoring and estimating tropical forest carbon stocks: making REDD a reality. – Environmental Research Letters 2(4): 45023-0.
[14] Huilin, G., Lihu, D., Fengri, L., et al. (2015): Evaluation of Four Methods for Predicting Carbon Stocks of Korean Pine Plantations in Heilongjiang Province, China. – Plos One 10(12): e0145017-.
[15] Intergovernmental Panel on Climate Change (IPCC) (2014): Summary for Policymakers. – In: Edenhofer, O., Madruge, R. P., Sokona, Y., Farahani, E., Kadner, S., Seyboth, K., Adler, A., Baum, I., Brunner, S., Eickemeier, P., et al. (eds.) Climate Change 2014: Mitigation of Climate Change; Contribution of Working Group III to the Fifth Assessment Report of the Intergovernmental Panel on Climate Change. Cambridge University Press, Cambrige, UK.
[16] Jenkins, J. C., Chojnacky, D. C., Heath, L. S., Birdsey, R. (2003): National-scale biomass estimators for United States tree species. – Forest Science 49(1): 12-35.
[17] Johansson, T. (1999): Biomass equations for determining fractions of pendula and pubescent birches growing on abandoned farmland and some practical implications. – Biomass Bioenergy 16: 223-238.
[18] Koh, L. P. Ghazoul, J. (2010): Spatially explicit scenario analysis for reconciling agricultural expansion, forest protection, and carbon conservation in Indonesia. – Pnatl Acad Sci USA 107(24): 11140-4.
[19] Li, H., Lei, Y., Zeng, W. (2011): Forest carbon storage in China estimated using forestry inventory data. – Scientia Silvae Sinicae. 47(7): 7-12 (in Chinese).
[20] Martínez, B., Gilabert, M. A. (2009): Vegetation dynamics from NDVI time series analysis using the wavelet transform. – Remote Sensing of Environment 113(9): 1823-1842.
[21] Mcroberts, R. E., Næsset, E., Gobakken, T. (2013): Inference for lidar-assisted estimation of forest growing stock volume. – Remote Sensing of Environment 128: 268-275.

http://www.aloki.hu ● ISSN 1589 1623 (Print) ● ISSN 1785 0037 (Online)
DOI: http://dx.doi.org/10.15666/aeer/1705_1252112535

[22] Menéndez-Miguélez, M., Canga, E., Barrio-Anta, M., et al. (2013): A three level system for estimating the biomass of Castanea sativa Mill. coppice stands in north-west Spain. – Forest Ecol. Manag. 291: 417-426.
[23] Moncada Rojas, O., Botero, V. (2013): En-masse removal identification on a regional scale through the use of time series of the MODIS-NDVI sensor. – Second International Conference on Agro-Geoinformatics, IEEE, pp. 547-549.
[24] Navar, J. (2009): Allometric equations for tree species and carbon storage for forests of northwestern Mexico. – Forest Ecol Manag 257(2): 427-434.
[25] Nunery, J. S., Keeton, W. S. (2010): Forest carbon storage in the northeastern United States: Net effects of harvesting frequency, post-harvest retention, and wood products. – Forest Ecology & Management 259(8): 1363-1375.
[26] Parresol, B. R. (1999): Assessing tree and stand biomass: a Review with examples and critical comparisons. – Forest Sci. 45: 573-593.
[27] Popescu, S. C. (2007): Estimating biomass of individual pine trees using airborne lidar. – Biomass & Bioenergy 31(9): 646-655.
[28] Porté, A., Trichet, P., Bert, D. L., et al. (2002): Allometric relationships for branch and tree woody biomass of Maritime pine (Pinus pinaster Ait). – Forest Ecol. Manag. 158: 71-83.
[29] Reed, D. Tomé, M. (1998): Total aboveground biomass and net dry matter accumulation by plant component in young Eucalyptus globulus in response to irrigation. – Forest Ecol. Manag 103: 21-32.
[30] Schmidt, A., Poulain, M., Klein, D., Krause, K., et al. (2009): Allometric above-belowground biomass equations for Nothofagus pumilio (Poepp. & Endl.) natural regeneration in the Chilean Patagonia. – Ann. Forest Sci. 66: 513.
[31] Tang, S., Lang, K., Li, H. (2008): Statistical and Biological Mathematical Model Calculation (ForStat Course). – Science Press, Beijing.
[32] Tang, X., Fehrmann, L., Guan, F., et al. (2016): Inventory-based estimation of forest biomass in Shitai County, China: a comparison of five methods. – Annals of Forest Research 59(1).
[33] Trishchenko, A. P., Cihlar, J., Li, Z. (2002): Effects of spectral response function on surface reflectance and NDVI measured with moderate resolution satellite sensors. – Remote Sensing of Environment 113(2): 335-341.
[34] Wang, X. K., Feng, Z. W., Ouyang, Z. Y. (2001): Vegetation carbon storage and density of forest ecosystems in China. – Chinese Journal of Applied Ecology 12(1): 13 (in Chinese).
[35] Wengsheng, C., Zhongke, F., Jingxin, Y. (2017): Development of generic standard volume model form factor model for major tree species and derived in China. – Transactions of the Chinese Society for Agricultural Machinery 48(3): 245-252 (in Chinese).
[36] Woodbury, P. B., Smith, J. E., Heath, L. S. (2007): Carbon sequestration in the U.S. forest sector from 1990 to 2010. – Forest Ecology & Management 241(1): 14-27.
[37] Yang, L., Feng, Z., Yue, D., Sun, J. (2017): Forest stock volume estimation model using textural and topographic factors of Landsat8OLI. – Spectrosc Spect Anal 37(7): 2140-2145 (in Chinese).
[38] Zeng, W. Tang, S. (2010): Research status and prospect of foreign biomass model of standing wood. – World Forestry Research 23(4): 30-35.
[39] Zeng, W., Tang, S., Huag, G., Zhang, M. (2010): Population classification and sample structure on modeling of single tree biomass equations for national biomass estimation in China. – Forest Resour. Manag. 3: 16-23.
[40] Zeng, W. S. (2011): Goodness evaluation and precision analysis of tree biomass equations. – Scientia Silvae Sinicae 47(11): 106-113 (in Chinese).

http://www.aloki.hu ● ISSN 1589 1623 (Print) ● ISSN 1785 0037 (Online)
DOI: http://dx.doi.org/10.15666/aeer/1705_1252112535

[41] Zhang, C., Xia, B., Lin, J. (2016): A basin-scale estimation of carbon stocks of a forest ecosystem characterized by spatial distribution and contributive features in the Liuxihe River basin of Pearl River Delta. – Forests 7(12): 299.
[42] Zhao M, Zhou, G. S. (2004): Carbon storage of forest vegetation and its relationship with climatic factors. – Scientia Geographica Sinica 24(1): 50-54.
[43] Zhao, M., Yue, T., Zhao, N., et al. (2014): Combining LPJ-GUESS and HASM to simulate the spatial distribution of forest vegetation carbon stock in China. – Journal of Geographical Sciences 24(02): 249-268.
[44] Zolkos, S. G., Goetz, S. J., Dubayah, R. (2013): A meta-analysis of terrestrial aboveground biomass estimation using lidar remote sensing. – Remote Sensing of Environment 128(1): 289-298.

http://www.aloki.hu ● ISSN 1589 1623 (Print) ● ISSN 1785 0037 (Online)
DOI: http://dx.doi.org/10.15666/aeer/1705_1252112535

MICROBIAL COMMUNITY FUNCTIONAL DIVERSITY IN AN ORGANOCHLORINE CONTAMINATED SITE AND EVALUATION OF BIODEGRADATION EFFICIENCY

ZHU, C.[1#] – WANG, D.[1#] – ZHANG, J. W.[2, 4] – QU, C. S.[1] – HUA, Z. L.[3] – ZHANG, M. C.[1] – WANG, S.[1*]

[1]*Key Laboratory of Environmental Engineering, Jiangsu Provincial Academy of Environmental Science, Nanjing, Jiangsu 210036, China*

[2]*School of the Environment, Nanjing University, Nanjing, Jiangsu 210036, China*

[3]*College of Resources and Environmental Sciences, Nanjing Agricultural University, Jiangsu 210036, China*

[4]*Department of Public Health, University of Copenhagen, Copenhagen, Denmark*

[#]*These authors have contributed equally to this article*

**Corresponding author*
e-mail: wangshui@jsaes.com; phone: +86-25-5852-7708; fax: +86-25-5852-7706

(Received 16th May 2019; accepted 16th Jul 2019)

Abstract. A typical chlorinated hydrocarbon contaminated site was selected as the research object in southern China. First, Gas Chromatography-Mass Spectrometer (GC-MS) was used to analyze the composition and concentration of pollutants in soil and groundwater samples. Then, we investigated the microbial community structure, composition, and abundance by high-throughput sequencing analysis. Principal component analysis and environmental factor correlation analysis were further used to illustrate the functional diversity of microbial communities. Eventually, the results showed that the composition and structure of the microbial community were significantly different due to the various degrees of pollution in the soil and groundwater. In the soil with high pollution degree, the functional diversity of the microbial community was notably different from that of non-polluted or slightly polluted soil. This indicated that soil microbial physiological activities and community functional diversity could be affected by the residual concentration of chlorinated hydrocarbons in contaminated soils. The dominant microbial community in the soil was Penicillium, which had a higher abundance in the soil environment, while the Phylum Firmicutes were more sensitive species. In addition, as stain-resistant bacteria, Brevundimonas, Rhizobium Frank, and Pseudomonas were observed in the groundwater, where Lasiodiplodia was the dominant microbial community, while Fusarium was more sensitive species.
Keywords: *chlorinated hydrocarbon, soil and groundwater microorganism, community structure, species diversity, degradation*

Introduction

Due to the rapid development of urbanization in China, local governments have promoted the strategic transformation of industrial structure and urban layout, revealing problems of abandoned industrial buildings and resources facing relocation. A large number of heavily polluting industrial enterprises have been moved into industrial parks, which were originally in the main urban areas.

Through the long-time production history, a large amount of toxic and harmful substances persist in the soil of site thanks to some heavily polluting enterprises, because of improper operations, leakages, insufficient environmental supervisions and some other reasons, adversely affecting the local ecological environment, the health of

http://www.aloki.hu ● ISSN 1589 1623 (Print) ● ISSN 1785 0037 (Online)
DOI: http://dx.doi.org/10.15666/aeer/1705_1253712549

local people as well as land redevelopment and utilization. Organic pollutants have always been the vital monitoring targets in the investigation of contaminated sites. Most of them are generally bio-accumulative, chronically toxic and have a "three-way" (carcinogenic, teratogenic and mutagenic) effect, which have been listed as priority pollutants in the world (Su et al., 2015). At present, the soil and groundwater pollution situation in China is severe. In addition, according to reliable data, most of the contaminated sites contain chlorinated hydrocarbons and aromatic hydrocarbons (Tan et al., 2017). Chlorinated hydrocarbons have been extensively studied for their high toxicity, refractory degradation, and strong accumulation. According to the survey, once chlorinated hydrocarbons enter the groundwater, if they are not effectively repaired, the pollution can last for decades, even hundreds of years (Wang, 2018).

Chlorobenzene and chlorinated alkane are common pollutants in the soil of chemical pollution sites in Jiangsu Province. In addition to chemical detection and analysis methods, biological diagnosis is also an important means to assess the environmental risks associated with organically contaminated soils (Gao, 2014). The community structure and functional diversity of microorganisms have long been regarded as important biological indicators in soil and groundwater environments, and have received extensive attention in recent years. Through laboratory testing of microbial indicators in contaminated sites, the composition, concentration and biological toxicity of pollutants in contaminated sites can be accurately determined, thus providing a detailed and accurate reference for the risk assessment and remediation of contaminated sites. The specific indicators are as follows: (1) in the soil environment, the routine indicators of microorganisms include microbial biomass, microbial community structure, microbial functional diversity, microbial genetic diversity, total soil DNA, total soil RNA, etc.; (2) in the groundwater environment, routine microbiological indicators include, number of coliforms, heat-resistant coliforms, Escherichia coli, and total number of colonies.

Soil and groundwater microbial community diversity is very sensitive to changes in soil chemical properties and can be used as an important biological indicator to measure soil and groundwater quality and to assess the sustainability of soil ecosystems. The site pollution habitat is a special habitat composed of site pollutants-soil-groundwater-microorganisms (Song, 2015). A series of physical and chemical changes, caused by external pollutants, will occur in the soil and groundwater, and profoundly affect the environmental and biological properties of the site. High-throughput sequencing technology can be applied to evaluate the functional diversity of microbial communities in the site (Zhang et al., 2018; Shi et al., 2018; Li et al., 2019), such as comparing different soil types (Luo et al., 2013), different plant species in the same soil (Nie, 2013), and the diverse functions of soil microbial communities in different vegetation rhizosphere (Liang et al., 2018; Qiu et al., 2019). However, studies on the functional diversity of soil and groundwater microbes in chlorinated benzene and chlorinated alkane-contaminated sites using high-throughput sequencing technology have rarely been reported.

We attempted to use high-throughput sequencing technology to analyze the soil and groundwater microbial community functions and diversity of chlorobenzene and chlorinated alkane-contaminated sites, and to study the relationship between soil and groundwater pollution levels and microbial activity. Therefore, the present study was aimed to provide details of the spatial variations of the bacterial communities in surface sediments collected from different locations within the contaminated site.

http://www.aloki.hu ● ISSN 1589 1623 (Print) ● ISSN 1785 0037 (Online)
DOI: http://dx.doi.org/10.15666/aeer/1705_1253712549

Materials and methods

Brief introduction of the sampling site

The soil and groundwater samples selected for this study were from a decommissioning industrial contaminated site that was used as a point of production for chemical products. The enterprise was located in Taizhou, Jiangsu province, China, and focused on new material industry, and engaged in chlorine alkali, methane chloride, and fine chemicals production in 1960 to 2017.

Collection and analysis of soil and groundwater samples

The samples were collected from an industrial site of a chemical plant in May 2017. Five-point sampling methods were adopted to collect soil samples, and the hardened parts on the surface were removed. The depth of sampling for soil analysis was at 4 m and 7 m of S1 and S11, respectively. Soils were air-dried in shade and sifted through 10 meshes for analysis. The groundwater table was 0.8 m, and depth of the groundwater monitoring well construction was 9 m. The water-table contour map shows that the direction of groundwater flow is west to east (*Fig. 1*). Groundwater samplings were from Groundwater well No.11, No.1 and No. 6, as shown in *Figure 1*.

Figure 1. *Groundwater flow direction of the contaminated site*

After extraction, centrifugation, activation and purification, the samples were placed in Gas Chromatography-Mass Spectrometer (GC-MS) for analysis with helium as carrier gas. According to the obtained mass spectrogram, the database was searched. The result shows that the main pollutants in the environment are halogenated aliphatic compounds and chlorinated hydrocarbons.

Soil contaminant

There are about 20 kinds of organic contaminants in the soil samples, including entachlorobenzene, hexachlorobenzene, hexachloroethane, hexachlorobutadiene, phenol, phenanthrene, quinone, total petroleum hydrocarbon, dichloromethane, carbon tetrachloride, pentachloroethane,1,2-dichloroethane, 1,1,2-trichloroethane, 1,1,2,2-

http://www.aloki.hu ● ISSN 1589 1623 (Print) ● ISSN 1785 0037 (Online)
DOI: http://dx.doi.org/10.15666/aeer/1705_1253712549

tetrachloroethane, cis-1,2-dichloroethylene, trichloroethylene, tetrachloroethylene, chlorobenzene, carbon disulfide, chloroform. The contaminant concentration of soil sample at depth 4 m was higher than that of 7 m soil sample, such as chloroform was over 10.5 times.

Compared with the "Site Soil Environmental Risk Assessment Screening Value" (DB11/T 811-2011) (industrial land), there were excessive levels of methylene chloride, carbon tetrachloride and chloroform in the soil. Their values were respectively 4.3 times, 26.6 times, and 207 times the standard.

Groundwater contaminant

About 29 organic substances were detected in groundwater, including hexachloroethane, hexachlorobutadiene, phenol, 2-methylphenol, 3-methylphenol, 4-methylphenol, total petroleum hydrocarbons, 1,2-dichloride Propane, vinyl chloride, 1,1-dichloroethylene, dichloromethane, trans-1,2-dichloroethylene, cis-1,2-dichloroethylene, carbon tetrachloride, 1,2-dichloroethane, trichloroethylene, 1,1,2-trichloroethane, 1,3-dichloropropane, tetrachloroethylene, 1,1,2,2-tetrachloroethane, 1,2,3-trichloropropane, pentachloroethane, toluene, ethylbenzene, m-xylene and o-xylene, o-xylene, carbon disulfide, chloroform. Compared with Regional Screening Level (RSL) Summary Table (TR = 1E-06, HQ = 1) April 2019. In the G3 groundwater sample, no pollutants other than the above organic substances were detected.

High-throughput sequencing analysis of soil and groundwater microorganisms

According to the manufacturer's protocols, Microbial DNA was extracted from soil and groundwater samples using the E.Z.N.A.S. tool DNA Kit (Omega Bio-tek, Norcross, GA, U.S.). The amplification of the V3-V4 region of 16S rDNA and the Internal Transcribed Space (ITS) region of Eukaryotic Ribosomal RNA gene were examined by Polymerase Chain Reaction (PCR). Purified amplicons were pooled in equimolar and paired-end sequenced (2 × 250) on an Illumina platform according to the standard protocols. Then low quality reads with less than 80% bases with quality (Q-value) of 20 or lower and/or over 10% bases unknown (N) were removed from each data set to gain more reliable results. After that, the clean reads of high quality from all soil and groundwater samples were merged together and assembled by using FLASH (v 1.2.11) with a minimum overlap of 10 bp and mismatch error rates of 2%. The resultant high-quality sequences were processed to generate operational taxonomic units (OTUs) by UPARSE pipeline at the 97% sequence similarity threshold. The taxonomic categorification was performed with the RDP classifier based on UNITE Database (Wu et al., 2018) (https://unite.ut.ee/) and SILVA Database (Rosselli et al., 2016) (https://www.arb-silva.de), respectively. Based on the species abundance of each sample in the OUT list, vegan packages are used in the R to calculate 3 types of microbial diversity index (Chao1, Shannon and Coverage), and ggplot2 packages are used in the R to perform the principal component analysis. Chao1 index presents the total number of OUT in the sample; Shannon index shows the degree of α-diversity of species in the microbial community; and Coverage index presents the Database's coverage rate for different sample.

http://www.aloki.hu ● ISSN 1589 1623 (Print) ● ISSN 1785 0037 (Online)
DOI: http://dx.doi.org/10.15666/aeer/1705_1253712549

Results

Analysis of bacterial diversity in site soil and groundwater

The contaminant concentration of GW3 sample was high. In particular, the concentration of GW1 sample, of which 1, 2-Dichloropropane, carbon tetrachloride and chloroform reached to 19.5 μg/L, 193 μg/L and 63 μg/L, respectively. The 1, 2-dichloroethane concentration of GW2 was 1.3 μg/L. GW1 served as control.

Through high-throughput sequencing data analysis, a total of 264259 high-quality and valid sequencing results, with an average length of 459, were obtained from soil and groundwater bacteria samples from six groups of contaminated sites. The sequence clustering was divided with 97% consistency to obtain 3,840 OTUs. *Table 1* presented the results of Unique Tags, OUT quantity and Alpha diversity index in the soil and groundwater bacteria samples from six pollution sites. The coverage of sample libraries in each group was higher than 99.5%, and the main distribution was between 99.66% and 99.72%. The gene sequences in the bacterial samples had high detection probability, and the sequencing results could well reflect the real situation of the bacteria community in the contaminated site soil and groundwater.

Table 1. *High-throughput sequencing results of the bacteria in groundwater and soil*

Treatments	OTUs	Unique tags	Chao1	Shannon	Coverage
CK	681	33532	977.39	5.05	0.9971
SD1	994	39555	1216.46	5.69	0.9966
SD2	1109	39657	1318.59	5.19	0.9968
GW1	1279	56658	1578.24	6.30	0.9968
GW2	842	47606	1093.45	5.57	0.9972
GW3	893	47288	1173.23	5.84	0.9971

CK group represented the blank control group for bacteria sequencing; SD1 and SD2 represented the control group with soil depth of 4 m and 7 m respectively; GW1, GW2, and GW3 represented the bacteria control group in groundwater when the contaminant content was low, medium, and high, respectively

Chao1 index is used to predict the total number of OUT (microbial species) in the sample, which reflects the abundance of bacterial population to some extent. The higher the Chao1 index is, the higher the richness of the bacterial community will be. As shown in *Table 1*, the bacterial abundance in soil showed little difference at different depths, i.e. different pollution levels, but there were significant differences in the bacterial abundance in groundwater at different pollution levels ($p < 0.05$). Under the condition of medium pollutant content and high pollutant content, the bacterial abundance in groundwater was significantly reduced ($p < 0.05$), while the bacterial abundance in soil was not different with the influence of soil pollutant concentration. It suggested that the bacteria in groundwater were more sensitive to the change between the pollutant concentration of GW1-GW2, and the bacteria abundance would be greatly changed.

The Shannon index reflects the degree of α-diversity of species in the microbial community, and the higher the value of Shannon index is, the higher the degree of diversity will be. From *Table 1*, it could be seen that different depths, i.e. different pollution degrees, had smaller differences in the diversity of bacteria in soil, but there

http://www.aloki.hu ● ISSN 1589 1623 (Print) ● ISSN 1785 0037 (Online)
DOI: http://dx.doi.org/10.15666/aeer/1705_1253712549

were also significant differences in the diversity of bacteria in groundwater with different pollution levels ($p < 0.05$). Under the condition of medium pollutant content, the bacterial diversity in groundwater was significantly reduced ($p < 0.05$), while the bacterial diversity in soil did not change significantly with the influence of soil pollutant concentration. This also indicated that the concentration of pollutants between GW1-GW2 will have a huge impact on the diversity of bacteria. The bacteria in groundwater were more sensitive to the change of pollutant concentration, which was consistent with the change of the abundance of the bacteria community mentioned above.

The results of the change of bacterial community abundance showed that Bacillus can promote the bio-abundance of Bacillus in medium level pollution (see *Fig. 2* for details). In addition, compared with the community abundance of the control group, Comamonadaceae and Methylophilaceae had higher community abundance at this stage, while in the stage of pollution, the community abundance was low and exhibited extreme sensitivity, which could be used as the signature microorganism at this stage. Rhizobium and Pseudomonas were found in highly contaminated soil as two types of high community abundance, and the community abundance was reduced in both pollution-free and low-pollution states. Lysobacter, as a marker of low pollution in groundwater, was low in other pollution levels. Hydrogenophaga and Bacillus could be used as indicators of moderate groundwater pollution, while Brevundimonas could be used as markers of bacteria in highly polluted groundwater. In this way, Brevundimonas, Rhizobium and Pseudomonas might also be pollutant degrading-bacteria.

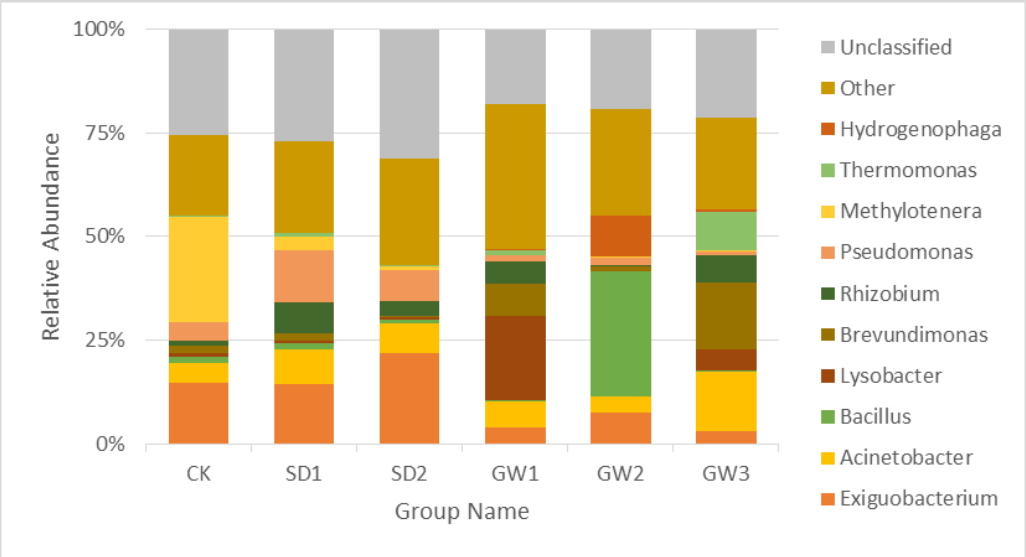

Figure 2. *Bacterial species abundance of soil and groundwater*

Through the primary ingredient analysis by OTU of bacteria in the control group and different environmental media, it could be seen (*Fig. 3*) that the cumulative contribution of bacteria in the first and second components of the six groups was 35.3% and 21.5%, respectively. The results showed that in different pollution levels and environmental media, the medium groundwater environment had the greatest impact on the diversity of communities, while the groundwater with high and low pollution levels did not show

http://www.aloki.hu ● ISSN 1589 1623 (Print) ● ISSN 1785 0037 (Online)
DOI: http://dx.doi.org/10.15666/aeer/1705_1253712549

apparent changes in the overall structure. For both soil and control groups, the diversity of their communities was generally similar.

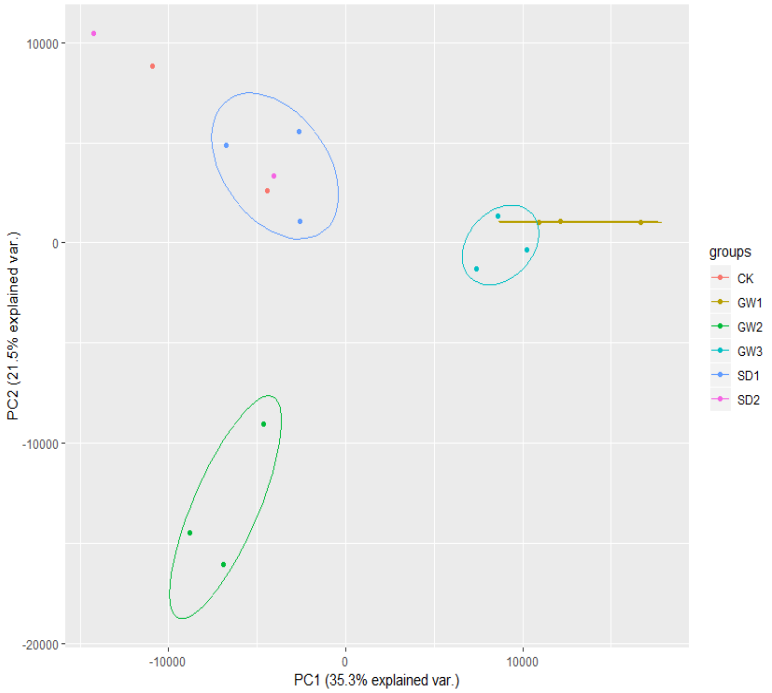

Figure 3. *OTU principal component analysis for the bacteria abundance in the control group and different environmental media*

Bacterial community of groundwater samples was analyzed by analyzing the main components of the group of bacteria OTU in the control group and the groundwater sample group under different pollution conditions. It could be seen (*Fig. 2*) that the accumulative contribution of bacteria in the first and second main components of the four samples was 42.8% and 21.4%, respectively. The control group and the contaminated groundwater sample group were separately clustered and far away, indicating that the pollution would lead to large differences in the diversity of bacteria in the groundwater environment. However, in the groundwater with different pollution levels, the bacteria group with medium pollution level was significantly separated from the bacteria group with high pollution level and the bacteria group with low pollution level in the first principal component. The distance was relatively far, indicating that the groundwater with medium pollution level would produce large and significant differences in the diversity of bacteria. Compared with the bacteria of high pollution level, the bacteria of low pollution level in groundwater were divided in the second principal component and did not coincide in the 95% confidence interval, indicating that the diversity of the bacterial community was also different between high and low pollution levels.

Analysis of fungi diversity in site soil and groundwater

A total of 103254 high quality and valid sequencing results, with an average length of 357, were obtained from soil and groundwater fungi samples in 6 groups by high-throughput sequencing data analysis. The sequence clustering was divided with 97% consistency, and 652 OTUs were obtained. *Table 2* showed the results of Unique Tags,

http://www.aloki.hu ● ISSN 1589 1623 (Print) ● ISSN 1785 0037 (Online)
DOI: http://dx.doi.org/10.15666/aeer/1705_1253712549

OUT quantity and Alpha diversity index in the soil and groundwater fungi samples of six pollution sites. The sample library coverage of each group was as high as 99.9%, and the main distribution was between 99.95% and 99.97%. The gene sequences in the fungi samples had a high probability of detection, and the sequencing results could well reflect the real situation of the fungi community in the contaminated site soil and groundwater.

Chao1 index is used to predict the total number of OUT (microbial species) in the sample, which reflects the fungi population abundance to a certain extent. The higher the Chao1 index is, the higher the richness of the fungi community will be. It could be seen from *Table 2* that the fungi abundance in soil was not significantly different with different depths, namely different pollution levels, and the fungi abundance in groundwater with different pollution levels was also similar.

Shannon index reflects the degree of diversity of species in the community of fungi, and the higher the value of Shannon index is, the higher the degree of diversity will be. It could be seen from *Table 2* that unless there was a significant difference in the diversity of fungi community in transenvironmental media, the diversity of fungi community was the same in soil and groundwater with different pollution levels. The extent of the contamination has caused a small change in the growth of the fungi population. Therefore, it could be seen that the changes of fungi abundance and diversity in contaminated soil and groundwater environments were not obvious in the large structure level, which further required investigation.

Table 2. *High-throughput sequencing results of the fungi of in groundwater and soil*

Sample name	OTUs	Unique tags	Chao1	Shannon	Coverage
CK	176	17728	204.07	2.69	0.9997
SD1	190	15245	240.89	2.13	0.9996
SD2	201	19651	224.80	3.71	0.9997
GW1	216	14908	258.73	4.08	0.9995
GW2	169	19009	227.81	3.12	0.9997
GW3	199	16713	235.30	3.55	0.9996

CK group represented the blank control group for bacteria sequencing; SD1 and SD2 represented the control group with soil depth of 4 m and 7 m bacteria; GW1, GW2, and GW3 represented the bacteria control group in groundwater when the contaminant content was low, medium, and high, respectively

Through high-throughput sequencing analysis of fungi samples in soil and groundwater, 652 OTUs belonged to 6 phyla, 16 classes, 35 orders, 67 families and 94 genera respectively. Alternaria of Pleosporaceae followed the above community abundance characteristics in groundwater, showing that the community abundance increased with the increase of pollution concentration in the environment. In addition, compared with each group, the community richness of the Penicillium in the highly polluted soil environment was higher, while that of the other environments was lower, which might indicate the characteristic expression of the Penicillium in the soil environmental pollution at this stage. However, Fusarium had a much higher abundance in low-concentration groundwater environment than that under other conditions. The abundance of Gibberella and Cladosporium in a moderately polluted groundwater environment was much higher than that under other conditions. The abundance of Lasiodiplodia in the groundwater environment with a high concentration of pollution

http://www.aloki.hu ● ISSN 1589 1623 (Print) ● ISSN 1785 0037 (Online)
DOI: http://dx.doi.org/10.15666/aeer/1705_1253712549

was much higher than that under other conditions (*Fig. 4*). All illustrate that these four strains could be as each phase of the identification of strains of bacteria and sign.

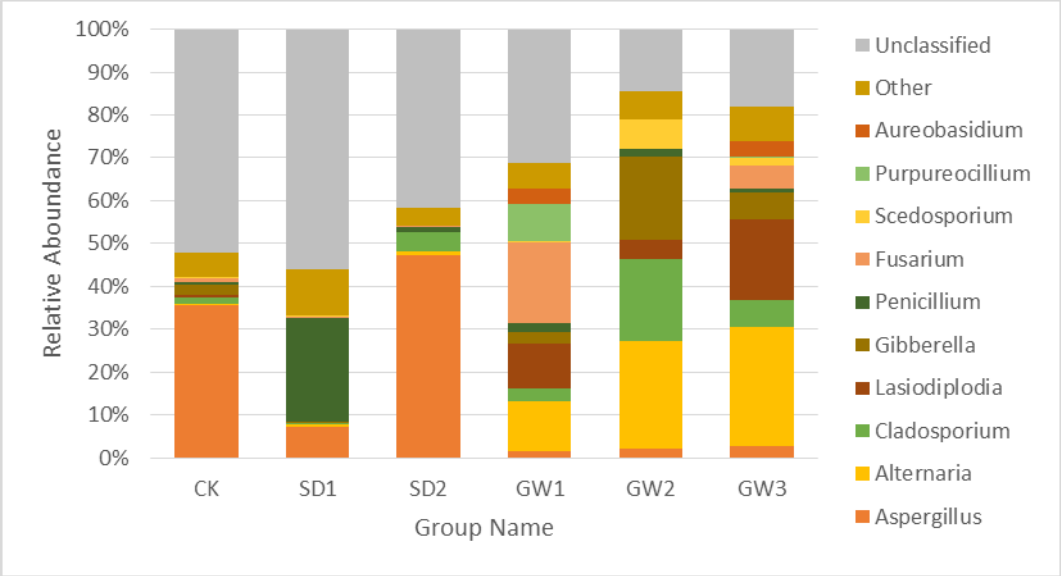

Figure 4. *Fungus abundance of soil and groundwater*

By principal component analysis of the OTU of the fungus in the control group and different environmental media, it could be seen (*Fig. 5*) that the accumulative contributions of fungi in the first and second main components of the six groups were 32.6% and 19.3%, respectively. The separation of the two groups was relatively distant, indicating that the pollutant would lead to the change of community diversity. Compared with the groundwater environment, the shallow soil environment with high pollution had more changes in the first principal component. The community diversity under three kinds of groundwater environment was not much different.

Discussion

Considering the diversity of microbial community structure and function, there is a huge potential value in investigating and assessing the risk of organic contaminated sites such as chlorinated hydrocarbons. In recent years, organizations and researchers at home and abroad have carried out a large number of related experiments and achieved remarkable results. Current experimental studies have found that the structure and functional diversity of microbial communities in contaminated sites are highly correlated with the degree of contamination in contaminated sites. For highly contaminated soil and groundwater environment, the microbial community structure will be destroyed by pollutants, and the diversity of microbial communities will decline significantly compared with natural soil (Goh et al., 1997; Fu, 2018). This study has shown that the composition and structure of the soil and groundwater with different pollution levels were significantly different. And no matter in the soil or the water environment, the higher the concentration of pollutants are, the lower the microbial community abundance is, which was consistent with the results of Fantroussi et al. (1999), Banerjee et al. (1997) and Teng et al. (2004). The site was heavily contaminated

http://www.aloki.hu ● ISSN 1589 1623 (Print) ● ISSN 1785 0037 (Online)
DOI: http://dx.doi.org/10.15666/aeer/1705_1253712549

with chlorinated hydrocarbons and the structural and functional diversity of the internal microbial population changed significantly. There are several reasons for this phenomenon. On the one hand, high concentrations of pollutants, such as chlorinated hydrocarbons, benzenes, heavy metals, etc., have poisoned and inhibited the physiological activities of microorganisms in the environment, resulting in changes in the community structure of microorganisms. Most of the sensitive microorganisms gradually died and the reproductive ability declined under the external high pollution environment, while other microorganisms with higher anti-pollution capabilities survived in the soil and groundwater. Eventually, the diversity of microbial in the environment declined. On the other hand, pollutants such as chlorinated hydrocarbons would gradually accumulate in microorganisms and some protozoa over time, which had a chronic toxic effect (Shi et al., 2010). Under the effect of bioaccumulation, the mortality rate of microorganisms and protozoa gradually increased and the reproduction rate gradually decreased, further causing changes in community structure and composition and aggravating the attenuation process of biodiversity.

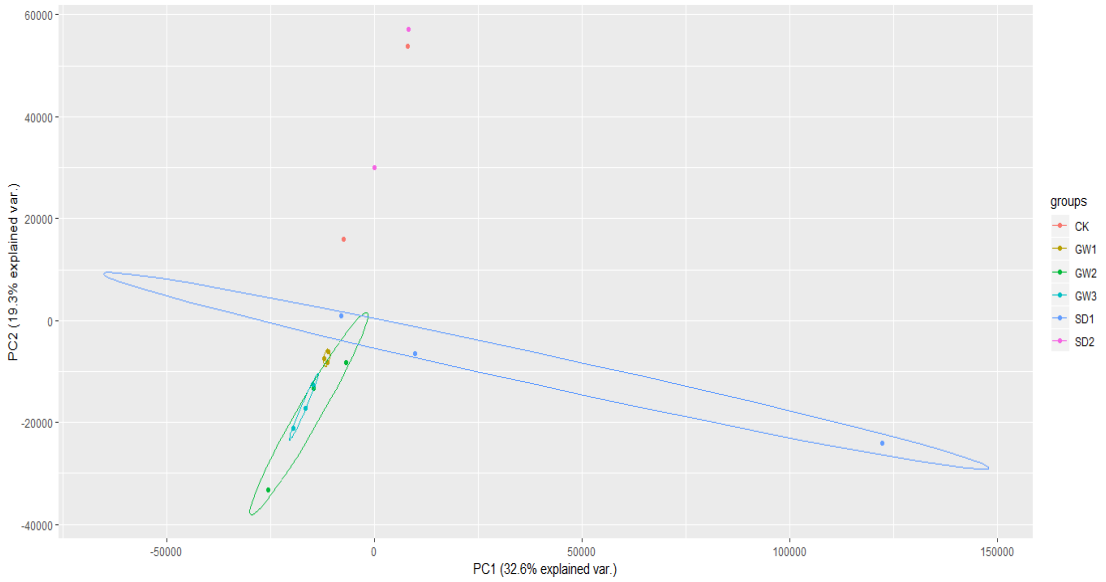

Figure 5. *OTU principal component analysis for the fungus abundance in the control group and different environmental media*

Besides, due to the residual effect of chlorinated hydrocarbon pollutants, there is a huge security threat to the sustainable development of human society and the balance of the natural environment. Through a large number of experimental studies, researchers and environmentalists at home and abroad have discovered that they can use the characteristics of microbial community structure and functional diversity to degrade chlorinated hydrocarbon organic pollution. As early as in the 1990s, Walter Reineke (Fritz et al., 1992) has studied the degradation of Pseudomonas to chlorobenzene and the toxicity of chlorobenzene to Pseudomonas. Shirley F (Nishino et al., 1987) reported that Pseudomonas putida could survive in soil and groundwater contaminated by chlorobenzene for a long time. This might be because that Pseudomonas was highly resistant to chlorobenzene toxicity, and they could use chlorobenzene as a carbon source for their own growth and reproduction, and absorb and degrade it to maintain their own

http://www.aloki.hu ● ISSN 1589 1623 (Print) ● ISSN 1785 0037 (Online)
DOI: http://dx.doi.org/10.15666/aeer/1705_1253712549

life activities (Song et al., 2007). In addition, Krausova et al. (2006) also found that a microbial community consisting of Acinetobacter and Pseudomonas can degrade methane in river water to more than 80% within six days. The experiment finds that the main types of anti-pollution bacteria in the groundwater were Brevunmdimonas, Pseudomonas and Rhizobium Frank. They were abundant in groundwater and could effectively degrade chlorinated hydrocarbon pollutants in water, which were consistent with the results of Walter Reineke (Fritz et al., 1992), Shirley F (Nishino et al., 1987), Krausova (2006) and Wright et al. (2017).

The existence of microorganisms is not only positive for remediation and limiting the expansion of pollution, but also the main influencing factor for determining the structure and functional diversity of microbial populations in contaminated sites. Under the original natural environmental conditions, the microbial community structure and functional diversity in soil and groundwater depend on the interaction between various microorganisms and the external environment. With the infiltration of external pollutants, the structure and diversity change. Some sensitive microorganisms tend to be inferior, and the remaining microorganisms with higher tolerance and ability to degrade external pollutants gradually take advantage, even by using pollutants as energy and nutrient sources to enhance the abundance of their communities. Wright et al. (2017) found that in the presence of methylene chloride and trichloroethylene, the relative abundance of Pseudomonas was significantly increased, and different levels of methylene chloride contamination in the site would cause different changes in microbial community structure. Taseli and Gokcay (2005) tested Penicillium's ability to degrade chlorinated compounds, and found it could remove not only the pentachlorophenol, but also the 2-chlorophenol and trichloroacetic acid, which all present great biodegrability. In addition to the bacteria, Fungus also show up their extraordinary ability in degrading chlorinated and polycyclic aromatic hydrocarbons, which even can be enhanced by oxidation (Marco-Urrea et al., 2015). The experimental analysis found that Penicillium was the dominant flora in the soil and had high abundance, while Phylum Firmicutes was a sensitive population, which was greatly affected by chlorinated hydrocarbon pollutants, and the result was consistent with the results of Carvalho M. B. et al. (2009). Additionally, the advantaged Fungi in the environment was Aspergillu, while Fusarium spp. was a more sensitive population.

But there also exist some limitations in this study. Through the high-throughput sequencing technology, we discovered the dominated and sensitive species in the chlorinated hydrocarbon contaminated site, which could provide some insights for assessment and remediation of organochlorine contaminated sites. However, limited by time and energy, more in-depth research is expected to be conducted on the selected species to explore its degradation mechanism and sensitivity threshold. In addition, the collection of samples from multiple regions can bring more general results and avoid the differences in community distribution levels caused by regional differences. In spite of that, this study still has its profound practical significance, and plays a connecting role in the future restoration of organochlorine contaminated sites.

Conclusion

The project analyzed the structural and functional diversity of microbial communities in chlorinated hydrocarbon contaminated sites, and selected microbial flora that could maintain its own advantages in the chlorinated hydrocarbon pollution environment and

http://www.aloki.hu ● ISSN 1589 1623 (Print) ● ISSN 1785 0037 (Online)
DOI: http://dx.doi.org/10.15666/aeer/1705_1253712549

have certain ability to degrade pollutants, which not only proved the analysis of the microbial indicators of the site can be used to assess the pollution degree and risk of the contaminated site, and provided a scientific and specific theoretical basis for the development and application of in situ bioremediation technology for chlorinated hydrocarbon contaminated sites. While in order to solid the results and make the conclusion taken into practice, further research will be necessary to select and cultivate microbial ability to degrade pollutants.

Acknowledgements. This work is supported by the Open Project of Jiangsu Key Laboratory of Environmental Engineering (ZX2016011), the Open Research Fund of Jiangsu Province Key Laboratory of Environmental Engineering (ZX2016012) and the Research project for environmental protection of Jiangsu Province (2017001). We thank Kai Sun at Southeast University for the constructive comments of this paper.

REFERENCES

[1] Banerjee, M. R., Burton, D. L., Depoe, S. (1997): Impact of sewage sludge application on soil biological characteristics. – Agriculture Ecosystems & Environment 66(3): 241-249.
[2] Carvalho, M. B., Martins, I., Leitão, M. C., Garcia, H., Rodrigues, C., Romão, V. S., McLellan, I., Hursthouse, A., Pereira, C. S. (2009): Screening pentachlorophenol degradation ability by environmental fungal strains belonging to the phyla Ascomycota and Zygomycota. – Journal of Industrial Microbiology and Biotechnology 36(10): 1249-1256.
[3] El Fantroussi, S., Verschuere, L., Verstraete, W., Top, E. M. (1999): Effect of phenylurea herbicides on soil microbial communities estimated by analysis of 16S rRNA gene fingerprints and community-level physiological profiles. – Applied and Environmental Microbiology 65(3): 982-8.
[4] Fritz, H., Reineke, W., Schmidt, E. (1992): Toxicity of chlorobenzene on Pseudomonas sp. strain RHO1, a chlorobenzene-degrading strain. – Biodegradation 2: 165-170.
[5] Fu, W. Y. (2018): Chemical Oxidation Remediation and Microbial Community Diversity Research of PAHs Contaminated Soil. – East China Normal University, Shanghai.
[6] Gao, H. P. (2014): Bioavailability Assessment and Biodegradation-Promoting Method for Persistent Organic Pollutants in Soil. – Dalian University of Technology, Liaoning.
[7] Goh, T. B., Banerjee, M. R. (1997): Vesicular arbuscular mycorrhizae -mediated uptake and translocation of P and Zn by wheat in calcareous soil. – Pedosphere 7: 317-324.
[8] Krausova, V. I., Robb, F. T., González, J. M. (2006): Biodegradation of dichloromethane in an estuarine environment. – Hydrobiologia 559: 77-83.
[9] Li, Y., Xu, X. X. (2019): Research progress of high-throughput sequencing technology. – China Medical Engineering 3: 32-37.
[10] Liang, J. G., Liu, P. C., Zhang, X. J. (2018): Impact of genetically modified crops on rhizosphere bacterial community structure based on 16S rDNA high-throughput sequencing. – Jiangsu Agricultural Science 46: 5-8.
[11] Luo, Q., Huang, B. L., Tang, Z. X., Lai, L. M., Wei, W., Zheng, Y. R. (2013): Carbon source utilization of microbes in saline soil of three vegetation types in Xinjiang, China. – Chinese Journal of Applied Environmental Biology 19: 96-104.
[12] Marco-Urrea, E., Garcia-Romera, I., Aranda, E. (2015): Potential of non-ligninolytic fungi in bioremediation of chlorinated and polycyclic aromatic hydrocarbons. – New Biotechnology. 32(6): 620-628.
[13] Nie, X. J. (2013): Preliminary Genomic Study of Two Non-Mondel Plants: Wheat (Triticum aesticum L) and Crofton Weed (Ageratina adenophora) through High-Throughput Sequencing Technology. – Northwest A&F University, Yangling.

http://www.aloki.hu ● ISSN 1589 1623 (Print) ● ISSN 1785 0037 (Online)
DOI: http://dx.doi.org/10.15666/aeer/1705_1253712549

[14] Nishino, S. F., Spain, J. C. (1987): Degradation of 1,4-dichlorobenzene by a Pseudomonas sp. – Applied and Environmental Microbiology 53: 1010-1019.
[15] Qiu, J., Hou, Y. L., Xu, L. L., Qian, Y, Ding, X. (2019): High-throughput sequencing analysis of rhizosphere soil bacteria diversity in different mulberry varieties. – Journal of Southern Agriculture 3: 585-592.
[16] Rosselli, R., Romoli, O., Vitulo, N., Vezzi, A., Campanaro, S., Pascale, F. D., Schiavon, R., Tiarca, M., Poletto, F., Concheri, G., Valle, G., Squartini, A. (2016): Direct 16S rRNA-seq from bacterial communities: a PCR-independent approach to simultaneously assess microbial diversity and functional activity potential of each taxon. – Scientific Reports 6: 32165.
[17] Shi, H. L., Su, Y., Xu, L., Wang, Y. (2018): The industry status and development trend of high-throughput sequencing. – Biotechnology 3: 6-12.
[18] Shi, Z., Zhang, D. W., Huang, X. P., Wang, F. (2010): Bioaccumulation of organochlorine pesticides in organisms and sediments in the western coastal waters of Guangdong province. – Journal of Tropical Oceanography 29: 114-119.
[19] Song, L., Wang, H., Jiang, J., Gao, J. S., Shi, H. C. (2007): Isolation, identification of 1,2,4-trichlorobenzene-degrading strain Pseudomonas nitroreducens J5-1 and cloning of chlorocatechol 1,2-dioxygenase gene. – Environmental Science 8: 1878-1881.
[20] Song, X., Lin, N., Yin, P. H. (2015): Contaminated site remediation industry in China: current state and future trends. – Soils 47: 1-7.
[21] Su, G. J., Huang, L. Y., Lu, H. J., Li, Q. Q. (2015): Preparation and application of nickel-cobalt-iron ternary composite nano-metal oxide: China, Research Center for Eco-Environmental Sciences. – Chinese Academy of Sciences, Beijing.
[22] Tan, L. L., Li, J. Z., Wu, H. X. (2017): Evaluation of soil and groundwater pollution in typical organic chemical plant. – Environment & Development 29: 68-69.
[23] Taseli, B. K., Gokcay, C. F. (2005): Degradation of chlorinated compounds by *Penicillium camemberti* in batch and up-flow column reactors. – Process Biochemistry 40(2): 917-923.
[24] Teng, Y., Huang, C. Y., Luo, Y. M., Long, J., Yao, H. Y. (2004): Microbial activities and functional diversity of community in soils polluted with Pb-Zn-Ag mine tailings. – Acta Pedologica Sinica 41(1): 113-119.
[25] Wang, H. P. (2018): Investigation and remediation of chlorinated hydrocarbon aromatics complex site. – China Resources Comprehensive Utilization 36: 141-142.
[26] Wright, J., Kirchner, V., Bernard, W., Ulrich, N., McLimans, C., Campa, M. F., Hazen, T., Macbeth, T., Marabello, D., McDermott, J., Mackelprang, R., Roth, K., Lamendella, R. (2017): Bacterial community dynamics in dichloromethane-contaminated groundwater undergoing natural attenuation. – Frontiers in Microbiology 8. DOI: 10.3389/fmicb.2017.02300.
[27] Wu, J. N., Liu, Y. X., Zhou, X., Wang, T. Y., Gao, Q., Gao, Y. H., Liu, S. X. (2018): Effects of long-term different fertilization on soil fungal communities in black soil based on the Illumina MiSeq platform. – Acta Microbiologica Sinica 58: 1658-1671.
[28] Zhang, X., Song, S. S., Huang, Y. P., Jia, Z. H., Huang, Y. Y., Song, C. (2018): Analysis of bacterial diversity in cultivated soils in middle and southern Hebei Province based on high-throughput sequencing. – North China Agricultural Journal 33: 196-203.

http://www.aloki.hu ● ISSN 1589 1623 (Print) ● ISSN 1785 0037 (Online)
DOI: http://dx.doi.org/10.15666/aeer/1705_1253712549

PREDICTION OF VEGETATION COVER INDEX ALONG HIGHWAYS IN HIGH-ALTITUDE AREAS USING MACHINE LEARNING

JIA, X. – LIU, F.* – WANG, D.

School of Highway, Chang'an University, Xi'an 710064, China
(e-mail: jiaxingli@chd.edu.cn, wangdang@179997689.com; phone: +86-134-6893-1646, +86-187-0090-7083)

**Corresponding author*
e-mail: liufabao@1950480311.com; phone: +86-183-0926-4289

(Received 16th May 2019; accepted 16th Jul 2019)

Abstract. The ecological environment in high-altitude areas are fragile. Improper highway construction or excessive vehicle emission may lead to irreparable damages to the natural environment in such areas. To ensure the sustainable development of the ecological environment in high-altitude areas, it is essential to evaluate the influence of highways construction and operation on the environment in such areas. In this article, using the normalized difference vegetation index (NDVI) to indicate environmental changes in the high-altitude areas road domain. Studying sections from Pengjiazhai Town to DaYagen, DaYagen to Dongxia Town and Dongxia Township to Riyue Tibetan Town along the National Highway G214, with the altitude ranging from 2620~3760 m. Four different machine learning methods including Extreme Learning Machine, Wavelet Neural Network, BP Neural Network and Cubic Smoothing Index are then applied to analyze the NDVI changes in study areas in order to build prediction models. The results of the MAE, WMAE, RMSE and R^2 value of the four different models show that the Wavelet Neural Network model works the best in predicting the NDVI in high-altitude areas. Based on this result, it is suggested that Wavelet Neural Network is more suitable for the intelligent prediction of road vegetation coverage in high-altitude areas.
Keywords: *normalized difference vegetation index (NDVI), prediction models; high-altitude highways, road land vegetation cover, machine learning*

Introduction

Due to the vulnerability and sensitivity of the ecological environment in high-altitude areas, it can be easily destroyed by engineering construction or other human activities compared to normal areas. Moreover, the ecological recovery ability of such areas is relatively weak and the recovery cycle is long. However, during the highways construction and operation process, the surrounding environment will be affected (Tu, 2016). For example, vehicle emission will cause the reduction of the surrounding vegetation coverage, which may further lead to soil degradation. In addition, the related indexes used to characterize the ecological environment of the highway domain are uncertain due to the particularity of the region and the data is usually classified. Therefore, it is essential to explore a certain algorithm that can be used to estimate and predict the environmental influence of highway on the surrounding environment in order to better reveal the environment change in road domain and to keep the sustainable development of the ecological environment in high-altitude areas. About vegetation indexes there are different kinds of vegetation indices that are commonly used, including Normalized Difference Vegetation Index (NDVI), ratio vegetation index, difference vegetation index, vertical vegetation index, environmental vegetation index and so on. Within which the NDVI is the most commonly used index in

http://www.aloki.hu ● ISSN 1589 1623 (Print) ● ISSN 1785 0037 (Online)
DOI: http://dx.doi.org/10.15666/aeer/1705_1255112571

vegetation research due to its advantages of detecting vegetation growth state, vegetation coverage and eliminating partial radiation errors. It is the best indicator of plant growth state and vegetation spatial distribution density, and can reflect the influence of plant canopy. Therefore, NDVI is selected to characterize the vegetation environment around the highway region in this study.

As for the research methods, five traditional prediction methods were used in previous research including empirical prediction method, trend extrapolation method, regression prediction method (Abutaqiya et al., 2019; Zhu et al., 2019), time series prediction method (Yang and Chen, 2019; Moews et al., 2019; Zhang et al., 2019), and gray prediction (Guo et al., 2019; Lin et al., 2018; Zhao and Zhou, 2018). The above five methods are more inclined to capture the data distribution characteristics through simple mathematical model. For instance, the regression prediction method and the gray theory fit more to the linear distributed data. Such prediction methods can not describe the characteristics of more complex nonlinear distributed data and can not reflect the accurate change of the dataset. On the other hand, with the continuous development of scientific information technology and the application of big data analysis, artificial intelligence prediction methods were used in environment-related research. For example, neural network (Chen, 2018; Leng et al., 2017), fuzzy logic (Xu et al., 2017) and multiple combination prediction methods (Mishra et al., 2015; Feng et al., 2015; Perez and Gramsch, 2016; Sun et al., 2013) were used to predict the concentration of PM2.5. In recent years, different machine learning models are introduced to predict wind, electricity, solar, coal and other resources. Cocchi et al. (2017) applied the time series analysis method, S-ARIMA, S-ARIMAX, extreme learning machine, support vector machine (SVR) and other methods in renewable energy market price bidding. It turned out that the accuracy of Support Vector Machines is superior to other methods. Liu et al. (2018) used wavelet decomposition, empirical mode decomposition and extreme learning machine methods to predict wind speed multi-step. Li et al. (2018) predicted energy consumption based on grey prediction theory and support vector machine that optimize through extreme learning machine. The results showed that the combination of SVR and ELM is more effective than single prediction method. Yi et al. (2019) applied the extreme learning machine to predict the growth of algae in the river. It was concluded that the ELM model had better prediction and generalization performance than the traditional BP neural network and adaptive neuro-fuzzy inference system. Fijani et al. (2019) employed a two-layer analysis method combined with a hybrid model formed by an extreme learning machine to monitor and predict the relevant quality parameters of water in the environment. By using the mixed model analysis, it was found that the results were more accurate than the single model in the prediction of results. Kisi et al. (2018) utilized the new wavelet combination model to establish a reference evaporation prediction model by comparing the wavelet extreme learning machine with the neural network. It was found that wavelet connection models usually had better precision than a single model, while WELM model was more suitable for predicting daily evaporation.

With the economic and infrastructure development in recent years, the demand for highway infrastructure in high-altitude areas is increasing. However, related research methods less attention were paid on the prediction of environmental indicators in highway regions. Considering the vulnerability and sensitivity of the ecological environment in high-altitude areas, it is important to explore the environmental influence of highway construction and operation in such areas. At the same time, it is

http://www.aloki.hu ● ISSN 1589 1623 (Print) ● ISSN 1785 0037 (Online)
DOI: http://dx.doi.org/10.15666/aeer/1705_1255112571

necessary to discuss which machine learning method can be applied to the road domain NDVI value in high-altitude areas. In addition to, the diversity and uncertainty of the factors affecting the road ecology asks for prediction models with higher ability and accuracy. Considering the characteristics of the discrete-distributed data, ELM, wavelet neural network, BP neural network and cubic smoothing index are considered to predict the NDVI along road domain. There methods are suitable for capturing the nonlinear characteristics and have good global learning ability. In this paper, spatial analysis of the NDVI along National Highway G214 were conducted using GIS. The extreme learning model, wavelet neural network, BP neural network and cubic smoothing index were applied to predict the vegetation index of high-altitude highway roads. This research explored the possibility of using machine learning method in exploring the ecological environmental impact of the road in the high-altitude areas. The results would help improve the sustainable development of the ecological environment in high-altitude areas.

Materials

In order to study and forecast the normalized difference vegetation index of highway in high-altitude region by using machine learning algorithm, G214 highway of Xi'ning City, Qinghai Province of China is selected for research and analysis. In this paper, we apply ArcGIS and ENVI tools to process and analyze the remote sensing image data in the research areas (101°20′~101°57′E; 36°55′~36°65′N). Remote sensing (RS) technology can quickly obtain the regional multi-factor surface information, and through combining the spatial analysis technology of GIS, can quickly get the required information for the target areas. On the satellite selection, the Landsat-8 satellite was chosen. The Landsat-8 satellite was launched on February 11, 2013 and is a follow-on satellite to the Landsat series of US terrestrial satellites. It is equipped with land imager (OLI) and thermal infrared sensor (TIRS). It has important applications in many fields, such as natural resource protection, energy exploration, environmental management, natural disaster monitoring and so on.

The starting point of the research data extraction is G214 Pengjiazhai Town, and the end point is the Riyue Tibetan Township. In order to reflect the particularity of the road environment indicators, the research range is divided into three sections, specifically Pengjiazhai Town~Dayagen; Dayagen~Dongxia Township; Dongxia Township~Riyue Tibetan Township, as shown in *Figure 1*.

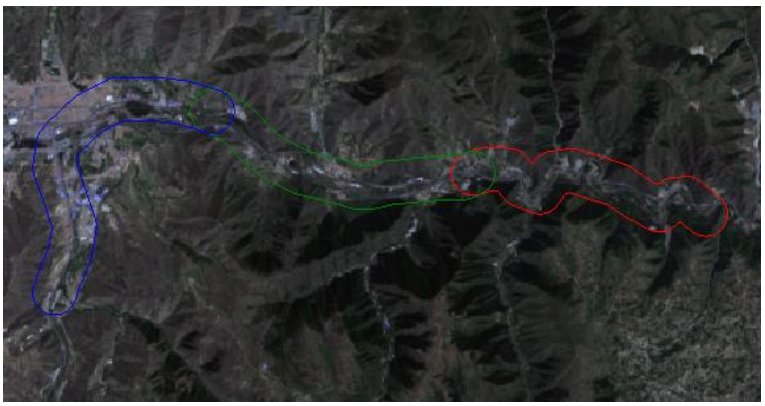

Figure 1. *Three sections of road research domain*

http://www.aloki.hu ● ISSN 1589 1623 (Print) ● ISSN 1785 0037 (Online)
DOI: http://dx.doi.org/10.15666/aeer/1705_1255112571

After the remote sensing image is processed by ArcGIS and ENVI, the image is clipped by ENVI. The main purpose is to eliminate unnecessary research areas. The range of the research road domain is 400 m on each side of the road of the G214 median line. The vector polygon of the study areas uses ArcGIS to analyze the spatial buffer of the road center line data, and the buffer radius is 400 m. Then the image clipping operation of ENVI software is used to obtain the image data of the research areas. The cropped remote sensing image is shown in *Figure 2*.

Figure 2. *The overall research domain obtained by clipping*

As for the research indicator of vegetation index, also known as spectral vegetation index, refers to the multi-spectral data obtained from remote sensing sensors, which are composed of linear and nonlinear combinations of various values that have certain indicative significance to vegetation (Wang, 2015). Because of the strong absorption of blue and red lights radiation by plant leaf tissue, but the strong reflection of near infrared radiation, the near infrared reflection increases with the increase of vegetation. Therefore, the linear or non-linear combination of red band and near infrared band is usually used to characterize the quantity distribution and quality of surface vegetation. This paper studies the vegetation coverage information by extracting NDVI to characterize the ecological environment in the G214 research areas.

As a remote sensing index reflecting the status of land cover vegetation, NDVI is defined as the quotient of the difference between the reflectivity of the near infrared band and the red band. The formula for calculating the difference between the reflectivity of the near infrared band and the red band is as follows:

$$NDVI = \frac{NIR - R}{NIR - R} = \frac{Band5 - Band4}{Band5 + Band4} \quad \text{(Eq.1)}$$

In the formula: Band4 and Band5 are the fourth (red) band luminance value and the fifth (near infrared) band luminance value of Landsat-8 remote sensing satellite OLI image, respectively. The calculation process is accomplished by ENVI remote sensing image processing software, and the NDVI is calculated by reflectivity image.

Specific Landsat-8 remote sensing satellite data selection from 2013~2018, according to the quarterly selection of one to two small cloud cover, small interference factors of Landsat8 remote sensing satellite map to establish a buffer radius of 400 m range of data extraction. The extracted data are shown in *Tables 1–3*.

http://www.aloki.hu ● ISSN 1589 1623 (Print) ● ISSN 1785 0037 (Online)
DOI: http://dx.doi.org/10.15666/aeer/1705_1255112571

Table 1. *Pengjiazhai Town ~ Dayagen NDVI data*

Pengjiazhai ~Dayagen	Jan	Feb	Apr.	June	Jul	Aug	Sep	Oct	Nov	Dec
2013	-	-	0.217734	0.579018	-	-	0.438763	-	-	0.117657
2014	-	0.099117	0.173993	-	-	0.491571	0.472169	0.350313	-	0.105011
2015	-	0.134264	0.134264	-	-	0.536533	-	0.326867	-	0.140341
2016	0.144673	0.184593	0.185297	-	-	0.53848	--	-	0.202526	-
2017	0.140669	-	0.19548	-	0.59262	-	-	-	0.147942	-
2018	0.137455	-	0.227371	-		-	-	-	-	-

Table 2. *Dayaegen ~ Dongxia Township NDVI data*

Dayaegen~ Dongxia Township	Jan	Feb	Apr.	June	Jul	Aug	Sep	Oct	Nov	Dec
2013	-	-	0.202384	0.511061	-	-	0.391358	-	-	0.114336
2014	-	0.096136	0.188883	-	-	0.353186	0.457984	0.351201	-	0.240173
2015	-	0.192425	0.200327	-	-	0.526266	-	0.343435	-	0.254257
2016	0.247882	0.306538	0.364527	-	-	0.557571	--	-	0.266581	-
2017	0.152848	-	0.365258	-	0.56718	-	-	-	0.208416	-
2018	0.184353	-	0.316285	-	-	-	-	-	-	-

Table 3. *Dongxia Township-Riyue Tibetan Township NDVI data*

Dongxia Township~ Riyue Tibetan Township	Jan	Feb	Apr	June	Jul	Aug	Sep	Oct	Nov	Dec
2013	-	-	0.22077	0.578396	-	-	0.444658	-	-	0.168276
2014	-	0.119978	0.218701	-	-	0.383716	0.538561	0.367532	-	0.240173
2015	-	0.192425	0.200327	-	-	0.567645	-	0.408466	-	0.254257
2016	0.247882	0.306538	0.364527	-	-	0.580294	-	-	0.271642	-
2017	0.152848	-	0.365258	-	0.566043	-	-	-	0.208416	-
2018	0.18822	-	0.316285	-	-	-	-	-	-	-

It can be known from the above tables that normalized difference vegetation index is extracted according to the range of road domain segments, and the results of NDVI extraction are limited to [-1,1], which avoids the inconvenience caused by too large or too small data. The negative value indicates that the surface cover is cloud, water, snow and so on, reflecting the height of visible light; zero means there are rocks or bare soil, Band4 and Band5 are approximately equal; positive value indicates vegetation cover, which increases with the increase of coverage. In general, there is a strong positive correlation between vegetation index and vegetation coverage. The higher the positive value of NDVI, the higher the vegetation coverage rate is, and the better the corresponding ecological background environmental quality is. In this study, taking the remote sensing satellite map of June in the second quarter of 2013 as an example, NDVI data extracted from ArcGIS are used to show the results of the data. Just showing in *Figure 3* of (a) is Pengjiazhai Town to Dayagen; (b) is Dayagen to Dongxia Township; (c) is Dongxia Township to Riyue Tibetan Township.

http://www.aloki.hu ● ISSN 1589 1623 (Print) ● ISSN 1785 0037 (Online)
DOI: http://dx.doi.org/10.15666/aeer/1705_1255112571

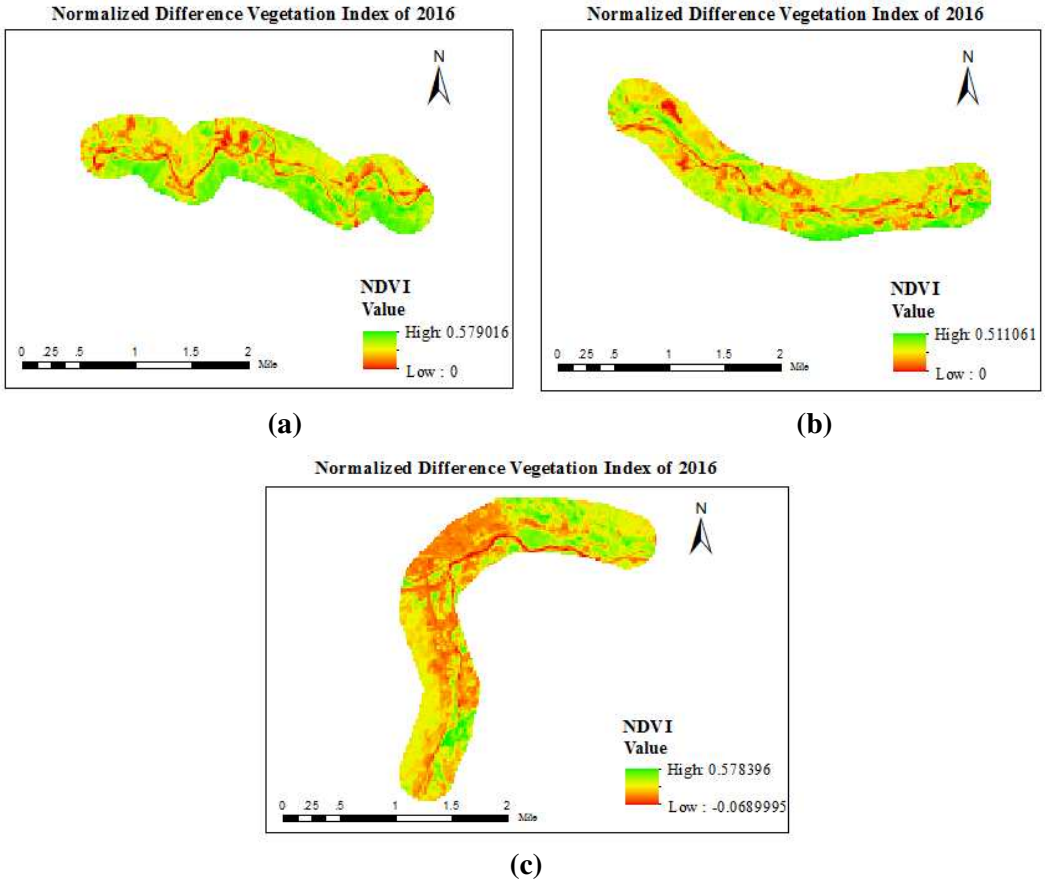

Figure 3. *(a) is NDVI value of Pengjiazhai Town to Dayagen; (b) is Dayagen to Dongxia Township; (c) is Dongxia Township to Riyue Tibetan Township*

Four types of methods

ELM

ELM is a new training algorithm for single hidden layer feed forward networks, (SLFNs) (Huang et al., 2006). Before the training begins, ELM algorithm selects the excitation function of hidden layer, and randomly selects the number of hidden layer nodes in the network, and inputs the weights. Let N different random data sample data are $G=\{(x_1,t_1),(x_2,t_2),\cdots,(x_N,t_N)\}$, $x_i=[x_{i1},x_{i2},\cdots,x_{in}]\in R^n$, $t_i=[t_{i1},t_{i2},\cdots,t_{in}]\in R^m$, $i=1,2,\cdots,N$. Single hidden layer number is L, and the excitation function $g(x)$ that standard SLFNs model just show as:

$$\sum_{i=1}^{L}\beta_i g_i(x_j)=\sum_{i=1}^{L}\beta_i g(a_i\bullet x_j+b_i)=t_j,\ j=1,2,\cdots,\ \mathrm{n} \qquad \text{(Eq.2)}$$

In the formula: $a_i=[a_{i1},a_{i2},\cdots,a_{in}]^T$ is the input weight vector that connects the node of the i hidden layer; b_i is the bias for i hidden layer nodes; $\beta_i=[\beta_{i1},\beta_{i2},\cdots,\beta_m]^T$ is an output weight vector connecting i hidden layer nodes; $a_i\bullet x_j$ represent the inner product of a_i and x_j. $g(x)$ contains L hidden layer nodes. Its standard SLFNs can approach L

http://www.aloki.hu ● ISSN 1589 1623 (Print) ● ISSN 1785 0037 (Online)
DOI: http://dx.doi.org/10.15666/aeer/1705_1255112571

training sample data infinitely, and there exists β, a_i and x_j can make it possible to build a formula like this.

Then we can set up the following extreme learning machines:

$$\sum_{i=1}^{L}\beta_i g\left(\alpha_i \bullet x_j + b_i\right) = t_j,\ j = 1,2,\cdots,\ \mathrm{n} \tag{Eq.3}$$

The above formula is transformed to form the following matrix:

$$H\beta = T \tag{Eq.4}$$

H is the hidden layer output matrix of the definite matrix network, Column i representation and input $x_1, x_2, \cdots, x_N$ as the output vector of the associated i hidden layer node, Line j represents the implicit layer output vector associated with the input.

In the formula:

$$H\left(\alpha_1,\alpha_2,\cdots,\alpha_l,b_1,b_2,\cdots,b_L,x_1,x_2,\cdots,x_N\right) = \begin{matrix} g\left(\alpha_1 - x_1 + b_1\right) & g\left(\alpha_2 - x_1 + b_2\right)\cdots g\left(\alpha_L - x_1 + b_L\right) \\ g\left(\alpha_1 - x_2 + b_1\right) & g\left(\alpha_2 - x_2 + b_2\right)\cdots g\left(\alpha_L - x_2 + b_L\right) \\ \vdots & \\ g\left(\alpha_1 \quad x_N + b_1\right) & g\left(\alpha_2 \quad x_2 + b_2\right)\cdots g\left(\alpha_L \quad x_N + b_L\right)_{N\times L} \end{matrix} \quad \beta = \begin{matrix} \beta_1^T \\ \beta_2^T \\ \vdots \\ \beta_L^T{}_{L\times m}; \end{matrix} \quad T = \begin{matrix} t_1^T \\ t_2^T \\ \vdots \\ t_L^T{}_{L\times m} \end{matrix} \tag{Eq.5}$$

Training SLFNs is equivalent to finding out least square solution of β for the $H\beta = T$ just like this: $\beta = \min_{\beta}\left\|T(a_1,\cdots,a_N,b_1,\cdots,b_N)\beta - T\right\|$.

And the Moore-Penrose generalized inverse matrix of the hidden layer output matrix H^+ can be expressed as follows: $H^+\beta = T$.

The solution is used as the weight parameter on the right side of the network. Overcoming the traditional artificial neural network prediction network prediction model some disadvantages such as the training time is long, and it is easy to produce over-fitting. The method mainly includes input layer, hidden layer and output layer, so when we are doing algorithmic calculations, it only needs to determine the number of neurons in the hidden layer to carry out the next operation, which overcomes the difficulty of determining multiple computational parameters and the complicated programming process of the traditional neural network system.

3.2. Wavelet neural network

Wavelet neural network (WNN) is a new type of neural network based on wavelet theory (Nian et al., 2001), which replaces the usual linear or nonlinear excitation function with wavelet basis which can scale and translate. The time-frequency local characteristic of wavelet transform is combined with the self-learning of neural network. Compared with the standard neural network, the structure of wavelet transform is simpler, the convergence is faster, and the blindness is effectively avoided.

In WNN, the number of input layer nodes, hidden layer wavelet elements and output layer nodes are M; J; N; respectively. The expansion coefficient of the j-th wavelet

http://www.aloki.hu ● ISSN 1589 1623 (Print) ● ISSN 1785 0037 (Online)
DOI: http://dx.doi.org/10.15666/aeer/1705_1255112571

element in the wavelet layer is a_j, translation coefficient is b_j, The weights of the m neurons in the input layer to the j wavelet elements in the hidden layer are ω_{mj}. The connection weights of the j-th wavelet element to the n-th output neuron is ω_{jn}. Output layer n-th node ideal output value is y_n^*. The wavelet layer uses non-orthogonal Morlet wavelet functions. The classical Tansig function is used in the output layer. WNN is a compact combination of wavelet analysis and BP neural network. Based on the structure of BP neural network, wavelet basis function is used to replace the traditional Sigmoid function as the transfer function of neuron nodes.

The input of the j-th wavelet element of the hidden layer is:

$$r_j = \sum_{m=1}^{M} \omega_{mj} X_m \quad \text{(Eq.6)}$$

The output of the j-th wavelet element is as follows:

$$c_j = \psi_{a_j,b_j}(r_j) = \cos(1.75\frac{r_j - b_j}{a_j}) \bullet \exp(-0.5(\frac{r_j - b_j}{a_j})^2) \quad \text{(Eq.7)}$$

The output layer's n-th node outputs as follows:

$$y_i = 1/(1+\exp(-\sum_{n=1}^{N} \omega_{jn} c_j)) \quad \text{(Eq.8)}$$

The network output error function is:

$$E = \frac{1}{N} \sum_{n=1}^{N} (y_n^* - y_n)^2 \quad \text{(Eq.9)}$$

The training of WNN is mainly aimed at ω_{mj}, a_j, b_j, ω_{jn} to optimized and selected. WNN has the advantage of faster convergence than the forward neural network. Firstly, the basic elements and the whole structure of the WNN are determined according to the wavelet analysis theory, which can avoid the blindness in the design of the structure such as BP neural network. Secondly, WNN has stronger learning ability and higher precision.

BP neural network

BP neural network is a multi-layer feedforward neural network trained according to the error reverse propagation algorithm. It was proposed by scientists led by Rumelhart and Mc Clelland in 1986 (Rumelhart et al., 1986). As one of the widely used prediction models, BP neural network is also called back propagation neural network. Its main model structure is composed of input layer, hidden layer and output layer. The number of hidden layers can be adjusted according to the actual needs. One or more layers can be used to realize all connections between the neurons between the adjacent upper and

http://www.aloki.hu ● ISSN 1589 1623 (Print) ● ISSN 1785 0037 (Online)
DOI: http://dx.doi.org/10.15666/aeer/1705_1255112571

lower layers, but there is no connection between the neurons in each layer. The BP neural network has better description ability for complex nonlinear problems, that is, good nonlinear mapping ability, function approximation ability and fault tolerance.

Cubic smoothing exponential model

Exponential smoothing method is proposed by Brown (2013). Brown thinks that the situation of time series is stable or regular, so the time series can be postponed reasonably. He believes that the recent past situation, to a certain extent, will continue into the future, thus putting a greater weight on the recent data. In the calculation of exponential smoothing method, the key is the value of α, but the value of α is easy to be subject to subjective influence, so how to reasonably determine the value of α is very important. Generally speaking, if the data fluctuates greatly, the value of α should be larger. It can increase the impact of recent data on the prediction results. If the data fluctuates steadily, the α value should be smaller. When the time series fluctuates, but the long-term trend changes little, we can choose a slightly larger α value, which is usually between 0.1~0.4. When the time series fluctuates greatly, the long-term trend changes greatly. In order to make the prediction model more sensitive and keep up with the change of data, it is advisable to choose a larger α value when the trend is obvious and rapid rise or fall, for example, the value can be chosen between 0.6~0.8, so as to make the prediction model more sensitive and able to keep up with the change of the data. The trial algorithm is usually used to determine the α value in the model. First of all, according to the specific time series analysis, referring to the empirical judgment method, to roughly determine the rated value range, and then take different α value for trial calculation, compare the prediction standard error under different α value. The minimum error α of prediction standard is chosen as the reasonable smoothing coefficient of the model. The basic formula for calculating the smoothing index is as follows.

$$Y_{t+1} = X_t + (1-\alpha)Y_t \tag{Eq.10}$$

In the formula, X_t is the actual value of period t, Y_t is the predicted value of phase t; α is an exponential smoothing coefficient.

The formula for calculating the cubic smoothing index is:

$$S_t^{(1)} = \alpha X_t + (1-\alpha)S_{t\ 1}^{(1)} \tag{Eq.11}$$

$$S_t^{(2)} = \alpha S_1^{(1)} + (1-\alpha)S_{t\ 1}^{(2)} \tag{Eq.12}$$

$$S_t^{(3)} = \alpha S_1^{(2)} + (1-\alpha)S_{t\ 1}^{(3)} \tag{Eq.13}$$

$$a_t = 3S_t^{(1)} - 3S_t^{(2)} + 3S_t^{(3)} \tag{Eq.14}$$

$$b_t = \frac{\alpha}{2(1-\alpha)^2}[(6-5\alpha)S_t^{(1)} - 2(5-4\alpha)S_t^{(2)} + (4-3\alpha)S_t^{(3)}] \tag{Eq.15}$$

http://www.aloki.hu ● ISSN 1589 1623 (Print) ● ISSN 1785 0037 (Online)
DOI: http://dx.doi.org/10.15666/aeer/1705_1255112571

$$c_t = \frac{\alpha}{2(1-\alpha)^2}(S_t^{(1)} - 2S_t^{(2)} + S_t^{(3)}) \quad \text{(Eq.16)}$$

When the forecast period is T year and the base year is the t year. The prediction model of Y_{T+t} cubic exponential smoothing method is as follows:

$$Y_{t+T} = a_t + b_t T + c_t T^2 \quad \text{(Eq.17)}$$

In the formula $S_t^{(1)}$ is the single exponential smoothing value; $S_t^{(2)}$ is the quadratic exponential smoothing value; $S_t^{(3)}$ is the cubic exponential smoothing values, a_t, b_t, c_t are the smoothing factor. The cubic smoothing index prediction model, it has the advantage of requiring a small amount of data to predict the desired results, and its main theoretical basis is a kind of time developed on the basis of moving average method. The method of inter-sequence analysis and prediction is compatible with the whole average and moving average without abandoning the data of the past.

Optimum architecture of model

(1) ELM model

Considering the output of ELM is influenced by weight and matrix, the prediction results are fluctuating. In order to make the prediction result more accurate, it is necessary to determine the optimal number of hidden layer nodes and neurons. Therefore, the normal mean square error (NMSE) is used as the criterion to select the optimal number of nodes and the number of neurons. When the smaller the value of NMSE, the higher the prediction accuracy of the model. Therefore, the ELM model need to determine number of neurons and input nodes to construct model. By repeated tests the trail number of neurons and the number of input nodes were 5; 10; 15; 20; 25; 30 and 2; 3; 4; 5; 6; 7; 8, respectively. The NMSE values of the output results of each experiment are calculated to compare the parameters, so as to obtain the most suitable number of neurons and input nodes. Its mathematical expression is:

$$NMSE = \frac{\sum_1^N (p_j - \hat{p}_j)^2}{\sum_1^N (p_j - p_j)^2} \quad \text{(Eq.18)}$$

In the formula, the $\hat{p}_j$ represents predictive NDVI value; the p_j represents the actual NDVI value; N for valid number $j = 1,2,\cdots N$.

According to *Table 4,* when the number of neurons is 25 and the number of input nodes is 6, the NMSE value can reach the minimum, which indicates that the prediction precision of ELM model is the best.

(2) WNN model

In the process of WNN training, the number of hidden layers and the number of iterations are mainly constructed. The standard variance is used as the evaluation index

http://www.aloki.hu ● ISSN 1589 1623 (Print) ● ISSN 1785 0037 (Online)
DOI: http://dx.doi.org/10.15666/aeer/1705_1255112571

to determine the number of the best hidden layers and the number of iterations, and the predicted value is compared with the actual standard variance. When the error between the two is the smallest, the prediction model is the best. The number of neurons used in this paper by the actual tests chose 5; 10; 15; 20; 25; 30, and the number of iterations is 10; 30; 50; 70; 90 just showing in *Table 5*.

Through the experiments showing in *Table 5*, we can see that when the number of neurons is 10 and the number of iterations is 50, the WNN can achieve the best prediction effect.

Table 4. *ELM experiment*

Trail	Cell	Input	NMSE	Trail	Cell	Input	NMSE
1	5	2	0.6613	22	20	5	0.4937
2	10	2	0.7067	23	25	5	0.6473
3	15	2	0.7528	24	30	5	0.6346
4	20	2	0.7476	25	5	6	0.5766
5	25	2	0.7759	26	10	6	0.8067
6	30	2	0.9280	27	15	6	0.3656
7	5	3	0.7740	28	20	6	0.3592
8	10	3	0.7723	29	25	6	0.3077
9	15	3	0.6767	30	30	6	0.1720
10	20	3	0.6107	31	5	7	1.0726
11	25	3	0.8229	32	10	7	0.5019
12	30	3	0.4532	33	15	7	0.5276
13	5	4	0.9184	34	20	7	0.4566
14	10	4	0.7812	35	25	7	0.486
15	15	4	0.5598	36	30	7	0.3515
16	20	4	0.7221	37	5	8	0.7423
17	25	4	1.0046	38	10	8	0.4724
18	30	4	1.3483	39	15	8	0.5642
19	5	5	0.9524	40	20	8	0.5394
20	10	5	0.5766	41	25	8	0.4017
21	15	5	0.6338	42	30	8	0.7695

(3) BP neural network

In the research process of this paper, when the double hidden layers algorithm model is constructed, the key parameters of the model need to determine the learning rate parameters, the number of training times, and the number of neurons in the double hidden layer. By repeating the test when the test parameters of learning rate parameter is set to 0.005, the precision requirement is set to 0.01, and the training times are 1000 meet the accuracy requirements. According to the characteristics of the neural network, the data type of this study belongs to the single-layer input and output type. Respectively, the input layer and output layer set to 1. In the experiment, when the double hidden layer numbers are set to 50 and 1 shown in *Figure 4,* the MSE value and the variance value shown in *Figure 5* are obtained, which meets the requirements of the test.

http://www.aloki.hu ● ISSN 1589 1623 (Print) ● ISSN 1785 0037 (Online)
DOI: http://dx.doi.org/10.15666/aeer/1705_1255112571

Table 5. *WNN experiment*

Trail	Cell	Iterations	R^2	Trail	Cell	Iterations	R^2
1	5	10	0.08028	19	5	70	0.1521
2	10	10	0.1669	20	10	70	0.1551
3	15	10	0.1648	21	15	70	0.1666
4	20	10	0.1631	22	20	70	0.1553
5	25	10	0.1599	23	25	70	0.1561
6	30	10	0.2094	24	30	70	0.1693
7	5	30	0.1455	25	5	90	0.1321
8	10	30	0.1431	26	10	90	0.1605
9	15	30	0.1562	27	15	90	0.1578
10	20	30	0.1649	28	20	90	0.1731
11	25	30	0.1627	29	25	90	0.1664
12	30	30	0.154	30	30	90	0.1621
13	5	50	0.1338	31	5	110	0.1596
14	10	50	0.156	32	10	110	0.152
15	15	50	0.1579	33	15	110	0.1564
16	20	50	0.1529	34	20	110	0.1577
17	25	50	0.1519	35	25	110	0.1541
18	30	50	0.1524	36	30	110	0.1671

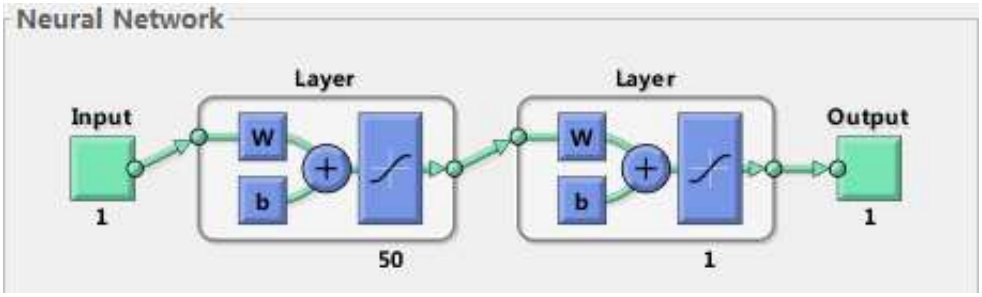

Figure 4. *Double implicit layers parameter*

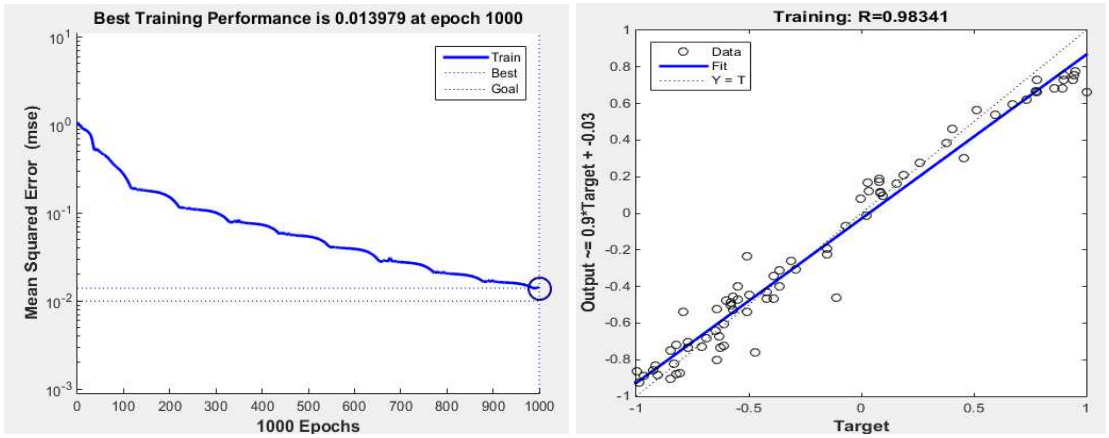

(a) **(b)**

Figure 5. *Training result diagram*

http://www.aloki.hu ● ISSN 1589 1623 (Print) ● ISSN 1785 0037 (Online)
DOI: http://dx.doi.org/10.15666/aeer/1705_1255112571

(4) Cubic smoothing exponential model

In this paper, after the construction of the cubic smoothing index algorithm, the results of the model can be obtained by determining the smoothing index of α. The extracted data show that the road domain NDVI values are fluctuating and the range of fluctuation is not very large. According to the characteristics of the algorithm, when the data series fluctuates, but the long-term trend changes little, we can choose a slightly larger α value, which is usually between 0.1~0.4. Therefore, the smoothing coefficients α are 0.05, 0.1, 0.15, 0.2, 0.25, 0.3, 0.35, 0.4, 0.45, 0.5, respectively, and the corresponding NMSE values are calculated. The details are shown in *Table 6*.

When the smoothing coefficient α is 0.35, the NMSE is 0.1597723, and the corresponding NMSE is larger when the smoothing coefficient is small or the smoothing coefficient is larger. Therefore, 0.35 is chosen as the best smoothing coefficient of the model.

Table 6. *Cubic smoothing index experiment*

Trail	α	NMSE
1	0.05	0.866579159
2	0.1	0.688243365
3	0.15	0.523380124
4	0.2	0.379448459
5	0.25	0.263479288
6	0.3	0.18579078
7	0.35	0.159723238
8	0.4	0.199460299
9	0.45	0.318450584
10	0.5	0.52758426

Application results of model

The optimal prediction models are obtained after the correlation parameters are determined by the above four kinds of prediction models. There are different indicators used to evaluate the prediction effect of the models, the MAE; WMAE; RMSE and R^2 (Goodness of Fit) of the test values and the real values are compared and analyzed to evaluate the prediction effect (Sun et al., 2013; Feng et al., 2015; Li et al., 2018; Yi et al., 2018).

MAE: it is defined as the average error of road domain NDVI prediction, and a smaller MAE value indicates that the prediction is more accurate. Its expression is as follows.

$$MAE = \frac{\sum_{1}^{N} \left| \hat{p}_j - p_j \right|}{N} \quad \text{(Eq.19)}$$

WMAE: it is the average relative error of road domain prediction, and the smaller average relative error represents more accurate prediction. Its expression is shown below.

http://www.aloki.hu ● ISSN 1589 1623 (Print) ● ISSN 1785 0037 (Online)
DOI: http://dx.doi.org/10.15666/aeer/1705_1255112571

$$WMAE = \frac{\sum_{1}^{N}\left|\hat{p}_j - p_j\right|}{\sum_{1}^{N} p_j} \quad \text{(Eq.20)}$$

RMSE: indicates the fluctuation range between the predicted values and the true values error. The smaller RMSE error indicates that the model is more suitable for this kind of prediction. Its expression is shown below.

$$RMSE = \sqrt{\frac{\sum_{1}^{N}\left|\hat{p}_j - p_j\right|^2}{N}} \quad \text{(Eq.21)}$$

R^2 (Goodness of Fit): it is for the predicted value of road field, it is shown that the predicted values are in good agreement with the actual situation, and the expression is as follows.

$$R^2 = \frac{SSR}{SST} = \frac{\sum_{1}^{N}\left|\hat{p}_j - p_j\right|^2}{\sum_{1}^{N}\left|p_j - p_j\right|} \quad \text{(Eq.22)}$$

Above the formula: $\hat{p}_j$ represents predictive NDVI values; p_j represents the actual NDVI values; p_j represents the average of the actual values, N for valid number $j = 1,2,\cdots N$.

Results

In this paper, the predicted and actual values of four machine learning models, such as ELM, WNN, double hidden layers BP neural network and cubic smoothing index, are programmed by MATLAB software. Using the above-mentioned extracted Pengjiazhai Town~Dayagen, Dayyagen~Dongxia Township, a total of 52 sets of data for machine learning training, another road Dongxia Township~Riyue Tibetan Township a total of 26 sets of data for prediction simulation test of the effect. Through training the output predictive values were outputted and compared with that of the real values, then the MAE; WMAE; RMSE; R^2 are calculated and analyzed respectively. In addition, the analysis compares the prediction effects of the four machine models and which model is more suitable for the prediction of the normalized difference vegetation index at high-altitude.

(1) Analysis of the results of ELM

After determining the optimal numbers of neurons in the ELM and the input nodes, apply the MAE, WMAE, RMSE; R^2 shown above and four indexes are used to describe the prediction effect of it. The comparison and analysis of the actual values and the

http://www.aloki.hu ● ISSN 1589 1623 (Print) ● ISSN 1785 0037 (Online)
DOI: http://dx.doi.org/10.15666/aeer/1705_1255112571

predicted values are shown in *Figure 6,* and the concrete values of the calculation results are shown in *Table 7*.

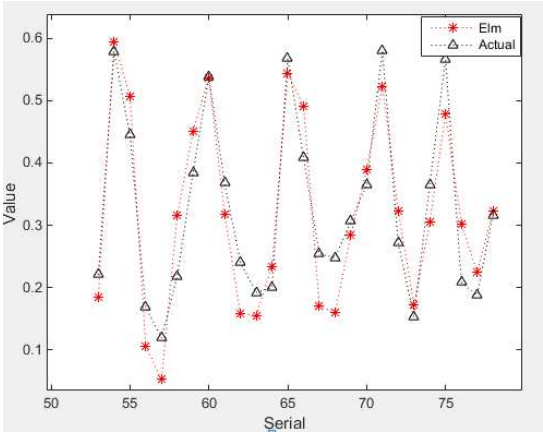

Figure 6. *Numerical comparison diagram of ELM prediction*

Table 7. *ELM specific indicator numerical table*

Cell	Input	MAE	WMAE	RMSE	R^2
30	6	0.05196807	0.159489669	0.001743194	0.809441907

(2) Analysis of the result of WNN

After determining the optimal number of neurons and the number of iterations, the WNN uses two sets of data to learn it. At the same time, in order to prevent the data overfitting, the minimum error is set to 10^{-3}. The prediction effect of WNN is compared as shown in *Figure 7,* and the calculation results are shown in *Table 8*.

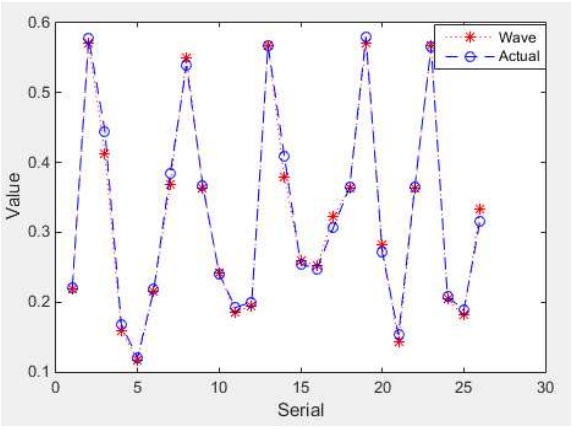

Figure 7. *Numerical comparison diagram of wavelet neural network prediction*

Table 8. *Numerical table of specific indexes of WNN*

Cell	Iterations	MAE	WMAE	RMSE	R^2
10	50	0.010790846	0.033117032	0.000139242	0.844069851

http://www.aloki.hu ● ISSN 1589 1623 (Print) ● ISSN 1785 0037 (Online)
DOI: http://dx.doi.org/10.15666/aeer/1705_1255112571

(3) Analysis of the results of BP neural network

Through the data training in the above process, the BP neural network determines the number of cycles and the hidden layer, and gets the comparison of the prediction effect of it as shown in *Figure 8,* and the concrete value of the calculation result is shown in *Table 9*.

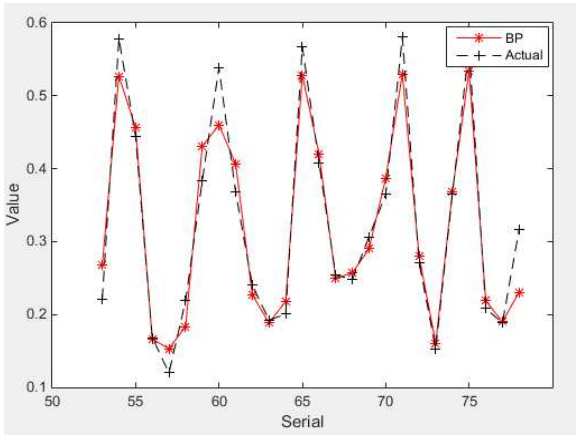

Figure 8. *Numerical comparison diagram of BP neural network prediction*

Table 9. *Numerical table of specific indexes of BP neural network*

The first cell	The second cell	Iterations	MAE	WMAE	RMSE	R^2
50	1	1000	0.0332575	0.108618413	0.001927419	0.8728

(4) Cubic smoothing index

It is known that the prediction effect can reach the best when the smoothing coefficient $\alpha = 0.35$ of the cubic smoothing index, so the corresponding index between the predicted value and the actual value can be calculated. The prediction effects of it compared as shown in *Figure 9*, and the calculated results are shown in *Table 10*.

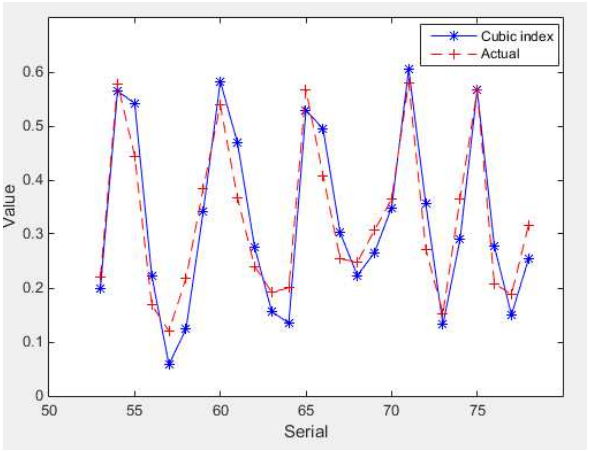

Figure 9. *Numerical comparison diagram of cubic smoothing index prediction*

http://www.aloki.hu ● ISSN 1589 1623 (Print) ● ISSN 1785 0037 (Online)
DOI: http://dx.doi.org/10.15666/aeer/1705_1255112571

Table 10. *Numerical table of specific indexes of cubic smoothing index*

α	MAE	WMAE	RMSE	R^2
0.35	0.045676	0.149187191	0.00139507	0.79231912

When evaluating the prediction quality and applicability of machine learning models, the MAE, WMAE, RMSE, and R^2 calculated above are usually employed. MAE and WMAE are utilized as the average error and the average relative error of the predicted value. The smaller the value, the higher the accuracy of the prediction. As the root mean square error of the predicted value, RMSE can reflect the fluctuation range between the predicted value and the actual value, and the smaller the value, the more suitable this kind of machine learning model is for this kind of research. R^2 can reflect the agreement between the predicted value and the real value in the overall effect, and the larger the value, the better fit the prediction of the whole range. The results of the four indexes are shown in *Table 11,* and the comparison between the true values and the predicted values of the four models are shown in *Figure 10*, the concrete values of the prediction results of the four models are shown in *Table 12*.

Discussion

Compared with the other three models, the MAE predicted by the ELM with a single hidden layer is the largest. The comparison from *Table 11* and the line chart shows that the average error of the model is 79.24% higher than that of the WMAE model. It is 36.0% higher than the BP neural network model and 12.11% higher than the cubic smoothing index model. In general, the superiority of ELM has been demonstrate in the previous literatures (Liu et al., 2018; Yi et al., 2018; Fijani et al., 2019) The comparison and analysis show that the average error of WNN is relatively small, which indicates that the accuracy of WNN is better. As for the mean relative error (WMAE) of the WNN, it is 79.24% higher than that of the ELM model, 69.51% higher than BP neural network, and 77.80% higher than cubic smoothing index. Compared with the WNN, the RMSE value of the ELM model and BP neural network model are significantly larger than it. The fluctuation range effect of WNN is 92.21% higher than that of ELM model, 92.78% higher than that of BP neural network, and 90.02% higher than cubic smoothing index. This shows that the fluctuation range between the predicted value and the actual value of the WNN is small, and there is no sudden change of the predicted value compared with the other three models, from the predicted comparison chart of the broken line fully proves it. According to some researches using wavelet transform to predict the results is more accurate (Feng et al., 2015; Kisi et al., 2018). In terms of the fit of the prediction effect, extreme learning machine's R^2 reaches 0.809441907; BP neural network is 0.8728, WNN is 0.844069851; the cubic smoothing index is 0.79231912, and the overall fit effect of the BP neural network is 7.26% higher than that of the ELM model, 3.29% higher than the WNN, and 9.22% higher than the cubic smoothing index. Although overall fit of BP neural network is superior to that of the other three types, the improvement effect is not very obvious, which shows that the four kinds of models all have better prediction results in terms of predicted fit degree.

http://www.aloki.hu ● ISSN 1589 1623 (Print) ● ISSN 1785 0037 (Online)
DOI: http://dx.doi.org/10.15666/aeer/1705_1255112571

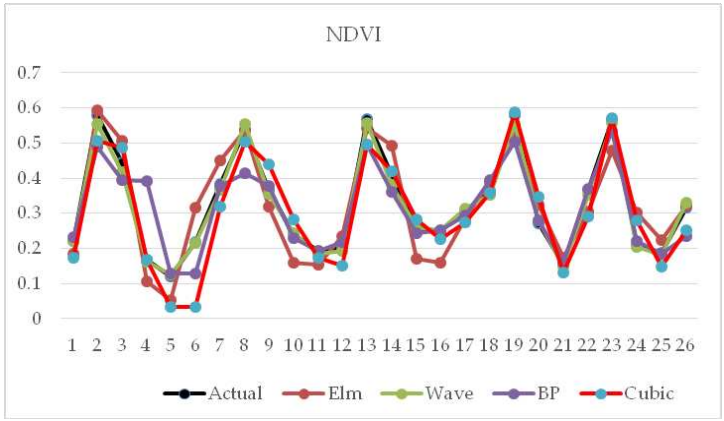

Figure 10. *Comparison chart between predicted values and actual values*

Table 11. *Comparison of four models for predicting effect indexes*

	ELM		**Wavelet neural network**		**BP neural network**		**Cubic smoothing index**
	Cell = 25	**Input = 6**	**Cell = 10**	**Iterations = 50**	**Cell (50, 1)**	**Iterations = 1000**	**α = 0.35**
MAE	0.051968077		0.010790846		0.0332575		0.045676
WMAE	0.159489669		0.033117032		0.108618413		0.1491872
RMSE	0.001743194		0.000139242		0.001927419		0.0013951
R^2	0.809441907		0.844069851		0.8728		0.7923191

Table 12. *Four models of predicting values*

Actual	0.22077	0.578396	0.444658	0.168276	0.119978	0.218701	0.383716	0.538561	0.367532	0.240173	0.192425	0.200327	0.567645	0.408466	0.254257	0.247882	0.306538	0.364527	0.580294	0.271642	0.152848	0.365258	0.566043	0.208416	0.18822	0.316285
Elm	0.1847	0.5942	0.5071	0.1066	0.05276	0.3151	0.4514	0.537	0.3182	0.1587	0.1549	0.2342	0.5427	0.4916	0.1707	0.1597	0.2843	0.3899	0.5228	0.3234	0.1719	0.3049	0.478	0.3026	0.2242	0.3221
Wave	0.2208	0.5545	0.418	0.1607	0.1264	0.216	0.3658	0.5542	0.3551	0.2424	0.1853	0.1942	0.5567	0.381	0.2595	0.2518	0.3137	0.3533	0.5541	0.2796	0.1474	0.3537	0.557	0.2036	0.1807	0.3296
BP	0.2307	0.4896	0.3949	0.3914	0.1278	0.1293	0.3789	0.4138	0.379	0.2285	0.1917	0.2178	0.4953	0.3613	0.2445	0.2528	0.2928	0.3952	0.5034	0.2792	0.1601	0.3692	0.5334	0.2201	0.1858	0.2336
Cubic	0.1733	0.5063	0.4862	0.1666	0.0344	0.0344	0.3187	0.5047	0.4405	0.2826	0.1721	0.1495	0.4962	0.4194	0.2837	0.2268	0.2747	0.3576	0.5876	0.3465	0.132	0.2918	0.5704	0.2798	0.1467	0.252

http://www.aloki.hu ● ISSN 1589 1623 (Print) ● ISSN 1785 0037 (Online)
DOI: http://dx.doi.org/10.15666/aeer/1705_1255112571

Conclusions

There is little research on predicting the normalized difference vegetation index (NDVI) of high-altitude highways by using relevant machine learning algorithm, but in the process of highways construction, especially, the highways operation and construction in the ecologically fragile areas at high-altitude will affect the surrounding ecological environment. Therefore, in this paper, four machine learning algorithms of ELM, WNN, BP neural network and cubic smoothing index are introduced to predict the normalized difference vegetation index (NDVI) of high-altitude highways to promote the sustainable development of the ecological fragile areas of the high-altitude environment and road construction.

Through research, it is found that WNN is more complex than ELM and cubic smoothing index in algorithm models, but compared with BP neural network, it is relatively simple and easy, an because of its multiple iterations and the continuous replacement of algorithm weight, the WNN is more complex than the ELM and the cubic smoothing index. Considering the weight effect of the whole data, the prediction precision is high. The prediction time of BP neural network is relatively longer when the condition of double hidden layer is adopted and the number of iterations is larger, so the efficiency of the neural network is greatly reduced. Under the condition of considering the weight of the data, the cubic smoothing index tries to have different smoothing coefficients, but it fails to solve the sudden change which is easy to produce a large value. The ELM as a single hidden layer is relatively simple, and its prediction effect is poor, the precision is not high, and it is easy to produce abrupt values. In the high-altitude areas, the road normalized difference vegetation index is more easily affected by the external factors, and the climate factors at high-altitude are more complex and changeable than in ordinary areas, and the data are characterized by fluctuating variability. Therefore, the model selection requires high precision, not easy to occur mutation, and can pay attention to the global factors and other characteristics. In this paper, compared with the other three models, WNN has higher overall prediction accuracy, closer to the actual value and no large deviation, thus showing a higher prediction level. Therefore, the WNN is more suitable for the prediction of road normalized difference vegetation index (NDVI) in high-altitude areas, which will helpful to the coordinated and sustainable development of ecological environment and highway construction in high-altitude areas. In the future research, we can pay attention to the method of comparison and selection is combined with the analysis and screening of the factors affecting the vegetation and the extent of roads, so as to find out the overall trend of the influence of highway on vegetation cover in road areas.

Data availability. The research data in this paper mainly downloaded the Landsat8 satellite data through the geospatial data cloud http://www.gscloud.cn/, and selected the available satellite data in the region where G214 is located through the geographic condition information, then made use of ENVI and GIS software to extract the data for this research as described in the article. The specific data extracted is shown in *Tables 1–3* in this paper.

Funding. The Project was Supported by Natural Science Basic Research Plan in Shaanxi Province of China (Program No. 2017JQ5122 and No. 2018JQ4009), and the Science and Technology Project of Transportation Department of Qinghai Province (Program No. 2016-03).

Conflict of interests. The authors declare no conflict of interests.

http://www.aloki.hu ● ISSN 1589 1623 (Print) ● ISSN 1785 0037 (Online)
DOI: http://dx.doi.org/10.15666/aeer/1705_1255112571

REFERENCES

[1] Abutaqiya, M. I. L., Sisco, C. J., Vargas, F. M. (2019): A linear extrapolation of normalized cohesive energy (LENCE) for fast and accurate prediction of the asphaltene onset pressure. – Journal of Fluid Phase Equilib 483: 52-69.
[2] Brown, R. G. (2013): Exponential smoothing. – Journal of Encyclopedia of Operations Research & Management Science 11: 537-539.
[3] Chen, Y. G. (2018): Prediction algorithm of PM2.5 mass concentration based on adaptive BP neural network. – Journal of Computing 100: 825-838.
[4] Cocchi, G., Galli, L., Galvan, G., Sciandrone, M., Cantu, M., Tomaselli, G. (2018): Machine learning methods for short-term bid forecasting in the renewable energy market: A case study in Italy. – Journal of Wind Energy 21: 357-371.
[5] Feng, X., Li, Q., Zhu, Y. J., Hou, J. X., Jin, L. Y., Wang, J. J. (2015): Artificial neural networks forecasting of PM2.5 pollution using air mass trajectory based geographic model and wavelet transformation. – Journal of Atmos Environ 107: 118-128.
[6] Fijani, E., Barzegar, R., Deo, R., Tziritis, E., Skordas, K. (2019): Design and implementation of a hybrid model based on two-layer decomposition method coupled with extreme learning machines to support real-time environmental monitoring of water quality parameters. – Journal of Sci. Total Environ 648: 839-853.
[7] Guo, X. J., Liu, S. F., Yang, Y. J. (2019): A prediction method for plasma concentration by using a nonlinear grey Bernoulli combined model based on a self-memory algorithm. – Journal of Comput. Biol. Med 105: 81-91.
[8] Huang, G., Zhu, Q., Siew, C. (2006): Extreme learning machine: Theory and applications. – Journal of Science Direct 70: 489-501.
[9] Kisi, O., Alizamir, M. (2018): Modelling reference evapotranspiration using a new wavelet conjunction heuristic method: Wavelet extreme learning machine vs wavelet neural networks. – Journal of Agric for Meteorol 263: 41-48.
[10] Leng, X. Z., Wang, J. H., Ji, H. B., Wang, Q. G., Li, H. M., Qian, X., Li, F. Y., Yang, M. (2017): Prediction of size-fractionated airborne particle-bound metals using MLR, BP-ANN and SVM analyses. – Journal of Chemosphere 180: 513-522.
[11] Li, M. L., Wang, W., De, G., Ji, X. H., Tan, Z. F. (2018): Forecasting carbon emissions related to energy consumption in Beijing-Tianjin-Hebei region based on grey prediction theory and extreme learning machine optimized by support vector machine algorithm. – Journal of Energies 11: 2475.
[12] Lin, C. C., He, R. X., Liu, W. Y. (2018): Considering multiple factors to forecast CO2 emissions: a hybrid multivariable grey forecasting and genetic programming approach. – Journal of Energies 11: 3432.
[13] Liu, H., Mi, X. W., Li, Y. F. (2018): An experimental investigation of three new hybrid wind speed forecasting models using multi-decomposing strategy and ELM algorithm. – Journal of Renew. Energy 123: 694-705.
[14] Mishra, D., Goyal, P., Upadhyay, A. (2015): Artificial intelligence based approach to forecast PM2.5 during haze episodes: a case study of Delhi, India. – Journal of Atmos Environ 102: 239-248.
[15] Moews, B., Herrmann, J. M., Ibikunle, G. (2019): Lagged correlation-based deep learning for directional trend change prediction in financial time series. – Journal of Expert Syst 120: 197-206.
[16] Nian, C., Hu, K., Li, S. (2001): Wavelet neural network and its application. – Journal of Chinese Stereology and Image Analysis 6: 239-245.
[17] Perez, P., Gramsch, E. (2016): Forecasting hourly PM2.5 in Santiago de Chile with emphasis on night episodes. – Journal of Atmos Environ 124: 22-27.
[18] Rumelhart, D. E., Hinton, G. E., Williams, R. J. (1986): Learning representations by back-propagating errors. – Journal of Nature 323: 533-536.

http://www.aloki.hu ● ISSN 1589 1623 (Print) ● ISSN 1785 0037 (Online)
DOI: http://dx.doi.org/10.15666/aeer/1705_1255112571

[19] Sun, W., Zhang, H., Palazoglu, A., Singh, A., Zhang, W. D., Liu, S. W. (2013): Prediction of 24-hour-average PM2.5 concentrations using a hidden Markov model with different emission distributions in Northern California. – Journal of Sci. Total Environ 443: 93-103.
[20] Tu, M. (2016): Comprehensive Evaluation of the Impact of Highway Construction on Ecological Environment in Southern Forest Region Based on GIS. – University Of Agriculture and Forestry in Fujian, China.
[21] Wang, G. F. (2015): Dynamic Monitoring of vegetation coverage based on remote Sensing Technology. – Journal of Shanxi agricultural science 43: 592-595.
[22] Xu, Y. Z., Du, P., Wang, J. Z. (2017): Research and application of a hybrid model based on dynamic fuzzy synthetic evaluation for establishing air quality forecasting and early warning system: a case study in China. – Journal of Environ Pollu 223: 435-448.
[23] Yang, H. F., Chen, Y. P. P. (2019): Hybrid deep learning and empirical mode decomposition model for time series applications. – Journal of Expert Syst 120: 128-138.
[24] Yi, H. S., Park, S., An, K. G., Kwak, K. C. (2018): Algal bloom prediction using extreme learning machine models at artificial weirs in the Nakdong River, Korea. – Journal of Int. J. Environ. Res. Public Health 15: 2078.
[25] Zhang, M. Q., Jiang, X., Fang, Z., Chen, H. et al. (2019): High-order hidden Markov Model for trend prediction in financial time series. – Journal of Physica A 517: 1-12.
[26] Zhao, L. M., Zhou, X. Y. (2018): Forecasting electricity demand using a new grey prediction model with smoothness operator. – Journal of Symmetry-Basel 10: 693.
[27] Zhu, M. T., Shi, T., Chen, Y. et al. (2019): Prediction of fatty acid composition in camellia oil by 1H NMR combined with PLS regression. – Journal of Food Chem 279: 339-346.

http://www.aloki.hu ● ISSN 1589 1623 (Print) ● ISSN 1785 0037 (Online)
DOI: http://dx.doi.org/10.15666/aeer/1705_1255112571

MULTILOCUS SEQUENCE TYPING (MLST) BASED GENETIC VARIATION ANALYSIS OF SHISHAM DIEBACK ASSOCIATED STRAINS OF *CERATOCYSTIS FIMBRIATA* SENSU LATO SPECIES COMPLEX IN PAKISTAN

UL HAQ, I.[1*] – IJAZ, S.[2] – LATIF, M. Z.[1]

[1]*Department of Plant Pathology, University of Agriculture, Faisalabad, Pakistan*

[2]*Centre of Agricultural Biochemistry and Biotechnology (CABB), University of Agriculture, Faisalabad, Pakistan*

**Corresponding author*
e-mail: imran_1614@yahoo.com; phone: +92-34-4445-3063

(Received 17th May 2019; accepted 16th Jul 2019)

Abstract. *Ceratocystis fimbriata* sensu lato species complex is a group of highly diverse cryptic species known to be associated with different diseases in a range of host plants. For the accurate identification of fungal pathogens belonging to this species complex, molecular approaches have been employed in juxtaposition with morphological characterization. Different DNA based methods have become the routine practice of mycologist community throughout the world. Among them, multilocus sequence typing (MLST) approach is gaining popularity. Four fungal taxonomy groups have been established MLST scheme for few fungi, to date. However, in *Ceratocystis fimbriata* species complex, no report on MLST based genotyping is available yet. Therefore, by considering this perspective, we attempted MLST method for genotyping and diversity analysis of this species complex. We investigated ITS and TEF1-α loci, for two multilocus sequence typing scheme. Allelic profile of each locus gave 23 sequence types (STs) and 22 Allele types (ATs). However, the typing efficiency of ITS region was high as compared to TEF1-α. The phylogenetic network parallelograms based on neighbor net algorithm also showed genetic diversity in studied isolates. This relationship study was further supported by generating phylogram, which resolved these isolates in three different clades showing unequivocal phylogenetic diversity and relatedness.

Keywords: *Ceratocystis fimbriata, Dalbergia sissoo, genotyping variation, sequence types (STs), allele types (ATs)*

Introduction

Ceratocystis fimbriata complex represents a group of cryptic species of sever plant pathogen(s) and saprobe(s) as well (Wyk, 2005). *C. fimbriata* complex parasitizes a wide range of plant families from herbaceous to woody plants. The *C. fimbriata* was first time reported in Sweet potato in 1890 (Halsted, 1890). Since 1980, several fungi of species were isolated and identified from a range of host plants from around the globe (Seifert et al., 1993; Wyk et al., 2005). *C. fimbriata* is widely accepted as a complex that comprised of Latin American, North American, Asian and the African clades that include many fungal species (Johnson et al., 2005; Heath et al., 2009). In past few decades, new taxa have been evolved extensively in this complex with special reference to advancement in DNA based identification methods (Fourie et al., 2015). Different *Ceratocystis* species in the *C. fimbriata* sensu lato species complex have been reported to date that are associated with different plant diseases (Harrington, 2000). The fungi of this species complex causes root rot, cankers and vascular wilts and staining in woody hosts (Wingfield et al., 1996; Marin et al., 2003; Al Adawi et al., 2013).

http://www.aloki.hu ● ISSN 1589 1623 (Print) ● ISSN 1785 0037 (Online)
DOI: http://dx.doi.org/10.15666/aeer/1705_1257312582

The pathogens belong to Ceratocystis fimbriata sensu lato species complex are soil borne with fruity odor characteristics. This feature facilitates their dispersal by insects and beetles (Wyk et al., 2005). With wide host rang, this species complex has been recognized as of diverse taxonomic entity. However, with the aid of molecular based studies, different taxa have been recognized and diverged as distinct species from this species complex. It has been documented by DNA based studies that Ceratocystis fimbriata species complex represents diverse and discrete grouping based on geography and host (Harrington, 2000; Baker et al., 2003). Previously, in this complex, species delineation was made based on single gene genealogy of ITS (internal transcribed spacer) region. Nevertheless, multiple gene genealogies and analyzing phylogenetic diversity had been attempted to specify species boundaries.

However, there are diverse molecular tools employing for genotypic diversity analysis. Whereas, multilocus sequence typing (MLST) tool has become more popular scheme for genetic diversity studies. In fungal molecular biology, so far established MLST schemes are for Fusarium species (Westerdijk Fungal Biodiversity Institute), Candida species (Imperial College), Aspergillus (Oxford University), Bipolaris species and Scedosporium apiospermum and S. boydii species (International Society of Human and Animal Mycology, ISHAM). However, in Ceratocystis species complex, MLST scheme has not been established yet. Although this complex is a cryptic species complex and there is a great room of genetic diversity. By considering this perspective, we have attempted two multilocus sequence typing (MLST) method for genotyping and analyzing genetic variation in Ceratocystis species complex. This may be used for further studies based on other loci. Hence, the data generated by MLST scheme could be used for epidemiological studies for which accurate recognition of different species, subspecies and strains are required.

Material and methods

Fungal isolates

We used 23 isolates of *Ceratocystis fimbriata* sensu lato from our collection of fungal isolates associated to dieback affected shisham (*Dalbergia sissoo*) plants. Each isolate was characterized based on its morphocultural characteristics and was labelled as FMB (Fungal Molecular Biology Laboratory-Culture Collection) with a unique identification number as given in *Table 1*.

DNA extraction

Fungal DNA was extracted with GeneJET Genomic DNA Purification Kit (Thermoscientific, USA). The DNA samples were quantified with a NanoDrop 8000 spectrophotometer (Thermofisher). However, DNA quality was checked on agarose gel electrophoresis and stored at -20 °C until further use.

Molecular biology and computational biology

We used two genes, internal transcribed spacer (ITS) and translation elongation factor 1 α (TEF1-α), for polymerase chain reaction (PCR), sequencing and phylogenetic analysis. PCR amplifications of these two genetic regions was carried out in Veriti^{TM} 96 wells thermalcycler (Applied Biosystems) using 25 µl reaction volume with the ITS (White et al., 1990) and TEF1-α (Oliveira et al., 2015; Li et al., 2017) sequence regions

http://www.aloki.hu ● ISSN 1589 1623 (Print) ● ISSN 1785 0037 (Online)
DOI: http://dx.doi.org/10.15666/aeer/1705_1257312582

based primer pairs. PCR products were purified using a FavorPrep PCR purification kit (Favorgen Biotech Corporation, Taiwan) and were sequenced in both directions (Eurofins Genomics DNA sequencing services, USA). High quality trimmed sequences were generated using BioEdit software version 7.2.6.1. For getting consensus sequences of sequences obtained using forward and reverse primers DNASTAR Lasergene v. 7.1.0 SeqMan pro (SeqManTMII) software package was used. These generated sequences were compared with the sequences available in NCBI database using BLASTn and were deposited in GenBank under accession numbers, given in the *Table 1*.

Table 1. *A list of isolates name, strain accession number and GenBank accession numbers of sequences of ITS and TEF1-α*

Sr #	Isolate name	Strain accession number	Location	GenBank accession numbers	
				ITS	TEF1-α
1	FMB-GHP1E-SD	FMB 0146	Punjab, Pakistan	MK816923	MK890310
2	FMB-GHP2E-SD	FMB 0147	Punjab, Pakistan	MK816925	MK890311
3	FMB-GHP3-SD	FMB 0148	Punjab, Pakistan	MK816928	MK890312
4	FMB-GHP4-SD	FMB 0149	Punjab, Pakistan	MK816929	MK890313
5	FMB-GHP5-SD	FMB 0150	Punjab, Pakistan	MK816932	MK890314
6	FMB-GHP6-SD	FMB 0160	Punjab, Pakistan	MK816933	MK890315
7	FMB-GHP7-SD	FMB 0161	Punjab, Pakistan	MK816934	MK890316
8	FMB-GHP8-SD	FMB 0162	Punjab, Pakistan	MK816957	MK890317
9	FMB-M12-SD	FMB 0033	Punjab, Pakistan	MF767443	MK890321
10	FMB-BWP-SD	FMB 0163	Punjab, Pakistan	MK811131	MK820654
11	FMB-VR-SD	FMB 0164	Punjab, Pakistan	MK813838	MK890320
12	FMB-ST-SD	FMB 0165	Punjab, Pakistan	MK813839	MK890322
13	FMB-BR-SD	FMB 0166	Punjab, Pakistan	MK811133	MK820656
14	FMB-FSD-SD	FMB 0167	Punjab, Pakistan	MK811134	MK850855
15	FMB-TTS-SD	FMB 0168	Punjab, Pakistan	MK811125	MK890319
16	FMB-BLCN-01	FMB 0169	Baluchistan, Pakistan	MK811095	MK850853
17	FMB-BLCN-02	FMB 0170	Baluchistan, Pakistan	MK811097	MK820655
18	FMB-Thatta-SD	FMB 0171	Sindh, Pakistan	MK811092	MK850852
19	FMB-Hyderabad-SD	FMB 0172	Sindh, Pakistan	MK811093	MK850851
20	FMB-Nosheroferoz-SD	FMB 0173	Sindh, Pakistan	MK811094	MK850850
21	FMB-GL-SD	FMB 0174	KPK, Pakistan	MK811103	MK890318
22	FMB-BZ1-SD	FMB 0175	KPK, Pakistan	MK811102	MK910747
23	FMB-PZ1-SD	FMB 0176	KPK, Pakistan	MK811101	MK850854

Genotyping variation analysis of ITS and TEF1-α genes

Nucleotide sequences of ITS and TEF1-α genes were used for genetic distance analysis. Genotypic variation of each locus was assessed using MLSTest v1.0 software. The allele types (ATs) number, sequence types (STs) number, number of polymorphism, typing efficiency and discrimination power at 95% confidence interval were computed using this software. Neighbor net algorithm was used to perform phylogenetic network of each loci by splitsTree4 V4.14.8 software.

http://www.aloki.hu ● ISSN 1589 1623 (Print) ● ISSN 1785 0037 (Online)
DOI: http://dx.doi.org/10.15666/aeer/1705_1257312582

Nucleotide sequences of both genes were concatenated using Geneious software v. 4.8.5 in the order as ITS and TEF1-α to generate concatenated dataset file. The best evolutionary model for concatenated dataset was selected from Bayesian Information Criterion (BIC) using MEGA 7.0 software. However, evolutionary model with lowest BIC value was selected to construct a maximum likelihood phylogram. Sequences were aligned with ClustalW for phylogenetic tree construction. A phylogenetic tree of the 23 aligned sequences based on best evolutionary model was obtained for the heuristic search in bootstrap analysis with 1000 replications by applying the Neighbor-Joining method to a matrix of pairwise distances estimated through Maximum Composite Likelihood (MCL) approach using MEGA7 (Molecular Evolutionary Genetics Analysis version 7.0) software.

Results

Twenty-three fungal isolates collected from dieback disease affected tissues of *Dalbergia sissoo* (Shisham) were characterized based on morphological and genomic investigations. These characterizations has set them under the *Ceratocystis* species complex. Molecular characterization was based on the direct sequencing of ITS and TEF1-α regions. The generated sequences of these isolates were subjected to BLASTn tool to search their homology with already available sequences of the type materials in NCBI database (https://blast.ncbi.nlm.nih.gov/Blast.cgi). The sequence similarity using BLASTn showed significant similarity with Ceratocystis species of *Ceratocystis fimbriata* sensu lato complex.

The Genotypic variation profiling of 23 isolates belongs to *Ceratocystis fimbriata* sensu lato complex was generated using MLSTest software. The analysis showed 23 best different sequence types (STs) numbers and 22 allele types (ATs) numbers of both loci (*Table 2*). However, the frequency of each allele types (ATs) numbers in each isolate is given in *Table 3*.

The allelic profile of both genes including number of alleles, discrimination power (95% confidential interval), typing efficacy and number of polymorphisms were calculated, given in the *Table 4*. A diverse genetic relationship was found among the genotyped variants of 23 *Ceratocystis fimbriata* sensu lato after analyzing phylogenetic network of each of the both loci (ITS and TEF1-α) using neighbor net algorithm (*Fig. 1*).

Among 24 calculated models of concatenated dataset, the best evolutionary model of concatenated dataset (ITS and TEF1-α) for maximum likelihood (ML) phylogenetic tree was K2 (Kimura 2-parameter) with BIC (Bayesian Information Criterion) score 2721.116. This model was selected based on the theory that evolutionary models with the lowest BIC values are considered to describe best substitution pattern. The phylogenetic tree (*Fig. 2*) with highest log likelihood (-1145.9648) was drawn to scale, with branch lengths measured in the number of substitutions per site. Codon positions included were 1st + 2nd + 3rd + Noncoding. There were 749 positions in the final dataset.

The evolutionary hierarchy was inferred using ML method based on the K2 model, which categorized these fungal isolates into three discrete clades. The phylogram showed that the clade III was outer group and comprised of FMB-BZ1-SD, FMB-M12-SD, FMB-Thatta-SD, FMB-ST-SD, FMB-GHP2E-SD, FMB-BLCN-01, and FMB-GHP1E-SD with 96% bootstrap support. However, Clade I and Clade II were shown to be evolutionary diverged from Clade III with 96% and 86% bootstrap support respectively (*Fig. 2*).

http://www.aloki.hu ● ISSN 1589 1623 (Print) ● ISSN 1785 0037 (Online)
DOI: http://dx.doi.org/10.15666/aeer/1705_1257312582

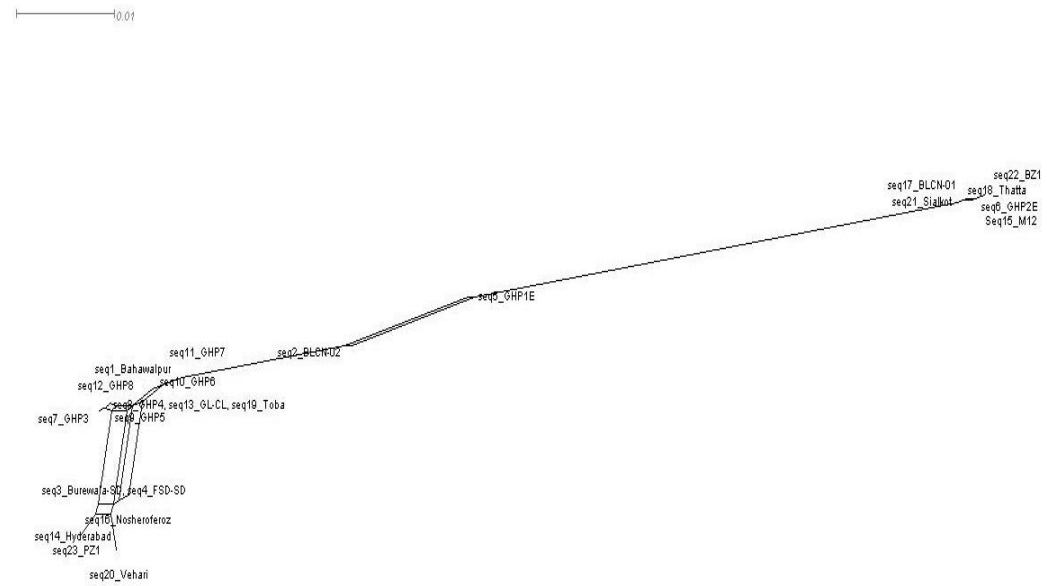

a

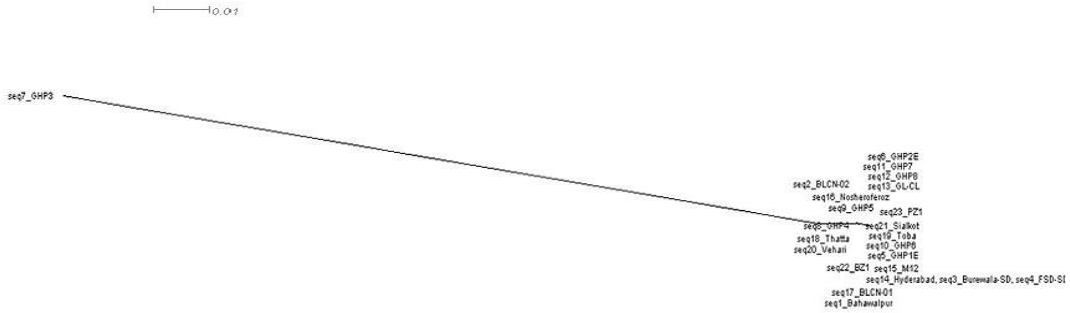

b

Figure 1. *Phylogenetic network of two loci, (a) ITS, (b) TEF1- α with neighbor net algorithm by split tree software*

Clade I majorly comprised of fungal isolates from Punjab (a province of Pakistan), as FMB-GHP3-SD, FMB-GHP4-SD, FMB-GHP5-SD, FMB-GHP6-SD, FMB-GHP7-SD, FMB-BWP-SD, and FMB-TTS-SD except FMB-BLCN-02, which was collected from Baluchistan (a province of Pakistan). These fungal isolates made cladding with 96% bootstrap support. However, in clade II fungal isolates from KPK, Sindh and Punjab (provinces of Pakistan) made grouping. In clade II, the isolate FMB-PZ1-SD (KPK) was evolutionary diverged from clade III with 86% bootstrap support. However, fungal isolates of this group, FMB-Nosheroferoz-SD, FMB-Hyderabad-SD (Sindh), FMB-BR-SD, FMB-FSD-SD and FMB-VR-SD (Punjab) were shown to diverged from FMB-PZ1-SD and grouped together in this clade with 67% bootstrap support (*Fig. 2*). Based on the phylogenetic networks of both loci and phylogenetic tree of concatenated dataset, among these 23 studied isolates, 9 isolates (FMB-BLCN-02, FMB-GHP3-SD FMB-GHP7-SD, FMB-PZ1-SD, FMB-FSD-SD, FMB-Nosheroferoz-SD, FMB-BZ1-SD, FMB-M12-SD and FMB-GHP1E-SD) were selected for phylogenetic analyses to delimit the species boundaries of Ceratocystis species associated to dieback disease of Dalbergia sissoo. These selected isolates showed more genotyping variation among all studied isolates by multilocus sequence typing (MLST) approach.

http://www.aloki.hu ● ISSN 1589 1623 (Print) ● ISSN 1785 0037 (Online)
DOI: http://dx.doi.org/10.15666/aeer/1705_1257312582

Table 2. *A list of sequence types (STs) numbers and allele types (ATs) numbers of ITS and TEF1-α loci in isolates of Ceratocystis fimbriata sensu lato complex*

Isolate name	Strain number	Allele types (ATs)		Sequence types (STs)
		TEF1-α	ITS	
FMB-BR-SD	FMB 0166	1	1	1
FMB-PZ1-SD	FMB 0176	2	2	2
FMB-FSD-SD	FMB 0167	3	3	3
FMB-Nosheroferoz-SD	FMB 0173	4	4	4
FMB-Hyderabad-SD	FMB 0172	5	5	5
FMB-VR-SD	FMB 0164	6	5	6
FMB-BLCN-02	FMB 0170	7	6	7
FMB-GHP8-SD	FMB 0162	8	7	8
FMB-GHP5-SD	FMB 0150	9	8	9
FMB-GHP4-SD	FMB 0149	10	9	10
FMB-GL-SD	FMB 0174	7	10	11
FMB-BWP-SD	FMB 0163	11	11	12
FMB-GHP7-SD	FMB 0161	12	12	13
FMB-GHP3-SD	FMB 0148	13	13	14
FMB-GHP6-SD	FMB 0160	14	14	15
FMB-TTS-SD	FMB 0168	15	15	16
FMB-GHP2E-SD	FMB 0147	16	16	17
FMB-BLCN-01	FMB 0169	17	17	18
FMB-M12-SD	FMB 0033	18	18	19
FMB-BZ1-SD	FMB 0175	19	19	20
FMB-Thatta-SD	FMB 0171	20	20	21
FMB-ST-SD	FMB 0165	21	21	22
FMB-GHP1E-SD	FMB 0146	22	22	23

Pertaining to allelic profile for multilocus sequence typing (MLST), typing efficiency of ITS locus was more (0.124) than TEF1-α (0.021). This genotyping supports the phylogram generated through concatenated dataset of both loci. This genotyping results have deduced that, the ITS region has more resolving and typing power than TEF1-α region to species identification and discrimination in case of Ceratocystis species of *Ceratocystis fimbriata* sensu lato complex. This is the first report of using two multilocus sequence typing (MLST) scheme for studying and typing genetic variation in Ceratocystis species complex.

Discussion

There are different approaches that have been employing for genotypic diversity studies. Among of them, multilocus sequence typing (MLST) has become more robust scheme. In the field of fungal molecular biology, MLST scheme Fusarium species, Candida species, Aspergillus, Bipolaris species and Scedosporium apiospermum and S. boydii species have been established by four working groups of Fungal taxonomy. However, in Ceratocystis species complex, MLST scheme has not been established yet. Although this complex is a cryptic species complex and there is a great room of genetic diversity. By considering this perspective, we have attempted two multilocus sequence typing (MLST) method in Ceratocystis species complex.

http://www.aloki.hu ● ISSN 1589 1623 (Print) ● ISSN 1785 0037 (Online)
DOI: http://dx.doi.org/10.15666/aeer/1705_1257312582

Table 3. *A list of allele types (ATs) numbers of ITS and TEF1-α with their frequency in each isolate*

Gene	ATs	Frequency	Isolate name
TEF1-α	1	1	FMB-BR-SD
	2	1	FMB-PZ1-SD
	3	1	FMB-FSD-SD
	4	1	FMB-Nosheroferoz-SD
	5	1	FMB-Hyderabad-SD
	6	1	FMB-VR-SD
	7	2	FMB-GL-SD, FMB-BLCN-02
	8	1	FMB-GHP8-SD
	9	1	FMB- GHP5-SD
	10	1	FMB-GHP4-SD
	11	1	FMB-BWP-SD
	12	1	FMB-GHP7-SD
	13	1	FMB-GHP3-SD
	14	1	FMB-GHP6-SD
	15	1	FMB-TTS-SD
	16	1	FMB-GHP2E-SD
	17	1	FMB-BLCN-01
	18	1	FMB-M12-SD
	19	1	FMB-BZ1-SD
	20	1	FMB-Thatta-SD
	21	1	FMB-ST-SD
	22	1	FMB-GHP1E-SD
ITS	1	1	FMB-BR-SD
	2	1	FMB-PZ1-SD
	3	1	FMB-FSD-SD
	4	1	FMB-Nosheroferoz-SD
	5	2	FMB-Hyderabad-SD, FMB-VR-SD
	6	1	FMB-BLCN-02
	7	1	FMB-GHP8-SD
	8	1	FMB- GHP5-SD
	9	1	FMB-GHP4-SD
	10	1	FMB-GL-SD
	11	1	FMB-BWP-SD
	12	1	FMB-GHP7-SD
	13	1	FMB-GHP3-SD
	14	1	FMB-GHP6-SD
	15	1	FMB-TTS-SD
	16	1	FMB-GHP2E-SD
	17	1	FMB-BLCN-01
	18	1	FMB-M12-SD
	19	1	FMB-BZ1-SD
	20	1	FMB-Thatta-SD
	21	1	FMB-ST-SD
	22	1	FMB-GHP1E-SD

http://www.aloki.hu ● ISSN 1589 1623 (Print) ● ISSN 1785 0037 (Online)
DOI: http://dx.doi.org/10.15666/aeer/1705_1257312582

Table 4. *Allelic profile including number of polymorphism, number of alleles, typing efficiency, discriminatory power of ITS and TEF1- α genes*

Locus	No. of alleles	No. of polymorphisms	Typing efficiency	Discrimination power (95% confidence interval)
ITS	22	177	0.124	0.996(0.985-1)
TEF1- α	22	1049	0.021	0.996(0.985-1)

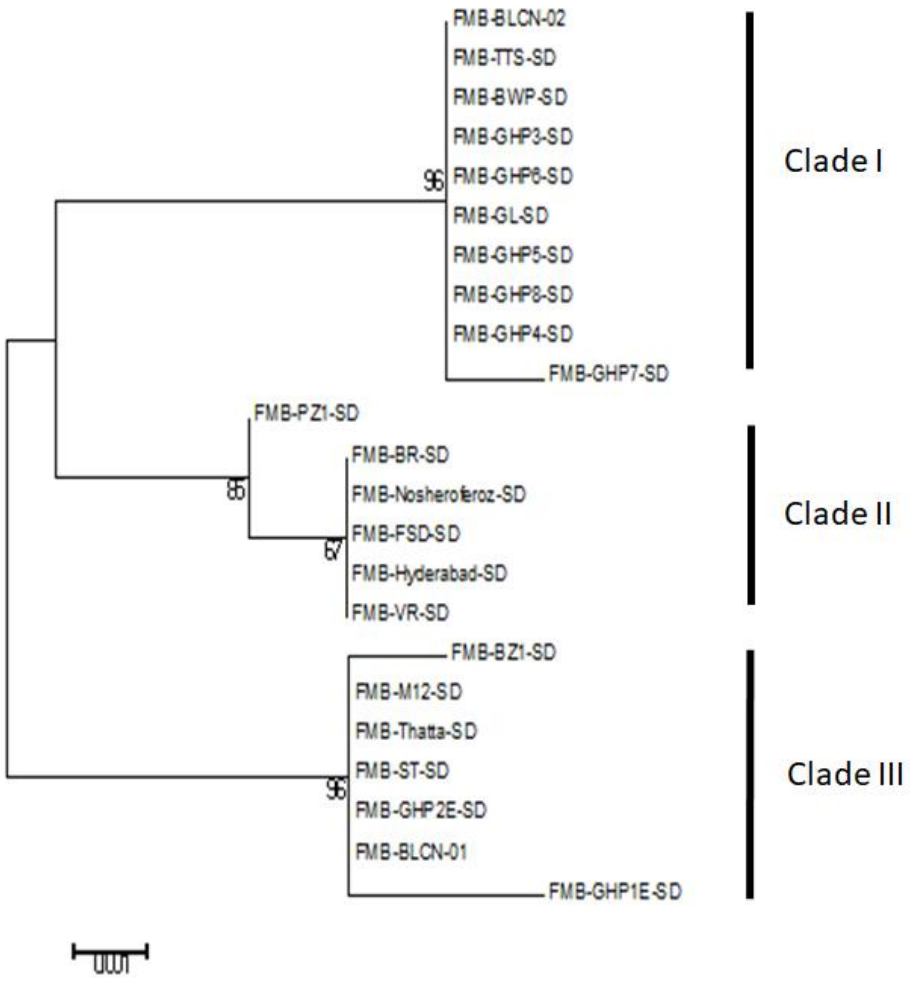

Figure 2. *A maximum likelihood (ML) phylogenetic tree of concatenated dataset of two loci (ITS and TEF1-α) based on evolutionary model K2 (Kimura 2-parameter)*

We have attempted to study the genetic variation and typing analysis among the isolates of Ceratocystis species. We have 23 isolates of this fungus collected from dieback tissues of Dalbergia sissoo. Initially we have used 2 loci, internal transcribed spacer (ITS) and translation elongation factor 1 α (TEF1-α), for MLST based genotyping analysis of *Ceratocystis fimbriata* sensu lato species complex. Successful sequencing of both loci in all isolates was attempted. We identified 23 STs (sequence types) in both loci. The number of polymorphism for each locus was varied which was 177 for ITS and 1049 for TEF1-α.

http://www.aloki.hu ● ISSN 1589 1623 (Print) ● ISSN 1785 0037 (Online)
DOI: http://dx.doi.org/10.15666/aeer/1705_1257312582

The sequences of 23 isolates of *Ceratocystis fimbriata* sensu lato species complex were analyzed by applying neighbor net algorithm using Splits-Tree software. The graph of ITS region-based sequences generated by Splits-Tree was shown as parallelogram, which implied all could be diverse but characters are shared by a set of species. However, the graph of TEF1-α showed the clustering of species at the one end of graphical string except FMB-GHP3-SD on its other end. The genetic network not shown to be able to describe genetic variation. This phylogenetic network results supported the allelic profiles generated by MLST tool which showed typing efficiency of ITS is more (0.124) as compared to TEF1-α (0.021), however, their discriminatory power was same (0.996). The sequence types (STs) number were 23 in case of both loci, which depicted that each isolates had one ST type. However, the allele types (ATs) number was 22 in both loci. Each isolates has one type of allele except FMB-GL-SD, FMB-BLCN-02 that have same type of allele of TEF1-α. Similarly, in case of ITS loci, each isolate has one type of allele except FMB-Hyderabad-SD, FMB-VR-SD that possess same type of allele.

In nutshell, here we have presented first two multilocus sequence typing (MLST) scheme based relationship analysis among *Ceratocystis fimbriata* sensu lato species complex associated to dieback disease in Dalbergia sissoo in Pakistan to studying and typing genetic variation in Ceratocystis species complex. In future, more loci may be explored for allelic profiling of these fungal isolates. Allele types (ATs) of those loci could be appraised to apprise sequence types (STs) numbers of these fungal isolates in way that is more precise.

Conclusion

Ceratocystis fimbriata sensu lato species complex is a group of cryptic species. Several species have been evolved and identified as discrete taxa. In Ceratocystis fimbriata species complex, no report on MLST based genotyping is available yet. We investigated two loci (ITS and TEF1-α) of 23 fungal isolates from dieback disease affected tissues of Dalbergia sissoo for MLST scheme. In allelic profile, the typing efficiency of ITS region was shown to be high by scoring the value of 0.124 as compared to TEF1-α with 0.021 typing score. This allelic profile result was supported by phylogenetic network parallelograms based on neighbor net algorithm, which showed genetic diversity in studied isolates though some were sharing characters. This relationship study was further supported by generating phylogram of concatenated dataset by applying K2 evolutionary model in maximum likelihood phylogenetic analysis, which resolved phylogenetic diversity and relatedness among these fungal isolates with maximum bootstrap support.

REFERENCES

[1] Al Adawi, A. O., Barnes, I., Khan, I. A., A Subhi, A. M. A., Jahwari, A. A., Deadman, M. L., Wingfield, B. D., Wingfield, M. J. (2013): Ceratocystis manginecans associated with a serious wilt disease of two native legume trees in Oman and Pakistan. – Australasian Plant Pathology 42(2): 179-193.

[2] Baker, C. J., Harrington, T. C., Krauss, U., Alfenas, A. C. (2003): Genetic variability and host specialization in the Latin American clade of Ceratocystis fimbriata. – Phytopathology 93(10): 1274-1284.

http://www.aloki.hu ● ISSN 1589 1623 (Print) ● ISSN 1785 0037 (Online)
DOI: http://dx.doi.org/10.15666/aeer/1705_1257312582

[3] Fourie, A., Wingfield, M. J., Wingfield, B. D., Barnes, I. (2015): Molecular markers delimit cryptic species in Ceratocystis sensu stricto. – Mycological Progress 14(1): 1020.
[4] Halsted, B. D. (1890): Some fungus diseases of the sweet potato. – New Jersey Agricultural College Experiment Station Bulletin (76): 25-27.
[5] Harrington, T. C. (2000): Host specialization and speciation in the American wilt pathogen. – Fitopatologia Brasileira 25: 262-263.
[6] Heath, R. N., Wingfield, M. J., Wingfield, B. D., Meke, G., Mbaga, A., Roux, J. (2009): Ceratocystis species on Acacia mearnsii and Eucalyptus spp. in eastern and southern Africa including six new species. – Fungal Diversity 34: 41-67.
[7] Johnson, J. A., Harrington, T. C., Engelbrecht, C. J. B. (2005): Phylogeny and taxonomy of the North American clade of the Ceratocystis fimbriata complex. – Mycologia 97(5): 1067-1092.
[8] Li, Q., Harrington, T. C., McNew, D., Li, J. (2017): Ceratocystis uchidae, a new species on Araceae in Hawaii and Fiji. – Mycoscience 58(6): 398-412.
[9] Marin, M., Castro, B., Gaitan, A., Preisig, O., Wingfield, B. D., Wingfield, M. J. (2003): Relationships of Ceratocystis fimbriata isolates from Colombian coffee-growing regions based on molecular data and pathogenicity. – Journal of Phytopathology 151(7-8): 395-405.
[10] Oliveira, L. S., Harrington, T. C., Ferreira, M. A., Damacena, M. B., Al-Sadi, A. M., Al-Mahmooli, I. H., Alfenas, A. C. (2015): Species or genotypes? Reassessment of four recently described species of the Ceratocystis wilt pathogen, Ceratocystis fimbriata, on Mangifera indica. – Phytopathology 105(9): 1229-1244.
[11] Seifert, K. A., Wingfield, M. J., Kendrick, W. B. (1993): A nomenclator for Described Species of Ceratocystis, Ophiostoma, Ceratocystiopsis, Ceratostomella and Sphaeronaemella. – American Phytopathological Society, St. Paul, Minnesota, pp. 269-287.
[12] Tamura, K., Stecher, G., Peterson, D., Filipski, A., Kumar, S. (2013): MEGA6: molecular evolutionary genetics analysis version 6.0. – Molecular Biology and Evolution 30(12): 2725-2729.
[13] Van Wyk, M., Al-Adawi, A. O., Wingfield, B. D., A-Subhi, A. M., Deadman, M. L., Wingfield, M. J. (2005): DNA based characterization of Ceratocystis fimbriata isolates associated with mango decline in Oman. – Australasian Plant Pathology. 34(4): 587-590.
[14] White, T. J., Bruns, T., Lee, S. J. W. T., Taylor, J. L. (1990): Amplification and Direct Sequencing of Fungal Ribosomal RNA Genes for Phylogenetics. – In: Innis, M. A., Gelfand, D. H., Sninsky, J. J., White, T. J. (eds.) PCR Protocols. A Guide to Methods and Applications. Academic Press, San Diego, pp. 315-322.
[15] Wingfield, M. J., D Beer, C., Visser, C., Wingfield, B. D. (1996): A new Ceratocystis species defined using morphological and ribosomal DNA sequence comparisons. – Systematic and Applied Microbiology 19(2): 191-202.

http://www.aloki.hu ● ISSN 1589 1623 (Print) ● ISSN 1785 0037 (Online)
DOI: http://dx.doi.org/10.15666/aeer/1705_1257312582

IMPACTS OF SALT STRESS ON THE PHYSIOLOGY OF PLANTS AND OPPORTUNITY TO REWATER THE STRESSED PLANTS WITH DILUTED WATER: A REVIEW

JAVED, Q.[1] – AZEEM, A.[1] – SUN, J.[1*] – ULLAH, I.[2] – JABRAN, K.[3] – ANANDKUMAR, A.[1] – PRABAKARAN, K.[1] – BUTTAR, N. A.[2] – DU, D.[1,2*]

[1]*Institute of Environment and Ecology, Academy of Environmental Health and Ecological Security, School of the Environment and Safety Engineering, Jiangsu University, Zhenjiang 212013, China*

[2]*Key Laboratory of Modern Agricultural Equipment and Technology, Ministry of Education, Institute of Agricultural Engineering, Jiangsu University, Zhenjiang, Jiangsu, China*

[3]*Department of Plant Production and Technologies, Faculty of Agricultural Sciences and Technologies, Niğde Ömer Halisdemir University, Niğde, Turkey*

**Corresponding authors*
e-mail: ddl@ujs.edu.cn (D. L. Du), zxsjf@ujs.edu.cn (J. F. Sun)

(Received 12th May 2019; accepted 16th Jul 2019)

Abstract. Water scarcity on a global scale declines the availability of fresh water for agricultural usage. This situation demands the urgent need of utilizing saline water as an alternative resource for irrigation. Stressful environments characterized by adverse natural conditions such as drought, salinity and heat impact the normal molecular, biochemical and physiological processes in crops. Plant stress responses to adverse environmental conditions are reviewed with emphasis on growth, physiological and electrophysiological mechanisms of plant tolerance. This review may also help in interdisciplinary studies to evaluate the photosynthetic threshold levels for rewatering of plant with diluted saline water. Furthermore, considering the goal of high plant production, the best rewatering time was found when plants undergo threshold levels. Therefore, this review provides a new method for dilution of saline irrigation based on plant physiology, which has a huge practical and theoretical importance for saline irrigation research.
Keyword: *photosynthetic traits, growth properties, plant tolerance, rewatering time, threshold levels*

Introduction

Salinity is a major abiotic constraint curtailing crop growth and yield all over the world. The soil salinity is a widespread global concern caused as a result of abundant seawater intrusion in coastal areas, occurrence of saline groundwater and inadequate irrigation and/or drainage (Souza Filho et al., 2003; Nadeem et al., 2014; Yepes et al., 2018). Salinity induced stress in crop plants is a severe environmental problem in many parts of the world, particularly arid and semi-arid (i.e., dry) regions (Rady et al., 2018). Increasing soil salinity issues in some parts of the arid and semi arid regions is due to the inadequate drainage facilities which obliges the use of poor-quality water for irrigation, which may cause 30% shrink in cultivable land within the next 25 years (Shahbaz and Ashraf, 2013). In the present scenario, the adverse effects of land salinization become evident for the fact that over 30 m ha of irrigated lands are significantly damaged by the salt build up and about 0.5 m ha are reported to be lost from farming annually (Singh, 2018). Salinity poses adverse effects to almost all growth stages and metabolic processes in plants starting from a reduction in seed germination, a

http://www.aloki.hu ● ISSN 1589 1623 (Print) ● ISSN 1785 0037 (Online)
DOI: http://dx.doi.org/10.15666/aeer/1705_1258312604

disruption of node formation, a retardation of plant development and finally ending up with a reduction in final crop yield (Munns and Tester, 2008). This reduction in crop yield will pose a severe threat to the global food security as the world populace is estimated to reach between 9 and 10 billion in 2050 (Lutz et al., 2017). Therefore, in order to feed the burgeoning world populace, sustainable irrigation practices should be adopted that improve the existing salinised agricultural lands (Flowers and Yeo, 1995; Biswas, 2008; Garcia, 2008).

Water scarcity and salinity are two major constraints which affect the agricultural production all over the world and the adoption of different irrigation regimes is the key requisite to improve water use efficiency in agricultural practices (Nangare et al., 2016; Mosaffa and Sepaskhah, 2018). Therefore, knowledge on the understanding of the physiological responses that define the plants' tolerance to surpass salinity stress is essential. By understanding the mechanism of the plants' stress tolerance, it is possible to develop water efficient irrigation regimes for agricultural activities (Zhang et al., 2011). Water saving agriculture is an effective approach to manage the ever increasing demand for food. Practically, this is achieved by amendments in different technological disciplines such as agronomy, biology and engineering. The engineering approaches include efficient utilization of existing water resources, water desalinization, and usage of brackish water or recycled sewage water for agricultural purposes. Meanwhile, agronomic and plant biology approaches include a wide range of innovative methods such as crop rotation, water conservation, water-fertilizer combination, physiological responses of plants, crop management and vegetative growth (Du et al., 2014, 2015).

In case of water scarcity, diluted saline water becomes the inevitable source for irrigation of plants. However, to ensure the safe use of saline water, effective crop management strategies are required to be developed in order to understand the response of crops to salinity (Bustan et al., 2004; Azeem et al., 2017a). The use of diluted saline water as an alternative resource for fresh water to irrigate the moderately salt tolerant crops will reduce irrigation cost, sustain agricultural productivity and save water resources. Thus, this comprehensive review aims to focus on the effect of rewatering or dilution of salted water on the photosynthetic responses in plants *growing* under saline stress (*Fig. 1*). Furthermore, this review emphasized the restoring abilities of plants from salt stress after re-watering or dilution of salted water.

Physiological response of plants to salt stresses

Photosynthetic characteristics

Salinity stress obstructs the physiological processes of plants (Negrão et al., 2017). It imposes a severe impact on the photosynthetic activity of plants (Sayed, 2003; Ashraf and Shahbaz, 2003; Kao et al., 2006; Munira et al., 2015; Habib et al., 2012; Hu et al., 2009). Photosynthesis is the most essential and complex functional process in all plants and a key factor in the development of plants. The stress induced by salinity impacts the overall capacity of photosynthesis (Ashraf and Harris, 2013). During salinity exposure, plants experience changes in photosynthetic characteristics, including transpiration rate (T_R), relative leaf water content (Lee et al., 2005) and photosynthetic pigments (Tort and Turkyilmaz, 2004; Murillo-Amador et al., 2007; Taffouo et al., 2010; Javed et al., 2017). However, the regulation of photosynthesis is being distressed through stomata limitation, thereby reducing T_R and leaf water potential (Ψ_L) (Azevedo Neto et al., 2004; Azeem et al., 2017b).

http://www.aloki.hu ● ISSN 1589 1623 (Print) ● ISSN 1785 0037 (Online)
DOI: http://dx.doi.org/10.15666/aeer/1705_1258312604

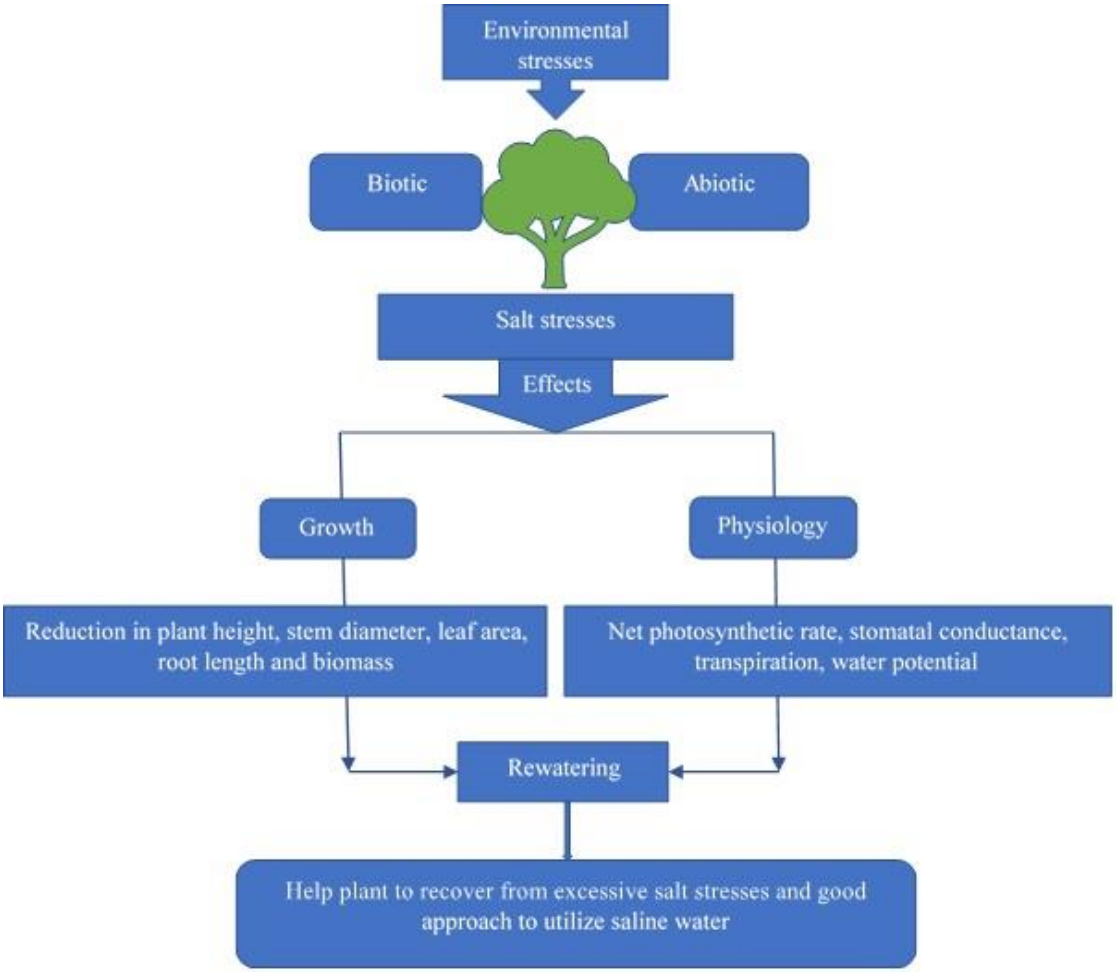

Figure 1. *Graphical representation of salt stress on plant and afterwards rewatering effects*

Stresses in plants inhibit the net photosynthetic rate (P_N) through stomatal opening-closing restrictions (Saibo et al., 2009; Rahnama et al., 2010), particularly in the case of green plants. Salt-stress in the leaves of tomato plants is increased through increased Na^+ concentration (Ullah et al., 2017). Salt stress of > 80 mM of NaCl strongly inhibited the P_N and stomata conductance (S_g). This indicated that the high salt concentration exhibited toxicity in the leaves of tomatoes, which is the main reason of reduction of S_g and P_N under high-stress (> 80 mM of NaCl) (Wang et al., 2011a). Limitation in S_g has been recorded usually at early stages of drought-stress, which in turn increases the water use efficiency (WUE). Stomatal closure has more inhibitory results on transpiration than diffusion of CO_2 into the leaf tissues (Sikuku et al., 2010). Though in comparison, under severe-stress dehydration takes place in mesophyll cells and initiating marked inhibition of necessary photosynthetic metabolic process as well as reduces WUE of plants (Damayanthi et al., 2011; Anjum et al., 2011). Yousif et al. (2010) examined the salt-tolerance difference mechanisms between water spinach (*Ipomoea aquatica* L.) and New Zealand spinach (*Tetragonia tetragonoides*). The P_N, S_g and T_R of both species are reduced with increasing salt-stress, but P_N, S_g and T_R in New Zealand spinach are maintained at 100 mM NaCl than in water spinach. Chartzoulakis et al. (2002a) observed the salt-stress caused by varying concentrations of NaCl (0, 25, 50, 100 and 200 mM) on the growth and photosynthetic traits of six olive

http://www.aloki.hu ● ISSN 1589 1623 (Print) ● ISSN 1785 0037 (Online)
DOI: http://dx.doi.org/10.15666/aeer/1705_1258312604

cultivars (Kalamata, Koroneiki, Mastoidis, Amphissis, Megaritiki and Kothreiki). The P_N and S_g of fully prolonged young leaves of all cultivars were reduced significantly at high concentrations of salinity > 100 mM. In all species, Kalamata showed the higher tolerance to salt stress at 100 mM NaCl, followed by Megaritiki and Kothreiki. Effects of abiotic stresses on plant physiology and their corresponding threshold values are shown in *Table 1*.

Table 1. *Effect of stresses on photosynthetic characteristics and their corresponding threshold values*

Stress	Plant species	Concentrations	P_N µmol m^2 s^{-1}	S_g mol m^{-2} s^{-1}	T_R mmol m^2 s^{-1}	Threshold levels	Resources
Salt-stress NaCl (mM)	New Zealand spinach (*Tetragonia tetragonoides*)	0	22.5	1.3	6.6	= 100	Yousif et al., 2010
		50	16.9	0.4	2.6		
		100	15.7	0.2	1.8	= 200	
		200	8.7	0.1	1.1		
Salt-stress NaCl (mM)	Water spinach (*Ipomoea aquatica* L.)	0	21.0	0.6	3.3	= < 100	Yousif et al., 2010
		50	11.9	0.1	1.4		
		100	10.7	0.08	0.9	= 200	
		200	0	0	0		
Salt-stress NaCl (mM)	Tomato	40	10	0.10	2.0	= < 120	Wang et al., 2011b
		80	7.8	0.07	1.8		
		120	6.0	0.05	1.5	> 120	
		160	5.0	0.04	1.45		
Salt-stress Ec (dsm^{-1})	*Brassica juncea* L. (*Varuna*)	0	20	0.07	3.2	= 4.2	Wani et al., 2013
		2.8	16	0.04	27		
		4.2	14	0.03	2.5	= 5.6	
		5.6	13	0.03	2.4		
Salt-stress Ec (dsm^{-1})	*Brassica juncea* L. (RH-30)	0	17	0.057	3.0	= < 4.2	Wani et al., 2013
		2.8	11	0.028	2.3		
		4.2	9	0.025	2.0	> 4.2	
		5.6	7	0.02	1.7		
Deficit irrigation ETc (%)	Cabbage (*Brassica oleracea* L.)	50			10	= 75	Xu and Leskovar, 2014
		75	18.6	0.357	12.1		
		100	21.6	0.472	14.4	= 50	
			23.6	0.673			
Drought stress (FC %)	*Medicago laciniata* saharian (Ml-90)	100	9.2	0.17	3.0	= 75	Yousfi et al., 2016
		75	6.3	0.11	1.8		
		35	4	0.07	1.6	= 35	
Drought stress (days of withheld irrigation)	Astragalus gombiformis Pomel	5	5.41	0.232	4.09	= 15	Boughalleb et al., 2016a
		10	5.61	0.229	4.00		
		15	5.04	0.205	3.58	= 20	
		20	4.95	0.171	3.19		
Irrigation water salinity	Barley cultivar [Morocco]	2	17.0	0.43	6.0	= 10	Mahlooji et al., 2018
		10	15.0	0.25	7.5		
		18	7.0	0.18	4.0		
	Barley cultivar [Nosrat]	2	16.0	0.38	6.9	> 10 < 18	
		10	24.5	0.27	8.5		
		18	14.2	0.25	6.7		
	Barley cultivar [Khatam]	2	22.0	0.35	5.8	= 18	
		10	19.4	0.28	7.4		
		18	19.2	0.26	5.5		

P_N is net photosynthetic rate; S_g is stomatal conductance; T_R is transpiration

http://www.aloki.hu ● ISSN 1589 1623 (Print) ● ISSN 1785 0037 (Online)
DOI: http://dx.doi.org/10.15666/aeer/1705_1258312604

Stomatal closure is one of the instant responses to water-stress. Generally the atmospheric vapor pressure and leaf turgor pressure can be disturbed because of reduction in stomatal opening in response to drought and salinity stress (Chaves et al., 2009; Javed et al., 2018). Therefore, reduction in P_N under traumatic conditions like drought, temperature, and salinity, is normally due to suppression in the mesophyll cells and stomatal opening-closing limitation (Flexas et al., 2004; Azeem et al., 2017a).

The research by Boughalleb et al. (2016a) on *Astragalus gombiformis Pomel*, found that P_N, S_g, T_R, and internal CO_2 concentration (Ci) was decreased significantly with water-stress duration as compared to that of well watered conditions. A Cerrado's native plant, *Campomanesia adamantinum* (*C. adamantium*) O. Berg, has a potential to exhibit stress tolerant abilities. It is susceptible to grow in an atmosphere of high temperature, dry land and water deficit region. During the experimental period, the photosynthetic factors are evaluated for *C. adamantium.* Seedlings are more stable for plants under control condition, and vast variations are noted in stress subjected plants. At the thirty-first day of water-deficit, S_g and T_R are reduced and P_N approaches to zero as 0.285 lmol m^{-2} s^{-1}. Consequently, WUE also reaches close to zero. Subsequently, the plants are rewatered to recover the photosynthetic metabolic activity (Junglos et al., 2016). Further, the threshold levels of photosynthetic capacity is explained by the extent to which the plants can withstand the stress imposed on the different features of photosynthesis, which can subsequently be used for rewatering of plants to regain the photosynthetic capacity affected by stresses.

Leaf water potential and carbonic anhydrase activity

The leaf water potential (Ψ_L) is termed as the energy status of water in the leaves. The comparative activity of S_g and P_N regulation is directed to water-use efficiency (Vos and Groenwold, 1989) and leaf water potential (Wani et al., 2013). Leaf water potential or leaf water status is a major factor affecting overall behavior and performance of stomata (Ruiz-Sýnchez et al., 1988). Salt-stress inhibits photosynthesis process by lowering Ψ_L (Parida and Das, 2005). Gorai et al. (2010) stated that limited supply of water reduced the dry weight of whole-plant, with a reduction in relative water content and Ψ_L. In certain studies, salt-stressed plants exhibit osmotic regulation due to changes in leaf water status (Kaymakanova and Stoeva, 2008; Gama et al., 2009). Among the different physiological parameters recommended to indicate water-status of vine, Ψ_L has been considered more feasible (Baeza et al., 2007) rather than S_g (Cifre et al., 2005) and temperature of leaf canopy (Bernard et al., 2004). However, there still exists some uncertainity as to which time plant shows the best water status, and what time of the day is optimum for measuring the water potential. (Deloire et al., 2004), used predawn Ψ_L as a standard to assess water-status at different stages of plants development in France. In Portugal, (Lopes, 1998), attained a very close relationship between P_N and predawn Ψ_L under water-stress conditions. Sato et al. (2006) checked the validity of predawn Ψ_L as an indicator for irrigation of wheat in northern Syria. Whereas, Intrigliolo et al. (2004) and Salón et al. (2005) measured Ψ_L during daylight and found that Ψ_L at mid-morning or at noon seem to execute the water-status better than predawn Ψ_L.

Williams and Araujo (2002) described that the measurements of plant water status are associated with plant physiology. According to Xiloyannis et al. (1997), olive plants (*Olea europaea*) adopt different strategies to survive under water-stress conditions as: (i) by lowering their Ψ_L and water content (WC) of leaf tissues, and then use soil water

http://www.aloki.hu ● ISSN 1589 1623 (Print) ● ISSN 1785 0037 (Online)
DOI: http://dx.doi.org/10.15666/aeer/1705_1258312604

up to −2.5 MPa; (ii) plants stop shoot's growth but not its P_N activity; (iii) adjustment of osmotic pressure, which is found to show a significant part in maintaining leaf cell activities. Generally, good positive relationships are found between S_g, Ψ_L and growth of plants. The growth of New Zealand spinach (*Tetragonia tetragonoides*) showed a notable reduction in Ψ_L and osmotic potential with increasing salinity. Water spinach showed tolerance and survived up to −1.99 Mpa (Yousif et al., 2010). Plant water status and stem water potential are used as indicators for irrigation scheduling, which requires the description of reference values or threshold values, in order to acheive the optimum irrigation levels. Depending on the response of plants in relationship with Ψ_L and WC, the obtained threshold values are −1.04 and −1.46 MPa, respectively for irrigation of apple varieties i.e., *Mutsu* and *CoxOrange* (De Swaef et al., 2009). Increasing salinity reduces the osmotic potential of the bean plants. This variation is considered as one of the defensive mechanism of plants to tolerate stresses. The values noticed indicate an inverse relationship between osmotic potential and salt stress in bean leaves. The statistical analysis revealed that the decline in osmotic potential is significant with increased NaCl concentration > 120 Mm (Qados, 2011).

A decline in water potential was noticed as a result of reducing relative WC (Kalapos, 1994; Bhatt et al., 2008). Therefore, some plants could convert intracellular HCO_3^- into CO_2 and H_2O by carbonic anhydrase activity (CA) to maintain water content. Carbonic anhydrase activity (CA) is very important in biological functions of plants that include reactions of carboxylation and decarboxylation and it is also takes part in the transporting of inorganic CO_2 to active photosynthetic cells (Henry, 1996). CA is a zinc containing enzyme activity, and is found in all living organisms. CA plays a dynamic role in assisting the transport of CO_2 and protons in intracellular spaces and in the layers of the extracellular space, across cell membranes. It is also involved in several other processes like photosynthesis and respiration. CA catalyzes the rapid inter conversion of HCO_3^- into CO_2 and H_2O. Meanwhile, CA activity is pretentious by deficiency of Zn and also takes part in sustaining the inorganic carbon levels (Tavallali et al., 2009). A reduction in CA activity caused by deficiency of Zn may contribute to the decrease in P_N (Hacisalihoglu et al., 2003).

CA activity helps plants to prevent from losses of water under traumatic environmental conditions (Hu et al., 2011). Kicheva and Lazova (1998) elucidated the reduction of CA activity in wheat seedlings in response to slight osmotic-stress. However, it increased rapidly under severe osmotic-stress conditions. It is noted that wheat cultivars differ in their response to drought stress with different CA activities (Guliyev et al., 2008). CA activities varied with plant species, osmotic-stress levels and stress durations. CA activity is higher in *Pharbitis nil* (*Linn.*) Choisy (*P. Nil*) than *Parthenocissus tricuspidata* (*Sieb. et Zucc.*) (*P. Tricuspidata*) and *Lonicera japonica* Thunb (*L. Japonica*) under drought-stress. CA activity is undetectable in *P. tricuspidata* but for *L. japonica*, CA activity is lower under medium or high stress, than that of the stress under low level. With an increase in drought stress duration, CA activity sharply decreases (Xing and Wu, 2012).

CA plays an important role in a number of physiological processes, such as maintaining acid-base balance, ion exchange, reactions of carboxylation and decarboxylation, and circulation of inorganic carbon between the cells (*Table 2*). CA regulates the photosynthetic mechanism in response to low stomata conductance (Wu and Xing, 2012). Xing and Wu (2015) examined the variations in CA activities with fluctuating nutrient levels for 3-climber species. *P. nil* showed higher CA activity when

http://www.aloki.hu ● ISSN 1589 1623 (Print) ● ISSN 1785 0037 (Online)
DOI: http://dx.doi.org/10.15666/aeer/1705_1258312604

compared with the other two species. While, *P. tricuspidata* showed the lowest and nearly undetectable CA activity. CA activity of *P. nil* under 1/2 and 1/4 strength nutrient solutions, is slightly higher than those under 1/16 and 1/32 strength nutrient solution. For *L. japonica*, CA activity is lower under control (full-strength nutrient solution) than those which are concealed under 1/4, 1/8, 1/16 and 1/32 strength nutrient solution. In previous studies, it is found that, by the regulation of CA activity P_N increased in *Orychophragmus violaceus (L.) O. E. Schulz* (*Orychophragmus violaceus*) and it is observed as a shade tolerant crop in comparison of other *Brassicaceae* species (Wu et al., 2007; Wu et al., 2005). Therefore, water status in crop can be maintained by the regulation of CA activity. As a result, carbon and water source are provided for the photosynthesis process by the plant (Hu et al., 2011). Hence, CA activity deeds for the survival of plants under stressed environments (Wu et al., 2011).

This section emphasized on two key factors *viz.,*(1) the water status and water potential of stem and leaves to indicate the threshold values for irrigation or rewatering of plants; (2) the role of CA activity for regulation of photosynthesis against stressful environments.

Table 2. *The role of CA activity during stress condition*

Plant species	Treatment	CA-activity role	Reference
Okra	Salt stress $NaCl + CaCl_2$	In moderate and low salt stress levels CA-activity play a main role to maintain plant water status	Azeem et al., 2017a
Orychophragmus violaceus (L.) O. E. Schulz and *Brassica napus* (*L.*)	Salt stress ($NaCl$, Na_2SO_4, $NaCl + Na_2SO_4$)	The CA-activity in plants showed good regulatory and was initially activated, when the leaves were under slight stress levels. A substantial increase of CA-activity noted under moderate-stress-levels. Due to regulation of CA-activity, photosynthetic activity was increase and showed development of growth parameters	Javed et al., 2018
Broussonetia papyrifera (L.) Vent. and *Morus alba* L.	Salt stress $NaHCO_3$	The stomatal opening and closing affected through variation in leaf-water potential, initiating an imbalance in gaseous exchange, and disturb the photosynthetic activity. To overcome this situation, CA-activity is become activated in leaves and providing partially carbon-water source to plants suffering from shortage of water	Wu and xing, 2012
Pharbitis nil (Linn.) Choisy, *Lonicera japonica* Thunb. and *Parthenocissus tricuspidata (Sieb. et Zucc.)*	Nutrient deficit (1/2,1/4,1/8,1/16,1/32)	CA-activity was increasing with nutrient deficit and activate when plant is going to stress due to nutrient deficit	Xing and Wu, 2015
Brassica napus (*L.*)	Drought stress (poly-ethylene glycol 6000 (i.e. 0, 20, 40 and 80 g L^{-1}))	CA-activity is also activated in drought stress when duration of drought was increasing. CA-activity helps plants during drought stress for H_20 and CO_2 regulation and maintain its growth	Xing et al., 2018

CA activity is carbonic anhydrase activity

Electrophysiological properties of plants

Plants are subjected to several diverse abiotic stresses throughout the growing season in the field (Tester and Bacic, 2005). Toxic effects imposed by salt stress decreased the production of new leaves and inhibited leaf expansion (Mansour and Salama, 2004). In plants, salt tolerance is attributed by structural and functional variations, such as plant growth regulation, Ψ_L and osmotic adjustment. Water deficiency and its stability in plants can be described through its electrophysiological properties, in which, Ψ_L of a plant was reflected by WC, capacitance and leaf air temperature.

http://www.aloki.hu ● ISSN 1589 1623 (Print) ● ISSN 1785 0037 (Online)
DOI: http://dx.doi.org/10.15666/aeer/1705_1258312604

A miniaturized, nondestructive sensor that employs a microwave micro strip ring resonator is developed for estimation of WC in single grain of wheat (Abraham et al., 2000) detected the amount of applied water/day, soil moisture content and leaf-air temperature based on electrical resistance. Koide (1991) revealed the relationship between Ψ_L with hydraulic resistance and capacitance of a plant. (Turner, 1988) used pressure chamber to calculte Ψ_L. While, Zhang et al. (2015) suggested the rapid measurement of drought resistance in the leaves of *Broussonetia papyrifera* (*B. Papyrifera*) and *Morus alba* (*M. Alba*) based on electrophysiological properties. A significant bonding is detected between physiological capacitance (C_p), WC and Ψ_L. The changes in physiological resistance and C_p, varied the water status in leaves (*Table 3*). Tensity of plant's leaf cell also can describe the status of water in leaf cells of plants, and that reflects the tolerance of plants to stress (Zhang et al., 2015). The outcomes of this review highlight the electrophysiological characteristics as rapid responses of plants to stress resistance. Furthermore, electrophysiological properties can be used to obtain precise information for irrigation and dilution of saline irrigation on the basis of water status in leaves.

Table 3. *Plants responses due to variation in water potential, physiological capacitance and leaf tensity under salt stress and re-watering*

Plant species	Salt treatments	Effect	Re-watering effect	Mechanism	Reference
Okra Abelmoschus esculentus	Salt stress (NaCl + $CaCl_2$)	Salt stress in every level reduces plant water potential and physiological capacitance	Recovery in the moderate and slow salt levels but could not recover in high salt stress	Plant stop to get water from root zone because of osmotic process	Azeem et al., 2017b
Orychophragmus violaceus (L.) O. E. Schulz and *Brassica napus* (L.)	Salt stress (NaCl + Na_2SO_4)	Physiological capacitance and leaf tensity of both species decline with increasing concentration of salts under single salts effect and a mixture of salts	Plant show better recovery during re-watering in single and mixture of salts, but single salts recover well	Due to excess amount of salts, plant leaf tissue loss the ability to hold water	Javed et al., 2017
Brassica napus (L.)	Drought stress poly-ethylene glycol 6000 (i.e. 0, 20, 40 and 80 g L^{-1})	Leaf water potential and physiological capacitance are decreased with increasing drought stress level	Re-water from 40-0 recover better, but 80-40 could not recover because higher drought damage plant leaf cell badly that could not recover during re-watering	During drought stomatal conductance decreased and effect the water regulation and sustainability	Xing et al., 2018

Plant growth features

Salinity is one of the key limiting factors affecting the physiological processes and its impacts may pose severe consequences on the growth of plants (Vilagrosa et al., 2003). The effect of salinity is different for different plant species and for different genotypes because plants exhibit unique tolerance mechanism (Memon et al., 2010; Gama et al., 2007). Salt stress inflicts biological disturbances in plants, causing adverse effects on plant growth, plant quality, and plant yield (Jouyban, 2012; Siddiqui et al., 2008; Qados, 2011). Mostly, species of brassica are considered to possess inbuilt salt tolerant mechanism because of their ability to cope up with salt-stress (Maggio et al., 2005; Hayat et al., 2007). This mechanism might be particularly significant with concerns for survival of salt tolerant plants. Previous studies point out the effects of salt stress on plant growth characteristics (Riccardi et al., 2014; Boughalleb et al., 2016b; Rameshwaran et al., 2016). Some researchers studied the relationship between the

http://www.aloki.hu ● ISSN 1589 1623 (Print) ● ISSN 1785 0037 (Online)
DOI: http://dx.doi.org/10.15666/aeer/1705_1258312604

reduction in plant length by increasing the concentrations of NaCl (Mustard and Renault, 2006; Jamil et al., 2007; Rui et al., 2009). Certain other studies elucidated the toxic effect of NaCl concentrations on leaf characteristics (Netondo et al., 2004; Chen et al., 2007; Yilmaz and Kina, 2008). The harmful effect of salinity on the number of leaves per plant also increases with increasing concentration of salts. Numerous studies have focused on the effect of varying concentration of salts on fresh and dry weight of plants, either positively or negatively, which is dependent on the nature of salt present (Bayuelo-Jimenez et al., 2002b; Niazi et al., 2005; Turan et al., 2007; Taffouo et al., 2009, 2010).

Drought-salt resistance in plants is explained by structural and functional adaptations, such as osmotic adjustment, Ψ_L, S_g limitations and growth regulation (Zollinger et al., 2007). Plants undergo different changes from the very onset period of salinity stress till maturity periods (Munns, 2002). The variations in the plant development differ with differing time scales after salinization. Quick response of salinity to plants result in dehydration of plant's cells and cell shrinkage, but some hours later on there occurs the regaining of cell volume. But this mechanism affects the cell elongation and division and thereby impacting the plant root growth and leaf size (Läuchli and Grattan, 2007). Understanding these times dependent mechanism of plants in response to salinity, lead to the accomplishment of "two-phase" growth responses to salinity (Munns, 2005).

Salinity exceeding 6 dS/m causes constriction in the length of stem and impacts severe consequences on fruit quality (Carter et al., 2005). Among cultivars, there are even dissimilarities with respect to the tolerance mechanism (Ahmad et al., 2005) and these differences are not parallel with seasonal tolerance, as explained by Nerson and Paris (1984) for melon, Heenan et al. (1988) rice, Bayuelo-Jimenez et al. (2002a) bean and Tajbakhsh et al. (2006) barley. The best growth of *Rhizophora mucronata Lam.* is attained at 50% seawater, and a further rise in salinity beyond this level scales down the growth (Aziz and Khan, 2001). Experimental results demonstrated that in a salt-stress condition, the mangrove *B. parviflora* shows optimal growth performance at 100 mM NaCl, however a further increase in NaCl concentration retards the growth of plant. A concentration of about 500 mM NaCl was found to be lethal to mangrove plants (Parida et al., 2004). The mangrove *Aegiceras corniculatum (L.) Blanco* shows tolerance up to 250 mM NaCl and is found to be dead beyond this concentration (Mishra and Das, 2003). Increased concentration of NaCl results in a significant reduction of root/shoot ratio and leaf growth biomass (Meloni et al., 2001). There is an overall trend found for the increase in the plant's lengths of the *Vicia faba* L. by using the concentrations of NaCl, 60 mM and 120 mM. More precisely, after treatment of 10 days, the increment is negatively correlated, by increasing NaCl concentration from 60 to 120 mM and consequently, 40% death of the plants occurs at initial stage by using highest concentration of 240 mM NaCl (Qados, 2011). Contrary results are recorded as well, such as Dantas et al. (2005) on cowpea (*Vigna unguiculata L.*), and Memon et al. (2010) on *Brassica campestris* L., specified that the usage of low concentrations of NaCl causes an increase in plant's height, whereas high NaCl concentrations affected the growth of plants. Studies on moth bean (*Vigna aconitifolia* L.) (Mathur et al., 2006), radish plant (*Raphanus sativus* L.) (Jamil et al., 2007) and *Vigna mungo* L. (Kapoor and Srivastava, 2010) indicated that increased NaCl concentrations causes a decline in plant's length.

http://www.aloki.hu ● ISSN 1589 1623 (Print) ● ISSN 1785 0037 (Online)
DOI: http://dx.doi.org/10.15666/aeer/1705_1258312604

In the light of the different tolerant mechanisms adopted by plants at their specific developmental stages against salinity, this review encompasses the reference levels or point for re-watering, the plants can endure after being exposed to salinity stress.

Effects of rewatering on the physiology of plants

Recovery of physiological parameters by rewatering

Photosynthetic responses to stresses are very complex and these include the chemistry of restrictions, taking place at diverse spots of leaf cell at different time periods in relation to the growth of plants (Boughalleb et al., 2016b). The stress intensity, duration and progression rate influence the plant responses to salinity and water shortage (Nohong and Nompo, 2015). These factors are associated with acclimation responses under drought stress, thereby affecting the photosynthetic rate indirectly. Under the influence of salinity, acclimation responses also include an adjustment in ion-transport such as uptake and extrusion of ions. These reactions are eventually clue to refurbishment of cellular homeostasis, shows survival of plants under stress (Chaves et al., 2009). Moreover, the carbon balance of plants during a period of water-stress and afterward regaining may depend as much on the recovery of P_N (Flexas et al., 2006). Overall, the plant recovers 40 to 60% of maximum photosynthetic rate only after rewatering, when subjected to extreme water-stress, and recovery is continued through the next days, but maximum P_N is not recovered always (Sofo et al., 2004). The strong influence of severe water-stress on P_N and its recovery has been established by Miyashita et al. (2005), in kidney bean and has been recommended by (Gómez-del-Campo et al., 2015), for *Vitis vinifera L.* plants.

Moreover, the recovery phase after stress release (e.g., irrigation or rewatering), becomes a major part of general plant biological responses to water-stress period. Recovery of the photosynthetic capability of plants from severe water-stress, defines the future growth development and survival of plants. Recently, this area is gaining much attention (Ennahli and Earl, 2005; Gallé et al., 2007; Xing et al., 2018; Javed et al., 2018; Azeem et al., 2017a). There is a need for further studies in order to understand the physiological basis and mechanism of recovery from water-stress. A method to assess the restriction of photosynthetic processes during water-stress time scales and then recovery has been suggested by Grassi and Magnani (2005), who recorded the results by dividing the total limitation into 3-parts: stomatal closure, diffusion of mesophyll and carboxylation activity. These outcomes highlight the importance of mesophyll conductance during stress periods and for further research, it suggests an important involvement in the overall plants adaptation to drought-stress. Additional short-term experiments on water stress revealed a reduction of mesophyll conductance (Galmés et al., 2007), indicating a general trend of stress and afterwards exhibits high resistance during rewatering. However, Badger and Price (1994) and Gillon and Yakir (2000) suggested that CA activity helps for regulation of mesophyll conductance during stress and facilitating diffusion of CO_2 at cellular level, and shows recovery (Flexas et al., 2008). *Campomanesia adamantinum O. Berg*, a salt tolerate plant, subjected to water deficit condition and rewatering which is done on day 31 from the onset of suspension of irrigation. The S_g and T_R began to drop from the 23rd day to 31st -day and photosynthetic rate approached to zero as 0.285 lmol m^{-2} s^{-1}. Therefore, WUE and Rubisco carboxylation activity are also reached to zero values. Subsequently, plants are rewatered to regain photosynthetic metabolism (Junglos et al., 2016). According to

http://www.aloki.hu ● ISSN 1589 1623 (Print) ● ISSN 1785 0037 (Online)
DOI: http://dx.doi.org/10.15666/aeer/1705_1258312604

Yousfi et al. (2016), there had been a small recovery after rewatering in some species of *Medicago laciniata L.* as a result of severe drought stress. During rewatering phase, the plants recovered their photosynthetic metabolism, with consequent increase rate of S_g, T_R and WUE (*Fig. 2*).

A small contribution is found in this aspect of study by Galle et al. (2009) in tobacco (*Nicotiana sylvestris*) and Flexas et al. (2009) for hybrid Richter-110 (*Vitis berlandieri* × *Vitis rupestris*), focusing on reduction of P_N under stress followed by rewatering to persuade recovery. In summary, the present literature strongly supports the important of rewatering and recovery of physiological parameters during rewatering as shown in *Figures 2* and *3*.

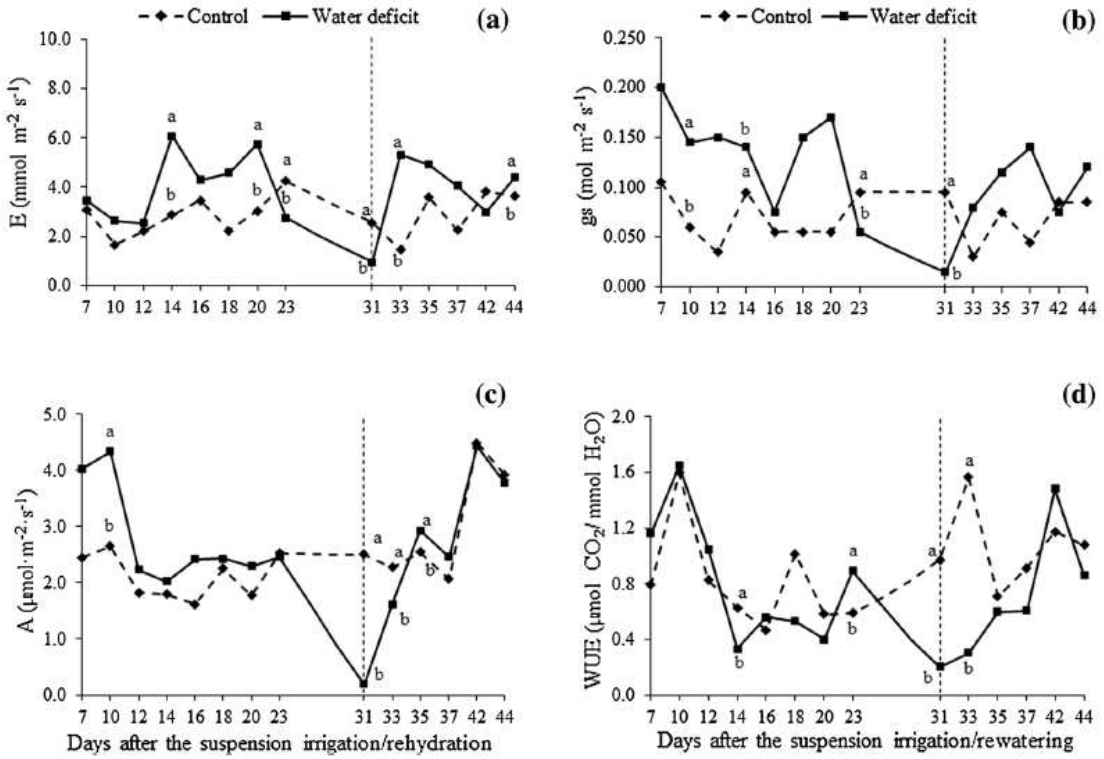

Figure 2. *Transpiration (TR = E) (a), stomatal conductance (Sg = gs) (b), photosynthetic rate (PN = A) (c), and water-use efficiency (WUE) (d) during different intervals when Campomanesia adamantium is grown in well-watered and water deficit condition (Junglos et al., 2016)*

Dilution of salt water

Generally, plants exhibit different physiological responses when subjected to slight, moderate and high salt stress. Many works have been done by researchers to check the response of different crops by using saline water (Turhan et al., 2014; Al-Harbi et al., 2015; Rameshwaran et al., 2016; Zhang et al., 2016; Martinez et al., 2018; de Cássia Alves et al., 2018; El-Mogy et al., 2018; Rodriguez-Ortega et al., 2017). Rewatering facilitates a positive response for plant water status and plant growth development. Over the last few years, many researchers have addressed the reaction of photosynthesis to rewatering after water-stress, which highlights the influence of salt stress and subsequent rewatering with pure water on plants (Hura et al., 2006; Pérez-Pérez et al.,

http://www.aloki.hu ● ISSN 1589 1623 (Print) ● ISSN 1785 0037 (Online)
DOI: http://dx.doi.org/10.15666/aeer/1705_1258312604

2007; Luo et al., 2008; Gomes et al., 2008). But none of these studies reflect the dilution of salted water or rewatering with saline water. However, by doing so it is possible to utilize the saline water resources for agricultural activities.

Moderately, salt-tolerant crop can be irrigated by diluted saline water, when freshwater resources are limited. Diluted saline water becomes the readily available water for irrigation of plants. The order of dilution or re-watering is that the plants are suffering in high concentration of salts irrigated with moderate concentration of salts. In another sense, at threshold levels, the plant can be re-watered with diluted saline water (Javed et al., 2017). The regime is considered very important in plants to adopt the behavior of salt tolerance under drought stress environment, at which P_N is sustained and recovered throughout the phases of water-stress (Chartzoulakis et al., 2002b). Junglos et al. (2016) rewatered *Campomanesia adamantinum O. Berg* plants when photosynthetic rate approached to zero. Therefore, it is essential for plants to be re-watered with diluted saline water prior to their wilting stages instead of applying direct saline-water to crops.

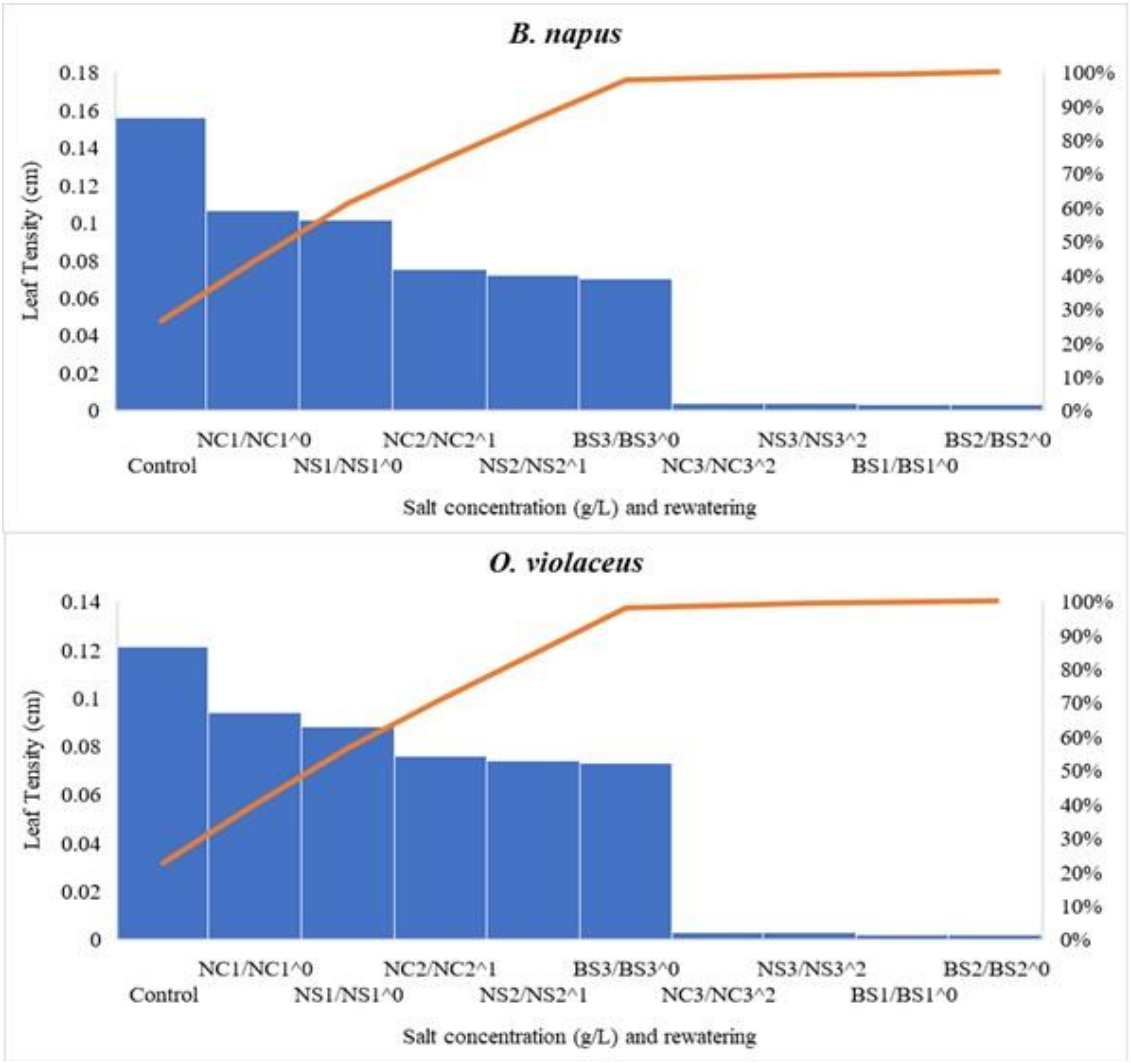

Figure 3. *Effect of salt stress on leaf tensity of Brassica napus and Orychophragmus violaceus under salt stress conditions followed by recovery during re-watering (Javed et al., 2017)*

http://www.aloki.hu ● ISSN 1589 1623 (Print) ● ISSN 1785 0037 (Online)
DOI: http://dx.doi.org/10.15666/aeer/1705_1258312604

This review thus suggested new insights in the agricultural field to design irrigation scheduling by considering the salt tolerant capability of crops as explained well in *Figure 4*.

Afterwards, irrigation water use efficiency can be ascertained through the application of precise irrigation quantity, based on the rewatering point. It would be an affirmative step, if implemented, to increase crop production in salt affected regions. It will aid in maintaining the stability between the irrigation amount and optimum crop water consumption and effective utilization of salt water, thereby reducing the everlasting demand fresh water resources for irrigation purposes.

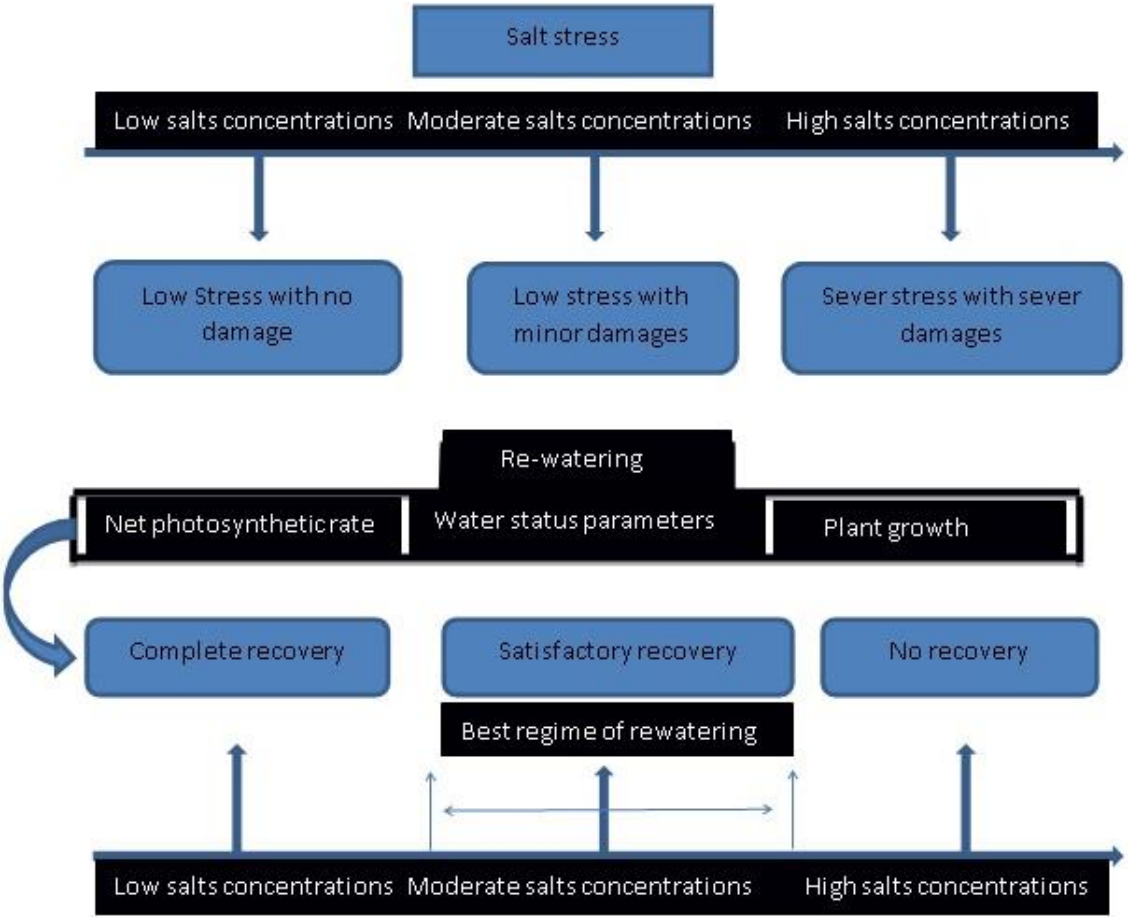

Figure 4. *Irrigation scheduling by considering the salt tolerant capability of crops*

Conclusion

This review briefly described the stress effects with respect to tolerance and physiological performances of plants. The review provides information for precise theoretical and practical irrigation based on physiological and electrophysiological characteristics. Efforts have been made to link the relative tolerance of several plant species to salt stress and subsequent rewatering with regard to toxicity under stress and their recoveries after rewatering. Present facts offer some strategies to counteract salt stress in crops through rewatering. Hence this review affirms the promising future of increasing crop production even under saline conditions. However, the vast majorities of research have focused on stress responses based on irrigation of plants. Plant

http://www.aloki.hu ● ISSN 1589 1623 (Print) ● ISSN 1785 0037 (Online)
DOI: http://dx.doi.org/10.15666/aeer/1705_1258312604

response to stresses and then rewatering with saline water is a good approach in the field of saline irrigation and is a boon for regions where fresh water resources are limited. Therefore, the effect of salinity in plant could be reduced by diluting the saline irrigation (re-watering) response to threshold growth and photosynthetic values. Application of dilution of saline irrigation could be helpful to save water resources, maintain crop productivity even in stressful environments and reduces irrigation cost. It is recommended based on findings of this review; short experiment in controlled environment can be done to determine the dilution point for re-watering of different crops before wilting. Afterwards, this information can be utilized for irrigation of open field crops with diluted water.

Acknowledgements. We would like to acknowledge that this work was supported by the State Key Research Development Program of China (2017YFC1200103). The National Natural Science Foundation of China (31570414, 31770446), Project Funded by the Priority Academic Program Development of Jiangsu Higher Education Institutions (PAPD), Jiangsu Collaborative Innovation Center of Technology and Material of Water Treatment.

REFERENCES

[1] Abraham, N., Hema, P., Saritha, E., Subramannian, S. (2000): Irrigation automation based on soil electrical conductivity and leaf temperature. – Agricultural Water Management 45: 145-157.

[2] Ahmad, S., Wahid, A., Rasul, E., Wahid, A. (2005): Comparative morphological and physiological responses of green gram genotypes to salinity applied at different growth stages. – Botanical Bulletin of Academia Sinica 46: 135-142.

[3] Al-Harbi, A. R., Al-Omran, A. M., Alenazi, M. M., Wahb-Allah, M. A. (2015): Salinity and deficit irrigation influence tomato growth, yield and water use efficiency at different developmental stages. – International Journal of Agriculture, Biology 17(2): 241-250.

[4] Anjum, S. A., Xie, X.-Y., Wang, L.-C., Saleem, M. F., Man, C., Lei, W. (2011): Morphological, physiological and biochemical responses of plants to drought stress. – African Journal of Agricultural Research 6: 2026-2032.

[5] Ashraf, M., Harris, P. (2013): Photosynthesis under stressful environments: an overview. – Photosynthetica 51: 163-190.

[6] Ashraf, M., Shahbaz, M. (2003): Assessment of genotypic variation in salt tolerance of early CIMMYT hexaploid wheat germplasm using photosynthetic capacity and water relations as selection criteria. – Photosynthetica 41: 273-280.

[7] Azeem, A., Wu, Y., Javed, Q., Xing, D., Ullah, I., Kumi, F. (2017a): Response of okra based on electrophysiological modeling under salt stress and re-watering. – Bioscience Journal 33.

[8] Azeem, A., Wu, Y., Xing, D., Javed, Q., Ullah, I. (2017b): Photosynthetic response of two okra cultivars under salt stress and re-watering. – Journal of Plant Interactions 12: 67-77.

[9] Azevedo Neto, A. D. D., Prisco, J. T., Enéas-Filho, J., Lacerda, C. F. D., Silva, J. V., Costa, P. H. A. D., Gomes-Filho, E. (2004): Effects of salt stress on plant growth, stomatal response and solute accumulation of different maize genotypes. – Brazilian Journal of Plant Physiology 16: 31-38.

[10] Aziz, I., Khan, M. A. (2001): Effect of Seawater on the Growth, Ion Content and Water Potential of *Rhizophora mucronata Lam.* – Journal of Plant Research 114: 369-373.

[11] Badger, M. R., Price, G. D. (1994): The role of carbonic anhydrase in photosynthesis. – Annual Review of Plant Biology 45: 369-392.

http://www.aloki.hu ● ISSN 1589 1623 (Print) ● ISSN 1785 0037 (Online)
DOI: http://dx.doi.org/10.15666/aeer/1705_1258312604

[12] Baeza, P., Sánchez-De-Miguel, P., Centeno, A., Junquera, P., Linares, R., Lissarrague, J. R. (2007): Water relations between leaf water potential, photosynthesis and agronomic vine response as a tool for establishing thresholds in irrigation scheduling. – Scientia Horticulturae 114: 151-158.
[13] Bayuelo-Jimenez, J. S., Craig, R., Lynch, J. P. (2002a): Salinity tolerance of species during germination and early seedling growth. – Crop Science 42: 1584-1594.
[14] Bayuelo-Jimenez, J. S., Debouck, D. G., Lynch, J. P. (2002b): Salinity tolerance in Phaseolus species during early vegetative growth. (Plant Genetic Resources). – Crop Science 42: 2184-2193.
[15] Bernard, N., Zebic, O., Deloire, A. (2004): Estimation de l'état hydrique de la vigne par la mesure de la température foliaire: Un outil au service des professionnels. – Le Progrès Agricole et Viticole 121: 539-542.
[16] Bhatt, M. J., Patel, A. D., Bhatti, P. M., Pandey, A. N. (2008): Effect of soil salinity on growth, water status and nutrient accumulation in seedlings of *Ziziphus mauritiana (rhamnaceae)*. – Journal of Fruit Ornamental and Plant Research 16: 383-401.
[17] Biswas, A. K. (2008): Integrated water resources management: is it working? – Water Resources Development 24: 5-22.
[18] Boughalleb, F., Abdellaoui, R., Brahim, N. B., Neffati, M. (2016a): Growth, photosynthesis, water use efficiency, and osmoregulation of the wild species *Astragalus gombiformis Pomel*. – Under water deficit. Brazilian Journal of Botany 39: 147-156.
[19] Boughalleb, F., Abdellaoui, R., Brahim, N. B., Neffati, M. (2016b): Growth, photosynthesis, water use efficiency, and osmoregulation of the wild species *Astragalus gombiformis Pomel*. – Under water deficit. Brazilian Journal of Botany 39: 147-156.
[20] Bustan, A., Sagi, M., De Malach, Y., Pasternak, D. (2004): Effects of saline irrigation water and heat waves on potato production in an arid environment. – Field Crops Research 90: 275-285.
[21] Carter, C., Grieve, C., Poss, J. (2005): Salinity effects on emergence, survival, and ion accumulation of *Limonium perezii*. – Journal of Plant Nutrition 28: 1243-1257.
[22] Chartzoulakis, K., Loupassaki, M., Bertaki, M., Androulakis, I. (2002a): Effects of NaCl salinity on growth, ion content and CO 2 assimilation rate of six olive cultivars. – Scientia Horticulturae 96: 235-247.
[23] Chartzoulakis, K., Patakas, A., Kofidis, G., Bosabalidis, A., Nastou, A. (2002b): Water stress affects leaf anatomy, gas exchange, water relations and growth of two avocado cultivars. – Scientia Horticulturae 95: 39-50.
[24] Chaves, M., Flexas, J., Pinheiro, C. (2009): Photosynthesis under drought and salt stress: regulation mechanisms from whole plant to cell. – Annals of Botany 103: 551-560.
[25] Chen, C., Tao, C., Peng, H., Ding, Y. (2007): Genetic analysis of salt stress responses in asparagus bean (*Vigna unguiculata (L.) ssp. sesquipedalis Verdc.*). – Journal of Heredity 98: 655-665.
[26] Cifre, J., Bota, J., Escalona, J., Medrano, H., Flexas, J. (2005): Physiological tools for irrigation scheduling in grapevine (*Vitis vinifera L.*): An open gate to improve water-use efficiency? – Agriculture, Ecosystems & Environment 106: 159-170.
[27] Damayanthi, M., Mohotti, A., Nissanka, S. (2011): Comparison of tolerant ability of mature field grown tea (*Camellia sinensis L.*) cultivars exposed to a drought stress in Passara Area. – Tropical Agricultural Research 22. DOI: 10.4038/tar.v22i1.2671.
[28] Dantas, B. F., Ribeiro, L. D. S., Aragão, C. A. (2005): Physiological response of cowpea seeds to salinity stress. – Revista Brasileira de Sementes 27: 144-148.
[29] De Cássia Alves, R., De Medeiros, A. S., Nicolau, M. C. M., De Assis Oliveira, F., Lima, L. W., Aroucha, E. M. M., Gratão, P. L. (2018): Influence of partial root-zone saline irrigation management on tomato yield and fruit quality from a potted-plant study. – HortScience 53: 1326-1331.

http://www.aloki.hu ● ISSN 1589 1623 (Print) ● ISSN 1785 0037 (Online)
DOI: http://dx.doi.org/10.15666/aeer/1705_1258312604

[30] De Swaef, T., Steppe, K., Lemeur, R. (2009): Determining reference values for stem water potential and maximum daily trunk shrinkage in young apple trees based on plant responses to water deficit. – Agricultural Water Management 96: 541-550.
[31] Deloire, A., Carbonneau, A., Wang, Z., Ojeda, H. (2004): Vine and water: a short review. – OENO One 38: 1-13.
[32] Du, T., Kang, S., Zhang, X., Zhang, J. (2014): China's food security is threatened by the unsustainable use of water resources in North and Northwest China. – Food and Energy Security 3: 7-18.
[33] Du, T., Kang, S., Zhang, J., Davies, W. J. (2015): Deficit irrigation and sustainable water-resource strategies in agriculture for China's food security. – Journal of Experimental Botany 66: 2253-2269.
[34] El-Mogy, M. M., Garchery, C., Stevens, R. (2018): Irrigation with salt water affects growth, yield, fruit quality, storability and marker-gene expression in cherry tomato. – Acta Agriculturae Scandinavica, Section B - Soil & Plant Science. DOI: 10.1080/09064710.2018.1473482.
[35] Ennahli, S., Earl, H. J. (2005): Physiological limitations to photosynthetic carbon assimilation in cotton under water stress. – Crop Science 45: 2374-2382.
[36] Flexas, J., Bota, J., Loreto, F., Cornic, G., Sharkey, T. (2004): Diffusive and metabolic limitations to photosynthesis under drought and salinity in C3 plants. – Plant Biology 6: 269-279.
[37] Flexas, J., Bota, J., Galmes, J., Medrano, H., Ribas-Carbó, M. (2006): Keeping a positive carbon balance under adverse conditions: responses of photosynthesis and respiration to water stress. – Physiologia Plantarum 127: 343-352.
[38] Flexas, J., Ribas-Carbo, M., Diaz-Espejo, A., Galmes, J., Medrano, H. (2008): Mesophyll conductance to CO2: current knowledge and future prospects. – Plant, Cell & Environment 31: 602-621.
[39] Flexas, J., Barón, M., Bota, J., Ducruet, J.-M., Gallé, A., Galmés, J., Jiménez, M., Pou, A., Ribas-Carbó, M., Sajnani, C. (2009): Photosynthesis limitations during water stress acclimation and recovery in the drought-adapted Vitis hybrid Richter-110 (V. berlandieri × V. rupestris). – Journal of Experimental Botany 60: 2361-2377.
[40] Flowers, T., Yeo, A. (1995): Breeding for salinity resistance in crop plants: where next? – Functional Plant Biology 22: 875-884.
[41] Galle, A., Florez-Sarasa, I., Tomas, M., Pou, A., Medrano, H., Ribas-Carbo, M., Flexas, J. (2009): The role of mesophyll conductance during water stress and recovery in tobacco (*Nicotiana sylvestris*): acclimation or limitation? – Journal of Experimental Botany 60: 2379-2390.
[42] Gallé, A., Haldimann, P., Feller, U. (2007): Photosynthetic performance and water relations in young pubescent oak (*Quercus pubescens*) trees during drought stress and recovery. – New Phytologist 174: 799-810.
[43] Galmés, J., Medrano, H., Flexas, J. (2007): Photosynthetic limitations in response to water stress and recovery in Mediterranean plants with different growth forms. – New Phytologist 175: 81-93.
[44] Gama, P., Inanaga, S., Tanaka, K., Nakazawa, R. (2007): Physiological response of common bean (*Phaseolus vulgaris L.*) seedlings to salinity stress. – African Journal of Biotechnology 6(2).
[45] Gama, P. B. S., Tanaka, K., Eneji, A. E., Eltayeb, A. E., Siddig, K. E. (2009): Salt-induced stress effects on biomass, photosynthetic rate, and reactive oxygen species-scavenging enzyme accumulation in common bean. – Journal of Plant Nutrition 32: 837-854.
[46] Garcia, L. E. (2008): Integrated water resources management: a 'small'step for conceptualists, a giant step for practitioners. – Water Resources Development 24: 23-36.
[47] Gillon, J. S., Yakir, D. (2000): Internal conductance to CO2 diffusion and C18OO discrimination in C3 leaves. – Plant Physiology 123: 201-214.

http://www.aloki.hu ● ISSN 1589 1623 (Print) ● ISSN 1785 0037 (Online)
DOI: http://dx.doi.org/10.15666/aeer/1705_1258312604

[48] Gomes, F. P., Oliva, M. A., Mielke, M. S., De Almeida, A.-A. F., Leite, H. G., Aquino, L. A. (2008): Photosynthetic limitations in leaves of young Brazilian Green Dwarf coconut (*Cocos nucifera L. 'nana'*) palm under well-watered conditions or recovering from drought stress. – Environmental and Experimental Botany 62: 195-204.
[49] Gómez-Del-Campo, M., Baeza, P., Ruiz, C., Sotés, V., Lissarrague, J. (2015): Effect of previous water conditions on vine response to rewatering. – *VITIS*-Journal of Grapevine Research 46: 51.
[50] Gorai, M., Hachef, A., Neffati, M. (2010): Differential responses in growth and water relationship of *Medicago sativa (L.) cv. Gabès* and *Astragalus gombiformis (Pom.)* under water-limited conditions. – Emirates Journal of Food and Agriculture 22: 1.
[51] Grassi, G., Magnani, F. (2005): Stomatal, mesophyll conductance and biochemical limitations to photosynthesis as affected by drought and leaf ontogeny in ash and oak trees. – Plant, Cell & Environment 28: 834-849.
[52] Guliyev, N., Bayramov, S., Babayev, H. (2008): Effect of Water Deficit on RUBISCO and carbonic Anhydrase Activities in Different Wheat Genotypes. – In: Allen, J. F. et al. (eds.) Photosynthesis. Energy from the Sun. Springer, Dordrecht.
[53] Habib, N., Ashraf, M., Ali, Q., Perveen, R. (2012): Response of salt stressed okra (*Abelmoschus esculentus Moench*) plants to foliar-applied glycine betaine and glycine betaine containing sugarbeet extract. – South African Journal of Botany 83: 151-158.
[54] Hacisalihoglu, G., Hart, J. J., Wang, Y.-H., Cakmak, I., Kochian, L. V. (2003): Zinc efficiency is correlated with enhanced expression and activity of zinc-requiring enzymes in wheat. – Plant Physiology 131: 595-602.
[55] Hayat, S., Ali, B., Hasan, S. A., Ahmad, A. (2007): Effect of 28-homobrassinolide on salinity-induced changes in *Brassica juncea.* – Turkish Journal of Biology 31: 141-146.
[56] Heenan, D., Lewin, L., Mccaffery, D. (1988): Salinity tolerance in rice varieties at different growth stages. – Animal Production Science 28: 343-349.
[57] Henry, R. P. (1996): Multiple roles of carbonic anhydrase in cellular transport and metabolism. – Annual Review of Physiology 58: 523-538.
[58] Hu, H., Boisson-Dernier, A., Israelsson-Nordström, M., Böhmer, M., Xue, S., Ries, A., Godoski, J., Kuhn, J. M., Schroeder, J. I. (2011): Carbonic anhydrases are upstream regulators of CO2-controlled stomatal movements in guard cells. – Nature Cell Biology 13: 734-734.
[59] Hu, L., Wang, Z., Huang, B. (2009): Photosynthetic responses of bermudagrass to drought stress associated with stomatal and metabolic limitations. – Crop Science 49: 1902-1909.
[60] Hura, T., Grzesiak, S., Hura, K., Grzesiak, M., Rzepka, A. (2006): Differences in the physiological state between triticale and maize plants during drought stress and followed rehydration expressed by the leaf gas exchange and spectrofluorimetric methods. – Acta Physiologiae Plantarum 28: 433-443.
[61] Intrigliolo, D., Castel, J., Perez, D. (2004): Water relations of field grown drip irrigated Tempranillo grapevines. – VII International Symposium on Grapevine Physiology and Biotechnology 689: 317-324.
[62] Jamil, M., Rehman, S., Rha, E. (2007): Salinity effect on plant growth, PSII photochemistry and chlorophyll content in sugar beet (Beta Vulgaris L.) and cabbage (*Brassica Oleracea Capitata L.*). – Pakistan Journal of Botany 39: 753-760.
[63] Javed, Q., Wu, Y., Xing, D., Azeem, A., Ullah, I., Zaman, M. (2017): Re-watering: An effective measure to recover growth and photosynthetic characteristics in salt-stressed *Brassica napus L.* – Chilean Journal of Agricultural Research 77: 78-86.
[64] Javed, Q., Wu, Y., Xing, D., Ullah, I., Azeem, A., Rasool, G. (2018): Salt-induced effects on growth and photosynthetic traits of *Orychophragmus violaceus* and its restoration through re-watering. – Brazilian Journal of Botany 41: 29-41.
[65] Jouyban, Z. (2012): The effects of salt stress on plant growth. – Tech J Engin & App Sci 2: 7-10.

http://www.aloki.hu ● ISSN 1589 1623 (Print) ● ISSN 1785 0037 (Online)
DOI: http://dx.doi.org/10.15666/aeer/1705_1258312604

[66] Junglos, F. S., Junglos, M. S., Dresch, D. M., Pereira, N. S., Kodama, F. M., De Paula Quintão Scalon, S. (2016): Recovery of the photosynthetic capacity of *Campomanesia adamantium (Myrtaceae)* after water deficit. – Brazilian Journal of Botany 39: 541-546.
[67] Kalapos, T. (1994): Leaf water potential-leaf water deficit relationship for ten species of a semiarid grassland community. – Plant and Soil 160: 105-112.
[68] Kao, W.-Y., Tsai, T.-T., Tsai, H.-C., Shih, C.-N. (2006): Response of three Glycine species to salt stress. – Environmental and Experimental Botany 56: 120-125.
[69] Kapoor, K., Srivastava, A. (2010): Assessment of salinity tolerance of Vinga mungo var. Pu-19 using ex vitro and in vitro methods. – Asian J. Biotechnol 2: 73-85.
[70] Kaymakanova, M., Stoeva, N. (2008): Physiological reaction of bean plants (*Phaseolus vulg. L.*) to salt stress. – General and Applied Plant Physiology (Special Issue) 34(3-4): 177-188.
[71] Kicheva, M., Lazova, G. (1998): Response of carbonic anhydrase to polyethylene glycol-mediated water stress in wheat. – Photosynthetica 34: 133-135.
[72] Koide, R. T. (1991): Nutrient supply, nutrient demand and plant response to mycorrhizal infection. – New Phytologist 117: 365-386.
[73] Läuchli, A., Grattan, S. (2007): Plant Growth and Development under Salinity Stress. – In: Jenks, M. A. et al. (eds.) Advances in Molecular Breeding Toward Drought and Salt Tolerant Crops. Springer, Dordrecht.
[74] Lee, G., Carrow, R. N., Duncan, R. R. (2005): Growth and water relation responses to salinity stress in halophytic seashore paspalum ecotypes. – Scientia Horticulturae 104: 221-236.
[75] Lopes, C. M. (1998): Relationships between leaf water potential and photosynthetic activity of field-grown grapevines under a Mediterranean environment. – I ISHS Workshop on Water Relations of Grapevines 493: 287-292.
[76] Luo, H., Zhang, Y., Zhang, W., Bai, H., He, Z., Du, M., Zhang, H. (2008): Effects of Rewatering after Drought Stress on Photosynthesis and Yield during Flowering and Boll-Setting Stage of Cotton Under-Mulch-Drip Irrigation in Xinjiang. – Acta Agronomica Sinica 34: 171.
[77] Lutz, W., Butz, W. P., Samir, K. E. (2017): World Population & Human Capital in the Twenty-First Century: An Overview. – Oxford University Press, Oxford.
[78] Maggio, A., De Pascale, S., Ruggiero, C., Barbieri, G. (2005): Physiological response of field-grown cabbage to salinity and drought stress. – European Journal of Agronomy 23: 57-67.
[79] Mahlooji, M., Sharifi, R. S., Razmjoo, J., Sabzalian, M., Sedghi, M. (2018): Effect of salt stress on photosynthesis and physiological parameters of three contrasting barley genotypes. – Photosynthetica 56: 549-556.
[80] Mansour, M. M. F., Salama, K. H. (2004): Cellular basis of salinity tolerance in plants. – Environmental and Experimental Botany 52: 113-122.
[81] Martinez, V., Nieves-Cordones, M., Lopez-Delacalle, M., Rodenas, R., Mestre, T. C., Garcia-Sanchez, F., Rubio, F., Nortes, P. A., Mittler, R., Rivero, R. M. (2018): Tolerance to stress combination in tomato plants: new insights in the protective role of melatonin. – Molecules 23: 535.
[82] Mathur, N., Singh, J., Bohra, S., Bohra, A., Vyas, A. (2006): Biomass production, productivity and physiological changes in moth bean genotypes at different salinity levels. – American Journal of Plant Physiology 1: 210-213.
[83] Meloni, D. A., Oliva, M. A., Ruiz, H. A., Martinez, C. A. (2001): Contribution of proline and inorganic solutes to osmotic adjustment in cotton under salt stress. – Journal of Plant Nutrition 24: 599-612.
[84] Memon, S. A., Hou, X., Wang, L. J. (2010): Morphological analysis of salt stress respose of pak choi. – Electronic Journal of Environmental, Agricultural & Food Chemistry 9: 248-254.

http://www.aloki.hu ● ISSN 1589 1623 (Print) ● ISSN 1785 0037 (Online)
DOI: http://dx.doi.org/10.15666/aeer/1705_1258312604

[85] Mishra, S., Das, A. (2003): Effect of NaCl on leaf salt secretion and antioxidative enzyme level in roots of a mangrove, *Aegiceras corniculatum*. – Indian Journal of Experimental Biology 41: 160-166.
[86] Miyashita, K., Tanakamaru, S., Maitani, T., Kimura, K. (2005): Recovery responses of photosynthesis, transpiration, and stomatal conductance in kidney bean following drought stress. – Environmental And Experimental Botany 53: 205-214.
[87] Mosaffa, H. R., Sepaskhah, A. R. (2018): Performance of irrigation regimes and water salinity on winter wheat as influenced by planting methods. – Agricultural Water Management. https://doi.org/10.1016/j.agwat.2018.10.027.
[88] Munira, S., Hossain, M., Zakaria, M., Ahmed, J., Islam, M. (2015): Evaluation of Potato Varieties against Salinity Stress in Bangladesh. – International Journal of Plant and Soil Science 6: 73-81.
[89] Munns, R. (2002): Comparative physiology of salt and water stress. – Plant, Cell & Environment 25: 239-250.
[90] Munns, R. (2005): Genes and salt tolerance: bringing them together. – New Phytologist 167: 645-663.
[91] Munns, R., Tester, M. (2008): Mechanisms of salinity tolerance. – Annual Review of Plant Biology 59: 651-681.
[92] Murillo-Amador, B., Yamada, S., Yamaguchi, T., Rueda-Puente, E., Ávila-Serrano, N., García-Hernández, J., López-Aguilar, R., Troyo-Diéguez, E., Nieto-Garibay, A. (2007): Influence of calcium silicate on growth, physiological parameters and mineral nutrition in two legume species under salt stress. – Journal of Agronomy and Crop Science 193: 413-421.
[93] Mustard, J., Renault, S. (2006): Response of red-osier dogwood (Cornus sericea) seedlings to NaCl during the onset of bud break. – Botany 84: 844-851.
[94] Nadeem, S. M., Ahmad, M., Zahir, Z. A., Javaid, A., Ashraf, M. (2014): The role of mycorrhizae and plant growth promoting rhizobacteria (PGPR) in improving crop productivity under stressful environments. – Biotechnology Advances 32: 429-448.
[95] Nangare, D., Singh, Y., Kumar, P. S., Minhas, P. (2016): Growth, fruit yield and quality of tomato (Lycopersicon esculentum Mill.) as affected by deficit irrigation regulated on phenological basis. – Agricultural Water Management 171: 73-79.
[96] Negrão, S., Schmöckel, S. M., Tester, M. (2017): Evaluating physiological responses of plants to salinity stress. – Annals of Botany 119: 1-11.
[97] Nerson, H., Paris, H. (1984): Effects of salinity on germination, seedling growth, and yield of melons. – Irrigation Science 5: 265-273.
[98] Netondo, G. W., Onyango, J. C., Beck, E. (2004): Sorghum and salinity. – Crop Science 44: 797-805.
[99] Niazi, B., Athar, M., Salim, M., Rozema, J. (2005): Growth and ionic relations of fodderbeet and seabeet under saline environments. – International Journal of Environmental Science & Technology 2: 113-120.
[100] Nohong, B., Nompo, S. (2015): Effect of water stress on growth, yield, proline and soluble sugars contents of Signal grass and Napier grass species. – American-Eurasian Journal of Sustainable Agriculture 9: 14-21.
[101] Parida, A. K., Das, A. B. (2005): Salt tolerance and salinity effects on plants: a review. – Ecotoxicology and Environmental Safety 60: 324-349.
[102] Parida, A. K., Das, A., Mittra, B. (2004): Effects of salt on growth, ion accumulation, photosynthesis and leaf anatomy of the mangrove, *Bruguiera parviflora*. – Trees 18: 167-174.
[103] Pérez-Pérez, J., Syvertsen, J. P., Botía, P., García-Sánchez, F. (2007): Leaf water relations and net gas exchange responses of salinized *Carrizo citrange* seedlings during drought stress and recovery. – Annals of Botany 100: 335-345.
[104] Qados, A. M. A. (2011): Effect of salt stress on plant growth and metabolism of bean plant *Vicia faba (L.)*. – Journal of the Saudi Society of Agricultural Sciences 10: 7-15.

http://www.aloki.hu ● ISSN 1589 1623 (Print) ● ISSN 1785 0037 (Online)
DOI: http://dx.doi.org/10.15666/aeer/1705_1258312604

[105] Rady, M. O., Semida, W. M., El-Mageed, T. A. A., Hemida, K. A., Rady, M. M. (2018): Up-regulation of antioxidative defense systems by glycine betaine foliar application in onion plants confer tolerance to salinity stress. – Scientia Horticulturae 240: 614-622.
[106] Rahnama, A., Poustini, K., Tavakkol-Afshari, R., Tavakoli, A. (2010): Growth and stomatal responses of bread wheat genotypes in tolerance to salt stress. – International Journal of Biology and Life Sciences 6: 216-221.
[107] Rameshwaran, P., Tepe, A., Yazar, A., Ragab, R. (2016): Effects of drip-irrigation regimes with saline water on pepper productivity and soil salinity under greenhouse conditions. – Scientia Horticulturae 199: 114-123.
[108] Riccardi, M., Pulvento, C., Lavini, A., D'andria, R., Jacobsen, S. E. (2014): Growth and ionic content of quinoa under saline irrigation. – Journal of Agronomy And Crop Science 200: 246-260.
[109] Rodriguez-Ortega, W., Martinez, V., Rivero, R., Camara-Zapata, J., Mestre, T., Garcia-Sanchez, F. (2017): Use of a smart irrigation system to study the effects of irrigation management on the agronomic and physiological responses of tomato plants grown under different temperatures regimes. – Agricultural Water Management 183: 158-168.
[110] Rui, L., Wei, S., Muxiang, C., Chengjun, J., Min, W., Boping, Y. (2009): Leaf anatomical changes of *Bruguiera gymnorrhiza* seedlings under salt stress. – Journal of Tropical and Subtropical Botany 17: 169-175.
[111] Ruiz-Sýnchez, M., Torrecillas, A., Del Amor, F., Leon, A., Abrisqueta, J. (1988): Leaf water potential and leaf conductance during the growing season in almond trees under different irrigation regimes. – Biologia Plantarum 30: 327-332.
[112] Saibo, N. J., Lourenço, T., Oliveira, M. M. (2009): Transcription factors and regulation of photosynthetic and related metabolism under environmental stresses. – Annals of Botany 103: 609-623.
[113] Salón, J. L., Chirivella, C., Castel, J. R. (2005): Response of cv. Bobal to timing of deficit irrigation in Requena, Spain: water relations, yield, and wine quality. – American Journal of Enology and Viticulture 56: 1-8.
[114] Sato, T., Abdalla, O. S., Oweis, T. Y., Sakuratani, T. (2006): The validity of predawn leaf water potential as an irrigation-timing indicator for field-grown wheat in northern Syria. – Agricultural Water Management 82: 223-236.
[115] Sayed, O. (2003): Chlorophyll fluorescence as a tool in cereal crop research. – Photosynthetica 41: 321-330.
[116] Shahbaz, M., Ashraf, M. (2013): Improving salinity tolerance in cereals. – Critical Reviews in Plant Sciences 32: 237-249.
[117] Siddiqui, Z. S., Khan, M. A., Kim, B.-G., Huang, J.-S., Kwon, T.-R. (2008): Physiological responses of *Brassica napus* genotypes to combined drought and salt stress. – Plant Stress 2: 78-83.
[118] Sikuku, P., Netondo, G., Onyango, J., Musyimi, D. (2010): Chlorophyll fluorescence, protein and chlorophyll content of three nerica rainfed rice varieties under varying irrigation regimes. – ARPN Journal of Agricultural and Biological Science 5: 19-25.
[119] Singh, A. (2018): Salinization of agricultural lands due to poor drainage: a viewpoint. – Ecological Indicators 95: 127-130.
[120] Sofo, A., Dichio, B., Xiloyannis, C., Masia, A. (2004): Effects of different irradiance levels on some antioxidant enzymes and on malondialdehyde content during rewatering in olive tree. – Plant Science 166: 293-302.
[121] Souza Filho, A., Alves, S., Figueiredo, F. (2003): Allelopathic effects of calopo according to its age and to seed density of the receiver plant. – Planta Daninha 21: 211-218.
[122] Taffouo, V., Wamba, O., Youmbi, E., Nono, G., Akoa, A. (2010): Growth, yield, water status and ionic distribution response of three bambara groundnut (*Vigna subterranea (L.) Verdc.*) landraces grown under saline conditions. – International Journal of Botany 6: 53-58.

http://www.aloki.hu ● ISSN 1589 1623 (Print) ● ISSN 1785 0037 (Online)
DOI: http://dx.doi.org/10.15666/aeer/1705_1258312604

[123] Taffouo, V. D., Kouamou, J. K., Ngalangue, L. M. T., Ndjeudji, B. A. N., Akoa, A. (2009): Effects of salinity stress on growth, ions partitioning and yield of some cowpea (*Vigna unguiculata L. Walp.*) cultivars. – International Journal of Botany 5: 135-143.
[124] Tajbakhsh, M., Zhou, M., Chen, Z., Mendham, N. (2006): Physiological and cytological response of salt-tolerant and non-tolerant barley to salinity during germination and early growth. – Animal Production Science 46: 555-562.
[125] Tavallali, V., Rahemi, M., Maftoun, M., Panahi, B., Karimi, S., Ramezanian, A., Vaezpour, M. (2009): Zinc influence and salt stress on photosynthesis, water relations, and carbonic anhydrase activity in pistachio. – Scientia Horticulturae 123: 272-279.
[126] Tester, M., Bacic, A. (2005): Abiotic stress tolerance in grasses. From model plants to crop plants. – Plant Physiology 137: 791-793.
[127] Tort, N., Turkyilmaz, B. (2004): A physiological investigation on the mechanisms of salinity tolerance in some barley culture forms. – JFS 27: 1-16.
[128] Turan, M. A., Katkat, V., Taban, S. (2007): Salinity-induced stomatal resistance, proline, chlorophyll and ion concentrations of bean. – International Journal of Agricultural Research 2: 483-488.
[129] Turhan, A., Kuşçu, H., Özmen, N., Demir, A. O. (2014): The effect of different salinity levels on the yield and some quality parameters of garlic (*Allium sativum L.*). – Journal of Agricultural Sciences (Turkey) 20(3): 280-287.
[130] Turner, N. C. (1988): Measurement of plant water status by the pressure chamber technique. – Irrigation Science 9: 289-308.
[131] Ullah, I., Hanping, M., Chuan, Z., Javed, Q., Azeem, A. (2017): Optimization of irrigation and nutrient concentration based on economic returns, substrate salt accumulation and water use efficiency for tomato in greenhouse. – Archives of Agronomy and Soil Science 63: 1748-1762.
[132] Vilagrosa, A., Bellot, J., Vallejo, V., Gil-Pelegrín, E. (2003): Cavitation, stomatal conductance, and leaf dieback in seedlings of two co-occurring Mediterranean shrubs during an intense drought. – Journal of Experimental Botany 54: 2015-2024.
[133] Vos, J., Groenwold, J. (1989): Genetic differences in water-use efficiency, stomatal conductance and carbon isotope fractionation in potato. – Potato Research 32: 113-121.
[134] Wang, R., Kang, Y., Wan, S., Hu, W., Liu, S., Liu, S. (2011a): Salt distribution and the growth of cotton under different drip irrigation regimes in a saline area. – Agricultural Water Management 100: 58-69.
[135] Wang, X., Geng, S., Ri, Y.-J., Cao, D., Liu, J., Shi, D., Yang, C. (2011b): Physiological responses and adaptive strategies of tomato plants to salt and alkali stresses. – Scientia Horticulturae 130: 248-255.
[136] Wani, A. S., Ahmad, A., Hayat, S., Fariduddin, Q. (2013): Salt-induced modulation in growth, photosynthesis and antioxidant system in two varieties of *Brassica juncea*. – Saudi Journal of Biological Sciences 20: 183-193.
[137] Williams, L., Araujo, F. (2002): Correlations among predawn leaf, midday leaf, and midday stem water potential and their correlations with other measures of soil and plant water status in *Vitis vinifera*. – Journal of the American Society for Horticultural Science 127: 448-454.
[138] Wu, Y., Xing, D. (2012): Effect of bicarbonate treatment on photosynthetic assimilation of inorganic carbon in two plant species of *Moraceae*. – Photosynthetica 50: 587-594.
[139] Wu, Y., Wu, X., Li, P., Zhao, Y., Li, X., Zhao, X. (2005): Comparison of photosynthetic activity of *Orychophragmus violaceus* and oil-seed rape. – Photosynthetica 43: 299-302.
[140] Wu, Y., Li, P., Zhao, Y., Wang, J., Wu, X. (2007): Study on photosynthetic characteristics of *Orychophragmus violaceus* related to shade-tolerance. – Scientia Horticulturae 113: 173-176.
[141] Wu, Y., Shi, Q., Wang, K., Li, P., Xing, D., Zhu, Y., Song, Y. (2011): An Electrochemical Approach Coupled with Sb Microelectrode to Determine the Activities

http://www.aloki.hu ● ISSN 1589 1623 (Print) ● ISSN 1785 0037 (Online)
DOI: http://dx.doi.org/10.15666/aeer/1705_1258312604

of Carbonic Anhydrase in the Plant Leaves. – In: Zeng, D. (ed.) Future Intelligent Information Systems. – Springer, Berlin.
[142] Xiloyannis, C., Dichio, B., Nuzzo, V., Celano, G. (1997): Defence strategies of olive against water stress. – III International Symposium on Olive Growing 474: 423-426.
[143] Xing, D., Wu, Y. (2012): Photosynthetic response of three climber plant species to osmotic stress induced by polyethylene glycol (PEG) 6000. – Acta Physiologiae Plantarum 34: 1659-1668.
[144] Xing, D., Wu, Y. (2015): Effects of low nutrition on photosynthetic capacity and accumulation of total N and P in three climber plant species. – Chinese Journal of Geochemistry 34: 115-122.
[145] Xing, D., Xu, X., Wu, Y., Liu, Y., Wu, Y., Ni, J., Azeem, A. (2018): Leaf tensity: a method for rapid determination of water requirement information in *Brassica napus L.* – Journal of Plant Interactions 13: 380-387.
[146] Xu, C., Leskovar, D. (2014): Growth, physiology and yield responses of cabbage to deficit irrigation. – HortScience (Prague) 41: 138-146.
[147] Yepes, L., Chelbi, N., Vivo, J.-M., Franco, M., Agudelo, A., Carvajal, M., Del Carmen Martínez-Ballesta, M. (2018): Analysis of physiological traits in the response of Chenopodiaceae, *Amaranthaceae, and Brassicaceae* plants to salinity stress. – Plant Physiology and Biochemistry 132: 145-155.
[148] Yilmaz, H., Kina, A. (2008): The influence of NaCl salinity on some vegetative and chemical changes of strawberries (*Fragaria x ananssa L.*). – African Journal of Biotechnology 7(18).
[149] Yousfi, N., Sihem, N., Ramzi, A., Abdelly, C. (2016): Growth, photosynthesis and water relations as affected by different drought regimes and subsequent recovery in *Medicago laciniata (L.)* populations. – Journal of Plant Biology 59: 33-43.
[150] Yousif, B. S., Nguyen, N. T., Fukuda, Y., Hakata, H., Okamoto, Y., Masaoka, Y., Saneoka, H. (2010): Effect of salinity on growth, mineral composition, photosynthesis and water relations of two vegetable crops; New Zealand spinach (*Tetragonia tetragonioides*) and water spinach (*Ipomoea aquatica*). – International Journal of Agriculture and Biology 12: 211-216.
[151] Zhang, L., Clarke, M., Steven, M., Jaggard, K. (2011): Spatial patterns of wilting in sugar beet as an indicator for precision irrigation. – Precision Agriculture 12: 296-316.
[152] Zhang, M., Wu, Y., Xing, D., Zhao, K., Yu, R. (2015): Rapid Measurement of Drought Resistance in Plants Based on Electrophysiological Properties. – Transactions of the ASABE 58: 1441-1446.
[153] Zhang, P., Senge, M., Dai, Y. (2016): Effects of salinity stress on growth, yield, fruit quality and water use efficiency of tomato under hydroponics system. – Reviews in Agricultural Science 4: 46-55.
[154] Zollinger, N., Koenig, R., Cerny-Koenig, T., Kjelgren, R. (2007): Relative salinity tolerance of intermountain western United States native herbaceous perennials. – HortScience 42: 529-534.

http://www.aloki.hu ● ISSN 1589 1623 (Print) ● ISSN 1785 0037 (Online)
DOI: http://dx.doi.org/10.15666/aeer/1705_1258312604

IMPACT OF VERTICAL LEVEL DISTRIBUTIONS ON SIMULATED STRATOSPHERIC CLIMATE

LIU, X. Y.[1*] – LU, C. C.[2]

[1]*College of Oceanography, Hohai University, Nanjing 210098, China*

[2]*College of Meteorology and Oceanography, National University of Defense Technology Nanjing 211101, China*

[*]*Corresponding author*
e-mail: xyliu@hhu.edu.cn

(Received 17th May 2019; accepted 16th Jul 2019)

Abstract. The climate of stratosphere was simulated with a spectral element model under two different vertical level distributions, one had 28 levels with 0.3 hPa at the top of the atmosphere and another 66 levels with 4.5×10^{-6} hPa at the top boundary. Simulation results were validated against ERA-Interim reanalysis dataset from ECMWF (European Center for Medium-Range Weather Forecasts) and the influence of vertical level distributions on the numerical simulation of stratospheric temporal mean state had been analyzed. It is shown that the lift of upper boundary can reduce the temperature error above the height of 100 hPa level significantly. It can also improve the simulation of seasonal variation of zonal mean zonal wind on 50 hPa in the northern high latitudes. In both configurations, cold biases of 10-year averaged zonal mean of temperature are mainly discerned at levels around 75 hPa at low latitudes and levels around 175 hPa at high southern latitudes. The simulated seasonal variation of westerly at 50 hPa in the northern hemisphere with 66-layer model coincides with results of ERA-Interim better.
Keywords: *spectral element, atmospheric model, vertical resolution, numerical modeling, middle atmosphere*

Introduction

With the advancement of observation technique, there have been more observations available in the stratosphere and their reliability has improved greatly as well. People have come to possess more knowledge of variation tendency of the stratospheric climate and have deepened their understanding on the anthropogenic and natural factors that contribute to the climate change. People also have a more comprehensive understanding of the connections in processes of dynamics and radiation thermodynamics between the changes in the stratosphere and that specific to the earth's surface. For example, it has been realized that temperature change in the stratosphere is an important component of the global climate change, and its trend can give evidence for the separation of natural and anthropogenic effects contributing to the climate change (Randel et al., 2009); the vapor in the stratosphere plays an important role in the radiation balance of troposphere (Held and Soden, 2000); the stratosphere can influence the climate of the earth surface as well as its variability through the remote response mechanism between the stratosphere and the troposphere (Baldwin et al., 2007; Mitchell et al., 2013); and so on. The researches on the stratospheric climate are getting more people's attention. Of which, numerical modeling is an important direction.

In atmospheric climate models, two discretization methods, which are finite difference and spectral approximation, are mostly used to solve the partial differential equations numerically. Other methods, such as finite element, finite volume and so on are also used in some models. The advantage of finite difference is that it is simple and

http://www.aloki.hu ● ISSN 1589 1623 (Print) ● ISSN 1785 0037 (Online)
DOI: http://dx.doi.org/10.15666/aeer/1705_1260512614

intuitive and easy for implementation of parallel computing. But it has the weakness of low accuracy compared to spectral approximation. The advantage of spectral method is that it has high accuracy. But since spectral approximation is carried out on the whole domain of computation, its local errors can disseminate to large area and it is hard to implement parallel computing basing on the idea of region splitting. The finite element method has the merits that it is suitable for seeking solution for domain of complex geometry; it is flexible and also easy for parallel computing. But it cannot give high accuracy solution as the spectral method does. The finite volume method can be used to construct discreet scheme more flexibly than the finite difference method and it share similar merits and weakness with the finite difference method. The spectral element method combines the merits of high accuracy from spectral approximation and flexibility from finite element discretization (Patera, 1984). The basic idea of performing computation with spectral element method is dividing the domain into finite elements and then solving the problem with spectral approximation within each of them. The spectral element method has been used widely in numerical modeling of geophysical fluid dynamics (Founier et al., 2004; Giraldo, 2005; Liu, 2011).

Many climate models used mainly for troposhere study cannot depict the stratosphere well due to their low height of top boundaries. In theses low top models, although reasonable mean climate can be reproduced through introducing damping at their top boundaries, which usually situate at the stratosphere, the simulated variability is small. There have been increasing evidences showing that the variability in the stratosphere has significant influence on the modes of climate variability in the troposphere and the earth surface (Norton, 2003; Charlton et al., 2004; Scaife et al., 2005). Besides, the influence of climate change on the stratospheric circulation is a hot topic in current scientific research, whereas the reactions of stratospheric circulation variation to ozone and earth surface climate are unclear to a large extent (Butchart and Scaife, 2001; Butchart et al., 2006; Abalos et al., 2015; Linz et al., 2017).

Since the paper of Boville (1984), many works on the influence of the middle atmosphere on the properties of the tropospheric simulation have been performed (for example, Boville and Cheng, 1988; Boville and Baumhefner, 1990; Sassi, 2010; Shaw and Perlwitz, 2010). Ruosteenoja (2006) studied the sensitivity of the simulations of tropospheric stationary waves to the height of the model top with a linear model. It is of necessity to study the influence of the height of model top on the simulation of stratosphere as well. In the paper, a model, in which the prognostic variables are discretized with spectral element method in the horizontal and the whole stratosphere is included, will be used to simulate the stratospheric climate under configuration of two different top boundary extensions; and, if a lid in the mesosphere versus one in the lower thermosphere makes any difference to the representation of climate in the stratosphere will be studied. The work will enrich the understanding on the sensitivity of the simulations of stratospheric climate to the height of the model top and contribute to the choice of model resolution for study of stratosphere.

Materials and Methods

The atmospheric general circulation model SEMANS (Spectral Element Model with Atmospheric Near Space resolved) (Liu et al., 2015) is used in the work. It uses a horizontal coordinate on the projection plane of cubed sphere (Ronchi et al., 1996) and a p-σ mixed vertical coordinate (Simmons and Burridge, 1981). The model prognostic

http://www.aloki.hu ● ISSN 1589 1623 (Print) ● ISSN 1785 0037 (Online)
DOI: http://dx.doi.org/10.15666/aeer/1705_1260512614

variables are discretized with spectral element method in the horizontal and finite difference in the vertical respectively. When spectral element discretization is used, a triangular or quadrilateral basic element (Giraldo, 2005; Liu, 2011) is often adopted. SEMANS adopts a quadrilateral basic element. By using of coordinate on the projection plane of cubed sphere, SEMANS can overcome the difficulty of polar problem which is unavoidable in longitude-latitude grids. Through using of p-$\boldsymbol{\sigma}$ mixed vertical coordinate, the model can treat topography easily and reduces the error from calculation of pressure gradient at high altitude of the atmosphere as well. Schemes used for physical processes are shown in *Table 1*.

Table 1. *Schemes used for physical processes*

Physical process	Scheme used
Deep convection	Zhang and McFarlane (1995)
Shallow convection	Park and Bretherton (2009)
Boundary layer parameterization	Nonlocal diffusion scheme (Holtslag and Boville, 1993)
Near surface constant flux over land	Monin-Obukhov similarity theory
Near surface constant flux over ocean water and sea ice	Bulk formula
Thermal radiation	Ramanathan et al.(1986)
Solar radiation for height below 60 km	δ-Eddington approximation (Briegleb, 1992)
Solar radiation for height above 100 km	Radiation heating rates from TIME-GCM (Thermosphere Ionosphere Mesosphere Electrodynamics General Circulation Model) (Marsh and Roble, 2002)
Solar radiation for height between 60 km and 100 km	Weighted average of TIME-GCM results and output of radiation transfer with δ-Eddington approximation

The low boundary value, initial value and the data for validation of simulation results are all from the ERA-Interim reanalysis datasets (Simmons et al., 2007). In model validation, the reanalysis data from 1997 to 2006 will be used.

Two numerical experiments were designed. In the first one (denoted by EXP1), the model atmosphere was divided into 28 layers and the air pressure of model top is 0.3 hPa (see *Fig. 1a*); in the second one (denoted by EXP2), the model atmosphere was divided into 66 layers and the air pressure of model top is 4.5×10^{-6} hPa (*Fig. 1b*). In both numerical experiments, every projected plane was divided into 81 basic elements (*Fig. 1c*) and the 8^{th} degree Gauss-Legendre-Lobatto interpolation polynomials were used to approximate the solution with spectral method within each basic element (*Fig. 1d*). Since the model atmosphere in EXP2 had extended beyond 100 km in altitude, the radiation transfer scheme in EXP1 was no longer valid for high level atmosphere. In EXP2, radiation heating rates from TIME-GCM (Thermosphere Ionosphere Mesosphere Electrodynamics General Circulation Model) (Marsh and Roble, 2002) were used in model layers above a certain height (approximately 100 km); in model layers below a certain height (approximately 65 km) radiation transfer scheme identical to that of EXP1 were used; in model layers between the two heights, weighted average of TIME-GCM results and radiation transfer results of EXP2 were used (chemical processes were not considered here). The atmospheric state at 0000 UTC 1 January 1997 from the ERA-Interim datasets was used as initial values. For model layers above the height of 1 hPa level, initial values of model variables are identical to those of the highest model layer just below the height of 1 hPa level. The low boundary

http://www.aloki.hu ● ISSN 1589 1623 (Print) ● ISSN 1785 0037 (Online)
DOI: http://dx.doi.org/10.15666/aeer/1705_1260512614

conditions (ground surface temperature, sea ice concentration, soil moisture etc) are all multi-year (1997-2006) means with monthly variations included. In each numerical experiment, the model was integrated for 20 years and monthly mean results were saved. If not noted specifically, the results for model output and reanalysis all denote 10 year mean case.

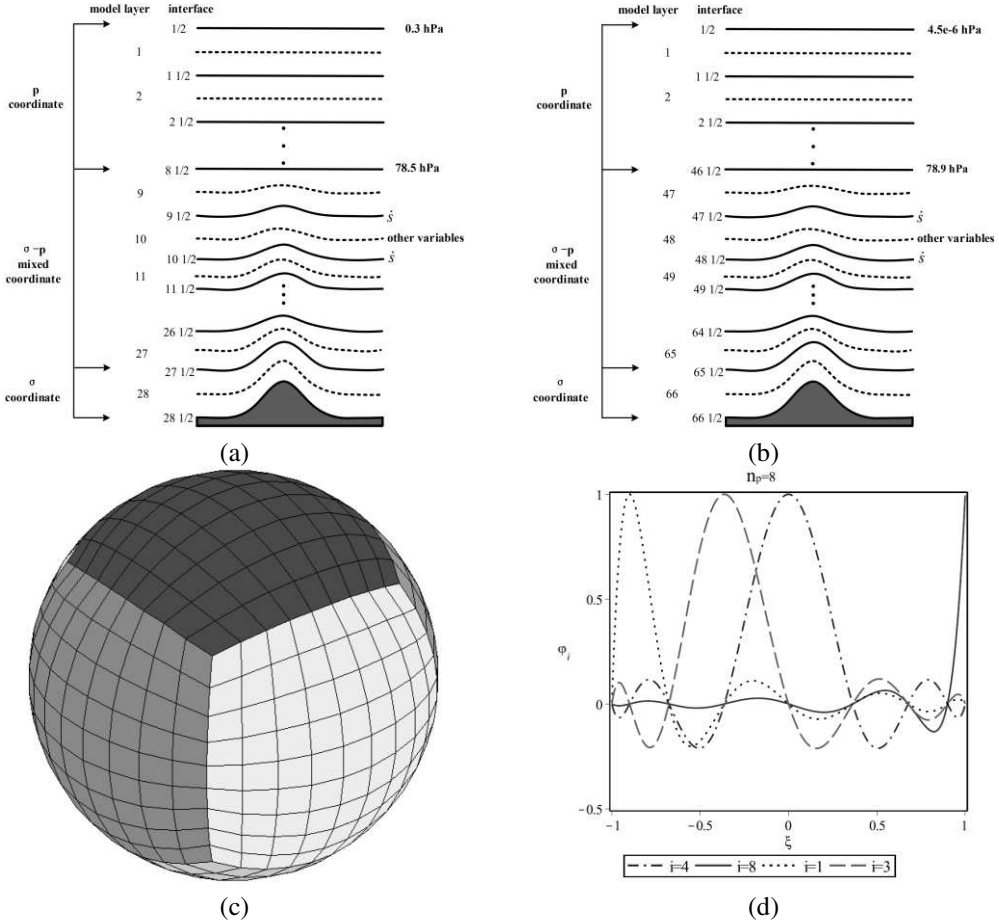

Figure 1. *Discretization of SEMANS. (a) vertical division of model atmosphere in version of 28 layers, (b) vertical division of model atmosphere in version of 66 layers, (c) projected grids on cubed sphere (81 elements in each face), (d) Gauss-Legendre-Lobatto interpolation polynomials in local coordinate from -1 to 1 (with a degree of 8)*

Results

The two numerical experiments all reproduce such features as the 2-wave pattern in the northern hemisphere and the 1-wave pattern in the southern hemisphere of geopotential at 20 hPa. The strength of simulated perturbation in the northern hemisphere is weaker than that of the reanalysis data and the strength of simulated perturbation in the northern hemisphere is close to that of the reanalysis data (see *Fig. 2*). The patterns of geopotential reproduced by both the 28 layer version and the 66 layer version of SEMANS are similar, whereas the values from the 28 layer version are bigger (compare *Fig. 2a* with *2b*). Compared to results from reanalysis dataset, the extent encircled by the 26400 geopotential meter contour is smaller (compare *Fig. 2a* with *2c*).

http://www.aloki.hu ● ISSN 1589 1623 (Print) ● ISSN 1785 0037 (Online)
DOI: http://dx.doi.org/10.15666/aeer/1705_1260512614

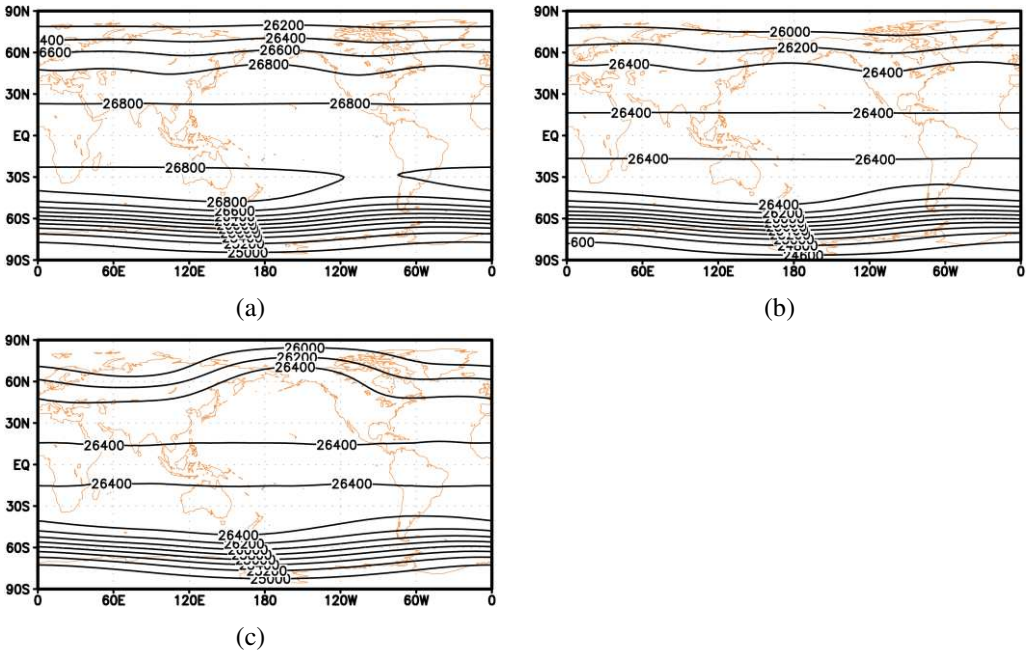

Figure 2. *Distribution of geopotential height at 20hPa (unit:gpm). (a) EXP1, (b) EXP2, (c) ERA-Interim. The horrizontal axis is longitude (°) and the vertical axis is latitude (°) in each panel*

From the 10-year averaged zonal mean temperature difference (*Fig. 3*), it can be seen that, the simulated climate features of temperature are similar from the two different configurations of SEMANS; the cold biases of zonal mean temperature in the low latitudes are mainly confined to the atmospheric levels around 75 hPa; there are cold biases above the height of 20 hPa level in the two polar regions and the biases from the 66-layer configuration are relatively smaller; there are also severe cold biases around the 175 hPa level in the southern high latitudes and the region near 45°N (compare *Fig. 3a* with *3b*).

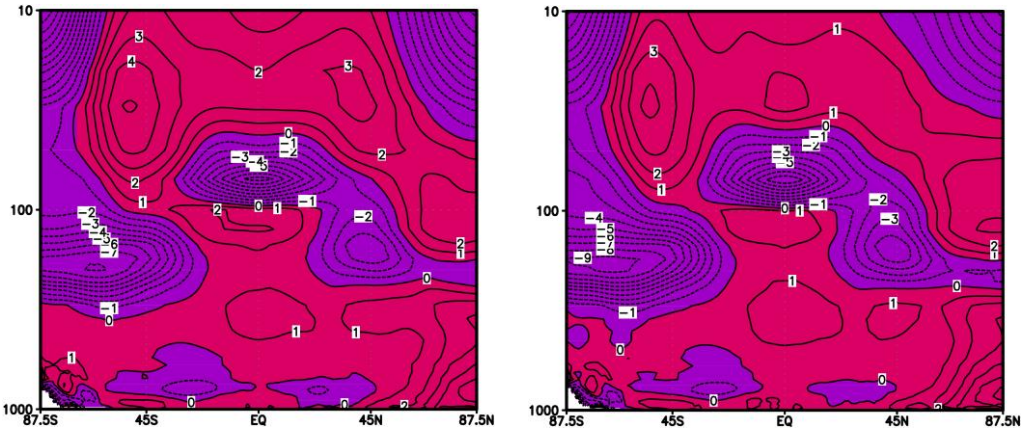

Figure 3. *Difference of zonal mean temperature (unit:K) between model results and ERA-Interim. (a) EXP1 minus ERA-Interim, (b) EXP2 minus ERA-Interim. The horrizontal axis is latitude (°) and the vertical axis is pressure (hPa) in each panel*

http://www.aloki.hu ● ISSN 1589 1623 (Print) ● ISSN 1785 0037 (Online)
DOI: http://dx.doi.org/10.15666/aeer/1705_1260512614

The divisions of model atmosphere are identical within the troposphere in the two configurations. But due to the influence of differences in the height of model top and divisions of model atmosphere at higher levels, there are also differences in the reproduced temperature of troposphere, which are quite smaller compared to that of stratosphere.

From the differences of regionally averaged temperature between model results and ERA-Interim (*Fig. 4*), it is clear that, the simulated temperature biases varies with height in the same manner for results in EXP1 and its counterpart in EXP2; the globally averaged annual mean temperature from the 66-layer model is colder than that from the 28-layer model (see *Fig. 4a*); in the winter, the simulated temperatures above the height of 100 hPa level in the high latitudes of both hemisphere are warmer in EXP2 (see *Fig. 4b* and *4d*); in the summer, the simulated temperatures above the height of 100 hPa level in the high latitudes of both hemisphere are colder in EXP2 (see *Fig. 4c* and *4e*). It's apparent that the biases of simulated temperature above the height of 100hPa level are smaller in EXP2. In contrast, the biases of simulated regionally averaged temperature in the high latitudes in both the spring and the autumn are smaller (figures not shown).

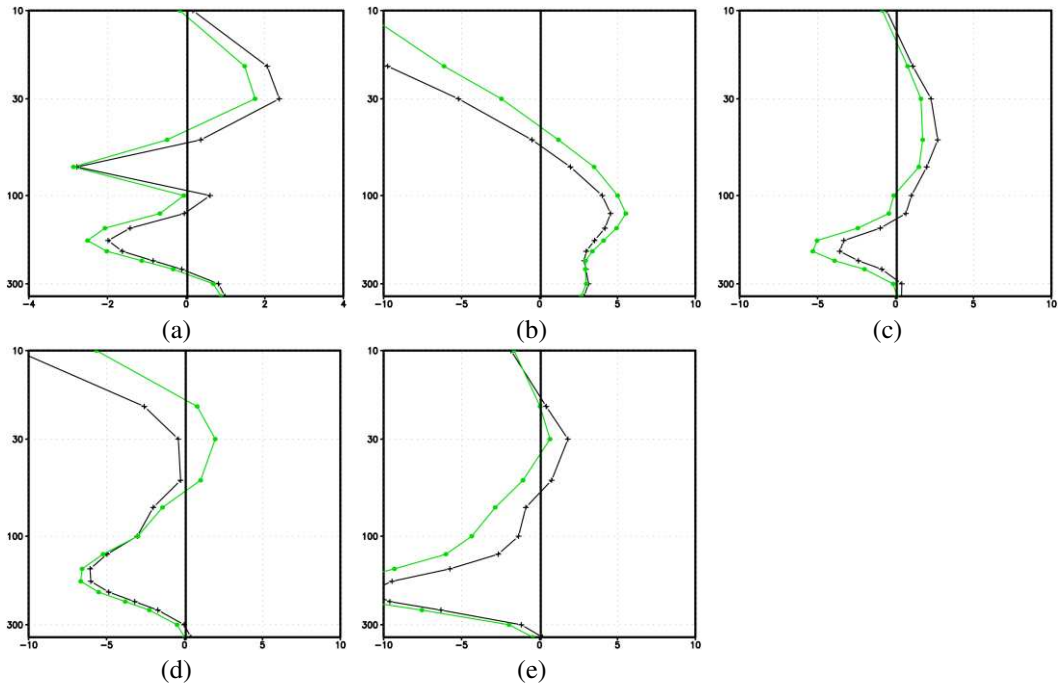

Figure 4. *Differences of regionally averaged temperature between model results and ERA-Interim. Cross and solid dot denote results from EXP1 minus ERA-Interim and EXP2 minus ERA-Interim respectively. (a)annual global average, (b) winter (December, January and February) 60−90°N average, (c) summer (June-August) 60−90°N average, (d) winter (June-August) 60−90°S average, (e) summer (December, January and February) 60−90°S average. The horrizontal axis is temperature difference (K) and the vertical axis is pressure (hPa) in each panel*

In both numerical experiments, the major features of zonal mean zonal wind distribution (such as position of westerly belts, easterly belts and centers of strong wind) at 50 hPa are consistent (see *Fig. 5a* and *5b*). Compared to that of ERA-Interim, the

http://www.aloki.hu ● ISSN 1589 1623 (Print) ● ISSN 1785 0037 (Online)
DOI: http://dx.doi.org/10.15666/aeer/1705_1260512614

simulated seasonal variation of westerly in the northern hemisphere and intensity of westerly wind in the southern hemisphere by the 66-layer model agrees with that of ERA-Interim better (compare *Fig. 5a* with *5b* and *5c*).

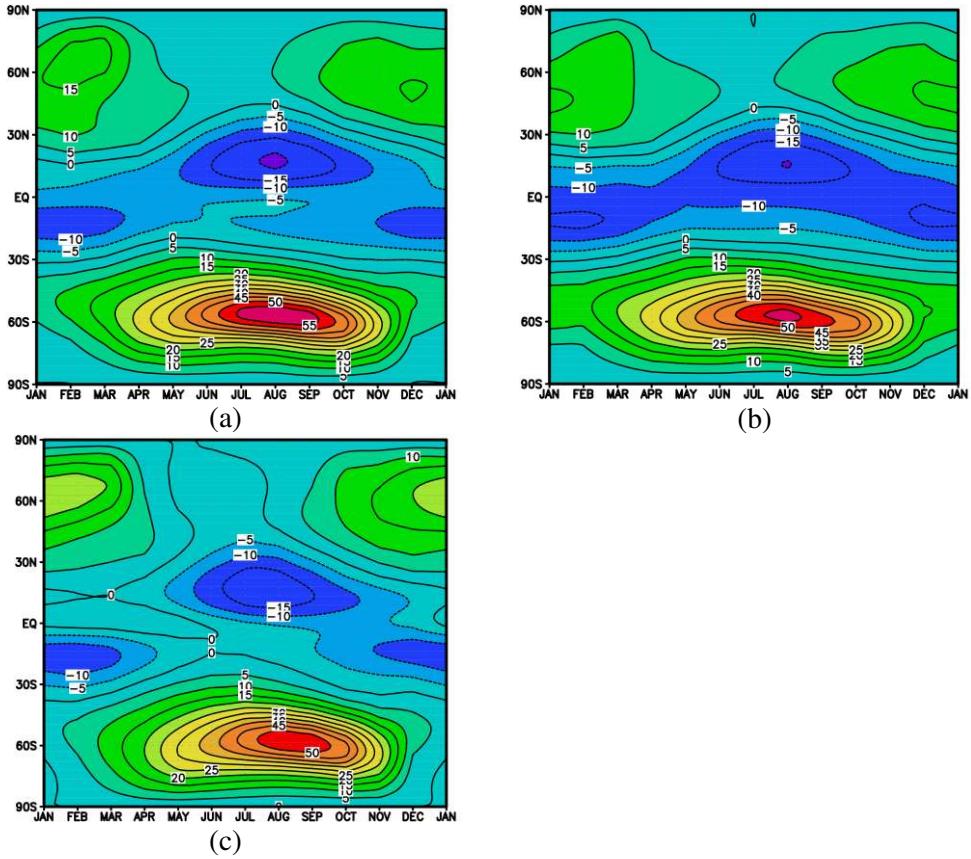

Figure 5. *Distribution of zonal mean zonal wind at 50hPa (unit: m/s). (a) EXP1, (b) EXP2, (c) ERA-Interim. The horrizontal axis is time (month) and the vertical axis is latitude (°) in each panel*

Discussion

In the study, a numerical atmospheric model with two configurations had been used to study the influence of vertical divisions of the model atmosphere on the simulation of stratospheric climate. All the employed schemes of physical processes except solar radiation are identical in the two configurations. There have been work on the effects of upper layer of atmosphere on simulations of stratosphere or troposphere based on results from different models (for example, Sassi et al., 2010). It would be difficult to deduce the reason of specific feature in simulated stratospheric climate from multiple models since there are many factors involved. In contrast, attribution is simple if simulations are from the same model. But work to study the influence of upper atmosphere on the simulation of stratospheric climate under the same dynamical framework are still less.

The analysis in the work was only on the mean climate. This is very limited. Any downward influence of the middle atmosphere on the troposphere is likely to happen during dynamically disturbed times. Thus, the time mean is not a sufficient measure to describe climate influence. More work of comparative analysis, such as the behavior of

http://www.aloki.hu ● ISSN 1589 1623 (Print) ● ISSN 1785 0037 (Online)
DOI: http://dx.doi.org/10.15666/aeer/1705_1260512614

the model during sudden stratospheric warming, the features of the penetration of stratospheric anomalies in the two models, and so on, should be done in future research.

No chemical process has been included in SEMANS and the radiation process scheme is rather simplified for atmosphere of high altitude (above 65 km). If the chemical processes and more complex radiation process scheme are considered, the simulation results may show new features. So, much further work needs to be done in the future research.

Conclusion

A numerical model named SEMANS had been used to study if a lid in the mesosphere versus one in the lower thermosphere makes any difference to the representation of climate in the stratosphere. It's shown that, there are apparent similarities in the simulation results from the two configurations; the cold biases of zonal mean temperature in the low latitudes are mainly confined to the atmospheric levels around 75 hPa; the globally averaged annual mean temperature from the 66-layer model is colder than that from the 28-layer model; the biases of simulated temperature above the height of 100 hPa level are smaller in results from 66-layer version model; the simulated seasonal variation of westerly in the northern hemisphere and intensity of westerly wind in the southern hemisphere by the 66-layer model agrees with that of ERA-Interim better.

Acknowledgements. The work is sponsored by "the Fundamental Research Funds for the Central Universities" in China (Grant No. 2019B00214). The ERA-Interim reanalysis datasets were downloaded from the ECMWF data server website.

REFERENCES

[1] Abalos, M., Legras, B., Ploeger, F., Randel, W. J. (2015): Evaluating the advective Brewer–Dobson circulation in three reanalyses for the period 1979–2012. – J. Geophys. Res. 120: 7534-7554.

[2] Baldwin, M. P., Dameris, M., Shepherd, T. G. (2007): How will the stratosphere affect climate change. – Science 316: 1576-1577.

[3] Boville, B. A. (1984): The influence of the polar night jet on the tropospheric circulation in a GCM. – J. Atmos. Sci. 41: 1132-1142.

[4] Boville, B. A., Cheng, X. (1988): Upper boundary effects in a general circulation model. – J. Atmos. Sci. 45: 2591-2606.

[5] Boville, B. A., Baumhefner, D. P. (1990): Simulated forecast error and climate drift resulting from the omission of the upper stratosphere in numerical models. – Mon. Wea. Rev. 118: 1517-1530.

[6] Briegleb, B. P. (1992): Delta-Eddington approximation for solar radiation in the NCAR Community Climate Model. – J. Geophys. Res. 97: 7603-7612.

[7] Butchart, N., Scaife, A. A. (2001): Removal of chlorofluorocarbons by increased mass exchange between the stratosphere and troposphere in a changing climate. – Nature 410: 799-802.

[8] Butchart, N., Scaife, A. A., Bourqui, M., de Grandpré, J., Hare, S. H. E., Kettleborough, J., Langematz, U., Manzini, E., Sassi, F., Shibata, K., Shindell, D., Sigmond, M. (2006): Simulations of anthropogenic change in the strength of the Brewer–Dobson circulation. – Climate Dynamics 27: 727-741.

http://www.aloki.hu ● ISSN 1589 1623 (Print) ● ISSN 1785 0037 (Online)
DOI: http://dx.doi.org/10.15666/aeer/1705_1260512614

[9] Charlton, A. J., Neill, A. O., Lahoz, W. A., Massacand, A. C. (2004): Sensitivity of tropospheric forecasts to stratospheric initial conditions. – Q. J. R. Meteorol. Soc. 130: 1771-1792.
[10] Founier, A., Taylor, M. A., Tribbia, J .J. (2004): The spectral element atmosphere model (SEAM): high-resolution parallel computation and localized resolution of regional dynamics. – Mon. Wea. Rev. 132: 726-748.
[11] Giraldo, F. X. (2005): Semi-implicit time-integrators for a scalable spectral element atmospheric model. – Q. J. R. Meteorol. Soc. 131: 2431-2454.
[12] Held, I. M., Soden, B. J. (2000): Water vapor feedback and global warming. – Annu. Rev. Energy Environ. 25: 441-475.
[13] Holtslag, A. A. M., Boville, B. A. (1993): Local versus nonlocal boundary-layer diffusion in a global climate model. – J. Climate 6: 1825-1842.
[14] Linz, M., Plumb, R. A., Gerber, E. P., Haenel, F. J., Stiller, G., Kinnison, D. E., Ming, A., Neu. J. L. (2017): The strength of the meridional overturning circulation of the stratosphere. – Nature Geoscience 10: 663-667.
[15] Liu, X. Y. (2011): Numerical simulation of typhoon movement with a regional spectral element barotropic atmospheric model. – Chinese Journal of Computational Physics 28: 35-40.
[16] Liu, X. Y., Liu, C. Y., Yao, S. S. (2015): A spectral element model with atmospheric near space resolved (SEMANS). – Chinese Journal of Computational Physics 32: 40-50.
[17] Marsh, D., Roble, R. (2002): TIME-GCM simulations of lower-thermospheric nitric oxide seen by the halogen occultation experiment. – J. Atmos. Solar Terr. Phys. 64: 889-895.
[18] Mitchell, D., Gray, L., Anstey, J., Baldwin, M., Charlton-Perez, A. (2013): The influence of stratospheric vortex displacements and splits on surface climate. – Geophys. Res. Lett. 26: 2668-2682.
[19] Norton, W. A. (2003): Sensitivity of northern hemisphere surface climate to simulation of the stratospheric polar vortex. – Geophys. Res. Let. 30: 1627.
[20] Park, S., Bretherton, C. S. (2009): The university of washington shallow convection and moist turbulence schemes and their impact on climate simulations with the community atmosphere model. – J. Climate 22: 3449-3469.
[21] Patera, A. T. (1984): A spectral element method for fluid dynamics: laminar flow in a channel expansion. – J. Comput. Phys. 54: 468-488.
[22] Ramanathan, V., Downey, P. A. (1986): Nonisothermal emissivity and absorptivity formulation for water vapor. – J. Geophys. Res. 91: 8649-8666.
[23] Randel, W. J., Shine, K. P., Austin, J., Barnett, J., Claud, C., Gillett, N. P., Keckhut, P., Langematz, U., Lin, R., Long, C., Mears, C., Miller, A., Nash, J., Seidel, D. J., Thompson, D. W. J., Wu, F., Yoden, S. (2009): An update of observed stratospheric temperature trends. – Journal of Geophysical Research 114: D02107.
[24] Ronchi, C., Iacono, R., Paolucci, P. S. (1996): The 'cubed sphere': A new method for the solution of partial differential equations in spherical geometry. – J. Comput. Phys. 124: 93-114.
[25] Ruosteenoja, K. (2006): The impact of the height of the model top on the simulation of tropospheric stationary waves. – Q. J. R. Meteorol. Soc. 125: 677-695.
[26] Sassi, F., Garcia, R. R., Marsh, D., Hoppel, K. W. (2010): The Role of the Middle Atmosphere in Simulations of the Troposphere during Northern Hemisphere Winter: Differences between High- and Low-Top Models. – J. Atmos. Sci. 67: 3048-3064.
[27] Scaife, A. A., Knight, J. R., Vallis, G. K., Folland, C. K. (2005): A stratospheric influence on the winter NAO and North Atlantic Surface Climate. – Geophys. Res. Let. 32: L18715.
[28] Shaw, T. A., Perlwitz, J. (2010): The Impact of Stratospheric Model Configuration on Planetary-Scale Waves in Northern Hemisphere Winter. – J. Climate 23: 3369-3389.

http://www.aloki.hu ● ISSN 1589 1623 (Print) ● ISSN 1785 0037 (Online)
DOI: http://dx.doi.org/10.15666/aeer/1705_1260512614

[29] Simmons, A. J., Burridge, D. M. (1981): An Energy and Angular-Momentum Conserving Vertical Finite-Difference Scheme and Hybrid Vertical Coordinates. – Mon. Wea. Rev. 109: 758-766.
[30] Simmons, A., Uppala, S., Dee, D., Kobayashi, S. (2007): ERA-Interim: New ECMWF reanalysis products from 1989 onwards. – ECMWF Newsletter 110: 25-35.
[31] Zhang, G. J., McFarlane, N. A. (1995): Sensitivity of climate simulations to the parameterization of cumulus convection in the Canadian Climate Centre general circulation model. – Atmosphere- Ocean 33: 407-446.

http://www.aloki.hu ● ISSN 1589 1623 (Print) ● ISSN 1785 0037 (Online)
DOI: http://dx.doi.org/10.15666/aeer/1705_1260512614

ASSOCIATION BETWEEN EXPOSURE TO FAMILY ENVIRONMENTAL TOBACCO SMOKE AND OBSTRUCTIVE SLEEP APNEA HYPOPNEA SYNDROME

HUANG, Q.[1] – ALI, S.[2] – ZHANG, J.[1*]

[1]*Department of Respiratory Medicine, Beijing Tian Tan Hospital, Capital Medical University, Beijing, China*

[2]*Department of Information Science, University of Education, Lahore, Pakistan*

**Corresponding author*
e-mail: ttyy_zj@163.com

(Received 23rd May 2019; accepted 4th Jul 2019)

Abstract. The objective of this study was to observe the relationship between levels of family environmental tobacco smoke (ETS) and obstructive sleep apnea hypopnea syndrome (OSAHS). Clinical datr AHI, lower oxygen saturation, longer apnea time, and lower ventilation time ($p < 0.05$). There was a correlation between EST and OSAHS. Compared with non-exposa of 209 patients who visited the respiratory department were retroactively collected. The data entailed gender, age, body mass index (BMI), family environmental smoke exposure, medical history, Epworth sleepiness scale (ESS) score, and polysomnography (PSG) indicators. Two groups of patients were studied: ETS-exposed group and non-ETS-exposed group. Using the apnea hypopnea index (AHI), OSAHS patients were classified as mild ($5 \leq AHI \leq 15$), moderate ($15 < AHI \leq 30$), and severe ($AHI > 30$). There were 148 cases in the OASHS group and 61 cases in the normal group. 56.66% of the OASHA group were ETS-exposed patients, which was significantly higher than that the normal group ETS-exposure of 31.57% . Compared to the OSAHS patients unexposed to ETS, the OSAHS patients with EST exposure had a greater degree of lethargy, greateed, the EST-exposed group was more susceptible to OSAHS, and the longer the time, the more severe the condition.
Keywords: *obstructive sleep apnea hypopnea syndrome, health effects, passive smoking, sleep apnea hypopnea index, ESS questionnaire*

Introduction

Environmental tobacco smoke (EST) exposure has become a worldwide health problem. Currently, there are 1.3 billion smokers worldwide, and a high number of people are exposed to family environmental tobacco smoke (Rando et al. 999; Aviado et al., 1996). Studies have shown that EST impairs the stability of the internal environment and affects normal physiological processes, leading to various chronic diseases. Obstructive sleep apnea hypopnea syndrome (OSAHS) accounts for most of sleep apnea hypopnea syndrome cases, a frequently-occurring disease (Muggli, 2004). In China, OSAHS affects about 4% of adults. The syndrome is characterized by snoring and repeated apnea resulting in sleep fragmentation, morning discomfort, dry mouth, daytime sleepiness, fatigue, dizziness, headache, decreased memory, and inattentiveness. These problems result in reduced work efficiency, increased risk of industrial accidents and traffic accidents, as well as sudden death during sleep (Davidson and Reed, 2018; Theweny, 2015). With improvement in living standards, ageing and incidence of obesity have increased significantly, and the incidence of OSAHS is increasing year by year, thereby posing an important public health problem. Since OSAHS and ETS often occur simultaneously, they may have common oxidative stress and inflammatory pathways, leading to metabolic disorders (Barnes et al., 2006; Elliott et al., 2007; Jenkins and Counts, 1999; Steenland, 1999; Thun et al., 1999). At

http://www.aloki.hu ● ISSN 1589 1623 (Print) ● ISSN 1785 0037 (Online)
DOI: http://dx.doi.org/10.15666/aeer/1705_1261512622

present, local and foreign scholars have studied the etiology and pathogenesis of OSAHS. Studies have suggested that ETS is one of the risk factors for OSAHS, but there are few studies on the relationship between ETS and OSAHS.

In the present study, the relationship between EST and OSAHS was studied by investigating the association between ETS exposure and the severity of OSAHS, so as to provide a theoretical basis for effective prevention and treatment of OSAHS.

Materials and methods

Materials

Setting and samples

The clinical data of 209 patients who visited the Department of Respiratory Medicine were retrospectively collected. The patients were divided into ETS-exposed group and non-ETS-exposed group. The ETS-exposed group was sub-divided into mid-ETS (tobacco smoke in the house but not in the same room as patient), and heavy-ETS (tobacco smoke in the same room as patient). Using the latest American Society of Sleep Medicine Standards (AASM) and AHI, patients with OSAHS were classified as mild ($5 \leq AHI \leq 15$), moderate ($15 < AHI \leq 30$), and severe ($AHI > 30$). The OSAHS classification is shown in *Table 1*.

Table 1. *Grading of OSAHS*

Classification	AHI (time/hour)	$LSaO_2$ (%)
Mild	5-15	85-90
Moderate	> 15-30	80- < 85
Severe	> 30	< 80

Inclusion criteria

Patients older than 18 years, patients who snored while sleeping at night and in daytime, and those with complete clinical data (including BMI, ESS score and PSG monitoring, etc.) were included in the study.

Exclusion criteria

Patients with loss of polysomnography, maxillofacial deformity, severe pneumonia, asthma, pulmonary interstitial disease, and chronic obstructive pulmonary disease were excluded. Moreover, those with severe heart failure, liver failure, renal failure, and neuromuscular diseases were excluded. Patients with central and mixed sleep apnea, and those on prolonged use of sleeping and sedative drugs were considered ineligible.

Methods

Polysomnography

Polysomnography (PSG) is the most important test for diagnosing OSAHS. Through continuous monitoring of night-time breathing, arterial oxygen saturation, electroencephalogram, electrocardiogram, heart rate and other indicators, you can know whether the snorer has apnea, the number of pauses, the time of suspension, the minimum arterial oxygen value at the time of suspension, and The extent of the impact on physical

http://www.aloki.hu ● ISSN 1589 1623 (Print) ● ISSN 1785 0037 (Online)
DOI: http://dx.doi.org/10.15666/aeer/1705_1261512622

health is an internationally recognized gold standard for the diagnosis of OSAHS. The polysomnography is the most commonly used sleep monitoring method and is the internationally recognized gold standard for diagnosing OSAHS. According to the results of polysomnography, not only can the diagnosis of OSAHS be made, but also the severity can be judged, and it is convenient to formulate clinical treatment plans and quantitatively evaluate the operation or other treatment effects. Polysomnography is used to measure various physiological signals during sleep. The parameters of the measurement include: (1) Breathing: The airflow monitor can find the length and frequency of sleep apnea syndrome. Stopping breathing for more than 10 s is called a pause. Insufficient breathing usually means that the respiratory airflow drops by more than 50%. (2) Oxygen saturation: A decrease in blood oxygen saturation is a key manifestation of OSAHS patients. (3) Muscle movement: Monitoring of chest movements can help diagnose whether the pause is central or obstructive. Other types of sleep disorders can be manifested as leg movements, jaw closures, and other characteristic sports. (4) Brain waves and eye movements: Sleep can be divided into different stages according to brain waves and eye movements, namely fast phase and slow phase (deep and light sleep). (5) Electrocardiogram (ECG): Some patients with OSAHS may have abnormal heart rhythms. (6) Position of the body: OSAHS is most likely to occur in the supine position, when the base of the tongue falls and it is easy to block the upper respiratory tract. Two of these assessment methods are often cited to summarize sleep monitoring outcomes: (1) Calculate the mean of the hourly breathing disorder by calculating the average of the sum of night-time sleep apnea syndrome and hypopneas, ie, breathing Pause the hypogastric index Apnea Hypopnea Index (AHI). Adult AHI greater than or equal to 5 can be defined as OSAHS. (2) The lowest oxygen saturation in sleep apnea syndrome, although there is no specific indication of sleep apnea syndrome, but less than 85% can determine sleep apnea syndrome. The PSG monitor with US Embla NN7000 (Jain, 2018) multi-lead sleep monitor was used to monitor the subjects for polysomnography ≥ 7 h overnight. At the same time, the subjects were advised to avoid drinking alcohol, coffee, tea, taking sleeping pills, and sedating drugs. The monitored parameters were EEG, ocular electricity, mandibular muscle power, nose and mouth airflow, chest and abdomen exercise, ECG, eye movement, body position, snoring, and fingertip oxygen saturation. The results were analyzed with computer software, and were strictly followed by professional physicians in accordance with the American Sleep Medicine Society. The sleep monitoring indicators selected for reflecting the objective severity of the patient's disease were AHI, minimum oxygen saturation, mean oxygen saturation, longest apnea time, and longest low ventilation time.

Tests and questionnaires

The clinical data of all selected subjects were collected. These were gender, age, height, weight, past medical history (hypertension, diabetes, cardiovascular and cerebrovascular diseases). The ESS score, AHI, minimum oxygen saturation, mean oxygen saturation, longest apnea time, and longest low ventilation time were recorded. The ESS shown in *Table 2* was used for the subjects. The ESS was assessed by a professional under the guidance of a questionnaire containing 8 questions, each with 0-3 points and 4 levels. The maximum score was 24 points. Determination of lethargy ESS score < 5 is normal, 5-9 is mild sleepiness, 10-15 is moderate sleepiness, 16-24 is severe sleepiness. The higher the score, the more severe the daytime sleepiness, and scores greater than 10 points were considered to be excessive daytime sleepiness.

http://www.aloki.hu ● ISSN 1589 1623 (Print) ● ISSN 1785 0037 (Online)
DOI: http://dx.doi.org/10.15666/aeer/1705_1261512622

Table 2. *The Epworth sleepiness scale (ESS) score chart*

ESS item	1	2	3	4
Sitting and reading				
Watching TV				
Sitting inactive in a public place (e.g., a theater or a meeting)				
As a passenger in a car for an hour without a break				
Lying down to rest in the afternoon when circumstances permit				
Sitting and talking to someone				
Sitting quietly after a lunch				
In a car, while stopped for a few minutes in traffic				

Statistical analysis

Normal distribution data are presented as mean ± standard deviation ($\bar{x} \pm s$). Statistical differences were analyzed with χ^2 test and *t*-test. All statistical analyses were performed using SPSS 23. Differences were assumed statistically significant at $p < 0.05$.

Results

Characteristics of participants

A total of 209 patients were included in the study, out of which 148 patients had OSAHS, comprising 111 males and 37 females. The remaining patients comprised 37 males and 24 females. The population of OSAHS patients with EST exposure formed 56.66%, which was significantly higher than that in the normal group (31.57%), and the OSAHS group had significantly higher BMI ($p < 0.05$). There were no significant differences in age, and in male and female distribution ($p > 0.05$; *Table 3*).

Table 3. *Characteristics of the OSAHS group and the normal group*

Parameter	OSAHS group	Normal group	Test value	*p*
Gender (male/female)	111/37	34/24	2.191	0.162
Age (years)	48.17 ± 12.41	46.71 ± 11.56	-0.659	0.427
BMI (kg/m^2)	29.58 ± 4.28	25.89 ± 1.37	3.179	0.001**
EST-exposed group (%)	87(58.89)	19(30.56)	5.728	0.009**

$^{*}p < 0.05$, $^{**}p < 0.01$

Comparative analysis of OSAHS with EST exposure and the non-ETS-exposed group

There were 87 cases in OSAHS group with EST exposure consisting of 77 males and 10 females. In the non-ETS-exposed OSAHS group, there were 61 subjects made up of 34 males and 27 females. Compared with OSAHS group without exposure to ETS, OSAHS group with EST exposure differed significantly in gender composition ($p = 0.000$), but there were no significant differences in age, BMI and past medical history between the two groups ($p > 0.05$). These results are shown in *Table 4*.

http://www.aloki.hu ● ISSN 1589 1623 (Print) ● ISSN 1785 0037 (Online)
DOI: http://dx.doi.org/10.15666/aeer/1705_1261512622

Table 4. *Clinical data of OSAHS group exposed to EST, and OSAHS group unexposed to ETS*

Parameter	OSAHS group with EST exposure	OSAHS group within no-exposed	Test value	*p*
Gender (male/female)	77/10	34/27	11.787	0.000**
Age (years)	45.26 ± 12.89	50.77 ± 14.69	0.658	0.482
BMI (kg/m^2)	29.98 ± 4.38	30.13 ± 4.32	0.075	0.768
EST-exposed group (%)	87(58.89)	19(30.56)	6.728	0.009*
Diabetes	12	5	0.967	0.355
Hypertension	25	31	3.005	0.079
Cardiovascular	21	13	0.074	0.783

*$p < 0.05$, **$p < 0.01$

Contrastive analysis of somnolence and PSG of OSAHS within the EST-exposed and non-exposed groups

Compared with non-exposed OSAHS group, OSAHS group exposed to EST had more somnolence, higher AHI, lower oxygen saturation, and longer apnea pause time and hypopnea time ($p < 0.05$; *Table 5*). The exposed group scored higher on the ESS than the non-exposed group, which said there was more drowsiness. The reported SD values are highly overlapping in case longest apnea time in *Table 5,* but statistical processing was reliable.

Table 5. *Comparison of ESS scores and PSG between OSAHS group exposed to EST and unexposed OSAHS group*

Parameter	OSAHS group exposed to EST	OSAHS group unexposed to ETS	Test value	*p*
Number	87	61		
ESS score	**9.65 ± 5.19**	**7.43 ± 4.79**	**2.359**	**0.022***
AHI (time/h)	**46.33 ± 21.03**	**35.78 ± 26.37**	**2.169**	**0.043***
$LSaO_2$ (%)	**72.88 ± 3.64**	**78.92 ± 8.48**	**22.28**	**0.001****
$MSaO_2$ (%)	**90.18 ± 4.32**	**92.25 ± 2.77**	**-2.417**	**0.017***
Longest apnea time (s)	**77.65 ± 37.35**	**61.02 ± 33.42**	**2.138**	**0.046***
Longest hypoventilation time (s)	**99.27 ± 43.21**	**78.88 ± 41.50**	**-2.250**	**0.040***

*$p < 0.05$, **$p < 0.01$

Comparison of characteristics, ESS scores and PSG in OSAHS with different exposure levels

The groups were divided into ETS-exposed group and the non-ETS-exposed group, and the ETS-exposed subjects were classified into mid-ETS (tobacco smoke in the house but not in the same room as patient) and heavy-ETS (tobacco smoke in the same room as patient). In the ETS-exposed group, 25 OSAHS subjects with mid-ETS exposure, and 62 OSAHS subjects with heavy-ETS exposure were included. There were no significant differences in age and BMI between the two groups. Compared with OSAHS patients with mid-ETS exposure, OSAHS patients with heavy-ETS exposure

http://www.aloki.hu ● ISSN 1589 1623 (Print) ● ISSN 1785 0037 (Online)
DOI: http://dx.doi.org/10.15666/aeer/1705_1261512622

had more ESS scores, greater AHI, lower oxygen saturation and longer apnea pause time ($p < 0.05$). There were no significant differences in longest hypopnea times ($p > 0.05$) between the two groups, as shown in *Table 6*.

Table 6. *Comparison of ESS scores and PSG between OSAHS group with mid-ETS exposure and OSAHS group with heavy-ETS exposure*

Parameter	OSAHS group with mid-ETS exposure	OSAHS group with heavy-ETS exposure	Test value	*p*
Number	25	62		
ESS score	**8.57 ± 5.88**	**9.66 ± 6.07**	**2.505**	**0.012***
AHI (time/h)	**38.39 ± 22.15**	**55.89 ± 2617**	**-2.447**	**0.022***
$LSaO_2$ (%)	**78.07 ± 12.83**	**68.87 ± 14.58**	**2.289**	**0.025***
$MSaO_2$ (%)	**89.97 ± 4.26**	**92.19 ± 2.73**	**-2.682**	**0.011***
Longest apnea time (s)	**63.57 ± 32.47**	**93.96 ± 37.55**	**-2.793**	**0.038***
Longest hypoventilation time (s)	**78.15 ± 42.26**	**97.87± 44.57**	**-2.001**	**0.073**

$^{*}p < 0.05$, $^{**}p < 0.01$

Discussion

Obstructive sleep apnea hypopnea syndrome (OSAHS) is a common sleep-disorder in the general population. It is one of the causes of drug resistance, refractory hypertension, and heart failure. If it is not treated effectively for a long time, it results in irreparable damage to multiple organs. The disorder seriously affects the quality of life and longevity of patients. The present study compared the ESS scores and AHI index of OSAHS patients exposed to ETS with those of OSAHS patients who were not exposed to ETS. In addition, the ESS score and PSG data of the OSAHS subjects exposed to mid-ETS were compared with those of OSAHS patients exposed to heavy-ETS. The study was aimed at providing scientific data and basis for adjunct clinical intervention in OSAHS. Long-term exposure to EST reduces the sensitivity of tissues to hypoxia and degrades the capacity to recover from conditions caused by hypoxia. These pathological changes impair the ability of the body to recover automatically from apnea when it occurs (Coggins, 2008; Owili et al., 2018; Van et al., 2018). This will result in a longer apnea and a long-term decline in blood oxygen saturation associated with it. It has been reported that patients with OSAHS exposed to mid-EST experienced longer and lower nocturnal hypoxemia than non-exposed OSAHS patients (Berman et al., 2018). In the treatment of OSAHS patients, doctors should, through joint interventions in multiple disciplines, pay attention to the patient's environmental status, and actively persuade them to improve the environment so as to reduce the occurrence of long-term complications of the disorder (Nachamkin, 2012; Li et al., 2018; Maskarinec et al., 2000). Improving the home environment can be used as an adjunct to conventional therapy for OSAHS.

The sample size used in this study was small. Moreover, retrospective studies may have recall bias. To obtain more reliable data, it is important to use a larger sample size and more representative study locations (Yang et al., 2018; Nurminen and Jaakkola, 2004). It is also important to apply more stringent control conditions in the study of EST and improvement of OSAHS. The relationship between ETS and OSAHS is expected to be further elucidated through animal experiments.

http://www.aloki.hu ● ISSN 1589 1623 (Print) ● ISSN 1785 0037 (Online)
DOI: http://dx.doi.org/10.15666/aeer/1705_1261512622

Conclusion

This study shows that there is a certain correlation between EST and OSAHS. Compared with subjects who were not exposed to ETS, patients exposed to EST are more susceptible to OSAHS, and the longer the exposure time, the more severe the condition. This study found that the BMI of the OSAHS group was significantly higher than that of the non-OSAHS group, which is consistent with the currently well-recognized high incidence of obesity and OSAHS. The study found that the ETS exposed group had higher ESS, higher AHI, lower oxygen saturation, and longer apnea time and hypopnea time. Compared with non-smokers, the current smoking population has longer sleep latency, shorter sleep time, longer I-stage sleep time, and slower slow-wave sleep time. The sleep characteristics of OSAHS patients are prolonged latency, sleep fragmentation, and prolonged stage I sleep. III stage IV sleep reduction. To a certain extent, this also explains the impact of ETS exposure on sleep.

Thus, OSAHS may be mitigated by improving the environment. Families are the main places where tobacco smoke is exposed. Public health policies need to focus on family smoking ban. To publicize and pay attention to the harm of EST, we should actively advocate smoking cessation, strengthen the publicity of the hazards of passive smoking, control the impact of EST on OSAHS, and have great significance in preventing OSAHS.

REFERENCES

[1] Aviado, D. M. (1996): Cardiovascular disease and occupational exposure to environmental tobacco smoke. – American Industrial Hygiene Association Journal 57(3): 285-294.

[2] Barnes, R. L., Hammond, S. K., Glantz, S. A. (2006): The tobacco industry's role in the 16 cities study of secondhand tobacco smoke: do the data support the stated conclusions? – Environmental Health Perspectives 114(12): 1890-1897.

[3] Berman, T., Barnettitzhaki, Z., Mery, N., Keinanboker, L., Shimony, T., Goldsmith, R., Göen, T., Geva, H., Rosen, L. (2018): Exposure to environmental tobacco smoke in non-smoking adults in Israel: results of the second Israel biomonitoring survey. – Israel Journal of Health Policy Research 7(1): 33.

[4] Coggins, C. R. E. (2008): The Osha review of Animal inhalation studies with environmental tobacco smoke. – Inhalation Toxicology 8(8): 819-830.

[5] Davidson, M., Reed, S. (2018): Preliminary assessment of real-time air quality instruments for monitoring environmental tobacco smoke. – British Actuarial Journal 3(2): 547-614.

[6] Elliott, L., Arbes, S. J., Harvey, E. S., Lee, R. C., Salo, P. M., Cohn, R. D., London, S. J., Zeldin, D. C. (2007): Dust weight and asthma prevalence in the National Survey of Lead and Allergens in Housing (NSLAH). – Environmental Health Perspectives 115(2): 215-220.

[7] Jain, R. B. (2018): Rates of exposure to environmental tobacco smoke from various indoor environments among US children and nonsmoker adolescents and adults. – Environmental Science & Pollution Research 25(4): 17002-17011.

[8] Jenkins, R. A., Counts, R. W. (1999): Occupational exposure to environmental tobacco smoke: results of two personal exposure studies. – Environmental Health Perspectives 107(2): 341-348.

[9] Li, M., Liu, X., Zhang, L. (2018): The relationship of indoor coal use and environmental tobacco smoke exposure with lung cancer in China: A meta-analysis. – Journal of Cancer Research & Therapeutics 14: 7-13.

http://www.aloki.hu ● ISSN 1589 1623 (Print) ● ISSN 1785 0037 (Online)
DOI: http://dx.doi.org/10.15666/aeer/1705_1261512622

[10] Maskarinec, M. P., Jenkins, R. A., Counts, R. W., Dindal, A. B. (2000): Determination of exposure to environmental tobacco smoke in restaurant and tavern workers in one US city. – Journal of Exposure Analysis & Environmental Epidemiology 10(1): 36.
[11] Muggli, M. E., Hurt, R. D., Repace, J. (2004): The tobacco industry's political efforts to derail the EPA report on ETS. – American Journal of Preventive Medicine 26(2): 167-177.
[12] Nachamkin, E. W. (2012): An examination of secondhand smoke in a sample of Atlanta hospitality venues and their compliance with the Georgia Smokefree Air Act. – Journal of Animal Science 84(2): 291-299.
[13] Nurminen, M. M., Jaakkola, M. S. (2004): On the estimation of lung cancer mortality caused by occupational exposure to environmental tobacco smoke in Finland. – Journal of Occupational & Environmental Medicine 46(2): 93-95.
[14] Owili, P., Muga, M., Kuo, H. W. (2018): Gender difference in the association between environmental tobacco smoke and birth weight in Africa. – International Journal of Environmental Research & Public Health 15(7): 1409.
[15] Rando, R., Poovey, H., Gibson, R., Lehrer, S. (1999): 136. Laboratory and field study of emission of environmental tobacco smoke from smokeless cigarette. – American Industrial Hygiene Conference and Exposition, Toronto, Ontario, June 5-11.
[16] Steenland, K. (1999): Risk assessment for heart disease and workplace ETS exposure among nonsmokers. – Environmental Health Perspectives 107(6): 859-863.
[17] Theweny, T. S. (2015): Measurement of thirdhand smoke in a casino: surface nicotine wipes pre and post smoking ban. – Thesis in partial fulfilment of the requirements for the degree Master of Social Work and Master of Public Health. San Diego State University, San Diego, CA.
[18] Thun, M., Henley, J., Apicella, L. (1999): Epidemiologic studies of fatal and nonfatal cardiovascular disease and ETS exposure from spousal smoking. – Environmental Health Perspectives 107(6): 841-846.
[19] Van, F. O., Jochems, S., Wesselius, A., Van, F. S., Bryan, R. T., Zeegers, M. P. (2018): A stratified meta-analysis of the association between exposure to environmental tobacco smoke during childhood and adulthood and urothelial bladder cancer risk. – International Journal of Environmental Research & Public Health 15(4): 569.
[20] Yang, H. S., Lim, H., Choi, J., Bae, S., Kim, Y., Kwon, H. J., Ha, M. (2018): Environmental tobacco smoke exposure at home and attributable problem behaviors in Korean children and adolescents for 2012-2014 in a nationally representative survey. – Journal of Korean Medical Science 33(36): 229.

http://www.aloki.hu ● ISSN 1589 1623 (Print) ● ISSN 1785 0037 (Online)
DOI: http://dx.doi.org/10.15666/aeer/1705_1261512622

COMPARATIVE ANALYSIS OF LAND SURFACE TEMPERATURE AND LAND COVER BASED ON GEOGRAPHICALLY WEIGHTED REGRESSION

XU, D. – GAO, J.*

Shanghai Normal University, School of Environmental and Geographical Sciences
Shanghai 200234, China

**Corresponding author*
e-mail: gaojunshnu@126.com

(Received 12th Jun 2019; accepted 12th Jul 2019)

Abstract. The relationship between land surface temperature (LST) and land use patterns has long been explored to understand the impact of urbanization on the urban heat island effect. This paper reports the geographically weighted regression method. The LST is derived from the radiation transfer model and the urban reflectance is grouped into three types from the linear spectral mixture in Nanjing City, China. The high LST on October 3, 2009 in the central city, suburbs, outer suburbs, and outer suburbs near water were 44, 40, 36, and 33°C, respectively. The LSTs of the central city in spring, summer, and autumn were 1–5°C higher than that of the suburbs. The high absorption coefficient of vegetation, substrate, and dark surfaces with LST were -0.80, 1.05, and -1.64, respectively. The promoting role of impervious surfaces is much higher than the cooling effects of vegetation on LST. Water surfaces have a more obvious effect on adjusting LST. If the landscape diversity index or the fragment index are low, the vegetation cover has a more noticeable negative correlation with LST. The way in which LST relates to land reflectance and to landscape provides a quantitative reference for urban planning of sustainable development in Nanjing.
Keywords: *spectral unmix, heat island, landscape indices, Nanjing, radiative transfer equation*

Introduction

The main feature of the urban heat island effect is that the LST in central urban areas is higher than that in the suburbs (Landsberg, 1831). In the study of the urban heat island pattern, remote sensing data for land surface temperature (LST) inversion were mainly gathered by the National Oceanic and Atmospheric Administration's Advanced Very-High-Resolution Radiometer (AVHRR), Moderate Resolution Imaging Spectroradiometer (MODIS), Landsat Thematic Mapper/Enhanced Thematic Mapper (Landsat TM/ETM), and Advanced Spaceborne Thermal Emission and Reflection Radiometer (ASTER). The urban area is firstly determined using the temperature difference between the urban and rural surface detected by AVHRR (Rao et al., 1972). Heat island intensities from AVHRR data are highest in the day time and in the warm season for towns in North America (Roth et al., 1989). Qin et al. (2001 a,b) proposed a single window algorithm for Landsat TM/ETM and modified the land temperature inversion algorithm for MODIS. ASTER data is optimized using a neural network algorithm (Mao et al., 2008). A split window algorithm is provided for Landsat 8 and the root mean square is determined as 0.93°C (Rozenstein et al., 2014). When the urban reflectance is known, the algorithms are divided into three types; the single-channel method (Coll et al., 2012), the multi-channel method (Atitar and Sobrino, 2009), and the multi-angle method (Sobrino and Jiménez-Muñoz, 2005). When the urban reflectance is not known, the algorithms are again divided into three types, but which differ from the preceding case; the stepwise retrieval method (Sobrino et al., 2008), simultaneous

http://www.aloki.hu ● ISSN 1589 1623 (Print) ● ISSN 1785 0037 (Online)
DOI: http://dx.doi.org/10.15666/aeer/1705_1262312638

retrieval (Hulley and Hook, 2011), and simultaneous retrieval with unknown atmospheric information (Wang et al., 2013).

In a related analysis of the spatiotemporal characteristics of LST, the urban heat island magnitude is considered to be inversely correlated with the rural temperature (Streutker, 2002). The intensity of the urban heat island reached a maximum during the summer and a minimum during the winter periods. The overall relationship between urban heat island and population density have been quantitatively explored (Li et al., 2012). The minimum temperature difference formed at the end of the cooling process increases with urban length and while wind speed is on the decline (Lee et al., 2012). The LST has been increasing in recent years, with an increase of LST in both rural and urban areas (Rajasekar and Weng, 2009; Alavipanah et al., 2015; Fu and Weng, 2016a; Haashemi et al., 2016).

By predicting the urban expansion pattern of cities in the Pearl River Delta of China and considering the LST and urban reflectance patterns, the radiation temperature is expected to increase by 13.01 K (Weng, 2001). LST possesses a more negative relation with the unmixed vegetation abundance than with the normalized difference vegetation index (NDVI) across the spatial resolution from 30 m to 960 m (Weng et al., 2004). The NDVI can be easily influenced by leaf area, view angle, and soil background, thus, it is not a suitable indicator for quantitative vegetation research (Small, 2001). The three-end members of substrate, vegetation, and dark surface, can represent more than 95% of the 30 million ETM+ image spectra with misfits of less than 0.04 (Small, 2004, 2005). There is a negative relation between LST and vegetation abundance, and a positive relation between LST and impervious surface. The rates of change of low and high temperatures differ depending on the impervious surface abundance (Small and Lu, 2006). The heat island effect is more noticeable in industrial and commercial areas (Zhang et al., 2012). The LST is expected to increase by 2.63°C by overall regression, and 3.17°C from geographically weighted regression, and additionally, according to an analysis of the accuracy the overall regression underestimates the heat island effect and its risks (Su et al., 2012). High-intensity urban land in Atlanta has the highest mean LST value of 294.9 K with a yearly amplitude of 17.4 K (Fu and Weng, 2016b). Information support systems for urban heat landscape have been proposed to simulate the urban heat island and mitigate these effects (Quattrochi et al., 2000). Landscape indices can also be used to predict the LST. The landscape dominance index and the landscape shape index account for 56% and 6–12% of the variance of the LST, respectively (Chen et al., 2014).

In spite of these significant studies, there are few studies of the regional arithmetical relation between LST and urban reflectance. Using Landsat TM/ETM imagery of Nanjing City, this study aims to illustrate the quantitative relation between LST and urban reflectance Specific objectives of this study are as follows: (1) to derive the LST and analyze its temporal, spatial, and fractal characteristics. (2) to apply linear spectral unmixing to analyze the urban reflectance of vegetation, substrate, and dark areas. (3) to investigate the relation between LST and vegetation, substrate and dark abundance using geographically weighted regression (GWR). This research also investigates the relation between LST and the enhanced vegetation index (EVI) under landscape diversity indices and fragment indices.

http://www.aloki.hu ● ISSN 1589 1623 (Print) ● ISSN 1785 0037 (Online)
DOI: http://dx.doi.org/10.15666/aeer/1705_1262312638

Materials and Methods

Study Sites

Nanjing City is in the central region of the Yangtze river downstream at 118°22′-119°14′E, 31°14′–32°37′N in Jiangsu province. The total area of Nanjing City was 6597 km^2, with 1427.81 km^2 of built area in 2018. Nanjing City has a humid subtropical climate. The average, maximum (summer), and minimum (winter) temperatures, are 15.4, 39.7, and -13.1°C, respectively. Rainfall averages 1006 mm per annum. Nanjing's geomorphology is primarily characterized by low mountains and low hillocks, with 3.5% low mountains, 4.3% hilly areas, 53% low hillocks, and 39.2% plains and rivers (Li et al., 2016). The natural vegetation is mixed deciduous forest and broadleaf evergreen forest. Nanjing includes seven districts, Central, Jiangning, Qixia, Pukou, Liuhe, Lishui, and Gaochun districts, respectively (*Fig. 1*).

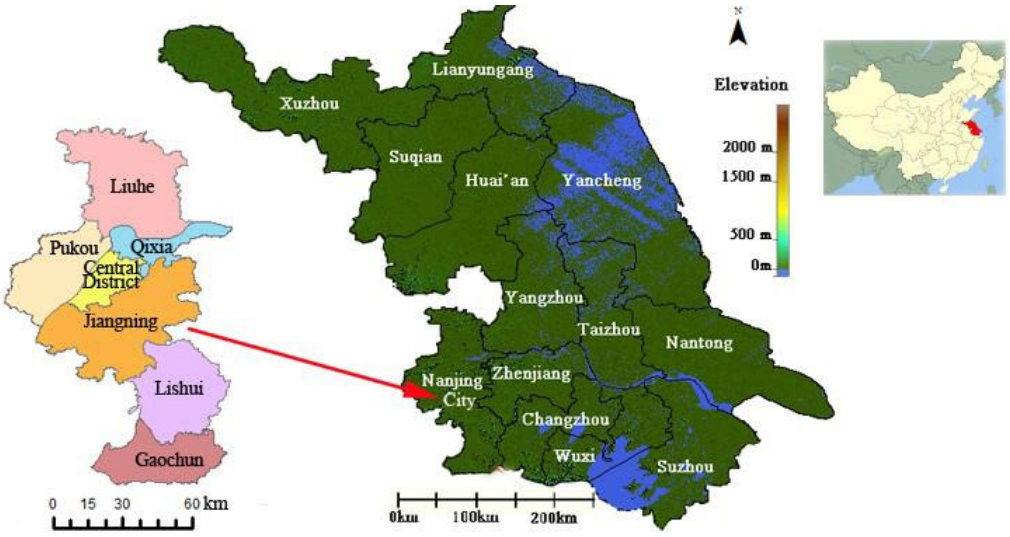

Figure 1. *Nanjing City of China. There are seven districts in Nanjing.*

Nanjing is the Capital of Jiangsu province with nearly 2000 years of history. The GDP of Nanjing was 972.08 billion yuan in 2015, ranking 11th in China. In 2015 Nanjing's industrial infrastructure account for 2.4% in primary industry, 40.3% in secondary industry, and 57.3% in tertiary industry. Nanjing's resident population in 2015 was 8.24 million and the urbanization rate was 81.4%. The reform and open policy of the 1980s produced a rapid urbanization phase and further encroachment on the countryside. The Nanjing Plan of 1991-2010 proposed new towns around the main old city (Jim and Chen, 2003).

Data

The data sets were downloaded from the United States Geological Survey (USGS) website (http://glovis.usgs.gov/ accessed 7th March 2019). 22 Landsat images are used to derive the LSTs in Nanjing (*Table 1*). The Landsat TM image obtained on May 20, 2006 is utilized to derive the landscape diversity indices and fragment indices. The Landsat image obtained on October 3, 2009 is utilized to derive the fractions of substrate, vegetation, and dark surface land cover by linear spectral unmixing.

http://www.aloki.hu ● ISSN 1589 1623 (Print) ● ISSN 1785 0037 (Online)
DOI: http://dx.doi.org/10.15666/aeer/1705_1262312638

Table 1. *Dataset of Landsat images used without cloud or less than 5% cloud*

Data set	Date
LandSat TM 5	04/17/2000
LandSat TM 5	10/10/2000
LandSat TM 5	0d4/04/2001
LandSat ETM 7	07/17/2001
LandSat ETM 7	02/10/2002
LandSat TM 5	07/12/2002
LandSat TM 5	09/30/2002
LandSat ETM 7	10/24/2002
LandSat ETM 7	11/09/2002
LandSat ETM 7	12/27/2002
LandSat ETM 7	01/28/2003
LandSat TM 5	02/08/2004
LandSat TM 5	11/22/2004
LandSat TM 5	12/08/2004
LandSat TM 5	04/02/2006
LandSat TM 5	05/20/2006
LandSat TM 5	03/20/2007
LandSat TM 5	05/07/2007
LandSat TM 5	10/03/2009
LandSat TM 5	08/19/2010
LandSat TIRS 8	08/11/2013
LandSat TIRS 8	10/14/2013

Methods

Radiative transfer equation

The LST is obtained using the radiative transfer equation from the following expression (Berk et al., 1987; Sobrino et al., 2004).

$$L_{sensor} = (\varepsilon L_\lambda + (1-\varepsilon)L_\downarrow)\tau + L_\uparrow \quad \text{(Eq.1)}$$

where L_{sensor} is the at-sensor radiance above the atmospheric radiance, ε is the urban relectance, τ is the total atmospheric transmissivity between the land surface and the sensor, $L_\downarrow$ and $L_\uparrow$ are the downwelling and upwelling atmospheric radiances, $L_\uparrow$and L_λ

is the blackbody radiance given by Planck's law.

The formula for the actual temperature, T is as follows:

$$T = \frac{K_2}{Ln(K_1/L_\lambda + 1)} \quad \text{(Eq.2)}$$

where K_1 and K_2 are constants. For Landsat TM, K1 = 607.66 and K2 = 1260.56, and for Landsat ETM, K1 = 666.09 and K2 = 1282.71.

$$NDVI = (TM4 - TM3)/(TM4 + TM3) \quad \text{(Eq.3)}$$

where TM4 and TM3 are the near the infrared and red bands, respectively.

$$F_V = [(NDVI - NDVI_S)/(NDVI_V - NDVI_S)] \quad \text{(Eq.4)}$$

$$\varepsilon surface = 0.9625 + 0.0614F_V - 0.046F_V^2 \quad \text{(Eq.5)}$$

http://www.aloki.hu ● ISSN 1589 1623 (Print) ● ISSN 1785 0037 (Online)
DOI: http://dx.doi.org/10.15666/aeer/1705_1262312638

$$\varepsilon built = 0.9589 + 0.086F_V - 0.0671F_V^2 \quad \text{(Eq.6)}$$

where F_V is the percentage of vegetation cover, and $\varepsilon surface$ and $\varepsilon built$ represent the emissivities corresponding to the natural and urban surfaces, respectively.

Linear spectral mixture model

The linear spectral mixture model assumes that the spectral reflectance of the field of view of a sensor can be expressed as a linear combination of the constituent end members (Small and Lu, 2006).

$$R(\lambda) = f_1E_1(\lambda) + f_2E_2(\lambda) + \cdots + f_nE_n(\lambda) \quad \text{(Eq.7)}$$

where $R(\lambda)$ is the observed reflectance, λ is the wavelength, $E_i(\lambda)$ is the spectrum of the end members, f_i is a coefficient representing the abundance of the corresponding end members.

The linear spectral mixture has two significant problems. One is to determine the number of end members related to surface reflectance. Another one is to determine the reflectance spectrum of end members. Linear spectral mixture models can be standardized by using end members that span the global mixing space. The mean substrate, vegetation, and dark end members can be used to define a global standard mixture model for Landsat spectra (Clement et al., 2009; Small and Milesi, 2013).

Geographically weighted regression

Geographic weighted regression is an extension of the traditional global regression because it allows for local regression rather than global parameter estimation (Fotheringham et al., 2001). The GWR method is also applied to LST and environmental driving factors (Buyantuyev and Wu, 2010; Zhou and Wang, 2011; Schwarz et al., 2012; Du et al., 2016).

The equation for the GWS model is:

$$y_i = \beta_0(u_i, v_i) + \sum_k \beta_k(u_i v_i)\, x_{ik} + \varepsilon_i \quad \text{(Eq.8)}$$

where (u_i, v_i) is the coordinate of the *i*-th point, $\beta_k(u_i v_i)$ is the *k*-th regression parameter of the *i*-th point, and ε_i is the random error of the *i*-th sample.

Data near the *i*-th point will have a more profound effect on $\beta_k(u_i v_i)$ than data further away.

$$\hat{\beta}(u,v) = (X^T W(u,v) X)^{-1} X^T W(u,v) y \quad \text{(Eq.9)}$$

http://www.aloki.hu ● ISSN 1589 1623 (Print) ● ISSN 1785 0037 (Online)
DOI: http://dx.doi.org/10.15666/aeer/1705_1262312638

where $\hat{\beta}(u,v)$ represents the unbiased estimate of β, $W(u, v)$ is a weight function, which ensures that observation points close to the specific point will have a large weight.

$$W_{ij} = \exp\left(\frac{d_{ij}^2}{b^2}\right) \quad \text{(Eq.10)}$$

where W_{ij} is the weight of observation point *j* related to the point *i*.

If the observation point *j* coincides with point *i*, the weight of point *j* is 1. If the distance between points *j* and *i* is greater than the bandwidth, the weight of point *j* is zero. Thus, the GWR model takes the bandwidth into account.

Landscape indices

The land surface is classified into five types by an un-supervised classification method and checked with Google Earth, including farmland, forest, water areas, construction land and other land. Based on the land classification, landscape diversity and Landscape fragmentation indices are calculated by fragstas.

Results

The Character of Urban Reflectance and LST

The urban reflectance is classified into three types by linear spectral unmixing, including the substrate fraction (*Fig. 2a*), vegetation fraction (*Fig. 2b*), and dark fraction (*Fig. 2c*). The LST is inversed by radiation transfer model in Nanjing City on October 3, 2009.

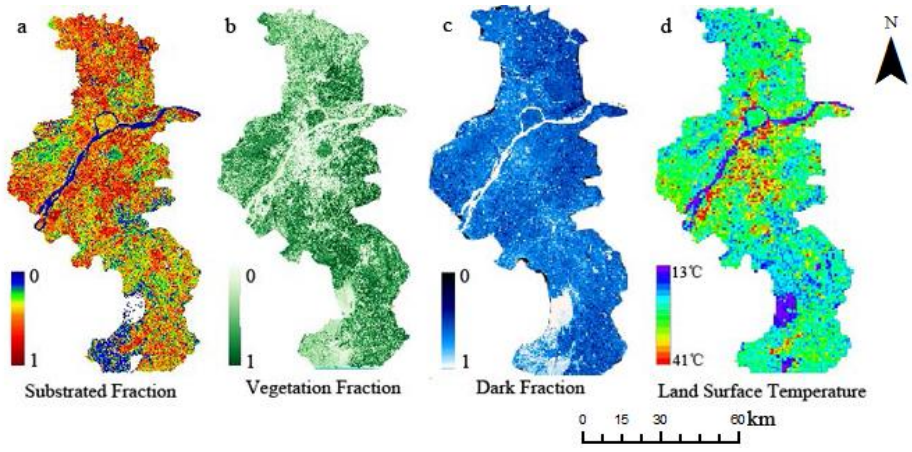

Figure 2. *The urban reflectance and LST in Nanjing City on October 3, 2009. The fraction of impervious surface from 0-100% (Fig.2a). Vegetation fraction (Fig.2b). Water Fraction (Fig.2c). LST (Fig.2d)*

High impervious surface fractions are mainly distributed in the middle and the north part of Nanjing City (*Fig. 2a*). The central city of Nanjing is in the center along the Changjiang river. With urbanization, the impervious surface is gradually extending in

http://www.aloki.hu ● ISSN 1589 1623 (Print) ● ISSN 1785 0037 (Online)
DOI: http://dx.doi.org/10.15666/aeer/1705_1262312638

the northerly direction. Low vegetation surface fractions are in the center of Nanjing City and some is also observed in the north (*Fig. 2b*). The vegetation in cultivated areas, forest parks, and undeveloped remote areas in the outer suburbs is less disturbed. High water surface fractions are in the middle and in the south, and correspond to the Yangtze river and Gucheng lake, respectively (*Fig. 2c*). Nanjing City with the high LST observed on October 3, 2009 is in the center of Nanjing (*Fig. 2d*). The high temperature area is larger than the area of the high impervious surface fraction. With the rapid progress of urban construction in Nanjing, the city is subject to a large number of anthropogenic heat sources, including fuel combustion, automobile exhaust, and air conditioning, increasing the air temperature. The development of commercial and service industries in Nanjing has resulted in business areas with dense population. These areas are have high densities so the heat is not easy to diffuse.

Characteristics of the spatial dimension of LST

Taking the city of Nanjing as the center, and extending to the north, east, south, and west we make a temperature profile for October 3, 2009 (*Fig. 3*). The LST profile serves to observe the general characteristics of LST and horizontal distribution trends. The section of the profile running from north to central urban (*Fig. 3a*), has a low temperature of approximately 24°C, corresponding to the Yangtze River basin, and the profile continues from central urban to the south (*Fig. 3b*).

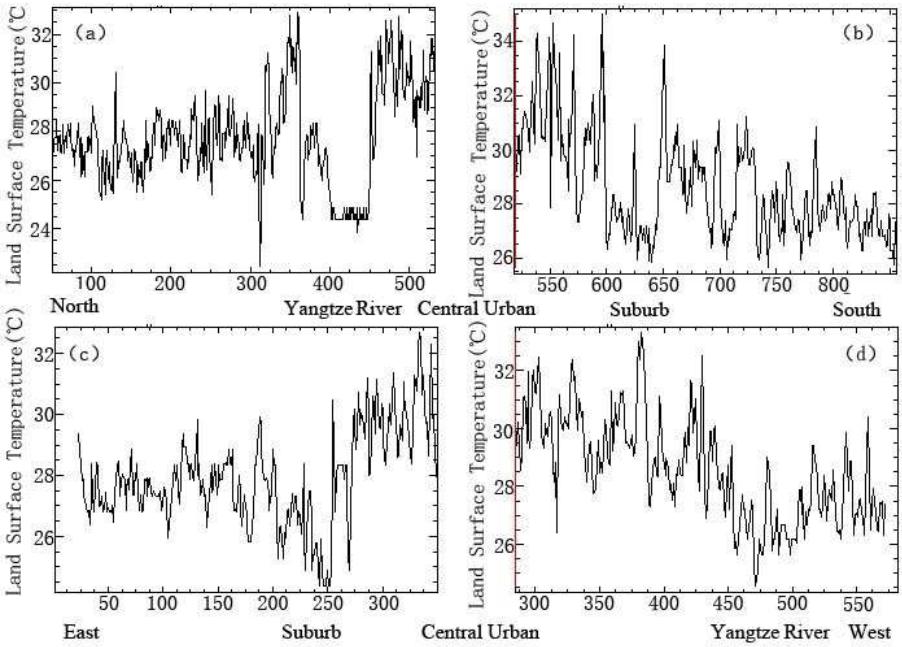

Figure 3. *Spatial sectional view of LST in Nanjing on October 3,2009. From north to Central direction (a). From central to south direction (b). From east to central direction (c). From central to west direction (d)*

The junction of the urban and rural areas has a low temperature because of high vegetation cover. The section of the profile running from east to central urban (*Fig. 3c*) and the corresponding place of low temperature is the junction of urban and rural areas. The section of the profile running from central urban to east (*Fig. 3d*) has a low

http://www.aloki.hu ● ISSN 1589 1623 (Print) ● ISSN 1785 0037 (Online)
DOI: http://dx.doi.org/10.15666/aeer/1705_1262312638

temperature of about 26°C. As a result, the temperature in central urban is higher by 8-6°C than that in Yangtze River and urban-rural junction with high vegetation cover.

Characteristics of the temporal dimension of LST

LST time series data from April 17, 2000 to October 14, 2013 is selected in the central city (*Fig. 4a*), the suburbs (*Fig. 4b*), the outer suburbs (*Fig. 4c*), and the outer suburbs near a lake (*Fig. 4d*) of Nanjing City (*Fig. 4e*). The high LST is 44°C in central city, 40°C in suburbs, 36°C in outer suburbs, and 33°C in outer suburbs near water. During the fourteen years of the presented time series data, urban development has expanded to the suburbs and impacted its LST. The land surface of the outer suburbs is less disturbed by humans and the LST is 5°C lower than that in central urban. The LST in the outer suburbs near the lake is lower than that in the outer suburbs, mainly because of the influence of the water surface.

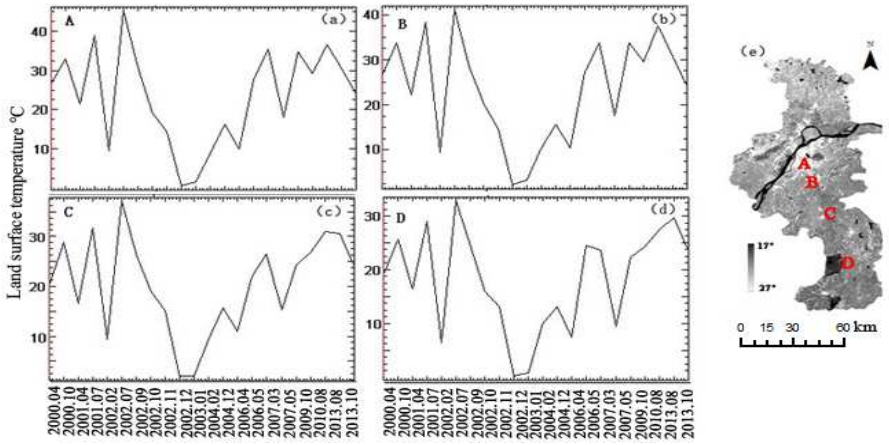

Figure 4. *Time series of LST in Nanjing from Year 2000-2013. Time series curve in central urban (Fig.4a). Time series curve in suburbs (Fig.4b).Time series curve in outer suburbs (Fig.4c). Time series curve in outer suburbs near lake (Fig.4d). Sample position map (Fig.4e)*

Characteristics of the fractal dimension of LST

From 2000 to 2010, the LST of the central city in spring, summer, and autumn was 1-5°C higher than that of the suburbs (Jiangning, Qixia, and Pukou districts) and outer suburbs (Liuhe, Lishui, and Gaochun districts), for example, on July 12, 2002 and May 7, 2007 (*Table 2*).

Table 2. *Zoning LST in Central urban, suburbs (Jiangning District, Qixia District, and Pukou District) and outer suburbs (Liuhe District, Lishui District, and Gaochun District) from 2000 to 2010. (Units: ℃)*

	District						
Date	**Central**	**Jiangning**	**Qixia**	**Pukou**	**Liuhe**	**Lishui**	**Gaochun**
2000/04/17	25.38	23.41	24.12	23.96	24.48	22.96	22.37
2000/10/10	32.63	30.74	31.02	31.77	31.02	31.74	31.73
2001/04/04	22.00	20.00	20.28	20.29	19.98	18.80	16.71
2001/07/17	35.43	31.67	33.34	32.04	31.35	31.58	29.60
2002/02/10	11.16	10.60	11.12	11.00	10.77	10.61	10.32
2002/07/12	41.33	36.16	40.56	36.15	35.53	37.60	35.98
2002/09/30	29.62	28.00	27.75	29.55	28.34	27.84	26.34

http://www.aloki.hu ● ISSN 1589 1623 (Print) ● ISSN 1785 0037 (Online)
DOI: http://dx.doi.org/10.15666/aeer/1705_1262312638

2002/10/24	20.90	20.01	19.68	20.65	20.03	20.09	20.80
2002/11/09	15.98	15.97	15.88	16.43	16.43	15.87	16.18
2002/12/27	2.11	2.57	2.30	2.60	1.92	2.61	2.00
2003/01/28	3.18	3.20	3.20	3.40	2.03	2.78	2.00
2004/02/08	11.74	12.60	12.34	12.65	11.66	12.18	12.10
2004/11/22	16.53	16.71	16.12	16.26	16.33	17.11	16.60
2004/12/08	11.85	11.71	11.98	11.97	11.40	11.82	11.40
2006/04/02	27.31	26.00	24.74	25.24	24.80	23.96	23.08
2006/05/20	32.30	30.65	30.27	30.68	31.67	30.00	30.62
2007/03/20	18.14	16.71	17.72	17.06	16.60	16.02	15.02
2007/05/07	33.74	29.65	30.30	29.87	30.43	28.51	26.00
2009/10/03	28.56	27.37	28.14	27.41	27.21	27.20	27.16
2010/08/19	34.22	30.52	32.68	30.60	29.75	29.63	29.54

In winter, the LST is less than or close to that of the suburbs and the outer suburbs, such as on December 27, 2002 and February 8, 2004.

Comparing the LST of different years, the intensity of the heat island effect is decreased on May 20, 2006 and October 3, 2009. During the period 2007-2010, the LST difference between central urban and outer suburbs is small because urbanization has led to the expansion of urban space, thus the intensity of the heat island effect is relatively weakened.

Relationship between LST and Land Cover

In the GWR method, local R^2 and standard residuals provide the criteria for judging the degree of fit to observational data. Local R^2, ranges from 0 to 1, and indicates the degree of local regression of the simulation for the observed values. Higher values indicate that the local regression model fits the results well, and lower values less-well. The coefficients represent the relationship between the two variables of LST and vegetation surface, and the related directions. The residual represents the difference between the observed and estimated values. The standard residual is zero.

Fig. 5 shows the correlation between LST and vegetation based on the GWR, in which the LST is the dependent variable and the vegetation abundance is the argument. High local R^2 represents a strong correlation, and mainly occurs in the central area of Nanjing and the suburbs (*Fig. 5a*).

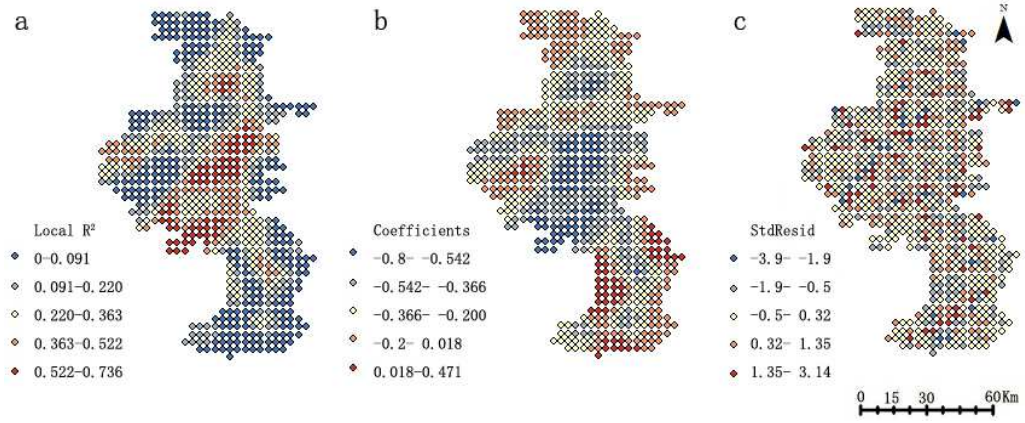

Figure 5. *Correlation between LST and vegetation based on geographically weighted regression model in October 2009 in Nanjing City. Fig.5a is Local R2. Fig.5b is Coefficients. Fig.5c is StdResid*

http://www.aloki.hu ● ISSN 1589 1623 (Print) ● ISSN 1785 0037 (Online)
DOI: http://dx.doi.org/10.15666/aeer/1705_1262312638

Lower local R^2 represents a relatively weak geographic linear correlation, and mainly occurs in the south and north of Nanjing. Vegetation in the Central district of Nanjing showed a stronger negative correlation with LST and the coefficient ranged from -0.8 to -0.542 (*Fig. 5b*). Vegetation abundance in the outer suburbs displayed a weak negative correlation with the LST. The distance from the central district has a significant impact on the relationship between vegetation and LST. Positive residuals represent a high predictive value and negative residuals a low value (*Fig. 5c*). On the whole, the standard residuals are distributed in an apparently random pattern, and all residual values are lower than four, thus the overall model fit well.

Figure 6 shows the correlation between LST and impervious surface abundance based on GWR. The high R^2 is mainly distributed in the central district and southern suburbs of Nanjing where the LST and impervious surface have a strong correlation (*Fig. 6a*). The coefficient of LST and impervious surfaces are all positive, showing a significant positive correlation (*Fig. 6b*). The coefficients in the urban center range from 0.803 to 1.045. The impervious surface has a significant impact on land surface warming. Absolute values of the majority of standard residuals are lower than 1, indicating that the model fit very well (*Fig. 6c*).

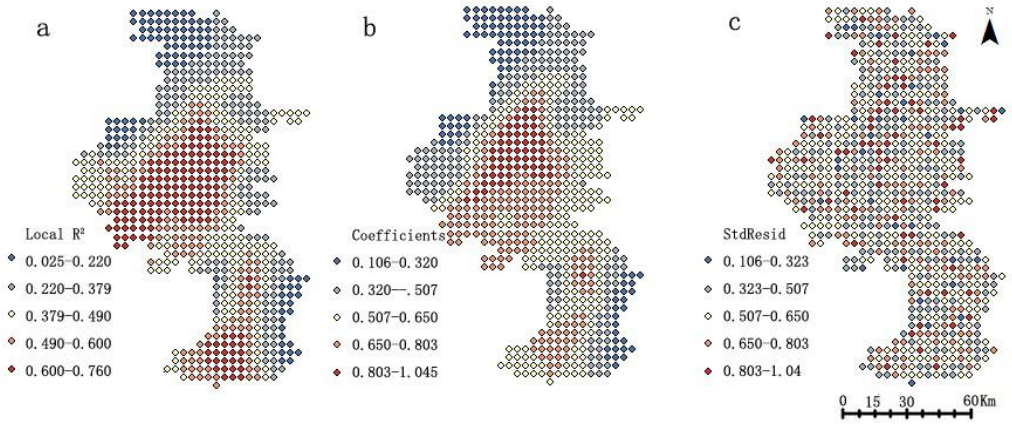

Figure 6. *Correlation between LST and impervious surface based on geographically weighted regression model in October 2009 in Nanjing City. Fig.6a is Local R2. Fig.6b is Coefficients. Fig.6c is StdResid*

Comparing *Fig. 5b* to *Fig. 6b*, the coefficients in the central district for vegetation and impervious surfaces range from -0.800 to -0.542 and from 0.803 to 1.045, respectively. The promoting role of impervious surface is much higher than the cooling effects of vegetation on LST.

Figure 7 shows the correlation between LST and water from GWR, in which the LST is the dependent variable and water abundance is the argument. The high R^2 is mainly distributed in the middle and north of Nanjing in the proximity of the Yangtze River and Gucheng Lake (*Fig. 7a*). The high local R^2 reaches 0.538 indicating that there is a good fit between LST and water. The coefficients in the south and middle of Nanjing are negative valued which signifies a negative correlation between LST and water (*Fig. 7b*). Along the Yangtze River, the coefficients are low (-1.64 to -1.07), thus, the Yangtze River forms a band which impedes heat transfer, and further slows down

http://www.aloki.hu ● ISSN 1589 1623 (Print) ● ISSN 1785 0037 (Online)
DOI: http://dx.doi.org/10.15666/aeer/1705_1262312638

the urban heat island effect. The absolute value of the standard residuals is less than four signifying that the model fit well (*Fig. 7c*).

Comparing *Fig. 5b* to *Fig. 7b*, the low coefficients for vegetation and water surface fitting with LST are -0.8 and -1.64, respectively, thus the water surface has a more obvious effect on adjusting the LST than the vegetation.

Relationship between LST and Landscape Indices

Landscape indices can describe the detailed pattern of the land surface. Landscape diversity indices include patch richness density and Shannon's diversity index. Landscape fragmentation indices include number of patches, patch density, division and splitting indices. These indicators are selected to reflect different aspects of landscape features and to verify the accuracy of the indicators (*Table 3*).

The Shannon's diversity index of the central city is 1.1691, and is the smallest of all districts. Diversity indices of the suburbs (Qixia, Pukou, and Jiangning districts) are 1.4072, 1.4287, and 1.4270. Diversity indices of the outer suburbs (Lishui, Liuhe, and Gaochun districts) are 1.4848, 1.4288, and 1.5037.

The division index of the central city is 0.7664, and is the smallest of all districts. Division indices of the suburbs (Qixia, Pukou, and Jiangning districts) are 0.8819, 0.9737, and 0.9777. Division indices of the outer suburbs (Lishui, Liuhe, and Gaochun districts) are 0.9853, 0.9723, and 0.9677.

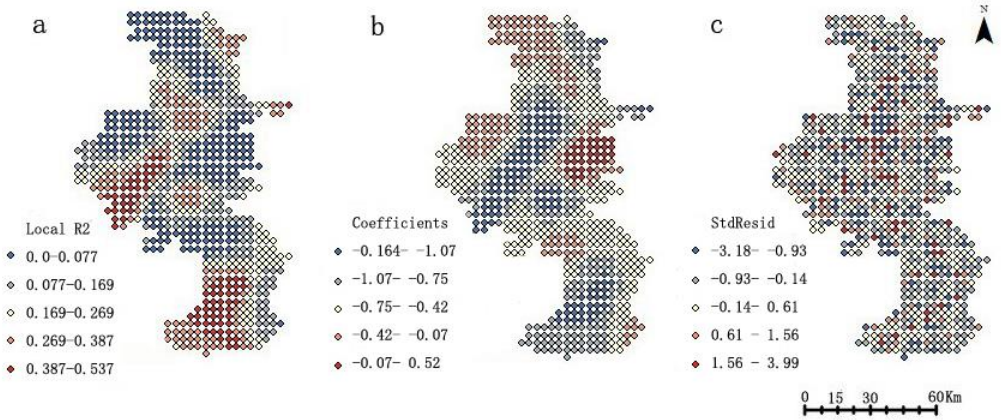

Figure 7. *Correlation between LST and water surface based on geographically weighted regression model in October 2009 in Nanjing City. Fig.7a is Local R2. Fig.7b is Coefficients. Fig.7c is StdResid*

Table 3. *Landscape index in Nanjing zones on May 20, 2006*

District	Landscape indices					
	Number of patches	Patch density	Division index	Splitting index	Patch richness density	Shannon's diversity index
Lishui	99019	92.93	0.9853	68.08	0.0047	1.4848
Liuhe	132821	90.08	0.9723	36.15	0.0034	1.4288
Pukou	80495	88.72	0.9737	37.96	0.0055	1.4287
Qixia	20283	51.79	0.8819	8.46	0.0128	1.4072
Central	18084	50.19	0.7664	4.28	0.0139	1.1691
Jiangning	147583	91.91	0.9777	44.84	0.0031	1.4270
Gaochun	69328	86.29	0.9677	30.95	0.0062	1.5037

http://www.aloki.hu ● ISSN 1589 1623 (Print) ● ISSN 1785 0037 (Online)
DOI: http://dx.doi.org/10.15666/aeer/1705_1262312638

The diversity index in the central city is lowest of all, and the LST and EVI display a significant negative correlation. Diversity indices in the suburbs are in the middle value of all. The LST and EVI have a weak negative correlation (*Fig. 8*). Diversity indices in the outer suburbs are the largest of all the sites, and the LST and EVI show substantially no linear correlation.

If the landscape diversity indices are smaller, the LST has a more obvious negative correlation with the vegetation index. Conversely, if the landscape diversity indices are greater, the LST response to the vegetation index is weaker.

Similarly, if landscape fragmentation indices are smaller, the LST has a more obvious negative correlation with the vegetation index. Conversely, if landscape fragmentation indices are greater, the LST response to the vegetation index is weaker.

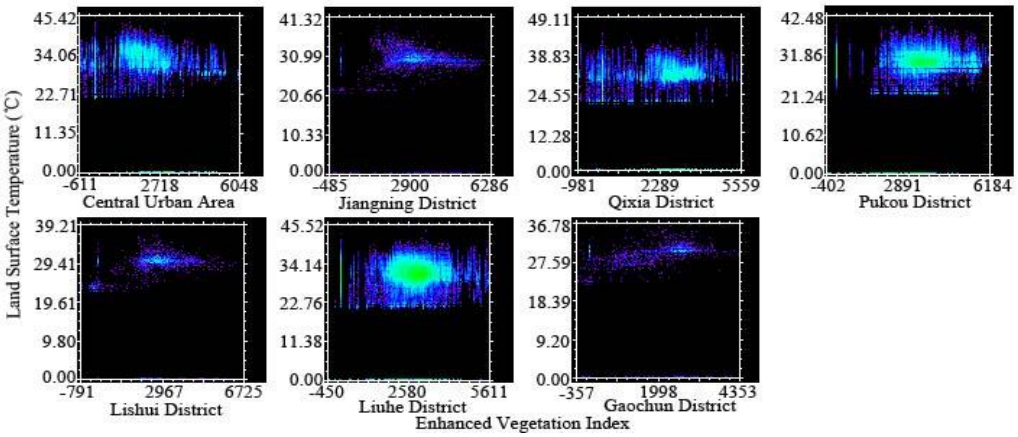

Figure 8. *The relation of LST and enhanced vegetation index (EVI) under different landscape indexes in Nanjing zones. X axis is enhance vegetation index and Y axis is LST*

Conclusions

In the spatial dimension, the high temperature is in the central city, and the low temperature is in the suburbs and the Yangtze River, and there was a 6-8°C temperature difference on October 3, 2009. In the temporal dimensional, the maximum LSTs in the central city, suburbs, outer suburbs and outer suburbs near water are 44, 40, 36, and 33°C, respectively. In the fractal dimension, the LST of the central city in spring, summer, and autumn is 1-5°C higher than that of the suburbs. In winter, the LST of the central city is less than or close to that of the suburbs.

In the quantitative relation between the LST and urban reflectance, vegetation in the Central District of Nanjing showed a stronger negative correlation with LST and the coefficient is -0.8. Impervious surface in the central district of Nanjing displayed an extinctive positive correlation with the LST and the highest coefficient is 1.045. The promoting role of impervious surface is considerably higher than the cooling effects of vegetation on LST. The water surface of Gucheng Lake had a negative correlation with LST and a low coefficient of -1.64. The water surface has a more obvious effect on adjusting the LST.

The landscape diversity indices and fragmentation indices have a negative relationship with both the LST and vegetation index. If the landscape diversity indices are smaller, the LST has a more noticeable negative correlation with the vegetation

http://www.aloki.hu ● ISSN 1589 1623 (Print) ● ISSN 1785 0037 (Online)
DOI: http://dx.doi.org/10.15666/aeer/1705_1262312638

index. Similarly, if the landscape fragmentation indices are smaller, LST has a more obvious negative correlation with the vegetation index.

Discussions

In this research, the GWR model is utilized to explore the scale-dependent and spatial non-stationary relationships between LST and urban reflectance. In the GWR model, the strength of the regression relationships increased significantly, with a mean of 59% of the changes in LST values explained by the predictors, compared with only 43% using the ordinary least squares model (Li et al., 2010). The most important problem for the GWR method is to set the local regression parameters and select a suitable bandwidth, which involves the problem of spatial autocorrelation. Here the local regression parameters are set to be adaptive and not consider the spatial autocorrelation factor. However, spatial autocorrelation is a key issue for future research. The land cover and land surface temperature have the same trend with the published paper (Liu et al., 2016; Wang et al., 2018).

Scaling is another important factor effecting the relationship between landscape patterns and LST. Thirty meters was found to be the optimal resolution in the study of the relationship between urban relectance and LST classes. Ninety meters was found to be the optimal spatial resolution for assessing the landscape-level relationship between land cover and LST patterns (Liu and Weng, 2009). Here the Landsat dataset of 30 meters resolution was selected to derive the LST.

The impact of urbanization on the urban heat island can be mitigated not only by balancing land use patterns, but also by optimizing the spatial landscape (Zhou et al., 2011). Landscape patterns can determine the land function. The same amount of vegetation cover in different landscape patterns will play a different role in slowing LST. The composition metric alone explains about 56% of the landscape mean LST. Whereas, adding a configuration explains approximately another 6–12% (Chen et al., 2014). Here we study the correlation between LST and vegetation index under different landscape index conditions; a focus of research on the quantitative relation between LST and urban landscape pattern.

Acknowledgements. The research was supported by the National Natural Science Foundation of China (Key Program) (41730642), National Natural Science Foundation of China (NSFC) project (no. 41401094) and Shanghai Normal University project (307-AC0302-19-005416). We thank the anonymous reviewers for the numerous helpful comments and suggestions.

Competing interests. The authors declare no competing interests.

REFERENCES

[1] Alavipanah, S., Wegmann, M., Qureshi, S., Weng, Q. H., Koellner, T. (2015): The Role of Vegetation in Mitigating Urban Land Surface Temperatures: A Case Study of Munich, Germany during the Warm Season. – Sustainability 7(4): 4689-4706.

[2] Atitar, M., Sobrino, J. A. (2009): A split-window algorithm for estimating LST from Meteosat 9 data: Test and comparison with in situ data and MODIS LSTs. – IEEE Geoscience and Remote Sensing Letters 6(1): 122-126.

http://www.aloki.hu ● ISSN 1589 1623 (Print) ● ISSN 1785 0037 (Online)
DOI: http://dx.doi.org/10.15666/aeer/1705_1262312638

[3] Berk, A., Bernstein, L., Robertson, D. C. (1987): MODTRAN: A moderate resolution model for LOWTRAN. – SPECTRAL SCIENCES INC BURLINGTON MA 9: 325.
[4] Buyantuyev, A., Wu, J. (2010): Urban heat islands and landscape heterogeneity: linking spatiotemporal variations in surface temperatures to land-cover and socioeconomic patterns. – Landscape ecology 25(1): 17-33.
[5] Chen, A., Yao, L., Sun, R. H., Chen, L. D. (2014): How many metrics are required to identify the effects of the landscape pattern on land surface temperature? – Ecological Indicators 45: 424-433.
[6] Clement, F., Orange, D., Williams, M., Mulley, C., Epprecht, M. (2009): Drivers of afforestation in Northern Vietnam: assessing local variations using geographically weighted regression. – Applied Geography 29(4): 561-576.
[7] Coll, C., Valor, E., Galve, J. M., Mira, M., Bisquert, M., García-Santos, V., Caselles, E., Caselles, V. (2012): Long-term accuracy assessment of land surface temperatures derived from the Advanced Along-Track Scanning Radiometer. – Remote Sensing of Environment 116: 211-225.
[8] Du, S. H., Xiong, Z. Q., Wang, Y. C., Guo, L. (2016): Quantifying the multilevel effects of landscape composition and configuration on land surface temperature. – Remote Sensing of Environment 178: 84-92.
[9] Fotheringham, A. S., Charlton, M. E., Brunsdon, C. (2001): Spatial variations in school performance: a local analysis using geographically weighted regression. – Geographical and Environmental Modelling 5(1): 43-66.
[10] Fu, P., Weng, Q. (2016a): Consistent land surface temperature data generation from irregularly spaced Landsat imagery. – Remote Sensing of Environment 184: 175-187.
[11] Fu, P., Weng, Q. (2016b): A time series analysis of urbanization induced land use and land cover change and its impact on land surface temperature with Landsat imagery. – Remote Sensing of Environment 175: 205-214.
[12] Haashemi, S., Weng, Q. H., Darvishi, A., Alavipanah, S. K. (2016): Seasonal Variations of the Surface Urban Heat Island in a Semi-Arid City. – Remote Sensing 8(4): 352.
[13] Hulley, G. C., Hook, S. J. (2011): Generating consistent land surface temperature and emissivity products between ASTER and MODIS data for earth science research. – IEEE Transactions on Geoscience and Remote Sensing 49(4): 1304-1315.
[14] Jim, C. Y., Chen, S. S. (2003): Comprehensive greenspace planning based on landscape ecology principles in compact Nanjing city, China. – Landscape and Urban Planning 65(3): 95-116.
[15] Landsberg, H. E. (1981): The urban climate. International Geophysics Series. – Academic Press, New York 28: 275.
[16] Lee, T. W., Lee, J. Y., Wang, Z. H. (2012): Scaling of the urban heat island intensity using time-dependent energy balance. – Urban Climate 2: 16-24.
[17] Li, S., Zhao, Z. Q., Xie, M. M., Wang, Y. L. (2010): Investigating spatial non-stationary and scale-dependent relationships between urban surface temperature and environmental factors using geographically weighted regression. – Environmental Modelling & Software 25(12): 1789-1800.
[18] Li, Y. Y., Zhang, H., Kainz, W. (2012): Monitoring patterns of urban heat islands of the fast-growing Shanghai metropolis, China: Using time-series of Landsat TM/ETM+ data. – International Journal of Applied Earth Observation and Geoinformation 19: 127-138.
[19] Li, B., Chen, D., Wu, S., Zhou, S., Wang, T., Chen, H. (2016): Spatio-temporal assessment of urbanization impacts on ecosystem services: Case study of Nanjing City, China. – Ecological Indicators 71: 416-427.
[20] Liu, H., Weng, Q. (2009): Scaling effect on the relationship between landscape pattern and land surface temperature. – Photogrammetric Engineering & Remote Sensing 75(3): 291-304.

http://www.aloki.hu ● ISSN 1589 1623 (Print) ● ISSN 1785 0037 (Online)
DOI: http://dx.doi.org/10.15666/aeer/1705_1262312638

[21] Liu, G., Zhang, Q., Li, G., Doronzo, D. M. (2016): Response of land cover types to land surface temperature derived from Landsat-5 TM in Nanjing Metropolitan Region, China. – Environmental Earth Sciences 75(20): 1386.
[22] Mao, K. B., Shi, J. C., Tang, H. J., Li, Z. L., Wang, X. F., Chen, K. S. (2008): A neural network technique for separating land surface emissivity and temperature from ASTER imagery. – IEEE Transactions on Geoscience and Remote Sensing 46(1): 200-208.
[23] Qin, Z., Dall'Olmo, G., Karnieli, A., Berliner, P. (2001a): Derivation of split window algorithm and its sensitivity analysis for retrieving land surface temperature. – Journal of Geophysical Research: Atmospheres 106(19): 22655-22670.
[24] Qin, Z., Karnieli, A., Berliner, P. (2001b): A mono-window algorithm for retrieving land surface temperature from Landsat TM data and its application to the Israel-Egypt border region. – International Journal of Remote Sensing 22(18): 3719-3746.
[25] Quattrochi, D. A., Luvall, J. C., Rickman, D. L., Estes Jr, M. G., Laymon, C. A., Howell, B. F. (2000): A decision support information system for urban landscape management using thermal infrared data: Decision support systems. – Photogrammetric Engineering and Remote Sensing 66(10): 1195-1207.
[26] Rajasekar, U., Weng, Q. (2009): Urban heat island monitoring and analysis using a non-parametric model: A case study of Indianapolis. – ISPRS Journal of Photogrammetry and Remote Sensing 64(1): 86-96.
[27] Rao, P. K., Smith, W. L., Koffler, R. (1972): Global sea-surface temperature distribution determined from an environmental satellite. – Monthly Weather Review 100(1): 10-14.
[28] Roth, M., Oke, T. R., Emery, W. J. (1989): Satellite-derived urban heat islands from three coastal cities and the utilization of such data in urban climatology. – International Journal of Remote Sensing 10(11): 1699-1720.
[29] Rozenstein, O., Qin, Z. H., Derimian, Y., Karnieli, A. (2014): Derivation of land surface temperature for Landsat-8 TIRS using a split window algorithm. – Sensors 14(14): 5768-5780.
[30] Schwarz, N., Schlink, U., Franck, U., Großmann, K. (2012): Relationship of land surface and air temperatures and its implications for quantifying urban heat island indicators—an application for the city of Leipzig (Germany). – Ecological Indicators 18: 693-704.
[31] Small, C. (2001): Estimation of urban vegetation abundance by spectral mixture analysis. – International Journal of Remote Sensing 22(7): 1305-1334.
[32] Small, C. (2004): The Landsat ETM+ spectral mixing space. – Remote Sensing of Environment 93(1-2): 1-17.
[33] Small, C. (2005): A global analysis of urban reflectance. – International Journal of Remote Sensing 26(4): 661-681.
[34] Small, C., Lu, J. W. (2006): Estimation and vicarious validation of urban vegetation abundance by spectral mixture analysis. – Remote Sensing of Environment 100(4): 441-456.
[35] Small, C., Milesi, C. (2013): Multi-scale standardized spectral mixture models. – Remote Sensing of Environment 136: 442-454.
[36] Sobrino, J. A., Jiménez-Muñoz, J. C., Paolini, L. (2004): Land surface temperature retrieval from LANDSAT TM 5. – Remote Sensing of Environment 90(4): 434-440.
[37] Sobrino, J. A., Jiménez-Muñoz, J. C. (2005): Land surface temperature retrieval from thermal infrared data: An assessment in the context of the Surface Processes and Ecosystem Changes through Response Analysis (SPECTRA) mission. – Journal of Geophysical Research: Atmospheres 110(16): 19.
[38] Sobrino, J. A., Jimenez-Munoz, J. C., Soria, G., Romaguera, M., Guanter, L., Moreno, J., Plaza, A., Martinez, P. (2008): Land surface emissivity retrieval from different VNIR and TIR sensors. – IEEE Transactions on Geoscience and Remote Sensing 46(2): 316-327.
[39] Streutker, D. R. (2002): A remote sensing study of the urban heat island of Houston, Texas. – International Journal of Remote Sensing 23(13): 2595-2608.

http://www.aloki.hu ● ISSN 1589 1623 (Print) ● ISSN 1785 0037 (Online)
DOI: http://dx.doi.org/10.15666/aeer/1705_1262312638

[40] Su, Y. F., Foody, G. M., Cheng, K. S. (2012): Spatial non-stationarity in the relationships between land cover and surface temperature in an urban heat island and its impacts on thermally sensitive populations. – Landscape and Urban Planning 107(2): 172-180.
[41] Wang, N., Li, Z. L., Tang, B. H., Zeng, F. N., Li, C. R. (2013): Retrieval of atmospheric and land surface parameters from satellite-based thermal infrared hyperspectral data using a neural network technique. – International Journal of Remote Sensing 34(9-10): 3485-3502.
[42] Wang, S., Ma, Q., Ding, H., Liang, H. (2018): Detection of urban expansion and land surface temperature change using multi-temporal landsat images. – Resources, Conservation and Recycling 128: 526-534.
[43] Weng, Q. (2001): A remote sensing? GIS evaluation of urban expansion and its impact on surface temperature in the Zhujiang Delta, China. – International Journal of Remote Sensing 22(10): 1999-2014.
[44] Weng, Q., Lu, D. S., Schubring, J. (2004): Estimation of land surface temperature–vegetation abundance relationship for urban heat island studies. – Remote Sensing of Environment 89(4): 467-483.
[45] Zhang, Y., Chen, Y. Y., Qing, D., Jiang, P. (2012): Study on urban heat island effect based on Normalized Difference Vegetated Index: a case study of Wuhan City. – Procedia Environmental Sciences 13: 574-581.
[46] Zhou, X., Wang, Y. C. (2011): Dynamics of Land Surface Temperature in Response to Land Use/Cover Change. – Geographical Research 49(1): 23-36.
[47] Zhou, W. Q., Huang, G. L., Cadenasso, M. (2011): Does spatial configuration matter? Understanding the effects of land cover pattern on land surface temperature in urban landscapes. – Landscape and Urban Planning 102(1): 54-63.

http://www.aloki.hu ● ISSN 1589 1623 (Print) ● ISSN 1785 0037 (Online)
DOI: http://dx.doi.org/10.15666/aeer/1705_1262312638

EFFECT OF CHICKEN MANURE ON YIELD AND YIELD CRITERIA OF ONION (*ALLIUM CEPA* L.) AS SECOND CROP

YOLDAS, F.[1*] – CEYLAN, S.[1] – MORDOGAN, N.[2]

[1]*Department of Organic Production, Ödemiş Vocational Training High School, Ege University 35750 İzmir, Turkey*

[2]*Department of Soil Science and Plant Nutrition, Faculty of Agriculture, Ege University 35100 İzmir, Turkey*

**Corresponding author*
e-mail: funda.yoldas@ege.edu.tr; phone: +90-542-322-5385; fax: +90-232-544-4356

(Received 13th May 2019; accepted 16th Jul 2019)

Abstract. This study was conducted to determine the residue effects of chicken manure on the yield and yield components of eight onion varieties as second crop after lettuce in field condition. Varieties (14-16, Burgaz, Karbeyazı, Naz, NWG, Perwana, Seyhan, Şampiyon) and also four different doses of chicken manure at the rates of 0, 20, 40, 60 t ha^{-1} with the recommended dose of NPK were used. A non-fertilized parcel was used as control. The experiment was laid out in split plot design and replicated three times. Yield and yield components were investigated. According to the results residual effect of chicken manures and onion varieties as second crop significantly affected the yield and bulb production in the field condition. The application of chicken manure significantly improved yield, bulb weight, bulb height, number of shoot tip, number of dried leaf compared to control. Highest yields (46.31 t ha^{-1}) were obtained in the parcels where the chicken manure was applied at a rate of 60 t ha^{-1}. The onion cultivar Burgaz was more responsive to the chicken manure compared to other onion cultivars. The best yield was shown by the Burgaz cultivar under 60 t ha^{-1} chicken manure treatment, thus this method is the most suitable for onion production.
Keywords: *onion, varieties, organic manure, NPK, yield*

Introduction

Onion (*Allium cepa* L.) is a vegetable that is widely consumed due to its flavoring and health-promoting properties. Onions have many possible health benefits including reducing the risk of obesity, heart disease, and cancer. Onion bulb is a rich source of minerals like phosphorus, calcium, magnesium, iron, manganese and carbohydrates. It also contains protein, Vitamin C, Vitamin B6, and antioxidants (Ware, 2017).

According to the statistics, Turkey's bulb onion production is 2131513 ton in 576918 ha area (Anonymous, 2017).

Healthy life and environmental consciousness are important today. In this case it caused to increase on natural feeding. Using of chemical matter was decreased and natural productions get importance. But soil fertility is important in this case. Organic matter improves soil's physical, chemical, biological properties and is also effect the availability of nutrient. But high level organic material in soils especially in dry conditions may be caused unable effects and also it can be create organo-mineral complex and it reduced the availability of some mineral (Sezen, 1995). Animal fertilizers are major source of organic matter for soil.

Boyhan and Hill (2008) found that fertilizer requirements were higher with organic fertilizer sources compared with conventional fertilizers presumably because nutrients were less available in organic compounds due to slow mineralization rates.

http://www.aloki.hu ● ISSN 1589 1623 (Print) ● ISSN 1785 0037 (Online)
DOI: http://dx.doi.org/10.15666/aeer/1705_1263912647

Work has been done to predict the availability of plant nutrients from organic sources over time. Whitmore (2007), for example, found that 40% of the total N from composted chicken manure was available in the first year, with the remainder available in subsequent years at a rate of 6 to 12% per year.

Many researchers reported that soil application of chicken manure increased yield and yield criteria of onion (Shaheen et al., 2007; Dina et al., 2010; El-Shatanofy and Manar, 2011; Yoldas et al., 2011; Ali et al., 2018).

Comparisons of conventional and organic farms matched by soil type indicated that organic practices improved soil fertility (Liebig and Doran, 1999). This included a 22% increase in organic matter, 20% more total N, lower bulk density and higher water holding capacity.

Many authors reported that the onion yield and bulb production was significantly affected by onion cultivars (Soleymani and Shahrajabian, 2012; Ali et al., 2018).

The objective of this study was to evaluate the residue effect of chicken manure on yield and yield criteria of onion as second crop in field condition.

Materials and methods

The study was carried out in experimental area of the Ödemiş Vocational School, at the Ege University, in İzmir (38°16'N, 27°59'E) during the 2017 year. The experimental designs were split plot with three replications. Before sowing of lettuce, the chicken manure were applied to soil at the rates of 0 – 20 – 40 – 60 t ha^{-1} and also recommended dose of NPK (150:100:150 kg ha^{-1}). Five different treatments with control and three replications were conducted in 15 plots. Lolla Rossa lettuce variety was sown and harvested at the end of vegetation. After harvesting the lettuce plant, onion varieties was sown in order to determine the residual effect of chicken manure and chemical fertilizer in field conditions. No nutrient addition was made for onion. In this study, during the growth period, weeds were removed by hand hoeing and irrigation was done on a regular basis.

Eight onion varieties called 14-16, Burgaz, Karbeyazı, Naz, NWG, Pewana, Seyhan, Şampiyon were used. *Allium cepa* L. was planted in each plot with 30 cm between rows and 15 cm above the rows. Total plot length is 11.5 m and plot width is 6.2 m.

The composition of chicken manure that residual effect investigated was analyzed according to Kacar (1995) and is presented in *Table 1*.

Table 1. *Some properties of chicken manure*

pH	8.55
Total salt (ms/cm)	2.47
Ash 550 °C (%)	79
Organic matter (%)	19.8
Organic carbon (%)	11.51
Total N (%)	0.95
C/N	12.1
P (%)	0.70
K (%)	1.02
Ca (%)	1.37
Mg (ppm)	3729
Na (ppm)	1248

http://www.aloki.hu ● ISSN 1589 1623 (Print) ● ISSN 1785 0037 (Online)
DOI: http://dx.doi.org/10.15666/aeer/1705_1263912647

Soil samples (0-30 cm) were collected from the individual experimental plots (15 samples) at the beginning of onion vegetation. The soil sample was air dried, ground, and passed through 2 mm sieve for the determination of chemical parameters. pH (Jackson, 1967), total soluble salt (Anonymous, 1951), $CaCO_3$ (Kacar, 1995), organic matter content (Reuterberg and Kremkurs, 1951) were determined in the soil. Total N was also analyzed according to Bremner (1965), the available K^+, was determined after extracting with 1 N NH_4OAc by flame photometer (Atalay et al., 1986) and available P was measured by colorimeter (Olsen et al., 1954).

At the end of the vegetation, the plants were harvested. Average bulb head weight, bulb height, bulb width and flesh thickness, number of storage leaf, number of shoot tip, and number of dried leaf were determined as growth and yield parameters.

Ten randomly selected plants were harvested from each plot (avoiding side effect) to record the data on data set for all characters. Bulb length and diameter refers to the height of the bulb and the average width at the widest point in the middle portion of the mature bulb measured using vernier caliper. Average bulb weight computed by weighing ten bulbs together and calculating the average.

Total bulb yield was computed based on the weight of matured bulbs yield per plot and converted in to hectare base and expressed in tones. Marketable bulb yield was determined after discarding bulbs smaller than 3 cm in diameter, splitted, thick necked, rotten and discolored. Split bulbs percentage was determined by counting the number of split bulbs per plot and expressed in percentage in reference to total number of normal bulbs per plot.

The collected data on various parameters were statistically analyzed. Analysis of variance was computed and LSD was used to compare means. Trial statistical evaluation result of data was done using software package TARIST (Açikgöz et al., 1993).

Results and discussion

Soil properties

The physical and chemical properties of soils before onion sowing are presented in *Tables 2* and *3*. pH, organic matter, lime values in the soil did not show any statistical difference between applications at the beginning of vegetation. On the contrary, the salt, N, P, Na, Fe content of the soil was significantly affected by the applications. The highest values were analyzed in the parcels which the chicken manure was applied as 60 t ha^{-1}.

Table 2. *Some chemical properties of field trial soils at the beginning of onion vegetation*

Treatment	pH	Salt (µS/cm)	O.M. (%)	$CaCO_3$ (%)
0	7.06	183 ab	0.66	0.63
NPK	7.00	160 b	0.89	0.84
20 t ha^{-1}	7.08	168 ab	0.83	0.69
40 t ha^{-1}	6.98	221 a	0.72	0.72
60 t ha^{-1}	7.02	185 ab	0.79	0.66
LSD	n.s.	57.25*	n.s.	n.s.

**$p < 0.01$; n.s.: not significant

http://www.aloki.hu ● ISSN 1589 1623 (Print) ● ISSN 1785 0037 (Online)
DOI: http://dx.doi.org/10.15666/aeer/1705_1263912647

Table 3. *Macro-micro nutrient contents of field trial soils at the beginning of vegetation*

Treatment	Total N (%)	P (mg kg^{-1})	K (mg kg^{-1})	Ca (mg kg^{-1})	Mg (mg kg^{-1})	Na (mg kg^{-1})
0	0.056 c	24.16 b	100.6	1056	224	16.26 d
NPK	0.090 b	34.56 a	98.0	1023	215	27.96 bc
20 t ha^{-1}	0.076 b	27.59 b	97.4	986	210	23.90 cd
40 t ha^{-1}	0.081 b	24.72 b	80.9	891	220	32.13 b
60 t ha^{-1}	0.110 a	35.50 a	106.7	1089	218	42.90 a
LSD	0.018**	5.92**	n.s.	n.s.	n.s.	8.15**

Treatment	Fe (mg kg^{-1})	Zn (mg kg^{-1})	Mn (mg kg^{-1})	Cu (mg kg^{-1})
0	3.38 b	1.06	3.68	0.64
NPK	3.75 a	1.19	4.03	0.63
20 t ha^{-1}	3.49 ab	1.16	4.13	0.67
40 t ha^{-1}	3.49 ab	3.03	4.04	0.65
60 t ha^{-1}	3.75 a	1.09	4.15	0.63
LSD	0.368*	n.s.	n.s.	n.s.

**$p < 0.01$; n.s.: not significant

Before onion sowing, field soil properties are neutral (6.6-7.3), humus (< 1%) and lime (0-2.5) poor. When the productivity status of the soil is investigated, N is moderate (0.05-0.1%); K (< 150 ppm), Ca (715-1430 ppm) poor; rich in P (3.26 ppm); Mg (large 114 ppm) is good; Fe (large 4.5 ppm); Zn (large 1 ppm), Mn (large 1 ppm), Cu (large 0.2 ppm) is determined to be sufficient according to Güneş et al. (2000).

Onion yield and yield characteristics

Residue effect of chicken manure on yield and some quality criteria of onion as second crop after the lettuce production are given in *Table 4*.

In the field condition, the results showed significant differences in yield amongst treatments ($p < 0.01$) (*Table 4*). Highest yields (46.31 t ha^{-1}) were obtained in the parcels which the chicken manure was applied as 60 t ha^{-1}. This application increased yield by 44% compared to the control plots. But there was no statistically significant difference in yield between mineral fertilizer and 60 t ha^{-1} of chicken manure application. Similarly Rumpel (1998), Sharma et al. (2003), Yoldas et al. (2011), Indira and Singh (2014), Zewde et al. (2018) found that animal manure applications increased onion yield. Organic manures activate many species of living organisms which release phytohormones and may stimulate the plant growth and absorption of nutrients (Arisha et al., 2003). Organic manures improved the water holding capacity of soil and provide nutrients for a long duration due to less leaching of nutrients and increase efficiency (Carol et al., 1999). Mahala et al. (2018) reported that the increased yield and yield parameters with poultry manure might be because of rapid availability and utilization of nitrogen for various internal plant processes for carbohydrates production. Later on these carbohydrates may undergo hydrolysis and get converted into reproductive sugars which ultimately helped in increasing yield.

http://www.aloki.hu ● ISSN 1589 1623 (Print) ● ISSN 1785 0037 (Online)
DOI: http://dx.doi.org/10.15666/aeer/1705_1263912647

Table 4. *Residue effect of chicken manure on yield and some quality criteria of onion as second crop in the field condition*

Treatment	Yield (t ha^{-1})	Bulb weight (g no^{-1})	Bulb width (cm)	Bulb height (cm)	Number of stored leaf (no)	Number of shoot tip (no)	Number of dried leaf (no)
0	32.13 bc	96.4 bc	4.4	6.7 ab	6.1	1.3.	2.6
NPK	44.06 a	132.0 a	4.9	7.2 a	6.5	1.2	3.1
20 t ha^{-1}	34.63 b	103.9 b	4.5	6.9 ab	6.5	1.4	2.9
40 t ha^{-1}	30.39 c	90.8 c	4.3	6.5 b	6.4	1.4	2.9
60 t ha^{-1}	46.31 a	138.9 a	4.9	6.8 ab	6.5	1.5	3.2
LSD	4.129 **	12.2 **	n.s.	0.5*	n.s.	0.18*	0.6**

**$p < 0.01$; *$p < 0.05$; n.s.: not significant

Yield

Similar to the results Velmurugan and Swarnam (2017), explained that rice grain yield were significantly affected by the residual effect of manures and Inorganic fertilizer to okra, different our results, Abdelrezzag (2002) reported that chicken manure tend to reduce onion yield for all levels in comperation with fertilizer and control.

In the study, the highest yield was observed Burgaz variety ($p < 0.01$) (*Table 5*). Highest yield after Burgaz obtained with Şampiyon variety. The differences in yield among varieties can be caused by differences in genetic characteristics of varieties (Khan et al., 2011).

The interaction between onion cultivars and treatment was found statistically significant on yield. Maximum yield was obtained in Burgaz variety with the 60 t ha^{-1} of chicken manure application as 79.87 t ha^{-1}. Hasan et al. (2018) reported similar results in their studies.

Bulb weight

Treatments, variety and the interaction between onion cultivars and treatment affected bulb weight of onion significantly ($p < 0.01$). Highest values (138 g) were obtained in the parcels which the chicken manure was applied as 60 t ha^{-1} in the field (*Table 4*). This application increased weight of onion by 44% compared to the control plots. But there was no statistically significant difference in bulb weight between mineral fertilizer and 60 t ha^{-1} of chicken manure application. Similarly, Yohannes et al. (2013) reported that farmyard manure and nitrogen fertilizer increased bulb weight. Organic fertilizers provide nutrients to the plants by decomposing and increase growth and yield. Manures improved the soil structure, fertile and availability of nutrient to the plant. Better nutrition of the plant; increase the cell division of plant tissues and the rate of photosynthesis. This is reflected in product growth and the bulb weight (Ewais et al., 2010).

Bulb weights of Burgaz variety (195.2 g) were higher than the others onion variety significantly (*Table 5*).

The interaction between onion cultivars and treatment for bulb weight was found statistically significant The highest bulb weights was obtained in Burgaz variety with mineral fertilizer as 268.7 g in the field condition.

http://www.aloki.hu ● ISSN 1589 1623 (Print) ● ISSN 1785 0037 (Online)
DOI: http://dx.doi.org/10.15666/aeer/1705_1263912647

Table 5. *Effect of variety on yield and same quality criteria of onion as second crop depending on residue effect of chicken manure in the field condition*

Variety	Yield (t ha^{-1})	Bulb weight (g no^{-1})	Bulb width (cm)	Bulb height (cm)	Number of storage leaf (no)	Number of shoot tip (no)	Number of dried leaf (no)
14-16	32.42 d	97.3 d	4.4 cde	6.8 bc	5.8 c	1.7 a	2.8 cd
Burgaz	65.06 a	195.2 a	5.8 a	7.9 a	7.4 a	1.3 bcd	4.7 a
Kar Beyazı	39.09 c	117.3 c	4.7 bc	7.5 ab	6.9 a	1.1 d	3.4 b
Naz	25.26 f	75.3 f	3.9 e	5.9 d	6.8 ab	1.1 cd	2.3 e
NWG	28.29 def	84.9 def	4.1 de	6.8 bc	5.5 c	1.5 ab	3.1 bc
Perwana	32.08 de	96.3 de	4.6 bcd	6.1 cd	6.9 ab	1.7 a	2.6 d
Seyhan	28.13 ef	84.1 ef	4.3 cde	6.3 cd	5.7 c	1.4 abc	1.8 f
Şampiyon	49.66 b	148.9 b	5.1 b	7.4 ab	6.2 bc	1.1 d	2.9 cd
LSD	4.228 **	12.7 **	0.56 **	0.8 **	0.7 **	0.3 **	0.5 **

**p < 0.01; *p < 0.05; n.s.: not significant

Bulb width

The residual effect of chicken manure and mineral NPK applications on onion bulb width not found significant (*Table 4*). Similarly, Yohannes et al. (2013) and Mekonnen et al. (2017) reported that farmyard manure did not affect bulb length of onion in their work.

The highest bulb width (5.8 cm) was observed Burgaz variety ($p < 0.01$) followed by the bulb width (5.1 cm) in Şampiyon variety (*Table 5*). The interaction between onion cultivars and treatment for bulb width was statistically important. Maximum bulb was obtained in Burgaz variety with the mineral NPK application as 6.60 cm.

The differences in the responses to the applications of onion varieties may be genetic variation and also depending on the adoptability of variety in specific environment (Shah et al., 2012; Ali et al., 2018).

Bulb height

Onion bulb height was significantly ($p < 0.01$) affected by the residual effect of chicken manure and mineral NPK applications (*Table 4*). The highest value (7.2 cm) was determined in mineral NPK application and followed bulb height (6.9 cm) by the application of chicken manure as 20 t ha^{-1}. Similarly, Yohannes et al. (2013) reported that application of FYM at a rate of 45 ton ha^{-1} gave the highest mean bulb diameter (5.99 cm). Consistent with the results Metwally and Bary (1999) suggested that the poultry manure improve the bulb growth by enhancing the soil properties and overcome the leaching of nutrients from the root zone. As different Mekonnen et al. (2017) reported that organic manure did not significantly influence bulb length.

In the study, bulb height of Burgaz variety (7.9 cm) was reported higher than other varieties ($p < 0.01$) (*Table 5*). The interaction between onion cultivars and treatment for bulb height was found non-significant.

Number of storage leaf

According to statistical analyzes, number of storage leaf was not affected from the treatments. But these characteristics have changed significantly in relation to the varieties

http://www.aloki.hu ● ISSN 1589 1623 (Print) ● ISSN 1785 0037 (Online)
DOI: http://dx.doi.org/10.15666/aeer/1705_1263912647

(*Tables 4* and *5*). Highest value was obtained in Burgaz variety (7.4 cm) followed Şampiyon variety (6.9) (*Table 5*). However, there was no statistically significant difference between Burgaz and Şampiyon variety. The interaction between onion cultivars and treatment had a significant effect on the number of storage leaf ($p < 0.01$). The number of storage leaf was higher in the application of mineral fertilizer and Burgaz variety.

Number of shoot tip

The results presented in (*Tables 4* and *5*) showed that treatment and onion variety had significantly affected number of shoot tip of onion, where the interaction had also significantly affected. The highest number of shoot tip (1.5) was observed with the application of chicken manure at the rate of 60 t ha^{-1}. While the lowest numbers of shoot tip (1.2) was observed in mineral NPK aplication. Among the onion variety highest number of shoot tip was recorded in variety 14-16 and Perwana.

Maximum number of shoot tip was obtained in 14-16 varieties with the 60 t ha^{-1} of chicken manure application as 20 t ha^{-1}.

Number of dried leaf

Treatments, variety and the interaction between onion cultivars and treatment affected number of dried leaf of onion significantly ($p < 0.01$) (*Tables 4* and *5*). Highest value (3.2) was obtained in the parcels which the chicken manure was applied as 60 t ha^{-1} in the field. Number of dried leaf of Burgaz variety (4.7) were higher than the others onion variety significantly (*Table 5*). The highest number of dried leaf was obtained in Burgaz variety with mineral fertilizer as 6.2.

Conclusion

As a result it was found that residual effect of chicken manures and onion varieties as second crop significantly affected the yield and bulb production in the field condition. Residual of chicken manure increased yield, bulb weight, bulb height, number of dry shell, number of shoots of onion varieties. The highest results were obtained especially with 60 t ha^{-1} of chicken manure application in the field condition. The onion varieties Burgaz gave more response to the organic manure as compare with other onion varieties in yield, bulb weight, bulb height, bulb width, number of storage leaf and number of dried leaf.

The interaction of chicken manure and onion cultivar also affected the yield of onion. The best yield was shown by Burgaz cultivar under 60 t ha^{-1} chicken manure treatment, thus this method is the most suitable for onion production.

In today's world, where healthy life and environmental consciousness is gaining importance, it should be aimed to increase the conscious use of natural organic fertilizers.

Acknowledgements. This research is a work supported by Scientific Research Project Commission of Ege University; Contact no: 2017/OMYO/001.

http://www.aloki.hu ● ISSN 1589 1623 (Print) ● ISSN 1785 0037 (Online)
DOI: http://dx.doi.org/10.15666/aeer/1705_1263912647

REFERENCES

[1] Abdelrazzag, A. (2002): Effect of chicken manure, sheep manure and inorganic fertilizer on yield and nutrients uptake by onion. – Pakistan J. Biol. Sci. 5(3): 266-268.
[2] Açıkgöz, N., Akka, M. E., Maghaddam, A., Özcan, K. (1993): Database dependent. – Congress of International Practice of Computer.
[3] Ali, M., Khan, N., Khan, A., Ullah, R., Naeem, A., Khan, M. W., Khan, K., Farooq, S., Rauf, K. (2018): Organic manures effect on the bulb production of onion cultivars under semiarid condition. – Pure Appl. Biol. 7(3): 1161-1170.
[4] Anonymous (1951): U. S. Soil Survey Staff, Soil Survey Manual. U. S. Dept. Agr. Handbook 18. – U. S. Govt. Printing Office, Washington DC, USA.
[5] Anonymous (2017): Plant Production Statistics. – www.tuik.gov.tr.
[6] Arisha, H. M. E., Gad, A. A., Younes, S. E. (2003): Response of some pepper cultivars to organic and mineral nitrogen fertilizer under sandy soil conditions. – Zagazig J. Agr. Res. 30: 1875-1899.
[7] Atalay, I. Z., Kılınç, R., Anaç, D., Yokaş, İ. (1986): Gediz havzası rendzina topraklarının potasyum durumu ve bu topraklarda alınabilir potasyum miktarlarının tayininde kullanılacak yöntemler. – Bilgehan Matbaası, İzmir.
[8] Boyhan, G. E., Hill, C. R. (2008): Organic fertility sources for the production of short-day organic onion transplants. – Hort. Technology 18: 227-231.
[9] Bremner, J. M. (1965): Total Nitrogen. – In: Black, C. A., Evans, D. D., White, J. L., Ensminger, L. E., Clark, F. E., Dinauer, R. C. (eds.) Methods of Soil Analysis. Part 2: Chemical and Microbiological properties. Am. Soc. of Agron., Madison, WI, pp. 1149-1237.
[10] Carol, M., Tanya, C., Tamera, F. (1999): A Manure Resource Guide for Farmers and Gardeners in Western Washington. – King Conservation, Renton, WA.
[11] Dina, M. S., Shafeek, M. R., Abdallah, M. M. F. (2010): Effect of different nitrogen sources and soil solarization on green onion productivity for exportation. – Annals of Agric. Sci., Cairo Univ. 55(1): 97-106.
[12] El-Shatanofy, Manar, M. E. (2011): Influence of organic manure and inorganic fertilizers on growth, yield and chemical contents of onion (*Allium cepa,* L.). – M.Sc. Thesis, Fac. of Agric., Alex. Univ., Alexandria.
[13] Ewais, M. A., Mahmoud, A. A., Khalil, A. A. (2010): Effect of nitrogen fertigation in comparison with soil application on onion production in sandy soils. – Alex J Agric Res 55(3): 75-83.
[14] Güneş, A., Alpaslan İnal, M. (2000): Bitki besleme ve gübreleme. – Ankara Üniversitesi Ziraat Fak. 1514: 199.
[15] Hassan, S. A. E., Elmehrat, H. G., Ragab, A. A., Abdel Megiud, M. A., Dahab, A. (2018): Growth, yield, bulb quality and storability of some onion cultivars response to compost, vermicompost and plant growth promoting Rhizobacteria. – Middle East J. Agric. Res. 7(2): 292-306.
[16] Indira, S., Singh, S. J. (2014): Effect of vermicompost and biofertilizer on yield and quality of rabi onion (Allium cepa L) CV. – Puna Red. Agric. Sci. Digest. 34(2): 144-146.
[17] Jackson, M. L. (1967): Soil Chemical Analysis. – Prentice Hall, New Delhi.
[18] Kacar, B. (1995): Toprak analizleri: Bitki ve toprağın kimyasal analizleri III. – Ankara Üni., Zir. Fak., Eğitim Araş. ve Geliştirme Vakfı Yayınları, pp.81-86.
[19] Khan, I. M., Hassan, G., Khan, I., Marwat, K. B. (2011): Testing of herbicides at various doses on the growth stages of wild onion grown in pots. – Sarhad J Agric 27(1): 85-91.
[20] Liebig, M. A., Doran, J. W. (1999): Impact of organic production practices on soil quality indicators. – J. Environ. Qual. 28: 1601-1609.

http://www.aloki.hu ● ISSN 1589 1623 (Print) ● ISSN 1785 0037 (Online)
DOI: http://dx.doi.org/10.15666/aeer/1705_1263912647

[21] Mahala, P., Chaudhary, M. R., Garhwal, O. P. (2018): Yield and quality of rabi onion (Allium cepa L.) influenced by integrated nutrient management. – Int. J. Curr. Microbiol. App. Sci. 7(5): 3313-3321.
[22] Mekonnen, D. A., Mihretu, F. G., Woldetsadi, K. (2017): Farmyard manure and intra-row spacing on yield and yield components of adama red onion (*Allium cepa* L.) cultivar under irrigation in Gewane district, Afar Region, Ethiopia. – J. Hortic. For. 9(5): 40-48.
[23] Metwally, S. M., Abdel-Bary, E. A. (1999): Assessment of application of amendments to sandy soils using a computer model. – Zagazig J Agric Res 2: 947-962.
[24] Olsen, S. R., Cole, C. V., Watanbe, F. S., Dean, L. A. (1954): Estimation of available phosphorus in soils by extraction with sodium bicarbonate. – USDA Cir. No. 939.
[25] Reuterberg, E., Kremkus, F. (1951): Bestimmung von Gesamthumus und alkalischen Humusstoffen im Boden, z. Pflanzenernaehr. Düng. und Bodenkd. – Verlag Chemie GmbH, Weinheim.
[26] Rumpel, J. (1998): Effect of long-term organic, mineral, and combined organic-mineral fertilization on yield of onions (*Allium cepa* L.) grown from seeds. – Biuletyn Warzywniczy 48: 5-15.
[27] Sezen, Y. (1995): Soil Chemistry. Edition of Ataturk University No: 790. – Atatürk Univ. Faculty of Agriculture, Erzurum.
[28] Shah, ST., Sajid, M., Alam, R., Rab, A., Mateen, A., Jan, I., Ali, A., Wahid, F. (2012): Comparative study of onion cultivars at Mardan, Khyber Pakhtunkhwa - Pakistan. – Sarhad J Agric 28(3): 399-402.
[29] Shaheen, A., Fatma, M., Rizk, A., Singer, S. M. (2007): Growing onion plants without chemical fertilization. – Res. J. Agr. Biol. Sci. 3(2): 95-104.
[30] Sharma, R. P., Datt, N., Sharma, P. K. (2003): Combined application of nitrogen, phosphorus, potassium and farmyard manure in onion under high hills, dry temperate conditions of North-Western Himalayas. – Indian J. Agr. Sci. 73: 4: 225-227.
[31] Soleymani, A., Shahrajabian, M. H. (2012): Effects of different levels of nitrogen on yield and nitrate content of four spring onion genotypes. – Inter. J. of Agric. and Crop Sci. 4(4): 179-182.
[32] Velmurugan, A., Swarnam, P. (2017): Nutrient uptake and residual effect of organic treatments applied to vegetable–rice system in an acid soil. – Journal of Plant Nutrition 40(12): 1755-1772.
[33] Ware, M. (2017): https://www.medicalnewstoday.com/articles/276714.php. – Accessed on: 15.2.2019.
[34] Whitmore, A. P. (2007): Determination of the mineralization of nitrogen from composted chicken manure as affected by temperature. – Nutr. Cycl. Agroecosyst. 77: 225-232.
[35] Yohannes, K. W., Belew, D., Debela, A. (2013): Effect of farmyard manure and nitrogen fertilizer rates on growth, yield and yield components of onion (Allium cepa L.) at Jimma, Southwest Ethiopia. – Asian Journal of Plant Sciences 12 (6-8): 228-234.
[36] Yoldas, F., Ceylan, S., Mordogan, N, Esetlili, B. C. (2011): Effect of organic and inorganic fertilizers on yield and mineral content of onion (*Allium cepa* L.). – African J. of Biotech. 10(55): 1148811492.
[37] Zewde, A., Mulatu, A., Astatkie, T. (2018): Inorganic and organic liquid fertilizer effects on growth and yield of onion. – International Journal of Vegetable Science 24(6): 567-573.

http://www.aloki.hu ● ISSN 1589 1623 (Print) ● ISSN 1785 0037 (Online)
DOI: http://dx.doi.org/10.15666/aeer/1705_1263912647

THE INFLUENCE OF BIOSTIMULANTS AND FOLIAR FERTILISERS ON THE PROCESS OF BIOLOGICAL NITROGEN FIXATION AND THE LEVEL OF SOIL BIOCHEMICAL ACTIVITY IN SOYBEAN (*GLYCINE MAX* L.) CULTIVATION

NIEWIADOMSKA, A.[1] – SULEWSKA, H.[2] – WOLNA-MARUWKA, A.[1] – RATAJCZAK, K.[2] – WARACZEWSKA, Z.[1] – BUDKA, A.[3] – GŁUCHOWSKA, K.[1]

[1]*Department of General and Environmental Microbiology, Poznań University of Life Sciences, ul. Szydłowska 50, 60-656 Poznań, Poland*

[2]*Department of Agronomy, Poznań University of Life Sciences, ul. Dojazd 11, 60-632 Poznań, Poland*

[3]*Department of Mathematical and Statistical Methods[3], Poznań University of Life Sciences, ul. Wojska Polskiego 28, 60-637 Poznań, Poland*

**Corresponding author*
e-mail: alicja.niewiadomska@up.poznan.pl

(Received 13th May 2019; accepted 16th Jul 2019)

Abstract. The aim of this study was to assess the influence of selected biostimulants (Tytanit, Rooter) and foliar fertilisers (Optysil, Metalosate Potassium, Bolero Bo, ADOB 2.0 Zn IDHA, ADOB B, ADOB 2.0 Mo) on the activity of dehydrogenases, acid and alkaline phosphatases and catalase, and their influence on the level of biological nitrogen fixation based on the nitrogenase activity in soybean cultivation. Between 2016 and 2018 a field experiment was conducted at the Gorzyń Experimental and Educational Station, Poznań University of Life Sciences in Poland. During the three years of the experiment the foliar fertilisers and biostimulants significantly stimulated the catalytic dehydrogenase activity (DHA) and alkaline phosphatase activity (PAL) in all the experimental variants, as compared to the control variant. The analysis of the results of acid phosphatase activity (PAC) during the entire soybean growing period showed that it decreased significantly compared to the control variant when Tytanit, Rooter and Bolero Mo preparations were applied. Additionally, the analysis of catalase activity (CAT) revealed that apart from Tytanit, all the preparations significantly stimulated this enzyme, as compared with the control variant. The field analyses of biological nitrogen fixation showed that the fertilisers and biostimulants significantly stimulated nitrogenase activity under the soybean plantation.
Keywords: *dehydrogenase activity, phosphatase activity, catalase activity, nitrogenase activity, BIF*

Introduction

In recent years agrotechnical treatments with pesticides as well as phosphorus and nitrogen fertilisation have become a threat to all elements of the ecosystems (Nardi et al., 2016). New sustainable, cost-effective and environment-friendly cultivation technologies that ensure high yield and quality of crops are being sought to limit the negative influence of these treatments on the soil environment (Vernieri et al., 2006). The application of environment-friendly practices is dictated by European Union law (EU Directive 2009/128) and recommendations concerning integrated protection/cultivation which have been in effect, in Poland since 2014. Moreover, due to the feed protein deficit in Europe and Poland (Borowska et al., 2016) there is a pressing need to search for opportunities to increase the yield of crops, especially legumes, which are a valuable sources of protein.

http://www.aloki.hu ● ISSN 1589 1623 (Print) ● ISSN 1785 0037 (Online)
DOI: http://dx.doi.org/10.15666/aeer/1705_1264912666

Legumes are becoming increasingly important in sustainable agriculture (Massawe et al., 2016). What speaks in favour of their cultivation is the fact that they improve the physicochemical properties of soil, enrich organic matter content by leaving large amounts of crop residue and reduce the consumption of nitrogen fertilisers. Soybean (*Glycine max* L.) is one of the most important crops in this group. Its seeds contain about 40% of protein with a favourable amino acid composition and 20% of fat, with the predominant share of unsaturated fatty acids. The cultivation of soybean is gaining popularity in Poland as a result of the changing climate and the introduction of new varieties (Gaweł, 2011; Florek et al., 2012; Stagnari et al., 2017).

One of the metabolic features of legumes is their ability to coexist with bacteria that fix atmospheric nitrogen (diazotrophy process) (Poole et al., 2018). As the content of valuable protein in a plant depends on the system formed between the plant and rhizobia, it seems right to look for agents that increase the efficiency of this symbiosis.

Biostimulants, which are defined as materials containing one or more active substances and/or microorganisms, are gaining increasing attention in scientific circles. They increase the uptake of nutrients by plants and tolerance to abiotic and biotic stress and they improve the yield quality (Calvo et al., 2014). Biostimulants can also stimulate the activity of rhizosphere microorganisms and soil enzymes, the production of hormones and increase photosynthesis (Giannattasio et al., 2013).

Intensified cultivation has caused foliar fertilisation to become an indispensable agrotechnical treatment. Among the large number of nutrients that are necessary for the proper growth of plants, some must be supplied in larger quantities, while others – in smaller or even trace amounts. Plants exhibit the highest demand for potassium and nitrogen (more than 200 kg when the yield per 1 ha is calculated), while they need only small amounts of zinc, boron, copper and molybdenum (only a few grams when the yield per 1 ha is calculated). This shows that foliar fertilisation is particularly effective when micronutrients need to be supplied to crops. In some situations, it is also recommended that macroelements such as nitrogen, and magnesium, and less frequently phosphorus, potassium, sulphur and calcium, should be sprayed onto leaves (Szewczuk and Sugier, 2009).

Each of the agrotechnical treatments applied to crops, i.e. fertilisers or biostimulants, may lead to changes in the soil environment. Many studies have shown the diverse effects of these treatments on the populations of selected groups of microorganisms and the level of soil enzymes they secrete (Karaca et al., 2010).

The determination of the biochemical activity of soil based on the activity of soil enzymes is an important tool in helping to assess soil quality. Enzymes are considered to be good and sensitive indicators because they quickly react to changes in the soil caused by natural and anthropogenic factors. Furthermore, they are easy to measure and their activity determines the main microbiological reactions occurring in the cycles of nutrients in the soil (Nannipieri et al., 2002; Karaca et al., 2010). Studies have shown that agrotechnical treatments affect enzymatic activity more than other biochemical parameters (Saviozzi et al., 2001).

The aim of this study was to assess the influence of selected biostimulants (Tytanit, Rooter) and foliar fertilisers (Optysil, Metalosate Potassium, Bolero Bo, ADOB 2.0 Zn IDHA, ADOB B, ADOB 2.0 Mo) on the activity of dehydrogenases, acid and alkaline phosphatases and catalase, and their influence on the level of biological nitrogen fixation based on the nitrogenase activity in soybean cultivation.

http://www.aloki.hu ● ISSN 1589 1623 (Print) ● ISSN 1785 0037 (Online)
DOI: http://dx.doi.org/10.15666/aeer/1705_1264912666

Materials and methods

Between 2016 and 2018 a field experiment was conducted at the Gorzyń Experimental and Educational Station, Poznań University of Life Sciences. The GPS coordinates of the experiment at the Gorzyń Station were as follows: N-52.56589, E-015.90556, 65 m AMSL. Each year one-factor experiments were conducted as randomised block design in four replications, with following nine factor levels: 1. control variant –not treated plants; 2. Tytanit; 3. Optysil; 4. Metalosate Potassium; 5. Rooter; 6. Bolero Mo; 7. ADOB Zn IDHA; 8. ADOB B; 9. ADOB 2.0 Mo (*Fig. 1*).

Figure 1. *Experimental culture at the plants' full growth (BBCH 35-40)*

Each fertiliser was applied in a timely manner, according to the manufacturer's recommendations (*Table 1*).

Soybean seeds, Merlin cultivar (SAATBAU) were used in the experiment. When seeds of this cultivar are purchased, they are already encapsulated with rhizobia of the *Bradyrhizobium* genus together with the polymer, which also acts as a preservative and protects the bacteria from sunlight.

The Merlin cultivar can be grown all over Poland. It is characterised by high yield (from 2.4 t ha^{-1} on poor quality soils up to 3.2 t ha^{-1} on good and very good quality soils), high resistance to lodging and high regeneration capacity.

The seeds were sown (25th April 2016, 24th April 2017 and 20th April 2018), on plots with an area of 21 m^2, with a distance between rows of 15 cm, and sowing density was 90 seeds per 1 m^2.

http://www.aloki.hu ● ISSN 1589 1623 (Print) ● ISSN 1785 0037 (Online)
DOI: http://dx.doi.org/10.15666/aeer/1705_1264912666

Table 1. *The terms and doses of biostimulants and fertilisers applied in the experiment*

Biostimulants/foliar fertilisers		Term and dose of biostimulant	Fertiliser characteristics
Biostimulants	Tytanit	I: leaf and shoot development (BBCH 13–29) - 0.3 dm^3 ha^{-1} II: inflorescence development (BBCH 51–59) - 0.3 dm^3 ha^{-1} III: beginning of pod development (BBCH 71) - 0.3 dm^3 ha^{-1}	Liquid, mineral stimulant containing titanium (Ti). It increases the yield volume and development of plants, improves yield quality parameters and increases plants' natural resistance to stress factors. Composition: 8.5 g Ti $(dm^3)^{-1}$
	Rooter	BBCH 13–14 - 1 dm^3 ha^{-1}	Biostimulant – it stimulates the growth of the root system, accelerates regeneration and improves the uptake of soil minerals. Composition: P_2O_5 13.0%; K_2O 5.0%
Foliar fertilisers	Optysil	I: leaf and shoot development (BBCH 15–29) - 0.5 dm^3 ha^{-1} II: inflorescence development (BBCH 51–55) - 0.5 dm^3 ha^{-1} III: beginning of pod development (BBCH 71–73) - 0.5 dm^3 ha^{-1}	Liquid, silicon antistressor stimulating the growth and development of plants, activating their natural immune systems and increasing tolerance to unfavourable cultivation conditions. Composition: 200 g SiO_2 $(dm^3)^{-1}$
	Metalosate Potassium	2-3 treatments every 10-14 days during intensive growth - 3 dm^3 ha^{-1}	Liquid foliar fertiliser containing an easily absorbable form of potassium, which supplements potassium deficit in plants with amino acids. Composition: K_2O 24%
	Bolero Mo	Before florescence - 1.5 dm^3 ha^{-1}	Liquid foliar fertiliser containing boron and molybdenum to supplement the deficit of these elements in plants. Composition: B 8.2%; Mo 0.8%
	ADOB 2.0 Zn IDHA	Before florescence - 1 dm^3 ha^{-1}	Foliar fertiliser containing zinc (Zn) fully chelated by biodegradable chelating agent IDHA. Composition: Zn 100 g kg^{-1} (weight percentage content 10, chelated by IDHA)
	ADOB B	I: before florescence - 2 dm^3 ha^{-1} II: after florescence on pods - 1 dm^3 ha^{-1}	Liquid, highly concentrated foliar fertiliser containing boron that regulates auxin activity and participates in cell division. Composition: N 78 g kg^{-1}; B 150 g kg^{-1}
	ADOB 2.0 Mo	Early stages of development - 0.15 dm^3 ha^{-1}	Liquid, single-component fertiliser which increases the rate and efficiency of use of nitrogen by plants and improves interaction with iron. Composition: Mo 20%

According to the FAO/WRB classification [IUSS Working Group WRB], the soil in the experimental plots is a typical luvisol soil formed from light loamy sands, deposited in a shallow layer on light loam (*Haplic Luvisols*) (*Table 2*). The soil texture was determined by means of sieving the sand fraction from the silt and clay fraction (Van Reeuwijk, 2002).

http://www.aloki.hu ● ISSN 1589 1623 (Print) ● ISSN 1785 0037 (Online)
DOI: http://dx.doi.org/10.15666/aeer/1705_1264912666

Table 2. *The texture of soil material sampled from a depth of 0-25 cm*

Percentage content of soil fractions %				Texture class
Fraction	Sand 2 – 0.05 mm	Silt 0.05-0.002	Clay < 0.002	
	78	18	4	LS

LS – loamy sand

The agrotechnical treatments were carried out as recommended for the specie tested. The following crop protection products were applied: herbicides: Stomp Aqua 455 CS (2.6 L ha^{-1}) in April and Pantera 040 EC (1.75 L ha^{-1}) in May; Piorun 200 SL (0.2 L ha^{-1}) in June or Fastac 100 EC 0.1 (L ha^{-1}) in August; fungicides: Korazzo 250 SC 1.0 (L ha^{-1}) in June.

Weather conditions

The weather course in the years of the study was presented as mean values of the Sielianinov (Stachowski, 2010) hydrothermal indicator (*Fig. 2*), calculated based on meteorological data registered in the Experimental Station. Interpretation of the indicator: K > 1.5 - excess moisture for plants, K = 1.0-1.5 - optimal humidity, K = 0.5-1.0 - insufficient humidity for plants, K < 0.5 - humidity below required for plants (drought). During the growing seasons in 2016 and 2017 the weather conditions were similar in terms of temperature and rainfall. During the growing season the highest average air temperature was noted in July both in 2016 (19.5 °C) and 2017 (18.9 °C), whereas the lowest temperature was noted in April, i.e. 8.7 °C in 2016 and 7.5 °C in 2017. However, the weather conditions in 2018 were different than in the previous years (*Fig. 1*). The highest average temperature was noted in August (21.2 °C), whereas the lowest was noted in May (12.7 °C). As far as the average monthly temperature from April to September is concerned, 2018 was the warmest – it was 2.9 °C warmer than 2016 and 1.7 °C warmer than 2017. In 2016 there was drought only at the end of the growing season. Likewise, in 2017 there was no rainfall deficit. On the contrary, it was a wet year, especially from June to August. On the other hand, in 2018 rainfall was unevenly distributed and there were droughts which were particularly unfavourable for plants in May, June and August.

Influence of fertilisers on nitrogenase activity (diazotrophy)

Plants representing each experimental variant (5 on average) were selected to measure the diazotrophy level. The analyses were made at the beginning of the flowering period. The nitrogenase activity (diazotrophy) was tested with the acetylene method on a CHROM5 gas chromatograph (Sawicka, 1983). The amount of acetylene reduced to ethylene was measured and expressed as nMC_2H_4 $plant^{-1}$ h^{-1}.

Microbial analyses

Soil samples collected from the arable layer (0-20 cm) were used as the research material for biochemical analyses. Each year they were collected at four terms: 1st term – at the plants' emergence (BBCH 5-10), 2nd term - at the plants' full growth (BBCH 35-40), 3rd term – at the plants' florescence (BBCH 51-59), 4th term – after harvest.

http://www.aloki.hu ● ISSN 1589 1623 (Print) ● ISSN 1785 0037 (Online)
DOI: http://dx.doi.org/10.15666/aeer/1705_1264912666

Soil samples were taken from five places of each experimental plot, in four replications for each of the nine variants of the experiment. In this way, at each analysis term we received 36 samples of soil, each of 1 kg.

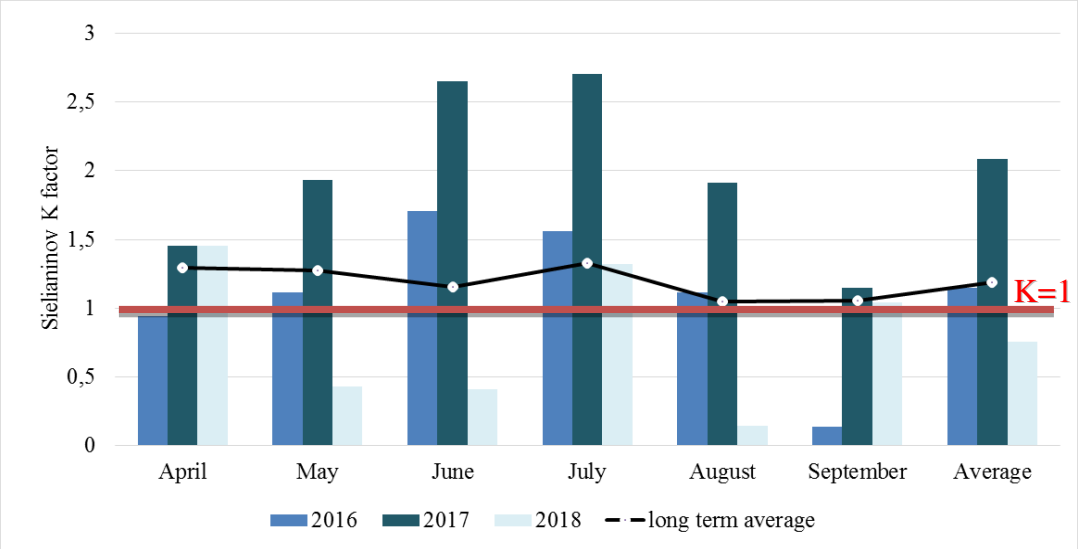

Figure 2. *Climate graph according to Sielianinov characterizing weather conditions in Gorzyń*

Soil enzymatic activity

The analyses of soil enzymatic activity in individual variants were based on the colorimetric method applied to measure dehydrogenase activity (DHA), where 1% triphenyl tetrazolium chloride (TTC) was used as the substrate. The activity was measured after 24-h incubation at a temperature of 30 °C and a wavelength of 485 nm and it was expressed as µmol triphenyl formazane (TPF) 24 h^{-1} g^{-1} dm of soil (Thalmann, 1968).

Additionally, acid phosphomonoesterase activity was measured (EC 3.1.3.2) (PAC) by means of the method developed by Tabatabai and Bremner (1969), where disodium p-nitrophenyl phosphate tetrahydrate was the substrate. The activity was measured after 1-h incubation at 37 °C and a wavelength of 400 nm. The results were converted into µmol (p-nitrophenol) PNP h^{-1} g^{-1} dm of soil.

Catalase activity was measured by means of permanganometry, according to the method developed by Johnsons and Temple (1964), where 0.3% H_2O_2 was the substrate. After 20-min incubation at room temperature (about 20 °C) 0.02 M $KMnO_4$ was titrated to a light pink colour and expressed as µmol H_2O_2 g^{-1} d.m. min^{-1}.

Biological index of fertility

The biological index of fertility (BIF) was calculated using the dehydrogenase activity (DHA) and catalase activity (CAT) in the following formula: (DHA + kCAT)/2, where k was the factor of proportionality and equalled 0.01 (Saviozzi et al., 2004).

Statistical analyses

The dynamics of changes in the soil enzymatic activity were analysed statistically. The results were analysed with two-way ANOVA using Statistica 9.1 software. The

http://www.aloki.hu ● ISSN 1589 1623 (Print) ● ISSN 1785 0037 (Online)
DOI: http://dx.doi.org/10.15666/aeer/1705_1264912666

fertilisation method and the term of analysis were the factors differentiating the traits under study. The significance of differences between the pairs of factors was checked with Tukey's test. Principal component analysis (PCA) was used to visualise the multidimensional dependencies between the soil biochemical activity and the types of fertilisation.

Results

The experiment showed the influence of biostimulants and foliar fertilisers on soil enzymatic activity and fertility (BIF) as well as nitrogenase activity under a soybean plantation. The two-way analysis of variance revealed the highly significant effect ($p = 0.001$) of foliar fertilisation/biostimulants and the term of tests on enzymatic activity and the biological index of fertility (BIF) of soil under the soybean plantation (*Table 3*).

Table 3. *F-test statistics and significance levels of two-way analysis of variance for soil bioactivity. Foliar fertilisation/biostimulants and the terms of tests were the factors influencing the traits under study*

Parameter	Treatment	Term	Interaction
Dehydrogenase	5.84^{***}	131.512^{***}	5.63^{***}
Alkaline phosphatase	14.94^{***}	146.6^{***}	4.62^{***}
Acid phosphatase	7.61^{***}	137.40^{***}	6.765^{***}
Catalase	16.9^{***}	142.82^{***}	16.66^{***}
BIF	14.06^{***}	192.4^{***}	14.065^{***}
Nitrogenase	7.08^{***}	-	-

F test statistics and significance levels of two-way analysis of variance for activity of enzymes associated with herbicides and terms research fixed factors. ***p = 0.001

Biological fixation of nitrogen under soybean plantation

The field analyses of biological nitrogen fixation showed that the fertilisers and biostimulants significantly stimulated nitrogenase activity under the soybean plantation. The diagram (*Fig. 3*) presents the average nitrogenase activity during the three years of the study. In comparison with the control sample, nitrogenase activity increased in all the experimental variants. The application of the Tytanit and Rooter biostimulants resulted in the highest nitrogenase activity. In comparison with the control plot, nitrogenase activity in these variants increased by 77% and 69%, respectively. Apart from the control sample, the lowest biological nitrogen fixation activity was observed in the Bolero Mo variant.

Analysis of soil biochemical activity

Figure 4 shows the results of the analysis of dehydrogenase activity in the soil under the soybean plantation. During the three years of the experiment the foliar fertilisers and biostimulants significantly stimulated the catalytic dehydrogenase activity in all the experimental variants, as compared with the control variant. The ADOB 2.0 Mo and Bolero Mo foliar fertilisers resulted in the highest dehydrogenase activity. The research

http://www.aloki.hu ● ISSN 1589 1623 (Print) ● ISSN 1785 0037 (Online)
DOI: http://dx.doi.org/10.15666/aeer/1705_1264912666

also showed that the highest dehydrogenase activity occurred at the second term of analyses, when the plants were at the phase of full growth (BBCH 35-40).

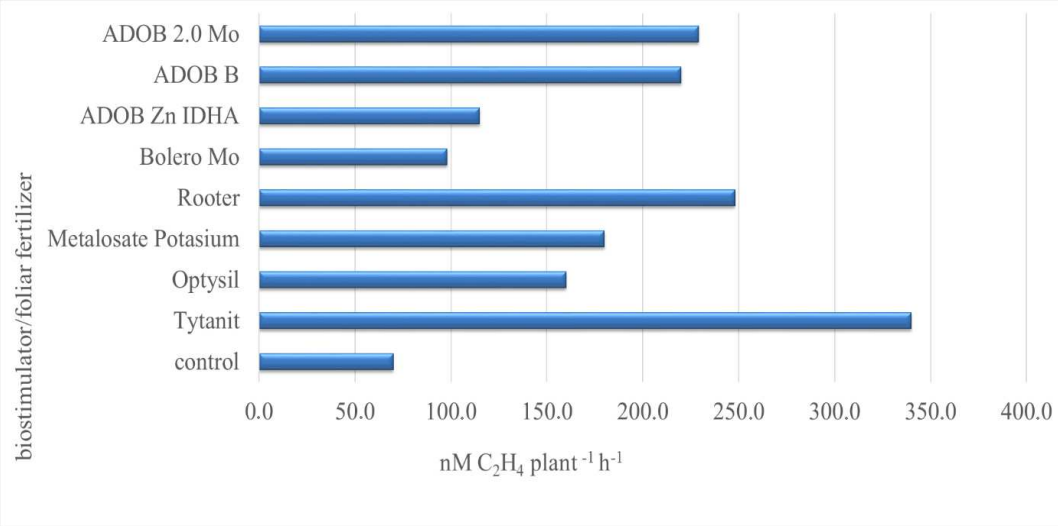

Figure 3. *The influence of the biostimulants and fertilisers on biological nitrogen fixation*

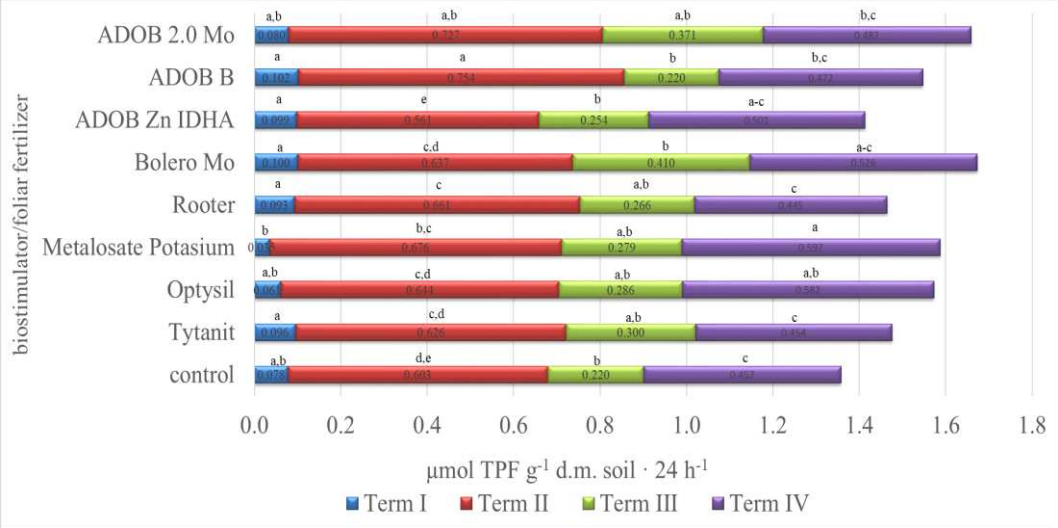

Figure 4. *The influence of biostimulants and fertilisers on dehydrogenase activity. (Note: data are represented as means of five replications. a, b, c, d, e – homogenous groups according to Tuckey's test; different letters denote statistical differences at level α = 0.05; n = 5, in the same term)*

The analysis of the results of acid phosphatase activity (PAC) during the entire soybean growing period showed that in comparison with the control variant it decreased significantly when Tytanit and Rooter biostimulants and Bolero Mo foliar fertiliser were applied (*Fig. 5*). This effect was not observed with the other foliar fertilisers, i.e. Optysil, Metalosate Potassium, ADOB Zn IDHA, ADOB B and ADOB 2.0 Mo. Moreover, at the second term of analyses, i.e. at the stage of full development of the plant just before flowering, acid phosphatase activity in all the experimental variants

http://www.aloki.hu ● ISSN 1589 1623 (Print) ● ISSN 1785 0037 (Online)
DOI: http://dx.doi.org/10.15666/aeer/1705_1264912666

was higher than in the control variant. The highest activity was observed after the application of ADOBE 2.0 Mo and Optysil foliar fertilisers (*Fig. 5*).

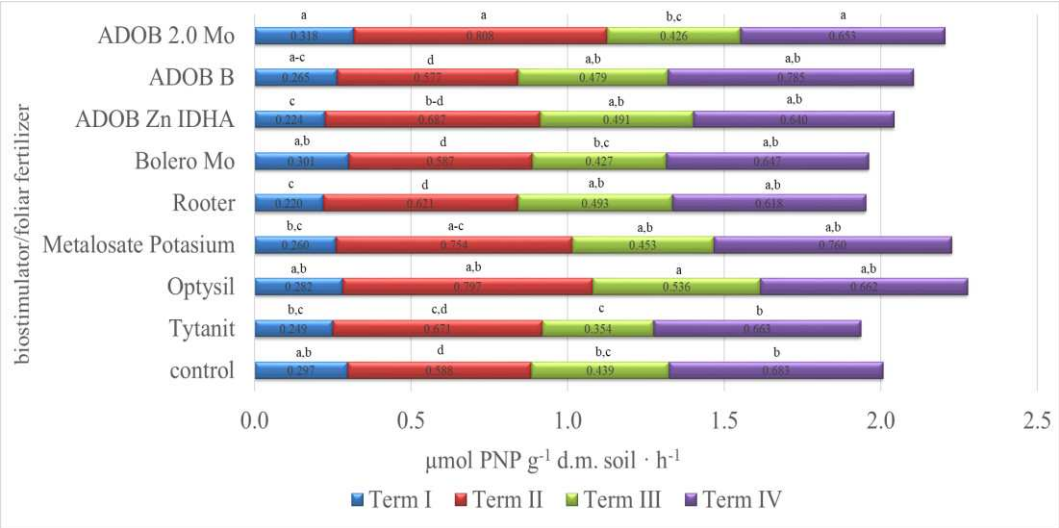

Figure 5. *The influence of the biostimulants and fertilisers on acid phosphatase activity. (Note: data are represented as means of five replications. a, b, c, d, e – homogenous groups according to Tuckey's test; different letters denote statistical differences at level α = 0.05; n = 5, in the same term)*

The analysis showed that in comparison with the control variant the biostimulants and most of the foliar fertilisers used in the research increased alkaline phosphatase activity (PAL) (*Fig. 6*). Metalosate Potassium and Bolero Mo foliar fertilisers stimulated enzyme activity particularly significantly. In comparison with the control variant, the Tytanit and Rooter biostimulants increased PAL activity by 6% and 5%, respectively. Similarly to dehydrogenase activity, alkaline phosphatase activity also increased significantly at the second term of analyses after the application of the fertilisers and biostimulants.

The analysis of catalase activity revealed that apart from Tytanit, all the preparations significantly stimulated this enzyme, as compared with the control variant (*Fig. 7*). The application of the Metalosate Potassium resulted in the highest catalase activity. The research also showed that the enzyme exhibited high activity at the fourth term of analyses, i.e. after the harvest in all experimental variants, where it ranged from 55.9 µmol H_2O_2 g $^{-1}$d.m. min^{-1} after treatment with Tytanit biostimulant to 149.7 µmol H_2O_2 g^{-1} d.m. min^{-1} after the application of Metalosate Potassium.

The biological index of soil fertility (BIF) calculated on the basis of the dehydrogenase and catalase activity was significantly greater after treatment with all the biostimulants and foliar fertilisers (*Fig. 8*). The highest value of the index was noted when Metalosate Potassium foliar fertiliser was applied to the soybean plantation. By contrast, ADOB 2.0 Mo foliar fertiliser resulted in the lowest BIF value. The BIF also had a very high value at the phase of the plants' florescence. It ranged from 2.77 after treatment with ADOB 2.0 Mo fertiliser to 8.34 after the application of Bolero Mo fertiliser. Treatment with ADOB Zn IDHA and ADOB B fertilisers also resulted in high BIF values.

http://www.aloki.hu ● ISSN 1589 1623 (Print) ● ISSN 1785 0037 (Online)
DOI: http://dx.doi.org/10.15666/aeer/1705_1264912666

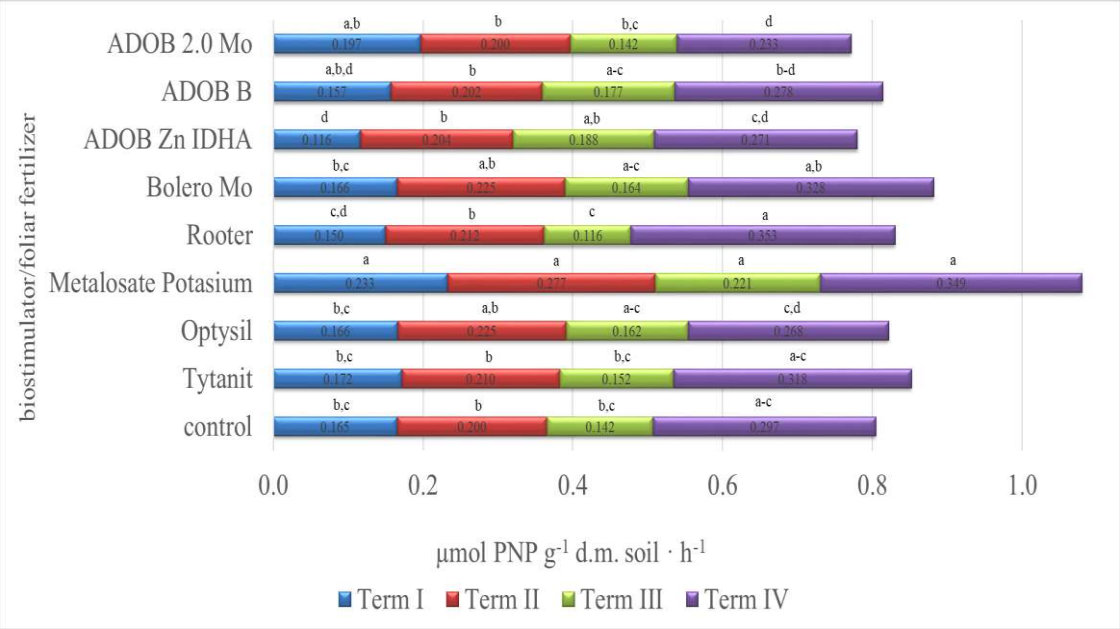

Figure 6. *The influence of the biostimulants and fertilisers on alkaline phosphatase activity. (Note: data are represented as means of five replications. a, b, c, d, e – homogenous groups according to Tuckey's test; different letters denote statistical differences at level α = 0.05; n = 5, in the same term)*

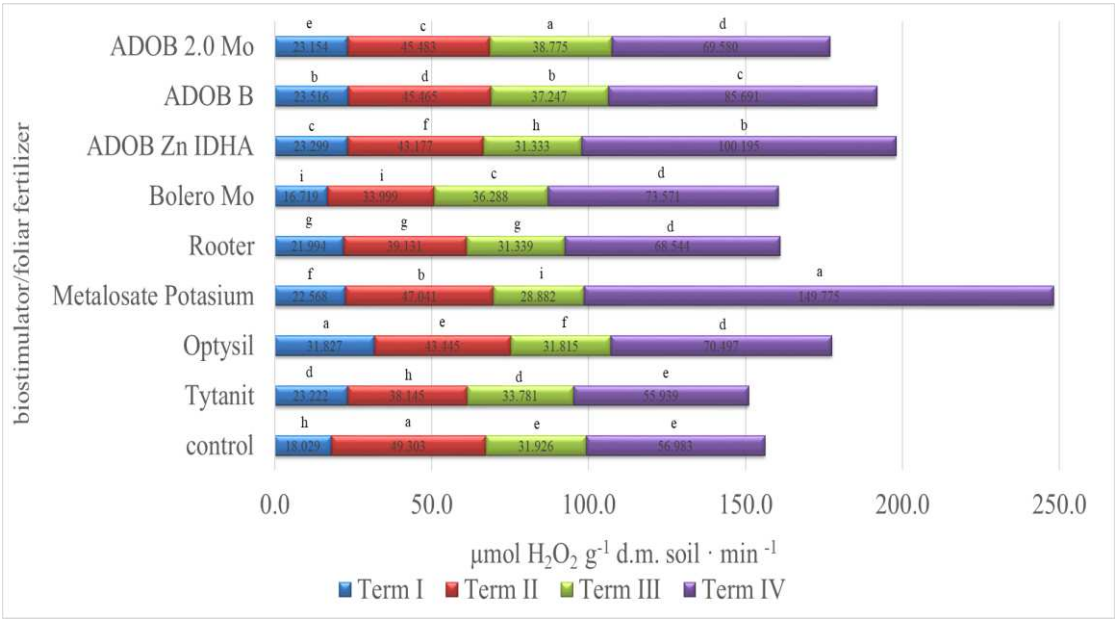

Figure 7. *The influence of the biostimulants and fertilisers on catalase activity. (Note: data are represented as means of five replications. a, b, c, d, e, f, g, h – homogenous groups according to Tuckey's test; different letters denote statistical differences at level α = 0.05; n = 5, in the same term)*

http://www.aloki.hu ● ISSN 1589 1623 (Print) ● ISSN 1785 0037 (Online)
DOI: http://dx.doi.org/10.15666/aeer/1705_1264912666

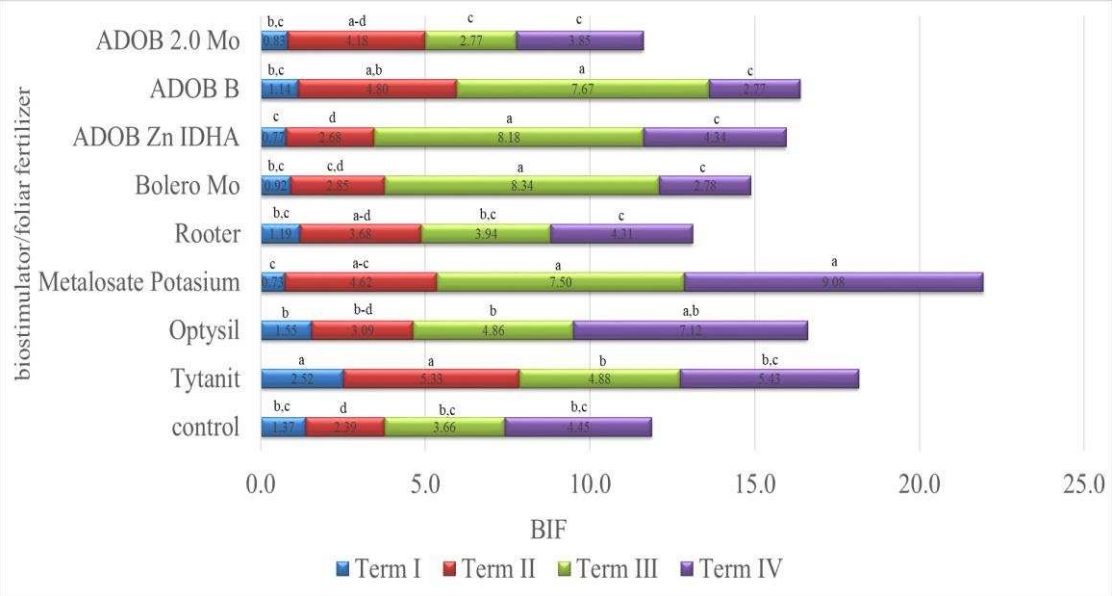

Figure 8. *The influence of the biostimulants and fertilisers on the BIF value. (Note: data are represented as means of five replications. a, b, c, d – homogenous groups according to Tuckey's test; different letters denote statistical differences at level α = 0.05; n = 5, in the same term)*

The influence of the foliar fertilisers and biostimulants applied to the soybean plantation at specific terms was subjected to principal component analysis (PCA) (*Fig. 9*). The first two main components explained more than 77.68% of the total variance. The parameters of soil biochemical activity in 2018 were considerably divergent from those observed in 2016 and 2017, probably as a result of the weather conditions (*Fig. 1*). The growing season in 2018 was the warmest of all the research years. In comparison with the previous years, the average temperature difference amounted to 2.9 °C in August and 1.7 °C in May. In 2016 and 2017 the thermal conditions were very similar so the PCA showed similar dependencies for those two years. In those years, at the phase of the plants' florescence (the 3rd term of analyses) and after the harvest (the 4th term of analyses), the biostimulants and foliar fertilisers significantly influenced alkaline phosphatase activity and the value of the biological index of fertility (BIF). In 2018, the 2nd and 4th terms of analyses influenced the catalytic activity of catalase (CAT) and dehydrogenase (DHA).

Discussion

Biological nitrogen fixation

The biostimulants and foliar fertilisers which increased the biological fixation of nitrogen under the soybean plantation contained the essential macro- or microelements for this process. According to scientific reports, the role of some chemical elements in the process of nitrogen fixation is very important.

Molybdenum, boron, iron, and cobalt are among the micronutrients that significantly affect plants' development and the nitrogen fixation process. Molybdenum and iron are particularly important elements. They are components of nitrogenase – the bacterial enzyme thanks to which the diazotrophy process is possible. Nitrogenase is a protein

http://www.aloki.hu ● ISSN 1589 1623 (Print) ● ISSN 1785 0037 (Online)
DOI: http://dx.doi.org/10.15666/aeer/1705_1264912666

composed of two subunits – the larger one containing the FeMo cofactor and the smaller one containing iron only (Symanowicz et al., 2005). The availability of molybdenum is naturally limited in acidic, moist, and poorly buffered soils. According to some reports, when the leaves of leguminous plants are treated with molybdenum in a field, the nitrogen fixation efficiency, the weight of root nodules, and the seed yield increase (Vieira, 1998; Weisany et al., 2013). This effect was also observed in our research when the ADOB 2.0 Mo fertiliser with high molybdenum content was applied. Although plants contain small amounts of boron, this microelement plays an important role in a wide range of physiological processes. It affects the separation of plant tissues and is necessary for the optimal growth of plants. Plants with boron deficit have fewer *Rhizobium* cells and infectious threads (Brown et al., 2002; Weisany et al., 2013). The significantly higher rate of biological nitrogen fixation after the application of the foliar fertiliser with boron (ADOB B - variant 8) could have caused the increase in the content of this parameter.

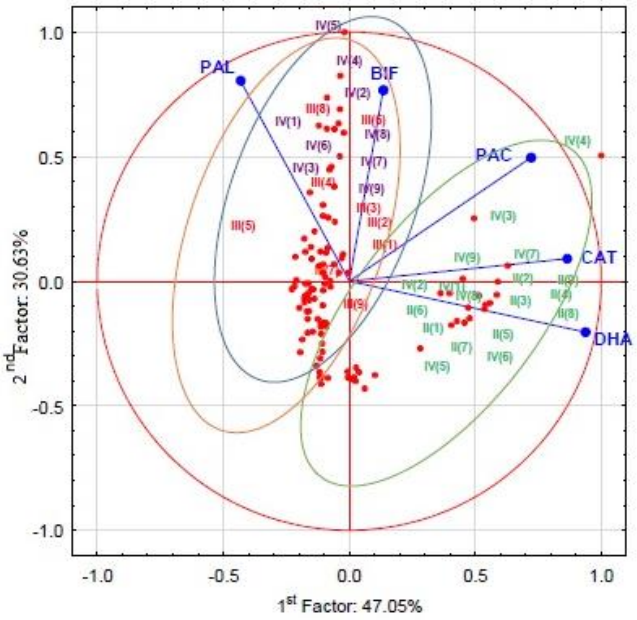

Figure 9. *The dependence between soil enzymatic activity for all variants with fertilisers and biostimulants at the terms of analyses; I - 1st term, II - 2nd term, III - 3rd term, IV - 4th term; (1) control sample – no biostimulants or foliar fertilisers; (2) Tytanit; (3) Optysil; (4) Metalosate Potassium (potassium + amino acids); (5) Rooter; (6) Bolero Mo - liquid suspension boron fertiliser with molybdenum; (7) ADOB Zn IDHA (chelated zinc); (8) ADOB B (high boron content); (9) ADOB 2.0 Mo (high molybdenum content); PAC - acid phosphatase; PAL- alkaline phosphatase; DHA - dehydrogenase; BIF - biological index of fertility*

The role of phosphorus in symbiotic systems has also been the subject of many studies which have confirmed its key importance for the efficiency of atmospheric nitrogen fixation (Bucher, 2007; Bonilla and Bolaños, 2009). The Rooter biostimulant, which contained phosphorus and potassium, had a highly stimulating effect on the nitrogen fixation process. Phosphorus participates in a wide range of molecular and biochemical processes, and some phosphate bonds carry the energy used in cells. The presence of phosphorus in soil affects plants' ability to form root nodules, especially the

http://www.aloki.hu ● ISSN 1589 1623 (Print) ● ISSN 1785 0037 (Online)
DOI: http://dx.doi.org/10.15666/aeer/1705_1264912666

weight and number of nodules (Abusuwar and Omer, 2011), which translates to the nitrogen fixation level.

When plants are deficient in phosphorus they are usually deficient in nitrogen too. The role of sulphur and potassium is less important for symbiotic systems than that of the abovementioned elements. Nevertheless, potassium ions are very desirable in saline soils because they function as osmolytes. In view of the fact that almost half of the irrigated soils around the world are considered to be saline, the addition of potassium helps to maintain the symbiotic system between bacteria and plants (Zahran, 1999; Bonilla and Bolaños, 2009).

Biochemical activity

Soil enzymes are a group of catalysts that play a permanent and major role in maintaining the ecological properties of the pedosphere, its physicochemical properties, fertility and health (Das and Varma, 2011; Utobo and Tewari, 2015; Niewiadomska et al., 2018b). These include both extracellular enzymes and those that can be found in microorganisms (both in proliferating cells and in sporulating forms). Enzymes are responsible for the course of all chemical reactions in microbial cells, including the synthesis of proteins, nucleic acids or carbohydrates (Błońska, 2011). On the other hand, soil enzymes participate in the decomposition of organic matter released into the soil during plants' growth, the formation and decomposition of humus as well as the release and transfer of mineral substances to plants. Although microbiological and biochemical properties are dynamic, enzymes are a precise and important determinant of soil fertility and they are of even greater significance when it is necessary to determine changes occurring in soil (Burns et al., 2013; Niewiadomska et al., 2018a).

When fertilisers are applied into soil, the enzymatic activity changes significantly. The direction and intensity of the change depends on the type and dose of fertiliser and on the enzyme in question (Selivanovskaya et al., 2006; Napora and Grobelak, 2014). Changes in the activity of soil enzymes reflect environmental disturbances, which influence both the soil and plants (Bielińska and Mocek-Płóciniak, 2012).

Dehydrogenases (DHA) are enzymes belonging to the group of oxidoreductases. They catalyse the oxidation of organic compounds. Active dehydrogenases can only be found inside living cells and their presence indicates the presence of physiologically active microorganisms. They are commonly found in the pedosphere, where they participate in the decomposition of organic compounds. The identification of dehydrogenase activity in soil indicates the intensity of the respiratory metabolism of soil microorganisms, mostly actinobacteria and eubacteria.

The study showed that the biostimulants and foliar fertilisers significantly stimulated dehydrogenase activity. The activity was high during the period of full growth of soybeans, i.e. at BBCH 30-45. It may have been caused by increased secretions from the root system at the time and it resulted in a greater count of microorganisms. Dehydrogenase activity also increased considerably after the harvest, which may have been caused by the fact that organic matter in the form of crop residue entered the soil. Kang et al. (2009) also observed a similar increase in dehydrogenase activity in the spring and autumn. In our study the activity of this enzyme in the spring may also have been stimulated by higher rainfall in June. Brzezińska et al. (2001) and Błońska et al. (2012) reached similar conclusions in their studies, where they proved that the high humidity of the substrate increased dehydrogenase activity. The macro- and microelements applied with the foliar fertilisers and biostimulants were also significant.

http://www.aloki.hu ● ISSN 1589 1623 (Print) ● ISSN 1785 0037 (Online)
DOI: http://dx.doi.org/10.15666/aeer/1705_1264912666

Bielińska et al. (2013) noticed that fertilisers containing nitrogen, phosphorus and potassium had a positive influence on the dehydrogenase content in the soil. Swędrzyńska et al. (2013) and Niewiadomska et al. (2018a) made similar observations in their studies on similar biological soil conditioners. According to Bilen et al. (2011) and Kumar et al. (2015), boron increases dehydrogenase activity. Taran et al. (2014) proved that molybdenum stimulated the production of these enzymes by the root nodules of leguminous plants and discussed a possible positive correlation between titanium and soil biochemistry.

The biostimulants used in the experiment (Tytanit and Rooter) had a positive effect on acid phosphatase activity because they reduced its level. Apart from the Bolero Mo, the other foliar fertilisers used in the experiment did not cause this effect. This shows that these biostimulants and the foliar fertiliser positively affected the plants' ability to absorb phosphorus. The acid phosphatase activity in the other experimental variants was higher than in the control variant. It is important to remember that when plants are exposed to phosphorus deficiency they increase the secretion of acid phosphatase through the root system into the soil. These dependencies were confirmed in the studies by Lemanowicz and Koper (2012) and Niewiadomska (2013), who investigated the effect of PRP SOL fertiliser containing phosphorus, potassium, zinc, boron and molybdenum under an alfalfa plantation. The research showed that the fertiliser decreased the catalytic activity of acid phosphatase by activating inaccessible compounds for plants. Bielińska and Mocek-Płóciniak (2009) made similar observations. Lemanowicz and Koper (2010) also observed higher activity of these enzymes in the experimental variant which was not fertilised with phosphorus. Rotaru (2015) found that the deficit of this macroelement stimulated plants' secretion of acid phosphatases.

As far as alkaline phosphatase is concerned, most of the foliar fertilisers significantly increased the activity of this enzyme. It may have been stimulated by increased activity of the soil microorganisms reacting to organic phosphorus compounds released by soybean plants into the soil. Lemanowicz and Koper (2010) proved the correlation between the content of organic forms of phosphorus and the activity of alkaline phosphatases in soil.

With the exception of Tytanit, the other preparations applied in the experiment significantly stimulated catalase activity. As early as 1963, Koter demonstrated higher catalase activity in plants fertilised with boron. Hu and Zhu (2008) observed that fertilisation with silicon increased the activity of catalase and dehydrogenases. Romanowicz and Krzepiłko (2013) indicated that soil oxygenation and temperature significantly affected catalase activity. According to Szymczak et al. (2011), the catalytic activity of this enzyme is a good marker of physiological stresses in plants.

The results of analyses of the catalase and dehydrogenase activity enabled the calculation of the biological index of soil fertility (BIF). The variants with Metalosate potassium and Tytanit preparations had a significant influence on the BIF values, as compared with the control sample. The former preparation resulted in particularly high BIF values in the soil samples collected after the harvest of soybean plants. This effect was caused by the significant influence of these fertilisers on the activity of catalase and dehydrogenases. According to Natywa et al. (2014), mineral fertilisation, which increases the yield of crops, indirectly affects the amount of crop residue and thus increases the biochemical activity of soil after harvest.

http://www.aloki.hu ● ISSN 1589 1623 (Print) ● ISSN 1785 0037 (Online)
DOI: http://dx.doi.org/10.15666/aeer/1705_1264912666

Conclusion

When foliar fertilisation is applied, the plant extracts the necessary elements mostly through the leaves, but also through the stem and the entire aerial system. However, it is necessary to remember that this method of 'feeding' cannot replace soil fertilisation. It only quickly provides the necessary ingredients to the plant at difficult phases so as not to slow down its growth. The biostimulants and foliar fertilisers applied in our research stimulated most of the parameters of soil biochemical activity and the process of nitrogen fixation under the soybean plantation. This may have been caused by the fact that the foliar application of nutrients to the plants increased the rate of their penetration and resulted in higher efficiency of their use. Macro- and micronutrients differ in their rate of penetration but foliar fertilisation accelerates this process several times. The disadvantage of foliar fertilisation is the limited amount of the fertiliser that can be provided to plants. Therefore, this method is particularly effective when it is necessary to supply them with the elements that they need in smaller amounts, e.g. iron, boron, and molybdenum. Apart from the increased efficiency of the foliar application of micronutrients, this method is also safer for the environment and for the plant itself. The search for methods that increase the yield and biochemical parameters of the soil environment is an important part of sustainable agriculture policy.

We can observe increasing importance of legumes in sustainable agriculture. The following facts speak in favour of cultivation of this group of plants: they improve the physicochemical properties of soil, enrich the content of organic matter and leave large amounts of crop residues with high content of nitrogen. Soybean (Glycine max L.) is one of the most important crops in this group of plants. Soybean seeds contain about 40% of protein with a favourable amino acid composition and 20% of fat, with the majority of unsaturated fatty acids. Conducting further research in the search for preparations supporting the yielding capacity of soybeans, while not affecting the environment, seems necessary in the realities of modern agriculture.

Acknowledgements. This research was financed by the Ministry of Agriculture and Rural Development of the Republic of Poland in the framework of the Multi-annual Program 'Increasing the use of domestic feed protein for the production of high quality animal products in conditions of balanced development' implemented at the Department of Agronomy of the University of Life Sciences in Poznan.

REFERENCES

[1] Abusuwar, A. O., Omer, E. A. (2011): Effect of intercropping, phosphorus fertilization and rhizobium inoculation on the growth and nodulation of some leguminous and cereal forages. – Agriculture and Biological Journal of North America 2: 109-124.

[2] Bielińska, E., Mocek-Płóciniak, A. (2009): Phosphatases in the Soil Environment. – UP Pub., Poznan.

[3] Bielińska, E., Mocek-Płóciniak, A. (2012): Impact of the tillage system on the soil enzymatic activity. – Archives of Environmental Protection 38(1): 75-82.

[4] Bielińska, E. J., Futa, B., Bik-Mołodzińska, M., Szewczuk, C., Sugier, D. (2013): The impact of fertilizing agents on the enzymatic activity of soils. – Journal of Research and Applications in Agricultural Engineering 58(3): 15-19 (in Polish).

[5] Bilen, S., Bilen, M., Bardhan, S. (2011): The effects of boron management on soil microbial population and enzyme activities. – African Journal of Biotechnology 10(27): 5311-5319.

http://www.aloki.hu ● ISSN 1589 1623 (Print) ● ISSN 1785 0037 (Online)
DOI: http://dx.doi.org/10.15666/aeer/1705_1264912666

[6] Błońska, E. (2011): Soil enzymes and their importance in assessing the biological activity of forest soils on the example of nature reserves in the Polish lowlands and uplands. – Soil Science Annual 62(4): 163-172.
[7] Błońska, E., Lasota, J., Januszek, K. (2012): Enzyme activity in forest gleysols. – Soil Science Annual 63(4): 3-8 (in Polish).
[8] Bonilla, I., Bolaños, L. (2009): Mineral nutrition for legume-rhizobia symbiosis: B, Ca, N, P, S, K, Fe, Mo, Co, and Ni. A review. – Organic Farming, Pest Control and Remediation of Soil Pollutants 1: 253-274.
[9] Borowska, M., Kaszkowiak, E., Prusiński, J. (2016): Production and economic effects of enhanced cultivation technology in white lupin (*Lupines albus* L.). – Problematic Notebooks about the Progress of Agricultural Sciences 585: 97-107.
[10] Brown, P. H., Bellaloui, N., Wimmer, M. A., Bassi, E. S., Ruiz, J., Hu, H., Pfeffer, H., Dannel, F., Römheld, V. (2002): Boron in plant biology. – Plant Biology 4: 205-223.
[11] Brzezińska, M., Stępniewska, Z., Stępniewski, W., Włodarczyk, T., Przywara, G., Bennicelli, R. (2001): Effect of oxygen deficiency on soil dehydrogenase activity (pot experiment with barley). – International Agrophysics 15: 3-7.
[12] Bucher, M. (2007): Functional biology of plant phosphate uptake at root and mycorrhiza interfaces. – New Phytollogist 173(1): 11-26.
[13] Burns, R. G., DeForest, J. L., Marxsen, J., Sinsabaugh, R. L., Stromberger, M. E., Wallenstein, M. D., Weintraub, M. N., Zoppini, A. (2013): Soil enzymes in a changing environment: current knowledge and future directions. – Soil Biology and Biochemistry 58: 216-234.
[14] Calvo, P., Nelson, L., Kloepper, J. W. (2014): Agricultural uses of plant biostimulants. – Plant and Soil 383: 3-41.
[15] Das, S. K., Varma, A. (2011): Role of Enzymes in Maintaining Soil Health. – In: Shukla, G., Varma, A. (eds.) Soil Enzymology, Soil Biology 22. Springer-Verlag, Berlin.
[16] Directive 2009/128/EC of the European Parliament and of the Council of 21 October 2009 Establishing a Framework for Community Action to Achieve the Sustainable Use of Pesticides.
[17] Florek, J., Czerwińska-Kayzer, D., Jerzak, M. A. (2012): The current status and use of legume crops. – Fragmenta Agronomica 29(4): 45-55 (in Polish).
[18] Gaweł, E. (2011): The role of small-seed leguminous plants on a farm. – Water-Environment-Rural Areas 11: 73-91 (in Polish).
[19] Giannattasio, M., Vendramin, E., Fornasier, F., Alberghini, S., Zanardo, M., Stellin, F., Concheri, G., Stevanato, P., Ertani, A., Nardi, S., Rizzi, V., Piffanelli, P., Spaccini, R., Mazzei, P., Piccolo, A., Squartini, A. (2013): Microbiological features and bioactivity of a fermented manure product (Preparation 500) used in biodynamic agriculture. – Journal of Microbiology and Biotechnology 23: 644-651.
[20] Hu, X. J., Zhu, Z. J. (2008): Effect of silicon on resistance of powdery mildew and the activities of antioxidative enzymes in leaf apoplast of cucumber. – Acta Agriculturae Zhejiangensis 20(1): 67-71.
[21] IUSS Working Group WRB (2007): World Reference Base for Soil Resources 2006. First Update 2007. – World Soil Resources Reports No.103. FAO, Rome.
[22] Johnson, J. L., Temple, K. L. (1964): Some variables affecting the measurement of "catalase activity" in soil 1. – Soil Science Society of America Journal 28(2): 207-209.
[23] Kang, H., Kang, S., Lee, D. (2009): Variations of soil enzyme activities in a temperate forest soil. – Ecological Research 24(5): 1137-1143.
[24] Karaca, A., Cetin, S. C., Turgay, O. C., Kizilkaya, R. (2010): Soil enzymes as indication of soil quality. – Soil Enzymology 22: 119-148.
[25] Koter, M. (1963): Research on the impact of boron on the growth and development of plants. – Soil Science Annual 13(1): 185-211.

http://www.aloki.hu ● ISSN 1589 1623 (Print) ● ISSN 1785 0037 (Online)
DOI: http://dx.doi.org/10.15666/aeer/1705_1264912666

[26] Kumar, N., Misra, R., Shankhdhar, S. C., Shankdhar, D. (2015): Effect of foliar application of boron on growth, yiels, chlorophyll, amylose and nitrate reductase activity in rice. – ORYZA - An International Journal on Rice 52(2): 123-130.
[27] Lemanowicz, J., Koper, J. (2010): Changes in the content of available phosphorus and soil phosphatase activity as a result of fertilization. – Soil Science Annual 61(4): 140-145 (in Polish).
[28] Lemanowicz, J., Koper, J. (2012): Activity of phosphatase and the content of phosphorus in soil under selected crops fertilised with slurry. – Proceedings of ECOpole 6(1): 239-243.
[29] Massawe, F., Mayes, S., Cheng, A. (2016): Crop diversity: an unexploited treasure trove for food security. – Trends in Plant Science 21(5): 365-368.
[30] Nannipieri, P., Kandeler, E., Ruggiero, P. (2002): Enzyme Activities and Microbiological and Biochemical Processes in Soil. – In: Burns, R. G., Dick, R. P. (eds.) Enzymes in the Environment. Activity, Ecology and Applications. Marcel Dekker, New York, pp. 1-33.
[31] Napora, A., Grobelak, A. (2014): Sewage sludge influence on microbiological and biochemical soil activity. – Engineering and Protection of Environmental 17(4): 619-630.
[32] Natywa, M., Selwet, M., Maciejewski, T. (2014): Effect of some agrotechnical factors on the number and activity soil microorganisms. – Fragmenta Agronomica 31(2): 56-63 (in Polish).
[33] Nardi, S., Pizzeghello, D., Schiavon, M., Ertani, A. (2016): Plant biostimulants: physiological responses induced by protein hydrolyzed-based products and humic substances in plant metabolism. – Scientia Agricola 73(1): 18-23.
[34] Niewiadomska, A. (2013): Assessment of the Impact of PRP SOL Fertiliser and Co-inoculation on the Process Diazotrophy, Biological and Chemical Properties of Soil and the Crop Condition under Clover and Alfalfa Cultivation. – UP, Poznań (in Polish).
[35] Niewiadomska, A., Sulewska, H., Wolna-Maruwka, A., Ratajczak, K., Głuchowska, K., Waraczewska, Z., Budka, A. (2018a). An assessment of the influence of co-inoculation with endophytic bacteria and rhizobia, and the influence of PRP SOL and PRP EBV fertilisers on the microbial parameters of soil and nitrogenase activity in yellow lupine (*Lupinus luteus* L.) cultivation. – Polish Journal of Environmental Studies 27(6): 2687-2702.
[36] Niewiadomska, A., Sulewska, H., Wolna-Maruwka, A., Waraczewska, Z., Budka, A., Ratajczak, K. (2018b): An assessment of the influence of selected herbicides on the microbial parameters of soil in maize (Zea mays) cultivation. – Applied Ecology and Environmental Research 16(4): 4735-4752.
[37] Poole, P., Ramachandran, V., Terpolilli, J. (2018): Rhizobia: from saprophytes to endosymbionts. – Nature Reviews Microbiology 16(5): 291-303.
[38] Romanowicz, A., Krzepiłko, A. (2013): Volumetric determination of catalase activity in various organs of the primocane-fruiting polana variety of raspberry *Rubus idaeus* L. and in soil it is grown on. – Polish Journal Agronomy 15: 49-53 (in Polish).
[39] Rotaru, V. (2015): Responses of acid phosphatase activity on the root surface and rhizospheric soil of soybean plants to phosphorus fertilization and rhizobacteria application under low water supply. – Scientific Papers-Series A, Agronomy 58: 295-300.
[40] Saviozzi, A., Levi-Minzi, R., Cardelli, R., Riffaldi, R. (2001): A comparison of soil quality in adjacent cultivated, forest and native grassland soils. – Plant and Soil 233: 251-259.
[41] Saviozzi, A., Cardelli, R., Levi-Minzi, R., Riffaldi, R. (2004): Evolution of biochemical parameters during composting of urban wastes. – Compost Science and Utilization 12(2): 153-160.
[42] Sawicka, A. (1983): The ecological aspects of dinitrogen fixation. – Annals of the University of Agriculture in Poznan. Scientific Dissertations 134: 1-57 (in Polish).

http://www.aloki.hu ● ISSN 1589 1623 (Print) ● ISSN 1785 0037 (Online)
DOI: http://dx.doi.org/10.15666/aeer/1705_1264912666

[43] Selivanovskaya, S. Y., Latypova, V. Z., Gubaeva, L. A. (2006): Microbiological processes in gray forest soil treated with sewage sludge compost. – European Journal of Soil Science 39(4): 443-449.
[44] Stachowski, P. (2010): Evaluation of meteorological droughts in post-mining areas in Poland in Konin area. – Central Pomeranian Scientific Society for Environmental Protection. Annual Set the Environ. Protect. 12: 587.
[45] Stagnari, F., Maggio, A., Galieni, A., Pisante, M. (2017): Multiple benefits of legumes for agriculture sustainability: an overview. – Chemical and Biological Technologies in Agriculture 4(1): 1-13.
[46] Swędrzyńska, D., Zielewicz, W., Przybył, P., Starzyk, J. (2013): Effect of bio soil conditioner on microbial state and enzymatic activity of soil under Lolium perenne cultivation. – Grassland Science in Poland 16: 111-128.
[47] Symanowicz, B., Pala, J., Kalembasa, S. (2005): Influence of biological reduction of N2 on the uptake of nitrogen by goat's rue (Galega orientalis Lam.). Acta Scientiarum Polonorum. – Agricultura 4(2): 93-99 (in Polish).
[48] Szewczuk, C., Sugier, D. (2009): General characteristics and types of foliar fertilizers offered on the Polish market. – Annales Universitatis Mariae Curie-Skłodowska, Agricultura 64(1): 29-36.
[49] Szymczak, J., Kłódka, D., Smolik, B., Pawlica, M. (2011): Effect of cadmium salt on the activity of oxidative stress enzymes in soil and maize (Zea mays var. saccharata). – Environmental Protection and Natural Resources 48: 210-215.
[50] Tabatabai, M. A., Bremner, J. M. (1969): Use of p-nitrophenyl phosphate for assay of soil phosphatase activity. – Soil Biology and Biochemistry 1(4): 301-307.
[51] Taran, N. Y., Gonchar, O. M., Lopatko, K. G., Batsmanova, L. M., Patyka, M. V., Volkogon, M. V. (2014): The effect of colloidal solution of molybdenum nanoparticles on the microbial composition in rhizosphere of Cicer arietinum L. – Nanoscale Research Letters 9(1): 289-297.
[52] Thalmann, A. (1968): Zur Methodik der Bestimmung der Dehydrogenase aktivität im Boden mittels triphenytetrazoliumchlorid (TTC). – Landwirtsch Forsch 21: 249-258.
[53] Utobo, E. B., Tewari, L. (2015): Soil enzymes as bioindicators of soil ecosystem status. – Applied Ecology and Environmental Research 13(1): 147-169.
[54] Van Reeuwijk, L. P. (2002): Procedures for Soil Analysis. 6th Ed. – ISRIC, Wageningen, Netherlands.
[55] Vernieri, P., Ferrante, A., Borghesi, E., Mugnai, S. (2006): Biostimulants: a tool for improving quality and yield (=Biostimolanti: uno strumento per migliorare la qualità delle produzioni). – Fertilitas Agrorum 1: 17-22.
[56] Vieira, R. F., Cardoso, E. J. B. N., Vieira, C., Cassini, S. T. A. (1998): Foliar application of molybdenum in common beans. I. Nitrogenase and reductase activities in a soil of high fertility. – Journal of Plant Nutrition 21: 169-180.
[57] Walter, H. (1976): Vegetation Zones and Climate. – PWRiL, Warszawa, pp. 26-31 (in Polish).
[58] Weisany, W., Raei, Y., Allahverdipoor, K. H. (2013): Role of some of mineral nutrients in biological nitrogen fixation. – Bulletin of Environment, Pharmacology and Life Sciences 2(4): 77-84.
[59] Zahran, H. H. (1999): Rhizobium-legume symbiosis and nitrogen fixation under severe conditions and in arid climate. – Microbiology and Molecular Biology Reviews 63(4): 968-989.

http://www.aloki.hu ● ISSN 1589 1623 (Print) ● ISSN 1785 0037 (Online)
DOI: http://dx.doi.org/10.15666/aeer/1705_1264912666